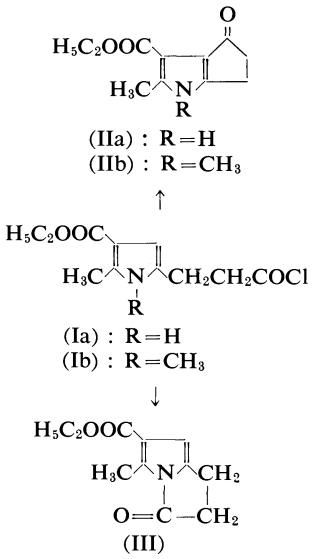
# The Reactions of Methyl β-(Substituted-2-pyrrolyl)-propionate and Ethyl β, β-Bis(substituted-2-pyrrolyl)-propionate with Some Formylating Reagents*

By Hiroyuki SHINOHARA, Masato SAWADA and Eiji IMOTO

(Received January 6, 1964)

In a preceding paper[1] we reported on an attempt to obtain cyclopenteno(b)pyrrole derivatives, the skeletal structure of which is present in chlorophyll-a and -b. The Friedel-Crafts cyclization of β-(3-ethoxycarbonyl-2-methyl-5-pyrrolyl)-propionyl chloride (Ia) failed to yield 3-ethoxycarbonyl-2-methyl-1, 4, 5, 6-tetrahydrocyclopenta(b)pyrrol-4-one (IIa) and this reaction gave an undesired product III, though in it β-(1, 2-dimethyl-3-ethoxycarbonyl-5-pyrrolyl)-propionyl chloride (Ib) afforded 1, 2-dimethyl-3-ethoxycarbonyl-4, 5, 6-trihydrocyclopenta(b)pyrrol-4-one (IIb).



(III)

As an alternative method of synthesizing a compound with a cyclopenteno(b)pyrrole ring, we propose to condense the active α-methylene group of the side chain of VIII or XII with a formyl group at the neighboring β-position of the pyrrole ring. The formylation of α, α', β'-trisubstituted pyrroles with such formylating reagents as (a) dimethylformamide and phosphorus oxychloride, (b) dichloromethyl ethyl ether and stannic chloride, or (c) dichloromethyl ethyl ether and boron trifluoride-etherate, is reported in this paper. As is shown in Fig. 1, these formylating reagents gave incoherent results. The formylating reagents a and b gave the normally formylated products V or VII respectively as the result of the reaction with ethyl 2, 5-dimethyl-3-pyrrolecarboxylate (IV)[2] or methyl β-(1, 2-dimethyl-3-ethoxycarbonyl-5-pyrrolyl)-propionate (VI),[1] but the reactions of these compounds with c resulted in the recovery of the starting materials. From methyl β-(3-ethoxycarbonyl-2-methyl-5-pyrrolyl)-propionate (VIII),[3] two different products were obtained. One is the normally formylated product IX, resulting from the reaction with a or b; the other is bis(4-ethoxy carbonyl-2-methoxycarbonylethyl-5-methyl-3-pyrrolyl)-carbinol (X), resulting from the reaction with c. From ethyl β, β-bis(4-ethoxycarbonyl-5-methyl-2-pyrrolyl)-propionate (XII)[4] two kinds of products were also derived; one is the normally formylated product XIII, resulting from the reaction with a, while the other is a compound, $C_{22}H_{28}N_2O_7$, the product of the reaction with a or b. The structures of all the normally formylated products, V, VII, IX and XIII, have been concluded to be as shown in Fig. 1 on the basis of the results of their elementary analyses, infrared spectra, the formation of 2, 4-dinitrophenylhydrazones, and elementary analyses of the 2, 4-dinitrophenylhydrazones. Moreover, the structure of the carbinol X has been assumed to be as given in the formula on the basis of the results of elementary analysis, the measurement of the molecular weight, and the infrared spectrum. Furthermore, the carbinol X gave a 2, 4-dinitrophenylhydrazone as the result of the reaction with 2, 4-dinitrophenylhydrazine in an acidic medium; this 2, 4-dinitrophenylhydrazone

* Studies of Pyrroles, Part IX. Part VIII: H. Shinohara and E. Imoto, *J. Chem. Soc. Japan, Pure Chem. Sec.* (*Nippon Kagaku Zasshi*), **83**, 945 (1962).

Part of the data given in this article were presented at the 14th Annual Meeting of the Chemical Society of Japan, Tokyo, April, 1961.

1) H. Shinohara, G. Shichijo and E. Imoto, *J. Chem. Soc. Japan, Pure Chem. Sec.* (*Nippon Kagaku Zasshi*), **83**, 615 (1962).

2) G. Korschun, *Ber.*, **37**, 2196 (1904).

3) A. Treibs and K. H. Michl, *Ann.*, **589**, 163 (1954).

4) H. Shinohara, H. Shiba, M. Sawada and E. Imoto, *J. Chem. Soc. Japan, Pure Chem. Sec.* (*Nippon Kagaku Zasshi*), **83**, 618 (1962).

TABLE I.

| Starting compound | Method* | Reaction temp., °C | Reaction time, min. | Resulting compound | Yield % |
|---|---|---|---|---|---|
| IV[2] | a | 50—55 | 30 | V | 84** |
| IV[2] | b | 0 | 15 | V | 40 |
| VI[1] | a | Room temp. | 30 | VII | 90 |
| VI[1] | b | 0 | 10 | VII | 14 |
| VIII[3] | a | 30 | 30 | IX | 56 |
| VIII[3] | b | 0 | 10 | IX | 4.5 |

* The procedures are shown in the synthesis of XIII and compound $C_{22}H_{28}N_2O_7$.
** This compound has been prepared by Fischer et al.[6] by the Gattermann formylation of IV with hydrogen cyanide and hydrogen chloride in yield of 75%.

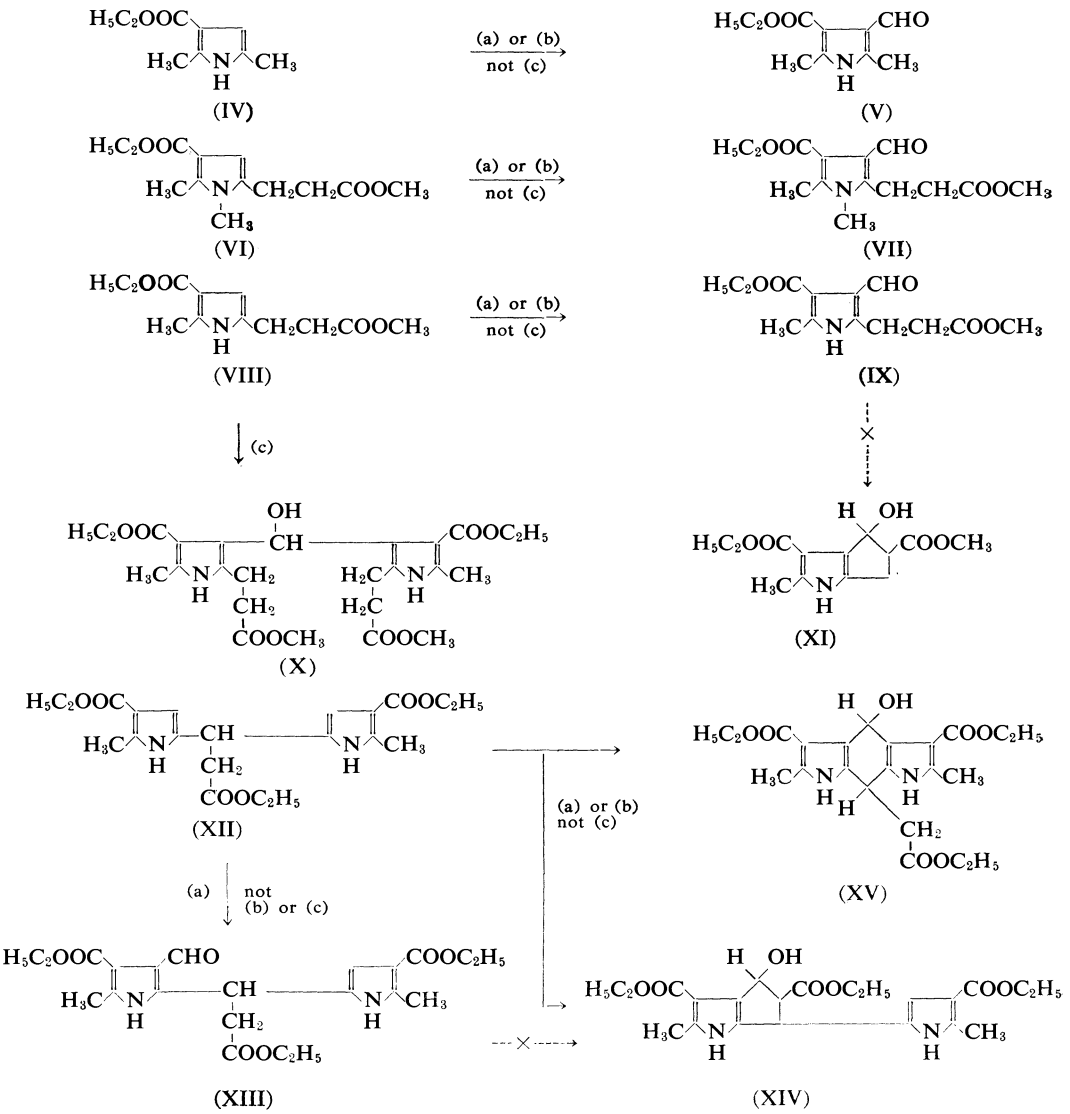



Fig. 1.

was identical with that derived from IX. This fact is also an evidence of the structure of X.

The compound $C_{22}H_{28}N_2O_7$ is an isomer of XIII, but it has no formyl group attached to the carbon atom or to the nitrogen atom of the pyrrole ring. Therefore, the structure of the compound $C_{22}H_{28}N_2O_7$ may be either XIV or XV.

The infrared spectrum definitely shows the presence of a hydroxyl group at 3500 $cm^{-1}$ and the compound $C_{22}H_{28}N_2O_7$ has a band at 3000 $cm^{-1}$ which should be assigned[5] to a stretching vibration of the C–H bond in the pyrrole ring. The compound $C_{22}H_{28}N_2O_7$ seems to have the structure formulated as XIV, because in the structure XV there is no hydrogen atom attached to the pyrrole nucleus. However, the NMR spectra of the compound $C_{22}H_{28}N_2O_7$ do not show a signal due to protons of the pyrrole ring. Attempts to derive XV from XIII in the presence of an acid as a catalyzer have also been unsuccessful, as have attempts to derive XIV from XIII in the presence of sodium methoxide as a catalyzer. From the results previously obtained, it is impossible to determine which structure should be assigned to the compound $C_{22}H_{28}N_2O_7$.

TABLE II.

| Compound | | M. p. °C | Analyses % Nitrogen Calcd. | Found |
|---|---|---|---|---|
| $C_{10}H_{13}NO_3$ | (V) | 149—151 | 7.74 | 7.76 |
| $C_{14}H_{19}NO_5$ | (VII) | 86—87 | 4.98 | 5.03 |
| $C_{13}H_{17}NO_5$ | (IX) | 113.5—114.5 | 5.24 | 5.38 |

2, 4-Dinitrophenylhydrazone of IX was prepared by the usual method. M. p. 202—205°C (decomp.)
Found: N, 15.68. Calcd. for $C_{19}H_{21}N_5O_8$: N, 15.44%.

## Experimental

**Bis(4-ethoxycarbonyl-2-methoxycarbonylethyl-5-methyl-3-pyrrolyl)-carbinol (X).**—To a cold mixture of 1 g. of VIII[3] and 4 g. of dichloromethyl ethyl ether, there was added 3 ml. of borontrifluoride-etherate under ice cooling. The reaction mixture was warmed to 49—50°C and stirred at this temperatue for 30 min., diluted with iced water, and neutralized to Congo red with a saturated solution of sodium acetate in order to precipitate crystals. These crystals were collected by filtration, washed with cold water, and recrystallized from aqueous ethanol repeatedly to give colorless needles with a m. p. of 150—151.5°C in a yield of 350 mg. (33%).
Found: C, 59.29; H, 6.66; mol. wt. (Rast), 508. Calcd. for $C_{25}H_{34}N_2O_9$: C, 59.30; H, 6.72%; mol. wt., 506.

**Reaction with 2, 4-Dinitrophenylhydrazine.** — A solution of 100 mg. of X was mixed with an acidic solution of 2, 4-dinitrophenylhydrazine, warmed for a short time, and allowed to stand in order to precipitate crystals, which were then recrystallized from ethanol. The m. p., 202—204°C (decomp.), was undepressed on admixture with 2, 4-dinitrophenylhydrazone of IX.

Found: N, 15.71. Calcd. for $C_{19}H_{21}N_5O_8$: N, 15.44%.

**Ethyl β-(4-Ethoxycarbonyl-3-formyl-5-methyl-2-pyrrolyl)-β-(4-ethoxycarbonyl-5-methyl-2-pyrrolyl)-propionate (XIII).** — To a cold solution of 3 g. of XII[4] in 3.1 g. of dimethylformamide, 2.3 g. of phosphorus oxychloride was added drop by drop at room temperature. The reaction mixture was stirred for 60 hr. at room temperature in order to precipitate a solid material stained by a resinous material, diluted with 70 ml. of a saturated solution of sodium acetate, and stirred for a further two days. After the aqueous layer of the reaction mixture had been removed by decantation, the solid material was repeatedly washed with water and then with a small amount of ethanol to remove the resinous material; then the material was collected by filtration, washed with water, and treated with boiling benzene. The insoluble part in benzene was recrystallized from ethanol to obtain the desired product, XIII, in a yield of 200 mg. (6.3%), m. p. 186—188°C (decomp.).
Found: C, 61.14; H, 6.57; N, 6.62. Calcd. for $C_{22}H_{28}N_2O_7$: C, 61.11; H, 6.49; N, 6.49%. 2, 4-Dinitrophenylhydrazone of XIII, m. p. 187~188°C.
Found: N, 13.78. Calcd. for $C_{28}H_{31}N_6O_{10}$: N, 13.67%.

**The Compound $C_{22}H_{28}N_2O_7$ XIV or XV.**—a) In to a mixture of 4 g. of XII[4] and 1.5 g. of dimethyl formamide, 1.53 g. of phosphorus oxychloride was gradually stirred at 40°C. After the addition, the reaction mixture was warmed to 60°C, kept at this temperature for 15 min., mixed with iced water, and then neutralized to Congo red with a saturated solution of sodium acetate. The precipitate thereby yielded was collected by filtration, washed with cold water, and recrystallized from aqueous ethanol. Yield, 1.2 g. Pale yellow crystals, m. p. 217—219°C (decomp.).

b) To a cold mixture of 1 g. of XII and 16 g. of dichloromethyl ethyl ether, 2 ml. of stannic chloride was added at once under ice cooling. After having been stirred for 10 min., the reaction mixture was poured into iced hydrochloric acid. Since the oily product which separated solidified slowly, it was collected by filtration, washed with cold water, and dissolved in warm ethanol. After the ethanolic solution had been treated with norite, it was diluted with water to reprecipitate the product. The product was then washed with a few drops of ethanol and repeatedly recrystallized from aqueous ethanol to obtain pale yellow crystals of the compound $C_{22}H_{28}N_2O_7$. M. p. 215—217°C (decomp.), undepressed with the sample obtained above at a) on admixture. Yield, 50 mg.
Found: C, 60.94; H, 6.50; N, 6.56. Calcd. for $C_{22}H_{28}N_2O_7$: C, 61.11; H, 6.49; N, 6.49%.

**An Attempt to Cyclize Methyl β-(4-Ethoxycarbonyl-3-formyl-5-methyl-2-pyrrolyl)-propionate (VII) into 3-Ethoxycarbonyl-5-methoxycarbonyl-2-methyl-1, 4, 5, 6-tetrahydrocyclopenta(b)pyrrol-4-ol (XI).**—a) To 100 ml. of an ethereal solution of sodium ethoxide prepared from 50 mg. of sodium 500 mg. of VII was added; the mixture was then refluxed for 5 hr. After the ether had been evaporated, the residue was dissolved in water and filtered.

5) A. R. Katrifzky, *Quart. Rev.*, **13**, 353 (1959).
6) H. Fischer and W. Zerweck, *Ber.*, **55**, 1942 (1922).

The filtrate was acidified to obtain a solid material. The solid material was washed with iced water and recrystallized from aqueous ethanol to obtain 180 mg. of β-(3-ethoxycarbonyl-4-formyl-2-methyl-5-pyrrolyl)-propionic acid, m. p. 166—167°C, which is soluble in an aqueous solution of sodium bicarbonate.

Found: N, 5.40. Calcd. for $C_{12}H_{15}NO_5$: N, 5.54%.

b) A mixture of 500 mg. of VII, 0.5 ml. of triethylamine, and 10 ml. of absolute ethanol was refluxed for 3 hr. and then poured into iced water to precipitate crystals. The crystals were collected by filtration, washed with water, and recrystallized from water to recover the starting material (about 500 mg.) with a m. p. of 113—114°C. Similarly, the reaction of VII with dispersed sodium in benzene at the refluxing temperature or with hydrogen chloride in absolute ethanol under reflux also resulted in the recovery of the starting material.

**Attempts to Cyclize XIII into XIV.**—a) To 80 ml. of an ethereal solution of sodium ethoxide prepared from 50 mg. of sodium, 300 mg. of XIII was added; the mixture was then refluxed for 3 hr. After it had evaporated, the residue was treated with iced hydrochloric acid and filtered. The solid material was washed with iced water and recrystallized from ethanol to recover the starting material.

b) The reaction of XIII with hydrogen chloride in absolute ethanol at reflux also resulted in the recover of the starting material.

*Infrared Spectra.* — These were recorded with a Hitachi EPI-2 spectrophotometer; the measurements were made on pressed disks of potassium bromide.

The authors wish to thank Dr. Naohiro Hayakawa of the Japan Atomic Energy Research Institute for his measurements and for invaluable advice on the assignment of NMR spectra.

*Department of Applied Chemistry*
*University of Osaka Prefecture*
*Sakai, Osaka*

# Poly-L-histidine and the Copolymer of L-Histidine with L-Glutamic Acid. Their Synthesis and Catalytic Activity on the Hydrolysis of *p*-Nitrophenyl Acetate*1

By Tomoo SAITO

(Received April 9, 1964)

It has previously been established that the histidine residue plays an important role in certain proteolytic enzymes. Poly-L-histidine is, therefore, an interesting material to use as a model compound in order to study the catalytic behavior of the histidine residue.

Poly-L-histidine has been prepared by Patchornik et al.[1] However, better results have been achieved in the present experiments, where the synthesis of homo- and co-polymers of L-histidine by the carbothiophenyl method[2] will be described. An attempt to polymerize 1-benzyl-$\alpha$, *N*-carbothiophenyl-L-histidine with $\gamma$-benzyl-L-glutamate *N*-carboxy anhydride (NCA) and their catalytic activities will also be described.

**The Synthesis and Properties of Poly-L-histidine.**—Two series of reactions are outlined in scheme A. In one process, the free imidazole group was used, and in the other, the imidazole imino group, which was protected by a benzyl group.

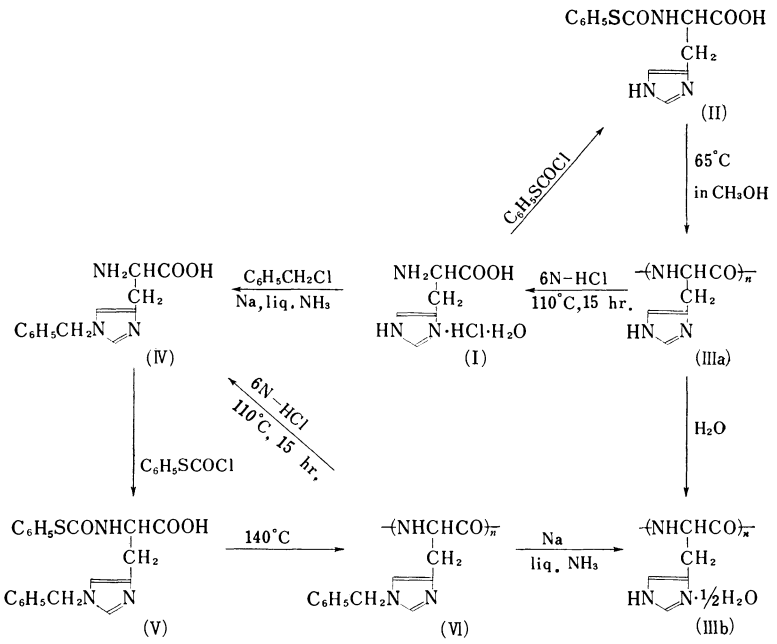
L-Histidine hydrochloride (I) was treated with sodium methylate to give free L-histidine, from which $\alpha$, *N*-carbothiophenyl-L-histidine (II) was obtained in a 43% yield by the action of carbothiophenyl chloride. II was polymerized in methanol at 65°C for 3 weeks to yield poly-L-histidine (mol. wt.$\fallingdotseq$2040, $n\fallingdotseq$15)*2 (IIIa). 1-Benzyl-$\alpha$, *N*-carbothiophenyl-L-histidine (V) was obtained from 1-benzyl-L-histidine (IV) in a 81% yield by a reaction with carbothiophenyl chloride in an anhydrous basic medium. In order to obtaine poly-1-benzyl-L-histidine (mol. wt.$\fallingdotseq$2830, $n\fallingdotseq$12.5)*2 (VI), V was polymerized at 140°C in vacuo for ten hours. The reduction of VI with metallic sodium in liquid ammonia gave poly-L-histidine (IIIb). Since the average degree of the polymerization of IIIb was shown to be ca. 13.3 (mol. wt.$\fallingdotseq$1940),*2 it was concluded that the average chain length of VI was unaffected by the reduction. The insolubility of

*1 T. Saito and J. Noguchi, Partially presented at the 15th Annual Meeting of the Chemical Society of Japan, Kyoto, April, 1962.

1) A. Patchornik, A. Berger and E. Katchalski, *J. Am. Chem. Soc.*, **79**, 5227 (1957).

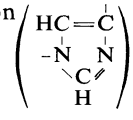
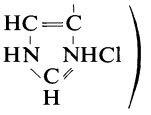
2) J. Noguchi, *J. Chem. Soc. Japan, Pure Chem. Sec.* (*Nippon Kagaku Zassi*), **74**, 961 (1953).

*2 The molecular weight was determined by a terminal end group titration with anhydrous sodium methylate.

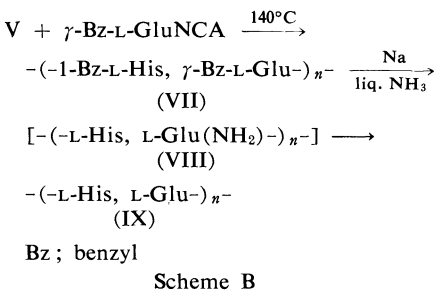


Scheme A

VI in an alkaline solution can perhaps be explained by the absence of any free imidazole group in VI, and the solubilities of IIIa and IIIb in a dilute acid and in a strongly alkaline solution (above 3 N) showed that they behaved as polyampholytes. IIIb contained half a molecule of crystalline water per histidine residue; this could not be removed by drying at 100°C for 5 hr. in vacuo on phosphorus pentoxide.[1] However, neither water nor methanol was contained in IIIa. When IIIa, ($[\alpha]_D = -19.5°$),[1] was hydrolyzed with acid, L-histidine hydrochloride monohydrate resulted; this was proved to be optically pure ($[\alpha]_D = +13.0°$).[3] The configuration of the histidine residue in IIIa was, therefore, unaffected in the process of the synthesis.

The ultraviolet absorption spectra of IIIa showed the absorption maximum at 294 mμ ($\varepsilon = 29.8$) in 1 N sodium hydroxide, and at 275 mμ ($\varepsilon = 12.8$) in 1 N hydrochloric acid respectively. The former absorption band may be attributed to the imidazolium ion  and the latter, to the imino group 

**The Synthesis of the Copolymer of L-Histidine with L-Glutamic Acid.**—The synthetic process of the copolymer is shown in scheme B.



Scheme B

The bulk copolymerization of the equi-molar V and γ-benzyl-L-glutamate NCA gave the copoly(1-benzyl-L-histidine, γ-benzyl-L-glutamate)$_n$ (1 : 1) (VII) with an average degree of polymerization of ca. 25 (mol. wt.≒11300)*2 and in a 86% yield. Copoly(L-histidine, L-glutamic acid)$_n$ (1 : 1) (IX) was obtained from VII by reduction with metallic sodium in liquid ammonia in order to remove the protected groups. Van Slyke terminal nitrogen analysis for IX indicated that neither a remarkable decrease in its chain length nor the cyclization of the *N*-terminal residue had taken place and that the average degree of the polymerization of IX was ca. 20 (mol. wt.≒5320). Poly-β-benzyl-L-aspartate was converted to the β-amide of the polymer (polyasparagine) by treatment with liquid ammonia,[4] analogously,

3) L-Histidine HCl $H_2O$: $[\alpha]_D^{24} = +13.15°$ (in 6 N hydrochloric acid), S. Akabori and S. Mizushima, "Protein Chemistry" (Tanpakushitu Kagaku), Vol. 1, Kyoritsu Shuppan K. K., Tokyo (1952), p. 112.

4) J. Noguchi, T. Saito and M. Asai, *J. Chem. Soc. Japan, Pure Chem. Sec.* (*Nippon Kagaku Zasshi*), **81**, 620 (1960).

poly-γ-methyl-L-glutamate was converted to the γ-hydrazide of the polymer by treatment with hydrazine.[5] The elementary analysis for IX, however, proved that the glutamate residues were reduced to free glutamic acid residues. The discrepancy mentioned above might be due to the fact that a possible intermediate, VIII, was hydrolyzed to give IX in an alkaline treatment during the isolation of IX.

**Catalytic Activity on the Hydrolysis of *p*-Nitrophenyl Acetate.** — In a previous work,[6] catalytic activity on the hydrolysis of *p*-nitrophenyl acetate was examined in many histidine-containing oligopeptides and some polypeptides, and it was found that amino acids which were adjacent to the *N*- or the *C*-terminal of histidine through the peptide linkage increased the activity of histidine. However, the activity was not increased by the polymerization of these oligomers. For example, the activity of carnosine (β-alanyl-L-histidine) was 2.40 times that of histidine, while that of ε-aminocaproylhistidine was much the same as that of histidine. Each of the polymers prepared from carnosine and ε-aminocaproylhistidine (i. e., polycarnosine (poly-β-alanyl-L-histidine) and poly ε-aminocaproylhistidine), had the same activity as its monomer.

The activities of IIIa and IX on the hydrolysis of *p*-nitrophenyl acetate were determined by on the basis of the rate of appearance of *p*-nitrophenylate ions. It was observed that the catalytic activities of IIIa and IX were, respectively, 1.43 and 1.45 times that of L-histidine. The ratio, 1.43 of IIIa which has an average degree of polymerization ($n \fallingdotseq 15$), agreed with that (1.40) of the low molecular weight preparation ($n \fallingdotseq 3.3$).[6],*3 The ratio of IX, 1.45, agreed approximately with the average of the ratios, 1.64 in L-glutamyl-L-histidine and 1.12 in L-histidyl-L-glutamic acid. The activation of the hydrolytic effect for the substrate was, therefore, not affected by the increase in the degree of polymerization. The results concerning IX, however, seemed to suggest that L-histidine and L-glutamic acid were arranged irregularly in the copolymer chain.

## Experimental

All melting points are uncorrected.

**α, *N*-Carbothiophenyl-L-histidine (II).** — L-Histidine hydrochloride monohydrate (10 g.) was added to 2 N sodium methylate in methanol (47.8 ml.) at 0—5°C, and then carbothiophenyl chloride (9.0 g.) was vigorously stirred into the solution at −5°C. The resulting precipitates were filtered, and from the filtrate, II (m. p. 165—167°C (decomp.)) was obtained in a 48% (6.0 g.) yield.

Found: C, 53.5; H, 4.50; N, 14.4; S, 11.3; equiv. wt. 286 and 149 (determined by anhydrous perchloric acid and sodium methylate titration respectively). Calcd. for $C_{13}H_{13}O_3N_3S$: C, 53.6; H, 4.48; N, 14.4; S, 11.0%; equiv. wt. 291.3, 145.6.

**Poly-L-histidine (IIIa).** — II (1.0 g.) was dissolved in anhydrous methanol (15 ml.), and the atmosphere was replaced with carbon dioxide. The polymerization was carried out in a sealed tube at 65°C for 3 weeks. The resulting precipitate was collected by centrifugation, washed with methanol, and dried to yield 0.3 g. (64%) of IIIa, which gave positive biuret and Pauli reactions, $[\alpha]_D^{32} = -19.5°$ (*c* 0.77, glacial acetic acid). IIIa was soluble in glacial acetic acid and dichloroacetic acid, but insoluble in alcohol, acetone, and ether. It also dissolved in dilute hydrochloric acid and 3 N sodium hydroxide, but it was insoluble in water.

Found: C, 52.1; H, 5.17; N, 30.2; equiv. wt. 135 (determined by perchloric acid titration). Calcd. for $C_6H_7ON_3$: C, 52.5; H, 5.15; N, 30.6%; equiv. wt. 137.

**1-Benzyl-α, *N*-carbothiophenyl-L-histidine (V).** — 1-Benzyl-L-histidine[7] (10 g.) was treated with carbothiophenyl chloride (7.7 g.) in the presence of 2 N sodium methylate in methanol (20.4 ml.) at −5°C. The precipitate was collected by filtration, washed with warm water and then with distilled water, and dried to yield 12.5 g. (81%) of V (m. p. 143°C).

Found: C, 62.5; H, 5.01; N, 11.1; S, 8.42; equiv. wt. 378 and 189 (determined by perchloric acid and sodium methylate titration respectively). Calcd. for $C_{20}H_{19}O_3N_3S$: C, 63.0; H, 4.99; N, 11.0; S, 8.40%; equiv. wt. 381.5, 190.7.

**Poly-1-benzyl-L-histidine (VI).** — V (2 g.) was added to dioxane (2 ml.), and the atmosphere was replaced with nitrogen. Polymerization was carried out at 140°C for 30 min., and then it was continued in vacuo at the same temperature for 10 hr. The solidified reaction mixture was triturated with acetone and ether. The precipitate was contrifugated, washed with ether, and dried to yield 1.1 g. (93%) of VI, which gave a negative Pauli reaction, $[\alpha]_D^{32} = +43.5°$ (*c* 1.86, benzyl alcohol), $[\alpha]_D^{25} = -20.3°$C (*c* 0.94, glacial acetic acid). VI was soluble in chloroform, *N*, *N*-dimethylformamide, benzyl alcohol, glacial acetic acid, and dichloroacetic acid. VI was dissolved in 0.1 N hydrochloric acid and precipitated from this solution by neutralization with alkali, but it was insoluble in concentrated hydrochloric acid and caustic alkali.

Found: C, 68.3; H, 5.83; N, 18.4; equiv. wt. 230 (determined by perchloric acid titration). Calcd. for $C_{13}H_{13}ON_3$: C, 68.7; H, 5.77; N, 18.5%; equiv. wt. 227.3.

**Poly-L-histidine Hemi-hydrate (IIIb).** — VI ($n \fallingdotseq 12.5$) (1.0 g.) was suspended in anhydrous liquid

5) V. Bruckner, J. Kovacs and K. Kovacs, *J. Chem. Soc.*, **1953**, 1512.

6) J. Noguchi and T. Saito, "Polyamino Acid, Polypeptides, and Proteins," Ed. by M. A. Stahmann, University of Wisconsin Press, Madison (1962), p. 313.

*3 In this case, each adjoining histidine residue is considered to be activated up from 1.00 to 1.40.

7) V. du Vigneaud and O. K. Behrens, *J. Biol. Chem.*, **117**, 27 (1937).

ammonia (50 ml.); finely divided metallic sodium (ca. 2 g.) was added to the mixture over a period of 15 min. until a blue color persisted for at least 5 min. The excess sodium was then discharged with ammonium chloride, and the ammonia was allowed to evaporate spontaneously. The residue was dissolved in 1 N hydrochloric acid (10 ml.). After the solution had been extracted with 20 ml. of ether, the aqueous layer was filtered and neutralized with 1 N sodium hydroxide. The precipitates were collected by centrifugation and washed with water. The product was dried in vacuo on phosphorus pentoxide at 100°C for 5 hr. to yield 0.5 g. (83%) of IIIb. which gave positive biuret and Pauli reactions, $[\alpha]_D^{32} = -13.3°$ (*c* 1.24, glacial acetic acid). The solubilities of IIIb were the same as those of IIIa.

Found: C, 48.8; H, 5.59; N, 28.9. Calcd. for $C_6H_7ON_3\,1/2\,H_2O$: C, 49.3; H, 5.50; N, 28.8%.

**The Hydrolysis of Poly-1-benzyl-L-histidine.**—A suspension of VI (0.1 g.) in 6 N hydrochloric acid (2.0 ml.) was heated at 110°C for 15 hr. in a sealed tube. From the hydrolysate, 0.08 g. of 1-benzyl-L-histidine melting at 241°C was obtained by neutralization with 6 N sodium hydroxide and recrystallization from water.

Found: Equiv. wt. 240 and 119 (determined by sodium methylate and perchloric acid titration respectively). Calcd. for $C_{13}H_{15}O_2N_3$: Equiv. wt. 245, 122.5.

**The Hydrolysis of Poly-L-histidine.**—IIIa (0.1 g.) was hydrolyzed under the same conditions as VI. When the hydrolysate was worked up in the usual manner, it gave L-histidine hydrochloride monohydrate (0.07 g., m. p. 160°C, $[\alpha]_D^{25} = +13.0°$ (*c* 1.15, 6 N hydrochloric acid)).

**Poly-L-histidine Hemi-hydrate (IIIb) from Poly-L-histidine (IIIa).**—IIIa (0.3 g.) was dissolved in 1 N hydrochloric acid (2.0 ml.) and the solution was filtered, then 1 N sodium hydroxide (2.0 ml.) was added to the filtrate. The precipitates were collected by centrifugation and washed with cold water. The analytical sample was dried on phosphorus pentoxide in vacuo at 100°C for 5 hr.

Found: C, 48.9; H, 5.54; N, 28.3; equiv. wt. 143 (determined by perchloric acid titration). Calcd. for $C_6H_7ON_3\,1/2\,H_2O$: C, 49.3; H, 5.50%; N, 28.8%; equiv. wt. 146.

**Copoly(1-Benzyl-L-histidine, γ-Benzyl-L-glutamate)$_n$ (1:1) (VII).**—A mixture of V (1.00 g.), γ-benzyl-L-glutamate NCA[8] (0.69 g.), and 2.0 ml. of dioxane was heated under a nitrogen atmosphere at 140°C for 24 hr. The product was triturated with acetone and ether, and collected by centrifugation to yield 1.0 g. (86%) of VII.

Found: C, 67.0; H, 5.93; N, 12.3; equiv. wt. 427 (determined by perchloric acid titration). Calcd. for $C_{25}H_{26}O_4N_4$: C, 67.3; H, 5.87; N, 12.6%; equiv. wt. 446.5.

**Copoly(L-Histidine, L-Glutamic Acid)$_n$ (1:1) (IX).**—To a suspension of VII (0.9 g.) in liquid ammonia (ca. 50 ml.), finely divided metallic sodium was added over a period of 15 min. until a blue color persisted for at least 5 min. The excess sodium was discharged with ammonium chloride, and the ammonia was allowed to evaporate spontaneously. The residue was then dissolved in water (20 ml.) and extracted twice with 20 ml. portions of ether. The aqueous layer was filtered and neutralized with 6 N hydrochloric acid to pH 6 and concentrated to dryness in vacuo. The residue was redissolved in water (20 ml.) and dialyzed. Then the solution was lyophilized to yield 0.4 g. (67%) of IX.

Found: C, 47.7; H, 5.51; N, 20.6; equiv. wt. 267 and 260 (determined by perchloric acid and sodium methylate titration respectively). Calcd. for $C_{11}H_{14}O_4N_4\,1/2\,H_2O$: C, 48.0; H, 5.45; N, 20.4%; equiv. wt. 275.3.

**The Determination of the Amino Acid Contents of IX.**—The histidine content of IX was determined by the reaction of the histidine residue with diazotized sulfanilic acid, followed by colorimetric analysis. After the hydrolysis of IX with 6 N hydrochloric acid at 110°C for 10 hr., both histidine and glutamic acid were assayed by the colorimetric determination of paper chromatography, using ninhydrine as a developer. It was demonstrated that they were in the ratio of ca. 1:1.

**The Determination of Catalytic Activity.**—The catalyst, IIIa or IX, in the concentration of 100 mg./l. and the substrate, *p*-nitrophenyl acetate, in the concentration of 3.311 mmol./l. were incubated for 30 min. at 25°C in a 1/30 mol. phosphate buffer solution of pH 6.4 containing 10% (V/V) acetone in order to dissolve the *p*-nitrophenyl acetate. The liberated *p*-nitrophenylate ions were determined by measuring the increases in optical density at 400 mμ using a Hitachi EPU type 2 spectrometer.

The author is very grateful to Professor Junzo Noguchi of the University of Hokkaido for his kind help.

*Department of Chemistry*
*Faculty of Science*
*Kanazawa University*
*Kanazawa-shi, Ishikawa*

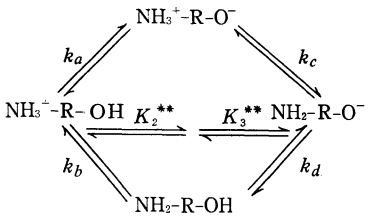
8) W. E. Hanby, S. G. Waley and J. Watson, *J. Chem. Soc.*, **1950**, 3239.

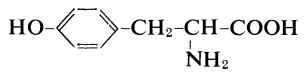
# The Ionization Constants of Organic Compounds. I. The Microscopic Ionization Constants of Tyrosine and Related Compounds*

By Futaba YAMAZAKI, Kiyoko FUJIKI and Yasue MURATA

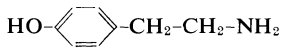
(Received April 10, 1964)

The object of this paper is to describe a method for evaluating microscopic ionization constants. Tyrosine (I), tyramine (II), 3-iodotyrosine (III), tyrosine methyl ester (IV), tyrosine ethyl ester (V), 3, 5-diiodotyrosine (VI), and 3, 5-dibromotyrosine (VII) will be investigated in the present work. The ionization of two protons from the phenolic and amino groups in these compounds may be represented by the following scheme:

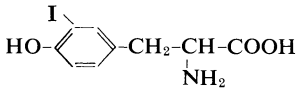


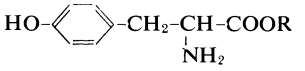
(I)



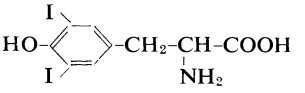
(II)



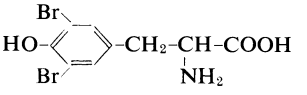
(III)



R=$CH_3$ (IV)
R=$C_2H_5$ (V)



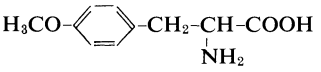
(VI)



(VII)

* Read in part at the Autumn Meeting of the Chemical Society of Japan, Tokyo, November, 1963, and at the 17th Annual Meeting of the Chemical Society of Japan, Tokyo, April, 1964.

** $K_2$ and $K_3$ should be properly replaced by $K_1$ and $K_2$ respectively for II, IV, and V.



(VIII)

The four compounds, I, III, VI, and VII, have a carboxyl group which corresponds to $pK_1$ as another ionizable group. However, as the $pK$ values of the carboxyl groups in these compounds are around 2, if we consider only the ionization which occurs at pH values above 4, it is safe to assume that the carboxyl group carries a negative charge in all the species under consideration.

The scheme is composed of two macroscopic constants, $K_2$ and $K_3$, and four microscopic constants, $k_a$, $k_b$, $k_c$ and $k_d$. Moreover, these constants are interrelated as follows:

$$K_2 = k_a + k_b \quad (1)$$

$$1/K_3 = 1/k_c + 1/k_d \quad (2)$$

$$K_2K_3 = k_ak_c = k_bk_d \quad (3)$$

The macroscopic constants of some of these compounds have been reported in the literature, but no discussion has been undertaken of the microscopic constants, except on I.[1]

We have reinvestigated the ultraviolet spectrum of I and confirmed that the maximum in the absorption spectrum shifts from 274 mμ to 294 mμ with an increase in the pH value of the solution (Fig. 1). On the other hand, *O*-methyltyrosine (VIII) displayed practically the same absorption at pH 6.10 and at pH 12.50 (see Experimental section). This behavior demonstrates that the ionization of the amino group does not affect the absorption spectra accordingly, it may be assumed that the molar extinction coefficient of the $NH_3^+$-R-$O^-$ form is identical with that of the $NH_2$-R-$O^-$ form. Furthermore, the molar extinction coefficients at 295 mμ and 300 mμ are practically zero for acidic media, where the OH group is un-ionized, whereas they are large in the alkaline media, where the OH group has been converted to $O^-$ ions. Therefore, the absorption at these wavelengths may be completely ascribed to $O^-$ species. The

1) J. T. Edsall, R. B. Martin and B. R. Hollingworth, *Proc. Natl. Acad. Sci.*, **44**, 505 (1958).

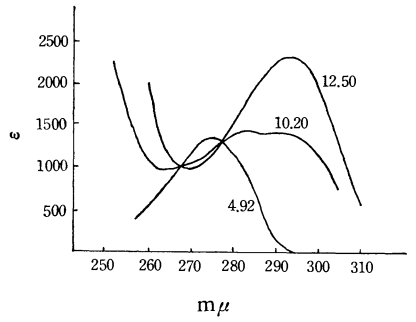



Fig. 1. Ultraviolet spectra of tyrosine at various pH (numbers besides curves).

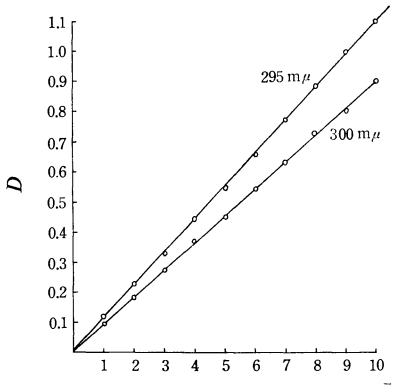



Fig. 2. Ultraviolet absorption of tyrosine at 295 mμ and 300 mμ in various dilution of 105 mg./l. solution at pH 12.50.

molar extinction coefficients of I in the completely ionized form (pH 12.50) were found to be independent of the concentration over the range less than 0.0005 M at these wavelengths (Fig. 2). Therefore, the fraction of all $O^-$ species in the solution at each pH can be determined from the extinction coefficient at 295 mμ and 300 mμ by dividing the maximum extinction coefficient at the same wavelength for the completely dissociated state (pH 12.50):

$$\alpha_{OH} = \varepsilon/\varepsilon_{max} \qquad (4)$$

where $\varepsilon$ and $\varepsilon_{max}$ represent the molar extinction coefficient at each pH and that at pH 12.50 respectively.

On the other hand, the fraction $\alpha_{OH}$ can be expressed as follows by making use of Eqs. 1—3:

$$\alpha_{OH} = \frac{(NH_3^+\text{-R-}O^-) + (NH_2\text{-R-}O^-)}{(NH_3^+\text{-R-OH}) + (NH_3^+\text{-R-}O^-) + (NH_2\text{-R-OH}) + (NH_2\text{-R-}O^-)} = \frac{k_a/(H^+) + K_2K_3/(H^+)^2}{1 + K_2/(H^+) + K_2K_3/(H^+)^2} \qquad (5)$$

Once macroscopic constants have been determined by independent titration, each value of $(H^+)$ with an associated value of $\alpha_{OH}$ from the ultraviolet absorption should fix the value of $k_a$ from Eq. 6, which is a modification of Eq. 5;

$$k_a = \alpha_{OH}[(H^+) + K_2] - (1-\alpha_{OH})K_2K_3/(H^+) \qquad (6)$$

A series of such $k_a$ values may be obtained and suitably averaged to obtain the most probable value of $k_a$. From this, the other microscopic constants may readily be determined from Eqs. 1—3. This method has been suggested by Edsall,[2] but no results have been reported. For the present work, the microscopic constants were studied by this procedure.

## Experimental and Calculations

**Materials.**—I, II, III, V, VI and VII were obtained from the Tokyo Kasei Co. and were recrystallized before use. IV was preared according to Fischer[3] from I. VIII was also prepared from I according to Beer[4] (monosulfate, $\lambda_{max}$: 274 mμ, log $\varepsilon$: 3.14 at pH 6.10, 3.16 at pH 12.50).

**Spectral Measurement.** — Spectral measurements were made with a Shimadzu QR-50 spectrophotometer and a Beckman DU spectrophotometer at 25±0.5°. For the measurement, 10 ml. of a 0.001 M solution of a compound were added to 10 ml. of buffer solution with an ionic strength of 0.01. The following buffers were used for the pH indicated: 6.10, 6.56, 7.13, 7.49, $Na_2HPO_4+NaH_2PO_4$; 8.10, $Na_2HPO_4+KH_2PO_4$; 8.60, $H_3BO_4+Na_2CO_3$; 9.15, 10.18, 10.60, 11.53, $Na_2CO_3+NaHCO_3$; 12.50, glycine + NaOH.—The absorption was determined immediately after mixing, the corresponding buffer being used as the blank.

**The Measurement of the pH.** — All pH measurements were carried out with a Horiba-Hitachi Model-P pH meter, equipped with a glass electrode and a double-junction sleeve-type caromel elctrode. The meter was calibrated with standard Horiba buffer solutions of pH 6.86 and 4.01 at 25°C.

**The Measurement of Macroscopic Constants.** — About a 0.001 M solution was titrated with 0.5 N sodium hydroxide. The titration solvent was a 0.05 M potassium nitrate solution in order to keep the ionic strength at 0.05. The vessel was maintained at 25±0.5°C in a water jacket with a stream from a thermo-circulator. The macroscopic constants were obtained from the titration curves, with reference to Albert.[5] The error is not greater than ±0.03 p$K$ units.

For the compounds other than I, it has also been assumed that the molar extinction coefficient of the $NH_3^+$-R-$O^-$ form is identical with that of the $NH_2$-R-$O^-$ form. The residual absorptions in acidic solutions, where the OH group is un-ionized, at a chosen wavelength were substantial in VI

2) J. T. Edsall and J. Wyman, "Biophysical Chemistry," Vol. I, Academic Press, New York (1958), p. 501.
3) E. Fischer and W. Scharanth, *Ann.*, **354**, 34 (1907).
4) L. D. Beer and H. F. Clark, *J. Am. Chem. Soc.*, **54**, 1630 (1934).
5) A. Albert, "Ionization Constants of Acid and Bases" Methuen & Co. (1962), Chap. II.

and VII. Therefore, the following formula was used instead of Eq. 4 to obtain $\alpha_{OH}$ in VI and VII:

$$\alpha_{OH} = (\varepsilon - \varepsilon_O)/(\varepsilon_{max} - \varepsilon_O)$$

Where $\varepsilon_O$ stands for the extinction coefficient in acidic media.

The values of $k_a$ were calculated in the region where $\alpha_{OH}$ is more than 0.1 and less than 0.9.

## Results and Discussion

**Tyrosine (I).**—The values of $\alpha_{OH}$ obtained at 295 m$\mu$ and 300 m$\mu$ appeared to be almost identical, supporting the validity of such an evaluation of $\alpha_{OH}$. The macroscopic and microscopic constants (Table I) agree with those of Edsall[1] when account is taken of the difference in the ionic strengths in the experiments. The values of $k_a$, $K_2$ and $K_3$ were used to construct a theoretical curve, which closely follows the experimental points (Fig. 3.) The ratio of $NH_3^+$–R–$O^-$ species to $NH_2$–R–OH species, $K_z$, becomes:

$$K_z = k_a/k_b \cong 1.1$$

This value shows that, in the course of the titration, comparable amounts of the two species are in equilibrium. Therefore, it is safe to say that $K_2$ and $K_3$ are almost completely hybridized and that, accordingly, a single assignment to the ionization of either the amino or the phenolic group is incorrect.

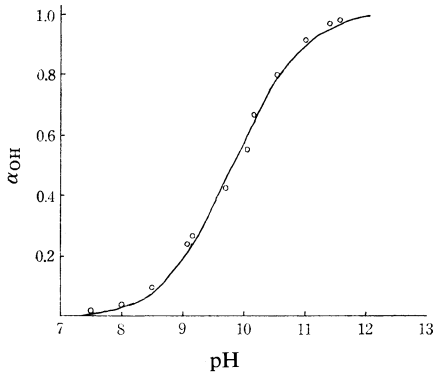



Fig. 3. Spectroscopic titration curve of tyrosine. The points are experimental, the line is calculated from the ionization constants.

The hydrogen ion concentration at $\alpha_{OH}=0.5$ is represented as follows from Eq. 5:

$$(H^+)_{\alpha=0.5} = \frac{2k_a - K_2 + [(K_2 - 2k_a)^2 + 4K_2K_3]^{1/2}}{2} \qquad (7)$$

This formula shows that, when a complete hybridization occurs in the ionization, i. e., $K_2 = 2k_a$, the value of pH at $\alpha_{OH}=0.5$ equals ($pK_2 + pK_3$)/2. The observed pH at $\alpha_{OH}=0.5$ for I was 9.82, which is approximately equal to ($pK_2 + pK_3$)/2. In the literature on I, the ultraviolet spectrometric $pK_{OH}$[6-8] values are significantly lower than the titrimetric $pK_3$ values.[9,10] Apparently the former is a composite value of $pK_2$ and $pK_3$, since in the procedure $pK_{OH}$ is determined as the pH value at $\alpha=0.5$.

Also in support of the present method, it was attempted to prove that the $K_2$ for *O*-methyltyrosine (VIII) should be nearly equal to the $k_b$ for I. The ionization constants of *O*-methyl derivatives of fatty acids and amino acids with hydroxyl groups appeared essentially to confirm the above statement.[11] The $pK_2$ for VIII was determined as 9.50 at an ionic strength of 0.05, which agrees with the $pk_b$ for I within the range of experimental error.

Benesch[12] was remarkably successful in solving Eq. 5 for $k_a$, $k_b$, and $k_d$ for cysteine by the substitution of the ultraviolet spectral $\alpha_{SH}$ and ($H^+$) values into three simultaneous equations. However, we have observed that in the case of I the ionization of the OH group was confined within a rather small pH range, and that the calculation error by his method became considerable.

**Tyramine (II).**—The values of $pK_1$ and $pK_2$ agree approximately with those obtained by Lewis[13] and by Ogston.[14] The microscopic constants are higher than the corresponding value for I by about 0.3 and 0.5 pH units respectively, as is to be expected from the elimination of the carboxyl group from I. From the results shown in Table I, the assignment of a single $pK_{OH}$ and a single $pK_{NH_3^+}$ is apparently unreasonable, as in the case of I, so each proton has an approximately equal chance to be ionized from either group.

**3-Iodotyrosine (III).** — The value of $K_z$, 5.0, shows that the hybridization in the ionization of the OH group and the $NH_3^+$ group is considerably less than those in I and II, and that the ionization of the OH group is mainly involved in $pK_2$. Herriot[15] has reported $pK'_{OH}$ as 8.20; he based his calculations on the ultraviolet absorption. The value is between $pK_2$ and $pK_3$, and it is obviously the composite constant of $pK_2$ and $pK_3$, Considerably lower values of $pK$ and $pk$, compared with those for I and II, apparently follow from the inductive effect of the iodine atom.

6) C. Tanford, *J. Am. Chem. Soc.*, **74**, 2509 (1952).
7) C. Fromageot, *Biochim. et Biophys. Acta*, **6**, 113 (1950).
8) A. Neuberger, *Biochem. J.*, **37**, 302 (1943).
9) H. Simms, *J. Gen. Physiol.*, **11**, 629 (1928).
10) A. Albert, *Bichem. J.*, **50**, 690 (1952).
11) Sec Ref. 2, p. 498.
12) R. E. Benesch and R. Benesch, *J. Am. Chem. Soc.*, **77**, 5877 (1955).
13) G. P. Lweis, *Brit. J. Pharmacol.*, **9**, 488 (1954).
14) A. G. Ogston, *J. Chem. Soc.*, **1936**, 1713.
15) R. M. Herriot, *J. Gen. Physiol.*, **31**, 18 (1947).

TABLE I

| | I | II | III | IV | V | VI | VII |
|---|---|---|---|---|---|---|---|
| $\lambda_{max}$(OH), mμ | 274 | 273 | 281 | 273 | 273 | 285 | 286 |
| (ε) | (1380) | (1462) | (2499) | (1222) | (1354) | (2650) | (2577) |
| $\lambda_{max}$($O^-$), mμ | 294 | 293 | 304 | 292 | 291 | 308 | 308 |
| (ε) | (2330) | (2594) | (3961) | (2154) | (2408) | (5695) | (5736) |
| Chosen wavelength, mμ | 295 / 300 | 307 | 307 | 296 | 296 | 310 | 310 |
| p$K_1$ | — | 9.55 | — | 7.24 | 7.28 | — | — |
| p$K_2$ | 9.26 | 10.87 | 7.92 | 10.16 | 10.12 | 6.44 | 6.29 |
| p$K_3$ | 10.37 | — | 9.60 | — | — | 9.36 | 9.22 |
| p$k_a$ | 9.55 | 9.70 | 8.00 | 8.41 | 8.43 | 6.44 | 6.29 |
| p$k_b$ | 9.57 | 10.09 | 8.70 | 7.27 | 7.31 | $k_b \ll k_a$ | $k_b \ll k_a$ |
| p$k_c$ | 10.08 | 10.72 | 9.52 | 8.99 | 8.97 | 9.36 | 9.22 |
| p$k_d$ | 10.06 | 10.33 | 8.82 | 10.13 | 10.09 | $k_d \gg k_c$ | $k_d \gg k_c$ |
| $K_z$ | 1.1 | 2.4 | 5.0 | 0.07 | 0.08 | very large | very large |
| pH ($\alpha$=0.5) | 9.82 | 9.91 | 9.18 | 10.05 | 10.05 | 6.44 | 6.29 |

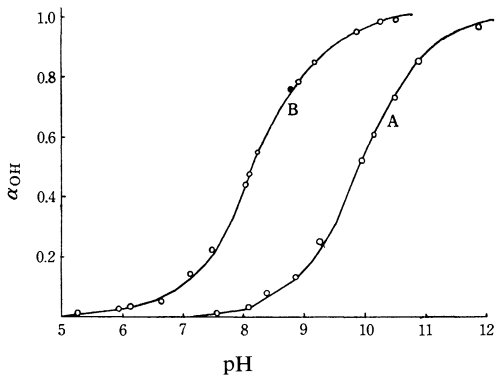



Fig. 4. Spectrophotometric titration curves of tyramine (A) and 3-iodotyrosine (B). The points are experimental, the lines are calculated from the constants given in Table I.

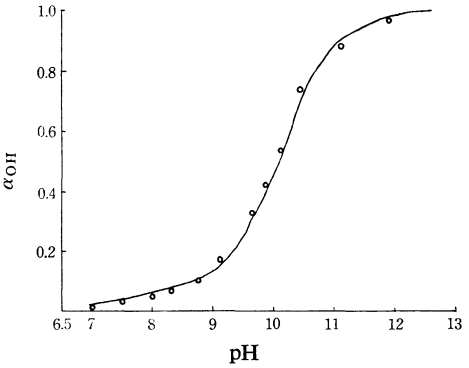



Fig. 5. Spectrophotometric titration curve of tyrosine methyl ester.

**Tyrosine Methyl Ester (IV) and Tyrosine Ethyl Ester (V).**—The ultraviolet spectra and ionization constants are identical within the range of experimental error in IV and V, as is to be expected from the nearly equal inductive effect of the methoxycarbonyl and ethoxycarbonyl groups. In these substances, $k_a \ll k_b$ and $k_b$ corresponds with $K_1$ within the range of experimental error. The Edsall method[15] is unsuitable for the cases where $k_a \ll k_b$ or where, conversely, $k_a \ll k_b$, but it is revealed that the present approach may be applied even in the former cases. In these compounds, p$K_1$ is reasonably shifted by nearly 2 pH units, compared with p$K_2$ of I, as a result of the removal of a negative charge on the carboxylate group. In conclusion, it is safe to say that $K_1$ and $K_2$ are mainly associated with the amino and the phenolic groups respectively in these compounds.

**3, 5-Diiodotyrosine (VI) and 3, 5-Dibromotyrosine (VII).**—In these compounds $k_a$ equals $K_2$ and corresponds to the pH value at which $\alpha_{OH}$ is exactly 0.5. It follows that the dissociation of the first proton is confined entirely to the OH group, and that $K_2$ and $K_3$ may be assigned exclusively to the ionization of the amino and phenolic groups respectively. It is revealed that when $k_a$ nearly equals $K_2$, $k_b$ and $k_d$ can not be estimated by the present method. The values of p$K_2$ are found to be lower than that of III, a natural result of the inductive effect of the second halogen atoms. Schmidt et al. determined the macroscopic constants from the solubility as p$K_2$=6.86, p$K_3$=7.82 for VI,[16] and p$K_2$=6.44, p$K_3$=7.58 for VII.[17] There is a significant discrepancy, especially in p$K_3$, between his values and those in Table I. However, the halogen atoms appear to be too separated from amino groups to exert such a large inductive effect as is shown by Schmidt's p$K_3$. It may be considered that the values of p$K_3$ in the present work are more reasonable.

16) J. D. Dalton, P. L. Kirk and C. L. A. Schmidt, *J. Biol. Chem.*, **88**, 589 (1933).
17) C. L. A. Schmidt and P. S. Winnek, *J. Gem. Physiol.*, **18**, 889 (1935).

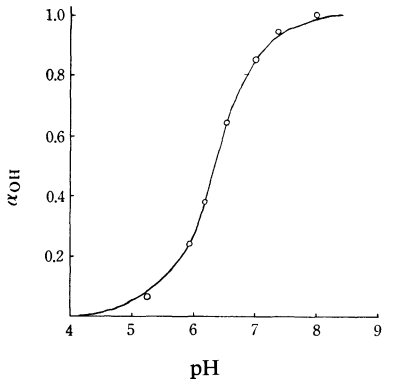



Fig. 6. Spectrophotometric titration curve of 3,5-dibromotyrosine

## Summary

A method has been formulated for the estimation of the microscopic ionization constants from spectroscopic data which measure the fractional ionization of one of the groups as a function of the pH value. This method has been applied at the ionic strength of 0.05 to the ionization of tyrosine (I), tyramine (II), 3-iodotyrosine (III), tyrosine methyl ester (IV), tyrosine ethyl ester (V), 3,5-diiodotyrosine (VI), and 3,5-dibromotyrosine (VII). The microscopic constants obtained are 9.55, 9.57, 10.08, 10.06 for I; 9.70, 10.09, 10.72, and 10.33 for II; 8.00, 8.70, 9.52 and 8.82 for III; 8.41, 7.27, 8.99 and 10.13 for IV, and 8.43, 7.31, 8.97 and 10.09 for V, in the order of p$k_a$, p$k_b$, p$k_c$, and p$k_d$. For VI and VII, the p$k_a$ values are 6.44 and 6.29, and the p$k_b$ values are 9.36 and 9.22, respectively. It has been illustrated that the method may be applied even in cases where $k_a \ll k_b$. This approach can probably be extended to other systems containing two dissociable protons, one of which affects the ultraviolet absorption and the other does not.

The authors wish to thank Miss Hisako Kimoto for her help in the experiments.

*Tokyo Kasei College*
*Itabashi-ku, Tokyo (F. Y. & Y. M.)*

*Department of Agriculture*
*Meiji University*
*Kawasaki-shi, Kanagawa (K. F.)*

# The Oxidation of Iodide to Iodite and the Reduction of Iodate to Iodite in Iodine Solutions of Permanganate and Some of the Carboxylic Acids

By Yugul Kishore GUPTA and Anand Prakash BHARGAVA

(Received April 21, 1964)

The oxidation of iodide at low concentrations has been the subject of much recent interest. A number of oxidation products are possible, but some of which might be unstable. Such a possibility has already been indicated by Kahn and Wahl[1] and by Eiland and Kahn[2] in the oxidation of iodine by dichromate and cerium(IV). A number of the oxidation products of iodine from +1 to +5 states are possible if the oxidation is suitably carried out. However, iodate seems to be one of the most important products in all the oxidations reported by the above authors, and also in those reported by Musakin and Puchkov[3] and by one of the present authors[4] in permanganate oxidations.

During a kinetic study of the reduction of permanganate by citric and malonic acids in the presence of low concentrations of iodide, it has been reported by Misra and Gupta[5] that the reaction mixtures, even after becoming colourless, have some oxidant which could be determined iodometrically. This was suspected to be iodite. This observation necessitated a systematic attempt to identify this oxidant and to ascertain the mechanism by which it is produced. Similar observations have been reported by a number of workers[6-10] in the oxidation of oxalic acid by permanganate in

1) M. Kahn and A. C. Wahl, *J. Chem. Phys.*, **21**, 1185 (1953).
2) H. M. Eiland and M. Kahn, *J. Phys. Chem.*, **65**, 1317 (1961).
3) A. P. Musakin and L. V. Puchkov, *Zh. Neorg. Khim.*, **4**, 483 (1959).
4) Y. K. Gupta, *J. Inorg. Nucl. Chem.*, **19**, 179 (1961).
5) Y. K. Gupta and D. D. Misra, *Bull. acad. polon. sci.*, **9**, 379 (1961).
6) Y. K. Gupta and S. Ghosh, *Z. physik. Chem.*, **208**, 368 (1958).
7) H. Taube, *J. Am. Chem. Soc.*, **70**, 1216 (1948).
8) F. Oberhauser and W. Hensinger, *Ber.*, **61B**, 521 (1928).
9) P. S. Macmohan and B. B. Lal, *J. Ind. Chem. Soc.*, **20**, 143 (1943).
10) H. Wieland and W. Zilg, *Ann.*, **530**, 257 (1937).

the absence of iodine, wherein hydrogen peroxide has been said to be formed.

Not much is known about iodite. Landolt[11] suspected the intermediate formation of iodite during the reduction of iodate. Lievin[12] and Guiseppe[13], from a study of the order of the conversion of hypoiodites into iodates, suspected the intermediate formation of iodite. Josien[14] found the existence of iodite in silver nitrate-iodine solutions by an analytical method. Kireev[15] reported the existence of silver iodite. The compound has not been isolated so far. Attempts have been made to discover a qualitative test to distinguish it from iodate or periodate, but no definite conclusions could be arrived at for want of this compound in the pure state.

It will be suggested in the present paper that, when permanganate is added to small amounts of iodide in aqueous solutions of citric or malonic acid, iodate is first formed and that this is subsequently reduced to iodite by the intermediate oxidation products of the acid. It will further be shown that iodate also is reduced to iodite in such solutions by the oxidation products of the acids.

## Experimental

All the chemicals were of B.D.H.A.R. quality; the malonic acid made by Riedel. Distilled water was freshly boiled and cooled for preparing stock solutions and reaction mixtures.

Requisite quantities of the citric or malonic acid and potassium iodide were mixed, a permanganate solution was added, and the mixture was thoroughly shaken. The reaction mixtures were preferably kept overnight, whereupon they became colourless. The oxidising capacity of the mixtures was determined iodometrically by titrating 10 ml. of the mixture against N/100 thiosulphate using a 10—15% solution of iodide and 2 N sulphuric acid. The temperature varied between 15—20°C.

In the case of citric acid and higher concentrations of iodide, when a precipitate was obtained the mixture was filtered and the oxidising capacities of the filtrate and of the precipitate were determined separately.

For reactions with iodate, permanganate and the organic acid were mixed and allowed to become colourless, and then a requisite quantity of iodate was added. Ten or twenty-five milliliters aliquots were determined for the oxidant iodometrically using 10% potassium iodide. The determinations were repeated after 8, 24 and 48 hr. Analytical measurements were also made in cases when iodate was added before the permanganate.

In the case of malonic acid, a few experiments were carried out by adding iodate to the reaction mixture when the permanganate colour had just disappeared and there remained a reddish orange colour.

When iodide is oxidised to iodite or iodate, iodine is the intermediate product; it may react with the organic acid or with its oxidation products (by permanganate). The substitution products may remain in the solution or may be thrown out of the solution, but all of them give back iodine in acidified solutions of potassium iodide and hence can be determined iodometrically. A few qualitative experiments were made to ascertain this, as Table I shows. Tests for iodate or iodide and iodometric measurements were made only in colourless solutions. In columns 4, 5 and 6 the permanganate and the acid were allowed to react in the presence of iodate or iodide or aqueous iodine, and then the tests were made. In the experiments of column 7, aqueous iodine was added after the permanganate-acid mixture had become colourless. The concentrations of the reactants used were as will be shown in subsequent tables.

It was found that malonic and pyruvic acids could immediately react with the aqueous iodine and give back the latter when acidified potassium iodide was added. The reaction of iodine with other acids is slow and photochemical. Such an oxidation of citric acid by iodine has been reported by a number of workers,[16-21] but little has been said about the reaction between iodine and the oxidation products of citric acid. Mecmohan and Srivastava[22] and Bakore and Bharadwaj[23] have mentioned the formation of tetraiodoacetone and hexaiodoacetone. Similarly, a number of workers[24-30] have studied the reaction between iodine and malonic acid, but nothing has been said about the oxidation products of malonic acid. Kappanna and Talati[31] reported a slower reaction between malonate ion and iodine in the presence of hydrogen or iodide ions — a fact which indicates that the reaction is reversible and that, under appropriate conditions, iodine may not react with malonic acid

11) H. Landolt, *Sitzber Akad. Bodin.*, **1885**, 249.
12) O. Lievin, Memoires et Travaux des Facultes Catholiques de Lille (1923).
13) D. Guiseppe, *Boll. Chim. farma.*, **78**, 117 (1939); *Chem. Abstr.*, **33**, 7652 (1939).
14) M. L. Josien, *Compt. rend.*, **216**, 842 (1943).
15) V. Kireev, *Acta Physicochem., U. R. R. S.*, **20**, 905 (1943).
16) P. S. Macmohan and T. N. Srivastava, *J. Ind. Chem. Soc.*, **20**, 307 (1943).
17) N. R. Dhar, *J. Chem. Soc.*, **111**, 699 (1917).
18) A. N. Dey and N. R. Dhar, *Z. Electrochem.*, **32**, 586 (1926).
19) R. P. Sanyal and N. R. Dhar, *Z. anorg. Chem.*, **139**, 161 (1924).
20) N. R. Subbaratnam and A. K. Bhattacharya, *Saugor Univ. J. (India)*, Part 2, Nos. 4, 5 (1954).
21) J. L. Mukherji and C. M. Kakati, *J. Ind. Chem. Soc.*, **24**, 361 (1947).
22) P. S. Macmohan and T. N. Srivastava, ibid., **23**, 261 (1946).
23) G. V. Bakore and S. D. Bharadwaj, *Proc. Natl. Inst. Sci. (India)*, **29A**, 90 (1963).
24) T. N. Srivastava, *Current Sci.*, **15**, 249 (1946).
25) R. W. West, *J. Chem. Soc.*, **1924**, 125.
26) J. O. Halford and L. C. Anderson, *J. Am. Chem. Soc.*, **58**, 736 (1936).
27) S. L. Bafna, K. P. Govindan and W. V. Bhagwat, *J. Sci. Industr. Res. (India)*, **IIB**, 376 (1952).
28) S. L. Bafna, W. V. Bhagwat and M. A. Tilak, ibid., **IIB**, 231 (1952).
29) V. M. Bhale, S. L. Bafna and W. V. Bhagwat, *Z. physik. Chem.*, **12**, 298 (1957).
30) R. M. Verma and S. Bose, *J. Ind. Chem. Soc.*, **38**, 899 (1961).
31) A. N. Kappanna and E. R. Talati, ibid., **28**, 675 (1951).

TABLE I.

| (1) Acid | (2) Reaction with iodate | (3) Reaction with aq. $I_2$ | (4) $KMnO_4$-Acid ($KIO_3$) test for | | (5) $KMnO_4$-Acid (KI) test for | | (6) $KMnO_4$-Acid (aq. iodine) test for | | (7) $KMnO_4$-Acid → colourless. aq·$I_2$ added. Whether $I_2$ obtained back from colourless solution |
|---|---|---|---|---|---|---|---|---|---|
| | | | Iodate (iodite) ? | Iodide | Iodate (iodite) ? | Iodide | Iodate (iodite) ? | Iodide | |
| Citric | No | Slow | Yes | No | Yes | No | Yes | No | Yes |
| Lactic | No | Slow | Yes | No | Yes | No | Yes | No | Yes |
| Maleic | No | Slow | No | Yes | No | Yes | No | Yes | — |
| Malic | No | Slow | Yes | No | Yes | No | Yes | No | Yes |
| Malonic | No | Fast* | Yes | No | Yes | No | Yes ? | No | Yes |
| Oxalic | No | Slow | No | Yes | No | Yes | No | Yes | — |
| Pyruvic | Slow | Fast* | No | No | No | No | No | Yes ? | — |
| Tartaric | No | Slow | No | Yes | No | Yes | No | Yes | — |

* Iodine was quantitatively obtained back from colourless solutions.

TABLE II. OVERALL VOLUME OF THE REACTION MIXTURE : 50 ml.

| $KMnO_4$ N | Malonic acid, M | Oxidant (N) for KI (N) | | | | Citric acid, M | | |
|---|---|---|---|---|---|---|---|---|
| | | $2\times10^{-4}$ | $4\times10^{-4}$ | $1\times10^{-3}$ | $2\times10^{-3}$ | | | |
| 0.02 | 0.08 | $8\times10^{-4}$ | $15.6\times10^{-4}$ | $3.92\times10^{-3}$ | $6.40\times10^{-3}$** | 7.6 | 15.8 | 3.58** |
| | 0.04 | 8 | 16.3 | 4.06 | 6.70** | 8.2 | 16.0 | 3.78** |
| | 0.02 | 8 | 15.8 | 4.06 | 6.78** | 8.2 | 16.2 | 3.90 |
| | 0.008 | 11.2* | 19.2* | 3.78** | 6.10** | 8.4 | 16.4 | 4.06 |
| 0.01 | 0.08 | 7.6 | 16.4 | 3.92 | 5.82** | 8.2 | 15.2 | |
| | 0.04 | 8.4 | 16.8 | 3.96 | 6.10** | 8.4 | 15.6 | |
| | 0.02 | 8.4 | 16.4 | 4.02 | 6.26** | 8.0 | 16.4 | |
| | 0.008 | 10.4* | 16.0 | 3.24** | 5.35** | 8.0 | 16.0 | |

* More than the expected four times the iodide.
** Less than the expected four times the iodide.

at all or that the reacted iodine may be set free from the substitution product.

Iodometric determinations in colourless mixtures are based on the above observations and on the fact that iodite, being an oxidising substance, will also liberate iodine from acidified iodine solution. However, a qualitative distinction between two such determinations can always be made. The organic acid is treated with the permanganate until the mixture becomes colourless. If iodine solution in water or dilute potassium iodide is then added, it reacts to give colourless solutions. These mixtures do not give back iodine when more potassium iodide is added, though the medium is acidic. Iodine is obtained only when dilute hydrochloric acid or dilute sulphuric and is added. On the other hand, colourless mixtures containing iodate liberate iodine instantaneously on the addition of potassium iodide. The two processes are quite different. In the latter there is an oxidant which liberates the iodine, whereas in the former it is a substitution product of the iodine which gives back iodine, probably by displacement.

## Results and Discussion

For low concentrations of iodide ($<10^{-3}$ N) the oxidant produced is always four times the original iodide. This points to the existence of iodite in these colourless solutions. These solutions do not respond to the test for iodide. Some mixtures show the presence of iodate, while others do not, but all of them respond to this test after a couple of days. Qualitative tests for iodite, though not yet known, are likely to be similar to those of iodate, and, hence, in all probability, a positive thiocyanate test[32] can be obtained in all cases. The test is not administered in some cases in the beginning because when citric or malonic acid is oxidised by permanganate, a number of stable and unstable products may be formed which may then exist in colourless solution. When the test is applied, liberated iodine reacts with one or more of these intermediate products, and the blue colour with the starch is not obtained or it appears for only a short time. Afterwards these unstable products decompose and disappear and iodate test produces a positive response.

The data for the reduction of iodate by the oxidation products of the organic acids is given in Tables III, IV and V. In almost all

32) F. Feigl, "Spot Tests in Inorganic Analysis," Elsvier Publishing Co. (1958).

TABLE III.

Citric acid : 0.08 M ; 5 ml. of $KIO_3 \equiv 3.08$ ml. of 0.05 N $Na_2S_2O_3$ ; $KIO_3$ added after the reaction mixture was colourless. Figure in parentheses give the oxidant values when $KIO_3$ was added before the addition of the permanganate

| $KIO_3$ in ml. of $Na_2S_2O_3$ | Oxidant in the reaction mixture after 24 hr. in ml. of $Na_2S_2O_3$ | | |
|---|---|---|---|
| | $KMnO_4$ : 0.01 N | $KMnO_4$ : 0.02 N | $KMnO_4$ : 0.04 N |
| 0.616 | 0.44 (0.42) | 0.42 (0.42) | — (0.42) |
| 1.23 | 0.89 (0.85) | 0.85 (0.83) | 0.82 (0.82) |
| 2.46 | 1.99* (1.68) | 1.71 (1.64) | 1.66 (1.64) |
| 4.93 | 3.90* (3.38) | 3.70* (3.30) | 3.37 (3.30) |
| 12.32 | — (9.28)* | 9.74* (8.30) | 8.30 (8.30) |
| 15.40 | — — | — (10.32) | 10.45 (10.28) |
| 18.48 | — — | — (12.30) | 12.37 (12.32) |

* More than the expected 2/3 of iodate added.

TABLE IV.

Malonic acid : 0.16 M ; $KIO_3$ added immediately after the disappearance of the pink colour of the permanganate

| $KIO_3$ in ml. of $Na_2S_2O_3$ | Oxidant after 24 hr. in ml. of $Na_2S_2O_3$ | | $KIO_3$ in ml. of $Na_2S_2O_3$ | Oxidant after 24 hr. in ml. of $Na_2S_2O_3$ | |
|---|---|---|---|---|---|
| | $KMnO_4$ : 0.02 N | $KMnO_4$ : 0.04 N | | $KMnO_4$ : 0.06 N | $KMnO_4$ : 0.08 N |
| 5.09 | 3.45 | 3.02** | 5.04 | 2.73** | 2.52** |
| 10.18 | 6.82 | 6.49 | 10.08 | 5.83** | 5.50** |
| 15.27 | 10.36 | 10.12 | 20.16 | 13.32 | 13.20 |
| 20.36 | 14.28 | 13.68 | 25.20 | 16.75 | 16.75 |
| 30.54 | 23.79* | 21.45 | 30.24 | 20.28 | 20.15 |
| 5 ml. of $KIO_3 \equiv 5.09$ ml. of 0.02 N thiosulphate | | | 5 ml. of $KIO_3 \equiv 5.04$ ml. of 0.02 N thiosulphate | | |

* More than the expected 2/3 of iodate.
** Less than the expected 2/3 of iodate.

TABLE V.

Malonic acid : 0.1 M ; 5 ml. of $KIO_3 \equiv 5.09$ ml. of 0.02 N $Na_2S_2O_3$ ; $KIO_3$ added before the addition of $KMnO_4$

| $KIO_3$ in ml. of $Na_2S_2O_3$ | Oxidant after 24 hr. in ml. of thiosulphate | | |
|---|---|---|---|
| | $KMnO_4$ : 0.01 N | $KMnO_4$ : 0.025 N | $KMnO_4$ : 0.05 N |
| 5.09 | 3.50 | 3.40 | 2.60** |
| 10.18 | 7.40* | 6.80 | 5.60** |
| 15.27 | 11.40* | 10.20 | 8.90** |
| 20.36 | 16.70* | 14.00 | 11.80** |
| 30.54 | 21.40 | 21.40 | 20.20 |

* More than the expected 2/3 of iodate.
** Less than the expected 2/3 of iodate.

cases, subject to the conditions of mixing and the concentration of the reactants, the oxidising capacity of the original iodate is reduced to 2/3 (oxidising capacity), a fact which points to the reduction of iodate to iodite.

Higher iodometric values than the expected 2/3 of the added iodate are obtained only in cases where the reducing intermediates (the oxidation products of the organic acid) are not present in sufficient concentration, i. e., when there is less permanganate or comparatively more original iodate. In a few cases (Tables IV and V) the reduction of iodate seems to have gone further than the stage of iodite and the iodometric values are less than the expected 2/3 of the original iodate. This obviously happens when there is less iodate and when the reducing intermediates are formed in sufficient concentration. The mixtures are colourless and do not respond to the tests

of iodide. Some of the iodate, therefore, appears to have been reduced to hypoiodite. A possibility of iodite disproportionating in a mixture of iodate and hypoiodite, with the same oxidising capacity as iodite, is ruled out because the reaction mixtures, even on heating, do not show any visible colour change or other reactions giving tests for iodide, a product which is well known to be formed by heating a solution of hypoiodite. An ammonia test[32] was negative.

The iodometric determinations were made 2, 8, 24 and 48 hr. after the addition of iodate. It was found that the reduction to iodite was not complete in two hours. It was, however, complete the next day. In the case of iodate experiments, difficulty was encountered in carrying out the iodometric titrations. The blue colour of the iodine-starch complex appeared again and again. However, no such difficulty was met with after 2 or 3 days nor in the case of malonic acid, even in the beginning. This difficulty is linked with the formation of the oxidation products of the organic acid. These products, existing in solution, react with the iodine liberated from the acidified potassium iodide for the purpose of titration; this iodine is retrieved only slowly. In the case of malonic acid, iodine is readily obtained even from the substituted products, and there is no difficulty during the titration. The oxidation products of citric acid disappear after 2 or 3 days, and once again there is no difficulty in titration.

The experiments with iodate were carried out by adding it after the permanganate-acid mixture had become colourless, and also by adding it to the acid before the addition of the permanganate. This was done in order to ascertain the degree of the stability of the oxidation products of the organic acid. It would appear from the results that the oxidation products of citric acid are more stable than those of the malonic acid. In the case of malonic acid, when iodate is added after the acid-permanganate mixture becomes colourless, a little iodate is reduced to iodite. Macmohan and Srivastava[16] have reported that acetone dicarboxylic acid — a product of oxidation of citric acid — is fairly stable, whereas the corresponding oxidation products of malonic acid are not stable.

Experiments were also carried out by adding iodate when the acid-permanganate mixtures had just lost the characteristic colour of the permanganate and become reddish orange, due probably to the formation of colloidal manganese dioxide[33] and tripositive manganese complexes.[34-38] The results were the expected 2/3 of the original iodate.

An interesting observation made in the case of malonic acid was the persistence of a light yellow colour when iodate was added in a sufficient concentration before the acid-permanganate mixture had become colourless. It was not due to iodine; probably manganese(III) complexes of malonic acid persisted in the solution. It, therefore, appears that the reduction of manganese(III) by malonic acid is very slow and that it is mainly brought about by its oxidation products. Irrespective of the nature of these products, whether they be radicals[37] or tartronic and glyoxalic acids,[39-41] they are all oxidised by iodate, and the colour of manganese(III) complexes tends to persist.

In the case of citric acid when higher concentrations ($>10^{-3}$ N) of iodide are employed, a light yellow precipitate is obtained, presumably a substitution product of citric acid with iodine, by a mechanism which will be given latter. This substance gives back its iodine in the presence of 15—20% potassium iodide and 1—2 N sulphuric acid, though not as quickly as the similar soluble product of malonic acid. The iodine in the yellow solid and the oxidising capacity of the filtrate are separately determined, and from this the total iodide is calculated. Table VI shows these results.

The fourth column gives the oxidant values of iodine in the +3 oxidation state (iodite), and column 6 gives those of iodine in its normal state (iodine-substituted oxidised species of the acid). The total of the iodine and iodide is obtained by dividing column 4 by four and adding it to column 6. The results show many deviations because of the crude method employed for the determination of iodine in the solid. The results of the individual columns are generally not reproducible, although those of the last column are fairly so in the 15—20°C temperature range (not at higher temperatures). Two or three iodine-substituted products are posssible in this case; if the concentration of such a soluble product is fairly comparable to that of the solid product, the present calculations would not give the expected results. However,

33) Y. K. Gupta and R. Dutta, *Bull. acad. polon. sci.*, **7**, 821 (1959).

34) G. H. Cartledge and R. M. Nichols, *J. Am. Chem. Soc.*, **62**, 3057 (1940).
35) J. Meyer and W. Schramm, *Z. anorg. Chem.*, **123**, 56 (1921).
36) H. Taube, *J. Am. Chem. Soc.*, **70**, 3926 (1948).
37) A. Y. Drummond and W. A. Waters, *J. Chem. Soc.*, **1954**, 2456.
38) T. N. Srivastava, *Z. anorg. u. allgem. Chem.*, **288**, 288 (1956).
39) W. H. Hatcher and C. R. West, *Trans. Roy. Soc., Canada*, **21** (III), 269 (1927).
40) M. Cantley, L. Hough and A. O. Pettit, *Chem. Ind.*, **1959**, 1126.
41) J. Courtois, *Ann. pharm. franc.*, **7**, 77 (1949).

TABLE VI.

Volume of the reaction mixture: 50 ml.; All values in ml. of 0.01 N thiosulphate

| KI in ml. of $Na_2S_2O_3$ | $KMnO_4$ N | Citric acid M | Oxidant in the filtrate ml. | Iodine in the filtrate (1/4 of 4th. column) | Oxidant or iodine in the ppt. | Total of iodide and iodine found | % Deviation |
|---|---|---|---|---|---|---|---|
| 10 | 0.02 | 0.08 | 29.80 | 7.45 | 2.70 | 10.1 | + 1.5 |
| | | 0.04 | 32.00 | 8.00 | 1.40 | 9.40 | − 6.0 |
| | | 0.02 | 34.48 | 8.62 | 0.26 | 8.88 | −11.2 |
| | 0.01 | 0.08 | 17.40 | 4.35 | 6.70 | 11.05 | +10.5 |
| | | 0.04 | 20.20 | 5.05 | 5.60 | 10.65 | + 6.5 |
| | | 0.02 | 22.52 | 5.64 | 3.37 | 9.00 | −10.0 |
| 20 | 0.02 | 0.08 | 28.20 | 7.05 | 17.40 | 24.45 | +22.20 |
| | | 0.04 | 31.00 | 7.75 | 14.40 | 22.15 | +10.75 |
| | | 0.02 | 41.20 | 10.30 | 8.50 | 18.80 | − 6.0 |
| | 0.01 | 0.08 | 4.40 | 1.10 | 19.80 | 20.90 | + 4.5 |
| | | 0.04 | 8.40 | 2.10 | 18.60 | 20.70 | + 3.5 |
| | | 0.02 | 12.00 | 3.00 | 15.00 | 18.00 | −10.0 |

the regular increase or decrease in the values of this table does point to the correctness of the procedure adopted for the calculation.

It may thus be seen that, for low concentrations of iodide, the oxidant is always four times the equivalents of initial iodide, indicating the presence of the +3 state of iodine. The following reactions appear to take place:

$$MnO_4^- + \text{organic acid} \rightarrow Mn^{3+} \text{ (complex)} + \text{oxidation products of acid} \quad (1)$$

$$I^- + MnO_4^- \rightarrow I^0 + MnO_2 \quad (2)$$

$$I^0 + MnO_4^- \rightarrow IO_3^- + MnO_2 \quad (3)$$

$$I^0 + \text{organic acid} \rightarrow \text{substitution products} \quad (4)$$

$$I^0 + \text{oxidation product of acid} \rightarrow \text{substitution products} \quad (5)$$

$$IO_3^- + \text{oxidation products of acid} \rightarrow IO_2^- \quad (6)$$

$$MnO_2 \text{ or } Mn(III) + \text{acid or its products} \rightarrow Mn(II) + \text{products} \quad (7)$$

It would be reasonable to conclude, from the experiments on iodate (Tables III to V) and from the fact that permanganate is a strong oxidant, that iodate is first formed and that it is subsequently reduced to iodite. This could have been verified had it been possible to make a number of determinations of the oxidant (Table II) immediately after the addition of permanganate to the iodide-acid mixture. The iodometric determinations could be made, however, only when coloured manganese(III) complexes were reduced to colourless manganese(II) or its complexes. By the time this happens, iodate, even if formed earlier, has been reduced to iodite. The presence of iodate has been found[42] also when small amounts of iodide are oxidised by the permanganate in a sulphuric acid solution.

The first reaction of the above scheme has been reported[18,19,33,37,43-46] to be slow, but 2 is fairly fast.[4,5] The fate of iodine is now determined by reaction 3 on one hand, and by reactions 4 and 5 on the other. Ordinarily if the concentration of iodide is low, reaction 3 is predominant, which through 6 yields iodite; but if the concentration of malonic acid is also low, reactions 1, 4, 5, 6 and 7 would be insignificant and iodate will be the final product, giving oxidant values higher than the expected value of four times the original iodide. In some such cases manganese(IV) oxide was also precipitated.

If the concentration of iodide is increased, more iodine is produced and reactions 4 and 5 compete with 3. Part of the iodine gives substitution products with the acid and its oxidised species and, hence, is not raised to the +5 state by the permanganate. Consequently, the iodometric results are lower than expected for higher concentrations of iodide.

Citric acid seems to yield at least two oxidation products, one of which gives a soluble substituted product and the other, an insoluble one. These two products are obtained together if the temperature of the reaction is 25°C or higher, but at 20°C or lower, only a solid product can be obtained if the concentrations of iodide and citric acid are high. This yellow

42) Y. K. Gupta, unpublished work.
43) Y. K. Gupta and R. S. Awasthi, *Proc. Natl. Acad. Sci. (India)*, **29A**, 331 (1960).
44) L. Cabrera and C. Del Rio, *Anales. real Soc. espan fis. y quim (Madrid)*, **49B**, 263 (1953).
45) V. M. Bhale, S. Mohammad, W. V. Bhagwat and S. L. Bafna, *J. Sci. Indust. Res. (India)*, **12B**, 521 (1953).
46) A. Y. Drummond and W. A. Waters, *J. Chem. Soc.*, **1953**, 453.

product has properties similar to the tetraiodoacetone[47] reported to be formed under very similar conditions. The oxidation products of citric acid[48,49] are acetone, and acetonedicarboxylic, formic and oxalic acids. The solid product may be an iodine compound of one of these. Further work on this compound is in progress. In the case of malonic acid, the substitution product is soluble and is reported to be diiodomalonic acid.[29,43] Thus citric and malonic acids provide the products for the reduction of iodate to iodite and also prevent the accumulation of manganese dioxide, a product obtained from the reduction of permanganate. The organic acids react with it, giving soluble manganese(III) complexes.

Experiments with malic acid give somewhat similar results, but under limited conditions. The concentration ranges studied were:

| Malic acid | $KMnO_4$ | KI |
|---|---|---|
| $4—32\times10^{-2}$ M | $1—4\times10^{-2}$ N | $2—20\times10^{-4}$ N |

In most cases the oxidant was found to be 4 to 6 times the original concentration of iodide, which corresponds to the situation of iodite or iodate or a mixture of the two, depending on the relative concentrations of malic acid and the permanganate. Permanganate should be more than ten times the concentration of iodide; otherwise the iodide is not likely to be oxidised beyond the stage of iodine. Reactions with iodate show its oxidising capacity reduced to 2/3 iodometric values only when the concentrations of the permanganate and the acid are high. At other concentrations, reduction does invariably take place in all cases, but not always to the extent expected.

Experiments with lactic acid and iodate reveal that the latter is not reduced by the permanganate-oxidation products of the acid. Experiments with iodine show that it is partly oxidised to iodate and partly to iodite.

47) T. N. Srivastava, *J. Ind. Chem. Soc.*, **22**, 253 (1945).
48) P. Fleury and J. Courtois, *Compt. rend.*, **223**, 633 (1946).
49) G. Deniges, ibid., **130**, 32 (1900).

## Summary

Permanganate oxidises small amounts of iodide to iodite in the presence of malonic, citric or malic acid. The colourless reaction mixtures always have an oxidising capacity equivalent to four times the concentration of the iodide originally taken. In mixtures of permanganate and one of these acids, iodate is reduced to its 2/3 oxidising capacity, showing the formation of iodite. A mechanism for this has been suggested. Iodine is the product in the first stage of the oxidation of iodide, which is further oxidised to iodite or iodate or which may react with the oxidation products of the organic acids. Citric acid probably gives a number of such iodinated products, one of which is solid.

One of the present authors (Y. K. G.) wishes to thank the Scientific Research Committee, Uttar Pradesh, for a contingency grant for part of this work done at the Department of Chemistry, M. N. Regional Engineering College, Allahabad.

*Department of Chemistry*
*University of Rajasthan*
*Jaipur, India*

# The Base-catalyzed Condensation of *o*-Nitroacetophenone. III. The Structure of Compound A, a Condensation Product

By Takeo SAKAN, Kousuke KUSUDA[1] and Toshio MIWA

(Received May 28, 1964)

In a previous paper,[2] compound A,[3] $C_{17}H_{14}O_5N_2$, an orange-red product of the base-catalyzed condensation of *o*-nitroacetophenone, has been shown to contain *o*-nitrophenyl and *N*-hydroxyindoline moieties.

The reduction of compound A methyl ether, $C_{18}H_{16}O_5N_2$, with sodium borohydride gave a colorless product, dihydro-compound A methyl ether, $C_{18}H_{18}O_5N_2$. The infrared absorption spectrum of this compound indicated that the nitro group of the original compound had survived during the reduction. The dihydro-compound, on acetylation with acetic anhydridepyridine, gave a monoacetyl derivative, $C_{20}H_{20}O_6N_2$. The infrared absorption spectrum

1) Present address: Research Institute of Atomic Energy, Osaka City University, Kita-ku, Osaka.
2) T. Sakan, K. Kusuda and T. Miwa, This Bulletin, 37, 1681 (1964).
3) T. Sakan, K. Kusuda and T. Miwa, ibid., 37, 1678 (1964).

of the latter has a peak at 3435 $cm^{-1}$, which should be assigned to a tertiary hydroxyl group of the indoline nucleus.[2] The formation of an acetylable hydroxyl group by the reduction seems to imply the presence of a carbonyl group in the original compound.

The catalytic hydrogenation of dihydro-compound A methyl ether in the presence of palladium-on-carbon gave an amine, $C_{17}H_{18}ON_2$. The ultraviolet absorption of the amine indicated the presence of an indole nucleus in it. The amine, on brief heating with acetic anhydride, was transformed into a monoacetyl derivative, whereas it was converted into an *O*, *N*-diacetyl derivative by treatment with acetic anhydride-pyridine. The latter derivative was obtained in the crystalline state with a molecule of benzene as a solvent of crystallization. The series of reductions will be represented by partial structures in Chart 1.

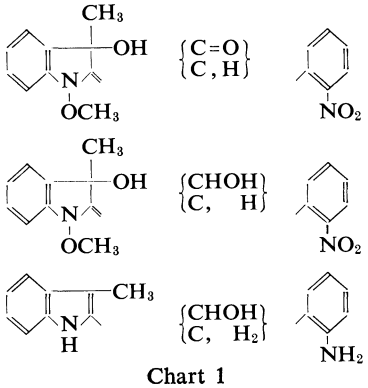
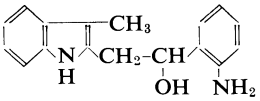


Chart 1

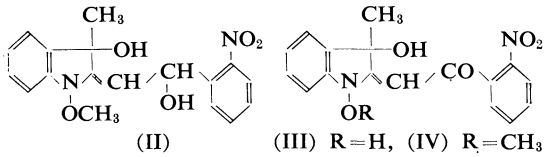
The fact that the catalytic hydrogenation of compound A methyl ether over Raney nickel at a high temperature and high pressure gave the same indole-amine confirmed that no skeletal change had occurred during the above reductions.

The indole-amine on alkali-fusion was cleaved to give 2, 3-dimethylindole and anthranilic acid in fairly good yields. The latter product was isolated as the *N*-acetyl derivative. Hence, structure I was assigned to the indole-amine.



(I)

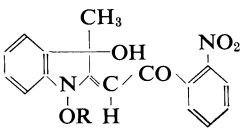
Consequently, dihydro-compound A methyl ether, compound A and its methyl ether possess structures, II, III and IV respectively.



(II) (III) R=H, (IV) R=$CH_3$

Loudon and Wellings[4] reported that the *O*-acetyl derivatives of cyclic hydroxamic acids exhibit an intense absorption near 1800 $cm^{-1}$. Interestingly, the acetyl derivative of compound A, a vinylog of hydroxamic acid, has a strong peak at 1796 $cm^{-1}$. The acetyl derivative decomposed gradually on being kept at room temperature for a long time.

The infrared spectra of compound A methyl ether and acetate give information on the stereochemistry around the double bond in these compounds. Both of the compounds in the solid state possess a very weak band near 3100 $cm^{-1}$ as a result of the tertiary hydroxyl group. The low wave number of the band is probably due to an intermolecular hydrogen bonding, for the band is shifted to about 3300 $cm^{-1}$ when the compounds are dissolved in carbon tetrachloride. The fact that this band of the methyl ether remains at 3300 $cm^{-1}$, even in a very dilute solution ($3.4\times10^{-4}$ M in carbon tetrachloride), suggests the presence of an intramolecular hydrogen bonding between the tertiary hydroxyl and the carbonyl of this compound, thus locating these groups on the same side of the double bond as shown in V. Compound A itself has the same configuration, for the mild conditions of the methylation should not change the stereochemistry around the double bond.

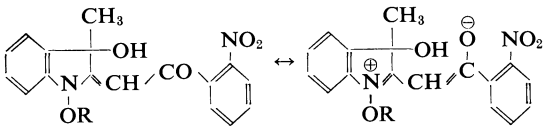


(V)

The carbonyl stretching absorption of compound A is quite obscure, as has been stated in a previous paper.[3] The infrared spectra of the methyl ether and the acetate also show quite unusual features in the region. Although they have a band of medium intensity at 1626 and 1632 $cm^{-1}$ respectively, it appears that these should be assigned to the double bond rather than to the carbonyl bond, the stretching band of the latter being considered to be shifted to about 1500 $cm^{-1}$ from the following reasons: (1) The bands at 1626 and 1632 $cm^{-1}$ are rather weak for the carbonyl bond; (2) the 1500 $cm^{-1}$ bands of these compounds are much broader than those of dihydro-compound A derivatives; (3) the 1500 $cm^{-1}$ bands show a shoulder near 1560 $cm^{-1}$ in a carbon tetrachloride solution. The unusual shift of the carbonyl absorption of compound A derivatives may be due to an intense interaction between

4) J. D. Loudon and I. Wellings, *J. Chem. Soc.*, **1960**, 3463.

the tertiary hydroxyl group and the carbonyl oxygen atom, which possesses a high electron density produced by the mesomerism VI ↔ VII.



(VI) (VII)

The characteristic ultraviolet spectra[3] of compound A and its alkyl ethers correspond to those of β-amino-α, β-unsaturated ketones.[5]

The base-catalyzed condensation of the homologous *o*-nitrophenyl ketones is currently being investigated. The mechanism for the formation of compound A will be discussed in a later paper.

## Experimental[6]

**The Sodium Borohydride Reduction of Compound A Methyl Ether. Dihydro-Compound A Methyl Ether (II).** — To a solution of 1.70 g. (5 mmol.) of compound A methyl ether[3] in 60 cc. of methanol 0.5 g. (13 mmol.) of sodium borohydride was added. The mixture was heated on a water bath for five minutes and diluted with 10 cc. of water, and the solvent was removed by distillation. The residue was then triturated with water, filtered, washed with water, and dried. The crude material weighed 1.25 g. (73%). A small portion of the material was recrystallized from aqueous methanol for analysis. A pure compound melts at 155°C. IR 3304, 3240 (OH), 1529, 1350, 855 ($NO_2$).

Found: C, 63.09; H, 5.83; N, 7.86. Calcd. for $C_{18}H_{18}O_5N_2$: C, 63.15; H, 5.30; N, 8.18%.

**Dihydro-Compound A Acetate.** — A mixture of 320 mg. (0.93 mmol.) of dihydro-compound A methyl ether, 1.5 cc. of acetic anhydride, and 7 drops of pyridine was shaken for three hours, left to stand overnight, and decomposed with water. The separated crystals were then filtered, washed with water, and dried. Crude acetate (m. p. 140.5—142°C) weighed 340 mg. (95%). Recrystallization from ethanol gave pure acetate melting at 145°C. IR 3435 (OH), 1718 (CO), 1522, 1355, 855 ($NO_2$).

Found: C, 62.33; H, 5.64; N, 7.34. Calcd. for $C_{20}H_{20}O_6N_2$: C, 62.49; H, 5.24; N, 7.29%.

**2-[2-(*o*-Aminophenyl)-2-hydroxyethyl]-3-methylindole (I).** — *The Catalytic Hydrogenation of Dihydro-Compound A Methyl Ether.* — Dihydro-compound A methyl ether (1.13 g., 3.3 mmol.) in 100 cc. of methanol was hydrogenated in the presence of 0.5 g. of 5% palladium-on-carbon. After the removal of the catalyst, the methanol was distilled and the residue dissolved in a small amount of hot benzene. On cooling, 0.63 g. (64%) of the indoleamine was obtained. The amine (m. p. 151—152°C) was found to be identical with the sample described below by an admixture test and by infrared spectroscopy.

*The High Pressure Hydrogenation of Compound A Methyl Ether.*—A solution of 1.0 g. (2.9 mmol.) of compound A methyl ether in 50 cc. of ethanol was hydrogenated over 1.0 g. of Raney nickel at a hydrogen pressure of 75 atm. and 125—145°C for three hours. The hydrogenation mixture was worked up as described above to give 0.2 g. of the amine melting at 146—148°C. The amine, after recrystallization from benzene, melted at 149.0—149.5°C. $\lambda_{max}$ 229—230 (4.61), 286 (4.02), 293 (3.99). IR 3390 (NH and OH).

Found: C, 76.60; H, 6.99; N, 10.30. Calcd. for $C_{17}H_{18}ON_2$: C, 76.66; H, 6.81; N, 10.52%.

***N*-Acetyl Derivative.**—A mixture of 0.46 g. (1.6 mmol.) of the amine and 0.8 cc. of acetic anhydride was heated to the boiling point, immediately cooled with water, and decomposed with 5 cc. of water. The separated solid was then filtered, washed with water, and dried. The acetate, after recrystallization from ethanol, melted at 154.5—155.5°C. IR 3400 (OH), 3210 (NH), 1645 (CO).

Found: N, 9.06. Calcd. for $C_{19}H_{20}O_2N_2$: N, 9.09%.

***O*, *N*-Diacetyl Derivative.**—To a solution of 240 mg. (0.8 mmol.) of the amine in 1 cc. of pyridine, 0.3 cc. of acetic anhydride was added at room temperature. The mixture was left to stand overnight and diluted with water, and the separated oil was triturated with 1 N hydrochloric acid until it became solid. The dried solid was recrystallized from benzene. The pure diacetyl derivative melts at 108°C. IR 3340 (NH), 1728, 1663 (C=O).

Found: C, 75.62; H, 6.64; N, 6.07. Calcd. for $C_{21}H_{22}O_3N_2$-$C_6H_6$: C, 75.67; H, 6.59; N, 6.54%.

**The Alkali-fusion of the Indole-amine I.** — A solution of 0.8 g. of the amine and 1.0 g. of potassium hydroxide in 3 cc. of methanol was heated under nitrogen to 180°C; at that temperature effervescence occurred. The mixture was kept at the temperature for a few minutes until the foaming subsided; then it was cooled and taken into water and ether. The aqueous layer was neutralized with 1 N hydrochloric acid until the solution had become slightly turbid, treated with two portions of 1 cc. of acetic anhydride each, acidified with hydrochloric acid to Congo red, and extracted with ether. The ether was then evaporated and the residue treated with benzene and petroleum ether to yield about 30 mg. of precipitates, which on recrystallization from water melted at 185.5°C. This material was identified with *N*-acetylanthranilic acid, m. p. 186—187°C, by the mixed melting point test with an authentic sample and by infrared spectroscopy. The original ethereal layer, on concentration, gave 180 mg. of crystals melting at 104—108°C. The crystals, after sublimation followed by recrystallization from petroleum benzine, melted at 107—108°C. This compound was identified as 2,3-dimethylindole, m. p. 106.5—107°C, by mixed melting point determination and by infrared spectral comparison.

**Compound A Acetate.**—An aqueous-alkaline solution of compound A was treated with acetic anhydride under ice-cooling. The precipitates formed

5) N. H. Cromwell and J. C. David, *J. Am. Chem. Soc.*, **82**, 2046 (1960).

6) All melting points are uncorrected. Unless otherwise noted, the ultraviolet spectra were taken in ethanol and the infrared spectra in Nujol mull; they are expressed in $\lambda_{max}$ mμ (log ε) and in IR $cm^{-1}$ respectively.

were dissolved in aqueous ethanol and the solution was condensed in a desiccator to give yellow crystals decompositing at 108—109°C. IR (in $CCl_4$) 3300 (OH), 1818 (C=O), 1525, 1346 850 ($NO_2$).

Found: C, 62.10; H, 4.57; N, 7.63. Calcd. for $C_{19}H_{16}O_6N_2$: C, 61.95; H, 4.38; N, 7.61%.

The authors are very much indebted to Dr. Hideo Kamio of the Research Laboratory of the Takeda Chemical Industries, Ltd., for his kind measurement of the infrared spectrum in high dilution, and also to Dr. Masao Yamaguchi of the Wakayama Prefectural Medical College for his valuable discussions about infrared spectroscopy. The present work was supported in part by a grant-in-aid from the Ministry of Education.

*Faculty of Science*
*Osaka City University*
*Sumiyoshi-ku, Osaka*

# An Electron Paramagnetic Resonance and Spectrophotometric Study of Titanium(III)-Chelate Compounds with Nitrilotricarboxylic Acid and Its Derivatives

By Maurice CODELL,* Shizuo FUJIWARA, Kozo NAGASHIMA and Tokuko SEKI

(Received June 9, 1964)

The EPR hyperfine structure of titanium(III) has recently been obtained with several chelating agents,[1] and the chemistry of mixed chelate compounds of titanium(III), EDTA and several complexing organic acids has recently been elucidated,[2] where titanium(III)-EDTA and oxalic, tartaric, citric, and lactic acids have been shown to form complexes which give EPR signals and can be spectrophotometrically identified. It has also been recently shown[3] that a complex formed between titanium(III), zinc and tartaric acid gives an EPR signal of two peaks.

The effect of varying numbers of carboxyl groups on chelating agents of a similar structure seemed of considerable interest, since experience with several chelating agents has shown that those agents with the largest numbers of coordinating groups are the most likely to give EPR signals showing the hyperfine structure of titanium(III). The chelating agents investigated were nitrilotriacetic acid (NTA) $N(CH_2COOH)_3$, hydroxyethyliminodiacetic acid (HEID) $N(CH_2COOH)_2CH_2CH_2OH$, Bishydroxyethyl glycine (BHEG) $N(CH_2OH)_2CH_2COOH$, and iminodiacetic acid (IDA) $HN(CH_2COOH)_2$. NTA gives the largest EPR signals, while IDA, which contains -H in place of $-CH_2CH_2OH$ in HEID, gives the smallest signals.

EPR spectra were obtained using capillary tubes containing solutions prepared by admixing the constituents and adjusting the pH. In the spectrophotometric establishment of the combining ratios of titanium(III) to NTA and HEID in an acid solution, the concentration range of the chelating agents was limited because of the slight solubility of the excessive agents.

**Apparatus and Reagents.**—The electron paramagnetic resonance spectrometer used was a model JES-118 manufactured by the Japan Electron Optics Company. The recording spectrophotometer used was a Cary Model 11. The spectrophotometers used were Hitachi, model EPU-2 and Hirama, model IIB, filter electrophotocolorimeters.

*Titanium(III) Chloride Solution.*—A pure grade of titanium sponge (courtesy of the Osaka Titanium Corporation, Amagasaki, Japan) was dissolved in hot 6 N hydrochloric acid. An excess of titanium sponge was added to the hydrochloric acid, and additional acid was added as the reaction progressed in order to prevent the acid concentration from falling to the point where hydrolysis could occur. The solution was decanted from the metal while the vigorous reaction was proceeding in order to prevent the formation of any appreciable quantity of titanium(IV). The solution was then maintained in an atmosphere of nitrogen. The final concentration of titanium(III) ions was determined volumetrically by titration with a ceric sulfate solution.

* On leave from the Pitman-Dunn Institute for Research, Philladelphia, Penna.

1) S. Fujiwara and M. Codell, This Bulletin, **37**, 49 (1964).

2) S. Fujiwara, K. Nagashima and M. Codell, ibid., in press.

3) S. Fujiwara, K. Nagashima and M. Codell, *J. Chem. Soc. Japan, Pure Chem. Sec.* (*Nippon Kagaku Zasshi*), **85**, 305 (1964).

*Chelating Reagents.* — The NTA and IDA used were commercial first-grade reagents (Wako Junyaku Co., Tokyo). The HEID and BHEG were synthetized for this investigation (courtesy of Daiichi Seiyaku Co., Ltd., Tokyo).

**Titanium(III)-NTA Complexes.** — Nitrilotriacetic acid (NTA) forms a complex with titanium(III), which is quite stable and which gives the largest EPR signals of the group studied in this investigation (Fig. 1). A 0.1 M

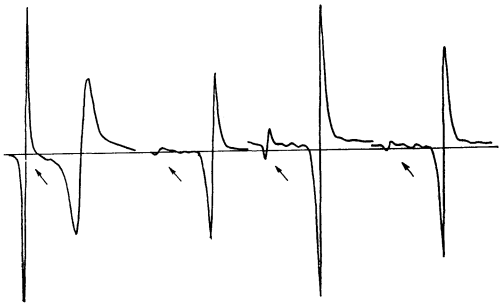



Fig. 1. EPR spectra for Ti(III)-NTA complexes. The concentration of Ti(III) is 0.2 M and the concentration of NTA is 0.4 M. The pH was adjusted with NaOH. Arrows designate DPPH.

titanium(III) solution of this complex gives signals at pH 1.7, although at pH 1.5 no signal was obtained. The signals become larger with increasing pH values up to approximately 4. Above pH 4, however, the signal intensity remains almost constant to a pH value of approximately 10.

Figure 2 shows a complex at pH 1 which gives a blue solution and exhibits a maximum absorbance at 600 m$\mu$, and another complex at pH 4.7 which gives a greenish yellow solution with a maximum absorbance at 710 m$\mu$.

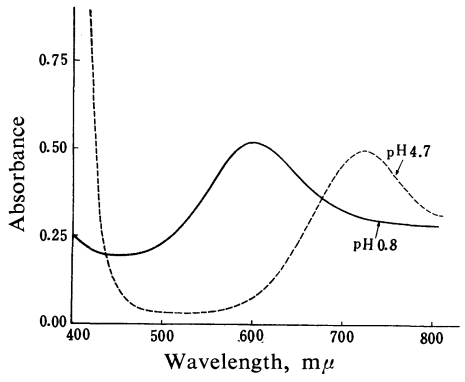



Fig. 2. Spectrophotometric curves of Ti(III)-NTA complexes in solution.

Figure 3 shows the change in the optical absorbance of each maximum with the changing pH value. The maximum, which occurs

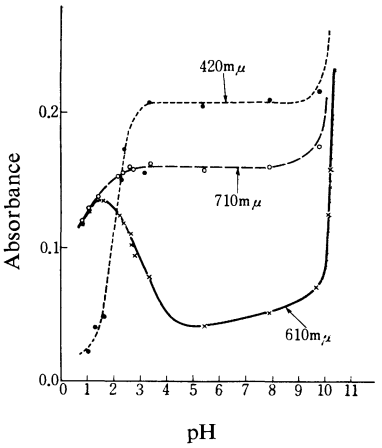



Fig. 3. Change of optical absorbance of Ti(III)-NTA solutions containing tartaric acid with change in pH values.

at 600 m$\mu$, increases with an increase in the pH value up to about pH 1.5, and then decreases from about pH 1.5 to about pH 4. A red filter whose absorbance curve reaches a peak at approximately 610 m$\mu$ was used to determine the above maximum. The points for pH values higher than 3.5 were extrapolated because of interference from the peak which shows a maximum absorbance at 710 m$\mu$. The maximum which occurs at 710 m$\mu$ increases with the increase in pH values. It attains the highest value at pH 3.5 and shows no further change with the increase in pH until a pH value of a little above 9 is attained, whereupon a rapid increase in absorbance occurs with the further increase in pH value.

The establishment of the ratios of titanium(III) to NTA are shown in Figs. 4a through

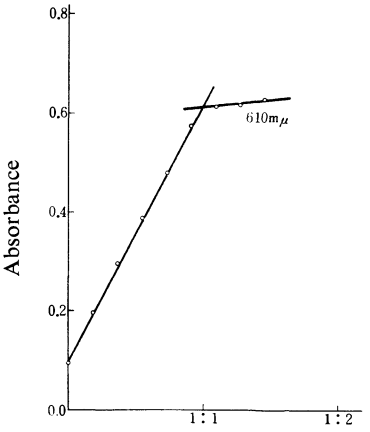



Fig. 4a. Establishment of the ratio of Ti(III) to NTA at pH 1.5 by the molar ratio method. Higher concentrations of NTA were not tested because of the limited solubility.

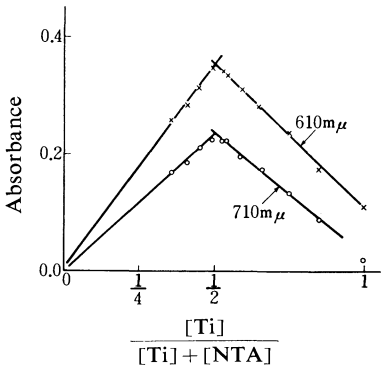



Fig. 4b. Establishment of the ratio of Ti(III) to NTA at pH 1.0 by the method of continuous variation.

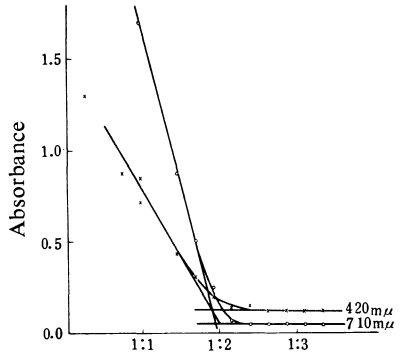



Fig. 4c. Establishment of the ratio of Ti(III) to NTA at pH 9.0 by the molar ratio method.

4c. Figure 4a shows the molar ratio method for determining the composition of the species which exists at pH 1.5 and which exhibits a maximum absorbance at 600 mμ. The red filter mentioned above was also used for this experiment. Figure 4b shows the method of continuous variation for establishing the ratio of the same species. The ratio is clearly shown to be 1 to 1 by both procedures. Figure 4c shows the molar ratio method for establishing the ratio of the species which appears at pH values between 3.5 and 9. Experiments were carried out at pH 9 in the presence of tartaric acid to prevent the hydrolysis of titanium(III). The strong blue color of the titanium(III)-tartrate compound becomes lighter upon the addition of increasing amounts of NTA. The absorbance curve changes abruptly at a ratio of 1 titanium(III) to 2 NTA, corresponding to the formation of the chelate. The species which exists in this solution shows a maximum absorbance at 710 mμ.

From the above discussion, the following complex species may be proposed;

| Formula | Optical absorbance at | Predominant at pH | g Value (EPR) |
|---|---|---|---|
| (1) $Ti(III)(NTA)_1$ | 600 mμ | 1.5 | unobservable |
| (2) $Ti(III)(NTA)_2$ | 710 mμ | 3.5—9 | $1.961 \pm 0.002$ |

**The Titanium(III)-HEID Complexes.**—Figure 5 shows the absorbance curves of a titanium(III)-HEID solution at different pH values. At pH 1.4 the solution is blue and the maximum absorbance is seen at 590 mμ. At pH 5.0 the solution is yellowish green and the maximum is shown at 720 mμ. At pH 9.2 the solution is purplish and the maximum appears at 540 mμ. Figure 6 shows the change in absorbance with the variation in pH values. It should be noted that the complex which shows a maximum absorbance at 590 mμ exhibits the highest intensity at pH 1.2 (traced with a 610 mμ filter). The complex which shows a maximum absorbance at 720 mμ shows a steady increase in intensity up to a pH value of about 3, and it remains constant to pH 5.5, after which an increase in intensity occurs until a pH of

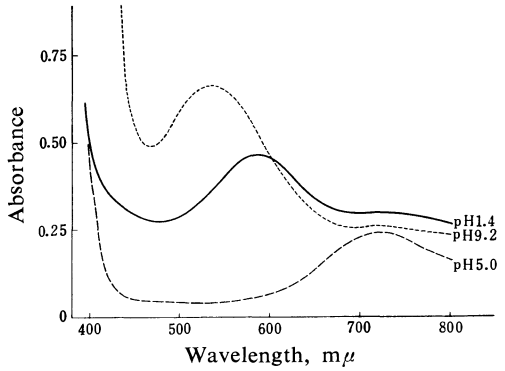



Fig. 5. Spectrophotometric curves of Ti(III)-HEID complexes in solution.

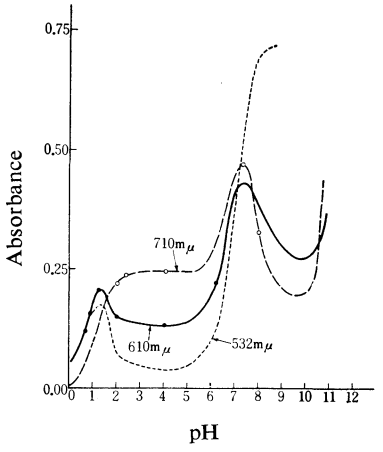



Fig. 6. Change of optical absorbance with pH of Ti(III)-HEID solutions.

about 7 is attained when a 710 mμ filter was used. At pH values above 7 a continual decrease is noted. The peculiar appearance of the curves at pH values above 8 is due to precipitation.

From Fig. 6 it may be seen that the complex which shows a maximum absorbance at 540 mμ (traced by using a 532 mμ filter) exhibits the highest intensity at pH 8, which indicates that this complex is the predominant species at higher pH values.

Figures 7a through 7c show the spectrophotometric determination of the ratios of titanium(III) to HEID. Filters which transmit the light of wavelengths close to the absorbance maxima of the complexes were used. The same procedures were applied for these determinations as for the titanium(III) to NTA ratios. Figure 7a shows that at pH 1.2 titanium(III) is combined with HEID in a 1 to 1 ratio. Two species were shown by the EPR spectra (Fig. 8) to exist at this pH, with one of the species being predominant.

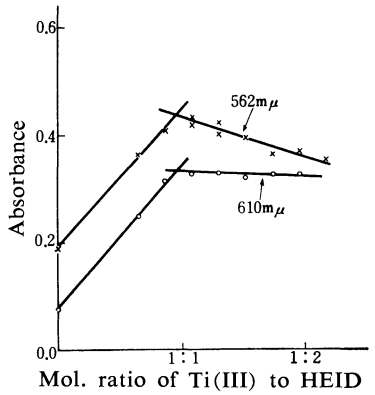



Fig. 7a. Establishment of the ratio of Ti(III) to HEID at pH 1.2 by the molar ratio method.

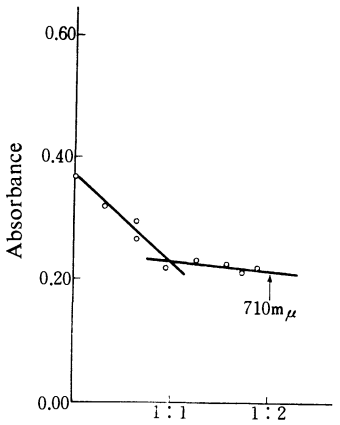



Fig. 7b. Establishment of the ratio of Ti(III) to HEID at pH 4.2 by the molar ratio method.

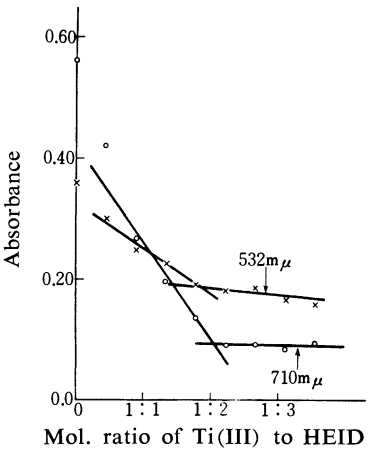



Fig. 7c. Establishment of the ratio of Ti(III) to HEID at pH 9.2 by the molar ratio method.

The minor species, which exhibits a maximum absorbance at 720 mμ and which is stable at higher pH values (pH 3—5.5) was shown, as is illustrated in Fig. 7b, to be in a 1 to 1 ratio. Thus, it must be concluded that the species which exhibits a maximum absorbance at 590 mμ and which is stable at the lower pH values (—pH 1.2) is composed of 1 to 1 proportions of titanium(III) and HEID. Figure 7b shows that at pH 4.2 a species composed of a 1 to 1 ratio is also predominant, while it may be seen in Fig. 7c that, at pH 9, a species composed of a 1 to 2 ratio predominates. The experiments illustrated in Fig. 7c were carried out in the presence of tartaric acid to prevent the hydrolysis of titanium(III). The strong blue color of the titanium(III)-tartrate compound becomes lighter upon the addition of increasing amounts of HEID. The absorbance curve changes abruptly at a ratio of 1 titanium(III) to 2 HEID.

Figures 7a through 7c show the decrease in the absorbances with an increase in the quantities of HEID. This is probably due to the

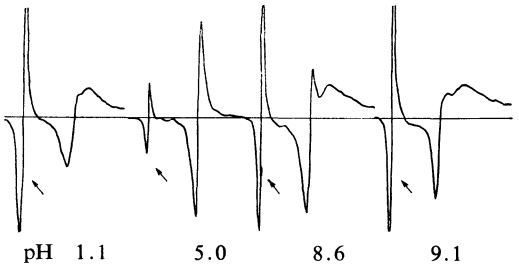



Fig. 8. EPR spectra for Ti(III)-HEID complexes. The concentration of $TiCl_3$ is 0.2 M and concentration of HEID is 0.4 M. The pH was adjusted with NaOH. Arrows designate DPPH.

oxidizing effect of some impurity in the reagent.

Figure 8 shows EPR spectra for the titanium(III)-HEID system. To obtain the EPR spectra at very low pH values a concentrated solution must be used, since the signal intensity is so low. At pH 1, two peaks are obtained. As the pH value is increased, however, only one peak is discernible. The signal intensity increases to pH 3.7, after which little change is noted until a pH of 7.5 is reached; a second peak then appears which is favored by higher pH values.

The following species may be proposed to represent the complexes which exist at the various pH values mentioned above.

| | Absorbance at | Predominant at pH | $g$ Value |
|---|---|---|---|
| (1) $Ti(III)_1$-$(HEID)_1$ | 590 m$\mu$ | 1.2 | 1.952± 0.002 |
| (2) $Ti(III)_1$-$(HEID)_1$ | 720 m$\mu$ | 3 to 5.5 | 1.952± 0.002 |
| (3) $Ti(III)_1$-$(HEID)_2$ | 540 m$\mu$ | >8 | 1.952± 0.002 |

Species 1 and 2 represent those species which are similar in composition but which are stable at different pH values and which exhibit different optical absorbances. Species 1 must be an acid complex in which the HEID is bidentate ($HEIDH^{-1}$) and one hydrogen of a carboxylic group remains unionized, and species 2, a complex in which HEID is tridentate and both hydrogens are ionized.

From Figs. 5 and 6 it may be seen that at pH 1 to 1.5 species 1 is predominant, but some absorbance at 720 m$\mu$ is observable. The EPR spectrum (spectrum at pH 1.1 of Fig. 8) shows a major species and a minor species which correspond to the species which were spectrophotometrically observed.

**Titanium(III)-BHEG, and -IDA Complexes.**— The absorbance curves obtained with the blue solutions of titanium(III) and BHEG are always very broad, with a considerable absorbance over the entire visible spectrum. This indicates some hydrolysis which precludes the establishment of formation ratios by the spectrophotometric technique. With titanium(III) and BHEG a very small EPR signal can be obtained at pH 5.2; the signal increases with an increase in pH values up to about 9, after which the signals decrease in size. Only one peak can be obtained, and no definite hyperfine structure is discernible.

Figure 9 shows that the signal obtained with a solution containing BHEG to titanium(III) in a ratio of 6 to 1 is definitely larger than that obtained with a 3 to 1 ratio. The presence of oxalic acid has no apparent effect on the signal size or shape.

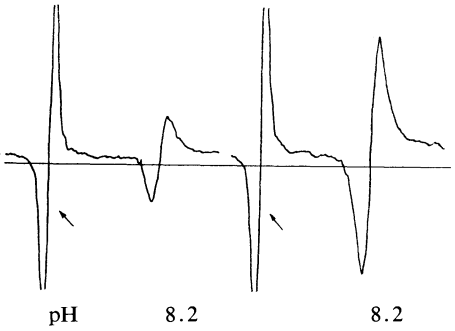



Fig. 9. EPR spectra for the Ti(III)-BHEG complex. The concentration of Ti(III) is 0.2 M and the concentration of BHEG is 0.6 M for the smaller spectrum and 1.2 molar for the larger spectrum. The pH was adjusted with NaOH. The chart speed for this figure is different than that used for Figs. 1 and 8. Arrows designate DPPH.

Solutions containing titanium(III) and IDA are blue and give EPR signals only over the narrow pH range of 7.5 to 9.0. Only one peak can be seen, and all the signals are very small. The presence of oxalic acid has a definite depressing effect on the signal intensity.

## Summary

Complexes formed by titanium(III) and agents which are similar in structure but varying in numbers of carboxyl groups have been studied by EPR and spectrophotometry. Among the reagents investigated, NTA, which posesses four coordinating groups, gives the largest EPR signals with a well-developed hyperfine structure. BHEG, which possesses two coordinating groups, gives much smaller signals, and even at the highest sensitivity setting of the instrument, no definite hyperfine structure can be detected. HEID, which posesses three coordinating groups, gives signals with two peaks, which indicates the simultaneous existance of two complexes in the solution. The ratios of the complexes of titanium(III) and NTA and HEID which exist in solution at various pH values have been spectrophotometrically determined.

The authors wish to express their thanks to Dr. Junzo Shinoda of the Daiichi Seiyaku Co., Ltd., Tokyo for his kindness in giving them reagents.

*Department of Chemistry*
*Faculty of Science*
*The University of Tokyo*
*Hongo, Tokyo*

# Life-time of the Propagating Radicals in the Radiation-Induced Telomerization of Ethylene with Propanol-2*

By Motoyoshi HATADA and Kozo HIROTA

(Received June 10, 1964)

In previous reports[1,2] the telomerization of an ethylene - propanol-2 mixture was investigated by using $\gamma$-rays as the initiating agent, and it was concluded that the telomers are produced by the following elementary reaction:

$$(CH_3)_2CHOH \rightsquigarrow (CH_3)_2\dot{C}OH$$

$$(CH_3)_2\dot{C}OH + C_2H_4 \longrightarrow (CH_3)_2C(OH)-CH_2-CH_2\cdot$$

$$\longrightarrow (CH_3)_2C(OH)CH_2-CH_3$$

$$\text{or } (CH_3)_2C(OH)-CH_2-CH_2-CH_2-CH_2\cdot$$

In the present research, the telomerization of the same system will be investigated by the use of electron beams from a Van de Graaff accelerator instead of $\gamma$-rays, adopting both intermittent and steady irradiation methods in order to determine the life-time of the chain-carrying radicals. The results will be given and compared with those of the previous reports.

## Experimental

**Materials.**—Propanol-2 was dried over calcium hydride and was distilled before each use. Commercial ethylene (99.8%) was used without any purification.

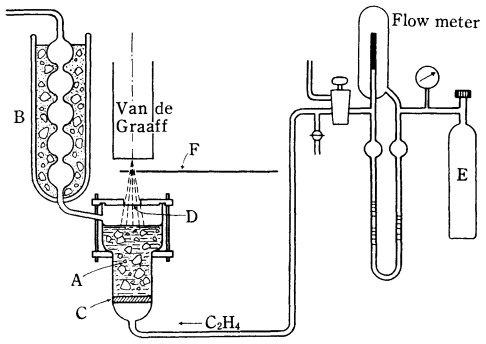



Fig. 1. Apparatus for electron beam irradiation.

**Irradiation Procedures.** — Figure 1 shows the apparatus for irradiation. Propanol-2 (80 ml.) was held in the irradiation vessel (A) (56 mm. $\phi$ in diameter) equipped with the condenser (B) kept at $-78°C$, a glass-filter (C) for bubbling ethylene into the vessel, and a window (D) made of aluminum film (0.1 mm. thick, 3.0 cm. in diameter), through which the electron beam penetrates into the irradiation vessel.

For the intermittent irradiation, the rotating sector method was used. A rotating aluminum disk (F) (4 mm. thick, 60 cm. in diameter) with two $\pi/6$ sector openings was placed between the irradiation windows of the Van de Graaff accelerator and the irradiation vessel. The ratio of the off-to-on time was kept constant at 5 throughout the experiments. The period of a whole cycle could be varied from 0.06 to 6.0 sec.

A spot electron beam (1.5 MeV, 100 $\mu$amp.) from the Van de Graaff accelerator (High Voltage Eng. Co.) was used for the irradiation. The dose rate was estimated to be $2.6\times10^{22}$ eV. $min^{-1}$ from the amount of oxalate ions produced by the irradiation of an aqueous solution of sodium formate, which was contained in a vessel with the same specifications as the irradiation vessel of propanol-2 and ethylene. This method was proposed and elaborately described by Hardwick and Guenter.[3]

**Analysis.**—After irradiation, samples were taken out and subjected to gas-chromatographic analysis. (Apparatus: Shimadzu GC1A)

## Results

In the sample irradiated, *t*-amyl alcohol could be identified by the use of a 3.0 m. column of dioctylphthalate. The higher telomers found in the previous reports were not identified in the present experiment. In Fig. 2, the amount of *t*-amyl alcohol produced is plotted against the irradiation time. Without any inhibitor, as is indicated by the open circles in the figure, the amount of telomer increases linearly with the irradiation time. By the addition of $3.66\times10^{-4}$ mol. of DPPH, some retardation was observed, as is indicated by the filled circles. The inclinations of the linear part of the two lines are equal, however.

By the use of a gas chromatograph equipped with a hydrogen flame ionization detector, several products other than *t*-amyl alcohol were

* Chain Telomerization Induced by Radiation. VII. Preliminary report: M. Hatada and K. Hirota, The 5th Meeting of Radiation Chemistry, Tokyo, 1962.

1) K. Hirota and M. Hatada, This Bulletin, **34**, 1644 (1961).

2) M. Hatada and K. Hirota, Proceedings of the 4th Conference on Radioisotopes, 294 (1961), Tokyo.

3) T. J. Hardwick and W. S. Guenter, *J. Phys. Chem.*, **63**, 897 (1961).

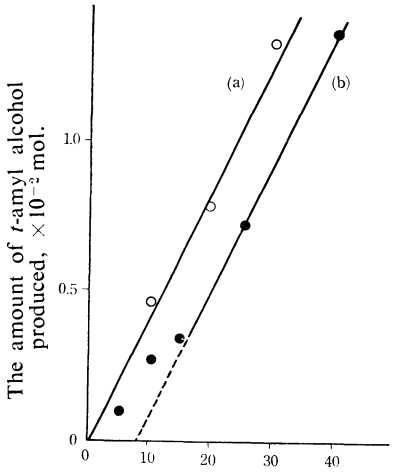



Fig. 2. The amount of *t*-amyl alcohol produced vs. irradiation time.
○ : without inhibitor
● : $3.6\times10^{-4}$ mol. DPPH
Electron accelerating voltage : 1.5 MeV.
Electron beam current : 100 $\mu$amp.
Dose rate : $2.5\times10^{22}$ eV./min.
Ethylene flow rate : 128 ml./min.

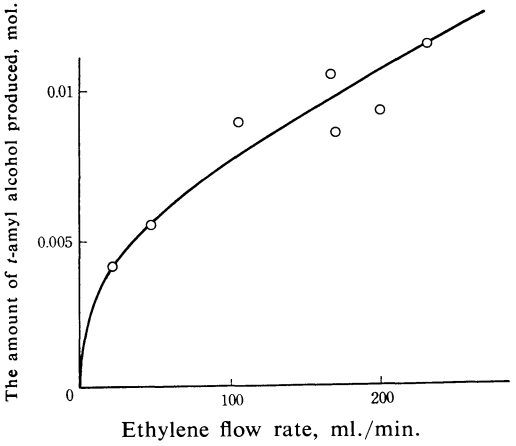



Fig. 3. The amount of *t*-amyl alcohol produced vs. flow rate of ethylene.
Isopropanol 80 ml.
Irradiation acc. volt : 1.5 MeV.
beem curr.: 100 $\mu$amp.
time : 30 min.

found to be produced. The details of the results will be published elsewhere.

In Fig. 3 the amount of the telomer produced after 30 min. of irradiation is plotted against the flow rate of ethylene. Up to the flow rate of 30 ml./min., the rate of telomer formation increases markedly with the flow rate of ethylene, but above this critical flow rate the rate of formation seems to increase linearly with the ethylene flow rate.

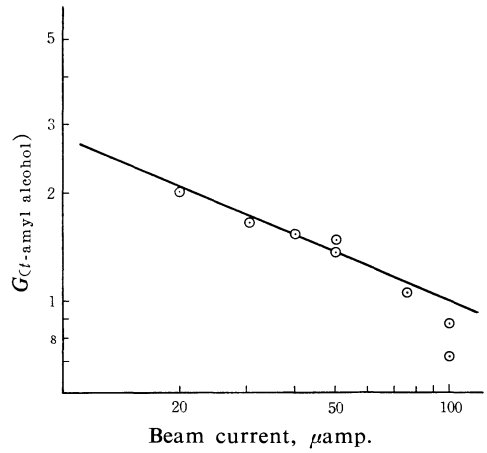



Fig. 4. $G_{(t\text{-amyl alcohol})}$ vs. electron beam current.
Ethylene flow rate : 128 ml./min.

In Fig. 4 the $G$ value for *t*-amyl alcohol formation is plotted against the electron beam current in logarithmic scales. Since the dose rate depends linearly on the beam current, the $G$ value for telomer formation is proportional to the $-1/2$ power of the dose rate.

The results of the sector experiment are shown in Fig. 5, in which the $R_0/R_s$ is plotted

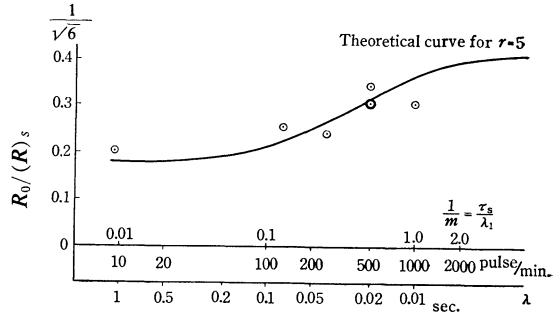



Fig. 5. Comparison of theoretical and experimental relative reaction rates.
Dose rate : $2.6\times10^{22}$ eV./min.
Ethylene flow rate : 128 ml./min.

against logarithms of the pulse frequency in pulses/min. as the abscissa, where $R_0$ and $R_s$ are the average radical concentration under intermittent and steady irradiations respectively and are assumed to be given by the amount of the telomer produced by irradiation. The theoretical curve shown in the same figure is plotted against $\lambda_1/\tau_s$ from the table by Burnett and Melville,[4] where $\lambda_1$ is the time when the beam is on, and $\tau_s$ is the mean life-time of the radicals.

4) G. M. Burnett and H. W. Melville, "Techniques of Organic Chemistry," Vol. IV, Interscience Publishers, New York (1953), p. 144.

## Discussion

As is shown in Fig. 2, the formation of *t*-amyl alcohol was not inhibited completely, but it was retarded by the addition of DPPH. This retardation may be caused by the fact that, because of the high concentration of radicals produced by the electron beams of a high dose rate, DPPH can not inhibit the telomer formation effectively.

On the other hand, this retardation might be considered to be a contribution of some reaction paths which are not affected by the presence of DPPH. However, in the present research, these paths were assumed to play little part in the telomer formation.

The rate of initiation, $v_i$, was estimated approximately to be of the order of $10^{-5}$ mol. $l^{-1}$ $sec^{-1}$ from the following equation:

$$v_i = -\frac{d[DPPH]}{dt} \simeq \frac{\Delta[DPPH]}{\Delta t}$$

Where [DPPH] is the initial concentration of diphenylpicrylhydrazyl in mol. $l^{-1}$ and $\Delta t$ is the induction period in sec. assumed to be given by the intercept of curve b.

From the $\lambda_1$ scale of Fig. 5, where $\lambda_1/\tau_s$ is unity, $\tau_s$ is estimated to be 0.01 sec. This value is a little smaller than that estimated by Clingman in a similar telomerization reaction between *n*-butylmercaptane and *n*-octene,[5] although the chain-carrying radicals and dose rates are different in the two cases.

However, there remain some ambiguities which may arise from the shape of the electron pulses. The electron pulses used in the present research were not exactly square in shape, but were rather complicated, because each pulse consisted of a number of trigonometrical waves of 400 c./sec., which might be induced by the rotating magnetic field (400 c./sec.) of the generator of the Van de Graaff accelerator. However, since the frequency of pulses was very low compared to 400 c./sec., the pulse shape can be regarded as square.

If the dissolving or diffusion rate, $k_s$, of ethylene into propanol-2 and the rate of reaction 2, $k$, in the following scheme:

$$(E)_g \overset{k_s}{\rightarrow} (E)_s \qquad (1)$$

$$(P\cdot) + (E)_s \overset{k}{\rightarrow} (PE\cdot) \qquad (2)$$

are assumed to have a significant role in the reaction, the plots in Fig. 5 might be explained in terms of $k_s$. However, since it has been reported that the diffusion rate did not affect the sector curve in the system of *n*-butylmercaptane and *n*-octene,[5] the diffusion rate was assumed to be negligible in the present research.

By the use of the data obtained, the average concentration of radicals, $R_s$, the kinetic chain length, $\nu$, and the rate constant of the termination reaction $k_t$, can be estimated to be of the order of $10^{-7}$ $mol^{-1}$, 10 and $10^9$ $mol^{-1}$ l. $sec^{-1}$ respectively from the following relations:

$$\tau_s = [R_s]/v_i, \quad [R_s] = (v_i/k_t)^{1/2} \text{ and } \nu = \frac{v_p}{v_i}$$

The $G$ value for telomer formation obtained in the present research is compared in Table I with that obtained in the $\gamma$-ray irradiation,

Table I. The effect of the dose rate on $G$(*t*-amyl alcohol)

| Radiation source | Electron beams from the Van de Graaff Accelerator | | $\gamma$-Rays from cobalt-60 |
|---|---|---|---|
| Dose rate, I (eV./min.) | $7.2\times10^{22}$ | $5\times10^{22}$ | $8\times10^{16}$ |
| $I_e/I\gamma$ | 960 | 780 | 1 |
| $G$(*t*-amyl alcohol) | 1.6$_7$ | 2.0 | 250 |

as has already been reported.[1] The $G$ value in the present paper is smaller than that in the former by a factor of $10^2$. This can be explained as being caused by a higher dose rate of the electron beam, considering that $G$ (telomer) depends on the $-1/2$ power of the dose rate. There are some ambiguities in this comparison, however, which come from the non-uniformity of the dose rate in the present system caused by the weaker penetrating power of the electron beams.

## Conclusion

It has been found that the 1 : 1 telomer, *t*-amyl alcohol, is produced by electron irradiation, and that it has a $G$ value smaller than that obtained by $\gamma$-irradiation. The average life-time of the radicals of the rate-determining step has been estimated to be 0.01 sec. by the rotating sector method.

The authors wish to thank Dr. Yohta Nakai for his operation of the Van de Graaff accelerator. Some of the expenses have been defrayed by a grant given by the ministry of Science and Technology, to which the authors' thanks are due.

*Japanese Association for Radiation Research on Polymers*
*Neyagawa, Osaka* (*M. H. & K. H.*)

*Department of Chemistry*
*Faculty of Science*
*Osaka University*
*Nakanoshima, Osaka* (*K. H.*)

5) W. H. Clingman, *J. Phys. Chem.*, **64**, 1355 (1960).

# The Reaction of Methyl Vinyl Ketone with Alkyl Grignard Reagents

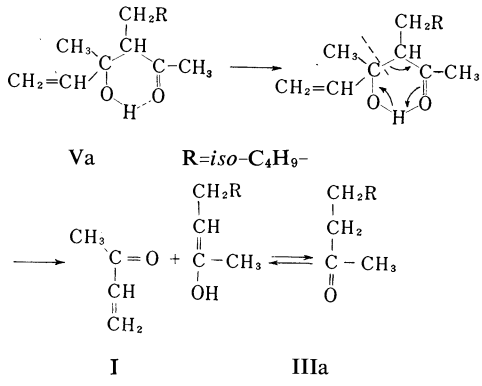
By Yoshie KURIHARA, Tatsuo HIGA, Kikumasa SATO and Shigehiro ABE

(Received June 11, 1964)

The reaction of methyl vinyl ketone (I) with acetylenic Grignard reagents has been reported[1,2] to afford almost exclusively the 1,2-addition product, ethynylcarbinol. However, Smith and Sprung[3] could not obtain a simple product in the reaction between laurylmagnesium bromide and the ketone I because of the polymerization of I. Sarycheva et al.[4] obtained the 1, 2-addition product in the reaction between the Grignard reagent from 5-bromo-2, 3-dimethylpentene-2 and I, but its infrared spectrum seems to indicate that the product is a mixture of the 1, 4- and 1, 2-addition products.

In a previous study,[5] isophytol was synthesized from pseudoionone and propargyl alcohol, and it was found that the ketone I reacted with laurylmagnesium bromide to yield the 1, 4-addition product rather than the 1, 2-addition product. The reactions of I with isobutylmagnesium bromide IIa or ethylmagnesium bromide IIb will be studied in the present paper to see whether or not the previous findings concerning 1, 4-addition indicate a general tendency in the reaction between methyl vinyl ketone and alkyl Grignard reagents.

The reactions were carried out at low concentrations of the reactants and at low temperatures in order to suppress the polymerization of I. The reaction between I and IIa at $-50°C$ gave two products as colorless liquids. The lower boiling substance was found to be the 1, 4-addition product, methylheptanone (IIIa), and 3-isoamyl-2-vinyl-2-pentanol-4-one (Va) was assigned to the higher boiling product. The spectrum of Va indicated the presence of tertiary hydroxyl, non-conjugated carbonyl, and vinyl groups. When Va was treated with semicarbazide by an ordinary method,[6] no precipitate was formed. When the mixture with semicarbazide was warmed for thirty minutes or allowed to stand at room temperature for a long time, the semicarbazone of IIIa was obtained. In this reaction, IIIa was supposed to be derived by the decomposition of Va. Actually the compound, Va, decomposed readily when heated at 150°C to afford IIIa and I quatitatively. Such a decomposition supported the assignment of structure Va for the higher-boiling product, and the decomposition probably proceeds through a cyclic transitional state, as is illustrated below. This decomposition occurred also in the presence of sulfuric acid to give IIIa in a high yield.



Va R=*iso*-$C_4H_9$-

I IIIa

Thus, the reaction of I with IIa has been shown to yield a mixture of IIIa and Va. The formation of IIIa and Va can reasonably be explained by assuming the following reaction mechanism (Fig. 1). The Grignard reagent, IIa, condenses with I by the 1, 4-addition process to form an enolate III'a of methylheptanone in the first step. The enolate is converted into IIIa by hydrolysis. On the other hand, when the enolate is added to the carbon atom of the carbonyl group of another molecule of I, compound V'a is formed; this is finally hydrolyzed to Va. These courses of the reaction are shown by pathways A and B in Fig. 1 respectively.

The reaction mechanism of the Grignard

1) J. Cymerman, I. M. Heilbron and E. R. H. Jones, *J. Chem. Soc.*, **1944**, 144.
2) N. A. Milas, F. X. Grossi, S. E. Penner and S. Kahn, *J. Am. Chem. Soc.*, **70**, 1292 (1948).
3) L. I. Smith and J. A. Sprung, ibid., **65**, 1276 (1943).
4) I. K. Sarycheva, G. A. Vorobyeva, L. G. Kucheryavenko and N. A. Preobrazhensky, *Zh. Obshch. Khim.*, **27**, 2994 (1957).
5) K. Sato, Y. Kurihara and S. Abe, *J. Org. Chem.*, **28**, 45 (1963).
6) R. L. Shriner and R. G. Fuson, "The Systematic Identification of Organic Compounds," John Wiley & Sons, New York, N. Y. (1948), p. 170.

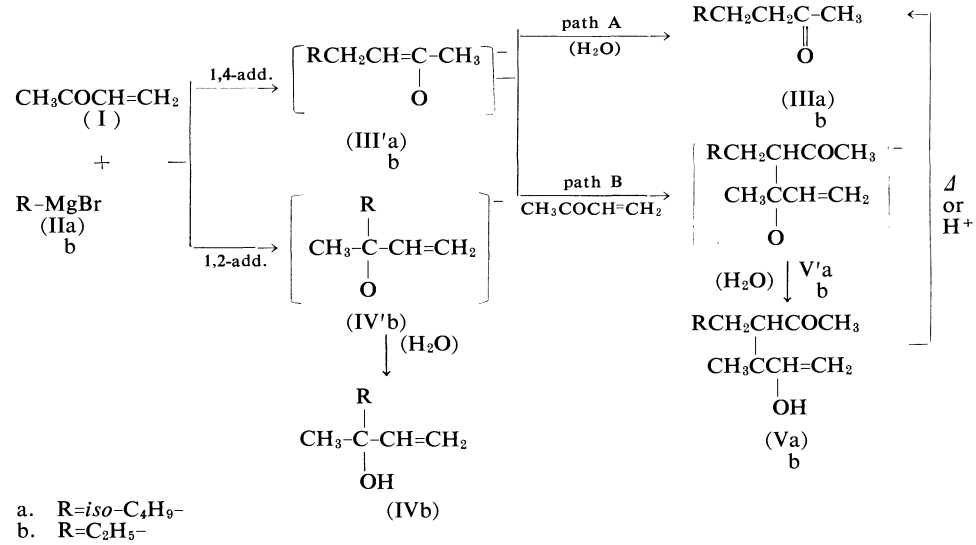



Fig. 1.

enolate ion with methyl vinyl ketone (pathway B) is supported by a number of investigations[7] of the condensation of ketones during the Grignard reaction. For example, Mosher and Lux[8] demonstrated that the interaction of methyl isopropyl ketone and *t*-butylmagnesium chloride led to the formation of not only the secondary alcohol to be expected from the reduction of the ketone but also of the ketol, 2, 3, 6-trimethyl-3-heptanol-5-one, which is a self-condensation product of methyl isopropyl ketone. According to the commonly accepted view,[7] the formation of this ketol may be explained as follows; the Grignard reagent causes the enolization of the ketone, as is already known, and the enolate thus formed is added to the carbon atom of the carbonyl group in a molecule of the corresponding keto form (Fig. 2).

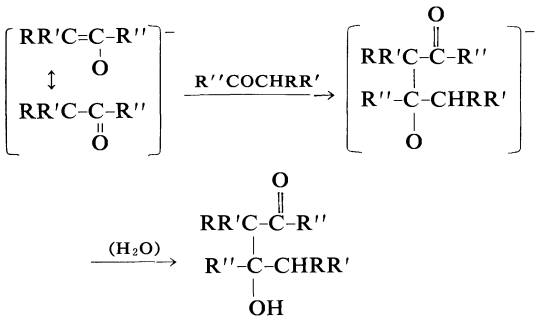



Fig. 2.

The yields of compound IIIa and compound Va were strongly influenced by the experimental conditions. The effect of varying the molar ratio of the reactants at −50°C was examined. When two moles of I per mole of IIa were used, the main product was Va, and only a trace of IIIa was obtained. When approximately equimolar amounts of I and IIa were used, both IIIa and Va were obtained in, respectively, 7.5% and 38% yields based on I. When half a mole of I was used, Va was again preferably obtained. Judging from these results, it seems likely that the reaction of the enolate, III'a, with I is faster than that of IIa with I. When the reaction temperature was raised to −15°C, only Va was obtained, even with equivalent moles of the reactants.

On the other hand, the reaction between equimolar amounts of I and ethylmagnesium bromide, IIb, at −50°C afforded 3-methyl-1-penten-3-ol (IVb, the 1, 2-addition product) contaminated with methyl *n*-butyl ketone (IIIa) and 3-propyl-2-vinyl-2-pentanol-4-one (Vb, the addition product between I and the 1, 4-addition product). The yields of IVb and Vb were, respectively, 6.6% and 17% based on I. The structure of IVb was established by infrared spectrum and by conversion into its 3, 5-dinitrobenzoate. The purification of IVb was unsuccessful, even by means of careful fractionation. Methyl *n*-butyl ketone as a contaminant was identified by gas chromatography using an authentic sample. The structure of Vb was established by means of elemental analysis and its infrared spectrum. Compound Vb may have been formed from III'b by a mechanism similar to that found in the formation of Va. It was decomposed into IIIb in

7) M. S. Kharasch and O. Reinmuth, "Grignard Reactions of Nonmetallic Substances," Prentice-Hall, New York, N. Y. (1954), pp. 174—181.
8) W. A. Mosher and A. R. Lux, *J. Am. Chem. Soc.*, **63**, 648 (1941).

the presence of sulfuric acid. Although the ratios of the reaction products were not studied under a variety of reaction conditions, it might be concluded from the above results that the reaction of I with IIb proceeds by both 1,2- and 1,4-addition, and that the 1,4-addition product III'b subsquently condenses with I to afford Vb. As has been described above, IIa gives only the 1,4-addition product. The reason for this difference in the reaction products has not been clariffied in the present study. It may, however, be worth noticing that, in the cases of both IIa and IIb, methyl vinyl ketone is added to their 1,4-addition products, whereas no further addition was previously observed in the case of laurylmagnesium bromide.

## Experimental[9]

**Materials.**—Methy vinyl ketone was prepared from γ-ketobutanol (78—80°C/18 mmHg, prepared from acetone and formalin) by dehydration with oxalic acid according to the method of Murata[10]; b. p. 80—82°C. Commercially available isobutyl bromide and ethyl bromide were used after purification (isobutyl bromide, b. p. 90—90.8°C; ethyl bromide, b. p. 38—39°C).

**The Reaction of Methyl Vinyl Ketone (I) with Isobutylmagnesium Bromide (IIa).—(a) At −50°C.**—*i) The Equimolar Ratio of I to IIa.*—The Grignard reagent was prepared from 54.8 g. of isobutyl bromide and 9.8 g. of magnesium in 300 ml. of anhydrous ether. To the solution, 22.4 g. of freshly-distilled methyl vinyl ketone in 150 ml. of anhydrous ether was added drop by drop at such a rate as to maintain the temperature at −50°C. After the reaction mixture had been continuously stirred for a further hour, it was decomposed with an ice-cooled saturated ammonium chloride solution and extracted with ether. The ether extract was washed with water and with a saturated sodium bicarbonate solution, dried, and evaporated. The residue was distilled fractionally; fraction I (5.5 g.) (b. p. 25—37.5°C/18 mmHg), fraction II (5 g.) (b. p. 27—50°C/4 mmHg), fraction III (14.5 g.) (b. p. 80—103°C/5 mmHg), and a residue (2.1 g.). By gas chromatographic analysis (column temp. 151°C; injection temp. 185°C; $N_2$ flow 12.8 ml./min.; silicon oil DC550, 2 m.), fraction I was found to be composed mostly of isobutyl alcohol (retention time 1.2 min.) contaminated with a small amount of methylheptanone (retention time 6 min.). These retention times were in good agreement with those for authentic samples. Fractions II and III were redistilled. Fraction II gave 3.0 g. (7.5% based on I) of methylheptanone, boiling at 30—31°C/4 mmHg, 166—167°C/760 mmHg, $n_D^{20}$ 1.4230 (lit.[11] $n_D^{19}$ 1.4144, b. p. 164—165°C/760 mmHg). The infrared spectrum indicated a band at 1715 $cm^{-1}$ (>C=O).

Found: C, 74.13; H, 12.71. Calcd. for $C_8H_{16}O$: C, 74.96; H, 12.58%.

The semicarbazone was recrystallized from $C_2H_5OH$ and $H_2O$ (1:1); m. p. 150.5—151°C (lit. m. p. 157°C,[11] m. p. 146°C[12]).

Found: C, 58.12; H, 10.45; N, 22.65. Calcd. for $C_9H_{19}ON_3$: C, 58.34; H, 10.34; N, 22.68%.

Fraction III gave 12.0 g. (38% based on I) of Va, boiling at 88—90°C/3 mmHg, $n_D^{20}$ 1.4602, $d_4^{20}$ 0.9223. The infrared spectrum of this substance showed bands at 1640, 1415, 990, 920 (-CH=$CH_2$), 3450, 1165 (tert. OH), and 1705 $cm^{-1}$ (C=O).

Found: C, 72.33; H, 10.97. Calcd. for $C_{12}H_{22}O_2$: C, 72.68; H, 11.18%.

*ii) The Molar Ratio of I to IIa (2:1).*—To the Grignard reagent (prepared from 54.8 g. of isobutyl bromide, 9.8 g. of magnesium and 300 ml. of anhydrous ether), 44.8 g. of I in 400 ml. of anhydrous ether was added at −50—−55°C. The reaction mixture was then treated by the same procedure as that described in part i. Methylheptanone (1.8 g.), b. p. 31—33°C/3 mmHg, the ketol (22.3 g.), b. p. 88—90°C/3 mmHg, and the residue (9.0 g.) were obtained. These materials were proved to be identical with the samples described in the preceding paragraph by gas chromatography or the refractive index.

*iii) The Molar Ratio of I to IIa (1:2).*—The same procedure as that described in the part i was employed. 3.4 g. of Va, b. p. 81—85°C/4 mmHg, and 0.2 g. of IIIa, b. p. 38—40°C/4 mmHg were obtained from 25.5 g. of isobutyl bromide, 4.8 g. of magnesium and 5.6 g. of I.

**(b) At −15°C.**—To the Grignard solution prepared from 27.4 g. of isobutyl bromide, 5.0 g. of magnesium in 150 ml. of anhydrous ether, 12.6 g. of I in 160 ml. of anhydrous ether was added. The oily product isolated was 5.8 g. of Va (b. p. 87—92°C/3 mmHg, redistilled, b. p. 97—100°C/5 mmHg). The refractive index of this substance agreed with that of the preceding sample.

**The Decomposition of 3-Isoamyl-2-vinyl-2-pentanol-4-one (Va).**—*a) By Sulfuric Acid.*—Three grams of Va, 2 ml. of ethyl alcohol and ten drops of diluted sulfuric acid (1:1) were placed in a flask; then the mixture was heated to 100°C while being stirred for half an hour. After cooling, the reaction mixture was neutralized with a sodium bicarbonate solution and extracted with ether. After the ether had been removed, the residual liquid was distilled under atmospheric pressure; b. p. 165—169°C (1.6 g.). The product gave the semicarbazone with a m. p. of 152°C, which did not depress the melting point of an authentic sample of IIIa.

*b) By Heating.*—The pyrolysis was carried out with a gas chromatograph apparatus (column temp. 150°C; injection temp. 181°C; $N_2$ flow 10.7 ml./min.; silicon oil DC 550, 2 m.). The two peaks

9) The boiling points and melting points are uncorrected. The infrared spectra and gas chromatograms were recorded with a Hitachi Model EPI-S2 spectrophotometer and a Hitachi Model KGL-2 gas chromatograph.

10) J. Murata, "Synthetic Methods of Monomers," Vol. 9, Kyoritsu Shuppan Co., Tokyo (1957) p. 183.

11) O. Wallach, *Ann.*, **381**, 86 (1911).

12) M. Guerbert, *J. Pharm. Chim.*, (7), **6**, 49 (1912); *Chem. Zentr.*, **83**, 1099 (1912 II).

in the chromatogram were found by the use of authentic samples to be methyl vinyl ketone (retention time 4.5 min.) and methylheptanone (retention time 9.8 min.) respectively.

**The Reaction of I with Ethylmagnesium Bromide (IIb).**—A procedure similar to that described for the reaction of I and IIa was adopted. To a Grignard reagent solution (prepared from 43.6 g. of ethyl bromide, 9.7 g. of magnesium and 150 ml. of anhydrous ether), freshly-distilled methyl vinyl ketone (39.6 g.) in 500 ml. of anhydrous ether was added in such a manner as to maintain the reaction temperature at −50—−55°C. The products were fractionated. Fraction I (3.7 g.) boiled at 33—35°C/17 mmHg. On redistillation, the sample was obtained at 117—119°C/760 mmHg; $n_D^{20}$ 1.4310 (lit.[13] b. p. 116°C/760 mmHg). The infrared spectrum showed bands at 3400 and 1160 (tert. OH), 1850, 1650, 1415, 995 and 920 (CH=$CH_2$), and 1715 $cm^{-1}$ (C=O, very weak). Two peaks appeared in the gas chromatogram (column temp. 96°C; injection temp. 120°C; $N_2$ flow 2.4 ml./min.; silicon oil DC 550, 2 m.). The peak corresponding to the ketone was increased when methyl *n*-butyl ketone was added (retention time 2.5 min.). The ratio of 3-methyl-1-penten-3-ol to methyl *n*-butyl ketone was estimated to be about 5 to 1. The 3, 5-dinitrobenzoate obtained from fraction I was recrystallized from ethyl alcohol, m. p. 91—92°C.

Found: N, 9.68. Calcd. for $C_{13}H_{14}N_2O_6$: N, 9.52%.

Fraction II (13.7 g.) boiled at 50—77°C/5 mmHg, and the residue amounted to 1.8 g. The redistillation of fraction II afforded 8.5 g. (17% based on I) of Vb, b. p. 73.5—75°C/3.5 mmHg, $n_D^{20}$ 1.4589. The infrared spectrum showed bands at 1650, 1420, 995, 920 (CH=$CH_2$), 3500, 1170 (tert. OH), and 1705 $cm^{-1}$ (C=O).

Found: C, 70.57; H, 10.84. Calcd. for $C_{10}H_{18}O_2$: C, 70.54; H, 10.66%.

The semicarbazone, m. p. 124°C (lit.[14] m. p. 122°C), obtained from Vb by the action of sulfuric acid as described in the case of Va, did not depress the melting point of methyl *n*-butyl ketone semicarbazone. No attempt was made to determine the structure of the residue.

13) *Chem. Zentr.*, **86**, 1223 (1915 II).
14) See Ref. 6, p. 262.

## Summary

The reactions of methyl vinyl ketone with isobutylmagnesium bromide and ethylmagnesium bromide have been studied. Methyl vinyl ketone reacts with isobutylmagnesium bromide to give methylheptanone and 3-isoamyl-2-vinyl-2-pentanol-4-one as a result of 1, 4-addition; the latter compound is formed from 2 mol. of ketone and one mole of the Grignard reagent. On the other hand, in the reaction of ethylmagnesium bromide with methyl vinyl ketone, both 1, 2- and 1, 4-addition take place, and 3-methyl-1-penten-3-ol and 3-propyl-2-vinyl-2-pentanol-4-one are obtained. These keto-alcohols have been decomposed to the corresponding ketones and methyl vinyl ketone by heating or by treatment with sulfuric acid.

The authors are grateful to Mr. Mohammad Raees for his help in carrying out the experiments.

*Department of Applied Chemistry*
*Faculty of Engineering*
*Yokohama National University*
*Minami-ku, Yokohama*

# On the Competition of Homogeneous and Heterogeneous Chain Terminations in Heterogeneous Photooxidation Catalysis by Zinc Oxide

By Akiko IKEKAWA, Mamoru KAMIYA, Yuzaburo FUJITA and Takao KWAN

(Received June 12, 1964)

It has previously[1] been shown that the photoexcited adsorption or desorption of oxygen takes place on zinc oxide when lights of 3650—4350 Å are irradiated. In connection with this finding, the photooxidation of isopropyl alcohol has been investigated on zinc oxide in the presence of oxygen, the products being identified as acetone and hydrogen peroxide exclusively.[2] The same photooxidation was investigated also by Kriascose and Markham[3] on zinc oxide in pure isopropyl alcohol and aqueous suspensions. The ratio

1) Y. Fujita and T. Kwan, This Bulletin, 31, 803 (1958).

2) I. Komuro, Y. Fujita and T. Kwan, ibid., 32, 884 (1959).

3) J. Kriascose and M. C. Markham, *J. Catalysis*, 1, 498 (1962).

of the oxygen uptake to the hydrogen peroxide formed was always greater than unity, especially when zinc oxide was suspended in pure liquid, suggesting that hydrogen peroxide is decomposing or participating in the oxidation of alcohol to a certain extent.

Despite the simple reaction, however, little is yet known about the photooxidation mechanism, probably because of the complex nature of the reactions occurring in the heterogeneous phase. In this paper we shall show some significant aspects of the photooxidation kinetics and then discuss them with respect to the competition of homogeneous and heterogeneous chain terminations.

## Experimental and Results

The photooxidation of isopropyl alcohol by zinc oxide in the presence of oxygen has been characterized by a certain induction period.[2] This can be eliminated, however, by stirring the zinc oxide - alcohol mixture in an oxygen atmosphere prior to photoirradiation. The initial steady-state rate for the consumption of oxygen was thus obtained within twenty minutes at the most. The apparatus and procedure for the measurements of the photooxidation catalysis were almost the same as those described previously.[2,4] The reaction was carried out at a constant oxygen pressure above 30 cmHg, where the rate of oxygen consumption was found to be independent of the oxygen pressure. The volume of oxygen consumed was determined by a conventional gas burette kept in a thermostat. Typical rate data, expressed by the volume of oxygen consumed upon irradiation, are shown in Fig. 1.

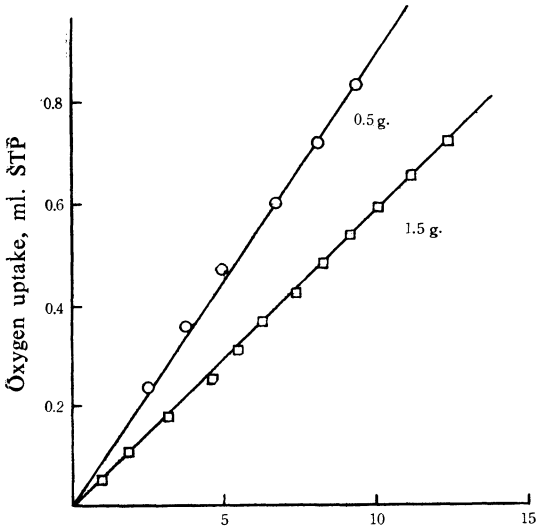



Fig. 1. Initial photooxidation rate of isopropyl alcohol on zinc oxide.
Isopropyl alcohol: 50 ml.
Partial pressure of oxygen: ca. 45 cmHg. Reaction temperature: 60°C.
Intensity of entering light $I_0$: $4.3^6\times10^{17}$ quanta/l. sec.

It was found in this way that the rate of oxygen uptake increases with the increase in the amount of zinc oxide added, suggesting that the light quanta absorbed increases with an increase in the concentration of photocatalysts. A further increase in the amount of zinc oxide, however, caused the rate of oxygen uptake to decrease gradually, hence giving rise to a maximum in the plot of the rate against the amount of zinc oxide present. Such a curve obtained at the reaction temperature of 60°C is illustrated in Fig. 2.

The quantum yield for the oxygen uptake is calculated in Table I at various amounts of zinc oxide.

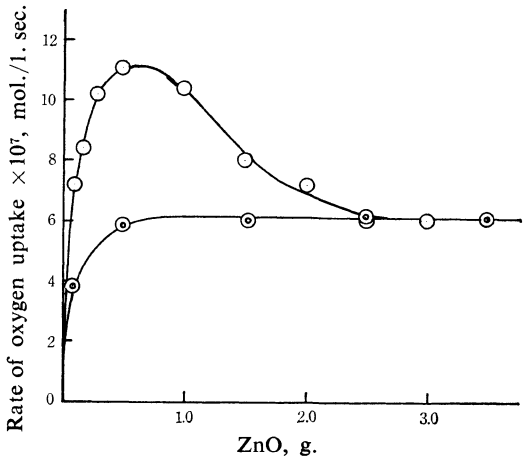



Fig. 2. The relationship between the rate of oxygen uptake and the amount of zinc oxide present.
Isopropyl alcohol: 50 ml.
$I_0$: $4.3^6\times10^{17}$ quanta/l. sec.
Reaction temperature; 40 and 60°C.
○ 60°C ◎ 40°C

Table I. Quantum yield for the oxygen uptake.
Intensity of entering light $I_0$ (determined by uranyl oxalate actinometry): $4.3^6\times10^{17}$ quanta/l. sec.
Reaction temp.: 60°C
Isopropyl alcohol: 50 ml.

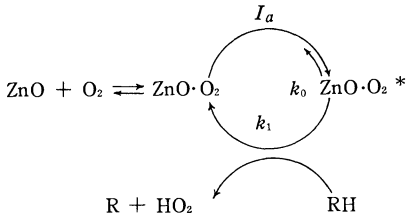
| ZnO g. | 0.1 | 0.2 | 0.5 | 1.0 | 2.0 | 3.0 |
|---|---|---|---|---|---|---|
| $\Phi$ | 1.0 | 1.1 | 1.5 | 1.4 | 1.0 | 0.8 |

4) M. Kamiya, Y. Fujita and T. Kwan, *Shokubai (Catalyst)*, 6, 15 (1964).

## Discussion

It is generally accepted that the liquid phase oxidation of alcohol at high temperature is of a chain character. It has already been shown[4] that the anthraquinone-sensitized oxidation of isopropyl alcohol proceeds with a chain mechanism above 50°C. The quantum yield given in Table I, probably showing the lower limit due to the light scattering on the suspensions and also to the light penetration through the liquid phase at lower concentrations of zinc oxide, may be indicative of the chain reaction participating to some extent.

The following mechanism is, therefore, assumed to be the principal process for the photooxidation of isopropyl alcohol on zinc oxide. The primary process may be schematically represented by:




where $I_a$ is the intensity of light absorbed or the rate of the excitation of oxygen on zinc oxide, $k_0$ and $k_1$ are rate constants of the respective steps, and RH denotes the isopropyl alcohol molecule. No description will be made at the moment regarding the adsorbed state of oxygen and the mechanism of photoexcitation; detailed investigations will soon be reported in association with adsorption, conductivity and ESR measurements of zinc oxide and adsorbed oxygen.[5] The steady state rate of the primary process may readily be derived as:

$$R_i = \frac{k_1 I_a (\mathrm{RH})}{k_0 + k_1 (\mathrm{RH})} \qquad (1)$$

The secondary process may be thermal, and the following steps are expected to participate at least:

$$\mathrm{R} + \mathrm{O_2} \xrightarrow{k_2} \mathrm{RO_2}$$

$$\mathrm{RO_2} \xrightarrow{k_3} \mathrm{CH_3}\rangle\mathrm{CO} + \mathrm{HO_2}$$
$$\mathrm{CH_3}$$

$$\mathrm{RH} + \mathrm{HO_2} \xrightarrow{k_4} \mathrm{R} + \mathrm{H_2O_2}$$

$$\mathrm{HO_2} + \mathrm{HO_2} \xrightarrow{k_5} \mathrm{H_2O_2} + \mathrm{O_2}$$

$$\mathrm{HO_2} + \mathrm{HO_2} \xrightarrow[\mathrm{M}]{k_5'} \mathrm{H_2O_2} + \mathrm{O_2}$$

where the last step indicates the heterogeneous chain termination effected on the third body, M, or on the surface of zinc oxide competing with the homogeneous bimolecular chain termination given just above.

The steady state treatment of the overall reaction yields the expression:

$$-\frac{\mathrm{d(O_2)}}{\mathrm{d}t} = R_i + \frac{k_4}{\sqrt{k_5}}\sqrt{R_i}\,(\mathrm{RH}) \qquad (2)$$

for the homogeneous chain termination. The substitution of $k_5'$ (M) for the $k_5$ of Eq. 2 gives, of course, the rate equation for the heterogeneous chain termination:

$$-\frac{\mathrm{d(O_2)}}{\mathrm{d}t} = R_i + \frac{k_4}{\sqrt{k_5'(\mathrm{M})}}\sqrt{R_i}(\mathrm{RH}) \qquad (3)$$

It seems more likely that the heterogeneous chain termination on zinc oxide is monomolecular rather than a third-body collision involving M. The rate of oxygen uptake is, then, given by:

$$-\frac{\mathrm{d(O_2)}}{\mathrm{d}t} = R_i + \frac{k_4}{k_5''(\mathrm{M})} R_i(\mathrm{RH}) \qquad (4)$$

The $\mathrm{RH} + \mathrm{HO_2} \rightarrow \mathrm{R} + \mathrm{H_2O_2}$ step requires a definite energy of activation, so the chain can not propagate around room temperature.[4] In other words, the second term on the right of Eq. 2 will only be significant at elevated temperatures. This may be applicable not only in the homogeneous phase but also in the heterogeneous phase provided the concentration of zinc oxide is low enough.

On the other hand, the chain will not propagate, according to Eq. 3 or 4 even at elevated temperatures in the heterogeneous phase, if sufficient amounts of M or zinc oxide are present, leaving only the first term in the rate expression. Thus, the rate of oxygen uptake may be expected to decrease with an increasing M value and finally to approach a limiting value which may be identified to $R_i$. The decreasing curve of Fig. 2 observed at high concentrations of zinc oxide may probably be ascribed to such a predomination of the heterogeneous chain termination.

A low temperatures, where the chain propagation is suppressed, the rate may be expected to increase monotonously with an increase in the amount of zinc oxide, finally attaining $R_i$ without showing any maximum. The supposition was supported by experiments at the temperature of 40°C, where the chain reaction was almost negligible.[4] As is shown by the double circles of Fig. 2, the results were found to be strikingly consistent with the expectation.

Mashio,[6] who studied the benzoyl peroxide-initiated oxidation of isopropyl alcohol above 80°C, estimated the temperature coefficient of

5) Y. Fujita and T. Kwan, *Shokubai* (*Catalyst*), **5**, 206 (1963).

6) F. Mashio, *J. Chem. Soc. Japan, Ind. Chem. Sec.* (*Kogyo Kagaku Zasshi*), **63**, 699 (1960).

$k_4/\sqrt{k_5}$ to be 9.8 kcal./mole. Hence, the temperature coefficient of the rate of oxygen uptake should assume a more or less rapid increase with a rise in the temperature from room temperature to, say, 80°C, because the reaction around room temperature is photochemical, involving radical recombinations, and so the rate should be little dependent on the temperature.

In the presence of excess zinc oxide, the rate of oxygen uptake was found actually to agree with that of the primary process. The temperature coefficient of the rate is, then, expected to be very small, even beyond the temperature where the chain propagation actively participates. On the other hand, such would not be the case when the amount of zinc oxide is sufficiently small; the temperature coefficient of the rate is expected to increase with the increasing temperature, much as in the homogeneous phase.

In Fig. 3 the plot of $\log(-\mathrm{d}(O_2)/\mathrm{d}t)$ vs. $1/T$ with 0.1 g. zinc oxide added on the one hand and that with 2.5 g. zinc oxide on the other hand are compared.

As can be seen from Fig. 3, the temperature coefficient of the oxidation rate increases distinctly from near zero to about 10 kcal./mole. at around 45°C when the amount of zinc oxide present was small, whereas it was nearly constant at a very small value on excess zinc oxide over the same temperature range.

The decreasing curve of Fig. 2, already explained as being due to the heterogeneous chain termination of $HO_2$, might resemble the effect of the third gases in the photochemical dissociation of the bromine or iodine molecule worked out by Rabinowitch and Wood[7] many years ago, although the increase in the third gases, in the latter reaction, serves to accelerate the homogeneous recombination of dissociated atoms and, hence, to decrease the concentration of halogen atoms.

The effect of the electronic properties of zinc oxide on the photocatalytic activity will be discussed next. It has previously been shown[2] that the rate of oxygen uptake continues, even when the light is interrupted, when a sample of oxidized zinc oxide is subjected to photo-oxidation catalysis. No such memory was perceptible on a reduced zinc oxide sample. Investigations of these phenomena led to the conclusion that the dark oxidation of isopropyl alcohol on oxidized zinc oxide is due to the hydrogen peroxide-initiated oxidation of alcohol.

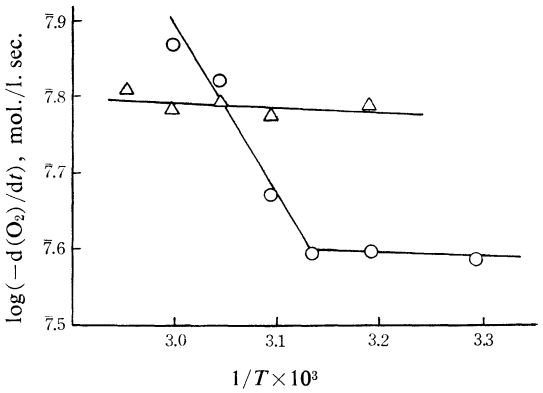



Fig. 3. The temperature coefficient of the photooxidation rate at low and high concentrations of zinc oxide.
○ ZnO 0.1 g. △ ZnO 2.5 g.

In view of the dual nature of the photoresponses for the oxygen adsorbed on reduced and oxidized zinc oxide samples on the one hand and on alumina-doped and lithia-doped zinc oxide samples on the other hand, it seemed of interest to find the difference in the activity in the photo-primary process using doped zinc oxide samples. Preliminary experiments have shown that the rate of oxygen uptake is much greater on lithia-doped zinc oxide than on an alumina-doped sample at the temperature of 60°C. The rate on the lithia-doped sample was autocatalytic, controlled even by the diffusion of oxygen into the liquid phase at the later stage of the reaction. It was considered that the thermal oxidation of isopropyl alcohol, initiated by the decomposition of hydrogen peroxide, occurs simultaneously on the surface of lithia-doped zinc oxide. At the initial stage of the photoreaction, the rate of oxygen uptake was greater on lithia-doped zinc oxide than on an alumina-doped sample; $ZnO(Li_2O) > ZnO(Al_2O_3)$.

It is interesting to note that the sequence of the activity is reversed at a lower temperature, i. e., at 30°C. The rate of oxygen uptake upon irradiation was the greatest on alumina-doped zinc oxide, as $ZnO(Al_2O_3) > ZnO > ZnO(Li_2O)$. Markham and Kuriacose did not investigate the effect of doping zinc oxide on the photocatalytic activity, but they noted that the addition of hydrogen peroxide to a zinc oxide suspension does not affect the rate of acetone formation at 25°C. If the decomposition of hydrogen peroxide to give oxygen and water is the only side reaction on zinc oxide samples around room temperature, then the activity sequence mentioned above may be quite natural, for Sedaka of this laboratory found that the decomposition of hydrogen

7) E. Rabinowitch and W. C. Wood, *J. Chem. Phys.*, **4**, 497 (1936). See also W. A. Noyes, Jr., and P. A. Leighton, "The Photochemistry of Gases," Reinhold Publishing Co., New York (1941), p. 195.

peroxide in an aqueous solution occurs more rapidly on lithia-doped zinc oxide than an alumina-doped sample. The decomposition of hydrogen peroxide on lithia-doped zinc oxide may compensate for the consumption of oxygen to some extent.

In this connection, reference may be made to the work by Bernas and Doo-Kingue.[8] Bernas reported that the photoirradiation of an aqueous suspension of zinc oxide produces hydrogen peroxide more efficiently on reduced zinc oxide than on an oxidized sample. The efficient production of hydrogen peroxide on zinc oxide of a reduced state, according to Bernas and Dook-Kingue, might be due to its inefficient activity in the thermal decomposition of hydrogen peroxide; this is in accordance with the finding by Sedaka.

In studying the photooxidation of carbon monoxide on zinc oxide, Stone[9] found that the relative catalytic activity is the sequence: $ZnO(Li_2O) > ZnO > ZnO(Cr_2O_3)$. A similar result was found concerning oxygen exchange catalysis on zinc oxide samples.[10] The activity of doped zinc oxide samples in the decomposition of hydrogen peroxide, as well as in the oxidation of isopropyl alcohol, may be correlated with the data available in the literature.

## Summary

The photooxidation catalysis of isopropyl alcohol on zinc oxide has been investigated with special reference to the chain termination mechanism. It has been proposed that homogeneous and heterogeneous chain terminations compete in this system. At a low concentration of zinc oxide, the homogeneous termination predominates, while at a high concentration the heterogeneous termination may come into play. As a result, a maximum may appear in the relation of the rate of oxygen uptake to the amount of zinc oxide present. With excess zinc oxide, chain reactions are suppressed, so no maximum may appear in the corresponding plot and the temperature coefficient should be very small. The experimental results have been found to be consistent with the expectations. The effect of doping zinc oxide on the photooxidation kinetics has been investigated and discussed, mainly on the basis of the data available on the formation and decomposition of hydrogen peroxide on doped zinc oxide samples.

It has been suggested that lithia-doped zinc oxide is more active than alumina-doped zinc oxide at higher temperatures because of the accompanying hydrogen peroxide-initiated oxidation of isopropyl alcohol on the former, while it is less active at lower temperatures because of the efficient decomposition of hydrogen peroxide, giving oxygen and water.

This work was supported in part by a grant of the Ministry of Education, to which the authors' grateful acknowledgements are made.

*Faculty of Pharmaceutical Sciences*
*The University of Tokyo*
*Hongo, Tokyo*

8) A. Bernas and M. Doo-Kingue, Photochemistry Symposium, March 27—29, 1963, Rochester.
9) F. Romero-Rossi and F. S. Stone, 2nd International Congress on Catalysis, 1960, Paris.
10) V. I. Gorgoraki, V. Yu. Levin and L. A. Kasatkina, *Kin. Kata.*, 4, 422 (1963).

# Kinetics of Methane Oxidation in Shock Waves*

By Hajime MIYAMA and Tetsu TAKEYAMA

(Received June 12, 1964)

The oxidation of methane at comparatively low temperatures has been extensively studied and its mechanism has been well established by Semenov[1] and others[2]. Although there have also been several papers[3-6] about the methane oxidation at higher temperatures, satisfactory results were not obtained because of experimental difficulties. However, the recent development of the shock tube technique has made possible such high temperature studies; Skinner and Ruehrwein[7] measured induction periods of visible light emission in the range of conditions, $1150 \leq T \leq 1740$°K and $0.25 \leq [O_2]/[CH_4] \leq 0.67$; he suggested that the initiating reaction is $CH_4 + O_2 \rightarrow CH_3 + HO_2$. Kistiakowsky and Richards[8] observed the emission of vacuum ultraviolet radiation from the shock-heated gas mixtures in the range of conditions, $1800 \leq T \leq 2700$°K and $0.5 \leq [O_2]/[CH_4] \leq 4.5$ and suggested that the step $H + O_2 \rightarrow OH + O$ controls the reaction rate during the induction period. On the other hand, Asaba et al.[9] measured the ignition delay by a pressure transducer over the wide range of conditions and proposed that the reaction $CH_3 + O_2 \rightarrow CH_2O + OH$ is rate-determining for methane-lean mixtures and that the reaction $CH_4 + O_2 \rightarrow CH_3 + HO_2$ is rate-determining for the methane-rich mixtures.

In the present study, in order to clarify the mechanism of methane oxidation, the induction period of the OH absorption (3067 Å) and that of the pressure increase were measured simultaneously, and also the reaction products of certain cases were analyzed by gas chromatography.

## Experimental

**Materials.** — Takachiho methane (99.9% min.), Nippon Sanso oxygen (99.5% min.), and Nippon Sanso argon (99.999% min.) were used without further purification. The gas mixtures were prepared manometrically in a reservoir and allowed to stand for at least 24 hr. before being used. Helium was used as the driver gas in the shock tube at pressures up to 11 atm.

**Shock Tube and Instrumentation.**—A schematic diagram of the apparatus is shown in Fig. 1. A

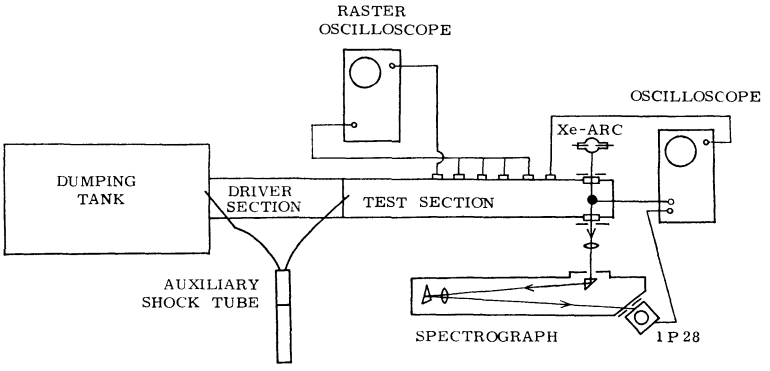



Fig. 1. Schematic diagram of apparatus.

* A part of this paper was presented at the 17th Annual Meeting of the Chemical Society of Japan, Tokyo, April, 1964, and at the Symposium on Chemical Reactions in Shock Tubes at Duke University, North Carolina, U. S. A., April, 1964.

1) N. N. Semenov, "Some Problems in Chemical Kinetics and Reactivity," Vol. II, Princeton University Press, New Jersey (1959), p. 217.
2) N. S. Enikolopyan, "7th Symposium (International) on Combustion," Butterworths, London (1959), p. 157; L. V. Karmilova, N. S. Enikolopyan and A. B. Nalbandyan, *Zhur. Fiz. Khim.*, **34**, 550 (1960).
3) B. P. Mullins, *Fuel*, **32**, 343 (1953).
4) J. H. Burgoyne and H. Hirsch, *Proc. Roy. Soc.*, **A227**, 73 (1954).
5) G. I. Kozlov, "7th Symposium (International) on Combustion," Butterworths, London (1959), p. 98.
6) H. Vandenabeele, R. Corbeels and A. van Tiggelen, *Combust. Flame*, **4**, 253 (1960).
7) G. B. Skinner and R. A. Ruehrwein, *J. Phys. Chem.*, **63**, 1736 (1959).
8) G. B. Kistiakowsky and L. W. Richards, *J. Chem. Phys.*, **36**, 1707 (1962).
9) T. Asaba, K. Yoneda, N. Kakihara and T. Hikita, "9th Symposium (International) on Combustion," Pergamon, New York (1963), p. 193.

single-pulse shock tube consisted of a 2.4 m.-long driver section and a 3.5 m. experimental section which were made of 7.6 cm. inside diameter precision-bore stainless steel tubing, and a dumping tank 90 cm. inside diameter and 3.6 m. long. One of six piezo gauges (Murata $BaTiO_3$ Ceramic Vibrator) was used to trigger the oscilloscopes, while the others were used to measure the shock velocities along the tube. The gauge signals were displayed on a raster-sweep oscilloscope (Iwasaki SS-5102), which permitted the measurement of the shock velocity in each gauge interval to a 0.5% accuracy. A quartz pressure transducer (Kistler Model 603) was installed 5.5 mm. from the end of the tube in order to measure the pressure change of the reacting system. Also, at the end of the tube, 5.5 mm. from the end plate, two quartz windows, each with a slit 2 mm. wide, were inserted to provide an optical path through the tube. The light source used was an Ushio 500 W. xenon arc lamp, the power for which was supplied by batteries. The other optics consisted of a Shimadzu QL-170 spectrograph with a $0.3\times8$ mm. entrance slit and a $0.5\times8$ mm. exit slit set a 3067 Å and an RCA 1P28 photomultiplier. The outputs of the pressure transducer and the photomultiplier were fed to a dual-beam oscilloscope (Iwasaki DS-5305) and recorded with a Polaroid camera. Before each run, the experimental section was evacuated to $10^{-3}$ mmHg and the lamp had been lit for at least 20 min. The measured leak rate of the shock tube was 3 $\mu$Hg per min.

**Gas Analysis.**—All the gas mixtures used and the produced gas mixtures, which were withdrawn through a valve near the end plate immediately after each run, were analyzed by gas chromatography. These analyses were performed with a Yanagimoto GCG-2 gas chromatograph at 50°C employing 1.5 m. columns of a molecular sieve 5A and silica gel, with helium as the carrier; the former column was used for the analysis of methane and carbon monoxide, and the latter, for ethane, ethylene, acetylene and carbon dioxide. The chromatograph was calibrated carefully for the peak area with pure gas specimens, using neon as an internal standard. The reproducibility of the analyses was maintained within an error of $\pm1\%$.

## Calculations

The temperatures, pressures and other parameters of the gas behind the reflected shock waves were calculated by means of the one-dimensional theory, assuming rotational and vibrational relaxations but no chemical relaxation. Numerical calculations were made by a USS 90 computor using Strehlow's method.[10]

Gas chromatographic analysis was applied to the reaction products of the methane-rich mixtures. For these mixtures, the second-order reaction was assumed by other researchers.[8,9] In order to evaluate the second-order rate constant from the analytical results of the reaction products, the following procedure was adopted, extending the method of Asaba et al.[11] The rate of the consumption of methane was considered to be given by Eq. 1:

$$dx/dt=k(a-x)(b-nx) \tag{1}$$

where $a$ and $b$ denote the initial concentrations of methane and oxygen respectively; $x$ and $nx$, the quantities of methane and oxygen respectively consumed during $t$, and $k$, the rate constant. In this equation, it is implicity assumed that, during the whole reaction time, methane reacts with $n$-fold oxygen; the value of $n$ can be determined by the material balance from the results of the analysis of the products. The integration of Eq. 1 gives:

$$x=\frac{ab\{1-\exp[(na-b)kt]\}}{b-na\exp[(na-b)kt]} \tag{2}$$

As is shown in Fig. 2, the dwell time of gas molecules exposed to a high temperature varies along the distance from the end plate; accordingly, the extents of reaction are not equal along all the distance. The quantity of methane decomposed at a distance of $l$ from the intersection of a reflected shock wave with a rarefaction wave may be expressed as follows by using Eq. 2:

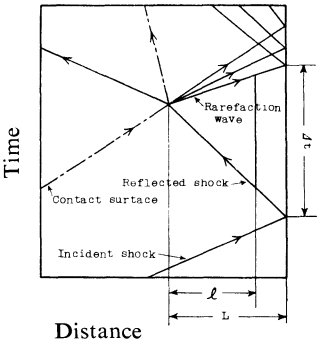



Fig. 2. Distance-time diagram.

$$x(l)=\frac{ab\left\{1-\exp\left[(na-b)k\frac{l\Delta t}{L}\right]\right\}}{b-na\exp\left[(na-b)k\frac{l\Delta t}{L}\right]} \tag{3}$$

Here, $\Delta t$ is the dwell time at the end plate and $L$, the distance from the intersection to the end of the tube. Thus, the average of $x(l)$ over the range $l=0$—$L$ is given by the equation:

10) R. A. Strehlow, Ballistic Research Laboratories Report No. 978, April, 1956, Aberdeen Proving Ground, Maryland, U. S. A.

11) T. Asaba, K. Yoneda and T. Hikita, *J. Chem. Soc. Japan, Ind. Chem. Sec.* (*Kogyo Kagaku Zasshi*), **64**, 1925 (1961).

$$\bar{x}=\frac{1}{L}\int_0^L x(l)\,\mathrm{d}l=a-\frac{1}{kn\Delta t}\times \ln\frac{b-na\exp[(na-b)k\Delta t]}{b-na} \quad (4)$$

Since $a$, $b$ and $\Delta t$ can be obtained from the experimental conditions combined with calculated shock parameters and $\bar{x}$ and $n$, from the analytical data of the reaction products, the rate constant, $k$, can be calculated from Eq. 4.

## Results

**The Methane-Lean Mixtures.**—A typical oscillogram, obtained for the mixture consisting of 70% argon, 9% methane and 21% oxygen, is shown in Fig. 3. The OH absorption appears

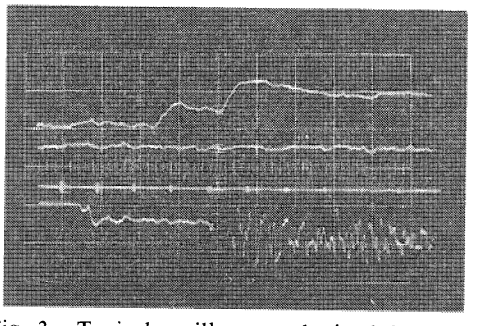


Fig. 3. Typical oscillogram obtained from the mixture of 70% Ar, 9% $CH_4$ and 21% $O_2$. The uppermost beam shows the change in the OH absorption, the second the noise level of Xe-lamp, the third timing markers and the lowest the pressure change. Sweep velocity is 100 $\mu$ sec./division.

after the induction time $\tau_1$. Its intensity increases exponentially to a limiting value, again increases as an explosive reaction starts, and decreases when the mixture is cooled by a rarefaction wave. On the other hand, the pressure increases suddenly after the induction time $\tau_2$ which is longer than $\tau_1$. The time of this pressure increase agrees with that of the second increase in OH absorption. From the data obtained in the range of conditions, $1050 \leq T \leq 2100$°K, $3 \leq p \leq 9$ atm. and $4.1\times10^{-3} \leq [O_2] \leq 1.5\times10^{-2}$ mol./l., it was found[12] that the logarithmic values of $\tau_1[O_2]$ and $\tau_2[O_2]$ are linearly proportional to $1/T$, but that other plots, such as $\log \tau_1[CH_4]$ or $\log \tau_1[CH_4][O_2]$, are not linearly proportional to $1/T$. Also, the apparent activation energies obtained from the slope of these straight lines are 21.5 and 33.8 kcal./mol. respectively.

A typical oscillogram obtained for the mixture of 30% methane and 70% oxygen without

12) H. Miyama and T. Takeyama, *J. Chem. Phys.*, **40**, 2049 (1964).

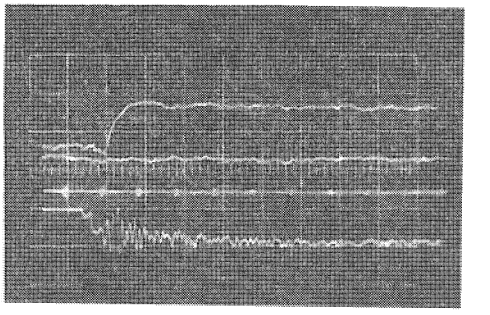


Fig. 4. Typical oscillogram obtained from the mixture of 30% $CH_4$ and 70% $O_2$. The four traces are the same as in Fig. 3.

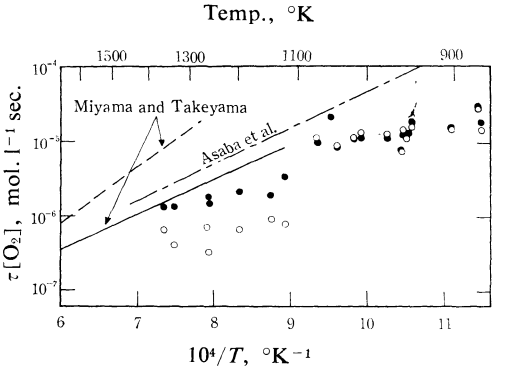



Fig. 5. Induction period vs. reciprocal temperature. Solid and open circles are from the pressure and OH-absorption measurements, respectively. Solid and dashed lines are obtained from the mixture with 70% Ar, measuring the OH-absorption and the pressure change, respectively.

argon is shown in Fig. 4. The OH absorption appears almost simultaneously with the pressure increase. Data obtained over the range of conditions, $870 \leq T \leq 1360$°K, $3.7 \leq p \leq 6.6$ atm. and $2.4\times10^{-2} \leq [O_2] \leq 6.0\times10^{-2}$ mol./l. are plotted in Fig. 5. Obviously, the data obtained for the mixtures without argon deviate markedly from those for the mixtures with a large amount of argon. Also, the data of Asaba et al.[9] obtained for the mixtures without argon are shown for purposes of comparison.

**The Intermediate Mixtures.**—The same measurements as have been described above were conducted for mixtures of 70% argon, 18% methane and 12% oxygen and those of 60% methane and 40% oxygen over the range of conditions $1420 \leq T \leq 2010$°K, $4.2 \leq p \leq 7.1$ atm. and $2.9\times10^{-3} \leq [O_2] \leq 2.2\times10^{-2}$ mol./l. The OH absorption and pressure change appeared at the same time in both mixtures. The induction periods measured are shown in Fig. 6 as a plot of $\log(\tau[CH_4][O_2])$ vs. $1/T$, which presents a fairly straight line in spite of the rather wide range of oxygen and methane concentrations, although the other

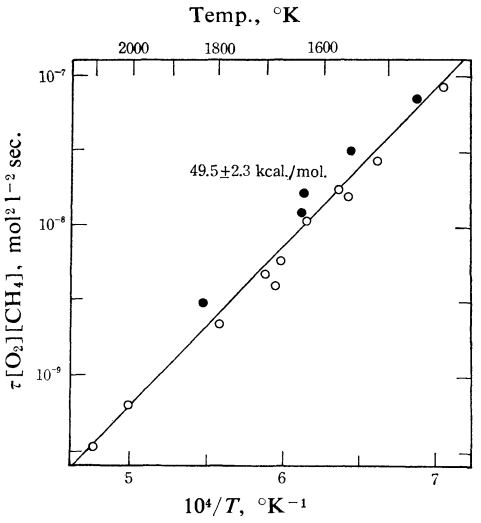



Fig. 6. Induction period vs. reciprocal temperature. Open and solid circles are obtained from mixture with and without argon, respectively. Solid line is a least-squares fit to these points.

plots, such as $\log(\tau[O_2])$ vs. $1/T$ and $\log(\tau[CH_4])$ vs. $1/T$, showed marked deviations of the measured points. The least-squares equation obtained for this line is:

$$\log \tau[CH_4][O_2] = -14.62\pm0.12+(10810\pm500)/T \quad (5)$$

From the slope of this line, the apparent activation energy is found to be 49.5±2.3 kcal./mol.

**The Methane-Rich Mixtures.** — Experiments were performed for mixtures of 86% argon, 12% methane and 2% oxygen and those of 86% methane and 14% oxygen. However, for the latter mixtures, it was very difficult to define the reaction temperature because the reflected shock wave interacted with the contact surface to produce a new shock wave and reheat the gas. Therefore, only the results obtained for the former mixtures will be reported. For the methane-rich mixtures, it was impossible to apply the above technique because the carbon precipitation obscured the OH absorption and the pressure increase was not appreciable. Therefore, the reaction products obtained by using a single pulse shock wave[13] were analyzed by gas chromatography.

The dwell time during which the reaction mixture was exposed to a high temperature was measured by a pressure transducer at the endplate and was adjusted to be about 1 msec. In Fig. 7, percentages of the products, based on the initial methane concentration, are plotted against the reaction temperatures. Using the analytical data shown in Fig. 7, the rate constants of methane oxidation were calculated on the assumptions[7,9] that the rate of consumption of methane is proportional to the product of methane and oxygen concentrations, and that the change in the concentration of various species during the cooling process in the rarefaction waves can be neglected.*

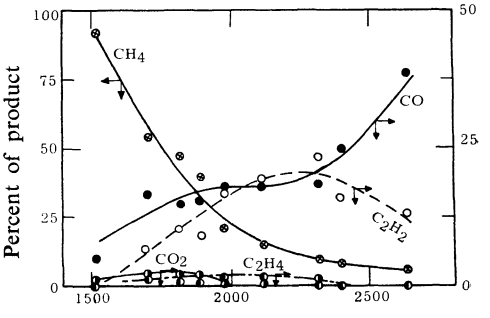



Fig. 7. Percentage composition of $CH_4$ and its products for various reaction temperatures.
⊗ $CH_4$, ○ $C_2H_2$, ● CO, ◐ $CO_2$, ◑ $C_2H_4$

TABLE I. DETAILS OF EXPERIMENTS AND CALCULATED SECOND-ORDER RATE CONSTANTS

| Run No. | $T$ °K | $P$ atm. | $a\times10^3$ mol./l. | $b\times10^3$ mol./l. | $\Delta t\times10^3$ sec. | $n$ | $\bar{x}\times10^3$ mol./l. | $k$ l./mol. sec. |
|---|---|---|---|---|---|---|---|---|
| 1 | 1617 | 6.250 | 5.652 | 0.9420 | 0.9 | 0.3474 | 0.4262 | $2.101\times10^5$ |
| 8 | 1703 | 5.318 | 4.568 | 0.7614 | 1.3 | 0.2075 | 2.062 | $2.355\times10^6$ |
| 9 | 1822 | 5.122 | 4.111 | 0.6852 | 1.3 | 0.1449 | 2.166 | $2.924\times10^6$ |
| 37 | 1975 | 4.866 | 3.605 | 0.6008 | 1.1 | 0.1222 | 2.858 | $1.229\times10^7$ |
| 38 | 2121 | 4.593 | 3.168 | 0.5280 | 1.1 | 0.1143 | 2.709 | $1.973\times10^7$ |
| 39 | 2320 | 3.728 | 2.350 | 0.3916 | 1.0 | 0.1071 | 2.141 | $4.593\times10^7$ |
| 43 | 1886 | 5.438 | 4.218 | 0.7030 | 0.8 | 0.1375 | 2.554 | $6.331\times10^6$ |
| 44 | 2400 | 3.287 | 2.003 | 0.3338 | 0.9 | 0.1348 | 1.838 | $8.231\times10^7$ |

13) H. S. Glick, W. Squire and A. Herzberg, "5th Symposium (International) on Combustion," Reinhold, Pittsburgh (1955), p. 393.

* The latter assumption is not justified for the reaction of a small activation energy. In the case of hydrazine decomposition,[14] the activation energy is 35 kcal./mol. and about 25% of the total reaction occurs in the cooling process. However, this assumption may be approximately applicable in the present case since the activation energy is 51 kcal./mol.

14) H. B. Palmer and B. E. Knox, *AIAA.* **1**, 1195 (1963).

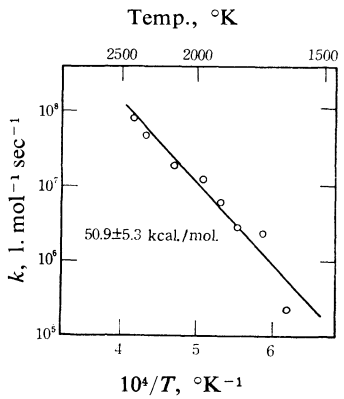



Fig. 8. Arrhenius plot of second-order rate constants. Solid line is a least-squares fit.

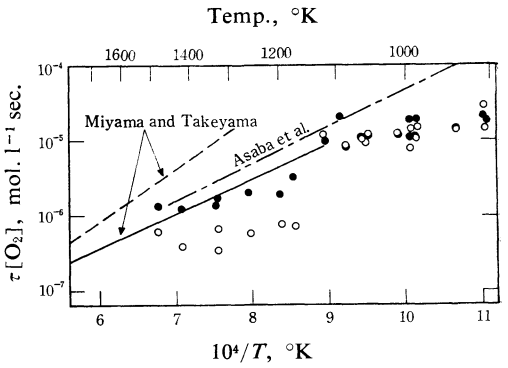



Fig. 9. Induction period vs. reciprocal temperature. The lines and symbols have the same significance as in Fig. 5. Temperatures were recalculated as described in the text.

Numerical calculations were conducted by using Eq. 4 combined with the values shown in Table I, where the calculated values of $k$ are also tabulated in the last column. Figure 8 shows an Arrhenius plot of these rate constants. The equation of the least-squares line is:

$$\log k = 12.56 \pm 0.21 + (-11070 \pm 1150)/T \quad (6)$$

The apparent activation energy obtained from the slope of this line is 50.9±5.3 kcal./mol. Further, the first-order rate constants were calculated in an analogous method, assuming that the rate of consumption of methane is proportional to the concentration of methane or oxygen. However, the Arrhenius plot did not show a straight line.

## Discussion

As is shown in Fig. 5, the data obtained for the methane-lean mixtures without argon deviate markedly from those for the mixtures with argon. At about 800°K, the vibrational relaxation time of oxygen molecule[15] is of almost the same order of magnitude as the induction periods described above, although that of methane is negligibly small.[16] Therefore, the temperatures and pressures of reflected shock waves were recalculated by assuming that the vibrational energy of the oxygen molecule is *frozen* but that the other relaxation conditions are the same as have been described above. The corrected data are plotted in Fig. 9. The agreement between the data for the mixtures with and without argon is thereby improved a little. However, there is still a large discrepancy. Other factors which possibly cause this discrepancy are considered to be as follows: when the mixture is not diluted with argon, the large concentrations of reactants release an appreciable amount of heat of reaction, even during the induction period; when the shock wave passes through the large concentration of polyatomic gases, bifurcation occurs as a result of the interaction between the reflected shock wave and the boundary layer;[17] and because of the high concentration of reactants, the abundance of reactive species such as radicals changes the reaction mechanism.

Since not enough data are available to explain the above-described discrepancies, however, the results obtained for the methane-lean mixtures without argon will not be discussed further.

According to Semenov,[1] the mechanism of methane oxidation at relatively lower temperatures may be considered to be as follows:

$$CH_4 + O_2 \rightarrow CH_3 + HO_2$$
(I) $E = 55$ kcal./mol.

$$CH_3 + O_2 \rightarrow CH_2O + OH$$
(II) $E = 20$ kcal./mol.

$$OH + CH_4 \rightarrow H_2O + CH_3$$
(III) $E = 8$ kcal./mol.

$$OH + CH_2O \rightarrow H_2O + HCO$$
(IV) $\Delta H = -38$ kcal./mol.

$$CH_2O + O_2 \rightarrow HCO + HO_2$$
(V) $E = 32$ kcal./mol.

$$HCO + O_2 \rightarrow CO + HO_2$$
(VI) $\Delta H = -20$ kcal./mol.

$$HO_2 + CH_4 \rightarrow H_2O_2 + CH_3$$
(VII) $E = 11$ kcal./mol.

15) D. R. White and R. C. Millikan, *J. Chem. Phys.*, **39**, 1803 (1963).
16) F. D. Rossini, "High Speed Aerodynamics and Jet Propulsion," Vol. I, "Thermodynamics and Physics of Matter," Princeton University Press (1955), p. 701.
17) R. A. Strehlow and A. Cohen, *J. Chem. Phys.*, **30**, 257 (1959).

$$HO_2 + CH_2O \rightarrow H_2O_2 + HCO$$
(VIII) $\Delta H = -12$ kcal./mol.

$$OH \xrightarrow{\text{wall}} \text{destruction}$$
(IX)

$$CH_2O \xrightarrow{\text{wall}} \text{destruction}$$
(X)

At higher temperatures in shock waves, Asaba et al.[9] proposed to adopt reactions I, II, III, V, VI and VII, and they concluded from the measurements of the ignition delay that the rate-determining step for a methane-rich mixture with a methane-oxygen ratio above unity is reaction I, while the rate-determining step for a methane-lean mixture with a methane-oxygen ratio below unity is reaction II.

The results described in the preceding section for the methane-rich mixtures and for the intermediate mixtures support their conclusion regarding rich mixtures; the consumption of methane is a second-order reaction with an activation energy of 50.9±5.3 kcal./mol., which is first order with regard to both methane and oxygen. However, in the case of methane-lean mixtures, it was found that the induction periods, $\tau_1$s and $\tau_2$s, were inversely proportional to the concentration of oxygen. In addition, apparent activation energies of 21.5±1.2 and 33.8±1.0 kcal./mol. were obtained from the plots of log ($\tau_1[O_2]$) vs. $1/T$ and log ($\tau_2[O_2]$) vs. $1/T$ respectively. In order to establish the actual meaning of these findings, it is assumed that, during the induction period $\tau_1$, OH, $HO_2$, HCO and $CH_2O$ are steady-state intermediates and that the principal chain carrier is the $CH_3$ radical. Therefore, the rate of increase of the $CH_3$ radical is expressed in Eq. 7:

$$\begin{aligned} d[CH_3]/dt &= k_1[CH_4][O_2] - k_2[CH_3][O_2] \\ &\quad + k_3[OH][CH_4] + k_7[HO_2][CH_4] \\ &= 2k_1[CH_4][O_2] + k_2[CH_3][O_2] \end{aligned} \quad (7)$$

The integration of Eq. 7 gives Eq. 8, assuming $[CH_4] = [CH_4]_0$ and $[O_2] = [O_2]_0$:

$$\frac{2k_1[CH_4][O_2] + k_2[CH_3][O_2]}{2k_1[CH_4][O_2] + k_2[CH_3]_0[O_2]} = \exp\{k_2[O_2](t - t_0)\} \quad (8)$$

Here, $t_0$ is any reference time following which Eqs. 7 and 8 are valid, and the subscript zero on a concentration denotes the value of that concentration at time $t_0$. Defining the origin of time as the time when the rate of reaction II becomes equal to that of initiation I, i. e., at $t=0$:

$$k_1[CH_4][O_2] = k_2[O_2][CH_3]_0 \quad (9)$$

Eq. 10 is obtained from Eq. 8.

$$[CH_3] = 3[CH_3]_0\{\exp(2k_2[O_2]t) - 2/3\} \quad (10)$$

The steady-state expression for [OH] in terms of $[CH_3]$ is:

$$[OH] = [CH_3](k_2[O_2]/k_3[CH_4]) \quad (11)$$

so [OH] also increases exponentially according to:

$$[OH] = 3[OH]_0\{\exp(2k_2[O_2]t) - 2/3\} \quad (12)$$

$[OH]_0$ is given by Eqs. 9 and 11.

Defining $[OH]_{\tau_1}$ and $[CH_3]_{\tau_1}$ as the concentrations of [OH] and $[CH_3]$ respectively at $t=\tau_1$, the following relations are obtained:

$$\begin{aligned} [CH_3]_{\tau_1}/[CH_3]_0 &= [OH]_{\tau}/[OH]_0 \\ &= 3\{\exp(2k_2[O_2]\tau_1 - 2/3\} \end{aligned} \quad (13)$$

It can be assumed, in analogy with the hydrogen-oxygen reaction,[18] that the ratio $[OH]_{\tau_1}/[OH]_0$ remains approximately constant over the temperature range studied. Therefore;

$$k_2[O_2]\tau_1 = \text{const.}$$

Thus, a plot of log ($\tau_1[O_2]$) vs. $1/T$ should give a straight line, the slope of which gives the activation energy of reaction II.

On the other hand, after the induction period $\tau_1$ formaldehyde can no longer be assumed to be a steady-state intermediate and its concentration accumulates, since reaction II is faster than reaction V. Hence, the rate of increase of $[CH_3]$ is:

$$d[CH_3]/dt = 2k_1[CH_4][O_2] + k_5[CH_2O][O_2] \quad (15)$$

Since the first term may be disregarded for the methane-lean mixtures,[9] Eq. 16 should approximately hold when Eq. 15 is integrated:

$$[CH_3]_{\tau_2} = k_5[O_2]\int_0^{\tau_2}[CH_2O]dt \quad (16)$$

Here, $[CH_3]_{\tau_2}$ is the concentration at the end of the induction periods $\tau_2$, and its value is considered to be approximately a constant which depends upon the detectability of the pressure transducer. Therefore, Eq. 17 may be obtained from Eq. 16:

$$[CH_3]_{\tau_2} = k_5[O_2]\tau_2[CH_2O]_{av} \quad (17)$$

where:

$$[CH_2O]_{av} = \frac{1}{\tau_2}\int_0^{\tau_2}[CH_2O]dt$$

If it is assumed that $[CH_2O]_{av}$ reaches a certain limiting value at the start of the explosive reaction, $\tau_2[O_2]$ is inversely proportional to $k_5$:

$$\tau_2[O_2] \propto 1/k_5 \quad (18)$$

Thus, a plot of log ($\tau_2[O_2]$) vs. $1/T$ should also give a straight line, the slope of which gives the activation energy of reaction V.

18) G. L. Schott and J. L. Kinsey, *J. Chem. Phys.*, **29**, 1177 (1958).

Therefore, the results presented in the previous paper[12] suggest that the rate-determining step for OH formation is reaction (II) and that that for the over-all reaction is reaction V. The discrepancy about the rate-determining step of the over-all reaction for the methane-lean mixtures between the present study and that of Asaba et al. might be explained by the difference in experimental conditions which was discussed at the beginning of this section. For the intermediate mixtures under the present experimental conditions, it may be considered from the value of the apparent activation energy and the distinct dependence of $\tau$s on the product of methane and oxygen concentrations that the over-all reaction is controlled also by the reaction $CH_4 + O_2 \rightarrow CH_3 + HO_2$.

According to the recent papers of Kistiakowsky and his coworkers,[19,20] the kinetics at lower partial pressures of reactants differ from those observed or proposed for reactions taking place at much higher partial pressures or at much lower temperatures; that is, ion molecules must be taken into account under the former conditions. In the present studies, the partial pressures of reactants ranged from 250 to 5000 mmHg and so are much higher than those chosen by them (a few mmHg). Thus, it may be reasonable to suppose that reactions I, II, III, V, VI and VII occur during the induction periods under the present experimental conditions, as has been proposed by Semenov as occurring at lower temperatures.

19) G. B. Kistiakowsky and J. V. Michael, ibid., **40**, 1447 (1964).

20) G. P. Glass and J. V. Michael, Lecture Delivered at the Symposium on Chemical Reactions in Shock Tubes, Duke University, North Carolina, U. S. A., April 21—23, 1964.

**Summary**

The mechanism of methane oxidation in reflected shock waves has been studied by measuring the induction period of the OH absorption and that of the pressure increase simultaneously, and also by using the single-pulse technique combined with gas chromatography.

As a result, it has been found under the present experimental conditions that the rate-determining step for the over-all reaction of the methane-rich mixtures with the ratio $[CH_4]/[O_2]=6$ is $CH_4 + O_2 \rightarrow CH_3 + HO_2$, and that the rate-determining step for the over-all reaction of the methane-lean mixtures with the ratio $[CH_4]/[O_2]=3/7$ is $CH_2O + O_2 \rightarrow HCO + HO_2$. Also, the rate-determining step for the OH formation of the lean mixtures has been found to be $CH_3 + O_2 \rightarrow CH_2O + OH$ under the present conditions. In the case of the intermediate mixtures with the ratio $[CH_4]/[O_2]=1.5$, the over-all reaction is considered to be controlled mainly by the reaction $CH_4 + O_2 \rightarrow CH_3 + HO_2$.

The authors wish to express their thanks to Mr. Akio Sawa for his help in the experiments and to Mr. Daisuke Miura and Mrs. Yukiko Takemura for their computations of shock parameters.

*Basic Research Laboratories*
*Toyo Rayon Company, Ltd.*
*Tebiro, Kamakura*

# The Oxidimetric Determination of Thioureas with Potassium Bromate

By Balwant SINGH, Balbir Chand VERMA and M. S. SARAN

(Received June 10, 1964)

Szebelledy and Madis[1] determined thiourea by titrating it with bromate in a hydrochloric acid medium at 40 to 50°C in the presence of potassium bromide and a little gold chloride. The end-point was marked by the appearance of a yellow colour which persisted only for 5 to 10 sec. On the other hand, Mahr[2] titrated thiourea with a standard bromate-bromide solution in a sulphuric acid medium at 35°C in the presence of potassium iodide and a little starch. The end-point was the appearance of a blue colour when thiourea was oxidised to formamidine disulphide. Rao and Neelakantam[3] found Mahr's method to be erratic and developed a method replacing

1) L. Szebelledy and V. Madis, *Z. anal. Chem.*, **114**, 253 (1938).
2) C. Mahr, ibid., **117**, 91 (1939).
3) K. B. S. R. P. S. P. Appa Rao and K. Neelakantam, *Ind. J. Pharm.*, **14**, 50 (1952).

potassium bromate by potassium permanganate and using a lower concentration of sulphuric acid and double the amount of potassium iodide.

However, no systematic study has so far been made regarding the oxidimetric determination of thiourea and its organic derivatives. In the present work an attempt will be made to use potassium bromate as a redox reagent for the determination of thioureas in a sulphuric acid medium at room temperature. In the presence of potassium iodide, the thiourea and its organic derivatives will be oxidised to their corresponding disulphides with this oxidant.

## Experimental

A known weight (10 to 60 mg.) of each compound was taken in a titration flask. In the case of thiourea and its alkyl derivatives, sufficient water and enough sulphuric acid to keep the acid concentration at 2 N were added. Each aryl derivative of thiourea was dissolved in 18 N sulphuric acid (10 to 15 ml.), and sufficient water (50 to 90 ml.) was added to keep the acid concentration between 2.5 to 4.0 N. To the solution of each compound a 0.40 ml. portion of 10% potassium iodide solution was added except in the case of the *p*-tolyl-, *p*-methoxyphenyl- and *p*-ethoxyphenyl thioureas, to which 0.10 ml. portions of 10% potassium iodide solution were added. The solution in each case was cooled to room temperature and titrated with standard (N/20) potassium bromate. The end-point in each case was detected visually as well as potentiometrically. In visual titrations,

Table I. The determination of thiourea and its organic derivatives with standard (N/20) potassium bromate

| Compound | Visual method | | Potentiometric method | |
|---|---|---|---|---|
| | Taken g. | Found g. | Taken g. | Found g. |
| $H_2N{\cdot}CS{\cdot}NH_2$ | 0.0152 | 0.0152 | 0.0152 | 0.0151 |
| | 0.0457 | 0.0459 | 0.0457 | 0.0458 |
| $CH_3NH{\cdot}CS{\cdot}NH_2$ | 0.0099 | 0.0099 | 0.0165 | 0.0165 |
| | 0.0449 | 0.0451 | 0.0513 | 0.0513 |
| $CH_3CH_2NH{\cdot}CS{\cdot}NH_2$ | 0.0124 | 0.0124 | 0.0226 | 0.0226 |
| | 0.0553 | 0.0550 | 0.0543 | 0.0543 |
| $(CH_3)_2CHNH{\cdot}CS{\cdot}NH_2$ | 0.0112 | 0.0112 | 0.0178 | 0.0178 |
| | 0.0554 | 0.0556 | 0.0488 | 0.0490 |
| $n\text{-}CH_3CH_2CH_2{\cdot}CH_2NH{\cdot}CS{\cdot}NH_2$ | 0.0105 | 0.0105 | 0.0263 | 0.0262 |
| | 0.0553 | 0.0550 | 0.0560 | 0.0561 |
| $(CH_3)_2CHCH_2NH{\cdot}CS{\cdot}NH_2$ | 0.0103 | 0.0103 | 0.0203 | 0.0202 |
| | 0.0502 | 0.0501 | 0.0555 | 0.0553 |
| $n\text{-}CH_3CH_2CH_2CH_2CH_2{\cdot}NH{\cdot}CS{\cdot}NH_2$ | 0.0102 | 0.0102 | 0.0147 | 0.0147 |
| | 0.0525 | 0.0522 | 0.0573 | 0.0572 |
| $o\text{-}(CH_3)C_6H_4{\cdot}NH{\cdot}CS{\cdot}NH_2$ | 0.0155 | 0.0155 | 0.0126 | 0.0126 |
| | 0.0500 | 0.0499 | 0.0608 | 0.0609 |
| $p\text{-}(CH_3)C_6H_4{\cdot}NH{\cdot}CS{\cdot}NH_2$ | 0.0103 | 0.0103 | — | — |
| | 0.0532 | 0.0530 | — | — |
| $o\text{-}(OCH_3)C_6H_4{\cdot}NH{\cdot}CS{\cdot}NH_2$ | 0.0165 | 0.0166 | 0.0184 | 0.0184 |
| | 0.0535 | 0.0536 | 0.0541 | 0.0544 |
| $p\text{-}(OCH_3)C_6H_4{\cdot}NH{\cdot}CS{\cdot}NH_2$ | 0.0202 | 0.0201 | — | — |
| | 0.0500 | 0.0497 | — | — |
| $o\text{-}(OC_2H_5)C_6H_4NH{\cdot}CS{\cdot}NH_2$ | 0.0142 | 0.0142 | 0.0096 | 0.0096 |
| | 0.0496 | 0.0493 | 0.0519 | 0.0517 |
| $p\text{-}(OC_2H_5)C_6H_4NH{\cdot}CS{\cdot}NH_2$ | 0.0107 | 0.0107 | — | — |
| | 0.0501 | 0.0498 | — | — |

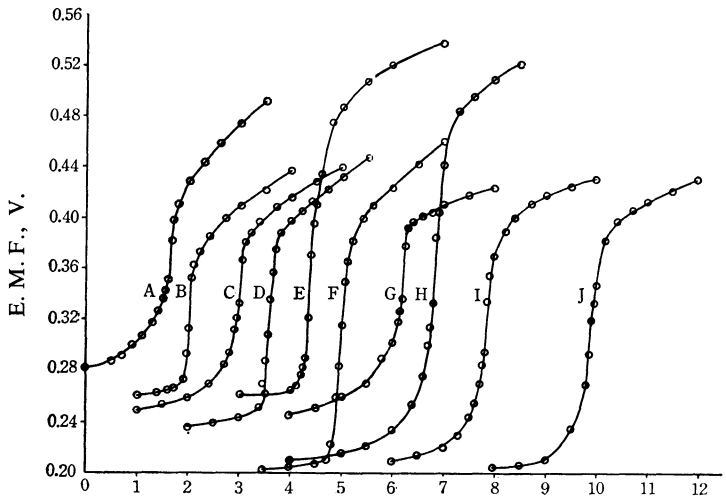



Fig. 1

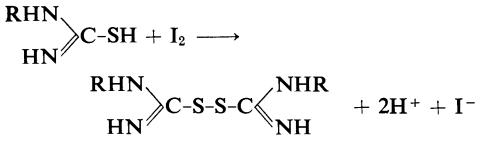
A *o*-Ethoxy phenyl thiourea
B *o*-Methoxy phenyl thiourea
C Isobutyl thiourea
D *o*-Tolyl thiourea
E Ethyl thiourea
F Thiourea
G Isopropyl thiourea
H *n*-Butyl thiourea
I *n*-Amyl thiourea
J Methyl thiourea

0.20 ml. of 1% amylose was used as an indicator, and the solution acquired a blue colour at the end-point. A series of potentiometric titrations was performed with different amounts of the compound in each case. The potentiometric titrations, one for each compound, are represented by curves A to J in Fig. 1.

From the volume of the standard (N/20) potassium bromate solution used corresponding to the end-point in each titration, the amount of each compound was calculated. Some typical results are given in Table I.

The results recorded in the table show that the listed compounds can be determined volumetrically by titrating them with standard (N/20) potassium bromate. Thiourea and its organic derivatives are oxidised by potassium bromate to their corresponding disulphides in the presence of potassium iodide in a sulphuric acid medium.

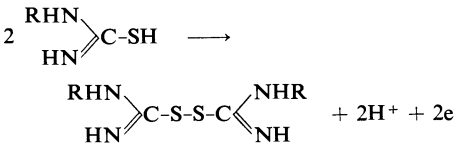
$$BrO_3^- + 6\,I^- + 6H^+ \longrightarrow Br^- + 3\,I_2 + 3\,H_2O$$



(R=hydrogen atom, alkyl or aryl group)

## Summary

Potassium bromate has been used as a redox reagent in the presence of potassium iodide for the visual and potentiometric determination of thiourea and its several alkyl and aryl derivatives in a sulphuric acid medium. In visual titrations, amylose, is used as a visual indicator, turning blue at the end-point. In the potentiometric method, a bright platinum wire is used as an oxidation-reduction electrode; this is coupled with a saturated calomel electrode. The thioureas are oxidised to their corresponding disulphides with a single electron-change:



(R=hydrogen atom, alkyl or aryl group)

This direct method is simple, accurate, instantaneous and widely applicable.

One of the present authors (B. C. V.) wishes to thank the Council of Scientific and Industrial Research, Rafi Marg, New Delhi, for the award of a Senior fellowship.

*Chemistry Department*
*Punjabi Univesity*
*Patiala, India*

# Electron Paramagnetic Resonance Absorption of Chromium Ions Dispersed on Silica-alumina. I. The Influence of Chemical Constitution of the Supporting Materials on the Dispersed State

By Akira MATSUMOTO, Hazime TANAKA and Nobuhisa GOTO

(Received June 12, 1964)

The electron paramagnetic resonance (EPR) absorption of chromium ions dispersed on supporting materials, principally silica, silica-alumina and gamma alumina, has been examined by several investigators for the purpose of clarifying their catalytic active sites in some chemical reactions.[1-11] Three types of resonance absorption have been confirmed. The first of these appears in the vicinity of 1500 oe. in the X-band and has been referred to as the $\delta$-line. This absorption has been interpreted as due to $Cr^{3+}$ ions well dispersed and electronically isolated.[4] The second resonance,

1) P. Cossee and L. L. Van Reijen, 2nd International Congress on Catalysis (Paris) 1960, paper no. 82.
2) Yu. I. Pecherskaya, V. B. Kazansky and V. V. Voevodsky, ibid., paper no. 108.
3) D. E. O'Reilly, *Advances in Catalysis*, **12**, 99 (1960).
4) D. E. O'Reilly and D. S. MacIver, *J. Phys. Chem.*, **66**, 276 (1962).
5) C. P. Poole, Jr., W. L. Kehl and D. S. MacIver, *J. Cat.*, **1**, 407 (1962).
6) F. M. Bukanaeva, Yu. I. Pecherskaya, V. B. Kazansky and V. A. Dzis'ko, *Kin. i Kat.*, **3**, 358 (1962).
7) V. V. Antuf'ev, M. P. Votinov, A. G. Sazhin, A. C. Cemenova and M. N. Peitman, ibid., **3**, 353 (1962).
8) V. B. Kazansky and Yu. I. Pecherskaya, ibid., **4**, 244 (1963).
9) A. A. Spinskin, E. A. Fedorovskaya and A. M. Rubinshtejn, ibid., **4**, 230 (1963).
10) K. Tarama, S. Teranishi and K. Yoshida, *Shokubai* **4**, 341 (1962).
11) D. G. Howard and R. H. Lindquist, *J. Chem. Phys.*, **38**, 573 (1963).

referred to as the $\beta$-line, is broad and centered at about 3400 oe. in the X-band. MacIver et al.[5] distinguished two kinds of $\beta$-lines, using coprecipitated chromia-alumina, and attributed them to $Cr^{3+}$ in small clusters of chromia in the amorphous phase and in the solid solution phase. The last resonance, whose $g$ value is almost the same as that of the $\beta$-line but whose width is narrower, has been referred to as the $\gamma$-line. This absorption has been generally attributed to $Cr^{5+}$.

The character of these absorptions varies with the supporting materials and the oxidation-reduction conditions and, though the various general explanations of their origin agree with each other fairly well, some uncertainty remains about the configurational state of the ions. In the present investigation, we intend to examine the structural change of chromium ions with the variation in the chemical constitution of the supporting material under the heat treatment, pursuing principally the behavior of the $\gamma$-lines and comparing their shapes with those of some chromium compounds.

## Experimental

**Materials and Treatment.** — As supporting materials pure silica gel, silica-alumina and gamma alumina were prepared by the hydrolysis of ethyl-orthosilicate, aluminum isopropoxide and their mixtures in order to avoid their containing impurities of transition elements. Aluminum isopropoxide was made from highly pure metallic aluminum. After having been crushed down to 30 mesh pass, they were heat-treated at 500°C for 17 hr. in a stream of dry air. Figure 1 shows their thermal variation, while Table I indicates the chemical composition, the surface area, and the results of qualitative analysis by the emission spectroscopy of the materials heat-treated. In some cases a commercial silica-alumina cracking catalyst (Davison Co.) was employed; the official specifications are also shown in Table I.

The impregnation of chromia was carried out with an aqueous solution of chromic anhydride of a special grade (Kanto Kagaku Co.). The supporting materials were immersed in the solution and strirred at 50°C for 2 hr. The excess solution was then filtered out, and the impregnated materials were dried for 24 hr. in an air bath at 120°C. The quantity of chromium was controlled by changing the concentration of the solution and the ratio of the supporting material to the solution. Table II indicates the impregnated samples used in the experiment. The heat treatment of the impregnated materials was carried out in a stream of dry air for 4 hr. at definite temperatures.

Chromic anhydride was also heat-treated without supporting material. This compound melts at a relatively low temperature, i.e., at 196°C, and it is changed into alpha chromia at about 400°C through a few intermediates. Various intermediate chromium oxides between CrO and $CrO_3$ have been

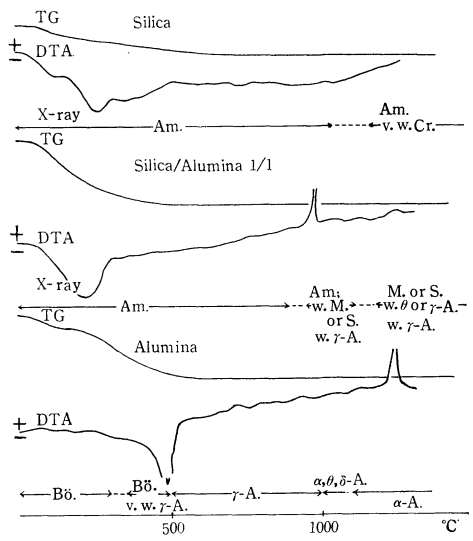



Fig. 1. Thermal transition of the supporting materials.
TG: thermogravimetry, DTA: differential thermal analysis, Am.: amorphous, Cr.: cristobalite, Bö.: boemite, A.: alumina, M.: mullite, S.: sillimanite, w.: weak, v. w.: very weak.
X-ray diffraction was measured after holding at each temperature for 4 hr.

Table I. Supporting materials used in the experiment

| No. | Material | $SiO_2/Al_2O_3$ mol. | BET surface area $m^2/g$. | Purity* |
|---|---|---|---|---|
| 1 | Silica gel | — | 634.6 | Al : N.D. |
| 2 | Silica-alumina I | 1 : 4 | 279.1 | Cu : ± |
| 3 | Silica-alumina II | 1 : 1 | 308.5 | |
| 4 | Gamma alumina | — | 233.4 | Si : + |
| 5 | Commercial silica alumina | 1 : 10 | >400 | |

* By emission spectroscopy, No. 1—4: Ca ±, Mg, Na, Fe, Ti, Cu, Mn, Cr N. D.

Table II. Impregnated samples used in the experiment

| Sample No. | Base material* | Cr cont., wt.% |
|---|---|---|
| 1 | 1 | 2.43 |
| 2 | 2 | 2.73 |
| 3 | 3 | 4.83 |
| 4 | 4 | 4.93 |
| 5-1 | 5 | 0.65 |
| 5-2 | 5 | 2.11 |
| 5-3 | 5 | 3.0 |
| 5-4 | 5 | 5.8 |
| 5-5 | 5 | 16.7 |

* Corresponds to the numbers indicated in Table I.

reported; however, their crystal structures are unknown except in a few cases. For the present work the chemical formulas of the thermal decomposition products were determined from the X-ray powder patterns obtained by Schwartz et al.[12]

The alkaline peroxychromates ($K_3CrO_8$, $Na_3CrO_8$ and $(NH_4)_3CrO_8$) were prepared using the method of Riesenfeld.[13] In one case they were prepared in the presence of supporting material.

**The Measurement of EPR Spectra.** — The EPR measurements were performed with a superheterodyne-type spectrometer, constructed by the Applied Electric Laboratory Co., which operated in the K-band (24 kMc./s.) using two klystrons (24 VlO) and 45 Mc./s. as I. M. F. The first derivatives of resonance spectra were recorded on a chart, using modulation amplitudes from 2 to 50 oe. The peak-to-peak width and the position of the spectra were measured with a proton magnetic resonance recorded on the same chart and corrected by the spectra of DPPH.

The relative intensity of the spectra was determined by comparing it with a resonance absorption of a piece of synthetic ruby fixed in the cavity. The absolute number of unpaired electrons in the sample was estimated from a comparison of this standard resonance with that of DPPH.

Most of the measurements were made at room temperature and in open air. It has been recognized that the width of the resonance in the X-band was affected by the partial pressure of oxygen over the sample.[2] We could not observe this effect when the sample sealed off with nitrogen after the heat treatment was exposed to air. Samples were put into quartz tubes 3 mm. in o. d. directly after the treatment and measured.

**Chemical Analysis.** — The portion of the chromium which dissolved out into distilled water was determined with several samples. About 100 mg. of the sample was boiled in 50 cc. of distilled water for 10 min. and then filtered. The chromium in the filtrate was determined colorimetrically.

The total chromium content was measured after the heat treatment using flux agents to make them all water soluble. In the course of this analysis, it was recognized that potassium-sodium carbonate and potassium sulfate were sufficient as the flux in most cases, but the silica-alumina II indicated in Table I fixed chromium strongly and it became difficult to make all chromium water soluble with this flux. For these exceptional cases sodium peroxide was used as the flux.

The oxidation number was also determined in some cases. About 100 mg. of the sample was immersed in 60 cc. of distilled water; 10 cc. of 1 : 4 hydrochloric acid and 1 g. of potassium iodide were added, and then the mixtures were kept still for 1 hr., after which time iodometry was carried out.

## Results

**The $\gamma$-Absorption of Dispersed Samples.** — *The Variation in $\gamma$-Line Shape with the Supporting Materials.* — The general features of the spectra obtained in the experiment agree with the results given in the preceding reports. The factor which has the greatest effect on the spectral shape is the constitution of the supporting material. The spectra of chromium

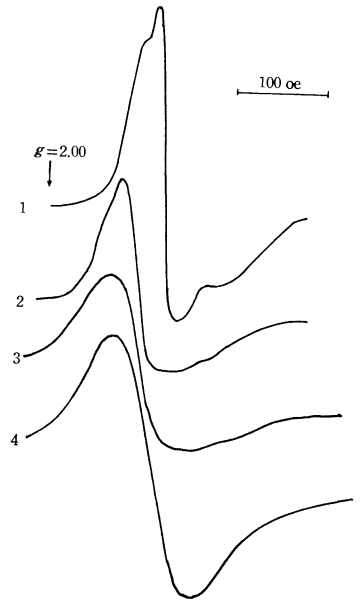
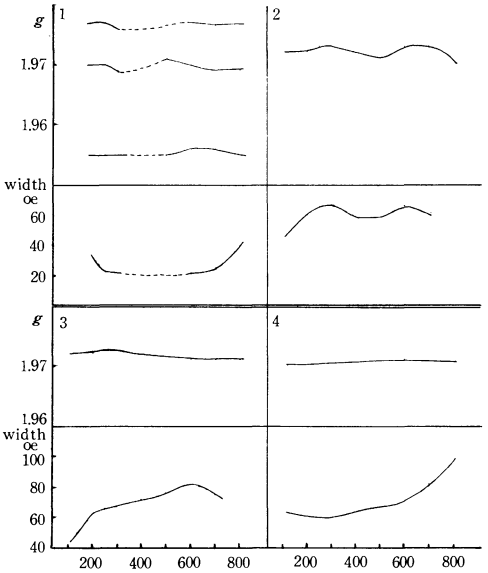



Fig. 2. Derivative of $\gamma$-absorption of chromium ions dispersed on different supporting materials (heat treated at 700°C for 4 hr.). Numbers indicate sample number in Table II.




Temp. of the heat treatment, °C

Fig. 3. The variation of $g$ value and width of the $\gamma$-absorption with the heat treatment. Base 1: silica-gel, 2: silica/alumina 4/1, 3: silica/alumina 1/1, 4: gamma alumina

12) P. S. Schwartz, I. Fankuchen and R. Ward, *J. Am. Chem. Soc.*, **74**, 1676 (1952).
13) E. H. Riesenfeld, H. E. Wohlars and W. A. Kutsch, *Ber.*, **38**, 1885 (1905).

ions on pure silica gel show typical asymmetric features; the three components of the $g$ tensor are distinct (Fig. 2). The addition of alumina to the base material makes the separation of the peak indistinct, and only the difference between $g_{//}$ and $g_{\perp}$ can be recognized. When the content of alumina reaches 50 mol.%, it becomes more difficult to see the separated peaks and the apparent symmetry of the spectra increases. Chromium ions on gamma alumina are similar. When the measurement is performed at the temperature of liquid nitrogen, the intensity of the absorption increases but the line shape hardly changes at all.

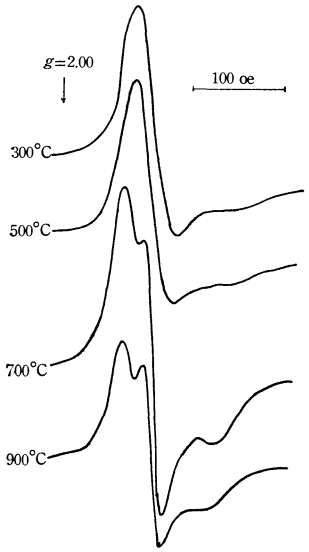



Fig. 4 (a). Variation of $\gamma$-absorption shape with heat treatment (Sample No. 5-2 in Table II).

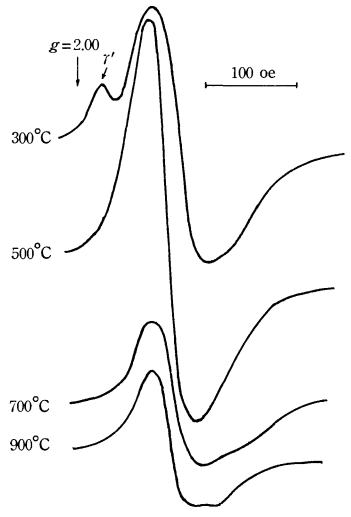



Fig. 4 (b). Variation of $\gamma$-absorption shape with heat treatment (Sample No. 5-1 in Table II).

The $g$ values and the width of the $\gamma$-line vary slightly with the temperature of the heat treatment (Fig. 3). The chromium content in the sample also affects the line shape (Fig. 4). When commercial silica-alumina is used as the supporting material and when the chromium concentration is low, a new resonance appears at a lower magnetic field, between 250 and 300°C, of the heat treatment. This resonance, indicated in Fig. 4b as the $\gamma'$-line, does not appear in other cases; here we will only note its appearance.

*The Variation in Intensity with Heat Treatment.*—The intensity of the $\gamma$-line varies with the temperature of heat treatment and shows a maximum value between 400 and 700°C (Figs. 5 and 6). If one compares the relative intensities of the different samples, two main inclinations may be recognized: first, the increase in chromium content decreases the portion of chromium which contributes to the $\gamma$-absorption (Fig. 6), and second, the chromium dispersed on the supporting material which contains more alumina makes many more sites of $\gamma$-absorption, though it remains difficult to compare the relative intensities of samples with different supporting materials because of the differences in spectral shape.

As is shown in Fig. 5, the sample of pure silica gel does not show a sharp maximum of intensity during the heat treatment, but it

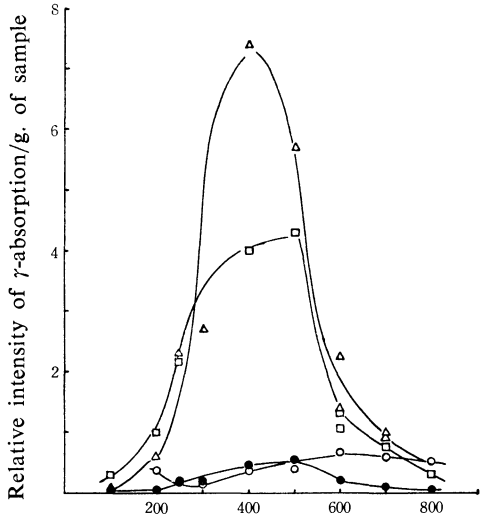



Fig. 5. Intensity variation of $\gamma$-absorption with different supporting materials.
○ 1: Base silica gel
● 2: Base silica/alumina 4/1
△ 3: Base silica/alumina 1/1
□ 4: Base gamma alumina

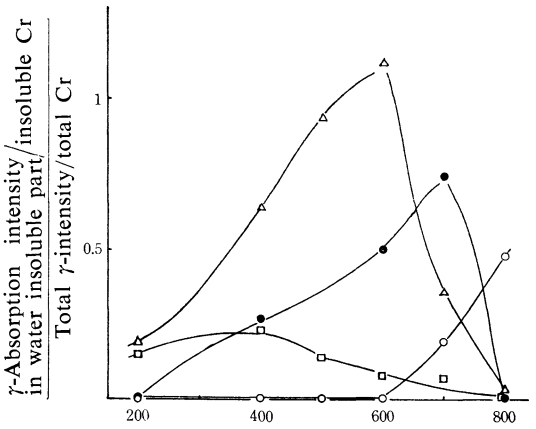



Fig. 9. γ-Absorption after dissolving out water soluble chromium.
○ 1 : Base silica gel
● 2 : Base silica/alumina 4/1
△ 3 : Base silica/alumina 1/1
□ 4 : Base gamma alumina

make the total chromium soluble using the flux which is effective in other cases.

In order to make it clear whether it is the water-soluble part of chromium or the insoluble part which contains the sites which give the γ-absorption, EPR measurements were also carried out of the residues of filtration in the analysis of water-soluble chromium. The results shown in Fig. 9 indicate that silica-alumina, particularly silica-alumina II, retains more sites of the resonance per chromium; i. e., the chromium ions which give the γ-line exist mainly in the water-insoluble part in these supporting materials. However, there remains some uncertainty whether the sites of the γ-absorption regenerate or disappear in the course of dissolving and drying.

The variation in oxidation number is shown in Fig. 10. On the silica-alumina II, the oxidation number is already low in the original impregnated sample. It is noticiable that

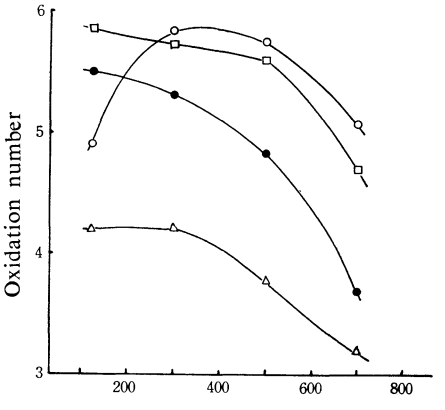



Fig. 10. Variation of the oxidation number with heat treatment.
○ 1 : Base silica gel
● 2 : Base silica/alumina 4/1
△ 3 : Base silica/alumina 1/1
□ 4 : Base gamma alumina

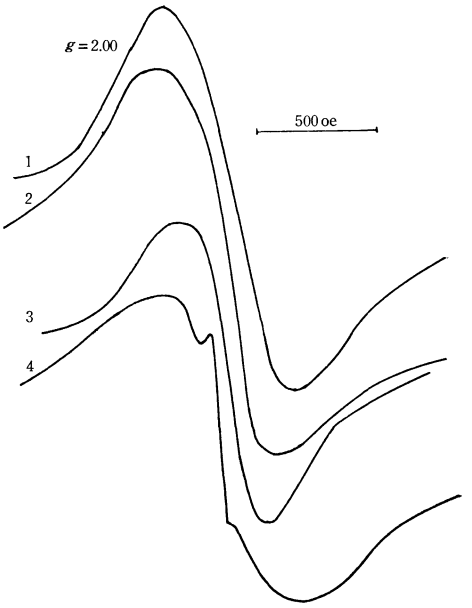



Fig. 11 (a). Derivative of EPR absorption of several chromium compounds.
1 : $Cr(OH)_3$
2 : $Cr(OH)_3$ on the silica gel
3 : $Cr_2(SO_4)_3$ on the silica gel
4 : $(NH_4)_3CrO_8$ (at room temp.)

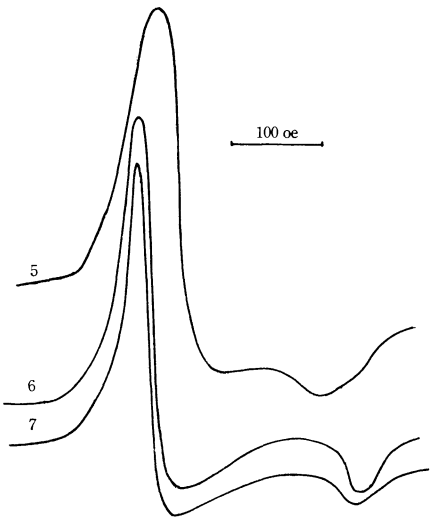



Fig. 11 (b). Derivative of EPR absorption of several chromium compounds.
5 : $Na_3CrO_8$
6 : $K_3CrO_8$ on the silica gel
7 : $K_3CrO_8$ on the silica/alumina 1/1

gamma alumina gives rather a high oxidation number, though the water-soluble chromium is poorest on this material.

**The EPR of Some Chromium Compounds.** — For the purpose of comparison, EPR measurements were made of some chromium compounds. The results are shown in Fig. 11 and Table IV. Alkaline peroxychromates give

TABLE IV. EPR ABSORPTION OF SEVERAL CHROMIUM COMPOUNDS MEASURED AT ROOM TEMPERATURE

| | | $g$ | Width, oe. |
|---|---|---|---|
| $Cr(OH)_3$ | Powder | 1.98 | 350 |
| $Cr_2(SO_4)_3$ | Dispersed on silica gel | 1.97 | 170 |
| $Ba_3(CrO_4)_2$ | Polycrystal | undetectable | |
| $K_3CrO_8$ | Dispersed on silica gel | $g_\perp$ 1.983 | (33.5) |
| | | $g_{//}$ 1.942 | |
| $Na_3CrO_8$ | Powder | $g_\perp$ 1.978 | |
| | | $g_{//}$ 1.949 | |

absorptions similar to the $\gamma$-line. These materials are unstable at room temperature, and $(NH_4)_3CrO_8$ shows a spectrum which is similar to a superposition of the $\beta$-line and the $\gamma$-line. These peroxychromates contain $Cr^{5+}$ ions; recently Swalen and Ibers[14] and McGarvey[15] discussed their electronic level scheme on the basis of the optical absorption and the EPR absorption. $Cr(OH)_3$ and $Cr_2(SO_4)_3$ dispersed on the supporting material give a resonance absorption like the $\beta$-line.

## Discussion

**An Analysis of the Line Shape.** — Cossee and VanReijen[1] first pointed out that the chemical composition of the supporting material affected the line shape of the $\gamma$-line. We intend here to consider the differences in the dispersed state of chromium ions on different supporting materials, working through a consideration of the variation in EPR spectral shape.

As is shown in Fig. 2, chromium ions on silica gel give an asymmetrical $\gamma$-line in which three peaks in the first derivative can be distinguished. The addition of alumina makes the separation of peaks obscure. On gamma alumina the ions give an apparently symmetrical $\gamma$-line, and the apparent width increases.

The origin of the $\gamma$-absorption has been ascribed to $Cr^{5+}$ ions, as has been cited. Indeed, alkaline peroxychromates containing $Cr^{5+}$ ions give a quite similar absorption line (Fig. 11). Garif'yanov,[16] however, using borosilica glass, observed a similar absorption which might contain dispersed $Cr^{5+}$ ions. The $g$ values of these lines agree well with each other.

The shoulder of the absorption in the low magnetic field in the case of silica gel had not previously been recognized. We think that the variation in the line shape, this shoulder, depends mainly on the $g$ anisotropy and the line width: the three principal values of $g$ tensor can be observed with $Cr^{5+}$ ions on silica gel, but the increase in the content of alumina in the supporting material makes it obscure and increases the apparent symmetry as a results of the increase in the width or the variation in $g$ anisotropy.

First, we will consider the variation in the line shape from this point of view, using a simple approximation. There have been several works[17-19] about the line shape, which must be given an assembly of crystallites randomly oriented but with a $g$ anisotropy. These works have used a $\delta$-function approximation or a Lorentzian line shape for the absorption of each crystallite. Here we employ the method of Kneubühl.[18] The assumptions in this calculation are as follows:

(a) Each chromium ion has an anisotropy of the $g$ tensor;

(b) The resonance absorption line of each crystallite is Lorentzian;

(c) The width is constant and independent of the orientation of the orientation of the crystallites;

(d) The orientations of the crystallites are at random;

(e) The spin Hamiltonian consists of the Zeeman, dipolar and exchange terms only.

The results of the calculation are shown in Fig. 12, where the parameter, $b$, is the half-width at the half-power of absorption which must be given by each individual crystallite. It must be noted that, as the three principal values of $g$ tensor, the values observed in the silica gel sample, which was heat-treated at 700°C, are used. Figure 13 shows how the half-width, maximum slope width and asymmetry, expressed by (half-width of low field side)/(half-width of high field side), change with $b$.

Figure 12 shows that the three components of the $g$ tensor are distinct until $b$ becomes 15 oe. When $b$ is over 20 oe., the existence of $g$ anisotropy can be recognized only from the asymmetric figures. From Fig. 12, it can also be seen that the position of the maximum of

14) J. D. Swalen and J. A. Ibers, *J. Chem. Phys.*, **37**, 17 (1962).
15) B. R. McGarvey, ibid., **37**, 2001 (1962).
16) N. S. Garif'yanov, *Solid State Phys. (SSSR)*, **4**, 2450 (1962).
17) J. A. Ibers and J. D. Swalen, *Phys. Rev.*, **127**, 1914 (1962).
18) F. K. Kneubühl, *J. Chem. Phys.*, **33**, 1074 (1960).
19) R. H. Sands, *Phys. Rev.*, **99**, 1222 (1955).

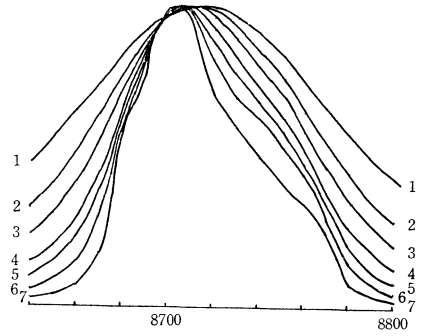



Fig. 12. Calculated absorption line shape.
The maximum values of the curves are set at unity.
The half-width at half power of each crystallite, $b$, is taken as a parameter.
1: $b$=60 oe. 2: $b$=40 oe. 3: $b$=30 oe.
4: $b$=20 oe. 5: $b$=15 oe. 6: $b$=10 oe.
7: $b$=5 oe.

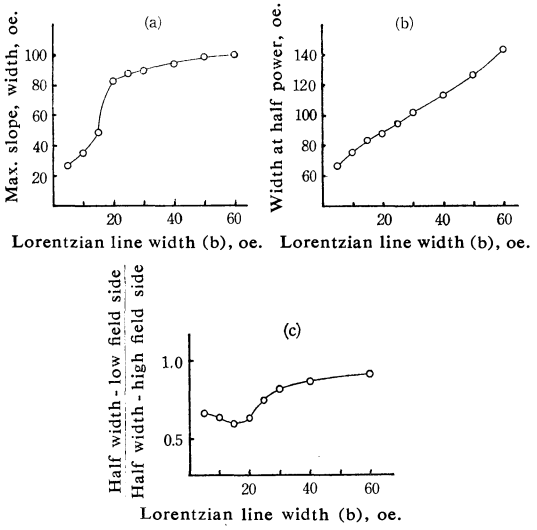



Fig. 13. Variation of line width and asymmetry as a function of Lorentzian line width, b (from the calculated curves in Fig. 12).

the absorption line goes up to a higher magnetic field with the increase in $b$. This inclination contradicts the experimental results shown in Fig. 3. If samples with the same supporting material are compared, the apparent $g$ value slightly decreases or is constant when the temperature of the heat treatment rises and the apparent width of the maximum slope increases. However, if samples with different supporting materials are compared, it is noticed that gamma alumina gives lines with somewhat larger apparent $g$ values than the $g_2$ values of those with silica gel. In the above calculations the definite $g$ components given in the silica gel sample are used, but it is doubtful that the principal values of th $g$ tensor remain constant among the different supporting materials. It is rather more probable that $g$ anisotropy decreases with the increase in the alumina content of the supporting materials.

Keeping this precaution in mind, we will try a rough comparison of the observed results shown in Fig. 3 with those of Fig. 13. The $\gamma$-line of samples with silica gel gives spectra which show the three components of $g$ distinctly and which have a maximum slope width of 30 oe. This corresponds to the calculated curves with $b < 10$ oe. The samples with silica/alumina 4:1 give $\gamma$-lines with maximum slope widths of 40—60 oe., indicating a still considerable asymmetry; they corresponds to the calculated curves with $b$=15—20 oe. Silica-alumina II produces samples which give $\gamma$-lines corresponding to those of $b$=20 oe. When gamma alumina is used as the supporting material, the width is about 60 oe. when the temperature of the heat treatment is low, but if the temperature of the heat treatment is over 700°C, the width increases up to about 100 oe.; this corresponds to the curves calculated with $b$=50—60 oe.

**The Dispersed State of Chromium Ions on the Different Supporting Materials.** — As has been described, three kinds of absorption, $\delta$, $\beta$ and $\gamma$, are observed with chromia dispersed on silica-alumina; the $\delta$-absorption has been attributed to $Cr^{3+}$ ions well dispersed and isolated. Howard[11] indicated that this $\delta$-absorption was not observed with chromia dispersed on silica gel. This means that there are few isolated chromia on silica gel. On the other hand, the decrease in $\gamma$-absorption and the increase in $\beta$-absorption occur with the same inclination during heat treatment, though the quantitative correspondence does not exist. This indicates that the sites of both absorptions may be in the same region on the sample. Eischens and Selwood[20] concluded from their susceptibility measurements that chromic anhydride dispersed on gamma alumina is deposited mainly three oxide layers thick.

The chromia dispersed on silica gel is almost entirely water-soluble, and the solubility is not affected by the heat treatment of a higher temperature. On the contrary, gamma alumina and silica-alumina II make insoluble chromium which increases remarkably in amount with the heat treatment. As is well known, alumina easily makes a solid solution with chromia; also, alumina crystallizes from hydroxide at about 500°C. On the other hand, the

20) R. P. Eischens and P. W. Selwood, *J. Am. Chem. Soc.*, **69**, 1590, 2698 (1947).

silica gel used in the present experiment does not produce a solid solution with chromia, at least below 1000°C, and it does not crystallize before 1000°C, according to the X-ray diffraction analysis. Chromic anhydride changes into alpha chromia at about 400°C, as has been mentioned before.

From these facts it may be considered that on silica gel chromia exists mainly in the form of clusters, probably several atomic layers thick. If 5 wt.% of chromium are dispersed homogeneously on the material with a surface area of 500 $m^2/g$., the distance between chromium atoms becomes about 10 Å. This means that, though the dispersed chromia exists in the form of clusters, their thickness may be rather thin if the affinity of chromia to the supporting material does not greatly differ from the affinity between them.

On gamma alumina and on silica-alumina II, the isolated dispersion of chromium occurs simultaneously and the interaction between the base materials and chromium is stronger. It is not clear at present whether $Cr^{5+}$ ions isolate from other chromium ions, but at least the variation in the $\gamma$-line shape with the variation in supporting materials indicates that the base materials can influence the electronic condition of chromium ions. Dereń et al.[21] reported that chromia gel also gave a variation of the water-soluble part under heat treatment similar to the present results obtained by dispersed chromia. However, in their experiment pure chromia gel showed a maximum value of water-soluble chromia at a lower temperature of heat treatment. One can consider pure chromia gel to be chromia dispersed on chromia.

As is shown in Figs. 5 and 6, the concentration of $Cr^{5+}$ ions in the samples is at most several percent of the total chromium content, and in the case of silica gel this concentration is particularly low. From this fact, it is natural to consider that $Cr^{5+}$ ions are separated from each other. If chromia exists almost entirely in the form of small clusters on the silica gel, the mean distance among $Cr^{5+}$ ions becomes small and their coordination is decided principally by the superficial condition of chromia. As is well known, gamma alumina has a spinel-like structure and it contains many lattice defects of a symmetrical coordination. If these defects take part in the fixation of chromium ions or if chromium ions replace aluminum ions because of compatibility between their oxides, they bring about a more stable fixation of the chromium and give them a more symmetrical crystal field. This will cause a reduction of the $g$ anisotropy. If the coordination becomes perfectly octahedral or tetrahedral, it is difficult to observe the EPR absorption at room temperature, as will be described below.

**A Further Consideration of the Line Width.**— The apparent width of $\gamma$-lines obtained in the present work by using the K-band wave is somewhat larger than those in the X-band reported by others. O'Reilly also pointed out this fact[3] in the case of gamma alumina. It shows that one of the causes of the line width is probably $g$ anisotropy.

At the same time another cause of the increase in line width must be considered: spin-lattice relaxation. Many investigations have been made of the electronic structure of the ion which has a $3d^1$ electron in various crystal fields. When the symmetry of the field is high, the first excited level is so close to the ground level that it is generally impossible to observe the EPR absorption at room temperature. Concerning the $Cr^{5+}$ ion, Carrington et al.[22] and Van Reijen et al.[23] showed that EPR observation of $(CrO_4)^{3-}$ and $Ba_3(CrO_4)_2$ respectively was not possible at room temperature. However, when $Cr^{5+}$ ions are placed in a field of tetrahedrally-distorted octahedron, as in the case of $(NH_4)_2CrCl_5$,[23] or in a field of dodecahedron, as in the cases of the above-mentioned alkaline peroxychromates, a narrow absorption can be observed, even at room temperature.

In the peroxychromates, $Cr^{5+}$ ions are situated in a field with an axial symmetry: $g_1 = g_2$. Swalen and Ibers,[17] using 25 oe. as the half width, $b$, showed that the observed line agrees with the calculated curve. As compared with the value of $b$ which was estimated in the preceding section for the samples dispersed on silica gel, this value is fairly large. It may arise from the dipole interaction. Indeed, McGarvey[15] indicated that the dilution of peroxychromate with peroxyniobate markedly reduced the apparent line width. In connection with this width, it is necessary to consider the possibility of motional narrowing in the dispersed samples.

At present it is impossible to evaluate the relative contribution of these effects to the line width. It will be useful to examine the variation in optical absorption, electrical conductivity, etc. in these materials.

Concerning the variation in $\gamma$-line with dissolution, some uncertainty remains, as has been mentioned before. There have been

21) J. Dereń, J. Haber, A. Podgórecka and J. Burzyk, *J. Cat.*, **2**, 161 (1963).

22) A. Carrington, D. J. E. Ingram, D. Scholand and M. C. R. Symons, *J. Chem. Soc.*, **1956**, 4710; **1957**, 203, 659.

23) L. L. Van Reijen, P. Cossee and H. J. VanHaren, *J. Chem. Phys.*, **38**, 572 (1963).

attempts to distinguish $Cr^{5+}$ from $Cr^{6+}$ by using the difference between them in the solubility in water, but when the base material changes, this method can not be applied, even for relative measurements. We will discuss the variation in $\gamma$-absorption sites under several chemical treatments in our next paper.

## Summary

Chromic anhydride has been dispersed on several supporting materials of silica-alumina of different compositions, and the so-called $\gamma$-line in the EPR of these samples has been observed. When the temperature of heat treatment rises, the intensity of this absorption becomes strong, but after reaching a maximum value it decreases again. The chemical composition of the base materials remarkably influences the behavior of the absorption. The variations in water soluble chromium and oxidation number show corresponding results. However, $\gamma$-absorption sites may be distributed in the water-insoluble part of chromium as well as in the water-soluble part. The ratio between them depends on the base materials.

Under the assumption of $g$ anisotropy, the observed absorption lines have been compared with the calculated curves and the half-width at the half power of the absorption with the crystallite in these samples. From these results and from the differences in behavior, the states of chromium ions in various samples have been compared. By comparing the present results with those of other investigators, it has been concluded that, on pure silica gel, chromia is dispersed mainly in the form of thin-layer clusters and that this dispersion gives the characteristic of this matter. On the contrary, an alumina-rich base produces a more dispersive state of chromium and the fixation of chromium rapidly becomes stronger with the heat treatment. The influence of the supporting material on dispersed chromium becomes great and the characteristics are affected by this fact. These differences may be caused principally by the differences among these materials in thermal stability and in the compatibility with chromia.

The authors wish to express their thanks to Professor Hidetaro Abe, The Institute for Solid State Physics, The University of Tokyo, for his kind advice. They also wish to thank Jiro Nishimura, Kunihiko Nakamura and Hiroshi Fukunaga for their help during the course of these experiments.

*The Central Research Laboratory*
*Showa Denko K. K.*
*Ota-ku, Tokyo*

# Corundum $\alpha$-$Al_2O_3$ Formation from the Dehydration of Boehmite $\gamma$-AlOOH under Hydrothermal Conditions. II. The Reaction Rates and the Mechanism*

By Goro YAMAGUCHI, Hiroaki YANAGIDA and Takeshi FUJIMARU

(Received June 26, 1964)

Aluminum hydroxide are transformed into corundum under hydrothermal conditions near 400°C. In the previous paper,[2] the present authors investigated the factors determining the grain size of the corundum produced from the hydrothermal dehydration of boehmite and proposed a scheme for the reaction mechanism. It seems essential that there be in the reaction a process for forming hydrated polyaluminate ions with a structure related to the lattice of the product phase, corundum in the present case. In the present work, the reaction rates of corundum formation will be measured for the purpose of further discussion of the reaction mechanism.

## Experimental

**Procedure.** — 1.20 or 3.60 g. of boehmite is weighed and laid in a Morey-type reactor, the inner volume being 10 ml., with an appropriate amount

* Subtitled "Investigations into the Processes of Solid Phase Formation." No. 3. The first one is "On the Reaction Mechanism of Boehmite Formation from the Dehydration of Gibbsite,"[1] while the second is Part I of the present main title: "Factors Determining the Grain Size of Corundum and a Proposal for the Formation Mechanism."[2]

1) G. Yamaguchi and H. Yanagida, *J. Chem. Soc. Japan, Ind. Chem. Sec.* (*Kogyo Kagaku Zasshi*), **66**, 770 (1963).

2) G. Yamaguchi and H. Yanagida, This Bulletin, **36**, 1155 (1963).

of the solvent, 0.1 or 1.0 N aqueous sodium hydroxide. The amount is calculated from Kennedy's table showing the relation among the P. V. T. values of water,[3] in order to produce a hydrothermal pressure of 1000 atm. at the reaction temperature. The reactor is heated up to the reaction temperature within 15 min. in an electric furnace and thereafter kept at that temperature for various periods; then it is quenched to room temperature within 5 min. The residues produced consist of grains of boehmite and/or corundum. The grains are washed with dilute hydrochloric acid and then with pure water, and dried at 110°C.

**The Determination of the Reaction Rates.**—The reaction rates of corundum formation are determined by measuring the ignition loss of the residues. The percentage of boehmite in a residue is calculated from the difference in weight before and after the residue has been heated at 1000°C for 1 hr. in air. In the present work, the ignition loss of boehmite treated at the temperature of 435—445°C under a hydrothermal pressure of 1000 atm. was found to be 16.18%, a value which corresponds to $Al_2O_3 : 1.08H_2O$. Boehmite is usually found in a non-stoichiometric form, $Al_2O_3 : (1+x)H_2O$.[4] The present authors will discuss the behavior of the non-stoichiometric water in a later paper.[5]

## Results

The results are shown in Figs. 1 to 5 and are summarized in Table I. The present authors determined the length of the induction period before the onset of the corundum formation by extrapolating the function $f(x, t) \equiv t_x - (t_{2x} - t_x)$ to $x=0$, where $t_x$ indicates the time (hours) required for the formation of corundum by $x$%.

**The Effect of the Initial Amount of Boehmite upon the Reaction Rates of Corundum Formation.**—The reaction rates were first measured under the following conditions: temperature 445°C; the solvent, 0.1 N sodium hydroxide; the pressure, 1000 atm. and the initial amount of boehmite, $B_0$, 1.20 or 3.60 g. without the addition of seed crystals of corundum. Figure 1 shows the results; here A-1 denotes the run of the initial amount of boehmite, $B_0$, 1.20 g., and A-3, that of 3.60 g. We can easily observe that the induction period of A-3 is shorter than that of A-1. The function $f(x, t)$ gives the induction period of the run A-1, 6.6 hr., and that of the run A-3, 2.8 hr. The induction period becomes shorter with the increase the initial amount of boehmite. The curves of the reaction rates after these induction periods are similar, except that a slight retardation of the reaction is noticeable in the curve A-3, especially in the last stage.

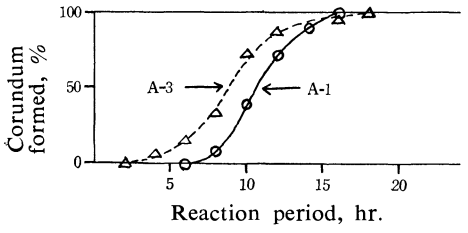



Fig. 1. The reaction rate of corundum formation; 445°C, 1000 atm., 0.1 N NaOH, A-1; $B_0$=1.20 g., A-3; $B_0$=3.60 g., No corundum seed added.

**The Effect of the Alkaline Concentration of the Solvent on the Reaction Rates.**—Next the reaction rates were measured under similar conditions to those of A-1 and A-3; that is, the temperature was 445°C, the pressure, 1000 atm., and the initial amount of boehmite, $B_0$, 1.20 or 3.60 g. without the addition of seed crystals of corundum, though in the present runs the alkaline concentration of the solvent was 1.0 N sodium hydroxide. The results are shown in Fig. 2, in which B-1 denotes the run of the initial amount of boehmite, $B_0$, 1.20 g., and B-3, that of 3.60 g. The induction period of B-3, 1.6 hr., is shorter than that of B-1, 3.6 hr. The induction period also becomes shorter with the increase in the initial amount of boehmite, as is true also in the A runs. The curves after both these induction periods are similar, as was also found in the A runs. Comparing the induction period of A-1 to that of B-1, and the length of A-3 to that of B-3, we find that the induction period becomes shorter with the increase in the alkaline concentration of the solvent.

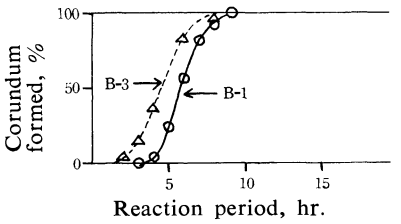



Fig. 2. The reaction rate of corundum formation; 445°C, 1000 atm., 1 N NaOH, B-1; $B_0$=1.20 g., B-3; $B_0$=3.60 g., No corundum seed added.

**The Effect of Seed Crystals of Corundum on the Reaction Rates.**—Third, the reaction rates were measured under conditions similar to those of A-1; that is, the temperature was 445°C; the pressure, 1000 atm.; the initial amount of boehmite, $B_0$, 1.20 g., and the solvent, 0.1 N sodium hydroxide, but here seed crystals of corundum with a surface area of about 1.5 $cm^2$ were added beforehand to the

3) G. C. Kennedy, *Am. J. Sci.*, **257**, 563 (1953).
4) B. C. Lippens, Ph. D. Thesis of Technische Hochschule, Delft (1961).
5) G. Yamaguchi and H. Yanagida, unpublished.

TABLE I. REACTION RATES OF CORUNDUM FORMATION UNDER SOME HYDROTHERMAL CONDITIONS

| No. of run | | A-1 | A-3 | B-1 | B-3 | AN-1 | AT-1 | ANT-1 |
|---|---|---|---|---|---|---|---|---|
| Temp., °C | | 445 | 445 | 445 | 445 | 445 | 435 | 435 |
| Pressure, atm. | | 1000 | 1000 | 1000 | 1000 | 1000 | 1000 | 1000 |
| Normality of NaOH | | 0.1 | 0.1 | 1.0 | 1.0 | 0.1 | 0.1 | 0.1 |
| Initial amount of boehmite, g. | | 1.20 | 3.60 | 1.20 | 3.60 | 1.20 | 1.20 | 1.20 |
| Seed crystal of corundum, $cm^2$ | | 0 | 0 | 0 | 0 | 1.5 | 0 | 1.5 |
| Reaction rates % corundum formed | 5 hr. | 0 | 8 | 25 | 69 | 18 | 0 | 0 |
| | 10 hr. | 40 | 72 | 100 | 100 | 84 | 0 | 20 |
| | 15 hr. | 83 | 95 | 100 | 100 | 100 | 0 | 65 |
| | 20 hr. | 100 | 100 | 100 | 100 | 100 | 0 | 100 |
| | 60 hr. | 100 | 100 | 100 | 100 | 100 | 0 | 100 |
| Induction period, hr. | | 6.6 | 2.8 | 3.6 | 1.6 | 3.4 | >60 | 8.1 |
| $t_{70\%}-t_{30\%}$, hr. | | 2.4 | 2.5 | 1.2 | 1.4 | 2.6 | ··· | 2.8 |

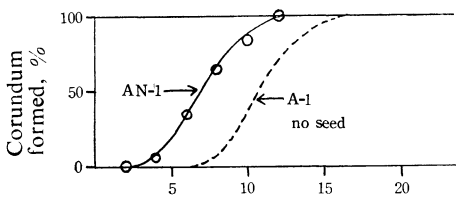



Fig. 3. The reaction rate of corundum formation; 445°C, 1000 atm., 0.1 N NaOH, AN-1 : $B_0$=1.20 g,, corundum seed 1.5 $cm^2$ added.

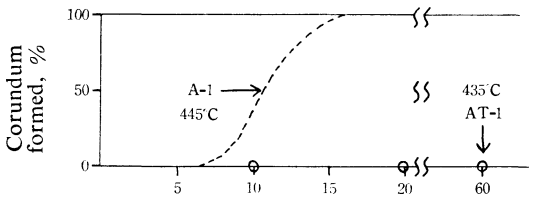



Fig. 4. The reaction rate of corundum formation; 435°C, 1000 atm., 0.1 N NaOH, AT-1 : $B_0$=1.20 g., No corundum seed added.

boehmite. The results are shown in Fig. 3, where they are denoted as AN-1; in this figure the run A-1 without any seeds is also shown as a reference. The seed crystals of corundum do shorten the induction period, 6.6 hr. for A-1 to 3.4 hr. for the present AN-1, but it does not have any remarkable effect upon the reaction rate after the induction period. Although the seed crystals grew by about 0.001 g./$cm^2$ hr. throughout the reaction, most of the grains of corundum were formed separately from the seeds.

**The Effect of the Reaction Temperature on the Reaction Rates without Seed Crystals.**—The residue of the run AT-1, obtained from the hydrothermal treatment of boehmite, initially 1.20 g. without any seed crystals of corundum, in 0.1 N sodium hydroxide under 1000 atm. at 435°C for up to 60 hr., was only boehmite grains. No crystals of corundum could be found with microscopic observation. Boehmite had been completely converted into corundum, however, with treatment similar to that of run A-1 at 445°C for less than 20 hr. The temperature difference, 10°C in the present case, had a remarkable effect on the initiation of corundum formation when no seed crystals of corundum had been added beforehand to the boehmite. The curves of the reaction rate of A-1 at 445°C and the present AT-1 at 435°C are shown in Fig. 4.

**The Effect of the Reaction Temperature on the Reaction Rates with the Addition of Seed Crystals of Corundum.**—The residues of the run ANT-1 obtained from the hydrothermal treatment of boehmite, initially 1.20 g. with addition of the seed crystals of corundum with a surface area of about 1.5 $cm^2$, in 0.1 N sodium hydroxide under 1000 atm. at 435°C and for various reaction periods have shown that the reaction of corundum formation takes place under the present conditions. The curve of the reaction rate of the run ANT-1 is shown in Fig. 5, where that of AN-1 at 445°C is also shown as a reference. The induction period of AN-1, 3.4 hr., has been lengthened to 8.1 hr.

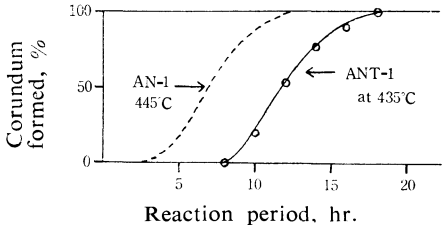



Fig. 5. The reaction rate of corundum formation; 435°C, 1000 atm, 0.1 N NaOH, ANT-1 : $B_0$=1.20 g., corundum seed 1.5 $cm^2$ added.

for the present ANT-1 by lowering the temperature by 10°C. The curve of the reaction rate of the run ANT-1 after the induction period is almost the same as that of the run AN-1. The temperature difference of 10°C had a noticeable effect on the initiation of the corundum formation, but it had no remarkable effect on the propagation of the reaction. The effects of the temperature, however, are different depending on whether or not the seed crystals have been added beforehand. At 435°C the initiation of corundum formation can take place in less than 10 hr. when the seed crystals of corundum have been added beforehand, as in the present ANT-1 run, but the reaction does not take place for up to 60 hr. when the seed crystals have not been added, as in the run AT-1.

## Discussion

With the measurements of the reaction rates of corundum formation under some hydrothermal conditions, we have established the following facts; 1) The induction period becomes shorter with an increase in the initial amount of boehmite (A-1 to A-3, B-1 to B-3). 2) The induction period becomes shorter with an increase in the alkaline concentration of the solvent (A-1 to B-1, A-3 to B-3). 3) The curves of the reaction rates after the induction periods are similar, independently of the initial amount of boehmite (A-1 and A-3, B-1 and B-3). 4) The addition of seed crystals of corundum shortens the induction period (A-1 to AN-1). 5) However, the reaction rates after the induction period are inifluenced by the addition of seed crystals (A-1 to AN-1). 6) When no seed crystals of corundum have been added beforehand, the induction period can be very remarkably lengthened by slightly lowering the reaction temperature. As in the present work without corundum seeds at 435°C, no corundum crystals can be formed from boehmite for up to 60 hr. At that temperature corundum phase is more stable than boehmite (A-1 to AT-1). 7) When seed crystals of corundum have been added beforehand, the induction period can be lengthened by lowering the reaction temperature (AN-1 to ANT-1). 8) The reaction rates after the induction periods are only slightly decreased by lowering the reaction temperature (AN-1 to ANT-1). 9) Although the seed crystals grow through the reaction, most of the grains are formed separately from the seed (AN-1 and ANT-1).

The present authors have proposed the reaction scheme for corundum formation which

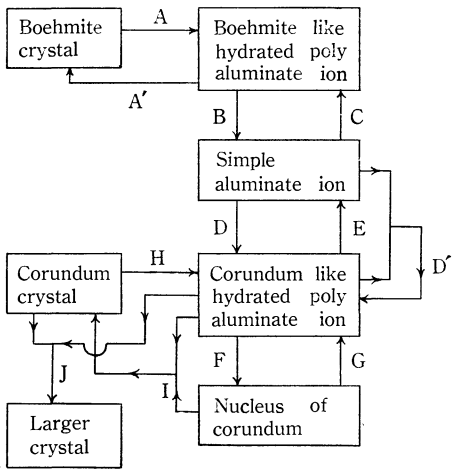



Fig. 6. The reaction scheme for corundum formation under hydrothermal condition.

is shown in Fig. 6, where a new process, D', is added to the previous scheme.[2] The present scheme, with the additional process, D', can explain the results of the reaction of the corundum formation better than the previous one[2] without the D'. The present results seem to support the mechanism.

Before the initiation of corundum formation, processes A, B, D and F should take place successively. The induction periods of the runs A-1, B-1, A-3, B-3 and AT-1, however, correspond to the time required for the onset of process D. The dissolution equation of aluminas under hydrothermal conditions[6] shows that processes A, A', B and C have been substantially in equilibrium when the boehmite grain in the reactor is heated up to the reaction temperatures. The grains of boehmite have a large enough specific surface area. Fact 1), therefore, shows that boehmite grains have a slight catalytic behavior in process D. On the basis of the dissolution equation, we can say that fact 2) is not due to the different times required for attaining the equilibrium in processes A, A', B and C. This may indicate that the concentration of simple aluminate ions in the liquid, not the relative concentration nor the supersaturation ratio, but the absolute one, determines the rate of process D. Fact 4) shows that the corundum grains added beforehand as seed crystals act as an effective catalyst for process D. The seed crystal supplies the corundum-like hydrated poly ions through process H. In the presence of the corundum-like hydrated poly ions in a solution, process D seems to take place easily. Note here that the corundum-like hydrated poly ion is characterized by a structure in which two adjacent aluminum ions are joined through

6) G. Yamaguchi, H. Yanagida and S. Soejima, This Bulletin, 35, 1789 (1962).

three oxygen atoms, as in the lattice of corundum. Interaction between the active sites of the poly ions and the simple aluminate ions may give new poly ions through process D' more easily than interaction among the simple ions themselves through process D. Fact 6) shows that a high reaction barrier exists against process D. Fact 7), on the other hand, shows that the barrier can be easily passed through another process, D', when the poly ions are supplied according to process H. Facts 6) and 7), therefore, may mean that the activation energy of process D is considerably higher than those of processes D', F, or H. In the runs when the seed crystals have been added beforehand, process D' or F may become the rate-determinant. Process F indicates a nucleation process through the further polymerization of the poly ions ; through it, the new crystal of corundum becomes precipitated separately from the seed. Process F, therefore, causes fact 9). After the induction periods, some of the runs show similar curves of the reaction rates, as can be seen in facts 3), 5) and 8), where corundum grain newly produced also becomes a new seed which supplies the poly ions through process H and process D is replaced by process D'. Fact 8) shows that the activation energy of the rate-determinant process after the induction periods is considerably lower than those before the onset of new corundum formation.

## Summary

The authors have measured the reaction rates of corundum formation from boehmite under some hydrothermal conditions for the purpose of discussing the reaction mechanism. They have proposed that, in such cases as the crystallization of corundum or boehmite, there exists the hydrated poly ion of the structure intimately related to the lattice of the product phase and that the formation process often becomes the rate-determinant if no seed crystals of the product phase have been added beforehand. The seed crystal supplies the poly ions which accelerate the simple ions to transform themselves into the poly ions. The mechanism has been illustrated schematically and discussed in detail.

*Department of Industrial Chemistry*
*Faculty of Engineering*
*The University of Tokyo*
*Hongo, Tokyo*

# Rearrangements of Tertiary Amine Oxides. XIII.* The Reactions of *p*-Nitrobenzenesulfenyl Chloride with Pyridine- and $\alpha$-Picoline *N*-Oxides

By Shigeru OAE and Katuyata IKURA

(Received June 26, 1964)

Since it was discovered in Professor Ochiai's Laboratories that the reaction between pyridine *N*-oxides and acetic anhydride leads to the formation of 2-acetoxypyridine,[1] many investigations have been made of the reactions between heteroaromatic *N*-oxides and acylating agents.[2]

Recently, by the aid of the $^{18}O$ tracer technique, the mechanistic features of these reactions have gradually been uncovered and it has become quite clear that one cannot draw any single common mechanistic scheme which can explain all these apparently similar reactions. The nature of the reaction may differ with the variation in *N*-oxides and in acylating agents and also in other reaction conditions, such as the change in solvent. For example, 2-picoline *N*-oxide has been considered to react with acetic anhydride via a free radical cage process,[3] while its isomer, 4-picoline *N*-oxide, apparently undergoes a nucleophilic SN2'-type replacement with the same reagent.[4] The reaction between pyridine *N*-oxide and acetic anhydride has been presumed to proceed through the initial nucleophilic addition of acetate ion at the $\alpha$-position to give $\alpha$-acetoxypyridine.[5]

* Part XII. S. Oae and S. Kozuka, *Tetrahedron*, in press.

1) M. Katada, *Yakugakuzashi*, **67**, 51 (1947).

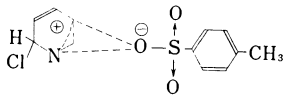
2) E. Ochiai, *Ann. Rept. ITSUU Lab.*, No. 12, 43 (1962).

3) S. Oae, T. Kitao and Y. Kitaoka, *J. Am. Chem. Soc.*, **84**, 3359 (1962).

4) S. Oae, T. Kitao and Y. Kitaoka, ibid., **84**, 3362 (1962).

5) J. H. Markgraf, H. B. Brown, Jr., S. C. Mohr and R. G. Peterson, ibid., **85**, 958 (1963).

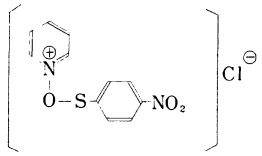
An especially interesing reaction is that of pyridine- or isoquinoline *N*-oxide with *p*-toluenesulfonyl chloride. Here, the mechanism, suggested as the result of $^{18}O$ tracer experiments, is very unusual and involves an intramolecular rearrangement via the $\alpha,\gamma$-intimate ion pair, as is shown below.[6]



The unique feature of this reaction may arise either in the intrinsic nature of sulfur-oxgen linkages or merely in the different bond strength of the acylated N–O bond. Thus, we have attempted to find some important information on the influence of the nature of sulfur-oxygen linkages on these reactions by reacting *N*-oxides of pyridine bases with arylsulfenyl and arylsulfinyl chlorides. This paper will deal with the reactions of *p*-nitrobenzenesulfenyl chloride with pyridine and α-picoline *N*-oxides.

## Results and Discussion

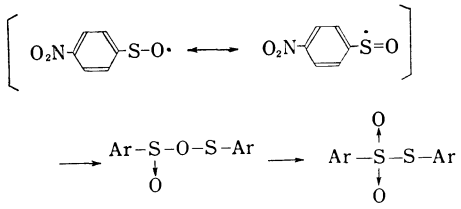
When equivalent amounts of pyridine *N*-oxide and *p*-nitrobenzenesulfenyl chloride were mixed in a benzene solution, colorless crystalline precipitates were formed immediately, with an evolution of heat. The crystals apparently has following structure (I); this structure is very hygroscopic, but it can readily be converted to its perchlorate, which has the correct analytical composition.



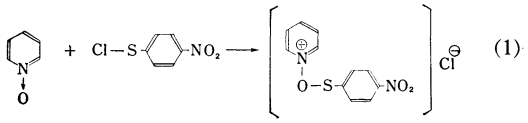
(I)

The salt I obtained after the thorough removal of the solvent benzene in a vacuum line was sealed in an ampoule; the ampoule was then heated at 150—160°C for five hours. It began to melt at around 80°C, at which point also color began to be formed, and at around 150°C the mixture became a dark, oily mass. Among the reaction products isolated were pyridine, *p*,*p*'-dinitrodiphenyl disulfide, *p*-nitrophenyl *p*-nitrobenzenethiolsulfonate and *p*-nitrobenzenesulfonic acid; these ingredients constituted more than 85% of the product mixture. Neither a ring-substituted rearrangement product nor unreacted pyridine *N*-oxide was found among the products. The evolution of hydrogen chloride was not observed when the salt was heated in an open vessel, unlike as in the case of pyridine *N*-oxide with tosyl chloride or *p*-nitrobenzoyl chloride.[7]

If the reaction followed a path similar to that of pyridine *N*-oxide with tosyl chloride, one would expect some pyridine ring-substituted compound among the products mixture, for the heterolytically-cleaved species, presumably nitrobenzenesulfinate ions, is considered to be more nucleophilic than tosylate and, hence, to react more readily with the other cleaved partner, 2-chloro-2-hydropyridinium cation, to give perhaps the sulfinyl product. On the other hand, if the N–O bond is assumed to cleave homolytically, the resulting radical, *p*-nitrosulfinyl, may not recombine with the other partner to give any pyridine ring-substituted compound, since the radical has been known to be quite stable, due to the electron-sharing 3d orbital resonance, as is shown below,[8] and to dimerize readily eventually yielding *p*-nitrophenyl *p*-nitrobenzenethiolsulfonate.[9]

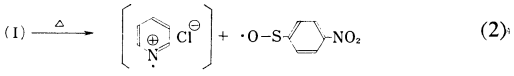


The lack of any heteroring-substituted product, together with the formation of *p*-nitrophenyl *p*-nitrobenzenethiolsulfonate, seems to favor the homolytic cleavage of the N–O bond of the salt I. Thus, the over-all reaction scheme may be formulated as is shown below:



(1)

(I)



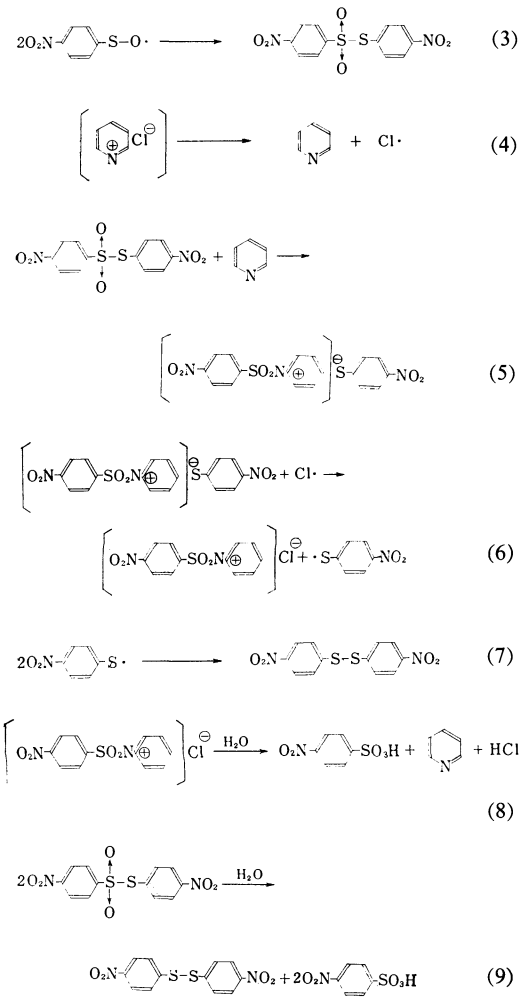
(2)

7) Our preliminary experiment suggests that *p*-nitrobenzoyl chloride reacts with pyridine *N*-oxide and similarly gives 3-acyloxypyridine as the main product.

8) S. Oae, "3d-Orbital Resonance Involving the Sulfur Atom in Organic Sulfides," in "Organic Sulfur Compounds," Vol. 4., Ed. by N. Kharasch, Pergamon Press, in press.

9) S. Oae and S. Kawamura, This Bulletin, **35**, 1156 (1962); H. J. Backer and H. Kloosterziel, *Rec. Trav. Chim.*, **73**, 129 (1954); R. N. Topping and N. Kharasch, *Chem. & Ind.*, **1961**, 178.

6) S. Oae, T. Kitao and Y. Kitaoka, *Tetrahedron*, **19**, 827 (1963).



(3)

(4)

(5)

(6)

(7)

(8)

(9)

The clear-cut ESR signals seen[10] during and shortly after the reaction also appear to suport the free radical mechanism.

Previously it was shown that the *p*-nitrobenzenesulfinyl radical, once formed, readily dimerized to give stable *p*-nitrophenyl *p*-nitrobenzenethiolsulfonate. However, the amount of this compound actually isolated was rather small as compared to those of the disulfide and *p*-nitrobenzenesulfonic acid. The latter two compounds were perhaps formed through steps 5—8.

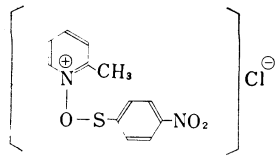
When *p*-nitrophenyl *p*-nitrobenzenethiolsulfonate was reacted with pyridine and the reaction mixture was quenched with water, both *p*-nitrobenzenesulfonic acid and *p*, *p'*-dinitrodiphenyl disulfide were actually obtained in substantial yields. Exactly the same compounds were also obtained when a mixture of the thiolsulfonate and pyridine hydrochloride was heated at 150°C and then quenched with water.

Some of the thiolsulfonate probably suffered hydrolysis during the treatment and was disproportionated to the disulfide and the sulfonic acid according to step 9.

Previously there was a case where the use of a solvent did change the reaction pathway. However, in this reaction of pyridine *N*-oxide with *p*-nitrobenzenesulfenyl chloride, the use of xylene as the solvent did not change the pattern of the reaction; it yielded essentially the same products.

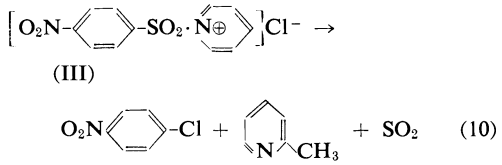
The same reaction was applied to $\alpha$-picoline *N*-oxide to see if the presence of the $\alpha$-methyl group would change the nature of the reaction as with acetic anhydride.

In this case, too, as soon as equimolar amounts of $\alpha$-picoline *N*-oxide and *p*-nitrobenzenesulfenyl chloride was mixed in a benzene solution, white crystalline precipitates formed, with an evolution of heat. The hygroscopic crystals were changed to its perchlorate, which was found by analysis to have the correct composition as derived from the salt, II.



(II)

The reaction conditions were nearly the same as in the case of pyridine *N*-oxide. Here again no detectable amount of any heteroring-substituted product was obtained among the reaction products. There was only one difference; that is, the formation of *p*-nitrochlorobenzene was observed in this case. Otherwise, the pattern product distribution was almost the same. Therefore, reaction also seems to proceed via the homolytic cleavage of the N–O bond of the salt II and the overall reaction scheme is considered to be very similar to the one previously obtained with pyridine *N*-oxide.



(III)

(10)

The formation of *p*-nitrochlorobenzene may be explained when one considers that this compound was formed through step 10, involving the nucleophilic attack of the chloride anion on the complex III.

10) A detailed study along this line is now underway by the group headed by Professor W. F. Forbes.

Indeed, *p*-nitrochlorobenzene was actually obtained when the mixture of *p*-nitrophenyl *p*-nitrobenzenethiolsulfonate and α-picoline hydrochloride was heated at around 150°C. The formation of *p*-nitrochlorobenzene in this case and not with pyridine *N*-oxide is fascinating; however, we have no way at present to explain it.

Apparently the overall pattern of the reaction was not much changed by the substitution of the α-methyl group. Even in alkaline conditions, where it was anticipated that the proton of the α-methyl group wolud be abstracted by base to form possibly an anhydrobase, there was no formation of any detectable amount of heteroring-substituted product. Thus, the reaction of the salt II in the presence of sodium ethoxide in ethanol was found to yield nearly the same compounds.

## Experimental

**Material.** — *Pyridine N-Oxide.* — Pyridine *N*-oxide was prepared by the oxidation of pyridine with hydrogen peroxide in glacial acetic acid, following the procedure used by Ochiai.[11]

B. p. 150—153°C (24 mmHg); lit.[11] 138—144°C (15 mmHg).

*Picoline N-Oxide.*—This *N*-oxide was also prepared by the same method.

B. p. 108—109°C (9 mmHg); lit.[12] 123—124°C (15 mmHg).

*p-Nitrosulfenyl Chloride.*—At first, *p, p'*-dinitrodiphenyl disulfide was prepared from sodium sulfide, sulfur,and *p*-nitrochlorobenzene,[13] m. p. 179~180°C (recrystallized from xylene) (lit.[13] 181°C).

Then this disulfide was chlorinated with dry chlorine gas in chloroform at room temperature until the solution turned yellow. The solvent was distilled off in a vacuum to obtain the chloride, m. p. 49—51°C (lit.[13] 52°C).

**The Reaction of Pyridine *N*-Oxide with *p*-Nitrobenzenesulfenyl Chloride.**—The benzene solutions of both pyridine *N*-oxide (1.00 g.) and *p*-nitrobenzenesulfenyl chloride (2.00 g.) were mixed at 10°C; then the solvent was distilled off and the crystalline residue was sealed in a vaccum line. This salt was heated at 150—160°C for five hours. It began to melt at around 80°C and turned dark red, while at around 150°C the reaction mixure became a dark, oily mass. After the reaction had been completed, dilute hydrochloric acid was added and the mixture was extracted with chloroform.

The removal of the solvent gave *p, p'*-dinitrodiphenyl disulfide (1.15 g.) and a mixture of *p, p'*-dinitrodiphenyl disulfide and *p*-nitrophenyl *p*-nitrobenzenethiolsulfonate (0.30 g.), m. p. 178—179°C and 154—155°C respectively.

The presence of *p*-nitrophenyl *p*-nitrobenzenethiolsulfonate was confirmed by the use of infrared spectra.

The aqueous layer was made neutral with sodium carbonate and extracted with chloroform. The removal of the solvent gave a colored liquid; then the residual liquid was converted into picrate. From its melting point and infrared spectrum, this picrate was confirmed to be the picrate of pyridine (0.67 g.), m. p. 164—165°C (lit.[14] 167°C).

Then, a 10% ethanol solution of benzylisothiourea hydrochloride salt was added to the aqueous mother solution from which pyridine had already been recovered, and the crystals thus precipitated was collected and recrystallized from a water-ethanol mixture. This was confirmed by elemental analysis, mixed melting point, and infrared spectra to be thiuronium salt of *p*-nitrosulfonic acid (0.21 g.), m. p. 205—206°C.

Found: N, 9.20. Calcd. for disulfide $C_{12}H_8N_2O_4S_2$: N, 8.92%.

Found: C, 45.71; H, 4.20; N, 11.78. Calcd. for thiuronium salt: C, 45.52; H, 4.09; N, 11.37%.

**The Isolation of 1-*p*-Nitrobenzenesulfinylpyridinium Perchlorate.** — In a separate experiment the hygroscopic crystalline precipitate obtained by reacting 0.5 g. of *p*-nitrobenzenesulfenyl chloride on 0.25 g. of pyridine *N*-oxide was treated with 0.43 g. of 60% perchloric acid at 0°C. The colorless crystals which precipitated immediately were washed well with water and dried; m. p. 160—170°C with decomposition.

Found: C, 40.09; H, 2.63; N, 8.04. Calcd. for $C_{11}H_9N_2O_7SCl$: C, 41.33; H, 2.58; N, 8.03%.

**The Reaction of α-Picoline *N*-Oxide with *p*-Nitrobenzenesulfenyl Chloride.**—α-Picoline *N*-oxide (1.00 g.) and *p*-nitrobenzenesulfenyl chloride (2.00 g.) were used. The reaction conditions and the treatment of the reaction products were exactly the same as in the case of pyridine *N*-oxide. The products from the chloroform layer were *p, p'*-dinitrodiphenyl disulfide (1.2 g.), *p*-nitrochlorobenzene (0.08 g.), and a mixture of *p, p'*-dinitrodiphenyl disulfide and *p*-nitrophenyl *p*-nitrobenzenethiolsulfonate (0.08 g.); m. p. 165—169°C. From the aqueous layer, α-picoline (0.62 g.), (picrate m. p. 160—163°C; (lit.[15] 164°C)) and *p*-nitrosulfonic acid (0.20 g.) (m. p. 204—205°C (thiuronium salt)) were obtained.

**The Isolation of 1-*p*-Nitrobenzenesulfinyl-2-picolinium Perchlorate.** — In a separate experiment the hygroscopic crystalline precipitate obtained by reacting 0.5 g. of *p*-nitrobenzenesulfenyl chloride on 0.25 g. of α-picoline *N*-oxide was treated with 0.42 g. of 20% perchloric acid at 0°C. The colorless crystals which precipitated immediately were washed well with water and dried; m. p. 128—150°C with decomposition.

Found: N, 8.43. Calcd. for $C_{12}H_{11}N_2O_7SCl$: N, 7.76%.

The slight discrepancy in the elemental analysis for salt II may be due to the instability of the salt, which could not be purified by recrystallization.

**The Reaction of Pyridine *N*-Oxide with *p*-Nitrosulfenyl Chloride in Xylenen.** — The salt I (3 g.) was placed in dry xylene (10 ml.) and refluxed

11) E. Ochiai, *J. Org. Chem.*, **18**, 534 (1953).
12) V. Boekelheide and W. J. Linn, *J. Am. Chem. Soc.*, **76**, 1286 (1954).
13) T. Zincke and S. Lenhardt, *Ann.*, **400**, 1 (1913).
14) "Daiyukikagaku," Vol. 16, Asakura, Tokyo (1959), p. 11.
15) Ibid., Vol. 16, Asakura, Tokyo (1959), p. 12.

for 5 hr. The reaction products were *p*, *p*'-dinitrodiphenyl disulfide (1.56 g.), *p*-nitrobenzenesulfonic acid (0.25 g.) and pyridine (0.61 g.).

**The Reaction of Salt II with Sodium Ethoxide in Ethanol.** — Sodium (0.26 g.) was added to anhydrous ethanol (10 ml.) and dissolved. Then the salt II (3 g.) was added at room temperature and warmed at 40°C for two hours. Finally the mixture was refluxed for three hours. The products isolated were *p*, *p*'-dinitrodiphenyl disulfide (0.91 g.), a mixture of *p*, *p*'-dinitrodiphenyl disulfide and *p*-nitrophenyl *p*-nitrobenzenethiolsulfonate (0.65 g.), and α-picoline (0.61 g.).

All the compounds were identified by mixed melting point, infrared spectra, and elemental analyses.

**Summary**

In the reactions of both pyridine and α-picoline *N*-oxides with *p*-nitrobenzenesulfenyl chloride, the N–O bonds of the intermediate salts appear to cleave homolytically, and the *p*-nitrosulfinyl radical which arises from the homolytic cleavage of the N–O bond is considered to be so stable that only the secondary reaction products from the sulfinyl radical, and no heteroring-substituted products, were obtained.

*Department of Applied Chemistry*
*Faculty of Engineering*
*Osaka City University*
*Sumiyoshi-ku, Osaka*

# The Mechanism of the Base-Promoted Rearrangement of *N*, *N*-Dichlorodiphenylethylamine to Desylamine

By Shigeru OAE and Naomichi FURUKAWA

(Received June 26, 1964)

Some years ago, Baugarten and his coworkers showed that the treatment of *N*, *N*-dichlorodiphenylethylamine with sodium methoxide, followed by that with aqueous hydrochloric acid, gave desylamine hydrochloride in a substantial yield.[1] They then successfully extended this remarkable reaction to various *N*, *N*-dichloro-*s*-alkylamines.[2] A similar rearrangement of *N*, *N*-dichlorocyclohexylamine to 2-aminocyclohexanone hydrochloride has also recently been reported.[3]

The following mechanism has been suggested for this reaction (Fig. 1):

Although this mechanism appears to be valid and although it is essentially the same as that of Neber Rearrangement of the corresponding oxime tosylate which was proposed earlier by Cram and Hatch,[4,5] there is no unequivocal evidence to support it. Meanwhile, since *N*-chloro compounds are known to halogenate the benzylic methylene group very readily,[6] and since the resulting halogenated benzylic compound would undergo a facile hydrolysis,[7] one can postulate another possible mechanism, namely, one involving the initial *gem*-dichlorination of 2-methylene and the subsequent hydrolysis, thus giving product as is shown below (Fig. 2).

One noticeable difference between these two mechanisms is that the former involves the 1, 2-migration of the amino group, while in the later the amino group remains in the original position.

Recently, an *N*-chloroimine intermediate similar to II was actually isolated in the case of *N*, *N*-dichlorocyclohexylamine;[3] also, the formation of the azirine ring III was strongly supported by the successful isolation of *cis*-2, 3-diphenylethyleneimine in the reduction of the reaction mixture of *N*, *N*-dichloro-1, 2-diphenylethylamine with lithium aluminum hydride.[2]

These two pieces of evidence seem to support very strongly the former mechanism, involving the 1, 2-migration of the amino group via the formation of the azirine ring. However, in strong alkaline conditions such as sodium methoxide in the methanol used in this

1) H. E. Baumgarten and F. A. Bowel, *J. Am. Chem. Soc.*, **76**, 4561 (1954).
2) H. E. Baumgarten and J. H. Petersen, ibid., **82**, 459 (1960).
3) G. H. Alt and W. S. Knowels, *J. Org. Chem.*, **25**, 2047 (1960).
4) D. J. Cram and M. S. Hatch, *J. Am. Chem. Soc.*, **75**, 33 (1953).
5) M. S. Hatch and D. J. Cram, ibid., **75**, 38 (1953).
6) For example see T. Takizawa and K. Hoshiai, *Mem. Inst. Sci. Ind. Research, Osaka Univ.*, **2**, 92 (1948); *Chem. Abstr.*, **45**, 11211 (1951).
7) A. Streitwieser, Jr., *Chem. Revs.*, **56**, 571—572 (1956).

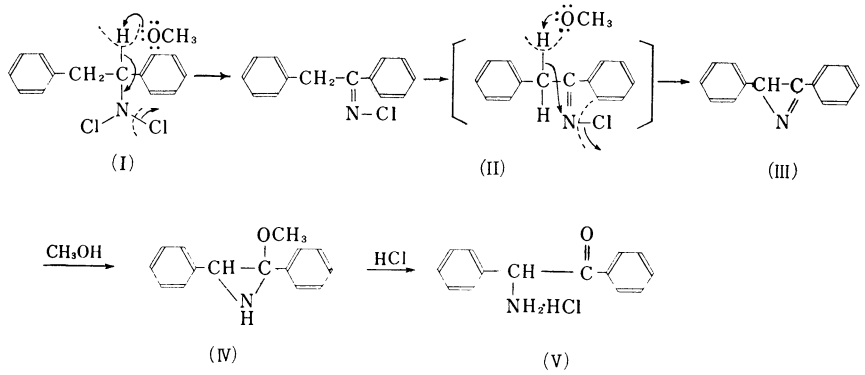


Fig. 1

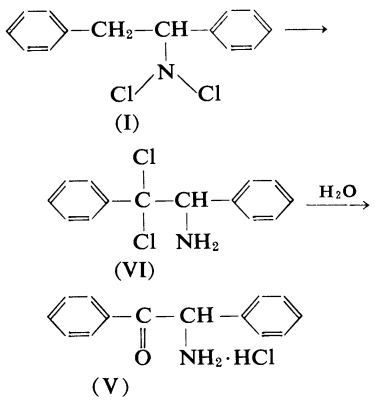


Fig. 2

reaction, one must also take into account the possibility of facile prototropy,[8] as is shown below (Fig. 3).

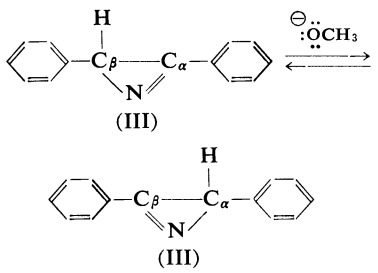


Fig. 3

If there were facile prototropy in III before the nucleophilic cleavage, the nucleophilic attack of the methoxy group could take place at both carbon atoms, $C_\alpha$ and $C_\beta$, with equal probability, yielding a fifty-fifty mixture of both 1,2-shifted and unshifted aminoketones.

All these unresolved problems can be readily answered by tracing the fate of a labeled carbon atom placed either at the $\alpha$ or the $\beta$-position of the original *N,N*-dichloro-1,2-diphenylethyl amine in the rearrangement.

Thus, *N,N*-dichloro-1,2-diphenylethylamine-1-$^{14}$C has been synthesized, and a series of succesive degradations has been carried out. This paper will present detailed accounts of the results and implications of these experiments.

The synthetic and degradative methods of $^{14}$C labeled desylamine may be shown as follows (Fig. 4).

## Experimental

**The Preparation of the *N,N*-Dichloro-1,2-diphenylethylamine-1-$^{14}$C.** — Phenylacetic acid-1-$^{14}$C[9] (VIII) was obtained by the carbonation of benzylmagnesium bromide which had been prepared from 1.3 g. of magnesium and 6.3 g. of benzylchloride with $^{14}CO_2$ which had been generated from 7.0 g. (1.0 mc.) of barium carbonate. The yield was 4.3 g. in 63%; m. p. 76°C.

Phenylacetic acid-1-$^{14}$C (4.3 g.) was converted to phenylacetyl chloride (IX) by treating it with 3 g. of phosphoroustrichloride; the phenylacetyl chloride thus prepared was then treated with 3.8 g. of aluminum chloride in a benzene solution. From the reaction mixture deoxybenzoin-1-$^{14}$C[10] (X) (4.3 g.) was obtained in a 75% yield; m. p. 56°C.

When deoxybenzoin-1-$^{14}$C (4.3 g.) was then allowed to react with a mixture of 6 g. of ammonium formate and 1 ml. of formic acid, 1,2-diphenylethylamine-$^{14}$C[11] (3.7 g.) was obtained in a 85% yield; b. p. 143°C/2.4 mmHg.

1,2-Diphenylethylamine-1-$^{14}$C (3.7 g.) was chlorinated with 5.5 g. of *t*-butylhypochlorite in dry benzene. The *N,N*-dichloro-1,2-diphenylethylamine-1-$^{14}$C[2] thus obtained was not isolated; the solution was used directly for the preparation of desylamine hydrochloride-*x*-$^{14}$C, as in the experiments of previous workers.[2]

8) C. K. Ingold, "Structure and Mechanism in Organic Chemistry," Cornell Univ. Press, New York (1953), pp. 530—575.

9) M. Calvin et al., "Isotopic Carbon," John Wiley and Sons, New York (1949), p. 180.

10) C. F. H. Allen and W. E. Barker, "Organic Syntheses," Coll. Vol. II, 156 (1943).

11) R. Adams, ed., "Organic Reactions," Vol. 5, John Wiley and Sons, New York (1949), p. 301.

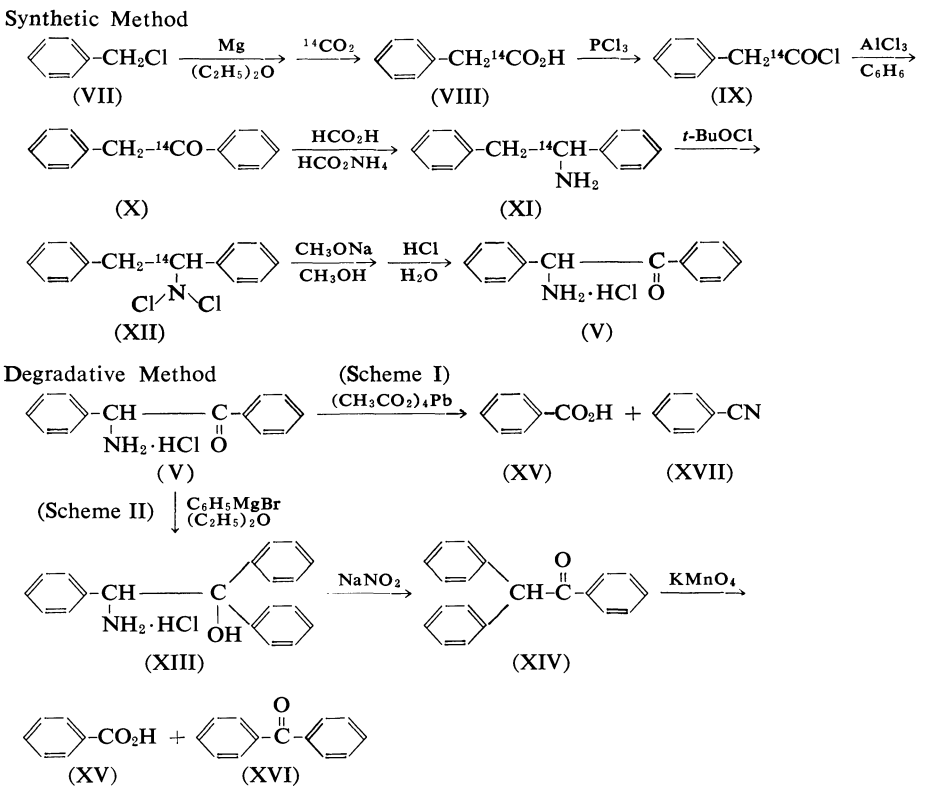



Fig. 4

**The Rearrangement of *N,N*-Dichloro-1,2-diphenylethylamine-1-$^{14}$C.** — The rearrangement of *N,N*-dichloro-1,2-diphenylethylamine-1-$^{14}$C was carried out following the procedure used previously.[2] Namely, the benzene solution of *N,N*-dichloro-1,2-diphenylethylamine-1-$^{14}$C prepared from 3.7 g. of 1,2-diphenylethylamine was treated in situ with 25 ml. of a methanol solution in which 2.5 g. of sodium had been dissolved. The yield was 1.7 g. (36%); m. p. 234°C.

**The Degradation of Desylamine-*x*-$^{14}$C.** — *Degradation Scheme I.* — In a 100 ml. three-necked flask equipped with a mechanical stirrer and a reflux condenser, 3.0 g. of desylamine hydrochloride-*x*-$^{14}$C was suspended in 50 ml. of dried benzene. To this mixture 10 g. of freshly prepared lead tetraacetate was added portion by portion, and then the mixture was heated for 2 hr. on a steam bath. After the mixture had cooled, the precipitated lead acetate was filtered off and washed with small portions of benzene. The combined benzene solution was extracted twice with 20 ml. of a 10% sodium carbonate solution. The aqueous extracts was acidified with concentrated hydrochloric acid. A white crystalline precipitate was thus obtained. Recrystallization from hot water gave hair-like crystals. These were identified as benzoic acid XV by a mixed melting point determination with authentic benzoic acid and by a study of the infrared spectrum. The yield was 1.0 g. (67.5%). The benzene solution was then evaporated and the residual oily substance (1.5 g.) distilled under reduced pressure to give benzonitrile XVI, which was identified by comparing its infrared spectrum with that of authentic benzonitrile. The yield was 0.3 g. (24%).

*Degradation Scheme II.*[12] — To a Grignard reagent prepared from 16 g. of bromobenzene and 2.4 g. of magnesium, 4.0 g. of powdered desylamine hydrochloride-*x*-$^{14}$C was added; 1,1,2-triphenyl-1-hydroxyethylamine hydrochloride-*x*-$^{14}$C was thus obtained in a 85% yield (4.5 g.).

1,1,2-Triphenyl-1-hydroxy-ethylamine hydrochloride-*x*-$^{14}$C (XIII) (4.5 g.) was deaminated by diazotization with 2.0 g. of sodium nitrite, followed by the migration of the phenyl group. Phenyldeoxybenzoin-*x*-$^{14}$C (XIV) was thus obtained (1.1 g.) in a 26% yield; m. p. 130—131°C.

The deoxybenzoin-*x*-$^{14}$C (0.25 g.) thus obtained was oxidized with 1.0 g. of potassium permanganate at room temperature; thus 50 mg. of benzoic acid (45%) and 0.17 g. of benzophenone (51%) were obtained. The benzoic acid XV was identified by mixed melting point determination. The benzophenone XVI thus obtained was derived to its 2,4-dinitrophenylhydrazone (m. p. 239°C).

**The Measurement of the Activities.**—*Scheme I.*— The activities of the $^{14}$C which were distributed in the compounds were measured by using a Packard-liquid scintilation spectrometer model 500B, Tricarb. The purified 1,2-diphenylethylamine-1-$^{14}$C

12) J. G. Burr, *J. Am. Chem. Soc.*, **75**, 1990 (1953); W. A. Bonner and C. J. Collins, ibid., **75**, 5372 (1953).

TABLE I. THE $^{14}C$ COUNTING OBTAINED IN SCHEME I

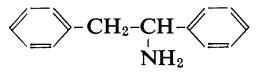
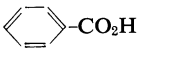
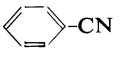
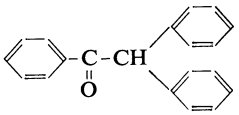
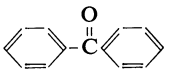
| |  |  |  |
|---|---|---|---|
| c. p. m./mmol. | $4.00\times10^5$ | $2.75\times10^5$ | $3.52\times10^3$ |
| % | (100%) | (68.8%) | (0.37%) |

TABLE II. THE $^{14}C$ COUNTING OBTAINED IN SCHEME II

| |  |  |  |
|---|---|---|---|
| c. p. m. | 1712 | 1663 | 19 |
| % | (100%) | (97.8%) | (1.1%) |
| c. p. m. | 1692 | 1656 | 15 |
| % | (100%) | (97.9%) | (0.90%) |

was chosen as a standard for the original total activity. The counting methods were as follows. Three samples, namely, 4.985 mg. of 1,2-diphenylethylamine-1-$^{14}C$, 3.176 mg. of benzoic acid, and 9.958 mg. of benzonitrile, were dissolved separately in 20 ml. each of toluene containing POP and POPOP as scintilators; then they were subjected to a Packard Tri-carb. The data obtained are shown in Table I.

*Scheme II.* — The measurements of the activities of the samples were carried out in this case by a JRC Aloka $2\pi$-gas flow proportional counter using Q-gas. Phenyl deoxybenzoin-*x*-$^{14}C$ was used as the standard sample of the total activity. A known amount of a sample was thoroughly oxidized by the Van-Slyke method, and all the carbon dioxide formed was converted to a barium carbonate pellet which was then subjected to $^{14}C$ counting. The respective pellets of barium carbonate obtained were, i. e., 158.1 mg. (98%) from phenyldeoxybenzoin (11.4 mg.), 120.5 mg. (96%) from benzoic acid (11.0 mg.), and 110 mg. (94%) from benzophenone-2,4-dinitrophenylhydrazone (11.4 mg). The counting data obtained are shown in Table II.

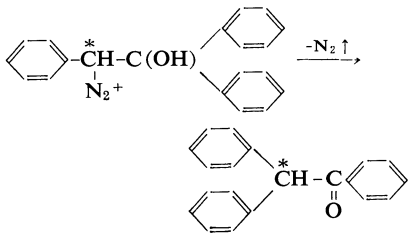
## Results and Discussion

The results of the degradations of the desylamine-*x*-$^{14}C$ obtained are shown in Tables I and II.

The first scheme of degradation involves the direct oxidation of desylamine hydrochloride with lead tetraacetate to yield benzoic acid and benzonitrile. The latter compound was obtained in rather a poor yield; however, it undoubtedly originated from the $\alpha$-amino benzylic portion of desylamine. It carries only a very small portion of the $^{14}C$ activity (0.87%) of the original activity of desylamine employed.

On the other hand benzoic acid was obtained in a substantial yield; it is the only compound isolated that carries a substantial amount of $^{14}C$ activity. However, its activity was somewhat reduced; e. g., in one experiment, it was 68.8% of that of the desylamine employed. This apparently diminished activity of the benzoic acid is assumed to be caused by the dilution of the $^{14}C$-active benzoic acid formed from the oxidation of the benzyl portion of desylamine with the non-active benzoic acid formed from the hydrolysis of benzonitrile during the treatment. Incidentally, this assumption seems to be quite valid in view of the results of the degradation by the second procedure. The very small amount of $^{14}C$ activity formed in the benzonitrile is quite significant, because it excludes both the $^{14}C$ scrambling that could be expected from the prototropy of the azirine ring III, and the *gem*-dichlorination hydrolysis mechanism. If the reaction were assumed to proceed according to the latter mechanism, all the $^{14}C$ activity would remain in the $\alpha$-amino benzylic carbon and, hence, the benzonitrile would carry the same amount of specific activity as the original amine. This was found not to be the case. Therefore, since it is considered that a portion of the benzoic acid originates in the hydrolysis of benzonitrile, the results of this degradation can serve as strong evidence in support of the mechanism proposed by Baumgarten.

The second degradation scheme is a beautiful product of Collins et al., who have demonstrated unequivocally through a $^{14}C$ tracer experiment that the deamination of 1,1,2-triphenyl-1-hydroxy-ethylamine by diazotization undergoes the following rearrangement:



Therefore, the only uncertainty, if any, is in the step of the reaction between desylamine and phenylmagnesium bromide to give 1, 1, 2-triphenyl-1-hydroxy-ethylaminehydrochloride, however, this step is a straightforward reaction involving the nucleophilic attack of the phenyl Grignard reagent on the carbonyl carbon. Thus, according to this degradative scheme, benzoic acid may be considered to originate from the benzoyl group and benzophenone, from the benzhydryl group. Here again the data indicates that the benzoic acid carries practically all the activity, while benzophenone is incorporated with almost no $^{14}C$ activity.

These data on $^{14}C$ distribution obtained by the second scheme are in accord with those obtained by the first scheme; they clearly exclude any mechanisms involving an initial *gem*-dihalogenation and subsequent hydrolysis, and also that one involving a rapid prototropic equilibrium of the azirine ring.

Therefore, the only remaining plausible mechanism is that suggested previously by Baumgarten et al.; this is essentially the same as that proposed originally by Cram and Hatch for the Neber rearrangement (Fig. 1).

**Summary**

*N*, *N*-Dichloro-1, 2-diphenylethylamine-1-$^{14}C$ has been treated with sodium methoxide in methanol and then with hydrochloric acid to yield $^{14}C$-labeled desylamine hydrochloride. Successive degradations have revealed that practically all the $^{14}C$ activity was found in the carbonyl carbon. From the $^{14}C$ distribution, it has been concluded that the reaction is essentially the same as that proposed for the Neber rearrangement, which involves the formation of the azirine ring intermediate.

*Department of Applied Chemistry*
*Faculty of Engineering*
*Osaka City University*
*Sumiyoshi-ku, Osaka*

# Studies of Mixed Cyano Cobalt(III) Complexes. I. The Cyano-Diamine Series

By Kuwako OHKAWA, Junnosuke FUJITA and Yoichi SHIMURA

(Received June 29, 1964)

Notwithstanding the strong tendency of cyanide to be coordinated to cobalt(III), a smaller number of mixed cyano cobalt(III) complexes have been known than of mixed ammine complexes. In particular, we know of extremely few cobalt(III) complexes which contain organic amines with cyanide.[1]

In the present paper, the preparation and the properties of mixed cyano complexes of a new type, $M[Co^{III}(CN)_4an]$ (an=en and tn),* which contains only one organic diamine molecule as a chelate ring, will be reported and discussed in comparison with those of the related bis(diamine) complexes, $[Co^{III}(CN)_2an_2]X$ (an=en, pn and tn).*

## Experimental

**Preparation.** — *Potassium Tetracyanoethylenediaminecobalt(III) Monohydrate: $K[Co(CN)_4en]\cdot H_2O$.*— Into a 200 ml. aqueous solution of 10 g. of *t*-$[CoCl_2(NH_3)_2en]Cl\cdot 1/2\,H_2O$,[2] 15 g. of potassium thiosulfate dissolved in 200 ml. of water was stirred. The greenish brown solution obtained was then warmed on a water bath until it gave a brownish red solution. Then 10 g. of potassium cyanide dissolved in 100 ml. of water was stirred drop by drop into this solution. An orange yellow solution evolving ammonia gas was obtained. After this had been warmed on a water bath for a while, it was filtered. The filtrate was concentrated to a volume of about 200 ml. on a water bath; then 18.2 g. of barium chloride dihydrate dissolved in 100 ml. of hot water was added to remove the thiosulfate ions as a precipitate of barium thiosulfate. This precipitate was filtered, and the filtrate was evaporated further to a volume of about 50 ml. and then cooled in ice. The crude orange crystals thus formed were filtered, washed with methanol, and dried in air.

The product of this was dissolved in a minimum amount of water, and about one-fourth the volume of methanol was added. After the mixture had cooled at 0°C for half an hour, the precipitate was removed by filtration. Methanol was added to the filtrate, and the mixture was cooled in ice. The pure

1) P. R. Rây and B. Sarma, *J. Indian Chem. Soc.*, **28**, 59 (1951).

* en=ethylenediamine $NH_2CH_2CH_2NH_2$
tn=trimethylenediamine $NH_2CH_2CH_2CH_2NH_2$
pn=propylenediamine $NH_2CH_2CH(CH_3)NH_2$

2) J. C. Bailar, Jr., and D. F. Peppard, *J. Am. Chem. Soc.*, **62**, 105 (1940).

product obtained by repeating the procedure three times was orange-colored crystalline plates which were effloresced on exposure to the air. The crystals freshly dried were analyzed for water of crystallization. The analyses for the other components were performed by using samples dehydrated in vacuo at 80°C.

Found: C, 26.96; H, 3.28; N, 31.10. Calcd. for $C_6H_8N_6KCo=K[Co(CN)_4en]$: C, 27.48; H, 3.18; N, 32.05%.

Found: $H_2O$, 6.42. Calcd. for $K[Co(CN)_4en]\cdot H_2O$: $H_2O$, 6.42%.

*Sodium Tetracyanoethylenediaminecobalt(III) 3.5 Hydrate: $Na[Co(CN)_4en]\cdot 3.5H_2O$.* — This was obtained by almost the same method as the potassium salt described above, using sodium thiosulfate and sodium cyanide.

The recrystallized orange crystals were soluble in methanol; therefore, ethanol was used for precipitation from the aqueous solution after the impurities had been removed by adding methanol.

Found: C, 28.07; H, 3.47; N, 33.29. Calcd. for $C_6H_8N_6NaCo=Na[Co(CN)_4en]$: C, 29.28; H, 3.28; N, 34.15%.

Found: $H_2O$, 20.39. Calcd. for $Na[Co(CN)_4en]\cdot 3.5H_2O$: $H_2O$, 20.39%.

*Dicyanobis(propylenediamine)cobalt(III) Thiosulfate Monohydrate; $[Co(CN)_2pn_2]_2S_2O_3\cdot H_2O$.*—This complex was prepared by almost the same method as that given by Rây and Sarma[1] for the preparation of $[Co(CN)_2en_2]_2S_2O_8\cdot H_2O$.

Into 150 ml. of an aqueous solution of 12.6 g. of *t*-$[CoCl_2pn_2]ClO_4$,[3] 16.6 g. of $Na_2S_2O_3\cdot 5H_2O$ dissolved in 150 ml. of water was stirred. After the green color of the solution had turned to brownish-violet, a 1:2 mixture of methanol and ethanol was added. When the mixture had cooled about 9 g. of bright brownish-violet crystals were formed. These were filtered, washed with methanol, and dried in air. These crystals (perhaps $Na[Co(S_2O_3)_2pn_2]$) were then dissolved in 150 ml. of water, and into the solution 13.2 g. of potassium cyanide dissolved in 150 ml. of water was stirred. The brownish yellow solution obtained was evaporated on a water bath until yellow crystals appeared. These crystals were filtered and recrystallized from hot water or from the aqueous solution by adding methanol.

Found: C, 30.19; H, 6.56; N, 26.21. Calcd. for $C_{16}H_{40}N_{12}O_3S_2Co_2=[Co(CN)_2pn_2]_2S_2O_3$: C, 30.47; H, 6.39; N, 26.66%.

Found: $H_2O$, 3.41. Calcd. for $[Co(CN)_2pn_2]_2S_2O_3\cdot H_2O$: $H_2O$, 3.39%.

*Dicyanobis(trimethylenediamine)cobalt(III) Thiosulfate: $[Co(CN)_2tn_2]_2S_2O_3$.*—To 100 ml. of an aqueous solution of 3.2 g. of *t*-$[CoCl_2tn_2]Cl$,[4] 5 g. of $Na_2S_2O_3\cdot 5H_2O$ dissolved in 50 ml. of water was added with continuous stirring, and then after ten minutes 50 ml. of an aqueous solution of 1 g. of potassium cyanide was added. The solution was concentrated on a water bath until crude dark yellow crystals began to appear. The crystals recrystallized from hot water were yellow and anhydrous.

Found: C, 30.15; H, 6.41; N, 26.99. Calcd. for $C_{16}H_{40}N_{12}O_3S_2Co_2=[Co(CN)_2tn_2]_2S_2O_3$: C, 30.47; H, 6.39; N, 26.66%.

*Trinitroamminetrimethylenediaminecobalt(III): $[Co(NO_2)_3(NH_3)tn]$.*—A mixture containing 10 g. of *m*-$[Co(NO_2)_3(NH_3)_3]$ and 30 ml. of a 10% aqueous solution of trimethylenediamine was heated gently on a free flame. After the evolution of ammonia gas had ended, the unreacted materials were separated by filtration. The filtrate was concentrated on a water bath until brownish-red needle crystals were formed. The crude crystals were then recrystallized from hot water containing a few drops of acetic acid.

Found: C, 12.73; H, 4.70; N, 30.83. Calcd. for $C_3H_{13}N_6O_6Co=[Co(NO_2)_3(NH_3)tn]$: C, 12.51; H, 4.55; N, 29.17%.

*Dichloroaquoamminetrimethylenediaminecobalt(III) Chloride Monohydrate: $[CoCl_2(OH_2)(NH_3)tn]Cl\cdot H_2O$.* Finely powdered $[Co(NO_2)_3(NH_3)tn]$ was dissolved in concentrated hydrochloric acid by warming it on a water bath. After the evolution of gas had ceased, a dark green solution was obtained; this was then cooled in ice. The dark green crystals thus obtained were filtered, washed with alcohol, and dried in air.

Found: C, 12.61; H, 6.19; N, 13.98. Calcd. for $C_3H_{15}N_3OCl_3Co\cdot H_2O=[CoCl_2(OH_2)(NH_3)tn]Cl\cdot H_2O$: C, 12.32; H, 5.86; N, 14.37%.

*Barium Tetracyanotrimethylenediaminecobalt(III) Tetrahydrate: $Ba[Co(CN)_4tn]_2\cdot 4H_2O$.*—To 200 ml. of an aqueous solution of 10 g. of $[CoCl_2(OH_2)(NH_3)tn]Cl\cdot H_2O$, 18.1 g. of $Na_2S_2O_3\cdot 5H_2O$ dissolved in 100 ml. of water was added, and then 7.2 g. of sodium cyanide in 150 ml. of water was stirred in drop by drop. The brownish yellow solution thus obtained was evaporated on a water bath to a volume of about 100 ml., and then 15 g. of $BaCl_2\cdot 2H_2O$ dissolved in 150 ml. of water was added and the mixture was cooled. After the filtration of barium thiosulfate, the mother liquor was concentrated further until crystals began to appear. These orange yellow crystals were then filtered and recrystallized from hot water.

In this preparation, an excess of barium chloride was used in order to convert potassium salt into the less soluble barium salt. The potassium salt which was prepared by the same method as the ethylenediamine complex was much contaminated by the barium salt.

Found: C, 24.43; H, 4.26; N, 24.91; $H_2O$, 10.32. Calcd. for $C_{14}H_{20}N_{12}BaCo_2\cdot 4H_2O=Ba[Co(CN)_4tn]_2\cdot 4H_2O$: C, 24.60; H, 4.13; N, 24.59; $H_2O$, 10.54%.

**Absorption Measurements.**—A Beckman DU and a Shimadzu QR-50 spectrophotometer were used to obtain visible and ultraviolet absorption spectra in the range from 30 to $150\times10^{13}$ $sec^{-1}$. All the complexes obeyed Beer's law in aqueous solutions in the $1-10^{-5}$ mol./l. range at room temperature. A Hitachi EPI-2G infrared spectrophotometer equipped with a potassium bromide foreprism and a grating double monochrometer was used to obtain infrared spectra in both the Nujol mull and the KBr disk methods.

3) A. Werner and A. Fröhlich, *Ber.*, **40**, 2228 (1907).
4) A. Werner and G. Lindenberg, *Ann.*, **386**, 271 (1912).

## Results and Discussion

**The Method of Preparation.**—In general, it has been recognized that the cobalt(III) complexes which coordinate one ethylenediamine molecule besides four unidentate ligands are rather difficult to prepare. The sulfitocomplex ion, $[Co(SO_3)_2(NH_3)_2en]^-$,[2] which is prepared[5] from $[Co(SO_3)_2(NH_3)_4]^-$ and ethylenediamine, is known as a starting material for the preparation of the complexes of this type.[6] The trans isomer of $[CoCl_2(NH_3)_2en]Cl$[2] which was used for the present preparation of tetracyanoethylenediaminecobalt(III) complex was prepared by warming this sulfito complex with hydrochloric acid, but the yield was rather low. The direct reaction of $[CoCl_2(NH_3)_2en]^+$ with cyanide gave no desired complex unless the chloro complex was transformed to the thiosulfato complex $[Co(S_2O_3)_2(NH_3)_2en]^-$. In the present work, the latter complex was not separated. Rây and Sarma[1] have prepared the dicyano complex $[Co(CN)_2en_2]^+$ from the bis(thiosulfato)complex $[Co(S_2O_3)_2en_2]^-$,[7] while Chan et al.[8] have reported that no mixed cyano complex was produced by the direct reaction of $[CoCl_2en_2]^+$ with cyanide in an aqueous solution.

An attempt to isolate a pure tetracyanopropylenediamine complex failed because of

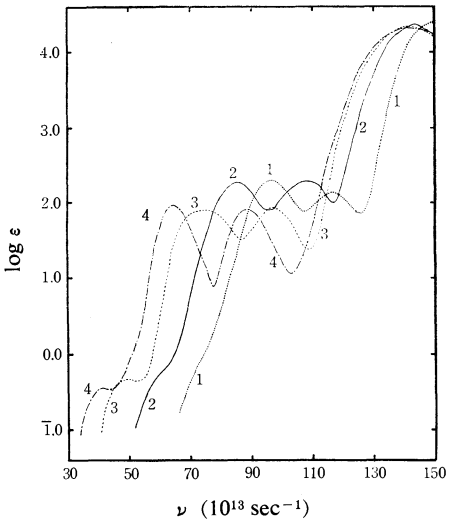



Fig. 1. Absorption curves of $[Co(CN)_{6-2x}(en)_x]^{2x-3}$ series.
1: $[Co(CN)_6]^{3-}$
2: $[Co(CN)_4en]^-$
3: *cis*-$[Co(CN)_2en_2]^+$
4: $[Co\ en_3]^{3+}$

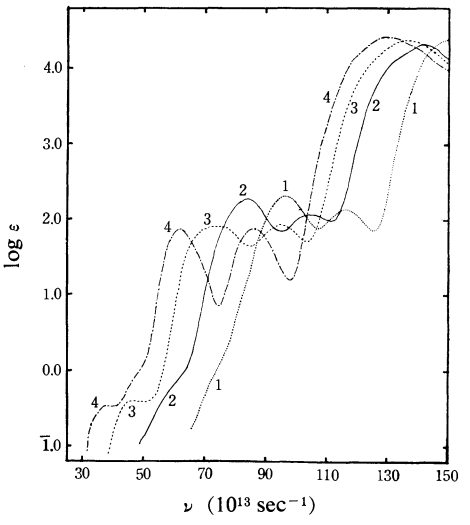



Fig. 2. Absorption curves of $[Co(CN)_{6-2x}(tn)_x]^{2x-3}$ series.
1: $[Co(CN)_6]^{3-}$
2: $[Co(CN)_4tn]^-$
3: *cis*-$[Co(CN)_2tn_2]^+$ (thiosulfate)
4: $[Co\ tn_3]^{3+}$

TABLE I. ABSORPTION DATA OF $[Co^{III}(CN)_{6-2x}(an)_x]^{2x-3}$ SERIES $\nu_{max}$ $10^{13}$ $sec^{-1}$(log ε)

| Complex | Spin-forbidden band | | Spin-allowed band | | Allowed band |
|---|---|---|---|---|---|
| | A | B | I | II | |
| $K_3[Co(CN)_6]$ | ca. 75(1.9) | — | 96.8(2.29) | 116.8(2.12) | 150 (4.28) |
| $K[Co(CN)en]\cdot H_2O$ | ca. 61(1.8) | — | 85.3(2.26) | 108.4(2.28) | 143.4(4.34) |
| $Ba_{1/2}[Co(CN)_4tn]\cdot 2H_2H$ | ca. 61(1.8) | — | 83.7(2.26) | 105.1(2.06) | 141.9(4.32) |
| *cis*-$[Co(CN)_2en_2]Cl$ | 49.7 (1.67) | — | 74.2(1.91) | 97.1(1.93) | 142.1(4.32) |
| *cis*-$[Co(CN)_2pn_2]_{1/2}(S_2O_3)_{1/2}\cdot 1/2H_2O$ | 50.6 (1.73) | — | 74.5(1.90) | 97.4(1.94) | 140.8(4.38) |
| *cis*-$[Co(CN)_2tn_2]_{1/2}(S_2O_3)_{1/2}$ | 47.2 (1.60) | — | 73.6(1.89) | 95.6(1.97) | 137.0(4.38) |
| $[Co\ en_3](ClO_4)_3$ | 41.5 (1.52) | ca. 52(1.8) | 63.9(1.94) | 88.4(1.90) | 141.8(4.32) |
| $[Co\ pn_3]Cl_3$ | 41.6 (1.65) | ca. 52(0.0) | 64.5(1.92) | 88.8(1.88) | 140.7(4.34) |
| $[Co\ tn_3](ClO_4)_3$ | 38.0 (1.54) | ca. 50(0.0) | 61.7(1.87) | 86.0(1.88) | 130.6(4.41) |

5) A. Werner and H. Grüger, *Z. anorg. Chem.*, **16**, 398 (1898).
6) Y. Shimura, This Bulletin, **31**, 311 (1958).
7) P. R. Rây and S. N. Maulik, *J. Indian Chem. Soc.*, **10**, 655 (1933).
8) S. C. Chan and M. L. Tobe, *J. Chem. Soc.*, 1963, 966.

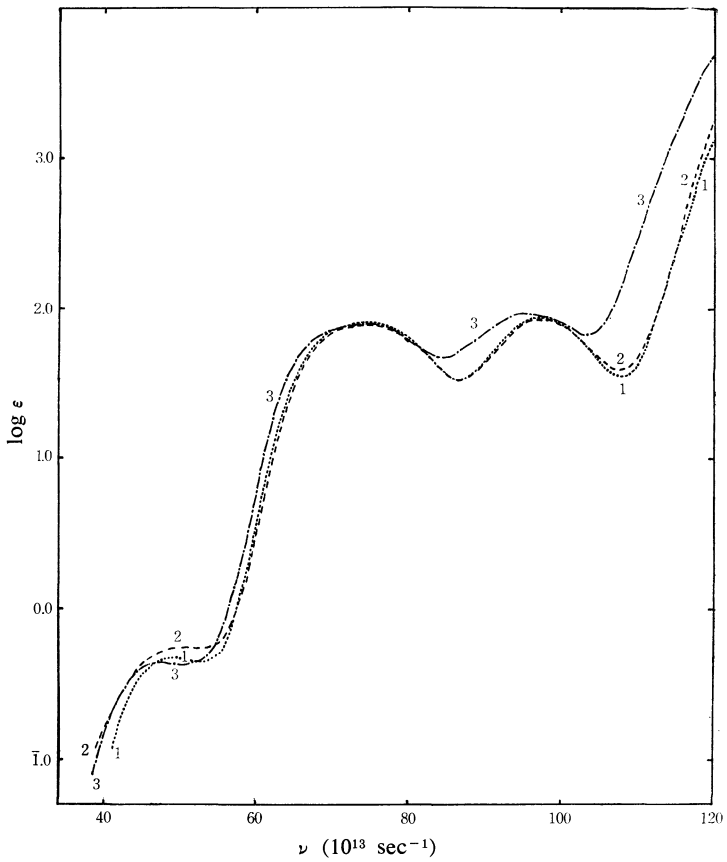



Fig. 3. Absorption curves of *cis*-$[Co(CN)_2an_2]^+$ complexes(thiosulfate).
1 : $[Co(CN)_2en_2]^+$ 2 : $[Co(CN)_2pn_2]^+$ 3 : $[Co(CN)_2tn_2]^+$

the extreme solubility of the complex.

For the preparation of the tetracyanotrimethylenediamine complex, a dark green complex, $[CoCl_2(OH_2)(NH_3)tn]^+$, was employed instead of $[CoCl_2(NH_3)_2tn]^+$, since the purification of the latter was hard.

The method for the preparation of dicyanobis(trimethylenediamine) and dicyanobis(propylenediamine) complexes was a modification of the method of Rây and Sarma described above for the corresponding ethylenediamine complex.

**Visible and Ultraviolet Absorption Spectra.**— Table I lists the numerical data of the absorption maxima of the complexes measured. In the table, the first four absorption bands are assigned to ligand field bands. The last strong band could be attributed to a characteristic absorption caused by the ligands, cyanides and diamines.

In a previous paper,[9] we have discussed the experimental relationships between the ligand field bands of cobalt(III) complexes, which also fit the complexes measured in the present work.

Figure 1 shows that the absorption frequencies of the first and second spin-allowed bands of the cyano-ethylenediamine series shift to shorter wavelengths in proportion to the number of ligand cyanides, as has been observed in the oxalato-ammine series.[10] The same relation is seen in the cyano-trimethylenediamine series. The absorption intensities of these cyano complexes, on the other hand, exhibit no such regular relation. The A bands of the weak spin-forbidden absorptions are observed on the longer wavelength side of the first spin-allowed bands. All the B bands of cyano complexes are hidden by the feet of the strong first bands.

Theoretically, two geometrical isomers, cis and trans, exist in the dicyanobis(ethylenediamine)cobalt(III) ion, but so far only one species has been obtained. Chan et al.[8] determined through the optical resolution that

9) J. Fujita and Y. Shimura, This Bulletin, **36**, 1281 (1963).

10) Y. Shimura and R. Tsuchida, ibid., **28**, 572 (1955).

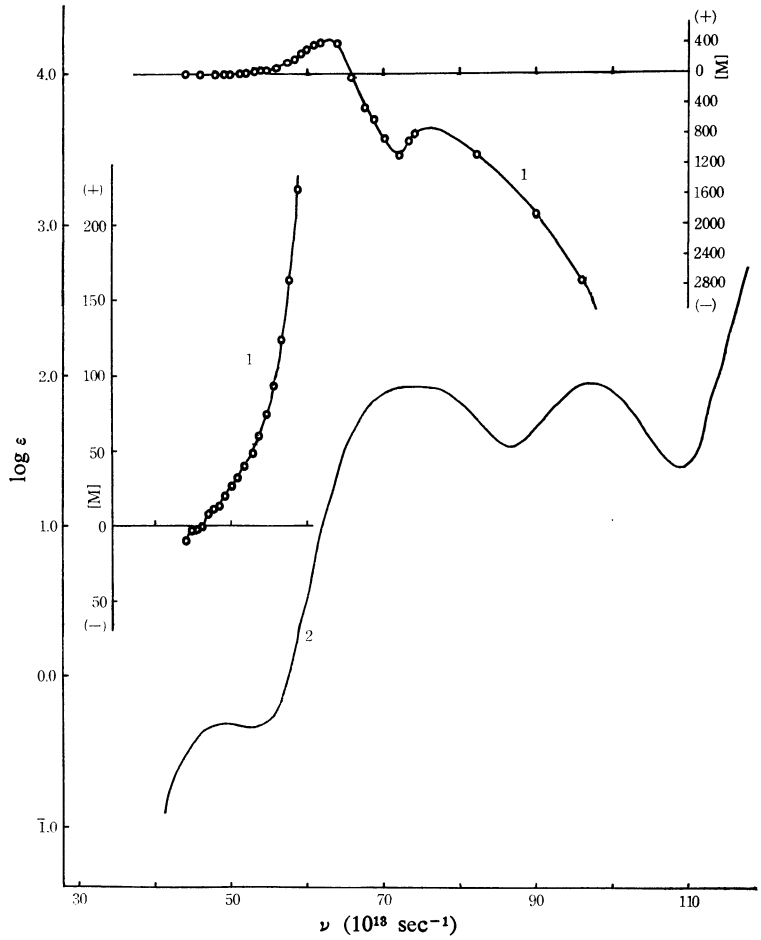



Fig. 4. Rotatory dispersion and absorption curves of $(+)_{546}$-*cis*-$[Co(CN)_2en_2]^+$.
1 Rotatory dispersion curves 2 Absorption curve

this complex takes the cis configuration. The absorption spectra of the dicyanobis(propylenediamine) and dicyanobis(trimethylenediamine) complexes closely resemble the ethylenediamine complex with the cis configuration. It may be concluded, therefore, that all three of the dicyano complexes prepared in this work correspond to the cis isomers.

**The Rotatory Dispersion of** $[Co(CN)_2en_2]^+$. —As has been described above, Chan et al.[8] have resolved the dicyanobis(ethylenediamine) cobalt(III) complex into its optically-active forms through its α-bromocamphor-π-sulfonate. In the present study, we have determined the rotatory dispersion of the $(+)_{546}$-isomer (Fig. 4). It exhibits a positive Cotton effect in the region of the first spin-allowed absorption band. The amplitude of this partial dispersion is as large as those of the same type of cobalt(III) complexes, such as $[CoCl_2en_2]^+$,[11] and $[Co(NO_2)_2en_2]^+$.[12]

It is interesting to note that no remarkable Cotton effect is shown in the region of the A spin-forbidden band of the complex. This might be because the Cotton effects are too weak to be measured, or because this small partial dispersion is hidden by the foot of the dispersion of the first spin-allowed absorption band. Mason[13] reported a very weak circular dichroism band ($\varepsilon_l - \varepsilon_r = +0.008$) in the region of the A spin-forbidden band of the $(+)_D$-$[Co\,en_3]^{3+}$ ion. Kling and Woldbye[14] have found several weak Cotton effects in the spin-forbidden bands of the tris(ethylenediamine) chromium (III) and related complexes.

**Infrared Spectra.**—Figure 5 shows the infrared absorption spectra of the C≡N stretching region for the cyano-diamine complexes. The

11) J. Hidaka, S. Yamada and R. Tsuchida, ibid., **31**, 921 (1958).

12) J. Hidaka, Y. Shimura and R. Tsuchida, ibid., **33**, 847 (1960).

13) S. F. Mason, *Quart. Rev.*, **17**, 20 (1963).

14) O. Kling and F. Woldbye, *Acta Chem. Scand.*, **15**, 704 (1961).

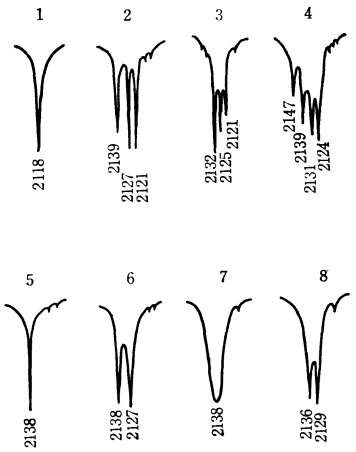



Fig. 5. Infrared absorption spectra in the region of $\nu(C\equiv N)$.
1 : $K_3[Co(CN)_6]$
2 : $K[Co(CN)_4en]$
3 : $Na[Co(CN)_4en]\cdot 3.5H_2O$
4 : $Ba[Co(CN)_4tn]_2\cdot 4H_2O$
5 : racemic *cis*-$[Co(CN)_2en_2]Cl$
6 : optically active *cis*-$[Co(CN)_2en_2]Cl\cdot H_2O$
7 : *cis*-$[Co(CN)_2pn_2]_2S_2O_3\cdot H_2O$
8 : *cis*-$[Co(CN)_2tn_2]_2S_2O_3$

complex ion $[Co(CN)_6]^{3-}$ which has an $O_h$ symmetry exhibits only one triply-degenerate C≡N stretching band,[15] while the mixed-diamine complex shows a group of C≡N stretching bands split by the lowering of the symmetry. The complex ion $[Co(CN)_4en]^-$ exhibits three C≡N stretching bands, although the theoretical number of this stretching band is four. The complex ion $[Co(CN)_4tn]^-$ distinctly shows four peaks. The optically-active dicyanobis(ethylenediamine) and racemic dicyanobis(trimethylenediamine) complexes, whose approximate symmetries are $C_{2v}$, exhibit two peaks, while the racemic dicyanobis(ethylenediamine) and dicyanobis(propylenediamine) complexes show no splitting. It is curious that there is a marked difference in the C≡N stretching band between the resolved and the racemic bis(ethylenediamine) complexes.

It is interesting to note that the magnitude of the splitting of the C≡N stretching bands in these cyanodiamine complexes is 1/10 those of the C=O stretching bands in several carbonyl complexes.[16] This suggests that the character of the bonding between the cyanide and the cobalt(III) ion in the former complexes would be considerably weak compared with that between the carbon monoxide and the metal atom in the latter ones.

## Summary

Several new mixed cyano-diamine complexes, $M[Co(CN)_4en]\cdot xH_2O$ ($M=K$, $x=1$; $M=Na$, $x=3.5$), $Ba[Co(CN)_4tn]_2\cdot 4H_2O$, $[Co(CN)_2pn_2]_2S_2O_3\cdot H_2O$ and $[Co(CN)_2tn_2]_2S_2O_3$, have been prepared, and their infrared, visible and ultraviolet absorption spectra have been determined. From these spectral results, it has been concluded that the two dicyano complexes are cis isomers.

No remarkable Cotton effect has been observed in the region of the spin-forbidden band of the *cis*-$[Co(CN)_2en_2]^+$.

The authors are indebted to Professor Nobuyuki Tanaka of Tohoku University for the use of the grating infrared spectrophotometer.

*Department of Chemistry*
*Faculty of Science*
*Osaka University*
*Nakanoshima, Osaka*

15) I. Nakagawa and T. Shimanouchi, *Spectrochim. Acta*, **18**, 101 (1962).

16) C. S. Kraihanzel and F. A. Cotton, *Inorg. Chem.*, **2**, 533 (1963).

# The Reaction of Tropoids and Quinone Derivatives. VI. On the Structures of the Reaction Products of *p*-Benzoquinonedibenzenesulfonimide with Phenol or Tropolone

By Yukio NISHIYAMA, Yusaku IKEGAMI and Shuichi SETO

(Received July 1, 1964)

Adams and Blomstrom[1] reported that the reaction of *p*-benzoquinonedibenzenesulfonimide (I) with phenols in the presence of triethylamine yielded the products exemplified by formula II.[2] The present authors[5] then applied this reaction to tropolone and reported that the product thereby obtained, which corresponded to an adduct of one molecule of I and one molecule of tropolone, would have structure III, as determined by analogy to the case of phenol.[1] Thereafter, as an extension of this reaction, the reaction of *o*-benzoquinonedibenzimide (IV) with phenol[6,7] or tropolone[8] was carried out, giving an adduct of one molecule of IV and one molecule of phenol or tropolone. The investigation of the structures of these adducts revealed that they were the *N*-(4-hydroxyphenyl)- and *N*-(tropolon-5-yl)-*o*-phenylenediamine derivatives V and VI respectively. Since this fact threw doubt upon the structures of the reaction products of I with phenol and tropolone, which had been previously assumed to be II and III respectively, the present authors attempted to reexamine these structures. This paper will present evidence showing that the structures previously assumed are erroneous and should be revised to the *N*-substituted derivatives VII and VIII.

The reaction of I with phenol in the presence of a catalytic amount of triethylamine gives colorless crystal (A), m. p. 227—228°C (decomp.). Adams et al. reported the melting points of 228.5—229.5°C (decomp.)[1] or 227—228°C (decomp.).[3] The methylation of A with diazomethane affords a methyl derivative (A), m. p. 136°C, which does not exhibit any absorption band due to the OH and NH groups in its infrared spectrum. In the NMR spectrum of B,[9] the signals for the protons of $NCH_3$ and $OCH_3$ groups appear at 6.85 and 6.21 $\tau$, respectively and have almost equal intensities. These facts show that B is not IX, but X. *N*-Methyl-*N'*-(4-methoxyphenyl)-*N*, *N'*-dibenzenesulfonyl-*p*-phenylenediamine (X) was then synthesized for purposes of comparison by an unequivocal route; the diamine obtained by the catalytic reduction of known 4-nitro-4'-methoxydiphenylamine[10] gives X on benzenesulfonylation followed by methylation. The compound X synthesized thus was found to be identical with the methyl derivative (B) through a mixed fusion test and by a comparison of the ultraviolet and infrared spectra. This evidence firmly establishes that, on the reaction of *p*-benzoquinonedibenzenesulfonimide (I) with phenol, the bond formation between the nitrogen atom of I and the carbon atom at the 4-position of phenol occurs, as in the case of the reaction with the *o*-benzoquinone derivative IV,[6] and that, consequently, the product is not 2-(4'-hydroxyphenyl)-*N*, *N'*-dibenzenesulfonyl-*p*-phenylenediamine (II), as was reported by Adams et al.,[1,3] but *N*-(4-hydroxyphenyl)-*N*, *N'*-dibenzenesulfonyl-*p*-phenylenediamine (VII). Adams and Braun[11] reported an example of such C–N bond formation by the reaction of the quinoneimide derivatives; the reaction of 2, 3, 5, 6-tetrachloro-*p*-benzoquinonedibenzenesulfonimide (XI) with aromatic amines, e. g., aniline and *N*-dimethylaniline, gave as products XII and XIII without a catalyst. The present authors carried out the reaction of XI with phenol in the presence of triethylamine and obtained a products XIV analogous to XII. On methylation with diazomethane, XIV affords a methyl derivative

1) R. Adams and D. C. Blomstrom, *J. Am. Chem. Soc.*, **75**, 3405 (1953).

2) It has been reported that the same types of products were obtained by the reaction of phenols with I, naphthoquinonedibenzenesulfonimide[1,3] or *p*-benzoquinonedibenzimide[4] in the presence of aluminum chloride or boron trifluoride.

3) R. Adams and K. R. Eilar, *J. Am. Chem. Soc.*, **73** 1149 (1951).

4) R. Adams and D. S. Acker, ibid., **74**, 5872 (1952).

5) S. Seto, H. Yamazaki and Y. Nishiyama, This Bulletin, **33**, 1081 (1960).

6) S. Seto and Y. Nishiyama, *J. Pharm. Soc. Japan.* (*Yakugaku Zasshi*), **82**, 590 (1962).

7) Y. Nishiyama, *Bull. Chem. Research Inst. of Non-Aqueous Solutions, Tohoku Univ.*, **12**, 55 (1963).

8) S. Seto and Y. Nishiyama, This Bulletin, **35**, 1010 (1962).

9) The NMR spectra were measured in deuteriochloroform, using a Varian 4301 high resolution NMR spectrometer (60 Mc.), by Assistant Professor Tsuneo Ikenoue of this Institute; to him the authors are indebted.

10) F. Ullmann and K. K. Jüngel, *Ber.*, **42**, 1077 (1909).

11) R. Adams and B. H. Braun, *J. Am. Chem. Soc.*, **74**, 5869 (1952).

(XV) whose NMR spectrum exhibits the signal at 6.78 and 6.20 $\tau$, due to the protons of the $NCH_3$ and $OCH_3$ groups respectively, with almost equal intensities.

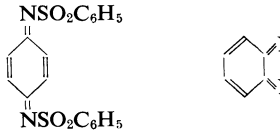
The reaction product (C)[12] of I with *o*-cresol was also methylated to a methyl derivative (D). The NMR spectrum of D shows the signals for the protons of $NCH_3$, $OCH_3$ and $CH_3$ at the position at 6.87, 6.21 and 7.84 $\tau$ respectively; their intensities are almost the same. These facts indicate that compounds C and D are XVI and XVII respectively, analogous to the case of the reaction product of I with phenol.

In the case of the reaction product (E)[5] of I with tropolone, the situation is very similar to that with phenols. The methylation of E with diazomethane gives a methyl derivative (F)[13], m. p. 190—191°C, whose infrared spectrum does not show any absorption band due to the OH or NH groups. To compound E, the introduction of two or three methyl groups may be expected, but the analytical figures do not permit the selection of the number of methyl groups in the case of a compound with a large molecular weight, such as F. Hence, the benzylation of E was undertaken; a monobenzyl derivative (XVIIIa) was thereby obtained. Its infrared spectrum shows the band due to the OH group, but it lacks that due to the NH group. The NMR spectrum of F shows the signals for the protons of $NCH_3$ and $OCH_3$ attached to the tropone nucleus at 6.84 and 6.04 $\tau$ respectively;[14] they have almost equal intensities. These facts suggest that product E is not III, but VIII.

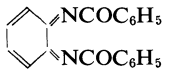
In order to confirm the structure further, the rearrangement of the tropolone ring in F into benzoic acid was attempted. The heating of F with sodium ethoxide in absolute ethanol, followed by hydrolysis, gave a benzoic acid derivative which was then converted into a methyl ester (G) by treatment with diazomethane. If product E is VIII and, consequently, F is XVIII, methyl ester G should be XIX. Therefore, the synthesis of XIX by an unequivocal route was carried out.

The treatment of known 4-amino-4'-methyldiphenylamine[15] with benzenesulfonyl chloride in pyridine gave XX, whose oxidation with potassium permanganate, followed by methylation with diazomethane, gave XIX. Methyl ester G showed no depression of its melting point on admixture with XIX, and the ultraviolet and infrared spectra of these two substances were in good agreement. Consequently, product E must be *N*-(tropolon-5-yl)-*N*, *N*'-dibenzenesulfonyl-*p*-phenylenediamine (VIII).

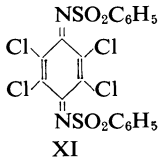
The reaction of XI with tropolone gave the tetrachloro-derivative XXI. The NMR spectrum of the methyl derivative of XXI shows the



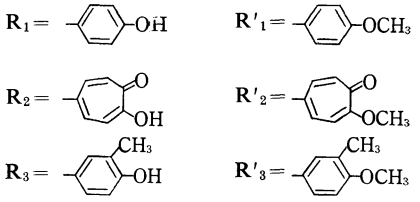
I

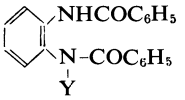


IV

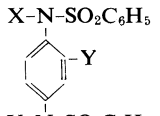


XI

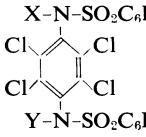


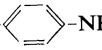


V : $Y=R_1$
VI : $Y=R_2$



II : X=H, $Y=R_1$
III : X=H, $Y=R_2$
IX : $X=CH_3$, $Y=R'_1$



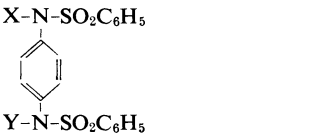
XII : X=H, 
XIII : X=H, 
XIV : X=H, $Y=R_1$
XV : $X=CH_3$, $Y=R'_1$
XXI : X=H, $Y=R_2$
XXII : $X=CH_3$, $Y=R'_2$

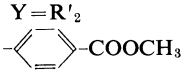
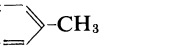
12) Adams and Blomstrom reported that this product also had a structure of type II.[1]

13) The authors previously described F as a monomethyl compound,[5] although its analytical values agreed rather with those of a dimethyl compound.

14) The proton signals of the $OCH_3$ group in 2-methoxytropones appear at a field lower by about 0.12—0.17 p.p.m. than those in methoxyphenyl groups, as a result of the magnetic anisotropy effect of the neighboring carbonyl group.

15) F. Ullmann and R. Dahmen, *Ber.*, **41**, 3751 (1908).



VII : X=H, Y=$R_1$
VIII : X=H, Y=$R_2$
X : X=$CH_3$, Y=$R'_1$
XVI : X=H, Y=$R_3$
XVII : X=$CH_3$, Y=$R'_3$
XVIII : X=$CH_3$, Y=$R'_2$
XVIIIa : X=$CH_2C_6H_5$, Y=$R_2$
XVIIIb : X=$CH_2C_6H_5$, Y=$R'_2$
XIX : X=$CH_3$, Y= 
XX : X=H, Y= 

signals for the protons of the $NCH_3$ and $OCH_3$ groups at 6.83 and 6.08 $\tau$ respectively, and they have almost equal intensities all indicating that the methyl derivative is XXII.

## Experimental[16]

***N*-(4-Hydroxyphenyl)-*N*, *N'*-dibenzenesulfonyl-*p*-phenylenediamine (VII).** — a) VII was prepared in the manner reported by Adams and Blomstrom,[1] using 1 g. of I and 600 mg. of phenol. Colorless crystals m. p. 227—228°C (decomp.) were obtained. Yield, 780 mg.

b) To a solution of 0.5 g. of I in 20 ml. of chloroform, a solution of 0.3 g. of phenol in 3 ml. of chloroform was added. The addition of 3 drops of boron trifluoride etherate changed the color of the solution temporarily to dark violet, but colorless crystals began to separate after a few minutes. The mixture was allowed to stand for 1 hr., and then the crystals were collected to give 530 mg. of VII. This compound was found to be identical with that prepared by method a) through a mixed fusion test and by a comparison of the ultraviolet and infrared spectra.

***N*-(4-Methoxyphenyl)-*N'*-methyl-*N*, *N'*-dibenzenesulfonyl-*p*-phenylenediamine (X).** — a) An ether solution of diazomethane was added to 100 mg. of VII suspended in 4 ml. of methanol; thereby, with the evolution of nitrogen the crystals dissolved once, and after a few minutes new colorless crystals began to separate out. After the mixture had been allowed to stand overnight, the crystals were collected and recrystallized from a mixture of methanol and chloroform to afford 65 mg. of X, m. p. 163—164°C.

Found: C, 61.19; H, 4.85; N, 5.54. Calcd. for $C_{26}H_{24}O_5N_2S_2$: C, 61.43; H, 4.72; N, 5.51%.

b) A suspension of 500 mg. of 4-nitro-4'-methoxydiphenylamine[10] in 40 ml. of ethanol, with 300 mg. of 5% palladium-carbon added, was shaken in a hydrogen atmosphere at an ordinary temperature. After the absorption of hydrogen had ended, a small amount of sodium dithionite was added to the mixture and the catalyst was removed by filtration. The filtrate was then evaporated to dryness under reduced pressure. The solid which formed on the addition of a small amount of water to the residue was collected to afford 400 mg. of 4-amino-4'-methoxydiphenylamine m. p. 98°C. To a solution of 200 mg. of this compound in 1 ml. of pyridine, 300 mg. of benzenesulfonyl chloride was added drop by drop. The color of the mixture changed to dark red and then to dark violet. After heating on a water bath for 3 hr., pyridine was evaporated under reduced pressure. The addition of ice water to the residue gave a solid which was recrystallized from ethanol to give 410 mg. of *N*-(4-methoxyphenyl)-*N*, *N'*-dibenzenesulfonyl-*p*-phenylenediamine, m. p. 187—188°C.

Found: C, 60.90; H, 4.44; N, 5.91. Calcd. for $C_{25}H_{22}O_5N_2S_2$: C, 60.74; H, 4.45; N, 5.66%.

To a suspension of 100 mg. of the *p*-phenylenediamine derivative obtained above in 5 ml. of ethanol, an ether solution of dizomethane was added. After the mixture had been allowed to stand overnight, the crystals were collected and recrystallized from methanol to give 95 mg. of colorless crystals, m. p. 163—164°C. The crystals thereby obtained did not show any depression of melting point on admixture with the compound obtained by method a), and the infrared spectra of the two were in good agreement.

***N*-(4'-Hydroxyphenyl)-*N*, *N'*-dibenzenesulfonyl-2, 3, 5, 6-tetrachloro-*p*-phenylenediamine (XIV).** — To 200 mg. of 2,3,5,6-tetrachloro-*p*-quinonedibenzenesulfonimide (XI) suspended in 4 ml. of chloroform, a solution of 130 mg. of phenol in 2 ml. of chloroform was added. On the addition of 2 drops of triethylamine to the mixture, the crystals of XI dissolved immediately, and then colorless crystals separated out. After the mixture had been allowed to stand overnight, the crystals were collected and recrystallized from chloroform to give 200 mg. of XIV as colorless crystals, m. p. 232—233°C.

Found: C, 46.72; H, 2.48; N, 4.70. Calcd. for $C_{24}H_{16}O_5N_2S_2Cl_4$: C, 46.64; H, 2.56; N, 4.53%.

**Dimethyl Derivative (XV) of XIV.** — An ether solution of diazomethane was added to 100 mg. of XIV suspended in 1 ml. of methanol. After the mixture had been allowed to stand for 1 hr., the crystals that separated out were collected and its solution in ethyl acetate was purified through an alumina column to give 30 mg. of XV, m. p. 228°C.

Found: C, 48.36; H, 2.78; N, 4.62. Calcd. for $C_{26}H_{20}O_5N_2S_2Cl_4$: C, 48.33; H, 3.09; N, 4.33%.

***N*-(4-Methoxy-3-methylphenyl)-*N'*-methyl-*N*, *N'*-dibenzenesulfonyl-*p*-phenylenediamine (XVII).** — To 150 mg. of XIV (the reaction product[1] of I with *o*-cresol) suspended in 5 ml. of methanol, an ether solution of diazomethane was added. After 24 hr. the solvent was evaporated and the residue was recrystallized from methanol to afford 135 mg. of colorless crystals (XVII), m. p. 158—160°C. The infrared spectrum of this compound did not show

16) All melting points are uncorrected. Microanalyses were carried out by the Misses Yoko Endo and Yukiko Endo in this Institute. Measurements of ultraviolet and infrared spectra were made, respectively, with a Hitachi EPU-2A type spectrophotometer and with a Perkin-Elmer 21 infrared spectrophotometer using a potassium bromide disk.

any absorption band due to the OH and NH groups.

Found: C, 62.31; H, 5.02; N, 5.51. Calcd. for $C_{27}H_{26}O_5N_2S_2$: C, 62.09; H, 4.98; N, 5.36%.

***N*-(2-Methoxytropon-5-yl)-*N'*-methyl-*N*, *N'*-dibenzenesulfonyl-*p*-phenylenediamine (XVIII).**—To 1 g. of VIII (the reaction product[5] of I with tropolone) suspended in 10 ml. of methanol, an ether solution of diazomethane was added. After the mixture had been allowed to stand overnight, the crystals that separated out were collected and recrystallized from a mixture of methanol and chloroform to give 950 mg. of XVIII, m. p. 190—191°C.

Found: C, 60.44; H, 4.35; N, 5.18. Calcd. for $C_{27}H_{24}O_6N_2S_2$: C, 60.46; H, 4.47; N, 5.22%.

**The Rearrangement Reaction of XVIII with Sodium Ethoxide.**—A mixture of 150 mg. of XVIII and sodium ethoxide prepared from 100 mg. of sodium and 2.5 ml. of absolute ethanol was heated at 120°C; thereby the crystals of XVIII once dissolved once, and after a while a solid separated out. After being heated for 1 hr., the mixture was cooled. The solid was collected by filtration and washed with ethanol. The solid (50 mg.) was heated in 2 ml. of 6 N hydrochloric acid on a water bath for 1 hr. After being cooled, the solid was collected, suspended in 2 ml. of methanol, and treated with an ether solution of diazomethane. After standing overnight, the solvent was evaporated. The residue was chromatographed on an alumina column, and elution with ethyl acetate afforded 20 mg. of colorless needles (XIX), m. p. 182—183°C.

Found: C, 60.69; H, 4.64; N, 5.51. Calcd. for $C_{27}H_{24}O_6N_2S_2$: C, 60.46; H, 4.47; N, 5.22%.

***N*-(4-Methoxycarbonylphenyl)-*N'*-methyl-*N*, *N'*-dibenzenesulfonyl-*p*-phenylenediamine (XIX).**—To a solution of 250 mg. of 4-amino-4'-methyldiphenylamine[14] in 2 ml. of pyridine, 390 mg. of benzenesulfonyl chloride was added drop by drop in a nitrogen atmosphere; the color of the mixture thereupon changed to a red dish purple and then, after 5 min., faded. The mixture was heated on a water bath for 30 min., and pyridine was removed under reduced pressure. The residue solidified on the addition of water. The solid thereby formed was collected and recrystallized from ethanol to give 400 mg. of *N*-(4-methylphenyl)-*N*,*N'*-dibenzenesulfonyl-*p*-phenylenediamine (XX) as colorless crystals, m. p. 175°C.

Found: C, 62.73; H, 4.27; N, 5.93. Calcd. for $C_{25}H_{22}O_4N_2S_2$: C, 62.77; H, 4.59; N, 5.85%.

To 50 mg. of XX suspended in a solution of 100 mg. of potassium hydroxide in 10 ml. of water, a solution of 50 mg. of potassium permanganate in 10 ml. of water was added. The mixture was then heated at 100°C for 1.5 hr. After the remaining potassium permanganate had been decomposed by the addition of methanol, the mixture was filtered to remove any manganese dioxide. The filtrate was then acidified, and the precipitate thereby formed was collected. The precipitate was added to an aqueous solution of sodium carbonate (30 mg. in 5 ml. of water), and an insoluble substance was removed by filtration. When the filtrate was acidified again, 35 mg. of the precipitate was collected. A solution of this precipitate in methaol was treated with an ether solution of diazomethane. The evaporation of the solvent gave 20 mg. of colorless needles, m. p. 183°C. This substance was identical with the compound (XIX) derived from the rearrangement reaction mentioned above.

Found: C, 60.61; H, 4.34; N, 5.04%.

***N*-(Tropolon-5'-yl)-*N*, *N'*-dibenzenesulfonyl-2, 3, 5, 6-tetrachloro-*p*-phenylenediamine (XXI).**—To 200 mg. of XI suspended in 4 ml. of chloroform, a solution of 100 mg. of tropolone in 2 ml. of chloroform was added. On the addition of one drop of triethylamine to the mixture, the orange crystals of XI dissolved immediately and colorless crystals separated out. After they had stood for 3 hr., the crystals (200 mg.) were collected. Recrystallization from a mixture of ethanol and chloroform gave 190 mg. of XXI as colorless crystals, m. p. 208—210°C (decomp.).

Found: C, 45.97; H, 2.73; N, 4.49. Calcd. for $C_{25}H_{16}O_6N_2S_2Cl_4$: C, 46.47; H, 2.48; N, 4.33%.

***N*-(2'-Methoxytropon-5'-yl)-*N'*-methyl-*N*, *N'*-dibenzenesufonyl-2, 3, 5, 6-tetrachloro-*p*-phenylenediamine (XXII).**—This compound was prepared by the treatment of 100 mg. of XXI with an ether solution of diazomethane in the same manner as in the case of XV. Colorless crystals; m. p. 228°C (decomp.).

Found: C, 47.96; H, 3.14; N, 4.21. Calcd. for $C_{27}H_{20}O_6N_2S_2Cl_4$: C, 48.10; H, 2.97; N, 4.15%.

***N*-(Tropolon-5-yl)-*N'*-benzyl-*N*, *N'*-dibenzenesulfonyl-*p*-phenylenediamine (XVIIIa).**—Into a solution of 300 mg. of VIII in aqueous potassium hydroxide (400 mg. in 12 ml. of water), 265 mg. of benzyl chloride was stirred at 30—40°C. After the treatment had been continued for 6 hr., the solid thereby formed was collected by filtration, suspended in a small amount of water, and acidified with dilute sulfuric acid. After the mixture had been stirred for a while, 160 mg. of the solid was collected; the recrystallization of this from a mixture of ethyl acetate and ethanol gave 120 mg. of the desired compound as colorless crystals, m. p. 220—222°C (decomp.). This compound showed a positive color reaction with ferric chloride.

Found: C, 64.78; H, 4.67; N, 4.82. Calcd. for $C_{32}H_{26}O_6N_2S_2$: C, 64.23; H, 4.35; N, 4.68%.

***N*-(2-Methoxytropon-5-yl)-*N'*-benzyl-*N*, *N'*-dibenzenesulfonyl-*p*-phenylenediamine (XVIIIb).**—The treatment of 50 mg. of the benzyl derivative prepared above with an ether solution of diazomethane gave 39 mg. of the methyl derivative; colorless needles, m. p. 204—205°C.

Found: C, 64.97; H, 4.65; N, 4.53. Calcd. for $C_{33}H_{28}O_6N_2S_2$: C, 64.72; H, 4.57; N, 4.57%.

***N*,*N'*-Dimethyl-*N*,*N'*-dibenzenesulfonyl-*p*-phenylenediamine.**—To 300 mg. of *p*-phenylenedibenzenesulfonamide suspended in 5 ml. of methanol, an ether solution of diazomethane was added. After the mixture had been allowed to stand overnight, the solvent was removed by evaporation. The residue was recrystallized from a mixture of chloroform and ethanol to afford 220 mg. of colorless crystals, m. p. 193—195°C.

Found: C, 58.43; H, 4.95; N, 6.84. Calcd. for $C_{20}H_{20}O_4N_2S_2$: C, 57.70; H, 4.80; N, 6.74%.

In its NMR spectrum, a singnal for the protons of $NCH_3$ appears at 6.84 $\tau$.

Some of the expenses for the present work were defrayed by funds from the Sankyo Co., Ltd., help which is gratefully acknowledged.

*The Chemical Research Institute of Non-Aqueous Solutions*
*Tohoku University*
*Katahira-cho, Sendai*

# The Chemiluminescence, Fluorescence and Absorption Spectra of 2, 4, 5-Triphenylimidazole

By Koko MAEDA, Heijiro OJIMA and Taro HAYASHI

(Received July 2, 1964)

In 1877 Radziszewski[1] found that 2, 4, 5-triphenylimidazole (lophine) exhibits chemiluminescence in ethanolic potassium hydroxide with oxygen at room temperature, yielding benzoic acid and ammonia. Trautz[2] later reported that lophine exhibited a brighter chemiluminescence with such ordinary oxidizing agents as aqueous solutions of hydrogen peroxide, chlorine, bromine and potassium ferricyanide. Cottman, Moffet and Moffet[3] and Cook and Jones[4] investigated the chemiluminescence of several substituted derivatives of lophine. However the mechanism of the chemiluminescence of lophine has never been studied. We have, therefore, studied the mechanism of the chemiluminescence of lophine for several years and have published[5] a mechanism involving the triphenylimidazolyl radical. molecular oxygen and peroxide. The details of our study of the mechanism of the chemiluminescence of lophine will be reported in the following papers.

Cottman and his collaborators[3] measured the chemiluminescence spectra of lophine and several of its substituted compounds with a photographic method and reported that those spectra were spread over 480—600 m$\mu$, with a single maximum near 530 m$\mu$. No details of the spectra, however, were shown. We measured the chemiluminescence spectra of lophine and several of its substituted compounds with a recording spectrophotometer and also measured the spectra of fluorescence and absorption. The present paper deals with the results obtained on those spectra of lophine.

1) B. Radziszewski, *Ber.*, **10**, 70 (1877).
2) M. Trautz, *Z. Physik. Chem.*, **53**, 86 (1905).
3) E. W. Cottman, R. B. Moffet and S. M. Moffet, *Proc. Indiana Acad. Sci.*, **47**, 133 (1938); *Chem. Abstr.*, **32**, 9081 (1938).
4) A. H. Cook and D. G. Jones, *J. Chem. Soc.*, **1941**, 278.
5) T. Hayashi and K. Maeda, This Bulletin, **35**, 2057 (1962).

## Experimental

Lophine was prepared by the method of Davidson, Weiss and Jelling.[6] It was recrystallized from ethanol as colorless fine needles, m. p. 271—272°C.

**The Chemiluminescence Spectrum.** — The chemiluminescence spectrum of lophine in 1 N ethanolic potassium hydroxide and oxygen was measured with the Hitachi recording spectrophotometer, EPS 2 type, equipped with an apparatus for measuring the chemiluminescence spectrum of a solution. The equipment and the procedure for measuring the chemiluminescence spectrum are as follows: lophine (0.5 g.) was added to 12 ml. of 1 N ethanolic potassium hydroxide in a quartz tube 1.5 cm. inner diameter and 25 cm. long. A cork at the upper end of the tube was provided with a small reflux condenser, a thermometer and a narrow glass tube for streaming gas into the solution in the tube. When the mixture in the tube was stirred by a nitrogen stream for a while, a pale yellow solution of lophine ($C=2.81\times10^{-1}$ mol./l.) was obtained. Then the tube containing the solution was put in a metallic tube, about 2 cm. in inner diameter, fixed in the center of a small metallic cylindrical thermostat which had been set in place of a light source. Hot water was circulated throughout this thermostat from another one in order to heat the solution in the tube at 70°C. Small windows both on an outer wall of the cylindrical thermostat and on a wall of the metallic tube containing the quartz tube which contained a solution of lophine, were connected with a narrow horizontal metallic tube, through which a light of chemiluminescence was introduced into the spectrophotometer. When the temperature of the solution of lophine became 70°C, a gentle stream of heated oxygen was passed into the solution. A chemiluminescence was exhibited at once; the spectrum was immediately measured by the recording spectrophotometer.

**The Fluorescence Spectra.** — The fluorescence spectra of lophine were measured with the spectrophotometer equipped with an apparatus for measuring fluorescence spectra. The 365 m$\mu$ line of a high

6) D. Davidson, M. Weiss and M. Jelling, *J. Org. Chem.*, **2**, 319 (1937).

pressure mercury lamp was used for the excitation.

**The Absorption Spectra.**—The absorption spectra of lophine were measured with the spectrophotometer.

## Results and Discussion

**The Chemiluminescence Spectra of Lophine.**—An ethanolic potassium hydroxide solution of lophine was used for measuring the chemiluminescence spectrum, since lophine was not dissolved in water. Like luminol and lucigenin, lophine exhibited chemiluminescence only in an alkaline medium. The light of the chemiluminescence of lophine with oxygen or with an aqueous solution of hydrogen peroxide was greenish blue, and the light could be detected even at the concentration of $10^{-5}$ mol./l. However, the intensity of chemiluminescence at room temperature was so weak that the chemiluminescence spectrum could not be measured by the recording spectrophotometer.

The intensity of the chemiluminescence with oxygen increased with a rise in the temperature. For example, a 2 N ethanolic potassium hydroxide solution of lophine ($C=1.6\times10^{-2}$ mol./l.) did not emit luminescence at $-15$°C. It did, however, emit a very weak luminescence at 0°C; the intensity increased with a rise in the temperature to about 80°C, at which point the solution began to boil, resulting in a rapid decrease in the intensity of the luminescence. Since the intensity was recovered by passing oxygen into the boiling solution, the rapid decrease in luminescence by boiling was obviously due to the loss of oxygen from the solution. These results indicated that the optimum temperature for measuring the chemiluminescence spectrum of lophine was 70—75°C.

In the chemiluminescence of lophine (concentration $10^{-1}$—$10^{-2}$ mol./l.) in 1—2 N ethanolic potassium hydroxide at room temperature, with oxygen which had previously been saturated, it was found that the logarithum of the total intensity of the chemiluminescence on an arbitrary scale linearly decreased with time for about ten minutes, that is at a rate probably of the first order with respect to the concentration of oxygen, whereas in the chemiluminescence with oxygen continuously passed into the solution, it was found that the total intensity hardly decreased at all for several minutes.

In view of these results, the chemiluminescence spectrum was measured by passing oxygen into a solution ($C=2.81\times10^{-1}$ mol./l.) in 1 N ethanolic potassium hydroxide at 70°C. The spectrum is shown in Fig. 1. It spreads over only a visible region, about 465—660 mμ, with a maximum at about 545 mμ. The time of the sweeping of the recorder from 450 to 680 mμ was 24 sec. Although it was found that the intensities of chemiluminescence just before and after measurement hardly decreased, resulting in no shift in the maximum, a part of the spectrum between about 520—590 mμ, centering about the maximum, was repeatedly measured with a sweeping time of 7 sec.; thus it was ascertained that the maximum was at 545 mμ.

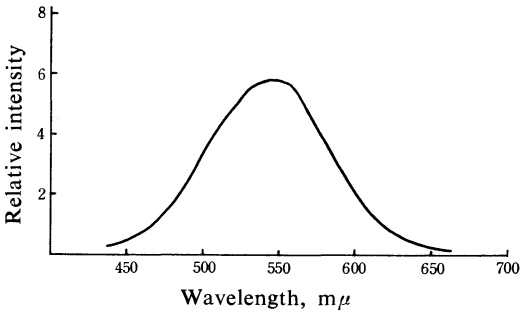



Fig. 1. The chemiluminescence spectrum of lophine in 1 N ethanolic potassium hydroxide ($C=2.81\times10^{-1}$ mol./l.) exhibited by passing oxygen through at 70°C.

The maximum wavelength, 545 mμ, in the chemiluminescence spectrum is more than 100 mμ longer the maximum wavelength, 441mμ, in the fluorescence spectrum of lophine and that, 440 mμ, of the fluorescence spectrum of benzoic acid, which is a product of the chemiluminescence of lophine. Therefore, the chemiluminescence of lophine is neither the fluorescence of lophine nor the fluorescence of benzoic acid. It is most likely a radiation emitted from some substance in an excited state which is probably produced by reactions involving the 2,4,5-triphenylimidazolyl radical produced from lophine and molecular oxygen. We now study the constitution of the intermediate compound emitting luminescence.

When a 1 N ethanolic potassium hydroxide solution of lophine was heated at 70°C on a water bath while being stirred by a stream of oxygen in the light, fine colorless crystals gradually appeared in the solution and ammonia was detected with a Nessler reagent in 0.1 N sulfuric acid by which the oxygen which had passed through the solution of lophine was washed. The fine crystals which separated were identified as potassium benzoate. In addition to benzoate and ammonia, sometimes a small quantity of fine colorless needles was isolated and then recrystallized from ethanol as fine needles, m. p. 231—232°C. This compound was identified as 2,4,6-triphenyl-1,3,5-triazine (cyaphenine). It was also obtained when chemiluminescence was exhibited with

ethanolic solution of bromine, its yield increasing when the solution of lophine was saturated with ammonia before the addition of bromine. These facts, and the formation of lophine by the reduction of cyaphenine with zinc dust in acetic acid,[4] suggest the formation of cyaphenine on the chemiluminescence is likely to be due to a reaction involving lophine and ammonia produced by the oxidation of lophine on the cheminescence.

The chemiluminescence spectrum with a 3% aqueous solution of hydrogen peroxide at 70°C was also measured with the recording spectrophotometer. Two milliliters of hydrogen peroxide heated at 70°C was quickly stirred into a solution of 0.72 g. of lophine in 12 ml. of 1 N ethanolic potassium hydroxide ($C=2.04\times10^{-1}$ mol./l.) heated at 70°C in the tube used for the measurement of the spectrum with oxygen; the spectrum was then immediately recorded. It spreads over 480—650 m$\mu$, with a maximum at 555 m$\mu$. When a 1 N ethanolic potassium hydroxide solution containing 0.5 g. lophine was heated at 70°C with 3% hydrogen peroxide for about 30 min. in another experiment, benzoic acid (0.3 g.) and ammonia were produced.

The measurement of the chemiluminescence spectrum with bromine was unsuccessful because of coloration by bromine. However, an important clue to the mechanism of chemiluminescence of lophine was obtained. When an ethanolic solution of bromine was added very slowly, drop by drop, to a hot solution of lophine in ethanolic potassium hydroxide without stirring, a reddish-purple color at once appeared around the part where a drop of a bromine solution was added; this color rapidly disappeared however, with the formation of a white precipitate, which was identified as potassium bromide. When a similar experiment was carried out in a dark room, chemiluminescence was observed around the part where a drop of a solution of bromine was added. The part where chemiluminescence was observed obviously corresponded to that where a reddish-purple color had appeared. In the chemiluminescence of lophine with a 2% aqueous solution of potassium ferricyanide, a reddish-purple color also appeared. When the dissolved oxygen in the solutions was removed, no chemiluminescence was observed, although the reddish-purple color appeared with the addition of bromine or potassium ferricyanide. Therefore, molecular oxygen was necessary for the chemiluminescence with bromine or potassium ferricyanide. From these facts and some other investigations concerning this coloration,[7] it was established that the reddish-purple color was due to the 2, 4, 5-triphenylimidazolyl radical produced by the oxidation of the lophine anion with bromine or potassium ferricyanide, and that the disapperance of the color was due to the combination of the free radical with oxygen in the solution to form an adduct which was probably in the following illuminating stage. The 2, 4, 5-triphenylimidazolyl radical was reasonably considered to be the intermediate also in the chemiluminescence with oxygen or hydrogen peroxide, although no reddish-purple color was observed in these cases.

**The Fluorescence Spectra of Lophine.** — The fluorescence spectra of lophine were measured at 20°C in ethanolic potassium hydroxide, in ethanol, and in ethanol containing acetic acid. In order to exclude a shift of the maximum of a spectrum by the oxidation of lophine, the dissolved oxygen in the solution was removed by a stream of nitrogen previously. The fluorescence spectra of lophine are shown in Fig. 2.

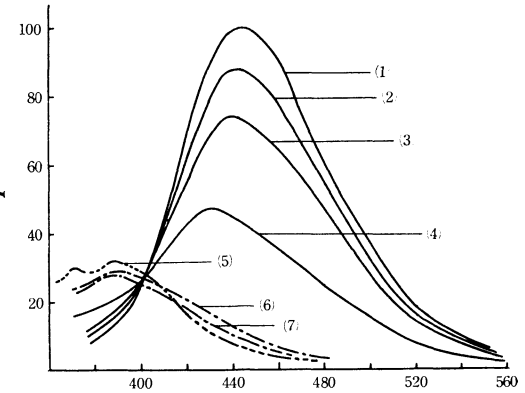



Fig. 2. The fluorescence spectra of lophine in ethanolic potassium hydroxide, in ethanol, and in ethanol containing acetic acid at 20°C.
$I$: relative intensity of fluorescence
Concn. of lophine: $C=4.05\times10^{-5}$ mol./l.
(1) 2 N KOH-$C_2H_5OH$, $\lambda_{max}$ 444 m$\mu$
(2) 1 N KOH-$C_2H_5OH$, $\lambda_{max}$ 441 m$\mu$
(3) 0.2 N KOH-$C_2H_5OH$, $\lambda_{max}$ 439 m$\mu$
(4) 0.02 N KOH-$C_2H_5OH$, $\lambda_{max}$ 432 m$\mu$
(5) $C_2H_5OH$, $\lambda_{max}$ 371 m$\mu$, 388 m$\mu$
(6) 1 N $CH_3COOH$-$C_2H_5OH$, $\lambda_{max}$ 391 m$\mu$
(7) 0.01 N $CH_3COOH$-$C_2H_5OH$, $\lambda_{max}$ 389 m$\mu$

The maximum intensity at 440 m$\mu$ of the fluorescence spectrum of lophine in 0.4 N ethanolic potassium hydroxide varied with the increase in the concentration of lophine at 25°C, as is shown in Fig. 3.

During the measurement of the fluorescence spectrum of lophine, a logarithum of the

7) T. Hayashi and K. Maeda, This Bulletin, 35, 2057 (1962).

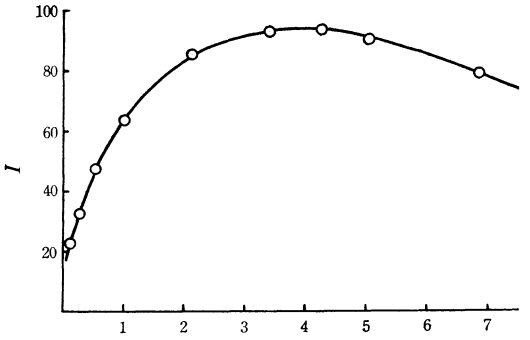



Fig. 3. The effect of the concentration of lophine on the intensity at 440 mμ of the fluorescence spectrum of lophine in 0.4 N ethanolic potassium hydroxide at 25°C.
*I*: relative intensity of fluorescence at 440 mμ
*C*: the concn. of lophine in a solution of 0.4 N ethanolic potassium hydroxide

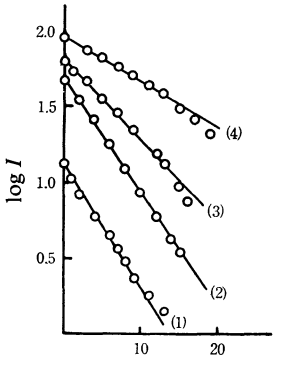



Fig. 4. The decrease with time in relative intensity at 440 mμ of the fluorescence spectrum of lophine in 0.4 N ethanolic potassium hydroxide at 25°C.
*I*: relative intensity of fluorescence at 440 mμ
Concn. of lophine:
(1) $5.05\times10^{-6}$ mol./l. (3) $1.01\times10^{-4}$ mol./l.
(2) $5.05\times10^{-5}$ mol./l. (4) $3.40\times10^{-4}$ mol./l.

maximum intensity at 440 mμ linearly decreased with the time of irradiation, as is shown in Fig. 4. When the dissolved oxygen in the solution was removed by a stream of nitrogen, no decrease in the intensity of fluorescence was observed, but when a stream of oxygen was passed into the solution, the rate of the decrease of fluorescence increased. Hence, the decrease of fluorescence is obviously involved with the oxidation with oxygen, and the rate of decrease is first order with respect to the concentration of oxygen in the solution.

The rate of the decrease of fluorescence was increased when the quantity of light illuminated was augmented by an increase in the area of a window on the wall of a cell containing the solution, but it was hardly affected by a rise in the temperature from 10 to 30°C. Therefore, the oxidation of the lophine responsible for the decrease in fluorescence was likely to be photochemical.

The tendency for the rate of the decrease of fluorescence to decrease with an increasing concentration of lopine, as shown in Fig. 4, can be understood from the relation between the relative intensity of fluorescence and the concentration of lophine which is shown in Fig. 3.

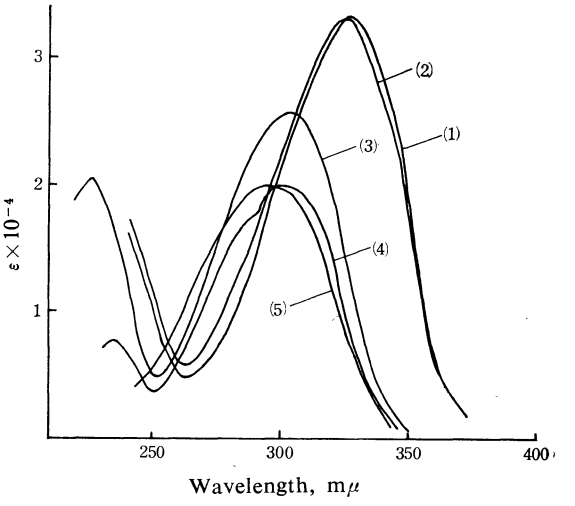



Fig. 5. The absorption spectra of lophine in ethanolic potassium hydroxide, and in ethanolic solutions of acetic acid at 20°C.
Concn. of lophine:
(1) $4.08\times10^{-5}$ mol./l. in 1 N KOH-$C_2H_5OH$
(2) $4.18\times10^{-5}$ mol./l. in 0.1 N KOH-$C_2H_5OH$
(3) $3.91\times10^{-5}$ mol./l. in ethanol
(4) $4.12\times10^{-5}$ mol./l. in 0.1 N $CH_3COOH$-$C_2H_5OH$
(5) $4.13\times10^{-5}$ mol./l. in 1 N $CH_3COOH$-$C_2H_5OH$

When the fluorescence of lophine in such a dilute ethanolic potassium hydroxide as 0.5 N was exhibited with or without a gentle stream of oxygen at room temperature, a small quantity of cyaphenine was isolated from a solution in which fluorescence had nearly ended. When fluorescence was exhibited in a rather concentrated ethanolic potassium hydroxide such as 1.8 N with a stream of oxygen at room temperature, a small quantity of benzoic acid was isolated and ammonia was detected. Cyaphenine was probably formed from lophine and ammonia which had been formed by the oxidation of lophine. Considering the facts that cyaphenine was very weakly fluorescent in the solution and that benzoic acid was also

weakly fluorescent, the decrease in the intensity of the fluorescence of lophine with time may be attributed to the photochemical oxidation of lophine with oxygen to give benzoic acid and ammonia.

**The Absorption Spectra of Lophine.** — The absorption spectra of lophine were measured in ethanol, in ethanolic potassium hydroxide, and in ethanolic solution of acetic acid at 20°C. The spectra are shown in Fig. 5.

The absorption maximum, $\lambda_{max}$ 303 m$\mu$ ($\varepsilon = 2.56\times10^4$), in ethanol was shifted to 326 m$\mu$ ($\varepsilon = 3.33\times10^4$) in 1 N ethanolic potassium hydroxide; conversely, 303 m$\mu$ was shifted to 295 m$\mu$ ($\varepsilon = 2.03\times10^4$) in a 1 N ethanolic solution of acetic acid. The shift in ethanolic potassium hydroxide is probably due to the dissociation of the NH of an imidazole ring.

## Summary

The chemiluminescence spectra of 2, 4, 5-triphenylimidazole (lophine) in 1 N ethanolic potassium hydroxide exhibited with oxygen and with hydrogen peroxide at 70°C have been measured. Both spectra spread over about 470—660 m$\mu$; the maximum wavelengths are 545 m$\mu$ and 555 m$\mu$ respectively.

The fluorescence spectra of solutions of lophine have been measured at 70°C. The maximum wavelengths are as follows: 371 m$\mu$, 388 m$\mu$ (ethanol), 441 m$\mu$ (1 N KOH–$C_2H_5OH$) and 391 m$\mu$ (1 N $CH_3COOH$–$C_2H_5OH$).

The absorption spectra of lophine have also been measured: $\lambda_{max}$ 303 m$\mu$ ($\varepsilon = 2.56\times10^4$) in ethanol: $\lambda_{max}$ 326 m$\mu$ ($\varepsilon = 3.33\times10^4$) in 1 N ethanolic potassium hydroxide, and $\lambda_{max}$ 295 m$\mu$ ($\varepsilon = 2.03\times10^4$) in a 1 N solution of acetic acid in ethanol.

The authors wish to express their hearty thanks to Dr. Hiroshi Midorikawa of the Institute of Physical and Chemical Research and Professor Ryojiro Iwaki of Aichi Gakugei University for their kind help, and to the Ministry of Education for the Scientific Research Expenditure Grant given to Mr. Hayashi.

*Department of Chemistry*
*Faculty of Science*
*Ochanomizu University*
*Bunkyo-ku, Tokyo (K.M. & T.H.)*

*Department of Chemistry*
*Aichi Gakugei University*
*Okazaki, Aichi Prefecture (H. O.)*

# The Effect of Sodium Triphosphate on the Nucleation of Strontium Sulfate

By Hiromitu NAONO and Masaji MIURA

(Received July 7, 1964)

Since the patent of Rosenstein[1] was first presented, several investigators[2] have considered the inhibiting action of condensed phosphates on the crystallization of several sparingly soluble inorganic salts from their supersaturated solutions. In our previous papers[3] it has been reported that a supersaturated solution of strontium sulfate is perfectly stabilized for an extended period in the presence of a minute amount of sodium triphosphate. The concentration of the coexisting triphosphate is several hundred times less than that of strontium sulfate, and so the decrease in the concentration of free strontium ions by forming a complex with triphosphate may be regarded as negligibly small, despite the fact that the triphosphate is known to form a stable and soluble complex with strontium ion.[4] Under such conditions, it can not be expected that the concentration of strontium sulfate solution will be so reduced by the addition of triphosphate as to be unable to form nuclei.

In order to explain such observations, it has been proposed by some authors[2] that the phosphate ions are adsorbed on the surface of crystal nuclei born in the solution and that

1) L. Rosenstein, U. S. Pat. 2038316 (1936).

2) G. B. Hatch and O. Rice, *Ind. Eng. Chem.*, **31**, 51 (1939); R. F. Reitemeier and T. F. Buehrer, *J. Phys. Chem.*, **44**, 535, 552 (1940); R. F. Reitemeier and A. D. Ayers, *J. Am. Chem. Soc.*, **69**, 2759 (1947); B. Raistrick, *Discussions Faraday Soc.*, **5**, 234 (1949); E. J. Burcik, *Producers Monthly*, **19**, No. 1 (1954), p. 42.

3) S. Otani, This Bulletin, **33**, 1544, 1549 (1960); M. Miura, S. Otani, M. Kodama and K. Shinagawa, *J. Phys. Chem.*, **66**, 252 (1962); M. Miura, S. Otani, Y. Abe and C. Fukumura, This Bulletin, **36**, 1091 (1963).

4) A. Roppongi and T. Kato, ibid., **35**, 1086 (1962).

they prevent the further growth of nuclei. Our previous investigation[3] has shown that the surface of strontium sulfate particles is completely covered by a monomolecular layer of adsorbed triphosphate in the vicinity of the concentration where the triphosphate exhibits the inhibiting action. This finding seems to indicate that the adsorption plays a predominant role in the action.

According to the above assumption, the number of nuclei should increase rapidly and, after an extended period, a large number of the nuclei should be accumulated in the supersaturated solution, while the growth of nuclei is prevented by the triphosphate adsorbed on them. Contrary to these expectations, however, a small number of large, distorted crystals of strontium sulfate were found to be deposited by the supersaturated solution when the concentration of triphosphate is slightly lower than that which makes the supersaturated solution stable. Therefore, there still remain some problems to be solved concerning the major effect of triphosphate on the nucleation of some inorganic salts.

In this paper, two physico-chemical methods are employed to investigate and clarify the problems described above: (1) a light-scattering study of the supersaturated solution of strontium sulfate stabilized in the presence of triphosphate, and (2) a study of the nucleation rate of strontium sulfate from its supersaturated solutions containing various amounts of triphosphate.

## Experimental

**Materials.**—The special grade reagents of strontium chloride and potassium sulfate were further purified by recrystallizing them from aqueous solutions. The method of the preparation and purification of sodium triphosphate has been described previously.[5]

**Light Scattering.**—The light-scattering measurements were performed at 25°C using a Shimadzu light-scattering photometer. All the solutions used in this work were filtered by a Cerafilter (its average pore diameter was 100—200 m$\mu$). The values of the turbidity and of the dissymmetry coefficient of water were $5.4\times10^{-5}$ cm$^{-1}$ and $1.00\pm0.01$ respectively at 436 m$\mu$. White light was used in place of monochromatic light in order to increase the intensity of the scattered light. Measurements were carried out in a semioctagonal cell for four samples: (1) 0.04 M $SrCl_2$; (2) 0.04 M $K_2SO_4$ containing $6\times10^{-5}$ M $Na_5P_3O_{10}$; (3) a mixed solution containing equal volumes of solutions (1) and (2), and (4) 0.02 M $SrCl_2$ containing $3\times10^{-5}$ M $Na_5P_3O_{10}$.

**Nucleation Kinetics.**—The rate of nucleation was measured by counting the number of crystals deposited from supersaturated solutions of strontium sulfate containing various amounts of sodium triphosphate. All the solutions used in this experiment were filtered according to the procedure used in the light-scattering measurements.

The supersaturated solution of strontium sulfate was prepared by adding 2.5 ml. of a 0.04 M strontium chloride solution to an equal volume of a 0.04 M potassium sulfate solution which also contained sodium triphosphate, the concentration of which varied from 0 to $3\times10^{-5}$ M. The solution thus obtained was allowed to form nuclei for an appropriate period (nucleation time), during which time the degree of supersaturation remained nearly constant.

Preliminary experiments showed that, in the strontium sulfate solution of the above-described concentration, containing $3\times10^{-5}$ M triphosphate, no crystals were formed for 1500 min., but the crystals placed in the solution grew slowly, although the number of crystals remained constant over the growth period. A solution of the same composition was used in this experiment as a growth medium. After the nucleation was over, the nuclei were transferred into a growth medium of a large volume and left to grow to crystals of a size large enough to be detected under a microscope (the growth time was about 1000 min.). The number of crystals thus grown was counted under a microscope using a Bürker counting room. In order to reduce the counting error, the average value of twenty-five runs was used to calculate the total number of crystals formed during nucleation.

## Results and Discussion

The results of the light-scattering measurements are shown in Tables I, II and III, where $i_\theta$ is the scattering intensity in the $\theta$ direction and $z_{45}$, the ratio of $i_{45}$ to $i_{135}$. As may be seen in Tables I and II, the value of $i_{90}$ for the supersaturated solution stabilized with triphosphate show no appreciable increase with the lapse of time and takes, within the range of experimental error, the same value as that for each solution from which the supersaturated solution is prepared. The nucleation of the solution may, therefore, be almost completely prevented by the presence of triphosphate. In contrast to $i_{90}$, the value of $z_{45}$ for the supersaturated solution changes with time. The two figures in the $z_{45}$ column in Table II indicate the maximum and minimum values for one minute. The fluctuation of the values of $z_{45}$ is mainly due to those of $i_{45}$. Even with the naked eye a small number of particles were observed to move at random by Brownian movement in the path of the incident beam. Scrupulous care was used to eliminate the traces of dusts in the solution, but the fluctuation in the values of $i_{45}$ did not disappear. As is shown in Table III, this phenomenon was not observed in the system containing

5) M. Miura, H. Naono and S. Otani, *J. Chem. Soc. Japan, Ind. Chem. Sec.* (*Kogyo Kagaku Zasshi*), **66**, 593 (1963).

TABLE I. LIGHT SCATTERING RESULTS OF THE SYSTEMS OF $SrCl_2$ (0.04 M) and $K_2SO_4$ (0.04 M)-$Na_5P_3O_{10}$ ($6\times10^{-5}$ M)

| System | $i_{90}$ | $z_{45}$ |
|---|---|---|
| $SrCl_2$ (0.04 M) | 13.5±0.2 | 1.00±0.01 |
| $K_2SO_4$ (0.04 M)-$Na_5P_3O_{10}$ ($6\times10^{-5}$ M) | 13.5±0.2 | 1.00±0.01 |

TABLE II. LIGHT SCATTERING RESULTS OF THE SYSTEM OF $SrCl_2$ (0.02 M)-$K_2SO_4$ (0.02 M)-$Na_5P_3O_{10}$ ($3\times10^{-5}$ M)

| Time min. | $i_{45}$ | $i_{90}$ | $i_{135}$ | $z_{45}$ |
|---|---|---|---|---|
| 20— 21 | 27.6—30.0 | 13.6 | 27.0 | 1.03—1.12 |
| 25— 26 | 27.5—27.8 | 13.6 | 26.8 | 1.03—1.04 |
| 30— 31 | 27.6—28.7 | 13.7 | 27.0 | 1.02—1.06 |
| 38— 39 | 27.2—28.1 | 13.5 | 26.8 | 1.02—1.05 |
| 50— 56 | 28.1—30.5 | 14.0 | 27.6 | 1.02—1.08 |
| 60— 61 | 29.3 | 13.9 | 27.6 | 1.06 |
| 103—104 | 27.8—32.5 | 13.9 | 27.8 | 1.00—1.17 |
| 110—111 | 28.4—32.5 | 13.9 | 27.2 | 1.05—1.19 |
| 330—331 | 28.8 | 13.8 | 27.4 | 1.05 |

TABLE III. LIGHT SCATTERING RESULTS OF THE SYSTEM OF $SrCl_2$ (0.02 M)-$Na_5P_3O_{10}$ ($3\times10^{-5}$ M)

| Time min. | $i_{45}$ | $i_{90}$ | $i_{135}$ | $z_{45}$ |
|---|---|---|---|---|
| 25— 26 | 26.3 | 13.0 | 26.0 | 1.01 |
| 45— 46 | 26.1 | 12.9 | 25.7 | 1.01 |
| 53— 54 | 26.4 | 12.9 | 26.1 | 1.01 |
| 145—146 | 26.6 | 13.2 | 26.4 | 1.01 |
| 153—154 | 26.8 | 13.0 | 26.4 | 1.01 |

both sodium triphosphate and strontium chloride. From these observation it has been concluded that the fluctuation is caused by a small number of crystallites of strontium sulfate formed in the supersaturated solution.

The effect of triphosphate upon the nucleation rate of strontium sulfate is shown in Table IV, where the nucleation rate, $J$, is defined as the rate of nuclei formation per unit volume (ml.) per unit time (sec.). In Fig. 1 the nucleation rate is plotted against the concentration of triphosphate in a log-log scale. The explosive formation of nuclei occurs in the absence of triphosphate, but the nucleation rate is markedly reduced by an increasing concentration of triphosphate. Within the concentrations of triphosphate ranging from $0.2\times10^{-5}$ M to $1.5\times10^{-5}$ M, the curve in Fig. 1 obeys the equation:

$$J=Kc^{-9.5}$$

where $K$ is a constant and $c$, the molar concentration of triphosphate. The equation shows that a tenfold increase in the concentration of triphosphate reduces the nucleation rate to approximately one-several thousand millionth.

TABLE IV. INFLUENCE OF TRIPHOSPHATE ON THE NUCLEATION RATE OF STRONTIUM SULFATE

| Concn. of triphosphate, M | Nucleation time, sec. | Nucleation rate ($J$) |
|---|---|---|
| 0 | 10 | $(8\ \pm3\ )\times10^{6}$ |
| $2.0\times10^{-6}$ | 30 | $(2.0\pm0.7)\times10^{6}$ |
| $5.0\times10^{-6}$ | 100 | $(1.0\pm0.5)\times10^{3}$ |
| $1.0\times10^{-5}$ | 180 | $(1.5\pm0.6)\times10^{-1}$ |
| $1.5\times10^{-5}$ | 600 | $(5\ \pm1\ )\times10^{-3}$ |

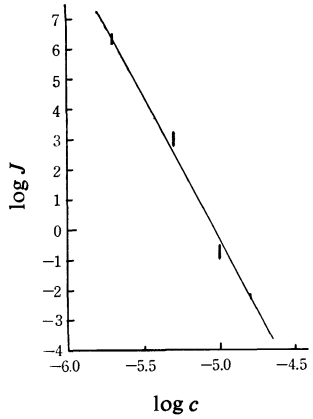



Fig. 1. Relation between the nucleation of strontium sulfate and the concentration of triphosphate.

It is now clear from these results that the minute amount of triphosphate greatly supresses the nucleation of strontium sulfate. In the previous papers of our laboratory[3,5] it was reported that the inhibiting action of condensed phosphates was closely related to the adsorption of phosphates onto the crystal surface in the cases of strontium sulfate and calcium carbonate.

By combining the finding concerning light scattering and the nucleation rate with those of adsorption, we may consider that the clusters of strontium sulfate with the embryonic dimension which are generated in the supersaturated solution may be broken into separated ions by the adsorption of triphosphate and that such a probability increases with the increase in the concentration of triphosphate.

## Summary

The nucleation from supersaturated solutions of strontium sulfate containing various amounts of triphosphate has been investigated by means of light scattering and nucleation kinetics. The nucleation rate is remarkably reduced by the increase in the concentration of triphosphate and may be represented by an empirical expression, $J=Kc^{-9.5}$. Light-scattering measurements have confirmed that practically no

nucleation occurs in the supersaturated solution stabilized in the presence of triphosphate.

The authors wish to express their thanks to Dr. Otani for his helpful discussions.

*Department of Chemistry*
*Faculty of Science*
*Hiroshima University*
*Hiroshima*

# On the Parameterization in the Semi-Empirical LCAO MO Method

By Takeshi NAKAJIMA

(Received July 10, 1964)

Although in the last decade Pariser and Parr's semi-empirical LCAO MO method[1] has been extensively and successfully used for the prediction of the electronic spectra of unsaturated molecules,[2] its applicability to the description of the ground-state electronic properties has not yet been clearly established. In fact, as will be shown in this paper, Pariser and Parr's approximation, with its original parameterization, if applied to benzene, gives the unexpected result that a skew structure ($D_{3h}$) is energetically favored as compared with the symmetric one ($D_{6h}$). In this paper we will, then, point out the origin of such an absurd result and propose a new parameterization applicable to the calculation of ground-state electronic properties as well as to the spectral calculation.

## The SCF-MO's of Benzene

The Pariser and Parr approximation, with its original parameterization, is applied to benzene in conjunction with the self-consistent field technique of Roothaan.[3] In computing interaction terms for adjacent atoms, the internuclear distances were predicted at each step of the iterative process from the $\pi$-bond orders, $p$, using the formula:[4]

$$r\,(\text{in Å}) = 1.520 - ap \tag{1}$$

with

$$a = 0.186 \tag{2}$$

However, nonneighbor internuclear distances were calculated by assuming the ring to be regular, with all bonds of an equal length (1.397Å). The Coulomb repulsion integrals $(pp/qq)$ were evaluated using the procedure of Pariser and Parr, and the core resonance integrals, $\beta$, for various distances were obtained from the Pariser and Parr curve;

$$\beta(r) = \beta_0 \exp[b(1.39 - r)] \tag{3}$$

with

$$\beta_0 = -2.39\ \text{eV. and}\ b = 5.6864\ \text{Å}^{-1} \tag{4}$$

The starting molecular orbitals used were of the Hückel type.

For the symmetric benzene ($D_{6h}$), the SCF-MO's are given directly by the Hückel type orbitals and are independent of parameterization. It is particularly noteworthy that the use of the above parameterization results also in the achievement of a self-consistency of molecular orbitals for an asymmetric benzene with the $D_{3h}$ molecular symmetry. The obtained self-consistent bond orders for the skew benzene indicate that the bond lengths vary considerably, the length of the shorter bonds being 1.347Å and that of the longer bonds 1.465Å. The refinement of the values of the Coulomb repulsion integrals (vide infra) leads to a further increase in skewness.

Now let us enquire which of the symmetric and asymmetric structures is more favorable in energy. It has been recognized[5,6] that a conclusion regarding the stability or the equilibrium configuration of a conjugated molecule cannot be based on $\pi$-electron calculations only; allowance for the effects of the $\sigma$-bond compression must also be made. Unfortunately, there is at present no theoretical method of estimating the $\sigma$-bond compression energy in the same degree of approximation as Pariser-Parr's. Longuet-Higgins and Salem's modification[5] of the Hückel MO theory is adopted here to obtain an estimate of the desired difference in energy between the two structures. According to Longuet-Higgins and Salem, the total binding energy of a conjugated molecule,

1) R. Pariser and R. G. Parr, *J. Chem. Phys.*, **21**, 446, 767 (1953).
2) R. G. Parr, "The Quantum Theory of Molecular Electronic Structure," W. A. Benjamin, New York (1963).
3) C. C. J. Roothaan, *Rev. Mod. Phys.*, **23**, 69 (1951).
4) T. Nakajima and S. Katagiri, *Mol. Phys.*, **7**, 149 (1963).
5) H. C. Longuet-Higgins and L. Salem, *Proc. Roy. Soc.*, **A251**, 172 (1959).
6) C. A. Coulson, *Tetrahedron*, **12**, 193 (1961); C. A. Coulson and A. Golebiewski, *Mol. Phys.*, **5**, 71 (1962).

taken to be the sum of the $\pi$-bond energy and the $\sigma$-bond energy, is given by:

$$V=E_\pi+E_\sigma=\sum_{p<q}2\int(\mathrm{d}p_{pq}/\mathrm{d}r)\bar{\beta}_{pq}(r)\mathrm{d}r \qquad (5)$$

where $\bar{\beta}(r)$, the resonance integral parameter in the Hückel MO theory, is interpreted as an "effective resonance integral" which includes an electron interaction term; it is assumed to be given as:*

$$\bar{\beta}_{pq}(r)=[2\beta_{pq}(r)-(p_{pq}/2)(pp/qq)]/2 \qquad (6)$$

Then, using Eqs. 1—4 and the Pariser and Parr quadratic formula:

$$(pp/qq)=0.2157r^2-2.625r+10.53 \qquad (7)$$

and integrating Eq. 5, we obtain:

$$V=\sum_{p<q}[1.8909\beta_{pq}(r)-0.7794r^4+14.2252r^3-104.9285r^2+231.3215r]+\text{const.} \qquad (8)$$

where the last term is the constant of integration, which is canceled in estimating the desired difference in $V$.

The total energy values thus calculated for the two structures indicate that the skew structure is more favorable in energy than the symmetric one, the deformation energy which favors the skew structure being 0.29 eV.—about 7 kcal./mol.—an appreciable amount.

## Stable Configurations in the $(4n+2)$ Cyclic Polyenes

In order to investigate the cause of the unreasonable results above, let us now examine the equilibrium configurations with respect to bond length distortion in cyclic polyenes generally having $(4n+2)$ carbon atoms. The Longuet-Higgins and Salems modification of the Hückel MO theory is again adopted to estimate the change in energy caused by the distortion.

At the outset, we define the bond alternation parameter, $k$, as

$$k=\bar{\beta}_\mathrm{s}/\bar{\beta}_\mathrm{d} \qquad (9)$$

where the subscripts s and d indicate the single and double bonds in an unexcited Kekulé structure respectively. As was taken in Longuet-Higgins and Salem's original theory, $\bar{\beta}(r)$ is now assumed to vary exponentially with $r$:

$$\bar{\beta}(r)=\bar{\beta}_0\exp[\bar{b}(1.39-r)] \qquad (10)$$

The total electronic energy, taken to be the sum of the $\pi$-bond energy and the $\sigma$-bond energy, is then given by:

$$V=(2/a\bar{b})\sum_{p<q}\bar{\beta}_{pq}(r)+\text{const.} \qquad (11)$$

For a given molecule, using Eqs. 1, 10 and 11, we can calculate the total electronic energies for various $k$ values (0—1), and the $V$-$k$ curve can be obtained.

The static equilibrium configurations of a given molecule are then given by the points of the $V$-$k$ curve where $\partial V/\partial k=0$; namely,

$$\exp[a\bar{b}(p_\mathrm{s}-p_\mathrm{d})]=k \qquad (12)$$

where

$$p_\mathrm{s}-p_\mathrm{d}=\sum_{l=-n}^{n}(k-1)\left(1-\cos\frac{2\pi l}{2n+1}\right)\Big/(2n+1)\left(1+2k\cos\frac{2\pi l}{2n+1}+k^2\right)^{1/2} \qquad (13)$$

It should be noted that Eq. 12 is nothing but the condition for the self-consistency of MO's with respect to $k$.

From Eq. 13 it follows at once that Eq. 12 is always satisfied by the point $k=1$, regardless of the value of $n$. It may be shown further that the sign of $(\partial^2V/\partial k^2)_{k\to1}$ coincides with that of the quantity:

$$A=1-a\bar{b}[\partial(p_\mathrm{s}-p_\mathrm{d})/\partial k]_{k\to1} \qquad (14)$$

where

$$[\partial(p_\mathrm{s}-p_\mathrm{d})/\partial k]_{k\to1}=\left(\frac{1}{2n+1}\right)\sum_{l=-n}^{n}\left|\sin\frac{\pi l}{2n+1}\tan\frac{\pi l}{2n+1}\right| \qquad (15)$$

Thus, if $A\geqq0$, the configuration $k=1$ is one of stable equilibrium, but if $A>0$, though it is one of static equilibrium, the configuration $k=1$ is one of unstable equilibrium. In the latter case a stable equilibrium is given by a point $k<1$, one in which $\partial V/\partial k=0$ and $\partial^2V/\partial k^2>0$.

For benzene the symmetric configuration with $k=1$ should, of course, be one of stable equilibrium. This yields

$$a\bar{b}\leqq1 \qquad (16)$$

This condition severely restricts our choice of $\bar{b}$ value, the value of $a$ being fairly narrowly determined empirically.

As was pointed out in the preceding section, the Pariser and Parr approximation, if applied to benzene, brings about the conclusions that the SCF MO's are achieved for the two symmetry types and that a skew structure is energetically favored as compared with the symmetric one. It is now clear that this absurd result is due to too large a value of $b$

* The resonance integral parameter, $\bar{\beta}_{pq}$, in the simple Hückel MO theory should explicitly be considered to be the arithmetic mean of the core resonance integral, $\beta_{pq}$, and the corresponding Fock matrix element, $\beta^\mathrm{F}_{pq}$ $(=\beta_{pq}-(p_{pq}/2)(pp/qq))$. If $\bar{\beta}_{pq}$ is interpreted merely as $\beta^\mathrm{F}_{pq}$, electron interactions are included twice in the total $\pi$-electronic energy.[7]

7) R. Daudel, R. Lefebvre and C. Moser, "Quantum Chemistry," Interscience, New York (1963), p. 303.

having being assigned by Pariser and Parr in their original parameterization. In fact, if we rewrite Eq. 6 in an approximately exponential form like Eq. 10, using the Pariser and Parr parameterization, the value of $\bar{b}$ turns out to be about $7\text{Å}^{-1}$,* which does not satisfy Eq. 16 when multiplied by $a=0.186$.

## A Refined Parameterization

Pariser and Parr's $b$ value was determined from $\beta$ values so adjusted as to reproduce the observed excitation energies of ethylene and benzene. Actually, at the time of the original development of the Pariser and Parr method the bond lengths of these molecules were not accurately known. In order to improve the $b$ value, we follow Pariser and Parr's procedure but use the recently observed bond lengths, 1.333 Å for ethylene[8] and 1.397 Å for benzene.[9] Moreover, the one-center electronic repulsion integral, given in the Pariser and Parr theory as $I_c-A_c$ is taken to be $11.54-0.46=11.08$ eV.[10] The two-center repulsion integrals were determined by the normal extrapolation procedure of Pariser and Parr.

Thus, adjusting the $\beta$ values of ethylene and benzene to fit the observed spectra, we obtain:

$$\beta(1.333\text{Å})=-2.80\text{ eV}. \quad (17)$$

and

$$\beta(1.397\text{Å})=-2.38\text{ eV}. \quad (18)$$

From these, we obtain $b=2.5801\text{Å}^{-1}$.* This value of $b$ is considerably smaller than Pariser and Parr's original value, and for benzene for use of this $b$ value results in the achievement of self-consistency only for the symmetric configuration. Furthermore, for butadiene the SCF MO's obtained by using the new parameterization lead to a good reproduction of experimental bond lengths and spectral data; the bond lengths for the double and single bonds are predicted to be 1.34 and 1.47 Å respectively, and the lowest singlet excitation energy is calculated to be 6.0 eV. If we rewrite Eq. 6 in an exponential form like Eq. 10, using the $b$ value obtained above, the value of $\bar{b}$ turns out to be about $4.5\text{Å}^{-1}$, which satisfies Eq. 16, and which is in good agreement with the value $4.5988\text{Å}^{-1}$,[4] which was determined by reference to the observed bond length alternation in butadiene. The latter $\bar{b}$ value has been successfully used in accounting for the ground-state electronic properties and electronic spectra of fundamental nonbenzenoid aromatic hydrocarbons.[12-14],**

*Department of Chemistry*
*Ibaraki University*
*Watari-cho, Mito*

* The SCF MO's obtained above for the skew benzene correspond to the MO's calculated by the simple Hückel method with $k=0.45$. To the degree of approximation, self-consistency is achieved for configurations with a static equilibrium, and for the skew benzene the $V$-$k$ curve should have a minimum at the point $k=0.45$. We obtain such a curve if we set $\bar{b}=6.7712\text{Å}^{-1}$, using $a=0.186$.

8) L. S. Bartell and R. A. Bonham, *J. Chem. Phys.*, **31**, 400 (1959).

9) A. Langseth and B. P. Stoicheff, *Can. J. Phys.*, **34**, 350 (1956); A. Almenningen, O. Bastiansen and L. Fernholt, *Kgl. Norske Vid. Selsk. Skr.*, No. 3 (1958).

10) H. D. Pritchard, *Chem. Revs.*, **52**, 529 (1955).

* Very recently Allinger[11] has proposed a value of $3.0323\text{Å}^{-1}$ for $b$. Allinger, however, predicted that the skew benzene would be more, though only slightly, stable than the symmetric one.

11) N. L. Allinger, *J. Org. Chem.*, **27**, 443 (1962).

12) T. Nakajima. Y. Yaguchi, R. Kaeriyama and Y. Nemoto, This Bulletin, **37**, 272 (1964).

13) T. Nakajima, "Molecular Orbitals in Chemistry, Physics, and Biology," Ed. by P. O. Löwdin and B. Pullman, Academic Press, New York (1964), p. 457.

14) T. Nakajima, T. Saijo and H. Yamaguchi, *Tetrahedron*, **20**, 2119 (1964).

** Recently Julg[15] has proposed a value of $5.26\text{Å}^{-1}$ for $\bar{b}$. This value was derived from the relation $a\bar{b}=1$ with $a=0.19$.

15) A. Julg, *Tetradron*, **19**, Suppl. 2, 25 (1963).

# The Electronic Spectra of Pyrene, Chrysene, Azulene, Coronene and Tetracene Crystals

By Jiro TANAKA

(Received July 14, 1964)

The theory of molecular exciton developed by Davydov and others has been widely used for the interpretation of the crystal spectrum, and a lot of results have been published which confirm a validity of the theory in general.[1] However, when a molecule has many excited levels, a mixing of excited states may occur between weak, medium and strong intensity bands and a spectrum may became so complicated that a simple correlation cannot be made between molecular and crystalline absorption bands.

In the present paper the electronic absorption spectra of single crystals of pyrene, chrysene, azulene, coronene and tetracene are reported in an attempt to affirm the theory; a particular effort will be made to find the mechanism of the intermolecular electronic interaction of the excited states in crystals.

The hydrocarbons cited above are characterized by having many strong absorptions in the near ultraviolet and relatively lower ionization potentials. The dipolar interaction between the excited levels might be very strong in such crystals, and the charge transferred level will be located at a relatively low energy region. The band splittings and intensities are calculated by including the configuration interaction between several excited states, and the results are compared with observed absorption bands.

Although the general features of the spectra can be explained very well, a discrepancy is noticed with some crystals, particularly in the intensities of very strong and very weak bands. The strong band is weakened and the weak band is strengthened more than would be expected from the dipole-dipole interaction scheme. The hypochromism of the stronger band may arise from the interaction with the ionization continuum level, and the hyperchromism of the weaker band may occur as a result of the higher order interaction with allowed transitions. Also the calculated splitting of some crystals does not agree completely

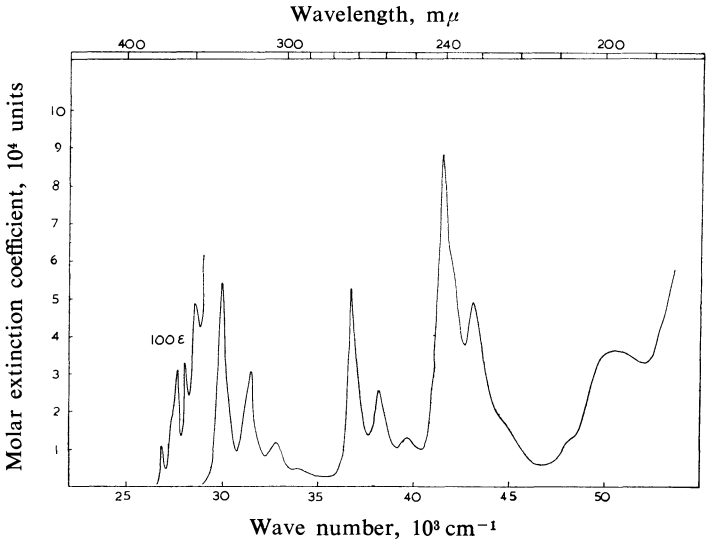



Fig. 1. Absorption spectrum of pyrene in *n*-heptane.

1) D. S. McClure, *Solid State Physics*, **8**, 1 (1958); J. Tanaka, *Prog. Theoret. Phys., Suppl.*, **12**, 183 (1959); A. S. Davydov, "Theory of Molecular Exciton" (translated by M. Kasha and M. Oppenheimer, Jr.), McGraw-Hill, New York (1962); D. P. Draig and S. H. Walmsley, "Physics and Chemistry of the Organic Solid State," Vol. I, Ed. by Fox, Labes and Weissberger, Interscience Publishers, New York (1963), p. 586.

with the experimental results; this may suggest a need for more elaborate calculations, including that of the electron overlap effect.

## Experimental

The ultraviolet and visible spectra of *n*-heptane solutions were measured by a Cary recording spectrophotometer, model 14. The crystal spectra were measured by an ultraviolet microspectrophotometer described in a previous paper.[2] All the samples were purified by recrystallization or chromatography, followed by sublimation. The thin crystals suitable for spectral measurement were prepared by sublimation. The thicknesses of these crystals were roughly estimated by means of the interference color as seen under a polarization microscope.

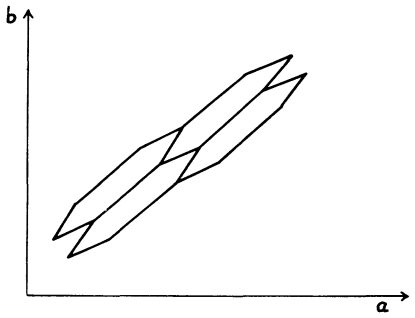



Fig. 2 (a). Projection of pyrene molecule onto the (001) plane.

## Pyrene

Five absorption bands have been observed in a *n*-heptane solution, as Fig. 1 and Table I show. Ham and Rudenberg[3] predicted that transitions to the $^1L_b$ and $^1B_a$ states are possible along the short-axis (M-axis) of the molecule, while the $^1L_a$ and $^1B_b$ transitions are active along the long-axis (L-axis). The crystalline spectrum (Fig. 2 (b)) has been recorded using a crystal about 0.4 $\mu$ thick* through the (001) plane and with a light polarized along the a- and b-axes. The projection of the molecules onto the (001) plane, based on the X-ray crystal analysis results of Robertson and White,[4] is shown in Fig. 2 (a). The wave functions of the crystalline exciton state are given by the following formula for each excited state:

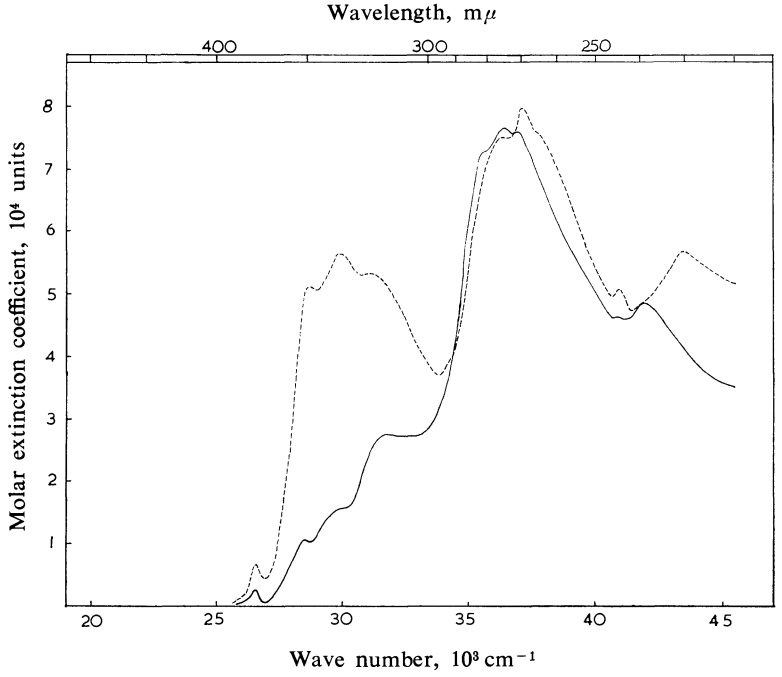



Fig. 2 (b). Polarized absorption spectrum of pyrene crystal.
—— The light polarized parallel to the b-axis
---- The light polarized parallel to the a-axis

2) J. Tanaka, This Bulletin, **36**, 833 (1963).

* The thickness of the crystal is estimated by means of the retardation color, assuming that the birefringence between the a- and b-axes is 0.125.

3) N. S. Ham and K. Rudenberg, *J. Chem. Phys.*, **25**, 14 (1956).

4) J. M. Robertson and J. G. White, *J. Chem. Soc.*, **1947**, 358.

TABLE I. ABSORPTION BANDS OF PYRENE

| | Solution | | | Crystal (Observed) | | | | Crystal (Calculated) | | | |
|---|---|---|---|---|---|---|---|---|---|---|---|
| | $cm^{-1}$ | $f$ | $\mu$, Å | a-axis | b-axis | splitting | $f_a : f_b$ (d. r.)* | a-axis | b-axis | splitting | $f_a : f_b$ (d. r.) |
| $^1L_b$ | 26880<br>27400<br>28050<br>28580 | 0.0016 | 0.074 | 26600 | 26600 | 0 | 0.0019 : 0.0011<br>(1.7 : 1.0) | 26884 | 26883 | 1 | 0.0015 : 0.0011<br>(1.35 : 1.0) |
| $^1L_a$ | 29920<br>31500<br>32850<br>34000 | 0.15<br>0.12<br>0.06 | 0.68<br>0.59<br>0.39 | 28570<br>29760<br>(31056)**<br>(31447) | 28328<br>29630<br>(31250)<br>(31847)<br>(32787) | 242<br>130<br>−200 | 0.12 : 0.03<br>(4.2 : 1.0) | 30158<br>31728<br>32968 | 29909<br>31485<br>32840 | 249<br>243<br>128 | 0.193 : 0.026<br>(7.4 : 1.0) |
| $^1B_a$ | 36710<br>38170<br>39700 | 0.35 | 0.935 | 35700<br>37070<br>37624 | 35138<br>36600<br>37067 | 562<br>470<br>563 | 0.20 : 0.19<br>(1.05 : 1.0) | 37395 | 37285 | 100 | 0.412 : 0.315<br>(1.3 : 1.0) |
| $^1B_b$ | 41480<br>43100<br>50500 | 0.85 | 1.36 | 42000 | 39500<br>40300 | 1700 | 0.15 : 0.12<br>(1.2 : 1.0) | 42826 | 41795 | 1020 | 0.58 : 0.43<br>(1.35 : 1.0) |

* d. r. is an abbreviation for the dichroic ratio.
** Those bands are regarded as the charge-transfer transitions.

$$\left.\begin{aligned}\Psi^{\alpha} &= \frac{1}{\sqrt{4N}}\Big(\sum_{i=1}^{N}\phi_{1i}' - \sum_{j=1}^{N}\phi_{2j}' \\ &\quad - \sum_{k=1}^{N}\phi_{3k}' + \sum_{l=1}^{N}\phi_{4l}'\Big); \quad B_u \\ \Psi^{\beta} &= \frac{1}{\sqrt{4N}}\Big(\sum_{i=1}^{N}\phi_{1i}' - \sum_{j=1}^{N}\phi_{2j}' \\ &\quad + \sum_{k=1}^{N}\phi_{3k}' - \sum_{l=1}^{N}\phi_{4l}'\Big); \quad A_u\end{aligned}\right\} \quad (1)$$

where $\phi_{1i}'$ denotes the excited state in which the 1st site molecule in the $i$-th cell is excited while the others are in the ground state. The coordinate of the molecule on each site is chosen following the notation of the International Table,[5] namely, 1 $(x, y, z)$, 2 $(\bar{x}, \bar{y}, \bar{z})$, 3 $(1/2-x, 1/2+y, \bar{z})$ and 4 $(1/2+x, 1/2-y, z)$. The first-order energy levels are given by Eq. 2 for each excited state:

$$\left.\begin{aligned}&E^{\alpha} = E_0 + V_{11} - 1/2V_{12} - 1/2V_{13} + 1/2V_{14} \\ &E^{\beta} = E_0 + V_{11} - 1/2V_{12} + 1/2V_{13} - 1/2V_{14} \\ &V_{kl} = \\ &\sum_{i=1}^{N}\int \phi_k^{*\prime}(1)\phi_{li}^{*}(2)\, V\phi_k(1)\phi_{li}'(2)\mathrm{d}\tau_1\mathrm{d}\tau_2\end{aligned}\right\} \quad (2)$$

where $E_0$ indicates the energy of the molecular excited state, including a small shift due to interaction between the excited state and the ground state. $V$ is the intermolecular potential, $\phi_k$ and $\phi_k'$ represent the ground- and the excited-state wave function of the $k$-th site molecule, and $\phi_l$ and $\phi_l'$ are those of $l$-th site molecule.

Actually, we have taken only the dipole-dipole interaction term, and the calculations have been carried out by the method of direct summation over molecules inside the restricted radius sphere. The ISSP Facom 202 computer has been used; the results are shown in Appendix I. It may be seen that the value obtained by the summation over a 30Å radius sphere is very close to the value of a 50Å radius sphere. Craig and Walmsley[1] published the results of similar calculations by the Ewald-Kornfeld's method; it is very interesting that the present results are in good agreement with their values in spite of the different computational procedures. The convergence of a direct summation seems to be sufficient if we take the summation within a 50Å radius sphere.

Since we are considering four excited levels in the present case, it might be necessary to calculate the second order interaction between those levels. The secular equation is given by:

$$\left.\begin{aligned}&\mathrm{Det}\,|H_{rs} - E\delta_{rs}| = 0 \\ &H_{rs} = \int \Psi_r{}^{\alpha} H \Psi_s{}^{\alpha}\,\mathrm{d}\tau, \\ \text{or}\quad &H_{rs} = \int \Psi_r{}^{\beta} H \Psi_s{}^{\beta}\,\mathrm{d}\tau \\ &H = H_0 + V,\ \delta_{rs} = 1 \text{ when } r = s, \\ &\delta_{rs} = 0 \text{ when } r \neq s\end{aligned}\right\} \quad (3)$$

where $H$ indicates the total Hamiltonian of the system, and $\Psi_r$ and $\Psi_s$ represent the $r$-th and $s$-th excited levels ($^1L_b$, $^1L_a$, $^1B_a$ or $^1B_b$ states). The interaction between $B_u$ and $A_u$-type functions vanishes for symmetry reasons. The diagonal element is taken as a first-order

5) "International Tables for X-ray Crystallography," Vol. I, Kynoch Press, Birmingham (1959).

exciton energy calculated by Eq. 2, while the off-diagonal term is calculated by a similar equation using the dipole approximation. For the $^1L_a$ band we have considered three vibrational levels separately; this implies a weak coupling between the $^1L_a$ state and other states. The secular equation is shown in Appendix II. Solving this equation, the wave function for the $L$-th crystal excited state is obtained as a linear combination of excited states $\Psi_r$:

$$\Psi_L{}^\alpha = \sum a_r \Psi_r{}^\alpha, \qquad \Psi_L{}^\beta = \sum b_r \Psi_r{}^\beta \tag{4}$$

and the transition moment, say, to the $\alpha$ state is given by a sum of the composite transition moments projected along the particular crystalline axis:

$$M_{OL}{}^\alpha = \int \Psi_0{}^* \boldsymbol{r} (\sum a_r \Psi_r{}^\alpha) \mathrm{d}r = \sum a_r M_{or} \cos\theta_{ar} \tag{5}$$

where $M_{or}$ is the magnitude of the transition moment to the $r$-th state, and $\theta_{ar}$ is the angle between the transition moment and the a-axis. The oscillator strength of the crystalline absorption band is calculated by Eq. 6:

$$f_{OL} = 3.25 \times 10^{-5} \times \nu \times (M_{OL}{}^\alpha)^2 \tag{6}$$

The second-order perturbation effect for the ground state (van der Waals force) has been disregarded. The results of the calculation are given in Table I and Fig. 3.

At room temperature the observation of the band splitting is not very feasible, but it may be clearly seen in Fig. 2(b) that both the $^1L_a$ and $^1B_a$ bands show appreciable splittings. By comparing the calculated intensity ratio with the observed spectrum, it is easy to prove the theoretical results of Ham and Rudenberg concerning the polarization of the bands. The first $^1L_b$ band, the weakest of all, might be influenced by the nearby stronger transition, and it shows the dichroic ratio $D_a : D_b = 1.7 : 1.0$, while the second-order calculation value is 1.35 : 1.0. The oriented gas value (the zeroth and first-order approximation) of 1.0 : 1.0 is improved by the second-order calculation, and it is almost certain that the $^1L_b$ state is short-axis polarized. The conclusion is in agreement with the earlier findings of Ferguson.[6]

The $^1L_a$ band shows four or more vibrational structures in the crystalline spectrum, the first and the second peaks being split about 240 $cm^{-1}$ and 130 $cm^{-1}$. The calculated values, 249 $cm^{-1}$ and 243 $cm^{-1}$ respectively, are in excellent agreement with the observed values. The splittings of the third and fourth peaks are reversed in sign; therefore, it might be possible that those peaks have a different origin. The charge-transfer transition might be very probable in such a crystal as pyrene, where molecules are placed in pairs, and it has been observed in the case of perylene.[7] The fluorescence of pyrene crystal has been established to originate from an excited dimeric state,[6] and the corresponding absorption should exist at a higher energy region. Following the recent theory of Murrell and Tanaka[8] on the spectra of the pyrene dimer, it is expected that the intermolecular charge-transfer band will appear in the 30000 $cm^{-1}$ spectral region when molecular planes are separated by about 3.5 Å. Therefore, the band near the 31000 $cm^{-1}$ region is regarded as charge-transfer band overlapped with the progression of the $^1L_a$ band. The polarization of the $^1L_a$ band is deduced from the dichroic intensity ratio to be long-axis, because the observed value of 4.2 : 1.0 is close to the calculated value of 7.4 : 1.0 (that of the zeroth and first-order value is 5 : 1), while the short-axis assignment will give a value of about 1.0 : 1.0.

The band system at about 35000 $cm^{-1}$ is clearly demonstrated by the intensity relations to be the short-axis polarized band. It shows splittings of 562, 470 and 563 $cm^{-1}$ for each vibrational progression; these values should be compared with the calculated value of 110 $cm^{-1}$ (strong coupling model). The first-order splitting was $-37$ $cm^{-1}$; therefore, the second-order calculation gives the right sign and the correct order of magnitude. The calculated intensity ratio, $D_a : D_b = 1.31 : 1.0$, is in good agreement with the observed value. The $^1B_b$ band is predicted to be at about 40000 $cm^{-1}$, but we see rather weaker absorptions in this region. Presumably the $^1B_b$ band is merged with the transitions to the ionization continuum state, and the original intensity is shared with the

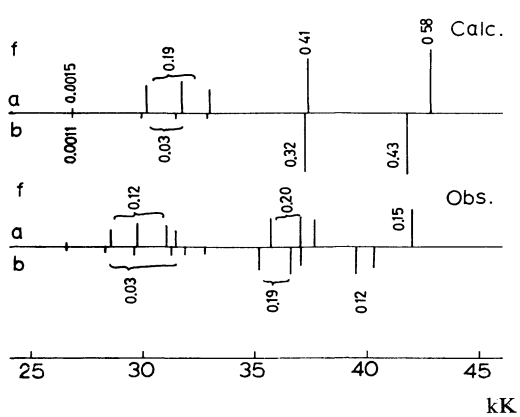



Fig. 3. Calculated and observed band positions of pyrene crystal.

6) J. Ferguson, *J. Chem. Phys.*, **28**, 765 (1958).
7) J. Tanaka, This Bulletin, **36**, 1237 (1963).
8) J. N. Murrell and J. Tanaka, *Mol. Phys.*, **7**, 363 (1964).

band at higher frequencies. The mechanism of this sort of interaction requires further investigation.

The thickness of the crystal could not be determined accurately enough to discuss the accurate value of the intensity of the crystal absorption; however, it seems certain that a hypochromism occurs in the $^1L_a$, $^1B_a$ and $^1B_b$ bands. Contrary to this the $^1L_b$ band intensity is nearly in agreement with the value of the second-order theory. Therefore, the deviations of the absorption intensities of the stronger band should be ascribed to a mechanism which has not been considered in the above treatment.

### Chrysene

Five absorption bands have been found in a *n*-heptane solution (Fig. 4); the band positions are tabulated in Table II, together with the theoretical assignment of Ham and Rudenberg.[3] The crystal structure analysis of chrysene was made by Iball;[9] the projection of molecules onto the (001) plane is pictured Fig. 5(a). The crystalline spectrum has been measured through the (001) plane by a polarized light (Fig. 4(b)). The thickness of the crystal has been estimated to be 0.25 $\mu$ by the use of optical data on the birefringence of Krc.[10] Since we are using a convergent light of a microscope lens, the absolute intensity of a band whose transition moment is vertical to the developed plane might not be accurate enough to discuss the direction of the transition moment on the basis of the dichroic intensity ratio. In the crystal spectrum the intensity is weaker with the light polarized along the a-axis than with that polarized along the b-axis for all absorption bands. Theoretical calculation[3] showed that the strongest $^1B_b$ band is polarized along the long-axis of the molecule and that the long-axis is nearly perpendicular to the b-axis; therefore, it seems to be unreasonable that the $^1B_b$ band is weaker along the a-axis than along the b-axis. This anomaly of intensity relation is clarified by the second-order calculations including interactions between $^1L_b$, $^1L_a$, $^1B_b$ and $^1B_a$ states. The crystal excited-state wave functions which are active along the a- and b-axes are:

$$\left.\begin{aligned}\Psi^{\alpha} &= \frac{1}{\sqrt{4N}}\left(\sum_{i=1}^{N}\psi_{1i}' + \sum_{j=1}^{N}\psi_{2j}' - \sum_{k=1}^{N}\psi_{3k}' - \sum_{l=1}^{N}\psi_{4l}'\right)\\ \Psi^{\beta} &= \frac{1}{\sqrt{4N}}\left(\sum_{i=1}^{N}\psi_{1i}' + \sum_{j=1}^{N}\psi_{2j}' + \sum_{k=1}^{N}\psi_{3k}' + \sum_{l=1}^{N}\psi_{4l}'\right)\end{aligned}\right\} \quad (7)$$

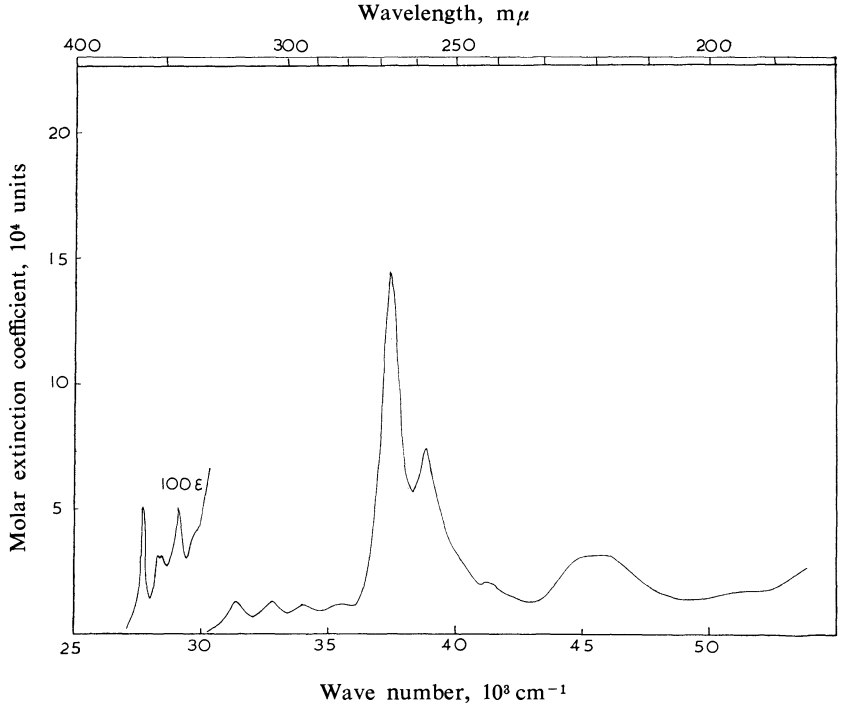



Fig. 4. Absorption spectrum of chrysene in *n*-heptane.

9) J. Iball, *Proc. Roy. Soc.*, **A146**, 140 (1934).

10) J. Krc, Jr., *Anal. Chem.*, **23**, 932 (1951).

TABLE II. ABSORPTION BANDS OF CHRYSENE

| | Solution | | | Crystal (Observed) | | | | Crystal (Calculated) | | | |
|---|---|---|---|---|---|---|---|---|---|---|---|
| | $cm^{-1}$ | $f$ | $\mu$ | a-axis | b-axis | splitting | $f_a : f_b$ (d. r.) | a-axis | b-axis | splitting | $f_a : f_b$ (d. r.) |
| | 27730 | 0.00076 | 0.05 | 27470 | 27470 | 0 | 0.0017 : 0.005 (1.0 : 3.2) | 27728 | 27728 | 0 | 0.00054 : 0.0013 (1.0 : 2.4) |
| $^1L_b$ | 28320 | | | 28120<br>28875 | 28120<br>28875 | | | | | | |
| | 31350 | 0.08 | 0.49 | 30580 | 30090 | 490 | 0.042 : 0.092 (1.0 : 2.2) | 31387 | 31170 | 217 | 0.136 : 0.382 (1.0 : 2.8) |
| $^1L_a$ | 32750<br>34030 | 0.07<br>0.06 | 0.44<br>0.40 | 31555<br>32880 | 31555<br>32980 | 0<br>−100 | | 32739<br>33981 | 32622<br>33929 | 117<br>52 | |
| | 35420 | 0.04 | 0.35 | | 34210 | | | 35333 | 35467 | −134 | |
| $^1B_b$ | 37320 | 0.95 | 1.58 | 36780 | 36780 | 0 | 0.17 : 0.295 (1.0 : 1.7) | 37517 | 37611<br>37839 | | 0.246 : 0.825 (1.0 : 3.3) |
| | 38860 | | | | | | 0.06 : 0.08 | 45863 | | | 0.164 |
| $^1B_a$ | 40000<br>41300 | 0.48 | 1.00 | 41400 | 40000 | | | | | | |
| | 45000 | 0.60 | 1.10 | 44200? | | | | | | | |

where $\psi_{1i}'$, $\psi_{2j}'$, $\psi_{3k}'$ and $\psi_{4l}'$ represent the excited state in which a molecule at the 1$i$-th, 2$j$-th, 3$k$-th or 4$l$-th site, respectively, is excited while the others are in their ground state. The coordinates of molecules are chosen following the space group notation of $C_{2h}^6$ I (2/C) : 1($x$, $y$, $z$), 2($1/2+x$, $1/2+y$, $1/2+z$), 3($1/2-x$, $1/2+y$, $z$) and 4($\bar{x}$, $y$, $1/2-z$). The diagonal and the off-diagonal elements of the energy matrix are give for $\alpha$ and $\beta$ states by:

$$\left.\begin{aligned}
&\int \Psi_m{}^{\alpha} H \Psi_m{}^{\alpha} d\tau = \\
&E_m + <m|V_{11} + 1/2 V_{12} - 1/2 V_{13} \\
&- 1/2\ V_{14}|m> \\
&\int \Psi_m{}^{\alpha} H \Psi_n{}^{\alpha} d\tau = \\
&<m|V_{11} + 1/2 V_{12} - 1/2 V_{13} \\
&- 1/2 V_{14}|n> \\
&\int \Psi_m{}^{\beta} H \Psi_m{}^{\beta} d\tau = \\
&E_m + <m|V_{11} + 1/2 V_{12} + 1/2 V_{13} \\
&+ 1/2\ V_{14}|m> \\
&\int \Psi_m{}^{\beta} H \Psi_n{}^{\beta} d\tau = \\
&<m|\ V_{11} + 1/2 V_{12} + 1/2 V_{13} \\
&+ 1/2 V_{14}|n>
\end{aligned}\right\} \quad (8)$$

where $\Psi_m{}^{\alpha}$ and $\Psi_n{}^{\alpha}$ denote the $m$-th and $n$-th excited states of the $\alpha$-type wave function (a-active), and $\Psi_m{}^{\beta}$ and $\Psi_n{}^{\beta}$ denote those of the $\beta$-type wave function (b-active). The intermolecular interaction terms, $V_{ij}$, have a similar meaning in Eq. 2; they have been evaluated using the direction of the transition moments predicted by Ham and Rudenberg ($l$, $m$, $n$ and $o$ for the $^1B_b$, $^1B_a$, $^1L_a$ and $^1L_b$ states respectively). The results of the calculation are shown in Appendix I; the terms $V_{ij}$ have been determined by the use of experimental values of the transition moment. We considered four vibrational sub-levels for the $^1L_a$ state; the resultant secular equation of the seventh degree is shown in Appendix II. The final result is compared with the observed values in Table II and Fig. 6.

For the first $^1L_b$ band the calculated small splitting is in accord with the observed value of nearly zero, but the crystalline band as a whole shifts to red about 400 $cm^{-1}$ from the calculated value. The observed intensity is larger than the calculated value by a factor of about 10 for both a- and b-axes.

The second $^1L_a$ band shows the vibrational structure in crystal, but the band splitting is unusual. The first 0-0 band shows a splitting of 490 $cm^{-1}$ (the a-axis is higher than the b-axis), while the second 0-1 band shows almost no splitting and the third 0-2 band shows a splitting of the reversed sign −100 $cm^{-1}$ (the a-axis is lower than the b-axis). Such results can not be explained by the first-order exciton theory, since the splitting should be proportional to the intensity of each vibrational level. Second-order calculations, including interaction with a higher state, give a better explanation for those splittings since the calculated value is reversed in sign for higher vibrational progressions. However, the magnitude of the calculated value for the 0-0 band is smaller than the observed value (217 $cm^{-1}$ compared with 490 $cm^{-1}$), while the first-order splitting is 530 $cm^{-1}$.

Another way of interpreting small splittings for higher vibrational levels might be to consider a strong coupling of the vibronic excited state with the internal vibration of the molecule, and to think that the vibrational relaxation precedes the excitation transfer. However,

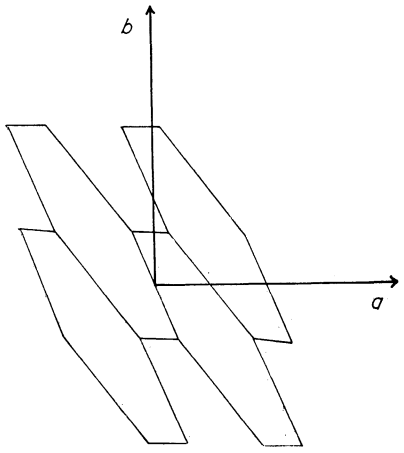



Fig. 5(a) Projection of chrysene molecule onto the (001) plane.

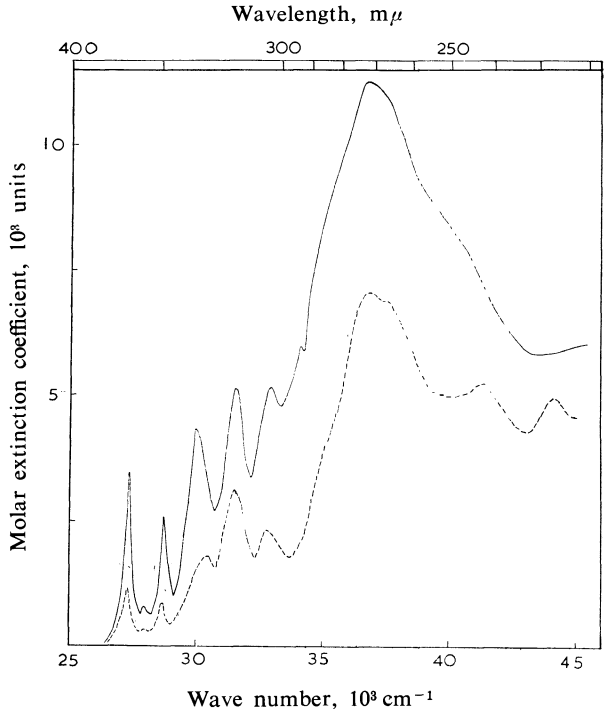



Fig. 5(b) Polarized absorption spectrum of chrysene crystal.

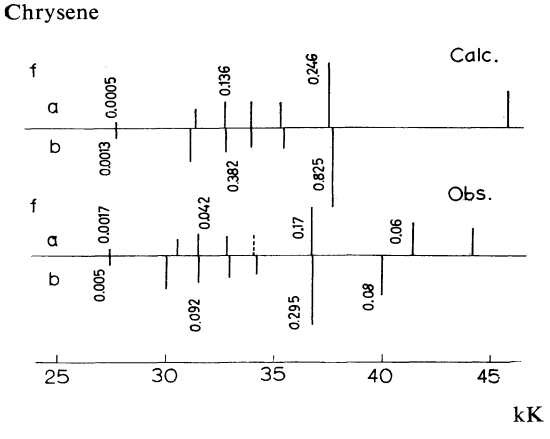



Fig. 6. Calculated and observed band positions of chrysene.

the change in the sign of the splitting can not be explained in this way.

The third $^1B_b$ band, which is the strongest of all the observed bands in solution, was predicted to be long-axis polarized and should be stronger along the a-axis than along the b-axis. However, both the first- and the second-order calculations show that the $^1B_b$ band will move to a higher frequency along tha a-axis, and that along the b-axis the $^1B_b$ and $^1B_a$ states will appear close together. Therefore, the interpretation of the spectrum in the 37000 $cm^{-1}$ region is that along the a-axis the $^1B_a$ band appears at a lower frequency than the $^1B_b$ band, and that the apparent intensity is weakened, since the $^1B_b$ band moves to a higher frequency. The intensity along the b-axis will be larger than along the a-axis since both $^1B_a$ and $^1B_b$ bands are expected to appear in the same region. The second-order calculations demonstrate that the b-axis intensity is stronger than the a-axis in this region and that two bands will be observed along the a-axis while one strong band will appear along b-axis. The observed crystalline spectrum is in fair agreement with this prediction (Fig. 6).

The confirmation of the theory of Ham and Rudenberg[3] concerning the direction of the transition moment is difficult for such an unsymmetrical molecule, because the second-order effect modifies the intensities and positions of each band. However, their theory seems to be correct, since the present calculations, based on their polarization direction, give a satisfactory explanation of the crystalline spectrum.

## Azulene

The ultraviolet and visible spectrum of azulene has been measured in a *n*-heptane solution (Fig. 7 (a), (b) and Table III). A theoretical assignment was made by Pariser;[11]

11) R. Pariser, *J. Chem. Phys.*, **25**, 1112 (1956).

his results are also included in Table III. The crystal structure of azulene was determined by Robertson, Shearer, Sim and Watson,[12] who established that the structure is disordered in such a way that successive azulene molecules are subject to a random reversal of direction. Such disorder in the crystal must be taken into account in the calculation of exciton-type interaction. However, it is verified that it is not necessary to change the usual treatment, since the allowed transition will occur when the molecular transition moments are taken in phase for the specified crystal directions. In Fig. 8 this situation is illustrated for the two molecules in an unit cell. The arrows in the figure indicate the direction of the transition moment reversed in the direction of the molecule B from Fig. 8(a) to Fig. 8(b). The allowed combination in Fig. 8 (a) is $\phi_A'\phi_B-\phi_A\phi_B'$ for the a-axis and $\phi_A'\phi_B+\phi_A\phi_B'$ for the b-axis, while in Fig. 8(b) it is $\phi_A'\phi_B+\phi_A\phi_B'$ for the a-axis and $\phi_A'\phi_B-\phi_A\phi_B'$ for the b-axis, where $\phi_A$ and $\phi_A'$ indicate the wave function of the A molecule in the ground and the excited states and $\phi_B$ and $\phi_B'$ are those for the B molecule. The sign of the dipolar interaction energy is reversed in Fig. 8(b) from Fig. 8(a); it follows that the splitting of the band is not changed by the reversal of the direction of the molecule. This relation can be extended for an infinite number of molecules in the crystal. The second-order calculation of band splitting is performed with a method similar to that described in the previous paragraphs. The calculated dipole-dipole interaction energy is shown in Appendix I, and the secular equation is given in Appendix II. The calculated rerults are compared with the experimental results in Fig. 9 and Table III.

For the first and the second bands, Sidman and McClure[13] had previously measured the polarization in the mixed crystal of azulene in naphthalene. Hunt and Ross[14] published a

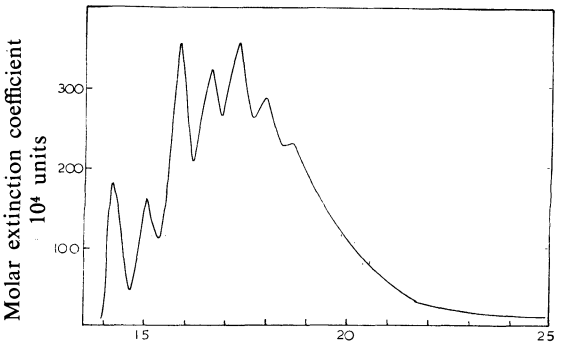



Fig. 7 (a). Visible absorption spectrum of azulene in *n*-heptane.

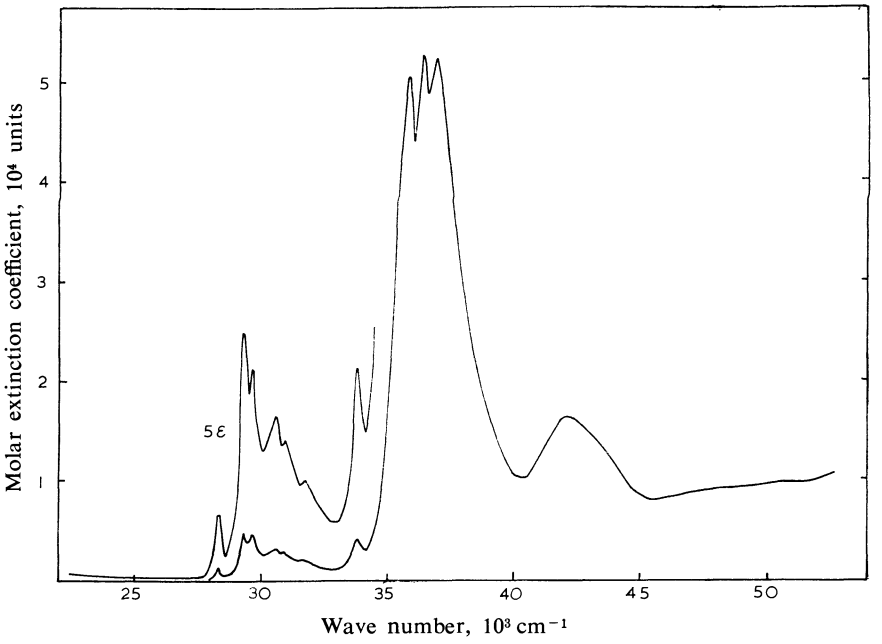



Fig. 7 (b). Ultraviolet absorption spectrum of azulene in *n*-heptane.

12) J. M. Robertson, H. M. M. Shearer, G. A. Sim and D. G. Watson, *Acta Cryst.*, **15**, 1 (1962).

13) J. Sidman and D. S. McClure, *J. Chem. Phys.*, **24** 757 (1955).

14) G. R. Hunt and I. G. Ross, *J. Mol. Spect.*, **9**, 50 (1962).

TABLE III. ABSORPTION BANDS OF AZULENE

| | Solution | | | Crystal (Observed) | | | Crystal (Calculated) | | |
|---|---|---|---|---|---|---|---|---|---|
| | $cm^{-1}$ | $f$ | $\mu$ | a-axis | b-axis | $f_a : f_b$ (d. r.)* | a-axis | b-axis | $f_a : f_b$ (d. r.) |
| | 14220 | | | 14500 | 14500 | | | | |
| | 15110 | | | 15250 | 15250 | | | | |
| | 15850 | | | 16000 | 16000 | | | | |
| $^1B$ | 16600 | 0.0065 | | 16750 | 16750 | 0.003 : 0.015 | | | 0.004 : 0.015 |
| | 17300 | | | 17300 | 17300 | (1.0 : 5.0) | | | (1.0 : 4.8) |
| | 17950 | | | 18100 | 18100 | | | | |
| | 18650 | | | 19000 | | | | | |
| | | | | 19600 | | | | | |
| | 28300 | | | | | | | | |
| | 29300 | | | 27540 | 27540 | | 29575 | 28593 | 0.0025 : 0.0013 |
| $^1A$ | 29630 | 0.048 | 0.40 | 29240 | 29540 | 0.014 : 0.036 | | | (1.9 : 1.0) |
| | 30650 | | | | 30230 | (1.0 : 2.5) | | | |
| | 31750 | | | | | | | | |
| $^1B$ | 33800 | 0.013 | 0.18 | 33530 | 33470 | 0.053 : 0.10 | 33757 | 32614 | 0.01 0.02 |
| | | | | 34750 | 34360 | (1.0 : 1.8) | | 33813 | 0.032 |
| | | | | | | | | | (1.0 : 5.2) |
| | 35830 | | | | | 0.077 | 41029 | | 0.260 |
| $^1A$ | 36400 | 0.765 | 1.40 | 40700 | | | | | |
| | 36960 | | | | | | | | |
| $^1B$ | 42100 | 0.27 | 0.77 | | 41400 | 0.225 | 43715 | 41849 | 0.036 : 0.635 |
| | | | | | | (1.0 : 3.0) | | | (1.0 : 2.5) |

* The oscillator strength $f$ for the crystal is estimated by using a value of 0.3 $\mu$ thickness for the crystal shown in Fig. 8(b).

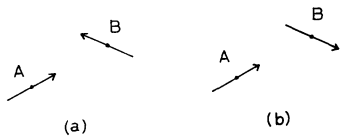



Fig. 8. Direction of transition moment in the azulene crystal.

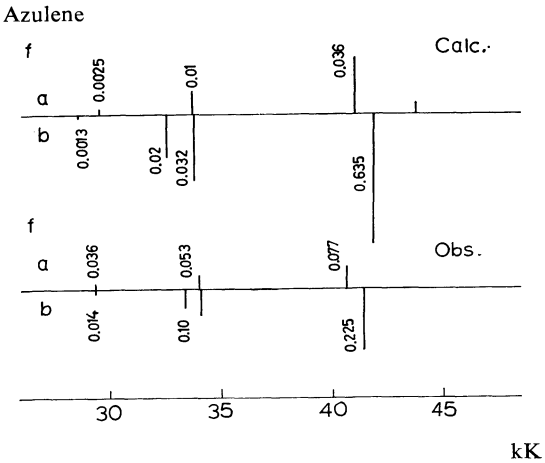



Fig. 9. Calculated and observed band positions of azulene.

pure crystal spectrum for the longer wavelength region; both pairs of authors concluded that the first band is polarized along the short-axis of the molecule. In the present study the pure crystal spectrum has been measured through the (001) plane by a polarized light, as is shown in Fig. 10(b). The projection of molecules according to X-ray results is pictured in Fig. 10(a). The band positions of the visible band are in good agreement with

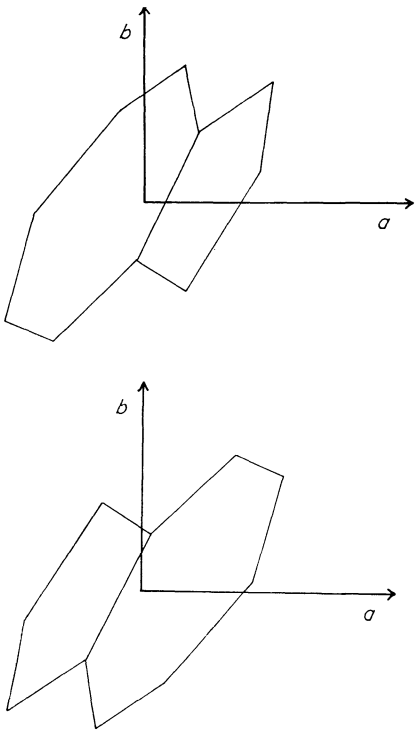



Fig. 10 (a). Projection of the azulene molecule onto the (001) plane.

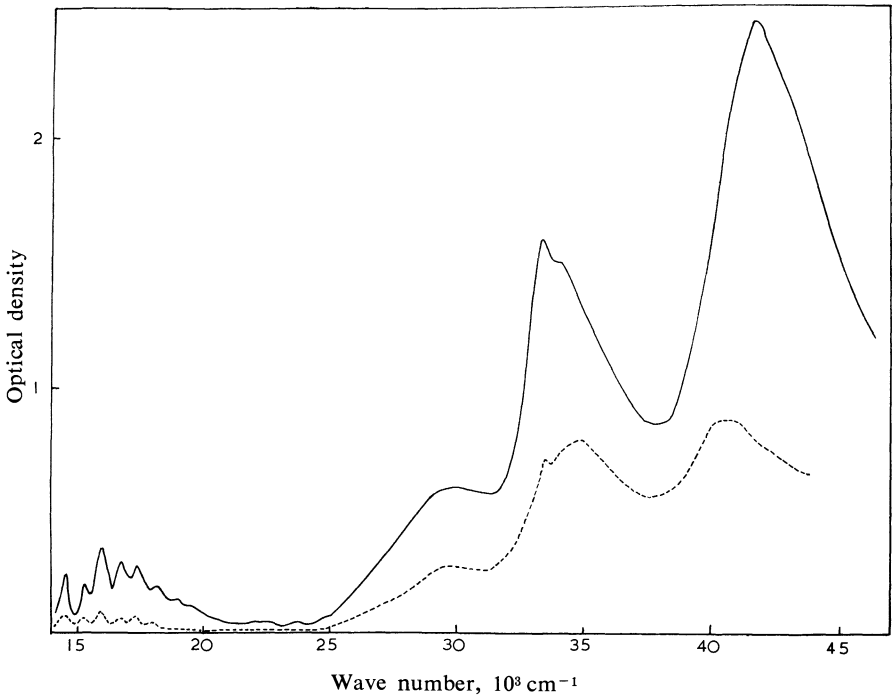



Fig. 10 (b). Polarized absorption spectrum of azulene crystal.

the results of Hunt and Ross within a range of experimental error of $\pm 50\,cm^{-1}$. The dichroic ratio is $D_b : D_a = 5 : 1$; this is in good agreement with the oriented gas value of the short-axis polarization ($D_b : D_a = 4.8 : 1.0$). Since the visible band is situated far from the stronger transitions at higher frequencies, it is possible to treat this band separately from the other transitions. The observed dichroic ratio is in good agreement with the short-axis polarization ratio, so the band may be deduced to be a B-type.

For the second band, Sidman and McClure[13] confirmed the polarization to be long-axis by mixed crystal measurement. Both the present results and the earlier results by Wolf[15] have shown that the absorption is stronger along the b-axis than along the a-axis. If we compare the intensity ratio obtained by the simple oriented gas model with our present results, the dichroic ratio is not in conformity with the long-axis polarization. By the second-order interaction calculation the calculated intensity is still stronger along the a-axis than along the b-axis, but the dichroic ratio is certainly improved. This is mainly due to the interaction with the strongest allowed transition (long-axis polarized), which increases the b-axis intensity and decreases the a-axis intensity. The observed intensity relation might be explained in this way; however, the calculated splitting of $980\,cm^{-1}$ is not clearly observed in the crystal spectrum.

The third band, which has been observed in solution as a shoulder on the tail of a very strong fourth band, is assigned by Pariser to a short-axis polarized B-type band. By a second-order calculation this band is calculated to appear at about $33800\,cm^{-1}$ in both the a- and b-axes, the latter being stronger than the former. In the observed crystal spectrum, the dichroic ratio is in good agreement with these predictions that the b-axis band is stronger than the a-axis and that they will appear at about $33500\,cm^{-1}$.

The fourth absorption band, which is the strongest of all, was shown by Pariser to be a long-axis polarized A-type band. The first order exciton splitting calculation shows that the band should be split very greatly and that the b-axis absorption should be lower in frequency than the a-axis. The second-order calculation shows that it will appear along the b-axis at about $32600\,cm^{-1}$ and along the a-axis at about $41030\,cm^{-1}$. Therefore, the spectrum of the crystal is explained in such a way that the b-axis band is overlapped with the third band and the a-axis band is removed to a higher frequency, at about $40500\,cm^{-1}$.

The fifth band, which was predicted to be of the short-axis polarized B-type, is expected to appear along the b-axis at about $41850\,cm^{-1}$

15) H. C. Wolf, *Solid State Physics*, **9**, 1 (1959).

with the largest intensity and along the a-axis at 43715 $cm^{-1}$ with a smaller intensity. The observed band at 41700 $cm^{-1}$ along the b-axis is assigned to this origin, but along the a-axis the band is not clearly seen because the shifted fourth band overlaps it in this region.

In this way, all the crystalline absorption bands are correlated with the calculated energy levels, but the changes from molecular levels to crystalline states are so complicated that it is difficult to give an explanation of the nature of the crystalline transition by a one-to-one correspondence with each molecular absorption band. The second-order calculation based on Pariser's assignment is shown to be satisfactory in explaining the whole pattern of the crystalline spectrum, but still there remain some discrepancies between the observed and the calculated splittings and intensities. The calculated intensities show a big difference between the

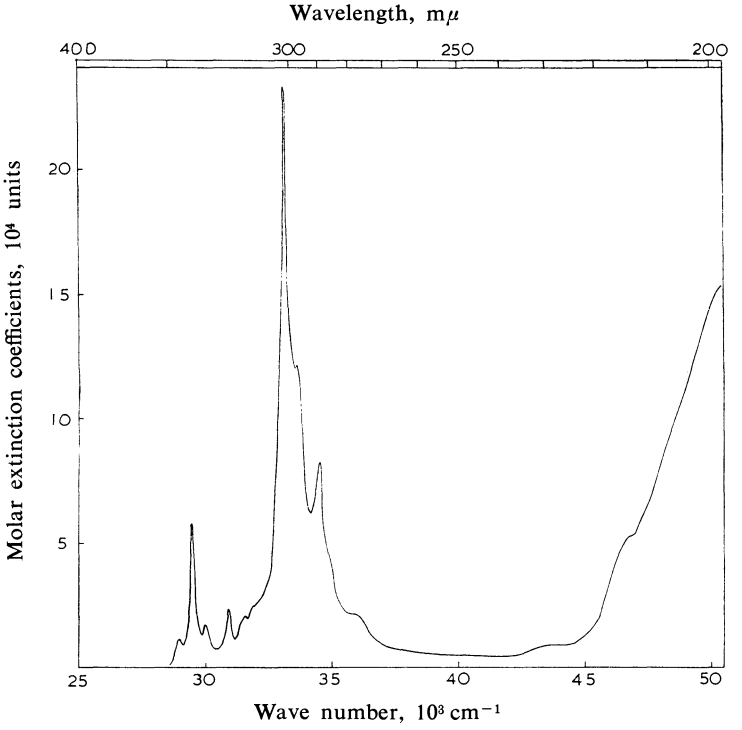



Fig. 11. Absorption spectrum of coronene in ethanol.

TABLE IV. ABSORPTION BANDS OF CORONENE

| | Solution | | | Crystal (Observed) | | | | Crystal (Calculated) | | | |
|---|---|---|---|---|---|---|---|---|---|---|---|
| | $cm^{-1}$ | $f$ | $\mu$ | a-axis | b-axis | splitting | $f_a : f_b$ (d. r.) | a-axis | b-axis | splitting | $f_a : f_b$ (d. r.) |
| $^1B_{2u}$ | | | | 22130<br>23250<br>24140<br>24600 | 22130<br>23250<br>24190<br>24640 | | | | | | |
| $^1B_{1u}$ | 29000<br>29490<br>30000<br>30930<br>31600<br>31950 | 0.100<br>0.090 | 0.56 | 27150<br>28250<br>29950 | 27250<br>28450<br>30230<br>31850 | 200 | 0.08 : 0.03<br>(2.7 : 1.0) | 29058 | 29497 | 439 | 0.39 : 0.03<br>(13 : 1) |
| $^1E_{1u}$ | 33200<br>33700<br>34600<br>35850 | 1.34 | 0.76<br>0.76 | 31410<br>33570<br>36440 | 34560 | 3200 | 0.33 : 0.23<br>(1.4 : 1.0) | 30359<br>39335 | 33129<br>36084 | 2770 | 1.06 : 0.87<br>(1.2 : 1.0)<br>0.002 : 0.01 |
| | 43900<br>46500 | | | | | | | | | | |

* The oscillator strength of crystal is tentatively determined by assuming the value of birefringence of 0.1 between the b- and a-axes.

strong and weak bands, but the observed spectrum shows a rather stronger mixing, so that there must be unknown mechanism which changes the intensity of the crystalline band.

## Coronene

The ultraviolet absorption spectrum of coronene has been measured in an ethanol solution; three strong absorption bands were observed, as Fig. 11 and Table IV show. In a benzene solution another weaker band is observed in the region of 23400 $cm^{-1}$. The crystal spectrum has been recorded through the (001) plane; it is shown in Fig. 12(b). The crystal structure was determined by Robertson and White,[16] and the projection of molecules onto the (001) plane is pictured in Fig. 12(a). The characteristics of the spectrum resemble these of benzene since coronene has a symmetry like that of $D_{6h}$. The first weak band at 23400 $cm^{-1}$ may correspond to the 2600 Å band of benzene ($^1B_{2u}$); the band in the 29000 $cm^{-1}$ region, to the 2000 Å band of benzene ($^1B_{1u}$), and the strongest band at 33000 $cm^{-1}$, to the 1800 Å band ($^1E_{1u}$).

In the free coronene molecule the transition to the $^1B_{1u}$ state is possible along the three two-fold symmetry axes passing through carbon atoms (three axes like m in Fig. 13), and the transition to the $^1B_{2u}$ state is possible along the other three two-fold axes (three axes like l in Fig. 13). Davydov[1] has discussed the relation between the symmetry of the molecular excited state and that of the crystalline state, but his argument may be justified only when the molecular symmetry axis coincides with the crystalline symmetry axis. In crystal coronene one of the m-axis (with the direction cosines of $m_a=0.7174$, $m_b=0.6865$ and $m_{c'}=-0.1188$) is nearly perpendicular to the c'-axis. Therefore, we will assume that this axis is the pseudo-two-fold unique symmetry axis of coronene in crystal. Namely, the crystal symmetry operation, $C_2^b$, may correspond to the transposition of the molecule

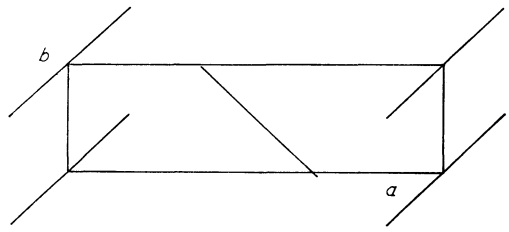



Fig. 12 (a). Projection of coronene molecule onto the (001) plane.

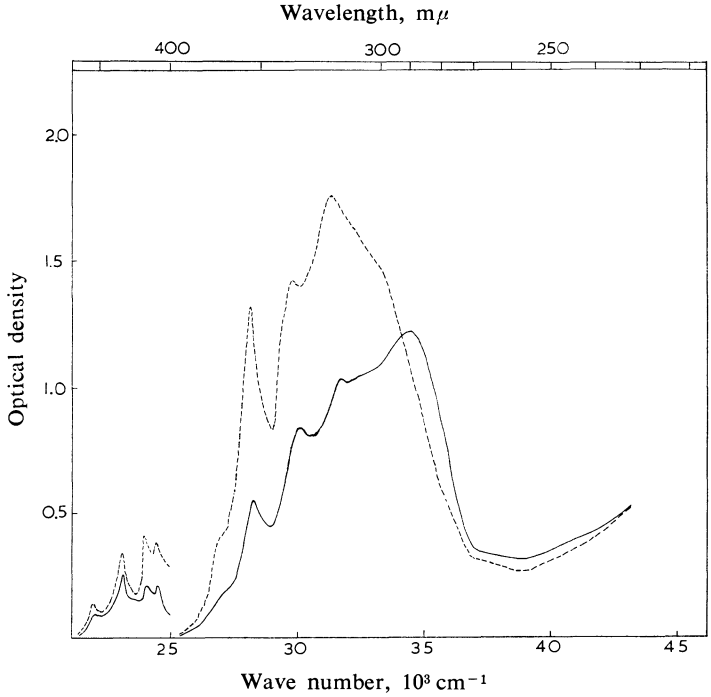



Fig. 12 (b). Polarized absorption spectrum of coronene crystal. (The retardation in the thin crystal (right curve) is about 25 mμ and that in the thick crystal (left curve) is 190 mμ.)

16) J. M. Robertson and J. G. White, *J. Chem. Soc.*, **1945**, 607.

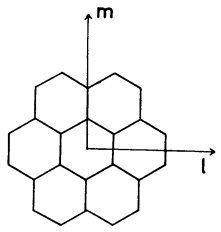



Fig. 13. Coronene.

at the origin to the (1/2, 1/2, 0) position, followed by a rotation of 180° around the m-axis and a rotation of about 90° around the l-axis. In this situation the degeneracy of the electronic transitions might be removed so that the m-axis may be taken as an axis along which the transition to the $^1B_{1u}$ state is possible. From the intensity relations observed in the crystal spectrum, it seems certainly correct to choose the m-axis as an unique two-fold symmetry axis, since the 29000 $cm^{-1}$ band is observed strongly in crystal, while the 22000 $cm^{-1}$ band is very weak. The 22000 $cm^{-1}$ band is supposed to be strengthened in intensity in crystal by mixing with stronger transitions, but in reality the band is observed very weakly in crystal; therefore, the direction of the transition moment is considered to be on the l-axis, which is nearly vertical to the (001) plane.

Lyons and Walsh[17] have calculated the first-order splitting of the $^1E_{1u}$ level, but they did not pay any particular attention to the interaction with the $^1B_{1u}$ state. Actually the observed band shows a mixing of the $^1B_{1u}$ state with the $^1E_{1u}$ state; namely, the intensity of the absorption band at 29000 $cm^{-1}$ is far less than that of the 33000 $cm^{-1}$ band in solution, while it becomes comparable in crystal. Therefore, it might be necessary to include the interaction between the $^1B_{1u}$ state and two $^1E_{1u}$ states. The first-order wave function for each excited states may be given by the following formulae:

$$\left.\begin{aligned}\Psi^{\alpha} &= \frac{1}{\sqrt{2N}}\left(\sum_{i=1}^{N}\phi_{1i}' - \sum_{j=1}^{N}\phi_{2j}'\right)\\ \Psi^{\beta} &= \frac{1}{\sqrt{2N}}\left(\sum_{i=1}^{N}\phi_{1i}' + \sum_{j=1}^{N}\phi_{2j}'\right)\end{aligned}\right\} \quad (9)$$

where $\Psi^{\alpha}$ and $\Psi^{\beta}$ represent the wave functions which are active along the a- and b-axes respectively. The functions $\phi_{1i}'$ and $\phi_{2j}'$ indicate that a molecule at the $1i$-th or $2j$-th site is excited and that the others are in their ground state. The dipole-dipole interaction energies have been calculated over molecules within 20 Å and 40 Å radius spheres; they are shown in Appendix I. The figures for the 40 Å radius summation are in excellent agreement with the values of Lyons and Walsh who employed the Ewald-Kornfeld method for infinite summation, so that the convergence of the summation seems to be sufficient by 40 Å for such a large molecule.

The assignment of the crystalline absorption bands is very much complicated by the presence of the vibrational structures. We have tentatively decided on the assignments shown in Table IV, taking the 31300 $cm^{-1}$ band along the a-axis and the 34500 $cm^{-1}$ band along the b-axis as the split $^1E_{1u}$ components. The other peaks around 28000—32000 $cm^{-1}$ are ascribed to the vibrational progressions of the $^1B_{1u}$ band. The first-order band splitting of the $^1E_{1u}$ level, considering the degeneracy of the band, is 3110 $cm^{-1}$, while the observed value will be 3200 $cm^{-1}$ if we follow the assignment mentioned above. The value suggested by Lyons and Walsh was 3615 $cm^{-1}$; their value might be larger than ours because they used a larger transition dipole moment.

As has been mentioned previously, a characteristic feature of the crystalline spectrum is the mixing of the $^1B_{1u}$ state with the $^1E_{1u}$ state; therefore, the second-order calculations have been made with the first $^1B_{1u}$ state and two degenerate $^1E_{1u}$ levels. The higher $^1B_{1u}$ progressions are disregarded since they are situated close to the $^1E_{1u}$ state. The first trial using the solution's intensity data gave too strong a coupling between the $^1B_{1u}$ and $^1E_{1u}$ states, so we have reduced the magnitude of the transition dipole for the $^1B_{1u}$ state to half of the observed value. The calculated results are compared with the experimental results in Fig. 14 and Tabe IV. It is found that the general pattern of the spectrum is

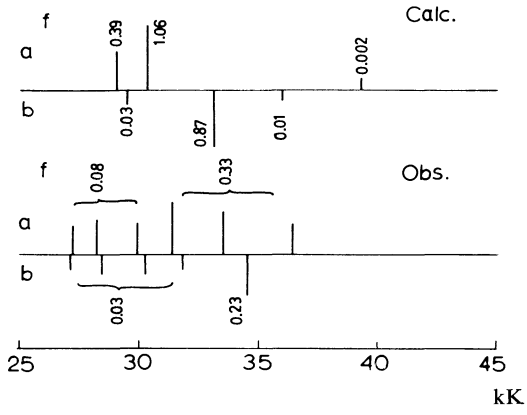



Fig. 14. Calculated and observed band positions of coronene.

17) L. E. Lyons and J. R. Walsh, ibid., 1959, 3447.

rather well reproduced in the calculations, particularly in intensity relations between the $^1B_{1u}$ and $^1E_{1u}$ states, but the splittings are slightly smaller than the observed values. Presumably a more complicated interaction will occur between the $^1B_{1u}$ and $^1E_{1u}$ states in crystal by the electron exchange or another effect, because the electron overlap along the b-axis is expected to be large.

The use of a smaller transition moment for the $^1B_{1u}$ state is possible if we think that the band is originally forbidden in character but appears through the vibrational coupling.

The absorption tail at about 38000 $cm^{-1}$, which continues to the shorter ultraviolet region, may involve a transition to the Rydberg series or to the continuous band.

## Tetracene

The electronic absorption spectrum of tetracence in ethanol and in a crystal has been measured as is shown in Figs. 15 and 16(b). Pariser[18] calculated the energy levels of the molecule; the bands at 21000 $cm^{-1}$ and 34000 $cm^{-1}$ were shown to be short-axis (M-axis) polarized, while the 36400 $cm^{-1}$ band is long-axis (L-axis) polarized. Another transition at about 60000 $cm^{-1}$ was also predicted to be an M-axis polarized band.

The crystal spectrum was measured by Bree and Lyons,[19] but they did not discuss the results with reference to the crystal structure. The present results are nearly in agreement with theirs; in addition, the shape of the 46000 $cm^{-1}$ band is confirmed to be at a shorter

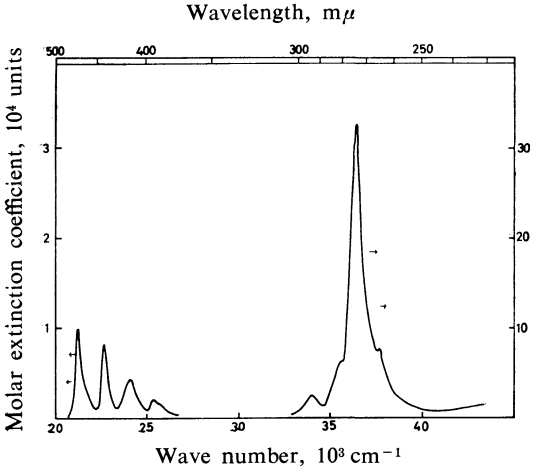



Fig. 15. Absorption spectrum of tetracene in ethanol.

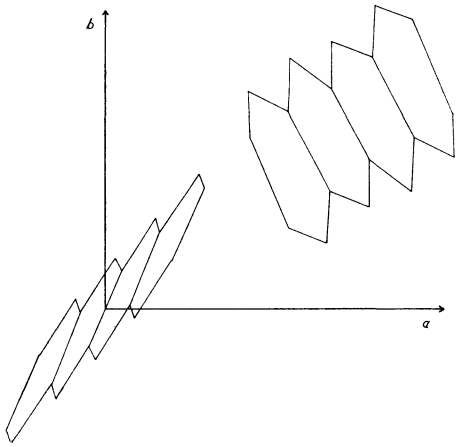



Fig. 16(a). Projection of tetracene molecules onto the (001) plane.

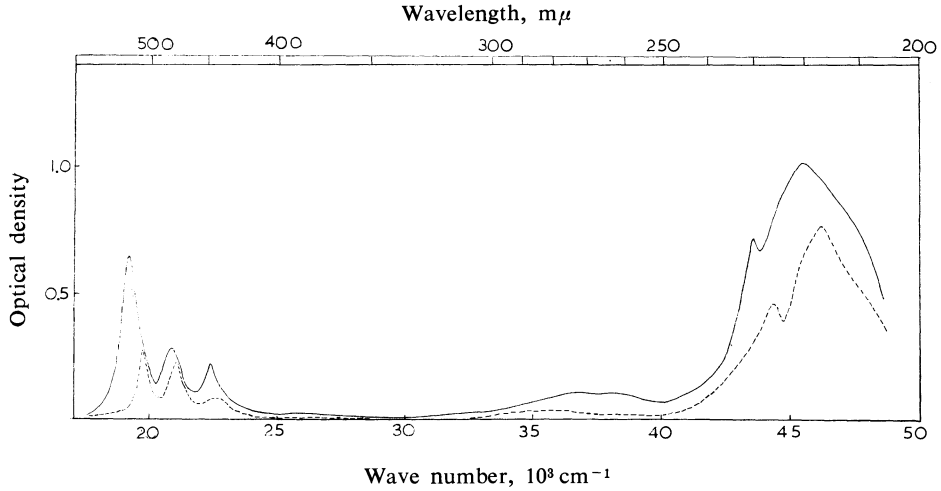



Fig. 16 (b). Polarized absorption spectrum of tetracene crystal.

18) R. Pariser, *J. Chem. Phys.*, **24**, 250 (1956).

19) A. Bree and L. E. Lyons, *J. Chem. Soc.*, **1960**, 5206.

TABLE V. ABSORPTION BANDS OF TETRACENE

| | Solution | | | Crystal (Observed) | | | | Crystal (Calculated I) | | | Crystal (Calculated II) | | | |
|---|---|---|---|---|---|---|---|---|---|---|---|---|---|---|
| | $cm^{-1}$ | $f$ | $\mu$ | a-axis | b-axis | split | $f_a : f_b$ | a-axis | b-axis | split. | a-axis | b-axis | split. | $f_a : f_b$ |
| $^1B_{2u}$ | 21200 | 0.025 | 0.33 | 19861 | 19231 | 630 | 0.007 : 0.027 | 21062 | 21032 | 30 | 21062 | 21045 | 17 | 0.012 : 0.058 |
| | 22620 | 0.020 | 0.29 | 21186 | 20964 | 222 | 0.006 : 0.014 | 22527 | 22509 | 18 | 22528 | 22516 | 12 | 0.009 : 0.047 |
| | 24100 | 0.017 | 0.26 | 22760 | 22607 | 153 | 0.004 : 0.006 (1.0 : 2.8) | 24030 | 24016 | 14 | 24030 | 24021 | 9 | 0.008 : 0.040 (1.0 : 5.1) |
| $^1B_{2u}$ | 34000 | 0.086 | 0.48 | 35670 | 34000 | | | 33747 | 30736 | | 33764 | 33369 | | |
| | | | | | 36400 | | | | 33650 | | | 33665 | | |
| $^1B_{3u}$ | 35600 | 1.3 | 1.81 | 44340 | 43480 | 860 | 0.15 : 0.24 | 50555 | 50555 | 0 | 43526 | 43526 | 0 | 0.25 : 0.25 |
| | 36400 | | | 46080 | 45455 | 625 | (1.0 : 1.6) | | | | | | | (1.0 : 1.0) |
| | 37650 | | | | | | | | | | | | | |

ultraviolet region. The crystal structure has been determined recently by Robertson, Sinclair and Trotter;[20] they have found that the crystal is triclinic with the space group of $P\bar{1}$ (cf. Fig. 16(a)). For this crystal symmetry the selection rule which is strict for the crystal of a higher symmetry does not hold, and possible transitions are observed in all directions of the crystal. The excited state wave functions are:

$$\Psi^{\alpha} = \frac{1}{\sqrt{2N}} \left( \sum_{i=1}^{N} \phi_{1i}' + \sum_{j=1}^{N} \phi_{2j}' \right)$$

$$\Psi^{\beta} = \frac{1}{\sqrt{2N}} \left( \sum_{i=1}^{N} \phi_{1i}' - \sum_{j=1}^{N} \phi_{2j}' \right)$$

where $\phi_{1i}'$ represents the state in which the molecule on the $1i$-th site is excited and the others are in their ground state. These two types of excited-state wave functions will behave differently in intensity relations. Following the crystal structure data, it is found that the M-axis polarized band is stronger for the $\Psi^{\alpha}$ state along the b-axis than along the a-axis, while for the $\Psi^{\beta}$ state the situation is reversed. The L-axis polarized band will appear only for the $\Psi^{\alpha}$ state in both a- and b-axes directions, and the band for the $\Psi^{\beta}$ state will be very weak. The dipole interaction energies have been calculated for every combination of directions of the transition moment on 1st-site and 2nd-site molecules, as Appendix I shows.

The band observed near 20000 $cm^{-1}$ is assigned to the M-axis polarized band on the basis of the dichroic intensity ratio. The b-axis polarized band is considered to be the transition to the $\Psi^{\alpha}$ state, while the a-axis band is regarded as arising from the $\Psi^{\beta}$ state. The first-order dichroic ratio is;

$$D_b : D_a = (\cos m_b(\mathrm{I}) + \cos m_b(\mathrm{II}))^2 / (\cos m_b(\mathrm{I}) - \cos m_b(\mathrm{II}))^2 = 5.1 : 1.0$$

where $m_b(\mathrm{I})$ indicates the angle between the b-axis and the M-axis of the 1st site molecule. The observed dichroic ratio is 2.8 : 1.0. The results of the calculation of splitting between the $\Psi^{\alpha}$ and $\Psi^{\beta}$ states are shown in Table V, where it is shown that the calculated value is less than 30 $cm^{-1}$ according to a weak coupling model. The observed value is as large as 630 $cm^{-1}$; even when a strong coupling model is employed, the calculated value does not exceed 130 $cm^{-1}$. Presumably the interaction involving electron exchange and the charge transfer effect might be important in explaining this splitting. Near the 37000 $cm^{-1}$ region in the crystal another band is observed which is regarded as the M-axis polarized band observed in solution at 34000 $cm^{-1}$.

The strongest L-axis polarized band, situated at 36000 $cm^{-1}$ in solution, is expected to split into $\Psi^{\alpha}$ and $\Psi^{\beta}$ states in the crystal. The first-order band shift is calculated to be about 14000 $cm^{-1}$ for the $\Psi^{\alpha}$ stated and $-6000$ $cm^{-1}$ for the $\Psi^{\beta}$ state. Actually, the $\Psi^{\alpha}$ state is shifted about 8000 $cm^{-1}$ to a higher frequency and the $\Psi^{\beta}$ state, although it can not be clearly seen, seems to be unchanged in position and to overlap with the M-axis polarized band. The $\Psi^{\beta}$ state is calculated to appear more strongly along the b-axis than along the a-axis, so that the extra band along the b-axis near 34000 $cm^{-1}$ might be explained by this origin. The observed smaller shift of the $\Psi^{\alpha}$ state can be explained if we use a smaller value of the transition dipole in crystal; the second-order calculation value using $1/\sqrt{2}$ of the solution's $f$-value is shown in Table V. The $\Psi^{\alpha}$ state shows a splitting of 800 $cm^{-1}$ between the b- and a-axes; such a result cannot be explained by the present calculations. A possible mechanism for this shift is interaction with the higher ionized state in the crystal.

With regard to the band position of the first $^1B_{2u}$ band, the present results are in good agreement with the earlier results of Bree and Lyons, but the present intensity is not in

20) J. M. Robertson, V. C. Sinclair and J. Trotter, *Acta Cryst.*, **14**, 697 (1961).

accordance with theirs. The prsent measuerement of the thickness of the crystal is not as accurate because we have determined the thickness by a retardation of the crystal as measured by a compensator, which might be in error by as much as 20%. The molar extinction coefficient of the first peak is estimated to be $\varepsilon_b = 6300$; this is a half of the value of Bree and Lyons. However, our oscillator strength is larger than theirs, since we have used the usual formula for the oscillator strength instead of that for the reduced oscillator strength. The theoretical intensities are compared with the experimental values in Table V; it is remarkable that the second calculation using the smaller transition dipole for the $^1B_{3u}$ state gives nearly the correct size of the oscillator strength in the crystal. The intensity of the first $^1B_{2u}$ state is smaller than the calculated value; therefore, it seems certain that a general hypochromism occurs in the crystal of tetracene.

## Discussion

When the observed band splittings and intensities are compared with the calculated values, the second-order theory, which includes interactions between several excited levels, is shown to be better than the first-order calculation. In crystals such as azulene and chrysene, the first-order intensity relations are so greatly changed that the direction of the transition moment can not be simply determined from the dichroic intensity ratio for each band. This is quite contrary to the case of substituted benzenes,[2] where the direction of the transition moment has been nicely determined from the intensity relations. When these two cases are examined in the off-diagonal ($H_{ij}$) and the diagonal matrix element ($H_{ii}$, $H_{jj}$) in the second-order secular equation, it is found that a big deviation occurs when the term

$$H_{ij}/H_{ii}-H_{jj}$$

becomes large enough to make for an efficient mixing of several excited states. In cases of substituted benzenes, the separation of each band, $H_{ii}-H_{jj}$, is relatively large, and the off-diagonal term is smaller because of the small magnitude of the transition moment; hence, the simple oriented gas model holds rather well. In the aromatic hydrocarbons described in the present paper, an efficient mixing of excited levels occurs under favorable conditions of large interaction terms and a narrow spacing of excited states. In this way the larger deviation of the intensity relation from the simple oriented gas rule in azulene and chrysene crystals can be explained.

However, there still remains some question unexplained by the dipolar interaction theory. Namely, in coronene and tetracene crystals the calculated splittings do not agree with the observed values. One possible reason for these difficulties might be our ignorance of electron overlap and charge transfer effects, which are certainly important in such crystals as pyrene and perylene.[7] The matrix element, including the electron overlap effect, has been disregarded in the present calculations; however, it would be significant if we consider the interaction between the exciton state and the charge transfer state.[8] Because of the small ionization potential and the large electron affinity of aromatic hydrocarbon molecules, the diagonal element of the charge-transfer state would be comparable in energy to some exciton state, and the off-diagonal term includes the energy which is first-order with the electron overlap. In recent notes[21] some authors have stressed the importance of electron exchange effect in triplet exciton, the magnitude of which has been estimated to be about 5 to 10 $cm^{-1}$, but the effect might be second-order to the electron overlap, which should be one to two orders of magnitude smaller than the present consideration of interaction energy. Therefore, the charge-transfer electron overlap effect may be important in the calculation of splitting, since its magnitude may reasonably be guessed to amount to several hundred reciprocal centimeters under favorable conditions. This point will be explored in a further study.

## Summary

The electronic absorption spectra of single crystals of pyrene, chrysene, azulene, coronene and tetracene have been measured by a polarized light. Some crystal absorption bands exhibit appreciable splittings and changes in intensity relations according to the simple exciton theory. Those results are explained by the use of the second-order exciton calculation without the inclusion of the electron overlap effect. The theoretical results give a fairly reasonable explanation of crystal spectra, and it has been shown that the second-order mixing of excited states plays an essential role in modifying the crystal spectra from the pattern of the free molecule.

The author would like to thank Professor Saburo Nagakura for his encouragement throughout this work. He would also like to express his gratitude to Professors Hideo Akamatu and Hiroo Inokuchi for their gifts

21) G. C. Nieman and G. W. Robinson, *J. Chem. Phys.*, 37, 2150 (1962); J. Jortner, S. Choi, J. L. Katz and S. A. Rice, *Phys. Rev. Let.*, 11, 323 (1963).

of samples, and to Professor David P. Craig for his kind communication on dipole interaction energies.

*The Institute for Solid State Physics*
*The University of Tokyo*
*Azabu, Tokyo*

## Appendix I

### Dipole Interaction Energies ($cm^{-1}/Å^2$)

*Pyrene**

| | l-l | m-m | n-n | l-m | l-n | m-n | N. S. |
|---|---|---|---|---|---|---|---|
| 1-1 | −19 | −59 | 81 | 371 | −338 | −185 | 510 |
| | (−26) | (−58) | (88) | (373) | (−332) | (−171) | 108 |
| 1-2 | −769 | −1731 | 2494 | 54 | −2043 | 126 | 504 |
| | (−767) | (−1741) | (2501) | (40) | (−2046) | (120) | 106 |
| 1-3 | −676 | −281 | −324 | 201 | −151 | −344 | 504 |
| | (−669) | (−292) | (−334) | (197) | (−152) | (−340) | 108 |
| 1-4 | 38 | −324 | −629 | −664 | 392 | 78 | 504 |
| | (32) | (−348) | (−650) | (−659) | (384) | (76) | 112 |

*Azulene**

| | l-l | m-m | n-n | l-m | l-n | m-n | |
|---|---|---|---|---|---|---|---|
| 1-1 | 648 | −813 | 172 | −48 | 146 | 735 | 1462 |
| | (658) | (−830) | 177 | (−68) | (139) | (751) | 304 |
| 1-2 | −2715 | 250 | 1976 | 855 | 1130 | 1074 | 1432 |
| | (−2759) | (236) | (1987) | (859) | (1134) | (1092) | 316 |

*Coronene***

| | l-l | m-m | n-n | l-m | l-n | m-n | |
|---|---|---|---|---|---|---|---|
| 1-1 | 1994 | −839 | −1157 | −41 | −671 | −3678 | 376 |
| | (2091) | (−883) | (−1211) | (−100) | (−629) | (−3671) | 42 |
| 1-2 | −497 | 903 | 957 | 440 | −293 | −257 | 372 |
| | (−536) | (868) | (912) | (405) | (−262) | (−276) | 48 |

*Tetracene**

| | l-l | m-m | l-m |
|---|---|---|---|
| 1-2 | 1175 | −981 | 907 |
| | (1156) | (−973) | (864) |
| 2-2 | 1235 | −1274 | 497 |
| | (1214) | (−1250) | (485) |
| 1-2 | 3030 | 22 | 81 |
| | (2998) | (34) | (80) |
| 2-1 | 3030 | 22 | 1615 |
| | (2998) | (34) | (1619) |

*Chrysene****

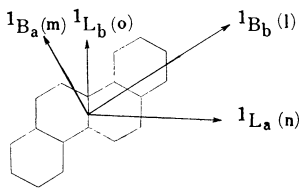
| | l-l | m-m | n-n | o-o | l-m | l-n | m-n | l-o | m-o | n-o |
|---|---|---|---|---|---|---|---|---|---|---|
| 1-1 | 1877 | −1483 | 792 | −260 | −378 | 1748 | 782 | 671 | −1378 | 1529 |
| 1-2 | −719 | 408 | −420 | 405 | 165 | −688 | −173 | −269 | 364 | −479 |
| 1-3 | −3523 | 78 | −2913 | −1000 | 709 | −3307 | 456 | −1492 | −4 | −1192 |
| 1-4 | 724 | 216 | 657 | 352 | −87 | 635 | −220 | 337 | 186 | 130 |

The directions of the transition dipoles are referred to the long (l), short (m) and normal (n) axes of the molecule for pyrene, azulene, coronene and teracene. The directions for chrysene are shown below. N. S. means the number of molecules summed.

* Numbers without bracket are for 50Å-radius summation and those in bracket are for 30Å-radius summation.

** Numbers without brackets are for 40Å-radius summation and those in brackets are 20Å-radius summation.

*** The summation was taken for a 30Å-radius sphere only.



## Appendix II

### Matrix Elements for the Secular Equations of the Excited States

*Pyrene*

*α*

| | | | | | | |
|---|---|---|---|---|---|---|
| $^1L_b$ | 26884 | | | | | |
| $^1L_a$(I) | −4 | 30236 | | | | |
| $^1L_a$(II) | −4 | 274 | 31739 | | | |
| $^1L_a$(III) | −3 | 181 | 157 | 32954 | | |
| $^1B_a$ | 54 | −56 | −49 | −32 | 37396 | |
| $^1B_b$ | −9 | 632 | 550 | 362 | −113 | 42748 |

*β*

| | | | | | | |
|---|---|---|---|---|---|---|
| $^1L_b$ | 26926 | | | | | |
| $^1L_a$(I) | 39 | 29941 | | | | |
| $^1L_a$(II) | 34 | 18 | 31516 | | | |
| $^1L_a$(III) | 22 | 12 | 11 | 32857 | | |
| $^1B_a$ | 57 | 494 | 428 | 283 | 37433 | |
| $^1B_b$ | 78 | 42 | 37 | 24 | 989 | 41565 |

*Chrysene*

*α*

| | | | | | | | |
|---|---|---|---|---|---|---|---|
| $^1L_b$ | 27730 | | | | | | |
| $^1L_a$ | 49 | 31760 | | | | | |
| | 44 | 369 | 33082 | | | | |
| | 40 | 335 | 301 | 34304 | | | |
| | 35 | 293 | 266 | 240 | 35628 | | |
| $^1B_b$ | −4 | 2120 | 1910 | 1730 | 1520 | 44610 | |
| $^1B_a$ | 60 | 283 | 254 | 231 | 202 | −960 | 37434 |

*β*

| | | | | | | | |
|---|---|---|---|---|---|---|---|
| $^1L_b$ | 27730 | | | | | | |
| $^1L_a$ | 20 | 31219 | | | | | |
| | 18 | −118 | 32644 | | | | |
| | 17 | −107 | −96 | 33943 | | | |
| | 15 | −94 | −84 | −71 | 35486 | | |
| $^1B_b$ | 97 | 57 | 47 | 43 | 38 | 37615 | |
| $^1B_a$ | 70 | 398 | 358 | 325 | 285 | 24 | 37728 |

*Azulene*

*α*

| | | | | |
|---|---|---|---|---|
| A | 29840 | | | |
| B | −65 | 33766 | | |
| A | 1880 | −228 | 43000 | |
| B | −278 | −147 | −975 | 41470 |

*β*

| | | | | |
|---|---|---|---|---|
| A | 28970 | | | |
| B | 58 | 33782 | | |
| A | −1152 | 204 | 32350 | |
| B | 248 | −78 | 870 | 41767 |

*Coronene*

*α*

| | | | |
|---|---|---|---|
| $^1B_{1u}$ | 29400 | | |
| $^1E_{1u}$(m) | −560 | 30100 | |
| $^1E_{1u}$(l) | −155 | −866 | 39253 |

*β*

| | | | |
|---|---|---|---|
| $^1B_{1u}$ | 29500 | | |
| $^1E_{1u}$(m) | 20 | 33315 | |
| $^1E_{1u}$(l) | 128 | 718 | 35895 |

*Tetracene*

*α*

| | | | | | |
|---|---|---|---|---|---|
| $^1B_{2u}$ | 21078 | | | | |
| | −110 | 22526 | | | |
| | −99 | −87 | 24024 | | |
| $^1B_{2u}$ | −182 | −160 | −144 | 33736 | |
| $^1B_{3u}$ | −87 | −77 | −69 | −127 | 30378 |

*β*

| | | | | | |
|---|---|---|---|---|---|
| $^1B_{2u}$ | 21083 | | | | |
| | −106 | 22529 | | | |
| | −95 | −83 | 24027 | | |
| $^1B_{2u}$ | −175 | −154 | −138 | 33746 | |
| $^1B_{3u}$ | 925 | 814 | 730 | 1350 | 50376 |

# Mean-Square Amplitudes and Force Constants of Tetrahedral Molecules. II. Silicon Tetrachloride*

By Yonezo MORINO and Yoshitada MURATA

(Received July 15, 1964)

In a preceding paper,[1] we have proposed a new method for determining the force field of molecules by the use of the mean-square amplitudes in addition to the vibrational frequencies, and have shown that the application of the method to germanium tetrachloride and carbon tetrachloride molecules provides reasonable sets of the force constants. In the present report, the results of the application of the same method to silicon tetrachloride will be shown, with a special emphasis on the estimation of the uncertainties of the results by a statistical consideration.

In order to use the mean-square amplitudes for the determination of the force field, it is essential to ascertain the precise experimental values of the amplitudes, with their uncertainties. Accordingly, possible sources of experimental errors are discussed in this paper.

The failure of the first Born approximation is often regarded as a serious error for an atom pair with very different atomic numbers. Fortunately, however, silicon tetrachloride has the advantage that the error caused by the Born approximation is negligibly small; the correction is only 1% for the Si–Cl pair, in contrast to about 20% for the Ge–Cl pair in germanium tetrachloride, or 10% for the C–Cl pair in carbon tetrachloride.[2] The finite sample size is another source of the error,[3,4] and presumably the largest one for this molecule. It is assumed in the theory of gas diffraction that the scattering occurs at an infinitesimal point, but in a practical experiment the diffracted beams come from a finite cross-section of the primary beam in the gas stream. A needle-type nozzle is, therefore, employed in this study in order to reduce the sample delocalization, and at the same time, the correction for the finite sample size was estimated on the basis of the distribution of the gas molecules along the primary beam, which was measured with a special device which will be described in detail in a following paper.[5]

The atomic distances in the silicon tetrachloride molecule have been determined by the visual method by Wierl,[6] Brockway and Wall,[7] Pauling and Brockway,[8] and Iwasaki et al.[9] The Si-Cl distances obtained are 2.02Å, 2.02Å, 2.00±0.02Å and 2.01±0.02Å respectively and the tetrahedral structure has been established, although the mean-square amplitudes have not been reported any of the above papers.

## Experimental

The apparatus used for the electron diffraction measurement is the same as that reported in a previous paper,[1] except for a few improvements. Diffraction photographs were obtained on Fuji Process Hard plates through an $r^3$-sector, with camera lengths of 11.8 cm. and 27.9 cm. The accelerating voltage was about 45—47 kV., and its fluctuation and drift were regulated to within 0.1%. The sample of silicon tetrachloride was kindly provided by the Shin-Etsu Chemical Industrial Co., Ltd. The gaseous sample was held in a glass flask of about 1 l. at a pressure of about 30 mmHg, and the gas flow was controlled by a needle valve at the rate of decrease in the gas pressure in the flask of about 1 mmHg/min. The exposure time was varied from 2 to 5 min. Two kinds of nozzles were used. One was of a drum-type, the same as that reported by Kuchitsu;[4] it is shown in Fig. 1. The other, a needle-type nozzle, was made of a straight tube of stainless steel with an inner diameter of 0.55 mm. The drum-type nozzle gives a wider spread of the gas distribution at the diffraction center, and it presumably leads to an apparent increase in the mean-square amplitudes. Therefore, the needle-type nozzle is more suitable for obtaining the precise values of the mean-square amplitudes. The drum-type nozzle was, then, used as an auxiliary nozzle for calibrating the scale factor of the needle-type nozzle, because the needle-type nozzle had no space

* A preliminary report on this work was presented at the International Conference on Magnetism and Crystallography, Kyoto, 1961.

1) Y. Morino, Y. Nakamura and T. Iijima, *J. Chem. Phys.*, **32**, 643 (1960).

2) L. S. Bartell and L. O. Brockway, *Nature*, **171**, 978 (1953).

3) I. L. Karle and J. Karle, *J. Chem. Phys.*, **18**, 963 (1950).

4) K. Kuchitsu, This Bulletin, **32**, 748 (1959).

5) Y. Morino and Y. Murata, ibid., **38**, 114 (1965).

6) R. Wierl, *Ann. Physik*, **8**, 521 (1931).

7) L. O. Brockway and F. T. Wall, *J. Am. Chem. Soc.*, **56**, 2373 (1934).

8) L. Pauling and L. O. Brockway, ibid., **57**, 2684 (1935).

9) M. Iwasaki, A Kotera, A. Tatematsu and K. Yamasaki, *J. Chem. Soc. Japan, Pure Chem. Sec.* (*Nippon Kagaku Zassi*), **69**, 104 (1948).

on which to attach a reference gold-foil without disturbing the gas flow near the nozzle.

The beam current was about 0.02 $\mu$amp. for the short camera length and about 0.005 $\mu$amp. for the long camera length when the drum-type nozzle was used. In the case of the needle-type nozzle, it was necessary to increase the beam current by five times. The photographs were developed at 20°C for 5 min. with an FD-131 developer diluted twice. The photographs were scanned with a Rigaku-Denki MP-3 microphotometer. The optical densites of the plates were regulated to be less than 0.6. It has been confirmed by Morino and Iijima[10] that the intensity is directly proportional to the photographic density in the range of density less than 0.6.

The wavelength of the electron beam was calibrated with reference to the diffraction pattern of the gold-foil on the assumption that the camera length for the gas pattern was equal to that for the gold-foil pattern. After a gas pattern had been taken, the gas nozzle was replaced by the gold-foil and the scattering pattern of the reference was taken on the same photographic plate, beside the gas pattern, by sliding the plate holder. In order to make a precise calibration, it was thought important to make sure that the reference gold-foil was placed in exactly the position of the gas diffraction center, and that the photographic plate was set in exactly the same position when the photographic plate was moved for the reference pattern to be taken; the latter test was necessary because the plate may not be exactly perpendicular to the beam axis due to a mechanical imperfection in the construction of our plate-holder.

For the former test, the gas pattern was taken at a reversed orientation where the nozzle, together with the gold-foil, was rotated around the axis by 180°, keeping their relative positions fixed (see Fig. 1.). The difference in the camera lengths, if there is any, should have a reverse effect by the same amount on the diffraction pattern at the reversed orientation. In fact, about a 0.22% increase in the atomic distance was observed after this reversal of the nozzle, as is shown in Table I. For the latter test, the difference in the camera length was measured by taking gold-foil patterns at the center of the photographic plate, where, in our normal operation, the gas pattern was taken, and also at the place where the reference pattern was normally taken; the difference in the camera length thus found was corrected for each gas pattern.

A slight blackening by an extraneous scattering was observed by a blank experiment near the outer periphery of the pattern. The density of the blank photograph was subtracted from each photograph in order to correct for the extraneous scattering.

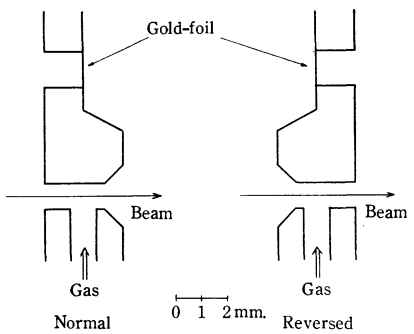



Fig. 1. Normal and reversed orientations of the drum-type nozzle.

10) Y. Morino and T. Iijima, This Bulletin, 35, 1661 (1962).

## Analysis

A small fluctuation from the defined opening, $\theta = cr^3$, was observed in the $r^3$-sector used in this experiment. The variations in the parameters caused by the correction for this sector deficiency were $-0.0013$Å and $+0.0009$Å for the Si–Cl and the Cl–Cl distances respectively, and $-0.0021$Å and $+0.0017$Å for the mean amplitudes of Si–Cl and Cl–Cl respectively. These corrections were especially important for the mean amplitudes in comparison with their total errors, even though the defects in the sector were less than 1%.

In order to calculate the molecular intensities, a correction for the so-called non-nuclear scattering was made by Bartell's method.[11] For the atomic scattering factors of the silicon and chlorine atoms, appropriate averages of the factors given by Viervoll and Ögrim[12] and those by Tomiie and Stam[13] were used. The values of the inelastic scattering factors were taken from the table given by Bewilogua,[14] and the values of $\Delta\eta(\theta)$, from the table of Ibers and Hoerni.[15]

The reduced molecular intensity curves thus obtained were compared with the theoretical expression:

$$qM(q) = \frac{10}{\pi} \sum_i \sum_j{}' k_{ij} \frac{1}{r'_{aij}} \frac{Z_i Z_j}{\sum_k (Z^2_k + Z_k)} \times \mu_{ij} \cos \Delta\eta_{ij} \exp\left(-\frac{1}{2}(l'_{aij})^2 s^2\right) \times \sin\left(sr'_{aij} - s^3\kappa_{ij}\right) \quad (1)$$

by a procedure essentially the same as that used in a previous paper:[1] the parameters to be determined by the least-squares calculation were the atomic distances, $r'_a$(Si–Cl) and $r'_a$(Cl–Cl), the mean amplitudes, $l'_a$(Si–Cl) and $l'_a$(Cl–Cl), and the indices of resolution, $k$(Si–Cl) and $k$(Cl–Cl). As was described in

11) L. S. Bartell, L. O. Brockway and R. H. Schwendeman, *J. Chem. Phys.*, 23, 1854 (1955).
12) H. Viervoll and O. Ögrim, *Acta Cryst.*, 2, 277 (1949).
13) Y. Tomiie and C. H. Stam, ibid., 11, 126 (1958).
14) L. Bewilogua, *Physik. Z.*, 32, 740 (1931).
15) J. A. Ibers and J. A. Hoerni, *Acta Cryst.*, 7, 405 (1954).

a previous paper,[16] the indices of resolution varied independently for each atomic pair. The $r'_a$ and $l'_a$ constants are not equal to the molecular constants, $r_a$ and $l_a$ respectively, since the effect of gas distribution at the diffraction center is involved in the former. The anharmonicity constants, $\kappa$(Si–Cl) and $\kappa$(Cl–Cl), were fixed at approximate values (perhaps a very crude one for $\kappa$(Cl–Cl)) as follows.

If a potential funtion of the Morse-type is assumed for the bonded Si–Cl pair,[17] the anharmonicity parameter, $\kappa$, and the so-called anharmonic term of the internuclear distance, $\langle \Delta z \rangle$, may be approximately represented by:[18]

$$\kappa = \frac{a}{6} l^4 \tag{2}$$

and

$$\langle \Delta z \rangle = \frac{3}{2} a l^2 \tag{3}$$

where $a$ is the asymmetry constant of the Morse function and may be obtained on the basis of the parameters given by Lippincott and Schroeder.[19] The parameter $\kappa$(Si–Cl) is thus found to be $1.21 \times 10^{-6}$ Å$^3$.

The anharmonicity parameter $\kappa$ for the non-bonded Cl–Cl pair may be obtained if the actual motion of the two chlorine atoms along the line connecting their equilibrium positions is approximated by a motion under a Morse potential. In such a case, the following relation is derived from relations 2 and 3:

$$\kappa = \frac{1}{9} l^2 \langle \Delta z \rangle \tag{4}$$

where $l$ is the mean amplitude of the atom pair and can be obtained by measurements. On the other hand, the $\langle \Delta z \rangle$ value for the pair is given by:

$$\langle \Delta z \rangle (\text{Cl–Cl}) = 2\sqrt{\frac{2}{3}} \langle \Delta z \rangle (\text{Si–Cl}) \tag{5}$$

since there is no totally symmetric deformation vibration for a tetrahedral molecule.[20] The parameter $\kappa$(Cl–Cl) thus obtained is $7.11 \times 10^{-6}$ Å$^3$.*

As will be mentioned in the next section, it is reasonable to assume that the weight matrix is given by a diagonal form when the observations are made in the interval of $\Delta q = 1$. Thus, the statistical weight given in Fig. 1(c) of Ref. 16 was used in the present analysis.

As is shown in Table I; the least-squares fit was carried out on several observed molecular intensity curves for each of the three kinds of nozzles; for the drum-type nozzle in the normal and reversed positions and for the needle-type nozzle. Ten sets of parameters with their standard deviations were obtained by making the respective least-squares outputs converge.[21] Table I shows the average values for each nozzle with the estimated standard deviations $\sigma_1$ and $\sigma_2$; $\sigma_1$ denotes the standard deviation for the average value of the atomic distances obtained by the least-squares fit, and $\sigma_2$, the standard deviation obtained from the deviations of the several observed values from the average value.[16] The calculation was carried out by means of two digital computers, PC-1 and PC-2, in the University of Tokyo.

It has already been mentioned that the atomic distances obtained by the reversed orientation of the nozzle were larger than those obtained by the normal orientation.** Because there are four observations corresponding to the normal position and two to the reversed position, the most probable values of the observed atomic distances may be given according to an ordinary statistical theory, by means of the arithmetic means of each averaged value, with their standard deviations $(\sqrt{3}/4\sqrt{2})(6\sigma_-^2 + \sigma_+^2)^{1/2}$, where $\sigma_-$ and $\sigma_+$ denote their standard deviations. However, the values of $\sigma_+$ obtained in this experiment is not considered to be reliable, because it was obtained

* In the analysis mentioned above, the anharmonicity constants were fixed as the estimated values. However, when they were taken as variable parameters in the least-squares analysis, the following values were obtained for the most probable values and their standard deviations (in $10^{-6}$ Å$^3$ units):

| | | Average | $\sigma_1$ | $\sigma_2$ |
|---|---|---|---|---|
| Needle-type nozzle: | $\kappa$(Si-Cl) | 2.2 | 1.3 | 0.3 |
| | $\kappa$(Cl-Cl) | 11.3 | 4.1 | 3.3 |
| Drum-type nozzle: | $\kappa$(Si-Cl) | −2.1 | 1.7 | 1.7 |
| | $\kappa$(Cl-Cl) | −1.1 | 5.9 | 6.3 |

The negative values of $\kappa$ obtained for the drum-type nozzle may be caused by the effect of finite sample distribution. When this nozzle is used, some of the scattered electrons are screened by the edge of the nozzle because of the finite spread of the gas molecules, and they do not reach the photographic plate at larger scattering angles. Therefore, the center of gravity of the distribution of gas molecules, by which electrons are scattered to a given point on the photographic plate, changes with the scattering angle; the change makes the effective $\kappa$ values significantly different from the ideal values. By using the distribution function of the gas molecule obtained for the drum-type nozzle,[5] the shift, $\kappa$, caused by the above shielding effect was approximately determined by a numerical calculation to be $-1 \times 10^{-5}$ Å$^3$ and $-2 \times 10^{-5}$ Å$^3$ for Si–Cl and Cl–Cl respectively. The deviations in atomic distances obtained in this analysis were taken into account in estimating the systematic errors caused by uncertainties in the assumed $\kappa$ values.

** This discrepancy may be explained by an asymmetric distribution of the gaseous sample, as will be described in a following paper.[5]

16) Y. Morino, K. Kuchitsu and Y. Murata, ibid., to be published.
17) K. Kuchitsu and L. S. Bartell, *J. Chem. Phys.*, **36**, 2470 (1962).
18) K. Kuchitsu and L. S. Bartell, ibid., **35**, 1945 (1961).
19) E. R. Lippincott and R. Schroeder, ibid., **23**, 1131 (1955).
20) Y. Morino, S. J. Cyvin, K. Kuchitsu and T. Iijima, ibid., **36**, 1109 (1962).
21) Y. Morino, K. Kuchitsu, T. Iijima and Y. Murata, *J. Chem. Soc. Japan, Pure Chem. Sec.* (*Nippon Kagaku Zasshi*), **83**, 803 (1962).

TABLE I. AVERAGE VALUES OF THE PARAMETERS
($r$ and $l$ in Å units)

| Nozzle-type | Parameter | Average | $\sigma_1$ | $\sigma_2$ |
|---|---|---|---|---|
| D-N | $r'_a$(Si-Cl) | 2.0159 | 0.0004 | 0.0011 |
| | $r'_a$(Cl-Cl) | 3.2893 | 0.0008 | 0.0021 |
| | $l'_a$(Si-Cl) | 0.0495 | 0.0008 | 0.0013 |
| | $l'_a$(Cl-Cl) | 0.0943 | 0.0011 | 0.0010 |
| | $k$(Si-Cl) | 0.998 | 0.010 | 0.043 |
| | $k$(Cl-Cl) | 0.979 | 0.016 | 0.027 |
| D-R | $r'_a$(Si-Cl) | 2.0204 | 0.0005 | 0.0003 |
| | $r'_a$(Cl-Cl) | 3.2963 | 0.0011 | 0.0029 |
| | $l'_a$(Si-Cl) | 0.0482 | 0.0011 | 0.0010 |
| | $l'_a$(Cl-Cl) | 0.0944 | 0.0016 | 0.0022 |
| | $k$(Si-Cl) | 0.992 | 0.013 | 0.012 |
| | $k$(Cl-Cl) | 0.989 | 0.022 | 0.030 |
| N | $r'_a$(Si-Cl) | 2.0182 | 0.0002 | — |
| | $r'_a$(Cl-Cl) | 3.2935 | 0.0005 | 0.0007 |
| | $l'_a$(Si-Cl) | 0.0479 | 0.0005 | 0.0006 |
| | $l'_a$(Cl-Cl) | 0.0905 | 0.0007 | 0.0009 |
| | $k$(Si-Cl) | 1.055 | 0.007 | 0.013 |
| | $k$(Cl-Cl) | 1.063 | 0.011 | 0.003 |

D-N : The drum-type nozzle in the normal direction.
Four observed curves were used to obtain the average values.
D-R : The drum-type nozzle in the reversed direction.
Two observed curves were used.
N : The needle-type nozzle.
Four observed curves were used.
$r'_a$ and $l'_a$: See text.

from only two observations. On the other hand, $\sigma_-$ is somewhat more reliable since it was obtained from four observations. Therefore, it seems more reasonable in this case to assume $\sigma_+^2 \sim 2\sigma_-^2$ since both experimental procedures are essentially the same, and the standard deviation for the most probable values is taken to be $(\sqrt{3}/2)\sigma_-$.

After the series of corrections mentioned above, the final results for the observed atomic distances and their standard deviations shown in Table II have been obtained. As has been mentioned above, the values obtained by using the needle-type nozzle are suitable for determining the mean amplitudes, while the average of all the observed values were used for the indices of resolution, because the latter are not influenced by the sample delocalization around the nozzle.[5]

The scale factor for the needle-type nozzle was adjusted to give the atomic distances consistent with those obtained with the drum-type nozzle. Fortunately, the apparent increment or decrement of the atomic distances in the drum-type nozzle, $\Delta r$, was in almost the same ratio for Si-Cl and Cl-Cl; the Cl-Cl distance obtained by the needle-type nozzle

TABLE II. FINAL RESULTS OF THE LEAST-SQUARES ANALYSIS
($r$ and $l$ in Å units)

| Parameter | Most probable value | $\sigma_1$ | $\sigma_2$ |
|---|---|---|---|
| $r_a$(Si-Cl) | 2.0182 | 0.0003 | 0.0010 |
| $r_a$(Cl-Cl) | 3.2928 | 0.0006 | 0.0018 |
| $l'_a$(Si-Cl) | 0.0479 | 0.0005 | 0.0006 |
| $l'_a$(Cl-Cl) | 0.0905 | 0.0007 | 0.0009 |
| $k$(Si-Cl) | 1.020 | 0.005 | 0.019 |
| $k$(Cl-Cl) | 1.015 | 0.009 | 0.017 |

was longer by 0.0007 Å than that obtained by the other nozzle, but this discrepancy is smaller than the uncertainty of the Cl-Cl distance.

The photographs taken with the long camera distance ($q=8-36$) were analyzed separately because their index of resolution was much larger than that derived from the photographs taken with the short camera distance. These results will be described in the Appendix.

## The Estimation of the Uncertainties of the Molecular Constants

**Atomic Distances.**—Let us first consider the uncertainties of the observed atomic distances. The standard deviation of each least-squares fit, $\sigma_1$, was found to be about 0.0003 Å and 0.0006 Å for the Si-Cl and the Cl-Cl pairs respectively (Table II), whereas the $\sigma$ values of the fluctuations among the mean values of the atomic distances obtained by the respective least-squares fit, $\sigma_2$, were 0.0010 Å and 0.0018 Å respectively. If the experimental conditions were kept strictly the same for all photographs, the latter should have been equal to the former. The difference between $\sigma_1$ and $\sigma_2$ may be attributed mainly to the difference between the accelerating voltages when the photographs of the sample and those of the gold-foil reference were taken, to the failure in locating the center of the halos when the plates were photometered, to the difference in the gas spread among different exposures, to the difference in the conditions of developing the photographic plates, and to random errors in the determination of the camera lengths for the sample and for the reference. In our present experiment, none of these sources of difference can be corrected for by the measurement of the deviations. All of them can occur randomly and, hence, they must be included in the random errors, $\sigma_2$, described above.

The systematic errors consist of all the uncertainties which do not occur at random and which can, in principle, be estimated. Uncertainties of various corrections made of the

observed values should also be included in these errors. For instance, the true lattice constant of the gold-foil used in this experiment may have been different from the assumed value, 4.070Å; this difference should give an uncertainty to the scale factor. It was reported by Morino and Iijima that the error of this origin may be 0.05%.[10] A gradual drift of the accelerating potential during the measurement may be another source of the uncertainty: it was found to be within 0.1%, corresponding to 0.05% in $\lambda$.

The inclination of the plates has been corrected for by the procedure described in the Experimental Section. The $\sigma$ in the measurement of the correction gives an uncertainty of 0.03% to the final result concerning the atomic distance.

Another error may originate from the difference in the camera lengths between the sample and the reference, as has been pointed out in the preceding section.

The failure in estimating the correct anharmonicity constants may possibly lead to some uncertainty in the final results, because the anharmonicity constant has an intensive correlation with the interatomic distance. In order to estimate these uncertainties, the parameters $\kappa$ were either taken as variable parameters or were fixed as constants of various estimated values. The uncertainties thus estimated are 0.0010Å and 0.0025Å for the Si–Cl and Cl–Cl distances respectively.

If the accuracy of the measurement be expressed by the limit of errors, two-and-a-half times the standard deviation plus the systematic errors, it corresponds to taking a 99% confidence interval. Because the individual errors are considered to be all mutually independent, the square roots of their squared sums, 0.0034Å and 0.0062Å (as is shown in Table III), are taken as the limit of errors of the Si–Cl and Cl–Cl pairs respectively.

TABLE III. ERRORS OF THE ATOMIC DISTANCES (in Å units)

| Source of error | $r$(Si–Cl) | $r$(Cl–Cl) |
|---|---|---|
| Random error ($2.5\sigma$) | 0.0025 | 0.0045 |
| Drift of voltage | 0.0010 | 0.0017 |
| Lattice constant | 0.0010 | 0.0017 |
| Inclination of plate | 0.0015 | 0.0025 |
| Effect of $\kappa$ | 0.0010 | 0.0025 |
| Total error | 0.0034 | 0.0062 |

**Mean-Square Amplitudes.** — The errors in the mean amplitudes are estimated in the following way. The standard deviations obtained by the least-squares method for each of the four molecular intensities, $\sigma_1$, were 0.0005Å and 0.0007Å for Si–Cl and Cl–Cl respectively, while those of the fluctuations from the mean values, $\sigma_2$, were found to be 0.0006Å and 0.0009Å respectively. As the standard deviations, $\sigma_1$ and $\sigma_2$, are almost equal in magnitude, either of them can be taken as a measure of the random error of the mean amplitude.

It should be mentioned in this connection that an appropriate interval of the observations, $\Delta q$, should be taken if a diagonal weight matrix is used in the least-squares analysis. It appears plausible to take the interval $\Delta q$ as unity in our experiment because of the following consideration.

(1) If the interval $\Delta q$ decreases, the standard deviation, $\sigma_1$, decreases while $\sigma_2$ is expected to remain almost invariant. Since the observations made at an unreasonably small interval can not be regarded as mutually independent, such a $\sigma_1$ value is of little statistical significance; for a proper treatment, a weight matrix with off-diagonal elements must be used in such a case.[22] In other words, only for the range of $\Delta q$ for which $\sigma_1$ is not smaller than $\sigma_2$ may the weight matrix be approximated by a diagonal form. (2) The standard deviations, $\sigma_1$, obtained by the least-squares analysis of $f(r)$ by using diagonal matrices are of almost the same magnitude as those shown in Table I(b) of Ref. 16, where the number of the observations was the same as in the case of the analysis of $qM(q)$, where the interval was taken to be $\Delta q=1$. It, therefore, seems likely that the observations are mutually independent if the interval is taken to be as small as unity.

The above arguments are based on somewhat indirect reasoning. It may, nevertheless, be a plausible approximation for the weight matrix in a diagonal form corresponding to $\Delta q=1$ to be taken in our experiment. The random errors obtained by taking two-and-a-half times the present standard deviations, 0.0015Å and 0.0023Å for Si–Cl and Cl–Cl respectively, will, therefore, be statistically adequate.

Of the uncertainties which belong to the systematic errors, those from the drift of the accelerating voltage and from the lattice constant are both about 0.05%, while that from the fluctuation of the camera length is 0.08%, as has already been described. The contribution from the multiple sacttering may not be important, because the indices of resolution were found to be roughly unity. Even if the multiple scattering were present, it would have a significant effect only on the effective damping factor in the range $q \lesssim 10$.[23] Since the

22) Y. Murata and Y. Morino, *Acta. Cryst.*, to be published.

23) J. A. Hoerni, *Phys. Rev.*, **102**, 1530 (1956).

mean amplitudes were determined in the range $q=18-100$, the effect of the multiple scattering on the mean amplitude may be ignored. The effect of the finite sample size has been corrected for by estimating the distribution of the gas molecules.[5] The uncertainty in the theoretical approximation for this procedure was estimated to be about 10%, as will be described in a following paper.[5] The uncertainty caused by the experimental error in the intensity measurement cannot be estimated in a reliable way. However, even if it were assumed to be 50%, which is certainly an overestimate, it would have no appreciable influence on the final results. The failure of the Born approximation, and the imperfection in the assumption of a linear relationship between the photographic darkness and the electron intensity, is so slight that the errors in their corrections are negligible. The error caused by the correction for the extraneous scattering is probably included in $\sigma_2$. The final values of the limit of errors are 0.0016 Å for Si–Cl and 0.0024 Å for Cl–Cl, as is shown in Table IV.

TABLE IV. ERRORS OF THE MEAN AMPLITUDES* (in Å units)

| Source of error | $l$(Si-Cl) | $l$(Cl-Cl) |
|---|---|---|
| Random error ($2.5\sigma$) | 0.0015 | 0.0023 |
| Sample size | 0.0005 | 0.0007 |
| Total error | 0.0016 | 0.0024 |

* Errors of negligible magnitude are excluded from the table.

The uncertainties in the indices of resolution are considered to arise from the same origins as those in the mean amplitudes, except for the finite sample size, which makes no appreciable contribution to the uncertainties in the former. The standard deviations obtained from the ten plates, $\sigma_2$, were 0.019 and 0.017, and the $\sigma_1$ values for each least-squares fit were 0.005 and 0.009 for $k$(Si–Cl) and $k$(Cl-Cl) respectively. The limit of errors in the indices of resolution are, therefore, taken to be 0.05 and 0.04.

## Results

**Atomic Distances and Mean-Square Amplitudes.** — The atomic distance obtained by the least-squares fit of the observed curve to the molecular intensity function, $qM(q)$, is neither the equilibrium distance, $r_e$, nor the mean value of the internuclear probability distribution function, $r_g$. When $r'_a$ is corrected to $r_a$ to compensate for the difference in the camera lengths, the observed distance, $r_a$, is approximately equal to the mean value with respect to the radial distribution function; it is related to $r_g$ as follows;[1]

$$r_g = r_a + l^2/r_a \tag{6}$$

The observed mean amplitude, $l_a$, for which the effect of the sample size is corrected, is approximately equal to $l_g$, the mean amplitude referred to $r_g$ as will be shown below. It is assumed that the internuclear probability distribution function is represented by:

$$P(r) = [1+\beta_1(r-r_e)+\beta_2(r-r_e)^2 + \beta_3(r-r_e)^3]\,P_h(r) \tag{7}$$

where $P_h(r)$ is a probability distribution function corrected to the harmonic oscillator. The observed mean-square amplitude, $l_a^2$, is represented by:

$$\begin{aligned} l_a^2 = l_\alpha^2 + l_\alpha^4\{&2(\beta_2+\gamma\beta_1)-(\beta_1+\gamma)^2 \\ &-6l_\alpha^2(\beta_3+r\beta_2)(\beta_1+\gamma) \\ &-9l_\alpha^4(\beta_3+\gamma\beta_2)^2\} + l_\alpha^4\{(1/r_e^2) \\ &+6l_\alpha^2(\beta_3+\gamma\beta_2)/r_e\} \end{aligned} \tag{8}$$

and $l_g^2$ is represented by:

$$\begin{aligned} l_g^2 = l_\alpha^2 + l_\alpha^4\{&2(\beta_2+\gamma\beta_1)-(\beta_1+\gamma)^2 \\ &-6l_\alpha^2(\beta_3+\gamma\beta_2)(\beta_1+\gamma) \\ &-9l_\alpha^4(\beta_3+\gamma\beta_2)^2\} \end{aligned} \tag{9}$$

where $\gamma = (\langle\Delta x^2\rangle + \langle\Delta y^2\rangle)/2\langle\Delta z^2\rangle r_e$ and $l_\alpha$ is the mean amplitude referred to the harmonic oscillator. The last term in Eq. 8 is of the order of $(l/r)^2$. Therefore, $l_a$ is approximately equal to $l_g$.[17] It may easily be shown that almost the same result can be obtained if the Morse potential is assumed, in which case the term of $(r-r_e)^6$ is significant.

It should also be noted that the difference in the observed mean amplitudes, $l_g$, from the amplitudes, $l_\alpha$, which refer to the harmonic oscillators, is negligibly small when it is compared with their experimental errors; accordingly, $l_g$ may be used directly for the computation of the force constants.

We have recently proposed an internuclear distance parameter, $r_\alpha$:[24]

$$r_\alpha = r_g - (\langle\Delta x^2\rangle + \langle\Delta y^2\rangle)/2r_e - \delta r \tag{10}$$

where $\delta r$ is the correction for the centrifugal distortion; it is negligibly small for this molecule. For a tetrahedral molecule, $XY_4$, the perpendicular amplitudes, $\langle\Delta x^2\rangle$ and $\langle\Delta y^2\rangle$, are given by,

for the X-Y pair:

$$\langle\Delta x_1^2\rangle = \langle\Delta y_1^2\rangle = \frac{\mu_Y}{4}\langle Q_2^2\rangle + \left\{\frac{2}{\sqrt{3}}\mu_X L^{-1}{}_{33} - \left(\frac{4}{\sqrt{3}}\mu_X + \frac{\sqrt{3}}{2}\mu_Y\right)L^{-1}{}_{34}\right\}^2\langle Q_3^2\rangle$$

24) Y. Morino, K. Kuchitsu and T. Oka, *J. Chem. Phys.*, 36, 1108 (1962).

$$+\left\{\frac{2}{\sqrt{3}}\mu_X L^{-1}{}_{43} - \left(\frac{4}{\sqrt{3}}\mu_X + \frac{\sqrt{3}}{2}\mu_Y\right)L^{-1}{}_{44}\right\}^2\langle Q_4^2\rangle \quad (11)$$

and for the Y–Y pair:

$$\langle \Delta x_2^2\rangle = \frac{2}{3}\mu_Y^2(L^{-1}{}_{33}+L^{-1}{}_{34})^2\langle Q_3^2\rangle + \frac{2}{3}\mu_Y^2(L^{-1}{}_{43}+L^{-1}{}_{44})^2\langle Q_4^2\rangle \quad (12)$$

$$\langle \Delta y_2^2\rangle = \mu_Y\langle Q_2^2\rangle, \quad (14)$$

where $\mu_i$ denotes the reciprocal mass and $L^{-1}{}_{ij}$ the $i$, $j$ element of the $\boldsymbol{L}^{-1}$ matrix. The x and y axes are taken to be as shown in Fig. 2. The values of $r_\alpha$ obtained in this way are shown in Table V. The uncertainties listed in Table V are the 99% confidence limit of errors, including the systematic errors, as has been discussed above.

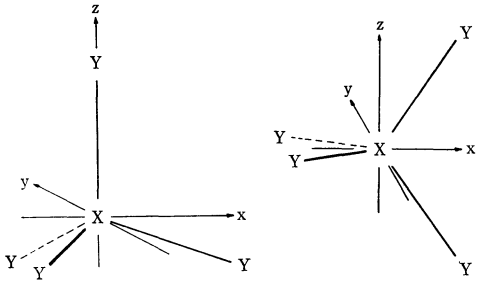



Fig. 2. Cartesian coordinates. The $z_i$ axes ($i$=1 or 2) are taken in the direction of the atomic pair at their equilibrium positions, the $x_i$ axes are taken on the plane Y-X-Y and perpendicular to $z_i$, and $y_i$ are perpendicular to $x_i$ and $z_i$.

TABLE V. FINAL RESULTS OF THE MOLECULAR CONSTANTS ($r$, $l$ and $\delta$ in Å units)

| | | |
|---|---|---|
| $r_g$ | 2.0193±0.0034 | 3.2953±0.0062 |
| $r_\alpha$ | 2.016 ±0.004 | 3.293 ±0.007 |
| $l_g$ | 0.0470±0.0016 | 0.0892±0.0024 |
| $k$ | 1.020 ±0.048 | 1.015 ±0.043 |
| $\delta_g$ | 0.0022±0.0032 | |

In this type of molecule, there is no totally-symmetric deformation mode; hence, the shrinkage of the Y–Y distance can be evaluated only by means of quadratic potential constants, just as in the case of linear molecules.[20] It is shown to be 0.0036Å for Cl–Cl. The observed shrinkage, $\delta_g$, on the other hand, is 0.0022±0.0032Å. It should be noted here that the shrinkage is not influenced by the uncertainty in the scale factor; it is given by the difference between two large quantities, both of which vary in the same ratio, when the scale factor changes.

The distance $r_\alpha$ does not show any shrinkage effect, because by definition it does not include the perpendicular vibration. The experimental result satisfies this requirement, although the uncertainty in the measurement does not give any clear evidence for the presence of the shrinkage effect in $r_g$ or for its absence in $r_\alpha$.

**Force Constants.**—It has already been pointed out that, in the tetrahedral molecules, all of the force constants in the general quadratic form cannot uniquely be determined from the vibrational frequencies alone. Accordingly, mean-square amplitudes cannot be calculated simply by using the frequencies. Since there are four frequencies in contrast to five constants, one degree of freedom is left undetermined. The two mean-square amplitudes which are compatible with the four vibrational frequencies, if taken as a set of coordinates, are given by a point on a closed curve given by the following set of relations:

$$l^2(\text{Si–Cl}) = \frac{1}{4}G_{11}\langle Q_1^2\rangle + \frac{3}{4}G_{33}\langle Q_3^2\rangle - \frac{3}{4}L_{34}^2(\langle Q_3^2\rangle - \langle Q_4^2\rangle) \quad (14)$$

$$l^2(\text{Cl–Cl}) = \frac{2}{3}G_{11}\langle Q_1^2\rangle + \frac{1}{9}G_{22}\langle Q_2^2\rangle + \frac{1}{6}(4G_{33}+4G_{34}+G_{44})\langle Q_3^2\rangle - \frac{1}{6}(2L_{34}+L_{44})^2(\langle Q_3^2\rangle - \langle Q_4^2\rangle) \quad (15)$$

$$(G_{33}-L_{34}^2)(G_{44}-L_{44}^2) = (G_{34}-L_{34}L_{44})^2 \quad (16)$$

where the $G_{ij}$'s are the elements of the $\boldsymbol{G}$-matrix, and the $\langle Q_i^2\rangle$'s are the squared mean

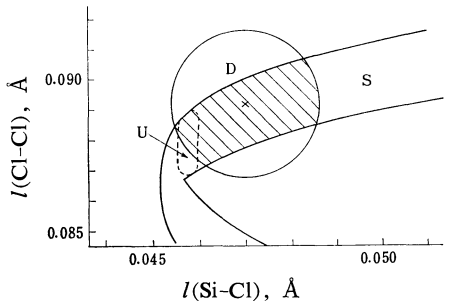


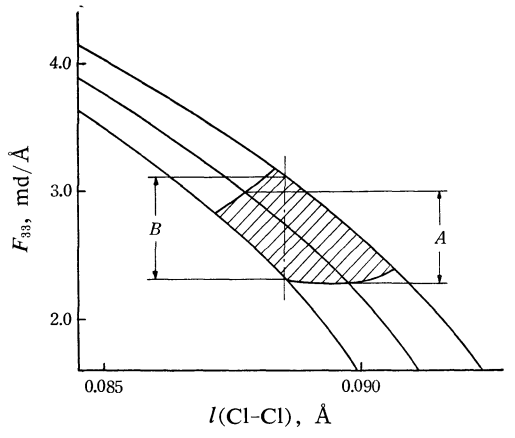

Fig. 3. Correlation curve of two mean amplitudes. The shaded area indicates the values which are compatible with both the diffraction and spectroscopic data.
D: Observed values by electron diffraction.
S: Calculated values from spectroscopic data.
U: Calculated values corresponding to the Urey-Bradley force field.

values of the displacements of the normal coordinates. The curve is shown in Fig. 3.

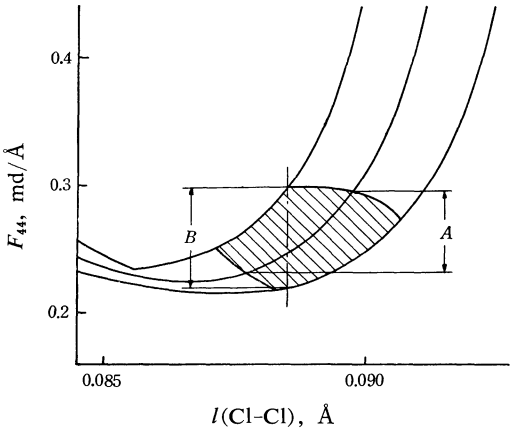
For the tetrahedral molecules, all fundamentals are Raman active, while only two frequencies of the symmetry $F_2$ are active in the infrared; for silicon tetrachloride one of them has a frequency too small to be observed by an ordinary infrared spectrometer. For the calculation of the force constants, we must use the normal frequencies of the molecule in the gaseous state. Since no observations of the Raman spectrum of this molecule in the vapor state had been reported, the measurement of the gaseous Raman spectrum was undertaken. The details of the experiment have beed reported elsewhere.[25] The vibrational frequencies obtained in this measurement are used in the calculations except for $\nu_3$, for which the fundamental frequency obtained by the infrared spectrum in the gaseous state[25] was used.

It is not practicable to make the correction of fundamental frequencies to the normal frequencies, because we have no exact knowledge on the anharmonicity factors of the potential function as a basis for calculating the correction. A tentative assumption regarding the potential function shows that the correction may be of the same order of magnitude as the uncertainties of the frequencies. The uncertainties in the frequencies cause the spread of the position and the size of the curve shown in Fig. 3. On the other hand, the mean amplitudes obtained by the electron diffraction experiment are expressed by an area enclosed by a circle which represents the limit of errors around the observed values. Thus, any point included in the overlapping area, the shaded portion in Fig. 3, is compatible with both the observed mean amplitudes and the observed vibrational frequencies within the limit of errors. As is clearly indicated in Figs. 4a and 4b, the uncertainties of the force constants originate from the mean amplitudes by the same order of magnitude as from the vibrational frequencies.

Table VI gives the force constants of the potential function in the general quadratic form in terms of the symmetry coordinates and of the internal coordinates. The force constants of the Urey-Bradley force field, with the additional assumption proposed by Shimanouchi that $F' = -(1/10)F$,[26] were computed by using the observed vibrational frequencies; the results are shown in Table VII. The possible range of the mean amplitudes




(a)




(b)

Fig. 4. Correlation curves of the force constants and $l$(Cl-Cl). The ranges $A$ indicate the limits of the force constants for which the errors of frequencies are disregarded, while the ranges $B$ show those for which the error of $l$(Cl-Cl) is ignored. Though only the diagonal elements of $F$-matrix are shown in this figure, the curve of $F_{34}$ is similar to $F_{44}$ in shape. (a) $F_{33}$, and (b) $F_{44}$.

TABLE VI. FORCE CONSTANTS OBTAINED BY USING THE MEAN AMPLITUDES
(in md./Å units)

| Symmetry coordinate system | | Internal coordinate system | |
|---|---|---|---|
| $F_{11}$ | 3.77 ±0.02 | $k_r$ | 2.97±0.34 |
| $F_{22}$ | 0.154±0.004 | $k_{rr}$ | 0.26±0.12 |
| $F_{33}$ | 2.71 ±0.45 | $k_\alpha - k_{\alpha\alpha'}$ | 0.26±0.04 |
| $F_{34}$ | 0.07 ±0.13 | $k_{\alpha\alpha} - k_{\alpha\alpha'}$ | 0.05±0.02 |
| $F_{44}$ | 0.26 ±0.04 | $k_{r\alpha} - k_{r\alpha'}$ | 0.05±0.10 |

calculated on the basis of these force constants is shown by the area enclosed in a broken ellipse in Fig. 3. Since a half of this area is located inside the limit of errors of the observed mean amplitudes, it may be inferred that the

25) Y. Morino, Y. Murata, T. Ito and J. Nakamura, *J. Phys. Soc. Japan*, **17**, Supplement B-II, 37 (1962).
26) T. Shimanouchi, *J. Chem. Soc. Japan, Pure Chem. Sec. (Nippon Kagaku Zassi)*, **74**, 266 (1953).

TABLE VII. FORCE CONSTANTS IN THE SYMMETRY-COORDINATE SYSTEM (in md./Å) AND MEAN AMPLITUDES (in Å) OBTAINED IN TERMS OF THE UREY-BRADLEY FORCE FIELD WITH THE ADDITIONAL ASSUMPTION THAT $F' = -(1/10)F$.

| | |
|---|---|
| $F_{11}$ | 3.77 ±0.02 |
| $F_{22}$ | 0.154 ±0.004 |
| $F_{33}$ | 3.02 ±0.03 |
| $F_{34}$ | 0.161 ±0.006 |
| $F_{44}$ | 0.23 ±0.01 |
| $l$(Si-Cl) | 0.0458±0.0002 |
| $l$(Cl-Cl) | 0.0877±0.0011 |

assumption of the Urey-Bradley type with $F' = -(1/10)F$ is approximately permissible in the case of silicon tetrachloride.

## Summary

The atomic distances and the mean-square amplitudes of silicon tetrachloride have been determined by the sector-microphotometer method. The possible sources of experimental errors have been thoroughly examined. The quadratic force constants of the potential function have been determined by the use of the mean-square amplitudes thus obtained, by combining them with the vibrational frequencies obtained from the Raman spectrum in the gaseous state. It has been shown that the errors of the force constants originate from those of the mean-square amplitudes by the same order of magnitude as from those of the frequencies.

The authors wish to express their gratitude to the Shin-Etsu Chemical Industrial Co., Ltd., for the supply of silicon tetrachloride, and to Professor Hidetoshi Takahashi of the Physics Department of the University of Tokyo for the use of the digital computer, PC-1. The expenses of the work were defrayed by the Ministry of Education, to which their thanks are also due.

*Department of Chemistry*
*Faculty of Science*
*The University of Tokyo*
*Hongo, Tokyo*

## Appendix

**The Analysis of Small-Angle Intensities.**—As has been described in this text, the atomic distances and the mean-square amplitudes of silicon tetrachloride have been determined precisely by the analysis of the electron diffraction halos taken by the short camera length, 11.8 cm. ($q$=18—97). On the other hand, the errors of the atomic distances and mean amplitudes are inversely proportional to $s$ and $s^2$ respectively, and the error caused by the uncertainty in the $\mu$-factor increases in the range of small $q$-values. It would be of interest to see what results can be obtained by the analysis of the photographs of silicon tetrachloride taken by the long camera distance at smaller scattering angles ($q$=8—36).

Since there are four humps in this range, as is shown in Fig. 5, reasonable background curves were obtained by Karle's method.[27] An analysis was made by the same procedure as that used in the analysis for the short camera distance except for the few points given below. In view of the limited number of observations (less than 30 for $\Delta q$=1), it was thought advantageous to make the number of variables for the analysis as small as possible. Therefore, by assuming that the Si-Cl and Cl-Cl distances have equal indices of resolution, the index was taken as one of the parameters instead of having both indices varied. A conventional weight function was used, since the use of other weight functions caused little change in this case. Four photographs were used for the analysis.

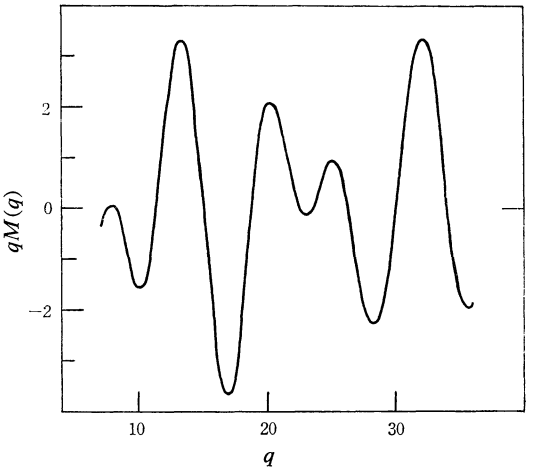



Fig. 5. Molecular intensity curve of $SiCl_4$ obtained by the long camera distance.

In the small-angle scattering ($s \lesssim 10$), the theoretical atomic form factor is strongly dependent on the original wave function used in the calculation. Therefore, the analysis of the intensity taken by the long camera distance, as separated from that taken by the short camera distance, was useful as a test of the effect of the atomic form factors on our analysis by using the various values listed below. The atomic form factors for silicon and chlorine have been obtained by Viervoll and Ögrim[12] on the basis of Hartree's wave function; by Ibers and Hoerni,[15] who reported $|f|$ based on the Thomas-Fermi model, and by Tomiie and Stam,[13] whose calculation was based on Slater's wave function. Three kinds of atomic form factor, were, threfore, used in the present analysis; (the first obtained by Viervoll and Ögrim, the second given by Tomiie and Stam for the silicon and chlorine atoms, and the third obtained by the

27) I. L. Karle and J. Karle, *J. Chem. Phys.*, **18**, 565 (1950).

arithmetic mean values of $f(Si^{4+})$ and $f(Si)$, and $f(Cl^-)$ and $f(Cl)$, for silicon and chlorine respectively, and given by Tomiie and Stam) since the Si-Cl bond in the silicon tetrachloride molecule is likely to have about a 50% ionic character at the chlorine atom, as estimated from the pure quadrupole resonance frequency[28] of $^{35}Cl$. Two kinds of the inelastic scattering factors which were obtained by Bewilogua[14] and Freeman[29] were used for calculating the $\mu$-factors. Unfortunately, however, the inelastic scattering factor for the chlorine atom was not calculated by Freeman; hence, an approximate value was estimated for our use.

Four sets of $\mu$-factors were obtained for Si-Cl and Cl-Cl, as is shown in Fig. 6; by using these

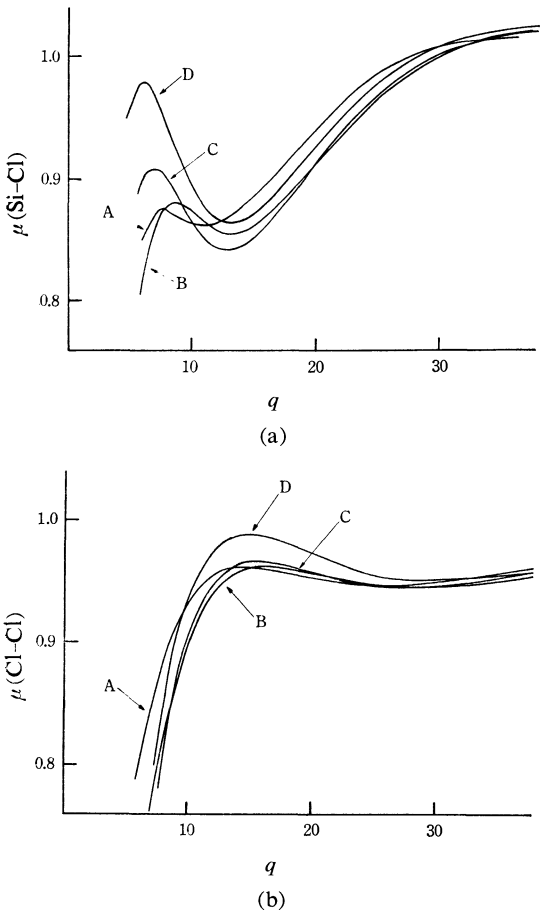



Fig. 6. The $\mu$-factors obtained by the combinations of the atomic form factors and the inelastic scattering factors shown in Table III. (a) Si-Cl, and (b) Cl-Cl.

28) H. C. Dehmelt, *J. Chem. Phys.*, **21**, 380 (1953); R. Livingston, *J. Phys. Chem.*, **57**, 496 (1953).
29) A. J. Freeman, *Acta Cryst.*, **12**, 929 (1959).

Table VIII. Dependence of parameters on the choice of variable $\mu$-factors ($r$ and $l$ in Å units)[a]

| | $r$(Si-Cl) | $\sigma_1$ | $\sigma_2$ | $r$(Cl-Cl) | $\sigma_1$ | $\sigma_2$ |
|---|---|---|---|---|---|---|
| A | 2.0173 | 0.0010 | 0.0028 | 3.2949 | 0.0012 | 0.0007 |
| B | 2.0175 | 0.0011 | 0.0028 | 3.2949 | 0.0012 | 0.0007 |
| C | 2.0172 | 0.0012 | 0.0029 | 3.2949 | 0.0013 | 0.0009 |
| D | 2.0172 | 0.0012 | 0.0028 | 3.2951 | 0.0014 | 0.0007 |
| | $l$(Si-Cl) | $\sigma_1$ | $\sigma_2$ | $l$(Cl-Cl) | $\sigma_1$ | $\sigma_2$ |
| A | 0.0520 | 0.0032 | 0.0018 | 0.0949 | 0.0021 | 0.0017 |
| B | 0.0520 | 0.0032 | 0.0018 | 0.0949 | 0.0021 | 0.0017 |
| C | 0.0520 | 0.0036 | 0.0017 | 0.0943 | 0.0024 | 0.0016 |
| D | 0.0467 | 0.0041 | 0.0019 | 0.0918 | 0.0025 | 0.0017 |
| | $k$ | $\sigma_1$ | $\sigma_2$ | | | |
| A | 1.098 | 0.011 | 0.018 | | | |
| B | 1.098 | 0.011 | 0.018 | | | |
| C | 1.096 | 0.012 | 0.019 | | | |
| D | 1.065 | 0.012 | 0.018 | | | |

a) The atomic form factors and the inelastic scattering factors used for calculating the $\mu$-factors were taken in the following combinations: A(a, d); B(b, d); C(c, d); and D(c, e).
a: The atomic form factor given by Viervoll and Ögrim.
b: The atomic form factor given by Tomiie and Stam.
c: The atomic form factor given by Tomiie and Stam in which the 50% ionic character was taken into account.
d: The inelastic scattering factor obtained by Bewilogua.
e: The inelastic scattering factor obtained by Freeman.

$\mu$-factors and each of the four observed intensity curves, the corresponding average values and the standard deviations of the parameters were obtained by the method of the least squares,[21] as is shown in Table VIII. It was found that the most probable values of the parameters in the first three sets were almost equal to one another, but that they are significantly different from the values obtained with the short camera distance, especially for the mean amplitudes. The last set agreed with the values obtained by the short camera distance. The $\mu$-factor is little affected by the change in the atomic form factor, since the change of the numerator is seemingly cancelled by that of the denominator. The inelastic scattering factor, on the other hand, is included only in the denominator of the $\mu$-factor, since, on the basis of the basic assumption, the inelastic scattering makes no contribution to the molecular term. The change in the inelastic scattering factor, therefore, has an appreciable effect on the molecular intensity in the small-angle region.

# The Distribution of Gas Molecules at the Diffraction Center in the Electron Diffraction Experiment*

By Yonezo MORINO and Yoshitada MURATA

(Received July 15, 1964)

The mean square amplitude determined by electron diffraction provides us with valuable information regarding the dynamical properties of molecules. Since, however, the values of the mean square amplitudes directly obtained from our measurements are strongly influenced by the delocalization of the sample, physically significant values cannot be obtained unless the correction for this effect is properly made. Moreover, the distribution of gas molecules depends on the shape of the nozzle, and sometimes a systematic error from this origin is introduced into the observed atomic distances.

The effect of a finite sample size has been discussed by Karle and Karle,[1] Harvey et al.,[2] and Kuchitsu.[3] Kuchitsu evaluated the distribution of gas molecules from a gradual decrease in the background curve at more than 80 in the $q$-scale. His basic idea was that the decrease was produced by the shielding of electron beams by the edge of the nozzle. The principle has been extended in the present experiment for a nozzle with an artificial diaphragm especially designed for the measurement of the distribution of gas molecules.

## The Measurement of the Distribution of Gas Molecules at the Diffraction Center

A diaphragm with a circular aperture at its center is attached immediately behind the nozzle. The main electron beam is adjusted to pass through the center of the aperture at a right angle to the plane of the diaphragm, as is shown in Fig. 1. If diffraction occurs in an infinitesimally small region at O, as assumed in the theoretical calculation, the diffraction intensity on the plate should be cut off sharply at point P, with no blackening beyond that point. However, as the gas stream has a finite width, some electrons diffracted at points nearer to the plate than O arrive at points farther away than P, resulting in a gradual

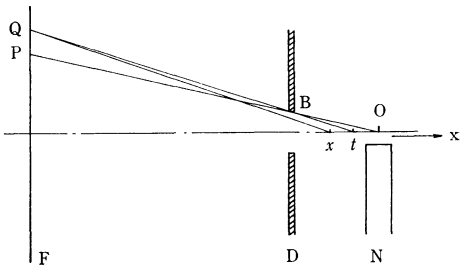



Fig. 1. Schematic representation of the arrangement for measurement of the gas distribution.
N: Nozzle D: Circular diaphragm
F: Photographic plate

change in the intensity. From the measurement of the change in the intensity near point P on the photograph, information is obtained regarding the distribution function, $f(x)$.

If multiple scattering is ignored, the scattered intensities with and without the diaphragm, $I_T{}^a$ and $I_T{}^b$ respectively, are given by the following expressions:

$$P(t)=\frac{I_T{}^a(s_0)}{I_T{}^b(s_0)}=\frac{\int_{-\infty}^{t} I_T(x, s_0)f(x)\mathrm{d}x}{\int_{-\infty}^{\infty} I_T(x, s_0)f(x)\mathrm{d}x} \qquad (1)$$

where $I_T(x, s_0)$ denotes the total intensity scattered at point $x$ along the main beam toward point Q, which corresponds to the direction, $s_0$, from the origin. The origin of the x axis is taken at a point above the center of the nozzle, while the negative direction of the x axis is taken from the nozzle towards the photographic plate. The function $f(x)$ denotes the linear density of gas molecules along the path of the primary electron beam. The upper limit of Eq. 1, $t$, designates the point at which line QB intersects the x axis, B being the edge of the diaphragm. The electrons diffracted before reaching point $t$ hit the diaphragm and do not arrive at the photographic plate.

When the main portion of the gaseous sample is localized in a small region near point O, $f(x)$ decreases steeply as $x$ increases. In such a case, $I(x, s_0)$ is supposed to be nearly constant in the range where $f(x)$ is of a significant magnitude, and Eq. 1 is simply

* Some preliminary results of this work were presented at the International Conference on Magnetism and Crystallography, Kyoto, 1961.

1) I. L. Karle and J. Karle, *J. Chem. Phys.*, **18**, 963 (1950).
2) R. B. Harvey, F. A. Keidel and S. H. Bauer, *J. Appl. Phys.*, **21**, 860 (1950).
3) K. Kuchitsu, This Bulletin, **32**, 748 (1959).

approximated by:

$$P(t)=\int_{-\infty}^{t} f(x)\mathrm{d}x \qquad (2)$$

when $f(x)$ is normalized as:

$$\int_{-\infty}^{\infty} f(x)\mathrm{d}x=1 \qquad (3)$$

The accuracy of such an approximation will be considered in Appendix II.

A diaphragm with an aperture 2.38 mm. in diameter was attached to the nozzle at a distance of 4.51 mm. The primary beam passed 0.41 mm. above the top of the nozzle. The surface of the diaphragm was coated with colloidal graphite powder in order to decrease the extraneous scattering.

A set of three photographs was taken by using silicon tetrachloride. The first photograph was taken for a blank test to make a correction for the extraneous scattering. The second was taken with the diaphragm, and the third, without it. The experimental conditions were the same as those in the case of the needle-type nozzle described in a previous paper.[4] The microphotometer tracings shown in Fig. 2 clearly indicate the decrease in

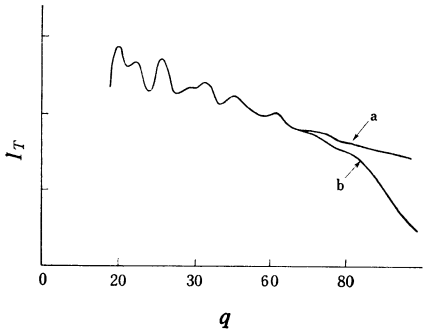



Fig. 2. Photometer curves of $SiCl_4$ with and without the diaphragm. The ordinate scale is in arbitrary units.
a: Without the diaphragm
b: With the diaphragm

intensity when the diaphragm was used. By the use of the dimension of the diaphragm and the observed ratio of the diffraction intensities at $s_0$, the function of $t$, $P(t)$, in Eq. 2 was derived. The $P(t)$ curve is shown in Fig. 3. The fact that the $P(t)$ curve was 1/2 at $t=0$ is consistent with the expectation derived from the assumption that the distribution of gas molecules is symmetric across the origin. It also indicates that the experimental arrangement conformed to our original plan. The plot of $\log(1-P(t))$ against $t$ was found to be closely approximated by two straight lines, as is shown in Fig. 4. It was

4) Y. Morino and Y. Murata, This Bulletin, 38, 105 (1965).

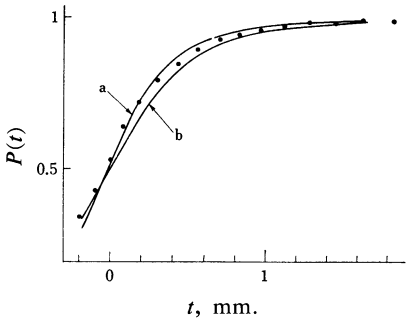



Fig. 3. Observed and calculated $P(t)$ curves. Observed values are shown in dots.
a: Calculated curve obtained by Eq. 9
b: Calculated curve obtained by Eq. 10

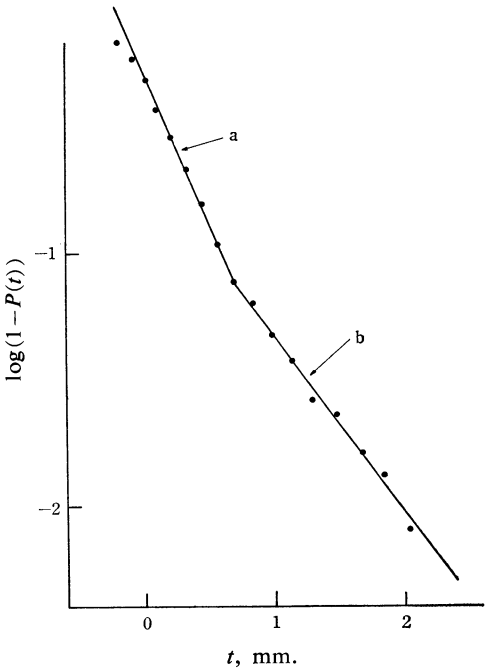



Fig. 4. Plots of $\log(1-P(t))$ vs. $t$; observed values are shown in dots. The straight lines a and b are represented by Eqs. 4a and 4b respectively. A break at $t=0.7$ is of little significance, since the lines a and b are only approximate representations of the original curve, which may lie on a smooth line. See descriptions in the text.

found that:

for

$$0.7 \geqq t \geqq 0, \quad P(t)=1-\frac{1}{2}\exp(-2.74t) \qquad (4a)$$

and for

$$t \geqq 0.7, \quad P(t)=1-0.224\exp(-1.59t) \qquad (4b)$$

when $t$ was measured in millimeter. By differentiating the above equations by $t$, the distribution function on the beam is represented

by:

for $0.7 \geqq x \geqq 0$,

$$f(x) = (2.74/2)\exp(-2.74x) \quad (5a)$$

and for $x \geqq 0.7$,

$$f(x) = 0.356\exp(-1.59x) \quad (5b)$$

where $x$ is also measured in millimeter. It may be possible to assume the same distribution function on the negative side of the x axis, because the value of $P(t)$ at $t=0$ was compatible with the assumption of the symmetric distribution around the origin. It seems strange that the density functions obtained above, 5a and 5b, are discontinuous at the intersection $x=0.7$. The sharp break results from the approximation that $\log(1-P(t))$ may be expressed by two straight lines.

As will be shown in Appendix I, the atomic distances and the index of resolution are little affected by the finite spread of gas molecules at the diffraction center, whereas the apparent increment in the root-mean-square amplitude, $\Delta l$, is given by:

$$\Delta l_{ij} = r_{ij}^2/l_{ij}\rho^2 L_0^2 \quad (6)$$

if the distribution function $f(x) = (\rho/2)\times \exp(-\rho|x|)$, with $\rho = 2.74\,\mathrm{mm}^{-1}$, is used through the whole range. The calculated values are listed in column a in Table I. In the range of $|x| \geqq 0.7$, the real distribution is slightly different from this function; it is expressed by another exponential function, 5b, which results in a 10% increase in the increment. The values of $\Delta l$ derived with this function are shown in column b of Table I.

TABLE I. CORRECTION FOR THE MEAN AMPLITUDES DUE TO THE FINITE SPREAD OF GAS MOLECULES (in Å units)

| | $l_a$(obs) | $\Delta l(a)$ | $\Delta l(b)$ |
|---|---|---|---|
| Si-Cl | 0.0479 | 0.0008 | 0.0009 |
| Cl-Cl | 0.0905 | 0.0012 | 0.0013 |

$\Delta l(a)$: Calculated by Eq. 6, on the assumption that the gas distritution is expressed by a simple distribution function 5a.
$\Delta l(b)$: Calculated by taking both functions 5a and 5b into account.

In the calculations described above, several approximations and assumptions were made. We will consider the validity of these approximations and assumptions below.

First, the assumption that the main portion of the gaseous molecules is confined to the range $|x/L_0| \ll 1$ is satisfied, because the value of $f(x)$ at $L_0 = 118$ mm. is very small, as is evident from Eq. 5. Next, the multiple scattering[5] can be disregarded in this experiment, because the indices of resolution were found to be unity or at least very close to unity.[4] This means that no "delocalization" of the gas molecules in the camera box[6] was recognized.

It will be shown in Appendix II that the approximation made in Eq. 2 is valid within 5% if we consider that $t$ is less than 2 mm. and $L_0 = 118$ mm.

## The Flow of Gas Molecules Emitted from the Nozzle

It is interesting to see what kind of gas flow is responsible for the distribution of gas molecules obtained above. The model to be considered first is the simplest one, in which the gas molecules are emitted from the center of the nozzle with an equal probability in all directions. The solid angle, $d\omega$, which corresponds to a rectangular area enclosed by the width, $d$, and the length of $dx$ on the beam is given by:

$$d\omega = ad\,dx/(x^2+a^2)^{3/2} \quad (7)$$

where $a$ is the distance from the top of the nozzle to the main beam ($a = 0.41$ mm.). Therefore, the normalized distribution function is represented by:

$$f(x) = a^2/2(x^2+a^2)^{3/2} \quad (8)$$

It follows that:

$$P(t) = (1/2)\,(1+t/(a^2+t^2)^{1/2}) \quad (9)$$

This formula, which denotes the integrated distribution of the gas molecules, contains only a measurable parameter, $a$. In Fig. 3, curve a shows the $P(t)$ which was obtained by inserting the actual dimension of $a = 0.41$ mm. into Eq. 9.

In the model described above, the drastic assumption was made that the flow of the molecules comes from a single point, i. e., from the center of the top of the nozzle. In the actual experiment, however, the molecules come out from the whole area of the nozzle exit. It is, accordingly, likely that the gas distribution near the nozzle is quite different from that derived above. Thus another model must be considered, one in which gas molecules are emitted from the entire opening of the nozzle with an equal probability in every direction. It is easy to show that, when the radius of the nozzle is $b$, the distribution function on the main beam is given by:

$$f(x) = \int_0^b \int_0^{2\pi} \frac{Aar\,dr\,d\theta}{(x^2+a^2+r^2-2xr\cos\theta)^{3/2}} \quad (10)$$

5) J. A. Hoerni, *Phys. Rev.*, **102**, 1530 (1956).

6) L. S. Bartell, *J. Appl. Phys.*, **31**, 252 (1960).

where $A$ is a normalization constant.

An approximate calculation was carried out by the use of a series expansion, instead of exact integration using the elliptic function of the second kind. The results are shown by curve b in Fig. 3. Both of the calculated $P(t)$ functions, a and b, are consistent with the observed $P(t)$, but a detailed comparison reveals that the first model is slightly better than the second. It may be considered from this finding that the gas flows faster in the central part than in the outer part of the nozzle; in other words, the flow is more or less viscous within the tube, even though the stream of gas molecules behaves as a molecular flow after leaving the nozzle. In fact, the mean free path in the nozzle is estimated to be 0.03 mm., much smaller than the diameter of the nozzle, 0.55 mm.

### The Effect of Asymmetric Distribution at the Nozzle

It was shown in the previous section that, in the case of the needle-type nozzle, the gas distribution has its center exactly over the nozzle and fades away symmetrically from the center in both directions. However, in the case of the drum-type nozzle, as is shown in Fig. 8 of Ref. 3, the distribution may be asymmetric with respect to the center of the nozzle, because the front edge of the nozzle was cut off in a cone-shape in order to secure a wide angle for the diffracted electrons. Hence, it is worthwhile measuring the difference in the distribution on both sides and estimating its influence on the observed molecular parameters.

For the needle-type nozzle, it was found in this study that the distribution may be represented by an exponential function, $C\exp(-\rho|x|)$. However, in the case of the drum-type nozzle, a Gaussian function is more suitable for the distribution. This is because the emitted gas molecules hit the upper wall of the nozzle and recoil to give an increased gas density near the center of the nozzle and an increased spread of the gas distribution. Accordingly, for a drum-type nozzle, the distribution may be fitted by two Gaussian functions with different parameters in the exponents, one for the positive side and the other for the negative side. It may be reasonable to take the maximum at $x=0$. Thus the distribution function in the regular orientation is assumed to be

$$f(x)=C_1\exp(-ax^2), \quad \text{for} \quad x>0 \tag{11a}$$

and

$$f(x)=C_2\exp(-bx^2), \quad \text{for} \quad x<0 \tag{11b}$$

If the functions are taken to be continuous at $x=0$ and are normalized to unity, then the coefficient is given by:

$$C_1=C_2=2(a/\pi)^{1/2}/(1+K) \tag{12}$$

where $K=(a/b)^{1/2}$ denotes the ratio of the half-widths. In order to estimate parameters $a$ and $b$, two photographs were taken, one at the regular orientation to obtain the constant $b$, and the other at the reversed orientation of the nozzle, i. e., by turning the other face of the nozzle to the plate, to obtain the constant $a$. Silicon tetrachloride was taken as a sample, and experimental conditions were chosen to be almost the same as in the case of the drum-type nozzle described in the previous paper.[4] For both regular and reversed orientations of the nozzle, the experimental background curves were compared with the theoretical curve.[3]

The observed $P(t)$ curve should fit with

$$P(t)=\frac{K}{1+K}+\frac{1}{1+K}\,\mathrm{Erf}(\sqrt{a}\,t) \tag{13a}$$

for the regular position, and

$$P(t)=\frac{1}{1+K}+\frac{K}{1+K}\,\mathrm{Erf}(\sqrt{b}\,t) \tag{13b}$$

for the reversed orientation. Parameters $a$ and $b$ cannot be determined separately, because both Eqs. 13a and 13b contain $K$, in addition to a single parameter, $a$ or $b$. Hence, by considering both curves simultaneously, the values of $a$ and $b$ were obtained to be $a=0.42\,\mathrm{mm}^{-2}$ and $b=0.67\,\mathrm{mm}^{-2}$, while $K=0.79$. It is interesting to notice that 0.79 is much larger than the value presumed from the geometrical dimension of the nozzle; if we assume that the half-width of each side of the distribution is proportional to the width of the nozzle wall, $K$ should be 0.53. The result indicates that the asymmetry of the gas distribution is smaller than the geometrical asymmetry of the nozzle.

As will be shown in Appendix I, the apparent increases in the atomic distances and in the root-mean-square amplitudes are given by:

$$\frac{\Delta r}{r}=-\frac{1-K}{\sqrt{\pi a}\,L_0} \tag{14}$$

and:

$$\frac{\Delta l}{l}=\frac{(1-K+K^2)}{4aL_0^2}\left(\frac{r}{l}\right)^2 \tag{15}$$

The values of $a$ and $b$ determined above lead to the result that $\Delta r$'s are $-0.0032$ Å and $-0.0052$ Å, while $\Delta l$'s are 0.0031 Å and 0.0045 Å for Si–Cl and Cl–Cl respectively.

On the other hand, a small discrepancy in the atomic distance was observed by reversing the orientation of the nozzle, as has been described in a previous paper.[4] Since the observed differences in the atomic distances, shown in Table I of Ref. 4, correspond to $2\Delta r$, the apparent increases, $\Delta r$ caused by the asymmetric distribution are shown to be $-0.0022$ Å

for Si–Cl and −0.0035 Å for Cl–Cl; they are in good agreement with the values obtained above by estimating the gas distribution.

It should be noted that the apparent increase in the mean amplitudes is much larger in the case of the drum-type nozzle than in the case of the needle-type nozzle. The mean amplitudes obtained by the drum-type nozzle, when corrected for the gas distribution given above, agree well with the values obtained by the needle-type nozzle, as Table II shows.

TABLE II. MEAN AMPLITUDES OBTAINED BY TWO TYPES OF NOZZLES (in Å units)

| | | $l$(Si–Cl) | $l$(Cl–Cl) |
|---|---|---|---|
| Needle-type | (a) | 0.0479 | 0.0905 |
| | (b) | 0.0470±0.0016 | 0.0892±0.0024 |
| Drum-type (regular orientation) | (a) | 0.0495 | 0.0943 |
| | (b) | 0.0464±0.0045 | 0.0898±0.0053 |

(a): Most probable values obtained by the method of least squares to each of four photographs.
(b): Final values. The errors associated with the drum-type nozzle caused by the estimation of the finite sample size were assumed to be 100% of the corrections.

## Summary

A method has been proposed for estimating the distribution of gas molecules at the diffraction center in order to evaluate the correction for finite sample size in gas electron diffraction. The distribution measured in this way has been interpreted by a simple model regarding the motion of the gas molecules in the vicinity of the nozzle. A slight asymmetry of the nozzle construction produces in the atomic distances a deviation which cannot be disregarded if an accurate measurement is desired.

The expenses of the work were defrayed by a grant from the Ministry of Education, to which the authors' thanks are due.

*Department of Chemistry*
*Faculty of Science*
*The University of Tokyo*
*Hongo, Tokyo*

## Appendix I

Let us consider the influence of the finite distribution of gas molecules at the diffraction center upon the atomic distances, mean square amplitudes, and index of resolution.

If the gas distribution is given by $f(x)$, the observed total intensity is expressed by:

$$I_T(s_0)=\int_{-\infty}^{\infty} I_T(x,s_0)f(x)\,dx \tag{A1}$$

and the observed molecular intensity function is given by:

$$M(s_0)=\int_{-\infty}^{\infty} I_M(x,s_0)f(x)\,dx \Big/ \int_{-\infty}^{\infty} I_B(x,s_0)f(x)\,dx \tag{A2}$$

where $I_M(x,s_0)$ and $I_B(x,s_0)$ are the functions of $x$ through $s$ and $L$:

$$I_M(x,s_0)=\sum_{ij} C_{ij}\frac{L}{(L^2+R^2)^{3/2}s^4}\frac{\sin sr_{ij}}{sr_{ij}} \times\exp(-\alpha_{ij}s^2) \tag{A3}$$

and

$$I_B(x,s_0)=\sum_{ij} C'_{ij}\frac{L}{(L^2+R^2)^{3/2}s^4} \tag{A4}$$

To the second order of approximation with regard to $z=x/L_0$ and $a^2=(R/L_0)^2$ ($L_0$ being the camera length from the origin of the x axis, and $R$, the radius of point P on the photographic plate), $s$ is given by:

$$s=s_0(1-\gamma z+\delta z^2) \tag{A5}$$

where

$$\gamma=1-\frac{3}{4}bs_0^2+\frac{1}{8}b^2s_0^4 \tag{A6}$$

$$\delta=1-\frac{15}{8}bs_0^2+\frac{41}{32}b^2s_0^4 \tag{A7}$$

and

$$L=L_0+x \tag{A8}$$

$$a^2=bs_0^2\left(1+\frac{3}{4}bs_0^2\right) \tag{A9}$$

Here $s_0$ denotes the $s$-value for the diffraction at the origin to point P and $b=\lambda^2/4\pi^2$. Expanding Eqs. A3 and A4 in terms of $x$ and $a^2$, and disregarding coefficients smaller than 1% of the largest one, it can be shown that:

$$\begin{aligned}M(s)=&\sum I_M(0,s_0)\Big[(1+\langle z\rangle+2\langle z^2\rangle-2\langle z\rangle^2)\\&+\Big(2\alpha\langle z\rangle-\frac{1}{2}r^2\langle z^2\rangle\Big)s_0^2\\&+\Big\{-\frac{3}{2}\alpha b\langle z\rangle+\Big(\frac{3}{4}br^2+2\alpha^2\Big)\langle z^2\rangle\Big\}s_0^4\Big]\\&+\sum I_M(0,s_0)\frac{\cos s_0r}{\sin s_0r}rs_0\Big[(-\langle z\rangle-2\langle z^2\rangle+2\langle z\rangle^2)\\&+\Big(\frac{3}{4}b\langle z\rangle-2\alpha\langle z^2\rangle\Big)s_0^2\\&+\Big(-\frac{1}{8}b^2\langle z\rangle+3\alpha b\langle z^2\rangle\Big)s_0^4\Big]\end{aligned} \tag{A10}$$

where

$$\langle z\rangle=\int_{-\infty}^{\infty} zf(x)\,dx \tag{A11}$$

On the other hand, if it is assumed that the diffraction intensity can be expressed by the usual diffraction formula with slightly modified molecular parameters:

$$M(s)=\sum kC\exp(-(\alpha+\Delta\alpha)s_0^2)\sin(s_0r+s_0\Delta r)/ s_0(r+\Delta r) \tag{A12}$$

a formula corresponding to Eq. A10 is obtained by expanding Eq. A12 with regard to the small quantities. Comparing the corresponding terms in $s_0$, the following relations are obtained:

$$1+\langle z\rangle+2\langle z^2\rangle-2\langle z\rangle^2=k(1-\Delta r/r) \tag{A13}$$

$$2\alpha\langle z\rangle-\frac{1}{2}r^2\langle z^2\rangle=-k(1-\Delta r/r)(\Delta\alpha+\Delta r^2/2) \quad \text{(A14)}$$

$$(3b/4)(-2\alpha\langle z\rangle+r^2\langle z^2\rangle)=k(1-\Delta r/r)\times(\Delta\alpha\Delta r^2/2+\Delta\alpha^2/2+\Delta r^4/4!) \quad \text{(A15)}$$

$$-r(\langle z\rangle+2\langle z^2\rangle-2\langle z\rangle^2)=k(1-\Delta r/r)\Delta r \quad \text{(A16)}$$

$$-r(2\alpha\langle z^2\rangle-\frac{3}{4}b\langle z\rangle)=-k(\Delta\alpha+\Delta r^2/6)(1-\Delta r/r)\Delta r \quad \text{(A17)}$$

and

$$r(3\alpha b\langle z^2\rangle-\frac{1}{8}b^2\langle z\rangle)=k(1-\Delta r/r)\Delta r\times(\Delta\alpha\Delta r^2/6+\Delta\alpha^2/2+\Delta r^4/5!) \quad \text{(A18)}$$

From Eqs. A13 and A16 we obtain:

$$\Delta r/r=-(\langle z\rangle+2\langle z^2\rangle-3\langle z\rangle^2) \quad \text{(A19)}$$

By inserting the result in Eq. A13, it is shown that:

$$k=1 \quad \text{(A20)}$$

and also in Eq. A14:

$$\Delta\alpha=\frac{1}{2}r^2\langle z^2\rangle-2\alpha\langle z\rangle-\frac{1}{2}r^2\langle z\rangle^2+2\alpha\langle z\rangle^2 \quad \text{(A21)}$$

**(I) The Case of a Symmetric Distribution.**—It was found that the distribution of gas molecules for the needle-type nozzle was symmetrical with respect to the origin $x=0$. In this case, $\langle z\rangle=0$, and Eqs. A19 and A21 are simplified as follows:

$$\Delta r/r=-2\langle z^2\rangle \quad \text{(A22)}$$

and

$$\Delta\alpha=\frac{1}{2}r^2\langle z^2\rangle \quad \text{(A23)}$$

Now, if the distribution function obtained above, $f(x)=(\rho/2)\exp(-\rho|x|)$, with $\rho=2.74\,\mathrm{mm}^{-1}$, is used over the whole range, the mean value of $z^2$ is given by:

$$\langle z^2\rangle=2/\rho^2L_0^2 \quad \text{(A24)}$$

and: $$\Delta r/r=-4/\rho^2L_0^2 \quad \text{(A25)}$$

The apparent increase in the mean amplitude is thus obtained by:

$$\Delta l=\Delta\alpha/l=r^2/l\rho^2L_0^2 \quad \text{(A26)}$$

**(II) The Case of Asymmetric Distribution.**—For the drum-type nozzle, we have evidence that the distribution of gas molecules is not symmetrical with respect to the origin. Therefore, correction must be made in such a case.

If the distribution function in the regular orientation is expressed by the following formulas:

$$f(x)=C\exp(-ax^2) \quad \text{for } x>0 \quad \text{(A27)}$$

and $$f(x)=C\exp(-bx^2) \quad \text{for } x<0 \quad \text{(A28)}$$

where $$C=2\sqrt{a}/\sqrt{\pi}\,(1+K) \quad \text{(A29)}$$

and $$K^2=a/b \quad \text{(A30)}$$

the means of $z$ and $z^2$ are expressed by:

$$\langle z\rangle=(1-K)/\sqrt{\pi a}\,L_0 \quad \text{(A31)}$$

and $$\langle z^2\rangle=(1-K+K^2)/2aL_0^2 \quad \text{(A32)}$$

The observed values of $a=0.418$, $K=0.787$ and $L_0=118$ lead to the results $\langle z\rangle=1.57\times10^{-3}$, and $\langle z^2\rangle=7.15\times10^{-5}$. Therefore, disregarding smaller terms, Eqs. A19 and A21 reduce to:

$$\Delta r/r=(K-1)/\sqrt{\pi a}\,L_0 \quad \text{(A33)}$$

and $$\Delta\alpha=(1-K+K^2)r^2/4aL_0^2 \quad \text{(A34)}$$

and $$\Delta l/l=(1-K+K^2)r^2/4l^2aL_0^2 \quad \text{(A35)}$$

Equations A15, A17 and A18 give further relations among $\Delta r$, $\Delta\alpha$ and $k$, but they are not always reasonable, because the basic assumption A12 does not hold exactly for such higher terms.

## Appendix II

It will be worthwhile to consider the uncertainty of the approximation used in Eq. 2; that is:

$$P(t)=\frac{\int_{-\infty}^{t}I_Tf(x)\mathrm{d}x}{\int_{-\infty}^{\infty}I_Tf(x)\mathrm{d}x}=\int_{-\infty}^{t}f(x)\mathrm{d}x \quad \text{(A36)}$$

Now the total scattering intensity is given by:

$$I_T=I_B(1+M) \quad \text{(A37)}$$

By expanding it in terms of $z$,

$$I_T\cong I_T^0(1+2z+z^2)+I_B^0\times\left[\left(\frac{dM}{dz}\right)_0z+2\left(\frac{dM}{dz}\right)_0z^2+\frac{1}{2}\left(\frac{d^2M}{dz^2}\right)_0z^2\right] \quad \text{(A38)}$$

while by assuming the symmetric distribution $f(x)=(\rho/2)\exp(-\rho|x|)$, the $P(t)$ function is shown to be as follows:

$$P(t)=\int_{-\infty}^{t}f(x)\mathrm{d}x(1+\Delta) \quad \text{(A39)}$$

where

$$\Delta=\frac{1}{L_0}\left(t-\frac{1}{\rho}\right)\left[2I_T^0+I_B^0\left(\frac{dM}{dz}\right)_0\right]\Big/\int_{-\infty}^{\infty}I_Tf(x)\mathrm{d}x \quad \text{(A40)}$$

By considering the fact that:

$$2/\rho^2L_0^2=2\times10^{-5}\ll1$$

$$I_B^0\cong I_T^0$$

$$\left|\left(\frac{dM}{dz}\right)_0\right|\cong1$$

$$\left|I_B^0\left(\frac{dM}{dz}\right)_0\frac{1}{\rho^2L_0^2}\right|\ll I_T^0$$

$$\left|\left(\frac{d^2M}{dz^2}\right)_0\right|<(rs_0+4\alpha s_0^2)$$

$$\left|I_B^0\left(\frac{d^2M}{dz^2}\right)_0\frac{1}{\rho^2L_0^2}\right|<\frac{1}{100}I_T^0$$

and that, therefore:

$$\int_{-\infty}^{\infty}I_Tf(x)\mathrm{d}x\cong I_T^0$$

Eq. A40 may be roughly evaluated as follows:

$$|\Delta|\cong\frac{2}{L_0}\left(t-\frac{1}{\rho}\right)\left(1+\frac{1}{2}\right)=\frac{3}{L_0}\left(t-\frac{1}{\rho}\right)\cong5\% \quad \text{(A41)}$$

In conclusion, the approximation made in Eq. 2 is satisfied within an uncertainty of 5%.

# A Synthesis of Oxytocin

By Shumpei SAKAKIBARA, Yoshibumi NOBUHARA,*
Yasutsugu SHIMONISHI and Reiko KIYOI

(Received July 27, 1964)

Oxytocin, which is well known as a hormone of the posterior pituitary gland, has been synthesized by many workers[1-6] in different ways since the first brilliant synthesis of the hormone by du Vigneaud et al. in 1953—1954[7]. In all cases, two protecting groups, *S*-benzyl for the cysteinyl residue and carbobenzoxy for the amino nitrogen, have been employed during the syntheses for the following reasons: (1) The *S*-benzyl group is comparatively stable during the peptide synthesis. (2) The carbobenzoxy group is, generally, the most convenient *N*-protecting group for peptide synthesis, and the selective removal of the *N*-protecting group from an *N*-carbobenzoxy-peptide derivative containing *S*-benzyl cysteine can be accomplished by using anhydrous hydrogen bromide without any complications in other parts of the peptide. (3) Both protecting groups can be removed simultaneously using sodium in liquid ammonia.

The sodium treatment of the protected peptide in liquid ammonia, however, is rather drastic, and some side-reactions may occur during the process. Moreover, it must be remembered that the removal of a protecting group from a larger peptide is, in general, more difficult than the removal of one from a smaller peptide. Actually, du Vigneaud et al. reported that the protected pre-oxytocic nona-peptide had been reduced in boiling liquid ammonia.[7] Nevertheless, the yield of active oxytocin from a large-scale sample (1.3 g.) of the protected nona-peptide was less than that from a small-scale sample (50 mg.) of the same intermediate.[5] This must be because it is difficult to remove the *S*-benzyl group with sodium in liquid ammonia. Therefore, an *S*-protecting group which is easier to remove has long been required in the preparation of such a complicated cysteine-peptide.

Only one different route to oxytocin has been reported, the method of Velluz.[3] In this the *S*-trityl group is used for the protection of the sulfhydryl group. Since, however, the *S*-trityl group is quite unstable against anhydrous hydrogen bromide, the use of the carbobenzoxy group for the protection of amino nitrogen during peptide synthesis is impossible, and the more labile *N*-trityl group is used. This limitation is fatal to the practical synthesis of the hormone, because the synthesis of *N*-trityl amino acids or peptides is, in general, much more complicated than that of carbobenzoxy derivatives.[8]

Recently, it was found by the present authors[9] that the *p*-methoxybenzyl (anisyl) group was valuable in protecting the thiol of cysteinyl residues; that is, the protecting group was stable against hydrogen bromide at room temperature, and it was easily cleaved from the final product by treatment with either sodium in liquid ammonia, or boiling trifluoroacetic acid. Moreover, it was found that the synthesis of *S*-*p*-methoxybenzyl cysteine was as easy as that of the *S*-benzyl derivative.

In the present paper, the synthesis of oxytocin using the *p*-methoxybenzyl group for the protection of cysteinyl residues will be described. For the synthesis of the hormone, the step-wise elongation method using carbobenzoxyamino acid *p*-nitrophenylesters was employed. *N*-Carbobenzoxy-*S*-*p*-methoxybenzyl-L-cysteine *p*-nitrophenylester (III) was synthesized by the dicyclohexylcarbodiimide method. Compound III was coupled with L-prolyl-L-leucylglycinamide,[10] and then the carbobenzoxy group was removed from the

* Present address: Dainippon Pharmaceutical Co., Ltd., Fukushima-ku, Osaka.

1) R. A. Boissonnas, S. Guttmann, P. A. Jaquenoud and J. P. Waller, *Helv. Chim. Acta*, **38**, 1491 (1955).
2) J. Rudinger, J. Honzl and M. Zaoral, *Chem. Listy*, **50**, 288 (1956); *Coll. Czech. Chem. Communs.*, **21**, 202 (1956).
3) L. Velluz, G. Amiard, J. Bartos, B. Goffinet and R. Heymès, *Bull. soc. chim. France*, **1956**, 1464.
4) M. Bodanszky and V. du Vigneaud, *J. Am. Chem. Soc.*, **81**, 2504 (1959).
5) M. Bodanszky and V. du Vigneaud, ibid., **81**, 5688 (1959).
6) H. C. Beyerman, J. S. Bontekoe and A. C. Koch, *Rec. trav. chim.*, **78**, 935 (1959).
7) V. du Vigneaud, C. Ressler, J. M. Swan, C. W. Roberts, P. G. Katsoyannis and S. Gordon, *J. Am. Chem. Soc.*, **75**, 4879 (1953); V. du Vigneaud, C. Ressler, J. M. Swan, C. W. Roberts and P. G. Katsoyannis, ibid., **76**, 3115 (1954).
8) L. Zervas and D. M. Theodoropoulos, ibid., **78**, 1359 (1956); L. Zervas, D. Borovas and E. Gazis, ibid., **85**, 3660 (1963).
9) S. Akabori, S. Sakakibara, Y. Shimonishi and Y. Nobuhara, This Bulletin, **37**, 433 (1964).
10) C. Ressler and V. du Vigneaud, *J. Am. Chem. Soc.*, **76**, 3107 (1954).

product, *N*-carbobenzoxy-*S*-*p*-methoxybenzyl-L-cysteinyl-L-prolyl-L-leucylglycinamide (IV), by treatment with hydrogen bromide in the normal way. A series of carbobenzoxyamino acid *p*-nitrophenylesters were then coupled one by one with the respective peptide amides after treatment with hydrogen bromide. No complications occurred with *S*-methoxybenzyl cysteine residues during the synthesis, and the final protected nona-peptide amide (IX) was obtained in a good yield.

H-CyS(MBz)-OH → Cbz-CyS(MBz)-OH →
(I) (II)

Cbz-CyS(MBz)-OPNP
(III)

III + H-Pro-Leu-Gly-$NH_2$ →

Cbz-CyS(MBz)-Pro-Leu-Gly-$NH_2$ (IV)

1) HBr/AcOH
2) Cbz-Asp($NH_2$)-OPNP → Cbz-Asp($NH_2$)-

CyS(MBz)-Pro-Leu-Gly-$NH_2$ (V)

1) HBr/AcOH
2) Cbz-Glu($NH_2$)-OPNP → Cbz-Glu($NH_2$)-

Asp($NH_2$)-CyS(MBz)-Pro-Leu-Gly-$NH_2$ (VI)

1) HBr/AcOH
2) Cbz-Ileu-OPNP → Cbz-Ileu-Glu($NH_2$)-

Asp($NH_2$)-CyS(MBz)-Pro-Leu-Gly-$NH_2$ (VII)

1) HBr/AcOH
2) Cbz-Tyr(Bz)-OPNP → Cbz-Tyr(Bz)-Ileu-

Glu($NH_2$)-Asp($NH_2$)-CyS(MBz)-

Pro-Leu-Gly-$NH_2$ (VIII)

1) HBr/AcOH
2) III → Cbz-CyS(MBz)-Tyr-Ileu-

Glu($NH_2$)-Asp($NH_2$)-CyS(MBz)-

Pro-Leu-Gly-$NH_2$ (IX)

1) $CF_3COOH$ or Na/$NH_3$
2) aeration → Oxytocin

MBz=*p*-Methoxybenzyl Cbz=Carbobenzoxy
PNP=*p*-Nitrophenyl

First, the protected nona-peptide (IX) was treated with boiling trifluoroacetic acid for two hours; it was confirmed that a total oxytocic activity of about 3300 units is obtained from 100 mg. of substance IX after the usual aeration procedure. Some hydrolysis of amide-bonds probably occurs during the process, and this is the main reason why the recovery of the active oxytocin is low. The trifluoroacetic acid procedure is now being improved in the laboratory. The usual procedure of sodium reduction in liquid ammonia, followed by aeration at pH 6.5, gave a high oxytocic activity, regardless of the quantity of material IX fed into the reaction (170000 units from 1 g. of substance IX, or 24000 units from 100 mg. of the same substance). This was surprising in view of the results of Bodanszky et al.,[5] who reported that 12500—15000 units were obtained from 50 mg. of a protected nona-peptide containing *S*-benzyl-cysteinyl residues, whereas 168000 units were obtained from 1.3 g. of the same material.

## Experimental*

***S*-*p*-Methoxybenzyl-L-Cysteine (I).** — This compound was prepared from L-cystine (50.0 g., 0.21 mol.) and *p*-methoxybenzyl chloride (72.0 g., 0.46 mol.) according to the procedure of du Vigneaud et al. for the synthesis of *S*-benzyl derivatives. The recrystallization of the crude product (107 g.) from water gave colorless plates; wt. 78.0 g. (78%), m. p. 198—199°C (decomp.), $[\alpha]_D^{25}$ +22.6° (*c* 1.02, N NaOH).

Found: C, 54.50; H, 6.33; N, 5.89; S, 13.05. Calcd. for $C_{11}H_{15}O_3NS$: C, 54.75; H, 6.26; N, 5.81; S, 13.29%.

***N*-Carbobenzoxy-*S*-*p*-methoxybenzyl-L-cysteine (II).**—A solution of I (12.1 g., 0.05 mol.) in a cold N sodium hydroxide solution (50 ml.) was treated with carbobenzoxy chloride (10.3 g., 0.06 mol.) and 2 N sodium hydroxide (30 ml.) alternately under vigorous stirring below 0°C. The stirring was continued for an additional hour without external cooling. When usual extraction procedures were then followed, an oily material was obtained which was solidified by adding petroleum ether (60—80°C). The crude material was recrystallizable from toluene; wt. 14.2 g. (76%), m. p. 62—65°C, $[\alpha]_D^{23}$ −45.5° (*c* 1.98, acetone).

Found: C, 61.11; H, 5.81; N, 3.68; S. 8.46. Calcd. for $C_{19}H_{21}O_5NS$: C, 60.78; H, 5.64; N, 3.73; S, 8.54%.

***N*-Carbobenzoxy-*S*-*p*-methoxybenzyl-L-cysteine *p*-nitrophenylester (III).**—A solution of II (109 g., 0.29 mol.) and *p*-nitrophenol (48.4 g., 0.348 mol.) in ethyl acetate (250 ml.) was cooled to −10°C, and dicyclohexylcarbodiimide (59.7 g., 0.29 mol.) in ethyl acetate (100 ml.) was stirred in. The mixture was allowed to react for an hour at −10°C, and then for two hours more at room temperature. The precipitated materials were filtered off and washed with a small amount of ethyl acetate. The filtrate and washings were combined and concentrated to dryness in vacuo. Crude material III was collected by using a mixture of ethanol and petroleum ether (60—80°C); wt. 18.5 g., m. p. 92—97°C. Recrystallization from ethanol gave colorless fine needles; wt. 110 g. (76%), m. p. 94—97°C, $[\alpha]_D^{21}$ −39.8° (*c* 2.06, dimethylformamide).

Found: C, 60.71; H, 4.80; N, 5.78; S, 6.68. Calcd. for $C_{25}H_{24}O_7N_2S$: C, 60.48; H, 4.87; N, 5.64; S, 6.46%.

***N*-Carbobenzoxy-*S*-methoxybenzyl-L-cysteinyl-L-prolyl-L-leucylglycinamide (IV).** — A solution of III (19.8 g., 0.04 mol.) and L-prolyl-L-leucylglycinamide[10] (11.4 g., 0.04 mol.) in dimethylformamide (20 ml.) was allowed to react overnight at room

* All melting points given are uncorrected. All samples for analyses were first dried in vacuo at 110°C for 2 hr.

temperature. Ethyl acetate (60 ml.) was then added to the reaction mixture to precipitate the product as crystals, which were collected by filtration. The crude product was recrystallized from hot methanol (300 ml.) and water (300 ml.); wt. 19.8 g. (77%), m. p. 165—167°C, $[\alpha]_D^{21}$ −55.4° (*c* 2, dimethylformamide).

Found: C, 59.90; H, 6.81; N, 10.59; S, 4.91. Calcd. for $C_{32}H_{43}O_7N_5S$: C, 59.88; H, 6.75; N, 10.91; S, 5.00%.

***N*-Carbobenzoxy-L-asparaginyl-*S*-*p*-methoxybenzyl-L-cysteinyl-L-prolyl-L-leucyl-glycinamide (V).**—A suspension of IV (15.09 g., 0.024 mol.) in acetic acid (25 ml.) was treated with 29% hydrogen bromide in acetic acid (120 g.). After one hour at room temperature, dry ether (1000 ml.) was added to the reaction mixture. The precipitated mass was separated by filtration, washed well with ether three times, and dried over sodium hydroxide. The dried material was dissolved in methanol (150 ml.), and ion exchange resin IRA-400 (in an OH cycle) was added until the bromine ions disappeared. Then the resin was filtered off and washed throughly with methanol. The filtrate and washings were combined and evaporated to dryness. The residue and *N*-carbobenzoxy-L-asparagine *p*-nitrophenyl-ester[5] (9.09 g., 0.024 mol.) were dissolved in dimethylformamide (30 ml.), and the mixture was allowed to react at room temperature for two days. The product was then precipitated by adding ethyl acetate (100 ml.), collected by filtration, washed with ethyl acetate and with ethanol, and dried; wt. 15.4 g. (87%), m. p. 211—212°C, $[\alpha]_D^{20}$ −50.5° (*c* 1, dimethylformamide). For analysis, a part of the product was recrystallized from 80% methanol; m. p. 213—214°C, $[\alpha]_D^{21}$ −51.9° (*c* 1, dimethylformamide).

Found: C, 57.14; H, 6.47; N, 12.68; S, 4.12. Calcd. for $C_{36}H_{49}O_7N_9S$: C, 57.20; H, 6.54; N, 12.97; S, 4.24%.

***N*-Carbobenzoxy-L-glutaminyl-L-asparaginyl-*S*-*p*-methoxybenzyl-L-cysteinyl-L-prolyl-L-leucylglycinamide (VI).**—A suspension of V (15.12 g., 0.02 mol.) in acetic acid (20 ml.) was treated with 29% hydrogen bromide in acetic acid (150 g.) for one hour at room temperature. Dry ether (1000 ml.) was added to the reaction mixture to precipitate the product, which was then separated and washed with ether three times and dried over sodium hydroxide. Then the dried mass was dissolved in methanol (200 ml.), and the bromine ions in the solution were removed by adding ion exchange resin IRA-400 (in an OH cycle). The bromine-free solution was concentrated to dryness in vacuo, and the residue was dissolved in dimethylformamide (30 ml.). *N*-Carbobenzoxy-L-glutamine *p*-nitrophenylester[5] (8.42 g., 0.021 mol.) was added to the solution, and the mixture was kept for two days at room temperature. Then the product was precipitated by adding ethyl acetate, which was collected by filtration and washed with ethyl acetate and ethanol. The yield was 13.51 g. (76%); m. p. 207—208°C, $[\alpha]_D^{21}$ −42.6° (*c* 1, dimethylformamide). For analysis, a part of the product was recrystallized from 80% methanol; m. p. 208—210°C, $[\alpha]_D^{21}$ −51.3° (*c* 1, dimethylformamide).

Found: C, 55.93; H, 6.79; N, 14.51; S, 3.43. Calcd. for $C_{41}H_{57}O_{11}N_9S$: C, 55.70; H, 6.50; N, 14.26; S, 3.63%.

***N*-Carbobenzoxy-L-isoleucyl-L-glutaminyl-L-asparaginyl-*S*-*p*-methoxybenzyl-L-cysteinyl-L-prolyl-L-leucylglycinamide (VII).**—A suspension of VI (9.72 g., 0.011 mol.) in 20 ml. of acetic acid was treated with 29% hydrogen bromide in acetic acid (80 g.) for one hour. The product was precipitated by adding dry ether (600 ml.), and the precipitate was washed three times with dry ether and dried. The dried product was dissolved in methanol (300 ml.), and the solution was treated with ion exchange resin IRA-400 (in an OH cycle) until bromine ions disappeared. The resin was filtered and washed well with methanol. The filtrate and washings were combined and concentrated to dryness in vacuo. The residue was dissolved in 25 ml. of dimethylformamide, and to the solution was added *N*-carbobenzoxy-L-isoleucine *p*-nitrophenyl-ester[5] (4.63 g., 0.012 mol.). The mixture was allowed to react for two days at room temperature. Ethyl acetate (200 ml.) was added to the reaction mixture, and the precipitates were collected by filtration and washed with ethyl acetate and then with ethanol. The yield was 8.56 g. (78%); m. p. 216—217°C, $[\alpha]_D^{20}$ −43.6° (*c* 1, dimethylformamide). The product was recrystallized from 80% methanol (500 ml.); wt. 6.93 g., m. p. 217—218°C, $[\alpha]_D^{18}$ −44.2° (*c* 1, dimethylformamide).

Found: C, 56.55; H, 7.07; N, 13.89; S, 3.10. Calcd. for $C_{47}H_{68}O_{12}N_{10}S$: C, 56.61; H, 6.87; N, 14.05; S, 3.22%.

***N*-Carbobenzoxy-*O*-benzyl-L-tyrosyl-L-isoleucyl-L-glutaminyl-L-asparaginyl-*S*-*p*-methoxybenzyl-L-cysteinyl-L-prolyl-L-leucylglycinamide (VIII).**—A suspension of VII (4.99 g., 0.005 mol.) in acetic acid (10 ml.) was treated with 29% hydrogen bromide in acetic acid (25 g.) for one hour. Dry ether (250 ml.) was added to the reaction mixture to precipitate the product, which was collected by filtration, washed with ether three times, and dried. The dried material was dissolved in methanol (500 ml.). Ion exchange resin IRA-400 (in an OH cycle) was added to the solution until bromine ions disappeared, and then the resin was filtered off. The filtrate was evaporated to dryness. The residue was dissolved in dimethylformamide (60 ml.), and *N*-carbobenzoxy-*O*-benzyl-L-tyrosine *p*-nitrophenyl ester[5] (2.63 g., 0.005 mol.) was added to the solution. After two days, ethyl acetate (300 ml.) was added to the reaction mixture to precipitate the product, which was then filtered off, washed with ethyl acetate and then with ethanol, and dried; wt. 5.33 g. (85%), m. p. 221—222°C, $[\alpha]_D^{18}$ −33.1° (*c* 1, dimethylformamide). For analysis, a part of the product was recrystallized from 80% methanol; m. p. 223—224°C, $[\alpha]_D^{18}$ −35.7° (*c* 1, dimethylformamide).

Found: C, 60.31; H, 6.54; N, 12.42; S, 2.63. Calcd. for $C_{63}H_{83}O_{14}N_{11}S$: C, 60.51; H, 6.69; N, 12.32; S, 2.57%.

***N*-Carbobenzoxy-*S*-*p*-methoxybenzyl-L-cysteinyl-L-tyrosyl-L-isoleucyl-L-glutaminyl-L-asparaginyl-*S*-*p*-methoxybenzyl-L-cysteinyl-L-prolyl-L-leucylglycinamide (IX).**—A suspension of VIII (5.00 g.,

0.004 mol.) in acetic acid (20 ml.) was treated with 29% hydrogen bromide in acetic acid (40 g.). After one hour, dry ether (400 ml.) was added to precipitate the product, which was then separated, washed with ether, and dried. The dried mass was dissolved in dimethylformamide (40 ml.) and triethylamine (6 ml.) was carefully added to the solution. Triethylamine hydrobromide which formed was filtered off, and III (2.38 g., 0.0048 mol.) was added to the filtrate. After three days, ethyl acetate (200 ml.) was added to the reaction mixture and the precipitate which formed was collected by filtration and washed with ethyl acetate and then with ethanol. The yield was 5.16 g. (93%); m. p. 218—220°C, $[\alpha]_D^{20}$ −41.1° (*c* 1, dimethylformamide). For analysis, a part of the product was recrystallized from 80% methanol; m. p. 223—224°C, $[\alpha]_D^{18}$ −43.7° (*c* 1, dimethylformamide).

Found: C, 58.19; H, 6.68; N, 12.29; S, 4.56. Calcd. for $C_{67}H_{90}O_{16}N_{12}S_2$: C, 58.15; H, 6.56; N, 12.15; S, 4.63%.

**Oxytocin.**—a) A solution of IX (100 mg.) and anisole (50 mg.) in trifluoroacetic acid (30 ml.) was gently refluxed for two hr. Then the solvent was evaporated off in vacuo, and the residue was dissolved in water (100 ml.). The pH was adjusted to 6.5 with diluted aqueous ammonia, and carbon dioxide free air was bubbled through the solution until the nitroprusside-test became negative. Then the solution was acidified to pH 4 with acetic acid, and the small amount of insoluble material was filtered out. The final solution showed a total oxytocic activity of 3300 units as determined by rat-uterine contractive activity.

b) Product IX was reduced with sodium in liquid ammonia, as described by Bodanszky and du Vigneaud,[4] and the final reduced material was aerated to oxytocin as has been described before. The total oxytocic activity obtained from 100 mg. of IX was 24500 units, while that from 1 g. IX was 180000 units.

## Summary

*N*-Carbobenzoxy-*S*-methoxybenzyl-L-cysteinyl-L-tyrosyl-L-isoleucyl-L-glutaminyl-L-asparaginyl-*S*-*p*-methoxybenzyl-L-cysteinyl-L-prolyl-L-leucylglycinamide (IX) was synthesized by the step-wise elongation method, and highly potent oxytocin was obtained from IX by treatment not only with sodium in liquid ammonia, but also with boiling trifluoroacetic acid, followed by the usual aeration procedure. It was demonstrated during the reactions that the newly introduced *S*-*p*-methoxybenzyl group could be cleaved more easily than the usual *S*-benzyl group, and that the new *S*-protecting group was useful in the preparation of complicated cysteinyl peptides.

The authors wish to express their thanks to Professor Shiro Akabori for his encouragement and valuable advice, and to Professor Shigeru Aonuma and to Dr. Keiji Nakamura of the Dainippon Pharmaceutical Co., Ltd. for determining the oxytocic activities of the synthetic materials.

*Peptide Center*
*Institute for Protein Research*
*Osaka University*
*Kita-ku, Osaka*

# The Preparations and the Electronic Spectra of Sexa-co-ordinate Molybdenum(III) Complexes

By Takashi KOMORITA, Seiko MIKI and Shoichiro YAMADA

(Received August 1, 1964)

It is interesting to compare the electronic spectra of the corresponding coordination compounds of molybdenum(III) and of chromium(III), both of which have a $d^3$-electronic configuration.

There have been a number of systematic studies of the spectra of chromium(III) complexes, and the band assignments have been well established,[1] as is schematically shown in Fig. 1, where quartet-quartet transitions are denoted with Roman numerals and quartet-doublet transitions, with letters of the alphabet.

In contrast with the case of chromium(III) complexes, however, such investigations of molybdenum(III) complexes have been so rare that only the hexachloro- and the pentachloroaquo-molybdate(III) ions appear to have been well investigated with regard to the inner d-shell bands. The absorption curves and the band assignments were reported by Jørgensen for these complexes.[1] According to these assignments and to the concept of

1) C. K. Jørgensen, "Absorption Spectra and Chemical Bonding in Complexes," Pergamon Press, Oxford (1962).

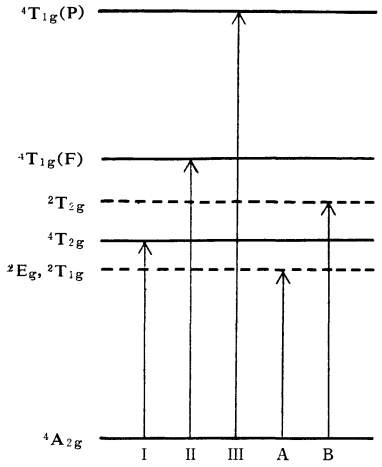



Fig. 1. Observed electronic transitions in $d^3$-system ($Cr^{3+}$) in octahedral field.

the spectrochemical series, the absorption spectra and band assignments by other authors for trichlorotripyridine- and "hexaquo-" molybdenum(III) complexes are doubtful.[2,3] Thus no systematic discussion of the electronic spectra of molybdenum(III) complexes has so far been presented because of a lack of available data.

The present paper is concerned with the preparation of and the electronic absorption spectra of several sexa-co-ordinate molybdenum(III) complexes, including three new compounds. Experimental results will be discussed, together with the available data on the corresponding chromium(III) complexes.

## Experimental

**Materials.**—The following molybdenum(III) compounds were prepared: $K_3[MoCl_6]$, $(NH_4)_2[MoX_5(H_2O)]$, $[MoX_3(urea)_3]$, $[Mo(urea)_6]Br_3$, $[MoX_3(dmf)_3]$, $[MoCl_3(tu)_3]$ and $[MoX_3(py)_3]$ (where dmf=*N*, *N*-dimethylformamide, tu=thiourea, py=pyridine and X=Cl and Br). Among these compounds, $[MoBr_3(urea)_3]$, $[MoCl_3(dmf)_3]$ and $[MoBr_3(dmf)_3]$ are new compounds, while $[MoCl_3(urea)_3]$, $[Mo(urea)_6]Br_3$* and $[MoCl_3(tu)_3]$ have been briefly reported on by Russian authors.[4] No description, however, has yet been given of their preparation methods.

*Trichlorotriureamolybdenum(III), $[MoCl_3(urea)_3]$.*—Five grams of $(NH_4)_2[MoCl_5(H_2O)]$ and five grams of urea, ground together in a mortar, were added to 30 ml. of ethanol in a nitrogen atmosphere; the reaction mixture was then stirred continuously at 50—55°C. As the reaction proceeded, the color of the precipitate gradually changed from orange to yellow. After 3.5 hr. the product was filtered in air, washed with water until the filtrate became colorless and then with ethanol, and dried at 60°C. A yellow powder was obtained. Yield, 2.5 g. (43%).

This crude product was recrystallized with a concentrated aqueous solution of urea to give as a pure product yellow, tetragonal plates. The yield of the recrystallization was rather poor (less than 20%) because of the predominant decomposition,

Found: C, 9.42; H, 3.26; N, 21.77. Calcd. for $[MoCl_3(urea)_3]$: C, 9.42; H, 3.16; N, 21.97%.

Preparation in an aqueous medium was also possible.

*Tribromotriureamolybdenum(III), $[MoBr_3(urea)_3]$.*—A saturated aqueous solution of urea was prepared at room temperature. Five grams of $(NH_4)_2[MoBr_5(H_2O)]$ and three grams of urea were dissolved in as small an amount as possible of the urea solution in a nitrogen atmosphere, and then the mixture was stirred continuously at 48—50°C. After about 15 min. a crystalline precipitate began to separate. For an additional 30 min. the stirring was continued; then the mixture was cooled to room temperature, poured into about 50 ml. of water in air, and stirred for about 15 min. The precipitate was filtered, washed with water and with ethanol, and dried at 60°C. Yield, 1.3 g. (28%).

Found: C, 7.02; H, 2.24; N, 16.78. Calcd. for $[MoBr_3(urea)_3]$: C, 6.99; H, 2.34; N, 16.29%.

This compound, which consists of fine, orange microcrystals, is soluble in a warm aqueous solution of urea with decomposition, but insoluble in cold water and in common organic solvents.

*Hexaureamolybdenum(III) Bromide, $[Mo(urea)_6]Br_3$.*—The initial procedure was the same as that described for $[MoBr_3(urea)_3]$. When the orange precipitate of $[MoBr_3(urea)_3]$ had separated out, the temperature of the reaction mixture was raised to 70°C. Soon the precipitate was dissolved, and about 10—20 min. after the dissolution a pale-colored crystalline precipitate separated slowly from the dark brown solution. When the amount of the precipitate no longer increased, the stirring was stopped and the mixture was allowed to cool at room temperature. The crystals, which separated abundantly, were filtered in air, washed with ethanol, and dried at 60°C. Yield, 2.2 g. (35%).

For the elemental analyses the crude crystals were added to a large amount of ethanol at 40°C and stirred continuously for 20 min., filtered, washed with cold ethanol, and dried at 30°C under reduced pressure over phosphorus pentoxide for half a day.

Found: C, 10.48; H, 3.75; N, 23.83. Calcd. for $[Mo(urea)_6]Br_3$; C, 10.35; H, 3.48; N, 24.15%.

The pale greenish yellow pillar-shaped crystals thus obtained were soluble in water with decomposition but insoluble in common organic solvents.

*Trichlorotris(N, N-dimethylformamide)molybdenum(III), $[MoCl_3(dmf)_3]$.*—To 50 ml. of a purified *N*, *N*-dimethylformamide[5] 15 g. of $(NH_4)_2[MoCl_5(HO_2)]$

2) E. König and H. L. Schläfer, *Z. phys. Chem., N. F.* **26**, 371 (1960).

3) H. Hartmann and H.-J. Schmidt, *Z. phys. Chem., N. F.*, **11**, 234 (1957).

* In the Russian paper it is described as a dihydrate, $[Mo(urea)_6]Br_3 \cdot 2H_2O$.

4) V. B. Evdokimov, V. V. Zelentsov, I. D. Kolli, Wen-Hsia T'ang and V. I. Spitsyn, *Dokl. Akad. Nauk S. S. S. R.*, **145**, 1282 (1962).

5) D. W. Meek, R. S. Drago and T. S. Piper, *Inorg. Chem.*, **1**, 285 (1962).

were added. The mixture was then stirred continuously for 12 hr. at 30—35°C in a nitrogen atmosphere. The insoluble red precipitate of the starting molybdate salt was slowly displaced by a white precipitate of ammonium chloride until the red color disappeared in the precipitate at the end of the reaction. This was separated with a glass filter, and the dark-brown filtrate was concentrated to a thick paste under reduced pressure below 35°C and preserved in an ice-box for several days. When the crystallization of the paste did not occur spontaneously, one of the following procedures was taken: (1) scratching by means of a magnetic stirrer, (2) dissolving the paste in ethanol at 50°C, followed by cooling the solution with an ice-bath as soon as possible and scratching,* or (3) dissolving the paste in ethanol or in acetone at room temperature and then preserving it in an ice-box for a few weeks. The yellow product separated was filtered and washed with ethanol. Yield of the crude product was about 60%. As the crude product was often contaminated with ammonium chloride, purification was performed by procedure 2 for the elemental analyses. The yellow powder produced was filtered, washed with ethanol several times, and dried at 35°C under reduced pressure over phosphorus pentoxide for 100 min. All the procedures were carried out in an oxygen-free atmosphere so far as possible.

Found: C, 26.13; H, 5.21; N, 10.36. Calcd. for $[MoCl_3(dmf)_3]$: C, 25.64; H, 5.02; N, 9.97%.

This compound is soluble with decomposition in water, ethanol, acetone, pyridine and chloroform, but insoluble in benzene; the color changes after a few days in moist air.

*Tribromotris(N, N-dimethylformamide)molybdenum(III), $[MoBr_3(dmf)_3]$*—Five grams of $(NH_4)_2[MoBr_5(H_2O)]$ were dissolved in 17 ml. of purified *N, N*-dimethylformamide; the mixture was then stirred continuously at 29—31°C for 6 hr. in a nitrogen atmosphere. After about 15 min. the color of the solution became blood-red. Near the end of the reaction, the white precipitate of ammonium bromide separated. This was filtered rapidly in air, and the filtrate was concentrated at 30°C under reduced pressure in an atmosphere of carbon dioxide until just enough of the solvent remained to moisten the crystalline product. All the contents were then poured into about 50 ml. of water, and the suspension was stirred for 20 min. at room temperature. The orange crystalline substance was filtered, washed with water and with methanol, and dried at about 30°C under reduced pressure over calcium chloride. Yield, 1.4 g. (28%).

Found: C, 19.55; H, 3.79; N, 7.97. Calcd. for $[MoBr_3(dmf)_3]$: C, 19.48; H, 3.81; N, 7.57%.

The orange-red hexagonal microcrystalline plates of the compound are soluble in chloroform, where they rapidly decompose; soluble in water and in acetone only with difficulty, and insoluble in ethanol and in ether. The color of the compound changes when it is left in moist air for several days.

*Trichlorotrithioureamolybdenum(III), $[MoCl_3(tu)_3]$.*—Fifteen grams of $(NH_4)_2[MoCl_5(H_2O)]$ and ten grams of thiourea were ground together in a mortar, added to about 200 ml. of ethanol, and the mixture was stirred continuously at 50°C for 20 hr. in a nitrogen atmosphere. The color of the solution gradually became dark brown. Then the reaction mixture was left at room temperature for 10 hr., and filtered. The crude precipitate was washed with cold and warm water until the reddish color faded from the filtrate; it was then washed with ethanol and dried at 60°C for several minutes. Yield, 8.5 g. (43%).

Found: C, 8.58; H, 2.84; N, 19.30. Calcd. for $[MoCl_3(tu)_3]$: C, 8.38; H, 2.81; N, 19.54%.

This compound, obtained as an orange-yellow microcrystalline powder, is soluble in *N, N*-dimethylformamide with decomposition, slightly soluble in water and in pyridine, and insoluble in common organic solvents. The compound is stable in air, at least for several days.

*Other Compounds.* — $K_3[MoCl_6]$, $(NH_4)_2[MoCl_5(H_2O)]$ and $(NH_4)_2[MoBr_5(H_2O)]$ were prepared according to the method of Hartmann and Schmidt[3] with slight modifications.

$[MoCl_3(py)_3]$ was prepared according to the method described in the literature.[6]

Found: C, 40.93; H, 3.35; N, 9.56. Calcd. for $[MoCl_3(py)_3]$: C, 40.98; H, 3.44; N, 9.56%.

$[MoBr_3(py)_3]$ was obtained by almost the same method as that used for $[MoCl_3(py)_3]$.

Found: C, 32.23; H, 2.34; N, 7.54. Calcd. for $[MoBr_3(py)_3]$: C, 31.44; H, 2.64; N, 7.33%.

**Measurements.**—Electronic absorption spectra in the solid state were measured with a Hitachi EPU-2A spectrophotometer equipped with a diffuse reflectance attachment, and the spectra in solution, with a Beckman DU spectrophotometer. A Hitachi EPS-2 self-recording spectrophotometer was employed for the measurement of $[Mo(urea)_6]Br_3$ in solution.

The infrared absorption spectra measurements of the three molybdenum(III) compounds containing urea and of hexaureachromium(III) chloride were made in the rock salt region by the KBr disk technique.

All the measurements of the ultraviolet and infrared spectra were carried out at room temperature.

## Results and Discussion

**The Ultraviolet Spectra and the Structures of the Molybdenum(III) Complexes.** — The main results of the ultraviolet measurements are given in Figs. 2—4 and in Table I. There are common features through all these absorption spectra: each spectrum has two sharp bands of a lower intensity near 9000 $cm^{-1}$ and 15000 $cm^{-1}$ and two more intense broad bands of a similar type in the higher wave number region, though these bands are partly embedded under

* This complex is rapidly decomposed in ethanol at 50°C.

6) H. B. Jonassen and L. J. Bailin, *Inorg. Syn.*, 7, 140 (1963).

much more intense bands in some spectra. This observation gives support to Jørgensen's band assignments, which are shown in Figs. 1—2,[1] and to the octahedral configuration in all these complexes. The corresponding bands of the molybdenum(III) compounds have been similarly assigned.

The absorption spectra of ammonium pentabromoaquomolybdate(III) were measured in the solid state, in 3 N hydrobromic acid and in 12 N hydrobromic acid (Fig. 2). The I- and II-bands in the 12 N hydrobromic acid solution are shifted by about 1000 $cm^{-1}$ to a lower wave number compared with those in the solid state, and they show almost no change during

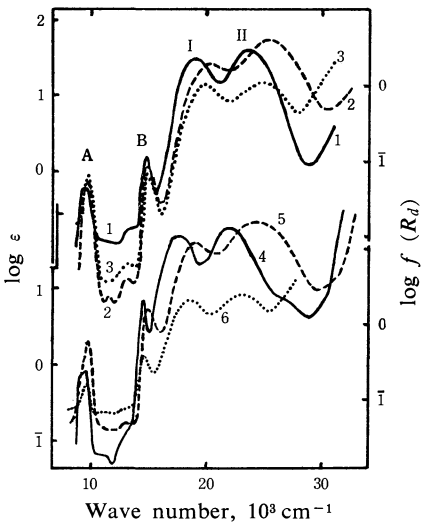



Fig. 2. Absorption spectra of: 1, $K_3[MoCl_6]$ in 12 N HCl; 2, in 3 N HCl; 3, $(NH_4)_2[MoCl_5(H_2O)]$ in solid state; 4, $(NH_4)_2[MoBr_5(H_2O)]$ in 12 N HBr; 5, in 3 N HBr; 6, in solid state.

the measurement. On the other hand, the corresponding bands in the 3 N hydrobromic acid solution are shifted to a higher wave number and show a considerable time dependency. The same behavior was observed among the spectra of the corresponding chlorocomplexes, such as $(NH_4)_2[MoCl_5(H_2O)]$ and $K_3[MoCl_6]$ (Fig. 2). Table I summarizes the corresponding band maxima in these spectra. From these observations it may be concluded that the spectra of $(NH_4)_2[MoBr_5(H_2O)]$ in 12 N hydrobromic acid and of $K_3[MoCl_6]$ in 12 N hydrochloric acid are due to the $[MoBr_6]^{3-}$ ion and to the $[MoCl_6]^{3-}$ ion respectively, and that considerable decomposition takes place in the 3 N hydrobromic acid solution of the bromomolybdate complex.

Since $[Mo(urea)_6]Br_3$ is rapidly decomposed, even in a concentrated aqueous solution of

TABLE I. SPIN-ALLOWED BANDS OF SOME MOLYBDENUM(III) COMPLEXES

| Complex | Condition | Band maxima and assignments I | II |
|---|---|---|---|
| $K_3[MoCl_6]$ | in 12 N HCl | 19.15 | 23.8 |
| $(NH_4)_2[MoCl_5(H_2O)]$ | Solid | 19.95 | 24.15 |
| $K_3[MoCl_6]$ | in 3 N HCl | 20.5 | 25.35 |
| $(NH_4)_2[MoBr_5(H_2O)]$ | in 12 N HBr | 17.7 | 22.0 |
| | Solid | 18.55 | 23.2 |
| | in 3 N HBr | 19.05 | 24.25 |
| $[Mo(urea)_6]Br_3$ | Solid | 25.9 | 31.0 |

wave number, $10^3$ $cm^{-1}$

urea (about 4 mol. urea), the spectrum was obtained within 15 min. after dissolution. Both the I- and II-bands are considerably (about 1000 $cm^{-1}$) shifted to a lower wave number compared with those of the solid state. Therefore, any structure in which the bromide ion is directly attached to the molybdenum ion is improbable for the compound in the solid state. Moreover, the pronounced intensity of the B-band common to the other bromide-containing complexes is not obvious in the spectra of the hexaurea compound. It is, therefore most likely that this contains the $[Mo(urea)_6]^{3+}$ ions.

It may obviously be concluded, on the basis of absorption spectra and chemical properties, that the two trihalotriurea complexes are not $[MoX_6]$ $[Mo(urea)_6]$ but $[MoX_3(urea)_3]$ (Figs. 2 and 3). The infrared absorption spectra of these three urea-containing compounds and of $[Cr(urea)_6]Cl_3$ were, therefore, measured in order to obtain further information on their molecular structure. The results are summarized in Table II.

Penland et al.[7] have studied the infrared spectra of many transition metal-urea complexes and found a method to determine the species of atom by which the central metal ion is coordinated in each of the complexes. This consists mainly of comparisons of NH-stretching frequencies and of CO-stretching frequencies coupled with $NH_2$ bending. According to this method, it may be concluded from Table II that urea is coordinated through the oxygen atom to the metal atom in the molybdenum complexes as well as in the chromium complex.

The trichloro- and tribromo-triureamolybdenum(III) have almost the same infrared patterns, while the pattern of hexaureamolybdenum(III) bromide is quite similar to that of hexaureachromium(III) chloride. The main differences between the spectra of these two

7) R. B. Penland, S. Mizushima, C. Curran and J. V. Quagliano, *J. Am. Chem. Soc.*, **79**, 1575 (1957).

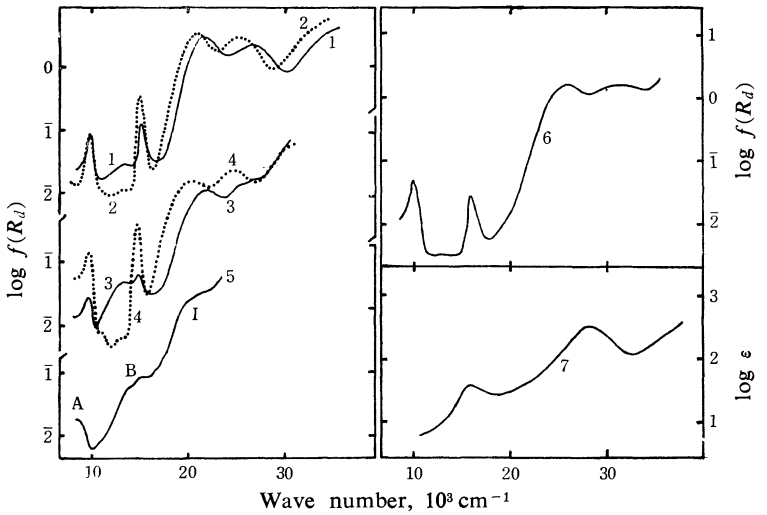



Fig. 3. Absorption spectra of: 1, $[MoCl_3(urer)_3]$; 2, $[MoBr_3(urea)_3]$; 3, $[MoCl_3(dmf)_3]$; 4, $[MoBr_3(dmf)_3]$; 5, $[MoCl_3(tu)_3]$; 6, $[Mo(urea)_6]Br_3$; 7, $Mo^{3+}$ in 4 N $H_2SO_4$ (Ref. 3).

TABLE II. INFRARED ABSORPTION MAXIMA OF THE UREA COMPLEXES OF Mo(III) AND Cr(III)

| $[MoCl_3(urea)_3]$ | $[MoBr_3(urea)_3]$ | $[Mo(urea)_6]Br_3$ | $[Cr(urea)_6]Cl_3$* | Assignments |
|---|---|---|---|---|
| 3460 s | 3450 s | 3430 s | 3440 s | free NH str. |
| 3350 s | 3340 s | 3320 s | 3340 s | |
| — | — | 3210m | 3190m | ? |
| 1660 sh | 1660 sh | 1660 sh | 1660 sh | CO str. |
| 1627 s | 1627 s | 1620 s | 1623 s | $+NH_2$bend. |
| 1130m | 1130m | 1160m | 1165m | $NH_2$ rock. |

Wave number, cm$^{-1}$
Abbreviations: s, strong; m, medium; sh, shoulder
* Our measurement virtually reproduced the Penland's data for this compound (Cf. Ref. 7).

couples are found in the bands near 3200 cm$^{-1}$ and near 1150 cm$^{-1}$. The former band is found only in the spectra of the hexaurea complexes; a corresponding band has also been found in hexaureairon(III) chloride.[7] On the other hand, both the frequency and the shape of the latter $NH_2$ rocking band are the same within each of the two pairs of compounds, but they are differentiated between the two pairs. These observations also support the presence of the $[Mo(urea)_6]^{3+}$ species in the hexaureamolybdenum(III) bromide.

Although the electronic absorption spectrum of the trichlorotris(*N*, *N*-dimethylformamide)-molybdenum(III) has some ambiguous features, which may be related to the difficulty of preparation (Fig. 3), the wave numbers of both the I- and II-bands of the two *N*, *N*-dimethylformamide complexes are not essentially different from those of the two corresponding triurea complexes, so the former two complexes, as well as the latter two, may be regarded as having the configuration $[MoX_3O_3]$.

The spectrum of trichlorotrithioureamolybdenum(III) appears to show at least four bands in the near infrared and visible region. These bands may be assigned to the A, B and I transitions, as is shown in Fig. 3. According to this assignment and to the spectrochemical series, this complex may be concluded to be of the $[MoCl_3S_3]$ type.

The spectra of trichlorotripyridinemolybdenum(III) have already been investigated by König and Schläfer[2]; one of them is shown in Fig. 4. However, our measurements for this compound gave slightly different absorption curves (Fig. 4), which show the spectral features common to the other sexa-co-ordinate molybdenum(III) complexes. The I- and the II-bands are most probably embedded under the much more intense charge transfer bands, because a part of the I-band appears on the lower wave number side of the charge transfer band in the spectra of the tribromotripyridinemolybdenum(III) (Fig. 4). A considerable splitting of the B-band was observed in the spectra of the two complexes, both in solution and in the solid state. On the contrary, a broad band at 12500 cm$^{-1}$ in the spectra of the trichlorotripyridine complex has an enhanced

TABLE III. LIGAND FIELD PARAMETERS, *Dq* AND *B*, AND NEPHELAUXETIC RATIO $\beta$ OF SOME OCTAHEDRAL COMPLEXES OF Mo(III) AND Cr(III)

| | | 6 $Br^-$ | 6 $Cl^-$ | 6 urea | 6 $H_2O$ |
|---|---|---|---|---|---|
| $Mo^{3+}$ | *Dq* | 1.77 | $1.91_5$ | 2.59 | — |
| | *B* | $0.39_0$ | $0.42_1$ | $0.45_3$ | — |
| | $\beta$ | 0.64 | 0.69 | 0.74 | — |
| $Cr^{3+}$ | *Dq* | — | a 1.318 / b $1.38_5$ | c 1.60 | c 1.74 |
| | *B* | — | a 0.575 / b $0.61_1$ | c 0.660 | c 0.725 |
| | $\beta$ | — | a 0.62 / b 0.67 | c 0.72 | c 0.79 |

*Dq* and *B*: $10^3\,cm^{-1}$

a) These values for $[Rh(ph)_3][CrCl_6]$ are quoted from Ref. 8.

b) These values were calculated from the unpublished spectral data for $K_3[CrCl_6]$ in Ref. 9.

c) These values are quoted from Ref. 1.

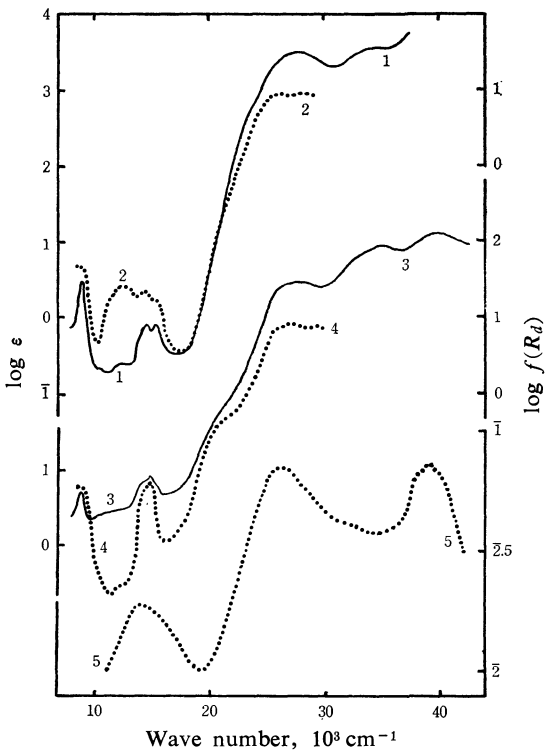



Fig. 4. Absorption spectra of: 1, $[MoCl_3(py)_3]$ in $CH_2Cl_2$; 2, in solid state; 3, $[MoBr_3(py)_3]$ in $CH_2Cl_2$; 4, in solid state; 5, $[MoCl_3(py)_3]$ in solid state, copied from Ref. 2.

intensity only in the solid state. More detailed investigations will be necessary to explain these phenomena.

**Spectrochemical Series and Nephelauxetic Series.**—From our spectral data the spectrochemical series for molybdenum(III) complexes was obtained as:

$$py \gtrsim (urea, dmf, and\ tu) > Cl^- > Br^-$$

This agrees with the series for complexes of other transition metal ions.

Using the wave numbers of the I- and II-bands, the Racah's parameter *B*'s of interelectronic repulsion were calculated for the three octahedral molybdenum(III) complexes. From these values nephelauxetic ratios $\beta$' were then obtained by assuming $B=0.61\,(10^3\,cm^{-1})$ for free molybdenum(III) ions, in accordance with the findings of Jrgøensen.[1] The results are tabulated in Table III. For the purpose of comparing these parameters for $3d^3$- and $4d^3$-complexes, the corresponding values for three octahedral chromium(III) complexes are also given in Table III.[1,8,9] The following nephelauxetic series were obtained:

$Br^- > Cl^- >$ urea for molybdenum(III) complexes, and Cr(III) > Mo(III) for the same ligands.

These series are in good agreement with those for the chromium(III) and other transition metal complexes.[1]

Approximating the transition energies for the first and the second spin-forbidden bands as $9B+3C$ and $15B+5C$ respectively, Racah's parameters *C*' were calculated for the three molybdenum(III) complexes. These give ratios $C/B$ between 4 and 5.

Hartmann and Schmidt[3] regarded the spectra of the green solutions obtained by the electrolytic reduction of diluted solutions of molybdenum oxide in various mineral acids as due to the "hexaquomolybdenum(III) ion"; a typical spectrum is shown in Fig. 3. This is apparently not a spectrum of the genuine hexaquomolybdenum(III) ion, in the light of the present investigation.

## Summary

Several sexa-co-ordinate molybdenum(III) compounds containing some of chloride ions, bromide ions, urea, thiourea *N*, *N*-dimethylformamide and pyridine as ligands have been

8) W. E. Hatfield, R. C. Fay, C. E. Pfluger and T. S. Piper, *J. Am. Chem. Soc.*, **85**, 265 (1963).

9) M. Nakahara, private communication.

10) Y. Tanabe and S. Sugano, *J. Phys. Soc. Japan*, **9**, 753 (1954).

prepared, and their electronic absorption spectra determined.

It has been shown that the spectrum of the sexa-co-ordinate molybdenum(III) compound generally has two spin-forbidden and two spin-allowed bands. The ligand field parameters of the octahedral molybdenum(III) complexes have been calculated and compared with those of the corresponding chromium(III) complexes.

We wish to express our sincere thanks to Dr. Masayoshi Nakahara of Rikkyo St. Paul's University for his valuable information on the spectrum of the hexachlorochromium(III) complex.

*Department of Chemistry*
*Faculty of Science*
*Osaka University*
*Nakanoshima, Osaka*

# Band Structure of Circumanthracene

By Yoshiya HARADA, Yusei MARUYAMA, Hiroo INOKUCHI and Noriko MATSUBARA

(Received August 14, 1964)

Considerable interest has developed in recent years in the theoretical interpretation of the electrical transport properties of organic molecular crystals. The characteristic nature of the crystals is their small mobilities. In fact, values of the order of $10^{-1}$—$10^{0}$ $cm^2/V.sec.$ were observed for both electrons and holes at room temperature.[1-3] In order to account for the electron and the hole mobilities, two mechanisms have so far been considered; the usual band model (the Bloch theory), and the hopping one (the Heitler-London approach).[4] When the mobility is much larger than 1 $cm^2/V.sec.$, the band model is applicable, while the hopping model may be better when the mobility is much smaller than 1 $cm^2/V.sec.$[4b] Since mobilities of the order of unity are on the borderline region between the two mechanisms, neither approach seems to be accurate enough.

The temperature dependence of the mobility also offers a condition under which one of the two models can be selected. In the usual band model the mobility should decrease with an increase in the temperature. On the other hand, the hopping model should lead to a mobility which increases exponentially with a rise in the temperature, because the thermally-activated charge carrier wanders through the crystal by jumping from one lattice site to another.* Although the mobility of anthracene decreases as the temperature increases, the situation is not favourable to the band model, because the decrement of the mobility due to the thermal expansion of the crystal has a comparable effect.[1b]

Recently, Toyozawa[5] has proposed an alternate model which is applicable to an intermediate between the above two mechanisms. He treated the carrier transport of the organic semiconductor by a localized picture and obtained, below room temperature, a mobility which is almost independent of the temperature.**

1) For anthracene: a) O. H. LeBlanc, *J. Chem. Phys.*, **33**, 626 (1960); b) R. G. Kepler, *Phys. Rev.*, **119**, 1226 (1960); R. G. Kepler, "Organic Semiconductors," Ed. by J. J. Brophy and J. W. Buttrey, The Macmillan Co., New York (1962), p. 1; c) I. Nakada and Y. Ishihara, *J. Phys. Soc. Japan*, **19**, 695 (1964).

2) For pyrene: a) O. H. LeBlanc, *J. Chem. Phys.*, **37**, 916 (1962); b) K. Ohki, H. Inokuchi and Y. Maruyama, This Bulletin, **36**, 1512 (1963).

3) For naphthalene: M. Silver, J. R. Rho, D. Olness and R. C. Jarnagin, *J. Chem. Phys.*, **38**, 3030 (1963).

4) a) F. J. Morin, *Phys. Rev.*, **93**, 1199 (1954); b) J. Yamashita and T. Kurosawa, *J. Phys. Soc. Japan*, **15**, 802 (1960); c) T. Kurosawa, ibid., **15**, 1211 (1960).

* In the case of the hopping model, the self-trapping due to the interaction of the carrier with the lattice may be necessary. Friedman (Ref. 4) suggested the absence of the self-trapping, judging from the estimation that the bandwidths are not small compared to the binding energy of the excess carrier on the mononegative anthracene ion due to the associated lattice deformation.

5) Y. Toyozawa, Private communication.

** His basic idea is as follows: The characteristic nature of organic semiconductors which can be clearly distinguished from inorganic ones is the existence of a large number of intramolecular vibrations. Since numerous vibronic levels resulting from these vibrational modes and their various combinations spread almost continuously over a pure electronic state (a state used for the construction of the band), and also since the distribution width of the vibronic energy states is larger than the values of the intermolecular resonance integrals, a non-localized treatment (band picture) may be a poor approach. On the other hand, since the interaction of the carrier with the lattice is relatively small (cf. preceding note), only a little activation energy may be required for the resonance transfer of the excess carrier between adjacent molecules (this is a difference from the hopping motion).

The intermolecular overlap integrals in the anthracene crystal were first calculated by Murrell.[6] Later calculations of this type were reported by Ohki et al.[2b] for pyrene. In these calculations the anisotropy of the mobility may be explained on the assumption that the overlap integrals are roughly proportional to the resonance integrals.

The tight-binding band approximation for the anthracene crystal was first calculated by LeBlanc[7] in order to describe the motion of excess charge carriers. The calculated mobility anisotropy agreed qualitatively with those experimentally observed, and the bandwidth was found to be approximately $0.56\,kT$ at room temperature.* Subsequently, Thaxton et al.[8] extended LeBlanc's method to homologs of anthracene: naphthalene, anthracene, tetracene and pentacene. Katz et al.[9] also calculated the band structure of naphthalene, anthracene, and several polyphenyls in the tight-binding band approximation. In the calculation of intermolecular resonance integrals they used the SCF carbon atomic orbital, represented in the form of a linear combination of four Slater wave functions.[10],* The bandwidths calculated by their method were about five times larger than those found by LeBlanc. Recently, Friedman[11] calculated the electrical and thermal transport properties of organic crystals from a Boltzmann equation treatment based on the tight-binding band structure. For anthracene the calculated mobility anisotropies in the ab plane were the same as those obtained by LeBlanc, but in the $c'$ direction a better agreement with the experiments was found.

We have already examined in a previous paper[12] the band structure of the anthracene crystal at atmospheric pressure and also at 160 kilobars. It was found that the increase in the mobility due to the decrease in the lattice constants was found to be several tens of times at 160 kilobars. In the case of a larger hydrocarbon, the distances between molecules in the crystal, are also expected to be shorter, in addition to the change in the distribution of the carriers in the molecule.

In this report, we will attempt to calculate the band structure of circumanthracene, $C_{40}H_{16}$ (Fig. 2), by the method used by LeBlanc. Since circumanthracene is a largest hydrocarbon in the polycyclic aromatics, the electrical properties of which have been experimentally investigated,[13] it may be worth-while to compare the band structure and the mobility properties of the compound with those of anthracene.

## Crystal Structure

The first step in the calculation of the band structure of the circumanthracene crystal is to estimate the coordinates of atoms in the crystal. Although the lattice constants of the crystal have been set up,[14] the orientation of the molecule in the crystal has not yet been determined. Hence, we will try to estimate the latter from the crystal structure of coronene.[15] A method of estimation is described in the Appendix. The crystal data of these two compounds, in addition to those of anthracene, are compared in Table I. The estimated orientation of the molecule in the

TABLE I. COMPARISON OF CRYSTAL DATA

| | Coronene[a] | Circum-anthracene[b] | Anthracene[c] |
|---|---|---|---|
| Space group | $C_{2h}^5-P2_1/a$ | $C_{2h}^5-P2_1/a$ | $C_{2h}^5-P2_1/a$ |
| a (Å) | 16.10 | 23.77 | 8.561 |
| b (Å) | 4.695 | 4.59 | 6.036 |
| c (Å) | 10.15 | 9.98 | 11.163 |
| $\beta$ | 110.8° | 99.9° | 124.7° |
| z | 2 | 2 | 2 |

a) Ref. 15.
b) Ref. 14.
c) V. C. Sinclair, J. M. Robertson and A. M. Mathieson, *Acta. Cryst.*, **3**, 241 (1950).

TABLE II. ESTIMATED ORIENTATION OF THE MOLECULE IN THE CRYSTAL

| | | |
|---|---|---|
| $\chi_L=44.1°$ | $\chi_M=107.6°$ | $\chi_N=128.7°$ |
| $\psi_L=54.8°$ | $\psi_M=104.2°$ | $\psi_N=38.7°$ |
| $\omega_L=67.2°$ | $\omega_M=22.9°$ | $\omega_N=90.0°$ |

6) J. N. Murrell, *Mol. Phys.*, **4**, 205 (1961).
7) O. H. LeBlanc, *J. Chem. Phys.*, **35**, 1275 (1961); O. H. LeBlanc, "Organic Semiconductors," Ed. by J. J. Brophy and J. W. Buttrey, The Macmillan Co., New York (1962), p. 21.
* In the calculation of the intermolecular resonance integrals, LeBlanc (and also Thaxton et al.) made some minor errors (cf. Ref. 9). The correct bandwidths obtained by his method are somewhat wide (cf. Table IV and also Figs. 5 and 6 in Text).
8) G. D. Thaxton, R. C. Jarnagin and M. Silver, *J. Phys. Chem.*, **66**, 2461 (1962).
9) J. I. Katz, S. A. Rice, S. Choi and J. Jortner, *J. Chem. Phys.*, **39**, 1683 (1963).
10) E. Clementi and C. C. J. Roothaan, *Phys. Rev.*, **127**, 1618 (1962).
* By this choice of the atomic orbital, the behaviour of the wave function was expressed properly at large internuclear distances relevant to this problem. The calculated values of the mobility anisotropy were in better agreement with the experimental data than the mobility calculated from the single Slater-type atomic orbital.
11) L. Friedman, *Phys. Rev.*, **133**, 1668 (1964).
12) Y. Harada, Y. Maruyama, I. Shirotani and H. Inokuchi, This Bulletin, **37**, 1378 (1964).
13) H. Inokuchi, N. Matsubara, Y. Maruyama and E. Clar, *Nature*, in press.
14) E. Clar, W. Kelly, J. M. Robertson and M. G. Rossman, *J. Chem. Soc.*, **1956**, 3878.
15) J. M. Robertson and J. G. White, ibid., **1945**, 607.

crystal is given in Table II,* where $\chi_L$, $\phi_L$, $\omega_L$; $\chi_M$, $\varphi_M$, $\omega_M$; $\chi_N$, $\psi_N$, $\omega_N$ are the angles which the molecular long (L) and short (M) axes and their perpendicular (N) make with the a and b crystal axes and with their perpendicular, c'. Furthermore, all the hexagons in circumanthracene were assumed to be regular ones with a radius of 1.39Å. Thus, the coordinates of atoms referred to orthogonal axes a, b and c' were estimated.** Although the above estimate of the coordinates of atoms lacks confirmation, it may be adequate for the calculation of the band structure, considerering the rather rough nature of the present theoretical treatment.

## Method of Calculation

The band structure and mobility tensors for circumanthracene are calculated by the method introduced by LeBlanc.[7]

Disregarding the interaction between carriers (electrons or holes), the Hamiltonian operator appropriate to an electron or a hole is expressed in the form:

$$\boldsymbol{H}=(-\hbar^2/2m)\nabla^2+\sum_n V_n(\boldsymbol{r}-\boldsymbol{r}_n) \tag{1}$$

where $V_n$ is the Hartree potential of an isolated molecule. Since the circumanthracene crystal has two molecules per unit cell, the wave function in the tight-binding band approximation is expressed by:

$$\Psi=C_1\psi_1+C_2\psi_2 \tag{2}$$

where

$$\begin{aligned}\psi_1&=\textstyle\sum_A \exp[i\boldsymbol{k}\cdot\boldsymbol{r}_A]\,\phi(\boldsymbol{r}-\boldsymbol{r}_A)\\ \psi_2&=\textstyle\sum_B \exp[i\boldsymbol{k}\cdot\boldsymbol{r}_B]\,\phi(\boldsymbol{r}-\boldsymbol{r}_B)\end{aligned} \tag{3}$$

in which $\phi(\boldsymbol{r})$ denotes the molecular wave function. In Eq. 3, the first sum is taken over the centre of the standard molecule and all the lattice points generated from it by primitive lattice translations; the second sum is similarly taken over the points generated from the centre of the reflected molecule at $(\boldsymbol{a}/2, \boldsymbol{b}/2)$. On the basis of variational principles, the band energy can be determined by the solution of a secular equation:

$$\begin{vmatrix} H_{11}-ES & H_{12} \\ H_{21} & H_{22}-ES \end{vmatrix}=0 \tag{4}$$

where

$$\begin{aligned}H_{11}&=H_{22}=\int \phi_1^* H\phi_1 d\tau\\ H_{12}&=H_{21}^*=\int \phi_1^* H\phi_2 d\tau\end{aligned} \tag{5}$$

Therefore, by disregarding overlap integrals, the solution of Eq. 4 becomes:

$$E=H_{11}\pm|H_{12}| \tag{6}$$

By disregarding three-centre integrals and overlap integrals, the substitution of Eq. 3 into 6 leads to:

$$\begin{aligned}E(\boldsymbol{k})=E_0+\sum_{n\,(r_n\neq 0)} E_n^\alpha+\sum_{l\,(r_l\neq 0)} E_l^\gamma \exp[-i\boldsymbol{k}\cdot\boldsymbol{r}_l]\\ \pm\Big|\sum_l E_{l+AB}^\gamma \exp[-i\boldsymbol{k}(\boldsymbol{r}_l+\boldsymbol{r}_{AB})]\Big|\end{aligned} \tag{7}$$

where

$$\left.\begin{aligned}E_0&=\int \phi^*(\boldsymbol{r}-\boldsymbol{r}_n)\,[(-\hbar^2/2m)\nabla^2+V_n]\\ &\quad\times\phi(\boldsymbol{r}-\boldsymbol{r}_n)d\tau\\ E_n^\alpha&=\int \phi^*(\boldsymbol{r})\,V_n(\boldsymbol{r}-\boldsymbol{r}_n)\,\phi(\boldsymbol{r})d\tau\\ E_l^\gamma&=\int \phi^*(\boldsymbol{r}-\boldsymbol{r}_l)\,V_l(\boldsymbol{r}-\boldsymbol{r}_l)\,\phi(\boldsymbol{r})d\tau\\ E_{l+AB}^\gamma&=\int \phi^*(\boldsymbol{r}-\boldsymbol{r}_l-\boldsymbol{r}_{AB})\\ &\quad\times V_{l+AB}(\boldsymbol{r}-\boldsymbol{r}_l-\boldsymbol{r}_{AB})\,\phi(\boldsymbol{r})d\tau\end{aligned}\right\} \tag{8}$$

in which $E^\alpha$ and $E^\gamma$ denote the coulomb and the intermolecular resonance integrals respectively. In Eq. 7, while the sum, $\sum_n$ is taken over all molecules except the one with a centre located at the origin, the sum, $\sum_l$, is carried out over the primitive lattice translations.

In the actual calculation of the circumanthracene crystal, $E^\gamma$'s with values of less than $10^{-16}$ erg were disregarded (cf. Table III). Therefore, Eq. 7 becomes

$$\begin{aligned}E(\boldsymbol{k})=&\text{const.}+2E_b\cos\boldsymbol{k}\boldsymbol{b}+2E_c\cos\boldsymbol{k}\boldsymbol{c}\\ &+2E_{b\bar{c}}\cos\boldsymbol{k}(\boldsymbol{b}-\boldsymbol{c})\\ &\pm|2E_{a/2\,b/2}[\cos\boldsymbol{k}(\boldsymbol{a}/2+\boldsymbol{b}/2)\\ &+\cos\boldsymbol{k}(\boldsymbol{a}/2-\boldsymbol{b}/2)]|\end{aligned} \tag{9}$$

which shows the interaction of the centre molecule with ten neighbouring ones (Fig.

---

* The inclination of molecules to the ac face and also the perpendicular distances between the planes of molecules overlying each other in the b axial direction are collected in the following table. Since ovalene, $C_{32}H_{14}$, has a molecular structure intermediate between those of coronene and circumanthracene, and also since its crystal structure is similar to that of coronene, the estimated data for circumanthracene may be regarded as appropriate.

| | Coronene[a] | Ovalene[b] | Circumanthracene[c] |
|---|---|---|---|
| Inclination of molecule | 43.7° | 42.7° | 38.7° |
| Distance between the molecular planes | 3.40 Å | 3.45 Å | 3.58 Å |

a) Ref. 15.
b) D. M. Donaldson and J. M. Robertson, *Proc. Roy. Soc.*, A220, 157 (1953).
c) Calculated from Table II.

** While, in the case of coronene, the shortest distance between carbon atoms of the standard molecule and those of the reflected molecule at $(\boldsymbol{a}/2, \boldsymbol{b}/2)$ is 3.77 Å, the corresponding distance of circumanthracene is found to be 3.90 Å, showing the estimated coordinates of atoms to be appropriate.

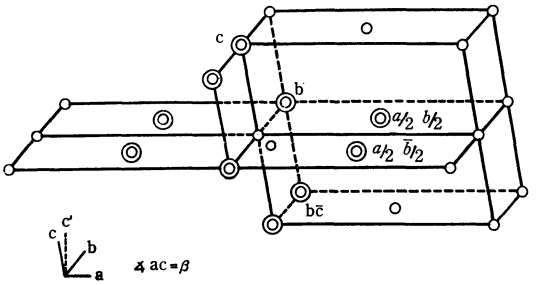



Fig. 1. The unit cell of the circumanthracene crystal. The interaction of the centre molecule (O) with molecules marked with double circles was considered.

1). The constant in Eq. 7 is immaterial to the determination of bandwidths and mobilities.

The molecular wave functions, $\phi$, are linear combinations of Slater-type $2p_z$ atomic orbitals:

$$\phi=\sum_i a_i\chi_i \tag{10}$$

with

$$\chi_i=(\alpha^5/\pi)^{1/2}r_i\cos\xi_i\exp(-\alpha r_i) \tag{11}$$

and

$$\alpha=1.64\text{ a. u.}=3.08\times10^8\text{ cm}^{-1}$$

The coefficients, $a_i$, are determined using the approximation of Hückel. Although the orbital energies and the bond orders of the circumanthracene molecule had already been investigated by Baudet and Pullman,[16] we recalculated the orbital coefficients (cf. Fig. 2), because the latter were not shown in their paper. In cases of multiple signs the upper signs are associated with the lowest antibonding orbital (for the electron) and the lower signs with the highest bonding orbital (for the hole).

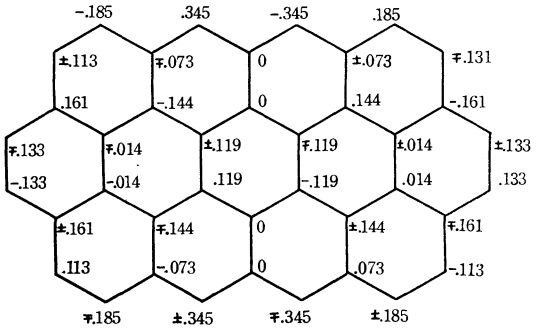



Fig. 2. Values of the coefficients for the Hückel wave functions. The magnitudes of these coefficients are the same for holes and electrons; when they differ in phase, the upper sign is for the electron and the lower for the hole.

16) J. Baudet and B. Pullman, *Compt. rend.*, **244**, 777 (1957).

The intermolecular resonance integrals, $E_b$, $E_c$, etc., were calculated by the method used by LeBlanc except that all of the two-centre interatomic integrals were considered for the evaluation of each intermolecular resonance integrals.

If we assume that the carrier-scattering can be described by the constant mean free time, $\tau(\boldsymbol{k})=\tau_0$, the mobility components are given by:

$$\mu_{ij}=e\tau_0\langle v_iv_j\rangle/\boldsymbol{kT} \tag{12}$$

where $v_i$ is the $i$th component of the carrier velocity, and is given by:

$$v=(1/h)\partial E(\boldsymbol{k})/\partial\boldsymbol{k} \tag{13}$$

The quantity $\langle v_iv_j\rangle$ is a statistical average over the band.

## Results of Calculation

The intermolecular resonance integrals of the circumanthracene crystal are given in Table III in comparison with those of anthracene.*

Table III. Intermolecular resonance integrals ($10^{-16}$ erg)

| | Circumanthracene* | | Anthracene | |
|---|---|---|---|---|
| | Electron | Hole | Electron | Hole |
| $E_b$ | −86.0 | −89.7 | 25.2 | −33.5 |
| $E_c$ | −34.0 | 34.8 | 0.802 | 0.167 |
| $E_{b\bar{c}}$ | 1.91 | −2.10 | −0.000100 | 0.000291 |
| $E_{a/2\ b/2}$ | −1.23 | −1.20 | −39.7 | −29.0 |
| $E_{a/2\ b/2\ c}$ | 0.207 | −0.282 | 1.02 | 6.64 |

* The values of some of other resonance integrals are in unit of erg; $E_a=0.494\times10^{-32}$, $E_{bc}=0.748\times10^{-16}$, $E_{a/2\ b/2\ \bar{c}}=-0.750\times10^{-23}$ for the electron; $E_a=-1.30\times10^{-31}$, $E_{bc}=-0.916\times10^{-16}$, $E_{a/2\ b/2\ \bar{c}}=0.571\times10^{-23}$ for the hole.

In the reduced zone scheme given by $-\pi<\boldsymbol{ka}, \boldsymbol{kb}, \boldsymbol{kc}<\pi$, the electron and hole band structures of circumanthracene in the reciprocal crystal axis direction are shown in Figs. 3 and 4. The origins of the energy scales are arbitrarily taken in both figures. The band structures of the anthracene crystal are also given in Figs. 5 and 6.

In Table IV we present the values of the bandwidths in the $\boldsymbol{a}^{-1}$, $\boldsymbol{b}^{-1}$, and $\boldsymbol{c}^{-1}$ directions,

* The band structure of the anthracene crystal was calculated by the same method. For the evaluation of the band energy, the interaction of the centre molecule with twelve neighbouring ones was considered (cf. Ref. 12):

$$E(\boldsymbol{k})=\text{const.}+2E_b\cos\boldsymbol{kb}+2E_c\cos\boldsymbol{kc}\pm[2E_{a/2\ b/2}[\cos\boldsymbol{k}(\boldsymbol{a}/2+\boldsymbol{b}/2)+\cos\boldsymbol{k}(\boldsymbol{a}/2-\boldsymbol{b}/2)]+2E_{a/2\ b/2\ c}[\cos\boldsymbol{k}(\boldsymbol{a}/2+\boldsymbol{b}/2)+\boldsymbol{c})+\cos(\boldsymbol{a}/2-\boldsymbol{b}/2+\boldsymbol{c})]]$$

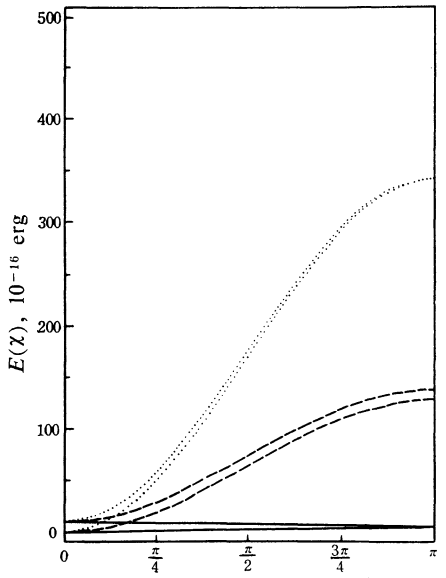



Fig. 3. Electron band structure of circumanthracene in the $a^{-1}$ (solid line), $b^{-1}$ (dotted line) and $c^{-1}$ (dashed line) directions.

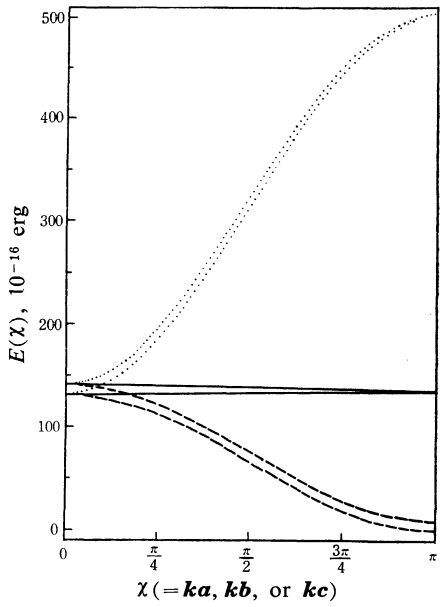



Fig. 4. Hole band structure of circumanthracene in the $a^{-1}$ (solid line), $b^{-1}$ (dotted line) and $c^{-1}$ (dashed line) directions.

TABLE IV. BANDWIDTHS AND SPLITTINGS IN THE $c^{-1}$ DIRECTION OF CIRCUMANTHRACENE AND ANTHRACENE ($10^{-4}$ eV.)

| | Circumanthracene | | Anthracene | |
|---|---|---|---|---|
| | Electron | Hole | Electron | Hole |
| $a_-^{-1}$ | 3.1 | 3.0 | 96.7 | 55.7 |
| $a_+^{-1}$ | 3.1 | 3.0 | 96.7 | 55.7 |
| $b_-^{-1}$ | 212.9 | 232.3 | 37.1 | 139.3 |
| $b_+^{-1}$ | 206.8 | 226.3 | 159.6 | 37.1 |
| $c_-^{-1}$ | 80.3 | 81.8 | 7.1 | 33.5 |
| $c_+^{-1}$ | 80.3 | 81.8 | 3.1 | 32.7 |
| $c_{\text{splitting}}^{-1}$ | 6.1 | 6.0 | 193.4 | 111.5 |

and also the splittings in the $c^{-1}$ direction. Since there are two branches in each band, the lower and the upper branches are shown by $-$ and $+$ suffices respectively.

The velocity components and the mean square velocities of circumanthracene are given in Table V, in addition to those of the anthracene crystal.

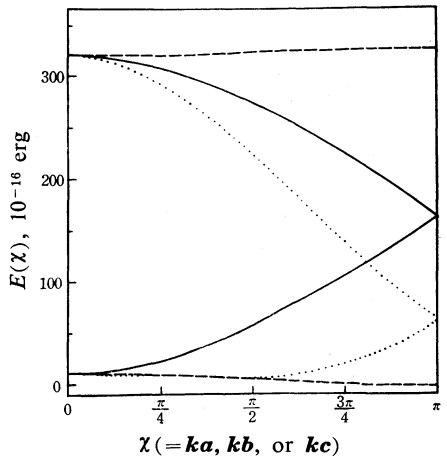



Fig. 5. Electron band structure of anthracene in the $a^{-1}$ (solid line), $b^{-1}$ (dotted line), and $c^{-1}$ (dashed line) directions.

## Discussion

**Band Structure.**—As is shown in Figs. 3—6, and also in Table IV, while the bandwidths of both the electrons and holes of circumanthracene are largest in the $b^{-1}$ direction (ca. $2\times10^{-2}$ eV.), the widths in the $a^{-1}$ direction are only $3\times10^{-4}$ eV. In the case of anthracene, the direction of the smallest bandwidth is that of $c^{-1}$. Moreover, the splittings between the upper lying bands and the lower ones of circumanthracene are smaller by a factor of 30 than those of the anthracene crystal. These relations may be due to the differences in molecular and crystal structure between these two hydrocarbons. In spite of a larger size of the molecular long axis, however, the c axis of the circumanthracene crystal is shorter than that of anthracene. This leads to far larger $E_c$ values of circumanthracene (Table III) and, accordingly, larger bandwidths in the $c^{-1}$ direction. On the

TABLE V. THE VELOCITY COMPONENTS AND THE MEAN SQUARE VELOCITIES ($10^{10}$ cm$^2$/sec$^2$)

| | Electron | | | Hole | | |
|---|---|---|---|---|---|---|
| | Circumanthracene | Anthracene | Ratio | Circumanthracene | Anthracene | Ratio |
| $\langle v^2_a \rangle$ | 0.69 | 10.4 | 0.06 | 0.72 | 5.60 | 0.13 |
| $\langle v^2_b \rangle$ | 28.0 | 9.34 | 3.00 | 30.5 | 10.2 | 3.00 |
| $\langle v^2_{c'} \rangle$ | 20.2 | 0.041 | 490 | 21.2 | 1.34 | 16 |
| $\langle v^2 \rangle$ | 49.0 | 19.8 | 2.5 | 52.4 | 17.1 | 3.1 |

TABLE VI. OBSERVED ELECTRICAL CONDUCTIVITY AT 15°C OF CIRCUMANTHRACENE AND ANTHRACENE

| Circumanthracene[a] (Single crystal, ∥ b axis) | | Anthracene[b] (powder) | | $n_{circum}/n_{anth}$ | $\mu_{circum}/\mu_{anth}$ |
|---|---|---|---|---|---|
| $\sigma_{15}$, $\Omega^{-1}\cdot cm^{-1}$ | $\Delta\varepsilon$, eV. | $\sigma_{15}$, $\Omega^{-1}\cdot cm^{-1}$ | $\Delta\varepsilon$, eV. | | |
| $1.7\times10^{-13}$ | 1.8 | $10^{-21}$ | 2.7 | $7.4\times10^{7}$ | 2 |

a) Ref. 13.
b) H. Inokuchi, unpublished.

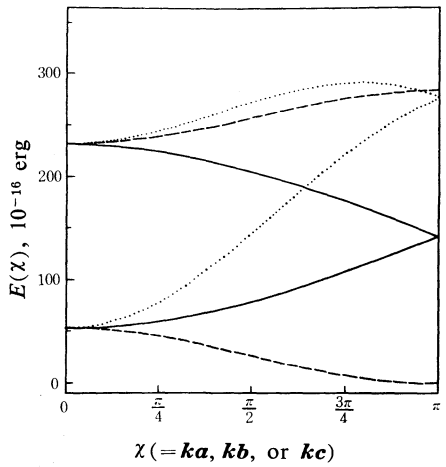



Fig. 6. Hole band structure of anthracene in the $a^{-1}$ (solid line), $b^{-1}$ (dotted line), and $c^{-1}$ (dashed line) directions.

other hand, the much longer a axis of circumanthracene brings about smaller $E_{a/2\,b/2}$ values, with the consequence that the bandwidths in the $a^{-1}$ direction and also the splittings between the upper and lower branches become very small (cf. Eq. 9). The large bandwidths in the $b^{-1}$ direction of circumanthracene may be due to the remarkably short b axis.

As is shown in Figs. 3—6, the total bandwidths are slightly larger for circumanthracene. The total widths of the electron and the hole band of circumanthracene are 0.021 eV. (0.82 $kT$) and 0.031 eV. (1.22 $kT$); the corresponding widths of anthracene are 0.020 eV. (0.79 $kT$) and 0.018 eV. (0.70 $kT$) respectively.

**Mobility Tensors.**—It can be noted from Table V that the anisotropy properties of the band structure also appear in the mobility anisotropy. In the case of circumanthracene, the largest mobilities of both electrons and holes are found in the $b$ direction, corresponding to the widest bands in the $b^{-1}$ direction. Moreover, the mobilities in the $a$ direction are found to be much smaller than those in the other directions, a corollary of the small bandwidths in the $a^{-1}$ direction. On the other hand, the mobilities of anthracene are fairly isotropic on the ab plane and smaller perpendicular to it, reproducing the anisotropy properties of the bandwidths in the reciprocal lattice directions. We may, therefore, conclude that the significant differences between the mobility anisotropies of the two compounds may also be due to the differences in their crystal geometry and molecular structure.

If we assume that the values of $\tau_0$ are comparable for these hydrocarbons, it can be seen, by comparing the values of their mean square velocities, that the mobility of circumanthracene is, on the whole, 2 or 3 times larger than that of anthracene. In general, as the resonance structure of aromatic compounds becomes larger, the electron and the hole densities at a carbon atom are smaller one side, while the distances between molecules in the crystal become shorter on the other side. The former effect may decrease the mobilities of the carriers, since it may reduce the electron and the hole densities at positions favourable to making the resonance integrals large. On the other hand, the latter effect may clearly lead to a larger mobility. Since the change in the molecular distances has a greater influence on the mobilities,* the latter effect may decide the variation in the mobility, as is found in the cases of circumanthracene and anthracene.

**A Comparison with Experimental Results.**—The experimental results for the electrical conductivity of circumanthracene and anthracene are summarized in Table VI. The

* In the case of anthracene, the one percent change of the lattice distances (corresponding to the application of a pressure of 3000 atm.) leads to an increase in the mobility by a factor of 1.1—1.4 (cf. Refs. 1b, 9 and 12).

conductivity of the former was measured in the direction parallel to the b axis of a single crystal. However, in the case of anthracene, the values of a powder specimen were used.* In Table VI the ratios of the number of carrier concentrations, $n_{\text{circum}}/n_{\text{anth}}$, and of the mobilities, $\mu_{\text{circum}}/\mu_{\text{anth}}$, are estimated from two relations, $n \propto \exp(-\Delta\varepsilon/2kT)$ and $\sigma \propto n\mu$. In Table V it is found that, assuming that the values of $\tau_0$ are comparable for both compounds, the mobilities of both the electrons and the holes of circumanthracene are three times larger than those of anthracene in the ***b*** direction, and also two or three times larger in the mean (corresponding to the mean square velocity). Thus, the calculated mobility ratio is roughly in agreement with the experimentally estimated one (Table VI), the values of the mobility of circumanthracene perhaps being several $cm^2/V.sec$. It is also pointed out from Table VI that, in the case of circumanthracene, while the increment of the conductivity due to the increase in the mobility is relatively small, the great increase in charge carriers due to the lowering of the energy gap value causes a sharp drop in the resistivity. When the organic crystal is compressed under high pressure, it behaves similarly.[12] The increase in the conductivity, which amounts to a factor of $10^4$—$10^6$ at high pressure, is also due mostly to the increase in the concentrations of carriers, $10^3$—$10^4$ times.

As for the mobility anisotrotropy of circumanthracene, although interesting properties are expected theoretically, no experimental confirmation has been obtained.**

Finally, it can be noted that, judging from the estimated magnitude of the mobility, the band model may be not satisfactory enough for us to understand the conduction in the circumanthracene crystal, as has been discussed in the introduction to the present paper. Although the substance is among the largest polycyclic aromatics, its conduction mechanism may still be distinguished from that of graphite, the electrical-transport properties of which can be satisfactorily explained by the band model.[17]

## Summary

The band structure and mobility tensors of circumanthracene have been calculated by the tight-binding band approximation.

The total bandwidths of the compound have been found to be slightly larger than those of anthracene; the total widths of the electron and the hole band being $0.82\,kT$ and $1.22\,kT$ room temperature.

The values of the calculated mobilities for the electron and the hole are comparable in the ***b*** and the ***c'*** directions, but the corresponding values in the ***a*** direction are smaller by a factor of about 30~40, reproducing the anisotropy properties of the bandwidths in the reciprocal lattice directions. Thus, the anisotropy of the band structure of the compound is considerably different from that of anthracene. This behaviour may be associated with the differences in their crystal geometry and molecular structure.

The magnitude of the mobility is three times larger than that of anthracene in the ***b*** direction, and two or three times larger in the mean, the calculated ratio being roughly in agreement with the experimentally-estimated one. Hence, it has been concluded the sharp drop in the resistivity in going from anthracene to circumanthracene is due mostly to the great increase in the concentrations of charge carriers, $10^7$ times, as a result of the lowering of the energy gap value.

Finally, it has been pointed out that, although circumanthracene is among the largest polycyclic aromatics, judging from the estimated magnitude of the mobility (several $cm^2/V.sec$), the band model may be not satisfactory enough for us to understand the conduction in the crystal.

We would like to thank Professor Yoshihiko Saito and Professor Yutaka Toyozawa for their helpful discussions.

*The Institute for Solid State Physics*
*The University of Tokyo*
*Azabu, Tokyo*

## Appendix

Both coronene and circumanthracene have a monoclinic unit cell containing two molecules, one at the corner and the other in the centre of the ab face. The very short b axis is a striking feature of the circumanthracene crystal structure. This periodicity and that of the c axis are almost identical with the corresponding axial lengths in coronene. On the other hand, the length of the a

* We adopted the values of anthracene given in Table VI for the following two reasons. Firstly, although various data for single crystals and powder specimens are found in the literature, few of them are reliable. Secondly, since the value of the conductivity of a powder specimen may be close to that on the ab plane of a single crystal, and also since the conductivity is almost isotropic on the plane, the values in Table VI may be taken as those in the b direction. In fact, Nakada's values, recently obtained on the ab plane of a single crystal, are near above-mentioned values.

** Since the single crystal used by Matsubara et al. was a fine needle developed in the b axial direction (0.2 ×0.2×5 mm.), the conductivity in other directions could not be observed.

17) C. A. Coulson, *Nature*, **159**, 265 (1947); P. R. Wallace, *Phys. Rev.*, **71**, 622 (1947); R. R. Hearing and S. Mrozowski, *Progress in Semiconductors*, **5**, 273 (1960).

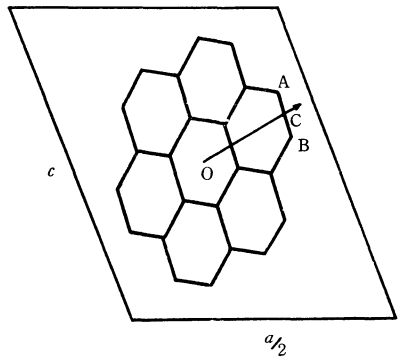



Fig. A1. Projection of the coronene structure on (010). C is the middle point of AB.

axis of circumanthracene is considerably longer that of coronene. These relations suggest that the orientations of molecules are similar in the two cases, and also that the long axis of the molecule is in the direction of the monoclinic a axis. The projection of the coronene structure on the ac face is shown in Fig. A1. In the estimation of the molecular orientation of circumanthracene, the molecule was first arranged in the same orientation as the coronene molecule, the molecular long axis being directed toward the OC axis of coronene, as is shown in Fig. A1. Then, since the circumanthracene crystal has a slightly shorter b axis, the molecule was rotated by 5° about the intersection of the molecular plane and the ac face, so as to reduce the inclination of the molecular planes to (010).

NOTES

# The Influence of pH on Mercuric Chloride Reduction under Ionising Radiations

By P. Srinivasa RAO*

(Received November 9, 1963)

The post-irradiation effects in the mercuric chloride - sodium oxalate reduction system under X, $\beta$, $\gamma$- and ultraviolet radiations have been shown earlier by the present author.[1] The present study will report data on the influence of pH on the radiation-induced reduction of the above system in the presence and in the absence of oxygen.

The aerated and $H_2$-saturated Eder's solutions (mercuric chloride - sodium oxalate) were prepared as described earlier.[1] The pH values were altered by the addition of pure concentrated hydrochloric acid and were determined by a Beckmann pH meter. These solutions of different pH values were then exposed to radiations from (1) an ultraviolet source (a quartz Hg vapour lamp run at 220 V. 0.12 amp. from a distance of 10 cm.), (2) 112 pkV. $-X$ rays ($5\times10^5$ r/hr.), and (3) 1 MeV. electrons ($2\times10^7$ r/hr.), for 20 min. at 30.5°C; the amount of mercurous chloride formed was calculated by titrating it against standard potassium iodate (using Jamieson's[2] procedure).

It may be seen from the figure that, in aerated solutions, the yields of mercurous chloride diminish with decreasing pH values and that at pH$\leqslant$1.9 the reduction is completely inhibited under ultraviolet, at pH$\leqslant$1.78, under X-rays, and at pH$\leqslant$1.62, with 1 MeV. electrons. It is significant that, in the presence of molecular $H_2$, the reduction is not completely inhibited.

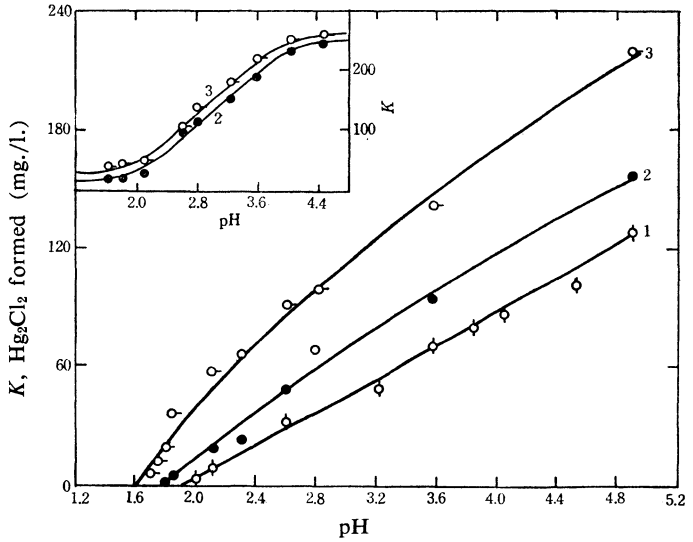



Fig. 1. Plots of $K$ vs. pH in the presence of $O_2$ and saturated with $H_2$ (inset).
1, UV 2, X-rays 3, 1 MeV. electrons

* Present Address: Radiation and Nuclear Chemistry Section, National Chemical Laboratory, Poona-8, India.

1) P. S. Rao, *Z. physik. Chem.*, **19**, 226 (1959).

2) A. I. Vogel, "A Text Book of Quantitative Inorganic Chemistry" (1961), p. 377.

The rate law[3] can be written as:

$$\frac{K_1[Hg_2Cl_2(C_2O_4)^{2-}]I}{P_1[1/pH]}$$

where $K_1$ is the rate of formation of $Hg_2Cl_2(K)$ in the absence of acid (in this system, at pH 4.9); $I$ is the intensity of the ionising radiation, and $P_1$ is the critical value of pH when $K=0$. The near linearity of the $K$ vs. reciprocal acidity (pH) plots and the diminution of $p$, with $I$ follows from the above relationship.

It is well known[4] that the complex $Hg_2Cl_2(C_2O_4)^{2-}$ formed by mercuric chloride and oxalate decomposes to mercurous chloride under both ultraviolet and ionising radiations as follows: $2Hg_2Cl_2(C_2O_4)^{2-}+h\nu \rightarrow 2HgCl+2Cl+2(C_2O_4)^{-}$ with $C_2O_4^-$ and probably $Hg^+$ acting as chain carriers. At high acid concentrations and under ultraviolet, it can be assumed that the chain carrier $C_2O_4^-$ is destroyed:

$$H^+ + C_2O_4^- \rightarrow HC_2O_4$$

Under ionising radiations, H atoms are produced by the disruption of $H_2O$ molecules:[5]

$$H_2O \rightsquigarrow H+OH$$

These can be removed in the presence of $O_2$ or by the $O_2$ formed by the interaction of OH radicals.

$$2OH \rightarrow H_2O+O$$

and

$$2O \rightarrow O_2$$

Thus, at high acid concentrations,

$$H+O_2 \rightarrow HO_2$$

$$HO_2+Hg^+ \rightarrow Hg^{2+}+HO_2^-$$

which might result in an inhibition of the reaction.

In the presence of molecular $H_2$, the possibility of H atoms exerting an oxidising effect on the present system can be shown if one assumes the formation of hydrated hydrogen molecular ions in the solution.[6]

$$H+H^+(\text{hydra.}) \leftrightharpoons H_2^+(\text{hydra.})$$

The $H_2^+$ ion has been shown to have an oxidising effect in the $FeSO_4$ system.[7]

Thus, the back reaction,

$$Hg^+ + H_2^+(\text{hydra.}) \rightarrow Hg^{2+}+H_2$$

might account for the observed inhibition of the reduction.

The author wishes to thank Professor F. H. Barlow of the Agricultural Engineering College, Michigan State University, for loaning 1 MeV.-electron irradiation facilities and Miss R. V. Gowramma of N. C. L., Poona, for her assistance.

*Banaras Hindu University*
*Varanasi-5, India*

3) E. A. Haussman and T. W. Davis, *J. Am. Chem. Soc.*, **76**, 5341 (1954).
4) G. H. Cartledge and S. L. Goldheim, *J. Am. Chem. Soc.*, **55**, 3583 (1933).
5) G. Stein, J. Weiss and R. Watt, *Trans. Faraday Soc.*, **48**, 1030 (1952).
6) J. Weiss, *Nature*, **165**, 728 (1950).
7) T. Rigg, G. Stein and J. Weiss, *Proc. Roy. Soc.*, **A211**, 377 (1952).

# Three Crystalline Forms of Iminodiacetic Acid*

By Yuko TOMITA, Takeshi ANDO and Keihei UENO

(Received May 16, 1964)

There have been reports on the polymorphism of such amino acids as glycine[1,2] and ethylenediaminetetraacetic acid (EDTA),[3] however, no mention has been made of the polymorphism of iminodiacetic acid (IDA).

During the course of our investigation of the infrared spectra of aminopolycarboxylic acid metal chelates, we have found new forms of IDA which do not match the standard spectrum of IDA. Chemical analyses have proved the compounds to be IDA with different spectra and X-ray diffraction patterns.

Further work has then been undertaken to substantiate these three crytsal forms of IDA.

## Experimental

When IDA is dissolved into hot water and the solution is allowed to cool to room temperature, the stable form of IDA ($\alpha$) is obtained. When the hot solution is rapidly chilled to 0°C, a metastable form ($\gamma$) is obtained. Another metastable form ($\beta$) is obtained by adding ethanol to an aqueous solution of IDA at room temperature. The results

* Contribution No. 67 from the Department of Organic Synthesis, Faculty of Engineering, Kyushu University.

1) J. D. Bernal, *Z. Krist.*, **78**, 363 (1931).

2) Y. Iitaka, *Proc. Japan Acad.*, **30**, 109 (1954).

3) R. B. LeBlanc and H. L. Spell, *J. Phys. Chem.*, **64**, 949 (1960).

of elementary analyses show the chemical identity of three forms:

| | Anal. Calcd. for IDA | Found for $\alpha$ | Found for $\beta$ | Found for $\gamma$ |
|---|---|---|---|---|
| C | 36.09% | 36.04% | 36.03% | 36.03% |
| H | 5.30% | 5.32% | 5.27% | 5.32% |

The melting point (232°C with decomposition) is also the same for the three forms.

The main differences between the three forms are observed in their infrared absorption spectra and X-ray diffraction patterns. The infrared absorption curves of the three forms in KBr disks are reproduced in Fig. 1, which indicates that the $\alpha$-, $\beta$-, and $\gamma$-forms of IDA have different crystalline structures. However, when their spectra were taken in a $D_2O$ solution using a cell with calcium fluoride windows, they gave an identical curve in 5000—1200 $cm^{-1}$ region, the only transparent region for a $D_2O$ solution.

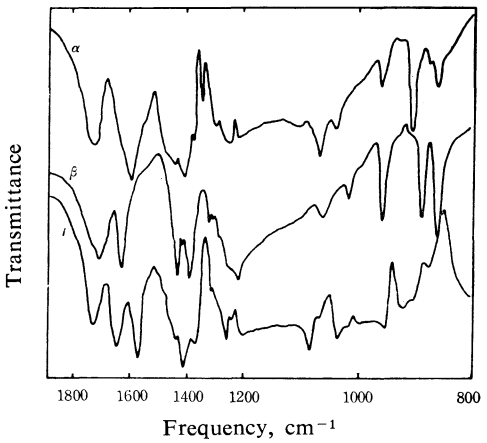



Fig. 1. Infrared spectra of three forms of iminodiacetic acid. (KBr disks)

TABLE I. X-RAY DIFFRACTION PATTERNS FOR THE THREE FORMS OF IMINODIACETIC ACID*

| $\alpha$ Form $d$, Å | $I/I_1$ | $\beta$ $d$, Å | $I/I_1$ | $\gamma$ $d$, Å | $I/I_1$ |
|---|---|---|---|---|---|
| 7.47 | ( 36) | 7.50 | ( 8) | 6.11 | ( 6) |
| 6.42 | ( 9) | 6.55 | ( 20) | 4.77 | ( 24) |
| 5.14 | ( 10) | 6.33 | ( 10) | 4.48 | ( 4) |
| 4.69 | ( 9) | 4.48 | ( 24) | 4.30 | (100) |
| 4.31 | ( 9) | 4.11 | ( 40) | 4.05 | ( 6) |
| 4.23 | ( 15) | 3.71 | ( 13) | 3.95 | ( 6) |
| 4.12 | ( 26) | 3.68 | ( 15) | 3.68 | ( 5) |
| 3.74 | (100) | 3.55 | ( 11) | 3.52 | ( 15) |
| 3.50 | ( 9) | 3.42 | (100) | 3.42 | ( 3) |
| 3.30 | ( 50) | 3.27 | ( 9) | 3.14 | ( 25) |
| 3.23 | ( 12) | 3.03 | ( 40) | 2.97 | ( 11) |
| 3.04 | ( 24) | 2.86 | ( 35) | 2.79 | ( 3) |
| 2.79 | ( 6) | 2.81 | ( 9) | 2.71 | ( 9) |
| 2.63 | ( 10) | 2.75 | ( 13) | 2.65 | ( 4) |
| 2.49 | ( 31) | 2.62 | ( 7) | 2.59 | ( 4) |
| 2.34 | ( 5) | 2.58 | ( 8) | 2.46 | ( 3) |
| 2.25 | ( 2) | 2.47 | ( 10) | 2.42 | ( 5) |
| | | 2.42 | ( 10) | 2.39 | ( 4) |
| | | 2.23 | ( 20) | | |

* The diffractions data were obtained with a Norelco X-ray diffractometer by using the copper $K\alpha$ radiation.

The data of X-ray diffraction which were taken on the powdered sample are shown in Table I; they also support the polymorphism of IDA.

Metastable $\beta$- and $\gamma$-forms can be converted to the stable $\alpha$-form by simple heating; their transitions are observed around 184°C under a polarized microscope. The transitions can also be observed by a differential thermal analysis, in which a broad weak peak can be noticed at around 180°C. The conversions from $\beta$- and $\gamma$-forms to the $\alpha$-form were confirmed by comparing the infrared spectra and X-ray diffraction patterns of the samples before and after heating. After heating, the samples gave spectral and X-ray diffraction patterns completely identical with those of the $\alpha$-form.

## Discussion

No difference in chemical properties was observed for the three forms of IDA, nor was any difference observed in the physical properties in a solution. In the case of glycine, three modifications are known to give different spectra; their differences can be attributed to the differences in the crystalline structures. By analogy, it seems reasonable to assume that the differences in the infrared spectra and X-ray diffraction patterns of IDA are caused by the differences in the crystalline structures. However, the change in the infrared spectra of the $\gamma$-form is so drastic compared with the other two forms that it seems also probable that the $\gamma$-form has a different molecular configuration rather than a different crystalline structure. As we have not been successful so far in obtaining single crystals which are large enough to give diffraction data for the crystalline structure analysis, no conclusive structure can be given for any of the forms.

Some of the expenses of the work reported on in this paper were supported by a research grant provided by the Ministry of Education, to whom the author's thanks are due.

*Department of Organic Synthesis*
*Faculty of Engineering*
*Kyushu University Hakozaki, Fukuoka*

# A Convenient Method of Determining the Stability of a 1:1 Complex in Solution by the Refractometric Method

By Zen-ichi YOSHIDA and Eiji ŌSAWA

(Received May 20, 1964)

Giles' method[1] of detecting complex formation in solution by the refractive index measurement is a well-established, simple and sensitive one, especially for detecting intermolecular hydrogen-bonding pairs, including the X–H$\cdots\pi$ electron type (X=O and N).[2] In this communication the possibility of estimating the equilibrium constant, $K$, of a 1:1 complex formation ($X+Y \leftrightarrows XY$) by this method will be described.

In the Giles method, a physical property (the square of the refractive index) of the solution of X and Y is plotted against the solute molar ratio, while the total concentration (X+Y) is kept constant. The deviation from the "additivity" line PQ (see Fig. 1) is

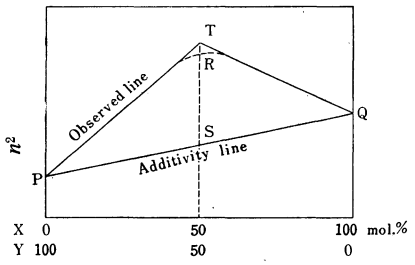



Fig. 1. Schematic representation of $n^2$ vs. molar ratio plot where 1:1 complex is formed between X and Y.

proportional to the concentration of the complex XY.[3] For an equimolar mixture of X and Y, where the deviation is the maximum value, $RS$[4], we can write:

$$RS=\alpha Z \tag{1}$$

where $Z$ is the maximum concentration of XY, and $\alpha$ is constant for the three substances X, Y and XY. When the total concentration, $C$, is changed to $C'$ and the same procedure repeated, we can obtain the similar relation:

$$R'S'=\alpha Z' \tag{2}$$

From Eqs. 1 and 2 we obtain:

$$RS/R'S'=Z/Z'=k \tag{3}$$

The equilibrium constant, $K$, is given by:

$$K=Z/(C/2-Z)^2=Z'/(C'/2-Z')^2 \tag{4}$$

From Eqs. 3 and 4,

$$K=2\sqrt{k}\{\sqrt{k}(C+C')-(C+kC')\}/(C-kC')^2 \tag{5}$$

Thus K can be calculated from Eq. 5.

A preliminary test of the utility of this equation was carried out using an Abbe refractometer. The results are summarized in Table I.

Because of the limited accuracy of the Abbe refractometer ($\pm 0.0002$), it was necessary to raise the concentration of the solute to $10^{-1}$ mol./l. in order to make the $k$ term large enough to fit Eq. 5. At these large concentrations, howerver, the data obtained are less reliable because of the self-association of the solutes (over 30%). Nevertheless, the orders of $K$ obtained are in agreement with the literature values: phenol-methyl acetate, $K_{20°}$ 13.4,[5] phenol-naphthalene $K_{27°}$ 4.6.[6] It will be possible to obtain reliable thermodynamic data on 1:1 association in solution by utilizing a differential refractometer of a higher precision.[7]

TABLE I. THE ESTIMATION OF THE $K$ VALUE BY REFRACTIVE INDEX MEASUREMENT

| X | Y | $C$, mol./l. | Temp., °C | $K$, l./mol. |
|---|---|---|---|---|
| Phenol | Methyl acetate | 0.20—0.15 | 19 | ca. 10 |
| Phenol | Naphthalene | 0.10—0.16 | 27 | ca. 5 |
| Ethanol | Naphthalene | 0.30—0.40 | 28 | ca. 5 |

*Department of Synthetic Chemistry*
*Faculty of Engineering*
*Kyoto University*
*Sakyo-ku, Kyoto*

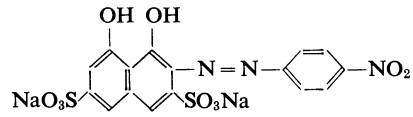
1) C. H. Giles and R. B. Mckay, *J. Biol. Chem.*, **237**, 3388 (1962), and the preceding papers of this series.
2) Z. Yoshida, E. Ōsawa and R. Oda, *J. Phys. Chem.*, **68**, 2895 (1964).
3) F. M. Arshid, C. H. Giles, E. C. McLure, A. Ogilve, T. J. Rose and J. C. Eaton, *J. Chem. Soc.*, **1955**, 67.
4) Practically RS is observed as TR, since the amount of TR is too small to be discerned.
5) S. Nagakura, *J. Chem. Soc. Japan, Pure Chem. Sec.* (*Nippon Kagaku Zassi*), **75**, 734 (1954).
6) R. West, Intern. Symp. Mol. Struc. Spectroscopy, 1962, Tokyo, D117.
7) A D.R. of a $7\times10^{-7}$ accuracy has been manufactured; see *Chem. Eng. News*, **38**, [31] (1960), p. 55.

# *p*-Nitrobenzene Azochromotropic Acid (Chromotrope 2B) as a Colorimetric Reagent for Thorium

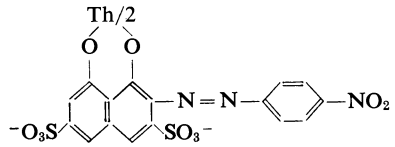
By Satendra P. SANGAL

(Received June 22, 1964)

Metal chelates of *p*-nitrobenzene azochromotropic acid (disodium salt), (Chromotrope 2 B, abbreviated as CTB) with copper,[1] thorium,[2] lanthanum[3] and rare earths have been extensively studied in these laboratories. Chromotrope 2 B has also been recommended as a metalochromic indicator in the EDTA titration of thorium.[4] The structure of the reagent is as follows:




The possibility of chelation with metals in the ligand is at 1 : 8 hydroxy groups; hence, the structure of the metal chelate of Chromotrope 2 B may be assigned as:




The composition of the thorium - Chromotrope 2 B chelate ($\lambda_{max}$ 550 m$\mu$), as reported by Banerji and Dey,[2] is 1 : 2. This communication report the results of the spectrophotometric determination of thorium using Chromotrope 2 B as a chromogenic reagent.

## Experimental

**Instruments.**—A Unicam SP 500 spectrophotometer operated by a Doran mains unit was employed for the absorbance measurements. The measuring glass cells, 1 cm. thick, were those supplied with the instrument.

A Leeds and Northrup direct reading pH indicator was employed for the adjustment of the hydrogen ion concentration.

**Reagents.**—Stock solutions of thorium chloride (B. D. H. AnalaR) and *p*-nitrobenzene azochromotropic acid (disodium salt) were prepared in distilled water and standardised by the usual methods. Solutions of various concentrations were obtained by suitable dilution. The other reagents used were also of the AnalaR grade.

## Results and Discussion

**The Rate of Colour Formation.**—The colour formation is almost immediate; it takes less than five minutes to assume the full colour intensity.

**The Influence of pH Value.**—Full coloration is obtained between pH 3.0 and 6.5 (Fig. 1).

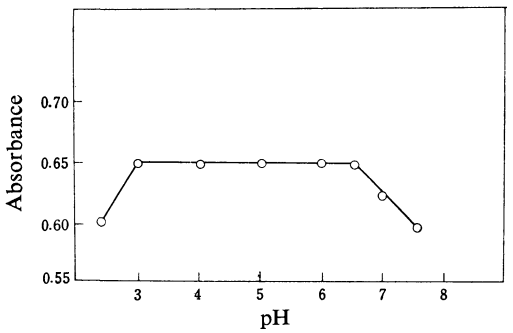



Fig. 1. The Effect of pH on the intensity of the colour.
CTB $2.0 \cdot 10^{-4}$ M
Thorium chloride $4.0 \times 10^{-5}$ M, 580 m$\mu$

**The Effect of the Temperature.**—The absorbance value of a mixture containing ($2.0 \times 10^{-4}$ M) Chromotrope 2 B and ($8.0 \times 10^{-5}$ M) thorium chloride was found to be constant, i. e., 0.820 at 580 m$\mu$, at temperatures from 5 to 95°C.

**Beer's Law.**—Varying quantities (1 ,2, 3, ....., 8, 9 ml.) of thorium chloride were added to an excess of the reagent and the volume was raised to 25 ml. after the pH had been adjusted to 3.5. The colour instensity was measured with a Unicam SP 500 spectrophotometer at 580 m$\mu$. It was found that the system adheres to Beer's law in the range from 0.74 p. p. m. to 16.6 p. p. m. of thorium (Fig. 2).

**Sensitivity.**—The sensitivity as defined by Sandell[5] was found to be 0.232 $\gamma$/cm$^2$. The practical sensitivity based upon an absorbance

1) S. P. Sangal and A. K. Dey, *Ind. J. Chem.*, **1**, 870 (1963).
2) S. K. Banerji and A. K. Dey, *J. Indian Chem. Soc.*, **38**, 139 (1961).
3) S. P. Sangal and A. K. Dey, ibid., **40**, 273 (1963); S. P. Sangal, *J. prakt. Chem.*, in press.
4) S. P. Sangal and A. K. Dey, *Z. anal. Chem.*, **183**, 178 (1961).
5) E. B. Sandell, "Colorimetric Determination of Traces of Metals," 2nd Ed., Inter. Sci., New York (1950).

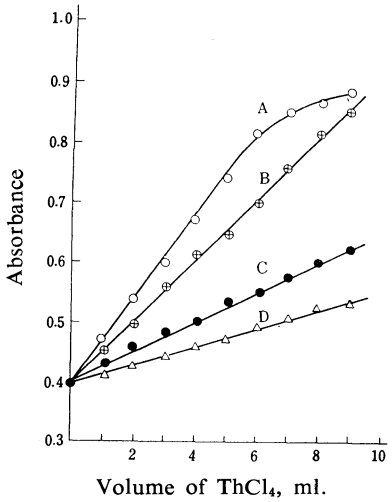



Fig. 2. Adherence to Beer's law.
(Total volume 25 ml.), pH 3~5, 580 mμ
Curve A 5 ml. ($1.0\times10^{-3}$ M) CTB + $x$ ml. ($4.0\times10^{-4}$ M) $ThCl_4$ + $(20-x)$ml. $H_2O$
Curve B 5 ml. ($1.0\times10^{-3}$ M) CTB + $x$ ml. ($2.0\times10^{-4}$ M) $ThCl_4$ + $(20-x)$ml. $H_2O$
Curve C 5 ml. ($1.0\times10^{-3}$ M) CTB + $x$ ml. ($1.0\times10^{-4}$ M) $ThCl_4$ + $(20-x)$ml. $H_2O$
Curve D 5 ml. ($1.0\times10^{-3}$ M) CTB + $x$ ml. ($8.0\times10^{-5}$ M) $ThCl_4$ + $(20-x)$ ml. $H_2O$

of 0.01 unit was found to be 2.32 $\gamma/cm^2$ at 580 mμ.

**Interference Due to Foreign Ions.**—The effect of various cations and anions was studied; it was found that silver, copper, beryllium, cadmium, titanium, zirconium, hafnium, tungsten, scandium, yttrium, lanthanum and rare earths, uranium, tartrate, oxalate, citrate, acetate and fluoride interfere.

**Recommended Procedure.**—For the determination of thorium from this method, the interfering substances must be removed. The pure solution of thorium chloride should then be added to an excess of the reagent and the pH adjusted to 3.5. The colour intensity is then measured by a spectrophotometer at 580 mμ.

## Summary

A method for the colorimetric determination of thorium with Chromotrope 2 B has been described. The composition of the coloured chelate ($\lambda_{max}$ 550 mμ) is $Th(Ke)_2$. The system adheres to Beer's law from 074 p. p. m. to 16.6 p. p. m. of thorium between pH 3.0 and 6.5 at all temperatures from 5 to 95°C. The sensitivities are 0.232 $\gamma/cm^2$ (Sandell) and 2.32 $\gamma/cm^2$ (practical) based on an absorbance of 0.01 unit at 580 mμ. The interference of some cations and anions has also been reported.

The author is thankful to Dr. A. K. Dey for his suggestions and to The Council of Scientific and Industrial Research for its financial aid.

*Chemical Laboratories*
*University of Allahabad*
*Allahabad, India*

# Photolysis of Butene-1 at 1849Å

By Noriho HARUMIYA, Shoji SHIDA and Shigeyoshi ARAI

(Received June 26, 1964)

The photolysis of gaseous olefins has been studied on ethylene[1,2] and propylene[3], but the study of the photolysis of butene-1 seems not to have been made. The mercury photosensitized decomposition of butene-1, however, has been studied by several workers. Gunning and Steacie[4] showed, from the pressure dependence of the reaction, that in the primary step an excited molecule of butene-1 is produced which either decomposes or is collisionally deactivated. Lossing et al.[5] and recently Cvetanović and Doyle[6] showed that there are two modes of primary dissociation involving the splittings of C–C and C–H bonds, the ratio being estimated to be 1.3—1.6. For the present work we have studied the photolysis of butene-1 with the light of 1849 Å and

1) M. C. Sauer and L. M. Dorfman, *J. Chem. Phys.*, **35**, 497 (1961).
2) H. Okabe and J. R. McNesby, ibid., **36**, 601 (1962).
3) Work done in this laboratory, to be published.
4) H. E. Gunning and E. W. R. Steacie, *J. Chem. Phys.*, **14**, 581 (1946).
5) F. P. Lossing, D. G. H. Mardsen and J. B. Farmer, *Can. J. Chem.*, **34**, 701 (1956).
6) R. J. Cvetanović and L. C. Doyle, *J. Chem. Phys.*, **37**, 543 (1962).

TABLE I. RELATIVE AMOUNTS OF PRODUCTS FORMED BY PHOTOLYSIS OF BUTENE-1 AT 1849Å, WITH REFERENCE TO $C_2H_6=10.0$

Time of irradiation: 2 min. Pressure range: 1.7—125 mmHg. The listed values are pressure-independent unless otherwise stated.

| | | | |
|---|---|---|---|
| $H_2$ | 1.7 | *iso*-$C_5H_{12}$ | 1.8 |
| $CH_4$ | 0.4 | 3-Methylbutene-1 | 0.8 |
| $C_2H_6$ | (10.0) | 2-$C_5H_{10}$ | 1.6 |
| $C_2H_2$ | 0.5 | 1-$C_5H_{10}$ | 1.1(1.7 mmHg) |
| $C_3H_8$ | 0.6 | | 1.0(125 mmHg) |
| $C_3H_6$ | 3.5(1.7 mmHg) | 1,5-Hexadiene | 5.8(1.7 mmHg) |
| | 1.1(20—125 mmHg) | | 6.8(30—125 mmHg) |
| $C_4H_{10}$ | 0.3 | 4-Methylhexene-1 | 2.8 |
| *trans*-$C_4H_8$-2 | 0.2 | 3-Methyl-1,5-hexadiene | 3.1 |
| *cis*-$C_4H_8$-2 | trace | 1,5-Heptadiene | |
| Methylcyclopropane | 0.0 | $C_8$ | trace |
| 1,3-Butadiene | 0.6 | | |

have compared the results with those obtained in the previous works on the mercury-photosensitized reaction. Only the main features of the reaction will be reported on here.

Butene-1 of a pure grade, supplied by the Takachiho-Shoji Co., was purified from mercury using gold foil and was then distilled several times in vacuo. The remaining impurities were 1,3-butadiene (0.09%) and *cis*-butene-2 (<0.05%). A quartz cell, 47 mm. in diameter and 13 mm. thick, was connected to a mercury-free vacuum line. All runs were made statically at room temperature, 22±2°C. An ordinary mercury resonance lamp was used as the light source. The absence of mercury in the system was confirmed by making runs using the light source with a filter which transmitted 2537Å but not 1849Å. A 20 m. DMS column was used for the gas chromatographic analysis of light hydrocarbon products ($C_2$—$C_5$) and a 10 m. DNP column for heavier ones. Hydrogen and methane were analyzed volumetrically as usual.

Some twenty products, shown in Table I, were analyzed. The amounts of major products were measured with varying irradiation times at a 20 mmHg pressure. Until 4 min. every product increased linearly with time, showing no measurable secondary reaction of the product at this stage of reaction, although the rates of the formation of some products gradually decreased with time after 4 min. The variation in the light intensity by the factor of ten had no effect on the relative amounts of products. The effect of pressure was examined in the range of 1.7 to 125 mmHg. The rates of the formation of all the products except 1,5-hexadiene and propylene were practically constant, irrespective of the pressure (Table I). This is remarkably different from the results in the photosensitized decomposition and suggests that different kinds of excited states are involved. Methylcyclopropane was not found in any appreciable amount,* and $C_8$ products were found only in a trace; both of these are products in the mercury photosensitization. The polymer formation was not measured, but it may be assumed to be of minor importance on the basis of several pieces of indirect evidence, such as the practical absence of $C_8$ products (dimer), no visible deposit on the cell wall, and the linearity of the product formation with the irradiation time. The addition of nitric oxide (0—15%) to butene-1 at 20 mm. did not change the amount of propylene, but in the low pressure region below 20 mmHg reduced it to the high pressure value, i.e., 1.1 in Table I. This result seems to indicate that a fraction of propylene is produced molecularly in the primary process.

To explain the above results we may assume the following two primary processes:

$$C_4H_8\text{-}1 + h\nu \rightarrow CH_3 + C_3H_5 \quad \text{(A)}$$

$$\searrow H + CH_2=CH-CH-CH_3 \quad \text{(or } CH_2-CH=CH-CH_3\text{)} \quad \text{(B)}$$

The hydrogen atoms thus formed are scavenged by butene-1 to give butyl radicals, $C_4H_9$. Conforming to Cvetanović's procedure, we assume only the recombination reactions of the free radicals thus produced; disproportionations are assumed to be of minor importance. $CH_3 + CH_3 \rightarrow C_2H_6$, $CH_3 + C_3H_5 \rightarrow C_4H_8$-1, $CH_3 + C_4H_7 \rightarrow$ 2-pentene or 3-methylbutene-1, $CH_3 + C_4H_9 \rightarrow$ isopentane, $C_3H_5 + C_3H_5 \rightarrow$ 1,5-hexadiene, $C_3H_5 + C_4H_7 \rightarrow$ 3-methyl-1,5-hexadiene or 1,5-heptadiene, $C_3H_5 + C_4H_9 \rightarrow$ 4-methylhexene-1. Then,

* In an experiment in which butene-1 was photolyzed by mercury photosensitization, methylcyclopropane was actually detected by gas chromatography. In this case the peak of methylcyclopropane was superposed on those of *trans*-butene-2 and isopentane using a DMS column, but it could be separated from the others using a benzylether column.

from the measured yields of products, we obtain the relative yields of radicals as follows: $CH_3$ 39.4, $C_3H_5$ 37.3 (mean value 38.3), $C_4H_7$ 5.5, and $C_4H_9$ 4.6, all with reference to $C_2H_6=10.0$. Judging from these results the relative importance of the two primary processes, A and B, are about 7 : 1. Thus, the C–C bond rupture is far more important in the direct photolysis at 1849Å than in the mercury-photosensitized decomposition. A similar trend has also been found in the photolysis of propylene at 1849Å.[3)]

The formation of propylene can not be explained uniquely in the present stage of study. Possible reactions are $C_4H_8\text{-}1+h\nu \rightarrow C_3H_6+CH_2$ and, in the low pressure region:

$$H+C_4H_8\text{-}1 \rightarrow C_4H_9' \xrightarrow{+M} C_4H_9$$
$$\searrow C_3H_6+CH_3$$

*Laboratory of Physical Chemistry*
*Tokyo Institute of Technology*
*Meguro-ku, Tokyo*

# Alkali Metal Hyperfine Splittings of *o*-Substituted Benzophenone Ketyls

By Rikuhei TANIKAGA, Kazuhiro MARUYAMA and Ryozo GOTO

(Received June 27, 1964)

Aromatic ketyls formed by the reaction of alkali and alkali earth metals with aromatic ketones exist as a contact ion-pair in ethers.[1,2] Their ESR spectra, therefore, show the lines due to splitting by metals as well as by protons. The metal hyperfine splitting of the ketyl generally decreases with an increasing dielectric constant of the solvent, as with other anion-radicals.[3] On the other hand, in a very polar solvent such as *N*, *N*-dimethylformamide, no metal splitting at all has been observed. This variation in the metal splitting can be attributed to charge separation in an ion-pair through solvation.

In the electronic spectrum of the ketyl, the wave number of the maximum absorption peak due to a $\pi \rightarrow \pi^*$ transition shifts towards the red as the radius of the metal cation and the dielectric constant of the solvent increase.[4,5] This spectral shift can be interpreted as a decrease in the cationic effect of a metal on a ketyl anion.[6] Consequently, we expected to find a relationship between the metal splitting, $a_M$, of the ESR spectra and the wave number, $\bar{\nu}_m$, of the maximum absorption peak of the electronic spectra. Indeed, a close relationship between them was observed; that is, $a_M$ increased with $\bar{\nu}_m$.

In the course of an investigation of the ion-pair structure, we have measured the ESR spectra and the electronic spectra of *o*- and *p*-substituted benzophenone ketyls, such as

TABLE I. METAL HYPERFINE SPLITTING CONSTANTS $a_M$ (GAUSS) AND WAVE NUMBERS $\bar{\nu}_m$ OF MAXIMUM ABSORPTION ($\times 10^3\,cm^{-1}$) OF KETYLS IN THF AT 18°C

| Benzophenone derivative | $a_M$ | | | $\bar{\nu}_m$ | | |
|---|---|---|---|---|---|---|
| | Li | Na | K | Li | Na | K |
| —— (I) | 0.32 | 1.18 | 0.24 | 15.3 | 14.7 | 14.0 |
| 4,4'-Me (II) | 0.33 | —* | 0.25 | —** | —** | —** |
| 2,6,2',6'-Me (III) | 0.07 | 0.16 | 0.04 | 14.5 | 13.4 | 12.7 |
| 2,6,2',6'-Et (IV) | 0.00 | 0.00 | 0.00 | 14.5 | 13.3 | 12.8 |

* Assignment of splittings was not possible because of the broadness of the spectrum.
** No measurement was made.

1) D. J. Morantz and E. Warhurst, *Trans. Faraday Soc.*, **51**, 1375 (1955).
2) F. C. Adam and S. I. Weissman, *J. Am. Chem. Soc.*, **80**, 1518 (1958).
3) H. Nishiguchi, Y. Nakai, K. Nakamura, K. Ishizu, Y. Deguchi and H. Takaki, *J. Chem. Phys.*, **40**, 241 (1964).
4) H. V. Carter, B. J. McClelland and E. Warhurst, *Trans. Faraday Soc.*, **56**, 455 (1960); D. G. Powell and E. Warhurst, ibid., **58**, 953 (1962).
5) J. F. Garst, C. Hewitt, D. Walmsley and W. Richards, *J. Am. Chem. Soc.*, **83**, 5034 (1961); J. F. Garst, D. Walmsley, C. Hewitt, W. R. Richards and E. R. Zabolotn, ibid., **86**, 412 (1964).
6) B. J. McClelland, *Trans. Faraday Soc.*, **57**, 1458 (1961).

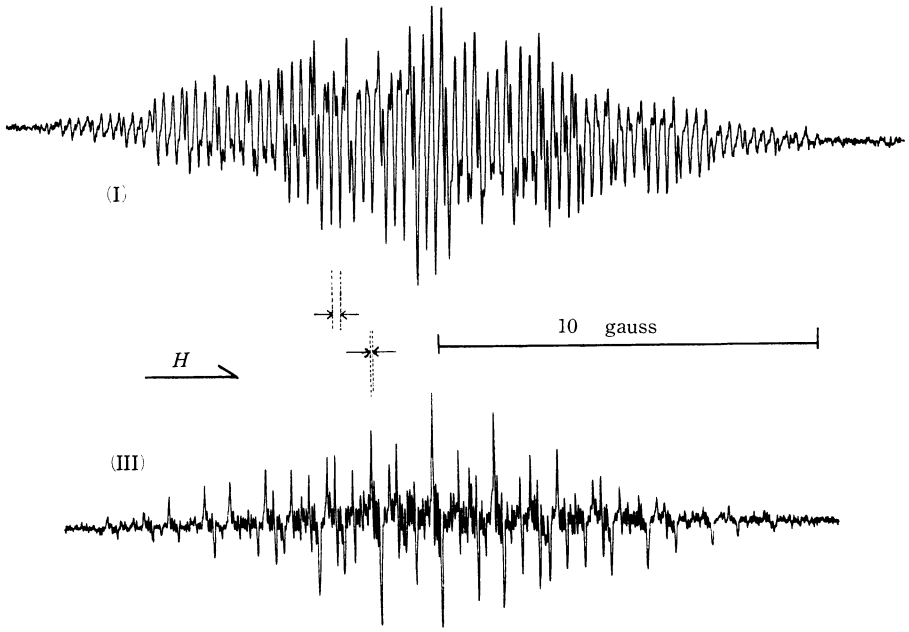



Fig. 1. Potassium splittings of benzophenone (I) and 2,6,2′,6′-tetramethylbenzophenone (III) ketyls in THF at 18°C.

benzophenone (I), 4,4′-dimethylbenzophenone (II), 2,6,2′,6′-tetramethylbenzophenone (III) and 2,6,2′,6′-tetraethylbenzophenone (IV). The preparation of metal ketyls and the method of ESR measurement were described in a previous paper.[7] The metal hyperfine splittings of ketyls in tetrahydrofuran (THF) are summarized in Table I, while representative spectra are shown in Fig. 1.

In the ketyl ion-pair the cation is mainly localized near the oxygen atom,[6,8] so that the decrease in the metal splitting shown in Table I can only be attributed to the steric effect of the *o*-substituents on the metal cation. Although in the case of the metal ketyl of IV the existence of a contact ion-pair is shown by the fact that the $\bar{\nu}_m$ value shifts regularly with the radius of a metal, no metal splitting is observed in its ESR spectrum. These facts indicate that the magnetic effect of a cation attached to an aromatic negative anion is only effective in rather close contact.

The proton hyperfine splittings of benzophenone ketyls will be discussed in subsequent publications.

*Department of Chemistry*
*Faculty of Science*
*Kyoto University*
*Sakyo-ku, Kyoto*

7) K. Maruyama, R. Tanikaga and R. Goto, This Bulletin, **36**, 1141 (1963).
8) W. Schlenk and T. Weickel, *Ber.*, **44**, 1182 (1911).

# The Conformation of *p*-Menthane-2, 3-diol*

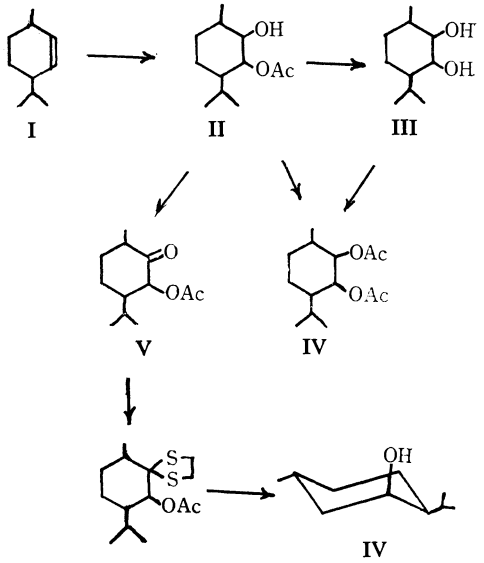
By Shin-ichi SASAKI and Shoei ITO

(Received July 10, 1964)

The hydroxylation of (+)-*p*-menth-2-ene (I) with an organic peracid, or the hydrolysis of its epoxide, affords *p*-menthane-2, 3-diol (II), which has its hydroxyls in the trans configuration. Infrared studies[1] have indicated that the diol adopts a conformation in which both the hydroxyls are axial; its spectrum exhibits the absorption (at 3635 $cm^{-1}$) due to free (non-bonded) hydroxyls only. We have arrived at the same conclusion in the investigation reported here.

(+)-*p*-Menth-2-ene (I), derived from (−)-menthol, after treatment with peracetic acid afforded a viscous liquid b. p. 120—128°C/3mmHg, which deposited crystals of 2-hydroxy-3-acetoxy-*p*-menthane (III), m. p. 114—116°C, $[\alpha]_D = +16.8°$ (methanol), after standing for several days at room temperature. The oily mother liquor, which is apparently a mixture of the diol and its partial acetate, was not separated but was treated with alkali, whereupon it afforded pure *p*-menthane-2, 3-diol (II) b. p. 98—100°C/0.1 mmHg, $[\alpha]_D = +66.4°$ (benzene), identical with that obtained by the hydrolysis of compound III. The diol II and its monoacetate III afforded the same diacetate, m. p. 48—50°C on acetylation. The monoacetate III, which is considered to be an intermediate in the formation of the diol, was used in the following conformational study.

The chromic acid oxidation of the monoacetate III yielded the acetoxy ketone V, m. p. 46—47°C, $[\alpha]_D = +37.1°$ (methanol). The thioketal derived from the ketone V, on desulfurization with Raney nickel, afforded an oil which was identified as (+)-neomenthol by a comparison of their *p*-nitrobenzoates (infrared spectrum and mixed melting point). (+)-Neomenthol has been shown to have the absolute configuration and conformation shown in VI[2]. The acetoxy ketone V is, therefore, 3-acetoxycarvomenthone, which has an axial acetoxyl group, and the conformation of the two oxygenated functions in III and II must be transdiaxial. This finding is in agreement with the ultraviolet spectrum of the monoacetate V, which shows a bathochromic shift of 9 mμ with respect to carvomenthone (see Table I), thus indicating[3] the presence of an axial acetoxyl group at the α-position in V. Consequently, III has axial hydroxyl and acetoxyl groups, and in II both hydroxyls are axial.




The ORD curve of V shows a strong positive Cotton effect in both methanol and in isooctane (see Fig. 1). It has been observed[4] that an α-acetoxyl group makes an irregular contribution to the Cotton effect. In our case the axial acetoxyl group probably does not make much contribution to the effect in both solvents, and the conformational mobility normally

TABLE I

| | $\lambda_{max}$ (mμ) | log ε |
|---|---|---|
| V in ethanol | 293 | 1.80 |
| Carvomenthone in ethanol | 284[5] | 1.35 |

The bathochromic shifts of the acetoxy ketone V

* The work was partly reported in a short communication in *Chem. & Ind.*, 1963, 1119.

1) P. R. Jefferies and B. Miligan, *J. Chem. Soc.*, 1956, 2363; A. R. H. Cole and P. R. Jefferies, ibid., 1956, 4391; T. Matsuura, T. Suge and T. Shishihori, The 16th Annual Meeting of the Chemical Society of Japan, April, Tokyo.

2) J. L. Simonsen, "The Terpenes," Vol. 1, Cambridge University Press (1953), p. 237.

3) C. Djerassi, "Optical Rotatory Dispersion," McGraw-Hill, New York (1960), p. 113.

4) C. Djerassi, O. Halpern, V. Halpern and O. Schindler, *Helv. Chim. Acta*, 41, 250 (1958).

5) T. M. Lowry and R. E. Lishmund, *J. Chem. Soc.*, 1935, 1313.

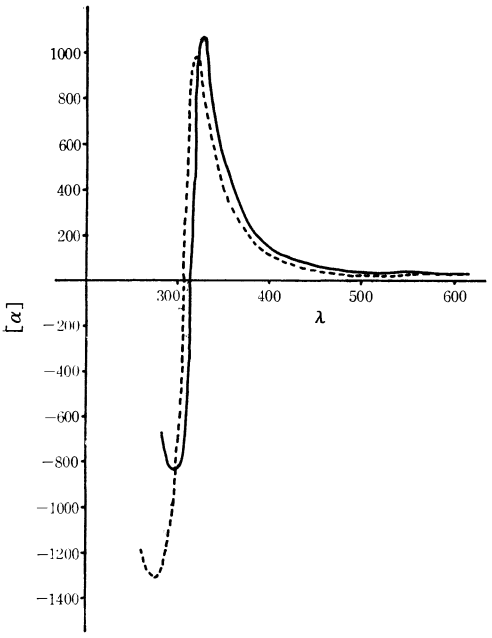



Fig. 1. ORD curves of the acetoxyketone (V).
—— in isooctane
- - - in methanol

dependent on the polarity of the solvents was not observed.

## Experimental

**The Hydroxylation of *trans-p*-Menth-2-ene (I) with Peracetic Acid.** — *trans-p*-Menth-2-ene (I), b. p. 55—56°C/15 mmHg, $d_4^{15}=0.8160$, $[\alpha]_D=+120.46$ (neat), was prepared from 1-menthyl tosylate.

I (15 g.) was added drop by drop over a half-hour period to a solution of 30% hydrogen peroxide (25 ml.) in acetic acid (120 ml.) containing a few drops of concentrated sulfuric acid and warmed at 50°C. After the addition of I, the reaction mixture was stirred for another hour. The acetic acid was then removed in vacuo. The residue was dissolved in ether, washed with saturated sodium bisulfite to destroy the excess peracid, and then washed with aqueous sodium carbonate. The evaporation of the dried (sodium sulfate) ether solution yielded a viscous liquid (14.5 g.), b. p. 120—128°C/3 mmHg. On standing at room temperature the liquid gradually deposited crystals of 2-hydroxy-3-acetoxymenthane (III) (1.5 g.) ; after recrystallization from ligroin, it had an m. p. of 114—116°C, $[\alpha]_D=+16.8°$ (*c* 2.10, methanol) (Found : C, 66.82; H, 10.52. $C_{12}H_{22}O_3$ requires C, 67.25 ; H, 10.35%). The acetylation of III with acetic anhydride and sodium acetate gave the diacetate IV, m. p. 48—50°C (Found : C, 65.82 ; H, 9.41. $C_{14}H_{24}O_4$ requires C, 65.59 ; H, 9.44%).

The filtrate (10 g.) was heated in 20% alcoholic potash (100 ml.) under reflux for an hour. After acidification with hydrochloric acid, the product was isolated by ether extraction to yield *p*-menthane-2,3-diol (II) (8 g.) b. p. 98—100°C/0.1 mmHg, $[\alpha]_D=+66.4°$ (*c* 2.12, benzene)). Diacetate : m. p. and mixed m. p. with acetate IV of III 48—50°C. Di-*p*-nitrobenzoate : m. p. 179—180°C (Found : N, 5.86. $C_{24}H_{26}O_8N_2$ requires N, 5.96%).

**The Chromic Acid Oxidation of 2-Hydroxy-3-acetoxymenthane (III).**—A solution of 2-hydroxy-3-acetoxymenthane (III) (3 g.) in pyridine (20 ml.) was added drop by drop to a suspension of chromic anhydride (4.5 g.) in pyridine (45 ml.). After the addition of III, the reaction mixture was stirred for five days at room temperature. After acidification with dilute sulfuric acid, the product was isolated by continuous extraction with ether (five days). The evaporation of the ether gave crude 3-acetoxycarvomenthone (V), which, after purification by vacuum sublimation (120°C (bath), 0.03 mmHg), had an m. p. of 46—47°C ; yield 2.1 g. (Found : C, 68.04 ; H, 9.85. $C_{12}H_{20}O_3$ requires C, 67.89; H, 9.50%). 2,4-Dinitrophenylhydrazone : m. p. 157°C (from alcohol) (Found : N, 14.16. $C_{18}H_{24}O_6N_4$ requires N, 14.28%).

The ORD curves were measured in methanol and in isooctane.

In methanol (*c* 0.1025) :
$[\alpha]_{318}=+975.6°$ (peak)
$[\alpha]_{280}=-1326.8°$ (trough)

In isooctane (*c* 0.1035) :
$[\alpha]_{322}=+1078.4°$ (peak)
$[\alpha]_{308}=-850.3°$ (trough)

**The Reduction of 3-Acetoxycarvomenthone (V).** —A mixture of 3-acetoxycarvomenthone (V) (2 g.), ethane dithiol (6.5 ml.) and boron trifluoride etherate (6.5 ml.) was allowed to stand for four hours at room temperature. After the addition of water, the product was extracted with ether. The ethereal solution was washed with dilute sodium hydroxide and dried over sodium sulfate. The evaporation of the ether yielded the thioketal of V. Without further purification the thioketal was heated with Raney nickel (from 30 g. of Raney alloy) in dioxane for five hours. After filtration and the removal of the solvent, the residue was treated with *p*-nitrobenzoyl chloride in pyridine at room temperature. The *p*-nitrobenzoate after recrystallization from alcohol showed an m. p. and mixed m. p. with *p*-nitrobenzoate of *d*-neomenthol of 96—99°C. The two *p*-nitrobenzoates showed identical infrared spectra.

*Department of Chemistry*
*Tohoku University*
*Katahira-cho, Sendai*

# Absorption Spectra of Quinoline Adsorbed on Nickel Plates in an Aqueous Solution

By Wataru SUËTAKA*

(Received July 6, 1964)

In a previous paper,[1] a remarkable decrease in the intensity of the absorption bands of thiourea and potassium iodide caused by the presence of nickel plates in aqueous solutions was observed and strong adsorptions on the metal was deduced. In the present investigation, the absorption spectrum of quinoline adsorbed on nickel plates was observed by means of the technique already reported.[1]

The absorption spectra of a solution of quinoline (b. p. 83.5—84.0°C/3 mmHg) in purified water, as measured with a reflection cell and a transmission cell, are shown in Fig. 1.

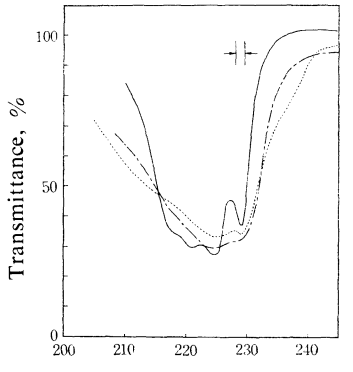



Fig. 1. Absorption spectra of quinoline in purified water measured with the reflection and transmission methods.
-·-·- : reflection (concentration of quinoline : $1.70\times10^{-5}$ mol./1.)
···· : transmission (concentration of quinoline : $1.70\times10^{-1}$ mol./1.)
—— : in isooctane (concentration : $2.09\times10^{-5}$ mol./1.)

In this figure, the absorption spectrum of an isooctane solution is also shown for purposes of comparison. The relative intensities of a peak at 220 mμ and shoulders at 233 mμ and 212 mμ evidently decreased the reflection measurements.

The nickel plates were probably covered with oxide or hydroxide, which could dissolve in the aqueous solution because the water contained carbonic acid. In consequence, the concentration of hydrogen ions in the solution probably diminished as a result of the immersion of the nickel plates, and the decrease in the hydrogen ion concentration might produce an intensity reduction of some absorption bands.

The spectra of quinoline in aqueous solutions containing hydrogen ions at various concentrations were observed (Fig. 2). The shoulder at

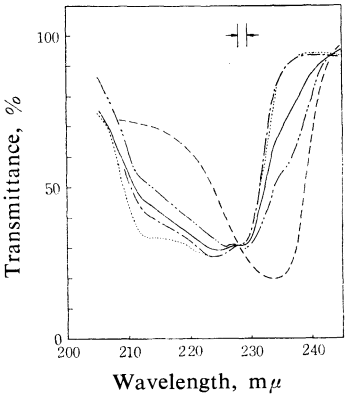



Fig. 2. Fffect of the hydrogen ion concentration on the spectrum of quinoline in aqueous solutions.
Concn. quinoline : $2.02\times10^{-5}$ mol./1.
····· : in $1\times10^{-2}$ N NaOH
-·-·- : in $1\times10^{-3}$ N NaOH
—— : in purified water
-···- : in $1\times10^{-5}$ N HCl
- - - : in $1\times10^{-3}$ N HCl

233 mμ, decreased in relative intensity with the decrease in the hydrogen ion concentration and can be assigned to quinolinium ions. Furthermore, the absorption spectrum of aqueous solution of quinoline was measured after the withdrawal of nickel plates which had been dipped in the solution for about twenty minutes a relative intensity reduction of the shoulder at 233 mμ was found.

On the basis of the results mentioned above, the intensity reduction of the shoulder at 233 mμ observed in the reflection measurement can be concluded to be due to the reduction of the quinolinium ion concentration in the solution as a result of the dissolution of nickel

* Present adress : Department of Chemistry, University of Virginia, Charlottesville, Va., U. S. A.
1) W. Suëtaka, This Bulletin, 37, 1121 (1964).

oxide or hydroxide, accompanied by a decrease in the hydrogen ion concentration.

The experimental results reported in the preceding paragraphs indicate that the decrease in the relative intensity of the peak at 229 mμ and more particularly that in the intensity of the shoulder at 212 mμ observed in the reflection measurements cannot be explained on the basis of the decrease in the hydrogen ion concentration in the solution. Since the complex formation of quinoline with nickel salts has been reported,[2] it may be considered that the spectral change in question arises from the complex formation in the solution. The spectrum of quinoline in an aqueous solution containing nickel sulfate of a relatively high concentration (1.0 mol./l.)* has shown, however, only a slight increase in the relative intensity of the shoulder at 212 mμ. It must be added that the shape of the absorption band due to quinoline in water did not change with the dipping of nickel plates in the solution, except for the minor variation produced by the decrease in quinolinium ion concentration. The change in the spectrum observed in the reflection measurements, therefore, cannot be the result of the formation of a quinoline-nickel salt complex in the solution.

As a result of the investigation described above, the change in the shape of absorption band in question can be attributed to the overlapping of an absorption band of adsorbed quinoline and a band of the same compound in solution. The absorption band of adsorbed quinoline is assumed to have the shape shown in Fig. 3. In drawing the assumed band, the shape of the band due to quinoline in solution is supposed to be the same as that observed for the aqueous solution of quinoline after the withdrawal of the dipped nickel plates. The similarity in the band shape between the hypothetical absorption band of adsorbed quinoline and that of quinolinium ions is very interesting, because it suggests that the adsorption might occur at the acid center of the surface oxide on the nickel plates.

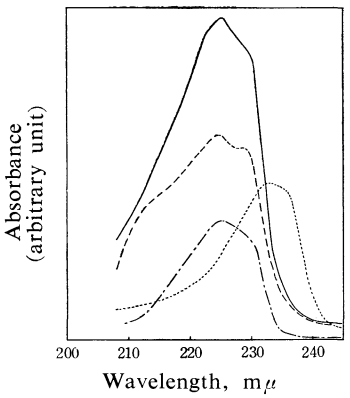



Fig. 3. Assumed absorption band of adsorbed quinoline.
——: absorption band observed with the reflection cell
– – –: quinoline in solution
–·–·–: adsorbed quinoline
------: quinolinium ion

*Research Institute for Iron, Steel and Other Metals*
*Tohoku University*
*Katahira-cho, Sendai*

* The pH-value of the solution was adjusted to 5.0 by the addition of sodium hydroxide so as to reduce the quinolinium ion concentration.

2) G. C. Bhattacharya and P. C. Sinha, *J. Indian Chem. Soc.*, **30**, 485 (1953).

# Temperature Effect in a Radiolytic System under Steady Irradiation

By Kenji FUEKI and John L. MAGEE

(Received July 23, 1964)

There are two types of temperature effects in a system under irradiation by high-energy radiation; one is a local temperature effect on a microscopic scale, and the other is a gross or macroscopic temperature effect. The former is initially confined to a small region of the system (spur) which cools rapidly.[1] No significant contribution from such effect can be expected in the case of low LET radiations. The latter effect is the temperature rise in the system when a thermally steady state is reached under irradiation; its magnitude depends upon dose rate, properties of the system, and chemical reactions involved. In this note we will describe the gross temperature effect and estimate average temperature rise, the time constant for approach to steady condition, and an effective rate constant in an irradiated system. This consideration is of interest in connection with the conditions under which irradiations can be taken to be isothermal.

Let us consider a spherical system with radius $r_m$ in a thermostat at a constant temperature, $T_0$.

The temperature of the system as a function of the space ($r$) and the time ($t$) is given by:

$$\frac{\partial T(r,t)}{\partial t}=\frac{\kappa}{\rho c_v}\nabla^2 T(r,t)+\frac{1}{\rho c_v}\left(qI+\frac{\partial(\Delta H)}{\partial t}\right) \tag{1}$$

where $T$, $\kappa$, $c_v$ and $\rho$ are the absolute temperature, the heat conductivity, the specific heat and the density, and $qI$ and $\Delta H$ are the dose rate and the heat of reaction per unit volume, respectively.

We put:

$$\frac{\partial(\Delta H)}{\partial t}=h,\quad \theta=\frac{T-T_0}{T_0},$$
$$\tau=\left(\frac{\kappa}{r_m^2\rho c_v}\right)t,\quad x=\frac{r}{r_m} \tag{2}$$

We can then solve Eq. 1 by using the boundary condition $T=T_0$ at $r=r_m$. The solution is given by:

$$\theta(x,\tau)=\frac{T(x,\tau)-T_0}{T_0}$$
$$=\frac{\lambda}{6}\left[1-x^2+\frac{12}{\pi^3 x}\sum_{n=1}^{\infty}\frac{(-1)^n}{n^3}(\sin\pi nx)\times\exp\left(-n^2\pi^2\tau\right)\right] \tag{3}$$

where $\lambda=-\dfrac{(qI+h)r_m^2}{\kappa T_0}$

Since the temperature at a steady state can be defined as that when $t$ approaches to infinity, we get:

$$\theta(x,\infty)=\frac{T(x,\infty)-T_0}{T_0}=\frac{\lambda}{6}(1-x^2) \tag{4}$$

Taking an average over space, we get:

$$\bar{\theta}=<\theta(x,\infty)>_{av}=-\frac{\lambda}{15} \tag{5}$$

where $\bar{\theta}$ represents the relative temperature rise of the system at a steady state.

In the case where $qI\gg h$, as is the case with most systems in radiation chemistry, $\bar{\theta}$ is given by:

$$\bar{\theta}\simeq\frac{qIr_m^2}{15\kappa T_0} \tag{6}$$

As an example, we have estimated $\bar{\theta}$ for liquid hydrocarbons as a function of the dose rate and the sample size. The results are shown in Fig. 1.

As we can see from Eq. 6, the relative temperature rise is proportional to $I$ and $r_m^2$ and inversely proportional to $T_0$ in the temperature

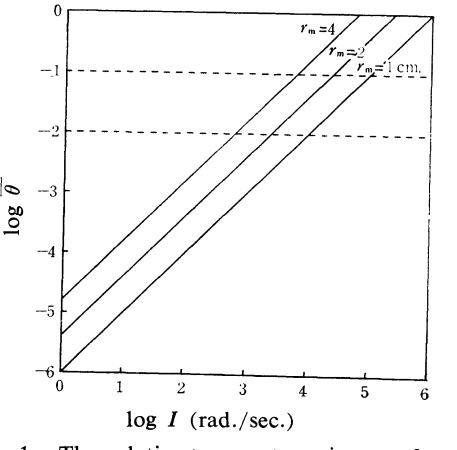



Fig. 1. The relative temperature rise as a function of dose rate and sample size.
$\kappa=4\times10^{-4}$ cal./cm. sec.°C; $\rho=0.8$ g./cm$^3$
$T_0=300$°K

range in which the physical constants do not change very much. Consequently, a smaller sample at a higher temperature is more favorable for maintaining isothermal conditions in an irradiated system, provided that the system is irradiated uniformly.

The time constant for approach to this steady state is given by the condition that the first term in the series in Eq. 3 falls to 1/e of its initial value:

$$\tau_c=\frac{1}{\pi^2}, \quad \text{or} \quad t_c=\frac{r_m^2\rho c_v}{\pi^2\kappa} \tag{7}$$

Putting numerical values into Eq. 7, we get:

$$t_c\simeq 100\ r_m^2\ \text{(sec.)}$$

where $r_m$ is in unit of cm. and $c_v$ is taken to be 0.5 cal./g.°C.

Let us consider the case where a rate constant is expressed by the Arrhenius equation. We define an effective rate constant as the rate constant averaged over space, since temperature is a function of space. Then, the ratio of the effective rate constant to the rate constant at the temperature $T_0$ is given by:

$$\frac{k_{eff}}{k_{T_0}}=3\ \exp\left(\frac{E}{RT_0}\right)\int_0^1 X^2 \times \exp\left[-\frac{E}{FT_0\{1+qIr_m^2(1-x^2)/6\kappa T_0\}}\right]dx \tag{8}$$

where $E$ is an activation energy and $R$ is the gas constant.

The ratio $k_{eff}/k_{T_0}$ calculated using Eq. 8 is shown in Fig. 2. At high dose rates the ratio deviates considerably from unity.

Thus care must be taken in application of simple kinetic techniques to systems irradiated at such high dose rates.

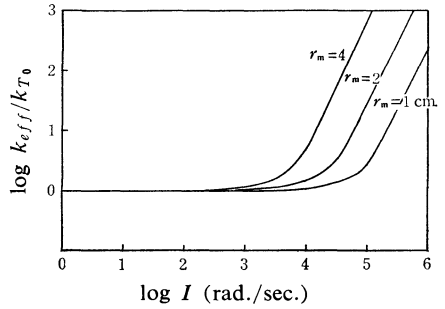



Fig. 2. The effective rate constant as a function of dose rate and sample size.
$E$=6 kcal./mol.; $T_0$=300°K

*Department of Synthetic Chemistry*
*Faculty of Engineering*
*Nagoya University*
*Chikusa-ku, Nagoya (K. F.)*

*Radiation Laboratory*
*University of Notre Dame*
*Notre Dame, Indiana, U. S. A. (J. L. M.)*

1) J. L. Magee, *Ann. Rev. Phys. Chem.*, **12**, 389 (1961).

## SHORT COMMUNICATIONS

# Neutron Diffraction Study of Deuterated Oxalic Acid Dihydrate, $(COOD)_2 \cdot 2D_2O$

By Fujiko FUKUSHIMA, Hitoshi IWASAKI, Yoshihiko SAITO, Shoichi SATO and Sadao HOSHINO

(Received October 27, 1964)

Crystals of deuterated oxalic acid dihydrate, $(COOD)_2 \cdot 2D_2O$, have been found not to be isomorphous[1,2] with those of $(COOH)_2 \cdot 2H_2O$.[3] The crystal structure of the former was determined by X-ray study.[1]

This isotope effect is expected to be closely related to the nature of the hydrogen bonds. A neutron diffraction study has thus been undertaken in order to determine the deuteron positions and to investigate the difference between the hydrogen bonds in the two structures.

Anhydrous oxalic acid was dissolved in $D_2O$

1) F. Fukushima, H. Iwasaki and Y. Saito, *Acta Cryst.*, in press; This Bulletin, to be published.
2) T. Chiba, *J. Chem. Phys.*, **41**, 1352 (1964).
3) J. M. Robertson and A. R. Ubbelohde, *Proc. Roy. Soc.*, **A170**, 222 (1939); F. R. Ahmed and D. W. J. Cruickshank, *Acta Cryst.*, **6**, 385 (1953); R. S. Garrett, Oak Ridge National Laboratory Report, No. 1745 (1954).

with warming, and the water was evaporated in vacuo. This procedure was repeated three times, then the rhomboidal crystals of $(COOD)_2 \cdot 2D_2O$ were obtained. A high concentration of $D_2O$ was necessary to the formation of these crystals.[2]

The crystal data obtained with X-rays (Cu$K\alpha$, $\lambda = 1.542$ Å) are listed in Table I.

TABLE I. CRYSTAL DATA

| | $(COOD)_2 \cdot 2D_2O$ | $(COOH)_2 \cdot 2H_2O$ |
|---|---|---|
| Crystal system | Monoclinic | Monoclinic |
| Space group | $P2_1/a$ | $P2_1/a$ |
| $a$ | $10.04 \pm 0.01$ Å | 11.88 Å |
| $b$ | $5.06 \pm 0.01$ | 3.60 |
| $c$ | $5.16 \pm 0.01$ | 6.12 |
| $\beta$ | $99°12' \pm 6'$ | 103.5° |
| $Z$ | 2 | 2 |

For the neutron diffraction work, crystals approximately $5 \times 5 \times 2$ mm$^3$ in dimensions were grown slowly from a supersaturated solution. They are colorless and unstable when exposed to air. The specimens were coated with a glyptal film and enclosed in glass tubes with a drop of mother liquor. The integrated intensities were measured at the JRR-2 reactor, Japan Atomic Energy Research Institute, Tokai, using the apparatus described by Miyake et al.[4] A neutron wavelength of 1.057 Å was obtained by means of a lead monochromator. The 27 reflections $0kl$ and the 26 reflections $h0l$ were observed in each zone for which $2\theta < 65°$.

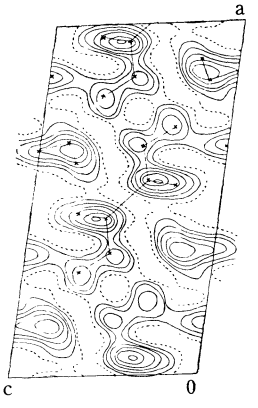



Fig. 1. Fourier projection along the b axis.

The approximate deuteron positions were found by the Fourier method, assuming the carbon and oxygen parameters derived from the X-ray analysis. Then $(F_o - F_{C,O})$ synthesis was carried out, where $F_{C,O}$ was the calculated contribution to the structure factor of all the atoms except deuteron. Figures 1 and 2 show

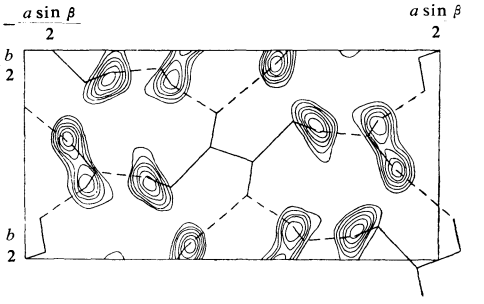



Fig. 2. $(F_o - F_{C,O})$ synthesis projected along the c axis.

the Fourier projection along the b axis and the $(F_o - F_{C,O})$ synthesis projected along the c axis respectively. The atomic co-ordinates are listed in Table II. They give the reliability index, $R = \sum ||F_o| - |F_c|| / \sum |F_o|$, of 0.19. These deuteron parameters agree with those obtained from the difference synthesis of X-ray data[1] and with the O–D directions suggested from the nuclear magnetic resonance study.[2]

TABLE II. ATOMIC CO-ORDINATES

| | $x$ | $y$ | $z$ |
|---|---|---|---|
| C | 0.052 | 0.023 | 0.404 |
| O (1) | 0.037 | 0.196 | 0.248 |
| O (2) | 0.150 | −0.157 | 0.438 |
| O (3) | 0.328 | −0.080 | 0.150 |
| D (1) | 0.205 | −0.113 | 0.294 |
| D (2) | 0.146 | 0.330 | 0.002 |
| D (3) | 0.112 | 0.548 | 0.788 |

Refinements are now going on. Further experiments are in progress to collect more reflection data. Full details will be reported later.

*The Institute for Solid State Physics*
*The University of Tokyo*
*Azabu, Tokyo*

4) S. Miyake, S. Hoshino, K. Suzuki, H. Katsuragi, S. Hagiwara, T. Yoshie and K. Miyashita, *J. Phys. Soc. Japan*, **17**, *Suppl.* B-II, 358 (1962).

# Radical Formation from the Intermediates of $S_N1$ Reacions. A One-Electron Transfer Reaction between a Carbonium-ion Type Intermediate and Nucleophiles

By Kunio OKAMOTO, Yoshihisa MATSUI and Haruo SHINGU

(Received November 5, 1964)

The recent work of Kerber et al.[1] on the transient formation of a radical anion, probably of E. Weitz's molecular-complex type,[2] during the course of the reaction of *p*-nitrobenzyl halides with a salt of 2-nitropropane prompts us to report on some of our previous work.[3] It has been found that reactions of benzhydryl halides with hindered nucleophiles, e. g., potassium 2, 6-di-*t*-butyl-4-methylphenoxide (I) and tri-*n*-butylamine, afford not the products anticipated for nucleophilic substitution, but rather products derived from benzhydryl radicals, i. e., *sym*-tetraphenylethane, diphenylmethane, and 1-(3′, 5′-di-*t*-butyl-4′-hydroxyphenyl)-2, 2-diphenylethane (II). The results are illustrated in Table I.

The structure of II, m. p. 113.0—115.0°C, was assigned on the basis of its elementary composition and spectral data (Found: C, 87.07; H, 8.76; mol. wt., 386 (cryoscopic measurements in benzene). Calcd. for $C_{28}H_{34}O$: C, 86.99; H, 8.87%; mol. wt., 386.6). Spectral peaks appeared at: infrared spectrum $\lambda_{max}$ (KBr pellet) 2.70 $\mu$ (OH, monomeric), no polymeric OH; 60 Mc. NMR (carbon tetrachloride) :[4] 1.28 p.p.m. (18-proton singlet, *t*-butyl methyls), 3.20 p.p.m. (2-proton doublet, methylene, $J$=7.7 c.p.s.), 3.93 p.p.m. (1-proton triplet, methine, $J$=7.7 c.p.s.), 4.78 p.p.m. (1-proton singlet, hydroxyl), 6.52 p.p.m. (2-proton singlet, tetra-substituted phenyl) and 7.10 p.p.m. (10-proton, mono-substituted phenyl).

For purposes of comparison the results of the reaction of benzhydryl chloride and potassium phenoxide in acetonitrile are also presented in Table I.

Despite their second-order kinetics (Table I), the $S_N1$ ionization character of the initiation of these reactions of hindered nucleophiles is supported by the following facts and considerations: (1) The reaction of unhindered potassium phenoxide displays characteristics typical of an $S_N1$ reaction with respect to the reaction-order and the products (Table I). Consequently, there would exist an $S_N1$ intermediate produced from a benzhydryl halide in acetonitrile in all reactions with hindered nucleophiles. (2) The nature of the reaction products can not be explained by the $S_N2$ mechanism. (3) The rates of these second-order reactions are sensitive to the natures of the solvents and of the leaving groups. The reaction of benzhydryl chloride and tri-*n*-butylamine proceeds more than 68% at about 150°C for 6.5 hr. (Table I), whereas the same reaction in decalin yields chloride ions less than 4% of the starting chloride under identical reaction conditions. Furthermore, it is estimated that bromide is about 5—30 times as reactive as the chloride (Table I) (4) These second-order reactions of benzhydryl chloride proceed with rates which do not exceed the rate of a typical $S_N1$ reaction of the chloride and potassium phenoxide (Table I).

On the basis of the above facts, (1)—(4), these reactions can be explained as a limiting case of an $S_N1$ reaction where the condition, $k_{-1} \gg k_2[Y]$, is satisfied in the following rate expression, which correspondes to the general reaction scheme of the $S_N1$ reaction:

$$RX \underset{k_{-1}}{\overset{k_1}{\rightleftarrows}} (R^{\delta+} \cdots X^{\delta-}) \xrightarrow{k_2[Y]} RY$$

$$\text{Rate} = \frac{k_1 k_2 [RX][Y]}{k_{-1} + k_2[Y]}$$

Namely, for hindered nucleophiles,

$$\text{Rate} = \frac{k_1 k_2}{k_{-1}} [RX][Y].$$

Therefore, we propose a bimolecular one-electron transfer mechanism for the transient formation of benzhydryl radicals in the reaction of the $S_N1$ intermediate and hindered nucleophiles. This is illustrated in the following scheme:

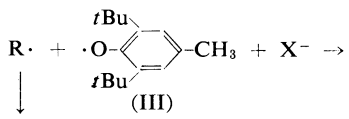
1) R. C. Kerber, G. W. Urry and N. Kornblum, *J. Am. Chem. Soc.*, **86**, 3904 (1964).
2) E. Weitz, *Angew. Chem.*, **66**, 658 (1954).
3) K. Okamoto, Y. Matsui and H. Shingu, Abstracts of the 17th Annual Meeting of the Chemical Society of Japan, Tokyo, April, 1964, p. 128.
4) We are indebted to Professor Kenichi Fukui and Mr. Isao Morishima for their assistance with the measurement of the NMR spectrum. The spectrum was taken with tetramethylsilane as an internal standard on a Varian Associates Model A-60 spectrometer.

TABLE I. PRODUCTS AND RATES IN THE REACTION OF BENZHYDRYL HALIDES AND NUCLEOPHILES IN ACETONITRILE

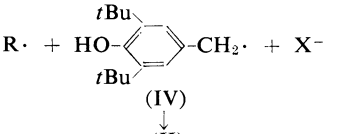
| Nucleophile | Temp. °C | Conversion %[a] (Reaction time, hr.) | Reaction products, %[b] | | | | | Rates[c] $k_1$ ($min^{-1}$) or $k_2$ ($min^{-1}\,M^{-1}$) |
|---|---|---|---|---|---|---|---|---|
| | | | *sym*-Tetraphenylethane | Diphenylmethane | II[g] | Benzhydrylphenyl ether | *p*-Benzhydrylphenol | |
| | | | Substrate: Benzhydryl chloride | | | | | |
| I[g] | 82— 85[d] | 82 (18.3) | 40.2 | 0.0 | 28.7 | — | — | $k_2$ (110.0°C) $6.82\times10^{-1}$ |
| $(n\text{-Bu})_3N$ | 146—156[e] | 68 (6.5) | 64.5 | 3.0 | — | — | — | $k_2$ (140.0°C) $3.66\times10^{-2}$ |
| Potassium phenoxide | 82[d] | 97 (2.5) | 0.0 | 0.0 | — | 93.2 | 3.1[h] | $k_1$ (70.0°C) $1.58\times10^{-2}$ |
| | | | Substrate: Benzhdryl bromide | | | | | |
| I | 82[d] | 97 (6.9) | 3.0 | 0.0 | 24.1 | — | — | — |
| $(n\text{-Bu})_3N$ | 90— 93[f] | 91 (18.3) | 22.8 | 34.4 | — | — | — | — |

a) Conversion of the halide, calculated from determination of the halide ions formed during the reaction.
b) Based on the halide.
c) Determined by sealed ampoule technique. Initial concentrations of the substrate and nucleophiles were 0.05—0.13 M.
d) Reflux temperature.
e) Reaction in a stainless-steel bomb.
f) Reaction in a sealed tube.
g) I; Potassium 2,6-di-*t*-butyl-4-methylphenoxide; II; 1-(3',5'-Di-*t*-butyl-4'-hydroxyphenyl)-2,2-diphenylethane.
h) Contaminated with the ortho-isomer.

$$RX \underset{\text{in } CH_3CN}{\rightleftharpoons} (R^{\delta+}\cdots X^{\delta-}) \xrightarrow{+(I)}$$



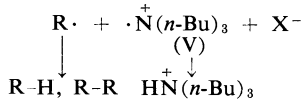
(III)



(IV)

(II)

$$RX \underset{\text{in } CH_3CN}{\rightleftharpoons} (R^{\delta+}\cdots X^{\delta-}) \xrightarrow{+(n\text{-}Bu)_3N}$$



(R=Benzhydryl)

It is known[5] that I easily undergoes oxidation to give the 2,6-di-*t*-butyl-4-methylphenoxy radical (III) and that III isomerizes rapidly to the 3,5-di-*t*-butyl-4-hydroxybenzyl radical (IV). In our experiments, a coupling product II between a benzhydryl radical and a radical IV has been isolated. It is also known that aliphatic tertiary amines, e.g., triethylamine, lose one electron to yield a charge-transfer complex with tetracyanoethylene[6a] and 7,7,8,8-tetracyanoquinodimethane.[6b] A part of the amminium ion radical (V) seems to be stabilized by forming tri-*n*-butylammonium ions, which have been isolated in our experiments as the halide with a yield of 50—60%. The source of the hydrogen atoms has not been established.

*Department of Fuel Chemistry*
*Faculty of Engineering*
*Kyoto University*
*Sakyo-ku, Kyoto*

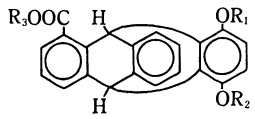
5) C. D. Cook, N. G. Nash and H. R. Flanagan, *J. Am. Chem. Soc.*, **77**, 1783 (1955).
6) a) O. W. Webster, W. Mahler and R. E. Benson, *J. Am. Chem. Soc.*, **84**, 3678 (1962); b) L. R. Melby, R. J. Harder, W. R. Hertler, W. Mahler, R. E. Benson and W. E. Mochel, ibid., **84**, 3374 (1962).

# The Optical Rotatory Dispersion of Triptycene Derivatives. The Direction of Electronic Polarization as a Determining Factor of the Sign of the RD Curve

By Fumio OGURA and Masazumi NAKAGAWA

(Received November 9, 1964)

In a previous paper,[1] the present authors have reported the synthesis and optical resolution of 7-carboxy-2,5-diacetoxy-triptycene (I). The acetyl groups at 2,5-positions could be replaced by different groups.[2] Various kinds of optically-active triptycenes thus prepared (II–X)* have the same configuration as that of the parent triptycene (I), as the rigid cage structure of triptycene excludes the occurrence of any racemization or Walden inversion during the course of the transformation. In view of their rigid structure, the series of optically-active triptycenes bearing different substituents seems to offer the best tool for studying the effect of substituents on the rotatory properties.




I: $R_1=R_2=CH_3CO$, $R_3=H$, m. p. 269~270°C
II: $R_1=R_2=CH_3CO$, $R_3=CH_3$, m. p. 200~202°C
III: $R_1=R_2=H$, $R_3=CH_3$, m. p. 294~297°C (decomp.)
IV: $R_1=H$, $R_2=R_3=CH_3$, m. p. 250~251°C
V: $R_1=R_3=CH_3$, $R_2=H$, m. p. 256~258°C
VI: $R_1=R_2=R_3=CH_3$, m. p. 261.5~262.5°C
VII: $R_1=CH_3CO$, $R_2=R_3=CH_3$, m. p. 270~271°C
VIII: $R_1=R_3=CH_3$, $R_2=CH_3CO$, m. p. 278~279°C
IX: $R_1=CF_3CO$, $R_2=R_3=CH_3$, m. p. 262~263.5°C
X: $R_1=R_3=CH_3$, $R_2=CF_3CO$, m. p. 241~243°C

The compounds II, III, VI, VII, VIII, IX and X used in the measurements of the rotatory dispersion were derived from the *d*-isomer of I, while IV and V were derived from its *l*-isomer. The compounds I, II, III, IV, V, and VI exhibit plain curves of the same sign in so far as they have identical configurations. In sharp contrast to this fact, the sign of the plain curves of VII and IX are positive, whereas VIII and X show negative plain curves in spite of having the same configuration as VII and IX. Some representative RD curves are given in Fig. 1. The electronic spectra of VII, VIII, IX and X were found to be almost superimposable over a wide range of wavelengths. The only difference between VII and VIII and between IX and X are the relative positions of the electron-donating methoxyl groups and electron-attracting acyloxy groups in the *p*-disubstituted benzene ring in the triptycene molecules.

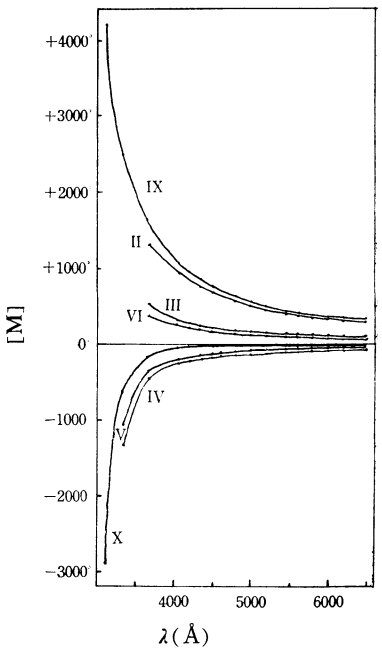



Fig. 1. The RD curves of the triptycenes.

These experimental results clearly indicate that the direction of electronic polarization is a determining factor in the sign of the RD curve. It seems evident that the inversion of the direction of electronic polarization exerts an inverse effect on the electric transition moment of the optically-active absorption band. However, the more extensive influence of the inversion of the direction of polarization is reflected in the fact that the RD curves of

1) A. Sonoda, F. Ogura and M. Nakagawa, This Bulletin, 35, 853 (1962).
2) F. Ogura, Y. Toshiyasu. K. Kimura, R. Fujishiro and M. Nakagawa, ibid., 37, 757 (1964).
* All compounds described in this paper gave satisfactory IR spectra and elemental analyses.

II, III, IV, V, VI, VII and IX can be expressed by a one-term Drude equation, whereas in the cases of VIII and X the plots of $1/[M]$ versus $\lambda^2$ give no straight lines.

In order to obtain more precise information, the authors are now preparing to measure the optical rotatory dispersion at a shorter wavelength region and to measure the circular dichroism of the triptycene derivatives.

*Department of Chemistry*
*Faculty of Science*
*Osaka University*
*Nakanoshima, Osaka*

# The Rearrangement Polymerization of Propenylbenzene: A Reinvestigation

By Shunsuke MURAHASHI, Shun'ichi NOZAKURA, Kazuhiko TSUBOSHIMA and Yahide KOTAKE

(Received November 20, 1964)

In a previous paper[1] the present authors studied the rearrangement polymerization of propenylbenzene, which had been proposed by Staudinger,[2] and reported a set of confirmative data. However, further study has revealed that the propenylbenzene used, which had been prepared by thermal cracking of ethylbenzyl acetate at 500°C,[3] contained a small impurity (ca. 5%), and that this impurity even in a minute quantity deeply influences the course of polymerization.

The impurity was, therefore, concentrated by preparative gas chromatography and identified with indene by a comparison of its infrared spectrum with that of an authentic sample.

Since indene is a monomer with a high cationic polymerizability, the presence of indene in propenylbenzene of a low activity influences the polymerization of propenylbenzene a great deal. Thus, i) the residual monomer, which was recovered after the initial polymerization (about 20% conversion) with a mild catalyst, $BF_3Et_2O$, is found to contain no indene. This means that indene has been consumed at an early stage of polymerization. ii) The initial rate of polymerization became larger upon the addition of a small amount of indene to pure propenylbenzene. iii) The initial polymer obtained with a $BF_3Et_2O$ catalyst using an indene-containing propenylbenzene yielded a methanol-insoluble polymer of a comparatively high molecular weight, as was reported in the previous paper. On the other hand, pure propenylbenzene yielded only a methanol-soluble polymer of a low molecular weight. Many differences are observed between the two polymers in infrared and NMR spectra. While the former shows a very weak $CH_3$ band at 2960 $cm^{-1}$ and a strong $CH_2$ band at 2925 $cm^{-1}$, and the ratio of the number of methyl protons to that of aromatic protons is found to be 0.26, the latter has a strong $CH_3$ band and a comparatively weak $CH_2$ band, and the ratio of methyl protons to aromatic protons is nearly 0.6, which corresponds to the theoretical value for polypropenylbenzene polymerized by a 1,2-opening. When a strong cationic initiator, such as $BF_3$, is used, the effect of the presence of a small amount of indene is masked by the rapid production of a large amount of polypropenylbenzene.

Table I shows a gas chromatographic analysis of relative amounts of impurities contained in samples of propenylbenzene prepared by three different methods.

In order to examine the existence of rearrangement polymerization in more detail, the polymerization was carried out under various conditions, including Staudinger's system. When toluene was used as a solvent, as in the case of Staudinger's original work, the resulting viscous polymer appeared to contain toluene residues ($\tau = 7.7$). This complicated the NMR analysis and made the apparent ratio of methyl protons ($\tau \sim 9.2$) to aromatic protons considerably lower than the theoretical value (0.4—0.5). When *n*-heptane or methylene chloride was used as the solvent and boron fluoride or titanium(IV) chloride as the initiator, the resulting polymers showed a ratio of methyl to aromatic protons of about 0.6, indicating

1) S. Murahashi, S. Nozakura, K. Tsuboshima and Y. Kotake, This Bulletin, 37, 706 (1964).
2) H. Staudinger and E. Dreher, *Ann.*, 517, 73 (1935).
3) C. G. Overberger and D. Tanner, *J. Am. Chem. Soc.*, 77, 369 (1955).

TABLE I. PROPENYLBENZENE PREPARED BY DIFFERENT METHODS

| Method of preparation | Allylbenzene %[a] | Propenylbenzene cis % | Propenylbenzene trans % | Indene % |
|---|---|---|---|---|
| Thermal cracking of ethylbenzyl acetate[3] | 5.4 | 20.2 | 66.3 | 8.1 |
| Dehydrochlorination of ethylbenzyl chloride with pyridine[1] | 0 | 1.5 | 98.5 | 0 |
| Catalytic dehydration of ethylbenzyl alcohol[b] | 4.7 | 30.5 | 64.8 | 0 |

a) Relative composition was calculated based on peak area of gas chromatogram.
b) Dehydration was carried out at about 300°C in a stream of $N_2$ using alumina as catalyst.

no sign of rearrangement during polymerization.[4]

The confirmative results reported in the previous paper must, therefore, be corrected; there was contamination by indene, which led the authors to a misunderstanding of the polymer structure.

4) Recently Kennedy stated a similar negative observation in a review article. J. F. Kennedy and A. W. Langer, Jr., *Fortschr. Hochpolym. Forsch.*, 3, 523 (1964).

*Faculty of Science*
*Osaka University*
*Nakanoshima, Osaka*

# The Crystal Structure of Hexachlorocyclopropane $C_3Cl_6$

By Tsunehiro TAKANO, Tohru CHIBA, Yoshio SASADA, Masao KAKUDO, Shun'ichi NOZAKURA and Shunske MURAHAHI

(Received November 26, 1964)

The crystal structure of the hexachlorocyclopropane synthesized at the laboratory of two of the authors was determined by X-ray analysis. Equi-inclination photographs around the b axis were taken with Mo-$K\alpha$ radiation ($k=0, \cdots\cdots, 5$).

The unit cell dimensions obtained are:

$a=12.60$, $b=6.13$, $c=10.94$ Å, $\beta=112.0°$.

The space group is $C_{2h}^5-P2_1/a$, and $Z=4$.

Intensities were measured by a visual comparison with an intensity scale and corrected for Lorentz and polarization factors. However, no correction for absorption was made. The Weissenberg photographs showed a characteristic distribution of intensities; the reflections were very weak for $h+k+l=2n+1$. This suggested that the arrangement of the molecules is approximately body-centered.

Two-dimensional Patterson synthesis projected along [010] and [001] were also computed. The crystal structure was derived uniquely from the Patterson maps and from the requirement of a psuedo-body-centered arrangement of the molecules.

The refinement of the structure projected on the (010) plane was carried out by the least-squares method. After several cycles, the discrepancy index, $R=\sum||F_o|-|F_c||/\sum|F_o|$, became 0.14.

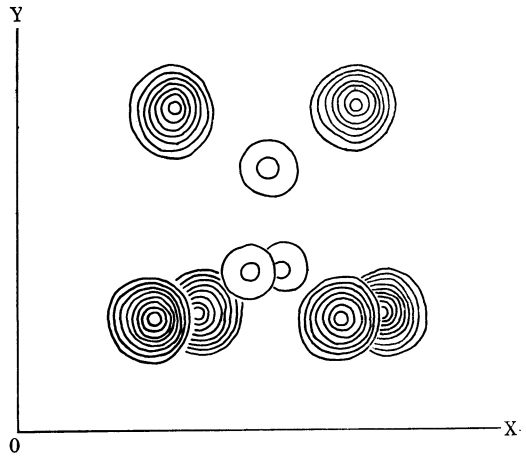



Fig. 1. Composite Fourier diagram of sections parallel to (001).

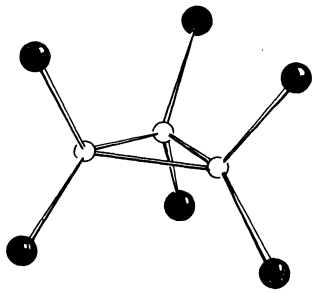


Fig. 2. The molecular configuration of hexachlorocyclopropane.

The three-dimensional Fourier synthesis is shown in Fig. 1. According to the Fourier map, the molecular configuration may be as is shown in Fig. 2.

Intermolecular contacts consist of the ordinary van der Waals distance between chlorine atoms.

The accuracy of the analysis at this stage of refinement is not sufficient to evaluate the bond lengths and bond angles. In order to obtain the details of the structure, a three-dimensional refinement of the atomic parameters is in progress by the least-squares method.

A fullpaper will be published soon.

*Institute for Protein Research*
*Osaka University*
*Kita-ku, Osaka*

*Faculy of Science*
*Osaka University*
*Kita-ku, Osaka (S. N. & S. M.)*

# The Cation Exchange Adsorption of Calcium and Strontium from an Ammonium Formate or Ammonium Acetate Solution in Mixtures of Organic Solvents and Water*

By Hiroyuki TSUBOTA

(Received March 20, 1963)

Several methods for separating calcium and strontium by cation exchange resin have been reported.[1-5] Most of them, however, have difficulty in handling a large sample. Although EDTA has been used for separating strontium from a large quantity of calcium,[6] it is not suitable for usual purposes because of the difficulty of the after-treatment of the effluent.

There are other possibilities for overcoming these difficulties, for example, the use of non-aqueous or mixed solvents as elutriants.[7-15] The results of studies of the anion exchange adsorption of anionic metal complexes have shown that the addition of an organic solvent to the system has a large effect on the exchange equilibrium when an ion exchange reaction is accompanied by a complex formation.[10-14] For a cation exchange system, Ionescou et al.[15] measured the distribution coefficients of some transition metals between a phenol - sulfonic acid - type cation exchange resin and an acetone-hydrochloric acid mixture, and used the results for the separation of these metals. Thus, a study of cation exchange equilibria when an organic solvent is added to a calcium or strontium solution containing a complexing agent would be of interest and would be useful for the separation of these metals. In this report, the selectivity coefficients of calcium-ammonium and strontium-ammonium exchange reactions have been measured in methanol-water, acetone-water and dioxane-water mixtures containing formate or acetate as a complexing agent. In addition, by using these complexing agents, the treatment of effluents is greatly simplified. Experiments by column operation have been also carried out to learn whether the expectation from the selectivity coefficient measurements can be actually applied to the separation of calcium and strontium.

## Experimental

**Chemicals.**—Air-dried Amberlite IR-120 (a sulfonated polystylene divinylbenzene cation exchange resin, 100—120 mesh) in ammonium form was used for batch measurement after thorough conditioning. The exchange capacity was 3.5 meq. for 1 g. of the air-dried resin. The organic solvents were used after purification, and calcium and strontium salts were purified by the ion exchange method.

A column of cation exchange resin, Amberlite IR-120, 100—200 mesh in hydrogen form, 10 cm. long and 1.1 cm. in diameter, was used for the column operation.

**Measurements.**—The adsorption of metal ions by the resin was measured by the equilibrium method, and the results were described in terms of the selectivity coefficients of the ion against the ammonium ion, $K^{M}_{NH_4}$, as defined by the following equation:

$$K^{M}_{NH_4} = \frac{[M^{2+}]_r[NH_4^+]_s}{[M^{2+}]_s[NH_4^+]_r}$$

where parentheses denote molarities, the suffixes r and s denote the resin phase and the outer solution phase respectively, and $M^{2+}$ denotes calcium or strontium ions, including their cationic complex ions.

Solutions with the following composition were prepared:

| | |
|---|---|
| $NH_4A$: | $(1-2a)$ mol./l. |
| $MA_2$: | $a$ mol./l. |
| Organic liquid: | $b$ % (v/v) |

* A part of this work was read at the 3rd Radiochemical Symposium, Shizuoka, October, 1959.

1) E. R. Tompkins, *J. Am. Chem. Soc.*, **70**, 3520 (1948).
2) M. Lerner and W. Rieman, III, *Anal. Chem.*, **26**, 610 (1954).
3) M. Honda, *Japan Analyst (Bunseki Kagaku)*, **3**, 132 (1954).
4) F. Nelson and K. A. Kraus, *J. Am. Chem. Soc.*, **77**, 801 (1955).
5) H. Tsubota and Y. Kitano, This Bulletin, **33**, 770 (1960).
6) P. S. Davis, *Nature*, **183**, 674 (1959).
7) H. Okuno, M. Honda and T. Ishimori, *Japan Analyst (Bunseki Kagaku)*, **2**, 428 (1953).
8) T. Sakaki, This Bulletin, **28**, 217, 220 (1955).
9) O. D. Bonner and J. C. Moorefield, *J. Phys. Chem.*, **58**, 555 (1954).
10) L. I. Katzin and E. Gebert, *J. Am. Chem. Soc.*, **75**, 801 (1953).
11) Y. Yoshino and Y. Kurimura, This Bulletin, **30**, 563 (1957).
12) E. W. Berg and J. T. Truemper, *Anal. Chem.*, **30**, 1827 (1958).
13) D. G. Tuck and G. A. Welch, *J. Inorg. Nucl. Chem.*, **9**, 302 (1959).
14) J. Kennedy and R. V. Davies, ibid., **12**, 193 (1959).
15) S. Ionescou, O. Constantinescou, D. Topor and E. Gârd, Proceedings of the Second United Nations International Conference on the Peaceful Uses of Atomic Energy, Geneva, Vol. 28, p. 58, United Nations (1958).

where A denotes a formate or acetate ion. The value of $a$ ranged from $1\times10^{-3}$ to $40\times10^{-3}$, but it was kept constant in each series of experiments. The percentage of the organic solvent, $b$, was in the 0—80 range for methanol and the 0—60 range for acetone and dioxane. Fifty milliliters of the calcium solution was shaken with 1.000 g. of the dried resin for 24 hr. in a constant temperature bath at 25°C. After an exchange equilibrium had been reached, the outer solution was rapidly separated from the resin with a glass filter, and the calcium concentration in the solution was measured by EDTA titration, using Eriochrome Black T as an indicator. The ammonium ion concentration in the outer solution was determined from the difference between the total concentration and the calcium concentration measured above, the former being measured by alkalimetry after the solution had been converted to acid with a hydrogen-form cation exchange column. The quantities of calcium and ammonium ions in the outer solution and the quantities of the ions in the resin phase were then calculated, with a correction for the swelling of the ion exchanger. The relative volume decrease in the solution caused by the swelling was determined by the quotient between the initial and the equilibrium total ion concentrations of the outer solution.

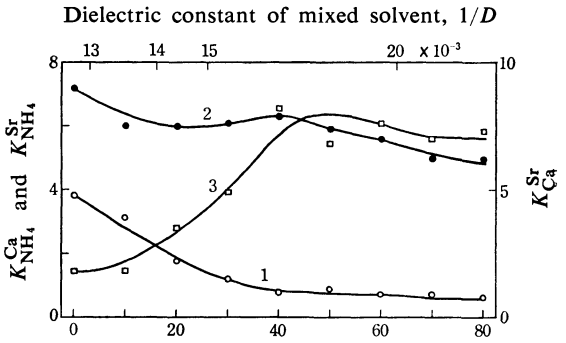
Since the selectivity coefficients will vary with the fraction of exchangeable sites occupied by calcium ions, they were measured at various loading-values, and the selectivity coefficients were normalized at a certain loading-value by interpolation or extrapolation. The selectivity coefficient of strontium was obtained in the same manner as calcium.

In the column operation, the calcium and strontium adsorbed on the column were eluted with various elutriants. The concentration of ammonium ions in the elutriants was kept at 1 mol./l. throughout the experiments. The effluents from the column were divided into 5 ml. fractions and the amount of calcium or strontium in each fraction was determined by EDTA titration.

## Results and Discussion

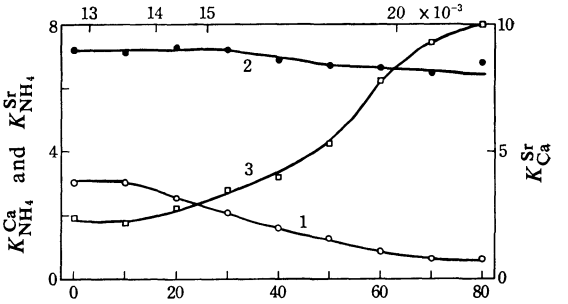
**The Selectivity Coefficients of Calcium and Strontium.**—In Figs. 1—6, the selectivity coefficients in an acetate solution containing methanol, acetone or dioxane are plotted against the percent concentration (v/v) of the organic solvent. Curves 1 and 2 in each figure show the selectivity coefficients of calcium and strontium against ammonium, $K^{Ca}_{NH_4}$ and $K^{Sr}_{NH_4}$, respectively, while curve 3 shows the ratio of the two coefficients, i. e., the selectivity coefficients of strontium against calcium, $K^{Sr}_{Ca}$, or the separation factor of these two ions.

In Figs. 7—10, the selectivity coefficients in a formate solution containing acetone or dioxane are plotted. The results are not shown for the solution containing methanol,




Content of methanol in the outer soln., vol. %

Fig. 1. Selectivity coefficients of calcium and strontium in 1 M ammonium acetate-methanol-water mixture.
(loading: 0.5%)
Curve 1 (○): $K^{Ca}_{NH_4}$ Curve 3 (□): $K^{Sr}_{Ca}$
Curve 2 (●): $K^{Sr}_{NH_4}$




Content of methanol in the outer soln., vol. %

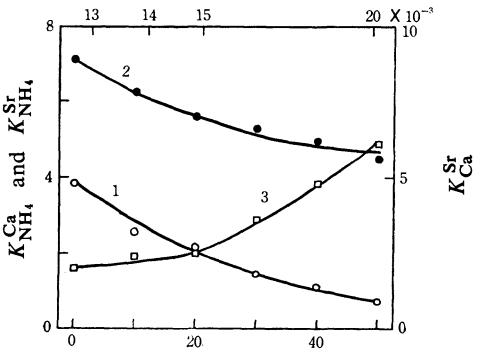
Fig. 2. Selectivity coefficients of calcium and strontium in 1 M ammonium acetate-methanol-water mixture.
(loading: 10%)
Curve 1 (○): $K^{Ca}_{NH_4}$ Curve 3 (□): $K^{Sr}_{Ca}$
Curve 2 (●): $K^{Sr}_{NH_4}$

because methyl formate was formed during 24 hr. shaking in the presence of the resin.*

The same tendencies are found in all figures, irrespective of the loading values and of the organic solvents. The selectivity coefficients of both calcium and strontium against ammonium decrease with an increasing concentration of the organic solvent. The decrease is greater for calcium than for strontium, and the separation factor between strontium and calcium increases with an increasing concentration of the organic solvent.

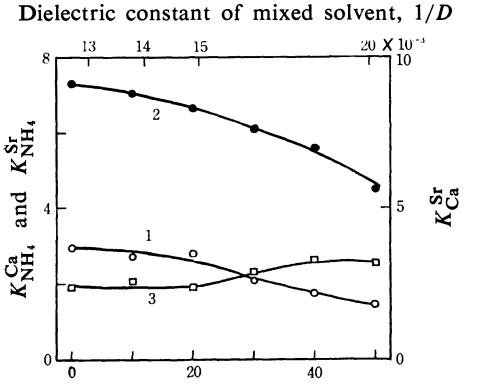
The causes for the variation in the selectivity coefficients with the concentration of organic

* The formation of the ester was estimated by its odor, the pH rise, and the decrease in the ammonium ion concentration. The phenomenon was not found in a mixture of methanol and an ammonium formate aqueous solution without the resin.



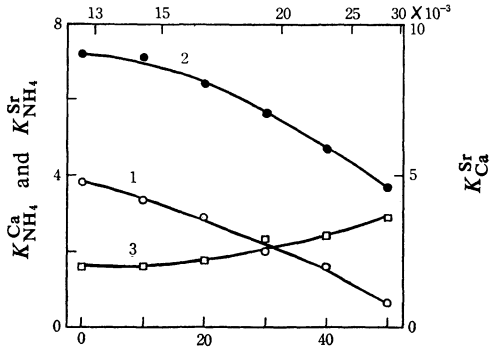

Content of acetone in the outer soln., vol. %

Fig. 3. Selectivity coefficients of calcium and strontium in 1 M ammonium acetate-acetone-water mixture.
(loading: 0.5%)
Curve 1 (○): $K^{Ca}_{NH_4}$ Curve 3 (□): $K^{Sr}_{Ca}$
Curve 2 (●): $K^{Sr}_{NH_4}$



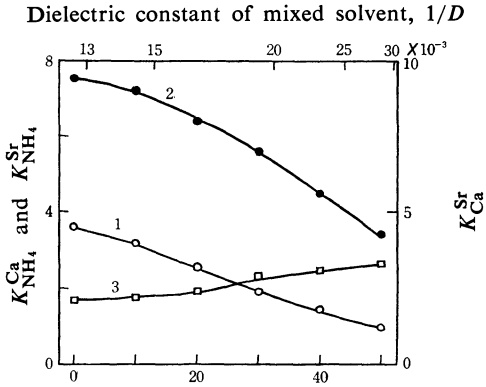

Content of acetone in the outer soln., vol. %

Fig. 4. Selectivity coefficients of calcium and strontium in 1 M ammonium acetate-acetone-water mixture.
(loading: 10%)
Curve 1 (○): $K^{Ca}_{NH_4}$ Curve 3 (□): $K^{Sr}_{Ca}$
Curve 2 (●): $K^{Sr}_{NH_4}$




Content of dioxane in the outer soln., vol. %

Fig. 5. Selectivity coefficients of calcium and strontium in 1 M ammonium acetate-dioxane-water mixture.
(loading: 10%)
Curve 1 (○): $K^{Ca}_{NH_4}$ Curve 3 (□): $K^{Sr}_{Ca}$
Curve 2 (●): $K^{Sr}_{NH_4}$




Content of dioxane in the outer soln,, vol. %

Fig. 6. Selectivity coefficients of calcium and strontium in 1 M ammonium acetate-dioxane-water mixture.
(loading: 5%)
Curve 1 (○): $K^{Ca}_{NH_4}$ Curve 3 (□): $K^{Sr}_{Ca}$
Curve 2 (●): $K^{Sr}_{NH_4}$

solvents can not be explained clearly. We can, however, say that the change in the selectivity coefficients in these systems depends on the following three factors: 1) *The variation in the formation constant of complex ions with the dielectric constant of the outer solution.* It is known that ion association generally increases with a decrease in the dielectric constant of the solution caused by the addition of an organic solvent. 2) *The variation in the affinities of metal and complex ions for the resin with the dielectric constants of the outer solution phase and the resin phase.* It is known that the distribution coefficients for a 1-1 exchange in a mixed solvent varies with the $1/D$ ($D$: dielectric constant) of the solution phase.[8,11] In the present work, however, we can not discover any clear relationship between $K^{Ca}_{NH_4}$ or $K^{Sr}_{NH_4}$ and $1/D$, and the correlation between $K^{Sr}_{Ca}$ and $1/D$[16] is rather uncertain, as is shown in Figs. 1—10. Ohtaki and his coworkers[17] explained their experimental results concerning the distribution coefficients for a 1-1 exchange in mixed solvents, in which an electrolyte existed, on the basis of the

16) B. E. Conway, "Electrochemical Data," Elsevier Pub., Amsterdam (1952).
17) H. Ohtaki, H. Kakihana and K. Yamasaki, *Z. Phys. Chem. Neue Folge*, **21**, 224 (1959).

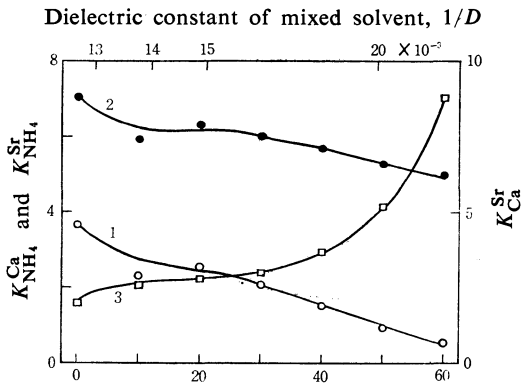



Fig. 7. Selectivity coefficients of calcium and strontium in 1 M ammonium formate-acetone-water mixture.
(loading: 1%)
Curve 1 (○): $K^{Ca}_{NH_4}$ Curve 3 (□): $K^{Sr}_{Ca}$
Curve 2 (●): $K^{Sr}_{NH_4}$

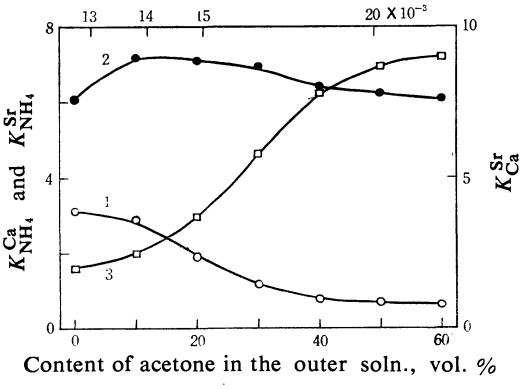



Fig. 8. Selectivity coefficients of calcium and strontium in 1 M ammonium formate-acetone-water mixture.
(loading: 10%)
Curve 1 (○): $K^{Ca}_{NH_4}$ Curve 3 (□): $K^{Sr}_{Ca}$
Curve 2 (●): $K^{Sr}_{NH_4}$

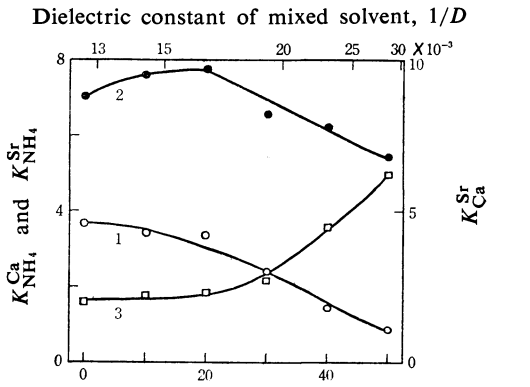



Fig. 9. Selectivity coefficients of calcium and strontium in 1 M ammonium formate-dioxane-water mixture.
(loading: 1%)
Curve 1 (○): $K^{Ca}_{NH_4}$ Curve 3 (□): $K^{Sr}_{Ca}$
Curve 2 (●): $K^{Sr}_{NH_4}$

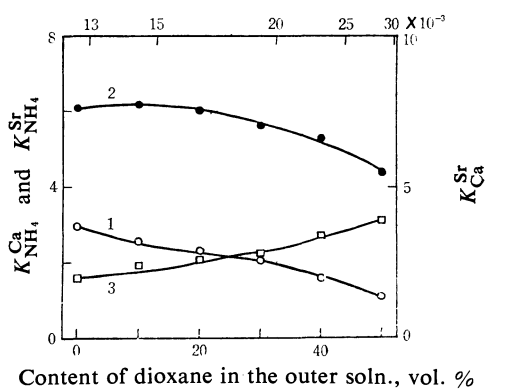



Fig. 10. Selectivity coefficients of calcium and strontium in 1 M ammonium formate-dioxane-water mixture.
(loading: 10%)
Curve 1 (○): $K^{Ca}_{NH_4}$ Curve 3 (□): $K^{Sr}_{Ca}$
Curve 2 (●): $K^{Sr}_{NH_4}$

calculated dielectric constants of the solution phase ($D_s$) and that of the resin phase ($D_r$). However, the method cannot be applied to such complicated cases as are discussed here, because $D_s$ and $D_r$, the formation constants of the complex ions, and the affinities of complex and metal ions to the exchanger are not yet known for the systems studied. 3) *The specific solvation effect on the metal and complex ions.* The variation in the selectivity coefficients with an organic solvent may be caused also by the solvation effect. The finding that dioxane, unlike cellosolves,[18] is not effective in separating calcium and strontium seems to correspond to the fact that dioxane shows no evident solvation effects[19] on these ions. When the cellosolves are used in the column operation, the separation of calcium and strontium is as excellent as can be expected, as is shown in Fig. 11. Thus, the solvation effect may be considered to be one of the factors strongly affecting the selectivity coefficients.

From these results, it may be expected that strontium can be easily separated from calcium by the column operation when an elutriant with a high separation factor, and, at the same time, a low selectivity coefficient

18) M. Izawa, H. Tsubota and A. Kasai, *Japan Analyst (Bunseki Kagaku)*, **10**, 1230 (1961).
19) G. Atkinson, Private communication.

TABLE I. COLUMN DIMENSION AND VOLUME OF ELUTRIANTS TO SEPARATE CALCIUM AND STRONTIUM

| Amount of sample mg. | | Column dimension | Volume of elutriant,* ml. | | | |
|---|---|---|---|---|---|---|
| | | | I | | II | |
| Ca | Sr | | for Ca | for Sr | for Ca | for Sr |
| 20 | 20 | 1.1$\phi$×10 cm. | 50 | 40 | 60 | 50 |
| 100 | 20 | 1.1$\phi$×12 cm. | 60(**) | 50 | 75 | 60 |
| 200 | 20 | 1.1$\phi$×15 cm. | 75** | 60 | 90(**) | 75 |
| 50 | 30 | 1.5$\phi$×10 cm. | 95 | 75 | 110 | 95 |
| 200 | 30 | 1.5$\phi$×12 cm. | 100(**) | 95 | 130 | 110 |
| 400 | 30 | 1.5$\phi$×15 cm. | 140** | 110 | 170(**) | 140 |
| 100 | 50 | 2.0$\phi$×10 cm. | 170 | 130 | 200 | 150 |
| 300 | 50 | 2.0$\phi$×12 cm. | 200(**) | 165 | 240 | 180 |
| 600 | 50 | 2.0$\phi$×15 cm. | 250** | 200 | 300(**) | 225 |

* Elutriant: I-Ca: Mixture of 2 M ammonium formate aqueous solution and acetone in equal volume
I-Sr: 2 M ammonium formate aqueous solution
II-Ca: Mixture of 2 M ammonium acetate aqueous solution and methanol in equal volume
II-Sr: 2 M ammonium acetate aqueous solution
** White precipitate is found in the column.
(**) White precipitate is sometimes found in the column.

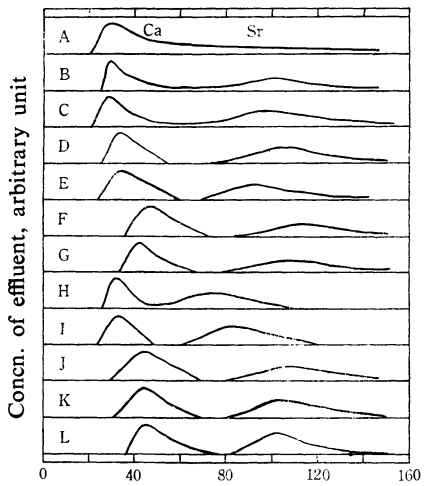



Fig. 11. Elution curves of calcium and strontium with various elutriants.
Column: Amberlite IR-120, 1.1$\phi$×10 cm.
Elutriants: Concentration of ammonium salts was kept 1 mol./l.
A: Ammonium acetate - 80% methanol
B: Ammonium acetate - 70% methanol
C: Ammonium acetate - 60% methanol
D: Ammonium acetate - 50% methanol
E: Ammonium acetate - 40% methanol
F: Ammonium acetate - water
G: Ammonium formate - water
H: Ammonium formate - 50% dioxane
I: Ammonium formate - 50% acetone
J: Ammonium formate - 50% methanol
K: Ammonium formate - 50% methanol cellosolve
L: Ammonium formate - 25% ethyl cellosolve

of calcium against ammonium is used. A 1 M acetate solution containing over 40% methanol and a 1 M ammonium formate solution containing about 60% acetone will meet this purpose. It is, however, very difficult to ascertain the most suitable concentration of the organic solvent, because the variation in selectivity coefficients with the percentage of organic solvents is different for different loading-values. The best can be found only by experiments in the future.

**The Separation of Calcium and Strontium.**— Figure 11 shows the elution curves of calcium and strontium (10 mg. each) with various elutriants, using a 10 cm. column of Amberlite IR-120. The most suitable elutriant is a 1 M ammonium formate solution containing 50% acetone, as is shown by curve I in the figure; the next was a 1 M ammonium acetate solution containing 50% methanol, shown by curve D, as has been expected from the results of the batch operation.

The elution curves by the same column with various amounts of calcium and strontium are shown in Fig. 12. A 1:1 mixture of a 2 M ammonium formate aqueous solution and acetone and a 1:1 mixture of a 2 M ammonium acetate aqueous solution and methanol were used as elutriants.* When the strontium and calcium added to the column were less than 25 mg. and 50 mg. respectively, the elution front of strontium remained unchanged and well separated from the calcium fraction.

* The results with these elutriants were essentially the same as those with the elutriants used for batch operation.

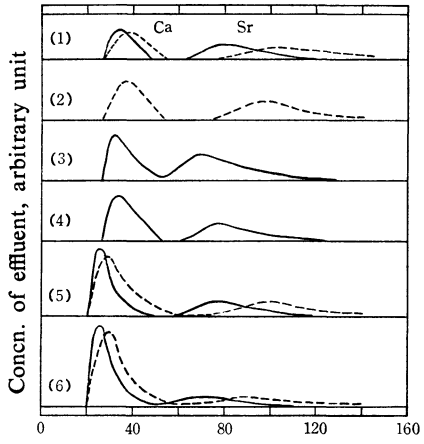



Fig. 12. Elution curves of various amounts of calcium and strontium.
Column : Amberlite IR-120, 1.1$\phi \times$10 cm.
Elutriants :
——: mixture of 2 M ammonium formate aqueous solution and acetone in equal volume
----: mixture of 2 M ammonium acetate aqueous solution and methanol in equal volume
(1) Ca 9.7 mg., Sr 10.0 mg.
(2) Ca 19.4 mg., Sr 20.0 mg.
(3) Ca 19.4 mg., Sr 50.0 mg.
(4) Ca 19.4 mg., Sr 25.0 mg.
(5) Ca 48.5 mg., Sr 25.0 mg.
(6) Ca 67.8 mg., Sr 25.0 mg.

When the amounts of calcium and of strontium increased further, however, strontium came to be soon eluted from the column, and the elution curves of calcium and of strontium overlapped to some extent.

The column dimensions and the volume of the elutriants necessary to treat various amounts of calcium and strontium were determined; they are shown in Table I. Allowance was made for small changes in column dimensions and in the concentration of elutriants. When a large quantity of calcium existed and an ammonium formate solution in acetone-water was used, a white precipitate was formed in the column, preventing the downward flow of the solution and the clear-cut separation of the two cations. The elution curves of strontium show a considerable tailing when the elutriant used to elute calcium is used, as is shown by the dotted curves in Fig. 13. Strontium can be completely eluted with a 2 M ammonium acetate or formate aqueous solution (without organic solvents). The volume of the elutriant necessary to elute strontium is shown in the same table, while the elution curves are shown in Fig. 13 by solid curves.

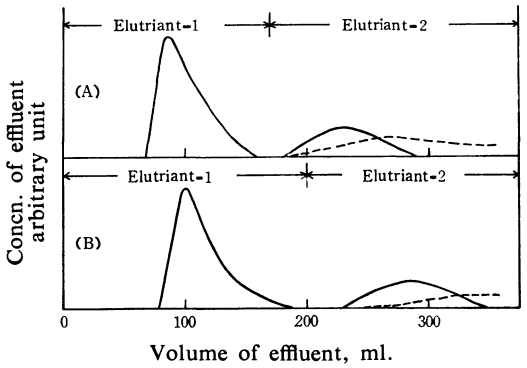



Fig. 13. Elution curves of calcium and strontium.
Column : Amberlite IR-120, 2.0$\times$10 cm.
Elutriant :
(A) 1 : mixture of 2 M ammonium formate aqueous solution and acetone in equal volume
2 : 2 M ammonium formate aqueous solution
(B) 1 : mixture of 2 M ammonium acetate aqueous solution and methanol in equal volume
2 : 2 M ammonium acetate aqueous solution
Dotted lines show the elution curves of strontium using elutriant-1.

## Summary

Ion exchange equilibria of calcium- and strontium-ammonium exchange systems have been studied in methanol-water, acetone-water and dioxane-water mixtures in which acetate or formate ions co-exist as a complexing anion. The selectivity coefficients of calcium against ammonium and those of strontium against ammonium decrease, while the separation factor between strontium and calcium increases, with an increase in the organic solvent concentration. Therefore, by the column operation, calcium can easily be eluted from the column, and strontium can be well separated from calcium when a suitable elutriant with a high separation factor between strontium and calcium and with a low selectivity coefficient of calcium against ammonium is selected. A 1 : 1 mixture of a 2 M ammonium formate aqueous solution and acetone or a 1 : 1 mixture of a 2 M ammonium acetate aqueous solution and methanol is recommended. When strontium in a large amount of calcium is to be analyzed, the latter elutriant is the most suitable.

The author wishes to thank Professor Hidetake Kakihana of the Tokyo Institute of Technology, Professor Hideo Yamatera of Rikkyo (St. Paul's) University, and Dr. Masami

Izawa of the National Institute of Radiological Sciences for their helpful discussions and advice.

*National Institute of Radiological Sciences*
*Kurosuna, Chiba*

# The Cation Exchange Investigation of Scandium Acetate and Sulfate Systems

By Akira TATEDA

(Received July 9, 1963)

Previously the present author[1] has reported on the adsorption of scandium ions on several adsorbents, showing that the concentrations and kinds of salts contained in the solution have an influence on the ratios of scandium adsorption. The aim of the present investigation is to make quantitative studies of the formation equilibria of the complexes in the scandium acetate and sulfate systems, in order to get some clue as to the mechanism of the influence described above.

A work[2] has recently reported on the scandium acetate system, in which, by the cation exchange method, scandium was separated from rare earth elements, using a 0.5 M ammonium acetate - acetic acid solution (pH 4.5) as an eluent. However, there has been no study of the composition of the eluted species.

In the present study, the compositions of the scandium acetate and sulfate complexes will be determined by the cation exchange method according to the procedures of Fronaeus,[3] with some simplification to be described below. Judging from the data obtained, species with scandium to ligand ratios of 1 : 1, 1 : 2 and 1 : 3 seem to be formed both in acetate solutions and in sulfate solutions at a constant ionic strength of $\mu=0.5$ and at 25°C. Then overall formation constants of the various complexes will be determined.

## Derivation of Equations

An equation for determining the compositions and the formation constants of metal complex species using cation exchange resin has been derived by Schubert.[4] Fronaeus[3] has applied the cation exchange method to the step to step equilibria between a divalent cation and a univalent complexing anion. In this investigation, an equation was derived for the complex systems of the $M^{3+}-A^{-}$ and $M^{3+}-B^{2-}$ types, and a graphical method developed by Banerjea and Tripathi[5] was used in evaluating the formation constants. According to the data of Biedermann[6] concerning the hydrolysis of scandium ions, the mononuclear complexes exist in an acid solution which contains a low concentration of scandium. As a small amount of radioactive scandium was used in these experiments, the formation of only the mononuclear complexes need to be considered.

The following equilibrium is obtained between a cation exchanger in the sodium form and a solution containing scandium ions, $Sc^{3+}$, and complex ions, $ScA_j^{3-j}$:

$$(3-j)\,Na_R^{+}+ScA_j^{3-j} = (3-j)\,Na^{+}+ScA_{jR}^{3-j};\ (j=0,\ 1,\ 2)$$

If the law of mass action is applied to this exchange equilibrium,

$$[ScA_j^{3-j}]_R/[ScA_j^{3-j}] = k_j[Na^{+}]_R^{3-j}/[Na^{+}]^{3-j}=l_j;\ (j=0,\ 1,\ 2) \quad (1)$$

where [ ] indicates the molar concentration and the subscript R indicates the resin phase.

In this experiment, the total concentration of the scandium ions is very low and the load of metal ions in the resin phase is very low compared with the total exchange capacity. Moreover, the ionic strengths of both the resin and the aqueous phase have been nearly constant. Under these conditions, $k_j$ and $l_j$ in Eq. 1 may be considered to be constant. The total concentration of scandium ions in the

1) J. Yoshimura and A. Tateda, *J. Chem. Soc. Japan, Pure Chem. Sec.* (*Nippon Kagaku Zasshi*), **83**, 1018 (1962).
2) J. Yoshimura, Y. Takashima and H. Waki, ibid., **79**, 1169 (1958).
3) S. Fronaeus, *Acta Chem. Scand.*, **5**, 859 (1951); **6**, 1200 (1952).
4) J. Schubert, *J. Colloid. Chem.*, **52**, 340 (1948); *J. Phys. Chem.*, **56**, 113 (1952).
5) D. Banerjea and K. K. Tripathi, *J. Inorg. Nucl. Chem.*, **18**, 199 (1961).
6) G. Biedermann, M. Kilpatrick, L. Pokras and L. G. Sillén, *Acta Chem. Scand.*, **10**, 1327 (1956).

resin phase, $C_{MR}$, and in solution, $C_M$, are considered to be as follows:

$$C_{MR}=[Sc^{3+}]_R+[ScA^{2+}]_R+[ScA_2^{+}]_R \quad (2)$$

and

$$C_M=[Sc^{3+}]+[ScA^{2+}]+\cdots\cdots+[ScA_N^{3-N}]$$
$$=[Sc^{3+}](1+\sum_{j=1}^{N}\beta_j[A^-]^j) \quad (3)$$

where a $N$ indicates a maximum ligand number bound to a scandium ion, and $\beta_j$ is the overall formation constant of $j$th complex, $ScA_j^{3-j}$, i. e. $\beta_j=[ScA_j^{3-j}]/[Sc^{3+}][A^-]^j$.

From Eqs. 1, 2 and 3, putting $l_1\beta_1/l_0=L_1$ and $l_2\beta_2/l_0=L_2$, the distribution coefficients of the scandium between the resin and the solution, $K_d$, can be represented by:

$$K_d=C_{MR}/C_M=l_0(1+L_1[A^-]+L_2[A^-]^2)/X \quad (4)$$

where

$$X=1+\sum_{j=1}^{N}\beta_j[A^-]^j$$

For determining the value of $L_1$, the following function, $f_1$, is introduced:

$$f_1=(K_d^{-1}-l_0^{-1})/[A^-] \quad (5)$$

The relation, Eq. 6, is derived by introducing the expression of $K_d$ from Eq. 4 into Eq. 5 and by extrapolating it to $[A^-]=0$;

$$\lim_{[A]\to 0} f_1=f_1^0=(\beta_1-L_1)/l_0 \quad (6)$$

When the ligand concentration, $[A^-]$ in Eq. 4, is very small, it may be assumed that the $L_1$ and $L_2$ terms can be disregarded. Then an approximate value of $\beta_1$ can be determined graphically by extrapolation to $[A^-]=0$, according to the following equation:

$$(l_0/K_d-1)/[A^-]=\beta_1+\beta_2[A^-]+\cdots\cdots$$
$$+\beta_N[A^-]^{N-1} \quad (7)$$

As $l_0$ is measurable or calculable, $L_1$ can be estimated from Eq. 6. $L_2$ can be determined in the same way. Another function, $f_2$, is also introduced as follows:

$$f_2=[f_1-(\beta_1-L_1)l_0]/[A^-] \quad (8)$$

Now the values of $f_1^0$, $L_1$ and $l_0$ and an approximate value of $\beta_2$ being known or calculated, the value of $L_2$ can be calculated from Eq. 9, obtained by extrapolating the $f_2$ function to $[A^-]=0$:

$$\lim_{[A^-]\to 0} f_2=f_2^0=[(\beta_2-L_2)-f_1^0l_0L_1]/l_0 \quad (9)$$

When $L_1$ and $L_2$ have been determined in this way, the function $X$ in Eq. 4 can be calculated, and from the corresponding values of $X_j$ and $[A^-]$ the formation constant can be computed from the relations:

$$X_1=(X-1)/[A^-]=\beta_1+\beta_2[A^-]$$
$$+\beta_3[A^-]^2+\cdots\cdots+\beta_N[A^-]^{N-1} \quad (10)$$
$$X_2=(X_1-\beta_1)/[A^-]=\beta_2+\beta_3[A^-]$$
$$+\beta_4[A^-]^2+\cdots\cdots+\beta_N[A^-]^{N-2} \quad (11)$$

This process is continued till the $X_N$ function independent of $[A^-]$ is obtained, where:

$$X_N=\beta_N$$

Hence a plot of $X_N$ versus $[A^-]$ will be a straight line parallel to the $[A^-]$ axis, indicating that the highest complex formed in the system is $ScA_N^{3-N}$.

In the case of a divalent complexing anion $B^{2-}$ such as the sulfate ion, it has only to be considered that the complex ions in the resin phase are $Sc^{3+}$ and $ScB^+$. Therefore, Eq. 4 can be rewritten as:

$$K_d=l_0(1+L_1[B^{2-}])/X \quad (12)$$

Since $L_1$ can be determined as has been described above, the function $X$ can be calculated and $\beta_j$ can be estimated.

## Experimental

**Reagents.** — Radioactive $^{46}Sc$ ($T_{1/2}$=85 days) in dilute hydrochloric acid, obtained from N. V. Philip-Duphar (Holland), was employed as a stock solution of scandium ($\sim 5\times10^{-4}$ M). In these experiments, a portion of the above solution was dried in a glass dish and then dissolved in dilute perchloric acid. When the solution was converted into a 0.5 M sodium perchlorate solution, the radioactivity corresponded to about one microcurie per ml. of solution.

The resin used in all the experiments was the sodium form of the cation exchanger, Amberlite IR-120, with a particle size of 60 to 100 mesh and with a capacity of 3.69 meq. per g. in hydrogen form.

The sodium acetate solution and the sodium sulfate solution used as sources of complexing anions were prepared from guaranteed reagents.

**Procedure.** — The adsorbability of the scandium ions was measured by a batch method as follows; To the solution which contained a known quantity of a 0.5 M ligand solution and 1.0 ml. of the scandium solution, 0.5 M sodium perchlorate solution was added until the volume of the solution reached 10 ml. in a small stoppered glass vessel. The ionic strength of the resultant solution was then made up to 0.5. Since a 0.5 M acetic acid-sodium acetate buffer solution (pH 4.5) was used as the ligand solution in the case of the acetate system, pH of the solution prepared above could be adjusted easily. In the case of the sulfate system, the pH of the solution was adjusted with a dilute perchloric acid. Each of these solutions was shaken with 0.2 g. of the resin for 24 hr. at 25°C. A portion of the supernatant solution was then taken with a pipet and dried in a glass dish. The radioactivity of the residue was measured, and the distribution coefficient was calculated from the difference in the scandium activity before and

after the achievement of equilibrium. The measurements of the radioactivity were carried out with a Toshiba Scintillation Detector, DDS-14301 type (NaI: $1''\phi \times 1''l$), attached to a Flow Counter Scaler, UDS-24204 type.

## Results and Discussion

**On the Formation of Scandium Acetate and Sulfate Complexes.**—In Fig. 1 the distribution coefficients, $K_d$, are plotted against pH values of scandium-perchlorate, -acetate and -sulfate solutions. The ionic strength of each solution was kept constant at 0.5 and, since the radioactive scandium used in this experiment was considered to form radiocollid or to precipitate hydroxide in an alkaline solution,[7,8] these experiments were carried out over the range of pH values from 1.0 to 7.0.

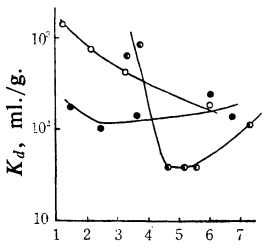



Fig. 1. Relation between the distribution coefficient and pH of the solutions.
Ionic strength: 0.5, Temp.: 25°C
—○— $NaClO_4$
—◐— $CH_3COONa + CH_3COOH$
—●— $Na_2SO_4$

It may be observed from Fig. 1 that $K_d$ values in the acetate solution in the pH range from 4.5 to 6.0 are smaller than that in the perchlorate solution and that $K_d$ values in the sulfate solution are also smaller than that in the perchlorate solution over a broad range of the acidic side of pH values. In the curve obtained with a perchlorate solution, $K_d$ decreases with an increase in the pH values. This phenomenon may be considered to be due to the hydrolysis of scandium ions. Since the concentrations of scandium ion used in these experiments are below $10^{-5}$ mol./l., there is little or no tendency to precipitate scandium hydroxide below pH 5, according to the data of the solubility product.[8] $K_{so}=[Sc^{3+}][OH^-]^3 = 10^{-27-30.1}$.

Moreover, the formation of the hydroxo complex ions, $Sc(OH)^{2+}$, $Sc(OH)_2^+$ and $Sc_2(OH)_2^{4+}$, were considered. From the values of the formation constants of these complex ions obtained by Biedermann et at.,*,[6] it has been found that only the scandium ion, $Sc^{3+}$, is a predominant species in the sulfate solution with pH=2.7 and that the hydroxo complex ions, $Sc(OH)^{2+}$ and $Sc(OH)_2^+$, form 26% and 7% of the total scandium concentration respectively in the acetate solution with pH=4.5. The polymerization of scandium ions is negligibly small in both cases.

On the other hand, the $K_d$ value without a ligand obtained by the graphical extrapolation of the relation between $1/K_d$ and $[A]^2$ to $[A]=0$ in the acetate or the sulfate system, agreed with the value $K_d$ obtained experimentally in the perchlorate solution with the same pH. In the case of acetate system, the numerical values of 204 ml./g. and 225 ml./g. respectively were obtained for the extrapolated and the experimental values at pH=4.5, while as regards the sulfate system, 545 ml./g. and 520 ml./g. respectively were obtained. Therefore, it has been proved, as has been shown by Feldman et al.,[9] that the species of the metal ion in the complexes are the same as that in the uncomplexed metal.

On the basis of these facts, it seems reasonable to assume that the decrease in the $K_d$ value in both the acetate and sulfate solutions as compared with the $K_d$ value of the perchlorate solution shows the occurrence of a considerable complex formation, since, although the resin adsorbs not only $Sc^{3+}$ ions but also the cationic complexes, the adsorption of the latter for the resin is small because of the lower charge on the cationic complex and its low concentration in each system.

**On the Composition and Formation Constants of Scandium Acetate Complexes.**—In the formation reaction between the scandium ion and the acetate ion, it must be taken into consideration that the scandium ion has been hydrolyzed in the solution with pH=4.5, as has been described above. Therefore, the following equilibria are considered in solution, assuming that: 1) the species of the scandium ions reacting with the acetate ion, $A^-$, are $Sc^{3+}$ and $Sc(OH)^{2+}$; 2) since only a few dihydroxo complex ions, $Sc(OH)_2^+$, are present in the solution under the experimental conditions, they can be disregarded as central metal ions; 3) the monohydroxo complex ion, $Sc(OH)^{2+}$, forms complexes with acetate ions. The formation of the hydroxo acetato complex ion, $Sc(OH)A_n^{2-n}$,

7) J. D. Gile, W. M. Garrison and J. G. Hamilton, *J. Chem. Phys.*, **18**, 1685 (1950).
8) J. Bjerrum, G. Schwarzenbach and L. G. Sillén, "Stability Constants of Metal-ion Complexes, Part II: Inorganic Ligands," The Chemical Society, London (1958).

* These values are used: $*K_1=[Sc(OH)^{2+}][H^+]/[Sc^{3+}] = 10^{-4.90}$, $*K_2=[Sc(OH_2)^+][H^+]/[Sc(OH)^{2+}]=10^{-5.1}$ and $\beta_{22}=[Sc_2(OH_2)^{4+}][H^+]^2/[Sc^{3+}]^2=10^{-5.9}$ (cf. Biedermann et al.[6]).
9) L. Feldman, T. V. Toribara, J. R. Havill and W. F. Neuman, *J. Am. Chem. Soc.*, **77**, 878 (1955).

may be supported by the finding[10] that Sc(OH)$A_2$ was precipitated from a hot and concentrated solution with pH=4.76 and 4.93.

$$Sc^{3+}+jA^-=ScA_j^{3-j}$$
$$\beta_j=[ScA_j^{3-j}]/[Sc^{3+}][A^-]^j$$
$$Sc^{3+}+H_2O=Sc(OH)^{2+}+H^+$$
$$*K_1=[Sc(OH)^{2+}][H^+]/[Sc^{3+}]$$
$$Sc(OH)^{2+}+nA^-=Sc(OH)A_n^{2-n}$$
$$\beta_n'=[Sc(OH)A_n^{2-n}]/[Sc(OH)^{2+}][A^-]^n$$

The exchange equilibrium in the resin phase is considered, along with that of Eq. 1, as follows:

$$(2-n)Na_R^+ + Sc(OH)A_n^{2-n} = (2-n)Na^+ + Sc(OH)A_{nR}^{2-n}$$
$$[Sc(OH)A_n^{2-n}]_R/[Sc(OH)A_n^{2-n}] = k_n'[Na^+]_R^{2-n}/[Na^+]^{2-n}=l_n' ;\ (n=0, 1) \quad (13)$$

From these equations, $K_d$ is represented as follows, by the same treatment from Eq. 1 to Eq. 4:

$$K_d=\frac{\left(\begin{array}{l} l_0+l_0'*K_1[H^+]^{-1}+l_1\beta_1[A^-]+ \\ l_1'\beta_1'*K_1[H^+]^{-1}[A^-]+l_2\beta_2[A^-]^2 \end{array}\right)}{\left(\begin{array}{c} (1+\sum_{j=1}^{N}\beta_j[A^-]^j)+ \\ *K_1[H^+]^{-1}(1+\sum_{n=1}^{M}\beta_n'[A^-]^n) \end{array}\right)}$$

$[H^+]$ is determined by the pH value in solution and a constant value in this experiment, while $*K_1$ is a known value.* Putting $l_0+l_0'*K_1[H^+]^{-1}=K_{d_0}$, $l_1\beta_1/*K_{d_0}=L_1$, $l_1'\beta_1'*K_1\cdot[H^+]^{-1}/*K_{d_0}=L_1'$ and $l_2\beta_2/*K_{d_0}=L_2$, $K_d$ can be represented by:

$$K_d=*K_{d_0}[1+(L_1+L_1')[A^-]+L_2[A^-]^2]/X'$$
$$X'=1+*K_1[H^+]^{-1}+B_1[A^-]+B_2[A^-]^2+\cdots\cdots \quad (14)$$

where $B$ represents $\beta_j+\beta_j'*K_1[H^+]^{-1}$ and gives a constant value when $[H^+]$ is kept constant. Since the distribution coefficients of $Sc^{3+}$ and $Sc(OH)^{2+}$ ions in the absence of an acetate ion, $K_{d_0}$, are obtained by the graphical extrapolation of $K_d$ to $[A^-]=0$, $*K_{d_0}$ can be calculated from the following equation:

$$K_{d_0}=*K_{d_0}/(1+*K_1[H^+]^{-1})$$
or $$*K_{d_0}=K_{d_0}(1+*K_1[H^+]^{-1}) \quad (15)$$

Equation 14 can be made analogous to Eq. 4 by substituting $L_1$ and $\beta_j$ for $(L_1+L_1')$ and $B_j$ respectively. Similarly, the following equations are obtained instead of Eqs. 5, 6, 7, 8 and 9 respectively:

$$f_1=(K_d^{-1}-K_{d_0}^{-1})/[A^-] \quad (16)$$
$$\lim_{[A]\to 0} f_1=f_1^0=[B_1-(L_1+L_1')\times(1+*K_1[H^+]^{-1})]/*K_{d_0} \quad (17)$$
$$[*K_{d_0}/K_d-(1+*K_1[H^+]^{-1})]/[A^-] = B_1+B_2[A^-]+\cdots\cdots \quad (18)$$
$$f_2=(f_1-f_1^0)/[A^-] \quad (19)$$
$$\lim_{[A]\to 0} f_2=f_2^0 = [B_2-L_2-(L_1+L_1')f_1^0*K_{d_0}]/*K_{d_0} \quad (20)$$

In the case of an acetate system, the ratios of ligands to scandium can be determined, but the chemical formulae and the formation constants for the corresponding complex ions can not be estimated unless either $\beta_j$ or $\beta_j'$ are estimated.

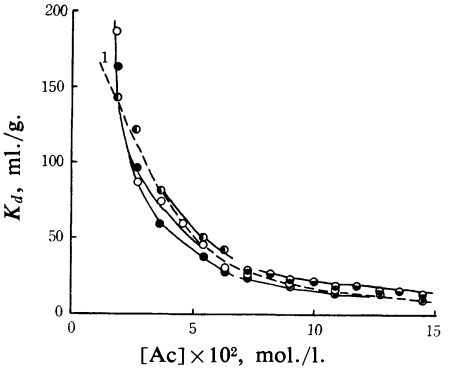



Fig. 2. $K_d$ as a function of acetate ion concentrations at different Sc(III) concentrations.
Ionic strength: 0.5, Temp.: 25°C, pH: 4.5
—⊙— Total concentration of Sc(III) added, $C_M'=1.17\times10^{-4}$ mol./l.
—●— $C_M'=8.1\times10^{-5}$ mol./l.
—○— $C_M'=5.0\times10^{-5}$ mol./l.
—◒— $C_M'=3.6\times10^{-5}$ mol./l.
—◐— $C_M'=2.9\times10^{-5}$ mol./l.
Broken line curve: Total concentration of Sc(III) in resin phase, $C_{MR}=1\times10^{-4}$ mol./l.

Figure 2 shows the dependence of $K_d$ on the acetate ion concentrations and the scandium concentrations, when the ionic strength is kept constant at 0.5 in a sodium perchlorate solution and at pH 4.5. The acetate ion concentration of the solution was calculated from the added acetate concentration, the pH of the solution and the dissociation constant of acetic acid.** In all of the above equations, $[A^-]$ represents the concentration of free acetate ions. However, since the total acetate ion concentration is very much larger than the total scandium

10) J. S. Sterba-Bohm and M. Melichar, *Collection Czechoslov. Chem. Commun.*, 7, 56 (1935).

** The dissociation constants of acetic acid used was the value, $K=1.75\times10^{-5}$, given by J. F. J. Dippy [*Chem. Revs.*, 25, 151 (1939)].

TABLE I. $K_d$, $X'$, $X_1'$, $X_2'$ AND $X_3'$ CORRESPONDING TO THE ACETATE ION CONCENTRATIONS
IONIC STRENGTH: $\mu=0.5$, Temp.: 25°C, pH: 4.5

| $[Ac^-]$ $10^{-2}$ mol. $l^{-1}$ | $K_d$ ml./g. | $X'$ | $X_1'$ $mol^{-1}$ l. | $X_2'$ $mol^{-2}$ $l^2$ | $X_3'$ $mol^{-3}$ $l^3$ |
|---|---|---|---|---|---|
| 0.00 | 204 | 1.40 | 22 | 1500 | 11000 |
| 1.81 | 143 | 2.32 | 51 | 1600 | — |
| 2.72 | 121 | 3.0 | 57 | 1300 | — |
| 3.63 | 80.0 | 4.8 | 93 | 2000 | 12000 |
| 5.44 | 47.1 | 9.1 | 140 | 2200 | 12000 |
| 6.35 | 37.1 | 12.3 | 172 | 2300 | 12000 |
| 7.26 | 29.6 | 16.4 | 207 | 2500 | 12000 |
| 9.07 | 21.0 | 24 | 258 | 2600 | 12000 |
| 10.90 | 16.4 | 35 | 306 | 2600 | 10000 |
| 12.70 | 14.4 | 42 | 324 | 2400 | — |
| 14.50 | 9.9 | 66 | 450 | 3000 | 10000 |

ion concentration, $[A^-]$ can be substituted for the total acetate ion concentration, $[Ac^-]$.

The scandium concentration in the resin phase was selected as $1\times10^{-4}$ mmol./g. resin, so that the total concentration in the resin phase might be kept constant. The relation between $K_d$ and the scandium concentration in the resin phase at a constant value of $[Ac^-]$ is presumed to be practically linear when graphically represented. Therefore, it is easy to determine the values of $K_d$ corresponding to a constant and low value of $C_{MR}$ by graphical interpolation. The resultant value of $K_d$ is shown as a broken-line curve in Fig. 2 and in the second column of Table I.

The value of $K_{d_0}$ was determined by graphical extrapolation. Since $1/K_d$ plotted against $[Ac^-]^2$ was shown to be a straight line at a low concentration of $[Ac^-]$, by extrapolation to $[Ac^-]=0$ the value of $K_{d_0}$ was found to be 204 ml./g. Therefore, $^*K_{d_0}$ was calculated from Eq. 15 to be 286 ml./g.

In order to get the values of $(L_1+L_1')$ and $L_2$, an approximate value of $B_1$ was calculated according to Eq. 18. The calculated values of approx. $X_1'=[^*K_{d_0}/K_d-(1+{}^*K_1[H^+]^{-1})]/[Ac^-]$ are plotted as a function of $[Ac^-]$ in curve 1 of Fig. 4; by graphical extrapolation to $[Ac^-]=0$, $B_1$ was found to be $22\pm10$ $mol^{-1}$ l. On the other hand, as is shown in Fig. 3, the relation between $f_1$ and $[Ac^-]$ is practically linear at $[Ac^-]\leq9.07\times10^{-2}$ mol./l., and $f_1^0$ was found to be $(30\pm6)\times10^{-3}$ g. $ml^{-1}$ $mol^{-1}$ l. Accordingly, the value of $(L_1+L_1')=9\pm2$ $mol^{-1}$ l. was obtained from Eq. 17.

Therefore, on substituting numerical value for the $L_1+L_1'$ quantity into Eq. 14 the $X'$ function may be shown as:

$$X'={}^*K_{d_0}(1+9[Ac^-])/K_d \qquad (21)$$

The values of $f_2$ calculated from Eq. 19 are plotted as a function of $[Ac^-]$ in Fig. 3. The $f_2^0$ value obtained by the extrapolation of $f_2$ to $[Ac^-]=0$ was $4.93\pm0.04$ g. $ml^{-1}$ $mol^{-2}$ $l^2$. On the other hand, the approximate value of $B_2$ at $[Ac^-]\leq9.07\times10^{-2}$ mol./l. was found to be $(15\pm7)\pm10^2$ $mol^{-2}$ $l^2$ by the extraporation of curve 4 in Fig. 4 plotted from the relation between $X_2'=(X_1'-22)/[Ac^-]$ and $[Ac^-]$. Then the value of $L_2$ was given as almost zero by calculating from Eq. 20.

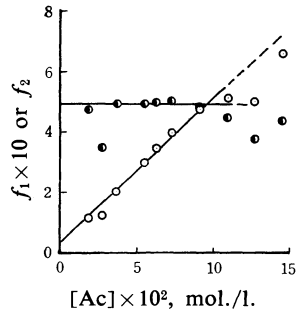



Fig. 3. $f_1$ and $f_2$ as a function of acetate ion concentration.
—○— $f_1$ —◐— $f_2$

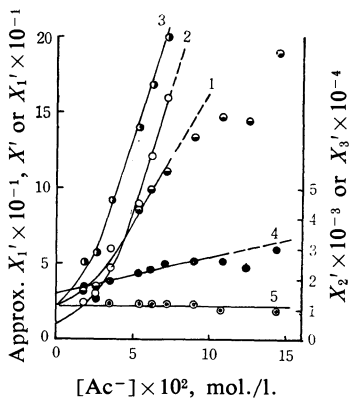



Fig. 4. Approximate $X_1'$ and $X_j'$ as a function of acetate ion concentration.
1: Approx. $X_1'$, 2: $X'$, 3: $X_1'$, 4: $X_2'$, 5: $X_3'$.

The functions $X'$ calculated are shown in Fig. 4 and in Table I. By the extrapolation of $X_1'$ and $X_2'$ to $[Ac^-]=0$, $B_1$ and $B_2$ agreed, of course, with the values of the first approximation. The function $X_3'$ in curve 5 of Fig. 4 and in the sixth column of Table I has been calculated for such $[Ac^-]$ values in which the difference $X_2'-B_2$ is not small compared with $B_2$. By the extraporation of $X_3'$ to $[Ac^-]=0$, $B_3$ was determined to be $(11\pm3)\times10^3$ mol.$^{-3}$ l$^3$. No value of $B_4$ can be obtained from this experiment.

From the results obtained it appears that the species with scandium to ligand ratios of 1 : 1, 1 : 2 and 1 : 3 are formed in an acetate solution with pH=4.5, while the species with the ratio of 1 : 2, $Sc(Ac)_2^+$ or $Sc(OH)(Ac)_2$ or both $Sc(Ac)_2^+$ and $Sc(OH)(Ac)_2$, appear to the predominant species in the acetate system under the experimental conditions, judging from the determined values of the formation constants.

**On the Compositions and Formation Constants of Scandium Sulfate Complexes.** — Figure 5 presents a plot of the $K_d$ value versus the sulfate ion concentration. The experiment was carried out at a constant ionic strength of $\mu=0.5$ and at pH 2.7. The values of $f_1$ calculated according to Eq. 5 are plotted as a function of $[SO_4^{2-}]$ in Fig. 6; the extrapolated value of $f_1$ was found to be $(6.8\pm0.1)\times10^{-2}$ g. ml$^{-1}$ mol$^{-1}$ l. The values of approx. $X_1=(l_0/K_d-1)/[SO_4^{2-}]$ versus $[SO_4^{2-}]$ are shown in Fig. 6. The approximate formation constant, $\beta_1=39.2\pm0.3$ mol$^{-1}$ l., was easily found by extrapolating the approx. $X_1$ to $[SO_4^{2-}]=0$ at $[SO_4^{2-}]\leq2.79\times10^{-2}$ mol./l. Then the value $L_1=3\pm1$ mol$^{-1}$ l. was calculated from Eq. 6.

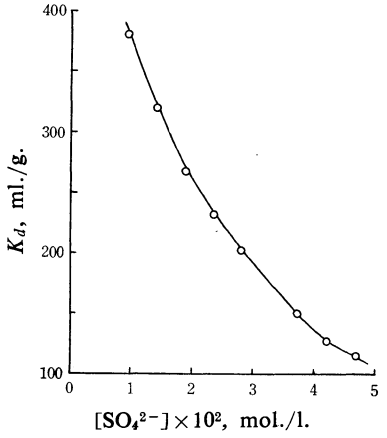



Fig. 5. $K_d$ as a function of sulfate ion concentration.
Ionic strength: 0.5, Temp.: 25°C, pH: 2.7

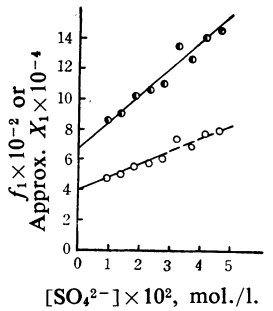



Fig. 6. $f_1$ and approximate $X_1$ as a function of sulfate ion concentration.
◐ $f_1$ ○ Approx. $X_1$

On substituting the value $L_1$ into Eq. 12, the function $X$ can be calculated; by the extrapolation of $X_1$ to $[SO_4^{2-}]=0$, the more accurate value of $\beta_1$ was found, $46\pm5$ mol$^{-1}$ l. Then the value $L_1=8\pm1$ mol$^{-1}$ l. was estimated. For the next approximation, the same procedure was repeated; the $\beta_1$ value obtained was practically the constant value. The function $X$ may, then, be shown as follows:

$$X=l_0(1+8[SO_4^{2-}])/K_d \qquad (22)$$

The functions $X$ calculated from Eq. 22 are shown in Table II and in Fig. 7. The $\beta_1$, $\beta_2$ and $\beta_3$ formation constants were found to be $46\pm5$ mol$^{-1}$ l., $(11\pm6)\times10^2$ mol$^{-2}$ l$^2$ and $(10\pm7)\times10^3$ mol$^{-3}$ l$^3$ respectively.

TABLE II. $K_d$, $X$, $X_1$, $X_2$ AND $X_3$ CORRESPONDING TO THE SULFATE ION CONCENTRATIONS
Ionic strength: $\mu=0.5$, Temp.: 25°C, pH: 2.7

| $[SO_4^{2-}]$ $10^{-2}$ mol. l$^{-1}$ | $K_d$ ml./g. | $X'$ | $X_1$ mol$^{-1}$ l. | $X_2$ mol$^{-2}$ l$^2$ | $X_3$ mol$^{-3}$ l$^3$ |
|---|---|---|---|---|---|
| 0.00 | 545 | 1.00 | 46 | 1100 | 10000 |
| 0.93 | 380 | 1.54 | 58.0 | — | — |
| 1.40 | 322 | 1.88 | 62.9 | 1200 | 7000 |
| 1.86 | 268 | 2.33 | 72 | 1400 | 16000 |
| 2.33 | 233 | 2.78 | 76 | 1300 | 9000 |
| 2.79 | 203 | 3.28 | 82 | 1300 | 7000 |
| 3.26 | 159 | 4.32 | 102 | 1700 | 15000 |
| 3.72 | 152 | 4.65 | 98 | 1400 | 8000 |
| 4.19 | 129 | 5.64 | 111 | 1600 | 10000 |
| 4.64 | 116 | 6.45 | 117 | 1500 | 9000 |

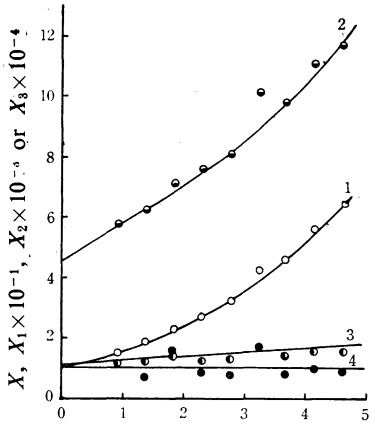



Fig. 7. $X_j$ as a function of sulfate ion concentration.
1: $X$, 2: $X_1$, 3: $X_2$, 4: $X_3$

## Summary

Ion exchange equilibria between the cation exchange resin, Amberlite IR-120, and an aqueous solution containing a small concentration of scandium ions and a relatively large concentration of acetate or sulfate ions have been measured at a constant ionic strength of $\mu=0.5$ and at 25°C. The values of the formation constants of the complexes in solution have been calculated by the application of the Fronaeus method[3] and by the graphical method.[5]

In the case of the acetate system, at an acetate ion concentration $[Ac]\leq14.5\times10^{-2}$ mol./l. and pH 4.5, species with scandium to ligand ratios of 1:1, 1:2 and 1:3 seem to be formed. However, since scandium exists mainly in two ionic species, $Sc^{3+}$ and $Sc(OH)^{2+}$, in the solution, the chemical formulae can not be determined; therefore, the formation constants have been estimated for the addition of each formation constant of two complexes with the same ligand ratio, $Sc(Ac)_j^{3-j}$ and $Sc(OH)(Ac)_j^{2-j}$. The values of $B_j=(\beta_j+\beta_j'{}^*K_1[H^+]^{-1})$ were $B_1=22\pm10$ mol$^{-1}$ l., $B_2=(15\pm7)\times10^2$ mol$^{-2}$ l$^2$ and $B_3=(11\pm3)\times10^3$ mol$^{-3}$ l$^3$ at pH 4.5. In the case of the sulfate system, three complex ions were formed at a sulfate ion concentration of $[SO_4^{2-}]\leq4.65\times10^{-2}$ mol./l. and pH 2.7: $Sc(SO_4^{2-})^+$, $Sc(SO_4^{2-})_2^-$ and $Sc(SO_4^{2-})_3^{3-}$. The formation constants were $\beta_1=46\pm5$ mol$^{-1}$ l., $\beta_2=(11\pm6)\times10^2$ mol$^{-2}$ l$^2$ and $\beta_3=(10\pm7)\times10^3$ mol$^{-3}$ l$^3$.

The author is grateful to Professor Jun Yoshimura, of Kyushu University, for his suggestions and encouragement; he also wishes to thank Mr. Tokio Aihara, Kurita Chemical Industry Co., Ltd., for his valuable assistance during the measurements.

*Department of Chemistry*
*Faculty of Literature and Science*
*Ehime University*
*Dogo, Matsuyama*

# Studies of Thio Acids. III.[1] The Ultraviolet Absorption Spectra of Thiostearic Acid and Related Compounds*1

By Yoshio HIRABAYASHI and Tetsuro MAZUME*2

(Received December 26, 1963)

The ultraviolet absorption spectrum of thioacetic acid has been studied by Hantzsch,[2] Cunneen[3] and Koch.[4] However, no studies of the ultraviolet absorption spectra of higher aliphatic thio acids have yet been published.

The present authors have, therefore, investigated the ultraviolet absorption spectra of thiostearic acid,[5] its derivatives, and thioacetic acid. An absorption maximum of thiostearic acid appears at 221 mμ in a cyclohexane solution, while a low-intensity absorption appears at 260—290 mμ. The latter is assumed to be an R-band due to the C=O group. Similar phenomena have been observed with thioacetic acid and methyl thiostearate. An absorption maximum of thiostearic acid appears at 223 mμ in an ethanol solution, and in lower concentrations another absorption maximum

1) Part II of this series: Y. Hirabayashi, M. Mizuta and T. Mazume, This Bulletin, **38**, 320 (1965).

*1 Most of this study was presented at the Symposium of Oils and Fats of the Chemical Society of Japan, Nagoya, November, 1956.

*2 Present address: Shimogamo-Kishimotocho, Sakyo-ku, Kyoto.

2) A. Hantzsch and E. Scharf, *Ber.*, **45**, 3570 (1913).

3) J. I. Cunneen, *J. Chem. Soc.*, **1947**, 134.

4) H. P. Koch, ibid., **1949**, 387.

5) Y. Hirabayashi, M. Mizuta and T. Mazume, This Bulletin, **37**, 1002 (1964).

appears at 250 mμ, which is probably due to the mesomeric anion produced by the dissociation. Similar phenomena have been observed with thioacetic acid and potassium thiostearate in ethanol.

## Results and Discussion

**The Spectra of the Solution in Cyclohexane.** —*Thiostearic Acid and Thioacetic Acid.*—The ultraviolet absorption spectrum of thiostearic acid in cyclohexane shows a band with its maximum at 221 mμ (ε, 1800).[5] The shape of the absorption curve is in good accord with that of thioacetic acid measured in cyclohexane by Cunneen.[3] However, at higher concentrations, an inflection was observed in the region 260—290 mμ (see Fig. 1). The ε value at 275 mμ is nearly 40. This low-intensity absorption band in the region 260—290 mμ is not due to impurities, as is proved by the following observations. The thiostearic acid used for the measurement has a purity of more than 99%; the impurities which could not be separated by recrystallization are stearic acid and distearoyl disulfide.[5] Distearoyl disulfide has an absorption in the region 260—290 mμ; $\lambda_{max}$=224 mμ, ε=4260 in cyclohexane (cf. Fig. 2). Distearoyl disulfide (10%) was added to the sample of thiostearic acid, and the ultraviolet absorption spectrum of the mixture in cyclohexane was measured (Fig. 1). The absorption band slightly shifts toward a longer wavelength and is intensified, but the inflection in the region 260—290 mμ is not intensified.

The ultraviolet absorption spectrum of thioacetic acid reported by Cunneen[3] indicated no absorption at 260—290 mμ. However, according to the present authors' measurements, in the ultraviolet absorption spectrum of thioacetic acid in cyclohexane as well (Fig. 2, $\lambda_{max}$=220 mμ, ε=1660), an inflection was observed in the region 260—290 mμ at higher concentrations (ε=24 at 270 mμ).

Koch[4] explained that the absorption band at 220 mμ is undoubtedly associated with the sulfur-carbonyl conjugation (between the non-bonding ($3p^2$) electron pair of the sulfur atom and the π electrons of the carbonyl group), involving contributions from the polar canonical structure*3 I in the excited state. As to the assignment of this band, the authors agree with Koch's opinion. However, the low-intensity absorption (inflection) at a longer wavelength measured by the present authors has never been discussed. The authors suppose that this absorption is an R-band due to the C=O group.

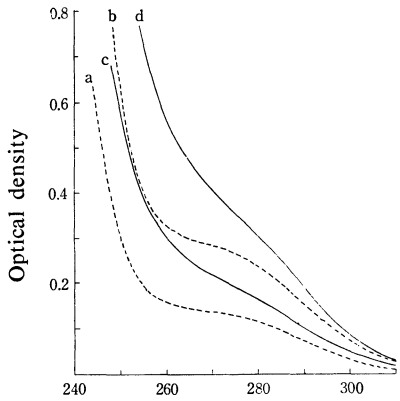



Fig. 1. Ultraviolet absorption spectra in cyclohexane.
Thiostearic acid (- - -): a, 1.0; b, 2.0 g./l. solution.
Thiostearic acid containing distearoyl disulfide (10%) (——): c, 1.0; d, 2.0 g./l. solution

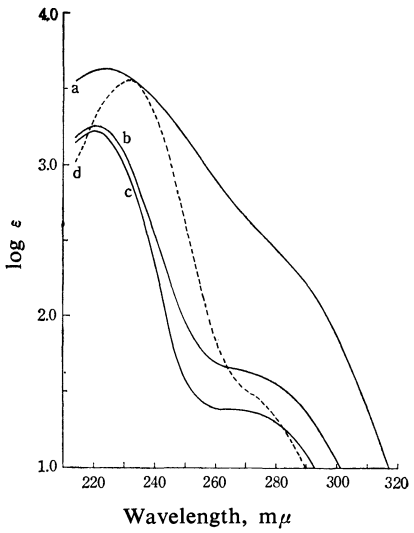
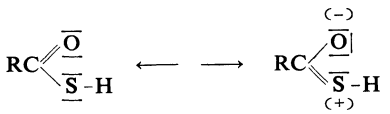



Fig. 2. Ultraviolet absorption spectra in cyclohexane.
a : Distearoyl disulfide
b : Thiostearic acid
c : Thioacetic acid
d : Methyl thiostearate




*3 Electron-diffraction bond-length measurements by Gordy suggest that I makes only a very slight contribution to the ground state of thioacetic acid (W. Gordy, *J. Chem. Phys.*, **14**, 560 (1946)).

*Methyl Thiostearate.*—The ultraviolet absorption spectrum of methyl thiostearate in cyclohexane is shown in Fig. 2 ($\lambda_{max}$=231 m$\mu$, $\varepsilon$=3560). The absorption band at 231 m$\mu$ is undoubtedly associated with the sulfur-carbonyl conjugation. Probably the low-intensity absorption (inflection) at 265—290 m$\mu$ is an R-band due to the C=O group.

**The Spectra of the Solution in Ethanol.**—*Thiostearic Acid and Thioacetic Acid.* — The ultraviolet absorption spectrum of thiostearic acid in ethanol (98 wt.%) is shown in Fig. 3. At lower concentrations, the position and intensity of the absorption band at 223 m$\mu$ remain almost unchanged and a large inflection appears near 250 m$\mu$. In further dilutions, the second absorption maximum (248 m$\mu$) appears; its intensity varies, depending on the concentration (see Table I).

These phenomena were found not only in such higher thio acids as thiostearic acid, but also in thioacetic acid. The ultraviolet absorption spectrum of thioacetic acid in ethanol is shown in Fig. 4. Absorption maxima appear in the regions 218—222 and 248—249 m$\mu$ as is shown in Table I.

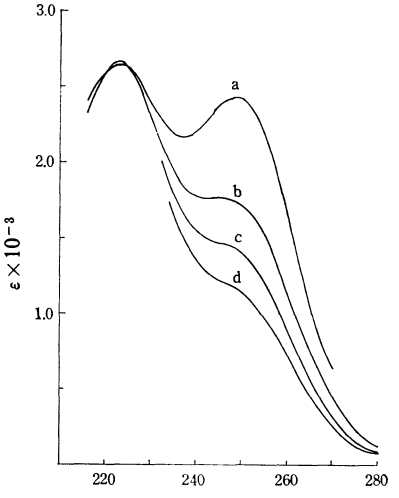



Fig. 3. Ultraviolet absorption spectra of thiostearic acid in ethanol.

Concn.: a : $0.83\times10^{-4}$ mol./l.
b : $1.67\times10^{-4}$ mol./l.
c : $3.33\times10^{-4}$ mol./l.
d : $6.67\times10^{-4}$ mol./l.

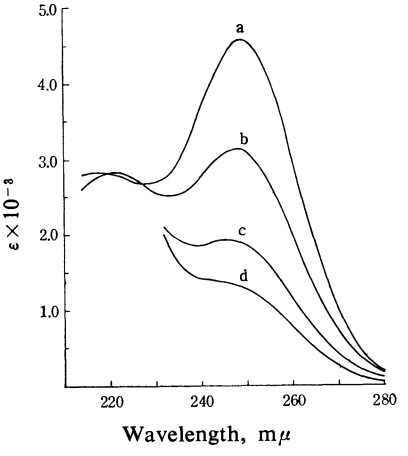



Fig. 4. Ultraviolet absorption spectra of thioacetic acid in ethanol.

Concn.: a : $0.82\times10^{-4}$ mol./l.
b : $1.64\times10^{-4}$ mol./l.
c : $3.29\times10^{-4}$ mol./l.
d : $6.58\times10^{-4}$ mol./l.

TABLE I. DATA OF ULTRAVIOLET ABSORPTION SPECTRA OF THIOSTEARIC ACID AND THIOACETIC ACID IN ETHANOL

| Concentration $10^{-4}$ mol./l. | 1st absorption | | 2nd absorption | |
|---|---|---|---|---|
| | $\lambda_{max}$, m$\mu$ | $\varepsilon$ | $\lambda_{max}$, m$\mu$ | $\varepsilon$ |
| Thiostearic acid | | | | |
| 1.67 | 223 | 2650 | 247 | 1760 |
| 0.83 | 223 | 2640 | 248 | 2440 |
| Thioacetic acid | | | | |
| 1.64 | 221 | 2830 | 248 | 3140 |
| 0.82 | 218 | 2820 | 249 | 4560 |

*Potassium Thiostearate.* — The ultraviolet absorption spectrum of potassium thiostearate in ethanol is shown in Fig. 5. At lower concentrations, only one absorption maximum appears, at 251 m$\mu$ ($c=9.30\times10^{-5}$ mol./l., $\varepsilon$=7610). At higher concentrations, another maximum appears in the region 290—350 m$\mu$.

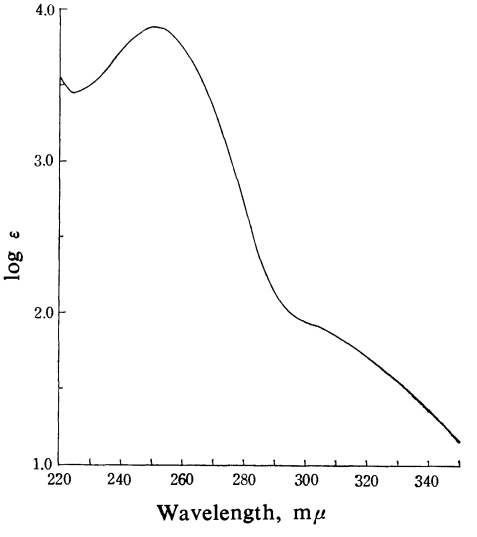



Fig. 5. Ultraviolet absorption spectrum of potassium thiostearate in ethanol.
Concn.: 220—280 m$\mu$, $9.30\times10^{-5}$ mol./l.
280—350 m$\mu$, $3.72\times10^{-3}$ mol./l.

The results obtained above show that in the spectra of thio acids or its salts, which are dissociable to $RC\overset{O}{\underset{S}{<}}(-)$ and $H^+$ or $K^+$, an absorption maximum appears at 250 mμ in ethanol. Furthermore, in the spectra of thiostearic acid and thioacetic acid, the absorption at 250 mμ does not obey Beer's law, but increases in intensity in higher dilutions. In view of thess facts, it may be concluded that, in ethanol, thio acids are partly dissociated to produce the mesomeric anion III, which in turn causes the absorption at 250 mμ. The water content in ethanol probably has a great effect on the dissociation. On the other hand, the absorption at 223 mμ due to undissociated acid (II) obeys Beer's law approximately within the range of measuring concentrations. This behavior of the absorption at 223 mμ would appear to be apparently inconsistent with the above conclusion. This apparent discrepancy can be satisfactorily explained by considering the following two reasons together: first, the degree of the disociation of thio acid in ethanol is very low, so that the decrease in undissociated acid caused by the increasing dilution is very small; secondly, the absorption band at 223 mμ is partially superposed by that of the mesomeric anion, which has a high-intensity absorption at 250 mμ.

Potassium thiostearate is more ionized in ethanol. The anomaly at 290—300 mμ in a higher concentration observed in the spectrum of potassium thiostearate is probably related to the thionic acid form reported by Hantzsch.[2] This problem will be discussed in the future.

$$\left[ RC\overset{\overline{O}}{\underset{\overline{S}\text{-}H}{<}}\ (K) \longleftrightarrow RC\overset{\overline{O}|^{(-)}}{\underset{\overset{(+)}{\overline{S}}\text{-}H}{<}}\ (K) \right]$$

(II)

$$\rightleftarrows RC\overset{O}{\underset{S}{<}}\ (-) + H^+(K^+)$$

(III)

## Experimental

**Ultraviolet Absorption Spectra.** — A Shimadzu quartz spectrophotometer, model QB-50, and a silica cell (1 cm.) were used (measuring temperature 26±1°C).

**Methyl Thiostearate.** — Thiostearic acid (3.5 g.) in absolute ethanol (350 ml.) was neutralized with ethanolic potassium hydroxide. Methyl iodide (15 g.) was added to the above solution, and the mixture was refluxed for 6 hr. and extracted with ether after the ethanol had been distilled off. The ether layer was washed with a diluted potassium carbonate solution and water succesively and dried over anhydrous sodium sulfate, and the ether was distilled off. The residue (yield 3.2 g.) was recrystallized from methanol to give colorless needles (m. p. 50.3—50.8°C) (yield 1.5 g.), which corresponded with the product obtained by Ralston in another way.[6]
(Found: S, 10.14. Calcd. for $C_{19}H_{38}OS$: S, 10.19%).

**Thioacetic Acid.** — Prepared from phosphorus pentasulfide and glacial acetic acid and purified by Kitamura's[7] method (b. p. 88.0—88.5°C).
(Found: S, 41.80 (Kitamura's method). Calcd. for $C_2H_4OS$: S, 42.13%).

*Department of Industrial Chemistry*
*Faculty of Engineering*
*Gifu University*
*Kagamigahara-shi, Gifu*

6) A. W. Ralston, E. W. Segebreckt and S. T. Bauer, *J. Org. Chem.*, 4, 502 (1939).
7) R. Kitamura, *J. Pharm. Soc. Japan* (*Yakugaku Zasshi*), 57, 31 (1937).

# Studies of Thio Acids. IV.[1] Dipole Moments of Methyl Thiostearate, Thiostearic Acid and Thioacetic Acid*1

By Yoshio HIRABAYASHI

(Received May 22, 1964)

The acyl-thiol structure, RCO·SH, of aliphatic thio acids previously studied, e.g., thioacetic acid[2,3] and thiostearic acid,[4] has been confirmed by infrared absorption and other physical data. Furthermore, their molecular structures have been elucidated by the bond-length measurements[5] of electron diffraction. However, no study of the dipole moments of thio acids and their esters has yet been reported.

In this paper, the dipole moments of thiostearic acid, methyl thiostearate, and thioacetic acid (each of which has the thiol form) are measured, and some discussion on their molecular structures will be presented.

## Experimental*2 and Results

**Materials.**—The samples used in the present investigation were prepared according to the procedure previously described and were carefully purified. They are:

Thiostearic acid:[4] m. p. 39.8—40.3°C; neutralisation value 186.0; S, 10.60%.

Methyl thiostearate:[1] m. p. 50.3—50.8°C; S, 10.14%.

Thioacetic acid[1]: b. p. 88.0—88.5°C; S, 41.80%.

All the solvents, *n*-hexane, benzene, and dioxane, used for the measurement of dipole moments were purified according to the methods given in "Organic Solvents."[6]

**Measurement.**—The densities, $d$, and the dielectric constants, $\varepsilon$, of solutions of various concentrations were measured with a picnometer and an apparatus which consists of a fixed-frequency (3 Mc.) crystal oscillator and a variable-frequency oscillator with a cell (ca. 45 pF in capacity) for the measurement of the dielectric constant. The tuning points of the variable-frequency oscillator with the fixed-frequency oscillator were determined by a Lissajous' figure on a cathode-ray oscilloscope. The frequency used for the measurements was 1 Mc., and all measurements were made at 30.0°C.

The specific solute polarization, $p_{2\infty}$, (at an infinite dilution) was calculated by the following

TABLE I. DIPOLE MOMENTS OF METHYL THIOSTEARATE, THIOSTEARIC ACID AND THIOACETIC ACID

| Solvent | $\varepsilon_\infty$ | $d_\infty$ (g./cc.) | $a$ | $b$ (g./cc.) | $p_{2\infty}$ (cc./g.) | $P_{2\infty}$ (cc.) | $\mu$ (D) |
|---|---|---|---|---|---|---|---|
| Methyl thiostearate | | | | | | | |
| H | 1.9059 | 0.6737 | 0.586 | 0.180 | 0.4212 | 132.5 | 1.30 |
| B | 2.2628 | 0.8685 | 0.501 | 0.008 | 0.4331 | 136.2 | 1.37 |
| D | 2.2903 | 1.0228 | 0.532 | −0.188 | 0.4325 | 136.1 | 1.37 |
| Thiostearic acid | | | | | | | |
| H | 1.9057 | 0.6735 | 1.17 | 0.181 | 0.5937 | 178.4 | 2.06 |
| B | 2.2630 | 0.8685 | 1.47 | 0.009 | 0.6170 | 185.4 | 2.14 |
| D | 2.2924 | 1.0229 | 1.82 | −0.189 | 0.6385 | 191.9 | 2.21 |
| Thioacetic acid | | | | | | | |
| H | 1.8920 | 0.6756 | 4.07 | 0.217 | 1.4238 | 109.8 | 2.12 |
| B | 2.2615 | 0.8683 | 6.20 | 0.137 | 1.4666 | 113.1 | 2.16 |
| D | 2.1950 | 1.0220 | 8.66 | 0.058 | 1.7072 | 131.7 | 2.36 |

H: *n*-Hexane, B: Benzene, D: Dioxane

$R'_D$(cc.): Methyl thiostearate, 98.3; Thiostearic acid, 93.4; Thioacetic acid, 19.1

*1 Presented at the Symposium held under the auspices of the Japan Oil Chemists' Society and the Tokai Branch of the Chemical Society of Japan, Nagoya, November, 1960.

1) Part III of this series: Y. Hirabayashi and T. Mazume, This Bulletin, 38, 171 (1965).

2) N. Sheppard, *Trans. Faraday Soc.*, 45, 693 (1949).

3) W. W. Crouch, *J. Am. Chem. Soc.*, 74, 2926 (1952).

4) Y. Hirabayashi, M. Mizuta and T. Mazume, This Bulletin, 37, 1002 (1964).

5) W. Gordy, *J. Chem. Phys.*, 14, 560 (1946).

*2 All melting points and boiling points are uncorrected.

6) A. Weissberger and E. S. Proskauer, "Organic Solvents" (Techniques of Organic Chemistry VII), Interscience Publishers, New York (1955).

formula, derived from Halverstadt-Kumler's method:[7]

$$p_{2\infty}=\frac{\varepsilon_\infty-1}{\varepsilon_\infty+2}\cdot\frac{1}{d_\infty}\left[1+\frac{3a}{(\varepsilon_\infty-1)(\varepsilon_\infty+2)}-\frac{b}{d_\infty}\right]$$
$$\varepsilon=\varepsilon_\infty+aw,\quad d=d_\infty+bw$$

where $\varepsilon_\infty$ and $d_\infty$ are extrapolated values, at the concentration of 0, for $\varepsilon$ and $d$ respectively. The values of $a$ and $b$ are the coefficients of the linear expansion of the dielectric constant and the density of the solution with respect to the weight fraction of the solute, $w$, respectively.

The dipole moment, $\mu$, is then given by the following equation:

$$\mu=0.0128\ [(P_{2\infty}-R'_D)\cdot T]^{1/2}$$

where $P_{2\infty}=M_2\cdot p_{2\infty}$ is the solute molar polarization at an infinite dilution, $M_2$ is the molecular weight of the solute, and $T$ is the absolute temperature. The sum of the electronic ($P_E$) and atomic ($P_A$) polarization was assumed to be equal to the molar refraction, $R'_D$, for the sodium D line calculated by adding the bond refractions[8] of the constituent atoms and bonds.

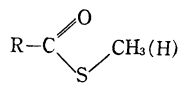
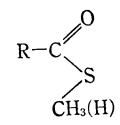
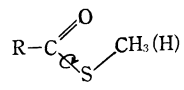
The results are shown in Table I.

## Discussion

The molecular structures of methyl thiostearate, thiostearic acid, and thioacetic acid may now be discussed on the basis of the dipole moments obtained by the above measurements.

Three models for the spacial configurations of thio acids and their methyl esters have been selected and are shown as I, II, and III of Table II. In configurations I and II, the

TABLE II. RESULTANT MOMENTS OF THIO ACID AND ITS ESTER

| Configuration | Resultant moment: Ester | Acid |
|---|---|---|
| I  | $1.1_8$ | $1.6_4$ |
| II  | $3.5_8$ | $2.9_5$ |
| III  | $2.3_4$ | $2.2_9$ |

C–C, C=O, C–S, and S–$C_{CH_3}$ or S–H bonds are all coplanar, and the S–$C_{CH_3}$ or S–H bond is fixed on the same side as the C=O bond in configuration I, while it is on the opposite side in configuration II. Configuration III corresponds to the case of free rotation about the C–S bond (the C–C(=O)–S group being assumed to be coplanar). The moments calculated by using the bond moments derived from the textbook of Smyth[9] and from the following valence angles are given in Table II for each configuration: H–C, 0.4; H–S, 0.68; C–S, 0.9; C=O, 2.3 D; the moment of $C_{17}H_{35}$–C or $CH_3$–C is assumed to be 0.4 D. The valence angles, ∠C–C=O (=125°), ∠C–C–S (=110°), and ∠O=C–S(=125°), are assumed to be the same as those of $CH_3COSH$,[10] and the valence angles, ∠C–S–$C_{CH_3}$(=105°) and ∠C–S–H(=100°), are set equal to the values of R–S–R[11] and R–SH[12] respectively.

**Methyl Thiostearate.**—The dipole moments ($\mu$) measured in the solvents were 1.30 D(H), 1.37 D(B), and 1.37 D(D). The orientation polarization is not very large; the observed values, therefore, depend relatively upon the assumed values of the $P_E+P_A$. When the sum of the $P_E$ and $P_A$ is assumed to be equal to the 1.05 $R'_D$ or 1.10 $R'_D$, the observed values become as follows:

$\mu'$(for 1.05 $R'_D$): 1.21 D(H); 1.28 D(B); 1.28 D(D)

$\mu''$(for 1.10 $R'_D$): 1.10 D(H); 1.18 D(B); 1.18 D(D)

Although these data are still insufficient to enable us to discriminate whether the solvent effect is positive or negative, the order of this effect may be estimated by the following values, which are obtained when a plot of $\mu$, $\mu'$, or $\mu''$ versus $(\varepsilon_\infty-1)^2$, or $(\varepsilon_\infty-1)/(\varepsilon_\infty+2)$ is extrapolated to $\varepsilon_\infty=1$:

For $(\varepsilon_\infty-1)^2$: $\mu_e=1.22$ D, $\mu'_e=1.13$ D, $\mu''_e=1.02$ D

For $(\varepsilon_\infty-1)/(\varepsilon_\infty+2)$: $\mu_{e'}=1.06$ D, $\mu'_{e'}=0.95$ D, $\mu''_{e'}=0.83$ D

As a result, the dipole moment of this molecule is found to be 1.1±0.3 D.

On the other hand, since the induction effect is left out of consideration for the calculated values given in Table II, the moments induced at each bond by the C=O dipole should, of course, be taken into consideration. While

7) I. F. Halverstadt and W. D. Kumler, *J. Am. Chem. Soc.*, **64**, 2988 (1942).
8) A. I. Vogel, W. C. Cresswell, G. H. Jeffery and J. Liecester, *J. Chem. Soc.*, **1952**, 514.
9) C. P. Smyth, "Dielectric Behavior and Structure," McGraw Hill, New York (1955), p. 224.
10) P. W. Allen and L. E. Sutton, *Acta Cryst.*, **3**, 46 (1950); W. Gordy, *J. Chem. Phys.*, **14**, 560 (1946).
11) L. O. Brockway and H. O. Jenkins, *J. Am. Chem. Soc.*, **58**, 2407 (1936).
12) R. W. Kilb, *J. Chem. Phys.*, **23**, 1736 (1955).

the quantitative values of these induced moments are not known at present, the calculated values given in Table II may not be grossly in error (possibly to within 20%) for the moments corresponding to configuration I since an intramolecular compensation of this effect seems to occur; the values for configurations II and III, on the other hand, will become somewhat larger than the values given in Table II, since no intramolecular compensation of this effect seems to occur with them.

On the basis of the above consideration of the observed and the calculated values, configuration I seems to be the most probable of the three possible configurations for methyl thiostearate. Furthermore, though it is still unknown whether or not the S–$C_{CH_3}$ bond is fixed in the  plane in configuration I, it seems reasonable, from a consideration of its resonance structures and of its electrostatic potential, to assume that the S–$C_{CH_3}$ bond is fixed in the  plane as in configuration I.

**Thiostearic Acid and Thioacetic Acid.**—Thiostearic acid is considerably stable and remains almost unchanged in solvents at room temperature. On the other hand, an authentic sample of thioacetic acid is rapidly changed with a decrease in its sulfur content. Even when much care was taken in the treatment of the latter, some change in the quality was inevitable.

The dipole moments measured were 2.06D(H), 2.14 D(B), and 2.21 D(D) for thiostearic acid, and 2.12 D(H), 2.16 D(B), and 2.36 D(D) for thioacetic acid. In carboxylic acids, the dipole moments measured in benzene or hexane have sometimes been different from those in dioxane, and it is known that two molecules of carboxylic acids associate in benzene or hexane by hydrogen bonds.[13] For thio acids, however, the presence of only a slight solvent effect in the observed dipole moments suggests that such association by hydrogen bonds does not take place to any appreciable extent.

In the case of thio acids, for which the orientation polarizations are large, the decreases in the observed values are only 0.1 D for thiostearic acid, and about 0.02 D for thioacetic acid, when the sum of $P_E$ and $P_A$ is assumed to be equal to $1.10\,R'_D$. Furthermore, by a treatment similar to that used in the case of methyl thiostearate, the following values are obtained:

For thiostearic acid: $\mu_e=1.95$ D; $\mu_{e'}=1.82$ D

For thioacetic acid: $\mu_e=1.96$ D; $\mu_{e'}=1.82$ D

The dipole moments are thus found to be $1.9\pm0.2$ D for both molecules.

The obtained values are somewhat too large and too small respectively for the  group to be planar with configurations I and II.

As for the structures of thio acids, either of the following four cases appears reasonable judging from their observed values: A. configuration I; B. a configuration in which the S–H bond is located at a certain angle to the  plane from configuration I;*3 C. the coexistence of configurations I and II; D. configuration III. However, the free rotation (D) is not probable in view of its electrostatic potential and in view of the fact that its resonance structures are similar to those of the ester. The other three structures (A, B, C) may be suitable; it seems difficult at present to determine which of the three is the most reasonable.

## Summary

The dipole moments of methyl thiostearate, thiostearic acid, and thioacetic acid have been measured in *n*-hexane, benzene, and dioxane solutions at 30°C. The values obtained are; methyl thiostearate, $1.3_0$ D (*n*-hexane), $1.3_7$ D (benzene), $1.3_7$ D (dioxane); thiostearic acid, $2.0_6$ D (*n*-hexane), $2.1_4$ D (benzene), $2.2_1$D (dioxane); thioacetic acid, $2.1_2$ D (*n*-hexane), $2.1_6$ D (benzene), $2.3_6$ D (dioxane). On the basis of the above results, a planar configuration similar to the cis configuration of carboxylic ester is considered to be the most probable structure of methyl thiostearate; three probable alternative configurations have been suggested for the structure of thio acid.

The author wishes to express his sincere appreciation to Mr. Kotobuki Watanabe and Mr. Hideo Uchihiro for their assistance in carrying out the experiments. He is also indebted to Dr. Tetsuro Mazume for his invaluable guidance and encouragement.

*Faculty of Engineering*
*Gifu University*
*Kagamigahara-shi, Gifu*

13) G. Briegreb, *Z. physik. Chem.* (*B*), **10**, 205 (1930).

*3 For the configuration in which the S-H bond is fixed on the plane perpendicular to the  plane, the resultant moment should be $2.3_9$D.

# The Near-infrared Absorption Spectra of Lanthanide Chlorides Dissolved in Molten LiCl-NaCl-KCl Eutectic

By Masato MAMIYA

(Received February 26, 1964)

The observation of the absorption spectra of fused metal salt with[1-12] or without[13-15] the addition of a diluent has recently become a powerful means for analyzing or identifying the metallic constituents of the salts.

This investigation is concerned with the determination of molar absorptivities for significant absorption bands from the near-infrared absorption spectra of lanthanide chlorides dissolved in molten alkali chloride eutectic solvents.

A previous report on the spectra of several lanthanide chlorides in a fused LiCl-KCl eutectic solution was limited to the visible and ultraviolet regions.[7] Similar studies in the visible region have been carried out in molten LiF-KF[5,6] and in $LiNO_3$-$KNO_3$ eutectics.[2] Recently, the near-infrared absorption spectra of lanthanides in molten $LiNO_3$-$KNO_3$ eutectic and in a deuterium perchloric acid solution have been observed by Carnall and his associates.[9]

There are, of course, many different fused salt systems in which a spectrophotometric study could be made; most of the work has thus far been done in alkali fluorides, chlorides, nitrates and sulfates. In this paper, the fused LiCl-NaCl-KCl eutectic was used because of the advantage of its optical transparency in the near-infrared region and its relatively low melting point (about 333°C).

Several characteristic absorption bands of praseodymium, neodymium, samarium, dysprosium holmium, erbium, thulium and ytterbium in this medium were observed in the region from 0.8 to 2.6 $\mu$. These near-infrared data will be compared with similar results which have been obtained in molten nitrate[9] and deuterium oxide solutions.[16]

## Experimental

**Apparatus.** — The spectral measurements were made using a Cary recording spectrophotometer, Model 14M, equipped with the high-temperature cell assembly described in a previous report by the present author.[12] The furnace was designed for high temperature investigation in the near-infrared region. Temperature control to ±2°C at 400°C was achieved with an electronic thermocouple control unit on a Chino automatic thermometer, Modell 600, and temperatures were measured with a platinum-platinum rhodium thermocouple (0°C cold junction) placed near the sample. The optical absorption cells used were fused quartz cells with 10.0 and 2.0 mm. light paths.

**Alkali Chlorides Eutectic.** — In most of the reported spectrophotometric studies of solutions of several chloride salts, a LiCl-KCl mixture with a composition close to that of eutectic (about 59 mol.% LiCl m. p. 350°C) has been used. The solvent used in this study was a eutectic mixture of LiCl-NaCl-KCl (49.0 - 17.3 - 33.7 mol.%, m. p. 333°C) which melts at a lower temperature than the above binary mixture.

In order to obtain clear sample solutions, free of oxidation and precipitation products, the eutectic had to be anhydrous. Since water has an appreciable solubility in the eutectic, even at 500°C, it is very difficult to achieve complete dehydration by vacuum fusion alone. Various techniques have been described for preparing anhydrous melts, techniques which involve treatment while dry hydrogen chloride gas is blown in to the molten salts.[3,17] The pure alkali chlorides eutectic pellets were dehydrated and purified by the bubbling method proposed by Gruen and McBeth.[2]

**Sample Preparation.**—The lanthanides used were obtained commercially in the form of oxides with a stated purity higher than 99.0%. The dried

1) D. M. Gruen, *Nature*, **178**, 1181 (1956).
2) D. M. Gruen, *J. Inorg. & Nucl. Chem.*, **4**, 74 (1957).
3) C. R. Boston and G. P. Smith, *J. Phys. Chem.*, **62**, 409 (1958).
4) D. M. Gruen and R. L. McBeth, *J. Inorg. & Nucl. Chem.*, **9**, 290 (1959).
5) J. P. Young and J. C. White, *Anal. Chem.*, **31**, 1658 (1959).
6) J. P. Young and J. C. White, ibid., **32**, 799 (1960).
7) C. V. Banks, M. R. Heusinkveld and J. W. O'Langhlin, ibid., **33**, 1235 (1961).
8) D. M. Gruen and R. L. McBeth, *J. Phys. Chem.*, **66**, 57 (1962).
9) W. T. Carnall, *Anal. Chem.*, **34**, 786 (1962).
10) W. T. Carnall, D. M. Gruen and R. L. McBeth, *J. Phys. Chem.*, **66**, 2159 (1962).
11) W. T. Carnall, ibid., **67**, 1206 (1963).
12) M. Mamiya, *J. Chem. Soc. Japan, Ind. Chem. Sec. (Kogyo Kagaku Zasshi)*, **66**, 1625 (1963).
13) E. Rhodes and A. R. Ubbelohde, *Proc. Faraday Soc.*, **A251**, 156, (1959).
14) G. P. Smith and C. R. Boston, *Discussions Faraday Soc.*, **32**, 14 (1961).
15) B. Cleaver, E. Rhodes and A. R. Ubbelohd, ibid., **32**, 22 (1961).
16) M. Mamiya, *Molecular Structure and Spectroscopy*, **A**, **402**, Tokyo (1962); *Japan Analyst (Bunseki Kagaku)*, **11**, 1262 (1962).
17) B. R. Sundheim and J. Greenberg, *J. Chem. Phys.*, **66**, 1056 (1958).

lanthanide oxides were weighed and then dissolved in a minimum of hydrochloric acid. These solutions were evaporated to dryness by heating them at 200°C for two hours under an atmosphere of flowing nitrogen gas. A weighed amount of the appropriate lanthanide chloride was placed in the spectrophotometer cell with the desired amount of the purified eutectic pellets, and the cell was heated to 400°C under the above conditions.

The lanthanide dissolved when the molten eutectic solution was stirred with bubbles of dry nitrogen gas from a tube inserted in the cell. If water and oxygen remain in the eutectic solvent, lanthanide chloride reacts with these, water, and oxygen to form lanthanide oxychloride, which is not soluble in the molten salt solution. This insoluble matter may, however, be brought into the solution by the addition of a few grams of ammonium chloride. This salt acts as an acid in the chloride melt and dissolves the insoluble lanthanide compound when nitrogen is bubbled at 450°C for 1 to 2 hr.

Figure 1 shows the absorption characteristics of

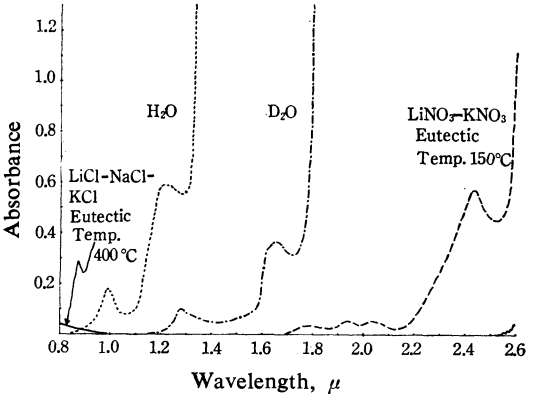



Fig. 1. Absorption characteristics of water, deuterium oxide, $LiNO_3$-$KNO_3$ and LiCl-NaCl-KCl in the near infrared region using quartz cell with 10.0 mm. path length.

the pure LiCl-NaCl-KCl eutectic melt in a 10.0 mm. fused quartz cell for the range between 0.8 and 2.6 $\mu$ at 350°C, together with the absorption characteristics of water, deuterium oxide, and $LiNO_3$-$KNO_3$ eutectic in this range. The pure alkali chloride eutectic mixture has no absorption band, and other solvents absorb strongly in the near-infrared region, but the deuterium oxide and molten alkali nitrate solvents were seen to have a wide range of transparency. The absorption increase in alkali chloride eutectic (shown in Fig. 2) at wavelengths shorter than 1.0 $\mu$ arises from the optical cell etching caused by the impurity in the eutectic salts at temperatures above 600°C, but below 550°C the polished quartz cell was not etched, even after repeated measurements. The effect of temperature on a blank run is not observed at temperatures below 500°C, but at high temperatures, above 550°C the polychromatic radiation from an emitting eutectic medium and furnace is accepted by the signal amplifier, resulting in increased transmittance signals.

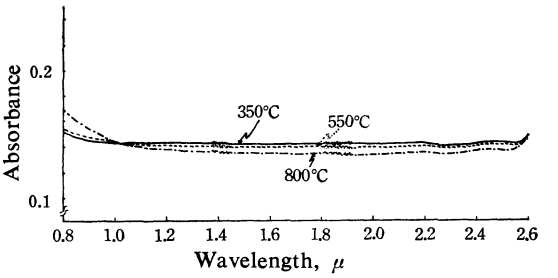



Fig. 2. Absorption base lines of LiCl-NaCl-KCl eutectic at several temperatures.

A correction for emission becomes necessary for wavelengths above approximately 1.0 $\mu$.

The ratio of the energy emitted by the furnace and the sample to that emitted by the light source is given in Plank's equation:

$$E_{\lambda T_1}/E_{\lambda T_2}=(e^{1.43/\lambda T_2}-1)/(e^{1.43/\lambda T_1}-1)$$

where $\lambda$ is the wavelength, $T_1$ the temperature of the light source, and $T_2$ the temperature of the furnace and the sample. This calculated value is not the same as the experimentally determined value.[8] The discrepancy undoubtedly is due to the fact that the assumption of equal emitting values made in Plank's equation is inadequate for this particular experiment.

The correction for radiation from the molten salts solution, cell and furnace at a high temperature was made by the base line method.[2]

The experimental results are plotted in terms of molar absorptivity, $\varepsilon=\log(I_0/I)cd$, where $I_0/I$ is the intensity ratio of the incident to the transmitted light beam, $c$ the molar concentration, and $d$ the light path length. Molar concentrations were calculated from density values of Van Artsdalen and Yaffe who have determined the values for the LiCl, NaCl, KCl and LiCl-KCl eutectics. Their value of 1.69 g. per cubic centimeter at 400°C was used in calculating the molarity of each molten LiCl-NaCl-KCl eutectic.

In each case, the absorption bands of lanthanide in the alkali chloride eutectic was determined by a comparison of the spectra of the sample and of the solvent. Thus, the blank run was measured by recording first the characteristic spectrum of a cell containing the pure eutectic solution vs. air as the reference, and then sample spectra were measured by running the same cell containing the desired concentration of the lanthanide vs. air. All the absorption bands were scanned at speeds commensurate with their sharpness to obtain a reliable value at the position of the absorbance maximum.

## Results and Discussion

The absorption spectra of fourteen lanthanide chlorides, from lanthanum to lutetium (except. promethium), in the molten LiCl-NaCl-KCl eutectic media have been measured at temperatures 400±2°C in the range from 0.8 to 2.6 $\mu$.

Of these, it was found that praseodymium, neodymium, samarium, dysprosium, holmium, thulium and ytterbium each have a characteristic absorption band, as is shown in Figs. 3 to 5. Near-infrared absorption bands of lanthanide ions arise from electronic transitions within the inner shell 4f-configurations, as is the case with their visible and ultraviolet absorption bands, with few exceptions.

Lanthanum and lutetium lie at the extremes of the lanthanide group, the former with no 4f-electrons and the latter with a completed 4f-electron shell. Trivalent ions of neither element showed any characteristic absorption band in the 0.8 to 2.6 $\mu$ range.

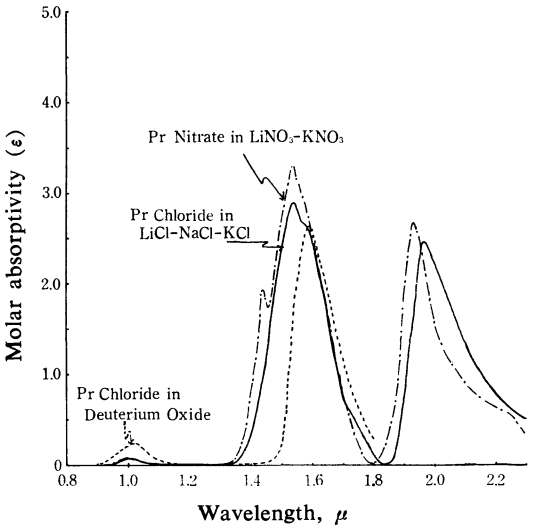



Fig. 3. Absorption spectra of praseodymium in the near-infrared region.

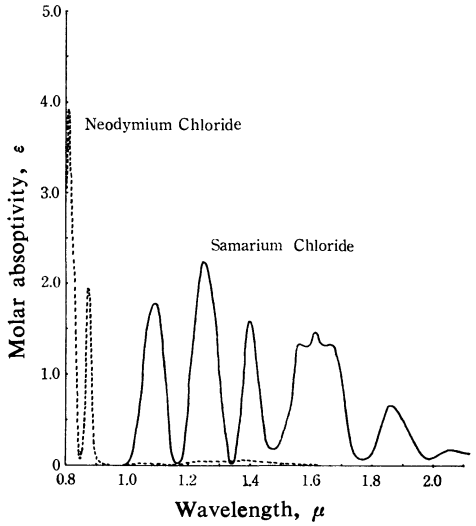



Fig. 4. Absorption spectra of neodymium and samarium chlorides in LiCl-NaCl-KCl eutectic.

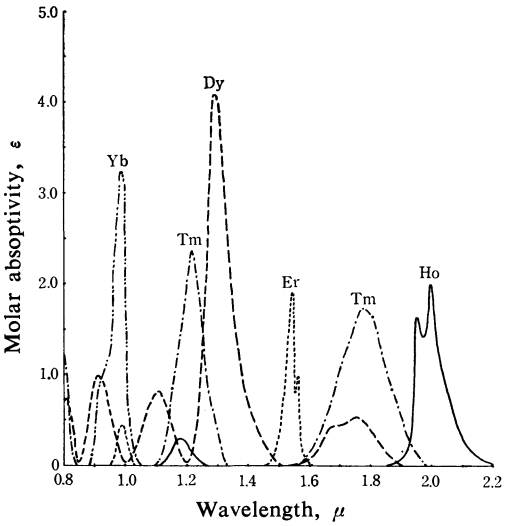



Fig. 5. Absorption spectra of dysprosium, holmium, erbium, thulium and ytterbium in LiCl-NaCl-KCl eutectic.

Trivalent cerium and gadolinium, whose absorption bands are observed only in the ultraviolet[7] and/or infrared regions,[19] have no bands in the wavelength range investigated in this study.

Promethium was excepted from the present experiment because this element is non-existent in natural lanthanide, and the absence of an absorption band in the near-infrared region in molten nitrate and deuterium oxide solutions has been indicated by Carnall[9] and Gruber.[20]

**Praseodymium Chloride.** — The absorption spectra in the near-infrared region of praseodymium chloride in fused LiCl-NaCl-KCl eutectic and of praseodymium ions at 400°C in the alkali chloride eutectic solution resemble the spectra at 150°C in molten nitrate media, in spite of the large differences in temperature and solvent effects. An absorption peak occurring at 1.445 $\mu$ in fused nitrate eutectic has been reported. This peak, however, has not been observed in alkali chloride eutectic and in a deuterium oxide solution. On the basis of these data, it seemed reasonable to assume that this absorption band is the O–H overtone of the water remaining in molten nitrate media as a result of incomplete dehydration.

**Neodymium Chloride.** — The trivalent neodymium ion in the LiCl-NaCl-KCl eutectic has only two absorption maxima, at 0.810 and 0.876 $\mu$, in the near-infrared region. These absorption maxima are quite comparable to

19) R. J. Lang, *Can. J. Res.*, **14**, 127 (1936).
20) J. B. Gruber and J. G. Conway, *J. Inorg. & Nucl. Chem.*, **14**, 303 (1960).

the absorption maxima of neodymium in LiCl-KCl eutectic, at 0.810 and 0.885 $\mu$, which have been reported by Sundheim and Harrington.[21] The effect of different solvents on these absorption bands is small; namely, the similar spectra are obtained in molten nitrate media[9] and in other solvents.[5]

**Samarium Chloride.** — The spectrum of samarium chloride in fused LiCl-NaCl-KCl eutectic is presented in Fig. 4. The wavelengths of the absorption bands below the 1.4 $\mu$ range obtained by the author in aqueous solution are almost the same as those reported by Carnall[9] in alkali nitrates eutectic. The absorption maxima beyond the 1.40 $\mu$ range were found to be located at different wavelengths due to the solvent effect. These absorption bands showed the formation of different species of the complex in each solvent.

**Europium Chloride.**—The europium chloride in molten LiCl-NaCl-KCl eutectic has no absorption peaks in the near-infrared range, and also no absorption band structure is reported in the visible range for europium chloride in fused LiCl-KCl eutectic.[7] However, the characteristic absorption bands of europium in molten nitrate media have been reported; the maximum absorbance was observed at 0.395, 0.465, 2.05 and 2.165 $\mu$ in the visible and near-infrared ranges by Carnall.[9]

In the visible range, the spectra of europium chloride in molten alkali chloride eutectic are similar to the spectra of $Eu^{2+}$ in an aqueous solution.[22] It is reported that $EuCl_2$ can be formed from $EuCl_3$ at about 270°C under an atmosphere of flowing hydrogen gas,[23] since the absorption spectrum obtained in the LiCl-NaCl-KCl eutectic melt may be due at least in part to $EuCl_2$ formed by the practical thermal decomposition of $EuCl_3$ or by reducing matter in the eutectic media. The difference between near-infrared absorption spectra in molten chloride and nitrate solutions is due to the existence of different valency ions and complex species in each solution.

**Terbium Chloride.**—The terbium chloride in fused LiCl-NaCl-KCl eutectic media has no absorption band in the range from 0.8 to 2.6 $\mu$. However, the characteristic absorption bands of terbium in molten nitrate media have been reported; maximum absorbance was observed at 1.837, 1.938 and 2.275 $\mu$ in the near-infrared region by Carnall.[9] The difference between the absorption spectra in the two molten salts solutions is due to the presence of different complex species in each solvent.

**Holmium Chloride.** — The near-infrared absorption spectrum of holmium chloride in the molten alkali chloride eutectic is presented in Fig. 5. The absorption band at 1.18 $\mu$ is identified in various fused salt media and in an aqueous solution. However, the absorption band at about 1.95 $\mu$ was found to be different in molten nitrate and chloride eutectic solvents; thus, the absorption bands have been determined to be located at 1.922 $\mu$ in $LiNO_3$-$KNO_3$ eutectic,[9] whereas, for holmium in LiCl-NaCl-KCl eutectic media, its two absorption peaks occur at 1.959 and 1.996 $\mu$. This discrepancy is due to the different species of complexes in the different molten salts solutions.

**Other Lanthanide Chlorides.**—The near-infrared absorption spectra of dysprosium, erbium, thulium and ytterbium chlorides in fused LiCl-NaCl-KCl eutectic media are presented in Fig. 5. The wavelengths of the maximum absorbances of these lanthanide chlorides in molten alkali chloride eutectic media at 400°C, in fused nitrate media at 150°C and in deuterium oxide solution[16] are substantialy comparable, considering the great differences in measurement conditions.

**Solvent Effect.** — A number of studies have been made concerning chlorocomplexes of metal ions in nitrate melts to which excess chloride ions have been added.[4] This method was here applied to lanthanide, that is, lithium chloride was added to the fused $LiNO_3$-$KNO_3$ eutectic lanthanide nitrates solution until the solution was saturated with the chloride ions. As a result, the author observed only an absorbance decrease on the characteristic absorption band of lanthanide nitrate in the wavelength range investigated. Most of the lanthanide complexes in fused nitrate media react with the chloride ions and water in

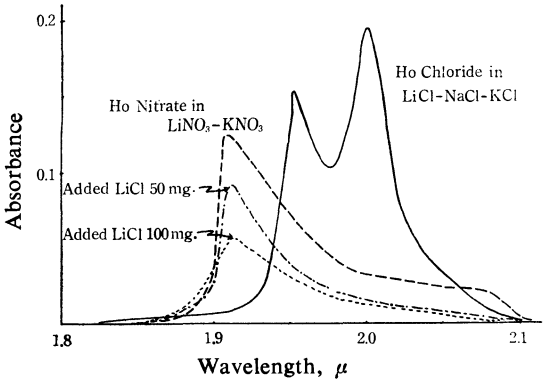



Fig. 6. The change of absorption spectra of holmium ion in $LiNO_3$-$KNO_3$ eutectic at 160°C by addition of several amounts of lithium chloride.

21) B. R. Sundheim and G. Harrington, *U. S. Atomic Energy Comm., Report* NYO-7742, March 9, 1959.
22) F. S. Butement, *Trans. Faraday Soc.*, **44**, 617 (1948).
23) Y. Shibata, "Inorganic Chemistry (Mukikagaku Zensho)," IX-2, Maruzen, Tokyo (1948), p. 685.

solvent to form insoluble compounds, oxychlorides. Thus, the absorbance on characteristic bands of lanthanide nitrate is decreased.

For example, the change in the absorption bands of holmium nitrate in fused $LiNO_3$-$KNO_3$ eutectic media upon the addition of lithium chloride is presented in Fig. 6. Thus, the chlorocomplex of lanthanides in molten nitrate media was not observed by this method. However, several different absorption bands have been observed in various solvents, such as molten nitrate, chloride and deuterium oxide solutions. These solvent effects could be attributed to the presence of different complex species in the various solvents, for the ligand field affects the 4f-electronic energy levels of the lanthanide elements.

**Temperature Effect.** — Most of the peaks of the near-infrared absorption bands of lanthanide chloride in fused LiCl-NaCl-KCl eutectic are slightly shifted to longer wavelengths when the temperature is increased from 400 to 800°C, and at the same time their absorbances decrease. For example, the temperature effect of the absorption bands of holmium chloride in molten alkali chloride media is shown in Fig. 7.

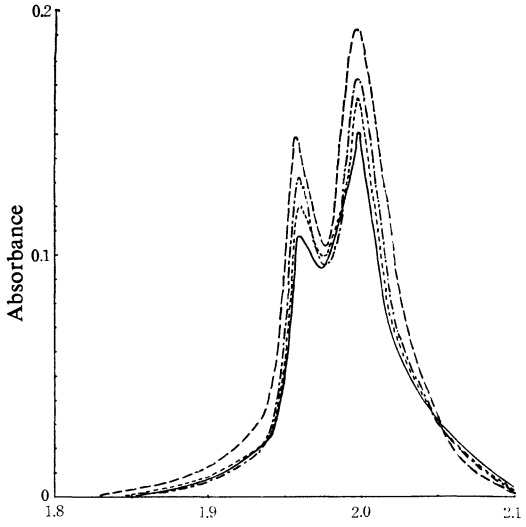



Fig. 7. Absorption spectra of holmium chloride in LiCl-NaCl-KCl eutectic at various temperatures.

| | Temp. | | Temp. |
|---|---|---|---|
| ------ | 400°C | ..... | 660°C |
| —·—· | 530°C | ——— | 800°C |

This observation is not comparable with the fact that in the study of the molten salt spectra absorption peaks have been observed to change with the chang of temperature.[3,12,24]

24) J. R. Morrey, *J. Chem. Phys.*, **66**, 2169 (1962).

Because the shifts of the absorption peaks are too small for the absorption species to be distinguished, the concentration of the lanthanide ions changes as the fluid expands and contracts, and also the absorption bands are broadened at high temperatures. Thus, the temperature effect of lanthanide absorption bands is due to a single absorbing species, the concentration and peak intensity of which change as a function of the temperature. However, in the narrow temperature range of 400±2°C, the temperature effect on the characteristic lanthanide absorption band is negligibly small.

**Analytically Principal Lanthanide Absorption Bands.**—As can be seen from the spectra and

TABLE I. MOLAR ABSORPTIVITIES OF PRINCIPAL LANTHANIDE ABSORPTION BANDS IN VARIOUS SOLVENTS IN THE NEAR-INFRARED REGION

| $D_2O$ or $H_2O$[16] 25°C | | $LiNO_3$-$KNO_3$[9] 150°C | | LiCl-NaCl-KCl 400°C | |
|---|---|---|---|---|---|
| $\mu$ | $\varepsilon$ | $\mu$ | $\varepsilon$ | $\mu$ | $\varepsilon$ |
| | | Pr | | | |
| 0.800 | 5.60 | $0.81_0$ | $3.8_5$ | 0.810 | 3.89 |
| 0.862 | 2.90 | $0.87_0$ | $0.9_5$ | 0.866 | 1.88 |
| — | — | 1.445 | 1.83 | — | — |
| 1.590 | 2.58 | 1.538 | 3.17 | 1.535 | 2.81 |
| | | Nd | | | |
| 0.803 | 5.42 | 0.798 | 3.80 | 0.810 | 3.89 |
| 0.868 | 2.57 | $0.87_0$ | $0.9_5$ | 0.876 | 1.88 |
| | | Sm | | | |
| 1.095 | 2.00 | 1.088 | 1.51 | 1.087 | 1.54 |
| 1.250 | 2.19 | 1.246 | 2.10 | 1.241 | 2.61 |
| 1.385 | 0.55 | 1.385 | 1.32 | 1.390 | 1.67 |
| 1.530 | 0.62 | 1.500 | 1.87 | 1.550 | 1.33 |
| — | — | 1.557 | 1.87 | 1.615 | 1.47 |
| | | Dy | | | |
| 0.810 | 1.50 | $0.80_5$ | $0.7_0$ | 0.803 | 0.69 |
| 0.911 | 2.04 | 0.910 | 1.16 | 0.910 | 0.99 |
| 1.102 | 1.83 | 1.108 | 1.06 | 1.110 | 0.81 |
| 1.300 | 1.24 | 1.290 | 4.20 | 1.290 | 4.07 |
| 1.670 | 0.85 | 1.691 | 1.05 | 1.670 | 0.42 |
| — | — | — | — | 1.750 | 0.52 |
| | | Ho | | | |
| 1.145 | 0.80 | — | — | — | — |
| 1.197 | 0.76 | $1.17_5$ | $0.7_0$ | 1.180 | 0.34 |
| — | — | 1.922 | 1.14 | 1.959 | 1.46 |
| — | — | — | — | 1.996 | 1.56 |
| | | Er | | | |
| 0.980 | 1.02 | $0.98_0$ | $0.6_5$ | 0.985 | 0.50 |
| 1.510 | 1.02 | 1.510 | 1.26 | 1.542 | 1.85 |
| — | — | — | — | 1.560 | 0.93 |
| | | Tm | | | |
| 1.220 | 1.09 | 1.212 | 1.38 | 1.222 | 2.36 |
| 1.720 | 1.13 | 1.740 | 1.79 | 1.775 | 1.72 |
| | | Yb | | | |
| 0.974 | 2.12 | 0.975 | 3.77 | 0.982 | 3.22 |

TABLE II. REPRODUCIBILTY OF SEVERAL ABSORPTION BANDS OF LANTHANIDE CHLORIDES DISSOLVED IN MOLTEN LiCl-NaCl-KCl EUTECTIC AT 400±2°C

| Element | Absorption peak, $\mu$ | Mean. value | Concn. range mg./5 g. | No. of readings | Std. error, % |
|---|---|---|---|---|---|
| Pr | 1.535 | 2.81±0.03 | 50—200 | 4 | 1.0 |
| Sm | 1.241 | 2.61±0.03 | 50—200 | 4 | 1.1 |
| | 1.615 | 1.47±0.04 | 50—200 | 4 | 2.7 |
| Ho | 1.939 | 1.46±0.02 | 50—150 | 3 | 1.4 |
| | 1.996 | 1.56±0.02 | 50—150 | 3 | 1.3 |

molar absorptivities, it would be practical to determine the concentrations of most of lanthanides dissolved in fused salts media by the use of the spectrophotometric technique. The wavelengths and molar absorptivities of the main absorption bands found in the spectra of eight of the lanthanide chlorides in fused LiCl-NaCl-KCl at 400±2°C are presented in Table I, along with the absorbance peaks which have been reported in a deuterium oxide solution and the lanthanide nitrates reported in molten $LiNO_3$-$KNO_3$ media. The reproducibility of all the absorption spectra of these lanthanide chlorides was good, with standard deviations below 3.0% (Table II), and the absorbances of these spectra obeyed Beer's law, indicating that these absorption bands could be used for the quantitative analysis of each lanthanide.

## Summary

Using a high temperature cell for molten salts, a spectrophotometric investigation in the near-infrared region from 0.8 to 2.6 $\mu$ and at temperatures from 400 to 800°C has been carried out with fourteen lanthanide chlorides dissolved in a LiCl-NaCl-KCl mixture of eutectic composition (49.0 - 17.3 - 33.7 mol.%, m. p. 333°C). Praseodymium, neodymium, samarium, dysprosium, holmium, erbium, thulium and ytterbium have characteristic absorption bands in this region. Most of the near-infrared absorption bands of lanthanide chlorocomplexes have been compared to similar spectra obtained in molten nitrate media. However, the several absorption bands have been found to be different in molten nitrate and chloride eutectics. Thus, the absorption bands of europium and terbium have been observed in nitrate, wheras their bands have not been found in chloride, and the absorption bands of praseodymium, samarium and holmium beyond the 1.4 $\mu$ range have been found to be located at different wavelengths. These solvent effects can be attributed to the existence of a different lanthanide complex in each solvent, for the ligand field affects the 4f-electronic energy levels of the above elements.

The absorption peaks of lanthanide ions decrease as the temperature increases, partly due to the change in the concentration of the ions associated with the volume change. However, all the characteristic absorption bands of lanthanide in the near-infrared region have stable molar absorptivities at a constant temperature. These absorption bands can be used for the investigation of chemical constitution and electronic structure, for analysis and for other purposes.

The author wishes to thank Mr. Hiroshi Fukuda for his kind cooperation in this research.

*Goverment Chemical Industrial Research Institute, Tokyo*
*Shibuya-ku, Tokyo*

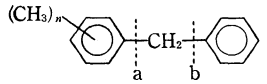
# Studies of Diarylalkanes. III.*[1] The Cleavage of Diarylmethanes under the Influence of Aluminum Chloride

By Otohiko TSUGE and Masashi TASHIRO

(Received March 13, 1964)

In the course of the study of the reaction of diarylalkanes with Friedel-Crafts catalysts, an investigation was carried out in order to find how various diarylmethanes cause cleavage under the catalytic influence of aluminum chloride.

It was reported in the preceding paper[1] that, under the influence of aluminum chloride, while diphenylmethane gives benzene, toluene, methyldiphenylmethane, dimethyldiphenylmethanes and anthracene, methyl-substituted diphenylmethanes give trimethylbenzene and dimethylanthracene beside the above products. It was also found that, in the case of methyldiphenylmethanes (I), the bond a is more easily cleft than the bond b and that the facility of the cleavage of the former is increased by increasing the number of methyl groups at the benzene ring, if the facility of the bond cleavage is estimated by the molar ratio of methylbenzene to the benzene which is formed by the cleavage. In other words, the higher the relative basicity of the methyl-substituted benzene ring in I, the more easily the bond a is cleft.




$n=1,2,3$

(I)

In the present work, the reaction of various diarylmethanes with aluminum chloride was studied in the absence of a solvent or by using excess aromatics as a solvent so that clearer information concerning the effect of the substituent could be obtained on the bond cleavage.

## Results and Discussion

Diphenylmethane (II), 4-methyl- (III), 4-ethyl- (IV), 4-isopropyl- (V), 4-hydroxy- (VI), 2-hydroxy- (VII), 4-methoxy- (VIII), 2-methoxy- (IX), 4-chloro- (X), 4-phenyldiphenylmethane (XI) and 1-benzylnaphthalene (XII) were treated with aluminum chloride under various

TABLE I. REACTION OF EQUIMOLAR AMOUNTS OF 4-ETHYL- (IV), 4-ISOPROPYL- (V) OR 4-CHLORODIPHENYLMETHANE (X) AND ALUMINUM CHLORIDE AT 27°C FOR 2 hr.[a]

| Run | Diphenylmethane | Product[b] | | | | | | |
|---|---|---|---|---|---|---|---|---|
| | | Benzene | Toluene | ArH[c] | ArH/Benzene | DPM[d] | $C_1$-DPM[d] | $C_2$-DPM[d] |
| 1 | IV | 25.02 | 2.75 | 25.82 | 1.03 | 5.78 | 0.90 | 1.79 |
| 2 | V | 22.65 | 4.02 | 19.46 | 0.86 | 5.33 | 0.84 | 5.41 |
| 3 | X | 16.54 | 1.55 | 40.72 | 2.46 | 4.16 | 0.43 | — |

| Run | Diphenylmethane | Product[b] | | | | | |
|---|---|---|---|---|---|---|---|
| | | $C_3$-DPM[d] | Cl-DPM[d] | $Cl_2$-DPM[d] | Anthracene | Unidentified | Residue[e] |
| 1 | IV | — | — | — | — | 13.97 (14)[f] | 47.19 |
| 2 | V | 3.70 | — | — | — | 14.60 (13)[f] | 39.35 |
| 3 | X | — | 14.78 | 3.30 | 1.45 | 1.09 (2)[f] | 36.99 |

a) Method A was applied to the analyses.
b) The amount of each product in this table and others is generally given as the mol. % to the starting material.
c) ArH: Ethyl-, isopropyl- and chlorobenzene are represented in the respective run.
d) DPM, $C_1$-DPM, $C_2$-DPM, $C_3$-DPM, Cl-DPM and $Cl_2$-DPM are represented diphenylmethane, methyl-, dimethyl-, trimethyl-, chloro- and dichlorodiphenylmethane respectively.
e) Weight % to the starting material.
f) Parentheses relate to a number of component.

* Presented in part at the 16th Annual Meeting of the Chemical Society of Japan, Tokyo, April, 1963.

1) Part II: O. Tsuge and M. Tashiro, *The Coal Tar (Koru Taru)*, **14**, 513 (1962).

TABLE II. REACTION OF VARIOUS DIARYLMETHANES WITH ALUMINUM CHLORIDE[a] AND RELATIVE REACTIVITIES OF AROMATIC COMPOUNDS

| Run | Diaryl-methane | Benzene | ArH | | ArH/ Benzene | Relative reactivity (ArH/Benzene) | Residue[b] |
|---|---|---|---|---|---|---|---|
| 4 | IV | 33.3 | 37.1 | Ethylbenzene | 1.11 | 2.42[f] | 35.9 |
| 5 | V | 34.7 | 29.3 | Isopropyl-benzene | 0.84 | 2.22[f] | 43.5 |
| 6 | VI | 17.5 | 25.7 | Phenol | 1.46 | 8.15[g] | 37.5 |
| 7[c] | VI | 30.4 | 71.5 | Phenol | 2.35 | — | 25.5 |
| 8 | VII | 25.8 | 39.8 | Phenol | 1.54 | — | 41.5 |
| 9[c] | VII | 29.1 | 70.9 | Phenol | 2.43 | — | 25.4 |
| 10 | VIII | 26.6 | 39.1[d] | Anisole | 1.45 | 6.77[g] | 45.3 |
| 11 | IX | 22.7 | 38.4[e] | Anisole | 1.69 | — | 33.8 |
| 12 | X | 15.7 | 51.2 | Chlorobenzene | 3.25 | 0.21[g], 0.24[f] | 35.4 |
| 13 | XI | 28.9 | 23.8 | Biphenyl | 0.82 | 3.85[g] | 41.8 |
| 14 | XII | 36.0 | 19.6 | Naphthalene | 0.55 | 16.95[g] | 59.7 |

a) Equimolar amounts of the diarylmethane and aluminum chloride were reacted at 100°C for 1 hr. and method A was used to the analyses.
b) Weight % to the starting material.
c) Three moles of aluminum chloride were used to hydroxydiphenylmethane.
d) Total mol.% of anisole (13.1), phenol (21.4) and cresols (4.6).
e) Total mol.% of anisole (14.3), phenol (17.4) and cresols (6.7).
f) Competitive benzylation by benzyl chloride and aluminum chloride - nitromethane complex (G. A. Olah, S. J. Kuhn and S. H. Flood, *J. Am. Chem. Soc.*, **84**, 1688 (1962)).
g) Competitive benzylation by benzyl chloride and aluminum chloride - nitrobenzene complex (Present work).

conditions and the products were analyzed by a quantitative gas-liquid chromatographic method.

**The Reaction in the Absence of a Solvent.**— The reaction of IV, V and X with aluminum chloride was carried out under conditions similar to those described previously.[1] The results are shown in Table I.

As Table I shows, various unidentified products were obtained from IV or V; hence, it is difficult to give the relative facility of the bond cleavage. The data for nine diarylmethanes (IV—XII) which may imply the approximate relative facility are shown in Table II.

The relative reactivities of the aromatic compounds which showed good agreement with the known order of the relative stabilities of aromatic $\pi$-complexes, toluene>ethylbenzene >propylbenzene,[2] are also listed in Table II. The relative facility of the bond cleavage in I and IV is in accordance with the relative basicities of the two aromatic rings.

In the case of V, however, the bond in the side of benzene exhibited a higher reactivity for the cleavage than the other; this is inconsistent with the relative basicities of benzene and propylbenzene. This discrepancy may be attributed chiefly to the secondary formation of benzene by the dispropotionation of the products, in addition to the formation of unidentified substances.

In the cases of VI, VII, VIII and IX (runs 6—11), the corresponding aromatic compound (phenol or anisole) was formed more than benzene in the corresponding case. The amount of the aromatic compound in the cases of VIII and IX, however, is given as the total mol. % of anisole, phenol and cresols, since the reaction of anisole with aluminum chloride under the same conditions was found to afford anisole, phenol and cresols in 28.0, 56.8 and 15.2 mol. % yields respectively.

As is shown in runs 7 and 9, the more severely the reaction condition was used, the larger the amount of lower boiling compounds formed and the smaller the amount of resinous material. This suggests that the resinous material consisting of a mixture of polybenzyls is partially decomposed to regenerate the corresponding aromatics. This seems to conform with the fact that diphenylmethane is regenerated by heating the mixture of polybenzyl and benzene with a large amount of aluminum chloride.[3]

In spite of the lower basicity of chlorobenzene than benzene, more chlorobenzene than benzene was obtained in the cleavage X, as is shown in runs 3 and 12. Moreover, the amount of unidentified substances was smaller than that in the cases of the alkyl derivatives mentioned above. This seems to be due to the stability of the chlorobenzene formed by the cleavage. When an equimolar

2) G. A. Olah, S. J. Kuhn and S. H. Flood, *J. Am. Chem. Soc.*, **84**, 1688 (1962).

3) "Organic Syntheses," Coll. Vol. II, 232 (1948).

Table III. Reaction of equimolar amounts of several diarylmethanes and aluminum chloride in the presence of solvent (10 mol.) at 70°C for 1 hr.[a]

| Run | Diaryl-methane | Solvent | Product | | | | | | | | |
|---|---|---|---|---|---|---|---|---|---|---|---|
| | | | Benzene | Cl-$C_6H_5$[b] | Naphtha-lene | DPM[b] | Cl-DPM[b] | 1-Bz-N[b] | $Cl_2$-DPM[b] | Anthra-cene | Re-sidue[c] |
| 15 | II | Chloro-benzene | 126.3 | 836.9 | — | 1.2 | 21.8 | — | 15.5 | 28.8 | 16.7 |
| 16 | X | Benzene | 923.9 | 53.7 | — | 66.8 | 7.4 | — | 1.7 | 0.5 | 8.0 |
| 17 | XII | Benzene | 970.5 | — | 56.4 | 60.6 | — | 9.7 | — | +[d] | 18.0 |

a) Method B was used to the analyses.
b) Cl-$C_6H_5$: Chlorobenzene, DPM: Diphenylmethane, Cl-DPM: Chlorodiphenylmethane, 1-Bz-N: 1-Benzylnaphthalene, $Cl_2$-DPM: Dichlorodiphenylmethane.
c) Weight % to the starting diarylmethane.
d) A plus-sign, +, means a trace amount.

amount of chlorobenzene and aluminum chloride was heated at 100°C for 1 hr. only unchanged chlorobenzene was recovered; this finding is also endorsed by Olah and his co-workers,[4] who reported that chlorobenzene was not disproportionated by water-promoted aluminum chloride.

In the cases of XI and XII (runs 13 and 14), less biphenyl and naphthalene, respectively which exhibit a higher basicity than benzene, were formed than benzene.

On the basis of the data mentioned above, it may be considered that the diarylmethanes are divided into two groups which exhibit different tendencies of the bond cleavage.

**The Reaction in the Presence of Excess Aromatic.**—As it may be considered that the resinous material is composed of polybenzyls, it is anticipated that the reaction in the excess benzene derivative will cause a decrease in its formation.

The data for some diarylmethanes which have been treated in excess benzene or chlorobenzene are shown in Table III. As expected, the amount of resinous material decreased definitely in comparison with the data in Table II.

In the reaction of II in excess chlorobenzene (run 15), the II was almost all consumed, and chloro-, dichlorodiphenylmethanes[5] and anthracene were obtained. It was also observed that the amount of benzene increased and that of chlorobenzene decreased. In the similar reactions of X and XII in excess benzene (runs 16 and 17), similar phenomena were observed, where X and XII were consumed and diphenylmethane was formed in yields of 66.8 and 60.8 mol.% respectively.

On the basis of these data, it may be considered that benzyl cation entities were formed as the intermediates in the cleavage process.[6] In run 15, furthermore, more anthracene was formed than in run 16 or 17. This fact may be interpreted as follows. The self-condensation of the benzyl cation to dihydroanthracene, which easily converts to anthracene,[7] can take place to some extent in chlorobenzene, since the attack of the benzyl cation on chlorobenzene is relatively slow as a result of the low basicity of chlorobenzene.

On the other hand, the attack of the benzyl cation on benzene is more predominant than the self-condensation in runs 16 and 17, because the basicity of benzene is higher than that of chlorobenzene.

From the data in runs 15 and 16, also, it seems reasonable to say that a reaction of this kind is reversible.

When 0.1 mol. of aluminum chloride and 20 mol. of benzene derivative were used with the diphenylmethanes, it was also observed that the bond cleavage took place and that only a small percentage of the resinous material was formed.[8] The results in the reactions of III, X, XI and XII in 20 mol. of benzene are shown in Fig. 1.

As is shown in Fig. 1, an incubation which had been reported in the Friedel-Crafts alkylation of aromatics at a low temperature[9,10] was observed, and toluene, chlorobenzene, biphenyl and naphthalene were formed in a ratio of about 5 mol. % to the benzene, respectively. It was also observed that diphenylmethane was invariably formed in a ratio of about 5 mol. % to the benzene in all cases.

4) G. A. Olah, W. S. Tolgyesi and R. E. A. Dear, *J. Org. Chem.*, **27**, 3441 (1962).
5) Dichlorodiphenylmethanes are considered to be a mixture of bis(chlorophenyl)methanes.
6) H. C. Brown and M. Grayson (*J. Am. Chem. Soc.*, **75**, 6285 (1953)) reported that a benzyl cation entity in the Friedel-Crafts benzylation is not an ionized form, such as $C_6H_5\overset{\oplus}{C}H_2$, but a polarized form, $C_6H_5\overset{\oplus}{C}H_2\cdots\overset{\ominus}{A}lCl_4$.
7) R. Scholl and C. Seer, *Ber.*, **54**, 330 (1922).
8) In order to obtain the reproducibiliy of data, a 0.025 molar ratio of water was added to aluminum chloride.
9) T. M. Berry and E. E. Reid, *J. Am. Chem. Soc.*, **49**, 3142 (1927).
10) E. M. Marks, J. M. Almand and E. E. Reid, *J. Org. Chem.*, **9**, 13 (1944).

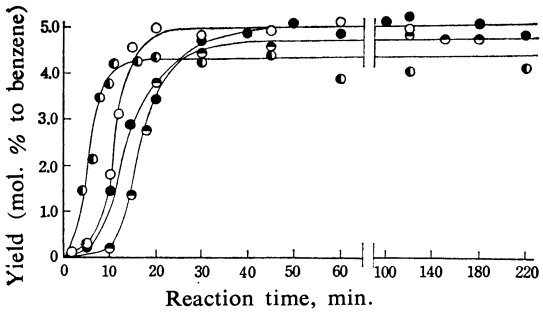



Fig. 1. Formation of the corresponding aromatic compounds by reactions of III, X, XI or XII (1.0 mol. respectively) with aluminum chloride (0.1 mol.) in the presence of benzene (20 mol.) at 50°C.
○ Toluene
● Chlorobenzene
◔ Biphenyl
◐ Naphthalene

On the basis of the apparent formation rates of the corresponding aromatics at the initial stage, the formation rate of chlorobenzene was considerably slower than those of naphthalene, toluene and biphenyl. This order is roughly in agreement with that of the relative basicity of the corresponding aromatic compounds.

In order to evaluate concurrently the effect of the two aromatic rings on the cleavage of the diarylmethane, the reactions of X in excess toluene and of III in excess chlorobenzene were carried out. The results are shown in Fig. 2.

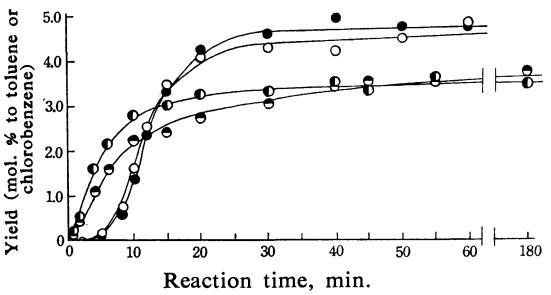



Fig. 2. Reactions of X (1.0 mol.) in toluene (20 mol.) and of III (1.0 mol.) in chlorobenzene (20 mol.) with aluminum chloride (0.1 mol.) at 50°C.
○ Benzene
● Chlorobenzene } in the reaction of X
◔ Benzene
◐ Toluene } in the reaction of III

Contrary to expectation, benzene and chlorobenzene were formed at nearly equal rates, as is shown in Fig. 2. However, the formation rate of toluene at the initial stage was faster than that of benzene. It may be considered that the contrast is due to the different strengths of the basicities of the chlorobenzene and toluene used as solvents.

Consequently, it is considered that the bond cleavage is affected by the basic strength of the benzene derivative which is present in the reaction system as well as by the relative basicities of the two aromatic rings in the diarylmethane.

Further investigation of the point in dispute is in progress; details will be published in the near future.

**Resinous Material.**—As has been mentioned above, the resinous material is composed of a mixture of polybenzyls. The resinous material in several runs was divided into three main fractions: the benzene-insoluble fraction ($F_1$), the benzene-soluble and petroleum ether-insoluble fraction ($F_2$) and the petroleum ether-soluble fraction ($F_3$). In general, $F_1$ was a higher melting black solid (m. p. above 200°C), $F_2$ was an orange-to-reddish brown powder (m. p. 60—100°C) and $F_3$ was an oily brown substance. As no suitable solvent of $F_1$ could be found, its molecular weight was not determined. The degree of the polymerization of $F_2$ and $F_3$ was about 5 to 8, like the polybenzyls, as judged by measuring their molecular weights by the Rast method.

## Experimental

**Materials.**—The diarylmethanes were prepared by the reported method and were purified by fractional distillation and/or recrystallization. Diphenylmethane:[3] b. p. 140—141°C/5 mmHg, m. p. 25°C, retention time (hereafter referred to as R.T.[11]), 4.6 min.

4-Ethyldiphenylmethane:[12] b. p. 121—123°C/2 mmHg, $n_D^{20}$ 1.5707, R.T., 7.0 min. 4-Isopropyldiphenylmethane:[13] b. p. 143—145°C/3 mmHg, $n_D^{20}$ 1.5650, R.T., 9.5 min., 2-Hydroxydiphenylmethane:[14] b. p. 156—159°C/6 mmHg, m. p. 53—54°C, R.T., 8.5 min. 4-Hydroxydiphenylmethane:[15] b. p. 141—143°C/4 mmHg, m. p. 84°C, R. T., 10.5 min. 2-Methoxydiphenylmethane:[14] b. p. 148—152°C/9 mmHg, m. p. 31°C, R.T., 7.6 min. 4-Methoxydiphenylmethane:[15] b. p. 155°C/4 mmHg, $n_D^{20}$ 1.5775, R.T., 9.1 min. 4-Chlorodiphenylmethane:[16] b. p. 130—135°C/3 mmHg, $n_D^{20}$ 1.5885, R.T., 7.9 min. 4-Phenyldiphenylmethane:[17] b. p. 180—188°C/2 mmHg, m. p. 83—84°C, R.T., 43.1 min. 1-Benzylnaphthalene:[17] b. p. 175—179°C/5 mmHg, m. p. 57—58°C, R.T., 22.0 min.

11) Column: 30% High vacuum silicon grease; Column temperature: 235°C; Carrier gas: $H_2$, 22 ml./min.
12) C. Söllscher, *Ber.*, **15**, 1680 (1882).
13) K. Allendorff, ibid., **31**, 1000 (1899).
14) L. Claisen, *Ann.*, **442**, 210 (1925).
15) W. F. Short and M. L. Steward, *J. Chem. Soc.*, **1929**, 555.
16) J. Blackwell and W. J. Hickinbotton, ibid., **1961**, 1405.
17) C. D. Nenitzescu, D. A. Isăcescu and C. N. Ionescu, *Ann.*, **491**, 210 (1931).

Aluminum chloride (reagent grade, of the Wako Pure Chemical Industries, Ltd.) was purified by sublimation.

**Procedure.**—The experiments were carried out in an apparatus similar to one described previously.[1] Aluminum chloride was stirred into the diarylmethane at a constant temperature. After the specified reaction time, the reaction was quenched with dilute hydrochloric acid under ice-cooling.

The quenched product was treated by the following methods according to the individual case.

*Method A.*—When the product was contaminated with a fairly large amount of a resinous material (runs 1 to 14), this method was used. After the quenched product was subjected to steam distillation, the distillate $f_1$ was extracted with ether. The ether solution was washed well with water, dried over sodium sulfate, and analyzed by gas chromatography. The ether-insoluble residue was separated by a distillation into three fractions, the fraction $f_2$ distilling below 150°C (bath temperature), the higher boiling fraction $f_3$ distilling below 240°C (bath temperature)/1—2 mmHg, and the residual fraction. The fractions $f_2$ and $f_3$ were analyzed by gas chromatography.

*Method. B.*—When the amount of a resinous material was relatively small (runs 15 to 17), this method was applied. After being quenched, the reaction mixture was extracted with ether. The ether solution was washed with water to remove traces of acid and dried over sodium sulfate. The solution was divided by a distillation into three fractions, the lower boiling fraction $f_1$, the higher boiling fraction $f_2$, and residual fraction, as above. The distillates $f_1$ and $f_2$ were analyzed by gas chromatography.

*Method C.*—This method was used in the case of a reaction mixture in which a little resinous material was contained (Figs. 1 to 2). After the quenched product had been extracted with ether, the ether solution was washed well with water, dried over sodium sulfate, and immediately analyzed by gas chromatography.

**Analytical Procedure.**—The analyses were carried out by gas-liquid chromatography. The conditions for the gas chromatographic analyses were as follows. For the lower boiling fraction: column, 30% high vacuum silicon grease (HVSG) 2 m., temperature, 150°C, carrier gas, hydrogen, 30 ml./min. For the higher boiling fraction: column, 30% HVSG, 2 m., temperature, 235°C, carrier gas, hydrogen, 22 ml./min.

From the areas of individual peaks, mol. % figures were calculated for each product after determining the relative response data by the internal standard method. Individual peaks were identified by means of the retention times of pure samples.

**The Measurement of Relative Basicity.**—The relative basicities of phenol, anisole, chlorobenzene, biphenyl and naphthalene to benzene were measured by a modification of Olah's method.[2]

Aluminum chloride (0.5 g.) dissolved in 20 ml. of nitrobenzene was vigorously stirred drop by drop into a mixture of benzyl chloride (8.7 mmol.), benzene (113 mmol.) and the corresponding aromatic compound (110 mmol.). After the addition of the aluminum chloride solution, the mixture was stirred at 30°C for another 30 min., and then it was quenched by the usual method. The quenched product was extracted with benzene, and the organic layer was washed well with water, dried over sodium sulfate, and analyzed by gas chromatography. The relative basicities of the corresponding aromatics were calculated by means of the molar ratio of the diarylmethane to diphenylmethane in each individual case.

## Summary

The reaction of several diarylmethanes (III—XII) with aluminum chloride under various conditions has been carried out in order to elucidate the effect of the substituent on the cleavage of diarylmethanes. It has been established that the bond between the aromatic ring and the methylene group is cleft and that the cleavage is affected by the relative basicities of the two aromatic rings in the diarylmethane as well as by the basic strength of the benzene derivative which is present in the reaction system.

The authors wish to thank Miss Akiko Kawano for her technical assistance.

*The Research Institute of Science and Industry*
*Kyushu University*
*Hakozaki, Fukuoka*

# The Reactivity of Hydrogen Atoms of Unsaturated Hydrocarbons in Metathetical Reactions

By Hiroshi KATO, Kenichi FUKUI and Teijiro YONEZAWA

(Received April 28, 1964)

In order to discuss quantum-mechanically the reactivity of the hydrogen atoms of unsaturated compounds in abstraction reactions, the stabilization energy due to $\pi$ conjugation occurring in the structure of the final product, which is calculated by the molecular orbital method, has been employed as a measure of the reactivity.[1] However, no attention has been paid to the behavior of the $\sigma$ electrons of the unsaturated compounds which must play the main part in these reactions. The present authors have previously proposed a new reactivity index—delocalizability, $D_r$—which has proved to be a satisfactory one for metathetical reactions of saturated hydrocarbons.[2] In the present paper, we will treat the $\sigma$ electronic system in various unsaturated hydrocarbons, such as olefins, alkylbenzenes and acetylenes, by the same method as that used in our previous paper[3] in order to show the calculated values of $D_r^{(R)}$ (delocalizability for radical reaction) at each hydrogen atom in these compounds. The results display a good correlation with experience and generally explain the high reactivity of $\alpha$ hydrogen atoms in unsaturated hydrocarbons.

## Theoretical

As has already been shown, the $\sigma$ electronic structure in unsaturated compounds is investigated by the LCAO MO method, taking only $\sigma$-electrons explicitly into consideration. Accordingly, the molecular orbitals in these molecules are represented by a linear combination of hydrogen 1s orbitals and carbon hybridized orbitals.

The values of the parameters used in the present paper are summarized as follows:

Coulomb integrals

$C(sp^3)$ : $\alpha$ $C(sp^2)$ : $\alpha+0.1\beta$

$C(sp)$ : $\alpha+0.2\beta$ H: $\alpha-0.2\beta$

resonance integrals

a) between adjacent carbon atoms:

$C(sp^3)$–$C(sp^3)$ : $\beta$ $C(sp^2)$–$C(sp^2)$ : $1.2\beta$

$C(sp)$–$C(sp)$ : $1.3\beta$ $C(sp^3)$–$C(sp^2)$ : $\beta$

$C(sp^3)$–$C(sp)$ : $1.1\beta$

b) between carbon and hydrogen atoms:

$C(sp^3)$–H: $1.1\beta$ $C(sp^2)$–H: $1.1\beta$

$C(sp)$–H: $1.2\beta$

c) between two orbitals in the same carbon atom:

$C(sp^3)$–$C(sp^3)$ : $0.34\beta$ $C(sp^2)$–$C(sp^2)$ : $0.40\beta$

$C(sp)$–$C(sp)$ : $0.70\beta$

where $\alpha$ and $\beta$ denote the Coulomb integral of an $sp^3$ carbon atom and the resonance integral between two $sp^3$ hybridized orbitals at the C–C $\sigma$ bond respectively.* This parameter system is convenient for comparing the value of the $D_r^{(R)}$ of unsaturated compounds with those of saturated compounds which have already been calculated.[2]

The reactivity index referred to as the delocalizability for the radical reaction, $D_r^{(R)}$, may then be given as:

$$D_r^{(R)}=\sum_i^{occ}\frac{(C_r^i)^2}{\lambda_i}+\sum_j^{unocc}\frac{(C_r^j)^2}{-\lambda_j}$$

where $C_r^i$ is the coefficient of the $r$th $\sigma$ orbital in the $i$th MO and $\lambda_i$ is given by $\varepsilon_i=\alpha+\lambda_i\beta$, in which $\varepsilon_i$ is the energy of $i$th MO.

## Results and Discussion

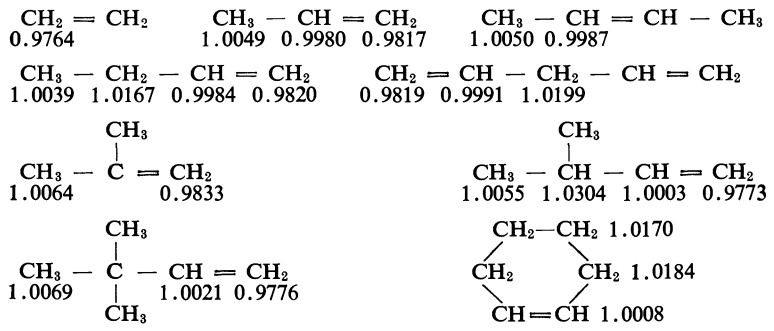
The calculated $D_r^{(R)}$ values of the hydrogen atoms in various unsaturated hydrocarbons are given in Figs. 1a, b, c and d. In Fig. 2 the calculated $D_r^{(R)}$ values of hydrogen atoms are plotted according to their grouping. A detailed discussion with regard to the variation in the $D_r^{(R)}$ in each group will be given in the following sections. As a general trend, it can be pointed out that the reactivity of a hydrogen atom bonded to an $sp^3$ carbon atom will be larger than that of hydrogen atoms attached to an $sp^2$ or sp carbon atom, and also larger than that of the same kind

1) E. g. G. W. Wheland, *J. Am. Chem. Soc.*, **63**, 2025 (1941); C. A. Coulson, *Discussions Faraday Soc.*, **2**, 9 (1947); A. Streitwieser, Jr., "Molecular Orbital Theory for Organic Chemists," John Wiley, N. Y. (1961).

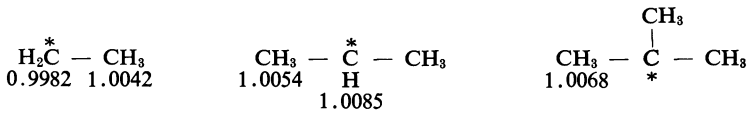
2) K. Fukui, H. Kato and T. Yonezawa, This Bulletin, **34**, 1111 (1961).

3) K. Fukui, H. Kato, T. Yonezawa, K. Morokuma, A. Imamura and C. Nagata, ibid., **35**, 38 (1962).

* In Ref. 3 we adopted a parameter system which was based on the $sp^2$ carbon atom, whereas in the present paper the system is based on the $sp^3$ carbon atom. No essential difference exists between these two parameter systems.

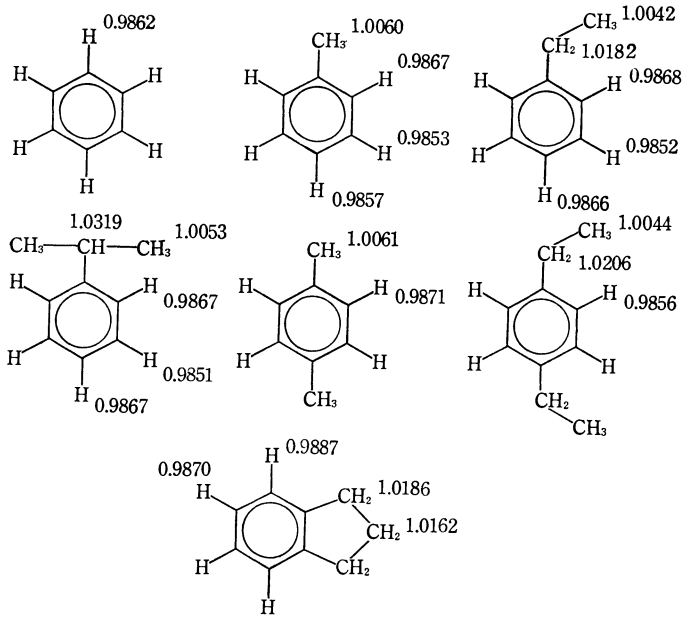



(a) Olefins

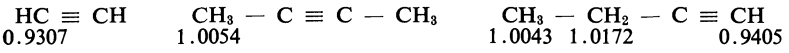



* C: $sp^2$ carbon atom

(b) Alkyl ions and radicals




(c) Alkylbenzenes




(d) Acetylenes

Fig. 1. The calculated values of $D_r^{(R)}$ of the H atoms in various unsaturated hydrocarbons.

(that is, primary, secondary or tertiary) in saturated hydrocarbons.

In particular, the large reactivity of hydrogen atoms in the $\alpha$-methylenic group is interpreted by $D_r^{(R)}$ values, for instance, in cyclohexenene and indane molecules.

**Olefins.**—The calculated $D_r^{(R)}$ values of hydrogen atoms in several olefinic compounds are summarized in Fig. 1a. The value of $D_r^{(R)}$ falls in a definite range for each type of hydrogen atom; the average $D_r^{(R)}$ value of hydrogen atoms of the same type, that is, of each primary, secondary and tertiary hydrogens, is compared in Table I with the rate

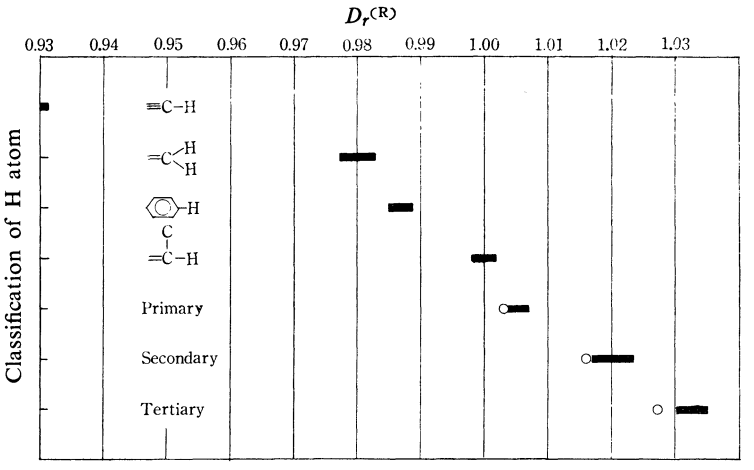



Fig. 2. The value of $D_r^{(R)}$ and the kind of hydrogen atoms.
■ : in unsaturated compounds
○ : in saturated compounds (average)

TABLE I. CHANGE OF AVERAGE OF $D_r^{(R)}$ AND OBSERVED RATE CONSTANTS ACCORDING TO THE TYPE OF THE HYDROGEN ATOM IN HYDROCARBONS

| Type of H atom | $D_r^{(R)}$ | | $k\times10^{-6}$ per atom at 182°C toward $CH_3$ radical[4] mol$^{-1}$ cc. sec$^{-1}$ | |
|---|---|---|---|---|
| | Olefins | Paraffins[2] | Olefins | Paraffins |
| Primary hydrogen | 1.006 | 1.003 | 5 | 0.3 |
| Secondary hydrogen | 1.017 | 1.016 | 17 | 2.1 |
| Tertiary hydrogen | 1.030 | 1.027 | 53 | 15 |

TABLE II. THE CALCULATED $D_r^{(R)}$ VALUES AND THE EXPERIMENTAL ACTIVATION ENERGIES AND REACTIVITIES IN $\alpha$ HYDROGEN ATOMS IN OLEFINIC HYDROCARBONS

| Compound | $D_r^{(R)}$ | Activation energy[a] kcal./mol. | | Reactivity per $\alpha$-hydrogen atom |
|---|---|---|---|---|
| | | Ref. 4 | Ref. 5* | Ref. 4 |
| $CH_2:CH_2$ | 0.9764 | 10.0 | — | 1.4 |
| $CH_3CH:CH_2$ | 1.0049 | 7.7 | 13.5[a] | 8 |
| $CH_3CH:CHCH_3$ | 1.0050 | 7.7 | — | 10 |
| $(CH_3)_2C:CH_2$ | 1.0064 | 7.3 | — | 8 |
| $(CH_3)_3CCH:CH_2$ | 1.0069 | — | — | — |
| $CH_3CH_2CH:CH_2$ | 1.0167 | 7.6 | 11.5[a] | 33 |
|  | 1.0184 | — | 9.5[a] | — |
| $(CH_3)_2CHCH:CH_2$ | 1.0304 | 7.4 | 8.1[b] | 102 |

* These values correspond to the average of the hydrogen atom with similar circumstances.
a) The attacking reagent is the $CH_3$ radical in Ref. 4 and olefinic peroxy radicals in Ref. 5.

constants characteristic of various types of hydrogen atoms in metathetical reaction by means of the methyl radical.[4] A parallelism is observed between these two and the calculated values of olefins are on an average larger than those of corresponding paraffins, although the differences between them are rather smaller than expected and the calculated orders of reactivity between the different types of hydrogen atoms in unsaturated and saturated hydrocarbons are inconsistent with the observed values. These discrepancies may result from the neglect of $\pi$ conjugation energies.

In Fig. 1a, the $D_r^{(R)}$ values of $\alpha$ methylenes in 1-butene, 1,4-pentadiene and cyclohexene are large, obviously corresponding to the large reactivities. That is, in cyclohexene the $D_r^{(R)}$

4) A. F. Trotman-Dickenson, *Quart. Revs.*, **7**, 198 (1953); A. F. Trotman-Dickenson and E. W. R. Steacie, *J. Chem. Phys.*, **19**, 329 (1951).

of the $\alpha$-hydrogen atom is 1.0184, while at the $\beta$-hydrogen atom it is 1.0170. In 1, 4-pentadiene, the hydrogen atom of the methylene has a value of 1.0199, which is larger than that of the average of methylenes in paraffins (ca. 1.016).

These $D_r^{(R)}$ values of hydrogen atoms on $\alpha$ carbon atoms in several olefinic molecules are listed in Table II, together with the observed activation energies[4,5] and experimental reactivities[4] in hydrogen abstraction reactions. (In Ref. 4, the values were obtained in the reactions with the methyl radical, and in Ref. 5, the values in the autoxidation reactions with benzoyl peroxide as an initiator were estimated by assuming frequency factors to be constant for all reactants). We can remark with a certain reservation that there is an apparent parallelism between calculated and observed values, since Trotman-Dickenson has pointed out that the rate in these type reactions does not depend on the magnitudes of the activation energy, but on that of frequency factor.[4] This point should be reinvestigated by future calculations and experiments.

**Alkyl Ions and Radicals.**—For the sake of comparison, calculated values of $D_r^{(R)}$ in some alkyl ion or radicals* are indicated in Fig. 1b. It is of interest to see that the reactivity of hydrogen atoms bonded to an $sp^3$ carbon atom is larger than that of the hydrogen atoms of an $sp^2$ carbon atom which had the same circumstances in a parent molecule. In this way, the change in the hybridization of a carbon atom from $sp^3$ to $sp^2$ causes a deactivation of the hydrogen atoms attached to this carbon atom and a simultaneous slight activation of the hydrogen atoms in other parts of the molecule.

**Alkylbenzenes.**—The calculation with respect to several alkylbenzenes was also made; the results are shown in Fig. 1c. The reactivity of $\alpha$ hydrogen atoms may be clearly recognized. For instance, in the indane molecule, the $D_r^{(R)}$ value of the $\alpha$ hydrogen atom is 1.0186 and that of the $\beta$ hydrogen atom is 1.0162, while it is about 0.99 at the hydrogen atoms on the benzene ring. Similarly, in ethylbenzene the value at the methylene group is 1.0184. These values correspond to the largest one among those of different positions in each hydrocarbon of this sort; such an order of magnitude is larger than that of the hydrogen atoms of the corresponding class (that is, primary, secondary or tertiary) in saturated hydrocarbons.

5) a) L. Bateman, *Quart. Revs.*, **8**, 147 (1954); b) J. L. Bolland, ibid., **3**, 1 (1948).

* If we neglect the behavior of $\pi$ electrons, the $\sigma$ electronic states of the ion and the radical are identical for the first approximation.

TABLE III. THE VALUES OF $D_r^{(R)}$ AND THE EXPERIMENTAL REACTIVITY OF $\alpha$-HYDROGEN TOWARD THE $CCl_3$ RADICAL IN VARIOUS ALKYLBENZENES

| Compound | Type of H atom | $D_r^{(R)}$ | Relative[6] rate per $\alpha$-hydrogen atom $k$ |
|---|---|---|---|
| Benzene | — | 0.9862 | — |
| Toluene | prim. | 1.0060 | 0.080 |
| *p*-Xylene | prim. | 1.0061 | 0.090 |
| Ethylbenzene | sec. | 1.0184 | 0.37 |
| Indan | sec. | 1.0186 | 0.57 |
| Diphenylmethane | sec. | 1.0231 | 0.958 |
| Isopropylbenzene | tert. | 1.0319 | 1.00 |
| Triphenylmethane | tert. | 1.0450 | 4.00 |

In Table III the $D_r^{(R)}$ values of $\alpha$ hydrogen atoms in these compounds are listed, together with the relative rates per hydrogen atom as summarized by Russell[6] in the hydrogen abstraction reaction. The parallelism between the calculated theoretical indices, $D_r^{(R)}$, and the experimental indices is almost sufficient. However, Russell and Desmond[7] recently pointed out that diphenylmethane is less reactive than ethylbenzene in reaction with the chlorine atom and with the bromine atom. This result seems to be inconsistent with the result indicated in Table III. This discrepancy will be discussed in the last part of the present paper.

**Acetylenic Compounds.**—Figure 1d illustrates some acetylenic compounds with their $D_r^{(R)}$. The acetylene hydrogen atom is the least reactive of the common hydrocarbon molecules. The hydrogen atoms in the methyl and methylene groups of alkyl derivatives of acetylene are in general more reactive than the corresponding atoms in saturated hydrocarbons, according to our calculation. The $D_r^{(R)}$ values of $\alpha$ hydrogen atoms in alkyl acetylenes are given in Table IV, together with the observed activation energies and reactivities obtained by Trotman-Dickenson.[4] The calculated reactivity is not parallel with the observed activation energy with respect to ethylacetylene and

TABLE IV. THE VALUE OF $D_r^{(R)}$ AND OBSERVED ACTIVATION ENERGY AND REACTIVITY OF $\alpha$-HYDROGEN ATOM IN SOME ALKYL ACETYLENES

| Compound | $D_r^{(R)}$ | Activation[4] energy kcal./mol. | Reactivity[4] toward $CH_3$ radical |
|---|---|---|---|
| $CH{\equiv}CH$ | 0.9307 | — | — |
| $CH_3C{\equiv}CCH_3$ | 1.0054 | 8.6 | 11 |
| $CH_3CH_2C{\equiv}CH$ | 1.0172 | 9.1 | 33 |

6) G. A. Russell, *J. Am. Chem. Soc.*, **78**, 1047 (1956).

7) G. A. Russell and K. M. Desmond, ibid., **85**, 365 (1963).

dimethylacetylene. However, it agrees with the observed reactivity as defined by Trotman-Dickenson.[4]

As has been described in preceding sections, a good parallelism is observed, with some exceptions, between the calculated magnitude of $D_r^{(R)}$ and the experimental reactivity in hydrogen abstraction reactions. However, we should not neglect the following problems, which have to be taken into account before accepting the theoretical results mentioned above as being of significance. One of these problems is: which is the more essential index in this type of reaction, the delocalizability, derived by considering the $\sigma$ type transition state, or the $\pi$ conjugation energy in the radical species formed as the result of a hydrogen abstraction.

The answer of this question may be dependent upon the model for the transition state. That is, in the scheme:

$$\mathrm{R:H} + \mathrm{X}\cdot \rightarrow \mathrm{R:H\cdot X} \rightarrow$$
(I)
$$\mathrm{R\cdot H:X} \rightarrow \mathrm{R}\cdot + \mathrm{H:X}$$
(II)

if model I happens to correspond to the actual transition state, the reactivity will be represented by $D_r^{(R)}$, whereas, for the transition state represented by model II, the $\pi$ conjugation energy will become a better index. Fortunately, the orders of reactivity predicted by these two indecies are almost parallel with each other in simple unsaturated hydrocarbons.[1]

The next problem is that an attacking radical which will bring about a large polarization to hydrocarbon molecules in its approach may yield a different order of reactivity from such a nonpolar radical as an alkyl radical.[6-8] This polar effect is explained by the procedure mentioned in our previous paper.[9] In deriving the index, $D_r^{(R)}$, the Coulomb energy of the orbital of an attacking reagent was assumed to be equal to that of the $sp^3$ hybridized orbital of the carbon atom. However, for polarizing radicals like chlorine and bromine this assumption has to be changed. We remember that in our previous paper[2] the Coulomb energies of chlorine and bromine atoms were taken as $\alpha+0.5\beta$ and $\alpha+0.45\beta$ respectively. We use these values, so that $D_r^{(R)}$ is given by the following equation:

$$D_r^{(R)}(\lambda_a) = \sum_i^{\mathrm{occ}} \frac{(C_r^i)^2}{\lambda_i-\lambda_a} + \sum_j^{\mathrm{unocc}} \frac{(C_r^j)^2}{-\lambda_j+\lambda_a}$$
$$= \frac{1}{2} D_r^{(E)}(\lambda_a) + \frac{1}{2} D_r^{(N)}(\lambda_a)$$

in which $\lambda_a$ is the coefficient in the Coulomb energy of the attacking reagent orbital, $\alpha+\lambda_a$, and $D_r^{(E)}$ and $D_r^{(N)}$ denote the delocalizability for the electrophilic attack and for the nucleophilic attack, respectively. For an electronegative reagent, the sign of $\lambda_a$ will be positive. In this way, with the electronegative reagent orbital, the magnitude of $D_r^{(E)}$ increases and at the same time that of $D_r^{(N)}$ decreases. That is, an electronegative reagent shows a more electrophilic character than otherwise in the reaction, thus changing the reactivity. For instance, the $D_r^{(E)}$, $D_r^{(N)}$ and $D_r^{(R)}$ values of the $\alpha$ hydrogen atom are 1.0288, 1.0080 and 1.0184 respectively in ethylbenzene, and 1.0178, 1.0284 and 1.0231 respectively in diphenylmethane. Hence, if the electrophilic character of the reaction is larger, the reactivity may be in the order; ethylbenzene>diphenylmethane, which was observed in the experiment of Russell and Desmond.[7],*

The numerical calculation has been carried out on the digital computer, KDC-I, of Kyoto University.

*Faculty of Engineering*
*Kyoto University*
*Sakyo-ku, Kyoto*

8) J. M. Tedder, *Quart. Revs.*, **14**, 336 (1960).
9) K. Morokuma, H. Kato and K. Fukui, This Bulletin, **36**, 542 (1963).

* The orders of magnitude of $D_r^{(N)}$ and $D_r^{(E)}$ are parallel with that of $D_r^{(R)}$ in olefinic compounds, and so the reactivity orders obtained by the above treatment do not vary from the order given in Table II.

# The Kinetics of the Phosphate-catalyzed Epoxidation of Styrenes with a Mixture of Nitrile and Hydrogen Peroxide*

By Yoshiro OGATA and Yasuhiko SAWAKI

(Received April 30, 1964)

The reaction of benzonitrile with alkaline hydrogen peroxide has been found to proceed by way of peroxycarboimidic acid (I) :[1]

$$RCN+OOH^- \xrightarrow[\text{slow}]{} R\text{-}\underset{\underset{OOH}{|}}{C}=N^-$$

$$\xrightarrow[\text{fast}]{H_2O} \underset{\underset{OOH}{|}}{RC}=NH+OH^- \qquad (1)$$

(I)

$$(I)+H_2O_2 \xrightarrow[\text{fast}]{} RCONH_2+O_2+H_2O \qquad (2)$$

Peroxycarboimidic acid can oxidize such other substrates as olefins,[2] and it is a favorable oxidant which acts under milder and alkaline conditions and avoids the Baeyer-Villiger reaction,[3] although the oxidation must be done under the controlled pH value (ca. 8).

The present authors have discovered that an aqueous methanolic mixture of nitriles and hydrogen peroxide can oxidize styrene in the presence of alkaline phosphate, giving a high yield (above 95%) of epoxide according to this stoichiometric equation[4]:

$$RCN+H_2O_2+C_6H_5CH=CH_2$$

$$\xrightarrow{HPO_4^{2-}} RCONH_2+C_6H_5\underset{\underset{O}{\diagdown\diagup}}{CH}\text{-}CH_2 \qquad (3)$$

The present paper summarizes the kinetic data which treats the effect of basicity of the reaction media and of substituent effects in benzonitrile and styrene. A probable mechanism is postulated from these data. The reaction of nitriles with hydrogen peroxide in the presence of borate was also studied to compare with the case of phosphate.

## Experimental

**Materials.**—Commercial benzonitrile, acetonitrile and styrene were purified by fractional distillations, b. p. 190°C, 83°C and 58°C (35 mmHg), respectively. Substituted benzonitriles were synthesized from the corresponding anilines:[5] *p*-tolunitrile, b. p. 107—110°C (23 mmHg); *p*-anisnitrile was recrystallized from ethanol, m. p. 60°C; *p*-chloro- and *p*-nitrobenzonitrile were purified by recrystallization from ethanol, m. p. 93°C and 140°C, respectively. Substituted styrenes were prepared by the dehydration of phenylmethylcarbinols[6] obtained from the corresponding acetophenones[7]: *p*-chlorostyrene, b. p. 54—55°C (3 mmHg); *p*-methylstyrene, b. p. 43—44 (5 mmHg); *m*-nitrostyrene, b. p. 100—103°C (5 mmHg).

Hydrogen peroxide, phosphate and other inorganic reagents were all of guaranteed grade. Commercial methanol was used without further purification, since no appreciable difference in the rates was found between purified methanol and the commercial one.

**The Analytical Method.**—Hydrogen peroxide was analyzed iodometrically, 10 ml. of a reaction mixture was added to 30 ml. of ca. 0.1 N aqueous sulfuric acid containing 0.2—0.3 g. of potassium iodide, and the mixture was titrated with 0.1 N aqueous sodium thiosulfate immediately after the addition of three drops of a 1% sodium molybdate solution, thus avoiding the reaction of iodine with styrene. Neither nitriles nor styrenes interfered with the analysis.

The concentration of styrene oxide produced was determined by adding a 10 ml. aliquot to aqueous saturated sodium chloride (40 ml.) in a separatory funnel, extracting it with three 10 ml. portions of chloroform. The organic layer was washed three times with water and dried with anhydrous sodium sulfate. Then the oxirane oxygen content was determined by the pyridinium chloride-chloroform method.[8] This method gave 90.0±1.0% of the recovery of styrene oxide and was not interfered with the presence of nitriles and styrene. The estimation of styrene oxide was corrected by the above value.

**A Typical Procedure for Rate Measurement.**—A 75% (v/v) methanolic solution containing nitrile and styrene of a known concentration was buffered by the addition of potassium dihydrogen phosphate-sodium hydroxide and then thermostated in a brown flask. The epoxidation was started by adding a thermostated solution of hydrogen peroxide of the desired concentration. Aliquots were taken out at appropriate intervals, and the remaining

* Contribution No. 62.

1) K. B. Wiberg, *J. Am. Chem. Soc.*, 75, 3961 (1953).
2) G. B. Payne, P. H. Deming and P. H. Williams, *J. Org. Chem.*, 26, 659 (1961).
3) G. B. Payne, *Tetrahedron*, 18, 763 (1962).
4) Y. Ogata and Y. Sawaki, ibid., 20, 2063 (1964).
5) H. T. Clarke and R. R. Read, "Organic Syntheses," Coll. Vol. I, 514 (1948).
6) C. G. Overberger and J. H. Saunders, ibid., Coll. Vol. II, 204 (1948).
7) Y. Ishii and Y. Inamoto, *J. Chem. Soc. Japan, Ind. Chem. Sec.* (*Kogyo Kagaku Zasshi*), 63, 765 (1960).
8) J. L. Jungnickel, E. D. Peters, A. Polgár and F. T. Weiss, "Organic Analysis," Vol. I, Interscience Publisher, New York, N. Y. (1953), p. 136.

hydrogen peroxide was estimated as has been described above. The oxirane content was also determined, if it was necessary. Most reactions were carried out to 40—50% conversion, and the constancy of rate constants was confirmed up to 80% conversion.

The decomposition of hydrogen peroxide itself was not appreciable, and its consumption in the presence of nitrile alone was so small that it was negligible in the calculation of the rate constants.

Table I. A typical third-order rate constant for the phosphate-catalyzed epoxidation in 75% methanol at 40°C

Initial concn., $[C_6H_5CN]=[H_2O_2]=0.100$ M; $[C_6H_5CH=CH_2]=0.200$ M; Buffer, $KH_2PO_4$-NaOH (4 : 5), pH=11.35

| Time min. | Conversion of $H_2O_2$, % | $k_4\times10^3$ $l^2\,mol^{-2}\,sec^{-1}$ |
|---|---|---|
| 45 | 15.2 | 3.54 |
| 130 | 33.2 | 3.54 |
| 180 | 41.1 | 3.51 |
| 240 | 47.3 | 3.65 |
| 330 | 54.2 | 3.60 |
| 420 | 60.0 | 3.69 |
| 540 | 65.2 | 3.61 |

## Results

**Rate Law.**—The rate of the epoxidation of styrene with nitrile and alkaline hydrogen peroxide catalyzed by phosphate in 75% methanol were determined by estimating the disappearence of hydrogen peroxide. The results of a typical kinetic run shown in Table I clearly indicate that the reaction is of third-order:

$$v=k_4[RCN][H_2O_2][C_6H_5CH=CH_2] \quad (4)$$

These third-order kinetics are satisfactory with various initial concentrations of reactants or phosphate (Table II-A). The slight decrease in the rate with increasing concentration of styrene may be attributed to the decrease in the polarity of the reaction mixture, as will be described below.

**The Effect of pH.**—The effect of pH on the rate was examined by changing the composition of the phosphate buffer (Table II-B). The rate of epoxidation increased only a little with the increasing pH except at pH values below 10, which is rather surprising if it is remembered that $\log k$ linearly increased with the pH value in the reaction of benzonitrile with hydrogen peroxide.[1] Although a small amount of hydrogen peroxide was consumed in the absence of styrene, the yields of styrene oxide based on the peroxide consumed were essentially the same (93—96%) in each pH examined.

**The Effect of the Polarity of Solvent.**—The rate of epoxidation was affected by the composition of the solvent (Table II-C). The higher water content in the reaction mixture tended to increase the rate. Compare methanolic solvents with 15% and 35% water. Hence, the slight decrease of rate with increasing initial concentration of styrene may be attributed to the decrease in the polarity of the reaction mixture. The addition of toluene also resulted in the same decrease in the rate.

**Substituent Effect.**—Substituent effects are shown in Table III-A and Fig. 1. The introduction of electron-attracting groups in benzonitrile increases the rate, the Hammett's $\rho$-value being 0.57, while substituents in styrene exhibit the reverse effect, giving a $\rho$-value of $-0.51$. These results suggest an electrophilic attack of the peroxycarboimidic acid intermediate.

For purposes of comparison, the reaction of substituted benzonitrile with alkaline hydrogen peroxide was also studied in the presence of borate (Table III-B and Fig. 1); the resulting $\rho$-value of 1.14 in 75% methanol is somewhat smaller than that obtained in 50% acetone.[9] This $\rho$-value is about two times greater than that in the phosphate-catalyzed epoxidation of

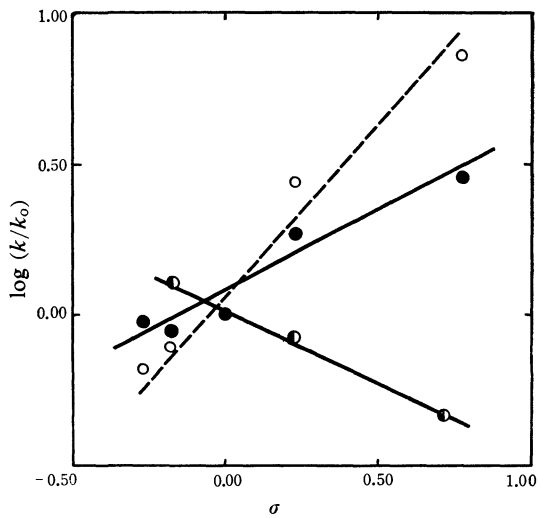



Fig. 1. Plots of logarithm of rate constants for the epoxidation of styrenes with benzonitriles and hydrogen peroxide in phosphate buffer at 40°C versus $\sigma$ (Hammett and Jaffé):
—●— Epoxidation of styrene with substituted benzonitriles
—◐— Epoxidation of substituted styrenes with benzonitrile
---○--- Reaction of substituted benzonitriles with hydrogen peroxide in borate buffer

9) K. B. Wiberg, *J. Am. Chem. Soc.*, 77, 2519 (1955).

TABLE II. PHOSPHATE-CATALYZED EPOXIDATION OF STYRENE WITH A MIXTURE OF NITRILE AND ALKALINE HYDROGEN PEROXIDE IN 75% (v/v) METHANOL BUFFERED WITH $KH_2PO_4$-NaOH AT 40°C

A) Effect of the initial concentration of reactants. Buffer solution: 0.2 M $KH_2PO_4$ - 0.2 N NaOH (4 : 5), pH = 11.35

| [RCN] M | $[H_2O_2]$ M | $[C_6H_5CH=CH_2]$ M | Buffer soln.[a] ml. | $k_4 \times 10^3$ $M^{-2}\,sec^{-1}$ |
|---|---|---|---|---|
| Benzonitrile | | | | |
| 0.100 | 0.100 | 0.100 | 15 | 4.01 |
| 0.100 | 0.150 | 0.100 | 15 | 4.00 |
| 0.200 | 0.100 | 0.100 | 15 | 4.13 |
| 0.100 | 0.100 | 0.200 | 15 | 3.59 |
| 0.100 | 0.100 | 0.300 | 15 | 3.25 |
| 0.100 | 0.100 | 0.100 | 10 | 3.90 |
| 0.100 | 0.100 | 0.100 | 20 | 4.15 |
| Acetonitrile | | | | |
| 0.100 | 0.100 | 0.100 | 15 | 1.21 |
| 0.200 | 0.100 | 0.100 | 15 | 1.15 |
| 0.300 | 0.150 | 0.150 | 15 | 0.94 |
| 0.150 | 0.150 | 0.150 | 15 | 0.98 |

B) Effect of pH. Initial concn.; $[C_6H_5CN] = [H_2O_2] = [C_6H_5CH=CH_2] = 0.100$ M, [buffer soln.] = 15 ml.[a]

| Buffer No. | 0.2 M $KH_2PO_4$ - 0.2 N NaOH | pH (glass electrode) | at $t$ = 5 hr. Conversion % | at $t$ = 5 hr. Consumption of $H_2O_2$ without styrene % | $k_4 \times 10^3$ $M^{-2}\,sec^{-1}$ |
|---|---|---|---|---|---|
| 1 | 4 : 3 | 9.34 | 23.6 | 0.10 | 1.88 |
| 2 | 4 : 4 | 10.40 | 32.6 | 0.35 | 3.40 |
| 3 | 4 : 5 | 11.35 | 37.4 | 0.70 | 4.01 |
| 4 | 4 : 6 | 11.80 | 38.9 | 1.34 | 4.17 |
| 5 | 4 : 8 | 12.00 | 40.7 | 2.90 | 4.48 |

C) Effect of the solvent composition. Initial concentration is same as that in buffer 3 in B.

| Solvent, vol. % Methanol | Ethanol | Water | Added toluene M | $k_4 \times 10^3$ $M^{-2}\,sec^{-1}$ |
|---|---|---|---|---|
| 75 | 0 | 25 | 0 | 4.01 |
| 75 | 0 | 25 | 0.1 | 3.78 |
| 75 | 0 | 25 | 0.2 | 3.61 |
| 55 | 20 | 25 | 0 | 3.48 |
| 45 | 30 | 25 | 0 | 3.40 |
| 85 | 0 | 15 | 0 | 2.65 |
| 65 | 0 | 35 | 0 | 6.00 |

a) Volume per 200 ml. of reaction solution.

styrene with a mixture of substituted benzonitriles and alkaline hydrogen peroxide. The energies and entropies of activation also substantially differ between these two reactions, 1 and 3.

## Discussion

The reaction of nitrile with alkaline hydrogen peroxide[10] ($RCN + 2H_2O_2 \rightarrow RCONH_2 + O_2 + H_2O$, Radziszewski's reaction) is suppressed by the presence of phosphate, yielding styrene oxide almost quantitatively on addition of styrene.[4] Our results may be summarized as follows: (1) The phosphate-catalyzed epoxidation of styrene with nitrile and alkaline hydrogen peroxide follows third-order kinetics, being first-order in each reactant. (2) The rate of epoxidation is essentially constant at various pH's, while the rate increases with the increasing polarity of the reaction mixture. (3) Electron-attracting substituents on the

10) B. Radziszewski, *Ber.*, **17**, 1389 (1884).

TABLE III. SUBSTITUENT EFFECTS IN BENZONITRILES AND STYRENES IN 75% METHANOLIC BUFFERS

| Substituent | | Temp., °C | | | $E_a$, kcal. mol$^{-1}$ | $\Delta S$ (40°C) e. u. |
|---|---|---|---|---|---|---|
| Benzonitrile | Styrene | 30.0 | 40.0 | 50.0 | | |
| A) Third-order rate constant ($M^{-2}$ sec$^{-1}$) for the epoxidation in phosphate buffer (pH=11.35)[a] | | | | | | |
| *p*-$CH_3O$ | H | 2.49 | 3.78 | 5.72 | 8.1 | −44 |
| *p*-$CH_3$ | H | 2.37 | 3.47 | 4.51 | 6.3 | −46 |
| H | H | 3.24 | 4.01 | 4.97 | 4.1 | −56 |
| *p*-Cl | H | 5.16 | 7.33 | 9.60 | 6.0 | −49 |
| *p*-$NO_2$ | H | — | 11.3 | — | — | — |
| H | *p*-$CH_3$ | 4.10 | 5.28 | 6.84 | 5.0 | −53 |
| H | *p*-Cl | 2.55 | 3.34 | 4.23 | 4.9 | −54 |
| H | *m*-$NO_2$ | 1.26 | 1.83 | 2.60 | 7.5 | −48 |
| $CH_3CN$[b] | H | 0.60 | 0.94 | 1.39 | 8.2 | −46 |
| B) Second-order rate constants ($M^{-1}$ sec$^{-1}$) for the reaction of benzonitriles with hydrogen peroxide in borate buffer (pH=9.02)[c] | | | | | | |
| *p*-$CH_3O$ | none | — | 1.28 | — | — | — |
| *p*-$CH_3$ | none | — | 1.52 | — | — | — |
| H | none | 0.763 | 1.95 | 4.61 | 17.5 | −19.8 |
| *p*-Cl | none | — | 5.45 | — | — | — |
| *p*-$NO_2$ | none | — | 14.2 | — | — | — |
| $CH_3CN$[b] | none | — | — | 0.264 | — | — |

a) $v=k_4$ [RCN][$H_2O_2$][$C_6H_5CH=CH_2$] ; initial concn. : [RCN]=[$H_2O_2$]=[$C_6H_5CH=CH_2$]=0.100 M
b) Acetonitrile instead of benzonitrile
c) $v=k$[RCN][$H_2O_2$] ; initial concn. : [RCN]=[$H_2O_2$]=0.100 M

benzonitrile accelerate the rate of epoxidation to give a Hammett's $\rho$-value of 0.57, while the Radziszewski's reaction results in the $\rho$-value of 1.14. (4) Electron-releasing groups in the styrene accelerate the rate, exhibiting a negative $\rho$-value of −0.51. (5) The energy of activation is low and the entropy of activation is highly negative, while with the Radziszewski's reaction the former is higher and the latter is less negative.

**Reaction Scheme.**—The kinetic data show that nitrile, hydrogen peroxide and styrene are involved in the transition state, while the phosphate catalysis suggests that the oxidizing intermediate stabilized by phosphate dianion is effective for an electrophilic attack on olefin. These results agree with the following mechanism:

$$H_2O_2+OH^- \overset{K_5}{\rightleftharpoons} HO_2^-+H_2O \qquad (5)$$

$$RCN+HO_2^- \overset{K_6}{\rightleftharpoons} \underset{\underset{\text{(II)}}{\overset{|}{OOH}}}{R-C=N^-} \qquad (6)$$

$$\text{(II)}+H_2O \overset{K_7}{\rightleftharpoons} \underset{\underset{\text{(I)}}{\overset{|}{OOH}}}{R-C=NH}+OH^- \qquad (7)$$

$$\text{(I)}^+ + \begin{matrix} {}^{-}O \\ {}^{-}O \end{matrix}\!\!>\!P\!<\!\begin{matrix} O \\ OH \end{matrix} \overset{K_8}{\rightleftharpoons} \underset{\underset{\text{(III)}}{}}{\begin{matrix} R-C=N\cdots H\cdots{}^{(-)}O \\ | \\ O-O\cdots H\cdots{}^{(-)}O \end{matrix}\!\!>\!P\!<\!\begin{matrix} O \\ OH \end{matrix}} \qquad (8)$$

$$\text{(III)}+PhCH=CH_2 \underset{\text{slow}}{\overset{K_9}{\longrightarrow}} PhCH\underset{O}{\overset{\diagup\diagdown}{-}}CH_2 + RCONH_2+HPO_4^{2-} \qquad (9)$$

Assuming that the concentrations of I and II are both very low and that equilibrium 8 is mobile and very favorable to the right side, the concentration of III may be expressed as:

$$[III]\cong\frac{K_7[II][H_2O]}{[OH^-]} \cong\frac{K_6K_7[H_2O][RCN]_s[HO_2^-]}{[OH^-]} \cong K_5K_6K_7[RCN]_s[H_2O_2]_s$$

Here, $k$ and $K$ are the rate and equilibrium constants of the subscripted steps, respectively, and [ ]$_s$ represents its stoichiometric concentration. Hence, the rate equation is:

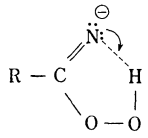
$$v=k_9[III][PhCH=CH_2] =k_9K_5K_6K_7[RCN]_s[H_2O_2]_s[PhCH=CH_2]_s \qquad (10)$$

Rate Eq. 10 is consistent with the observed third-order kinetics and also with the independence of the rate on the hydroxide ion concentration (pH).

The mechanism assumes that II is not so active as to epoxidize styrene and that I is rapidly stabilized by phosphate to prohibit the reaction with hydrogen peroxide.

**Active Epoxidizing Species.**—Phosphoric acid should exist exclusively in the form of

dianion, $HPO_4^{2-}$, in these pH's in view of the dissociation constant. The interaction of the dianion with the intermediate anion II is less probable because of the electrostatic repulsion. While the intermediate I may easily form with the nucleophilic phosphate dianion, the intermediate III is so deactivated as to fail to oxidize hydrogen peroxide. The epoxidizing species is thought to be stabilized by the electron-releasing interaction of the phosphate dianion.



(II')

The intermediate anion, II, presumably has a chelate structure II', resembling that of peroxyacid,[11-13] where the electrophilicity of the oxygen atom is increased by internal hydrogen bonding. However, the electophilicity of peroxide oxygen should be greatly decreased with the anion II' by the presence of a negative charge. Although the intramolecular activation of II' by hydrogen bonding may actually exist, this effect would not surpass the electron-releasing power of the imide anion, since hydrogen bonding may contribute much less than does the inductive effect.

When boric acid was added to the phosphate buffer, the Radziszewski's reaction[10] occurred in spite of the presence of an exess of phosphate and the rate increased with increasing amount of the added acid, although the pH's of the reaction mixture decreased.[4] This promotion of the Radziszewski's reaction by boric acid is probably due to the ability of the acid to combine with the unshared electron pair of the nitrogen atom, decreasing the electron density on the peroxide oxygen atom.

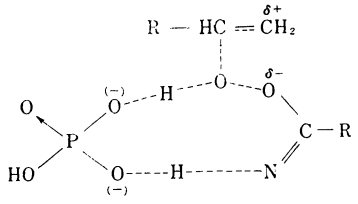
**Substituent Effects.**—The substituent effects on both benzonitrile and styrene imply an electrophilic attack of III on the doubly-bound carbon atoms. The same effects have been observed with the peroxybenzoic acid epoxidation of olefins.[14] The Hammett's $\rho$-value for the epoxidation with substituted benzonitriles is about one-half of that for the Radziszewski's reaction, indicating a lower sensitivity to the polar effect. This lower value of $\rho$ can be well understood by considering the effect on equilibrium 7 reverse to that on equilibrium 6, thus leading to the decrease in total $\rho$-value.

The Hammett's plot for epoxidation with substituted benzonitriles in Fig. 1 shows a little departure from linearity especially for the *p*-methoxy group, while the plot for the Radziszewski's reaction is more satisfactory. The deviation of the former plot may be attributed to the overestimation of the resonance effect, since II should be less resonance-stabilized than the benzoate anion; hence, the above deviation is conceivable.

As for the epoxidation of substituted styrenes, the Hammett's plot is much more satisfactory, but it has a slight deviation as to *p*-substituents. According to the correction for $\sigma$-value using the $\gamma$ parameter,[15] $\sigma = \sigma + \gamma \times \Delta_{\sigma R}$, the value for $\rho$(meta) is calculated to be $-0.48$ from the rates for unsubstituted and *m*-nitrostyrene and the $\gamma$'s are 0.62 for *p*-methyl- and 0.59 for *p*-chlorostyrene. The $\gamma$-value of 0.61 (average) is similar to 0.48 for the perbenzoic acid epoxidation of styrenes,[7] suggesting a similar resonance effect in the transition state.

**The Approach of the Reagent to Substrate.**—The rate of epoxidation increased in solvents with higher dielectric constants, which seems to mean that an increase of polarity may increase the degree of dissociation of III, resulting in the regeneration of the stronger oxidant (I). This was confirmed by the fact that the reaction rate of benzonitrile with hydrogen peroxide alone increased with the increasing water content of methanol.[4]

Considering the above discussion, the transition state may be expressed as IV:



(IV)

As is to be expected, IV, a highly-crowded transition state, would require a highly negative entropy of activation, reflecting the hindered motion of each reactant. Thus, the present reaction is considered to be slowed down by the highly negative entropy of activation in spite of the low energy of activation. The less negative entropy of activation for the Radziszewski's reaction can be well explained by the less crowded transition state containing

11) B. M. Lynch and K. H. Pausacker, *J. Chem. Soc.*, 1955, 1525.
12) T. W. Findley, D. Swern and J. T. Scanlan, *J. Am. Chem. Soc.*, **67**, 412 (1945).
13) G. J. Minkoff, *Proc. Roy. Soc.*, **A224**, 176 (1954).
14) D. Swern, *Chem. Revs.*, **45**, 1 (1949); "Organic Reactions," Vol. 7, John Wiley & Sons, New York, N. Y. (1953), p. 378.
15) Y. Yukawa and Y. Tsuno, This Bulletin, **32**, 971 (1959).

only two species, e. g., nitrile and hydroperoxide ion.

## Summary

The phosphate-catalyzed epoxidation of styrenes with a mixture of nitriles and alkaline hydrogen peroxide have been studied kinetically in 75% methanol. The reactions satisfy third-order kinetics, being first-order in nitrile, hydrogen peroxide and styrene. The rate is essentially constant at various pH's, while it increases with the increasing polarity of the reaction medium. The energy of activation is low (6—8 kcal. $mol^{-1}$), and the entropy of activation is highly negative (−50 e. u.). The effect of substituent in benzonitrile is to give a Hammett's $\rho$-value of 0.57, while that in styrene resulted in a negative $\rho$-value of −0.51. It is probable that the peroxycarbimidic acid (I), produced by mobile equilibria from nitrile and hydroperoxide ion, is stabilized by an intermolecular hydrogen bonding with the phosphate dianion, and that this species contributes mostly to the epoxidation of styrene in the following, rate-determining step.

*Department of Applied Chemistry*
*Faculty of Engineering*
*Nagoya University*
*Chikusa-ku, Nagoya*

# Application of Electrostatic Models to the Colloidal Behavior of Plate-shaped Particles

By E. St. A. JORDINE, B. J. STEEL and J. D. WOLFE

(Received June 4, 1964)

The approach to many colloidal problems has usually been based on the equilibrium assumption, that is, of a Boltzmann distribution of ions around the macromolecular surface in question. It would appear however, that certain electrostatic models may give only an approximate but yet more useful description of systems which possess some symmetry. The two methods are in a way analogous to the equilibrium and orbit theories of plasma physics.

While the use of electrostatic models seems to be valid only for perticle-particle separations which are no greater than 20 to 30 Å, it is precisely in this region that the equilibrium approach fails catastrophically.

The idea of specific attractive forces between the counter ions and charged macromolecules was first proposed by Langmuir.[1] He first considered the colloid system as a whole instead of the two interacting particles. This approach has been severely criticised by Verwey and Overbeek (Ref. 2, p. 195). Actually, as will be seen in the present work, where two particles are considered with the aid of an electrostatic model, fairly good results are obtained.

Langmuir[1] believed that unipolar coacervation was due to Coulomb forces and suggested that a repulsive force, possibly hydration, was needed in order to counter-balance the tendency of the colloid system as a whole to contract under the influence of attractive Coulomb forces. This casts serious doubt on the exact role of the long-range London-van der Waals attractive force.

That this repulsive force has eluded most investigators has been due mainly to two factors: The belief that the Boltzmann distribution of ions always exists, and the gross simplification of treating the macromolecule either as a conductor or as a point charge. It is well known that, even for fairly ideal systems, such as are found in the gas phase, the first assumption has been found to fail. Now, to regard the macromolecule as a point charge means to ignore the important surface and dipole effects, while the assumption that it is a conductor is equivalent to assigning a value of infinity to the dielectric constant. This last factor will be shown to be of considerable importance.

As has been pointed out by McEwan[3] and Norrish[4], for small separations of two large plate-shaped particles the counter ions may be

1) I. Langmuir, *J. Chem. Phys.*, **6**, 873 (1938).
2) E. J. W. Verwey and J. T. G. Overbeek, "Theory of Stability of Lyophobic Colloids," Elsevier Publishing Co. Inc., New York (1948).
3) D. M. MacEwan, *Nature*, **162**, 935 (1948).
4) K. Norrish, *Discussions Faraday Soc.*, **18**, 120 (1954).

regarded as being ordered between the particles. The counter ions may, therefore, be considered to a first approximation as having specific areas of interaction with additive effects, quite analogous to the specific orbits describing the interactions in plasma physics. Derjaguin[5] makes a similar assumption concerning the volume elements of polarization which he justifies for small particle-particle separations. The main requirement for this model to hold is that the macromolecules should have relatively large surface areas per counter ion. While edge effects are important, montmorillonite or vermiculite platelets with surface areas of the order of millions of square angstroms[6] should be very suitable systems for treatment in the crystalline region of swelling.

Recently Jordine, Bodman and Gold[6] and Jordine[7] have applied the method of the electrostatic images of an infinite dielectric slab to montmorillonite systems. Only an approximate solution was obtained, however, since several terms were ignored. A rigorous solution of a point charge located between two charged slabs of dielectric will now be given. It will be seen that a repulsive image force arises quite naturally, and in such a way as to contribute to a minimum in the potential energy curve. A major problem, however, is that of assigning the correct effective dielectric constant to the intervening solvent medium. Nevertheless, as in Ref. 6 and Ref. 7, dielectric saturation has been taken into account.

The problem will be solved for the midway position*[1] of the charge between the dielectric slabs. It will also be outlined how a generalised crystal lattice theory of images can be developed to treat the system as a whole without making any assumptions concerning specific areas of interaction by the interlayer ions.

Lastly, a detailed theory of the mechanism of swelling will be proposed.

**A Statement of the Problem of the Point Charge between Two Charged Dielectric Slabs (Montmorillonite, Vermiculite, Mica).** — As a starting point for the model, consider that in Fig. 1 of Ref. 6 another platelet is placed symmetrically so as to form a plane ($-2D$, yz). This will be quite similar to Norrish's model (Ref. 4, Fig. 8) except that the platelets are not regarded as conductors.

In terms of electrostatics, the problem may be stated as the interaction between two dielectric interfaces and an array of charges. Thus, we have for $x<-2D$ and $x>0$ two regions mL and mR respectively of the dielectric constant $K_m$, while there is for $-2D<x<0$ a region w of the dielectric constant $K_w$. A set of point charges is located along the plane $x=-D$, and the interfaces $x=-2D$ and $x=0$ have a uniform surface charge of density, $\sigma$. We shall, for purposes of simplification in what follows, regard the interaction of the point charges as additive and, hence, consider only a given point charge $e^*$ located at $(-D, 0, 0)$. In other words, we will consider a cell model, as has been discussed in the introduction.

**A Solution of the Problem.**—The differential equations which must be solved to obtain the potential $V$ and, hence, the electrostatic energy of interaction are:

$$\nabla^2 V=0 \tag{1}$$

in the regions mL and mR and

$$\nabla^2 V=-\frac{4\pi}{K_w}\sum_{j=1} e_j^*\delta(x+D)\delta(y-y_j)\delta(z-z_j) \tag{2}$$

in the region w.

Since we are interested in a single cell, we may consider only one point charge; therefore, Eq. 2 may be written as:

$$\nabla^2 V=-\frac{4\pi}{K_w}\sum e_j^*\delta(x+D)\delta(y)\delta(z) \tag{3}$$

In addition to satisfying Eqs. 1 and 2, the potential must satisfy the usual electrostatic boundary conditions at the interfaces and at infinity.[6]

Since Eqs. 1 and 2 are linear, by a well-known theorem the potential can be written as $V=V_i+V_\sigma$, where $V_i$ denotes the potential due to the point charge and its images, and $V_\sigma$, that due to the surface charge. We can choose $V_\sigma$ as follows:

$$\left.\begin{aligned} V_\sigma &= \frac{2\pi\sigma x}{K_w} && -D<x<0 \\ &= -\frac{2\pi\sigma x}{K_m} && 0<x<\infty \\ &= -\frac{2\pi\sigma(2D+x)}{K_w} && -2D<x<-D \\ &= \frac{2\pi\sigma(2D+x)}{K_m} && -\infty<x<-2D \end{aligned}\right\} \tag{5}$$

Strictly speaking, since the platelets are only effectively infinitive, $V_\sigma$ must be cut off for $x$ at a value sufficiently large so that it tends to zero as $x$ tends to $\infty$.

5) B. V. Derjaguin, ibid., **18**, 85 (1954).
6) E. St. A. Jordine, G. B. Bodman and A. H. Gold, *Soil Sci.*, **94**, 371 (1962).
7) E. St. A. Jordine, ibid., **96**, 149 (1963).
*[1] In a forthcoming paper (Hurst and St. A. Jordine, *J. Chem. Phys.*, **41**, November 1 (1964)) it is shown that the midway position is favored energetically. See also experimental studies by Brown.[8]
8) G. A. Brown, *Mineralog. Soc. Gr. Britain Clay Mineral Bull.*, **4**, 109 (1950); Quoted in R. E. Grim, "Clay Mineralogy," McGraw-Hill Book Co. Inc., New York, Toronto, London (1953), p. 134.

Applying the method of images in dielectrics we get, for the potential due to the ion and its images in w, mL and mR respectively:

$$V_w - V_\sigma = \sum_{n=0} \frac{\alpha^n e^*/K_w}{\sqrt{[x+(2n+1)D]^2+y^2+z^2}} + \sum_{n=1} \frac{\alpha^n e^*/K_w}{\sqrt{[x-(2n-1)D]^2+y^2+z^2}} \quad (6)$$

$$V_{mL} - V_\sigma = \sum_{n=0} \frac{\alpha^n 2e^*/(K_w+K_m)}{\sqrt{[x-(2n-1)D]^2+y^2+z^2}} \quad (7)$$

$$V_{mR} - V_\sigma = \sum_{n=0} \frac{\alpha^n 2e^*/(K_w+K_m)}{\sqrt{[x+(2n+1)D]^2+y^2+z^2}} \quad (8)$$

where

$$\alpha = (K_w - K_m)(K_w + K_m)^{-1}$$

Having obtained the potential functions for the various regions we can now obtain the energies of interaction, designated $U_w$ and $U_m$.

With the aid of Green's theorem (Ref. 9, p. 160) the energy may be written in general as:

$$U_w = \frac{K_w}{8\pi} \iiint (\nabla V_w)^2 dx dy dz = -\frac{K_w}{8\pi} \Sigma \iint V_w \frac{\partial V_w}{\partial n_i} ds_i \quad (9)$$

$$U_m = \frac{K_m}{8\pi} \iiint (\nabla V_m)^2 dx dy dz = -\frac{K_m}{8\pi} \Sigma \iint V_m \frac{\partial V_m}{\partial n_i} ds_i \quad (10)$$

The significant interaction-energy terms will be those arising from the following cross terms:

a) The real charge with all the images. These are images with respect to the real charge; hence, the integration is only over the surface of the real charge.

b) An image with the successive image induced by it. The first image functions as a virtual charge and as such has an integrable surface.

c) Cross interaction between the two symmetric image sets, but not between images within a given set located behind a platelet or slab.

d) Interaction between images on the left with the free charge or the slab on the right, and vice versa. These terms are quite symmetric.

e) Interaction between the real point charge and the free charge on the two surfaces.

f) Interaction between the free charges on the two platelets. This is a more difficult problem then it would appear; hence, it will be treated in conjunction with e).

g) For the energy of the field in the platelets, the interaction terms follow from the equations for $V_{mR}$ and $V_{mL}$. The terms involving the surfaces of the images are, as in d), fictitious and, hence, zero.

On carrying out the appropriate integrations and putting $e^* = ze$, we obtain:

$$U_w = \frac{z^2e^2}{2DK_w}\left\{-\left(2+\frac{1}{2|1-\alpha^2|}\right)\ln(1-\alpha) + \frac{1}{|1-\alpha^2|}\left(\frac{1}{2}\ln(1+\alpha) - \alpha - \frac{\alpha^3}{3}\right) - \alpha\right\} + \frac{ze\pi\sigma}{K_w}\sum_{n=1}(\alpha^n[\sqrt{(2n+1)^2D^2+ze/2\pi\sigma} - (2n+1)D) + \frac{ze\pi\sigma}{2K_w}(\sqrt{D^2+ze/2\pi\sigma}+D) \quad \text{ergs/ion} \quad (11)$$

and

$$U_m = \frac{2ze\pi\sigma}{(K_w+K_m)}\sum_{n=0}(\alpha^n[\sqrt{(2n+1)^2D^2+ze/2\pi\sigma} - (2n+1)D) \quad \text{ergs/ion} \quad (12)$$

The total electrostatic energy of interaction, designated $U_E$, is:

$$U_E = U_w + U_m \quad (13)$$

In view of the discussion following Eq. 5, it can be shown that, when $2D \to \infty$, the last two terms of Eq. 11 become:

$$\frac{ze\pi\sigma}{K_w}\sum_{n=0}(\alpha^n[\sqrt{(2n+1)^2D^2+ze/z\pi\sigma} - (2n+1)D) \quad (14)$$

Thus eliminating the problem of an energy term which becomes indefinitely large as $2D$ increases.

**The Mechanism of Swelling and the Role of the Hydration Energy of the Interlayer Ions.** — Before applying Eq. 13 to obtain potential energy curves, it is necessary to consider the mechanism of expansion. According to Barshad,[10-12] in the dry montmorillonite, vermiculite, or other expanding clay mineral the platelets are sandwiched together, with interlayer ions present in the cavities of the oxygen framework which forms the boundary of the platelets. It is known that the presence of the interlayer ions is essential to swelling, and that this process is dependent on the size and charge of the ion. An important role is also played by the dielectric constant of the solvent medium. In the crystalline region of swelling a few essential things seem to cccur. Firstly, the solvent molecules, those of water,

9) J. Jeans, "Mathematical Theory of Electricity and Magnetism," 5th ed., Cambridge University Press, Cambridge, England (1960).

10) I. Barshad, *Am. Min.*, **34**, 675 (1949).
11) I. Barshad, *Soil Sci. Soc. Am., Proc.*, **16**, 176 (1952).
12) I. Barshad, *Clays and Clay Technology, California Div. of Mines, Bull.*, **169**, 70 (1955).

for instance, must be adsorbed to the external surface of the crystal; thereafter water molecules penetrate the platelets with the concomitant removal of the ions from the cavities of the platelets and the subsequent coordination of the water molecules by the ions.

In terms of solid state physics, the foregoing process may be considered to be the creation of negative holes in the montmorillonite crystal as a result of the removal of the ions from the cavities. The interlayer ion now functions as a nucleus for the coordination of water molecules to give a heterogeneous crystal of montmorillonite-water. The creation of holes in the montmorillonite and the movement apart of the platelets require energy which must be yielded to the montmorillonite. On the other hand, the incorporation of water into the crystal requires that the water molecules release energy. The processes are, therefore, seen to be complementary, the ions being the main intermediary agents, extracting energy from the water molecules to be yielded to the montmorillonite and to contribute to the swelling potential. All this may be stated more concisely; swelling or crystal growth is a consequence of a defect or imperfection in the montmorillonite crystal. The foregoing essentially describes the process in the region of platelet separation, $0 \leqslant 2D \leqslant 5.4$ Å, corresponding to two complete and continuous monomolecular layers of water between any two platelets.

In order to relate the energy extracted from the water molecules to the hydration energy of the ion, it is necessary to consider the following equation of Bernal and Fowler[13] for the hydration energy of an ion with a valence $z$ and a radius $r$:

$$U_h = \frac{(K_w - 1)z^2e^2}{2K_wR_z} + (nP_{(r,z)} - u_w) \qquad (15)$$

where the symbols have the some meaning as in Ref. 13. The first term in the above equation arises quite logically from the general electric field equations, while the second terms is an empirical relation representing the potential energy change of the water molecules due to coordination by an ion. The term due to the electric field equations has already been partially computed in the general expression for $U_w$, that is, Eq. 11. In addition, the diameter $2R_z$ of the saturation sphere which is the lower boundary of integration takes values such that it coincides with $2D$. From Table VII of Ref. 13, $2R_z = 5.8$, 7.2 and 9.2 Å for $z = 1$, 2 and 3 respectively. This would make the first term zero, since the platelet separation $2D$ corresponds to the upper boundary or the physical infinity. Thus, the first term is, for practical purposes, zero. Herein could lie a partial explanation for the lower heats of the solution of ions when bound to montmorillonite reported by Janert.[14] It must also be borne in mind that some of the energy abstracted from the polar solvent is yielded to the montmorillonite crystal. Jordan,[15] for example, showed that even after the separation of 12 Å had been attained it was still necessary to add polar solvents to commercial montmorillonite-organic complexes in order to obtain further expansion and gelation. This would suggest an energy requirement of the montmorillonite before extensive separation can occur. As has been shown by Barshad,[11] the dielectric constant of the solvent plays a key role. Other factors, such as the size and type of interlayer ions and solvent molecules, are also important, as has been shown by Granquist and McAtee.[16] Whatever the interlayer ion may be, it appears that the solvent should have a high dielectric constant and the ability to solvate the interlayer ion, thus releasing energy, as has been discussed above.

There is no rigorous way of representing the mutual potential energy of the coordination of the water molecules by the ion. Intuitively, this may be represented by an integral function, such as:

$$(nP_{(r,z)} - u_w) = (nP_{(r,z)} - u) \int_0^\infty f(\rho)\,\mathrm{d}\rho$$

Clearly, $f(\rho) = e^{-\rho}$

Proceeding in this empirical manner, the contribution to the total potential energy of the system at any interplatelet separation $2D$ may now be defined as:

$$U_C = (nP_{(r,z)} - u_w) \frac{\int_{D-1}^{D} f(\rho)\,\mathrm{d}\rho}{\int_0^\infty f(\rho)\,\mathrm{d}\rho} \qquad (16)$$

$$= (nP_{(r,z)} - u_w) \int_{D-1}^{D} e^{-\rho}\,\mathrm{d}\rho$$

Since $f(\rho) = e^{-\rho}$,

$$U_C = (nP_{(r,z)} - u_w)(e-1)e^{-D}; \quad (D \geqslant 1) \qquad (17)$$

The interpretation of Eqs. 16 and 17 is that the fraction of the energy under the curve between $(\rho - 1)$ and $\rho$ contributes to the potential energy at $\rho = D$. In a way, the function bears some similarity to a Dirac $\delta$-function.

13) J. D. Bernal and R. H. Fowler, *J. Chem. Phys.*, **1**, 515 (1933).

14) H. Janert, *J. Agri. Sci.*, **24**, 136 (1934): Quoted in R. E. Grim, "Clay Mineralogy," McGraw-Hill Book Co. Inc., New York, Toronto, London (1953), p. 187.

15) J. W. Jordan, *J. Phys. & Colloid Chem.*, **53**, 194 (1948).

16) W. T. Cranquist and J. L. McAtee, *J. Colloid Sci.*, **18**, 409 (1963).

There should also be a term similar to $(nP_{(r,z)}-u_w)$ for the energy yielded to the montmorillonite platelets in order to remove the ion from the cavity. This term could be developed empirically as above for $U_C$, but the sign should be negative. An attempt is now being made to estimate this term theoretically. A possibility exists, however, of estimating its value experimentally. If, for example, montmorillonite flakes of varying ratios of high to low hydration energy ions such as $K^+$; $Na^+K^+$; $Li^+Cs^+$; $Li^+$ are prepared and then allowed to swell, there may exist a critical ratio of ions at which the interplatelet separation takes a value $\geqslant 9$Å. In this way the critical average hydration energy per ion could be obtained and related to the crystal energy term. This term should to all appearances be much less than $(nP_{(r,z)}-u_w)$ for most ions possessing large hydration energies, but it would never be completely satisfied for those ions with relatively small hydration energies.

**Potential Energy Curves and Extensions.**— Except for the unknown term describing the energy of creating a hole in the montmorillonite platelets, it is now possible to obtain potential energy curves from Eq. 13 and its sum with Eq. 17. These are shown below in Figs. 1, 2 and 3 for $z=1$, 2 and 3 respectively. The numerical values of the various parameters in Eqs. 13 and 17 are given in Ref. 7 and 13 respectively.

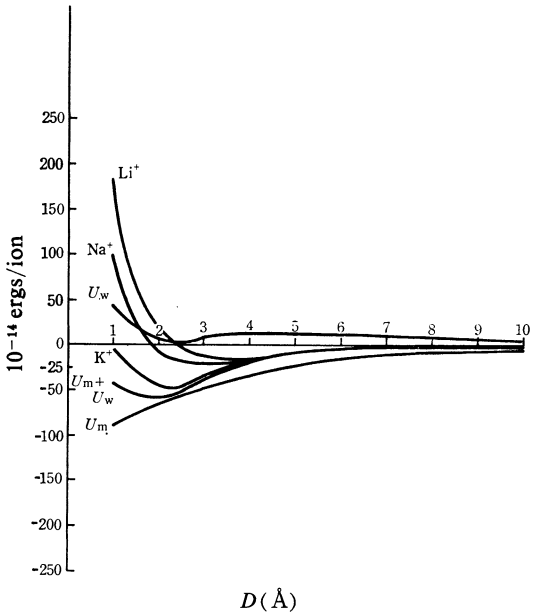



Fig. 1. Energy of interaction between two faces of montmorillonite and monovalent interlayer ions in relation to distance of separation, calculated for varying values of $K_w$ as in Eqs. 13 and 14.

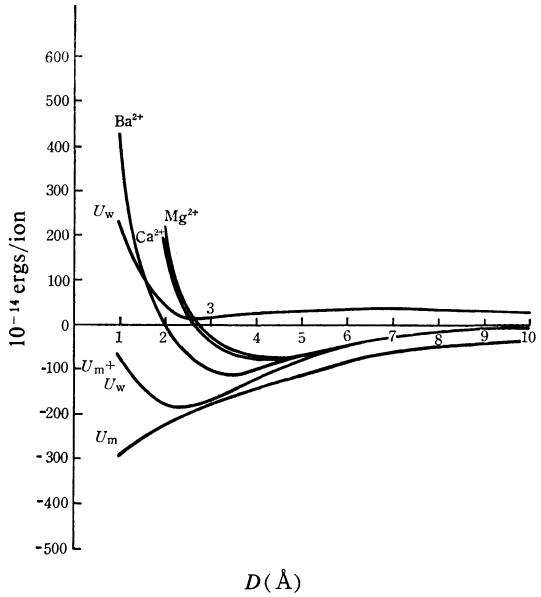



Fig. 2. Energy of interaction between two faces of montmorillonite and divalent interlayer ions in relation to distance of separation, calculated for varying values of $K_w$ as in Eqs. 13 and 14.

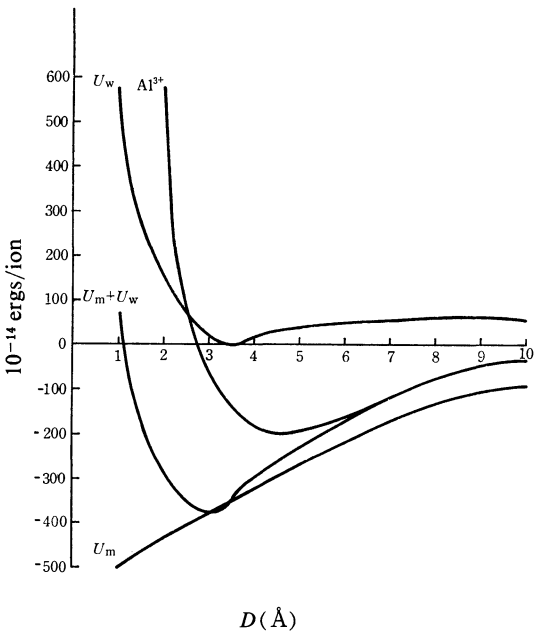



Fig. 3. Energy of interaction between two faces of montmorillonite and trivalent interlayer ions in relation to distance of separation, calculated for varying values of $K_w$ as in Eqs. 13 and 14.

It must be stressed that Eq. 13 is not strictly valid except for $2D \geqslant 5$Å, since the development postulates two complete and continuous

monomolecular layers of water, one on either side of the interlayer ion. In addition, Eq. 17 is completely empirical.

It may be noted that, if the first term in the image series is taken, Eq. 11 reduces to:

$$U_w = \frac{K_w - K_m z^2 e^2}{(K_w + K_m) K_w 2D} + \frac{\pi \sigma z e}{2K_w}(\sqrt{D^2 + ze/2\pi\sigma} + D) \qquad (18)$$

This expression, which is the first order approximation, yields a curve quite similar to that given by Ref. 15, Eq. 8 in Ref. 6, Fig. 2. If, now, the platelets were replaced by uncharged conductors $U_w$ would reduce to:

$$U_w = -\frac{z^2 e^2}{2DK_w} \ln 2 \qquad (19)$$

This result indicates that the energy for small $D$ would always be attractive if the montmorillonite platelets are assumed to be conductors.

From Eqs. 11 and 19 it is clear that the image problem we have solved is essentially that of a one-dimensional ionic crystal lattice. With extensions for computing the lattice sums, it is possible to extend this to a two-dimensional lattice and thus treat several ions and their images as one system. This would indeed yield a more rigorous solution to the problem. For the present, however, Eq. 13 is adequate for both montmorillonite and vermiculite systems.

Lastly, the problem as solved represents the case for two dielectric faces or for two slabs of an infinite thickness. In the work referred to in Footnote *1, a solution is given which takes into account the thickness of the platelets, giving a small correction term to the energy.

## Discussion

From Eq. 13 and its representation in Figs. 1, 2 and 3, it would appear that the electrostatic energy of interaction is such a function of the distance as to exhibit a minimum or an energy well. This minimum arises from the combined effects of dielectric image or polarisation energy terms and Coulombic terms. The experimental values of the equilibrium separation for some of the various ionic forms of montmorillonite are given in Ref. 4 as $D=1.9$Å for $Cs^+$, $D=2.5$Å for $K^+$, $D=6$Å for $Li^+$, and $D=4.5$Å for $Na^+$, $Ba^{2+}$, $Ca^{2+}$, $Mg^{2+}$ and $Al^{3+}$. It would appear from the curves of Eq. 13 in the figures that some other repulsive energy term must be operative. After adding $U_C$ to $U_E$, the total potential energy curves are obtained for the various ions. As was anticipated, the best agreement seems to be obtained for $Al^{3+}$, since the larger the surface element $ze/2\sigma$ the more ideal the image model becomes. From the depth of the minimum in the total potential energy curve for $Al^{3+}$, the binding energy is seen to be about 30 kcal. per mole of ions, a value which is about sixteen per cent that of the sodium chloride crystal. These correlations indicate conclusively why aluminum-montmorillonite does not exhibit macroscopic swelling. On the other hand, the curves for $Li^+$ and $Na^+$ show binding energies of the order of 3 to 4 $kT$. Such minima are shallow enough to permit macroscopic sweelling, as experiment confirms.[4]

Since the binding energies of the various ions determine the potential energy of the surface, this feature may have general biochemical implications. In Figs. 1 and 2 there is a marked difference between the biologically important ions, such as $K^+$, $Na^+$, $Mg^{2+}$ and $Ca^{2+}$, and $Li^+$ and $Ba^{2+}$. Thus, $K^+$ and $Ca^{2+}$, which assist in maintaining the osmotic and structural integrity of living cells, have high binding energies and would thus maintain the surface in a state of stable potential energy. Of course, at the other extreme is $Cs^+$, which would virtually immobilise the surface. $Ca^{2+}$ has perhaps ideal properties for biological functions in that, while it facilitates a good turnover of water, it also has a high binding energy. This could explain its well-known regulatory influence on, for example, the uptake of some other ions by excised plant and animal tissues. These correlations cannot be taken too far, but there does seem to be some relationship between these properties and the potential energy spectrum displayed in the figures.

From the curves representing $U_m$, $U_w$ and $U_E$, it may be seen that in the region of separation under study $U_m$ is the leading term of $U_E$ for $z=1, 2$ and 3 respectively. This evidence does seem to favor the theory of swelling proposed, that there is an energy requirement of the montmorillonite platelets which must be satisfied by cooperative processes between the solvent medium, the interlayer ion, and the platelets before any appreciable expansion can proceed. It may be noted that, if the platelets were conductors $U_m$ would be zero.

In Figs. 1, 2 and 3 the curves of Eqs. 11, 13 and 13+17 all have the typical appearance of potential energy curves for molecular systems. The explosion to a gel by montmorillonite or vermiculite crystals may be regarded as the probability of skating out of the energy well. There is, therefore, a statistical problem concerning a distribution function for the number

of platelets which escape the barrier to demonstrate macroscopic swelling. This is borne out by the X-ray date of Norrish (Ref. 4, Fig. 2) and Norrish and Rausell-Colom (Ref. 17, Fig. 3). It is well to note that the expansion of the first few platelets will act as a trigger mechanism for others, leading to an explosive avalanching process.

Let us consider now the mechanism of this explosive process, known as macroscopic swelling.[4] In an earlier section of this work, an approximation was made in computing the energy terms, e) and f); as soon as the interlayer ions lose their ordered arrangement, the shielding effect is considerably reduced and f) is no longer zero. In other words, the free surface charges of a like sign on adjacent platelets repel each other, since, as has been pointed out earlier, they now act as sinks for sources at infinity. Support for this proposal is found in Ref. 17 and in Weies' work.[18] These workers have shown that, within certain limits, the macroscopic swelling for a variety of clay minerals with various interlayer ions is greater and more explosive the greater the surface charge density. In the second instance, the authors, by perturbing the mobile interlayer ions of lithium-vermiculite with an electric field of a few V./cm., stimulated lithium-vermiculite to exhibit macroscopic swelling almost instantaneously. These crystals thereafter exhibited unexplained electrical properties similar to those described by Garrent and Walker.[19]

Before giving an explanation to the electrical phenomena in 18, it is of interest to describe briefly the procedure for preparing what appears to be lithium-vermiculite. By applying much higher voltages for short intervals to a native sodium-vermiculite crystal immersed in water, the crystal was stimulated to swell some three to four times its original volume within a few minutes. The water was then replaced by a dilute lithium chroride solution, and the perturbation field was maintained for a few more minutes. The crystal was then left overnight in lithium chloride solution, a procedure which is perhaps not essential. It would appear, therefore, that the laborious method of prolonged heat treatment used by many workers in preparing lithium-vermiculite can be simplified. The heat serves largely to increase the ionic conductivity as it would for any ionic crystal lattice. The swollen sodium-vermiculite, when left for a few hours in air, always contracted to one-and-a-half times its original thickness.

17) K. Norrish and J. A. Rausell-Colom, *Clays and Clay Minerals*, **10**, 123 (1963).
18) A. Weies, ibid., **10**, 191 (1963).
19) W. G. Garret and G. F. Walker, ibid., **10**, 557 (1963).

The explanation for all these electrical phenomena seems to lie in a model presented in Ref. 6, that is, the consideration of the vermiculite platelets with the interlayer ions as a pile of plate-shaped conductors. If an electric field is now applied, the mobile interlayer ions or positive charge carriers migrate in the direction of the field and can thus be replaced by other positive-charge carriers. This perturbation destroys the equilibrium distribution of the ions over the surface; hence, towards the anode there is an increased interaction between the surface charge of adjacent platelets leading to repulsion and the growth of the crystal. By applying an a.c. field of a sufficiently low frequency, the mechanical response time of the system could be determined. Preliminary studies by the authors suggest a value of 0.06 sec. The possibility of a permanent dipole moment may be ruled out since there is no preferential direction in the plane of the crystal for growth. It follows the field completely.

## Conclusion

The general theory of images in dielectrics has yielded results which convincingly support Langmuir's[1] preliminary ideas. All the evidence from theory and from current experimental knowledge suggests that, within the limits set by the type and size of solvent and interlayer ion, the swelling and many other colloidal properties of clay minerals are wholly determined by the electrical properties of the system. The influence of the surface density of the charge on the swelling, which was reported in Refs. 17 and 18, points to the fact that double-layer theory should not be applied without reservations to clay mineral systems. As further proof of the importance of the dielectric constant of the medium between the platelets, a comparison may be made of Table VII of Ref. 11 and Table I of Ref. 18. Here it is seen that a calcium-saturated montmorillonite immersed in a mixture of octanol and *n*-pentane gives almost the same X-ray spacing as a montmorillonite saturated with *n*-octylammonium ions in a mixture of *n*-octanol and *n*-octylamine. This result would indicate that, in this range of dielectric constants of the solvent, the alkylammonium ions behave much like any other ions; support is also given to Barshad's[11] proposal regarding the formation of complexes between the solvent and the platelets of montmorillonite. Moreover, these complexes should be regarded as heterogeneous crystals.

Finally, Figs. 1, 2 and 3 provide convincing evidence that the image model describes the system adequately.

## Summary

The method of images in dielectrics is applied to a model consisting of two infinite dielectric slabs and a point charge. When specific effects of the ions such as hydration energies are taken into account, the model describes the electrical aspects of the swelling of the clay minerals satisfactorily. In addition, a detailed theory of the mechanism of swelling is proposed and is shown to be favored by preliminary experimental studies of vermiculite.


One of the present authors (E. St. A. J.) wishes to express his appreciation to Dr. G. H. Cashen for his stimulating critism of a previous work[6] and to Dr. C. A. Hurst for his helpful discussions.

*Department of Physical and Inorganic Chemistry*
*The University of Adelaid*
*South Australia (E. St. A. J. & B. J. S.)*

*Reliance Chemical Co.*
*Richmond, California, U. S. A. (J. D. W.)*

## Appendix I

In order to demonstrated further the agreement between theory and experiment, we may compare Barshad's (Ref. 20, Figs. 2 and 3) experimental results for $\Delta F_w$ with its equivalent, $\partial(U_C+U_w)/\partial D$, or even $\Delta F_m$ (Ref. 20, Fig. 6) with $\partial U_m/\partial D$. Though the units are different, the respective families of curves can be shown to be identical except for units and scale. The units used in Ref. 20 are not obvious, hence no exact comparison can be made until they are clarified and converted to ours. Both experiment and theory agree that the free-energy change of the water is a path of decreasing potential energy as $D$ increases, while for the montmorillonite it is a path of increasing potential energy, rapidly approaching zero from negative values. The total potential energy, $U_C+U_E$, will, therefore, tend to demonstrate a minimum followed by a maximum as $D$ increases. These features can be deduced from the potential energy curves and expressions. The value of $D$ at the maximum increases as the valence of the ions increases. For monovalent ions the maximum occurs at about $D=9$ Å, whereas for polyvalent ions it is greater. This is not surprising, since no polyvalent ion exhibits macroscopic swelling (at least as far as current experiments indicate).

20) I. Barshad, ibid., 8, 84 (1960).

## Appendix II

The case of the added electrolyte has already been treated,*[1] but experimental evidence can be presented to show that excess salt exerts only a secondary influence on the swelling process. In Figs. 5 and 7 of Ref. 4, which depict the experimental X-ray spacings of sodium-montmorillonite in sodium chloride solutions and water respectively, similar progressive interlayer separations of $2D=0$, 9 and 30 Å are demonstrated.

Clearly, though the added electrolyte can inhibit swelling, the primary mechanism of the swelling process is essentially due to the counter ions which neutralise the charge on the platelets. This is the basis of the theory developed in this work.

# Photoreduction of Methylene Blue and Thionine in Ethanol

By Yoshiharu USUI

(Received June 17, 1964)

Studies of the photoreduction of xanthene dyes in alcohol were started by Imamura and Koizumi,[1] and the mechanism has been clarified to some extent since then. However, as for the similar photoreduction of thiazine dyes, there seem to have been no kinetic studies undertaken with the aim of elucidating its mechanism, although a few reports, rather qualitative, have been made, including those of Kutsaya and others.[2]

There are two reasons why the author has started the present investigation. One is to add to our knowledge concerning the photochemical behavior of various dyes is alcohol and, in particular, to compare thiazine dyes with xanthene dyes and acridine, which have been already investigated.[3] The other is to examine the peculiar behavior of the thiazine dyes, which are known to undergo photoreduction in an aqueous solution in the absence of

1) M. Imamura and M. Koizumi, This Bulletin, **28**, 117 (1955).

2) B. F. Kutsaya and Ya. B. Dain., *Ukrain. Khim. Zhur.*, **17**, 820 (1951).

3) S. Kato, S. Minagawa and M. Koizumi, This Bulletin, **34**, 1026 (1961); S. Niizuma and M. Koizumi, ibid., **36**, 1629 (1963).

a reducing agent.[4] It has been found, in sharp contrast to the behavior of xanthene dyes and acridine, that this reaction is second order in respect to the dye. The mechanism is discussed on the basis of the hypothesis proposed by Koizumi et al.[5]

## Experimental

**Materials.** — *Methylene Blue (MB).* — Grübler's reagent was purified according to the procedure described before.[4] The molar absorbance at the 655 mμ peak was $8.8\times10^4$ for an ethanol solution.

*Thionine (Th).*—Merck's reagent was recrystallized twice from purified ethanol and dried under a vacuum. The molar absorbance in an ethanol solution was $7.12\times10^4$ at $\lambda_{max}$ (605 mμ).

*Ethanol.*—Wako Pure Chemical Industry's G.R. grade ethanol was used. After removing traces of aldehyde, water, etc., by the ordinary method, it was fractionally distilled three times. Such a sample, however, did not show, spectroscopically, any noticeable difference compared with the twice-fractionally distilled sample; the ultraviolet spectra of these two samples were essentially identical, thus assuring their purity.*

*Acetaldehyde.*—To obtain an absolute aldehyde, a commercial 80% acetaldehyde aqueous solution (Junsei Chemical Co.) was submitted several times to distillation from a dry-ice methanol to a liquid air bath under a high vacuum.

**Procedure.**—The alcoholic solution of methylene blue was degassed in vacuo four or five times, and then irradiated with a 500 W.-85 V. tungsten projection lamp at 25.0±0.1°C. In the case of methylene blue, the light shorter than 620 mμ was eliminated by means of a Walz WR-2 cut-off filter. For thionine, a Matzuda SO56 filter was used to cut off the light shorter than 560 mμ. The reaction was followed by measuring the change in optical density at the absorption peak by the use of an interference filter. The absorption spectra were measured on a Hitachi EPU-2A or EPS autorecording spectrophotometer. The reaction cell was a quartz spectrophotometer cell ($1\times1\times4$ cm³), the upper part of which was connected to an ampule by a quartz-telex-SB-grade tube.

## Results

**Some General Features of the Reaction.**—*Photobleached Product.* — Figure 1 shows the spectral change of an irradiated solution of methylene blue and thionine in the ultraviolet and visible region. The introduction of the air into the bleached sample restored the original absorption spectra almost completely in both cases. This is considered to be strong evidence that the dye was photoreduced to its leuco form. Further evidence was obtained from a comparison of the absorption spectrum of the photobleached product with that of the chemically prepared leuco dye. The latter compound was prepared by reducing methylene blue with Pd–$H_2$, and its spectrum was measured in a hydrogen atmosphere. Table I gives a comparison of the two spectra.

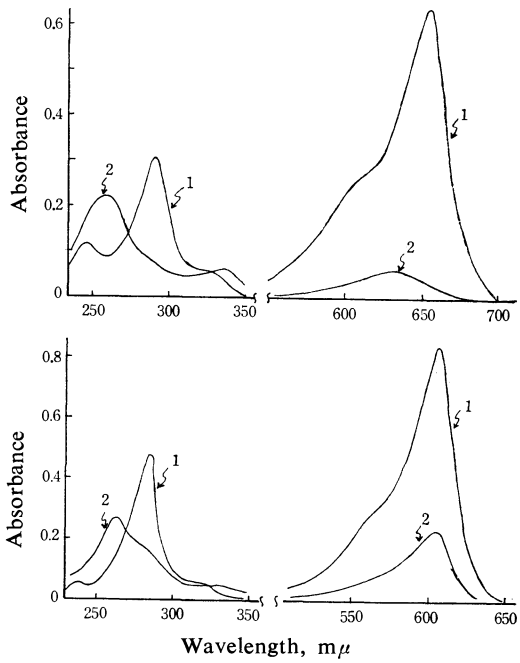



Fig. 1. The absorption spectra of the irradiated ethanol solution of methylene blue (upper) and thionine (lower) in vacuo.
$[MB]_{init}=8.0\times10^{-6}$ M
$[Th]_{init}=1.15\times10^{-5}$ M
1 Before irradiation
2 After irradiation

TABLE I

| | Chemically prepared leuco methylene blue | Photobleached product |
|---|---|---|
| Absorption peak | 261(s)* 315(w) | 261(s) 320(?) |
| $\varepsilon_{max}$ | $3.0\times10^3$ | $3.2\times10^3$ |
| % of recovery by air-introduction | 100 | 90—100 |

* s, strong; w, weak

From the agreement of the position and intensity of the absorption and from the fact that the response is quite similar to the admittance of oxygen or hydrogen peroxide, there is scarcely any doubt that the photobleached product in question consists mainly

4) Y. Usui, H. Obata and M. Koizumi, ibid., **34**, 1048, 1651 (1961).
5) M. Koizumi, H. Obata and S. Hayashi, ibid., **37**, 108 (1964).
* It appeared that the purity or the age of ethanol had a very delicate effect on the reaction rate, even when the solvent was optically pure. In the present investigation, such an obstacle was avoided by using alcohol from the same source.

of leuco dye. Furthermore, aldehyde was detected among the reaction products by gas chromatography. Thus, the overall reaction can safely be written as follows:

$$D^{+*} + C_2H_5OH \rightarrow DH + CH_3CHO + H^+$$

*The Influence of the Addition of Acetaldehyde.* —Since acetaldehyde is produced by the reaction and since a trace of it might have been present as a contaminant in the ethanol used, its effect on the rate of the reaction was examined. It was found that the rate of bleaching increased about six times when 1.16 M acetaldehyde was added to the solution (Fig. 2). On the basis of this experiment, it can safely be said that the small quantity of acetaldehyde produced during the reaction does not affect the rate appreciably. As Fig. 2 shows, the original dye is reformed when the bleached sample is kept in the dark. This is probably due to the gradual oxidation of the leuco dye by acetaldehyde.

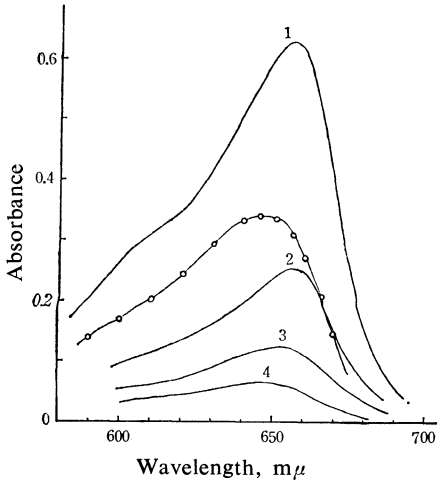



Fig. 2. Spectral changes of methylene blue in deaerated ethanol containing acetaldehyde (1.16 M).

1 Before irradiation
2 2 min-irradiation
3 5 min-irradiation
4 10 min-irradiation
-○- After keeping for 14 hr. in the dark

**Kinetic Studies.** — *Rate Formula.* — Although the photoreduction of xanthene dyes and acridine, as has already been reported,[1,3] proceeds at a rate simply proportional to the absorption of light, the same can not necessarily be expected with thiazine dyes. In view of the peculiar behavior of thiazine dyes, namely, that they are photoreduced without the addition of any reducing agent, and further, in view of the fact that this reaction in the case of methylene blue and toluidine blue in a phosphate buffer proceeds as a simple second order reaction with regard to the dye concentration,[5] it is necessary in particular to compare the applicability of the first order and the second order rate formula.* As Fig. 3 shows, the second order rate formula is far more satisfactory than the first order one. Although this result by itself appears quite extraordinary, it is not really so if one recalls that the general scheme of the photoreduction of such dyes proposed by Koizumi et al., i. e., the scheme that electron transfer occurs between the excited and the ground state dye molecules, is supported by the flash experiment to some extent.[6] Next, the effect of various factors upon the second order rate constant $k$ (rate$=kC^2$) was examined.

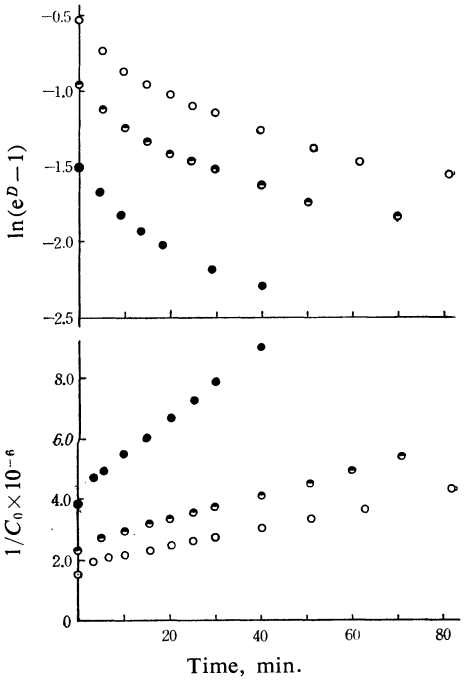



Fig. 3. Comparison of the following two rate formules; second order in dye concentration (lower), and proportional to the absorption of light (upper).

○ $C_0=6.2\times10^{-6}$ M
◓ $C_0=4.5\times10^{-6}$ M
● $C_0=2.7\times10^{-6}$ M

*The Effect of the Light Intensity.* — The intensity of the incident light was varied by means of neutral filters by a factor of about ten. The plot of $k$ against the relative intensity, as may be seen from Fig. 4, gives a good straight line. This implies that the

* The absorption of light is approximately proportional to the dye concentration, since the concentration is low.

6) S. Kato, M. Morita and M. Koizumi, This Bulletin, 37, 117 (1964).

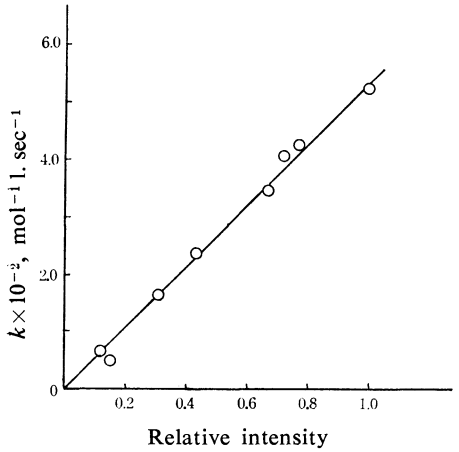



Fig. 4. Intensity effect on the overall rate constant for the second order reaction. ([MB]$=10^{-5}$ M)

net rate is essentially controlled by the interaction of the excited dye and the ground state dye, because the overall rate is of the second order with regard to the dye concentration.

*Quantum Yield.*—The quantum yield ($\Phi$) for the initial stage was evaluated from the inclination of the plot of the dye concentration against the time, together with the number of photons absorbed by the solution in a unit time ($I_{ab}$).

The latter quantity was measured with a combination of a Moll and Burger thermopile and a Shimadzu K2 potentiometer. For $5.95\times10^{-6}$ M methylene blue, $I_{ab}$ was measured as $4.8\times10^{18}$ photons $l^{-1}$ sec$^{-1}$, and the value of $\Phi$ was found to be $1-3\times10^{-3}$ (at 25°C). For $8.5\times10^{-6}$ M thionine, $I_{ab}$ was $3.6\times10^{18}$ photons $l^{-1}$ sec$^{-1}$ and $\Phi$ was $1.1\times10^{-3}$ at 25°C.

**Further Studies of the Basis of the Second Order Rate Formula.**—As has been stated above, the photobleaching of methylene blue in ethanol was accompanied with some degree of demethylation, which caused a slight shift of the absorption maximum toward a shorter wavelength. Although the minimum ratio method was employed in order to exclude the absorption of the demethylated dye, this procedure made the kinetic treatment less exact. In the case of thionine, on the other hand, such a shift does not occur and the kinetic treatment is expected to be simpler and more accurate.

Therefore, a more detailed investigation was carried out, using thionine as well as methylene blue. First, the effect of the initial dye concentration on the rate was examined quantitatively, and second, the effect on the rate of the addition of the leuco dye was investigated quantitatively in order to establish the reaction mechanism. Lastly, the photobleaching in a mixed solvent of water and ethanol was studied.

*The Effect of the Initial Dye Concentration.*—The initial dye concentration, $C_0$, was varied in the region $10^{-6}$—$10^{-5}$ M for both methylene blue and thionine. It was found that the overall second order rate constant, $k$, decreases with the increase in $C_0$ (Table II).

Figures 5a, 5b and 5c give plots of $1/k$ or $1/\Phi$* against $C_0$. The latter plot gives a good straight line; this leads to the following equation:

$$1/k=\alpha C_0(C_0+\beta) \qquad (1)$$

in which $\alpha$ and $\beta$ are constants. The kinetic

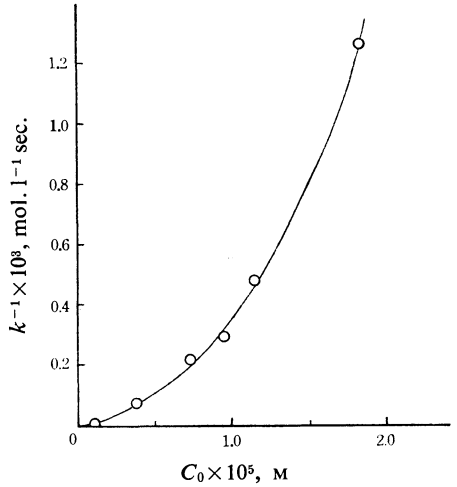



Fig. 5a. Dependence of $k^{-1}$ on the initial concentration ($C_0$) of thionine.

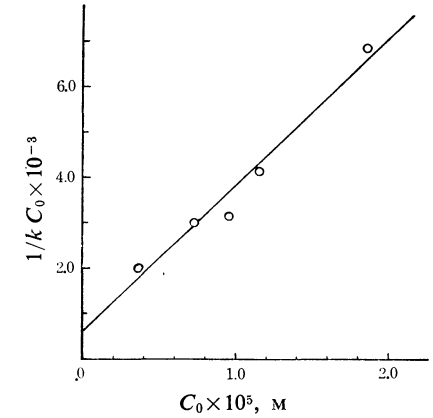



Fig. 5b. Dependence of $(kC_0)^{-1}$ on the initial concentration of thionine.
(Slope, $S_k=3.36\times10^{3}$, intercept, $I_k=4.5\times10^{2}$)

* When $C_0$ is small enough for the initial stage, $\Phi$ is proportional to $kC_0$.

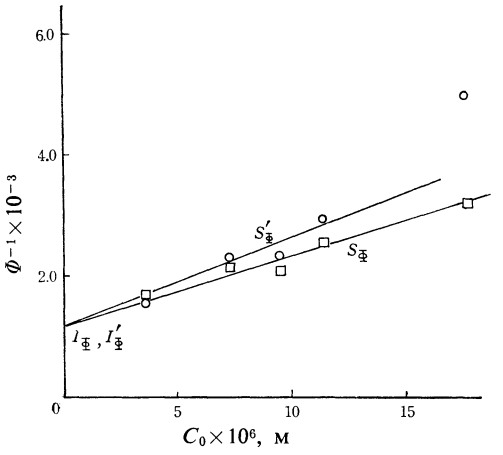



Fig. 5c. Dependence of $\Phi^{-1}$ on the initial concentration of thionine.
-○- : the plot evaluated by the approximation $I_{ab}\approx I_0\tilde{\varepsilon}C_0$
-□- : the plot evaluated by $I_{ab}=I_0(1-e^{-\tilde{\alpha}C_0})$

TABLE II. THE INITIAL CONCENTRATION EFFECT ON THE SECOND ORDER RATE CONSTANT

Thionine

| $C_0$ M | $k$ mol$^{-1}$ l. sec$^{-1}$ | $\Phi$ |
|---|---|---|
| $1.14\times10^{-6}$ | $1.24\times10^{4}$ | (0.02) |
| $3.80\times10^{-6}$ | $1.38\times10^{2}$ | $6.8\times10^{-4}$ |
| $7.30\times10^{-6}$ | $4.64\times10$ | $4.7\times10^{-4}$ |
| $9.56\times10^{-6}$ | $3.42\times10$ | $4.5\times10^{-4}$ |
| $1.15\times10^{-5}$ | $2.12\times10$ | $3.4\times10^{-4}$ |
| $1.84\times10^{-5}$ | $0.79\times10$ | $2.0\times10^{-4}$ |

Methylene blue

| $C_0$ M | $k$ mol$^{-1}$ l. sec$^{-1}$ | $\Phi$ |
|---|---|---|
| $2.39\times10^{-6}$ | $1.29\times10^{3}$ | $4.6\times10^{-3}$ |
| $3.44\times10^{-6}$ | $1.40\times10^{3}$ | $7.2\times10^{-3}$ |
| $4.95\times10^{-6}$ | $2.16\times10^{2}$ | $1.6\times10^{-3}$ |
| $6.02\times10^{-6}$ | $1.71\times10^{2}$ | $1.5\times10^{-3}$ |
| $9.59\times10^{-6}$ | $1.53\times10^{2}$ | $2.2\times10^{-3}$ |
| $1.04\times10^{-5}$ | $4.81\times10$ | $7.5\times10^{-4}$ |
| $1.9\times10^{-5}$ | $1.76\times10$ | $5.0\times10^{-4}$ |

results so far obtained are quite similar to those for methylene blue and toluidine blue in the phosphate buffer solution.

*The Retarding Effect of the Leuco Dye.*—As has already been stated, acetaldehyde, which is a reaction product, was found to have no significant influence on the rate. The effect of the leuco dye on the rate is more difficult to examine,* since the leuco dye is very sensitive to oxygen and is easily oxidized to the original form.

The procedure employed was as follows. The leuco dye, which was synthesized by reducing thionine with Pd–$H_2$ in alcohol in the dark, was added to the deaerated solution of thionine in vacuo. Using this solution, the experiment was performed and the results were compared with those for an ordinary solution with no leuco dye added. The comparisons are summarized in Table III, in which $k_L$ and $k_0$ are, respectively, the second order rate constants for the solutions with or without the leuco dye.

It is evident that the addition of the leuco dye causes a marked reduction in the rate.

*The Photoreduction of Thionine in a Mixed Solvent of Ethanol and Water.*—The absorption maximum for thionine in an aqueous solution differs from that in ethanol by only 5 m$\mu$. Furthermore, the dye exists solely in the monomeric form when the concentration of ethanol is more than 25% (v/v). These features are thought to make the results easier to interpret.

Once again, the second order rate formula could be applied satisfactorily to all the results, except for a small deviation in the initial stage. Table IV gives the maximum wavelength, its molar absorbance, and the overall second order rate constant ($k$) and the quantum yield ($\Phi$) for various compositions ($C_0=8.0\times10^{-6}$ M).

The values of the quantum yield are plotted against the molar fraction of ethanol ($\chi_R$) in Fig. 6. Evidently, there is a good linear relation between them. Thus, experimentally,

$$\Phi = \Phi^0_{H_2O} + (\Phi^0_R - \Phi^0_{H_2O})\chi_R$$

where $\Phi^0_{H_2O}$ and $\Phi^0_R$ are the quantum yields in the pure aqueous solution and in an ethanol solution respectively.

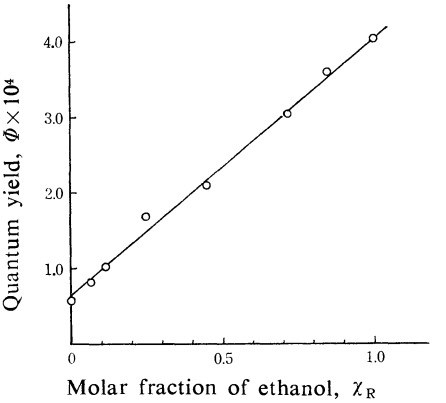



Fig. 6. The effect of water on the quantum yield for a mixed solvent.
$[Th]_0=1\times10^{-5}$ M

* When the deaerated ethanol solution of leucothionine and thionine was kept in the dark for a few days, a queer phenomenon was observed; the peak of the absorption shifted from 605 m$\mu$ to 635 m$\mu$, and the absorption in the wavelength region above 500 m$\mu$ increased. This phenomenon becomes more pronounced when the solution is illuminated.

TABLE III. THE RETARDING EFFECT OF LEUCO THIONINE

| Exp. No. | [Th] | [LTh] | $k_L$ mol$^{-1}$ l. sec$^{-1}$ | $k_0$ mol$^{-1}$ l. sec$^{-1}$ | $k_L/k_0$ |
|---|---|---|---|---|---|
| i | $6.88\times10^{-6}$ | $4.48\times10^{-6}$ | 59.6 | 52.6 | (1.12) |
| ii | $8.06\times10^{-6}$ | $8.77\times10^{-6}$ | 33.7 | 39.6 | 0.86 |
| iii | $8.80\times10^{-6}$ | $2.43\times10^{-5}$ | 17.8 | 32.2 | 0.55 |
| iv | $1.10\times10^{-5}$ | $3.80\times10^{-4}$ | 0.65 | 21.2 | 0.03 |

TABLE IV. KINETIC DATA IN THE MIXED SOLVENT

| $\chi_R$ | | $\lambda_{max}$ mμ | $\varepsilon_{max}\times10^{-4}$ | $k$ l. mol$^{-1}$ sec$^{-1}$ | $\Phi$ $(kC_0/I_0\tilde{\varepsilon})$ |
|---|---|---|---|---|---|
| 0 | (100)* | 600 | 3.98 | 2.5 | $4.3\times10^{-5}$ |
| 0.077 | (80) | 602 | 4.99 | 5.9 | $8.0\times10^{-5}$ |
| 0.125 | (70) | 602 | 5.06 | 7.4 | $10.0\times10^{-5}$ |
| 0.247 | (50) | 605 | 5.59 | 12.2 | $15.5\times10^{-5}$ |
| 0.430 | (29.9) | 605 | 5.90 | 17.4 | $21.5\times10^{-5}$ |
| 0.740 | (9.95) | 605 | 6.58 | 25.1 | $30.5\times10^{-5}$ |
| 0.846 | (5.0) | 605 | 6.76 | 29.0 | $36.4\times10^{-5}$ |
| 1.000 | (0) | 605 | 7.38 | 34.1 | $40.3\times10^{-5}$ |

* Volume percentage of water

From the above results, it is reasonable to assume that similar mechanisms prevail throughout the whole range of composition.

**A Flash Experiment on the Ethanol Solution of Methylene Blue.** — Flash experiments were performed only to compare the transients in alcohol with those in the phosphate buffer solution. Figure 7 shows the transient spectra in the degassed ethanol solution at various delay times. The present results resemble those for the aqueous solution[6] so closely that there is scarcely any doubt that the strong band at ~420 mμ and the weak shoulder at ~520 mμ correspond, respectively, to a half-reduced form and a half-oxidized form. Although it is believed that the triplet state absorption superposes at an early stage, the above two absoptions decay at about the same rate in the latter stage, suggesting that most of the half-reduced and the half-oxidized states revert to the original two dye molecules by the backward reaction.

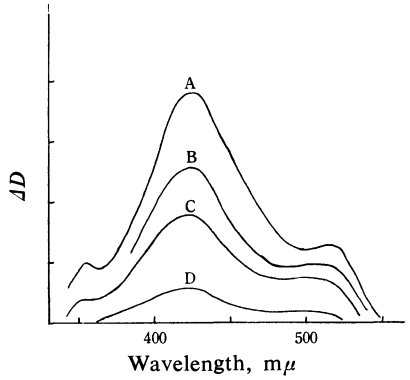



Fig. 7. The absorption spectra of the transient species in ethanol.
$[MB]_0=1\times10^{-5}$ M, $\Delta D$ is the difference in the blackness of two plates.
A : After 20 μsec.
B : After 100 μsec.
C : After 200 μsec.
D : After 400 μsec.

All the results obtained thus support the view that the mechanism of the photoreduction in an alcoholic solution is quite similar to that in an aqueous solution.

**The Effect of Dissolved Oxygen.**—The effect of the oxygen concentration on the rate of the irreversible decomposition of methylene blue in a plain aqueous solution was studied a few years ago.[7] It was found that the quantum yield of the irreversible decomposition of dye by oxygen increased with the rise in oxygen concentration but reached a constant maximum value above a certain oxygen concentration, suggesting that the reaction is competitive with the self-deactivation of the triplet state dye. A similar behavior had been observed for an aqueous solution of xanthene dyes.[1,8] On the other hand, quite a different observation had been made of an alcoholic solution of eosine.[9] When a very small amount of oxygen was added to this solution, the photobleaching was inhibited almost completely, but after a certain induction period, the length of which was proportional to the amount of oxygen, the reaction commenced at almost the same rate as in the

7) H. Obata, K. Kogasaka and M. Koizumi, This Bulletin, **32**, 125 (1958).
8) M. Imamura, *J. Inst. Polytech., Osaka City Univ.*, **5**, 85 (1956).
9) M. Imamura and M. Koizumi, This Bulletin, **29**, 899 (1956).

deoxygenated solution. This result was interpreted as being due to a very prompt attack of oxygen on the semiquinone of the dye.

In view of the bimolecular nature of the present reaction, it was thought interesting to investigate the oxygen effect on the photoreduction of an alcoholic solution of methylene blue. The concentration of dye was $8.0\times10^{-6}$ M in all cases. This reaction, however, proved rather complicated. Thus, the rate of the photobleaching decreased with an increase in the oxygen concentration. However, in this case the bleaching was interpreted as consisting of the reversible photobleaching as well as the irreversible decomposition of dye, because the introduction of air after the reaction caused a partial recovery of the dye. Besides, when the partially bleached solution was kept in the dark, the color was restored a little, perhaps due to the oxidation of leuco dye by the existent oxygen. The reversible photobleaching could occur even in the air-saturated solution; its extent was estimated to reach about ten per cent of the total bleaching.

Another feature which complicated the reaction was that significant demethylation accompanied the decoloration. As Fig. 8 shows, the degree of demethylation increases gradually with the progress of bleaching. In spite of all these complicating factors, the general effect of oxygen can be seen from Fig. 9, which gives the rate of bleaching at an initial stage as a function of the concentration of oxygen. A notable fact is that a rather rapid fall of the rate caused by a small amount of oxygen is followed by a very gradual decrease in the range of oxygen concentration beyond that of the dye.

Table V. Initial rates at various oxygen concentrations

| $O_2$ Concn., M | $(\Delta C/\Delta t)_{t=0}$, M sec$^{-1}$ |
|---|---|
| 0 | $3.6\times10^{-8}$ |
| $8.6\times10^{-6}$ | $3.6\times10^{-8}$ |
| $1.7\times10^{-5}$ | $1.5\times10^{-8}$ |
| $2.6\times10^{-5}$ | $5.6\times10^{-9}$ |
| $4.7\times10^{-5}$ | $2.2\times10^{-9}$ |
| $9.2\times10^{-5}$ | $1.8\times10^{-9}$ |
| $1.2\times10^{-4}$ | $1.4\times10^{-9}$ |
| $1.7\times10^{-4}$ | $0.7\times10^{-9}$ |
| $\sim2\times10^{-3}$ (air sat.) | $0.5\times10^{-9}$ |

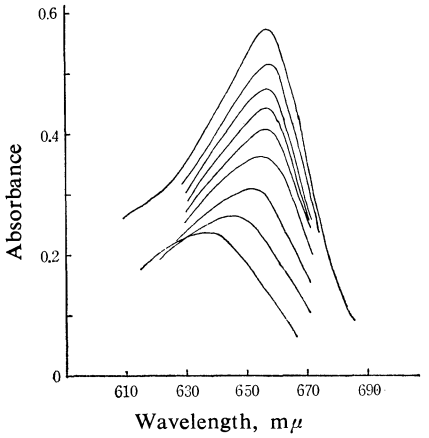



Fig. 8. An example of spectral changes in the oxygen pressure effect.
$[MB]_0=6.46\times10^{-6}$ M, $[O_2]=2.6\times10^{-5}$ M

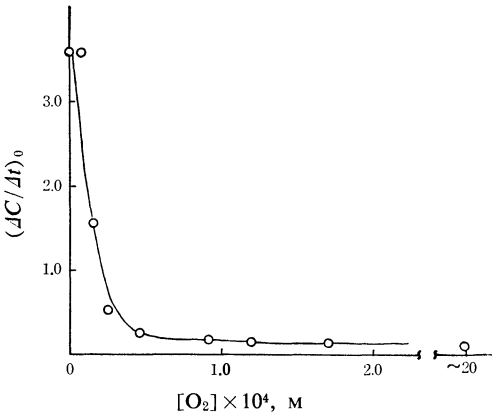
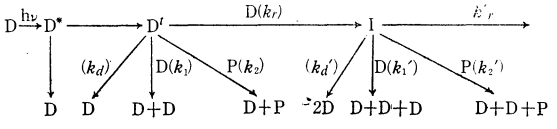



Fig. 9. Dependence of initial rate $(\Delta C/\Delta t)_0$ on oxygen concentration ($[MB]_0=8\times10^{-6}$ M).

## Discussion

In an alcoholic solution, the kinetic result is quite similar to that obtained for methylene blue and toluidine blue in a phosphate buffer solution. Hence, one can feel confident in discussing the results on the basis of a similar scheme. The scheme involves an electron transfer between the triplet dye ($D^t$) and the ground state dye, which produces another transient species (I) consisting of a half-oxidized and a half-reduced dye. Further, both $D^t$ and I are presumed to be deactivated by the ground state dye (D) and the resultant leuco dye (P), the processes being controlled by diffusion.

The above scheme can be written schematically as follows:




Scheme A

From the above scheme, one can easily derive the following equation by means of the steady state method:

$$-\frac{dC}{dt}=\frac{\alpha k_r k_r' C^2}{\left\{\begin{array}{l}\{k_d+k_1^s C+k_2(C_0-C)\}\times\\ \{k_d'+k_r'+k_1' C+k_2'(C_0-C)\}\end{array}\right\}} \quad (2)$$

where $\alpha$, the rate constant for the production of the triplet dye, can be expresse alternatively by $\alpha=\tilde{\varepsilon}\phi_{s-t}I_0$, and where $k_1^s$ is $(k_1+k_r)$. Putting $k_1^{s(\prime)}=k_2'$ and $k_d(k_d'+k_r')\approx 0$, one gets:

$$-\frac{dC}{dt}=\frac{\alpha k_r k_r' C^2}{(k_d+k_2C_0)(k_d'+k_r'+k_2'C_0)}\equiv kC^2 \quad (2')$$

$$k=\frac{\alpha k_r k_r'}{\{(k_d k_2'+k_2 k_d'+k_2 k_r')+k_2 k_2' C_0\}C_0} \quad (3)$$

This is just the same form as experimental relation 1. From relation 3:

$$\frac{1}{kC_0}=\frac{(k_d' k_2+k_2 k_r'+k_2' k_d)}{\alpha k_r k_r'}+\frac{k_2 k_2' C_0}{\alpha k_r k_r'} \quad (4)$$

Alternatively, by multipling $I_0\tilde{\varepsilon}$*:

$$\frac{1}{\Phi}=\frac{k_d' k_2+k_2 k_r'+k_2' k_d}{\phi_{s-t}\ k_r k_r'}+\frac{k_2 k_2' C_0}{\phi_{s-t} k_r k_r'} \quad (4')$$

The values of the slopes and the intercepts of the plots in Figs. 5b and 5c are given in Table VI. From these one may discuss the rate constant of each elementary reaction to some extent.

TABLE. VI. THE CONCENTRATION EFFECT OF DYE

| | Methylene blue | Thionine |
|---|---|---|
| $S_k$ (l. mol$^{-1}$ sec.) | $1.68\times10^8$ | $3.36\times10^8$ |
| $S'\phi$ (l. mol$^{-1}$) | $1.1\times10^8$ | $2.3\times10^8$ |
| $S\phi$ (l. mol$^{-1}$) | $\sim1\times10^8$ | $2.1\times10^8$ |
| $I_k$ (sec.) | $\sim10$ | $4.5\times10^2$ |
| $I'\phi$, $I\phi$ | $\sim6.7$ | $1.2\times10^3$ |
| $S_k/I_k$ | $\sim10^7$ | $7.5\times10^5$ |
| $S\phi/I\phi$ | $(\sim10^7)$ | $2\times10^5$ |

i) The slopes; $S_k$, $S\phi$ and $S\phi'$, and the intercepts, $I_k$, $I\phi$ and $I\phi'$, of each line in Figs. 5b and 5c refer to the same experimental data.

ii) For methylene blue, the values of the intercepts are too small to be treated quantitatively.

If one tentatively assumes $k_2\approx k_2'=10^{10}$—$10^9$ (l. mol$^{-1}$ sec$^{-1}$), which is the value for a diffusion controlled process, then for thionine $k_d+k_d'+k_r'=1.3\times10^4$ (sec$^{-1}$)** and $\phi_{s-t}k_r k_r'=5\times10^{11}$ (l. mol$^{-1}$ sec$^{-2}$), and for methylene blue, $k_d+k_d'+k_r'\approx10^3$ (sec$^{-1}$) $\phi_{s-t}k_r k_r'\sim1\times10^{12}$ (l. mol$^{-1}$ sec$^{-2}$). Inserting $\phi_{s-t}\approx10^{-1}$ as a plausible value, the $k_r k_r'$ values for thionine and methylene blue are, respectively, $5\times10^{12}$ and $10^{13}$. Since the $k_r'$ values for thionine and methylene blue are, respectively, less than $10^4$ and $\sim10^3$, the lowest limits of the $k_r$ value for the two dyes are, respectively, $10^9$ and $\sim10^{10}$. These data conform well with the fact that in the flash experiment a rather large quantity of the intermediate I is produced and that its life is of the order of a millisecond. They also seem to be consistent with the results obtained in the photoreduction of thiazine dyes in the phosphate buffer solution.[5] So far, Scheme A is quite satisfactory.

Next, the effect of leuco dye on the reaction rate will be discussed. According to Scheme A, the following rate formula should hold for the case in which a definite quantity of leuco dye is added beforehand:

$$-\frac{dC}{dt}=k_L C^2=\frac{\alpha k_r k_r' C^2}{\left\{\begin{array}{l}(k_d k_2'+k_d' k_2+k_2 k_r')\{[\mathrm{LTh}]_0+[\mathrm{Th}]_0\}\\ +k_2 k_2'\{[\mathrm{LTh}]_0+[\mathrm{Th}]_0\}^2\end{array}\right\}}$$

For the solution to which no leuco dye is added:

$$-\frac{dC}{dt}=k_0 C^2=\frac{\alpha k_r k_r' C^2}{(k_d+k_2[\mathrm{Th}]_0)(k_d'+k_r'+k_2'[\mathrm{Th}]_0)}$$

where $[\mathrm{LTh}]_0$ and $[\mathrm{Th}]_0$ are, respectively, the initial concentrations of leuco thionine and thionine. Using the value $k_2k_2'/(k_2k_d'+k_2'k_d+k_2k_r')=7.5\times10^5$, $k_L$ can easily be calculated from $k_0$. The values thus obtained are compared with the observed values in the following table:

| Exp. No. in Table III | $(k_L/k_0)_{obs}$ | $(k_L/k_0)_{calcd}$ |
|---|---|---|
| ii | 0.86 | 0.22 |
| iii | 0.55 | 0.10 |
| iv | 0.03 | 0.0009 |

Since the observed effect is much smaller than the calculated one, one can not say that the effect of the addition of the leuco dye is consistent with the proposed scheme. In connection with this discrepancy, it should be noted that a relation quite similar to that of

* $\tilde{\alpha}$ is the average molecular absorption coefficient defined by the relation:

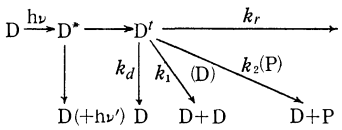
$$I_{ab}=I_0\ (1-e^{-\tilde{\alpha}cd})$$

and $\tilde{\alpha}$ is $2.303\tilde{\varepsilon}$.

From the measurement of $I_0$ and $I_{ab}$ by means of a thermopile, the values of $\tilde{\varepsilon}$ were determined for methylene blue and thionine to be $3\times10^4$ and $2.1\times10^4$ respectively. In view of the magnitude of $\tilde{\alpha}$, one may safely use the approximation, $I_{ab}=I_0\tilde{\varepsilon}C_0$, when $C_0$ is less than $\sim7\times10^{-6}$ M. The $I_0\tilde{\varepsilon}$ values used for MB and Th were 0.67 and 0.71 respectively.

** According to Parker, the $k_d$ value of thionine in an aqueous acidic solution is $5\times10^4$ sec$^{-1}$ (C. A. Parker, *J. Phys. Chem.*, **63**, 26 (1959)).

4 can be derived even when the reaction scheme is such that the primary process consists of the attack of an alcohol molecule on $D^t$. Thus, if one adopts the following scheme:




Scheme B

then:

$$-\frac{dC}{dt}=\frac{I_{ab}\phi_{s-t}k_r}{k_d+k_r+k_1C_0}$$

on the assumption that $k_1\approx k_2$.

Hence,

$$\frac{1}{\Phi}=\frac{k_d+k_r}{\phi_{s-t}k_r}+\frac{k_1C_0}{k_r\phi_{s-t}} \qquad (6)$$

This is formally the same as 4'. In other words, the values for $S\phi$ and $I\phi$ experimentally obtained according to Scheme B are written as follows:

$$S\phi=k_1/k_r\phi_{s-t} \quad I\phi=(k_r+k_d)/k_r\phi_{s-t}$$

Inserting the proper values, one gets, for thionine, $k_1/(k_d+k_r)=2\times10^5$ and $k_r\phi_{s-t}=10^2$. If one assumes that $\phi_{s-t}$ for thionine is of the $10^{-1}$ order, $k_r$ is $\sim10^3\,sec^{-1}$.

The effect on $k$ of the addition of leuco thionine should be as follows, according to Scheme B:

| Exp. No. in Table III | $(k_L'/k_0)_{calcd}$ |
|---|---|
| ii | 0.51 |
| iii | 0.42 |
| iv | 0.033 |

Thus, as far as the effect of leuco dye is concerned, Scheme B seems to be more satisfactory than A.

However, the value for $k_r$ on the basis of Scheme B is unreasonable if one takes the oxygen effect into consideration (the result given in Fig. 9). The reason is as follows.

A rapid decrease in the bleaching caused by a small concentration of oxygen is interpreted by the competition of $D^t+O_2$ (mainly deactivation) and $D^t+D\rightarrow$ according to Scheme A, while only the latter process needs to be replaced by $D^t+alc\rightarrow$ for Scheme B. In either case, it is very plausible to assume that the deactivation of $D^t$ by oxygen is an encounter-rate-determining process. If so, the effect of oxygen should become appreciable at the oxygen concentration given by the following relation:

for Scheme A $\quad k_r[D]\approx k_{diff}[O_2]$ (7)

for Scheme B $\quad k_r\approx k_{diff}[O_2]$ (8)

The $k_r$ values in Eqs. 7 and 8 have the meanings given in Scheme diagrams A and B, and $k_{diff}$ is the rate constant for the diffusion controlled process and is of the order of $10^9$—$10^{10}$ l. $mol^{-1}\,sec^{-1}$.

For Scheme B, the value of $k_r$, $\sim10^3\,sec^{-1}$ requires that the concentration of oxygen in question be $10^{-6}$—$10^{-7}$ M. As Fig. 9 shows, however, the real concentration of oxygen necessary to compete with the reductive bleaching is more than $\sim10^{-5}$ M, a value much larger than the above value. In addition, the fact that a reversible photoreduction takes place to a measurable extent, even in an air-saturated solution, is quite difficult to understand when the above line of reasoning is followed.

For Scheme A, there is no such inconsistency if the value of $k_r$ is large enough; this is plausible, as has already been shown.

Summing up all the results, one cannot decide conclusively whether Scheme A or Scheme B predominates. Yet, Scheme A seems more plausible on the basis of the various results so far obtained. The inconsistency between the second order rate formula and the effect of the leuco dye is the only question which needs to be further studied.

It is to be hoped that more extensive studies of the dye concentration effect on the rates for the degassed solution and the aerated solution will give a more definite conclusion.

Lastly, let us add a brief discussion of the results obtained for a mixed solvent. If the attack of the water molecule and the alcohol molecule on I (in the case of Scheme A) or on $D^t$ (in the case of Scheme B) occurs according to the mass-action law, the rate would be given by:

$$\text{Rate}=\text{const.}\times\frac{k^r_w[H_2O]+k^r_{alc}[C_2H_5OH]}{k^s_w[H_2O]+k^s_{alc}[C_2H_5OH]}$$

where $k^r$ and $k^s$ refer, respectively, to the rate constant of the genuine reaction of I or $D^t$ as the case may be, and the rate constant for the disappearance (the sum of the deactivation and the genuine reaction of I or $D^t$). If $k^s_w=k^s_{alc}$ holds approximately, then the expected rate formula would result.

## Summary

The photochemical behavior of methylene blue and thionine in ethanol is quite different from that of eosine in the same solvent. They are compared from several viewpoints below.

From the preliminary flash experiment and the kinetic results by steady illumination, it has been concluded that interaction between

| | Methylene blue | Eosine |
|---|---|---|
| % of leuco dye | About 100% leuco | Above 50% leuco |
| Quantum yield | $1-3\times10^{-3}$ | $5.6\times10^{-4}$ |
| Air introduction | Complete recovery | No recovery |
| Intensity ($I_0$) effect | Proportional to $I_0$ | Proportional to $I_0$ |
| Rate formula | Second order in dye concentration | Proportional to the absorption of light |
| $O_2$ effect | Very complex oxidative and reductive bleaching simultaneously occur | The reaction is completely suppressed by a trace of $O_2$. |

the ground state and the excited state dye is essential for photoreduction.

It is most probable that the overall scheme for the photoreduction of thiazine dyes in alcohol is similar to that in the case of the same dyes in a phosphate buffer solution.

The author would like to express his deep thanks to Professor Masao Koizumi for his encouragement and many valuable discussions throughout this work. He also wishes to express hearty thanks to Professor Shunji Kato for his helpful advice.

*Department of Chemistry*
*Faculty of Science*
*Tohoku University*
*Katahira-cho, Sendai*

# The Synthesis of *N*-Terminal Acetylpeptides of Ovalbumin and Mammalian Heart Cytochrome c

By Yoshihiko BABA, Fumio SAKIYAMA, Koiti TITANI and Kozo NARITA

(Received June 18, 1964)

In previous publications from our laboratory,[1,2] it has been reported that *N*-acetylglycylserine and *N*-acetylglycylserylglycylisoleucylalanine can be isolated from the enzymatic hydrolysates of ovalbumin; it has also been suggested that these *N*-acetylpeptides are derived from the *N*-terminal position of the protein, because many attempts over the past ten years, to find the terminal group by the usual analysis methods have been unsuccessful. It seems to be important to confirm the structure of such an unusual *N*-terminal peptide by chemical synthesis. *N*-Acetylglycyl-L-serine and *N*-acetyl-L-serylglycine have thus been synthesized. Comparisons of their chromatographic behaviors and of the products of the N→O acyl shift reaction with those of the natural acetylpeptide have been made.

Like ovalbumin, for the *N*-terminal group of mammalian (bovine and equine) heart cytochrome c, conflicting results had also been presented until *N*-acetylglycylaspartylvalylglutamic acid was isolated in a fairly good yield from the enzymatic digest of the cytochrome.[3] The structure of the isolated *N*-acetyltetrapeptide was confirmed by comparison with the synthetic material. The synthesis of the acetyltetrapeptide will be described and the troubles encountered during its synthesis will be discussed in the present communication.

## Experimental[4]

**The Synthesis of Acetylpeptide.**—*N-Chloroacetyl-O-benzyl-L-serine.*—*O*-Benzyl-L-serine[5] (9.8 g.) was dissolved in a mixture of 2 N sodium hydroxide and 2 N sodium carbonate (55 ml.); then into this solution chloroacetyl chloride (8.5 g.) was stirred portion by portion at 0—5°C. After the addition was complete, the reaction mixture was stirred at room temperature for half an hour. The pH of the solution was adjusted to 2.8 with 6 N hydrochloric acid, and white precipitates were collected as a waxy material. Yield, 11 g. (80%). Recrystallization from ethylacetate gave fine crystals. M. p. 114—115°C.

Found: N, 4.77. Calcd. for $C_{12}H_{14}O_4NCl \cdot H_2O$: N, 4.83%.

*N-Glycyl-O-benzyl-L-serine.* — Absolute methanol (200 ml.) in an ice-salt bath was saturated with

1) K. Narita, *Biochem. Biophys. Res. Comm.*, **5**, 160 (1961).
2) K. Narita and J. Ishii, *J. Biochem.*, **52**, 367 (1962).
3) K. Titani, K. Narita and K. Okunuki, *J. Biochem.*, **51**, 350 (1962).
4) All melting points are uncorrected. The $R_f$ values listed were measured on a paper chromatogram developed with *n*-butanol-acetic acid-water (4:1:1, v/v). The specific optical rotation was measured in an acetic acid solution.
5) K. Okawa, This Bulletin, **29**, 486 (1956).

dry ammonia, and pulverized *N*-chloroacetyl-*O*-benzyl-L-serine (9 g.) was added. *N*-Chloroacetyl-*O*-benzyl-L-serine is soluble in pure methanol, but sparingly soluble in the methanol-ammonia. Thus the suspension in a stoppered bottle was allowed to stand at room temperature for thirteen days with occasional shaking. The insoluble material (2.6 g.), which was the starting material, was removed by filtration. When the filtrate was concentrated in vacuo, a crystalline material was obtained. Yield, 4.3 g. When the above recovered starting material was subjected to further amination, an additional 2.2 g. of the dipeptide derivative was obtained. The total yield was 78%. Recrystallization from water-acetone gave fine crystals. M. p. 192—193°C.

Found: C, 57.87; H, 6.39; N, 10.82. Calcd. for $C_{12}H_{16}O_4N_2$: C, 57.13; H, 6.39; N, 11.11%.

*N-Acetylglycyl-O-benzyl-L-serine.*—Glycyl-*O*-benzyl-L-serine was acetylated in a usual manner using acetic anhydride and aqueous alkali. The acetylated dipeptide derivative was recrystallized from water. Yield, 74%. M. p. 105—108°C.

Found: N, 8.73. Calcd. for $C_{14}H_{18}O_5N_2 \cdot H_2O$: N, 8.97%.

*N-Acetylglycyl-L-serine.* — *N*-Acetylglycyl-*O*-benzyl-L-serine (2g.) was hydrogenated on palladium-charcoal in 75% *t*-butanol (60 ml.) in a 90% yield. Recrystallization from water gave pure acetyldipeptide. M. p. 166—167.5°C (decomp.).

Found: C, 40.80; H, 5.96; N, 13.45. Calcd. for $C_7H_{14}O_5N_2$: C, 41.17; H, 5.92; N, 13.72%.

*Carbobenzoxy-L-serylglycine Benzyl Ester.*—Carbobenzoxy-L-serine (6.4 g.) was dissolved in a warm chloroform-dioxane mixture (2 : 1, v/v, 45 ml.) and was coupled with glycine benzyl ester by dicyclohexylcarbodiimide (5.4 g.). After the mixture had been kept at room temperature overnight, dicyclohexylurea (4.6 g.) was filtered off. The filtrate was then concentrated and the residue dissolved in ethylacetate (150 ml.). The solution was washed successively with 0.6 N hydrochloric acid, 5% sodium hydrogen carbonate and water, and finally dried. After the removal of additional precipitates of the urea derivative, the solution was partly evaporated and petroleum ether was added. When the crude product (9.1 g.) was recrystallized from ethylacetate, 7.4 g. (72%) of the product was obtained. M. p. 109—110°C (lit. m. p. 102°C[6]).

Found: C, 62.84; H, 6.09; N, 7.14. Calcd. for $C_{20}H_{22}O_6N_2$: C, 62.16; N, 5.74; N, 7.25%.

*N-Acetyl-L-serylglycine.*—L-Serylglycine (m. p. 204—207°C, decomp.) was obtained from the carbobenzoxydipeptide benzylester by catalytic hydrogenation on palladium-charcoal in 75% *t*-butanol for 5 hr. Into an aqueous triethylamine solution (15% solution, 10 ml.), L-serylglycine (570 mg.) was dissolved, and then acetic anhydride (0.55 g.) was added. The reaction mixture was stirred for half an hour at 0—2°C and then kept for an additional thirty minutes at room temperature. The syrupy product which was obtained by the concentration of the above mixture below 38°C was dissolved in water (2 ml.) and placed on the top of a column of Dowex 50-X2 (H-form, 1×14 cm.). The column was then washed with water until the effluent became neutral. The effluent (30 ml.) was lyophilized. Yield, 480 mg. (68%). M. p. 161—163°C (decomp.).

Found: C, 40.98; H, 5.93. Calcd. for $C_7H_{12}O_5N_2$: C, 41.17; H, 5.92%.

*Carbobenzoxy-L-valyl-L-glutamic Acid Dibenzyl Ester.*—Crystalline carbobenzoxy-L-valine (6.6 g.) and L-glutamic acid dibenzyl ester *p*-toluenesulfonate (15.8 g.) were dissolved in methylene chloride (40 ml.) containing triethylamine (1.5 g.). Into this solution, dicyclohexylcarbodiimide (5.5 g.) in a small amount of the same solvent was then added on an ice-bath. Dicyclohexylurea precipitated immediately. After it had been allowed to stand in an ice-bath, the reaction mixture was left at room temperature for an additional fifteen hours. The urea derivative was removed by filtration, and the filtrate was successively washed with 0.1 N hydrochloric acid, water, 5% sodium hydrogen carbonate and water. It was then dried over anhydrous sodium sulfate, and the solution was evaporated to dryness in vacuo. The crystalline residue was recrystallized from ethylacetate. Yield, 11.2 g. (76.2%). M. p. 148°C. $[\alpha]_D^{27}$ −23.9° (*c* 2.0).

Found: C, 68.66; H, 6.76; N, 5.09. Calcd. for $C_{32}H_{36}O_7N_2$: C, 68.55; H, 6.47; N, 5.00%.

*L-Valyl-L-glutamic Acid.*—Carbobenzoxy-L-valyl-L-glutamic dibenzyl ester (10 g.) was reduced in 70% acetic acid (150 ml.) in the presence of 10% palladium on charcoal (1.0 g.) for two hours. After the removal of the catalyst by filtration, the filtrate was concentrated under reduced pressure. In order to remove the acetic acid completely, the solid residue was dissolved in a minimal volume of water and the solution evaporated to dryness. The above treatment was repeated, and then the crystalline residue was recrystallized from water-ethanol. Yield, 3.7 g. (84.2%). M. p. 227°C (decomp.). $[\alpha]_D^{27}$ +17.4° (*c* 1.4). $R_f$. 0.38.

Found: C, 48.84; H, 7.63; N, 11.30. Calcd. for $C_{10}H_{18}O_5N_2$: C, 48.76; H, 7.37; N, 11.38%.

*L-Valyl-L-glutamic Acid Dibenzyl Ester p-Toluenesulfonate.*—L-Valyl-L-glutamic acid (2.5 g.) *p*-toluenesulfonic acid hydrate (2.2 g.) and benzyl alcohol (20 ml.) were mixed in chloroform (100 ml.), and the mixture was refluxed with Wieland's apparatus (silica gel was used as a desiccant). Within a few hours the partly-insoluble starting material was dissolved entirely. Reflux was continued for ten hours, and then the solvent and the excess benzyl alcohol were removed in vacuo. When the syrupy residue was triturated in ether (150 ml.), a crystalline solid precipitated. It was recrystallized from ethanol-ether. Yield, 5.6 g. (91.8%). M. p. 108~109°C. $[\alpha]_D^{27}$ +0.0° (*c* 2.0). $R_f$ 0.81.

Found: C, 61.66; H, 6.54; N, 4.80. Calcd. for $C_{31}H_{38}O_8N_2S$: C, 62.19; H, 6.40; N, 4.68%.

*Carbobenzoxy-L-aspartyl-L-valyl-L-glutamic Acid Tribenzyl Ester.* — A mixture of L-valyl-L-glutamic acid dibenzyl ester *p*-toluenesulfonate (3.0 g.), triethylamine (0.5 g.), carbobenzoxy-L-aspartic acid β-benzyl ester[7] (1.6 g.) and dicyclohexylcarbodiimide (1.0 g.) was dissolved in methylene chloride

6) J. S. Fruton, *J. Biol. Chem.*, **146**, 463, (1942).

7) A. Berger and E. Katchalski, *J. Am. Chem. Soc.*, **73**, 4083 (1951).

(30 ml.); this solution was then allowed to stand for fifteen hours at room temperature. The precipitated dicyclohexylurea was filtered off and the filtrate was evaporated to dryness. The residue crystallized immediately. It was recrystallized from methanol. Yield, 2.4 g. (63.2%). M. p. 131°C. $[\alpha]_D^{27}$ −24.0° (*c* 1.9).

Found: C, 66.97; H, 6.34; N, 4.99. Calcd. for $C_{43}H_{47}O_{10}N_3 \cdot CH_3OH$: C, 66.73; H, 6.35; N, 5.19%.

*L-Aspartyl-L-valyl-L-glutamic Acid.*—Carbobenzoxy-L-aspartyl-L-valyl-L-glutamic acid tribenzyl ester (2.4 g.) was suspended in 70% acetic acid (100 ml.). Hydrogen gas was bubbled into the above solution for three hours in the presence of 10% palladium on charcoal (0.5 g.). The starting tripeptide derivative was dissolved within fifteen minutes. The catalyst was removed by filtration, and the filtrate was evaporated to dryness in vacuo. The residue was dissolved into water and lyophilized. (Attempts to crystallize it were unsuccessful.) Yield, 1.0 g. (89.0%). M. p. 165°C (decomp.). $[\alpha]_D^{27}$ −6.9° (*c* 1.0). $R_f$ 0.18.

Found: C, 45.46; H, 6.84; N, 11.20. Calcd. for $C_{14}H_{23}O_8N_3 \cdot 1/2\ H_2O$: C, 45.39; H, 6.35; N, 11.34%.

*L-Aspartyl-L-valyl-L-glutamic Acid Tribenzyl Ester p-Toluenesulfonate.*—L-Aspartyl-L-valyl-L-glutamic acid (0.8g.), *p*-toluenesulfonic acid hydrate (0.45 g.) and benzyl alcohol (1.0 ml.) were mixed in chloroform (20 ml.). The mixture was then refluxed with Wieland's apparatus. The solvent and the excess benzyl alcohol were distilled off in a high vacuum. The syrupy residue was dissolved in ether (2 ml.), and *n*-hexane was slowly added until crystalline precipitates appeared. These precipitates were collected and recrystallized from ether-*n*-hexane. Yield, 1.35 g. (78.3%). M. p. 181°C. $[\alpha]_D^{27}$ −21.0° (*c* 2.2). $R_f$ 0.85.

Found: C, 62.97; H, 6.10; N, 5.33. Calcd. for $C_{42}H_{49}O_{11}N_3S$: C, 62.95; H, 6.14; N, 5.23%.

*Acetylglycyl-L-aspartyl-L-valyl-L-glutamic Acid Tribenzyl Ester.*—Into an ice-cooled solution of acetylglycine (0.21 g.) in freshly-distilled dimethylformamide (10 ml.), carbonyldiimidazole (0.3 g.) was stirred. After ten minutes, a solution of L-aspartyl-L-valyl-L-glutamic acid tribenzyl ester *p*-toluenesulfonate (1.2 g.) and an equivalent amount of triethylamine in dimethylformamide (10 ml.) were added. The reaction mixture was then left for four hours at room temperature and diluted with water (20 ml.). The gelatinous product separated was collected by centrifugation, followed by filtration with suction. This was recrystallized from hot ethanol as fine needles. Yield, 0.7 g. (64.2%). $[\alpha]_D^{27}$ −13.0° (*c* 2.1).

Found: C, 63.85; H, 6.20; N, 8.00. Calcd. for $C_{39}H_{46}O_{10}N_4$: C, 64.09; H, 6.36; N, 7.67%.

*Acetylglycyl-L-aspartyl-L-valyl-L-glutamic Acid.*—Acetylglycyl-L-aspartyl-L-valyl-L-glutamic acid tribenzyl ester (0.5 g.) was reduced over 10% palladium on charcoal (0.2 g.) in 50% acetic acid (20 ml.) for two hours. The catalyst was then removed by filtration, and the filtrate was concentrated in vacuo. The residue was dissolved in water, (20 ml.) and Amberlite IR-120 (H-form, 3 ml.) was poured in while it was being stirred and cooled. The resin was removed by filtration and washed with three 5 ml. portions of water. The combined filtrate and washings were then lyophilized. The colorless, fluffy material which remained was negative to the ninhydrin reaction. It contained three equivalents of carboxyl groups, as determined by titration with sodium methoxide.[8] M. p. 192°C (decomp.). $[\alpha]_D^{27}$ −29° (*c* 1.3). $R_f$ 0.55 (detected with bromocresol green; the paper strip must be free from acetic acid). Amino acid analysis with automatic equipment gave a molar ratio of 0.9 : 1.0 : 1.1 : 1.1 for glycine, aspartic acid, valine and glutamic acid.

Found: C, 44.62; H, 6.35; N, 11.82. Calcd. for $C_{18}H_{28}O_{10}N_4$: C, 45.19; H, 6.32; N, 11.71%.

**The N→O Acyl Shift Reaction of *N*-Acetylglycylserine and *N*-Acetylserylglycine.** — About 2 mg. of the peptide was suspended in 5 ml. of dry dioxane, and hydrogen bromide gas was passed through until the mixture became clear.[2] The solution was refluxed for a few minutes to complete the N→O shift reaction and then evaporated to dryness in vacuo. The residue was dissolved in a minimum volume of water, and an aliquot was used for paper chromatography (*n*-butanol - acetic acid - water 4 : 1 : 1, v/v). The remaining aliquot was made alkaline by the addition of 5% ammonium hydroxide, and then the solution was kept for 2 hr. at room temperature in order to reverse the shifted products (O→N acyl shift). The solution was evaporated at room temperature in an evacuated desiccator. The characterization of the products of the O→N acyl shift reaction was performed by paper chromatography.

**The Carboxypeptidase A Digestion of the Acetylglycylaspartylvalylglutamic Acid.**—To compare the natural acetyltetrapeptide with the synthetic one, the rate and the extent of the release of amino acids from the peptides by the action of carboxypeptidase A were measured. The crystalline enzyme was purchased from the Worthington Biochemical Corp. (Freehold, New Jersey) and used after three recrystallizations. As has been reported previously,[3] the enzyme hydrolyzed the acetyltetrapeptide most at pH 6.0, in contrast to the usual optimum of pH 8.0, and the digestion was carried out at pH 6.0 (M/7 sodium acetate - M/7 sodium barbiturate - N/10 hydrochloric acid - 8.5% sodium chloride buffer) and at room temperature in the substrate to the enzyme ratio of 1 : 1 by weight. The amino acids released were characterized and estimated as their dinitrophenyl derivatives by paper chromatography.

## Results and Discussion

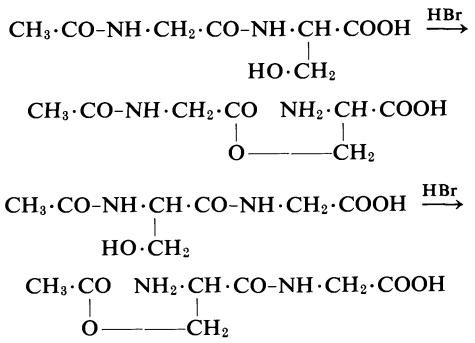
Although it was quite clear from the structural analysis that the acetyldipeptide isolated from the pronase (the trade name of a protease of *Streptomyces griseus*) digest of ovalbumin was acetylglycylserine,[1,2] two acetyldipeptides, which have opposite amino acid sequences were prepared in order to compare them with the natural acetyldipeptide.

8) J. S. Fritz and N. M. Lisicki, *Anal. Chem.*, **23**, 589 (1951).

Unfortunately, the two synthetic acetyldipeptides behaved identically on a paper chromatogram with the natural peptide ($R_f$ 0.46, *n*-butanol - acetic acid - water, 4 : 1 : 1, v/v) ; moreover, the chromatograms of the hydrazinolysates of the three acetyldipeptides, synthetic and natural, were all the same, showing acetylhydrazide ($R_f$ 0.63, pyridine-aniline-water, 9 : 1 : 4, v/v ; 0.45, collidine-picoline-water, 5 : 3 : 2, v/v), glycine hydrazide ($R_f$ 0.37 ; 0.11) and serine hydrazide ($R_f$ 0.46 ; 0.16).[1,2]

In order to distinguish *N*-acetylglycylserine from *N*-acetylserylglycine, the N→O acyl shift reaction was explored in anhydrous dioxane by passing hydrogen bromide gas through. It may be expected that *O*-[acetylglycyl]-serine will be produced from *N*-acetylglycylserine by the shift reaction[2] while *O*-acetylserylglycine is obtained from *N*-acetylserylglycine, and that the $R_f$ values of the above two products are probably different from one another on a paper chromatogram.

The $R_f$ values of the reaction products of the two synthetic and one natural acetyldipeptides are listed in Table I. It is clear from the table that the shift reaction under the conditions was accompanied by some side reactions. The products of the N→O acyl shift reaction may be recovered as the starting compound by the reverse O→N acyl shift



reaction in an alkaline medium, whereas the products by the side reaction will not be changed under the conditions. As can be seen in Table I, free amino acid resulted from the *C*-terminal amino acid, in some extent as a result of the hydrolytic side reaction. An additional unknown side reaction product, which is ninhydrin-positive, was observed in both cases, but it is not known whether or not the unknown product from acetylglycylserine is the same as that from acetylserylglycine, although their $R_f$ values are quite similar.

At any rate, the behavior of the products of the N→O acyl shift reaction of the natural acetyldipeptide was identical with that of the synthetic acetylglycyl-L-serine. Thus, the

TABLE I. $R_f$ VALUES OF THE PRODUCTS OF N→O ACYL SHIFT REACTION OF *N*-ACETYLGLYCYLSERINE AND *N*-ACETYLSERYLGLYCINE*

| | Standard | Reaction products of N→O acyl shift | | | | |
|---|---|---|---|---|---|---|
| | | Synthetic *N*-acetylglycylserine | | Natural *N*-acetylglycylserine | Synthetic *N*-acetylserylglycine | |
| | | Before O→N shift | After O→N shift | Before O→N shift | Before O→N shift | After O→N shift |
| Glycylserine | 0.14 | | | | | |
| Serine | 0.16 | 0.16 | 0.16 | 0.16 | | |
| Serylglycine | 0.17 | | | | | |
| Glycine | 0.18 | | | | 0.18 | 0.18 |
| *O*-[Acetylglycyl]-serine | 0.20 | 0.20 | | 0.20 | | |
| *O*-Acetylserine | 0.31 | | | | | |
| *O*-Acetylserylglycine | 0.34 | | | | 0.33 | |
| *N*-Acetylglycylserine | *0.46* | | *0.46* | | | |
| *N*-Acetylserylglycine | *0.46* | | | | | *0.46* |
| *N*-Acetylserine | *0.56* | | | | | |
| Unknown** | | 0.67 | 0.67 | 0.60—0.70 | 0.66 | 0.66 |

* *n*-Butanol-acetic acid-water (4 : 1 : 1, v/v) was used as a solvent for descending paper chromatography. The ninhydrin reagent was used for the detection of the products. When quite enough amount of *N*-acetyl derivatives are present on a paper and when prolonged heating with an iron after spraying the reagent was used, they colored as pinkish purple. In this experiment, the chlorine-iodide-starch reaction was also employed after the ninhydrin reaction to identify *N*-acetyl derivatives sharply ($R_f$ values are shown as italic figures). *O*-[Acetylglycyl]-L-serine was a generous gift from Dr. Shumpei Sakakibara of the Institute for Protein Research, Osaka University and the other standard peptides were synthesized by the present authors.

** Color intensity of an unknown spot was weak, especially in the case of the reaction product of *N*-acetylserylglycine.

structure deduced for the natural acetyldipeptide isolated from ovalbumin[1] was confirmed without any ambiguity.

We have demonstrated that cytochromes c from bovine and equine hearts terminated at acetylglycylaspartylvalylglutamic acid.[3] At almost same time Margoliash et al.[9] determined the complete amino acid sequence of equine heart cytochrome, their results are consistent with the *N*-terminal sequence we have described above. In order to confirm the *N*-terminal structure of the cytochrome, we attempted the synthesis of *N*-acetylglycyl-L-aspartyl-L-valyl-L-glutamic acid. The first route to synthesize the acetyltetrapeptide of the problem was as follows:

Cbz-L-aspartic acid β-methyl ester + L-Valyl-L-glutamaic dimethyl ester —DCCD→

Cbz-L-aspartyl-L-valyl-L-glutamic acid trimethyl ester

M. p. 171°C, $[\alpha]_D^{22}$, −19.40 (*c* 0.62, acetic acid), 71%

—$H_2$/Pd→ L-Aspartyl-L-valyl-L-glutamic acid trimetyl ester + Cbz-glycine —DCCD→

Cbz-glycyl-L-aspartyl-L-valyl-L-glutamic acid trimethyl ester

M. p. 130—137°C, $[\alpha]_D^{22}$ −36.6° (*c* 0.82), 64%

—$H_2O$→ Cbz-glycyl-L-aspartyl-L-valyl-L-glutamic acid

M. p. 100—111°C, $[\alpha]_D^{22}$ −4.20 (*c* 1.18), 81%

—$H_2$/Pd→ Glycyl-L-aspartyl-L-valy-L-glutamic acid

$[\alpha]_D^{22}$ +4.7° (*c* 0.64), 89%

—Acetic anhydride→ Acetylglycyl-L-aspartyl-L-valyl-L-glutamic acid

M. p. 140°C, $[\alpha]_D^{22}$ −5.1° (*c* 0.78), 83%

(Cbz and DCCD are the abbreviations for the carbobenzoxy group and for dicyclohexylcarbodiimide respectively.)

The acetylglycyl-L-aspartyl-L-valyl-L-glutamic acid thus synthesized (this acetyltetrapeptide is designated as I to distinguish it from the acetyltetrapeptide II which is prepared by the method described in the "Experimental" section) was shown by amino acid analysis to contain an equimolar amount of the constituent amino acids. The chromatographic behavior ($R_f$ 0.72, *n*-butanol - acetic acid - water, 4 : 1 : 1, v/v) of the synthetic acetyltetrapeptide I on a paper was identical with that of the natural acetyltetrapeptide obtained from bovine and equine heart cytochromes c. *C*-Terminal analyses of both the peptides by the hydrazinolysis method gave only glutamic acid. However, when the synthetic acetyltetrapeptide I was incubated with carboxypeptidase A at pH 6.0, the expected amount of glutamic acid and an unexpectedly small amount of valine were liberated, whereas from the natural acetyltetrapeptide almost quantitative amounts of glutamic acid and valine were released. Therefore, we have considered that the valine residue might be partly racemized during its synthesis. Thus, a bioassay of the valine in the acid hydrolysate of the acetyltetrapeptide I was performed.[10] The estimate showed that it was the natural form. Then the products of partial acid hydrolysate (concentrated hydrochloric acid at room temperature for 48 hr.) of the synthetic acetyltetrapeptide I were compared with those of the natural peptide by paper chromatography and electrophoresis. As is schematically represented in Fig. 1, one main spot, aspartylvalylglutamic acid, could be revealed with the ninhydrin reagent in the case of the natural acetyltetrapeptide. However, in the case of the synthetic peptide I, the aspartylvalylglutamic acid spot was quite faint, and another bluish-green spot appeared with the ninhydrin reagent at a slightly lower $R_f$ value on the chromatogram. This bluish-green spot was located at a more negatively-charged position on the paper electrophoregram at pH 3.6 than that of the tripeptide derived from the natural acetylpeptide. The amino acid analysis of this abnormal spot demonstrated that it also contained equimolar amounts of aspartic acid, valine and glutamic acid. Therefore, it seems to be β-aspartylpeptide, since the p*K'* value

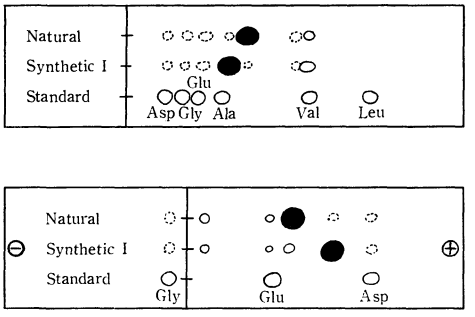



Fig. 1. Paper chromatogram and paper electrophoregram of partial acid hydrolysates of natural and synthetic acetylglycylaspartylvalylglutamic acid I.

Paper chromatography was carried out by descending way using *n*-butanol - acetic acid - water (4 : 1 : 1, v/v). Paper electrophoregram was made after migration for 120 min. at a potential of 3000 V./60 cm. at pH 3.6. Black spot represents aspartylvalylglutamic acid.

9) E. Margoliash, E. L. Smith, G. Kreil and H. Tuppy, *Nature*, **192**, 1125 (1961).

10) The bioassay of valine was kindly performed by the Ajinomoto Research Laboratory.

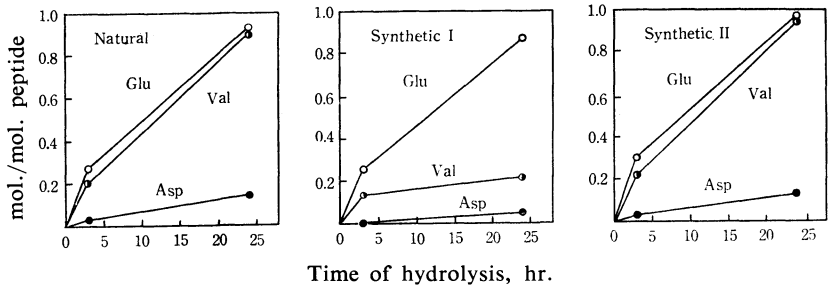



Fig. 2. Releases of amino acids from natural and synthetic acetylglycylaspartylvalylglutamic acids I and II by the action of carboxypeptidase A at pH 6.0. Released amino acids were estimated as their dinitrophenyl derivatives.

of the $\alpha$-carboxyl group (1.995)[11] is lower than that of the $\beta$-carboxyl group (3.910)[11] and the former is more negatively charged than the latter at an acidic medium (pH 3.6). The $\beta$-linkage might be produced during the saponification step of the ester groups of carbobenzoxyglycyl-L-aspartyl-L-valyl-L-glutamic acid trimethyl ester via an assumed succinimide-type linkage.[12] It appears probable that the synthetic acetyltetrapeptide I is acetylglycyl-$\beta$-L-aspartyl-L-valyl-L-glutamic acid.

Thus we next explored the synthesis of the acetyltetrapeptide II, excluding the saponification step of the ester of the side chain of the aspartyl residue, as is described in the "Experimental" section. Namely, only the benzyl ester was used as the protection of the carboxyl groups, and it was removed by catalytic hydrogenation. Furthermore, to avoid alkaline conditions throughout the synthesis, acetylglycine was coupled with the tripeptide tribenzyl ester, in contrast to the use of acetic anhydride under the alkaline conditions to introduce the acetyl group to the tetrapeptide in the previous synthesis of the acetyltetrapeptide I.

The synthesized acetyltetrapeptide II showed behavior identical to that of the natural one in every respect examined. The releases of amino acids from the three acetyltetrapeptides, natural, synthetic I and II, by the action of carboxypeptidase A at pH 6.0 are shown in Fig. 2.

The infrared absorption spectra of the two synthetic acetylpeptides I and II were the same in the 4000—650 $cm^{-1}$ region, but an appreciable difference could be observed between the two in the 900—400 $cm^{-1}$ region. Such a difference should probably be attributed to the difference in the mode of linkage in aspartic acid residues in the synthetic acetyltetrapeptides.

## Summary

In previous studies acetylglycylserine and acetylglycylaspartylalylglutamic acid had been isolated from the enzymatic digests of ovalbumin and cytochromes c of bovine and equine hearts, respectively. Here, in order to confirm the structures of the acetylpeptides isolated, acetylglycyl-L-serine and acetylglycyl-L-aspartyl-L-valyl-L-glutamic acid have been synthesized. It has been proved that the natural acetylpeptides are identical with the synthetic ones in every respect examined. Some troubles encountered during the synthesis of the acetyltetrapeptide have been discussed.

The authors are grateful to the Ajinomoto Co., Ltd., and to Dr. Kunio Fukushima for performing the bioassay of L-valine and the infrared absorption analysis respectively.

*Institute for Protein Research*
*Osaka University*
*Kita-ku, Osaka*

11) J. T. Edsall and J. Wyman, "Biophysical Chemistry," Vol. I, Academic Press (1958), p. 453.
12) M. Goodman and G. W. Kenner, *Adv. in Protein Chem.*, 12, 498 (1957).

# The Radiation-induced Addition of Hydrogen Sulfide to Olefins*

By Ken'ichi SUGIMOTO, Wataru ANDO and Shigeru OAE

(Received June 18, 1964)

In a previous investigation of the radiation-induced addition of hydrogen sulfide to propylene,[1] the formation of *n*-propyl mercaptan and of di-*n*-propyl sulfide have been observed. The radiation-induced addition of hydrogen sulfide to propylene took place very readily, and was completed at room temperature with a relatively small radiation dose. The *G*-values of this reaction were found to be more than ten thousand, while the addition followed the anti-Markownikov rule. Apparently the reaction proceeds through a free radical chain process, where the sulfhydryl radicals formed in the initial step of the radiolysis of hydrogen sulfide undergo a radical addition to the propylene in the following chain propagating step:

$$H_2S \longrightarrow HS\cdot + \cdot H \qquad (1)$$

$$HS\cdot + CH_2{=}CH{-}CH_3 \rightarrow \underset{\displaystyle SH}{CH_2{-}\dot{C}H{-}CH_3} \qquad (2)$$

$$\underset{\displaystyle SH}{CH_2{-}\dot{C}H{-}CH_3} + H_2S \rightarrow \underset{\displaystyle SH}{CH_2{-}CH_2{-}CH_3} + HS\cdot \qquad (3)$$

In the present work, the radiation-induced addition of hydrogen sulfide to propylene has been extended to other various gaseous olefins.

## Experimental

**Irradiations.**—The gamma radiation was provided by a 1000-curie or a 5000-curie cobalt-60 source.[2] Samples were irradiated at fixed positions at which the dose rates were $1.9\times10^5$, $2.8\times10^4$, $1.1\times10^4$, and $5.7\times10^3$ r./hr. respectively. The dose rates were obtained by means of a Fricke ferrous sulfate dosimeter, taking *G* as 15.6.[3]

**Reaction Vessel.**—The irradiation vessel used for this gaseous reaction was a Pyrex tube 25 mm. in outside diameter and 20 cm. long and equipped with a breakoff seal.

**Materials.**—All the olefins except butadiene were purchased from the Takachiho Chemicals Co., Tokyo, and hydrogen sulfide, from the Seitetsu Chemicals Co., Kakogawa; both were purified by vacuum distillations. Butadiene was obtained from the Japan Synthetic Rubber Co., Yokkaichi. The impurities in both the olefins and hydrogen sulfide used were found to be less than 0.5% by gas chromatographic analysis.

**Analysis.**—Conventional high-vacuum techniques were employed throughout the investigation. All the analyses of the irradiated samples were carried out by a combination of fractional distillation and gas chromatographic separation.

*Isobutene with Hydrogen Sulfide.*—The samples were analyzed by the same procedure as was used in the case of propylene.[1]

*cis- and trans-2-Butene with Hydrogen Sulfide.*—The procedure will be explained in the following paper.[4]

*Various Olefins with Hydrogen Sulfide.*—The irradiated samples were first passed through a series of dry ice-acetone cooled traps and then through a liquid nitrogen-cooled trap. The fraction condensed in the dry ice-acetone cooled trap was analyzed qualitatively by a gas chromatograph (Hitachi type KGL-2A), using a 90 m. Golay column coated with squalane. The amount of thiols in this fraction was determined by potentiometric titration with silver nitrate in isopropyl alcohol.[5]

## Results and Discussion

Various amounts of olefins were mixed with hydrogen sulfide, and these mixtures were irradiated at several radiation doses in static systems.

**The Radiation-induced Addition of Hydrogen Sulfide to Isobutene.**—The mixtures of hydrogen sulfide and isobutene were irradiated with cobalt-60 gamma rays; these results are shown in Table I. The addition is undoubtedly initiated by the decomposition of hydrogen sulfide, as is shown by:

$$H_2S \longrightarrow HS\cdot + \cdot H \qquad (1)$$

Then the sulfhydryl radical thus formed attacks isobutene:

$$HS\cdot + CH_2{=}\underset{\displaystyle CH_3}{\overset{\displaystyle CH_3}{C}} \rightarrow HSCH_2{-}\underset{\displaystyle CH_3}{\overset{\displaystyle CH_3}{\dot{C}}}\cdot \qquad (4)$$

* The Study of the Radiation Chemistry of Organic Sulfur Compounds. Part VII. Presented at the 17th Annual Meeting of the Chemical Society of Japan, Tokyo, April, 1964.

1) K. Sugimoto, W. Ando and S. Oae, This Bulletin, **37**, 365 (1964).

2) T. Azuma et al., *Ann. Rept. Radiation Center Osaka Pref.*, **2**, 56 (1961).

3) C. J. Hochanadel and J. A. Ghormley, *J. Chem. Phys.*, **21**, 880 (1953).

4) K. Sugimoto, W. Ando and S. Oae, This Bulletin, **38**, 224 (1965).

5) M. W. Tamele and L. B. Ryland, *Ind. Eng. Chem., Anal. Ed.*, **8**, 16 (1936).

The adduct radical formed can react with hydrogen sulfide, yielding 2-methylpropylmercaptan:

$$HSCH_2-\overset{CH_3}{\underset{CH_3}{C}}\cdot + H_2S \rightarrow HSCH_2-\overset{CH_3}{\underset{CH_3}{CH}} + HS\cdot \quad (5)$$

or with isobutene, giving the propagating radical:

$$HSCH_2-\overset{CH_3}{\underset{CH_3}{C}}\cdot + CH_2=\overset{CH_3}{\underset{CH_3}{C}} \rightarrow HSCH_2-\overset{CH_3}{\underset{CH_3}{C}}-CH_2-\overset{CH_3}{\underset{CH_3}{C}}\cdot \quad (6)$$

Steps 4 and 5 are the chain-carrying steps of the addition of hydrogen sulfide to isobutene, while step 6 is the propagating step of telomer production. The experiments indicate that reaction 5 proceeds in preference to reaction 6.

TABLE I. THE RESULTS OF THE RADIATION-INDUCED ADDITION OF HYDROGEN SULFIDE TO ISOBUTENE

| Dose rate r./hr. | Product | Amount of product mmol. Irrd. time 24 hr. | Irrd. time 48 hr. |
|---|---|---|---|
| $2.8\times10^4$ | 2-Methylpropylmercaptan | 1.53(24%) | 1.35(21%) |
| | Di(2-methylpropyl) sulfide | 1.88(59%) | 2.47(78%) |
| $1.1\times10^4$ | 2-Methylpropylmercaptan | | 1.53(29%) |
| | Di(2-methylpropyl) sulfide | | 2.22(70%) |
| $5.7\times10^3$ | 2-Methylpropylmercaptan | | 1.26(20%) |
| | Di(2-methylpropyl) sulfide | | 1.68(53%) |

Sample: Isobutene, 980 mmHg, 6.33 mmol.; $H_2S$, 700 mmHg, 4.50 mmol.

The telomer was not found in the products. The reactivity of isobutene with hydrogen sulfide is nearly equal to that of propylene with hydrogen sulfide, while that of *trans* or *cis*-2-butene with hydrogen sulfide is one-tenth of that of propylene or isobutene, as shown in Tables II and III. The difference between these reactivities might depend on the reactivity of each olefin. The radiation-indcued polymerization of isobutene did take place and was easy to follow, while no polymerizations of *cis*- and *trans*-2-butenes were recognized. Under the conditions of cationic polymerization,[6] at room temperature, isobutene has been shown to polymerize much more readily than 2-butenes.

**The Radiation-induced Addition of Hydrogen Sulfide to *trans*- or *cis*-2-Butene.**—The results of the radiation-induced addition of hydrogen sulfide to 2-butenes are shown in Tables II and III. In the addition reaction of *trans*- or *cis*-2-butene, a rapid isomerization of 2-butene was found to take pleace simultaneously; hence, in Table II the amounts of *cis*-2-butene isomerized from *trans*-2-butene are also shown. The radiation-induced equilibriation of *trans*- and *cis*-2-butene with hydrogen sulfide is readily, attained. The cis-trans ratio reaches a limiting value, 28 to 72, under various conditions. On the other hand, the *G*-values of the 1-methylpropylmercaptan formed are $4—9\times10^3$, and the rate of reaction has been shown to be linear to the square root of the dose rate.

**The Formation of Thiols by the Radiation-induced Reaction of Hydrogen Sulfide with Olefins.**—When one wants to obtain thiols, it is desirable to employ a large excess of hydrogen sulfide, or to separate the thiols at an early stage of the radiation-induced reaction.[1] Thiols were the only products obtained when the amount of hydrogen sulfide added was 6—8 times more than that of an unsaturated compound in this radiation-induced addition

TABLE II. THE RESULTS OF THE RADIATION-INDUCED ADDITION OF HYDROGEN SULFIDE TO *trans*-2-BUTENE

| Does rate, r./hr. | Product | *G*-value | Amount of product, mmol. Irrd. time 24 hr. | Irrd. time 48 hr. |
|---|---|---|---|---|
| $2.8\times10^4$ | 1-Methylpropylmercaptan | $4.1\times10^3$ | 0.18 (2.6%) | 0.26 (3.7%) |
| | *cis*-2-Butene | | 1.67 (24%) | 1.60 (23%) |
| $1.1\times10^4$ | 1-Methylpropylmercaptan | $7.1\times10^3$ | 0.15 (2.2%) | 0.23 (3.3%) |
| | *cis*-2-Butene | | | 1.60 (23%) |
| $5.7\times10^3$ | 1-Methylpropylmercaptan | $8.5\times10^3$ | | 0.18 (2.6%) |
| | *cis*-2-Butene | | | 1.74 (25%) |

Sample: *trans*-2-Butene, 6.95 mmol.; $H_2S$, 4.10 mmol.

6) W. H. T. Davison, S. H. Piwner and R. Worrall, *Proc. Roy. Soc.*, **A252**, 187 (1959).

TABLE III. THE RESULTS OF THE RADIATION-INDUCED ADDITION OF HYDROGEN SULFIDE TO *cis*-2-BUTENE

| Dose rate r./hr. | Product | Amount of product, mmol. Irrd. time 24 hr. |
|---|---|---|
| | 1-Methylpropylmercaptan | 0.19 (2.7%) |
| $2.8\times10^4$ | Di(1-methylpropyl) sulfide | 0.50 (14%) |
| | *trans*-2-Butene | 4.17 (60%) |
| | 1-Methylpropylmercaptan | 0.17 (2.4%) |
| $1.1\times10^4$ | Di(1-methylpropyl) sulfide | 0.49 (14%) |
| | *trans*-2-Butene | 4.31 (62%) |
| | 1-Methylpropylmercaptan | 0.20 (2.9%) |
| $5.7\times10^3$ | Di(1-methylpropyl) sulfide | |
| | *trans*-2-Butene | |

Sample : *cis*-2-Butene, 6.95 mmol. ; $H_2S$, 4.10 mmol.

TABLE IV. THE FORMATION OF THIOLS BY THE RADIATION-INDUCED REACTION OF HYDROGEN SULFIDE TO OLEFINS

| Olefin | Amount of thiol formed, mmol. |
|---|---|
| Ethylene | 1.45 |
| Propylene | 1.40 |
| 1-Butene | 0.94 |
| Isobutene | 0.75 |
| *cis*-2-Butene | 0.52 |
| *trans*-2-Butene | 0.50 |
| Butadiene | 0.00 |
| Acetylene | 0.18 |

Dose rate : $1.9\times10^5$ r./hr. Radiation dose : $5.7\times10^5$ r.
Sample : Olefin, 2.15 mmol. ; $H_2S$, 12.6 mmol.

reaction. Here, the addition follows the anti-Markownikov rule. The experiment of the addition of hydrogen sulfide has been extended to various olefins; the results of the radiation-induced addition are listed in Table IV.

Apparently the reactivities of various olefins toward hydrogen sulfide are different in this addition reaction, and the radical chain of these reactions seems to decrease with an increase in the carbon number of olefins. However, all the olefins apparently underwent a similar radical chain process, and the *G*-value dependence of dose rate is also similar to the case of propylene with hydrogen sulfide.[1]

The radiation-induced addition of hydrogen sulfide to butadiene was not observed. The addition of hydrogen sulfide to butadiene was substantially more difficult than that to other olefins. Similar phenomena have been reported by Sivertz[7] in the photo-initiated addition of methyl mercaptan. The photo-initiated addition of methyl mercaptan to isobutene, ethylene and butadiene in the gas phase has yielded overall negative activation energies of $-8900$, $-8800$, $-7900$ and $+2800$ respectively. The rate-determining step is thought to be hydrogn abstraction, for which the activation energy is estimated to lie between 2 and 3 kcal. for all except butadiene, which is considerably higher, about 6 kcal.

## Summary

The radiation-induced free radical addition of hydrogen sulfide to olefins to give the corresponding thiols has been studied. The addition of the thiols to olefins has been found to undergo a free radical chain reaction, readily yielding the corresponding sulfides in the succeeding step. However, the thiols were found to be the only component when an excess of hydrogen sulfide was used. The reactivity of the radical chain reaction decreases with an increase in the carbon number of $\alpha$-olefins.

*Research Laboratory*
*Kurashiki Rayon Co., Ltd.*
*Kurashiki, Okayama* (*K. S*)

*Department of Chemistry*
*Radiation Center of Osaka Prefecture*
*Sakai, Osaka* (*W. A.*)

*Department of Applied Chemistry*
*Faculty of Engineering*
*Osaka City University*
*Sumiyoshi-ku, Osaka* (*S. O.*)

7) C. Sivertz, W. Andrews, W. Elsdon and K. Grabam, *J. Polymer Sci.*, **19**, 587 (1956).

# The Radiation-induced cis-trans Isomerization of 2-Butenes by Hydrogen Sulfide*

By Ken'ichi SUGIMOTO, Wataru ANDO and Shigeru OAE

(Received June 18, 1964)

The radiation-induced free radical addition of hydrogen sulfide to olefins is a reaction which has been often studied;[1-4] it is considered to involve the following chain propagating steps:

$$H_2S \xrightarrow{\gamma} HS\cdot + H \quad (1)$$

$$HS\cdot + CH_2{=}CHR \rightarrow HS\dot{C}H_2{-}CHR \quad (2)$$

$$HSCH_2{-}\dot{C}HR + H_2S \rightarrow HSCH_2{-}CH_2R + HS\cdot \quad (3)$$

The thiols, once formed, undergo further reaction with olefins to give the corresponding sulfides. The free radical addition of thiols to olefins is considered to involve the following similar chain-propagating steps:[5,6]

$$RCH_2CH_2SH \xrightarrow{\gamma} RCH_2{-}CH_2S\cdot + H \quad (4)$$

$$RCH_2{-}CH_2S\cdot + CH_2{=}CHR \rightarrow RCH_2{-}CH_2S\dot{C}H_2{-}CHR \quad (5)$$

$$RCH_2{-}CH_2S\dot{C}H_2{-}\dot{C}HR + RCH_2{-}CH_2SH \rightarrow (RCH_2{-}CH_2)_2S + RCH_2{-}CH_2S\cdot \quad (6)$$

In a previous paper[7] of this series, evidence was presented for the abstraction of hydrogen atoms from hydrocarbons either by sulfhydryl radicals or thiyl radicals; that is, the reactions which are essentially the reverse of 3 and 6 can occur with ease in certain systems. There is also good reason to believe that reactions 2 and 5 may be reversible as well, in view of several previous works on similar thiol-addition reactions to olefins.[7,8] In studying the addition of methanethiol to isobutene, propylene and ethylene in the gas phase, Sivertz et al.[9] have found negative overall activation energies of 8 to 9 kcal. The photoisomerization of *cis*- and *trans*-2-butenes in the presence of methanethiol has also been studied recently.[10] Especially interesting is the work by Skell and Allen, who demonstrated that the orientation of the free radical addition of $CH_3SD$ is controlled by the strength of the deuterium-bound bond.[11] Meanwhile, experiments in our work[2] have demonstrated the reversibility of the radical-addition reaction in the gas-phase mixtures of hydrogen sulfide and olefins by the rapid isomerization of unreacted olefin during the irradiations at room temperature. This paper will present more detailed data on this reversibility.

## Experimental

**Irradiations.**—The gamma radiation was provided either by a 100-curie or a 1000-curie cobalt-60 source.[12] The dose rates were obtained from the Fricke ferrous sulfate dosimeter, taking $G$ as 15.6,[13] and from the Victoreen rate meter. The $G$-values were calculated from the relation of the products formed and the absorption energy of the gaseous sample. The absorption energies of 2-butenes and of hydrogen sulfide were corrected in electron density from the absorption of air, 83.8 erg./g./r.; 2-butenes correspond to 95.7 erg./g./r., and hydrogen sulfide, to 88.7 erg./g./r. All the irradiations were carried out at room temperature.

**Reaction Vessel.**—The irradiation vessel used for these gaseous reactions was a Pyrex tube 25 mm. in outside diameter and 20 cm. long and equipped with a breakoff seal.

**Materials.**—*cis*-2-Butene and *trans*-2-butene were purchased from the Takachiho Chemicals Co., Tokyo, and hydrogen sulfide, from Seitetsu Chemicals Co., Kakogawa; both were purified by fractional distillations. The impurities in both the 2-butenes and the hydrogen sulfide used were found to be less than 0.5% by gas chromatographic analysis.

**Analyses.**—Conventional high-vacuum techniques

* The Study of the Radiation Chemistry of Organic Sulfur Compounds. Part VIII.

1) K. Sugimoto, W. Ando and S. Oae, This Bulletin, **37**, 365 (1964).
2) K. Sugimoto, W. Ando and S. Oae, ibid., **38**, 221 (1965).
3) J. F. Harris, Jr., and F. W. Stacey, *J. Am. Chem. Soc.*, **85**, 794 (1963).
4) Dow Chemical Co., British Pat. 842277 (1960).
5) A. Fontijn and J. W. T. Spinks, *Can. J. Chem.*, **35**, 1384, 1397, 1410 (1957).
6) K. Araki, *J. Chem. Soc. Japan, Pure Chem. Sec. (Nippon Kagaku Zasshi)*, **81**, 808 (1960).
7) W. Ando, K. Sugimoto and S. Oae, This Bulletin, **37**, 353, 360 (1964).
8) See details in S. Oae, *Chem. Ind.*, **15**, No. 5. 435-443 (1964); cf. also W. A. Pryor, "Mechanisms of Sulfur Reactions," Chapters 3-5, McGraw-Hill, N. Y. (1962), pp. 64-94.
9) C. Sivertz, W. Andrew, W. Elsdon and K. Graham, *J. Polymer Sci.*, **19**, 587 (1956).
10) C. Walling and W. Helmerich, *J. Am. Chem. Soc.*, **81**, 1144 (1959).
12) T. Azuma et al., *Ann. Rept. Rad. Center Osaka Pref.*, **2**, 56 (1961).
13) C. J. Hochanadel and J. A. Ghormley, *J. Chem. Phys.*, **21**, 880 (1953).

were employed throughout the investigation. All the analyses of the irradiated samples were carried out by a combination of fractional distillation and gas chromatographic separation.

The irradiated sample was passed first through a series of dry ice - acetone cooled traps, then through carbon disulfide - cooled traps, and finally through liquid nitrogen traps. The fraction condensed in dry ice - acetone cooled traps was found to be a mixture of 2-butanethiol and di-2-butyl sulfide. The condensed gas at the carbon disulfide - cooled traps was identified as a mixture of unreacted and isomerized 2-butene. This portion was measured by gas chromatography (Hitachi type KGL-2A), using a 90 m. Golay column coated with squalane and operated at room temperature with a He carrier at 1.5 kg./cm$^2$. The condensed gas at liquid nitrogen was identified as unreacted hydrogen sulfide.

## Results and Discussion

Samples of mixtures consisting of various amounts of pure *trans*-2-butene and hydrogen sulfide were irradiated in a static system as has been described in the "Experimental" section. These were then periodically analyzed by gas chromatography. The results of such experiments are shown in Table I. The isomerized mixtures show the compositions of 72% and 28% for *trans*- and *cis*-2-butenes respectively. Similar experiments carried out on pure *cis*-2-butene gave the results shown in Table I. Here again, the values obtained for trans-cis are nearly identical, i. e., 73%-27%. The radiation-induced equilibrium of *trans*- and *cis*-butenes by hydrogen sulfide obtained under various conditions are shown in Table I; the cis-trans isomerization readily reaches an equilibrium and gives a mixture of 28% and 72% of *cis*- and *trans*-2-butenes. Meanwhile, the *G*-value of 2-butanethiol formation was found to be about $4-9\times10^3$, and the rate was shown to be linear to the square root of the dose rate.

To determine the yield of the radiation-induced cis-trans isomerization in somewhat more detail, mixtures of various amounts of *cis*-2-butene and hydrogen sulfide were subjected to small doses of irradiation. The results of these experiments are shown in Fig. 1. Within these irradiation doses, the amount of

Table I. The radiation-induced isomerization of *cis*- and *trans*-2-butene by hydrogen sulfide

| Dose rate r./hr. | *trans*-Butene* 24 hr. | *trans*-Butene* 48 hr. | *cis*-Butene* 48 hr. |
|---|---|---|---|
| $2.8\times10^4$ | trans 72% cis 28% | trans 72% cis 28% | trans 73% cis 27% |
| $1.1\times10^4$ | | trans 72% cis 29% | trans 73% cis 27% |
| $5.7\times10^3$ | | trans 71% cis 29% | |

* Composition of reaction mixtures : 2-butenes, 1140 mmHg ; $H_2S$, 670 mmHg

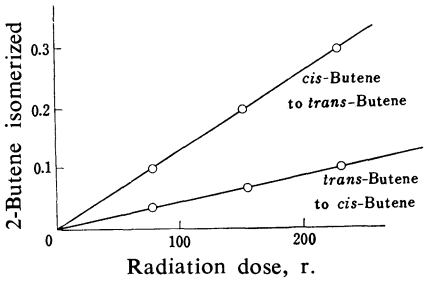
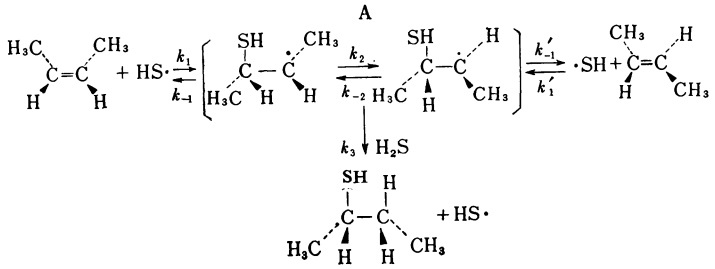



Fig. 1. The radiation-induced isomerization of *trans*- and *cis*-2-butene with hydrogen sulfide. (Sample : 2-butene 2.48 mmol., $H_2S$ 0.90 mmol.)

trans-isomerization is proportional to the energy absorbed, and no thiol and sulfide were detected among the products.

The radiation-induced isomerizations of *cis*-2-butene alone, without any addent, namely direct isomerizations, were also performed. The *G*-value of the direct isomerization is 300, while the *G*-value of the isomerization by sulfhydryl radicals was found to be around $2.5\times10^5$. These results can be well explained by the formation of intermediate radicals (A) by the attack of the sulfhydryl radical on 2-butene.

If one assumes that the initial step of the reaction is the attack of the sulfhydryl radical on 2-butene, one can write the scheme for the reaction as in 7, where $k_3$, the rate of hydrogen abstraction, is much smaller than $k_2$ or $k_{-2}$, the rate of the equilibration of the incipient radical A.




(7)

The intermediate incipient radical presumably readily regenerates the equibrium mixture of *cis*- and *trans*-2-butenes by losing the sulfhydryl radical.

Since the reaction of sulfhydryl radicals with 2-butenes to form the incipient radical A is presumed to be reversible, the trans isomer appears in the unreacted 2-butene in the addition reaction of hydrogen sulfide to *cis*-2-butene by gamma irradiations. It was found that the *G*-value for the formation of *trans*-2-butene from the composite radical was 50 times that of the formation of the addition product by the hydrogen transfer from hydrogen sulfide. The *G*-value for *cis*-2-butene formation is 20 times that for the formation of the addition product. Therefore, the decomposition of the incipient radical into the sulfhydryl radical and 2-butenes is very rapid compared to the hydrogen transfer reaction with hydrogen sulfide.

In this respect, the $\gamma$-ray induced isomerization of 2-butenes by $H_2S$ is essentially the same as that by photochemical isomerization with methanethiol,[10] and it involves the reversible formation of an incipient radical intermediate, as has been described in Eq. 2. The larger *G*-value of the isomerization from *cis*-2-butene than that from the trans isomer seems to suggest that the initial addition and the final loss of the sulfhydryl radical are very fast and that the rate is controlled by the rotation barrier in A. Meanwhile, the rate-determining step in the formation of the addition product is thought to be 3, the activation energy for which is estimated to lie between 2 and 3 kcal.[14]

## Summary

Radiation-induced free radical isomerizations of 2-butenes with hydrogen sulfide at room temperature gave identical mixtures of about 72% *trans*- and 28% *cis*-butenes. The *G*-value of the isomerization is 20 to 50 times larger than that of the formation of the addition product. With gamma irradiation, 2-butenes in the presence of hydrogen sulfide were rapidly isomerized, even with a very small radiation dose. This ready isomerization indicates the ease of the reversibility of the first step of the sulfhydryl-radical addition reactions.

*Research Laboratories*
*Kurashiki Rayon Co., Ltd.*
*Kurashiki, Okayama (K. S.)*

*Department of Chemistry*
*Radiation Center of Osaka Prefecture*
*Sakai, Osaka (W. A.)*

*Department of Applied Chemistry*
*Faculty of Engineering*
*Osaka City University*
*Sumiyoshi-ku, Osaka (S. O.)*

14) R. Back, G. Trick, C. McDonald and C. Sivertz, *Can. J. Chem.*, 32, 1078 (1954).

# The Radiation-induced Isomerization of 2-Butenes

By Wataru ANDO, Ken'ichi SUGIMOTO and Shigeru OAE

(Received June 18, 1964)

The cis-trans isomerization of 2-butenes has been investigated under various conditions in order to obtain some critical information about the nature and reactivity of the double bond. Gas-phase thermal isomerization has been known to be of a unimolecular reaction, in which there is a transition to an excited state, which can then undergo a radiationless transition to the ground state with isomerization.[1]

The cis-trans isomerization of 2-butenes through the triplet state provides a straightforward means of conducting the multiplicity exchange:

Sensitizer (triplet) + 2-Butene (singlet) ⟶ 2-Butene (triplet) + Sensitizer (singlet) (1)

Hammond, Leermarkers and Turro[2] have suggested that it is possible to study the mechanisms of various photochemical reactions by determining the formation of the triplet intermediates from the reactants in the presence of such a sensitizer as benzophenone. Cundall and Palmer[3] have also studied the gas-phase

1) B. S. Rabinovitch and K. W. Michel, *J. Am. Chem. Soc.*, **81**, 5065 (1959).

2) G. S. Hammond, P. A. Leermarkers and N. J. Turro, ibid., **83**, 2395 (1961).

3) R. B. Cundall and T. F. Palmer, *Trans. Faraday Soc.*, **56**, 1211 (1960).

isomerization of 2-butene in the presence of various photosensitizers, such as mercury, sulfur dioxide, benzene and a variety of other organic photosensitizers, and have shown that the multiplicity exchanges that lead to the isomerization can be accomplished if the photosensitizing species have energy in excess of approximately 60 kcal. mol.$^{-1}$ above the ground state. If this latter condition is satisfied, reaction 1 occurs at every collision.

It has long been known that a trace of bromine or iodine initiates the cis-trans isomerization of such substances as dimethyl maleate and stilbene; early works in this field have been reviewed by Mayo and Walling.[4] Such an isomerization has been suggested to be a radical-chain process, and the isomerization of dimethyl maleate to dimethyl fumarate by bromine in carbon tetrachloride is known to be induced by light. Thus the isomerization takes place through the reversible addition of bromine atoms, which occurs in the initial step of the reaction:

$$\mathrm{Br}\cdot + \begin{matrix} X \\ H \end{matrix}\!\!>\!C{=}C<\!\!\begin{matrix} X \\ H \end{matrix} \longrightarrow \left[\mathrm{BrCHX\text{-}\dot{C}HX}\right]$$

$$\longrightarrow \begin{matrix} X \\ H \end{matrix}\!\!>\!C{=}C<\!\!\begin{matrix} X \\ H \end{matrix} + \begin{matrix} X \\ H \end{matrix}\!\!>\!C{=}C<\!\!\begin{matrix} H \\ X \end{matrix} + \cdot\mathrm{Br}$$

Since the incipient radical formed can readily rotate around the C–C bond axis, the elimination of the halogen atom gives both isomers, although the more stable isomer is yielded preferentially. The same incipient intermediate radical is also involved in the addition reaction; therefore, the addition reaction usually competes with the isomerization reaction.

In high-energy radiation chemistry, a similar situation arises. The radiation-induced reactions involve a transfer of electronic excitation from one molecule to another. Moreover, all possible excited states, ions and electrons may be produced, and so little or no selectivity can be expected in the product formation. In the process of being thermalized, an electron may induce the excitation of a molecule to a triplet state, and the number of such states may also result from the neutralization of positive ions by electrons, or indirectly by transition from higher excited states. Radicals can also be made by various processes, and different radicals may display different chemical behavior in the overall reaction process.

It, therefore, appears of interest to study a system where such a species leads to the cis-trans isomerization of 2-butenes by either chemical change or energy degradation.

4) F. R. Mayo and C. Walling, *Chem. Revs.*, **27**, 351 (1940).

## Experimental

**Materials.**—*cis* and *trans*-2-Butenes were Takachiho research-grade materials. The *trans*-2-butene contained less than 0.05% of the cis material, and the *cis*-2-butene contained less than 0.05% of the trans isomer and 0.05% of butane. 1-Butene, purchased in a cylinder, was purified by repeated distillations in a vacuum. The purities of these materials were confirmed by gas chromatography. Spectrally-pure argon, helium, nitrogen, hydrogen, oxygen, carbon dioxide and carbon monoxide supplied by Takachiho Chemical were used without any further purification. Benzene was washed with sulfuric acid, water and sodium carbonate solution, dried with calcium chloride, and purified by bulb-to-bulb distillation. Ethyl bromide was distilled and stored under vacuum. Nitric oxide and sulfur dioxide were dried with phosphorus pentoxide and purified by repeated vacuum distillations. Diphenyl disulfide, obtained from Tokyo Kasei, was purified by repeated recrystallizations in ethyl alcohol. All the other chemicals used were purified by conventional methods.

**Apparatus and Procedure.** — A conventional vacuum apparatus was employed. The radiation-induced reactions were carried out in a Pyrex glass bulb 20 to 30 ml. in size. The sample in the gas phase was irradiated by a cylinder-type cobalt 60 source giving a radiation dose rate of $1.0\times10^{6}$ roentgen per hour. The dose rate was obtained from the Fricke ferrous-sulfate dosimeter, taking the *G*-value as 15.6, and from the Victoreen rate meter. All the irradiations were carried out at 45±1°C. At the end of the irradiation, the materials were removed for analysis from the reaction bulb to a system consisting of a series of traps and a manometer. The measured samples were analyzed with a Hitachi FID gas chromatograph, with a 90 m. squalane column at room temperature. The chromatograph was capable of handling a sample of $10^{-7}$ mol. with an accuracy of better than 2%.

## Results and Discussion

**The Radical Isomerization of 2-Butene.**—The gamma irradiation of *trans*-2-butene was studied under various conditions. At room temperature and atmospheric pressure, the reaction did not occur markedly. The gas evolved consisted mainly of hydrogen and methane, together with a small amount of butene isomers. A detailed examination of the isomerization by the irradiation of *trans*-2-butene with a dose of $2.4\times10^{7}$ r. showed that little isomerization (only 0.7%) from trans to cis occured. Even the addition of hydrogen, nitrogen, helium, argon, carbon dioxide, carbon monoxide, oxygen or nitrous oxide had only a little effect on the isomerization of *trans*-2-butene, when the pressure was between 10 and 100 mmHg.

Recently the radiation-induced radical isomerization of 2-butene with hydrogen sulfide

has been reported by this laboratory.[5] The cis-trans isomerization (ratio: 0.39) takes place through the formation of an incipient radical intermediate, together with the formation of small amounts of butyl mercaptan and butyl sulfide.

Usually in such a system there arises competition between addition and isomerization. Therefore, the radical isomerization of 2-butene in the vapor phase has been studied by using a variety of radicals formed by the irradiation of gamma rays. Figure 1 gives typical data for the conversion of 2-butene by the bromine radical as a function of the dose.

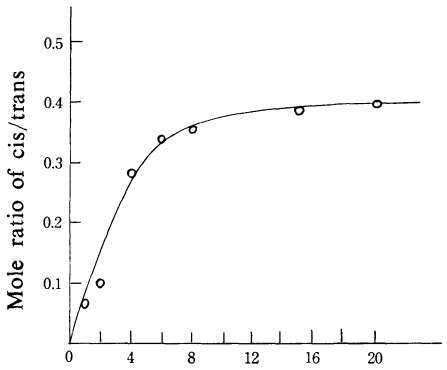



Fig. 1. Effects of ethyl bromide upon *trans*-2-butene as function of dose. (Ethyl bromide, 30 mmHg; *trans*-2-Butene, 100 mmHg)

The effect of the concentration of ethyl bromide upon the isomerization was examined at a constant dose. The isomerization of 2-butene took place very readily and was not affected by the change in the concentration of ethyl bromide, as Table I shows, suggesting that the reaction is a radical-chain process initiated by the bromine atom.

TABLE I. EFFECTS OF ETHYL BROMIDE ON THE 2-BUTENE ISOMERIZATION

| *trans*-2-Butene mmHg | $C_2H_5Br$ mmHg | cis/trans | 1-Butene/*trans*-2-Butene $\times 10^{-2}$ |
|---|---|---|---|
| 100 | 10 | 0.40 | 0.82 |
| 100 | 20 | 0.366 | 1.13 |
| 100 | 30 | 0.394 | 1.11 |
| 100 | 40 | 0.389 | 0.89 |

Irraidiation dose: $1.5 \times 10^7$ r.

It is important to notice also that a very small quantity of bromine-containing by-products were observed.

The addition of an atom or a free radical to an olefin produces a vibrationally-excited adduct radical which contains all the energy of the newly-formed bond and the activation energy required for the reaction. However, such a radical may decompose without requiring any activation energy, or it may be deactivated by a suitable collision.[6] Its lifetime is substantially longer than the period of the internal rotation around the C–C bond, and the isomerization ensues. The work of Dainton shows that such a situation arises upon the addition of a Cl atom to dichloroethylenes; therefore, the isomerization observed in our experiments is explicable if one assumes that it is caused by a bromine atom.

$$C_2H_5Br \xrightarrow{r} C_2H_5\cdot + \cdot Br$$

$$Br\cdot + \textit{trans}\text{-2-Butene} \longrightarrow \cdot C_4H_8Br$$

$$\cdot C_4H_8Br \rightarrow \textit{cis}\text{- or } \textit{trans}\text{-2-Butene} + \cdot Br$$

This mechanism may be supported by the formation of small amounts of 1-butene and other by-products containing bromine.

The radical isomerization for 2-butene was investigated further in a heterogeneous or a homogeneous system. The results are shown in Table II. The relative rate of the isomerization of 2-butene with halogenated compounds decreased in the order, Br>Cl>I, being small with chlorine and less with iodine.

As we have seen in the bromine system, the isomerization caused by a reversible Cl-atom addition is extremely rapid. However, in contrast to the cases with chlorine and bromine, the radical addition of iodine to 2-butene is a marginal proposition. The heat of formation[7] of the $C_4H_8I$ radical may be very roughly estimated as 25 kcal. $mol^{-1}$.* Therefore, the radical formed from 1-butene may be said to be quite unstable, and that formed from 2-butene, slightly more so. On the other hand, Christie et al.[8] have found values of a few kcal. $mol^{-1}$ for the heat of formation of several complexes formed by the interaction of an iodine atom and a hydrocarbon molecule. Rand and Strong[9] have also found a complex formation between an iodine atom and benzene when iodine was flash-photolyzed in a benzene solution.

If the mechanism of the isomerization may be described by the following reactions:

5) K. Sugimoto, W. Ando and S. Oae, This Bulletin, **38**, 224 (1965).

6) P. B. Ayscough, A. J. Cooker and F. S. Dainton, *Trans. Faraday Soc.*, **58**, 284 (1962).

7) M. H. Back and R. J. Cvetanovic, *Can. J. Chem.*, **41**, 1396 (1963).

8) M. I. Christie, R. G. Norrish and G. Porter, *Proc. Roy. Soc.*, **A216**, 152 (1953).

9) J. Rand and R. L. Strong, *J. Am. Chem. Soc.*, **82**, 5 (1960).

* Values used in this estimation; $H_{f25}(C_4H_{10}) = -29.8$, $D(s\text{-}C_4H_9\text{-}H) = D(s\text{-}C_3H_7\text{-}H) = 94$, $D(H_2) = 103.2$, $D(I_2) = 35.35$, $D(s\text{-}C_4H_9\text{-}I) = 48$, $D(s\text{-}C_4H_8I\text{-}H) = D(s\text{-}C_4H_9\text{-}H)$.

Table II. Radical isomerization of 2-butene in the gamma irradiation

| Radical source | mmHg | cis/trans | 1-Butene / *trans*-2-Butene |
|---|---|---|---|
| $C_2H_5I$ | 30 | 0.0127 | 0.0091 |
| $C_2H_5Br$ | 30 | 0.394 | 0.0111 |
| $C_2H_5Cl$ | 30 | 0.0654 | — |
| $CCl_4$ | 30 | 0.025 | — |
| $CHCl_3$ | 30 | 0.0213 | — |
| $(C_6H_5S)_2$ | 1 g. | 0.365 | — |

*trans*-2-Butene, 100 mmHg; Irradiation dose, $1.5\times10^7$ r.

$$C_2H_5I \xrightarrow{\gamma} C_2H_5\cdot + \cdot I \quad (1)$$

Isomerization

$$\begin{cases} I\cdot + \textit{trans}\text{-2-Butene} \rightarrow C_4H_8I \text{ (radical)} & (2) \\ C_4H_8I \text{ (radical)} \rightarrow I\cdot + \alpha\ \textit{trans}\text{-2-Butene} + (1-\alpha)\ \textit{cis}\text{-2-Butene} & (3) \end{cases}$$

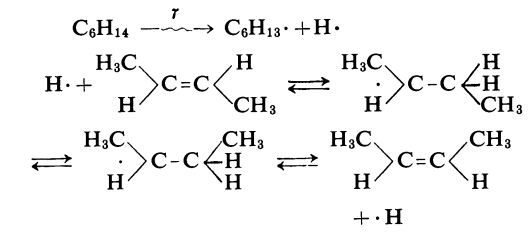
No isomerization

$$\begin{cases} I\cdot + \textit{trans}\text{-2-Butene} \rightarrow C_4H_8I\ (\pi\text{-complex}) & (4) \\ \pi\text{-Complex} \longrightarrow \textit{trans}\text{-2-Butene} + I\cdot & (5) \\ \pi\text{-Complex} + I\cdot \rightarrow \textit{trans}\text{-2-Butene} + I_2 & (6) \end{cases}$$

the complex formed in 4 may be more stable than the radical and have a lower energy barrier for formation. The easy formation of a $\pi$-complex is in agreement with the low isomerization of 2-butene.

Other chemical systems have also been examined for the radical isomerization, with special attention being paid to the effect of radiation-sensitive hydrocarbons. Particularly interesting is the isomerization of 2-butene in hexane or cyclohexane, because they readily liberate hydrogen atoms on irradiation and would eventually lead to the isomerization of 2-butene (Table III).

The hydrogen atom formed from hexane or cyclohexane was found to attack the double bond of *trans*-2-butene, and the formation of new C–H bond easily expelled the other hydrogen atom of 2-butene.



Steinmetz and Noyes,[10] by measuring the relative rates of exchange and isomerization, concluded that the rate constant for the exchange process is about twice that for the rotation process that lead to the isomerization, but that the two have almost identical activation energies of somewhat greater than 3 kcal. The difference is probably caused by the barrier to rotation in the intermediate radical.

10) H. Steinmetz and R. M. Noyes, *J. Am. Chem. Soc.*, **74**, 4141 (1952).

Table III. The effects of hydrocarbon on the isomerization

| *trans*-2-Butene mmHg | $C_6H_{14}$ mmHg | cyclo-$C_6H_{12}$ mmHg | Mole ratio cis/trans | 1-Butene / *trans*-2-Butene |
|---|---|---|---|---|
| 100 | 25 | | 0.1005 | 0.0060 |
| 100 | | 25 | 0.1025 | 0.0051 |

Irradiation dose: $2.4\times10^7$ r.

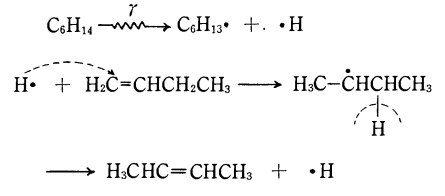
To demonstrate these possibilities, the exchange of the hydrogen atom was studied by investigating the isomerization of 1-butene in hexane or cyclohexane in the gas phase. The results are shown in Table IV.

Table IV. Isomerization of butene-1 in hydrocarbon

| 1-Butene mmHg | $C_6H_{14}$ mmHg | cyclo-$C_6H_{12}$ mmHg | Mole ratio: *trans*-2-Butene / 1-Butene | Mole ratio: *cis*-2-Butene / 1-Butene |
|---|---|---|---|---|
| 100 | 25 | | 0.0777 | 0.00142 |
| 100 | | 25 | 0.0481 | 0.00231 |

Irradiation dose: $2.4\times10^7$ r.

If the hydrogen exchange reaction does not occur, the isomerization from 1-butene to *trans*- or *cis*-2-butene should not take place. The results showed the rapid isomerization of 1-butene to 2-butene, leading us to the conclusion that the hydrogen-exchange reaction is actually involved. If one assumes the isomerization of 1-butene as arising from the exchange of hydrogen, the reaction involved may be diagramed as:



A similar path can probably account for the isomerization of 1-butene in cyclohexane vapor, and also the fact that hydrogen exchanges in the 1-butene isomerization lead to a similar process for the isomerization of 2-butene. With other hydrocarbons, therefore, one can also find similar processes for isomerization.

**The Isomerization Involving Transfer of Electronic Energy.**—There are a large number of known elementary processes which involve

atoms or molecules in excited electronic states.

Benzene photosensitzation has been successfully applied by Sato et al.[11] to the isomerization of 2-butene. Cundall and Criffiths[12] have also reported that a large amount of benzene triplets are formed during the irradiation of a benzene solution with varying concentrations of *cis*-2-butene, and they have presented strong evidence for the energy transfer from benzene to *cis*-2-butene.

Similar experiments have thus been carried out in the gas phase. The results for the benzene - *trans*-2-butene system are shown in Fig. 2 as function of the dose. The conversion of *trans*-2-butene to the cis isomer increased with the irradiation dose; equilibrium was attained at a cis/trans ratio of around 0.33. Even when the benzene pressure was varied with respect to that of *trans*-2-butene, the rate of isomerization remained nearly constant, as may be seen in Table V.

The process in the gas phase isomerization *of 2-butene is not simple in contrast to the case* in a solution. As we have seen in the previous section, a considerable isomerization of 2-butene was observed with hexane or cyclohexane. Therefore, if hydrogen atoms are formed in the irradiation of benzene, the isomerization should occur in the radical-chain process. However, as Cundall and Mine have suggested,[13] if the isomerization takes place by an energy transfer mechanism involving the benzene triplet, the triplet 2-butene formed by intersystem crossing would not isomerize to 1-butene or isobutene. The possibility of radical-chain reaction in causing isomerization can be seen from the formation of a small amount of 1-butene. In order to study this problem further, experiments were also carried out using 1-butene and benzene (Table VI).

Some isomerization to the other isomer did occur from 2-butene, but in view of other evidence, it seems that the radical-chain reaction is not the main process in the isomerization.

TABLE V. EFFECT OF BENZENE ON *trans*-2-BUTENE

| *trans*-2-Butene mmHg | $C_6H_6$ mmHg | Mole ratio | |
|---|---|---|---|
| | | cis/trans | 1-Butene / *trans*-2-Butene |
| 100 | 5 | 0.244 | 0.00762 |
| 100 | 10 | 0.152 | 0.00562 |
| 100 | 20 | 0.171 | 0.00445 |
| 100 | 30 | 0.216 | 0.00308 |
| 100 | 40 | 0.166 | 0.00338 |

Irradiation dose $1.5\times10^7$ r.

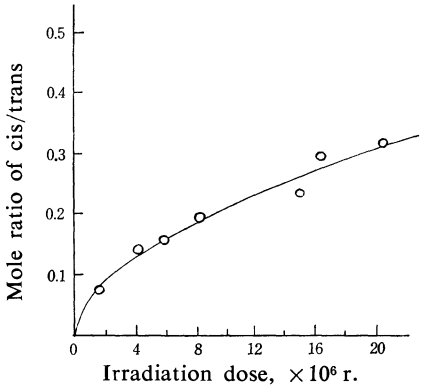



Fig. 2. Effect of dose upon 2-butene with benzene. (*trans*-2-Butene, 100 mmHg; Benzene, 30 mmHg)

TABLE VI. EFFECT OF BENZENE ON 1-BUTENE

| 1-Butene mmHg | $C_6H_6$ mmHg | Mole ratio | |
|---|---|---|---|
| | | *trans*-2-Butene / 1-Butene | *cis*-2-Butene / 1-Butene |
| 100 | 5 | 0.00228 | 0.00076 |
| 100 | 10 | 0.00166 | 0.00088 |
| 100 | 20 | 0.00318 | 0.00159 |
| 100 | 40 | 0.00556 | 0.00185 |

Irradiation dose: $1.5\times10^7$ r.

These experiments demonstrate that a large number of triplets are formed during the irradiation of benzene and that the energy transfer appears to occur in preference to the radical-chain process for the isomerization of 2-butene. The mechanism which accounts for this is the following:

$$\text{Benzene} \xrightarrow{r} \text{Benzene (triplet)}$$

$$\text{Benzene (triplet)} + \textit{trans}\text{-2-Butene (singlet)} \rightarrow \text{2-Butene (triplet)} + \text{Benzene (singlet)}$$

$$\text{2-Butene (triplet)} \rightarrow \textit{cis}\text{- or } \textit{trans}\text{-2-Butene}$$

Similar experiments were carried out in the gas phase using a variety of organic compounds. The data are summarized in Table VII.

The use of toluene and acetone illustrates a similar energy transfer process for the 2-butene isomerization. Here the case is, however, less unambigous and involves a partial contribution by the radical-chain process to the isomerization. Meanwhile, the effect of acetophenone or acetaldehyde on the isomerization does not seem to be through a clear process of energy transfer. The formation of a large amount of

11) S. Sato, K. Kikuchi and M. Tanaka, *J. Chem. Phys.*, **38**, 239 (1963).
12) R. B. Cundall and P. A. Griffiths, *J. Am. Chem. Soc.*, **85**, 1211 (1963).
13) R. P. Cundall and D. G. Mine, ibid., **83**, 3902 (1961).

Table VII. Effect of organic substances on *trans*-2-butene

| Substance | mmHg | Mole ratio | |
|---|---|---|---|
| | | cis/trans | *trans*-2-Butene / 1-Butene |
| $C_6H_6$ | 50 | 0.348 | 0.0033 |
| $C_6H_5CH_3$ | 10 | 0.288 | 0.0046 |
| $(CH_3)_2CO$ | 30 | 0.195 | 0.0044 |
| $CH_3COC_6H_5$ | 1 ml. | 0.0368 | 0.0286 |
| $CH_3CHO$ | 50 | 0.0203 | 0.0187 |
| $(CH_3CO)_2$ | 50 | — | 0.0147 |

*trans*-2-Butene, 100 mmHg; Irradiation dose $2.4\times10^7$ r.

1-butene may be brought about by the radical-chain process.

The possibility of the triplet states of naphthalene and anthracene causing the isomerization of 2-butene in the irradiation was studied. It is probably safe to assume that energy transfer will not take place readily in these heterogerneous systems; therefore, it is likely that the isomerization proceeds through the radical-chain process by means of a hydrogen atom formed in the irradiation of naphthalene and anthracene.

**The Effects of Inorganic Substances on the Isomerization.**—It has been suggested that the radiation-induced isomerization of 2-butene can take place either by a free-radical chain process or by the energy transfer with a triplet state of an organic molecule with $\pi$-electrons, or by both.

It is, therefore, interesting to see the effect of simple inorganic compounds in the radiation-induced isomerization. Recent work of Cundall and Palmer on the sulfur dioxide-photosensitized isomerization is very interesting in this connection; they have regarded it as involving the triplet state of sulfur dioxide.[3] Their results are in agreement with those of Dainton and Ivin,[14] who showed that the

Table VIII. Sulfur dioxide induced isomerization of *trans*-2-butene

| *trans*-2-Butene mmHg | cis/trans $\times10^{-2}$ | 1-Butene / *trans*-2-Butene $\times10^{-3}$ |
|---|---|---|
| 10 | 15.3 | 7.13 |
| 20 | 10.6 | 6.25 |
| 40 | 8.69 | 2.67 |
| 60 | 7.58 | 2.31 |
| 80 | 7.08 | 3.44 |
| 100 | 6.64 | 0.833 |

Sulfur, dioxide 50 mmHg; Irradiation dose, $1.5\times10^7$ r.

14) F. S. Dainton and K. J. Ivin, *Trans. Faraday Soc.*, **46**, 374 (1950).

Table IX. Sulfur dioxide induced isomerization of 1-butene

| 1-Butene mmHg | *trans*-2-Butene / 1-Butene $\times10^{-3}$ | *cis*-2-Butene / 1-Butene $\times10^{-3}$ |
|---|---|---|
| 10 | 9.37 | — |
| 20 | 5.26 | — |
| 40 | 4.50 | 0.45 |
| 60 | 4.66 | 0.66 |
| 80 | 3.45 | 1.14 |
| 100 | 2.89 | 0.48 |

Sulfur dioxide, 50 mmHg; Irradiation dose, $1.5\times10^7$ r.

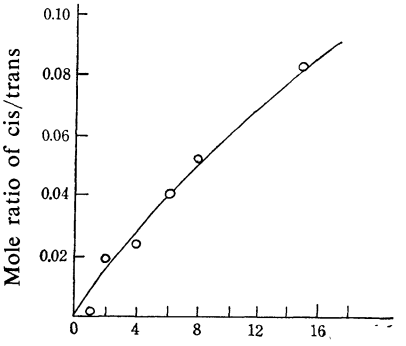



Fig. 3. Effects of sulfur dioxide upon *trans*-2-Butene as function of irradiation dose. (Sulfur dioxide, 100 mmHg; *trans*-2-Butene, 100 mmHg)

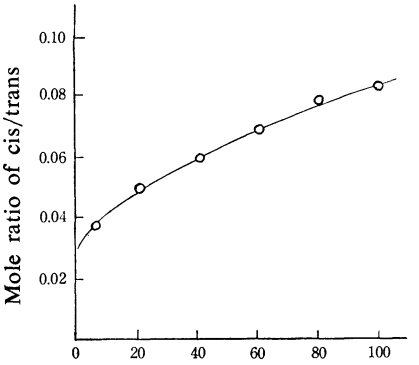



Fig. 4. Effects of sulfur dioxide upon the *trans*-2-butene isomerization (*trans*-2-butene, 100 mmHg; irradiation dose, $15\times10^6$ r.).

photochemical reactions of sulfur dioxide are due to the formation of the first triplet state (73.4 kcal. $mol.^{-1}$.[15]).

A similar experiment was applied to radiation chemistry with gamma rays. The effects of sulfur dioxide upon the isomerization were

15) A. D. Walsh, *J. Chem. Soc.*, 1953, 2266.

examined in a mixture of *trans*-2-butene and sulfur dioxide (Tables VIII and IX).

A marked isomerization was found to occur from trans to cis, but little isomerization to 1-butene was found to take place. The isomerization from 1-butene to *trans*- or *cis*-2-butene was also almost negligible. Further observations as to the function of the dose and the pressure of sulfur dioxide are shown in Figs. 3 and 4.

The isomerization can be explained similary by the following mechanism, which assumes the interaction of the triplet state of sulfur dioxide:

$$SO_2 \xrightarrow{\gamma\sim} SO_2 \text{ (triplet)}$$

$$SO_2 \text{ (triplet)} + \textit{trans}\text{-2-Butene (singlet)} \rightarrow \text{2-Butene (triplet)} + SO_2 \text{ (singlet)}$$

$$\text{2-Butene (triplet)} \rightarrow \textit{cis}\text{- or } \textit{trans}\text{-2-Butene}$$

However, the formation of small amounts of sulfinic acid and of the polymer on the walls of reaction vessels in the case of both 2-butene and 1-butene seems to suggest that at least a portion of the isomerization proceeds via the chain process shown below:

$$\textit{trans}\text{-2-Butene} + SO_2^* \rightarrow \cdot C_4H_8SO_2 \cdot$$

$$\cdot C_4H_8SO_2 \cdot \rightarrow \textit{trans}\text{- or } \textit{cis}\text{-2-Butene} + \text{1-Butene} + SO_2$$

$$\cdot C_4H_8SO_2 \cdot + M \rightarrow \text{Products}$$

Experiments were also conducted with nitric oxide and carbon disulfide. Nitric oxide has been used extensively as a free-radical trap in gas kinetics, and recently the possibility of an attack of nitric oxide on substrate molecules has been considered.[16,17] The effects of nitric oxide upon the isomerization are shown in Tables X and XI, with the function of the dose and the pressure of butene respectively.

These results, as well as others, indicate that the mechanism for the isomerization appears to be similar to that with sulfur dioxide; when 2-butene encounters unpaired electrons, transitions otherwise forbidden may be induced, and the addition to the double bond, followed by dissociation, may occur.

A brief study of the effect of carbon disulfide was made upon the mixture and 1-butene or 2-butene.

With 1-butene, some isomerization to 2-butene did occur, but a major portion underwent

TABLE X. EFFECTS OF NITRIC OXIDE UPON *trans*-2-BUTENE

| Dose ($\times 10^6$ r.) | 1 | 2 | 4 | 6 | 8 | 24 |
|---|---|---|---|---|---|---|
| cis/trans ($\times 10^{-2}$) | 10.3 | 14.5 | 13.3 | 15.1 | 13.8 | 16.5 |

Nitric oxide, 100 mmHg; *trans*-2-Butene 100 mmHg

TABLE XI. EFFECTS OF NITRIC OXIDE UPON *trans*-2-BUTENE AND 1-BUTENE

| *trans*-2-Butene mmHg | cis/trans $\times 10^{-2}$ | 1-Butene / *trans*-2-Butene $\times 10^{-3}$ |
|---|---|---|
| 10 | 27.3 | 5.05 |
| 20 | 24.4 | — |
| 40 | 16.0 | 5.33 |
| 60 | 14.2 | 3.57 |
| 80 | 9.61 | 4.63 |
| 100 | 8.13 | 3.33 |

| 1-Butene mmHg | *trans*-2-Butene / 1-Butene $\times 10^{-3}$ | *cis*-2-Butene / 1-Butene $\times 10^{-3}$ |
|---|---|---|
| 10 | — | — |
| 20 | 2.22 | 1.11 |
| 40 | 3.75 | 1.25 |
| 60 | 1.66 | 0.83 |
| 80 | 1.11 | 0.55 |
| 100 | 0.724 | 0.36 |

Nitric oxide, 50 mmHg; Irradiation dose, $3.5 \times 10^6$ r.

TABLE XII. EFFECTS OF CARBON DISULFIDE UPON *trans*-2-BUTENE

| *trans*-2-Butene mmHg | Carbon disulfide mmHg | cis/trans $\times 10^{-1}$ | 1-Butene / *trans*-2-Butene $\times 10^{-3}$ |
|---|---|---|---|
| 100 | 10 | 1.24 | 1.32 |
| 100 | 20 | 1.50 | 1.51 |
| 100 | 30 | 1.71 | 2.38 |
| 10 | 50 | 2.65 | 3.34 |
| 20 | 50 | 2.74 | 2.18 |
| 40 | 50 | 2.47 | 3.75 |
| 60 | 50 | 2.28 | 1.20 |
| 100 | 50 | 2.77 | 7.55 |

Irradiation dose: $1.5 \times 10^7$ r.

TABLE XIII. EFFECTS OF CARBON DISULFIDE UPON 1-BUTENE

| 1-Butene mmHg | *trans*-2-Butene / 1-Butene $\times 10^{-3}$ | *cis*-2-Butene / 1-Butene $\times 10^{-3}$ |
|---|---|---|
| 10 | 7.14 | — |
| 20 | 10.0 | 2.0 |
| 40 | 3.8 | 0.95 |
| 60 | 3.86 | 0.77 |
| 80 | 5.13 | 1.71 |
| 100 | 3.84 | 0.96 |

Irradiation dose: $1.5 \times 10^7$ r.
Carbon disulfide: 50 mmHg

16) B. W. Wojciechowski and K. Laidler, *Can. J. Chem.*, **38**, 1027 (1960); *Proc. Roy. Soc.*, **A260**, 103 (1961).
17) R. Blackmore and Sir C. Hinshelwood, ibid., **A268**, 21 (1962).

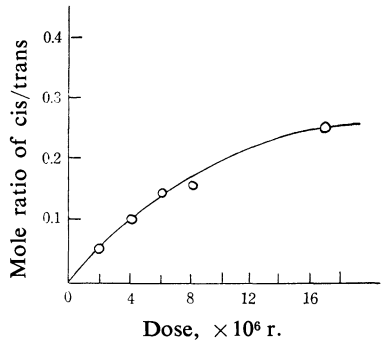



Fig. 5. Effect of dose of irradiation upon 2-butene by carbon disulfide. (Carbon disulfide, 25 mmHg; *trans*-2-butene, 100 mmHg)

decomposition. With 2-butene, carbon disulfide caused some isomerization, and here again the main product was a large amount of by-products, which consisted of some organo-sulfur compounds and elemental sulfur (Tables XII, XIII and Fig. 5).

The effect of gaseous carbon disulfide in the isomerization has not been reported previously. However, it has been shown that, under flash-photolysis conditions, the absorption spectrum taken a few millisenonds after the illumination of gaseous carbon disulfide gave the characteristic bands of $S_2$ and CS.[18,19] Therefore, one can safely assume the initial interaction of the double bond with the sulfur atom formed by the irradiation of carbon disulfide. The formation of by-products indicates that the isomerization must be carried out through interaction with CS and S, since S is formed in the primary act, while CS is formed both in the primary:

$$CS_2 \xrightarrow{r} CS + S$$

and the secondary acts:

$$CS_2 + S \longrightarrow CS + S_2$$

The sulfur atom thus formed presumably induces isomerization by a direct radical attack on the double bond. The following basic processes may be proposed to explain the action of the sulfur atom in the induced isomerization:

$$\textit{trans}\text{-2-Butene} + S \rightarrow \cdot C_4H_8S\cdot$$

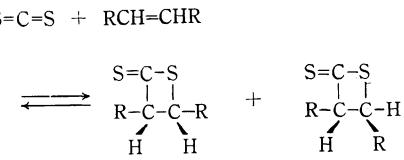
$$\cdot C_4H_8S\cdot \rightarrow \textit{cis}\text{- or } \textit{trans}\text{-2-Butene} + S$$

$$\cdot C_4H_8S\cdot + CS \rightarrow \textit{cis}\text{- or } \textit{trans}\text{-2-Butene} + CS_2$$

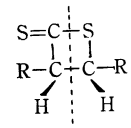
$$\cdot C_4H_8S\cdot + CS_2 \rightarrow \textit{cis}\text{- or } \textit{trans}\text{-2-Butene} + CS + S_2$$

A similar reaction scheme can be postulated with CS, another radical formed by the initial irradiation of $CS_2$. Isomerization induced by the sulfur molecule would involve the formation of the free radical by the homolytic cleavage of the sulfur, with the subsequent addition of the free radical to the double bond. However, the contribution of this process would not be very large. The explanation of the isomerization mechanism involves the formation of a $\pi$-complex between sulfur and the double bond, as has been suggested for the thermal isomerization of polybutadiene with sulfur.[20] However, this mechanism does not reveal the exact nature of the bonding, either in the radical attack or the $\pi$-complex formation. The $\pi$-complex possibly involves the $\pi$-orbital of the olefin and the anti-bonding $\pi$-orbital of sulfur, but this is a mere conjecture; until further evidence is available, the discussion of the exact nature of bonding in such a complex will not be fruitful.

Another interesting mechanism is the one involving initial addition, followed by subsequent dissociation, as is shown below:




Here, the formation of a large amount of sulfur containing by-products can be also explained if one assumes that the dissociation takes place by A-type cleavage. A similar addition-dissociation was reported very recently




(A)

in the photochemical reaction between thiobenzophenon and olefins.[21] At present, it is difficult to single out the most plausible mechanism for this carbon disulfide-catalyzed isomerization. A detailed investigation of the nature of the by-products would, however, shed further light on the probable pathway of this reaction.

## Summary

A detailed study of the radiation-induced trans-cis isomerization of 2-butenes has been made. The effects of halogenated compounds

18) R. G. Norrish and G. Porter, ibid., **A200**, 284 (1950).
19) G. Porter, *Discussions Faraday Soc.*, **9**, 60 (1950).
20) W. A. Bishop, *J. Polymer Sci.*, 55, 827 (1961).
21) E. T. Kaiser and T. F. Wulfers, *J. Am. Chem. Soc.*, **86**, 1898 (1964).

upon 2-butene can be explained by the attack of the halogen radicals formed in irradiation, and a radical chain process can be suggested for the isomerization.

The addition of hexane or cyclohexane to 2-butene in the gas phase has shown a rapid isomerization of trans to cis; it has been suggested that this is caused by the hydrogen atom formed in the irradiation of hexane or cyclohexane. The facile isomerization of 1-butene to *trans*-2-butene by the presence of such hydrocarbons suggests that the hydrogen is readily exchanged with the other hydrogen of olefin, thus leading to the isomerization.

Radiation-induced isomerizations brought by benzene, sulfur dioxide, nitric oxide, carbon disulfide and other molecules have also been examined. The effect of benzene on the trans-cis isomerization of 2-butene has been explained by production of vibrationally-excited triplet states. Results with sulfur dioxide have shown that radiation-induced isomerization is due not only to the formation of the first triplet state, but also to the addition to the double bond, followed by dissociation.

*Department of Chemistry*
*Radiation Center of Osaka Prefecture*
*Sakai, Osaka (W. A.)*

*Research Laboratory*
*Kurashiki Rayon Co., Ltd.*
*Kurashiki, Okayama (K. S.)*

*Department of Applied Chemistry*
*Faculty of Engineering*
*Osaka City University*
*Sumiyoshiku, Osaka (S. O.)*

# The Formation Constants and the Rate Constants of the Electrode Processes of Thiocyanato-Indium(III) Complexes with the Dropping Mercury Electrode*

By Yoshio NARUSAWA,*1 Jinzo HASHIMOTO*2 and Hiroshi HAMAGUCHI*3

(Received June 20, 1964)

Few authors[1,2] have reported investigations of the formation constants of indium(III) thiocyanate complexes. Sunden[1] has, however, determined the formation constants of thiocyanato-indium(III) complexes potentiometrically. The potentiometric method and the polarographic method, though they have a wide applicability, generally include uncertainties arising from the estimations of a liquid junction potential and those of the activity coefficients of the complex ions present.

The polarographic method proposed by DeFord and Hume[3] for the formation constants, though it has an unknown liquid junction potential, is applicable when the electrode processes are reversible at the dropping mercury electrode.

In the present paper, the formation constants and rate constants of the electrode processes of thiocyanato-indium(III) complexes are presented. Analyses of the present data will show the existence of the mono-, di-, tri- and tetra-coordinated species in a solution, and each consecutive formation constant will be calculated. The rate constants, $(k_0)_B$ and $(k_1)_B$ at the standard potential and $k^0_{f,h}$ at 0 V. vs. NHE, will also be determined.

## Experimental

**Reagents.** — A commercial sodium thiocyanate was dissolved in water and standardized against the standard silver nitrate solution by volumetric titration with uranin as the indicator. An appropriate amount of indium perchlorate, prepared from a commercial indium sesquioxide, was dissolved in water and standardized gravimetrically. A solution of sodium perchlorate was prepared by dissolving a commercial reagent and was standardized by the ion exchange method. A solution of geratine was freshly prepared every time it was used. All the other chemicals were of a reagent grade and were used without further purification. The composition of the solution was obtained by mixing indium(III) ions, perchlorate and variable amounts of thiocyanate solutions, the ingredients being so chosen

* Presented partly at the 12th Annual Meeting of the Chemical Society of Japan, Kyoto, April, 1959.

*1 Present address: Department of Chemistry, Rikkyo (St. Paul's) University, Ikebukuro, Tokyo.

*2 Present address: Hitotsubashi University, Kunitachi-machi, Tokyo.

*3 Present address: Department of Chemistry, The University of Tokyo, Hongo, Tokyo.

1) N. Sundén, *Svensk Kem. Tidskr.*, **66**, 50 (1954).

2) T. P. Radhakrishnan and A. K. Sundaram, *J. Electroanal. Chem.*, **5**, 124 (1963).

3) D. D. DeFord and D. N. Hume, *J. Am. Chem. Soc.*, **73**, 5321 (1951).

that the total ionic strength was kept constant at 2.0 mol./l.

**Apparatus.**—A Yanagimoto PB-105 pen-recording polarograph was used for the measurement of the current-potential curves. The usual polarographic technique was used in this study. The capillary used was $m=1.28$ mg./sec., $\tau=3.74$ sec./drop and 1.47 $mg^{2/3} sec^{-1/2}$ for $m^{2/3} \tau^{1/6}$ (where $m$ is the flow rate of mercury and $\tau$, the drop time) in a solution to be examined at $-0.7$ V. vs. SCE at a height of 70 cm. of the mercury reservoir. The sample solution was connected to the reference electrode through the series of successive bridges of an agar-sodium nitrate, a saturated sodium nitrate solution, and an agar-potassium chloride. The resistance of the cell was found to be 95 ohms when measured by an a. c. bridge. This resistance is very small and it did not change noticeably as the composition of the thiocyanate-perchlorate mixture was varied, so it was neglected in measuring the half-wave potential. Toa-Dempa HM-5 pH meter was used for pH measurements. The pH of the solution of this system measured was about 3.0. All polarographic measurements were made at $25\pm0.1$°C unless otherwise stated. Purified hydrogen gas was used for removing oxygen from a solution before polarograms were obtained.

**Measurements of the Half-Wave Potential.**—The polarograph was always set with an initial voltage of $-0.4$ V. vs. SCE and a span voltage of 0.5 V. The sensitivity used was 0.06 $\mu$amp./mm., without condenser damping. Using the Leeds and Northrup K-type potentiometer as an external potentiometer, the inital and final potentials were measured to within 0.5 mV. All the current measurements used in the calculations were of the average current of an individual oscillation of the polarogram. The average current was taken simply as one-half of the oscillation (the maximum pen excursion).

The half-wave potentials were found by plotting the logarithm of $\bar{i}/(\bar{i}_d-\bar{i})$ (where $\bar{i}$ is the current corresponding to a given potential and $\bar{i}_d$, the diffusion current corrected for the residual current) versus the applied potential. A point was plotted for each individual small oscillation on the polarogram, and at least twelve values were used along the mid-portion of the curve. The plots of the $\log \bar{i}/(\bar{i}_d-\bar{i})$ versus the applied potentials yielded a slightly curved line in a lower half and a straight line in an upper half in perchlorate and/or thiocyanate media (see Fig. 1). These curves of the log-plot are typical of those obtained for the "quasi"-reversible electrode processes. The reversible half-wave potential, $E_{1/2}{}^r$, was calculated by applying the Matsuda-Ayabe theory.[4] Duplicate experiments showed that the reproducibility of the half-wave potential was within 1 mV. Measurements were made with four separately-prepared samples containing 1.09 mmol./l. indium(III) ion, 0.5 mol./l. thiocyanate, 1.5 mol./l. perchlorate and 0.005% gelatine; the individual half-wave potentials obtained were $-0.5670$, $-0.5688$, $-0.5688$ and $-0.5692$ V. vs. SCE respectively. The observed half-wave potentials involve an unknown liquid junction potential. The junction potential is a composite of the potential across the saturated potassium chloride - saturated sodium nitrate boundary and the saturated sodium nitrate - sodium perchlorate, sodium thiocyanate boundary. Although the correct value is unavailable, it will be taken into consideration in the future if it is determined for this system.

4) H. Matsuda and Y. Ayabe, *Z. Elektrochem.*, 63, 1164 (1959).

## Results

**The Effect of Maximum Suppressors and of the Concentrations of the Supporting Electrolyte.**—When the total ionic strength of the solution was 2.0 mol./l. indium(III) simple ion and thiocyanato-indium(III) complexes, in perchlorate and in thiocyanate media respectively, showed pronounced maxima which could be depressed in the presence of 0.005 per cent gelatin, and "well-defined" waves were obtained. When the concentration of the supporting electrolyte (sodium thiocyanate) was smaller than 0.1 mol./l., the maximum appeared even in the presence of 0.005 per cent gelatine. That the maximum does not appear in the presence of positively-charged gelatine in an acid solution of the pH 3 when the concentration of thiocyanate is greater than 0.1 mol./l., while in the concentration of thiocyanate lower than 0.1 mol./l., the fact that the maximum which appears in the positive branch of the electrocapillary curve can not be eliminated by gelatine means that the maximum is of the first kind.

**The Effect of Mercury Height.**—A typical limiting diffusion current should be proportional to the square root of the effective height of the mercury.[5] At four various applied heights of the mercury column, 70, 60, 50 and 40 cm., the value of $\bar{i}_d/h_{corr}{}^{1/2}$ (where $h_{corr}$ is an effective height of mercury) was found to be $0.785\pm0.005$ $\mu$amp./$cm^{1/2}$ for a solution of 1.09 mmol./l. indium(III), 0.5 mol./l. thiocyanate, 1.5 mol./l. perchlorate and 0.005 per cent gelatine. In these experiments the half-wave potentials were constant within $\pm0.3$ mV. These results indicate that the limiting current is diffusion-controlled.

**The Effect of Temperature.**—From the results with a solution of 2.0 mol./l. potassium thiocyanate, 0.941 mmol./l. indium(III) and 0.005 per cent gelatine, the temperature coefficient of limitting current near 25°C was calculated to be 1.37 per cent/deg.

This value is in fairly good agreement with the usual diffussion-controlled current[6a]. The

5) See, e. g., I. M. Kolthoff and J. J. Lingane, "Polarography," Vol. I, Interscience Publishers, New York (1952), p. 85.

6) *a*, *b*, See, e. g., Ref. 5, pp. 92, 234.

half-wave potential became less negative with an increase in the temperature, and the value of $dE_{1/2}/dT$ was 3.4 mV./deg. The positive temperature coefficient which has been seen for the several hydrated metal ions implies that an appreciable activation energy is required in the electrode reaction.[6)b]

**The Calculation of the Reversible Half-Wave Potential, $E_{1/2}{}^r$, According to the Matsuda-Ayabe Theory.** — Figure 1 shows the plot of $\log \bar{i}/(\bar{i}_d-\bar{i})$ versus the applied potential, with a solution 1.09 mmol./l. indium(III) ion, 0.005 per cent gelatine and various thiocyanate concentrations of (0, 0.5 and 2.0 mol./l.). The plots of the upper halves of the curves show straight lines, while the lower halves of the plots are curved lines. The log-plots for all other cases were similar to those shown in Fig. 1. According to the Matsuda-Ayabe theory,[4)] the curves shown in Fig. 1 are considered to be typical of a "quasi"-reversible electrode process, and in such cases $\Lambda\sqrt{\tau}$ (where $\Lambda$ is a kinetic parameter of an electrode process) is obtained from Eq. 1 and falls in the range between 30 and $10^{-2}$. The reversile half-wave potential, $E_{1/2}{}^r$ can also be obtained as follows;

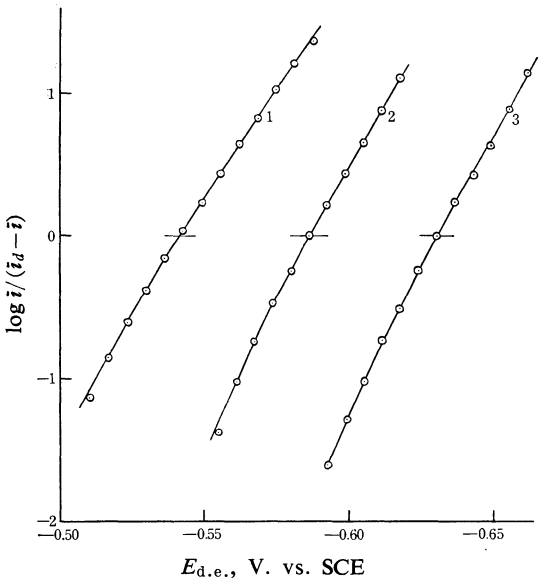



Fig. 1. A log-plot of 1.09 mmol./l. indium(III) ion in the presence of 0.005 per cent of gelatin and various thiocyanate concentration. Curves 1, 2 and 3: 0, 0.50 and 2.0 mol./l. $C_{SCN^-}$, respectively.

$$\log \Lambda = \frac{\alpha nF}{2.3RT}(E_{1/2}' - E_{1/2}{}^r) + \log(\bar{i}_l/\bar{i}_d) - \frac{1}{2}\log\tau + 0.053 \quad (1)$$

$$E_{1/2}{}^r = E_{1/\nu+1} - 2.3\frac{RT}{nF}\left\{\log\left[\nu - \exp\frac{\alpha nF}{RT} \times (E_{1/\nu+1} - E_{1/2}')\right] - \log(\bar{i}_l/\bar{i}_d)\right\} \quad (2)$$

where $E_{1/\nu+1}$ and $E_{1/2}'$ are the potentials corresponding to $-\log\nu$ and zero on the ordinate respectively, $\bar{i}_l$ and $\bar{i}_d$ are average limiting and diffusion currents respectively, and $\alpha$ is the transfer coefficient in the electrode reaction. As the limitting current, $\bar{i}_l$ ($7.02_0$ $\mu$amp.), of simple indium(III) ions in $1.08_6$ mmol./l. agrees fairly well with the value ($7.09_2$ $\mu$amp.) calculated from the original Ilkovic equation, assuming the diffusion coefficient $D$ to be $5.97 \times 10^{-6}$ cm$^2$/sec. (which is the average value calculated from the equivalent conductivity at an infinite dilution of many other trivalent ions such as ferric[7a)] chromic[7a)], aluminium[7a)] and rare earth metal ions[7b)]), the ratio of $\bar{i}_l$ to $\bar{i}_d$ must be unity. For complex ions, $\bar{i}_l$ gradually becomes smaller than $\bar{i}_d$ with an increase in the concentration of thiocyanate. Table I shows some of the experimentally-obtained potentials, $E_{1/2}'$, $E_{1/11}$ and the diffusion currents, together with the results calculated from Eqs. 1 and 2. As is shown in Table I $\Lambda\sqrt{\tau}$ was 0.3 to 0.1, which is in the range of 30 to $10^{-2}$. This means that the electrode process of the indium(III)-thiocyanate system is "quasi"-reversible.

Table I. Calculations of $E_{1/2}{}^r$ and $\Lambda\sqrt{\tau}$

| $C_{SCN^-}$ mol./l. | $\bar{i}_l$ $\mu$amp. | $\alpha$ | $-E_{1/2}'$ | $-E_{1/11}$ V. vs. SCE | $-E_{1/2}{}^r$ | $\Lambda\sqrt{\tau}$ |
|---|---|---|---|---|---|---|
| 0 | 7.020 | 0.614 | 0.5415 | 0.5134 | 0.5213 | 0.238 |
| 0.01998 | 7.026 | 0.627 | 0.5477 | 0.5204 | 0.5286 | 0.250 |
| 0.4994 | 6.744 | 0.701 | 0.5870 | 0.5612 | 0.5664 | 0.180 |
| 0.9988 | 6.618 | 0.730 | 0.6081 | 0.5829 | 0.5863 | 0.149 |
| 1.498 | 6.594 | 0.730 | 0.6198 | 0.5949 | 0.5997 | 0.171 |
| 1.998 | 6.534 | 0.732 | 0.6309 | 0.6057 | 0.6090 | 0.145 |

7) a) J. D'Ans and E. Lax, "Taschenbuch für Chemiker und Physiker" (1949), p. 1237.
b) F. H. Spedding, P. E. Porter and J. M. Wright, *J. Am. Chem. Soc.*, **74**, 2055, 2778, 2781 (1952); F. H. Spedding and I. S. Yaffe, ibid., **74**, 4751 (1952); F. H. Spedding and J. L. Dye, ibid., **76**, 879 (1954); F. H. Spedding and S. Jaffe, ibid., **76**, 882, 884 (1954).

**The Relation between Half-Wave Potentials and Logarithms of Thiocyanate Concentration.** —A relation of the half-wave potentials, $E_{1/2}{}^r$, to the logarithms of thiocyanate is given in Fig. 2; the ligand number can be estimated from the slope of the curve. Figure 2 also shows by a broken line the theoretical slopes corresponding to the ligand number. This indicates that the tetra-coordinated species is present in a solution of an ionic strength of 2.0 mol./l. The slope of the last part, 3.8, is slightly smaller than the theoretical value of 4; this deviation is considered to be due to overlapping with that of the lower ligand numbers, or with di- and tri-coordinated complexes.

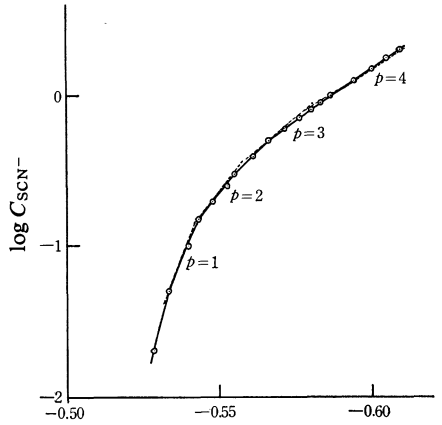



Fig. 2. A relation between $E_{1/2}{}^r$ and log $C_{SCN^-}$. The broken lines indicate the theoretical slopes corresponding to the respective ligand number.

**An Analysis of the DeFord-Hume Function.**— The following paragraph will describe the method of analysis of DeFord and Hume.[3]

The method is applicable when the following conditions are satisfied: (1) the electrode processes of a hydrated metal ion, as well as of a complex ion, are reversible at the dropping mercury electrode; (2) the metal reduced at the electrode is soluble in mercury, or forms an amalgam, and (3) the formation constants are not very large.

The indium(III)-thiocyanate system satisfies these conditions except that the electrode processes of the simple indium(III) ion, like those of complex ions, are "quasi"-reversible in the reduction at the electrode, and the method of DeFord and Hume[3] is supposed to be applicable for this system by the aid of the reversible half-wave potential, $E_{1/2}{}^r$, which is calculated from the experimentally-observable values according to the Matsuda-Ayabe theory.[4]

For the calculation of DeFord-Hume function $F_j(X)$, $E_{1/2}{}^r$ was taken as the half-wave potential of a simple or complex ions. According to the DeFord and Hume's theory,[3] $F_j(X)$ functions are defined as follows;

$$F_0(X) = \sum_{j=0}^{N} \frac{K_j (C_X)^j (f_X)^j}{f_{MX_j}}$$

$$= \text{antilog}\left[0.434 \frac{nF}{RT}\{(E_{1/2}{}^r)_s - (E_{1/2}{}^r)_c\} + \log \frac{I_s}{I_c}\right] \quad (3)$$

$$F_j(X) = [F_{j-1}(X) - (K_{j-1}/f_{MX_{j-1}})]/C_X f_X \quad (j=1, 2, \cdots\cdots, N) \quad (4)$$

where $K_j$ is the formation constant of complex $MX_j$, $C_X$ is the concentration of ligands, $f$'s are the activity coefficients of corresponding ions, $I$'s are diffusion current constants, subscripts $s$ and $c$ refer to simple and complex ions, respectively, and other symbols are used with their usual significances. Substituting the experimentally-measurable quantity on the right-hand side of Eq. 3, the $F_0(X)$ function is calculated. The logarithm of $I_s/I_c$ was so small in comparison with the first term of the bracket of Eq. 3 in the range of ligand concentrations from 0 to 2.0 mol./l. that it was disregarded in the calculation of the $F_0(X)$ function. Furthermore, the $F_j(X)$ functions were calculated from the previous $F_{j-1}(X)$ function by the aid of Eq. 4.

Figure 3 shows the plot of the $F_j(X)$ functions calculated from Eqs. 3 and 4 against the thiocyanate concentration, $C_X$.

By extrapolating the $F_j(X)$ function to $C_X=0$, the value of $K_j$ is obtained as an intersection The formation constant, $K_0$, is the value of $F_0(X)$ corresponding to the zero concentration of ligand; it is unity. The extraporation of the plot of $F_1(X)$, $F_2(X)$, $F_3(X)$ and $F_4(X)$ to zero thiocyanate concentration yielded the values of $K_1$, $K_2$, $K_3$ and $K_4$ respectively. Besides, a value of $F_j(X)$ at zero thiocyanate concentration or a value of $K_j$ is equal to the initial slope of the curve of a previous $F_{j-1}(X)$ function. Equation 4 indicates that $F_j(X)$ is a function of the concentration of ligands, $C_X$. When $F_{j-1}(X)$ is a function of the first power of $C_X$ or is linear with a positive slope against $C_X$, $F_j(X)$ becomes parallel against the $C_X$ axis, and the value of $F_j(X)$ gives that of $K_j$. As is shown in Fig. 3, a tetra-coordinated complex is explicitly present in the solution with the higher ligand concentration, in accordance with the result of Fig. 2. Bock[8] has shown the presence of the tetra-coordinated species $In(SCN)_4^-$ in diethylether by the distribution method. Accordingly, it

8) R. Bock, *Z. anal. Chem.*, 133, 110 (1951).

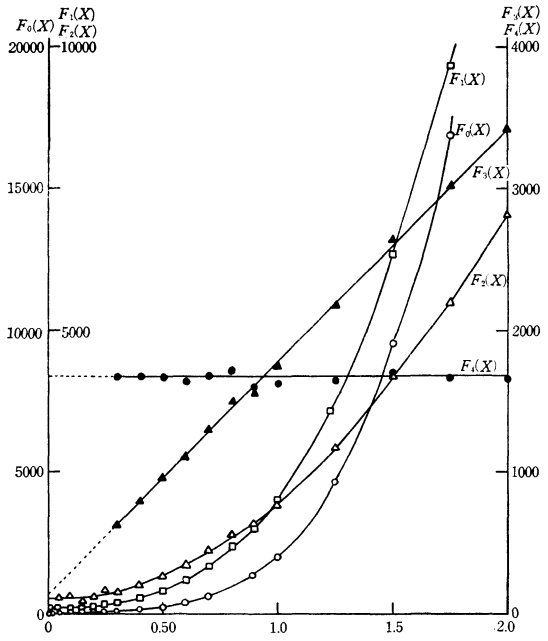



Fig. 3. A relation between $F_j(X)$ and $C_{SCN^-}$.

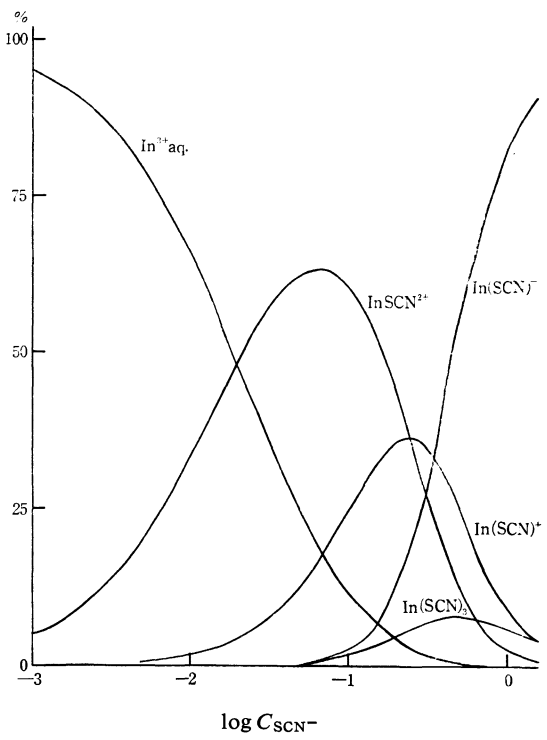



Fig. 4. Concentration distribution of each complex species.

may be reasonable to assume the presence of $In(SCN)_4^-$ in an aqueous solution. The extrapolation of the plot of $F_1(X)$, $F_2(X)$, $F_3(X)$ and $F_4(X)$ to zero thiocyanate concentration yielded values of 50, 200, 120 and 1670 for $K_1$, $K_2$, $K_3$ and $K_4$ respectively. Moreover, the values of 45 to 55, 190 to 220, 110 to 130 and 1650 to 1660 for $K_1$, $K_2$, $K_3$ and $K_4$ were obtained from the initial slopes of the curves. These values are in good agreement with the extrapolated values.

Experimental errors in the determination of $\Delta E_{1/2}{}^r$ were cumulative in the successive calculations of $F_j(X)$; particularly for low concentrations (below 0.3 mol./l.) of a complexing agent, the values of $F_3(X)$ and $F_4(X)$ were so scattered that they were disregarded. As is shown in Fig. 3, however, these plots resulted in a linear relation with a higher thiocyanate concentration than 0.3 mol./l., and a better point at the intersection was obtained by extrapolation.

From the data of Fig. 3, the concentration distribution of each species may be calculated from the following equations.

Indium(III) ions are associated with the excess of thiocyanate as follows:

$$In_{aq}^{3+} + jSCN^- \rightleftarrows In(SCN)_j^{(3-j)+} \qquad (5)$$

The formation constant $K_j$ is given in the following equation:

$$K_j = \frac{[C_{MX_j} f_{MX_j}]}{[C_M f_M][(C_X)^j (f_X)^j]} \qquad (6)$$

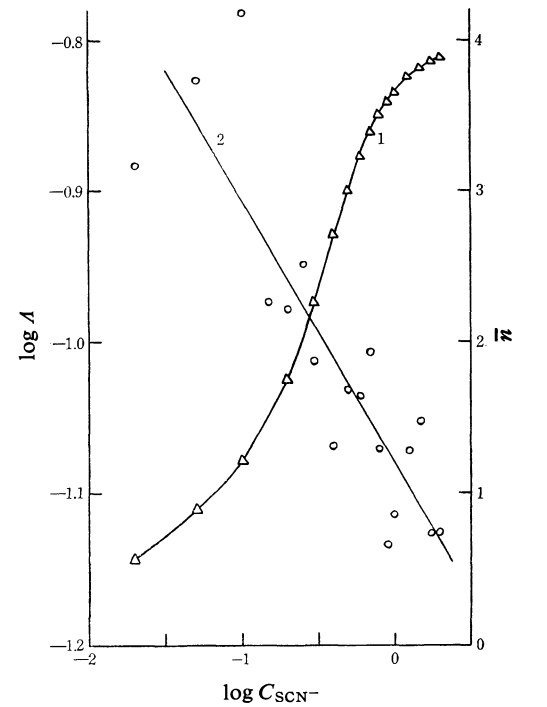



Fig. 5. The mean ligand number $\bar{n}$ (curve 1) and log $\Lambda$ (curve 2) against log $C_{SCN^-}$.

where $[C_M]$ is the simple indium(III) ion non-coordinated in the solution and is written as follows:

$$[C_M]=\frac{\sum_{j=0}^{N}[C_{MX_j}f_{MX_j}]}{\sum_{j=0}^{N}K_j[C_X]^j[f_X]^j[f_M]} \quad (7)$$

Therefore, the concentration of a complex species, $[C_{MX_j}]$, is written is the following equation:

$$[C_{MX_j}]=K_j[C_Mf_M][C_X]^j[f_X]^j/f_{MX_j} \quad (8)$$

In Fig. 4, the distributions of the concentration of all the species calculated from Eqs. 7 and 8 for $\sum_{j=0}^{N}[C_{MX_j}f_{MX_j}]=100\%$ are plotted against $\log C_{SCN^-}$. The activity coefficients, $f$'s, were all assumed to be unity. As is obviously shown in Fig. 4, when the concentration of thiocyanate is greater than 1.5 mol./l, more than 90 per cent of all the species present in the solution exist as tetra-coordinated form $In(SCN)_4^-$. In Fig. 5, the mean values of the ligand number, $\bar{n}$, obtained from the data in Fig. 4 are plotted against $\log C_{SCN^-}$, and also the relation between $\log \Delta$ and $\log C_{SCN^-}$ is shown. The slope, $-0.174$, for the latter curve was obtained by the aid of the least-square method.

## Discussion

Sundén[1] has reported the overall formation constants obtained potentiometrically for $K_1$, $K_2$ and $K_3$ to be $3.8\times10^2$, $4.0\times10^3$ and $4.4\times10^4$ respectively, at an ionic strength of 2.0 mol./l. at 20.0°C. The polarographically-obtained values reported by Radhakrishnan et al.[2] for $K_1$, $K_2$, $K_3$, $K_4$, $K_5$ and $K_6$ are $1.2\times10^2$, $1.6\times10^3$, $1.75\times10^4$, $1.7\times10^4$, $6.5\times10^4$ and $6.9\times10^4$ respectively, at an ionic strength of 2.0 mol./l. at 30°C. On the other hand, the $K_1$, $K_2$, $K_3$ and $K_4$ values obtained from the present data are 50, 200, 120 and 1670 respectively. This discrepancy from the values obtained by Sundén[1] may be largely due to the adsorption of thiocyanate ions on the electrode surface. Furthermore, the slight enhancement of the limiting current, especially in the lower thiocyanate concentration, may be attributed to this adsorption of thiocyanate ions (see Table I). As is shown in Fig. 2, the tetra-coordinated species is evidently present in the higher ligand concentration. Moreover, as Fig. 3 shows, the value of the tetra-coordinated form, $K_4$, is obtained from the analysis of the DeFord and Hume function. Sundén[1] has not obtained the value of $K_4$, and Radhakrishnan et al.[2] have reported the values of $K_5$ and $K_6$. Though the values of $K_5$ and $K_6$ can be obtained by the analysis of DeFord and Hume function, they may include errors because of an obscurity in the half-wave potential measurement.

For the sake of simplicity, it is assumed that one of the complexes, $In(SCN)_p^{(3-p)+}$ ($p=4, 3, 1, 2, 0$), is present predominantly in a solution; it is reduced to an amalgam as follows:

$$In(SCN)_p^{(3-p)+}+3e^-+Hg \rightleftarrows In(Hg)+pSCN^- \quad (p=4, 3, \cdots\cdots, 0) \quad (9)$$

where the following consecutive dissociation and association reactions proceed very fast:

$$In(SCN)_p^{(3-p)+} \rightleftarrows In(SCN)_{p-1}^{(4-p)+}+SCN^- \quad (p=4, 3, 2, 1) \quad (10)$$

The ligand number, $p$, in the electrode reaction is given by the following equation:[4]

$$p=\beta N+\frac{\Delta \log \Delta}{\Delta \log (C_Xf_X)} \quad (10)$$

where $\beta=1-\alpha$, and $N$ is the maximum value of the ligand number of a complex present in a given solution. By substituting the values $\beta=0.27$, $N=3.9$ and the slope $\Delta \log \Delta/\Delta \log (C_Xf_X)=-0.174$ obtained from Fig. 5 into the above equation, $p=0.88$ was obtained at $C_{SCN^-}\simeq2.0$ mol./l. On the other hand, at the concentration of about 0.02 mol./l., $p$ was 0.03, which is nearly equal to zero. This means that two kinds of ions, $InSCN^{2+}$ and $In^{3+}$, are reduced at the D.M.E.

In fact, various complexes $In(SCN)_p^{(3-p)+}$ ($p=4, 3, \cdots\cdots, 0$) are present in a given solution and are reduced to an amalgam at different rates; therefore, the analysis of an individual rate constant is complicated.

According to the Matsuda-Ayabe theory,[9] however, the rate constants, $(k_p)_B$, ($p=4, 3, \cdots\cdots, 0$) at the standard potential, $(E^0)_B$, can be calculated as follows:

$$\Delta \exp\frac{(1-\alpha)n\boldsymbol{F}}{\boldsymbol{RT}}[(E_{1/2}{}^r)_s-(E_{1/2}{}^r)_c]=(1+\sum_{j=0}^{N}K_j)^{1-\alpha}(f_s/\sqrt{D_s})^{1-\alpha}(f_a/\sqrt{D_a})^{\alpha}\times\sum_{p=0}^{N}(k_p)_B(f_XC_X)^p \quad (12)$$

$$(E^0)_B=E_{1/2}{}^r-2.3\frac{\boldsymbol{RT}}{n\boldsymbol{F}}\log\frac{f_N/\sqrt{D_N}}{f_a/\sqrt{D_a}}-2.3N\frac{\boldsymbol{RT}}{n\boldsymbol{F}}\log(f_XC_X) \quad (13)$$

9) H. Matsuda and Y. Ayabe, *Z. Elektrochem., Ber. Bunsenges. physik. Chem.*, **66**, 469 (1962).

where $D_s$, $D_N$ and $D_a$ are the diffusion coefficients of simple indium(III) ions, indium(III) complex ions with the ligand number, $N$, and indium metal in mercury respectively, $f$'s are activity coefficients, and the other symbols are used with the usual significance. Although the half-wave potential of simple indium(III) ions was determined to be $-0.531 \pm 0.003$ V. vs. SCE by Moorhead and MacNevin[10] from the analysis of the log-plot, it was found by the precise analysis of the present data that the reduction of indium(III) ions at the electrode implies some overpotentials. The value, $E_{1/2}{}^r$ ($=-0.5213$ V. vs. SCE), of the simple indium(III) ions obtained by taking the overpotential into consideration is more valid than that of Moorhead and MacNevin.[10] It is, however, not the standard potential of the reaction of $In^{3+}+3e^- + Hg \rightarrow In(Hg)$. The standard potential of the above reaction is unavailable; therefore, it is assumed to be closely equal to the potential ($-0.5138$ V. vs. SCE) calculated from Eq. 13, in which the concentration of thiocyanate is 0.02 mol./l.

As is obviously shown in Eq. 12, the logarithm of the left-hand side must be a linear function of $\log C_{SCN^-}$ if one complex species is present predominantly. In Fig. 6, $\log \Lambda + \{(1-\alpha)nF/2.3RT\}[(E_{1/2}{}^r)_s-(E_{1/2}{}^r)_c]$ are plotted in respect to $\log C_{SCN^-}$; as is shown, the linear relation was not obtained. This indicates that two or more complex species are involved in the electrode reaction.

Further, the left-hand side of Eq. 12 is the experimentally-measurable quantity, which is defined as the $H_0(X)$ function. By extrapolating the $H_0(X)$ function to $(f_X C_X)=0$, the limiting value is given as follows:

$$\lim_{f_X C_X \to 0} H_0(X) = (1+\sum_{j=1}^{N} K_j)^{1-\alpha} \times (f_s/\sqrt{D_s})^{1-\alpha}(f_a/\sqrt{D_a})^{\alpha}(k_0)_B \qquad (14)$$

In general, $H_p(X)$ is defined as follows:

$$H_p(X) = [H_{p-1}(X) - \lim H_{p-1}(X)]/(f_X C_X) \qquad (15)$$

By extrapolating $H_p(X)$ to $(f_X C_X)=0$, the following equation is obtained:

$$\lim_{f_X C_X \to 0} H_p(X) = (1+\sum_{j=1}^{N} K_j)^{1-\alpha} \times (f_s/\sqrt{D_s})^{1-\alpha}(f_a/\sqrt{D_a})^{\alpha}(k_p)_B \qquad (16)$$

The relation of Eqs. 12 and 15 is shown in Fig. 7, in which $H_0(X)$ is linear with a positive slope with respect to the $C_X$ axis. The slope and the intersection of the straight line

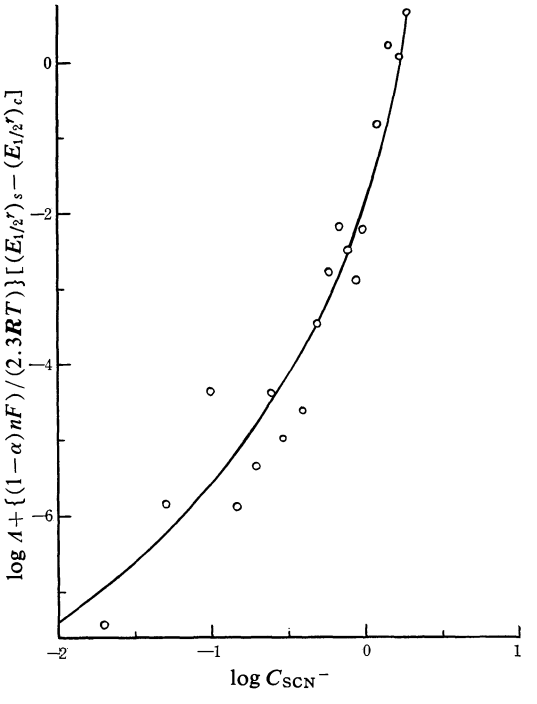



Fig. 6. The logarithmic relation of the left-hand side of Eq. 12 in respect to $\log C_{SCN^-}$.

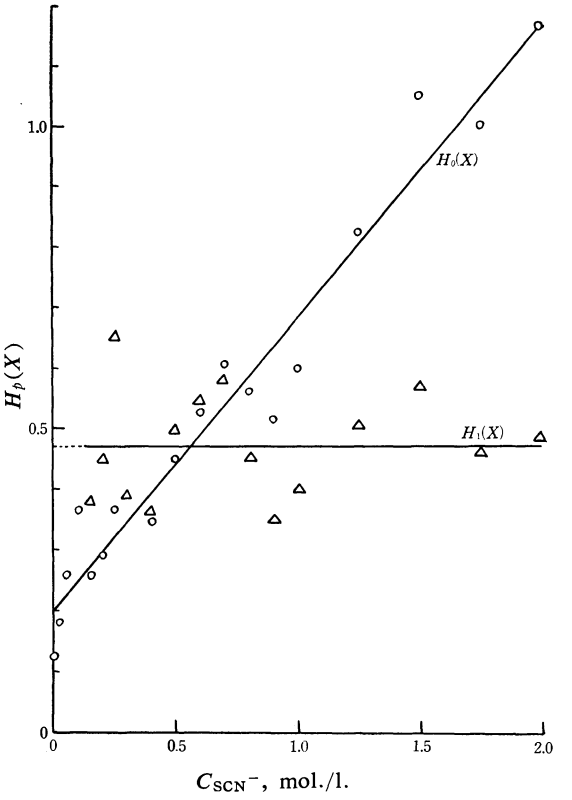



Fig. 7. The relation of $H_p(X)$ functions to $C_{SCN^-}$.

10) E. D. Moorhead and W. M. MacNevin, *Anal. Chem.*, 34, 269 (1962).

with the ordinate were obtained by the least-square method. This relation indicates that $H_0(X)$ is a linear function of $C_{SCN^-}$; $H_1(X)$ is, therefore, constant irrespective of $C_{SCN^-}$, and higher $H_p(X)$ functions are equal to zero. By extrapolating $H_0(X)$ and $H_1(X)$ to $(f_X C_X)=0$, the following values were obtained:

$$\lim_{f_X C_X \to 0} H_0(X) = 0.20 \pm 0.05$$

$$\lim_{f_X C_X \to 0} H_1(X) = 0.47 \pm 0.06$$

$$\lim_{f_X C_X \to 0} H_p(X) \simeq 0 \qquad (p=2,\ 3 \text{ and } 4)$$

From Eqs. 14 and 16, $(k_0)_B$ and $(k_1)_B$ at the standard potential, $(E^0)_B = -0.2678$ V. vs. NHE, are calculated as follows;

$$(k_0)_B = (0.64 \pm 0.16) \times 10^{-4} \text{ cm./sec.}$$

$$(k_1)_B = (1.5 \pm 0.2) \times 10^{-4} \text{ (cm./sec.)/(mol./l.)}$$

$$(k_p)_B \simeq 0 \quad (p=2,\ 3 \text{ and } 4)$$

where the values of $D_s = 5.85 \times 10^{-6}$ cm$^2$/sec., calculated from the Ilkovic equation, and $D_a = 1.47 \times 10^{-5}$ cm$^2$/sec. (at 22°C)[11] were used, and $f_s$ and $f_a$ were assumed to be unity. The $(k_0)_B$ and $(k_1)_B$ values are the rate constants for $p=0$ and 1 respectively in the reaction given by Eq. 9. This means that two kinds of complexes, $In_{aq}^{3+}$ and $InSCN^{2+}$, are reduced at the electrode; the presence of two kinds of complexes is in accordance with the results calculated from Eq. 11.

The logarithm of the forward rate constant, $k_{f,h}$, according to the Koutecky treatment[12] was plotted against the potential in NHE as is shown in Fig. 8 for the data of the simple indium(III) ion. As is shown in Fig. 8, the plot in a less negative potential deviates from a straight line. This deviation is due chiefly to the effect of the backward rate constant, $k_{b,h}$, in the range of this potential. In the range of the potential for the linear portion, however, $k_{b,h}$ may be neglected with respect to $k_{f,h}$.

By extrapolating the linear portion to the standard potential of −0.2678 V. vs. NHE and the potential of 0 V. vs. NHE, the logarithms of the rate constants, $(k_0)_s$ and $k^0_{f,h}$ respectively, are obtained from the following equation:

$$\log k_{f,h} = \log k^0_{f,h} - \frac{\alpha n F}{2.3RT} E \qquad (17)$$

The values of $(k_0)_s = 1.58 \times 10^{-4}$ cm./sec. and $k^0_{f,h} = 4.77 \times 10^{-12}$ cm./sec. were obtained by

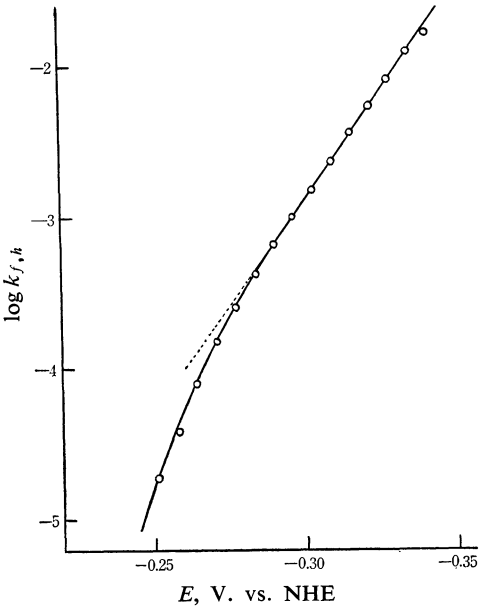



Fig. 8. The potential dependence of the rate constant of the electrode process for indium-(III) simple ion in perchlorate medium.

extrapolating the linear portion in Fig. 8 to −0.2678 V. and 0 V. vs. NHE respectively. The value of $(k_0)_B = (0.64 \pm 0.16) \times 10^{-4}$ cm./sec. is in good agreement with that of $(k_0)_s = 1.58 \times 10^{-4}$ cm./sec. when we consider that the scattering of the points in Fig. 7 is due largely to the errors of $E_{1/2}{}^r$, $A$ and $\alpha$. The latter value, $4.77 \times 10^{-12}$ cm./sec., agrees fairly well with the walue of $4.7 \times 10^{-12}$ cm./sec. (at 26.5°C) determined by Inouye and Imai[13] polarographically. Furthermore, from the slope of the straight line, $\alpha n$ was calculated to be 1.66, from which $\alpha = 0.55$ was obtained by assuming $n$ to be 3. Although the agreement of $k^0_{f,h}$ was fairly good, the polarographic wave obtained by Inouye and Imai[13] was a totally irreversible one whose half-wave potential was about −1.0 V. and whose product $\alpha n$ was 0.66, while the wave obtained in the present paper is "quasi"-reversible, and the half-wave potential and the product $\alpha n$ are about −0.5 V. and 1.66 respectively. Inouye and Imai,[13] however, pointed out that when a chloride, iodide or acetate ion is added to the simple indium-(III) ion, the irreversible wave, $E_{1/2} = -1.0$ V., is changed to a reversible one with $E_{1/2} = -0.5$ V. Likewise, the increase in perchlorate may cause the increase in the reversibility of the wave because the simple indium(III) ion in 2.0 mol./l. perchlorate is reduced at about −0.5 V. in the present paper.

11) M. von Stackelberg and V. Toome, *Z. Elektrochem.*, **58**, 226 (1954).

12) See, e.g., P. Delahay, "New Instrumental Methods in Electrochemistry," Interscience Publishers, 2nd Ed., New York (1958), Chap. 4.

13) S. Inouye and H. Imai, This Bulletin, **33**, 149 (1960).

## Summary

The formation constants, $K_j=[\mathrm{In(SCN)}_j^{(3-j)+}]/[\mathrm{In}^{3+}][\mathrm{SCN}^-]^j$ ($j=1$, 2, 3, 4), have been determined to be 50, 200, 120 and 1670 respectively. The electrode reaction proceeds as follows:

(1) At a higher ligand concentration;

$$\mathrm{In(SCN)}_p^{(3-p)+} \rightleftarrows \mathrm{InSCN}^{2+} + (p-1)\mathrm{SCN}^- \quad \text{(fast)} \quad (p=2,\ 3 \text{ and } 4)$$

$$\mathrm{InSCN}^{2+} + 3e^- + \mathrm{Hg} \rightarrow \mathrm{In(Hg)} + \mathrm{SCN}^- \quad \text{(rate constant } (k_1)_B)$$

(2) At a lower ligand concentration:

$$\mathrm{InSCN}^{2+} \rightleftarrows \mathrm{In}_{aq}^{3+} + \mathrm{SCN}^- \quad \text{(fast)}$$

$$\mathrm{In}_{aq}^{3+} + 3e^- + \mathrm{Hg} \rightarrow \mathrm{In(Hg)} \quad \text{(rate constant } (k_0)_B)$$

The rate constants, $(k_0)_B$ and $(k_1)_B$, at the standard potential are $(0.64\pm0.16)\times10^{-4}$ cm./sec. and $(1.5\pm0.2)\times10^{-4}$ (cm./sec.)/(mol./l.) respectively. The rate constant, $k^0_{f,h}$, at 0 V. vs. NHE was $4.77\times10^{-12}$ cm./sec.


The authors wish to thank Dr. Kunio Nakano and Dr. Kenichi Morinaga, Professors of Rikkyo University, Tokyo, for their interest in this work and their ardent discussions.

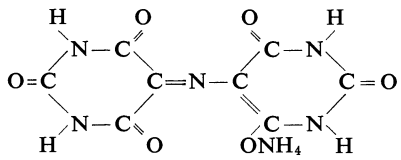
*Department of Chemistry*
*Faculty of Science*
*Tokyo University of Education*
*Koishikawa, Tokyo*

# The Colloidal Behaviour of Ammonium Purpurate (Murexide) in an Aqueous Solution

By Satendra P. SANGAL

(Received June 22, 1964)

Ammonium purpurate (murexide), which has the following structure:



has been used extensively in the complexometric titrations of calcium. Sangal and Dey[1] used the reagent as a chelatochrome indicator in thorium - ethylenediaminetetraacetic acid titrations also. Murexide gives coloured chelates with scandium and rare earths. During the investigations of the composition and stability of these chelates, it was found that, when the solutions of the reagent used were not very dilute, deviations in the composition from true stoichiometry were observed. Similar deviations had been observed earlier by Mukherji and Dey[2] during their studies of the metal chelates of aluminium; by Srivastava, Seth and Dey during their studies of the metal chelates of sulphodichlorohydroxydimethylfuchson dicarboxylate,[3] *p*-nitrobenzene-azochromotropic acid,[4] and 7-iodo-8-hydroxyquinoline-5-sulphonic acid (ferron),[5] and by Sangal and Dey during their studies of metal chelates of Thoron[6] with different metal ions. It appears, therefore, that murexide, like the above reagents, behaves as a colloidal electrolyte and does nos obey Beer's law in concentrated solutions.

The present communication records the results of our studies of the colloidal behaviour of murexide in an aqueous solution.

## Experimental

Electrical conductance measurements were carried with a Leeds and Northrup Kohlrausch slide wire with an audiofrequency oscillator in the circuit, operated by a 220 V./50 cycl. a. c. mains and using a measuring cell of the dip type, with a cell constant of 0.5875.

All solutions were freshly prepared in conductivity water using a B. D. H. sample of murexide.

1) S. P. Sangal and A. K. Dey, *Talanta*, in press.
2) A. K. Mukherji and A. K. Dey, *J. Colloid Sci.*, **13**, 99 (1958).
3) S. C. Srivastava, P. L. Seth and A. K. Dey, ibid., **17**, 86 (1963).
4) S. C. Srivastava, R. L. Seth and A. K. Dey, *J. Indian Chem. Soc.*, in press.
5) S. C. Srivastava, R. L. Seth and A. K. Dey, *Kolloid.-Z.*, **181**, 137 (1962).
6) S. P. Sangal and A. K. Dey, *J. Sci. Ind. Research (India)*, **21B**, 600 (1962).

## Results and Discussion

The electrical conductance of a series of solutions of murexide was measured at different dilutions at 25C°. A graph was then plotted between the square root of the concentration and the molar conductance (Fig. 1). The curve thus obtained was found to be similar to the curves of the colloidal electrolytes as recorded by McBain.[7] If the solution of Murexide had behaved like true electrolytes, the curve would have been linear and the Debye-Hückel equation would have been applicable.

The specific conductance of murexide was also determined at six temperatures, and by the extrapolation of the curves obtained by plotting the specific conductance against the temperature (Fig. 2), the temperature of the zero conductance was found to be −20°C. This observation confirms the findings of Mushran and Prakash,[8] who described, during their studies on colloidal systems, how although generally the temperature of the zero conductance of true electrolytes lies near −40°C, in the colloidal systems this temperature ranges between −15°C and −35°C.

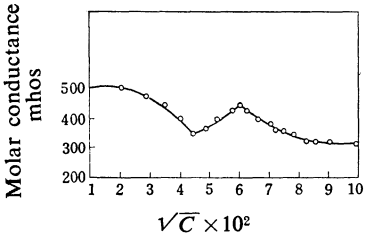



Fig. 1. Variation of molar conductance with concentration.

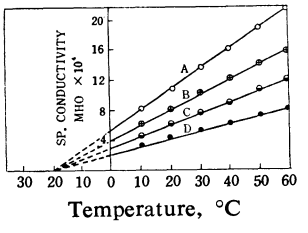



Fig. 2. Variation of specific conductance of murexide with temperature.
Curve A: Concn. of murexide 0.02 M
Curve B: Concn. of murexide 0.01 M
Curve C: Concn. of murexide 0.005 M
Curve D: Concn. of murexide 0.003 M

The temperature coefficients per 1°C per hundred of the conductance at 35°C have also been calculated; the results are as follows:

TABLE I. THE TEMPERATURE COEFFICIENT OF THE CONDUCTANCE

| Cocn. M | Specific conductance at 35°C (from graph) mhos×10⁴ | Temperature coefficient per 1°C | Temperature coefficient per hundred of the conductance |
|---|---|---|---|
| 0.003 | 5.8 | 0.050 | 0.86 |
| 0.005 | 8.4 | 0.100 | 1.19 |
| 0.010 | 11.2 | 0.150 | 1.34 |
| 0.020 | 15.2 | 0.250 | 1.65 |

These results also serve to establish the colloidal nature of murexide in concentrated solutions, as Shivapuri and Prakash[9] reported that usually the temperature coefficient per degree centigrade per hundred of the conductance at 35°C in a colloidal system is found to be below 2.0.

Thus, it may be concluded that murexide behaves as a colloidal electrolyte in concentrated solutions. For physico-chemical measurements, it is advisable, therefore, to work with very dilute solutions of the reagent for only then will the reagent behave as a true solution, as has also been suggested by Dey.[10]

## Summary

By electrical conductance studies it has been found that ammonium purpurate behaves as a colloidal electrolyte and does not obey Beer's law in concentrated solutions. The curve between the square root of the concentration and the molar conductance is not linear and resembles that of a colloidal electrolyte. The temperature of zero conductance has also been determined to be −20°C. The temperature coefficient per degree centigrade per hundred of the conductance at 35°C ranges between 0.86 and 1.65.

The author is thankful to Dr. A. K. Dey for his suggestions and to the Council of Scientific and Industrial Research for the award of a fellowship.

*Chemical Laboratories*
*University of Allahabad*
*Allahabad, India*

7) J. W. McBain, "Colloid Science," D. C. Heath and Co., Boston (1950).
8) S. P. Mushran and S. Prakash, *J. Phys. Chem.*, **50**, 251 (1946).
9) T. N. Shivapuri and S. Prakash, *Current Sci. (India)*, **18**, 403 (1949).
10) A. K. Dey, *J. Colloid Sci.*, **3**, 473 (1948).

# The Formylation of Amino Acids with Acetic Formic Anhydride

By Ichiro MURAMATSU, Masahiro MURAKAMI, Takahiro YONEDA and Akira HAGITANI

(Received June 29, 1964)

The formyl group has been used as a blocking substituent of the amino moiety of amino acids in peptide syntheses[1,2] or in optical resolutions of amino acids. In these procedures, *N*-formylamino acids have been prepared with formic acid[3] or with formic acid and acetic anhydride.[2,4,5] The latter method has been widely used, since the formylation gives good yield without any accompanying racemization.

These methods, however, have the common defect that too much of the reagents are necessary compared with the amount of amino acids employed. It has been presumed that, in the formylation of amino acids with formic acid and acetic anhydride, acetic formic anhydride or formic anhydride may be formed first and that then the anhydride may react with the amino groups to yield *N*-formylamino acids. Therefore, the present authors have tried to formylate amino acids directly with pure acetic formic anhydride. In addition to the ketene - formic acid method,[6] this anhydride has been successfully and conveniently prepared by the reaction of acetyl chloride with sodium formate. In many instances, it has been found that the formylation of amino acids by the present method can be performed in a very simple way under mild conditions, and that only a 2 to 3-molar excess of the reagent is required.

## Results

Acetic formic anhydride was prepared by the following reactions:

$$CH_3COCl + HCOONa \rightarrow HCO\text{-}O\text{-}COCH_3 + NaCl \quad (1)$$

$$HCOOH + CH_2{=}C{=}O \rightarrow HCO\text{-}O\text{-}COCH_3 \quad (2)$$

In method 1, although the purity of acetyl chloride and atmospheric humidity exerted a great influence upon the yield, the anhydride was generally obtained in a 75—91% yield. In method 2,[6] the anhydride was constantly obtained in a 80—90% yield. The refractive indices and the infrared spectra of the anhydrides prepared by the two methods are in agreement with each other (Fig. 1). This anhydride is stable in a refrigerator, but it is decomposed with the evolution of carbon monoxide above about 60°C, above room temperature in formic acid, or even at 0°C in the presence of a small amount of pyridine.

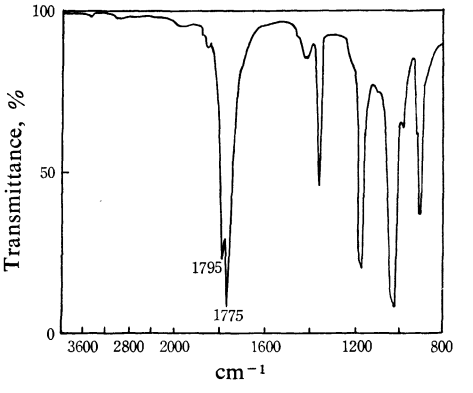



Fig. 1. Infrared absorption spectrum of acetic formic anhydride in carbon tetrachloride.

The formylation of amino acids with acetic formic anhydride was carried out using formic acid as a solvent. The temperature of the reaction was maintained below 10°C during the exothermic period in the reaction by means of an ice bath. After the stirring had been continued subsequently for two hours at room temperature, the mixture was concentrated to a solid mass or syrup under reduced pressure, and the residue was crystallized from a suitable solvent. Even when acetic acid was used as a solvent, formylation took place but acetylation did not. Monoamino monocarboxylic acids (glycine, DL-alanine, L-valine, L-leucine, L-methionine, L-phenylalanine, L-tyrosine and β-alanine) were generally formylated in good yields (70—94%), as was the alanine ester, and their optical activities were retained. The formylation of

1) S. G. Waley, *Chem. & Ind.*, **1953**, 107.
2) J. C. Sheehan and D. D. H. Yang, *J. Am. Chem. Soc.*, **80**, 1154 (1958).
3) E. Fischer and O. Warburg, *Ber.*, **38**, 3997 (1905).
4) V. du Vigneaud, R. Dorfmann and H. S. Loring, *J. Biol. Chem.*, **98**, 577 (1932).
5) J. S. Fruton and H. T. Clarke, ibid., **106**, 667 (1934).
6) R. E. Dunbar and F. C. Garven, *J. Am. Chem. Soc.*, **77**, 4161 (1955).

glutamic acid by the present method was difficult to carry out with a good yield, unlike that of the amino acids mentioned above. The formylation of other amino acids with three or more functional groups was not attempted in our studies. Special methods[7,8] may be required for the monoformylation of basic amino acids.

## Experimental[9]

**Acetic Formic Anhydride.** — *Method 1.* — Into a solution of 445 ml. of acetyl chloride in 250 ml. of dry ether, 500 g. of sodium formate was added in several portions in such a way that the temperature did not exceed 27°C. The mixture was kept from moisture and vigorously shaken. After the shaking had been continued for 5.5 hr. at 25—27°C, the salt was filtered off. The filtrate was then evaporated under water-pump pressure below 20°C (bath temperature) in order to remove the ether and the remaining reagent. The residual liquid weighed 502 g. (91%). A small amount of free acid was found, by a study of the infrared spectrum, to be present in the anhydride prepared in this way, but the crude anhydride was successfully used in the formylation of amino acids without further purification. When impure acetyl chloride was used, the product decomposed gradually, with forming, during the above procedure.

*Method 2.*—Ketene was prepared from acetone in a ketene lamp which delivered about 0.5 mol. of ketene per hour. The solution of 2 mol. of formic acid (98—100%, E. Merck AG.) in 300 ml. of ether was saturated with ketene in an ice bath. After the evaporation of ether, the residue was fractionated under reduced pressure, and the fractions boiling between 30°C/24 mmHg ($n_D^{20}$ 1.386) and 24°C/9 mmHg ($n_D^{20}$ 1.388) were collected; yield, 163 g. (93%). These fractions were successfully employed for the formylation of amino acids. From the infrared spectra of the distillates, it was found that the first runnings contained only a trace of free acid, while the last ones a small amount of acetic anhydride. The main fraction boiled at 30°C/19 mmHg ($n_D^{20}$ 1.387) (in the lit.,[6] b. p., 27—28°C/10 mmHg, $n_D^{20}$ 1.388); its infrared spectrum is shown in Fig. 1. This spectrum shows absorption bands at 1795, 1775, 1380, 1178, 1037 and 924 $cm^{-1}$ (in carbon tetrachloride). It is very interesting that the difference (20 $cm^{-1}$) between the wave numbers of the two carbonyl bands (1795 and 1775 $cm^{-1}$) of acetic formic anhydride is less than those of ordinary acid anhydrides (about 60 $cm^{-1}$).[10]

***N*-Formylglycine.** — To a solution of 3.76 g. (50 mmol.) of glycine in 20 ml. of formic acid (90%), 13.2 g. (150 mmol.) of acetic formic anhydride was added. The reaction mixture was stirred at a temperature maintained below 10°C by means of an ice bath. After 40 min., the bath was removed. Stirring was continued for a further 80 min., and then the solution was concentrated to dryness under reduced pressure. The solid residue was twice recrystallized from a mixture of ethyl acetate (75 ml.) and ethanol (25 ml.). *N*-Formylglycine was obtained as white crystals; 4.39 g. (85%); m. p. 151—153°C (lit[8] m. p. 153—154°C). (Found: N, 13.41%).

When acetic acid was used as the solvent instead of formic acid in the above instance, *N*-formylglycine was also obtained in a 76% yield.

***N*-Formyl-DL-alanine.** — After 3.57 g. (40 mmol.) of DL-alanine had been acylated with 10.57 g. (120 mmol.) of acetic formic anhydride by a method similar that of to the formylation of glycine in formic acid, the product was recrystallized from ethyl acetate - ethanol to yield 4.41 g. (94%) of pure crystals (m. p. 145—148.5°C; lit.[11] m. p. 147—148°C). (Found: C, 40.93; H, 6.17; N, 11.97%).

***N*-Formyl-L-valine.**—After 3.52 g. (30 mmol.) of L-valine had been treated with 10 g. (113 mmol.) of the anhydride in a similar way, the product was twice recrystallized from ethanol to yield 3.65 g. (84%) of pure crystals. M. p. 150—151°C, $[\alpha]_D^{21}$ +11.7° (*c* 3.97, ethanol); lit.[12] m. p. 156°C, $[\alpha]_D^{20}$ +13.1° (*c* 9.0, ethanol). (Found: C, 49.21; H, 7.81; N, 9.59%).

***N*-Formyl-L-leucine.** — L-Leucine (3.94 g., 30 mmol.) was formylated with the anhydride (7.93 g., 90 mmol.) in 20 ml. of formic acid. The recrystallization of the product from ethyl acetate gave 3.35 g. (70%) of crystals; m. p. 139—141°C. The analytical sample was prepared by further recrystallization from the same solvent; m. p. 140.5—142°C, $[\alpha]_D^{20}$ −17.7° (*c* 4.97, ethanol): lit.[3] $[\alpha]_D^{20}$ −18.4° (*c* 10, ethanol). (Found: C, 52.76; H, 8.30; N, 8.86%).

***N*-Formyl-L-methionine.** — L-Methionine (3.0 g., 20 mmol.) was treated with the anhydride (5.4 g., 60 mmol.) in 4 ml. of formic acid. The crude product obtained in a similar manner was twice recrystallized from ethyl acetate - petroleum ether to give 2.73 g. (77%) of pure crystals; m. p. 86—87°C, $[\alpha]_D^{24.5}$ −10.0° (*c* 2.41, water); lit. m. p. 86—87°C,[13] $[\alpha]_D^{25}$ −10.0° (*c* 0.8, water).[14]

***N*-Formyl-L-phenylalanine.**—L-Phenylalanine (2.65 g., 16 mmol.) was formylated with the anhydride (2.7 g., 30 mmol.) in 4 ml. of formic acid. The first crop of *N*-formyl-L-phenylalanine was taken out by filtration from the reaction mixture, while the second crop was obtained from the mother liquor. They were then washed with water, dried, and combined. Yield, 2.58 g. (83%); m. p. 165—166°C. The analytical sample was obtained by recrystallization from water. M. p. 165.5—166°C,

7) K. Hofmann, E. Stutz, G. Spühler, H. Yajima and E. T. Schwartz, ibid., **82**, 3727 (1960).
8) K. Okawa and S. Hase, This Bulletin, **36**, 754 (1963).
9) All melting points are uncorrected. The infrared spectra were recorded on a Shimadzu model IR 27-B spectrophotometer. The authors are grateful to the staff of the Central Research Laboratory of the Mitsui Chemical Industry Co., Ltd., for the elementary analyses, and to the Ajinomoto Co., Inc., for its gift of amino acids, L-valine, L-leucine, L-phenylalanine and L-glutamic acid.
10) L. J. Bellamy, "The Infra-red Spectra of Complex Molecules," Methuen & Co., London (1958), p. 127.
11) E. Biilmann, K. A. Jensen and H. B. Jensen, *Bull. soc. chim. France*, [5] **1**, 1661 (1934).
12) E. Fischer, *Ber.*, **39**, 2320 (1906).
13) J. R. Spies, *J. Biol. Chem.*, **182**, 439 (1950).
14) W. Windus and C. S. Marvel, *J. Am. Chem. Soc.*, **53**, 3490 (1931).

$[\alpha]_D^{20}$ +72.5° (*c* 1.58, ethanol); lit.[15] m. p. 167°C, $[\alpha]_D^{20}$ +75.2° (*c* 4, ethanol). (Found: N, 7.43%).

***N*-Formyl-L-tyrosine.**—To a suspension of 7.25 g. (40 mmol.) of L-tyrosine in 10 ml. of formic acid, 10.5 g. (120 mmol.) of the anhydride was added. The mixture was allowed to react for 2 hr., water was added thereto, and the solution was concentrated to dryness under reduced pressure. An ice cold *N*-hydrochloric acid was then added to the residue in order to dissolve the remaining tyrosine. The product was collected by filtration and washed with water. 7.05 g. (84%) of *N*-formyl-L-tyrosine was obtained; it melted at 166°C. The recrystallization from ethanol gave an anhydrous compound; m. p. 167°C, $[\alpha]_D^{20}$ +89.7° (*c* 1.78, ethanol), $[\alpha]_D^{20}$ +56.3° (*c* 1.33, water); lit.[16] m. p. 170—171°C, $[\alpha]_D^{10}$ +89.4° (*c* 1.74, ethanol).

Found: C, 57.29; H, 5.51; N, 7.11. Calcd. for $C_{10}H_{11}NO_4$: C, 57.41; H, 5.30; N, 6.70%.

The recrystallization from water generally gave a hydrated compound;[17-19] m. p. 166°C (sinters at 90°C), $[\alpha]_D^{20}$ +53.0° (*c* 1.52, water).

Found: $H_2O$, 7.88% (dried in vacuo at 100°C for 3 hr.). Calcd. for $C_{10}H_{11}NO_4 \cdot H_2O$; $H_2O$, 7.92%.

***N*-Formyl-L-glutamic Acid.** — L-Glutamic acid (4.42 g., 30mmol.) in 6.5 ml. of formic acid was formylated with the anhydride (3.36 g., 38 mmol.). The crude product was recrystallized from ethyl acetate to yield pure crystals of *N*-formyl-L-glutamic acid (1.85 g., 35%). M. p. 110—112°C, $[\alpha]_D^{20.5}$ −7.4° (*c* 2.02, water): lit.[20] m. p. 112—113°C, $[\alpha]_D^{20}$ −7.25° (*c* 2, water). Better yields have been reported in the literature[20,21] from the usual formic acid - acetic anhydride method.

***N*-Formyl-β-alanine.**—β-Alanine (3.1 g., 35 mmol.) was formylated with acetic formic anhydride (11.2 g., 130 mmol.) in a similar manner. The crystallization of the product from ethyl acetate yielded 3.24 g. (79%) of crystals (m. p. 73—74°C; lit.[22] m. p. 75—76°C).

***N*-Formyl-DL-alanine Ethyl Ester.**[23]—Into a solution of 91 g. of DL-alanine ethyl ester in 91 ml. of formic acid, 118 ml. of acetic formic anhydride was added with stirring in an ice bath. After the mixture had been stirred for 3 hr. at room temperature, the mixture was distilled under reduced pressure to afford the formylated ester; yield, 95.3 g. (85%); b. p. 98°C/1 mmHg (lit.[24] b. p. 100°C/1 mmHg).

## Summary

The formylation of amino acids with acetic formic anhydride has been studied. This anhydride is prepared by the reaction of acetyl chloride with sodium formate or, preferably, from ketene and formic acid. When various monoamino monocarboxylic acids are treated with acetic formic anhydride by a simple procedure and under mild conditions, *N*-formyl-amino acids were obtained in satisfactory yields.

*Department of Chemistry*
*Faculty of Science*
*Rikkyo (St. Paul's) University*
*Ikebukuro, Tokyo*

15) E. Fischer and W. Schoeller, *Ann.*, **357**, 1 (1907).
16) N. Izumiya and A. Nagamatsu, This Bulletin, **25**, 265 (1952).
17) E. Fischer, *Ber.*, **40**, 3716 (1907).
18) S. G. Waley and J. Watson, *Biochem. J.*, **57**, 529 (1954).
19) The sample was dried in a vacuum desiccator at room temperature.
20) H. Tabor and A. H. Mehler, *J. Biol. Chem.*, **210**, 559 (1954).
21) B. A. Borek and H. Waelsch, ibid., **205**, 459 (1953).
22) I. Muramatsu and A. Hagitani, *J. Chem. Soc. Japan, Pure Chem. Sec.* (*Nippon Kagaku Zasshi*), **80**, 1497 (1959).
23) We are indebted to Mr. Masakatu Hirose for this experiment.
24) E. E. Harris, R. A. Firestone, K. Pfister, III, R. R. Boettcher, F. J. Cross, R. B. Curie, M. Monaco, E. R. Peterson and W. Reuter, *J. Org. Chem.*, **27**, 2705 (1962).

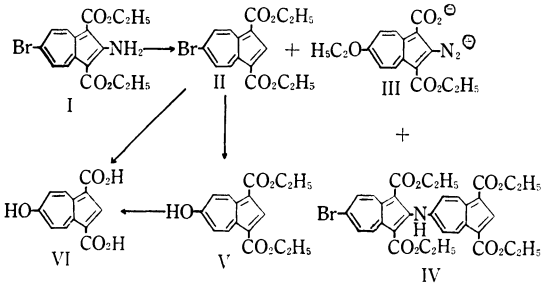
# The Anionoid Substitution Reaction of Diethyl 6-Bromoazulene-1, 3-dicarboxylate*

By Tetsuo NOZOE, Kahei TAKASE and Masao TADA

(Received July 3, 1964)

In previous papers[1-3] we have reported on the synthesis of some 5- and 6-substituted azulene derivatives from 5-aminotropolone and 4-acetyltropolone derivatives as a part of a general scheme of the synthetic study of azulenes with the functional group on a seven-membered ring. For synthesizing some 6-substituted azulenes, the present authors studied the anionoid substitution reactions of diethyl 6-bromoazulene-1, 3-dicarboxylate (II), which is the deaminated product of diethyl 2-amino-6-bromoazulene-1, 3-dicarboxylate (I);[4] this paper will describe the results.

The diazotization reaction of I was accomplished in dioxane by the use of a large excess of sulfuric acid and sodium nitrite and without cooling. The decomposition of diazonium salt to yield the corressponding deaminated product was achieved by letting the salt stand at room temperature in the presence of sodium hypophosphite. Thus, diethyl 6-bromoazulene-1, 3-dicarboxylate (II) was obtained in a 25% yield, accompanied by two by-products (III and IV), one of which, III, was a 6-ethoxyazulene derivative, being the intramolecular diazonium-salt type reported by Asao et al.[5] The other one, IV, obtained in a 2% yield, was assumed to be diethyl 2-(1, 3-diethoxycarbonylazulen-6-yl)amino-6-bromoazulene-1, 3-dicarboxylate on the basis of the infrared spectrum, the analytical values and the chemical reactivities of II, as will be described below. The ultraviolet spectrum of II is shown in Fig. 1.



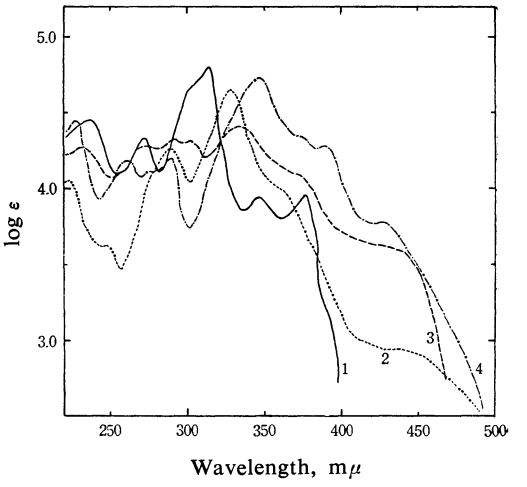




Fig. 1. Ultraviolet absorption spectra in methanol.
1 Diethyl 6-bromoazulene-1, 3-dicarboxylate (II)
2 Diethyl 6-hydroxyazulene-1, 3-dicarboxylate (V)
3 Diethyl 6-hydrazinoazulene-1, 3-dicarboxylate (X)
4 Diethyl 6-[di(2-hydroxyethyl)amino]-azulene-1, 3-dicarboxylate (XIV)

A mild alkaline treatment of II resulted in the replacement of the bromine atom by the hydroxyl group, thus forming diethyl 6-hydroxyazulene-1, 3-dicarboxylate (V), which, on being treated with acetic anhydride, gave an acetate with an absorption at 1764 $cm^{-1}$ for the acetoxy group. However, under more severe conditions, not only V but also II gave 6-hydroxyazulene-1, 3-dicarboxylic acid (VI). Since the alkaline treatment of I give only 2-amino-6-bromo-1, 3-dicarboxylic acid,[4] these results show the bromine atom at the 6-position in II to be more active than in I. The treatment of II with sodium ethoxide or

* Presented at the 16th Annual Meeting of the Chemical Society of Japan, Tokyo, April, 1963.

1) T. Nozoe, K. Takase and M. Tada, This Bulletin, 36, 1006 (1963).

2) T. Nozoe, K. Takase and M. Tada, ibid., 36, 1010 (1963).

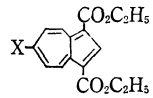
3) T. Nozoe, K. Takase and M. Tada, ibid., 36, 1016 (1963).

4) T. Nozoe, *Croat. Chem. Acta*, 29, 201 (1957); T. Nozoe and S. Ito, *Frotschr. Chem. org. Naturstoffe*, 19, 33 (1961); T. Nozoe, S. Seto and S. Matsumura, This Bulletin, 35, 1990 (1962); S. Matsumura, *Chem. Pharm. Bull.*, 10, 1024 (1962).

5) T. Asao, J. Tsunetsugu and M. Kobayashi, Presented at the 15th Annual Meeting of the Chemical Society of Japan, Kyoto, April, 1962.

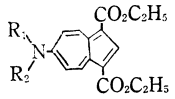
sodium hydrogen sulfide afforded diethyl 6-ethoxyazulene-1, 3-dicarboxylate (VII) or diethyl 6-mercaptoazulene-1, 3-dicarboxylate (VIII) respectively in a good yield.

The reaction of II with liquid ammonia afforded diethyl 6-aminoazulene-1, 3-dicarboxylate (IX), which was identical with an authentic specimen synthesized from 5-amino-2-methoxytropone.[1] Recently, Hafner et al.[6] reported that the reaction of 4, 8-dimethyl-6-chloroazulene with sodium azide, in the presence of dimethyl sulfoxide, afforded 4, 8-dimethyl-6-aminoazulene. In the same way, IX was also obtained from II.

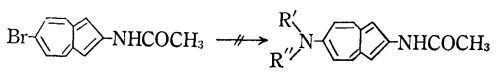


VII: X=$OC_2H_5$
VIII: X=SH
IX: X=$NH_2$

The bromine atom of II was easily replaced, when heated for a short period, with various amines, such as hydrazine, dimethylamine, diethylamine, ethanolamine, diethanolamine, diallylamine, ethyleneimine, pyrrolidine, piperidine, morpholine, aminopropylmorpholine and aniline, and the corresponding *N*-substituted amino derivatives of IX (X—XXI) were obtained in good yields. Under the same conditions, however, the bromine atom of 2-acetamido-6-bromoazulene (XXII)[4] was not replaced by various amines.



X: $R_1=NH_2$; $R_2=H$
XI: $R_1=R_2=CH_3$
XII: $R_1=R_2=C_2H_5$
XIII: $R_1=CH_2CH_2OH$; $R_2=H$
XIV: $R_1=R_2=CH_2CH_2OH$
XV: $R_1=R_2=CH_2CH=CH_2$
XVI: $R_1+R_2=$ 
XVII: $R_1+R_2=$ 
XVIII: $R_1+R_2=$ 
XIX: $R_1+R_2=$ 
XX: $R_1=CH_2CH_2CH_2-N$  ; $R_2=H$
XXI: $R_1=C_6H_5$; $R_2=H$



XXII

6) K. Hafner, H. Patzelt and H. Kaiser, *Ann.*, **656**, 24 (1962).

These facts can be understood by reference to the electrophilic nature of the seven-membered ring in azulene, enhanced by the presence of two ethoxycarbonyl groups at positions 1 and 3. This reaction path is shown in Chart I.

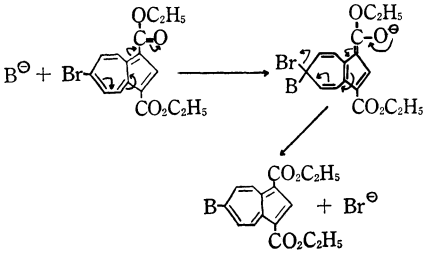
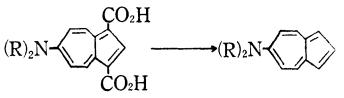


Chart I.

The alkaline hydrolysis of the 6-dimethylamino compound (XI) and the 6-diethylamino compound (XII) gave dicarboxylic acid (XXIII) and (XXIV), both of which, when heated in pyridine, caused decarboxylation, thus giving 6-dimethylaminoazulene (XXV) and 6-diethylaminoazulene (XXVI) respectively. Compared with 6-aminoazulene,[1] XXV and XXVI are more stable and do not change on being left



XXIII: R=$CH_3$ XXV: R=$CH_3$
XXIV: R=$C_2H_5$ XXVI: R=$C_2H_5$

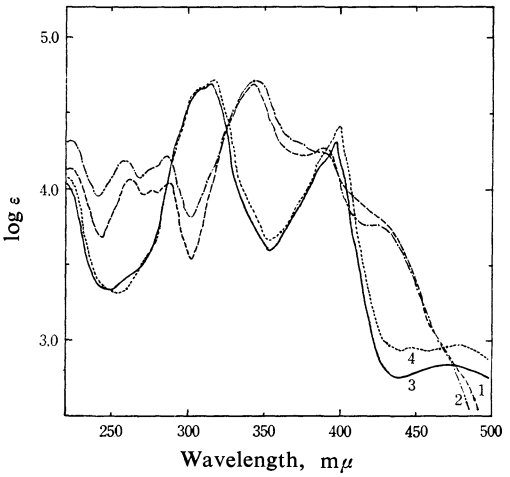



Fig. 2. Ultraviolet absorption spectra in methanol.
1 Diethyl 6-dimethylaminoazulene-1, 3-dicarboxylate (XI)
2 Diethyl 6-diethylaminoazulene-1, 3-dicarboxylate (XII)
3 6-Dimethylaminoazulene (XXV)
4 6-Diethylaminoazulene (XXVI)

in air for a long period of time. The ultraviolet spectra of these compounds are shown in Fig. 2.

The reactions of II with active methylene reagents are being investigated and will be reported on in the future.

## Experimental[7]

**The Deamination of I.** — Into a solution of I (2.0 g.) in dioxane (120 ml.) and concentrated sulfuric acid (12 ml.), a solution of sodium nitrite (1.0 g.) in water (5 ml.) was stirred at room temperature. After the solution had been stirred for 50 min., sodium hypophosphite (20 g.) was added to this diazotized solution and the mixture was vigorous stirred for 4 hr. After it had stood overnight, the solution was diluted with water (300 ml.) and extracted with benzene. The extract was washed with water, dried over anhydrous sodium sulfate, and passed through a column of alumina, and then the column was eluted with benzene. From the first effluent, crude crystals of diethyl 6-bromoazulene-1, 3-dicarboxylate (II), m. p. 198—199°C, 0.5 g.), were obtained. The recrystallization from ethanol gave purplish red micro-needles, m. p. 206—207°C.

Found: C, 54.85; H, 4.21. Calcd. for $C_{16}H_{15}O_4Br$: C, 54.70; H, 4.27%.

UV $\lambda_{max}^{MeOH}$ mμ (log ε): 235 (4.45), 270 (4.30), 312 (4.80), 345 (3.95), 375 (3.95). IR (Nujol): 1684 $cm^{-1}$.

The second effluent gave yellow needles (200 mg.), which showed no depression of melting point on admixture with III and the infrared spectrum of which was identical with that of III.[5]

From the third effluent, crude crystals (15 mg.) were obtained. Recrystallization from a mixture of benzene and ethanol afforded diethyl 2-(1, 3-diethoxycarbonylazulen-6-yl)amino-6-bromoazulene-1, 3-dicarboxylate (IV) as red micro-prisms, m. p. 159—160°C; 10 mg.

Found: C, 59.38; H, 4.75; N, 2.20. Calcd. for $C_{32}H_{30}O_8NBr$: C, 59.44; H, 4.54; N, 2.14%.

IR (Nujol): 3175, 1695, 1684, 1658 $cm^{-1}$.

**Diethyl 6-Hydroxyazulene-1, 3-dicarboxylate (V).** —Into a solution of potassium hydroxide (300 mg.) in 50% aqueous ethanol (8 ml.), II (100 mg.) was stirred, and then the mixture was warmed on a water bath for 5 min. This was diluted with water (25 ml.) and acidified with diluted sulfuric acid. The crystals (80 mg.) which separated were recrystallized from aqueous ethanol to give brownish yellow crystals of V (m. p. 201—201.5°C).

Found: C, 66.84; H, 5.98. Calcd. for $C_{16}H_{16}O_5$: C, 66.66; H, 5.59%.

UV $\lambda_{max}^{MeOH}$ mμ (log ε): 221 (4.07), 246.5 (3.64), 288 (4.28), 329 (4.67), 357 (4.05)sh, 433 (2.95)sh.

IR (KBr disk): 3260, 1701, 1647 $cm^{-1}$.

*The Acetate of V.*—A solution of V (50 mg.) in acetic anhydride (2 ml). was refluxed for 6 min. The residue obtained by the evaporation of the solvent was recrystallized from aqueous ethanol to give reddish orange crystals (m. p. 129—130°C; 30 mg.).

Found: C, 65.37; H, 5.55. Calcd. for $C_{18}H_{18}O_6$: C, 65.44; H, 5.49%.

IR (Nujol): 1764, 1695, 1681, 1669 $cm^{-1}$.

**6-Hydroxyazulene-1,3-dicarboxylic Acid (VI).**— To a solution of potassium hydroxide (400 mg.) in 80% aqueous ethanol (10 ml.), II (200 mg.) was added. After it had been refluxed for 3 hr., the mixture was diluted with water (30 ml.) and acidified with 6 N sulfuric acid. The separated crystals were dissolved in a diluted potassium hydroxide aqueous solution and reprecipitated with 2 N hydrochloric acid. After these crystals had been washed with water, a dark brown powder (140 mg.) of VI was obtained; m. p. 174—175°C (decomp.).

Found: C, 61.75; H, 4.11. Calcd. for $C_{12}H_8O_5$: C, 62.07; H, 3.47%.

IR (Nujol): 3125, 1653 $cm^{-1}$.

V (200 mg.) also gave VI (140 mg.) under the same treatment.

**Diethyl 6-Ethoxyazulene-1,3-dicarboxylate (VII).** —To a solution prepared from sodium (50 mg.) and absolute ethanol (12 ml.), fine powdered II (400 mg.) was added. After it had been refluxed for 10 min. on a water bath, the mixture was evaporated to dryness under reduced pressure. The residue was dissolved in benzene, and the benzene solution was passed through a column of alumina, giving orange needles (300 mg.; m. p. 129—130°C). The substance was identified with an authentic specimen[6] of VII by a comparison of the infrared spectra.

**Diethyl 6-Mercaptoazulene-1, 3-dicarboxylate (VIII).**—II (50 mg.) and a 27% sodium hydrogen sulfide aqueous solution (4 ml.) were dissolved in ethanol (20 ml.). The solution was then heated on a water bath for 15 min. After it had stood overnight at room temperature, the reaction mixture was diluted with water, acidfied with 6 N sulfuric acid, and extracted with benzene. The extract was washed with water and dried over anhydrous sodium sulfate. The residue obtained by the evaporation of the solvent was recrystallized from benzene, yielding VIII (30 mg.; m. p. 222—224°C) red crystals.

Found: C, 63.45; H, 4.76. Calcd. for $C_{16}H_{16}O_4S$: C, 63.14; H, 5.30%.

IR (Nujol): 2519, 1689 $cm^{-1}$.

**Diethyl 6-Aminoazulene-1, 3-dicarboxylate (IX).** —*a) With Liquid Ammonia.*—A suspension of II (100 mg.) in liquid ammonia was allowed to stand for a week at room temperature. The residue obtained by the evaporation of the ammonia was recrystallized from ethanol to give orange scales (45 mg.), which showed no depression of melting point on admixture with an authentic specimen[1] of IX.

*b) With Sodium Azide.*—A mixture of II (100 mg.) and sodium azide (0.4 g.) in dimethyl sulfoxide (5 ml.) was heated on a water bath for 15 hr. After dilution with water, this reaction mixture was extracted with ethyl acetate and the extract was passed through a column of alumina, yielding IX (30 mg.).

7) All melting points are uncorrected. Shoulders in the UV spectral data are designated by "sh."

**Diethyl 6-Hydrazinoazulene-1,3-dicarboxylate (X).**—To a solution of 80% hydrazine hydrate (2 ml.) in ethanol (2 ml.), II (50 mg.) was added. The mixture was then refluxed for 10 min. on a water bath. After the addition of water (20 ml.), the precipitate thereby formed was recrystallized from ethanol to give X (30 mg.; m. p. 237°C) as brilliant yellow scales.

Found: C, 63.48; H, 6.06; N, 9.64. Calcd. for $C_{16}H_{18}O_4N_2$: C, 63.56; H, 6.00; N, 9.27%.

UV $\lambda_{max}^{MeOH}$ mμ (log ε): 233 (4.26), 273 (4.28), 289.5 (4.32), 301 (4.32), 333 (4.42), 367 (4.13)sh, 420 (3.65)sh.

IR (Nujol): 3330 (broad), 1642 $cm^{-1}$.

*Acetate of X.*—Pale yellow micro-prisms (from aqueous ethanol), m. p. 232—233°C.

Found: N, 7.85. Calcd. for $C_{18}H_{20}O_5N_2$: N, 8.14%.

UV $\lambda_{max}^{MeOH}$ mμ (log ε): 224 (4.33), 254 (4.02)sh, 275 (4.17)sh, 282.5 (4.23), 337 (4.73), 371 (4.32), 428 (3.68).

IR (Nujol): 3520, 3330, 3260, 1689, 1656 $cm^{-1}$.

**Diethyl 6-Dimethylaminoazulene-1,3-dicarboxylate (XI).**—To a solution of a 40% dimethylamine aqueous solution (3 ml.) in ethanol (5 ml.), II (100 mg.) was added. The mixture was refluxed for 20 min. on a water bath. After the addition of water, the precipitate thereby formed was recrystallized from ethanol to give XI (75 mg.; m. p. 161—162°C) as yellow silky needles.

Found: N, 4.22. Calcd. for $C_{18}H_{21}O_4N$: N, 4.44%.

UV $\lambda_{max}^{MeOH}$ mμ (log ε): 225 (4.15), 262 (4.08), 277 (3.99), 288 (4.05), 343 (4.69), 390 (4.27).

IR (Nujol): 1669 $cm^{-1}$.

**Diethyl 6-Diethylaminoazulene-1,3-dicarboxylate (XII).**—To a solution of diethylamine (2 ml.) in ethanol (10 ml.), II (200 mg.) was added. The mixture was then refluxed for 20 min. on a water bath. After the addition of water, the crystals separated were recrystallized from aqueous ethanol to give XII (130 mg.; m. p. 171—172°C) as yellow needles.

Found: N, 3.96. Calcd. for $C_{20}H_{25}O_4N$: N, 4.08%.

UV $\lambda_{max}^{MeOH}$ mμ (log ε): 225 (4.32), 260 (4.20), 279.5 (4.15)sh, 288 (4.22), 347 (4.71), 373 (4.30)sh, 390 (4.26), 423 (3.77).

IR (Nujol): 1669 $cm^{-1}$.

**Diethyl 6-(2-Hydroxyethylamino)azulene-1,3-dicarboxylate (XIII).**—To a solution of ethanolamine (2 ml.) in ethanol (8 ml.), II (50 mg.) was added. The mixture was then treated as in the case of XI to give XIII (30 mg.; m. p. 165—167°C) as yellow crystals.

Found: N, 3.86. Calcd for $C_{18}H_{21}O_5N$: N, 4.23%.

UV $\lambda_{max}^{MeOH}$ mμ (log ε): 225.5 (4.17), 253.5 (4.23), 285 (4.23), 332 (4.66), 367 (4.03)sh, 424 (3.90), 476 (3.31)sh.

IR (KBr disk): 3550, 3340, 1678, 1656 $cm^{-1}$.

**Diethyl 6-[Di(2-hydroxyethyl)]aminoazulene-1,3-dicarboxylate (XIV).**—To a solution of diethanolamine (2 ml.) in ethanol (8 ml.), II (50 mg.) was added. The mixture was then treated as in the case of XII to give XIV (25 mg.; m. p. 125—126°C) as brilliant yellow needles.

Found: N, 3.55. Calcd. for $C_{20}H_{25}O_6N$: N, 3.73%.

UV $\lambda_{max}^{MeOH}$ mμ (log ε): 226 (4.45), 260.5 (4.18), 277 (4.12), 287.5 (4.21), 346 (4.74), 377 (4.33)sh, 391 (4.28), 423 (3.79).

**Diethyl 6-Diallylaminoazulene-1,3-dicarboxylate (XV).**—To a solution of diallylamine (1 ml.) in ethanol (5 ml.), II (50 mg.) was added. The mixture was then refluxed for 20 min. on a water bath. After dilution with water, the reaction mixture was extracted with benzene. The extract was then washed with water and dried over anhydrous sodium sulfate. The residue obtained by the evaporation of the solvent was recrystallized from aqueous ethanol to give XV (20 mg.; m. p. 103—104°C) as brownish yellow crystals.

Found: N, 3.66. Calcd. for $C_{22}H_{25}O_4N$: N, 3.81%.

UV $\lambda_{max}^{MeOH}$ mμ (log ε): 225 (4.35), 258.5 (4.17), 276.5 (4.12)sh, 286.5 (4.22), 346.5 (4.78), 376 (4.39), 389 (4.31), 425 (3.71).

**Diethyl 6-Ethyleneiminoazulene-1,3-dicarboxylate (XVI).**—To a solution of ethyleneimine (1 ml.) in ethanol (5 ml.), II (50 mg.) was added. The mixture was then refluxed for 10 min. on a water bath. After dilution with water, the reaction mixture was extracted with benzene, and the extract was washed with water. After it had been dried over anhydrous sodium sulfate, this was passed through a column of alumina and the column was eluted with ethyl acetate. From the first effluent, an oily substance was obtained; the yellow crystals obtained from the second effluent were recrystallized from aqueous ethanol to give XVI (15 mg.; m. p. 160—161°C) as yellow fine crystals.

Found: N, 4.56. Calcd. for $C_{18}H_{19}O_4N$: N, 4.47%.

UV $\lambda_{max}^{MeOH}$ mμ (log ε): 224 (4.18), 260 (4.03), 276 (4.05)sh, 286 (4.11), 340.5 (4.69), 388 (4.15).

**Diethyl 6-Pyrrolidinoazulene-1,3-dicarboxylate (XVII).**—A solution of II (60 mg.) and pyrrolidine (2 ml.) in ethanol (10 ml.) was refluxed for 20 min. on a water bath and concentrated to 1/3 volume under reduced pressure. After the addition of water, the solution was extracted with ethyl acetate and the extract was washed with 2 N acetic acid and water. After the removal of the solvent, the extract gave crude crystals (35 mg.), which were recrystallized from ethanol to give XVII (25 mg.; m. p. 194—195°C (decomp.)) as dark yellow micro-prisms.

Found: C, 69.98; H, 6.49; N, 3.83. Calcd. for $C_{20}H_{23}O_4N$: C, 70.36; H, 6.79; N, 4.10%.

UV $\lambda_{max}^{MeOH}$ mμ (log ε); 225 (4.30), 260 (4.22), 288 (4.20), 345 (4.77), 388 (4.34).

IR (KBr disk): 1669 $cm^{-1}$.

**Diethyl 6-Piperidinoazulene-1,3-dicarboxylate (XVIII).**—A solution of II (60 mg.) and piperidine (2 ml.) in ethanol (10 ml.) was treated as in the case of XVII to give XVIII (25 mg.; m. p. 103—103.5°C) as orange micro-needles.

Found: N, 3.56. Calcd. for $C_{21}H_{25}O_4N$: N, 3.94%.

UV $\lambda_{max}^{MeOH}$ mμ (log ε): 251 (4.22), 338 (4.63), 458 (3.96).

**Diethyl 6-Morpholinoazulene-1,3-dicarboxylate (XIX).**—A solution of II (60 mg.) and morpholine (2 ml.) in ethanol (10 ml.) was treated as in the case of XII to give XIX (20 mg.; m. p. 101—102°C) as brilliant yellow scales.

Found: N, 3.57. Calcd. for $C_{20}H_{23}O_5N$: N, 3.92%.

UV $\lambda_{max}^{MeOH}$ mμ (log ε): 228.5 (4.26), 263 (4.18), 287 (4.04), 345 (4.68), 396 (4.32).

IR (KBr disk): 1689, 1669 $cm^{-1}$.

**Diethyl 6-(3-Morpholinopropyl)aminoazulene-1,3-dicarboxylate (XX).**—A solution of II (50 mg.) and aminopropylmorpholine (2 ml.) in ethanol (8 ml.) was refluxed for 30 min. on a water bath. After dilution with water, the solution was extracted with ethyl acetate, and the extract was washed with 2 N acetic acid and water. After it had been dried over anhydrous sodium sulfate, the extract was evaporated to dryness. The residue that was dissolved in benzene was passed through a column of alumina, and the column was eluted with benzene to give yellow crystals (25 mg.). Recrystallization from aqueous ethanol afforded reddish yellow micro-prisms (m. p. 109—110°C).

Found: N, 6.57. Calcd. for $C_{23}H_{30}O_5N_2$: N, 6.76%.

UV $\lambda_{max}^{MeOH}$ mμ (log ε): 224 (4.27), 286 (4.25), 341 (4.79), 370 (4.30)sh, 420 (3.84).

IR (KBr disk): 3380, 1678, 1664 $cm^{-1}$.

**Diethyl 6-Anilinoazulene-1,3-dicarboxylate (XXI).**—A solution of II (50 mg.) and aniline (1 ml.) in ethanol (9 ml.) was refluxed for 1.5 hr. on a water bath and then concentrated to half volume. After the addition of water (5 ml.), the precipitate thereby formed was recrystallized from ethanol to give XXI (20 mg.; m. p. 182—183°C) as reddish yellow leaflets, and II (5 mg.) was recovered.

Found: N, 3.43. Calcd. for $C_{22}H_{21}O_4N$: N, 3.85%.

UV $\lambda_{max}^{MeOH}$ mμ (log ε): 227 (4.36), 270 (4.25), 347 (4.69), 399 (4.33).

IR (KBr disk): 3310, 1689, 1658 $cm^{-1}$.

**6-Dimethylaminoazulene-1,3-dicarboxylic Acid (XXIII).**—A solution of XI (150 mg.) and potassium hydroxide (300 mg.) in 60% aqueous ethanol (10 ml.) was refluxed for 3 hr. on a water bath. The solution was then concentrated to half volume under reduced pressure, and this was diluted with water (15 ml.) and acidified with 6 N sulfuric acid. The precipitate was collected by filtration and repeatedly washed with water, by which process XXIII was obtained as a brown crystalline powder; m. p. 167—168°C (decomp.), 100 mg.

**6-Diethylaminoazulene-1,3-dicarboxylic Acid (XXIV).**—When XII (300 mg.) was treated as in the above experiment, XXIV was obtained as brown crystals (200 mg.; m. p. 180°C (blacken)).

**6-Dimethylaminoazulene (XXV).**—A solution of XXIII (100 mg.) in pyridine (2 ml.) was heated at 125—130°C to effect decarboxylation. The residue produced by the evaporation of the excess pyridine was dissolved in benzene, the solution was passed through a column of alumina, and the column was eluted with benzene. From the effluent, orange crystals (15 mg.) were obtained, and recrystallization from benzene afforded pale red scales (m. p. 163—164.5°C) of XXV. The infrared spectrum of XXV shows no absorption for $\nu_{C=O}$ and $\nu_{N-H}$.

Found: N, 7.86. Calcd. for $C_{12}H_{13}N$: N, 8.18%.

UV $\lambda_{max}^{MeOH}$ mμ (log ε): 307 (4.66)sh, 316(4.70), 390 (4.20)sh, 397 (4.32), 472 (2.84).

*The Picrate of XXV.*—Dark green micro-prisms (from ethanol); m. p. above 280°C.

Found: N, 13.60. Calcd. for $C_{18}H_{16}O_7N_4$: N, 14.00%.

**6-Diethylaminoazulene (XXVI).**—When a solution of XXIV (180 mg.) in pyridine (2.5 ml.) was treated as in the above experiment, XXVI (15 mg.) was obtained. Recrystallization from ethanol afforded pale red scales (m. p. 71—71.5°C). The infrared spectrum of XXVI shows no absorption for $\nu_{C=O}$ and $\nu_{N-H}$.

Found: N, 6.61. Calcd. for $C_{14}H_{17}N$: N, 7.03%.

UV $\lambda_{max}^{MeOH}$ mμ (log ε): 309 (4.68)sh, 318 (4.72), 392 (4.26)sh, 399 (4.41), 443 (2.94), 476 (2.95).

Expenses for the present series of experiments were defrayed by a grant-in-aid for Scientific Research from the Ministry of Education. The infrared spectra in this paper were measured by using a Shimadzu infrared spectrophotometer IR-27 purchased by a grant-in-aid for Scientific Research from the Toyo Rayon Co., Ltd. The authors wish to express their deep gratitude for these contributions.

*Department of Chemistry*
*Faculty of Science*
*Tohoku University*
*Katahira-cho, Sendai (T. N. & K. T.)*

*The Research Institute for*
*Tuberculosis, Leprosy and Cancer*
*Tohoku University*
*Kitayoban-cho, Sendai (M. T.)*

# Chlorination by Sulfuryl Chloride. IV.[1] The Effect of Substituents in the Radical Chlorination of Benzaldehydes

By Mannosuke ARAI

(Received July 10, 1964)

In a previons peper of this series,[1] the author has shown that the polar effect of reactant molecules exerts an influence on the reaction rate, an influence based on the relative reactivity of the C–H bond toward the radical chlorination by sulfuryl chloride.

In the present work, the author will investigate whether or not the chlorination of substituted benzaldehydes to the corresponding acid chlorides is governed by the Hammett equation; this will be done in order to estimate the polar effect of substituents. The study was extended to alkylbenzaldehydes with both alkyl and formyl groups on the same benzene-ring in order to establish the change in the reactivity of the groups compared with alkylbenzene or benzaldehyde.

## Experimental

**Materials and Reagents.**—Toluene, of reagent grade, was purified in advance by fractional distillation, and the constantly boiling fraction was redistilled before use.

Substituted benzaldehydes, except *p*-isopropylbenzaldehyde and *p*-*t*-butylbenzaldehyde, all of reagent grade, were fractionated in an atmosphere of nitrogen; constantly boiling fraction was used.

Sulfuryl chloride, of first grade, was fractionally distilled, stored in a bottle wrapped with aluminum foil, and kept in a desiccator.

*p*-Isopropylbenzaldehyde was prepared by the chloromethylation of cumene, followed by heating with hexamethylenetetramine according to Blanc's method.[2] The product was purified through a sodium hydrosulfite adduct, b. p. 91°C/7 mmHg. Semicarbazone, m. p. 210—211°C. Found: N, 20.72. Calcd. for $C_{11}H_{15}ON_3$: N, 20.47%

*p*-*t*-Butylbenzaldehyde was similarly prepapred by the chloromethylation of *t*-butylbenzene, followed by heating with formaldehyde and hexamethylenetetramine following Schaklett and Smith's method;[3] b. p. 129—130°C/27 mmHg. 2,4-Dinitrophenylhydrazone, m. p. 250—251°C. Found: N, 16.25. Calcd. for $C_{17}H_{17}O_4N_4$: N, 16.37%.

**General Procedure for Chlorination.**—The materials to be chlorinated competitively were weighed in a 50 ml. round-bottomed flask equipped with a stirrer, a dropping funnel, and a reflux condenser with a calcium chloride tube on the top. After the air in the system had been replaced by dry nitrogen, benzoyl peroxide (0.1% of the weight of the sulfuryl chloride used) was added to the flask and the system was then heated to 80±1°C. Upon the gradual stirring in of sulfuryl chloride through the dropping funnel, the evolution of gas was observed after some induction period. Heating was continued until the gas evolution ceased. After cooling, the hydrogen chloride formed was driven off by passing nitrogen through.

**Analytical Procedures.** — The reaction mixture obtained by the method described above was weighed, and any loss of weight during the reaction was distributed among the starting materials according to the relative ratio of vapor pressure.

The total amount of chlorides was determined by the procedure described in Part III in the cases of all substituted benzaldehydes except chlorobenzaldehyde. In the case of chlorobenzaldehyde, since Rauscher's method could not be applied, 2 ml. of the reaction mixture was heated under reflux for 2 hr. with 10 ml. of 0.5 N sodium hydroxide in 30 ml. of ethanol, and the chloride liberated was determined by a silver nitrate solution (Mohr's method). Under these conditions, benzoyl chloride is also hydrolyzed quantitatively.

The amount of benzoyl chloride produced was also determined by the procedure described in Part III.

**Chlorination Products of *p*-Tolualdehyde.**—The reaction of 0.2349 mol. of *p*-tolualdehyde and 0.0481 mol. of sulfuryl chloride gave 4.75 g. of *p*-toluoyl chloride, b. p. 72—74°C/4 mmHg. Toluanilide, m. p. 140°C was derived quantitatively. Found: N, 6.80. Calcd. for $C_{14}H_{13}ON$: N, 6.81%. The residue of the above distillation (2.53 g.; positive in a Beilstein test) was boiled in water. Some needles, m. p. 82°C, were obtained. Found: C, 70.78, H, 6.10. Calcd. for $C_5H_5O_2$: C, 70.59; H, 5.88%

## Results and Discussion

As it was experimentally difficult to determine each component in the acid chloride mixture as a result of the direct competitive reaction between benzaldehyde and substituted benzaldehydes, the substituent effect was derived indirectly as follows: the relative reactivity of substituted benzaldehydes was determined against toluene by competitive chlorination at 80°C, and then these values were compared with those obtained by the similar reaction of unsubstituted benzaldehyde and toluene.

1) Part III: M. Arai, This Bulletin, 37, 1280 (1964).
2) G. Blanc, *Bull. soc. chem. France*, [4] 33, 313 (1923).
3) C. D. Shacklett and H. A. Smith, *J. Am. Chem. Soc.*, 75, 2654 (1933).

The relative reactivity of the benzaldehydes to toluene was calculated by by the following equation:

$$ArCHO + \cdot SO_2Cl \xrightarrow{k} ArCO\cdot + HCl + SO_2$$

$$C_6H_5CH_3 + \cdot SO_2Cl \xrightarrow{k_T} C_6H_5CH_2\cdot + HCl + SO_2$$

$$\frac{k}{k_T} = \frac{\log\left([ArCHO]_{int}/[ArCHO]_{fin}\right)}{\log\left([C_6H_5CH_3]_{int}/[C_6H_5CH_3]_{fin}\right)}$$

where $[\ ]_{int}$ and $[\ ]_{fin}$ denote the initial and final concentrations of ArCHO and $C_6H_5CH_3$ respectively.

The value of 3.23 was used for $k_O/k_T$, in which $k_O$ was the $k$ value of unsubstituted benzaldehyde, as was shown in Part III of

TABLE I. COMPETITIVE CHLORINATION OF *p*-NITROBENZALDEHYDE AND TOLUENE AT 80°C[a]

| Reactant | mol. | mol. |
|---|---|---|
| *p*-Nitrobenzaldehyde | 0.0662 | 0.0543 |
| Toluene | 0.1656 | 0.2494 |
| Sulfuryl chloride | 0.0247 | 0.0247 |
| Product | | |
| Total chlorides | 0.0245 | 0.0248 |
| *p*-Nitrobenzoyl chloride | 0.0082 | 0.0059 |
| Benzyl chloride[b] | 0.0163 | 0.0189 |
| *p*-Nitrobenzaldehyde[c] | 0.0580 | 0.0484 |
| Toluene[c] | 0.1493 | 0.2305 |
| $k/k_T$ | 1.28 | 1.46 |
| $k/k_O$ | 0.40 | 0.45 |
| mean | 0.43 | |

a) In the presence of benzoyl peroxide
b) Total chlorides minus *p*-nitrobenzoyl chloride
c) Initial quantity minus the amount substituted and the amount vaporized

TABLE II. COMPETITIVE CHLORINATION OF *m*-NITROBENZALDEHYDE AND TOLUENE AT 80°C[a]

| Reactant | mol. | mol. |
|---|---|---|
| *m*-Nitrobenzaldehyde | 0.0687 | 0.0651 |
| Toluene | 0.1357 | 0.2583 |
| Sulfuryl chloride | 0.0247 | 0.0247 |
| Product | | |
| Total chlorides | 0.0243 | 0.0241 |
| *m*-Nitrobenzoyl chloride | 0.0095 | 0.0059 |
| Benzyl chloride[b] | 0.0148 | 0.0182 |
| *m*-Nitrobenzaldehyde[c] | 0.0592 | 0.0592 |
| Toluene[c] | 0.1209 | 0.2401 |
| $k/k_T$ | 1.29 | 1.31 |
| $k/k_O$ | 0.40 | 0.41 |
| mean | 0.41 | |

a) In the presence of benzoyl peroxide
b) Total chlorides minus *m*-nitrobenzoyl chloride
c) Initial quantity minus the amount substituted and the amount vaporized

TABLE III. COMPETITIVE CHLORINATION OF *p*-CHLOROBENZALDEHYDE AND TOLUENE AT 80°C[a]

| Reactant | mol. | mol. |
|---|---|---|
| *p*-Chlorobenzaldehyde | 0.0698 | 0.0614 |
| Toluene | 0.1270 | 0.1526 |
| Sulfuryl chloride | 0.0247 | 0.0247 |
| Product | | |
| Total chlorides | 0.0251 | 0.0248 |
| *p*-Chlorobenzoyl chloride | 0.0143 | 0.0121 |
| Benzyl chloride[b] | 0.0108 | 0.0127 |
| *p*-Chlorobenzaldehyde[c] | 0.0555 | 0.0493 |
| Toluene[c] | 0.1162 | 0.1399 |
| $k/k_T$ | 2.58 | 2.53 |
| $k/k_O$ | 0.80 | 0.78 |
| mean | 0.79 | |

a) In the presence of benzoyl peroxide
b) Total chlorides minus *p*-chlorobenzoyl chloride
c) Initial quantity minus the amount substituted and the amount vaporized

TABLE IV. COMPETITIVE CHLORINATION OF *m*-CHLOROBENZALDEHYDE AND TOLUENE AT 80°C[a]

| Reactant | mol. |
|---|---|
| *m*-Chlorobenzaldehyde | 0.0826 |
| Toluene | 0.1012 |
| Sulfuryl chloride | 0.0247 |
| Product | |
| Total chlorides | 0.0243 |
| *m*-Chlorobenzoyl chloride | 0.0155 |
| Benzyl chloride[b] | 0.0088 |
| *m*-Chlorobenzaldehyde[c] | 0.0671 |
| Toluene[c] | 0.0924 |
| $k/k_T$ | 2.29 |
| $k/k_O$ | 0.71 |

a) In the presence of benzoyl peroxide
b) Total chloride minus *m*-chlorobenzoyl chloride
c) Initial quantity minus the amount substituted and the amount vaporized

TABLE V. COMPETITIVE CHLORINATION OF ANISALDEHYDE AND TOLUENE AT 80°C[a]

| Reactant | mol. | mol. |
|---|---|---|
| Anisaldehyde | 0.0543 | 0.0819 |
| Toluene | 0.1914 | 0.1112 |
| Sulfuryl chloride | 0.0247 | 0.0247 |
| Product | | |
| Total chlorides | 0.0245 | 0.0232 |
| Anisoyl chloride | 0.0110 | 0.0153 |
| Benzyl chloride[b] | 0.0135 | 0.0079 |
| Anisaldehyde[c] | 0.0433 | 0.0666 |
| Toluene[c] | 0.1779 | 0.1033 |
| $k/k_T$ | 3.10 | 2.80 |
| $k/k_O$ | 0.96 | 0.87 |
| mean | 0.92 | |

a) In the presence of benzoyl peroxide
b) Total chloride minus anisoyl chloride
c) Initial quantity minus the amount substituted and the amount vaporized

this series.[1] The results obtained in the cases of *m*- and *p*-nitrobenzaldehydes, *m*- and *p*-chlorobenzaldehydes, and anisaldehyde are listed in Tables I—V.

A linear relation was found between log $k/k_0$ and Hammett's $\sigma$ values,[4] as is shown in Fig. 1, where $\rho = -0.48$, excepting for anisaldehyde.

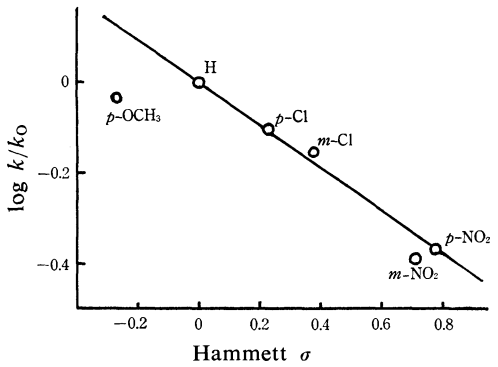



Fig. 1. Correlation of relative reactivities of substituted benzaldehydes with Hammett $\sigma$ values.

As reasons for the deviation of the value for the *p*-methoxy group, (1) the inadequacy of using the $\sigma$ value (the application of the $\sigma^+$ value, etc. should also be considered) and (2) the occurrence of a considerable side-reaction are both conceivable. As for the first factor, it is stated the $\sigma^+$ value is better than the $\sigma$ value when the reactivity of the electron-releasing group is greater than the value expected from the log $k/k_0$—$\sigma$ line determined by the other substituents. The experimental results show the smaller log $k/k_0$ value for the *p*-methoxy group. Although the application of Yukawa's modified Hammett relationship[5] can also be considered, no conclusion can be drawn before more experimental results are available regarding other electron-releasing groups. As the second factor, there is a possibility of chlorination at the methoxy group, since the methylenedioxy group suffers from radical chlorination, as has been shown in Part II of this series.[6]

The chlorination reaction of benzaldehyde by sulfuryl chloride is, by nature, a radical reaction.[7] However, since the reaction follows Hammett rule, the polar effect of substituents is also recognized in the reaction. This effect can easily be understood on the assumption of the following activated complex I:

$$\mathrm{ArC(=O)-H} + \cdot\mathrm{SO_2Cl} \rightarrow \mathrm{Ar\overset{\delta+}{C}(=O)\cdots\dot{H}\cdots\overset{\delta-}{S}O_2Cl} \rightarrow \quad \text{(I)}$$

$$\mathrm{ArC(=O)\cdot} + \mathrm{SO_2} + \mathrm{HCl}$$

I would be more easily formed in the case of the formyl group has more electrons around it, and then, the reaction would be accelerated.

Next, in order to compare the reactivity of the formyl group with that of various alkyl groups at the *p*-position, the reaction was carried out with *p*-tolualdehyde, cuminaldehyde and *p*-*t*-butylbenzaldehyde, using about 1/5 mol. of sulfuryl chloride. The results are smmarized in Tables VI—VIII.

TABLE VI. ISOMER DISTRIBUTION IN THE CHLORINATION OF *p*-TOLUALDEHYDE AT 80°C[a]

| Reactant | mol. | mol. |
|---|---|---|
| *p*-Tolualdehyde | 0.2349 | 0.2496 |
| Sulfuryl chloride | 0.0481 | 0.0506 |
| Product | | |
| Total chlorides | 0.0478 | 0.0502 |
| *p*-Toluoyl chloride | 0.0345 | 0.0375 |
| *p*-Chloromethylbenzaldehyde[b] | 0.0133 | 0.0127 |
| Reactivity of $-CH_3$ group[c] | 0.39 | 0.34 |
| mean | 0.37 | |

a) In the presence of benzoyl peroxide
b) Total chlorides minus *p*-toluoyl chloride
c) Reactivity of -CHO group assumed to be 1.00

TABLE VII. ISOMER DISTRIBUTION IN THE CHLORINATION OF CUMINALDEHYDE AT 80°C[a]

| Reactant | mol. |
|---|---|
| Cuminaldeyde | 0.1301 |
| Sulfuryl chloride | 0.0247 |
| Product | |
| Total chlorides | 0.0250 |
| (HCl)[b] | 0.0233 |
| $\beta$-Chloride of $-CH(CH_3)_2$ group[c] | 0.0017 |
| $\alpha$-Chloride of $-CH(CH_3)_2$ group[d] | 0.0115 |
| *p*-Isopropylbenzoyl chloride[e] | 0.0118 |
| Reactivity of $-CH(CH_3)_2$ group[f] | 1.11 |

a) In the presence of benzoyl peroxide
b) The amount of HCl by hydrolyzed with 80% EtOH — *p*-isopropylbenzoyl chloride and $\alpha$-chloride of $-CH(CH_3)_2$ group
c) Total chlorides minus (HCl)
d) 6.80 times $\beta$-chlride[1]
e) (HCl) minus $\alpha$-chloride
f) Reactivity of -CHO group assumed to be 1.00

4) D. H. McDaniel and H. C. Brown, *J. Org. Chem.*, 23, 420 (1958).
5) Y. Tsuno, T. Ibata and Y. Yukawa, This Bulletin, 32, 960 (1959); Y. Yukawa and Y. Tsuno, ibid., 32, 965, 971 (1959).
6) M. Arai, This Bulletin, 35, 1272 (1962).
7) M. Arai, *J. Chem. Soc. Japan, Pure Chem. Sec.* (*Nippon Kagaku Zasshi*), 81, 1450 (1960).

TABLE VIII. ISOMER DISTRIBUTION IN THE CHLORINATION OF *p-t*-BUTYLBENZALDEHYDE AT 80°C[a)]

| Reactant | mol. |
|---|---|
| *p-t*-Butylbenzaldehyde | 0.1558 |
| Sulfury chloride | 0.0408 |
| Product | |
| Total chlorides | 0.0406 |
| *p-t*-Butylbenzoyl chloride | 0.0298 |
| Chloride of $-C(CH_3)_3$ group[b)] | 0.0108 |
| Reactivity of $-C(CH_3)_3$ group[c)] | 0.36 |

a) In the presence of benzoyl peroxide
b) Total chlorides minus *p-t*-butylbenzoyl chloride
c) Reactivity of -CHO group assumed to be 1.00.

Furthermore, two kinds of chlorination products, *p*-toluoyl chloride and *p*-chloromethylbenzaldehydes, were obtained in the reaction of *p*-tolualdehyde. The results are listed in Table VI.

As is shown in Tables VI—VIII, the relative reactivities of the methyl, isopropyl and *t*-butyl groups toward the formyl group are 0.37, 1.11 and 0.36 respectively. These values are close enough to those (0.31, 1.37 and 0.25) resuling from the reaction of toluene, cumene and *t*-butylbenzene toward benzaldehyde.[1)] In the reaction of alkylbenzaldehydes, it is considered that the reactivity of the formyl group is increased by the presence of the alkyl group, while the reactivity of the alkyl group is decreased by the presence of the formyl group. Therefore, the reactions in this series show that the modified reactivity of groups is due to mutual electronic interaction.

The author wishes to express his gratitude to Professor Mamoru Yamaguchi of Tohoku University for his constant guidance through the course of this work.

*College of General Education*
*Tohoku University*
*Kawauchi, Sendai*

# The Cyclization of Diethyl 3, 6-Dioxo-azelate

By Choji KASHIMA, Kungtu KUO, Yoshimori OMOTE and Noboru SUGIYAMA

(Received July 15, 1964)

1, 4, 7-Cyclononanetrione (XIX) has many active methylenes and seems to be structurally interesting compound, but its convenient synthesis cannot be found in the literature. It has only obtained in the form of trioxime in a poor yield.[1] In this paper the synthesis of XIX will be attempted through the acyloin condensation[2,3] of the bisethylene ketal derivative (XI) of diethyl 3, 6-dioxo-azelate (I).

It is well-known that diesters of aliphatic dicarboxylic acids afford the corresponding cyclic acyloin by the action of sodium. However, when XI was subjected to this reaction, the reaction product was not the expected acyloin (XVIII). This anomalous result stimulated the present authors to examine these reactions further. Though the ultimate synthesis of XIX was unsuccessful, the synthesis of I and its anomalous cyclization reactions will be reported in this paper.

## Results and Discussion

I was obtained through two synthetic routes. In one route, furyl-acrylic acid (VII) was changed into diethyl 4-oxo-pimelate (II),[4] which was then partially hydrolyzed[5] and converted to an ester chloride (IV). IV was derived into I through malonic ester synthesis.[6] However, it was difficult to obtain pure I by this method. Even after repeated distillation, the product showed infrared absorptions at 1780 ($\nu_{C=O}$, $\gamma$-lactone), 1740 ($\nu_{C=O}$, ester), 1720 ($\nu_{C=O}$, ketone) and 1600 $cm^{-1}$ ($\nu_{C=C}$), indicating the presence of an unsaturated $\gamma$-lactone (X).[7]

1) S. Kawai, S. Tanaka, K. Terai. M. Tezuka and T. Nishiwaki, This Bulletin, **33**, 251 (1960).

2) V. Prelog, L. Frenkiel, M. Kobelt and P. Barman, *Helv. Chim. Acta*, **30**, 1741 (1947); M. Stoll, J. Hulstkamp and A. Rouvé, ibid., **31**, 543 (1948); A. T. Blomquist, L. H. Liu and J. C. Bohrer, *J. Am. Chem. Soc.*, **74**, 3643 (1952); P. D. Gardner, G. R. Haynes and R. L. Brandon, *J. Org. Chem.*, **22**, 1206 (1957); N. L. Allinger, "Organic Syntheses," Vol. 36, 79 (1956).

3) J. C. Sheehan, R. A. Coderre and P. A. Cruickshank, *J. Am. Chem. Soc.*, **75**, 6231 (1953).

4) W. S. Emerson and R. I. Longley, Jr., "Organic Synthese," Vol. 33, 25 (1953).

5) W. Marckwald, *Ber.*, **21**, 1402 (1888).

6) D. S. Breslow, E. Baumgarten and C. R. Hauser, *J. Am. Chem. Soc.*, **66**, 1286 (1944).

7) F. A. Kuehl, Jr., R. P. Linstead and B. A. Orkin, *J. Chem. Soc.*, **1950**, 2213.

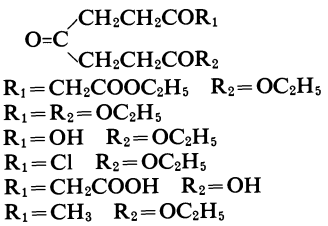
In the other route, I was obtained by the ring opening of ethyl furyl-acryloyl-acetate (IX),[8] which was synthesized from VII by malonic ester synthesis.[6] It was shown by gas chromatography that the reaction product of IX with hydrogen chloride in ethanol consisted of I and ethyl 4,7-dioxo-octanoate (VI),[9] and that I and VI were separated by distillation. I showed strong infrared absorptions at 1740 ($\nu_{C=O}$, ester) and 1720 $cm^{-1}$ ($\nu_{C=O}$, ketone) and produced the corresponding dibasic acid (V) on hydrolysis with an aqueous sodium hydroxide solution.

Before the acyloin cyclization of I is carried out, its keto groups must be protected.[10] Therefore, I was changed into the bis-ethylene ketal derivative (XI). XI showed no infrared absorption at 1720 ($\nu_{C=O}$, ketone), but it did show one at 1740 $cm^{-1}$ ($\nu_{C=O}$, ester).

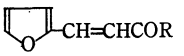
A dilute xylene solution of XI was added very slowly, through a capillary tube and with vigorous stirring, to xylene in which sodium had been dispersed. After 24 hr. the reaction mixture was then neutralized by acetic acid. The isolated product was proved to be not an acyloin (XVIIII), but 2-ethoxycarbonyl-4,4-ethylenedioxy-1,7-cyclooctanedione (XXII), a partially hydrolyzed compound of a Dieckmann condensation product (XXII).

The structure of XXIII was deduced as follows. XXIII gave a positive ferric chloride test, but a negative Fehling test, indicating the absence of the acyloin structure in XXIII. The infrared absorption spectrum of XXIII showed absorptions at 1740 ($\nu_{C=O}$, ester; keto form), 1720 ($\nu_{C=O}$, ketone; keto form), 1660 ($\nu_{C=O}$, ester; enol form) and 1610 $cm^{-1}$ ($\nu_{C=C}$; enol form), the last two being attributed to the enolizable $\beta$-ketoester.[11] The ultraviolet absorption spectrum of XXIII showed $\lambda_{max}^{EtOH}$ 255 ($\varepsilon$, 4500) and $\lambda_{max}^{alkali\ EtOH}$ 287 m$\mu$ ($\varepsilon$, 10800).

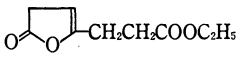
The NMR spectra[12] of XXIII in carbon tetrachloride were assigned to the ethyl group of the ester at 5.71 (quartet) and 8.68$\tau$ (triplet, $J$ 7.0 c.p.s.), to the enolized hydroxyl group at $-2.30\tau$ (singlet), to 4 protons of methylene groups neighbor carbonyl groups at 7.46—7.64$\tau$ (multiplet), to 4 protons of the other methylenes at 7.81—8.35$\tau$ (multiplet), and to 4 protons of the ethylene ketal group at 6.04$\tau$ (singlet).[13] These data indicate that



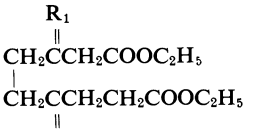
I $R_1=CH_2COOC_2H_5$ $R_2=OC_2H_5$
II $R_1=R_2=OC_2H_5$
III $R_1=OH$ $R_2=OC_2H_5$
IV $R_1=Cl$ $R_2=OC_2H_5$
V $R_1=CH_2COOH$ $R_2=OH$
VI $R_1=CH_3$ $R_2=OC_2H_5$



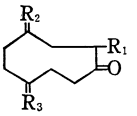
VII R=OH
VIII R=Cl
IX $R=CH_2COOC_2H_5$



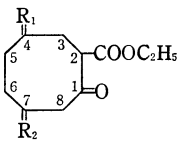
X



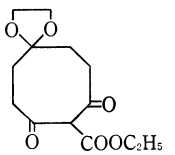
XI $R_1=R_2=OCH_2CH_2O$
XII $R_1=H_2$ $R_2=O$
XIII $R_1=H_2$ $R_2=OCH_2CH_2O$
XIV $R_1=O$ $R_2=H_2$
XV $R_1=OCH_2CH_2O$ $R_2=H_2$
XVI $R_1=O$ $R_2=OCH_2CH_2O$
XVII $R_1=OCH_2CH_2O$ $R_2=O$



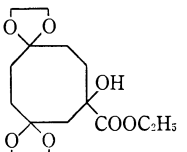
XVIII $R_1=OH$ $R_2=R_3=OCH_2CH_2O$
XIX $R_1=H$ $R_2=R_3=O$
XX $R_1=OH$ $R_2=H_2$ $R_3=OCH_2CH_2O$
XXI $R_1=OH$ $R_2=OCH_2CH_2O$ $R_3=H_2$



XXII $R_1=R_2=OCH_2CH_2O$
XXIII $R_1=OCH_2CH_2O$ $R_2=O$
XXIV $R_1=H_2$ $R_2=OCH_2CH_2O$



XXV



XXVI

8) J. English, Jr., and L. J. Lapides, *J. Am. Chem. Soc.*, **65**, 2466 (1943).
9) F. L. Breush and E. Ulusay, *Rev. faculté sci. univ. Istanbul*, **13A**, 51 (1948); *Chem. Abstr.*, **42**, 5850h (1948).
10) E. J. Salmi, *Ber.*, **71**, 1805 (1938).
11) S. J. Rhoads, J. C. Gilbert, A. W. Decora, L. R. Garland, R. J. Spangler and M. J. Urbigkit, *Tetrahedron*, **19**, 1625 (1963).
12) NMR spectra were measured on a Varian A-60 megacycle spectrometer by courtesy of Dr. S. Yoshida of Sankyo Co. Ltd.
13) E. Capsi, Th. A. Wittstruck and D. M. Piatak, *J. Org. Chem.*, **27**, 3183 (1962).

one of the ethylene ketal groups at C-7 was hydrolysed to a ketone.

In order to find a reasonable explanation why only the Dieckmann condensation reaction occurred in this case, diethyl azelate was subjected to the same treatment as above; 2-hydroxy-cyclononanone (azeloin)[2] was obtained in about a 25% yield. Even in the presence of ethanol, azeloin was obtained, but in this case, the product was contaminated with a small amount of a Dieckmann condensation product, 2-ethoxycarbonyl-cyclooctanone.

The different behavior of XI and diethyl azelate could be attributed to the presence of two ethylene ketal groups in the former. It is suspected that the relative position of the ketal group and the ethoxycarbonyl group might influence their behavior. In fact, this was proved by the reaction of the ethylene ketal of 4-oxo-azelate (XII)[14] and 3-oxo-azelate (XIV) under the same conditions.

From XIII, the ethylene ketal of XII, acyloin (XX) was obtained. XX gave a positive Fehling test. Its infrared absorption spectrum showed absorptions at 3400 ($\nu_{OH}$) and 1705 $cm^{-1}$ ($\nu_{C=O}$, ketone). Its ultraviolet absorption spectrum showed $\lambda_{max}^{EtOH}$ 260 m$\mu$ ($\varepsilon$, 2600), which shifted to $\lambda_{max}^{alkali\ EtOH}$ 310 m$\mu$ ($\varepsilon$, 3800).

On the other hand, from XV, the ethylene ketal of XIV, a Dieckmann condensation product (XXIV) was obtained instead of the corresponding acyloin (XXI). The structure of XXIV was deduced from the following facts. The product obtained gave a positive ferric chloride test, but a negative Fehling test. Its infrared absorption spectrum showed absorptions at 1705 ($\nu_{C=O}$, ketone) and 1730 $cm^{-1}$ ($\nu_{C=O}$, ester).

Now let us discuss when and why one of the ethylene ketal groups was hydrolyzed in the reaction of XI to XXIII. In the first place, the hydrolysis may be presumed to occur after the ring closure. If it had occurred before the ring closure, the intermediate compound, XVI or XVII, must be subjected to the condensation reaction. Of these two intermediates, only XVI can produce XXIII. However, methylene at C-2 in XVI would be more reactive than methylene at C-8, and the reaction from XVI to XXV must be predominant over the reaction from XVI to XXIII. As the experimental results were not in accord with this reasoning, the formation of the cyclic intermediate (XXII) must precede the hydrolysis of one member of the ethylene ketal group.

Next, let us consider the partial hydrolysis of XXII. The ethylene ketal group at C-7 seems to be less stable than that at C-4, because of the effect of the $\beta$-carbonyl group at C-1 or because of the steric effect of the other ethylene ketal group at C-4 in the medium-size ring. As a model compound of ethylene ketal with a $\beta$-carbonyl group, 4,4-ethylenedioxy-2-pentanone[15] was prepared, and the hydrolysis of the ketal with acetic acid was studied. It was found that only a small amount of 2,4-pentanedione was produced. Therefore, the partial hydrolysis of XXII during the neutralization of the reaction mixture with acetic acid, seems to be effected mainly by the steric hindrance, not by the electron displacement.

As a modified acyloin condensation, liquid ammonia has been used[3] instead of xylene. The acyloin condensation reaction of XI in the presence of sodium in liquid ammonia gave a product different from XXIII. On the basis of infrared spectra at 3400 ($\nu_{OH}$) and 1740 $cm^{-1}$ ($\nu_{C=O}$, ester), a negative Fehling test, and a positive ferric chloride test, the structure of the product was tentatively proposed to be 1-ethoxycarbonyl-3,3,6,6-bisethylenedioxy-1-cyclooctanol (XXVI). The details of this reaction will be reported elsewhere.

## Experimental

All melting points are uncorrected.

**6-Ethoxycarbonyl-4-oxo-hexanoic Acid (III).**—A solution of 120 g. of diethyl 4-oxo-pimelate and 26 g. of potassium hydroxide in 2 l. of ethanol was allowed to stand overnight at room temperature. After the reaction mixture had been concentrated under reduced pressure, it was poured into cold water, acidified with hydrochloric acid, and extracted with benzene. The benzene solution was then dried over anhydrous sodium sulfate. After the benzene had been removed, 10 g. of crude III was obtained. This was recrystallized from benzene-petroleum ether as colorless plates; m. p. 70.5°C. IR: $\nu$ 1730, 1700 $cm^{-1}$.

**6-Ethoxycarbonyl-4-oxo-hexanoyl Chloride (IV).**—A mixture of 10 g. of III and 15 g. of thionyl chloride was allowed to stand overnight at room temperature. After the excess thionyl chloride had been removed, IV was obtained as a colorless oil; b. p. 171—176°C/17 mmHg, yield 6.5 g.

**Ethyl Furyl-acryloyl-acetate (IX).**—To 0.56 g. of magnesium were added 0.5 ml. of absolute ethanol, a few drops of carbon tetrachloride, and 10 ml. of anhydrous ether. After a few minutes, 4.3 g. of ethyl *t*-butyl malonate, 2 ml. of absolute ethanol, and 18 ml. of anhydrous ether were added, and the mixture was refluxed for 4 hr. with stirring. To the mixture, 3.7 g. of furylacryloyl chloride (b. p.

14) S. Hünig and W. Lendle, *Chem. Ber.*, **93**, 913 (1960).

15) P. C. Dutta, P. K. Dutta and K. N. S. Sastry, *J. Indian Chem.*, **31**, 881 (1954); *Chem. Abstr.*, **50**, 838h (1956).

119—120°C/19 mmHg)[8] in 15 ml. of anhydrous ether was then added slowly and the solution refluxed for one hour. The mixture was acidified with 1.8 N sulfuric acid and washed with water. After the ether had been removed, the residue was dissolved in benzene and refluxed for 4 hr. with 100 mg. of *p*-toluenesulfonic acid. The benzenene solution was washed with water, and the solvent was removed. IX was obtained as pale yellow oil; b. p. 77—107°C/3.5 mmHg, IR: $\nu$ 3080, 1730, 1640, 1540 $cm^{-1}$; UV: $\lambda_{max}^{EtOH}$ 342 m$\mu$.

2, 4-Dinitrophenylhydrazone was prepared and recrystallized from ethanol-ethyl acetate; m. p. 179°C.

Found: C, 52.17, 52.26; H, 3.91, 3.97; N, 13.90, Calcd. for $C_{17}H_{16}N_4O_7$: C, 52.58; H, 4.15; N, 14.43%.

**Diethyl 3, 6-Dioxo-azelate (I).**—1) I was obtained from IV in about a 35% yield by a procedure similar to the one described for IX.

2) Dry hydrogen chloride was passed for 45 min. through a hot solution of 25 g. of ethyl furyl-acryloyl-acetate in 70 ml. of 95% ethanol. After the ethanol had been removed under reduced pressure, the residue was poured into an aqueous solution of sodium carbonate and extracted with benzene, and the benzene layer was dried over sodium sulfate. After the benzene had been removed, the residue was distilled under reduced pressure; b. p. 134—135°C/0.8 mmHg, yield 12 g.

Dibenzylamide, m. p. 177°C.

Found: C, 70.68; H, 6.53. Calcd. for $C_{23}H_{16}N_2O_4$: C, 70.03; H, 6.64%.

**3, 6-Dioxo-azelaic Acid (V).**—I was added to an aqueous 3 N sodium hydroxide solution, and the mixture was heated until a clear solution was obtained. After it had cooled, the solution was acidified with dilute hydrochloric acid and extracted with ether. The ether layer was separated and dried over sodium sulfate. After the ether had been removed, the free dibasic acid (V) was obtained; it was then recrystallized from benzene-ethanol; m. p. 139°C, IR: $\nu$ 3050, 1720, 1700 $cm^{-1}$.

Found: C, 48.19, 48.09; H, 5.82, 5.47. Calcd. for $C_9H_{12}O_6 \cdot 1/2H_2O$: C, 48.00; H, 5.82%.

**Diethyl 3, 3, 6, 6-Bisethylenedioxy-azelate (XI).**—The solution of 29.7 g. of I and 15 ml. of ethylene glycol in 200 ml. of benzene was refluxed with 300 mg. of *p*-toluenesulfonic acid under azeotropic distillation for 7 hr. The mixture was washed with water and dried over sodium sulfate. After the benzene had been removed under reduced pressure, XI was obtained as a colorless oil; b. p. 146—154°C/2.5 mmHg, yield 22.4 g.

Found: C, 57.31, 57.09; H, 7.90, 7.98. Calcd. for $C_{17}H_{28}O_8$: C, 56.65; H, 7.83%.

**The Acyloin Condensation of Diethyl Azelate.**—1) With freshly dispersed sodium: In a 200 ml., three-necked, round-bottom flask equipped with a sealed stirrer, a reflux condenser, and a dropping-funnel, 5.2 g. of sodium and 90 ml. of dry xylene were placed. The mixture was refluxed and stirred (3600 r. p. m.) for 10 min. To the mixture was then added 11 g. of diethyl azelate in 50 ml. of xylene over a 24 hr. period, with sufficient stirring under reflux. After all of the xylene solution of diethyl azelate had been added, the reaction mixture was refluxed for another hour, and cooled with water and then with an ice bath. A mixture of 20 ml. of acetic acid and 20 ml. of xylene was then added. All these procedures were carried out during stirring and under a nitrogen atmosphere. The reaction mixture was washed with water and dried over anhydrous sodium sulfate. After the xylene had been removed under reduced pressure, the residue was distilled. 1.4 g. of 2-hydroxy-cyclononanone (azeloin) was thus obtained; b. p. 124—139°C/17 mmHg; IR: $\nu$ 3450, 1700 $cm^{-1}$; UV: $\lambda_{max}^{EtOH}$ 262, $\lambda_{max}^{alkali\ EtOH}$ 286 m$\mu$.

2) With commercial dispersed sodium: Into a mixture of 80 ml. of boiling xylene and 12.0 g. of commercial dispersed sodium in toluene (40%), 10.3 g. of diethyl azelate in 45 ml. of xylene was stirred in over a 24 hr. period. After the solution had been treated as has been described above, 700 mg. of azeloin was obtained.

**The Reaction of XI with Dispersed Sodium.**—The reaction of XI with freshly dispersed sodium was carried out according to the procedure described for azeloin, but no acyloin was detected in the product by a study of its infrared spectrum. The reaction of 11.5 g. of XI and 10 g. of commercial dispersed sodium (40% in toluene) in xylene afforded 1.8 g. of the crude reaction product. By distillation, XXIII was isolated; b. p. 133—137°C/3 mmHg.

Found: C, 58.21, 58.17; H, 6.98, 7.00. Calcd. for $C_{13}H_{18}O_6$: C, 57.77; H, 6.71%.

Bis-2, 4-dinitrophenylhydrazone of XXIII was prepared and recrystallized from ethanol-ethyl acetate; m. p. 167°C.

Found: N, 18.09. Calcd. for $C_{25}H_{26}N_8O_{12}$: N, 17.77%.

**Diethyl 4, 4-Ethylenedioxy-azelate (XIII).**—By refluxing the mixture of 15.7 g. of ketone (XII), 5 ml. of ethylene glycol, and 100 mg. of *p*-toluenesulfonic acid in 150 ml. of benzene, 13.9 g. of XIII was obtained; b. p. 146—151°C/0.13 mmHg, IR: $\nu$ 1740 $cm^{-1}$.

Found: C, 59.62, 59.45; H, 8.93, 8.87. Calcd. for $C_{15}H_{26}O_6$: C, 59.58; H, 8.67%.

**The Reaction of XIII with Dispersed Sodium.**—By the reaction of 3.2 g. of XIII and 4.5 g. of commercial dispersed sodium (40% in toluene) in 50 ml. of xylene, 200 mg. of the corresponding acyloin (XX) was obtained; b. p. 80—90°C/0.02 mmHg.

**6-Ethoxycarbonylhexanoyl Chloride.**—From 8.0 g. of 6-ethoxycarbonylhexanoic acid[16] and 6.2 ml. of thionyl chloride, 7.8 g. of the acid chloride was obtained; b. p. 138—141°C/17.5 mmHg, IR: $\nu$ 1800, 1740 $cm^{-1}$.

**Diethyl 3-Oxo-azelate (XIV).**—The malonic ester synthesis was carried out by a procedure similar to that described for the synthesis of IX. From 650 mg. of magnesium, 0.1 ml. of carbon tetrachloride, 3.6 g. of absolute ethahol, 5 ml. of ethyl *t*-butyl malonate, and 5.4 g. of 6-ethoxy-carbonyl-hexanoyl chloride in 31 ml. of anhydrous

16) J. Walker and J. S. Lumsden, *J. Chem. Soc.*, **79**, 1197 (1901).

ether, 1.5 g. of XIV were obtained; b. p. 105—106°C/0.5 mmHg, IR: $\nu$ 1740, 1720 $cm^{-1}$.

Found: C, 60.13, 60.24; H, 9.24, 9.31. Calcd. for $C_{13}H_{22}O_5$: C, 60.44; H, 8.59%.

**Diethyl 3, 3-Ethylenedioxy-azelate (XV).** — By the same procedure as was used for XI, XV was obtained from 1.3 g. of XIV; b. p. 95—110°C/0.24 mmHg, yield 0.6 g., IR: $\nu$ 1740 $cm^{-1}$.

Found: C, 59.45, 59.49; H, 8.70, 8.75. Calcd. for $C_{15}H_{26}O_6$: C, 59.58; H, 8.67%.

**The Reaction of XV with Dispersed Sodium.**— The reaction of 0.6 g. of XV and 0.5 g. of dispersed sodium (40% in toluene) in xylene afforded only a trace of the product; b. p. 82—87°C/0.05 mmHg; UV: $\lambda_{max}^{EtOH}$ 250 m$\mu$ ($\varepsilon$, 1300).

**The Acyloin Condensation of XI in Liqid Ammonia.**—0.8 g. of sodium was stirred in a nitrogen atmosphere and thus dissolved into a mixture of 200 ml. of anhydrous ether and about 300 ml. of liquid ammonia cooled in an acetone - dry ice bath. To this solution was then added 1.9 g. of XI in 180 ml. of anhydrous ether over a 2 hr. period. After the ammonia had been removed, 2 ml. of methanol and 75 ml. of 5% hydrochloric acid were added slowly. The ethereal solution was then washed with water and dried over anhydrous sodium sulfate. The ether was removed, and the residue was distilled to give 100 mg. of XXVI; b. p. 70—110°C/2 mmHg. XXVI was treated with 2, 4-dinitrophenylhydrazine acidified with sulfuric acid. Bis-2, 4-dinitrophenylhydrazone was prepared and recrystallized from ethanol - ethyl acetate; m. p. 147°C.

Found: N, 19.81. Calcd. for $C_{23}H_{24}N_8O_{11}$: N, 19.04%.

*Department of Chemistry*
*Tokyo Kyoiku University*
*Otsuka, Tokyo*

# A Deuteron Magnetic Resonance Study of Urea-$d_4$

By Takehiko CHIBA

(Received July 27, 1964)

Urea is perhaps one of the few compounds whose crystal structure has been extensively investigated. Recent structure analyses of urea include a neutron diffraction study by Worsham, Levy and Peterson[1] and X-ray studies by Vaughan and Donohue,[2] and by Sklar, Senko and Post.[3] The last-named paper includes a study at $-140°C$. The temperature factors determined from these studies are anisotropic and quite large, especially for the nitrogen and hydrogen atoms. This is considered to be due to librational motion about one or more axes in urea. After the present work had been completed, another paper on the X-ay analysis of urea was published by Caron and Donohue.[4] These authors were able to derive mean amplitudes of the translational and librational motion from the temperature factors. On the other hand, from the proton magnetic resonance (PMR) linewidth transition centered at about 50°C, Kromhout and Moulton[5] deduced the setting-in of a free rotational motion of the $NH_2$ group about the C–N bond. In a more recent PMR investigation using a single crystal, Emsley and Smith[6] showed that the angular dependence of the second moment when the crystal is rotated about the c axis can be accounted for not by such a motion, but, instead, by a reorientation of the whole molecule about the C=O bond. They showed that the observed line shape is also consistent with the presence of a reorientation about the C=O axis, but that the line shape could not show whether or not a reorientation about the C–N bond is also present. Though their experimental evidence is quite convincing, the reorientational motion of a large molecule as a whole about the C=O axis seems rather unusual. Since deutron magnetic resonance (DMR) provides a powerful means for the study of the motion of a group with hydrogen atoms,[7] the present study was undertaken in the hope that new information could be obtained concerning both the molecular motion of urea and deuteron quadrupole coupling in amides which has not been observed so far.

1) J. E. Worsham, H. A. Levy and S. W. Peterson, *Acta Cryst.*, **10**, 319 (1957).
2) P. Vaughan and J. Donohue, ibid., **5**, 530 (1952).
3) N. Sklar, M. E. Senko and B. Post, ibid., **14**, 716 (1961).
4) A. Caron and J. Donohue, ibid., **17**, 544 (1964).
5) R. A. Kromhout and W. G. Moulton, *J. Chem. Phys.*, **23**, 1673 (1955).
6) J. W. Emsley and J. A. S. Smith, *Trans. Faraday Soc.*, **57**, 1233 (1961).
7) a) T. Chiba, *J. Chem. Phys.*, **36**, 1122 (1962); b) **39**, 947 (1963).

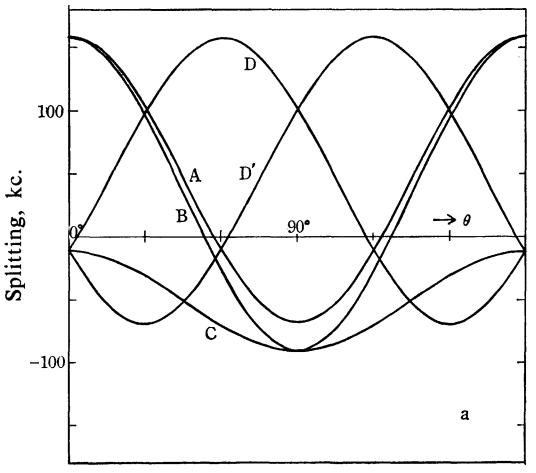



Fig. 1a.

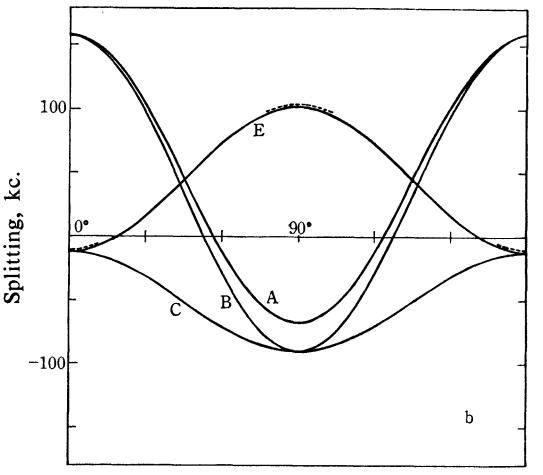



Fig. 1b.

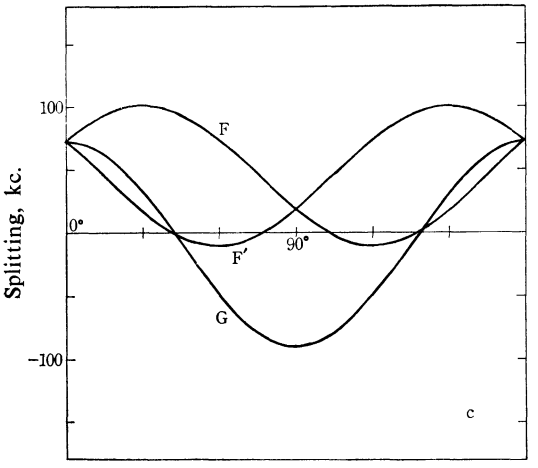



Fig. 1c.

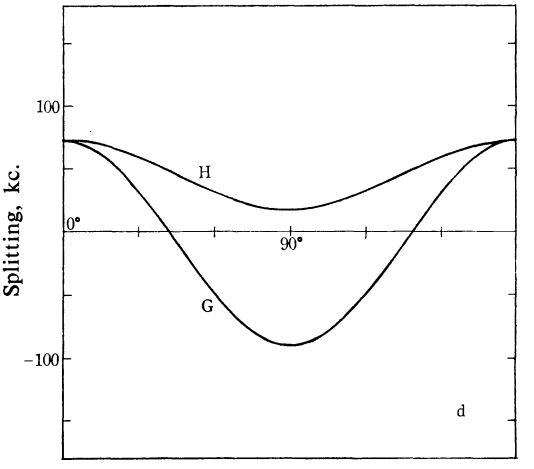



Fig. 1d.

Fig. 1. Calculated rotation patterns of the deuteron quadrupole splitting of urea-$d_4$ crystal assuming, (a) a stationary molecule, (b) a molecule reorienting about the C=O axis, (c) a molecule reorienting about C–N axis, (d) a molecule reorienting about the C=O and C–N axes, with $H_0$ in the (110) plane. $\theta$ is the angle between $H_0$ and the c-axis direction. The other member of the satellite pair, which is a mirror image of the one in this figure with respect to the zero-splitting, is not shown.

## Experimental

A single crystal of urea-$d_4$ was prepared by the gradual cooling of a saturated solution of urea-$d_4$ in methanol-d. Urea-$d_4$ was prepared by repeated evaporation of urea solution in heavy water. Methanol-d was prepared by refluxing dimethyl oxalate with potassium carbonate and heavy water,[8] followed by a fractionation. A small amount of deuterated ammonium bromide (a small percentage of the urea) was added to the solution to prevent the urea crystal from growing as long needles.[9]

The apparatus and the procedure of the measurement of DMR have been described elsewhere.[7] Measurements were made at the field strength of 16.6 kgauss.

## Results

**Observation at Room Temperatue.** — Urea crystallizes in a tetragonal form belonging to the space group $D_{2d}^3$–P$\bar{4}$ $2_1$m.[1] All urea molecules in the lattice are in equivalent positions. The planar molecule lies on a plane parallel either to (110) or to (1$\bar{1}$0). At room temperature, the spin-lattice relaxation time, $T_1$, is sufficiently short to give lines with good signal-to-noise ratio while at lower temperature

8) J. Beersmans and J. C. Jungers, *Bull. soc. chim. Belges.*, **56**, 81 (1947).
9) E. A. Andrew and D. Hyndman, *Discussions Faraday Soc.*, **19**, 195 (1955).

only poor signal is obtained because of a strong saturation, indicating a long $T_1$. The spectra are observed as a function of the angle of the crystal about the axis perpendicular to the applied dc field. DMR was first observed with the crystal rotated about the c axis. Since the crystal structure is simple, the angular dependence of quadrupole splitting lines could be easily interpreted by assuming a quadrupole tensor in each N–D bond direction, with a small asymmetry parameter. Approximate $eqQ$ and $\eta$ values derived in this way are then used to set up a rotation pattern of quadrupole splitting when the crystal is rotated in the [110] direction. All subsequent observations are made at this crystal orientation. The expected rotation pattern of the quadrupole splitting for the molecule (a) at rest, (b) reorienting about the C=O bond, (c) reorienting about the C–N bond, and (d) reorienting about both the C=O and C–N bonds, are shown in Fig. 1. The observed rotation pattern at room temperature agreed completely with Fig. 1(a), the stationary molecule. $eqQ$, and $\eta$ values and the principal axis directions of $q$-tensor are listed in Table I.

TABLE I. OBSERVED DEUTERON QUADRUPOLE COUPLING, ASYMMETRY PARAMETER AND PRINCIPAL-AXIS DIRECTIONS OF THE FIELD GRADIENT[a] IN UREA-$d_4$

Room temperature

$D_1$ $eqQ/h=210.8\pm1.0$ kc./sec, $\eta=0.139\pm0.010$.
$q_I$, 60.2° from [001] direction, in (110) plane (molecular plane), $q_{II}$ in [1$\bar{1}$0] direction, and $q_{III}$, 28.8° form [001] direction, in (110) plane.

$D_2$ $eqQ/h=210.7\pm1.0$ kc./sec., $\eta=0.146\pm0.010$.
$q_I$, in [001] direction, $q_{II}$ in [110] direction, and $q_{III}$ in [1$\bar{1}$0] direction.

117°C

$D_2$ $eqQ/h=206.3\pm1.2$ kc./sec., $\eta=0.138\pm0.010$.

a) $q_I$, $q_{II}$, $q_{III}$ are the principal components of a field gradient tensor such that $|q_I|>|q_{II}|>|q_{III}|$.

**Observation at Elevated Temperatures.** — As the temperature is raised, the lines D and D' except at $\theta=0°$ and 90°, where $\theta$ is the angle of the rotation of the crystal measured from its c axis parallel to $H_0$, disappear at about 36°C. (The signal of line D already manifests slight broadening at room temperature). Above 100°C the signal corresponding to line E of Fig. 1 (b) begins to appear near $\theta=0°$ and 90°, as is shown by the broken line in the figure, where the frequency separation between line D and line D' is small. This can be explained by the motion assumed in (b), namely, a reorientation about the C=O axis, but not by a free rotational motion. A further raising of the temperature (above 110°C), however, results in a collapse of the line E pattern, even at $\theta=0°$ or 90°, while the intensity and line-width of line C at $\theta=90°$ remains almost unchanged. This can be reasonably explained by assuming the onset of an additional reorientation about the C–N bond, since this motion, which interchanges $D_1$ and $D_2$, alters all the line patterns except the one at $\theta=90°$ of line C. Because of this behavior, the observations of the line-width change due to the reorientation about the C=O bond could only be made over a small range of temperature. Likewise, for the motion about the C–N bond, the behavior of the line-width transition could only be observed on the low temperature side, limited by its melting point of 135°C. The exchange rates derived from these observations, by the procedure described in a previous report,[7b] are shown in Fig. 2. These observations

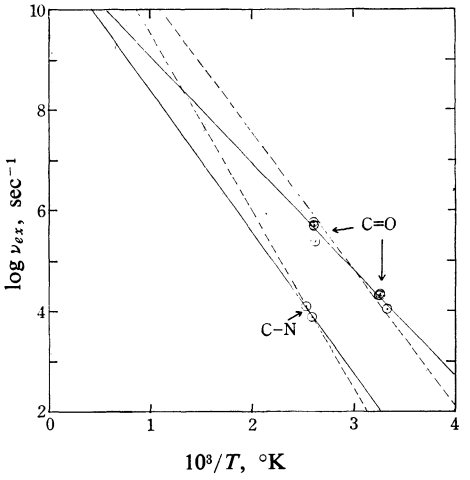



Fig. 2. Observed exchange rate with temperature, for reorientation about the C=O bond and that about the C–N bond. Solid lines are drawn assuming a frequency factor of $10^{11.1}$/sec. and broken line assuming that of $10^{13}$/sec.

are not sufficient for the accurate determination of the potential barriers. However, assuming a frequency factor of $10^{13}$, the order of magnitude often found in the case of hydration water, the barrier height is 12.5 kcal. and 16.1 kcal./mol. for the motion about C=O and for that about C–N respectively. Or, assuming frequency factor of $10^{11.1}$, which best fits the C=O reorientation data, 9.8 and 13.0 kcal./mol. are obtained for the two motions. Therefore, a reasonable estimate would be $11\pm2$ kcal./mol. for the motion about the C=O bond and $15\pm3$ kcal./mol. for that about the C–N bond.

The temperature dependence of the splitting frequency is examined for line A at $\theta=0°$ and

for line D (or E) at $\theta=90°$. The splitting frequency decreases about 3.5 kc. from 0°C to 100°C in the former case and about 2.5 kc. in the latter. $eqQ$ has also been determined for $D_2$ at 117°C, as is listed in Table I. The line structure due to dipolar coupling with the directly-bonded nitrogen atom is observable in some orientations. The three-line structure at $\theta=0°$ of line A or at $\theta=90°$ of line D, which are actually more complicated with the D–D coupling and possibly also with H–D coupling from incomplete deuteration, are observed. The structure becomes obscured at about 70—80°C and coalesces to a broad single peak at about 100°C.

## Discussion

The $eqQ$'s of $D_1$ and $D_2$ are almost identical, and they are close to that of $ND_3$ (200 kc.).[10] The $q_{II}$ direction (see footnote to Table I) is perpendicular to the $ND_2$ plane in accord with the rule observed in the XOD bond.[11] $eQ(q_{III}-q_{II})$ is about 30 kc., a similar magnitude to those found in the OD bond.[11] The direction of the $q_I$ of the $D_1$ deviates 1° from the N–D direction. The direction of the $q_I$ of the $D_2$ is found to be along the c axis, whereas the N–D direction determined by neutron diffraction deviates 3.4° from the c axis (Fig. 3). If the $q_I$ direction of the $D_2$ deviates only slightly from the c axis, the reorientational motion about the C=O bond of even a relatively slow exchange rate can average out the frequency splitting, resulting in an averaged $q_I$ along the c axis. To see if this is the case, an observation of the pattern at −20°C is made of lines A and C, where, judging from Fig. 2, the exchange rate must be about $10^3$/sec. or less. No additional splitting in these lines is found. Therefore, it may be concluded that the $q_I$ of $D_2$ is indeed along the c axis within the limit of 1°.

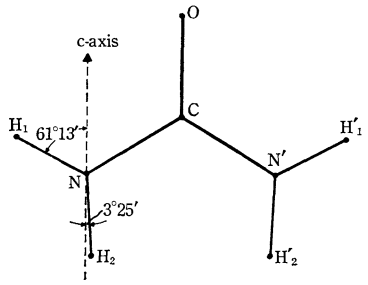



Fig. 3. Molecular structure of urea in the crystal (Ref. 1).

The reorientational motion about the C=O bond, as concluded from the temperature dependence of the line shape, is in agreement with the conclusion of the PMR study by Emsley and Smith. The estimated barrier height though not very accurate for the reason stated earlier, is in fair agreement with that estimated from the PMR, that is, 9 kcal.[6] If one urea molecule rotates 90° about the C=O bond, with all the neighboring molecules fixed, the closest-neighbor H–H distance will be 1.5 Å ($H_1$, $H_2'$) or 1.8 Å ($H_2$, $H_2'$) which is much less than the van der Waals' distance. Therefore, the motion is considered to be some sort of a correlated one which gears in neighboring molecucles as one molecule rotates. Since no phase transitions of the urea crystal in the temperature range of present interest has been reported, such correlated motion would involve a small number of molecules instead of the crystal as a whole. The potential barrier may be considered to be a sum of the hydrogen bond energy of N–D···O and the steric energy. The barrier arising from the hydrogen bond energy may not be greater than a few kcal., and the main origin of potential must be due to the steric effect. Therefore, we can expect a flatness of the potential at the bottom. We can also expect that the potential is somewhat dependent on the temperature, since the expansion of the lattice with the temperature is rather large.[3] The barrier of about 15 kcal./mol. to the motion about the C–N bond is mainly due to the partial double-bond character of the C–N bond. It should be noted that the present value is in fair agreement with the value of 12.24 kcal./mol. calculated by Das.[12]

The decrease in the splitting frequency from 0°C to 100°C for line D at $\theta=90°$ due to a simple torsional oscillation about the C=O bond, assuming that the potential curve $V=(V_0/2)\cdot(1-\cos 2\varphi)$, where $\varphi$ is the angle of the rotation of the molecule, with $V_0=11$ kcal./mol., is calculated to be 1.7 kc., which is in fair agreement with the observed decrease of 2.5 kc. The r. m. s. amplitude of oscillation about the C=O bond obtained by Caron and Donohue is 13.13°,[4] which, by harmonic oscillation approximation gives 3.3 kc. for this frequency decrease, or corresponds to a $V_0$ value of 5.8 kcal. for the $\cos 2\varphi$ type potential. Such an apparent low $V_0$ value seems to indicate the flatness of the potential curve at the bottom, as has been mentioned earlier The torsional oscillation about the C=O bond would not give the temperature dependence of the frequency of line A at $\theta=0°$. On the other hand,

10) G. Herrmann, *J. Chem. Phys.*, **29**, 875 (1958).
11) T. Chiba, ibid., **41**, 1352 (1964).
12) T. P. Das, ibid., **35**, 1897 (1961).

that about the C–N bond can give rise to this frequency change, assuming that the $V_0$ of 15 kcal./mol. amounts to only 0.7 kc. from 0°C to 100°C. Caron and Donohue obtained a mean amplitude for the oscillation about the axis parallel to N–N' of 6.08°, which can give rise to 0.9 kc. for the corresponding frequency decrease. Therefore, these effects can explain only half of the observed value of 3.5 kc. The reason for this is not clear.

The collapse of the line structure due to the dipolar coupling between N and D at 70—80°C is consistent with the PMR findings,[6] that is, at temperatures above the line-width transition the proton second moment indicates no coupling between N and H. The temperature at which N–D coupling disappears is considerably higher than the temperature at which the $^{14}N$ pure quadrupole line disappears.[13] A similar situation in PMR has been already pointed out and discussed by Emsley and Smith, who presented some mechanisms which possibly account for the situation. The vanishing of the $^{14}N$ line at about 22°C is likely to be associated with the reorientation about the C=O bond, as these authors point out. The effect on the $^{14}N$ PQR frequency of this motion can be estimated as follows. The direction of the field gradient tensor at N in urea are not known, but we can reasonably assume that the $q_I$ is perpendicular to the molecular plane and that the $q_{II}$ is along the C–N bond. The reorientation about the C=O bond does not change the $q_I$ provided that the time during the flip is sufficiently short. However, this motion changes the $q_{II}$ and $q_{III}$ directions, and $\eta$ decreases from the 0.32[14] of the stationary molecule to 0.16 in the limit of rapid reorientation. The corresponding change in PQR frequency will be 0.14 Mc. This is of the same order with the corresponding frequency change in the D resonance line due to this motion. The difficulty lies in determining why the $^{14}N$ line should vanish at a temperature more than 10°C below that where the D resonance line vanishes. It is clear this is not due to a $T_1$ broadening of $^{14}N$ because N–D coupling is observable at higher temperatures. The reason is not well understood. However, it can be said that since the absolute magnitude of $^{14}N$ quadrupole coupling is much larger (3.5 Mc.)[14] than that of D, the fluctuation of the field gradient due to the motion may be more effective in broadening the $^{14}N$ line.

13) T. Chiba, M. Toyama and Y. Morino, *J. Phys. Soc. Japan*, **14**, 379 (1959).

14) M. Minematsu, ibid, **14**, 1030 (1959).

## Summary

A deuteron magnetic resonance study has been made on a single crystal of urea-$d_4$. At room temperature deuteron quadrupole coupling corresponding to a stationary molecule is obtained. The $eqQ$ and $\eta$ values determined are: $eqQ/h=210.8\pm1.0$ kc./sec. and $\eta=0.139\pm0.010$ for $D_1$, and $eqQ/h=210.7\pm1.0$ kc./sec. and $\eta=0.146\pm0.010$ for $D_2$ at room temperature, and $eqQ/h=206.3\pm1.2$ kc./sec., $\eta=0.138\pm0.010$ for $D_2$ at 117°C. In both cases the maximum field gradient component and the N–H direction are in good agreement.

The onset of reorientational motion about the C=O bond of a whole molecule has been concluded from the line-width change at high temperatures. Above 110°C the effect on the line-width of the reorientation about C–N bond has also been observed. The barrier heights for these motions are estimated to be $11\pm2$ kcal./mol. for the reorientation about the C=O bond and $15\pm3$ kcal./mol. for that about the C–N bond. The temperature dependence of the quadrupole splitting and that of the dipole coupling between $^{14}N$ and D have been observed and dicussed in relation to the motion of the urea molecule.

The author wishes to thank Professor Yoshinobu Kakiuchi for reading the manuscript and for his helpful discussions.

*The Institute for Solid State Physics*
*The University of Tokyo*
*Azabu, Tokyo*

# Absorptinon Spectra of Dyes. VIII.[1] The Correlation between Thermodynamic Quantities and Chemical Structure in Complex Formation*

By Yoshié TANIZAKI, Toshihiko HOSHI and Noboru ANDO

(Received July 27, 1964)

Previously,[1] the present authors have discussed the ease of the formation of complexes between Chrysophenine G and Chlorazol Sky Blue FF and similar skeletal dyes, from the viewpoints of the magnitudes of the equilibrium constant and of the spectral change. According to the conclusion reached, the partner dyes (to be abbreviated to P) of G (Chrysophenine G) have a negative effect on the complex formation when the P dyes have sulfonic groups at the positions adjacent to azo groups on the naphthalene rings. Further, the larger the number of effective auxochromes of P, the easier the formation of the complex, and the OH groups make the complex formation easier than $NH_2$ does. The above problem may be worth considering from the view-points of the strength of the connection between the component molecules forming a complex, and of the degree of the steric deformation and the restriction inflicted upon the molecule before and after the formation of a complex. Therefore, with the purpose of discussing again the above conclusion on a more rigid foundation, the authors measured a similar sample series at various temperatures. According to the free energy change, enthalpy change and entropy change thus obtained, the above-mentioned problem will be discussed for a 1 : 1 and a 1 : 2 complex formed between P and G.

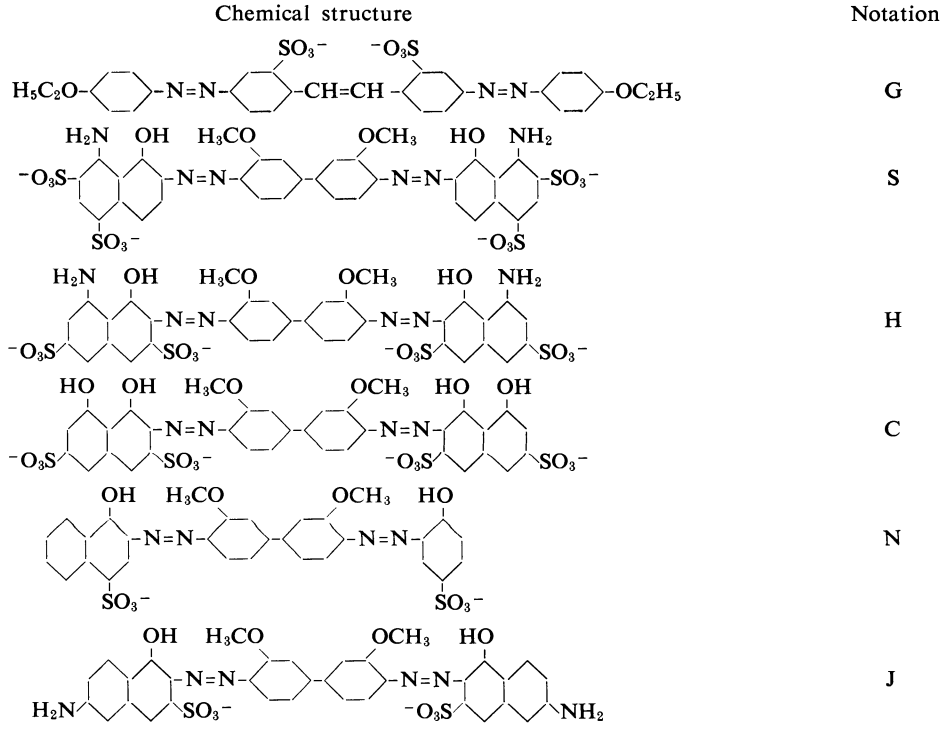



Fig. 1. Chemical structures and their notations.

* Presented at the 15th Annual Meeting (April, 1962) and at the Chūgoku-Shikoku Meeting (August, 1962) of the Chemical Society of Japan.

1) Part VII of this series: T. Kobayashi, K. Saito, Y. Tanizaki and N. Ando, This Bulletin, 35, 935 (1962).

## Experimental

The chemical structures of the dyes used are shown in Fig. 1, along with the notations to be used here. Excepting G (Chrysophenine G), the notations are taken from the names of the coupling components. These are the same as the purified dyes used in the previous investigations.[1,2]

Water was used as the solvent. The dye solutions were prepared by using a mother solution of about $10^{-4}$ mol./l. All of the concentrations were determined by weight.

The absorption spectra were measured with a Shimadzu QR-50 spectrophotometer, the cell chamber of which was replaced by a larger one which contains cylindrical cells. The temperature of the cells was regulated by a specially-designed apparatus, and so could be kept within ±0.2°C of the desired temperature. The optical path of the cell is 20 mm. long, but it can be used, if necessary, as a 10 mm. path cell by the insertion of spacers.

At each 10°C interval in the 20—60°C temperature range, the absorption spectra of the sample solutions were measured after they had been kept intact more than overnight after having been prepared. It has been confirmed that the temperature of the solution reaches the adjusted point within twenty minutes. All the measurements, therefore, were standardized so as to be started about twenty

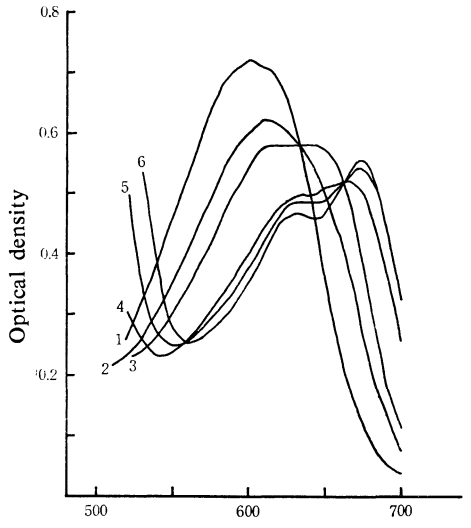



Fig. 2. Absorption spectra of C-G aqueous solutions: temp., 20°C; cell, 1 cm.

| | G, mol./l. | C, mol./l. |
|---|---|---|
| 1 | 0 | $9.293\times10^{-6}$ |
| 2 | $4.375\times10^{-6}$ | $9.293\times10^{-6}$ |
| 3 | $9.007\times10^{-6}$ | $9.293\times10^{-6}$ |
| 4 | $71.81\times10^{-6}$ | $9.293\times10^{-6}$ |
| 5 | $180.6\times10^{-6}$ | $9.293\times10^{-6}$ |
| 6 | $718.7\times10^{-6}$ | $9.293\times10^{-6}$ |

2) T. Kobayashi, Y. Tanizaki and N. Ando, This Bulletin, 33, 913 (1960).

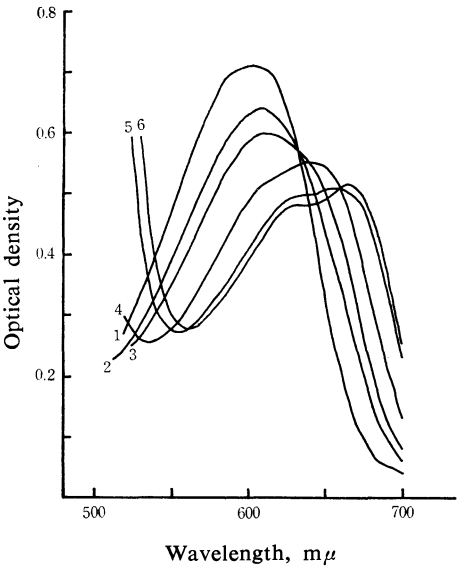



Fig. 3. Absorption spectra of G-C aqueous solutions: temp., 40°C; cell, 1 cm.

| | G, mol./l. | C, mol./l. |
|---|---|---|
| 1 | 0 | $9.293\times10^{-6}$ |
| 2 | $4.375\times10^{-6}$ | $9.293\times10^{-6}$ |
| 3 | $9.007\times10^{-6}$ | $9.293\times10^{-6}$ |
| 4 | $71.81\times10^{-6}$ | $9.293\times10^{-6}$ |
| 5 | $360.6\times10^{-6}$ | $9.293\times10^{-6}$ |
| 6 | $718.8\times10^{-6}$ | $9.293\times10^{-6}$ |

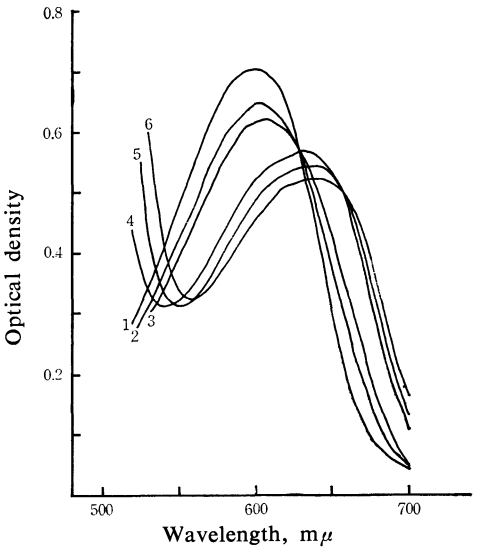



Fig. 4. Absorption spectra of G-C aqueous solutions: temp., 60°C; cell, 1 cm.

| | G, mol./l. | C, mol./l. |
|---|---|---|
| 1 | 0 | $9.293\times10^{-6}$ |
| 2 | $9.007\times10^{-6}$ | $9.293\times10^{-6}$ |
| 3 | $17.72\times10^{-6}$ | $9.293\times10^{-6}$ |
| 4 | $180.6\times10^{-6}$ | $9.293\times10^{-6}$ |
| 5 | $360.7\times10^{-6}$ | $9.293\times10^{-6}$ |
| 6 | $718.8\times10^{-6}$ | $9.293\times10^{-6}$ |

minutes after the solution had been kept at a constant temperature.

## Results

Figures 2, 3 and 4 indicate the spectral change of the binary mixture of C and G when the concentration of C is varied, at 20, 40 and 60°C respectively. In every case well-defined isosbestic points exist at about 630 mμ and 660 mμ. The same tendency for the spectra to change was also found for the S-G system, and the appearance was the same as in the result already reported (ca. 27°C).[2] As has already been shown,[1] the first isosbestic points (ca. 630 mμ) of Figs. 2—4 indicate the co-existence of G and CG (1 : 1 complex), and the second, that of G and $CG_2$ (1 : 2). A quite similar tendency was observed for the binary mixture of G with any other dyes used. It is a matter of course, however, that the shapes of the individual bands and positions of the isosbestic points, etc., differed from one another according to the kinds of partner dyes.

Let P stand for the partner dye of G. If the following equilibriums exist for the 1 : 1 and 1 : 2 complex formation between P and G;

$$P + G = PG \qquad (K_1) \qquad (1)$$

$$PG + G = PG_2 \qquad (K_2) \qquad (2)$$

and if the mass action law can be applied, the respective equilibrium constants are expressed as follows;

$$K_1 = [PG]/[P][G] \qquad (3)$$

$$K_2 = [PG_2]/[PG][G] \qquad (4)$$

where [P], [G], etc. represent the respective equilibrium concentrations. $K_1$ and $K_2$ were calculated following the method described in the Appendix. The data are shown in Tables I and II respectively. In the usual way, the free energy change ($-\Delta F$) was obtained from the values of $K_1$ and $K_2$ shown in Tables I and II. The results obtained are given in Tables III and IV respectively. The relation between $\ln K$ and $1/T$ ($T$: absolute temperature) was plotted in Figs. 5 and 6. By the application of the method of least squares,

TABLE I. EQUILIBRIUM CONSTANTS FOR THE 1 : 1 COMPLEX FORMATIONS AT VARIOUS TEMPERATURES

| | $K_1\times10^{-5}$, $mol^{-1}l$. | | | | |
|---|---|---|---|---|---|
| P | 20°C | 30°C | 40°C | 50°C | 60°C |
| S | 600 | 210 | 61 | 14 | 5.3 |
| H | 35 | 7.0 | 1.8 | 0.58 | 0.18 |
| C | — | 50 | 7.0 | 2.4 | 0.77 |
| N | 5.3 | 4.4 | 2.3 | 1.7 | 1.1 |
| J | — | 1.4 | 0.73 | 0.32 | 0.22 |

TABLE II. EQUILIBRIUM CONSTANTS FOR THE 1 : 2 COMPLEX FORMATIONS AT VARIOUS TEMPERATURES

| | $K_2\times10^{-5}$, $mol^{-1}l$. | | | | |
|---|---|---|---|---|---|
| P | 20°C | 30°C | 40°C | 50°C | 60°C |
| S | 2.8 | 1.0 | 0.29 | 0.12 | — |
| H | 0.048 | 0.022 | 0.0067 | 0.0025 | — |
| C | 0.31 | 0.12 | — | — | — |
| N | 0.80 | 0.65 | 0.36 | — | — |
| J | — | 0.031 | 0.020 | 0.0086 | 0.0070 |

TABLE III. FREE ENERGY-, ENTHALPY- AND ENTROPY- CHANGES FOR THE 1 : 1 COMPLEX FORMATIONS

| | $-\Delta F_1$, kcal./mol. | | | | | $-\Delta H_1$ kcal./mol. | $-\Delta S_1$ e. u. |
|---|---|---|---|---|---|---|---|
| P | 20°C | 30°C | 40°C | 50°C | 60°C | | |
| S | 10.4 | 10.1 | 9.7 | 9.1 | 8.7 | 24 | 44 |
| H | 8.8 | 8.1 | 7.5 | 7.0 | 6.5 | 25 | 57 |
| C | — | 9.3 | 8.4 | 7.9 | 7.4 | 27 | 60 |
| N | 7.7 | 7.7 | 7.7 | 7.7 | 7.7 | 7.4 | −1 |
| J | — | 7.1 | 7.0 | 6.7 | 6.6 | 13 | 19 |

TABLE IV. FREE ENERGY-, ENTHALPY- AND ENTROPY-CHANGES FOR THE 1 : 2 COMPLEX FORMATIONS

| | $-\Delta F_2$, kcal./mol. | | | | | $-\Delta H_2$ kcal./mol. | $-\Delta S_2$ e. u. |
|---|---|---|---|---|---|---|---|
| P | 20°C | 30°C | 40°C | 50°C | 60°C | | |
| S | 7.3 | 6.9 | 6.4 | 6.0 | — | 20 | 45 |
| H | 4.9 | 4.6 | 4.1 | 3.6 | — | 19 | 47 |
| C | 6.0 | 5.7 | — | — | — | 19 | 40 |
| N | 6.6 | 6.7 | 6.5 | — | — | 6.7 | 0 |
| J | — | 4.9 | 4.7 | 4.3 | 4.3 | 11 | 20 |

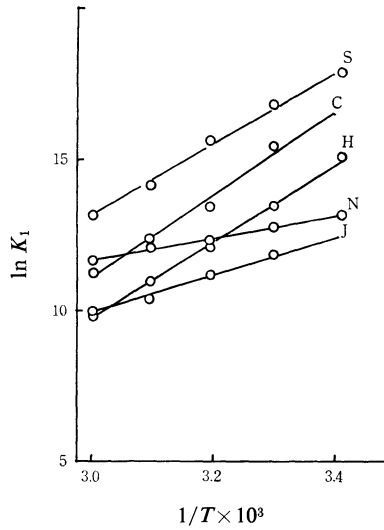



Fig. 5. Plots of $\ln K_1$ vs. $1/T$ for the 1 : 1 P-G molecular complex formations.

regarding the relation as linear, we obtained the enthalpy change ($-\Delta H$) and the entropy change ($-\Delta S$) from, respectively, the values

of the slope and the intercept of the straight line and the $\ln K$ axis. The results for a 1 : 1 and a 1 : 2 complex are shown in the corresponding columns of Tables III and IV respectively.

## Discussion

**The Free Energy Change.**—A criterion of the facility of the complex formation in the system under consideration has already been made by means of the magnitude of the equilibrium constant[1] in the relationship $-\Delta F=RT \ln K$. As the free energy change is combined with the equilibrium constant, $-\Delta F$ as well as $K$ can be adopted as a measure of the criterion of the complex formation. In this paper, the discussion will be made in terms of $-\Delta F$.

The plotting of the $-\Delta F$ values against the temperature in Tables III and IV gives the

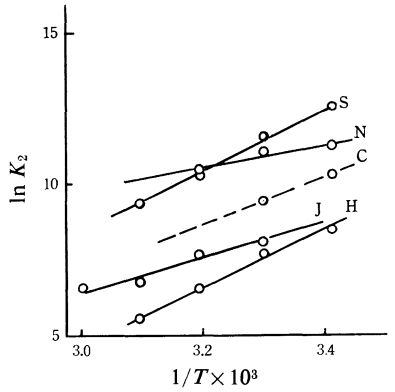



Fig. 6. Plots of $\ln K_2$ vs. $1/T$ for the 1 : 2 P-G molecular complex formations.

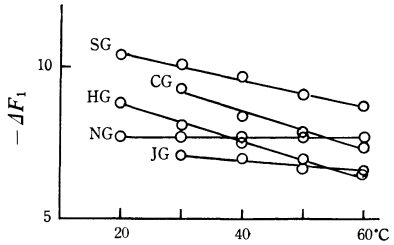



Fig. 7. Relation of $-\Delta F$ vs. temperature.

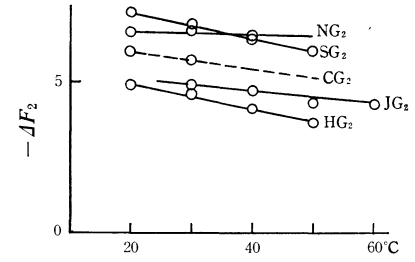



Fig. 8. Relation of $-\Delta F$ vs. temperature.

relations shown in Figs. 7 and 8 respectively. In each case the relation is regarded as linear. According to Fig. 7 the inclinations of lines of S, C and H are large in about the same order, while those of N and J are nearly horizontal. By comparing the chemical structures of these two classes shown in Fig. 1, it may be seen that S, C and H each has four sulfonic groups and two effective auxochromes, while the class of N and J has only two sulfonic groups and two effective terminal auxochromes.[1] It seems that there is some correlation between this fact and the behavior of the $-\Delta F$ value against the temperature.

There are also the following differences among the dyes of the respective classes. The magnitudes of the $-\Delta F$ values at any temperature are in the order of S, C and H (Fig. 7), and the difference in the chemical structures may be seen in the location of the sulfonic group and the sort of auxochrome. The facility of the 1 : 1 complex formation had already been discussed in terms of the difference in chemical structure.[1] Moreover, the conclusion derived from the discussion comes into existence over the temperature range observed here. Again, the relation between the difference of the $-\Delta F$ values of N and J and the positions of the sulfonic groups may be interpreted in terms of conclusion mentioned above.

It is clear from an inspection of Fig. 8 that there is also approximately the same relationship as above in the case of the 1 : 2 complex formation.

The so-called standard affinity ($-\Delta\mu^\circ$) has been used extensively as a measure of the substantivity of dyes. However, $-\Delta\mu^\circ$ and $-\Delta F$ are identical in physical meaning. The expression of $-\Delta\mu^\circ$ involves a quantity which represents a surface volume in the substrate.[3] This can be regarded as a parameter for matching the dimensions of the dye concentrations in both phases of the solution and in the substrate of cellulose. However, it is not always easy to estimate the surface volume. In any case, Table V illustrates the affinity values of S (Chlorazol Sky Blue FF) and G (Chrysophenine G) quoted from those obtained for various cellulose-substrates. If the relation of $-\Delta\mu^\circ$ and temperature is plotted using the

Table V. Standard affinities ($-\Delta\mu^\circ$, cal./mol.) and heats of dyeing ($-\Delta H^\circ$, kcal./mol.)

| D | 60°C | 70°C | 80°C | 90°C | 100°C | $-\Delta H^\circ$ |
|---|---|---|---|---|---|---|
| S | 7500 | 6600 | 6300 | 6100 | 5900 | 22 |
| G | 3800 | 3400 | 3200 | 3000 | 2600 | 14 |

3) T. Vickerstaff, "The Physical Chemistry of Dyeing," 2nd Ed., Oliver and Boyd, London (1954), p. 195.

values in Table V, a tendency similar to that of Fig. 7 will be obtained. The heat of the dyeing ($-\Delta H°$) of S and G are, respectively, 22 and 14 kcal. (Table V). The values for many other direct dyes are also in the same order and correspond to the magnitude of $-\Delta H$ in Tables III and IV. Accordingly, the relative order of substantivity can be compared by the use of $-\Delta F$ values for the complex formation or by the use of $-\Delta H$ values, without using the standard affinity involving various problems.

**The Enthalpy Change.**—The magnitudes of the enthalpy change for the class of S, C, and H, and the class of N and J, classified in the foregoing section apparently differ from each other, as may be seen from Tables III and IV. According to the comparison of the mean values for the respective classes, the $-\Delta H_1$ and $-\Delta H_2$ values for the former class are 2—2.5 times as large as those for the latter. As is well known, the dyeing mechanism of direct dyes believed in at the present time involves mainly the formations of the hydrogen bond and the dispersion force. The magnitude of the dispersion force is considered to be dependent upon the extension of the electron cloud on the faced molecules, namely, in this case the dimensions of the confronted molecular surface. However, such a difference may not be so large with regard to the partner dyes used here. In the meanwhile, the formation of the intermolecular hydrogen bond in the complex under consideration is impossible in the usual way. However, if the auxochromes contribute to the complex formation in some way other than hydrogen bonding, the fact that the class of S, C and H has twice as many auxochromes as the class of N and J corresponds well with the fact that the former class produces an 2—2.5 times as much energy of formation as the latter. In this case, therefore, it is considered that the lone paired electrons on the functional group (auxochrome) play an important role in forming the complex.

The only difference in the chemical structures of C and H is that the OH groups are the auxochromes for the former, while the $NH_2$ groups are for the latter in the same positions. For that reason, the bonding energies should be compared with respect to the distinction of the auxochromes. Unfortunately, however, no conclusion could be obtained for the subject just mentioned because of the small number of proper samples used in the the present experiment.

**The Entropy Change.**—By the use of the entropy change, the degree of the restriction of the partner dye in the complex formation will be compared, and also the deformation of the sterical structure will be discussed. It is a matter of course that the G molecule undergoes a similar change through a complex formation, but the degree of change should be correlated with that of the partner dye. Because G is the common ingredient, it is possible to regard the apparent entropy change as a relative measure of the entropy change of the partner dye itself. The magnitudes of the $-\Delta S$ values in Tables III and IV are divided again into the class of S, C, and H and the class of N and J. The magnitudes of the former class are much larger than those of the latter. This fact may be interpreted as due to the following reason. As has been described above, all of the former, which have twice as many functional groups as the latter, can form a more compact complex, so the component in a complex undergoes the stronger restriction. The freedom is decreased, therefore, and $-\Delta S$ is necessarily increased. Among the classes of S, C and H, S and H differ from each other only in the attached positions of the sulfonic groups, while C and H differ only in the kinds of functional groups (Fig. 1). As for the $-\Delta S_1$ value for a 1 : 1 complex, in Table III the value for S is about 44 e. u. while those of C and H are, respectively, about 57 e.u. and 60 e.u. which are regarded as nearly equal and are considerably larger than that of S. This great difference must be due to the location of the sulfonic groups. The same situation is found in N and J. In the case of a 1 : 2 complex (Table IV), the same relationship can be seen if the result of C which was based on only two experimental values ($-\Delta F_2$) is excluded because of its weak support.

The sulfonic groups of J and those in the inner position of C and H (see Fig. 1) make the plane of the naphthalene nuclei deviate largely from the molecular plane.[2] Accordingly, if it is assumed that all the partner dyes take a similar sterical configuration in the complex state, the above-mentioned difference in $-\Delta S_1$ suggests that partner molecule is more planar in the 1 : 1 complex state than in the free state. This is because a larger deformation is required for C and H than for S to be brought to the similar planar structure. The same thing can be said for the case of N and J.

It may be noticed in Tables III and IV that the $-\Delta S$ values for N are nearly zero through the formation of a 1 : 1 and 1 : 2 complex. In the foregoing discussion solvation has not been taken into account. The effect of solvation should be included naturally in the $-\Delta S$ (and $-\Delta H$) values obtained here. Therefore, the fact that the absolute entropy in the N-G

system is not changed by the complex formation might suggest that, in the course of the complex formation, the solvent molecules which lie between G and N are removed, and that the intermolecular force between G and N formed instead of the hydration restricts the system to the same degree as the hydrated state.

## Summary

1) Using five kinds of dyes of Sky Blue FF and of similar structures, the equilibrium constants for a 1 : 1 and a 1 : 2 complex formed with Chrysophenine G have been determined by means of spectroscopy in the intervals of 20—60°C.

2) A new method of calculating the equilibrium constant has been proposed.

3) The free energy change ($-\Delta F$), the enthalpy change ($-\Delta H$) and the entropy change ($-\Delta S$) for the complex formation have been obtained.

4) The correlation between these quantities and the chemical structure has been discussed and the following facts clarified: The larger the number of effective auxochromes ($NH_2$, OH), the greater $-\Delta H$ and $-\Delta S$ become. The sulfonic group contributes to $-\Delta S$ through the location of that group. The dye molecule in the complex state is more planar than in the free state.

This work was supported in part by a Scientific Research Grant of the Ministry of Education (405108, 405119, 405143), to which the authors' thanks are due.

*Laboratory of Physical Chemistry*
*Tokyo Institute of Technology*
*Ookayama, Tokyo*

## Appendix

As the method of determining the equilibrium constant by utilizing the change in spectra, the Benesi-Hildebrand method[4] has been applied most extensively. Various other methods are also known. In the case of the present investigation, however, the equilibrium constants can be evaluated easily and precisely by utilizing the two isosbestic points, and by following the treatment described below.

When P, G, PG and $PG_2$ species are in equilibrium and the respective absorption coefficients are $\varepsilon_P$, $\varepsilon_G$, etc. at any wavelength, the optical density, $D$, of the system is expressed as follows:

$$D=[P]\varepsilon_P+[G]\varepsilon_G+[PG]\varepsilon_{PG}+[PG_2]\varepsilon_{PG2} \quad (5)$$

Two isosbestic points appear for the system under consideration. In the wavelength region at which the component G does not absorb light, $\varepsilon_G$ is zero. In this region, and yet in the concentration range in which the first isosbestic point is kept, $[PG_2]=0$; hence, Eq. 5 is simplified to Eq. 6:

$$D=[P]\varepsilon_P+[PG]\varepsilon_{PG} \quad (6)$$

Expressing the initial concentration by $P_0$, the optical density ($D_0$) before G is added is:

$$D_0=P_0\varepsilon_P \quad (7)$$

Hence, we obtain from Eqs. 6 and 7:

$$\Delta D=D_0-D=(P_0-[P])\varepsilon_P-[PG]\varepsilon_{PG}$$
$$=[PG](\varepsilon_P-\varepsilon_{PG})$$

or
$$\Delta D=\varepsilon_1[PG] \quad (8)$$

were $\varepsilon_P-\varepsilon_{PG}=\varepsilon_1$. From Eqs. 3 and 8, therefore, the equilibrium constant, $K_1$, becomes:

$$K_1=\Delta D/\varepsilon_1(P_0-\Delta D/\varepsilon_1)(G_0-\Delta D/\varepsilon_1) \quad (3')$$

where $P_0$ and $G_0$ stand for the respective initial concentrations of P and G.

Next, in the concentration range in which the second isosbestic point is kept, $[P]=0$ because all of the species must be completely changed to the complexes. Therefore, Eq. 5 becomes:

$$D=[PG]\varepsilon_{PG}+[PG_2]\varepsilon_{PG2} \quad (6')$$

By putting $D_0'$ as the optical density for the initial concentration of the PG component corresponding to Eq. 2, and by taking into account the fact that the difference between that initial concentration and [PG] is $[PG_2]$, we obtain the following equation, corresponding to Eq. 8:

$$\Delta D'=D_0'-D=[PG_2](\varepsilon_{PG}-\varepsilon_{PG_2})$$

or
$$\Delta D'=\varepsilon_2[PG_2] \quad (8')$$

where $\varepsilon_2=\varepsilon_{PG}-\varepsilon_{PG2}$. The equilibrium constant, $K_2$, for Eq. 4 may then be expressed as follows:

$$K_2=\Delta D'/\varepsilon_2(P_0-\Delta D'/\varepsilon_2)(G_0-P_0-\Delta D'/\varepsilon_2) \quad (4')$$

Now, when $K_1$ and $K_2$ are evaluated according to Eqs. 3' and 4', the question arises of how $\varepsilon_1$ and $\varepsilon_2$ are determined. This problem can be solved simply by utilizing the isosbestic points as described below. At first, the second isosbestic point (a letter II will be affixed to indicate the position of that wavelength) is noticed in order to determine $\varepsilon_1$. Thus, Eq. 6' holds for the optical density, and besides $\varepsilon^{II}_{PG}=\varepsilon^{II}_{PG2}$; therefore,

$$D^{II}=([PG]+[PG_2])\varepsilon^{II}_{PG} \quad (9)$$

Taking into account that $([PG]+[PG_2])=P_0$ is true in the concentration range where the second isosbestic point is kept, Eq. 9 may be rewritten as Eq. 10;

$$\varepsilon^{II}_{PG}=D^{II}/P_0 \quad (10)$$

On the other hand, as $\varepsilon^{II}_P$ is obtained directly by Eq. 7, $\varepsilon^{II}_P-\varepsilon^{II}_{PG}=\varepsilon^{II}_1$ is determined. Consequently, by substituting $\varepsilon^{II}_1$ and the density-difference $\Delta D^{II}$ at the wavelength of the second isosbestic point, respectively, into $\varepsilon_1$ and $\Delta D$ of Eq. 3', $K_1$ may be evaluated. Similarly, $K_2$ can be calculated by utilizing the first isosbestic point. That is to say, in this case, Eq. 6 holds, $\varepsilon^{I}_P=\varepsilon^{I}_{PG}$, and $([P]+[PG])=P_0$, so that the relation $\varepsilon^{I}_{PG}=D^{I}/P_0$ is derived. On the other hand, with the condition $P_0 \ll G_0$, $\varepsilon^{I}_{PG2}$

4) H. A. Benesi and J. H. Hildebrand, *J. Am. Chem. Soc.*, 71, 2703 (1949).

can be determined as the quotient of the optical density, $D^{I}$, at the wavelength of the first isosbestic point divided by $P_0$. From Eq. 4', $K_2$ can be calculated by using the $\varepsilon^{I}_{2}$ ($=\varepsilon^{I}_{PG}-\varepsilon^{I}_{PG2}$) value thus obtained and the density-difference, $\Delta D^{I}$, at the same wavelength.

# The Rotatory Dispersion and Stereochemistry of Organic Compounds. VII.[1] Monosulfides and Disulfides Derived from Glucose and Glucosamine

By Yojiro TSUZUKI, Koko TANABE, Masuo AKAGI and Setsuzo TEJIMA

(Received July 27, 1964)

In previous papers[1-3] the rotatory dispersion (RD) and stereochemistry of sugar xanthates have been studied, and it has been shown that the Cotton effect is due to the weak absorption band of the $-S-\overset{S}{\overset{\|}{C}}-$ group.

The present paper deals with the studies made of some monosulfides as well as disulfides containing an -S-S- group with the object of investigating the rotatory contribution of the sulfur atoms.

Since it has often been observed[4-7] that optically active disulfides in general are characterized by anomalously large rotations, it appears that it would be particularly interesting to investigate, by means of RD, how the -S-S- group contributes to the optical activity of the disulfides newly synthesized from D-glucose and D-glucosamine.

The following compounds will be investigated:

Bis(2-acetamido-2-deoxy-β-D-glucopyranosyl)-sulfide (compound I),

Bis(2-acetamido-2-deoxy-3, 4, 6-tri-*O*-acetyl-β-D-glucopyranosyl)sulfide (compound II),

Bis(2-acetamido-2-deoxy-β-D-glucopyranosyl)-D-disulfide (compound III),

1, 6-Anhydro-1, 6-sulfide-2, 3, 4-tri-*O*-acetyl-β-glucopyranose (compound IV),

Bis(2, 3, 4, 6-tetra-*O*-acetyl-β-D-glucopyranosyl) sulfide (compound V),

Bis(2, 3, 4, 6-tetra-*O*-acetyl-β-D-glucopyranosyl) disulfide (compound VI).

## Results and Discussion

The structural formulas of compounds I—VI and their molecular rotations (of the D-line) are shown in Fig. 1.

The RD curves of the glucosamine derivatives (compounds I, II and III) are shown in Fig. 2, and those of the glucose derivatives (IV, V and VI) in Fig. 3. The ultraviolet absorption curves of compounds I—VI are shown in Fig. 4.

As may be seen in Fig. 2 and Fig. 3, they

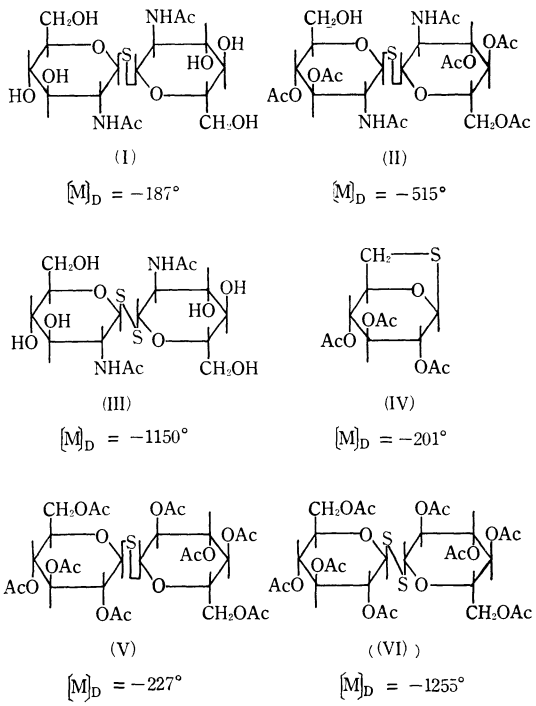



*Fig. 1. Structural formulas and [M]D.*
Ac=COCH3

1) Part VI: Y. Tsuzuki, K. Tanaka, K. Tanabe, M. Akagi and S. Tejima, This Bulletin, 37, 730 (1964).
2) Y. Tsuzuki, K. Tanaka and K. Tanabe, ibid., 35, 1614 (1962).
3) Y. Tsuzuki, K. Tanabe, M. Akagi and S. Tejima, ibid., 37, 162 (1964).
4) W. J. Kauzmann and H. Eyring, *J. Chem. Phys.*, 9, 41 (1941).
5) L. F. Fieser, *Rec. trav. chim.*, 69, 410 (1950).
6) A. Fredga, *Acta Chem. Scand.*, 4, 1307 (1950).
7) C. Djerassi, A. Fredga and B. Sjöberg, ibid., 15, 417 (1961).

all exhibit negative, plain, rotatory dispersion curves, since in the measured wavelength region (from 265 mμ to 700 mμ) these compounds have no optically active absorption bands.

As is evident from Fig. 4, the monosulfides **I**, II and V show no absorption maxima in the measured wavelength region (from 225 mμ to 340 mμ), in accordance with the observations that dialkyl sulfides exhibit strong absorption bands ($\log \varepsilon \sim 3$) only below 210 mμ.[8] Even these "monothiodisaccharides" may be expected to have optically active absorption bands at a shorter wavelength region when we reflect upon the situation described above as well as the detailed considerations[9,10] of the ultraviolet absorption spectra of various sulfides. However, it is natural that the RD curves of I, II and V are plain in the measured wavelength region.

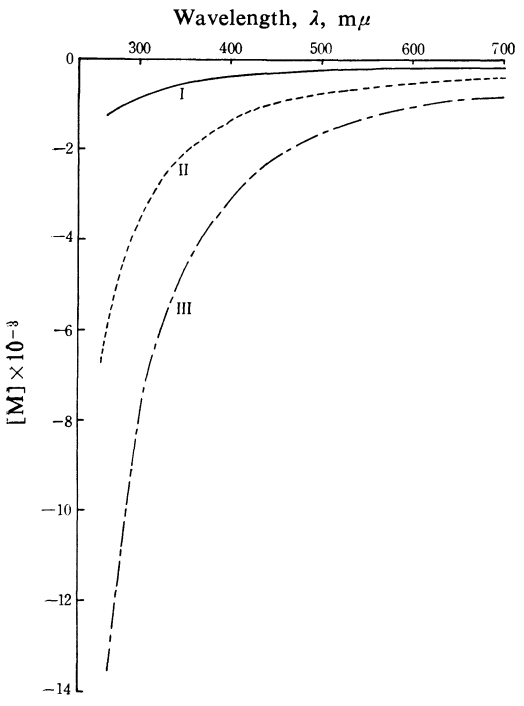



Fig. 2. RD of I—III.

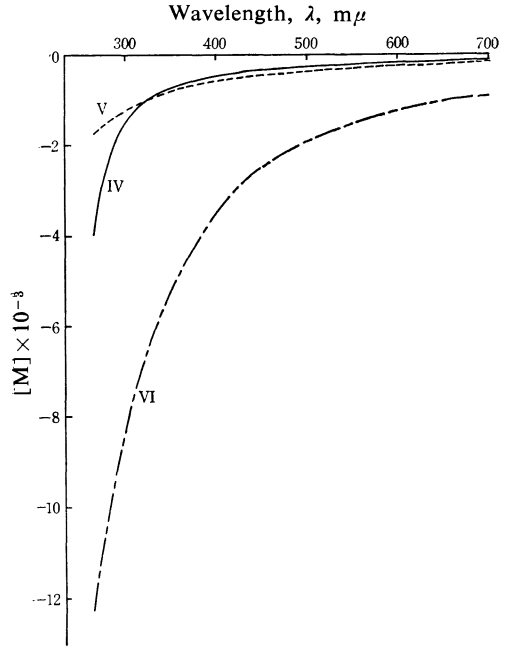



Fig. 3. RD of IV—VI.

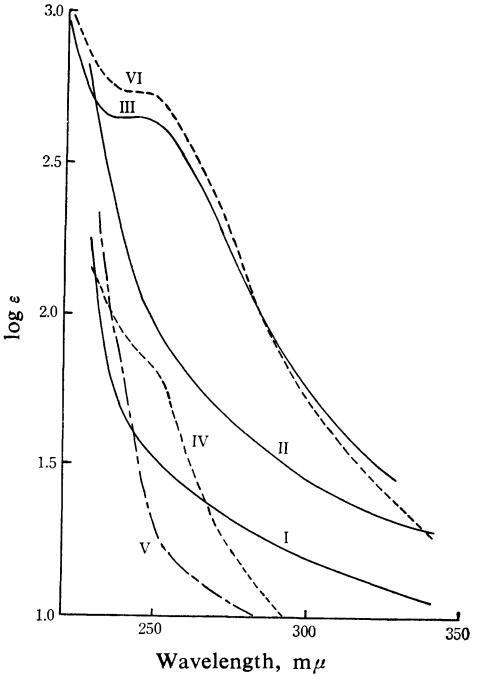



Fig. 4. UV absorption spectra.

Although the absorption due to the $n \rightarrow \pi^*$ transition of the S–S bond varies from 230 mμ to 370 mμ according to the molecular eviron-ment, it has been reported[8,10] that dialkyl disulfides exhibit broad maxima ($\log \varepsilon \sim 2.6$) in the neighborhood of 250 mμ. Compounds III and VI exhibit slight absorption maxima at 235 to 250 mμ, as may be seen in Fig. 4. It is, however, uncertain whether these absorptions are optically active or inactive. Really the dispersion curves of compounds III and VI are plain up to the possible limit of the experiment as compared with the RD curves

8) S. Ishida, *J. Chem. Soc. Japan* (*Nippon Kwagaku Kwaishi*), **64**, 177, 179, 382 (1943); See also N. Kharasch, "Organic Sulfur Compounds," Vol. I, Pergamon Press, Oxford (1961), p. 51.

9) H. H. Jaffé and Milton Orchin, "Theory and Applications of Ultraviolet Spectroscopy," John Wiley & Sons, Inc., New York (1962), p. 474.

10) G. Bergson. G. Claeson and L. Schotte, *Acta Chem. Scand.*, **16**, 1159 (1962).

of the other compounds, but they are very steep and their terminals closely approach the first extremes of the possible Cotton effects associated with the absorption bands of the disulfides.

The fact that all the RD curves (I—VI) are negative in sign may be due to the $\beta$-configuration of the $C_1$ of the $\beta$-D-glucopyranosides. The negative rotation of compound II is distinctly greater in value than that of compound I, probably because the optically active absorption is deeper in the former than in the latter, for its acetoxyl group has a larger polarizability than the hydroxyl group.

The following two examples will illustrate the noticeable effect of the sulfur atom in comparison with the oxygen atom on optical rotation. As may be seen in Fig. 3, the RD curve (IV) is plain; however, its absorption curve shows a shoulder near 250 m$\mu$ (Fig. 4, IV), quite in harmony with the fact that heterocyclic sulfur compounds usually show bathochromic shifts in comparison with simple sulfides.[8] The negative RD curve (Fig. 3, IV) also descends steeply toward the absoption region, and its terminal nearly approaches the extreme of the shoulder. In this respect the thiolevoglucosan (compound IV) is distinguished from other simple sulfides. It may be stated positively that this "heterocyclic" sulfur atom contributes a strong negative rotation to thiolevoglucosan, as is evident from a comparison with levoglucosan, its corresponding oxygen compound (1, 6-anhydro-2, 3, 4-triacetyl-$\beta$-D-glucopyranose):

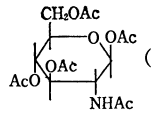
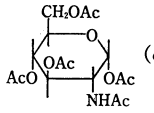
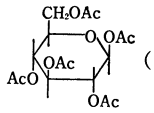
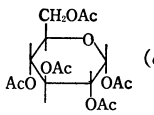
| | $[\alpha]_D$ | $[M]_D$ |
|---|---|---|
| Thiolevoglucosan triacetate | $-65.9°$ | $-201°$ |
| Levoglucosan triacetate | $-45.5°$[11] | $-131°$ |

Next compound V ($\beta$, $\beta$-thiotrehalose octaacetate) was compared with its corresponding oxygen compound, $\beta$, $\beta$-trehalose octaacetate:

| | $[\alpha]_D$ | $[M]_D$ |
|---|---|---|
| $\beta$, $\beta$-Thiotrehalose octaacetate | $-32.6°$ | $-227°$ |
| $\beta$, $\beta$-Trehalose octaacetate | $-18.4°$[12] | $-125°$ |

The negative value of the molecular rotation of the former (V) $[M]_D=-227°$ is far greater than that of the latter, $[M]_D=-125°$. This fact indicates that the sulfur atom of the $C_1$-$\beta$-configuration contributes to a greater negative rotation, as can be expected from the bathochromic shift of the $C_1$-S-$C_1$ group.

TABLE I. THE OPTICAL SUPERPOSITION OF PENTAACETATES OF GLUCOSE AND GLUCOSAMINE

| | | $[\alpha]_D^{20}$ | $[M]_D$ | |
|---|---|---|---|---|
|  | ($\beta$) | + 1.2° | + 4.7= $-A+B$ | $A=180$ $B=184$ |
|  | ($\alpha$) | + 93.5° | +364= $A+B$ | |
|  | ($\beta$) | + 3.8° | + 15= $A+B'$ | $A=191$ $B'=206$ |
|  | ($\alpha$) | +101.6° | +396= $A+B'$ | |

One may get a glimpse into the effect of the acetamido group-$NHCOCH_3$ from a comparison of the glucosamine derivative (II) with the glucose derivative (V). Their configurations differ from each other only in $C_2$.

From Figs. 2 and 3 it is evident that the former compound shows a far stronger RD curve of a negative sign. This fact can be interpreted as follows:

In the first place, the values of $A$ and $B$ of the pentaacetates of glucose and glucosamine must be taken into consideration; they are given by Hudson's rule of optical superposition.[13]

As may be seen in Table I, the values of $B$ and $B'$ are both positive in sign, and the $B'$ value of glucose pentaacetate is distinctly larger than the $B$ value of glucosamine pentaacetate. This fact indicates that the partial rotation of the group $C_2$-NHAc is lower than that of $C_2$-OAc. In a similar way, the $B$ value of compound II is found, by applying Hudson's rule, to be smaller than that of compound V, implying that here also $C_2$-NHAc is lower than $C_2$-OAc in partial rotatory power. Thus, it is reasonable that compound II exhibits a stronger negative RD curve.

### Dispersions Constants

It is to be expected that the dispersion data can be expressed by a single-term Drude equation, since the dispersions exhibit only plain curves.

11) C. Tanret, *Compt. rend.*, **119**, 158 (1894); P. Karrer and A. P. Smirnoff, *Helv. Chim. Acta*, **4**, 819 (1921).
12) C. M. McClosky, R. E. Pyle and G. H. Coleman, *J. Am. Chem. Soc.*, **66**, 349 (1944); "Advances in Carbohydrate Chemistry," Vol. VI, Acad. Press, New York (1951), p. 75.
13) C. S. Hudson and J. K. Dale, *J. Am. Chem. Soc.*, **38**, 1433 (1916).

$$[M]=\frac{R}{\lambda^2-\lambda_0^2}$$

Table II shows the dispersion constants obtained by the usual method of calculation from the dispersion data.

TABLE II. DISPERSION CONSTANTS

| Compound | $R$ | $\lambda_0^2$ |
|---|---|---|
| I | − 56.95 | $0.151^2$ |
| II | −157.26 | $0.212^2$ |
| III | −341.00 | $0.220^2$ |
| IV | − 59.38 | $0.201^2$ |
| V | − 75.43 | $0.196^2$ |
| VI | −380.40 | $0.218^2$ |

As may be seen in Table II, all the values of $\lambda_0$ except that of I are reasonable, representing the most probable, optically active absorption maxima. The dispersion data of III and VI in particular are precisely expressed with the single-term Drude equation, and the relations between $\lambda^2$ and 1/[M] become quite rectilinear (Fig. 5). Moreover, it is noticeable that the factors of the rotational strength, $R$, are especially high in these compounds. This fact suggests that the their ultraviolet absorptions at 235—250 m$\mu$ make so predominant contributions to the optical activity that the minor residual rotations due to other asymmetric centers may practically be ignored.

On the other hand, the dispersion data of compounds I, II, IV and V can not be so precisely expressed by the single-term equation, for the differences between the observed and the calculated values sometimes rise to five per cent, and the relations between $\lambda^2$ and 1/[M] deviate more or less from straight lines, rather drawing slightly convex curves. These facts suggest that the more hypsochromic $C_1$–S–$C_1$ group contributes relatively little to the optical rotation as compared with the disulfide group. Moreover, the residual partial rotation may make a considerable contribution. To elucidate this problem, however, further detailed inquiries should be made in this shorter wavelength region.

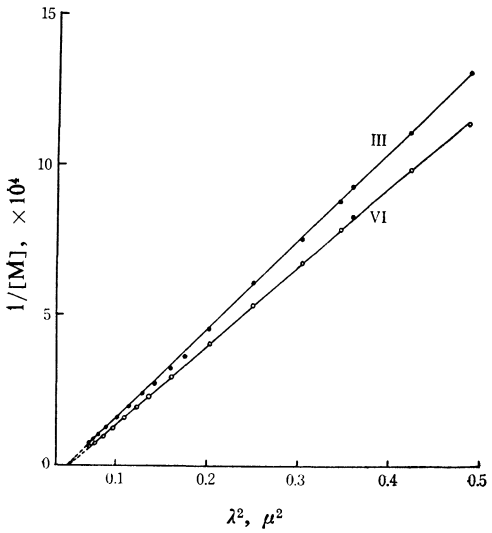



Fig. 5. Rotatory dispersion of disulfides represented as 1/[M] in function of $\lambda^2$.

## Experimental

The rotatory dispersion was measured with a Rudolph spectropolarimeter over the wavelength region from 265 to 700 m$\mu$. The ultraviolet absorption was measured in the same solvent as with RD measurements made with a self-recording spectrophotometer of the Hitachi EPU-II type.

*Bis(2-acetamido-2-deoxy-β-D-glucopyranosyl)sulfide (Compound I).*[14] — Colorless powder, m. p. 219—220°C. $[\alpha]_D^{16}=-36.7°$ (*c* 1.0, $H_2O$).[14] The RD was measured at 22°C in water (*c* 0.3064). $[\alpha]_{700}^{22}$ −32.6°, $[\alpha]_{589}$ −42.4°, $[\alpha]_{265}$ −277°.

*Bis(2-acetamido-2-deoxy-3,4,6-tri-O-acetyl-β-D-glucopyranosyl)sulfide (Compound II).*[14]—Needles, m. p. 314—316°C (decomp.). $[\alpha]_D^{16}=-146.4°$ (*c* 0.8, $CHCl_3$).[14] The RD was measured at 20.6°C in chloroform. $[\alpha]_{700}^{20.6}$ −52.8°, $[\alpha]_{589}$ −74.5°, $[\alpha]_{260}$ −973°.

*Bis(2-acetamido-2-deoxy-β-D-glucopyranosyl)disulfide (Compound III).*[14]—Fine crystals, m. p. 212—213°C. $[\alpha]_D=-223°$ (*c* 0.90, $H_2O$).[14] The RD was measured at 22°C in water (*c* 0.2293). $[\alpha]_{700}^{22}$ −161°, $[\alpha]_{589}$ −243°, $[\alpha]_{270}$ −2843°.

*1,6-Anhydro-1,6-sulfide-2,3,4-tri-O-accetyl-β-D-glucopyranose (Compound IV).*[15]—Colorless crystals, m. p. 93—94°C. $[\alpha]_D^{23}=-25.2°$ (*c* 1.1, $CHCl_3$).[15] The RD was measured at 17.3°C in tetrahydrofuran (*c* 0.2883). $[\alpha]_{700}^{17.3}$ −46.5°, $[\alpha]_{589}$ −65.9°, $[\alpha]_{265}$ −1297°.

*Bis(2,3,4,6-tetra-O-acetyl-β-D-glucopyranosyl)sulfide (Compound V).*[16]—Colorless crystals, m. p. 175—176°C. $[\alpha]_D^{18}=-38.0°$ (*c* 1.0, $CHCl_3$).[16] The RD was measured at 17.3°C in tetrahydrofuran (*c* 0.3586). $[\alpha]_{700}^{17.3}$ −27.3°, $[\alpha]_{589}$ −32.6°, $[\alpha]_{265}$ −248°.

*Bis(2,3,4,6-tetra-O-acetyl-β-D-glucopyranosyl)disulfide (Compound VI).*[17] — Colorless crystals, m. p. 143—144°C. $[\alpha]_D=-160°$ (*c* 6.0, $CHCl_3$).[17] The RD was measured at 17.3°C in tetrahydrofuran (*c* 0.3875). $[\alpha]_{700}^{17.3}$ −122°, $[\alpha]_{589}$ −173°, $[\alpha]_{265}$ −1679°.

## Summary

Measurements have been made ot the rotatory dispersions (265 to 700 m$\mu$) and ultraviolet absorptions (225 to 340 m$\mu$) of various thiosugars, namely, there monothiodisaccharides (I, II, V), two dithio disaccharides (III, VI),

14) M. Akagi, S. Tejima and M. Haga, *Chem. & Pharm. Bull.*, **9**, 360 (1961).
15) M. Akagi, S. Tejima and M. Haga, ibid., **11**, 58 (1963).
16) M. Akagi, S. Tejima and M. Haga, ibid., **11**, 1081 (1963).
17) W. Schneider and A. Bonsa, *Ber.*, **64**, 1321 (1931).

and thiolevoglucosan (IV), in order to investigate the effect of sulfur atoms on optical activity.

The monosulfides, I, II and V, exhibit no absorption maxima and plain, negative RD curves. The disulfides, III and VI, exhibit absorption maxima at 235 to 250 m$\mu$. Their negative RD curves are, accordingly, very steep, approaching the first extremes of the possible Cotton effect.

Thiolevoglucosan (IV), containing a "heterocyclic" sulfur atom, shows more bathochromic shifts than simple sulfides, and a stronger optical activity than levoglucosan. The strong rotatory contribution of the sulfur atom is also observed in acetylated thiotrehalose (V).

In thiosugars the acetamido group also shows a smaller rotatory contribution than the acetoxyl group.

The dispersion data have been analyzed by means of the Drude equation, and the physical significance of the dispersion constants has been discussed.

*Department of Chemistry*
*Tokyo College of Science*
*Kagurazaka, Tokyo*
*(Y. T. & K. T.)*

*Faculty of Pharmaceutical Sciences*
*School of Medicine*
*Hokkaido University*
*Sapporo (M. A. & S. T.)*

# The Rotatory Dispersion and Stereochemistry of Organic Compounds. VIII.[1] Mono- and Dinitrates of Glucopyranose (Preliminary Report)

By Yojiro TSUZUKI, Koko TANABE and Kikuhiko OKAMOTO

(Received August 17, 1964)

In previous papers it has been reported that the chromophores containing sulfur atoms exercise predominant roles in the rotatory dispersion (RD) of sugar xanthates[2-4] and sugar sulfides[1]. This paper will report on similar studies of the rotatory contribution of a nitrogen-containing chromophore $-O-NO_2$ (nitrate).

Although the nitrate chromophore has never been studied with respect to the RD, it has been reported by Mitchell et al.[5] that dinitrocamphane exhibits an intense negative Cotton effect, and some interesting information has been obtained with several nitro-compounds with regard to the RD.[6,7] Recently Djerassi et al.[8] have studied the circular dichroism and RD of compounds containing a nitro chromophore.

On the other hand, it has been shown with aliphatic nitro-compounds[9,10] that the nitro group exhibits an intense absorption band around 210 m$\mu$ and a weak band around 270 m$\mu$ due to the $n\rightarrow\pi^*$ transition. Similarly, some alkyl nitrates have also been shown to have a feeble absorption band due to the $n\rightarrow\pi^*$ transition.[9] Thus, it can be expected that with sugar nitrates also the nitrate chromophore will exhibit an optically active absorption. In this paper the following compounds will be investigated with the object of studying how the $C_2$- and $C_3$-$ONO_2$ groups affect the RD of glucose:

Methyl 4:6-*O*-benzylidene-$\alpha$-D-glucopyranoside 3-nitrate (compound I),

Methyl 4:6-*O*-benzylidene-$\alpha$-D-glucopyranoside 2,3-dinitrate (compound II),

Methyl 4:6-*O*-benzylidene-$\alpha$-D-glucopyranoside (compound III),

3,4,6-Tri-*O*-acetyl-2-*O*-nitro-$\alpha$-D-glucopyranosyl chloride (compound IV),

1,3,4,6-Tetra-*O*-acetyl-2-*O*-nitro-$\alpha$-D-glucopyranoside (compound V),

3,4,6-Tri-*O*-acetyl-$\alpha$-D-glucopyranosyl chloride (compound VI),

Pentaacetyl-$\alpha$-D-glucose (compound VII).

1) Part VII: Y. Tsuzuki, K. Tanabe, M, Akagi and S. Tejima, This Bulletin, **38**, 270 (1965).
2) Y. Tsuzuki, K. Tanaka and K. Tanabe, ibid., **35**, 1614 (1962).
3) Y. Tsuzuki, K. Tanabe, M. Akagi and S. Tejima, ibid., **37**, 162 (1964).
4) Y. Tsuzuki, K. Tanaka, K. Tanabe, M. Akagi and S. Tejima, ibid., **37**, 730 (1964).
5) S. Mitchell and R. R. Gordon, *J. Chem. Soc.*, **1936**, 853.
6) N. Kornblum, L. Fishbein and R. A. Smiley, *J. Am. Chem. Soc.*, **77**, 6261 (1955).
7) A. Bowers, M. B. Sánchez and H. T. Ringold, ibid., **81**, 3702 (1959).
8) C. Djerassi, H. Wolf and E. Bunnenberg, ibid., **85**, 2835 (1963).
9) H. E. Ungade and R. A. Smiloy, *J. Org. Chem.*, **21**, 993 (1956).
10) A. Balasubramanian and C. N. R. Rao, *Chem. & Ind.*, **1960**, 1025.

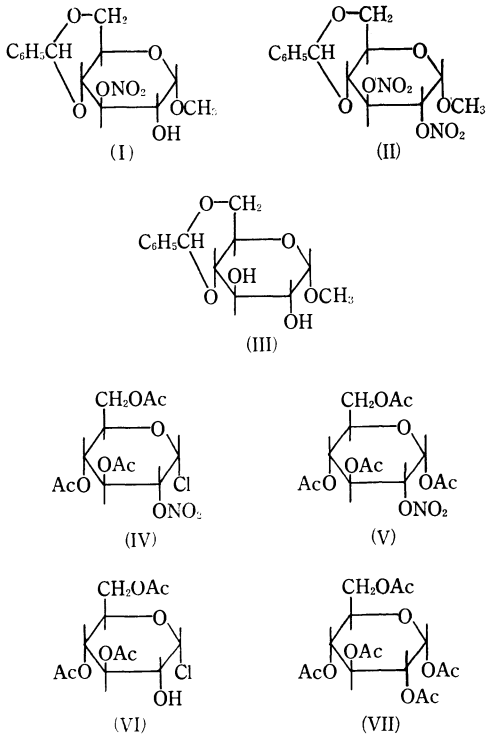



Fig. 1. Structural formulas of investigated glucopyranosides.

## Results and Discussion

The RD curves of compounds I, II and III are shown in Fig. 2. Curve III is considered to represent the background rotation of curves I and II. As is shown in Fig. 4, the ultraviolet absorption spectra of compounds I and II are found to have the $\lambda_{max}$ at 250—270 m$\mu$, and their absorption is optically active.

As is evident from Fig. 2, compound I ($C_3$-nitrate) exhibits a positive Cotton effect (the peak at 300 m$\mu$), while compound II (2, 3-dinitrate) shows a very feeble negative Cotton effect. The broad peak around 335 m$\mu$ of curve II is produced from the positive background RD of curve III superposed by a slight negative Cotton effect, the peak of which appears at 295 m$\mu$, nearly identical with the peak (300 m$\mu$) of the Cotton effect of curve I.

Thus, the $C_3$-$ONO_2$ group may be supposed to give rise to a positive Cotton effect, as the $C_3$-xanthate group does in glucose,[2,4] even though the $C_3$-group of glucose is usually believed to make a levo-rotatory contribution because of the $\beta$-type of $C_3$-configuration (i. e., the inversion of the sign of rotation).

In comparing the $C_2$-$ONO_2$ group with the 3-nitrate in rotatory contribution, the value of the $[\alpha]_D$ of the 2, 3-dinitrate (compound II) is lower than that of the 3-nitrate (compound I),

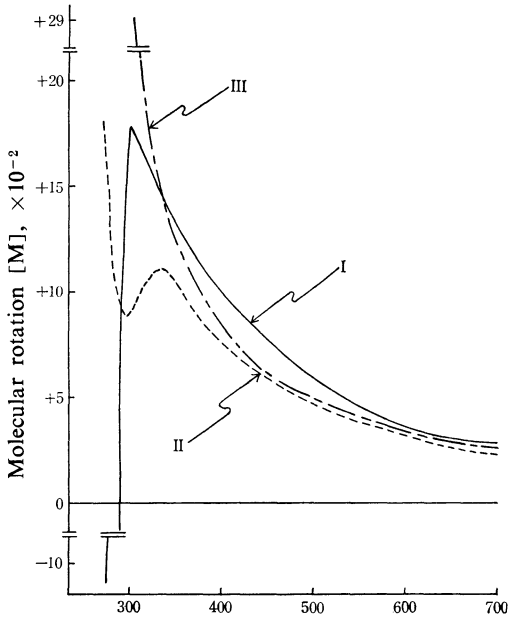



Fig. 2. RD of I—III.

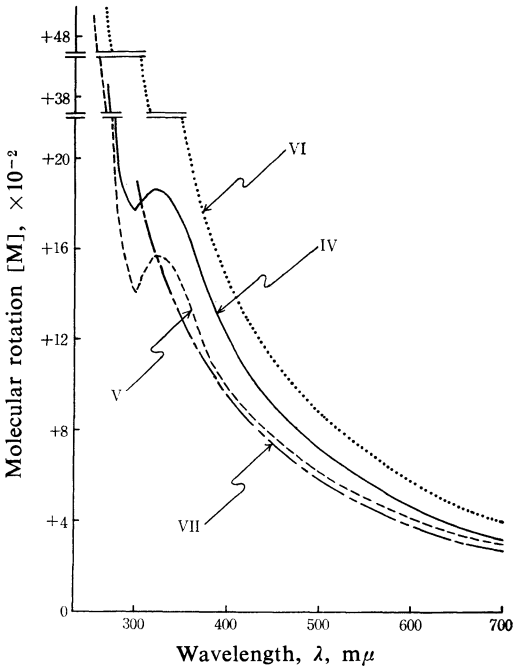



Fig. 3. RD of IV—VII.

and Honeyman et al.[11] have given a value of 104° to the specific rotation of methyl 4 : 6-*O*-benzylidene-$\alpha$-D-glucopyranoside 2-nitrate, which is also lower than that of the corresponding 3-nitrate. These facts suggest that the

11) J. Honeyman and J. W. W. Morgan, *J. Chem. Soc.*, 1955, 3669.

$C_2$-$ONO_2$ group contributes somewhat to the negative rotation.

In order to make a further study of the rotatory contribution of the $C_2$-$ONO_2$ group, compounds IV and V have also been studied.

The RD curves of compounds IV and V are shown in Fig. 3, together with those of VI and VII as illustrations of the background curves. As may be seen in Fig. 2, the absorption maxima appear at the region of 295—300 mμ in the RD due to the nitrate chromophore. The peaks around 325 mμ on the curves of IV and V are properly to be attributed to a small Cotton effect (negative peak around 300 mμ) overlapped on the positive background RD curves. Thus, the Cotton effects of compounds IV and V are to be judged negative in sign, the negative peaks being located respectively at 295 and 300 mμ, quite in coincidence with those of compounds I and II (Fig. 2).

In a previous paper[4] it has been shown that the $C_2$-$OCOCH_3$ group in D-mannose exhibits a negative rotatory contribution; accordingly, the $C_2$ group of D-glucose (of α-configuration) may be presumed to contribute to the positive rotation. However, the Cotton effects of IV and V due to the nitrate group in the $C_2$ position are to be considered negative in sign, as has already been stated and as may be seen in Fig. 3, so the nitrate group may also be assumed to exhibit an inversion effect in the sign of rotation, as has already been observed and pointed out with several xanthates.[2,3]

The ultraviolet absorption spectra of compounds I and II are given in Fig. 4, and those of IV and V, in Fig. 5. The first two curves are distinguished in that both exhibit fine structures in the region of 250—270 mμ, the forms of which structure are almost entirely identical in chloroform as well as in tetrahydrofuran. It is worthy of note that the ultraviolet absorption curves of I and II rather resemble those of alkyl nitrates,[9] although the nitrites exhibit weak absorption bands (ε ~80) of fine structures in the longer wavelength region around 370 mμ.

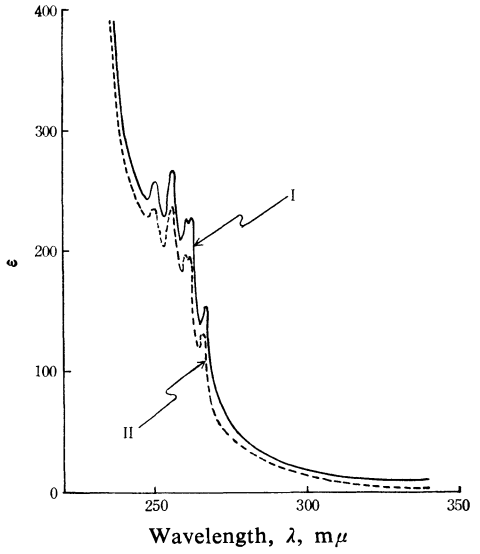



Fig. 4. UV absorption spectra of I and II.

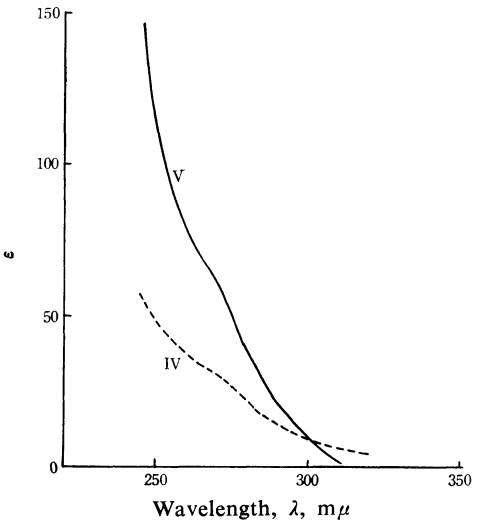



Fig. 5. UV absorption spectra of IV and V.

Compounds IV and V do not exhibit any noticeable ultraviolet absorption in tetrahydrofuran; although in chloroform their curves do show slight anomalies, they do not exhibit so distinct inflections as are observed in alkyl nitrates,[9] which occur around 270 mμ (ε ~20.[12])

Apparently the ultraviolet absorption curves of these compounds (IV and V) have no relation to the behaviors of RD, but it is worthy of attention that the RD curves exhibit optically active absorptions at longer wavelengths of 295—300 mμ, and that also in some nitrites the first peaks of the Cotton effects are situated at longer wavelengths than are the ultraviolet absorption maxima[8] by 10—20 mμ.

With the nitro-chromophore such red shifts have also been observed as with the first peaks of RD, which are displaced toward longer wavelengths from the ultraviolet absorption maxima.

It is thus reasonable, in view of the above-stated facts, to assume that the peaks of the Cotton effects due to the nitrate chromophore are observed at wavelengths about 20 mμ

12) It is likely that distinct absorption maxima will result if the spectra are taken in less polar solvents. See C. N. R. Rao, "Ultra-violet and Visible Spectroscopy," Butterworths, London (1961), p. 22.

longer than the ultraviolet absorption maxima.

Finally, it should be noted that the authors, as usual, have tried to express the RD by means of the equations of Drude, but the complex RD curves could not successfully be expressed. This is probably because the shapes of the curves are peculiar, and because the falls between the peaks of the feeble Cotton effects are too small. The values of the dispersion constants obtained by the usual calculation method often fail to give proper physical significance. Further detailed studies will be necessary for a quantitative analysis and for more comprehensive treatment of the dispersion data.

## Experimental

The derivatives of glucose were prepared according to the methods of the literature. The rotatory dispersion was measured with a Rudolph spectropolarimeter over a wavelength region from about 265 mμ to 700 mμ. The ultraviolet absorption was measured with a self-recording spectrophotometer of Hitachi EPU-II type.

*Methyl 4 : 6-O-Benzylidene-α-D-glucopyranoside 3-Nitrate (Compound I).*[11] — Colorless crystals, m. p. 168—169°C. The RD was measured at 22.5°C in tetrahydrofuran (*c* 0.0939). $[\alpha]_{700}^{22.5}$ +87.3°, $[\alpha]_{589}$ +118°, $[\alpha]_{500}$ +179°, $[\alpha]_{400}$ +305°, $[\alpha]_{300}$ +544° (peak), $[\alpha]_{275}$ −330°.

*Methyl 4 : 6-O-Benzylidene-α-D-glucopyranoside 2 : 3-Dinitrate (Compound II).*[11] — Needles, m. p. 122—123°C. The RD was measured at 22°C in tetrahydrofuran (*c* 0.9623). $[\alpha]_{700}^{22}$ +66.1°, $[\alpha]_{589}$ +90.5°, $[\alpha]_{500}$ +127°, $[\alpha]_{400}$ +202°, $[\alpha]_{335}$ +297° (broad extreme), $[\alpha]_{295}$ +241° (negative peak), $[\alpha]_{270}$ +483°.

*Methyl 4 : 6-O-Benzylidene-α-D-glucopyranoside (Compound III).*[13] — Needles, m. p. 163—164°C. The RD was measured at 20°C in chloroform (*c* 0.1). $[\alpha]_{650}$ +95.0°, $[\alpha]_{589}$ +123°, $[\alpha]_{400}$ +320°, $[\alpha]_{305}$ +1101°.

*3,4,6-Tri-O-acetyl-2-O-nitro-α-D-glucopyranosyl Chloride (Compound IV).*[14] — Syrup. The RD was measured at 21°C in chloroform (*c* 0.5935). $[\alpha]_{700}^{21}$ +85.1°, $[\alpha]_{589}$ +132°, $[\alpha]_{500}$ +192°, $[\alpha]_{400}$ +333°, $[\alpha]_{325}$ +505° (broad extreme), $[\alpha]_{295}$ +492° (negative peak), $[\alpha]_{265}$ +1054°.

*1,3,4,6-Tetra-O-acetyl-2-O-nitro-α-D-glucopyranose (Compound V).*[14] — Needles, m. p. 91°C. The RD was measured at 21°C in chloroform (*c* 1.2886). $[\alpha]_{700}^{21}$ +77.5°, $[\alpha]_{589}$ +108°, $[\alpha]_{500}$ +154°, $[\alpha]_{400}$ +252°, $[\alpha]_{320}$ +403° (broad extreme), $[\alpha]_{300}$ +358° (negative peak), $[\alpha]_{255}$ +1242°.

*3,4,6-Tri-O-acetyl-α-D-glucopyranosyl Chloride (Compound VI).*[15] — Needles, m. p. 93—94°C. The RD was measured at 21°C in chloroform (*c* 0.9374). $[\alpha]_{700}^{21}$ +126°, $[\alpha]_{589}$ +184°, $[\alpha]_{500}$ +268°, $[\alpha]_{400}$ +465°, $[\alpha]_{300}$ +1038°, $[\alpha]_{250}$ +1900°.

*Pentaacetyl-α-D-glucopyranoside (Compound VII).*[16] —Colorless crystals, m. p. 112—113°C. The RD was measured at 21°C in chloroform (*c* 1.0820). $[\alpha]_{700}^{21}$ +68.6°, $[\alpha]_{589}$ +102°, $[\alpha]_{500}$ +146°, $[\alpha]_{400}$ +245°, $[\alpha]_{300}$ +486°.

## Summary

The RD and ultraviolet absorption have been observed with some derivatives of glucose carrying a nitrate group in the $C_2$ and $C_3$ positions in order to study the optical contributions of the $C_2$- and $C_3$-ligands with respect to their configurations.

*Department of Chemistry*
*Tokyo College of Science*
*Kagurazaka, Tokyo*

13) K. Freudenberg, H. Toeppffer and C. C. Andersen, *Ber.*, **61**, 1750 (1928).

14) M. L. Wolfrom, A. Thompson and D. R. Lineback, *J. Org. Chem.*, **28**, 1930 (1963).

15) R. U. Lemieux and G. Huber, *Can. J. Chem.*, **31**, 1040 (1953).

16) C. S. Hudson and J. K. Dale, *J. Am. Chem. Soc.*, **37**, 1264 (1915).

# The Behavior of Fission Products Captured in Graphite Powder by Nuclear Recoil. VIII. Further Studies of Iodine-131 Diffused out of Graphite

By Seishi YAJIMA, Koreyuki SHIBA and Muneo HANDA

(Received July 29, 1964)

In the sixth and seventh papers of this series,[1-2] the chemical state of fission iodine-131 diffusing out of various kinds of ceramic fuels was studied by using a thermochromatograph, and the following experimental results were reported:

1) The fission iodine-131 diffusing out of uranium dioxide, thorium dioxide, and a mixture of graphite and uranium dioxide, all containing fission products, was not an elementary iodine but was composed of iodine compounds.

2) The iodine compounds were fairly stable at high temperatures in a helium atmosphere; i. e., the compound diffusing out of uranium dioxide and the mixture of graphite and uranium dioxide was able to exist as a solid at 580°C; the compound from thorium dioxide was of two kinds of states, one in a solid at 530°C and the other at 430°C.

3) From the behavior of iodine compounds in solvent extraction, it was found that the chemical state of the compounds was iodide.

4) As iodide is a chemical form, it should be thought that iodine combined with other fission products, with impurities in uranium dioxide, thorium dioxide, graphite, etc., or with the fissionable material, i. e., uranium or thorium. Of the above possibilities, that that the fission iodine-131 combined with impurities was eliminated, because the fission iodine-131 diffusing out of the uranium dioxide and that diffusing out of the mixture of graphite and uranium dioxide, the impurities in the two differing from one other, were stable at 580°C in a solid form. The theory that the fission iodine-131 combined with other fission products was weakened by the fact that there was a difference between the fission iodine-131 from uranium dioxide and that from thorium dioxide at the temperature where the iodide existed as solid, even if the fission products yield curves of uranium were different from that of thorium.

On the basis of the above facts, it was assumed that the fission iodine-131 combined with the fissionable material, uranium or thorium. To prove directly the chemical forms of these iodine compounds by the chemical or physical methods was, however, very difficult. This was because the amount of fission iodine-131 in the irradiated sample was extremely small ($\mu\mu$g. level) and, further, because, if the fission iodine-131 existed as a uranium iodide or thorium iodide, these compounds were considerably unstable in the atmosphere.

The present paper will describe further studies made to prove the combining of the fission iodine-131 with fissionable material. A uranium tetraiodide was prepared by the reaction of uranium metal powder with iodine labeled with iodine-131. The behavior of uranium tetraiodide was compared with that of the fission iodine-131 by using a thermochromatograph. The uranium tetraiodide deposited on the same place in a thermochromatotube as the fission iodine-131, in an inert gas atmosphere. Further, the chemical behavior of the uranium tetraiodide toward the oxygen contained in a small amount in the helium stream was compared with that of the fission iodine-131 diffused out of the graphite. The behavior of the uranium tetraiodide toward the oxygen was the same as that of the fission iodine-131. On the basis of above results, it seemed reasonable to assume that the fission iodine-131 diffused out from the graphite as uranium tetraiodide. As for the chemical behavior of the uranium tetraiodide toward the oxygen, it was clarified that the uranium tetraiodide was oxidized to triuranium octoxide and iodine through three intermediates, which deposited on the silica powders heated at temperatures of about 400°C, 300°C and 200°C respectively.

## Experimental and Results

**The Preparation of Samples.** — *Sample No. I (A mixture of natural graphite powder and uranium dioxide containing fission products).*—Natural graphite powder degassed (in a vacuum, 1000°C, 24 hr.) was mixed with a stoichiometric uranium dioxide powder in the weight ratio of 2 : 1, in a glove box filled with purified helium gas. About 100 mg. of

1) S. Yajima, K. Shiba and M. Handa, This Bulletin, **36**, 253 (1963).
2) S. Yajima, K. Shiba and M. Handa, ibid., **36**, 258 (1963).

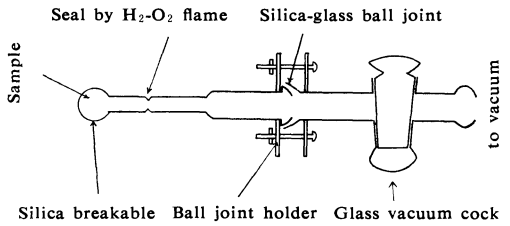



Fig. 1. Assembly to prepare the sample packed in a silica breakable.

the mixture was packed in a silica breakable equipped with a ball joint, a joint which is shown in Fig. 1. Then a cock was attached to the breakable with a ball-joint holder, and the whole assembly was taken out of the glove box. The helium gas in the breakable was evacuated, and the part containing the sample was sealed by an oxygen-hydrogen flame. Then the mixture of graphite and uranium dioxide sealed in the silica breakable was neutron-irradiated in the JRR-1 (a water boiler-type reactor with a thermal neutron flux of about $5\times10^{11}$ n/cm$^2$·sec.) for 15 hr. After irradiation, the mixture was cooled for 5 days to allow the other short-lived isotopes of iodine, as well as the mostly precursor of iodine-131, to decay out. The fission iodine-131 diffusing out of this sample mixture when it was heated was determined to be the iodine-131 contained in the graphite, because about 70% of the fission iodine-131 was captured in the graphite by nuclear recoil[3] and the diffusion coefficient of the fission iodine-131 in the graphite was far larger than in the uranium dioxide.

*Sample No. 2 (Uranium tetraiodide labeled with iodine-131).*—Potassium iodide was added to a commercial aqueous solution of iodine-131, and the potassium iodide was oxidized to an elementary iodine with nitric acid. The iodine labeled with iodine-131 was washed with water to eliminte a potassium nitrate and was dried in a desiccator containing an anhydrous calcium chloride.

By the use of this elementary iodine, uranium tetraiodide labeled with iodine-131 was prepared by the method reported by Gregory.[4] About 100 mg. of the uranium tetraiodide was packed in a silica breakable in a way similar to that used for sample No. 1.

**Packing Material for the Thermochromato-tube.**—Natural graphite powder, with particle sizes less than one micron, or silica powder, twenty-to-thirty mesh, was degassed by heating it in a vaceuum at 1000°C for 24 hr. The treated graphite or silica was kept in a helium gas atmosphere before being used in the experiment.

**Apparatus.**—The apparatus used is shown schematically in Fig. 2. The automatic Toepler pump was attached to the thermochromatograph reported on earlier.[1] The apparatus was modified in order to circulate the carrier gas through the apparatus. A trap for the mercury, cooled with a mixture of alcohol and dry-ice, was installed at the entrance and exit of the thermochromato-tube; the mercury

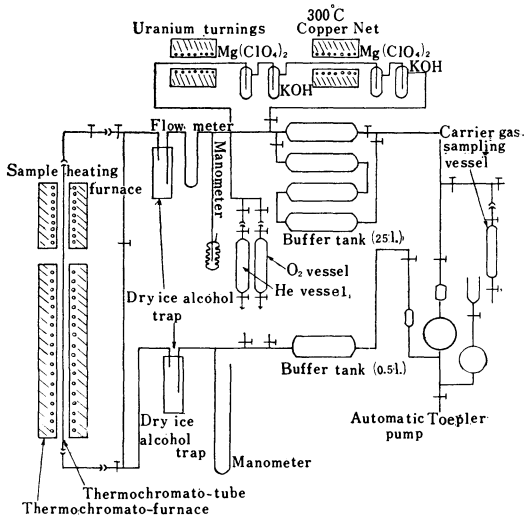



Fig. 2. Thermochromatograph.

was used in the automatic Toepler pump. A buffer tank was set at the entrance and exit of the automatic Toepler pump in order to stabilize the flow rate of the carrier gas; the volumes of the buffer tanks were 0.5 l. and 25 l. respectively. The apparatus had a bypass gas-purification system and made possible the experiments with purified helium carrier gas. The thermochromato-tube was externally heated by a nichrome wire to produce the linear temperature gradient of 600°C to room temperature; the temperature gradient is shown in Fig. 3. The gradient was obtained by changing the

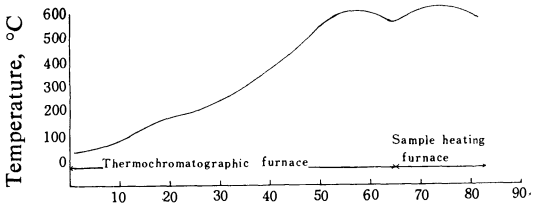



Fig. 3. Condition of two electric furnace (thermochromato-furnace and sample heating furnace) when an equilibrium was attained.

number of windings for each part of the furnace. The thermochromato-tube used was the same as in the previous study, with a transparent silica tube (0.6 cm. in inner diameter and 100 cm. long). Twenty-to-thirty mesh silica powder or fine natural graphite powder was used as the packing material in the thermochromato-tube. The sample-heating furnace was divided in two halves at the center of the furnace, so that the breakable in the thermochromato-tube could be broken from outside with a magnet.

**Procedure.**—Silica powder or graphite powber was packed into the thermochromato-tube. The sample in the silica breakable and its breaker (an iron bar sealed in a silica tube) were located in the center

3) T. Nakai, S. Yajima, K. Shiba, J. Osugi and D. Shinoda, This Bulletin, 33, 494 (1960).
4) N. W. Gregory, UCRL, RL-4, 6, 272 (1944).

of the sample-heating furnace on the packing material in the thermochromato-tube. Then the whole apparatus was evacuated by a rotary pump, and the thermochromato-furnace was heated for 2 hr. to remove the impurity gases adsorbed on the packing powders. Arbitrary volumes of helium and oxygen were introduced into the apparatus to a one-tenth atmosphere; these were then completely mixed by circulating them 5 hr. through the apparatus with the automatic Toepler pump. On the other hand, when the experiment was carried out in an inert atmosphere, only helium was introduced into the apparatus; it was purified by circulating 5 hr. through the gas purification system with the automatic Toepler pump. In both cases, the heating of the sample-heating furnace was then started. After the temperature of the sample-heating furnace reached 600°C, the circulation of the carrier gas was continued for a further 2 hr. The thermochromato-tube was cooled and surveyed along the whole length in order to locate the iodine-131 activities. An RCL-256 channel gamma-ray spectrometer connected with an NaI(Tl) crystal (a lead slit 1 cm. wide was set) was used for measuring the iodine-131 activity.

**Thermochromatograms.** — The thermochromatograms of the fission iodine-131 diffused out of the mixture of graphite and uranium dioxide, and that diffused out of the uranium tetraiodide prepared in a laboratory, for the pure helium carrier gas, are shown in Figs. 4 and 5 respectively. The results obtained for the two samples under various oxygen partial pressures are shown in Figs. 6 and 7 respectively. In the thermochromatograms in Figs. 4 to 7, the axis of the abscissa is shown by the temperature. These thermochromatograms were obtained by replacing each position of the thermochromato-tube with the temperature of the thermochromato furnace, according to Fig. 3.

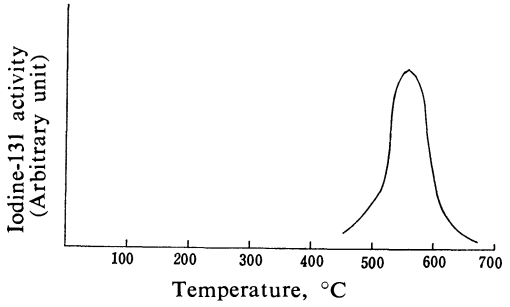



Fig. 4. Thermochromatograms.
Sample: No. 1 (Mixture of graphite and uranium dioxide)
Packing: Natural graphite powder
Time: 2 hr.
Carrier: Pure helium

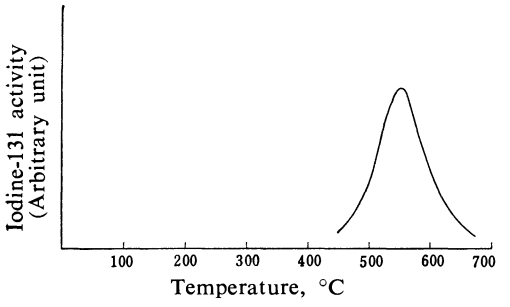



Fig. 5.
Sample: No. 2 (Uranium tetraiodide)
Packing: Natural graphite powder
Time: 2 hr.
Carrier: Pure helium

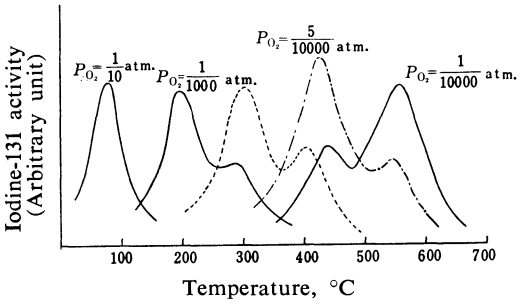



Fig. 6.

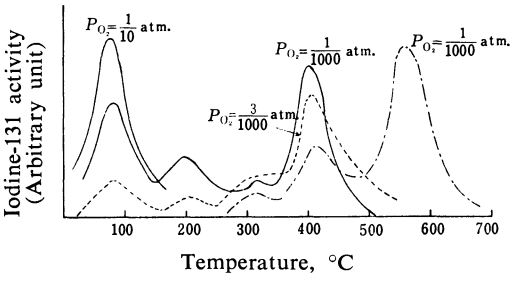



Fig. 7.
Sample: No. 2 (Uranium tetraiodide)
Packing: Silica powder
Time: 2 hr.
Carrier: $O_2$-He mixture

## Discussion

As is shown in Fig. 4, when thoroughly purified helium was used as the carrier gas (the partial pressure of oxygen was less than $10^{-5}$ atmosphere), the fission iodine-131 deposited on the graphite powder heated at 550°C,*

* In a previous report,[1] it was reported that the fission iodine-131 deposited on the graphite powder heated at 580°C. The deposition temperature of the fission iodine-131 in the thermochromato-tube was mainly influenced by two factors, i. e., the flow rate of the carrier gas in the thermochromato-tube and the temperature gradient of the thermochromato-furnace. In the present experiment the thermochromatograph was modified considerably compared with the previous one, and so the location of the deposition of the fission iodine-131 shifted to a low temperature; it was deposited on graphite powder heated at 550°C. However, when the same thermochromatograph was used for the experiment, the deposition temperature of the fission iodine-131 was reproducible within ±20°C at the same experimental conditions.

temperature near the melting point of the uranium tetraiodide (the melting point of uranium tetraiodide reported in the literature is 506—518°C[5,6]). On the other hand, the uranium tetraiodide prepared in a laboratory deposited on the graphite powder heated at 550°C under the same experimental conditions as that of the fission iodine-131. The data shown in Fig. 6 indicate that, at a constant temperature, the reaction between the fission iodine-131 and oxygen is governed by the partial pressure of the oxygen in the carrier gas. The position of the fission pressure of the oxygen in the carrier gas increased.

When the partial pressure of oxygen was one-tenth atmosphere, the fission iodine-131 was oxidized to an elementary iodine and deposited at the position of 100°C (the melting point of iodine is 113.6°C). The results for the reaction of uranium tetraiodide with oxygen under the same experimental conditions, which are shown in Fig. 7, were the same as those obtained with the thermochromatograms for the fission iodine-131. From the above results, it must be considered that the fission iodine-131 diffusing out of the neutron-irradiated mixture of graphite and uranium dioxide is not an elementary iodine but is in the chemical form of uranium tetraiodide.

To prove the above facts directly, uranium must be detected at the position of the deposition of the fission iodine-131 by neutron activation analysis. These experiments are now planned in the author's laboratory. The intermediates which deposited at 400°C, 300°C and 200°C are thought to be either compounds of uranium and iodine (for example, $UI_6$ and $UI_5$) or compounds of uranium, iodine, and oxygen (for example, $UO_2I_2$ and $UOI_2$), but the existence of these compounds in the solid state is not reported in any literature. The mechanism of the formation of these compounds is thought to be the oxidation, decomposition or disproportionation of uranium tetraiodide or their combinations; the chemical forms and the types of crystallization are now being investigated.

Recently, Hudswell[7] confirmed that the fission iodine diffusing out of uranium-carbide fuel dopsited on the surface of graphite heated at the temperature of 350°C in a helium gas atmosphere. It is thought that Hudswell found one of the intermediates confirmed by the authors. The phenomenon that the fission iodine diffuses out in the chemical form of uranium tetraiodide from ceramic fuels, such as uranium dioxide or a mixture of uranium carbide and graphite, is important in connection with uranium migration in nuclear ceramic fuels; therfore, the mechanism of the formation of uranium tetraiodide in the fuels must be studied further.

*The Research Institute for Iron, Steel and Other Metals*
*Tohoku University*
*Katahira-cho, Sendai* (*S. Y.*)

*Division of Nuclear Engineering*
*Reactor Fuel Laboratory*
*Japan Atomic Energy Research Institute*
*Tokai, Ibaraki* (*K. S. & M.H.*)

5) J. J. Katz and E. Rabinowitch, "The Chemistry of Uranium; The Element, Its Binary and Related Compounds," Dover Publications, New York (1951), p. 536.
6) M. M. Popov and M. D. Senin, *Zhur. Neorganichskoi Khimii*, 2, 1479 (1957).
7) F. H. Hudswell, Unpublished work.

# The Dipole Moments of Some Sesquifulvalene Quinones and Related Compounds

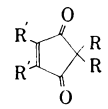
By Shigeyoshi KATAGIRI, Ichiro MURATA,* Yoshio KITAHARA* and Hiroshi AZUMI

(Received August 7, 1964)

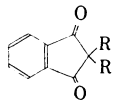
Although it is considered probable, from theoretical considerations, that sesquifulvalene is a highly polar molecule due to a charge transfer from the electron-donating seven-membered ring towards the electron-accepting five-membered ring, experimental evidence for this conclusion has not yet been provided because sesquifulvalene is not stable and easily polymerizes.[1-4] Recently Kitahara et al.[5] have synthesized some stable quinone derivatives of sesquifulvalene—sesquifulvalene-1, 4-quinone (VII) and 2, 3-benzosesquifulvalene-1, 4-quinone (VIII). Each of these quinones has two electron-withdrawing carbonyl groups in the five-membered ring, so that a considerable amount of charge transfer should be expected between the two rings. Accordingly, their dipole moments should provide some information with respect to this charge transfer. In order to obtain more detailed information, however, an investigation of the dipole moments of some diones related to the above quinones must also be undertaken. Therefore, besides those for the sesquifulvalene quinones, the dipole moments were measured for several compounds not having a heptafulvene structure—cyclopentene-3, 5-dione, indane-1, 3-dione, and their halogeno and tropyl derivatives.

## Experimental

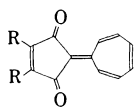
The following samples were used: cyclopentene-3, 5-dione (I), m. p. 37—38°C,[6] 4, 4-ditropylcyclopentene-3, 5-dione (II), m. p. 121—122°C,[5] 1, 2-dichlorocyclopentene-3, 5-dione (III), m. p. 163°C,[7] 1, 2-dichloro-4,4-ditropylcyclopentene-3,5-dione (IV), m. p. 103—104°C[5], indane-1, 3-dione (V), m. p. 132—133°C,[8] 2, 2-ditropylindane-1, 3-dione (VI), m. p. 167.5—168°C[5] [reported m. p. 173—174°C[9]]), sesquifulvalene-1, 4-quinone (VII), m. p. 179—180°C,[5] 2, 3-benzosesquifulvalene-1, 4-quinone (VIII), m. p. 244—245°C,[5] and 2, 3-dichlorosesquifulvalene-1, 4-quinone (IX), m. p. 263°C (decomp.).[5]



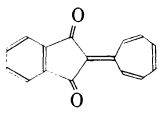
I R=R'=H
II R=$C_7H_7$; R'=H
III R=H; R'=Cl
IV R=$C_7H_7$; R'=Cl



V R=H
VI R=$C_7H_7$



VII R=H
IX R=Cl



VIII

The dipole moments of these substances were measured in benzene at 25°C using a high-inpedance a. c. bridge method described previously.[10] The benzene was purified as before.[10] The dipole moments were calculated using the method and equation of Halverstadt and Kumler:[11]

$$P_{2\infty}=(\varepsilon_1-1)/(\varepsilon_1+2)\cdot(v_1+\beta)M_2 + 3\alpha v_1 M_2/(\varepsilon_1+2)^2$$

$$\mu=0.012812\sqrt{(P_2-R_D)T}$$

The plots of $\varepsilon_{12}$ versus $w_2$ and $v_{12}$ versus $w_2$ were straight lines within the limits of experimental error. The values of $\varepsilon_1$ and $v_1$ were obtained by the method of least squares. The molar refractions, $R_D$, were calculated from the bond refraction data.[12] For 1, 2-dichlorocyclopentene-3, 5-dione and 1, 2-dichloro-4, 4-ditropylcyclopentene-3, 5-dione, however, because of their low dipole moments, the refractive indices at the D-line were measured using a Purflich refractometer, and the molar refractions were obtained from the following equa-

* Present address: Department of Chemistry, Faculty of Science, Tohoku University, Sendai.

1) A. Streitwieser, "Molecular Orbital Theory for Organic Chemists," John Wiley & Sons, New York, N. Y. (1961), p. 300.
2) H. Prinzbach and W. Rosswog, *Angew. Chem.*, **73**, 543 (1961).
3) A. J. Silbestri, L. Goodman and J. A. Dixon, *J. Chem. Phys.*, **36**, 148 (1962).
4) T. Nakajima and S. Katagiri. This Bulletin, **35**, 109 (1962); *Mol. Phys.*, **7**, 149 (1963).
5) Y. Kitahara, I. Murata and T. Asano, This Bulletin, **34**, 589 (1961); ibid., **37**, 924 (1964),
6) C. H. DePuy and E. F. Zaweski, *J. Am. Chem. Soc.*, **79**, 3923 (1957); ibid., **81**, 4920 (1959).
7) A. Roedig and L. Hörnig, *Chem. Ber.*, **88**, 2003 (1955).
8) L. F. Fieser, "Experiments in Organic Chemistry," 3rd ed., D. C. Heath and Company, Boston (1957), p. 127.
9) N. W. Jordan and I. W. Elliott, *J. Org. Chem.*, **27**, 1445 (1962).
10) S. Katagiri, *Sci. Repts. Tohoku Univ.*, I, **44**, 165 (1960).
11) I. F. Halverstadt and W. D. Kumler, *J. Am. Chem. Soc.*, **64**, 2988 (1942).
12) J. W. Smith, "Electric Dipole Moments," Butterworth Scientific Publications, London (1955).

TABLE I. THE DIPOLE MOMENT DATA IN BENZENE AT 25°C

(I) Sesquifulvalene-1, 4-quinone

| $10^4 w_2$ | $\varepsilon_{12}$ | $v_{12}$ | | |
|---|---|---|---|---|
| 0.8815 | 2.2731 | 1.14474 | $\varepsilon_1=2.2732$ | $\alpha=4.987$ |
| 2.8899 | 2.2748 | 1.14464 | $v_1=1.14475$ | $\beta=-0.331$ |
| 7.2037 | 2.2773 | 1.14448 | $P_{2\infty}=217.42$ | $R_D=51.27$ calcd. |
| 12.0515 | 2.2791 | 1.14435 | $\mu=2.85$ D. | |
| 18.4768 | 2.2822 | 1.14415 | | |

(II) 2, 3-Benzosesquifulvalene-1, 4-quinone

| | | | | |
|---|---|---|---|---|
| 2.2029 | 2.2740 | 1.14475 | $\varepsilon_1=2.2733$ | $\alpha=3.213$ |
| 5.2757 | 2.2750 | 1.14462 | $v_1=1.14483$ | $\beta=-0.414$ |
| 10.7722 | 2.2767 | 1.14438 | $P_{2\infty}=192.57$ | $R_D=66.59$ calcd. |
| 19.5782 | 2.2794 | 1.14400 | $\mu=2.48$ D. | |
| 27.7886 | 2.2823 | 1.14370 | | |

(III) 2, 3-Dichlorosesquifulvalene-1, 4-quinone

| | | | | |
|---|---|---|---|---|
| 3.7649 | 2.2771 | 1.14444 | $\varepsilon_1=2.2730$ | $\alpha=10.685$ |
| 5.0349 | 2.2782 | 1.14431 | $v_1=1.14463$ | $\beta=-0.545$ |
| 6.8195 | 2.2804 | 1.14430 | $P_{2\infty}=553.56$ | $R_D=60.93$ calcd. |
| 9.2968 | 2.2829 | 1.14410 | $\mu=4.91$ D. | |

(IV) Cyclopentene-3, 5-dione

| | | | | |
|---|---|---|---|---|
| 2.1889 | 2.2734 | 1.14560 | $\varepsilon_1=2.2728$ | $\alpha=3.623$ |
| 5.7821 | 2.2751 | 1.14543 | $v_1=1.14563$ | $\beta=-0.317$ |
| 12.6409 | 2.2772 | 1.14519 | $P_{2\infty}=89.25$ | $R_D=22.70$ calcd. |
| 21.0662 | 2.2806 | 1.14494 | $\mu=1.80$ D. | |
| 34.2452 | 2.2851 | 1.14454 | | |

(V) 4, 4-Ditropylcyclopentene-3, 5-dione

| | | | | |
|---|---|---|---|---|
| 0.2586 | 2.2725 | 1.14511 | $\varepsilon_1=2.2726$ | $\alpha=1.320$ |
| 1.8458 | 2.2730 | 1.14504 | $v_1=1.14510$ | $\beta=-0.286$ |
| 10.0227 | 2.2741 | 1.14478 | $P_{2\infty}=139.35$ | $R_D=80.79$ calcd. |
| 16.4297 | 2.2748 | 1.14463 | $\mu=1.69$ D. | |
| 25.0302 | 2.2759 | 1.14439 | | |

(VI) Indane-1, 3-dione

| | | | | |
|---|---|---|---|---|
| 3.5277 | 2.2745 | 1.14468 | $\varepsilon_1=2.2728$ | $\alpha=5.506$ |
| 6.7824 | 2.2766 | 1.14460 | $v_1=1.14479$ | $\beta=-0.310$ |
| 12.5974 | 2.2800 | 1.14439 | $P_{2\infty}=187.72$ | $R_D=35.43$ calcd. |
| 23.1803 | 2.2854 | 1.14408 | $\mu=2.73$ D. | |

(VII) 2, 2-Ditropylindane-1, 3-dione

| | | | | |
|---|---|---|---|---|
| 0.3809 | 2.2727 | 1.14524 | $\varepsilon_1=2.2728$ | $\alpha=2.723$ |
| 2.4533 | 2.2736 | 1.14519 | $v_1=1.14525$ | $\beta=-0.300$ |
| 8.7616 | 2.2752 | 1.14500 | $P_{2\infty}=249.44$ | $R_D=96.11$ calcd. |
| 17.0778 | 2.2775 | 1.14470 | $\mu=2.74$ D. | |
| 24.5799 | 2.2794 | 1.14454 | | |

(VIII) 1, 2-Dichlorocyclopentene-3, 5-dione

| $10^3 w_2$ | $\varepsilon_{12}$ | $v_{12}$ | $n^2_{12}$ | | |
|---|---|---|---|---|---|
| 1.1253 | 2.2729 | 1.14405 | — | $\varepsilon_1=2.2726$ | $\alpha=0.470$ |
| 3.5924 | 2.2745 | 1.14278 | 2.24484 | $v_1=1.14463$ | $\beta=-0.516$ |
| 6.0176 | 2.2756 | 1.14154 | 2.24517 | $n_1^2=2.24448$ | |
| 8.3489 | 2.2763 | 1.14032 | 2.24535 | $\gamma=0.107$ | |
| | | | | $P_{2\infty}=45.48$ | |
| | | | | $R_D=33.77$ (32.37 calcd.) | |
| | | | | $\mu=0.76$ D. (0.80 D.)* | |

(IX) 1, 2-Dichloro-4, 4-ditropylcyclopentene-3, 5-dione

| | | | | | |
|---|---|---|---|---|---|
| 1.4302 | 2.2734 | 1.14422 | — | | |
| 2.4639 | — | 1.14384 | — | $\varepsilon_1=2.2730$ | $\alpha=0.427$ |
| 2.6318 | 2.2744 | | 2.24496 | $v_1=1.14479$ | $\beta=-0.394$ |
| 3.5235 | 2.2747 | 1.14339 | — | | |
| 4.8600 | 2.2749 | 1.14287 | 2.24541 | $n_1^2=2.24444$ | |
| 6.4273 | 2.2756 | 1.14226 | 2.24571 | $\gamma=0.198$ | |
| 10.1467 | 2.2774 | 1.14079 | — | $P_{2\infty}=107.68$ | |
| | | | | $R_D=91.34$ (90.46 calcd.) | |
| | | | | $\mu=0.88$ D. (0.92 D.)* | |

* The moment values in parentheses were obtained using the $R_D$ value calculated from bond refraction data.

tion, which is similar to Halverstadt and Kumler's:

$$R_D = (n_1^2-1)/(n_1^2+2)\cdot(v_1+\beta)M_2 + 3\gamma v_1 M_2/(n_1^2+2)^2$$

Where $\gamma$ is the slope of $n_1^2$ against $w_2$. The values of $n_1^2$ and $\gamma$ were also obtained by the method of least squares. The molar refractions thus obtained were in substantial agreement with the calculated values. The data are shown in Table I. The dipole moments of the diones and sesquifulvalene quinones are listed in Tables II and III respectively.

TABLE II. THE DIPOLE MOMENTS OF CYCLOPENTENE DIONE, INDANE DIONE AND SOME DERIVATIVES

| Compound | $\mu$, D. |
|---|---|
| Cyclopentene-3, 5-dione | 1.80 |
| 4, 4-Ditropylcyclopentene-3, 5-dione | 1.69 |
| 1, 2-Dichlorocyclopentene-3, 5-dione | 0.76 |
| 1, 2-Dichloro-4, 4-ditropylcyclopentene-3, 5-dione | 0.88 |
| Indane-1, 3-dione | 2.73 |
| 2, 2-Ditropylindane-1, 3-dione | 2.74 |

TABLE III. THE DIPOLE MOMENTS OF SESQUIFULVALENE QUINONE AND ITS DERIVATIVES

| Compound | $\mu$, D. | $\Delta\mu$, D. |
|---|---|---|
| Sesquifulvalene-1, 4-quinone | 2.85 | 4.27 |
| 2, 3-Benzosesquifulvalene-1, 4-quinone | 2.48 | 3.90 |
| 2, 3-Dichlorosesquifulvalene-1, 4-quinone | 4.91 | |

## Results and Discussion

**Cyclopentene- and Indane-diones.**—The fact that the dipole moment of 1, 2-dichlorocyclopentene-3, 5-diones is ca. 1 D. lower than that of unsubstituted cyclopentene-3, 5-dione evidently indicates that the moment of cyclopentene-3, 5-dione is directed towards the methylenic carbon from the center of the ring, the same direction as the carbonyl resultant moment.

In the case of cyclopentene-3, 5-dione, the substitution of two tropyl groups on the methylenic carbon results in a decrease of ca. 0.1 D. (1.69 D. compared with 1.80 D.), whereas with its dichloro derivatives an increase of almost the same value is revealed (0.88 D. compared with 0.76 D.). This indicates that the tropyl resultant moment is in the same direction as the C–Cl resultant and that these two moments are in the direction opposite to that of the C=O resultant; the moment of 1, 2-dichlorocyclopentene-3, 5-dione is, therefore, directed towards the C–Cl resultant. The moment of the tropyl group, therefore, seems to be ca. 0.1 D. larger than the C–H moment when the positive pole of the C–H moment is assumed to lie on the hydrogen atom. On the other hand, in the case of indane-1, 3-dione there is scarcely any change in the moment for a similar substitution of the tropyl groups (2.74 D. compared with 2.73 D.).

If one assumes the five-membered ring to be a regular pentagon, the two C=O groups make an angle of 144°. Using the bond moments $\mu_{C-H}=0$ and $\mu_{C=O}=2.3$ D.,[13] the moments of both cyclopentene-3, 5-dione and indane-1, 3-dione are calculated to be 1.4 D. The observed moments are both larger than those calculated, the difference being 0.4 D. with the former molecule and 1.3 D. with the latter. Such an increase in the moment, called the mesomeric moment, may be attributed to the charge transfer brought about through the resonance interaction from the ethylene or benzene group to the C=O groups, such as:



These values are very close to the incremental moments in going from maleic anhydride (3.91 D.[14]) to succinic anhydride (4.2 D.[15]) and from the latter to phthalic anhydride (5.27 D.[15]).

**Sesquifulvalene Quinone.**—If a change transfer does not occur between the five- and seven-membered rings, one would expect the dipole moments of sesquifulvalene-1, 4-quinone and its benzo derivative to be close to those of the corresponding diones which have been dealt with above. The experimental results for benzosesquifulvalene quinone seem nearly to bear this out, for it has a moment of 2.48 D. compared to the moment of 2.73 D. of indane-1,3-dione. On the contrary, the dipole moment of sesquifulvalene quinone is very high compared with that of cyclopentene dione, the difference in the moment being ca. 1 D. Thus these facts strongly suggest the possibility of a charge transfer interaction between the two rings present in these quinones. Regarding the direction of such a transfer, there are two possibilities to be considered, but one of them, transfer at the charge towards the seven-membered ring, is evidently in contradiction with the experimental data, as can be seen from a comparison of the moment of benzosesquifulvalene quinone with that of the corresponding indane dione. On the other hand, assuming that the transfer is oppositely

13) C. P. Symth, "Dielectric Behavior and Structure," McGraw-Hill Book Co., New York (1955), p. 245.
14) L. G. Wesson, "Tables of Electric Dipole Moments," The Technology Press, Cambridge, Mass. (1948).
15) M. G. A. Rau and N. Anantanarayanan, *Proc. Indian Acad. Sci.*, A5, 185 (1937).

directed towards the five-membered ring and that the moments due to it are 4.7 and 5.2 D. respectively, values which are very large compared with those of the diones, then the observed relationship between sesquifulvalene quinones and the corresponding diones may be satisfactorily explained. Accordingly, the decrease in the moment of sesquifulvalene quinone upon the addition of a fused benzene ring may be understood as being due to the increase in the moment opposed to the charge transfer from the seven-membered ring. If the above reasoning is correct, one would expect a very large moment for the 2, 3-dichloro disubstituted derivative of sesquifulvalene quinone because the C–Cl resultant takes the same direction as the moment of sesquifulvalene quinone. Theoretical calculation predicts a moment of 4.95 D. for such a compound, using the bond moment $\mu_{C-Cl}=1.3$ D. deduced from the moment of *o*-dichlorobenzene (2.26 D.).[14] In fact, a value of 4.91 D. was observed for this quinone, a value in good agreement with the predicted one.

Thus one arrives at the conclusion that a remarkably large amount of charge transfer takes place from the seven-membered ring towards the five-membered ring in these sesquifulvalene quinones and that, consequently, their dipole moments are as a whole in the same direction as the charge transfer, and opposite to the C=O resultant.

By making the reasonable assumption that the five-membered rings of these quinones have regular pentagonal structures, as in cyclopentene dione and indane dione, the C=O resultant is calculated to have a value of 1.4 D., as before. Accordingly, the increase from this value, $\Delta\mu=\mu_{total}-2\mu_{C=O}$, is calculated to be 4.3 D. for sesquifulvalene quinone and 3.9 D. for its benzo derivative by subtracting vectorially the C–O resultant from each observed value; surprisingly, they are both very large and directed from the seven-membered ring towards the five-membered ring, the former being 1.1 times higher than the latter. These incremental moments may be ascribed to the contribution of such polar structures as:



When the inductive effects due to the C=O groups are disregarded, it follows that:

$$\Delta\mu=\mu_{total}-2\mu_{C=O}=\mu^{\pi}{}_{total}-2\mu^{\pi}{}_{C=O}$$

Even though various values, ranging from 1.5 D. to 0.3 D.,[1] have been estimated for the $\pi$-moment of a C=O group ($\mu^{\pi}{}_{C=O}$), it can only be said that the $\pi$-moment of sesquifulvalene-1, 4-quinone should be greater than that of benzosesquifulvalene-1, 4-quinone.

The charge transfer moment towards the five-membered ring may be obtained as follows. Taking the moments opposed to it as equal to 0.4 D. and 1.3 D., which have been found in the dione compounds, then the required transfer moments turn out to be 4.7 D. for sesquifulvalene quinone and 5.2 D. for its benzo derivative, the latter value being 1.1 times higher than the former. Although the above assumption regarding the magnitudes of the opposite moments is open to question, it seems very likely that the charge transfer from the seven-membered ring would be larger in benzosesquifulvalene quinone. The greatest part of these transfer moments may, of course, be considered to be due to the migration to the C=O groups, as may be seen from the contribution of the various polar structures. The charge migration in these sesquifulvalene quinones are also shown by the molecular orbital calculations. The electronic structures and the spectral data of these compounds will be discussed in detail later.

## Summary

The dipole moments of some quinone derivative of sesquifulvalene, the corresponding dione compounds and their several derivatives have been measured in benzene at 25°C. The moments of cyclopentene-3, 5-dione and indane-1, 3-dione are in the same direction as the carbonyl resultant, the mesomeric moments being 0.4 D. and 1.3 D. respectively. On the other hand, the direction of the moments of sesquifulvalene-1, 4-quinone and its 2, 3-benzo derivative is just reversed because of a large transfer from the seven-membered ring towards the five-membered ring, presumably towards the carbonyl groups. The incremental moments, the difference between the observed and the carbonyl resultant, in these quinones are 4.2 and 3.9 D. respectively, while the moments due to the transfer from the seven-membered ring are 4.7 and 5.2 D., suggesting that such a charge transfer is greater in benzosesquifulvalene quinone.

*Department of Chemistry*
*Faculty of Science*
*Tohoku University*
*Katahira-cho, Sendai (S. K. & H. A.)*

*The Chemical Research Institute of*
*Non-Aqueous Solutions*
*Tohoku University*
*Katahira-cho, Sendai (I. M. & Y. K.)*

# The Crystal Structure of Monoclinic Phenylhydrazine Hydrochloride, $C_6H_5NHNH_3Cl$

By Chung Hoe Koo*

(Received August 10, 1964)

Crystal structures of hydrazonium salts containing the $N_2H_6^{2+}$ ion, such as hydrazonium fluoride, $N_2H_6F_2$,[1] chloride, $N_2H_6Cl_2$,[2] and sulfate, $N_2H_6SO_4$,[3] and also hydrazinium salts containing the $N_2H_5^+$ ion, such as hydrazinium bromide, $N_2H_5Br$,[4] and chloride, $N_2H_5Cl$,[5] have hitherto been determined by X-ray methods. However, few of the structures of the substituted hydrazine salts have yet been examined. In order to obtain further information about the relationship among these structures of crystals, the substituent effects, and the nature of the chemical bonds in hydrazine salts, the present author has attempted to investigate the crystal structure of phenylhydrazine hydrochloride by means of X-ray analysis. During the preparation of the sample, it was found that this substance was dimorphous, one modification being monoclinic and the other orthorhombic. The crystal structure of the monoclinic modification was first determined; it will be reported on in the present paper and its structure discussed. The structure of the orthorhombic modification will be reported on shortly.

## Experimental

Single crystals for this work were obtained from saturated aqueons solution by slow evaporation at room temperature. The crystals were thin plates elongated along direction of the monoclinic c axis and showed an excellent cleavage parallel to the crystal plane (010).

Ni-filtered Cu$K\alpha$ radiation was employed in all X-ray experiments. The specimens used had the following cross-sections at right angles to the axes of rotation: $0.1\times0.15$ mm. for the c axis rotation, and $0.15\times0.2$ mm. for the a axis. Crystallographic data were obtained from oscillation and from Schiebold-Sauter and Weissenberg photographs of the equatorial and layer lines about two crystallographic axes (c and a). Photographs of the ($hk0$), ($0kl$) and ($hkl$) reflections were taken by means of an integrating Weissenberg camera for each zone, using the multiple-film technique. Intensities were estimated visually with the aid of standard intensity scales prepared by the exposure time method. The intensity ratios among the multiple-films were determined by the Geiger-Müller counter method. The corrections for polarization and Lorentz factors were made in the usual way. Relative values of the observed structure factors were then deduced by the ordinary procedure. No correction for the absorption was made because samll crystals were employed.

## Determination of the Structure

**Unit Cell and Space Group.**—X-Ray examinations show that the crystal belongs to the monoclinic system and has the following cell dimensions:

$$b=7.82\pm0.03\ \text{Å}$$
$$a=30.80\pm0.06\ \text{Å}$$
$$c=3.87\pm0.02\ \text{Å}$$
$$\beta=130.3^\circ\pm0.5^\circ$$

The space group was uniquely determined to be $C_{2h}^5-P2_1/a$ by the observed rules of absent reflections. Though accurate density measurement was difficult and the value thus obtained was rather poor, it was sufficient for the determination of the number of formula units in a cell-four formula units per unit cell. The calculated density is 1.344 g. $cm^{-3}$.

**Approximate Structure.** — Direct sign determination of the structure factors, using Harker-Kasper inequalities and Sakurai's chart,[6] gave only the signs of a few structure factors. Since the crystal has a heavy atom (chlorine), the position of this atom was easily determined by the interpretation of the two-dimensional peak-sharpened Patterson projections along the a and c axes. Further, since the lengths of the a and c axes are short, the positions of the phenylhydrazine group could be determined by a carerful interpretation of these Patterson maps. The approximate position of the chlorine atom was found to be (1/4, 0.05, 0). Ignoring the end nitrogen atom (in the present investigation, $N_{(2)}$), we can consider a symmetry axis of the phenylhydrazine group.

* Present address: Department of Chemistry, College of Liberal Arts and Science, Seoul National University, Seoul, Korea.

1) M. L. Kronberg and D. Harker, *J. Chem. Phys.*, **10**, 309 (1942).
2) J. Donohue and W. N. Lipscomb, ibid., **15**, 115 (1947).
3) I. Nitta, K. Sakurai and Y. Tomiie, *Acta Cryst.*, **4**, 289 (1951).
4) K. Sakurai and Y. Tomiie, ibid., **5**, 289 (1952).
5) K. Sakurai and Y. Tomiie, ibid., **5**, 293 (1952).
6) K. Sakurai, ibid., **5**, 546 (1952).

This axis was found to be approximately on (3/4, $y$, 0). The contribution of each atom except the end nitrogen atom $N_{(2)}$ to $F(hk0)$ and $F(0kl)$ of $k=2n+1$ was essentially zero for these approximate atomic parameters. However, by putting the $N_{(2)}$ atom in an appropriate position, the signs of a sufficient number of structure factors with $k=2n$ and a few signs of structure factors with $k=2n+1$ could be determined, so that the calculation of preliminary Fourier projections $\rho(xy)$ and $\rho(yz)$ could be carried out. After each three successive syntheses of Fourier projections along the c and a axes, it was found that the agreement between $F_o$ and $F_c$ in $F(hk0)$ and in $F(0kl)$ with $k=2n$ was much improved, whereas there still remain large discrepancies with $k=2n+1$, suggesting that either the chlorine atom or the symmetry axis of phenylhydrazine, or both, may not lie precisely on the special lines mentioned above.

**Refinement of the Structure.**—*xy-Projection.*—The refinement of the coordinates was carried out by the trial and error method at the first stage to find out the direction of the chlorine atom and the symmetry axis of the phnylhydrazine group from the two-fold screw axes, (1/4, $y$) and (3/4, $y$) respectively. The further refinement of this projection was carried out by successive $(F_o-F_c)$ syntheses. No attempt was made to introduce individual temperature factors. The temperature factor finally employed for all atoms in this projection was $\exp(-3.8\sin^2\theta/\lambda^2)$. The atomic scattering factors used in the calculation of the structure factors were those given by Berghuis et al.[7] The final value of the discrepancy index, $\sum||F_o|-|F_c||/\sum|F_o|$, was 0.15 for all ($hk0$)'s, and 0.10 if the unobserved $F_o$ was omitted. The final electron density map is shown in Fig. 1.

*yz-Projection.*—The refinement of the coordinates was carried out by the trial-and-error method and Fourier syntheses, but no $(F_o-F_c)$ synthesis was tried since all of the atoms in this projection were unresolved. After laborious work, the best $z$ coordinates were finally determined. The values of the discrepancy factor for this zone were 0.16 and 0.12 (if the unobserved $F_o$ was omitted). The temperature factor finally employed for this zone was $\exp(-3.6\sin^2\theta/\lambda^2)$. The final electron density map is shown in Fig. 2.

Two possible structures can be considered from the combinations of atomic coordinates which are determined independently from $\rho(xy)$ and $\rho(yz)$. The best agreement between

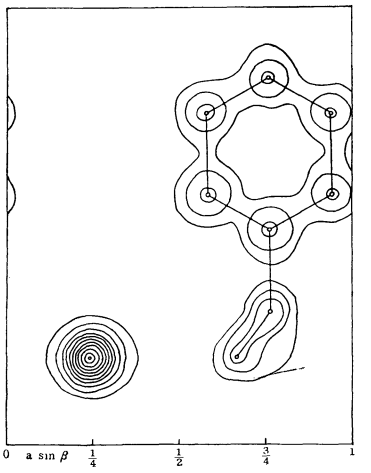



Fig. 1. Electron density distribution projected along the c axis. Contours are at every 2 e. Å$^{-2}$.

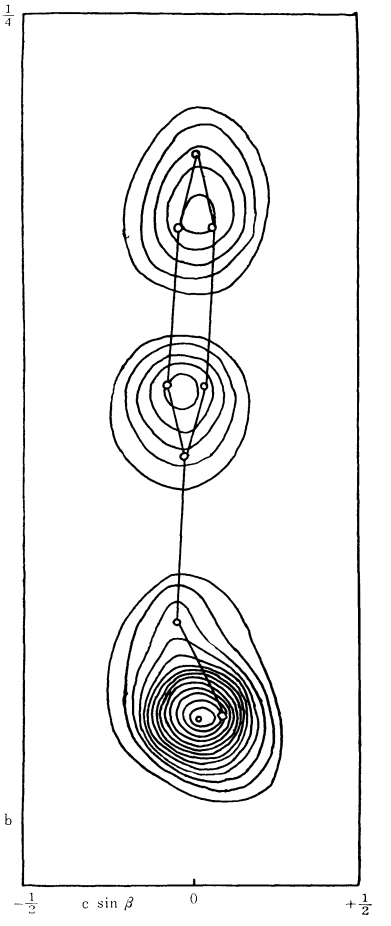



Fig. 2. Electron density distribution projected along the a axis. Contours are at every 2 e. Å$^{-2}$, the contour at the 2e. Å$^{-2}$ level being omitted.

7) J. Berghuis, IJ. M. Haanappel, M. Potters, B. O. Loopstra, C. H. MacGillavry and A. L. Veenendaal, ibid.. **8**, 478 (1955).

$F_o$ and $F_c$ for $F(hkl)$ in these cases was sought so as to find out one reasonable final combination of parameters. Thus, the three dimensional atomic parameters were determined to be as given in Table I.

Table I. Atomic parameters

| Atom | $x$ | $y$ | $z$ |
|---|---|---|---|
| $C_{(1)}$ | 0.7608 | 0.1225 | −0.0233 |
| $C_{(2)}$ | 0.9400 | 0.1429 | 0.0433 |
| $C_{(3)}$ | 0.9367 | 0.1888 | 0.0650 |
| $C_{(4)}$ | 0.7575 | 0.2092 | 0.0083 |
| $C_{(5)}$ | 0.5800 | 0.1883 | −0.0483 |
| $C_{(6)}$ | 0.5833 | 0.1425 | −0.0700 |
| $N_{(1)}$ | 0.7633 | 0.0754 | −0.0500 |
| $N_{(2)}$ | 0.6667 | 0.0492 | 0.0900 |
| Cl | 0.2433 | 0.0480 | 0.0167 |

The interatomic distances and bond angles calculated from the atomic parameters given in Table I are listed in Table II.

**The Accuracy of the Numerical Results.**—The standard deviations of the atomic coordinates estimated from the observed $\rho(xy)$ values are $\sigma(x_C)=0.006$, $\sigma(x_N)=0.005$ and $\sigma(x_{Cl})=0.002$ Å while those from the observed $\rho(yz)$ values are $\sigma(z_C)=0.013$, $\sigma(z_N)=0.012$ and $\sigma(z_{Cl})=0.005$ Å. The standard deviations of the C–N and N–N distances derived from these values are $\sigma(\text{C–N})=0.008$ and $\sigma(\text{N–N})=0.012$ Å.

## Discussion

Figure 3 shows the atomic arrangement in the crystal projected along the c axis. The figure shows the values of the interatomic distances. The N–N distance is 1.432 Å, with the standard deviation of 0.012 Å. This is significantly shorter than the N–N single bond found in the hydrazine molecule (1.47 Å in the gaseous state[8] and 1.46 Å in a crystal[9]). The value seems to be slightly larger than that in $N_2H_6^{2+}$ (1.40—1.42 Å) and smaller than that in $N_2H_5^+$ (1.45 Å), but such differences may not be significant in view of probable uncertainty of these values. Therefore, it is difficult to say that the N–N distance found in the phenylhydrazine ion is really affected by the substituted phenyl group.

The phenyl group has ordinary dimensions in this crystal. The C–N bond distance in the phenylhydrazine ion is 1.455 Å, the standard deviation being 0.008 Å. This is slightly shorter than the C–N single bond distance, 1.475 Å, given by Cox and Jeffrey[10] from a survey of many experimental values. Since this shortening is probably significant, there may exist a slight conjugation effect between the lone orbital on the nitrogen atom $N_{(1)}$ and the $\pi$-bond orbital on the carbon atom of the phenyl group. From the results of conjugation, the nitrogen atom $N_{(1)}$ has a positive net charge and, therefore, the proton affinity will become weak. Thus, when phenylhydrazine acts as a monoacidic base, the end nitrogen, $N_{(2)}$, will attract the acid proton, forming an $-NH_3^+$ group, and $N_{(1)}$ will remain as an imino –NH– group. This is in accord with the results of the present experiment; i. e., the distances of N···Cl show that $N_{(1)}$ should be the imino –NH– group and $N_{(2)}$, the amino $-NH_3^+$ group.

The direction of the N–N bond deviates far from the plane formed by the phenyl group and the N–C bond, the azimuthal angle being 67.2°. This shows that the conjugation between the phenyl $\pi$-orbital and the lone pair orbital on $N_{(1)}$ occurs to a certain extent. As a matter of fact, if the conjugation between the phenyl group and the lone pair on $N_{(1)}$ were sufficiently strong, three bond directions of the imino nitrogen atom (and hence the N–N

Table II. Interatomic distances and bond angles (in Å unit)

| | | | | | | |
|---|---|---|---|---|---|---|
| $C_{(1)}$—$N_{(1)}$ | 1.455 | $N_{(2)}$···$N_{(1)}$ | 3.007 | | | |
| $N_{(1)}$—$N_{(2)}$ | 1.432 | $N_{(2)}$···Cl | 3.134, | 3.162, | 3.224, | 3.498 |
| $C_{(1)}$—$C_{(2)}$ | 1.399 | $N_{(1)}$···Cl | 3.356, | 3.430, | 3.690, | 3.805 |
| $C_{(2)}$—$C_{(3)}$ | 1.415 | Cl···Cl | 3.870, | 4.755, | 4.404 | |
| $C_{(3)}$—$C_{(4)}$ | 1.417 | $C_{(5)}$···$C_{(3)}$ | 4.052 | | | |
| $C_{(4)}$—$C_{(5)}$ | 1.411 | $C_{(5)}$···$C_{(4)}$ | 4.134 | | | |
| $C_{(5)}$—$C_{(6)}$ | 1.415 | $C_{(4)}$···$C_{(4)}$ | 4.649 | | | |
| $C_{(6)}$—$C_{(1)}$ | 1.419 | $C_{(4)}$···$C_{(3)}$ | 4.116 | | | |

| | | | |
|---|---|---|---|
| $C_{(6)}$—$C_{(1)}$—$C_{(2)}$ | 127.5° | $C_{(5)}$—$C_{(6)}$—$C_{(1)}$ | 118.7° |
| $C_{(1)}$—$C_{(2)}$—$C_{(3)}$ | 113.9° | $C_{(6)}$—$C_{(1)}$—$N_{(1)}$ | 118.7° |
| $C_{(2)}$—$C_{(3)}$—$C_{(4)}$ | 119.2° | $C_{(2)}$—$C_{(1)}$—$N_{(1)}$ | 113.8° |
| $C_{(3)}$—$C_{(4)}$—$C_{(5)}$ | 126.6° | $C_{(1)}$—$N_{(1)}$—$N_{(2)}$ | 120.1° |
| $C_{(4)}$—$C_{(5)}$—$C_{(6)}$ | 114.1° | | |

8) P. A. Giguère and V. Schomaker, *J. Am. Chem. Soc.*, 65, 2025 (1943).
9) R. L. Collin and W. N. Lipscomb, *Acta Cryst.*, 4, 10 (1951).
10) E. G. Cox and G. A. Jeffrey, *Proc. Roy. Soc.*, A207, 110 (1951).

bond) would be coplanar with the phenyl group. Although the N–N bond deviates from the plane formed by the phenyl group, as has been observed, and the N–H bond lies on this plane, the conjugation is still possible should the –NH– group have a tetrahedral arrangement.

The phenyl group is significantly distorted. The C–C–C angles at $C_{(1)}$ and $C_{(4)}$ are 127.5° and 126.6° respectively; they are significantly larger than 120°. The C–C–C angles at $C_{(2)}$ and $C_{(5)}$ are significantly smaller than those at $C_{(1)}$ and $C_{(4)}$.

The end nitrogen atom, $N_{(2)}$, has three nearest chlorine neighbors, the N···Cl distances being 3.134, 3.162 and 3.224 Å. Besides, $N_{(2)}$ is in contact with the $N_{(1)}$ belonging to the neighboring molecule, the distance being 3.007 Å. Two of the $N_{(2)}$···Cl contacts, with 3.134 and 3.162 Å, and the $N_{(2)}$···$N_{(1)}$ contact with 3.007 Å may be hydrogen bonds. This arrangement more or less resembles that formed in $N_2H_5Cl$,[5] although the hydrogen bonds in the latter are slightly stronger than those of the former. From the point of view of atomic arrangement, the $N_{(2)}$···Cl with the distance of 3.224 Å is not a hydrogen bond. It is of interest to see that the $-NH_3^+$ groups in aniline hydrochloride[11] and cyclohexylamine hydrochloride[12] have no neighboring chlorine ion which is linked by a hydrogen bond.

The nitrogen atom, $N_{(1)}$, which is linked to the phenyl group has two nearest chlorine neighbors, the N···Cl distances being 3.356 and 3.430 Å. Although these distances are not short enough, the directions connecting $N_{(1)}$ with the two chlorine atoms in question extend in the same proper directions as the NH···Cl bonds. Since only one NH···Cl hydrogen bond is possible for $N_{(1)}$, we must decide which direction is the proper hydrogen bond. If the former is the direction of NH···Cl, the lone pair on the $N_{(1)}$ will lie nearly on the plane formed by the phenyl group, and, hence, the conjugation will not occur. On the other hand, if the latter is the NH···Cl hydrogen bond, the lone pair on the $N_{(1)}$ can reserve a tendency to conjugate with the phenyl group. Therefore, it may be reasonable that the N···Cl with the distance of 3.430 Å should be the weak hydrogen bond required by $N_{(1)}$ and that the N···Cl with the distance of 3.356 Å should be a van der Waals contact. Such very weak hydrogen bonds are also found in the crystal of hydrazinium chloride, where the $-NH_2$ group of $N_2H_5^+$ ion has three chlorine neighbors, and two of the N···Cl have proper directions as NH···Cl hydrogen bonds, the distances being 3.43 and 3.49 Å.

The slightly positive net charge on the $N_{(1)}$ atom due to some conjugation effect, as has been mentioned before, will decrease the proton affinity of $N_{(1)}$. This can explain the fact that the NH···N hydrogen bond (3.007 Å) in this crystal is slightly longer than that found in $N_2H_5Cl$, where the distace is 2.96 Å.

Phenylhydrazine ions are linked by the NH···N hydrogen bonds, which form an infinite zig-zag chain along the c axis. This type of linkage is different from that found in $N_2H_5Cl$ and $N_2H_5Br$, where the NH···N hydrogen bond makes infinite spiral chains.

The projections of the crystal structure along the c and a axes are illustrated in Figs. 3 and 4 respectively. The figures given show the interatomic distances. Each two phenylhydrazine and chlorine ions are linked into a pair by $NH^+$···Cl hydrogen bonds approximately on the (001) plane. Such dimers of

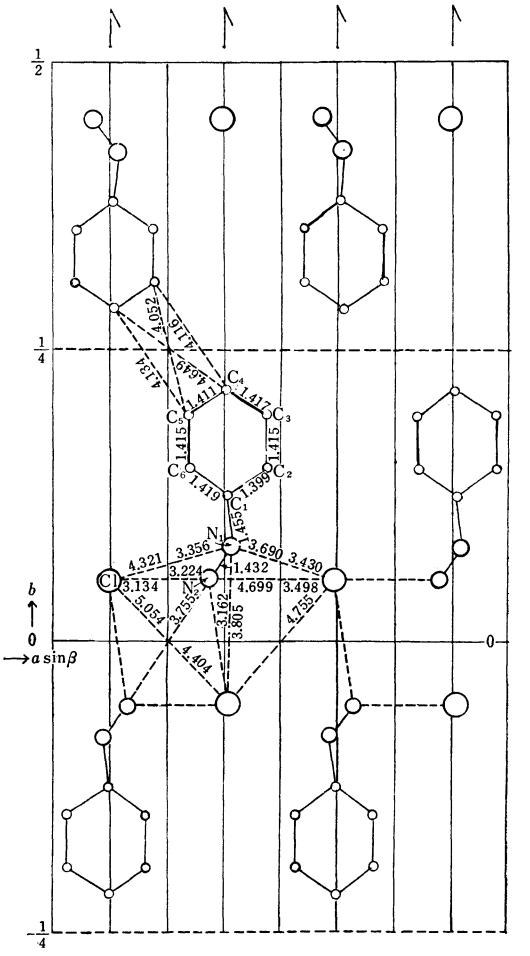



Fig. 3. Atomic arrangement in the crystal projected along the c axis giving interatomic distances.

11) C. J. Brown, *Acta Cryst.*, **2**, 228 (1949).
12) A. Shimada, Y. Okaya and M. Nakamura, ibid., **8**, 819 (1955).

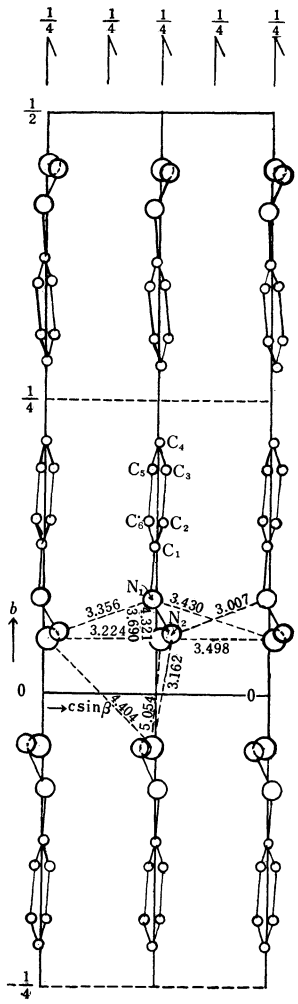



Fig. 4. Atomic arrangement in the crystal projected along the a axis giving interatomic distances.

positive and negative ions linked by hydrogen bonds are found in tropolone hydrochloride.[13] These pairs are linked by weak NH···N hydrogen bonds and are piled up into columns in the c axis direction. Such columns are linked by weak NH···Cl hydrogen bonds formed by $N_{(1)}$ atoms in the a axis direction.

As for the b axis direction, the phenyl groups are in contact with other phenyl groups by van der Waals force only; therefore, the cohesive force is not strong in this direction. This structural feature is compatible with the observed remarkable cleavage along the (010) plane.

It is of interest to compare the structure of the present crystal with those of aniline hydrochloride[11] and cyclohexylamine hydrochloride[12]. The structure of aniline hydrochloride is of a distorted caesium chloride arrangement, such as is also found in the structures of lower-membered alkylamine hydrochloride. On the other hand, cyclohexylamine hydrochloride crystallizes in a layer structure derivable from the sodium chloride arrangement, which is common in the structures of higher-membered alkylamine hydrochloride. It should be noted that the structure of phenylhydrazine hydrochloride has a remarkable layer structure, like cyclohexylamine hydrochloride, that each phenylhydrazine group is surrounded by six chlorine ions, and that each chlorine ion has six phenylhydrazine rings as its first neighbors. The packing is thus closely related to the sodium chloride type.

The author wishes to express his thanks to Professors Isamu Nitta, Tokunosuke Watanabé and Yujiro Tomiie for their continuous guidance and helpful discussions during the course of this research. This investigation was partly supported by a grant from the Ministry of Education. The author is also grateful for a scholarship awarded by the Korean Scholarship Foundation in Japan.

*Department of Chemistry*
*Faculty of Science*
*Osaka University*
*Nakanoshima, Osaka*

13) Y. Sasada and I. Nitta, This Bulletin, 30, 62 (1957).

# Heats of Mixing for Binary Mixtures. II. The 1, 3-Butanediol-Methylethylketone System

By Mitsumasa TAKAMI, Sachio MURAKAMI and Ryoichi FUJISHIRO

(Received August 22, 1964)

In the previous paper,[1] we measured the heats of mixing of monoalcohol-ketone systems and estimated the value of the hydrogen-bond energy of the type O–H···O= to be about 4 kcal.

In order to make a further study of the interaction between alcohol and ketone, we measured the heats of mixing of the 1, 3-butanediol-methylethylketone system, together with those of the ethanol-methylethylketone system, in which an ethanol molecule may be regarded as a monomer of a butanediol molecule.

This paper will describe the results of the measurement and will discuss the existence of the intramolecular hydrogen bond in butanediol.

## Experimental

The apparatus used in this study was the one described in the previous paper,[1,2] except for a slight improvement in the calorimeter to make the handling easier. The calorimeter is shown schematically in Fig. 1.

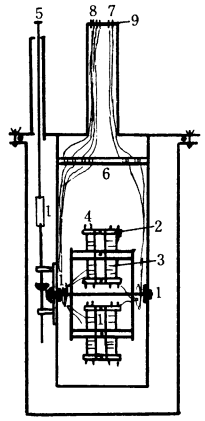



Fig. 1. Calorimeter.
1 Thermal insulater (Teflon)
2 Mixing vessel holder
3 Heater
4 Thermocouple
5 Handle
6 Thermal damper (brass)
7 Lead wire of the thermocouple
8 Lead wire of the heater
9 Harmetic seal

Commercial 1, 3-butanediol was distilled with a Stedman column through nitrogen gas under reduced pressure, and over the molecular sieves in a vaccum. Ethanol and methylethylketone were purified according to the method described in the literature[3] and were finally distilled over the molecular sieves through a long column.

## Results and Discussion

The heats absorbed when 1, 3-butanediol and methylethylketone were mixed in various proportions were measured at the temperature of 25.0±0.01°C; the results are shown in Table I, Fig. 2 and Fig. 3. The heats of mixing per mole of solution are shown as

TABLE I. HEATS OF MIXING OF 1, 3-BUTANEDIOL (1) AND METHYLETHYLKETONE (2)

| Mole fraction of alcohol ($x_1$) | $\Delta H^M$ cal./mol. of solution | $\Delta H^M_{x_1}$ kcal./mol. of 1 |
|---|---|---|
| 0.0473 | 80.11 | 1.69 |
| 0.0999 | 157.4 | 1.57 |
| 0.1363 | 201.1 | 1.48 |
| 0.1654 | 239.0 | 1.44 |
| 0.2047 | 280.3 | 1.37 |
| 0.2126 | 295.5 | 1.39 |
| 0.2184 | 291.4 | 1.33 |
| 0.2452 | 293.5 | 1.20 |
| 0.2855 | 347.9 | 1.22 |
| 0.3134 | 367.5 | 1.17 |
| 0.3391 | 394.4 | 1.16 |
| 0.3418 | 378.1 | 1.10 |
| 0.4333 | 383.0 | 0.884 |
| 0.4512 | 371.5 | 0.823 |
| 0.4522 | 386.3 | 0.854 |
| 0.4806 | 370.3 | 0.770 |
| 0.4899 | 389.6 | 0.795 |
| 0.5217 | 362.6 | 0.695 |
| 0.5721 | 364.6 | 0.637 |
| 0.6508 | 303.8 | 0.467 |
| 0.6527 | 323.1 | 0.495 |
| 0.7023 | 281.9 | 0.401 |
| 0.7402 | 286.0 | 0.386 |
| 0.8295 | 186.1 | 0.224 |

1) S. Murakami, K. Amaya and R. Fujishiro, This Bulletin, 37, 1776 (1964).
2) K. Amaya and R. Fujishiro, ibid., 34, 1271 (1961).
3) A. Weissberger and E. S. Porskauer, "Organic Solvents," Interscience Publishers Inc., New York (1955).

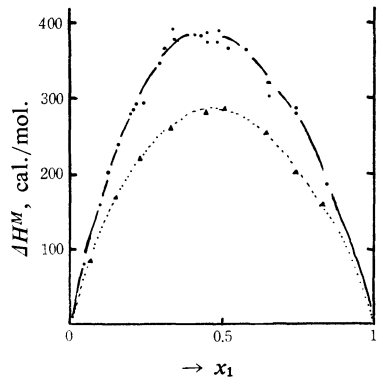



Fig. 2. The plots of $\Delta H^M$ vs. mole fraction of alcohol.
—— 1, 3-Butanediol-methylethylketone
····· Ethanol-methylethylketone

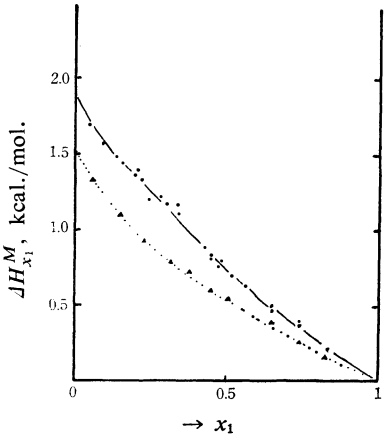



Fig. 3. The plots of $\Delta H^M_{x_1}$ vs. mole fraction of alcohol.
—— 1, 3-Butanediol-methylethylketone
····· Ethanol-methylethylketone

$\Delta H^M$, and those per mole of butanediol as $\Delta H^M_{x_1}$, where $x_1$ indicates the mole fraction of butanediol. $\Delta H^M$ and $\Delta H^M_{x_1}$ versus $x_1$ are expressed, respectively, by the following equations:

$$\Delta H^M = x_1(1-x_1)\,[1185.8+693.5(1-x_1)]$$

$$\Delta H^M_{x_1} = \Delta H^M/x_1 = (1-x_1)\,[1185.8+693.5(1-x_1)]$$

which are shown by the full lines in Fig. 2 and Fig. 3.

We also measured the heats of mixing of ethanol and methylethylketone in various concentrations at the same temperature; the results are shown in Table II and are depicted by the dotted line in Figs. 2 and 3 against the mole fraction of ethanol. They are expressed by the following equations, which agree well with the experimental data:

TABLE II. HEATS OF MIXING OF ETHANOL (1) AND METHYLETHYLKETONE (2)

| Mole fraction of alcohol ($x_1$) | $\Delta H^M$ cal./mol. of solution | $\Delta H^M_{x_1}$ kcal./mol. of 1 |
|---|---|---|
| 0.0636 | 84.56 | 1.33 |
| 0.1546 | 169.5 | 1.10 |
| 0.2361 | 218.1 | 0.924 |
| 0.3340 | 263.3 | 0.788 |
| 0.3866 | 280.7 | 0.726 |
| 0.4565 | 280.2 | 0.614 |
| 0.5083 | 285.0 | 0.561 |
| 0.6514 | 254.2 | 0.390 |
| 0.7397 | 198.3 | 0.268 |
| 0.8150 | 160.4 | 0.170 |

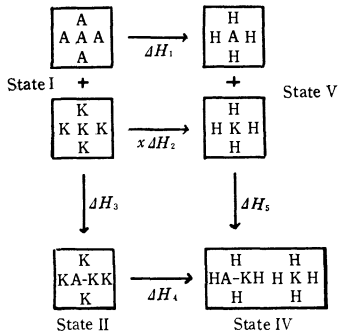



Fig. 4. The thermochemical cycle.

$$\Delta H^M = x_1(1-x_1) \times [1497.2-1673.5(1-x_1)+1698.7(1-x_1)^2]$$

$$\Delta H^M_{x_1} = \Delta H^M/x_1 = (1-x_1) \times [1497.2-1673.5(1-x_1)+1698.7(1-x_1)^2]$$

From these results, the $\lim_{x_1\to 0} \Delta H^M_{x_1}$ values of the butanediol-methylethylketone and ethanol-methylethylketone systems are found to be 1.88 and 1.52 kcal. respectively.

In the previous paper,[1] we estimated the intermolecular hydrogen bond energy of the type O–H···O= for the monoalcohol-ketone system by the use of the following equation, derived from the thermochemical cycle, as in Fig. 4:

$$\Delta H_5 = -\Delta H_1 - x\Delta H_2 + \Delta H_3 + \Delta H_4 \qquad (1)$$

$\Delta H_5$ is the intermolecular hydrogen-bond energy between alcohol and ketone molecules. $\Delta H_1$ is the energy needed to break the hydrogen bonds of pure alcohol by adding a large quantity of hexane, and $x\Delta H_2$ is the heat of dilution of $x$ moles of ketones by a large amount of hexane. $\Delta H_3$ is the energy of transfer from the pure alcohol state to one in which each alcohol molecule makes a hydrogen bonding with a ketone molecule and in which such complexes are surrounded with a

TABLE III. PHYSICAL CONSTANTS OF ALCOHOL-KETONE COMPLEX NECESSARY FOR THE CALCULATION OF DIPOLAR ENERGIES AND CALCULATED VALUES OF $\Delta G_i$ AND $\Delta H_i$ FOR THE ETHANOL-METHYLETHYLKETONE SYSTEM

| $\mu$ D. | $t$ °C | $\alpha$ $\times 10^{23}$ | $a^3$ $\times 10^{23}$ ml. | kcal./mol. $\Delta G_K$ | $\Delta H_K$ kcal./mol. | $\Delta G_H$ kcal./mol. | $\Delta H_H$ kcal./mol. |
|---|---|---|---|---|---|---|---|
| | 15 | 1.3311 | 5.8293 | 2.4377 | | 0.8527 | |
| | | | | | 3.83 | | 1.42 |
| 4.11 | 20 | 1.3321 | 5.8648 | 2.4135 | | 0.8429 | |
| | | | | | 3.80 | | 1.42 |
| | 25 | 1.3331 | 5.9010 | 2.3892 | | 0.8328 | |
| | | | | Av. | 3.82 | | 1.42 |

| Dielectric contant $t$, °C | 15 | 20 | 25 |
|---|---|---|---|
| *n*-Hexane | 1.897 | 1.890 | 1.883 |
| Methylethylketone | 18.98 | 18.51 | 18.07 |

* $\mu$, $\alpha$ and $a$ are dipole moment, the polarizability and the molecular radius of the alcohol-ketone complex, respectively. They are estimated in the same way as that described in the previous paper (Ref. 1). $\Delta G$ and $\Delta H$ are the stabilization free energy and the stabilization enthalpy of the complex molecule in the medium. The suffixes K and H represent the media of ketone and hexane, respectively.

large amount of the ketone medium. $\Delta H_4$ consists of two energy changes. The first one is equal to $(x-1)\Delta H_2$. The second one is due to the different dipolar stabilization energies of the dipole of an alcohol-ketone complex arising from the reaction field with different media.

For the ethanol-ketone system, each $\Delta H_i$ term ($i=1$, 2, 3 and 4) in Eq. 1 may be estimated as follows. The heat of mixing for monoalcohol-hexane systems was measured and reported by Elbe[4] to be 5.8 kcal. at an infinite dilution, which is adopted as $\Delta H_1$ for ethanol. For $\Delta H_2$, we use 1.90 kcal., as measured in the previous paper.[1] $\Delta H_3$ is 1.52 kcal., which was obtained in this study. The dipolar part of the energy change in $\Delta H_4$ is calculated by the method described in the previous paper.[1] The necessary data in this calculation and the results obtained are summarized in Table III.

By using estimated values of $\Delta H_1$ to $\Delta H_4$ and Eq. 1, $\Delta H_5$ is calculated for the ethanol-methylethylketone system as:

$$\Delta H_5 = -5.80 - 1.90x + 1.52 + 2.40 + 1.90(x-1)$$
$$= -3.8 \text{ kcal.}$$

This energy is nearly the same as those derived in the previous paper.[1]

Butanediol is insoluble in any non-polar solvent, and the thermochemical cycle can not be applied to this system. Therefore, we must study the behavior of butanediol from the heats of mixing with ketone. If two hydroxyl groups in a butanediol molecule behave independently of each other, this molecule may be regarded as two ethylalcohol molecules, and the $\lim_{x_1 \to 0} \Delta H_{x_1}^M$ value for the butanediol-ketone system may be expected to be twice that for the ethylalcohol-ketone one, that is, $2 \times 1.52 = 3.04$ kcal., because each of these hydroxyl groups has a possibility of making a hydrogen bond with a ketone molecule. However, the actual value of $\lim_{x_1 \to 0} \Delta H_{x_1}^M$ for the butanediol system is 1.88 kcal., which is 1.16 kcal. ($=3.04-1.88$) lower than the expected value. This decrease may be ascribed to the interaction of two hydroxyl groups in the butanediol molecule. It is not unreasonable to say that a 1, 3-butanediol molecule has so favorable a molecular structure as to make the strong intramolecular hydrogen bond by its two hydroxyl groups, the energy of which may be estimated to be of the same order as that of the intermolecular one. Therefore, if the intramolecular hydrogen bonds are perfectly formed in the ketone medium (an infinitly diluted solution of butanediol in ketone) and are excluded in the pure butanediol state, $\lim_{x_1 \to 0} \Delta H_{x_1}^M$ must be 1.52 kcal., and the corresponding decrease of $\lim_{x_1 \to 0} \Delta H_{x_1}^M$ from the expected value will also be 1.52 kcal., because upon the perfect formation of intramolecular hydrogen bonds of butanediol in the ketone medium there remains only one hydroxyl group available to form a hydrogen bond with a ketone molecule for each butanediol molecule.

Assuming that there are no intramolecular hydrogen bonds in the pure butanediol state and that the energy of the intramolecular hydrogen bond is nearly the same as that of the intermolecular one, the fraction of the intramolecular hydrogen-bonded form will amount to 80% ($=1.16/1.52$) in the ketone medium.

4) G. von Elbe, *J. Chem. Phys.*, **2**, 73 (1934).

In order to confirm the assumption that hardly any intramolecular hydrogen bonds are formed in the pure butanediol, we must estimate the probability that butanediol molecules exist as the intramolecular hydrogen-bonded form. Since a butanediol molecule takes an intramolecular form or an intermolecular one, the probability of the former form is represented in the liquid state of butanediol as:

$$w_A = f_A \exp(-E_A/RT) / [f_{AA} \exp(-E_{AA}/RT) + f_A \exp(-E_A/RT)] \quad (2)$$

where $f_A$ and $f_{AA}$ are the weights at which the intramolecular and intermolecular forms occur, and $E_A$ and $E_{AA}$ are the intra- and inter-hydrogen-bonded energies of alcohol, respectively.

If we replace the butanediol medium which surrounds the butanediol molecule by ketone, we can obtain the state in which the butanediole molecule is surrounded by the ketone medium. This state corresponds to an infinitely dilute solution of butanediol in ketone. In this state, the probability of the intramolecular form is derived in a similar way as:

$$w_B = f_A \exp(-E_A/RT) / [f_{AK} \exp(-E_{AK}/RT) + f_A \exp(-E_A/RT)] \quad (3)$$

where $f_{AK}$ is the weight at which the intermolecular form with a ketone molecule occurs, and $E_{AK}$ is the intermolecular energy between alcohol and ketone molecules. If we tentatively put $E_A = -6$ kcal., $E_{AK} = -4$ kcal. and $w_B = 0.8$ in Eq. 3, we can obtain $f_{AK}/f_A \simeq 10$. To find $w_A$, we must estimate the order of $f_{AA}$. Since $f_{AA}$ and $f_{AK}$ are the weights of an intermolecular form in the alcohol and the ketone media respectively, they may not be very different in magnitude. If we put $f_{AA}/f_{AK} = 2$, that is, $f_{AA}/f_A \simeq 20$, in Eq. 2, considering that a butanediol molecule has a chance of making more intermolecular hydrogen-bonds (usually twice, as a proton donor and an accepter) in the pure state than in the ketone medium, $w_A$ may be estimated to be 5%.

The fact that butanediol liquid is very viscous and insoluble in any non-polar solvent may suggest that strong intermolecular forces act in the liquid state, overcoming the intramolecular forces. Therefore, we may say that, in the pure liquid state of butanediol, the amount of the intramolecular form will be in the range of a few %.

The discussion just mentioned was based on the assumption that the energies of both the inter- and the intra-molecular hydrogen bondings of butanediol are $-6$ kcal. It may easily be shown that as $E_A$ falls off from 6 kcal., the $\lim_{x_1 \to 0} \Delta H^M_{x_1}$ value of the butanediol-ketone system must move from 1.52 to 3.04 kcal. The actual value of 1.88 kcal. may indicate that $E_A$ is nearly equal to or a little less than $E_{AA}$.

Consequently, we may conclude that, in the ketone medium, a considerable amount of butanediol molecules or, rather, nearly all the molecules have intramolecular hydrogen-bonded forms, although in the pure state they are hydrogen-bonded with each other.

## Summary

The heats of mixing of 1, 3-butanediol and ethanol with methylethylketone have been measured. The results obtained for these two systems have been compared with each other, and it has been found that there exist a considerable number of intramolecular hydrogen bonds of butanediol molecules in the ketone medium.

For the ethanol-methylethylketone system, the energy of the intermolecular hydrogen bond with ketone has been estimated to be about 4 kcal. by using the thermochemical cycle; this value is nearly the same as those obtained for other monoalcohol-ketone systems in the previous paper.[1]

The authors wish to thank Dr. Ko Kimura for his kind advice. The cost of this work has been partly defrayed by a grant from the the Ministry of Education.

*Department of Chemistry*
*Faculty of Science*
*Osaka City University*
*Sumiyoshi-ku, Osaka*

# Perchloro-(3,4-dimethylenecyclobutene)

By Akira FUJINO, Yoshikuni NAGATA and Takeo SAKAN

(Received July 6, 1964)

The dechlorination of perchloropropene in an anhydrous ether solution with several kinds of aluminum (chips, granules or powder) principally produces perchloro-(3,4-dimethylenecyclobutene) (I)[1-3] in quite good yields. In the sufficiently high dechlorination degree range, I is the only reaction product isolated in many runs. This result is remarkably different from that of Roedig's report,[4] in which perchlorofulvene (II), two perchlorohexatrienes ($\alpha$-: IIIa and $\beta$-: IIIb, respectively) and perchloro-4-methylenecyclopentene (IV) were given as the ordinary products duplicating the carbon atom number of this substrate, and in only two particular runs was there the poorly reproducible formation of I on the dechlorination of perchloropropane with granulated aluminum. Depending mainly on the reaction conditions, I in the product mixture is sometimes accompanied by perchloro-(3,4-dimethylenecyclobutane) (V),[1-5] m. p. 93°C, the dechlorination intermediate first obtained directly from perchloropropene. The identification of V has been established by comparing it with the specimen synthesized from 1,1,2,3,3-pentachloropropene.[6] It has also been found that V is easily dechlorinated with aluminum - aluminum chloride to give I.[1,3]

The aluminum metal used for the dechlorination is a comparatively pure one (ca. 99% for chips), with which alone the reaction does not start readily, as Roedig noted; a small amount of anhydrous aluminum chloride must first be added to the system. Even with this initiation, the autocatalytic acceleration of reaction is so mild that the whole system is necessarily heated to a violent refluxing. It has been found, however, that the pre-amalgamation of aluminum makes the reaction proceed far more smoothly, without the addition of the catalyst, and causes a remarkable increase in the yield of I up to 44% (chips, $D^*=54\%$), 51% (granules, $D=51\%$) and 62% (powder, $D=66\%$). In general, the incomplete corrosion-treament requires a prolonged reaction time, followed by the partial formation of V. The careful examination of Roedig's dechlorination of perchloropropene with the granulated aluminum - aluminum chloride available in the authors' laboratory has unexpectedly resulted in the random production of either I or II. Perchlorohexa-1,5-diene (VI), a primary coupling product of perchloropropene in Prins' method,[7] was not dechlorinated at all to yield I by amalgamated aluminum, but it was dechlorinated quantitatively to yield IIIa.

I (m. p. 147—148°C, colorless prisms with a slightly irritative odor, crystallized in the triclinic system from ether) is stable in the solid state, whereas it gradually decomposes with the evolution of hydrogen chloride, when allowed to stand in such solvents as ether, benzene and carbon tetrachloride; some of these solvents are, however, applicable in its recrystallization. The ultraviolet light irradiation (principally 2537Å) also destroyed I in

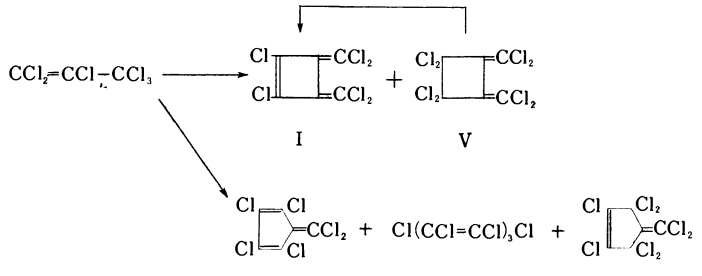



Chart I

1) The establishment of the structure was reported by the authors at 14th Annual Meeting of the Chemical Society of Japan, Tokyo, April, 1961. Abstracts p. 320.
2) A. Roedig and F. Bischoff, *Naturwissenschaften*, **49**, 448 (1962); J. Brandmüller, E. Ziegler and A. Roedig, ibid., **49**, 1466 (1962).
3) A. Roedig, F. Bischoff, B. Heinrich and G. Märkl, *Ann.*, **670**, 8 (1963).
4) A. Roedig, *Ann.*, **569**, 161 (1950).
5) A. Roedig and P. Bernemann, ibid., **600**, 1 (1956).
6) H. J. Prins, *Rec. trav. chim.*, **68**, 898 (1949).
* Dechlorination degree defined by Roedig in Ref. 4.
7) H. J. Prins, ibid., **68**, 419 (1949).

hexane at a markedly rapid rate. The detailed work on both the autodegradation in solution and the photochemistry will be reported later.

Contrary to the disordered results observed in the molecular weight determination of I by the Rast method,[8] the cryoscopic measurement with a fresh benzene solution afforded consistent values, which, however, confusedly became higher even after being stored for only 1/2 hr. The observed dipole moment is 0.43 D. This value is not, however, fully reliable as a result of the instability of the material in carbon tetrachloride.

By long heating with concentrated sulfuric acid at 100°C, I was partially converted, with the evolution of hydrogen chloride, to a carboxylic acid, m. p. 146—147°C, one which has not been yet characterized. A mild alkali-fusion test showed no indication that I has suffered from the degradation. I also resisted the bromine addition in chloroform, as commonly observed in perchloro-polyolefins, but it consumed permanganate in acetone almost instantly.

With a small excess of liquid chlorine in a sealed tube, I was converted in low yield to a chlorocarbon, $C_5Cl_6$ (VII), m. p. 77—78°C, to which the structure of perchloro-(3-methylenecyclobutene) has been assigned. When chlorinated with a large excess of the reagent for a short period, three crystalline products and an oily fraction were obtained: $C_6Cl_{10}$, perchloro-(1,2-dimethylcyclobutene), (VIII), m. p. 146—148°C, $C_5Cl_8$, perchloro-(1-methylenecyclobutane) (IX), m. p. 73—74°C; $C_{12}Cl_{18}$, possibly a dimeric chlorinated product (X), m. p. 163°C (decomp.), and an oil, b. p. 110—130°C(bath temp.)/0.008 mmHg. The purity of the oil remains equivocal.

An attempt to reduce I with zinc and alcohol to some hydrocarbon equivalent has been unsuccessful; the product was merely an amorphous solid mass, which had hardly been purified to serve as an analyltical sample.

The oxidation of I with potassium permanganate in acetone, chromic oxide in acetic acid, or fuming nitric acid always gave the same dicarboxylic acid (XII), $C_6Cl_4H_2O_4$, m. p. 215°C (decomp.), always in very low yields. The rate of oxidation is seemingly decreased in this order of reagents. No definite neutral products have been isolated in the first two cases, whereas, in the slowest nitric acid oxidation, a neutral nitrogeneous material (XIII), $C_6Cl_6N_2O_4$, m. p. 114—115°C (decomp.), was obtained. XII is doubtlessly perchloro-(dimethylenesuccinic) acid; it was converted, by refluxing it with acetic anhydride, to the corresponding anhydride (XIV), m. p. 119—120°C. which was then smoothly hydrolyzed to the original acid by heating it with an aqueous bicarbonate solution. Chart II summarizes the reaction schemes related to I.

## Discussion

Obviously, the most interesting feature of the preceding results is the course of reaction, which is distinctly different from that described by Roedig, whose extensive work pioneering this kind of dechlorination has mainly been concentrated on studies of the production of five-membered ring compounds and of acyclic olefinics. The purity of Roedig's aluminum chips has been reported to be 85—87% (with copper, silicon and zinc as the major impurities, in quantities of 4—5, 3—5 and 2—4% respectively), while the authors' chips in the routine use contain far less impurities (Cu, 0.04; Fe, 0.51; Si, 0.25%). Although Roedig noted the unsuitability of pure aluminum for the reaction, it has been

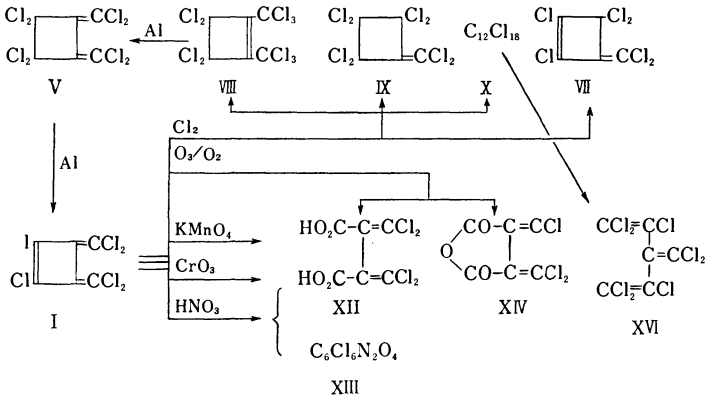
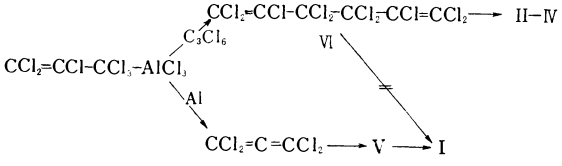



Chart II

8) The observed values are disorderly low as seen in the experimental. Although Roedig reported the value of 279[3] as observed by Rast, it seems highly probable that, with camphor, the thermal decomposition of I above 170°C will affect the determination result.

proved that even a high grade aluminum (99.99%) reacts, after amalgamation, with perchloropropene to give I (in a 55% yield) under essentially the same conditions. It is, therefore, possible to point out that the leading cause of the different results in the dechlorination reactions can be attributed to the quality of the metal, in which some foreign element might function specifically at an early stage of the reaction. The fact that I has not been produced in the dechlorination of VI by the amalgamation procedure strongly excludes the possibility that VI might be an intermediate in the process of the formation of I from perchloropropene. Thus, it is most likely that perchloroallene (XV) is an unstable precursor of V, the formation and the chemical behavior of which have recently been shown in the elaborate synthetic work[3] related to the dehydrochlorination of 1,1,2,3,3-pentachloropropene.




XV

It is also reasonable to assume that the formation of a four-membered ring could be possible only under some specifically accommodated participation of the allene components.[9] This mechanistic speculation would not, however, contradict the observation that I and II have seemed to be incompatible in the product of the Roedig's dechlorinations closely-reexamined with aluminum granules, since, particularly in this case, the metal reagent possibly has a lower and less homogeneous purity than the chips and also a wide-ranging size distribution, both of which more or less affect the reaction process.

The *D*-values determined and the yield of I are illustrated in Table I. So far as the aluminum chips are concerned, the whole reaction appears basically to proceed in a way similar to that of Roedig's reaction in terms of *D*-values (approximately 50—60%). In the runs with granules the *D*-values are much higher than those (less than 5%) reported, and no particular difference has been observed between the "amalgamated" and the "with aluminum chloride." Remarkable indeed is the difference between the two runs with aluminum powder, where the amalgamation causes a tremendous increase in *D* as well as in the yield of I.

Some interesting problems in the course of the structure investigations of I and other related compounds will be briefly discussed below.

The structure of VII is derived from the observation of the very close relationship of the ultraviolet spectral feature of this compouud and that of I, with only a small hypsochromic shift of $\lambda_{max}$ in the former, and from the fact that its infrared spectrum exhibits the $\nu_{C=C}$ doublet (1680 and 1580 $cm^{-1}$)** instead of the

Table I. The dechlorination of perchloropropene with aluminum metal

| Sort of Al | Amalgamated or with $AlCl_3$ | Reactants $C_3Cl_6$ mol. | Reactants Al mol. | Reaction periods hr. | *D* % | Yield of I % |
|---|---|---|---|---|---|---|
| Al-chips[a] | A[b] | 0.32 | 0.74 | 5 | 54 | 44 |
| | A | 0.32 | 0.74 | 5 | 59 | 41 |
| | A | 0.32 | 0.74 | 5 | 47 | 39 |
| | A | 0.32 | 0.74 | 5 | 58 | 37 |
| | A | 0.32 | 0.74 | 5 | 15 | 21[c] |
| | A | 0.32 | 0.74 | 10 | 61 | 38 |
| | A | 0.32 | 0.74 | 35 | 67 | 25 |
| Al-granules | A | 0.08 | 0.19 | 6 | 51 | 51 |
| | B | 0.08 | 0.19 | 6 | 50 | 46 |
| | B | 0.15 | 0.37 | 35 | — | 8.6[d] |
| Al-powder | A | 0.08 | 0.19 | 8 | 66 | 62 |
| | A | 0.08 | 0.19 | 5 | 63 | 56 |
| | A | 0.08 | 0.19 | 6 | 58 | 45[e] |
| | B | 0.08 | 0.19 | 12.5 | 22 | 0 |

a) Chips are small, cross-shaped pieces of the metal stamped out from thin plates.
b) A and B indicate "amalgamated" and "with $AlCl_3$" respectively.
c) The low yield is due to insufficient amalgamation and/or inefficient stirring.
d) The yield of II. The *D* value was not determined in this run.
e) The figure does not include the additional crop composed of I and V.

9) J. D. Roberts and C. M. Sharts, "Organic Reactions," Vol. 12, 24 (1962).

** All IR spectra have been measured with Nujol mull unless noted.

triplet (1695, 1625 and 1550cm$^{-1}$ (KBr)) in I. The first $\nu_{C=C}$ band of I is noteworthy because of its extremely high frequency, which is probably next to the 1810 cm$^{-1}$ value in perchlorocyclopropene,[10] the highest ever observed in the chlorocarbon series. Conceivably, this band is connected with the presence of the endocyclic double bond involved in a four-membered ring. This interpretation further explains the respective presence and lack of band in the corresponding high frequency region in VII and IX. Special caution must be taken before assigning the 1625 cm$^{-1}$ band for VIII, since in position it coincides with the band in IX and rather seems to be for an exocyclic structure. The first reason to favor VIII, however, is its very weak intensity in contrast to the strong one for the double bond of the exocyclic type, as in IX. A >C=C< bond with no chlorine-substituent is suggested here. Secondly, if it has an exocyclic double bond, a considerably intense band can be expected to arise in the 930—900 cm$^{-1}$ range with reference to the $-\underset{|}{C}=CCl_2$ group in the molecule.[11] Only three weak peaks (955 vw, 905 vw and 895 w (cm$^{-1}$)) are practically found in this vicinity, however. In additional consideration of the chemical evidence for the skeletal structure of VIII, established through its dechlorinative conversion to V, the double bond in question can most easily be located at the $C_{1-2}$ position.

The assumption of an exocyclic double bond in IX could also be justified by interpreting the strong 910 cm$^{-1}$ band as characteristically arising from the $-\underset{|}{C}=CCl_2$ group. Although the complete elucidation of the structure of X is a future problem, it may be worth noting here that this chlorocarbon is decomposed above its melting point, or even at a lower temperature under a vacuum, to ε-$C_6Cl_8$ (XVI), m. p. 45°C, which was recently proposed to be perchloro-3-methylene-1, 4-pentadiene by Roedig[2] on the basis of its Raman spectroscopic analysis.

The structure of perchloro-(dimethylenesuccinic) acid was earlier suggested for a carboxylic acid, with an m. p. of 219°C (decomp.), obtained by the alkaline hydrolysis of α, α'-bis-trichloromethylsuccinic acid (XVII),[12] a minor by-product in the reaction of diethyl maleate with benzoyl peroxide in carbon tetrachloride. The re-investigated runs of this reaction have not, however, reproduced XVII and so made the final identification of XII impossible. Nevertheless, the interpretation of the infrared spectrum of XIV leaves little doubt about the structure of XII, since the possible alternatives may all be excluded on the basis of either extremely high carbonyl frequencies (1835 and 1765 cm$^{-1}$) and the magnitude of $\Delta\nu_{C=C}$[13] (70 cm$^{-1}$), or two closely-located bands (930 and 920 cm$^{-1}$) assigned to the two exocyclic dichloromethylene groups. Roedig reported the production of only chloropicrin and oxalic acid dihydrate in the nitric acid oxidation of I, but the small amount of XII and XIII may have been overlooked. The application of ozone to I also affords XII and XIV. It is, however, obscure whether or not the real attack of ozone has occurred in this degradation, because I is very readily decomposed to XII, even with oxygen in some moistened organic solvents, as will be reported in the succeeding paper.

The formation of XIII in the oxidation is interesting enough to mention, since it would be the first case that I is converted to a nitrogeneous compound without losing any chlorine atom in the molecule. The infrared absorption band at 1580 vs and 1315 s (cm$^{-1}$) reveals at least one nitro-group attached to the carbon with two chlorine atoms.[14] The very high intensity of the former band is partially due to the $\nu_{C=C}$ absorption. The investigation is present under way to clarify the structure of XIII.

The ultraviolet absorption spectra data do not seem capable of giving sufficient information about the structural problem of the products mentioned above unless some more compounds of various and appropriate types of four-membered cyclic chlorocarbons are available. However, it is interesting to emphasize that the estimated wavelength values for VII and VIII are in good accordance with those observed, if, on the basis of the available data, the bathochromic displacement factors caused by chlorine substitution (+8.5 mμ for a vinylic substituent,[15] +7.5 mμ for an allylic one,[16] and +10 mμ for a trichloromethyl group attached to the unsaturated carbon,[16]) are taken into account. An extraordinarily large bathochromic shift (+64 mμ) of the $\lambda_{max}$ in the K band from 1, 2-dimethylenecyclobutane[17] to V can also be rationally explained by the con-

10) S. W. Tobey and R. West, *Tetrahedron Letters*, **1963**, 1179.

11) Unpublished. From the accumulated IR data of perchlorocarbons it may be noted that the compounds holding $-\underset{|}{C}=CCl_2$ group in the molecule generally give a strong absorption band in the range of 930—900 cm$^{-1}$, while those with $-\underset{Cl}{\underset{|}{C}}=CCl_2$ group absorb in some higher frequency range, 965—940 cm$^{-1}$.

12) C. S. Marvel, E. J. Prill and D. F. DeTar, *J. Am. Chem. Soc.*, **69**, 52 (1947).

13) R. G. Cook, *Chem. & Ind.*, **1955**, 142.

14) J. F. Brown, Jr., *J. Am. Chem. Soc.*, **77**, 6341 (1955).

15) A. Roedig and E. Klappert, *Ann.*, **605**, 126 (1957).

16) Unpublished.

17) A. T. Blomquist and J. A. Verdol, *J. Am. Chem. Soc.*, **77**, 1806 (1955).

sideration that such a larger increment is due to the allylic chloro-substitution on the four-membered ring carbon rather than to that (less than $+5m\mu$) in the case of five-membered cyclic compounds.[18]

Roedig et al.[3] suggested the lack of an extended conjugation in I on the basis of the close relationship between the K bands in the ultraviolet spectra of I and those of the corresponding hydrocarbon,[19] which also exists as a cross-conjugated form. The particularly high reactivity of the $C_{1-2}$ double bond in I suffices to reflect this indication. It is, therefore, eagerly desirable to make, in the near future, an extensive stereochemical study of whether or not the whole molecule, or, more interestingly, the cyclobutene ring itself, of I is twisted under the influence of its vicinal dichloromethylene groups. If the van der Waals radius of 1.80 Å for the chlorine atom operates in I, it is not possible to keep all four chlorine atoms in the groups coplanar; in addition, its spacial requirement appears to be too large to afford the distortion of only two severely interacting C–Cl bonds (one bending up and one down, from the $sp^2$ plane of each methylene carbon).

## Experimental

**Starting Materials.**—Hexachloropropene was prepared from 1,1,1,2,2,3,3-heptachloropropane[20] by dehydrochlorination according to the literature[21]; b. p. 103—104°C/28 mmHg.

*Aluminum Amalgam.*[22]—A necessary amount of aluminum was corroded thrice with 4 ml./g. (Al) of a 10% aqueous solution of sodium hydroxide and then amalgamated thrice with 5 ml./g. (Al) of a 0.5% aqueous mercuric chloride solution. After having been carefully washed with water, ethanol, ether and anhydrous ether, the compound metal was immediately covered with anhydrous ether in the volume necessary for the reaction.

**The Dechlorination of Perchloropropene. The Production of Perchloro-(3, 4-dimethylenecyclobutene) (I) (An example).**—In a three-necked, round-bottomed, 500 ml.-flask, fitted with a mechanical stirrer and a reflux condenser, the top of which was connected to a calcium chloride tube, an aluminum amalgam (5.0 g. Al) was prepared as has been mentioned above; then 20.2 g. (0.081 mol.) of perchloropropene was vigorously stirred into the contents. The volume of the solvent was 75 ml., including that for rinsing. The exothermic reaction soon occurred, and the solution came to have a tinge of yellow. After an 8-hr. refluxing, the reaction mixtre was allowed to cool; it was then separated into the dark brown muddy material and an ether solution by filtration. The former was decomposed with 10% nitric acid, and the latter with water. The residual dark brown amorphous solid was repeatedly extracted with ether.

The combined ethereal solution was washed with water, shaken with the saturated aqueous sodium bicarbonate solution, and dried over calcium chloride. On the removal of the solvent, the residual oil began to crystallize and afforded the crude product of I (7.2 g.; 62% of the theoretical yield). Vacuum sublimation (110—120°C/5 mmHg) and recrystallization from ether produced the analytical sample as colorless prisms; m. p. 147—148°C.

Found: C, 25.57; H, 0.49; Cl, 74.93. Calcd. for $C_6Cl_6$: C, 25.30; H, 0.00; Cl, 74.70%. Mol. Wt. Found: 238, 230 (Rast method with camphor); 289, 278 (cryoscopic method with benzene). Calcd. for $C_6Cl_6$: 285.

The aqueous solutions were combined, and 5 ml. taken from the whole was titrated with a N/10-silver nitrate solution, using uranine as an indicator to determine the degree of dechlorination.

After having been recovered from the bicarbonate solution by acidification and ether extraction, the acidic fraction gave a small amount of a white crystalline solid, which was recrystallized twice from ligroin; m. p. 74—75°C (perchloroacrylic acid[4]; m. p. 76—77°C).

**The Formation of Perchloro-(1, 2-dimethylenecyclobutane) (V).**—In some runs similar to the above, the sublimate of the crude product showed a lower melting point with a wide range (e. g., 118—134°C). The crops collected from the mother liquor in the course of recrystallizations from ether furnished, after several recrystallizations from benzene, hexagonal plates of V with an m. p. of 92—93°C. Although I is a little more volatile than V, an attempted separation of I from V by means of fractional vacuum sublimation was not successful.

Found: C, 20.52; H, 0.69; Cl, 80.38. Calcd. for $C_6Cl_8$: C, 20.26; H, 0.00; Cl, 79.74%.

**The Synthesis of V from 1, 1, 2, 3, 3-Pentachloropropene.**—According to Prins' method,[23] 1,1,1,2,3,3-hexachloropropane (65 g.), b. p. 95—97°C/14 mmHg, $n_D^{24}$ 1.5213, was obtained from chloroform (300 g.), trichloroethylene (131 g.) and aluminum chloride (30 g.). Subsequent dehydrochlorination[24] in carbon tetrachloride (65 ml.) with aluminum chloride (0.78 g.) at 30—40°C for 1/2 hr., followed by refluxing for 4 hr., gave 1, 1, 2, 3, 3-pentachloropropene (44 g., 80%), b. p. 75—76.5°C/19 mmHg. Further dehydrochlorination with the base-paste (potassium hydroxide, 36.9 g.; calcium oxide, 26.3 g., and water, 7.4 g.) suspended in benzene (70 ml. in all) in accordance with the manner previously described[6] resulted in the production of V (17 g., 36.5%). Recrystallization from trichloroethylene-ethanol afforded white prisms, with an m. p. of 91—92°C, which were identical in all respects (mixture m. p. test, ultraviolet and infrared absorption spectra) with those obtained from perchloropropene.

18) J. D. Idol, Jr., C. W. Roberts and E. T. McBee, *J. Org. Chem.*, **20**, 1743 (1955).
19) A. T. Blomquist and P. M. Maitlis, *Proc. Chem. Soc.*, **1961**, 332.
20) M. W. Farlow, "Organic Syntheses," Coll. Vol. II, 312 (1948).
21) P. Fritsch, *Ann.*, **297**, 314 (1897).
22) J. Houben, "Die Methoden der organischen Chemie," Vol. II, Verlag Georg Thieme, Leipzig (1925), p. 256.
23) H. J. Prins, *J. Prakt. Chem.*, **89**, 414 (1914).
24) H. J. Prins, *Rec. trav. chim.*, **65**, 455 (1946).

**The Chlorination of I.**—*a) With a Small Excess of Chlorine.*—In a thick-walled sealed glass tube, 3.0 g. of I and 2.0 g. (a 2.8 mol. equivalent) of liquid chlorine were allowed to stand for 3 weeks. After the evaporation of the unreacted chlorine, the residue (4.05 g.) was separated into two parts: 0.09 g. of crystals, m. p. 63—76°C, and the filtrate, from which the second crop (1.05 g.) of the solid material crystallized out. The former was repeatedly recrystallized from ethanol until it became a pure sample, with an m. p. of 78—79°C. UV: $\lambda_{max}^{EtOH}$ 236 (32000), 278 (7000), $\lambda_{sh}$ 228 (26000), 244 (22000), $\lambda_{min}$ 256 (5500) mμ (ε).

Found: Cl, 78.34. Calcd. for $C_5Cl_6$: Cl, 77.99%.

The second crystals, after having been washed with ethanol, melted at 43—60°C. Either vacuum sublimations or recrystallizations from methanol and ethanol gave unpurified samples which showed a fairly intense absorption peak at 310 mμ. The filtered viscous oil was 0.98 g.

*b) With a Large Excess of Chlorine.* — The same amount of I was treated with about three times as much liquid chlorine as in the experiment above. The total content was ca. 6 ml. The reaction mixture became clear in 72 hr., after which period the sealed tube was opened. By passing nitrogen gas through, a viscous crystal sludge was obtained. After filtration, 1.2 g. of a solid, white material was recrystallized from benzene-ethanol as VIII, m. p. 146—148°C. 0.35 g.

Found: C, 17.17; H, 0.39; Cl, 83.18. Calcd. for $C_6Cl_{10}$: C, 16.89; H, 0.00; Cl, 83.11%. UV: $\lambda_{max}^{EtOH}$ 223 mμ (ε 8200).

Methanol was added carefully to a slightly greenish yellow viscous filtrate (3.2 g.) dissolved in benzene. The deposited mass was filtered and recrystallized from ether to afford a colorless pure sample of X, m. p. 163°C (decomp.). 0.20 g.

Found: C, 18.78; H, 0.33; Cl, 81.48. Calcd. for $(C_4Cl_6)_x$: C, 18.42; H, 0.00; Cl, 81.58%. UV: $\lambda_{max}^{EtOH}$ 224 mμ (ε 12000); IR: $\nu_{C=C}$ 1600 s cm$^{-1}$.

After the removal of the solvent, the oily fraction was distilled; b. p. 110—130°C (bath temp.)/0.008 mmHg; a colorless clear distillate.

Found: C, 17.76; H, 0.64; Cl, 81.66%.

This sample turned turbid very gradually. When it was stored over two years about one-fifth of the oil crystallized. The separated solid (0.30 g.) melted at 73—74°C after recrystallization from ether-methanol.

Found: C, 17.47; H, 0.61; Cl, 83.07. Calcd. for $C_5Cl_8$: C, 17.47; H, 0.00; Cl, 82.55%. UV: $\lambda_{max}^{EtOH}$ 223 mμ (ε 6500).

The residual oil weighed 1.50 g.

**The Oxidation of I.**—*a) With Potassium Permanganate.*—Into a solution of 50 g. of I in 350 ml. of acetone, 10.1 g. of potassium permanganate dissolved in 510 ml. of the same solvent was stirred at room temperature. The decolorization of the reagent occurred very quickly. Manganese dioxide was removed by filtration and boiled thrice with 100 ml. of water. The filtrate was, after the evaporation of acetone, dissolved in ether in order to be shaken with a saturated aqueous sodium bicarbonate solution. One gram of crude I was recovered from the dried ether solution. The acidified bicarbonate solution and the concentrates of the combined hot water extracts gave, through separate ether extractions, 45 mg. and 11 mg. of perchloro-(dimethylenesuccinic acid), XII, which were combined and recrystallized from ether to a pure sample; m. p. 214°C (decomp.).

Found: C, 26.41; H, 0.92; Cl, 51.08. Calcd. for $C_6Cl_4H_2O_4$: C, 25.75; H, 0.72; Cl, 50.67%.

*b) With Chromic Trioxide.*—To the 100 ml.-solution of acid containing 1.40 g. of chromic trioxide and a trace of water, 1.00 g. of I was added and the mixture was allowed to stand for 48 hr. After the reduction of the excess oxidizing reagent with methanol, the solvent was removed under diminished pressure. A small amount of water was added, and the product was isolated in the usual manner. The acidic fraction gave only a trace of crystals, m. p. 214°C (decomp.) which were pressed on the clay plate, washed with chloroform, and identified with the XII obtained by the nitric acid oxidation of I through infrared sepectra comparison.

*c) With Fuming Nitric Acid.* — Five grams of I was oxidized with 1.0 ml. of fuming nitric acid (sp. gr. 1.52) by warming it on a steam bath until all the excess oxidizing reagent was evaporated off. The ether solution of the remaining oil gave, after being shaken with a bicarbonate solution and upon the evaporation of the solvent, a viscous oil (0.69 g.), from which the pale yellow crystals were precipitated on cooling. The crystals were collected by filtration; 2.27 g. of XIII; m. p. 103—108°C. Recrystallization from methanol elevated its m. p. to 114—115°C (decomp.).

Found: C, 19.47; H, 0.56; N, 7.48; Cl, 56.31. Calcd. for $C_6Cl_6N_2O_4$: C, 19.12; H, 0.00; N, 7.43; Cl, 56.41%. UV: $\lambda_{max}^{EtOH}$ 318 (14500); $\lambda_{sh}$ 328 (13500); $\lambda_{min}$ 265 (2700) mμ (ε). IR: $\nu_{C=C}$ 1610 m, 1580 vs cm$^{-1}$.

0.13 g. of crystals of m. p. 215°C (decomp.) were obtained from the acidified bicarbonate solution.

Found: C, 26.14, H, 1.44; Cl, 51.13%. UV: $\lambda_{max}^{EtOH}$ 230 mμ (ε 13900); IR: $\nu_{C=O}$ 1790 s; $\nu_{C=C}$ 1580 s, 1560 s cm$^{-1}$.

The oily acidic fraction weighed 1.12 g.

**Anhydride (XIV) Formation from perchloro-(dimethylenesuccinic) Acid.**—Thirty milligrams of XII was refluxed at 140—145°C with 0.5 ml. of acetic anhydride for 1/2 hr. in a small tubing vessel equipped with a cold finger. After the reaction had been completed, the cold finger was taken off and the unreacted acetic anhydride and acetic acid were thoroughly removed by heating the mixture on a steam bath under reduced pressure. Vacuum sublimation was applied to the residue. At ca. 100°C (bath temp.)/5 mmHg, 25 mg. of white crystals were obtained. Repeated sublimations gave a pure sample with an m. p. of 119—120°C.

Found: C, 27.83; H, 0.37; Cl, 54.01. Calcd. for $C_6Cl_4O_3$: C, 27.52; H, 0.00; Cl, 54.15%. UV: $\lambda_{max}^{cyclohexane}$ 227 (13300), 300—303 (12400); $\lambda_{min}$ 250 (3700) mμ (ε); IR: $\nu_{C=O}$ 1835 m, 1765 s; $\nu_{C=C}$ 1580 s, 1543 s cm$^{-1}$.

XIV was heated with a saturated aqueous sodium

bicarbonate solution until the all crystals had dissolved completely. The regenerated material was extracted with ether from the acidified solution, followed by the usual procedure. The acid thus obtained melted at 212°C (decomp.) and gave an infrared chart identical with that of XII.

**The Ozonolysis of I.**—A stream of ozone was passed for 5 hr. under cooling (0°C) through a 40 ml.-chloroform solution in which 2.0 g. of I was dissolved. The removal of the solvent under reduced pressure gave a greenish yellow oil which began to evolve hydrogen chloride when it was left in the air. When heated with a small amount of water for 10 min., the ozonide was thoroughly decomposed.

By the usual procedure, 108 mg. of the crystalline product, XIV, with an m. p. of 119—120°C, was obtained from the neutral oil. The acidic fraction (662 mg.) also partly crystallized to the carboxylic acid, m. p. 215°C(decomp.), identical with that of XII.

**The Dechlorination of V to I.**—In a three-necked, 50 ml.-flask, 360 mg. of I was dissolved in 15 ml. of anhydrous ether. Fifteen milligrams of aluminum powder and 2—3 mg. of anhydrous aluminum chloride were then added to the solution, and the solution was refluxed for 3 hr. under vigorous stirring. The same treatment as the usual dechlorination furnished 276 mg. (95%) of white crystals, m. p. 146—148°C, which were in all respects identical with I.

**The Partial Dechlorination of Perchloro-(1, 2-dimethylcyclobutene) (VIII) to V.**—A mixture of 170 mg. of VIII, 250 mg. of aluminum powder, and 30 mg. of anhydrous aluminum chloride in 15 ml. of anhydrous ether was heated under refluxing for 5 hr. After ordinary handling, the neutral oil was kept in a refrigerator for 5 days. The crstallized solid was filtered and purified by vacuum sublimation. White crystals; m. p. 120—127°C; 40 mg. From ultraviolet and infrared spectra it was inferred that the mixing ratio of V to VIII was ca. 0.8.

**The Dechlorination of Perchlorohexa-1, 5-diene (VI) with Amalgamated Aluminum.**—A mixture of 1.50 g. of VI, synthesized by the action of cuprous chloride on perchloropropene in methanol-water,[7] 0.150 g. of amalgamated aluminum chips (99.99% pure) and 30 ml. of anhydrous ether was stirred for 1.5 hr. at room temperature and then heated under refluxing for the same period. The neutral product was distilled at 110—120°C (bath temp.)/0.09 mmHg. The infrared spectrum of this distillate was identical with the IIIa synthesized by the dechlorination of VI with alcoholic potassium hydroxide in acetone.[25]

The authors wish to express their thanks to Mr. Junichi Goda of Osaka City University, Miss Kiku Koike of the Institute for Protein Research (Osaka University), and Dr. Junichi Kawanami of the Shionogi Pharmaceutical Co. for their elemental analyses; to Miss Hiromi Tokuda of Osaka City University for her infrared spectra measurements, and Dr. Ko Kimura of Osaka City University for the dipole moment datum.

*Organic Chemistry Division*
*Research Institute for Atomic Energy*
*Osaka City University*
*Kita-ku, Osaka (A. F. & T. S.)*

*Department of Chemistry*
*Faculty of Science*
*Osaka City University*
*Sumiyoshi-ku, Osaka (Y. N.)*

25) A. Roedig, G. Voss and E. Kuchinke, *Ann.*, **580**, 24 (1955).

# The Synthesis and Some Reaction of 3-Acetonyltropolones

By Kahei TAKASE

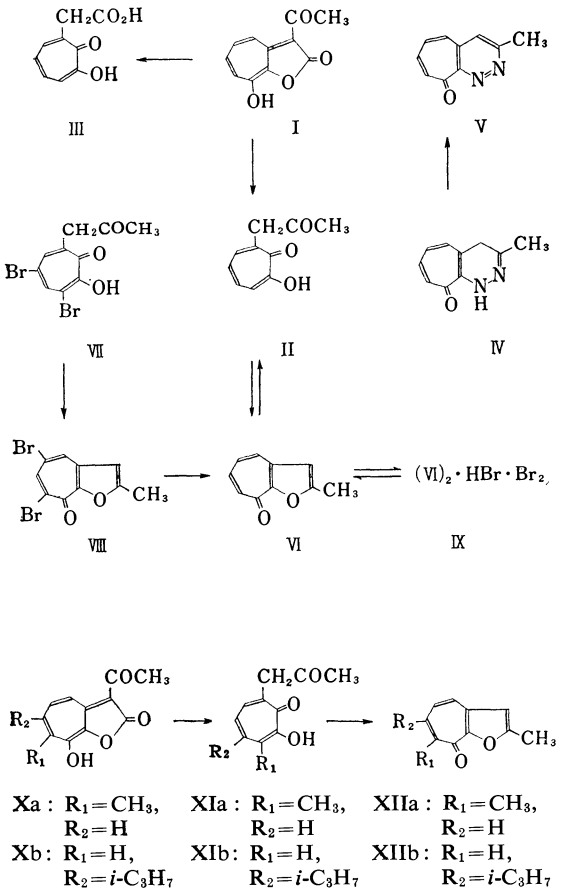
(Received August 19, 1964)

In a previous paper,[1] it was described how 3-acetyl-8-hydroxy-1-oxaazulan-2-one (3-acetyl-8-hydroxy-2*H*-cyclohepta[b]furan-2-one) (I) was obtained by the condensation reaction of 3-bromotropolone and ethyl acetoacetate. By the extension of this reaction to alkyl derivatives of 3-bromotropolone, the alkyl derivatives of I were also synthesized.[1] During the studies of the examination of their chemical behavior, it has been found that the alkaline hydrolysis of I affords 3-acetonyltropolone (II). Since the tropolone derivatives with a carbonyl function in their side-chain are very interesting in the synthetical studies of troponoid, the synthesis and some reactions of 3-acetonyltropolones have now been examined.

When 3-acetyl-8-hydroxy-1-oxaazulan-2-one (I) was heated in hydrobromic acid, it was converted into 3-carboxymethyltropolone (III), as has been reported.[1] However, when heated

1) K. Takase, This Bulletin, 37, 1460 (1964).

in a potassium hydroxide or sodium hydroxide solution, the compound I gave a ketonic compound II, from which an oxime, a semicarbazone, a phenylhydrazone and a 2,4-dinitrophenylhydrazone were derived. The tropolonic nature of II was shown from the facts that it was soluble in alkali, showed a positive ferric chloride coloration, and gave a green copper chelate. Its ultraviolet absorption spectrum, which is similar to that of 3-methyltropolone,[1] also supports its tropolonic structure. From these evidences and its elemental analysis, II is assumed to be 3-acetonyltropolone, produced by the hydrolysis of the lactone ring of I, followed by decarboxylation. It is interesting that, when heated with a sodium methoxide solution, I did not hydrolize into II, but was converted into 3-carboxymethyltropolone (III). It is known that the treatment of acetoacetic esters with dilute alkali gives ketones by ketonic hydrolysis, but with sodium alcoholate, esters are obtained by acidic hydrolysis.[2] In the case of I, it was found that a similar cleavage was also caused by sodium methoxide.




Xa: $R_1=CH_3$, $R_2=H$ XIa: $R_1=CH_3$, $R_2=H$ XIIa: $R_1=CH_3$, $R_2=H$

Xb: $R_1=H$, $R_2=i\text{-}C_3H_7$ XIb: $R_1=H$, $R_2=i\text{-}C_3H_7$ XIIb: $R_1=H$, $R_2=i\text{-}C_3H_7$

Although II produced the normal carbonyl derivatives in the reaction with the usual carbonyl reagents, as has been mentioned above, when heated with hydrazine it gave a bicyclic compound: 1,4-dihydro-3-methylpyridazo[3,4-b]tropone (IV). Its structure was deduced on the basis of the facts that it was insoluble in alkali and showed a negative ferric chloride coloration. Its ultraviolet absorption spectrum is similar to those of alkylidene derivatives of 2-hydrazinotropones,[3] as is shown in Fig. 1, and its infrared spectrum shows the absorption of an N–H stretching vibration of secondary amine at 3270 $cm^{-1}$. The compound IV was dehydrogenated by treatment with nitric acid, affording 3-methylpyridazo[3,4-b]tropone (V), whose ultraviolet absorption spectrum is shown in Fig. 1.

When heated in concentrated sulfuric acid or hydrochloric acid, II gave a basic compound VI, which in turn produced a picrate and a styphnate. This compound did not show the tropolonic enolone or the carbonyl nature;

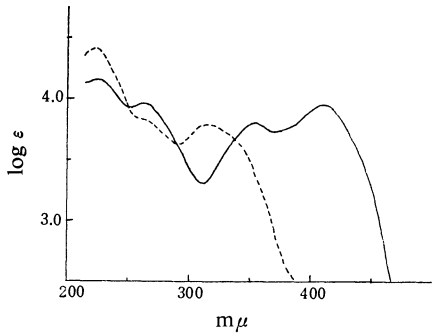



Fig. 1. The ultraviolet absorption spectra of 1,4-dihydro-2-methylpyridazo[3,4-b]tropone (IV); ——, and of 2-methylpyridazo[3,4-b]-tropone (V); ----, in methanol.

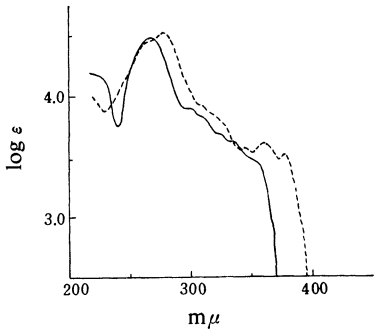



Fig. 2. The ultraviolet absorption spectra of 2-methylfuro[2,3-b]tropone (VI); ——, and of 5,7-dibromo-2-methylfuro[2,3-b]tropone (VIII); ----, in methanol.

2) C. R. Hauser and B. E. Hudson, Jr., "Organic Reactions," Vol. 1, pp. 266-302.

3) K. Takase, This Bulletin, 37, 1288 (1964); T. Nozoe and J. Shin, to be published.

it was insoluble in alkali, showed a negative ferric chloride coloration, and did not give any carbonyl derivative. In its infrared spectrum in KBr, no absorption appears in the region of the stretching vibration of the tropolonic hydroxyl or of the carbonyl of the acetonyl group. However, when VI was heated in a dilute alkali solution, the tropolone (II) was reproduced. These facts show that VI has the same carbon-skeleton as II, but the tropolonic hydroxyl group and the carbonyl group in the side-chain are masked. From these evidences and its elemental analysis, VI is assumed to be 2-methylfuro[2,3-b]tropone produced from II by ring formation under dehydration. Its ultraviolet absorption spectrum, as is shown in Fig. 2, is considerably different from those of tropones or tropolones in the long wave region (300—400 m$\mu$). This fact shows that VI belongs to a new aromatic ring system.

The behavior of II in relation to some cationoid reagents, such as aryldiazonium salt or bromine, was also examined. When treated with a *p*-toluenediazonium chloride solution, II gave an azo compound, in which the position of the azo group is assumed to be at the 5-position, in analogy to the other azotropolone.[4]

The bromination of II in methanol, in the presence of sodium acetate, afforded a dibromo compound VII, which is assumed to be 5,7-dibromo-3-acetonyltropolone since it is soluble in alkali, shows a positive ferric chloride coloration, and gives a 2,4-dinitrophenylhydrazone. The positions of the bromines were inferred from the following evidence. It was expected that the compound which brominated in the acetonyl side-chain would be unstable to alkali, but this compound was stable. On the other hand, it is well-known that the bromination of the tropolone nucleus is easily attained at the 3, 5 or 7-position.[4] When the bromination of II was undertaken in methanol without the presence of sodium acetate, VII could not be obtained, but a dibromo compound VIII was produced, accompanied with the formation of VI. The dibromo compound VIII was also obtained when VII was heated with concentrated sulfuric acid. The ultraviolet absorption spectrum of VIII is similar to that of VI, as is shown in Fig. 2. The reductive debromination of VIII afforded VI. From these facts, VIII is assumed to be 5,7-dibromo-2-methylfuro[2,3-b]tropone. Since VI did not gave any brominated compound under these conditions, the formation of VIII from II is considered to proceed through VII, which is produced by the bromination of II and which then forms the furan ring by the action of hydrogen bromide in a way similar to that of II.

The furo[2,3-b]tropone (VI) changed to 3-acetonyltropolone (II) by alkali, as has been mentioned before, but it was very stable to acid. It resists the action of the cationoid reagents, such as nitric acid, nitrous acid or aryldiazonium salts. The bromination of VI in acetic acid did not give the brominated compound, but it produced a complex compound IX, which easily reproduced VI when treated with a sodium hydrogen sulfite solution. Similar complex compounds of tropone[5] or tropolone[6] and bromine have been known, but IX is more stable than the corresponding tropone- or tropolone-complex; the former could not be converted into an addition or substitution product, while the latter could. When treated with *N*-bromosuccinimide, VI gave a monobromo compound, which is considered from its ultraviolet absorption curves to be a bromo-substituted derivative of VI but the position of the substitution is not yet clear.

The alkyl derivatives of I, 3-acetyl-7-methyl-8-hydroxy-1-oxaazulan-2-one (Xa) and 3-acetyl-6-isopropyl-8-hydroxy-1-oxaazulan-2-one (Xb)[1] also gave 3-acetonyltropolone derivatives (XIa and XIb) by alkaline hydrolysis. These compounds showed a positive ferric chloride coloration and reacted with carbonyl reagents in a manner similar to II. When they were treated with concentrated sulfuric acid, furo[2,3-b]-tropone derivatives (XIIa and XIIb) were obtained. The chemical behaviors of these compounds were similar to those of VI; they were insoluble in alkali and gave a picrate and a styphnate respectively. Their ultraviolet absorption curves are also similar to that of VI.

## Experimental[7]

**3-Acetonyltropolone (VI).** — A solution of I (1.00 g.) in a 2 N potassium hydroxide solution (10 ml.) was heated under reflux for 3 hr., and then the mixture was acidified with 6 N hydrochloric acid and extracted with chloroform. The solvent was evaporated and the residue was recrystallized from cyclohexane to give II (550 mg.) as colorless needles, m. p. 86—87°C.

4) Cf. T. Nozoe, *Fortschr. Chem. organ. Naturstoffe*, **13**, 233 (1956); T. Nozoe et al., "Dai Yuki Kagaku" ("Comprehensive Organic Chemistry"), Vol. 13, Chapters 5, 6, 8 and 9, Asakura Shoten, Tokyo (1960).

5) T. Nozoe, T. Mukai and K. Takase, *Sci. Repts. Tohoku Univ.*, I, **39**, 164 (1956).

6) T. Nozoe, S. Seto, T. Mukai, K. Yamane and A. Matsukuma, *Proc. Japan Acad.*, **27**, 224 (1951).

7) All melting points are uncorrected.

Found: C, 67.09; H, 6.09. Calcd. for $C_{10}H_{10}O_3$: C, 67.40; H, 5.66%. $\lambda_{max}^{MeOH}$ mμ (log ε): 240 (4.27), 330 (3.95), 392 (3.92).

The same treatment of I (200 mg.) with a 2 N sodium hydroxide solution (2.5 ml.) also afforded II (90 mg.).

*Copper Chelate:* m. p. 253°C, green crystals.

*Oxime:* m. p. 127—128°C, colorless prisms (from ethanol).

Found: C, 61.88; H, 5.70; N, 7.28. Calcd. for $C_{10}H_{11}O_3N$: C, 62.16; H, 5.74; N, 7.25%.

*Semicarbazone:* m. p. 189—189.5°C, colorless silky needles (from ethanol).

Found: C, 56.37; H, 5.59; N, 18.00. Calcd. for $C_{11}H_{13}O_3N_3$: C, 56.16; H, 5.57; N, 17.86%.

*Phenylhydrazone:* m. p. 138 — 138.5°C, yellow needles (from benzene).

Found: C, 71.88; H, 5.88; N, 10.59. Calcd. for $C_{16}H_{16}O_2N_2$: C, 71.62; H, 6.01; N, 10.44%.

*2, 4-Dinitrophenylhydrazone:* m. p. 170.5—171°C, reddish orange needles (from ethanol).

Found: C, 53.37; H, 4.18; N, 15.77. Calcd. for $C_{16}H_{14}O_6N_4$: C, 53.63; H, 3.94; N, 15.64%.

**The Reaction of I with Sodium Methoxide.**—To a sodium methoxide solution prepared from sodium (100 mg.) and methanol (4 ml.), I (200 mg.) was added, and the mixture was heated under reflux for 6 hr. The solvent was then evaporated, and the residue was dissolved in water and acidified with 6 N hydrochloric acid. Continuous extraction with ether for 8 hr. afforded 3-carboxymethyltropolone (III) (120 mg.), m. p. 171°C (decomp.).

**1, 4-Dihydro-3-methylpyridazo[3,4-b]tropone (IV).**—When mixture of II (200 mg.), 80% hydrazine hydrate (150 mg.) and ethanol (1 ml.) was allowed to stand for 2 hr. at room temperature, yellow hydrazine salt (150 mg., m. p. 119°C), was separated out.

Found: C, 54.20; H, 6.60; N, 23.14. Calcd. for $C_{10}H_{16}O_2N_4$: C, 53.55; H, 7.19; N, 24.98%.

This mixture was heated under reflux for 30 min. and then allowed to cool; the crystals thereby obtained were recrystallized from ethanol to give IV (100 mg.) as yellow plates, m. p. 145—146°C.

Found: C, 68.67; H, 5.49; N, 15.98. Calcd. for $C_{10}H_{10}ON_2$: C, 68.95; H, 5.79; N, 16.08%. $\lambda_{max}^{MeOH}$ mμ (log ε): 225 (4.16), 265 (3.94), 350 (3.78), 414 (3.98).

**3-Methylpyridazo[3, 4-b]tropone (V).**—A mixture of IV (90 mg.) and concentrated nitric acid (0.5 ml.) was stirred at room temperature. After the evolution of gas had ceased, the mixture was neutralized with a 2 N potassium hydroxide solution and extracted with chloroform. The crystals obtained after the removal of the solvent were recrystallized from benzene to give V (20 mg.) as pale yellow prisms, m. p. 189°C (decomp.).

Found: C, 69.72; H, 5.01; N, 16.08. Calcd. for $C_{10}H_8ON_2$: C, 69.79; H, 4.68; N, 16.27%. $\lambda_{max}^{MeOH}$ mμ (log ε): 225 (4.40), 315 (3.77).

**2-Methylfuro[2, 3-b]tropone (VI).**—After a mixture of II (200 mg.) and concentrated sulfuric acid (0.5 ml.) had been heated at 100°C for 5 min., it was diluted with water (3 ml.) and extracted with chloroform. The removal of the solvent gave an oily substance, which was solidified by cooling. Sublimation under reduced pressure and recrystallization from a mixture of benzene and petroleum ether gave VI (180 mg.) as colorless needles, m. p. 49—50.5°C.

Found: C, 70.99; H, 5.24; $H_2O$, 5.18. Calcd. for $C_{10}H_8O_2 \cdot 1/2H_2O$: C, 70.99; H, 5.36; $H_2O$, 5.32%. $\lambda_{max}^{MeOH}$ mμ (log ε): 251 (4.48), 300 (3.90), 335 (3.62).

The same result was obtained with concentrated hydrochloric acid in place of sulfuric acid.

*Picrate:* m. p. 142—143°C, yellow needles (from ethanol).

Found: C, 49.31; H, 3.05; N, 11.25. Calcd. for $C_{10}H_8O_2 \cdot C_6H_3O_7N_3$: C, 49.36; H, 2.85; N, 10.80%.

*Styphnate:* m. p. 164 — 165°C, yellow prisms (from ethanol).

Found: C, 47.39; H, 2.87; N, 9.94. Calcd. for $C_{10}H_8O_2 \cdot C_6H_3O_8N_3$: C, 47.42; H, 2.74; N, 10.37%.

**The Reaction of VI with Alkali.**—A mixture of VI (100 mg.) and 2 N potassium hydroxide solution (1.5 ml.) was heated under reflux for 2 hr., it was then acidified with 6 N hydrochloric acid and extracted with chloroform. The solvent was evaporated and residue was recrystallized from cyclohexane to give II (50 mg.), m. p. 86—87°C.

**5-(*p*-Tolylazo)-3-acetonyltropolone.**—To a stirred solution of II (100 mg.) in pyridine (3 ml.), a solution of *p*-toluenediazonium chloride, prepared from *p*-toluidine (70 mg.) in the usual manner, was added, and the mixture was stirred for 1 hr. Water was added, and the crystals obtained were recrystallized from cyclohexane to give the azo compound (160 mg.) as reddish-orange prisms, m. p. 133—134°C.

Found: C, 69.29; H, 5.43; N, 9.84. Calcd. for $C_{17}H_{16}O_3N_2$: C, 68.90; H, 5.44; N, 9.45%. $\lambda_{max}^{MeOH}$ mμ (log ε): 232 (4.31), 290 (4.08), 400 (4.43), 435 (4.41).

**5, 7-Dibromo-3-acetonyltropolone (VII).** — To a suspension of II (90 mg.) and sodium acetate (100 mg.) in methanol (2 ml.), bromine (160 mg.) was added, and the mixture was stirred for 3 hr. under cooling. Water was added, and the crystals thereby obtained were recrystallized from methanol to give VII (120 mg.) as pale yellow needles, m. p. 155—156°C.

Found: C, 35.75; H, 2.54. Calcd. for $C_{10}H_8O_3Br_2$: C, 35.74; H, 2.40%. $\lambda_{max}^{MeOH}$ mμ (log ε): 262 (4.43), 347 (4.10), 428 (3.85).

*2, 4-Dinitrophenylhydrazone:* m. p. 198 — 199°C, orange scales (from ethanol).

Found: C, 37.55; H, 2.51; N, 10.54. Calcd. for $C_{16}H_{12}O_6N_4Br_2$: C, 37.22; H, 2.34; N, 10.85%.

**5, 7-Dibromo-2-methylfuro[2, 3-b]tropone (VIII).**—*a) By the Heating of VII with Sulfuric Acid.*—A mixture of VII (100 mg.) and concentrated sulfuric acid (0.3 ml.) was heated at about 100°C for 5 min. and diluted with water to give VIII (70 mg.). Recrystallization from ethanol afforded colorless needles, m. p. 209°C (decomp.).

Found: C, 37.72; H, 2.05. Calcd. for $C_{10}H_6O_2 \cdot Br_2$: C, 37.65; H, 1.09%. $\lambda_{max}^{MeOH}$ mμ (log ε): 278 (4.52), 362 (3.61), 378 (3.51).

*b) By the Bromination of II.*—To a solution of

II (100 mg.) in methanol (1.5 ml.), bromine (200 mg.) was added, and the mixture was stirred for 1 hr. under cooling. When the solvent was removed and the residue was recrystallized from ethanol, VIII (50 mg.) was obtained as colorless needles, m. p. 209°C (decomp.).

From the mother liquor, an oily substance (40 mg.) was obtained by extraction with chloroform. This oil gave a picrate, m. p. 143°C, undepressed by admixture with the picrate of VI.

**The Debromination of VIII.** — A solution of VIII (120 mg.) and sodium acetate (100 mg.) in methanol (4 ml.) was shaken with hydrogen in the presence of 5% palladium on carbon; 19.4 ml. (at 20°C) of hydrogen was absorbed during 5 hr. After had been filtered off the catalyst, the evaporation of the solvent left an oily substance (50 mg.), which gave a picrate, m. p. 143°C, undepressed by admixture with the picrate of VI.

**The Reaction of VI with Bromine.**—To a solution of VI (160 mg.) in glacial acetic acid (1 ml.), bromine (170 mg.) was added, and the mixture was stirred for 1 hr. under cooling. The complex compound (IX) (200 mg.) was obtained as orange needles, m. p. 135—136°C.

Found: C, 43.00; H, 3.29. Calcd. for $(C_{10}H_8O_2)_2 \cdot HBr_3$: C, 42.81; H, 3.05%.

This compound (100 mg.) was shaken with a sodium hydrogen sulfite solution and extracted with chloroform to give an oily substance (60 mg.), which gave a picrate, m. p. 143°C, undepressed by admixture with the picrate of VI.

**The Reaction of VI and *N*-Bromosuccinimide.**—A solution of VI (500 mg.), *N*-bromosuccinimide (570 mg.) and benzoyl peroxide (10 mg.) in carbon tetrachloride (15 ml.) was heated under reflux for 2 hr. The solvent was then evaporated, and the residue was extracted with chloroform. The evaporation of the solvent left an oily substance containing some crystals. The addition of methanol gave crystals (260 mg.), m. p. 145—150°C, which were recrystallized from methanol to give bromo-2-methylfuro[2, 3-b]tropone as colorless needles, m. p. 169—170°C.

Found: C, 50.57; H, 3.02. Calcd. for $C_{10}H_7O_2Br$: C, 50.24; H, 2.95%. $\lambda_{max}^{MeOH}$ mμ (log ε): 220 (4.17), 278 (4.32).

**3-Acetonyl-7-methyltropolone (XIa).**—A solution of 3-acetyl-7-methyl-8-hydroxy-1-oxaazulan-2-one (Xa) (100 mg.) in a 2 N potassium hydroxide solution (2 ml.) was heated under reflux for 3 hr. The mixture was then acidified with 6 N hydrochloric acid and extracted with chloroform. The evaporation of the solvent and the recrystallization of the residue from cyclohexane gave XIa (60 mg.) as colorless needles, m. p. 106—107°C.

Found: C, 68.90; H, 6.50. Calcd. for $C_{11}H_{12}O_3$: C, 68.73; H, 6.29%. $\lambda_{max}^{MeOH}$ mμ (log ε): 245 (4.45), 323 (3.82), 355 (3.77), 370 (3.77).

*2, 4-Dinitrophenylhydrazone:* m. p. 173 — 174°C, orange needles (from ethanol).

Found: C, 55.22; H, 4.43; N, 14.89. Calcd. for $C_{17}H_{16}O_6N_4$: C, 54.84; H, 4.33; N, 15.05%.

**3-Acetonyl-6-isopropyltropolone (XIb).**—A solution of 3-acetyl-6-isopropyl-8-hydroxy-1-oxaazulan-2-one (Xb) (1.00 g.) in a 2 N potassium hydroxide solution (20 ml.) was treated in a manner similar to that used in the above experiment. Recrystallization from methanol gave XIb (590 mg.) as colorless needles, m. p. 101—102°C.

Found: C, 70.73; H, 7.29. Calcd. for $C_{13}H_{16}O_3$: C, 70.89; H, 7.32%. $\lambda_{max}^{MeOH}$ mμ (log ε): 245 (4.47), 328 (3.91), 355 (3.86), 370 (3.84).

*Oxime:* m. p. 125—126°C, colerless scales (from methanol).

Found: C, 66.43; H, 6.95; N, 5.83. Calcd. for $C_{13}H_{17}O_3N$: C, 66.36; H, 7.28; N, 5.95%.

*Semicarbazone:* m. p. 129—130°C, colorless microneedles (from ethanol).

Found: C, 60.35; H, 6.77; N, 15.31. Calcd. for $C_{14}H_{19}O_3N_3$: C, 60.63; H, 6.91; N, 15.15%.

*Phenylhydrazone:* m. p. 110—111°C, yellow needles (from ethanol).

Found: C, 73.41; H, 6.95; N, 9.15. Calcd. for $C_{19}H_{22}O_2N_2$: C, 73.52; H, 7.14; N, 9.03%.

*2, 4-Dinitrophenylhydrazone:* m. p. 162 — 163°C, orange microneedles (from ethanol).

Found: C, 56.91; H, 4.88; N, 14.18. Calcd. for $C_{19}H_{20}O_6N_4$: C, 56.99; H, 5.04; N, 13.99%.

**5-(*p*-Tolylazo)-3-acetonyl-6-isopropyltropolone.**—To a stirred solution of XIb (200 mg.) in pyridine (5 ml.), a solution of a *p*-toluenediazonium chloride solution, prepared from *p*-toluidine (100 mg.) in the usual manner, was added under cooling, and the mixture was stirred for 2 hr. Water was added, and the crystals obtained were recrystallized from benzene to give the azo compound (250 mg.) as reddish silky needles, m. p. 154—155°C.

Found: C, 70.72; H, 6.58; N, 8.28. Calcd. for $C_{20}H_{22}O_3N_2$: C, 70.98; H, 6.55; N, 8.28%. $\lambda_{max}^{MeOH}$ mμ (log ε): 235 (4.29), 295 (4.05), 390 (4.35).

**2, 7-Dimethylfuro[2, 3-b]tropone (XIIa).**—A mixture of XIa (100 mg.) and concentrated sulfuric acid (1 ml.) was heated at about 100°C for 5 min., then diluted with water and extracted with chloroform. The evaporation of the solvent and the recrystallization of the residue from cyclohexane gave XIIa (80 mg.) as colorless prisms, m. p. 62—64°C.

Found: C, 76.07; H, 5.51. Calcd. for $C_{11}H_{10}O_2$: C, 75.84; H, 5.79%. $\lambda_{max}^{MeOH}$ mμ (log ε): 225 (4.12), 268 (4.44), 337 (3.61), 352 (3.49).

*Picrate:* m. p. 110°C, yellow needles (from ethanol).

Found: C, 50.82; H, 3.10; N, 10.66. Calcd. for $C_{11}H_{10}O_2 \cdot C_6H_3O_7N_3$: C, 50.63; H, 3.25; N, 10.42%.

*Styphnate:* m. p. 100 — 101°C, yellow needles (from ethanol).

Found: C, 48.84; H, 3.10; N, 10.24. Calcd. for $C_{11}H_{10}O_2 \cdot C_6H_3O_8N_3$: C, 48.69; H, 3.13; N, 10.02%.

**6-Isopropyl-2-methylfuro[2, 3-b]tropone (XIIb).**—A mixture of XIb (200 mg.) and concentrated sulfuric acid (0.5 ml.) was treated in a manner similar to that used in the above experiment, and the product was distilled under reduced pressure to give XIIb (180 mg.) as a pale yellow oil.

Found: C, 74.00; H, 6.98. Calcd. for $C_{13}H_{14}O_2 \cdot 1/2H_2O$: C, 73.91; H, 7.16%. $\lambda_{max}^{MeOH}$ mμ (log ε): 230 (4.23), 270 (4.39).

*Picrate:* m. p. 158—159°C, yellow scales (from ethanol).

Found: C, 52.64; H, 3.69; N, 9.90. Calcd. for

$C_{13}H_{14}O_2 \cdot C_6H_3O_7N_3$: C, 52.90; H, 3.97; N, 9.74%.

*Styphnate:* m. p. 150 — 151°C, yellow needles (from ethanol).

Found: C, 51.06; H, 3.99; N, 9.25. Calcd. for $C_{13}H_{14}O_2 \cdot C_6H_3O_8N_4$: C, 51.01; H, 3.83; N, 9.39%.

The author wishes to express his sincere gratitude to Professor Tetsuo Nozoe for his kind guidance throughout the course of this study. He is also grateful to Mr. Masaru Ogata for his cooperation in these experiments.

*Department of Chemistry*
*Faculty of Science*
*Tohoku University*
*Katahira-cho, Sendai*

# The Reaction of Aminotropones with Diketene. I. On the Synthesis of 3-Acetyl-1-azaazulenes and Related Reactions

By Kyozo OGURA, Hiroko SASAKI and Shuichi SETO

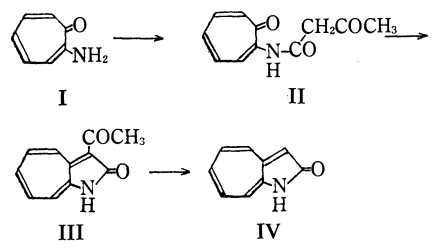
(Received July 11, 1964)

It has previously been shown that 2-aminotropones react with diethyl malonate in the presence of sodium alkoxide to afford directly 3-ethoxycarbonyl-1-azaazulan-2-ones, from which various 1-azaazulenes can be synthesized.[1-3]



The present authors have now examined the reaction of diketene with some aminotropones and aminotropolones, and have found that the reaction products are useful for the synthesis of 3-acetyl-1-azaazulenes.

When 2-aminotropone (I) was treated with a large excess of diketene, 2-acetoacetamidotropone (II) was obtained in a good yield. The treatment of II with sodium ethoxide gave 3-acetyl-1-azaazulan-2-one (III), whose structure was confirmed from the infrared and ultraviolet absorption spectra and from the chemical evidence that III was transformed to the known 1-azaazulan-2-one (IV)[1] by the action of acid. The treatment of III with phosphorus oxychloride under the usual conditions[1-3] gave two kinds of 1-azaazulene derivatives, yellow needles (V) ($C_{11}H_8ONCl$) and red prisms (VI) ($C_{11}H_7NCl_2$). The former, V, shows a strong absorption band at 1640 $cm^{-1}$ due to a carbonyl group, while the latter shows bands at 1630 and 895 $cm^{-1}$ due to terminal methylene moiety. The ultraviolet spectra of these products are of the 1-azaazulene type,[1-3] as is shown in Fig. 1. From these facts and from the NMR spectra, which will be described later, it was learned that V and VI were 3-acetyl-2-chloro-and 3-(α-chlorovinyl)-2-chloro-1-azaazulene respectively. It may also be observed that the vinyl derivative VI, compared with the acetyl derivative V, shows a bathochromic shift in the visible region and a hypsochromic shift in the ultraviolet region.



I II III IV



V VI

The NMR spectrum of V exhibits a signal for the acetyl group at 7.20τ, while that of VI shows two doublets of the AB type at 4.40 and 4.08τ, with a coupling constant of 1.2 c.p.s. due to the α-chlorovinyl group. Furthermore, a marked difference in the influence by these two substituents at the 3-position is also apparent in the chemical shifts of the protons at the 4-position of V and VI. The signals for the protons on the seven-membered ring of V consist of three parts of a multiplet with an intensity ratio of 3 : 1 : 1, centered at 2.0, 1.4 and 0.3τ respectively. The components at the abnormally low field (0.3τ) can be assigned to the $H_4$, because only this proton is

1) T. Nozoe, S. Seto, S. Matsumura and T. Terasawa, *Chem. & Ind.*, **1954**, 1356.
2) T. Nozoe, S. Seto and S. Nozoe, *Proc. Japan Acad.*, **32**, 172 (1956).
3) S. Seto and S. Nozoe, ibid., **32**, 756 (1956).

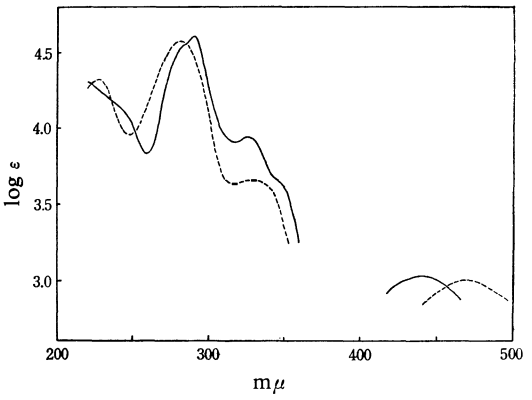



Fig. 1. UV spectra of V (——) and VI (- - -) in methanol.

situated at such a position where the magnetic anisotropy of the acetyl group can be effective. The bands at 1.4$\tau$ may be due to the $H_8$, the nearest proton to the nitrogen atom, since the figure of the splitting closely resembles that of the $H_4$, which has almost the same environment in terms of spin coupling. This assignment is also consistent with that to be expected from the order of electron density in 1-azaazulene reported by Kon.[4] Furthermore, it is also supported, as will be described later, by the analysis of the spectra of other derivative bearing substituents on the seven-membered ring. Therefore, the components at the highest field can be assigned to the three protons at the 5, 6 and 7-positions.

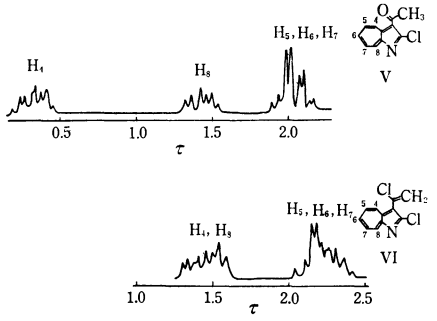
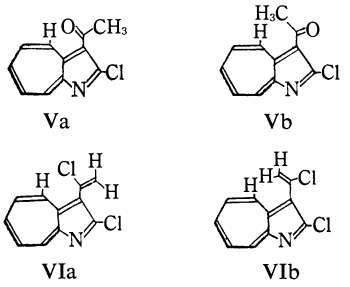



Fig. 2. NMR spectra of V and VI in $CDCl_3$.

The spectrum of VI shows two separated multiplets, centered nearly at 2.2 and 1.5$\tau$, with an intensity ratio of 3 : 2, corresponding to the protons at the 5, 6 and 7-positions and to the protons at the 4 and 8-positions respectively.

The coplanarity of the acetyl and the $\alpha$-chlorovinyl group with the azaazulene nucleus was suggested by the ultraviolet spectra, and the remarkable effect of these substituents in the NMR spectra noted above indicates that the acetyl group must have predominantly the Va, conformation which is sterically preferable to the other one, Vb. The $\alpha$-chlorovinyl derivative VI also probably prefers VIa to VIb.



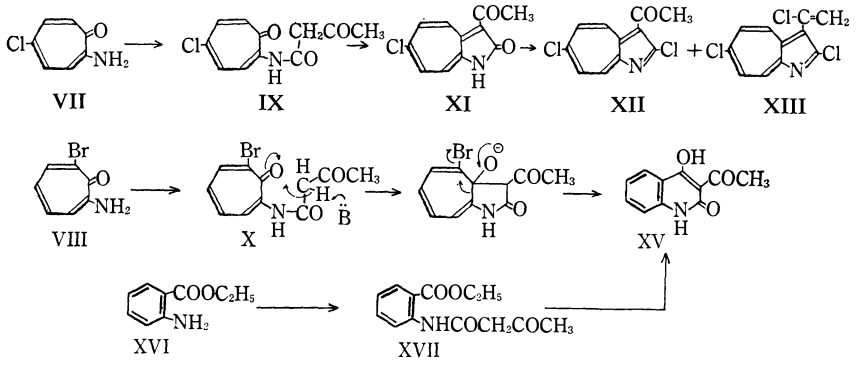

Although the mechanism of the formation of VI from III can not be understood with certainty, it is clear that VI is not produced via V, since any treatment of V with phosphorus oxychloride resulted only in the recovery of V.

2-Amino-5-chlorotropone (VII) and 2-amino-7-bromotropone (VIII) reacted with diketene under somewhat more severe conditions than in the case of I to afford the corresponding *N*-acetoacetyl derivatives, IX and X, while 2-amino-3-bromotropone was quite unreactive under the reaction conditions. The reaction of IX with sodium ethoxide gave 3-acetyl-6-chloro-1-azaazulan-2-one (XI), which in turn afforded 3-acetyl-2,6-dichloro-1-azaazulene (XII) by the action of phosphorus oxychloride as a major product. Only a small amount of red crystals that seemed to be the $\alpha$-chlorovinyl derivative XIII was obtained. The structure of XII was determined by the analysis of the spectra in the same way as for V. The NMR spectrum of XII exhibits a signal for the acetyl group at 7.3$\tau$ and less complicated bands in the 2.1—0.3$\tau$ region than those of V and VI due to the ring protons. These bands can be considered to be two sets of a doublet of the AB type to a first approximation; the first doublet in the lower field (0.40$\tau$) and the second at 1.45$\tau$ can be assigned to the $H_4$ and the $H_8$ respectively, while the signals for the $H_5$ and the $H_7$ consist of two just-overlapping doublets at 1.95$\tau$. No splitting by spin coupling between these two protons is observed since these chemical shifts are just the same. The coupling constants, $J(H_4, H_5)$ and $J(H_7, H_8)$, are almost equal, 11.8 c. p. s.

For the sake of comparison, the spectrum of 2, 6-dichloro-1-azaazulene (XIV)[5] was also determined. In this case, the signal for the $H_4$ is moved upfield, as compared with that

4) H. Kon, *Sci. Repts., Tohoku Univ., First Series*, **38**, 67 (1954).

5) T. Toda, to be published.



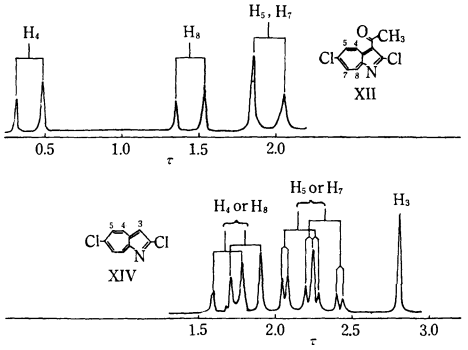


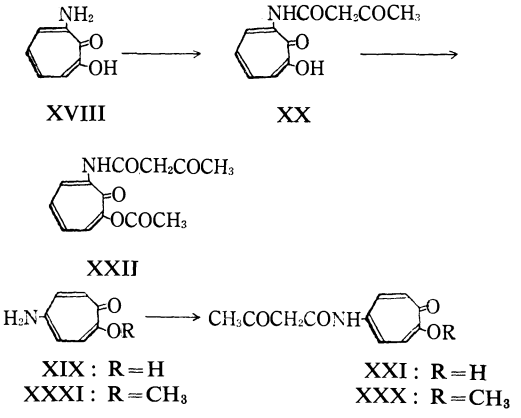
Fig. 3. NMR spectra of XII and XIV in $CDCl_3$.

of XII, and is incorporated among the signals for the $H_8$.

Although the chemical shift for each proton can not be determined, the signals at 2.1—2.5$\tau$, which consist of a pair of a quartet, may be assigned to the $H_5$ and the $H_7$ ($J(H_4, H_5) = J(H_7, H_8) = 11.0$; $J(H_5, H_7) = 2.1$ c.p.s.) (Fig. 3). The singlet at 2.80$\tau$ must correspond to the $H_3$.

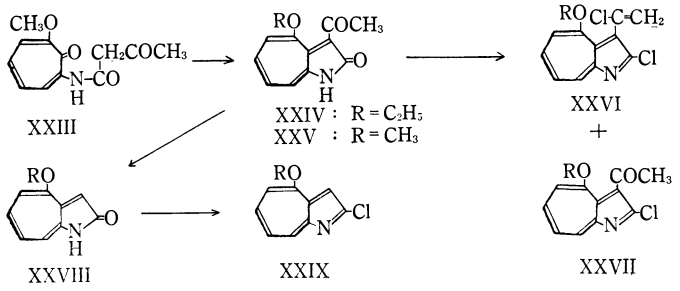
The treatment of 2-acetoacetamido-7-bromotropone (X) with alkali gave a product which was not a 1-azaazulanone derivative. This product was found to be 3-acetyl-4-hydroxycarbostyril (XV) by comparison with an authentic specimen prepared from ethyl anthranilate (XVI). It was reported that the reaction of ethyl anthranilate (XVI) with ethyl acetoacetate gave an *N*-acetoacetyl derivative (XVII) and that the heating of XVII in dry xylene in the presence of powdered sodium afforded XV.[6] The authors also found that the reaction of diketene with XVI gave the corresponding *N*-acetoacetyl derivative XVII under rather mild conditions, this could then be converted into XV in a fairly good yield, even by mild treatment with alcoholic alkali.

3-Aminotropolone (XVIII) and 5-aminotropolone (XIX) also reacted easily with diketene to afford 3-acetoacetamido- (XX) and 5-acetoacetamidotropolone (XXI) respectively. The compound XX itself did not give any cyclization product on treatment with sodium alkoxide, and the reaction of XX with acetic anhydride gave only its acetate XXII. When



a methyl ether XXIII, obtained by the reaction of XX with diazomethane was treated with sodium ethoxide, a 1-azaazulanone derivative XXIV, $C_{13}H_{13}O_3N$, was obtained. The fact that the treatment of XXII with sodium methoxide gave another 1-azaazulanone derivative XXV, $C_{12}H_{11}O_3N$, suggested that anionoid substitution by alkoxide at the 4-position of the azaazulanone ring might occur during this reaction. The existence of an ethoxy group in XXIV was verified by the NMR spectra of the 1-azaazulene derivative XXVI derived from XXIV. The treatment of XXIV with phosphorus oxychloride gave orange needlers XXVI and a small amount of yellow crystals XXVII. The latter was found from its infrared spectrum to be a likely 3-acetyl derivative. The appearance of a triplet at 8.36$\tau$ and a quartet at 5.66$\tau$ ($J$, 6.4 c. p. s.) in the NMR spectrum of XXVI indicates the presence of the ethoxy group, while two doublets at 4.61

6) K. Tomita, *J. Pharm. Soc. Japan*, **71**, 1100 (1951).




and 4.82$\tau$ ($J$, 0.9 c. p. s.) seem to be attributable to the two protons of the $\alpha$-chlorovinyl group.

It is noteworthy that XXIV was deacetylated with surprising ease when treated with acid at room temperature to give 4-ethoxy-1-azaazulan-2-one (XXVIII). This compound was converted into 2-chloro-4-ethoxy-1-azaazulene (XXIX), whose infrared spectrum indicated the absence of an acetyl group. It was also observed that the introduction of an ethoxy group to the 4-position of both 1-azaazulan-2-one and 2-chloro-1-azaazulene causes a hypsochromic shift (about 15 m$\mu$) of the band in the shorter-wavelength region in the ultraviolet spectrum.

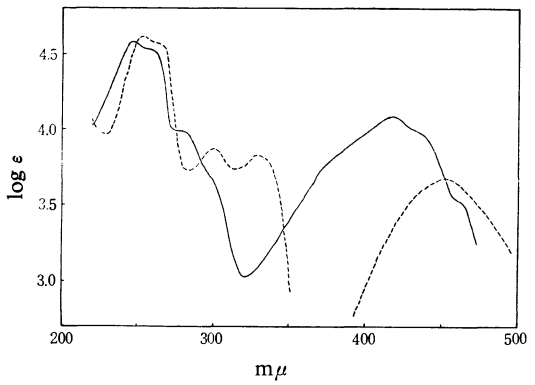
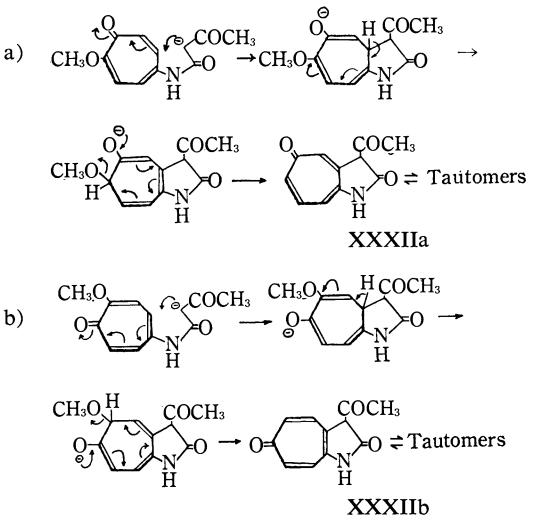



Fig. 4. UV spectra of XXVIII (——) and XXIX (- - -) in methanol.

A methyl ether XXX which had been prepared either by the treatment of XXI with diazomethane or by the reaction of 5-amino-2-methoxytropone (XXXI) with diketene gave yellow crystals XXXII when treated with sodium ethoxide. It is sparingly soluble in organic solvents and shows a characteristic absorption in the ultraviolet spectrum. The treatment of XXXII with acetic anhydride gave a diacetate XXXIII, which has an ultraviolet absorption curve of the 1-azaazulanone type. The infrared spectrum of XXXIII exhibits four bands for the carbonyl group, at 1755, 1710, 1700 and 1650 $cm^{-1}$, suggesting that XXXIII might be an *N*-acetyl-1-azaazulan-2-one derivative, bearing an acetyl group and an acetoxy group on the azaazulanone ring. This was also supported by a spectral comparison between XXXIII and the *N*-acetyl-1-azaazulan-2-one derivative XXXIV prepared from III. Two kinds of structure (XXXIIa and XXXIIb) for XXXII may be expected from a consideration of the reaction mechanism of this abnormal substitution:



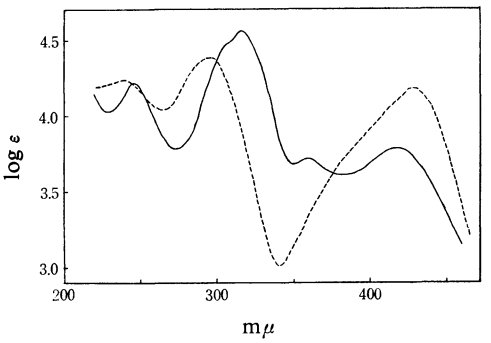




Fig. 5. UV spectra of XXXII (——) and XXXIII (- - -) in methanol.

If the product XXXII had the structure XXXIIb, it would be converted into 3-acetyl-2, 6-dichloro-1-azaazulene (XII) by treatment

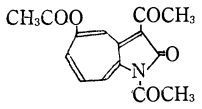
with phosphorus oxychloride. The treatment of XXXII, however, gave 3-acetyl- (XXXV) and 3-$\alpha$-chlorovinyl derivatives (XXXVI) of 2, 5-dichloro-1-azaazulene derivatives, whose structures were strongly supported by the analysis of the NMR spectra. Consequently, XXXII must have the structure XXXIIa and XXXIII must be *N*, 3-diacetyl-5-acetoxy-1-aza-azulan-2-one.



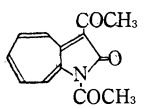
XXXV



XXXVI



XXXIII



XXXIV

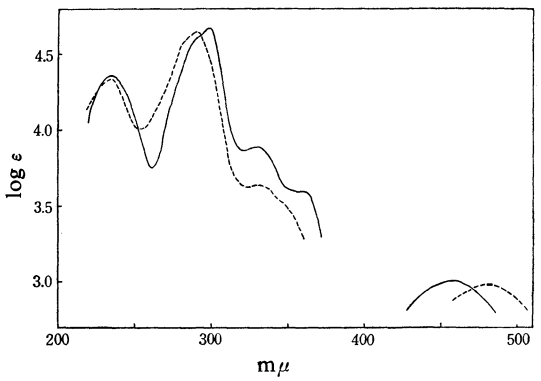
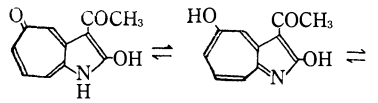
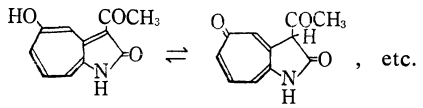



Fig. 6. UV spectra of XXXV (——) and XXXVI (- - -) in methanol.

Although the situation of the tautomerism in XXXII can not be strictly stated, the ultraviolet and infrared spectra indicate that the A form may be predominant.



(A) (B)



(C) (D)

In the NMR spectrum of XXXV the pattern arising from the protons at the 6, 7 and 8-positions of XXXV can be approximately described as an ABX system, where X corresponds to the $H_8$. The lower-field components must arise from the $H_6$, since they show additional splitting by coupling with the $H_4$, which corresponds to a doublet at 0.2$\tau$ ($J$, 2.4 c. p. s.), and the higher-field quartet can be assigned to the $H_7$. A first-order analysis of this spectrum gives the following values:

$J(H_6, H_7) = 10.0$, $J(H_6, H_8) = 1.5$,

$J(H_7, H_8) = 9.3$ c. p. s.

$H_4 = 0.2$, $H_8 = 1.5$, $H_6 = 1.9$, $H_7 = 2.2\tau$

The spectrum of XXXVI also displays almost the same pattern for the protons at the 6, 7 and 8-positions, but the doublet due to the $H_4$ is moved upfield (1.3$\tau$). The signal for the acetyl group of XXXV appears at 7.2$\tau$, and the signals for the $\alpha$-chlorovinyl group in XXXVI represent an AB system at 4.0 and 4.4$\tau$ ($J$, 1.5 c. p. s.). A schematical illustration of these spectra is given in Fig. 7.

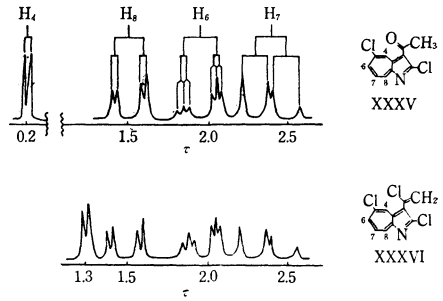



Fig. 7. NMR spectra of XXXV and XXXVI in $CDCl_3$.

The only structures for XXXV and XXXVI that can account for these spectra are 3-acetyl-2, 5-dichloro-1-azaazulene and 2, 5-dichloro-3-($\alpha$-chlorovinyl)-1-azaazulene respectively.

Additional work is in progress to make a further extension of these reactions; it will be reported on in the near future.

## Experimental*

**2-Acetoacetamidotropone (II).**—A solution of 2-aminotropone (2 g.) in diketene (10 ml.) was heated on a water bath for 2 hr.; the complete evaporation of the excess diketene then left colorless crystals, which were collected and recrystallized from methanol to give colorless needels, m. p. 118—121°C. Yield, 3.1 g.

Found: C, 64.12; H, 5.62; N, 6.33. Calcd. for $C_{11}H_{11}O_3N$: C, 64.38; H, 5.40; N, 6.83%.

* All melting points are uncorrected. The microanalyses were carried out by Misses Yôkô Endo and Yukiko Endo of this Institute, to whom the authors are indebted. The measurements of the ultraviolet and infrared spectra were made, respectively, with a Hitachi EPU-2A type spectrophotometer and with a Hitachi EPI Model S-2 spectrophotometer. The NMR spectra were measured with a Varian 4301 high resolution NMR spectrometer.

**3-Acetyl-1-azaazulan-2-one (III).** — A mixture of II (1 g.) and sodium (0.4 g.) in absolute ethanol (50 ml.) was refluxed for 1.5 hr., and then the ethanol was distilled off. When the residual crystals were dissolved in water and neutralized with diluted hydrochloric acid, yellow crystals precipitated; these were collected and recrystallized from ethanol to give yellow needles, m. p. 265—270°C. Yield, 650 mg.

Found: C, 70.90; H, 4.68; N, 7.85. Calcd. for $C_{11}H_9O_2N$: C, 70.58; H, 4.85; N, 7.48%.

**The Deacetylation of III.** — After 50 mg. of III had been heated in hydrobromic acid (1 ml.) at 100°C for 2 hr., the solution was neutralized with sodium carbonate and extracted with ethyl acetate to give yellow needles (25 mg.) of IV.

**3-Acetyl-2-chloro-1-azaazulene (V) and 2-Chloro-3-(α-chlorovinyl)-1-azaazulene (VI).** — A mixture of III (200 mg.) and phosphorus oxychloride (6 ml.) was heated at 85°C for 15 min. After the excess phosphorus oxychloride had been removed under reduced pressure, cracked ice was added to the residue. The solution was then neutralized with sodium bicarbonate and extracted with benzene. The deep yellow crystals obtained by the evaporation of the solvent were chromatographed on an alumina colum, after which elution with benzene-petroleum ether gave red prisms of VI and yellow needles of V. The respective recrystallizations from benzene-petroleum ether afforded red prisms of VI (35 mg.), m. p. 76—77°C and yellow needles of V (140 mg.), m. p. 159—160°C.

V: $\lambda_{max}^{MeOH}$ mμ (log ε): 291 (4.62), 326 (3.95), 440 (3.03).

Found: C, 64.26; H, 3.89; N, 6.67. Calcd. for $C_{11}H_8ONCl$: C, 64.24; H, 3.92; N, 6.81%.

VI: $\lambda_{max}^{MeOH}$ mμ (log ε): 228 (4.32), 281 (4.58), 330 (3.66), 470 (2.99).

Found: C, 59.35; H, 3.16; N, 6.71. Calcd. for $C_{11}H_7NCl_2$: C, 58.96; H, 3.15; N, 6.25%

**2-Acetoacetamido-5-chlorotropone (IX).**—A solution of VII (270 mg.) in diketene (8 ml.) was heated at 100—120°C for 2 hr. The evaporation of the excess diketene left brownish yellow crystals, which were collected and recrystallized from acetone to afford pale yellow needles, m. p. 145°C. Yield, 325 mg.

Found: C, 55.36; H, 3.87; N, 6.15. Calcd. for $C_{11}H_{10}O_3NCl$: C, 55.10; H, 4.21; N, 5.85%.

**2-Acetoacetamido-7-bromotropone (X).** — A solution of VIII (150 mg.) in diketene (1.5 ml.) was heated at 95—98°C for 4 hr. After the evaporation of the excess diketene, the crystals were recrystallized from methanol to give colorless needles, m. p. 114—115°C. Yield, 130 mg.

Found: C, 46.76; H, 3.36; N, 5.23. Calcd. for $C_{11}H_{10}O_3NBr$: C, 46.40; H, 3.89; N, 4.93%.

**3-Acetyl-6-chloro-1-azaazulan-2-one (XI).**—When IX (115 mg.) was added to a sodium ethoxide solution (sodium, 80 mg.; absolute ethanol, 20 ml.), orange crystals appeared immediately. While the mixture was then refluxed for 2 hr., however, the crystals dissolved gradually. After the removal of the solvent, the residue was acidified with 6 N sulfuric acid and adjusted to pH 2; the yellow crystals which had been deposited were collected and recrystallized from methanol to give yellow needles, m. p. 278°C (decomp.). Yield, 185 mg.

Found: C, 59.11; H, 3.44; N, 6.40. Calcd. for $C_{11}H_8O_2NCl$: C, 59.59; H, 3.64; N, 3.22%.

**3-Acetyl-2, 6-dichloro-1-azaazulene (XII).** — A mixture of XI (115 mg.) and phosphorus oxychloride (8 ml.) was warmed at 80°C for 2 hr. After the evaporation of the excess phosphorus oxychloride under reduced pressure, the residue was neutralized with an aqueous sodium bicarbonate solution, adjusted to pH 8, and extracted with ethyl acetate. The solution, after being dried on sodium sulfate, was passed through an alumina column. Elution with benzene gave yellow needles of XII. Recrystallization from benzene gave yellow needles, m. p. 183°C (decomp.). Yield, 100 mg. $\lambda_{max}^{MeOH}$ mμ (log ε): 298 (4.65), 340 (4.04), 450 (3.07).

Found: C, 55.05; H, 2.64; N, 5.97. Calcd. for $C_{11}H_7ONCl_2$: C, 55.00; H, 2.92; N, 5.84%.

Red crystals of XIII were also obtained from the effluent, but in a very poor yield.

**The Reaction of X with Alkali.** — A solution of X (20 mg.) in an alcoholic potassium hydroxide solution (potassium hydroxide, 70 mg.; ethanol, 1 ml.; water, 2 drops) was warmed on a water bath for 30 min. The acidification of the solution with diluted hydrochloric acid caused colorless crystals to precipitate; they were collected and recrystallized from ethanol to give colorless needles, m. p. 246—247°C. This substance was found to be identical with 3-acetyl-4-hydroxycarbostyril (XV) by comparison with an authentic sample.

**Ethyl 2-Acetoacetamidobenzoate (XVII).** — A mixture of ethyl anthranilate (1 g.) and diketene (2.5 ml.) was warmed at 70—80°C for 1.5 hr. After the complete removal of the excess diketene, the resultant oily residue was dissolved in ether and the solution was shaken with diluted hydrochloric acid to remove any unreacted starting material. The concentration of the ether solution gave colorless crystals, which were recrystallized from petroleum ether to yield granular crystals, m. p. 163—165°C. Yield, 1 g.

**3-Acetyl-4-hydroxycarbostyril (XV).**—A solution of XVII (20 mg.) in an alcoholic potassium hydroxide solution (potassium hydroxide, 70 mg; ethanol, 1 ml.; water, 2 drops) was warmed on a water bath for 30 min. After the evaporation of the ethanol, the solution was acidified with diluted hydrochloric acid. The colorless precipitate which was thus deposited was collected and recrystallized from ethanol to afford colorless needles, m. p. 244—247°C. Yield, 10 mg. This product was found, by a comparison of their infrared spectra, to be identical with an authentic sample prepared by Tomita's method.[6]

**3-Acetoacetamidotropolone (XX).** — A mixture of XVIII (500 mg.) and diketene (2.5 ml.) was heated on a water bath for 2 hr. After the removal of the excess diketene under reduced pressure, the residual crystals were recrystallized from methanol to afford colorless needles, m. p. 93—95°C. Yield, 680 mg. IR 3180, 1700, 1680 $cm^{-1}$ (KBr).

Found: C, 59.31; H, 5.17; N, 6.42. Calcd. for $C_{11}H_{11}O_4N$: C, 59.72; H, 5.01; N, 6.33%.

**5-Acetoacetamidotropolone (XXI).** — A mixture

of 5-aminotropolone (4 g.) and diketene (20 ml.) was heated at 80°C for 2 hr. The colorless crystals that separated when the mixture was cooled to room temperature were collected and washed with ether. Recrystallization from acetone-methanol afforded colorless needles (4.16 g.), m. p. 138—139°C.

Found: C, 59.49; H, 4.72; N, 6.45. Calcd. for $C_{11}H_{11}O_4N$: C, 59.72; H, 5.01; N, 6.33%.

**The Acetate (XXII) of XX.** — A solution of XX (50 mg.) in acetic anhydride (0.4 ml.) was heated at 120°C for 4 hr., and then the excess acetic anhydride was removed under reduced pressure. The recrystallization of the residue from methanol gave colorless scales, m. p. 146—148°C. Yield, 30 mg. IR 3270, 1750, 1690 $cm^{-1}$ (KBr).

Found: C, 59.49; H, 4.83; N, 6.37. Calcd. for $C_{13}H_{13}O_5N$: C, 59.31; H, 4.98; N, 5.32%.

**The Methyl Ether (XXIII) of XX.** — To a suspension of XX (630 mg.) in a mixture of ether (18 ml.) and methanol (3 ml.), ethereal diazomethane was added until the evolution of nitrogen ceased. The end point of the reaction was determined by a coloration test with ferric chloride. During this reaction, the crystals (XX) dissolved gradually and colorless needles newly appeared. The needles were collected and recrystallized from ethanol to give colorless needles, m. p. 163—166°C. Yield, 360 mg. IR 3240, 1710, 1675 $cm^{-1}$ (KBr).

Found: N, 6.18. Calcd. for $C_{12}H_{13}O_4N$: N, 5.96%.

**3-Acetyl-4-ethoxy-1-azaazulan-2-one (XXIV).** — A suspension of XXIII (100 mg.) in a sodium ethoxide solution (sodium, 40 mg.; ethanol, 4 ml.) was refluxed for 4 hr., and then the yellow solution thus obtained was concentrated under reduced pressure. When the residue was dissolved in water (2 ml.) and neutralized with diluted hydrochloric acid, yellow crystals separated. The recrystallization of the crystals from methanol yielded yellow needles, m. p. 220—225°C. Yield, 70 mg. $\lambda_{max}^{MeOH}$ mμ (log ε): 252 (4.57), 440 (4.14). IR 1690, 1630 $cm^{-1}$ (KBr).

Found: C, 68.14; H, 6.14; N, 5.72. Calcd. for $C_{13}H_{13}O_3N$: C, 67.52; H, 5.67; N, 6.06%.

**3-Acetyl-4-methoxy-1-azaazulan-2-one (XXV).** — A suspension of XXIII (50 mg.) in a sodium methoxide solution (sodium, 20 mg.; absolute methanol, 3 ml.) was refluxed for 3.5 hr. After the evaporation of the solvent, the residue was neutralized with dilute hydrochloric acid and extracted with ethyl acetate. The removal of the sovlent left yellow crystals, which were then collected and recrystallized from methanol to give yellow needles, m. p. 200—220°C (decomp.). Yield, 20 mg. IR 1690, 1625 $cm^{-1}$ (KBr).

Found: C, 65.82; H, 4.85; N, 6.65. Calcd. for $C_{12}H_{11}O_3N$: C, 66.35; H, 5.10; N, 6.45%.

**2-Chloro-3-(α-chlorovinyl)-4-ethoxy-1-azaazulene (XXVI).** — A mixture of XXIV (100 mg.) and phosphorus oxychloride (3 ml.) was heated at 95—98°C for 1 hr., after which the excess phosphorus oxychloride was removed under reduced pressure. To the residue, ice-cooled water was added, and the solution was neutralized with sodium bicarbonate, adjusted to pH 8, and extracted with benzene. The crystals obtained from the extract were chromatographed on an alumina column, and elution with benzene afforded orange crystals. Recrystallization from benzene-petroleum ether gave orange needles, m. p. 109—111°C. Yield, 95 mg. $\lambda_{max}^{MeOH}$ mμ (log ε): 253 (4.52), 270 (4.51), 304 (399), 332 (3.93), 455 (3.64). IR 1640, 885 $cm^{-1}$ (KBr).

Found: C, 58.51; H, 3.48; N, 5.25. Calcd. for $C_{13}H_{11}ONCl_2$: C, 58.23; H, 4.14; N, 5.22%.

**4-Ethoxy-1-azaazulan-2-one (XXVIII).** — When a solution of XXIV (100 mg.) in concentrated hydrochloric acid (1 ml.) was allowed to stand at room temperature, yellow crystals began to separate out in a few minutes. After it had been allowed to stand for 1 hr., the mixture was neutralized with a sodium bicarbonate solution and the crystals were collected. Recrystallization from methanol gave yellow needles, m. p. 180—183°C. Yield, 80 mg. $\lambda_{max}^{MeOH}$ mμ (log ε): 246 (4.58), 417 (4.09). IR 1670 $cm^{-1}$ (broad) (KBr).

Found: C, 69.66; H, 5.65; N, 7.44. Calcd. for $C_{11}H_{11}O_2N$: C, 69.82; H, 5.86; N, 7.40%.

**2-Chloro-4-ethoxy-1-azaazulene (XXIX).** — A mixture of XXVIII (40 mg.) and phosphorus oxychloride (1.5 ml.) was heated at 90—95°C for 1 hr. The evaporation of the excess phosphorus oxychloride left a dark red residue, which was then dissolved in cold water (5 ml.) and neutralized with sodium bicarbonate. The precipitate which was thus deposited was collected and chromatographed on an alumina column. Elution with benzene gave orange crystals. Recrystallization from benzene-petroleum ether afforded orange needles, m. p. 120—122°C. Yield, 30 mg. $\lambda_{max}^{MeOH}$ mμ (log ε): 252 (4.62), 300 (3.88), 328 (3.84), 452 (3.69).

Found: C, 63.99; H, 4.51; N, 6.99. Calcd. for $C_{11}H_{10}ONCl$: C, 63.62; H, 4.85; N, 6.75%.

**Methyl Ether (XXX) of XXI.**—a) To a suspension of XXI (3.5 g.) in methanol (40 ml.), ethereal diazomethane was added until a portion of the mixture no longer showed coloration with ferric chloride. The colorless crystals that appeared were collected and recrystallized from acetone to give colorless crystals, m. p. 164°C (decomp.). Yield, 2.4 g.

Found: C, 61.06; H, 5.52; N, 5.79. Calcd. for $C_{12}H_{13}O_4N$: C, 61.27; H, 5.57; N, 5.96%.

b) To a solution of 5-aminotropolone (100 mg.) in methanol, ethereal diazomethane was added until a portion of the solution no longer colored with ferric chloride. After the evaporation of the solvent, the addition of a small amount of acetone brought the residue to crystallization. The crystals were collected and recrystallized from acetone to give yellow crystals of 110 mg. of 5-amino-2-methoxytropone (XXXI), m. p. 95—105°C. A mixture of XXXI (110 mg.) and diketene was warmed at 60°C for 20 min., and the crystals that separated out on cooling were collected and recrystallized from acetone to afford colorless crystals of XXX. Yield, 80 mg.

**3-Acetyl-2-hydroxycyclohepta[b]pyrrol(1*H*)-5-one (XXXII).** — After a suspension of XXX (1.5 g.) in a solution of sodium ethoxide (sodium, 600 mg.; absolute ethanol, 84 ml.) was refluxed for 3 hr., the solvent was removed. The residue was then

dissolved in 20 ml. of water, acidified with diluted sulfuric acid, and adjusted to pH 4, and the yellow crystals that separated were collected. Recrystallization from methanol gave yellow crystals, m. p. >300°C. Yield, 800 mg. $\lambda_{max}^{MeOH}$ mμ (log ε): 245 (4.21), 316 (4.56), 360 (3.71), 418 (3.78).

Found: C, 63.47; H, 4.70; N, 6.62. Calcd. for $C_{11}H_9O_3N$: C, 65.02; H, 4.46; N, 6.89%.

***N*, 3-Diacetyl-5-acetoxy-1-azaazulan-2-one (XXXIII).**—A mixture of XXXII (40 mg.), pyridine (0.7 ml.) and acetic anhydride (1 ml.) was warmed at 80—90°C for 10 min. The yellow needles that separated out on cooling were collected and recrystallized from benzene to give yellow needles, m. p. 177—179°C. Yield, 25 mg. $\lambda_{max}^{MeOH}$ mμ (log ε): 245 (4.21), 316 (4.56), 360 (3.71), 418 (3.78).

Found: C, 62.84; H, 4.73; N, 5.59. Calcd. for $C_{15}H_{13}O_5N$: C, 62.71; H, 4.56; N, 4.88%.

***N*, 3-Diacetyl-1-azaazulan-2-one (XXXIV).** — A mixture of III (50 mg.), acetic anhydride (1.5 ml.) and pyridine (1 drop) was heated on a water bath for 10 min. After the mixture had then been cooled to room temperature, the yellow needles that separated out were collected and recrystallized from benzene to give yellow needles, m. p. 190—191°C. Yield, 30 mg. IR 1710, 1695, 1640 $cm^{-1}$ (KBr).

Found: C, 68.23; H, 4.77; N, 6.56. Calcd. for $C_{13}H_{11}O_3N$: C, 68.11; H, 4.84; N, 6.11%.

**3-Acetyl-2,5-dichloro-1-azaazulene (XXXV) and 2,5-Dichloro-3-(α-chlorovinyl)-1-azaazulene (XXXVI).** — A mixture of XXXII (200 mg.) and phosphorus oxychloride (15 ml.) was heated at 80°C for 2 hr., after which the excess phosphorus oxychloride was removed under reduced pressure. The residue was dissolved in water, and the pH was adjusted to 8 with sodium bicarbonate. The extraction of the solution with ethyl acetate afforded orange crystals of a mixture of XXXV and XXXVI. The mixture was chromatographed on an alumina column, and elution with benzene-petroleum ether gave red plates (XXXVI) and yellow needles (XXXV). Recrystallizations from benzene (for XXXV) and benzene-petroleum ether (for XXXVI) gave yellow needles of XXXV, m. p. 179—180°C (35 mg.) and red plates of XXXVI, m. p. 127—128°C (50 mg.).

XXXV: $\lambda_{max}^{MeOH}$ mμ (log ε): 235 (4.36), 298 (4.69), 332 (3.88), 460 (3.00).

Found: C, 55.06; H, 3.14; N, 6.01. Calcd. for $C_{11}H_7ONCl_2$: C, 55.00; H, 2.94; N, 5.84%.

XXXVI: $\lambda_{max}^{MeOH}$ mμ (log ε): 234 (4.34), 290 (4.66), 330 (3.64), 480 (2.97).

Found: C, 51.36; H, 2.61; N, 5.81. Calcd. for $C_{11}H_6NCl_3$: C, 51.08; H, 2.34; N, 5.42%.

The present authors wish to express their thanks to Professor Taro Isobe for his guidance in the analyses of the NMR spectra and to Assistant Professor Tsuneo Ikenoue for his measurement of and advice on the NMR spectra. They are also grateful to Dr. Takashi Toda for the gift of the sample of 2,6-dichloro-1-azaazulene and to the Sankyo Co., Ltd., which defrayed a part of the expense for the present work.

*The Chemical Research Institute of Non-Aqueous Solutions*
*Tohoku University*
*Katahira-cho, Sendai*

# The Electrical Conduction of Iodine Complexes of Aromatic Diamines*

By Hideaki KUSAKAWA and Shun-ichiro NISHIZAKI

(Received July 14, 1964)

In our previous work[1], we have studied the electrical properties of the *p*-phenylenediamine (*p*-PDA) - iodine complex system. The magnitude and the temperature dependence of the electrical resistivity of this system is dependent upon the iodine content.

As part of the study of a series of aromatic diamine - iodine complex systems, in this paper we have studied the electrical properties of iodine complexes of aromatic diamines, which contain two benzene rings. To examine the effects of the molecular structures of donors, we have selected four compounds from three different types of aromatic diamines: (a) 1, 5-naphthylenediamine (NDA), from diaminopolyacenes, (b) benzidine (BEN) and *o*-tolidine (TOL), from polyphenylenediamines, and (c) *p*, *p*'-diaminodiphenylmethane (APM), from non-conjugated diamines.

## Experimental

**Materials.** — The aromatic diamines and iodine were purified by means of two recrystallizations or sublimations. The complexes were prepared in the following way. A diamine and iodine were dissolved separately in benzene, and then the two

* Presented in part at the 17th Annual Meeting of The Chemical Socity of Japan, Tokyo, April, 1964.

1) S. Nishizaki and H. Kusakawa, This Bulletin, **36**, 1681 (1963).

solutions were mixed in four different proportions, so that the mole ratios of iodine to diamine in the mixtures were 3/4, 4/4, 5/4 and 6/4 respectively. After the mixtures had been kept standing for one day, the precipitates were collected by filtration and dried. In the case of the APM-iodine system, however, no precipitate could be obtained from the solution. Thus to prepare this complex system, the two components were blended in a test tube and heated to the melting point. The iodine contents of the complexes prepared from the solutions were determined by the microanalytical method.

**Resistivity Measurements.** — The experimental method and the conditions for the measurement of the magnitude and the temperature dependence of the electrical resistivity were similar to those described in the previous paper[1] except that, in the present case, the temperature range was from −70°C to 20°C, and carbon electrodes were used instead of the metal electrodes for BEN and TOL complexes. All specimens of the APM and iodine systems are of flowage, so only the resistivity at room temperature was obtained.

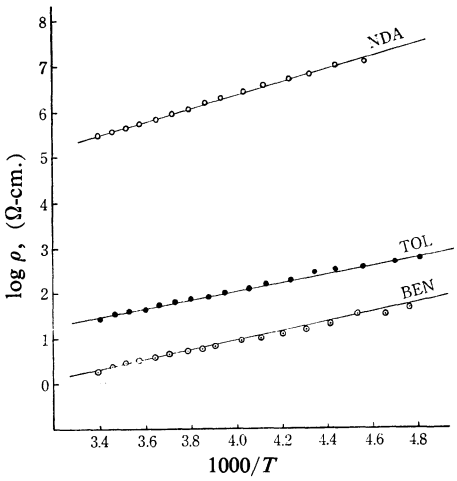



Fig. 1. Temperature dependence of conductivity of aromatic diamine complexes: for determination of thermal activation energy for conduction.

## Results and Discussion

The aromatic diamine - iodine complexes do not have a constant coordination number, and their resistivities are dependent on their iodine content. The correlation of resistivities at room temperature with iodine content is shown in Table I.

Examples of the experimental data on the temperature dependence of the electrical resistivity are shown in Fig. 1. The mole ratio of iodine in the examples shown this figure are 1.01 in the NDA-iodine system, 1.26 in the BEN-iodine system, and 1.29 in the TOL-iodine system. The activation energy, $E_c$, was determined from the experimental data according to the following equation:

$$\rho = \rho_0 \exp(E_c/kT) \qquad (1)$$

The results obtained are listed in the last column of Table I. The resistivity of the complex of BEN with iodine is not in agreement with that obtained by van der Hoek and his coworkers.[2] When metal electrodes were used, however, we also obtained a value similar to that reported by them ($10^2\Omega$-cm. at 20°C). It seems that a reaction takes place between metal electrodes and the specimen during the resistivity measurement, thus causing a high resistivity region in the neighborhood of the electrodes, and hence, an increase in the apparent resistivity.

For the *p*-PDA-iodine system both the resistivity and the activation energy showed

TABLE I. IODINE CONTENTS OF SPECIMENS AND THEIR ELECTRICAL RESISTIVITIES AND ACTIVATION ENERGIES

| Donor | $I_2$/diamine mixed mole ratio | Iodine content | Resistivity at 20°C Ω-cm. | Activation energy, eV. |
|---|---|---|---|---|
| NDA | 0.75 | 0.70 | $6.1\times10^{7}$ | 0.66 |
| | 1.00 | 0.86 | $1.6\times10^{6}$ | 0.42 |
| | 1.25 | 0.90 | $1.0\times10^{6}$ | 0.40 |
| | 1.50 | 1.01 | $3.1\times10^{5}$ | 0.32 |
| BEN | 0.75 | 0.78 | $1.6\times10^{5}$ | 0.34 |
| | 1.00 | 0.94 | $6.2\times10^{2}$ | 0.19 |
| | 1.25 | 1.26 | $2.2\times10^{0}$ | 0.19 |
| | 1.50 | 1.49 | $1.2\times10^{1}$ | 0.19 |
| TOL | 0.75 | 0.94 | $3.5\times10^{3}$ | 0.27 |
| | 1.00 | 1.02 | $2.9\times10^{2}$ | 0.24 |
| | 1.25 | 1.29 | $2.9\times10^{1}$ | 0.18 |
| | 1.50 | 1.53 | $9.1\times10^{1}$ | 0.18 |
| APM | 0.75 | — | $8\times10^{10}$ | — |
| | 1.00 | — | $3\times10^{9}$ | — |
| | 1.25 | — | $2\times10^{8}$ | — |
| | 1.50 | — | $6\times10^{7}$ | — |

2) J. A. van der Hoek, J. H. Lupinski and L. J. Oosterheff, *Mol. Phys.*, 3, 299 (1960).

TABLE II. CORELATION BETWEEN *Ec* AND $\rho_0$ ON AROMATIC DIAMINE IODINE COMPLEXES

| Donor | *p*-PDA | NDA | BEN | TOL |
|---|---|---|---|---|
| Activation energy, eV. | 0.41 | 0.32 | 0.19 | 0.18 |
| $\rho_0$ in Eq. 1, Ω-cm. | $2.6\times10^{-2}$ | $8.0\times10^{-1}$ | $1.2\times10^{-3}$ | $2.3\times10^{-2}$ |
| Iodine content | 0.82 | 1.01 | 1.26 | 1.29 |

minimum values at an iodine mole ratio of 0.8. In the cases of these aromatic diamines, the minimum appears at a mole ratio above 1.0. This is reasonable because the molecules of these aromatic diamines are longer than that of *p*-PDA.

When a non-conjugated diamine such as APM is used as the electron donor, the charge transfer complex of iodine does not possess a high electrical conductivity at room temperature. In this case, there was no minimum in the resistivity vs. iodine content curve in a 3/4—6/4 range of the mole ratio of iodine to amine. The resistivity of this system decreases with an increase in the iodine content, as with polyiodides.[3]

The results shown in Table II demonstrate that the activation energy, $E_c$, increases in the order; TOL, BEN, NDA and *p*-PDA, but this order is not in agreement with the order of their specific resistivities at room temperature. A linear relation can often be found between the activation energy, $E_c$, and the logarithm of $\rho_0$ in Eq. 1,[4,5] but such a relation can not be observed for aromatic diamine-iodine complexes.

The results obtained in this investigation indicate that polyphenylenediamines, such as BEN and TOL, are better than diaminopolyacenes, represented by NDA, as electron donors for iodine. It is well known that the charge transfer complex, which shows the remarkable electrical conduction, can be formed from the interaction of a strong electron donor with a strong electron acceptor. In the case of aromatic hydrocarbon, the ionization potential of naphthalene is lower than those of biphenyl[6] and benzene.[7] However, not only is the NDA-iodine complex poor in electrical conduction but also its energy of charge transfer transition[8] in the solid state is large compared with that of the BEN-iodine complex. Considering these facts, it is imaginable that the pendant amino group of polyacenes does not interact with iodine so strongly as does that of polyphenylene diamines.

Foster and Thompson have reported[9] that for chloranil, the donor character of *N,N,N',N'*-tetramethylbenzidine is as strong as that of *N,N,N',N'*-tetramethyl-*p*-phenylenediamine. In the case of non-substituted compounds for iodine, BEN is a very strong donor compared with *p*-PDA. On the other hand, if chloranil is used as the acceptor, BEN and TOL behave as weak donors,[10] but the *p*-PDA-chloranil complex shows a conspicuous signal of electron-spin resonance.[11] Concerning the charge transfer complexes of a given donor, its strength of charge transfer interaction seems to vary with the acceptor molecule, depending on its molecule, depending on its molecular size and other properties.

## Summary

The magnitudes and temperature dependence of the electrical resistivities of aromatic diamine - iodine complexes have been studied on four aromatic diamines; 1,5-naphthylenediamine (NDA), benzidine (BEN), *o*-tolidine (TOL) and *p,p'*-diaminodiphenylmethane (APM).

As the donor is a non-conjugated molecule, the electrical conductivity of its iodine complex is inferior to that of the conjugated diamine.

BEN and TOL, which are polyphenylenediamines, are better electron donors for iodine than NDA, a diaminopolyacene; the characteristics of the electron donor for iodine of NDA are as strong as those of *p*-PDA.

The resistivity shows a minimum value at an iodine mole ratio above 1.0 in the cases of the conjugated aromatic diamine which involve two benzene rings. These iodine contents are higher than the corresponding value *p*-PDA-iodine, 0.8.

The authors wish to thanks Mr. Osamu Hashimoto for microanalysis of the aromatic diamine - iodine complexes.

*The Central Research Laboratories*
*Mitsubishi Electric Corporation*
*Amagasaki, Hyogo*

3) S. Kusabayashi, H. Mikawa, S. Kawai, M. Uchida and R. Kiriyama, This Bulletin. **37**, 811 (1964).
4) V. L. Talrose and L. A. Bromenfeld, *Doklady Akad. Nauk SSSR*, **135**, 1450 (1960).
5) W. Z. Heldt and C. P. Weis, *J. Phys. Chem.*, **67**, 1392 (1963).
6) J. D. Morrison and A. J. C. Nicholson, *J. Chem. Phys.*, **20**, 1021 (1952).
7) R. S. Becker and W. E. Wentworta, *J. Am. Chem. Soc.*, **85**, 2210 (1963).
8) H. Kusakawa, unpublished.
9) R. Foster and T. J. Thomson, *Trans. Faraday Soc.*, **59**, 1059 (1963).
10) H. Kusakawa, unpublished.
11) A. Offenberg, C. J. Hoffman and J. Osiecki, *J. Chem. Phys.*, **38**, 1898 (1963).

# Properties of the Dilute Solution of Poly-2-methyl-5-vinylpyridine

By Masaji MIURA, Yukio KUBOTA and Teruaki MASUZUKAWA

(Received July 21, 1964)

Polyvinylpyridine has been used as a source material for polyelectrolytes and polysoaps, and several studies[1,2] have given some information on its molecular dimensions. Poly-2-methyl-5-vinylpyridine (PMVP), a derivative of polyvinylpyridine, has been studied by Sato and his co-worker[3] by means of osmotic pressure measurements, but its molecular dimensions are not yet known. It is of interest, therefore, to study the properties of the dilute solution of PMVP by viscosity and light-scattering measurements.

The purpose of this investigation is (1) to establish the relationship between the intrinsic viscosity and the molecular weight of PMVP; (2) to estimate the extension of the polymer chain with the aid of recent theories on the solution behavior of high polymers,[4,5] and (3) to compare the results with those for other vinylpyridine polymers and polystyrene.

## Experimental

**The Preparation of PMVP.**—2-Methyl-5-vinylpyridine was distilled immediately before use, and a middle fraction (b. p. 69.8—71.2°C/13 mmHg) was collected. The polymerization was carried out at 70°C for five days in a nitrogen atmosphere; the conversion rate was found to be about 40%. The polymer produced was first dissolved in methanol and then precipitated by pouring the methanol solution into a large amount of water. This was repeated twice more in order to remove the monomer which remained in the product, and then the precipitate was isolated by filtration; finally this purified material was fractionally precipitated, with methanol as a solvent and water as a precipitant. At first six fractions were obtained from a 3% methanol solution and then each fraction was separated into three to five subfractions by the same procedure, for a total of twenty subfractions; nine of these were finally selected for the viscosity and light-scattering measurements. The results of nitrogen analyses of fractions F-1-2, F-2-2 and F-6-1 were found to be 11.80, 11.94 and 11.97% respectively. These values were in good agreement with the calculated value, 11.76%.

**Solvents.**—The solvents used in this work were purified by the usual methods.

**Viscosity.**—The viscosity was measured at 25± 0.01°C with two Ubbelohde dilution viscometers, whose flow times for methanol were 114.4 sec. and 123.2 sec. The intrinsic viscosities were obtained by extrapolating the plots of the reduced viscosity, $\eta_{sp}/C$, vs. the concentration to infinite dilution.

**Light Scattering.** — The intensity of scattered light was measured at 25°C with both unpolarized blue (4358Å) and green light (5460Å), using a Brice-type light-scattering photometer manufactured by Shimadzu Seisakusho. All solvents and solutions were filtered into a clean semi-octagonal cell through a "Cellafilter fein or mittel" (Membranfiltergesellshaft, Göttingen) under applied pressure. Scattered intensities were measured at angles 45, 90 and 135° to the incident beam, and the data obtained were analyzed according to the usual procedure.[6] The depolarization was found to be negligible. All dissymmetries were corrected for the back reflection of the incident light.[7]

The instrument was calibrated according to two procedures; one refers to the values in the literature for the Rayleigh ratio, $R_{90}$, of benzene,[8] while the other utilizes standard opal glass.[9] With these calibrations, the molecular weight of the standard polystyrene sample was found to be in satisfactory agreement with the value in the literature.[10]

The refractive index increments, $dn/dc$, were measured at 25°C using a Debye-type differential refractometer manufactured by Shimadzu Seisakusho. The $dn/dc$ values of PMVP in methanol were 0.273 and 0.257 at 436 and 546 mμ respectively, both at 25°C.

## Results and Discussion

Abnormal light-scattering behavior, probably due to the ionization of the pyridine nitrogen, was found for all PMVP fractions in methanol. A typical example is shown in Fig. 1. Accordingly, dry ammonia gas was introduced to methanol in order to suppress any possible

1) A. Boyes and U. P. Strauss, *J. Polymer Sci.*, **22**, 463 (1956).
2) J. B. Berkowitz, M. Yamin and R. M. Fuoss, ibid., **28**, 69 (1958).
3) H. Sato and T. Yamamoto, *J. Chem. Soc. Japan, Pure Chem. Sec. (Nippon Kagaku Zasshi)*, **80**, 1393 (1959).
4) M. Kurata, W. H. Stockmayer and A. Roig, *J. Chem. Phys.*, **33**, 151 (1960).
5) W. H. Stockmayer and M. Fixman, *J. Polymer Sci., Part C*, No. 1, 137 (1963).
6) P. Doty and R. F. Steiner, *J. Chem. Phys.*, **18**, 1211 (1950).
7) A. Oth, J. Oth and V. Desreux, *J. Polymer Sci.*, **10**, 551 (1953).
8) C. I. Carr and B. H. Zimm, *J. Chem. Phys.*, **18**, 1616 (1950).
9) B. A. Brice, M. Halwer and R. Speiser, *J. Opt. Soc. Am.*, **40**, 768 (1950).
10) Research Group of Light Scattering Standard Sample, *Chem. High Polymers (Kobunshi Kagaku)*, **17**, 216 (1960).

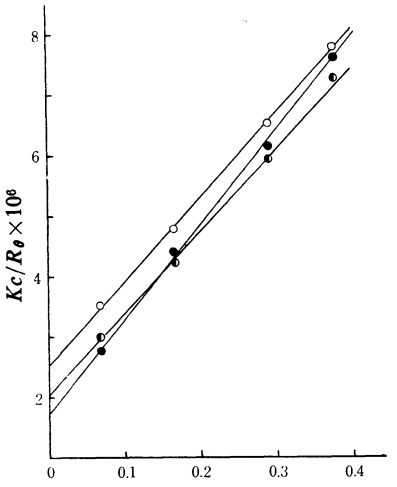



Fig. 1. Light scattering behavior of fraction F-3-2 in methanol at 4358Å.
-○-: 135° -◐-: 90° -●-: 45°

ionization (0.02 M $NH_3$).[2] By this procedure the normal plots were obtained. The term *methanol* used hereafter denotes that methanol which contains ammonia in the amount described above. Figure 2 shows the reciprocal reduced intensity, $Kc/R_{90}$, of PMVP fractions in methanol at 4358Å. The results of the viscosity and light-scattering measurements are summarized in Table I. Since the light-scattering properties are in good agreement at both wavelengths, the average values are used in the following discussion. The

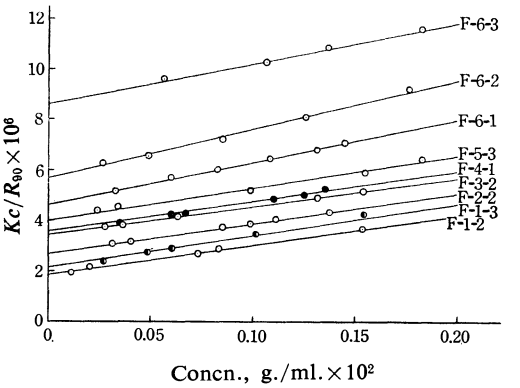



Fig. 2. Reciprocal reduced intensity, $Kc/R_{90}$, of PMVP fractions in methanol at 4358Å.

results of the behavior of PMVP in various solvents are summarized in Table II. There is a satisfactory agreement of the weight average molecular weight, $M_w$, in various solvents.

**The Relation between the Intrinsic Viscosity and the Molecular Weight.**—The log-log plots of the intrinsic viscosity and the molecular weight are shown in Fig. 3. In the range of the molecular weights of our samples, the plots are seen to be on a straight line. The relation between the intrinsic viscosity and the molecular weight is usually represented by the equation:

$$[\eta] = KM^a \qquad (1)$$

The constants $K$ and $a$ were calculated by the method of least squares, and the following equations were obtained:

Table I. The results of the viscosity and light-scattering measurements of PMVP

| Fraction | $[\eta]_{methanol}$ (100cc./g.) | $M_w \times 10^{-5}$ | | | $(\bar{R}^2)^{1/2}$ in Å | | | $A_2 \times 10^4$ | | | $[\eta]_{MEK}$ (100cc./g.) | $[\eta]_{toluene}$ (100cc./g.) |
|---|---|---|---|---|---|---|---|---|---|---|---|---|
| | | 4358Å | 5460Å | Av. | 4358Å | 5460Å | Av. | 4358Å | 5460Å | Av. | | |
| F-1-2 | 2.53 | 8.61 | 8.99 | 8.80 | 1074 | 1105 | 1090 | 5.50 | 5.65 | 5.58 | 1.07 | 0.580 |
| F-1-3 | 2.05 | 6.71 | 6.92 | 6.82 | 955 | 958 | 957 | 6.00 | 6.00 | 6.00 | | |
| F-2-2 | 1.70 | 4.83 | 5.08 | 4.96 | 837 | 845 | 841 | 5.80 | 6.00 | 5.90 | 0.778 | 0.435 |
| F-3-2 | 1.46 | 3.88 | 3.97 | 3.93 | 726 | 739 | 732 | 5.75 | 6.00 | 5.88 | | |
| F-4-1 | 1.35 | 3.62 | 3.69 | 3.66 | 719 | 695 | 707 | 6.00 | 6.05 | 6.03 | 0.572 | 0.370 |
| F-5-3 | 1.22 | 3.19 | 3.20 | 3.20 | 670 | 652 | 661 | 6.20 | 6.15 | 6.18 | | |
| F-6-1 | 1.00 | 2.57 | 2.58 | 2.58 | 559 | 564 | 562 | 7.65 | 7.55 | 7.60 | 0.490 | 0.307 |
| F-6-2 | 0.80 | 1.98 | 2.00 | 1.99 | 496 | 506 | 501 | 8.00 | 7.90 | 7.95 | | 0.275 |
| F-6-3 | 0.585 | 1.27 | 1.27 | 1.27 | 408 | 420 | 414 | 7.50 | 7.60 | 7.55 | 0.302 | 0.218 |

Table II. The results of the viscosity and light-scattering measurements of fraction F-3-2 in various solvents

| Solvent | d$n$/dc | $M_w \times 10^{-5}$ | $(\bar{R}^2)^{1/2}$ in Å | $A_2 \times 10^4$ | $[\eta]$ | $k'$* |
|---|---|---|---|---|---|---|
| Methanol | 0.273 | 4.96 | 841 | 5.90 | 1.70 | 0.353 |
| Dioxane | 0.180 | 4.46 | 644 | 2.35 | 0.97 | 0.353 |
| MEK | 0.219 | 4.33 | 552 | 1.65 | 0.778 | 0.617 |
| Toluene | 0.0951 | 4.94 | 471 | −0.10 | 0.435 | 1.93 |

* $k'$: Huggins' constant

$$[\eta] = 0.80 \times 10^{-4} M_w^{0.76}$$
in methanol at 25°C (2)

$$[\eta] = 1.39 \times 10^{-4} M_w^{0.65}$$
in MEK at 25°C (3)

**The Dependence of the Root-Mean-Square End-to-End Distance, $(\overline{R^2})^{1/2}$, and the Second Virial Coefficient, $A_2$, on the Molecular Weight.** —Figure 4 shows the relation between $(\overline{R^2})^{1/2}$ and $M_w$. The following equation was obtained by the method of least squares:

$$(\overline{R^2})^{1/2} = 0.49 M_w^{0.57}$$
in methanol at 25°C (4)

As may be seen in Table I, $A_2$ decreases with an increase in the molecular weight. The log-log plot of $A_2$ and $M_w$ in Fig. 5 gives the following relation, which is consistent with the results found for many other polymers:

$$A_2 \propto M_w^{-0.20} \quad (5)$$

**Unperturbed Dimensions.**—As is well known, the unperturbed dimensions may be evaluated from the data of viscosity and light scattering at the theta point.[11] The relations are:

$$[\eta]_\theta = K_0 M^{1/2} \quad (6)$$

$$K_0 = \Phi_0 (\overline{R_0^2}/M)^{3/2} \quad (7)$$

where $[\eta]_\theta$ is the intrinsic viscosity in the theta solvent, $\Phi_0 = 2.87 \times 10^{21}$, and $\overline{R_0^2}$ is the unperturbed mean square end-to-end distance. As our work was not done at the theta point, the values of $[\eta]_\theta$ were not obtained directly from the experiment; $[\eta]_\theta$, however, may be determined on the basis of the $[\eta]$ and $A_2$ values obtained in several solvents.[12] In Fig. 6 $[\eta]$ is plotted against $A_2$ for fraction F-3-2 using the data in Table II. The value of $[\eta]_\theta$ was 0.46. Substituting the values for $[\eta]_\theta$ and $M(4.69 \times 10^5)$ into Eq. 6, we found $K_0$ to be $6.7 \times 10^{-4}$. This value is in good agreement with the results obtained below (cf. Table III).

The recent theories of polymer solutions made it possible to estimate both the unperturbed dimensions and the excluded volume effect from the data in any solvent, good or

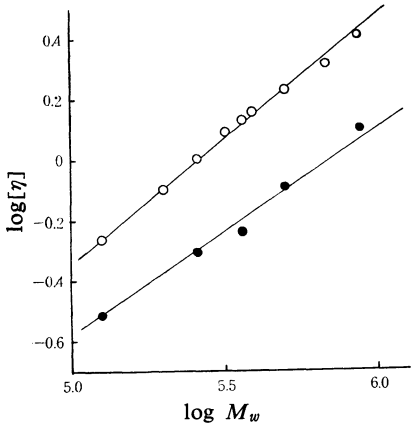



Fig. 3. Relation between intrinsic viscosity and molecular weight.
-○-: PMVPM-ethanol -●-: PMVP-MEK

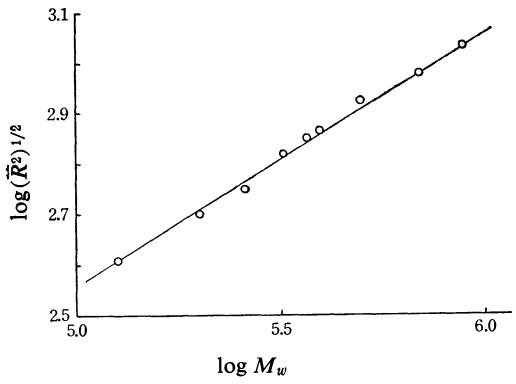



Fig. 4. Relation between root-mean-square end-to-end distance and molecular weight.

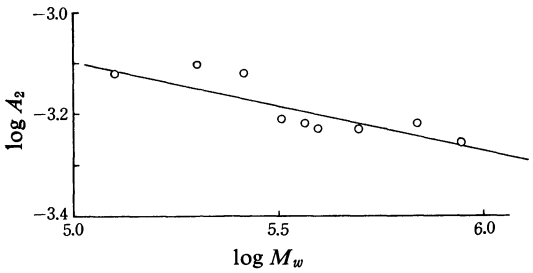



Fig. 5. Dependence of second virial coefficient on molecular weight.

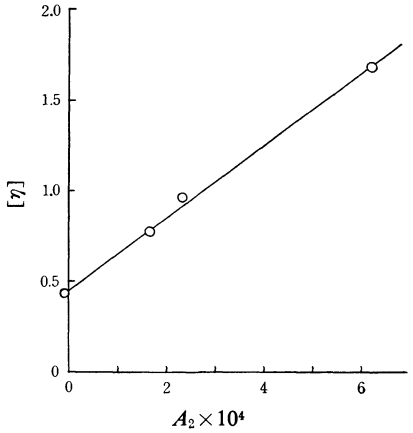



Fig. 6. Relation between $[\eta]$ and $A_2$ for fraction F-3-2 in various solvents.

11) P. J. Flory and T. G. Fox, *J. Am. Chem. Soc.*, **73**, 1904 (1951).
12) W. R. Krigbaum, *J. Polymer Sci.*, **18**, 315 (1955).

TABLE III. COMPARISON OF UNPERTURBED MOLECULAR PARAMETERS OF VARIOUS POLYMERS

| Polymer | Temp. °C | $K_0\times10^4$ | $(\bar{R}^2_0/M)^{1/2}\times10^{11}$ | $(\bar{R}^2_{0f}/M)^{1/2}\times10^{11}$ | $(\bar{R}^2_0/\bar{R}^2_{0f})^{1/2}$ | Ref. |
|---|---|---|---|---|---|---|
| PMVP | 25 | 6.9±0.5 from Eq. 8<br>7.0±0.5 from Eq. 11 | 652±15 | 282 | 2.31±0.05 | Present work |
| Poly-4-vinylpyridine | 25 | 8.1 | 686 | 301 | 2.28 | 1 |
| Poly-2-vinylpyridine | 25 | 7.9 | 680 | 301 | 2.26 | 14 |
| Polystyrene | 34 | 8.2 | 688 | 302 | 2.28 | 15 |

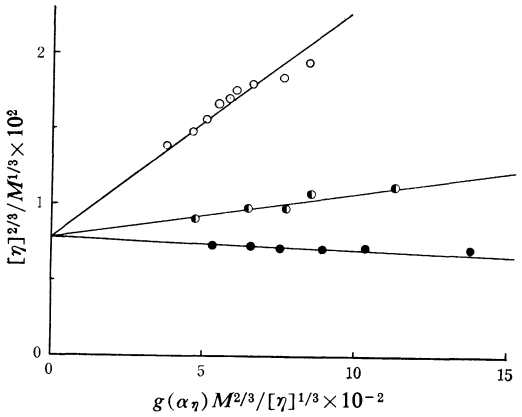



Fig. 7. $g(\alpha_\eta)M^{2/3}/[\eta]^{1/3}$ vs. $[\eta]^{2/3}/M^{1/3}$ for PMVP.
-○-: Methanol -◐-: MEK
-●-: Toluene

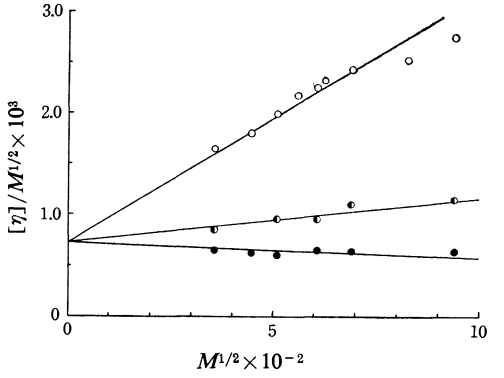



Fig. 8. $[\eta]/M^{1/2}$ vs. $M^{1/2}$ for PMVP.
-○-: Methanol
-◐-: MEK
-●-: Toluene

poor. According to the theory of Kurata-Stockmayer-Roig,[4]

$$[\eta]^{2/3}/M^{1/3} = K_0^{2/3}+0.363\Phi_0 B[g(\alpha_\eta)M^{2/3}/[\eta]^{1/3}] \quad (8)$$

$$g(\alpha_\eta)=8\alpha_\eta^3/(3\alpha_\eta^2+1)^{3/2} \quad (9)$$

where

$$\alpha_\eta^3=[\eta]/[\eta]_\theta \quad (10)$$

and where $B$ is the parameter of the excluded volume effect. Figure 7 shows the plots of $[\eta]^{2/3}/M^{1/3}$ against $g(\alpha_\eta)M^{2/3}/[\eta]^{1/3}$ as obtained in the usual manner.[13]

Very recently Stockmayer and Fixman[5] proposed the following equation:

$$[\eta]M^{1/2}=K_0+0.51\Phi_0 BM^{1/2} \quad (11)$$

where $K_0$ is the intercept of the plots of $[\eta]/M^{1/2}$ against $M^{1/2}$. The plots are shown in Fig. 8. The $K_0$ values obtained by both Eqs. 8 and 11 are in close agreement, and using the average value the unperturbed molecular parameters were calculated. The results are shown in Table III, together with those of other vinylpyridine polymers and polystyrene.

The quantity $(\bar{R}_0^2/\bar{R}^2_{0f})^{1/2}$ may be used as a measure of the extension of the polymer chain. Here $\bar{R}^2_{0f}$ is the unperturbed mean square end-to-end distance in the absence of any hindrance about each single bond; its value was calculated by assuming a C–C bond length to be 1.54Å and the tetrahedral angle to be 109.5°.

As is shown in Table III, the value of $(\bar{R}^2_0/\bar{R}^2_{0f})^{1/2}$ for PMVP is slightly higher than the values for the other polymers, but the difference is within the range of experimental error. Thus, it can be concluded that the degree of the extension of PMVP is almost the same as those of the other polymers. This is perhaps to be expected from the fact that the methyl substituent of PMVP is relatively small in size and is located at the farthest position with regard to the carbon atom of the main chain. Therefore, the methyl group may make only a minor contribution to the internal rotation about the C–C bonds of the polymer chain.

## Summary

Nine fractionated samples of poly-2-methyl-5-vinylpyridine (PMVP) have been investigated by viscosity and light-scattering measurements at 25°C. In the range of the molecular weights from about $1\times10^5$ to $1\times10^6$, the following relationship between the intrinsic viscosity and

13) M. Kurata and W. H. Stockmayer, *Fortschr. Hochpolymer. Forsch.*, 3, 196 (1963).
14) S. Arichi, private communication.
15) W. R. Krigbaum and P. J. Flory, *J. Polymer Sci.*, 11, 37 (1953).

the molecular weight in methanol has been obtained: $[\eta]=0.80\times10^{-4}M_w^{0.76}$. The unperturbed molecular dimensions have been obtained using the recent theories of the solution behavior of high polymers. The results have been compared with those of other vinylpyridine polymers and polystyrene, and it has been found that the degree of the extension of PMVP is almost the same as those of the other polymers.

The authors wish to express their thanks to Mr. Shizuo Arichi of this University for his helpful discussions throughout this work. They also wish to thank the Institute of Takeda Yakuhin Co. for making the elementary analysis.

*Department of Chemistry*
*Faculty of Science*
*Hiroshima University*
*Hiroshima*

# NOTES

## Studies of Thio Acids. II.[1] The Reaction of Stearic Esters with Sodium Hydrosulfide*1

By Yoshio HIRABAYASHI, Masateru MIZUTA and Tetsuro MAZUME*2

(Received December 26, 1963)

Thio acids can be synthesized as follows: (1) By heating carboxylic acids with phosphorus pentasulfide.[2,3] (2) By saponifying phenyl esters of carboxylic acids with sodium hydrosulfide in absolute alcohol.[4] (3) By treating acid chlorides with alkali hydrosulfide.[1] (4) By treating carbon oxysulfide with a Grignard reagent. (5) By treating carboxylic acid anhydrides with phosphorus sulfide.

It was reported that thio acids were not obtained, while carboxylic acids and mercaptans were obtained, by method 2 when alkyl esters of carboxylic acids were used in place of phenyl esters.[4] The present authors have now treated phenyl, methyl, β-chloroethyl, and cetyl stearates with sodium hydrosulfide in absolute ethanol, and obtained ethyl stearate and stearic acid from alkyl stearates, and thiostearic acid, distearoyl disulfide, ethyl stearate, and a trace of stearic acid from phenyl stearate.

### Experimental and Results

**Stearic Acid Esters.**—Methyl stearate was prepared by the reaction of stearic acid with methanol in the presence of concentrated sulfuric acid as a catalyst; it was then purified by recrystallization (m. p. 38.0—39.0°C).

Phenyl stearate and β-chloroethyl stearate were prepared by the reactions of stearoyl chloride[1] with phenol and ethylene chlorohydrine respectively, and were purified by recrystallization (m. p. 52.0—52.5°C for phenyl stearate and 49.5—50.5°C for β-chloroethyl stearate).

Cetyl stearate was prepared from stearoyl chloride, cetyl alcohol and polished magnesium ribbon according to the directions of Paquot and Boquet;[5] it was then recrystallized from ethanol (m. p. 60.5—61.5°C, saponification value 110.2 (110.2 by calcd.)).

TABLE I. ACID VALUES AND SULFUR CONTENTS OF PRODUCT

| Product | Acid value | Sulfur content, % (iodine method) |
|---|---|---|
| I | 106.4 | 5.2 |
| II | 108.5 | 0 |
| III | 138.5 | 1.4 |
| IV | 29.6 | 0 |

*1 Most of this study was presented at the Symposium of Oils and Fats of the Chemical Society of Japan, Nagoya, October, 1957.

*2 Present address: Shimogamo-kishimotocho, Sakyo-ku, Kyoto.

1) Part I of this series: Y. Hirabayashi, M. Mizuta and T. Mazume, This Bulletin, 37, 1002 (1964).

2) F. A. Kekulé, *Ann.*, 90, 311 (1854).

3) R. Kitamura, *J. Pharm. Soc. Japan*, 57, 31 (1937).

4) V. Auger and M. Billy, *Compt. rend.*, 136, 555 (1903).

5) C. Paquot and F. Boquet, *Bull. soc. chim. France*, 1947, 321.

TABLE II. COMPOSITION OF PRODUCTS OBTAINED BY REACTION OF STEARIC ACID ESTERS WITH ETHANOL - SODIUM HYDROSULFIDE

| Stearic acid ester ($R=C_{17}H_{35}-$) | Composition of product |
|---|---|
| $RCOOC_6H_5$ | RCOOH(10%), $RCOOC_2H_5$(20%), RCOSH(50%), RCOSSOCR(20%) |
| $RCOOCH_3$ | RCOOH(54%), $RCOOC_2H_5$(46%) |
| $RCOOCH_2CH_2Cl$ | RCOOH(75%), $RCOOC_2H_5$(20%), sulfur compound[a] |
| $RCOOC_{16}H_{33}$ | RCOOH, $RCOOC_2H_5$, $C_{16}H_{33}OH$, $RCOOC_{16}H_{33}$[b] |

a) A trace of a compound with SH group, confirmed to be not thiostearic acid, was detected in some ethyl stearate-fraction.
b) Too much losses were inevitable during the process of isolation, and an attempt to determine material balance among the components was unsuccessful.

**An Ethanol Solution of Sodium Hydrosulfide.**—This was prepared by the method described in the previous paper.[1]

**The Reaction of Phenyl, Methyl, β-Chloroethyl, Cetyl Stearates with Sodium Hydrosulfide.**—About a 2 N sodium hydrosulfide-ethanol solution (80 ml., or 0.167 mol. NaSH (50 ml., or 0.1 mol. NaSH to the cetyl ester only)) was added to the phenyl ester (12.4 g.), the methyl ester (9.9 g.), the β-chloroethyl ester (11.6 g.) (0.033 mol. for each), or the cetyl ester (10.2 g., or 0.02 mol.). Each mixture was refluxed for 3 hr. under a current of dried nitrogen. The ethanol was then distilled off under reduced pressure, and water was added to the residue. The mixture was acidified with dilute hydrochloric acid and extracted with ether. The ether layer was washed with water and dried over anhydrous sodium sulfate, and the ether was distilled off. The acid value*3 and sulfur content of the products are shown in Table I, in which I refers to the product from phenyl ester, II refers to that from methyl ester, III refers to that from β-chloroethyl ester, and IV refers to that from cetyl ester.

The data evidently indicate that mercaptan or thio acid is not contained in products II and III.

**The Identification of Products.**—Each product was recrystallized repeatedly from hexane, benzene, ether, methanol, or ethanol, giving nine fractions from I, four fractions from II, seven fractions from III and more than ten fractions from IV. The melting points, ultraviolet absorption spectra, neutralization values, saponification values, acetyl values, and sulfur contents (by iodine method and Kitamura's method) of these fractions were measured. The identified products and their yield are shown in Table II.

## Discussion

Auger and Billy[4] reported that sodium salts of carboxylic acids and mercaptans were formed when alkyl esters of carboxylic acids (RCOOR') were treated with absolute ethanol - sodium hydrosulfide at 180°C, while thio acids were formed when phenyl esters ($RCOOC_6H_5$) were used, and, further, that heating at 80°C or 120°C was insufficient for the achievement of these reactions. Hence, from their experimental results, it is deduced that splitting may occur between O and R' in RCOOR' and between C and O in $RCOOC_6H_5$.

$$RC(=O)O + R' + NaSH \rightarrow RC(=O)ONa + R'SH \quad (1)$$

$$RC(=O)O-C_6H_5 + NaSH \rightarrow RC(=O)SNa + C_6H_5OH \quad (2)$$

However, in the author's experiments, the products shown in Table II were obtained. It was not investigated whether the methyl ester would form methyl mercaptan or not. In order to examine the formation of mercaptans from alkyl esters, the authors investigated the reaction of the cetyl ester, but compounds with an S-H group were not obtained. After all, in these experiments, the reaction shown in Eq. 1 did not occur, though our conditions for the reaction were slightly different from those of Auger's experiments; that is, a trace of water*4 (principally in alcohol) was present, and heating was at nearly 78°C.

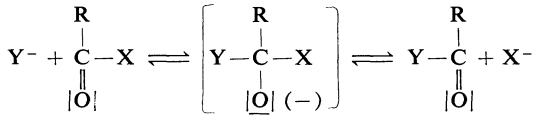
Wiberg[6] states that, in the mechanism of the hydrolysis of carboxylic acid esters by the base $Y^-$ (Eq. 3), the initial addition depends on the nucleophilicity of $Y^-$, but the partitioning of the addition compound to form reactants or products depends on the relative stabilities of $Y^-$ and $X^-$. If $Y^-$ is a weaker base than $X^-$, the reaction will not proceed, but if $Y^-$ is stronger than $X^-$, the reaction will proceed. Accordingly, ester hydrolysis by a general basic catalysis may be expected to occur when the anion formed from the ester is of a basicity at least comparable to the attacking base; therefore, when such esters are chosen in which the

*3 The acid value of the product varies with the concentration of sodium hydrosulfide added and with the heating time.

*4 In Auger's experiments, the water content is unknown, since the method of preparing absolute alcohol is not described.

6) K. B. Wiberg, *J. Am. Chem. Soc.*, 77, 2519 (1955).

alcoholic portion (HX) is more acidic than YH, a general basic catalysis will occur.



(3)

Although it is not a hydrolysis in the strict sense, the above mechanism will be applied to the authors' reaction.

In these experiments, those substances corresponding to HX are $CH_3OH$, $ClCH_2CH_2OH$, $C_{16}H_{33}OH$, and $C_6H_5OH$, in which phenol is more acidic than in the former three. The bases ($Y^-$) present in the sodium hydrosulfide - ethanol solution are $SH^-$, $C_2H_5O^-$, and $OH^-$ (NaSH, $C_2H_5OH$, and $H_2O$) ; for their relative basicities, the sequence $OH^- > C_2H_5O^-(RO^-) > SH^-$ should be taken, while for their nucleophilicities, the sequenee $SH^- > C_2H_5O^-(RO^-) > OH^-$ should be taken.

There is not a great difference between the basicities of $OH^-$ and $OR^-$. Hence, esters of $CH_3OH$, $ClCH_2CH_2OH$, and $C_{16}H_{33}OH$ are replaced by those of $C_2H_5O^-$ or $OH^-$. However, for $SH^-$ basicity ($X^- = (RO^-) > SH^-$), the difference between $X^-$ and $SH^-$ is too large to prompt the reaction. In phenyl ester, it is supposed that $C_6H_5O^-$ is weakly basic and replaced by $SH^-$, $C_2H_5O^-$, $OH^-$, etc.; the quantities of substituted products will depend on their nucleophilicities and concentrations. The results obtained in the experiments are well explained by the above mechanism.

*Department of Industrial Chemistry*
*Faculty of Engineering*
*Gifu University*
*Kagamigahara-shi, Gifu*

# Heats of Adsorption of Hydrogen and Catalytic Activities of Hydrogenation of Ethylene on Powdered Copper-Nickel Alloys

By Toyosaburo TAKEUCHI

(Received June 15, 1964)

A previous paper[1] on copper-nickel alloys prepared from copper and nickel nitrates demonstrated that the heat of adsorption of hydrogen and the catalytic activity of the hydrogenation of ethylene are closely related to the composition of alloys. In this note we are concerned with the correlation of the heat of adsorption of hydrogen to the rate of hydrogenation of ethylene and the activation energy, which were not discussed in the previous paper.

The correlation may be represented on the basis of the data in the previous paper as in Fig. 1, where the rates of reaction and the activation energies are plotted against the heats of adsorption of hydrogen at a sparse coverage of the corresponding alloy. The activation energies were obtained from further study at various reaction temperatures (100—160°C), study which was carried out in order to supply the deficiency in the previous study. The composition (Ni%) to which each point corresponds is indicated in the figure. Of particular interest is the fact that the correlation of the rate to the heat of the adsorption of hydrogen can be represented as a straight

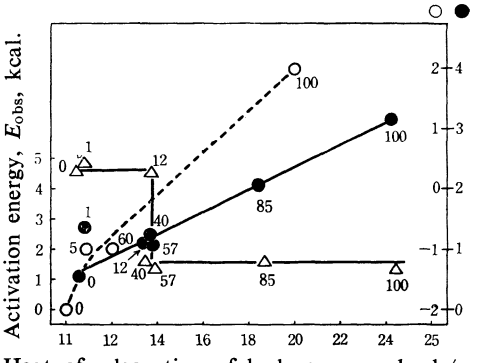



Fig. 1. Relations of the heat of hydrogen adsorption to the rate of catalytic hydrogenation of ethylene and the activation energy of the reaction.
—△— Activation energy.
—●— Rate of hydrogenation of ethylene (120°C) $K$/min.cm$^2$×10$^7$ outside scale of ordinate
—○— Rate of *p*-hydrogen interconversion (−196°C) log $K$ inside scale of ordinate
(Russell et. al.[4,5])

1) T. Takeuchi, M. Sakaguchi, I. Miyoshi and T. Takabatake, This Bulletin, 35, 1390 (1962).

line, and that the rate increases with an increase in the heats of adsorption, unlike the results on pure metals obtained by Beeck[2] and Schuit.[3] A similar correlation has, however, been obtained by Russell and his co-workers[4,5] from their study of the reaction of *p*-hydrogen interconversion and that of the heat of the adsorption of hydrogen on the same type of catalyst.

Since the observed activation energy in our study did not change continuously, notwithstanding the continuous change in the heat of adsorption of hydrogen, the correlation between the rate and the heat of adsorption can not be explained by the following equation obtained from the Langmuir-Hinshelwood kinetics:

$$E_{obs} = E_{true} - q_h - q_e$$

where $E_{obs}$ is the observed activation energy, $E_{true}$, the true activation energy, and $q_h$ and $q_e$, the heats of adsorption of hydrogen and ethylene respectively.

In view of this situation, we attempted to explain the occurrence of the discrepancy of the correlation between alloys and pure metals on the basis of the following hypothesis. If the surface of the catalyst is assumed to be nonuniform with respect to the adsorption of hydrogen and if the distribution of the bond strength of the adsorbed hydrogen against the coverage can be represented as the two cases shown in Fig. 2, and if, moreover, the bond strength of the hydrogen available for the reaction is restricted in the $E \sim E+dE$ range, the available amount of hydrogen on catalyst B in case 1 will be greater than that on catalyst A, when the greater inclination of the distribution curve can be given by the catalyst with the greater initial heat of adsorption. On the other hand, if the inclination is represented as in case 2, the available amount of hydrogen on catalyst A* will be greater than that on B*. Inasmuch as the available amount of hydrogen rules the rate of hydrogenation as well as that of *p*-hydrogen interconversion, it may suffice to say, consequently, that the reaction on pure metals and that on copper-nickel alloys correspond to those in case 1 and case 2 respectively. It was found in the study[6] using tritium as a tracer that the hydrogen adsorbed very strongly and/or very weakly on nickel did not react readily with ethylene. Unfortunately, we have no positive evidence that the heats of adsorption of hydrogen on the alloys can be given as case 2, for the measurement was made only on the sparse coverage. However, the heats on pure metals measured by Beeck[2] may be regarded to be approximately as in case 1.

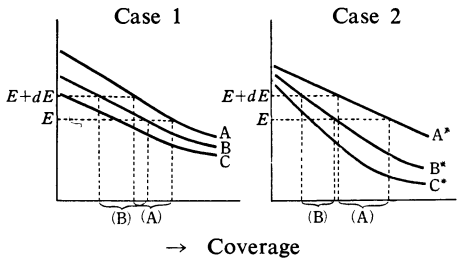



Fig. 2. Possible forms for the variation of bond strength ($E$) of adsorbed hydrogen.

The activation energies can be represented by the distinct series of different values, i.e., about 4.5 kcal. and 1.5 kcal. respectively. Such a discontinuous variation in activation energy is very similar to that found by Couper and Eley[7] in the *p*-hydrogen interconversion on palladium-gold alloys, if the expression of the axis of the abscissa can be replaced by the concentration of nickel on the surface of the alloy. Our previous studies[8,9] indicated that the concentration of nickel on the surface of the powdered copper-nickel alloy differed from that in the interior. It would be possible, however, to assume that the concentration of nickel on the surface increases with an increase in the average concentration of alloy and that the increase in the concentration increases the heat of adsorption of hydrogen. The figure shows that the composition which changed the activation energy is in the range from 12 to 40% nickel. Such a composition is approximately in accord with that to be expected from the proposal by Dowden and Reynolds,[10] even though the compositions indicated in the figure do not mean those of the surface. The activation energies in our study are quite small compared with those which have been reported by many other researchers.[11-16] No

2) O. Beeck, *Discussions Faraday Soc.*, **8**, 118 (1950).
3) G. C. A. Schuit, ibid., **8**, 205 (1950).
4) P. B. Shallcross and W. W. Russell, *J. Am. Chem. Soc.*, **81**, 4132 (1959).
5) L. S. Shield and W. W. Russell, *J. Phys. Chem.*, **64**, 1592 (1960).
6) D. Miyatani, R. Yamaguchi and T. Takeuchi, 1st Symposium on Isotopes, Japan (1964); to be published shortly.
7) A. Couper and D. D. Eley, *Discussions Faraday Soc.*, **8**, 172 (1950).
8) S. Yamaguchi and T. Takeuchi, *Z. anorg. u. allgem. Chem.*, **294**, 254 (1958).
9) T. Takeuchi, F. Shibata and M. Sakaguchi, *Z. physik. Chem., N. F.*, **14**, 339 (1958).
10) D. A. Dowden and P. W. Reynolds, *Discussions Faraday Soc.*, **8**, 184 (1950).
11) E. K. Rideal, *J. Chem. Soc.*, **121**, 309 (1922).
12) O. Toyama, *Rev. Phys. Chem., Japan*, **11**, 153 (1937).
13) O. Beeck, *Rev. Mod. Phys*, **17**, 61 (1945).
14) R. J. Best and W. W. Russell, *J. Am. Chem. Soc.*, **76**, 838 (1954).
15) W. K. Hall and P. H. Emmett, *J. Phys. Chem.*, **63**, 1102 (1959).
16) J. Tuul and H. E. Farnsworth, *J. Am. Chem. Soc.*, **83**, 2247 (1961).

confident explanation for this occurrence of small values can be offered. It can be recalled, however, that the rate of the hydrogenation of ethylene has an optimum at the temperature range of about 150°C.[17] The reaction temperature of our study includes this transition range. This might give the small activation energies.

17) H. Zur Strassen, *Z. physik. Chem.*, **A169**, 81 (1934); cf. G. C. Bond, "Catalysis by Metals," Academic Press, New York (1962), p. 243.

*Faculty of Literature and Science*
*Toyama University*
*Gofuku, Toyama*

# The Separation of the Main Constituents of Hiba Oil by Nitromethane Extraction

By Masaaki Ito and Kazuo Abe

(Received June 26, 1964)

Thujaplicin is a valuable terpenoid compound used industrially in a very small amount as a constituent of Thujopsis dolabrata. On the contrary, thujopsene is quantitatively the main constituent. Katsura et al.[1] showed in 1959 that thujaplicin can be isolated by the phosphoric acid treatment of an acidic oil which has been extracted with alkali.

Judging from the results reported by one of the present authors,[2] it is probable that terpene hydrocarbons are insoluble and that terpenoids, except for *l*-menthol and a few other compounds, are soluble in nitromethane. In this paper, the authors will propose a nitromethane method for the separation of the constituents of Hiba oil. It has been found that thujaplicin, can be isolated as a soluble part of the solvent, while thujopsene remains in the insoluble part. Therefore, a nitromethane-*n*-hexane system has been developed for the same separating purpose, because thujaplicin is insoluble and thujopsene is soluble in *n*-hexane, in contrast to nitromethane.

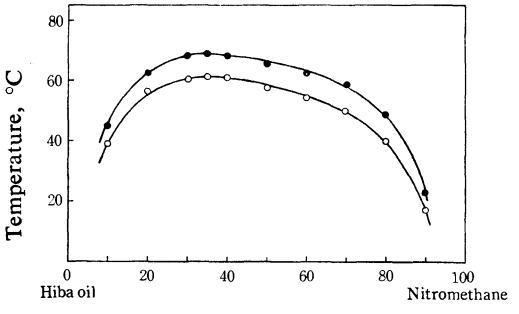



Fig. 1. The Hiba oil - nitromethane system.
○ Natural oil, ● Rectified oil

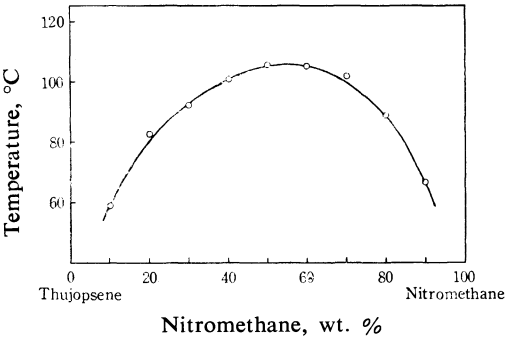



Fig. 2. The thujopsene-nitromethane system.

The mutual solubility curves between Hiba oil, thujopsene and nitromethane are shown in Figs. 1 and 2. The consolute temperature and the corresponding composition for these systems may be recorded as follows:

| System | Consolute temperature °C | Composition | |
|---|---|---|---|
| | | Oil wt. % | Nitomethane wt. % |
| Hiba oil - nitromethane | 61.0 | 35 | 65 |
| Rectified oil - nitromethane | 68.3 | 37 | 63 |
| Thujopsene - nitromethane | 105.8 | 53 | 47 |

The distribution of β-thujaplicin and thujopsene in the nitromethane - *n*-hexane system is shown in Tables I and II.

The extraction of an imitation oil (contents: β-thujaplicin 4.98%, thujopsene 95.02%) with the nitromethane - *n*-hexane system was carried out in order to confirm this separating

1) S. Katsura and A. Komatsu, Japanese Pat. 3794 (1959).
2) M. Ito, *J. Chem. Soc. Japan, Ind. Chem. Sec.* (*Kogyo Kagaku Zassi*), **59**, 981 (1956); ibid., **60**, 375 (1957).

Table I. Distribution of β-thujaplicin between nitromethane and *n*-hexane

| Temp., °C | Distribution of: Nitromethane layer, wt. % | *n*-Hexane layer, wt. % |
|---|---|---|
| 30 | 89.11 | 10.20 |
| 0 | 90.91 | 8.21 |
| −10 | 93.40 | 5.41 |

Table II. Distribution of thujopsene between nitromethane and *n*-hexane

| Temp., °C | Distribution of: Nitromethane layer, wt. % | *n*-Hexane layer, wt. % |
|---|---|---|
| 30 | 3.74 | 95.43 |
| 0 | 1.86 | 97.47 |
| −10 | 1.20 | 98.37 |

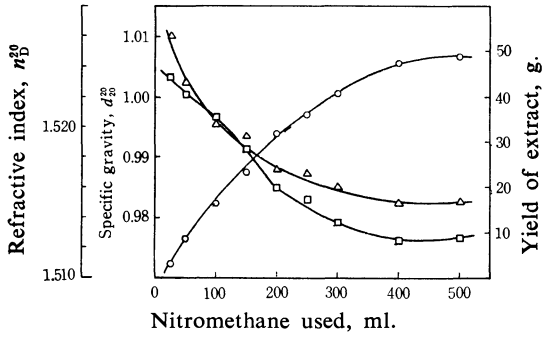



Fig. 3. Extraction of the Hiba oil by nitromethane.
○ Yield of extract, △ Specific gravity, □ Refractive index

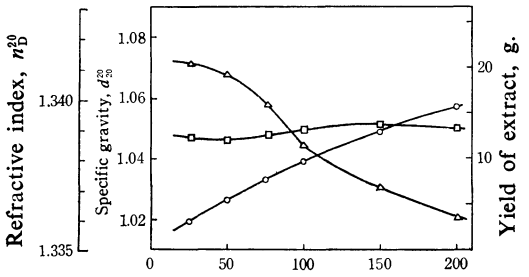



Fig. 4. Extraction of the Hiba oil by nitromethane - *n*-hexane system.
○ Yield of extract, △ Specific gravity, □ Refractive index

method. The crude thujaplicin and thujopsene were recovered quantitatively.

Subsequently, the nitromethane treatment and the nitromethane - *n*-hexane treatment of Hiba oil were carried out. The results are shown in Figs. 3 and 4. The results of the extractions were checked by the measurement of the specific gravity and the refractive index.

The residual oil in the nitromethane extraction and the *n*-hexane layer in the nitromethane - *n*-hexane system treatment was distilled under reduced pressure and rectified through a fractionating column (the number of the theoretical plate, 80) at 10 mmHg. The recovered thujopsene is of good quality.

## Experimental

**Hiba Oil.**—This was obtained by the steam-distillation from sawdust of Thujopsis dolabrata Sieb.; $d_{20}^{20}$ 0.9594, $n_D^{20}$ 1.5117.

**Rectified Hiba Oil.**—This was obtained by the steam-distillation of the above natural oil; $d_{20}^{20}$ 0.9485, $n_D^{20}$ 1.4955.

**Thujopsene.**—This was isolated from Hiba oil by the nitromethane method and then rectified; b. p. 119—120°C/10 mmHg, $d_{20}^{20}$ 0.9362, $n_D^{20}$ 1.5033, $[\alpha]_D^{20}$ −93.68.

**The Distribution of β-Thujaplicin and Thujopsene in the Nitromethane - *n*-Hexane System.**—A sample was distributed in nitromethane - *n*-hexane in a separating funnel which had been dipped into a thermostat. The solvent in each layer was evaporated, and the residual solute was weighed.

**The Extraction of an Imitation Oil with the Nitromethane - *n*-Hexane System.**—The nitromethane - *n*-hexane system (20 ml. of each) was added to the imitation oil (20 g.) and left to stand at −20°C overnight. The nitromethane layer was separated and evaporated. The crude thujaplicin was recovered in about a 100% yield. When it was then recrystallized from petroleum ether, its yield amounted to 70.3%. Also, thujopsene was recovered quantitatively from the *n*-hexane layer.

**The Nitromethane Treatment of Hiba Oil.**—Hiba oil (100 g.) was extracted with a definite volume of nitromethane at 20°C.

**The Nitromethane - *n*-Hexane System Treatment of Hiba Oil.**—A definite volume of nitromethane was added to a mixture of Hiba oil (100 g.) and *n*-hexane (100 ml.) in a separating funnel at 20°C. After the mixture had been shaken, the nitromethane layer was separated and then evaporated.

The authors are very grateful to the Takasago Perfumery Co. for its financial support and to the Hokusyu Wood Co. for the donation of Hiba oil. Also, the authors are indebted to Mr. Kunihiko Sasaki for his eager collaboration.

*Department of Applied Chemistry*
*Kitami College of Technology*
*Kitami, Hokkaido*

# A New Spectrophotometric Determination of Gallium with Capri Blue*

By Tsutomu MATSUO, Shunsuke FUNADA and Mikio SUZUKI

(Received July 20, 1964)

It is well known that, when gallium is spectrophotometrically determined with acid dyes, the chlorogallate ion $[GaCl_4]^-$ produced in strong hydrochloric acid media (ca. 6N) reacts with acid dyes to produce chelates, which are then extracted with organic solvents.[1] In previous papers,[2,3] triphenylmethaneamino derivative dyes were used to determine some metal ions. Jankovský[4] and other workers[5] reported that gallium is determined spectrophotometrically with the following two dyes; Malachite green and Brilliant green. We considered, however, that the dyes employed by them were probably unsuitable for this determination because of the small values of their apparent dissociation constants.

Capri blue (3-diethylamino-7-dimethylamino-2-methyl phenazoxonium chloride) is stable in a strong hydrochloric acid solution because its apparent dissociation constant is large.[6] However, it has not yet been applied to the determination of metal ions.

In this paper, a new method is described for the spectrophotometric determination of small amounts of gallium. It is based on the formation of a colored complex of gallium with Capril blue in a hydrochloric acid solution. The complex is extracted with benzene.

## Experimental

**Reagents.**—*Gallium Stock Solution.*—About 3 g. of gallium nitrate crystal ($Ga(NO_3)\cdot 8H_2O$ Mitsuwa Yakuhin Co.) was dissolved in 100 ml. of 6 N hydrochloric acid and titrated with an EDTA standard solution, using Cu-PAN[7] as an indicator. The working solution containing 1 $\mu$g./ml. was prepared from this solution by successive dilution with 6 N hydrochloric acid.

*Capri Blue.*—Two grams of commercial Capri blue (Tokyo Kasei Co.) was dissolved in 100 ml. of 6 N hydrochloric acid.

*Benzene.*—Commercial benzene was purified in the usual manner.

**Apparatus.**—The spectrophotometric absorbances were measured with a Shimadzu spectrophotometer Model QB-50 and a Hitachi photometer Model EPW-4, with 1 cm. cells.

**Procedure.**—Transfer the sample solution (less than 20 $\mu$g. Ga) in 6 N hydrochloric acid to a separate funnel and add 3 ml. of 2% Capri blue in a 6 N hydrochloric acid solution. Shake the solution for 1 min. with 20 ml. of benzene. Make up the benzene layer to 25 ml. with benzene. Centrifuge for 1 min. and measure the absorbance at 655 m$\mu$ (Filter 66) with the reagent blank solution as a reference. Determine the amount of gallium in the sample from a calibration curve prepared similarly.

## Results

**The Effect of the Acidity of Hydrochloric Acid and the Absorption Spectra.**—The absorbance of the sample solution was measured in the 500—680 m$\mu$ range, using the reagent as a

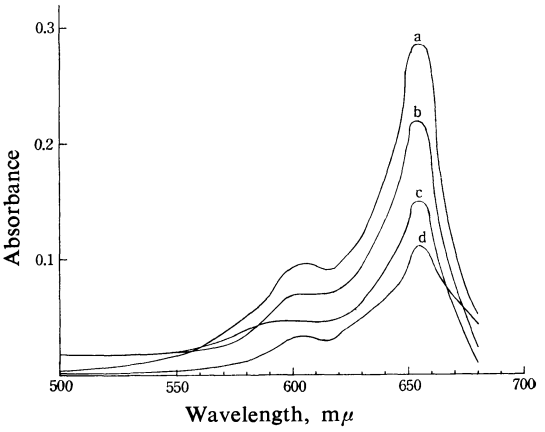



Fig. 1. Absorption spectra of Capril blue and its gallium complex benzene solution.
Ga $10^{-4}$ M, 3 ml.+Dye soln. 2%, 3 ml./25 ml. Benzene, 25 ml.
a: 6 N HCl vs. reagent blank
b: 4 N HCl vs. reagent blank
c: 8 N HCl vs. reagent blank
d: Reagent blank vs. benzene.

* Presented at the 16th Annual Meeting of the Chemical Society of Japan, Tokyo, April, 1963.

1) E. B. Sandell, "Colorimetric Determination of Traces of Metals," Interscience Publishers, Inc., New York (1959), p. 473.
2) T. Matsuo, Y. Kuroyanagi and S. Meguro, *Japan Analyst (Bunseki Kagaku)*, **12**, 515, 521 (1963).
3) T. Matsuo, S. Funada, H. Koide and M. Suzuki, ibid., **13**, 763 (1964).
4) J. Jankovský, *Talanta*, **2**, 29 (1959).
5) V. K. Kuzunetsova, N. A. Tananaev, *Referat. Zhur. Khim.*, No. 86097 (1959); *Anal. Abstr.* **7**, 4162, (1960); K. Hagiwara, M. Nakane, Y. Osumi, E. Ishii and Y. Miyake, *Japan Analyst (Bunseki Kagaku)*, **10**, 1374 (1962).
6) G. N. Lewis, J. Bigeleisen, *J. Am. Chem. Soc.*, **65**, 1144 (1943).
7) K. Ueno, "Kireto Tekitei" (Chelatometric Titration) (in Japanese), Nankodo, Tokyo (1960), p. 267.

TABLE I. MOLAR EXTINCTION COEFFICIENTS OF VARIOUS DYES

| Dye | Gallium: Concn. mol. | Gallium: Added ml. | Absorbance | Measured wavelength mμ | Molar extinction coefficient |
|---|---|---|---|---|---|
| Capri blue | $5\times10^{-5}$ | 2 | 0.226 | 655 | $5.6\times10^{4}$ |
| Rhodamine b*[1] | $1\times10^{-4}$ | 3 | 0.385 | 570 | $3.2\times10^{4}$ |
| Malachite green*[4] | $1\times10^{-4}$ | 5 | 0.580 | 635 | $2.9\times10^{4}$ |
| Brilliant green*[5] | $1\times10^{-4}$ | 5 | 0.300 | 640 | $1.5\times10^{4}$ |

* Data was obtained by ref. described procedure.

TABLE II. EFFECT OF AMOUNT OF DYE SOLUTION ADDED

| Gallium $5\times10^{-5}$ M ml. | Capri blue: Concn. % | Capri blue: Added ml. | Absorbance | Blank value |
|---|---|---|---|---|
| 2.0 | 2.0 | 2.0 | 0.219 | 0.080 |
| 2.0 | 2.0 | 3.0 | 0.227 | 0.098 |
| 2.0 | 2.0 | 4.0 | 0.228 | 0.101 |

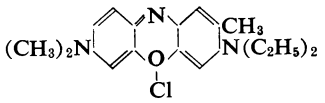


TABLE III. STABILITY OF GALLIUM-CAPRI BLUE COLORED BENZENE SOLUTION

| Standing time, min. | 0 | 30 | 60 | 90 | 120 |
|---|---|---|---|---|---|
| Absorbance | 0.226 | 0.226 | 0.226 | 0.226 | 0.226 |

Gallium taken: 2 ml. ($5\times10^{-5}$ M); Dye soln.: 2%, 3 ml.

reference. The extractability of a gallium-Capri blue complex, with benzene as a function of hydrochloric acid, is shown in Fig. 1. The maximum absorbance of the complex is at about 655 mμ. The absorbance of the sample solution is the greatest, and the absorbance of the blank solution is the smallest, when the complex is extracted from a 6 N hydrochloric acid solution.

The molar extinction coefficient of the gallium-Capri blue complex in benzene is about $5.6\times10^{4}$ at 655 mμ. The molar extinction coefficients of various complexes used for the colorimetric determination of gallium are compared in Table I; the Capri blue complex is very sensitive.

**The Effect of the Amount of the Dye and the Stability of the Colored Complex.** — The amount of Capri blue solution added was varied, the other factors remaining unchanged. The results are shown in Table II. The absorbance is constant on the addition of more than 3 ml. of a 2% Capri blue solution. When too much is added, however, the absorbance of the reference increases. The stability of the colored complex in a benzene solution was investigated as shown in Table III. The complex is stable in benzene for 2 hr.

**Calibration Curve.**—Various amounts of a standard gallium solution containing more than 1 μg. of gallium were used in the manner

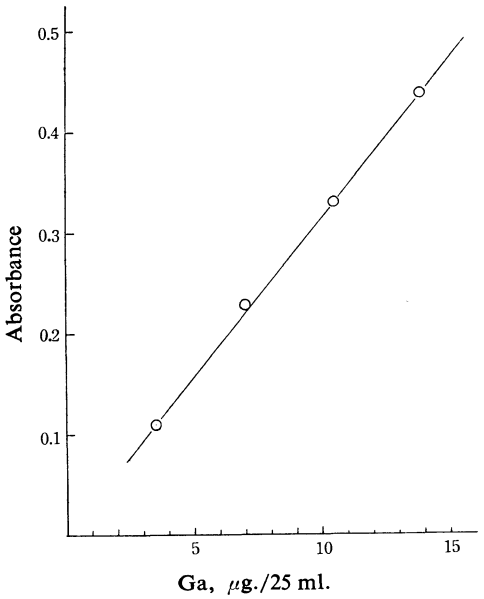



Fig. 2. Calibration curve.
Dye soln.: 2%, 3 ml., measured at 655 mμ

described above. The relationship between the absorbance and the amount of gallium obeys Beer's law for 1—15 $\mu$g. of gallium as is shown in Fig. 2.

**The Effect of Foreign Ions.**—The effect of foreign ions was studied with a solution containing 2 ml. of $5\times10^{-5}$ mol. (8.7 $\mu$g.) of gallium and various ions. Alkali metal salts of the anions were used. Cations were added as chloride or nitrate.

Under these conditions no interference was observed from about fifty-fold (0.5 mg.) amounts of aluminum, antimony, calcium, cadmium, cobaltous, cupric, magnesium, manganese, indium or thallium ions. However, even a minute quantity of iron (both II and III) interferes seriously. Five millimicrograms of iron, for instance, doubled the apparent gallium content. Of the few anions examined, large excesses (1 mg.) of nitrate and sulafte were without effect.

*Yamagata Technical Junior College*
*Yamagata University*
*Yonezawa, Yamagata-ken*

# The Dye-sensitized Photopolymerization of Vinyl Acetate in the Presence of Benzoyl Peroxide

By Koichi TAKAKURA and Gozo TAKAYAMA

(Received July 21, 1964)

Oster[1] reported that the dye-sensitized photopolymerization of vinyl monomers can easily occur in the presence of oxygen when a suitable combination of a dye and a reducing agent is used. Since then, many studies have been made concerning polymerization by means of such sensitizing systems.[2-8] One of the present authors previously found[4] that the riboflavin-sensitized photopolymerization of acrylamide in an aqueous solution was initiated by free radicals arising from the photoredox process between the photoreduced dye and the peroxidic compound produced during an induction period, and, furthermore, that this polymerization readily occurred at or below room temperature, even in the complete absence of oxygen, when a small amount of a peroxide, such as hydrogen peroxide or potassium persulfate, was added to the monomer mixture.

1) G. Oster, *Nature*, **173**, 300 (1954).
2) K. Nakatsuka, *Chemistry* (*Kagaku*), **11**, 218 (1956).
3) H. Oba and I. Fujita, *Chem. High Polymers, Japan* (*Kobunshi Kagaku*), **15**, 445 (1958).
4) Y. Nishijima, K. Takakura, T. Hayahara and Y. Ohno, presented at the 12th Annual Meeting of the Chemical Society of Japan, Kyoto, April, 1959; K. Takakura, Master Thesis, Dept. of Polymer Chem., Kyoto University, March, 1959.
5) G. Takayama, *Chem. High Polymers, Japan* (*Kobunshi Kagaku*), **17**, 644 (1960).
6) G. Delzenne, S. Toppet and G. Smets, *J. Polymer Sci.*, **48**, 347 (1960).
7) G. Delzenne, W. Dewinter, S. Toppet and G. Smets, *J. Polymer Sci.*, **A2**, 1069 (1964).
8) Y. Nishijima, T. Fujimoto and K. Shimabayashi, presented at the 17th Annual Meeting of the Chemical Society of Japan, Tokyo, April, 1964.

These sensitizing systems, including peroxide, seem to be superior to the previous one in that there is no induction period and polymerization can be easily controlled by varying the amounts of the peroxide added. For this reason, the present work was undertaken.

## Experimental

The sample solution, a mixture of the monomer and methanol (80 : 20 by volume), was deaerated by flushing it with purified nitrogen. Then the solution was irradiated with a 500-W. tungsten projector lamp through a color filter which removed the light of wavelengths shorter than 3000 Å.

## Results and Discussion

Table I shows the effects of several organic peroxides on the photopolymerization sensitized by riboflavin and acriflavine at 24°C. The polymerization was markedly accelerated by the addition of small amounts of such peroxides. The polymerization in the dark scarcely occurred under identical conditions, however. The rates of photopolymerization induced by the reaction between BPO and acetamide and by BPO itself are of an order of magnitude lower than that in the presence of both the dye and BPO. In all cases, the fading of the dye commenced immediately on irradiation, and then polymerization occurred. The conversion was increased with the increase in BPO concentration, whereas the polymerization

TABLE I. EFFECT OF BPO AND ITS DERIVATIVES ON THE DYE-SENSITIZED PHOTOPOLYMERIZATION OF VAc

| Dye-sensitizer mol./l. $\times 10^5$ | | Peroxide mol./l. $\times 10^4$ | | Acetamide[a] mol./l. | Conversion % | DP[b] |
|---|---|---|---|---|---|---|
| RF[c] | 4 | | 0 | 0.34 | 1.7 | 3440 |
| | 4 | BPO | 8.3 | 0.42 | 14.6 | 4000 |
| | 40 | BPO | 8.3 | 0.42 | 4.7 | 1270 |
| | 4 | BPO | 8.3 | 0 | 10.7 | 3860 |
| AF[d] | 2 | BPO | 2.1 | 0 | 9.6 | 4060 |
| | 2 | BPO | 4.2 | 0 | 13.7 | 3650 |
| | 2 | BPO | 8.3 | 0 | 15.2 | 3650 |
| | 4 | BPO | 8.3 | 0 | 23.4 | 4020 |
| | 2 | Bis(*p*-ClB)PO[f] | 8.3 | 0 | 16.6 | 4450 |
| | 2 | Bis(*o*-methoxyB)PO[g] | 8.3 | 0 | 21.7 | 4300 |
| | 4 | LPO[e] | 10.0 | 0 | 30.0 | 3860 |
| | 0 | BPO | 8.3 | 0.25 | 2.7 | 4640 |
| | 0 | Bis(*o*-methoxyB)PO[g] | 8.3 | 0 | 3.0 | 5200 |

a) Mild reducing agent. b) Degree of polymerization of PVAc determined viscometrically. c) Riboflavin-5'-phosphate sodium salt. d) Acriflavine. e) Lauroyl peroxide. f) Bis-(*p*-chlorobenzoyl)peroxide. g) Bis(*p*-methoxybenzoyl)peroxide.
Irradiation time, 2 hr.; temp., 24°C

TABLE II. EFFECT OF BPO ON THE DYE-SENSITIZED PHOTOPOLYMERIZATION OF SEVERAL MONOMERS IN ORGANIC SOLUTIONS

| Monomer | Dye-sensitizer mol./l. $\times 10^5$ | | BPO mol./l. $\times 10^4$ | Irradiation time hr. | Conversion % |
|---|---|---|---|---|---|
| MMA | AF | 2 | 0 | 8 | 2.9 |
| | AF | 2 | 8.3 | 8 | 13.0 |
| | AF | 2 | 8.3 | 8 | 15.7 |
| | | 0 | 8.3 | 8 | 4.2 |
| AN | RF | 2 | 8.3 | 2 | 10.5 |
| | AF | 2 | 0 | 2 | 0.5 |
| AAm | RF | 2 | 0 | 3/4 | 2.0 |
| | RF | 2 | 8.3 | 3/4 | 41.5 |
| | | 0 | 8.3 | 3/4 | 5.0 |

MMA, methyl methacrylate : benzene : methanol = 40 : 40 : 20 (by vol.)
AN, acrylonitrile : DMSO : methanol = 20 : 60 : 20 (by vol.)
AAm, acrylamide in methanol, 5 g./dl.
Temp., 24°C in nitrogen

was markedly retarded at higher dye concentrations. The BPO-catalyzed polymerization of VAc at 60°C in the dark was almost entirely inhibited when riboflavin was present.

Figure 1 shows the course of the polymerization performed at three different temperatures. The overall activation energy was calculated to be 7.4±0.5 kcal./mol., a value which was in good agreement with that of a previous study.[5]

On irradiation the absorption spectra of the reaction mixture in the visible regions began to disappear. The original color of the dye could no longer be recovered by admitting air into the irradiated system. It should be noted that such a spectral change in the polymerizing system was not observed in the dark, even at a high temperature. Therefore, it may be suggested that the photo-excited dyes or some derived species would react with BPO and undergo irreversible decomposition to produce some active free radicals.

Among the dyes examined, fluorescein sodium, acriflavine, rhodamin B and riboflavin

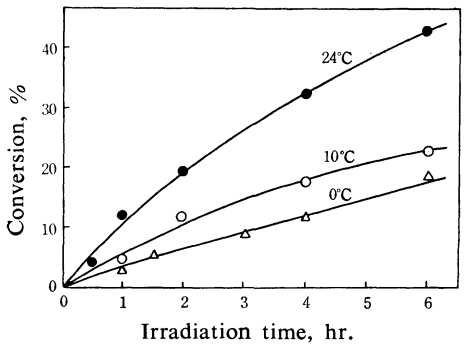



Fig. 1. Time-conversion curve for the photopolymerization of VAc sensitized by acriflavine-BPO: (Acriflavine) $=2.4\times10^{-5}$ mol./l., (BPO) $=8.3\times10^{-4}$ mol./l., (Acetamide) $=0.68$ mol./l.; VAc : methanol $=80:20$ (by vol.), under nitrogen.

are particularly effective. All of them are photoreducible dyes and are characterized by their fluorescence.[9]

This sensitizing system has been successfully applied to the photopolymerization of other vinyl monomers in organic solutions. The preliminary results are summarized in Table II. The effect of BPO is pronounced here also, and the polymerization is always accompanied by the photobleaching of the dye.

The results obtained may be explained in terms of a photo-redox mechanism by which the photoreduced dye is irreversibly oxidized with BPO to produce active initiating radicals.

The authors wish to thank Dr. Masakazu Matsumoto and Dr. Junji Ukida of our laboratory for their helpful discussions during this work.

*Research Laboratory*
*Kurashiki Rayon Co., Ltd.*
*Sakazu, Kurashiki*

9) For example, M. Koizumi, "An Introduction to Photochemistry" (Kokagaku Gairon), Asakura Shoten, Tokyo (1963), p. 346.

# The Reaction of Organolithium Compounds with Nickel Carbonyl*

By Song Kwang Myeong, Yoshihiko Sawa, Membo Ryang and Shigeru Tsutsumi

(Received August 3, 1964)

In previous papers we reported that organolithium compounds reacted smoothly with iron pentacarbonyl at −50—−40°C in an ether solution, giving ketones and acyloins as major produts.[1,2] This communication will deal with similar reactions of organolithium compounds with nickel carbonl.

Organolithium compounds were prepared by the ordinary methods, and nickel carbonyl was added to the ether solutions of organolithium compounds at −70°C. The reaction mixture was hydrolyzed with ethanol and hydrochloric acid.

The results of this reaction are given in Table I.

As a general tendency, acyloins were produced from arillithiums and symmetrical ketone alkyllithiums.

Table I.

| Organolithium compound | Main product | Yield* % |
|---|---|---|
| Phenyllithium | Benzoin | 36 |
| *m*-Tolyllithium | *m*-Toluoin | 61 |
| *p*-Tolyllithium | *p*-Toluoin | 71 |
| *p*-Methoxyphenyllithium | *p*-Anisoin | 15 |
| | *p*-Anisil | 23 |
| 2,6-Dimethylphenyllithium | 2,6-Dimethylbenzaldehyde | 22 |
| | 2,2',6,6'-Tetramethylbenzil | 23 |
| *n*-Butyllithium | Di-*n*-butyl ketone | 29 |

* The calculations of yields are based on the amounts of organic halides used.

Whereas the reaction mixture obtained from the reaction of *p*-tolyllithium with nickel carboyl at −70°C gave *p*-toluoin in a 71% yield on hydrolysis with ethanol - 6N hydrochloric acid at −70°C, the extraction of the reaction mixture with anhydrous benzene in a dry nitrogen box at room temperature, i. e., the isolation of the products without hydrolysis, yielded di-*p*-tolyl ketone in a 29% yield.

* This work was presented at the 17th Annual Meeting of the Chemical Society of Japan, Tokyo, April, 1964.

1) M. Ryang, Y. Sawa, H. Masada and S. Tsutsumi, *J. Chem. Soc. Japan, Ind. Chem. Sec.* (*Kogyo Kagaku Zasshi*), 66, 1086 (1963).

2) M. Ryang, I. Rhee and S. Tsutsumi, This Bulletin, 37, 341 (1964).

When the reaction time was prolonged by stirring for a further 5 hr. at 30—60°C, the subsequent hydrolysis gave *p*-toluoin and di-*p*-tolyl ketone in yields of 36 and 25% respectively (at 35°C) and in yields of 34 and 38% respectively (at 60°C). Thus it is evident that the reaction products were markedly affected by the methods of treating the reaction mixtture.

The present findings suggest that the ketones and acyloins were produced from the same intermediate complexes, but that the acyloins were produced via the dimerization of the intermediate, followed by hydrolysis, while the ketones were produced by the thermal decomposition of the same intermdiates. Hence, the complicated results in the reaction of organolithium compounds with iron pentacarbonyl or nickel carbonyl can be explained by considering the thermal stabilities and chemical reactivities of the intermediates. As for the intermediates, the following three unstable complexes can be postulated:

(a) $R-\underset{\underset{O}{\|}}{C}-Ni(CO)_x$ (b) $[R-\underset{\underset{O}{\|}}{C}-Ni(CO)_x]^-Li^+$

(c) $R-\underset{\underset{O}{\|}}{C}-Li$

The mechanistic aspects of this reaction will be discussed in detail in a forthcoming paper.

*Department of Chemical Technology*
*Faculty of Engineering*
*Osaka University*
*Miyakojima-ku, Osaka*

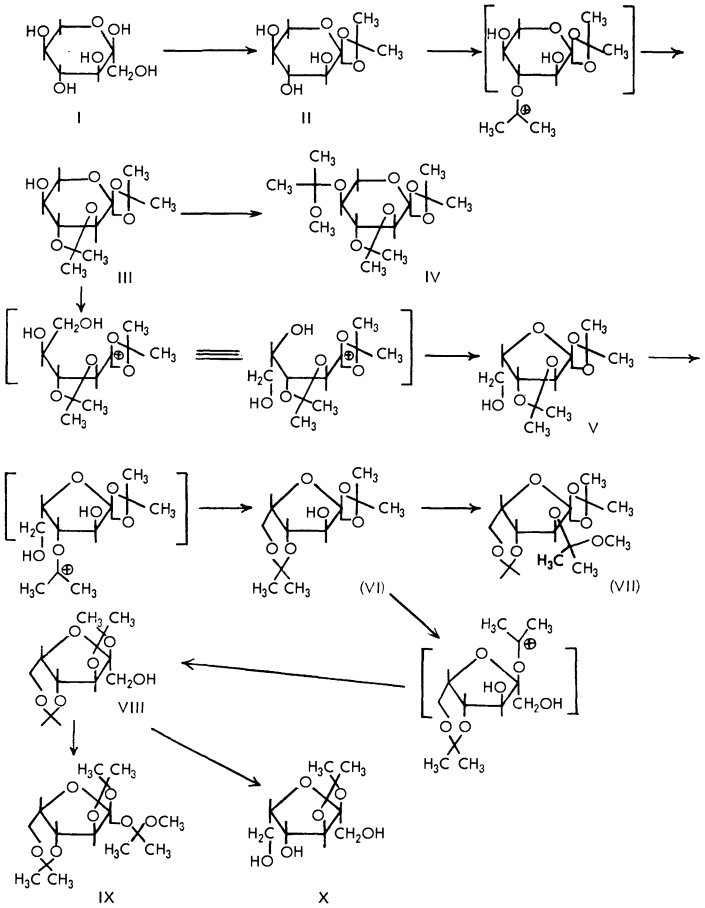
## SHORT COMMUNICATIONS

# Reaction Mechanism of the Acetonation of L-Sorbose by Ketal Interchange

By Takasi MAEDA, Masumi KIYOKAWA and Kanji TOKUYAMA

(Received December 14, 1964)

The acetonation of L-sorbose (I) is a very important reaction for the production of L-ascorbic acid. Previously we reported that, from the point of view of the reaction mechanism, the acetonation with acetone ketal[1] is different from the process of the acetonation with acetone,[2] and established the mechanism of the latter as I→1, 2-*O*-isopropylidene-α-L-sorbopyranose (II)[3] → the dimer of II → 2, 3 : 4, 6-di-*O*-isopropylidene-α-L-sorbofuranose



Scheme 1

1) K. Tokuyama and E. Honda, This Bulletin, 37, 591 (1964).

2) K. Tokuyama, E. Honda and N. Hōki, *J. Org. Chem.*, 29, 133 (1964).

3) H. Ohle, *Ber.*, 71, 762 (1938).

(VIII)[4]+I, in which the last element I takes this route further. In this paper, we present a reaction mechanism of the former acetonation.

The reaction of I with 2,2-dimethoxypropane (acetone dimethyl ketal) in the presence of *p*-toluenesulfonic acid gave a mixture syrup whose thin layer chromatogram exhibited multiple spots. The relative concentrations of the spots varied with the reaction conditions employed. Each component was separated in a pure state by thin-layer and fractional-gas chromatography, and their structures were determined to be 1,2-*O*- (II), 1,2:3,4-di-*O*- (III) and 5-*O*-1'-methoxyisopropyl-1,2:3,4-di-*O*-isopropylidene-α-L-sorbopyranose (IV), and 1,2:3,4-di-*O*- (V), 1,2:4,6-di-*O*- (VI),[1] 3-*O*-1'-methoxyisopropyl-1,2:4,6-di-*O*- (VII), 2,3:4,6-di-*O*- (VIII), 1-*O*-1'-methoxyisopropyl-2,3:4,6-di-*O*- (IX) and 2,3-*O*-isopropylidene-α-L-sorbofuranose (X),[5] respectively, by the infrared and NMR spectra and by the optical rotations. The analytical data are summarized below. III: colorless needles, m.p. 103—105°C (recrystallized from *n*-hexane), $[\alpha]_D^{27.5}$ −91.2 (*c* 1.051, acetone). Found: C, 55.75; H, 7.78. Calcd. for $C_{12}H_{20}O_6$: C, 55.37; H, 7.75%. IV: colorless needles, m.p. 133—135°C (recrystallized from *n*-hexane), $[\alpha]_D^{24.0}$ −82.2 (*c* 1.017, chloroform). Found: C, 57.77; H, 8.37; $CH_3O$, 9.03. Calcd. for $C_{16}H_{28}O_7$: C, 57.81; H, 8.49; $CH_3O$, 9.38%. V: m.p. 80—83°C, $[\alpha]_D^{24.0}$ −69.3 (*c* 1.090, chloroform). Found: C, 55.85; H, 7.91. Calcd. for $C_{12}H_{20}O_6$: C, 55.37; H, 7.75%. VII: syrup, $[\alpha]_D^{24.0}$ +17.5 (*c* 0.561, acetone). Found: C, 57.61; H, 8.26. Calcd. for $C_{16}H_{28}O_7$: C, 57.81; H, 8.49. IX: colorless syrup, $[\alpha]_D^{26.0}$ −10.9 (*c* 1.118, acetone). Found: C, 57.54; H, 8.55%. Calcd. for $C_{16}H_{28}O_7$: C, 57.81; H, 8.49%.

The above acetonated sugars (II→X) were also obtainable by the reaction of II with 2,2-dimethoxypropane; the mild acetonation of I gave II as a major product. On the other hand, the acetonation of X by ketal interchange gave only two products, VIII and IX. Therefore, the first intermediate of the acetonation process must be II.

On the basis of the above facts and the changes with time in the thin layer and gas chromatograms throughout the course of the acetonation by ketal interchange, the acetonation mechanism may be concluded to be as shown in Scheme 1.

*Shionogi Research Laboratory*
*Shionogi & Co. Ltd.*
*Fukushima-ku, Osaka*

4) T. Reichstein, *Helv. Chim. Acta*, **17**, 3111 (1934).
5) T. I. Temnikova and V. V. Sklyarava, *Zh. Prikl. Khim.*, **21**, 1131 (1954).

# The Radiolysis of Crystalline Oxalatocobalt(III) Complex Salts

By Hirotoshi SANO, Noriko MATSUBARA* and Nobufusa SAITO

(Received October 21, 1964)

Many attempts have already been made to investigate the hot-atom effect in neutron-irradiated metal complex salts.[1-3] The study of radiation effect is quite important in hot-atom chemistry. However, little attention has so far been paid to the radiolysis of these complex salts. Sugimori and Tsuchihashi have studied the radiolysis in trioxalato complex salts of trivalent metals, such as cobalt, chromium, iron, aluminum.[4] The present authors have recently reported that ninety per cent

TABLE I. $G(Co^{2+})$ VALUES ESTIMATED

| Compound | $G(Co^{2+})$ value[a] |
|---|---|
| $[Co(en)_3](NO_3)_3$ | $0.4\pm0.1$ |
| $[Co(NH_3)_6](NO_3)\cdot H_2O$ | $1.1\pm0.2$ |
| $[Co(NH_3)_6](C_2O_4)_3\cdot 4H_2O$ | $2.9\pm0.2$ |
| $[Co(C_2O_4)(NH_3)_4]NO_3\cdot H_2O$ | $3.1\pm0.2$ |
| $[Co(C_2O_4)(NH_3)_4]Cl$ | $4.3\pm0.2$ |
| $NH_4[Co(C_2O_4)_2(NH_3)_2]\cdot 2H_2O$ | $8.9\pm0.05$ |
| $K_3[Co(C_2O_4)_3]\cdot 3H_2O$ | $11._6\pm0.2$ |

a) From least squares analysis of plot of log (retention of complex) vs. dose.

* Present adress: The Institute for Solid State Physics, The University of Tokyo, Azabu, Tokyo.

1) N. Saito, H. Sano and T. Tominaga, This Bulletin, **33**, 20, 120 (1960); *Chem. & Ind.*, **1961**, 1796.

2) "Proceedings of International Symposium on Chemical Effects of Nuclear Transformation," IAEA, Vienna (1962).

3) N. Saito, T. Tominaga and H. Sano, *J. Inorg. and Nucl. Chem.*, **24**, 1539 (1962); *Nature*, **194**, 466 (1962); This Bulletin, **36**, 230, 232 (1963).

4) A. Sugimori and G. Tsuchihashi, This Bulletin, **34**, 449 (1961).

or more of radiocobalt atoms are found as cationic divalent species after the dissolution of the neutron-irradiated oxalatocobalt(III) complex salts.[5] In this paper, the radiolysis of the oxalatocobalt(III) complex salts will be reported.

The seven kinds of crystalline complex salts listed in Table I were irradiated with Co-60 gamma rays at room temperature, at a dose rate of $2.2-3.0\times10^5$ r./hr. in the presence of air. The irradiated salts were dissolved in water or dilute hydrochloric acid. The amount of cationic cobalt(II) species was determined by the $\beta$-nitroso-$\alpha$-naphthol method[6] or the nitroso-R salt method,[7] after the separation of cobalt(II) species from parent cobalt(III) complex ions by procedures includiding anion exchange or solvent extraction. The results were practically the same irrespective of the analytical method employed.

It was found that the amount of cobalt(II) species produced increases with an increase in the gamma-ray dose. Table I shows the estimated $G(Co^{2+})$ values. It should be mentioned that the $G$ value depends on the content of oxalate ions in the nearest coordination sphere, and that the $G$ value of hexamminecobalt(III) oxalate is definitely greater than that of hexamminecobalt(III) nitrate. The results may be explained by assuming the electron transfer process from oxalate to cobalt ions during the radiation-induced decomposition of complex salts.

*Department of Chemistry*
*Faculty of Science*
*Ochanomizu University*
*Otsuka, Bunkyo-ku, Tokyo (H. S.)*

*Department of Chemistry*
*Faculty of Science*
*The University of Tokyo*
*Hongo, Tokyo (N. M. & N. S.)*

5) N. Saito, H. Sano and T. Tominaga, *Chem. & Ind.*, 1964, 1622.
6) E. B. Sandell, "Colorimetric Determination of Traces of Metals," 3rd Ed., Interscience Publishers, Inc., N. Y. (1959), p. 420.
7) Ibid., p. 415.

# The Synthesis of 2-(1, 8-Dihydroxy-3, 6-disulfo-2-naphthylazo)-phenoxyacetic Acid as a New Reagent and Its Thorium Complex

By Kyoji TÔEI, Haruo MIYATA, Toshiya SHIBATA* and Sadao MIYAMURA**

(Received November 14, 1964)

Neo-thorin (2-(1, 8-dihydroxy-3, 6-disulfo-2-naphthylazo)-benzenearsonic acid)[1,2] has been applied as a reagent for the determination of thorium, zirconium and uranium. The arsono group, $-AsO_3H_2$, is most interesting as a functional group for thorium. The oxyacetic acid group, $-OCH_2COOH$, is also reactive with this element.

The present paper will describe the preparation of 2-(1, 8-dihydroxy-3, 6-disulfo-2-naphthylazo)-phenoxyacetic acid, and the determination of the acid dissociation constant of the reagent by the spectrophotometric method. The complex of the reagent with thorium will also be studied spectrophotometrically.

**The Synthesis of the Reagent.**—The acetylation of *o*-aminophenol with acetic anhydride afforded the acetyl derivative, which was converted into *o*-acetaminophenoxyacetic acid[3] by reaction with monochloroacetic acid in an alkaline medium.

The potassium salt of *o*-aminophenoxyacetic acid[4] was prepared by the reaction of potassium hydroxide and the lactam of *o*-aminophenoxyacetic acid, which had been obtained by the hydrolysis of *o*-acetaminophenoxyacetic acid with hydrochloric acid.

2-(1, 8-Dihydroxy-3, 6-disulfo-2-naphthylazo)-phenoxyacetic acid was prepared by the coupling of chromotropic acid with diazotized potassium *o*-aminophenoxyacetate. Greenish needles of the disodium salt of the product were obtained by recrystallization from water.

**The Spectral Properties of the Reagent and Its Acid Dissociation Constant.**—The absorption

* Present address: Osaka Gas Co., Ltd., Osaka.
** Present address: Nippon Synthetic Chemical Industry Co., Ltd., Uto-shi, Kumamoto-ken.

1) V. I. Kuznetsov, *Reports of Academii (USSR)*, **31**, 895 (1941).

2) K. Emi, K. Tôei and K. Furukawa, *J. Chem. Soc. Japan, Pure Chem. Sec. (Nippon Kagaku Zasshi)*, **79**, 681 (1958).

3) W. A. Jacobs and M. Heidelberger, *J. Am. Chem. Soc.*, **39**, 2190 (1917).

4) A. Thate, *J. prak. Chem.*, **29**, 180 (1884).

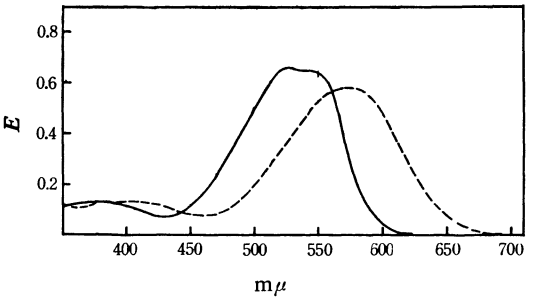



Fig. 1. Absorption spectra of the reagent and its thorium complex (broken line).
—— $2.0\times10^{-5}$ mol./l., pH 2.9
---- Thorium concn. to the reagent concn. =4 : 1, pH 2.9

spectra of the reagent solution ($2.0\times10^{-5}$ mol./l., pH 2.9), as well as its thorium complex, are shown in Fig. 1.

The first and second dissociation constants of the reagent, $pK_{a_1}$ and $pK_a$, have been estimated spectrophotometrically to be $2.9_9$ and $9.7_6$ (25°C, $\mu=0.1$) respectively.

**The Spectral Properties of the Thorium Complex.**—On the addition of thorium to the reagent solution, the absorption maxima (525 mμ) shifted toward longer wavelengths. The curve shows an absorption maximum at 575 mμ.

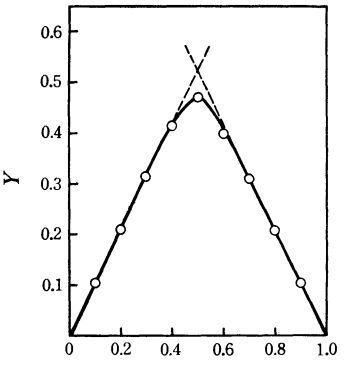



Fig. 2. Continuous variation method. Thorium concn.+the reagent concn. $=5.0\times10^{-5}$ mol./l. pH 2.7, 600 mμ

The mole ratio of thorium to the reagent was confirmed by the continuous variation method (Fig. 2) and by the mole ratio method at the pH values of 2.7 and 3.2 respectively; the results obtained indicate the formation of a 1 : 1 complex.

*Department of Chemistry*
*Faculty of Science*
*Okayama University*
*Tsushima, Okayama*

# A Polymerization of Isophthalonitrile Di-*N*-oxide by 1, 3-Dipolar Cycloaddition Reaction

By Yoshio IWAKURA, Masayasu AKIYAMA and Shinsaku SHIRAISHI

(Received December 14, 1964)

We wish to report a novel polymerization of isophthalonitrile di-*N*-oxide with diolefins, *m*-phenylenebismaleimide, ethylene dimethacrylate and biallyl. The polymerization proceeded by the repetition of the so-called 1, 3-dipolar cycloaddition between a nitrile *N*-oxide and a carbon-carbon double bond, forming a 4*H*-isoxazoline ring.[1] The 1, 3-dipolar cycloaddition resembles the Diels-Alder reaction in many respects;[2] on the other hand, it has been shown that polymerizations by the Diels-Alder reaction produce high-molecular-weight polymers.[3,4]

Isophthalonitrile di-*N*-oxide (m. p. 92—94°C decomp.) was prepared by the same method as was terephthalonitrile di-*N*-oxide.[5] The conditions of the polymerizations and the properties of the polymers obtained are presented in Tables I and II.

A typical polymerization is as follows: Into a solution of 0.402 g. (0.002 mol.) of *m*-phenylenebismaleimide (m. p. 201°C) in 4.0 ml. of dimethylformamide, 0.320 g. (0.002 mol.) of isophthalonitrile di-*N*-oxide was added portion

1) R. Huisgen, *Proc. Chem. Soc.*, **1961**, 357; *Angew. Chem.*, **75**, 604 (1963).
2) R. Huisgen, ibid., **75**, 742 (1963).
3) W. J. Bailey and J. Economy, Abstracts of papers presented at the 126th Meeting of the Ammerican Chemical Society, (1954), p. 195.
4) J. K. Stille, *Fortschr. Hochpolym. Forsch.*, **3**, 48 (1961); J. K. Stille and J. Anoys, *J. Polymer Sci.*, **A2**, 1487 (1964).
5) Y. Iwakura, M. Akiyama and K. Nagakubo, This Bulletin, **37**, 767 (1964).

TABLE I. POLYMERIZATION OF ISOPHTHALONITRILE DI-*N*-OXIDE WITH DIOLEFINS
In each run, 0.002 mol. of the di-*N*-oxide and 0.002 mol. of a diolefin were used.

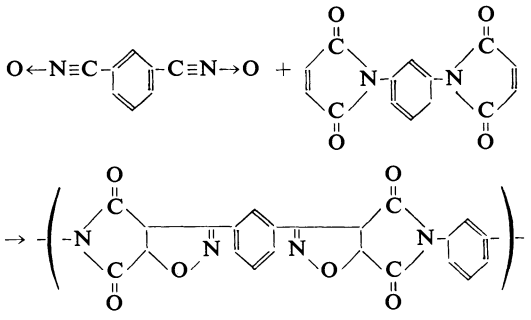
| Polymer | Diolefin | Solvent ml. | Temp. °C | Time hr. | Yield % | Polymer melt temp. °C | $\eta_{inh}$*1 | Analysis, % Found C | H | N | Calcd. C | H | N |
|---|---|---|---|---|---|---|---|---|---|---|---|---|---|
| I | *m*-Phenylene bismaleimide | 26*2 | 25 | 24 | 77 | 400 | 0.17 | | | | | | |
| I | *m*-Phenylene bismaleimide | 4.0*3 | 25 | 2.5 | 92 | | 0.19 | 59.06 | 3.40 | 12.09 | 61.68 | 2.82 | 13.08 |
| I | *m*-Phenylene bismaleimide | 4.0*3 | 75 | 2.5 | 93 | | 0.26 | 60.03 | 3.45 | 11.29 | | | |
| II | Ethylene dimethacrylate | 2.6*2 | 20 | 24 | 55 | 170 | 0.21 | 60.25 | 5.17 | 8.09 | 60.33 | 5.06 | 7.82 |
| III | Biallyl | 2.0*3 | 20 | 24 | 86 | 200 | 0.10 | 67.55 | 5.79 | 10.24 | 69.40 | 5.83 | 11.56 |

*1 Measured at a concentration of 0.5 g./100 ml. of dimethylformamide at 30°C.
*2 Dioxane
*3 Dimethylformamide

TABLE II. INFRARED ABSORPTTION MAXIMA OF POLYMERS
Nujol mulls

| Polymer | Absorption maxima, $cm^{-1}$ |
|---|---|
| I | 1790, 1725(s), 1605, 1490, 1375, 1310(w), 1180(s) 905, 795 and 685. |
| II | 1740(s), 1600(w), 1340, 1300, 1175, 910, 795 and 685. |
| III | 1640(w), 1580(s), 1440, 1335, 910, 795 and 685. |

by portion, over a period of 30 min. at room temperature. The mixture was then stirred for an additional two hours and poured into methanol. The polymer separated was washed with hot dioxane and hot methanol and dried under vacuum at 110°C, to give an almost colorless powder (90% yield) which did not melt up to 400°C. The polymer showed the infrared absorptions at 1790 and 1725 $cm^{-1}$ characteristic of an imide group, those at 1605 and 1490 $cm^{-1}$ characteristic of a phenyl group, and those at 795 and 685 $cm^{-1}$ characteristic of an *m*-phenylene group. It also gave at 905 $cm^{-1}$ the strong band which was common to all the other polymers obtained in these experiments and which was assigned tentatively to the isoxazoline ring. Absorptions of isophthalonitrile di-*N*-oxide at 2320, 1350 and 1080 $cm^{-1}$, and those of *m*-phenylenebismaleimide at 1150, 830 and 700 $cm^{-1}$, disappeared in the polymer. The infrared spectral data and the high yield of the product strongly support the theory that the polymerization of isophthalonitrile di-*N*-oxide with *m*-phenylenebismaleimide takes place according to Eq. 1.



(1)

Further detailed studies are now in progress.

*Department of Synthetic Chemistry*
*Faculty of Engineering*
*The University of Tokyo*
*Hongo, Tokyo (Y. I. & S. S.)*

*Tokyo Institute of Technology*
*Meguro-ku, Tokyo (M. A.)*

# A New Spectrophotometric Method for the Determination of Magnesium with Sodium *p*-Aminobenzene-azo-1, 8-dihydroxynaphthalene-3, 6-disulfonate

By Katsuya UESUGI

(Received October 13, 1964)

A new spectrophotometric method for the determination of traces of magnesium has been developed. It is based upon the formation of a stable bluish-violet magnesium complex of sodium *p*-aminobenzene-azo-1, 8-dihydroxynaphthalene - 3, 6 - disulfonate (pontacyl violet 4BSN).

The absorption spectra of the complex are shown in Fig. 1. At pH 11, the maximum absorbance is at 580 m$\mu$. The complex is formed by adding a microgram of magnesium to the mixture of 5.0 ml. of an ammonium chloride - ammonia buffer solution and 2.5 ml. of a 0.2% reagent solution in a 25 ml. volumetric flask. The solution is diluted to the mark with distilled water and thoroughly mixed. The full color develops within five minutes, and its stability is quite adequate for the determination of magnesium. As may be seen in Fig. 2., the magnesium complex has a maximum absorbance in the pH range from 10.8 to 11.3 ($\lambda_{max}$ 580 m$\mu$). Beer's law is obeyed up to a magnesium concentration of 1.0 p. p. m. (Fig. 3, curve 1). At 580 m$\mu$, the molar extinction coefficient is about 19300, and the sensitivity is 0.0013 $\mu$g. Mg/cm$^2$ that corresponds to log $I_0/I$=0.001.

The presence of acetone increases the sensitivity of the reagent to magnesium about 60%. In the addition of 20% vol./vol. with respect to acetone, Beer's law is obeyed up to a magnesium concentration of at least 0.8 p. p. m.

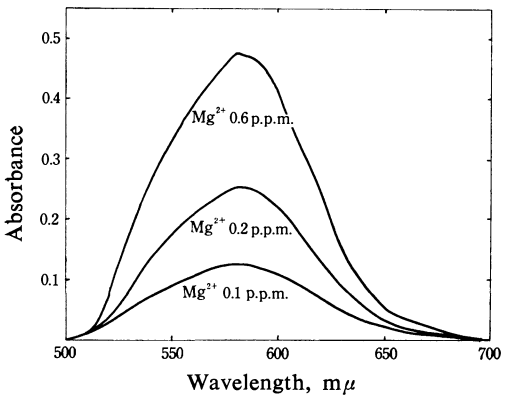



Fig. 1. Absorption spectra on the Mg-complex.
pH 11, reagent 200 p. p. m., against reagent blank.

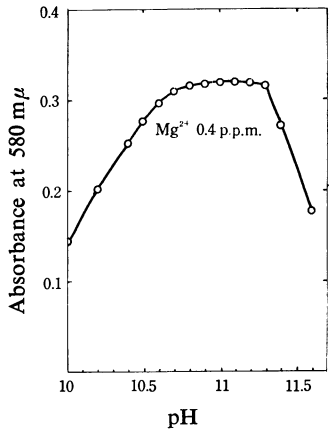



Fig. 2. Effect of pH on the absorbance of the Mg-complex.

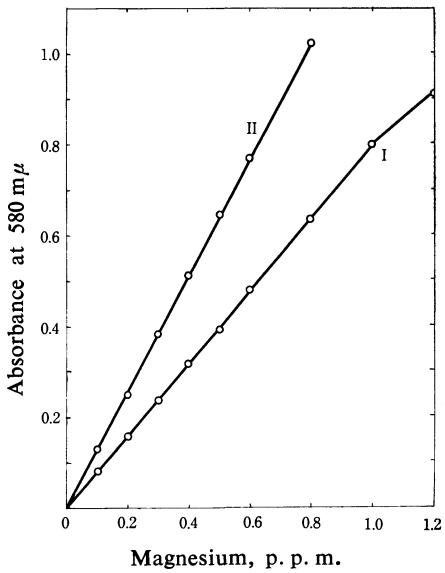



Fig. 3. Beer's law curve.
pH 11. I acetone — II acetone 20%

(Fig. 3, curve II). At 580 m$\mu$, the molar extinction coefficient is about 31300, and the sensitivity is 0.0008 $\mu$g. Mg/cm$^2$ that corresponds to log $I_0/I=0.001$.

Strontium and barium in concentrations up to 10 p. p. m. do not interfere. Calcium in amounts up to 2 p. p. m. also does not interfere; however, the presence of more than that causes a positive error. Chloride, sulfate, and nitrate in concentrations up to 500 p. p. m. have no effect. More than 1000 p. p. m. of chloride leads to poor results.

The details of this study will be reported elsewhere.

*Himeji Technical Institute*
*Idei-600, Himeji*

# The Synthesis of Local Anaesthetics

By Prithwi Nath BHARGAVA and Phulgan RAM

(Received May 2, 1964)

In view of the significant biological properties exhibited by thiazoles[1] and benzothiazoles[2], the preparation of some 2-(*N*-benzimidazolyl-acetylamino) benzothiazoles and their hydrochlorides was examined in order to ascertain their local anaesthetic properties.

The starting compound, 2-aminobenzothiazole, was prepared by the action of liquid bromine on asymmetrical phenylthiourea in an inert solvent such as chloroform.[3] Similarly, various substituted benzothiazoles have been prepared from the corresponding substituted asymmetrical thioureas. These 2-aminobenzothiazoles were condensed with chloroacetylchloride in dry benzene to obtain the corresponding 2-chloroacetylaminobenzothiazoles, which subsequently, on condensation with benzimidazole and 2-methylbenzimidazole, gave various substituted 2-(*N*-benzimidazolylacetylamino)benzothiazoles. Hydrochlorides of the above mentioned benzothiazoles have been prepared, and their local anaesthetic activity has been tested.[4]

A study of the pharmacological screening has shown that not a single compound is active. The values obtained for these compounds are more than those obtained for procaine-hydrochloride probably because of a heavier hydrophylic end in these compounds.

## Experimental

**2-Chloroacetylaminobenzothiazole.**—To a solution of 2-aminobenzothiazole (20 g.) dissolved in dry benzene (150 ml.), a solution of chloroacetylchloride (10 ml.) in dry benzene (50 ml.) was

TABLE I. 2-CHLOROACETYLAMINOBENZOTHIAZOLES

| 2-Chloroacetylamino | M. p. °C | Molec. formula | N, % | | S, % | |
|---|---|---|---|---|---|---|
| | | | Found | Calcd. | Found | Calcd. |
| -benzothiazole | 156 | $C_9H_7N_2OSCl$ | 12.32 | 12.36 | 14.21 | 14.13 |
| -(4-methyl)-benzothiazole | 181 | $C_{10}H_9N_2OSCl$ | 11.46 | 11.64 | 13.61 | 13.30 |
| -(5-methyl)-benzothiazole | 185 | $C_{10}H_9N_2OSCl$ | 11.42 | 11.64 | 13.49 | 13.30 |
| -(6-methyl)-benzothiazole | 183 | $C_{10}H_9N_2OSCl$ | 11.48 | 11.64 | 13.71 | 13.30 |
| -(4-chloro)-benzothiazole | 182 | $C_9H_6N_2OSCl_2$ | 10.67 | 10.73 | 12.61 | 12.26 |
| -(5-chloro)-benzothiazole | 184 | $C_9H_6N_2OSCl_2$ | 10.39 | 10.73 | 12.31 | 12.26 |
| -(6-chloro)-benzothiazole | 198 | $C_9H_6N_2OSCl_2$ | 10.48 | 10.73 | 12.57 | 12.26 |
| -(6-bromo)-benzothiazole | 204 | $C_9H_6N_2OSClBr$ | 9.10 | 9.16 | 10.61 | 10.47 |
| -(6-methoxy)-benzothiazole | 188 | $C_{10}H_9N_2O_2SCl$ | 10.46 | 10.91 | 12.71 | 12.48 |
| -(6-ethoxy)-benzothiazole | 174 | $C_{11}H_{11}N_2O_2SCl$ | 10.63 | 10.35 | 11.70 | 11.82 |

TABLE II. 2-(*N*-BENZIMIDAZOLYLACETYLAMINO)BENZOTHIAZOLES

| 2-(*N*-Benzimidazolyl-acetylamino) | M. p. °C | Molec. formula | N, % | | S, % | |
|---|---|---|---|---|---|---|
| | | | Found | Calcd. | Found | Calcd. |
| -benzothiazole | 245 | $C_{16}H_{12}N_4OS$ | 18.00 | 18.18 | 10.61 | 10.39 |
| -(4-methyl)-benzothiazole | 260 | $C_{17}H_{14}N_4OS$ | 17.03 | 17.39 | 10.21 | 9.93 |
| -(5-methyl)-benzothiazole | 262 | $C_{17}H_{14}N_4OS$ | 17.41 | 17.39 | 10.18 | 9.93 |
| -(6-methyl)-benzothiazole | 210 | $C_{17}H_{14}N_4OS$ | 17.01 | 17.39 | 10.32 | 9.93 |
| -(4-chloro)-benzothiazole | 266 | $C_{16}H_{11}N_4OSCl$ | 16.46 | 16.35 | 9.61 | 9.34 |
| -(5-chloro)-benzothiazole | 228 | $C_{16}H_{11}N_4OSCl$ | 16.18 | 16.35 | 9.66 | 9.34 |
| -(6-chloro)-benzothiazole | 192 | $C_{16}H_{11}N_4OSCl$ | 16.20 | 16.35 | 9.51 | 9.34 |
| -(6-bromo)-benzothiazole | 230 | $C_{16}H_{11}N_4OSBr$ | 14.00 | 14.47 | 8.30 | 8.26 |
| -(6-methoxy)-benzothiazole | 265 | $C_{17}H_{14}N_4O_2S$ | 16.19 | 16.57 | 9.83 | 9.46 |
| -(6-ethoxy)-benzothiazole | 244 | $C_{18}H_{16}N_4O_2S$ | 15.80 | 15.92 | 9.44 | 9.09 |

1) P. N. Bhargava and P. R. Singh, *J. Indian Chem. Soc.*, 37, 241 (1960).
2) P. N. Bhargava and S. C. Sharma, This Bulletin, 35, 942 (1962).
3) A. Hugershoff, *Ber.*, 36, 3121 (1903).
4) E. Bülbring and I. Wajda, *J. Pharmacol.*, 85, 78 (1945).

TABLE III. 2-[*N*-(2'-METHYLBENZIMIDAZOLYL)ACETYLAMINO]BENZOTHIAZOLES

| 2-[*N*-(2'-Methylbenzimidazolyl)acetylamino] | M. p. °C | Molec. formula | N, % | | S, % | |
|---|---|---|---|---|---|---|
| | | | Found | Calcd. | Found | Calcd. |
| -benzothiazole | 160 | $C_{17}H_{14}N_4OS$ | 17.32 | 17.39 | 10.10 | 9.93 |
| -(4-methyl)-benzothiazole | 200 | $C_{18}H_{16}N_4OS$ | 16.42 | 16.66 | 9.98 | 9.52 |
| -(5-methyl)-benzothiazole | 193 | $C_{18}H_{16}N_4OS$ | 16.39 | 16.66 | 9.71 | 9.52 |
| -(6-methyl)-benzothiazole | 183 | $C_{18}H_{16}N_4OS$ | 16.58 | 16.66 | 9.86 | 9.52 |
| -(4-chloro)-benzothiazole | 158 | $C_{17}H_{13}N_4OSCl$ | 15.63 | 15.71 | 8.68 | 8.97 |
| -(5-chloro)-benzothiazole | 191 | $C_{17}H_{13}N_4OSCl$ | 15.73 | 15.71 | 9.21 | 8.97 |
| -(6-chloro)-benzothiazole | 193 | $C_{17}H_{13}N_4OSCl$ | 15.48 | 15.71 | 9.03 | 8.97 |
| -(6-bromo)-benzothiazole | 218 | $C_{17}H_{13}N_4OSBr$ | 13.48 | 13.96 | 8.41 | 7.98 |
| -(6-methoxy)-benzothiazole | 214 | $C_{18}H_{16}N_4O_2S$ | 15.87 | 15.92 | 9.60 | 9.09 |
| -(6-ethoxy)-benzothiazole | 198 | $C_{19}H_{18}N_4O_2S$ | 15.00 | 15.30 | 8.69 | 8.74 |

TABLE IV. HYDROCHLORIDES OF 2-(*N*-BENZIMIDAZOLYLACETLYLAMINO)BENZOTHIAZOLES

| Hydrochlorides of 2-(*N*-benzimiazolylacetylamino) | M. p. °C | Molec. formula | N, % | | S, % | |
|---|---|---|---|---|---|---|
| | | | Found | Calcd. | Found | Calcd. |
| -benzothiazole | 200 | $C_{16}H_{13}N_4OSCl$ | 16.10 | 16.26 | 9.46 | 9.28 |
| -(4-methyl)-benzothiazole | 204 | $C_{17}H_{15}N_4OSCl$ | 15.49 | 15.63 | 9.31 | 8.92 |
| -(5-methyl)-benzothiazole | 191 | $C_{17}H_{15}N_4OSCl$ | 15.43 | 15.63 | 9.19 | 8.92 |
| -(6-methyl)-benzothiazole | 188 | $C_{17}H_{15}N_4OSCl$ | 15.61 | 15.63 | 9.41 | 8.92 |
| -(4-chloro)-benzothiazole | 263 | $C_{16}H_{12}N_4OSCl_2$ | 14.81 | 14.78 | 8.51 | 8.44 |
| -(5-chloro)-benzothiazole | 183 | $C_{16}H_{12}N_4OSCl_2$ | 14.39 | 14.78 | 8.36 | 8.44 |
| -(6-chloro)-benzothiazole | 202 | $C_{16}H_{12}N_4OSCl_2$ | 14.61 | 14.78 | 7.99 | 8.44 |
| -(6-bromo)-benzothiazole | 219 | $C_{16}H_{12}N_4OSClBr$ | 13.21 | 13.22 | 7.63 | 7.55 |
| -(6-methoxy)-benzothiazole | 197 | $C_{17}H_{15}N_4O_2SCl$ | 14.87 | 14.95 | 8.41 | 8.54 |
| -(6-ethoxy)-benzothiazole | 164 | $C_{18}H_{17}N_4O_2SCl$ | 14.48 | 14.42 | 8.63 | 8.23 |

TABLE V. HYDROCHLORIDES OF 2-[*N*-(2'-METHYLBENZIMIDAZOLYL)ACETYLAMINO]BENZOTHIAZOLES

| Hydrochlorides of 2-[*N*-(2'-methylbenzimidazolyl)acetylamino] | M. p. °C | Molec. formula | N, % | | S, % | |
|---|---|---|---|---|---|---|
| | | | Found | Calcd. | Found | Calcd. |
| -benzothiazole | 166 | $C_{17}H_{15}N_4OSCl$ | 15.55 | 15.63 | 9.41 | 8.92 |
| -(4-methyl)-benzothiazole | 193 | $C_{18}H_{17}N_4OSCl$ | 14.98 | 15.03 | 8.67 | 8.59 |
| -(5-methyl)-benzothiazole | 211 | $C_{18}H_{17}N_4OSCl$ | 14.88 | 15.03 | 8.37 | 8.59 |
| -(6-methyl)-benzothiazole | 168 | $C_{18}H_{17}N_4OSCl$ | 15.13 | 15.03 | 8.57 | 8.59 |
| -(4-chloro)-benzothiazole | 182 | $C_{17}H_{14}N_4OSCl_2$ | 14.16 | 14.25 | 8.79 | 8.14 |
| -(5-chloro)-benzothiazole | 199 | $C_{17}H_{14}N_4OSCl_2$ | 14.00 | 14.25 | 8.44 | 8.14 |
| -(6-chloro)-benzothiazole | 195 | $C_{17}H_{14}N_4OSCl_2$ | 14.23 | 14.25 | 8.58 | 8.14 |
| -(6-bromo)-benzothiazole | 257 | $C_{17}H_{14}N_4OSClBr$ | 12.88 | 12.79 | 7.18 | 7.31 |
| -(6-methoxy)-benzothiazole | 158 | $C_{18}H_{17}N_4O_2SCl$ | 14.31 | 14.42 | 8.63 | 8.23 |
| -(6-ethoxy)-benzothiazole | 183 | $C_{19}H_{19}N_4O_2SCl$ | 13.87 | 13.92 | 8.28 | 7.95 |

gradually added. The reaction mixture was then warmed at 70°C on a water bath for 1.5 hr. The benzene was distilled off, and the residue was washed with a sodium bicarbonate solution and water and then dried. The product was crystallized from alcohol; m. p. 156°C.

Similarly other substituted 2-aminobenzothiazoles were converted into 2-chloroacetylamino-derivatives. Their melting points and analytical data are recorded in Table I.

**2-(*N*-Benzimidazolylacetylamino)benzothiazole.**—To 2-chloroacetylaminobenzothiazole (6 g.) dissolved in absolute ethanol (50 ml.), benzimidazole (3 g.) was added, and the mixture refluxed for 8 hr. After the alcohol had been recovered and the residue washed with a sodium bicarbonate solution and water, the product was crystallized from alcohol as brown crystals; m. p. 245°C.

Similarly, various substituted 2-(*N*-benzimidazolylacetylamino)- and 2-[*N*-(2'-methylbenzimidazolyl)-acetylamino]-benzothiazoles were prepared. Their melting points and analytical data are listed in Tables II and III.

**The Preparation of Hydrochlorides.**—The hydrochlorides of the above-mentioned bases were prepared as usual. Their melting points and analytical data are recorded in Tables IV and V.

**Pharmacological Screening.**—The hydrochlorides prepared above were screened for local anaesthetic activity by the method using a frog's sciatic plexus.

TABLE VI. LOCAL ANAESTHETIC ACTIVITY OF HYDROCHLORIDES OF 2-(*N*-BENZIMIDAZOLYLACETYLAMINO)BENZOTHIAZOLES

| Hydrochlorides of 2-(*N*-benzimidazolylacetylamino) | Onset of anaesthesia (min.) with administration of anaesthetic* in hydrochloric acid of strength | | |
|---|---|---|---|
| | 0.05 N | 0.1 N | 0.2 N |
| -benzothiazole | 22 | 40 | 58 |
| -(4-methyl)-benzothiazole | 20 | 36 | 55 |
| -(5-methyl)-benzothiazole | 26 | 39 | 56 |
| -(6-methyl)-benzothiazole | 28 | 41 | 58 |
| -(4-chloro)-benzothiazole | 30 | 40 | 55 |
| -(5-chloro)-benzothiazole | 25 | 38 | 53 |
| -(6-chloro)-benzothiazole | 23 | 36 | 55 |
| -(6-bromo)-benzothiazole | 24 | 42 | 52 |
| -(6-methoxy)-benzothiazole | 27 | 39 | 58 |
| -(6-ethoxy)-benzothiazole | 26 | 41 | 56 |
| Procaine-hydrochloride | 12 | 15 | 20 |

* Concentration of anaesthetic, 0.2%

TABLE VII. LOCAL ANAESTHETIC ACTIVITY OF HYDROCHLORIDES OF 2-[*N*-(2'-METHYLBENZIMIDAZOLYL)ACETYLAMINO]BENZOTHIAZOLES

| Hydrochloride of 2-[*N*-(2'-methylbenzimidazolyl)-acetylamino] | Onset of anaesthesia (min.) with administration of anaesthetic* in hydrochloric acid of strength | | |
|---|---|---|---|
| | 0.05 N | 0.1 N | 0.2 N |
| -benzothiazole | 22 | 40 | 56 |
| -(4-methyl)-benzothiazole | 19 | 37 | 51 |
| -(5-methyl)-benzothiazole | 22 | 40 | 56 |
| -(6-methyl)-benzothiazole | 25 | 39 | 56 |
| -(4-chloro)-benzothiazole | 23 | 41 | 52 |
| -(5-chloro)-benzothiazole | 26 | 39 | 55 |
| -(6-chloro)-benzothiazole | 18 | 42 | 56 |
| -(6-bromo)-benzothiazole | 21 | 39 | 58 |
| -(6-methoxy)-benzothiazole | 22 | 30 | 55 |
| -(6-ethoxy)-benzothiazole | 28 | 41 | 53 |
| Procaine-hydrochloride | 12 | 15 | 20 |

* Concentration of anaesthetic, 0.2%

The compounds were tested at the concentration of 0.2%, and the time taken by a given concentration of a local anaesthetic to fail to provoke the withdrawal of a foot was recorded. The results are shown in Tables VI and VII.

## Results

A study of the pharmacological screening has shown that not a single compound is active.

Thanks are due to the authorities of the Banaras Hindu University for providing necessary facilities and to the University Grants Commission for the award of a Junior Research Fellowship to one of us (P. R.).

*Department of Chemistry*
*Science College*
*Banaras Hindu University*
*Varanasi, India*

# The Synthesis of Some *S*-Substituted-2-mercapto-3-aryl-4-quinazolones

By Prithwi Nath BHARGAVA and Phulgan RAM

(Received May 2, 1964)

Several 4-quinazolone derivatives and 2- or 4-sulphanilamido-quinazolines have been reported to be therapeutically active.[1,2] Several potential antimalarials belonging to substituted quinazolones and quinazolines have been screened against blood-induced *P. gallinaceum* infection in 7-day-old chicks. Gujral et al. observed the hypnotic activity of 2-alkyl-3-aryl-4(3*H*)-quinazolones in rats.[3]

The above findings have led the authors to prepare *S*-substituted-2-mercapto-3-aryl-4-quinazolones[4,5] as possible antimalarials. In the present investigation, the synthesis of *S*-substituted-2-mercapto-3-aryl-4-quinazolones from anthranilic acid, arylisothiocyanates and alkyl halides has been studied.

## Experimental

**2-Mercapto-3-*m*-chlorophenyl-4-quinazolone.**—A mixture of *m*-chlorophenylisothiocyanate (15 g.), *o*-aminobenzoic acid (15 g.) and absolute ethanol (150 ml.) was refluxed on a water bath for about 2 hr. The product was washed with ethanol, dissolved in 10% sodium hydroxide, precipitated with dilute hydrochloric acid, filtered, and after washing with water, dried.

Similarly, various 2-mercapto-3-aryl-4-quinazolones were prepared from the corresponding arylisothiocyanates and *o*-aminobenzoic acid. Their yields, melting points, and analytical data are listed in Table I.

**2-Ethylthio-3-*m*-chlorophenyl-4-quinazolone.**—To a solution of sodium hydroxide (5 g.) in (85 ml.) of 50% aqueous ethanol, 2-mercapto-3-*m*-chlorophenyl-4-quinazolone (7.5 g.) was added. The solution was then stirred, filtered and treated with ethyl iodide (4 ml.); after being stirred again for an hour, the solution gave a crystalline product which was washed first with water and then with ethanol. Long needles were obtained on crystallization form ethanol.

Similarly, various *S*-substituted-2-mercapto-3-aryl-4-quinazolones have been prepared. Their yields,

TABLE I. 2-THIO-3-ARYL-4-QUINAZOLONES

| Aryl group | Yield % | M. p. °C | Molec. formula | N, % | | S, % | |
|---|---|---|---|---|---|---|---|
| | | | | Found | Calcd. | Found | Calcd. |
| *m*-Chlorophenyl- | 90 | 292 | $C_{14}H_9N_2OSCl$ | 9.66 | 9.70 | 11.21 | 11.09 |
| *p*-Chlorophenyl- | 90 | 320 | $C_{14}H_9N_2OSCl$ | 9.73 | 9.70 | 11.14 | 11.09 |
| *p*-Bromophenyl- | 90 | 320 | $C_{14}H_9N_2OSBr$ | 8.52 | 8.41 | 9.86 | 9.61 |
| *o*-Methoxyphenyl- | 75 | 265 | $C_{15}H_{12}N_2O_2S$ | 9.73 | 9.86 | 11.40 | 11.27 |
| *p*-Methoxyphenyl- | 80 | 275 | $C_{15}H_{12}N_2O_2S$ | 9.75 | 9.86 | 11.32 | 11.27 |
| *p*-Ethoxyphenyl- | 90 | 335 | $C_{16}H_{14}N_2O_2S$ | 9.28 | 9.39 | 10.82 | 10.74 |
| Benzyl- | 75 | 248 | $C_{15}H_{12}N_2OS$ | 10.51 | 10.45 | 12.01 | 11.94 |
| $\alpha$-Naphthyl- | 70 | 266 | $C_{18}H_{12}N_2OS$ | 9.33 | 9.21 | 10.61 | 10.52 |

TABLE II. *S*-SUBSTITUTED-2-MERCAPTO-3-*m*-CHLOROPHENYL-4-QUINAZOLONES

| 2-Substituent | Yield % | M. p. °C | Molec. formula | N, % | | S, % | |
|---|---|---|---|---|---|---|---|
| | | | | Found | Calcd. | Found | Calcd. |
| 2-Methylthio- | 86 | 156 | $C_{15}H_{11}N_2OSCl$ | 9.33 | 9.25 | 10.70 | 10.58 |
| 2-Ethylthio- | 70 | 124 | $C_{16}H_{13}N_2OSCl$ | 8.81 | 8.84 | 10.31 | 10.11 |
| 2-Butylthio- | 70 | 88 | $C_{18}H_{17}N_2OSCl$ | 8.20 | 8.12 | 9.50 | 9.28 |
| 2-Allylthio- | 75 | 178 | $C_{17}H_{13}N_2OSCl$ | 8.47 | 8.52 | 9.87 | 9.73 |
| 2-$\alpha$-Methylallylthio- | 60 | 94 | $C_{18}H_{15}N_2OSCl$ | 8.21 | 8.17 | 9.42 | 9.34 |
| 2-Benzylthio- | 80 | 106 | $C_{21}H_{15}N_2OSCl$ | 7.28 | 7.39 | 8.57 | 8.45 |
| 2-*p*-Nitrobenzylthio- | 70 | 162 | $C_{21}H_{14}N_3O_3SCl$ | 9.87 | 9.91 | 7.63 | 7.55 |
| 2-Carboxymethylthio- | 75 | 180 | $C_{16}H_{11}N_2O_3SCl$ | 8.20 | 8.08 | 9.41 | 9.23 |

1) F. G. Wolf, U. S. Pat. 2473931 (1949); *Chem. Abstr.*, **43**, 7042 (1949).
2) B. R. Baker, F. J. McEvoy, R. E. Schaub, J. P. Joseph and J. H. Williams, *J. Org. Chem.*, **18**, 178 (1953).
3) M. L. Gujral, P. N. Saxena and R. S. Tiwari, *Indian J. Med. Res.*, **43**, 637 (1955); *Chem. Abstr.*, **50**, 6662 (1956).
4) Br. Pawlewski, *Ber.*, **38**, 131 (1905).
5) T. N. Ghosh, *J. Indian Chem. Soc.*, **7**, 981 (1390).

TABLE III. *S*-SUBSTITUTED-2-MERCAPTO-3-*p*-CHLOROPHENYL-4-QUINAZOLONES

| 2-Substituent | Yield % | M. p. °C | Molec. formula | N, % | | S, % | |
|---|---|---|---|---|---|---|---|
| | | | | Found | Calcd. | Found | Calcd. |
| 2-Methylthio- | 90 | 178 | $C_{15}H_{11}N_2OSCl$ | 9.21 | 9.25 | 10.65 | 10.58 |
| 2-Ethylthio- | 80 | 150 | $C_{16}H_{13}N_2OSCl$ | 8.78 | 8.84 | 10.24 | 10.11 |
| 2-Isopropylthio- | 85 | 152 | $C_{17}H_{15}N_2OSCl$ | 8.16 | 8.47 | 9.90 | 9.68 |
| 2-Butylthio- | 85 | 113 | $C_{18}H_{17}N_2OSCl$ | 8.11 | 8.12 | 9.32 | 9.28 |
| 2-Allylthio- | 80 | 137 | $C_{17}H_{13}N_2OSCl$ | 8.45 | 8.52 | 9.69 | 9.73 |
| 2-*α*-Methylallylthio- | 85 | 134 | $C_{18}H_{15}N_2OSCl$ | 8.10 | 8.17 | 9.39 | 9.34 |
| 2-Benzylthio- | 95 | 183 | $C_{21}H_{15}N_2OSCl$ | 7.32 | 7.39 | 8.63 | 8.45 |
| 2-*p*-Nitrobenzylthio- | 75 | 218 | $C_{21}H_{14}N_3O_3SCl$ | 9.79 | 9.91 | 7.48 | 7.55 |
| 2-Carboxymethylthio- | 80 | 218 | $C_{16}H_{11}N_2O_3SCl$ | 8.19 | 8.08 | 9.46 | 9.23 |
| 2-Amylthio- | 75 | 102 | $C_{19}H_{19}N_2OSCl$ | 7.76 | 7.80 | 9.31 | 8.92 |

TABLE IV. *S*-SUBSTITUTED-2-MERCAPTO-3-*p*-BROMOPHENYL-4-QUINAZOLONES

| 2-Substituent | Yield % | M. p. °C | Molec. formula | N, % | | S, % | |
|---|---|---|---|---|---|---|---|
| | | | | Found | Calcd. | Found | Calcd. |
| 2-Methylthio- | 90 | 208 | $C_{15}H_{11}N_2OSBr$ | 8.00 | 8.07 | 9.51 | 9.22 |
| 2-Ethylthio- | 85 | 146 | $C_{16}H_{13}N_2OSBr$ | 7.69 | 7.75 | 8.91 | 8.86 |
| 2-Butylthio- | 85 | 121 | $C_{18}H_{17}N_2OSBr$ | 7.30 | 7.20 | 8.33 | 8.22 |
| 2-Allylthio- | 85 | 148 | $C_{17}H_{13}N_2OSBr$ | 7.43 | 7.50 | 8.63 | 8.57 |
| 2-*α*-Methylallylthio- | 80 | 131 | $C_{18}H_{15}N_2OSBr$ | 7.33 | 7.23 | 8.43 | 8.26 |
| 2-Benzylthio- | 95 | 182 | $C_{21}H_{15}N_2OSBr$ | 6.58 | 6.62 | 7.81 | 7.56 |
| 2-*p*-Nitrobenzylthio- | 75 | 230 | $C_{21}H_{14}N_3O_3SBr$ | 8.82 | 8.97 | 6.57 | 6.83 |
| 2-Carboxymethylthio- | 80 | 214 | $C_{16}H_{11}N_2O_3SBr$ | 7.23 | 8.19 | 9.50 | 9.35 |

TABLE V. *S*-SUBSTITUTED-2-MERCAPTO-3-*o*-METHOXYPHENYL- AND *S*-SUBSTITUTED-2-MERCAPTO-3-BENZYL-4-QUINAZOLONES

| Compound | Yield % | M. p. °C | Molec. formula | N, % | | S, % | |
|---|---|---|---|---|---|---|---|
| | | | | Found | Calcd. | Found | Calcd. |
| 2-Methylthio-3-*o*-methoxyphenyl-4-quinazolone | 88 | 134 | $C_{16}H_{14}N_2O_2S$ | 9.32 | 9.39 | 10.69 | 10.74 |
| 2-Ethylthio-3-*o*-methoxyphenyl-4-quinazolone | 72 | 114 | $C_{17}H_{16}N_2O_2S$ | 8.79 | 8.97 | 10.32 | 10.28 |
| 2-Butylthio-3-*o*-methoxyphenyl-4-quinazolone | 70 | 141 | $C_{19}H_{20}N_2O_2S$ | 8.31 | 8.23 | 9.67 | 9.41 |
| 2-Allylthio-3-*o*-methoxyphenyl-4-quinazolone | 60 | 98 | $C_{18}H_{16}N_2O_2S$ | 8.58 | 8.64 | 9.99 | 9.87 |
| 2-Methylthio-3-benzyl-4-quinazolone | 75 | 94 | $C_{16}H_{14}N_2OS$ | 9.88 | 9.93 | 11.52 | 11.34 |
| 2-Ethylthio-3-benzyl-4-quinazolone | 70 | 83 | $C_{17}H_{16}N_2OS$ | 9.56 | 9.46 | 10.94 | 10.81 |
| 2-Allylthio-3-benzyl-4-quinazolone | 70 | 93 | $C_{18}H_{16}N_2OS$ | 9.12 | 9.09 | 10.64 | 10.39 |

TABLE VI. *S*-SUBSTITUTED-2-MERCAPTO-3-*p*-METHOXYPHENYL-4-QUINAZOLONES

| 2-Substituent | Yield % | M. p. °C | Molec. formula | N, % | | S, % | |
|---|---|---|---|---|---|---|---|
| | | | | Found | Calcd. | Found | Calcd. |
| 2-Methylthio- | 84 | 148 | $C_{16}H_{14}N_2O_2S$ | 9.41 | 9.39 | 10.62 | 10.74 |
| 2-Ethylthio- | 75 | 170 | $C_{17}H_{16}N_2O_2S$ | 8.81 | 8.97 | 10.34 | 10.28 |
| 2-Butylthio- | 75 | 122 | $C_{19}H_{20}N_2O_2S$ | 8.40 | 8.23 | 9.53 | 9.41 |
| 2-Allylthio- | 70 | 160 | $C_{18}H_{16}N_2O_2S$ | 8.56 | 8.64 | 9.78 | 9.87 |
| 2-*α*-Methylallylthio- | 50 | 113 | $C_{19}H_{18}N_2O_2S$ | 8.32 | 8.28 | 9.56 | 9.46 |
| 2-Benzylthio- | 80 | 153 | $C_{22}H_{18}N_2O_2S$ | 7.63 | 7.48 | 8.80 | 8.55 |
| 2-*p*-Nitrobenzylthio- | 70 | 188 | $C_{22}H_{17}N_3O_4S$ | 10.10 | 10.02 | 7.81 | 7.61 |
| 2-Carboxymethylthio- | 80 | 182 | $C_{17}H_{14}N_2O_4S$ | 8.23 | 8.19 | 9.50 | 9.35 |

TABLE VII. *S*-SUBSTITUTED-2-MERCAPTO-3-*p*-ETHOXYPHENYL-4-QUINAZOLONES

| 2-Substituent | Yield % | M. p. °C | Molec. formula | N, % | | S, % | |
|---|---|---|---|---|---|---|---|
| | | | | Found | Calcd. | Found | Calcd. |
| 2-Methylthio- | 90 | 158 | $C_{17}H_{16}N_2O_2S$ | 8.98 | 9.00 | 10.11 | 10.29 |
| 2-Ethylthio- | 85 | 139 | $C_{18}H_{18}N_2O_2S$ | 8.48 | 8.59 | 9.99 | 9.81 |
| 2-Butylthio- | 80 | 140 | $C_{20}H_{22}N_2O_2S$ | 8.01 | 7.91 | 9.20 | 9.03 |
| 2-Allylthio- | 80 | 152 | $C_{19}H_{18}N_2O_2S$ | 8.17 | 8.28 | 9.39 | 9.46 |
| 2-$\alpha$-Methylallylthio- | 65 | 134 | $C_{20}H_{20}N_2O_2S$ | 7.88 | 7.95 | 9.00 | 9.09 |
| 2-Benzylthio- | 85 | 241 | $C_{23}H_{20}N_2O_2S$ | 7.13 | 7.21 | 8.38 | 8.24 |
| 2-*p*-Nitrobenzylthio- | 70 | 186 | $C_{23}H_{19}N_3O_4S$ | 9.57 | 9.69 | 7.44 | 7.39 |
| 2-Carboxymethylthio- | 80 | 202 | $C_{18}H_{16}N_2O_4S$ | 7.77 | 7.82 | 9.01 | 8.99 |

melting points, and analytical data are recorded in Tables II to VII.

**2-Carboxymethylthio-3-*m*-chlorophenyl-4-quinazolone.**—An equimolecular quantity of sodium monochloroacetate was added to an alkaline solution of 2-mercapto-3-*m*-chlorophenyl-4-quinazolone, and the mixture was shaken for 6 hr. It was then acidified with dilute hydrochloric acid, and the precipitate obtained was dissolved in sodium bicarbonate solution and reprecipitated with diluted hydrochloric acid. The product was crystallized from ethanol.

Similarly, other 2-carboxymethylthio derivatives of -3-*p*-chlorophenyl-, -3-*p*-bromophenyl-, -3-*p*-methoxyphenyl- and -3-*p*-ethoxyphenyl-4-quinazolones were prepared. Their yields, melting points, and analytical data are also recorded in Tables II, III, IV, VI, and VII.

Thanks are due to the authorities of the Banaras Hindu University for providing necessary facilities and also to the University Grants Commission for the award of Junior Research Fellowship to one of us (P. R.).

*Department of Chemistry*
*College of Science*
*Banaras Hindu University*
*Varanasi, India*

# Solid State Polymerization of Binary Component System

By Masatoshi MIURA, Takako HIRAI and Shunji KAWAMATSU

(Received May 16, 1964)

During the past few years it has been reported that various vinyl[1-3] and cyclic compounds[4-6] can be polymerized in a solid state by high-energy ionizing radiation. However, there have been few reports on the solid state polymerization of a binary component system. In the solid of a binary component system, there are various states of aggregation, such as a solid solution or mixed crystals, and these states are expected to affect the polymerization and the polymer structure. The present study was undertaken to elucidate the correlation of the polymerization with those aggregation states. Various oxetane derivatives polymerize in a solid state, and the mixture of these may be expected to give solid solution because of the similarity of the molecular structures. Therefore, in this investigation, mixtures of 3-chloromethyl-3-ethyloxetane (CMEO), with 3-fluoromethyl-3-ethyloxetane (FMEO) and with 3,3-bis(chloromethyl)-oxetane (BCMO) were chosen as the binary component system of a solid solution. As the mixed crystals, mixtures of CMEO with diketene and with trioxane were chosen. All of these cyclic compounds have been reported to polymerize in the solid state,[4-6] and the crystal states of these monomers play important roles in the solid state polymerization. Recently Okamura and his co-workers have independently from our study reported[7]

1) A. Chapiro and V. Stannett, *J. chim. phys.*, **56**, 830 (1959).
2) N. Sobue and Y. Tabata, *J. Polymer Sci.*, **43**, 459 (1960).
3) T. A. Fadner and H. Morawetz, ibid., **45**, 475 (1960).
4) S. Okamura, K. Hayashi and Y. Kitanishi, ibid., **58**, 925 (1962).
5) S. Nakashio, M. Kondo and H. Tsuchita, *Makromol. Chem.*, **52**, 79 (1962).
6) M. Miura, T. Aoyagi and T. Hirai, *J. Chem. Soc. Japan, Ind. Chem. Sec.* (*Kogyo Kagaku Zasshi*), **67**, 485 (1964).
7) K. Hayashi, H. Watanabe and S. Okamura, *J. Polymer Sci.*, B1, 3971 (1963).

the radiation-induced polymerization of the solid solution of oxetane derivatives. However, no detailed studies of the polymerization behavior of the solid solution have yet been published.

## Experimental

**Monomer.**—CMEO and FMEO were prepared by the method reported previously,[6] while commercially available BCMO (Kōei Chemicals) and diketene (Tokyo Chem. Ind.) were used. All the oxetanes were purified by dehydration with $CaH_2$ and redistillation under reduced pressure in a nitrogen anhydrous stream before use. Diketene was purified, in the same manner as has been described above, using anhydrous sodium sulfate as a drying agent. Trioxan (Tokyo Chem. Ind.) was recrystallized two times from methylene chloride.

The phase diagram of the monomer mixture was made from the freezing or melting curves of the mixtures of various compositions. The rate of cooling or heating was about 0.3°C/min.

**Polymerization.** — *γ-Ray-induced Polymerization.* — The monomer mixture in a glass ampoule was degassed by three successive freezing-by-melting procedures and then sealed. The mixture of CMEO and trioxane was not degassed because of the sublimation tendency of trioxane. The ampoule was set in a Dewar vessel containing a suitable cooling agent and irradiated at an appropriate distance from a source of $^{60}Co$. The cooling agents were as follows: Dry ice-methanol (−80°C). Dry ice-acetone (−86°C), such freezing materials as benzene (5°C), ethyleneglycol (−15.6°C) and 1,2-dichloroethane (−35°C), and cryohydrates of $BaCl_2$ (−8°C), KCl (−11°C), NaCl (−21°C), $CuNO_3$ (−24°C) and $CaCl_2$ (−55°C). The sample irradiated was extracted with methanol and dried in vacuo. To determine the polymer yield, the extraction was performed below the irradiation temperature so as to prevent post-polymerization.

*$BF_3$-catalyzed Copolymerization.* — In a reaction vessel containing 25 g. of the CMEO-BCMO mixture and 75 g. of chloroform, 15 g. of a 1.4 wt. % solution of $BF_3$-etherate was added at room temperature under a gentle stream of nitrogen. The reaction was stopped with less than 10% conversion by the addition of methanol. The polymer obtained was purified by the manner described above. The copolymerization of CMEO and FMEO was carried out by the same procedure with 10 g. of a monomer mixture, 90 g. of chloroform, and 9 g. of a $BF_3$-solution.

**The Characterization of the Polymer.** — The infrared absorption spectra were obtained with an Hitachi EPI-2 Type spectrophotometer. The composition of the copolymer of CMEO and FMEO was determined by measuring the intensities of absorptions at 730 $cm^{-1}$ (C-Cl stretching vibration) and 1010 $cm^{-1}$ (C-F stretching vibration). The composition of the coploymer of CMEO and BCMO was calculated from the chlorine content of the elemental analysis. An X-ray diffraction diagram was obtained by means of the Rigaku D-3F Type diffractometer.

The viscosities of the polymer solution were measured at 42±0.02°C in a chloroform solution. The intrinsic viscosities were calculated by the single-point determination method at a concentration of 0.2 g./100 cc. The melting points of the polymers were determined by means of a hot-stage microscope. The fractionation of the copolymers was carried out using chloroform as a solvent and acetone as a nonsolvent. The polymer blend was fractionated by extracting it with dimethylformamide containing 1% β-naphthylamine as an antioxidant under a nitrogen stream at 50°C.

## Results and Discussion

**The CMEO-FMEO Binary Component System.**—The phase diagram given in Fig. 1 indicates that the binary component system forms a solid solution over the whole range of the composition. γ-Ray-induced polymerization was carried out at −86°C with the solid solution crystallized at a temperature about 5°C below its melting point. Figure 2 shows the melting points of the polymers obtained with 311-hr. radiation at $1.5\times10^4$ r./hr. The melting point is as sharp as that of the polymer obtained from each single component crystal.

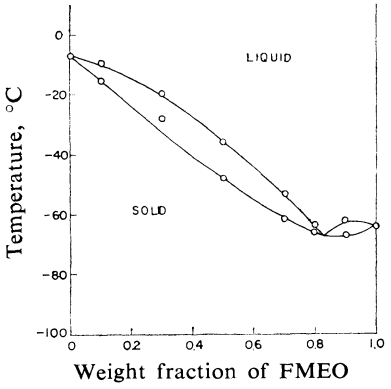



Fig. 1. Phase diagram of CMEO-FMEO binary component system.

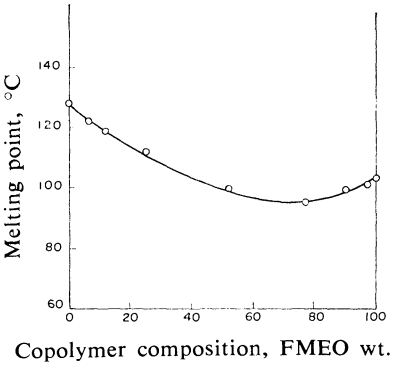



Fig. 2. Melting point of CMEO-FMEO copolymers.

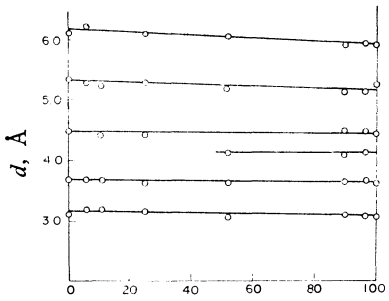



Fig. 3. X-Ray diffraction pattern of CMEO-FMEO copolymer.

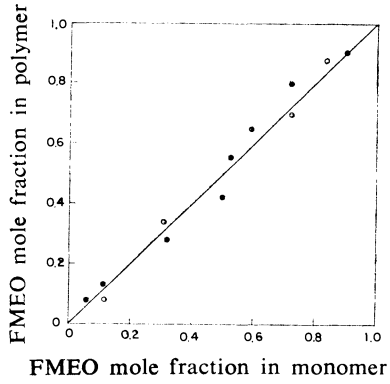



Fig. 4. Copolymer composition curve for CMEO-FMEO binary component system (●) $\gamma$-ray induced solid state polymerization, (○) $BF_3$-catalized liquid state polymerization.

Figure 3 gives the interplanar distances of the polymers as determined by X-ray diffractometry. Figure 3 suggests that all polymers have the same crystal structures, regardless of their compositions, whereas the interplanar distance varies a little. From the facts shown in Figs. 2 and 3, it may be concluded that a copolymer is formed from the solid solution by irradiation of $\gamma$-rays. Figure 4 shows the composition curve of the copolymer obtained by the procedure described above. The composition of the polymer is the same as that of the corresponding initial monomer mixture. $BF_3$-catalyzed copolymerization also seems to give the same result, as is shown in the same figure. However, this agreement is only apparent. A detailed discussion of the polymerization of a solid solution will be given in the following section.

**The CMEO-BCMO Binary Component System.**—The phase diagram of the binary component system is shown in Fig. 5. The system also crystallizes to a solid solution. The solid solution with a 1 : 1 composition by weight was irradiated at 0°C. As is shown in Figs. 6 and 7, the polymerization rate, the saturation polymer yield and the molecular weight of the polymer are all higher in a large crystal grown by slow cooling than in a small crystal. Figure 8 shows that similar behavior is also observed with the solid solu-

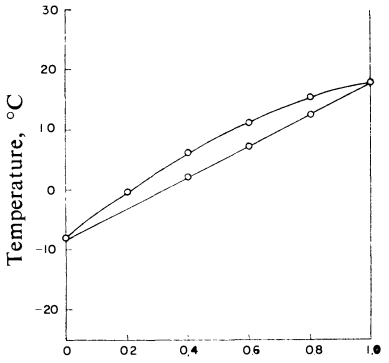



Fig. 5. Phase diagram of CMEO-BCMO binary component system.

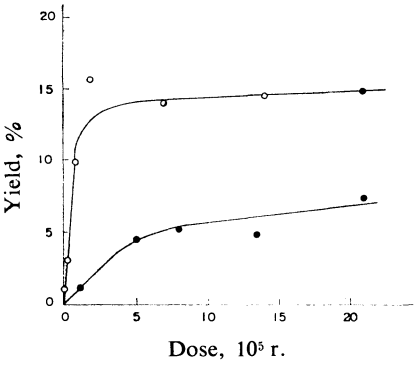



Fig. 6. Solid state polymerization of CMEO-BCMO binary component system at the composition 1 : 1 : crystallization temperature (○) 0°C, (●) −196°C, irradiation temperature 0°C, dose rate $4.3\times10^4$ r./hr.

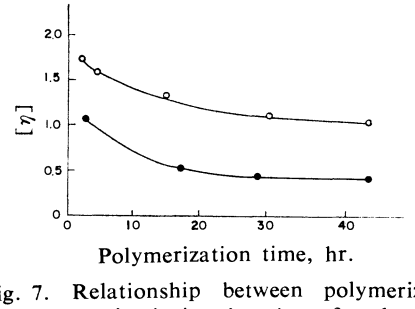



Fig. 7. Relationship between polymerization time and intrinsic viscosity of polymer in the solid state polymerization of CMEO-BCMO binary component system at the composition 1 : 1 : crystallization temperature (○) 0°C, (●) −196°C; irradiation temperature 0°C; dose rate $4.3\times10^4$ r./hr.

tion of a 9 : 1 composition, but that both the rate and the yield are less than those of a 1 : 1 composition. However, in order to compare the results of Figs. 8 and 6, the influence of the irradiation temperature on the polymer yield should be taken into consideration. Figure 9 represents the relation between the irradiation temperature and the polymer yield at various monomer compositions. Each monomer mixture was crystallized at a temperature about 5°C below its melting point. In any composition, the maximum yield was obtained at a temperature 10—20°C lower than the melting point of the corresponding solid solution. The polymerization behavior in Figs. 6 and 9 agrees with that of each single component crystal,[5,6] and its also comfirmed by the fact that crystal structure of the solid solution is almost the same as that of each single component. Figure 10 shows the

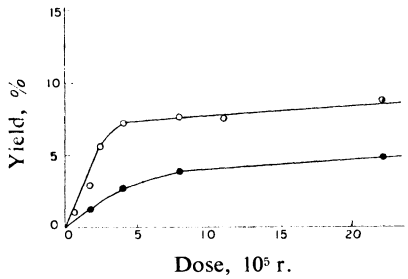



Fig. 8. Solid state polymerization of CMEO-BCMO binary component system at the composition 9 : 1 : crystallization temperature (○) −11°C, (●) −196°C; irradiation temperature −21°C; dose rate $1.3\times10^5$ r./hr.

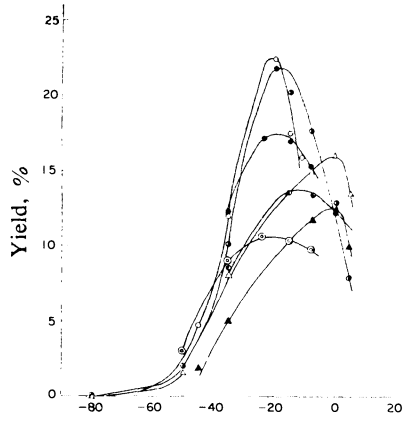



Fig. 9. Influence of irradiation temperature on polymer yield at various composition: irradiation dose, $9\times10^5$ r.; crystallization temperature, about 5°C below its melting point; composition of solid solution (CMEO-BCMO) (○) 10 : 0, (◎) 9 : 1, (●) 7 : 3, (◑) 5 : 5, (◐) 3 : 7, (▲) 1 : 9, (△) 0 : 10.

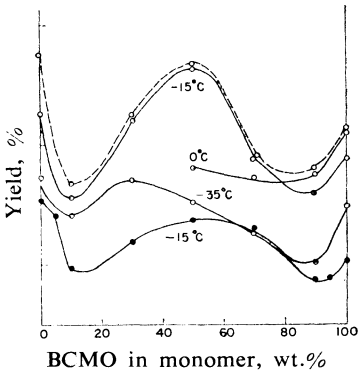



Fig. 10. Influence of monomer composition on polymer yield at various irradiation temperatures in CMEO-BCMO binary component system : irradiation dose $9.1\times10^5$ r.; crystallization temperature, (○) about 5°C below its melting point, (●) −196°C; -○- maximum yield at the each composition; irradiation temperatures are shown in the figure.

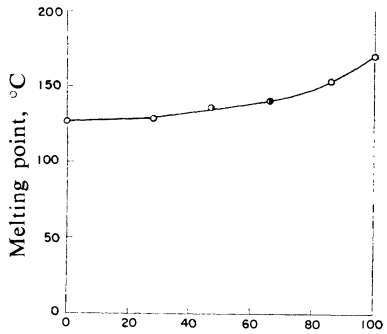



Fig. 11. Relationship between composition and melting point of CMEO-BCMO copolymer.

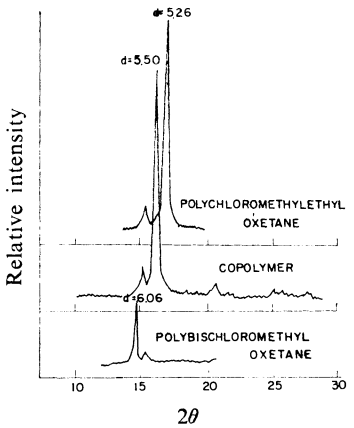



Fig. 12. X-Ray diffraction peaks of polymer. $d$: interplanar distance
Copolymer composition: (BCMO : CMEO 7 : 3)

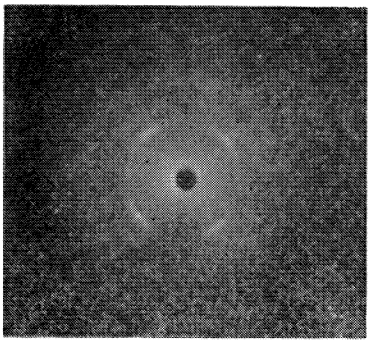


Fig. 13. X-Ray diffraction pattern of CMEO-BCMO copolymer.

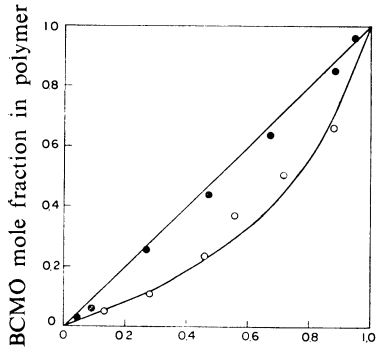



Fig. 14. Copolymer composition curve for CMEO-BCMO binary component system: (●) $\gamma$-ray induced solid state polymerization, (○) $BF_3$-catalyzed liquid state polymerization.

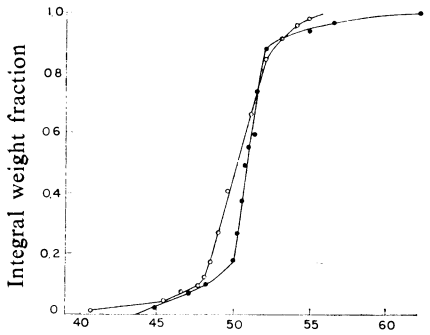



Fig. 15. Integral composition distribution curve of CMEO-BCMO copolymer; (○) copolymer from large crystal, (●) copolymer from small crystal.

polymer yield versus the monomer composition curves at various irradiation temperatures. In the same figure, the maximum yield is plotted against the composition. The polymer yield was at a minimum in the composition with a small quantity of the second component. This can be explained by the

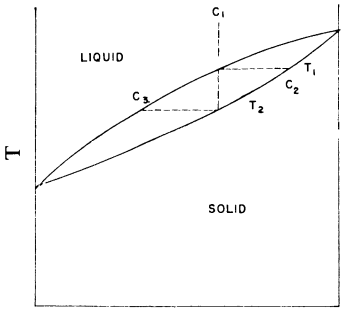



Fig. 16. Phase diagram of binary component system to form a solid solution.

effect of the composition on the crystal state of the solid solution. The sizes and structures of the two component molecules are not exactly the same, so the introduction of the second component in a small quantity may cause a disorder of the crystal lattice to some extent and result in a decrease in the polymer yield. On the other hand, the existence of both the components in equal quantities may give preferable conditions for the crystallization, because the differences in the molecular size are compensated for each other in the lattice. Also, the temperature difference between the starting and the final points of the crystallization of the monomer mixture may help the crystallization into a preferable state; this difference is at a maximum in a 1 : 1 composition. However, the complete elucidation of those phenomena seems to be difficult at the present stage; the further experimental efforts are hoped for.

Furthermore, the characteristics of the polymer obtained were examined. From the investigations of the melting point, X-ray diffraction and fractionation of the polymer, it has been concluded that a random copolymer is formed from the solid solution. As Fig. 11 shows, the melting point of the coploymer is as sharp as that of the homopolymer and decreases with an increase in the CMEO content. Figure 12 shows the X-ray diffraction diagrams of the copolymer and each component homopolymer. The crystallinity of the copolymer was proved to be as high as that of the homoploymer, and the interplanar distance corresponding to the highest peak in the copolymer is located between those in the two homopolymers. The X-ray diffraction pattern of the raw polymer obtained from the irradiated crystal by an extraction of the unreacted monomer is shown in Figure 13. It suggests the orientation of growing chains in the solid solution. This fact was also observed by means of the polarizing microscope. A similar result

has been reported in the polymerization of a single-component crystal.[4]

Figure 14 presents the composition curve of the copolymer obtained from the small crystal with an irradiation dose of $9.1\times10^5$ r. at $-15°C$. The composition of the copolymer obtained from the solid solution is the same over the whole range as that of the monomer mixture within experimental error. On the other hand, the copolymer obtained by $BF_3$ in the liquid state has a composition rich in CMEO, as is shown in the same figure. Those facts suggest that the propagating chain can grow only in a unique way controlled by the crystal lattice and that the difference in reactivities between monomers has little influence on the path of propagation in the solid solution. The above-mentioned mechanism is supported also by the orientation of the polymer chain in the irradiated solid solution.

The integral composition distribution curves of the coploymer are shown in Fig. 15. It is found that the width of the distribution is narrower in the copolymer obtained from a small crystal grown by rapid cooling than in that obtained from a large crystal by slow cooling. The difference would seem responsible for the difference in the distribution of monomer components in the solid solution. As is shown in Fig. 16, a liquid mixture of the composition $C_1$ begins to crystallize at $T_1$ and the initial segregating crystal has the composition $C_2$. When the temperature gets to $T_2$, crystallization is complete; the composition of the portion crystallized at the final stage is $C_3$. The solid solution obtained in such a manner should have a composition distribution from $C_2$ to $C_3$. However, the rapid cooling hinders the fractional crystallization to give a more homogeneous solid solution than does the slow cooling. It is clear that the copolymer obtaned from a more homogeneous crystal has a narrower distribution.

**The CMEO-Diketene Binary Component System.**—From the phase diagram in Fig. 17 it was found that this binary component system formed a mixed crystal. The binary component system polymerized at any composition when it was exposed to $\gamma$-ray at $-35°C$, which was below the eutectic point. The polymer obtained was determined by fractionation to be a blend of two component homopolymers. Infrared spectrum studies have proved that the dimethylformamide-soluble portion was polydiketene and the insoluble portion, polyoxetane. Figure 18 represents the yields of the unfractionated polymer and the fractionated polyoxetane respectively, plotted against the mole fraction of oxetane in the mixed crystal. The results

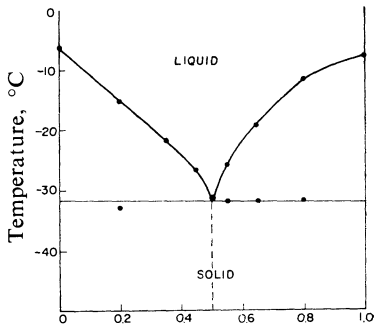



Fig. 17. Phase diagram of CMEO-diketene binary component system.

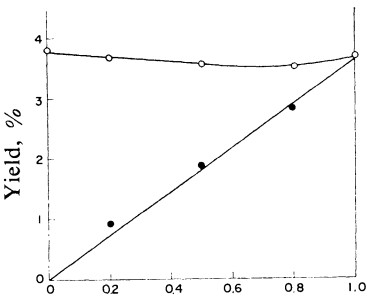



Fig. 18. Influence of monomer composition on polymer yield in the solid state polymerization of CMEO-diketene binary component system: crystallization temperature $-35°C$; irradiation temperature $-35°C$; irradiation dose $2.6\times10^5$ r.; (○) unfractionated polymer yield, (●) fractionated polyoxetane yield.

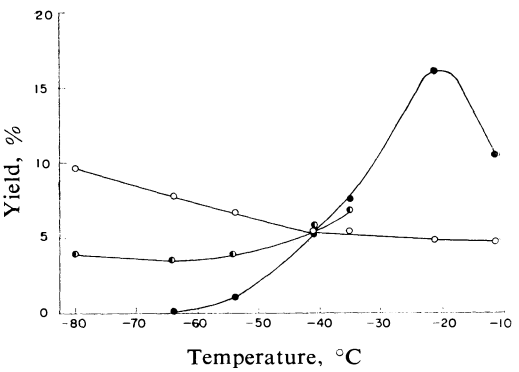



Fig. 19. Influence of irradiation temperature on polymer yield: crystallization temperature, single system $-11°C$, eutectic mixture $-35°C$; irradiation dose $5\times10^5$ r.; (●) 3-chloromethyl-3-ethyloxetane, (○) diketene, (◐) eutectic mixture (composition 1 : 1 mole fraction).

show that yields of polyoxetane and polydiketene are proportional to the mole fraction of the corresponding monomer. Furthermore,

the influence of the irradiation temperature on the polymer yield was examined; it is shown in Fig. 19. The relation between the yield and the temperature is a superposition of those two single component systems. These results suggest that in the mixed crystal the polymerization of each component takes place independently, even in the eutectic mixture.

**The CMEO-Trioxane Binary Component System.**—The phase diagram in Fig. 20 shows that this system also forms a mixed crystal and that its eutectic point is in the side of oxetane. From the infrared spectrum and the elemental analysis, it was found that the mixed crystal gave only polyoxetane at any composition when it was irradiated at −21°C, which was below the eutectic point. As Fig. 21 shows, the polymer yield is proportional to the mole fraction of oxetane, except for a range close to pure oxetane, and the molecular weight of the polymer is not affected by the existence of trioxane. The

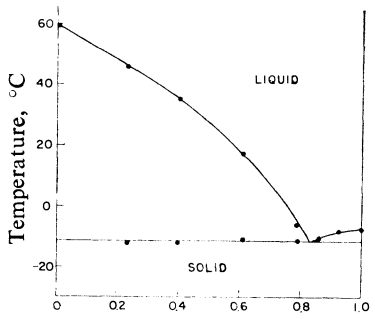



Fig. 20. Phase diagram of CMEO-trioxane binary component system.

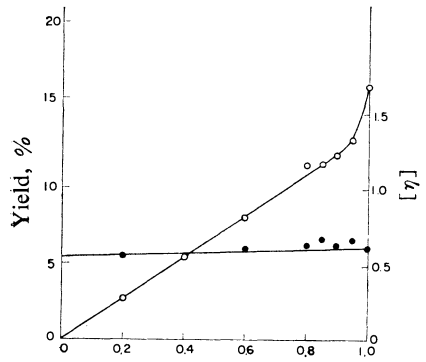



Fig. 21. Influnce of composition on polymer yield and molecular weight in CMEO-trioxane binary component system: crystallization temperature −16°C; irradiation temperature −21°C; irradiation dose $1.7\times10^6$ r.; (○) polymer yield, (●) intrinsic viscosity.

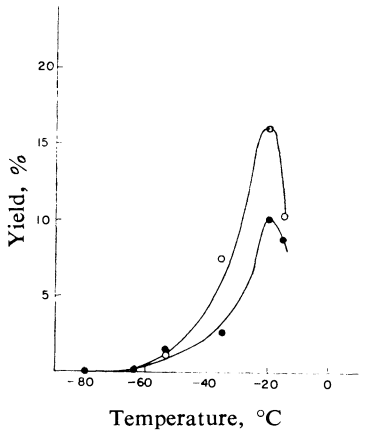



Fig. 22. Influence of irradiation temperature on polymer yield: (●), eutectic mixture of CMEO and trioxane, crystallization temperature −11°C, irradiation dose $9\times10^5$ r.; (○) CMEO crystallization temperature −11°C, irradiation dose $9\times10^5$ r.

data given in Fig. 21 indicate that the temperature dependence of the yield in the eutectic mixture is similar to that obtained in CMEO. When irradiation was done at room temperature, only trioxane was polymerized.

Okamura and his co-workers[8] have reported that trioxane polymerized only in the solid state above 0°C. The temperature range in which trioxane polymerizes is above the melting point of oxetane, whereas oxetane scarcely polymerizes at all in a liquid state.[6] If polymerization occurs independently in each component crystal, it should be impossible to polymerize two components at the same time.

## Summary

The γ-ray irradiation of a solid solution of 3-chloromethyl-3-ethyloxetane and 3,3-bis-(chloromethyl)oxetane has given a copolymer with the same composition as that of the initial monomer mixture, while a $BF_3$-catalyzed copolymerization has formed a copolymer with a different composition from that of the initial monomer mixture. In the polymerization, the solid solution has behaved like each single component crystal in respect to the relation of polymer yield to the irradiation temperature and to the crystal state of the monomers. The copolymer obtained from small crystals grown by rapid cooling has been found to have a narrower distribution of composition than that obtained from large crystals. With a solid solution of 3-chloromethyl-3-ethyloxetane

8) S. Okamura, K. Hayashi and Y. Nakamura, *Isotopes and Radiation*, 3, 416 (1960).

and 3-fluoromethyl-3-ethyloxetance, the polymerization has been studied and similar results obtained.

The mixed crystal of 3-chloromethyl-3-ethyloxetane and diketene gives a polymer blend. The curve of the polymer yield versus the irradiation temperature is a superposition of those in the each component crystal. The mixed crystal of 3-chloromethyl-3-ethyloxetane and trioxane gives only a homopolymer of oxetane, and the temperature dependence of the yield is similar to that of oxetane, even in an eutectic composition.

The authors wish to thank Dr. Hiroshi Kitagawa for his continued interest and encouragement; acknowledgment is also due to Mr. Akimasa Ōyama for his irradiations and Mr. Tetsuo Ino for his assistance in this experiment.

*Hitachi Central Research Laboratory*
*Kokubunji, Tokyo*

# The Growth Reaction of an $\alpha,\omega$-Dialuminoalkane Compound

By Go HATA and Akihisa MIYAKE

(Received May 27, 1964)

It is well known that ethylene undergoes a stepwise addition to trialkylaluminum to form a long-chain alkylaluminum[1]:

$$R\text{-al}+n C_2H_4 \rightarrow R\text{-}(C_2H_4)_n\text{-al} \quad (\text{al}=1/3\text{Al})$$

If this growth reaction can be applied to an organoaluminum compound with two aluminum atoms attached to both ends of a polymethylene chain, it is expected to synthesize long-chain bifunctional compounds by adding ethylene to the above-mentioned organoaluminum compound; and converting the resulting aluminum compound into other product (diolefin, diol).

With the object of synthesizing an $\alpha,\omega$-dialuminoalkane compound, various attempts have been made by several workers to add dialkylaluminum hydride to $\alpha,\omega$-dienes. Ziegler[2] reported that the reaction of 1, 5-hexadiene with diisobutylaluminum hydride afforded a cyclopentylmethylaluminum compound, instead of the expected 1, 6-dialuminohexane derivative. Zakharkin[3] reported that the reaction of butadiene with diethylaluminum hydride yielded mainly polymeric (di- and trimeric) hydrocarbons, accompanied by a small amount of a 1, 4-dialuminobutane derivative. The present authors[4] previously investigated the reaction between diisobutylaluminum hydride and $\alpha,\omega$-dienes with carbon numbers from five to eleven (molar ratio 1 : 1) and found that the facile ring-closure reaction is specific only to 1, 5-hexadiene and that other $\alpha,\omega$-dienes gave the $\alpha,\omega$-dialuminoalkane compounds. Especially, the 1, 7-dialuminoheptane derivative is stable at the temperature of the growth reaction of alkylaluminum.

These facts suggest that the growth reaction of the 1, 5-dialuminopentane derivative by means of the addition of ethylene can be carried out without forming cyclic compounds. We confirmed, as expected, that the growth reaction of this compound proceeds without ring closure.

## Results and Discussion

The 1, 5-dialuminopentane derivative*1 was prepared by the addition of diisobutylaluminum hydride to 1, 4-pentadiene. The growth reaction of this compound was carried out at an ethylene pressure of 130 kg./cm$^2$ at 100°C for five hours. To avoid the influence of the metal surface of the autoclave which catalyses the displacement reaction of alkylaluminum by ethylene, a glass tube with a small hole was used as the reaction vessel. On hydrolysis, the reaction product

1) K. Ziegler, H. G. Gellert, K. Zosel, E. Holzkamp, J. Schneider, M. Söll and W. R. Kroll, *Ann.*, **629**, 121 (1960).
2) K. Ziegler, "Organometallic Chemistry," Ed. by H. Zeiss, Reinhold Publishing Corp., New York, N. Y. (1960), p. 234.
3) L. I. Zakharkin, L. A. Savina and L. M. Antipin, *Bull. Acad. Sci. U. S. S. R.*, **6**, 931 (1962).
4) G. Hata and A. Miyake, *J. Org. Chem.*, **28**, 3237 (1963).

*1 The initial product from the reaction of 1,4-pentadiene with diisobutylaluminum hydride should be 1,5-bis(diisobutylalumino)pentane (I),

$$(i\text{-Bu})_2\text{Al-}(CH_2)_5\text{-Al}(i\text{-Bu})_2 \quad \text{(I)}$$

which, however, might be converted through alkyl exchange reaction to a mixture of $(i\text{-Bu})_3\text{Al}$, $(i\text{-Bu})_2\text{Al-}(CH_2)_5\text{-Al}(i\text{-Bu})_2$, $(i\text{-Bu})_2\text{Al}\langle^{(CH_2)_5\text{-Al}(i\text{-Bu})_2}_{(CH_2)_5\text{-Al}(i\text{-Bu})_2}$, etc. This sort of alkyl exchange reaction occurs readily at room temperature (K. Ziegler, W. R. Kroll, W. Larbig and O. W. Steudel, *Ann.*, **629**, 53 (1960)). For the sake of simplicity, the product is hereafter called 1, 5-dialuminopentane derivative and written as al-$(CH_2)_5$-al.

afforded a mixture of *n*-pentane, *n*-heptane, *n*-nonane, *n*-undecane, *n*-tridecane and higher hydrocarbons with odd carbon numbers. In addition to the *n*-paraffins, small amounts of 1-pentene (10% of $C_5$ hydrocarbons) and 1-heptene (4% of $C_7$ hydrocarbons) were formed. However, no appreciable amount of $\alpha,\omega$-diene was found. The formation of these *n*-paraffins indicates the occurrence of the following growth reaction (Eq. 1) :

$$\text{al-(CH}_2)_5\text{-al} \xrightarrow{n\text{C}_2\text{H}_4} \text{al-(CH}_2)_5\text{-(C}_2\text{H}_4)_n\text{-al} \quad (1)$$
$$\downarrow \text{H}_2\text{O}$$
$$\text{CH}_3\text{-(C}_2\text{H}_4)_{n+1}\text{-CH}_2\text{CH}_3$$

$$\text{al-(CH}_2)_5\text{-al} \xrightarrow{\text{C}_2\text{H}_4} \text{al-(CH}_2)_3\text{-CH=CH}_2 + \text{al-CH}_2\text{CH}_3$$
$$\downarrow \text{H}_2\text{O} \quad (2)$$
$$\text{CH}_3\text{CH}_2\text{CH}_2\text{CH=CH}_2$$

1-Pentene was formed by the displacement of the 1, 5-dialuminopentane derivative by one mole of ethylene (Eq. 2). The formation of 1-heptene is due to the displacement of the 1, 7-dialuminoheptane derivative by one mole of ethylene and/or to the addition of ethylene to the 4-pentenylaluminum derivative.

The distribution of the hydrocarbons produced by hydrolysis was determined by gas chromatographic analysis. In this procedure, hydrocarbons higher than *n*-heneicosane were neglected, since they were present in very small amounts. The results are shown in Table I and Fig. 1. The average number of added ethylene per aluminum-carbon bond of the 1, 5-dialuminopentane derivative was 1.1.

Table I. Distribution of hydrocarbons obtained by hydrolysis of the product from al-$(CH_2)_5$-al+1.1$C_2H_4$

| Hydrocarbon | Composition, mol. % | |
|---|---|---|
| | Obs. | Calcd. |
| $C_5$[a] | 15.5 | 12.6 |
| $C_7$[b] | 22.5 | 26.1 |
| $C_9$ | 25.8 | 27.2 |
| $C_{11}$ | 19.9 | 18.8 |
| $C_{13}$ | 10.2 | 9.7 |
| $C_{15}$ | 4.2 | 4.0 |
| $C_{17}$ | 1.5 | 1.4 |
| $C_{19}$ | 0.4 | 0.4 |

a) *n*-pentane 90%, 1-pentene 10%
b) *n*-heptane 96%, 1-heptene 4%

In order to compare the distribution of the grown chains from the 1, 5-dialuminopentane derivative with that of those from trialkylaluminum, the results of the growth reaction of the *n*-pentylaluminum derivative under the same reaction conditions are shown in Table II and Fig. 2.

Table II. Distribution of hydrocarbons obtained by hydrolysis of the product from al-$(CH_2)_4$-$CH_3$+1.5$C_2H_4$

| Hydrocarbon | Composition, mol. % | |
|---|---|---|
| | Obs. | Calcd. |
| $C_5$[a] | 23.3 | 23.4 |
| $C_7$ | 34.2 | 34.0 |
| $C_9$ | 24.6 | 24.7 |
| $C_{11}$ | 12.1 | 11.9 |
| $C_{13}$ | 4.2 | 4.3 |
| $C_{15}$ | 0.3 | 0.3 |
| $C_{17}$ | 0.1 | 0.1 |

a) *n*-pentane 95%, 1-pentene 5%

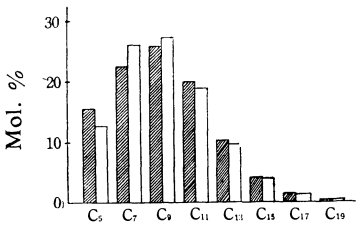



Fig. 1. Distribution of hydrocarbons by hydrolysis of the product from al-$(CH_2)_5$-al+1.1 $C_2H_4$.

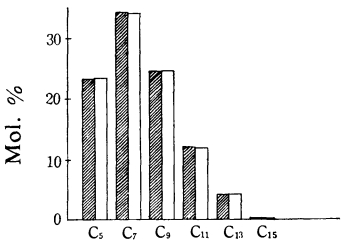



Fig. 2. Distribution of hydrocarbons by hydrolysis of the product from al-$(CH_2)_4$-$CH_3$+1.5 $C_2H_4$.
▨ Observed value
□ Calculated value

Ziegler[1] reported that the distribution of the different chains resulting from the addition of ethylene to trialkylaluminum was found to be very close to that calculated on the assumption that all aluminum-carbon bonds present in the reaction mixture have the same probability of being added to ethylene during the entire period of the reaction (Poisson distribution). If the addition of ethylene to the 1, 5-dialuminopentane derivative proceeds in the same manner as is assumed above, the theoretical distribution of the grown chains can be given by the following equations:

$$X_r = \sum_{p=0}^{r} X_p X_{(r-p)}$$

$$X_p = \frac{n^p e^{-n}}{p!} \qquad X_q = \frac{n^q e^{-n}}{q!}$$

In these equations, $X_r$ is mole fraction of the chain $-(C_2H_4)_p-(CH_2)_5-(C_2H_4)_q-$ in which $p+q$ is equal to $r$ and $n$ is defined, according to the equation $al-(CH_2)_5-al \xrightarrow{2nC_2H_4} al-(C_2H_4)_n-(CH_2)_5-(C_2H_4)_n-al$, as the average number of moles of ethylene taken up per aluminum-carbon bond. The theoretical values in the case of $n=1.1$ are given in Table I and Fig. 1. As may be seen from Fig. 1, the agreement between the observed and the theoretical distributions is relatively good. The slight discrepancies in $C_5$ and $C_7$ hydrocarbons indicate that conditions are somewhat unfavorable for the formation of $C_7$ chain from a $C_5$ chain.

By the displacement of the growth product of the 1, 5-dialuminopentane derivative by ethylene in the presence of a nickel catalyst, $\alpha$, $\omega$-dienes with odd carbon atoms (1, 4-pentadiene, 1, 6-heptadiene, 1, 8-nonadiene and 1, 10-undecadiene) were obtained (Eq. 3):

$$al-(CH_2)_5-(C_2H_4)_r-al \xrightarrow[C_2H_4]{Ni(acac)_2} 2alCH_2CH_3 + H_2C=CH-CH_2-(C_2H_4)_r-CH=CH_2 \quad (3)$$

The two aluminum-carbon bonds of the 1, 5-dialuminopentane derivative are not displaced completely by ethylene, unlike those of the 1, 7-dialuminoheptane derivative and the 1, 9-dialuminononane derivative. The composition of those hydrocarbons with the same carbon number is shown in Table III.

Further investigation is necessary of these different reactivities of the 1, 5-dialuminopentane derivative in growth reaction and in displacement reaction.

TABLE III. DISPLACEMENT REACTION OF THE GROWTH PRODUCT BY ETHYLENE (HYDROLYZED PRODUCTS)

| Carbon number | Products (composition %)[a] | | |
|---|---|---|---|
| | $\alpha,\omega$-Diene | $\alpha$-Olefin | *n*-Paraffin |
| $C_5$ | 1,4-Pentadiene (70) | 1-Pentene (22) | *n*-Pentane (8) |
| $C_7$ | 1,6-Heptadiene (93) | 1-Heptene (7) | — |
| $C_9$ | 1,8-Nonadiene (94) | 1-Nonene (6) | — |

a) Ratio of peak area of gas chromatogram.

## Experimental

**The Growth Reaction of the 1, 5-Dialuminopentane Derivative.** — The 1, 5-dialuminopentane derivative was prepared from 1, 4-pentadiene (0.03 mol.) and diisobutylaluminum hydride (0.063 mol.) by a method previously reported.[4] The 1, 4-dialuminopentane derivative in 10 ml. of *n*-hexane was introduced into a glass tube with a small hole. This glass tube was then set in an autoclave. The pressure of ethylene and the reaction temperature were kept at 130 kg./cm$^2$ and 100°C respectively for 5 hr. while the mixture was being shaken. The reaction product was decomposed by the successive addition of ethanol, water and 6 N hydrochloric acid. The organic layer was washed with water and dried over sodium sulfate. The hydrocarbons*2 thus produced were analyzed by gas chromatography, using either a squalane column (2.5 m.) or a silicone DC 550 column (2.5 m.). *n*-Pentane, *n*-heptane, *n*-nonane and *n*-undecane were identified by a comparison of their gas chromatographic retention times and infrared spectra with those of authentic samples. *n*-Tridecane, 1-pentene and 1-heptene were identified by gas chromatographic comparison.

**$\alpha,\omega$-Dienes from the Growth Product.**— To the growth product obtained under the same reaction conditions as have been described above, 8 mg. of nickel acetylacetonate and 80 mg. of phenylacetylene in 5 ml. of *n*-hexane were added. The pressure of ethylene and the temperature were kept at 55 kg./cm$^2$ and 70°C respectively for 2 hr. The reaction product was then hydrolyzed and the organic layer separated by gas chromatography, using a squalane column. 1, 4-Pentadiene 1, 6-heptadiene, 1, 8-nonadiene and 1, 10-undecadiene were identified by comparing their gas chromatographic retention times and infrared spectra with those of authentic samples prepared by the method previously reported.[4] 1-Pentene, *n*-pentane, 1-heptene and 1-nonene were identified by gas chromatographic comparison.

**The Growth Reaction of the *n*-Pentylaluminum Derivative.**—*n*-Pentylaluminum derivative was prepared from the reaction of 0.07 mol. of 1-pentene with 0.09 mol. of diisobutylaluminum hydride at 70°C for 16 hr. The growth reaction of this compound was carried out under the same reaction conditions as have been described above.

*Basic Research Laboratories*
*Toyo Rayon Company, Ltd.*
*Kamakura*

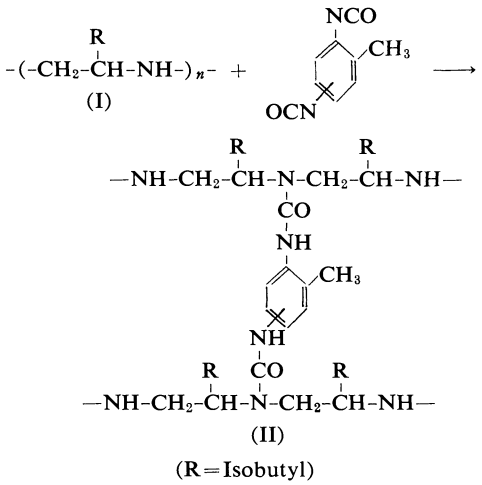
*2 The hydrocarbons derived from the growth reaction of isobutyl group are completely distinguished from those with odd carbon atoms by gas chromatography.

# Catalytic Asymmetric Benzaldehyde Cyanohydrin Synthesis with Synthetic Optically Active Polymer. II. Cross-linked Poly-(s)-isobutylethylenimine

By Sei TSUBOYAMA

(Received May 28, 1964)

In the previous paper,[1] an asymmetric synthesis of benzaldehyde cyanohydrin performed in the presence of the basic catalyst of several optically active polymers was described. With poly-(s)-isobutylethylenimine (I), the optical yield of the produced (−)-cyanohydrin was relatively high, about 20%. In the present work, an insoluble polymer, obtained from poly-(s)-isobutylethylenimine by cross-linking with tolylene diisocyanate (TDI), was used. The insoluble polymer catalyst can be separated from the reaction mixture containing unstable and viscous compounds and reused. Besides, the cross-linking seems to stabilize the conformation.



(I) (II)

(R=Isobutyl)

**The Cross-linking of Poly-(s)-isobutylethylenimine.**—Among the cross-linking agents tested so far, only TDI gave an insoluble product from the polymer I, while with the others the polymer did not even gelatinize. The TDI cross-linked polymer (II) swells in benzene or toluene, but it repels water in spite of the presence of hydrophilic amino groups; this property seems to be useful for a catalyst in organic solvents. The exchange capacities of the cross-linked polymers are listed in Table I. The infrared spectrum of the polymer reveals the presence of a –NH–CO–N= group by absorptions at 1655 $cm^{-1}$ and at 1525 $cm^{-1}$ as similar to that of phenyl isocyanate-modified polymer (Fig. 1).

TABLE I. CROSS-LINKING OF POLY-(S)-ISOBUTYLETHYLENIMINE WITH TOLYLENE DIISOCYANATE

| Sample No. | TDI weight mg./polymer g. | –NCO/=NH | Capacity meq./g. |
|---|---|---|---|
| 1 | 150 | 0.17 | 3.68 |
| 2 | 174 | 0.20 | 3.00* |
| 3 | 261 | 0.30 | 2.71 |
| 4 | 348 | 0.40 | 2.18 |
| 5 | 700 | 0.80 | 1.70 |
| 6 | 280 | 0.32 | 3.57** |

* Found: C, 67.83; H, 10.65; N, 13.10. Calcd. for $(C_6H_{13}N)\cdot(C_9H_6N_2O_2)_{0.20/2}$: C, 71.09; H, 11.76; N, 14.42%.

** Molecular weight of the original polymer is 3300, the others are 1050. Analytical data as hydrochloride;
Found: C, 58.90; H, 9.66; N, 11.67; Cl, 11.55.
Calcd. for $(C_6H_{13}N)\cdot(C_9H_6N_2O_2)_{0.32/2}\cdot(HCl)_{1-0.32}$: C, 58.85; H, 9.72; N, 12.18; Cl, 15.88%.

**Benzaldehyde Cyanohydrin Synthesis with Cross-linked Polymer.**—The asymmetric synthesis and analysis of the product were carried out in a similar way to those described in the previous paper.[1]

The data in Table II show that the product with the cross-linked polymer and that with the original linear polymer are completely reversed in the sign of the optical rotation. This reversal of sign is independent of whether or not the reaction system is homogeneous, for we observe the same result when a solvent-soluble catalyst partly modified with phenyl or methyl isocyanate is used instead of TDI. Since *symm-n*-butylphenylurea had no catalytic activity for cyanohydrin formation in a benzene solution, the –NH–CO–N= groups themselves may not be related directly to this reversal.

**The Contribution of –NH–CO–N= Groups to the Asymmetric Synthesis.**—In order to elucidate the reversal of sign, several polymers

1) S. Tsuboyama, This Bulletin, 35, 1004 (1962).

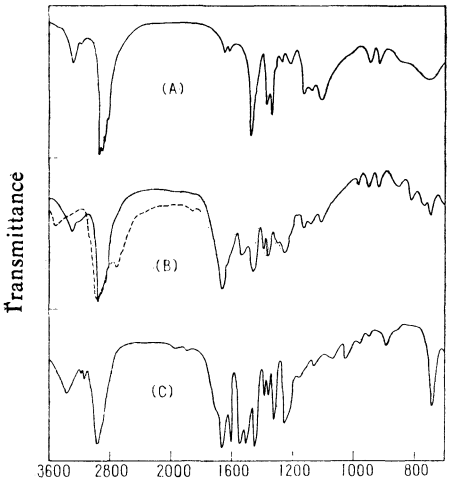



Fig. 1. Infrared absorption spectra: (A) poly-(s)-isobutylethylenimine (I), (B) solid line; TDI cross-linked polymer (II), dotted line; its HCl salt, (C) phenyl isocyanate modified polymer.

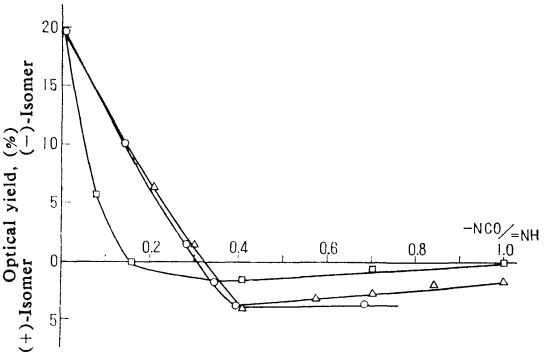



Fig. 2. Effect of introducing -NH-CO-N= group into the polymer I on the optical yield of the asymmetric synthesis.
—○— Tolylene diisocyanate
—△— Phenyl isocyanate
—□— Methyl isocyanate

containing R-NH-CO-N= groups in various ratios were prepared by the addition of TDI, phenyl or methyl isocyanate to the linear polymer, and the asymmetric cyanohydrin formation was carried out with each of them as a catalyst. The optical yields of the product obtained with various modified polymers as catalysts are given in Table III and illustrated in Fig. 2. In the figure, the optical yield is plotted against the mole ratio of the isocyanate group to the amino group, -NCO/=NH, on the assumption that the added isocyanate had reacted stoichiometrically. It may be seen from the results that: (1) with respect to the TDI series, the optical yield decreases continuously with the additional amount of isocyanate, and the sign of the optical rotation of the product changes from negative to positive. The curve shows that the optical yield reaches a maximum at approximately the ratio of 0.4 and that thereafter it is independent of the ratio, suggesting that TDI reacts with the linear polymer to some extent but not further, for its taking part in the reaction seems to be hindered by the net work structure formed. The benzene solution of the polymer emulsifies near 0.34 and is gelatinized at the ratio of 0.40 (Table III); (2) the curve concerning phenyl isocyanate is similar to that of TDI at values lower than 0.4, but at values over this ratio, the optical yield of the (+)-isomer decreases with the increase in the ratio. As the polymer modified with phenyl isocyanate has no net work, phenyl isocyanate seems to be introduced more easily than TDI into the polymer. However, even when the ratio is 1, the minor amino groups, which are capable of catalyzing, are still likely to remain in the polymer. In any case, both these polymers have almost identical efficiencies for the steric course of the asymmetric reaction, regardless of the reaction phase; (3) in the methyl isocyanate series, the cross-over point of

Table II. Asymmetric synthesis with cross-linked poly-(s)-isobutylethylenimine*

| Catalyst | Catalyst wt. mg. | Cyanohydrin | | | |
|---|---|---|---|---|---|
| | | Yield, % | $\alpha_D$** | $[\alpha]_D$ | P%*** |
| Polymer I | 100 | 51.5 | −2.15 | −8.34 | 19.0 |
| 1 | 270 | 86.0 | +0.30 | +0.68 | 1.5 |
| 3 | 400 | 65.0 | +0.15 | +0.45 | 1.0 |
| 3 | 40 | 24.5 | +0.30 | +2.41 | 5.5 |
| 5 | 500 | 64.1 | +0.42 | +1.29 | 2.9 |
| 6 | 300 | 84.4 | +0.62 | +1.42 | 3.3 |

* These reactions were performed with benzaldehyde (0.1 mol.) and hydrogen cyanide (0.1 mol.) in the presence of the polymer catalyst (1 mmol.) in benzene at 20°C for 20 hr.
** $c$ 1—4, 2 dm. tube.
*** Optical yield; percentage of specific rotation of the product to the absolute value of the rotation of optically pure cyanohydrin in benzene, $[\alpha]_D^{25}$+43.75 ($c$ 5.006).

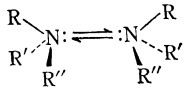
TABLE III. ASYMMETRIC SYNTHESIS WITH POLY-(S)-ISOBUTYLETHYLENIMINE MODIFIDE BY SEVERAL ISOCYANATES

| -NCO/=NH | Apparent reaction phase | Polymer $\alpha_D$* | Cyanohydrin | | |
|---|---|---|---|---|---|
| | | | $\alpha_D$** | $[\alpha]_D$ | P% |
| Tolylene diisocyanate | | | | | |
| 0.136 | Homogeneous | +0.32 | −1.30 | −4.42 | 10.0 |
| 0.273 | Homogeneous | +0.07 | −0.20 | −0.68 | 1.6 |
| 0.340 | Emulsive | | +0.20 | +0.78 | 1.8 |
| 0.395 | Gelatinous | | +0.30 | +1.67 | 3.8 |
| 0.682 | Heterogeneous | | +0.30 | +1.68 | 3.8 |
| Phenyl isocyanate | | | | | |
| 0.200 | Homogeneous | | −1.40 | −2.89 | 6.6 |
| 0.286 | Homogeneous | +0.14 | −0.22 | −0.65 | 1.5 |
| 0.400 | Homogeneous | | +0.66 | +1.79 | 4.1 |
| 0.571 | Homogeneous | +0.16 | +0.32 | +1.32 | 3.2 |
| 0.700 | Homogeneous | | +0.36 | +1.07 | 2.5 |
| 0.840 | Homogeneous | +0.22 | +0.10 | +0.96 | 1.9 |
| 1.000 | Homogeneous | +0.28 | +0.11 | +0.72 | 1.7 |
| Methyl isocyanate | | | | | |
| 0.075 | Homogeneous | +0.26 | −0.64 | −2.55 | 5.8 |
| 0.158 | Homogeneous | +0.20 | 0.00 | 0.00 | 0 |
| 0.270 | Homogeneous | +0.11 | +0.12 | +0.45 | 1.0 |
| 0.404 | Homogeneous | 0.00 | +0.22 | +0.69 | 1.7 |
| 0.700 | Homogeneous | −0.20 | +0.05 | +0.16 | 0.4 |
| 1.000 | Homogeneous | | 0.00 | 0.00 | 0 |

* The optical rotation of the original linear polymer, $\alpha_D$ +0.60.
** *c* 1—4, 2 dm. tube.

the curve comes at a value of the ratio lower than those the cases of the former two, and then P% gradually approaches zero by way of a maximum at about 0.4. If the reversal in the sign of the cyanohydrin produced by these polymers depends on only the size of the introduced group, the first two series must be more effective than the methyl isocyanate series, at least within the range of small values of the ratio, and the curves of the former must be steeper than the curve of the latter. However the result obtained refute this assumption; some other explanation, therefore, should be considered.

One possible interpretation is as follow. Amines, and presumably amine polymers, may be converted at a very high rate and with a very low energy to their enantiomers by a molecular vibration of the type known in $NH_3$ molecule (as is shown in the scheme).



In this reaction, therefore, when the carbonyl reagent approaches equivalently to either side of the amine which is vibrating, the cyanohydrins produced at the two sides become enantiomers with each other. Consequently, the selectivity of the reaction may not be recognized. Only when the accessibilty of the reagent is different on the two sides of interconverting amine, as a result of a steric requirement, the reaction will be performed asymmetrically. In the steric requirement, even if the absolute configuration of the polymer remains the same, the accessibility of the reagent and even the direction of its approach appear to change as a result of the change produced by the modification in the arrangement at the circumference of the catalytic center. Each conformation of these modified polymers may be very unlike the original one because of such interaction as intra- and inter-molecular hydrogen bonding between introducing groups or between the amino group and the introducing group. To the newly-formed conformation, the approach of the reagent may become easier on the side opposite to what would the approach be originally. In all cases, it seems that the arrangement of these modified polymers changes markedly until the ratio reaches 0.4 but that thereafter the conformation undergoes no appreciable change. Although the conformation of these polymers has not yet been analyzed, it should be noted that the configuration and

the optical yield of the product in the asymmetric synthesis are not always controlled by the absolute configuration of the catalyst but by the conformation of the circumference of the catalytic center.

## Experimental

**Cross-linking of Poly-(s)-isobutylethylenimine with Tolylene Diisocyanate.**—To an ice-cooled solution of 1.0 g. of the linear polymer I in 25 ml. of toluene was added dropwise a known volume of toluene solution containing 1% of tolylene diisocyanate* with vigorous stirring. The viscous or opaque jelly-like solution formed was then stirred for about 5 hr. at 60°C and allowed to stand overnight at room temperature. The insoluble polymer was filtered off and washed with hot toluene, benzene, ethanol and ether. The pale yellow solid obtained was then ground and screened to 20—40 mesh. To regenerate it, the dried polymer was made to swell thoroughly with benzene and then washed with ethanol, N hydrochloric acid, 4% ammonium hydroxide and finally with deionized water. The exchange capacity was measured for the wet polymer in the presence of N/10 hydrochloric acid and N sodium chloride (Table I).

Other cross-linking agents for the amine polymer, such as ethylene dichloride[2] epichlorohydrine,[3] formaldehyde, tetra- and pentamethylene dibromide, *symm*-dichloroacetone, *p*-xylylene dichloride, and their various combinations, were applied under various conditions. Every mixture of the linear polymer and an agent was heated in a sealed glass tube at 100—180°C for 24—72 hr., but no insoluble product was obtained.

**Phenyl Isocyanate-modified Polymer.**—A solution of a slight excess of phenyl isocyanate in benzene was added with stirring into a solution of the linear I polymer in benzene, and the mixture was left standing overnight at room temperature. The benzene solution was then washed with water to remove the excess of isocyanate. The pale yellow solution obtained was freeze-dried; m. p. 143°C. $[\alpha]_D^{23}$ +71.01 (*c* 2.056, benzene).

Found: C, 71.95; H, 8.36; N, 10.84. Calcd. for $(C_{13}H_{18}N_2O)_n$: C, 71.52; H, 8.31; N, 12.83%.

***symm*-*n*-Butylphenylurea.**—To an ice-cooled solution of 0.7 g. (0.01 mol.) of *n*-butylamine in 5 ml. of heptane, a solution of 1.2 g. (0.01 mol.) of phenyl isocyanate in heptane was added slowly with stirring. The product, *symm*-*n*-butylphenylurea, separated as needle crystals which weighed 1.7 g. and melted at 129—130°C after recrystallization from ethanol.

Found: C, 68.92; H, 8.12. Calcd. for $C_{11}H_{16}N_2O$: C, 68.72; H, 8.39%.

**Asymmetric Synthesis with Several Isocyanate-modified Polymers.**—To every solution of 50 mg. of the linear polymer in benzene was added an appropriate, known volume of benzene solution containing ca. 1% of one of TDI, phenyl and methyl isocyanate (b. p. 39.5—40.5°C),[4] dropwise, with vigorous stirring, and each solution thus prepared was then filled up to 10 ml. with benzene. After 3 hr., the rotation of each solution was measured, and the asymmetric synthesis and analysis of cyanohydrin were carried out in a way similar to that described in the previous report.[1] For the measurment of the optical rotation, all the samples except the gelatinized ones were purifled by distillation.

## Summary

Asymmetric benzaldehyde cyanohydrin synthesis with TDI cross-linked poly-(s)-isobutylethylenimine has been studied. The cyanohydrin obtained was (+)-isomer; its sign is opposite to what it is in the case of the linear polymer. With the linear and soluble polymer which contains some –NH–CO–N= groups, the (+)-isomer was also found to be produced. These results suggest that (1) the reversal of the sign is independent of the reaction phase, and (2) the configuration of the product is not always controlled by the configuration of the asymmetric carbon in the catalyst but by the conformation of the catalytic center.

The author wishes to thank Dr. Masaya Yanagita for many valuable discussions and suggestions.

*Laboratory of Polymer Chemistry*
*The Institute of Physical and Chemical Research*
*Komagome, Bunkyo-ku, Tokyo*

* Hodogaya Chem. Co., Ltd., 2,4-isomer: 2,6-isomer = 80:20. distilled at 97—97.5°C/3 mmHg, $n_D^{28}$ 1.5634.

2) F. J. Shepherd and J. A. Kitchener, *J. Chem. Soc.*, **1957**, 86.

3) G. Manecke and K. F. Bonhoffer., *Z. Electrochem.*, **55**, 475 (1951).

4) J. Colucci, *Can. J. Research*, **23B**, 111 (1945).

# Some Cationoid Reactions of 4-Ethyltropolone

By Tetsuo NOZOE, Kahei TAKASE and Keiji UMINO

(Received June 1, 1964)

Since the steric effect of the side-chain in troponoid compounds is generally larger than in benzenoid compounds, because of a planar, seven-membered ring, tropolone and its homologs often show interesting unexpected behavior in some reactions[1] in which benzenoid compounds react normally. Although the chemical and physical properties of 4-methyl- and 4-isopropyl-tropolone have extensively been studied,[2] the properties of 4-ethyltropolone have scarcely been known; it has been synthesized only in a poor yield from 4-ethylcycloheptane-1, 2-dione.[3] In this paper, we wish to report on a new synthesis of 4-ethyltropolone (I) and on some of its reactions.

4-Ethyltropolone (I) was synthesized from 4-acetyltropolone (II)[4] by the Huang-Minlon reduction. When heated with hydrazine, II afforded the hydrazone (III), which gave I when heated with potassium hydroxide in ethylene glycol. The yield of I from II was about 60%. When the reduction was carried out without the isolation of the hydrazone, I was not obtained, but a polymerized substance was formed. Besides the known copper chelate,[3] I gave a cyclohexylamine and dicyclohexylamine salts.

The azo-coupling of I with *p*-toluenediazonium chloride gave a *p*-tolylazo compound (IV).[3] The nitration of I gave a mononitro (V) or dinitro compound (VI), according to the variation in the reaction conditions. The action of 1–3 molar equivalents of fuming nitric acid on I afforded V, while 1–4 molar equivalents of concentrated nitric acid gave mainly VI. However, in one experiment, in which one molar equivalent of concentrated nitric acid was used, a trinitro compound (VII) was isolated in a poor yield, although these results could not be reproduced. The amino compound (VIII) obtained by the catalytic reduction of V was identical with that derived from the azo compound (IV) by similar reduction. Since IV has an azo group at the 5-position,[5] V and VIII were assumed to be 4-ethyl-5-nitro- and 5-amino-4-ethyltropolone respectively. The amine (VIII) was easily diazotized by sodium nitrite and an acid, and 5-chloro-4-ethyl- (IX) and 5-bromo-4-ethyltropolone (X) were prepared by Sandmeyer reaction. The heating of the dinitro compound (VI) in methanol for a few minutes afforded a colorless neutral compound (XI) in a good yield. On the basis of its ultraviolet absorption spectrum, this compound is considered to be a benzenoid compound produced by the rearrangement reaction. From such a similarity in chemical behavior between VI and 4-methyl-5, 7-dinitro-[6] or 4-isopropyl-5, 7-dinitrotropolone,[7] which afforded methyl 3-methyl-4, 6-dinitrobenzoate and methyl 3-isopropyl-4, 6-dinitrobenzoate in the same treatment, the dinitro compound (VI) and the rearranged product (XI) were assumed to be 4-ethyl-5, 7-dinitrotropolone and methyl 3-ethyl-4, 6-dinitrobenzoate respectively. The trinitro compound (VII) was assumed to be 4-ethyl-3, 5, 7-trinitrotropolone from its ultraviolet and infrared spectra, which are similar to those of 3, 5, 7-trinitrotropolone,[8] although it showed a negative ferric chloride coloration and was stable when heated with alcohol.

The bromination of 4-ethyltropolone (I) with a molar equivalent of bromine in methanol afforded as the main product a monobromo compound (XII)[9] which was different from the monobromo compound (X), besides a dibromo compound (XIII) and a tribromo compound (XIV). On the other hand, when two molar equivalents of bromine were used, besides XIV an isomeric dibromo compound (XV) was obtained in a good yield. When three molar equivalents of

1) T. Nozoe, *Nature*, 167, 1055 (1951); *Fortschr. Chem. org. Naturstoffe*, 13, 233 (1956).

2) Cf. T. Nozoe et al., "Dai Yuki Kagaku (Comprehensive Organic Chemistry)," Vol. 13, Chapters 5–9, Asakura Shoten, Tokyo (1960), esp. pp. 156, 160.

3) T. Nozoe, T. Mukai and S. Matsumoto, *Proc. Japan Acad.*, 27, 110 (1951).

4) T. Nozoe, K. Takase and M. Ogata, *Chem. & Ind.*, 1957, 1070.

5) It is known that the azo-coupling to a tropolone ring usually occurs at the 5-position.[1]

6) T. Nozoe, T. Mukai, M. Kunori, T. Muroi and K. Matsui, *Sci. Repts. Tohoku Univ., I*, 35, 242 (1951); T. Muroi, *Bulletin Yamagata University, Natural Science*, 3, 155 (1954); R. D. Haworth and P. R. Jefferies, *J. Chem. Soc.*, 1951, 2067.

7) T. Nozoe, Y. Kitahara, E. Kunioka and K. Doi, *Proc. Japan Acad.*, 26 (9), 38 (1950); E. Sebe, *Sci. Repts. Tohoku Univ.*, I, 36, 99 (1952).

8) T. Nozoe, M. Oyama and K. Kikuchi, This Bulletin, 36, 168 (1963).

9) This compound, m. p. 67.5–69°C, was identical with the monobromo compound, m. p. 66°C, formerly obtained by the bromination of 4-ethylcycloheptane-1,2-dione.[3]

bromine were used in the presence of sodium acetate, the tribromo compound (XIV) was obtained in a good yield. The monobromo compound (XII) is assumed to be 7-bromo-4-ethyltropolone on the basis of the following evidence. The azo-coupling of XII gave a crystalline azo compound (XVI).[5] The infrared spectrum of XII is quite similar to that of 7-bromo-4-isopropyltropolone[10] in the region of out-of-plane C-H deformation vibrations. The dibromo compound (XV) is assumed to be 3, 7-dibromo-4-ethyltropolone, since it was also obtained by the bromination of XII and gave a crystalline azo compound (XVII) by azo-coupling. Therefore, another dibromo compound (XIII) is assumed to be 5, 7-dibromo-4-ethyltropolone. The tribromo compound (XIV) is considered to be 3, 5, 7-tribromo-4-ethyltropolone since it was obtained from X, XII and XV by bromination. The formation of the tribromo derivative (XIV) by the bromination of I shows that the steric hindrance of the ethyl group is smaller than that of the isopropyl group,[11] as was expected. On the other hand, the formation of the dibromo compound (XIII) is similar in tendency to the bromination of 4-isopropyltropolone[2,10] rather than to that of 4-methyltropolone.[2]

The treatment of I with iodine, in the presence of potassium carbonate, afforded 4-ethyl-7-iodotropolone (XVIII), the structure of which was based on the following evidence. The azo-coupling of XVIII gave a crystalline azo compound (XIX),[5] and it was known that the iodination of tropolones, under these conditions, generally give 3 (or 7)-iodotropolones. Furthermore, the infrared spectrum of XVIII is similar to that of 7-iodo-4-isopropyltropolone[12] in the region of out-of-plane C-H deformation vibrations.

When heated in acetic acid or ethanol, the 5-arylazo derivatives of 4-isopropyltropolone are known to give, especially in the presence of acid or benzoquinone, the reddish-purple "hinopurpurine," whose structure was established to be 2-aryl-3, 3-dimethyl-2, 3, 5, 6-tetrahydro-5, 6-cyclohepta[c]pyrazoledione (XX).[13] On the other hand, it has been reported[3] that 4-ethyl-5-(*p*-tolylazo)tropolone (IV) gives, on heating in acetic acid in the presence of hydrochloric acid, no hinopurpurin-like, highly colored compound, but an unidentified brown crystals with a m. p. of 210°C. The reexamination of this reaction gave pale yellow needles with a m. p. of 203°C, which were proved

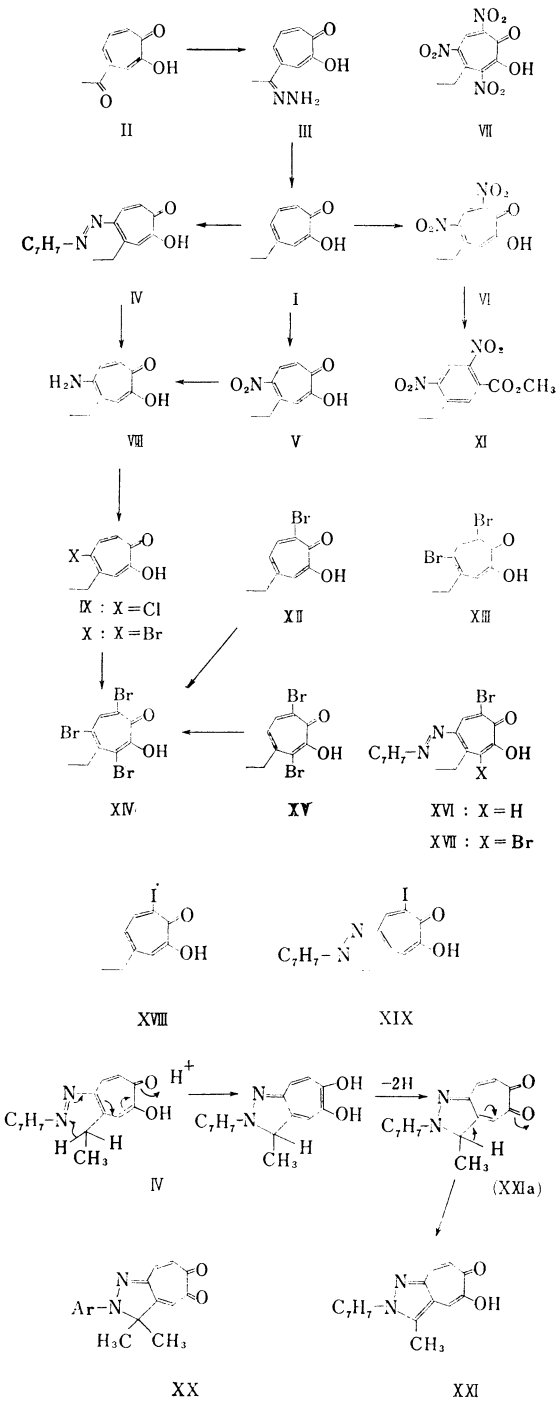



Chart 1. The mechanism of the cyclization reaction of 4-ethyl-5-(*p*-tolylazo)tropolone (IV).

10) T. Nozoe, E. Sebe, S. Mayama and S. Iwamoto, *Sci. Repts. Tohoku Univ., I*, **36**, 184 (1952).

11) 3,5,7-Tribromo-4-isopropyltropolone was only obtained by the heating of the bromine-addition product of 4-isopropyltropolone; T. Nozoe, K. Takase and M. Yasunami, to be published.

12) T. Nozoe, E. Sebe, L. S. Cheng, S. Mayama and T. J. Hsü, *Sci. Repts., Tohoku Univ., I*, **36**, 299 (1952); Y. Kitahara and T. Arai, *Proc. Japan Acad.*, **27**, 423 (1951).

13) T. Nozoe, T. Ikemi and T. Ozeki, *Proc. Japan Acad.*, **31**, 455 (1955) and the references therein cited.

to be identical with 5-hydroxy-3-methyl-2-(*p*-tolyl)-6(2*H*)-cyclohepta[c]pyrazolone (XXI)[14] obtained by the ring closure of the *p*-tolylazo derivatives of 4-(1-hydroxyethyl)- or 4-(1-acetamidoethyl)tropolone. The mechanism of the formation of XXI from IV is thought to be similar to that of the hinopurpurin-formation,[13] as is shown in Chart 1, the reaction is facilitated in the presence of iodine or benzoquinone, as was to be expected from the inevitable dehydrogenation process. In this case, however, the hinopurpurin-like diketone (XXIa) easily tautomerizes to the more stable enolic form (XXI), since XXIa, being different from hinopurpurin, has a mobile hydrogen at the 3-position.

## Experimental[15]

**4-(1-Hydrazonoethyl)tropolone (III).**—A mixture of 4-acetyltropolone (II) (16.4 g.), ethanol (20 ml.), and 80% hydrazine hydrate (9 ml.) was heated while being stirred in a boiling-water bath until the orange crystals turned yellow. After they had been allowed to cool, the crystals were collected by filtration and washed with ethanol to give III (16.6 g.) as yellow needles, m. p. 193°C (decomp.).

Found: C, 60.51; H, 5.37; N, 15.50. Calcd. for $C_9H_{10}O_2N_2$: C, 60.66; H, 5.66; N, 15.72%.

*N-Acetyl Derivative:* M. p. 188—189°C, yellow prisms (from glacial acetic acid).

Found: C, 60.43; H, 5.19; N, 12.22. Calcd. for $C_{11}H_{12}O_3N_2$: C, 59.99; H, 5.49; N, 12.72%.

**4-Ethyltropolone (I).**—To a solution of potassium hydroxide (8.8 g.) in ethylene glycol (40 ml.), III (16.6 g.) was added; the mixture was then heated at 140—150°C for 10 hr. The reaction mixture was poured into water (600 ml.) and acidified with 6 N hydrochloric acid, and the oily substance which separated out was extracted three times with chloroform. The solvent was evaporated and the residue was recrystallized from petroleum ether to give I (4.83 g.) as colorless rhombic prisms, m. p. 42—43°C; reported[3] m. p. 42°C.

Found: C, 72.05; H, 6.55. Calcd. for $C_9H_{10}O_2$: C, 71.98; H, 6.71%. $\lambda_{max}^{MeOH}$ mμ (log ε); 240 (4.48), 327 (3.87).

*Copper Chelate:* m. p. 157—158°C, reported[3] m. p. 156°C, pale green crystals (from ethanol).

Found: C, 59.39; H, 4.80. Calcd. for $(C_9H_9O_2)_2$-Cu: C, 59.74; H, 5.01%.

*Cyclohexylamine Salt.:* m. p. 159—160°C pale yellow crystals (from cyclohexane).

Found: C, 72.64; H, 9.44; N, 5.65. Calcd. for $C_{15}H_{23}O_2N$: C, 72.25; H, 9.30; N, 5.62%.

*Dicyclohexylamine Salt.:* m. p. 118—119°C, yellow crystals (from cyclohexane).

Found: C, 76.07; H, 9.61; N, 3.59. Calcd. for $C_{21}H_{33}O_2N$: C, 76.09; H, 10.03; N, 4.23%.

**4-Ethyl-5-(*p*-tolylazo)tropolone (IV).**—Into a solution of I (750 mg.) in pyridine (10 ml.) a solution of *p*-toluene diazonium chloride, prepared by diazotizing *p*-toluidine (600 mg.) in the usual manner, was stirred while the mixture was being cooled an azo compound began to separate during the addition. After the mixture had been stirred for an additional 2 hr., water (10 ml.) was added, and the crystals thereby formed were collected and recrystallized from benzene to give IV (1.27 g.) as red needles m. p. 142—143°C; reported[3] m. p. 141—142°C.

Found: C, 71.38; H, 5.89; N, 10.49. Calcd. for $C_{16}H_{16}O_2N_2$: C, 71.62; H, 6.01; N, 10.44%. $\lambda_{max}^{MeOH}$ mμ (log ε); 233 (4.42), 292 (4.07), 395 (4.43).

**4-Ethyl-5-nitrotropolone (V).**—Into a solution of I (300 mg.) in glacial acetic acid (1 ml.), fuming nitric acid (sp. gr. 1.50, 0.1 ml.) was stirred while the mixture was being cooled; a yellow nitro compound began to separate out. After it had been stirred for an additional 2 hr., the reaction mixture was diluted with water (3 ml.) to give V (70 mg.), m. p. 157—163°C, which was recrystallized from methanol to afford pale yellow needles, m. p. 162.5—163°C.

Found: C, 55.51; H, 4.44; N, 6.98. Calcd. for $C_9H_9O_4N$: C, 55.38; H, 4.65; N, 7.18%. $\lambda_{max}^{MeOH}$ mμ (log ε); 245 (4.57), 325 (4.17), 400 (4.19).

**4-Ethyl-5, 7-dinitrotropolone (VI).**—Into a solution of I (300 mg.) in glacial acetic acid (1 ml.), concentrated nitric acid (sp. gr. 1.38, 0.5 ml.) was stirred while the mixture was being cooled; yellow crystals then began to separate out. After stirring for an additional 2 hr., water (5 ml.) was added to give VI (150 mg.), m. p. 123—125°C, which was recrystallized from benzene, affording yellow prisms, m. p. 127—128°C.

Found: C, 45.12; H, 3.16; N, 11.45. Calcd. for $C_9H_8O_6N_2$: C, 45.01; H, 3.36; N, 11.67%. $\lambda_{max}^{MeOH}$ mμ (log ε); 246 (4.44), 405 (4.14).

**4-Ethyl-3, 5, 7-trinitrotropolone (VII).**—To a solution of I (300 mg.) in glacial acetic acid (1 ml.), concentrated nitric acid (sp. gr. 1.38, 0.15 ml.) was added, and the mixture was stirred for 2 hr. with cooling. After dilution with water, the crystals (100 mg.), m. p. 75—82°C, thereby formed were collected and recrystallized from methanol to give VII as pale yellow prisms, m. p. 84—85.5°C.

Found: C, 37.77; H, 2.49; N, 14.58. Calcd. for $C_9H_7O_8N_3$: C, 37.90; H, 2.47; N, 14.74%. $\lambda_{max}^{MeOH}$ mμ (log ε); 255 (3.99), 357 (4.15).

Another experiment under the same conditions gave the dinitro compound (VI) in a poor yield.

**5-Amino-4-ethyltropolone (VIII).**—*a) From the Azo Compound (IV).*—A suspension of IV (1.07 g.) in methanol (12 ml.) was shaken, in the presence of platinum oxide (20 mg.), with hydrogen at room temperature and at atmospheric pressure; 205 ml. of hydrogen was absorbed after 1 hr. The catalyst was filtered off, the solvent was evaporated, and the residue was recrystallized from methanol to give VIII (530 mg.) as yellow needles, m. p. 168—169°C.

Found: C, 65.39; H, 6.54; N, 8.48. Calcd. for $C_9H_{11}O_2N$: C, 65.44; H, 6.71; N, 8.48%. $\lambda_{max}^{MeOH}$ mμ (log ε); 240 (4.38), 360 (4.13), 390 (4.15).

*b) From the Nitro Compound (V).*—A solution

14) T. Nozoe, K. Takase and K. Suzuki, This Bulletin, **38**, 362 (1964).

15) All melting points are uncorrected.

of V (40 mg.) in methanol (5 ml.) was shaken with hydrogen in the presence of platinum oxide; 17 ml. of hydrogen was absorbed after 17 min. The catalyst and the solvent were removed, and the residue was recrystallized from methanol to give VIII (20 mg.) as yellow needles, m. p. 168—169°C.

**5-Chloro-4-ethyltropolone (IX).**—To a solution of VIII (330 mg.) in 50% aqueous dioxane (5 ml.), concentrated sulfuric acid (0.3 ml.) was added, and then a solution of sodium nitrite (150 mg.) in water (0.5 ml.) was stirred in while the mixture was being cooled. After additional stirring (30 min.), the diazotized solution was stirred into a solution of cuprous chloride (680 mg.) in concentrated hydrochloric acid (3.8 ml.). After additional stirring (1 hr.), the mixture was diluted with water (25 ml.); the copper chelate thereby formed was collected and dried (480 mg.). This copper chelate was suspended in chloroform, hydrogen sulfide gas was passed throughly and the copper sulfide thereby formed was filtered off. The evaporation of the solvent from the filtrate left crystals, which were then recrystallized from methanol to give IX (300 mg.) as pale yellow needles, m. p. 128—129°C.

Found: C, 58.51; H, 4.92. Calcd. for $C_9H_9O_2Cl$: C, 58.54; H, 4.91%. $\lambda_{max}^{MeOH}$ mμ (log ε); 243 (4.50), 336 (4.12), 365 (3.81), 379 (3.82).

**5-Bromo-4-ethyltropolone (X).** — A diazotized solution of VIII (330 mg.), prepared as described in the above experiment, was stirred into a solution of cuprous bromide (700 mg.) in concentrated hydrobromic acid (3.8 ml.). The copper chelate thereby formed was decomposed with hydrogen sulfide as described in the above experiment, and the crystals thereby obtained were recrystallized from methanol to give X (350 mg.) as yellow needles, m. p. 128—129°C.

Found: C, 46.69; H, 4.08. Calcd. for $C_9H_9O_2Br$: C, 47.18; H, 3.96%. $\lambda_{max}^{MeOH}$ mμ (log ε); 244 (4.46), 340 (4.20), 383 (3.79), 401 (3.78).

**Methyl 3-Ethyl-4, 6-dinitrobenzoate (XI).** — A solution of VI (100 mg.) in methanol (1 ml.) was heated for 2 min., affording XI (80 mg.) as colorless prisms, m. p. 64—65°C, after recrystallization from ether.

Found: C, 47.56; H, 3.81; N, 10.90. Calcd. for $C_{10}H_{10}O_6N_2$: C, 47.25; H, 3.97; N, 11.02%.

**The Bromination of I.**—*a) With a Molar Equivalent of Bromine.*—Into a solution of I (1.00 g.) in methanol (5 ml.), bromine (1.07 g.) in methanol (2 ml.) was stirred while the mixture was being cooled. After additional stirring (3 hr.), the mixture was allowed to stand overnight and then diluted with water. The crystals (1.47 g.) thereby formed were collected by filtration and fractionally recrystallized from methanol to give *7-bromo-4-ethyltropolone (XII)* (560 mg.), m. p. 63—66°C, which was further recrystallized from petroleum ether, affording colorless needles, m. p. 67.5—69°C, reported[3] m. p. 66°C.

Found: C, 47.23; H, 3.74. Calcd. for $C_9H_9O_2Br$: C, 47.18; H, 3.96%. $\lambda_{max}^{MeOH}$ mμ (log ε); 256 (4.59), 330 (3.91), 380 (3.84).

The crystalline substance, obtained from the filtrate by the evaporation of the solvent, was dissolved in benzene and shaken with a 5% sodium hydrogen carbonate solution; the sparingly soluble sodium salt thereby formed was then collected by filtration. This salt was dissolved in hot water and acidified with 6 N hydrochloric acid, and the crystals thereby formed were collected and recrystallized from methanol to give *5, 7-dibromo-4-ethyltropolone (XIII)* (20 mg.) as pale yellow needles, m. p. 115—116°C.

Found: C, 35.44; H, 2.52. Calcd. for $C_9H_8O_2Br_2$: C, 35.02; H, 2.61%.

The benzene layer left after the removal of the sodium salt was shaken with a 5% sodium carbonate solution, and the sodium salt thereby formed was collected by filtration. This salt was dissolved in hot water and acidified with 6 N hydrochloric acid, and the crystals thereby formed were collected and recrystallized from methanol to give *3, 5, 7-tribromo-4-ethyltropolone (XIV)* (20 mg.) as greenish yellow prisms, m. p. 96.5—97°C.

Found: C, 28.09; H, 1.65. Calcd. for $C_9H_7O_2Br_3$: C, 27.94; H, 1.82%. $\lambda_{max}^{MeOH}$ mμ (log ε); 272 (4.35), 352 (3.93), 430 (3.80).

*b) With Two Molar Equivalents of Bromine.*—Into a solution of I (450 mg.) in methanol (10 ml.), bromine (960 mg.) in methanol (2 ml.) was stirred while the mixture was being cooled. After the mixture had been allowed to stand overnight, the solvent was evaporated and the residue was recrystallized from petroleum ether to give *3, 7-dibromo-4-ethyltropolone (XV)* (350 mg.) as pale yellow prisms, m. p. 90—90.5°C.

Found: C, 35.38; H, 2.51. Calcd. for $C_9H_8O_2Br_2$: C, 35.02; H, 2.61%. $\lambda_{max}^{MeOH}$ mμ (log ε); 267 (4.48), 339 (3.73), 383 (3.59), 415 (3.64).

The crystals obtained by the removal of the solvent from the mother liquor were fractionally recrystallized from methanol to give XIV (20 mg.).

*c) With Three Molar Equivalents of Bromine.*—Into a solution of I (300 mg.) and sodium acetate (820 mg.) in methanol (6 ml.), bromine (960 mg.) in methanol (4 ml.) was stirred while the mixture was being cooled. After additional stirring (3 hr.), the mixture was allowed to stand overnight; the crystals thereby formed were collected and recrystallized from methanol to give XIV (550 mg.) as greenish yellow prisms, m. p. 96.5—97°C.

The crystals obtained by the removal of the solvent from the mother liquor were fractionally recrystallized from methanol to give a small amount of XV.

**The Bromination of 5-Bromo-4-ethyltropolone (X).**—To a solution of X (100 mg.) in methanol (3 ml.), bromine (70 mg.) was added, and the mixture was stirred for 3 hr. The crystals obtained by the addition of water were fractionally recrystallized from petroleum ether to give XIV (40 mg.) as greenish yellow prisms, m. p. 96—97°C; together with the X (40 mg.) was also recovered.

**The Bromination of 7-Bromo-4-ethyltropolone (XII).**—To a solution of XII (100 mg.) in methanol (3 ml.), bromine (70 mg.) was added, and the mixture was stirred for 3 hr. The crystals obtained by the addition of water were recrystallized from

petroleum ether to give XV (60 mg.); m. p. 96—97°C.

**The Bromination of 3, 7-Dibromo-4-ethyltropolone (XV).**—To a solution of XV (100 mg.) in methanol (3 ml.), bromine (60 mg.) was added in the presence of sodium acetate (100 mg.); the mixture was then stirred for 3 hr. with cooling. The crystals obtained by the addition of water were collected and recrystallized from methanol to give XIV (40 mg.), m. p. 96—97°C.

**4-Ethyl-7-iodotropolone (XVIII).**—Into a solution of I (300 mg.) and potassium carbonate (610 mg.) in water (1.5 ml.), a solution of iodine (560 mg.) and potassium iodide (560 mg.) in water (1.5 ml.) was stirred while the mixture was being cooled; the potassium salt separated out. After additional stirring (1 hr.), the excess iodine was destroyed by the addition of sodium sulfite and a yellow potassium salt was collected by filtration. This salt was dissolved in hot water and acidified with 6 N hydrochloric acid; the crystals thereby formed were collected and recrystallized from petroleum ether to give XVIII (490 mg.) as yellow needles, m. p. 76—76.5°C.

Found: C, 38.56; H, 3.38. Calcd. for $C_9H_9O_2I$: C, 39.15; H, 3.28%. $\lambda_{max}^{MeOH}$ (log $\varepsilon$); 230 (4.12), 260 (4.32), 265 (4.33), 340 (3.91), 383 (3.88).

***p*-Tolylazo Compounds of XII, XV and XVIII.**—They were obtained by the treatment described in the experiment with 4-ethyl-5-(*p*-tolylazo)tropolone (IV).

*a) 7-Bromo-4-ethyl-5-(p-tolylazo)tropolone (XVI).*—This was obtained from XII as red needles (from benzene), m. p. 181.5—182°C, in a 78% yield.

Found: C, 55.52; H, 4.24; N, 7.97. Calcd. for $C_{16}H_{15}O_2N_2Br$: C, 55.33; H, 4.32; N, 8.07%.

*b) 3, 7-Dibromo-4-ethyl-5-(p-tolylazo)tropolone (XVII).*—This was obtained from XV as reddish orange needles (from benzene), m. p. 151°C, in an 85% yield.

Found: C, 45.09; H, 3.04; N, 6.61. Calcd. for $C_{16}H_{14}O_2N_2Br_2$: C, 45.06; H, 3.31; N, 6.57%.

*c) 4-Ethyl-7-iodo-5-(p-tolylazo)tropolone (XIX).*—This was obtained from XVIII as dark red needles (from methanol), m. p. 181—182°C, in an 85% yield.

Found: C, 48.14; H, 3.68; N, 7.07. Calcd. for $C_{16}H_{15}O_2N_2I$: C, 48.73; H, 3.81; N, 7.11%.

**5-Hydroxy-3-methyl-2-(*p*-tolyl)-6(2*H*)-cyclohepta[*c*]pyrazolone (XXI).**—To a solution of IV (100 mg.) in ethanol (10 ml.), 6 N hydrochloric acid (0.3 ml.) was added; this mixture was then heated under reflux for 6 hr. The solvent was evaporated, and the residue was recrystallized from ethanol to give XXI (30 mg.) as pale yellow needles, m. p. 202—203°C; this was identified with an authentic specimen[14] by admixture and by a comparison of their infrared spectra.

When this reaction was carried out with the addition of iodine, XXI was obtained in a 50% yield.

The authors wish to express their sincere gratitude to the Sankyo Co., Ltd., which defrayed a part of the expenses of the present work.

*Department of Chemistry*
*Faculty of Science*
*Tohoku University*
*Katahira-cho, Sendai*

# 2-Aryl-5-hydroxy-3-methyl-6(2*H*)-cyclohepta[c]pyrazolones: The Cyclization Products of 5-Arylazo-4-ethyltropolone and Its Related Compounds

By Tetsuo NOZOE, Kahei TAKASE and Katsumi SUZUKI

(Received June 1, 1964)

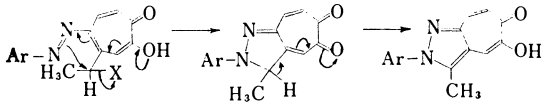
In our laboratory, a process has recently been developed for the preparation of 4-ethyltropolone[1] and 4-(1-hydroxyethyl)tropolone[2] from 4-acetyltropolone (I),[3] and the reactions of these tropolones have been investigated.[1,2] During these studies it has been observed that the 5-arylazo derivatives of these tropolones undergo a facile change upon heating, especially in the presence of a mineral acid; thus, 4-ethyl-5-(*p*-tolylazo)tropolone (II) afforded a pale yellow compound (III) with a m. p. of 203°C when heated in an alcoholic solution in the presence of hydrochloric acid.[1] 4-(1-Hydroxyethyl)-5-(*p*-tolylazo)tropolone (IV) also gave the same product (III) when merely heated over its melting point or when heated in an alcoholic solution in the presence of hydrochloric acid.[2] The present authors have prepared 4-(1-acetamidoethyl)-5-(*p*-tolylazo)-tropolone (V) from 4-acetyltropolone (I) and found that this azo compound also afforded the same product (III) when heated in alcohol. The rather curious behavior of these

1) T. Nozoe, K. Takase and K. Umino, This Bulletin, **38**, 358 (1965).
2) T. Nozoe, K. Takase, K. Shimizu and M. Yasunami, to be published.
3) T. Nozoe, K. Takase and M. Ogata, *Chem. & Ind.*, **1957**, 1070.

azo compounds prompted us to examine the structure of III. The account of the structural elucidation of III will be described herein, together with the record of some reactions of 4-(1-acetamidoethyl)tropolone.

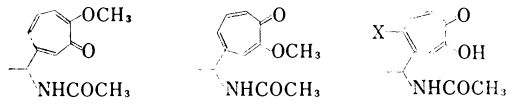
The catalytic reduction of 4-(1-hydroxyiminoethyl)tropolone (VI)[3] in the presence of palladized charcoal gave an amino compound (VII). The acetylation of VII afforded 4-(1-acetamidoethyl)tropolone (VIII), the structure of which was clear from the positive ferric chloride coloration and from the presence of the amide band at 1667 $cm^{-1}$ in its infrared absorption spectrum. The tosylation of the amine (VII) with *p*-toluenesulfonyl chloride also gave the corresponding sulfonamide (IX).

The treatment of VIII with *p*-toluenediazonium chloride gave a *p*-tolylazo compound (V), the position of the azo group being assumed to be at the 5-position by analogy with the other azotropolones.[4] The heating of the azo compound (V) in ethanol gave pale yellow crystals with a m. p. of 203°C, which was found to be identical with the compound (III) obtained earlier from the azo compound (II and IV). The compound (III), whose elemental analysis corresponds to the formula $C_{16}H_{14}O_2N_2$, gives an orange sodium salt, and, in its ultraviolet absorption spectrum, shows a bathochromic shift of the absorption maxima in an alkaline solution, as is shown in Fig. 1. These results indicate that III is an acidic compound. The presence of the $\alpha$-enolone system was suggested by the positive ferric chloride coloration and by the formation of an orange copper chelate, as well as by the presence of $\nu_{OH}$ at 3350 $cm^{-1}$ in its infrared absorption spectrum. No hydroxyl group was observed in the infrared absorption spectra of its acetyl and



X=OH or $NHCOCH_3$ (IIIa) III

Chart 1. The reaction mechanism of the ring closure of the 5-arylazo derivatives of 4-(1-hydroxyethyl)- and 4-(1-acetamidoethyl)tropolone.



XVI$_a$ XVI$_b$ XVII: X=$NH_2$

XVIII: X=Cl

XIX: X=Br

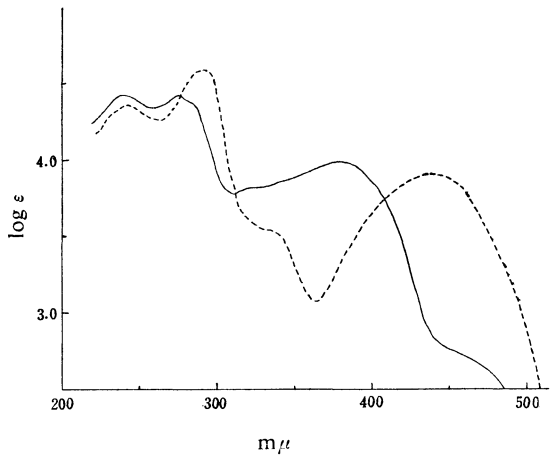



Fig. 1. The ultraviolet absorption of III in methanol (——) and in 0.1 N sodium hydroxide solution (- - -).

tosyl derivatives, which were neutral and lacked the ferric chloride coloration.

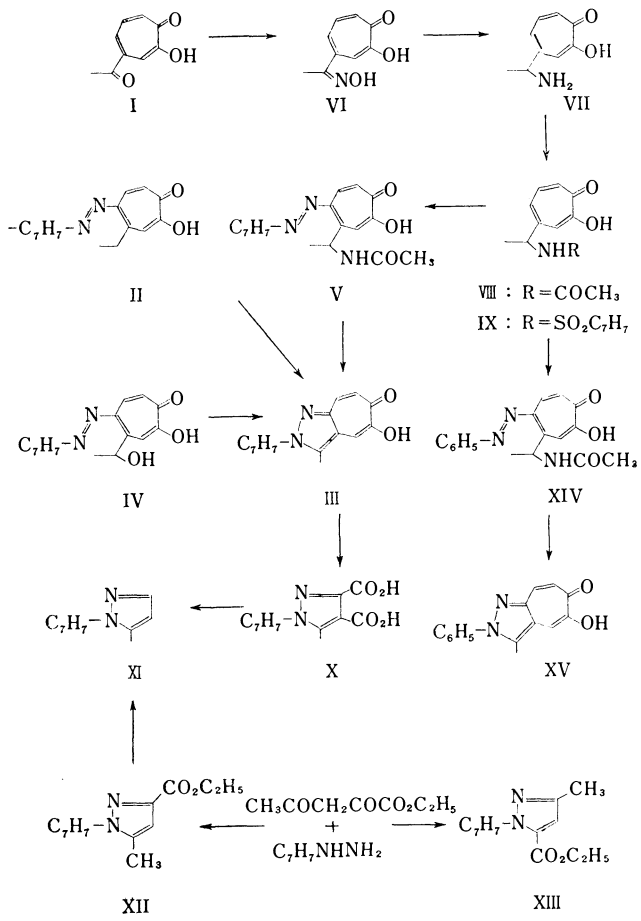
The alkaline permanganate oxidation of III gave a dicarboxylic acid (X). The decarboxylation of X by heating gave an oily substance, which was identified with 5-methyl-1-(*p*-tolyl)-pyrazole (XI)[5] by a direct comparison of their infrared absorption spectra and by an admixture of their picrates. An authentic specimen of XI was synthesized by a modified Finar and Hurlock method[6] as follows: The reaction of ethyl acetopyruvate and *p*-tolylhydrazine gave two isomeric condensation products, ethyl 5-methyl-1-(*p*-tolyl)pyrazole-3-carboxylate (XII) and ethyl 3-methyl-1-(*p*-tolyl)pyrazole-5-carboxylate (XIII). The alkaline hydrolysis of XII, followed by decarboxylation, gave XI. This result shows that the dicarboxylic acid (X) is 5-methyl-1-(*p*-tolyl)pyrazole-3,4-dicarboxylic acid;[5] therefore, the compound (III) contains a pyrazole ring. From the above-mentioned evidence, only one structure, 5-hydroxy-3-methyl-2-(*p*-tolyl)-6(2*H*)-cyclohepta-[c]pyrazolone, is deduced for the compound (III).

4-(1-Acetamidoethyl)-5-phenylazotropolone (XIV), which was obtained by treating VIII with benzenediazonium chloride, also gave a pale yellow compound (XV) when heated in an alcoholic solution. From the elemental analysis, the positive ferric chloride coloration and the ultraviolet absorption spectrum, which are similar to those of III, it seems that the structure of XV is best represented by 5-hydroxy-3-methyl-2-phenyl-6(2*H*)-cyclohepta[c]pyrazolone. The infrared absorption spectrum also supported this structure.

4) T. Nozoe, *Nature*, **167**, 1055 (1951); *Fortschr. Chem. org. Naturstoffe.*, **13**, 233 (1956).

5) C. Bulow and A. Schlesinger, *Ber.*, **33**, 3365 (1900).

6) I. L. Finar and R. J. Hurlock, *J. Chem. Soc.*, **1958**, 3260.




The formation of the cyclohepta[c]pyrazolone derivatives (III and XV) from the azo compounds (V and XIV) is mechanistically conceivable, as Chart 1 shows. The formation of the same product (III) from the azo compound (IV) can also be explained by the same mechanism. This mechanism is apparently different from the mechanism of the formation of III from 4-ethyl-5-(*p*-tolylazo)tropolone (II), in which the inevitable dehydrogenation process accompanies the ring closure.[1] In the present case, the yield of the cyclization product showed no change upon the addition of the oxidant.[1,7] The reaction path, therefore, is the initial elimination of the acetamido or hydroxyl group, followed by the ring closure to afford the diketone (IIIa), which then enolizes to III.

The methylation of the acetamido compound (VIII) with diazomethane gave two isomeric methyl ethers, XVIa and XVIb. The structures of these ethers were determined by an examination of their infrared absorption spectra, in which the characteristic absorptions appeared at 791 $cm^{-1}$ and at 828 $cm^{-1}$ respectively.[8] These ethers are of interest in that they possess partial structures of colchicine and isocolchicine[9] respectively. The catalytic reduction of the azo compound (V) gave 4-(1-acetamidoethyl)-5-aminotropolone (XVII), from which 5-chloro (XVIII) and 5-bromo (XIX) derivatives were prepared by a Sandmeyer reaction.

## Experimental[10]

**4-(1-Aminoethyl)tropolone (VII).**—To a suspension of 4-(1-hydroxyiminoethyl)tropolone (VI) (1.58 g.) in methanol (25 ml.), concentrated hydrochloric acid (5 ml.) was added. The mixture was then shaken with hydrogen, in the presence of 5% palladium on carbon (300 mg.), at room temperature and at atmospheric pressure; after 4 hr., 430 ml. of hydrogen was absorbed. The catalyst was removed, the

7) T. Nozoe, T. Ikemi and T. Ozeki, *Proc. Japan Acad.*, **27**, 110 (1951).

8) 2,4- and 2,6-Disubstituted tropones show the characteristic absorption in the 810—840 $cm^{-1}$ and 770—800 $cm^{-1}$ ranges respectively; T. Nozoe, K. Takase and M. Yasunami, to be published.

9) E. J. Forbes, *Chem. & Ind.*, **1956**, 192.

10) All melting points are uncorrected.

solution was concentrated to a small volume and adjusted to pH 5 with potassium hydroxide solution, and the potassium chloride thereby precipitated was filtered off. The filtrate was adjusted to pH 7, and the crystals thereby formed were collected by filtration and recrystallized from methanol to give the monohydrate of VII (1.35 g.) as yellow needles, m. p. 220°C (decomp.).

Found: C, 59.10; H, 6.86; N, 7.54. Calcd. for $C_9H_{11}O_2N \cdot H_2O$: C, 59.00; H, 7.15; N, 7.65%.
$\lambda_{max}^{MeOH}$ mμ (log ε); 243 (4.39), 335 (3.97), 395 (3.68).

**4-(1-Acetamidoethyl)tropolone (VIII).**—A mixture of VII (8.2 g.) and acetic anhydride (9 ml.) was allowed to stand for 1 hr. at room temperature. Water (9 ml.) was then added, and the crystals thereby formed were collected by filtration to give VIII (5.6 g.), m. p. 156°C. From the filtrate, further crops (2.64 g.) of VIII were obtained by extraction with ethyl acetate. Recrystallization from ethanol gave colorless prisms, m. p. 166°C. VIII is green in water or ethanol and red in chloroform with a ferric chloride solution.

Found: C, 63.83; H, 6.00; N, 6.63. Calcd. for $C_{11}H_{13}O_3N$: C, 63.75; H, 6.32; N, 6.76%.
$\lambda_{max}^{MeOH}$ mμ (log ε); 241 (4.43), 324 (3.89).

**4-[1-(*p*-Toluenesulfonamido)ethyl]tropolone (IX).**—To stirred solution of VII (170 mg.) in a 0.5 N sodidum hydroxide solution (5.5 ml.), *p*-toluenesulfonyl chloride (210 mg.) was added at room temperature. After being stirred for 4 hr., the mixture was acidified with 6 N hydrochloric acid, and the brown gummy material thereby formed was triturated in order to crystallize it. Recrystallization from ethanol gave IX (90 mg.) as colorless prisms, m. p. 176—177°C.

Found: C, 60.18; H, 5.37; N, 4.39. Calcd. for $C_{16}H_{17}O_4NS$: C, 59.69; H, 5.34; N, 4.61%.
$\lambda_{max}^{MeOH}$ mμ (log ε); 230 (4.47), 325—330 (3.88).

**4-(1-Acetamidoethyl)-5-(*p*-tolylazo)tropolone (V).**—To a stirred solution of VIII (2.10 g.) in pyridine (20 ml.), a *p*-toluenediazonium chloride solution prepared from *p*-toluidine (1.10 g.) was added with the mixture was being cooled in an ice bath; orage red crystals were separated out during stirring. After 30 min., water (100 ml.) was added and the crystals were collected by filtration and washed with water to give V (2.90 g.); m. p. 153—155°C. Recrystallization from benzene gave orange red needles, m. p. 167°C (decomp.).

Found: C, 66.13; H, 5.61; N, 12.77. Calcd. for $C_{18}H_{19}O_3N_3$: C, 66.44; H, 5.89; N, 12.97%.
$\lambda_{max}^{MeOH}$ mμ (log ε); 235 (4.33), 291 (3.95), 404 (4.36).

**5-Hydroxy-3-methyl-2-(*p*-tolyl)-6(2*H*)-cyclohepta[c]pyrazolone (III).**—A solution of V (1.00 g.) in ethanol (30 ml.) was heated under reflux for 3 hr. On cooling, III (700 mg.) was obtained as pale yellow needles, m. p. 203°C, which showed no depression on admixture with the specimen obtained from 4-ethyl-5-(*p*-tolylazo)tropolone (II)[1] or 4-(1-hydroxyethyl)-5-(*p*-tolylazo)tropolone (IV).[2] Their infrared spectra were also identical.

Found: C, 71.83; H, 5.26; N, 10.59. Calcd. for $C_{16}H_{14}O_2N_2$: C, 72.16; H, 5.30; N, 10.52%.
$\lambda_{max}^{MeOH}$ mμ (log ε); 239 (4.43), 275 (4.44), 379 (3.99).
$\lambda_{max}^{0.1N\ NaOH}$ mμ (log ε); 242 (4.36), 292 (4.58), 435—440 (3.09).

*Acetate*: Obtained by treatment with acetic anhydride in the presence of sulfuric acid; colorless needles (from ethanol); m. p. 205—206°C.

Found: C, 69.98; H, 4.89; N, 9.35. Calcd. for $C_{18}H_{16}O_3N_2$: C, 70.11; H, 5.23; N, 9.35%.
$\lambda_{max}^{MeOH}$ mμ (log ε); 235 (4.42), 263 (4.47), 335—340 (4.20).

*Tosylate*: Obtained by treatment with *p*-toluenesulfonyl chloride in pyridine; pale yellow prisms (from benzene), m. p. 195—196°C.

Found: C, 66.42; H, 4.82; N, 6.76. Calcd. for $C_{23}H_{20}O_4N_2S$: C, 65.69; H, 4.79; N, 6.66%.

**The Permanganate Oxidation of III.**—To a stirred suspention of III (1.06 g.) in a mixture of a N potassium hydroxide solution of (8 ml.) and water (30 ml.), powdered potassium permanganate was added in small portions at room temperature; 3.2 g. of permanganate was consumed during 3 hr. After decomposing an excess of permanganate by the addition of methanol, manganese dioxide was filtered off and washed with water. The combined filtrate and washing were acidified with 6 N sulfuric acid, and the crystals thereby formed were collected by filtration and recrystallized from aqueous ethanol to give *5-methyl-1-(p-tolyl)pyrazole-3, 4-dicarboxylic acid (X)* (600 mg.) as colorless prisms, m. p. 243°C (decomp.).

Found: C, 59.84; H, 4.38; N, 10.59. Calcd. for $C_{13}H_{12}O_4N_2$: C, 59.99; H, 4.65; N, 10.59%.

**5-Methyl-1-(*p*-tolyl)pyrazole (XI).**—*a) From Ethyl 5-Methyl-1-(p-tolyl)pyrazole-3-carboxylate (XII).*—A mixture of XII (8.0 g.), a 2 N potassium hydroxide solution (25 ml.) and ethanol (15 ml.) was heated under reflux for 30 min. The reaction mixture was concentrated to a small volume and acidified with concentrated hydrochloric acid to give *5-methyl-1-(p-tolyl)pyrazole-3-carboxylic acid.* Recrystallization from aqueous ethanol afforded colorless rods of monohydrate (7.2 g.), m. p. 170°C.

Found: C, 61.88; H, 5.86; N, 12.04. Calcd. for $C_{12}H_{12}O_2N_2 \cdot H_2O$: C, 61.52; H, 6.02; N, 11.96%.

This acid (3.0 g.) was heated at 240—260°C for 10 min., and the oily substance thereby formed was distilled to give XI (1.1 g.) as a colorless oil, b. p. 137°C/5 mmHg, b. p. 272°C, reported[5] b. p. 270—280°C.

Found: C, 76.43; H, 6.93; N, 16.10. Calcd. for $C_{11}H_{12}N_2$: C, 76.71; H, 7.02; N, 16.27%.

*Picrate*: m. p. 121°C, yellow needles (from ethanol).

Found: C, 50.91; H, 3.55; N, 17.61. Calcd. for $C_{17}H_{15}O_7N_5$: C, 50.87; H, 3.77; N, 17.45%.

*b) From 5-Methyl-1-(p-tolyl)pyrazole-3, 4-dicarboxylic Acid (X).*—X (250 mg.) was heated at 250—255°C for 15 min., and the oily substance thereby formed was distilled to give a colorless oil. The infrared spectrum of this oil was identical with that of XI, and the picrate of this oil, m. p. 121°C, showed no depression on admixture with the picrate of XI.

**Ethyl 5-Methyl-1-(*p*-tolyl)pyrazole-3-carboxylate (XII) and Ethyl 3-Methyl-1-(*p*-tolyl)pyrazole-5-carboxylate (XIII).**—To a stirred solution of ethyl

acetopyruvate (28 g.) in glacial acetic acid (45 ml.), a solution of *p*-tolylhydrazine (21.6 g.) in the same solvent (20 ml.) was added at room temperature, and the mixture was heated under reflux for 2 hr. After it had been cooled, the mixture was poured into water (270 ml.) and extracted 4 times with ether, and the combined extract was washed with a 10% sodium carbonate solution (30 ml.×3). The solvent was evaporated, and the residue was fractionally recrystallized from ethanol. The sparingly soluble part gave XII (21.7 g.) as colorless scales, m. p. 77°C.

Found: C, 68.68; H, 6.36; N, 11.54. Calcd. for $C_{14}H_{16}O_2N_2$: C, 68.83; H, 6.60; N, 11.47%.

The more soluble part gave XIII (5.2 g.) as colorless needles, m. p. 65°C.

Found: C, 69.01; H, 6.50; N, 11.40. Calcd. for $C_{14}H_{16}O_2N_2$: C, 68.83; H, 6.60; N, 11.47%.

The heating of XIII with potassium hydroxide in aqueous ethanol gave *3-Methyl-1-(p-tolyl)pyrazole-5-carboxylic acid* as colorless needles, m. p. 203°C (decomp.) (from aqueous ethanol).

Found: C, 66.65; H, 5.59; N, 12.96. Calcd. for $C_{12}H_{12}O_2N_2$: C, 66.61; H, 5.34; N, 12.97%.

**4-(1-Acetamidoethyl)-5-phenylazotropolone (XIV).**—To a stirred solution of VIII (420 mg.) in pyridine (5 ml.), a benzene-diazonium chloride solution prepared from aniline (190 mg.) was added while the mixture was being cooled in an ice bath. After being stirred for 1 hr., the mixture was diluted with water and the crystals thereby formed were collected by filtration and recrystallized from benzene to give XIV (540 mg.) as orange red needles, m. p. 141°C.

Found: C, 66.05; H, 5.46; N, 13.53. Calcd. for $C_{17}H_{17}O_3N_3$: C, 65.58; H, 5.50; N, 13.50%. $\lambda_{max}^{MeOH}$ mμ (log ε); 232 (4.35), 288 (4.03), 392 (4.35).

**5-Hydroxy-3-methyl-2-phenyl-6(2*H*)-cyclohepta[c]pyrazolone (XV).**—A solution of XIV (100 mg.) in ethanol (3 ml.) was heated under reflux for 1.5 hr. and allowed to cool. The crystals thereby formed were recrystallized from ethanol to give XV (50 mg.) as pale yellow prisms, m. p. 230—231°C.

Found: C, 71.26; H, 4.75; N, 10.90. Calcd. for $C_{15}H_{12}O_2N_2$: C, 71.41; H, 4.80; N, 11.11%. $\lambda_{max}^{MeOH}$ mμ (log ε); 241 (4.37), 275 (4.43), 378—381 (3.95).

**The Methylation of VIII.**—To a stirred solution of VIII (560 mg.) in methanol (20 ml.), an ethereal solution of diazomethane was added while the mixture was being cooled in an ice bath; the mixture was then stirred for an additional 3 hr. The evaporation of the solvent left an oily substance, which was dissolved in ethyl acetate and chromatographed through an alumina column. The crystal obtained by evaporation of the solvent from the effluent were fractionallized from ethyl acetate to give *6-(1-acetamidoethyl)-2-methoxytropone (XVIa)* (100 mg.) as colorless prisms, m. p. 153.5°C.

Found: C, 65.08; H, 6.85; N, 6.33. Calcd. for $C_{12}H_{15}O_3N$: C, 65.14; H, 6.83; N, 6.33%. $\lambda_{max}^{MeOH}$ mμ (log ε); 240 (4.41), 322 (3.88).

The more soluble part gave *4-(1-acetamidoethyl)-2-methoxytropone (XVIb)* (90 mg.) as colorless prisms, m. p. 162—163°C.

Found: C, 64.91; H, 6.73; N, 6.23. Calcd. for $C_{12}H_{15}O_3N$: C, 65.14; H, 6.83; N, 6.33%. $\lambda_{max}^{MeOH}$ mμ (log ε); 240 (4.39), 346 (3.87).

**4-(1-Acetamidoethyl)-5-aminotropolone (XVII).**—A suspension of V (1.0 g.) in methanol (15 ml.) was shaken with hydrogen in the presence of platinum oxide (50 mg) at room temperature and at atmospheric pressure; 124 ml. of hydrogen was absorbed. After the removal of the catalyst, the solvent was evaporated and the residue was washed with a small amount of benzene and recrystallized from ethanol to give XVII (590 mg.) as yellow needles, m. p. 203°C (decomp.).

Found: C, 59.60; H, 6.15; N, 12.75. Calcd. for $C_{11}H_{14}O_3N_2$: C, 59.45; H, 6.35; N, 12.60%. $\lambda_{max}^{MeOH}$ mμ (log ε); 239 (4.36), 359 (4.11), 388 (4.10).

**4-(1-Acetamidoethyl)-5-chlorotropolone (XVIII).**—To a stirred solution of XVII (220 mg.) in a mixture of dioxane (1 ml.) and 12% sulfuric acid (1.4 ml.), a solution of sodium nitrite (70 mg.) in water (0.4 ml.) was added while the mixture was being cooled in an ice bath. After being stirred for 30 min., the mixture was poured into a solution of cuprous chloride (250 mg.) in concentrated hydrochloric acid (2 ml.); the stirring was then continued for 4 hr. The reaction mixture was diluted with water (15 ml.) and extracted with chloroform, and the chloroform solution was saturated with hydrogen sulfide gas. The copper sulfide thereby formed was filtered off and the solvent was evaporated to give crystals. Recrystallization from methanol gave XVIII (30 mg.) as yellow microneedles, m. p. 227°C.

Found: C, 55.00; H, 5.11; N, 5.79. Calcd. for $C_{11}H_{12}O_3N_2Cl$: C, 54.66; H, 5.01; N, 5.80%. $\lambda_{max}^{MeOH}$ mμ (log ε); 244 (4.37), 330 (3.99).

**4-(1-Acetamidoethyl)-5-bromotropolone (XIX).**—A diazotized solution of XVII (100 mg.) prepared as in the above experiment was poured into a solution of cuprous bromide (150 mg.) in concentrated hydrobromic acid (1 ml.). After being stirred for 5 hr., the mixture was treated with hydrogen sulfide gas as in the above experiment, and the crystals thereby obtained were recrystallized from methanol to give XIX (30 mg.) as yellow needles, m. p. 201°C (decomp.).

Found: C, 46.99; H, 4.28; N, 4.78. Calcd. for $C_{11}H_{12}O_3NBr$: C, 46.17; H, 4.23; N, 4.90%. $\lambda_{max}^{MeOH}$ mμ (log ε); 244 (4.36), 330 (4.03).

The authors wish to express their deep gratitude to the Sankyo Co., Ltd., which defrayed a part of the expenses for the present work.

*Department of Chemistry*
*Faculty of Science*
*Tohoku University*
*Katahira-cho, Sendai*

# Electron Transfer between Anion Radicals and Neutral Molecules as Revealed by Electron Spin Resonance Spectra

By Akira ISHITANI and Saburo NAGAKURA

(Received June 1, 1964)

Recently the anion radicals of various aromatic molecules have been prepared and their electron spin resonance and electronic absorption spectra extensively studied from both experimental and theoretical points of view. Anion radicals may be expected to possess low ionization potentials and, therefore, to be strong electron donors. This means that they may be able to form Mulliken type charge-transfer complexes with some electron acceptors.[1] Moreover, there may be a possibility that the complexes of this kind will exhibit interesting electric and magnetic properties. With these expectations, we have undertaken to study the interaction of some anion radicals with neutral aromatic molecules, mainly by measuring electron spin resonance spectra.

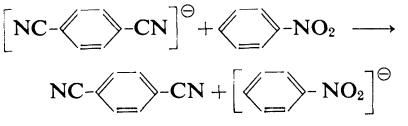
## Experimental

**Materials.** — Commercial pyridine, benzonitrile and nitrobenzene of the G. R. grade were purified by distillation. Commercial *p*-dinitrobenzene, *p*-nitrotoluene, $\alpha$-nitronaphthalene and 9-nitroanthracene of the G. R. grade were purified by repeated recrystallizations from ethanol. Their melting points are 173.5°C, 53.5°C, 61.5°C and 146°C respectively. Commercial terephthalonitrile was purified by repeated sublimations in vacuo; m. p. 222°C. Pyromellitonitrile was synthesized from pyromellitic acid through the following route. Pyromellitimide was obtained by heating ammonium pyromellitate[2] which had been prepared by neutralizing pyromellitic acid with aqueous ammonia. This pyromellitimide was then converted into pyromellitamide by aqueous ammonia. Pyromellitonitrile finally obtained by the dehydration of pyromellitamide was purified by repeated recrystallizations from ethanol. Nitrosobenzene was synthesized by the mild oxidation of phenylhydroxylamine with sodium chromate and purified by recrystallization from ethanol; m. p. 67.5°C. $\beta$-Nitronaphthalene was synthesized from the diazonium sulfate of $\beta$-naphthylamine by the addition of copper(I) oxide. Dimethoxyethane used as a solvent in the present experiment was carefully purified by the method described in a previous paper.[3]

**The Preparation of Anion Radicals and the Measurement of ESR Spectra.** — Anion radicals were prepared by the alkali metal reduction method in vacuo, as has been described in a previous paper.[3] Neutral molecules were added to the anion radical solutions in vacuo by the use of breakable joints. ESR spectra were measured at room temperature with a Hitachi ESR spectrometer model-18 (X band, 100 kc. modulation).

## Results and Discussion

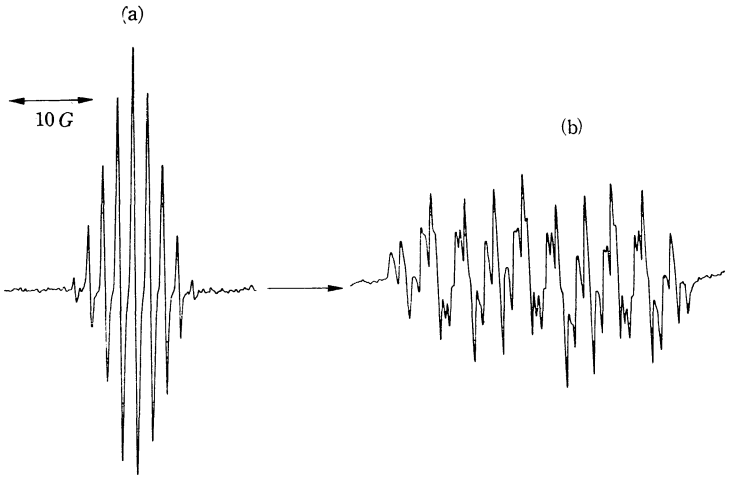
Let us take the nitrobenzene-terephthalonitrile system as an example and explain how the ESR spectrum of an anion radical changes upon the addition of a neutral molecule. First, the terephthalonitrile anion was prepared and the ESR spectrum was measured. The observed hyperfine structure was completely consistent with that obtained by Carrington and Todd[4] (see Fig. 1a). Thereafter, neutral nitrobenzene was added through the breakable joint in vacuo, and the ESR spectrum of the mixed solution was measured. The results are shown in Fig. 1b. The hyperfine structure of the terephthalonitrile anion disappeared and a new pattern, which could safely be assigned to that of the nitrobenzene anion,[5] was observed. At the same time, the color of the solution changed immediately from yellow (the color of the terephthalonitrile anion) to reddish purple (the color of the nitrobenzene anion). This clearly shows that the following electron transfer reaction occurs:



(1)

On the other hand, when neutral terephthalonitrile was added to the solution of the nitrobenzene anion, the hyperfine structure and the color of the solution remained unchanged. The above-mentioned experimental results lead to the conclusion that electron transfer does not occur from the nitrobenzene anion to the terephthalonitrile molecule but takes place only

1) R. S. Mulliken, *J. Am. Chem. Soc.*, **74**, 811 (1952).
2) H. Meyer and K. Steiner, *Monatsch. Chem.*, **35**, 391 (1914).
3) A. Ishitani, K. Kuwata, H. Tsubomura and S. Nagakura, This Bulletin, **36**, 1357 (1963).
4) A. Carrington and P. F. Todd, *Mol. Phys.*, **6**, 161 (1956).
5) R. L. Ward, *J. Chem. Phys.*, **82**, 1296 (1961).




$$(\text{Terephthalonitrile})^- \xrightarrow{\text{Nitrobenzene}} (\text{Nitrobenzene})^-$$

Fig. 1. The change in the ESR spectrum of the terephthalonitrile anion in dimethoxyethane by the addition of nitrobenzene.

in the direction shown in Eq. 1, and that, therefore, nitrobenzene is a stronger electron acceptor than terephthalonitrile is.

Similar experiments were carried out with more than ten systems. Typical examples are shown in Table I. All of them failed to show a tendency toward charge transfer complex formation, but, in all, the complete electron transfer occurred under the present experimental conditions. This may conceivably be due to the fact that the anion radicals are surrounded by polar solvent molecules and are stabilized largely by solvation energies. A similar electron transfer phenomenon from the naphthalene anion radical to anthracene has been reported by Wertz.[6]

TABLE I. ELECTRON TRANSFER BETWEEN SOME AROMATIC ANION RADICALS AND NEUTRAL MOLECULES

(a) $\left[\text{C}_6\text{H}_5\text{NO}\right]^- + \text{C}_6\text{H}_5\text{NO}_2 \rightarrow \text{C}_6\text{H}_5\text{NO} + \left[\text{C}_6\text{H}_5\text{NO}_2\right]^-$

(b) $\left[\text{C}_6\text{H}_5\text{NO}_2\right]^- + \text{C}_6(\text{CN})_6 \rightarrow \text{C}_6\text{H}_5\text{NO}_2 + \left[\text{C}_6(\text{CN})_6\right]^-$

(c) $\left[\text{NC-C}_6\text{H}_4\text{-CN}\right]^- + \text{C}_6(\text{CN})_6 \rightarrow \text{NC-C}_6\text{H}_4\text{-CN} + \left[\text{C}_6(\text{CN})_6\right]^-$

(d) $\left[\text{CH}_3\text{-C}_6\text{H}_4\text{-NO}_2\right]^- + \text{C}_6\text{H}_5\text{NO}_2 \rightarrow \text{CH}_3\text{-C}_6\text{H}_4\text{-NO}_2 + \left[\text{C}_6\text{H}_5\text{NO}_2\right]^-$

(e) $\left[\text{C}_{10}\text{H}_7\text{NO}_2\right]^- + \text{C}_{10}\text{H}_7\text{NO}_2 \rightarrow \text{C}_{10}\text{H}_7\text{NO}_2 + \left[\text{C}_{10}\text{H}_7\text{NO}_2\right]^-$

(f) $\left[\text{C}_6\text{H}_5\text{NO}_2\right]^- + \text{N-C}_6\text{H}_4\text{-NO}_2 \rightarrow \text{C}_6\text{H}_5\text{NO}_2 + \left[\text{N-C}_6\text{H}_4\text{-NO}_2\right]^-$

From the experimental results given in Table I, we could determine the order of the electron accepting abilities of various aromatic molecules. The results are shown below:

1) Pyridine < Benzonitrile < Terephthalonitrile < Nitrosobenzene < Nitrobenzene < Pyromellitonitrile < *m*-Dinitrobenzene
2) *p*-Nitrotoluene < Nitrobenzene
3) Nitrobenzene < 4-Nitropyridine
4) $\alpha$-Nitronaphthalene < $\beta$-Nitronaphthalene
5) Nitrobenzene < $\alpha$-Nitronaphthalene < 9-Nitroanthracene

Series 1 shows the effect of substituent groups upon the electron accepting ability. From this it may be inferred that the substituent groups increase the electron accepting ability of the benzene ring in the following order: $-CN < -NO < -NO_2$. In particular, it is noticeable that terephthalonitrile with two CN groups is a weaker electron acceptor than nitrobenzene or nitrosobenzene.

The order in series 2 can be understood by considering the electron releasing hyperconjugation effect of the methyl group. It is noticeable that the electron moves so completely between the two species, notwithstanding so small a difference in electron affinity,

6) J. Wertz, *Chem. Revs.*, 55, 922 (1955).

as in the system of nitrobenzene and *p*-nitrotoluene. Series 3 indicates that the pyridine nucleus is more electron attracting than is the benzene nucleus.

The results in series 4 can be explained by the fact that the nitro group at the $\beta$-position of the naphthalene nucleus is more sterically free and more strongly conjugated with the nucleus than is the nitro group at the $\alpha$-position. This explanation may be said to be supported by the X-ray crystal analysis data showing that the nitro group of 1,5-dinitronaphthalene is twisted by 67° from the aromatic ring plane,[7] while the group of $\beta$-nitronaphthalene is coplanar with the naphthalene nucleus. Series 5 indicates that the electron affinity increases with an increase in the number of conjugated rings. This result seems to be consistent with the order of the magnitudes of the electron affinities evaluated theoretically with benzene, naphthalene and anthracene.[8]

In this stage of the experiments, we can obtain only qualitative information about the electron affinities of aromatic molecules. However, by measuring the ESR spectra at various temperatures it may be possible to obtain some quantitative knowledge about the equilibrium of the $A^- + B \rightleftarrows A + B^-$ type, as was done by Hausser[9] with the diphenylpicryl hydrazyl-tetramethyl-*p*-phenylenediamine system.

The authors wish to express their thanks to Miss Yasuko Maruyama for her kind help in preparing pyromellitonitrile.

*The Institute for Solid State Physics*
*The University of Tokyo*
*Azabu, Tokyo*

7) J. Trotter, *Acta Cryst.*, **13**, 95 (1960).

8) N. S. Hush and J. A. Pople, *Trans. Faraday Soc.*, **51**, 600 (1955).

9) K. H. Hausser, *Naturwiss.*, **21**, 597 (1959).

# A Study of the Interaction between the Stearic Acid Monolayer and the Calcium Ions by the Radiotracer Method

By Akira MATSUBARA, Ryohei MATUURA and Hideo KIMIZUKA

(Received June 5, 1964)

The composition of the calcium stearate formed on the surface of water through the interaction between the stearic acid monolayer and calcium ions has been studied by several authors.[1-3] Langmuir and Schaefer[1] and Havinga[2] collected the monolayer spread on a solution containing calcium ions and ascertained the composition by means of chemical analysis. Later, Sobotka et al.[3] measured the composition of the built-up film by using radioactive calcium. The composition of the calcium stearate in the film thus measured was discussed by these authors as a function of the pH of the underlying solution.

However, these methods involve the disturbing of the monolayer, i.e., "skimming off" or "building up" the monolayer. It has not yet been confirmed whether or not the composition of the film determined by these methods is the same as that on the surface of water itself. Thus it is necessary to measure the calcium content of the monolayers directly, without disturbing the system. The radiotracer method has, therefore, been used in this study; the state of the monolayer has also been discussed.

## Experimental

**Materials.** — Non-radioactive stearic acid was purified from a commercial sample by fractional distillation through a rectifying column of 65 plates at a reflux ratio of 15, followed by repeated recrystallizations from ethanol. The fraction distilled at 225—225.5°C/10 mmHg was collected. Its melting point was 67.2°C. Radioactive stearic acid, labeled with $^{14}C$, was obtained from Daiichi Pure Chemicals, Tokyo, Japan. Because of the very minute amount of radioactive stearic acid, we followed the method of purification developed by Gaines,[4] which consists of dissolving the sample in reagent grade *n*-hexane and extracting the impurities first with 1 N hydrochloric acid and then

1) I. Langmuir and V. J. Schaefer, *J. Am. Chem. Soc.*, **58**, 284 (1936); **59**, 2400 (1937).
2) E. Havinga, *Rec. trav. chim.*, **71**, 72 (1952).
3) H. Sobotka, M. Demeny and J. D. Chanley, *J. Colloid Sci.*, **13**, 565 (1958).
4) G. L. Gaines, Jr., ibid., **15**, 321 (1960).

with several portions of water. Monolayers of radioactive and non-radioactive stearic acids gave almost the same pressure-area ($\Pi$-$A$) curve, indicating the purity of radioactive stearic acid. The specific activity of this radioactive stearic acid was 2 mc./mmol.

Calcium chloride of a guaranteed grade was purified by recrystallization from its aqueous solution. $^{45}$Ca-labeled calcium chloride, with a specific activity of 275 mc./g., was obtained from the Oak Ridge National Laboratory, Oak Ridge, Tennessee, U. S. A. The $\Pi$-$A$ curve of the stearic acid monolayer on a solution containing radioactive calcium ions was exactly the same as that on a solution containing purified non-radioactive calcium ions.

The pH of the substrate solution was adjusted by sodium carbonate, sodium bicarbonate and hydrochloric acid, all of which were guaranteed reagents. The water used for these studies was redistilled with a quartz still.

**Method.**—The procedure of measuring the surface excess by the radiotracer technique was essentially the same as one described previously.[5] The apparatus used in the present experiment is shown in Fig. 1. A brass trough A, 15×30 cm$^2$ in inner area, was made, and its surface was plated by chromium. An end-window Geiger-Müller tube B, with a mica window 1.5 mg./cm$^2$ thick was supported by a brass cylinder, C, over the surface of the trough. A brass mount D, with a hole 2 cm. in diameter, was placed on the edges of the trough, A, as is shown in Fig. 1, so that the reproducibility of the geometrical condition could be realized with ease. The inside of the trough and the glass barriers, F, were covered by a thin paraffin film and rinsed with water overnight before use. A radioactive calcium chloride solution of a known concentration and pH was then poured into the trough. The surface of the solution was swept by the barriers, a Geiger-Müller tube was put down to the measuring arrangement and the radioactive counting was started. The same procedure was also carried out after the monolayer of stearic acid had been spread on the surface of the solution.

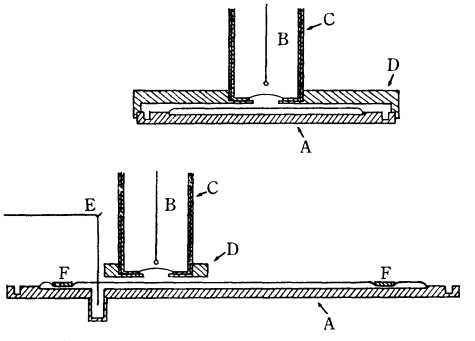



Fig. 1. The measuriug apparatus.

The amount of calcium adsorbed by the stearic acid monolayer, $\Gamma_{Ca}$, in mole per cm$^2$, was calculated according to this equation:

$$\Gamma_{Ca}=\frac{I_m-I}{SA} \qquad (1)$$

where $I$ is the intensity, in count./min., of the radiation due to the substrate without film; $I_m$, the intensity of the radiation due to that with the stearic acid monolayer; $S$, the specific activity, in count./min./mol., of the radioactive calcium in the film and $A$, the surface area, in cm$^2$ within which the radiation is detectable with the Geiger-Müller tube in the present apparatus. Of these quantities, $S$ and $A$ were determined by using a point source, as has been reported already.[5] $\Gamma_{Ca}$ was hence obtained from the measurement of $I$ and $I_m$.

The measurement of the surface pressure of the monolayer was simultaneously carried out by a modified Wilhelmy-type surface balance,[6] E, as is shown in Fig. 1.

All the experiments were carried out at a fixed concentration of calcium ions, 5×10$^{-5}$ mol./l. The temperature of the experiment was ca. 10°C. By preliminary experiments it was confirmed that the variation in temperature from 5 to 15°C modified the $\Pi$-$A$ curves slightly, although the change in the surface excess of calcium with the temperature was within the range of experimental error.

## Results and Discussion

The $\Pi$-$A$ curves of the stearic acid monolayers on the aqueous solutions of calcium

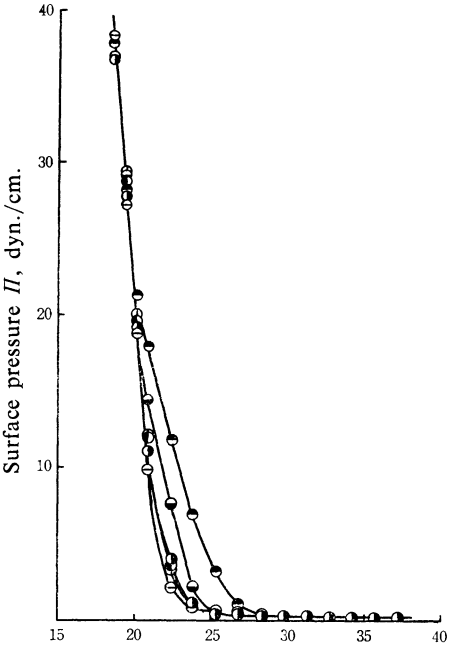



Fig. 2. The $\Pi$-$A$ curves for the stearic acid monolayers on the 5×10$^{-5}$ mol./l. $CaCl_2$ solution at pH=5.90 ◓; 6.51 ◒; 7.05 ◑; 7.95 ◐; 8.77 ⊖ and 9.69 ⓘ.

5) R. Matuura, H. Kimizuka, S. Miyamoto and R. Shimozawa, This Bulletin, 31, 532 (1958).

6) R. Matuura and I. Hayashi, *Memoirs Fac. Sci., Kyushu Univ., C*, 1, 31 (1948).

chloride of varying pH values are shown in Fig. 2. The general features are the same as those measured by Sasaki and Matuura.[7] It is obvious from this figure that the condensation of the stearic acid monolayer by calcium ions increases with the increase in the pH of the substrate. This effect has been explained as being due to the formation of calcium stearate, $Ca(St.)_2$.[8]

In the measurement of the surface excess of calcium, the values of $I$ were almost time-independent. On the other hand, the values of $I_m$ increased at once and fluctuated for about thirty minutes or, occasionally, more after the monolayer had been spread. Then, thirty minutes after spreading, the monolayer was compressed at the rate of 1 cm. of a trough scale/min. and at 3 min. intervals and the surface excess of calcium was measured as a function of the surface concentration of stearic acid. In Fig. 3 the amounts of calcium

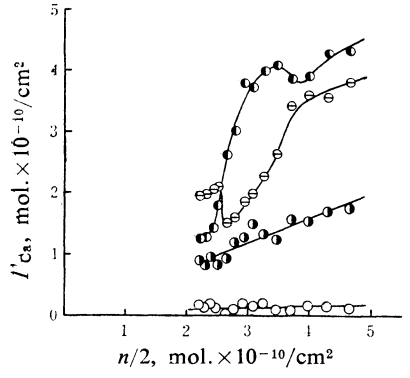



Fig. 3. $\Gamma_{Ca}$ vs. $n/2$ curves at pH=5.30 ○; 6.45 ◑; 8.00 ⊖ and 10.6 ◐.

adsorbed on the stearic acid monolayer, $\Gamma_{Ca}$, are plotted against a half of the surface concentration of the stearyl chain, $n/2$ in mol./cm$^2$, for the typical pH values. If it is assumed that the mole ratio of calcium stearate to stearic acid is constant at a given pH, and, in addition, that the film is homogeneous and compressed uniformly, $\Gamma_{Ca}$ should increase with an increase in the surface concentration of the monolayer along a straight line passing through the point of origin, the slope of the line depending on the pH of the substrate solution. The experimental points in Fig. 3, however, scatter randomly at smaller surface concentrations, especially when the pH of the substrate is high.

The irregularity of the experimental points observed at a smaller surface concentration should be attributed to the inhomogeneity of the monolayer. Harkins et al.[9] has pointed out the existence of a two-phase region by means of surface potential measurements. Some other authors have also confirmed the inhomogeneity of the stearic acid monolayer at low surface pressures by the electron microscopic[10] and radiotracer[11] methods. Unfortunately, these authors have not referred to the large islands of the monolayer. We observed large islands in the present experiment as follows. The $^{14}C$-labeled stearic acid was spread over an area of 37.2Å$^2$/molec. on the surface of a solution containing non-radioactive calcium ions at pH=8.60, and the counting rate as a function of the position was measured by moving the Geiger-Müller tube horizontally and uni-directionally over the surface film. The results are shown in Fig. 4. It may be seen in this figure that the monolayer is localized as large islands, especially around the position where the spreading solution has been dropped. The inhomogeneity of the monolayer found at lower pH values was less pronounced than that at higher pH's. Thus, it is evident that the monolayer consists of concentrated and dilute regions. As the monolayer is compressed, the area of the dilute region decreases until, finally, the monolayer becomes a homogeneous one composed of closely-packed molecules. The surface pressure increases suddenly from this point.

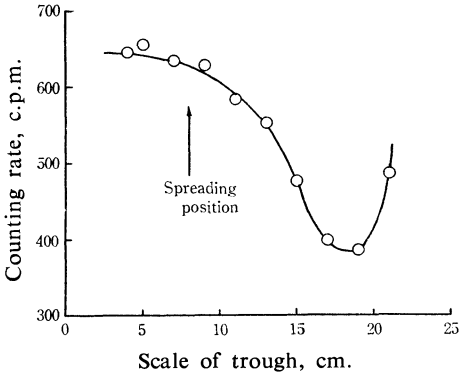



Fig. 4. The radiation from the various position of the $C^{14}$-labeled stearic acid monolayer at $A$=37.2 Å$^2$/molec. on the $5\times10^{-5}$ mol./l. $CaCl_2$ solution at pH=8.60. The measurement was carried out 30 min. after spreading.

7) T. Sasaki and R. Matuura, This Bulletin, **24**, 274 (1951).
8) W. D. Harkins and R. J. Myers, *Nature*, **139**, 367 (1937); W. D. Harkins and E. Boyd, *J. Phys. Chem.*, **45**, 20 (1941).
9) W. D. Harkins and E. K. Fischer, *J. Chem. Phys.*, **1**, 852 (1933).
10) H. E. Ries, Jr., and W. A. Kimball, *Nature*, **181**, 901 (1958); H. E. Ries, Jr., and D. C. Walker, *J. Colloid Sci.*, **16**, 361 (1961).
11) J. R. Ryan and J. W. Sheppard, *J. Phys. Chem.*, **59**, 1181 (1955); G. L. Gaines, Jr., *J. Colloid Sci.*, **15**, 321 (1960).

From these facts it is clear that the surface excess at each limiting area should be taken into account in determining the true composition of the film. At this area the fraction of the stearyl chain neutralized by, the calcium in the monolayer, $\Phi_{Ca}$ is given by:

$$\Phi_{Ca}=\frac{\Gamma_{Ca}}{n/2} \tag{2}$$

The calculated values of $\Phi_{Ca}$ are plotted against the pH of the substrate solution in Fig. 5. The results obtained by Langmuir and Schaefer[1] and Sobotka et al.[2] are also shown in this figure. The present result is similar to that obtained by Sobotka et al. with regard to the pH range where $\Phi_{Ca}$ sharply changes. It may also be seen in this figure that the curve is shifted to the alkaline side as compared to the dissociation curve of fatty acids. Such a kind of shift has frequently been observed in surface chemical phenomena[12] and has been explained there by regarding the pH at the interface as being lower than that in the bulk of the solution.

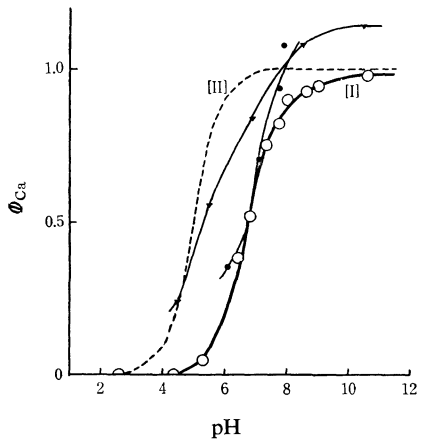



Fig. 5. $\Phi_{Ca}$ vs. pH curves. ○ by the present experiment; ▼ by Langmuir and Schaefer; ● by Sobotka et al. The broken line [II] represents the dissociation curve in bulk for fatty acids.

The monolayer of calcium stearate condenses more than that of stearic acid. Furthermore, it has been pointed out already that the more the formation of calcium stearate increases, the more easily the film forms islands, and even over a large area the molecules in these islands are in a closely-packed state. These facts clearly suggest that the cohesive force between calcium stearate molecules is stronger than that between stearic acid molecules. Hence, the energy of the mixing of stearic acid molecules with calcium stearate molecules in the monolayer should not be zero.

For the following relation:

$$2HSt.+Ca^{2+}=Ca(St.)_2+2H^+$$

$$a_{Ca^{2+}}/a_{H^+}^2=Ka_{Ca(St.)_2}/a_{HSt.}^2 \tag{3}$$

where $K$ is the equilibrium constant and $a$'s are the activities. If this monolayer is assumed to be a mixture not athermal, $a_{Ca(St.)_2}$ and $a_{HSt.}$ are represented by:

$$a_{Ca(St.)_2}=\Phi_{Ca}\exp\{2w(1-\Phi_{Ca})^2\} \tag{4}$$

$$a_{HSt.}=(1-\Phi_{Ca})\exp(w\Phi_{Ca}^2) \tag{5}$$

where $w$ is the interchange energy. Then, by substituting Eqs. 4 and 5 into Eq. 3 the following equation is obtained:

$$a_{Ca^{2+}}/a_{H^+}^2=K'\{\Phi_{Ca}/(1-\Phi_{Ca})^2\}\exp(-4w\Phi_{Ca}) \tag{6}$$

where $K'$ is a constant. For an athermal mixture in which $w$ is equal to zero, the following equation is obtained:

$$a_{Ca^{2+}}/a_{H^+}^2=K'\Phi_{Ca}/(1-\Phi_{Ca})^2 \tag{7}$$

According to Eq. 6, if $a_{Ca^{2+}}$ is constant, $\log\{(1-\Phi_{Ca})^2/a_{H^+}^2\Phi_{Ca}\}$ must be linear against $\Phi_{Ca}$ and, according to Eq. 7, $\log\{\Phi_{Ca}/(1-\Phi_{Ca})^2\}$ must be linear against pH. The former relation was confirmed by the present experimental data as Fig. 6 shows, although the latter one was not confirmed.

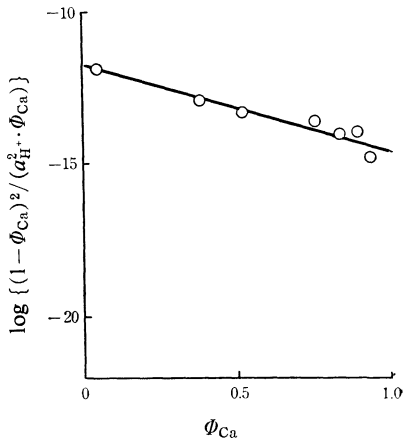



Fig. 6. The test of Eq. 6.

## Summary

Direct measurement by the radiotracer method has been carried out in order to determine the surface excess of calcium on the stearic acid monolayer. It did not provoke any disturbance in the monolayer, such as "skimming off" or "building up". At higher pH values the stearic acid monolayer spread

12) R. A. Peters, *Proc. Roy. Soc.*, **A133**, 140 (1931); J. F. Danielli, ibid., **B122**, 155 (1937), etc.

on a calcium chloride solution shows a very remarkable inhomogeneity. It has been pointed out that this inhomogeneity must be taken into consideration in determining the composition of the monolayer.

The mixed monolayer of stearic acid and calcium stearate satisfies the equation derived by assuming this monolayer to be a mixture not athermal.

*Department of Chemistry*
*Faculty of Science*
*Kyushu University*
*Fukuoka*

# The Micelle Formation of Some Alkyl Sulfates in a Dioxane-Water Mixture

By Keishiro SHIRAHAMA and Ryohei MATUURA

(Received August 24, 1964)

The formation of the micelles of surfactants in aqueous solutions has been known to be affected by various kinds of additives. The effect of added salts has been fully studied by many investigators. As for organic additives, Shinoda[1] and Ooshika[2] showed the decrease in the critical micelle concentration (CMC) of surfactants which resulted when some alcohols were added, correlating it with the number of carbon atoms in an alcohol molecule and in a surfactant molecule. The addition of hydrocarbons also depresses the CMC.[3] However, such substances as lower alcohols, acetone and ethylene glycol are known to increase the CMC.[3-5] Flockhart[4] suggested that the increase is due to the increasing "solvent power" of an ethanol-water mixture. Mukerjee[6] reported the increase in the CMC of dodecylpyridinium iodide in a urea-water mixture and pointed out that this probably results from the urea breaking the "iceberg" structure around the nonpolar part of the surfactant molecule. However, no quantitative explanation of any kind has yet been given of the factors that increase the CMC.

Dioxane is completely miscible with water, just as lower alcohols are, and varies the dielectric constant of its aqueous solution considerably. Therefore, it would be interesting to know how these specific characters of a dioxane-water mixture affect the solutional behavior of surfactants. In the present paper we will report the CMC's of sodium dodecyl sulfate (SDS), sodium tetradecyl sulfate (STS) and sodium hexadecyl sulfate (SHS) in a dioxane-water mixture, and a theoretical consideration will be given to the change in CMC by adding dioxane to aqueous solutions of these surfactants.

## Experimental

**Materials.**—Sodium alkyl sulfates were synthesized from corresponding pure long chain alcohols (obtained by fractional distillation) and sulfuric acid by the method reported earlier.[7] They were purified by repeated recrystallization from butanol and water, and finally extracted by ether for more than 40 hr. Their purity was checked by elementary analysis and surface tension measurements. Dioxane was distilled after refluxing it for more than 8 hr. on metallic sodium. Water was twice distilled.

**Method.**—The CMC's were determined by the electric conductivity method. Solubilities were determined from the weight of the solid deposited by drying up a known amount of a saturated surfactant solution obtained by the mechanical shaking of the solution in the presence of a solid phase for more than 8 hr. at a constant temperature and then filtering it through a glass filter.[8] The titration analysis using bromphenol blue was also used to check the solubilities. The results of the two methods agreed well with each other.

## Results and Discussion

The CMC, determined from a break point on the equivalent conductivity vs. square root of molar concentration curves, is plotted against the concentration of dioxane in the

1) K. Shinoda, This Bulletin, 26, 101 (1953).
2) Y. Ooshika, *J. Colloid Sci.*, 9, 254 (1954).
3) W. D. Harkins, R. Mittelman and M. L. Corrin, *J. Phys. & Colloid Chem.*, 53, 1350 (1949).
4) B. D. Flockhart, *J. Colloid Sci.*, 12, 557 (1957).
5) A. W. Ralston and D. N. Eggenberger, *J. Phys. & Colloid Chem.*, 52, 1494 (1948).
6) P. Mukerjee and A. Ray, *J. Phys. Chem.*, 67, 190 (1963).
7) R. Matuura, H. Kimizuka, S. Miyamoto and R. Shimozawa, This Bulletin, 31, 532 (1958).
8) S. Miyamoto, ibid. 33, 371 (1960).

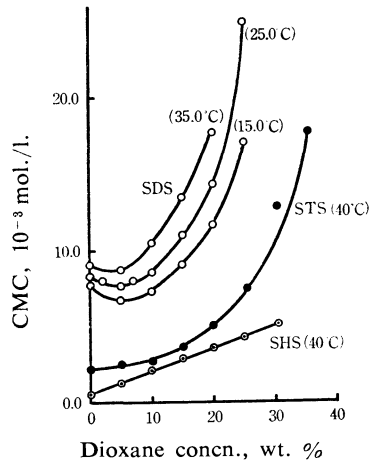



Fig. 1. The CMC of sodium alkyl sulfates (SDS, STS and SHS) as a function of dioxane concentration.

solvent in Fig. 1. No maximum was found around CMC on the conductivity curve at any dioxane concentration, but the break point became obscure as the dioxane concentration increased and eventually faded out. The CMC could not be detected in the region of dioxane more concentrated than that shown in Fig. 1. It should be noted that the CMC of SDS shows a slight minimum and then increases markedly, while that of STS and SHS increases monotonically, even linearly in the case of SHS. The CMC of SDS increases as the temperature rises at any dioxane concentration.

The results may be discussed from two points of view.

**The Solubilization of Dioxane.**—In spite of a strong affinity with water, dioxane is considered to be solubilized partly in the micelle of the surfactant, as in the case of alcohols, resulting in a lowering of the CMC. Shinoda[1] derived an equation which expresses the lowering of the CMC of soap solutions resulting from the solubilization of alcohols. The equation is as follows:

$$\ln(-\mathrm{dCMC}/\mathrm{d}x) = -0.64\,mw/kT + m'w/kT + \text{const.} \qquad (1)$$

where $x$ is the concentration of alcohols, $m$ and $m'$ are the number of carbon atoms in soap and alcohol molecules respectively, and $w$ is the free energy change per methylene group when transferred from water into the micelle phase. Judging from the assumptions included in Eq. 1, it is not unreasonable to apply the same type of equation to the alkyl sulfates-water-dioxane system, which may be expressed as:

$$\ln(-\mathrm{dCMC}/\mathrm{d}x) = -gmw/kT + \text{const.} \qquad (2)$$

where $g$ is a constant (calculated as 0.68) for homologues of sodium alkyl sulfates. Equation 2 means that $-\mathrm{dCMC}/\mathrm{d}x$ decreases as $m$ increases. This effect of lowering the CMC probably competes with a solvent effect, i.e., the effect of raising the CMC, which increases with an increase in the dioxane concentration. The details of this solven effect will be referred to later. It is because of these two compensating effects that the CMC vs. dioxane concentration curve for SDS passes through a minimum. In the case of STS and SHS, the value of $-\mathrm{dCMC}/\mathrm{d}x$ is not so large as to show a minimum on the CMC vs. dioxane concentration curve, even at the lower concentration of dioxane. Indeed, we could determine the unknown constant by substituting the value of $-\mathrm{dCMC}/\mathrm{d}x$ for SDS into Eq. 2 and in turn obtain the values for STS and SHS of $0.386\times10^{-3}$ and $0.089\times10^{-3}$ respectively. These are quite small compared with the $1.72\times10^{-3}$ for SDS.

In order to compare the CMC-lowering effect of dioxane on SDS with that of some lower alcohols, $\log(-\mathrm{dCMC}/\mathrm{d}x)$ is plotted against the number of carbon atoms in an alcohol molecule, and the value of $\log(-\mathrm{dCMC}/\mathrm{d}x)$ for dioxane is placed on this plot, as Fig. 2* shows. We see from this figure that dioxane corresponds, with regard to the CMC-lowering effect, to "an alcohol with one and a half carbon atoms."

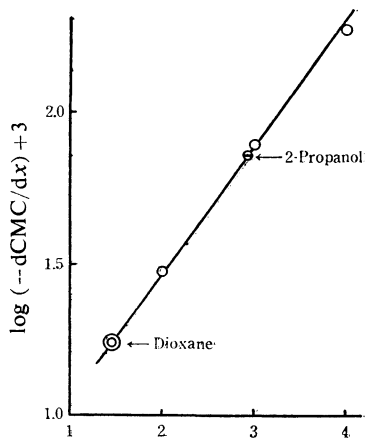



Fig. 2. log $(-\mathrm{dCMC}/\mathrm{d}x)$ vs. number of carbon atoms in an alcohol molecule. The points for dioxane and 2-propanol were placed in order to obtain corresponding number of carbon atoms of straight chain alcohols.

* The data in Fig. 2 for ethanol and propanol were taken from Flockhart's paper (Ref. 4 and B. D. Flockhart and A. R. Ubbelohde, *J. Colloid Sci.*, 8, 428 (1953)) and those for butanol, from Tomoto's (unpublished).

**The Solvent Power of the Dioxane-Water Mixture.**—In the micellar solution the chemical potential of surfactant molecules in the bulk solution is equal to that in the micelle phase. Therefore,

$$\mu_s^\circ + 2RT\ln C = \mu_m^\circ + RT\ln Xf \qquad (3)$$

where $\mu_s^\circ$ and $\mu_m^\circ$ are the standard chemical potential of the surfactant in the bulk solution and that in the micelle phase respectively; $C$ is the CMC, and $X$ and $f$ are, respectively, the mole fraction and the activity coefficient of surfactant in the mixed micelle, both of which become unity when the solvent is pure water. Hereafter, the subscript $x$ refers to the dioxane concentration in the solvent and 0, to pure water.

Then, from Eq. 3;

$$2RT\ln C_x = -(\mu_{sx}^\circ - \mu_m^\circ) + RT\ln X + RT\ln f \qquad (4)$$

Equation 4 becomes simpler, when no solubilized substance is present, as follows:

$$2RT\ln C_0 = -(\mu_{s0}^\circ - \mu_m^\circ) \qquad (5)$$

Subtracting Eq. 5 from Eq. 4 we obtain:

$$2RT\ln(C_x/C_0) = -(\mu_{sx}^\circ - \mu_{s0}^\circ) + RT\ln X + RT\ln f \qquad (6)$$

Equation 6 is quite a general expression for the solvent effect on the micelle formation. Shinoda[1] and Ooshika[2] explained the CMC-lowering effect of alcohols in terms of the entropy of mixing and the reduction of charge density of micelles on adding alcohols, factors which correspond to the second and the third term of the right hand side of Eq. 6 respectively. Namely, in their theory the effect due to the first term is neglected.

In order to evaluate $\mu_{sx}^\circ - \mu_{s0}^\circ$, which is often called the free energy of transfer, solubility measurements are employed. For a 1:1 electrolyte the free energy of transfer, $\Delta F_{tr}$, is correlated with the solubility as:

$$\Delta F_{tr} = \mu_{sx}^\circ - \mu_{s0}^\circ = -2RT\ln(a_x/a_0) \qquad (7)$$

where $a_x$ and $a_0$ are activities of the saturated solution of the electrolyte in mixed and pure solvents respectively. Here, in the case of a micellar solution, we assume that a single surfactant ion in the presence of micelle behaves very much like a surfactant ion in the presence of a solid phase just below the Krafft point. For SHS we see, as has already been stated, that the CMC-lowering effect, and accordingly, the solubilization of dioxane in surfactant micelles, is so small as to be neglected and that only the solvent effect should be considered. We are concerned primarily with this case. Then, combining Eq. 6 with Eq. 7:

$$\Delta F_{tr} = -2RT\ln(a_x/a_0) = -2RT\ln(C_x/C_0) \qquad (8)$$

Taking the accuracy of measurement into account, we can safely use the solubility in place of the activity. The solubility of SHS in a dioxane-water mixture is plotted against the concentration of dioxane at 20, 25 and 30°C in Fig. 3. The result of the numerical calculations of the free energy of transfer from pure water to 20% dioxane-water using (a) solubility data and (b) CMC data is shown in Table I as an example. The rather good agreement between the values from (a) and (b) suggests that the assumptions made above are correct.

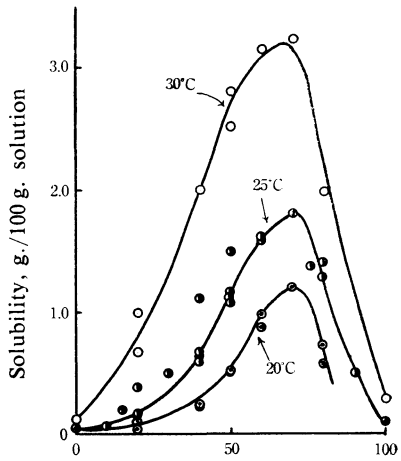



Fig. 3. Solubility of SHS in dioxane-water mixture at 20.0, 25.0 and 30.0°C.

Table I. The free energy of transfer for SHS from pure water to a 20% dioxane-water mixture

| Dioxane % | (a) Solubility g./100g. solvent | | (b) CMC mmol./l. |
|---|---|---|---|
| | 25°C | 30°C | 40°C |
| 0.0 | 0.027 | 0.117 | 0.52 |
| 20.0 | 0.15 | 0.672 | 3.54 |
| $-\Delta F_{tr}$ kcal./mol. | 2.23 | 2.30 | 2.58 |

Now let us try to represent $\Delta F_{tr}$ as an explicit function of the dioxane concentration. In the process of solution an electrolyte experiences various kinds of energy changes, among which the factors that affect the unitary term are given by:

$$\mu_{sx}^\circ = K_1/D + K_2 \qquad (9)$$

where $K_1$ and $K_2$ are constants, and $D$ is the

dielectric constant of the solvent.[9] Equation 9 means that the unitary term can be divided into two parts, i.e., one dependent on, and one independent of, the dielectric constant of the solvent. In fact, for simple inorganic electrolytes the logarithm of solubility is nearly linear against $1/D$ (Born's equation). However, in the case of an amphipathic compound like SHS, the solubility increases at first and then decreases with the dioxane concentration, as is shown in Fig. 3. This suggests that an appreciable hydrophobic contribution must be included in the $K_2$ in Eq. 9. Thus, we should rewrite Eq. 9 as:

$$\mu_{sx}^{\circ} = K/D + L + M \tag{10}$$

where $K$ is a constant, dependent on the geometry of ions; $L$ is a term representing hydrophobic contributions, and $M$ is a constant independent of the nature of the solvent.

In order to express $L$ as a function of the dioxane concentration, we may tentatively utilize the regular solution theory of Hildebrand.[10] In a regular ternary solution the partial molar heat of mixing for component 1 (here the surfactant), $\overline{E}_m$, is expressed as:

$$\overline{E}_m = V_1(\delta_1 - \delta_0)^2\phi_0^2 \tag{11}$$

where $V_1$ is the molar volume and $\delta_1$ is the solubility parameter, each for component 1. $\phi_0$ and $\delta_0$ are given by:

$$\phi_0 = \phi_2 + \phi_3, \quad \delta_0 = \frac{\delta_2\phi_2 + \delta_3\phi_3}{\phi_2 + \phi_3}$$

where the $\phi$'s and $\delta$'s are the volume fractions and solubility parameters respectively, each for the subscript component. When component 1 is extremely dilute, Eq. 11 becomes:

$$\overline{E}_m = V_1\{(\delta_1 - \delta_2) - (\delta_3 - \delta_2)\phi_3\}^2 \tag{12}$$

Neglecting a slight volume contraction on mixing, we can substitute $\phi_3$ for $x$, since the specific gravity of dioxane is about 1.03 at 25°C. Then Eq. 12 may be put into the following form:

$$L(x) = L_0(1 - rx)^2 \tag{13}$$

where $L_0$ is a hydrophobic contribution in pure water and $r$ is a constant correlating with the solubility parameters. $L_0$ may be approximated by the free energy of transfer for hexadecane from water to pure hexadecane, which can be obtained by extrapolating published data for some lower alkanes[11] (Fig. 4). The value is 14.5 kcal./mol.

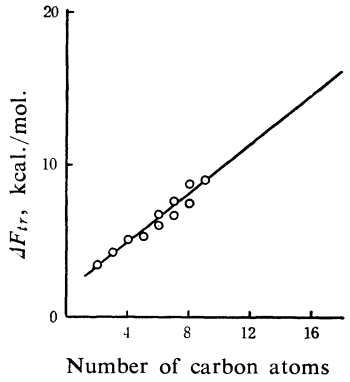



Fig. 4. Free energy of transfer ($\Delta F_{tr}$) for some alkanes from pure liquid to water.

The dielectric constant of a dioxane-water mixture is a nearly linear function of the weight fraction of dioxane, which is expressed empirically as follows:[12]

$$D(x) = 78.6(1 - 0.975\,x) \tag{14}$$

Combining Eqs. 13 and 14 with Eq. 10, we obtain:

$$\mu_{sx}^{\circ} = K/78.6(1 - 0.975\,x) + 14.5(1 - rx)^2 + M \tag{15}$$

Then we have:

$$\Delta F_{tr} = \mu_{sx}^{\circ} - \mu_{s0}^{\circ} = (K/78.6)\{1/(1 - 0.975x) - 1\} + 14.5\{(1 - r\,x)^2 - 1\} \tag{16}$$

The unknown parameters, $K$ and $r$, could be determined by using the data of $\Delta F_{tr}$ from pure water to 20% and 40% dioxane-water mixtures. The values found were $K = 2.1 \times 10^2$ kcal. and $r = 0.61$. Thus, finally we obtain:

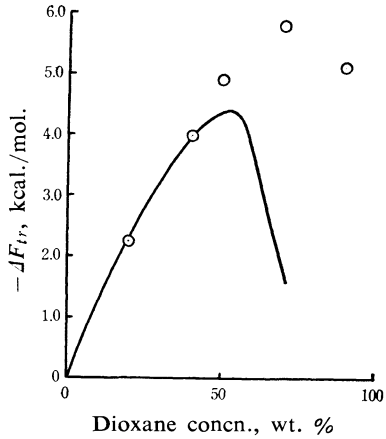



Fig. 5. Comparison of $\Delta F_{tr}$ from solubility data with that from Eq. 17 (solid line) at 25°C.

9) R. W. Gurney, "Ionic Processes in Solution," McGraw-Hill, New York (1953).
10) J. H. Hildebrand and R. L. Scott, "The Solubility of Non-electrolytes," Reinhold, New York (1950), p. 198.
11) G. Nemethy and H. A. Scheraga, *J. Chem. Phys.*, **36**, 3401 (1962).
12) J. B. Hasted, G. H. Haggis and P. Hutton, *Trans. Faraday Soc.*, **47**, 577 (1951).

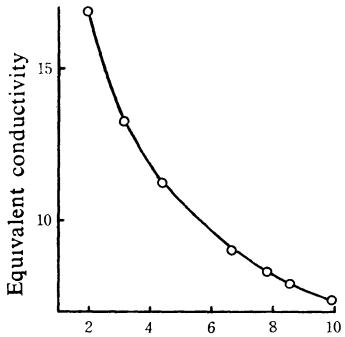



Fig. 6. Equivalent conductivity of SDS in an 80% dioxane-water mixture at 25.0°C.

$$\Delta F_{tr} = (2.1 \times 10^2/78.6)\{1/(1-0.975x) - 1\} + 14.5\{(1-0.61x)^2 - 1\} \quad (17)$$

In Fig. 5 the experimental value of $\Delta F_{tr}$ obtained from the solubility data is compared with the value calculated by using Eq. 17. The agreement is as expected in the dioxane concentration region of less than 50 per cent. Over 50 per cent the experimental values are higher than the theoretical. This may be caused by several factors, one of which is the imperfect dissociation effect. For example, as is shown in Fig. 6, the equivalent conductivity vs. the square root of concentration for SDS in an 80% dioxane-water mixed solvent gives a curved line, while there should be a straight line in a solvent with a higher dielectric constant. The same behavior is expected for SHS. This is probably caused by the imperfect dissociation of the surfactant molecules in a solvent with a low dielectric constant, leading to the diminution of coefficient 2 of Eq. 8 towards unity. Therefore, the effect of imperfect dissociation should reduce the experimental value of $-\Delta F_{tr}$ leading to a better agreement with the predicted value. Another factor which is considered to cause the discrepancy between the theoretical and the experimental values of $\Delta F_{tr}$ in the higher concentration region of dioxane is the effect of selective solvation.

The values of CMC can now be calculated from $\Delta F_{tr}$ of Eq. 17 for each dioxane concentration by using Eq. 8. In Fig. 7 the calculated values of CMC are compared with the observed. For SHS solutions the agreement is satisfactory. For STS, especially for SDS solutions, the same result can not be expected, since in these cases the CMC-lowering effect of dioxane, i. e., the solubilization of dioxane by the surfactant micelles, is not negligible. When the dioxane concentration is large, the formation of the micelles of sodium alkyl

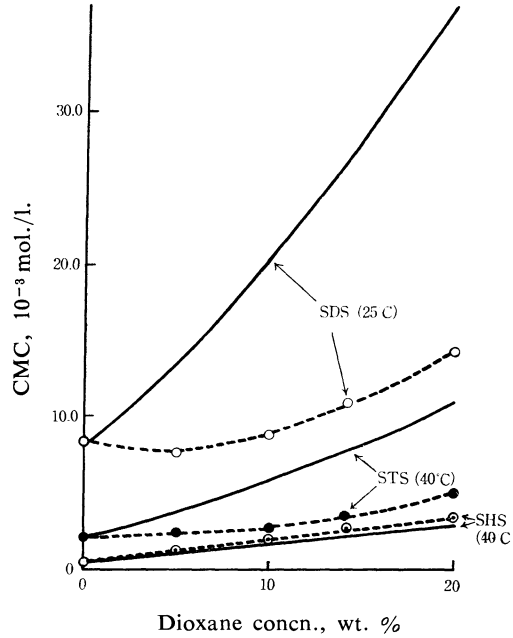



Fig. 7. Comparison of CMC values of sodium alkyl sulfates (SDS, STS and SHS) in dioxane-water mixture with those calculated by using Eq. 17 (solid line).

sulfates is not observable, so the comparison of the theoretical with the experimental values of CMC becomes impossible. However, from the standpoint of the hydrophobic contribution of Eq. 13, we can confirm that the present theory of the solvent power of a dioxane-water mixture is reasonable. For example, in the 50% dioxane solution the calculated value of the hydrophobic contribution is 7.0 kcal., which corresponds to the value of hexane on the plot in Fig. 4. The micelle formation of polar-nonpolar compounds with six carbon atoms has not been believed to be appreciable in an aqueous solution. This corresponds to the fact that the surfactants used in the present study do not seem to form micelles in 50% or more concentrated dioxane-water mixtures, as has been shown in these experiments.

## Summary

The CMC values of three sodium alkyl sulfates with the number of carbon atoms 12, 14 and 16 in a dioxane-water mixture have been measured. The CMC-lowering effect of dioxane, especially appreciable in the case of sodium dodecyl sulfate, has been explained in terms of Shinoda's equation. The CMC-raising effect of dioxane, which is the main effect in the case of sodium hexadecyl sulfate, has been explained by the decrease in the standard chemical potential, i. e., the free energy

of transfer, $\Delta F_{tr}$, of the surfactant. An equation has been derived which expresses $\Delta F_{tr}$ as a function of the dioxane concentration by applying Born's equation and Hildebrand's regular solution theory.

*Department of Chemistry*
*Faculty of Science*
*Kyushu University*
*Hakozaki, Fukuoka*

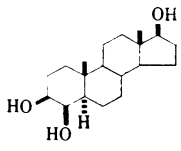
# The Preparation of 5α-Androstane-3β,4α,17β-triol through a Hydroboration Reaction[1]

By Hisao NAKATA

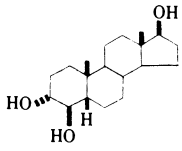
(Received June 29, 1964)

Although the syntheses of a number of androgenic steroids have been reported, only two androstane-3,4,17-triols have been described in the literature. Thus, 5α-androstane-3β,4β,17β-triol (I) was obtained by the catalytic reduction[2] of androst-5-ene-3β,4β,17β-triol, which, in turn, was prepared from androst-5-ene-3β,17β-diol either by direct oxidation with selenium dioxide[2,3] or by the treatment of its dibromo derivatives with bases.[4,5] An isomeric 5β-androstane-3α,4β,17β-triol (II) was prepared[6] by the reduction of 4β,5-epoxy-5β-androstan-17β-ol-3-one 17-acetate with lithium aluminum hydride.

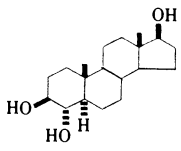
In connection with other steroid studies,[7] we have had occasion to synthesize another isomer of the triol from easily-available starting materials; this paper will deal with the preparation and configurational assignment of the previously unknown 5α-androstane-3β,4α,17β-triol (III).




(I)




(II)




(III)

When testosterone benzoate (IV) was treated with sodium borohydride in methanol, the reduction of the carbonyl group readily took place and androst-4-ene-3β,17β-diol 17-benzoate (V) was obtained in a fairly good yield. The configuration of the 3-hydroxyl group is assigned as such on the basis of the steric course of similar reactions.[8-16] The assignment was confirmed by the fact that, after the benzoate group had been removed by saponification, the product was identical with the known androst-4-ene-3β,17β-diol (VI).[17] A small amount of an isomeric alcohol was also isolated from the reaction mixture. This alcohol is probably androst-4-ene-3α,17β-diol 17-benzoate (VII).

The introduction of an oxygen function at $C_4$ of the steroid nucleus has been accomplished in many ways,[18,19] but the application of the recently-reported hydroboration reaction[20-22] seems most promising because the reaction usually proceeds in a highly stereospecific manner and gives an excellent yield. Thus, the hydroboration of the allylic alcohol (V) yielded a triol monobenzoate as the sole product. Since it is well-established that the

1) This work was initiated at the Department of Medicine, C. Roswell Park Memorial Institute, Buffalo, N. Y., and completed at the Chemical Institute, Nagoya University.

2) L. Ruzicka and P. A. Plattner, *Helv. Chim. Acta*, **20**, 809 (1939).

3) R. E. Marker, H. M. Crooks, Jr., and E. L. Wittbecker, *J. Am. Chem. Soc.*, **63**, 777 (1941).

4) M. Hosoi, *J. Pharm. Soc. Japan*, **67**, 129 (1947).

5) M. Hosoi, Japanese Pat. 177658, (1949).

6) B. Camerino and D. Cattapan, *Farmaco (Pavia) Ed. Sci.*, **13**, 39 (1958); *Chem. Abstr.*, **52**, 13767 (1958).

7) H. Nakata, *Tetrahedron*, **19**, 1959 (1963).

8) W. G. Dauben, R. A. Micheli and J. F. Eastham, *J. Am. Chem. Soc.*, **74**, 3852 (1952).

9) W. W. Zorbach, ibid., **75**, 6344 (1953).

10) M. Gut, *J. Org. Chem.*, **21**, 1327 (1956).

11) F. Unger, M. Gut and R. I. Dorfman, *J. Biol. Chem.*, **224**, 191 (1957).

12) O. H. Wheeler and J. L. Mateos, *Can. J. Chem.*, **36**, 1049 (1958).

13) F. Sondheimer and Y. Klibansky, *Tetrahedron*, **5**, 15 (1959).

14) B. Pelc, *Coll. Czeck. Chem. Comm.*, **25**, 309 (1960).

15) D. Kupfer, *Tetrahedron*, **15**, 193 (1961).

16) W. G. Dauben and A. C. Ashcraft, *J. Am. Chem. Soc.*, **85**, 3673 (1963).

17) A. Butenandt and A. Heusner, *Ber.*, **71**, 198 (1938).

18) L. F. Fieser and M. Fieser, "Steroids," Reinhold, New York, N. Y. (1959).

19) C. Djerassi, ed., "Steroid Reactions," Holden-Day, San Francisco, California (1963).

20) H. C. Brown, *Tetrahedron*, **12**, 117 (1961).

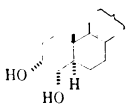
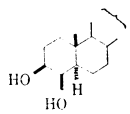
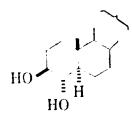
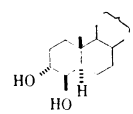
21) H. C. Brown, "Hydroboration," W. A. Benjamin, New York, N. Y. (1962).

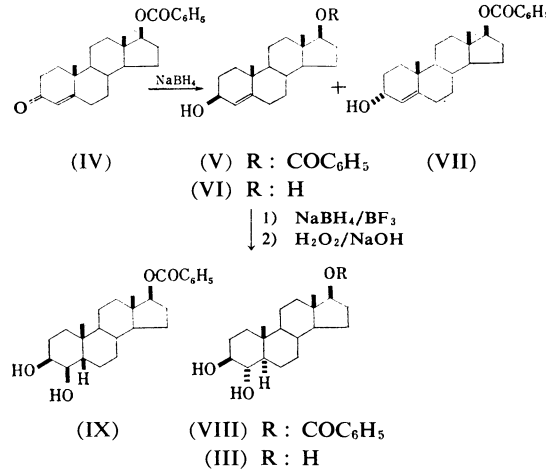
22) G. Zweifel and H. C. Brown, in A. C. Cope, ed., "Organic Reactions," Vol. 13, John Wiley & Sons, New York, N. Y. (1963), p. 1.

hydroboration reaction is anti-Markownikoff cis-addition and that the attack takes place from the less-hindered side of a given molecule,[20-22] the product may be formulated as 5α-androstane-3β, 4α, 17β-triol 17-benzoate (VIII). A less probable alternative is 5β-androstane-3β, 4β, 17β-triol 17-benzoate (IX).

To discriminate these two possibilities, the rate of lead tetraacetate consumption was measured. Unfortunately, the kinetic data for the 3β, 4α-glycol system have not been found in the literature and so no direct comparisons of the present experiment with references could be made. However, as may be seen from Table I, the observed rate constant, $7.43\times10^{-3}$ l. $mol^{-1}$ $sec^{-1}$, is quite compatible as a steroidal trans-glycol system when compared with the data so far available in the literature.[23,24] If the two hydroxyl groups were cis to each other, as in IX, the rate constant would be expected to be much larger than is actually observed. It is, therefore, safe to conclude that the product is 5α-androstane-3β, 4α, 17β-triol 17-benzoate (VIII).[25] The free triol (III) was obtained after removing the benzoate group by saponification.

TABLE I. RATES OF $Pb(OAc)_4$ CONSUMPTION OF 3,4-DIOLS AT 25°C

| 3,4-Diol | Configuration | $10^3k$ (l. $mol^{-1}$ $sec^{-1}$) | Ref. |
|---|---|---|---|
|  | 3α, 4α- | 112.6 | 23 |
|  | 3β, 4β- | 91.3 | 23 |
|  | 3β, 4α- | 7.43 | Present study |
|  | 3α, 4β- | 0.0357 | 23 |




The physiological properties of the new androstane-triol (III) are now being investigated; the results will be reported elsewhere.

## Experimental

The melting points were determined on a micro hot stage and are uncorrected. The ultraviolet spectra have been measured with a Beckman DK-2 spectrophotometer, while the infrared spectra were taken on a Koken IR-S spectrometer.

**The Reduction of Testosterone Benzoate (IV) with Sodium Borohydride.**—About 5 g. of sodium borohydride was gradually added into a suspension of 5.00 g. of testosterone benzoate (m. p. 191—192°C) in 100 ml. of methanol. After it had been stirred for 2 hr., the mixture became a clear solution. The mixture was then neutralized with a methanolic solution of acetic acid and poured into 300 ml. of water. The precipitated white solid (4.95 g.) was collected. Five recrystallizations from aqueous acetone gave 2.94 g. of androst-4-ene-3β, 17β-diol 17-benzoate (V) as colorless needles, m. p. 173—174°C. $\lambda_{max}^{EtOH}$ 230 mμ (ε 12050), $\nu_{max}^{KBr}$ 1718, 1660 $cm^{-1}$.

Found: C, 79.14; H, 8.67. Calcd. for $C_{26}H_{34}O_3$: C, 79.15; H, 8.69%.

From the mother liquor of the recrystallization, a small amount of the 3α-isomer was obtained. Recrystallization from aqueous methanol gave a pure specimen of androst-4-ene-3α, 17β-diol 17-benzoate (VII) as colorless needles, m. p. 153—154°C. $\lambda_{max}^{EtOH}$ 230 mμ (ε 12000), $\nu_{max}^{KBr}$ 1722, 1658 $cm^{-1}$.

Found: C, 79.24; H, 8.81. Calcd. for $C_{26}H_{34}O_3$: C, 79.15; H, 8.69%.

**The Saponification of Androst-4-ene-3β, 17β-diol 17-Benzoate (V).**—A solution of 0.023 g. of the benzoate (V) (m. p. 173—174°C) in 5 ml. of methanol was refluxed for 5 hr. with a methanolic solution of potassium hydroxide (1 g./10 ml.). The mixture was then diluted with 10 ml. of water, and the product was extracted with chloroform. The evaporation of the solvent and the recrystallization of the residue from aqueous methanol gave 0.012 g. of androst-4-ene-3β, 17β-diol (VI) as

23) C. Djerassi and R. Ehrlich, *J. Org. Chem.*, **19**, 1351 (1954).
24) S. J. Angyal and R. J. Young, *J. Am. Chem. Soc.*, **81**, 5251, 5467 (1959).
25) The preparation of 5α-cholestane-3β,4α-diol by a similar route has recently been reported.[26,27]
26) L. Caglioti and G. Cainelli, *Atti Accad. Nazl. Lincei, Rend., Classe Sci. Fis., Mat. e Nat.*, **29**, 555 (1960); *Chem. Abstr.*, **56**, 7386 (1962).
27) M. Nussim, Y. Mazur and F. Sondheimer, *J. Org. Chem.*, **29**, 1120 (1964).

colorless plates, m. p. 153—154°C. The reported melting point[17] is 153—154°C.

Found: C, 78.39; H, 10.22. Calcd. for $C_{19}H_{30}O_2$: C, 78.57; H, 10.41%.

**The Hydroboration Reaction of Androst-4-ene-3β, 17β-diol 17-Benzoate (V).**—A solution of 2.488 g. (6.31 mmol.) of androst-4-ene-3β, 17β-diol 17-benzoate (V) (m. p. 172—174°C) in 50 ml. of diglyme and 0.823 g. of sodium borohydride (purity 82%, 17.83 mmol.) were placed in a three-necked flask equipped with a magnetic stirrer, a pressure-equilibrated dropping funnel, a nitrogen inlet and outlet, and a reflux condenser. The reaction flask was flushed out with nitrogen, and a solution of freshly-distilled boron trifluoride etherate (2 ml., 15.83 mmol.) in 20 ml. of diglyme was added drop by drop over a period of 30 min. After the addition was complete, the mixture was stirred for 18 hr. under nitrogen at 30—40°C.

The reaction mixture was then hydrolyzed with 30 ml. of water. When the evolution of hydrogen had ceased, 20 ml. of 3 N sodium hydroxide was added, and the oxidation reaction was carried out by adding 30 ml. of 30% hydrogen peroxide. The mixture was allowed to cool, 30 ml. of water was added, and then the mixture was extracted with five 100 ml.-portions of methylene chloride. The extracts were combined, washed with water, and dried over sodium sulfate. The removal of the solvent gave a crystalline solid. Recrystallization from aqueous acetone afforded 1.132 g. of colorless needles, m. p. 237—238°C (first crop), and 0.522 g., m. p. 229—231°C (second crop). Repeated recrystallizations gave a specimen with an m. p. of 239—240°C. $\lambda_{max}^{EtOH}$ 230 mμ (ε 12100), $\nu_{max}^{KBr}$ 1710 $cm^{-1}$. The analytical figure shows that this specimen was a mono-hydrate of the desired 5α-androstane-3β, 4α, 17β-triol 17-benzoate (VIII).

Found: C, 72.80; H, 9.07. Calcd. for $C_{26}H_{36}O_4 \cdot H_2O$: C, 72.52; H, 8.90%.

The pure anhydrous sample of VIII, m. p. 239—240°C, was obtained after drying it over phosphorus pentoxide under a high vacuum at 110°C for 36 hr.

Found: C, 75.50; H, 8.72. Calcd. for $C_{26}H_{36}O_4$: C, 75.69; H, 8.80%.

**5α-Androstane-3β, 4α, 17β-triol (III).**—A solution of 0.037 g. of the benzoate (VIII) (m. p. 239—240°C) in 10 ml. of methanol was refluxed for 5 hr. with a methanolic solution of potassium hydroxide (1 g./10 ml.). The mixture was then concentrated to 5 ml. under reduced pressure and diluted with 20 ml. of water. The product was collected (0.029 g.) and recrystallized from aqueous methanol as colorless needles of 5α-androstane-3β, 4α, 17β-triol (III), m. p. 248—250°C.

Found: C, 73.98, H, 10.39. Calcd. for $C_{19}H_{32}O_3$: C, 73.98; H, 10.46%.

**The Kinetic Measurement of Lead Tetraacetate Oxidation.**—Essentially the same procedure as that reported in the literature[28] was used. The lead tetraacetate solution was prepared by dissolving 1.9 g. of lead tetraacetate in 50 ml. of glacial acetic acid. The sample of 5α-androstane-3β, 4α, 17β-triol 17-benzoate (VIII) (m. p. 239—240°C) (208.42 mg., 0.505 mmol.), dissolved in 20 ml. of acetic acid, was then mixed with 20 ml. of the lead tetraacetate solution (ca. 1.7 mmol.), and the volume was adjusted to 100 ml. with glacial acetic acid. Periodically an aliquot (10.0 ml.) was taken and added to 25 ml. of an aqueous solution of 0.5 g. of sodium iodide and 5 g. of sodium acetate, the liberated iodine being titrated with a 0.025 N sodium thiosulfate solution. The oxidation was carried out at 25°C, and the appropriate blank was used with each titration.

The rate constant for the oxidation was calculated in the following manner.[29] The $\log [a(b-x)/b(a-x)]$ was plotted against the time, $t$, where ($a$ is the initial concentration of the sample (VIII) $0.00505_2$ mol./l.), $b$ is the initial concentration of lead tetraacetate (0.0168 mol./l.), and $x$ is the amount reacted at time $t$. The slope of the resultant straight line was calculated and substituted into the equation: $k = (2.303 \times \text{slope})/(b-a)$ l. $mol^{-1}$ $sec^{-1}$ The numerical data are shown in Table II, from which one can obtain the rate constant as $7.43 \times 10^{-3}$ l./$mol^{-1}$ $sec^{-1}$.

Table II. Kinetic measurement of $Pb(OAc)_4$ consumption

| Time sec. | Thiosulfate titre, ml. Sample | Blank | $Pb(OAc)_4$ consumption mol./l. | $\log \frac{a(b-x)}{b(a-x)}$ |
|---|---|---|---|---|
| 0 | 13.37 | 13.42 | $0.063 \times 10^{-3}$ | 0.0038 |
| 480 | 13.21 | 13.40 | 0.238 | 0.0148 |
| 1020 | 12.90 | 13.41 | 0.638 | 0.0418 |
| 1620 | 12.63 | 13.41 | 0.975 | 0.0671 |
| 2400 | 12.35 | 13.41 | 1.325 | 0.0964 |
| 3300 | 12.11 | 13.37 | 1.575 | 0.1195 |
| 4980 | 11.50 | 13.34 | 2.300 | 0.1861 |
| 8580 | 10.79 | 13.30 | 3.138 | 0.3317 |

The author is indebted to Professor Yoshimasa Hirata of Nagoya University for his encouragement during this work. The author is also grateful to Professor Michio Shiota of Ochanomizu University for his helpful discussion at the earlier stage of the present study.

*Chemical Institute*
*Faculty of Science*
*Nagoya University*
*Chikusa-ku, Nagoya*

28) R. C. Hockett, M. T. Dienes and H. E. Ramsden, *J. Am. Chem. Soc.*, 65, 1474 (1943).
29) J. P. Cordner and K. H. Pausacker, *J. Chem. Soc.*, 1953, 102.

# The Structure and Stereochemistry of Four New Sesquiterpenes Isolated from the Wood Oil of "Kaya" (*Torreya nucifera*)

By Tsutomu SAKAI, Kiichi NISHIMURA and Yoshio HIROSE

(Received July 2, 1964)

In a previous communication,[1] we reported on the composition of volatile oil obtained from the leaves of *Torreya nucifera* Sieb. et Zucc. and on the identity of the torreyol isolated by Shinozaki[2] with δ-cadinol. We have subsequently studied the composition of the volatile wood oil of this species. As has previously been described in a short paper,[3] the wood oil was quite different from the leaf oil, containing four new sesquiterpenes without even trace amounts of ordinary terpenes.

**The Composition of the Neutral Volatile Oil.**—The following components were isolated by the adsorption chromatography of the wood oil on silica gel.

The first eluate was pure dendrolasin (I), which had been isolated previously from the ant *Lasius (Dendrolasius) fuliginosus* Latr. by Quilico et al.[4] and from the sweet potato fusel oil in our laboratory.[5] From the second and third fraction, two new sesquiterpene aldehydes were isolated; for these we propose the names nuciferal (II) and torreyal (III). Two new sesquiterpene alcohols were eluted after the aldehyde fractions. Since it was found that they were the alcohols corresponding to nuciferal and torreyal, they are named nuciferol (IV) and neotorreyol* (V). The last fraction consisted of *o*-methoxycinnamic aldehyde (VI), which had been isolated by Chiba[6] from this oil in the past.

TABLE I. THE COMPOSITION OF THE TRUNK AND ROOT OILS

| Compound | Trunk oil | | Root oil |
|---|---|---|---|
| | Nara Pref. | Hyōgo Pref. | Takarazuka City |
| Yield | % | % | % |
| | 0.46 | 0.13 | 0.09 |
| Dendrolasin (I) | 4 | 11 | — |
| Nuciferal (II) | 8 | — | 6 |
| Torreyal (III) | 27 | 17 | 2 |
| Nuciferol (IV) | 28 | 4 | 11 |
| Neotorreyol (V) | 2 | 5 | — |
| *o*-Methoxycinnamic aldehyde (VI) | 21 | 18 | 71 |
| Rest | 10 | 45 | 10 |

For purposes of comparison, the composition of the root oil of this species was investigated at the same time. These results are listed on Table I.

**The Structures of Nuciferal and Nuciferol.**—The molecular formula of nuciferal was determined to be $C_{15}H_{20}O$ by mass spectrometry (molecular weight=216) and by the elemental analysis of its 2,4-dinitrophenylhydrazone (m. p. 138—139°C) and semicarbazone (m. p. 160—161°C). Nuciferal shows the characteristics of an α,β-unsaturated aldehyde group in the ultraviolet ($\lambda_{max}^{EtOH}$ 222.5 mμ (ε, 15700)) and infrared spectra ($\nu_{max}^{film}$ 2720 (C–H), 1690 (conj. C=O) and 1645 $cm^{-1}$ (conj. C=C)), and gives a positive Tollens reagent test. Since the other ultraviolet bands ($\lambda_{max}^{EtOH}$ 264.5 mμ (ε, 950); 266.5 (880); 273 (800) and 279.5 (370)) and infrared bands ($\nu_{max}^{film}$ 1519 and 818 $cm^{-1}$) are similar to those of α-curcumene, it may be considered that nuciferal is an α,β-unsaturated aldehyde containing the α-curcumene skeleton.

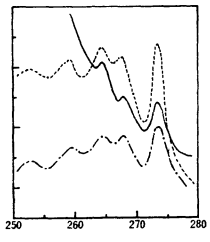
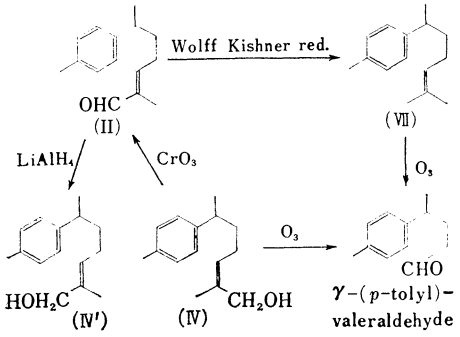



Fig. 1. UV spectra of nuciferal, nuciferol and α-curcumene.
——— Nuciferal ····· α-Curcumene
—·—· Nuciferol

1) T. Sakai, K. Nishimura, H. Chikamatsu and Y. Hirose, This Bulletin, **36**, 1261 (1963).
2) E. Shinozaki, *J. Soc. Chem. Ind.* (*Kōgyō-Kwagaku Zasshi*), **25**, 768 (1922).
3) T. Sakai, K. Nishimura and Y. Hirose, *Tetrahedron Letters*, No. 18, p. 1171 (1963).
4) A. Quilico, F. Piozzi and M. Pavan, *Tetrahedron*, **1**, 177 (1957).
5) Y. Hirose, M. Abu and Y. Sekiya, *J. Chem. Soc. Japan, Pure Chem. Sec.* (*Nippon Kagaku Zasshi*), **82**, 725 (1961).
6) K. Chiba, *Nippon Kagaku Sōran*, **1**, 6, 185 (1923).

* Since a sesquiterpene alcohol isolated from the leaves of the same plant had already been named "torreyol,"[2] the name of the present alcohol has been revised from "torreyol"[3] to neotorreyol. We wish to thank Professor H. Erdtman and Dr. V. Herout for their suggestions.

The Wolff-Kishner reduction of nuciferal afforded a hydrocarbon, which was identical with α-curcumene* (VII) as checked by infrared spectrometry and gas chromatography. Thus, it may be concluded that nuciferal is 2-methyl-6-(*p*-tolyl)hepten-2-al.




Nuciferol (IV) also shows the characteristic absorptions of a *p*-disubstituted benzene ring and a hydroxy group in the infrared ($\nu_{max}^{film}$ 3340 (OH), 1518 and 819 $cm^{-1}$ (aromatic)) and ultraviolet spectra (Fig. 1). On oxidation with chromium trioxide in pyridine, nuciferol afforded the corresponding aldehyde, which was identical with natural nuciferal. On the other hand, the reduction of nuciferal with lithium aluminum hydride in tetrahydrofuran afforded an alcohol (IV') the infrared, ultraviolet and MS spectra of which were superimposable on those of natural nuciferol. NMR evidence (mentioned below) indicated natural nuciferol (IV) and the alcohol (IV') obtained from nuciferal to be cis-trans isomers with regard to the double bond. These results demonstrate that nuciferol is the corresponding alcohol of nuciferal, and that an isomerization of the double bond occurs upon treatment with chromium trioxide and can be represented by formula IV.

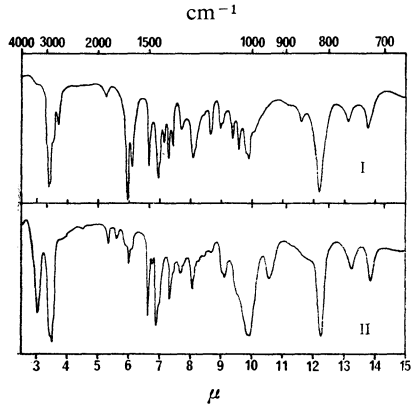



Fig. 2. IR spectra of nuciferal and nuciferol.
I, Nuciferal II, Nuciferol

The structures of nuciferal and nuciferol were confirmed by their mass spectra, in which the presence of a series of prominent peaks at *m/e* 77, 91, 105, 119 and 133 supported the α-curcumene skeleton, for these peaks are also predominant in the fragmentation pattern of α-curcumene.

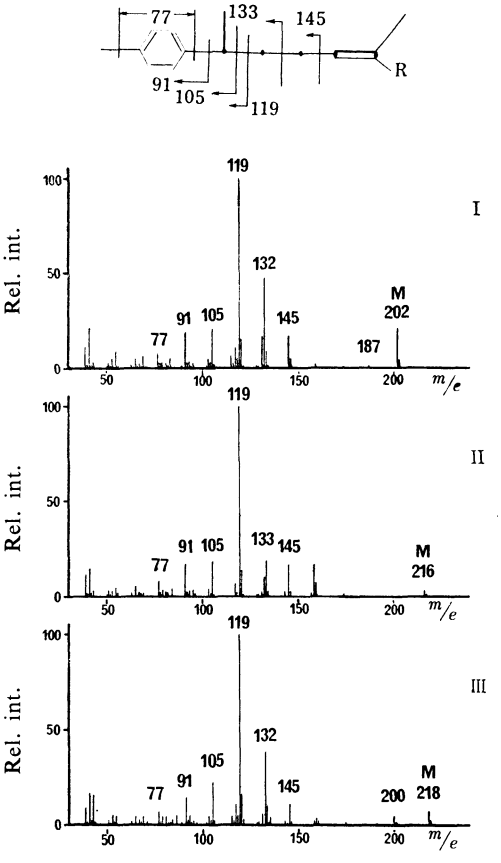


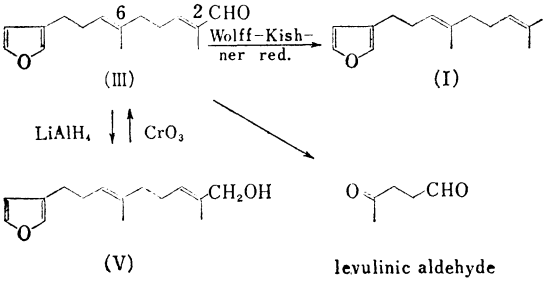

Fig. 3. Mass spectra of α-curcumene type compounds.
I, α-Curcumene II, Nuciferal III, Nuciferol

**The Structures of Torreyal and Neotorreyol.** —Molecular weight determination by mass spectrometry (parent peak at *m/e* 232) and the elemental analysis of its crystalline derivatives (2, 4-dinitrophenylhydrazone, m. p. 111—112°C; semicarbazone, m. p. 132—133°C) established the formula $C_{15}H_{20}O_2$ for torreyal. The ultraviolet ($\lambda_{max}^{EtOH}$ 224 mμ (ε, 15940)) and infrared spectra ($\nu_{max}^{film}$ 2720 (C–H), 1690 (conj. C=O) and 1645 $cm^{-1}$ (conj. C=C)) and the positive Tollens reagent test showed the presence of an α, β-unsaturated aldehyde group. The characteristic infrared bands at 1570, 1504, 1164, 1028, 874 and 779 $cm^{-1}$ (similar to dendrolasin) and

* This compound was isolated by fractional distillation and adsorption chromatography from a commercial ginger oil (Polack & Schwarz Co.).

the positive Ehrlich's color test suggested the presence of a furan ring in torreyal.

When torreyal was also subjected to Wolff-Kishner reduction, it afforded dendrolasin in an excellent yield. On the ozonolysis of torreyal, levulinic aldehyde was isolated as its bis-2, 4-dinitrophenylhydrazone (m. p. 238—239°C), but acetone was not detected. These results demonstrate that the aldehyde group conjugated with the ethylenic double bond is not located at C-6 but at C-2. Therefore, the structure of torreyal was deduced to be 2, 6-dimethyl-9(3-furyl)nonadien-2, 6-al.




Neotorreyol (V) is the corresponding alcohol of torreyal, because oxidation with chromium trioxide in pyridine led to torreyal, and the reduction of torreyal with lithium aluminum hydride in tetrahydrofuran yielded neotorreyol. Unlike the case of nuciferal-nuciferol, no isomerization about the double bond took place upon treatment with chromium trioxide. Its infrared spectra data are $\nu_{max}^{film}$ 3360 (OH), 1670 $\left(\begin{matrix}R\\R'\end{matrix}\right)$>C=C<$\left(\begin{matrix}R''\\H\end{matrix}\right)$, 1570, 1504, 1164, 1028, 874 and 779 $cm^{-1}$ (furan).

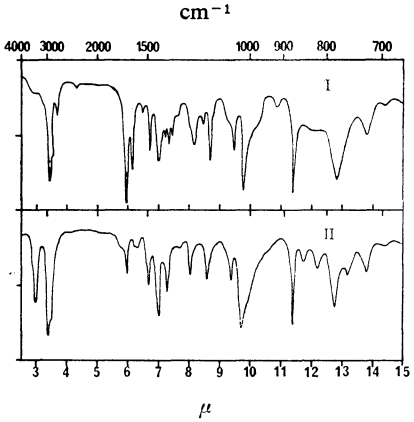
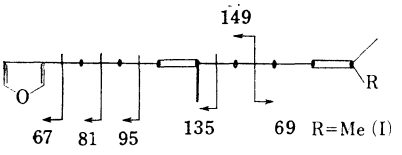



Fig. 4. IR spectra of torreyal and neotorreyol.
I, Torreyal II, Neotorreyol

The structures of torreyal and neotorreyol can be further confirmed by mass spectrometry. The predominance of the peaks at *m/e* 67, 81, 95 are common in alkylated furan compounds.[7] The peak at *m/e* 69, which, in dendrolasin and many other familiar terpenes containing the dimethylallyl group, often constitutes the base peak, is weak in the fragmentation of torreyal and neotorreyol; this suggests that the functional groups are located at the terminal position in both cases.



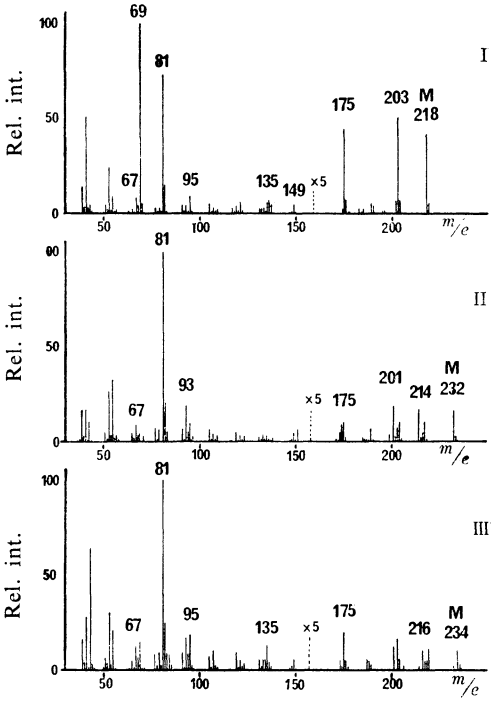




Fig. 5. Mass spectra of dendrolasin type compounds.
I, Dendrolasin II, Torreyal
III, Neotorreyol

**The Stereochemistry of Nuciferal and Nuciferol.**—There are two points of stereochemical interest in nuciferal and nuciferol, namely, the configurations at the asymmetric center, C-6, and at the ethylenic double bond.

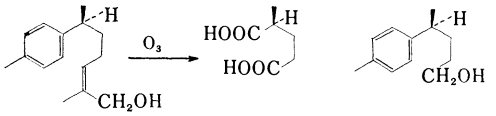
The configuration of the asymmetric center was established by the ozonization of nuciferol, which yielded *S*-(+)-α-methylglutaric acid (VIII), which was identical with an authentic sample.*

As nuciferal, nuciferol and α-curcumene isolated from ginger oil show a positive optical

7) Unpublished observation.

* We wish to thank Dr. H. Minato, Shionogi Pharmaceutical Institute, for his kind supply of (+)-α-methylglutaric acid.

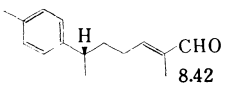
rotation, it may be suggested that they have the same S configuration. This conclusion was further supported by the calculations using the conformational asymmetry method of Brewster,[8] which was used by Marvell and Wiman[9] for the determination of the configuration of the 4-(*p*-tolyl)-1-pentanol (IX) isolated from the product of pulping Douglas fir.



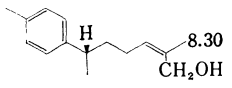

(IV) (VIII) (IX)

The configuration at the side-chain double bond was deduced from the NMR spectral data. Natural nuciferol shows in the NMR spectrum a singlet peak at 8.30 $\tau$, due to the methyl group attached to the double bond, and triplet peaks at 4.87 $\tau$, the vinyl proton. These peaks of the alcohol reduced from nuciferal shift to 8.50 and 4.72 $\tau$, respectively. Usually, in a system of the $X \cdot CH_2C(CH_3)=CHCH_2 \cdot Y$ type, the $\tau$ value of *cis*-methyl (the cis relationship between the methyl group and the vinyl proton) is 8.32 ($J$=1.0—1.5 c. p. s.), lower (by $\tau$ 0.07) than that of *trans*-methyl.[10]

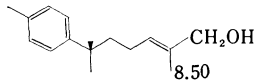
Thus, natural nuciferol was assigned a cis-isomer configuration, and the alcohol reduced from nuciferal, a trans-isomer configuration, they are illustrated by the following formulas:*




Natural nuciferal (II)

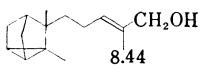



Natural nuciferol (IV)

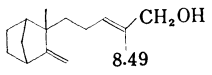



Alcohol reduced from nuciferal (IV')

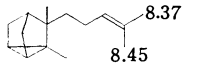
8) J. M. Brewster, *J. Am. Chem. Soc.*, **81**, 5475 (1959).
9) E. N. Marvell and R. Wiman, *J. Org. Chem.*, **28**, 1542 (1963).
10) R. B. Bates, R. H. Carinighan, R. O. Rakutis and J. H. Schauble, *Chem. & Ind.*, **1962**, 1020.
* The configuration of $\alpha$- and $\beta$-santalol was determined by Brieger[11] by an NMR spectral comparison of the corresponding hydrocarbons, $\alpha$- and $\beta$-santalene. They are in good agreement with our assignment.



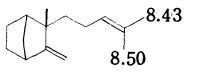

$\alpha$-Santalol




$\beta$-Santalol




$\alpha$-Santalene




$\beta$-Santalene

($\tau$ values in $CS_2$ with $Me_4Si$ internal reference)

11) G. Brieger, *Tetrahedron Letters*, No. 30, p. 2123 (1963).

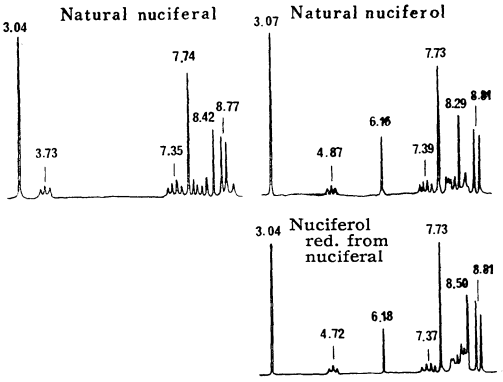
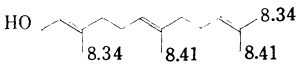


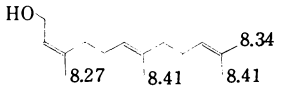

Fig. 6. NMR spectra of nuciferal and nuciferol.

**The Stereochemistry of Torreyal and Neotorreyol.**—As the interconversions between torreyal and neotorreyol involved no isomerization with respect to the configuration of the ethylenic double bond, it is suggested that they have the same configuration.

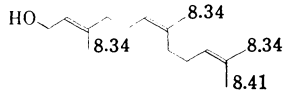
Recently, Bates et al.[12] examined the NMR spectra of four isomeric farnesols; the assigned methyl signals are shown in the following formulas:



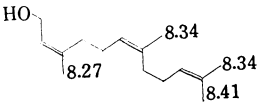

trans-trans




cis-trans

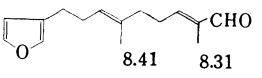



trans-cis



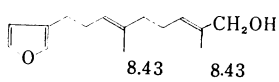

cis-cis

On the basis of these results and by comparison with dendrolasin, it may be concluded that torreyal and neotorreyol are trans-trans isomers which are represented by the following formulas:

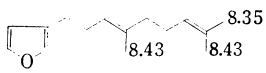



Torreyal (III)

12) R. B. Bates, D. M. Gale and B. J. Gruner, *J. Org. Chem.*, **28**, 1086 (1963).




Neotorreyol (V)




Dendrolasin (I)

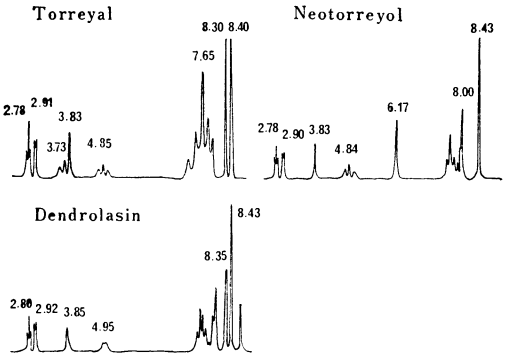



Fig. 7. NMR spectra of dendrolasin, torreyal and neotorreyol.

## Experimental*1

**The Preparation of the Volatile Oil.** — Crushed chips of a trunk of Kaya (498 kg.) which grew in Nara Prefecture were steam-distilled. The steam-volatile oil (2.3 kg.) was obtained in a yield of 0.46%. This oil was diluted with ether, washed with 5% potassium hydroxide, and dried over sodium sulfate. After the removal of the solvent, the neutral volatile oil (2.1 kg.) was obtained.

Another sample of a trunk (5 kg.) which grew in Hyōgo Prefecture were extracted with methanol. The methanol was evaporated off, and the residue was steam-distilled to give the volatile oil (6.5 g.).

The volatile oil (3.2 g.) from the root (3.4 kg.) was obtained by the same procedure.

**The Separation of the Oil.**—The neutral volatile wood oil (5 g.) was chromatographed on a silica gel column (70 g.). An example of the course of isolation is shown in Table II.

Their properties are recorded and presented below.

Nuciferal (II), b. p. 107.5—108.5°C/0.03 mmHg, $[\alpha]_D^{20}$ +62.07° (*c* 16.55, $CHCl_3$), 2,4-dinitrophenylhydrazone, m. p. 138—139°C (Found: C, 63.60; H, 6.06; N, 14.04. Calcd. for $C_{21}H_{24}N_4O_4$: C, 63.62; H, 6.10; N, 14.13%.), semicarbazone, m. p. 160—161°C (Found: C, 70.24; H, 8.50; N, 15.30. Calcd. for $C_{16}H_{23}N_3O$: C, 70.29; H, 8.48; N, 15.34%.).*3

Torreyal (III), b. p. 124—126°C/0.05 mmHg, $[\alpha]_D^{20}$ +1.90°, 2,4-dinitrophenylhydrazone, m. p. 111—112°C (Found: C, 61.67; H, 5.67; N, 13.74. Calcd. for $C_{21}H_{24}N_4O_5$: C, 61.15; H, 5.87; N, 13.59%.), semicarbazone, m. p. 132—133°C (Found: C, 67.09; H, 8.13; N, 14.48. Calcd. for $C_{16}H_{23}N_3O$: C, 66.41; H, 8.01; N, 14.52%.).

Nuciferol (IV), b. p. 131—132°C/0.05 mmHg, $[\alpha]_D^{20}$ +41.06°.

Neotorreyol (V), b. p. 117—119°C/0.03 mmHg, $[\alpha]_D^{20}$ 0°.

Attempts to prepare crystalline derivatives of the two alcohols were both unsuccessful.

**The Kishner Reduction of Nuciferal.**—The Cook and Linstead procedure[13] was followed. Nuciferal (0.8 g.) was converted into the semicarbazone, which was then heated with a free flame in a distilling flask with solid potassium hydroxide (2 g.). The mass fused, ammonia and nitrogen were given off, and then oily droplets of hydrocarbon began to distill. The residue was dissolved in water and extracted with ether. The distillate and the ether extract were combined, the solvent was removed in vacuo, leaving an oil, and the oil was purified by chromatography over silica gel to yield α-curcumene (0.5 g.), which was identical with an authentic sample isolated from ginger oil. The specific retention time relative to β-elemene (1.00) was 1.76 in GLC at 170°C.

**The Reduction of Nuciferal with Lithium Aluminum Hydride.**—A solution of nuciferal (0.8 g.) in dry tetrahydrofuran (10 ml.) was stirred drop

Table II. The separation of the neutral volatile wood oil

| Eluting solvent | Fr. No. | Eluate, g. | Component |
|---|---|---|---|
| 3% Ether in hexane | 1— 2 | 0.20 | Dendrolasin (I) |
| 3% Ether in hexane | 6—10 | 0.40 | Nuciferal (II) |
| 3% Ether in hexane | 11—20 | 1.34 | Torreyal (III) |
| 10% Ether in hexane | 24—40 | 1.38 | Nuciferol (IV) |
| 20% Ether in hexane | 41—43 | 0.12 | Neotorreyol (V) |
| 30% Ether in hexane | 44—51 | 1.05 | *o*-Methoxycinnamic aldehyde (VI) |
| Methanol | 52 | 0.50 | Rest |

*1 M. ps. and b. ps. are uncorrected. The IR spectra were taken with a Perkin-Elmer (Model 137) and a Hitachi (Model EPI-2) infracord spectrophotometer. The UV absorption spectra were measured in an ethanol solution with a Hitachi (Model FPS-2) spectrophotometer. The NMR spectra were determined in a $CCl_4$ solution with $Me_4Si$ as an internal standard, using a Varian (Model A-60) spectrometer.*2 The mass spectra were measured with a Hitachi (Model RMU-6) mass spectrometer: ionizing voltage, 80 eV.; ion-accelarating voltage, 2 kV.; temp. of ionization chamber, 250°C; vaporizing temp. of sample, 150°C. The GLC was carried out with a Shimadzu (Type GC-2B) gas chromatograph: column, Celite-Carbowax 1500 (10:2), 3 m.; temp., 170°C; carrier gas, $N_2$. For adsorption chromatography Mallinckrodt's silica gel was used.

*2 We wish to thank the Shionogi Pharmaceutical Institute and the Research Laboratory of Takeda Pharmaceutical Industries for their NMR measurements.

*3 The analyses were performed in the Microanalytical Laboratory of the Institute of Polytechnics, Osaka City University.

13) A. H. Cook and R. P. Linstead, *J. Chem. Soc.*, **1934**, 946.

by drop into a suspension of lithium aluminum hydride (0.4 g.) in dry tetrahydrofuran (10 ml.), and then the mixture was heated under reflux for 30 min. The mixture was decomposed by the addition of water in a ice bath and extracted with ether. The solvent was evaporated, and the residue was chromatographed on silica gel to yield a colorless oil (0.68 g.), the infrared and MS spectra of which were identical with that of nuciferol.

**The Oxidation of Nuciferol with Chromium Trioxide.** — (a) A solution of nuciferol (2 g.) in glacial acetic acid (6 ml.) was stirred drop by drop into a solution of chromium trioxide (0.8 g.) in glacial acetic acid (6 ml.) at room temperature. The mixture was then heated on a water bath for 20 min., cooled, poured into water (100 ml.), and extracted with ether. The ether extract was washed with saturated aqueous sodium hydrogen carbonate, dried over sodium sulfate, and evaporated to leave an oil. This residual oil was then dissolved in hexane and chromatographed on silica gel. Elution with 3% ether in hexane yielded an aldehyde (0.6 g.). Its infrared and MS spectra were identical with those of nuciferal, and the melting point of its semicarbazone was undepressed on admixture with an authentic sample.

(b) Chromium trioxide (2 g.) was stirred into pyridine (20 ml.) in an ice bath to give a chromium trioxide-pyridine complex. A solution of nuciferol (1 g.) in pyridine (10 ml.) was added to the complex prepared above in an ice bath and left overnight at room temperature. The reaction mixture was then poured into ice-water and extracted with ether. The ether extract was washed with dilute hydrochloric acid and water, dried over sodium sulfate, and evaporated. The residue was chromatographed on silica gel to yield nuciferal (0.8 g.).

**The Ozonolysis of Nuciferol.** — (a) Nuciferol (3 g.) was dissolved in methyl acetate (10 ml.) and ozonized at 0°C. The ozonide was decomposed by heating it with water (10 ml.) for 10 min., and methyl acetate was distilled off. The distillation residue was extracted with ether and then evaporated in vacuo to leave an aldehyde (1.5 g.). Its 2,4-dinitrophenylhydrazone had a m. p. of 94—95°C (Found: C, 60.13; H, 5.77; N, 15.70. Calcd. for $C_{18}H_{20}N_4O_4$: C, 60.66; H, 5.66; N, 15.72%.), which was identical with that of an authentic sample of $\gamma$-(*p*-tolyl)valeraldehyde 2,4-dinitrophenylhydrazone (prepared from $\alpha$-curcumene).

(b) A stream of ozone was passed into a solution of nuciferol (2 g.) in 90% acetic acid (10 ml.) at room temperature for 50 hr. To the mixture was then added 30% hydrogen peroxide (2 ml.), and the mixture was allowed to stand overnight at room temperature. After water (20 ml.) had been added, the excess hydrogen peroxide was decomposed by heating it with a small amount of a Pd-C catalyst on a water bath for 2 hr. After the usual work-up $\alpha$-methylglutaric acid (0.2 g., m. p. 79—80°C, $[\alpha]_D^{20}$ +17.0° (*c* 0.10, MeOH), was obtained. Its melting point was not depressed by admixture with an authentic sample.

**The Kishner Reduction of Torreyal.** — By the reduction of semicarbazone prepared from torreyal (1.2 g.) in the manner described above for nuciferal, dendrolasin (0.6 g.) was obtained. It was identified by a comparison of its infrared spectra and gas chromatographic retention times with those of an authentic sample. The specific retention time relative to $\beta$-elemene (1.00) is 2.97 in GLC at 170°C.

**The Reduction of Torreyal with Lithium Aluminum Hydride.** — Torreyal (1 g.) in tetrahydrofuran was reduced with lithium aluminum hydride by the procedure described above for nuciferal. When it was worked-up in the usual manner, an alcohol (0.83 g.) was obtained. This was found to be identical with neotorreyol by infrared and MS spectroscopy.

**The Oxidation of Neotorreyol with Chromium Trioxide.** — A mixture of neotorreyol (1 g.) and a chromium trioxide - pyridine complex was allowed to stand overnight at room temperature. The reaction mixture was then treated in the same manner as nuciferol, thus yielding torreyal (0.6 g.).

**The Ozonolysis of Torreyal.**—Torreyal (1 g.) in chloroform (10 ml.) was ozonized at 0°C. After the addition of water (10 ml.) to decompose the ozonide, the mixture was heated on a water bath for 10 min. By distillation on a water bath, a chloroform solution (A) was obtained, while distillation on a free flame produced an aqueous solution (B). From A, no carbonyl derivatives were obtained at all, but from B the presence of levulinic aldehyde was proved as its bis-2,4-dinitrophenylhydrazone (0.2 g., m. p. 238—239°C. Found: C, 44.40; H, 3.54; N, 23.61. Calcd. for $C_{17}H_{16}N_8O_8$: C, 44.35; H, 3.50; N, 24.34%.). The melting point of this derivative was not depressed by admixture with an authentic sample prepared from $\alpha$-methylfuran.

**The Identification of *o*-Methoxycinnamic Aldehyde.**—*Oxidation with Silver Oxide.*—A hot solution of aldehyde (1.7 g.) in ethanol (5 ml.) was added to a suspension of silver oxide prepared from silver nitrate (1.7 g.) in aqueous 10% sodium hydroxide (20 ml.) heated at 55—60°C. The mixture was then heated while being stirred for 10 min. The black precipitate was filtered off and washed with hot water. The filtrate was acidified with hydrochloric acid, and the precipitated acid was collected by filtration. The product was recrystallized from ethanol to furnish needles (0.8 g.; m. p. 184—185°C), identified as *o*-methoxycinnamic acid by mixed melting point determination with an authentic sample.

*Oxidation with Potassium Permanganate.*—To a suspension of *o*-methoxycinnamic aldehyde (1 g.) in water (10 ml.), an alkaline 10% potassium permanganate solution was added; the mixture was then heated while being stirred on a water bath for 30 min. The reaction mixture was worked up by the usual manner to give a crude acid. The crude crystall was recrystallized from hot water to yield *o*-methoxybenzoic acid, m. p. 94—95°C, which was identified by a mixed melting point determination with an authentic specimen.

## Summary

Four new sesquiterpenes, nuciferal (II), nuciferol (III), torreyal (IV) and neotorreyol (V),

together with dendrolasin and *o*-methoxycinnamic aldehyde, have been isolated from the neutral volatile wood oil of Kaya (*Torreya nucifera* Sieb. et Zucc.) by adsorption chromatography on silica gel.

The structures and stereochemistry of these new compounds have been confirmed by infrared, ultraviolet, NMR and MS spectrometry, as well as by chemical methods.

*The Institute of Food Chemistry*
*Kita-ku, Osaka*

# The Intramolecular Interaction between the N–H Group and π-Electrons. II.[1] Intramolecular Interaction in *N*-Phenethylanilines

By Michinori Ōki and Kiyoshi Mutai

(Received July 13, 1964)

In a previous paper[1] the authors have reported that there is an interaction between the N–H group and π-electrons of the benzyl group in *N*-benzylaniline, this fact being confirmed by infrared spectroscopy.

The same type of interaction, i. e., O–H···π interaction, has been reported in a variety of aliphatic and aromatic hydroxylic compounds with π-electrons in appropriate positions.[2] Since both N–H and O–H groups are known to be hydrogen donors, it is expected that the N–H···π interaction may be possible in a compound analogous to a hydroxylic compound which shows the O–H···π interaction.

Phenethyl alcohol and some derivatives of 3-phenylpropyl alcohol,[2e] as well as benzyl alcohol,[2d] have been reported to show the interaction; hence, it may be reasonable to begin with the investigation of *N*-phenethylaniline. Such a study will provide some data on X–H···π interaction in general and will make it possible to compare O–H···π and N–H···π cases.

## Experimental

**Spectral Measurement and Calculation.** — The infrared spectra were recorded on a Perkin-Elmer model 112-G double-pass high precision-grating infrared spectrometer, provided with a 2 cm. quartz cell and a spectral slit width being 1.0 $cm^{-1}$ in the N–H stretching region. Eastman Kodak spectrograde or redistilled carbon tetrachloride was used as a solvent. The concentration of the solution was 0.005—0.007 mol./l., which was dilute enough to exclude associated solute molecules. The temperature was 25±2°C.

The obtained bands were, if necessary, separated into two or more component bands, assuming that each one was expressed by Lorentz function. The integrated intensities were calculated according to the following equation:

$$A = (\pi/2) \cdot \Delta\nu^{a}_{1/2} \cdot \ln(I_0/I)_{max} \cdot l^{-1} \cdot c^{-1}$$

where $A$ is the integrated intensity; $\Delta\nu^{a}_{1/2}$, the half-band width; $c$, the concentration of the solution (mol./l.), and $l$, the cell length.

The errors in the values analyzed, especially in the absorption maximum position and the half-band width, are difficult to estimate, since the curves were divided by the "trial and error" method. The band shape was an important factor in determining the ease of division. Thus, the spectrometer allowed an accuracy of 0.1 $cm^{-1}$ for an apparent band maximum, but the analyzed values mentioned above were obtained with an accuracy of only ca. ±0.5 $cm^{-1}$.

**Materials.**—The compounds used in the present study were known, unless otherwise stated, and were purified through known methods. Their physical constants agreed well with those reported.

*N-Phenethylanilines.*—Two procedures were adopted for the preparation of this series of compounds; (a) Phenethyl chloride or bromide (0.1 mol.) and a substituted aniline (0.1 mol.) were heated with 30 ml. of 20% aqueous sodium hydroxide for 30 min. After the unreacted halide and aniline had been removed by steam distillation, the residue was taken up in ether and distilled under reduced pressure; (b) A substituted phenylacetanilide (0.05 mol.), recrystallized from 70% ethyl alcohol, was added in small portions into a stirred solution of 4.0 g. (0.105 mol.) of lithium aluminum hydride in 100 ml. of dry ether. The solution was then further stirred at a refluxing temperature for 6—8 hr., and the excess of lithium aluminum hydride was decomposed with ethyl acetate. The reaction mixture was poured into 150 ml. of 30% aqueous sodium hydroxide and extracted with ether. After the solvent had been distilled off, the residue was distilled under reduced pressure.

The physical constants and elemental analyses of

1) Part I: M. Ōki and K. Mutai, This Bulletin, **33**, 784 (1960).

2) M. Ōki and H. Iwamura, ibid., a) **31**, 770 (1958); b) **32**, 307 (1959); c) **32**, 567 (1959); d) **32**, 955 (1959); e) **32**, 1135 (1959); f) **33**, 681 (1960).

*N*-(2-Arylethyl)aniline ($RC_6H_5CH_2CH_2NHPh$)

| R | Method | B. p./mmHg | $n_D$ | Carbon, % | | Hydrogen, % | | Nitrogen, % | | Yield, % |
|---|---|---|---|---|---|---|---|---|---|---|
| | | | | Calcd. | Found | Calcd. | Found | Calcd. | Found | |
| *p*-$CH_3$ | b | 178—179°C /8.5 | 1.5891 (18°C) | 85.26 | 85.27 | 8.11 | 8.18 | | | 43 |
| *p*-Cl | b | 158—160°C /3 | 1.6040 (18°C) | 72.47 | 72.44 | 6.08 | 6.11 | 6.04 | 5.85 | 56 |
| *m*-Cl | b | 150—151°C /3 | 1.6112 (18°C) | 72.47 | 72.39 | 6.08 | 6.23 | 6.04 | 5.87 | 65 |
| *N*-Arylphenethylamine ($PhCH_2CH_2NHC_6H_4R$) | | | | | | | | | | |
| *p*-MeO | a | 159—161°C /2 | 1.5956 (16°C) | 79.26 | 79.50 | 7.54 | 7.52 | 6.16 | 6.13 | * |
| *p*-$CH_3$ | a | 140—144°C /2 | 1.5896 (20°C) | 85.26 | 85.25 | 8.11 | 8.26 | | | * |
| *m*-$CH_3$ | a | 154—156°C /2 | 1.5936 (14°C) | 85.26 | 85.49 | 8.11 | 8.10 | | | * |
| *p*-$C_6H_5$ | b | 47— 48°C (m. p.) | | 87.87 | 87.58 | 7.01 | 7.17 | | | 61 |
| *p*-Cl | a | 150—154°C /3 | 1.6072 (18°C) | 72.47 | 72.42 | 6.08 | 6.15 | 6.04 | 5.93 | * |
| *m*-Br | a | 175—177°C /3 | 1.6240 (18°C) | 60.88 | 60.62 | 5.11 | 5.20 | 5.07 | 5.16 | * |

* Generally 20—35%

the new compounds are summarized in the following table.

## Results and Discussion

***N*-(2-Arylethyl)aniline.** — The *N*-phenethylaniline derivatives containing substituents at the *m*- or *p*-position of phenethyl groups were selected for spectral inspection to avoid the formation of the N-H···X hydrogen bond, which is possible in *o*-substituted compounds. The apparent absorption curves in the N-H stretching region for *N*-phenethylaniline, *N*-(*p*-chlorophenethyl)aniline, and *N*-(*p*-nitrophenethyl)aniline are shown in Fig. 1.

Three curves show that two apparent maxima

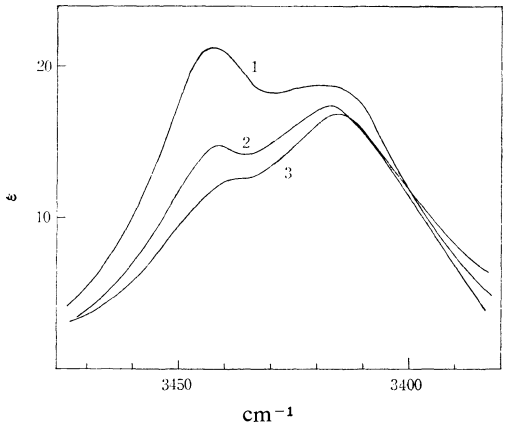



Fig. 1. $\nu_{N-H}$ Absorption of *N*-(*p*-nitrophenethyl)aniline (1), *N*-(*p*-chlorophenethyl)aniline (2) and *N*-phenethylaniline (3).

are present, suggesting that there are at least two bands and, therefore, two isomers. It might be an attractive explanation that they are simple rotational isomers due to the difference in steric conditions caused by the rotation of the N-H hydrogen atom around the N-$CH_2$ bond axis. The positions of the absorption maxima of the divided bands (see Table I) are at nearly the same wave numbers as those of the rotational isomers in *N*-ethylaniline;[1] this fact may be regarded as supporting evidence for the explanation.

However, it should be noted that a substituent effect is observed in the spectra; the extinction coefficient of the higher wave number band increases at the expense of the lower one as the electron-withdrawing power of the substituent increases. This effect suggests that N-H···$\pi$ interaction is the more probable interpretation of the presence of two N-H stretching bands, since a *m*- or *p*-substituent in the phenethyl group should not cause an appreciable difference in steric effect on the N-H group. In order to get firmer evidence for this interpretation, the curves of five *N*-(2-arylethyl)anilines were divided, assuming that they were the overlaps of two symmetrical ones expressed by Lorentz function. The results are shown in Table I.

From Table I, it is evident that the $A_i/A_f$ ratio, where $A_i$ is the integrated intensity of the absorption due to the interacting form and $A_f$, that of the free form, varies with the electron-donating or electron-withdrawing nature of the substituent, and this tendency is indicative of interaction between the N-H

TABLE I. $\nu_{N-H}$ ABSORPTION OF *N*-(2-ARYLETHYL)ANILINES, $RC_6H_4CH_2CH_2NHPh$

| R | Band | $\nu_{max}$ cm$^{-1}$ | $\Delta\nu_{max}$ cm$^{-1}$ | $\Delta\nu^a_{1/2}$ cm$^{-1}$ | $A\times10^{-3}$ mol$^{-1}\cdot$l$\cdot$cm$^{-2}$ | $\log(A_i/A_f)$ |
|---|---|---|---|---|---|---|
| *p*-$CH_3$ | i[a] | 3414.8 | 31.9 | 54.4 | 3.52 | 0.936 |
| | f[b] | 3446.7 | | 23.4 | 0.41 | |
| H | i | 3415.2 | 30.6 | 50.2 | 2.92 | 0.832 |
| | f | 3445.8 | | 25.0 | 0.43 | |
| *p*-Cl | i | 3416.6 | 29.7 | 48.2 | 2.85 | 0.636 |
| | f | 3446.3 | | 24.4 | 0.66 | |
| *m*-Cl | i | 3415.7 | 29.8 | 44.0 | 2.56 | 0.458 |
| | f | 3445.5 | | 29.0 | 0.89 | |
| *p*-$NO_2$ | i | 3415.0 | 29.5 | 41.8 | 2.34 | 0.148 |
| | f | 3444.5 | | 29.0 | 1.68 | |

a) i denotes interacting form of N-H group.
b) f denotes free form of N-H group.

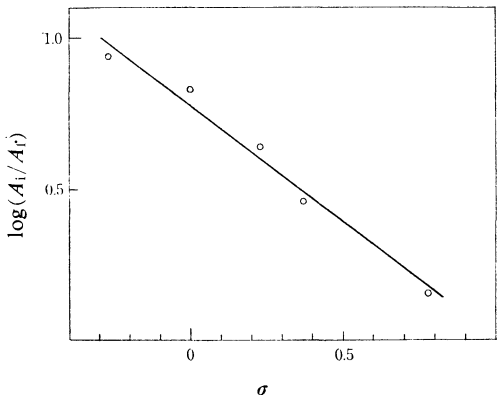



Fig. 2. The relationship between $\sigma$-constant and $\log(A_i/A_f)$ for *N*-(2-arylethyl)aniline.

group and $\pi$-electrons. The summation of the integrated intensities due to the two forms also changes slightly with the substituent, but this is not a significant factor in comparing the $A_i/A_f$ ratio, since the substituent seems to have nearly the same effect on both intensities.

The $\log(A_i/A_f)$ value was plotted against the Hammett $\sigma$ value[3] of the substituent. The $\sigma$ value is believed to be closely related to the electron density[4] at an appropriate carbon atom in a substituted benzene nucleus. As may be seen in Fig. 2, a linear relationship is gained when the $\sigma$ value is so taken as to represent the reactivity of the ring carbon atom which is attached to the anilinoethyl group. As the $A_i/A_f$ ratio corresponds to an equilibrium constant of the system between the two forms and changes with the electron density, the two component bands should be assigned to the interacting and the free forms of the N-H group, the forms corresponding to the higher and lower wave number bands respectively, as denoted in Table I.

A difference may be found between the data in Table I and those obtained with phenethyl alcohol derivatives. The displacement ($\Delta\nu_{max}$) of the absorption maximum of the O-H group by the O-H···π interaction has a tendency to increase as the $\sigma$ value of the substituent decreases, the phenomenon being far more evident than in *N*-phenethylaniline; when the substituent varies from *p*-$CH_3$ to *p*-$NO_2$, the difference of $\Delta\nu_{max}$ is 12.2 cm$^{-1}$ in the O-H···π interaction, while the corresponding difference in the N-H···π interaction is only 2.4 cm$^{-1}$, though the change is in the same direction. There has been general acceptance of a proposal that $\Delta\nu_{max}$ provides an index of the strength of the hydrogen bond ($\Delta H$, the enthalpy of hydrogen bonding),[5] though exceptions to this rule are not rare and the matter should be treated carefully. A comparison of the $\Delta H$'s of the O-H···π interaction in several hydroxylic compounds[6] with those of some derivatives of *N*-benzylaniline[7] has shown that there is no remarkable difference between the two groups. Thus, it must be emphasized that the $\Delta\nu_{max}$ difference between O-H and N-H groups cannot be directly related to the interaction energy.

Another striking difference is the value of $\log(A_i/A_f)$. In *N*-phenethylaniline, even the value of the most unfavorable derivative for the interaction among the compounds investigated, i.e., *N*-(*p*-nitrophenethyl)aniline, does not fall to the minus region. This means that if the absorption strength per molecule is the same for both free and interacting forms, the

3) L. P. Hammett, "Physical Organic Chemistry," McGraw-Hill Book Co., New York (1940); H. H. Jaffé, *Chem. Revs.*, 53, 191 (1953); D. M. McDaniel and H. C. Brown, *J. Org. Chem.*, 23, 420 (1958).
4) H. H. Jaffé, *J. Chem. Phys.*, 20, 279, 778, 1554 (1952); H. H. Jaffé *J. Am. Chem. Soc.*, 76, 5843 (1954).
5) For instance, G. C. Pimentel and A. L. McClellan, "The Hydrogen Bond," W. H. Freeman and Co., San Francisco, Cal. (1960). pp. 67—141.
6) M. Ōki and H. Iwamura, This Bulletin, 33, 717, 1599 (1960).
7) M. Ōki and K. Mutai, Presented at the 14th Annual Meeting of the Chemical Society of Japan, Tokyo, April, 1961.
8) M. Ōki and H. Iwamura, This Bulletin, 32, 950 (1959).

interacting form is always favored over the free one. On the contrary, in phenethyl alcohol the interaction is of little advantage and a fairly strong electron-donating group such as a *p*-amino substituent can only make the interacting form exceed the free one by a factor of 1.14.

To discuss the matter more fully, some comments should be made on the rotamer ratio in the corresponding compounds with no $\pi$-electron system available for interaction. The $A$(C–H)/$A$(H–H) ratio in *N*-ethylaniline is 8.7[1] and that in ethyl alcohol,[8] 0.56, where $A$(C–H) denotes the integrated intensity of the rotamer which has its X–H group hydrogen between carbon and hydrogen in the Newman projection (Fig. 3, I), and $A$(H–H), one with the X–H hydrogen between two hydrogens (Fig. 3, II).

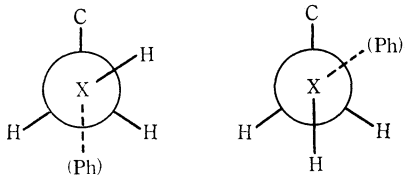



Fig. 3. Possible rotamers with regard to $CH_2$–X bond in C–$CH_2$–X–H.

The band at ca. 3445 $cm^{-1}$ shown in Table I should be assigned to the rotamer II. The fact that the ratio in *N*-ethylaniline is greater by the factor of ca. 15 than that of the alcohol may reasonably be explained by the steric effect of the phenyl group attached to the nitrogen, since the conformation with phenyl between two hydrogens (I) will be favored over one with the group between carbon and hydrogen (II) on account of the greater steric repulsion in the latter.

A comparison of the data in Table I with those of *N*-benzylanilines also shows two interesting points. First, the slope of the line obtained by plotting $\log(A_i/A_f)$'s against Hammett $\sigma$ values is remarkably steeper in *N*-phenethylaniline ($\rho=-0.85$) than that in *N*-benzylaniline ($\rho=-0.40$). Second, the $\log(A_i/A_f)$ values for the latter take both positive and negative signs, but those for the former take only the positive. These are rather abnormal phenomena, because in the *N*-phenethyl derivative the N–H group is separated farther by a methylene group when compared with benzylaniline and, therefore, the situation is unfavorable for the interaction (vide supra). The reasons for these unexpected results can be one or more of the following three: (1) The lower frequency band assigned to the interacting form is, in fact, composed of two bands, due to the interacting form and to the free rotamer, with the absorption maxima of the two at nearly the same position. (2) The absorption intensity per molecule of the interacting form is considerably higher than that of the free form. (3) On establishing the interaction, four- and five-membered rings are formed in *N*-benzyl- and *N*-phenethylaniline respectively. In view of ring strain and the bond angle of $p_\pi$–H–N in the rings, electronic interaction may be more fully effected in the larger ring, the effect leading to a real increase in the number of interacting molecules in spite of the statistical disadvantage.

The maximum positions of the bands due to the rotamers in *N*-ethylaniline are at 3445.2 and 3421.4 $cm^{-1}$, the latter being shifted to a wave number higher by ca. 6 $cm^{-1}$ than the maximum position of the interacting form in *N*-phenethylaniline. If this type of rotamer really exists, especially with a broad band width, it will be difficult to distinguish the bands at 3421 and 3415 $cm^{-1}$. It is even possible that they might in the calculations be regarded as one band in view of the technical uncertainties involved in dividing composite spectra. However, it is noteworthy that Fig. 2 shows a good linear correlation between $\log(A_i/A_f)$ and $\sigma$ values. This may reflect the fact that the contribution of the rotamer to the intensity $A_i$ is small for the reasons to be elucidated below. Let us consider an equilibrium:

$$f_1 \overset{K_i}{\rightleftharpoons} f_2 \overset{K_f}{\rightleftharpoons} i$$

where f and i denote the free and the interacting states respectively, and $f_1$ corresponds to the rotamer I and $f_2$ to the rotamer II in question. $K_f$ and $K_i$ are equilibrium constants. If it is true that the band at the lower wave number corresponds to the sum of the interacting and the free $f_2$ forms, $(f_2+i)/(f_1)$ rather than $(i)/(f_1+f_2)$ should be adopted as $A_i/A_f$. Therefore, $(A_i/A_f)=(f_2+i)/(f_1)=[K_f(f_1)+K_fK_i(f_1)]/(f_1)=K_f(1+K_i)$. In the above equation it is $K_i$ which is directly dependent on the substituent. On the other hand, $K_f$ changes indirectly and may be only a little dependent on the effect. Therefore, the conformity to a linear correlation for the wide range of $\log(A_i/A_f)$ values, as observed in Fig. 2, probably indicates the absence or the presence in only a small portion of $f_2$ in the equilibrium; at any rate the amount of $f_2$ cannot lead to the destruction of the linearity. However, there remains a possibility that $K_f$ and $K_i$ change so that $\log K_f(1+K_i)$ is linear with $\sigma$. Hence, postulate 1 cannot be obviated completely, but it probably is not a major factor.

Postulate 2 is very improbable. If the absorption intensity per molecule of the interacting form were appreciably larger than that of the free form, the sum of the intensities, i.e., $A_1+A_f$, should have increased with the increasing proportion of the interacting form. As is seen in Table I, however, the total intensities of the *p*-methoxyl and *p*-nitro derivatives are $3.93\times10^3$ and $4.02\times10^3$ $mol^{-1}\cdot l.\cdot cm^{-2}$ respectively, within the limit of experimental uncertainties. Hence, the postulate may be disregarded.

On the other hand, the remaining explanation, (3), seems to be more probable. A scale model shows a larger angle of $p_\pi$-N-H for *N*-phenethylaniline. Unfortunately, no literature has been published concerned with the experimental correlation between the hydrogen bond energy and the linearity of the bond in the non-crystalline state, but some theoretical estimations[9] seem to lend support to the explanation that in the hydrogen bond, the larger the deviation angle from linearity, the less the bond energy. The explanation is really consistent with the data obtained. It is probably the most significant factor in the effects; at least it is a major factor.

One further difference between the spectral characteristics of these homologs is concerned with $\Delta\nu_{max}$ values. In *N*-benzylanilines the values range from 30 to 42 $cm^{-1}$, whereas in *N*-phenethylanilines the range is from 29 to 32 $cm^{-1}$. This sharp contrast in the $\Delta\nu_{max}$ range may serve as a key to elucidate the mechanism of the interaction, but no convincing explanation has been obtained so far.

**N-Arylphenethylamines.** — Since the intramolecular interaction between the N-H group and π-electrons has been proved to exist in *N*-phenethylanilines, it seemed of interest to introduce various kinds of substituents into the aniline ring of the compound. The substituents might have an effect on the N-H group through resonance and induction, and, in turn, the effect may appear in the property of the interaction. For this purpose, four derivative were synthesized and their spectra investigated. Their absorption curves are shown in Fig. 4.

A comparison of Fig. 4 with Fig. 1 shows some differences between the spectral features of these series of derivatives. The absorption curves in Fig. 4 do not show two clear maxima. the presence of the latter two having been one of the characteristics of the interaction between the N-H group and the π-electrons. Additionally, three apparent characteristics can be pointed

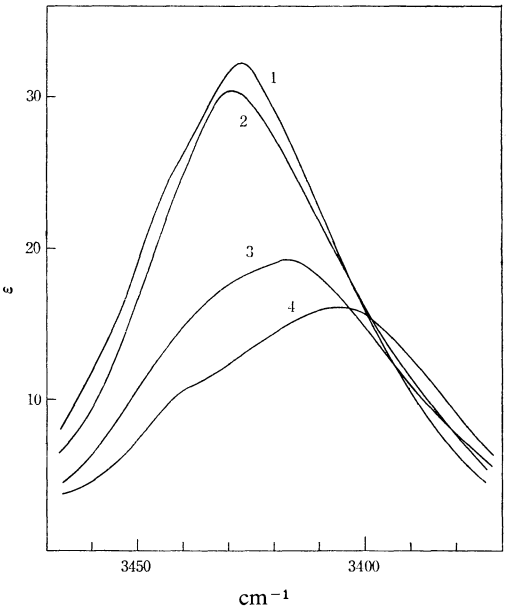



Fig. 4. $\nu_{N-H}$ Absorptions of *N*-(*m*-bromophenyl)- (1), *N*-(*p*-chlorophenyl)- (2), *N*-*p*-tolyl- (3) and *N*-*p*-anisyl-phenethylamines (4).

out in relation to the electronic effect of the substituent; as the electron-withdrawing power of a substituent increases (as the Hammett σ value inrceases), (a) the maximum intensity increases, (b) the half-band width decreases, and (c) the apparent maximum position shifts to a higher wave number. These characteristics, however, are not always peculiar to the N-H···π interaction, because they are also observed in *N*-arylethylamines, which lack a π-electron source for the interaction, as is shown in Fig. 5, and in *N*-methylanilines.[10] Although the substituent effects reveal just the same trend, a close examination of the change in band shape draws attention to the fact that the introduction of a phenyl group to the ethyl group in *N*-arylethylamines produces some changes in shape. The absorption curve of an *N*-arylphenethylamine shows a broader band with a little lower maximum intensity than that of an *N*-arylethylamine with the same substituent. This difference seems to come from the different shape of the side band which appears in the lower wave number region. In *N*-arylethylamines the shape of the band is due to a rotamer, as has already been discussed. On the other hand, the band should be assigned to the interacting N-H group in *N*-arylphenethylamine, though a band due to the free rotamer absorbing in nearly the same region may be a contributing factor.

9) G. C. Pimentel and A. L. McClellan, "The Hydroggen Bond," W. H. Freeman and Co., San Francisco, Cal. (1960), pp, 242–245.

10) P. J. Krueger and H. W. Thompson, *Proc. Roy. Soc.*, A243, 143 (1957).

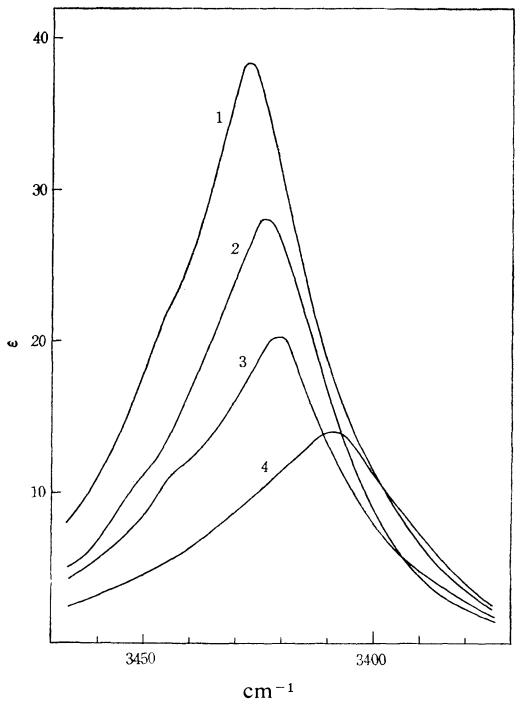



Fig. 5. $\nu_{N-H}$ Absorptions of *m*-bromophenyl- (1), *p*-chlorophenyl- (2), phenyl- (3) and *p*-anisyl-ethylamines (4).

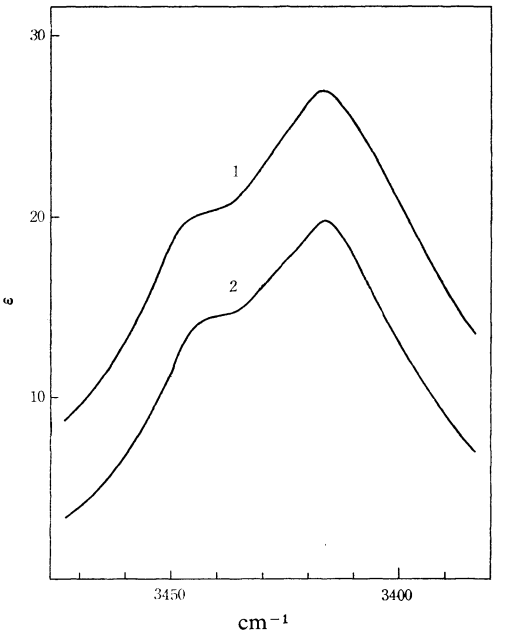



Fig. 6. $\nu_{N-H}$ Absorptions of *N*-*m*-tolyl-(1) and *N*-*p*-biphenylyl-phenethylamines (2). Curve (1) is displaced upward by 5 units.

The different features of the curves in Figs. 1 and 4 deserve comment. As has been reported previously,[1] the half-band width of the interaction band and the $\Delta\nu_{max}$ value in *N*-arylbenzylamine increase as a substituent becomes more electron-donating. Assuming that this relation still holds true in *N*-arylphenethylamine, a derivative with an electron-donating substituent should show a broader interaction band, with a larger $\Delta\nu_{max}$. The overlapping of the interaction band with the free results in a band with only one apparent maximum, on account of a broad band width in the case of an electron-donating substituent. On the other hand, although the half-band width is small in the case of an electron-withdrawing substituent, $\Delta\nu_{max}$ is also small, thus giving the apparent one band. Consequently, *p*-chloro and *m*-bromo derivatives show apparent narrower curves with an obscure shoulder in the higher wave number region, while *p*-methyl and *p*-methoxy derivatives show apparent broad curves. Although clear evidence for these explanations could be obtained by dividing the curves into their components, the band shape precludes this approach. Moreover, even if the division could be made, the experimental uncertainties could not be reduced to a level sufficiently low to permit a confident discussion of the results.

It should, in addition, be noted that the derivatives with a substituent of a nearly zero $\sigma$ value, e. g., *p*-phenyl ($-0.01$) and *m*-methyl ($-0.07$), show band shapes similar to that of unsubstituted *N*-phenethylaniline (see Fig. 6). This phenomenon suggests that the fact that the two maxima are indistinguishable in *N*-arylphenethylamine is not caused by a loss of a hydrogen atom from the benzene ring, but by the electronic effect of a substituent.

The authors are indebted to Professor Yoshiyuki Urushibara and Professor Takehiko Shimanouchi for their valuable discussions and encouragement. The authors are also indebted to the Ministry of Education for a grant-in-aid for Fundamental Scientific Research.

*Department of Chemistry*
*Faculty of Science*
*The University of Tokyo*
*Hongo, Tokyo*

# The Intramolecular Interaction between the N–H Group and π-Electrons. III.[1] Intramolecular Interaction in N-(ω-Phenylalkyl)anilines

By Michinori Ōki and Kiyoshi Mutai

(Received July 13, 1964)

In the previous papers of this series the existence of intramolecular interaction between the N–H group and π-electrons has been reported for *N*-benzylaniline[2] and *N*-phenethylaniline.[1] The predominance of the interacting form over the free form in the latter has now prompted the authors to investigate the higher homologs of *N*-(ω-phenylalkyl)aniline, $Ph\cdot(CH_2)_nNHPh$. In the alcoholic analogs, benzyl[3] and phenethyl[4] alcohols have been reported to show the same type of interaction.

In 3-phenylpropyl alcohol the interaction is absent unless the electron density is raised by the introduction of an electron-donating substituent into the benzene ring.[4] It would be interesting to know the limitation of the interaction by the chain length, since the N–H in an anilino group is known to be favorable toward the interaction.[1] Thus, the present paper is concerned with the determination of the limit of the chain length (the number, *n*) for the interaction and with an examination of its characteristics.

## Experimental

**Spectral Measurements and Calculations.**—They were performed as has been described previously.[1]

**Materials.**—The materials used for the measurement are known compounds, unless otherwise stated. Their physical constants agreed with those in the literature.

*N-(ω-p-Nitrophenylalkyl)anilines.*—All nitro derivatives of this type was prepared by the following method. A corresponding ω-phenylalkyl chloride or bromide was nitrated with a mixture of nitric acid and sulfuric acid. The ω-nitrophenylalkyl halide (*o*- and *p*-isomeric mixture) thus obtained was heated with ca. 4 equivalents of aniline at 180—200°C for 1—1.5 hr. The unreacted aniline was then removed by steam distillation, and the residue was extracted with ether. The solvent was distilled off, and the remaining oil was charged on a column of alumina. Elution with a petroleum ether - benzene mixture gave the desired product in a first eluate. The melting points and the results of elemental analyses are given in the following table.

*N-(3-Arylpropyl)- and N-(4-Arylbutyl)aniline.*—An appropriate hydrocinnamic acid or γ-phenylbutyric acid was heated with ca. 2 equivalents of aniline at a refluxing temperature to give anilide. This anilide, structure of which was confirmed by its infrared spectrum, was then recrystallized from 70% ethyl alcohol and reduced with lithium aluminum hydride, as has been described in a previous paper.[1] Probably because of the poor solubility of the anilide in ether, the yields were generally low.

The physical constants and the results of elemental analyses are given in the following table.

*N-(4-Phenylbutyl)aniline.*—4-Phenylbutyl chloride (12.0 g. or 0.07 mol.) was heated with 25 ml. of aniline at 190—200°C for 1 hr. The reaction mixture was neutralized with an aqueous sodium carbonate solution, the unreacted aniline was removed by steam distillation, and the organic layer was extracted with ether. After the solvent had been removed on a water-bath, the residue was distilled under reduced pressure, affording 8.3 g. (51% yield) of a pale yellow oil; b. p. 158—163°C (2.5 mmHg), $n_D^{22}$ 1.5836.

Found: C, 85.38; H, 8.73. Calcd. for $C_{16}H_{19}N$: C, 85.28; H, 8.50%.

*N-(5-Phenylpentyl)aniline.*—This compound was prepared by the same procedure as was *N*-(4-phenylbutyl)aniline. Pale yellow oil. Yield, 48%. B. p. 160—165°C (2.5 mmHg). $n_D^{22}$ 1.5740.

Found: C, 85.45; H, 9.00. Calcd. for $C_{17}H_{21}N$: C, 85.30; H, 8.84%.

*N-(7-Phenylheptyl)aniline.*—This compound was

$p\text{-}NO_2C_6H_4(CH_2)_nNHPh$

| *n* | M. p. °C | Carbon, % Calcd. | Carbon, % Found | Hydrogen, % Calcd. | Hydrogen, % Found | Nitrogen, % Calcd. | Nitrogen, % Found | Yield % |
|---|---|---|---|---|---|---|---|---|
| 3 | 52—53 | 70.29 | 70.44 | 6.29 | 6.40 | 10.93 | 10.97 | 48 |
| 4 | 105—106 | 71.09 | 71.32 | 6.71 | 6.80 | 10.36 | 10.29 | 33 |
| 5 | 59—60 | 71.75 | 71.80 | 7.36 | 7.09 | 9.73 | 9.85 | 23 |
| 7 | 52—53 | 73.04 | 72.84 | 7.74 | 7.87 | 8.97 | 8.79 | 36 |

1) Part II: M. Ōki and K. Mutai, This Bulletin, **40**, 387 (1965).
2) M. Ōki and K. Mutai, ibid., **33**, 784 (1960).
3) M. Ōki and H. Iwamura, ibid., **32**, 955 (1959).
4) M. Ōki and H. Iwamura, ibid., **32**, 1135 (1959).

*N*-(3-Arylpropyl)aniline $RC_6H_4(CH_2)_3NHPh$

| R | B. p. °C/mmHg | $n_D$ | Carbon, % | | Hydrogen, % | | Nitrogen, % | | Yield % |
|---|---|---|---|---|---|---|---|---|---|
| | | | Calcd. | Found | Calcd. | Found | Calcd. | Found | |
| *p*-MeO | 175—181/2 | 1.5848 (25°C) | 79.63 | 79.83 | 7.94 | 8.10 | 5.80 | 5.91 | 63 |
| *p*-$CH_3$ | 170—173/3 | 1.5760 (25°C) | 85.28 | 85.52 | 8.50 | 8.70 | | | 39 |
| *p*-Cl | 181—186/3 | 1.5910 (23°C) | 73.32 | 73.50 | 6.52 | 6.70 | 5.70 | 5.72 | 53 |

*N*-(4-Arylbutyl)aniline $RC_6H_4(CH_2)_4NHPh$

| | | | | | | | | | |
|---|---|---|---|---|---|---|---|---|---|
| *p*-MeO | 194—199/3 | 1.5742 (20°C) | 79.96 | 80.23 | 8.29 | 8.41 | 5.23 | 5.49 | 48 |
| *p*-Cl | 183—189/3 | 1.5841 (22°C) | 73.99 | 74.02 | 6.94 | 7.05 | 5.35 | 5.57 | 40 |

prepared from crude 7-phenylheptananilide (m. p. 71—75°C) by reduction with lithium aluminum hydride; it was obtained as a pale yellow oil. Yield, 45%; b. p. 180—185°C (2 mmHg), $n_D^{22}$ 1.5599.

Found: C, 85.13; H, 9.69. Calcd. for $C_{19}H_{25}N$: C, 85.34; H, 9.42%.

## Results and Discussion

***N*-(3-Arylpropyl)anilines.**—Three of the absorption curves measured in the N–H stretching region are shown in Fig. 1.

The shapes of the curves are similar to those of *N*-phenethylanilines. The two apparent maxima and the change in the relative absorption coefficients of the two with the substituent suggest the presence of the N–H$\cdots\pi$ interaction. Each curve was divided into two symmetric bands, each obeying the Lorentz function. No additional band was necessary to achieve a complete division. The data are summarized in Table I, in which the lower wave number band is assumed to be the interaction band.

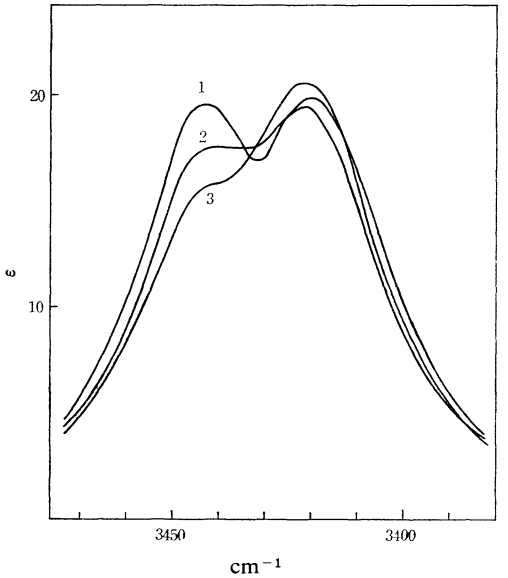



Fig. 1. $\nu_{N-H}$ Absorptions of *N*-(3-arylpropyl)-anilines: (1) *p*-nitro, (2) *p*-chloro and (3) *p*-methoxy.

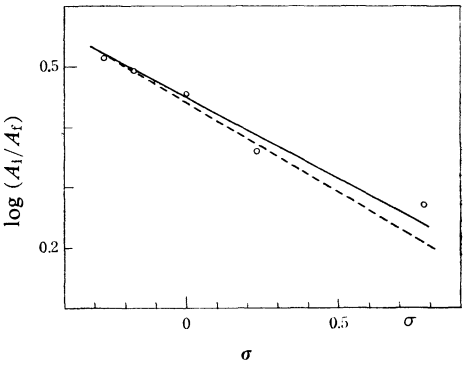



Fig. 2. The relationship between $\sigma$ value and log $(A_i/A_f)$ for *N*-(3-arylpropyl)aniline. Solid line; the value for *p*-nitro derivative ($\sigma=0.78$) is included. Broken line; the value for *p*-nitro derivative is excluded.

In the conventional approach, the $\log(A_i/A_f)$ value is compared with the Hammett $\sigma$ value[5] and, as Fig. 2 shows, a linear correlation is obtained. Hence, it may be said that the interaction exists in this compound.

A comparison of the data in Table I with those for *N*-phenethylanilines shows some interesting points: (1) the straight line is obtained only when the $\sigma$ value is so adopted as to indicate the interaction on the ring carbon atom attached to the aliphatic side chain*; (2) the slope ($\rho=-0.24$ for the solid line) of the line in Fig. 2 is gentler than that observed for *N*-phenethylaniline ($\rho=-0.85$);

5) L. P. Hammett, "Physical Organic Chemistry," McGraw-Hill Book Co., New York (1940); H. H. Jaffé, *Chem. Revs.*, 53, 191 (1953); D. M. McDaniel and H. C. Brown, *J. Org. Chem.*, 23, 420 (1958).

* This linearity may have to be discussed with some reserved significance, since the contribution of a free from to the absorption at a lower wave number cannot be neglected, as will be discussed later.

TABLE I. $\nu_{N-H}$ ABSORPTION OF N-(3-ARYLPROPYL)ANILINES
$RC_6H_4(CH_2)_3NHPh$

| R | Band | $\nu_{max}$ cm$^{-1}$ | $\Delta\nu_{max}$ cm$^{-1}$ | $\Delta\nu^a_{1/2}$ cm$^{-1}$ | $A\times10^{-3}$ mol$^{-1}$·l.·cm$^{-2}$ | log $(A_i/A_f)$ |
|---|---|---|---|---|---|---|
| p-$CH_3O$ | i[a] | 3420.4 | 27.1 | 37.6 | 2.58 | 0.516 |
| | f[b] | 3447.5 | | 25.0 | 0.79 | |
| p-$CH_3$ | i | 3420.5 | 26.7 | 36.6 | 2.88 | 0.493 |
| | f | 3447.2 | | 27.2 | 0.92 | |
| H | i | 3420.5 | 26.2 | 35.8 | 2.85 | 0.457 |
| | f | 3446.7 | | 26.2 | 0.99 | |
| p-Cl | i | 3420.5 | 25.9 | 39.0 | 2.40 | 0.362 |
| | f | 3446.4 | | 26.8 | 1.04 | |
| p-$NO_2$ | i | 3418.2 | 27.9 | 39.6 | 2.48 | 0.272 |
| | f | 3446.1 | | 27.2 | 1.32 | |

a) i denotes interacting form of N-H group.
b) f denotes free form of N-H group.

(3) the half-band width of the band assigned to the interacting form is narrower than that in N-phenethylanilines; (4) $\Delta\nu_{max}$ does not change appreciably with the substituent, but, again, it is smaller than that observed for N-phenethylanilines by ca. 4 cm$^{-1}$, and (5) log $(A_i/A_f)$ is positive even when a nitro group is introduced to the ring of the π-electron source, but the value is smaller than that of N-phenethylaniline with any corresponding substituent except the nitro derivative.

A comparison of the log $(A_i/A_f)$'s for N-(3-phenylpropyl)anilines with those for N-phenethylanilines show that the formation of a six-membered ring is less likely than that of a five-membered ring. The steeper slope for the latter ($n$=2) may be the result of the more sufficient overlap of the orbitals belonging to the N-H group with those of π-electrons in the five-membered ring. That is, the higher interaction energy is sensitively affected by a little change in π-electron density. Of the derivatives of N-phenethylaniline and N-(3-phenylpropyl)-aniline, only log $(A_i/A_f)$ value which is higher in the higher homolog is obtained for the p-nitro derivative.

This result seems inconsistent with the consideration established above. This anomaly may be explained in the following way. As was noted in an earlier paper,[2] the free form can take two different states, corresponding to the two rotamers observed for N-ethylaniline, one of which absorbs at ca. 3420 cm$^{-1}$. As the electron-withdrawing power of the substituent increases in N-(3-arylpropyl)aniline, the number of the N-H group in the free form increases. In the p-nitro derivative the population of one of the rotamers, the presence of which can be regarded as negligible in lower homologs, may become sufficiently noticeable in the spectrum and may contribute to the intensity to an appreciable extent. Thus, the band assigned to the interacting form in the derivative may be in fact a composite of the interacting form and the free form, both absorbing at nearly the same position. There is supporting evidence for this explanation. As is illustrated in Fig. 2, the value for the p-nitro derivative falls above the line. This deviation suggests an overestimation of $A_i$, to which the intensity due to one of the free forms contributes as well as that of the interacting form. Accordingly, the correlation line in Fig. 2 should be drawn with a modification of the slope (the broken line). By a least-square method, disregarding the p-nitro derivative, the slope is −0.31.

The ratio of the free form to the interacting form in $A_i$ will not be large enough to preclude the presence of the interaction in the derivative, since the log $(A_i/A_f)$ of N-(7-p-nitrophenylheptyl)aniline (see Table III), which is free from the interacting N-H group, is appreciably greater than that of this lower homolog.

**N-(4-Arylbutyl)anilines.**—The data on N-(4-arylbutyl)anilines are given in Table II.

As is shown by the filled circles in Fig. 3, a plot with $\sigma_p$'s for p-substituents does not allow a correlation significant enough to confirm the presence of the interaction. On the other hand, a plot with $\sigma_m$'s changes the situation fairly favorable for its presence. As the open circles in Fig. 3 show, the log$(A_i/A_f)$'s are in the order of corresponding σ values, though not linear. Since one of the free rotamers doubtlessly makes a certain contribution to the intensity assigned to the interaction band, it would be rash to conclude that the improvement of the σ–log $(A_i/A_f)$ relationship by the adoption of the $\sigma_m$ value reflects the actual site of the interaction. Nevertheless, it may be safe to conclude that the interaction does exist in N-(4-phenylbutyl)-anilines, for a comparison of the log $(A_i/A_f)$'s of

Table II. $\nu_{N-H}$ Absorption of *N*-(4-arylbutyl)anilines
$RC_6H_4(CH_2)_4NHPh$

| R | Band | $\nu_{max}$ cm$^{-1}$ | $\Delta\nu_{max}$ cm$^{-1}$ | $\Delta\nu^a_{1/2}$ cm$^{-1}$ | $A\times10^{-3}$ mol$^{-1}$·l.·cm$^{-2}$ | log $(A_i/A_f)$ |
|---|---|---|---|---|---|---|
| *p*-$CH_3O$ | i[a] | 3422.2 | 26.0 | 35.6 | 2.26 | 0.414 |
| | f[b] | 3448.2 | | 31.2 | 0.87 | |
| H | i | 3421.2 | 25.7 | 39.4 | 3.13 | 0.540 |
| | f | 3446.9 | | 31.0 | 0.90 | |
| *p*-Cl | i | 3421.8 | 25.4 | 36.2 | 2.22 | 0.396 |
| | f | 3447.2 | | 26.4 | 0.89 | |
| *p*-$NO_2$ | i | 3420.8 | 25.7 | 36.8 | 2.44 | 0.326 |
| | f | 3446.5 | | 27.6 | 1.15 | |

a) i denotes interacting form of N-H group.
b) f denotes free form of N-H group.

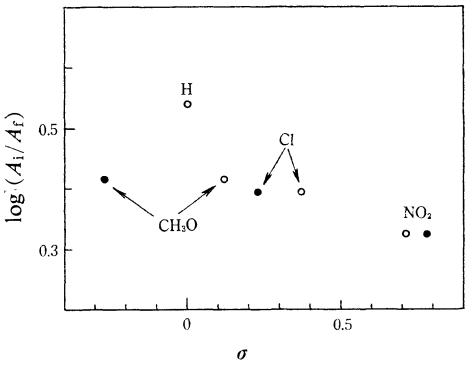



Fig. 3. The relationship between $\sigma$ value and log $(A_i/A_f)$ for *N*-(4-arylbutyl)aniline. Filled circles, $\sigma_p$; open circles, $\sigma_m$.

unsubstituted (0.540) and *p*-nitro (0.326) derivatives shows a significant difference, one which cannot be explained by any other reason than the N-H$\cdots\pi$ interaction.

This conclusion is important in that, in the hydroxy analog, $C_6H_5(CH_2)_4OH$, no O-H$\cdots\pi$ interaction was observed[4]. Although the conditions for the interaction, especially the distance between the X-H group and the $\pi$-electron source, seem to be unfavorable in these compounds, the following may be added as supporting evidence.

Martin and Gleicher[6] determined the NMR spectra of $\omega$-phenyl-2-methyl-2-alkenes, $C_6H_5\cdot(CH_2)_nCH{=}C(CH_3)_2$. They concluded from the chemical shift of the terminal *cis*-methyl group that the group spends a considerable portion of the time over the plane of the benzene ring in those compounds in which *n* is 2 and 3. This conclusion suggests the likely importance of the number of the ring member in the X-H$\cdots\pi$ interaction and, at the same time, the significance of the restriction of the rotation around the $CH_2$-XH bond, which may be the main reason for the different behavior of the OH and NHPh groups in the interaction.

**Higher Homologs with $n=5$ and 7.**—As an extention, the infrared spectra of *N*-(5-phenylpentyl)- and *N*-(7-phenylheptyl)anilines and of *p*-nitro derivatives were recorded. The N-H stretching absorption curves are shown in Figs. 4 and 5, and the analyzed data, in Table III. The observed spectra (Fig. 4) for *N*-(5-phenylpentyl)aniline and its nitro derivative are slightly different in the higher wave number band, with a higher intensity for the *p*-nitro derivative. The data given in Table III indicate this point more clearly. The log $(A_i/A_f)$ of the *p*-nitro derivative is smaller than that of the unsubstituted compound, but nearly

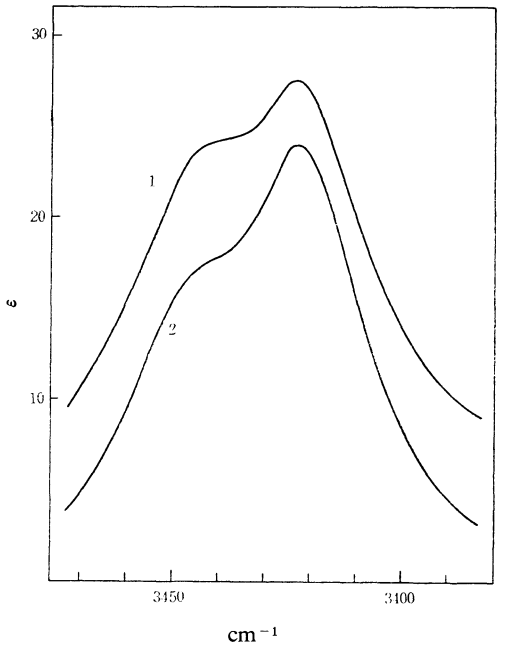



Fig. 4. $\nu_{N-H}$ Absorptions of *N*-(5-*p*-nitrophenylpentyl)- (1) and *N*-(5-phenylpentyl)anilines (2). Curve (1) is displaced upward by 5 units.

6) M. M. Martin and G. J. Gleicher, *J. Am. Chem. Soc.*, **86**, 238 (1964).

TABLE III. $\nu_{N-H}$ ABSORPTION OF HIGHER HOMOLOGS OF $RC_6H_4(CH_2)_nNHPh$ ($n$=5 and 7)

| $n$ | R | Band | $\nu max$ cm$^{-1}$ | $\Delta\nu max$ cm$^{-1}$ | $\Delta\nu^a_{1/2}$ cm$^{-1}$ | $A\times10^{-3}$ mol$^{-1}$·l.·cm$^{-2}$ | log ($A_i/A_f$) or log ($A_I/A_{II}$) |
|---|---|---|---|---|---|---|---|
| 5 | H | i[a] | 3421.6 | 25.2 | 33.4 | 2.63 | 0.428 |
| | | f[b] | 3446.8 | | 27.4 | 0.98 | |
| 5 | *p*-$NO_2$ | i | 3421.6 | 25.2 | 36.4 | 2.59 | 0.361 |
| | | f | 3446.8 | | 27.6 | 1.13 | |
| 7 | H | I | 3422.7 | 25.6 | 33.8 | 2.12 | 0.421 |
| | | II | 3448.3 | | 26.8 | 0.81 | |
| 7 | *p*-$NO_2$ | I | 3422.4 | 25.3 | 34.4 | 2.68 | 0.450 |
| | | II | 3447.7 | | 26.2 | 0.95 | |

a) i denotes interacting form of N-H group.
b) f denotes free from of N-H group.

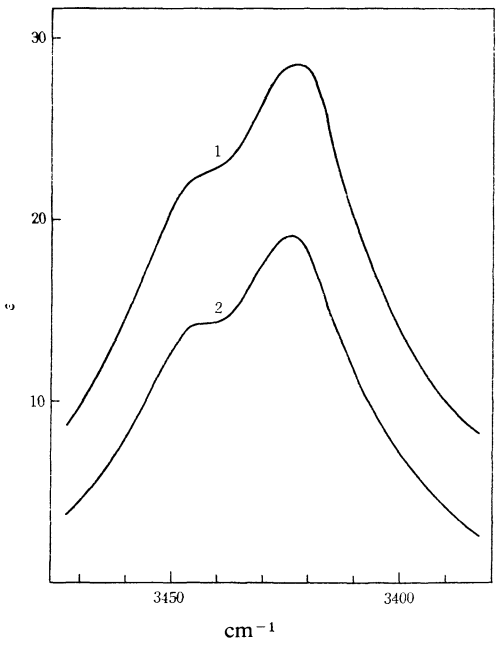



Fig. 5. $\nu_{N-H}$ Absorptions of *N*-(7-*p*-nitrophenylheptyl)- (1) and *N*-(7-phenylheptyl)anilines (2). Curve (1) is displaced upward by 5 units.

within the range of experimental error (ca. 0.05). If the observed effect of the substituent is meaningful, that fact should be interpreted as a reflection of the presence of the N-H···π interaction. Although the matter should be treated with great care, it seems that the apparent spectrum which shows the stronger absorption at higher wave number for the nitro compound suggests the existence of such interaction.

Two absorption curves of the higher homolog ($n$=7) (Fig. 5) indicate no substantial difference. Analyzed data also show the same result. The log ($A_i/A_f$)'s for two derivatives are similar within the range of experimental error. From these data, it can safely be concluded that the interaction is absent in *N*-(7-phenylheptyl)aniline.

**General Discussion.**—In summarizing the data for this series of compounds, $Ar(CH_2)_nNHPh$, one can conclude that the intramolecular interaction of the N-H group with π-electrons is present in the cases where $n$ is 1, 2, 3 and 4, and possibly 5. In contrast to this, in the hydroxy analog, $Ar(CH_2)_nOH$, it has been reported[3,4] that the O-H···π intramolecular interaction is present only in the cases where $n$ is 1, 2 and 3. From these results, it is tempting to conclude that the N-H group is more favorable for the interaction with π-electrons than is the O-H group, at least in these species.

As for chemical reactivity, the O-H group is more reactive and has more proton-releasing power than the N-H group. Additionally, and more significantly, it is generally accepted that the tendency of amines to associate is less than that of hydroxylic compounds.[7] The association of aniline in the liquid phase has been investigated by several workers[8-12] by infrared spectroscopy; it has been concluded that the shift of the N-H stretching bands of aniline with a change in concentration is due to N-H···N hydrogen bonding, with a very low energy. Recent ultraviolet spectroscopic studies[13] also show that hydrogen bonding in aniline is not very strong. Although Bellamy and Williams[14] have postulated that the steady shift of the bands to lower frequencies with

7) M. L. Huggins, *J. Org. Chem.*, 1, 407 (1936).
8) E. L. Kinsey and J. W. Ellis, *J. Chem. Phys.*, 5, 399 (1937).
9) W. Gordy, ibid., 7, 167 (1939).
10) E. Williams, R. Hofstadter and R. C. Herman, ibid., 7, 802 (1939).
11) A. N. Buswell, J. R. Downing and W. H. Rodebush, *J. Am. Chem. Soc.*, 62, 2759 (1940).
12) N. Fuson, M. L. Josien, R. L. Powell and E. Utterback, *J. Chem. Phys.*, 20, 145 (1952).
13) J. C. Dearden and W. F. Forbes, *Can. J. Chem.*, 38, 896 (1960).
14) L. J. Bellamy and R. L. Williams, *Spectrochim. Acta*, 9, 341 (1957).

an increase in the concentration can be explained by dielectric constant and dipolar effects in the liquid, Rao and his co-workers[15] studied the problem by NMR spectroscopy and confirmed the presence of a N-H···N hydrogen bond in aniline with quite a low energy. All these data suggest that the N-H group, especially in aniline, is much less proton-donating in hydrogen bonding than is the O-H group.

These opposing pieces of evidence raise the question of whether or not the bands observed in the N-H stretching region can be assigned to free and N-H···$\pi$ interacting forms with certainty. Other possible causes affecting two bands may be the Fermi resonance, or the presence of an overtone or a combination band. An inspection of the spectra of some compounds used in this series of papers in the sodium chloride region indicates that such effects cannot be expected for the compounds; on normal vibration band appears between 1650 and 2900 $cm^{-1}$, and it has been reported that there are two N-D stretching bands in *N*-deuterio-*N*-benzylaniline.[16]

Additional evidence for the equality of N-H and O-H groups as hydrogen donors was obtained by the determination of the interaction energy ($\Delta H$). The energies in the intramolecular O-H···$\pi$ interaction reported so far do not, in general, exceed 2.0 kcal./mol. The values for the N-H group have also been found, by a brief study of the energetics of *N*-benzylanilines,[17] to be within the same limits. Hence, O-H and N-H groups should be regarded as, at least, equally affecting functions for intramolecular interaction with $\pi$-electrons.

Probably one of the factors which result in the N-H group being equal with or having the advantage over the O-H group is the different extent of populations of rotamers caused by the rotations around the $CH_2$-NH and the $CH_2$-OH bands in the corresponding compounds. Taking *N*-ethylaniline and ethyl alcohol as reference compounds, the ratios of the state of possible interaction to that of the impossible are 8.7[2] and 0.57[18] respectively. The discrepancy, by a factor of more than 15, may reasonably be attributed to the large steric requirement of the phenyl group.

Finally, mention should be made of the interesting features of the spectra for this series of compounds in connection with the

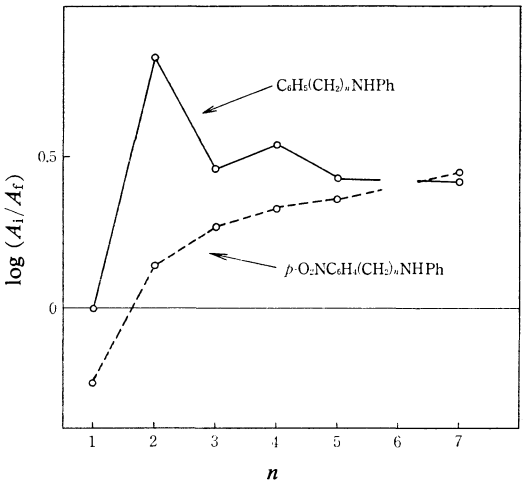



Fig. 6. The relationship between the number of the side chain carbon ($n$) and log ($A_i/A_f$) *N*-($\omega$-arylalkyl)aniline, $RC_6H_4(CH_2)_nNHPh$.

change in log ($A_i/A_f$) with the substituent and the chain length. The values for non-substituted and *p*-nitro derivatives are especially worthy of consideration. As is shown in Fig. 6, log ($A_i/A_f$)'s for *N*-($\omega$-phenylalkyl)anilines change in a zigzag fashion with the number of chain carbon atoms ($n$) and approach a limited value with a decreasing amplitude. The prominent peak at $n=2$ is the reflection of the highly favorable conditions for the N-H···$\pi$ interaction in this homolog. The following zigzag change with a small amplitude is interesting, but experimental uncertainties do not at present allow any unambiguous explanation for this.

On the other hand log ($A_i/A_f$)'s for *p*-nitro derivatives increase with increasing $n$ values and reach a limit. It may seem strange that the curve gives the impression that the longer the chain, the greater the ratio of the interacting form. However, as has been discussed, the $A_i$'s for higher homologs are overestimated when the intensity due to a free form is included. The gradual decrease of $\Delta\nu_{max}$ and its approach to the value for the compound lacking the interaction may be cited as support for this interpretation. The values for $n=3$, 4 and 5 can be explained on this basis, because no complete Hammett correlation is observed for them. The values for $n=1$ and 2 should be regarded as true ratios of $A_i$ and $A_f$, because the plots of log ($A_i/A_f$) against the $\sigma$ value yield good linear correlations.

A comparison of the log ($A_i/A_f$) values for *p*-nitrobenzyl- and *p*-nitrophenethylanilines gives an interesting picture of the molecular conformation. The value for the former, $-0.244$, is appreciably lower than that for the

15) B. D. N. Rao, P. Venkateswarlu, A. S. N. Murthy and C. N. R. Rao, *Can. J. Chem.*, **40**, 963 (1960).
16) A. G. Moritz, *Spectrochim. Acta*, **16**, 1176 (1960).
17) M. Ōki and K. Mutai, Presented at the 14th Annual Meeting of the Chemical Society of Japan, Tokyo, April, 1961.
18) M. Ōki and H. Iwamura, This Bulletin, **32**, 950 (1959).

latter, 0.148. This remarkable discrepancy may be partly the consequence of the preference for the five membered ring conformation in the interacting states. However, the free form absorbing at ca. 3450 $cm^{-1}$ in the *p*-nitrobenzyl derivative should be the conformer with two phenyl groups at an eclipsed or nearly-eclipsed position (see Ref. 2). In this conformation considerable repulsive forces will operate to prevent the two phenyls from becoming eclipsed; therefore, the state will be unstable compared with the interacting form in which phenyls are at trans and which is additionally stabilized by the interaction.

An explanation of this phenomenon will be published in a forthcoming paper.

The authors are indebted to Professor Yoshiyuki Urushibara and Professor Takehiko Shimanouchi for their valuable discussions and encouragement. They are also indebted to the Ministry of Education for a grant-in-aid for Fundamental Scientific Research.

*Department of Chemistry*
*Faculty of Science*
*The University of Tokyo*
*Hongo, Tokyo*

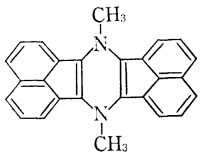
# Studies of Acenaphthene Derivatives. XI.[1] The Reaction of Acenaphthenequinone with Aliphatic Amines

By Otohiko TSUGE and Masashi TASHIRO

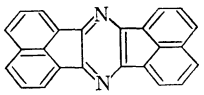
(Received July 23, 1964)

In an earlier paper[2] dealing with the reaction between acenaphthenequinone (I) and ammonia, it was shown that the structure of red crystals (II) is neither acenaphthenequinonimide anhydride[3] nor acenaphthazine,[4] but acenaphtho [1, 2-b] isoimidazole-2-spiro - 2' - acenaphthenone.

It had been shown by Rule and Thompson[5] that the reaction of I with aqueous methylamine at 100°C in a sealed tube afforded brown needles (III) (m. p. over 360°C); for these *N, N'* - dimethyldihydroacenaphthazine (IIIa) was assumed on the basis of the nitrogen value and the structure of acenaphthazine (IIIb) suggested by Schönberg and Nedzati[4] for II.



(IIIa)



(IIIb)

1) Part X: O. Tsuge and M. Tashiro, The Reports of the Research Institute of Science and Industry (Seisan Kagaku Kenkyusyo Hōkoku), Kyushu University, No. 36, 1 (1963).

2) O. Tsuge and M. Tashiro, This Bulletin, **36**, 970 (1963).

3) C. Graebe and E. Gfeller, *Ann.*, **276**, 1 (1893).

4) A. Schönberg and F. Nedzati, *Ber.*, **54**, 238 (1921).

5) H. G. Rule and S. B. Thompson, *J. Chem. Soc.*, **1937**, 1761.

Since Rule and Thompson's assumption of the structure of IIIa is incorrect, however, it is doubtful whether the structure of III is IIIa or not.

It was also found that naphthalimide was formed, even if the reaction of I with ammonia was carried out under mild conditions. Accordingly, I may be expected to result easily in the formation of the corresponding naphthalimide derivative by an aliphatic amine with a higher basicity than that of ammonia. However, little information is available regarding the formation of *N*-methylnaphthalimide by the reaction of I with methylamine.

The present paper deals with the results of a reexamination of the structure of III and of the reaction of I with methyl-, ethyl- and benzylamine.

## Results and Discussion

The reaction of I with 30% aqueous methylamine at 100°C in a sealed tube according to the Rule and Thompson procedure afforded yellow needles (III), m. p. over 400°C, and *N*-methylnaphthalimide (IV) in low yields due to the formation of a resinous material.

The elemental analytical data on III were in agreement with the formula $C_{24}H_{12}N_2$, whose infrared spectrum did not reveal any bands ascribed to the aliphatic C–H and N–H bonds. As Fig. 1 shows, its ultraviolet spectrum is

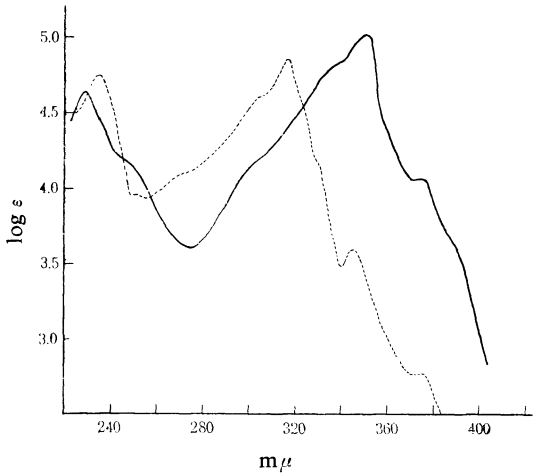



Fig. 1. UV spectra of IIIb and acenaphtho-[1,2-b]quinoxaline in dioxane.
—— IIIb
---- Acenaphtho[1,2-b]quinoxaline

very similar to that of the known compound, acenaphtho[1,2-b]quinoxaline.[6] In addition, the oxidation of III with sodium dichromate in boiling glacial acetic acid resulted in the recovery of III, so it might be considered that III has a stable structure for the oxidation.

These observations are accommodated much better by the structure of acenaphthazine (IIIb) than by IIIa. The mechanism of the formation of IIIb will be discussed below.

On the other hand, IV was identical with an authentic sample prepared by the reaction of naphthalic anhydride and methylamine.[7]

In treatment at room temperature for a long period, IV was formed as the main product, along with a small amount of IIIb.

In view of the fact that IIIb was obtained in the reaction of I with methylamine, it may well be doubted whether or not IIIb can be formed in the reaction of other amines than methylamine with two hydrogen atoms on the α-carbon atom. If IIIb is formed in the reaction with such amines, the structure of IIIb for III is more probable.

In the case of the reaction of I with 70% aqueous ethylamine at 80°C for 15 min., as had been expected, IIIb and *N*-ethylnaphthalimide (V) were obtained in yields of 17.5 and 42.5% respectively. V was proved, by the admixed melting point and by the infrared spectrum, to be identical with an authentic sample prepared by the reaction of naphthalic anhydride and ethylamine.[7]

In the reaction of I with 40% aqueous benzylamine or 100% benzylamine, also, IIIb and *N*-benzylnaphthalimide (VI) were formed in low yields as a result of the formation of a resinous material. Although the reported melting point of VI was 95—96°C,[8] the VI which was obtained by the reaction and by the condensation of potassium naphthalimide and benzyl bromide melted at 195—195.5°C.

Furthermore, benzaldehyde was isolated and and identified as the 2,4-dinitrophenylhydrazone in the reaction with benzylamine. This fact suggests the mechanism of the formation of IIIb in the reaction of I with an amine having two hydrogen atoms on the α-carbon atom.

The formation of IIIb may be as shown in Chart I. That is, *N*-alkylacenaphthenequinonimine (VII), the product of I and one equivalent of amine, rearranges to the Schiff base (VIII). The subsequent hydrolysis of the Schiff base would yield the aldehyde and 1,2-aminoacenaphthenole (IX). The self-condensation of IX leads to the formation of dihydroacenaphthazine (X), which easily dehydrogenates to IIIb.

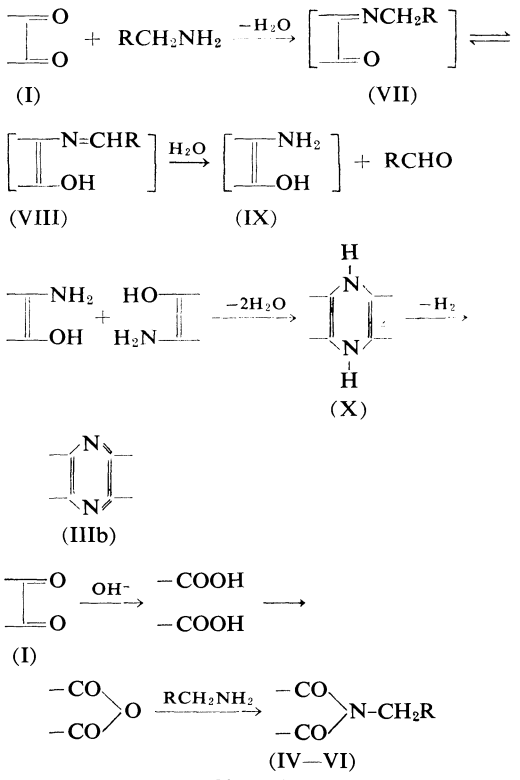



Chart 1.

In the reaction of I with ammonia, acenaphthenequinone monoimine corresponding to

6) This compound was prepared by the condensation of I and *o*-phenylenediamine. (G. Ampola and V. Recchi, *Atti R. Accad. dei Lincei Roma* [5], **8**, 209; *Chem. Zentr.*, **1899**, II, 338.)

7) G. F. Jaubert, *Ber.*, **28**, 360 (1895).

8) S. M. A. Devereux, S. N. J. M. and H. B. Donahoe, *J. Org. Chem.*, **25**, 457 (1960).

VII was isolated.[2] Since the monoimine can not be rearranged to the corresponding Schiff base, it might be considered that the self-condensation of the monoimine resulted in the formation of the isoimidazole derivative mentioned above.

On the other hand, *N*-alkylnaphthalimide is assumed to be formed through naphthalic acid and naphthalic anhydride, as has been shown in a previous paper.[2]

## Experimental[9]

**The Reaction of I with Aqueous Methylamine.**—*a) By the Rule and Thompson Procedure.*—A mixture of 2.0 g. of I and 5 ml. of 30% aqueous methylamine was heated in a sealed tube at 100°C for 6 hr. After it had cooled, the mixture was poured into water and the resinous precipitate was collected; then this was extracted with 100 ml. of methanol, leaving 0.5 g. (28%) of brown crystals, m. p. over 360°C. Recrystallization from nitrobenzene or sublimation afforded acenaphthazine (IIIb) as yellow needles, m. p. over 400°C.

Found: C, 87.79; H, 3.83; N, 8.57. Calcd. for $C_{24}H_{12}N_2$: C, 87.78; H, 3.68; N, 8.53%.

UV $\lambda_{max}^{Dioxane}$ m$\mu$ (log $\varepsilon$): 228.5 (4.64), 348 (5.03).

After the extract had been evaporated, there remained a resinous material, which was then dissolved in benzene and chromatographed on alumina. From the benzene eluate, *N*-methylnaphthalimide (IV) was obtained in the form of colorless needles (Found: C, 74.16; H, 4.32; N, 6.56%). Yield, 0.15 g. (6.3%); m. p. 205°C (lit.[7] m. p. 205°C). This compound was identical with the authentic sample prepared from naphthalic anhydride and methylamine.

*b) At Room Temperaure.*—A suspension of 2.0 g. of I in 20 ml. of 30% aqueous methylamine was stirred in a closed vessel at room temperature for 24 hr. During this time the mixture turned brown. After the reaction mixture had been poured into water, the precipitate was collected, washed with water, dried, and extracted with 50 ml. of hot ethanol, leaving 0.5 g. (28%) of brown crystals, m. p. over 360°C. Recrystallization from nitrobenzene gave yellow needles whose infrared spectrum was superimposable with that of IIIb.

After the ethanol extract had cooled, filtration afforded 1.4 g. (60.3%) of colorless needles, m. p. 195—198°C. Recrystallization from ethanol gave colorless needles, m. p. 205°C, which were proved, by the admixed melting point and infrared spectrum, to be identical with IV.

**The Reaction of I with Aqueous Ethylamine.**—A solution of 2.0 g. of I in 20 ml. of 70% aqueous ethylamine was heated at 80°C for 15 min. The color of the solution turned from green to reddish brown within a few minutes. The reaction mixture was then poured into water, and the precipitate collected, washed with water, dried, and extracted with 200 ml. of ether. The ether-extract was evaporated to give 1.05 g. (42.5%) of pale brown crystals, m. p. 140—145°C. Recrystallization from ethanol afforded pale yellow prisms, m. p. 154—155°C (lit.[8] m. p. 154°C. This compound was found to be identical with the *N*-ethylnaphthalimide (V) which was prepared from naphthalic anhydride and ethylamine.

The ether-insoluble residue was washed with hot benzene, leaving 0.63 g. (17.5%) of brown crystals, m. p. over 360°C. Recrystallization from nitrobenzene or sublimation afforded yellow needles which were identical with IIIb. The benzene-washing was then evaporated, leaving a resinous material which was not investigated further.

**The Reaction of I with Benzylamine.**—*a) With a 40% Aqueous Solution.*—When a solution of 2.0 g. of I in 20 ml. of 40% aqueous benzylamine was heated at 80°C for 1 hr., similar phenomena were observed. The reaction mixture was poured into water to precipitate a brown resinous substance. The precipitate was then collected, washed with water, dried and extracted with ether, leaving brown crystals. The ether-insoluble brown crystals were washed with 100 ml. of hot benzene, leaving 0.2 g. (7.2%) of brown crystals, m. p. over 360°C. Recrystallization from nitrobenzene afforded yellow needles whose infrared spectrum was superimposable on that of IIIb.

The benzene-washings was evaporated to leave 0.8 g. (25.8%) of pale brown crystals. Recrystallization from isopropyl alcohol afforded pale yellow needles m. p. 195—195.5°C.

Found: C, 79.47; H, 4.59; N, 4.91. Calcd. for $C_{19}H_{13}O_2N$: C, 79.43; H, 4.56; N, 4.88%.

This compound was identical with the *N*-benzylnaphthalimide prepared from potassium naphthalimide and benzyl bromide.

Although a reddish violet resinous material was obtained from the ether-washings, it was not investigated further.

*b) With 100% Benzylamine.*—A mixture of 2.0 g. of I and 4 ml. of benzylamine was heated at 80°C for 1 hr. After the mixture had been cooled, filtration afforded a brown precipitate which, on being washed with hot benzene, left 0.4 g. (14.3%) of brown crystals, m. p. over 360°C. Recrystallization from nitrobenzene afforded yellow needles which were identical with IIIb. The combined solution of the filtrate and the benzene-washings was then dried over sodium sulfate and chromatographed on alumina. To the first fraction of the red benzene eluate, a solution of 0.1 g. of 2, 4-dinitrophenylhydrazine in ethanol and then one drop of concentrated hydrochloric acid were added. The resultant solution was heated on a water bath for 30 min. and then cooled. Filtration gave orange crystals (50 mg.), m. p. 235°C, which were proved, by the admixed melting point and by the infrared spectrum, to be identical with benzaldehyde-2, 4-dinitrophenylhydrazone.

From the next fraction of the benzene eluate, *N*-benzylnaphthalimide (VI) was obtained as pale brown crystals. Yield, 0.4 g. (17.9%); m. p. 190—193°C. Recrystallization from isopropyl alcohol afforded pale yellow needles, m. p. 195—195.5°C. Although a resinous material was obtained from the other fractions of the benzene-ethanol eluate, it was not investigated.

9) All melting points are uncorrected.

***N*-Benzylnaphthalimide.**[8] — A mixture of 0.5 g. of potassium naphthalimide, which had been prepared from naphthalimide and potassium hydroxide according to the method of Mattocks and Hutchinson,[10] and 0.4 g. of benzyl bromide in 10 ml. of dimethylformamide was heated on a water bath for 1 hr. After the reaction mixture had been poured into water, filtration gave 0.55 g. (86.7%) of pale yellow crystals, m. p. 189—192°C. Recrystallization from isopropyl alcohol afforded pale yellow needles, m. p. 195—195.5°C (lit.[8] 95—96°C).

10) A. M. Mattocks and O. S. Hutchinson, *J. Am. Chem. Soc.*, **70**, 3474 (1948).

The authors wish to express their gratitude to the Kaisei Aid Association for providing the funds for this investigation, and also to the Yawata Chemical Co. for the supply of acenaphthene. They are indebted to the staff of the Analytical Service Centre of this university for the microanalyses.

*The Research Institute of Science and Industry*
*Kyushu University*
*Hakozaki, Fukuoka*

# The Spectrophotometric Determination of Anions by Solvent Extraction with Metal Chelate Cations. VI. A New Method for the Determination of Mercury(II)

By Keiya KOTSUJI

(Received July 23, 1964)

Margerum and Banks[1] have reported that the 1, 10-phenanthroline iron(II) chelate cation is extracted as the perchlorate complex into nitrobenzene. Diamond and Tuck[2] and Kuznetsov[3] have recently described how a large anion, such as $ClO_4^-$, $I^-$ or $NCS^-$, can be extracted into nitrobenzene with a large cation of the phenanthroline iron(II) chelate. In a similar fashion, Tribalat and Beydon[4-7] have shown that a large anion, such as $ReO_4^-$ or $TcO_4^-$, can be extracted into a polar solvent with a large cation of an onium compound, such as $Ph_4As^+$ or $Ph_4P^+$.

On the other hand, in the first paper[8] of this series, it has been shown how the 2, 2'-dipyridyl iron(II) chelate cation is extracted into nitrobenzene from an aqueous solution containing perchlorate ion. Moreover, as has previously been reported,[9] mercury(II) can be extracted into 1, 2-dichloroethane with the dipyridyl iron(II) chelate if the aqueous solution contains a large excess of iodide ions; the intensity of the red color of this extract is proportional to the amount of mercury(II). A consideration of these findings led to the present study, which is concerned with the optimum conditions for the determination of mercury(II).

This paper will report on a new spectrophotometric method for the determination of mercury(II) with the 2, 2'-dipyridyl iron(II) chelate, based upon a solvent extraction of the associated complex formed between the colored dipyridyl iron(II) chelate cation and the colorless tetra-iodo-mercury(II) complex anion, and upon the estimation of the chelate absorbance in the organic phase.

For the colorimetric determination of mercury, the dithizone method[10] is most familiar, but other methods are known in the literature, using diethyldithiocarbamate[11] and diphenylcarbazone[12]. Karas and Pinter[13] have shown that the intensity of the red color of the dipyridyl iron(II) chelate is inversely proportional to the amount of mercury(II), since

1) D. W. Margerum and C. V. Banks, *Anal. Chem.*, **26**, 200 (1954).
2) R. M. Diamond and D. G. Tuck, "Progress in Inorganic Chemistry," Vol. II, Interscience Publishers, New York (1960), pp. 139—150.
3) B. I. Kuznetsov, "The Chemical Basis for the Photometric Method by Solvent Extraction in Analytical Chemistry," State Printing Office of USSR, Moscow (1963), p. 11.
4) S. Tribalat, *Anal. Chim. Acta*, **3**, 113 (1949).
5) S. Tribalat, ibid., **4**, 228 (1950).
6) S. Tribalat, ibid., **5**, 115 (1951).
7) S. Tribalat and J. Beydon, ibid., **6**, 96 (1952).
8) Y. Yamamoto and K. Kotsuji, This Bulletin, **37**, 785 (1964).
9) Y. Yamamoto and K. Kotsuji, ibid., **37**, 594 (1964).
10) E. B. Sandell, "Colorimetric Determination of Traces of Metals," Interscience Publishers, New York (1950), p. 441.
11) E. A. Hakkila and G. R. Waterbury, *Anal. Chem.*, **32**, 1340 (1960).
12) H. Seno and Y. Kakita, *J. Chem. Soc. Japan, Pure Chem. Sec. (Nippon Kagaku Zasshi)*, **82**, 452 (1961).
13) V. Karas and T. Pinter, *Crat. Chem. Acta*, **30**, 141 (1958); *Anal. Abstr.*, 1650 (1959).

mercury replaces iron as the dipyridyl mercury chelate. Goto and Suzuki[14] have determined mercury by extracting the tetra-iodo-complex of mercury(II) with isoamylalcohol and by then measuring the absorbance at 305 mμ. Jackwerth and Spekker[15] have also investigated the extraction of this complex with cyclohexanone.

Therefore, the proposed method is different from the previously known methods in the mechanism of the color reaction.

## Experimental

**Apparatus and Reagents.** — Unless otherwise stated, the apparatus and reagents were the same as those described in the preceding paper.[8]

*Standard Mercury Solution.*—Guaranteed mercuric chloride was dissolved in hydrochloric acid and diluted with distilled water to a concentration of 1000 p. p. m. of mercury. Ths standard solution was then diluted to the concentration required for the experiments.

1,2-Dichloroethane was purified according to the method described in the literature.[16]

All the other reagents of an analytical grade were used without further purification.

**Procedure.**—Mix 2,2'-dipyridyl ($8\times10^{-3}$ M), ferrous ammonium sulfate ($2\times10^{-3}$ M), sodium acetate (3 M), potassium iodide (0.3 M) and a standard mercury solution in the proper concentration. Adjust the pH of the solution to the required value with a dilute sulfuric acid or a dilute sodium hydroxide solution, and dilute it to 25 ml. with distilled water. To this, add 10.0 ml. of dichloroethane and shake the solution for 6 min. After the solution has stood for 20 min., transfer the organic layer into a flask containing 1 g. of anhydrous sodium sulfate and shake it vigorously in order to make the solution transparent. Then transfer it into a 10 mm. cell. Measure the absorbance of the solution at 526 mμ, using a reagent blank solution or dichloroethane as a reference. Measure the pH of the aqueous layer after the separation.

## Results and Discussion

**Absorption Spectrum.**—The spectral absorbance curves using dichloroethane as a reference are shown in Fig. 1. They were measured for a dichloroethane solution obtained by extraction from one aqueous solution which contained mercury(II) and one which did not. It was observed that the presence of mercury(II) ions leads to a considerable increase in the absorbance and that both curves have a maximum absorbance at 526 mμ. The absorbance maximum of the chelate cation in the aqueous solution was at 522 mμ, a value which coincides with that found in the literature.[17] This slight red shift in the organic layer may be attributed to the effect of the association between the chelate cation and the complex anion in dichloroethane. Feigl[18] has shown that the 2,2'-dipyridyl iron(II) chelate can be precipitated as red crystals with a divalent complex anion, such as tetraiodo-mercury(II) or cadmium. On the basis of these facts, the chemical formula of the extracted species is assumed to be $Fe(Dip.)_3\cdot HgI_4$.

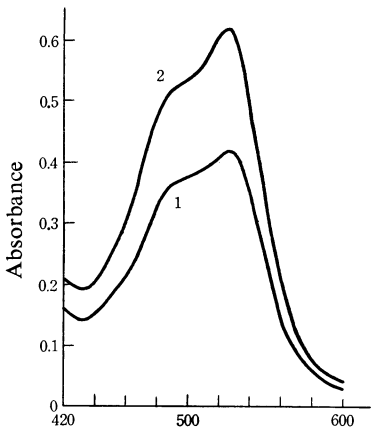



Fig. 1. Absorption spectra.
Reference: Dichloroethane, pH: 6.3
Curve 1: Spectrum of organic phase extracted from the aqueous solution (25 ml.) contained Dip. $9.6\times10^{-4}$ M, Fe(II) $2.4\times10^{-4}$ M, NaAc 0.24 M, KI $8.4\times10^{-2}$ M but Hg is absent.
Curve 2: Spectrum of organic phase extracted from the aqueous solution (25 ml.) containing 2 p. p. m. of Hg in addition to the same component as that of curve 1.

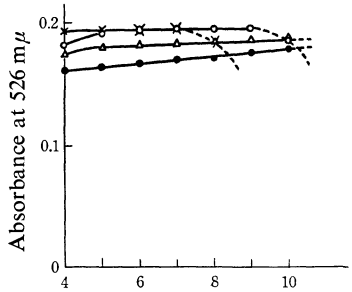
The maximum difference in the absorbance between curve 1 and curve 2 is found at 526 mμ. Therefore, the measurement of the absorbance was carried out at this wavelength.

**The Effect of Reagents.**—*A) The Effect of the Ferrous Ammonium Sulfate and Potassium Iodide Concentrations.* — The formation of extractable species is governed mainly by the concentration of the 2,2'-dipyridyl iron(II) chelate cation as well as of the tetra-iodo-mercury(II) complex anion. Moreover, the solution must contain a large excess of potassium iodide for the quantitative formation of the tetra-iodo-mercury(II) complex. The effect

14) H. Goto and S. Suzuki, *J. Chem. Soc. Japan, Pure Chem. Sec. (Nippon Kagaku Zassi)*, **74**, 142 (1953).
15) E. Jackwerth and H. Spekker, *Z. anal. Chem.*, **167**, 269 (1959).
16) L. F. Fieser, "Experiments in Organic Chemistry," Heath and Co., Boston (1957), p. 288.
17) M. L. Moss and M. G. Mellon, *Ind. Eng. Chem., Anal. Ed.*, **14**, 826 (1942).
18) F. Feigl, "Spot Test, Part I, Inorganic Application," Elsevier Publishing Company, New York (1954), p. 90.

of such variables on the extraction was investigated.

To a solution containing a constant amount of mercury(II), various amounts of potassium iodide, ferrous ammonium sulfate, and 2,2'-dipyridyl, in which the mole ratio of dipyridyl to ferrous iron was kept constant, were added. The mole ratio was kept at 4 to 1 because a slight excess of the dipyridyl seemed to be necessary for the stoichiometric formation of the chelate cation. The pH of the solutions was kept at 6.3, and the extraction procedure was carried out for such solutions. The results are shown in Fig. 2. If the final concentration



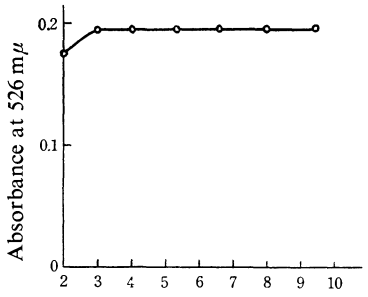

Concn. of potassium iodide $x$ ($\times 1.2\times10^{-2}$ M)

Fig. 2. Effect of ferrous ammonium sulfate and potassium iodide concentrations.
The concentration of acetate in the final solutions was 0.24 M.
Concentration of mercury, 2 p. p. m.
pH of aqueous layer, 6.3
Shaking time, 6 min.
Reference, Reagent blank

| | Concn. of Dip., M | Concn. of Fe(II), M |
|---|---|---|
| —×— | $1.6\times10^{-3}$ | $4.0\times10^{-4}$ |
| —○— | $9.6\times10^{-4}$ | $2.4\times10^{-4}$ |
| —△— | $6.4\times10^{-4}$ | $1.6\times10^{-4}$ |
| —●— | $3.2\times10^{-4}$ | $8.0\times10^{-5}$ |

of the ferrous ammonium sulfate is lower than $1.6\times10^{-4}$ M,* a rather low recovery is observed, although the recovery is improved with increasing concentration of potassium iodide. When the concentration of ferrous ammonium sulfate is kept in the range of $2.4\times10^{-4}$—$4.0\times10^{-4}$ M, the recovery reaches a maximum when the iodide concentration is higher than $7.2\times10^{-2}$ M. However, large excess of iodide or the chelate causes a decrease in the absorbance. Therefore, the concentrations of the ferrous ammonium sulfate and the potassium iodide were kept at $2.4\times10^{-4}$ M and $8.4\times10^{-2}$ M respectively in this work.

*B) The Effect of the 2,2'-Dipyridyl Concentration.*—While keeping other variables constant, a different amount of the dipyridyl was added, and the extraction was carried out according to the procedure described above. Figure 3 shows that the mole ratio of the dipyridyl to iron(II) has to be kept higher than 3. This mole ratio was therefore kept at 4 in this work.




Mole ratio of Dip. to Fe(II)

Fig. 3. Effect of mole ratio of Dip. to Fe(II).
The concentrations of iron(II), iodide, and acetate in the final solutions were $2.4\times10^{-4}$ M, $8.4\times10^{-2}$ M, and 0.24 M respectively.
Concentration of mercury, 2 p. p. m.
pH of aqueous layer, 6.3
Shaking time, 6 min.
Reference, Reagent blank

*C) The Effect of the Sodium Acetate Concentration.* — Sodium acetate was effective in keeping the solution at a constant pH. When the acetate concentration was maintained at 0.2 to 0.3 M in the solution to be extracted, no effect on the recovery was observed. The concentration of the acetate was kept at 0.24 M in this work

**The Effect of the Shaking Time.**—The shaking time for the extraction was varied from 2 to 20 min., while the other variables were kept

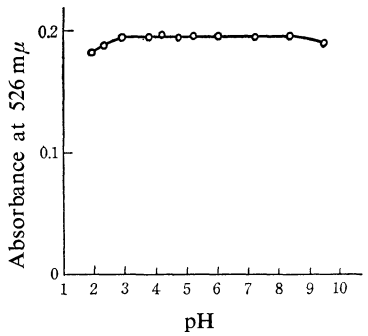



Fig. 4. Effect of pH.
The concentrations of dipyridyl, iron(II), iodide, and acetate in the final solutions were $9.6\times10^{-4}$ M, $2.4\times10^{-4}$ M, $8.4\times10^{-2}$ M, and 0.24 M respectively.
Concentration of mercury, 2 p. p. m.
Shaking time, 6 min.
Reference, Reagent blank

* The concentration of ferrous iron is approximately equal to that of the 2,2'-dipyridyl iron(II) chelate because of the high stability of the chelate.

constant. When the shaking time was shortened to less than 4 min., a lower recovery was noticed. The shaking time of 6 min. was thus chosen in this work.

**The Effect of pH.**—The effect of the pH of the aqueous layer on the extraction is shown in Fig. 4. Low recoveries are obtained in the pH ranges below 3 and above 8.5. The pH of the solution was adjusted to 6.3 in this work.

**The Stability of the Color.**—Color developed immediately at room temperature and was not influenced by the temperature at 10—17°C. The effect of the time of standing on the dichloroethane extract in a transmission cell with a stopper was investigated. The results are shown in Fig. 5. The absorbance remains constant for 60 min. After that the absorbance begins to decrease slightly.

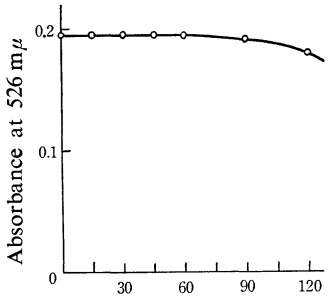



Fig. 5. Stability of color.
The concentrations of dipyridyl, iron(II), iodide, and acetate in the final solutions were $9.6\times10^{-4}$ M, $2.4\times10^{-4}$ M, $8.4\times10^{-2}$ M, and 0.24 M respectively.
Concentration of mercury, 2 p. p. m.
pH of aqueous layer, 6.3
Shaking time, 6 min.
Reference, Reagent blank

**The Choice of Organic Solvent.**—As has been pointed out by Diamond and Tuck[2], not only the size of the cation and the anion, but also the dielectric nature of the solvent, govern the extractivity of the associated complex. Various water-immiscible solvents were tested as extraction solvents. 1, 2-dichloroethane, chloroform, carbon tetrachloride, isoamylalcohol, methylisobutylketone, cyclohexanone, benzene, and nitrobenzene. Among them the most favorable degree of separation occured in 1, 2-dichloroethane. As has previously been reported,[8,19] nitrobenzene is the most available solvent in these systems and behaves similarly to 1, 2-dichloroethane in this case. Unfortunately, the reagent blank was too high to obtain a satisfactory net absorbance value.

19) Y. Yamamoto and S. Kinuwaki, This Bulletin, 37, 434 (1964).

**The Percentage of Extraction.**—The degree of the extraction of mercury(II) was calculated from a measurement of the mercury(II) concentration in the aqueous layer after the extraction. The amount of residual mercury(II) was determined as follows. To the aqueous layer, 20 ml. of a 30% sodium hypophosphite solution and 4 ml. of concentrated hydrochloric acid were added. The mixture was then diluted with distilled water to 50 ml. and was extracted with 10 ml. of isoamylalcohol. The absorbance of the isoamylalcohol extract was measured at 305 mμ, as has been described by Goto and Suzuki.[14] The degree of the extraction using 10.0 ml. of dichloroethane was about 98%.

**Calibration Curve.**—Three milliliters of the 2, 2'-dipyridyl solution, 3 ml. of the ferrous ammonium sulfate solution, 2 ml. of the sodium acetate solution, 7 ml. of the potassium iodide solution, and varying amounts (1—6 ml.) of the standard mercury solution (10 p. p. m.) were mixed and diluted to 25 ml. with distilled water. Then 10.0 ml. of dichloroethane was added, and the mixture was treated according to the procedure previously described. The absorbance for each set of the extract was measured at 526 mμ against the reagent blank. As Fig. 6 shows, Beer's law is followed in the 0.4—2.4 p. p. m. range of mercury(II) ions.

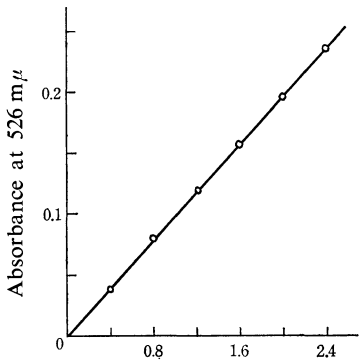



Fig. 6. Calibration curve at 526 mμ.
The concentrations of dipyridyl, iron(II), iodide, and acetate in the final solutions were $9.6\times10^{-4}$ M, $2.4\times10^{-4}$ M, $8.4\times10^{-2}$ M and 0.24 M, respectively.
pH of aqueous layer, 6.3
Shaking time, 6 min.
Reference, Reagent blank

**The Effect of Diverse Ions.** — A study was made of the effects of several cations and anions. Absorbance measurements were made for the dichloroethane extracts from solutions containing various amount of diverse ions with 2 p. p. m. of mercury(II). The results are given

TABLE I. EFFECT OF DIVERSE IONS ON EXTRACTION AND DETERMINATION OF MERCURY(II)
(2 p. p. m. of mercury taken in each case)

| Ion | Ion concn., p. p. m. | Absorbance at 526 mμ | Relative error, % |
|---|---|---|---|
| None | — | 0.196* | |
| $Zn^{2+}$ | 40 | 0.197 | + 0.5 |
| $Zn^{2+}$ | 80 | 0.212 | + 8.2 |
| $Pb^{2+}$ | 0.4 | 0.197 | + 0.5 |
| $Pb^{2+}$ | 0.8 | 0.203 | + 3.6 |
| $Cd^{2+}$ | 0.4 | 0.266 | +35.8 |
| $Cd^{2+}$ | 0.8 | 0.339 | +73.0 |
| $Bi^{3+}$ | 0.4 | 0.227 | +15.8 |
| $Bi^{3+}$ | 0.8 | 0.255 | +30.0 |
| $Cu^{2+}$ | 0.4 | 0.178 | − 9.2 |
| $Cu^{2+}$ | 0.8 | 0.160 | −18.4 |
| $SO_4^{2-}$ | 1150 | 0.197 | + 0.5 |
| $SO_4^{2-}$ | 2300 | 0.210 | + 7.2 |
| $NO_3^-$ | 1200 | 0.196 | ± 0.0 |
| $NO_3^-$ | 2400 | 0.201 | + 2.6 |
| $Cl^-$ | 170 | 0.196 | ± 0.0 |
| $Cl^-$ | 425 | 0.192 | − 2.0 |
| $Br^-$ | 150 | 0.195 | − 0.5 |
| $Br^-$ | 200 | 0.193 | − 1.5 |

pH of aqueous layer: 6.3, other variables were the same as that of the calibration curve.
* The absorbance of 2 p. p. m. of mercury(II) without diverse ions.

in Table I. Nitrate and sulfate do not interfere when the concentration is as high as 1000 p. p. m. but at a very large concentration higher results are obtained. The positive errors for zinc(II), cadmium(II), lead(II), and bismuth(III) may be due to the behavior of the iodo complex of these ions being similar to that of the tetra-iodo-mercury(II) complex anion. In order to eliminate the interferences of the diverse ions, the use of ethylenediaminetetraacetate is suggested, because the tetra-iodo-mercury(II) complex[20] is more stable than the mercury(II) chelate of ethylenediaminetetraacetate.[21] Favorable results were obtained when 1 ml. of a 0.05 M disodium ethylenediaminetetraacetate solution was added as a masking agent to the solution to be extracted, as is shown in Table II.

TABLE II. EFFECT OF DIVERSE IONS ON EXTRACTION AND DETERMINATION OF MERCURY(II) IN THE PRESENCE OF EDTA
(2 p. p. m. of mercury taken in each case)

| Ion | Ion concn., p. p. m. | Absorbance at 526 mμ | Relative error, % |
|---|---|---|---|
| None | — | 0.196* | ±0.0 |
| $Zn^{2+}$ | 80 | 0.196 | ±0.0 |
| $Pb^{2+}$ | 40 | 0.196 | ±0.0 |
| $Pb^{2+}$ | 80 | 0.206 | +5.1 |
| $Cd^{2+}$ | 40 | 0.196 | ±0.0 |
| $Cd^{2+}$ | 80 | 0.212 | +8.2 |
| $Bi^{3+}$ | 8 | 0.197 | +0.5 |
| $Bi^{3+}$ | 20 | 0.205 | +4.6 |
| $Cu^{2+}$ | 8 | 0.195 | −0.5 |
| $Cu^{2+}$ | 12 | 0.186 | −5.1 |

pH of aqueous layer: 6.3, concn. of EDTA: $2\times10^{-3}$ M, other variables were the same as that of the calibration curve.
* The absorbance of 2 p. p. m. of mercury(II) without diverse ions.

## Summary

A new method for the determination of mercury(II) has been proposed. The method is based upon the solvent extraction of the associated complex formed between the 2,2'-dipyridyl iron(II) chelate cation and the tetra-iodo-mercury(II) complex anion and upon the estimation of the absorbance belonging to the chelate cation in the organic phase. The interference of diverse ions is eliminated by using ethylenediaminetetraacetate as a masking agent.

The author wishes to express his thanks to Professor Yuroku Yamamoto of Hiroshima University for his kind guidance and encouragement throughout this work. He is also grateful to Professor Shigehiko Hayashi for his kind advice and to Mr. Toshiyuki Sakurai for his assistance in this work.

*Faculty of Liberal Arts*
*Fukui University*
*Makinoshima, Fukui*

20) J. Bjerrum, G. Schwarzenbach and L. G. Sillén, "Stability Constants," Part II, The Chem. Soc., Burlington House, London (1958), p. 121.
21) T. Goffart, G. Michel and G. Dnychaerts, *Anal. Chim. Acta*, 9, 184 (1953).

# Electrolytic Thermocouple for the Determining Soret Coefficients and Heats of Transfer of Hydrochloric Acid

By Toshio IKEDA

(Received July 29, 1964)

It is impossible to determine the Soret coefficients or the ionic heats of transfer directly from the initial thermoelectric power of a thermocell alone, though there is an intimate relation between them. It is possible, however, to determine the value of one electrolyte relative to the other electrolyte when two thermocells with a common electrode system are coupled. This procedure was employed on hydrochloric acid in the present work.

**General Relations.**—We used an electrolytic thermocouple of the following system:

$$\begin{array}{c}\mathrm{Hg/HgCl,\ KCl}(m),\\ T\end{array}$$

$$\begin{array}{ccc}\mathrm{HgCl/Hg/HgCl,\ HCl}(m), & \mathrm{HgCl/Hg} & (1)\\ T+\Delta T & T & \end{array}$$

The initial thermoelectric powers, $\varepsilon_0^{\mathrm{KCl}}$ and $\varepsilon_0^{\mathrm{HCl}}$, for two thermocells constituting the left and right halves of cell system 1 can be written, respectively, as follows:[1]

$$\boldsymbol{F}\varepsilon_0^{\mathrm{KCl}} = -t_{\mathrm{K^+}}^{\mathrm{KCl}}\frac{Q_{\mathrm{K^+}}^{*\mathrm{KCl}}}{T} + t_{\mathrm{Cl^-}}^{\mathrm{KCl}}\frac{Q_{\mathrm{Cl^-}}^{*\mathrm{KCl}}}{T} + S_{\mathrm{Cl^-}}^{\mathrm{KCl}} + S_{\mathrm{Hg}} - S_{\mathrm{HgCl}} - S_{\mathrm{el}} - \frac{Q_{\mathrm{el}}^{*}}{T} \quad (2)$$

and

$$\boldsymbol{F}\varepsilon_0^{\mathrm{HCl}} = -t_{\mathrm{H^+}}^{\mathrm{HCl}}\frac{Q_{\mathrm{H^+}}^{*\mathrm{HCl}}}{T} + t_{\mathrm{Cl^-}}^{\mathrm{HCl}}\frac{Q_{\mathrm{Cl^-}}^{*\mathrm{HCl}}}{T} + S_{\mathrm{Cl^-}}^{\mathrm{HCl}} + S_{\mathrm{Hg}} - S_{\mathrm{HgCl}} - S_{\mathrm{el}} - \frac{Q_{\mathrm{el}}^{*}}{T} \quad (3)$$

where $\boldsymbol{F}$ is the Faraday; $T$ is the absolute temperature; $t_{\mathrm{K^+}}^{\mathrm{KCl}}$ and $Q_{\mathrm{K^+}}^{*\mathrm{KCl}}$ are, respectively, the transport number and the ionic heat of transfer of potassium ions in an aqueous solution of potassium chloride at the molality of $m$, and $t_{\mathrm{Cl^-}}^{\mathrm{KCl}}$ and $Q_{\mathrm{Cl^-}}^{*\mathrm{KCl}}$ are the similar quantities for the chloride ions; $S_{\mathrm{Cl^-}}^{\mathrm{KCl}}$ represents the partial molar entropy of the chloride ions in an aqueous $m$ molal solution of potassium chloride; $S_{\mathrm{Hg}}$ and $S_{\mathrm{HgCl}}$ are, respectively, the molar entropies of the liquid mercury and of the solid mercurous chloride of the calomel electrode, and $S_{\mathrm{el}}$ and $Q_{\mathrm{el}}^{*}$ are, respectively, the molar entropy and the molar heat of transfer of electrons in the metallic leads of the electrodes. Equation 3 may be read in a similar fashion.

Now, if the following two conditions:

$$Q_{\mathrm{Cl^-}}^{*\mathrm{KCl}} = Q_{\mathrm{Cl^-}}^{*\mathrm{HCl}} \text{ and } S_{\mathrm{Cl^-}}^{\mathrm{KCl}} = S_{\mathrm{Cl^-}}^{\mathrm{HCl}} \quad (4)$$

are allowed simultaneously, the resultant initial thermoelectric power, $(\mathrm{d}E/\mathrm{d}T)_0$, for the electrolytic thermocouple of system 1 may be written as follows:

$$\boldsymbol{F}\left(\frac{\mathrm{d}E}{\mathrm{d}T}\right)_0 = -t_{\mathrm{K^+}}^{\mathrm{KCl}}\frac{Q_{\mathrm{K^+}}^{*\mathrm{KCl}} + Q_{\mathrm{Cl^-}}^{*\mathrm{KCl}}}{T} + t_{\mathrm{H^+}}^{\mathrm{HCl}}\frac{Q_{\mathrm{H^+}}^{*\mathrm{HCl}} + Q_{\mathrm{Cl^-}}^{*\mathrm{HCl}}}{T} \quad (5)$$

where the identity conditions, $t_{\mathrm{K^+}}^{\mathrm{KCl}} + t_{\mathrm{Cl^-}}^{\mathrm{KCl}} = 1$ and $t_{\mathrm{H^+}}^{\mathrm{HCl}} + t_{\mathrm{Cl^-}}^{\mathrm{HCl}} = 1$, are used. Further, Eq. 5 can be rewritten in terms of the Soret coefficients, $\sigma^{\mathrm{KCl}}$ and $\sigma^{\mathrm{HCl}}$, as follows:

$$\boldsymbol{F}\left(\frac{\mathrm{d}E}{\mathrm{d}T}\right)_0 = 2t_{\mathrm{K^+}}^{\mathrm{KCl}}\,\boldsymbol{RT}\sigma^{\mathrm{KCl}}B^{\mathrm{KCl}} - 2t_{\mathrm{H^+}}^{\mathrm{HCl}}\,\boldsymbol{RT}\sigma^{\mathrm{HCl}}B^{\mathrm{HCl}} \quad (6)$$

where

$$\left.\begin{aligned}\sigma^{\mathrm{KCl}} &= -(Q_{\mathrm{K^+}}^{*\mathrm{KCl}} + Q_{\mathrm{Cl^-}}^{*\mathrm{KCl}})/2\boldsymbol{RT}B^{\mathrm{KCl}}\\ \sigma^{\mathrm{HCl}} &= -(Q_{\mathrm{H^+}}^{*\mathrm{HCl}} + Q_{\mathrm{Cl^-}}^{*\mathrm{HCl}})/2\boldsymbol{RT}B^{\mathrm{HCl}}\\ B^{\mathrm{KCl}} &= 1 + (\mathrm{d}\ln\gamma_{\pm}{}^{\mathrm{KCl}}/\mathrm{d}\ln m)_{\mathrm{T,P}}\\ B^{\mathrm{HCl}} &= 1 + (\mathrm{d}\ln\gamma_{\pm}{}^{\mathrm{HCl}}/\mathrm{d}\ln m)_{\mathrm{T,P}}\end{aligned}\right\} \quad (7)$$

$\boldsymbol{R}$ is the gas constant, and $\gamma_{\pm}{}^{\mathrm{KCl}}$ and $\gamma_{\pm}{}^{\mathrm{HCl}}$ are the mean ion activity coefficients of potassium chloride and of hydrochloric acid in aqueous $m$ molal solutions respectively.

If the Soret coefficient is known accurately for an aqueous $m$ molal solution of potassium chloride, for example, then one may obtain, by means of Eq. 6, the Soret coefficient of hydrochloric acid at the same concentration and at the same temperature, and may further calculate the heats of transfer by the aid of Eq. 7.

## Experimental

All solutions were prepared from G. R. chemicals by using ordinary distilled water. The concentration of the solution was checked by titration and

1) E. g., H. J. V. Tyrrell, "Diffusion and Heat Flow in Liquids," Butterworths, London (1961).

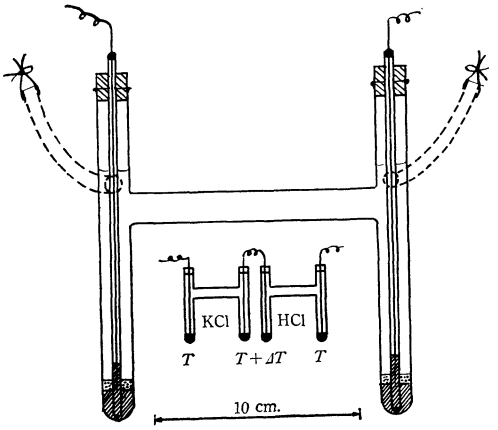



Fig. 1. Cell system, the parts drawn with dotted line representing the side tubes on the front of paper.

was adjusted to yield definite values in molality, values accurate within ±1% in the present work. Two H-shaped glass cells were convenient for the present purpose (Fig. 1). Two H-shaped calomel thermocells involving, respectively, the solutions of potassium chloride and hydrochloric acid at the same concentration were joined together by the legs and then placed in water thermostated in two respective Dewar vessels. The temperature was changed from 17°C to 32°C on only one side of of these two Dewar vessels by adding cold or hot water to yield the mean 25°C, while the temperature on the colder side was always fixed at 17°C. Under a moderate agitation with air bubbling, the thermal equilibrium of the cell system was attained in about ten minutes after the change of the temperature of thermostat water in the Dewar vessels. The temperature was read with a calibrated mercury thermometer with 0.1°C divisions. The terminals of two thermocells were joined together electrically on the warmer side, and the remaining terminals on the colder side were served to the measurements of the e. m. f. The e. m. f., $E$, of cell system 1 was measured for a given temperature difference, $\Delta T$, by the use of a Yokogawa precision potentiometer (Type P-7, for low voltage use, with a sensitivity as low as 0.1 $\mu$V.) by the use of a sensitive galvanometer as a zero indicator.

Here, the sign convention for e. m. f. of system (1) was taken as positive if the sign of the electrode on the colder side of hydrochloric acid was found be positive against the sign of the electrode on the colder side of potassium chloride.

In measuring every care was taken to get accurate and reproducible data. Even the best-prepared thermocells were let stand for about three days after having been prepared in order to bring them to a stationary state. A battery, the electric source, must be connected to the potentiometer for at least three hours prior to measurement so that the normalized state of the potentiometer does not drift. The shielding of the system from inconvenient heat effects is also important.

## Results and Discussion

The plots of the e. m. f., $E$, of 1 against the applied temperature difference, $\Delta T$, fell on a straihgt line, with a definite slope depending on the concentration. Here, the non-linear data were abandoned because they were taken when the system was not in a steady state. The results are presented in Figs. 2 and 3. The initial thermoelectric power, $(dE/dT)_0$, was found to be positive at the present sign

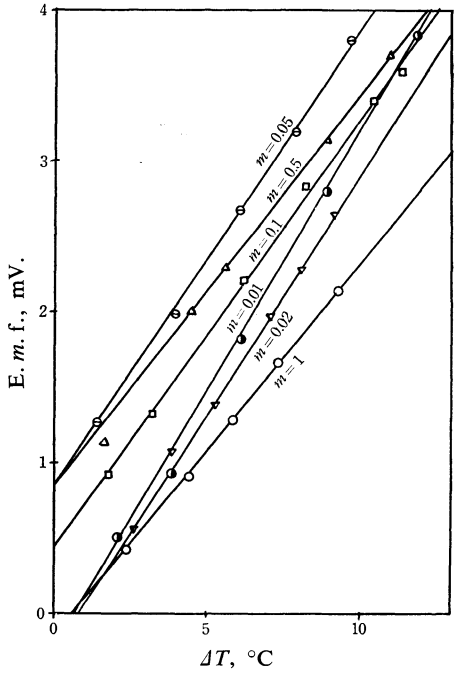



Fig. 2. E. $m$. f.'s of electrolytic thermocouple system of KCl/HCl with respect to temperature difference $\Delta T$, for different molalities $m$, at 25°C.

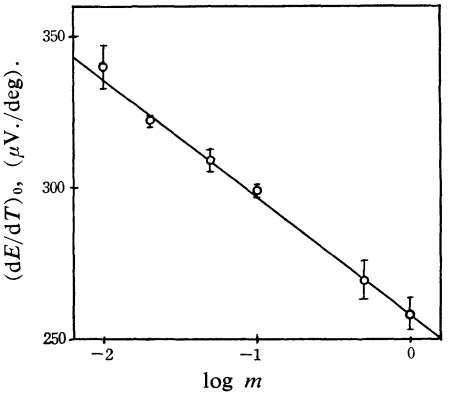



Fig. 3. Relation between the initial thermoelectric powers of electrolytic thermocouple of KCl/HCl and logarithm of molality at 25°C.

TABLE I. INITIAL THRMOELECTRIC POWER, $(dE/dT)_0$, OF THE ELECTROLYTIC THERMOCOUPLE SYSTEM OF KCl/HCl, AND THE ESTIMATION OF THE SORET COEFFICIENTS AND HEATS OF TRANSFER OF HYDROCHLORIC ACID AT 25°C

$$Q^*_{HCl} \equiv Q^{*HCl}_{H^+} + Q^{*HCl}_{Cl^-}$$

| $m$ | $t^{KCl}_{K^+}$ | $B^{KCl}$ | $t^{HCl}_{H^+}$ | $B^{HCl}$ | $-\sigma^{KCl} \times 10^3$ deg$^{-1}$ | $\left(\frac{dE}{dT}\right)_0$ $\frac{\mu V.}{deg.}$ this work | $-\sigma^{HCl} \times 10^3$ deg$^{-1}$ calcd. | obs. | obs.[e] | obs.[f] | $Q^*_{HCl}$ $\frac{cal.}{mol.}$ |
|---|---|---|---|---|---|---|---|---|---|---|---|
| 0.01 | 0.4902 | 0.954 | 0.8251 | 0.958 | 1.43[a] | 340±7 | 9.21 | 9.01[a] | 11 | 8.4 | 3120 |
| 0.02 | 0.4901 | 0.941 | 0.8266 | 0.946 | 1.22[b] | 322±3 | 8.73 | 7.8[d] | 8.2 | — | 2920 |
| 0.05 | 0.4899 | 0.925 | 0.8292 | 0.942 | 0.99[b] | 309±4 | 8.23 | — | 6.4 | 6.3 | 2740 |
| 0.1 | 0.4898 | 0.909 | 0.8314 | 0.943 | 0.86* | 299±3 | 7.90 | — | 5.6 | 5.3 | 2630 |
| 0.2 | 0.4894 | 0.900 | 0.8337 | 0.956 | 0.76* | — | — | — | 5.0 | — | — |
| 0.5 | 0.4888 | 0.892 | 0.838 | 1.044 | 0.79* | 269±7 | 6.36 | 6.71[c] | 6.2 | — | 2350 |
| 1.0 | 0.4882 | 0.931 | 0.841 | 1.160 | 0.94[c] | 258±5 | 5.58 | 5.82[c] | 6.0 | — | 2280 |

a) Ref. 3.
b) Ref. 2.
c) Ref. 4.
d) E. D. Eastman, *J. Am. Chem. Soc.*, **50**, 283, 292 (1928)
e) Values at 40°C, Ref. 5.
f) Values at 35°C, Ref. 6.
* Interpolation.

convention; it seems to diminish linearly with the logarithms of molality, as is indicated in Fig. 3.

Early data on the Soret coefficients are not very reliable, but fairly accurate data are available in recent reports, particularly those by Snowdon and Turner.[2,3] These authors determined the Soret coefficients directly by the conductometric method for a number of electrolytes at 25°C. The Soret coefficients at higher concentrations were formerly given by Tanner[4] at a mean temperature of 32°C. Data for medium concentrations are lacking at present.

In the present work, we calculated the Soret coefficient for hydrochloric acid at 25°C by using known $\sigma$ values for potassium chloride and the initial thermoelectric powers for system 1. The results are compared with the literature values in Table I, where the Sasaki values cited for comparison are those observed at the mean temperatures of 40°C[5] and 35°C[6]. Since the Soret coefficient is rather sensitive to the Soret coefficient is rather sensitive to the mean temperature at which it is measured, increasing with an increase in that temperature, it is inappropriate, strictly speaking, to make a direct comparison between Soret coefficients determined at different temperatures. However, as may be seen in Table I, the calculated values and the literature values were found to agree roughly in their magnitudes in a satisfactory manner, apart from details. Calculations for the medium concentrations could not be performed to yield correct values of the Soret coefficients for hydrochloric acid because of a lack of basic data on the Soret coefficients of potassium chloride in the corresponding region of concentration; therefore, tentative calculations were made by using the interpolated values of the Soret coefficients of potassium chloride for 0.1 and 0.5 M. No such peak as those reported by Chipman,[7] Hirota[8] and Sasaki[5] on the Soret coefficient of hydrochloric acid could be found here in the concentration range between 0.5 and 1.0 M. This might be either because the values of the Soret coefficients of potassium chloride used for the calculation were inadequate at higher concentrations, or becanse the basic conditions indicated in 4 can no longer hold at higher concentrations, or to both reasons. At any rate, the present method is likely to be applicable for determining the Soret coefficients at lower concentrations for any electrolyte that can form a thermocell with a convenient electrode system.

2) P. N. Snowdon and J. C. R. Turner, *Trans. Faraday Soc.*, **56**, 1 (1960).
3) P. N. Snowdon and J. C. R. Turner, ibid., **56**, 1409 (1960).
4) C. C. Tanner, ibid., **23**, 75 (1927).
5) K. Sasaki, *J. Chem. Soc. Japan, Pure Chem. Sec. (Nippon Kagaku Zasshi)*, **83**, 236 (1962).
6) K. Sasaki, ibid., **83**, 368 (1962).
7) J. Chipman, *J. Am. Chem. Soc.*, **48**, 2577 (1926).
8) K. Hirota, *J. Chem. Soc. Japan (Nippon Kwagaku Kwaisi)*, **63**, 105, 999 (1942).

**Summary**

We have studied an electrolytic thermocouple formed by coupling two thermocells, consisting of electrodes of the same nature, and with different electrolytes, either hydrochloric acid or potassium chloride, but both of the same concentration; we have demonstrated that the Soret coefficient of hydrochloric acid relative to that of potassium chloride can be estimated from the initial thermoelectric powers of this electrolytic thermocouple, as long as the entropies as well as the heats of the transfer of the chloride ions may be assumed to be the same between these two electrolytes.

Agreements between calculations and observations have been roughly good in the range of concentration between 0.01 M and 1 M, though there are some uncertainties about the Soret coefficients of potassium chloride at higher concentrations. This method may have general applicability, particularly in the dilute region.

*Department of Chemistry*
*Shizuoka University*
*Oiwa, Shizuoka*

# Thermal Decomposition of Acetaldehyde in the Presence of Hydrogen Chloride

By Naomi IMAI, Takeshi FUJII and Osamu TOYAMA

(Received August 1, 1964)

Hydrogen chloride and bromide have been shown to catalyze decompositions of a number of alcohols and other substances in the gas phase.[1,2] The present paper reports, as an additional example of hydrogen halide catalysis, the hydrogen chloride-catalyzed decomposition of acetaldehyde. The study of this reaction was undertaken in connection with our previous work on the hydrogen sulfide-catalyzed decomposition of acetaldehyde and dimethyl ether.[3-7]

The catalytic action of hydrogen sulfide on the pyrolysis of acetaldehyde has been attributed to the replacement of the chain-propagating reactions 8 and 6:

$$CH_3 + CH_3CHO \rightarrow CH_4 + CH_3CO \quad (8)$$

$$CH_3CO \rightarrow CH_3 + CO \quad (6)$$

in the decomposition of acetaldehyde alone, by the faster-propagating cycle of reactions 9, 10 and 6:

$$CH_3 + H_2S \rightarrow CH_4 + HS \quad (9)$$

$$HS + CH_3CHO \rightarrow H_2S + CH_3CO \quad (10)$$

both reactions, 9 and 10, being faster than reaction 8. The methanethiol-catalyzed pyrolysis of acetaldehyde[8] and the hydrogen sulfide-catalyzed pyrolysis of dimethyl ether[6] have been explained by similar mechanisms.

Hydrogen chloride may be expected to exert a similar catalytic effect in the pyrolysis of acetaldehyde if reactions 4 and 5:

$$CH_3 + HCl \rightarrow CH_4 + Cl \quad (4)$$

$$Cl + CH_3CHO \rightarrow HCl + CH_3CO \quad (5)$$

proceed faster than reaction 8, as was the case with reactions 9 and 10. That such a situation is very probable may be seen by a comparison of the following reported expressions for the rate constants (in $mol^{-1}$ cc. $sec^{-1}$):

$k_4$: $10^{11.7}\exp(-2100/RT)$[9]
$10^{12.2}\exp(-4500/RT)$[10]
$k_5$: $10^{13.3}\exp(-5000/RT)$[11]
$k_8$: $10^{11.3}\exp(-6800/RT)$[12]

1) A. Maccoll and V. R. Stimson, *J. Chem. Soc.*, **1960**, 2836; K. G. Lewis and V. R. Stimson, ibid., **1960**, 3087; R. A. Ross and V. R. Stimson, ibid., **1960**, 3090; V. R. Stimson and E. J. Watson, ibid., **1960**, 3920; V. R. Stimson and E. J. Watson ibid., **1961**, 1392; R. L. Failes and V. R. Stimson, ibid., **1962**, 653; R. A. Ross and V. R. Stimson, ibid., **1962**, 1602; M. Flowers, L. Batt and S. W. Benson, *J. Chem. Phys.*, **37**, 2662 (1962).
2) K. H. Anderson and S. W. Benson, ibid., **39**, 1677 (1963).
3) N. Imai and O. Toyama, This Bulletin, **33**, 1120 (1960).
4) N. Imai, Y. Yoshida and O. Toyama, ibid., **35**, 752 (1962).
5) N. Imai, Y. Yoshida and O. Toyama, ibid., **35**, 758 (1962).
6) N. Imai and O. Toyama, ibid., **34**, 328, (1961).
7) N. Imai and O. Toyama, ibid., **35**, 860 (1962).
8) N. Imai and O. Toyama, ibid., **33**, 1408, (1960).
9) R. J. Cvetanivic and E. W. R. Steacie, *Can. J. Chem.*, **31**, 158 (1953).
10) H. O. Pritchard, J. B. Pyke and A. F. Trotman-Dickenson, *J. Am. Chem. Soc.*, **77**, 2629 (1955).
11) Estimated from W. A. Alexander and H. J. Schumacher, *Z. physik. Chem.*, **B44**, 57 (1939).
12) P. Ausloos and E. W. R. Steacie, *Can. J. Chem.*, **33**, 31 (1955).

## Experimental

**Materials.** — Acetaldehyde was supplied commercially, purified by repeated bulb-to-bulb distillations, and stored as a liquid below 20°C. Hydrogen chloride was prepared by vaporizing it from concentrated hydrochloric acid, drying it by passing it through phosphorus pentoxide and a trap at −78°C, and purifying it by bulb-to-bulb distillations. The auramine used to absorb the hydrogen chloride was a commercial sample.

**Apparatus and Procedure.**—An ordinary static method was used in this work. The pyrolysis was carried out in a cylindrical glass vessel of about 181 cc. placed in an electric furnace, which was controlled to ±0.5°C by means of a thermocouple-activated controller.

The thermal decomposition was started by introducing the reactant vapor into a reaction vessel already kept at the reaction temperature; the total pressure rise with time due to decomposition was then followed. In some runs, the reaction mixture after the pyrolysis was passed through a trap at the temperature of liquid air and the non-condensable fraction was collected by a Toepler pump. This fraction, consisting exclusively of methane and carbon monoxide, was analyzed by a gas chromatograph on a 2-m Molecular Sieve 5 column at room temperature in use of hydrogen as the carrier. In order to determine the amount of hydrogen chloride remaining unconsumed in the pyrolysis, the condensate in the trap was warmed up to about −120°C and the vaporized fraction was collected by a Toepler pump and measured. This fraction was identified as hydrogen chloride, having been almost completely absorbed by the auramine.

## Results

In Fig. 1 are plotted against time the amounts of methane and carbon monoxide formed by the pyrolysis of a mixture of acetaldehyde and hydrogen chloride, and the amount of hydrogen chloride remaining in the mixture during the pyrolysis. The curve in the figure shows the total pressure rise. It may be seen that the total pressure increase is equal to the pressure of the methane formed as well as to that of carbon monoxide, and also that hydrogen chloride is not consumed during the pyrolysis, its amount remaining constant within 1%. No appreciable amount of hydrogen was detected by gas chromatographic analysis using a nitrogen carrier. These facts indicate that the stoichiometry of the pyrolysis of acetaldehyde,[13] i. e.,

$$CH_3CHO \rightarrow CH_4 + CO$$

13) C. N. Hinshelwood and W. K. Hutchson, *Proc. Roy. Soc.*, **A111**, 380 (1929); C. J. M. Fletcher and C. N. Hinshelwood, ibid., **A141**, 41 (1933); C. A. Winkler and C. N. Hinshelwood, ibid., **A149**, 355 (1935); R. V. Seddon and M. W. Travers, ibid., **A156**, 234 (1936); E. Leifer and H. C. Urey, *J. Am. Chem. Soc.*, **64**, 994 (1942).

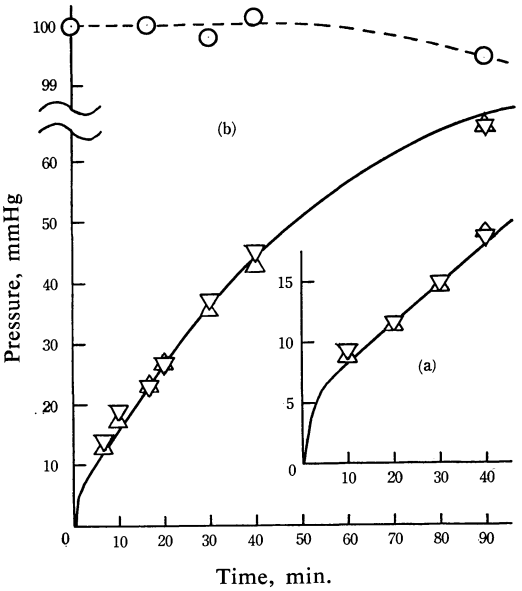



Fig. 1. Pyrolysis of acetaldehyde in the presence of hydrogen chloride.
(a) 401°C; $CH_3CHO$: 100 mmHg; HCl: 50 mmHg
(b) 423°C; $CH_3CHO$: 100 mmHg; HCl: 100 mmHg
▽, $CH_4$; △, CO; ○, HCl. Solid line represents total pressure rise.

is not affected by the presence of hydrogen chloride. Similar results had been obtained in previous studies with hydrogen sulfide[4] and methanethiol[8].

Figure 1 also shows that, at the beginning of the pyrolysis, the rate of decomposition is abnormally higher than in the following period. This initial period with a high rate is fairly long with a fresh vessel, but it is shortened with a "seasoned" one. The phenomenon may be attributed to a chain initiation on the wall, which is poisoned by the progress of pyrolysis or inactivated by seasoning.

Figure 2 shows the dependence of the decomposition rate on hydrogen chloride pressure in the decomposition of 100 mmHg acetaldehyde in the range of temperature from 401 to 433°C. The rate increases with the hydrogen chloride pressure until it attains a constant value, which is about seven times the rate in the absence of hydrogen chloride. This ratio of about seven compares with that of about ten previously found for dimethyl ether decomposition catalyzed by hydrogen chloride[2] and by hydrogen sulfide.[6]

Figure 3 shows the relations between the pressure of acetaldehyde and the rate of decomposition in the presence of 100 mmHg of hydrogen chloride at 401 and 423°C.

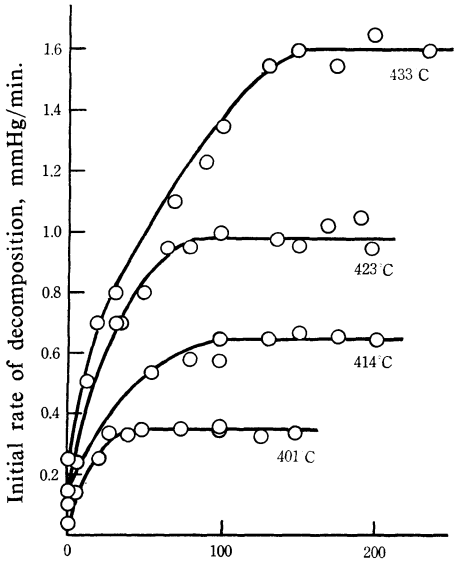



Fig. 2. Dependence of the rate of decomposition on hydrogen chloride pressure.
$CH_3CHO$ : 100 mmHg

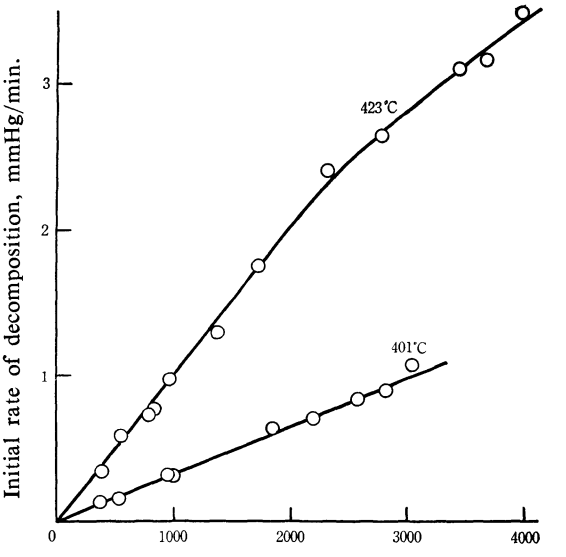



Fig. 3. Dependence of the rate of decomposition on acetaldehyde pressure.
HCl : 100 mmHg

Figures 2 and 3 indicate that the reaction is of the 3/2 order in the aldehyde and is independent of hydrogen chloride when the ratio of the hydrogen chloride pressure to that of the aldehyde is sufficiently high.

## Discussion

A probable reaction scheme that explains the 3/2 order kinetics given above may be presented as follows:

$$CH_3CHO + M \rightarrow CH_3 + CHO + M \quad (1)$$

$$CHO \rightarrow CO + H \quad (2)$$

$$H + HCl \rightarrow H_2 + Cl \quad (3)$$

$$CH_3 + HCl \rightarrow CH_4 + Cl \quad (4)$$

$$Cl + CH_3CHO \rightarrow HCl + CH_3CO \quad (5)$$

$$CH_3CO \rightarrow CH_3 + CO \quad (6)$$

$$Cl + Cl + M \rightarrow Cl_2 + M \quad (7)$$

Applying a steady-state treatment to this scheme, one obtains:

$$-d[CH_3CHO]/dt = k_1^{1/2}k_5k_7^{-1/2}[CH_3CHO]^{3/2} \quad (I)$$

which is in agreement with the experimental results.

Since the chain-propagating steps are reactions 4, 5 and 6, the steady-state condition requires that:

$$k_4[CH_3][HCl] = k_5[Cl][CH_3CHO] \quad (II)$$

or

$$\frac{[Cl]}{[CH_3]} = \frac{k_4[HCl]}{k_5[CH_3CHO]} \quad (III)$$

If the right hand side of Eq. III is very large, the concentration of chlorine atoms is much higher than that of methyl radicals and the chain terminates solely by reaction 7, as is assumed in the above scheme. On the contrary, when the right hand side of Eq. III is small, or when the concentration of methyl radicals is large, the combination of methyl radicals or that of methyl radicals and chlorine atoms will be important in chain termination. The rate then should be smaller than that which can be expected from Eq. I. Thus it is explained why the plots deviate from the straight lines in Figs. 2 and 3 when the relative amount of hydrogen chloride is low. The difference in activation energies $E_4-E_5$ is negative, as may be seen in the expressions of rate constants cited above. This explains the fact that the higher the temperature, the greater is the [HCl]/[$CH_3CHO$] ratio at which Eq. I begins to be applicable, as may be seen in Figs. 2 and 3.

The chain-initiation step given above (reaction 1) is represented as a second-order process. The order of such a chain-initiation step, together with those for the chain termination and decomposition of intermediate radicals, has been discussed by a number of workers. The overall order of the present catalyzed decomposition depends upon the orders of these elementary steps; various possibilities,

TABLE I. RATE EXPRESSIONS FOR VARIOUS MECHANISMS

| | | | | | |
|---|---|---|---|---|---|
| Order | Initiation | 1 | | | |
| | Termination | 2 | | 3 | |
| | Decomposition of $\mu$ | 1 | 2 | 1 | 2 |
| Termination | $\mu\beta$ | $[A]^{1/2}[B]^{1/2}$ | $[A]^{1/2}[B]^{1/2}[M]^{1/2}$ | $[A]^{1/2}[B]^{1/2}[M]^{-1/2}$ | $[A]^{1/2}[B]^{1/2}$ |
| | $\mu\beta'$ | $[A]$ | $[A][M]^{1/2}$ | $[A][M]^{-1/2}$ | $[A]$ |
| | $\beta\beta$ | $[A]^{1/2}[B]$ | | $[A]^{1/2}[B][M]^{-1/2}$ | |
| | $\beta\beta'$ | $[A][B]^{1/2}$ | | $[A][B]^{1/2}[M]^{-1/2}$ | |
| | $\beta'\beta'$ | $[A]^{3/2}$ | | $[A]^{3/2}[M]^{-1/2}$ | |
| Order | Initiation | 2 | | | |
| | Termination | 2 | | 3 | |
| | Decomposition of $\mu$ | 1 | 2 | 1 | 2 |
| Termination | $\mu\beta$ | $[A]^{1/2}[B]^{1/2}[M]^{1/2}$ | $[A]^{1/2}[B]^{1/2}[M]$ | $[A]^{1/2}[B]^{1/2}$ | $[A]^{1/2}[B]^{1/2}[M]^{1/2}$ |
| | $\mu\beta'$ | $[A][M]^{1/2}$ | $[A][M]$ | $[A]$ | $[A][M]^{1/2}$ |
| | $\beta\beta$ | $[A]^{1/2}[B][M]^{1/2}$ | | $[A]^{1/2}[B]$ | |
| | $\beta\beta'$ | $[A][B]^{1/2}[M]^{1/2}$ | | $[A][B]^{1/2}$ | |
| | $\beta'\beta'$ | $[A]^{3/2}[M]^{1/2}$ | | $[A]^{3/2}$ | |

as worked out by Goldfinger, Letort and Niclause,[14] are listed in Table I. Here, following the original terminology of Goldfinger et al., $\mu$ denotes a chain-propagating radical that decomposes ($CH_3CO$ in the present case); $\beta$, a chain-propagating atom or radical in the uncatalyzed decomposition that does not decompose further ($CH_3$); and $\beta'$, such an atom or radical formed by hydrogen abstraction from a catalyst molecule by a $\beta$-radical (Cl). A refers to the reactant to be decomposed ($CH_3CHO$); B to the catalyst (HCl), and M to a third body ($CH_3CHO$ and HCl). Since in the case of $\mu\mu$ termination the rate is not enhanced by the presence of a catalyst except by its effect as a third body, this case is omitted in Table I.

The rate expression that best conforms to the experimental results is obviously $[A]^{3/2}$, derived from the $\beta'\beta'$ termination, but $[A][M]^{1/2}$, resulting from the $\mu\beta'$ termination, might as well explain the result when $[M]\approx[A]$. However, the results obtained show that the $[A]^{3/2}$ kinetics does not hold when the ratio [B]/[A] is low, and, moreover, that the $\mu$-radical, i.e., the acetyl radical, is so unstable[15] above 400°C that its participation in the termination may be ruled out.

Table I shows that the overall rate proportional to $[A]^{3/2}$ is given by either of two different combinations of initiation and termination processes. However, the one involving a second-order termination is improbable, since the $\beta'$-radicals are here chlorine atoms. The reaction sequence 1 to 7 thus seems to be the most probable one to explain the 3/2 order kinetics.

The second-order initiation step as given in reaction 1 is further supported by the work of Trenwith,[16] who, in the pyrolysis of acetaldehyde alone, has found a rate of the formation of hydrogen proportional to the square of acetaldehyde pressure.[17]

Table II shows the values of $k_1^{1/2}k_5k_7^{-1/2}$ in Eq. I as determined from the constant values

TABLE II. VALUES OF $k_1^{1/2}k_5k_7^{-1/2}$

| Temp. °C | $k_1^{1/2}k_5k_7^{-1/2}$ ($mol^{-1/2}\,cc^{1/2}\,sec^{-1}$) from Fig. 2 | from Fig. 3 |
|---|---|---|
| 401 | 0.0376 | 0.0363 |
| 414 | 0.071 | |
| 423 | 0.099 | 0.101 |
| 433 | 0.172 | |

of the rates in Fig. 2 and from the slopes of the straight lines in Fig. 3. The values obtained by the two different methods agree within the range of experimental error. The Arrhenius expression obtained from Table II is:

$$k_1^{1/2}k_5k_7^{-1/2}=10^{13.0}\exp(-44000/RT)$$

$$mol^{-1/2}\,cc^{1/2}\,sec^{-1}$$

14) P. Goldfinger, M. Letort and M. Niclause, Volume Commémoratif Victor Henri: "Contribution à l'Etude de la Structure Moléculaire," Liège: Desoer (1948), p. 283.

15) C. A. McDowell and J. H. Thomas, *J. Chem. Soc.*, **1949**, 2217.

16) A. B. Trenwith, ibid., **1963**, 4426.

17) The hydrogen sulfide-catalyzed pyrolysis of acetaldehyde was previously explained with a reaction scheme involving a first order initiation step, $CH_3CHO \rightarrow CH_3+CHO$. In view of the present work and that of Trenwith, it seems preferable to replace this first order initiation by the second order process given in reaction 1. This replacement causes no changes in the other arguments, if the chain termination $CH_3+CH_3 \rightarrow C_2H_6$, at the same time, is replaced by a third order process.

Combining $k_1 = 10^{20} \exp(-73800/RT)$ $mol^{-1}$ cc. $sec^{-1}$ as reported by Trenwith[16] with $k_5 = 10^{13.3}\exp(-5000/RT)$ $mol^{-1}$ cc. $sec^{-1}$ [11] and $k_7 = 10^{17.4}$ $mol^{-2}$ $cc^2$ $sec^{-1}$,[18] one obtains:

$$k_1^{1/2}k_5k_7^{-1/2} = 10^{14.4}\exp(-41900/RT)$$
$$mol^{-1/2}\ cc^{1/2}\ sec^{-1}$$

which is in good agreement with the experimental expression given above.

## Summary

The thermal decomposition of acetaldehyde in the presence of hydrogen chloride has been investigated over the temperature range from 401 to 433°C. Hydrogen chloride, though it is not consumed, enhances the rate of decomposition to carbon monoxide and methane, thus acting as a catalyst. The rate law which holds when the [HCl]/[$CH_3CHO$] ratio is sufficiently high is the same as that which holds in the absence of hydrogen chloride, being represented as $k[CH_3CHO]^{3/2}$ independent of the hydrogen chloride pressure. The most probable reaction scheme for explaining this rate law is $CH_3CHO + M \rightarrow CH_3 + CHO + M$ (1), $CHO \rightarrow CO + H$ (2), $H + HCl \rightarrow H_2 + Cl$ (3), $CH_3 + HCl \rightarrow CH_4 + Cl$ (4), $Cl + CH_3CHO \rightarrow HCl + CH_3CO$ (5), $CH_3CO \rightarrow CH_3 + CO$ (6), and $Cl + Cl + M \rightarrow Cl_2 + M$ (7), yielding the overall rate $k_1^{1/2}k_5k_7^{-1/2}[CH_3CHO]^{3/2}$. The Arrhenius expression obtained from the experimental results, $k_1^{1/2}k_5k_7^{-1/2} = 10^{13.0}\exp(-44000/RT)$ $mol^{-1/2}$ $cc^{1/2}$ $sec^{-1}$, is in harmony with those for $k_1$, $k_5$, and $k_7$ available in the literature.

*Department of Applied Chemistry*
*College of Engineering*
*University of Osaka Prefecture*
*Sakai, Osaka*

18) Estimated from $K_7 = 10^{16.4}$ $mol^{-2}$ $cc^2$ $sec^{-1}$ for the reaction $Cl + Cl + Cl_2 \rightarrow Cl_2 + Cl_2$ (L. W. Bader and E. A. Ogryzlo, *Nature*, **201**, 491 (1964)).

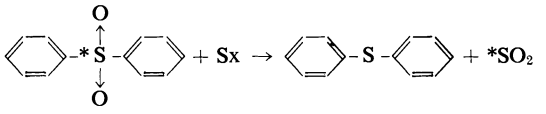
# The Reaction of Elemental Sulfur with Organic Compounds. II. The Reaction of Dibenzyl Sulfide, Sulfoxide and Sulfone, and Their Related Dibenzyl Compounds[1)]

By Waichiro TAGAKI, Sadanori KISO and Shigeru OAE

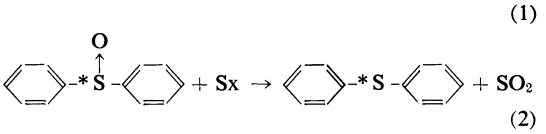
(Received August 4, 1964)

For many years, the reactions of elemental sulfur with organic compounds at elevated temperatures have been a subject of extensive investigation.[2)] Aromatization, vulcanization and Wilgerodt reactions are only a few of many well-known applications of these reactions. However, many of the mechanistic features of these reactions are yet to be clarified. For example, even in simple reactions of sulfur with olefins, it is not certain whether the reaction proceeds through the heterolytic or the homolytic pathway. Nor do we know whether the reaction is initiated by the abstraction of hydrogen or by the addition of sulfur to the double bond.[2c)]

Many years ago, the reaction of diphenyl sulfone with sulfur was found to give diphenyl sulfide and sulfur dioxide.[3)] Recently, we have investigated the mechanism of this reaction using a $^{35}S$-labeled compound.[1a)] As is illustrated in Eq. 1, the apparent reduction of the S–O bond was found actually to involve the cleavage of the phenyl-S bond and the replacement of the $SO_2$ group by sulfur to the extent of 70—80%:



(1)



(2)

1) a) Paper I; S. Oae and S. Kawamura, This Bulletin, **36**, 163 (1963); b) This work was supported by a grant from the Petroleum Research Fund administered by the American Chemical Society. Grateful acknowledgement is hereby made to the donors of this fund.

2) a) W. A. Pryor, "Mechanisms of Sulfur Reactions," McGraw-Hill, New York (1962), Chap. 5; b) L. Bateman and C. G. Moore, "Reactions of Sulfur with Olefin," in "Organic Sulfur Compounds," Vol. I, Ed. by N. Kharasch, Pergamon Press, New York (1961); c) S. Oae, *Kagaku (Chemistry)*, **18**, 779 (1963).

3) F. Kraft and W. Vorster, *Ber.*, **26**, 2813 (1893).

Meanwhile we have found that the corresponding diphenyl sulfoxide is also reduced to diphenyl sulfide. In this case, however, the reaction is a straightforward reduction of the SO group, involving the cleavage of the S–O bond, as is shown in Eq. 2. These different paths were ascribed to the weaker bond strength of the S–O bond in sulfoxide than in sulfone. We now turn our attention to the problem of how the reaction proceeds when a methylene group is inserted between a benzene ring and a sulfur group, i. e., the reaction with a benzylic compound. Here the reaction depends on the relative importance of hydrogen abstraction and of the cleavage of either the C–S or S–O bond, or both.

Therefore, we have investigated the reactions of sulfur with dibenzyl sulfide, sulfoxide, sulfone, ether and ketone, and this paper will present a detailed account of the investigation.

## Results and Discussion

The reaction was carried out by heating a mixture of starting compounds and elemental sulfur under a slow stream of nitrogen gas. The evolution of hydrogen sulfide usually started at around 160°C, and the reaction temperature was maintained near 200°C, substantially lower than that used in the reactions of diphenyl sulfoxide and sulfone (~300°C[1a]). An important though unexpected result was the failure to detect any sulfur dioxide which had been evolved quantitatively in the reactions of diphenyl sulfoxide and sulfone.[1a] In place of sulfur dioxide, a few drops of water were usually observed in all of the oxygen compounds except for dibenzyl ketone. The oily and solid products were separated into pure forms by a combination of gas-, thin-layer-, and column chromatographies and were identified by means of spectroscopic and elemental analyses. The results are shown in Table I and Chart 1.

**The Products from Dibenzyl Sulfoxide.**—Dibenzyl sulfoxide seems to undergo all the possible reactions conceivable for the compound, i. e., hydrogen abstraction, rearrangement, elimination and cleavage reaction. Therefore, a detailed discussion of the reactions of this compound would be most fruitful, for the reactions of the other compounds can then be discussed by referring to their differences from those of dibenzyl sulfoxide.

As is shown in Table I, the reaction products of dibenzyl sulfoxide were hydrogen sulfide (trapped as lead sulfide) (37.2%), oils (38%), solids (39%) and a small amount of water.

Since sulfur is known to yield a sulfur free radical at above 150°C, it is reasonable to consider that the initial step of this reaction involves the formation of the sulfoxide free radical, II-3, by the abstraction of benzylic hydrogen by the sulfur free radical, as Eq. 3 illustrates. The radical, II-3, would then undergo a variety of reactions.

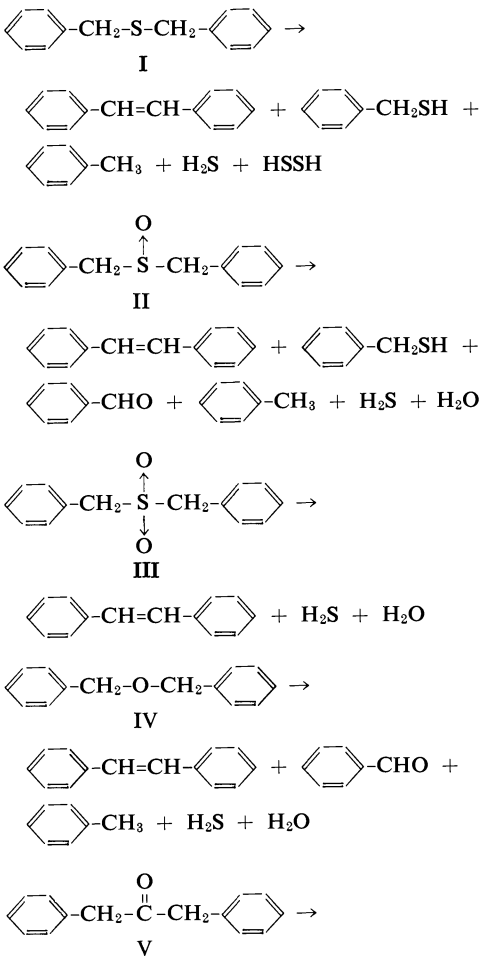
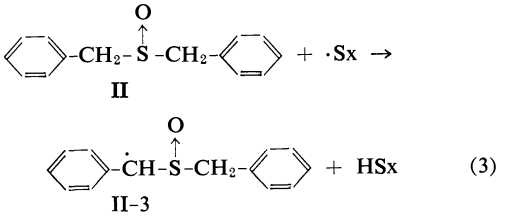



Chart 1. Species of the reaction products.

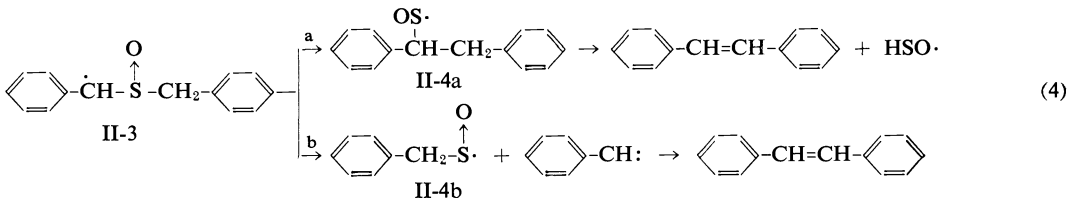



The major portion of the solid product (obtained in a 39% yield) was found to be stilbene. Two possible pathways are conceivable for the formation of stilbene. One is through the rearrangement and elimination of II-3, as is shown in Eq. 4a, and the other is via the

TABLE I. REACTION CONDITIONS AND THE YIELD OF THE PRODUCTS

| Compd. | Reaction temp. °C | Reaction time hr. | Weight of the reaction mixture: Compd. mg. | Weight of the reaction mixture: Sulfur mg. | Yield of the products,[a] mg. and per cent: PbS | Oils | Solid | $H_2S_2$ | water | $SO_2$ | Residue |
|---|---|---|---|---|---|---|---|---|---|---|---|
| $(C_6H_5CH_2)_2S$ (I) | 210 | 6.5 | 1073 | 162 | 472 (39.3) | 291[b] (27.2) | 375[e] (41.5) | +[g] | – | – | 198 |
| $(C_6H_5CH_2)_2SO$ (II) | 205 | 5.0 | 1157 | 160 | 445 (37.2) | 442[e] (38) | 354[e] (39) | – | + | – | 367 |
| $(C_6H_5CH_2)_2SO_2$ (III) | 250 | 7.0 | 3695 | 481 | 1152 (32) | — | 1818[e] (68) | – | + | – | 1236 |
| $(C_6H_5CH_2)_2O$ (IV) | 210 | 6.0 | 5940 | 971 | 739 (10.2) | 3562[d] (60) | 775[e] (14.4) | – | + | – | 1495 |
| $(C_6H_5CH_2)_2CO$ (V) | 230 | 7.0 | 4210 | 640 | 3477 (72.7) | — | 2030[f] | – | – | – | 1890 |

a) Percent yields are shown in the parentheses.
b) Mixture of toluene and benzylmercaptan.
c) Mixture of toluene, benzylmercaptan and benzaldehyde.
d) Mixture of toluene and benzaldehyde.
e) Mainly stilbene.
f) Mainly starting ketone.
g) About 200 mg. containing one drop of toluene and benzylmercaptan.

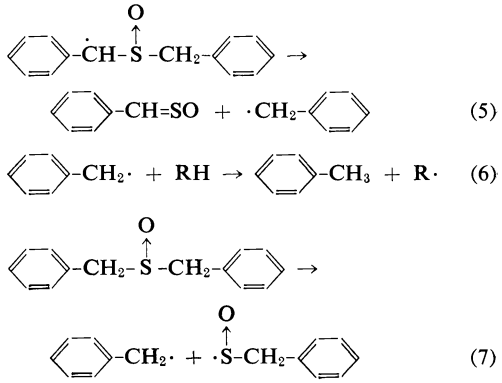



(4)

carbene intermediate, as is illustrated in Eq. 4b. The pathway 4a is a rearrangement involving the C–S bond cleavage of II-3, as in the formation of benzaldehyde, where sulfoxide S–O bond cleavage takes place as is postulated below (Eq. 8). The carbene intermediate leading to stilbene was also postulated in the base-catalyzed carbanion reaction of sulfonyl[4] and sulfonium compounds.[5]

Although there is no conclusive evidence for making any particular choice between these two pathways, we favor the former path, 4a, for the following reasons. A free radical of the Ar–S–O· type has been said to be very stable[6] and has been known to undergo disproportionation to give the corresponding thiolsulfonate.[7] Since the free radical, II-4b, is isoelectronic with Ar–SO·, it would give the thiolsulfonate. However, no such product was detected in the present reaction. Moreover, it also seems difficult for the carbene pathway to account for the reactions of the dibenzyl sulfide and the ether, as will be discussed later.

The oily product (38%) was found to be a mixture of toluene, benzaldehyde and benzyl mercaptan in a ratio of 1 : 8 : 13. The formation of toluene can be explained either by the decomposition of II-3 (Eq. 5—6) or by the direct homolysis of the C–S bond of the starting sulfoxide (Eq. 7), although the latter pathway is rather unlikely. The formation of



(5)

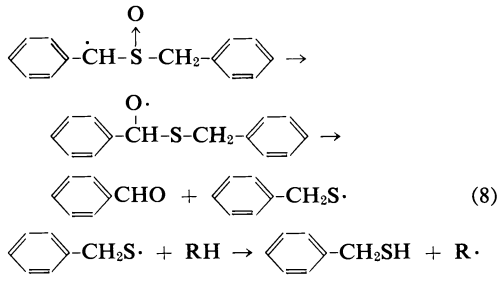
(6)

(7)

benzaldehyde and benzyl mercaptan can be readily explained by assuming an intramolecular migration of sulfoxide oxygen to the benzylic carbon, followed by the homolytic

4) J. F. King and T. Durst, *Tetrahedron Letters*, 585 (1963).
5) A. W. Johnson, V. J. Hruby and T. L. Williams, *J. Am. Chem. Soc.*, **86**, 918 (1964).
6) S. Oae, "3d Orbital Resonance Involving the Sulfur Atom in Organic Sulfides" in "Organic Sulfur Compounds" Vol. IV, Ed. by N. Kharasch, Pergamon Press, New York, in press.
7) a) R. M. Topping and N. Kharasch, *Chem & Ind.*, 1961, 178; b) S. Oae and K. Ikura, This Bulletin, **38**, 58 (1965).

cleavage of the C–S bond, as is shown in Eqs. 8 and 9. The relative importance of these reactions (Eqs. 4—9) will be discussed in a later section.



(8)



(9)

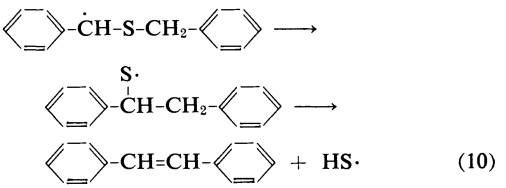
A small amount of water seems to be formed by the reduction with hydrogen sulfide, although it is not clear whether the compound to be reduced is the starting sulfoxide or one of the oxygen-containing intermediates shown in the foregoing equations. Related is the finding by Toland and his co-workers that a carboxylic acid or a nitrile is reduced to a hydrocarbon with hydrogen sulfide.[8]

The yield of the residual solid in the reaction flask was 27.8%, based on the original weight of the reactants. Alumina column chromatography and infrared analyses showed that this was mainly composed of elemental sulfur and the starting sulfoxide, and that there was no detectable amount of the other products which could be expected if species such as $C_6H_5CH_2SO$ and $C_6H_5CH{=}SO$ were the real intermediates.

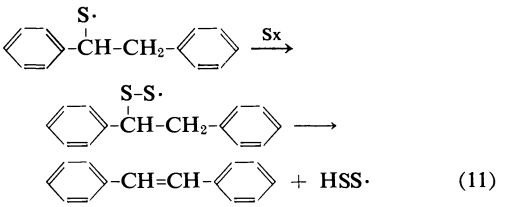
**The Products from the Other Dibenzyl Compounds.**—The mechanism of the reactions with the other compounds appear to be essentially similar to those with dibenzyl sulfoxide, i. e., the initial abstraction of hydrogen by a sulfur-free radical, followed by several competing reactions of the resulting free radicals. The relative importance of such competing reactions, however, varies depending on the nature of the dibenzyl compounds.

The products from the reaction with dibenzyl sulfide were hydrogen sulfide (39.3%), hydrogen persulfide, toluene, benzyl mercaptan and stilbene (41.5%). The formation of toluene, in an amount about equal to that of benzyl mercaptan, suggests three pathways; one is the direct splitting of the C–S bond, such as in Eq. 7, while the others are decompositions of the initially-formed free radical, such as in Eqs 5 and 4b. The direct splitting, however, seems unlikely, and the carbene pathway also fails to account for the yield of toluene, which should be smaller than that of benzyl mercaptan since the carbene would readily dimerize to stilbene. The pathway similar to Eq. 5 would, however, predict the formation of benzthioaldehyde. A related reaction to form benzaldehyde was actually observed in the reaction of dibenzyl ether, as will be described below. However, in the reaction of dibenzyl sulfide, infrared and gas chromatographic analyses failed to detect the formation of such thioaldehyde. Probably thioaldehyde, even when formed, was readily reduced to the corresponding mercaptan by hydrogen sulfide.

An interesting observation was the formation of hydrogen persulfide. The reaction leading to this product seems to be unique only to dibenzyl sulfide, since hydrogen persulfide was not detected in the reactions of the other dibenzyl compounds. Probably the following reactions, 10 and 11, are competing in the formation of stilbene:



(10)



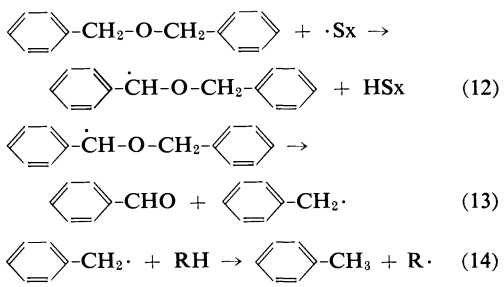
(11)

The products of dibenzyl sulfone were hydrogen sulfide (32%), stilbene (68%) and a small amount of water. Although the reaction was carried out several times, in no case was the evolution of sulfur dioxide detected. This observation seems strange when one recalls the quantitative formation of sulfur dioxide in the reaction of diphenyl sulfone.[1a] In this connection, it is interesting to compare the relative yields of lead sulfide and stilbene obtained from the three dibenzyl sulfur compounds. In the case of both sulfide and the sulfoxide, the yields of the two compounds were nearly the same, while the yield of lead sulfide from the reaction with the sulfone was about half of that of stilbene. The formation of water and no evolution of sulfur dioxide undoubtedly indicate that hydrogen sulfide was used for the reduction of the $SO_2$ group.

The major products in the case of dibenzyl ether were hydrogen sulfide (10.2%), benzaldehyde, toluene (60%), stilbene (14.4%), and a small amount of water. The formation of

8) W. G. Toland and R. W. Campbell, *J. Org. Chem.*, **28**, 3124 (1963).

toluene and benzaldehyde can be readily explained by means of Eqs. 12—14, which indicate the initial formation of a free radical, followed by its decomposition. As is illustrated



(12)

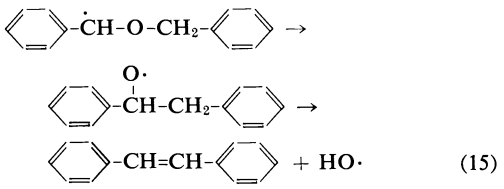


(13)



(14)

in Eqs. 7 and 4b, if the reaction is initiated by the direct splitting of the C–O bond or by the decomposition of the initially-formed free radical to give carbene, we might expect the formation of benzyl alcohol. However, the formation of benzyl alcohol was not detected by infrared and gas chromatographic analyses. These observations, together with the formation of a small amount of water, strongly indicate that the reaction to form stilbene proceeds through the pathway shown in Eq. 15:

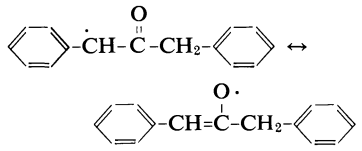


(15)

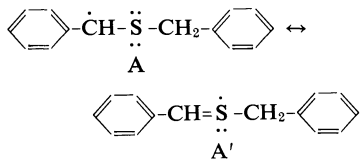
A remarkable feature of the reaction of dibenzyl ketone was the high yield of hydrogen sulfide (72.7%) as compared with the yields of less than 40% for the other compounds. This implies fewer fragmentation products, such as toluene and ketone, than would be expected if reactions of the type shown in Eqs. 5—6 or in Eqs. 12—14 took place. Actually, infrared spectra and alumina column chromatography failed to detect any fragmentation products except for the starting ketone and unidentified polyketones. These observations suggest that the initially-formed free radical is so stable that it undergoes dimerization or polymerization with less fragmentation than in the case of the other compounds.

**General Remarks.** — As has been described above, all these reactions appear to be initiated by the abstraction of benzylic hydrogen by the sulfur free radical. For the present five dibenzyl compounds, the total yield of stilbene plus fragmentation products (the yield of lead sulfide in the case of dibenzyl ketone) amounts to about 70%: i. e., all the compounds appear to undergo a facile abstraction of hydrogen. This is undoubtedly due to the very active nature of the benzylic hydrogen atom. For compounds having less active hydrogen, the reaction somewhat different from those of the dibenzyl compounds. Our preliminary experiments on the reactions of di-*n*-butyl sulfide, sulfoxide and sulfone indicate that these compounds undergo hydrogen abstruction to a much lesser extent than do the dibenzyl compounds under similar reaction conditions.[9] Extreme are the cases of the reaction of diphenyl sulfoxide and sulfone,[1a] as has been described before. The fate of the initially-formed free radical depends on its stability and also on the relative ease of the bond breakings of C–C, C–S, C–O and S–O linkages.

The following resonance stabilization of the initial free radical seems to be responsible for the apparent lack of fragmentation in the reaction with dibenzyl ketone. The dependence of the fragmentation reaction on the stability



of the initial free radical seems also to be manifested in the reactions of dibenzyl sulfide and ether. The free radical of the sulfide (A) can be stabilized by the 3d-orbital resonance of sulfur (A′) as well as by the resonance



stabilization by the phenyl ring, whereas such stabilization is impossible in the ether. This difference seems to be partly responsible for the higher yield of stilbene from the sulfide than from the ether and for the higher yield of fragmentation products from the ether than from the sulfide.

The same view can be derived from the reaction of benzyl cyanide. Recently, Mayer and Scheithauer found that the reaction of benzyl cyanide with sulfur above 175°C gave hydrogen sulfide and *trans*-dicyanostilbene as the major products and a small amount of 1, 2-dicyanodiphenylethane.[10] Although no mechanistic interpretation has been made, the reaction seems to be initiated by the abstraction of benzylic hydrogen by the sulfur free radical, and the initially-formed free radical

9) Unpublished work of these laboratories.
10) R. Mayer and St. Scheithauer, *J. Prakt. Chem.*, **21**, 214 (1963).

seems to be so stable that it readily dimerizes to give 1,2-dicyanodiphenylethane, which is then transformed to dicyanostilbene.

Although it is not easy to compare the relative ease of the bond breakings of C–C, C–O and C–S bonds from the product analyses, the product distribution can often serve as a measure for the comparison of some particular bonds. A good example is the case of the S–O bond in sulfoxide and sulfone. The formation of benzaldehyde and benzyl mercaptan clearly indicates the S–O bond breaking in dibenzyl sulfoxide, while no such bond breaking was detected in the corresponding sulfone except for the formation of water. In the reactions of di-*n*-butyl sulfoxide and sulfone, the S–O bond breaking in the former compound resulted in the formation of di-*n*-butyl sulfide, while no such reaction was observed with the latter compounds.[9] The most clear-cut case is the comparison between those of diphenyl sulfoxide and the sulfone.[1] In all these cases, the S–O bonds in the sulfoxides are found to be much weaker than those of the corresponding sulfones and to be readily cleaved, as had been predicted.[11]

## Experimental

**The Synthesis of the Starting Compounds.**—Dibenzyl sulfide was prepared by the reaction of benzyl chloride with sodium sulfide; m. p. 49°C (lit., 49°C),[12] recrystallized from 70% aqueous ethanol. Dibenzyl sulfoxide was prepared by the oxidation of the sulfide with hydrogen peroxide in acetic acid, m. p. 136—137°C (lit., 132—133°C),[12] recrystallized from *n*-hexane. Dibenzyl sulfone was prepared by the chromic acid oxidation of the sulfide in acetic acid, m. p. 150—151°C (lit., 149.5—150°C),[12] recrystallized from *n*-hexane-benzene.

Dibenzyl ether was prepared by the reaction of benzyl chloride with sodium benzyl alkoxide in dioxane, m. p. 148°C/6 mmHg (lit., 170°C/16 mmHg).[13]

Dibenzyl ketone was prepared by the reaction of benzylcyanide with benzyl magnesium chloride in anhydrous ether, followed by the decomposition of the resulting imino complex with water; m. p. 34—35°C (lit., 35°C),[14] recrystallized from *n*-hexane.

**General Procedure for the Reaction with Elemental Sulfur.** — The reaction apparatus (Fig. 1) was essentially the same as that employed in the previous reactions of diphenyl sulfoxide and sulfone, but here modified to trap volatile products and hydrogen sulfide.

Equimolecular amounts of the starting compound

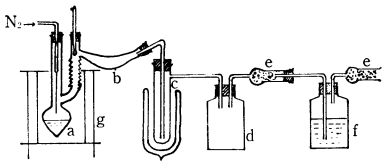



Fig. 1

a, Reaction flask; b, trap for solid or oils; c, trap for volatile oils; d, empty bottle; e, calcium chloride drying tube; f, trap for hydrogen sulfide containing lead acetate.

and sulfur were thoroughly mixed and placed in a Säbel-type flask with a short fractionating column (a) (in Fig. 1). The whole system was first flushed with nitrogen gas at room temperature for about 10 min. The reaction flask was then heated in an air bath (g) under a slow stream of nitrogen. At around 160°C, the evolution of hydrogen sulfide was usually observed. After the temperature had been slowly raised to about 200°C, this temperature was maintained for five to nine hours. The oily or solid product was trapped in (b) (in Fig. 1), the volatile product was trapped in (c) (in Fig. 1), which was cooled in a dry ice-acetone bath (below −50°C), and the hydrogen sulfide was trapped in a vessel as lead sulfide. After the evolution of hydrogen sulfide was no longer observed, the substance which remained in the reaction flask (a) (Fig. 1) was vacuum-distilled. The oily and solid products thus obtained were purified by a combination of gas-liquid and column elution chromatographies and identified by spectroscopy and by elemental analysis. At least three runs were carried out for each compound in order to (test the reproducibility). A typical run with dibenzyl sulfide is described in the next paragraph. Table I gives one representative run for each compound.

**The Reaction of Dibenzyl Sulfide.** — After the reaction had been completed, the hydrogen sulfide trapped as lead sulfide was filtered, washed with water, dried and weighed; it was found to amount to 472 mg. (39.3%). A volatile product in the trap c, was found to be a mixture of hydrogen persulfide and a very small fraction of benzylmercaptan plus toluene as two immiscible liquids. This mixture was mechanically separated from hydrogen persulfide with a syringe and analyzed by gas chromatography and infrared spectrometry. The gas chromatography was carried out using a high-vacuum silicone column and hydrogen carrier gas, at the column temperature of 88.5°C. The retention times of toluene and benzyl mercaptan were 5.2 and 40 min. respectively, and no other component was detected. The oils in trap b were also found to be a mixture of toluene and benzyl mercaptan by infrared and gas chromatographic analyses; the yield was 291 mg. (27.2%). The hydrogen persulfide was identified by its boiling point 73—74°C (lit., 74.5°C and its ultraviolet spectra ($\lambda_{max}$, 261, 268 m$\mu$ in EtOH).

After the mixture of toluene and benzyl mercaptan had been removed from the trap b, the brown residue in the reaction flask was vacuum-distilled to give a pale yellow solid, which was found to be

11) C. C. Price and S. Oae, "Sulfur Bonding," Ronald Press, New York (1962), Chapters 3 and 4.
12) R. L. Shriner, H. C. Struck and W. J. Jorison, *J. Am. Chem. Soc.*, **52**, 2060 (1930).
13) G. M. Bennett and G. H. Willis, *J. Chem. Soc.*, **1928**, 2305.
14) H. Adkins, R. M. Elofson, A. G. Rossow and C. C. Robinson, *J. Am. Chem. Soc.*, **71**, 3629 (1949).

mainly composed of stilbene. The analysis was first made by alumina thin-layer chromatography, using *n*-hexane as the developing solvent. The chromatogram after iodine coloration showed a main spot of stilbene and three other small faint spots. The alumina elution chromatography was carried out using a *n*-hexane-benzene (7 : 3 v/v) mixture as the developing solvent. Over 90% of the eluted fractions was found to be stilbene on the basis of their having the same melting point and the same infrared spectra as those of authentic stilbene. The fractions corresponding to the small spots on the thin-layer chromatogram were not detected by this column chromatography.

The dark brown residue in the reaction flask amounted to 198 mg., and its infrared spectra were found to be almost identical with those of the starting sulfide. This residue was probably composed of the starting sulfide, elemental sulfur and small amounts of unknown products.

**The Reaction of Dibenzyl Sulfoxide.**—Three runs were performed. In each case, the attempt to detect $SO_2$ failed. Hydrogen sulfide was obtained as lead sulfide, as has been described before. The oily product was found to be composed of toluene, benzaldehyde and benzyl mercaptan by infrared spectra and gas chromatography, which was carried out under conditions similar to those described above. The retention times of toluene, benzaldehyde and benzyl mercaptan at 85°C were 5.4, 24.2 and 45.6 min. respectively. The infrared spectra of the oil showed a strong band at 1730 $cm^{-1}$ due to benzaldehyde. The identification of benzaldehyde was also made converting it to the 2,4-dinitrophenylhydrazone m. p. 238—239°C (mixed melting point, 237—239°C). The solid product, m. p. 117—120°C was analyzed by alumina column chromatography to give stilbene as the major fraction and a trace of a yellow solid. Stilbene was identified by the infrared spectra, elemental analysis and a mixed melting point determination with an authentic sample :

Found : C, 92.65 ; H, 6.85. Calcd. : C, 93.33 ; H, 6.60%.

The above unknown yellow solid showed the following properties ; m. p. 116—119°C.

Found : C, 49.65 ; H, 4.45%.

A small amount of white crystals gradually adhered on the inner walls of the trap c as the reaction proceeded. This melts near 0°C and is miscible with water. The presence of the O-H band in the infrared spectra of the non-dried oily product (in the trap b) and the indication of water on the gas chromatogram of the same oily product indicated that the product in the trap c was water.

The identification of the black residue in the reaction flask was attempted. The infrared spectrum was very similar to the starting sulfoxide. This residue was probably mainly composed of the starting sulfoxide and elemental sulfur.

**The Products of the Other Compounds.** — The reaction conditions and the yields of the products are shown in Table I. The analytical methods were essentially the same as those described above.

*Department of Applied Chemistry*
*Faculty of Engineering*
*Osaka City University*
*Sumiyoshi-ku, Osaka*

# Surface Chemistry of the Polyamide Series. I. Effect of Hydrogen Bonding on the Nature of Poly-$\alpha$-amino Acid Monolayers

By Takuya YAMASHITA* and Toshizo ISEMURA

(Received August 5, 1964)

The conformation of protein is maintained mainly by the hydrogen bonding between $\rangle C{=}O$ and $H{-}N\langle$ groups of the peptide linkages. In this connection, the monolayers of poly-$\alpha$-amino acids, or polypeptides as model substances of protein, have been studied by many workers.[1-11] It has been found[8,9] that the monolayers of poly-$\alpha$-amino acids with nonionic side chains are condensed and that their surface viscosities appear at larger areas than the crose-packed areas when they are spread at the air/water interface. This finding has been interpreted by assuming that the polypeptide chain is rigid as a result of the

* Present address: Department of Chemistry, Faculty of Science, Osaka University, Nakanoshima, Kita-ku, Osaka.

1) C. W. N. Cumper and A. E. Alexander, *Trans. Faraday Soc.*, **46**, 235 (1950).
2) T. Isemura and K. Hamaguchi, This Bulletin, **25**, 40 (1952).
3) T. Isemura and K. Hamaguchi, ibid., **26**, 424 (1953).
4) T. Isemura and K. Hamaguchi, ibid., **27**, 125 (1954).
5) J. T. Davies, *Trans. Faraday Soc.*, **49**, 949 (1953).
6) J. T. Davies, *Biochim. Biophys. Acta*, **11**, 165 (1953).
7) D. F. Cheesman and J. T. Davies, *Adv. Protein Chem.*, **9**, 439 (1954).
8) T. Isemura and S. Ikeda, This Bulletin, **32**, 178 (1959).
9) S. Ikeda and T. Isemura, ibid., **32**, 659 (1959).
10) T. Yamashita and T. Isemura, ibid., **35**, 929 (1962).
11) Y. Kinoshita, *Makromol. Chem.*, **33**, 1 (1959).

hydrogen bonding between the peptide linkages of backbones. They are spread in a $\beta$-configration. On the other hand, the monolayers of prolyl polypeptides are of the expanded type and the appreciable surface viscosities are manifested at much smaller areas than their close-packed areas.[8,9] Their chain configurations have been considered to be flexible as a result of the weak interaction due to the decrease in the number of hydrogen bonds between peptide groups. Thus, the hydrogen bonds between $\rangle C{=}O$ and $H{-}N\langle$ groups of peptide linkages are important for understanding the nature of the monolayers of polypeptides, or proteins. Further, such a hydrogen bonding is assumed to play a major role in the stability of the configuration of polyamides of the nylon type.[11] The monolayers of nylons have been studied by some workers,[1,2,4,12-15] but the effect of the number of $CH_2$ groups on polyamide monolayers has never been investigated.

In the studies of this series, the effect of hydrogen bonding on the nature of the monolayers of poly-$\alpha$-amino acids and polyamides of the nylon type have been studied at the air/water and oil/water interfaces in order to elucidate the role of hydrogen bonding in the configurations of the polymers and proteins.

It appears that sarcosyl polypeptides are suitable for the present study, because the sarcosyl residue (that is, the *N*-methyl glycyl residue) cannot form a hydrogen bond with a carbonyl group of another residue, as in the case of the prolyl residue, because it lacks a hydrogen atom to be hydrogen-bonded. Accordingly, in the present work, the effect of hydrogen bonding on the polypeptide monolayers has been studied at the air/water and oil/water interfaces with polysarcosine, copoly-1 : 1-(glycine, sarcosine) and copoly-1 : 1-(DL-alanine, sarcosine). For the sake of comparison, the monolayers of poly-L-alanine and poly-DL-alanine have also been studied. Further, poly-$\alpha$-aminoisobutyric acid has been studied in order to investigate the steric hindrance to the hydrogen bond formation.

## Experimental

**Samples.**—The samples used in the present study were prepared by the polymerization or copolymerization of the *N*-carboxyanhydrides of the corresponding amino acids, using sodium methoxide as an initiator, according to the usual method.[16] The average degree of polymerization was determined by end-group analysis. Poly-DL-alanine ($n$=40), polysarcosine ($n$=27), copoly-1 : 1-(glycine, sarcosine) ($n$=33) and copoly-1 : 1-(DL-alanine, sarcosine) ($n$=40) were spread from solutions in a mixed solvent, water-isopropyl alcohol (1 : 1, v/v). The spreading solvents for poly-L-alanine and poly-$\alpha$-aminoisobutyric acid were trifluoroacetic acid and a mixture of dichloroacetic acid and benzene (3 : 7, v/v) respectively.

**Methods.**—At the air/water interface, the surface pressure was measured using surface balances of both the float and hanging-plate types. The trough used was made of polymethyl methacrylate, the rim of which was coated with purified paraffin.

The surface potential was measured by the ionizing air-electrode method, using polonium as a radiation source. The potential was detected by a Cary Model-31 vibrating reed electrometer. The accuracy was $\pm 3$ mV. The surface moment of the film, $\mu$, was calculated from the observed surface potential, $\Delta V$, utilizing the Helmholtz formula, $\mu = \Delta V A/4\pi$, where $A$ is the area per residue.

The surface viscosity was measured by the rotatory oscillation of a suspended disk on the surface of the liquid; it was calculated by the following formula;[17]

$$\eta_s = \Delta\lambda_{10}\frac{2.303\,I}{2\pi P}\left(\frac{1}{a^2}-\frac{1}{b^2}\right)$$

where $I$ is the moment of inertia of the disk; $P$, the period of oscillation; $\Delta\lambda_{10}$, the difference between logarithm decrements of oscillation in the presence of film and in its absence; $a$, the radius of the disk, and $b$, the radius of the film surrounding the oscillation disk. In the apparatus used in the present experiments, $I$ was 30.25 g. cm.; $P$, 13.06 sec.; $a$, 1.00 cm., and $b$, 4.00 cm.

The compression of the film at the air/water interface was started 20 minutes after the polymer was spread; the film was compressed at the rate of 12 $cm^2$/min.

At the oil/water interface, the interfacial pressure was measured by the ring method. The interfacial concentration of the polymer was changed by the successive injection method, corrected by the Thomas theoretical correction formula.[10,18,19] The diameter of the ring was 3.014 cm. Petroleum ether (b. p. 85—115°C) was used as an oil phase. The interfacial tension at the interface of petroleum ether and distilled water was 49.6 dyn./cm. at 23°C. The measurement of the interfacial pressure was carried out five minutes after each injection. It was ascertained that the interfacial pressure-area curve of polyvinyl acetate agrees closely with that reported by Hotta[13] at the oil/distilled water interface.

All the measurements were performed at room temperature. The change of temperature, however, never exceeded one degree during the course of an experiment.

12) D. J. Crisp, *J. Colloid Sci.*, **1**, 161 (1946).
13) H. Hotta, ibid., **9**, 504 (1954).
14) K. Inokuchi, This Bulletin, **29**, 490 (1956).
15) G. E. Hibberd and A. E. Alexander, *Proc. 3rd Int. Cong. Surface Activity*, **2**, 144 (1960).
16) E. Katchalski and M. Sela, *Adv. Protein Chem.*, **13**, 243 (1958).
17) L. G. Fourt and W. D. Harkins, *J. Phys. Chem.*, **42**, 897 (1938).
18) A. G. Thomas, *Nature*, **179**, 776 (1957).
19) E. G. Cockbain, K. J. Day and A. I. McMullen, *Proc. 2nd Int. Cong. Surface Activity*, **1**, 56 (1957).

## Results

The surface pressure-area ($\Pi$-$A$), the surface moment-area ($\mu$-$A$) and the surface viscosity-area ($\eta_s$-$A$) curves of poly-DL-alanine on distilled water are shown in Fig. 1. The $\Pi$-$A$ curve of poly-L-alanine is also represented in the same figure. The surface viscosity of poly-DL-alanine was first detected at the area where the surface pressure is sufficiently low. The area per residue of poly-DL-alanine was much smaller than that of poly-L-alanine.

The effects of sulfuric acid on the surface pressure and surface moment of poly-DL-alanine are shown in Fig. 2. On aqueous sulfuric acid, the film was expanded and an increase in surface moment was observed.

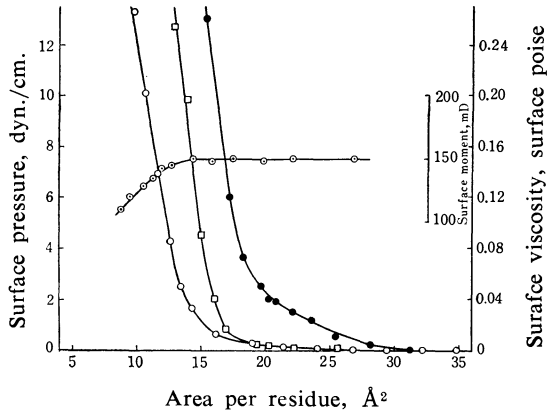



Fig. 1. Monolayers of poly-L-alanine and poly-DL-alanine on distilled water:
poly-L-alanine (15°C)—□, surface pressure
poly-DL-alanine (20°C)—○, surface pressure
⊙, surface moment; ●, surface viscosity.

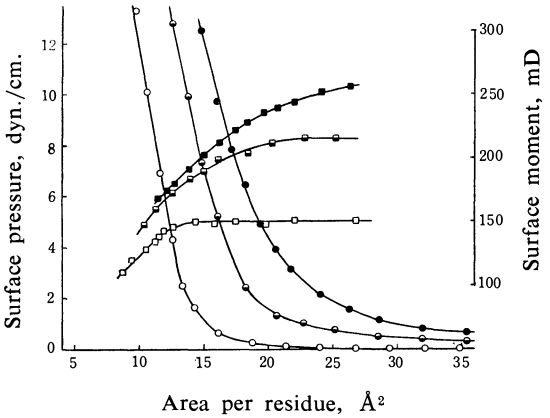



Fig. 2. Surface pressure-area and surface moment-area curves of poly-DL-alanine on distilled water (○, □) at 20°C and on the subsolutions of 3 N $H_2SO_4$ (◒, ◨) and 6 N $H_2SO_4$ (●, ■) at 20°C.

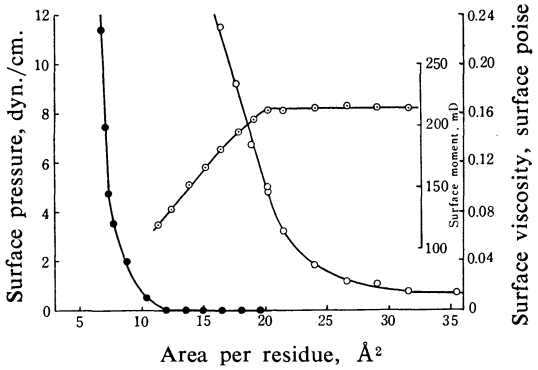



Fig. 3. Monolayer of poly-$\alpha$-aminoisobutyric acid on distilled water at 17°C: ○, surface pressure; ⊙, surface moment; ●, surface viscosity.

The $\Pi$-$A$, $\mu$-$A$ and $\eta_s$-$A$ curves of poly-$\alpha$-aminoisobutyric acid on distilled water are shown in Fig. 3. The film of this polypeptide is much more expanded than that of polyalanine on distilled water, and a higher surface moment was obtained. In contrast with polyalanine, the surface viscosity was found first at a small area where the surface pressure is markedly high.

Figure 4 shows the $\Pi$-$A$ and $\mu$-$A$ curves of copoly-1 : 1-(DL-alanine, sarcosine) on the 3 M potassium chloride solution. The film was of the expended type. The surface viscosity was not detected with our present apparatus because of its lower sensitivity. The surface moment was considerably lower than that of poly-DL-alanine. This might be caused by the partial dissolution of polymer chains in the aquous phase.

The film characteristics of the polymers described above are summarized in Table I, where $A_\delta$ is the area per residue at the minimum compressibility of the film; $A_{\Pi\to 0}$, the

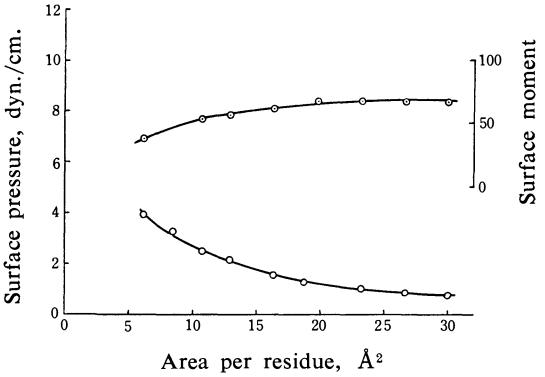



Fig. 4. Monolayer of copoly-1 : 1-(DL-alanine, sarcosine) on 3 M potassium chloride at 17°C: ○, surface pressure; ⊙ surface moment.

TABLE I. FILM CHARACTERISTICS OF POLYMERS AT THE AIR/WATER INTERFACE

| Polymer | Subphase | $A_\delta$ Å²/res. | $A_{\Pi\to 0}$ Å²/res. | $A_\eta$ Å²/res. | $A_\mu$ Å²/res. | $\mu$ mD |
|---|---|---|---|---|---|---|
| Poly-L-alanine | DW | 15.0 | 15.9 | | | |
| Poly-DL-alanine | DW | 13.2 | 14.2 | 31 | 14.2 | 150 (c) |
| | 3 N $H_2SO_4$ | 15.0 | 17.8 | | 22.8 | 215 (c) |
| | 6 N $H_2SO_4$ | 17.0 | 21.0 | | | 256 (at 26 Å²) |
| Poly-$\alpha$-aminoisobutyric acid | DW | 20.0 | 23.0 | 12 | 20.0 | 214 (c) |
| Copoly-1 : 1-(DL-alanine, sarcosine) | 3 M KCl | | | No viscosity | | 66 (at 20 Å²) |

DW: Distilled water

area per residue where the straight portion of the $\Pi$-$A$ curve is extraporated to $\Pi=0$; $A_\mu$, the area per residue where the surface moment, $\mu$, begins to decrease; $\mu(c)$, the constant value of the surface moment, and $A_\eta$, the area per residue where the surface viscosity is first detected or begins to rise.

Although polysarcosine could not be spread as a monolayer at the air/water interface, even on the 3 M potassium chloride subsolution, because of its high solubility, a stable film was obtained at the oil/water interface. Figure 5 shows the interfacial pressure-area ($\Pi_i$-$A$) curves of polysarcosine, copoly-1 : 1-(glycine, sarcosine), and copoly-1 : 1-(DL-alanine, sarcosine), as well as that of poly-DL-alanine. The film of poly-DL-alanine was slightly expanded in a lower surface-pressure region, and above the pressure of 3 dyn./cm., the interfacial, pressure was nearly identical with the surface pressure in the same areas. The $\Pi_i$-$A$ curve of copoly-1 : 1-(DL-alanine, sarcosine) agreed fairly well with that of polysarcosine. Both films can be considerably expanded and compressible. Copoly-1 : 1-(glycine, sarcosine) also gave an expanded film, although the area per residue was much smaller than that of polysarcosine.

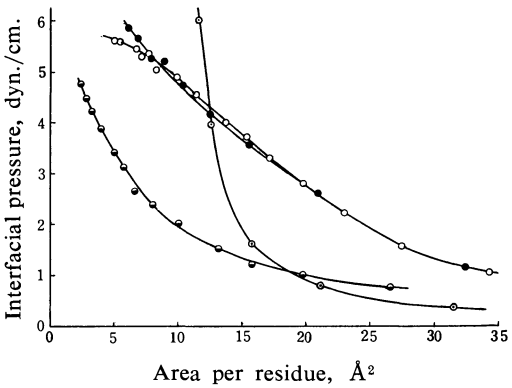



Fig. 5. Interfacial pressure-area curves of poly-DL-alanine (⊙), polysarcosine (○), copoly-1 : 1-(glycine, sarcosine) (◒) and copoly-1 : 1-(DL-alanine sarcosine) (●) at petroleum ether/distilled water interface (15°C).

## Discussion

**The Air/Water Interface.** — *Polyalanine on Disrilled Water.* — The films of poly-L-alanine and poly-DL-alanine on distilled water are of the condensed type. The $\pi$-$A$ curve of poly-DL-alanine is in good agreement with those reported by Isemura et al.[20] and by Glazer and Dogan,[21] and the $\mu$-$A$ curve, with Isemura and Ikeda's.[8] The surface viscosity of this polypeptide is first detected at a much larger area than its limiting area ($A_\delta$ or $A_{\Pi\to 0}$), as Fig. 1 and Table I show, and, accordingly, at the area where the surface pressure is sufficiently low. Similar results have been obtained by Ikeda and Isemura,[9] and by MacRitchie and Alexander.[22] Generally, a monolayer of the condensed type exibits such a suface viscosity-surface pressure relation.[9] In the monolayer of polyalanine, polypeptide chains are probably held together tightly, and the motion of residues or segments is strongly inhibited by the hydrogen bonding and by the partial double-bond nature of the peptide bonds.

It has been generally accepted[1-10] from the measurements of surface pressure, surface potential (or surface moment) and surface viscosity that on the aqueous sufaces poly-$\alpha$-amino acids with nonionic side chains are spread in a $\beta$-configuration, with an alternation of side chains up and down to the surface. The data shown in Table I suggest that such a configuration is also plausible for the monolayers of poly-L-alanine and poly-DL-alanine.

It has been found[3] that the area per residue of the film of poly-$\gamma$-benzyl-L-glutamate is much smaller than that of its DL-isomers.

20) T. Isemura, S. Ikeda, F. Tokiwa and J. Noguchi, This Bulletin, 34, 1236 (1961).
21) J. Glazer and M. Z. Dogan, *Trans. Faraday Soc.*, 49, 448 (1953).
22) F. MacRitchie and A. E. Alexander, *J. Colloid Sci.*, 16, 57 (1961).

Such a difference in area is to be ascribed to the much closer packing of L-polypeptide chains. On the contrary, poly-DL-alanine occupied a much smaller area in the film than poly-L-alanine. The $A_\delta$ value of the former is 13.2 Å$^2$ per residue, much smaller than the area calculated for the film in the $\beta$-form, (ca. 15 Å per residue), while that of the latter is 15.0 Å$^2$ per residue. As is well known, poly-DL-alanine is the only water-soluble polypeptide with nonpolar side chains, whereas poly-L-alanine is insoluble in almost all the solvents. Accordingly, the fact that the area of the film of poly-DL-alanine is smaller than that of its L-isomer may be ascribed to the greater solubility of the former film in the aqueous subphase. In the area, $A_\delta$, a part of the alanyl residues of the DL-isomer might be already submerged into the aqueous subphase, even though in a $\beta$-form. The size of the side chains of polyalanine is smallest in poly-$\alpha$-amino acids, and the van der Waals attractive force between side chains which contribute to the film stability will be quite weak, as will be discussed in a later section. Therefore, the smaller area of the DL-isomer, will be due to its greater solubility, caused by the partial presence of hydrogen bonds between the peptide group and the water molecule, because there may be some irregularity in the chain configuration.

*The Effect of Sulfuric Acid on the Monolayer of Poly-DL-alanine.*—The effect of concentrated sulfuric acid on the nylon monolayers has been studied by Crisp,[12] and by Hibberd and Alexander.[15] The expansion of films[12,15] and the increase in surface moments[15] have been observed by them on the concentrated sulfuric acid subsolutions. These findings were interpreted in terms of the weakening of hydrogen bonds between peptide groups. In the present study, as Fig. 2 and Table I show, a pronounced effect of sulfuric acid on the monolayer of poly-DL-alanine was observed on the 3 N and 6 N solutions. The expansion of the film of this polymer is caused by the increase in the flexibility of the polypeptide chain due to the breaking of hydrogen bonds, as in the case of nylon monolayers. The increase in surface moment seem to be caused by a similar reason. The breaking of hydrogen bonds will make the carbonyl groups more vertical as regards the interface, as was pointed out by Davies[5,7]; as a result, the surface moment increases.

*Poly-α-aminoisobutyric Acid.*—The monolayer of this polypeptide on distilled water is much more expanded than that of polyalanine. The shape of the *Π-A* curve is similar to those of poly-DL-alanine on the sulfuric acid subsolutions. As Table I shows, the discrepancy between the areas at $A_\delta$ and $A_{\Pi\to 0}$ is much greater than those of poly-L- and -DL-alanine on distilled water, as in the case of poly-DL-alanine on the acid subsolutions. In contrast with poly-DL-alanine on distilled water, the $\mu(c)$ value is quite high (214 mD), and the surface viscosity is first detected at a far smaller area than $A_\delta$ or $A_{\Pi\to 0}$ and, consequently, at the area where the surface pressure is sufficiently high.

In general, the monolayers of high polymers are of the condensed type under a strong interaction between constituent monomer units, while of the expanded type under a weak interaction.[8,9] The facts shown above indicate that the interaction between the monomer units or the polymer chains of poly-$\alpha$-aminoisobutyric acid is very weak.

The steric hindrance to the hydrogen bond formation between peptide bonds has been studied with nylon monolayers by Hibberd and Alexander.[15] They found that nylon obtained from the condensation of sebacic acid with $\alpha:\alpha:\alpha':\alpha'$-tetramethyl tetramethylenediamine (Nylon TeMe 410) gives an expanded monolayer with no rigidity, while Nylons 210, 410 and 610 cause condensed monolayers. The anomaly of the film of Nylon TeMe 410 must arise from the considerable steric hindrance to the –CO·NH– groups afforded by the four $\alpha$-substituted methyl groups. Poly-$\alpha$-aminoisobutyric acid possesses two $\alpha$-substituted methyl groups. Therefore, the steric hindrance to peptides bonds must be quite great, as in the case of Nylon TeMe 410. The expanded monolayer with a low surface viscosity can be obtained with this polypeptide because the formation of the hydrogen bonds between peptide groups is hindered. The higher value of the constant surface moment (214 mD) here than that of poly-DL-alanine on distilled water (150 mD) also suggests that there are few hydrogen bonds, as in the case of poly-DL-alanine film on the acid subsolutions.

*Copoly-1 : 1-(DL-alanine, sarcosine).*—This copolymer gives an expanded film on the 3 M potassium chloride solution, one with no viscosity. The sarcosyl residue has no hydrogen atom to be hydrogen-bonded like the prolyl residue in the polypeptide chain. The nature of the film observed is probably caused by the increase in the flexibility of the polymer chain due to the decreases in the number of hydrogen bonds between monomer units and in the double-bond nature of main chain. It has been found[8,9] that the films of prolyl polypeptides are of the expanded type and that their surface viscosities are observed at small areas per residue where the surface pressures are quite

high in contrast with those of nonionic polypeptides. This fact has been ascribed to the decrease in the number of hydrogen bonds between peptide linkages due to the presence of prolyl residues, and it is in good agreement with the results of our present investigation.

**The Oil/Water Interface.**—At the oil/water interface, the film of poly-DL-alanine was expanded slightly in the lower-pressure region, and under a higher pressure the $\Pi_i$-$A$ curve was found to be nearly identical with the $\Pi$-$A$ curve. The expansion of the film at this interface is much less than in the case of poly-DL-phenylalanine.[10] Poly-DL-alanine is a polypeptide with the smallest side chain. Therefore, the van der Waals attraction between side chains is rather weak. This is probably responsible for the slight expansion of the film of this polypeptide at the oil/water interface.

The behavior of the monolayer of polysarcosine is markedly different from that of poly-DL-alanine, even though these polymers have the same side chains. The film of polysarcosine is rather expanded and compressible. Methyl groups attach to nitrogen atoms of the polymer chain in polysarcosine, but to $\alpha$-carbon atoms in poly-DL-alanine. Evidently, the difference between these polymer films is to be ascribed to the absence or presence of hydrogen bonds between monomer units. The absence of the hydrogen bonds makes the polymer chains more flexible. Consequently, the monolayer of polysarcosine is considerably expanded and conpresible. The lack of a double-bond nature in polymer chain might also be responsible for the expansion of the polysarcosine film. On the other hand, the film of poly-DL-alanine is rather condensed, even at the oil/water interface, because its polypeptide chains are held together rigidly by the hydrogen bonds and by the partial double-bond nature of the peptide bonds.

Copoly-1 : 1-(DL-alanine, sarcosine) gives a $\Pi_i$-$A$ curve which is nearly identical with that of polysarcosine. The monolayer of copoly-1 : 1-(glycine, sarcosine) is also of the expanded type, although the area occupied per residue is much smaller. The effect of hydrogen bonding is small with these polymers because of the presence of sarcosyl residues.

## Summary

The effect of hydrogen bonding on the nature of poly-$\alpha$-amino acid monolayers has been studied at the air/water and oil/water interfaces with poly-L-alanine, poly-DL-alanine, polysarcosine, copoly-1 : 1-(glycine, sarcosine), copoly-1 : 1-(DL-alanine, sarcosine) and poly-$\alpha$-aminoisobutyric acid.

Poly-L-alanine and poly-DL-alanine gave monolayers of the condensed type on distilled water, and the surface viscosity of poly-DL-alanine was first detected at a much larger area than its close-packed area where the surface pressure was sufficiently low. This fact suggests that there exists a strong interaction between peptide bonds of polyalanine. Both polymers would assume a $\beta$-configration. On the concentrated sulfuric acid subsolutions, the film of poly-DL-alanine was expanded and an increase in surface moment was observed because of the breaking of hydrogen bonds between peptide linkages.

A steric hindrance to the hydrogen bond formation was observed with the film of poly-$\alpha$-amino isobutyric acid. This polypeptide gave an expanded monolayer on distilled water, and its surface viscosity could be first detected at a very small area where the surface pressure was remarkably high.

The film of copoly-1 : 1-(DL-alanine, sarcosine) was of the expanded type on the 3 M potassium chloride subsolution because of the decrease in the number of hydrogen bonds and that in the double-bond nature of the main chain.

At the oil/distilled water interface, a marked difference was found between the monolayers of poly-DL-alanine and polysarcosine, although these polymers have the same side chains. Poly-DL-alanine gave a considerably condensed monolayer, even at the oil/water interface. On the other hand, the film of polysarcosine was of the expanded type. The difference between the films of these polymers is mainly to be ascribed to the presence or the absence of hydrogen bonds. The 1 : 1-copolymer of sarcosine with glycine or DL-alanine also gave an expanded monolayer.

The authors are grateful to Professor Junzo Noguchi of Hokkaido University and to Dr. Sanshiro Kume of Osaka University for their kind guidance in preparing the polymer samples and in making the ionizing air-electrode respectively.

*Institute for Protein Research*
*Osaka University*
*Kita-ku, Osaka*

# Surface Chemistry of the Polyamide Series. II. Effect of the Sarcosyl Residue on the Monolayer of Polyleucine

By Takuya YAMASHITA* and Toshizo ISEMURA

(Received August 6, 1964)

The role of the prolyl residue in polypeptide monolayers has been studied by Isemura and Ikeda.[1,2] The surface viscosity of the poly-DL-alanine monolayer, which is of the condensed type, was found to rise at larger area than its close-packed area. This result was interpreted by assuming that the polypeptide chain is rigid because of the hydrogen bonds between peptide groups. On the other hand, the monolayers of prolyl peptides are of the expanded type, and the appreciable surface viscosities are manifested at much smaller areas than their close-packed areas. Their chain configuration are considered to be rather flexible as a result of the lack of hydrogen bonds between peptide groups.

In the preceding paper,[3] the view that the hydrogen bonds between peptide groups remarkably affect the nature of polypeptide monolayers has been supported by the results of studies of the monolayers of polysarcosine and of the copolymer of sarcosine with DL-alanine or glycine.

In the present investigation, the effect of hydrogen bonding on the polypeptide monolayers has been studied at the air/water and oil/water interfaces with copolypeptides of L-leucine with sarcosine of different compositions. The difference between monolayers of poly-L-leucine and its DL-isomer has also been studied.

## Experimental

**Samples.** — Poly-L-leucine, poly-DL-leucine and polysarcosine were prepared by the polymerization of the N-caboxyanhydride of the respective amino acid, using sodium methoxide as an initiator.[4] Copolymers of L-leucine, with sarcosine of different compositions, were prepared from the mixtures of *N*-carboxyanhydrides of sarcosine and L-leucine by the same method. The spreading solution and the average degree of polymerization of each polymer are shown in Table I.

Table I. Average degrees of polymerization of samples and their spreading solvents

| Polymer | $n$ | Solvent |
|---|---|---|
| Poly-L-leucine | | TFA |
| Poly-DL-leucine | | TFA |
| Copoly-3 : 1-(L-leucine, sarcosine) | | DCA+TFA+IPA (5 : 2 : 3, v/v) |
| Copoly-1 : 1-(L-leucine, sarcosine) | 20 | DCA+TFA+IPA (4 : 3 : 3, v/v) |
| Copoly-1 : 3-(L-leucine, sarcosine) | 28 | DCA+TFA+IPA (5 : 2 : 3, v/v) |
| Polysarcosine | 27 | $H_2O$+IPA (1 : 1, v/v) |

TFA Trifluoroacetic acid
DCA Dichloroacetic acid
IPA Isopropyl alcohol
$n$ was determined by the end group analysis.

**Methods.** — The surface pressure, the potential and the viscosity were measured by a surface balance of the float type, an ionizing air-electrode and an oscillating rotatory disk respectively. The surface moment was calculated from the surface potential using the Helmholtz equation. The interfacial pressure was measured by the ring method. The details of these experimental methods have been described in the preceding paper.[3]

## Results

The surface pressure-area ($\Pi$-$A$), surface moment-area ($\mu$-$A$) and surface viscosity-area ($\eta_s$-$A$) curves of poly-L-leucine and the 3 : 1-, 1 : 1- and 1 : 3-copolymers of L-leucine with sarcosine on distilled water are shown in Figs. 1—4 respectively. $\Pi$-$A$ curve of poly-DL-leucine is also illustrated in Fig. 1.

The film characteristics of these polymers are summarized in Table II, where $A_\delta$ is the area at the minimum compressibility of the film; $A_{\Pi\to 0}$, the area where the straight portion of the $\Pi$-$A$ curve is extraporated to $\Pi=0$; $A_\mu$, the area where the surface moment, $\mu$, begins to decrease; $\mu(c)$, the constant value of the surface moment; $A_\eta$, the area where the surface viscosity begins to rise, and $\Pi_\eta$, the pressure at $A_\eta$.

Poly-L-leucine and poly-DL-leucine gave monolayers of the condensed type. The area per residue of the former at the limiting area, $A_\delta$, was much smaller than that of the latter.

* Present address: Department of Chemistry, Faculty of Science, Osaka University, Nakanoshima, Kita-ku, Osaka.

1) T. Isemura and S. Ikeda, This Bulletin, **32**, 178 (1959).
2) S. Ikeda and T. Isemura, ibid., **32**, 659 (1959).
3) Part I of this series: T. Yamashita and T. Isemura, This Bulletin, **38**, 420 (1965).
4) E. Katchalski and M. Sela, *Adv. Protein Chem.*, **13**, 243 (1958).

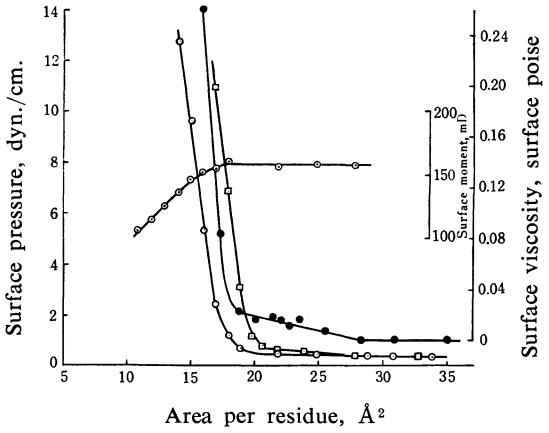



Fig. 1. Monolayers of poly-L-leucine and poly-DL-leucine on distilled water at 16°C: poly-L-leucine— ○, surface pressure; ⊙, surface moment; ●, surface viscosity: poly-DL-leucine— □, surface pressure.

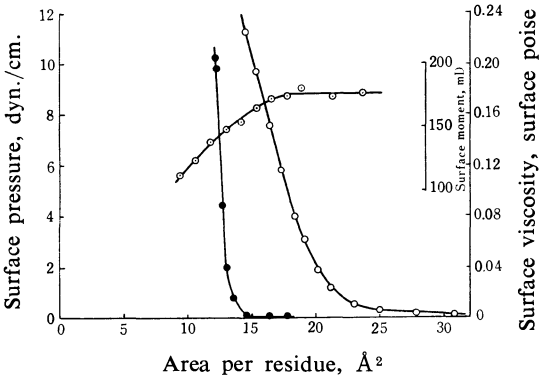



Fig. 2. Monolayer of copoly-3 : 1-(L-leucine, sarcosine) on distilled water at 16°C: ○, surface pressure; ⊙, surface moment; ●, surface viscosity.

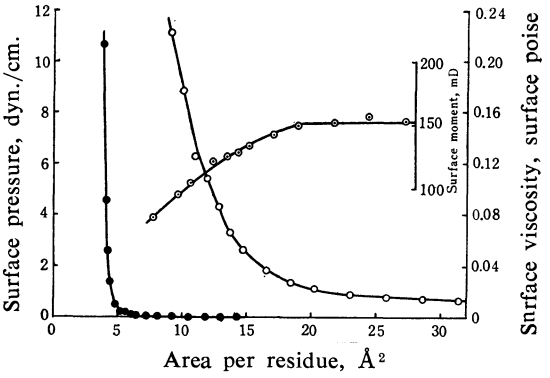



Fig. 3. Monolayer of copoly-1 : 1-(L-leucine, sarcosine) on distilled water at 16°C: ○, surface pressure; ⊙, surface moment; ●, surface viscosity.

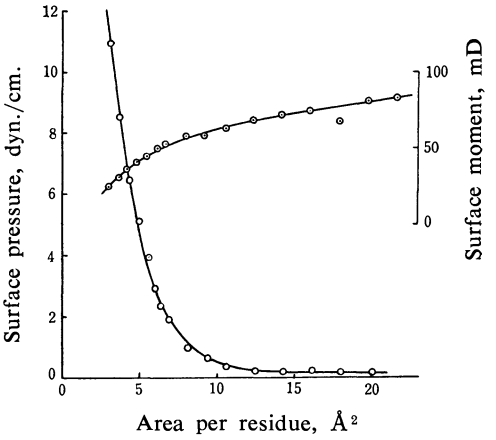



Fig. 4. Monolayer of copoly-1 : 3-(L-leucine, sarcosine) on distilled water at 16°C: ○, surface pressure; ⊙, surface moment.

The surface viscosity of poly-L-leucine was manifested at a larger area than $A_\delta$ and $A_{\Pi\to 0}$. The film characteristics of poly-L-leucine were noticeably affected by the incorporation of the sarcosyl residue in the polypeptide chain. The monolayer of copoly-3 : 1-(L-leucine, sarcosine) was expanded much more than that of poly-L-leucine. In contrast, the surface viscosity could be detected at a much smaller area than $A_\delta$ and $A_{\Pi\to 0}$. The monolayer of copoly-1 ; 1-(L-leucine, sarcosine) was much more compressible than those of the two polymers cited above. The viscosity was first detected at a very small area (5.5 Å² per residue). The *Π-A* curve of copoly-1 : 3-(L-leucine, sarcosine) shifted to a smaller area than that of 1 : 1-copolymer, and the viscosity

TABLE II. FILM CHARACTERISTICS OF POLYLEUCINE AND SARCOSYL POLYPEPTIDES AT THE AIR/WATER INTERFACE

| Polymer | $A_\delta$ Å²/res. | $A_{\Pi\to 0}$ Å²/res. | $A_\mu$ Å²/res. | $\mu(c)$ mD | $A_\eta$ Å²/res. | $\Pi_\eta$ dyn./cm. |
|---|---|---|---|---|---|---|
| Poly-L-leucine | 17.0 | 17.6 | 17.5 | 158 | 28.0 | 0.4 |
| Poly-DL-leucine | 19.0 | 19.6 | | | | |
| Copoly-3 : 1-(L-leucine, sarcosine) | 18.0 | 20.3 | 18.0 | 176 | 14.5 | 10.5 |
| Copoly-1 : 1-(L-leucine, sarcosine) | 11.5 | 14.0 | 19.0 | 152 | 5.5 | 19.0 |
| Copoly-1 : 3-(L-leucine, sarcosine) | 4.4 | 6.5 | | 80* | no viscosity | |

* Surface moment at 20 Å² per residue.

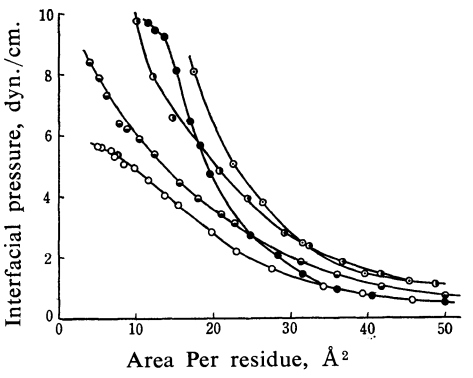



Fig. 5. Interfacial pressure-area curves of copolymers of L-leucine with sarcosine at the petroleum ether/distilled water interface at 17°C: ●, poly-L-leucine; ⊙, copoly-3 : 1-(L-leucine, sarcosine); ◑, copoly-1 : 1-(L-leucine, sarcosine); ◒, copoly-1 : 3-(L-leucine, sarcosine); ○, polysarcosine (15°C).

could not be detected. The low $A_\delta$ and surface moment values suggest that the polymer chain is partially dissolved in the aqueous subphase.

The interfacial pressure-area ($\Pi_i$-$A$) curves of poly-L-leucine and the copolymers of L-leucine with sarcosine (3 : 1, 1 : 1, 1 : 3) at the oil/distilled water interface are shown in Fig. 5. All the films are expanded much more than at the air/water interface. The film of poly-L-leucine was found to be rather condensed in comparison with those of polysarcosine and copolymers containing the sarcosyl residue, although poly-L-leucine is also much more expanded at this interface than at the air/water interface. The compressibility of the copolymer film increased with the increasing content of the sarcosyl residue in the polymer chain; the polysarcosine film was highly compressible.

## Discussion

**Air/Water Interface.**—*Polyleucine.*—The monolayers of poly-L-leucine and poly-DL-leucine are of the condensed type. As is shown in Table II, the $A_\delta$ and $A_{\Pi\to 0}$ values for these films agree fairly well with each other, as in the case of poly-L-alanine and poly-DL-alanine,[3] whereas $A_\delta$ differs to some extent from $A_{\Pi\to 0}$ with the films of sarcosyl polypeptides. The $\mu(c)$ value of poly-L-leucine agrees fairly well with that of poly-DL-alanine (150 mD[3]). The surface viscosity of poly-L-leucine is first detected at a much larger area than $A_\delta$ and $A_{\Pi\to 0}$, as in the case of the poly-DL-alanine monolayer,[2,3] and the surface pressure is quite low at $A_\eta$. These facts suggest that the interaction between the monomer units or the polymer chains of polyleucine is very strong. The polypeptide chains of polyleucine are probably tightly held together, the motion of the residues or segment being strongly inhibited by the hydrogen bonding and by the partial double bond nature of peptide bonds. Judging from the data in Table II, poly-L-leucine is spread in a $\beta$-configuration, as in most polypeptide films,[1,2,3,5,6,9,10] orientating the side chains alternatively up and down in relation to the interface. Poly-DL-leucine is probably also in a $\beta$-form in the monolayer, as has been suggested by Cheesman and Davies,[9] although the area per residue is much larger than that of poly-L-leucine.

The $A_\delta$ value of poly-L-leucine is 17.0 Å² per residue, while that of poly-DL-leucine is 19.0 Å² per residue. The larger area of the L-isomer may be ascribed to the closer packing of the L-polypeptide chains, as in the case of the isomers of poly-$\gamma$-benzylglutamate.[6]

*Copolymers of L-Leucine with Sarcosine.*—The film characteritics of poly-L-leucine are markedly changed by the incorporation of the sarcosyl residue in the polypeptide chains, as Table II shows. The films of the 3 : 1- and 1 : 1- copolymers of L-leucine with sarcosine are of the expanded type. In Fig. 6, the $A_\eta$ and $\Pi_\eta$ values of sarcosyl polyeptides are plotted against the sarcosyl residue content

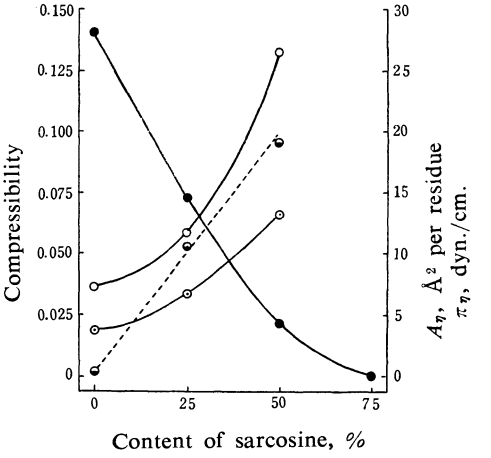



Fig. 6. Variations of compressibilites at 2 dyn./cm. (○) and 5 dyn./cm. (⊙), and of $A_\eta$ (●) and $\Pi_\eta$ (◒) with content of sarcosyl residue in polypeptide chain (at the air/distilled water interface).

5) C. W. N. Cumper and A. E. Alexander, *Trans. Faraday Soc.*, **46**, 235 (1950).
6) T. Isemura and K. Hamaguchi, This Bulletin, **27**, 125 (1954).
7) J. T. Davies, *Trans. Faraday Soc.*, **49**, 949 (1953).
8) J. T. Davies, *Biochim. Biophys. Acta*, **11**, 165 (1953).
9) D. F. Cheesman and J. T. Davies, *Adv. Protein Chem.*, **9**, 439 (1954).
10) T. Yamashita and T. Isemura, This Bulletin, **35**, 929 (1962).

in the polymer chain, together with the compressibilities of the film at 2 dyn./cm. and 5 dyn./cm. With the increase in the ratio of the sarcosyl residue in copolymers, the compressibility of the film and the $\Pi_\eta$ value are increased, whereas the area at which the surface viscosity is first manifested is decreased.

In general, a monolayer of a polymer is of the condensed type and the surface viscosity is first observed in a region where the surface pressure is quite low as the result of strong interaction between polymer chains, while a film is of the expanded type and the surface viscosity is first detected in a high surface-pressure region. Ikeda and Isemura[2] found that the films of polypeptides are of the expanded type, and that the viscosities are detected in areas where the surface pressures are quite high. They attributed this finding to the decrease in the number of hydrogen bonds between polymer chains.

The results shown in Fig. 6 suggest that the interaction between polymer chains decreases with an increase in sarcosyl content. The number of hydrogen bonds between peptide groups is decreased when sarcosyl residues are copolymerized in the polypeptide chain because they lack the hydrogen atoms to be hydrogen-bonded in the residues. This is responsible for the weak interaction which has been observed with sarcosyl polypeptides. The flexibility of the segments or the polymer chain will be increased by the decrease in the number of hydrogen bonds and by the decrease in the double-bond nature of the main chain. The view[1-3] that the condensation and the expansion of the polypeptide films primarily depend on the hydrogen bonding between peptide groups has thus been confirmed by the present investigation.

The $A_\mu$ value of poly-L-leucine (17.5 Å$^2$ per residue) is nearly equal with the $A_\delta$ (17.0 Å$^2$ per residue). On the other hand, the film of copoly-1 : 1-(L-leucine, sarcosine) gives a much smaller $A_\delta$ value than $A_\mu$. The $A_\delta$ and the $A_\mu$ of the 1 : 1-copolymer are 11.5 Å$^2$ per residue and 19.0 Å$^2$ per residue respectively. At the $A_\mu$ the electric dipole of the repeating unit begins to change its orientation. The sarcosyl residues of this copolymer begin to be submerged into the aqueous phase at $A_\mu$, accompanying the decrease in surface moment. The $A_\delta$ of the 1 : 1-copolymer corresponds to the area occupied by the leucyl residues and by the sarcosyl residues remaining at the surface as a result of the effect of the hydrophobic leucyl residues. The sarcosyl residues of copoly-3 : 1-(L-leucine, sarcosine) will be more stable at the interface than those of the 1 : 1-copolymer because of the coexistence of a higher leucyl-residue content. This may be the cause of the lack of discrepancy between the $A_\delta$ and the $A_\mu$ values.

Copoly-1 : 3-(L-leucine, sarcosine) gives a somewhat condensed film. The $A_\delta$ value is quite small (4.4 Å$^2$ per residue). The surface moment is low compared with the other polymer films shown in Table II and decreases with compression. When the film is compressed, the sarcosyl residues of this polymer are submerged in the aqueous pahse; at $A_\delta$, only leucyl residues remain at the surface. The $A_\delta$ value agrees closely with the area occupied by the remaining leucyl residues at the surface ($A_\delta$ of poly-L-leucine/4=4.3 Å$^2$ per residue).

**The Oil/Water Interface.** — A pronounced difference has been found[3] between the monolayers of poly-DL-alanine and polysarcosine at the oil/water interface, although the two polymers have the same side chains. The monolayer of poly-DL-alanine was rather condensed, even at the oil/water interface, while polysarcosine gave an expanded monolayer. The difference may be primarily ascribed to the presence or absence of hydrogen bonds between monomer units.

The monolayer of poly-L-leucine is of the expanded type at the oil/water interface. The film of this polypeptide is much more expanded than that of poly-DL-alanine at this interface. This expansion of the film is pbobably caused by the release of van der Waals force between side chains. The effect is much greater because the side chain is much larger than that of poly-DL-alanine.

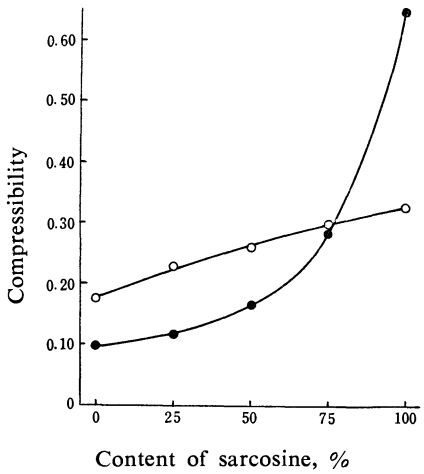



Fig. 7. Variations of compressibilities at 2 dyn./cm. (○), and 5 dyn./cm. (●) with content of sarcoyl residue in polypeptide chain (at the petroleum ether/distilled water interface).

The film of poly-L-leucine, however, is slightly more condensed than those of sarcosyl polypeptides.

Copoly-3 : 1-(L-leucine, sarcosine) gives a much more expanded film than poly-L-leucine, as well as at the air/water interface. A further increase in sarcosyl content increases the film compressibility, even at the oil/water interface, as Fig. 7 shows. This fact suggests that the polymer chain increases in flexibility as a result of the decrease in the number of hydrogen bonds between polymer chains and the decrease in the double-bond nature of the main chain.

## Summary

The effect of hydrogen bonding on the nature of poly-$\alpha$-amino acid monolayers has been studied at air/water and oil/water interfaces with poly-L-leucine, poly-DL-leucine, and the 3 : 1-, 1 : 1- and 1 : 3-copolymers of L-leucine with sarcosine.

Poly-L-leucine and poly-DL-leucine have been found to give condensed monolayers on distilled water. The surface viscosity of poly-L-leucine was first detected at a larger area than its close-packed area. The strong interaction between polymer chains of polyleucine was suggested by these findings.

On the other hand, at both air/water and oil/water interfaces, the compressibility of the film is increased much more by the incorporation of the sarocosyl residue in the polymer chain. At the air/water interface, the films of 3 : 1- and 1 : 1- copolymers of L-leucine with sarcosine are of the expanded type, and the surface viscosities have first been detected at much smaller areas than their close-packed areas. These findings suggest that the interaction between polymer chains diminishes because of the decrease in the number of intermolecular hydrogen bonds.

The authors wish to express their hearty thanks to Professor Junzo Noguchi of Hokkaido University for his kind guidance in preparing the samples.

*Institute for Protein Research*
*Osaka University*
*Kita-ku, Osaka*

# Surface Chemistry of the Polyamide Series. III. Monolayers of Nylons from $\omega$-Aminocarboxylic Acids at the Air/Water Interface

By Takuya YAMASHITA*

(Received August 13, 1964)

Polyamides of the nylon type are prepared from diamines and dicarboxylic acids or from $\omega$-aminocarboxylic acids, and they are commonly designated by the numbers of carbon atoms per monomer unit. For example, polyhexamethylene sebacamide, $(-HN(CH_2)_6NHCO(CH_2)_8CO-)_n$, and polyundecanamide, $(-NH(CH_2)_{10}CO-)_n$, are Nylon 610 and Nylon 11 respectively. It has been found that the melting points of nylons with odd numbers of $CH_2$ groups per monomer unit are lower than those with even numbers.[1-4] This fact has been ascribed to the deficient hydrogen bond formation of the former nylons.[1,2] Kinoshita[5,6] has shown that the odd number of $CH_2$ groups in polyamides does not lead to a deficient hydrogen bond formation, but that it in general gives rise to a configuration somewhat similar to the pleated sheets structure proposed by Pauling and Corey[7] for the structure of polypeptide. This configuration was called the $\gamma$-form. On the other hand, polyamides with even numbers of $CH_2$ groups usually contain two different crystalline forms, $\alpha$ and $\beta$, which have the same chain repeat distance and differ only in the side-by-side arrangement of molecules.

In this connection, it is interesting to study the effect of the numbers of $CH_2$ groups on

* Present address: Department of Chemistry, Faculty of Science, Osaka University, Nakanoshima, Kita-ku, Osaka.

1) G. Champetier and R. Aélion, *Bull. soc. chim. France*, **1948**, 683.
2) R. Hill and E. E. Walker, *J. Polymer Sci.*, **3**, 609 (1948).
3) D. D. Coffman, G. J. Berchet, W. R. Peterson and E. W. Spanagel, ibid., **2**, 306 (1947).
4) D. D. Coffman, N. L. Cox, E. L. Martin, W. E. Mochel and F. J. Van Natta, ibid., **3**, 85 (1948).
5) Y. Kinoshita, *Makromol. Chem.*, **33**, 1 (1959).
6) Y. Kinoshita, ibid., **33**, 21 (1959).
7) L. Pauling and R. B. Corey, *Proc. Nat. Acad. Sci. U. S. A.*, **39**, 253 (1953).

the nature of the monolayers of a series of nylons. Although the monolayers of several nylons have been studied,[8-15] no studies have been carried out along this line. Accordingly, in the present work, a series of nylons with 2 to 11 $CH_2$ groups per monomer unit (Nylons 3 to 12) prepared from $\omega$-aminocarboxylic acids have been studied at the air/water interface in order to investigate the correlation of the film porperties with the numbers of $CH_2$ groups per monomer unit. The film of Nylon 9 at the oil/water interface and that of polyurea, polynonamethylene urea $(-(CH_2)_9-HNCONH-)_n$, at the air/water interface have also been studied in order to prove the role of the van der Waals attractive force between hydrocarbon groups in polyamide monolayers.

## Experimental

**Materials.** — Nylon 3 (poly-$\beta$-alanine) prepared from acrylamide was supplied by Professor S. Murahashi of Osaka University. The insoluble fraction in boiling water was used in the present experiment. Its intrinsic viscosity was 0.432 (in 90% formic acid at 25°C). Nylon 4 ($n$=87) were prepared from pyrrolidone by Dr. Y. Joh of the Mitsubishi Rayon Co., and Nylon 5 ($n$<25), from piperidone by Mr. T. Konomi of the Toyo Spinning Co. Nylons 7, 8 and 10 were supplied by Dr. Y. Kinoshita and Nylon 12 by Dr. M. Ito of the Toyo Rayon Co. The intrinsic viscosities of these nylons were more than 0.9 (in cresol at 25°C). Nylons 7, 8 and 10 were the same samples as those used in Kinoshita's investigation.[5] Nylon 11 ($m$=16000) was a gift from Dr. V. Ambekar of L'école Supérieure de Physique et de Chimie de Paris. Nylon 6 (Amilan), Nylon 9 and polynonamethylene urea were commercial products.

Nylons 3, 4 and 5 were used without further purification. Nylon 6 was purified by precipitation from a solution in formic acid by adding water. The chips or fibers of Nylons 7 to 12 and polyurea were immersed in benzene for 24 hr. and then in ethyl alcohol for the same length of time. All the samples were dried at 80°C in vacuo for 3—4 hr.

Nylons 3 to 9 were spread from solutions in 90% formic acid, Nylons 10, 11 and 12, from solutions in a 1 : 1-mixture (v/v) of dichloroacetic acid and trifluoroacetic acid, and polyurea, from trifluoroacetic acid. Nylon 9 was also spread from a solution in trifluoroacetic acid. The concentrations of these solutions were 0.2—0.3 mg./ml.

A subsolution containing 40% ammonium sulfate or concentrated sulfuric acid was treated with active charcoal before use in order to remove any surface-active contaminants.

**Methods.** — The surface pressure was measured by the Wilhelmy methods; the surface potential, by the ionizing air-electrode method; the surface viscosity, by the rotatory oscillation method, and the interfacial pressure, by the ring method. The surface moment was calculated from the surface potential using the Helmholtz equation. The details of the experimental methods have already been described in Part I of this series.[16]

## Results

Nylons 3, 4 and 5 were spread on a 40% ammonium sulfate subsolution because stable films were not obtained on distilled water. For the sake of comparison, Nylon 6 was also spread on the same subsolution. The surface pressure-area ($\Pi$-$A$) curves of these nylons are shown in Fig. 1. The film of Nylon 3 was of the condensed type, while those of Nylons 4, 5 and 6 were of the expanded type.

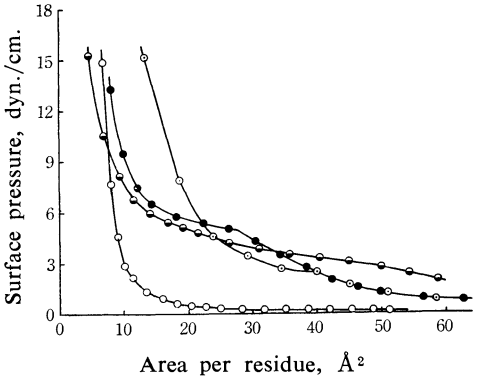



Fig. 1. Surface pressure-area curves of Nylon 3 (○), Nylon 4 (●), Nylon 5 (◒) and Nylon 6 (⊙) on 40% ammonium sulfate at 23°C.

The $\Pi$-$A$, surface moment-area ($\mu$-$A$) and surface viscosity-area ($\eta_s$-$A$) curves of Nylons 6 to 12 on distilled water are shown in Figs. 2 to 8 respectively. The interfacial presssure-area ($\Pi_i$-$A$) curve of Nylon 9 at the petroleum ether/water interface is also shown in Fig. 5. The $\Pi$-$A$ and $\mu$-$A$ curves of Nylons 6 to 9 on the concentrated sulfuric acid subsolutions (3 N and 6 N) are shown in the corresponding figures.

The film of Nylon 6 on distilled water was of the expanded type. The area per residue was somewhat smaller than that on 40% ammonium sulfate. The film of Nylon 7 on distilled water was rather more condensed than that of Nylon 6, although the film was of the expanded type.

8) D. J. Crisp, *J. Colloid Sci.*, **1**, 161 (1946).
9) C. W. N. Cumper and A. E. Alexander, *Trans. Faraday Soc.*, **46**, 235 (1950).
10) T. Isemura and K. Hamaguchi, This Bulletin, **25**, 40 (1952).
11) T. Isemura and K. Hamaguchi, ibid., **27**, 125 (1954).
12) H. Hotta, *J. Colloid Sci.*, **9**, 504 (1954).
13) K. Inokuchi, This Bulletin, **28**, 453 (1955).
14) K. Inokuchi, ibid., **29**, 490 (1956).
15) G. E. Hibberd and A. E. Alexander, *Proc. 3rd Int. Cong. Surface Activity*, **2**, 144 (1960).
16) Part I of this series: T. Yamashita and T. Isemura, This Bulletin, **38**, 420 (1965).

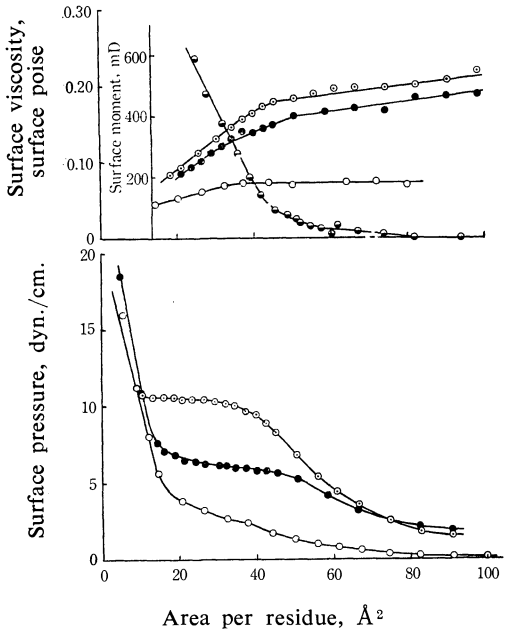



Fig. 2. Surface pressure-area and surface moment-area curves of Nylon 6 on distilled water (○) and on sulfuric acid (3 N, ●; 6 N, ⊙), and its surface viscosity-area curve on distilled water (◒) at 22°C.

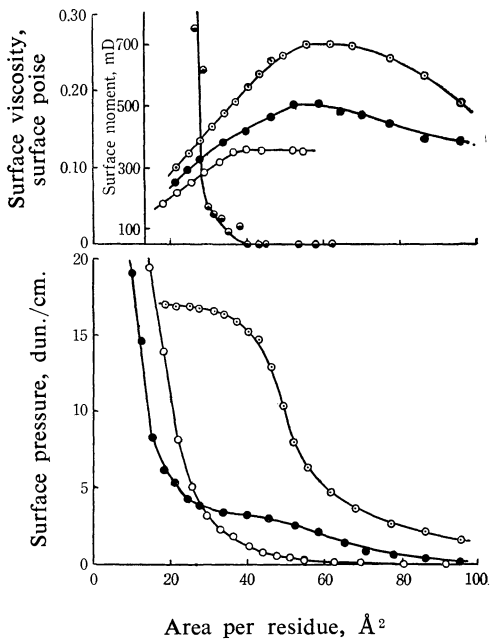



Fig. 3. Surface pressure-area and surface moment-area curves of Nylon 7 on distilled water (○) and on sulfuric acid (3 N, ●; 6 N, ⊙) at 21°C, and its surface viscosity-area curve on distilled water (◒) at 17°C.

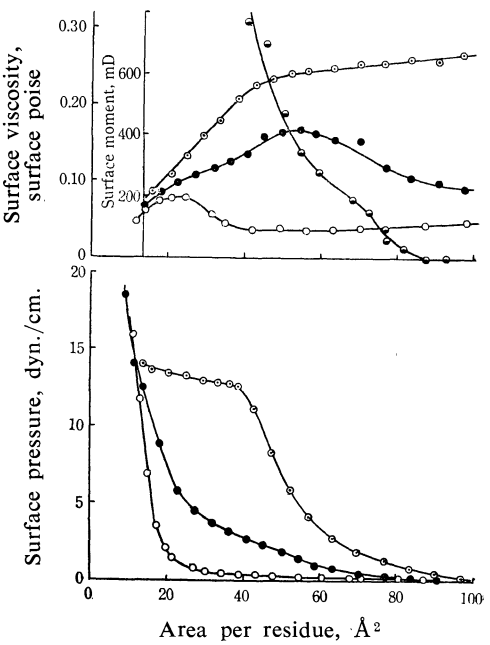



Fig. 4. Surface pressure-area and surface moment-area curves of Nylon 8 on distilled water (○) and on sulfuric acid (3 N, ●; 6 N, ⊙), and its surface viscosity-area curves on distilled water (◒) at 21°C.

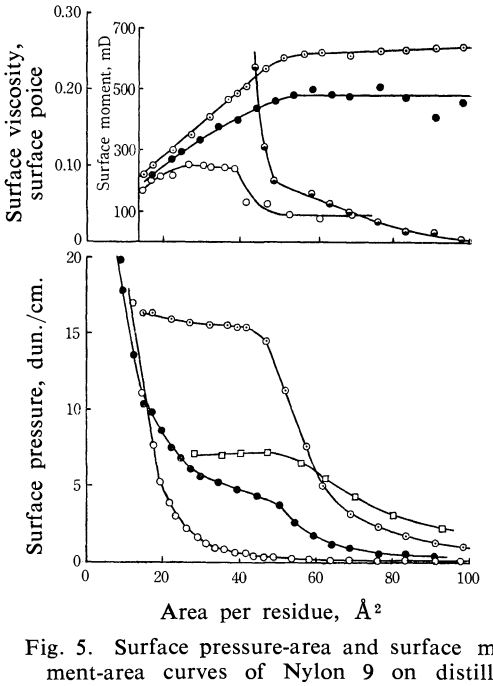



Fig. 5. Surface pressure-area and surface moment-area curves of Nylon 9 on distilled water (○) and on sulfuric acid (3 N, ●; 6 N, ⊙) at 24°C, and its surface viscosity-area curve on distilled water (◒) at 24°C and interfacial pressure-area curves at the petroleum ether/distilled water interface (□) 18°C.

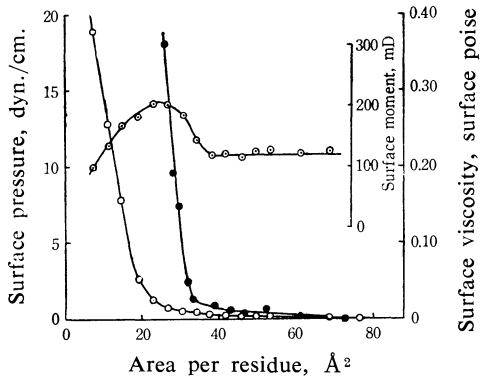



Fig. 6. Surface pressure-area (○), surface moment-area (⊙) and surface viscosity-area (●) curves of Nylon 10 on distilled water at 21°C.

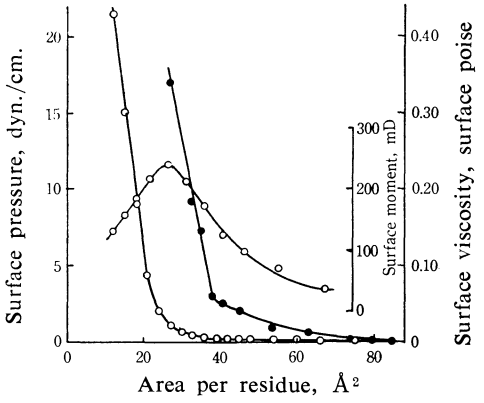



Fig. 7. Surface pressure-area (○), surface moment-area (⊙) and surface viscosity-area (●) curves of Nylon 11 on distilled water at 21°C.

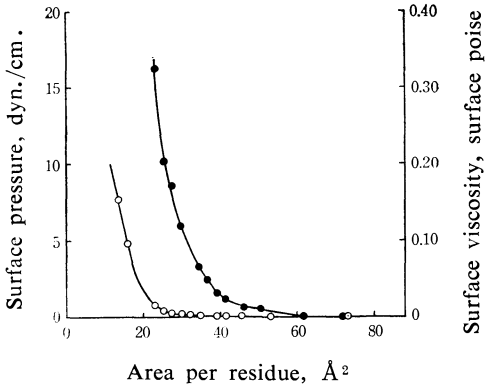



Fig. 8. Surface pressure-area (○), surface viscosity-area (●) curves of Nylon 12 on distilled water at 17.5°C.

The films of Nylons 8 to 12 were of the condensed type on distilled water, and their areas per residue were quite small. Trifluoroacetic acid is one of the strongest hydrogen bond-breaking agents. The film of Nylon 9 spread from a solution in this solvent gave a *Π-A* curve on distilled water (not shown in Fig. 5) completely identical with that spread from a solution in formic acid on the same subsolution (shown in Fig. 5). Further, the *Π-A* curve of this nylon spread from a solution in formic acid on 40% ammonium sulfate (not shown in the figure) was nearly identical with that on distilled water, and the change in the initial spreading areas of Nylons 8 to 12 did not affect practically the *Π-A* relations on distilled water. Judging from these facts, the poor spreadiag of Nylons 8 to 12 seems to be the result of neither the presence of an insoluble fraction in the spreading solution nor the dissolution of polymers in the aqueous phase.

Constant values of surface moments were not obtained with the films of Nylons 8 to 12 on distilled water. The surface moments increased with the compression of the films and they reached the maxima. The surface moment of Nylon 12 was not reproducible. The maximum value, however, was lower than that of Nylon 11.

On the 3 N and 6 N sulfuric acid subsolutions, a remarkable expansion of films and an increase in the surface moment were found with Nylons 6 to 9. The stronger the acidity, the greater the effect.

The *Π-A*, $\mu$-*A* and $\eta_s$-*A* curves of polynonamethylene urea on distilled water are shown in Fig. 9. This polymer also gave a condensed film.

The film characteristics of Nylons 6 to 12 and polyurea are summarized in Table I, where $A_\delta$ is the area per residue at the minimum compressibility of the film; $A_{\Pi\to 0}$,

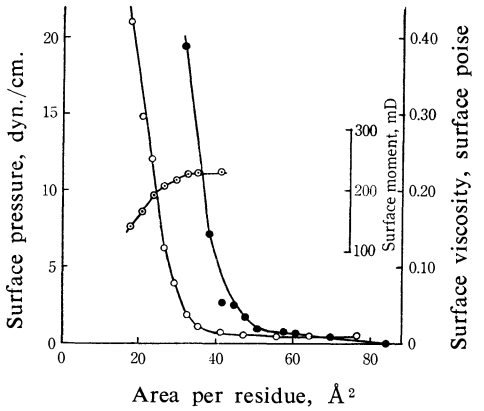



Fig. 9. Surface pressure-area (○), surface moment-area (⊙) and surface viscosity-area (●) curves of polynonamethylene urea on distilled water at 20°C.

TABLE I. FILM CHARACTERISTICS AND CALCULATED CLOSE-PACKED AREAS OF NYLONS 6 TO 12 AND POLYNONAMETHYLENE UREA

| Polymer | Subphase | $A_\delta$ Å²/residue | $A_{\pi\to 0}$ Å²/residue | $A_\mu$ Å²/residue | $\mu$ Dm | $A_\eta$ Å²/residue | Calculated close-packed area Å²/residue |
|---|---|---|---|---|---|---|---|
| Nylon 6 | DW | 14.4 | 20.0 | 37 | 180 (c) | 82 | $\frac{17.24}{2}\times\frac{9.56}{2}=41.2$ |
| | 3 N $H_2SO_4$ | | | | 400 (at 51 Å²/res.) | | |
| | 6 N $H_2SO_4$ | | | | 445 (at 46 Å²/res.) | | |
| Nylon 7 | DW | 22.0 | 27.0 | 40 | 355 (c) | 40 | $9.85\times 4.9\times\sin 77^\circ=47.0$ |
| | 3 N $H_2SO_4$ | | | 52 | 502 (m) | | |
| | 6 N $H_2SO_4$ | | | 56 | 700 (m) | | |
| Nylon 8 | DW | 17.6 | 19.0 | 25 | 198 (m) | 87 | $1.23\times 9\times 4.77=52.8$ |
| | 3 N $H_2SO_4$ | | | 54 | 420 (m) | | |
| | 6 N $H_2SO_4$ | | | | 600 (at 52 Å²/res.) | | |
| Nylon 9 | DW | 19.2 | 22.8 | 26 | 252 (m) | 104 | $1.23\times 10\times 4.77=58.7$ |
| | 3 N $H_2SO_4$ | | | 54 | 480 (c) | | |
| | 6 N $H_2SO_4$ | | | | 615 (at 56 Å²/res.) | | |
| Nylon 10 | DW | 18.0 | 20.0 | 25 | 205 (m) | 72 | $1.23\times 11\times 4.77=64.5$ |
| Nylon 11 | DW | 21.5 | 23.0 | 26 | 240 (m) | 85 | $14.9\times 4.9\times\sin 77^\circ=71.1$ |
| Nylon 12 | DW | 18.0 | 20.0 | | | 61 | $1.23\times 13\times 4.77=76.3$ |
| Polynonamethylene urea | DW | 27.2 | 30.0 | 32 | 255 (c) | 84 | $1.23\times 12\times 4.77=70.4$ |

DW: Distilled water.

the area per residue where the straight portion of $\Pi$-$A$ curve is extraporated to $\Pi=0$; $A_\mu$, the area per residue where the surface moment begins to decrease; $\mu(m)$ and $\mu(c)$, the maximum and the constant values of the surface moment respectively, and $A_\eta$, the area per residue where the surface viscosity is first detected.

For the sake of comparison with the observed limiting areas per residue, namely, the values of $A_\delta$ or $A_{\Pi\to 0}$, the close-packed areas for $\alpha$- or $\beta$-forms of Nylons 6 to 12 were calculated from the unit cell dimensions of their crystals as estimated from X-ray diffraction data. The results are shown in Table I, where the distance between chain atoms of Nylons 6 to 12, and polyurea, with the exception of Nylons 6,[17] 7[18] and 11[18] (for which the X-ray diffraction data are available), is assumed to be 1.23 Å for fully extended chains, judging from the distance between chain atoms of Nylon 6$\left(\frac{17.24^{17)}}{2\times 7}=1.231\text{ Å}\right)$, Nylon 7$\left(\frac{9.35^{18)}}{8}=1.231\text{ Å}\right)$, Nylon 11$\left(\frac{14.9^{18)}}{12}=1.24\text{ Å}\right)$, and Nylon 66$\left(\frac{17.2^{19)}}{14}=1.23\text{ Å}\right)$. The distance between neighboring chains is assumed to be $4.9\times\sin 77^\circ=4.77$ Å on the basis of those of Nylons 7,[18] 11[18] and 66.[19] These values are also used for the calculation of close-packed areas of Nylon 3, Nylon 4 and polynonamethylene urea.

## Discussion

**Nylon 3.**—Nylon 3 gives a film of the condensed type on 40% ammonium sulfate. Its $A_\delta$ and $A_{\Pi\to 0}$ values are 8.2 Å² per residue and 9.0 Å² per residue respectively. These values are much smaller than the calculated close-packed area for a fully extended chain (23.5 Å² per residue). It has been found[20,21] that polyglycine cannot be spread under any conditions because glycyl residues are particularly strongly hydrogen-bonded because of the absence of side chains. As Nylon 3 also lacks side chains, and as the chain repeat distance is rather short, the hydrogen bonds would be very

17) D. R. Holmes, C. W. Bunn and D. J. Smith, *J. Polymer Sci.*, **17**, 159 (1955).
18) W. P. Slichter, ibid., **36**, 259 (1959).
19) C. W. Bunn and E. V. Garner, *Proc. Roy. Soc.*, **A189**, 39 (1947).
20) J. T. Davies, *Trans. Faraday Soc.*, **49**, 949 (1953).
21) T. Yamashita and T. Isemura, This Bulletin, **35**, 929 (1962).

strong, as in the case of polyglycine. This might be the cause of the poor spreading and the condensation of the Nylon 3 film.

**Nylons 4, 5 and 6.** — In contrast with the condensed film of Nylon 3, the films of Nylons 4, 5 and 6 are of the expanded type on a 40% ammonium sulfate subsolution. Nylon 6 also gives an expanded film on distilled water. Kink points are found in the *Π-A* curves of Nylons 4 and 6.

The kink point of the *Π-A* curve of Nylon 6 appears at 37.5 Å$^2$ per residue on distilled water and at 40 Å$^2$ per residue on 40% ammonium sulfate. The *π-A* curve of this nylon on distilled water has already been reported by some workers.[10,12,14] The present result is in general agreement with theirs. The kink point was also found by them at nearly the same area as in the present study. The surface moment of Nylon 6 on distilled water begins to decrease at 37 Å$^2$ per residue, which is in good agreement with the area at kink point and the $A_\mu$ values reported by Hotta[12] and Inokuchi.[14] The surface viscosity of this nylon begins to rise at 82 Å per residue. This value is much smaller than that found by Isemura and Hamaguchi.[11] The larger area found by them seems to be caused by the interaction between polymer and solvent because they used a mixture of cresol and benzene as a spreading solvent. They, however, found a characteristic area at 80 Å$^2$ per residue, which agrees well with the $A_\eta$ value in the present study.

It has been found[16] that poly-α-aminoisobutyric acid gives a monolayer of the expanded type. A striking difference, however, exists in the surface viscosities between the films of this polymer and Nylon 6. The surface viscosity of the former first appears at an area (12 Å$^2$ per residue) considerably smaller than its limiting area ($A_\delta$=20.0 Å$^2$ per residue), where the surface pressure is remarkably high, while that of the latter is detected at a larger area (82 Å$^2$ per residue) than the calculated close-packed area for fully-extended chains (41.2 Å$^2$ per residue), where the surface pressure is sufficiently low. In the film of the former, interaction between polymer chains is scarce because it is difficult for the hydrogen bonds between keto and imino groups to be formed because of the steric hindrance of α-disubstituted methyl groups. On the other hand, the much larger $A_\eta$ value of Nylon 6 suggests that the interaction between polymer chains is quite strong. Near the $A_\mu$, the polymer molecules at the surface begin to come in contact with each other to construct a loose network structure because of the hydrogen bonding between amide groups.

The areas at the kink points of the *Π-A* curves of Nylon 4 (ca. 28 Å$^2$ per residue on 40% ammonium sulfate) and Nylon 6 (37.5 Å$^2$ per residue on distilled water, 40 Å$^2$ per residue on 40% ammonium sulfate) agree fairly well with the calculated close-packed areas (29.3 Å$^2$ per residue for Nylon 4, 41.2 Å$^2$ per residue for Nylon 6). All the chain atoms of these polymers would lie on the water surface above the areas at the kink points. No kink point is found in the *Π-A* curve of Nylon 5. This polymer, however, might be spread in a state similar to those of Nylon 4 and Nylon 6, because the film is remarkably expanded. The polymer chains of Nylons 4, 5 and 6 are quite flexible at the surface because of the effect of the increased $CH_2$ groups. This might be the cause of the expansion of the films of these nylons.

There is some difference among the films of Nylons 4, 5 and 6 on the 40% ammonium sulfate subsolution, although they are all of the expanded type. Below the surface pressure of ca. 4 dyn./cm., the film of Nylon 5 is most expanded, as Fig. 1 shows. The surface pressure of Nylon 6 is much lower than that of Nylon 5 over the same area. The pressure reduction in the film of Nylon 6 is probably caused by the increased van der Waals attractive force between hydrocarbon groups. The van der Waals force plays an important role in the films of Nylons 7 to 12, as will be discussed in later sections.

**Nylon 7.**—The film of Nylon 7 on distilled water is of the expanded type. The film, however, is somewhat more condensed than that of Nylon 6 on the same subsolution. This is the result of the increased van der Waals attractive force between hydrocarbon groups. The film of Nylon 7 might be in an intermediate state between the expanded films obtained with Nylons 4, 5 and 6, and the condensed films obtained with Nylons 8 to 12.

The surface moment of this nylon is remarkably high, the highest among those of the nylons investigated. The $A_\mu$ value is 40 Å$^2$ per residue, which agrees with the $A_\eta$ value. The surface moments of polyamides of the nylon type are mainly contributed by the C=O dipoles, as in the case of poly-α-amino acid with only hydrocarbon side chains.[22] The more vertical the C=O dipoles become in relation to the interface, the closer the surface moment will approach the maximum value of 360 mD.[23] The observed surface moment of Nylon 7 ($\mu(c)$=355 mD) is in good agreement with this value. Therefore, the C=O groups

22) J. T. Davies, *Biochim. Biophys. Acta*, **11**, 165 (1953).
23) A. E. Alexander and J. H. Schulman, *Proc. Roy. Soc.* **A161**, 115 (1937).

of Nylon 7 might orientate rather vertically to the interface. In such an orientation of C=O groups, the hydrogen bonds can hardly be formed between amide linkages in the area above $A_\mu$. It has already been found for the monolayers of poly-$\alpha$-aminoisobutyric acid[16] on distilled water, and poly-DL-alanine[16] and poly-DL-leucine[20] on the acid subsolutions that the surface moment increases if the number of hydrogen bonds is reduced.

The surface viscosities of polymers primarily depend on the number of hydrogen bonds between different groups, as has been found with prolyl polypeptides,[24] poly-$\alpha$-aminoisobutyric acid[16] and sarcosyl polypeptides.[16,25] The agreement of $A_\mu$ with $A_\eta$ supports the view that hardly any hydrogen bonds can be formed between amide groups in the area larger than $A_\mu$ because the orientation of C=O groups is unfavorable for the hydrogen bond formation.

**Differences in Film Properties between Odd- and Even-Numbered Nylons.** — It has been found[1-5] that the melting points of nylons with odd and even numbers of $CH_2$ groups are quite different from each other. Some film characteristics of Nylons 6 to 12 on distilled water are shown in Fig. 10 against the number of carbon atoms per monomer unit. There exist striking differences between odd- and even-numbered nylons as in melting points. It should be noted here that the amino acid nylons with even numbers of $CH_2$ groups are described by odd numbers, and vice versa.

It is striking that the the *Π-A* curves of Nylons 8, 10 and 12 are nearly identical. Accordingly, the limiting areas, namely, the

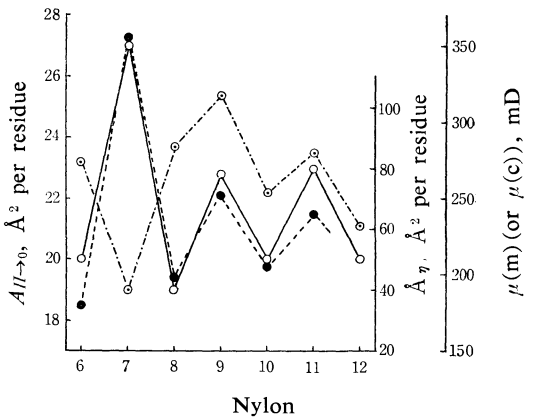



Fig. 10. Plots of $A_{II\to 0}$(○), $A_\eta$(⊙) and $\mu(m)$ (or $\mu(c)$) (●) values against the number of nylon.

$A_\delta$'s or $A_{II\to\phi}$'s of these nylons, are all nearly the same per residue, is as is shown in Table I. Nylon 9 and Nylon 11 also have nearly the same limiting areas per residue, although the areas are somewhat larger than those of even-numbered nylons. The maximum values of the surface moments of odd-numbered nylons are somewhat high compared with those of even-numbered nylons. The surface moment of Nylon 12 is not shown in Table I and Fig. 10 because of its poor reporducibility. Its maximum value, however, is lower than that of Nylon 11. The surface viscosities of odd-numbered nylons, with the exception of Nylon 7, begin to rise at larger areas than those of even-numbered nylons. These differences in film properties between odd- and even-numbered nylons will be discussed in the succeeding sections.

**The Condensation of the Films of Nylons 8 to 12.**—In contrast with the condensed films of Nylon 9 at the air/water interface, the film of this polymer at the oil/water interface is highly expanded, as Fig. 5 shows. It has been found that the films of poly-$\alpha$-amino acids[9,21] and some vinyl polymers[12] are expanded much more at the oil/water interface than at the air/water interface because of the release of van der Waals force between hydrocarbon groups. Accordingly, it seems that the van der Waals attractive force between hydrocarbon groups plays an important role in the remarkable condensation of these nylon films.

The hydrogen bonds between keto and imino groups of amide linkages is also responsible for the condensation of these films, because the film properties of nylons are remarkably affected on a concentrated sulfuric acid subsolution, thus causing the breaking of hydrogen bonds, and the surface viscosities of Nylons 8 to 12 are manifested at quite large areas, as will be discussed in the succeeding sections.

Thus, it seems that both the van der Waals force between hydrocarbon chains and the hydrogen bonds between keto and imino groups of amide linkages are responsible for the remarkable condensation of the films of Nylons 8 to 12 on distilled water.

Holt and Went[26] reported that, with the compression of the films, the hydrophilic amide groups of polyamide films remain at the surface, but that the polymethylene groups are, presumably, pushed out of the surface. The consistency of the observed small limiting areas per residue among even- or odd-numberd nylons suggests that the hydrocarbon chains leave the surface with the compression of the

24) S. Ikeda and T. Isemura, This Bulletin, **32**, 659 (1959).

25) Part II of this series: T. Yamashita and T. Isemura, This Bulletin, **38** (1965).

26) P. F. Holt and C. W. Went, *Proc. 3rd Int. Cong. Surface Activity*, **2**, 49 (1960).

films and are folded because of the van der Waals attractive force between them. The hydrogen bonding between amide groups might also play a significant role in the stability of such folded structures. Similar folded structures have been found by Isemura and Hotta[27] for adsorbed films of long-chain dibasic acids. If the hydrocarbon groups leave the surface and are folded, the contributions of monomer units of even- or odd-numbered nylons to the limiting areas should be identical with each other. The somewhat larger areas of odd-numbered nylons than those of even-numbered ones might be due to the difference in the packings of folded chains. The difference in maximum surface moments between the two series of nylons is caused by the same factor.

The maximum values of the surface moments of Nylons 8 to 11 are between 200 and 250 mD. These values are somewhat higher than the constant values of the surface moments of poly-$\alpha$-amino acids, which are in the range from 150 mD to 180 mD on neutral subsolutions;[16,20-22,25] It has been found that[16], for poly-$\alpha$-aminoisobutyric acid on distilled water and poly-DL-alanine on a acid subsolution (3 N sulfuric acids), the constant values of surface moments are increased to ca. 210 mD because the hydrogen bonds between keto and imino groups are scarce in these films. Probably, the higher $\mu(m)$ values of Nylons 8 to 11 on distilled water than the $\mu(c)$ values of poly-$\alpha$-amino acids on the neutral subsolutions is not caused by a small number of hydrogen bonds, but by a somewhat different orientation of C=O and H-N groups from that in poly-$\alpha$-amino acids, accompanied by a remarkable change in the orientation of these groups during the folding process, because the presence of hydrogen bonds is proved, as has been and will be described in this paper.

**The Surface Viscosities of Nylons 8 to 12.**—The surface viscosities of Nylons 8 to 12 begin to rise at much larger areas than their limiting areas, as Table I shows. Near the area at $A_\eta$, the polymer chains of these nylons begin to come in contact with each other to form a network structure because of the interaction between keto and imino groups of different amide groups.

The $A_\eta$ values of odd-numbered nylons are much larger than those of even-numbered nylons. This fact suggests that hydrogen bond formation between amide groups takes place more easily in the former nylons than in the latter nylons. It also seems that above the areas at $A_\eta$ almost all the chain atoms of these nylons lie on the water surface, because the $A_\eta$ values are larger than the calculated close-packed areas with the exception of Nylon 12, and with a higher compression of films the hydrocarbon groups would leave the surface and be folded.

It has been reported by several authors,[1,2,4,18] concerning the crystals of nylons, that in the fully-extended chains of nylons with even numbers of $CH_2$ groups, all the amide groups on one chain lie directly next to the amide groups on neighboring chains, so that the maximum degree of coupling is attained, while in the fully-extended chains of nylons with odd numbers of $CH_2$ groups, the parallel array leads to a close coupling of only half of the polar groups, although the antiparallel array allows the coupling of all the amide groups. The difference in $A_\eta$ values in the present study between odd- and even-numbered nylons might be related to the difference in the probabilities of hydrogen bond formation between the two series of nylons. Although the deficient hydrogen-bond formation in crystals of nylons with odd numbers of $CH_2$ groups was denied by Kinoshita,[5,6] it might have some effect on the areas where surface viscosities appear because these areas are closely related to the initial stage of hydrogen-bond formation.

**Polynonamethylene Urea.**—The monolayer of this polymer has been investigated in order to prove the role of the van der Waals attractive force between hydrocarbon groups for the stabilization of a folded structure of polyamides of the nylon type. Polyurea, like Nylons 8 to 12, was found to give a condensed film on distilled water, although the limiting area is somewhat larger than those for nylons. The constant value of the surface moment was obtained over a very narrow range; it was 225 mD, which is of the same order of magnitude as the $\mu(m)$ values of Nylons 8 to 12. From these facts, this polyurea is considered to assume a folded structure near the limiting area, like even-numbered nylons, because this polymer contains 9 $CH_2$ groups per residue. Somewhat larger values of $A_\delta$ (27.2 Å$^2$ per residue), $A_{II\to 0}$ (30 Å$^2$ per residue) and $A_\mu$ (32 Å per residue) are probably due to the contribution from another N-H group in the residue. At 84 Å$^2$ per residue, the surface viscosity was first detected. Near this area, the polymer molecules begin to come in contact and to interact with each other. With further compression, the hydrocarbon groups will be folded. The folded structure might be maintained both by the van der Waals attractive force and by hydrogen bonds.

27) T. Isemura and H. Hotta, This Bulletin, 23, 193 (1950).

**The Effect of Sulfuric Acid on the Monolayers of Nylons.**—As has been shown in Figs. 2—5 and in Table I, on concentrated sulfuric acid, a remarkable expansion of films and increase in surface moments are found with Nylons 6 to 9. The stronger the acidity, the greater the effect. It has been reported in Part I of this series[16] that, on concentrated sulfuric acid, poly-DL-alanine film is expanded much more than on distilled water, and that its surface moment increases from 150 mD ($\mu(c)$) to 215 mD ($\mu(c)$) and 256 mD (at 26 Å$^2$ per residue) on the 3 N and 6 N solutions respectively. These changes are due to the breaking of hydrogen bonds between keto-imino groups. The poly-$\alpha$-aminoisobutyric acid monolayer,[16] in which hardly any hydrogen bonds are formed because of the steric hindrance of $\alpha$-disubstituted methyl groups, also gives a high surface moment ($\mu(c)$, 214 mD) compared with poly-DL-alanine on distilled water. The surface moments of nylons on acid subsolutions are much higher than that of poly-DL-alanine on the acid, that of poly-$\alpha$-aminoisobutyric acid on distilled water,[16] and the maximum contribution from the C=O group (360 mD).[23] Accordingly, a different cause must be sought for the remarkably high moments besides the breaking of hydrogen bonds. Such a high surface moment has also been found by Hibberd and Alexander[15] for Nylon 610 (1038 mD per two amide groups at the maximum on 3 N sulfuric acid).

The adsorption of hydrochloric acid by nylon fibers has been studied as a function of the acid concentration.[28] In the concentrated hydrochloric acid solutions, nylon absorbs more acid than would be expected from the number of amino groups present. This excess absorption has been attributed to the interaction of the acid with amide linkages. The amide groups of nylon behave as a base in an acid medium. The interaction of hydrochloric acid with –CONH– groups of nylon has been proved by Larose[29,30] from measurements of the infrared and near-infrared spectra of nylon treated with hydrochloric acid.

The addition of acid to the –CONH– group of nylon can be represented by:

$$-CONH- + H^+ \rightarrow -CONH^+-.$$

Thus, nylon film would be charged positively. As a result of the protonation to amide linkage, the surface moments are increased remarkably.

The folded structures of higher nylons on distilled water are unfolded on the subsolutions of sulfuric acid because the hydrogen bonds which would stabilize the folded structure are broken. The repulsion between charged groups causes a remarkable expansion of the film. The polymer chains are in a rather flexible state.

28) F. T. Wall and A. Beresniewicz, *J. Phys. Chem.*, **60**, 692 (1956).
29) P. Larose, *Can. J. Chem.*, **35**, 1239 (1957).
30) P. Larose, ibid., **39**, 2394 (1961).

## Summary

The surface films of a series of nylons prepared from $\omega$-aminocarboxylic acids and with 2 to 11 $CH_2$ groups per monomer unit (Nylons 3 to 12) have been studied at the air/water interface in order to investigate the correlation of the film properties with the numbers of $CH_2$ groups. The film of Nylon 9 at the oil/water interface and that of polynonamethylene urea at the air/water interface have also been studied.

The film of Nylon 3 on the 40% ammonium sulfate subsolution was of the condensed type and the area occupied per residue was quite small, probably because of the especially strong hydrogen bonds between amide groups. On the other hand, the films of Nylons 4, 5 and 6 on 40% ammonium sulfate and that of Nylon 6 on distilled water were of the expanded type. These polymers might be spread in rather flexible states because of the effect of the increased number of $CH_2$ groups.

Nylons 8 to 12 and polyurea gave condensed films on distilled water, their limiting areas per residue being much smaller than the areas calculated for the fully extended chains. The condensation of the films might be primarily caused by the increased van der Waals attractive force between hydrocarbon groups, as has been proved by the remarkable expansion of Nylon 9 film at the petroleum ether/distilled water interface. The small limiting areas of these polymer films have been interpreted by assuming that the hydrocarbon chains are folded near these areas. Nylon 7 was found to give an intermediate film between expanded films, such as Nylons 4 to 6, and condensed films, such as Nylons 8 to 12.

Interesting differences in the film properties of odd- and even-numbered nylons have been found with Nylons 8 to 12. Odd-numbered nylons occupied somewhat larger areas per residue than even-numbered nylons, and the maximum surface moments of the formers were higher than those of the latters. This is the result of the difference in shapes of the folded chains between the two series of nylons.

The surface viscosities of Nylons 8 to 12, with the exception of the last, were first detected at larger areas than the close-packed areas calculated for the fully-extended

chains. The areas found for even-numbered nylons were much smaller than those for odd-numbered ones. This may be attributed to the difference in modes of hydrogen bond formation between amide groups.

A remarkable effect of the concentrated sulfuric acid subsolution on the film properties of Nylons 6 to 9 has been found, and interpreted as being due to the protonation to the amide linkages.

The author wishes to express his gratitude to Professor Toshizo Isemura of Osaka University for his kind guidance throughout the present work, and to Dr. Shoichi Ikeda of the same University for his helpful discussions. He is also indebted to Dr. Yukio Kinoshita and Dr. Masatoshi Ito of the Toyo Rayon Co., Professor Shunsuke Murahashi of Osaka University, Dr. Yasushi Joh of the Mitsubishi Rayon Co., Mr. Tsuyoshi Konomi of the Toyo Spinning Co., and Dr. Vassant Ambekar of L'école Superieure de Physique et de Chimie de Paris for the supply of samples.

*Institute for Protein Research*
*Osaka University*
*Kita-ku, Osaka*

# Equilibrium Study of Propylenediaminetetraacetato Complexes of Some Divalent Metal Ions

By Nobuyuki TANAKA and Hiroshi OGINO

(Received August 5, 1964)

Smith has reported the stability constants of propylenediaminetetraacetato complexes.[1] However, the experimental details were not given and the values seem to be somewhat questionable.

In this laboratory, the equilibria of substitution reactions involving ethylenediaminetetraacetato complexes have been investigated and the equilibrium constants of these reactions have been determined.[2,3] In this paper, the method developed previously[2] is applied to the systems involving propylenediaminetetraacetato complexes, and the results are compared with the values reported in literature[1] and discussed.

## Experimental

**Reagents.** — Standard solutions of nickel(II) nitrate, copper(II) nitrate, lead(II) nitrate, cadmium(II) nitrate[2,3] and zinc(II) nitrate[4] were obtained by the same procedures as reported previously. To remove a small amount of contaminant of nickel, a standard solution of cobalt(II) nitrate was prepared in the following way: Hexamminecobalt(III) chloride which was recrystallized three times from water was heated at 400°C in an electric furnace. The residue was dissolved into a dilute nitric acid solution, evaporated to dryness and the same procedure was repeated several times to convert cobalt(II) chloride to cobalt(II) nitrate. Cobalt(II) nitrate thus obtained was dissolved into distilled water and the residue was removed by filtration. The concentration of cobalt(II) was determined with a standardized EDTA (disodium dihydrogen ethylenediaminetetraacetate) solution by amperometric titration.

Propylenediaminetetraacetic acid ($H_4$pdta) was prepared according to the method of Dwyer and Garvan.[5] The stock solution of $Na_2H_2$pdta was prepared from equimolar quantities of $H_4$pdta and sodium carbonate. The concentration of PDTA was determined with all of the standard metal nitrate solutions mentioned above by amperometric titration. The values thus obtained were consistent with each other within experimental error and were in good agreement with the value expected from the weight of $H_4$pdta. Therefore, it may be considered that PDTA can be used in complexometric titration in the same way as in the case of EDTA.

All other chemicals used were of analytical reagent grade.

**Apparatus and Procedure.**—A Yanagimoto PB-4 pen-recording polarograph was used for the measurement of the current-voltage and current-time curves. The dropping mercury electrodes used had the characteristics given in Table I, being measured in an air-free 0.2 M potassium nitrate solution containing 0.01% gelatin at 25°C.

1) R. L. Smith, "The Sequestration of Metals," Chapman and Hall, London (1959).
2) N. Tanaka and K. Kato, This Bulletin, 33, 417 (1960).
3) N. Tanaka, M. Kamada, H. Osawa and G. Satô, ibid., 33, 1412 (1960).
4) N. Tanaka and H. Ogino, ibid., 36, 175 (1963).
5) F. P. Dwyer and F. L. Garvan, *J. Am. Chem. Soc.*, 81, 2955 (1959).

TABLE I. CHARACTERISTICS OF THE DROPPING MERCURY ELECTRODES

| | Flow rate of mercury ($m$) mg./sec. | Drop time ($t_d$), sec. |
|---|---|---|
| Electrode A*1,2 | $2.13_7$ | 3.96 |
| Electrode B*3 | $1.99_5$ | 4.13 |

*1 This electrode was used for the systems containing cobalt(II) ions.
*2 Measured at 63.9 cm. of the mercury height.
*3 Measured at 64.8 cm. of the mercury height.

The measurements of the diffusion currents of copper(II) in acetate buffer solutions were carried out with the following five reaction mixtures at 25°C:

(a) copper(II)-cobalt(II)-PDTA
(b) copper(II)-nickel(II)-PDTA
(c) copper(II)-zinc(II)-PDTA
(d) copper(II)-cadmium(II)-PDTA
(e) copper(II)-lead(II)-PDTA

The ionic strength was adjusted to be 0.2 with potassium nitrate. Gelatin was added as a maximum suppressor by 0.01% in concentration.

It was found in the preliminary experiments that the substitution reactions between copper(II) ions and various kinds of metal(II)-PDTA complexes were more sluggish than those of the corresponding reactions involving EDTA.[2,3] In Fig. 1, a typical example is given. Therefore, in system b, reaction mixtures were kept in a thermostat for 50 days before being subjected to the polarographic measurements. In other systems, as the substitution reactions were completed within 7 hrs., measurements were made after the solutions prepared had been kept overnight.

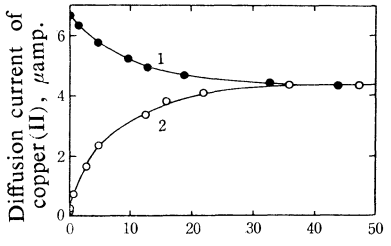



Fig. 1. Diffusion currents of copper(II) as a function of time in the forward (curve 1) and the reverse (curve 2) reactions of the substitution reaction $Cu^{2+}+NiY^{2-} \rightleftarrows CuY^{2-}+Ni^{2+}$, measured in acetate buffer solutions of pH $5.4_5$ at 25°C. Total concentrations are: $[Cu]_t=1.00\times10^{-3}$ M; $[Ni]_t=1.00\times10^{-3}$ M; $[PDTA]_t=0.99_0\times10^{-3}$ M.

## Results

In the acetate buffer solution which contains two different metal ions, $M^{m+}$ and $M'^{m'+}$, and propylenediaminetetraacetate ions, there exist the following equilibria:

$$\begin{Bmatrix} M^{m+} \\ \uparrow\downarrow \\ M(OAc)_n^{(m-n)+} \end{Bmatrix} + \begin{Bmatrix} M'Y^{(m'-4)+} \\ \uparrow\downarrow \\ M'HY^{(m'-3)+} \end{Bmatrix} \rightleftarrows \begin{Bmatrix} MY^{(m-4)+} \\ \uparrow\downarrow \\ MHY^{(m-3)+} \end{Bmatrix} + \begin{Bmatrix} M'^{m'+} \\ \uparrow\downarrow \\ M'(OAc)_{n'}^{(m'-n')+} \end{Bmatrix} \quad (1)$$

where $Y^{4-}$ denotes quadrivalent PDTA ions.

The values of $[Cu^{2+}]_{app}$ in the reaction mixtures of systems a to e which are given by[2]

$$[Cu^{2+}]_{app}=[Cu^{2+}]+\sum_1^n[Cu(OAc)_n^{(2-n)+}] \quad (2)$$

were determined at various concentrations of acetate. Then, the apparent equilibrium constants for Eq. 1,

$$K^M_{M',app}=\frac{[M'^{m'+}]_{app}\{[MY^{(m-4)+}]+[MHY^{(m-3)+}]\}}{[M^{m+}]_{app}\{[M'Y^{(m'-4)+}]+[M'HY^{(m'-3)+}]\}} \quad (3)$$

were calculated and plotted against the acetate ion concentration. These plots for systems a to e are shown in Fig. 2 to Fig. 4.

$K^M_{M',app}$ is rewritten as[2]

$$K^M_{M',app}=K^M_{M'}\frac{\alpha_{MHY(H)}}{\alpha_{M'HY(H)}}\times\frac{1+\sum_1^{n'}K_{M'(OAc)_{n'}}[OAc^-]^{n'}}{1+\sum_1^{n}K_{M(OAc)_n}[OAc^-]^n} \quad (4)^*$$

where

$$\alpha_{MHY(H)}=1+K^H_{MHY}[H^+] \quad (5)$$

$$\alpha_{M'HY(H)}=1+K^H_{M'HY}[H^+] \quad (6)$$

$$K^M_{M'}=\frac{[M'^{m'+}][MY^{(m-4)+}]}{[M^{m+}][M'Y^{(m'-4)+}]} \quad (7)$$

$K_{M(OAc)_n}$ and $K_{M'(OAc)_{n'}}$ represent the overall formation constants of $M(OAc)_n^{(m-n)+}$ and

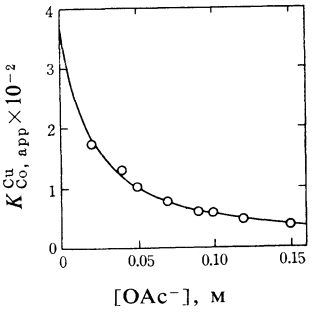



Fig. 2. $K^{Cu}_{Co,app}$ at pH 4.56 as a function of acetate ion concentration.

* $\beta$ and $\beta'$, the symbols that are given in previous papers[2,3] are replaced by $\alpha_{MHY(H)}$ and $\alpha_{M'HY(H)}$ respectively.

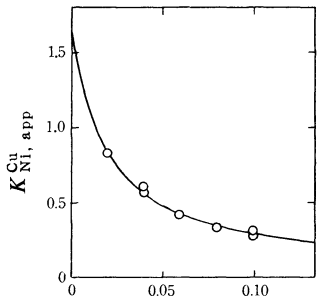



Fig. 3. $K^{Cu}_{Ni,\,app}$ at pH 4.9 as a function of acetate ion concentration.

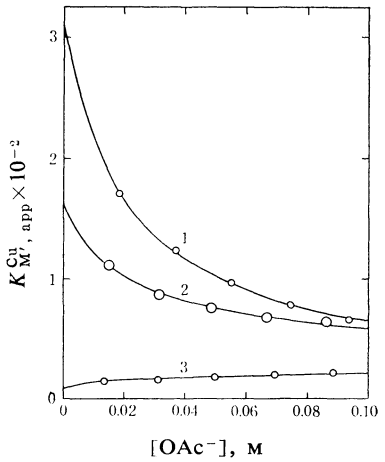



Fig. 4. $K^{Cu}_{Zn,\,app}$ (1), $K^{Cu}_{Cd,\,app}$ (2) and $K^{Cu}_{Pb,\,app}$ (3) at pH 5.4 as a function of acetate ion concentration.

$M'(OAc)_{n'}^{(m'-n')+}$, respectively, and $K^{M}_{M'}$ means the equilibrium constant of reaction given by the equation

$$M^{m+} + M'Y^{(m'-4)+} \rightleftarrows MY^{(m-4)+} + M'^{m'+} \quad (8)$$

It may be reasonable to consider the values of $\alpha_{MHY(H)}/\alpha_{M'HY(H)}$ as being approximately unity under these experimental conditions (pH 4.5—5.5), because this is true in the case of the EDTA complexes,[6] to which the PDTA complexes are closely related.

The experimental values in Figs. 2 to 4 were treated by a least square method with the aid of Eq. 4 and the formation constants of acetato complexes obtained previously,[2,3,7] the values of the equilibrium constants for Eq. 8 ($K^{Cu}_{M'}$) were determined. They are given in Table II.

Table II. Equilibrium constants for the substitution reaction (Eq. 8) involving PDTA complexes at 25°C and ionic strength 0.2

| $K^{Cu}_{Co}$ | $K^{Cu}_{Ni}$ | $K^{Cu}_{Zn}$ | $K^{Cu}_{Cd}$ | $K^{Cu}_{Pb}$ |
|---|---|---|---|---|
| $3.7\times10^{2}$ | $1.6_6$ | $3.2\times10^{2}$ | $1.6_1\times10^{2}$ | 8.8 |

The values of $K^{Cu}_{M',\,app}$ can be calculated as a function of acetate concentration using the $K^{Cu}_{M'}$ values given in Table II, the formation constants of acetato complexes[2,3,7] and Eq. 4. The solid curves in Figs. 2 to 4 are the calculated ones, which are in satisfactory agreement with the $K^{Cu}_{M',\,app}$ obtained experimentally at various acetate concentrations. This fact indicates that the values of the formation constants of acetato complexes obtained previously[2,3,7] are reliable.

## Discussion

Equation 7 means that $K^{M}_{M'}$ is equal to the ratio of the stability constant of the $M^{m+}$-PDTA complex to that of the $M'^{m'+}$-PDTA complex:

$$K^{M}_{M'} = \frac{K_{MY}}{K_{M'Y}} \quad (9)$$

For the sake of comparison, the $K^{Cu}_{M'}$ values in Table II are converted to the relative stability constants to the stability constant of zinc(II)-PDTA complex and the resulting values are given in Table III.

Smith has reported the stability constants of various PDTA complexes.[1] The $K^{M}_{Zn}$ values

Table III. The values of $K^{M}_{Zn}$ of PDTA complexes

| | Temp. °C | Ionic strength | $K^{Co}_{Zn}$ | $K^{Ni}_{Zn}$ | $K^{Cu}_{Zn}$ | $K^{Zn}_{Zn}$ | $K^{Cd}_{Zn}$ | $K^{Pb}_{Zn}$ |
|---|---|---|---|---|---|---|---|---|
| I | 25 | 0.2 | 0.85 | $1.9_0\times10^{2}$ | $3.2\times10^{2}$ | 1 | $1.9_6$ | $3.6\times10$ |
| II | 20 | 0.1 | $1.6\times10^{-2}$ | $1.0_0\times10^{-2}$ | $3.2\times10$ | 1 | 0.63 | $1.2_6\times10$ |

I. Values obtained in the present investigation.
II. Values calculated from the Smith's values.[1]

6) G. Schwarzenbach, R. Gut and G. Anderegg, *Helv. Chim. Acta*, **37**, 937 (1954).

7) N. Tanaka and K. Kato, This Bulletin, **32**, 516 (1959).

obtained from his stability constants are also given in Table III. Table IV shows the $K^{M}_{Zn}$ values calculated from the $K^{M}_{M'}$ values of the EDTA complexes obtained previously.[2,3] The $K^{M}_{Zn}$ values of the PDTA complexes obtained in this study do not agree with those calculated from the Smith's data, but are quite similar to the $K^{M}_{Zn}$ values of the EDTA complexs given in Table IV.

TABLE IV. THE VALUES OF $K^{M}_{Zn}$ OF EDTA COMPLEXES AT 25°C AND IONIC STRENGTH 0.2[2,3]

| $K^{Co}_{Zn}$ | $K^{Ni}_{Zn}$ | $K^{Cu}_{Zn}$ | $K^{Zn}_{Zn}$ | $K^{Cd}_{Zn}$ | $K^{Pb}_{Zn}$ |
|---|---|---|---|---|---|
| 0.59 | $1.5\times10^2$ | $3.3\times10^2$ | 1 | 1.1 | $6.6\times10$ |

Recently, the stability constants of alkaline earth chelates and the acid dissociation constants (p$K$) of PDTA have been determined by Grimes et al.[8] They reported that the fourth dissociation constant (p$K_4$) of PDTA is higher than that of EDTA, and the stability constants of alkaline earth chelates of PDTA are larger than those of EDTA,[8] explaining that these are attributed to the inductive effect of the methyl group in PDTA.

Nevertheless, it is considered that the increase of stability constants in the presence of methyl group is considered to affect slightly the values of $K^{M}_{M'}$, because it may be considerably compensated. Actually, the change in the stability constants of alkaline earth chelates of PDTA[8] with increase in atomic number is parallel to those of EDTA[9] as shown in Fig. 5. Therefore, the similarity between our data of $K^{M}_{M'}$ values of PDTA complexes and those of EDTA complexes seems to be reasonable.

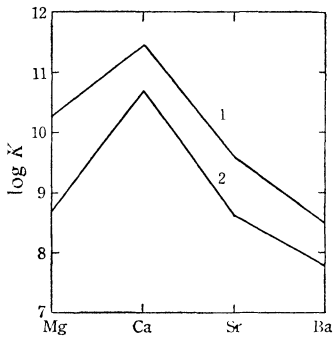



Fig. 5. Logarithms of the stability constants of alkaline earth chelate at ionic strength 0.1: (1) PDTA chelate at 30°C,[8] (2) EDTA chelate at 20°C.[9]

The values reported by Smith are considered to be somewhat erroneous, because his values for $K^{Co}_{Zn}$, $K^{Ni}_{Zn}$ and $K^{Cu}_{Zn}$ are too small.

## Summary

The relative stability constants of propylenediaminetetraacetato complexes ($K^{M}_{M'}=K_{MY}/K_{M'Y}$) of six metal ions were determined at 25°C and ionic strength 0.2 by the polarographic method reported previously.[2] The values obtained are $K^{Cu}_{Co}=3.7\times10^2$, $K^{Cu}_{Ni}=1.6_6$, $K^{Cu}_{Zn}=3.2\times10^2$, $K^{Cu}_{Cd}=1.6_1\times10^2$ and $K^{Cu}_{Pb}=8.8$ and are quite similar to the corresponding values of the ethylenediaminetetraacetato complexes respectively.

The authors wish to thank the Ministry of Education for the financial support granted for this research.

*Department of Chemistry*
*Faculty of Science*
*Tohoku University*
*Katahira-cho, Sendai*

8) J. H. Grimes, A. J. Huggard and S. P. Wilford, *J. Inorg. Nucl. Chem.*, **25**, 1225 (1963).
9) G. Schwarzenbach and H. Ackermann, *Helv. Chem. Acta*, **30**, 1798 (1947).

# Vibration-Rotation Spectra, the Coriolis Coupling Constants and the Intramolecular Force Field of Symmetric Top Molecules. I. The E-type Fundamental Bands of Methyl and Methyl-$d_3$ Halides

By Yonezo MORINO and Junko NAKAMURA*

(Received August 10, 1964)

It is a current problem in the determination of the intramolecular force field that a set of force constants must be chosen in such a way that they may reproduce not only the vibrational frequencies but also all the available observables that are related to the force field. Many attempts have been made to determine the intramolecular force field by using observed data of the Coriolis coupling constants as additional observables, especially in the case of molecules with methyl groups.[1a,b] As for the methyl halide molecules, however, the reported values of the Coriolis coupling constants are considered to be neither complete nor precise enough for the present purpose.[2-16] A systematic reinvestigation of infrared spectra has, therefore, been undertaken in the present study for the six species of methyl halides ($CH_3Cl$, $CD_3Cl$, $CH_3Br$, $CD_3Br$, $CH_3I$ and $CD_3I$). The present report is limited to the experimental results on the E-type fundamental bands. The results of the force-field calculation and the analyses of overtones and combination bands will be reported in the succeeding papers of this series.

Eighteen vibration-rotation spectra, $\nu_4$, $\nu_5$ and $\nu_6$ of six molecules, were resolved in the present study, and some of the previous subband assignments were revised. Analyses of the vibration-rotation bands gave the Coriolis coupling constants, the rotational constants and the frequencies of the vibrational band origins. A few bands show peculiar features which indicate the presence of perturbations, which probably influence some of the resulting data. Nevertheless, the "parallel nature" observed for the molecules investigated suggests the certainty of the present results. The assumption of the "parallel nature" was also extensively used to estimate the rotational correction terms through which the $r_0$ and $r_e$ structures were estimated.

## Experimental

**Preparation of Samples.** — All the compounds except $CH_3I$ were prepared by the direct halogenation of $CH_3OH$ or $CD_3OH$. Commercial $CH_3I$ was used after low-temperature distillation in vacuo through a U-tube packed with grained potassium hydroxide and calcium chloride. $CD_3OH$ was synthesized by the method described by Edgell and Parts[17] with some modifications; Ethylene carbonate, prepared from sodium ethylene glycolate and ethyl chloroformate, was reduced with $LiAlD_4$ to a complex compound which was then decomposed to $CD_3OH$ with monobutylcarbitol in diethylcarbitol. About 1.6 g. of $CD_3OH$ was obtained by this method starting from 2 g. of $LiAlD_4$.

$CH_3Cl$ ($CD_3Cl$) and $CH_3Br$ ($CD_3Br$) were prepared from alcohols by halogenation with phosphorus trichloride and phosphorus tribromide respectively. Sample gases were purified with potassium hydroxide, concentrated sulfuric acid and phosphorus pentoxide. $CH_3OH$ was iodized to $CD_3I$ by means of hydroiodic acid after the method of Cox, Tunner and Warner.[18]

The purities of the starting and the intermediate reagents as well as of the last products were examined by their physical constants, elemental analyses and spectroscopic analyses. The percentage of deuterium in $CD_3X$ samples was not tested, but the existence of serious impurities ($CH_2DX$, $CHD_2X$,

* Present address: The Institute of Physical and Chemical Research, Komagome, Bunkyo-ku, Tokyo

1) a) I. Nakagawa and T. Shimanouchi, *J. Chem. Soc. Japan, Pure Chem. Sec.* (*Nippon Kagaku Zasshi*), **80**, 128 (1959); b) I. M. Mills, *Spectrochim. Acta*, **16**, 35 (1960); **18**, 1073 (1962); **19**, 1967 (1963).
2) W. H. Bennett and C. F. Meyer, *Phys. Rev.*, **32**, 888 (1928).
3) A. H. Nielsen and E. F. Barker, ibid., **46**, 970 (1934).
4) E. K. Plyler and E. F. Barker, *J. Chem. Phys.*, **3**, 367 (1935).
5) H. H. Nielsen and A. H. Nielsen, *Phys. Rev.*, **56**, 274 (1939); **68**, 99 (1954); *Rev. Mod. Phys.*, **16**, 241 (1944).
6) B. T. Darling and D. M. Dennison, *Phys. Rev.*, **57**, 128 (1940).
7) H. D. Noether, *J. Chem. Phys.*, **10**, 664 (1942).
8) R. T. Lageman and H. H. Nielsen, ibid., **10**, 668 (1942).
9) C. P. Courtoy, *Ann. Soc. Sci. Bruxelles*, **LX**, 122 (1946).
10) F. Halverson, *Rev. Mod. Phys.*, **19**, 87 (1947).
11) M'me R. Mathis Noel, *Compt rend.*, **230**, 2168 (1950). *J. phys. Radium*, **12**, 550 (1951).
12) P. F. Fenlon, F. F. Cleveland and A. G. Meister, *J. Chem. Phys.*, **19**, 156 (1951).
13) I. L. Mador and R. S. Quinn, ibid., **20**, 1837 (1952).
14) R. B. Bernstein, F. F. Cleveland and F. L. Voelz, ibid., **22**, 196 (1954).
15) H. B. Weissman, R. B. Bernstein, S. E. Rosser, A. G. Meister and F. F. Cleveland, *J. Chem. Phys.*, **23**, 544 (1955).
16) F. A. Andersen, Private communication.
17) W. F. Edgell and L. Parts, *J. Am. Chem. Soc.*, **77**, 5515 (1955).
18) J. D. Cox, M. S. Tunner and R. J. Warner, *J. Chem. Soc.*, **1950**, 3167.

$CH_3X$, $CD_3OH$, HX, etc.) was not detected in their infrared spectra.

**Spectrometer.**—A Perkin-Elmer 112G grating infrared spectrometer was used throughout the investigation. $CH_3X$ and $CD_3X$ fundamentals were observed with a cell 10 cm. long. In the case of $CH_3X$, a long-path cell (with a net length of about 6 m.) was also used. The pressure of the gas was controlled in each case, ranging from 5 mmHg to some hundreds of mmHg. The resolution of the Perkin-Elmer 112G spectrometer is about 0.6 $cm^{-1}$ at 15 $\mu$ and 0.8 $cm^{-1}$ at 3$\mu$. Because the spectrometer has a slingle-beam system, the presence of water and carbon dioxide in the air seriously disturbs the observation. This difficulty was partially removed by an introduction of the stream of air free from water and carbon dioxide into the whole apparatus, but some bands were still obscured by the bands of residual water or carbon dioxide.

## Results for the E-type Fundamental Bands

All of the E-type fundamental bands were observed as a series of finely-resolved $Q$ branch subbands, with the intensity alternation to be expected for the $C_{3v}$ symmetric top molecules. As has already been pointed out, the origin of the subband peak (the position corresponding to the $J=K$ of ${}^{R}Q_K$ and ${}^{P}Q_K$) should be at the foot of the steeper side of the absorption curve. The observed curves are, however, more or less deformed by the limited resolving power of the instrument, the effect of the slit function, the pressure broadening, and other reasons. Therefore, it is almost impossible to determine the position of the subband origins precisely. The "peak frequencies," namely, the frequencies of the maximum absorption points, were accordingly measured; they correspond to those for $J_m$ in Eq. 24. (See Appendix I)

The criteria for finding the ${}^{R}Q_0$ for the E-type bands have already been discussed by several authors, especially by Overend and Crawford.[19] In many of the present investigations, however, it was found difficult to apply the method recommended by them, for the bands, the ${}^{R}Q_0$ of which could not be easily determined, were apparently irregular or in some cases, only half of the members of the series were observed; under such conditions, the measurement and the summing up of the band intensity were impossible. Consequently, the ${}^{R}Q_0$'s were determined according to the following features of the band:

1) The intensity alternation caused by the statistical spin weight, depending upon the $K$ numbers (strong for the subbands of $K=3m$, weak for $K\neq 3m$, where $m$ is an integer).

2) The gradual increase and decrease in the intensity of the subbands, with a maximum at ${}^{R}Q_0$ (besides the spin weight mentioned above). There may be the cases where the ${}^{R}Q_0$ peaks are abruptly weakened in intensity, but the survey of the peak intensities as a whole offers a reliable criterion.

3) The series of the molecules investigated must have parallel spectroscopic natures as the attached halogen atom changes from Cl to Br and to I.

Typical absorption curves are shown in Figs. 1—3. Observed peak frequencies and the assignments are listed in columns 2 and 3 of Tables I—XVIII respectively. These values were obtained as the most probable values out of several observations with different conditions. The asterisks in the tables show the peaks which were omitted from the least-squares calculations because they either are obscured by the presence of foreign bands, such as those of carbon dioxide and water, or are at apparently irregular positions.

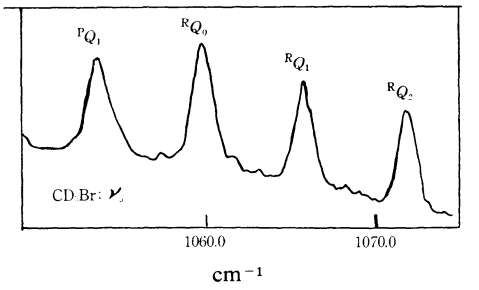



Fig. 1. $CD_3Br$; Part of $\nu_5$ ($\perp$).

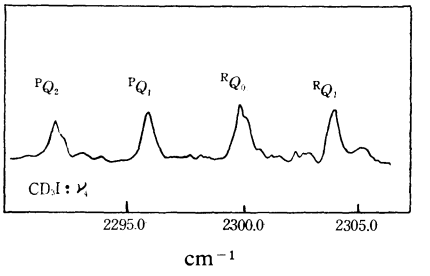



Fig. 2. $CD_3I$; Part of $\nu_4$ ($\perp$).

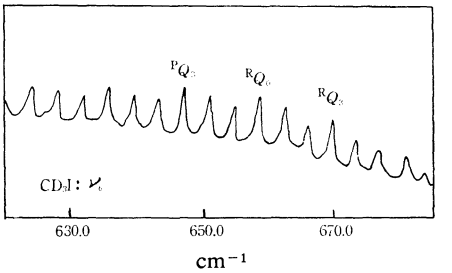



Fig. 3. $CD_3I$; $\nu_6$ ($\perp$).

19) J. Overend and B. Crawford Jr., *J. Chem. Phys.*, **29**, 1002 (1958).

If one ignores the effect of the centrifugal distortion and a slight change in the $J_m$ number in the different $K$ subbands, we should be able to fit, the observed peak frequencies to a quadratic equation of $K$, Eq. 1 :

$$\nu^{sub}=C_0+C_1K+C_2K^2 \quad (1)$$

and the separations of the successive $Q$ branches ($\Delta\nu_K$) plotted against their $K$ numbers should give a straight line with a tangent twice the coefficient $C_2$ (Fig. 4). The values of $\Delta\nu_K$ are listed in column 4 of Tables I—XVIII.

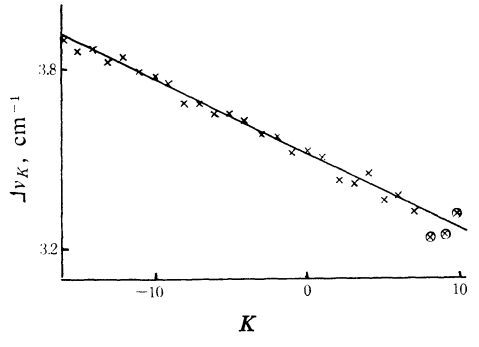



Fig. 4. $\Delta\nu_K=(Q_{K+1}-Q_K)$ : $CD_3Cl$ : $\nu_4(\perp)$ ⊗ : Overlapped with a $CO_2$ absorption.

Some peculiar features observed by the examination of $\Delta\nu_K$'s are as follows :

**(i) The $\nu_4$ Band of $CH_3Cl$.**—Figure 5 shows the irregular nature of the $\nu_4$ band of $CH_3Cl$. As has already been mentioned, each subband the $K$ number of which is a multiple of three has a greater absorption intensity than its neighbors, thus making a series of intensity alternations : strong, weak, weak, strong, etc. In the $\nu_4$ band of $CH_3Cl$, however, the sequence is apparently perturbed at about 3070 cm$^{-1}$. After a rather regular series of peaks assigned as $^RQ_{12}$—$^RQ_3$, three somewhat deformed and broad peaks follow, with a stronger peak as a fourth, from which another sequence of strong, weak, weak, starts. The separations, $\Delta\nu_K$, also change abruptly in this region, and, moreover, the tangents of the two sequences mentioned above differ beyond the range of error of the measurement. These features clearly show the existence of a certain perturbation which has not been considered before.

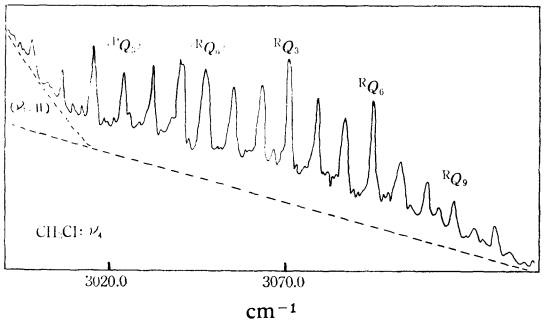



Fig. 5. $CH_3Cl$ : $\nu_4$ ($\perp$).

A similar type of irregularity takes place in the combination bands related to $\nu_4$ (the perpendicular band of $2\nu_4$,[20] and $\nu_1+\nu_4$). For the present, the peak at 3071.30 cm$^{-1}$ was assigned

TABLE I. FINE STRUCTURE OF THE $\nu_4$ BAND OF $CH_3Cl$

| No. | $\nu_{obs}$ | Assignment | $\Delta\nu_K$ | $\nu_{calcd}$ | $\nu_{obs}-\nu_{calcd}$ |
|---|---|---|---|---|---|
| 1 | 2989.57* | ($^PQ_7$) | | 2987.74 | (+1.83) |
| 2 | 2998.08* | ($^PQ_6$) | | 2995.31 | (+2.77) |
| 3 | 3006.64* | ($^PQ_5$) | | 3003.85 | (+2.79) |
| 4 | 3012.37* | ($^PQ_4$) | | 3012.37 | ( 0.00) |
| 5 | 3023.84* | ($^PQ_3$) | | 3020.87 | (−2.97) |
| 6 | 3031.86* | ($^PQ_2$) | | 3029.33 | (+2.53) |
| 7 | 3040.26* | ($^PQ_1$) | | 3037.78 | (+2.48) |
| 8 | 3047.41* | $^RQ_0$ | 7.47 | 3046.20 | (+1.21) |
| 9 | 3054.88* | $^RQ_1$ | 8.21 | 3054.59 | (+0.29) |
| 10 | 3063.09* | $^RQ_2$ | 8.21 | 3062.96 | (+0.10) |
| 11 | 3071.30 | $^RQ_3$ | 8.31 | 3071.30 | 0.00 |
| 12 | 3079.61 | $^RQ_4$ | 8.27 | 3079.61 | 0.00 |
| 13 | 3087.88 | $^RQ_5$ | 8.28 | 3087.90 | −0.02 |
| 14 | 3096.16 | $^RQ_6$ | 8.28 | 3096.16 | 0.00 |
| 15 | 3104.44 | $^RQ_7$ | 8.16 | 3104.40 | +0.04 |
| 16 | 3112.60 | $^RQ_8$ | 8.20 | 3112.62 | −0.02 |
| 17 | 3120.80 | $^RQ_9$ | 8.52 | 3120.80 | 0.00 |
| 18 | 3129.52* | $^RQ_{10}$ | 7.99 | 3128.96 | +0.36 |
| 19 | 3137.31* | $^RQ_{11}$ | 7.99 | 3137.10 | +0.20 |
| 20 | 3145.30* | $^RQ_{12}$ | | 3145.21 | +0.09 |

TABLE II. FINE STRUCTURE OF THE $\nu_5$ BAND OF $CH_3Cl$

| No. | $\nu_{obs}$ | Assignment | $\Delta\nu_K$ | $\nu_{calcd}$ | $\nu_{obs}-\nu_{calcd}$ |
|---|---|---|---|---|---|
| 1 | 1386.30* | $^PQ_6$ | 12.54 | 1386.02 | +0.28 |
| 2 | 1398.84* | $^PQ_5$ | 12.20 | 1398.57 | +0.27 |
| 3 | 1411.04 | $^PQ_4$ | 12.28 | 1411.03 | +0.01 |
| 4 | 1423.32 | $^PQ_3$ | 12.33 | 1423.39 | −0.07 |
| 5 | 1435.65 | $^PQ_2$ | 12.26 | 1435.65 | 0.00 |
| 6 | 1447.91* | $^PQ_1$ | 11.51 | 1447.82 | +0.09 |
| 7 | 1459.42* | $^RQ_0$ | 12.49 | 1459.89 | −0.47 |
| 8 | 1471.91 | $^RQ_1$ | 11.84 | 1471.86 | +0.05 |
| 9 | 1483.75 | $^RQ_2$ | 11.70 | 1483.74 | +0.01 |
| 10 | 1495.45 | $^RQ_3$ | 11.68 | 1495.52 | −0.07 |
| 11 | 1507.13 | $^RQ_4$ | 11.67 | 1507.21 | −0.08 |
| 12 | 1518.80 | $^RQ_5$ | 11.58 | 1518.79 | +0.01 |
| 13 | 1530.38 | $^RQ_6$ | 11.21 | 1530.29 | +0.09 |
| 14 | 1541.59* | $^RQ_7$ | 11.42 | 1541.68 | −0.09 |
| 15 | 1553.01 | $^RQ_8$ | 11.13 | 1552.99 | +0.02 |
| 16 | 1564.14 | $^RQ_9$ | 11.18 | 1564.19 | −0.05 |
| 17 | 1575.32 | $^RQ_{10}$ | 10.98 | 1575.30 | +0.02 |
| 18 | 1586.30 | $^RQ_{11}$ | | 1586.31 | −0.01 |

20) R. G. Brown and T. H. Edwards, ibid., **28**, 384 (1958).

TABLE III. FINE STRUCTURE OF THE $\nu_6$ BAND OF $CH_3Cl$

| No. | $\nu_{obs}$ | Assignment | $\Delta\nu_K$ | $\nu_{calcd}$ | $\nu_{obs}-\nu_{calcd}$ |
|---|---|---|---|---|---|
| 1 | 959.19 | $^PQ_9$ | 6.54 | 959.20 | −0.01 |
| 2 | 965.73 | $^PQ_8$ | 6.63 | 965.73 | 0.00 |
| 3 | 972.36 | $^PQ_7$ | 6.57 | 972.32 | +0.04 |
| 4 | 978.93 | $^PQ_6$ | 6.64 | 978.94 | −0.01 |
| 5 | 985.57 | $^PQ_5$ | 6.80 | 985.62 | −0.05 |
| 6 | 992.37 | $^PQ_4$ | 6.73 | 992.35 | +0.02 |
| 7 | 999.10 | $^PQ_3$ | 6.87 | 999.12 | −0.02 |
| 8 | 1005.97 | $^PQ_2$ | 6.90 | 1005.94 | +0.03 |
| 9 | 1012.87 | $^PQ_1$ | 6.83 | 1012.81 | +0.06 |
| 10 | 1019.70 | $^RQ_0$ | 7.01 | 1019.73 | −0.03 |
| 11 | 1026.71 | $^RQ_1$ | 7.05 | 1026.69 | +0.02 |
| 12 | 1033.76 | $^RQ_2$ | 6.93 | 1033.71 | +0.05 |
| 13 | 1040.69 | $^RQ_3$ | 7.13 | 1040.77 | −0.08 |
| 14 | 1047.82 | $^RQ_4$ | 7.25 | 1047.88 | −0.06 |
| 15 | 1055.07 | $^RQ_5$ | 7.13 | 1055.03 | +0.04 |
| 16 | 1062.50 | $^RQ_6$ | 7.30 | 1062.24 | −0.04 |
| 17 | 1069.50 | $^RQ_7$ | 7.33 | 1069.49 | +0.01 |
| 18 | 1076.83 | $^RQ_8$ | 7.18 | 1076.79 | +0.04 |
| 19 | 1084.01 | $^RQ_9$ | 7.54 | 1084.14 | −0.13 |
| 20 | 1091.55 | $^RQ_{10}$ | 7.37 | 1091.54 | +0.01 |
| 21 | 1098.92 | $^RQ_{11}$ | 7.60 | 1098.98 | −0.06 |
| 22 | 1106.52 | $^RQ_{12}$ | | 1106.48 | +0.04 |

TABLE IV. FINE STRUCTURE OF THE $\nu_4$ BAND OF $CH_3Br$

| No. | $\nu_{obs}$ | Assignment | $\Delta\nu_K$ | $\nu_{calcd}$ | $\nu_{obs}-\nu_{calcd}$ |
|---|---|---|---|---|---|
| 1 | 2996.61 | $^PQ_7$ | 9.33 | 2996.60 | +0.01 |
| 2 | 3005.94 | $^PQ_6$ | 9.35 | 3005.97 | −0.03 |
| 3 | 3015.29 | $^PQ_5$ | 9.22 | 3015.27 | +0.02 |
| 4 | 3024.51 | $^PQ_4$ | 9.24 | 3024.51 | 0.00 |
| 5 | 3033.75 | $^PQ_3$ | 9.05 | 3033.69 | +0.06 |
| 6 | 3042.80 | $^PQ_2$ | 9.02 | 3042.80 | 0.00 |
| 7 | 3051.82 | $^PQ_1$ | 9.00 | 3051.84 | −0.02 |
| 8 | 3060.82 | $^RQ_0$ | 8.89 | 3060.82 | 0.00 |
| 9 | 3069.71 | $^RQ_1$ | 8.82 | 3069.73 | −0.02 |
| 10 | 3078.53 | $^RQ_2$ | 8.87 | 3078.58 | −0.05 |
| 11 | 3087.40 | $^RQ_3$ | 8.67 | 3087.37 | +0.03 |
| 12 | 3096.07 | $^RQ_4$ | 8.59 | 3096.08 | −0.01 |
| 13 | 3104.66 | $^RQ_5$ | 8.65 | 3104.73 | −0.07 |
| 14 | 3113.31 | $^RQ_6$ | 8.61 | 3113.32 | −0.01 |
| 15 | 3121.92 | $^RQ_7$ | 8.48 | 3121.84 | +0.08 |
| 16 | 3130.40 | $^RQ_8$ | 8.31 | 3130.30 | +0.10 |
| 17 | 3138.71 | $^RQ_9$ | 8.27 | 3138.69 | +0.02 |
| 18 | 3146.98 | $^RQ_{10}$ | 8.23 | 3147.01 | −0.03 |
| 19 | 3155.21 | $^RQ_{11}$ | 8.00 | 3155.27 | −0.06 |
| 20 | 3163.21* | $^RQ_{12}$ | 8.23 | 3163.46 | −0.25 |
| 21 | 3171.44* | $^RQ_{13}$ | | 3171.59 | −0.15 |

to $^RQ_3$, because this choice of $K$-numbering seems most reasonable according to the three criteria mentioned above. Three coefficients of Eq. 1 were thus estimated from the data for the bands $^RQ_3$—$^RQ_9$ for convenience.

TABLE V. FINE STRUCTURE OF THE $\nu_5$ BAND OF $CH_3Br$

| No. | $\nu_{obs}$ | Assignment | $\Delta\nu_K$ | $\nu_{calcd}$ | $\nu_{obs}-\nu_{calcd}$ |
|---|---|---|---|---|---|
| 1 | 1338.56 | $^PQ_9$ | 12.73 | 1338.38 | +0.16 |
| 2 | 1351.29 | $^PQ_8$ | 12.58 | 1351.21 | +0.08 |
| 3 | 1363.87 | $^PQ_7$ | 12.62 | 1363.94 | −0.07 |
| 4 | 1376.49 | $^PQ_6$ | 12.44 | 1376.57 | −0.08 |
| 5 | 1388.93 | $^PQ_5$ | 12.55 | 1389.11 | −0.18 |
| 6 | 1401.48 | $^PQ_4$ | 12.40 | 1401.55 | −0.07 |
| 7 | 1413.88 | $^PQ_3$ | 12.19 | 1413.89 | −0.01 |
| 8 | 1426.07 | $^PQ_2$ | 12.16 | 1426.13 | −0.06 |
| 9 | 1438.23 | $^PQ_1$ | 11.99 | 1438.28 | −0.05 |
| 10 | 1450.22 | $^RQ_0$ | 12.15 | 1450.33 | −0.11 |
| 11 | 1462.37 | $^RQ_1$ | 11.91 | 1462.28 | +0.09 |
| 12 | 1474.28 | $^RQ_2$ | 11.82 | 1474.14 | +0.14 |
| 13 | 1486.10 | $^RQ_3$ | 11.50 | 1485.90 | +0.20 |
| 14 | 1497.60 | $^RQ_4$ | 11.64 | 1497.57 | +0.03 |
| 15 | 1509.24 | $^RQ_5$ | 11.30 | 1509.13 | +0.11 |
| 16 | 1520.54 | $^RQ_6$ | 11.43 | 1520.60 | −0.06 |
| 17 | 1531.97 | $^RQ_7$ | 11.16 | 1531.97 | 0.00 |
| 18 | 1543.13 | $^RQ_8$ | 11.26 | 1543.25 | −0.12 |
| 19 | 1554.39 | $^RQ_9$ | 10.86 | 1554.43 | −0.04 |
| 20 | 1565.25* | $^RQ_{10}$ | 11.40 | 1565.50 | −0.28 |
| 21 | 1576.65* | $^RQ_{11}$ | 10.23 | 1576.49 | +0.16 |
| 22 | 1586.88* | $^RQ_{12}$ | | 1587.38 | +0.50 |

TABLE VI. FINE STRUCTURE OF THE $\nu_6$ BAND OF $CH_3Br$

| No. | $\nu_{obs}$ | Assignment | $\Delta\nu_K$ | $\nu_{calcd}$ | $\nu_{obs}-\nu_{calcd}$ |
|---|---|---|---|---|---|
| 1 | 871.86* | $^PQ_{12}$ | 6.68 | 871.72 | +0.14 |
| 2 | 878.54 | $^PQ_{11}$ | 6.90 | 878.54 | 0.00 |
| 3 | 885.44 | $^PQ_{10}$ | 6.89 | 885.42 | +0.02 |
| 4 | 892.33 | $^PQ_9$ | 7.07 | 892.34 | −0.01 |
| 5 | 899.40 | $^PQ_8$ | 6.98 | 899.33 | +0.07 |
| 6 | 906.38 | $^PQ_7$ | 7.01 | 906.37 | +0.01 |
| 7 | 913.39 | $^PQ_6$ | 7.12 | 913.46 | −0.07 |
| 8 | 920.51 | $^PQ_5$ | 7.31 | 920.61 | −0.10 |
| 9 | 927.82 | $^PQ_4$ | 7.25 | 927.81 | +0.01 |
| 10 | 935.07 | $^PQ_3$ | 7.36 | 935.07 | 0.00 |
| 11 | 942.43 | $^PQ_2$ | 7.30 | 942.38 | +0.05 |
| 12 | 949.73 | $^PQ_1$ | 7.42 | 949.74 | −0.01 |
| 13 | 957.15 | $^RQ_0$ | 7.49 | 957.17 | −0.02 |
| 14 | 964.64 | $^RQ_1$ | 7.52 | 964.64 | 0.00 |
| 15 | 972.16 | $^RQ_2$ | 7.61 | 972.17 | −0.01 |
| 16 | 979.77 | $^RQ_3$ | 7.62 | 979.76 | +0.01 |
| 17 | 987.39 | $^RQ_4$ | 7.75 | 987.40 | −0.01 |
| 18 | 995.14 | $^RQ_5$ | 7.72 | 995.09 | +0.05 |
| 19 | 1002.86 | $^RQ_6$ | 7.78 | 1002.84 | +0.02 |
| 20 | 1010.64 | $^RQ_7$ | 7.86 | 1010.64 | 0.00 |
| 21 | 1018.50 | $^RQ_8$ | 7.96 | 1018.50 | 0.00 |
| 22 | 1026.46 | $^RQ_9$ | 7.90 | 1026.42 | +0.04 |
| 23 | 1034.36 | $^RQ_{10}$ | 7.95 | 1034.38 | −0.02 |
| 24 | 1042.31* | $^RQ_{11}$ | 8.00 | 1042.41 | −0.10 |
| 25 | 1050.31* | $^RQ_{12}$ | | 1050.40 | −0.09 |

Table VII. Fine structure of the $\nu_4$ band of $CH_3I$

| No. | $\nu_{obs}$ | Assignment | $\Delta\nu_K$ | $\nu_{calcd}$ | $\nu_{obs}-\nu_{calcd}$ |
|---|---|---|---|---|---|
| 1 | 2999.66 | $^PQ_7$ | 9.40 | 2999.50 | +0.16 |
| 2 | 3009.06 | $^PQ_6$ | 9.38 | 3009.04 | +0.02 |
| 3 | 3018.44 | $^PQ_5$ | 9.36 | 3018.51 | −0.07 |
| 4 | 3027.80 | $^PQ_4$ | 9.43 | 3027.90 | −0.10 |
| 5 | 3037.23 | $^PQ_3$ | 9.25 | 3037.23 | 0.00 |
| 6 | 3046.48 | $^PQ_2$ | 9.09 | 3046.49 | −0.01 |
| 7 | 3055.57 | $^PQ_1$ | 9.19 | 3055.68 | −0.11 |
| 8 | 3064.76 | $^RQ_0$ | 9.05 | 3064.81 | −0.05 |
| 9 | 3073.81 | $^RQ_1$ | 9.06 | 3073.86 | −0.05 |
| 10 | 3082.87 | $^RQ_2$ | 8.99 | 3082.84 | +0.03 |
| 11 | 3091.86 | $^RQ_3$ | 8.79 | 3091.75 | +0.11 |
| 12 | 3100.65 | $^RQ_4$ | 8.71 | 3100.59 | +0.06 |
| 13 | 3109.36 | $^RQ_5$ | 8.81 | 3109.37 | −0.01 |
| 14 | 3118.17 | $^RQ_6$ | 8.55 | 3118.07 | +0.10 |
| 15 | 3126.72 | $^RQ_7$ | 8.60 | 3126.71 | +0.01 |
| 16 | 3135.32 | $^RQ_8$ | 8.48 | 3135.27 | +0.05 |
| 17 | 3143.80 | $^RQ_9$ | 8.39 | 3143.77 | +0.03 |
| 18 | 3152.19 | $^RQ_{10}$ | 8.25 | 3152.20 | −0.01 |
| 19 | 3160.44 | $^RQ_{11}$ | 8.40 | 3160.56 | −0.12 |
| 20 | 3168.84 | $^RQ_{12}$ | | 3168.84 | 0.00 |

Table VIII. Fine structure of the $\nu_5$ band of $CH_3I$

| No. | $\nu_{obs}$ | Assignment | $\Delta\nu_K$ | $\nu_{calcd}$ | $\nu_{obs}-\nu_{calcd}$ |
|---|---|---|---|---|---|
| 1 | (1299.77) | | | | |
| 2 | (1311.95) | | | | |
| 3 | (1323.96) | | | | |
| 4 | (1335.42) | | | | |
| 5 | (1346.50) | | | | |
| 6 | (1356.97) | | | | |
| 7 | (1366.98) | | | | |
| 8 | (1376.12) | | | | |
| 9 | 1377.73* | $^PQ_6$ | 10.32 | | |
| 10 | (1384.68) | | | | |
| 11 | 1388.05* | $^PQ_5$ | 11.01 | | |
| 12 | (1393.07) | | | | |
| 13 | 1399.06* | $^PQ_4$ | 11.29 | | |
| 14 | (1401.55) | | | | |
| 15 | 1410.35* | $^PQ_3$ | 11.64 | | |
| 16 | 1421.99* | $^PQ_2$ | 11.83 | | |
| 17 | 1433.82* | $^PQ_1$ | 11.63 | | |
| 18 | 1445.45* | $^RQ_0$ | 12.16 | | |
| 19 | 1457.61* | $^RQ_1$ | 11.46 | | |
| 20 | 1469.07 | $^RQ_2$ | 11.94 | 1469.09 | −0.02 |
| 21 | 1481.01 | $^RQ_3$ | 11.84 | 1480.99 | +0.02 |
| 22 | 1492.85 | $^RQ_4$ | 11.58 | 1492.78 | +0.07 |
| 23 | 1504.43 | $^RQ_5$ | 11.58 | 1504.47 | −0.04 |
| 24 | 1516.01 | $^RQ_6$ | 11.46 | 1516.05 | −0.06 |
| 25 | 1527.47 | $^RQ_7$ | 11.49 | 1527.53 | −0.06 |
| 26 | 1538.96 | $^RQ_8$ | 11.22 | 1539.00 | −0.04 |
| 27 | 1550.18 | $^RQ_9$ | 11.15 | 1550.16 | +0.02 |
| 28 | 1561.33 | $^RQ_{10}$ | 11.07 | 1561.32 | +0.01 |
| 29 | 1572.40 | $^RQ_{11}$ | 10.90 | 1572.38 | +0.02 |
| 30 | 1583.30 | $^RQ_{12}$ | | 1583.32 | −0.02 |

( ): Peaks of the $(\nu_3+\nu_6)$ band.

Table IX. Fine structure of the $\nu_6$ band of $CH_3I$

| No. | $\nu_{obs}$ | Assignment | $\Delta\nu_K$ | $\nu_{calcd}$ | $\nu_{obs}-\nu_{calcd}$ |
|---|---|---|---|---|---|
| 1 | 825.83* | $^PQ_8$ | 7.29 | 825.91 | −0.08 |
| 2 | 833.12 | $^PQ_7$ | 7.27 | 833.12 | 0.00 |
| 3 | 840.39 | $^PQ_6$ | 7.35 | 840.39 | 0.00 |
| 4 | 847.74 | $^PQ_5$ | 7.39 | 847.72 | +0.02 |
| 5 | 855.13 | $^PQ_4$ | 7.43 | 855.13 | 0.00 |
| 6 | 862.56 | $^PQ_3$ | 7.57 | 862.60 | −0.04 |
| 7 | 870.13 | $^PQ_2$ | 7.61 | 870.14 | −0.01 |
| 8 | 877.74 | $^PQ_1$ | 7.69 | 877.75 | −0.01 |
| 9 | 885.43 | $^RQ_0$ | 7.73 | 885.42 | +0.01 |
| 10 | 893.16 | $^RQ_1$ | 7.83 | 893.16 | 0.00 |
| 11 | 900.99 | $^RQ_2$ | 7.83 | 900.97 | +0.02 |
| 12 | 908.82 | $^RQ_3$ | 7.95 | 908.84 | −0.02 |
| 13 | 916.77 | $^RQ_4$ | 8.06 | 916.78 | −0.01 |
| 14 | 924.83 | $^RQ_5$ | 8.04 | 924.79 | +0.04 |
| 15 | 932.87 | $^RQ_6$ | 8.15 | 932.87 | 0.00 |
| 16 | 941.02 | $^RQ_7$ | 8.18 | 941.01 | +0.01 |
| 17 | 949.20 | $^RQ_8$ | 8.28 | 949.22 | −0.02 |
| 18 | 957.48 | $^RQ_9$ | 8.05 | 957.49 | −0.01 |
| 19 | 965.53* | $^RQ_{10}$ | | 965.84 | −0.31 |

Table X. Fine structure of the $\nu_4$ band of $CD_3Cl$

| No. | $\nu_{obs}$ | Assignment | $\Delta\nu_K$ | $\nu_{calcd}$ | $\nu_{obs}-\nu_{calcd}$ |
|---|---|---|---|---|---|
| 1 | 2225.15 | $^PQ_{16}$ | 3.89 | 2225.11 | +0.04 |
| 2 | 2229.04 | $^PQ_{15}$ | 3.86 | 2229.03 | +0.01 |
| 3 | 2232.90 | $^PQ_{14}$ | 3.87 | 2232.92 | −0.02 |
| 4 | 2236.77 | $^PQ_{13}$ | 3.82 | 2236.78 | −0.01 |
| 5 | 2240.59 | $^PQ_{12}$ | 3.84 | 2240.62 | −0.03 |
| 6 | 2244.43 | $^PQ_{11}$ | 3.79 | 2244.43 | 0.00 |
| 7 | 2248.22 | $^PQ_{10}$ | 3.77 | 2248.22 | 0.00 |
| 8 | 2251.99 | $^PQ_9$ | 3.76 | 2251.99 | 0.00 |
| 9 | 2255.75 | $^PQ_8$ | 3.68 | 2255.73 | +0.02 |
| 10 | 2259.43 | $^PQ_7$ | 3.69 | 2259.44 | −0.01 |
| 11 | 2263.12 | $^PQ_6$ | 3.65 | 2263.13 | −0.01 |
| 12 | 2266.77 | $^PQ_5$ | 3.65 | 2266.80 | −0.03 |
| 13 | 2270.42 | $^PQ_4$ | 3.64 | 2270.43 | −0.01 |
| 14 | 2274.06 | $^PQ_3$ | 3.59 | 2274.05 | +0.01 |
| 15 | 2277.65 | $^PQ_2$ | 3.57 | 2277.64 | +0.01 |
| 16 | 2281.22 | $^PQ_1$ | 3.52 | 2281.20 | +0.02 |
| 17 | 2284.74 | $^RQ_0$ | 3.53 | 2284.74 | 0.00 |
| 18 | 2288.27 | $^RQ_1$ | 3.52 | 2288.26 | +0.01 |
| 19 | 2291.79 | $^RQ_2$ | 3.42 | 2291.74 | +0.05 |
| 20 | 2295.21 | $^RQ_3$ | 3.41 | 2295.21 | 0.00 |
| 21 | 2298.62 | $^RQ_4$ | 3.45 | 2298.65 | −0.03 |
| 22 | 2302.07 | $^RQ_5$ | 3.37 | 2302.06 | +0.01 |
| 23 | 2305.44 | $^RQ_6$ | 3.37 | 2305.45 | −0.01 |
| 24 | 2308.81 | $^RQ_7$ | 3.33 | 2308.81 | 0.00 |
| 25 | 2312.14 | $^RQ_8$ | 3.23 | 2312.15 | −0.01 |
| 26 | 2315.37* | $^RQ_9$ | 3.25 | 2315.47 | −0.10 |
| 27 | 2318.62* | $^RQ_{10}$ | 3.32 | 2318.76 | −0.14 |
| 28 | 2321.94* | $^RQ_{11}$ | 3.17 | 2322.02 | −0.08 |
| 29 | 2325.11* | $^RQ_{12}$ | 3.30 | 2325.26 | −0.15 |
| 30 | 2328.41* | $^RQ_{13}$ | 3.22 | 2328.47 | −0.06 |
| 31 | 2331.63* | $^RQ_{14}$ | 2.87 | 2331.66 | −0.03 |
| 32 | 2334.50* | $^RQ_{15}$ | | 2334.82 | −0.32 |

TABLE XI. FINE STRUCTURE OF THE $\nu_5$ BAND OF $CD_3Cl$

| No. | $\nu_{obs}$ | Assignment | $\Delta\nu_K$ | $\nu_{calcd}$ | $\nu_{obs}-\nu_{calcd}$ |
|---|---|---|---|---|---|
| 1 | 1045.97* | $^PQ_3$ | 5.94 | 1045.30 | +0.67 |
| 2 | 1051.91* | $^PQ_2$ | 6.22 | 1051.63 | +0.28 |
| 3 | 1058.13* | $^PQ_1$ | 5.91 | 1057.91 | +0.22 |
| 4 | 1064.04* | $^RQ_0$ | 6.29 | 1064.15 | −0.11 |
| 5 | 1070.33 | $^RQ_1$ | 6.24 | 1070.35 | −0.02 |
| 6 | 1076.57 | $^RQ_2$ | 6.04 | 1076.51 | +0.06 |
| 7 | 1082.61 | $^RQ_3$ | 6.07 | 1082.63 | −0.02 |
| 8 | 1088.68 | $^RQ_4$ | 6.02 | 1088.70 | −0.02 |
| 9 | 1094.70 | $^RQ_5$ | 6.03 | 1094.74 | −0.04 |
| 10 | 1100.73 | $^RQ_6$ | 5.95 | 1100.73 | 0.00 |
| 11 | 1106.68 | $^RQ_7$ | 5.92 | 1106.68 | 0.00 |
| 12 | 1112.60 | $^RQ_8$ | 5.94 | 1112.59 | +0.01 |
| 13 | 1118.54 | $^RQ_9$ | 5.81 | 1118.46 | +0.08 |
| 14 | 1124.35 | $^RQ_{10}$ | 5.70 | 1124.29 | +0.06 |
| 15 | 1130.05 | $^RQ_{11}$ | 5.70 | 1130.08 | −0.03 |
| 16 | 1135.75 | $^RQ_{12}$ | 5.74 | 1135.82 | −0.07 |
| 17 | 1141.49 | $^RQ_{13}$ | 5.73 | 1141.52 | −0.03 |
| 18 | 1147.22 | $^RQ_{14}$ | 5.60 | 1147.19 | +0.03 |
| 19 | 1152.82 | $^RQ_{15}$ | 5.42 | 1152.81 | +0.01 |
| 20 | 1158.24* | $^RQ_{16}$ | | | |

TABLE XII. FINE STRUCTURE OF THE $\nu_6$ BAND OF $CD_3Cl$

| No. | $\nu_{obs}$ | Assignment | $\Delta\nu_K$ | $\nu_{calcd}$ | $\nu_{obs}-\nu_{calcd}$ |
|---|---|---|---|---|---|
| 1 | 736.19 | $^PQ_{10}$ | 3.21 | 736.19 | 0.00 |
| 2 | 739.40 | $^PQ_9$ | 3.17 | 739.38 | +0.02 |
| 3 | 742.57 | $^PQ_8$ | 3.26 | 742.58 | −0.01 |
| 4 | 745.83 | $^PQ_7$ | 3.22 | 745.81 | +0.02 |
| 5 | 749.05 | $^PQ_6$ | 3.19 | 749.05 | 0.00 |
| 6 | 752.24 | $^PQ_5$ | 3.32 | 752.31 | −0.07 |
| 7 | 755.55 | $^PQ_4$ | 3.38 | 755.60 | −0.05 |
| 8 | 758.93 | $^PQ_3$ | 3.37 | 758.90 | +0.03 |
| 9 | 762.30 | $^PQ_2$ | 3.28 | 762.22 | +0.08 |
| 10 | 765.58 | $^PQ_1$ | 3.41 | 765.57 | +0.01 |
| 11 | 768.99 | $^RQ_0$ | 3.32 | 768.93 | +0.06 |
| 12 | 772.31 | $^RQ_1$ | 3.38 | 772.31 | 0.00 |
| 13 | 775.69 | $^RQ_2$ | 3.40 | 775.72 | −0.03 |
| 14 | 779.09 | $^RQ_3$ | 3.48 | 779.14 | −0.05 |
| 15 | 782.57 | $^RQ_4$ | 3.48 | 782.58 | −0.01 |
| 16 | 786.05 | $^RQ_5$ | 3.44 | 786.04 | +0.01 |
| 17 | 789.49 | $^RQ_6$ | 3.55 | 789.52 | −0.03 |
| 18 | 793.04 | $^RQ_7$ | 3.52 | 793.03 | +0.01 |
| 19 | 796.56 | $^RQ_8$ | 3.51 | 796.55 | +0.01 |
| 20 | 800.07 | $^RQ_9$ | 3.59 | 800.09 | −0.02 |
| 21 | 803.66 | $^RQ_{10}$ | 3.77 | 803.65 | +0.01 |
| 22 | 807.43* | $^RQ_{11}$ | | 807.23 | +0.20 |

**(ii) The $\nu_5$ Band of $CH_3I$.**—In the region from 1300 to 1600 $cm^{-1}$, two series of absorbing peaks were observed. One series, which was assigned to the fundamental band $\nu_5$ covers the region from 1378 to 1585 $cm^{-1}$. The $\Delta\nu_K$'s for this series, shown in Fig. 6 as

TABLE XIII. FINE STRUCTURE OF THE $\nu_4$ BAND OF $CD_3Br$

| No. | $\nu_{obs}$ | Assignment | $\Delta\nu_K$ | $\nu_{calcd}$ | $\nu_{obs}-\nu_{calcd}$ |
|---|---|---|---|---|---|
| 1 | 2239.17* | $^PQ_{15}$ | 4.22 | 2239.23 | +0.06 |
| 2 | 2243.39 | $^PQ_{14}$ | 4.04 | 2243.32 | +0.07 |
| 3 | 2247.43 | $^PQ_{13}$ | 4.01 | 2247.38 | +0.05 |
| 4 | 2251.44 | $^PQ_{12}$ | 4.00 | 2251.42 | +0.02 |
| 5 | 2255.44 | $^PQ_{11}$ | 3.95 | 2255.43 | +0.01 |
| 6 | 2259.39 | $^PQ_{10}$ | 3.95 | 2259.41 | −0.02 |
| 7 | 2263.34 | $^PQ_9$ | 3.89 | 2263.37 | −0.03 |
| 8 | 2267.23 | $^PQ_8$ | 3.94 | 2267.30 | −0.07 |
| 9 | 2271.17 | $^PQ_7$ | 3.89 | 2271.21 | −0.04 |
| 10 | 2275.06 | $^PQ_6$ | 3.87 | 2275.09 | −0.03 |
| 11 | 2278.93 | $^PQ_5$ | 3.83 | 2278.94 | −0.01 |
| 12 | 2282.76 | $^PQ_4$ | 3.78 | 2282.77 | −0.01 |
| 13 | 2286.54 | $^PQ_3$ | 3.76 | 2286.57 | −0.03 |
| 14 | 2290.30 | $^PQ_2$ | 3.74 | 2290.34 | −0.04 |
| 15 | 2294.04 | $^PQ_1$ | 3.76 | 2294.09 | −0.05 |
| 16 | 2297.80 | $^RQ_0$ | 3.74 | 2297.82 | −0.02 |
| 17 | 2301.54 | $^RQ_1$ | 3.69 | 2301.52 | +0.02 |
| 18 | 2305.23 | $^RQ_2$ | 3.66 | 2305.10 | +0.04 |
| 19 | 2308.89 | $^RQ_3$ | 3.62 | 2308.83 | +0.06 |
| 20 | 2312.51 | $^RQ_4$ | 3.56 | 2312.45 | +0.06 |
| 21 | 2316.07 | $^RQ_5$ | 3.55 | 2316.05 | +0.02 |
| 22 | 2319.62 | $^RQ_6$ | 3.59 | 2319.61 | +0.01 |
| 23 | 2323.21 | $^RQ_7$ | 3.53 | 2323.15 | +0.06 |
| 24 | 2326.74 | $^RQ_8$ | 3.45 | 2326.67 | +0.07 |
| 25 | 2330.19 | $^RQ_9$ | 3.46 | 2330.16 | +0.03 |
| 26 | 2333.65 | $^RQ_{10}$ | 3.37 | 2333.62 | +0.03 |
| 27 | 2337.02 | $^RQ_{11}$ | 3.38 | 2337.06 | −0.04 |
| 28 | 2340.40 | $^RQ_{12}$ | 3.39 | 2340.47 | −0.07 |
| 29 | 2343.79 | $^RQ_{13}$ | | 2343.86 | −0.07 |

TABLE XIV. FINE STRUCTURE OF THE $\nu_5$ BAND OF $CD_3Br$

| No. | $\nu_{obs}$ | Assignment | $\Delta\nu_K$ | $\nu_{calcd}$ | $\nu_{obs}-\nu_{calcd}$ |
|---|---|---|---|---|---|
| 1 | 1015.24 | $^PQ_7$ | 6.44 | 1015.17 | +0.07 |
| 2 | 1021.68 | $^PQ_6$ | 6.40 | 1021.59 | +0.09 |
| 3 | 1028.08 | $^PQ_5$ | 6.32 | 1028.03 | +0.05 |
| 4 | 1034.40 | $^PQ_4$ | 6.37 | 1034.45 | −0.05 |
| 5 | 1040.77 | $^PQ_3$ | 6.36 | 1040.83 | −0.06 |
| 6 | 1047.13 | $^PQ_2$ | 6.31 | 1047.18 | −0.05 |
| 7 | 1053.44 | $^PQ_1$ | 6.10 | 1053.50 | −0.06 |
| 8 | 1059.54* | $^RQ_0$ | 6.46 | 1059.79 | −0.25 |
| 9 | 1066.00* | $^RQ_1$ | 6.29 | 1066.04 | −0.04 |
| 10 | 1072.29 | $^RQ_2$ | 6.22 | 1072.27 | +0.02 |
| 11 | 1078.51 | $^RQ_3$ | 6.13 | 1078.47 | +0.04 |
| 12 | 1084.64 | $^RQ_4$ | 6.14 | 1084.63 | +0.01 |
| 13 | 1090.78 | $^RQ_5$ | 6.10 | 1090.77 | +0.01 |
| 14 | 1096.88 | $^RQ_6$ | 6.05 | 1096.87 | +0.01 |
| 15 | 1102.93 | $^RQ_7$ | 6.00 | 1102.94 | −0.01 |
| 16 | 1108.93 | $^RQ_8$ | 6.02 | 1108.98 | −0.05 |
| 17 | 1114.95 | $^RQ_9$ | 5.99 | 1114.99 | −0.04 |
| 18 | 1120.94 | $^RQ_{10}$ | 5.96 | 1120.97 | −0.03 |
| 19 | 1126.90 | $^RQ_{11}$ | 5.95 | 1126.92 | −0.02 |
| 20 | 1132.85 | $^RQ_{12}$ | 5.79 | 1132.83 | +0.02 |
| 21 | 1138.64* | $^RQ_{13}$ | | 1138.72 | −0.08 |

Table XV. Fine structure of the $\nu_6$ band of $CD_3Br$

| No. | $\nu_{obs}$ | Assignment | $\Delta\nu_K$ | $\nu_{calcd}$ | $\nu_{obs}-\nu_{calcd}$ |
|---|---|---|---|---|---|
| 1 | 671.40* | $^PQ_{12}$ | 3.32 | 671.57 | −0.17 |
| 2 | 674.72* | $^PQ_{11}$ | 3.75 | 675.03 | −0.31 |
| 3 | 678.47* | $^PQ_{10}$ | 3.62 | 678.51 | −0.04 |
| 4 | 682.09 | $^PQ_9$ | 3.49 | 682.02 | +0.07 |
| 5 | 685.58 | $^PQ_8$ | 3.49 | 685.55 | +0.03 |
| 6 | 689.07 | $^PQ_7$ | 3.60 | 689.10 | −0.03 |
| 7 | 692.67 | $^PQ_6$ | 3.56 | 692.67 | 0.00 |
| 8 | 696.23 | $^PQ_5$ | 3.61 | 696.27 | −0.04 |
| 9 | 699.84 | $^PQ_4$ | 3.65 | 699.88 | −0.04 |
| 10 | 703.49 | $^PQ_3$ | 3.71 | 703.53 | −0.04 |
| 11 | 707.20 | $^PQ_2$ | 3.66 | 707.19 | +0.01 |
| 12 | 710.86 | $^PQ_1$ | 3.73 | 710.88 | −0.02 |
| 13 | 714.59 | $^RQ_0$ | 3.71 | 714.59 | 0.00 |
| 14 | 718.30 | $^RQ_1$ | 3.78 | 718.32 | −0.02 |
| 15 | 722.08 | $^RQ_2$ | 3.77 | 722.08 | 0.00 |
| 16 | 725.85 | $^RQ_3$ | 3.78 | 725.85 | 0.00 |
| 17 | 729.63 | $^RQ_4$ | 3.88 | 729.65 | −0.02 |
| 18 | 733.51 | $^RQ_5$ | 3.83 | 733.48 | +0.03 |
| 19 | 737.34 | $^RQ_6$ | 3.90 | 737.33 | +0.01 |
| 20 | 741.24 | $^RQ_7$ | 3.89 | 741.19 | +0.05 |
| 21 | 745.13 | $^RQ_8$ | 3.88 | 745.09 | +0.04 |
| 22 | 749.01 | $^RQ_9$ | 3.94 | 749.00 | +0.01 |
| 23 | 752.95 | $^RQ_{10}$ | 3.95 | 752.94 | +0.01 |
| 24 | 756.90 | $^RQ_{11}$ | 3.94 | 756.90 | 0.00 |
| 25 | 760.84 | $^RQ_{12}$ | 4.02 | 760.88 | −0.04 |
| 26 | 764.86 | $^RQ_{13}$ | | 764.89 | −0.03 |

Table XVI. Fine structure of the $\nu_4$ band of $CD_3I$

| No. | $\nu_{obs}$ | Assignment | $\Delta\nu_K$ | $\nu_{calcd}$ | $\nu_{obs}-\nu_{calcd}$ |
|---|---|---|---|---|---|
| 1 | 2264.55 | $^PQ_9$ | 4.02 | 2264.52 | +0.03 |
| 2 | 2268.57 | $^PQ_8$ | 3.98 | 2268.57 | 0.00 |
| 3 | 2272.55 | $^PQ_7$ | 4.05 | 2272.61 | −0.06 |
| 4 | 2276.60 | $^PQ_6$ | 4.01 | 2276.61 | −0.01 |
| 5 | 2280.61 | $^PQ_5$ | 3.96 | 2280.59 | +0.02 |
| 6 | 2284.57 | $^PQ_4$ | 3.91 | 2284.54 | +0.03 |
| 7 | 2288.48 | $^PQ_3$ | 3.83 | 2288.46 | +0.02 |
| 8 | 2292.31 | $^PQ_2$ | 3.91 | 2292.35 | −0.04 |
| 9 | 2296.22 | $^PQ_1$ | 3.80 | 2296.21 | +0.01 |
| 10 | 2300.02 | $^RQ_0$ | 3.85 | 2300.05 | −0.03 |
| 11 | 2303.87 | $^RQ_1$ | 3.85 | 2303.86 | +0.01 |
| 12 | 2307.72* | $^RQ_2$ | 3.84 | 2307.64 | +0.08 |
| 13 | 2311.56* | $^RQ_3$ | | 2311.39 | +0.17 |

plotted against $K$, show a remarkable irregularity; i.e., the tangent of the $\Delta\nu_K$'s for the half of the peaks with larger wave numbers is different in value and opposite in sign from that for the other half of the peaks with smaller wave numbers.

Another series which appears in the region 1300—1400 $cm^{-1}$ is slightly weaker in intensity than the previous one. The strongest peak is at 1356.97 $cm^{-1}$. A plot of $\Delta\nu_K$ to $K$ gives a straight line with a large tangent, as is shown in Fig. 6. Three peaks in this series (1346.50, 1356.97 and 1366.98 $cm^{-1}$) coincide with those reported by Bennett and Meyer,[2] Mador and Quinn[13] and Cleveland et al.[14] They did not discriminate these three peaks from those of

Table XVII. Fine structure of the $\nu_5$ band of $CD_3I$

| No. | $\nu_{obs}$ | Assignment | $\Delta\nu_K$ | $\nu_{calcd}$ | $\nu_{obs}-\nu_{calcd}$ |
|---|---|---|---|---|---|
| 1 | 975.14* | $^PQ_{12}$ | 6.48 | 974.86 | +0.28 |
| 2 | 981.62* | $^PQ_{11}$ | 6.80 | 981.60 | +0.02 |
| 3 | 988.42* | $^PQ_{10}$ | 6.28 | 988.30 | +0.12 |
| 4 | 994.70* | $^PQ_9$ | 6.97 | 994.97 | −0.27 |
| 5 | (996.94) | ($Q$ of $2\nu_3$) | | | |
| 6 | 1001.67 | $^PQ_8$ | 6.57 | 1001.61 | +0.06 |
| 7 | 1008.24 | $^PQ_7$ | 6.56 | 1008.21 | +0.03 |
| 8 | 1014.80 | $^PQ_6$ | 6.49 | 1014.79 | +0.01 |
| 9 | 1021.29 | $^PQ_5$ | 6.54 | 1021.34 | −0.05 |
| 10 | 1027.83 | $^PQ_4$ | 6.49 | 1027.85 | −0.02 |
| 11 | 1034.32 | $^PQ_3$ | 6.42 | 1034.33 | −0.01 |
| 12 | 1040.74 | $^PQ_2$ | 6.45 | 1040.78 | −0.04 |
| 13 | 1047.19 | $^PQ_1$ | 6.28 | 1047.20 | −0.01 |
| 14 | 1053.47 | $^RQ_0$ | 6.48 | 1053.59 | −0.12 |
| 15 | 1059.95 | $^RQ_1$ | 6.31 | 1059.95 | 0.00 |
| 16 | 1066.26 | $^RQ_2$ | 6.39 | 1066.28 | −0.02 |
| 17 | 1072.65 | $^RQ_3$ | 6.25 | 1072.57 | +0.08 |
| 18 | 1078.90 | $^RQ_4$ | 6.16 | 1078.83 | +0.07 |
| 19 | 1085.06 | $^RQ_5$ | 6.24 | 1085.07 | −0.01 |
| 20 | 1091.30 | $^RQ_6$ | 6.24 | 1091.27 | +0.03 |
| 21 | 1097.54 | $^RQ_7$ | 6.06 | 1097.44 | +0.10 |
| 22 | 1103.60 | $^RQ_8$ | 6.03 | 1103.58 | +0.02 |
| 23 | 1109.63 | $^RQ_9$ | 6.10 | 1109.68 | −0.05 |
| 24 | 1115.73 | $^RQ_{10}$ | 6.08 | 1115.76 | −0.03 |
| 25 | 1121.81 | $^RQ_{11}$ | 5.97 | 1121.80 | +0.01 |
| 26 | 1127.78 | $^RQ_{12}$ | 5.73 | 1127.82 | −0.04 |
| 27 | 1133.51* | $^RQ_{13}$ | 6.00 | 1133.80 | −0.29 |
| 28 | 1139.51* | $^RQ_{14}$ | 6.04 | 1139.75 | −0.24 |
| 29 | 1145.55* | $^RQ_{15}$ | | 1145.67 | −0.12 |

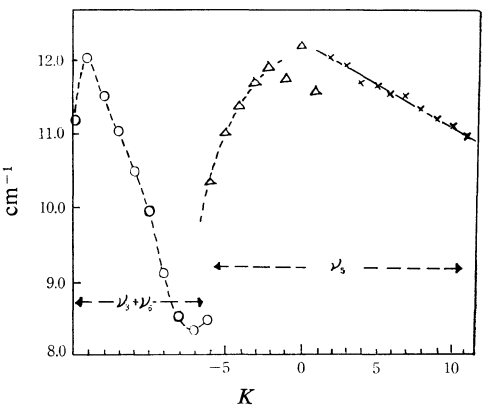



Fig. 6. $\Delta\nu_K=(Q_{K+1}-Q_K)$ : $CH_3I$ : $\nu_5$, $\nu_3+\nu_6$.
○, △ Perturbed peaks
× Less perturbed peaks

TABLE XVIII. FINE STRUCTURE OF THE $\nu_6$ BAND OF $CD_3I$

| No. | $\nu_{obs}$ | Assignment | $\Delta\nu_K$ | $\nu_{calcd}$ | $\nu_{obs}-\nu_{calcd}$ |
|---|---|---|---|---|---|
| 1 | 616.24* | $^PQ_{11}$ | 3.76 | 616.45 | −0.21 |
| 2 | 620.00* | $^PQ_{10}$ | 3.68 | 620.05 | −0.05 |
| 3 | 623.68 | $^PQ_9$ | 3.65 | 623.67 | +0.01 |
| 4 | 627.33 | $^PQ_8$ | 3.70 | 627.32 | +0.01 |
| 5 | 631.03 | $^PQ_7$ | 3.67 | 631.00 | −0.03 |
| 6 | 634.70 | $^PQ_6$ | 3.73 | 634.71 | −0.01 |
| 7 | 638.43 | $^PQ_5$ | 3.74 | 638.44 | +0.01 |
| 8 | 642.17 | $^PQ_4$ | 3.80 | 642.19 | −0.02 |
| 9 | 645.97 | $^PQ_3$ | 3.79 | 645.97 | 0.00 |
| 10 | 649.76 | $^PQ_2$ | 3.85 | 649.78 | −0.02 |
| 11 | 653.61 | $^PQ_1$ | 3.87 | 653.62 | −0.01 |
| 12 | 657.48 | $^RQ_0$ | 3.87 | 657.48 | 0.00 |
| 13 | 661.35 | $^RQ_1$ | 3.98 | 661.37 | −0.02 |
| 14 | 665.33 | $^RQ_2$ | 3.90 | 665.29 | +0.04 |
| 15 | 669.23 | $^RQ_3$ | 3.98 | 669.23 | 0.00 |
| 16 | 673.21 | $^RQ_4$ | 3.99 | 673.19 | +0.02 |
| 17 | 677.20 | $^RQ_5$ | 3.97 | 677.19 | +0.01 |
| 18 | 681.17 | $^RQ_6$ | 4.12 | 681.21 | −0.04 |
| 19 | 685.29 | $^RQ_7$ | 4.02 | 685.25 | +0.04 |
| 20 | 689.31 | $^RQ_8$ | 4.12 | 689.32 | −0.01 |
| 21 | 693.43 | $^RQ_9$ | 4.13 | 693.42 | +0.01 |
| 22 | 697.56 | $^RQ_{10}$ | 4.15 | 697.55 | +0.01 |
| 23 | 701.71 | $^RQ_{11}$ | 4.14 | 701.70 | +0.01 |
| 24 | 705.85* | $^RQ_{12}$ | 4.08 | 705.88 | −0.03 |
| 25 | 709.93* | $^RQ_{13}$ | 4.13 | 710.08 | −0.15 |
| 26 | 714.06* | $^RQ_{14}$ | 4.43 | 714.31 | −0.25 |
| 27 | 718.49* | $^RQ_{15}$ | 3.82 | 718.57 | −0.08 |
| 28 | 722.31* | $^RQ_{16}$ | | 722.85 | −0.54 |

$\nu_5$ and treated all peaks as members of $\nu_5$. Lageman and Nielsen[8] also observed the $\nu_5$ band of $CH_3I$, but they did not extend the region of research beyond 1380 $cm^{-1}$. This series of subbands, first observed in the present study, should perhaps be assigned to a binary combination band, $\nu_3+\nu_6$ ($E$). Many other experimental results suggest that the frequency of methyl deformation is in the region from 1440 to 1460 $cm^{-1}$, and the parallel nature of the methyl halide molecules indicates that the band origin of the $\nu_5$ of $CH_3I$ is at about 1435 —1440 $cm^{-1}$, while the observed values for the fundamental $\nu_3$ and $\nu_6$ of $CH_3I$ are 532.8 and 883.0 $cm^{-1}$ respectively. Consequently, a Fermi resonance is expected between the two vibrational states $\nu_5$ and $\nu_3+\nu_6$. This offers a reasonable explanation for the rather strong absorption intensity of the $\nu_3+\nu_6$ combination band. This type of Fermi resonance is expected, however, only in the case of $CH_3I$, because, for the other molecules, the separations $\delta=\nu_5-(\nu_3+\nu_6)$ are too large for any appreciable resonance to take place.

There is as yet no satisfactorily rigorous explanation for the anomaly of the rotational fine structures of these bands in terms of the rotational resonance; hence, only half the members of the subbands, $^RQ_2$—$^RQ_{12}$, were used to estimate the coefficients of Eq. 1 for the $\nu_5$ fundamental band. The values thus obtained are not precise. It is, nevertheless, likely that they do not differ very much from the values expected on the basis of the parallelism of six species of methyl halides.

**(iii) The Determination of $^RQ_0$ of $\nu_5$.**—All the $\nu_5$ fundamental bands of the molecules studied were found to be more or less disturbed, so the determinations of $K$ numbers for the observed peaks were difficult. The first unfavorable situation lies in the fact that the centers of the $\nu_5$ and of the $\nu_2$ ($CH_3$ or $CD_3$ sym. deform.) bands lie close together. As the absorption range of the $\nu_5$ band usually spreads over 180—250 $cm^{-1}$ because of the wide separations of the $Q$ branches, a part of the $^PQ_K$ subbands are more or less overlapped with the strong $R$ branch of the $\nu_2$ band and can, at best, scarcely be observed. This situation occurs most severely in the case of $CD_3I$, where only three subbands of $^PQ_K$ were observed. This is the main reason why the number of the observed peaks is smaller for the $\nu_5$ than for other bands. Secondly, the experimental results show that the $^RQ_0$ lines of $\nu_5$ for $CH_3Cl$, $CH_3I$, $CD_3Cl$, $CD_3Br$ and $CD_3I$ are narrower and weaker than expected and that those for $CD_3Br$ and $CD_3I$ are shifted slightly to a longer wavelength side from the expected positions. The reason for this anomaly has not yet been clarified.

Thirdly the shorter wavelength side of the $\nu_5$ band for the $CH_3X$ molecules more or less overlaps with the absorption of water vapor in the air. The overlapping region is the widest in the case of $CH_3Cl$ and the narrowest in $CH_3I$.

**(iv) The $\nu_5$ and $2\nu_3$ Band of $CD_3I$.**—A weak line with its peak at 996.9 $cm^{-1}$ was observed and assigned to the $Q$ branch of $2\nu_3$. As the $\nu_5$ state has the E symmetry and the $2\nu_3$ state, the A symmetry, no coupling is to be expected between the vibrational energy levels of $\nu_5$ and $2\nu_3$. The observed frequencies and the intensities of the neighboring four subbands which belong to $\nu_5$ are, however, perturbed in this region, perhaps through the second-order rotational resonance, and so the data for them were omitted from the least-squares calculation.

**(v) A Summary of the Observed Data.**—Taking into account the irregularities mentioned above, the coefficients in Eq. 1 were calculated by the least-squares method by using the precisely-determined wave numbers of the subbands. The results may be summarized as follows:

$CH_3Cl$, $\nu_4$; $\nu = 3046.20 \pm 8.405K - 0.0128K^2$ (2)

$\nu_5$; $\nu = 1459.89 \pm 12.022K - 0.0481K^2$ (3)

$\nu_6$; $\nu = 1019.82 \pm 6.942K + 0.0237K^2$ (4)

$CH_3Br$, $\nu_4$; $\nu = 3060.82 \pm 8.946K - 0.0327K^2$ (5)

$\nu_5$: $\nu = 1450.33 \pm 12.002K - 0.0485K^2$ (6)

$\nu_6$; $\nu = 957.16 \pm 7.448K + 0.0273K^2$ (7)

$CH_3I$, $\nu_4$; $\nu = 3064.80 \pm 9.086K - 0.0347K^2$ (8)

$\nu_5$; $\nu = 1444.98 \pm 12.162K - 0.0527K^2$ (9)

$\nu_6$; $\nu = 885.42 \pm 7.707K + 0.0335K^2$ (10)

$CD_3Cl$, $\nu_4$; $\nu = 2284.74 \pm 3.527K - 0.0125K^2$ (11)

$\nu_5$; $\nu = 1064.15 \pm 6.221K - 0.0207K^2$ (12)

$\nu_6$; $\nu = 768.93 \pm 3.373K + 0.0099K^2$ (13)

$CD_3Br$, $\nu_4$; $\nu = 2297.82 \pm 3.710K - 0.0130K^2$ (14)

$\nu_5$; $\nu = 1059.79 \pm 6.273K - 0.0155K^2$ (15)

$\nu_6$; $\nu = 714.59 \pm 3.721K + 0.0114K^2$ (16)

$CD_3I$, $\nu_4$; $\nu = 2300.05 \pm 3.822K - 0.0140K^2$ (17)

$\nu_5$; $\nu = 1053.59 \pm 6.373K - 0.0156K^2$ (18)

$\nu_6$; $\nu = 657.48 \pm 3.875K + 0.0131K^2$ (19)

The wave numbers for the subbands calculated by the use of these equations are shown in column 5 of Tables I—XVIII. The differences between the observed and the calculated wave numbers, shown in column 6, are negligibly small.

**(vi) The "Parallel Nature" of the Methyl Halide Molecules.**—It seems worthwhile to mention here the "parallel nature" of the three coefficients in Eqs. 2—19. As the compounds treated in the present study have a common structure, composed of a methyl group and a halogen atom, their physical constants may be expected to take analogous values with the systematic changes which originate from the nature of the substituents (H ⇄ D and X ⇄ Cl, Br, and I). Therefore, if a set of three arbitrary positions corresponding to the three halogen atoms (Cl, Br and I) is chosen on the abscissa, and if the coefficients are plotted on the ordinate, they make, as expected, parallel lines, depending on whether they are of $CH_3X$ or of $CD_3X$ type and on the vibrational modes shown in Figs. 7—9. The "parallel nature" of these molecules in the sense noted above was used throughout the present investigation to exclude the uncertainties and apparent irregularities of the data. However, serious deviations from the linear relation always occur for the coefficients of the $\nu_4$ band of $CH_3Cl$; this fact again suggests that the coefficients in Eq. 2 do not represent the unperturbed state of the $\nu_4$ band. If the parallel nature of the coefficients among the six species is extensively assumed, Eq. 2 might be replaced by Eq. 20

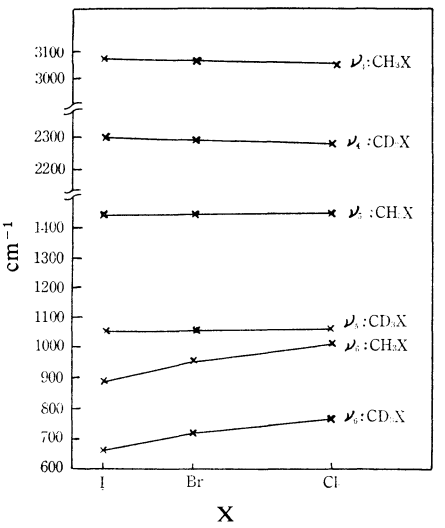



Fig. 7. "Parallel nature" of methyl halides $C_0$ of Eq. 1.

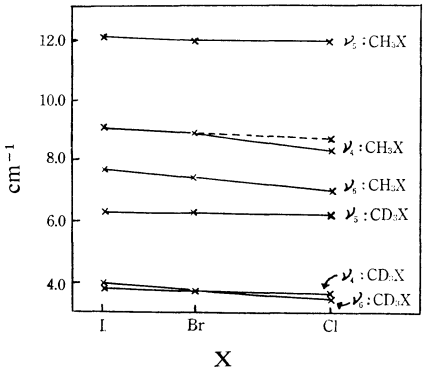



Fig. 8. "Parallel nature" of methyl halides $C_1$ of Eq. 1.

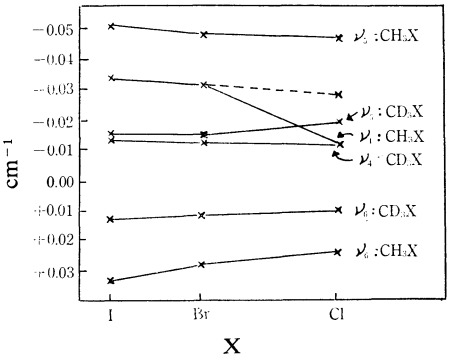



Fig. 9. "Parallel nature" of methyl halides $C_2$ of Eq. 1.

so as to fit the values of the coefficients indicated by the dotted lines in Figs. 8 and 9.

$CH_3Cl$, $\nu_4$; $\nu = 3046.20 \pm 8.720K - 0.0290K^2$ (20)

The values for the $\nu_5$ band of $CH_3I$ show an

accidental coincidence with the expected linearity, even though they are of a perturbed state.

### Coriolis Coupling Constants and Rotational Constants

The vibration-rotation energy levels of a symmetric top molecule in its ground and first-excited states are expressed, to the second order of approximation and by neglecting the effects of centrifugal distortion, by :[21]

$$E_0 = W_0 + B_0 J(J+1) + (A_0 - B_0) K^2 \qquad (21)$$

for the ground state, and

$$E_v = W_v + B_v J(J+1) + (A_v - B_v) K^2 - 2A_v \zeta_v K l_v + A_v (\zeta_v l_v)^2 \qquad (22)$$

for the first excited state, where $W$ denotes the vibrational energies ; $A$ and $B$, the rotational constants about the axes parallel and perpendicular, respectively, to the molecular axis ; $\zeta_v$, the effective Coriolis coupling constant of the degenerate mode (see Appendix II), and $l_v$, the quantum number of the vibrational angular momentum, which is taken as unity for the first excited states of the degenerate vibrations and zero for the non-degenerate vibrations.

The frequencies of the ${}^{R}Q_K$ or ${}^{P}Q_K$ subbands are then expressed as follows when the selection rule, $\Delta J=0$ and $\Delta K=\pm 1$ is taken into account :

$$\nu = \nu_0 + (B_v - B_0) J(J+1) + A_v (1-\zeta_v)^2 - B_v \pm 2[A_v(1-\zeta_v) - B_v] K + [(A_v - A_0) - (B_v - B_0)] K^2 \qquad (23)$$

where the signs + and − before the fourth term refer to the ${}^{R}Q_K$ and ${}^{P}Q_K$ branches respectively.

The experimental conditions are such that the actually-observed frequencies are "peak frequencies" which correspond to the maximum absorbing points of the peaks with certain values of $J$ (denoted as $J_m$). Thus the peak frequencies are expressed as follows :

$$\nu_m = \nu_{0K} + (B_v - B_0) J_m (J_m + 1) \qquad (24)$$

where

$$\nu_{0K} = \nu_0 + A_v (1-\zeta_v)^2 - B_v \pm 2(A_v(1-\zeta_v) - B_v) K + ((A_v - A_0) - (B_v - B_0)) K^2 \qquad (25)$$

The second term of Eq. 24 has a finite value determined by the Boltzmann distribution and the experimental conditions. It would affect the terms in the expression of $\nu_{0K}$ since the $J_m$ is dependent on the $K$ numbers (see Appendix I). Such an effect can, however, be expected to be negligibly small compared with the uncertainty in the measurement of the peak positions, so the second term in Eq. 24 was neglected and the observed data were analyzed according to Eq. 25.

Now the frequencies of the successive $Q$ branches are expressed by the $K$-dependent equation, the coefficients of which are composed of the molecular parameters, $\nu_0$, $A_0$, $B_0$, $A_v$, $B_v$ and $\zeta_v$. Nevertheless, it is impossible to obtain individual values of these parameters directly from a comparison of Eq. 25 with the observed relations, Eqs. 2—19, because there are more than three unknown parameters. At this stage, therefore, various conventional approximations have been proposed. In the present investigation, two alternative methods were tested.

**Method I.**—In the first method of approximation, the following assumptions were used in order to minimize the number of unknown molecular parameters :

i) The Coriolis sum rule was approximated as $\zeta_4 + \zeta_5 + \zeta_6 = B_0/2A_0$.[22]

ii) The coefficient of $K$ in Eq. 25 was replaced by $2(A_v - B_0 - A_0\zeta_v)$.

iii) The values of $B_0$ were taken from the data obtained by the analyses of microwave spectra[23] listed in Table XIX.

iv) The term $B_v - B_0$ was assumed to be zero.

TABLE XIX. THE $B_0$ VALUES OF METHYL HALIDES ($cm^{-1}$)

| | $CH_3Cl$ | $CH_3Br$ | $CH_3I$ | $CD_3Cl$ | $CD_3Br$ | $CD_3I$ |
|---|---|---|---|---|---|---|
| $B_0$ | 0.4434 | 0.3186 | 0.2502 | 0.3616 | 0.2568 | 0.2015 |

Assumptions i and ii are made for the sake of simplicity. Assumption iii requires the use of the effective atomic weights of chlorine and bromine since the microwave results are given for isotopic species. As no band splittings were observed for the isotopic species of $^{35}Cl$ and $^{37}Cl$, nor for those of $^{79}Br$ and $^{81}Br$, in the degenerate bands, the observed bands of $CH_3Cl$ and $CD_3Cl$ were assigned to those of the $^{35}Cl$ species, (accordingly, the $B_0$ values are those of the $^{35}Cl$ species), whereas the $B_0$ values of methyl bromide were taken as the average of the $^{79}Br$ and $^{81}Br$ species because the contributions of these two species to the intensities of the absorption bands were expected to be equal in the case of bromides.

By the use of these assumptions, the coefficients of Eqs. 2—19 lead to the values of $A_0$, $A_v$, $\zeta_v$ and $\nu_0$ shown in Table XX. Set 1 of

21) M. Johnston and D. M. Dennison, *Phys. Rev.*, **48**, 868 (1935) ; W. H. Shaffer, *J. Chem. Phys.*, **10**, 1 (1940) ; H. H. Nielsen, *Rev. Mod. Phys.*, **23**, 90 (1951).

22) F. A. Anderson, B. B. Bak and S. Brodersen, *J. Chem. Phys.*, **24**, 989 (1956).

23) S. L. Miller, L. C. Aamodt, G. Dousmanis, C. H. Townes and J. Kraitchman, ibid., **20**, 1112 (1952).

TABLE XX. $A_0$, $A_v$, $\zeta_v$ AND $\nu_0$ VALUES OF METHYL HALIDES (method I)

| | | $A_0$ cm$^{-1}$ | $A_v$ cm$^{-1}$ | $\zeta_v$ | $\nu_0$ cm$^{-1}$ |
|---|---|---|---|---|---|
| $CH_3Cl$, (1) | $\nu_4$ | | 5.078 | 0.085 | 3042.4 |
| | $\nu_5$ | 5.091 | 5.043 | −0.277 | 1452.1 |
| | $\nu_6$ | | 5.115 | 0.236 | 1017.3 |
| $CH_3Cl$, (2) | $\nu_4$ | | 5.120 | 0.062 | 3042.1 |
| | $\nu_5$ | 5.149 | 5.101 | −0.263 | 1452.2 |
| | $\nu_6$ | | 5.173 | 0.244 | 1017.3 |
| $CD_3Cl$ | $\nu_4$ | | 2.600 | 0.182 | 2283.4 |
| | $\nu_5$ | 2.613 | 2.522 | −0.337 | 1059.9 |
| | $\nu_6$ | | 2.623 | 0.220 | 767.7 |
| $CH_3Br$ | $\nu_4$ | | 5.090 | 0.058 | 3056.6 |
| | $\nu_5$ | 5.123 | 5.074 | −0.243 | 1442.8 |
| | $\nu_6$ | | 5.150 | 0.216 | 954.3 |
| $CD_3Br$ | $\nu_4$ | | 2.576 | 0.179 | 2296.3 |
| | $\nu_5$ | 2.589 | 2.574 | −0.316 | 1055.6 |
| | $\nu_6$ | | 2.601 | 0.187 | 713.1 |
| $CH_3I$ | $\nu_4$ | | 5.101 | 0.060 | 3060.5 |
| | $\nu_5$ | 5.136 | 5.083 | −0.243 | 1437.4 |
| | $\nu_6$ | | 5.169 | 0.208 | 882.4 |
| $CD_3I$ | $\nu_4$ | | 2.572 | 0.178 | 2298.1 |
| | $\nu_5$ | 2.586 | 2.570 | −0.316 | 1049.3 |
| | $\nu_6$ | | 2.599 | 0.178 | 655.9 |

$CH_3Cl$ was calculated by the use of Eqs. 2, 3 and 4, and set 2, by the use of Eqs. 3, 4 and 20.

**Method II.**—It may readily be seen that a more clear-cut treatment is possible if all the rotational correction terms $(A_v-A_0)$ and $(B_v-B_0)$ are known. The knowledge of these values is also indispensable for the determination of the molecular structures at their equilibrium state. Theoretically, the $A_v$ and $A_0$ are expressed as follows:

$$A_v=A_e-\sum_i \alpha_i(v_i+g_i/2)$$

and

$$A_0=A_e-\sum_i \alpha_i(g_i/2) \qquad (26)$$

where $\alpha_i$ is the correction term connected with the $i$th vibrational mode and is a function of the anharmonic terms in the potential function. Similar relations hold for $B_v$ and $B_0$ when we replace $\alpha_i$ with $\beta_i$. Efforts were also made to obtain information about the values of $\alpha_i$ and $\beta_i$. The results obtained to date for the methyl halide molecules are summarized in Table XXI (see Appendix III for the experimental sources). The precise values of $A_e$ and $B_e$ can not be obtained until Table XXI is filled up with appropriate values. However, a close examination of Table XXI suggests the possibility of obtaining rough values of $(B_e-B_0)$ and $(A_e-A_0)$. An interesting relation was obtained when the $\alpha_i/A_0$ and $\beta_i/B_0$ ratios were calculated for all the observed values of $\alpha_i$ and $\beta_i$; that is, the ratios are characteristic of the $i$th vibrational mode and similar for the six species of methyl halides, the deviations being within ±0.1% of $A_0$ (or $B_0$). Therefore, the $\sum_i \alpha_i g_i/2$ and $\sum_i \beta_i g_i/2$ sums can be estimated for all the six species by using the observed data of $A_0$ and $B_0$, with a possible error of only ±0.6%, if at least six $\alpha_i$'s and six $\beta_i$'s for the six normal vibrations are known. An estimate was made as follows in the present case:

TABLE XXI. THE OBSERVED VALUES OF $\alpha_i$ AND $\beta_i$ (cm$^{-1}$)

| | $CH_3Cl$ | $CH_3Br$ | $CH_3I$ | $CD_3Cl$ | $CD_3Br$ | $CD_3I$ |
|---|---|---|---|---|---|---|
| $\alpha_1$ | +0.0547[a-I] | + | + | + | + | + |
| $\alpha_2$ | − | − | − | − | − | − |
| $\alpha_3$ | + | + | + | + | + | + |
| $\alpha_4$ | +0.013 | +0.033 | +0.035 | +0.013 | +0.013 | +0.014 |
| $\alpha_5$ | +0.048 | +0.048 | +0.055 | +0.021 | +0.015 | +0.016 |
| $\alpha_6$ | −0.024 | −0.027 | −0.033 | −0.010 | −0.011 | −0.013 |
| $\beta_1$ | −0.00010[a-I] | | | | | |
| $\beta_2$ | +0.005[a-I] | | | | | |
| $\beta_3$ | +0.00484[b-M] | +0.0026[b-M] | +0.0018[c-M] | +0.0028[M] | | |
| $\beta_4$ | −0.00022[d-O] | −0.00008[e-O] | −0.0001[e-O] | − | − | − |
| $\beta_5$ | −0.0021[a-O] | − | − | − | − | − |
| $\beta_6$ | +0.001635[b-M] | + | + | + | + | + |

a = Ref. 26, b = Ref. 24, c = Ref. 25, d = Ref. 20, e = Ref. 27
I = Infrared
M = Microwave
O = Infrared Overtone
others: the present study. See Appendix III.

Note added in proof: Recently the authors have been informed by Dr. E. Jones that all the fundamentals, and many overtones and combination parallel and perpendicular bands of methyl halides have been measured and analyzed at Oxford.

1) As for $\beta$'s, all six values from $\beta_1$ to $\beta_6$ are available for $CH_3Cl$. By the use of these values, $B_4$, $B_5$, $B_6$ and $B_e$ were assumed for all the species as follows:

$$B_4 = B_0(1+0.0005)$$
$$B_5 = B_0(1+0.0048)$$
$$B_6 = B_0(1-0.0037)$$

and

$$B_e = B_0(1+0.0082)$$

where the $B_0$ values were taken from Table XIX.

2) There is no information about the absolute values of $\alpha_2$ and $\alpha_3$. However, an examination of the $Q$-branch shapes suggests that these terms have almost the same values but opposite signs ($\alpha_2 < 0$, $\alpha_3 > 0$); $\alpha_2+\alpha_3$ was consequently assumed to be zero.

3) The values of $\alpha_1$ was taken to be 1% of $A_0$.

4) For $\alpha_4$, $\alpha_5$ and $\alpha_6$, the observed values were used.

5) Assumptions 1 to 4 made it possible to estimate all the necessary values of the rotational constants, if another assumption on the Coriolis sum rule, $\zeta_4+\zeta_5+\zeta_6 = B_e/2A_e$, was made together with Eq. 25.

By using these estimated values, the molecular parameters, $A_e$, $A_0$, $A_v$ and $\zeta_v$, of $CH_3X$ and $CD_3X$ can be independently calculated from the observed data of the coefficients $C_0$, $C_1$ and $C_2$. The resultant values of $A_e(H)$ and $A_e(D)$ must satisfy the relation $A_e(H)m_H = A_e(D)m_D$. In the present results, however, the relation did not strictly hold and the deviation from the expected ratio of $A_e(H)/A_e(D)$ was largest for the case 1 of chlorides and was negligibly small for iodides. This inconsistency arose partly because the estimates of $(A_e-A_0)$ and $(B_e-B_0)$ include uncertainties and partly because the experimental data on $CH_3X$ (especially on $CH_3Cl$) include anomalies, so that the $A_e$ and $A_0$ values obtained by using these data must be influenced by the anomalies through the Coriolis sum rule used in the analysis.

At present, therefore, the values $A_e$, $A_v$, $A_0$ and $\zeta_v$ of $CD_3X$ (of which less anomaly was observed in the spectra) were first determined by the method mentioned above. The $A_e(D)$ values thus obtained were then reduced by the $A_e(H)m_H = A_e(D)m_D$ relation to $A_e(H)$, from which the $B_e/2A_e$ ratio and, henceforth, a set of $A_v$s and $\zeta_v$s for $CH_3X$ were so determined as to satisfy the Coriolis sum rule, $\zeta_4+\zeta_5+\zeta_6 = B_e/2A_e$. The final results are shown in Table XXII.

A comparison of the values in Tables XX and XXII provides the useful suggestion that method I, which is simpler than method II,

TABLE XXII. $A_e$, $A_0$, $A_v$ AND $\zeta_v$ VALUES OF METHYL HALIDES (method II)

| | | $A_e$ cm$^{-1}$ | $A_0$ cm$^{-1}$ | $A_v$ cm$^{-1}$ | $\zeta_v$ |
|---|---|---|---|---|---|
| $CH_3Cl$, (1) | $\nu_4$ | | | 5.084 | 0.086 |
| | $\nu_5$ | (5.304) | 5.148 | 5.080 | −0.278 |
| | $\nu_6$ | | | 5.119 | 0.236 |
| $CH_3Cl$, (2) | $\nu_4$ | | | 5.135 | 0.065 |
| | $\nu_5$ | (5.304) | 5.148 | 5.107 | −0.265 |
| | $\nu_6$ | | | 5.170 | 0.243 |
| $CD_3Cl$ | $\nu_4$ | | | 2.606 | 0.184 |
| | $\nu_5$ | 2.654 | 2.618 | 2.599 | −0.337 |
| | $\nu_6$ | | | 2.627 | 0.221 |
| $CH_3Br$ | $\nu_4$ | | | 5.094 | 0.059 |
| | $\nu_5$ | (5.237) | 5.127 | 5.080 | −0.244 |
| | $\nu_6$ | | | 5.153 | 0.216 |
| $CD_3Br$ | $\nu_4$ | | | 2.578 | 0.181 |
| | $\nu_5$ | 2.620 | 2.591 | 2.576 | −0.318 |
| | $\nu_6$ | | | 2.601 | 0.186 |
| $CH_3I$ | $\nu_4$ | | | 5.107 | 0.061 |
| | $\nu_5$ | (5.228) | 5.141 | 5.090 | −0.244 |
| | $\nu_6$ | | | 5.174 | 0.207 |
| $CD_3I$ | $\nu_4$ | | | 2.573 | 0.179 |
| | $\nu_5$ | 2.616 | 2.587 | 2.572 | −0.318 |
| | $\nu_6$ | | | 2.599 | 0.177 |

( ); estimated values: see text.

is a good approximation as far as the determination of $\zeta_v$ is concerned. A third, and the simplest, method of analysis is to use the values of $A_0$ calculated with the structure parameters determined by other experimental methods. This method is, however, less desirable because the uncertainty of $A_0$ values directly influences the value of $\zeta_v$, and, as will be discussed in the next section, the values of $A_0$ estimated by the analysis of microwave spectra differ considerably from those of the present investigation.

When all of the $\zeta_v$ values can be observed, the use of the Coriolis sum rule has the merit that a set of self-consistent molecular parameters, including the observed values of $A_e$ (or at least $A_0$), can be obtained from the analysis of the vibration-rotation spectra. An unfavorable point, however, lies in the fact that the irregularity or uncertainty of one vibrational mode affects all the other values through the sum rule, as was observed in the case of $CH_3Cl$.

## The Structures of Methyl Halides

In the preceding section, the rotational constants, $A_e$, $B_e$, $A_0$ and $B_0$, of the six species of methyl halides were obtained with a number of empirical assumptions and approximations. These rotational constants are related to the moments of inertia, $I_a$ and $I_b$, about the axes

parallel and perpendicular to the molecular axis, respectively, by the equations;

$$A_e = h/(8\pi^2 c I_a{}^e)$$

and

$$B_e = h/(8\pi^2 c I_b{}^e) \quad (27)$$

The terms $I_a{}^e$ and $I_b{}^e$ are, in turn, expressed by the molecular parameters of the equilibrium configuration of the molecule:

$$I_a{}^e = 2m_H r_{He}{}^2(1-\cos\theta_e)$$
$$I_b{}^e = m_H r_{He}{}^2(1-\cos\theta_e) + m_H(m_C+m_X) \times r_{He}{}^2(1+2\cos\theta_e)/M + m_X r_{Xe}[(3m_H + m_e) r_{Xe} + 6m_H r_{He}((1+2\cos\theta_e)/3)^{1/2}]/M \quad (28)$$

where $m_H$, $m_C$ and $m_X$ denote the masses of the atoms H, C and X respectively. $\theta_e$ is the angle HCH of the equilibrium configuration, and $M=(3m_H+m_C+m_X)$ is the total mass of the molecule. Analogous relations hold for $A_0$ and $B_0$. It should be noted that $A_0$ and $B_0$ include terms originating both from the coupling of vibration and rotation and from the anharmonicity of the potential function. Moreover, they have these terms as a result of taking an average of $1/r^2$ over the ground vibrational state. Thus the determination of the so-called "$r_0$ structure" is by no means the final goal of our structure determination. However, it seems interesting to compare the $r_0$ structures of methyl halides estimated from microwave spectra[23] with those estimated by the use of the present $A_0$ values.

Since there are three unknown parameters, $r_{H_0}$, $r_{X_0}$ and $\theta_0$, they can not be determined from the $A_0$ and $B_0$ values alone. On the other hand, the $r_0$ structures obtained from microwave spectra depend on the changes in $B_0$ resulting from the substitution of the isotopes in the molecule, and, although they are uncertain because of the neglect of the changes in the zero-point contributions, the $r_{X_0}$ values are usually determined more precisely than those of $r_{H_0}$ and $\theta_0$. Therefore, the values of $r_{X_0}$ were taken, for the sake of convenience, from the microwave data.[23] Assuming the same values of $r_{X_0}$ for the $CH_3X$ and $CD_3X$ molecules, the other parameters were obtained by the use of the $A_0$ and $B_0$ values determined above. The results are shown in Table XXIII, where the values for $CH_3Cl(1)$ and $CH_3Cl(2)$ correspond to the use of Eqs. 2 and 20 respectively.

TABLE XXIII. THE $r_0$ STRUCTURES OF METHYL HALIDES

| | $r_{X_0}$, Å | PR | | M | |
|---|---|---|---|---|---|
| | | $r_{H_0}$, Å | $\theta_0$ | $r_{H_0}$, Å | $\theta_0$ |
| $CH_3Cl$ (1) | (1.7810) | 1.1050 | 110°12′ | 1.113 | 110°31′ |
| $CH_3Cl$ (2) | (1.7810) | 1.0995 | 110°00′ | | |
| $CD_3Cl$ | (1.7810) | 1.0912 | 110°11′ | 1.104 | 110°43′ |
| $CH_3Br$ | (1.9391) | 1.0978 | 110°46′ | 1.113 | 111°14′ |
| $CD_3Br$ | (1.9391) | 1.0908 | 111°00′ | 1.104 | 111°26′ |
| $CH_3I$ | (2.1392) | 1.0956 | 110°53′ | 1.113 | 111°25′ |
| $CD_3I$ | (2.1392) | 1.0900 | 111°14′ | 1.104 | 111°37′ |

( ): assumed.
PR: Present investigation.
M: Ref. 23.

The structures proposed by Miller et al.[23] (shown for comparison in columns 2, 5 and 6 of Table XXIII) are those determined on the assumption that the difference $r_{H_0}-r_{D_0}=0.009$ Å for all the pairs of $CH_3X$ and $CD_3X$, irrespective of the halogen atoms. The results of the present investigation show, however, that the values of $r_{H_0}-r_{D_0}$ differ slightly according to the change in halogen atoms if the $r_X$ is taken as common for the two species, $CH_3X$ and $CD_3X$. The absolute values of $r_H$ and $r_D$ are smaller than those in column 5. As for the bond angles, the conclusion of Miller et al. that the angle HCH is larger than the tetrahedral one was again confirmed. As a whole, the $A_0$ values estimated by using the $r_H$ and $\theta$ values by Miller et al. are considerably larger than those observed in the present study.

When the configurations of $CH_3X$ and $CD_3X$ in their equilibrium state is assumed to be the same, the $r_e$ structures of methyl halides are obtained from the values of $A_e$ and $B_e$ without further assumptions, as is shown in Table XXIV.

TABLE XXIV. THE $r_e$ STRUCTURES OF METHYL HALIDES

| | $r_{X_e}$, Å | $r_{H_e}$, Å | $\theta_e$ |
|---|---|---|---|
| $CH_3Cl$, $CD_3Cl$ | 1.779 | 1.079 | 110°43′ |
| $CH_3Br$, $CD_3Br$ | 1.936 | 1.080 | 111°35′ |
| $CH_3I$, $CD_3I$ | 2.136 | 1.079 | 112°00′ |

Since the values of $A_e$ and $B_e$ employed are uncertain, these parameters should also include large errors, yet the general tendency, ($r_{Xe} < r_{X_0}$ and $r_{He} < r_{H_0}$) seems reasonable when the anharmonicity of the potential field is thought to have such a form as is expressed by the Morse function. The error of 1% in the $A_e$ value corresponds to the change of $\pm 0.003$ Å in $r_{He}$ and that of $\pm 10'$ in $\theta_e$. The effect of the errors in the $B_e$ values should be more serious.

## Discussion

The theoretical and numerical calculations of the intramolecular force field using the Coriolis coupling constants[1] have proved that these constants are useful observables for the

determination of the force field. This fact, however, means in turn that the experimental values of the Coriolis coupling constants must be determined precisely enough to give a critical check of the force field. The present investigation shows that the accuracy of the observed values of the Coriolis coupling constants is influenced by many factors, such as

1) The accuracy of the spectral measurement,

2) The approximations used in the course of the analysis,

3) The assignment of the $K$ numbering, the existence of the Fermi resonance, and other interactions, and

4) The effect of anharmonicity.

**1)** The first factor depends almost entirely on the uncertainties of the optical instrument used. The minimum requirement is that the individual $Q$ branches are well resolved and that the accuracy of the measurement of peak frequencies is such that the $K$-dependence of the successive $Q$ branch separations can be observed. The methyl halide molecules, of which the three off-axial atoms are all hydrogen or all deuterium, have the largest $A_0$ values among the symmetric top molecules; yet a grating spectrometer of medium dispersion is necessary for the observation of their spectra to satisfy the above requirement.

The maximum uncertainty of the observed frequencies is $\pm 0.1\ \mathrm{cm}^{-1}$. The coefficients of Eqs. 2—20 are determined by the least-squares method, using the observed data, so the accuracy of $C_0$, $C_1$ and $C_2$ in Eq. 1 is a function of the number of observed peaks. The standard deviations of these coefficients are estimated to be of the following orders of magnitude:

$$\sigma(C_0) = \pm 0.05, \qquad \sigma(C_1) = \pm 0.005$$

and $$\sigma(C_2) = \pm 0.0005\ \mathrm{cm}^{-1}$$

The effect of these deviations on the $\zeta$ values is estimated to be less than 0.001.

**2) a)** "*Peak Frequency.*"—The uncertainties due to the "peak frequency" measurement are discussed in Appendix I. As the final result depends on the slit function of the instrument, the estimation of the error is difficult. The upper limit of the error may, however, be $(B_v - B_0)(kT/hB_0)^{1/2}$ for the $C_1$ in the case of ${}^{R}Q_0 - {}^{R}Q_n$. This term amounts to $\pm 0.042\ \mathrm{cm}^{-1}$ for the $\nu_5$ band of $CD_3Cl$, and this leads to an error of $-0.008$ for $\zeta_5$.

**2) b)** *The Approximation of* $(\zeta_v^{(z)})'$ *to* $\zeta_v^{(z)}$.—The difference is of the order of 0.004, as will be estimated in Appendix II.

**2) c)** *The Reducction of the Molecular Parameters from the Observed Coefficients in Eq. 1.* —As the theoretical expression of the subband frequencies (Eq. 25) consists of many molecular parameters, approximations must be introduced so as to determine them by using the observed data. A comparison of two alternative treatments in the preceding section (Tables XX and XXII) will show, however, that the $\zeta$ values are little affected by the method of analysis as long as the value $(A_v - A_0)$ is taken into account and the Coriolis sum rule is used. The difference in the $\zeta$'s given in Tables XX and XXII is less than 0.003.

**3) a)** *The Assignment of the K Numbering.* —As has been discussed in the preceding section, the determination of the $K$ numbers in a series of $Q$ branches is very difficult and, therefore, there sometimes remains an ambiguity in the assignment. The change of assignment, however, results in a fairly large variation in the $\zeta$ values. Revision of the assignment $Q_K$ to $Q_{K+1}$ leads to the change of $C_1$ to $(C_1 - 2C_2)$. The magnitude of $C_2$ is $0.01$—$0.05\ \mathrm{cm}^{-1}$ for the fundamental bands of methyl halides. (Some of the combination bands have greater $C_2$ values.) Accordingly, a revision of $Q_K$ to $Q_{K\pm 3}$ (which occurs rather frequently), with large $C_2$ values, results in a change in $\zeta$ of up to $\pm 0.03$.

**3) b)** *The Effect of Resonance.* — When a series of $Q$ branches is well resolved but has an irregular feature, the existence of rotational resonances must be suspected (e.g., the $\nu_4$ of $CH_3Cl$ and the $\nu_5$ of $CH_3I$). Complete analyses of such bands have not yet been reported. Therefore, the values can not be determined with certainty. For example, Cleveland et al.[14] obtained a value of the $\zeta_5$ of $CH_3I$ ($\zeta_5 = -0.208$) by making all the data fit a quadratic equation of $K$ with equal weights. The present result ($\zeta_5 = -0.244$) is based on the less-perturbed part of the series.

These two factors, a) and b), include errors of an "unknown" order; they may amount to large values if the band in question alone is investigated. In the present investigation, however, the consideration of the "parallel nature" partly excludes such uncertainties, so that the accuracy of the final result may be estimated, after all the factors mentioned are taken into account, to be $\pm 0.02$ in the absolute value of the Coriolis coupling constants.

The last factor, "anharmonicity," represents the question of whether the observed $\zeta$ values can be regarded as $\zeta_e$, in other words, whether the Coriolis coupling constants can be expressed by the equations:

$$\zeta = \zeta_e + \sum_{i,j} \Delta\zeta_{ij}(v_i + g_i/2)(v_j + g_j/2) \qquad (29)$$

or

$$\zeta = \zeta_e + \sum_{i} \Delta\zeta_{i}(v_i + g_i/2) \qquad (29')$$

as in the case of the vibrational or rotational

anharmonic terms. This problem has not yet been elucidated either theoretically or experimentally; the discussion will be postponed to our coming paper on the analysis of the combination bands of methyl halides.

## Summary

The infrared spectra of $CH_3X$ and $CD_3X$ (X=Cl, Br and I) have been observed with a high-resolution instrument in the region 500 —3300 $cm^{-1}$. The rotational fine structures of all the E-type fundamental bands have been resolved and analyzed, giving the Coriolis coupling constants, the rotational constants and the frequencies of the band origins. The uncertainties of the observed molecular constants have been discussed. On the basis of the observed data for the rotational constants and their changes by the excitation of vibration, the structures of methyl halide molecules have been determined.

The authors are greatly indebted to Dr. Chi Matsumura for his kind help in the course of their experiments. This work was supported by a grant-in-aid for fundamental scientific research from the Ministry of Education, to which the authors' thanks are also due.

*Department of Chemistry*
*Faculty of Science*
*The University of Tokyo*
*Hongo, Tokyo*

## Appendix I

The definition of the "peak frequency" is simply the frequency of the maximum absorption point of a peak. The observed values of individual subbands included in Tables I—XVIII are, as mentioned in the text, the "peak frequencies." Strictly speaking, however, the absolute value of the "peak frequency" is influenced by many factors. A certain peak of the $^RQ_K$ or $^PQ_K$ of a symmetric top molecule consists of many lines labelled by the $J$ numbers and is located at the position $\nu=\nu_{0K}+(B_v-B_0)J(J+1)$, and the intensity ratio of these lines is given by:

$$\left.\begin{aligned} I_{^RQ_K} &\propto 2(2J+1)\frac{(J+1+K)(J-K)}{J(J+1)} \\ &\quad \times e^{-F(J\cdot K)hc/kT} \\ I_{^PQ_K} &\propto 2(2J+1)\frac{(J+1-K)(J+K)}{J(J+1)} \\ &\quad \times e^{-F(J\cdot K)hc/kT} \end{aligned}\right\} \quad (30)$$

Cleveland et al.[14] applied these relations directly to the case of methyl halides and gave $J_{max}$ values which depend on the $K$ numbers of the subbands and the rotational constants of the molecule. Such a treatment is, however, correct only if the individual lines of different $J$ numbers are resolved.

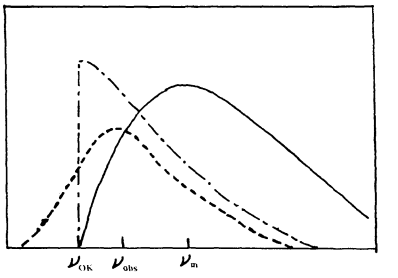



Fig. 10. E type $^RQ_0$ branch (schematic).
———: Intensity distribution by Eq. 30
– – – –: "Averaged" intensity distribution by Eq. 31
– – – –: Observed (re-averaged over the slit function)

In the case of a lower dispersion, the intensity of the lines are averaged over the unequal separations of successive $J$ number lines ($(B_v-B_0)\times(2J+1)$), and, accordingly, the $(2J+1)$ factor of Eq. 30 must be dropped out (See Fig. 10). Thus, the "averaged intensity" is expressed as follows:

$$\left.\begin{aligned} I_{av}(^RQ_K) &\propto \frac{2(J+1+K)(J-K)}{J(J+1)} \\ &\quad \times e^{-F(J\cdot K)hc/kT} \\ I_{av}(^PQ_K) &\propto \frac{2(J+1-K)(J+K)}{J(J+1)} \\ &\quad \times e^{-F(J\cdot K)hc/kT} \end{aligned}\right\} \quad (31)$$

The $K$-dependence of the $J_m$ number for the maximum intensity in Eq. 24 can be derived, after the differentiation of Eq. 31, as:

$$J_m(J_m+1)=(kT/hB_0)^{1/2}(K(K+1))^{1/2} + (1/2)K(K+1) \quad (32)$$

The "peak frequency" in the sense of Eq. 31 is given, instead of as Eq. 24, as follows:

$$\begin{aligned} {}^RQ_K:\ \nu &= \nu_0+(A_v(1-\zeta_v)^2-B_v)+2(A_v(1-\zeta_v)-B_v)K \\ &\quad +((A_v-A_0)-(B_v-B_0))K^2 \\ &\quad +(B_v-B_0)((kT/hB_0)^{1/2}(K(K+1))^{1/2} \\ &\quad +(1/2)K(K+1)) \\ &= \nu_0+(A_v(1-\zeta_v)^2-B_v)+2(A_v(1-\zeta_v) \\ &\quad -B_0-(3/4)(B_v-B_0))K+((A_v-A_0) \\ &\quad -1/2(B_v-B_0))K^2+(B_v-B_0)(kT/hB_0)^{1/2} \\ &\quad \times(K(K+1))^{1/2} \end{aligned} \quad (33)$$

The expression for the $^PQ_K$ is consistent with that for the $^RQ_K$ when $(K+1)$ is replaced by $(K-1)$, except for the sign of the last term. These equations may be visualized thus: the "peak" of the E-type subbands is shifted towards the lower or higher frequency, depending on whether the sign of $(B_v-B_0)$ is negative or positive, and the magnitude of the shift is nearly proportional to $|K|$. The separations of the successive $Q$ branches plotted against their $K$ numbers will, in this case, not lie on a straight line but have a break around the band center, as Fig. 11 shows. The conventional

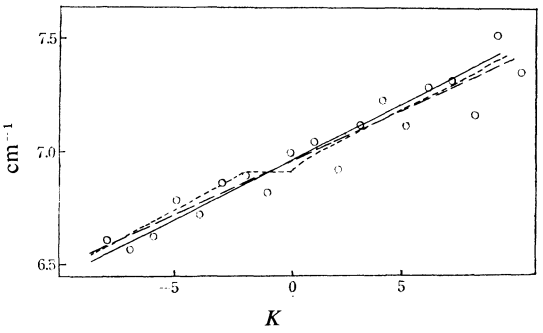



Fig. 11. Effect of the "peak-frequency" measurement.
$\Delta\nu_K=(Q_{K+1}-Q_K)$ : $CH_3Cl$ : $\nu_6$
——: From the subband origin $\nu_{0K}$ of Eq. 25
----: From the "peak frequency" $\nu_m$ of Eq. 24
– – –: Least-squares fit of the observed data to Eq. 1
○ : Observed

fitting of the "peak frequencies" to the quadratic equation of $K$, as was made in the preceding section, will result in small uncertainties for the three coefficients, $C_0$, $C_1$ and $C_2$, of Eq. 1, and the magnitude of the errors depends on the numbers of the observed subbands. For example, the observation of the ${}^RQ_n$ to ${}^PQ_n$ subbands leads to the errors of:

$(3/16)(B_v-B_0)(kT/hB_0)^{1/2}n$ for $C_0$

0 for $C_1$ and

$(kT/hB_0)^{1/2}/(K+1/2)$ for $C_2$.

In another case, that of ${}^RQ_0$ to ${}^RQ_n$, the errors are:

0 for $C_0$

$(kT/hB_0)^{1/2}$ for $C_1$ and

0 for $C_2$.

The above discussion must, however, be again modified when the slit function of the instrument is taken into account. An optimistic expectation is that the effect of the last term in Eq. 33 will be made much smaller after the re-average of the band intensity over the slit function is made. Practically speaking, the dispersions of the observed "peak frequencies" are comparable to or greater than the estimated theoretical "errors," as is shown in Fig. 11; therefore, the contribution of the "peak" measurement is disregarded in the present investigation. The cited values of $\nu_0$ do not include such corrections; corrections of $\pm 0$—$0.4\,cm^{-1}$ should be added to those $\nu_0$ values where the upper sign is for the band origins of $\nu_4$ and $\nu_5$, and the lower sign, for the $\nu_6$.

## Appendix II

According to Nielsen,[21] the energy level of a symmetric top molecule can be expressed as follows:

$$E/hc=W_v+B_vJ(J+1)+(A_v-B_v)K^2\mp 2\tilde{A}_v(\sum l_s\zeta_v^{(z)})K \qquad (34)$$

where $W_v$ is the vibrational energy; $A_v$ and $B_v$ are the rotational constants about the axes parallel and perpendicular to the molecular axis respectively; $z$ denotes the direction parallel to the molecular axis; and $J$ and $K$ are the rotational quantum numbers. $A_v$, $\tilde{A}_v$ and $B_v$ have the following expressions:

$$A_v=A_e-\sum_{s\sigma}\alpha_{s\sigma}(v_s+g_s/2)$$

$$\tilde{A}_v=A_e-\sum_{s\sigma}\tilde{\alpha}_{s\sigma}(v_s+g_s/2)$$

$$B_v=B_e-\sum_{s\sigma}\beta_{s\sigma}(v_s+g_s/2)$$

$$A_e=h/(8\pi^2cI_a^e)$$

$$B_e=h/(8\pi^2cI_b^e)$$

$$\tilde{\alpha}_{s\sigma}=\alpha_{s\sigma}+2\sum_{s'\sigma'}A_e(A_e/g_s\omega_s)\times[(3\lambda_s+\lambda_{s'})/(\lambda_s-\lambda_{s'})](\zeta_{s\sigma s'\sigma'}^{(z)})^2 \qquad (35)$$

where the $\alpha_{s\sigma}$ and $\beta_{s\sigma}$ are correction terms to $A_v$ and $B_v$ respectively, and $v_s$ and $g_s$ are the quantum number and the degeneracy of the $s$-th vibrational mode respectively.

Since the terms $A_v$ and $\tilde{A}_v$ differ slightly from each other, $\zeta_v^{(z)}$ must be modified to $(\zeta_v^{(z)})'$ if Eq. 34 is rewritten in such a way as to include only $A_v$ and $B_v$ as the rotational constants:

$$E/hc=W_v+B_v(J+1)J+(A_v-B_v)K^2\mp 2A_v(\sum l_v(\zeta_v^{(z)})')K \qquad (34')$$

$$(\zeta_v^{(z)})'=\zeta_v^{(z)}[1-2\sum_{s\sigma}\sum_{s'\sigma'}(A_e/g_s\omega_s)\times((3\lambda_s+\lambda_{s'})/(\lambda_s-\lambda_{s'}))(\zeta_{s\sigma s'\sigma'}^{(z)})^2(v_s+g_s/2)] \qquad (36)$$

The non-vanishing elements of $\zeta_{s\sigma s'\sigma'}^{(z)}$ are, in the case of methyl hadides, as follows:

$$\zeta_{4a5b}^{(z)},\ \zeta_{4a6b}^{(z)},\ \zeta_{5a6b}^{(z)}\neq 0$$

Accordingly, a numerical calculation shows that the second term in the brackets of Eq. 36 amounts, for example, to 0.004 in the case of the $\zeta_4$ of $CH_3Cl$; therefore, the difference between $\zeta_v^{(z)}$ and $(\zeta_v^{(z)})'$ is negligibly small when compared with the experimental errors included in the absolute values of $\zeta_v$. Thus, Eq. 34' is used in the present investigation instead of Eq. 34, in which $(\zeta_v^{(z)})'$ is simply expressed as $\zeta_v$.

## Appendix III

Experimental methods for obtaining the correction terms of the rotational constants ($\alpha_i$ and $\beta_i$ of Eq. 26) will be briefly discussed here. Table XXI includes the $\alpha_i$'s and $\beta_i$'s hitherto observed. The superscripts I, M and O designate the experimental methods used (I: infrared, M: microwave, O: infrared overtone), while a)—e) indicate the authors.

An analysis of the microwave spectra gives extremely precise values of $B_0$ and, in some cases, $B_v$. However, the application of this method is limited to the "$\beta_i$" of lower vibrational frequencies, about $2000\,cm^{-1}$ at most.

An analysis of the fine structures of the infrared and Raman spectra also gives the rotational constants, but such an analysis is usually restricted by the low resolving power of the instrument. Accurate values of $\alpha_i$ or $\beta_i$ can be obtained by this method only if the individual rotational lines are well resolved.

For non-degenerate vibrational modes, $\beta_i$ is obtained from a separation of resolved P- and R-branch lines ($\Delta K=0$, $\Delta J=\pm 1$), and $\alpha_i$, from the $K$-dependence of center $Q$-branch lines ($\Delta K$, $\Delta J=0$).

For degenerate vibrations, the values of $\alpha_i$ are obtained from the $K$-dependence of ${}^{R}Q_K$ and ${}^{P}Q_K$ separations ($\Delta J=0$, $\Delta K=\pm 1$). The $\beta_i$'s of the E-type might be obtained if the ${}^{R}P_K$, ${}^{R}R_K$, ${}^{P}P_K$ and ${}^{P}R_K$ lines are resolved. This is the case for the high-resolution studies of $NH_3$, $ND_3$, etc. However, in most cases of the E-type bands of methyl halides, these lines are weak and unresolved, making a smooth background for the prominent ${}^{R}Q_K$ and ${}^{P}Q_K$ lines. Recently, Brown and Edwards[28] observed these lines for some of the combination bands of $CH_3Br$ and $CH_3I$. The resultant values of $\beta$ are, however, not included in Table XXI because these values can not be reduced to those of the individual fundamental modes.

Overtone bands of a degenerate mode are sometimes useful for determining the $\beta_i$ because an overtone band of E-type fundamentals consists of an A- and an E-type band, and the resolved A-type band gives the value $2\beta_i$. The values in Table XXI with the "O" superscripts and referred to as "overtone" in the footnote are one half of the $\beta_{2\nu i}$ values.

When the individual lines are not resolved when their contours are observed (e.g., the $Q$ branch of an A-type band, the ${}^{R}Q_K$ or ${}^{P}Q_K$ peaks of an E-type band, etc.), precise values of $\alpha_i$ or $\beta_i$ are not obtained, as has been discussed in Appendix I. The sign of $\alpha_i$ or $\beta_i$ is, however, known from the shape of the peaks; that is, $\alpha_i$ or $\beta_i$ take a negative sign when the slope is steeper on the lower frequency side of the peak, and a positive sign in the opposite case. The terms in Table XXI with a + or − sign alone indicate that only the signs of $\alpha_i$ or $\beta_i$ were determined in this way by the present investigation. The accuracy of the $\alpha_i$ and $\beta_i$ values depends partly on the precision of the measurement. Another source of error lies, however, in the theoretical treatment; that is, apparent values of the rotational constants can not, in some cases, be expressed by such ordinary equations as are given in Eq. 26.

Two such cases are the rotational higher-order anharmonicity and the resonance through an accidental degeneracy of vibrational modes. Practically, therefore, the $\beta_{\nu i}$ of an E-type fundamental band is not always just one-half of the $\beta_{2\nu i}$, while some of the observed $\alpha_i$ or $\beta_i$ values might be perturbed ones (e.g., the $\alpha_5$ of $CH_3I$). Preliminary work on the effect of rotational resonance on $\alpha_i$, according to the formulation of Nielsen,[21] suggests that the perturbation is fairly large even if the two resonating bands are separated by more than 50 $cm^{-1}$ from each other. Similar situations have been recognized in microwave spectra.

24) I. A. Kraitchman and B. P. Dailey, *J. Chem. Phys.*, **22**, 1477 (1954).
25) T. Oka, private communication.
26) J. Pickworth and H. W. Thompson, *Trans. Faraday Soc.*, **50**, 218 (1954).
27) T. A. Wiggins, E. D. Shull and D. H. Rank, *J. Opt. Soc. Am.*, **43**, 157 (1953); *J. Chem. Phys.*, **21**, 1368 (1953).
28) R. G. Brown and T. H. Edwards, ibid., **37**, 1029 (1962); ibid., **37**, 1035 (1962).

# Vibration-Rotation Spectra, the Coriolis Coupling Constants and the Intramolecular Fore Field of Symmetric Top Molecules. II. Analysis of the Overtones and Combination Tones of Methyl Bromide

By Yonezo MORINO, Junko NAKAMURA* and Seiya YAMAMOTO

(Received August 10, 1964)

The infrared spectra of the overtones and combination tones of methyl bromide, $CH_3Br$, have been studied by many investigators;[1-4] six $A_1$-type bands and ten E-type bands have been observed. For the bands, $2\nu_4$, $\nu_1+\nu_4$, $\nu_1+\nu_5$, $\nu_2+\nu_4$, $\nu_4+\nu_5$ and $\nu_4+2\nu_5$, in particular, the rotational fine structures have been analyzed.

It seems, however, that no study has yet been undertaken with the particular intention of determining the second-order molecular parameters, that is, the vibrational anharmonic terms ($x_{ij}$), the rotational correction terms ($\alpha_i$ and $\beta_i$), and the effective Coriolis coupling constants ($\zeta_{eff}$). The primary object of this paper will be, therefore, to measure the

* Present address: The Institute of Physical and Chemical Research, Komagome, Bunkyo-ku, Tokyo

1) C. P. Courtoy, *Ann. Soc. Sci. Bruxelles*, **LX**, 122 (1946).

2) D. H. Rank, H. D. Rix and T. A. Wiggins, *J. Opt. Soc. Am.*, **43**, 157 (1953).

3) H. B. Weissman, R. B. Bernstein, S. E. Rosser, A. G. Meister and F. F. Cleveland, *J. Chem. Phys.*, **23**, 544 (1955).

4) R. G. Brown and T. H. Edwards, ibid., **37**, 1029 (1962); ibid., **40**, 2740 (1964).

infrared spectra of methyl bromide for this purpose. The parameters obtained in the present work will be used later to investigate the harmonic and anharmonic potential constants of this molecule.

## Experimental

A commercial sample of methyl bromide was dried by passing it through phosphorous pentoxide. Infrared spectra were recorded on a Perkin-Elmer 112G grating spectrometer, which has a resolution of about 0.6 $cm^{-1}$, an accuracy of the absolute frequency of about 0.5 $cm^{-1}$, and an accuracy of the relative frequency of about 0.05 $cm^{-1}$. A long-path cell (about 6 m. long) was used with a sample pressure varying from 100 to about 760 mmHg.

## Theory

The methyl bromide molecule has the $C_{3v}$ symmetry and six normal modes; three of them belong to the $A_1$-type, and the other three to the E-type. The energy level of the molecule is, to a second order of approximation, given by:[6]

$$T=G(v_1,\ v_2,\cdots)+F_v(J,\ K) \tag{1}$$

where $G$ is the vibrational energy and $F$ is the rotational energy, including the vibration-rotation interactions:

$$\begin{aligned}G=&\sum_i \omega_i(v_i+d_i/2)\\&+\sum_i\sum_{j\geq i} x_{ij}(v_i+d_i/2)(v_j+d_j/2)\\&+\sum_t\sum_{t'\geq t} g_{tt'}\,|l_t|\cdot|l_{t'}|\end{aligned} \tag{2}$$

and

$$\begin{aligned}F=&B_vJ(J+1)+(A_v-B_v)K^2-D_JJ^2(J+1)^2\\&-D_{JK}J(J+1)K^2-D_KK^4-2A_v\sum_t\zeta_tl_tK\\&+A_v(\sum_t\zeta_tl_t)^2\end{aligned} \tag{3}$$

The term $G$ can be referred to the ground state $G(0,\ 0,\ \cdots)$,

$$\begin{aligned}G_0=&\sum_i \omega_i{}^0v_i+\sum_i\sum_{j\geq i} x_{ij}v_iv_j\\&+\sum_t\sum_{t'\geq t} g_{tt'}|l_t|\cdot|l_{t'}|\end{aligned} \tag{4}$$

Where

$$\omega_i{}^0=\omega_i+x_{ii}d_i+1/2\sum_{j\neq i} x_{ij}d_j \tag{5}$$

Here $\omega_i$ is the normal frequency of the $i$th mode: $v_i$, its vibrational quantum number, and $d_i=1$ or 2, depending on whether $i$ refers to a totally symmetric or to a doubly-degenerate vibration. The suffix $t$ denotes a doubly-degenerate mode, and the vibrational angular momentum, $|l_t|$, takes the values $v_t$, $(v_t-2),\cdots$, 1 or 0. The coefficients $x_{ij}$ and $g_{tt'}$ are the vibrational anharmonic terms, and $A_v$ and $B_v$ are the rotational constants which depend on the vibrational state, $v$. The coefficients $D_J$, $D_{JK}$ and $D_K$ are the centrifugal distortion constants and do not depend on the vibrational state in this approximation.[7] The $\zeta_t$ is a first-order Coriolis coupling constant, which does not appear when no doubly-degenerate vibrations are excited.

As may be seen from Eq. 4, the band center of a fundamental $(\nu_i)$ is given by:

$$(\nu_i)=\omega_i{}^0+x_{ii},\ \text{for the } A_1\text{-type mode} \tag{6}$$

and

$$(\nu_t)=\omega_t{}^0+x_{tt}+g_{tt},\ \text{for the E-type mode} \tag{7}$$

If the centrifugal distortion terms are ignored because of their small size, the rotational structure for a parallel band is given by the selection rules $\Delta K=0$ and $\Delta J=0,\ \pm1$:

$$\begin{aligned}{}^QR_{|K|}(J)=&\nu_i+[(A'-A'')-(B'-B'')]K^2\\&+2B'+(3B'-B'')J+(B'-B'')J^2\\{}^QQ_{|K|}(J)=&\nu_i+[(A'-A'')-(B'-B'')]K^2\\&+(B'-B'')J(J+1)\\{}^QP_{|K|}(J)=&\nu_i+[(A'-A'')-(B'-B'')]K^2\\&-(B'+B'')J+(B'-B'')J^2\end{aligned} \tag{8}$$

where $J$ denotes the quantum number of the lower level, and the symbols '' and ' indicate the lower and upper states respectively.

For a perpendicular band whose selection rules are $\Delta K=\pm1$ and $\Delta J=0,\ \pm1$, the rotational structure is given by:

$$\begin{aligned}{}^P_RR_{|K|}(J)=&{}^P_R\nu_o{}^{\text{sub}}+2B'+(3B'-B'')J\\&+(B'-B'')J^2\\{}^P_RQ_{|K|}(J)=&{}^P_R\nu_o{}^{\text{sub}}+(B'-B'')J(J+1)\\{}^P_RP_{|K|}(J)=&{}^P_R\nu_o{}^{\text{sub}}-(B'+B'')J+(B'-B'')J^2\end{aligned} \tag{9}$$

where

$$\begin{aligned}{}^P_R\nu_o{}^{\text{sub}}=&\nu_t+[A'(1-\zeta_t)^2-B']\mp2[A'(1-\zeta_t)\\&-B']|K|+[(A'-A'')-(B'-B'')]K^2\end{aligned} \tag{10}$$

and $J$ and $K$ are the values of the lower state. In Eq. 10, the upper sign corresponds to the $P$ branch, and the lower sign, to the $R$ branch.

**Overtones and Combination Tones.** — The features of the overtones of the fundamentals belonging to the $A_1$-type symmetry are similar to those of the fundamentals since $(a_1)^2=A_1$. The band center of the overtone, $(2\nu_i)$, is given by:

5) Y. Morino and J. Nakamura, This Bulletin, **38**, 443 (1965).

6) G. Herzberg, "Infrared and Raman Spectra II," D. Van Nostrand Company, Inc., Princeton, New Jersey (1945).

7) H. H. Nielsen, *Revs. Mod. Phys.*, **23**, 90 (1951).

$$(2\nu_i)=2(\nu_i)+2x_{ii} \tag{11}$$

The overtones of the E-type fundamentals have two components, $A_1$ and E, since $(e)^2=A_1+E$. The band center of the $A_1$-type component is:

$$(2\nu_t)=2(\nu_t)+2x_{tt}-2g_{tt} \tag{12}$$

and that of the E-type component is:

$$(2\nu_t)=2(\nu_t)+2x_{tt}+2g_{tt} \tag{13}$$

It is important to note that in this case the $\zeta_t$ in Eq. 10 must be replaced by:[8]

$$\zeta_{\text{eff}}=-2\zeta_t \tag{14}$$

Since $a_1\cdot a_1=A_1$, the fine structure of a combination tone between two different $A_1$-type modes is similar to that of the fundamentals, and

$$(\nu_i+\nu_j)=(\nu_i)+(\nu_j)+x_{ij} \tag{15}$$

The fine structure of the combination tone between an $A_1$- and an E-type mode is similar to that of the E-type fundamental, since $a_1\cdot e=E$,

$$(\nu_i+\nu_t)=(\nu_i)+(\nu_t)+x_{it} \tag{16}$$

and

$$\zeta_{\text{eff}}=\zeta_t \tag{17}$$

The combination tones between two E-type modes have two components, since $e\cdot e=A_1+A_2+E$, the $A_2$-type not being infrared-active. The band center is given, for both of the $A_1$ and E components, by:

$$(\nu_t+\nu_{t'})=(\nu_t)+(\nu_{t'})+x_{tt'}+g_{tt'} \tag{18}$$

and, for the E component, by:

$$\zeta_{\text{eff}}=-(\zeta_t+\zeta_{t'}) \tag{19}$$

**The Method of the Analysis of the Observed Bands.**—If we assume that $B'=B''$, the Eqs. 8 for parallel bands become:

$$^{Q}R_{|K|}(J)=\nu_i+(A'-A'')K^2+2B''(J+1) \tag{20}$$
$$^{Q}Q_{|K|}(J)=\nu_i+(A'-A'')K^2$$
$$^{Q}P_{|K|}(J)=\nu_i+(A'-A'')K^2-2B''J$$

The line spacing due to the $J$ value is $2B''$ in the $P$ and R branches, and all lines of different $J$ values coincide with the band center, $\nu_i$, in the $Q$ branch. The spacing due to the $K$ value, on the other hand, is $(A'-A'')(2K+1)$ in the $P$, $Q$, and $R$ branches. In the case of methyl bromide, the value of $(A'-A'')$ is about $0.05\,\text{cm}^{-1}$, though those of different bands are not equal. The value of $2B''$ is $0.63\,\text{cm}^{-1}$. Since the resolving power of the spectrometer used is about $0.6\,\text{cm}^{-1}$, there may be a splitting of the lines which have different $J$ values, and, in fact, the splittings have been observed in several bands. The $K$ splitting may not be observed in the region of small $K$ numbers. In fact, most of the bands did not show their fine structures, and only the envelopes of the $P$, $Q$, and $R$ branches were observed. The $Q$ branches showed two types of envelopes, depending on whether $(A'-A'')$ is positive or negative. When $(A'-A'')$ was negative, the intensity of the absorption increased slowly from the lower frequency side, reached a maximum, and decreased rapidly toward the higher frequency side. The band origin of this band was determined by measuring the frequency at which the absorption disappeared at the higher frequency side. The case must be reversed if $(A'-A'')$ is positive, and the band origin determined at the lower frequency side. Since the envelopes of the $P$ and $R$ branches intersect near the band origin, the frequencies determined by the above method were proved consistent.

For perpendicular bands, if $B'=B''$, then Eq. 9 becomes:

$$^{P}_{R}R_{|K|}(J)=^{P}_{R}\nu_o^{\text{sub}}+2B''(J+1)$$
$$^{P}_{R}Q_{|K|}(J)=^{P}_{R}\nu_o^{\text{sub}}$$
$$^{P}_{R}P_{|K|}(J)=^{P}_{R}\nu_o^{\text{sub}}-2B''J \tag{21}$$

With a few exceptions, no bands show the $J$ splitting in the $P$ and $R$ branches, and lines which originate from different $J$ values form a background for the absorption curve. In the $Q$ branch, all lines of different $J$ values appear at nearly the same point, $^{P}_{R}\nu_o^{\text{sub}}$; therefore, they show a sub-bands series, which have much stronger intensities than the lines of the $P$ and $R$ branches, as peaks above the background with an interval of about $2[A'(1-\zeta)-B'']$. Naturally, they have an unresolved $J$ structure and show envelopes like the $Q$ branches of the parallel bands, due to $(B'-B'')$ and also to a slit function characteristic of the spectrometer used.

If $^{P}_{R}\nu_o^{\text{sub}}$ is rewritten as $\nu(m)$, where $m=-|K|$ in $^{P}Q_{|K|}$ and $m=|K|$ in $^{R}Q_{|K|}$, then:

$$\begin{aligned}\Delta\nu(m)&=\nu(m+1)-\nu(m)\\&=2[(A'-A'')-(B'-B'')]m\\&\quad+2[A'(1-\zeta_{\text{eff}})-B']\\&\quad+[(A'-A'')-(B'-B'')]\end{aligned} \tag{22}$$

If $\Delta\nu(m)$ is plotted against $m$, it lies on a straight line, and $[(A'-A'')-(B'-B'')]$ and $[A'(1-\zeta_{\text{eff}})-B']$ can be determined from the slope and $\Delta\nu(-1/2)$ respectively. If the values of $A''$ and $B''$ are known and if $B'$ is assumed to be equal to $B''$, the parameters $A'$, $\zeta$, and $\nu_t$ can then be determined.

The frequencies of the subbands at the

8) D. R. J. Boyd and H. C. Longuet-Higgins, *Proc. Roy. Soc.*, A 231, 55 (1952).

maximum intensities were measured, and the method described above was taken as a first step of the analysis. The assignment of $m$ was made by the use of the fact that the sub-bands whose $m$ numbers are a multiple of 3 have stronger intensities than the others. The values of $\zeta_{eff}$ obtained in this way were compared with the values to be expected from those of the fundamentals. This procedure confirms whether or not the vibrational assignment is correct. The coefficients of $m$ in Eq. 22 and the values of $A'$, $\zeta$, and $\nu_t$ were then determined by the method of least squares.

The values of $A''$ and $B''$ are taken to be 5.127 $cm^{-1}$ from the results of the analysis of the fundamentals,[5] and 0.3186 $cm^{-1}$ from the results of the microwave spectroscopy[9].

## Experimental Results

**a) Parallel Bands.**—The overtone and combination tone bands of the $A_1$-type fundamentals were all observed. Moreover, the $A_1$ components of the overtones $2\nu_4$ and $2\nu_5$, and the combination tone $\nu_4+\nu_6$, were also observed. Most of them, however, showed only envelopes, and no fine structures were resolved. The bands $\nu_1+\nu_2$ and $\nu_4+\nu_6$ showed fine structures, as Fig. 1 and Fig. 2 show, but the analysis has not been made in detail. For the band of $\nu_1+\nu_3$ it seems that the $Q$ branch was split into fine structures (Fig. 3), but it was difficult to distinguish each line because of the noise,

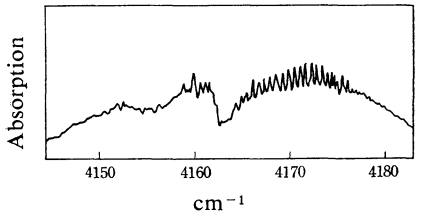



Fig. 1. The parallel band $\nu_1+\nu_2$ of $CH_3Br$.

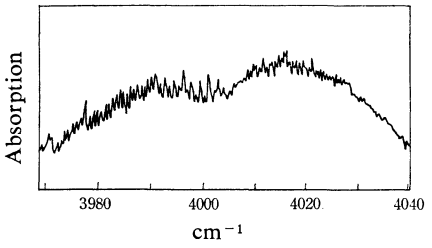



Fig. 2. The parallel band $\nu_4+\nu_6$ of $CH_3Br$.

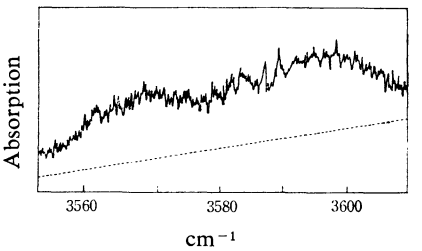



Fig. 3. The parallel band $\nu_1+\nu_3$ of $CH_3Br$. The dotted curve represents the blank curve.

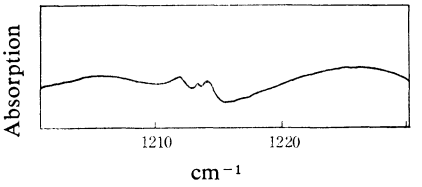



Fig. 4. The parallel band $2\nu_3$ of $CH_3Br$.

so the band center was determined from the point of intersection of the envelopes of the $P$ and $R$ branches. Two $Q$ branches observed in the band $2\nu_3$ (Fig. 4) are probably due to $^{79}Br$ and $^{81}Br$. The results are summarized in Table I.

**b) Perpendicular Bands.** — All the E-type bands of the overtones and the combination tones except $\nu_3+\nu_4$, $\nu_3+\nu_5$, $\nu_3+\nu_6$, $\nu_4+\nu_6$ and $2\nu_5$ were observed.

*1) Region 1500 — 2000 $cm^{-1}$.*—A perpendicular band was observed and assigned to $2\nu_6$ (1869 $cm^{-1}$). The quality of the spectra of this region was poor for the following reasons. First, this band has a weak intensity. This band was observed at the pressure of about 760 mmHg. Second, this region was interfered with by a strong absorption band of water. Finally, on the higher frequency side there was an absorption of the $A_1$-type band $\nu_2+\nu_3$. The observed frequencies and molecular constants are given in Table XII.

*2) Region 2000 — 2500 $cm^{-1}$.* — Two bands were observed in this region. They were assigned to $\nu_2+\nu_6$ (2256 $cm^{-1}$) and $\nu_5+\nu_6$ (2389 $cm^{-1}$). These bands were disturbed by the absorption of carbon dioxide. The higher

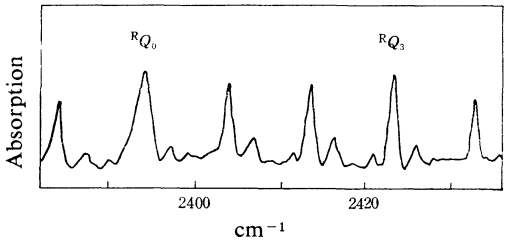



Fig. 5. The perpendicular band $\nu_5+\nu_6$ of $CH_3Br$.

9) W. J. O. Thomas, J. F. Cox and W. Gordy, *J. Chem. Phys.*, **22**, 1718 (1954).
10) I. A. Kraitchman and B. P. Dailey, ibid., **22**, 1477 (1954).
11) C. Hirose, Private communication.

frequency side of $\nu_2+\nu_6$ and the lower frequency side of $\nu_5+\nu_6$ were overlapped by a band of carbon dioxide. Between the lines of the band $\nu_5+\nu_6$, there were other lines (Fig. 5) which were considered to be a hot band or lines due to isotopic species; they are left unassigned. The observed frequencies are given in Tables VIII and XI.

*3) Region 2500—3000 cm$^{-1}$.*—There was one band, which was assigned to $\nu_2+\nu_5$. The observed frequencies are given in Table VII.

*4) Region 3500—4000 cm$^{-1}$.* — One E-type band was observed and assigned to $\nu_1+\nu_6$. This band was disturbed by the absorption of water. The observed frequencies of the sub-bands could not be described by an ordinary quadratic function of $K$ (Fig. 6). It is not clear whether or not this situation originated from an overlapping with the absorption of water alone. The constants were, tentatively, calculated from the observed frequencies of ${}^{P}Q_1$, ${}^{R}Q_0$ and ${}^{R}Q_1$. The observed frequencies are given in Table V.

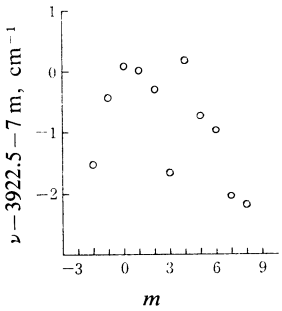



Fig. 6. The observed frequencies vs. $m$ for the perpendicular band $\nu_1+\nu_6$ of $CH_3Br$.

*5) Region 4000—4500 cm$^{-1}$.*—Three E-type bands were observed and assigned to $\nu_2+\nu_4$ (4352 cm$^{-1}$), $\nu_1+\nu_5$ (4411 cm$^{-1}$) and $\nu_4+\nu_5$ (4483 cm$^{-1}$). Brown et al.[4] measured this region with a high resolution spectrometer. Although their first assignments were different from those of this work, their revised values are in good agreement with the present results. An ambiguity lies, however, in the assignment of the ${}^{R}Q_0$ subband. For the band $\nu_1+\nu_5$, two subbands at 4418.25 cm$^{-1}$ and 4452.66 cm$^{-1}$ have about the same intensity. If one takes the latter as the ${}^{R}Q_0$, $\zeta_5$ becomes $-0.18$, whereas the assignment of the former to the ${}^{R}Q_0$ leads to the $\zeta_5$ value of $-0.22$. Therefore, the latter assignment (${}^{R}Q_0=4418.25$ cm$^{-1}$) was preferred in view of the knowledge of the fundamental $\zeta_5$ value of $-0.244$. The ${}^{P}Q_{|K|}$ lines in $\nu_1+\nu_5$ show an anomaly, as Fig. 7 shows. The origin of this anomaly is unknown. The observed frequencies are given in Tables IV, VI and X.

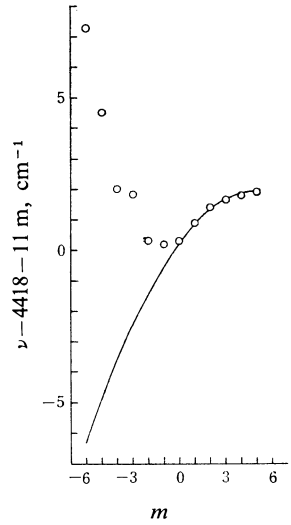



Fig. 7. The observed frequencies vs. $m$ for the perpendicuclar band $\nu_1+\nu_5$ of $CH_3Br$. The solid curve represents the calculated one.

*6) Region 5500—6500 cm$^{-1}$.*—In this region, four perpendicular bands were observed. They were assigned to $\nu_2+\nu_4+\nu_5$ (5781 cm$^{-1}$), $\nu_4+2\nu_5$ (5879 cm$^{-1}$), $\nu_1+\nu_4$ (5941 cm$^{-1}$) and $2\nu_4$ (6095 cm$^{-1}$). The bands $\nu_4+2\nu_5$, $\nu_1+\nu_4$ and $2\nu_4$ have also been observed by Rank et al.[2] Their results are in good agreement with those obtained in the present work.

The spectrum of the band $\nu_2+\nu_4+\nu_5$, given in Fig. 8, shows that the band is disturbed on the higher-frequency side by other absorption lines.

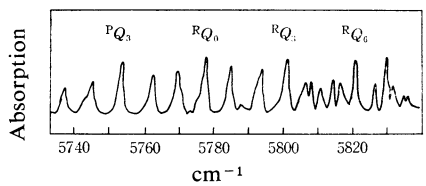



Fig. 8. The perpendicular band $\nu_2+\nu_4+\nu_5$ of $CH_3Br$.

For $\nu_4+2\nu_5$, since $e\cdot(e)^2=A_1+A_2+E+E$, there are two E-type components, that is, the state where $l_4=1$, $l_5=0$ and the state where $l_4=-1$, $l_5=2$. For the former, the predicted value of $\zeta_{eff}$ is 0.059, and for the latter it is $-0.547$. The observed value is $-0.021$; therefore, the observed transition is probably related to the former state, even though the difference between the observed and the predicted values of $\zeta$ is appreciable. There is presumably a resonance among these states. It seems that, because of this resonance, the ternary combination bands, $\nu_4+2\nu_5$ and $\nu_2+\nu_4+\nu_5$, appeared with sufficient intensities.

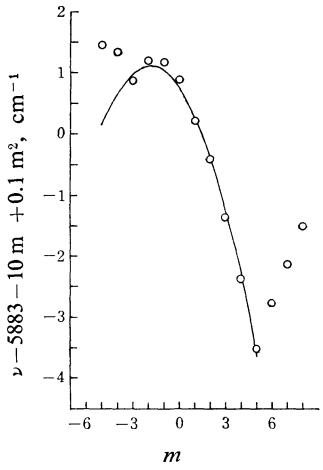



Fig. 9. The observed frequencies vs. $m$ for the perpendicular band $\nu_4+2\nu_5$ of $CH_3Br$. The solid curve represents the calculated one.

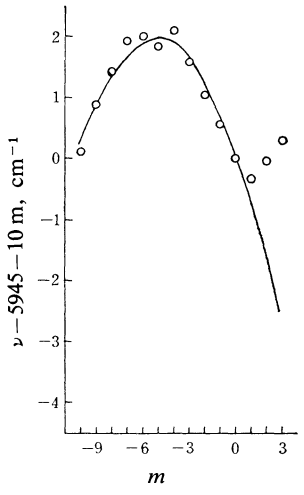



Fig. 10. The observed frequencies vs. $m$ for the perpendicular band $\nu_1+\nu_4$ of $CH_3Br$. The solid curve represents the calculated one.

The observed frequencies are given in Tables III, IX, XIII and XIV. Those of $\nu_4+2\nu_5$ and $\nu_1+\nu_4$ are shown graphically in Figs. 9 and 10 respectively. The anomalies shown in the figures may also be the result of the resonance.

*7) Summary.*—The results described above are summarized in Table XV. The errors associated with the molecular constants given in Tables III through XIV are taken to be 2.5 $\sigma$, where $\sigma$ is the standard deviation; 2.5 $\sigma$ is the 99% confidence interval, and it is thought to be a reasonable limit of error. However, these results do not include systematic errors; for example, the frequencies of the band centers are uncertain by an order of 0.1 $cm^{-1}$, since they are derived from the assumption that $B'=B''$. The values in the brackets in the tables show the subbands which were omitted from the least-squares calculations because they are either obscured by the presence of foreign bands, such as those of carbon dioxide and water, or are at apparently irregular positions.

## Discussion

It can be seen from Table XV that the differences between the observed and the predicted values of $\zeta$ are about 0.03. These differences indicate that the $\zeta$ values of the overtones and combination tones can not be expressed by the sums of those of the corresponding fundamentals. However, before concluding whether this is true or not, one must take into account the resonances among various vibrational states; this has not been done, and it would require complicated computations. The results of this work simply show that the values of the overtones and the combination tones can be expressed by the sums of the corresponding fundamentals, with proper signs, to within 0.03 in the case of $CH_3Br$.

The vibrational anharmonic terms obtained in this work are given in Table XVI. These values are still tentative, because the observed frequencies of the E-type bands are the frequencies of the maximum intensity; they must be corrected for the band origins, as has been discussed in the previous section.

The effective rotational constants for a given vibrational state can be expressed by the following relations:[6,7]

$$A_v=A_e-\sum_i\alpha_i(v_i+d_i/2)$$
$$B_v=B_e-\sum_i\beta_i(v_i+d_i/2)$$

where $A_e$ and $B_e$ are the rotational constants for the equilibrium position and $\alpha_i$ and $\beta_i$ are the rotational correction terms. The value of $(A'-A'')-(B'-B'')$ is obtained as the coefficient of $K^2$ from the analysis of the perpendicular band, and it is rewritten in terms of $\alpha_i$ and $\beta_i$ as follows:

$-\alpha_i+\beta_i$ for the $i$th fundamental,

$-2\alpha_i+2\beta_i$ for the overtone of the $i$th vibration,

$-(\alpha_i+\alpha_j)+(\beta_i+\beta_j)$ for the combination tone between the ith and $j$th vibrations.

The observed values are summarized in the third column of Table XVII. The values due to $(B'-B'')$ are shown in the fifth column. The values $\beta_i$ used are given in Table XVIII. It can be seen that the largest value of $(B'-B'')$ is 0.003 $cm^{-1}$ for $\nu_2+\nu_6$; nevertheless, this is within the range of error of the measurement of $(A'-A'')-(B'-B'')$. Therefore, the assumption that $B'=B''$, which was used in

the analysis of the perpendicular band, seems reasonable.

The appropriate combinations of observed values and the already-known values of $\alpha_i$ or $\beta_i$ determine some unknown rotational correction terms, $\alpha_i$.

The most probable values for $\alpha_i$ are given in Table XVIII. The values $(A'-A'')-(B'-B'')$ calculated by using $\alpha_i$ and $\beta_i$ in Table XVIII are given in the fourth column of Table XVII. They are in rather good agreement with the observed values.

## Summary

The infrared spectra of most of the overtones and combination tones of methyl bromide have been obtained. In the perpendicular band, the rotational fine structures have been observed. The values of the Coriolis coupling constants obtained from the analysis of the rotational fine structures are consistent with those obtained from the analysis of the fundamentals. It has been seen that, if one takes 0.03 as the error of the observed values of the Coriolis coupling constants, one can use the observed values to calculate the force constants.

Most of the vibrational anharmonic terms, $x_{ij}$, have been obtained, but they are tentative yet.

The rotational correction terms, $\alpha_1$ and $\alpha_2$ have been estimated from the combination-bands analyses.

This work was supported by a grant-in-aid for fundamental scientific research from the Ministry of Education, to which the authors' thanks are due.

*Department of Chemistry*
*Faculty of Science*
*The University of Tokyo*
*Hongo, Tokyo*

TABLE I. THE OBSERVED FREQUENCIES OF THE PARALLEL BANDS OF $CH_3Br$

| | $\nu_0^{obs}$ cm$^{-1}$ | $\nu_0^{pred}$ cm$^{-1}$ | $\Delta$ cm$^{-1}$ |
|---|---|---|---|
| $2\nu_1$ | 5882 | 5944 | −62 |
| $\nu_1+\nu_2$ | 4163 | 4277 | −114 |
| $\nu_1+\nu_3$ | 3582 | 3583 | −1 |
| $2\nu_2$ | 2596 | 2610 | −14 |
| $\nu_2+\nu_3$ | 1911 | 1916 | −5 |
| $2\nu_3$($^{79}$Br) | 1215 | 1222 | −8 |
| ($^{81}$Br) | 1213 | | |
| $2\nu_4$ | 6046 | 6113.2 | −67 |
| $\nu_4+\nu_6$ | 4003 | 4010.9 | −8 |
| $2\nu_5$ | 2863 | 2885.6 | −23 |

TABLE II. VIBRATIONAL FREQUENCIES AND CORIOLIS COUPLING CONSTANTS OF THE FUNDAMENTALS FOR $CH_3Br$[3,5]

| | $\nu_0$, cm$^{-1}$ | $\zeta$ |
|---|---|---|
| $\nu_1$ | 2972 | — |
| $\nu_2$ | 1305 | — |
| $\nu_3$ | 611 | — |
| $\nu_4$ | 3056.6 | 0.059 |
| $\nu_5$ | 1442.8 | −0.244 |
| $\nu_6$ | 954.3 | 0.216 |

TABLE III. THE OBSERVED AND CALCULATED FREQUENCIES OF THE BAND $\nu_1+\nu_4$

| $m$ | $\nu^{obs}$ cm$^{-1}$ | $\nu^{calcd}$ cm$^{-1}$ | $\Delta$ cm$^{-1}$ |
|---|---|---|---|
| −10 | 5845.09 | 5845.26 | −0.17 |
| −9 | 55.87 | 55.88 | −0.01 |
| −8 | 66.42 | 66.35 | 0.07 |
| −7 | 76.92 | 76.69 | 0.23 |
| −6 | 87.00 | 86.88 | 0.12 |
| −5 | 96.84 | 96.94 | −0.10 |
| −4 | 5907.09 | 5906.85 | 0.24 |
| −3 | 16.54 | 16.62 | −0.08 |
| −2 | 26.01 | 26.26 | −0.25 |
| −1 | 35.53 | 35.75 | −0.22 |
| 0 | 44.98 | 45.10 | −0.12 |
| 1 | 54.65 | 54.31 | 0.34 |
| 2 | (64.94) | 63.38 | (1.56) |
| 3 | (75.26) | 72.31 | (2.95) |

$\nu_0+[A'(1-\zeta)^2-B']=5945.1\pm0.3$ cm$^{-1}$
$2[A'(1-\zeta)-B']=9.3\pm0.1$ cm$^{-1}$
$(A'-A'')-(B'-B'')=-0.07\pm0.01$ cm$^{-1}$
$\nu_0=5940.6\pm0.3$ cm$^{-1}$
$\zeta=0.01_9\pm0.01_2$

TABLE IV. THE OBSERVED AND CALCULATED FREQUENCIES OF THE BAND $\nu_1+\nu_5$

| $m$ | $\nu^{obs}$ cm$^{-1}$ | $\nu^{calcd}$ cm$^{-1}$ | $\Delta$ cm$^{-1}$ |
|---|---|---|---|
| −6 | (4359.23) | 4345.53 | (13.70) |
| −5 | (67.49) | 58.02 | (9.47) |
| −4 | (76.00) | 70.36 | (5.64) |
| −3 | (86.81) | 82.55 | (4.26) |
| −2 | (96.28) | 94.60 | (1.68) |
| −1 | (4407.12) | 4406.50 | (0.62) |
| 0 | 18.25 | 18.26 | −0.01 |
| 1 | 29.88 | 29.87 | 0.01 |
| 2 | 41.35 | 41.33 | 0.02 |
| 3 | 52.66 | 52.65 | 0.01 |
| 4 | 63.76 | 63.82 | −0.06 |
| 5 | 74.88 | 74.85 | 0.03 |

$\nu_0+[A'(1-\zeta)^2-B']=4418.3\pm0.1$ cm$^{-1}$
$2[A'(1-\zeta)-B']=11.68\pm0.09$ cm$^{-1}$
$(A'-A'')-(B'-B'')=-0.07\pm0.02$ cm$^{-1}$
$\nu_0=4411.1\pm0.2$ cm$^{-1}$
$\zeta=-0.22\pm0.01$

TABLE V. THE OBSERVED FREQUENCIES OF THE BAND $\nu_1+\nu_6$

| $m$ | $\nu^{obs}$, cm$^{-1}$ |
|---|---|
| −2 | 3906.99 |
| −1 | 15.09 |
| 0 | 22.60 |
| 1 | 29.52 |
| 2 | 36.24 |
| 3 | 41.84 |
| 4 | 50.67 |
| 5 | 56.78 |
| 6 | 63.54 |
| 7 | 69.46 |
| 8 | 76.33 |

TABLE VI. THE OBSERVED AND CALCULATED FREQUENCIES OF THE BAND $\nu_2+\nu_4$

| $m$ | $\nu^{obs}$ cm$^{-1}$ | $\nu^{calcd}$ cm$^{-1}$ | $\Delta$ cm$^{-1}$ |
|---|---|---|---|
| −8 | 4283.91 | 4283.74 | 0.17 |
| −7 | 92.69 | 92.86 | −0.17 |
| −6 | 4301.86 | 4301.97 | −0.11 |
| −5 | 11.07 | 11.07 | 0.00 |
| −4 | 20.18 | 20.15 | 0.03 |
| −3 | 29.20 | 29.22 | −0.02 |
| −2 | 38.33 | 38.28 | 0.05 |
| −1 | 47.50 | 47.33 | 0.17 |
| 0 | 56.50 | 56.36 | 0.14 |
| 1 | 65.40 | 65.38 | 0.02 |
| 2 | 74.34 | 74.39 | −0.05 |
| 3 | 83.17 | 83.38 | −0.21 |
| 4 | 92.27 | 92.36 | −0.09 |
| 5 | 4401.25 | 4401.33 | −0.08 |
| 6 | 10.50 | 10.29 | 0.21 |
| 7 | | 19.23 | |
| 8 | (28.84) | 28.16 | (0.68) |

$\nu_0+[A'(1-\zeta)^2-B']=4356.4\pm0.2$ cm$^{-1}$
$2[A'(1-\zeta)-B']=9.03\pm0.02$ cm$^{-1}$
$(A'-A'')-(B'-B'')=-0.006\pm0.005$ cm$^{-1}$
$\nu_0=4352.1\pm0.1$ cm$^{-1}$
$\zeta=0.057\pm0.005$

TABLE VII. THE OBSERVED AND CALCULATED FREQUENCIES OF THE BAND $\nu_2+\nu_5$

| $m$ | $\nu^{obs}$ cm$^{-1}$ | $\nu^{calcd}$ cm$^{-1}$ | $\Delta$ cm$^{-1}$ |
|---|---|---|---|
| −10 | 2629.03 | 2628.98 | 0.05 |
| −9 | 41.59 | 41.51 | 0.08 |
| −8 | 54.01 | 53.98 | 0.03 |
| −7 | (66.11) | 66.39 | (−0.28) |
| −6 | 78.61 | 78.74 | −0.13 |
| −5 | 90.91 | 91.03 | −0.12 |
| −4 | 2703.11 | 2703.26 | −0.15 |
| −3 | 15.38 | 15.44 | −0.06 |
| −2 | 27.59 | 27.55 | 0.04 |
| −1 | 39.58 | 39.60 | −0.02 |
| 0 | 51.59 | 51.59 | 0.00 |
| 1 | (63.72) | 63.52 | (0.20) |
| 2 | 75.47 | 75.39 | 0.08 |
| 3 | (87.41) | 87.21 | (0.20) |
| 4 | 98.97 | 98.96 | 0.01 |
| 5 | 2810.53 | 2810.65 | −0.12 |
| 6 | 22.25 | 22.28 | −0.03 |

$\nu_0+[A'(1-\zeta)^2-B']=2751.59\pm0.07$ cm$^{-1}$
$2[A'(1-\zeta)-B']=11.96\pm0.02$ cm$^{-1}$
$(A'-A'')-(B'-B'')=-0.030\pm0.003$ cm$^{-1}$
$\nu_0=2744.13\pm0.11$ cm$^{-1}$
$\zeta=-0.236\pm0.005$

TABLE VIII. THE OBSERVED AND CALCULATED FREQUENCIES OF THE BAND $\nu_2+\nu_6$

| $m$ | $\nu^{obs}$ cm$^{-1}$ | $\nu^{calcd}$ cm$^{-1}$ | $\Delta$ cm$^{-1}$ |
|---|---|---|---|
| −9 | 2194.75 | 2194.73 | 0.02 |
| −8 | 2201.44 | 2201.48 | −0.04 |
| −7 | (08.03) | 08.33 | (−0.30) |
| −6 | 15.35 | 15.27 | 0.08 |
| −5 | 22.33 | 22.32 | 0.01 |
| −4 | 29.39 | 29.47 | −0.08 |
| −3 | 36.63 | 36.71 | −0.08 |
| −2 | (44.31) | 44.06 | (0.25) |
| −1 | 51.59 | 51.50 | 0.09 |
| 0 | 58.99 | 59.04 | −0.05 |
| 1 | 66.73 | 66.68 | 0.05 |
| 2 | 74.49 | 74.42 | 0.07 |
| 3 | 82.26 | 82.26 | 0.00 |
| 4 | 90.08 | 90.20 | −0.12 |
| 5 | 98.28 | 98.24 | 0.04 |

$\nu_0+[A'(1-\zeta)^2-B']=2259.04\pm0.07$ cm$^{-1}$
$2[A'(1-\zeta)-B']=7.59\pm0.02$ cm$^{-1}$
$(A'-A'')-(B'-B'')=0.050\pm0.004$ cm$^{-1}$
$\nu_0=2256.09\pm0.08$ cm$^{-1}$
$\zeta=0.205\pm0.003$

TABLE IX. THE OBSERVED AND CALCULATED FREQUENCIES OF THE BAND $2\nu_4$

| $m$ | $\nu^{obs}$ cm$^{-1}$ | $\nu^{calcd}$ cm$^{-1}$ | $\Delta$ cm$^{-1}$ |
|---|---|---|---|
| −8 | (6013.55) | 6012.13 | (1.42) |
| −7 | 23.77 | 23.69 | 0.08 |
| −6 | 35.10 | 35.14 | −0.04 |
| −5 | 46.39 | 46.48 | −0.09 |
| −4 | 57.62 | 57.70 | −0.08 |
| −3 | 68.80 | 68.81 | −0.01 |
| −2 | 79.93 | 79.81 | 0.12 |
| −1 | 90.80 | 90.70 | 0.10 |
| 0 | 6101.51 | 6101.48 | 0.03 |
| 1 | 12.17 | 12.15 | 0.02 |
| 2 | 22.66 | 22.70 | −0.04 |
| 3 | 33.10 | 33.14 | −0.04 |
| 4 | 43.47 | 43.47 | 0.00 |
| 5 | 53.57 | 53.69 | −0.12 |
| 6 | 63.81 | 63.80 | 0.01 |
| 7 | 73.88 | 73.79 | 0.09 |
| 8 | 83.58 | 83.68 | −0.10 |
| 9 | 93.52 | 93.45 | 0.07 |
| 10 | (6203.29) | 6203.11 | (0.18) |
| 11 | (12.25) | 12.66 | (−0.41) |
| 12 | (19.98) | 22.09 | (−2.11) |

$\nu_0+[A'(1-\zeta)^2-B']=6101.48\pm0.07$ cm$^{-1}$
$2[A'(1-\zeta)-B']=10.72\pm0.01$ cm$^{-1}$
$(A'-A'')-(B'-B'')=-0.056\pm0.002$ cm$^{-1}$
$\nu_0=6095.44\pm0.09$ cm$^{-1}$
$\zeta=-0.120\pm0.005$

TABLE X. THE OBSERVED AND CALCULATED FREQUENCIES OF THE BAND $\nu_4+\nu_5$

| $m$ | $\nu^{obs}$ cm$^{-1}$ | $\nu^{calcd}$ cm$^{-1}$ | $\Delta$ cm$^{-1}$ |
|---|---|---|---|
| −9 | 4410.50 | 4410.44 | 0.06 |
| −8 | 19.35 | 19.46 | −0.11 |
| −7 | 28.32 | 28.31 | 0.01 |
| −6 | 37.02 | 37.01 | 0.01 |
| −5 | 45.62 | 45.55 | 0.07 |
| −4 | 53.94 | 53.93 | 0.01 |
| −3 | 62.23 | 62.16 | 0.07 |
| −2 | 70.10 | 70.23 | −0.13 |
| −1 | 78.14 | 78.14 | 0.00 |
| 0 | 85.92 | 85.89 | 0.03 |
| 1 | 93.49 | 93.48 | 0.01 |
| 2 | 4500.86 | 4500.92 | −0.06 |
| 3 | 08.19 | 08.20 | −0.01 |
| 4 | (15.15) | 15.32 | (−0.17) |
| 5 | 22.29 | 22.29 | 0.00 |
| 6 | 29.14 | 29.09 | 0.05 |
| 7 | (36.17) | 35.74 | (0.43) |

$\nu_0+[A'(1-\zeta)^2-B']=4485.89\pm0.07$ cm$^{-1}$
$2[A'(1-\zeta)-B']=7.67\pm0.01$ cm$^{-1}$
$(A'-A'')-(B'-B'')=-0.079\pm0.002$ cm$^{-1}$
$\nu_0=4482.79\pm0.07$ cm$^{-1}$
$\zeta=0.177\pm0.003$

TABLE XI. THE OBSERVED AND CALCULATED FREQUENCIES OF THE BAND $\nu_5+\nu_6$

| $m$ | $\nu^{obs}$ cm$^{-1}$ | $\nu^{calcd}$ cm$^{-1}$ | $\Delta$ cm$^{-1}$ |
|---|---|---|---|
| −6 | (2335.15) | 2336.27 | (−1.12) |
| −5 | (45.37) | 45.91 | (−0.54) |
| −4 | (55.09) | 55.55 | (−0.46) |
| −3 | (64.83) | 65.20 | (−0.37) |
| −2 | (74.48) | 74.86 | (−0.38) |
| −1 | 84.51 | 84.53 | −0.02 |
| 0 | 94.23 | 94.21 | 0.02 |
| 1 | 2403.95 | 2403.90 | 0.05 |
| 2 | 13.57 | 13.59 | −0.02 |
| 3 | 23.27 | 23.29 | −0.02 |
| 4 | 32.99 | 33.00 | −0.01 |
| 5 | 42.67 | 42.72 | −0.05 |
| 6 | 52.47 | 52.44 | 0.03 |
| 7 | 62.25 | 62.18 | 0.07 |
| 8 | 71.88 | 71.92 | −0.04 |

$\nu_0+[A'(1-\zeta)^2-B']=2394.21\pm0.07$ cm$^{-1}$
$2[A'(1-\zeta)-B']=9.68\pm0.04$ cm$^{-1}$
$(A'-A'')-(B'-B'')=0.004\pm0.005$ cm$^{-1}$
$\nu_0=2389.40\pm0.09$ cm$^{-1}$
$\zeta=-0.005\pm0.005$

TABLE XII. THE OBSERVED AND CALCULATED FREQUENCIES OF THE BAND $2\nu_6$

| $m$ | $\nu^{obs}$ cm$^{-1}$ | $\nu^{calcd}$ cm$^{-1}$ | $\Delta$ cm$^{-1}$ |
|---|---|---|---|
| −6 | (1791.62) | 1795.70 | (−4.08) |
| −5 | 1809.01 | 1809.38 | −0.37 |
| −4 | 23.63 | 23.14 | 0.49 |
| −3 | 37.02 | 36.97 | 0.05 |
| −2 | 50.77 | 50.88 | −0.11 |
| −1 | 64.91 | 64.86 | 0.05 |
| 0 | 78.75 | 78.91 | −0.16 |
| 1 | 93.19 | 93.04 | 0.15 |
| 2 | | 1907.24 | |
| 3 | 1921.52 | 21.51 | 0.01 |
| 4 | 35.56 | 35.86 | −0.30 |
| 5 | 50.31 | 50.28 | 0.03 |
| 6 | 64.93 | 64.77 | 0.16 |

$\nu_0+[A'(1-\zeta)^2-B']=1878.9\pm0.3$ cm$^{-1}$
$2[A'(1-\zeta)-B']=14.09\pm0.06$ cm$^{-1}$
$(A'-A'')-(B'-B'')=0.04\pm0.02$ cm$^{-1}$
$\nu_0=1868.8\pm0.3$ cm$^{-1}$
$\zeta=-0.426\pm0.009$

TABLE XIII. THE OBSERVED AND CALCULATED FREQUENCIES OF THE BAND $\nu_2+\nu_4+\nu_5$

| $m$ | $\nu^{obs}$ cm$^{-1}$ | $\nu^{calcd}$ cm$^{-1}$ | $\Delta$ cm$^{-1}$ |
|---|---|---|---|
| −6 | 5728.62 | 5728.57 | 0.05 |
| −5 | 37.27 | 37.22 | 0.05 |
| −4 | 45.69 | 45.71 | −0.02 |
| −3 | 53.95 | 54.05 | −0.10 |
| −2 | 62.16 | 62.23 | −0.07 |
| −1 | 70.21 | 70.26 | −0.05 |
| 0 | 78.02 | 78.13 | −0.11 |
| 1 | (85.23) | 85.85 | (−0.62) |
| 2 | 93.53 | 93.41 | 0.12 |
| 3 | 5801.05 | 5800.81 | 0.24 |
| 4 | 08.15 | 08.06 | 0.09 |
| 5 | 14.90 | 15.15 | −0.25 |
| 6 | (22.21) | 22.09 | (0.12) |

$\nu_0+[A'(1-\zeta)^2-B']=5778.1\pm0.2$ cm$^{-1}$
$2[A'(1-\zeta)-B']=7.80\pm0.03$ cm$^{-1}$
$(A'-A'')-(B'-B'')=-0.08\pm0.01$ cm$^{-1}$
$\nu_0=5781.1\pm0.2$ cm$^{-1}$
$\zeta=0.165\pm0.005$

TABLE XIV. THE OBSERVED AND CALCULATED FREQUENCIES OF THE BAND $\nu_4+2\nu_5$

| $m$ | $\nu^{obs}$ cm$^{-1}$ | $\nu^{calcd}$ cm$^{-1}$ | $\Delta$ cm$^{-1}$ |
|---|---|---|---|
| −6 | (5820.85) | 5819.53 | (1.32) |
| −5 | (31.81) | 31.17 | (0.64) |
| −4 | 42.26 | 42.39 | −0.13 |
| −3 | 53.31 | 53.22 | 0.09 |
| −2 | 63.76 | 63.65 | 0.11 |
| −1 | 73.78 | 73.67 | 0.11 |
| 0 | 83.20 | 83.29 | −0.09 |
| 1 | 92.47 | 92.51 | −0.04 |
| 2 | 5901.21 | 5901.33 | −0.12 |
| 3 | 09.70 | 09.74 | −0.04 |
| 4 | 17.85 | 17.75 | 0.10 |
| 5 | (27.71) | 25.36 | (2.35) |
| 6 | (37.23) | 32.57 | (4.66) |
| 7 | (46.59) | 39.38 | (7.21) |

$\nu_0+[A'(1-\zeta)^2-B']=5883.3\pm0.2$ cm$^{-1}$
$2[A'(1-\zeta)-B']=9.42\pm0.04$ cm$^{-1}$
$(A'-A'')-(B'-B'')=-0.201\pm0.005$ cm$^{-1}$
$\nu_0=5878.6\pm0.2$ cm$^{-1}$
$\zeta=-0.021\pm0.005$

TABLE XV. VIBRATIONAL FREQUENCIES AND CORIOLIS COUPLING CONSTANTS OF THE PERPENDICULAR BANDS OF $CH_3Br$

| | Observed values | | Predicted values | | $\nu_0^{obs}-\nu_0^{pred.}$ |
|---|---|---|---|---|---|
| | $\nu_0$, $cm^{-1}$ | $\zeta$ | $\nu_0$, $cm^{-1}$ | $\zeta$ | $cm^{-1}$ |
| $\nu_1+\nu_4$ | 5940.6 | 0.02 | 6029.0 | 0.059 | −88.4 |
| $\nu_1+\nu_5$ | 4411.1 | −0.22 | 4415.2 | −0.244 | −4.1 |
| $\nu_1+\nu_6$ | 3920 | 0.23 | 3926.7 | 0.216 | −7 |
| $\nu_2+\nu_4$ | 4352.1 | 0.057 | 4361.6 | 0.059 | −9.5 |
| $\nu_2+\nu_5$ | 2744.13 | −0.236 | 2747.8 | −0.244 | −3.7 |
| $\nu_2+\nu_6$ | 2256.1 | 0.205 | 2259.3 | 0.216 | −3.2 |
| $2\nu_4$ | 6095.44 | −0.120 | 6113.2 | −0.118 | −17.8 |
| $\nu_4+\nu_5$ | 4482.79 | 0.177 | 4499.4 | 0.185 | −16.6 |
| $\nu_5+\nu_6$ | 2389.40 | −0.005 | 2397.1 | 0.028 | −7.7 |
| $2\nu_6$ | 1868.8 | −0.426 | 1908.6 | −0.432 | −39.8 |
| $\nu_2+\nu_4+\nu_5$ | 5781.1 | 0.165 | 5804.4 | 0.185 | −23.3 |
| $\nu_4+2\nu_5$ | 5878.6 | −0.021 | 5942.2 | −0.547<br>0.059 | −63.6 |

TABLE XVI. VIBRATIONAL ANHARMONIC TERMS OF $CH_3Br$, $cm^{-1}$

| | | | |
|---|---|---|---|
| $x_{11}$ | −31 | $x_{13}$ | −1 |
| $x_{12}$ | −114 | $x_{23}$ | −5 |
| $x_{22}$ | −7 | $x_{33}$ | −4 |
| $x_{44}+g_{44}$ | −8.9 | $x_{56}+g_{56}$ | −7.7 |
| $x_{45}+g_{45}$ | −16.6 | $x_{66}+g_{66}$ | −19.9 |
| $x_{46}+g_{46}$ | −8 | | |
| $x_{44}-g_{44}$ | −34 | | |
| $x_{55}-g_{55}$ | −12 | | |
| $x_{44}$ | −21 | | |
| $g_{44}$ | +12 | | |
| $x_{14}$ | −88 | $x_{24}$ | −10 |
| $x_{15}$ | −4 | $x_{25}$ | −4 |
| $x_{16}$ | −7 | $x_{26}$ | −3 |

TABLE XVII. THE OBSERVED AND CALCULATED VALUES FOR $(A'-A'')-(B'-B'')$ OF $CH_3Br$, $cm^{-1}$

| | | $(A'-A'')-(B'-B'')$ | | $-(B'-B'')$ |
|---|---|---|---|---|
| | | obs. | calcd. | |
| 1 | $\nu_1+\nu_4$ | −0.07 | −0.06 | −0.00009* |
| 2 | $\nu_1+\nu_5$ | −0.07 | −0.08 | −0.00066* |
| 3 | $\nu_2+\nu_4$ | −0.006 | −0.008 | 0.00191 |
| 4 | $\nu_2+\nu_5$ | −0.030 | −0.027 | 0.00134 |
| 5 | $\nu_2+\nu_6$ | 0.050 | 0.050 | 0.0031 |
| 6 | $2\nu_4$ | −0.056 | −0.060 | −0.00018 |
| 7 | $\nu_4+\nu_5$ | −0.079 | −0.079 | −0.00075 |
| 8 | $\nu_5+\nu_6$ | 0.004 | −0.020 | 0.00044 |
| 9 | $2\nu_6$ | 0.04 | 0.056 | 0.0022 |
| 10 | $\nu_2+\nu_4+\nu_5$ | −0.08 | −0.057 | 0.00125 |
| 11 | $\nu_4+2\nu_5$ | −0.201 | −0.127 | −0.00141 |

* It is assumed that $\beta_1=0$.

TABLE XVIII. THE ROTATIONAL CORRECTION TERMS OF $CH_3Br$, $cm^{-1}$

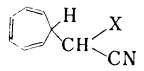
| | | |
|---|---|---|
| $\alpha_1$ | 0.03 | the present work |
| $\alpha_2$ | −0.020 | the present work |
| $\alpha_3$ | | |
| $\alpha_4$ | 0.030 | Morino et al.[5], Rank et al.[2], the present work |
| $\alpha_5$ | 0.048 | Brown et al.[4] with $\alpha_4=0.030$, Morino et al.[5], the present work |
| $\alpha_6$ | −0.027 | Morino et al.,[5] the present work |
| $\beta_1$ | | |
| $\beta_2$ | 0.00200 | Brown et al.[4] with $\beta_4=-0.00009$ |
| $\beta_3$ | 0.0024 | Kraitchman et al.[10] |
| $\beta_4$ | −0.00009 | Rank et al.[2] |
| $\beta_5$ | −0.00066 | Brown et al.[4] with $\beta_4=-0.00009$ |
| $\beta_6$ | 0.0011 | Hirose[11] |

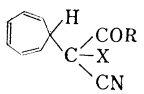
# The Reaction of Tropylmalononitrile and Ethyl Tropylcyanoacetate with Acyl Chloride[1]

By Toshio MUKAI and Tsutomu MIYASHI

(Received August 12, 1964)

The acylation of tropylmalononitrile (I) or ethyl tropylcyanoacetate (II) would be expected to give a compound of type (A), which, under basic conditions, might be hydrolyzed to a tropyl derivative different from the starting material, might form a heptafulvene by the elimination of hydrogen cyanide, or might give a styrene-type compound through rearrangement.[2] However, the treatment of I or II with acyl chloride in a basic medium led to an unexpected result, which will be described in this paper.





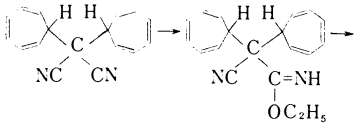
(A)

I : X=CN
II : X=$COOC_2H_5$

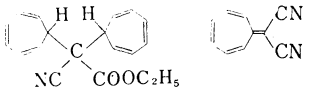
X=CN or $COOC_2H_5$
R=$C_6H_5$ or $CH_3$

The reaction of equimolar proportions of benzoyl chloride and I in a pyridine solution afforded compound (III), $C_{17}H_{14}N_2$, and benzoylcyanoacetamide. The former compound was also obtained when I was treated with acetyl chloride in pyridine. The ultraviolet spectrum of III showed a maximum at 255 m$\mu$ (log $\varepsilon=3.81$) due to the tropyl group;[3] the infrared spectrum had a band at 2260 $cm^{-1}$ (CN group). III may, therefore, be supposed to be ditropylmalononitrile. This was comfirmed by a mixed melting point determination with an authentic sample.[4] In the above reaction, and in several of those following, the products were isolated by chromatography on aluminum oxide,[5] which led to the partial conversion of compound (III) into ditropylcyanoacetamide (IV), which was identical with the compounds obtained by reaction of tropylcyanoacetamide with tropylium ions.

The sodio compound of I, in ethanol, also reacted with acetyl or benzoyl chloride to afford III in a fairly good yield, along with ethyl ditropylcyanoacetate[4] (V). The reaction of I with acyl chlorides in ethanol, in the presence of two molar equivalents of sodium ethoxide, gave compound (VI) $C_{19}H_{20}ON_2$ and 8,8-dicyanoheptafulvene[4] (VII), besides compounds III, IV and V; the yields are given in Table I. The infrared spectrum of VI showed bands at 2240 (CN), 3345 (NH) and 1658 $cm^{-1}$ (C=N). The mild treatment of VI with acid gave V. Furthermore, VI could be obtained from the reaction of III with sodium ethoxide. From these facts, VI is concluded to be ethyl ditropylcyanoacetimidate.



III VI



V VII

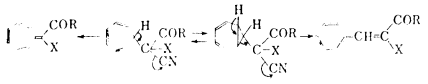
It is assumed that 8,8-dicyanoheptafulvene (VII) originates not from the intermediate (A), but from dehydrogenation of I, because the preferential elimination of hydrogen cyanide from A should give 8-cyano-8-acylheptafulvene. Indeed, it was found that the treatment of I with one molar equivalent of sodium ethoxide afforded tropylcyanoacetamide, together with a trace of VII, which is probably formed by the dehydrogenation of I with air.

The reaction of ethyl tropylcyanoacetate (II) with benzoyl or acetyl chloride in pyridine afforded ethyl ditropylcyanoacetate (V). The acylation of a sodio compound of II, in ethanol, also afforded V in the yield shown in Table II.

The formation of the ditropyl compounds (III, V, etc.) in the acylation reaction of I or

1) Presented at the 15th Annual Meeting of the Chemical Research Institute of Non-Aqueous Solutions, Tohoku University, October, 1963.

2) The following reactions would be expected:



Cf. C. R. Ganellin and R. Pettit, *J. Chem. Soc.*, **1958**, 576.

3) K. Conrow, *J. Am. Chem. Soc.*, **81**, 5461 (1959).

4) T. Nozoe, T. Mukai, K. Osaka and N. Shishido, This Bulletin, **34**, 2385 (1961).

5) This transformation did not occur when a neutralized aluminum oxide was used.

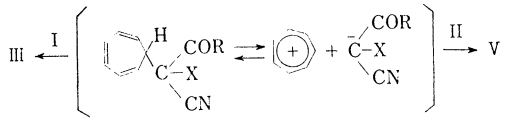
TABLE I. THE RESULTS OF THE ACYLATION OF I

| Medium | Reagent | Yield of products, % III | IV | V | VI | VII |
|---|---|---|---|---|---|---|
| In pyridine | $C_6H_5COCl$ | 82 | 14 | | | |
| | $CH_3COCl$ | 58 | 6.3 | | | |
| In ethanol 1 mol. equiv. of $NaOC_2H_5$ | $C_6H_5COCl$ | 89 | 7 | 4 | | |
| | $CH_3COCl$ | 67 | 5.4 | | | |
| In ethanol 2 mol. equiv. of $NaOC_2H_5$ | $C_6H_5COCl$ | 35 | | 5.5 | 2.6 | 1.5 |
| | $CH_3COCl$ | | 21 | 1.4 | 20 | 0.5 |

TABLE II. THE YIELDS (%) OF V IN ACYLATION OF II

| Reagent | In pyridine | In ethanol 1 mol. equiv. of $NaOC_2H_5$ | In ethanol 2 mol. equiv. of $NaOC_2H_5$ |
|---|---|---|---|
| $C_6H_5COCl$ | 45 | 64 | 21 |
| $CH_3COCl$ | 3.6 | 50 | 30 |

II can be explained as is shown in the following scheme, the first step of which is assumed to be the formation of compound A. The presence of three electron-with drawing groups in A, and the stabilization of the resulting tropylium ions, constitute a strong driving force for the cleavage of A to tropylium ions. The products III or V can result from the reaction of the tropylium ions with I or II.[4] As another pathway to III or V, a nucleophilic attack of I or II on A before its cleavage is also possible.



(A)

It has been pointed out previously that, in general, the fragmentation of tropyl derivatives is brought about by attack Lewis acids[3] or electrophilic reagents.[6] However, it should be emphasized that, in this case, the formation of tropylium ions (or their precursors) occurs readily, even in a basic medium, during the reaction of I or II with acyl chloride.

Attempted acylation of other tropyl compounds containing active methylenes, such as diethyl tropylmalonate, tropylacetylacetone and tropyldibenzoylmethane, did not afford any ditropyl compound, but it did result in the recovery of the starting materials. This is of interest when compared with the fact that diethyl tropylmalonate did not react with tropylium ions.[4]

6) T. Mukai and H. Tsuruta, This Bulletin, 37, 1018 (1964).

## Experimental[7,8]

**The Reaction of Tropylmalononitrile (I) with Acyl Chloride in Pyridine.**—*a) With Benzoyl Chloride.*—To a solution of 1 g. (6 mmol.) of I in 3 ml. of pyridine, 0.9 g. (6 mmol.) of benzoyl chloride was added under cooling with ice. After it had been stirred for 20 hr. at room temperature, the reaction mixture was poured into water and extracted with benzene. The benzene-extract was then washed with 2 N hydrochloric acid and 2 N sodium hydroxide successively, dried over sodium sulfate, and evaporated to give 1.92 g. of a brown oil. This oil was dissolved in benzene and chromatographed, using 60 g. of aluminum oxide (Grade I). The evaporation of the benzene-elute gave 650 mg. of colorless crystals (m.p. 103—105°C), which, on recrystallization from ethanol, afforded ditropylmalononitrile (III)[8] as colorless crystals (m. p. 106—108°C). The evaporation of the elute with benzene-methanol (5 : 1) gave 115 mg. of colorless crystals (m. p. 155—162°C), which, on recrystallization from petroleum ether-benzene, gave colorless crystals (m. p. 167°C). They were found to be identical with ditropylcyanoacetamide (IV), which was synthesized as will be described later. The alkaline washings were acidified with 6 N hydrochloric acid and extracted with ether. The ether-extract was dried over sodium sulfate and evaporated to give colorless crystals (m. p. 98—105°C), which, on recrystallization from benzene, gave 30 mg. of colorless crystals (m. p. 134—135°C), assumed to be benzoylcyanoacetamide.

Found: C, 64.03; H, 4.12; N, 14.51. Calcd. for $C_{10}H_8O_2N_2$: C, 63.82; H, 4.29; N, 14.89%.

*b) With Acetyl Chloride.*—The reaction of 2.0 g. (13 mmol.) of I and 1.02 g. (13 mmol.) of acetyl chloride was carried out in a pyridine solution as has been described in a). The evaporation of the benzene extract gave 1.1 g. of a neutral oil, which crystallized when allowed to stand. The recrystallization of crystals from ethanol gave 572 mg. of ditropylmalononitril (m. p. 105—107°C). The mother liquor was then evaporated, and the residue was dissolved in benzene and chromatographed by passing it through a column containing 15 g. of aluminum oxide (Grade I). A further 350 mg. of III (m. p. 105—107°C) were obtained from the benzene elute, and 107 mg. IV (m. p. 165—167°C),

7) All melting points are uncorrected.

8) The microanalyses were carried out by Miss A. Iwanaga and Miss M. Suzuki, to whom the authors wish to express their gratitude.

from the elute with ether-methanol (5 : 1). The alkaline washings were acidified and extracted with ether. The evaporation of the ether-extract gave 320 mg. of an acidic, viscous oil.

**The Synthesis of Tropylcyanoacetamide and Ditropylcyanoacetamide (IV).**—a) To a solution of 6.5 g. (30 mmol.) of tropyl bromide dissolved in 15 ml. of water, 2.5 g. (30 mmol.) of cyanoacetamide was added. The reaction mixture was neutralized to pH 6 by the addition of a 6 N sodium hydroxide solution and stirred at room temperature for 2 hr., during which time colorless crystals separated out. Filtration, followed by recrystallization from benzene, afforded 4.8 g. of tropylcyanoacetamide as colorless needles (m. p. 144—145°C).

Found: C, 69.21; H, 5.44; N, 15.74. Calcd. for $C_{10}H_{10}ON_2$: C, 68.95; H, 5.79; N, 16.08%.

b) To a solution of 77 mg. (0.45 mmol.) of tropyl bromide in 3 ml. of pyridine, 50 mg, (0.3 mmol.) of tropylcyanoacetamide was added, and the reaction mixture was allowed to stand for 12 hr. at room temperature. After the pyridine had been evaporated under reduced pressure, the residue was poured into water and extracted with benzene. The benzene-extract was washed with dilute hydrochloric acid and then with water and dried over sodium sulfate. The evaporation of benzene gave crystals, which, on recrystallization from ethanol, gave 76 mg. of ditropylcyanoacetamide (IV) as colorless crystals (m. p. 167°C).

Found: C, 76.83; H, 5.90; N, 9.99. Calcd. for $C_{17}H_{16}ON_2$: C, 77.25; H, 6.10; N, 10.60%.

Ditropylcyanoacetamide (IV) was also obtained in the chromatography of III using aluminum oxide. A benzene solution of 200 mg. of III was passed through a column containing 6 g. of alumina (Grade 1). From the benzene elute, 170 mg. of III was recovered, while 25 mg. of IV (m. p. 165—167°C) was obtained from the elute with ether-methanol (1 : 1).

**The Reaction of a Sodio Compound of Tropylmalononitrile (I) with Acyl Chloride in Ethanol.**—*a) With Benzoyl Chloride.*—To a solution of sodium ethoxide prepared from 450 mg. (19 mmol.) of sodium and 20 ml. of absolute ethanol, 3 g. (19 mmol.) of I was added; the mixture was then stirred for 1 hr. at room temperature. Under cooling with ice, 2.7 g. (19 mmol.) of benzoyl chloride was added, drop by drop, to the solution. After it had been stirred for 24 hr. at room temperature, the reaction mixture was poured into water and extracted with benzene. The benzene extract afforded 3.51 g. of a neutral oil by the usual treatment. The oil crystallized on standing; these crystals, on recrystallization from ethanol, afforded 705 mg. of III (m. p. 104—105°C). The filtrate was evaporated, and the residue was dissolved in benzene and chromatographed using 60 g. of aluminum oxide (Grade I). The evaporation of the benzene elute gave 1.50 g. of III as colorless prisms (m. p. 105—106°C). The ether elute gave 125 mg. of V as colorless needles (m. p. 125—126°C). From the elute with ether-methanol (5 : 1), 197 mg. of IV (m. p. 167—169°C) was obtained. The alkaline solution, after the extraction with benzene, was acidified with 6 N hydrochloric acid and extracted with ether. From the ether-extract, 770 mg. of an acidic oil was obtained in the usual way; this crystallized on standing. Filtration, followed by recrystallization from benzene, gave 705 mg. of benzoylcyanoacetamide (m. p. 134—135°C).

*b) With Acetyl Chloride.*—In the same way as in a), 2.3 g. of neutral oil and 100 mg. of an acidic oil were obtained from the reaction of 2 g. (13 mmol.) of I, 300 mg. (13 mmol.) of sodium in ethanol and 1.02 g. (13 mmol.) of acetyl chloride. On being allowed to stand, the neutral oil gave crystals, which, on recrystallization from ethanol, gave 630 mg. of III (m. p. 105°C). The filtrate was evaporated, dissolved in benzene, and chromatographed by passing it through a column containing 23 g. of aluminum oxide (Grade I). The benzene elute gave 480 mg. of III (m. p. 105—106°C). Elution with ether-methanol (10 : 1) afforded 90 mg. of IV (m. p. 166°C).

**The Reaction of Tropylmalononitrile (I) with Acyl Chloride in the Presence of 2 Molar Equivalents of Sodium Ethoxide.**—*a) With Benzoyl Chloride.*—To a solution of sodium ethoxide prepared from 584 mg. (26 mmol.) of sodium and 20 ml. of absolute ethanol, 1.95 g. (13 mmol.) of I and then 1.5 ml. (13 mmol.) of benzoyl chloride were added drop by drop under cooling with ice. After it had been stirred for 21 hr. at room temperature, the reaction mixture was treated in the usual way to give 2.46 g. of a neutral oil containing crystals. The addition of a small amount of ethanol, followed by filtration, afforded 496 mg. of colorless crystals, (m. p. 101—107°C), which, on recrystallization from ethanol, yielded 385 mg. of VI as colorless prisms (m. p. 114—115°C).

Found: C, 77.99; H, 6.33; N, 9.31. Calcd. for $C_{19}H_{20}ON_2$: C, 78.05; H, 6.90; N, 9.58%.

The combined filtrate was evaporated, dissolved in benzene, and chromatographed using 70 g. of aluminum oxide (Grade I). The evaporation of the benzene elute gave 530 mg. of colorless crystals, (m. p. 95—102°C), which, on recrystallization from ethanol, gave 140 mg. of III (m. p. 106—107°C). Elution with benzene-ether (5 : 1) gave 150 mg. of crystals with an oil, which, on recrystallization from ethanol, gave 30 mg. of red crystals (m. p. 140—170°C) from the scarcely soluble portion and 103 mg. of colorless crystals (m. p. 121—124°C) from the easily soluble portion. The recrystallization of the former from ethanol gave 8, 8-dicyanoheptafulvene (VII) (m. p. 199°C), while the latter gave V (m. p. 125°C). Elution with ether-methanol (10 : 1) afforded 300 mg. of crystals (m. p. 130—140°C), which, on recrystallization from ethanol, gave tropylcyanoacetamide (m. p. 140—142°C).

*b) With Acetyl Chloride.*—As has been described in a), 1.75 g. of a neutral oil was obtained from the reaction of 1.95 g. (13 mmol.) of I with 1.02 g. (13 mmol.) of acetyl chloride in the presence of 2 mol. equivalents of sodium ethoxide in an ethanolic solution. The oil crystallized partly when allowed to stand. Filtration, followed by recrystallization from ethanol, afforded 360 mg. of VI as colorless needles (m. p. 114—115°C). The filtrate

was then evaporated, dissolved in benzene and chromatographed by passing it through a column containing 50 g. of aluminum oxide (Grade I). The evaporation of the elute with benzene-ether (5 : 1) yielded 450 mg. of an oil, which crystallized on standing. The recrystallization of the crystals from ethanol gave 250 mg. of the starting material (I) (m. p. 60—62°C) as colorless prisms. Elution with ether gave 70 mg. of orange crystals, which, on recrystallization from benzene, afforded 10 mg. of red needles (m. p. 140—170°C), mainly composed of 8, 8-dicyanoheptafulvene (identified by its infrared spectrum). The benzene filtrate was evaporated to give crystals which, on recrystallization from ethanol, afforded 25 mg. of V (m. p. 120—123°C). The evaporation of the elute with ether-methanol (1 : 1) afforded 350 mg. of crystals (m. p. 140—142°C), which, on recrystallization from ethanol, gave IV (m. p. 168—169°C).

**The Hydrolysis and Synthesis of Ethyl Ditropylcyanoacetimidate (VI).**—*a) The Hydrolysis of VI.*—A solution of 100 mg. of VI dissolved in a mixture of 1 ml. each of 2 N hydrochloric acid and ethanol was refluxed for 30 min. After neutralization with 2 N sodium hydroxide, the reaction mixture was extracted with benzene. The benzene extract was then washed with water, dried over sodium sulfate, and evaporated to give 60 mg. of an yellow oil, which crystallized on cooling. Recrystallization from ethanol gave V as pale yellow needles (m. p. 126—127°C).

*b) The Synthesis of VI.*—To a solution of sodium ethoxide prepared from 600 mg. (24 mmol.) of sodium and 20 ml. of absolute ethanol, 500 mg. (2 mmol.) of III was added; the reaction mixture was stirred at room temperature for 20 hr., during which time colorless crystals separated out. After the evaporation of the ethanol, the reaction mixture was poured into water and extracted with benzene. The extract was washed with water, dried over sodium sulfate, and evaporated to give colorless needles, which, on recrystallization from ethanol, afforded 150 mg. of VI as colorless needles (m. p. 110—111°C). The residue from the mother liquor was recrystallized from ethanol to give 153 mg. of IV (m. p. 167°C).

**The Reaction of Tropylmalononitrile (I) with Sodium Ethoxide in Ethanol.**—To a solution of sodium ethoxide prepared from 46 mg. (2 mmol.) of sodium and 4 ml. of absolute ethanol, 312 mg. (2 mmol.) of I was added under cooling with ice. After it had been stirred for 24 hr. at room temperature, the solution was poured into water and extracted with ether; the usual treatment of the ether-extract then gave 300 mg. of an oil. The oil was dissolved in benzene and chromatographed by passing it through a column containing 9 g. of aluminum oxide (Grade I). The evaporation of the benzene elute gave 73 mg. of the starting material (I) (m. p. 62°C). Elution with benzene-ether gave 20 mg. of 8, 8-dicyanoheptafulvene (VII) (m. p. 199°C), while elution with ether-methanol gave 120 mg. of tropylcyanoacetamide (m. p. 145°C).

**The Reaction of Ethyl Tropylcyanoacetate (II) with Acyl Chloride in Pyridine.**—*a) With Benzoyl Chloride.*—To a solution of 2 g. (11 mmol.) of II dissolved in 4 ml. of pyridine, 1.55 g. (11 mmol.) of benzoyl chloride was added drop by drop under cooling with ice. The mixture was stirred under cooling for 1 hr. and at room temperature for 20 hr. The solution was then poured into water and extracted with benzene. The benzene-extract was successively washed with 2 N hydrochloric acid, 2 N sodium hydroxide and water, dried over sodium sulfate, and evaporated to give 2 g. of a brown oil, which crystallized on standing. Filtration, followed by recrystallization from ethanol, gave 485 mg. of ethyl ditropylcyanoacetate (V) (m. p. 125—127°C).[8] The ethanolic filtrate was evaporated, dissolved in benzene, and chromatographed using aluminum oxide. The evaporation of the benzene elute gave 143 mg. of V (m. p. 124—126°C), and the following benzene elute gave 95 mg. of a brown oil, which was identified with the starting material (II) by a comparison of their infrared spectra.

*b) With Acetyl Chloride.*—The reaction of 2 g. (11 mmol.) of II and 0.865 g. (11 mmol.) of acetyl chloride was carried out as in a). Only 52 mg. of V was obtained as colorless crystals (m. p. 127—128°C). The acidification of the alkaline washings, followed by extraction with ether and the usual treatment of the ether-extract, gave 1.12 g. of an acidic oil which contained the starting material (II) (identified from the infrared spectrum).

**The Reaction of a Sodio Compound of Ethyl Tropylcyanoacetate (II) with Acyl Chloride in Ethanol.**—*a) With Benzoyl Chloride.*—A sodio compound of II was obtained from 253 mg. (11 mmol.) of sodium and 2 g. (11 mmol.) of II in 10 ml. of absolute ethanol. To this solution, 1.55 g. (11 mmol.) of benzoyl chloride was added under cooling with ice. After it had been stirred for 20 hr. at room temperature, the mixture was poured into water and extracted with benzene. The benzene extract was washed with water, dried over sodium sulfate, and evaporated to give 2.1 g. of an oil, which crystallized on cooling. Filtration, followed by recrystallization from ethanol, gave 510 mg. of V as colorless crystals (m. p. 124—125°C). The ethanolic filtrate was evaporated, and the residue was dissolved in benzene and chromatographed using 40 g. of aluminum oxide (Grade I). The evaporation of the benzene elute gave 380 mg. of V (m. p. 124—125°C). After the mother liquor from the benzene extract had been acidified and extracted with ether, the ether-extract was dried over sodium sulfate and evaporated to give 587 mg. of an acidic oil containing crystals of ethyl benzoylcyanoacetate (m. p. 39.5—40.0°C)[9]

*b) With Acetyl Chloride.*—When the reaction of 2 g. (11 mmol.) of II with 0.864 g. (11 mmol.) of acetyl chloride was carried out in the same way as in a), and 1.4 g. of a neutral oil was obtained; this crystallized partly. Filtration, followed by recrystallization from ethanol, afforded 605 mg. of V (m. p. 126—127°C). The filtrate was evaporated, dissolved in benzene, and chromatographed using aluminum oxide (Grade I) to give 106 mg. of V and 150 mg. of II.

9) M. Haller, *Bull. soc. chim. France* [2], **45**, 271 (1886).

**The Reaction of Ethyl Tropylcyanoacetate (II) and Acyl Chloride in Ethanol in the Presence of 2 Molar Equivalents of Sodium Ethoxide.**—*a) With Benzoyl Chloride.*—To a solution of 506 mg. (22 mmol.) of sodium dissolved in 15 ml. of absolute ethanol, 2 g. (11 mmol.) of II was added, and then 1.55 g. (11 mmol.) of benzoyl chloride was added under cooling with ice. The usual treatment of the reaction mixture afforded 1.40 g. of a neutral oil, which crystallized partly, and 1.26 g. of an acidic oil. The former was filtered and recrystallized from ethanol to give 298 mg. of V as colorless needles (m. p. 124—125°C).

*b) With Acetyl Chloride.*—As has been described in a), 2 g. (11 mmol.) of II was acetylated with 0.864 g. (11 mmol.) of acetyl chloride in the presence of 2 molar equivalents of sodium ethoxide. From the reaction mixture, 760 mg. of a neutral oil, which crystallized partly, and 690 mg. of an acidic oil were obtained. When the crystals obtained from the neutral oil by chromatography were recrystallized from ethanol, 415 mg. of V (m. p. 126—127°C) were obtained.

The authors wish to express their deep gratitude to Professor Tetsuo Nozoe for his kind guidance throughout the course of this work. They also wish to thank the Sankyo Co. for its donation of research funds to cover a part of the expenses of their work. The infrared and ultraviolet spectrophotometers used in this work were purchased with a grant-in-aid for Fundamental and Technical Research from the Toyo Rayon Co., to whom the authors are grateful.

*Department of Chemistry*
*Faculty of Science*
*Tohoku University*
*Katahira-cho, Sendai*

# Photoelectric Emission and Electrical Conductivity of the Cesium Complex with Pyrene Derivatives

By Kyohei OGINO, Satoshi IWASHIMA, Hiroo INOKUCHI and Yoshiya HARADA

(Received August 17, 1964)

The efficiency of the photoelectric emission of an alkali metal was promoted by the evaporation of a hydrocarbon, naphthalene or anthracene onto a sodium (or potassium) film.[1]

In the 1950's, Ubbelohde investigated the electronic properties of the solid-state complexes of polycyclic aromatics involving an alkali metal; sodium, potassium or lithium.[2]

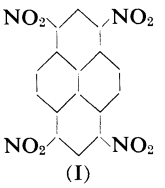
Recently, we have found a strong photoelectric emission and a high quantum efficiency of the complexes between cesium and polycyclic aromatic compounds in the region with wavelengths shorter than 600 m$\mu$.[3]

On the basis of the charge transfer process of the complexes, the selection of the types of the two components—the electron donor and the acceptor—may help to yield a group of materials with higher conductivities. In this article, we will discuss the photoemission and the electronic conduction of the cesium complexes with pyrene derivatives in an attempt to understand better the mechanism of the charge transfer process.

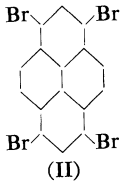
1) R. Suhrmann, *Z. Phys.*, **94**, 742 (1935); **111**, 18 (1937).
2) W. A. Holmes-Walker and A. R. Ubbelohde, *J. Chem. Soc.*, **1954**, 720; G. C. Martin, N. D. Parkyns and A. R. Ubbelohde, ibid., **1961**, 4958.
3) H. Inokuchi and Y. Harada, *Nature*, **198**, 477 (1963).

## Experimental Procedures

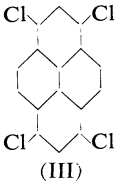
Though preparations of the pyrene derivatives have already been reported,[4] the descriptions are not reliable. The pyrene derivatives applied in this experiment were synthesized as follows:



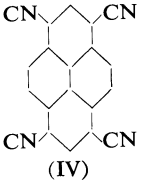
(I)



(II)



(III)



(IV)

**1, 3, 6, 8-Tetranitropyrene** ($TNO_2P$) (**I**). — One hundred grams of nitric acid ($d$=1.5) was added slowly to a 300 ml. nitrobenzene solution containing 30 g. of pyrene. With the addition of nitric oxide, yellow needle crystallites were deposited.

4) H. Vollmann, H. Becker, M. Corell and H. Streeck, *Ann.*, **531**, 1 (1937).

TABLE I. THE CHANGE OF COLOUR BY THE FORMATION OF THE COMPLEXES

| Complex | | Change of colour | |
|---|---|---|---|
| Donor | Acceptor | After formation 30 min. | 1 day |
| Cs | Pyrene (white) | Pink | Blue |
| Cs | $TNO_2P$ (orange yellow) | Dark brown | Dark brown |
| Cs | TCNP (yellow) | Orange yellow | Dark violet |
| Cs | TClP (pale yellow) | Bluish brown | Bluish brown |
| Cs | TBrP (pale yellow) | Dark brown | Dark brown |

After the solution had been stirred for 4—5 hr. at 110—120°C, the crystallites were separated with a glass-filter. Through sublimation in vacuo, purified crystallites, m. p. 334—336°C, were obtained.

**1, 3, 6, 8-Tetrabromopyrene (TBrP) (II).**—Twenty grams of pyrene was dissolved in 300 ml. of nitrobenzene. Seventy grams of bromine was then stirred drop by drop into the solution. Through continuous shaking at 120—125°C, pale yellow crystallites separated from the solution as precipitates. These crystallites were filtered and washed with ethanol. The melting point of tetrabromopyrene, which was purified by sublimation under a pressure of $10^{-4}$ mmHg, was 399—404°C.

**1, 3, 6, 8-Tetrachloropyrene (TClP) (III).**—Thirty-eight grams of 1, 3, 6, 8-tetranitropyrene (I) and 150 g. of phosphorus pentachloride were dissolved in 150 ml. of trichlorobenzene and heated at around 150°C for 8—9 hr. while being continuously stirred. During the operation, a large amount of gas was removed from the solution and the colour of solution changed from pale brown to dark brown. Dark brown crystallites were separated from the solution as precipitates. Through vacuum sublimation, purified compounds, for which the melting point was 358—360°C, were pale yellow-coloured crystallites.

**1, 3, 6, 8-Tetracyanopyrene (TCNP) (IV).**—Twelve grams of tetrabromopyrene (II) and 90 g. of copper cyanide (CuCN) were dissolved in 120 ml. of benzyl cyanide ($C_6H_5CH_2CN$) which had been purified by vacuum distillation. The solution was heated at 100°C for half an hour and then at 234°C (the boiling point of benzyl cyanide) for 4 hr. while being continuously stirred. Through these reactions, the color of the solution changed from pale brown to dark brown. One hundred millilitres of ethanol was added to the solution at 80—90°C for 1—1.5 hr. with stirring continuously. The precipitates which separated from the solution were washed with 30 per cent nitric acid to eliminate the residue of copper and then repeatedly washed with ethanol. The melting point of compound, sublimed in vacuo, was 445—448°C.

**The Preparation of a Cesium Complex Photocell (Fig. 1).**—A vapour of cesium metal (8), prepared from a reaction between cesium chloride and calcium metal, was brought in contact with a thin film (3) of pyrene derivatives which had previously been deposited on the surface of a glass plate with two aluminium electrodes. By the contact between the aromatic compound and cesium vapour, an abrupt change in the colour occurred, as Table I shows.

The formation of a complex was terminated by the saturation of the cesium metal involved. All preparations of the complexes were carried out at room temperature except that of the cesium-pyrene complex. In the latter, the thin film of the hydrocarbon had to be kept at a low temperature (around 0°C) in order to decrease the vapour pressure of the compound. The ratio of the components of cesium-tetranitropyrene, $Cs/TNO_2P$, was found to be two by chemical analysis.

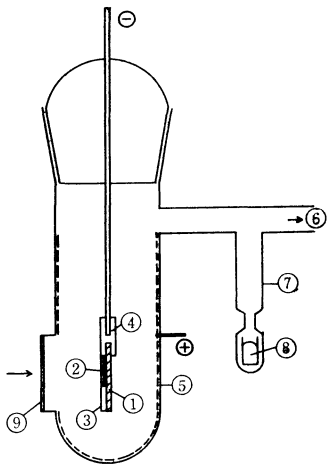



Fig. 1. The cesium complex photocell: 1, glass plate; 2, aluminium electrode; 3, organic thin film; 4, electrode connector; 5, collector (silver film); 6, to connect vacuum system, 7, annex glass for reaction; 8, CsCl+Ca mixture; 9, quartz window.

Under illumination by a visible and an ultraviolet light from a Hitachi spectrometer through a quartz window (9), a strong photoemission from the surface of the complex was found when an electric field (1—30 V.) between a specimen and a collector (5), deposited as a silver film, was applied.

**The Observation of the Quantum Yield of Photoemission.**—The quantum efficiency ($Y$) derives from the ratio between a number of incident photons ($n_p$) and a number of emissive electrons ($n_e$) observed in a photocurrent;

$$Y = \frac{n_e}{n_p} \qquad (1)$$

The photocurrent, $10^{-14}$—$10^{-6}$ amp., was observed by means of a Cary model 32 vibrating reed electrometer.*

* One ampere corresponds to $1.6\times10^{19}$ electrons/sec. in this experiment.

The incident photons ($n_p$) were measured by means of the thermoelectric power of the thermopile:

$$n_p = \frac{V\lambda}{vch} \times 10^7 \text{ photons/sec.} \quad (2)$$

where $v(\mu V./\mu W.\,cm^2)$ is the sensitivity of the thermopile, $V$ is an applied potential on the photocell, $\lambda$ is a wavelength of light, $c$ is the light velocity and $h$ is Plank's constant.

When a Nipponbunko thermopile was applied (its sensitivity was $7.0\times10^2\ \mu V./\mu W.\,cm^2$), the spectral response of the quantum efficiency of cesium-aromatics complexes in the wavelength range from 200 m$\mu$ to 900 m$\mu$ was obtained.

**The Measurement of the Electrical Resistivity of the Complexes.**—The thin organic film evaporated on a silica plate, with two aluminium electrodes as a surface-type cell, came in contact with the vapour of cesium gas in vacuo. The resistivity of the cell was measured with a Kawaguchi Denki model MMA III-13 vibrating reed electrometer.

The absorption spectra of the thin complex films were observed with a Cary recording spectrometer model 14.

## Experimental Results

A variation in the emission current as a function of the applied potential for a Cs-(TBrP) photocell under illumination by monochromatic light (550 m$\mu$), its intensity being $3.6\times10^{11}$ photons/sec., is illustrated in Fig. 2. From an irregularity in the geometrical arrangement of the photocell, as is shown in Fig. 1, the saturation potential of the photoemission was found to be around ten volts. Therefore, the observation has been carried out under an applied potential of 10 V. An ageing of the emission was found.

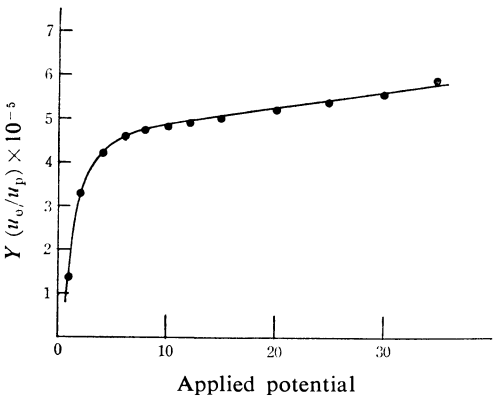



Fig. 2. The variation of photoemission as a function of applied potential for Cs-TBrP.

The spectral responses of the photo-emissive current were curves decreasing gradually from the short wavelength side to the long wavelength side as Fig. 3 shows. However, the response curves changed with time at an initial stage of the complex formation, as is shown in the figure, and converged to the stable state.

The electrical resistivity of the complexes, which was observed with a surface-type cell,[5] possessed a wide range of values, depending on the pyrene derivatives applied as acceptors. The temperature dependence of the resistivity was semiconductive in character ($\rho=\rho_0 \exp \Delta\varepsilon/2KT$), as Table II demonstrates.

Table II. The semiconductivity of pyrene-cesium complexes

| Complex | $\rho$, $\Omega$ cm. at 15°C | $\Delta\varepsilon$, eV. |
|---|---|---|
| Pyrene-Cs | $2.1\times10^4$ | 0.42 |
| TClP-Cs | 8 | 0.34 |
| TBrP-Cs | $1.6\times10^1$ | 0.35 |
| $TNO_2P$-Cs | $2\times10^6$ | 0.94 |
| TCNP-Cs | $6\times10^5$ | 0.70 |

## Discussion

The threshold values of the spectral response of the photoemission of the cesium complexes which correspond to the ionization potential are situated around $1.6\times10^4\ cm^{-1}$. The pure cesium metal has a strong response peak at around $2.5\times10^4\ cm^{-1}$. Further, the threshold value of the photoemission of pyrene was reported to be around $4.7\times10^4\ cm^{-1}$.[6] Therefore, it is reasonable to consider that the emission from a cesium-aromatics system, observed in the experiment, occurs from new compounds.

The formation of complexes demonstrated an increase in the quantum yield of photoemission from $10^{-3}$—$10^{-4}$, the values for pure cesium metal and also for pure aromatic compounds, to $10^{-1}$—$10^{-2}$, an increase shown in Fig. 3. These promotions may take place from the electron transfer from a cesium metal to a partner molecule.

The transfer charge carriers depends roughly on the energy difference between the ionization potential of metal, 1.9 eV. for cesium, and the electron affinity of the acceptor, pyrene derivatives. On the basis of organic chemistry, the order of the values of electron affinity is;

tetracyanopyrene > tetranitropyrene > tetrabromopyrene $\geqq$ tetrachloropyrene > pyrene

The velocity of complex formation followed the above relation qualitatively, and also the quantum yield of the photoemission was increased in roughly the above order. The spin

5) H. Inokuchi, "Organic Semiconductors," Maki-shoten, Tokyo (1964), p. 45.
6) L. E. Lyons and G. C. Morris, *J. Chem. Soc.*, **1960**, 5192.

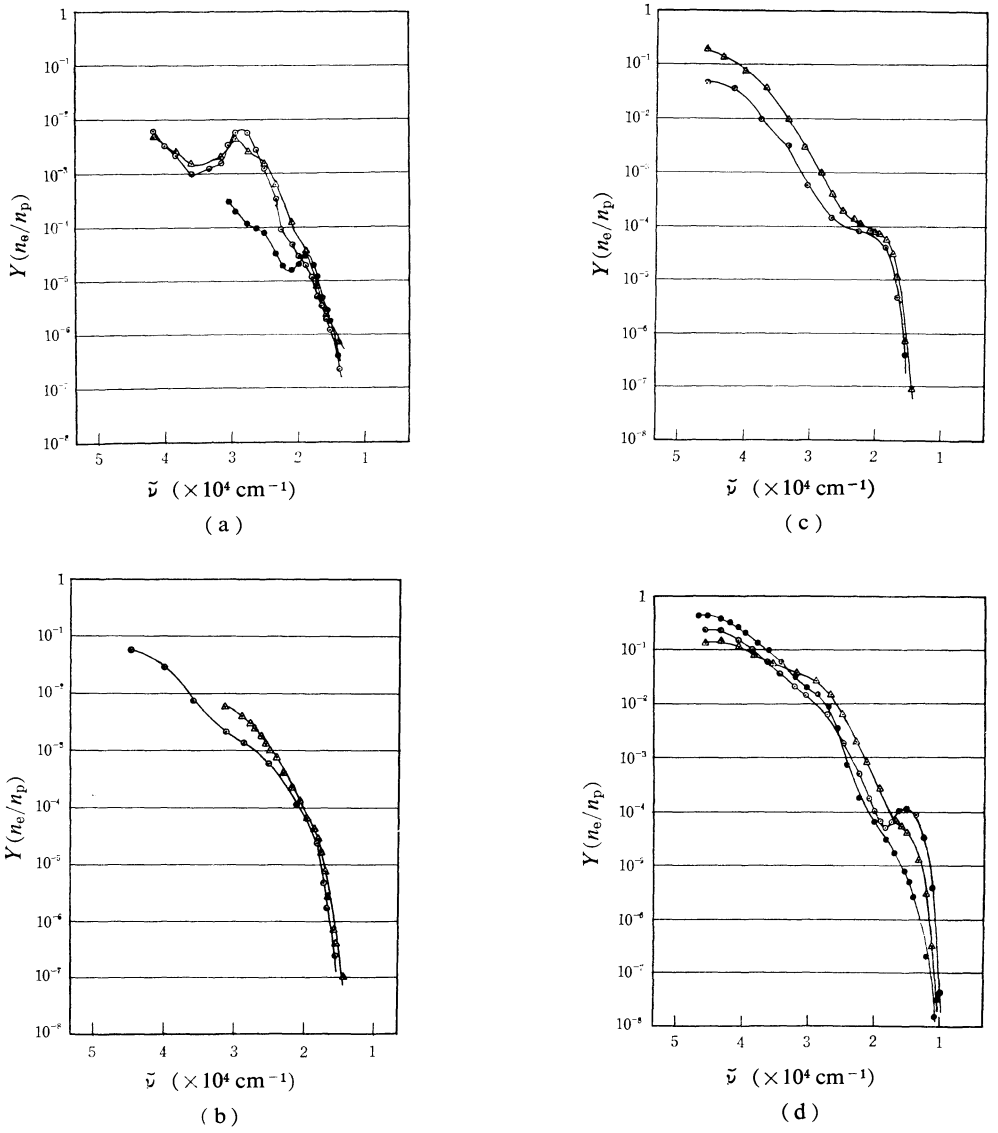



Fig. 3. The spectral response of the photoemission.
(a) Cs-pyrene: ● immediately after reaction, ⊙ 3 days, △ 4 days
(b) Saturated photoemission curve for ⊙ Cs-TBrP and △ for Cs-TClP
(c) Cs-$TNO_2P$: △ immediately after reaction, ⊙ 3 days
(d) Cs-TCNP: ● immediately after reaction, ⊙ 2 days, △ 10 days

concentrations of the Cs-complexes, which will be reported elsewhere,[7] were also increased in the order of the above relation.

As mentioned above, the changed in the spectral response of the photoemission occured gradually. In the case of cesium-tetracyanopyrene, the response peak, around $1.7\times10^4$—$1.8\times10^4$ $cm^{-1}$, was found during the formation of the complex, as Fig. 3 shows. This peak may be produced by cesium metal and was disappeared with time. Sometimes, the peak around $2.8\times10^4$ $cm^{-1}$ was found in the spectral response of the photoemission and was independent of the nature of the organic acceptors applied. Similar peaks, $2.87\times10^4$ $cm^{-1}$ for naphthalene-Cs and $2.87\times10^4$ $cm^{-1}$ for hydrogenated cesium, have already been observed by Suhrmann.[1] The source of the peak may be atomic cesium dispersed in the acceptors.

The absorption spectra of the Cs-aromatics complexes in th solid phase also gradually changed with time; a strong new absorption

7) K. Ohigashi, S. Iwashima and H. Inokuchi, Private Communication.

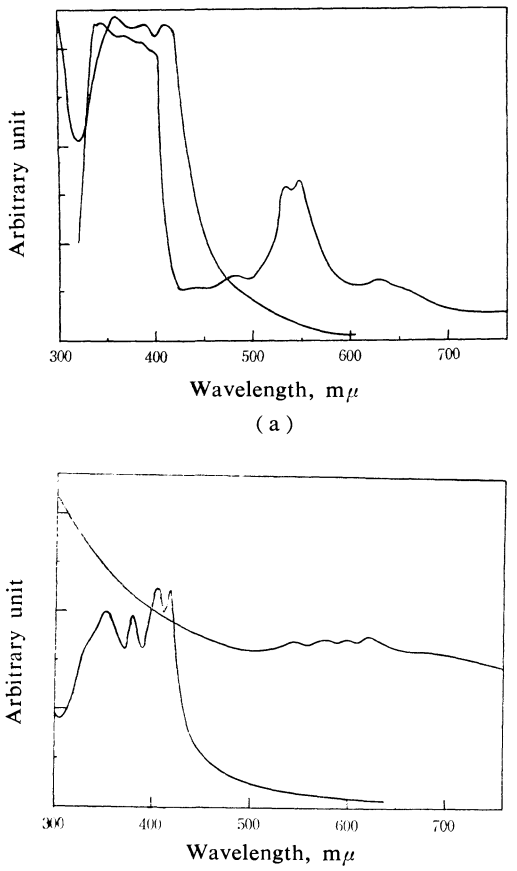



Fig. 4. The absorption spectra of the thin film of Cs-aromatics complex and its aromatic component.
(a) Cs-TCNP; curve I aromatic component and II the complex
(b) Cs-TBrP; curve I aromatic component and II the complex

peak, $1.7\times10^{4}$ cm$^{-1}$ for (TCNP) or $1.85\times10^{4}$ cm$^{-1}$ for ($TNO_2P$), was found after the complex formation had been completed. However, only a very weak peak for (TBrP) was detected or no new peak for (TClP) (Fig. 4). The behaviour is also explained by the order of the electron affinity of the organic compounds.

The charge-transfer absorption peaks resemble to that of the mono-negative pyrene ion;[8] that is, the results suggest that the components in the complex are charged as [$Cs^+$] [aromatics$^-$], as was described in our previous work.[3]

The electrical resistivity of the complexes has a fairly strange result, as is illustrated in Table II. The electrical conduction of (TBrP)-Cs or (TClP)-Cs is higher than that of ($TNO_2P$)-Cs or (TCNP)-Cs; in the case of the latter, the contribution of the dative-bond character to the interaction between donor and acceptor may be larger than the contributions of the former compounds. Because of the strong coupling between two components, it may be expected that the mobile carriers contributing to the electronic conduction will decrease.

## Summary

On the basis o the charge transfer process of the complexes, the photoemission and the electronic conduction of the complexes between cesium and pyrene derivatives, tetranitropyrene ($TNO_2P$), tetrachloropyrene (TClP), tetrabromopyrene (TBrP) and tetracyanopyrene (TCNP) have been measured. A strong increase in the quantum yield of photoemission, from $10^{-3}$—$10^{-4}$ to $10^{-1}$—$10^{-2}$, resulting from the formation of the complexes, has been found. The promotion may take place by means of an electron transfer from cesium metal to a partner molecule; [$Cs^+$] [Aromatics$^-$]. The assumption is supported by the findings concerning electron spin resonance absorption and charge-transfer spectra.

The electrical resistivity of the complexes, $\rho$ at 15°C of pyrene-Cs$=2.1\times10^{4}$ Ωcm., (TClP)-Cs$=8$Ωcm., (TBrP)-Cs$=1.6\times10^{1}$Ωcm., ($TNO_2P$)-Cs$=2\times10^{6}$ Ωcm. and (TCNP)-Cs$=6\times10^{5}$ Ωcm., is strongly affected by the contribution of the dative-bond character of the complexes.

*The Institute for Solid State Physics*
*The University of Tokyo*
*Azabu, Tokyo*

8) P. Balk, S. de Bruijn and G. J. Hoijtink, *Rec. Trav. Chim.*, **76**, 907 (1957).

# A Kinetic Study of the Isotopic Exchange of Thallium(III) between the Thallium(III) Ion and the Thallium *N*-2-Hydroxyethyl-ethylenediamine-*N*, *N'*, *N'*-triacetate Complex in Water

By Michiko TSUCHIMOTO

(Received August 19, 1964)

The kinetic study of isotopic exchange involving co-ordinated compounds with a $d^{10}$ structure, will in this paper be extended to thallium(III), with $^{204}Tl$ as tracer. The exchange of thallium in its *N*-2-hydroxyethyl-ethylenediamine-*N*, *N'*, *N'*-triacetate (henceforth written as EDTA-OH with the formula $H_3Z$) is very fast in strongly basic and acid solutions. The rate is measurable in the pH regions from 4 to 6 and from 7 to 10 under appropriate experimental conditions. This paper will give the results of kinetic studies of the thallium EDTA-OH complex $[TlZ\cdot OH_2]\cdot H_2O$ with thallium(III), in basic, neutral and acid media separately, and the mechanisms will be discussed.

Unlike the cases involving corresponding gallium and indium complexes, tervalent thallium is very unstable and is readily reduced to thallium(I) or precipitated as thallium(III) oxide. Hence, the exchange kinetics can be studied only in the presence of triethanolamine and chloride; their contribution to the reaction kinetics was precisely examined, as will be seen below. The thallium(III) ion will be present in a rather complicated form in the given solutions, but the state does not appear important in discussing the reaction mechanism. The rate constant is independent of the concentration of uncomplexed thallium, although it is proportional to that of the complex throughout these regions. Hence, it is written in the chemical equations in rather arbitrary forms, such as $[Tl(TEA)_x]^n$ or $[Tl(TEA)_xCl_y]^n$.

## Experimental

**The Preparation of the Complex.**—The processed radioisotope $^{204}Tl$ (half life 3.56*y*, Radio Chemical Centre, Amersham) with a specific activity about 0.15 mc./mg. was diluted to produce radioactive thallium with a specific activity of 0.4 $\mu$c./mg. Commercial univalent thallium nitrate in water (extra pure grade) was oxidized by bromine in an acid solution and precipitated with an aqueous ammonia solution as thallium(III) oxide. The precipitate was then filtered off, dried for about 2 hr. at 120°C, weighed, and dissolved in 6 N nitric acid to give a thallium(III) nitrate solution. The absence of thallium(I) was confirmed with a potassium chromate solution.

The thallium EDTA-OH complex was formed instantaneously on mixing a thallium(III) nitrate solution in nitric acid with an equivalent amount of EDTA-OH in water. The labeled complex was prepared immediately before use from a radioactive thallium(III) nitrate solution with a suitable specific activity and an equivalent amount of EDTA-OH in water. When titrated with a sodium hydroxide solution, an aqueous solution of this complex gave the titration curve shown in Fig. 1. From analogy

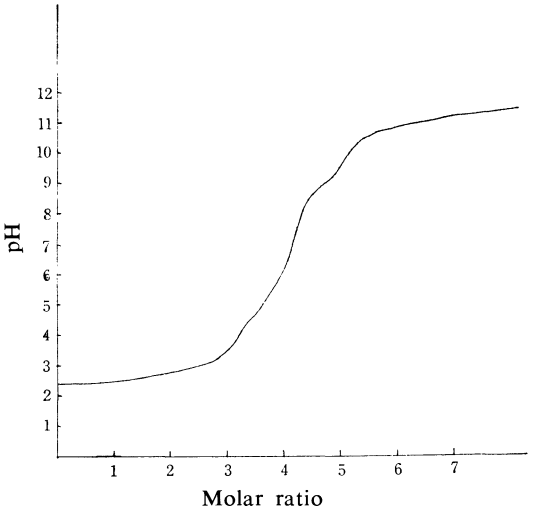



Fig. 1. Titration of $[Tl\cdot EDTA\text{-}OH\cdot OH_2]\cdot H_2O$ with sodium hydroxide.
$[TlZ\cdot OH_2]\cdot H_2O$, $1.2\times10^{-4}$ M;
$\mu=0.20$ ($KNO_3$); 25°C

to the corresponding gallium and indium homologue[2,3] and thallium(III) EDTA complex,[5] it is very probable that the [TlZ] complex contains one mole of co-ordinated water. The first rise in the curve will correspond to the neutralization of the $H^+$ liberated from $H_3Z$, and the second, to that of the $H^+$ liberated from the co-ordinated water.

1) H. A. C. Mckay, *Nature*, **142**, 997 (1938).
2) K. Saito and M. Tsuchimoto, *J. Inorg. Nucl. Chem.*, **23**, 71 (1961).
3) K. Saito and M. Tsuchimoto, This Bulletin, **36**, 1073 (1963).
4) K. Saito and M. Tsuchimoto, *J. Inorg. Nucl. Chem.*, **25**, 1245 (1963).
5) M. Tsuchimoto and K. Saito, ibid., in press.

$$H_3Z + Tl^{3+} \text{ aq.} \rightleftarrows [TlZ\cdot OH_2] + 3H_2O$$

$$[TlZ\cdot OH_2] \rightleftarrows H^+ + [TlZ\cdot OH]^-$$

**Buffers.**—Since thallium(III) is readily reduced to the thallium(I) state, only a few varieties of buffers are useful. The tartrate and citrate used in the studies with gallium and indium are not useful. In basic media *p*-hydroxybenzoate, glycine, ammonia, and barbiturate were used, whereas in the neutral region only barbiturate was useful. In the weakly acid region acetate was used. Their participation in the kinetics was carefully examined, as will be seen in the next section.

**The Procedure for Kinetic Runs.**—An aqueous thallium(III) nitrate solution (not radioactive) was mixed with potassium nitrate (or potassium chloride and nitric acid in the acid region), triethanolamine and the buffer in order to give it an appropriate pH value and ionic strength. A radioactive thallium(III) nitrate solution was mixed with an equivalent amount of EDTA-OH, potassium hydroxide (or nitric acid), and potassium chloride, and the pH value was made approximately the same as that of the thallium(III) solution with which the isotopic exchange is studied. Both solutions were mixed in a thermostat. An aliquot was taken at selected intervals, and a part of the initially-inactive thallium(III) precipitated with 8-quinolinol in ethanol, less than the equivalent of that of the initially-inactive thallium(III), the pH being adjusted to 5—7 with diluted nitric acid (or an aqueous ammonia solution). The precipitate was swiftly filtered through a filter paper of fine texture, washed with water, and dried under an infrared lamp. The composition of the thallium(III) 8-quinolinol complex remained unchanged in the presence of an excess of thallium(III) and the thallium(III) EDTA-OH complex. The pH value of the reaction mixture was measured carefully with a glass electrode pH meter from time to time during the kinetic runs in order to confirm the maintenance of the chemical equilibrium.

**The Measurement of Radioactivity.**—The Geiger-Müller counting method was adopted. $^{204}Tl$ gives $\beta$ rays of a maximum energy, 0.764 MeV. Dried thallium(III) oxinate on the filter paper was placed about 27.5 mm. below a Geiger-Müller tube, and the counting rate was measured. It was proportional to the amount of radioactive thallium on the filter.

**The Measurement of the Thallium.**—After the measurement of the radioactivity, the precipitate on the filter paper was placed in a flask containing a few drops of 6 N hydrochloric acid and treated with 50 ml. of hot water and a known excess of a disodium EDTA solution. After the pH had been adjusted to 4—5 with an ammonium acetate solution, excessive EDTA was back-titrated with an indium nitrate solution, using xylenol orange as an indicator. The specific activity was calculated from the titrated amount of thallium(III). The direct titration of thallium(III) with disodium EDTA was not successful because of the precipitation of thallium(III) oxide and the 8-quinolinol complex.

The fractional exchange, $F$, is expressed by:

$$F = (x_i - x_0)/(x_\infty - x_0)$$

where $x_\infty$, $x_i$ and $x_0$ are the specific activities at infinite time, time $i$ and time zero respectively, the last being about 5—30 min. after the solution is mixed.

The reaction was very slow in a neutral solution at 25°C, and so the kinetics was mainly studied at 40°C.

## Results and Discussion

The rate of exchange, $R$, is expressed by McKay's[1] formula:

$$R = -2.303 \cdot \frac{a\cdot b}{a+b} \cdot \frac{\log(1-F)}{t}$$

where $a$ and $b$ are the molar concentrations of the uncomplexed thallium (initially inactive) and of the thallium EDTA-OH respectively; $t$ is the lapse of time in seconds, and $F$, the fractional exchange.

The $R$ values are independent of the concentration of uncomplexed thallium ions ($a$)

Table I. Relationship between the exchange rate and the concentration of uncomplexed thallium and thallium EDTA-OH complex

| $a$ $10^{-3}$ M | $b$ $10^{-3}$ M | $R$ $10^{-8}$ mol. $l^{-1}\cdot sec^{-1}$ | $k$ $10^{-5}\cdot sec^{-1}$ |
|---|---|---|---|
| in weakly basic media | | | |
| 0.80 | 1.20 | 3.22 | 2.68 |
| 2.00 | 1.20 | 3.53 | 2.94 |
| 1.20 | 0.72 | 1.88 | 2.61 |
| 1.20 | 1.92 | 5.21 | 2.54 |
| $\mu$=0.20 ($KNO_3$); 25°C; TEA 0.1205 M; KCl 0.0015 M; pH 9.70; ammonia 0.2 M (0.032 M $NH_4Cl$); | | | |
| 0.80 | 1.20 | 1.84 | 1.54 |
| 2.00 | 1.20 | 1.72 | 1.43 |
| 1.20 | 0.72 | 1.14 | 1.58 |
| 1.20 | 1.92 | 2.75 | 1.43 |
| $\mu$=0.20 ($KNO_3$); 25°C; TEA 0.1205 M; KCl 0.0015 M; pH 8.50; barbiturate 0.05 M; | | | |
| in neutral media, near pH 7 | | | |
| 0.80 | 1.20 | 0.560 | 0.467 |
| 2.00 | 1.20 | 0.537 | 0.447 |
| 1.20 | 1.20 | 0.547 | 0.456 |
| 1.20 | 2.40 | 1.13 | 0.471 |
| $\mu$=0.20($KNO_3$); 40°C; TEA 0.1205 M; KCl 0.0015 M; barbiturate 0.025 M; | | | |
| in acid media, pH 4.40 | | | |
| 0.70 | 1.20 | 5.36 | 4.47 |
| 2.00 | 1.20 | 5.56 | 4.63 |
| 1.20 | 0.60 | 2.35 | 3.92 |
| 1.20 | 2.40 | 9.71 | 4.05 |
| $\mu$=0.20(KCl); 25°C; TEA 0.0268 M; NaAc 0.025 M; | | | |

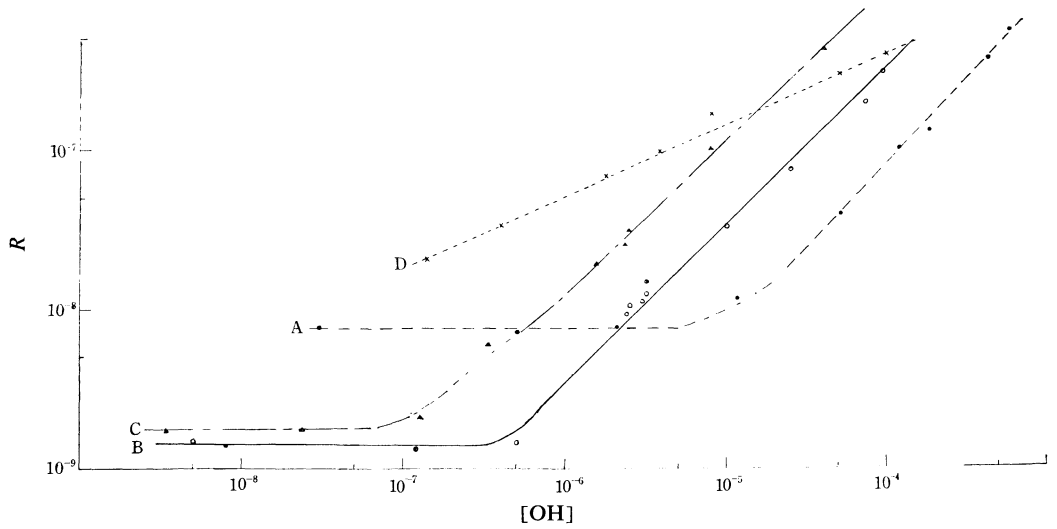



Fig. 2. Relationship between $[OH^-]$ and the exchange constant $R$.
$\mu$=0.2 ($KNO_3$) ; 25°C ; (*a*), 1.20×10⁻³ M ; (*b*), 1.20×10⁻³ M ; TEA, 0.1205 M ; KCl 0.0015 M
A: --●-- ammonia 0.2 M (0.032 M $NH_4Cl$) B: —○— barbiturate 0.05 M
C: —△— glycine 0.0625 M D: ---×--- *p*-hydroxybenzoate 0.0125 M

and proportional to the concentration of the thallium EDTA-OH complex (*b*), regardless of the pH value in the given range, as is shown in Table I. Hence, the rate constant, $k$, is expressed by $R/b$ and has a dimension of $t^{-1}$ under the experimental conditions.

The kinetics is very different in the acid, the neutral, and the basic regions; these regions will be discussed separately below. Tervalent thallium easily gives a precipitate of thallium(III) oxide over pH 1.5. Triethanolamine and potassium chloride were added to keep the thallium(III) and thallium EDTA-OH complexes respectively in the aqueous phase. Their participation in the exchange kinetics will be discussed in detail below.

**Isotopic Exchange in a Weakly Basic Solution.**—Figure 2 illustrates the relationship between $k$ and the $OH^-$ ion concentration, and Fig. 3, that between $k$ and the concentration of triethanolamine in various buffer solutions. In barbiturate, glycine, and ammonia buffers, the rate constant, $k$, is proportional to $[OH^-]$ and to the concentration of triethanolamine (henceforth written as TEA) :

$$R = k' \cdot b \cdot [OH^-] \cdot [TEA]$$

where [TEA] denotes the total concentration of TEA. Different ionization states of TEA do not affect the kinetic expression, because this formula is valid at various pH values, where TEA is present in different states. At a given temperature, $k$ is little influenced by the concentrations of the buffering agents, ammonia and barbiturate, and it is almost

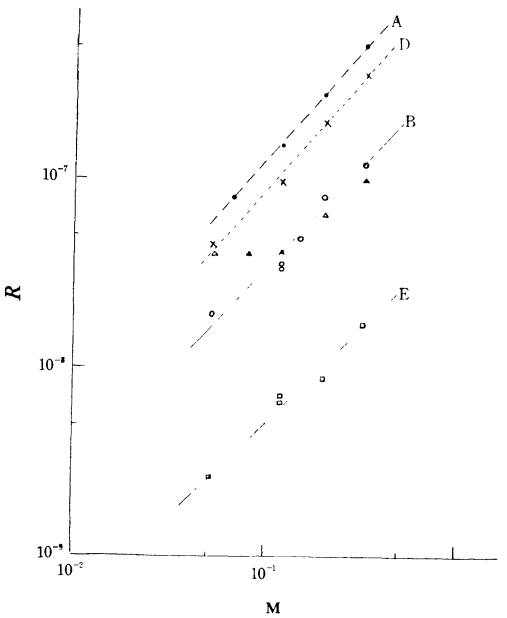



Fig. 3. Relationship between the concentration of triethanolamine and the exchange constant $R$.
$\mu$=0.2 ($KNO_3$) ; 25°C ; (*a*), 1.2×10⁻³ M ; (*b*), 1.2×10⁻³ M ; KCl, 0.0015 M ;
A: --●-- ammonia 0.2 M (0.032 M $NH_4Cl$) pH 9.70
B: —○— barbiturate 0.05 M
C: —△— glycine 0.0625 M } pH 8.50
D: ---×--- *p*-hydroxybenzoate 0.0125 M
E: —□— barbiturate 0.025 M near pH 7 (40°C)

TABLE II. INFLUENCE OF BUFFER, TRIETHANOLAMINE, POTASSIUM CHLORIDE, AND IONIC STRENGTH ($KNO_3$) UPON THE EXCHANGE RATE

| Concn. of reagents, M | | KCl | $\mu$ ($KNO_3$) | $k$ $10^{-5}$ sec$^{-1}$ |
|---|---|---|---|---|
| in weakly basic media | | | | |
| ammonia ($NH_4Cl$) pH 9.70 | | | | |
| 0.12 | (0.019) | 0.0015 | 0.33 | 3.54 |
| 0.60 | (0.096) | 0.0015 | 0.33 | 3.28 |
| 0.20 | (0.032) | 0.0015 | 0.33 | 3.22 |
| 0.20 | (0.032) | 0.0015 | 0.83 | 3.46 |
| 0.20 | (0.032) | 0.0005 | 0.33 | 3.70 |
| 0.20 | (0.032) | 0.0150 | 0.33 | 3.51 |
| barbiturate pH 8.50 | | | | |
| 0.025 | | 0.0015 | 0.33 | 2.26 |
| 0.20 | | 0.0015 | 0.33 | 1.04 |
| *p*-hydroxybenzoate pH 8.50 | | | | |
| 0.025 | | 0.0015 | 0.33 | 8.19 |
| 0.188 | | 0.0015 | 0.33 | 7.50 |
| glycine pH 8.50 | | | | |
| 0.025 | | 0.0015 | 0.33 | 2.97 |
| 0.0625 | | 0.0015 | 0.33 | 4.22 |
| 0.1875 | | 0.0015 | 0.33 | 14.9 |
| 0.25 | | 0.0015 | 0.33 | 21.7 |
| 25°C; (*a*), $1.2\times10^{-3}$ M; (*b*), $1.2\times10^{-3}$ M; | | | | |
| in neutral media | | | | |
| barbiturate near pH 7 | | | | |
| 0.05 | | 0.0015 | 0.33 | 0.306 |
| 0.125 | | 0.0015 | 0.33 | 0.344 |
| 0.025 | | 0.0015 | 0.33 | 0.368 |
| 0.025 | | 0.0015 | 0.83 | 0.356 |
| 0.025 | | 0.0010 | 0.33 | 0.390 |
| 0.025 | | 0.015 | 0.33 | 0.350 |
| 40°C; (*a*), $1.2\times10^{-3}$ M; (*b*), $1.2\times10^{-3}$ M; | | | | |
| in acid media | | | | |
| sodium acetate pH 4.40 | | | | |
| | TEA(M) | KCl | | |
| 0.025 | 0.0268 | 0.20 | 0 | 5.21 |
| 0.025 | 0.201 | 0.20 | 0 | 4.97 |
| 0.125 | 0.0268 | 0.20 | 0 | 5.25 |
| 0.025 | 0.0268 | 0.20 | 0.50 | 4.93 |
| 25°C; (*a*), $1.2\times10^{-3}$ M; (*b*), $1.2\times10^{-3}$ M; | | | | |

completely independent of the ionic strength and of the concentration of chloride (Table II). The temperature dependence of $R$ is shown in Fig. 4. The Arrhenius activation energy is calculated to be 29 kcal. mol$^{-1}$ in barbiturate and ammonia solutions.

The concentration of triethanolamine contributes to the exchange rate. The thallium(III) EDTA-OH complex is most likely present in the aqueous phase in a mixed complex anion form, containing EDTA-OH and TEA in the ligand.

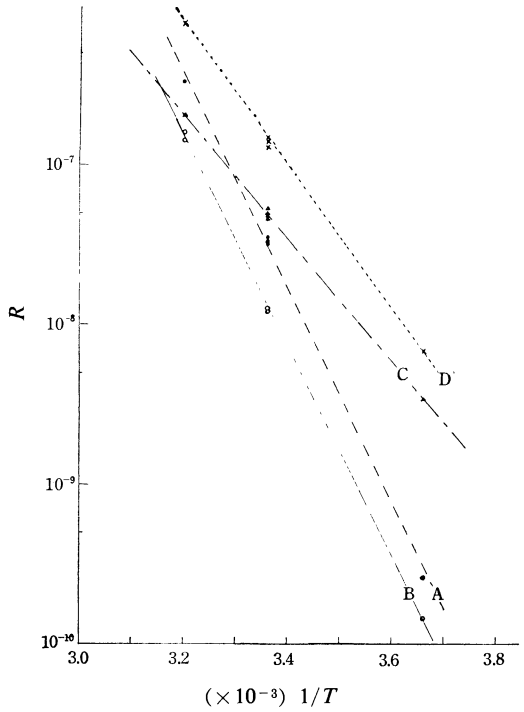



Fig. 4. Temperature dependence of the exchange constant $R$ in weakly basic media.
$\mu$=0.2 ($KNO_3$); (*a*), $1.2\times10^{-3}$ M; (*b*), $1.2\times10^{-3}$ M
TEA, 0.1205 M; KCl 0.0015 M
A: --●-- ammonia 0.2 M (0.032 M $NH_4Cl$) pH 9.70
B: —○— barbiturate 0.05 M
C: —△— glycine 0.0625 M
D: ---×--- *p*-hydroxybenzoate 0.0125 M
} pH 8.50

$$[^*TlZ\cdot OH_2]+N\equiv(-CH_2CH_2OH)_3 \rightleftarrows [^*TlZ\cdot TEA]+H_2O \qquad (1)$$

Despite their different structures, barbiturate and ammonia give the same kinetics as that mentioned above. Hence, the exchange mechanism would involve the exchange of EDTA-OH, -TEA mixed complexes, as will be shown below. Equilibrium 2 should be shifted towards the right-hand side with a rise in pH, bringing about the de-protonation of triethanolamine:

$$[^*TlZ\cdot TEA]+OH^- \rightleftarrows [^*TlZ\cdot TEA']+H_2O$$

equilibrium to form a conjugate base (2)

$$\left\{ N\equiv(CH_2CH_2OH)_3 = N=(CH_2CH_2O)^-{}_2H + H^+ \right\}$$

(TEA) (TEA')

$$^*[TlZ\cdot TEA']^- + [Tl(TEA)_x]^n \rightleftarrows [TlZ\cdot TEA']^- + [^*Tl(TEA)_x]^n \qquad (3)$$

In the case of corresponding gallium[2] and

indium[3] complexes, labile conjugate bases are formed by the de-protonation of the co-ordinated water molecule. However, the reaction mechanism does not appear to differ much. Similar values of the Arrhenius activation energies and the insignificant influence of the ionic strength (Table II) seem to support such a view. Other buffers, *p*-hydroxybenzoate and glycine seem to accelerate the exchange reaction.

In the glycine buffer, the reaction becomes more complex, and the rate constant, $k$, depends on the concentrations of both glycine and triethanolamine. It appears that glycine would replace co-ordinated triethanolamine, at least partly, in the presence of a large amount of glycine, and the exchange reaction proceeds in quite a different manner. Such a complication in the presence of glycine was also observed with indium EDTA[3] and EDTA-OH[4] and thallium EDTA[5] complexes.

In a *p*-hydroxybenzoate buffer solution, the rate of exchange, $R$, is apparently proportional to $[OH^-]^{1/2}$; therefore, the exchange reaction would involve both [TlZ·TEA] and [TlZ·TEA']$^-$.

As will be shown in the next section, the former complex undergoes a slow exchang with thallium(III) independent of the $[OH^-]$ concentration, and its contribution would be negligible in a high pH region, where the latter complex gives a greater exchange rate. However, in the presence of *p*-hydroxybenzoate, the former exchange would be accelerated so that its contribution would remain significant in a high pH region, thus giving such a complicated kinetic form.

**Isotopic Exchange in Neutral Solutions.**—In the pH region near 6—7.5, the rate constant little influenced by pH. The exchange rate constant, $k$, is proportional to the concentration of triethanolamine, and it is independent of the concentrations of barbiturate and potassium chloride and also of the ionic strength (Table II):

$$R = k'' \cdot b' \cdot [\mathrm{TEA}]$$

The temperature dependence of $k$, which is illustrated in Fig. 5, indicates that the Arrhenius activation energy is 22 kcal./mol. Thus, the exchange seems to proceed as follows:

$$[{}^*\mathrm{TlZ}\cdot\mathrm{OH_2}] + \mathrm{N}{\equiv}(\mathrm{CH_2CH_2OH})_3 \xrightleftharpoons{\text{equilibrium}} [{}^*\mathrm{TlZ}\cdot\mathrm{TEA}] + \mathrm{H_2O} \quad (4)$$

$$[{}^*\mathrm{TlZ}\cdot\mathrm{TEA}] + [\mathrm{Tl(TEA)}_x]^n \overset{\text{slow}}{\rightleftarrows} [\mathrm{TlZ}\cdot\mathrm{TEA}] + [{}^*\mathrm{Tl(TEA)}_x]^n \quad (5)$$

In this pH range, the thallium EDTA-OH complex is present mainly in the aquo complex form, as may be seen in Fig. 1, so the triethanolamine complex [*TlZ·TEA] is formed by the replacement of co-ordinated water.

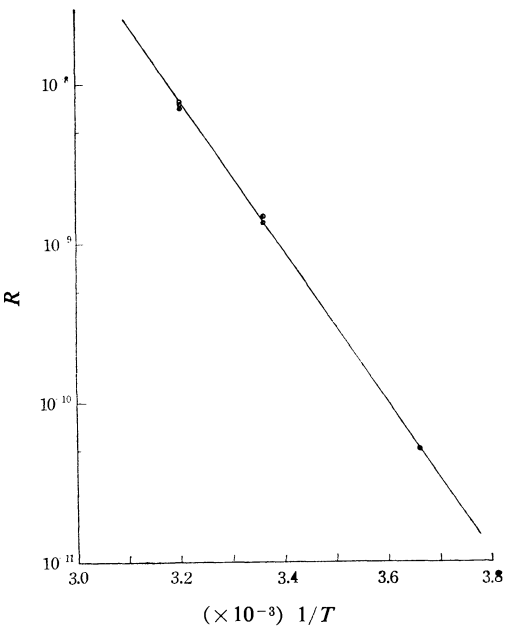



Fig. 5. Temperature dependence of the exchange constant, in neutral media.
$\mu$=0.2 ($KNO_3$); (*a*), $1.2\times10^{-3}$ M; (*b*), $1.2\times10^{-3}$ M TEA, 0.1205 M; KCl, 0.0015 M; barbiturate, 0.025 M

Ammonia and *p*-hydroxybenzoate are not useful buffers in neutral media, and glycine reduces thallium(III) to thallium(I). Hence, only barbiturate was used as a buffer.

With a rise in pH, the co-ordinated TEA liberates protons to give a de-protonated ligand, and the isotopic exchange proceeds through the conjugate base, as Eqs. 2 and 3 show. The $OH^-$ concentration that is independent of the exchange in neutral media would also promote the reaction in basic media with a pH of more than 8, but it would be overwhelmed by the faster exchange through the conjugate base, giving an apparent first-order dependence upon the hydroxide ion concentration.

**Isotopic Exchange in an Acid Solution.**—In the absence of chloride in acid solutions, a white precipitate is formed when thallium(III) nitrate and a disodium EDTA solution are mixed. When the concentration of chloride is of the same order as that of uncomplexed thallium(III), a homogeneous exchange rate is measurable near pH 3.5. However, the relationship between $R$ and $a$ and $b$ is very complicated, and the rate, $R$, is not expressed in a simple formula. This may be due to the

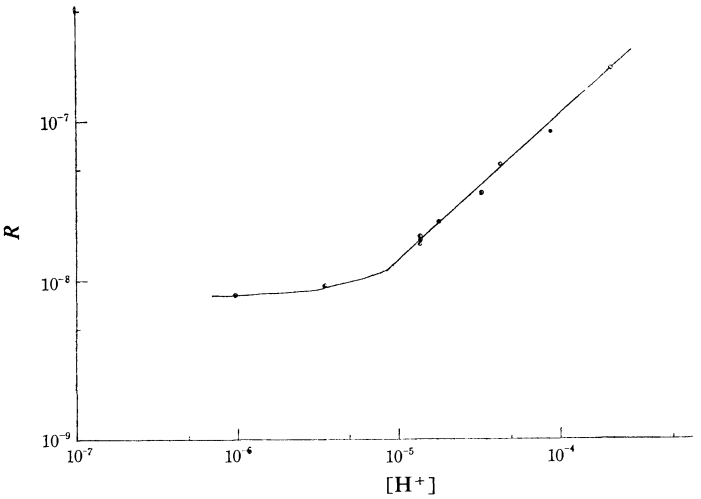



Fig. 6. Relationship between $[H^+]$ and the exchange constant in acid media.
$\mu=0.2$ (KCl); 25°C; TEA, 0.0268 M; NaOAc, 0.025 M; (*a*), $1.2\times10^{-3}$ M; (*b*), $1.2\times10^{-3}$ M

formation of chloro-complexes, such as $[TlCl_2]^+$ and $[TlCl_4]^-$,[6] with different labilities. In the presence of a large excess of chloride, the rate, $R$, is expressed by $R=k\cdot b$, and it is independent of $a$ at pH values from 4 to 6. The following discussion deals with the exchange under such conditions, the ionic strength being adjusted by potassium chloride. Figure 6 shows the relationship between $k$ and the $[H^+]$. The $k$ is proportional to $[H^+]$ and apparently to $[Cl^-]^{1.5}$, as Fig. 7 illustrates, so the rate constant, $k$, is expressed as $k=k'\cdot[H^+][Cl^-]^{1.5}$. The influence of the concentrations of triethanolamine and sodium acetate (see Experimental section) is not significant. The temperature dependence of $R$ is shown in Fig. 8, from which the Arrhenius activation energy is calculated to be 11 kcal./mol.

In the acid solution both aquo- and chloro-mixed EDTA-OH complexes could be present and participate in the exchange reaction.

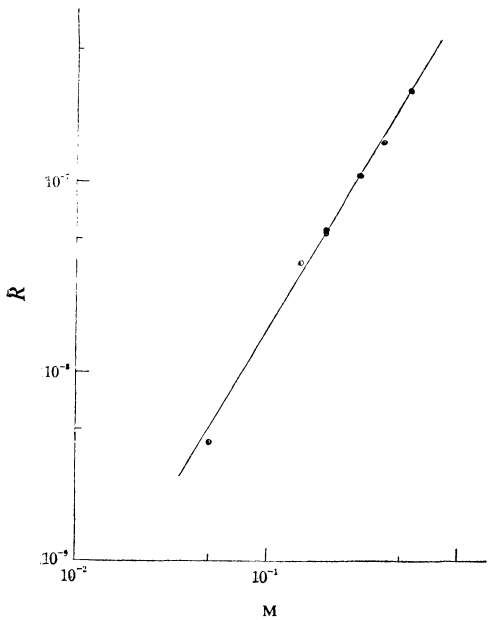



Fig. 7. Relationship between the concentration of potassium chloride and the exchange constant $R$, in acid media
25°C; TEA, 0.0268 M; NaOAc 0.025 M; pH 4.40; (*a*), $1.2\times10^{-3}$ M; (*b*), $1.2\times10^{-3}$ M

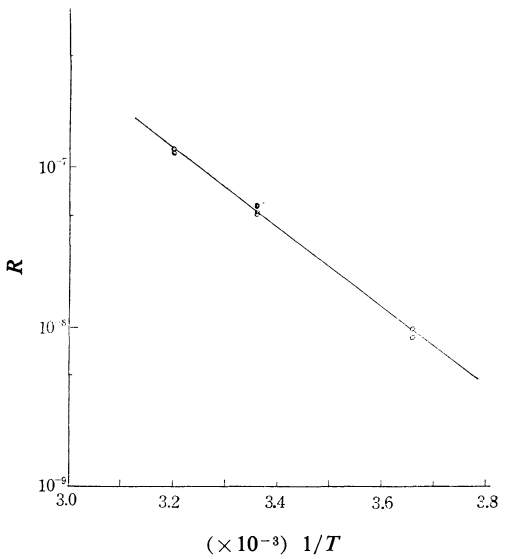



Fig. 8. Temperature dependence of the exchange rate, in acid media.
$\mu=0.2$ (KCl); TEA, 0.0268 M; NaOAc, 0.025 M
(*a*) $1.2\times10^{-3}$ M; (*b*), $1.2\times10^{-3}$ M

6) G. Harbottle and R. W. Dodson, *J. Am. Chem. Soc.*, 73, 2442 (1951).

TABLE III. COMPARISON OF KINETIC DATA FOR GALLIUM, INDIUM, THALLIUM COMPLEXES

| | Ga·EDTA | Ga·EDTA-OH | In·EDTA | In·EDTA-OH | Tl·EDTA | Tl·EDTA-OH |
|---|---|---|---|---|---|---|
| $K_2$ | $1.2\times10^{-6}$ | $1.5\times10^{-5}$ | $1.6\times10^{-9}$ | $1.5\times10^{-6}$ | $3.2\times10^{-7}$ | $2.5\times10^{-9}$ |
| in weakly basic media | | | | | | |
| $k$ | $k'\cdot[OH^-]$ | $k'\cdot[OH^-]$ | $k'\cdot[OH^-]^2$ | $k'\cdot[OH^-]$ | $k'\cdot\frac{[OH^-]}{[TEA]}$ | $k'\frac{[OH^-]}{[TEA]}$ |
| $k'$ | 11.3 (l./mol./sec.) | 37 (l./mol./sec.) | 52 ($l^2$/$mol^2$/sec.) | $1.1\times10^{-1}$ (l./mol./sec.) | 3.4 (l./mol./sec.) | 0.49 (ammonia) 2.7 (barbiturate) (l./mol./sec.) |
| $E_A$ (kcal.) | 25 | 27 | 25 | 25 | 22 | 29 |
| in neutral media | | | | | | |
| $k$ | | | | $k'$ | | $k'\cdot[TEA]$ |
| $k'$ | | | | $1.3\times10^{-5}$ ($sec^{-1}$) | | $9.8\times10^{-6}$ ($sec^{-1}$) |
| $E_A$ (kcal.) | | | | 19 | | 22 |
| in acid media | | | | | | |
| $k$ | $k'\cdot[H^+]^{2.4}$ | $k'\cdot[H^+]^{2.4}$ | $k'\cdot[H^+]^3$ | $k'\cdot[H^+]$ | $k'\cdot\frac{[H^+]^{1.4}}{[Cl^-]^{1.5}}$ | $k'\cdot[H^+][Cl^-]^{1.5}$ |
| $k'$ | $4.5\times10^{-3}$ ($l^{2.4}$/$mol^{2.4}$/sec.) | $1.8\times10^{-2}$ ($l^{2.4}$/$mol^{2.4}$/sec.) | $4.3\times10$ ($l^3$/$mol^3$/sec.) | $1.0\times10^{-2}$ (l./mol./sec.) | 2.7 ($l^{1.4}$/$mol^{1.4}$/sec.) | 12 (l./mol./sec.) |
| $E_A$ kcal. | 15 | 16 | 18 | 11 | 8.5 | 11 |

$$[*TlZ\cdot H_2O]+Cl^- \rightleftarrows [*TlZ\cdot Cl]^-+H_2O \quad (6)$$

$$[*TlZ\cdot Cl]^-+Cl^- \rightleftarrows [*TlZ\cdot Cl_2]^{2-} \quad (7)$$

However, when the chloride ions overwhelm the Tl-EDTA-OH complex, the $[*TlZ\cdot Cl]^-$ complex would predominate to make the relation between $R$ and $b$ simpler. The exchange reaction would proceed through the two chlorinated forms side by side:

$$[*TlZ\cdot Cl]^-+H^+ \rightleftarrows [*TlHZ\cdot Cl] \quad (8)$$

$$[*TlZ\cdot Cl_2]^{2-}+[H^+] \rightleftarrows [*TlHZ\cdot Cl_2]^- \quad (9)$$

$$[*TlHZ\cdot Cl]+[Tl\cdot Cl_x(TEA)_y]^n \rightleftarrows [TlHZ\cdot Cl]+[*Tl\cdot Cl_x(TEA)_y]^n \quad (10)$$

$$[*TlHZ\cdot Cl_2]^-+[Tl\cdot Cl_x(TEA)_y]^n \rightleftarrows [TlHZ\cdot Cl_2]^-+[*Tl\cdot Cl_x\cdot(TEA)_y]^n \quad (11)$$

At a higher pH than 4.5, the rate is too small to be measured. In the neutral region at pH near 7, the $k$ is independent of $[Cl^-]$ but dependent on [TEA]. Since TEA is present in the ammonium ion form in the pH region $<8$, its co-ordinating ability would be very small and would increase with a rise in pH. At pH values near 7, TEA in its basic form will replace co-ordinated chloride to give a rather labile mixed complex $[TlZ\cdot TEA]$ (Eq. 4).

Hence, Eq. 4 is more properly written as:

$$[TlZ\cdot Cl]^-+TEA \rightleftarrows [TlZ\cdot TEA]+Cl^- \quad (4')$$

The chloro-complexes, such as $[TlZ\cdot Cl]^-$ and $[TlZ\cdot Cl_2]^{2-}$, seem to undergo isotopic exchange only through the protonated complex as an intermediate, so the rate is very small in the pH range from 4.5 to 6.

The kinetic data of the EDTA-OH complexes are summarized in Table III. The gallium complex gives kinetics different from that of indium or thallium, but it is rather similar to the EDTA complexes of these three elements. The thallium complex gives kinetic data very similar to those of the indium complex, whereas the thallium-EDTA complex gives kinetics similar to those of the gallium-EDTA complex rather than to the indium complex. Further discussion will be given elsewhere, including the exchange data of the corresponding EDTA complexes.[7]

## Summary

1) The kinetics of the isotopic exchange of the thallium(III) EDTA-OH complex with uncomplexed thallium(III) has been studied in acid, neutral and weakly basic solutions, with $^{204}Tl$ as tracer.

7) K. Saito and M. Tsuchimoto, VIII International Conference on Co-ordination Chemistry, Vienna, 1964.

2) The exchange rate is independent of the concentration of uncomplexed thallium and proportional to that of the EDTA-OH complex, giving the relationship $R=k\cdot b$ under appropriate conditions throughout the pH range.

3) In a basic solution buffered by ammonia or barbiturate, the $k$ is proportional to $[OH^-]$ and [TEA] and is little affected by the concentration of buffers. The Arrhenius activation energy is 29 kcal./mol.

4) In a neutral solution, near pH 7, the rate is small but measurable. It is independent of the pH value but proportional to the concentration of TEA, and it is little affected by the concentration of barbiturate. The activation energy is 22 kcal./mol.

5) In an acid solution buffered by acetate, the $k$ is proportional to $[H^+]$, and $[Cl^-]^{1.5}$ and is little influenced by the concentration of acetate. The Arrhenius activation energy is 11 kcal./mol.

6) The features of the isotopic exchange of the thallium EDTA-OH complex are very similar to those of the thallium(III) EDTA complex.[5]

The author wishes to thank Dr. Kazuo Saito (Department of Chemistry, Faculty of Science, Tohoku University, Sendai) for his many helpful discussions and suggestions during this work and the Ministry of Education for its grant-in-aid.

*Institute for Nuclear Study*
*The University of Tokyo*
*Tanashi, Tokyo*

# Adsorption of Trimethylamine, Ammonia and Pyrrole on Amorphous Silica-alumina

By Yosisato TEZUKA and Toyosaburo TAKEUCHI

(Received August 20, 1964)

It is evident from many studies[1] that the catalytic property of silica-alumina closely depends upon the nature of the acidity of its surface; the adsorption of basic gases on the catalyst has therefore been carried out to clarify the nature of the acidity from the standpoint of surface structure. The basicity of the gaseous molecule depends upon the electronegativity of the nitrogen atom of the molecule, such as trimethylamine and ammonia; the nitrogen atom of trimethylamine is regarded as being more basic than that of ammonia, since the electron cloud of three carbon atoms of the molecule concentrates more densely around the nitrogen atom than around the hydrogen atoms of ammonia. Pyrrole is considered to be neutral, because the $\pi$ electrons of the nitrogen of the compound are incorporated into the sextet and so cannot coordinate with an acid without disrupting the "aromatic sextet." Richardson and Benson[2] investigated the adsorption of trimethylamine on silica-alumina by means of a spring balance included in an adiabatic calorimeter. They presented the correlations of the acidity and the catalytic activity with the heat of the adsorption of trimethylamine. Their results, however, were ambiguous in establishing the correlation of the heat of adsorption with the coverage, a correlation which is important in determining the amount of acid point. Clark et al.[3] have obtained the heats of the adsorption of ammonia on various silica-alumina from the adsorption isotherms. It is impossible, however, to compare these results because of the differences in the preparation of these samples. The present paper will report the results of the study of the surface nature of silica-alumina by means of the adsorption of gases of different basicities, i.e., trimethylamine, ammonia and pyrrole on silica, alumina and silica-alumina.

## Experimental

The amorphous silica which was used for the column packing of the gas chromatography was furnished by the Kotaki Co. and was 120-mesh. Silica-alumina containing 2% alumina (SA-2) was

1) A. G. Obald, T. H. Milliken, Jr., and G. A. Mills, "Advances in Catalysis," Vol. 3, Academic Press, New York (1951), p. 199.

2) R. L. Richardson and S. W. Benson, *J. Phys. Chem.*, **61**, 405 (1959).

3) A. Clark, V. C. F. Holm and D. M. Blackburn, *J. Catalysis*, **1**, 244 (1962).

prepared in the usual way by co-precipitation from solutions of sodium silicate and sodium aluminate.

Silica-alumina containing 13% alumina (SA-13) was furnished by the Davison Chemical Co. Silica-alumina containing 26% alumina (SA-26) was furnished by the Nikki Chemical Co. It was in tablet form. Trimethylamine and pyrrole were carefully purified by means of a vacuum distillation. Ammonia was distilled by pumping it after freezing.

The apparatus used for testing trimethylamine and ammonia was the same as that described elsewhere.[4] The volume of the reaction vessel, including the McLeod gauge, was about 350 cc. An adsorption spring balance made of quartz was used for testing the pyrrole. The reaction vessel of this experiment was a modification of that used by Richardson an Benson.[2] The diameter of the reaction vessel and its length were 30 mm. and 550 mm. respectively. Helix elongation was measured by a cathetometer, giving measurements within 0.05 mm., while the sensibility $Y$ (mm.) of helix was expressed as $Y=0.220X+0.004$, where $X$ denotes the gravity (mg.) of the sample. Prior to the adsorption measurement, the sample was degassed at a constant temperature of 200 and 500°C for about 20 hr. to remove physically adsorbed water or constitutional water from the sample. After the pressure had attained the order of $10^{-6}$ mmHg, the temperature was lowered to the reaction temperature. In the cases of trimethylamine and ammonia, the gas was admitted and the decrease in pressure was followed by the McLeod gauge until the equilibrium pressure was obtained. The temperature of the reaction vessel was raised or lowered at 20-degree intervals in the range from 100 to 140°C. In the case of pyrrole, the amount of gas still remaining on the surface after the evacuation was measured using the spring balance. That is, a certain amount of pyrrole was admitted into the reaction vessel and the mixture was kept for about one hour ; then the vessel was evacuated under a constant temperature until the helix elongation indicated a constant value. The sample was changed anew for every series of adsorption studies on the sample evacuated at a certain temperature.

The BET areas were measured by means of nitrogen adsorption at −196°C. The loss of the water included in each such sample was measured by the spring balance. The titration of the acidity of silica-alumina was made in anhydrous benzene, using *p*-dimethylaminoazobenzene as an indicator in the same way as has been described by Tamele.[5]

## Results

The adsorption isotherms of trimethylamine on silica and alumina evacuated at 200 and 500°C are shown in Fig. 1. The adsorption on silica was reversible in all the regions investigated, and the Langmuir equation could be approximately adapted to the isotherms; however, it could not be adapted for the isotherms on alumina, though the adsorption occurred reversibly. Figures 2—6 show the adsorption isotherms of trimethylamine on SA-2, SA-13 and SA-26, and those of ammonia on SA-13 and SA-26, respectively. Every isotherm shows a steep rise in an initial region but then enters a region of slow rise. The dependence of the adsorption amount on the temperature in the region of steep rise was conspicuously small. The velocity of the desorption by the evacuation or by the elevation of the temperature in this region was very slow, as if the adsorption were irreversible. It was determined, however, that the adsorption of this region was reversible, because the amount of adsorption on a virgin sample was practically equal to that of the sample which had been preliminarily covered by a certain

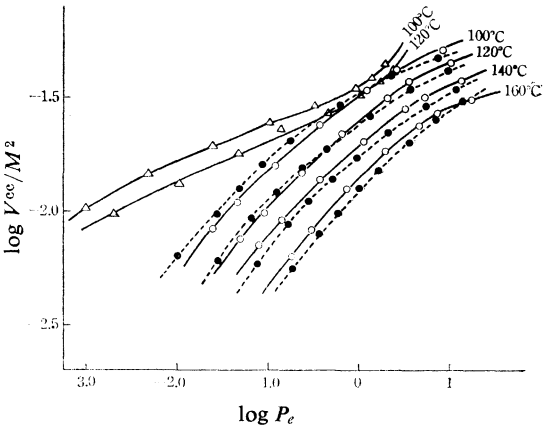



Fig. 1. Adsorption isotherms of trimethylamine on silica and alumina.

-△- Alumina evacuated at 200°C
-○- Silica evacuated at 200°C
-●- Silica evacuated at 500°C

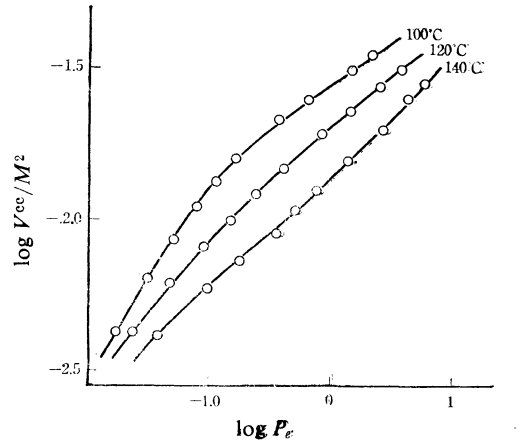



Fig. 2. Adsorption isotherms of trimethylamine on SA-2 evacuated at 200°C.

4) T. Takeuchi and M. Sakaguchi, This Bulletin, **30**, 182 (1957).
5) M. W. Tamele, *Discussions Faraday Soc.*, **8**, 270 (1950).

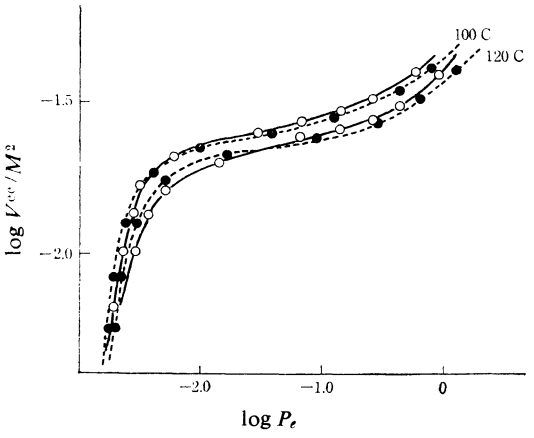



Fig. 3. Adsorption isotherms of trimethylamine on SA-13.
-○- Evacuated at 200°C
-●- Evacuated at 500°C

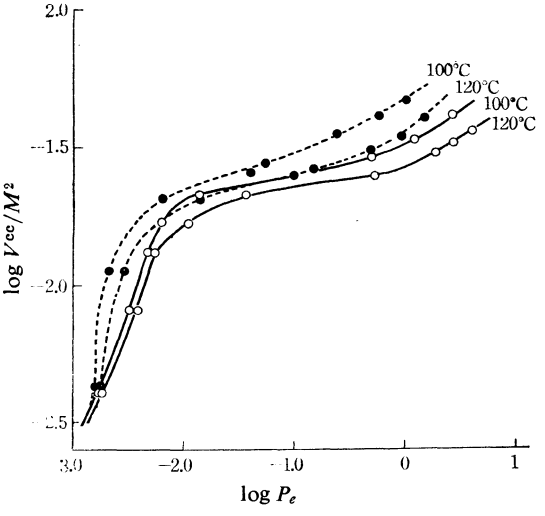



Fig. 4. Adsorption isotherms of trimethylamine on SA-26.
-○- Evacuated at 200°C
-●- Evacuated at 500°C

amount of gas, if the samples were kept under the same conditions of temperature and equilibrium pressure.

The heats of the adsorption of trimethylamine on silica and alumina obtained from the isotherms by adapting the Clausius-Clapeyron equation are summarized in Fig. 7. The heat of adsorption on silica was not practically affected by the variation in the coverage and the temperature of evacuation. However, that on alumina decreased markedly with an increase in the coverage. The heats of the adsorption of trimethylamine and ammonia on silica-alumina are summarized in Figs. 8 and 9. The heats always increased

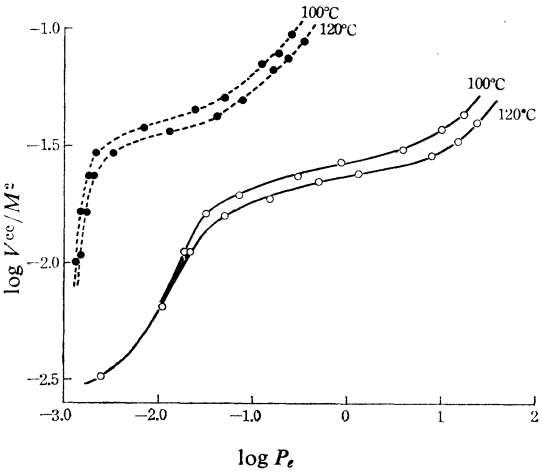



Fig. 5. Adsorption isotherms of ammonia on SA-13.
-○- Evacuated at 200°C
-●- Evacuated at 500°C

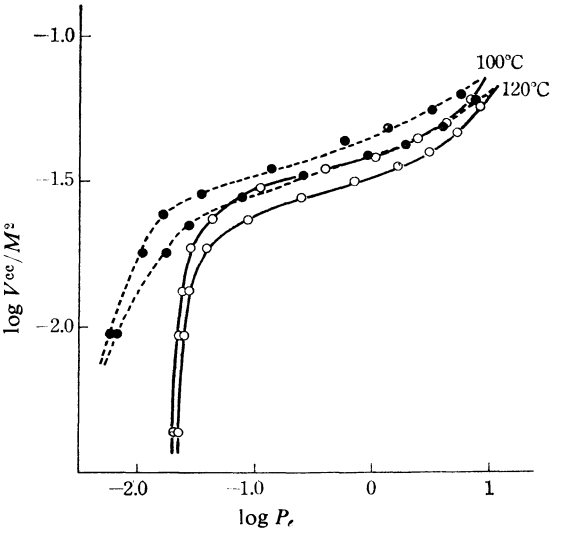



Fig. 6. Adsorption isotherms of ammonia on SA-26.
-○- Evacuated at 200°C
-●- Evacuated at 500°C

markedly with an increase in the coverage, but then decreased gradually. The coverages which gave the maximum heat varied with the samples in the order of the alumina concentration. The shift is toward the greater coverage by the elevation of the evacuation temperature. Table I shows the amount of pyrrole remaining on silica-alumina after the evacuation had been made, the amount of acid point measured by the titration,* the amounts

* The amount of the acid point of SA-26 could not be determined by the titration, because the decolorization of the surface by *n*-butylamine was not uniform.

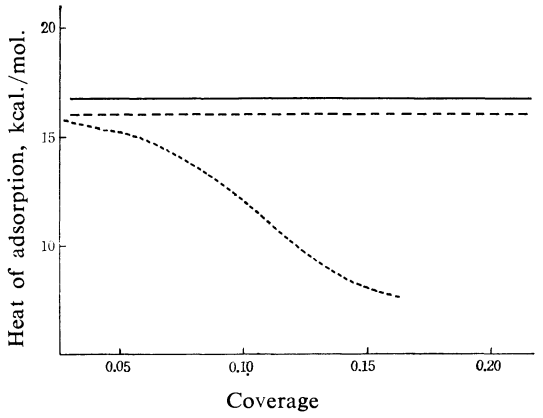



Fig. 7. The heats of adsorption of trimethylamine on silica and alumina.

—— Silica evacuated at 200°C
– – – Silica evacuated at 500°C
····· Alumina evacuated at 200°C

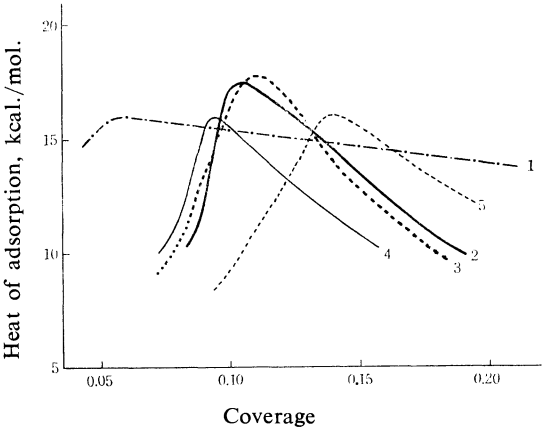



Fig. 8. The heats of adsorption of trimethylamine on silica-alumina.

1: SA-2 evacuated at 200°C
2: SA-13 evacuated at 200°C
3: SA-13 evacuated at 500°C
4: SA-26 evacuated at 200°C
5: SA-26 evacuated at 500°C

TABLE I. AMOUNTS OF THE ACID POINT MEASURED BY THE ADSORPTION OF GAS AND THE TITRATION

| % of alumina | 2 | 13 | | 26 | |
|---|---|---|---|---|---|
| Temp. evacuated, °C | 200 | 200 | 500 | 200 | 500 |
| BET area, $m^2/g.$ | 305 | 405 | 339 | 295 | 262 |
| Amount adsorbed mol. $10^7$ | | | | | |
| Pyrrole | | 0.90 | 1.05 | | |
| Trimethylamine | 0.63 | 0.91 | 1.05 | 1.10 | 1.43 |
| Ammonia | | 1.41 | 2.14 | 1.30 | 1.75 |
| *n*-Butylamine | | 0.94 | 1.15 | | |

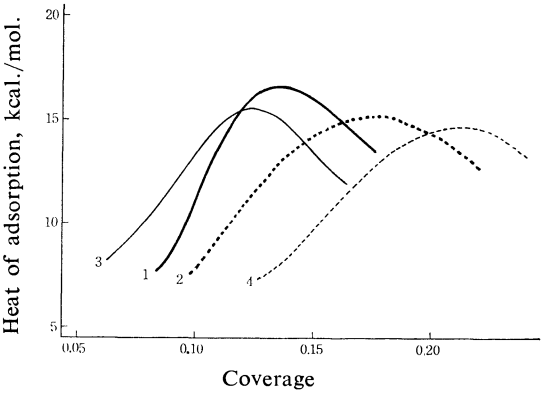



Fig. 9. The heats of adsorption of ammonia on silica-alumina.

1: SA-13 evacuated at 200°C
2: SA-13 evacuated at 500°C
3: SA-26 evacuated at 200°C
4: SA-26 evacuated at 500°C

of trimethylamine and ammonia adsorbed up to the steep rise of every isotherm, and the BET areas of the samples.

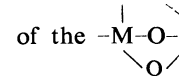
## Discussion

The heat of adsorption at the region near zero coverage could not be obtained in this study because of the difficulty of accurately reading pressures of less than $10^{-4}$ mmHg. Richardson and Benson[2] have reported that the initial heats of the adsorption of trimethylamine on two kinds of silica-alumina were about 38 kcal. and 33 kcal. respectively, and that they decreased with an increase in the amount of gas adsorbed. Clark et al.[3] reported that the heat of adsorption of ammonia on silica-alumina of various compositions began at more than 40 kcal. These, and the reports published recently by other authors,[6,7] suggest that the peak of heat on silica-alumina in our study should succeed the decrease after the initial great heat. Therefore, we call the peak the "secondary peak."

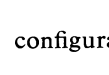
Table I indicates that the amount of gas adsorbed at the secondary peak of the heat in each silica-alumina is approximately equal to the amount of acid point measured by the titration. Such coincidence suggests that the secondary peak of the heat is caused by the complete occupation of the basic gas to both Lewis and Brønsted acid points. Beebe[8] and Rhodin[9] had found that the heat of the

6) V. Kevorkian and R. O. Steiner, *J. Phys. Chem.*, 67, 545 (1963).
7) P. Y. Hsieh, *J. Catalysis*, 2, 211 (1963).
8) R. A. Beebe and D. M. Young, *J. Phys. Chem.*, 58, 93 (1954).
9) T. N. Rhodin, *J. Am. Chem. Soc.*, 72, 5691 (1950).

physical adsorption of gas is increased by the interaction of gas near the completion of the monolayer. In our results, however, the coverage which gave the secondary peak was far less than unity. Moreover, the distance between aluminum atoms seems too large for mutual interaction due to the van der Waals force if the acid points are assumed to exist uniformly on the surface. Danforth[10] had proposed that silica-alumina is formed by the interconnecting rings of six silica tetrahedra, whose silicon atoms on the outer side are replaced by aluminum atoms keeping the distance of 5 Å. Though such a structure might be suitable for silica-alumina, the silica-alumina of our experiment should be considered to be formed by the mixture of perfect and inperfect structures, comprising the structures of pure silica and alumina. In view of the above situation, it can be proposed that the acid points, both Brønsted and Lewis acid points, exist in clusters, and that such acidic domains will be covered preferentially by basic gas at the initial stage of the adsorption. If these domains are regarded as aggregations of acidic points with different strengths, the adsorption occurs probably in an order of strength indicating a gradual decrease of heat, and the secondary peak of the heat would depend upon the mutual attraction of molecules adsorbing closely to one another.

The coverage of the secondary peak of the heat on ammonia was greater than that of trimethylamine and approached toward unity by the elevation of the evacuation temperature. These facts would reveal that ammonia is adsorbed partly on non-acid points as well as on acid points, before the completion of the monolayer on the acidic domains. Ammonia seems to adsorb more readily than trimethylamine and pyrrole on silica-alumina in virtue of the formation of a hydrogen bridge between its hydrogen atom and the lone pair electron of the oxygen of the adsorbent. Zettlemoyer and Chessick[11] proposed, as had been assumed by Young,[12] that the elevation of the evacuation temperature causes water to be removed from silica-alumina and produces surface sites of the  , where M and M* indicate silicon and aluminum atoms respectively. The increase of the oxygen on the surface would increase the amount of adsorption due to the hydrogen bridge. If the adsorption of ammonia occurs when the electron is switched to the acid point, the polarization will be accelerated by the shift of the electron of hydrogen atoms toward the nitrogen atom, and the attractive force between ammonia molecules will be strengthened; as a result, the piled-up adsorption of ammonia may be considered to occur. It is considered impossible, in view of their structure, for the hydrogen atoms of trimethylamine and pyrrole to form the hydrogen bridge.

The heat of the adsorption of trimethylamine on pure silica was approximately constant over the wide region of coverage, and it was practically the same as that of the secondary peak in silica-alumina catalysts. This fact reveals that the adsorption of trimethylamine initiated at active points, such as holes, crevices or crystal defects, as had been discussed by de Boer,[13] and spread gradually from these points to form two-dimensional layers by the van der Waals force of the adsorbing molecules. The heat of the adsorption of trimethylamine on SA-2 was approximately constant, except for the initial region of small heat. This might be explained combining the conceptions of the surface nature of silica and silica-alumina which have been proposed above. Most of the surface of SA-2 would be similar to that of silica, and the basic gas would begin the adsorption from the acid point then on the surface of the silica type, behaving in the way which has been proposed above. The correlation between the heat of trimethylamine and the coverage on alumina would reveal that the adsorption is of the chemical type, and suggests that the surface is substantially different from that of silica.

The unexpected characteristics of pyrrole in the adsorption on silica-alumina may be explained as follows. Two out of the six $\pi$ electrons in the ring of pyrrole are localized toward the nitrogen atom when it adsorbs on the acid point, and they fill one of four $sp^3$ orbitals forming a lone pair in a pyramidal configuration,  . Consequently, the nitrogen atom of pyrrole can behave like that of trimethylamine or ammonia on the surface.

## Summary

The adsorptions of trimethylamine, pyrrole and ammonia on pure silica, alumina and three silica-aluminas with (2%, 13% and 26% of alumina) have been studied. Isosteric heats have been obtained from adsorption isotherms at 100 and 120°C. A conspicuous rise, followed

10) J. D. Danforth, "Advances in Catalysis," Vol. 9, Academic Press, New York (1957), p. 558.
11) A. C. Zettlemoyer and J. J. Chessick, *J. Phys. Chem.*, **64**, 1131 (1960).
12) G. J. Young, *J. Colloid Sci.*, **13**, 67 (1958).
13) J. H. de Boer, "Advances in Catalysis," Vol. 8, Academic Press, New York (1956), p. 17.

by a gradual fall, was observed at an early stage of the heat curve obtained from the isotherm on silica-alumina, but not from those on silica and alumina. At the peak of the curve, the amount of the adsorption of trimethylamine agreed with that of pyrrole, both of which, again, agreed with the amount of the acid point as measured by the titration using *n*-butylamine. The amount of ammonia was twice as large as that of the acid point. The acid points of silica-alumina are assumed to exist in clusters on the surface. The rise of heat is due to the mutual interaction of the adsorbed molecules, the peak indicating the completion of the monolayer on such acid domains.

The authors are indebted to Dr. Tai Yokoyama and Dr. Kiyoyasu Kawai for several useful discussions. The assistance of Mr. Toyoki Kitayama, Mr. Yutaka Wada and Miss Yoko Yotsuya in the experimental measurements is also gratefully acknowledged.

*Faculty of Literature and Science*
*Toyama University*
*Gofuku, Toyama*

# D and $^{14}N$ Quadrupole Interaction in the Ammonium Ion of Ammonium Dihydrogen Phosphate

By Takehiko CHIBA

(Received August 25, 1964)

The deutron magnetic resonance (DMR) of $ND_4$ in a single crystal of $ND_4D_2PO_4$ (ADP) was measured in the paraelectric phase at room temperature and in the antiferroelectric phase at about $-40°C$. The $^{14}N$ resonance of ADP was also measured at room temperature. The observed quadrupole couplings are given in Table I. Lowering the temperature through the phase-transition temperature shatters a single crystal, but the fragments are held together, keeping the original crystal shape. It is known[1] that each fragment is oriented with its a or b axis parallel to the axis direction of the original high-temperature form. The spectra, therefore, correspond to a superposition of those two crystals which are oriented perpendicular to each other. It was then possible to determine $eqQ$ and the orientation of the field gradient (f. g.) tensor of the low temperature phase, except that there remains a choice of two alternatives of the a and b axes to which the f. g. tensor is referred, from the observed spectra with the help of symmetry considerations and the powder spectrum.[2]

Table I. Quadrupole coupling, asymmetry parameter and the direction cosines of field gradient tensor observed in ammonium dihydrogen phosphate

Ammonium D

Room temp. $eqQ/h=3.4$ kc., $\eta=0$.
F. g. parallel to c axis.

$-40°C$ $eqQ/h=6.0$ kc., $\eta=0.89$.

| F. g. component* | $a$ (or $b$) | $b$ (or $a$) | $c$ |
|---|---|---|---|
| 1 | 0.226 | 0.413 | 0.882 |
| 2 | 0.681 | 0.580 | −0.447 |
| 3 | −0.696 | 0.702 | −0.150 |

And three other sets of f. g. direction cosines which differ from the one listed by the sign of either $a$, or $b$, or $c$ axis components.

$^{14}N$

Room temp. $eqQ/h=24.6$ kc. ($NH_4H_2PO_4$) $\eta=0$.
F. g. parallel to c axis.
$eqQ/h=27.3$ kc. ($ND_4D_2PO_4$)

* F. g. components 1, 2 and 3 are in the order of the largest absolute value.

In general, except at very low temperatures, a large part of the quadrupole coupling of the D of an $ND_4^+$ ion is cancelled because of the rapid interchanges of its four deuterons, leaving the small fraction due to the deviation from the exact tetrahedral symmetry of the ion. On some ammonium salts DMR was measured and the results compared with the calculated f. g. from the point charge approximation, assuming a net charge located at the center of $ND_4^+$. The results were not in agreement with the observed value, although the magnitude of the calculated f. g. was of the right order. In the paraelectric phase of

1) E. A. Wood, W. J. Merz and B. T. Matthias, *Phys. Rev.*, **87**, 544 (1952).
2) T. Chiba, *J. Chem. Phys.*, **36**, 1122 (1962).

ADP the hydrogen positions have been determined by neutron-diffraction study.[3] The point charge calculation was carried out, taking hydrogen positions into account, to see if any better result can be obtained. In the present case the f. g. at a deuteron of $ND_4^+$ is axially symmetric about the c axis, so that only the f. g. component in that direction need be considered. The calculation was made* by taking all atoms within a sphere of 46Å (6-unit-cell distance) into account, by assuming charges for $NH_4$, H (acid), and $PO_4$ of $+e$, $+e$ and $-3e$ respectively, and by assuming parameter $\alpha$ to be the fraction of $+e$ on N and $\beta$, that of $-3e$ on P ($1 \geq \alpha$, $\beta \geq 0$). For those atoms outside 25Å (3-unit-cell distance), $\alpha$ and $\beta$ are set equal to zero. The same calculation was made at a nitrogen position. For the f. g. at a hydrogen position the effect of the directly-bonded nitrogen atom was excluded. Similarly for the f. g. at a nitrogen atom, the effect of directly-bonded hydrogens was excluded. The results are given by $V_h$ and $V_{h'}$ at hydrogen and by $V_n$ at nitrogen in the following equations (in units of $e/Å^3$).

$$V_h = -0.0079 - 0.0022\alpha - 0.0903\beta \quad (1)$$

$$V_{h'} = -0.0152 + 0.0051\alpha - 0.0403\beta \quad (2)$$

$$V_n = -0.0534 - 0.0033\alpha - 0.0612\beta \quad (3)$$

$V_h$ gives the value without the contribution to f. g. from the three hydrogen atoms which are bonded to the same nitrogen atom, and $V_{h'}$, that including it. The fact that the difference between the values of the calculated f. g. for a hydrogen and for a nitrogen ($V_h$ and $V_n$) is rather large indicates the strong dependence of this quantity on the atomic coordinates. The order of magnitude of the calculated f. g. is about the same as that in the previous paper. The observed $eqQ$ of 3.4 kc. corresponds to a field gradient of ($\pm$) 0.035 if the polarization effect[2] is disregarded. This can be fitted by Eq. 1 or 2 with reasonable values of parameters $\alpha$ and $\beta$. The difficulty arises when one compares Eq. 3 with the observed values. For nitrogen, the antishielding factor is not well known. However, Kanda gave an estimate of about 47 in the state of the $NH_4^+$ ion.[4] If one assumes this value, the observed f. g. will be ($\pm$)0.0006.** Equation 3 gives far too large an f. g. with any set of $\alpha$ and $\beta$ for the experimental value to be accounted for. Point charges at the four directly-bonded hydrogen atoms make an f. g. contribution of $-0.031(1-\alpha)$ at nitrogen, which only increases the discrepancy. This means an inadequacy of the point charge approximation in the present case. The reason why it fails most likely lies in the evaluation of the contribution from the neighboring atoms. However, there might be another reason, namely, that the charge distribution is diffuse in nature, as has been noted in the crystal analysis of ammonium bifluoride,[5] so that the f. g. arising from the crystalline field is actually much smaller. Therefore, it may be more reasonable to relate the observed $eqQ$ of deuteron, simply neglecting the effect of the long-range crystalline field, as in the previous paper, to the f. g. in each N–D bond direction which deviates from that of a regular tetrahedron by 2.0° as determined by neutron diffraction. That is, $3.4\ \text{kc.} = (eq_0Q_D/h) \times 2\sqrt{2/3} \times 2.0\pi/180$, which leads to $eq_0Q_D/h = 130$ kc. Considering the facts that an N–D···O hydrogen bond is present[3] and that a hydrogen bond tends to decrease $eqQ$, this value appears reasonable. For the f. g. at nitrogen, the observed value is so small that one needs to take the f. g. contribution from the crystalline field into consideration. Then one has to assume that there is a rather accidental cancellation of this effect by that due to the electronic configuration of the $NH_4^+$ ion. This point may be cleared up if the $eqQ_N$ values of other ammonium salts are measured.

Although the displacements of atoms in the ADP crystal due to the transition from the para- to the antiferroelectric phase have been determined for heavier atoms,[6] those for the hydrogen atoms are not known. Therefore, the calculation of f. g. values for the antiferroelectric phase could not be made. However, the large quadrupole coupling seems to indicate a greater distortion of the $ND_4^+$ ion in this phase than in the paraelectric one.

*The Institute for Solid State Physics*
*The University of Tokyo*
*Azabu, Tokyo*

3) L. Tenzer, B. C. Frazer and R. Pepinsky, *Acta Cryst.*, **11**, 505 (1958).

* The PC-2 electronic computer was used for the calculation.

4) T. Kanda, presented at the 1962 Fall Meeting of the Physical Society of Japan.

** A $Q_{14}$ value of $0.02 \times 10^{-24}$ cm$^2$ is assumed.

5) T. R. R. McDonald, *Acta Cryst.*, **13**, 113 (1960).

6) R. O. Keeling, R. Pepinsky, *Z. Krist.*, **106**, 236 (1955).

# The Effect of Several Condensed Phosphates on the Dissolution of Strontium Sulfate

By Masaji MIURA and Hiromitu NAONO

(Received September 3, 1964)

The subject of the retarding action of several condensed phosphates on the crystallization of such sparingly soluble inorganic salts as strontium sulfate,[1-4] calcium carbonate[5] and calcium sulfate[6] has been investigated in our laboratory. It has been found that the retarding action is closely correlated with the adsorption of condensed phosphates on the crystal surface. In continuation of these works, we have studied the dissolution of strontium sulfate in the dilute solutions of several condensed phosphates and have found that the dissolution is considerably retarded in the presence of phosphates and inhibited almost completely under suitable conditions. Such a phenomenon as the inhibition of dissolution has not yet been investigated, however, although the retarding action of some additives on the dissolution of such crystals as lithium fluoride[7] and silver chloride[8] has been studied. In the present paper, some results will be given on the effect of condensed phosphates on the dissolution of strontium sulfate, and the mechanism of the dissolution will be discussed.

## Experimental

**Materials.**—An analytical-grade reagent of sodium dihydrogen orthophosphate was further purified by recrystallization from its aqueous solution. Sodium pyro-, tri- and trimetaphosphate were prepared and then purified by the same procedure as has been described previously.[2,5] The powder of the strontium sulfate was the same as that used in the previous work ;[2] its specific surface area was 0.29 $m^2$/g.

**Dissolution.** — The dissolution process was followed by the conductance method at 25°C. Thirty milliliters of the phosphate solution was poured into a conductivity cell and then left to reach thermal equilibrium in a thermostat ; then 1 ml. of the strontium sulfate sol was quickly added to the solution, the concentration of the sol being 1 mg. $SrSO_4$/ml. While the cell was being shaken continuously, the conductivity of the solution was measured at regular intervals.

**Adsorption.** — The adsorption of triphosphate on strontium sulfate was measured by the radio tracer method at 25°C with the aid of triphosphate labelled with $^{32}P$. A known weight of the strontium sulfate powder was then added to 30 ml. of the triphosphate solution. The rate of the adsorption was determined by measuring the decrease in the radioactivity of the solution at intervals.

## Results

The effect of ortho-, pyro-, tri- and trimetaphosphate on the dissolution of strontium sulfate is shown in Figs. 1—4, which give the increase in the specific conductance arising from the dissolution of strontium sulfate in the presence of various amounts of the phosphates. Curve A in each figure indicates the dissolution into pure water. The effect of these phosphates on the dissolution of strontium sulfate is summarized in Fig. 5, where the increase in the specific conductance after 50 min. is plotted against the phosphate concentration.

The adsorption rate of triphosphate on the surface of the strontium sulfate is shown in

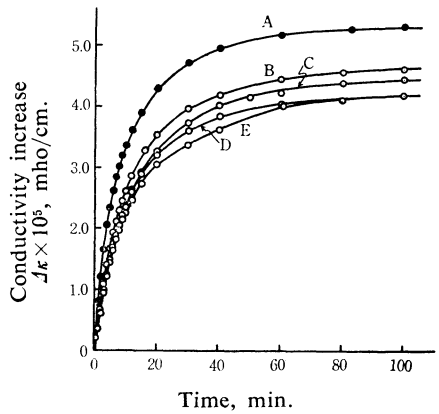



Fig. 1. Effect of sodium dihydrogen orthophosphate on the dissolution of strontium sulfate.
Concentration of orthophosphate :
A) 0, B) $1.0\times10^{-5}$ M, C) $4.0\times10^{-5}$ M,
D) $1.0\times10^{-4}$ M, E) $4.0\times10^{-4}$ M

1) S. Otani, This Bulletin, 33, 1544, 1549 (1960).
2) M. Miura, S. Otani, M. Kodama and K. Shinagawa, *J. Phys. Chem.*, 66, 252 (1962).
3) M. Miura, S. Otani, Y. Abe and C. Fukumura, This Bulletin, 36, 1096 (1963).
4) H. Naono and M. Miura, ibid., 38, 80 (1965).
5) M. Miura, H. Naono and S. Otani, *J. Chem. Soc. Japan, Ind. Chem. Sec. (Kogyo Kagaku Zasshi)*, 66, 593 (1963).
6) M. Miura, Unpublished data.
7) J. J. Gilman, W. G. Jhonston and G. W. Sears, *J. Appl. Phys.*, 29, 747 (1958) ; G. W. Sears, *J. Chem. Phys.*, 32, 1317 (1960).
8) C. W. Davies and G. H. Nancollas, *Trans. Faraday Soc.*, 51, 823 (1955).

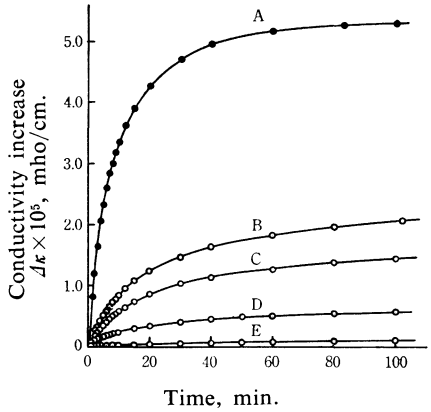



Fig. 2. Effect of sodium pyrophosphate on the dissolution of strontium sulfate.
Concentration of pyrohosphate:
A) 0, B) $5.0\times10^{-6}$ M, C) $1.0\times10^{-5}$ M,
D) $2.0\times10^{-5}$ M, E) $4.0\times10^{-5}$ M

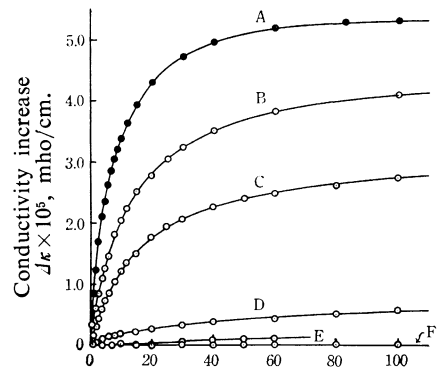



Fig. 3. Effect of sodium triphosphate on the dissolution of strontium sulfate.
Concentration of triphosphate:
A) 0, B) $5.0\times10^{-7}$ M, C) $1.0\times10^{-6}$ M,
D) $5.0\times10^{-6}$ M, E) $2.0\times10^{-5}$ M,
F) $4.0\times10^{-5}$ M

Fig. 6, where the initial concentration of triphosphate is $1.0\times10^{-5}$ M, the equilibrium concentration, $3.6\times10^{-6}$ M, and the weight of strontium sulfate, 150 mg.

## Discussion

As may be seen in Figs. 1—4, pyro- and triphosphate, even in their dilute solutions, exert a profound influence upon the dissolution of strontium sulfate, and an increase in the concentration of these phosphates brings about an increase in the retarding action until finally it practically inhibits the dissolution. Moreover, when a small amount of triphosphate is added to a system in which strontium sulfate has been dissolving in water, the dissolution of the substance is immediately and almost completely inhibited, as may be seen in Fig. 7. On the other hand, the effect of

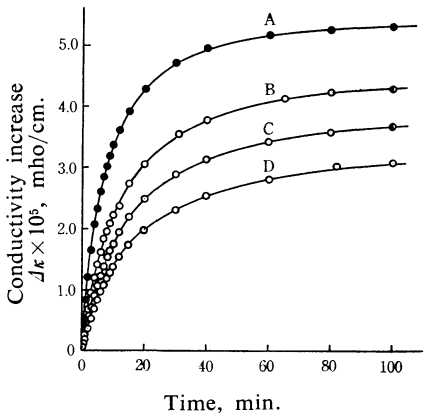



Fig. 4. Effect of sodium trimetaphosphate on the dissolution of strontium sulfate.
Concentration of trimetaphosphate:
A) 0, B) $2.5\times10^{-5}$ M, C) $1.0\times10^{-4}$ M,
D) $2.0\times10^{-4}$ M

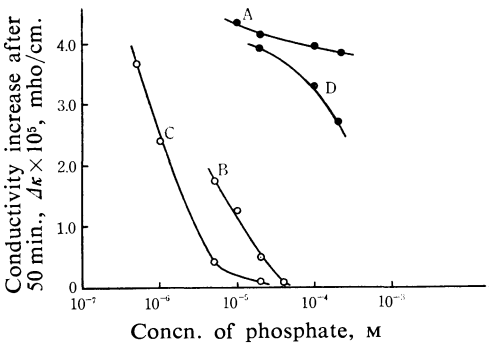



Fig. 5. The retarding action of several condensed phosphates on the dissolution of strontium sulfate.
A) ortho-, B) pyro-, C) tri-,
D) trimetaphosphate

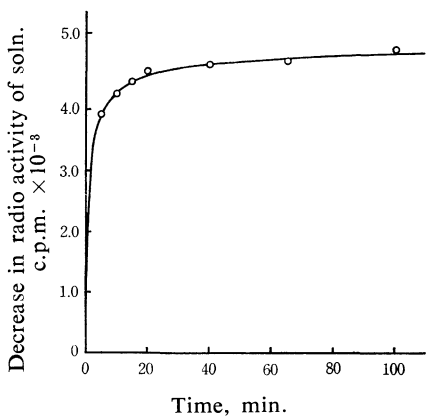



Fig. 6. Adsorption rate of triphosphate on the surface of strontium sulfate.

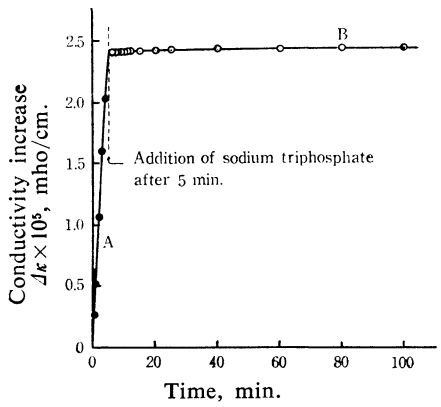



Fig. 7. Effect of sodium triphosphate on the dissolution of strontium sulfate.
Concentration of triphosphate:
A) 0, B) $1.0\times10^{-5}$ M

ortho- and trimetaphosphate is not so large as that of the other phosphates.

From Fig. 5 it may be seen that the retarding action of these four phosphates increases in the order of ortho-, trimeta-, pyro- and triphosphate and that there is a great difference in the retarding action between the former two phosphates and the latter two ones. The same tendency has been observed in the retarding action of these phosphates on the crystallization of strontium sulfate.[2]

The retarding action of phosphates may be considered to be caused by the covering of the surface of particles by the phosphates adsorbed, thus preventing the escape of ions from the surface of crystal into the solution. The adsorption of phosphates on the surface of crystal seems, then, to play a predominant role in the retarding action. According to the results of the measurements of the adsorption of these phosphates on the strontium sulfate particles previously reported,[2] the adsorbed amount of tri- or pyrophosphate is much larger than that of trimeta- or orthophosphate. The results of the adsorption reveal that the retarding action on the dissolution of strontium sulfate is closely related to the adsorption of phosphates.

It is of much interest to discuss the retarding action by combining the dynamic behavior of the dissolution of strontium sulfate with the rate of the adsorption of phosphate. Let us now consider the case where 1 mg. of strontium sulfate is dissolved in 30 ml. of a solution. The initial slope of the dissolution curve in water gives the initial rate of the dissolution. From the initial rate, the increase in the concentration of strontium sulfate in the solution is calculated to be $1.9\times10^{-4}$ M per minute, where a linear relationship is assumed between the specific conductance and the concentration. On the other hand, the average area occupied per ion pair of strontium sulfate on the (001), (010) and (100) faces of its crystal was found to be 23.2 Å$^2$.[3] The suface area of 1 mg. of strontium sulfate was also found to be $2.9\times10^{-4}$ m$^2$ from its specific surface area.[2] If the outermost layer of the crystal surface dissolves into 30 ml. of the solution, it can be calculated from the above two data that the increase in the concentration of strontium sulfate is $6.9\times10^{-8}$ M. The time necessary for removing the outermost layer of the particle surface is approximately $3.6\times10^{-4}$ min., by which time the surface layer of particles is uniformly removed by the dissolution. As is shown in Fig. 6, the amount of adsorbed triphosphate increases rapidly within the first few minutes, but it needs at least more than ten minutes to reach the adsorption equilibrium.

From these results, it is clear that there is an extremely large difference between the time required to remove one layer of the crystal surface of strontium sulfate by dissolution and that required to cover the surface by a monomolecular layer of triphosphate. In spite of such a large difference between these two times, the dissolution is greatly retarded. In order to explain such facts, the following mechanism may tentatively be proposed for the dissolution of strontium sulfate.

The surface of crystal may not be uniform; the special places may play a predominant role for the dissolution. On the other hand, the fact that the adsorption isotherm of triphosphate on strontium sulfate approaches the saturation point in an extremely dilute concentration, namely, ca. $10^{-6}$ M, shows that a strong interaction exists between the surface of strontium sulfate and triphosphate. The adsorbed triphosphate may form a fairly strong bond with the strontium ions of the crystal surface, presumably forming a compound such as the surface complex. When such places as the active sites for the dissolution are covered by the adsorption of triphosphate, the dissolution may be remarkably retarded. Such places may be kinks or steps on the crystal surface, as has been presumed by Sears et al.[7] in the case of the dissolution of lithium fluoride poisoned by a trace of ferric fluoride. It may be inferred that the adsorption on the kinks or steps prefers the adsorption on the flat surface of the crystals. The probability that such places are covered increases with the increase in the concentration of triphosphate, resulting in the strong retarding action. A similar consideration may be applied to the case of pyrophosphate.

The insignificant effect of ortho- and trimetaphosphate may be attributed not only to

the small adsorption amount, but also to the weak bond between these phosphates and the crystal surface in comparison with the case of tri- or pyrophosphate.

**Summary**

The effect of ortho-, pyro-, tri- and trimetaphosphate on the dissolution of strontium sulfate has been studied. Pyro- and triphosphate remarkably retard the dissolution, even in an extremely dilute solution, while ortho- and trimetaphosphate exhibit only an insignificant effect. From the results of the measurements of the adsorption of these phosphates onto the crystal surface, it is considered that the retarding action of these phosphates is to be attributed to the adsorption. The kinetic treatments of the dissolution and adsorption lead to the conclusion that the dissolution may be controlled by the specific places on the crystal surface and that such places may be the rate-determining sites for the dissolution.

The authors wish to thank Dr. Sadaichi Otani for his valuable advice on and discussions of this work.

*Department of Chemistry*
*Faculty of Science*
*Hiroshima University*
*Higashisenda, Hiroshima*

# NOTES

## The Synthesis of Ethyl 4-Carbethoxy-3-keto-2-tetrahydrothiophenevalerate, the Synthetic Intermediate of Biotin

By Hirozo SEGAWA and Eiji IMOTO

(Received June 15, 1964)

Biotin has previously been synthesized by Cheney and his co-workers through the diethylester of 4-carboxy-3-keto-2-tetrahydrothiophenevaleric acid[1] and by Baker and his coworkers through the corresponding dimethylester.[2] Although these synthetic intermediates were prepared by the same investigators, many steps were involved in their methods, and hence the yields were poor.

This paper will describe an improved method of synthesizing ethyl 4-carbethoxy-3-keto-2-tetrahydrothiophenevalerate, a method in which five steps are involved, as is shown in Fig. 1.

The starting compound, cyclohexanone, was first converted to 2-carbethoxycyclohexanone (II) and then to 6-bromo-2-carbethoxycyclohexanone (III) by Brenner's method.[3] Compound III condensed readily with ethyl β-mercaptopropionate in the presence of sodium ethoxide to produce 2-carbethoxy-6-(β-carbethoxyethylthio)cyclohexanone (IV), which gave an intense purple color with ferric chloride in ethanol.

The treatment of IV with a strong alkali gave a ring-opening product, 2-carboxyethyl 1,5-dicarboxyamyl sulfide (V), along with a by-product, 2-(β-carboxyethylthio)cyclohexanone (IX). The isolation and purification of V and IX were not attempted in this step, since their boiling points were too high for them to be distilled, even under reduced pressure. The esterification of a mixture of V and IX gave the corresponding esters, 2-carbethoxyethyl 1,5-dicarbethoxyamyl sulfide (VI) and 2-(β-carbethoxyethylthio)cyclohexanone (X). The by-product, X, was identified by means of a comparison of its infrared spectrum and the melting point of its 2,4-dinitrophenyhydrazone with those of an authentic sample prepared from 2-chlorocyclohexanone (VIII) and ethyl β-mercaptopropionate, as is shown in Fig. 2.

The yields of VI and X varied to some

1) L. C. Cheney et al., *J. Am. Chem. Soc.*, **66**, 1040 (1944); **67**, 729 731, 2213, 2252 (1945).
2) B. R. Baker et al., *J. Org. Chem.*, **12**, 138, 155, 160, 167, 174, 186, 322, 328, 475, 483 (1947); **13**, 123 (1948).
3) J. E. Brenner, ibid., **26**, 22 (1961).

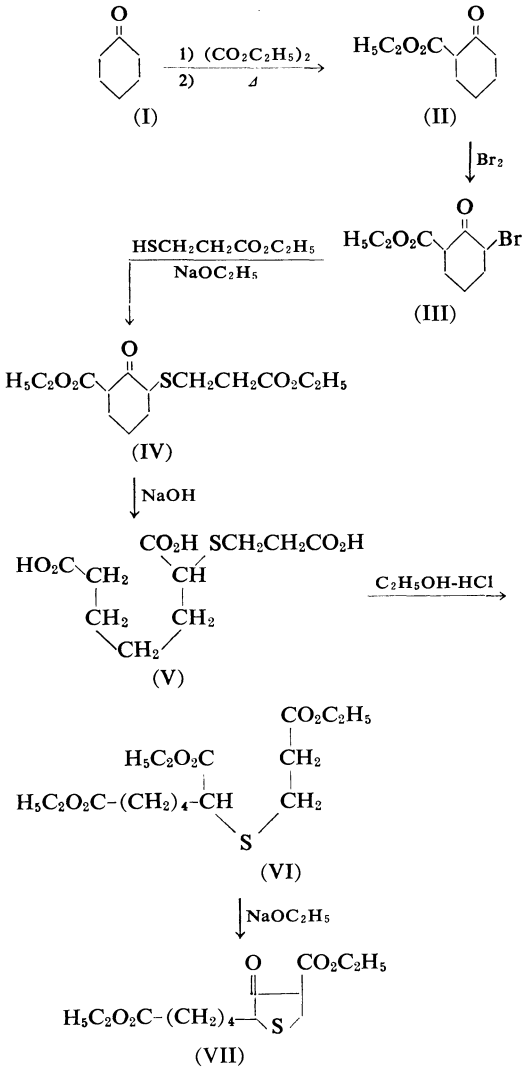



Fig. 1.

extent in each experiment. Compound VI was obtained in a 64% yield based on IV under the reaction conditions described in the "Experimental" section.

The Dieckmann cyclization of VI was performed by Cheney's method to produce VII. The melting point of its copper chelate compound agreed satisfactorily with the literature value.[1]

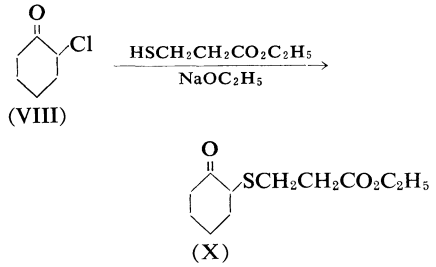



Fig. 2.

## Experimental*

**2-Carbethoxy-6-(β-carbethoxyethylthio)-cyclohexanone (IV).** — To a solution of sodium ethoxide (4.6 g. of sodium and of 70 ml. absolute ethyl alcohol), a solution of 27 g. of ethyl β-mercaptopropionate in 10 ml. of absolute ethyl alcohol was added. After this mixture had been cooled in a dry ice-acetone bath to −20°C, a solution of 50 g. of 6-bromo-2-carbethoxycyclohexanone in 20 ml. of ethyl alcohol was stirred drop by drop into the mixture under nitrogen. After the addition had been completed, stirring was continued for two hours at room temperature. During this period sodium bromide precipitated. After it had stood for fifteen hours at room temperature, the mixture was concentrated under reduced pressure to about 70 ml. The residue was poured into water, and the oily layer obtained was separated. The aqueous layer was then extracted three times with ether. The oily compound and the extracts were combined, washed with sodium bicarbonate solution, and dried over sodium sulfate. The ether was removed, and the residue was distilled to give 51 g. (84%) of IV as a colorless oil; b. p. 141—142°C/0.1 mmHg.

Found: C, 55.67; H, 7.42. Calcd. for $C_{14}H_{22}O_5S$: C, 55.61; H, 7.33%.

**2-Carbethoxyethyl 1,5-Dicarbethoxyamyl Sulfide (VI).**—In a 300 ml. three-necked flask equipped with a stirrer, a dropping funnel, a reflux condenser, a gas inlet tube and a thermometer were placed 50 g. of sodium hydroxide, 40 g. of water and 110 g. of ethyl alcohol. The stirred mixture was then heated for half an hour in a water bath at 50°C under nitrogen. A solution of 20 g. of 2-carbethoxy-6-(β-carbethoxyethylthio)cyclohexanone in 40 ml. of ethyl alcohol was then added to the mixture over a period of twenty minutes. The resulting mixture was heated further for five hours at 50°C. After this mixture had been diluted with 100 ml. of water, ethyl alcohol was removed under reduced pressure. The residue was washed with 50 ml. of ether, and the aqueous layer was made acidic to Congo red with concentrated hydrochloric acid. The mixture was continuously extracted with ether for forty hours, and the extract was dried over sodium sulfate. The ether was removed, and the residual, thick, oily compound was dissolved in 150 ml. of absolute ethyl alcohol. The solution was cooled in an ice-bath, saturated with dry hydrogen chloride, and refluxed for half an hour. Ethyl alcohol was then evaporated to about 50 ml. The residue was diluted with 200 ml. of water, and the oily compound obtained was separated. The aqueous layer was extracted with ether. The oily compound and the extracts were combined and washed with a sodium bicarbonate solution and then with water.

After the ether had been removed, the VI, distilling at 178.5—180°C/0.25 mmHg., weighed 14.8 g. (64%). The redistillation of the lower boiling

* All boiling and melting points are uncorrected.

distillate gave 1.9 g. (13%) of 2-(β-carbethoxyethylthio)cyclohexanone, b. p. 149—151°C/1 mmHg.

**2-(β-Carbethoxyethylthio)cyclohexanone (X).** — To a solution of 3.5 g. of sodium in 80 ml. of absolute ethyl alcohol, 20 g. of ethyl β-mercapto-propionate in 10 ml. of ethyl alcohol was added. To the stirred solution 20 g. of 2-chlorocyclohexanone in 40 ml. of ethyl alcohol was then added over a period of half an hour while the temperature was maintained at −20°C. After it had stood for fifteen hours at room temperature the mixture was diluted with 300 ml. of water and extracted three times with ether. The combined extract was then washed successively with aqueous sodium bicarbonate and dilute hydrochloric acid. After the ether had been removed, 31 g. (89%) of an oil was obtained; b. p. 151—152°C/1 mmHg.

Found: C, 57.48; H, 8.02. Calcd. for $C_{11}H_{18}O_3S$: C, 57.36; H, 7.88%.

The 2,4-dinitrophenylhydrazone prepared in the usual manner was separated as orange-yellow crystals from ethyl alcohol; m. p. 103—104°C.

**Ethyl 4-Carbethoxy-3-keto-2-tetrahydrothiophenevalerate (VII).** — According to the method of Cheney,[3] 3 g. of 2-carbethoxyethyl-1,5-dicarbethoxyamylsulfide (VI) in dry benzene was treated with sodium ethoxide at room temperature. The light-brown oil thus obtained gave a deep-red color when treated with ferric chloride in an alcoholic solution. The oil was converted into a copper chelate compound by treating it with a saturated cupric acetate solution. The recrystallization of the chelate compound from ether-petroleum ether yielded 2.6 g. (90.5%) of fine, light-green crystals, m. p. 120—121°C.

Found: C, 50.60; H, 6.55. Calcd. for $(C_{14}H_{22}O_4S)_2$-Cu: C, 50.32; H, 6.63%.

The authors are indebted to Mr. Noboru Matsumura for the microanalyses.

*Department of Applied Chemistry*
*College of Engineering*
*Univeresity of Osaka Prefecture*
*Sakai-shi, Osaka*

# Recalculation of the Bond Moments and the Bond Derivatives of the Dichloromethane Molecule

By Utako KANBAYASHI*1 and Kenkichi NUKADA*2

(Received August 19, 1964)

Straley[1] measured the absolute intensities of perpendicular bands of dichloromethane in vapor, expessed $\partial\mu/\partial Q_i$ (where $\mu$ is the dipole moment and $Q_i$ is the normal coordinates of the molecule) in terms of the bond moments ($\mu_{CH}$, $\mu_{CCl}$) and the bond derivatives ($(\partial\mu/\partial r)_{CH}$ and $(\partial\mu/\partial r)_{CCl}$), and calculated the values of the bond moments and the bond derivatives. (The results are given in column I of Table I.) In this case, one half of the observed intensity of the doublet centered at 2995 $cm^{-1}$, was allotted to the intensity of $\nu_6$ (the antisymmetrical stretching vibration).

Several recent studies[2-5] have shown, however, that it is reasonable to assign the doublet centered at 2995 $cm^{-1}$ to the P and R branch maxima of $\nu_1$ (the symmetrical stretching vibration) and that $\nu_6$ is not observed because of its very weak intensity in vapor. The present authors have, therefore, recalculated the bond moments and the bond derivatives by using the new assignment; the method is described below, and the results are shown in Table I.

1) The values in column II are the result of the recalculation made by following the process of Ref. 1 except that $A_6$ is set at zero. These values agree with those in column I except that the absolute value of $(\partial\mu/\partial r)_{CH}$ is smaller than that in column I.

2) When the above calculations (Ref. 1 and 1)) were made, it was assumed that the vector sum of the all bond moments obtained by infrared work was equal to the total dipole moment determined by dielectric measurements. However, this assumption is not valid, particularly if there are lone-pairs present, as Coulson indicated.[6] Therefore, the recalculation was made without using this assumption. The results are shown in column III.

3) Finally, the authors made more rigorous

*1 Present address: Ochiai;shataku, Nakoso-shi, Fokushima-ken

*2 Present address: Basic Research Laboratories, Toyo Rayon Co., Ltd., Kamakura-shi.

1) J. W. Straley, *J. Chem. Phys.*, **23**, 2183 (1955).

2) T. Shimanouchi and I. Suzuki, *J. Mol. Spectry.* **8**, 222 (1962).

3) R. E. Kagarise, *Spectrochim. Acta*, **19**, 1371 (1963).

4) M.-T. Forel, A. Lafaix, P. Saumagne and M.-L. Josien, *J. Chim. Phys.*, 875 (1963).

5) U. Kanbayashi, This Bulletin, **36**, 1173 (1963).

6) C. A. Coulson, *Spectrochim. Acta*, **14**, 161 (1959).

TABLE I. BOND MOMENTS AND BOND DERIVATIVES OF THE DICHLOROMETHANE MOLECULE CALCULATED FROM THE PERPENDICULAR BANDS

| | I | II | III | IV |
|---|---|---|---|---|
| $A_6$ (c. p. s./cm. at NTP) | $48.0\times10^{10}$ | 0 | 0 | 0 |
| $\mu_{CH}$ ($D$) | +0.45 | +0.45 | +0.60 | +0.58 |
| $\mu_{CCl}$ ($D$) | −0.95 | −0.95 | −1.4 or −3.0 | −1.4 or −3.0 |
| $(\partial\mu/\partial r)_{CH}$ ($D/A$) | +0.3 or −0.2 | +0.06 | +0.09 or +0.24 | +0.11 or +0.23 |
| $(\partial\mu/\partial r)_{CCl}$ ($D/A$) | +3.7 | +3.7 | ±3.8 | ±4.5 |

calculations of $\partial\mu/\partial Q_i$ by using the newest data on the normal vibrations of the dichloromethane molecule[7] and so got the following relations:

$$\pm\frac{\partial\mu}{\partial Q_6} = 1.679x + 95.525x' + 7.444y \quad (3081\ \mathrm{cm}^{-1}) \quad (1)$$

$$\pm\frac{\partial\mu}{\partial Q_7} = 54.539x + 4.458x' + 14.625y \quad (901\ \mathrm{cm}^{-1}) \quad (2)$$

$$\pm\frac{\partial\mu}{\partial Q_8} = 108.708x + 2.085y + 0.496y' \quad (1264\ \mathrm{cm}^{-1}) \quad (3)$$

$$\pm\frac{\partial\mu}{\partial Q_9} = 18.602x + 6.518y + 28.182y' \quad (747\ \mathrm{cm}^{-1}) \quad (4)$$

$$\pm\frac{\partial\mu}{\partial Q_1} = 11.661x + 62.514\chi' + 3.504y + 2.637y' \quad (3019\ \mathrm{cm}^{-1}) \quad (5)$$

where $x=\mu_{CH}$ (Debye), $x'=(\partial\mu/\partial r)_{CH}$ (Debye/Å), $y=\mu_{CCl}$ (Debye), and $y'=(\partial\mu/\partial r)_{CCl}$ (Debye/Å). (The numbers in parentheses reprsent the calculated frequencies.)

After Straley's observed values of $\partial\mu/\partial Q_7$ (±11.7), $\partial\mu/\partial Q_8$ (±63.1) and $\partial\mu/\partial Q_9$ (±123.0), and zero for $\partial\mu/\partial Q_6$ had been introduced into Eqs. 1—4, the bond moments and the bond derivatives for the perpendicular bands were calculated; they are given in column IV. It is interesting that the values of column IV based on the more accurate data agree approximately with those of column III.

The value of $\partial\mu/\partial Q_1$ calculated from Eq. 5 using the values in column IV was 20—25 (if $(\partial\mu/\partial r)_{CCl}=+4.5\ D/A$) or $\partial\mu/\partial Q_1=-3--2$ (if $(\partial\mu/\partial r)_{CCl}=-4.5\ D/A$). Neither of these values coincides with the value determined from the intensity of the doublet centered at 2995 $\mathrm{cm}^{-1}$ observed by Straley[1] (±32). In this case, the values of the bond moments and the bond derivatives calculated from the perpendicular bands are different from those calculated from the parallel bands, as has previously been pointed out.[8-10]

*Government Chemical Industrial Research Institute, Tokyo*
*Shibuya-ku, Tokyo*

7) I. Suzuki and T. Shimanouchi, *J. Mol. Spectry.*, 6, 277 (1961).

8) D. F. Hornig and D. C. McKean, *J. Phys. Chem.*, 59, 1133 (1955).

9) G. M. Barrow and D. C. McKean, *Proc. Roy. Soc.*, 213A, 27 (1952).

10) H. W. Thompson, "Molecular Spectroscopy," The Petroleum Institute (1955), p. 94.

# The Spectrophotometric Determination of Anions by Solvent Extraction with Metal Chelate Cations. VII.* A New Method for the Determination of Pentachlorophenol

By Yuroku YAMAMOTO, Keiya KOTSUJI and Sadayasu TANAKA

(Received August 21, 1964)

In the course of our study of the solvent extraction of an anion with a metal chelate cation,[1] it has been observed that not only inorganic anions, such as iodide, perchlorate and tetra-iodo-mercury(II) or cadmium, but also organic anions, such as trichloroacetate, or pentachlorophenolate (PCP), can be extracted into an organic solvent as nitrobenzene if the aqueous solution contains an excess of phenanthroline or dipyridyl iron(II) chelates cations.

This study will present a method for the determination of PCP based on solvent extraction with the tris-phenanthroline iron(II) chelate. Figure 1 shows the absorption spectra of the extracts against nitrobenzene as a reference. Curve 1 is a spectum of the extracts with PCP, while curve 2 is that of the extract when PCP is absent. It is shown that, when a small amount of PCP is present, the chelate cation is quite extractable into the organic layer. The absorbance maximum of the associated species, which may be assumed to be $[Fe(phen)_3][PCP]_2$, is found at 514 mμ. A maximum extraction is obtained in the range of pH 6.0—12.0, when the molar concentration of the chelate is kept five times that of PCP. The recommended procedure for the calibration curve is as follows.

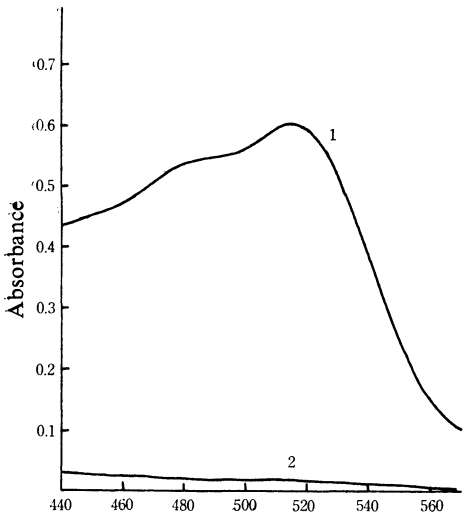



Fig. 1. Absorption spectra (reference: nitrobenzene).
Curve 1: Spectrum of organic phase extracted from the aqueous solution (25 ml.) containing $[Fe(phen)_3](2\times10^{-4}$ M), borax ($1\times10^{-2}$ M) and PCP ($4\times10^{-5}$ M), pH 10.0.
Curve 2: Spectrum of organic phase extracted from the aqueous solution (25 ml.) containing $[Fe(phen)_3](2\times10^{-4}$ M), borax ($1\times10^{-2}$ M), but PCP is absent, pH 10.0.

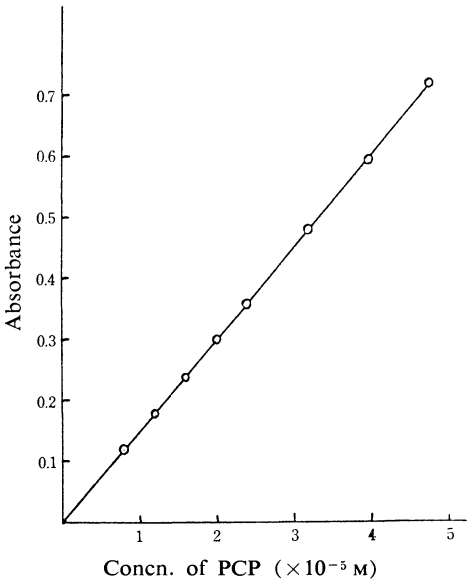



Fig. 2. Calibration curve at 514 mμ. $[Fe(phen)_3]^{2+}$ ($2\times10^{-4}$ M), borax ($1\times10^{-2}$ M), PCP ($8\times10^{-6}$—$5\times10^{-5}$ M), pH 10.0, reference: reagent blank

Mix 5 ml. of a tris-phenanthroline-iron(II) sulfate solution ($1\times10^{-3}$ M), 5 ml. of a borax buffer solution ($5\times10^{-2}$ M, pH 10.0), and varying amounts of the standard PCP solution, and then dilute to 25 ml. with distilled water. Shake the solution with 10.0 ml. of nitrobenzene (3 min.). Transfer the organic layer to a flask containing 1 g. of anhydrous sodium sulfate, and measure the absorbance at 514 mμ

* VI: K. Kotsuji, This Bulletin, 38, 402 (1965).
1) Y. Yamamoto et al., ibid., 37, 434, 594, 785 (1964).

using a reagent blank as a reference. Beer's law is followed in the range from $8\times10^{-6}$ to $5\times10^{-5}$ M. The presence of diverse ions, such as chloride, phosphate, sulfate and nitrate does not interfere with the determination, even when their amounts are about 1000 times that of PCP, but the same amount of tetrachlorophenol as that of PCP gives a slight positive error.

Although several methods,[2-4] based on the colorimetric estimation of the product obtained by the oxidation of PCP, have recently been reported, the method proposed here is based on a different mechanism of the color development and has a higher sensitivity and a better accuracy.

*Department of Chemistry*
*Faculty of Science*
*Hiroshima University*
*Higashisenda, Hiroshima*

2) T. Akisada, *Japan Analyst*, **12**, 611 (1963).
3) W. Deichmann and L. J. Schafer, *Ind. Eng. Chem., Anal. Ed.*, **14**, 310 (1942).
4) J. R. Lane, *J. Agr. Food Chem.*, **6**, 667 (1958).

# The Application of Brown Reduction to an $\alpha, \beta$-Unsaturated Keto-steroid

By Hisao NAKATA

(Received August 25, 1964)

Recently Brown and Brown[1,2] have reported a simple and convenient procedure for the catalytic hydrogenation of olefins[3-5] and aromatic nitro compounds.[6] The method utilizes the new active platinum metal catalysts prepared by the in situ treatment of platinum metal salts with sodium borohydride.[3,4,7] It is of interest to examine whether or not the Brown reduction may be undergone also with olefins that have other functional groups, such as oxo or formyl groups. We now wish to report a successful application of the Brown reduction to the double bond of an $\alpha, \beta$-unsaturated keto-steroid.

The platinum metal catalyst was prepared as reported,[5] and the reaction was tested with $\Delta^{16}$-5$\alpha$-pregnene-3$\beta$-ol-20-one, using sodium borohydride and acetic acid as a hydrogen source. At room temperature, the absorption of hydrogen took place smoothly, and the expected saturated ketone, 5$\alpha$-pregnane-3$\beta$-ol-20-one, was obtained in a good yield.

The results indicate that the Brown reduction may be expected to be applicable to a wide variety of compounds that have functional groups susceptible to reduction with sodium borohydride.

## Experimental

The procedure of the reduction followed that of Brown and Brown.[5] The platinum catalyst was prepared by adding 3 ml. of a standard stabilized solution of sodium borohydride[5] to an ethanolic solution of chloroplatinic acid (0.120 g./10 ml.). After the mixture had been acidified with 5 ml. of acetic acid, the solution of 0.442 g. (1.40 mmol.) of $\Delta^{16}$-5$\alpha$-pregnene-3$\beta$-ol-20-one (m. p. 207—208°C) in 20 ml. of ethanol was added and the reduction was carried out by adding 10 ml. of a 0.203 M solution of sodium borohydride in ethanol.

After it had been stirred for two hours, the reaction mixture was filtered to remove the catalyst and then concentrated to 25 ml. under reduced pressure. The solution was diluted with 30 ml. of ether and washed with a dilute sodium hydroxide solution. The evaporation of the solvent gave 0.427 g. of a white solid. Recrystallization from aqueous methanol afforded 0.425 g. of colorless needles; m. p. 189—190°C. Yield, 96%.

In order to remove a persistent impurity, 0.272 g. of this material in benzene was chromatographed on 10 g. of Florisil (10×150 mm.-column). Fractions eluted with 2% acetone-benzene were collected, and the removal of the solvent gave 0.251 g. of the white solid. Recrystallization from aqueous methanol yielded 0.210 g. of a pure specimen of 5$\alpha$-pregnane-3$\beta$-ol-20-one as colorless needles; m.p. 193—194°C. $\nu_{max}^{CHCl_3}$ 1708 cm$^{-1}$. The reported m.p. of 5$\alpha$-pregnane-3$\beta$-ol-20-one (17-normal, i.e., 17$\alpha$-H) is 194°C.[8,9]

1) C. A. Brown and H. C. Brown, *J. Am. Chem. Soc.*, **84**, 2829 (1962).
2) H. C. Brown, K. Sivasankaran and C. A. Brown, *J. Org. Chem.*, **28**, 214 (1963).
3) H. C. Brown and C. A. Brown, *J. Am. Chem. Soc.*, **84**, 1494 (1962).
4) H. C. Brown and C. A. Brown, ibid., **84**, 2827 (1962).
5) H. C. Brown and C. A. Brown, ibid., **84**, 1495 (1962).
6) H. C. Brown and K. Sivasankaran, ibid., **84**, 2828 (1962).
7) H. C. Brown and C. A. Brown, ibid., **84**, 1493 (1962).
8) W. Taylor, *Biochem. J.*, **60**, 380 (1955).
9) W. Taylor, ibid., **62**, 332 (1956).

An isomeric 17-iso compound (i. e., 17$\beta$-H) has an m. p. of 147—148°C[10,11] or 138—139°C[12].

Found: C, 79.23; H, 10.42. Calcd. for $C_{21}H_{34}O_2$: C, 79.19; H, 10.76%.

10) A. Butenandt and G. Fleischer, *Ber.*, **70**, 96 (1937).
11) A. Butenandt and L. Mamoli, ibid., **68**, 1847 (1935).
12) C. W. Shoppee, *J. Chem. Soc.*, **1949**, 1671.

The author is indebted to Professor Yoshimasa Hirata of Nagoya University for his encouragement during this work.

*Chemical Institute*
*Faculty of Science*
*Nagoya University*
*Chikusa-ku, Nagoya*

# ESR Studies of the Reactions of Triphenylamine with Alkali Metals

By Masamoto IWAIZUMI and Taro ISOBE

(Received August 26, 1964)

In secent years, many organic radicals have been prepared by reactions of the conjugated compounds with alkali metals in tetrahydrofuran (THF), 1, 2-dimethoxyethane (DME) and in solvents with similar properties.[1] Most of these radicals have been shown to be anion radicals formed by the transfer of an electron from the alkali metals to the conjugated compounds, and ESR studies of these radicals have yielded much interesting information about these molecules.

This work was undertaken to study the reactions of triphenylamine with alkali metals in DME and THF by ESR techniques. It has been found that the reactions are not simple one-electron reductions but that they proceed through the cleavage of C-N bonds and the subsequent recombination to yield a biphenyl anion radical as one of the reaction products.

## Experimental and Results

The reactions of triphenylamine with alkali metals (lithum, sodium and potassium) were undertaken in THF or DME as a solvent in vacuo. The reactions at $-70°C$ and at room temperature gave the same results. It was observed that, if a solution of triphenylamine in THF or DME was allowed to contact with an alkali metal, a deep green solution was obtained, a solution which exhibited an ESR absorption as is shown in Fig. 1. The measurements of ESR spectra were carried out with a Hitachi X-band ESR spectrometer, model MPU-3B, employing a field modulation at a frequency of 100 kc./s.

The spectrum can be explained by the couplings with three sets of equivalent protons, via., the coupling with two equivalent protons with the coupling constant of 5.33 gauss, four equivalent protons which have half the coupling of the former, and four equivalent protons with a smaller coupling constant, 0.43 gauss. Namely, the hyperfine structure can be interpreted as arising from the protons of two benzene rings, and no structures resulting from a nitrogen nucleus and the remaining five protons are evident. Recently, Hanna[2] has

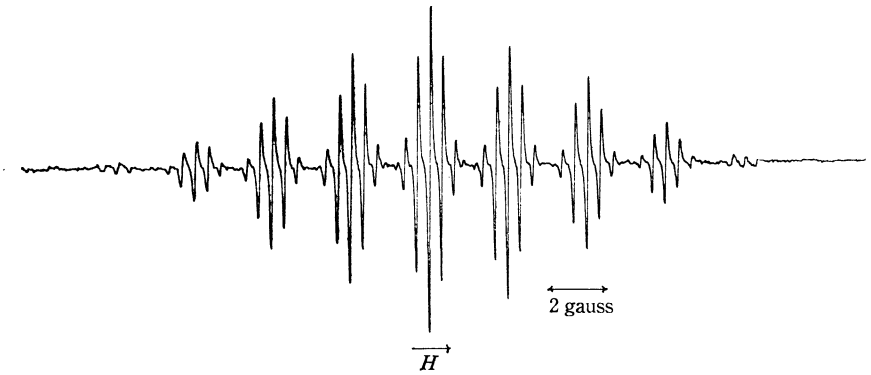



Fig. 1. ESR spectrum of the reaction product of triphenylamine with potassium in DME.

1) A. Carrington, *Quart. Revs.*, 17, 67 (1963).

2) M. W. Hanna, *J. Chem. Phys.*, 37, 685 (1962).

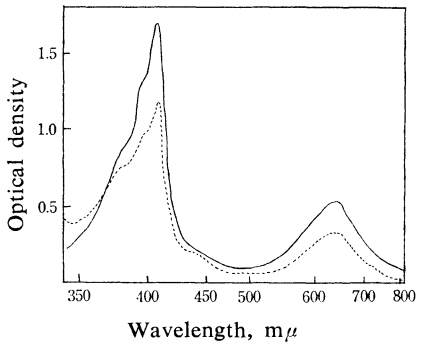



Fig. 2. Electronic absorption spectra of the reaction product of triphenylamine with potassium (----) and biphenyl anion radical (——) in THF.

reported that the odd-electron distribution in the triphenylphosphine anion is restricted to one benzene ring, and that the ESR spectrum can be interpreted by assuming the couplings with a phosphine nucleus and only four protons. He attributed this to the Jahn-Teller distortion. In the case of triphenylamine, because of its threefold symmetry, its anion radical was expected to be subjected to the Jahn-Teller distorsion. However, the ESR spectrum of the radical formed from triphenylamine agrees well with that of the biphenyl anion radical already reported by Carrington et al.[3]

We also observed the electronic absorption spectrum of the product formed upon the reaction of triphenylamine with potassium and that of the biphenyl anion radical obtained by the reduction with potassium using THF as a solvent. As Fig. 2 shows, the two spectra resemble each other very closely except that the spectrum of the reaction product triphenylamine exhibits an additional absorption at 430 mμ.

Gilman et al.[4] have reported that triphenylamine is cleaved by lithium at reflux in THF to yield, upon carbonation, diphenylamine in a low yield. However, from the agreement of the ESR and the electronic absorption spectra of triphenylamine with those of the biphenyl anion radical, it seems most reasonable to conclude that the radical formed on the reactions of triphenylamine with alkali metals under our experimental conditions was the biphenyl anion radical, though the mechanism of the reactions is unknown to us at the present time. The additional absorption band at 430 mμ of the reaction product of triphenylamine must be due to some other species.

Also, in the case of tri-*p*-tolylamine, the radical formed on the reactions with alkali metlas was the anion radical of the biphenyl derivative, the *p,p'*-bitolyl anion radical; its ESR spectrum, which is shown in Fig. 3, was identical with that of the *p,p'*-bitolyl anion radical previously reported by Ishizu.[5]

*Chemical Research Institute of*
*Non-Aqueous Solutions*
*Tohoku University*
*Katahira-cho, Sendai*

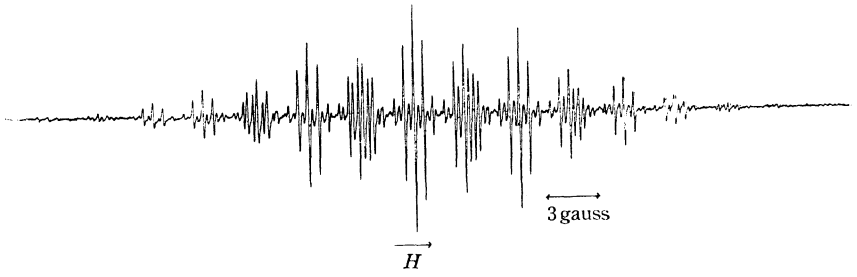



Fig. 3. ESR spectrum of the reaction product of tri-*p*-tolylamine with potassium in DME.

3) A. Carrington and J. Dos Santos-Veiga, *Mol. Phys.*, 5, 21 (1962).

4) H. Gilman and J. J. Dietrich, *J. Am. Chem. Soc.*, 80, 380 (1958).

5) K. Ishizu, This Bulletin, 36, 938 (1963).

## SHORT COMMUNICATIONS

# Ein neues Pteridin aus *Bombyx mori lem*

Von Miki GOTO, Masaki KONISHI und Motoo TSUSUE

(Eingegangen am 3. Dezember, 1964)

Aus 400 g Epidermis von *Bombyx mori lem* konnten 2 mg eines intensiv grün fluoreszierenden neuen Pteridins (I) isoliert werden. Die Ultraviolett Spektren von I sind mit denen von 2-Amino-4-hydroxy-6-lactoyl-7, 8-dihydropteridin (Sepiapterin)[1] sehr ähnlich. Bei der Behandlung mit Natriumborhydrid und der Rückoxydation mit Luft entstehen drei fluoreszierende Stoffe II, III und IV. III ist eine Säure; beim Erhitzen (250°C, 3 Std) entsteht II. Bei der Behandlung mit $KMnO_4$ oder $KJO_4$ sowie durch Bestrahlung oder Behandlung mit Natronlauge wird die Substanz I leicht zu III oxydiert; dies wird durch Papierchromatographie, Dünnschichtchromatographie und Elektrophorese festgestellt. II sowie III sind jeweils sehr ähnlich mit 2-Amino-4-hydroxypteridin und mit 2-Amino-4-hydroxy-pteridin-6-carbonsäure, jedoch nicht identisch. Es wird hierbei zum Vergleich 2-Amino-4-hydroxy-8-methylpteridin V durch Kondensation von 2,5-Diamino-4-methylamino-6-hydroxypyrimidin und Glyoxal hergestellt. Ebenfalls wird 2-Amino-4-hydroxy-8-methyl-pteridin-6-carbonsäure (VI) durch Kondensation von 2,5-Diamino-4-methylamino-6-hydroxypyrimidin und $\beta$-Bromobrenztraubensäure synthetisiert. Es werden keine Unterschiede in den Ultraviolett Spektren (Abb. 1), $R_f$-Werten und dem elektrophoretischen Verhalten (s. unten) zwischen dem synthetischen Material und dem durch Hydrierung erhaltenen Produkt (II oder III) beobachtet. Diese Tatsachen zeigen, dass die Substanz I ein 6-Derivat des 2-Amino-4-hydroxy-8-methylpteridins ist. Beim Schütteln von I mit 5% iger Boraxlösung ergibt sich Milchsäure und ein gelb fluoreszierender Stoff VII. Die Ultraviolett Spektren von VII sind fast identisch mit denen von 7,8-Dihydroxanthopterin.[2] Die Menge der dabei entstandenen Milchsäure wird spektrophotometrisch bestimmt;[3] ein Mol Milchsäure entsteht aus 1 Mol von I (Molekulargewicht als 251 gerechnet). Aufgrund dieser Ergebnisse wird die Konstitution 2-Amino-4-hydroxy-6-lactoyl-8-methyl-7, 8-dihydropteridin für I vorgeschlagen. IV und VII sind nicht identifiziert, jedoch kommen dazu wahrscheinlich die Konstitutionen von 8-Methyl-7, 8-dihydrobiopterin und 8-Methyl-7, 8-dihydroxanthopterin.

Chromatographie: $R_f$-Werte in Lösungsmittelsystem

| | A | B | C | D | E | F |
|---|---|---|---|---|---|---|
| I | 0,24 | 0,54 | 0,42 | 0,50 | 0,43 | 0 |
| II | 0,31 | 0,45 | 0,45 | 0,55 | 0,59 | 0 |
| V | 0,31 | 0,45 | 0,45 | 0,55 | 0,59 | 0 |
| III | 0,15 | 0,28 | 0,32 | 0,35 | 0,58 | 48 |
| VI | 0,15 | 0,28 | 0,32 | 0,35 | 0,58 | 48 |

Lösungsmittelsysteme: A = *n*-Butanol/Eisessig/Wasser (4 : 1 : 1); B=Isopropanol/1% iges Ammoniak in Wasser (2 : 1); C=*sek*-Butanol/Ameisensäure/Wasser (8 : 2 : 5); D=*n*-Propanol/2%ige Ammoniumacetat-Lösung (1 : 1); E=3%ige Ammoniumchlorid-Lösung. *Wanderung der Pteridine zur

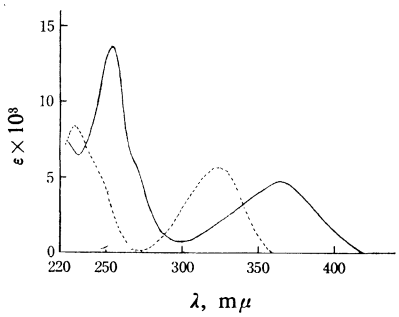
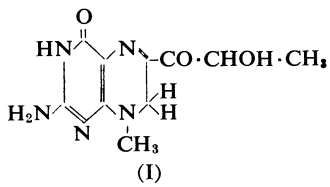



Abb. 1. UV-Spektren von II und V
—— pH 12, ---- pH 2




(I)

1) S. Nawa, Dieses Bulletin, **33**, 1555 (1960).
2) B. L. O'Dell, J. M. Vandenbelt, E. S. Bloom und J. J. Pfiffner, *J. Am. Chem. Soc.*, **69**, 250 (1947).
3) S. B. Barker und W. H. Summerson, *J. Biol. Chem.*, **138**, 535 (1941).

Anode (mm) nach einer Elektrophorese von 1 Std bei einer Spannung von 36 V/cm (0,05-M Essigsäure/Na-acetat; pH 4,5).

Es wird neuerdings gezeigt, dass die Tetrahydroform von Sepiapterin, Biopterin und 2-Amino-4-hydroxy-6,7-dimethylpteridin eine Funktion als Cofaktor bei der enzymatischen Hydroxylierung von Phenylalanin zu Tyrosin hat.[4,5] Die Konstitution I weist darauf hin, dass es auch bei Wasserstoffübertragungen in einem System Tetrahydropteridin $\rightleftarrows$ Dihydropteridin als Cofaktor wirkt; die Untersuchungen in dieser Hinsicht werden fortgesetzt.

4) S. Kaufman, *J. Biol. Chem.*, **237**, PC 2712 (1962).
5) S. Kaufman, ebenda, **239**, 332 (1964).

*Chemisches Institut der Gakushuin Universität*
*Mejiro, Tokyo* (*M. G. & M. K.*)

*Biologisches Institut der Tokyo*
*Metropolitan Universität*
*Setagaya, Tokyo* (*M. T.*)

# Chemical Effects Following the Isomeric Transition of $^{80m}Br$ in Pentamminecobalt(III) Bromides

By Nobufusa SAITO, Shizuko ITO and Takeshi TOMINAGA

(Received December 9, 1964)

In the course of an investigation of the behavior of hot radiobromine atoms produced by (n, $\gamma$) reaction in cobaltammine bromides, two of the present authors (N. S. and T. T.) found that the percentage of such energetic radiobromine atoms finally complexed with cobalt (i.e., the ligand yield) was related to the chemical or physical properties of the ligands in the target complexes.[1] In order to clarify the mechanism of such recoil reactions, it seemed worthwhile to compare chemical effects following different nuclear reactions. Therefore, they have studied the recoil reactions following the isomeric transition of $^{80m}Br$ in $^{80m}Br$-labeled cobaltammine bromides and have compared the results with those obtained with (n, $\gamma$) reaction.

TABLE I. LIGAND YIELD OF $^{80}Br$ PRODUCED IN ISOMERIC TRANSITION OF $^{80m}Br$

| No. | $^{80m}Br$-labeled complex salt | Ligand yield, % In dry ice-ethanol | Ligand yield, % In liquid nitrogen |
|---|---|---|---|
| 1 | $[Co(NH_3)_6]Br_3$ | 7.6±1.7 | 7.5±0.4 |
| 2 | $[Co(NH_3)_5NCS]Br_2$ | 6.1±0.9 | 4.9±0.9 |
| 3 | $[Co(NH_3)_5NO_2]Br_2$ | 6.1±1.3 | 7.8±0.3 |
| 4 | $[Co(NH_3)_5OH_2]Br_3$ | 10.9±2.1 | 9.5±1.0 |
| 5 | $[Co(NH_3)_5ONO]Br_2$ | 6.7±1.4 | 10.0±0.7 |
| 6 | $[Co(NH_3)_5ONO_2]Br_2$ | 8.0±1.2 | 8.9±1.5 |
| 7 | $[Co(NH_3)_5F]Br_2$ | 8.6±1.0 | 10.0±1.4 |
| 8 | $[Co(NH_3)_5Cl]Br_2$ | 12.3±3.0 | 14.2±1.4 |
| 9 | $[Co(NH_3)_5Br]Br_2$ | 11.7±1.4 | 13.8±1.3 |
| 10 | $[Co(NH_3)_5I]Br_2$ | 11.3±1.4 | 13.0±0.6 |

1) N. Saito, T. Tominaga and H. Sano, This Bulletin, 35, 63 (1962).

The ten kinds of pentamminecobalt bromides listed in Tabel I have been investigated.* The $^{80m}Br$-labeled bromide of each complex was precipitated from an aqueous solution by the addition of radioactive ammonium bromide irradiated in a nuclear reactor, filtered, washed

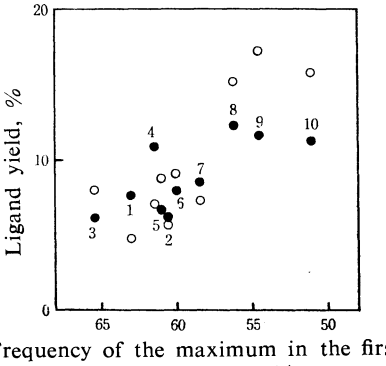



Fig. 1. The relationship between the ligand yield and the frequency of the maximum in the first absorption band.
● Isomeric transition; ○ (n, $\gamma$) reaction
Numbers in Fig. 1 correspond to those in Table I.

* Bisethylenediaminecobalt bromides, $[Co(en)_2X_2]Br_{1,3}$, have also been studied, and apparent ligand yields of about 2—10%, obtained. Unlike as in pentamminecobalt bromides, however, it appears that 2—5% of $^{80}Br$ is not complexed with cobalt but presumably bound in the ligand molecule (i.e., the ethylenediamine molecule).

and dried in air. After it had stood for 3 hr. in a mixture of dry ice and ethanol, or in liquid nitrogen, each salt was dissolved in water at 0°C, and cations (radiobromine complexed as ligands) and anions (bromide ions) were separated by means of ion-exchange resins. The radioactivities in both fractions were measured with a G-M counter, and the distribution of $^{80}Br$ was determined.

Table I shows the percentage of $^{80}Br$ complexed with cobalt (i.e., the ligand yield). For convenience of comparison, the ligand yields of radiobromine obtained in the (n, $\gamma$) reaction and the isomeric transition are plotted together in Fig. 1 against the frequency of the maximum in the first absorption band of the complex ion. The results may be summarized as follows:

1) Regarding the relationship between the ligand yield and the stability of the ligand, the ligand yield of $^{80}Br$ produced in the isomeric transition also tends to increase with the decrease in the frequency of the maximum in the first absorption band. Although this trend is very similar to that observed in the case of the (n, $\gamma$) reaction, the inclination is less pronounced for the former than for the latter.

2) Comparing ligand yields in the two reactions for the same salt, a higher ligand yield is generally obtainable in the (n, $\gamma$) reaction.

3) No remarkable difference is found between ligand yields obtained after storage in dry ice - ethanol and in liquid nitrogen.

*Department of Chemistry*
*Faculty of Science*
*The University of Tokyo*
*Hongo, Tokyo*

# The Radiolysis of Cobaltammine Complexes

By Nobufusa SAITO and Takeshi TOMINAGA

(Received December 12, 1964)

It has been found that the recoil and subsequent reactions in cobaltammine complexes irradiated with thermal neutrons are greatly influenced by such chemical factors as the chemical composition and stability as ligand of the outer anion.[1] Although a systematic study of the stability with regard to the ionizing radiations of these complex is also needed for the purpose of elucidating the intricate mechanism of such reactions, very few investigations have so far been made of the radiolysis of cobalt complexes in the solid state.[2,3] Therefore, the present authors have studied the radiolysis of the 23 kinds of crystalline cobaltammine complexes listed in Table I.

The cobaltammine complexes were irradiated with Co-60 gamma rays at an ambient temperature and at a dose rate of about $1.6\times10^5$ r./hr., up to a total dose of about $2\times10^8$ r., in

TABLE I. $G(Co^{2+})$ VALUES OF COBALTAMMINE COMPLEXES

| No. | Complex | $G(Co^{2+})$ |
|---|---|---|
| 1 | $[Co(NH_3)_6]F_3$ | $3.65\pm0.30$ |
| 2 | $[Co(NH_3)_6](NO_3)_3$ | $2.73\pm0.40$ |
| 3 | $[Co(NH_3)_6](NO_2)_3$ | $1.52\pm0.22$ |
| 4 | $[Co(NH_3)_6]Cl_3$ | $0.82\pm0.02$ |
| 5 | $[Co(NH_3)_6]Br_3$ | $0.32\pm0.06$ |
| 6 | $[Co(NH_3)_6]I_3$ | $0.21\pm0.07$ |
| 7 | $[Co(NH_3)_5NO_2](NO_3)_2$ | $1.39\pm0.17$ |
| 8 | $[Co(NH_3)_5NO_2](NO_2)_2$ | $0.93\pm0.12$ |
| 9 | $[Co(NH_3)_5NO_2]Cl_2$ | $0.48\pm0.02$ |
| 10 | $[Co(NH_3)_5NO_2]Br_2$ | $0.16\pm0.04$ |
| 11 | *cis*-$[Co(NH_3)_4(NO_2)_2]NO_3$ | $0.59\pm0.07$ |
| 12 | *trans*-$[Co(NH_3)_4(NO_2)_2]NO_3$ | $0.22\pm0.03$ |
| 13 | *cis*-$[Co(NH_3)_4(NO_2)_2]Cl$ | $0.30\pm0.04$ |
| 14 | *trans*-$[Co(NH_3)_4(NO_2)_2]Cl$ | $0.30\pm0.03$ |
| 15 | $[Co(NH_3)_3(NO_2)_3]$ | $0.37\pm0.05$ |
| 16 | $NH_4[Co(NH_3)_2(NO_2)_4]$ | $0.26\pm0.04$ |
| 17 | $[Co(NH_3)_5NO_3]Br_2$ | $0.48\pm0.04$ |
| 18 | $[Co(NH_3)_5F]Br_2$ | $1.28\pm0.10$ |
| 19 | $[Co(NH_3)_5Cl]Br_2$ | $0.65\pm0.04$ |
| 20 | $[Co(NH_3)_5Br]Br_2$ | $2.43\pm0.18$ |
| 21 | $[Co(NH_3)_5I]Br_2$ | $4.05\pm0.30$ |
| 22 | $[Co(NH_3)_5Cl]Cl_2$ | $2.13\pm0.08$ |
| 23 | $[Co(NH_3)_5Br]Cl_2$ | $3.05\pm0.25$ |

1) N. Saito, T. Tominaga and H. Sano, This Bulletin, 35, 365 (1962); ibid., 36, 230, 232 (1963); *J. Inorg. & Nucl. Chem.*, 24, 1539 (1962).

2) A. Sugimori and G. Tsuchihashi, This Bulletin, 34, 449 (1961).

3) N. Saito, H. Sano and N. Matsubara, paper presented at the 7th Symposium on Radiochemistry, Sendai, October, 1963.

the presence of air. After irradiation, each complex was dissolved in water, and the cobalt-(II) present in the solution was determined spectrophotometrically, by means of solvent extraction into chloroform, as β-nitroso-α-naphtholato-complex. The $G(Co^{2+})$ values obtained are shown in Table I. For convenience of comparison, the $G(Co^{2+})$ values of nitroamminecobalt complexes are plotted against the number of $NO_2$ groups contained in ligands of a complex in Fig. 1, while the $G(Co^{2+})$ values of pentamminecobalt complexes are plotted against the frequency of the maximum in the first absorption band in Fig. 2.

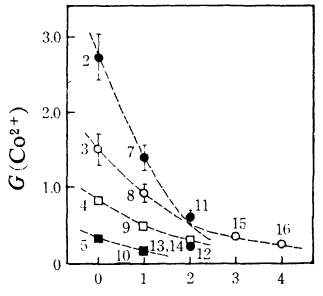



Fig. 1. The $G(Co^{2+})$ value of nitroammine complexes.
-●- Nitrates ; -○- Nitrites ;
-□- Chlorides ; -■- Bromides
(Numbers in Figs. 1 and 2 correspond to those in Table I.)

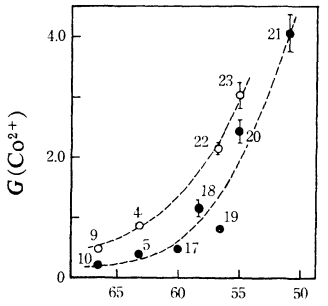



Fig. 2. The $G(Co^{2+})$ value of pentammine complexes.
-●- $[Co(NH_3)_5X]Br_{2,3}$
-○- $[Co(NH_3)_5X]Cl_{2,3}$

The following conclusions may be drawn from the experimental results:

1) For a series of nitroammine complexes which contain the same outer anion (those plotted on the curves in Fig. 1), the $G(Co^{2+})$ value decreases with the increase in the number of $NO_2$ groups in the ligands. Hence, it may be tentatively assumed that the stability of nitroammine complexes towards gamma irradiation increases with the increase in the thermodynamic stability of these complexes.[4]

2) For a series of pentammine complexes containing the same outer anion and a different acidic ligand, X ($[Co(NH_3)_5X]Br_{2,3}$ and ($[Co(NH_3)_5X]Cl_{2,3}$), the $G(Co^{2+})$ value decreases with the increase in the stability in the spectrochemical series.

3) In a group of salts composed of the same complex cation and a different outer anion, the $G(Co^{2+})$ value is greatly affected by the kind of outer anion. For hexammine complex salts, the $G(Co^{2+})$ value increases with the variation in the outer anion in the order: $I < Br < Cl < NO_2 < NO_3 < F$. For nitropentammine and other complex salts, the $G(Co^{2+})$ value increases in a similar order.

*Department of Chemistry*
*Faculty of Science*
*The University of Tokyo*
*Hongo, Tokyo*

4) M. Mori, R. Tsuchiya and H. Fukuda, This Bulletin, 33, 1503 (1960).

# The Reduction of Gamma-Irradiated Nickel Oxide by Hydrogen

By Toshiro YAMASHINA and Takaaki NAGAMATSUYA

(Received December 23, 1964)

In the process of reducting nickel oxide by hydrogen, it has been observed by several investigators that the reduction started after an induction period.[1-3] According to Hauffe,[1] the induction period should correspond to the period required for the nuclei formation of metallic nickel. Parravano[2] investigated the reduction process of nickel oxide from the view point of the electronic state of the semiconductor. Because the nickel oxide is a p-type semiconductor containing excess oxygen, it may be expected that the reduction process of nickel oxide could be affected by its physical properties, such as the electronic state and its non-stoichiometry. In this work, a gamma-irradiated nickel oxide will be found to behave in an unusual manner in the reduction process by hydrogen, depending upon the radiation dose.

Pure nickel oxide samples were obtained by decomposing and firing c. p. nickel nitrate in an atmosphere of air for five hours at 500°C. The reduction velocities were measured in an all-glass, closed system of a Gulbransen-type microbalance[4] with a sensitivity of $7.21\times10^{-7}$ g./div. The reaction temperature was 190°C

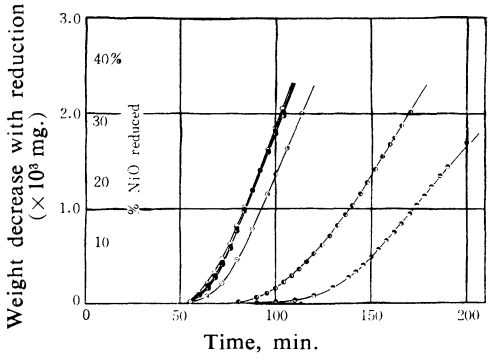



Fig. 1. The reduction curves of gamma-irradiated nickel oxide by hydrogen.

○ not irradiated ● $2.93\times10^5$ r.
◑ $1.0\times10^7$ r. ◉ $5.85\times10^7$ r.
◐ $8.5\times10^7$ r. ◓ $1.07\times10^8$ r.

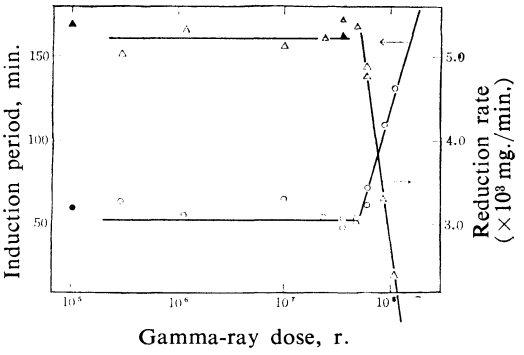



Fig. 2. Induction period and reduction rate as a function of irradiation dose.

▲, ● not irradiated

and the hydrogen pressure, 60 mmHg. The hydrogen used in these experiments was prepared by diffusing it through a palladium film. The irradiation was carried out with Co-60 gamma-rays, the intensity of which was $5.85\times10^5$ r./hr.; the total dose reached about $2\times10^8$ r.

The reduction curves of the irradiated nickel oxide are presented in Fig. 1. The reduction velocities were found to decrease with the radiation dose, being remarkable over a total dose of $5.8\times10^7$ r. The induction periods and the reduction rates are plotted as a function of the irradiation dose in Fig. 2, for which the induction periods were obtained by extraporating the curves in Fig. 1 to the time axis while the reduction rates were estimated from the slope of the linear part after the induction period. It is to be noted that both values changed abruptly at irradiation doses above $5\times10^7$ r. In order to explain the above phenomena, other measurements with a change of irradiation dose were made. The measurement of chemisorbed oxygen by means of iodometry[5,6] showed the same tendency as that in the induction periods and the reduction rates with irradiation; in other words, no change in the excess oxygen in nickel oxide was revealed up to irradiation dose of $5\times10^7$ r., while an abrupt increase of excess oxygen was

1) K. Hauffe and A. Rahmel, *Z. physik. Chem. N. F.*, 1, 104 (1954).
2) G. Parravano, *J. Am. Chem. Soc.*, 74, 1194 (1952).
3) Y. Iida and K. Shimada, This Bulletin, 33, 8 (1960).
4) T. Shibata and G. Okamoto, *Denki Kagaku*, 32, 293 (1964).
5) S. W. Weller and S. E. Volts, *J. Am. Chem. Soc.*, 76, 4695 (1954).
6) M. Nachman, I. Maxim and T. Braun, *J. Phys. Chem. Solids*, 20, 307 (1961).

observed above $1\times10^8$ r. The excess oxygen in nickel oxide was found to be 0.04—0.05 atm. % in the case of both unirradiated and irradiated less than $5\times10^7$ r., while 0.12 atm. % in that of $2\times10^8$ r. irradiated. No differences in BET surface area were observed in any case.

On the basis of results presented above, it may be concluded that the reduction of nickel oxide by hydrogen is greatly influenced by non-stoichiometry with gamma-irradiation. Detailed observations, such as hydrogen adsorption and catalysis by the gamma-irradiated nickel oxide, are now being made.

*Faculty of Engineering*
*Hokkaido University*
*Sapporo*

# Proton Magnetic Resonance of Thianaphthenes. II.* The Long-range Coupling between 2- and 6-Hydrogens

By Kensuke TAKAHASHI, Tatsuo KANDA, Fusaji SHOJI and Yasuo MATSUKI

(Received December 24, 1964)

In a previous communication, we have shown the long-range coupling between 3- and 7-hydrogens in some thianaphthenes and have also suggested, from the observation of the line width, the presence of another long-range coupling connected with 2-hydrogen.[1] In this report we will clear up this point. In the spectrum of 5-bromothianaphthene in a 5 mol. % solution in acetone, the signal of the 6-hydrogen consists of eight lines, as is shown in Fig. 1a; therefore, we must consider the coupling between 6-hydrogen and one of the hydrogens in the five-membered ring. The signals of 2- and 3-hydrogens also show second-order splittings by about 0.5 and 0.75 c. p. s. respectively. We have also examined the spectrum of 3,5-dibromothianaphthene in a 1.5 mol. % solution in cyclohexane. In this spectrum, the signal of the 6-hydrogen in question is overlapped with the signal of 2-hydrogen by nearly half, but the other half of it clearly consists of four lines, as was observed in the former compound. On the other hand, the signal of 2-hydrogen is unresolved and broad. Therefore, we can conclude that the 2-hydrogen is coupled to the 6-hydrogen in thianaphthenes. Recently, Black et al. have also suggested the presence of a similar 2,6-coupling in indolizine.[2]

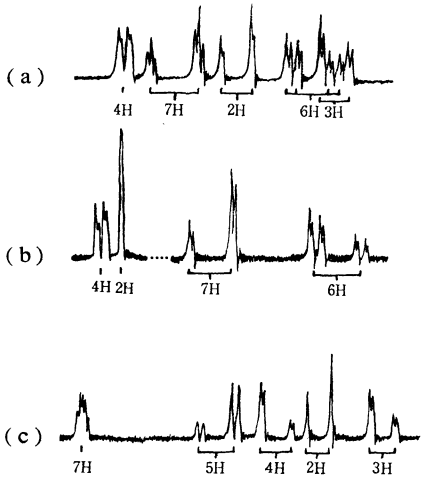



Fig. 1. The ring proton spectra of (a) 5-bromothianaphthene in a 5 mol.% solution in acetone, (b) 3-acetyl-5-bromothianaphthene in a 5 mol.% solution in acetone and (c) 6-carbomethoxythianaphthene in a 3 mol.% solution in carbon tetrachloride. Applied magnetic field increases from left to right in all figures.

It is said that there is a straight zig-zag path or some stereospecificity that gives facilities for coupling to hydrogens.[3] This 2,6- or 3,7-coupling in thianaphthenes is also a typical example in which the interacting hydrogens are located in such a straight zig-zag path as is shown in the following figure by the bold line. Although this kind of zig-zag path is found in some other aromatic compounds,

* Part II in this series (see Ref. 1 for Part I).

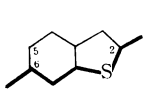
1) K. Takahashi, T. Kanda and Y. Matsuki, This Bulletin, 37, 768 (1964).

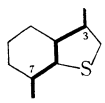
2) P. J. Black, M. L. Heffernan, L. M. Jackman, Q. N. Porter and G. R. Underwood, *Austr. J. Chem.*, 17, 1128 (1964).

3) C. N. Banwell and N. Sheppard, *Discussions Faraday Soc.*, 34, 115 (1963); G. Karabatsos and F. M. Vane, *J. Am. Chem. Soc.*, 85, 3886 (1963).

TABLE I. PMR DATA OF SOME THIANAPHTHENE DERIVATIVES, REFERRED TO CYCLOHEXANE AT 60 Mc./sec.

| Substituent | Chemical shift, p. p. m. | | | | | | | Coupling, c. p. s. | |
|---|---|---|---|---|---|---|---|---|---|
| | $CH_3$ | 2-H | 3-H | 4-H | 5-H | 6-H | 7-H | $J_{37}$ | $J_{26}$ |
| 5-Br | — | 5.93 | 5.74 | 6.45 | — | 5.94 | 6.21 | $0.7_5$ | 0.5 |
| 3,5-$Br_2$ | — | 5.97 | — | 6.50 | — | 6.03 | 6.22 | — | 0.6 |
| 3-$CH_3CO$, 5-Br | 1.10 | 6.71 | — | 7.37 | — | 5.97 | 6.15 | — | 0.6 |
| 2-$CH_3CO$, 5-Br | 1.15 | — | 6.30 | 6.52 | — | 6.07 | 6.26 | 0.7 | — |
| 6-$COOCH_3$ | 2.47 | 6.13 | 5.88 | 6.35 | 6.54 | — | 7.13 | $0.7_5$ | — |
| 3-Br, 6-$COOCH_3$ | 2.49 | 6.12 | — | 6.36 | 6.59 | — | 7.07 | — | — |
| 3-Br, 6-$COCH_3$ | 1.17 | 6.13 | — | 6.35 | 6.50 | — | 6.94 | — | — |




such as naphthalene, quinoline, benzofuran, etc., the coupling across the six bonds found here has not yet been reported in these compounds except in *N*-benzylthieno[3,2-b]-pyrrole.[4] The 2,5-hydrogens in thianaphthenes are also located in such a position, but no 2,5-coupling has yet been resolved, so any such coupling may be assumed to be smaller than 0.5 c. p. s. if one exists at all. The difference in condition between 2,5- and 2,6-couplings in thianaphthene is mainly due to the presence or absence of the intervening sulfur atom. The sulfur atom seems to play an important role in the transmission of this long-range coupling.

For the verification of our new finding in thianaphthenes, we have also examined some other compounds. The expected 2,6-coupling is also observed in the spectrum of 3-acetyl-5-bromothianaphthene, as Fig. 1b shows. On the other hand, the signal of 6-hydrogen in 2-acetyl-5-bromothianaphthene consists of four lines, as usual. In the spectra of 6-carbomethoxy-, 3-bromo-6-carbomethoxy- and 3-bromo-6-acetylthianaphthenes, no resolved structures were observed in the signals of 2-hydrogens. Table I lists the observed PMR data of our first-order analyses; the observed second-order splitting gives $J_{26}$ ~0.5 c. p. s. Figure 1 shows some typical spectra of these compounds. The chemical shifts were measured in solutions concentrated 0.1 g./cc. or less in carbon tetrachloride containing 0.5 wt. % cyclohexane as an internal reference.

*The Chemical Research Institute of Non-Aqueous Solutions*
*Tohoku University*
*Katahira-cho, Sendai*

4) H. S. Gutowsky and A. L. Porte, *J. Chem. Phys.*, 35, 839 (1961).

# Temperature Dependency of the ESR Absorption of the Diphenylamine Polymer with Reference to Its Electric Conductivity*

By Keiji KUWATA, Yoichi KAGEYAMA and Kozo HIROTA

(Received January 5, 1965)

As has been reported, a deep-brownish polymeric product can be obtained by oxidizing diphenylamine with vanadium pentoxide. This polymer is semiconductive and shows a sharp ESR absorption line.[1] Its specific conductivity, $\lambda$, and the number of unpaired electrons increases by several orders of magnitude if its complexes are formed with several electron acceptors.[2] In the present note, the temperature dependence of the number of unpaired electrons in the polymer will be reported on, as well as that of its conductivity.

Since the polymer is powdery, samples for conductivity measurement were pressed at more than 80 kg./cm$^2$. The apparatus used in the measurement was kindly provided by Dr. Seiichi Kanda of our University. The molecular weight of sample A (softening pt.=ca. 150°C) was ca. 3000, while that of sample B (softening pt.=ca. 200°C) was estimated to be higher than 3000 on the basis of its low solubility in ordinary solvents. The data obtained were very reproducible, irrespective of the order of measurement. In Fig. 1, the $\log \lambda$ of both samples is plotted against the reciprocal of the measuring temperature, $T$. Since a linear relation is given over the range between 32—120°C, we can determine the constants $\lambda_0$ and $\varepsilon_0$ in Eq. 1, where $k$ is the Boltzmann constant:

$$\lambda = \lambda_0 \exp(-\varepsilon_0/2kt) \qquad (1)$$

For samples A and B, $\varepsilon_0$ is given as 1.1 and 0.7$_9$ eV. respectively. These numerals show the magnitude of $\lambda$, which corresponds to the semiconductive nature of the samples.

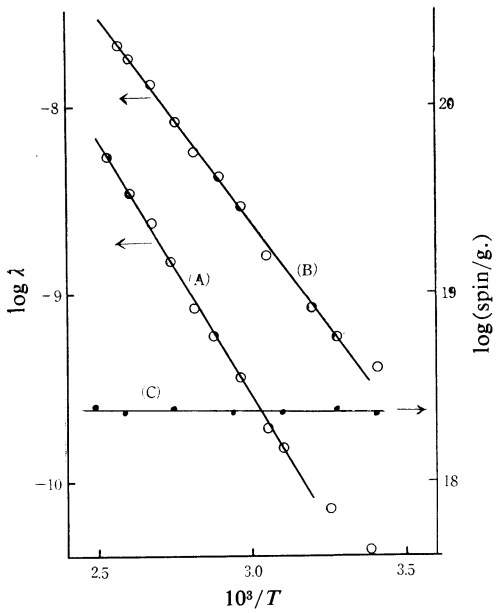



Fig. 1. Temperature variation of specific conductivity and spin concentration.
Softening pt.
(A) 150°C
(B) 200°C
(C) 220°C

The ESR measurement was the same as was hitherto adopted,[1,2] except that the rectangular cavity of the multiple mode, $H_{014}$, was used so as to determine the spin concentration with a greater reliability. The standard substance containing the free-radical, DPPH, was always inserted in the part of the cavity kept at room temperature, while the sample was placed in the part where the temperature could be varied independently of the standard. By the repeated determination of the spin concentration on sample C (sintering temp. 220°C and $\lambda = 1.83 \times 10^{-10}$ ohm$^{-1}$·cm$^{-1}$ at 24°C; $\varepsilon_0 = 1.07_6$ (24—80°C)), it was found to be constant, $2.4 \times 10^{18}$ spin/g., over the temperature range investigated (20—130°C), as Fig. 1 shows.

The results obtained above may be important, because they give us information which clarifies the conduction mechanism of organic semiconductors.

*Department of Chemistry*
*Faculty of Science*
*Osaka University*
*Nakanoshima, Osaka*

* This investigation was mostly done before Ref. 2 was published.

1) K. Hirota and Y. Kageyama, This Bulletin, 37, 793 (1964).
2) K. Kuwata, Y. Sato and K. Hirota, ibid., 37, 1391 (1964).

# Change in the Structure of Evaporated Aluminum Chloride by Adsorbing Several Substances

By Toshinobu IMANAKA and Kozo HIROTA

(Received January 5, 1965)

The catalytic polymerization of propylene on evaporated aluminum chloride has been studied in the absence of a solvent by spectroscopic methods and a kinetic method[1-4] in order to make clear the reaction mechanism.

During the course of these studies, it was found that the infrared spectrum of evaporated aluminum chloride is changed slowly by the adsorption of benzene derivatives, cyclohexene, and nitromethane. Therefore, infrared spectrum of crystallized aluminum chloride was measured for the sake of comparison and in order to make clear this phenomenon.

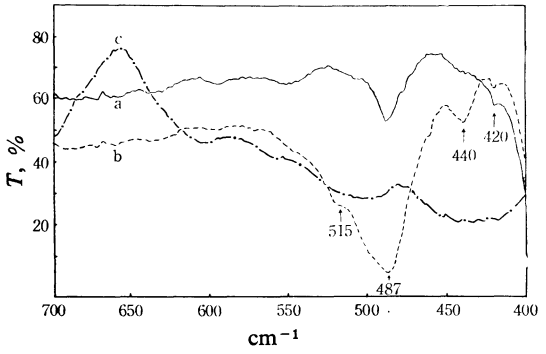



Fig. 1. Infrared absorption spectrum of evaporated aluminum chloride absorbing *p*-xylene.

a ——— Evaporated aluminum chloride alone
b ------ Evaporated aluminum chloride adsorbing *p*-xylene
c —·—· Crystallized aluminum chloride

In Fig. 1, curves a and b show a change in the infrared spectrum of evaporated aluminum chloride by adsorbing *p*-xylene. The band near 487 $cm^{-1}$ increased remarkably in intensity and in width with the lapse of time. Furthermore, new bands were observed near 520—500, 440 and 420 $cm^{-1}$. Even if this system was evacuated until the infrared bands due to *p*-xylene vanished, these bands did not change. However, these bands did disappear upon the addition of water. The same phenomenon was also observed with the adsorption of benzene, toluene, mesitylene, cyclohexene, and nitromethane. On the other hand, the phenomenon was not observed in the case of the adsorption of nitrogen or cyclohexane.

Curve c shows the infrared spectrum of crystallized aluminum chloride, which can be observed by mixing aluminum chloride with Nujol, putting the mixture between two potassium bromide plates, and painting vacuum grease around the potassium bromide plates. This spectrum shows that very broad absorption bands exist near 600, 500 and 450—420 $cm^{-1}$. Aluminum chloride was recently evaporated onto a platinum plate at −195°C by Perkampus and Baumgarten,[5] who observed its reflective absorption spectrum. By annealing the evaporated aluminum chloride, they found that the bands near 606 (very strong) and 467 $cm^{-1}$ (strong) shifted to a lower wavelength, i. e., 599 (very strong) and 440 $cm^{-1}$ (very strong), while the 508 $cm^{-1}$ band increased in intensity.

In view of this fact, the appearance of the infrared bands near 520—500 and 440 $cm^{-1}$ may be due to the crystallization of the evaporated aluminum chloride. When aluminum chloride is evaporated onto a potassium bromide plate at room temperature, the band near 487 $cm^{-1}$ increases remarkably in intensity. On the other hand, when aluminum chloride is evaporated onto the platinum plate at −196°C, the band does not even seem to exist, judging from the above data. This band was assigned by Klempeler to the dimer structure of gaseous aluminum chloride. This finding may suggest that the increase in the band near 487 $cm^{-1}$ is due to the dispersed state of the evaporated aluminum chloride.

On the basis of these data, it seems reasonable to assume that the absorbates which have such an action exist as compounds of the

1) T. Imanaka and K. Hirota, *J. Chem. Soc. Japan, Pure Chem. Sec. (Nippon Kagaku Zasshi)*, **84**, 193 (1963).
2) K. Hirota and T. Imanaka, ibid., **84**, 960 (1963).
3) T. Imanaka and K. Hirota, ibib., **85**, 359 (1964).
4) T. Imanaka and K. Kishimoto, ibid., **85**, 819 (1964).
5) H. H. Perkampus and E. Baumgarten, *Ber. der Bunsenges.*, **67**, 576 (1963).

$\pi$-electron system, and that the interaction between aluminum chloride and $\pi$-electrons promotes the crystallization and the dispersion of evaporated aluminum chloride.

*Department of Chemistry*
*Faculty of Science*
*Osaka University*
*Nakanoshima, Osaka*

# The Catechol Group in Lignosulfonate

By Akira HAYASHI and Yoshifumi NAMURA

(Received January 5, 1965)

The catechol group was proposed by Hayashi[1] as a functional group in lignosulfonate for the gelling reaction with dichromate. This assignment was also supported by a similarity in the reactivity of lignosulfonate with catechol.[2] Recently, several authors have also suggested the catechol group in lignosulfonate or in other lignin preparation.[3] These works, however, have dealt with the catechol group only by means of indirect methods, and this group did not yet have general support.

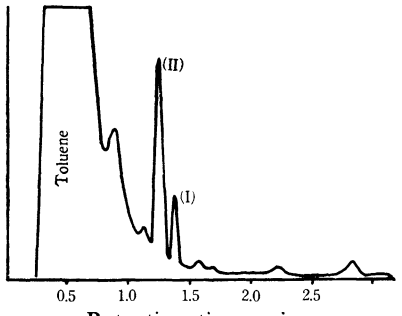
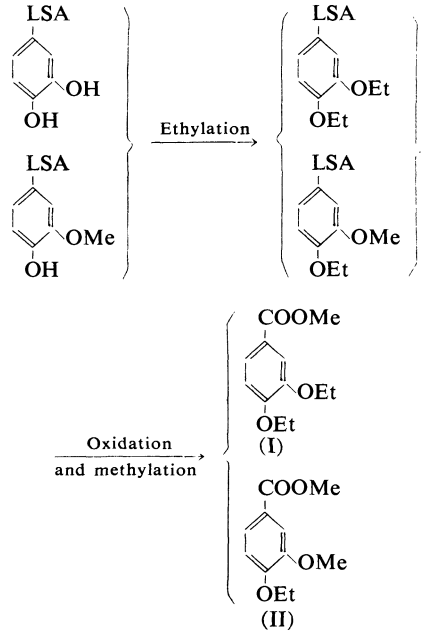



Fig. 1. Gas chromatogram of oxidation product of lignosulfonate.
Column: Apiezon Grease L 2.0 m.
Column temp.: 250°C
Carrier gas: $H_2$, 50 cc./min.

In order to establish the catechol group directly, softwood lignosulfonate was ethylated with diethyl sulfate, oxidized with potassium permanganate,[4] and methylated with methanol; then the resultant products were examined by means of gas chromatography. An Apiezon Grease L column was used at 250°C. The chromatogram obtained is given in Fig. 1.

Sufficient methyl 3,4-diethoxy-benzoate (I) was detected, along with methyl 3-methoxy-4-ethoxy-benzoate (II). Compounds I and II were derived from the pendant catechol group and the guaiacyl group in lignosulfonate respectively according to the following reaction scheme:




Thus the catechol group was directly confirmed in the lignosulfonate molecule by the formation of compound I.

Vanillyl alcohol was cooked in sulfite cooking liquor in order to ascertain the mechanism of catechol group formation. Methanol was obtained from the cooked liquor by gas chromatography, which corresponded to the 4% demethylation of the methoxyl group in vanillyl alcohol. I was also obtained from the

1) A. Hayashi, *J. Japan Wood Research Soc.*, in contribution (Studies on Lignosulfonate XX).
2) A. Hayashi, ibid., in contribution (Studies on Lignosulfonate XXI and XXII).
3) I. Croon and B. Swan, *Svensk Papperstidn.*, **66**, 812 (1963); C. Steelink, T. Reid and C. Tollin, *J. Am. Chem. Soc.*, **85**, 4048 (1963); J. Marton, *Tappi*, **47**, 713 (1964).
4) K. Freudenberg, *Chem. Ber.*, **86**, 155 (1953).

cooked liquor treated in a method similar to that used for lignosulfonate. These results indicate that the catechol group results from the demethylation of the free guaiacyl group in lignin during the sulfite cooking process.

A detailed and quantitative investigation will be reported soon.

*Department of Chemistry*
*Ritsumeikan University*
*Kita-ku, Kyoto*

# Polymerizations by 1, 3-Dipolar Cycloaddition Reactions. II. $\alpha, \alpha'$-(*p*-Phenylene)bis(*N*-phenylnitrone)

By Yoshio IWAKURA, Masayasu AKIYAMA and Shinsaku SHIRAISHI

(Received January 12, 1965)

In a previous communication,[1] a 1, 3-dipolar cycloaddition polymerization of isophthalonitrile di-*N*-oxide with diolefins was reported. Hitherto extensive studies have been made on the chemistry of nitrones,[2-4] and some bisnitrones have been prepared for dialdehyde syntheses.[3,5] This communication will describe a new polymerization of $\alpha, \alpha'$-(*p*-phenylene)-bis(*N*-phenylnitrone) (I) with diolefins, *m*-phenylenebismaleimide and ethylene dimethacrylate, by the 1,3-dipolar cycloaddition reaction.

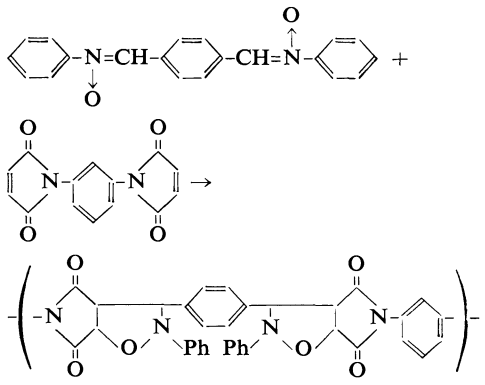
A new bisnitrone, I, was obtained by the reaction of terephthalaldehyde with phenylhydroxylamine[6] (yield, 66%), and recrystallized from dimethylformamide; m. p. 227—228°C (decomp.). Found: C, 75.71; H, 4.97; N, 9.11. Calcd. for $C_{20}H_{16}O_2N_2$: C, 75.93; H, 5.10; N, 8.86%.

I gave an infrared spectrum similar to that of $\alpha$, *N*-diphenylnitrone.

Two bisadducts of I were prepared as model compounds. I (0.414 g.) was refluxed in methyl methacrylate to yield 1, 4-bis(2'-phenyl-5'-methyl-5'-methoxycarbonyl-3'-isoxazolidinyl)-benzene (II) as colorless needles (0.186 g.); m. p. 188—190°C (from ethylacetate). Found: C, 69.67; H, 6.26; N, 5.38. Calcd. for $C_{30}H_{32}O_6N_2$: C, 69.75: H, 6.24; N, 5.42%.

By the addition reaction of I (0.316 g.) with *N*-phenylmaleimide (0.346 g.) in dimethylformamide at 120°C for 3 hr., 3, 3'-(*p*-phenylene)-bis(2-phenylisoxazolidine-4, 5-dicarboxyphenylimide) (III) was obtained (0.620 g.); m. p. 228—229°C (from benzene), (Found: C, 72.35; H, 4.69; N, 8.25. Calcd. for $C_{40}H_{30}O_6N_4$: C, 72.49; H, 4.56; N, 8.46%).

A typical polymerization of I with *m*-phenylenebismaleimide is as follows. 0.473 g. (0.0015 mol.) of I, 0.402 g. (0.0015 mol.) of *m*-phenylenebismaleimide, 0.005 g. of phenyl-$\beta$-naphthylamine and 8.0 ml. of dimethylformamide were placed in a glass ampule; the mixture was then sealed under an atmosphere of nitrogen, heated for 30 hr. at 95°C, and poured into diethyl ether. The polymer (IV) which separated was washed with ether, dried under vacuum (yield, 90%), and reprecipitated from dimethylformamide with ether. The inherent viscosity was 0.19 (0.5 g./100 ml. of dimethylformamide at 30°C). IV did not melt up to 300°C. Found: C, 69.88; H, 4.37; N, 9.32. Calcd. for $C_{34}H_{24}O_6N_4$: C, 69.85; H, 4.14; N, 9.59%. The infrared spectrum of IV exhibited the following absorption bands: 1790(w), 1720(s), 1600, 1490, 1450, 1365(broad), 1180-(broad), 1020(w), 755 and 688 $cm^{-1}$ (KBr disk), and showed good agreement with that of III. These data strongly suggest that the polymerization proceeds by a repetition of the 1, 3-dipolar cycloaddition reaction, as in the equation below:



1) Y. Iwakura, M. Akiyama and S. Shiraishi, This Bulletin, **38**, 335 (1965).
2) L. I. Smith, *Chem. Revs.*, **23**, 193 (1938).
3) J. Hamer and A. Macaluso, ibid., **64**, 473 (1964).
4) R. Huisgen, *Angew. Chem.*, **75**, 604 (1963).
5) T. Sone, This Bulletin, **37**, 1197 (1964).
6) O. H. Wheeler and P. H. Gore, *J. Am. Chem. Soc.*, **78**, 3363 (1956).

A similar polymerization of I with ethylene dimethacrylate was carried out in hexamethylphosphoramide at 140°C for 4 hr. The yield of the polymer (V), obtained as an ether-insoluble fraction, was 11%; m. p. 100—107°C, and the inherent viscosity, 0.09. Found: C, 69.89; H, 5.76; N, 5.43. Calcd. for $C_{30}H_{30}O_6N_2$: C, 70.02; H, 5.88; N, 5.44%. The infrared spectrum of V displayed the following maxima: 2940, 2850(w), 1735(s), 1600, 1490, 1453, 1375 (w), 1280(broad), 1175(s), 1125—1095, 1030(w), 753 and 690 $cm^{-1}$ (KBr disk), and was essentially identical with that of II.

Further investigations are now in progress.

*Department of Synthetic Chemistry*
*Faculty of Engineering*
*The University of Tokyo*
*Hongo, Tokyo (Y. I. & S. S.)*

*Tokyo Institute of Technology*
*Meguro-ku, Tokyo (M. A.)*

# On Glumamycin, a New Antibiotic. V.* The Steric Configuration of α, β-Diaminobutyric Acid

By Masahiko FUJINO, Michitaka INOUE, Jisaburo UEYANAGI and Akira MIYAKE

(Received October 7, 1963)

The authors[1] previously isolated α, β-diaminobutyric acid (α, β-Dab) from the acid hydrolysate of glumamycin, an acidic peptide-type antibiotic. About the same time, Martin et al.[2] reported the separation of α, β-Dab from Aspartocin, an antibiotic resembling glumamycin. Although the two products seem to have the same configuration, judging from their optical rotation, this question has so far not been studied.

In a previous paper of this series[3] it was shown that glumamycin contains two moles of α, β-Dab and that only one β-amino group of the α, β-Dab is free. These facts were then utilized to determine the steric configuration of α, β-Dab.

The configuration of the α-carbon of α, β-Dab has been studied by the conversion of the free β-amino group of glumamycin into a hydroxyl group and by subsequent hydrolysis to α-amino-β-hydroxybutyric acid, and that of the β-carbon of α, β-Dab, by the oxidation of α, β-Dab to alanine.

That is, glumamycin was treated with sodium nitrite in 80% acetic acid to convert the free amino group into hydroxyl, and then the resulting deamino-glumamycin was hydrolyzed with hydrochloric acid. The reaction mixture was developed on a column of Dowex 50 with an ammonium formate buffer (pH 3.4),[4] after which a crystalline substance was obtained from the threonine fraction. The product was found to be a mixture of threonine and allothreonine by paper chromatography with *n*-butanol - acetone - ammonia - water (50 : 6.25 : 6.25 : 37.5)[5] and by a study of its infrared spectrum (Fig. 1).

Fortunately, it is known that DNP-L-threonine and DNP-L-allothreonine exhibit the same optical rotation, $[M]_D^{25} = +305°$ (4% sodium bicarbonate).[6] The above product was converted into its DNP derivative by the method of Levy[7] and then submitted to column chromatography on Amberlite IRC-50, according to the method of Seki,[8] in order to remove the DNP-OH which was formed as a by-product. The DNP derivative showed an optical rotation of $[M]_D^{24} = -294° \pm 14$ (*c* 0.48, 4% sodium bicarbonate), and its yield was 92%. The results mentioned above show that the threonine and allothreonine obtained in the present work take the D-configuration; consequently, the α-carbon of α, β-Dab with the free β-amino group belongs to the D series. Further, as the α, β-Dab obtained from the hydrolysate of deamino-glumamycin and that obtained from the hydrolysate of glumamycin have the same optical rotation and physical properties, the two moles of α, β-Dab in glumamycin evidently have the same steric configuration.

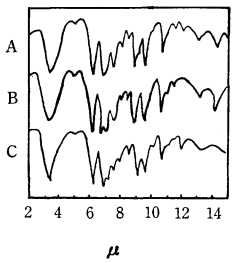



Fig. 1. Infrared-Spectra of α-amino-β-hydroxybutyric acid.
A: α-Amino-β-hydroxybutyric acid from deamino-glumamycin
B: L-Threonine
C: L-Allothreonine

Next, in order to establish the configuration at the β-carbon of α, β-Dab, it was oxidized with hydrogen peroxide according to the method of Dakin.[9] That is, the compound was allowed to react with 2 mol. of 3% hydrogen peroxide at 50°C for one hour in the presence of a small amount of ferrous sulfate. The reaction mixture was then passed

* Part XXXIV of a series entitled "Studies on Antibiotics," Ed. by Sueo Tatsuoka.

1) M. Inoue, H. Hitomi, K. Mizuno, M. Fujino, A. Miyake, K. Nakazawa, M. Shibata and T. Kanzaki, This Bulletin, **33**, 1014 (1960).
2) J. H. Martin and W. K. Hausmann, *J. Am. Chem. Soc.*, **82**, 2079 (1960).
3) M. Inoue, This Bulletin, **35**, 1557 (1962).
4) C. H. W. Hirs, S. Moore and W. H. Stein, *J. Biol. Chem.*, **159**, 669 (1952).
5) K. N. F. Shaw and S. W. Fox, *J. Am. Chem. Soc.*, **75**, 3421 (1953).
6) K. R. Rao and H. A. Sober, ibid., **76**, 1328 (1954).
7) A. L. Levy, *Nature*, **174**, 126 (1954).
8) T. Seki, *Chemistry of Proteins (Tokyo)*, **4**, 209 (1956).
9) H. D. Dakin, *J. Biol. Chem.*, **1**, 171 (1905); **4**, 63 (1908).

through a column of Amberlite IR-120 ($H^+$), and the adsorbed substance was eluted with N ammonia, the effluent giving D-alanine. Thus, it was found that the configuration at the $\beta$-carbon of $\alpha,\beta$-Dab belongs to the D series and that, consequently, $\alpha,\beta$-Dab takes the D-erythro-configuration.

## Experimental

**Deamino-glumamycin.**—Into a solution of 10 g. (ca. 7.7 mmol., mol. wt. taken as 1300*) of glumamycin in 100 ml. of 80% acetic acid, 1.06 g. (ca. 15.4 mmol.) of sodium nitrite and 11.6 ml. of N hydrochloric acid were stirred alternately over a period of 5 hr. at 0°C; the mixture was then left standing at room temperature for 12 hr.

The reaction mixture was concentrated to 20 ml. under reduced pressure, and water was added to separate the deamino-glumamycin. The precipitate was washed three times with water to remove the unchanged glumamycin, which is soluble in water; it was dissolved in acetone and reprecipitated by the addition of water. The product was washed twice with water and dried, giving 8 g. of deamino-glumamycin**.

**The Hydrolysis of Deamino-glumamycin with Hydrochloric Acid.** — Two grams of deamino-glumamycin was hydrolyzed by heating it with 40 ml. of 6 N hydrochloric acid at 110°C for 20 hr. in an oil bath. The hydrolysate was concentrated in vacuo, water was added to the residue, and the mixture was evaporated to dryness under reduced pressure.

**The Isolation of the Threonine Faction.**—The above residue was dissolved in 100 ml. of water, the solution was passed through a column (3×10 cm.) of Amberlite IR-4B (OH form) to remove acidic substances, and the effluent was evaporated to dryness in vacuo.

The residue was dissolved in 10 ml. of an ammonium acetate buffer (pH 5.0), and the solution was passed through a column (7×20 cm.) of Dowex-50×8 (200—400 mesh) treated beforehand with the same buffer.

The effluent was collected in 50-ml. fractions and examined by paper chromatography. All the neutral amino acids constituting deamino-glumamycin were then eluted out in 100—300 ml. of the effluent.

This portion of the effluent was evaporated to dryness under reduced pressure. The residue was dissolved in 10 ml. of an ammonium formate buffer (pH 3.4), and the solution was again passed through a column (6×60 cm.) of Dowex-50×4 (200—400 mesh) bufferized at pH 3.4. The fraction of the effluent showing the same $R_f$-value as threonine by paper chromatography with *n*-butanol - acetic acid - water (120 : 30 : 50) was collected and poured on a column of Amberlite IR-120 (H form). The adsorbed portion was eluted with N ammonia. The eluate was concentrated to give crude crystals, which were purified by recrystallization from aqueous ethanol, yielding 104 mg. of a mixture of threonine and allothreonine.

Found: C, 40.06; H, 7.81; N, 11.70. Calcd. for $C_4H_9O_3N$: C, 40.33; H, 7.62; N, 11.76%.

**The Isolation of $\alpha,\beta$-Dab.**—When the above column of Dowex-50×8 (pH 5.0) was further eluted with 0.25 N aqueous ammonia, it was found by paper chromatography that 230—300 ml. of the effluent contained $\alpha,\beta$-Dab. This fraction was evaporated under reduced pressure. The residue was dissolved in a small amount of hydrochloric acid, and the ethanol was added to the solution, giving colorless needles which were purified by recrystallization from aqueous ethanol (yield, 130 mg.).

Found: C, 31.24; H, 6.88; N, 17.96; Cl, 22.41. Calcd. for $C_4H_{10}O_2N_2 \cdot HCl$: C, 31.06; H, 6.48; N, 18.11; Cl, 22.95%. $[\alpha]_D^{23} = +20$ ($c$ 1, 6 N HCl).

The isolation of $\alpha,\beta$-Dab from the hydrolysate of glumamycin was previously reported.[3]

**The Dinitrophenylation and Optical Rotation of the DNP Derivative.** — According to Levy's method, 10.42 mg. of the mixture of threonine and allothreonine obtained above was dissolved in 5 ml. of water; 200 mg. of sodium carbonate and 0.2 ml. of 2,4-dinitrofluorobenzene were added to the solution, and the mixture was kept at 40°C for 20 min. while being vigorously stirred. The reaction mixture was diluted with 10 ml. of water, shaken three times with each half volume of ether to remove the excess 2,4-dinitrofluorobenzene, and, after being made acidic, again shaken with ether to extract DNP-threonine and DNP-allothreonine. The extract was evaporated to dryness and developed on a column (4×30 cm.) of Amberlite CG-50 (type II) with 1% hydrochloric acid-ethyl methyl ketone (75 : 25). In this case, the simultaneously-produced DNP-OH was developed half as slow as DNP-threonine and DNP-allothreonine, so the former was completely separated from the latter. The fraction containing DNP-threonine and DNP-allothreonine was evaporated under reduced pressure, and the residue (yield, 92%*) was dissolved in 2 ml. of a 4% sodium bicarbonate solution. The optical rotation of the solution is $[\alpha]_D^{24} = -102° \pm 5$, and from this the molecular rotation is calculated to be $[M]_D^{24} = -294° \pm 14$.

**Oxidation with Hydrogen Peroxide.**—To a solution of 1 g. of $\alpha,\beta$-Dab·HCl in 14.5 ml. of 3% hydrogen peroxide, about 5 mg. of ferrous sulfate was added; the mixture was then kept at 50°C for one hour with stirring. The reaction mixture was diluted with 2 vol. of water and passed through a column of Amberlite IR-120 ($H^+$ form). The column was eluted with N ammonia, the eluate was evaporated to dryness, and the residue was recrystallized from aqueous ethanol to give 120 mg. of D-alanine, $[\alpha]_D^{20} = -16°$ ($c$ 1, 6N HCl).

Found: C, 40.51; H, 7.88; N, 15.44. Calcd. for $C_3H_7O_2N$: C, 40.44; H, 7.92; N, 15.72%.

* The mol. wt. of the glumamycin determined by the method of the Vapor Pressure Osmometer is 1285 (sample, 13.400 mg.; solvent, 1 ml. of water; mole concentration, 0.01043), which is in good agreement with the min. mol. wt. (1, 300) obtained by means of amino acid analysis.[3]

** The DNP derivative was not obtained by Sanger's method.

* This yield was calculated from the ultraviolet-absorption at 360 m$\mu$.

## Summary

Glumamycin has been treated with nitrous acid to convert the free amino group into hydroxyl, and the resulting deamino-glumamycin has been hydrolyzed with hydrochloric acid. A mixture of threonine and allothreonine has then been isolated from this hydrolysate. The DNP derivative of the product shows an optical rotation $[M]_D^{24} = -294° \pm 14$ (*c* 0.48, 4% sodium bicarbonate). This fact shows that the above product is a mixture of D-threonine and D-allothreonine.

Further, as the $\alpha, \beta$-diaminobutyric acid obtained from the hydrolysate of deamino-glumamycin and that obtained from the hydrolysate of glumamycin have the same optical rotation, it may be concluded that the two moles of $\alpha, \beta$-diaminobutyric acid in glumamycin have the same steric configuration.

On the other hand, the product obtained by the oxidation of $\alpha, \beta$-diaminobutyric acid with hydrogen peroxide is in agreement with D-alanine. Thus, it has been found that the $\alpha$- and $\beta$-carbons of $\alpha, \beta$-diaminobutyric acid belong to the D series and that, consequently, $\alpha, \beta$-diaminobutyric acid takes the D-erythro-configuration.


The authors are grateful to Dr. Sueo Tatsuoka, the Director of Research Laboratories, and Drs. Satoru Kuwada, Kikichi Sato and Kuniyoshi Tanaka for their guidance and encouragement, and to Drs. Koichi Nakazawa and Motoo Shibata for their kind advice.

*Research Laboratories*
*Takeda Chemical Industries, Ltd.*
*Higashiyodogawa-ku, Osaka*

# On Glumamycin, a New Antibiotic. VI.*1 An Approach to the Amino Acid Sequence

By Masahiko FUJINO

(Received October 21, 1963)

In previous papers,[1-3] it was reported that glumamycin ($C_{59}H_{91}O_{20}N_{13}$, M. W. 1300[4]) was an acidic peptide consisting of 3-ITA[2] (1 mol.), L-Asp (3 mol.), L-MeAsp (1 mol.), Gly (2 mol.), L-Pro (1 mol.), L-Val (1 mol.), D-Pip (1 mol.) and $\alpha,\beta$-Dab (2 mol.), and that, of the 2 mol. of $\alpha,\beta$-Dab contained in glumamycin, the $\alpha$- and $\beta$-amino groups of one molecule take part in the peptide combination, while the $\beta$-amino group of the other is free.

As the glumamycin was resistant to such enzymes as pepsin, trypsin, chymotrypsin and pronase, the antibiotic was subjected to partial hydrolysis with hydrochloric acid. The present paper deals with experiments designed to determine the amino acid sequence of glumamycin.

*1 Part XL of a series entitled "Studies on Antibiotics," Ed. by Sueo Tatsuoka.

*2 The abbreviations used are: 3-ITA, 3-isotridecenoic acid; MeAsp, $\beta$-methylaspartic acid; Pip, pipecolic acid; $\alpha,\beta$-Dab, $\alpha,\beta$-diaminobutyric acid; DNFB, 2,4-dinitrofluorobenzene; DNP, 2,4-dinitrophenyl.

1) M. Inoue, This Bulletin, 35, 1249 (1962).
2) M. Inoue, ibid., 35, 1255 (1962).
3) M. Inoue, ibid., 35, 1557 (1962).
4) M. Fujino, M. Inoue, J. Ueyanagi and A. Miyake, ibid., 38, (1965).

## Experimental

**The Partial Hydrolysis of Glumamycin with N Hydrochloric Acid.** — One gram of glumamycin purified by the method reported in a previous paper[5] was heated with 10 ml. of N hydrochloric acid in an oil bath at 100°C for 4 hr. The mixture became turbid in about 2 hr., and an oily substance separated in 4 hr. The reaction mixture was then diluted with 40 ml. of water and extracted with three 30 ml.-portions of ethyl acetate and a 30 ml.-portion and two 20 ml.-portions of *n*-butanol in order to remove the oily substance. The aqueous layer (W-fraction) was lyophilized, and 100 mg. of this substance was dissolved in 2 ml. of 0.5 N acetic acid and poured on a column (2×40 cm.) Dowex-1×4 (200—400 mesh). The column was washed with 0.5 N acetic acid, and the effluent was collected in 5 ml.-portions with a fraction collector (Fig. 1).

The ethyl acetate layer was extracted three times with 20 ml. of a 2% sodium hydrogen carbonate solution, and the aqueous layer, after being adjusted to pH 2 with 2 N hydrochloric acid, was extracted again with ethyl acetate. The ethyl acetate

5) M. Shibata, T. Kanzaki, K. Nakazawa, M. Inoue, H. Hitomi, K. Mizuno, M. Fujino and A. Miyake, *J. Antibiotics* (*A*), 15, 1 (1962).

extract was evaporated to dryness, and the residue was washed with petroleum ether to give the E substance. The *n*-butanol extract was treated in the same manner to give the B substance.

**The Partial Hydrolysis of Glumamycin with 6 N Hydrochloric Acid.**—Four hundred milligrams of glumamycin was heated with 8 ml. of 6 N hydrochloric acid in a sealed tube at 100°C for 80 min.; the contents became turbid in about 40 min., and an oily substance separated in 60 min. The reaction mixture was diluted with 5 vol. of water and extracted with ethyl acetate to remove the fatty acid; after it had been diluted further with two times its volume of water, it was passed through a column (2×25 cm.) of Amberlite IR-120 (H-form) in order to adsorp the amino acids and peptides. The colum was washed with water to remove the hydrochloric acid and then eluted with 0.5 N aqueous ammonia, and the eluate was evaporated to dryness under reduced pressure at 35°C to give a sample for investigation by paper ionophoresis.

**The Partial Hydrolysis of DNP-glumamycin.**—On hundred milligrams of DNP-glumamycin obtained by Sanger's method (described in Part IV[3]) was dissolved in 2 ml. of concentrated hydrochloric acid and they hydrolyzed by being heated in a seald tube at 80°C for 2 hr. The hydrolysate was diluted with 11 volumes of water, and an oily substance was removed by extraction with ethyl acetate. The aqueous layer was poured on a talc-celite (2 : 1) column (2×20 cm.),[6] whereby all the yellow substance were adsorbed. The column was washed with N hydrochloric acid, and the washings were concentrated to yield non-DNP-peptides. The yellow zone of the column was eluted with N hydrochloric acid-ethanol (1 : 4), and the eluate was evaporated to dryness to give DNP-peptides.

**The Separation of Peptide Fragments by Paper Chromatography and Ionophoresis.**—The mixture of peptide fragements (30—40 mg.) described above was applied, in the form of a narrow band, to Toyo Roshi No. 526 (10×40 cm.) and was submitted to ionophoresis in a pyridine-acetate buffer of pH 6.5[7] (300—400 V., 2—4.5 hr.). In this manner the various peptide fragments were separated and were located by dipping narrow guide strips cut from both long edges of the paper in a 0.25% ninhydrin solution in acetone. The bands were then eluted with 5% acetic acid (0.5 ml.), and the solutions were taken to dryness in vacuo over potassium hydroxide pellets and stored at 0°C. A portion of each peptide fraction was tested for homogeneity by paper chromatograph in *n*-butanol - acetic acid - water (12 : 3 : 5, solvent A) and *n*-butanol - acetic acid - pyridine - water (15 : 10 : 3 : 12, solvent B). If more than one component was revealed in a peptide fraction by either of these solvents, it was refractionated and the additional peptide components were isolated as has been described above.

**The Characterization of Purified Peptides; Amino Acid Composition.** — The amino acid components of each peptide were determined, after hydrolysis with 6 N hydrochloric acid in a sealed tube at 105°C for 20 hr., by paper chromatography using solvent A and *n*-butanol - pyridine - water (1 : 1 : 1, solvent C), and by paper ionophoresis in 2 N acetic acid at 300—400 V. for 3 hr. Quantitative amino acid analyses of peptides were performed according to Levy's method[8] as described in a previous paper.[2] The paper chromatography of fatty acid and its related compound was carried out in *n*-butanol saturated with 2N aqueous ammonia (solvent D) and located by a pH indicator (bromophenol blue).

***N*-Terminal Analyses.**—0.3—1.0 mg. of a peptide and 2 mg. of sodium hydrogen carbonate were dissolved in 0.2 ml. of water in a small test tube, and then 0.4 ml. of a 5% ethanolic solution of DNFB was added. After 2 hr., the reaction mixture was diluted with 0.6 ml. of water, extracted with ether to remove the unreacted DNFB, and, after being adjusted to pH 2 with 4 N hydrochloric acid, extracted three times with 1 ml. of ethyl acetate. (All the DNP-peptides treated in the present work were extractable with ethyl acetate.) The ethyl acetate extract was then washed twice with 0.5 ml. of water and evaporated to dryness in a small test tube. The residue was sealed in a tube with 6 N hydrochloric acid and heated at 100°C for 6—8 hr. The hydrolysate was dried over potassium hydroxide in a desiccator to remove hydrochloric acid, dissolved in 1 ml. of water, and shaken three times with ether to extract DNP-amino acid for paper chromatographic identification. The paper chromatography of DNP-amino acids was conducted by the two-dimensional ascending method using solvent C and a 1.5 M phosphate buffer (pH 6.0).

***C*-Terminal Analyses.**—1—3 mg. of a dried peptide was heated with 0.1—0.2 ml. of anhydrous hydrazine in a sealed tube at 100°C for 4—6 hr. The reaction mixture was dried over sulfuric acid in a desiccator to remove the excess hydrazine, and the free amino acid therein was determined by paper chromatography and paper ionophoresis after the amino acid hydrazide has been removed by enanthaldehyde.

**The Hydrazinolysis of Glumamycin.**—Ten milligrams of glumamycin was dried with 65 mg. of hydrazine sulfate over phosphorus(V) oxide in a desiccator for 2 days, sealed together with 0.5 ml. of anhydrous hydrazine in a tube, and heated at 60°C for 16 hr. Another hydrazinolysis was conducted in a similar manner except that hydrazine sulfate was not added and the reaction was effected at 100°C for 10 hr. In both cases, the reaction mixture was dried over sulfuric acid in a desiccator, the residue was dinitrophenylated by Sanger's method, and the reaction mixture was extracted fractionally and subjected to paper chromatography. In all cases, no DNP-amino acid deriving from the *C*-terminus was detected. As a control, glumamycin was hydrazinolyzed in the presence of several moles of glycine per mole of glumamycin, but in this case only DNP-Gly was clearly detected.

6) F. Sanger, *Biochem. J.*, **45**, 503 (1949).
7) F. Sanger and H. Tuppy, ibid., **49**, 463 (1951).
8) A. L. Levy, *Nature*, **174**, 126 (1954).

## Results and Discussion

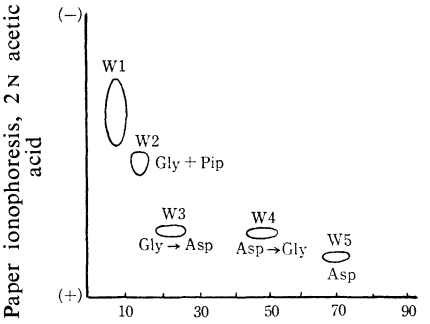
**The Partial Hydrolysis of Glumamycin with N Hydrochloric Acid.**—The partial hydrolysate of glumamycin with N hydrochloric acid was extracted successively with ethyl acetate (E-fraction) and *n*-butanol (B-fraction). The E-fraction was negative to the biuret and ninhydrin reactions and showed a fatty acid-like property, and on its paper chromatogram using solvent system D, only a spot of an acidic substance with an $R_f$ value of 0.32 was detected. Next, the E-substance was completely hydrolyzed with hydrochloric acid and extracted with ether; it was found with the ether extract that the $R_f$ 0.32 spot disappeared, while instead a spot ($R_f$ 0.61) corresponding to 3-ITA was detected. When the aqueous layer of the ether extraction was subjected to paper chromatography using solvent systems A and B, a spot corresponding to Asp was detected. The E-substance gave no DNP-derivative by Sanger's method;[9] its hydrazinolysis by Akabori's method[10] released Asp (0.4 mol./mol., uncorrected) and in this case no di-DNP-Asp monohydrazide was detected by paper chromatography. From the facts mentioned above, the structure of E-substance was found to be 3-ITA→Asp.

The B-fraction was positive to the biuret reaction and weakly positive to the ninhydrin reaction, and its acid hydrolysis gave all the components of glumamycin. Therefore, sequence studies of the B-fraction were not carried out.

Paper ionophoresis of the aqueous fraction of the *n*-butanol extraction mentioned above (W-fraction) detected many ninhydrine positive substance assumed to be amino acids and peptides. Therefore, the fraction was developed on a column of Dowex-1×4 with 5 N acetic acid in order to separate it into a basic (W1), a neutral (W2) and three acidic fractions (W3—W5), as is shown in Fig. 1. Further, the basic fraction, W1, was fractionated by a combination of paper ionophoresis in a pyridine-acetate buffer (pH 6.5) (Fig. 2) and paper chromatography in solvent systems A and B. The chromatographically-pure peptides obtained in this way analyzed for constituent amino acids and *N*- and *C*-terminal groups. The results obtained are summarized in Table I. From the results concerning the W1 fraction, a partial structure of glumamycin could be deduced as follows:

H·Gly→$\alpha$, $\beta$-Dab→Val→Pro→$\alpha$, $\beta$-Dab(→Pip)

9) F. Sanger, *Biochem. J.*, **39**, 50 (1945).
10) S. Akabori, K. Ohno, T. Ikenaka, Y. Okada, H. Hanafusa, I. Haruna, A. Tsugita, K. Sugae and T. Matsushima, This Bulletin, **29**, 507 (1956).




Effluent of Dowex-1×4 chromatography with 0.5 N acetic acid (×5 ml.)

Fig. 1. Separation of partial acid (N HCl) hydrolysate by Dowex-1×4 column (2×40 cm) chromatography.
Each fraction of the effluent was subjected to paper ionophoresis in 2 N acetic acid (400 V., 2 hr.). W2—W5 were identified by making use of their authentic samples by paper chromatography and infrared spectrum.

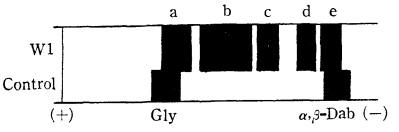



Fig. 2. Separation of W1 fraction by paper ionophoresis in pyridine-acetate buffer, pH 6.5, 300 V., 4.5 hr.

**The Partial Hydrolysis of Glumamycin with 6 N Hydrochloric Acid.**—The partial hydrolysate of glumamycin with 6 N hydrochloric acid was extracted with ethyl acetate in a manner similar to that used in the extraction of the partial hydrolysate with N hydrochloric acid. The aqueous fraction was passed through a column of Amberlite IR-120 (H-form), the absorbed substances were eluted with 0.5 N aqueous ammonia, and the eluted substances were fractionated by paper ionophoresis in a pyridine-acetate buffer (pH 6.5) (Fig. 3), followed by paper chromatography using solvent systems A and B. The components and the *N* terminal residues of the peptides thus separated were further investigated, as has been mentioned before; the results obtained are summarized in Table II.

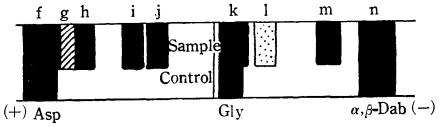



Fig. 3. Separation of partial acid (6 N HCl) hydrolysate by paper ionophresis in pyridine-acetate buffer, pH 6.5, 300 V., 5 hr.

TABLE I. AMINO ACID SEQUENCE OF PEPTIDES ISOLATED FROM PARTIAL ACID (N HCl) HYDROLYSATE OF GLUMAMYCIN

Fractions (W1 : a—e) obtained by ionophoresis at pH 6.5 (Fig. 2) were separately chromatographed in *n*-butanol - acetic acid - water (solvent A) or *n*-butanol - pyridine - acetic acid - water (solvent B). Fractions c and d were chromatographically pure, e was separated into $e_1$ and $e_2$; a and b were not identified.

| Peptide | | $R_f$ in A | $R_f$ in B | Amino acid composition* and deduced partial structure** |
|---|---|---|---|---|
| W1 : | a | | | all the amino acids constituting glumamycin were detected |
| | b | | | |
| | c | 0.36 | 0.34 | Gly·(α, β-Dab, Val)·Pro |
| | d | 0.34 | 0.28 | Gly·α, β-Dab·Val |
| | e : 1 | 0.21 | 0.21 | Gly·(α, β-Dab, Val, Pro)·α, β-Dab |
| | e : 2 | 0.41 | 0.45 | Gly·(α, β-Dab, Val, Pro, α, β-Dab, Pip) |

* Analyzed by paper chromatography and ionophoresis.
** *N*-Terminal was analyzed by Sanger's DNP-method and *C*-terminal was analyzed by hydrazinolysis.

TABLE II. PEPTIDES AND AMINO ACIDS ISOLATED FROM PARTIAL ACID (6N HCl) HYDROLYSATE OF GLUMAMYCIN

Fractions obtained by ionophoresis at pH 6.5 (Fig. 3) were separately chromatographed in *n*-butanol - acetic acid - water (solvent A) or *n*-butanol - pyridine - acetic acid - water (solvent B) and gave the additional components as shown.

| Peptide and amino acid | | $R_f$ in A | $R_f$ in B | Amino acid composition* | Deduced partial structure** |
|---|---|---|---|---|---|
| f | | 0.20 | 0.17 | Asp | — |
| g | | 0.22 | 0.25 | MeAsp, Asp | MeAsp·Asp |
| h : | 1 | 0.12 | 0.13 | Gly (1), Asp (1) | Gly·Asp |
| | 2 | 0.15 | 0.13 | Asp (1), Gly (1) | Asp·Gly |
| i | | 0.12 | 0.16 | MeAsp, Asp (2), Gly (1) | MeAsp·(Asp, Gly, Asp) |
| j | | 0.19 | 0.24 | Asp (2), Gly (1) | Asp·(Gly, Asp) |
| k | | — | — | | |
| l | | — | — | | |
| m : | 1 | — | 0.23 | α, β-Dab, Val, Pro | α, β-Dab·(Val, Pro) |
| | 2 | — | 0.27 | α, β-Dab, Val, Pro | ? |
| n : | 1 | — | 0.16 | Gly, α, β-Dab | Gly·α, β-Dab |
| | 2 | — | 0.20 | α, β-Dab | — |

* Analyzed by paper chromatography and ionophoresis. Molar ratio of amino acids was determined by Levy's DNP-method.
** *N*-Terminal was analyzed by Sanger's DNP-method.

TABLE III. PEPTIDES AND AMINO ACID OBTAINED FROM PARTIAL ACID HYDROLYSATE OF DNP-GLUMAMYCIN

| DNP-peptide (Fig. 5) | | Amino acid composition* | Deduced partial structure** |
|---|---|---|---|
| DNP-C : | a | β-DNP-α, β-Dab Val, Pro | β-DNP-α, β-Dab·(Val, Pro) |
| | b | β-DNP-α, β-Dab Val, Pro, α, β-Dab | β-DNP-α, β-Dab·(Val, Pro, α, β-Dab) |
| Non-DNP - Pertide (Fig. 6) | | | |
| n : | 1 | Val, Pro, α, β-Dab, Pip | Val·(Pro, α, β-Dab, Pip) |
| | 2 | α, β-Dab | — |

* Analyzed by paper chromatography and ionophoresis.
** *N*-Terminal was analyzed by Sanger's DNP-method. Non-*N*-terminal α, β-Dab was detected as β-mono-DNP-α, β-Dab by paper chromatography in the analysis of peptides DNP-C·b and n·1 respectively.

From the results on peptides f—j summarized in Table II, and also from the results of the partial hydrolysis with N hydrochloric acid shown in Fig. 1, the presence of the H·MeAsp →Asp→Gly→Asp·OH sequence was presumed. Results on the other peptides, m and n in Table II, were in accord with the sequence deduced from the results of the partial hydrolysis with N hydrochloric acid.

**The Partial Hydrolysis of DNP-glumamycin with Concentrated Hydrochloric Acid.** — DNP-Glumamycin prepared by Sanger's method[8] was hydrolyzed partially with concentrated hydrochloric acid, and the resulting oily substance was removed with ethyl acetate. The DNP-peptides were separated from non-DNP-peptides on a column packed with a mixture of talc and celite (2 : 1) and subjected to paper chromatography to give four yellow spots, as Fig. 4 shows. All the amino acids

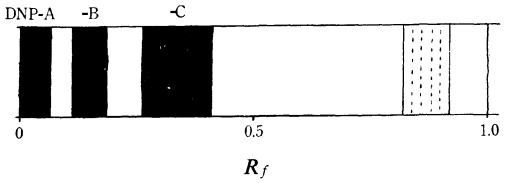



Fig. 4. Paper chromatogram of DNP-peptides obtained from partial acid hydrolysate of DNP-glumamycin.
Solvent system : *n*-butanol saturated with 2 N aqueous ammonia

constituting glumamycin were detected in the hydrolysate of DNP-A and -B and Val, Pro, α, β-Dab, β-DNP-α, β-Dab and a small amount of the other amino acids in that of DNP-C. The DNP-C was subjected to paper ionophoresis using a pyridine-acetate buffer (pH 6.5). It was separated into a neutral (DNP-C·a) and a basic (DNP-C·b) fraction, as is shown in Fig. 5. Analyses of these fractions are

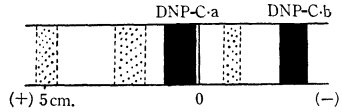



Fig. 5. Separation of DNP-C fraction by paper ionophoresis in pyridine-acetate buffer, pH 6.5, 300 V., 6 hr.

shown in Table III. From the results described above and from those of the partial hydrolysis of glumamycin, it was possible to formulate the partial sequence in the neighborhood of the free β-amino group in glumamycin as follows:

$$\rightarrow \alpha\text{-Dab} \rightarrow \text{Val} \rightarrow \text{Pro} \rightarrow \underset{\beta\text{-NH (free)}}{\alpha\text{-Dab}} \rightarrow \underset{\beta\text{-NH}}{\alpha\text{-Dab}} \leftarrow$$

Next, the non-DNP-peptide fraction from the above-mentioned talc-celite column was passed through a column of Amberlite IR-4B (OH form) in order to remove acidic amino acids and peptides. Peptides and amino acids in the effluent were adsorbed on a colum of Amberlite IR-120 (H from) and eluted with 0.5 N aqueous ammonia to give a sample for paper ionophoresis. The results are shown in Fig. 6. Analyses of the isolated substances are shown in Table III.

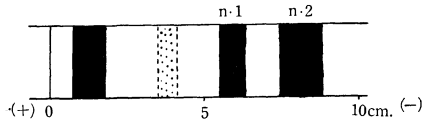



Fig. 6. Separation by paper ionophoresis of non-DNP-peptides obtained from partial acid hydrolysate of DNP-glumamycin.
Pyridine-acetate buffer, pH 6.5, 300 V., 3.5 hr.

From the results summarized in Table III, the structure of non-DNP-peptide n·1 may be as follows;

$$\text{H-Val} \rightarrow \text{Pro} \rightarrow \underset{\beta\text{-NH}_2}{\alpha\text{-Dab}} \rightarrow \text{Pip-OH}$$

**The Elucidation of the Sequence.**—The partial structure of glumamycin, inferred from the sequence of amino acids in the peptide fragments obtained by the partial hydrolysis of glumamycin and DNP-glumamycin, may be represented by 3-ITA→Asp·(OH), (H)·Gly→ $\underset{\beta\text{-NH}_2}{\alpha\text{-Dab}}\rightarrow\text{Val}\rightarrow\text{Pro}\rightarrow\underset{\beta\text{-NH}_2}{\alpha\text{-Dab}}\rightarrow$Pip·(OH) and (H)·MeAsp→Asp→Gly→Asp·(OH). All the amino acid residues constituting glumamycin are contained in the above three peptides. Glumamycin was subjected to the hydrazinolysis-DNP method of Akabori in the presence and in the absence of hydrazine sulfate, but no DNP-amino acid derived from *C*-terminal was detected in either case. Therefore, the three peptides above are presumed to be arranged in a cyclic form in glumamycin.

From these facts, the structure of glumamycin may be supposed to be one of the following two;

$$\text{(A)}\quad \text{3-ITA} \rightarrow \text{Asp} \rightarrow \text{Gly} \rightarrow \underset{\beta\text{-NH}_2}{\alpha\text{-Dab}} \rightarrow \text{Val} \rightarrow \text{Pro} \rightarrow \alpha,\beta\text{-Dab} \begin{cases} \nearrow \text{Pip} \rightarrow \text{MeAsp} \searrow \\ \nwarrow \text{Asp} \quad\rightarrow\quad \text{Gly} \swarrow \end{cases} \text{Asp}$$

$$\text{(B)}\quad \text{3-ITA} \rightarrow \text{Asp} \rightarrow \alpha,\beta\text{-Dab} \begin{cases} \nearrow \text{Pip} \rightarrow \text{MeAsp} \rightarrow \text{Asp} \rightarrow \text{Gly} \searrow \\ \nwarrow \text{Pro} \leftarrow \text{Val} \leftarrow \underset{\beta\text{-NH}_2}{\alpha\text{-Dab}} \leftarrow \text{Gly} \swarrow \end{cases} \text{Asp}$$

Fundamentally these structures of glumamycin are similar to those of the antibiotics of the polymixin series[11,12] but they are reverse in the relation of functional groups; that is, in the former, one amino group and four carboxyl groups are free, while in the latter only the amino groups are free. It is interesting to compare these points with their antibacterial spectra; glumamycin is active only to Gram-positive microorganisms, and the antibiotics of polymixin, only to Gram-negative microorganisms.

## Summary

To elucidate the amino acid sequence of glumamycin, glumamycin and DNP-glumamycin have been partially hydrolyzed with hydrochloric acid, and various peptides have been isolated by column chromatography on ion-exchange resin or talc-celite, paper chromatography and paper ionophoresis. From the structures of the peptides, two possible structures (A and B) for glumamycin have been presumed.

The author wishes to express his thanks to Dr. Sueo Tatuoka, the Director of the Research Laboratories, Dr. Satoru Kuwada and Dr. Kuniyoshi Tanaka for their guidance and encouragement, and to Drs. Koichi Nakazawa, Akira Miyake, Jisaburo Ueyanagi, Michitaka Inoue and Motoo Shibata for their kind advice.

*Research Laboratories*
*Takeda Chemical Industries, Ltd.*
*Higashiyodogawa-ku, Osaka*

11) W. Hausmann, *J. Am. Chem. Soc.*, **78**, 3663 (1956).
12) K. Vogler, R. O. Studer, W. Lergier and P. Lanz, *Helv. Chim. Acta*, **43**, 1751 (1960).

# The Extractional Behavior of Cerium with Acetylacetone

By Shōhachirō Ōki*

(Received December 10, 1963)

In previous papers[1,2] we have studied some details of the solvent extraction of cerium with acetylacetone—the conditions for the extraction, the interfering substances, and the application of the extraction technique to the separation of cerium-144 from the mixture of fission products.

In this paper we hope to make clear the extractional behavior of cerium in the form of the acetylacetonate. The oxidation number of cerium will be estimated, and the effects of the concentration of acetylacetone and temperature on the extraction will be studied.

## Experimental

**Reagents.**—Commercial acetylacetone was purified by washing it with dilute ammonia water and then with distilled water, followed by distillation under the reduced pressure of 47 mmHg; the 56—57°C fraction was then collected. The purity of the product was checked by gas chromatography.

The carrier-free cerium-144 was imported from Amersham, England, in the form of cerous trichloride in a hydrochloric acid solution, which was dissolved in 2 N perchloric acid and then stored.

Benzene was purified by washing it with sulfuric acid and then with distilled water; it was then distilled.

The other chemicals used are all of a guaranteed reagent grade.

**Distribution Measurements.** — The distribution ratio of acetylacetone was determined as follows: A mixture of 5 ml. of an acetylacetone benzene solution of a known concentration and 5 ml. of an aqueous solution of 0.1 M sodium perchlorate at various pH values was mechanically shaken for 30 min. in order to attain the distribution equilibrium of acetylacetone at a regulated temperature. After the phases had settled, the volumes of the two phases, the concentration of acetylacetone and the pH in the aqueous phase were measured. The distribution ratio was defined as the ratio of the concentration of acetylacetone in the organic phase to the concentration in the aqueous phase.

The concentration of acetylacetone in the aqueous phase was determined by adding a large excess of an aqueous solution of ferric sulfate at pH 0.5 to an aliquot (1 ml.) of the sample solution, while the absorption at 650 mμ was measured by a spectrophotometer. The pH measurements were carried

* Present address: Department of Industrial Chemistry, Faculty of Engineering, Shizuoka University, Hamamatsu.

1) N. Suzuki and S. Oki, This Bulletin, 35, 233 (1962).

2) N. Suzuki and S. Oki, This Bulletin, ibid., 35, 273 (1962).

out within an accuracy of 0.01 pH unit with a glass electrode pH meter.

The distribution ratio of cerium was determined as follows: A mixture of 5 ml. of an acetylacetone benzene solution of a known concentration, which had extracted cerium at pH 6—7 beforehand, and 5 ml. of an aqueous solution of 0.1 M sodium perchlorate at various pH values was mechanically shaken for an hour in order to attain the distribution equilibrium at a regulated temperature. The initial concentration of cerium in the organic phase was the tracer concentration, the order of $10^{-9}$ M. After the phases had settled, an aliquot (1 ml.) was taken out from each phase into each polyethylene test tube in order to count the gamma activity of cerium-144. Measurements of the gamma activity were carried out by a well-type NaI(Tl) scintillation countor, after a period of time, for the radioactive equilibria of cerium-144 and praseodymium-144.

**Symbols and Formulae.**—The following symbols and formulae are used:

[ ]=concentration in the aqueous phase

[ ]$_o$=concentration in the organic phase

HA=acetylacetone

$D_A$=distribution ratio of acetylacetone

$$D_A=[HA]_o/\{[HA]+[A^-]+[H_2A^+]\} \quad (1)$$

$D_A^\circ$=distribution coefficient of acetylacetone

$$D_A^\circ=[HA]_o/[HA] \quad (2)$$

$K_a$=acid dissociation constant of acetylacetone

$$K_a=[H^+][A^-]/[HA] \quad (3)$$

$K_b$=base dissociation constant of acetylacetone

$$K_b=[H_2A^+]/[H^+][HA] \quad (4)$$

$D_c$=distribution ratio of cerium

$D_c^\circ$=distribution coefficient of ceric acetylacetone

$$D_c^\circ=[CeA_4]_o/[CeA_4] \quad (5)$$

$K_n$=formation constant of the chelate $CeA_n$

$$K_n=[CeA_n^{4-n}]/[Ce^{4+}][A^-]^n \quad (6)$$

$k_m$=formation constantant of the compounds $CeA_4\cdot mHA$ in the organic phase

$$K_m=[CeA_4\cdot mHA]_o/[CeA_4]_o[HA]_o^m \quad (7)$$

## Results and Discussion

**The Distribution of Acetylacetone.** — The equilibrium distribution ratio of acetylacetone varies with the pH of the aqueous phase. The variation depends on the dissociation of acetylacetone as an acid or a base. When it is assumed that ions are not extracted, the distribution ratio will be given as Eq. 1 or:

$$D_A=D_A^\circ/\{1+K_a/[H^+]+K_b[H^+]\} \quad (8)$$

Equation 8 indicates that $D_A$ has a maximum value equal to $D_A^\circ/(1+2\sqrt{K_a\cdot K_b})$ at pH$=(pK_a-pK_b)/2$.

Since the prodct $K_a\cdot K_b$ is much smaller than unity, the maximum distribution ratio is reduced to $D_A^\circ$. A plot of $D_A$ vs. pH at 25°C is given in Fig. 1. The distribution ratio is found to be almost constant in the pH range from 1.5 to 7, and $D_A^\circ$ is determined graphically by Fig. 1. The distribution coefficients at various temperatures were determined in the same way; the results are summarized in Table I.

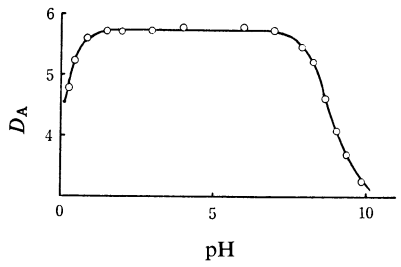



Fig. 1. Distribution curve of acetylacetone.

TABLE I. EQUILIBRIUM CONSTANTS OF ACETYLACETONE AT VARIOUS TEMPERATURES

| Temp., °C | $D_A^\circ$ | p$K_a$ |
|---|---|---|
| 10 | 5.5 | $8.9_0$ |
| 25 | 5.4 | $8.8_8$ |
| 40 | 5.3 | $8.8_6$ |

When the term of $K_b[H^+]$ is small enough to be negligible compared with $K_a/[H^+]$, Eq. 8 is rewritten as:

$$D_A=D_A^\circ/\{1+K_a/[H^+]\},$$

or

$$\log\{(D_A^\circ-D_A)/D_A\}=pH-pK_a$$

A plot of $\log\{(D_A^\circ-D_A)/D_A\}$ as ordinate against pH as abscissa is given in Fig. 2. The pH value where $D_A$ is equal to $D_A^\circ/2$ will be the p$K_a$ of acetylacetone. The dissociation constants at various temperatures were obtained in the same way and are summarized in Table I; they are in good agreement with the literature.[3,4] The decrease in the distribution ratio is observed in the pH range below 1. Acetylacetone is assumed to be present in an acid form such as $H_2A^+$ in strong acid solutions.[4] The decrease in the distribution ratio may be attributed partially to the fact that the ionic strength in the pH range below 1 was not maintained constant, but mainly to the gradual transformation of acetylacetone into an acid form or a cationic form with a decreasing pH, which is incapable of being extracted with benzene.

**The Distribution of Cerium.**—The distribution ratio of cerium increases with an increase in the concentration of acetylacetone in the

3) J. Rydberg, *Svensk Kem. Tid.*, **65**, 37 (1953).

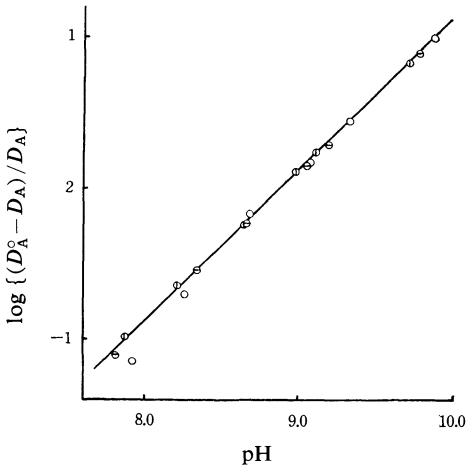



Fig. 2. Determination of p$K_a$ of acetylacetone.
⊖ 10°C ○ 25°C ⊕ 40°C

organic phase, as is shown in Fig. 9, which suggests the presence of such compounds as $CeA_N \cdot mHA$ $(m, N \geqq 0)$ in the organic phase. Accordingly, the distribution ratio of cerium may be given as:

$$D_c = \sum_{m=0} [CeA_N \cdot mHA]_o / \sum_{n=0} [CeA_n^{N-n}] \qquad (11)$$

where $N$ is the number of the acetylacetonate ligand coordinated to cerium. In Eq. 11 it is assumed that the ionic species are not extracted in the organic phase.

The distribution curves of cerium are given in Figs. 3, 4, and 5 at 10, 25, and 40°C respectively. Fortunately, the distribution ratio of acetylacetone was proved to be constant under these experimental conditions, and the concentration of acetylacetone can easily be maintained constant, while changing that of the acetylacetonate ion in the aqueous phase, by changing the pH. In either Figs. 3, 4, or 5, straight lines with fourth-power dependence of the concentration of a hydrogen ion are obtained in the lower pH region. With an increase in the pH, however, the experimental values show a discrepancy from the straight lines downwards. If the tendency were due to the hydrolysis of cerium, the discrepancy would disappear when the concentration of acetylacetone in the system was increased against the experimental results. In Figs. 6, 7, and 8 the distribution of cerium is plotted against p$A$, $-\log[A^-]$. Straight lines with fourth-power dependence of the concentration of the acetylacetonate ion in the higher p$A$ region are also given. The distribution curves are observed to give the same slopes at the

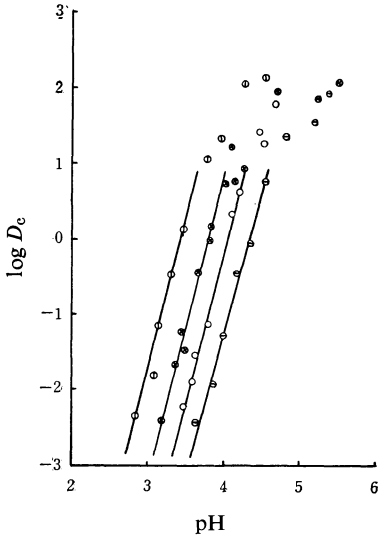



Fig. 3. Disrtibution curves of cerium as a function of pH at 25°C.
$[HA]_o$, M: ⊕ 0.866, ⊗ 0.438, ○ 0.302, ⊖ 0.199

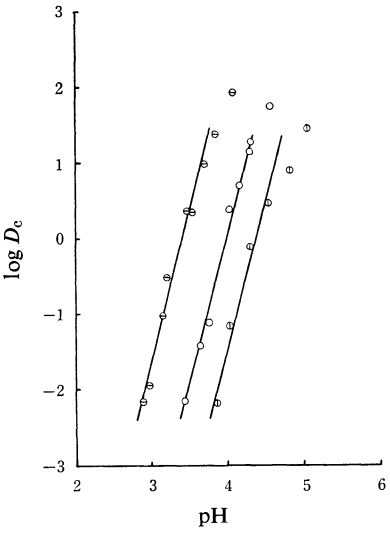



Fig. 4. Distribution curves of cerium as a function of pH at 10°C.
$[HA]_o$, M: ⊖ 0.897, ○ 0.310, ⊕ 0.167

same p$A$ value. The distribution ratio, however, increases with an increase in the concentration of acetylacetone in the organic phase. These results are adequately explained by Eq. 11, where $N$ is substituted for 4, or Eq. 12;

$$D_c = \sum_{m=0} [CeA_4 \cdot mHA]_o / \sum_{n=0} [CeA_n^{4-n}] \qquad (12)$$

Equation 12 is also supported by the early experimental results;[1] cerium(III) is not extracted, while in the presence of bromate cerium is extracted. By combining Eqs. 5, 6,

4) N. P. Rudenko and I. Stray, *Chem. Abstr.*, **53**, 3971 (1959).

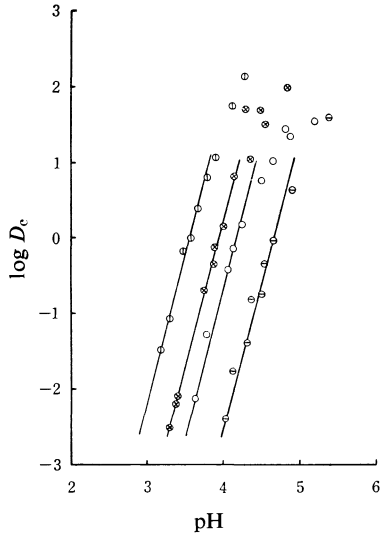



Fig. 5. Distribution curves of cerium as a function of pH at 40°C.
$[HA]_o$, M: ⊕ 0.904, ⊗ 0.437, ○ 0.302
⊖ 0.155

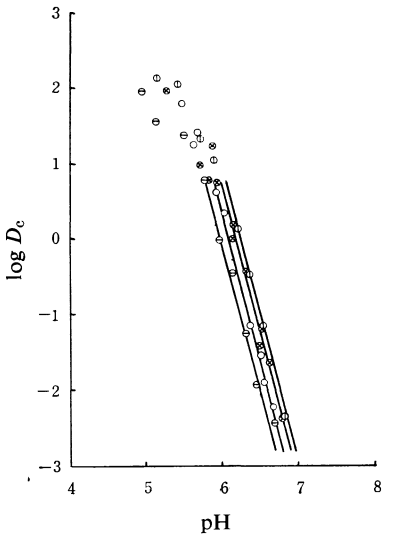



Fig. 5. Distribution curves of cerium as a function of pH at 25°C.
$[HA]_o$, M: ⊕ 0.866, ⊗ 0.438, ○ 0.302
⊖ 0.199

7, and 12, $D_c$ may be rewritten as:

$$D_c = D_c^\circ K_4 [A^-]^4 \{ \sum_{m=0} k_m [HA]_o^m \sum_{n=0} K_n [A^-]^n \} \quad (13)$$

When the p$A$ is high enough to make the products $K_n[A^-]$ ($n \geqq 1$) negligible compared with unity in the denominator in Eq. 13, that equation is reduced to:

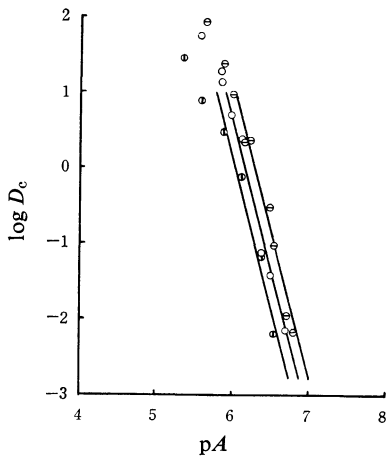



Fig. 7. Distribution curves of cerium as a function of p$A$ at 10°C.
$[HA]_o$, M: ⊖ 0.897, ○ 0.310, ⊕ 0.167

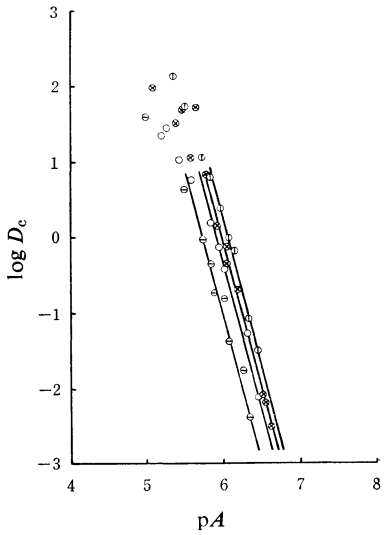



Fig. 8. Distribution curves of cerium as a function of p$A$ at 40°C.
$[HA]_o$, M: ⊕ 0.904, ⊗ 0.437, ○ 0.302
⊖ 0.155

$$D_c = D_c^\circ K_4 [A^-]^4 \sum_{m=0} k_m [HA]_o^m \quad (14)$$

Equation 14 indicates that in the higher p$A$ region the distribution ratio of cerium is proportional to the fourth power of the concentration of the acetylacetonate ion for a constant concentration of acetylacetone in the organic phase. The reason why the distribution ratio is observed to bend gradually downwards may be explained by Eq. 13 to be the result of the gradual formation of ceric acetylacetonate, $CeA_n^{4-n}$ ($n \geqq 1$), in the aqueous phase, because distribution curves at the respective

concentrations of acetylacetone seem to give the same slope at the same p$A$ values in Figs. 6, 7, and 8. The distribution data, however, were considerably scattered, and the reproducibility was somewhat poor in the higher pH region, where gradual hydrolysis may take place. Therefore, the stoichiometric treatments were not applied in the lower p$A$ regions.

The variations in the distribution ratio with the concentration of acetylacetone in the organic phase are given in Fig. 9, which was obtained by interpolating the distribution curves of Figs. 6, 7, and 8 at p$A$ 6.25. The increase in the distribution ratio of cerium with an increase in the concentration of acetylacetone in the organic phase is comprehensible as the results of the formation of the compounds, $CeA_4 \cdot mHA$ in the organic phase, which is explained by Eq. 14 (Fig. 9). Since the distribution ratio is proportional to the square of the concentration of acetylacetone below 0.5 M, it may be concluded that a molecule of cerium acetylacetonate combines

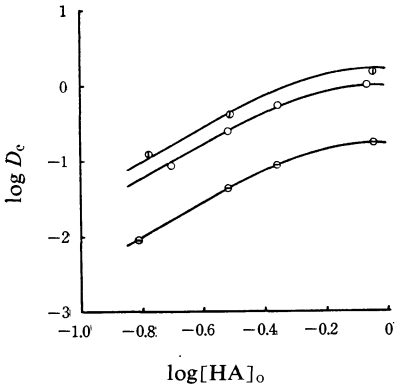



Fig. 9. Distribution curves of cerium as a function of $[HA]_o$ at p$A$ 6.25.
Temp., °C: ① 10, ○ 25, ⊖ 40

with two molecules of acetylacetone to form a compound $CeA_4 \cdot 2HA$ in the organic phase.

The effects of the temperature on the distribution ratio of cerium are given in Fig. 9. The effects of the temperature are small for reactions 1, 2, and 3. Supposing that reactions 5 and 6 are not so much influenced by the temperature as usual, reaction 7 has to be influenced by the temperature. The enthalpy change of reaction 7 was calculated to be −13 kcal. from Fig. 9 on the above assumption ($\Delta \log D_c = 1$ for $\Delta T = -30°$). If the interaction between benzene and $CeA_4$ does not amount to any appreciable amount, the enthalpy change is regarded as the binding energy between $CeA_4$ and 2HA. The magnitude of the energy needed for a molecule of acetylacetone to bind with $CeA_4$ is 6.5 kcal., which corresponds to the energy of hydrogen bond. The discrepancy from the straight line in the higher concentration regions is assumed to be the result of the saturation of hydrogen bonds for $CeA_4$ to combine with molecules of acetylacetone, or to be the result of changes in the solvent properties of benzene resulting from an increase in the concentration of acetylacetone in the organic phase.

## Summary

The extraction behavior of tracer amounts of cerium-144 with acetylacetone has been studied. The distribution ratio of acetylacetone between benzene and a 0.1 M sodium perchlorate solution is constant in the pH range 1.5−7, and the distribution coefficients have been determined to be 5.5, 5.4, and 5.3 at 10, 25, and 40°C respectively. The distribution ratio of cerium has been shown to be proportional to the fourth power of the concentration of the acetylacetonate ions and to the square of that of acetylacetone in the organic phase. From these results, it has been concluded that cerium exists as a tetravalent ion in the system and that the chemical form of cerium extracted in the organic phase is $CeA_4 \cdot 2HA$. Two molecules of acetylacetone are assumed to combine with $CeA_4$ forming hydrogen bonds.

The author wishes to express his thanks to Professors Takanobu Shiokawa and Nobuo Suzuki of Tohoku University for their helpful advice.

*Department of Chemistry*
*Faculty of Science*
*Tohoku University*
*Katahira-cho, Sendai*

# The Dielectric Properties of Some Alkyl Thiol

By Seiichi KONDO

(Received July 13, 1964)

As has already been studied by some authors, molecular crystals with a spherical molecular shape sometimes possess a small entropy of fusion, and such physical properties as nuclear magnetic resonance, dielectric properties, and X-ray diffraction can be well explained by the assumption of molecular rotation on the crystalline lattice site.

2-Methyl-2-propanethiol and 2-methyl-2-butanethiol also have small entropies of fusion,[1] 2.16 cal./deg. mol. and 0.86 cal./deg. mol. respectively, and the X-ray diffraction study of the plastic phase IV (the highest temperature solid phase) of 2-methyl-2-propanethiol shows a random orientation of molecules on the face-centered-cubic crystal lattice sites.[2] These facts lead us to the assumption that molecules on the lattice sites would make rotational motion as a whole, in spite of the possibility of interactions between thiol groups revealed by infrared spectroscopy of other compounds in liquid states.[3] It is of interest to compare the properties of such compounds with those of 2-methyl-2-propanol, which forms a stronger intermolecular hydrogen bond between hydroxyl groups than do thiols and which is not a plastic crystal.

Similarly, it is also interesting to compare the properties of cyclohexanethiol with those of cyclohexanol, which shows many properties characteristic of plastic crystals[2] in spite of the existence of a hydrogen bond between molecules. It is questionable whether or not cyclohexanethiol, which is supposed to have a weaker intermolecular interaction between thiol groups, is a plastic crystal. The dielectric study of these compounds has, therefore, been carried out, in both liquid and solid states, in respect to the dipole interaction of these molecules in condensed states, as one of the series of dielectric investigations of plastic crystals.

## Experimental

**Sample Preparation and Measuring Apparatus.**—2-Methyl-2-propanethiol and 2-methyl-2-butanethiol were supplied in vacuum-sealed glass ampules with breakable joints by the U. S. Bureau of Mines, through the courtesy of Dr. J. P. McCullough. These were vacuum-sublimed, dried with magnesium perchlorate, and then placed in glass dielectric cells with platinum electrodes. All these procedures were carried out in the same vacuum system without any exposure to air. The melting points of these materials after repurification are equal to those obtained by McCullough and others[1] within the range of experimental error. Cyclohexanethiol was synthesized in this laboratory from cyclohexanol and purified by the same method. However, the purity of this sample was not as high as that of the others, as may be seen in the curve near the melting point in Fig. 3, partly because of the difficulty in drying.

The measuring circuit used in this study is a low-frequency bridge with a frequency range from $10^2$ to $10^4$ c. p. s. It has been described elsewhere.[4] The dielectric constant was determined by a comparison of the electric capacity with purified organic liquids, such as benzene, ethyl ether and acetone, with accurate dielectric constant values.

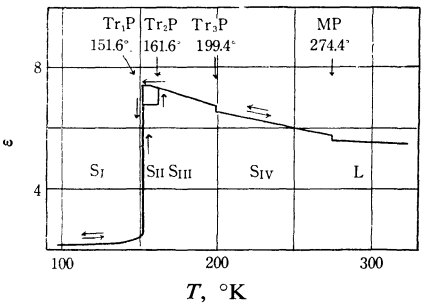



Fig. 1. The dielectric constant versus temperature curve of 2-methyl-2-propanethiol.

## Results and Discussion

**2-Methyl-2-propanethiol.**—The variation in the dielectric constant of this material with the temperature is illustrated schematically in Fig. 1. The value of the dielectric loss, tan $\delta$, was less than $10^{-3}$. This value, together with that of the dielectric constant, showed no detectable frequency effect within our temperature range. The dipole moment, $\mu$, of

1) J. P. McCullough, D. W. Scoff, H. L. Finke, W. N. Hubbard, M. E. Gross, C. Katz, R. E. Pennington, J. F. Messerpy and G. Waddington, *J. Am. Chem. Soc.*, **75**, 1818 (1953).

2) S. Kondo, *Memoirs of Osaka Gakugei University*, **B, 6**, 25 (1957).

3) R. A. Spurr and H. F. Byer, *J. Phys. Chem.*, **62**, 425 (1958). M. O. Bulanin, G. S. Denisov and R. A. Pushkina, *Optics and Spectroscopy*, **VI**, 491 (1959).

4) S. Kondo and T. Oda, This Bulletin, **27**, 567 (1954).

this molecule in the liquid state at 20° C can be calculated by using the Onsager equation[5] for pure polar liquid,

$$\frac{(\varepsilon-n^2)(2\varepsilon+n^2)M}{\varepsilon(n^2+2)^2 d}=\frac{4\pi N}{3}\frac{3kT}{\mu^2}$$

With $T=293°$ K, dielectric constant $\varepsilon=5.55$, density $d=0.8002$ g./cm$^3$,[6] and refractive index $n=1.4232$, the value of $\mu$ is calculated to be 1.67 D. This is almost equal to that of ethanethiol, 1.56 D, in the gas phase,[7] suggesting that the molecular association through the intermolecular hydrogenbond is very small.

The dipole moment of the plastic Phase IV, as calculated in the same manner, is 1.6 D, equal to that of the liquid. This suggests that the degree of molecular dipole rotation in the plastic phase is almost the same as that in the liquid state, as has been seen in other plastic crystals studied elsewhere.[2] The high symmetry of this crystal phase (face-centered-cubic structure) as shown by X-ray diffraction work,[2] compared with the low molecular symmetry of this compound, can be explained by the molecular rotation.

The same order of magnitude of the dielectric constant in phases III and II indicates the existence of some kind of molecular rotation in these phases. A thermal hysteresis of phase change was observed in phase II, as may be seen in Fig. 1. Careful thermal treatment shows that this is a sort of supercooling phenomenon probably accompanied by the molecular rearrangement process in this temperature region. The dielectric constant of phase I is nearly equal to the square of the refractive index of this material, suggesting the absence of the rotation of the molecular dipole in this phase.

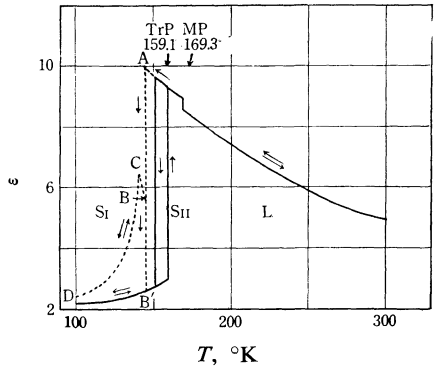



Fig. 2. The dielectric constant versus temperature curve of 2-methyl-2-butanethiol.

**2-Methyl-2-butanethiol.**—The dielectric constant versus the temperature relation is shown in Fig. 2. No anomalous dispersion has been observed in the present frequency and temperature range. As the application of the Onsager equation to the liquid and crystalline phase II of this material in the same manner as was done with 2-methyl-2-propanethiol gives, in both states, the value of 1.6 D as the dipole moment, this seems to be reasonable in comparison with those of other aliphatic thiols. This fact, and the very low entropy of fusion of this material, indicate the existence of molecular rotation in phase II. As may be seen in Fig. 2, this material shows a large thermal hysteresis on the phase transition from phase II to phase I; this hysteresis depends upon the cooling velocity. With a cooling rate smaller than 0.2 deg./min., the phase change occurs in accordance with the full line in Fig. 2. More rapid cooling gives rise to complicated behavior such is shown by the dotted line "A-B-C-D". Heating this sample from point "D" leads to the change "D-C-B-B'," and from point "B'" the system follows the full line. These facts seem to indicate the existence of a supercooled crystalline phase. McCullough and others observed a very small $\lambda$-type heat capacity anomaly at about 145°K which is likely to coincide with our point "C" in Fig. 2. The small value of the dielectric constant in phase I suggests the cessation of the rotation of the molecular dipole in this phase.

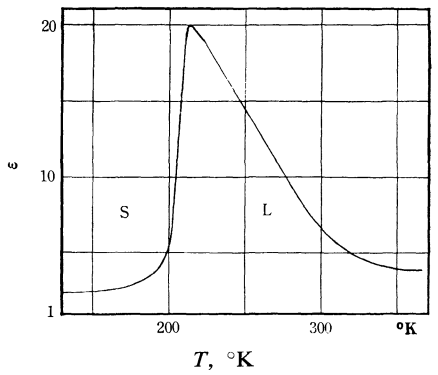



Fig. 3. The dielectric constant versus temperature curve of cyclohexanethiol.

**Cyclohexanethiol.**—In Fig. 3, the dielectric constant of this material decreases to about 2 in the solid phase upon being frozen, and no further marked change in the dielectric constant which indicates the phase change, has been observed within the present temperature and frequency range.

The curve of Fig. 3 near the melting point is somewhat ambiguous, as has been described

5) L. Onsager, *J. Am. Chem. Soc.*, **58**, 1486 (1936).
6) J. P. McCullough, *Private communication.*
7) M. Kubo, *Sci. Papers Inst. Phys. Chem. Research (Tokyo)*, **29**, 122 (1936).

in the section on sample preparation, because of the low purity of the sample. Therefore, no more detailed discussion will be made on this material beyond the suggestion that this material is not a plastic crystal.

The infrared absorption spectroscopy of this material by Kozima and Koda[8] shows the existence of a weak hydrogen bond in both the liquid and solid phases. They also concluded on the basis of an analysis of SH group vibration frequencies in these two states, that the molecule assumes both "a" and "e" forms in liquid phase but only "a" form in the solid phase. These properties of cyclohexanethiol are in marked contrast to those of cyclohexanol, which is a plastic crystal.

## Summary

It has been concluded that both 2-methyl-2-propanethiol and 2-methyl-2-butanethiol are plastic crystals and that, in their highest temperature crystalline phases, molecules perform a rotational motion on the lattice sites. The intermolecular S-H···S hydrogen-bond, which might possibly exist in these phases, seems to be too weak to hinder the molecular rotation. Cyclohexanethiol does not seem to be a plastic crystal, probably because of its low molecular symmetry in the solid phase and its intermolecular hydrogen bond.

The author wishes to express his thanks to Dr. J. P. McCullough of the U. S. Bureau of Mines for the supply of the samples of 2-methyl-2-propanethiol and 2-methyl-2-butanethiol and for his helpful discussions. Thanks are also due to Dr. Tsutomu Oda, Mr. Masaru Matsumoto and Mr. Kaoru Kawabe for their useful discussions and for their help with some of the measurements.

*Laboratory of Physical Chemistry*
*Osaka University*
*of Liberal Arts and Education*
*Tennoji, Osaka*

8) K. Kozima and Y. Kada, Presented at the 12th Annual Meeting of the Chemical Society of Japan, 1959.

# The Quenching Action of Benzoic Acid and Methyl Benzoate on the Fluorescence of Naphthalene Derivatives

By Takuji MIWA and Masao KOIZUMI

(Received July 16, 1964)

In a previous paper,[1] the present authors investigated the quenching action of pyridine and quinoline on the fluorescence of naphthylamine and naphthol and their related compounds, in connection with the effect of intermolecular hydrogen bonding on the fluorescence power. A high degree of quenching was observed in the system consisting of naphthylamine or naphthol as a fluorescer and pyridine or quinoline as a quencher; this was just what had been expected from Mataga's finding[2] that a fluorescer loses its emissivity when hydrogen-bonded directly with another conjugated system. A notable result then found was that a rather large quenching was observed in the system consisting of *N*, *N*-dimethyl-2-naphthylamine or 2-naphthyl methyl ether (fluorescer) and pyridine or quinoline (quencher), where no hydrogen bonding is conceivable. These phenomena were explained by assuming an intermolecular charge transfer between the excited fluorescer and the quencher. Although analogous mechanisms of quenching have long been postulated, no confirmative evidence had been presented until recently, when Weller,[3] by means of a flash photolytic technique, succeeded in providing strong support for this mechanism holding in the perylene - amine system. However, from the standpoint of a charge-transfer mechanism, there seems to be very little work which has succeeded in correlating the quenching constants with such properties of fluorescers and quenchers as the ionization potential or electron affinity. Among recent articles, the works

1) T. Miwa and M. Koizumi, This Bulletin, **36**, 1619 (1963).

2) E. g. N. Mataga, ibid., **31**, 481 (1958).

3) H. Leonhardt and A. Weller, *Z. Phys. Chem., NF*, **29**, 277 (1961); "Luminescence of Organic and Inorganic Materials," Ed. by Kallman and Spruch, John Wiley and Sons, New York (1962), pp. 74—82; *Ber. Bunsges. Phys. Chem.*, **61**, 791 (1963).

of Weller[4] and Majumder et al.[5] are prominent. The former compared the quenching action of various aliphatic amines on the fluorescence of an aqueous acridine solution, while the latter investigated the fluorescence power of some condensed aromatic compounds, such as anthracene, dissolved in benzene, toluene, xylene, and mesitylene. Still fewer have been the systematic studies of various systems undertaken from this point of view.

We became interested in undertaking such a study in the expectation that it would make our proposed mechanism more concrete. In this paper, the first in a series devoted to the above study, we will describe the quenching action of benzoic acid and its methyl ester, both chosen as weak electron acceptors, on the fluorescence of naphthalene derivatives, including *N,N*-dimethylnaphthylamine and naphthyl methyl ether.

It will be shown that the benzoic acid dimer has a rather large quenching action on the above-mentioned compounds; the molecular mechanism will also be discussed.

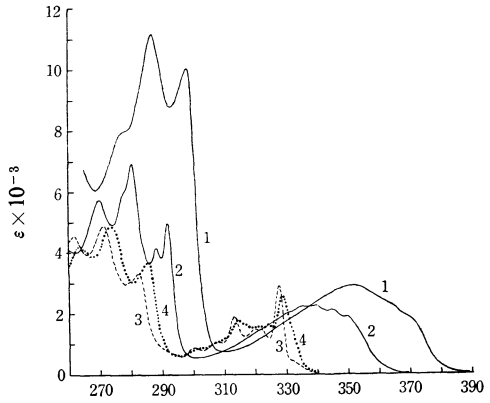



Fig. 1. Absorption spectra in cyclohexane.
1 *N,N*-Dimethyl-2-naphthylamine
2 2-Naphthylamine
3 2-Naphthyl methyl ether
4 2-Naphthol

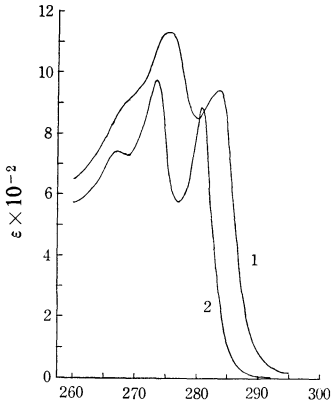



Fig. 2. Absorption spectra in cyclohexane.
1 Benzoic acid: $5\times10^{-4}$ M
2 Methyl benzoate: $6.4\times10^{-4}$ M

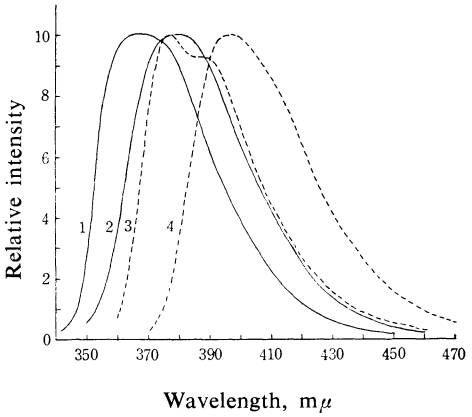



Fig. 3. Fluorescence spectra.
1 2-Naphthylamine $10^{-4}$ M/l. in cyclohexane
2 2-Naphthylamine $10^{-4}$ M/l. in benzene
3 *N,N*-Dimethyl-2-naphthylamine $10^{-4}$ M/l. in cyclohexane
4 *N,N*-Dimethyl-2-naphthylamine $10^{-1}$ M/l. in benzene

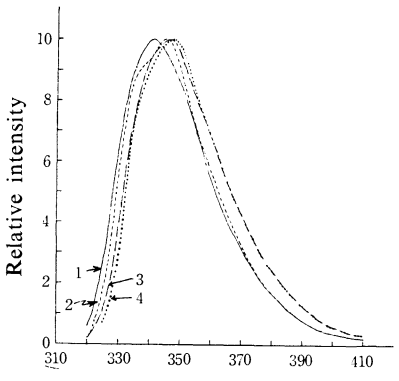



Fig. 4. Fluorescence spectra.
1 2-Naphthyl methyl ether $2\times10^{-4}$ M/l. in cyclohexane
2 2-Naphthol $2\times10^{-4}$ M/l. in cyclohexane
3 2-Naphthyl methyl ether $2\times10^{-4}$ M/l. in benzene
4 2-Naphthol $2\times10^{-4}$ M/l. in benzene

4) A. Weller, "Reaction Kinetics," Vol. I, Ed. by G. Porter, Pergamon Press, New York (1961), p. 195.
5) D. K. Majumdar and S. Basu, *J. Chem. Phys.*, 33, 1199 (1960).

## Experimental

**Materials.**—*Benzoic Acid.*—The standard sample for calorimetry, obtained from the Shigen Gijutsu Shikenjo (Natural Resources Institute), was recrystallized three times from benzene.

*Methyl Benzoate.* — Commercial material was treated twice with a concentrated aqueous potassium carbonate solution to remove the free acid, dehydrated over potassium carbonate (for more than a week), and finally distilled twice under reduced pressure.

*Cyclohexane and Other Materials.*—The procedure for purification was the same as that described in a previous paper.[1)]

**Apparatus and Procedure.** — The absorption spectra were measured with a Hitachi EPS or EPU spectrophotometer. The fluoresecence intensity was measured with a fluorometer made by the Narumi Shokai (the details of the apparatus were given in the previous paper[1)]) or an Aminco-Bowman spectrophotofluorometer. In the former apparatus, only the exciting light is monochromatized by a prism while the entire (not monochromatized) fluorescence or a part of it (through a filter) is caught by a photomultiplier. Intensities were measured on a photometer. In the latter apparatus both the exciting light and the fluorescence are monochromatized with a diffraction monochromator. The action spectra as well as the fluorescence spectra can be recorded automatically. The fluorescence intensity of the sample solution containing a quenching substance was compared with that of the reference solution, measurement of which was performed immediately before and after the measurement of the sample solution. All the measurements were made at room temperature without degassing. Integrated fluorescence spectra or the height of the maxima in the fluorescence spectra were used for the analysis. A suitable correction was made when necessary, for example, when the addition of a quenching substance changed the optical density at the exciting wavelength or affected the fluorescence spectra to an appreciable extent. The absorption spectra and the fluorescence spectra of the substances employed are given in Figs. 1—4. The error in wavelength is about $\pm 0.5\ m\mu$ for absorption and about $\pm 3\ m\mu$ for fluorescence spectra.

## Results

**Quenching Action of Methyl Benzoate.**—*N, N-Dimethyl-2-naphthylamine in Cyclohexane.*—Upon the addition of 0.2 M of quencher, the absorption spectra undergo a distinct red shift, which increases with the concentration of the quencher and which, at the same time, causes a broadening of all the features of the spectra. This phenomenon may be attributed to the so-called solvent effect. The fluorescence spectra show similar changes in the concentration range 0—2 M of the quencher. The fluorescence intensity decreases only a little with the addition of 0.2 M of quencher. In the region 0—2 M, the $F_0/F-1$ vs. [Q] (Q=quencher) plot does not obey the Stern-Volmer relation, but resembles the curve of the second degree, as Fig. 5 shows. The quenching constant was estimated to be $k<0.8$ from the tangent at $[Q]\rightarrow 0$.

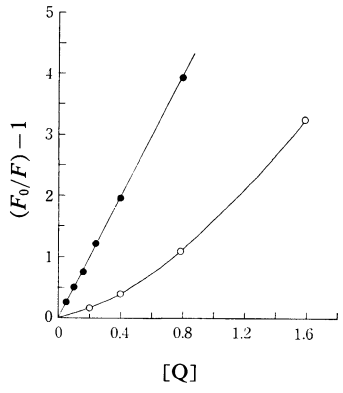



Fig. 5.

○ *N,N*-Dimethyl-2-naphthylamine ($1.00\times10^{-4}$ M/l.) - methyl benzoate in cyclohexane
● *N,N*-Dimethyl-2-naphthylamine ($1.00\times10^{-4}$ M/l.) - methyl benzoate in benzene
Q Methyl benzoate

*N, N-Dimethyl-2-naphthylamine in Benzene.* — This solution shows qualitative features similar to those of the cyclohexane solution, but the Stern-Volmer relation holds exactly in the range 0—2 M of [Q], as Fig. 5 shows. The value of the quenching constant is 5.

*2-Naphthyl Methyl Ether in Cyclohexane.*—With the addition of the quencher, the absorption spectra become a little diffused and suffer a slight red shift. The fluorescence spectra show a similar change, but the intensity is not practically affected, even by the addition of as much as 8 M of quencher (i. e., $k\approx 0$).

*2-Naphthylamine in Cyclohexane.* — With the addition of the quencher, the absorption spectra show a change characteristic of intermolecular hydrogen bonding, as Fig. 6 shows. The results can be analyzed by using the well known Eq. 1, where $K$ is the equilibrium constant, where $[Q_0]$ and $[A_0]$ denote the total concentrations of quencher and fluorescer respectively, where $d$ and $d_0$ are the optical densities at a certain wavelength in the presence and in the absence of the quencher respectively, and where $\varepsilon$ is the molar extinction coefficient of the hydrogen-bonded species at the same wavelength:

$$\frac{d-d_0}{[Q_0]}=\varepsilon K[A_0]-Kd \qquad (1)$$

The value of $K$ obtained is 0.7. Thus, the strength of the hydrogen bond is so weak that its effect on the absorption spectra may be

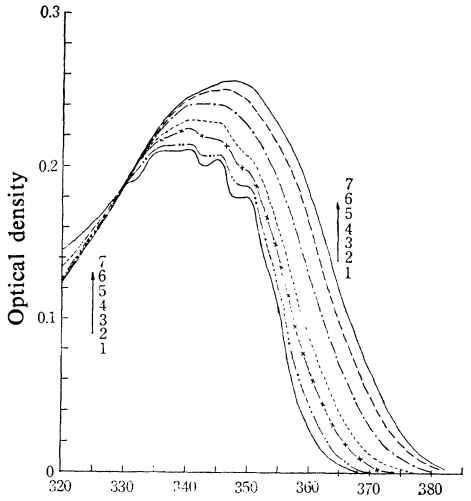



Fig. 6. Absorption spectra of 2-naphthylamine ($0.998\times10^{-4}$ M/l.) - methyl benzoate in cyclohexane. The concentrations of methyl benzoate are; 1) 0 M/l.; 2) $1.60\times10^{-1}$ M/l.; 3) $4.00\times10^{-1}$ M/l; 4) $8.01\times10^{-1}$ M/l.; 5) 2.40 M/l.; 6) 4.80 M/l.; 7) 8.00 M/l.

considered to be of the same degree as the solvent effect. In such situations, the change in the absorption spectra cannot be attributed only to hydrogen bonding, and hence, the above value may be an underestimation.

The fluorescence spectra do not change essentially with the addition of the quencher up to 0.2 M; beyond this value, they do show a slight red shift, but the intensity becomes so weak that one cannot say much about the spectral features. In any case, the hydrogen-bonded species is considered to be completely or almost completely non-fluorescent. The quenching constant obtained from the Stern-Volmer formula, which holds in this case up to $10^{-2}$ M (Fig. 7a), is 84. Beyond $1.6\times10^{-2}$ M, the $(F_0/F-1)/[Q]$ vs. [Q] plot becomes linear, as Fig. 7b shows. This indicates that the hydrogen-bonded species is non-fluorescent or negligibly fluorescent. It may be concluded that the quenching mechanism obeys the following scheme:

$$\begin{array}{ccc} & \mathrm{A^*} + \mathrm{Q} \underset{k_{-Q}}{\overset{k_Q}{\rightleftarrows}} \mathrm{A^*Q} & \\ k_f + k_d \downarrow\uparrow & & \uparrow\downarrow k_f' + k_d' \\ & \mathrm{A} + \mathrm{Q} \underset{}{\overset{K}{\rightleftarrows}} \mathrm{AQ} & \end{array} \qquad (2)$$

with $k_d' \gg k_{-Q}, k_f'$

From this scheme, the following relation can easily be derived:

$$\{(F_0/F)-1\}/[Q]=\left\{k+\left(\frac{\varepsilon'}{\varepsilon}\right)K\right\}+k\left(\frac{\varepsilon'}{\varepsilon}\right)K[Q];$$

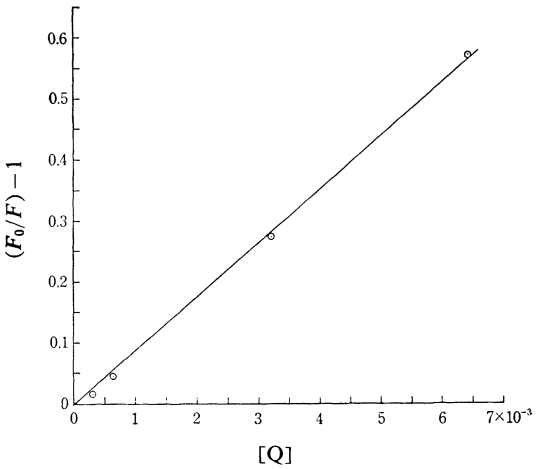



Fig. 7a. 2-Naphthylamine ($0.998\times10^{-4}$ M/l.) - methyl benzoate in cyclohexane.
Q: Methyl benzoate

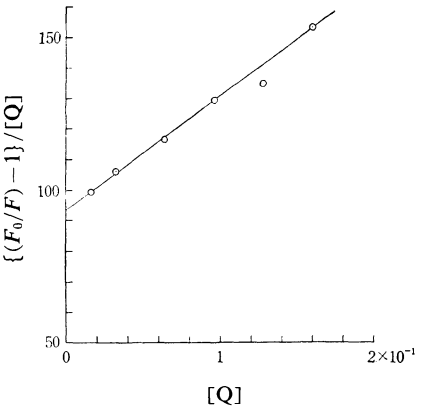



Fig. 7b. 2-Naphthylamine ($0.998\times10^{-4}$ M/l.) - methyl benzoate in cyclohexane.
Q: Methyl benzoate

$$k=\frac{k_Q}{k_f+k_d+k_Q}$$

where $\varepsilon$ and $\varepsilon'$ are, respectively, the molar extinction coefficient of the free species and of the hydrogen-bonded species at the exciting wavelength. It should be noted that actually the exciting wavelength was chosen at the position where $\varepsilon=\varepsilon'$. From the inclination and the intercept of the plot in Fig. 7b, one gets the quenching constant $k$ of 89, while the equilibrium constant $K$ for the hydrogen bonding (in the ground state) is 4. The former value agrees well with the quenching constant obtained from the inclination at $[Q]\rightarrow0$, and the latter value is consistent with the view that the hydrogen-bonding equilibrium constant obtained from the absorption spectra was underestimated.

*2-Naphthol in Cyclohexane.*—The absorption spectra show a typical change due to hydrogen bonding with isosbestic points at 315 and 330 mμ. From measurements of the optical densities at a fixed wavelength (334 mμ) of solutions of various compositions and by analyzing the data with Eq. 1, one gets the hydrogen-bonding equilibrium constant $K$ in the ground state of 11.5 (at 22.6°C).

The fluorescence spectra are scarcely affected at all by the addition of the quencher up to $5\times10^{-1}$ M, and at higher concentrations the fluorescence intensity is too weak for the spectra to be measured. By the application of the Stern-Volmer equation, which holds for quencher concentrations up to $8.0\times10^{-3}$ M, the quenching constant, $k$, was found to be 87 (Fig. 8a). At higher concentrations, the $\{(F_0/F)-1\}/[Q]$ vs. [Q] plot shows a linear relation, as may be seen in Fig. 8b. The values of $k$ and $K$ as determined from both the intercept and the slope were found to be 78 and 15 respectively. These data are quite consistent with one another, and there is no doubt that the hydrogen-bonded species is non-fluorescent or very poorly fluorescent and that the fluorescence phenomena obey Scheme 1.

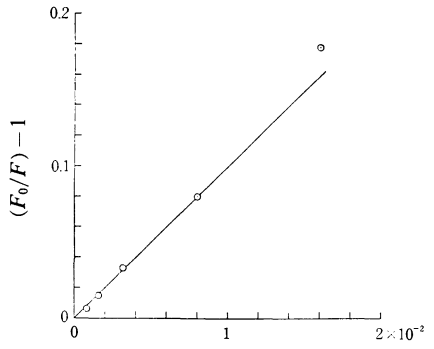



Fig. 8a. 2-Naphthol ($1.99\times10^{-4}$ M/l.) - methyl benzoate in cyclohexane.
Q: Methyl benzoate

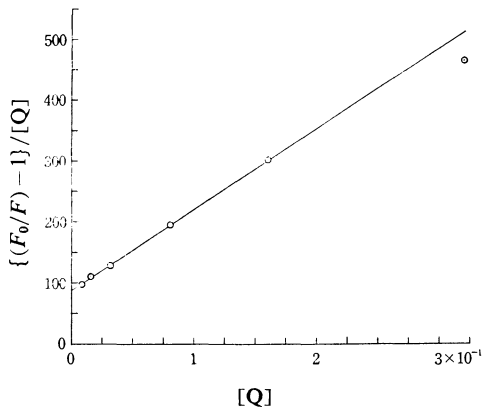



Fig. 8b. 2-Naphthol ($1.99\times10^{-4}$ M/l.) - methyl benzoate in cyclohexane.

**Quenching Action of Benzoic Acid.**—*i) N, N-Dimethyl-2-Naphthylamine in Cyclohexane: ii) N, N-Dimethyl-2-Naphthylamine in Benzene: iii) 2-Naphthyl Methyl Ether in Cyclohexane: iv) 2-Naphthyl Methyl Ether in Benzene.*—In none of these systems are either the absorption or the fluorescence spectra essentially affected by the addition of benzoic acid within the region of the concentrations used. An appreciable quenching of fluorescence occurs, and it is well reproduced by the Stern-Volmer relation. The quenching constants obtained for

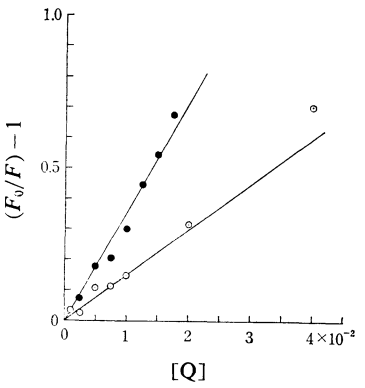



Fig. 9a.

○ 2-Naphthyl methyl ether ($2.01\times10^{-4}$ M/l.) - benzoic acid in cyclohexane
● *N,N*-Dimethyl-2-naphthylamine ($1.00\times10^{-4}$ M/l.) - benzoic acid in cyclohexane

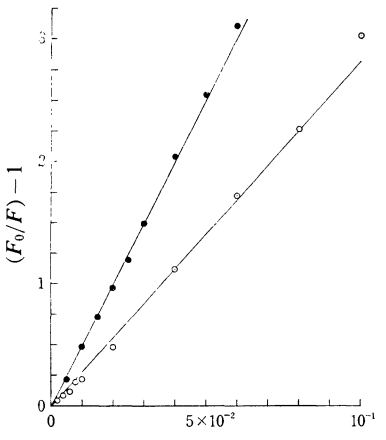



Fig. 9b.

○ 2-Naphthyl methyl ether ($2.00\times10^{-4}$ M/l.) - benzoic acid in benzene
● *N,N*-Dimethyl-2-naphthylamine ($1.00\times10^{-4}$ M/l.) - benzoic acid in benzene
Q: Benzoic acid

the systems i, ii, iii and iv are, respectively, 36, 50, 16 and 32 with reference to the monomer unit. Some examples are shown in Fig. 9.

*v) 2-Naphthylamine in Cyclohexane.* — The addition of the quencher causes a slight blue shift of the absorption spectra. The fluorescence are not essentially affected, and the quenching obeys the Stern-Volmer relation, from which one gets $k=52$.

*vi) 2-Naphthylamine in Benzene.*—The absorption spectra show a clearer blue shift than in cyclohexane. The fluorescence spectra are scarcely affected at all. The Stern-Volmer relation holds up to $5\times10^{-2}$ M of the quencher.

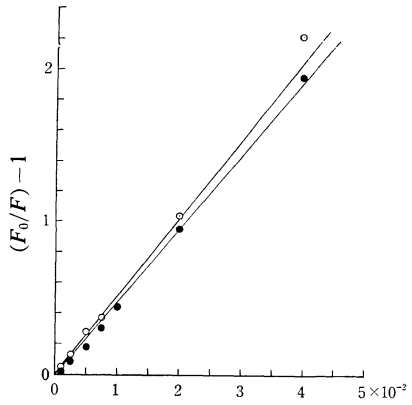



Fig. 10a.

○ 2-Naphthylamine ($0.998\times10^{-4}$ M/l.) - benzoic acid in cyclohexane
● 2-Naphthol ($1.99\times10^{-4}$ M/l.) - benzoic acid in cyclohexane

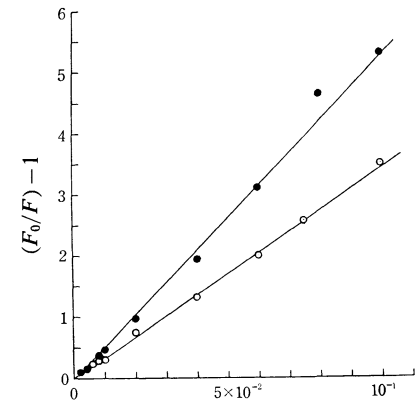



Fig. 10b.

● 2-Naphthylamine ($1.00\times10^{-4}$ M/l.) - benzoic acid in benzene
○ 2-Naphthol ($2.00\times10^{-4}$ M/l.) - benzoic acid in benzene
Q: Benzoic acid

In the higher concentration region the $\{(F_0/F)-1\}/[Q]$ vs. [Q] plot is linear and one gets $k=48$.

*vii) 2-Naphthol in Cyclohexane: viii) 2-Naphthol in Benzene.*—In these systems, neither the fluorescence nor the absorption spectra show any essential change. Quenching occurs and is well reproduced by the Stern-Volmer equation in both cases. The quenching constants $k$ are, respectively, 39 and 35. Some examples for v, vi, vii and viii are shown in Fig. 10.

## Discussion

A summary of the above results is given in Tables IA, IB and IC. The results in Table IA can be interpreted, for the most part, on the basis of hydrogen bonding. Thus, a remarkable difference in the magnitude of quenching between naphthylamine and naphthol, on the one hand, and their methyl derivatives, on the other, is without doubt due to the existence of intermolecular hydrogen bonding in the former case and the non-existence of it in the latter case.

The results conform quite well to Mataga's view-point, and one can say that such a compound as benzoic acid ester, which has a conjugated system of $\pi$-electrons extended to the side chain, can act as a quencher by forming a hydrogen bond with the fluorescer at the side-chain oxygen atom. The finding that a slight quenching occurs in the *N,N*-dimethyl-2-naphthylamine - benzoic acid ester system, but not in the 2-naphthyl methyl ether - benzoic acid ester system, may be interpreted by means of the charge transfer mechanism proposed in the previous paper, because naphthylamine derivatives are expected to act as stronger donors than naphthol derivatives.

Tables IB and IC contain the results for the systems in which benzoic acid is used as a quencher. They all show quenching phenomena to some extent. It is well-known that benzoic acid has a strong tendency to dimerize in non-polar solvents, and since the dimerization constant is so large,[6] practically all the molecules of benzoic acid are considered to exist as dimers under the present experimental conditions. Hence, there is no doubt that the quenching action of benzoic acid is phenomenologically to be attributed to its dimer. As for the detailed mechanism, however, no definite picture can be given at the present stage of investigation. Discussion of possible mechanisms will, however, be given below: the fluorescers being classified into two

6) For example, according to M. Ito (*J. Mol. Spectry*, 4, 144, (1960)) the value is of the order of $10^4$.

TABLE IA. QUENCHING ACTION OF METHYL BENZOATE (Q)

| Solvent | Fluorescer | Absorption spectra | | Fluorescence spectra | | |
|---|---|---|---|---|---|---|
| | | [Q] M/l. | Spectra | [Q] M/l. | Spectra | Quenching constant |
| Cy | $-NC(CH_3)_2$ | 0—8.01 | Red shift $\Delta\tilde{\nu}=630$ | 0—2 | Red shift | <0.8 |
| B | $-NC(CH_3)_2$ | 0—8.01 | Red shift $\Delta\tilde{\nu}=160$ | 0—2 | Red shift | 5 |
| Cy | $-NH_2$ | 0—8.01 | Red shift $\Delta\tilde{\nu}=680$ H.B.; $K>0.7$ | 0—8.01 | Ambiguous | 86 |
| Cy | $-OCH_3$ | 0—8.01 | Red shift $\Delta\tilde{\nu}=190$ | 0—8.01 | Red shift | ~0 |
| Cy | -OH | 0—8.01 | Red shift $\Delta\tilde{\nu}=390$ H.B.; $K=11.5$ (22.5°C) | 0—8.01 | Ambiguous | 87 |

Cy: Cyclohexane, B: Benzene, $-NC(CH_3)_2$: *N*,*N*-Dimethyl-2-naphthylamine, $-NH_2$: 2-Naphthylamine, -OCH: 2-Naphthyl methyl ether, -OH: 2-Naphthol, H.B.: Hydrogen bond formation, *K*: H.B. formation constant.

TABLE IB. QUENCHING ACTION OF BENZOIC ACID (Q)

| Solvent | Fluorescer | [Q] M/l. | Absorption spectra | Fluorescence spectra | Quenching constant |
|---|---|---|---|---|---|
| Cy | $-NC(CH_3)_2$ | $0—1.75\times10^{-2}$ | No change | No change | 36 |
| B | $-NC(CH_3)_2$ | $0—4\times10^{-1}$ | No change | No change | 50 |
| Cy | $-OCH_3$ | $0—4\times10^{-2}$ | No change | No change | 16 |
| B | $-OCH_3$ | $0—4\times10^{-1}$ | No change | No change | 22 |

Abbreviations are the same as before. Quenching constants are referred to a monomer unit.

TABLE IC. QUENCHING ACTION OF BENZOIC ACID (Q)

| Solvent | Fluorescer | [Q] M/l. | Absorption spectra | Fluorescence spectra | Quenching constant |
|---|---|---|---|---|---|
| Cy | $-NH_2$ | $0—4\times10^{-2}$ | Slight blue shift | No change | 52 |
| B | $-NH_2$ | $0—4\times10^{-1}$ | Blue shift H.B.; $K=11$ | No change | 48 |
| Cy | -OH | $0—4\times10^{-2}$ | No change | No change | 39 |
| B | -OH | $0—4\times10^{-1}$ | No change | No change | 35 |

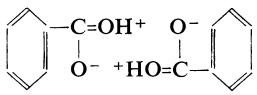
Abbreviations are the same as before. Quenching constants referred to a monomer unit.

groups: B; the fluorescers that cannot act as hydrogen donors; and C; those that can act as hydrogen donors.

It seems plausible to attribute the quenching phenomena observed in group B entirely to a charge transfer mechanism in which the fluorescer acts as an electron donor and the benzoic acid dimer acts as an acceptor.

The reason will be given below. Firstly, the possibility of hydrogen bonding in this group is limited to the case in which a fluorescer and a quencher act, respectively, as a hydrogen acceptor and a donor. However, since a rather strong intermolecular hydrogen bonding is present in the benzoic acid dimer, the dimer itself is expected to have little or no power to act as a hydrogen donor. In fact, no significant change is observed in the absorption spectra of systems made up of this group. Moreover, the formation constant of hydrogen bonding of this type is expected to be smaller in the excited state than in the ground state. In accord with this, there is, in fact, no change in the fluorescence spectra. Hence, one may safely rule out the possibility of hydrogen bonding between the excited fluorescer and the ground-state benzoic acid dimer. Thus, the mechanism of quenching must be of another type, and a charge-transfer mechanism, with charge transfer taking place between the fluorescer and benzoic acid dimer, seems to be the most plausible alternative. If charge transfer

were to take place between the benzoic acid monomer and the fluorescer, then the quenching constants for free acid and the $CH_3$-ester should be of the same order of magnitude, since the accepting powers of these two substances are not very different. The present result, however, shows that the quenching constant for free acid is far greater than that for the methyl ester. This may be interpreted as follows. According to the general view, the effect of hydrogen bonding on the $\pi$-electronic configuration is somewhat similar, though to a lesser extent, to that of acid dissociation, which in the present case is represented as follows*:



In other words, the delocalization of $\pi$-electrons in the carboxyl group is increased to some extent in the hydrogen-bonded system. Hence, the vacant level of this group is lowered, and a dimer is expected to be a better electron acceptor than a monomer. Furthermore, the following results can be easily comprehended on the basis of the above point of view: a) The quenching constant for *N*, *N*-dimethyl-2-naphthylamine is larger than that for 2-naphthyl methyl ether. This is because the dimethyl-amino group has a larger electron-releasing power than the methoxy group. b) The fluorescence of *N*, *N*-dimethyl-2-naphthylamine and 2-naphthyl methyl ether is quenched by benzoic acid much more than by methyl benzoate. The reason for this has already been stated above.

Turning to group C, the fluorescer is now free amine or free acid. In these cases there are two types of hydrogen bonding conceivable. One is type-a, in which the fluorescer is a donor and the quencher is an acceptor, and the other is type-b, in which their roles in the hydrogen bonding are reversed.

However, if one assumes that type-b hydrogen bonding is of no importance in the quenching phenomenon, as has been established already, then only type-a remains to be considered. However, in this connection it should be noted that the absorption spectra of naphthylamine display a slight blue shift after the addition of benzoic acid and that such a blue shift is usually related to type-b hydrogen bonding. This might imply that the formation constant of the hydrogen bond between naphthylamine and benzoic acid is large enough to compete with the dimerization of the acid. However, it is still open to question whether this is really true or whether the phenomenon is due to other unknown causes. On the other hand, the fluorescence spectra still display either a red shift or no change at all, which suggests the existence of type-a hydrogen bonding in the excited state. This is consistent with the expectation that this type of hydrogen bonding will become stronger in the excited state. Thus, one may safely assume that type-b does not take part in the quenching phenommena, whereas it is plausible that the hydrogen bond of type a participates in the quenching to some extent. However, there is a question about how the hydrogen bond is formed in this case; thus it is quite unknown whether such a hydrogen bond is formed between the fluorescer and benzoic dimer as it is, or whether the hydrogen bond formation is accompanied by a partial or a complete dissociation of the dimer molecules. The view that quenching really occurs through hydrogen bonding is supported by the fact that the quenching constant for naphthylamine and naphthol is somewhat larger than that for their methyl derivatives. However, on the basis of the discussion of group B, there is no doubt that the charge transfer mechanism also takes part in the quenching. The view that both the mechanisms are taking part in this group is supported by the following findings: a) The quenching constant of benzoic acid is larger for naphthylamine than for naphthol, while the quenching constant of methyl benzoate is of the same magnitude for naphthylamine and naphthol. This can be interpreted by taking account of the charge transfer mechanism in the former case, since the hydroxyl group is a stronger hydrogen donor than the amino group, while the amino group is a stronger electron-releasing group than the hydroxyl group. b) Benzoic acid quenches the fluorescence of naphthylamine more than it does that of dimethylnaphthylamine, and that of naphthol more than that of naphthyl methyl ether. This can be interpreted as being due to hydrogen bonding in the cases of the free amine and phenol. c) Methyl benzoate is a stronger quencher than benzoic acid toward naphthylamine and naphthol. This may be due to the fact that benzoic acid is a weaker hydrogen accepter than the ester, as has already been stated. It should be noted, however, that the quenching constants of benzoic acid in Tables 7B and 7C are given in terms of the monomer unit. If they are expressed in terms of the dimer unit, the values become twice as large and the statement in c) is not so decisive.

To summarize, only the charge transfer

* The contribution of this structure is inferred from the charge-transfer mechanism of the hydrogen bonding.[7]

7) S. Nagakura and M. Gouterman, *J. Chem. Phys.*, **26**, 881 (1957).

mechanism need be considered for group B, while the charge transfer mechanism and the hydrogen-bonding mechanism simultaneously take place in group C. It is apparent, however, that more confirming evidence is necessary before the charge transfer mechanism can be fully accepted.

## Summary

1) The quenching action of benzoic acid (dimer) (BA) and methyl benzoate (MB) on the fluorescence of 2-naphthol (I), 2-naphthylamine (II), 2-naphthyl methyl ether (III) and *N*, *N*-dimethyl-2-naphthylamine (IV) in benzene and in cyclohexane has been studied.

2) MB has little or no quenching effect on the fluorescence of III and IV, whereas it shows a significant quenching action on I and II. The latter is due to the intermolecular hydrogen bonding between the fluorescer and the quencher (the H.B. mechanism).

3) BA shows quite a large quenching action on III and IV. All the results can be interpreted on the basis of a charge transfer mechanism for quenching (the C.T. mechanism).

4) The quenching action of BA is larger on I than on III, and larger on II than on IV, except for benzene solutions of II and IV, in which case the magnitudes are equal within the range of experimental error. These results has been discussed on the basis of a simultaneous occurrence of the C.T. and H.B. mechanisms.

The authors wish to express their thanks to Professor Shunji Kato for his kind advice.

*Department of Chemistry*
*Faculty of Science*
*Tohoku University*
*Katahira-cho, Sendai*

# The NMR Spectra of Triethylsilane and Triethylhalogenosilane

By Osamu YAMAMOTO and Kikuko HAYAMIZU

(Received July 17, 1964)

The proton magentic resonance spectra of a number of metal ethyl compounds have been studied, and attempts have been made to correlate the internal chemical shift, $\delta$, between the methyl and the methylene protons in the ethyl group ($\nu_{CH_3}-\nu_{CH_2}$) with the electronegativity, $x$, of the metal attached to the ethyl group. Although the empirical relationship between $\delta$ and $x$ proposed by Dailey and Shoolery[1] approximately holds over a wide variety of metals, considerable deviations are observed when one of the ethyl group in the metal compounds is replaced by a halogen atom.[2,3] This is due to the magnetic anisotropy of the halogen atom or the C-X bond, where X denotes a halogen atom. Since the order of magnitude of the magnetic anisotropy effect of halogens in aliphatic compounds has been observed to increase with an increase in their atomic weight,[4] the deviation of the $\delta$ value from the simple Dailey and Shoolery relationship will increase in the order of fluorine, chlorine, bromine and iodine. Hence, when a more electronegative halogen atom substitutes on the metal, the $\delta$ value decreases in a manner contrary to that expected from the simple inductive mechanism. This trend has been observed in diethylaluminum monohalides.[3]

In connection with this, the NMR spectra of triethylsilane and triethylhalogenosilane were studied in the present work, and accurate $\delta$ and $J$ (coupling constant) values were given through a rigorous analysis of the spectra. Althought triethylchloro- and triethylbromosilane show the $A_3B_2$ spectra for their ethyl groups, which can be analyzed in the manner described in the previous paper,[3] triethylsilane and triethylfluorosilane give the $A_3B_2X$ spectra. The analysis of the $A_3B_2X$ system has been already made by Narasimhan and Rogers[5] using the model of the composite spin particles which have total spin angular momenta of 3/2, 1, and 1/2 respectively. In the present work this method is also followed, though the spin-spin coupling between A and X is also taken

1) B. P. Dailey and J. N. Shoolery, *J. Am. Chem. Soc.*, 77, 3977 (1955).
2) P. T. Narasimhan and M. T. Rogers, ibid., 82, 5983 (1960).
3) O. Yamamoto, This Bulletin, 36, 1463 (1963).
4) L. M. Jackman, "Applications of Nuclear Magnetic Resonance Spectroscopy in Organic Chemistry," Pergamon Press, New York (1959), p. 53.
5) P. T. Narasimhan and M. T. Rogers, *J. Chem. Phys.*, 33, 727 (1960).

into account. (This corresponds to the coupling between the methyl protons and fluorine or hydrogen directly attached to silicon.) While such a long-range coupling can be, practically speaking, extremely small in most organic compounds, it may not be negligible when such an atom as fluorine is present in the coupling system.[6]

Hereafter, in the notations $A_3B_2$ and $A_3B_2X$, A and B refer to methyl and methylene protons in an ethyl group respectively, and X to hydrogen or fluorine directly attached to silicon. Thus, for example, $J_{AB}$ means the coupling constant between the methyl and the methylene protons in the ethyl group.

## Experimental

Triethylsilane was prepared from trichlorosilane and ethylmagnesium bromide ;[7] triethylfluorosilane and triethylchlorosilane were prepared by adding the corresponding ammonium halide to hexaethyldisiloxane in concentrated sulfuric acid[8] triethylbromosilane was prepared by dropping liquid bromine into phenyltriethylsilane.[9] The purity of the samples was examined by means of their infrared absorption spectra and by gas chromatography.

The NMR spectra of the compounds were obtained by means of a Varian Associates DP-60 spectrometer at 60, 40, and 15 Mc./sec., together with a Varian HR-100 spectrometer at 100 Mc./sec. for the pure liquid samples degassed in a high-vacuum apparatus.

## Results and Discussion

The spectra for all of the compounds obtained at 60 Mc./sec. are illustrated in Fig. 1—4, together with the calculated spectral lines (shown at the bottoms of the figures). In addition, the spectra at 40 and at 100 Mc./sec. were also obtained for triethylsilane and triethylfluorosilane, which show the more complex spectra due to the $A_3B_2X$ spin system than do the other two, with the $A_3B_2$ pattern.

The analyses of the spectra as an $A_3B_2$ or $A_3B_2X$ system were accomplished with a NEAC-2101 digital computor. The procedure was the same for the $A_3B_2$ system as that described in the previous paper.[3] For the analysis of the $A_3B_2X$ system, the calculations were repeated until a good agreement in the coupling constants and the chemical shift values was obtained among 40, 60, and 100 Mc./sec. spectra by using the least-squares method.

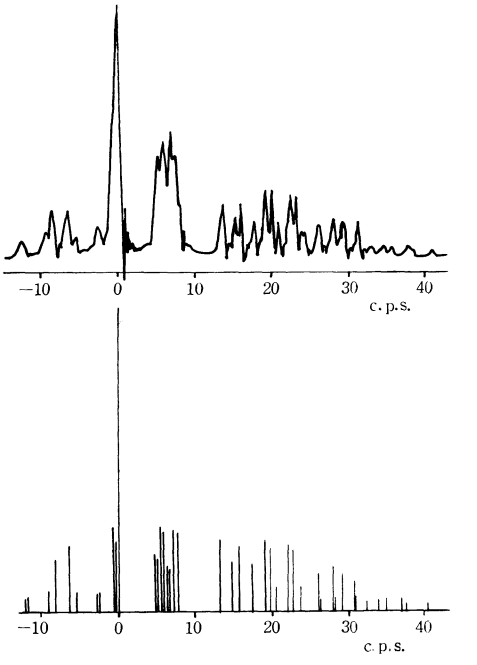



Fig. 1. The observed and the calculated spectra of $SiH(C_2H_5)_3$ at 60 Mc./sec.

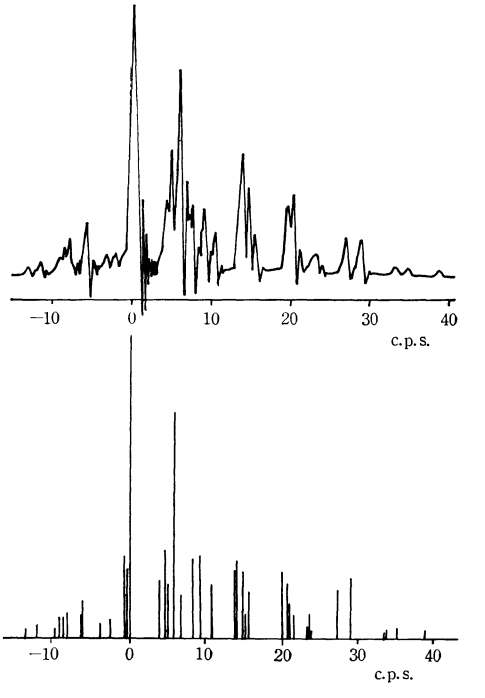



Fig. 2. The observed and the calculated spectra of $SiF(C_2H_5)_3$ at 60 Mc./sec.

The coupling constants and chemical shift values thus obtained are shown in Table I. The numerical details of the calculations for triethylsilane and triethylfluorosilane at 60

6) D. D. Elleman, L. C. Brown, and D. Williams, *J. Mol. Spectry.*, **7**, 322 (1961).
7) F. C. Whitmore, E. W. Pietrusza and L. H. Sommer, *J. Am. Chem. Soc.*, **69**, 2108 (1947).
8) P. A. Di Giorgio, W. A. Strong, L. H. Sommer and F. C. Whitmore, ibid., **68**, 1380 (1946).
9) B. O. Pray, L. H. Sommer, G. M. Goldberg, G. T. Kerr, P. A. Di Giorgio and F. W. Whitmore, ibid., **70**, 433 (1948).

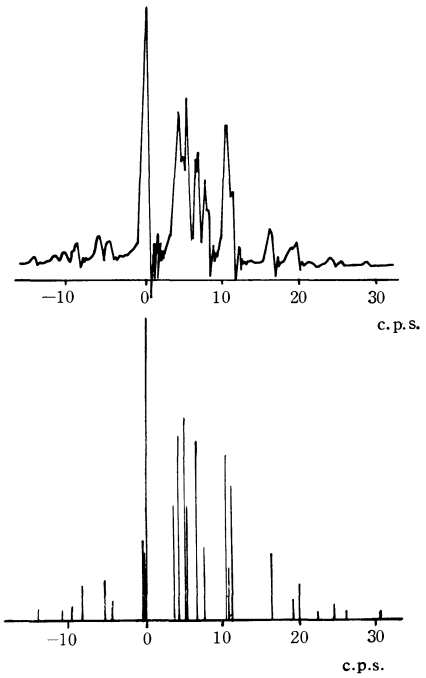



Fig. 3. The observed and the calculated spectra of $SiCl(C_2H_5)_3$ at 60 Mc./sec.

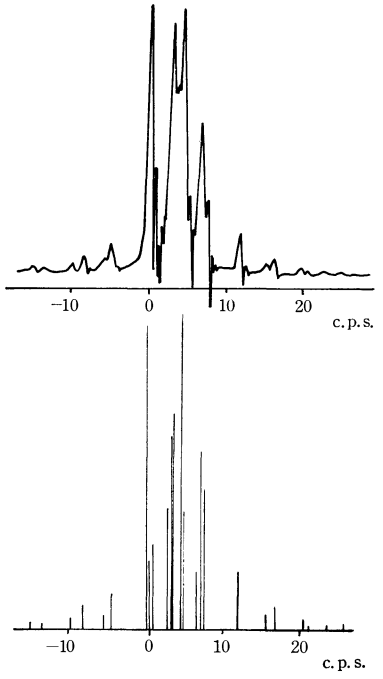



Fig. 4. The observed and the calculated spectra of $SiBr(C_2H_5)_3$ at 60 Mc./sec.

Mc./sec. are given in Tables II and III respectively. Similar good agreements between the observed and the calculated spectra were also obtained at other resonant frequencies.

The coupling constants, $J_{BX}$, can also be obtained from the X part of the $A_3B_2X$ spectra. As is shown in Table I, the observed values are in agreement with the values obtained from the $A_3B_2$ part of the spectra within the range of experimental error.

**Coupling Constants in Triethylfluorosilane.**— In triethylsilane the long-range coupling constant, $J_{AX}$, is practically zero, as is usually observed for two protons which are more than three bonds removed from each other in aliphatic compounds. In triethylfluorosilane, however, $J_{AX}$ definitely has a non-zero value, as may be seen from Table I. In fact, the calculations taking no account of $J_{AX}$ were tried at first, but in this case no overall agreement of the calculated coupling constants and chemical shift values was obtained among the spectra different in resonant frequencies.

The long-range coupling between protons and fluorines which are separated through four bonds from each other has been reported for fluorocarbon derivatives.[6] The order of magnitude of such coupling constants is from about 0.4 to 1.5 c.p.s., which is comparable with the value obtained, $J_{AX}$, for triethylfluorosilane. Further evidence for the long-range coupling is obtained from the 15 Mc./sec. spectrum of this compound. The most intense central line in the $A_3B_2$ spectrum splits into two lines of equal

Table I. Chemical shifts and coupling constants of triethylsilane and triethylhalogenosilane

| | $SiH(C_2H_5)_3$ | $SiF(C_2H_5)_3$ | $SiCl(C_2H_5)_3$ | $SiBr(C_2H_5)_3$ |
|---|---|---|---|---|
| $\delta_{AB}$* (p. p. m.) | 0.40 | 0.32 | 0.22 | 0.16 |
| $J_{AB}$ (c. p. s.) | $7.9_2$ | $8.0_5$ | $7.9_8$ | $7.7_7$ |
| $J_{BX}$ (c. p. s.) | $3.0_6$ | $5.8_6$ | | |
| $J_{AX}$ (c. p. s.) | $0.0_7$ | $0.3_9$ | | |
| Observed values from the X part of the spectrum | | | | |
| $\delta_{AX}$ (p. p. m.) | −2.70* | 116.8** | | |
| $J_{BX}$ (c. p. s.) | 3.0 | 5.7 | | |

* Referred to the methyl signal. Thus these values have opposite signs to the internal chemical shifts $\delta$.

** $^{19}F$ resonance from $CFCl_3$.

TABLE II. OBSERVED AND CALCULATED SPECTRA OF TRIETHYLSILANE AT 60 Mc./sec.

| Transition No. | Frequency c. p. s. Calcd. | Obs. | Relative intensity Calcd. | Obs. |
|---|---|---|---|---|
| $CH_3$-transition | | | | |
| 1 | −12.1 | −11.9 | 1.1 | 2.2 |
| 2 | −11.6 | | 1.2 | |
| 3 | − 9.1 | − 9.0 | 1.0 | 4.9 |
| 4 | − 8.9 | | 1.1 | |
| 5 | − 8.2 | − 8.1 | 2.0 | |
| 6 | − 8.2 | | 2.2 | |
| 7 | − 6.4 | − 6.3 | 1.3 | 4.5 |
| 8 | − 6.4 | | 2.0 | |
| 9 | − 6.3 | | 1.9 | |
| 10 | − 5.3 | − 5.4 | 1.6 | |
| 11 | − 2.7 | − 2.4 | 1.4 | 2.7 |
| 12 | − 2.4 | | 1.5 | |
| 13 | − 0.8 | 0.0 | 3.4 | 36.2 |
| 14 | − 0.7 | | 3.3 | |
| 15 | − 0.4 | | 2.8 | |
| 16 | − 0.3 | | 2.8 | |
| 17 | − 0.0 | | 12.0 | |
| 18 | 0.0 | | 12.0 | |
| 19 | 4.7 | 5.1 | 4.4 | 35.8 |
| 20 | 5.1 | | 4.2 | |
| 21 | 5.5 | 5.9 | 6.6 | |
| 22 | 5.9 | | 6.3 | |
| 23 | 6.3 | 6.8 | 3.6 | |
| 24 | 6.6 | | 3.4 | |
| 25 | 6.9 | | 6.6 | |
| 26 | 7.3 | 7.4 | 6.1 | |
| $CH_2$-transition | | | | |
| 1 | 13.0 | 12.9 | 5.7 | 4.7 |
| 2 | 14.8 | 14.6 | 4.0 | 7.7 |
| 3 | 15.6 | 15.6 | 5.1 | |
| 4 | 17.4 | 17.5 | 3.7 | 3.6 |
| 5 | 18.9 | 18.9 | 5.7 | 12.5 |
| 6 | 19.7 | 19.6 | 5.1 | |
| 7 | 20.5 | 20.4 | 2.0 | |
| 8 | 21.9 | 21.8 | 5.3 | 12.4 |
| 9 | 22.6 | 22.7 | 4.9 | |
| 10 | 23.6 | 23.6 | 2.0 | |
| 11 | 26.0 | 26.0 | 3.0 | 4.4 |
| 12 | 26.3 | 26.8 | 1.0 | |
| 13 | 28.0 | 28.0 | 1.2 | 4.8 |
| 14 | 28.0 | | 2.4 | |
| 15 | 28.2 | | 1.2 | |
| 16 | 29.1 | 29.1 | 3.0 | 3.2 |
| 17 | 30.9 | 30.8 | 2.5 | 3.6 |
| 18 | 31.0 | | 1.2 | |
| 19 | 32.5 | 32.5 | 0.8 | 1.2 |
| 20 | 33.9 | 33.7 | 0.9 | 1.0 |
| 21 | 34.9 | 34.8 | 0.9 | 0.9 |
| 22 | 37.0 | 37.1 | 0.9 | 2.2 |
| 23 | 37.5 | | 0.7 | |
| 24 | 40.3 | 40.2 | 0.7 | 0.8 |

TABLE III. OBSERVED AND CALCULATED SPECTRA OF TRIETHYLFLUOROSILANE AT 60 Mc./sec.

| Transition No. | Frequency c. p. s. Calcd. | Obs. | Relative intensity Calcd. | Obs. |
|---|---|---|---|---|
| $CH_3$-transition | | | | |
| 1 | −13.4 | −13.1 | 0.8 | 0.5 |
| 2 | −12.0 | −11.7 | 1.1 | 1.1 |
| 3 | − 9.6 | − 9.5 | 0.8 | 5.2 |
| 4 | − 9.0 | | 1.0 | |
| 5 | − 8.9 | − 8.8 | 0.8 | |
| 6 | − 8.5 | | 1.7 | |
| 7 | 8.1 | − 8.0 | 2.1 | |
| 8 | − 6.2 | − 5.9 | 1.4 | 4.8 |
| 9 | − 6.1 | | 1.7 | |
| 10 | − 6.1 | | 1.9 | |
| 11 | − 3.7 | − 3.3 | 1.2 | 1.8 |
| 12 | − 2.5 | − 2.7 | 1.4 | 2.0 |
| 13 | − 0.5 | 0.0 | 3.3 | 36.1 |
| 14 | − 0.4 | | 3.2 | |
| 15 | − 0.3 | | 2.7 | |
| 16 | − 0.2 | | 12.0 | |
| 17 | − 0.1 | | 2.8 | |
| 18 | 0.2 | | 12.0 | |
| 19 | 4.0 | 4.3 | 4.6 | 45.0 |
| 20 | 4.7 | 5.2 | 7.1 | |
| 21 | 5.1 | | 4.3 | |
| 22 | 5.8 | 6.3 | 4.1 | |
| 23 | 5.9 | | 6.5 | |
| 24 | 5.9 | | 7.5 | |
| 25 | 6.7 | 7.0 | 3.5 | |
| 26 | 7.3 | 7.6 | 6.5 | |
| $CH_2$-transition | | | | |
| 1 | 9.2 | 9.2 | 6.6 | 7.0 |
| 2 | 10.7 | 10.7 | 4.3 | 4.8 |
| 3 | 13.8 | 14.0 | 5.4 | 20.0 |
| 4 | 14.1 | | 6.2 | |
| 5 | 15.0 | 14.9 | 5.3 | |
| 6 | 15.2 | | 2.1 | |
| 7 | 15.5 | 15.7 | 3.8 | |
| 8 | 19.9 | 20.1 | 5.4 | 12.9 |
| 9 | 20.5 | 20.9 | 4.9 | |
| 10 | 21.0 | | 2.9 | |
| 11 | 21.4 | 21.6 | 1.9 | |
| 12 | 23.3 | 23.5 | 1.1 | 3.6 |
| 13 | 23.6 | | 2.0 | |
| 14 | 24.0 | | 0.6 | |
| 15 | 27.0 | 27.4 | 2.9 | 3.2 |
| 16 | 27.1 | | 1.0 | |
| 17 | 28.9 | 29.1 | 1.1 | 4.0 |
| 18 | 29.0 | | 2.3 | |
| 19 | 29.1 | | 0.8 | |
| 20 | 29.1 | | 0.6 | |
| 21 | 33.4 | 33.6 | 0.5 | 1.2 |
| 22 | 33.5 | | 0.7 | |
| 23 | 35.0 | 35.2 | 0.8 | 0.8 |
| 24 | 38.7 | 38.9 | 0.6 | 0.7 |

intensity in the $A_3B_2X$ system due to the coupling between the A and X spins, the separation between the two lines being just equal to $J_{AX}$ (see Appendix). However, if $J_{AX}$ is too small to be resolved under the conditions of a given magnetic field, the splitting is not observed. This is the case for the resonant frequency of 40 Mc./sec. or higher. The inhomogeneity, $\Delta H$, of the field may be reduced by decreasing the static field, $H_0$, in such a manner that $\Delta H/H_0 \sim$constant.[10] Thus, at the low static field, it may be possible to ovserve the splitting of two lines which can not be resolved in the higher field. As Fig. 5 shows, the two split lines are clearly realized at 15 Mc./sec., the separation of them being

10) A. Abragam, "The Principles of Nuclear Magnetism," Oxford University Press, London (1961), p. 64.

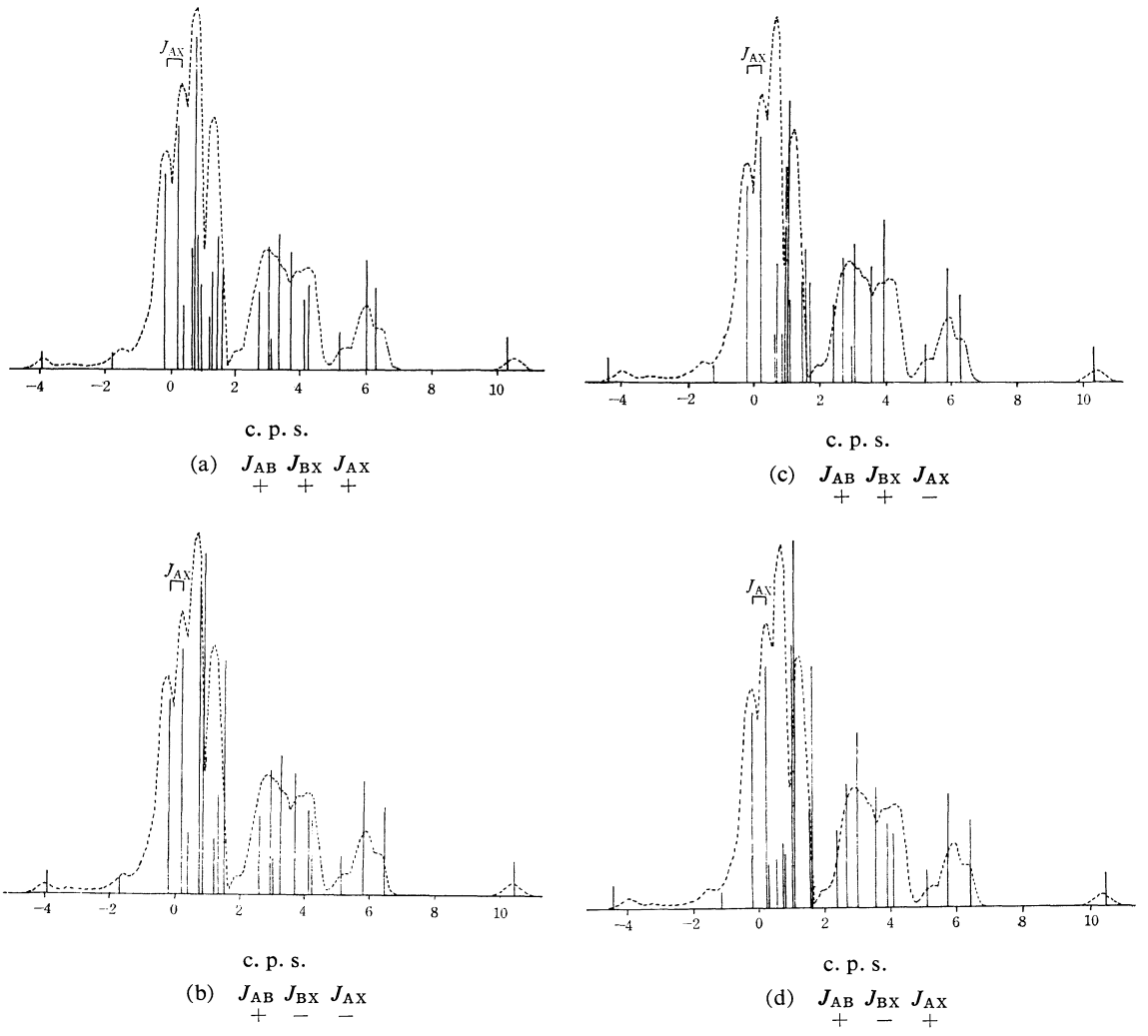



Fig. 5. The calculated spectra of $SiF(C_2H_5)_3$ at 15.085 Mc./sec. for possible four combinations of the signs of $J_{AX}$ and $J_{BX}$ with positive $J_{AB}$. The observed spectrum (dotted lines) is superposed on each calculated spectrum for comparison.

just the coupling constant, $J_{AX}$, calculated from the spectra at the higher resonant frequencies. Thus, it seems reasonable to assume the existence of the long-range coupling between the methyl protons and fluorine in this compound.

In the $A_3B_2X$ system the relative sign determination of the coupling constants is possible in principle.[5] Whether it is really possible or not, however, depends upon the relative order of magnitude between the $J$'s and $\delta$'s. Tentative calculations show that at 15 Mc./sec. the spectrum is sufficiently altered in its appearance by changing the signs of the couping constants, thus permitting an unambiguous determination of the relative signs for triethylfluorosilane, though not for triethylsilane. It can be assumed that $J_{AX}$ is positive on the basis of the theoretical considerations by Karplus[11] and by McConnell.[12] Thus, it is sufficient to consider the possible four cases with positive $J_{AB}$ values. In Fig. 5 the calculated spectra for triethylfluorosilane at 15 Mc./sec. are shown for possible combinations of the signs for $J_{BX}$ and $J_{AX}$ using the $J$'s and the $\delta_{AB}$ obtained from the spectra of other resonant frequencies. A close inspection of Figs. 5a—5d suggests that the best fit is obtained when all the signs are alike, i.e., when $J_{AB}$, $J_{BX}$, and $J_{AX}$ are all positive. To make the conclusion more unambiguous, NMR measurements on other similar compounds involving the double resonance experiment will be required. We are now planning to study further along these lines.

11) M. Karplus, *J. Chem. Phys.*, **30**, 11 (1959).
12) H. M. McConnell, ibid., **24**, 460 (1956).

**The Internal Chemical Shift, $\delta$.**—The additivity for the $\delta$ value in the $Si(C_2H_5)_4-SiCl_3(C_2H_5)$ series was pointed out by Narasimhan and Rogers.[2] They derived the empirical equation:

$\delta$ for $SiCl_n(C_2H_5)_{4-n} = -0.420+0.205\,n$ (in p.p.m.)

from the observed values for $Si(C_2H_5)_4$ and its di- and trichloro-derivatives. It is interesting, as they pointed out, to compare the value predicted for triethylchlorosilane from the above equation with the observed value. The predicted value is $-0.215$ p.p.m., while the observed value obtained in this work is $-0.22$ p.p.m.; thus, a good agreement is obtained.

The effect of the number of the substituents on the $\delta$ value in this case can be interpreted on the basis of the inductive mechanism, as has been mentioned by Narasimhan and Rogers.[2] The increase in the number of the substituents causes the metal atom to withdraw more electrons and results in less shielding on the methylene protons, which in turn leads to a larger $\delta$ value (including the sign) than that of the compound with fewer substituents.

The result can also be interpreted, however, in terms of the magnetic anisotropy effect. It was pointed out by Spiesecke and Schneider[13] that the anisotropy contributions to the methyl and the methylene protons in the ethyl halides, $CH_3CH_2X$, are in the same direction and of comparable magnitude; thus, on taking the difference (the $\delta$ value), the effects are largely cancelled. In the present case, the X group is a metal, and in the halides an additional substituent, Y (i.e., a halogen atom), is further attached to the X group. In this instance, the situation is rather different. The $\alpha$ and the $\beta$ protons from the metal are now at the $\beta$- and the $\gamma$-positions respectively in relation to the Y substituent. The $\gamma$ protons will be little affected by the secondary magnetic field generated by the diamagnetic circulation of electrons at the X-Y bond; therefore, they will suffer no appreciable contribution to shift to a lower field by the Y substituent.[14] There is no proton at the $\alpha$-position relative to the Y substituent. Thus, only the $\beta$ protons are subjected to a lower field shift, the extent increasing as the number of substituents increases. Thus, the above linear relation only states that the extent of the decrease in the $\delta$ value is proportional to the number of the Y substituent. The origin of the decrease may be either the inductive or the anisotropy effect, or it may perhaps be both.

On the contrary, the present study clearly indicates that the effect of the nature of the substituents attached to the metal on the $\delta$ value results from the magnetic anisotropy of the Y substituent. As may be seen in Table I, there is also a tendency for the $\delta$ values of the compounds to increase in the descending order of the electronegativity of the Y substituents in the triethylhalogenosilane, as in the case of diethylaluminum monohalides.[3] On the basis of the inductive mechanism, it would be expected that the $\delta$ values would become larger when a halogen atom with a larger electronegativity is substituted into the metal, and the order for the $\delta$ value would be reverse to the above results. Since the magnitude of the magnetic anisotropy effect of halogens increases with an increase in their atomic weight, as has been mentioned earlier, the tendency of the $\delta$ value can be elucidated on the basis of the anisotropy effect stated above in the triethylhalogenosilanes also.

The authors express their hearty thanks to Mr. Atsuo Tokutake for his assistance in the experimental work.

*Government Chemical Industrial Research Institute, Tokyo*
*Shibuya-ku, Tokyo*

## Appendix

The transitions which give the two central lines in question are shown in Table IV, in which such abbreviations for the spin functions as $A_{I_A,m_A}\cdot B_{I_B,m_B}X_{I_X,m_X}$, are used where $I_A$ and $m_A$ are the total spin and $z$-component of the angular momentum for the A nuclei respectively. The spin product functions of the states corresponding to these transitions are characterized by containing a $B_{0,0}$ term. In the $A_3B_2X$ system, $\delta_{AX}$ $(=\nu_X-\nu_A)$ is large compared with $J_{AX}$, so we have for transition 1:

$$\frac{1}{2}\delta_{AX}+J_{AX}-\frac{1}{2}\sqrt{(\delta_{AX}+J_{AX})^2+3J_{AX}^2}$$
$$=\frac{1}{2}(\nu_X-\nu_A)+J_{AX}-\frac{1}{2}(\nu_X-\nu_A+J_{AX})$$
$$\times\left\{1+\frac{3}{2}\left(\frac{J_{AX}}{\nu_X-\nu_A+J_{AX}}\right)^2+\cdots\cdots\right\}$$
$$=\nu_A+\frac{1}{2}J_{AX}$$

In a similar way, all of the first four transitions in Table IV give the frequency of $\nu_A+\frac{1}{2}J_{AX}$, and the other four $\nu_{AX}-\frac{1}{2}J_{AX}$. Thus, the transitions between these energy levels give two intense lines separated by $J_{AX}$ from each other, the center being at $\nu_A$. The relative intensities of the two lines can be shown to be equal. In the $A_3B_2$ system, however, the corresponding states, such as $A_{3/2,\,3/2}B_{0,0}$,

13) H. Spiesecke and W. G. Schneider, ibid., 35, 722 (1961).
14) J. R. Cavanaugh and B. P. Dailey, ibid., 34, 1099 (1961).

are themselves a stationary state, and all of the transitions between them give a single line at $\nu_A$, which forms the most intense central line in the $A_3B_2$ pattern.

TABLE IV. A-TRANSITION CONCERNED WITH $B_{0,0}$ SPIN STATES

| | Transition in the limit $J_{AX} \to 0$ | Frequency |
|---|---|---|
| 1 | $A_{3/2,1/2}B_{0,0}X_{1/2,1/2} \rightarrow A_{3/2,3/2}B_{0,0}X_{1/2,1/2}$ | $\frac{1}{2}\delta_{AX} + J_{AX} - \frac{1}{2}\sqrt{(\delta_{AX} + J_{AX})^2 + 3J_{AX}^2}$ |
| 2 | $A_{3/2,-1/2}B_{0,0}X_{1/2,1/2} \rightarrow A_{3/2,1/2}B_{0,0}X_{1/2,1/2}$ | $\frac{1}{2}\left(\sqrt{(\delta_{AX} + J_{AX})^2 + 3J_{AX}^2} - \sqrt{\delta_{AX} + 4J_{AX}^2}\right)$ |
| 3 | $A_{3/2,-3/2}B_{0,0}X_{1/2,1/2} \rightarrow A_{3/2,-1/2}B_{0,0}X_{1/2,1/2}$ | $\frac{1}{2}\left(\sqrt{\delta_{AX}^2 + 4J_{AX}^2} - \sqrt{(\delta_{AX} - J_{AX})^2 + 3J_{AX}^2}\right)$ |
| 4 | $A_{1/2,-1/2}B_{0,0}X_{1/2,1/2} \rightarrow A_{1/2,1/2}B_{0,0}X_{1/2,1/2}$ | $\frac{1}{2}\left(\delta_{AX} + J_{AX} - \sqrt{\delta_{AX}^2 - J_{AX}^2}\right)$ |
| 5 | $A_{3/2,1/2}B_{0,0}X_{1/2,-1/2} \rightarrow A_{3/2,3/2}B_{0,0}X_{1/2,-1/2}$ | $\frac{1}{2}\left(-\sqrt{(\delta_{AX} + J_{AX})^2 + 3J_{AX}^2} + \sqrt{\delta_{AX}^2 + 4J_{AX}^2}\right)$ |
| 6 | $A_{3/2,-1/2}B_{0,0}X_{1/2,-1/2} \rightarrow A_{3/2,1/2}B_{0,0}X_{1/2,-1/2}$ | $\frac{1}{2}\left(-\sqrt{\delta_{AX}^2 + 4J_{AX}^2} + \sqrt{(\delta_{AX} - J_{AX})^2 + 3J_{AX}^2}\right)$ |
| 7 | $A_{3/2,-3/2}B_{0,0}X_{1/2,-1/2} \rightarrow A_{3/2,-1/2}B_{0,0}X_{1/2,-1/2}$ | $\frac{1}{2}\delta_{AX} - J_{AX} - \frac{1}{2}\sqrt{(\delta_{AX} - J_{AX})^2 + 3J_{AX}^2}$ |
| 8 | $A_{1/2,-1/2}B_{0,0}X_{1/2,-1/2} \rightarrow A_{1/2,1/2}B_{0,0}X_{1/2,-1/2}$ | $\frac{1}{2}\left(\delta_{AX} - J_{AX} - \sqrt{\delta_{AX}^2 - J_{AX}^2}\right)$ |

# Sulfoxides. V.[1] The Ionization of Sulfoxides in Sulfuric Acid[2]

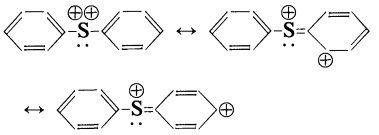
By Shigeru Oae, Teijiro Kitao and Yoshinori Kitaoka

(Received July 18, 1964)

Some years ago, Szmant and Brost[3] investigated the cryoscopic behaviors of several organic sulfur compounds in sulfuric acid and presented, among other things, the interesting observation that diphenyl sulfoxide gave a large and reproducible freezing point depression with an *i*-factor of 4.7 with the formation of a brilliant green solution. They theorized that diphenyl sulfoxide ionizes in 100% sulfuric acid according to the following Eq. 1:

$$(C_6H_5)_2\text{-}SO + 3H_2SO_4 \rightleftarrows \underset{\text{(I)}}{(C_6H_5)_2\overset{\oplus\oplus}{S}:} + H_3\overset{\oplus}{O} + 3HSO_4^{\ominus} \quad (i=5) \tag{1}$$

The green color of the double positive species, "diphenyl sulfidonium ion," I, was assumed to result from the contribution of such resonance structures as II. They also indicated that this species, I, in the presence of water



(II)

restored the original sulfoxide according to Eq. 2:

$$(C_6H_5)_2\text{-}\overset{\oplus\oplus}{S}: + 3H_2O \rightarrow (C_6H_5)_2\text{-}SO + 2H_3\overset{\oplus}{O} \tag{2}$$

1) a) Paper I: S. Oae, T. Kitao and Y. Kitaoka, *Chem. & Ind.*, **1961** 291; b) II: S. Oae and S. Kawamura, This Bulletin, **36**, 163 (1963); c) III: S. Oae, T. Kitao, S. Kawamura and Y. Kitaoka, *Tetrahedron*, **19**, 817 (1963); b) IV: S. Oae, T. Kitao and S. Kawamura, ibid., **19**, 1783 (1963).

2) a) Preliminary Communication; see Ref 1a; d) The early part of this work was performed at the Department of Chemistry, Brookhaven National Laboratory, under the auspices of the U. S. Atomic Energy Commission, while S. O. was a visiting chemist there. We wish to thank Dr. David R. Christman for some of the $^{18}O$ analyses. Appreciation is also expressed to Mr. Motoyoshi Hatada for his generous collaborations in the mass-spectroscopic analyses.

3) H. H. Szmant and G. A. Brost, *J. Am. Chem. Soc.*, **73**, 4175 (1951).

This conclusion was later challenged,[4] and it was claimed that the *i*-factor of this green solution was 2.0, that this gradually changed to about 3 when the solution was left standing and that the original sulfoxide could not be recovered after some time when its freezing point had become approximately constant.[5]

A convenient way to test the rather attractive Szmant & Brost's hypothesis of the presence of the doubly-charged "sulfidonium ion" I in sulfuric acid is to determine the $^{18}O$ incorporation into the resulting sulfoxide recovered by quenching the green solution by $^{18}O$-enriched water. When diphenyl sulfoxide was dissolved in 97% sulfuric acid and this brilliant green solution was diluted with a large excess of $^{18}O$-enriched water (0.6 atom % $^{18}O$), the original sulfoxide was recovered in almost a quantitative yield. However, the sulfoxide recovered was found to be incorporated with no excess of $^{18}O$, contrary to what one would expect from the conclusion by the previous workers.[3]

| | |
|---|---|
| $^{18}O$ for Ph-SO-Ph | 0.208% |
| $^{18}O$ for tank $CO_2$ | 0.211% |

Since this $^{18}O$ tracer experiment clearly excludes the hypothesis of the presence of the "diphenyl sulfidonium ion" in sulfuric acid, the other alternative would be that the ionization of the sulfoxide in sulfuric acid takes place according to Eq. 3, as was suggested by Gillespie *et al.*[4] Accordingly, the cryoscopic determinations were made on diphenyl sulfoxide and

$$(C_6H_5)_2S \rightarrow O + H_2SO_4 \rightleftarrows (C_6H_5)_2\overset{\oplus}{S}\text{-}OH + \overset{\ominus}{HSO_4} \quad (i=2) \qquad (3)$$

other related sulfoxides with about 99% sulfuric acid. Although some of the sulfoxides, e. g., phenyl benzyl sulfoxide and phenyl methyl sulfoxide, gradually decomposed in sulfuric acid, others were recovered in satisfactory yields when treated within an hour. Even the unstable sulfoxides could be recovered in satisfactory yields when the solutions were treated within ten to fifteen minutes. Therefore, with these compounds, the cryoscopic determinations were carried out in such short periods. The results obtained are shown in Table I.

An inspection of the results in Table I indicates that none of the sulfoxide measured gave an *i*-factor as large as 4 or 5; all the values fall around two, within the range of experimental error, suggesting that the sulfoxide in general ionizes according to Eq. 4, possibly with only the exception of thianthrene monoxide.[6]

TABLE I. CRYOSCOPIC *i*-FACTORS AND COLORS OF VARIOUS SULFOXIDES IN 99.5% SULFURIC ACID

| Compound | *i*-Factor | Color of solution |
|---|---|---|
| Ph-SO-Ph | 2.15 | Deep green |
| 4-$MeC_6H_4$-SO-$C_6H_4$-$NH_2$-4′ | 2.15 | Deep green |
| Ph-SO-$CH_2$Ph | 1.95 | Red |
| Ph-SO-$CH_3$ | 2.10 | Pale orange |
| $CH_3$-SO-$CH_3$ | 1.90 | None |

$$\underset{\underset{O}{\downarrow}}{R\text{-}\ddot{S}\text{-}R} + H_2SO_4 \rightleftarrows \underset{\underset{O\text{-}H}{|}}{R\text{-}\overset{\oplus}{S}\text{-}R} + \overset{\ominus}{HSO_4} \qquad (4)$$

Although we cannot offer any satisfactory explanation for the different colors associated with different compounds in sulfuric acid, these colors are probably related to the ease of charge-transfer. The sulfoxides bearing a $\pi$-electron system of a benzene ring at the $\alpha$-position appear to give deeper colors.

Earlier, it was suggested that the *i*-factor changes in value from 2 to 3 when diphenyl sulfoxide was kept in sulfuric acid for hours. We also confirmed this. It should be mentioned here also that the recovery of diphenyl sulfoxide was better from the green solution of less concentrated sulfuric acid, while the recovery became negligible and a large amount of a gummy, brown substance was formed when the sulfoxide was dissolved in over 100% of sulfuric acid. Even with 100% sulfuric acid, however, the yield of the recoverable sulfoxide was very small.

## Experimental

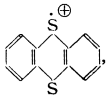
**Materials.** — *Diphenyl sulfoxide* purchased from K and K Laboratories, Inc., was recrystallized from a mixture (1 : 1) of benzene and ligroin. White crystals (m. p. 70.5—71°C) were used.

*Dimethyl Sulfoxide.*—The oxidation of dimethyl sulfide was performed by the method reported by R. L. Shriner et al.,[7] using 30% hydrogen peroxide in an acetone solution. The fraction boiling at 90—91°C/26 mmHg was used.

*Benzyl Phenyl Sulfoxide.* — The oxidation of benzyl phenyl sulfide was carried out in a similar way.[7] To the sulfide (52 g., 0.26 mol.) in 250 ml. of acetone 40 g. of 30% $H_2O_2$ was added. The

4) R. J. Gillespie and J. A. Leisten, *Quart. Rev.*, **8**, 40 (1954).

5) R. J. Gillespie and R. C. Passerini, *J. Chem. Soc.*, **1956**, 3850.

6) H. J. Shine and L. Piette have reported (*J. Am. Chem. Soc.*, **84**, 1798 (1962)) that thianthrene monoxide dissociates to form an ion radical.  , in 96—97% sulfuric acid. This view seems to be favored by our preliminary $^{18}O$-tracer experiment, a full account of which will be reported shortly.

7) R. L. Shriner, H. C. Struck and W. J. Jorison, *J. Am. Chem. Soc.*, **52**, 2060 (1930).

mixture was shaken and allowed to stand at room temperature for 72 hr. After the acetone had been removed, the oil which remained immediately solidified upon cooling. The solid was recrystallized from 60% ethanol. The yield was 40 g. (70%). After repeated recrystallization, white crystals m. p. 122—123°C were used.

*Phenyl Methyl Sulfoxide.*[8]—Phenyl methyl sulfide was prepared by treating thiophenol with dimethyl sulfide under alkaline conditions. Phenyl methyl sulfoxide was obtained by an oxidation similar to that described above, and the fraction boiling at 91—92°C/12 mmHg was collected and used.

*d,l-4-Amino-4'-methyldiphenyl Sulfoxide.*[9]—A mixture of *p*-toluenesulfinic acid (1 part) and aniline (4 parts) was heated at 110—115°C for 30 hr. The excess of aniline was removed by steam distillation, and the non-volatile residue was filtered, washed with ether, and recrystallized from ethanol. Pure d, l-4-amino-4'-methyldiphenyl sulfoxide m. p. 169.5—170.5°C was obtained in a 45% yield.

**Cryoscopic Measurements.**—The apparatus used for the cryoscopic measurements was essentially the same as that reported by Newman et al.[10]

Near 100% sulfuric acid was prepared by mixing extra pure concentrated sulfuric acid and fuming sulfuric acid. The concentration of sulfuric acid was checked by measuring the freezing point, which was determined by a Beckmann-type thermometer.

The thermometer was calibrated each time by a standard thermometer. All the determinations were carried out in an air-conditioned room which was kept at around 20°C with a humidity of slightly less than 40%. In all the runs, the freezing points of the acids were in the 9.80—10.20°C range. The samples taken to lower the freezing point of the solution were about $(1.0—2.0)\times10^{-2}$ mol./l.; they were kept in very thin glass ampules. After the acid had been kept in the apparatus for a few hours, the freezing point of the solvent was determined; then the solute in the ampule was put in as rapidly as possible through one of the three necks of the apparatus, and the apparatus was closed with a glass stopper. The ampule was broken with a glass-rod stirrer, and the solute was thoroughly dissolved by stirring it at room temperature. The system was then cooled in an ice-salt bath. The temperature of the solution was read every minute, and the freezing point was graphically recorded. The calculation of the van't Hoff factor was made by the equation where $\Delta m$ is the molarity of the solute, $\Delta\theta$ is the freezing point depression, and $\theta$ is the total freezing point depression:

$$i=\frac{\Delta\theta}{\Delta m\times 6.154\ (1-0.0047\theta)}$$

The average *i*-values of three to five runs are shown in Table II.

Table II. *i*-Factors of the Sulfoxides in Sulfuric Acid

| Compound | Initial f. p. °C | $\Delta w$, g. | $\Delta m$ (mol./1.) $\times10^2$ | $\Delta\theta$ °C | *i* |
|---|---|---|---|---|---|
| Ph-SO-Ph | 10.15 | 0.1134 | 1.404 | 0.186 | 2.15 |
| 4-Me$C_6H_4$-SO-$C_6H_4$-$NH_2$-4' | 10.00 | 0.1033 | 1.118 | 0.148 | 2.15 |
| Ph-SO-$CH_2$Ph | 10.20 | 0.1070 | 1.242 | 0.149 | 1.95 |
| Ph-SO-$CH_3$ | 9.82 | 0.08224 | 1.468 | 0.190 | 2.10 |
| $CH_3$-SO-$CH_3$ | 9.95 | 0.0542 | 1.737 | 0.203 | 1.90 |

**The Oxygen Exchange Reaction of Diphenyl Sulfoxide.**—Diphenyl sulfoxide (1.0 g.; 5 mmol.) was dissolved in 10 ml. of 98.99% sulfuric acid, prepared by adding fuming sulfuric acid to c. p.-grade 93.5% sulfuric acid under ice-cooling. A brilliant blue-green color formed immediately. After this ice-cooled solution had been kept for from five to ten minutes, the solution was poured into 25 ml. of frozen $^{18}O$-enriched water (0.6 atom% $^{18}O$). The pale yellow precipitate which formed was collected on a sintered-glass filter, washed once with 5 ml. of a cold, diluted, alkaline solution of the same $^{18}O$-enriched water, washed three times with 5 ml. of the same $^{18}O$-enriched water, and then dried. The dried sample (0.95 g.), recovered in nearly a quantitative yield, was recrystallized from ethanol to give colorless crystals with a m. p. of 70—71°C; the mixed melting point with an authentic sample was 70—71°C. This sample was subjected to $^{18}O$ analysis.

**Isotopic Analysis.**—The analysis of the $^{18}O$ content of the sulfoxide was performed by an adaptation of the method of Rittenberg and Ponticorvo.[11] The compound (50 mg.) was introduced, together with a 1:1 mixture (300 mg.) of mercuric chloride and mercuric cyanide, in to an 8 mm. A-top tube (27 cm.) with a break off-seal at one end and a seal-off construction at the other. The tube was vacuum-sealed and then heated at 500°C for 3—5 hr. After it had then been cooled, the tube was opened in a vacuum line and the hydrogen chloride which had formed was removed by adding a few drops of quinoline, while the hydrogen sulfide which had formed was removed by passing the gas through a glass-wool-packed tube absorbing a small amount of lead acetate. The gases which had formed were condensed by cooling the gas with liquid nitrogen, and the non-condensable gases which had formed were pumped off. After repeated fractionations, the carbon dioxide was collected and subjected to mass-spectrometric analysis. The atom % $^{18}O$ was calculated from the peak of mass 44 and 46 according to the following equation:

$$\text{Atom \% } ^{18}O=\frac{\text{Peak 46/Peak 44}}{2+\text{Peak 46/Peak 44}}$$

## Summary

Contrary to the earlier claim that diphenyl sulfoxide ionizes in nearly 100% sulfuric acid to give a "diphenyl sulfidonium" ion, which

8) van Hove, *Bull. soc. chim. Belg.*, **36**, 556 (1927).
9) P. W. B. Harrison, J. Kenyon and H. Phillips, *J. Chem. Soc.*, **1926**, 2079.
10) M. S. Newman, H. G. Kuivila and A. B. Garrett, *J. Am. Chem. Soc.*, **67**, 704 (1945).
11) D. Rittenburg and L. Ponticorvo, *J. Appl. Rad. Isotopes*, **I**, 208 (1956).

can then return to the original sulfoxide when quenched with water, the $^{18}O$ tracer experiment and a new set of cryoscopic determinations of a few sulfoxides have revealed that the dissociation of the sulfoxide takes place in a concentrated sulfuric acid in the following manner:

$$\underset{\underset{O}{\downarrow}}{R\text{-}S\text{-}R} + H_2SO_4 \rightleftarrows \underset{\underset{O\text{-}H}{|}}{R\text{-}\overset{\oplus}{S}\text{-}R} + \overset{\ominus}{HSO_4}$$

*Department of Applied Chemistry*
*Osaka City University*
*Kita-ku, Osaka* (*S. O.*)

*Department of Chemistry*
*Radiation Center of Osaka Prefecture*
*Sakai, Osaka* (*T. K. & Y. K.*)

# Sulfoxides. VI.[1] The Oxygen Exchange Reaction of Sulfoxides in Sulfuric Acid[2]

By Shigeru OAE, Teijiro KITAO, Yoshinori KITAOKA and Shunichi KAWAMURA

(Received July 18, 1964)

Unlike those in sulfone groups, the sulfur-oxygen links in sulfoxides are known to be considerably weak. A number of reactions are known to involve the facile cleavage of the S-O bonding.[3] A typical illustration of the weaker S-O bonding in sulfoxide than that in sulfone can be seen in the following $^{35}S$-tracer experiment. Diphenyl sulfone reacts sluggishly with sulfur above 300°C to give diphenyl sulfide, with a replacement of the sulfur atom of the sulfone group involving the cleavage of the C-S bond, while diphenyl sulfoxide is reduced quantitatively to the sulfide via the cleavage of the S-O bond by heating it with sulfur at 280°C.[4]

Another marked difference between the sulfoxide group and the sulfone group is that the former still retains a lone electron pair on the sulfur atom. Because of this lone electron pair, the sulfur atom of the sulfoxide is still nucleophilic in nature in spite of the positive charge. Thus, dimethyl sulfoxide is known to react with methyl iodide to yield trimethylsulfoxonium iodide.[5]

An interesting reaction in this connection is the oxygen exchange reaction of sulfoxides in sulfuric acid;[2] this paper will present detailed accounts of this rather unusual reaction.

## Results and Discussion

It was shown in the previous paper[1] that diphenyl sulfoxide ionized in concentrated sulfuric acid in the following manner, giving a deep green solution:

$$(C_6H_5)_2\ddot{S}\rightarrow O + H_2SO_4 \rightleftarrows (C_6H_5)_2\overset{\oplus}{\ddot{S}}-OH + H\overset{\ominus}{SO_4} \quad (1)$$

When diphenyl sulfoxide was dissolved in a large excess of concentrated $^{18}O$-enriched sulfuric acid for five to ten minutes at around 0°C, and the resulting green solution was diluted with normal water and $^{18}O$-enriched water (0.6 atom% $^{18}O$), and it was found that

Table I. $^{18}O$ Concentrations of diphenyl sulfoxides recovered from the green solution with $^{18}O$-enriched $H_2SO_4$

| | |
|---|---|
| Ph-SO-Ph (Quenched with $^{18}O$-enriched water, 0.6 atom% $^{18}O$) | 0.412% |
| Ph-SO-Ph (Quenched with normal water) | 0.426% |
| $H_2SO_4$ | 0.480% |
| Natural $CO_2$ | 0.212% |

1) Part V; S. Oae, T. Kitao and Y. Kitaoka, This Bulletin, **38**, 543 (1965).

2) a) Preliminary Communication; see S. Oae, T. Kitao and Y. Kitaoka, *Chem. & Ind.*, **1961**, 291. b) The early part of this work was performed at the Department of Chemistry, Brookhaven National Laboratory, under the auspices of the U. S. Atomic Energy ammission, when S. O. was a visiting chemist there. We wish to thank Dr. David R. Christman of the B. N. L. for some $^{18}O$ analysis. We are also grateful to Mr. Motoyoshi Hatada and Dr. Keiji Kuwata for their generous collaborations in mass spectric and ESR analyses.

3) For details see Chapter 4 of "Sulfur Bonding," by C. C. Price and S. Oae, Ronald Press., N. Y. (1962), or S. Oae, *Chemistry* (*Kagaku*), **19**, 220—229 (1964).

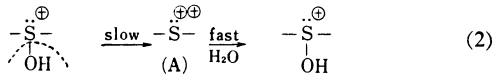
4) S. Oae and S. Kawamura, This Bulletin, **36**, 164 (1963).

5) R. Kuhn and H. Tischmann, *Ann.*, **611**, 117 (1958).

the recovered diphenyl sulfoxide was incorporated with a similar concentration of $^{18}O$. A typical run is shown in Table I.

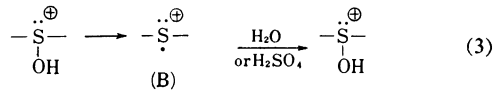
Among a number of mechanisms that could be considered, the following are a few mechanisms that are conceivable for this $^{18}O$ exchange reaction:

a) $SN_1$-Type:



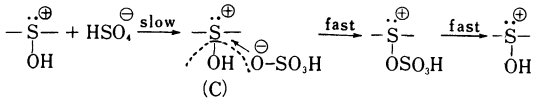
(2)

b) Free Radical Type:



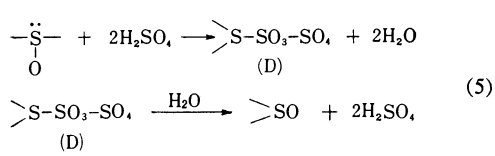
(3)

c) SNi-Type:



(4)

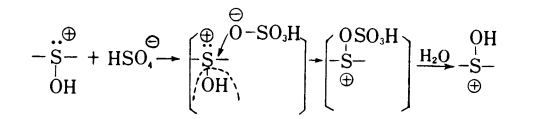
d) Oxidative Adduct Formation and Subsequent Hydrolysis:



(5)

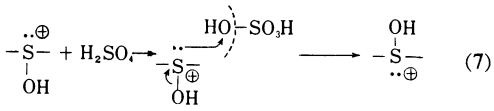
e) $SN_2$-type:

*1) Nucleophilic Attack on Sulfoxide by Sulfate Ion:*



(6)

*2) Nucleophilic Attack on Sulfuric Acid by Sulfoxide:*



(7)

**$SN_1$-Type Mechanism.** — Although Szmant's hypothesis of the formation of the diphenyl sulfidonium ion in the deep green solution was excluded by the $^{18}O$ tracer experiment[1] and by the careful determination of the i-factor[1], the $SN_1$-type mechanism still remains acceptable if one assumes that the formation of the sulfidonium ion (A) is the slow, rate-determining step and that the sulfidonium ion hydrolyzes to give the sulfoxide in the subsequent fast step. Here, the facile $^{18}O$ exchange of diphenyl sulfoxide can be explained on the basis of the resonance stabilization of the incipient sulfidonium ion, just as in the case of the facile solvolysis of benzhydryl compounds. The replacement of a phenyl group by an alkyl or an aralkyl substituent would retard the $^{18}O$ exchange. However, such was not found to be the case. Especially, the facile $^{18}O$ exchange of dimethyl sulfoxide, where the formation of the corresponding sulfidonium ion would be very difficult, does not seem to favor the mechanism. (See Table II).

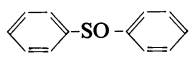
It is known that $SN_1$ reactivity increases if the starting substance has a steric strain and the strain is relieved in going to the transition state. Thus, 2, 4, 6-trimethyl-$\alpha$-phenethyl chloride reacts far faster (ca. 2000 fold.) than $\alpha$-phenethyl chloride in ethanolysis.[6]

A similar steric acceleration in the $SN_1$ reaction was observed in the ethanolyses of substituted benzhydryl chlorides[6].

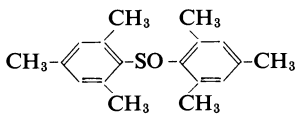
Table II. $^{18}O$-Exchange of various sulfoxides with 97% $^{18}O$-labeled sulfuric acid at 0°C for five minutes

| Compound | Color of solution | $^{18}O$ Incorporation |
|---|---|---|
| $C_6H_5$-SO-$C_6H_5$ | Deep green | 0.42 |
| $C_6H_5$-SO-$CH_2C_6H_5$ | Red | 0.42 |
| $C_6H_5$-SO-$CH_3$ | Pale orange | 0.42 |
| $CH_3$-SO-$CH_3$ | Colorless | 0.45 |
| $H_2SO_4$ | | 0.48 |
| Tank $CO_2$ | | 0.21 |

Table III. Rates of $^{18}O$ exchange of diaryl sulfoxides with $^{18}O$-labeled 94.5% sulfuric acid at 0°C



$3.4\times10^{-4}$ sec$^{-1}$

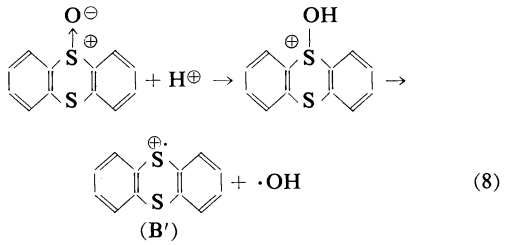


$1.0\times10^{-5}$ sec$^{-1}$

A similar comparison of rates between diphenyl sulfoxide and dimesityl sulfoxide has therefore been carried out; the results are shown in Table III. An inspection of the data clearly excludes the $SN_1$-type mechanism for this $^{18}O$ exchange, since in this case the sterically-strained dimesityl sulfoxide was found to be much less reactive than diphenyl sulfoxide this is contrary to what one would expect from the $SN_1$-type mechanism.

6) E. L. Eliel, "Substitution at Saturated Carbon Atoms," in "Steric Effects in Organic Chemistry," Ed. by M. S. Newman, John Wiley and Sons, N. Y. (1965), pp. 88—89.

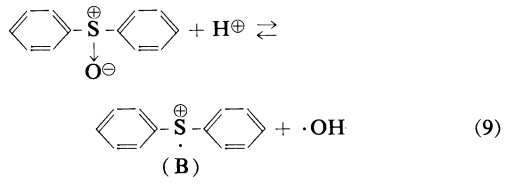
**Free Radical Mechanism.**—Hirshon, Gardner and Fraenkel[7] have reported that the sulfuric acid solutions of certain sulfur-containing aromatic compounds show electron spin resonance and contain free radicals in substantial concentrations. German workers have reported recently[8] that the sulfuric acid solutions of aryl sulfoxides are paramagnetic. Especially well-studied are the solutions of diphenyl disulfide, thianthrene and thianthrene oxides.[9,10] It has been suggested that the species present in the sulfuric acid solution of thianthrene oxide on thiantrene is the positive ion-radical (B'), as is shown below:



(8)

(B')

A similar mechanism could be adopted in this case. If the hydroxyl radical thus formed would transfer with either water or sulfuric acid to regenerate an alternative hydroxyl radical, the recombination between the positive ion-radical (B) and the hydroxyl radical will give rise to the sulfoxide in which the original oxygen atom is exchanged. However, it is unlikely that a substantial amount of radical transfer takes place between the hydroxyl radical and water or sulfuric acid, or both. If there were the following dissociation (Eq. 9),



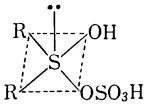
(9)

(B)

the presence of the radical ion (B) could be detected by a conventional electron spin-resonance spectroscopy. When diphenyl sulfoxide was dissolved in 93—98% sulfuric acid at various concentrations and the solutions were subjected to ESR spectroscopic analysis, however, no noticeable signal was detected, contrary to the early claim by German workers.[11] None of the other sulfoxides, used for this $^{18}O$ exchange study, showed a noticeable ESR signal. Therefore, it is not likely that such a free radical dissociation takes place in sulfuric acid.

Another remaining possibility in the free radical mechanism is the process which involves a rate-determining dissociation of protonated diphenyl sulfoxide into the radical ion (B) and the hydroxyl radical, followed by the subsequent recombination of the two radicals. This is also rather unlikely, since the hydroxyl radical so formed would attack not only the sulsur atom but also benzenoid carbon atoms, usually giving some rearranged products,[12] if there were any radical transfer of the hydroxyl radical during the process. Moreover, the radical ion would accept an electron to be reduced back to the sulfide more easily than it would one to recombine to yield the original sulfoxide. In fact, thianthrene monoxide, which is believed to give the radical ion, B', in sulfuric acid, showing clear ESR signals, is reduced back to thianthrene chiefly when the solution is quenched with water.[10,13] Obviously, a different reaction is taking place in the case of thianthrene.

**$SN_i$-Type Mechanism Involving 3d Orbitals of Sulfur Atom.**—Since the sulfur atom can utilize its 3d orbitals for forming an extra bond, expanding its valence shell beyond the octet, especially when the central sulfur atom bears positive charge, such as in the sulfoxide or sulfonium group,[14] the formation of an incipient intermediate, (C), is possible. If the intermediate (C) has a square pyramidal structure, stereochemical considerations will predict a net retention of the original configuration:



(C)

In fact, retention was found to be the case in some of the various nucleophilic substitutions involving tetracovalent phosphorous compounds,[15] and moreover, a similar nucleophilic addition-elimination process was suggested in the reaction of sulfonium compounds with phenyllithium.[16]

This mechanism can be readily tested by using

7) J. M. Hirshon, K. M. Gardner and G. K. Fraenkel, *J. Am. Chem. Soc.*, **75**, 4115 (1953).
8) V. Schmidt, K. Kabitze and K. Markau, *Angew. Chem.*, **72**, 708 (1960).
9) A. Fava, P. B. Sogs and M. Calvin, *J. Am. Chem. Soc.*, **79**, 1078 (1957).
10) H. J. Shine and L. Piette, ibid., **84**, 4798 (1962).
11) See Footnote 18 of Ref. 10.
12) A similar reaction can be found in the photochemical rearrangement of azoxybenzene to 2-hydroxyazobenzene. S. Oae, T. Fukumoto and M. Yamagami, This Bulletin, **36**, 601 (1963).
13) A detailed study is now under way in these laboratories.
14) C. C. Price and S. Oae, "Sulfur Bonding," Chapters 4 and 5.
15) a) W. E. McEwen et al., *J. Am. Chem. Soc.*, **82**, 2396, 2646, 5503 (1960); b) F. Ramirez et al., ibid., **82**, 2651, 2652, 5703 (1960); **82**, 429 (1961); **84**, 4588 (1962).
16) a) V. Franzen and C. Mertz, *Angew. Chem.*, **72**, 416 (1960); b) J. Bornstein and J. H. Supple, *Chem. & Ind.*, **1960**, 1333.

an optically-active sulfoxide. Thus, an optically-active sulfoxide, *d*-4-methyl-4-amino-diphenyl sulfoxide,[17] $[\alpha]_D^{30}$ +105.9 ($c$=1.10, $l$=2.0) in 98% ethanol, was synthesized and subjected to the $^{18}O$-exchange. When the blue green solution of the *d*-isomer sulfoxide $^{18}O$-enriched sulfuric acid was diluted with water, the compound recovered was found to be racemized completely to the *d, l*-isomer, while there was a usual amount of $^{18}O$ incorporation in the racemized sulfoxide, as Table IV shows.

Table IV. $^{18}O$ Exchange of *d*-4-amino-4'-methyldiphenyl sulfoxide in 97% $^{18}O$-enriched sulfuric acid at 0°C for five minutes

| | |
|---|---|
| $^{18}O$ for 4-$NH_2$-$C_6H_4$-SO-$C_6H_4$-$CH_3$-4' | 0.45% |
| $^{18}O$ for $H_2SO_4$ | 0.48% |
| $^{18}O$ for tank $CO_2$ | 0.21% |

This data clearly excludes the possibility of a $SN_i$-type process involving the incipient nucleophilic adduct intermediate, C.

**The Oxidative Formation of Adduct and Subsequent Hydrolysis.**—Very recently, it has been reported by Mislow, Simmons, Melillo and Ternay that sulfoxides are readily racemized in the presence of hydrochloric acid accompanied by oxygen exchange with solvent water. The mechanism suggested for this reaction involves the initial oxidative adduct formation (Eq. 10) and the subsequent hydrolysis of the adduct (Eq. 11), as is shown below:[18]

$$R_2SO + 2HCl \rightleftarrows R_2SCl_2 + H_2O \quad (10)$$

$$R_2SCl_2 + H_2{}^{18}O \rightleftarrows R_2S^{18}O + 2HCl \quad (11)$$

The reversible formations of dibromo compounds[19] or dichloro compounds[20] from the corresponding sulfoxides by the treatment of hydrobromic acid or hydrochloric acid have been known for some time. In fact, some dibromo compounds were successfully isolated, and the subsequent treatment of the dibromo compounds with $^{18}O$-enriched water was found to give the corresponding sulfoxides labeled with $^{18}O$.[21] However, unlike hydrohalous acid, sulfuric acid is not a good nucleophile and cannot be oxidized so readily by such a weak oxidizing agent. Meanwhile, it has been suggested that concentrated sulfuric acid dissociates to form sulfur trioxide and water.[22] Sulfur trioxide is a powerful electrophile and possibly coordinates with the sulfur atom of sulfoxide, replacing oxygen, as is shown by Eq. 5, to form perhaps the incipient intermediate (D), which would immediately react with water to give the original sulfoxide. If this were the case, then sulfides, being more nucleophilic in nature, would react more readily with sulfur trioxide to form the corresponding sulfoxides, as in the case of the bromine oxidation of sulfides and their corresponding sulfoxides.[21] However, the reaction of diphenyl sulfide in concentrated sulfuric acid or in oleum is very sluggish; only when the red solution of the sulfide was kept in sulfuric acid for a long time, was the formation of a small amount of the sulfoxide observed.[23] On the other hand, the $^{18}O$ exchange reaction of the sulfoxide is very fast in concentrated sulfuric acid; it is usually completed within a few minutes at 0°C. Therefore, it is likely that the $^{18}O$ exchange reactions of sulfoxides in concentrated sulfuric acid do not follow a path — oxidative adduct formation and subsequent hydrolysis — similar to that of the reactions with hydrohalous acids.

**The Nucleophilic Attack on Sulfoxide by the Hydrogen Sulfate Ion or Water.** — Since both sulfate and hydrogen sulfate ions are known to be very weak nucleophiles, it is difficult to accept the mechanism involving the nucleophilic attack of hydrogen sulfate or sulfate ion. Recently, however, Leonard and Johnson[24] have

Table V. Rates of the $^{18}O$ exchange of diphenyl sulfoxide and dimesityl sulfoxide with $^{18}O$-labeled sulfuric acid

| | Atom% $^{18}O$ of recovered sulfoxide | | | | | |
|---|---|---|---|---|---|---|
| Time, sec. | 300 | 600 | 1800 | 3600 | 7200 | |
| Diphenyl sulfoxide | 0.26 | 0.31 | 0.45 | 0.60 | — | $k_{ex}=3.4\times10^{-4}$ sec$^{-1}$ |
| Dimesityl sulfoxide | 0.206* | 0.21 | — | 0.22 | 0.24 | $k_{ex}=1.0\times10^{-5}$ sec$^{-1}$ |

* The Natural abundance of $^{18}O$ was 0.204 atom%.

17) P. W. B. Harrison, J. Kenyon and H. Phillips, *J. Chem. Soc.*, **1926**, 2079.
18) K. Misolow, T. Simmons, J. T. Melillo and A. L. Ternay, Jr., *J. Am. Chem. Soc.*, **86**, 1452 (1964).
19) T. Zincke and W. Frohneberg, *Ber.*, **43**, 837 (1909).
20) a) K. Fries and W. Vogt, *Ann.*, **381**, 337 (1911); b) E. Fromm, ibid., **396**, 75 (1913); c) K. Issleib, M. Tzschach, *Z. anorg. u. allegem. Chem.*, **305**, 198 (1960).
21) Unpublished works in our laboratories.
22) T. C. Hoering and J. W. Kennedy, *J. Am. Chem. Soc.*, **79**, 56 (1957).
23) R. J. Gillespie and R. C. Passerini, *J. Chem. Soc.*, **1956**, 3850.
24) N. J. Leonard and C. R. Johnson, *J. Am. Chem. Soc.*, **84**, 3701 (1962).

presented a case in which the sulfur atom of a cyclic sulfoxide, 1-thiacycloocta-5-one, was presumed to be attacked by a water molecule in the presence of 2, 2-dimethoxypropane and 70% perchloric acid. When diphenyl sulfoxide was treated with 70% perchloric acid, however, it was found not to exchange with oxygen, but to be oxidized to the sulfone when it was kept at 0°C for four hours. Therefore, it appears that this nucleophilic attack of water on the sulfur atom is limited to the reactions of the particular thiacyclooctanone and possibly some related ones, and that it is not a general reaction to ordinary sulfoxides.

Moreover, if one assumes the nucleophilic attack of hydrogen sulfate or water on the sulfur atom of sulfoxides, the same nucleophilic attack may also be considered to take place on the nitrogen atom of *N*-oxides as well as on the phosphor atom of tertiary phosphine oxides, since these semipolar linkages are known to have a magnitude of force constants similar to that of diphenyl sulfoxide, $7\times10^5$ dyn./cm. Thus, phenazine *N*-oxides, whose force constant of the N-O bond is $7.0\times10^5$ dyn./cm. and triphenylphosphine oxide ($8\times10^5$ dyn./cm.) were subjected to the $^{18}O$ exchange experiment. However, neither phenazine *N*-oxide nor triphenyl phosphine oxide was found to exchange oxygen in concentrated sulfuric acid. Diphenyl sulfone, which bears a double positive charge to attract nucleophilic attack[25] but has a stronger S-O bond (force constants $9.6\times10^5$ dyn./cm.), also failed to exchange oxygen. Furthermore, a more nucleophilic hydroxide ion also failed to attack the sulfur atom of diphenyl sulfoxide to exchange oxygen in a dioxane-water solution under prolonged refluxing. Thus, the mechanism involving the nucleophilic attack of the hydrogen sulfate ion or the water molecule on the sulfur atom of the sulfoxide cannot be accepted either as likely for this $^{18}O$ exchange reaction.

**The Nucleophilic Attack on Sulfuric Acid by Sulfoxide.**—One noteworthy fact which characterizes the sulfoxide bond is that the sulfur atom still bears a lone electron pair for nucleophilic reactions, unlike the hetero atoms in phenazine *N*-oxide, triphenylphosphine oxide and sulfones. Therefore, one can safely assume that the sulfur atom would undergo a nucleophilic attack on sulfuric acid, as is shown by Eq. 7. Meanwhile, this nucleophilic attack is considered to be suppressed by bulky substituents around the neighborhood of the reaction center. In fact, it was found that the rate of the $^{18}O$ exchange of dimesityl sulfoxide was 34 times slower than that of diphenyl sulfoxide. The extremely facile $^{18}O$ exchange of other sulfoxides tested can also be explained on the basis of the nucleophilic nature of the sulfur atoms of these sulfoxides, whose lone pair electrons are less delocalized and thus more nucleophilic than that of diphenyl sulfoxide. Therefore, this appears to be the only surviving, and hence the most favorable, mechanism for the $^{18}O$ exchange reactions.

As an outcome of the stereochemical considerations of this nucleophilic mechanism, one would expect that the rate of $^{18}O$ exchange will be exactly half of that of the racemization. Unfortunately, however, the kinetic control is very difficult with the optically-active sulfoxide, namely *d*-4-amino-4-methyldiphenyl sulfoxide, and only very crude, not very reproducible results were obtained. In several runs with different concentrations of sulfuric acid, it was found that the ratio of the rate of exchange ($k_e$) vs. that of racemization ($k_r$), $k_e/k_r$, fluctuates between 1/2—1/3.5, but that it is always less than 1/2 and never comes to 1. Although the $k_e/k_r$ value lies in the right direction and is close to the 1/2 which is predicted from this mechanism, this cannot serve as foolproof evidence for this mechanism, since it was thought that a kind of acid-catalyzed racemization[26] was taking place independently. Thus, the optically-active sulfoxide was dissolved in 50% sulfuric acid and kept at 0°C for five hours and a half; however, there was no racemization in the recovered sulfoxide. In more concentrated acids in which oxygen exchange occurs, however, it seems that an independent process of racemization takes place to cause a rate of racemization twice as fast as that of $^{18}O$ exchange. More careful kinetic studies with less reactive systems are necessary for more accurate evaluations of both rates of $^{18}O$ exchange and rates of racemization.[27]

## Experimental

**Materials.**—The manners of preparing the sulfoxides were similar to those previously reported. *Phenazine N-oxide*[28] was prepared by reacting aniline and nitrobenzene in the presence of sodium hydroxide. Yellow crystals with a m. p. of 221—222°C were used. *Triphenylphosphine oxide*[29] was prepared by reacting phenyl magnesium bromide with phosphorus oxychloride. The sample was repeatedly recrystallized from ethyl acetate to obtain colorless crystals with a m. p. of 157—157.5°C.

**The Preparation of Dimesityl Sulfoxide.**—A mixture of mesitylene (155 g.) and thionyl chloride (33 g.) was cooled in an ice-salt bath. To this

25) D. R. Christman and S. Oae, *Chem. & Ind.*, **1959**, 1251.

26) H. F. Herbrandson and R. T. Dickerson, Jr., *J. Am. Chem. Soc.*, **81**, 4102 (1959).

27) Studies are now underway in these laboratories.

28) A. Wohl and W. Aue, *Ber.*, **34**, 2442 (1901).

29) G. M. Kosolapoff, *J. Am. Chem. Soc.*, **64**, 2984 (1942).

mixture anhydrous aluminum chloride (60 g.) was added in portions over a period of two hours. Then mesitylene (60 g.) was added and the solution refluxed until no further hydrochloric acid gas was evolved. After the mixture had been allowed to stand at room temperature for one or two hours, it was poured slowly onto 600 g. of ice. After a vigorous reaction had taken place, the white solids which had separated were collected and washed with water. Recrystallization from acetone gave 64 g. (25%) ; m. p. 153.5—154°C.

Found : C, 75.57 ; H, 7.67. Calcd. for $C_{18}H_{22}OS$: C, 75.52 ; H, 7.69.

**$^{18}O$-Enriched Sulfuric Acid.** — The apparatus shown in Fig. 1 was used for the preparation of

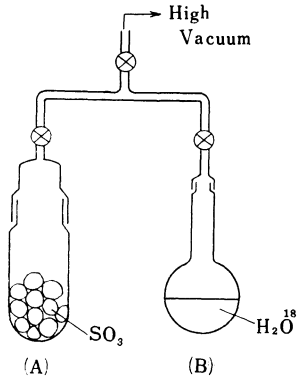



Fig. 1.

$^{18}O$-enriched sulfuric acid. An aliquot of sulfur trioxide distilled in a vacuum line was placed in one of the containers (A) and an equimolar amount of $^{18}O$-enriched water in the other (B). Both were first repeatedly frozen and degassed. Then the vessel (A) was warmed in a water bath at 50—60°C, while the other vessel (B) was cooled with dry-ice-acetone. By this procedure sulfur trioxide was introduced into the $^{18}O$-enriched water. After about twenty minutes, the introduction was stopped and the cooled trap was removed. The system was gradually warmed up to room temperature. After it had stood for a few minutes at room temperature, the vessel (A) was cooled once more and the other system (B) was warmed. By repeating this procedure, the introduction of sulfur trioxide into water was achieved. The concentration of the resulting sulfuric acid was determined by measuring the freezing point.

**The Resolution of *d, l*-4-Amino-4'-methyldiphenyl Sulfoxide**[17]. — The *d,l*-sulfoxide was prepared by reacting *p*-toluenesulfinic acid and aniline.[1] The *d,l*-sulfoxide (55 g.) was dissolved in 100 ml. of a hot water solution containing 60 g. of *d*-camphor sulfonic acid. Upon cooling, crude *d*-4-amino-4'-methyldiphenyl sulfoxide *d*-camphorsulfonate came out. After twenty recrystallizations (with 2% fresh *d*-camphor sulfonic acid added each time), the resolved salt was decomposed by ammonia and the sulfoxide obtained was recrystallized from ethanol. The *d*-isomer of the sulfoxide was thus obtained ; m. p. 150.5—151°C, with $[\alpha]_D^{30°}$ +105.9° in a 98% ethanol solution ($c$=1.10, $l$=2.0), +80.5° in a chloroform solution ($c$=1.15, $l$=2.0).

**$^{18}O$-Exchange Reactions in $^{18}O$-Enriched Sulfuric Acid.** — *Diphenyl Sulfoxide.* — Diphenyl sulfoxide (0.53 g.) was dissolved in 5.95 g. of 97% $^{18}O$-enriched sulfuric acid while the mixture was being cooled with ice, and the deep green solution was kept for fifteen minutes. From the deep green solution, about a half was quenched with 20 ml. of $^{18}O$-enriched water (ca. 0.6 atom% $^{18}O$), while the rest was quenched with 25 ml. of ordinary water. The precipitates were collected, washed with dilute alkali and water, and dried as usual. The two crude sulfoxide samples thus obtained were recrystallized from ethanol, and the samples with a m. p. of 70—71°C were subjected to $^{18}O$ analysis.

*Sulfoxides in General.*—An aliquot amount of sulfoxide was dissolved in a 10 molar equivalent of $^{18}O$-enriched sulfuric acid, and the solution was kept at the desired temperature for the desired period. Then the solution was poured into a large excess of ice-water, and the precipitate was washed with dilute alkali and then water. Solid samples were collected and recrystallized from either ethanol or benzene, while liquid samples were extracted with ether, and from the ether layer the samples were collected either by crystallization or by distillation. The samples thus collected, identified by their correct m. p.(s) or b. p.(s), were subjected to $^{18}O$-analysis.

*Phenazine N-Oxide.*—Phenazine *N*-oxide (200 mg.) was dissolved in 1.5 ml. of $^{18}O$-enriched 97% sulfuric acid (0.70 atom% $^{18}O$) ; the red solution was then allowed to stand at 0°C for 20 min. This solution was neutralized with 28% ammonia under cooling and then poured into 30 g. of ice-water. The precipitates were filtered and recrystallized from 99% ethanol, and the crystals m. p. 221—222°C were subjected to $^{18}O$ analysis.

*Triphenylphosphine Oxide.* — The oxide (1.0 g.) was dissolved in 5.0 ml. of $^{18}O$-enriched sulfuric acid (0.70 atom% $^{18}O$) and allowed to stand at 0°C for 10 minutes. The solution was then poured onto ice-water, and the resulting precipitates were collected and recrystallized repeatedly from ethyl acetate m. p. 157°C. They were used for the usual oxygen-18 analysis.

*Diphenyl Sulfone.*—Diphenyl sulfone (0.5 g.) was dissolved in 5 ml. of $^{18}O$ sulfuric acid (0.70 atom% $^{18}O$) ; the solution was kept at room temperature for 20 min. and then poured onto ice-water. The precipitate was collected and dried. Recrystallization from benzene gave colorless crystals with a m. p. of 128°C ; they were subjected to $^{18}O$-analysis.

| | | |
|---|---|---|
| Analysis : | Ph-$SO_2$-Ph | 0.209% |
| | Tank $CO_2$ | 0.211% |

**The Reaction of Diphenyl Sulfoxide With 70% Perchloric Acid.**—Diphenyl sulfoxide (0.5 g.) was dissolved in 10 ml. of 70% perchloric acid. The mixture was allowed to stand at 0°C for 4 hr. Then the mixture was poured into water, and the resulting solid was separated. Repeated recrystallizations from a mixture of benzene and ligroin gave a product the m. p. of which agreed with that of diphenyl sulfone. A mixed melting point determined with an authentic sample of diphenyl sulfone was

not depressed.

**$^{18}$O-Exchange of Diphenyl Sulfoxide in an Alkaline Solution.** — Diphenyl sulfoxide (1.01 g.) was dissolved in 60 ml. of a 70% dioxane solution, made by diluting 42 ml. of absolute dioxane with $^{18}$O-enriched water (0.61 atom% $^{18}$O) to 60 ml. of the solution. To this solution was added 0.28 g. of $^{18}$O-enriched potassium hydroxide (0.61 atom% $^{18}$O). Then the whole mixture was sealed in an ampoule and heated at 90°C for 8 hours and a half. After the ampoule had been broken and neutralized with hydrochloric acid, the solvent was distilled off. The precipitate was recrystallized from benzene, and the sample of sulfoxide m. p. 71°C was subjected to $^{18}$O-analysis.

| | | |
|---|---|---|
| Analysis: | Ph-SO-Ph | 0.214% |
| | Tank $CO_2$ | 0.212% |

**ESR Spectra.** — Sulfuric acid solutions (93.6%) containing $1.0\times10^{-2}$—$1.0\times10^{-4}$ mol./l. of the compounds, such as diphenyl sulfoxide, diphenyl sulfone, 4-amino-4'-methyldiphenyl sulfoxide and phenazine *N*-oxide, were subjected to ESR spectroscopy. However, none of the solutions of these compounds except phenazine *N*-oxide gave any sign of the presence of a free radical.

**Kinetic Studies of the Oxygen Exchange Reactions of Diphenyl Sulfoxide and Dimesityl Sulfoxide.**—To compare the rate constants of diphenyl sulfoxide and dimesityl sulfoxide, exchange reactions of both the sulfoxides were carried out under the same conditions. Both sulfoxides ($4.0\times10^{-2}$ mol.) were dissolved in 40 g. of $^{18}$O-enriched 94.5% sulfuric acid (0.57 atom% $^{18}$O) at 0°C. Aliquot portions (5.0 ml.) of the solutions were taken up after 5, 10, 30, 60 and 120 min., and each portion was quenched with ice-water. The precipitates were collected, recrystallized, and then subjected to $^{18}$O analyses. From the incorporation values of $^{18}$O in the recovered compounds, the rate constants of the oxygen exchange reactions were calculated.

**The Rate Constants of the Racemization and $^{18}$O-Exchange Reaction of *d*-4-Amino-4'-methyldiphenyl Sulfoxide in $^{18}$O-Enriched Sulfuric Acid.** —The kinetic studies of the rates of $^{18}$O exchange reaction and racemization were carried out in $^{18}$O-enriched 93% sulfuric acid (0.76 atom% $^{18}$O). The reaction conditions and the procedure of the separation were similar to those used with the diphenyl sulfoxide. However, in this case a portion of the sample was decomposed to give colored substances. In a separate experiment, it was confirmed that no change in the optical activity was observed when the *d*-isomer was treated with activated charcoal. Therefore, the recovered substance was refluxed with activated charcoal in order to purify it. The samples taken for $^{18}$O-analysis and for measuring the optical activity were repeatedly recrystallized from ethanol until the correct m. p. values were obtained. A solution containing 0.11 g. of the sample in 10 ml. of 98% ethanol was used for each measurement of the optical rotation. The same experiment was performed three times, but the rate constant of the racemization fluctuated from $2.5\times10^{-5}$ sec$^{-1}$ to $4.2\times10^{-5}$ sec$^{-1}$. Meanwhile, the $^{18}$O analyses of the same sample were done by the usual methods, and the rate constant, $k_{ex}=1.2\times10^{-5}$ sec$^{-1}$, was obtained.

Sulfoxides in general have been shown to exchange oxygen very readily in concentrated sulfuric acid. On the other hand, sulfones, *N*-oxides and phosphine oxides, with no lone electron pair, have been shown not to exchange oxygen with concentrated sulfuric acid. This oxygen exchange was accompanied by racemization and retarded by adjacent bulky substituents. All these observations seem to indicate that the oxygen exchange reaction proceeds by the nucleophilic attack of sulfoxide on sulfuric acid, as is depicted by Eq. 7.

*Department of Applied Chemistry*
*Faculty of Engineering*
*Osaka City University*
*Kita-ku, Osaka (S. O.)*

*Department of Chemistry*
*Radiation Center of Osaka Prefecture*
*Sakai, Osaka (T. K. & Y. K.)*

# Particle-size Determination of Suspensions or Emulsions by Viscometry*

By Sachio MATSUMOTO

(Received July 20, 1964)

The purpose of this work is to evaluate the particle-size distribution in the subsieve range of disperse systems, either suspensions or emulsions, by determining the relation between the relative viscosity of the system ($\eta_{rel}$) and the volume fraction of the particles ($\phi$). The measuring apparatus is an assembly of a modified Maron-Belner-type capillary viscometer[1] and a sedimentation tube, which provides a means for the measurement of the viscosity change with time at a fixed position in the bulk resulting from the sedimentation or ascension of dispersed particles.

In addition, this method seems to be useful for the viscosity measurement of dispersions with either quickly-sedimenting or -ascending particles.

## Apparatus and Theoretical

**Equipment.**—Figure 1 shows a sketch of the measuring apparatus, which is composed of two glass units; one is a sedimentation tube (S), and the other is essentially a capillary viscometer, consisting of a capillary tube (C) and a manometer tube (M). The two units are connected by a rubber stopper at the end of the sedimentation tube.

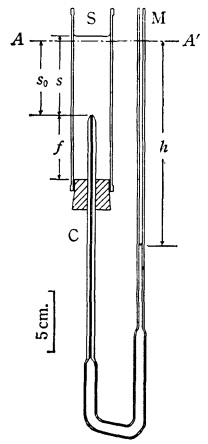



Fig. 1. Measuring apparatus.
A—·—A': Liquid level of the hydrostatic balance.

In the present study, an apparatus was employed in which the inner radii of the sedimentation tube ($R_S$), the capillary tube ($R_C$) and the manometer tube ($R_m$) were $1.47_8$ cm., $0.0249_2$ cm. and $0.304_4$ cm. respectively, while the length of the capillary tube ($L$) was 19.90 cm. The height of the capillary in the sedimentation tube, presented as $f$ in Fig. 1, can be changed from 0 to 10 cm. in accordance with the movements of the dispersed particles.

Although the dimensions of all the sections can be assembled interchangeably, the ratio $(R_C/R_m)^4$ must be kept in all instances below 0.004 in order to make negligible the resistance of flow in the manometer tube compared to that in the capillary tube.[1]

**Operation.**—The two units are joined as shown in Fig. 1 and are held vertically in place by means of a clamp. The sample is next introduced into the sedimentation tube, and the sample flows to the manometer tube through the capillary. During this flow, the times corresponding to the liquid meniscus in the manometer tube are recorded.

It may be desired that the above procedure be made in a thermostat since the viscosity changes remarkably with the temperature.

**The Theory of Measurement.**—The measuring apparatus is designed on the basis of a linear relationship between $\log \eta_{rel}$ and $\phi$ in the low dispersion concentrations.[2] Moreover, if the value of $\eta_{rel}$ is measured at a fixed position in the sedimentation tube containing the dispersion, this value will decrease with time as a result of the sedimentation or ascension of dispersed particles. The decreasing curve of $\log \eta_{rel}$ against time may correspond to the cumulative curve for the volume frequency of dispersed particles against the particle sizes.

The proper selection of suspending fluid to be used depends on various factors, as has been illustrated in the ordinary sedimentation method.[3]

Typical observations obtained by using the measuring apparatus are schematically presented

* Presented at the 16th Colloid Symposium, Osaka, November, 1963.

1) S. H. Maron and R. J. Belner, *J. Appl. Phys.*, **26**, 1457 (1955).
2) R. Rutgers, *Rheologica Acta*, **2**, 305 (1963).
3) R. D. Cadle, "Particle Size Determination," Interscience Publisher, New York (1955), p. 202.

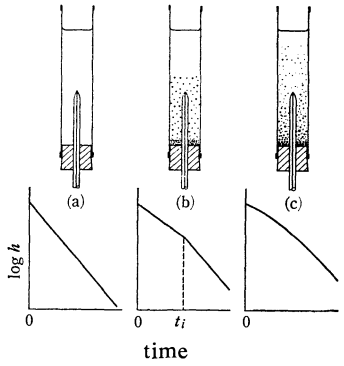



Fig. 2. Schematic curves of $\log h$ vs. time for suspending fluid (a), mono (b) and polydispersed (c) suspensions.

in Fig. 2, where $h$ denotes the difference in the meniscus of the fluid between the manometer tube and the hydrostatic balance, as is shown in Fig. 1. In the case of a suspending medium (Newtonian fluid), $\log h$ against time reveals a linear relationship, as is shown in Fig. 2(a), while the broken line at time $t_i$ in (b) is obtained with a monodispersed suspension. At time $t_i$, the boundary part between the dispersion and its suspending fluid may pass down or up to the end of the capillary tube. In the case of a polydispersed suspension, which is the most frequent case in practice, the plot of $\log h$ against time shows an upward convex curve, as may be seen in c.

In the same manner as has been established by Maron and Belner[1] for the capillary tube viscometer, the viscosity of the suspending fluid ($\eta_0$) with the present apparatus may be given by

$$\eta_0 = -\{R_c^4 \alpha / 8(2.303) L R_m^2\} \rho_0 / m_0 \qquad (1)$$

or

$$\mathrm{d}\log h/\mathrm{d}t = -m_0 = -B\rho_0/\eta_0 \qquad (2)$$

where $\rho_0$ is the density of the suspending fluid, $m_0$ is the slope of $\log h$ against time, and $\alpha$ and $B$ are the constants of the apparatus, as Eqs. 3 and 4 show:

$$\alpha = g\{1 + (R_m^2/R_s^2)\} \qquad (3)$$

$$B = R_c^4 \alpha / 8(2.303) L R_m^2 \qquad (4)$$

where $g$ is the gravitational constant, and $R_c$, $R_m$, $R_s$ and $L$ are the dimensions of the apparatus, as has been described above.

When a monodispersed suspension flows in the capillary tube, the slope of $\log h$ against time, presented as $m$, is smaller than $m_0$ and will agree with $m_0$ after time $t_i$. On the other hand, the slope of a polydispersed suspension approaches $m_0$ with time, so that the $\eta_{rel}$ value of this system will approach unity with a decrease in the dispersion concentration. If the relation of Eq. 2 is expanded for a given time, $t$, the ratio of the slope of the suspending fluid to that of the dispersion at time $t$ should be expressed as Eq. 5:

$$m_0/m = \eta\rho_0/\eta_0\rho \simeq \eta_{rel} \propto \phi \qquad (5)$$

where $\eta$ is the viscosity, $\rho$ is the density, and $\phi$ is the volume fraction of dispersed particles of the system at the end of the capillary tube at time $t$ respectively. Figure 3 shows the schematic plots of the ratio $m_0/m$ corresponding to the times for mono- and polydispersed systems.

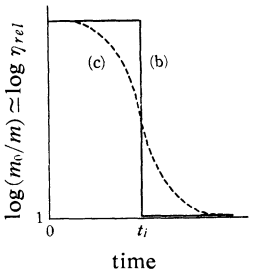



Fig. 3. Schematic curves of $m_0/m$ vs. time for mono (b) and polydispersed (c) suspensions.

In the case of a monodispersed suspension, the time $t_i$ corresponds to the dispersed particle size according to Stokes' equation:

$$t = 18x\eta_0/(\rho - \rho_0) g D^2 \qquad (6)$$

where $D$ is the particle diameter, and $x$ agrees with the distance of the sedimentation (equal to $s$ in Fig. 1) or ascension (equal to $f$ in Fig. 1) of dispersed particles. On the other hand, the size distribution of the particles of a polydispersed suspension may be reflected in the results over the entire measuring times; therefore, the decreasing curve c in Fig. 3 reminds us of a cumulative curve for the volume frequency of dispersed particles against the particle sizes, and of the possibility of obtaining the size distribution curve. The distribution function of the particle size frequency for the volume concentration is shown in Eq. 7:

$$F(D) = -4t/\mathrm{d}\cdot t/\mathrm{d}t\cdot(\phi_D/\phi) \qquad (7)$$

where $\phi_D$ is the cumulative volume fraction of a particle diameter below $D$.

When the particle sediments, the adjustment must be made for the sedimentation distance, $s$, as in Eq. 8, because $s$ decreases with an increase in the sample meniscus in the manometer tube:

$$\mathrm{d}(s - s_0)/\mathrm{d}t = -\mathrm{d}\log h/\mathrm{d}t\cdot(R_m^2/R_s^2) \qquad (8)$$

where $s_0$ is the distance from the end of the capillary tube to the sample position at a hydrostatic balance in the sedimentation tube, as is shown in Fig. 1.

## Experimental Results

**Potato Starch Granule.**—As an example of the sedimentation of dispersed particles, the potato starch granule was used, since it has such advantages as a large specific volume, a relatively spherical shape and a wide range of particle-size distribution.

The starch granule was extracted from fresh potatoes and then stored in a desiccator over calcium chloride until used. Suspensions of various concentrations were prepared with a 2 wt.% Tween 20 (polyoxyethylene sorbitan monolaurate) aqueous solution immediately before measurement.

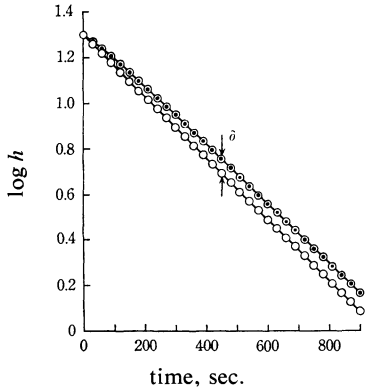



Fig. 4. Log $h$ vs. time plots for 3.91 vol. % potato starch granule suspension (⊙) and its suspending fluid (○) at 32°C.

Figure 4 shows the plots of log $h$ against time at 32°C for a 3.91 vol.% suspension and for a 2 wt.% Tween 20 aqueous solution. As may be seen in Fig. 4, these fluids do not show large differences of slopes from one another at the entire measuring times; hence, the d log $h$/d$t$ procedure may not be directly applied with accuracy. To avoid this difficulty, the so-called "$\delta$ method"[1] was employed. That is to say, a straight line of the suspending fluid was assumed as the standard line; then the differences, $\delta$, were measured between the curve of the suspension flow and the assumed line at the experimental values of $t$. When $\delta$ is plottod against $t$ and the curve is differentiated at $t$, d$\delta$/d$t$ is obtained; from this quantity, d log $h$/d$t$ is calculated.

Figure 5 gives the plots of log ($m_0/m$) against time deduced in this manner by using the data obtained from the relation between log $h$ and $t$ for a 2 wt.% Tween 20 aqueous solution and potato-starch-granule suspensions in various dispersion concentrations. Figure 6 shows the particle-size distribution of the potato starch granule, which was calculated from the decreasing curve in Fig. 5.

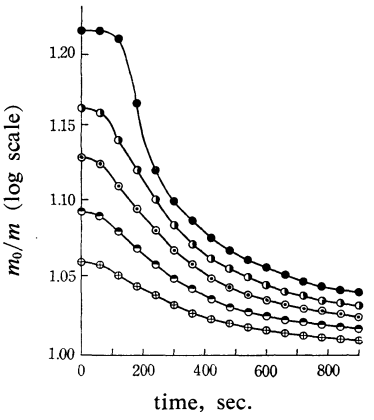



Fig. 5. $m_0/m$ vs. time plots for potato starch granule suspensions of 5.75 vol. % (●), 4.84 vol. % (◑), 3.91 vol. % (⊙), 2.96 vol. % (◓) and 1.99 vol. % (⊕) at 32°C.

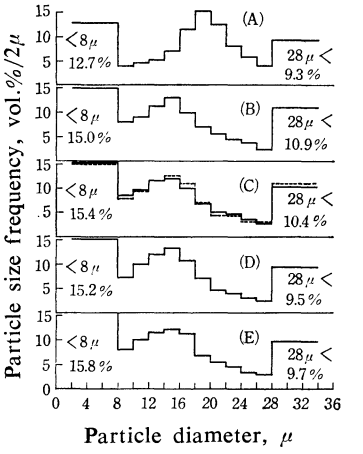



Fig. 6. Particle size distribution curves for potato starch granule suspensions of 5.75 vol. % (A), 4.84 vol.% (B), 3.91 vol.% (C), 2.96 vol.% (D) and 1.99 vol.% (E), calculated from $m_0/m$ vs. time plots in Fig. 5. Broken line represents a result by using Wiegner's tube method.

The distribution curves differ slightly from each other in the shape but they all correspond to the maximum for the frequency, except for the suspension with a 5.75 vol.% concentration. From these results, it may be understood that the upper limit of the dispersion concentration for the determination is below about 5 vol.%. On the other hand, the lower limit of the dispersion concentration for the determination depends on the accuracy of viscosity measurement.

For the suspension of a 3.91 vol.% dispersion concentration, the result obtained by this method was compared with that obtained by Wiegner's

tube method,[4] which is shown as a broken line in Fig. 6.

**Oil in Water Emulsions.**—Emulsions of 1-hexanol, benzene or *n*-hexane in water, stabilized by 1 wt.% SDS (sodium dodecyl sulfate), were used for viscosity and particle-size determinations, as in the case of ascending particles.

These emulsions were readily prepared by shaking mixtures of the 9.1 vol.% oil phase and the residual water phase; the shakings were done under similar conditions so as to give products of the same dispersion state. However, the plots of $\log h$ against $t$ for the emulsions differ according to the kind of dispersed liquids, as Fig. 7 shows. From these results, it is evident that the viscosity and the particle size of oil in a water emulsion are dependent on the nature of the dispersed substance, as Figs. 8 and 9 show. More detailed experimental results have been presented in a previous article.[5]

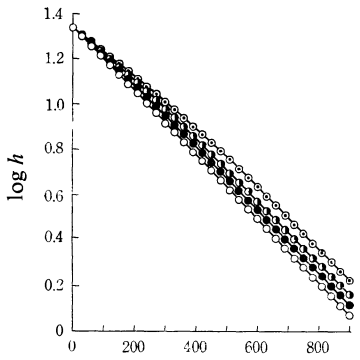



Fig. 7. Log $h$ vs. time plots for emulsions of 1-hexanol (⊙), benzene (◑) or *n*-hexane (●) in water, stabilized by sodium dodecyl sulfate, and these spending fluid (○) at 32°C; dispersion concentration are 9.1 vol.% in all the systems.

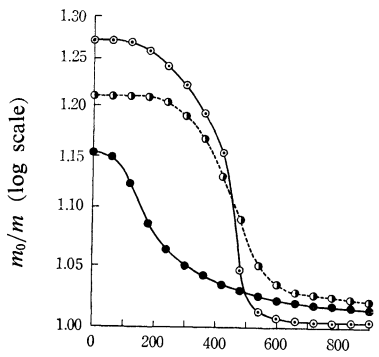



Fig. 8. $m_0/m$ vs. time plots for emulsions of 1-hexanol (⊙), benzene (◑) or *n*-hexane (●) in water at 32°C.

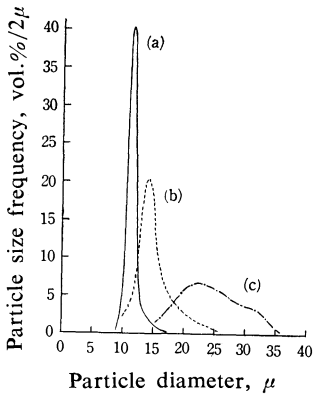



Fig. 9. Particle size distribution curves for emulsions of 1-hexanol (a), benzene (b) or *n*-hexane (c) in water.

As for the application, the advantage of this method is that it enables one to obtain the viscosity of dispersions with quickly-sedimenting or -ascending particles. The viscosity appears in the initial slope of $\log h$ against the $t$ curve where the original dispersion concentration is held.

Although independent of the particle size determination, the relation between the shearing stress and the rate of shear on the fluid may also be obtained from the measurements made during a single run,[1,6] so the apparatus can be used for the observation of the non-Newtonian flow.

## Summary

An apparatus for sedimentation analysis by the viscometric method, making possible the measurement of viscosity change with time at a fixed position in the bulk due to the sedimentation or ascension of dispersed particles, has be constructed. The new method has been examined with both a potato-starch-granule suspension and oil-in-water emulsions.

The author is very grateful to Professor Sôzaburo Ono and Dr. Takehiko Watanabe for their many helpful discussions and suggestions during this work. Thanks are also due to Professor Shû Nagayama for his continued interest and support.

*Department of Chemistry*
*College of General Education*
*University of Osaka Prefecture*
*Sakai, Osaka*

4) W. Ostwald and F. V. Hahn, *Kolloid-Z.*, **30**, 26 (1922).

5) S. Matsumoto, *J. Chem. Soc. Japan, Pure Chem. Sec.* (*Nippon Kagaku Zasshi*), **85**, 741 (1964).

6) I. M. Kriger and S. H. Maron, *J. Appl. Phys.*, **25**, 72 (1955).

# Nature of the Longest Wavelength Absorption Bands of *N*-Substituted Maleimides*

By Taku MATSUO

(Received July 29, 1964)

In spite of the considerable progress in recent years in understanding the absorption spectra of many $\pi$-electron systems, not much knowledge has been obtained as to the spectra of cyclic imides derived from anhydrides. For example, the absorption spectra of several imides have been reported in some papers without any theoretical consideration of the nature of each band.[1] The present paper will study the effects of *N*-substitution on the electronic spectra of maleimide derivatives from both the theoretical and experimental points of view.

## Experimental

The compounds used for the measurement of the absorption spectra were obtained in the same way as reported in the previous paper in which the infrared spectra of the carbonyl groups of maleimide and its *N*-substituted derivatives were discussed.[2]

The spectra were measured with a Hitachi model EPS-2U recording spectrophotometer.

## Experimental Results and Discussion

The absorption spectra of the compounds investigated are shown in Figs. 1 and 2 as measured in *n*-hexane. Since the main interest was concentrated on the longest wavelength absorption band of each compound, the highly intense bands in the shorter wavelength region are not shown in the figures. These high intensity bands are due to electronic transitions of a nature different from that discussed in this paper. The same could be said about the medium intensity band of *N*-(*p*-methoxyphenyl)-maleimide at 275 m$\mu$, which shows less solvent effect than does the lower intensity band at 350 m$\mu$, as will be discussed later. Also excluded from the present discussion are the bands with some fine structures around 260 m$\mu$

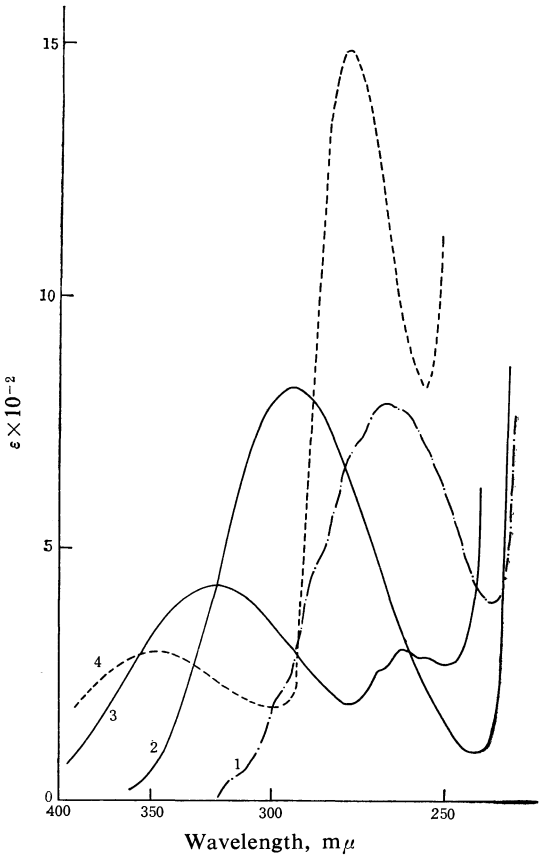



Fig. 1. Electronic absorption spectra of maleimide and its *N*-substituted derivatives in *n*-hexane.
1 Maleimide
2 *N*-Ethylmaleimide
3 *N*-Phenylmaleimide
4 *N*-(*p*-Methoxyphenyl)-maleimide

in the spectra of those compounds with a phenyl group as the constituent of their substituents. Obviously the bands are due to the transitions localized at the phenyl group, not to the characteristics of cyclic imides.

The longest wavelength absorption bands in question are classified into four groups according to their intensities and the wavelengths of the absorption maxima. The corresponding *N*-substituents of the four groups are found to be as follows:

* Contribution No. 72 from the Department of Organic Synthesis, Faculty of Engineering, Kyushu University. Presented, in part, at the 17th Annual Meeting of the Chemical Society of Japan, Tokyo, April, (1964).

1) a) W. R. Roderick, *J. Am. Chem. Soc.*, **79**, 1710 (1957); b) M. P. Grammaticakis, *Compt. rend.*, **251**, 1790 (1960); c) C. M. Lee and W. D. Kumler, *J. Am. Chem. Soc.*, **83**, 4586 (1961); d) C. M. Lee and W. D. Kumler, *J. Org. Chem.*, **27**, 2055 (1962).

2) T. Matsuo, This Bulletin, **37**, 1844 (1964).

Group 1: hydrogen,
Group 2: ethyl, cyclohexyl and benzyl,
Group 3: phenyl, *p*-tolyl and *p*-chlorophenyl, and
Group 4: *p*-methoxyphenyl.

The groups are numbered in the order of the increasing wavelength, or of the decreasing intensity, of the absorption maximum of the band concerned.

The difference between the classes given above becomes more evident when a comparison is made in terms of their solvent effects, shown in Figs. 3, 4 and 5. The solvent effect is also summarized in Table I. A strong bathochromic shift is observed for group 1 when the measurement is made in polar solvents. The bathochromic effect is very small or almost negligible in the case of group 2. The effect of the polar solvent becomes hypsochromic in group 3, and this same effect is further pronounced in group 4.

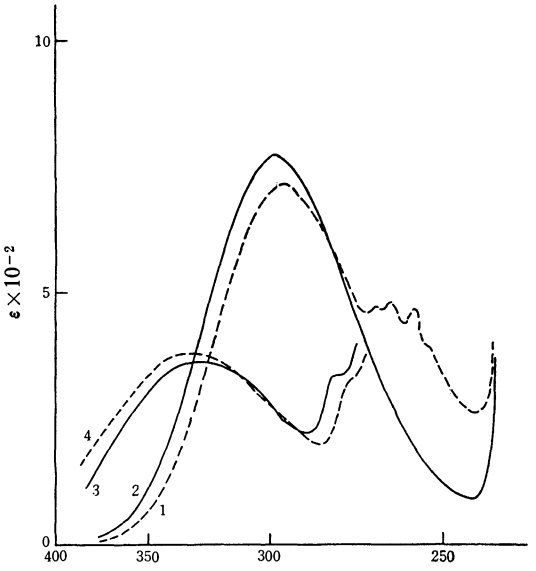



Fig. 2. Electronic absorption spectra of *N*-substituted maleimides in *n*-hexane.
1 *N*-Benzylmaleimide
2 *N*-Cyclohexylmaleimide
3 *N*-(*p*-Chlorophenyl)-maleimide
4 *N*-(*p*-Tolyl)-maleimide

TABLE I. THE WAVELENGTHS* AT MAXIMUM ABSORPTION OF THE LONGEST WAVELENGTH BANDS OF *N*-SUBSTITUTED MALEIMIDES IN VARIOUS SOLVENTS

| Substituent | *n*-Hexane | Acetonitrile | Ethanol | Methanol |
|---|---|---|---|---|
| Hydrogen | 265 | 272 | 274 | 275 |
| Ethyl | 294 | 296 | | 300 |
| Cyclohexyl | 299 | 302 | | |
| Benzyl | 296 | 296 | | |
| Phenyl | 322 | 307 | 298 | |
| *p*-Chlorophenyl | 327 | 311 | | |
| *p*-Tolyl | 330 | 312 | | |
| *p*-Methoxyphenyl | 348 | 317 | | |

* In mμ units.

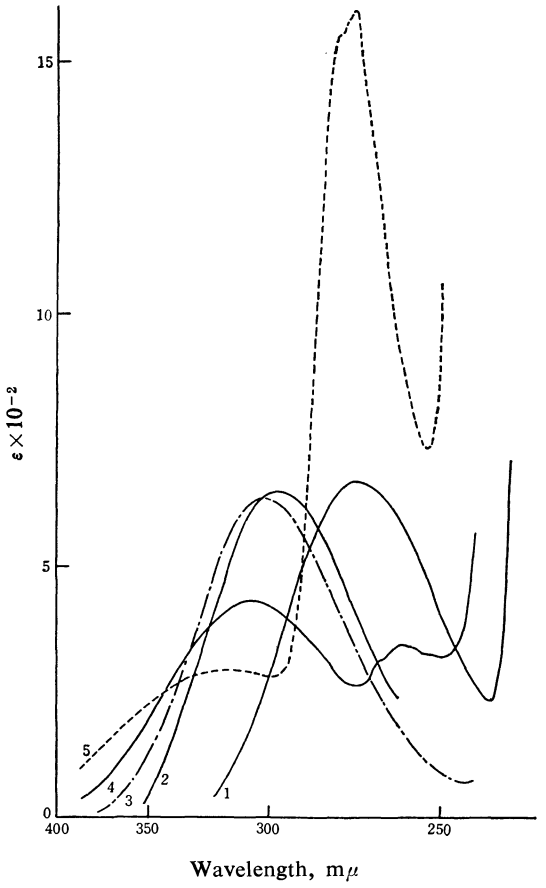
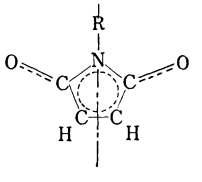



Fig. 3. Electronic absorption spectra of maleimide and its *N*-substituted derivatives in acetonitrile.
1 Maleimide
2 *N*-Etylmaleimide
3 *N*-Cyclohexylmaleimide
4 *N*-Phenylmaleimide
5 *N*-(*p*-Methoxyphenyl)-maleimide

Attempts were made to interpret the above experimental results by means of the Hückel LCAO-MO theory. The calculations were made by assuming a $C_{2v}$ symmetry and parameters for the imide system:




$\alpha_{\dot{O}} = \alpha_C + h_{\dot{O}}\beta$
$\alpha_{\ddot{N}} = \alpha_C + h_{\ddot{N}}\beta$
$\beta_{CO} = k_{CO}\beta$
$\beta_{CN} = k_{CN}\beta$

The effect of the expansion of conjugated systems on their energy levels was first examined by using the coplanar, axial structures and parameters shown in Fig. 6. When the substituent, R, is an aryl group, a new highest-occupied $\pi$-electron level appears. The lowest unoccupied energy level, on the other hand, is not affected at all, since the orbital is localized at the carbonyl groups and at the double bond connecting them. A decrease in the energy difference between the highest-occupied and the lowest-unoccupied levels results, therefore, when an aryl group is attached to the nitrogen atom. The decrease in the separation of the two $\pi$-electron energy levels argees qualitatively with the trend observed in the behavior of the longest-wavelength absorption bands of the four groups described above. This agreement, however, is not the true answer to the present problem, as may be seen by the following arguments. First of all, the oscillator strength of the pure $\pi \rightarrow \pi^*$ transition implied by the energy diagram may be expected to be much larger

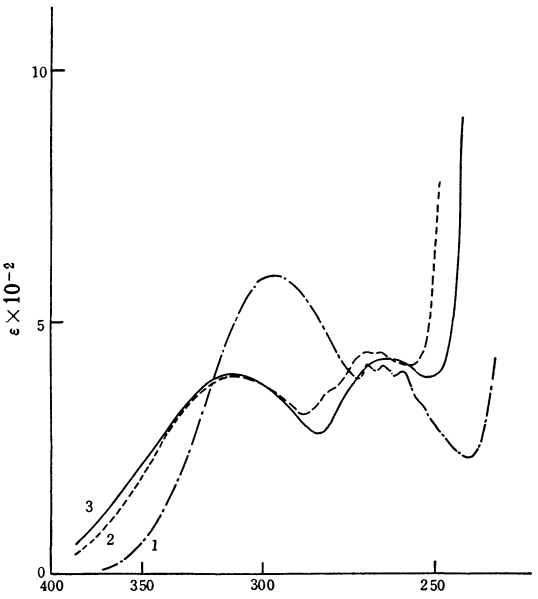



Fig. 4. Electronic absorption spectra of *N*-substituted maleimides in acetonitrile.
1 *N*-Benzylmaleimide
2 *N*-(*p*-Chlorophenyl)-maleimide
3 *N*-(*p*-Tolyl)-maleimide

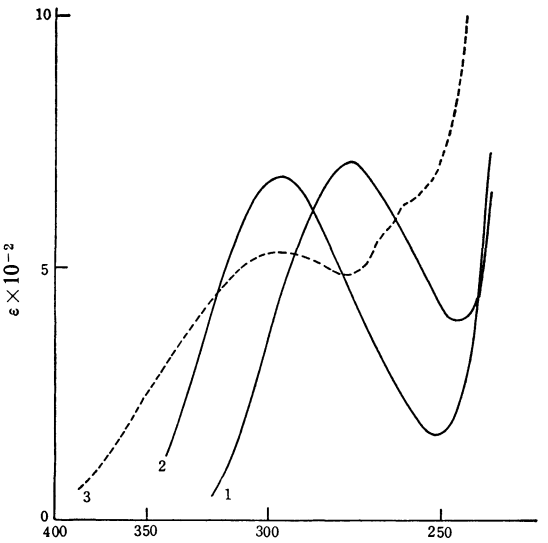



Fig. 5. Electronic absorption spectra of (1) maleimide (in methanol), (2) *N*-ethylmaleimide (in methanol), and (3) *N*-phenylmaleimide (in ethanol)

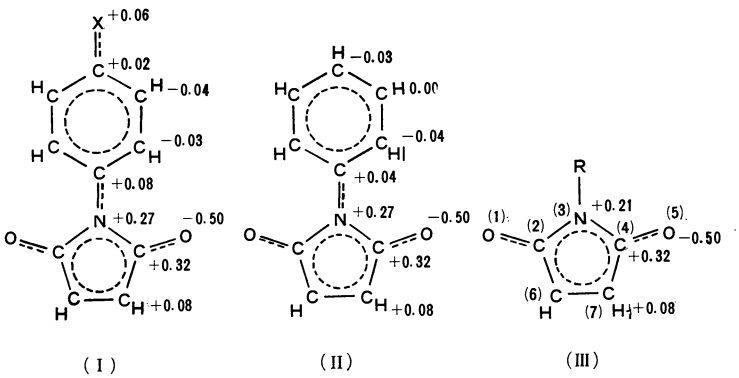



Fig. 6(a). The charge distributions in *N*-(*p*-methoxyphenyl)-maleimide (I), *N*-phenylmaleimide (II), and *N*-alkylmaleimide (III), as calculated by the Hückel LCAO method under the assumptions of coplanar, axial structures and the following parameters,
$h_O = k_{CO} = 1.0$, $h_N = 1.5$, $k_{CN} = 0.8$, $h_X = 2.0$ and $k_{CX} = 0.8$.
The parameters were chosen from the values recommended in the table given by Streitwieser.[3)]

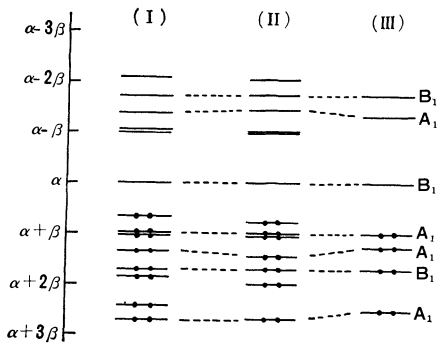



Fig. 6(b). The energy levels of the systems given in Fig. 6(a).

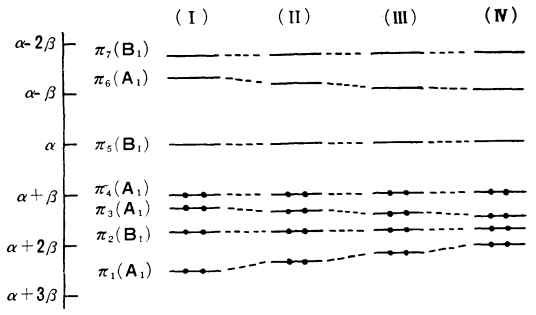



Fig. 7. The energy levels for maleimide systems as calculated by the use fo various $k_{CN}$ values.
(I) : $k_{CN}=0.8$ (II) : $k_{CN}=0.6$
(III) : $k_{CN}=0.4$ and (IV) : $k_{CN}=0.2$.
See the caption for Fig. 6(a) for the rest of the parameters used in the calculation.

TABLE II. CHARGE DENSITIES CALCULATED FOR MALEIMIDE SYSTEMS WITH VARIOUS $k_{CN}$ VALUES*

| Atom | $k_{CN}=0.8$ | $k_{CN}=0.6$ | $k_{CN}=0.4$ | $k_{CN}=0.2$ |
|---|---|---|---|---|
| N | +0.21 | +0.13 | +0.06 | +0.02 |
| O | −0.50 | −0.48 | −0.47 | −0.46 |
| $C_{C=O}$ | +0.32 | +0.33 | +0.33 | +0.33 |
| $C_{C=C}$ | +0.08 | +0.10 | +0.11 | +0.12 |

* See the caption for Fig. 7 for the rest of parameters used in the calculation.

than the largest observed values (of the order of $10^{-2}$) for the longest-wavelength absorption bands of *N*-alkylmaleimides. In the case of *N*-arylmaleimides, the molecular orbital of the highest-occupied $\pi$-electron energy level is localized at the aryl group. Therefore, the transition from that level to the lowest-unoccupied energy level has a strong character of charge-transfer absorption. An appreciable bathochromic shift may be expected, then, when the absorption band is measured in polar solvents. The experimental results are just the opposite of this prediction. In short, the absorption band in question can not be explained as due to a pure $\pi\rightarrow\pi^*$ transition.

The extent of the contribution of the nitrogen atom to the conjugated system was examined explicitly in the next calculations. In the cases of *N*-substituted phthalimides, their dipole moments indicate that the hybridization of the nitrogen orbital for the N-R bond changes from $sp^3$ to $sp^2$ types as the substituent is changed from hydrogen to methyl and then to phenyl groups.[4] Correspondingly, the orbital for the lone pair electrons of the nitrogen atom changes from a $sp^3$ to a pure p orbital in the order of the substituents given above. The same situation may be expected for *N*-substituted maleimides. In the Hückel LCAO-MO method, the above change in the hybridization of atomic orbitals corresponds to a modification of the parameters to be used in the calculations. In order to minimize any further complications, only $k_{CN}$ was varied in examining the effect of the isolation of the nitrogen atom from the conjugated system. The results are summarized in Fig. 7 and Table II. It shoud be noted that the electron densities at the nitrogen and oxygen atoms decrease and increase respectively as the $k_{CN}$ value increases. The increased electron density at the oxygen atom raises the energy level, *En*, of the lone pair electrons on the atom. Therefore, an interpretation of the absorption band as being due to the $n\rightarrow\pi^*$ transition of the carbonyl groups becomes possible, even though the lowest unoccupied level is not affected for the first approximation. Assuming that the nitrogen and the four carbon atoms make a completely coplanar system and that $k_{CN}$ is linearly proportional to the overlap integral, the $k_{CN}$ value is estimated to decrease approximately by a factor of 0.7 as a change is made from pure p to $sp^3$ orbitals for the nitrogen atom. A further reduction in $k_{CN}$ is expected if the nitrogen atom rises a little above the plane made by the carbonyl groups and the double bond. A close examination of the lowest unoccupied level reveals that it is also affected by the delocalization of the electrons of the nitrogen atom, as will be shown below. The molecular orbital of this level is:

$$\phi_5=\frac{1}{\sqrt{6}}(\phi_1-\phi_2+\phi_4-\phi_5-\phi_6+\phi_7) \qquad (1)$$

and its energy is given by:

$$E_5=\int\phi H\phi d\tau=\alpha_C+\frac{1}{3}(h_O-1)\beta+\frac{2}{3}(1-k_{CO})\beta \qquad (2)$$

3) A. Streitwieser, Jr., "Molecular Orbital Theory," John Wiley & Sons, Inc., New York (1961), p. 135.
4) a) H. Lumbroso and R. Dabard, *Bull. soc chim. France*, **1959**, 749; b) A. Arcoria, H. Lumbroso and R. Passerini, ibid., **1959**, 754.

The delocalization of the electrons to carbonyl groups increases the contribution of an ionic structure where the oxygen atom is bonded to the carbon atom through a single bond. Therefore, $k_{CO}$ becomes less than when the contribution of the ionic structure is small. The increased electron density at the oxygen atom in the ionic structure causes a reduction in the value of $h_O$ which appears in Eq. 2. The net results of these corrections are minor, however, in comparison with the change in *En*. Therefore, the increase in $k_{CN}$, or the contribution of the ionic structures, makes the separation between *En* and $E_5$ narrower than before after all.

The results obtained above agree qualitatively with the observed shift of the wavelength of the absorption band under discussion when the before-mentioned group is advanced from 1 to 4. However, neither the difference in the solvent effects of the four groups nor the relatively large intensities of the absorptions can be explained by a simple $n\rightarrow\pi^*$ transition of the carbonyl groups. Thus, it is clear that some modification of the above discussion are required. This modification is brought about quite naturally when the interaction between the $n\rightarrow\pi^*$ and other transitions of the system is taken into consideration.

A fairly large number of $\beta,\gamma$-unsaturated ketones have been known to show extraordinarily strong $n\rightarrow\pi^*$ transitions.[5,6] According to Labhart and Wagniere, the high intensities observed for these $n\rightarrow\pi^*$ transitions are due to a perturbation of the absorptions by the $\pi\rightarrow\pi^*$ transitions through the overlap of the oxygn 2p lone-pair orbital with the $\beta$-carbon $2p_\pi$ orbital.[6] Quite similar situations may be expected for the maleimide derivatives under discussion. Using Mulliken's table[7] and the geometry assumed for maleimide as shown in Fig. 8, the overlap integral between the oxygen 2p orbital and the nitrogen $sp^3$ orbital has been calculated to be 0.013. The overlap becomes small as the nitrogen orbital approaches a pure p orbital corresponding to the presumed cases of *N*-arylmaleimides. The nitrogen orbital, on the other hand, plays an important role in the $\pi$-electronic system of the imide group. As is shown in Table III, a large contribution of the nitrogen atomic orbital, to the third energy level $\pi_3$ of the imide systems given in Fig. 7 is observed. Therefore, a considerable interaction between the two transitions, $n$-$\pi^*$ and $\pi_3\rightarrow\pi^*$, may be expected when a noticeable

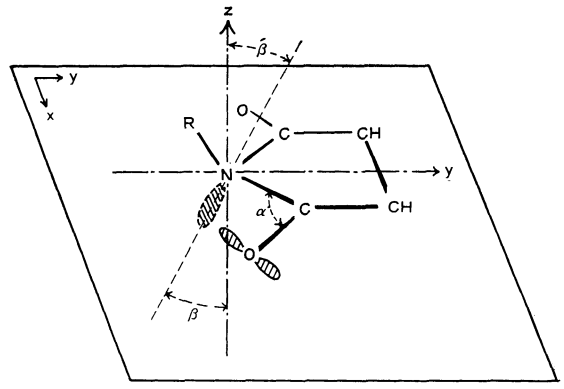



Fig. 8. Steric arrangement of atoms and the orbitals assumed for maleimide and its *N*-alkylsubstituted derivatives. The oxygen 2p orbitals are in the xy plane. The N—R bond and the nitrogen orbital as indicated by the shadowed area are directed up and down, respectively, from the xy plane. The following bond distance and bond angles were assumed in the calculation described in the text.
$r_{CN}=r_{CO}=1.25$Å, $\alpha=125°$, and $\beta=35°$

TABLE III. THE COEFFICIENTS FOR ATOMIC ORBITALS IN THE THIRD MOLECULAR ORBITAL $\pi_3$ SHOWN IN Fig. 7

| Atom | $k_{CN}=0.8$ | $k_{CN}=0.6$ | $k_{CN}=0.4$ | $k_{CN}=0.2$ |
|---|---|---|---|---|
| N | −0.709 | −0.781 | −0.863 | −0.952 |
| O | 0.346 | 0.304 | 0.242 | 0.146 |
| $C_{C=O}$ | 0.097 | 0.104 | 0.099 | 0.069 |
| $C_{C=C}$ | 0.346 | 0.304 | 0.242 | 0.146 |

overlap exists between the oxygen 2p orbital and the nitrogen orbital. Unfortunately, the $\pi_3\rightarrow\pi^*$ transition could not be identified in the present experiment. The oscillator strength of the corresponding absorption band, however, is estimated theoretically to be of the order of $10^{-1}$, since it is a possible $\pi\rightarrow\pi^*$ transition. Therefore, the overlap between the oxygen 2p lone-pair orbital and the nitrogen orbital as estimated above is large enough to explain the intensification of the $n\rightarrow\pi^*$ transition of the carbonyl groups by the perturbation. Furthermore, the $\pi_3\rightarrow\pi^*$ transition has a strong charge-transfer absorption character as is obvious from an inspection of the molecular orbitals concerned. Therefore, it is quite natural that a bathochromic shift is observed for the longest-wavelength absorption band of maleimide and its *N*-alkyl substituted derivatives when the spectra are measured in polar solvents. The overlap described above decreases rapidly as the nitrogen orbital approaches a pure p orbital. A decrease in intensity and a change in solvent effect are

5) R. C. Cookson and N. S. Wariyar, *J. Chem. Soc.*, **1956**, 2302.
6) H. Labhart and G. Wagniere. *Helv. Chim. Acta*, **42**, 2219 (1959).
7) R. S. Mulliken, C. A. Rieke, D. Orloff and H. Orloff, *J. Chem. Phys.*, **17**, 1248 (1949).

expected, accordingly, for the longest-wavelength absorption band of *N*-arylmaleimide.

In the case of *N*-arylmaleimide, an interaction of the oxygen 2p orbital with the $\pi$ orbital on the phenyl group must also be taken into consideration. This type of interaction is expected to have a small effect upon the longest-wavelength absorption for the following two reasons. The overlap between the oxygen lone-pair orbital and the $\pi$ orbital of the phenyl group is strongly dependent on the twisting angle, $\theta$, of the phenyl group around the $C_2$ axis, as is shown in Fig. 9. For the best situation, where $\theta$ is 90°, the overlap between the oxygen 2p orbital and the highest-occupied orbital of the phenyl group is estimated to be 0.01 or so. Actually, the phenyl group does not stay at the perpendicular position relative to the imide plane. Thus, the real or average value of the overlap integral is less than 0.01. Secondly, moment of the transition from the $\pi$ orbitals on the phenyl group to $\pi^*$ is expected to be small when $\theta$ is different from zero. Therefore, the $\pi \rightarrow \pi^*$ transition under discussion is not intensified very much by the perturbation through the interaction of the oxygen lone-pair orbital with $\pi$ orbitals of the phenyl group.

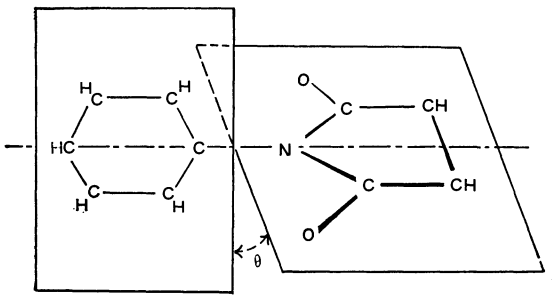



Fig. 9. Orientation of the plane of phenyl group with respect to the imide plane. The angle of twisting is indicated by $\theta$.

In conclusion, the longest-wavelength absorption bands of *N*-substituted maleimides are found to be essentially due to the $n \rightarrow \pi^*$ transition of the carbonyl group. When the hydrogen on the nitrogen atom is replaced by alkyl and aryl groups, the nitrogen lone-pair electrons delocalize more and more to the carbonyl groups and the absorption bands in question shift to longer wavelengths. In the case of maleimide, the $n \rightarrow \pi^*$ transition is perturbed strongly by the $\pi \rightarrow \pi^*$ transition of the cyclic imide system, and an appreciable intensification of the absorption band and its bathochromic shift in the polar solvents result. The perturbation decreases rapidly in the order of *N*-alkyl- and *N*-arylmaleimides, and the absorption approaches a pure $n \rightarrow \pi^*$ transition.

The author wishes to express his gratitude to Dr. Mitsuo Ito of the Department of Chemistry, Faculty of Science, Kyushu University, for his interest in this work and his continuous encouragement. He is also indebted to Miss Katsumi Mera for measuring the spectra reported in this paper.

*Department of Organic Synthesis*
*Faculty of Engineering*
*Kyushu Univertity*
*Hakozaki, Fukuoka*

# Quinoxaline Derivatives. V.[1] Some Reactions of 2-Cyano-3-hydroxyquinoxaline 1-Oxide

By Yusuf AHMAD, M. S. HABIB,* M. IQBAL and ZIAUDDIN

(Received July 30, 1964)

The presence of a nitrile group and an *N*-oxide function, side by side in the same molecule, confers some unusual properties on 2-cyano-3-hydroxyquinoxaline 1-oxide (Ia), as has been reported in an earlier paper.[2] It is recovered unchanged when it is refluxed with phosphorus trichloride. All atempts to deoxygenate it to 2-cyano-3-hydroxyquinoxaline (II: R=R'=H; R''=CN) by reduction with sodium dithionite in acetic acid (or aqueous ethanol), zinc and acetic acid, or by catalytic hydrogenation in the presence of Pd-C, were unsuccessful. Instead of the expected deoxygenated base (II: R=R'=H; R''=CN), the

* C/o Burroughs Wellcome & Co. (Pakistan), Ltd., D/43 S. I. T. E., Karachi, Pakistan.

1) Part IV: Y. Ahmad, M. S. Habib, Ziauddin and N. Bashir, *Tetrahedron*, **21**, April (1965).

2) Part III; Y. Ahmad, M. S. Habib and Ziauddin, ibid., **20**, 1107 (1964).

product isolated in each case was 2-hydroxyquinoxaline (II: R=R'=R''=H), indicating that although deoxygenation had been achieved, it was accompanied by a simultaneous loss of the nitrile group.

During the reaction of 3-hydroxyquinoxaline-2-carboxyamide 1-oxide (III) with aniline (or *N*-methylaniline) to obtain 3-hydroxyquinoxaline-2-carboxyanilide (or *N*-methylanilide) 1-oxide (III: CONHPh or CONMePh for $CONH_2$), it was observed that if the reactants were heated together for only a few minutes the product obtained in both cases was 3-hydroxyquinoxaline-2-carboxyamide (II: R=R'=H; R''=$CONH_2$), whereas if the heating was prolonged for 24 hr., 3-hydroxyquinoxaline-2-carboxyanilide (II: R=R'=H; R''=CONHPh) and 3-hydroxyquinoxaline-2-carboxy-*N*-methylanilide (II: R=R'=H; R''=CONMePh) respectively were obtained. This indicated that these amines deoxygenated the *N*-oxide (III) and that the resulting amide reacted further to give the corresponding anilides (II: R=R'=H; R''=CONHPh or CONMePh). This observation, combined with the fact that amines are known[3] to deoxygenate heterocyclic *N*-oxides, prompted us to try the action of amines on the *N*-oxide (Ia) to obtain 2-cyano-3-hydroxyquinoxaline (II: R=R'=H; R''=CN) which was needed in connection with another investigation.

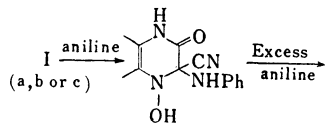
The *N*-oxide (Ia), on being heated with *N*-methylaniline, gave a product which also seemed to have lost the nitrile group (the infrared absorption peak at 2240 $cm^{-1}$ for CN was missing). Its constitution was established as 3-hydroxy-2-(*N*-methylanilino)quinoxaline (IIb) on the basis of the following evidence:

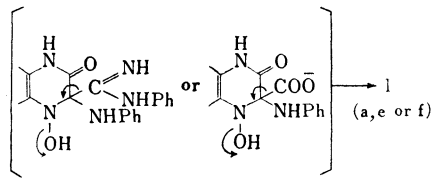
(i) Its elementary analysis agrees with $C_{15}H_{13}N_3O$.

(ii) On methylation with methyl sulphate in acetone in the presence of potassium carbonate, it was converted to 3,4-dihydro-4-methyl-2-(*N*-methylanilino)-3-oxoquinoxaline (IIc), identical (infrared spectra and mixed melting point) with an authentic sample prepared[4] by heating 2-chloro-3,4-dihydro-4-methyl-3-oxoquinoxaline and *N*-methylaniline together in methanol.

Aniline and cyclohexylamine also reacted similarly with the *N*-oxide (Ia) and yielded the corresponding amino-derivatives (IIa and d). 7-Chloro- and 7-ethoxy-derivatives (Ib and c) of 2-cyano-3-hydroxyquinoxaline 1-oxide also behaved similarly and with aniline gave anilino-derivatives (IIe and f) of the same type. The structures of these amino-derivatives (IIa and d-f) followed by analogy and on the basis of their elementary analysis. This reaction of bases on the *N*-oxides (Ia-c) can be compared to asimilar action of aqueous potassium hydroxide, described in Part III,[2] wherein the highly-developed electrophilicity of the $C_{(2)}$ of the *N*-oxide (Ia), on account of its attachment to two strong electron-withdrawing functions (i. e., CN and *N*-oxide), is considered to be responsible for the attack of the OH anion and, thereby, the displacement of the nitrile group.

The bases similarly attack the electron-deficient $C_{(2)}$. However, no free CN anions were detected in the reaction mixture, as in the case of the action of aqueous potassium hydroxide on I (a, b or c). Therefore, the amines (e. g. aniline) probably react further with the nitrile group and result in a simultaneous deoxygenation, as is shown below: **




3-Hydroxy-2-phenylquinoxaline 1-oxide[1] (Ia: Ph for CN), when heated under reflux with fuming hydrobromic acid, is quantitativly deoxygenated[5] to 3-hydroxy-2-phenylquinoxaline (II: R=R'=H; R''=Ph). This interesting transformation led us to study the effect of fuming hydrobromic acid on the *N*-oxide (Ia). On being refluxed with this reagent for two hours, Ia gave, in a 30% yield, a product which contained bromine in a non-reactive form. Its infrared spectrum resembled that of 2,3-dihydroxyquinoxaline. Elementary analysis agreed well with a monobromo-derivative of 2,3-dihydroxyquinoxaline. The position of bromine was established as follows:

(a) Its infrared spectrum was identical with that of 6-bromo-2,3-dihydroxyquinoxaline (IVa), which was synthesised by the condensation of 4-bromo-*o*-phenylenediamine with ethyl oxalate as described by Curd et al.[6]

(b) The mono-bromo compound, on methylation with methyl sulphate and aqueous alkali,

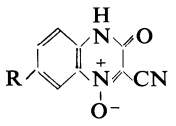
3) I. J. Pachter and M. C. Kloetzel, *J. Am. Chem. Soc.*, **74**, 971 (1952).

4) J. W. Clark-Lewis, *J. Chem. Soc.*, **1957**, 439.

** The authors wish to thank the referee for this suggestion, which accounts for the loss of the nitrile group with the simultaneous deoxygenation of the compounds.

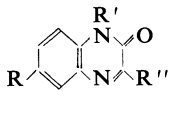
5) Unpublished work.

6) F. H. S. Gurd, D. G. Davey and G. J. Stacey, *J. Chem. Soc.*, **1949**, 1271.



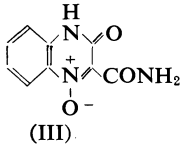
(I)

(a) R=H
(b) R=Cl
(c) R=EtO

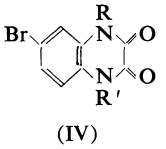


(II)

| | R | R′ | R″ |
|---|---|---|---|
| (a) | H | H | NHPh |
| (b) | H | H | NMePh |
| (c) | H | Me | NMePh |
| (d) | H | H | HN(S) |
| (e) | Cl | H | NHPh |
| (f) | EtO | H | NHPh |



(III)



(IV)

(a) R=R′=H
(b) R=R′=Me
(c) R=Me; R′=H

gave a dimethyl derivative, m. p. 205—207°C, which was identical (infrared spectra and mixed melting point) with an authentic sample of 6-bromo-1, 2, 3, 4-tetrahydro-1, 4-dimethyl-2, 3-dioxoquinoxaline (IVb) synthesised by the methylation of 6-bromo-2, 3-dihydroxyquinoxaline or 6-bromo-3, 4-dihydro-4-methyl-3-oxoquinoxaline (IVc). This unusual formation of 6-bromo-2, 3-dihydroxyquinoxaline from 2-cyano-3-hydroxyquinoxaline 1-oxide (Ia) probably takes place in two steps. The *N*-oxide (Ia) is first converted to 2, 3-dihydroxyquinoxaline through the sequence (cyano *N*-oxide (Ia) → amide *N*-oxide (III) → carboxylic acid *N*-oxide (III, $CO_2H$ for $CONH_2$) → decarboxylation to 3-hydroxyquinoxaline 1-oxide → rearrangement to 2, 3-dihydroxyquinoxaline) as was previously envisaged[2] in its reaction with a mixture of concentrated sulphuric acid and acetic acid. Bromination takes place later with bromine, which is either generated in situ by the consumption of a part of the *N*-oxide or by the aerial oxidation of hydrobromic acid itself. This is supported by the fact that 2, 3-dihydroxyquinoxaline (IVa: H for Br) itself gives 6-bromo-2, 3-dihydroxyquinoxaline (IVa) (a) on prolonged heating with fuming hydrobromic acid or (b), far more quickly and in a quantitative yield on the addition of an aqueous solution of potassium bromate (to generate one equivalent of bromine) to its solution in hydrobromic acid.

In contrast to this is the observation that the *N*-oxide (Ia) is recovered unchanged even after eight hours boiling with a mixture of concentrated hydrochloric acid and acetic acid.

7) A. H. Cowenlock, G. T. Newbold and F. S. Spring, ibid., **1945**, 622.

## Experimental

Infrared spectra were measured in Nujol mull. The light petroleum used had a 60—80°C boiling range.

**2-Anilino-3-hydroxyquinoxaline (IIa).**—2-Cyano-3-hydroxyquinoxaline 1-oxide[2] (Ia) (1g.) and aniline (20 ml.) were heated together under reflux for 4 hr. The reaction mixture was allowed to cool and then diluted with light petroleum. The solid thus separated was crystallised from ethanol as pale yellow micro-needles of the anilinoquinoxaline (IIa), yield, 90%; m. p. 247—248°C (Found: C, 69.6; H, 4.4; N, 17.5. Calcd. for $C_{14}H_{11}N_3O$: C, 70.8; H, 4.6; N, 17.7%).

**3-Hydroxy-2-(*N*-methylanilino)quinoxaline (IIb).**—Similarly, the *N*-oxide (Ia) in an excess of *N*-methylaniline gave, in a 40% yield, colourless cubes (from ethanol) of the *N*-methylanilinoquinoxaline (IIb), m. p. 180—182°C (Found: N, 16.5. Calcd. for $C_{15}H_{13}N_3O$: N, 16.7%). The compound IIb (0.13 g.), on methylation with methyl sulphate (0.1 ml.) in the presence of anhydrous potassium carbonate (0.5 g.) and acetone (heated under reflux), gave, in a 50% yield, 3, 4-dihydro-4-methyl-2-(*N*-methylanilino)-3-oxoquinoxaline (IIc), m. p. 145—146°C (Found: N, 15.95. Calcd. for $C_{16}H_{15}N_3O$: N, 15.8%). Its melting point was not depressed by admixture with a sample (m. p. 143—144°C) prepared by the method of Clark-Lewis[4] by the condensation of 2-choro-3, 4-dihydro-4-methyl-3-oxoquinoxaline with *N*-methylaniline in boiling methanol.

**2-Cyclohexylamino-3-hydroxyquinoxaline (IId).**—Similarly, the *N*-oxide (Ia), on being treated with cyclohexylamine, gave, in a 90% yield, yellow needles (from ethanol) of the cyclohexylaminoquinoxaline (IId), m. p. 246°C (Found: C, 63.8; H, 7.1; N, 16.3. Calcd. for $C_{14}H_{17}N_3O \cdot H_2O$: C, 64.3; H, 7.2; N, 16.1%).

**2-Anilino-7-chloro-3-hydroxyquinoxaline (IIe).**—7-Chloro-2-cyano-3-hydroxyquinoxaline 1-oxide[2] (Ib) with aniline gave, in a good yield, yellow cubes (from glacial acetic acid) of the anilinochloroquinoxaline (IIe), m. p. 318—319°C (Found: Cl, 13.15; N, 15.3. Calcd. for $C_{14}H_{10}ClN_3O$: Cl, 13.1; N, 15.5%).

**2-Anilino-7-ethoxy-3-hydroxyquinoxaline (IIf).**—2-Cyano-7-ethoxy-3-hydroxyquinoxaline 1-oxide[2] (Ic) with aniline gave in a good yield, yellow needles (from ethanol) of the anilinoethoxyquinoxaline (IIf), m. p. 260—261°C (Found: C, 67.65; H, 5.4; N, 15.0. Calcd. for $C_{16}H_{15}N_3O$: C, 68.3; H, 5.4; N, 14.9%).

**The Reduction of 3-Hydroxyquinoxaline-2-carboxyamide (III).**—The amide *N*-oxide[2] (III), on being heated under reflux with aniline or *N*-methylaniline for 3 min., gave 3-hydroxyquinoxaline-2-carboxyamide (II: R=R′=H; R″=$CONH_2$), m. p. 308—310°C (decomp.) in a quantitative yield. Its melting point was not depressed by admixture with a sample[7] (m. p. 308—310°C) obtained by the action of concentrated ammonium hydroxide on ethyl 3-hydroxyquinoxaline-2-carboxylate. The infrared spectra of the compounds obtained by the two methods were also identical.

**6-Bromo-2, 3-dihydroxyquinoxaline (IVa).**—a) The *N*-oxide (Ia) (1 g.) or amide *N*-oxide (III) (1 g.) in fuming hydrobromic acid (30 ml.) was heated under reflux for 2 hr. The reaction mixture was then allowed to cool. On dilution with water, a yellow solid separated which crystallised from dimethylformamide-ethanol as colourless cubes of the bromoquinoxaline (IVa), m. p. >350°C, yield 30% (Found: N, 11.8. Calcd. for $C_8H_5BrN_2O_2$; N, 11.6 %). This was identical (infrared spectra) with an authentic sample of 6-bromo-2, 3-dihydroxyquinoxaline.[6] The *N*-oxide (Ia) was recovered unchanged on being heated under reflux for 8 hr. with a mixture (1 : 1) of HCl and AcOH or on being heated under reflux with acetylchloride in a sealed tube at 100°C for 72 hr. The amide *N*-oxide (III), on the other hand, gave 2, 3-dihydoxyquinoxaline on being heated with a mixture (1 : 1) of HCl and AcOH.

b) A mixture of 2, 3-dihydroxyquinoxaline (1 g.) and fuming hydrobromic acid (50 ml.) was heated under reflux for 8 hr. The solid separated during the reaction was collected and crystallised from dimethylformamide-ethanol as colourless cubes of the monobromo-2, 3-dihydroxyquinoxaline (20% yield, m.p. >350°C, identical (infrared spectra) with a sample obtained under a). Curd, Davey and Stacey[6] have reported this compound, but have not given any melting point for it.

c) The addition of a calculated amount of aqueous potassium bromate to a solution of 2, 3-dihydroxyquinoxaline in hot fuming hydrobromic acid immediately precipitated, in a quantitative yield, the monobromo-2, 3-dihydroxyquinoxaline, which was then collected and crystallised from dimethylformamide-ethanol as colourless cubes, m. p. >350°C (The infrared spectrum was identical with that of 6-bromo2, 3-dihydroxyquinoxaline.).

**6-Bromo-1, 2, 3, 4-tetrahydro-1, 4-dimethyl-2, 3-dioxoquinoxaline (IVb).**—6-Bromo-2, 3-dihydroxyquinoxaline (obtained under a, b or c; see above) (1 g.), anhydrous potassium carbonate (2 g.) and methyl sulphate (0.5 ml.) in acetone (50 ml.) were heated under reflux for 3 hr. The reaction mixture was then filtered, and the filtrate on concentration gave a solid which crystallised from ethanol as white needles of the tetrahydroquinoxaline (IVb), m. p. 205—206°C, in a good yield. It was identical (infrared spectra and mixed melting point with a synthetic sample prepared by the methylation of 6-bromo-3, 4-dihydro-2-hydroxy-4-methyl-3-oxoquinoxaline (IVc) (see below) with methyl sulphate and aqueous sodium hydroxide. Curd, Davey and Stacey[6] recorded its m. p. as 205—206°C.

**6-Bromo-3, 4-dihydroxy-2-hydroxy-4-methyl-3-oxoquinoxaline (IVc).**—Without being isolated from its ethanolic solution, 4-bromo-2-methylaminoaniline prepared by the hydrogenation of 4-bromo-2-methylamino-1-nitrobenzene (5 g.) in ethanol (60 ml.) over Pd-C was condensed with ethyl oxalate (20 g.) by heating them together under reflux for 3.5 hr. The solid which separated was collected and crystallised from acetic acid as colourless micro-needles of the bromoquinoxaline (IVc), m. p. 325—327°C (Found: Br, 31.05; N, 10.7. Calcd. for $C_9H_7BrN_2O_2$: Br, 31.4; N, 11.0%).

## Summary

2-Cyano-3-hydroxyquinoxaline 1-oxide (Ia), and its 7-chloro- or 7-ethoxy-derivatives (Ib, c), on treatment with aniline, are deoxygenated, with a simultaneous displacement of the nitrile group, resulting in the formation of 2-anilinoquinoxalines (IIa, e and f). Ia undergoes similar transformations with *N*-methylaniline and cyclohexylamine.

The *N*-oxide (Ia), on being heated with fuming hydrobromic acid, yields 6-bromo-2, 3-dihydroxyquinoxaline (IVa), the mechanism of formation of which has been outlined.

We wish to thank Dr. S. Siddiqui, F. R. S., Chairman of the Pakistan Council of Scientific and Industrial Research, for his interest and encouragement. The analyses were carried out by M/S. Pascher & Pascher, Germany, and the Microanayltical Section, Central Laboratories, Pakistan Council of Scientific and Industrial Research Karachi.

*Chemical Research Division*
*Central Laboratories*
*Pakistan Council of Scientific and Industrial Research*
*Karachi, Pakistan*

# The Electrokinetic Potential of Lead(II) Sulfate

By Tetsuo MORIMOTO, Yutaka HIRATA and Shigeharu KITTAKA

(Received July 30, 1964)

It was reported in a previous paper that the signs of the electrokinetic potentials of sparingly soluble salts in water generally agree with those of the excess ions used when the salts are prepared. Lead(II) sulfate, however, was observed to be an exception.[1] Samples of lead sulfate which were prepared using either excess lead or sulfate ions both had positive charges. Buchanan and Heymann[2] observed that lead sulfate possesses a positive charge in a saturated solution. In the present paper, further studies of the electrokinetic behaviors of lead sulfate have been carried out in order to determine the origin of its positive electrokinetic potential. The electrokinetic potentials have been determined by applying the streaming potential method to samples prepared by different methods and treated at various temperatures, and the surface acidities of the samples have been investigated by the dye-adsorption method.

## Experimental

**Materials.** — Two solutions containing 0.005 M lead nitrate and 0.005 M sodium sulfate were mixed at room temperature in a large flask. In mixing, one reagent was used in a 5% excess over the other. The precipitations occurred after the solutions had been vigorously mixed for one minute or less. The pH values of the supernatant liquids were in the range from 4.60 to 4.74. The precipitates formed were washed with conductivity water by decantation and filtration until the pH values and the conductivities of the supernatant liquids attained limiting values. After these procedures the final pH values were 6.10—6.20 at 25°C. Finally, the samples were dried at 110°C for three hours. Parts of each sample were treated at 300, 500 and 700°C in an electric oven for an hour each.

**Electrokinetic Measurements.** — The streaming potential method was used for the determination of the electrokinetic potentials (ζ-potentials). For the measurement of the streaming potentials, an apparatus and techniques similar to those described in previous papers[1,3] were employed. The specific conductivity of the cell packed with the powdered sample was obtained by using the conductometer made by the Toa Dempa Co. The streaming potentials produced on the electrodes placed at the ends of the diaphragm were read by a precision potentiometer and were plotted against the pressure applied on the liquids flowing through the diaphragm. The linear relation obtained between them made possible the calculation of the ζ-potentials by using the Helmholtz-Smoluchowski equation. All the measurements were carried out at 15—20°C.

**Surface Acidity.**—In order to test the surface acidities, the dye-adsorption method was employed. 0.3 g. samples of the powders were shaken with 4 cc. of an isooctane solution containing 0.01% of methyl red.[4] After the adsorption of the dye molecules, the powders were separated and dried in air. The color of the adsorbed molecules on the surface of the powders was analyzed against magnesia as a reference by means of a Shimadzu spectrophotometer.

## Results and Discussion

The ζ-potentials obtained in water are summarized, together with those of the samples used, in preliminary experiments, in Table I. These values are equilibrium values obtained after a long streaming of water.

It may be seen from Table I that all the values of the ζ-potential of lead sulfate have a positive sign, irrespective of the kinds of reagents used, of the excess ions, and of the pH values of the solutions. It was found in a previous paper that the surfaces of lead(II) chromate, barium sulfate and barium chromate have charges of the same sign as that of the excess ion used in the preparation.[1] This suggests that the lattice ions extensively occupy the lattice points on the surface and that it is very difficult to remove them by washing. However, this is not true for lead sulfate.

The ζ-potentials, obtained from measurements on the samples at intervals of about one hour, of lead sulfate, treated at different temperatures, vary slowly with time to an equilibrium value which is positive, as is shown in Figs. 1 and 2. The equilibrium ζ-potentials are plotted against the treatment temperatures in Fig. 3. The ζ-values decrease

1) T. Morimoto, This Bulletin, 37, 386 (1964).
2) A. S. Buchanan and E. Heymann, *J. Colloid Sci.*, 4, 137 (1949).
3) T. Morimoto and M. Sakamoto, This Bulletin, 37, 719 (1964).
4) K. Tanabe and M. Katayama, *J. Res. Inst. Catalysis, Hokkaido Univ.*, 7, 106 (1956); C. Walling, *J. Am. Chem. Soc.*, 72, 1164 (1950).

TABLE I. ζ-POTENTIALS OF LEAD SULFATE IN WATER

| Sample | Reagent | | pH of solution | ζ-Potential |
|---|---|---|---|---|
| 1 | 0.005 M $Na_2SO_4$ 1900 ml. | 0.005 M $Pb(NO_3)_2$ 2000 ml. | 4.60 | +31.0 |
| 2 | 0.005 M $Na_2SO_4$ 2000 ml. | 0.005 M $Pb(NO_3)_2$ 1900 ml. | 4.74 | +28.6 |
| 3 | 1 M $Na_2SO_4$ 200 ml. | 1 M $Pb(NO_3)_2$ 180 ml. | 2.65 | +23.6 |
| 4 | 1 M $Na_2SO_4$ 200 ml. | 1 M $Pb(NO_3)_2$ 180 ml. | 1.04* | +21.2 |
| 5 | 1 M $Na_2SO_4$ 180 ml. | 1 M $Pb(NO_3)_2$ 200 ml. | 2.50 | +32.9 |
| 6 | 1 M $Na_2SO_4$ 200 ml. | 1 M $PbAc_2$ 180 ml. | 6.70 | +12.5 |
| 7 | 1 M $Na_2SO_4$ 180 ml. | 1 M $PbAc_2$ 200 ml. | 6.53 | +13.1 |

* Nitric acid was added to the lead nitrate solution prior to the preparation of the precipitate.

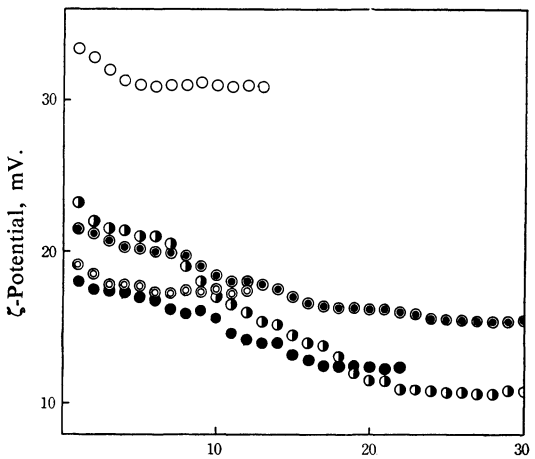



Fig. 1. ζ-Potentials of lead sulfate prepared from excess lead ions and treated at: ○ no heat treatment, ◎ 100°C, ⊙ 300°C, ◑ 500°C, ● 700°C.

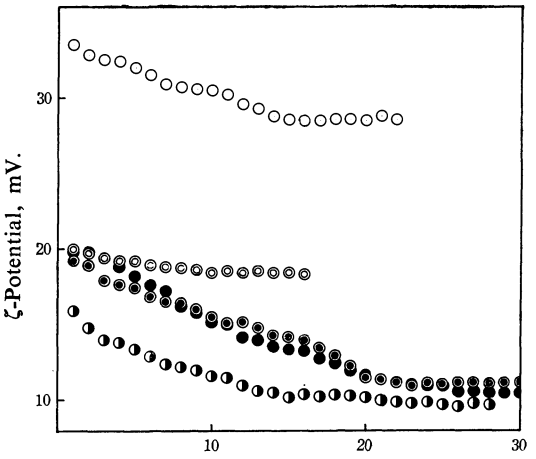



Fig. 2. ζ-Potentials of lead sulfate prepared from excess sulfate ions and treated at: ○ no heat treatment, ◎ 100°C, ⊙ 300°C, ◑ 500°C, ● 700°C.

initially to an almost constant value, irrespective of the kinds of excess ions used in the preparation of the samples.

Figure 4 shows the reflectance spectrum of lead sulfate, which adsorbed the molecules of methyl red. The yellow colors of the samples treated at higher temperatures indicate a decrease in the surface acidities with a rise in the treatment temperature. The same tendency has been seen in samples prepared from both excess lead ions and excess sulfate ions.

When the samples treated at higher temperatures were exposed to water vapor, the surfaces of the samples recovered their original acidities. It may be seen from Fig. 5 that the longer the time of exposure to water vapor, the deeper the red color of the adsorbed dye molecules, and, therefore, the stronger the acidity of the surface.

If lead sulfate is hydrolyzed in an aqueous solution, the following relations will hold in equilibrium at 25°C:

$$[Pb^{2+}]\,[SO_4^{2-}] = K_S{}^{5)} = 1.58\times10^{-8} \quad (1)$$

$$[Pb^{2+}]\,[OH^-]^2 = K_B{}^{6)} = 3\times10^{-20} \quad (2)$$

$$[H^+]\,[OH^-] = K_W = 10^{-14} \quad (3)$$

$$2[Pb^{2+}] + [H^+] = 2[SO_4^{2-}] + [OH^-] \quad (4)$$

The hydrogen ion concentration which can satisfy these four equations is $10^{-6.2}$ at 25°C. The pH value of the saturated solution of

5) J. A. Cowperthwaite and V. K. LaMer, ibid., 53, 4342 (1931).
6) P. Deschamps and B. Charreton, *Compt. rend.*, 232, 162 (1951).

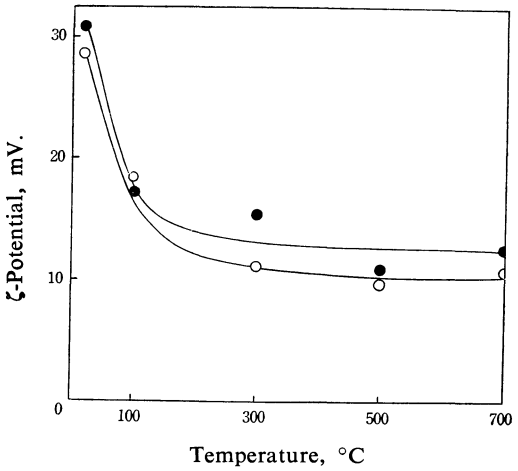



Fig. 3. Dependence of the ζ-potential of lead sulfate on the pretreatment temperature.
● lead ion excess, ○ sulfate ion excess

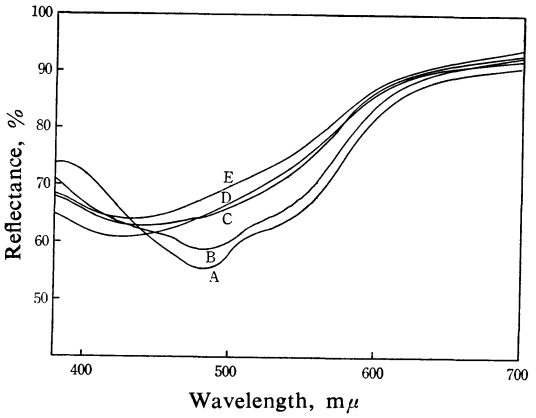



Fig. 4. Reflection spectra of methyl red adsorbed on lead sulfate treated at: A, no treatment; B, 100°C; C, 300°C; D, 500°C; E, 700°C.

lead sulfate should, therefore, be 6.2. The experimental pH values of the saturated solution of lead sulfate were 6.10—6.20, in good agreement with the calculated value. This suggests that the surface hydrolysis of lead sulfate leaves lead hydroxide on its surface although the saturated solution becomes acidic. From these considerations, it seems plausible that the lead sulfate produced from an aqueous phase and dried at lower temperatures has an acidic surface due to surface hydrolysis in the presence of adsorbed water. If the sample is treated at higher temperatures, the sulfuric acid will be removed, a solid surface being a basic characteristic of adsorbed dye molecules. The inversion of the surface acidity of the sample by water adsorption or by immersion in water can probably be explained by additional hydrolysis on the surface. In the measurement of the ζ-potentials on such hydrolyzed samples of lead sulfate, the solid surface may largely act like lead hydroxide.

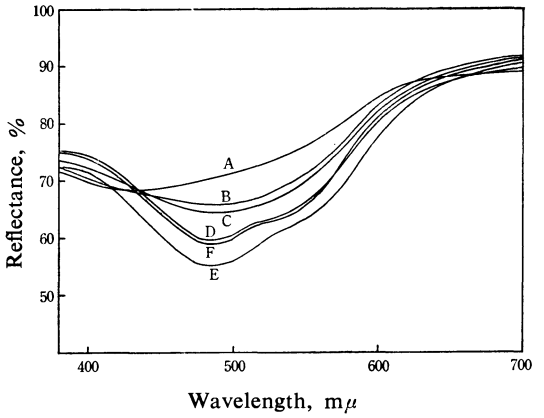



Fig. 5. Reflection spectra of methyl red adsorbed on lead sulfate treated at 700°C (A) and then exposed to saturated water vapor at 22°C for 1 hr. (B), 3 hr. (C), 24 hr. (D), 30 hr. (E). Sample F was immersed in water for 3 days and after that dried at 110°C for 1 hr.

In order to test the ζ-potential of lead hydroxide, a sample was prepared in the following way: in order to produce lead oxide pure lead oxalate was decomposed in an electric oven held at 600°C for an hour. The ζ-potential of this sample was found to be +10.1 mV. in water. Lead oxide can be hydrated to form surface hydroxyl groups in water. The fact that the surface of lead oxide has a positive charge is probably the result of the dissociation of surface hydroxyl groups thus formed:

$$-PbOH \rightarrow -Pb^{+} + OH^{-}$$

These considerations appear to indicate why the ζ-potential of lead sulfate is always positive in water. In this case, the preferential adsorption of hydrogen ions produced by surface hydrolysis may more or less contribute to the surface charge of lead sulfate. By progressive treatment at higher temperatures, the ζ-potentials decrease to a constant value, probably because the lead oxide produced by heat treatment by the condensation of surface hydroxyl groups, or by the decomposition of lead sulfate, can not be easily rehydrated on immersion in water, resulting in a decrease in the charge density on the surface.

## Summary

The ζ-potential of lead sulfate has been studied by applying the streaming potential

method to samples obtained by various preparative methods and subjected to various temperature treatments. All the ζ-potentials measured have a positive sign, irrespective of such conditions as the kinds of reagents and excess ions used in the preparation or the pH value of the reacting solution. It has been postulated that the surface of lead sulfate is hydrolysed to produce lead hydroxide, whose ζ-potential is explicit in the measurement of the streaming potential of lead sulfate. This is supported by the pH value of the saturated solution of lead sulfate. The surface behavior of lead sulfate in relation to the dye adsorption can also be explained in this way.

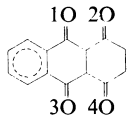
*Department of Chemistry*
*Faculty of Science*
*Okayama University*
*Tsushima, Okayama*

# Electronic Spectra of 1, 4, 9, 10-Anthradiquinone and Its Complexes with Aromatics

By Akira KUBOYAMA and Kōichi WADA*

(Received July 30, 1964)

The electronic spectra of quinones and carbonyl compounds have previously been studied by one of the present authors.[1] Moreover, Hartmann and Lorenz[2] reported on the electronic spectrum of 1, 4, 9, 10-anthradiquinone[3] in dioxane, together with the absorption spectra of many quinones. Except for these reports, however, the electronic spectrum of ADQ has never been studied. Since ADQ has four carbonyl groups in its conjugated system, as is shown below, its electronic spectrum and the charge-transfer absorption bands of ADQ complexes with aromatic compounds are of great interest to us. Accordingly, these spectra were studied. The results obtained will now be reported.




## Experimental

**Materials.**—ADQ was synthesized by the cautious oxidation of quinizarin(1,4-dihydroxy-anthraquinone) with lead tetraacetate in acetic acid, according to the method of Dimroth et al.[4] ADQ is so easily reduced to quinizarin that special caution is needed in its purification. Reddish-brown ADQ crystals dissolved in benzene at room temperature were separated from the solution by the addition of a large volume of isooctane. This procedure was repeated several times. The ADQ crystals obtained were straw-yellow needles. The melting point was consistent with that described in the literature.[5] Commercially-available, special-grade hydroquinone dimethyl ether, pyrene, and anthracene were purified by recrystallization from ethanol. The solvents were purified according to the methods described in our previous works.[1b,1d]

**Measurements.**—The absorption spectra were measured with a Cary 14M recording spectrophotometer with 1 and 5 cm.-path, fused quartz cells.

## Results

After leaving ADQ one day after synthesis, we found in the electronic spectra of ADQ solutions a slight absorption band of quinizarin near 480m$\mu$, an absorption which is characterized by a sharp vibrational structure in *n*-heptane. Therefore, each time ADQ was synthesized in the morning and the electronic spectra of its solutions were measured that afternoon. The electronic spectra of ADQ obtained in various solvents are shown in Figs. 1—4. The wavelengths ($\lambda_{max}$) and the molar absorption coefficients ($\varepsilon_{max}$) of the peaks of these spectra are shown in Table I. The wavelengths of the peaks of the charge transfer absorption bands[6] of ADQ complexes with aromatic compounds in carbon tetrachloride

* On leave of absence from the Yokohama Custom House, Yokohama.

1) A. Kuboyama, a) This Bulletin, **31**, 752 (1958); ibid., **32**, 1226 (1959); ibid., **33**, 917 (1960). b) ibid., **33**, 1027 (1960); *Rep. Gov. Chem. Ind. Res. Inst., Tokyo*, **57**, 541 (1962). c) This Bulletin, **35**, 295 (1962). d) ibid., **37**, 1540 (1964).

2) H. Hartmann and E. Lorenz, *Z. Naturforsh.*, **7b**, 360 (1952).

3) In the following, 1,4,9,10-anthradiquinone is abbreviated as ADQ.

4) O. Dimroth, O. Friedmann and H. Kämmerer, *Ber.*, **53**, 484 (1920).

5) O. Dimroth and E. Schultze, *Ann.*, **A411**, 345 (1916).

6) In the following, the term "charge transfer absorption bands" is abbreviated as CT bands.

are shown in Table II, together with those of the complexes between other quinones and aromatic compounds which were obtained in our previous work.[7] In Table II, the values

TABLE. I. THE PEAKS IN THE ELECTRONIC SPECTRA OF ADQ IN VARIOUS SOLVENTS

| Solvent | $\lambda_{max}$ mμ | $\varepsilon_{max}$ |
|---|---|---|
| Dioxane | 592 | 22 |
| | 344 | 2650 |
| | 227.5 | 29800 |
| Chloroform | 596 | 20 |
| | 363 | 2090 |
| | 232.5 | 28900 |
| Carbon tetrachloride | 598 | 20 |
| | 351 | 2080 |
| Carbon disulfide | 605 | 23 |

TABLE II.[a] THE CT BANDS OF THE QUINONE COMPLEXES IN CARBON TETRACHLORIDE

| Acceptor | Donor: Hydroquinone dimethyl ether | Pyrene | Anthracene |
|---|---|---|---|
| α-Naphthoquinone | | 428(mμ) (2550) | 435 (3050) |
| *p*-Benzoquinone | 418 (3200) | 448 (2350) | 457 (2400) |
| Chloranil | 545 (2700) | 599 (2000) | 623 (1880) |
| ADQ | 559 (2810) | 598 (2040) | 620 (2010) |

a) The values in parentheses are the distances (in wave number) between the peaks of the CT bands and the positions which situate on the longer wavelength sides of the peaks, and the intensities of which are one-half the intensities of the peaks.

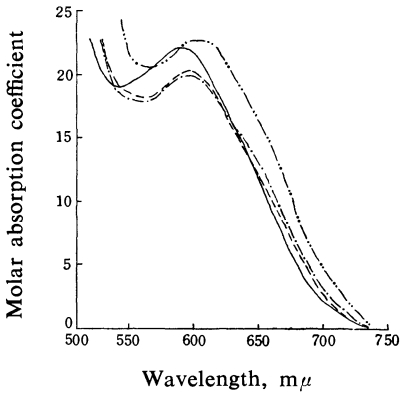



Fig. 1. ADQ, Solvent, —— Dioxane, - - - Chloroform, — — — Carbon tetrachloride, — — — — Carbon disulfide.

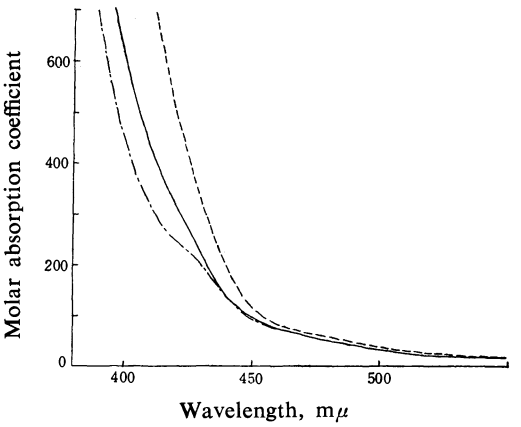



Fig. 2. ADQ, Solvent, —— Dioxane, - - - Chloroform, — — — Carbon tetrachloride.

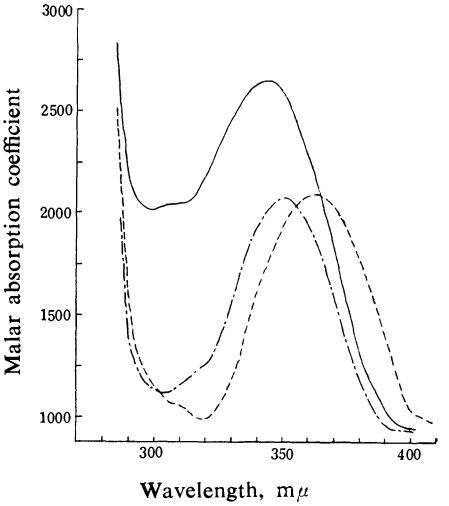



Fig. 3. ADQ, Solvent, —— Dioxane, - - - Chloroform, — — — Carbon tetrachloride.

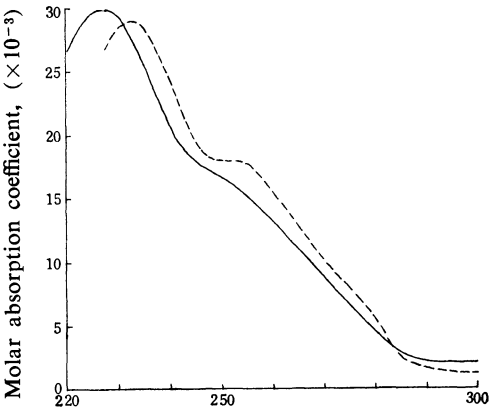



Fig. 4. ADQ, Solvent, —— Dioxane, - - - Chloroform, — — — Carbon tetrachloride.

7) A. Kuboyama, a) *J. Chem. Soc. Japan, Pure Chem. Sec.* (*Nippon Kagaku Zasshi*), **81**, 558 (1960); *Rep. Gov. Chem. Ind. Res. Inst., Tokyo*, **57**, 546 (1962). b) *J. Chem. Soc. Japan, Pure Chem. Sec.* (*Nippon Kagaku Zasshi*), **83**, 375 (1962); *Rep. Gov. Chem. Ind. Res. Inst., Tokyo*, **85**, 1 (1964).

in parentheses are thought to be nearly parallel to the half-widths of the CT bands and to be representative of the broadness of the CT bands.

## Discussion

Comparing Figs. 1—4 with the absorption spectrum reported by Hartmann and Lorenz,[2] two distinct differences between these two absorption spectra can be found. One is that, in the absorption spectrum reported by Hartmann and Lorenz, the weak absorption band near 600 m$\mu$ shown in Fig. 1 is not found. The other is that, in the absorption spectrum reported by them, an absorption band near 480 m$\mu$ ($\varepsilon_{max}\sim150$) is found, while in Fig. 2 no such absorption band is found. As has been described before, this absorption band near 480 m$\mu$ is thought to be that of quinizarin contained in ADQ.

The weak absorption band near 600 m$\mu$ in Fig. 1 may reasonably be assigned to an $n\rightarrow\pi^*$ band judging from its position and intensity. The fact that this band in carbon disulfide is found at longer wavelengths than in other solvents is characteristic of the $n\rightarrow\pi^*$ bands of the quinones, as has been studied in our previous work.[1b] From this fact, the band near 600 m$\mu$ may safely be assigned to an $n\rightarrow\pi^*$ band. The fact that this band in dioxane is found at shorter wavelengths than in other solvents may be attributed to the relatively strong charge transfer interaction between ADQ and dioxane.[1b] Indeed, as is shown in Table II, the CT bands of the ADQ complexes and of the chloranil complexes are at nearly the same position in a fixed electron-donor. Accordingly, the electron affinity of ADQ is thought to be nearly the same as that of chloranil, which is a strong electron-acceptor. The CT band of the ADQ complex with pyrene or anthracene is at almost the same position as that of the corresponding chloranil complex, while the CT band of the ADQ complex with hydroquinone dimethyl ether is at considerably longer wavelengths than that of the corresponding chloranil complex. This fact is thought to be due to the fact that the charge transfer interaction between ADQ and pyrene or anthracene is stronger than that between ADQ and hydroquinone dimethyl ether.[8] In Table II the values in parentheses which are representative of the broadness of the CT bands, in general become larger with an increase in the energies of the CT bands in a fixed electron-donor. The large values of this quantity in hydroquinone dimethyl ether in comparison with those ones in other electron-donors are thought to be related to the fact that the molecular structure of hydroquinone dimethyl ether is not so rigid because of the methoxyl groups not being fixed in this compound.

It is thought that ADQ has the four filled molecular orbitals, consisted of the lone pair orbitals of the four oxygen atoms, $((n_1+n_2)\pm(n_3+n_4)$ and $(n_1-n_2)\pm(n_3-n_4))$,[9] where $n_i$ denotes the lone pair orbital of the $i$-th oxygen atom in ADQ. Therefore, it may be expected that ADQ will show some $n\rightarrow\pi^*$ bands except for the band near 600 m$\mu$. In Fig. 2, the non-selective absorption band in the range from 550 m$\mu$ to 450 m$\mu$ is thought to contain some of these $n\rightarrow\pi^*$ bands. In Fig. 2, the spectrum of ADQ in carbon tetrachloride shows a shoulder near 425 m$\mu$. In other solvents the corresponding shoulders are masked by the absorption bands at the shorter wavelengths. Therefore, the solvent effect for this shoulder cannot be examined, and it is difficult to determine whether this shoulder should be interpreted as an $n\rightarrow\pi^*$ band or not.

In Fig. 3 a distinct peak near 350 m$\mu$ and a slight shoulder near 310 m$\mu$ are found, while in Fig. 4 a shoulder near 255 m$\mu$ and a strong peak near 230 m$\mu$ are found. In Figs. 3 and 4, all the absorption bands except for the slight shoulder near 310 m$\mu$ are assigned to $\pi\rightarrow\pi^*$ bands on the basis of their large intensities. The shoulder near 310 m$\mu$ may be assigned to an $n\rightarrow\sigma^*$ band on the basis of its weak intensity. Regarding Fig. 3, two points should be noticed about the distinct absorption band near 350 m$\mu$. First, this band in chloroform is found at far longer wavelengths than in other solvents. It is thought that this fact should be attributed mainly to the hydrogen bond formation between ADQ and chloroform. Second, the intensity of this band in dioxane is far larger than in other solvents. Since, as has been described before, ADQ is nearly as strong as chloranil as an electron-acceptor and since the CT band of the chloranil complex with dioxane is found near 330 m$\mu$,[7a] the CT band of the ADQ complex with dioxane is also expected to appear near 330 m$\mu$. Therefore, this CT band is thought to contribute much to the large intensity of the band near 350 m$\mu$ of ADQ in dioxane.

## Summary

The electronic spectrum of 1,4,9,10-anthradiquinone, and the charge transfer absorption bands of molecular complexes between

8) A. Kuboyama, *J. Am. Chem. Soc.*, **86**, 164 (1964).

9) The normalizing factor is omitted.

1, 4, 9, 10-anthradiquinone and aromatic compounds in solutions, have been studied. The weak absorption band near 600 m$\mu$ ($\varepsilon_{max}\sim 20$) of 1, 4, 9, 10-anthradiquinone has been assigned to an $n\rightarrow\pi^*$ band. The charge transfer absorption bands of the molecular complexes are found at nearly the same positions as those of the corresponding chloranil complexes. From this fact it has been concluded that the electron affinity of 1, 4, 9, 10-anthradiquinone is nearly the same as that of chloranil.

*Government Chemical Industrial Research Institute, Tokyo*
*Shibuya-ku, Tokyo*

# The Mass Transfer Rate through the Liquid-Liquid Interface. I. Potential Barriers near the Interface

By Teruya SHIMBASHI and Tadao SHIBA

(Received April 10, 1964)

In the treatment of mass-transfer through phases, the two concentrations immediately next to the interface have been assumed to be in distribution-equilibrium. In recent years, however, efforts have been made to obtain the true relation between these concentrations,[1-13] and some workers reported that there is a resistance in mass-transfer through the interface, so that the two concentrations are not in equilibrium.[1,3,8,13] Sinfelt and Drickamer[8] observed a high interfacial resistance by a static experiment on the diffusion of molecular sulfur across liquid-liquid interfaces; they associated this with the hydrogen bonding of liquids. On the other hand, Ward and Brooks[4] studied the diffusion of carboxylic acids statically across the water-toluene interface by the Lamm scale method; no distinct interfacial resistance was observed, but they carefully stated that this type of experiment does not detect an activation barrier to the crossing of the interface unless it is very high. Quinn and Jeannin[13] more recently studied the diffusion of isobutanol into the laminar aqueous isobutanol-water jet and found an interfacial resistance of approximately 80 cm./sec.

One of the factors that fix the rate of mass-transfer may be the amount of adsorption as well as the two concentrations immediately next to the interface at a constant temperature, although this aspect has been rather neglected. The present work is concerned with some relations between these three quantities.

Both phases, one of which is a pure solvent and the other a solution of a surface-active transfer-material in a different solvent, and the two solvents are mutually-immiscible, are brought into contact with each other. The adsorption of the transfer-material from the solution onto the interface takes place after the contact, and, consequently, the amount of adsorption increases quickly; the concentrations immediately next to the interface vary at the same time, so that the initial uniformity is destroyed and a new distribution of concentration appears at every moment until equilibrium. This variation in local concentration is originated only by the chemical potential gap obtained by comparing the zero amount of adsorption on the interface with the concentration of the solution immediately next to the interface at the beginning, and so it spreads out from the interface to the interiors of both bulks. That is, this variation in a sufficiently small lapse of time is practically limited to the vicinity of the interface, because the diffusion in liquid is rather slow. Consequently, it can be considered to be nearly independent of the thickness and shape of the layers.

1) J. T. Davies, *J. Phys. and Colloid. Chem.*, **54**, 185 (1950).
2) E. J. Scott, L. H. Tung and H. G. Drickamer, *J. Chem. Phys.*, **19**, 1075 (1951).
3) L. H. Tung and H. G. Drickamer, ibid., **20**, 6, 10 (1952).
4) A. F. H. Ward and L. H. Brooks, *Trans. Faraday Soc.*, **48**, 1124 (1952).
5) F. H. Garner and A. H. P. Skelland, *Ind. Eng. Chem.*, **46**, 1255 (1954).
6) P. L. Auer and E. W. Murbach, *J. Chem. Phys.*, **22**, 1054 (1954).
7) J. B. Lewis, *Chem. Eng. Sci.*, **3**, 248, 260 (1954).
8) J. H. Sinfelt and H. G. Drickamer, *J. Chem. Phys.*, **23**, 1095 (1955).
9) J. B. Lewis, *Chem. Eng. Sci.*, **8**, 295 (1958).
10) P. Raimondi and H. L. Toor, *A. I. Ch. E. Journal*, **5**, 86 (1959).
11) S. H. Chiang and H. L. Toor, ibid., **5**, 165 (1959).
12) J. T. Davies and J. B. Wiggill, *Proc. Roy. Soc.*, **A255**, 277 (1960).
13) J. A. Quinn and P. G. Jeannin, *Chem. Eng. Sci.*, **15**, 243 (1961).

The net rate of adsorption generally decreases, and so the amount of adsorption becomes nearly constant with an increase in the time of contact. This state is usually reached in a very short time when the molecule of the transfer-material is sufficiently small. The first stage, where the net rate of adsorption is high enough, is called the "adsorption stage," while the second, where the rate is nearly zero and the amout of adsorption is nearly constant, is called the "transfer stage" hereafter. The "transfer stage" will be discussed in this work.

A curve of the time dependence of the transfer-amount extrapolated to zero time does not necessarily coincide with that of the real process when all the observations are in the "transfer stage." The imaginary process obtained from this extrapolation, which has no "adsorption stage," is now called the "ideal process" in contrast with the real one. In other words, a curve of the time dependence of the transfer-amount in the "ideal process" does not necessarily start from the point of origin, and the amount of transfer in the initial state of the "ideal process" is not necessarily zero, but rather may apparently have a finite value in contrast with that in the real process, which is undoubtedly zero. It is assumed that the initial state of the "ideal process" holds a relation in the "transfer stage" and that it is independent of the thickness and the shape of the layers. This assumption is quite valid if the "adsorption stage" ceases in a short enough time, as has been described above. We will concentrate on the initial state of the "ideal process," because we can thus not only obtain the amount of adsorption, the two concentrations immediately next to the interface, and the transfer rate in this state, as will be described later, but also it is the most appropriate method for detecting the deviation from the equilibrium relation of the concentrations because of the high transfer rate.

## Experimental

An aqueous solution of *n*-butyric acid of a certain volume and concentration was placed in a glass vessel (I), shown in Fig. 1; at the same time, carbon tetrachloride was placed in another vessel (II), which had the same shape as vessel I. The temperature of vessels I and II was kept constant at 30°C by circulating jacket-water supplied from a thermostat. After the vessels had stood for 1 hr., carbon tetrachloride equal in volume to the aqueous *n*-butyric acid solution in vessel I was quickly taken out with a syringe from vessel II and introduced into vessel I, beneath the aqueous layer, much care being taken not to disturb the upper

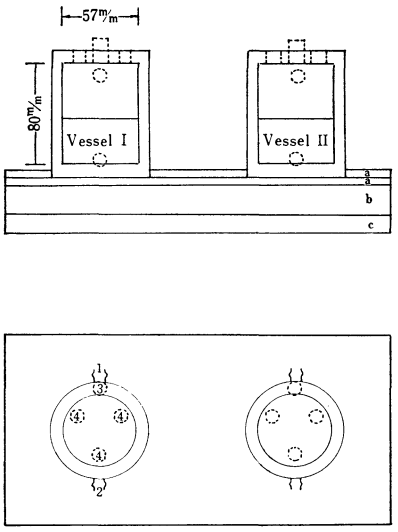



Fig. 1. Apparatus for the "layer absorption method."
a: Rubber sheet b: Iron plate
c: Rubber cushion
1: Inlet of water-jacket
2: Outlet of water-jacket
3: Thermometer hole
4: Sample-inlets and beaker-supporter

layer. Vessel I had been mounted on a stand to which a foam-rubber cushion was attached in order to insulate it from outside vibrations. *n*-Butyric acid was allowed to transfer from its aqueous solution into the carbon tetrachloride layer. After a certain lapse of time, the carbon tetrachloride layer was thoroughly taken out with a syringe, and the amount of *n*-butyric acid transferred into the carbon tetrachloride layer was determined by titration. This operation, now referred to as the "layer absorption method," was repeated with various volumes and concentrations of the aqueous *n*-butyric acid solution at definite periods of elapsed time after the contact of the two layers.

When benzene was used in place of carbon tetrachloride, benzene was placed in vessel I and the aqueous solution of *n*-butyric acid, in vessel II, and then the latter was introduced beneath the benzene layer in vessel I. After a definite period of time, the aqueous layer was separated from the benzene layer and the titration was made on the latter.

The amount of *n*-butyric acid adsorbed at the interface was determined by the pendant drop method.[14] A drop of the denser phase was hung from a capillary tip (0.1 mm. I. D. and 3 mm. O. D.) which was attached to a syringe, and the silhouette of the drop was obtained by parallel-ray photography. This procedure was repeated with various concentrations of *n*-butyric acid at definite time intervals.

In order to recognize whether observations have

14) J. M. Andreas, E. A. Hauser and W. B. Tucker, *J. Phys. Chem.*, **42**, 1001 (1938).

been made in the "transfer stage" or not, the variation in the amount of adsorption in very early stages must be determined, strictly, but, conventionally, recognized as follows. The "adsorption stage" takes place, but the "transfer stage" does not, when a new interface is made in the pendant drop method if the two phases have been previously brought into transfer-equilibrium. Consequently, this means that the observation has been made in the "adsorption stage" when the interfacial tension in the above experiment varies with time; on the contrary, the "adsorption stage" has ceased when no variation occurs, though only an approximate relation is obtained if the result is applied in the non-equilibrium system as it is.

The partition-equilibria of *n*-butyric acid in the water - carbon tetrachloride and water - benzene systems were determined by titrating equilibrated solutions.

## Results

Examples of the amounts of *n*-butyric acid in organic solvents transferred from the aqueous phase in the "layer absorption method" are plotted against the time in Figs. 2a and 2b. All the observations were made in the "transfer stage," because its "adsorption stage" ended within 1 min., as was established by determining the variation of interfacial tension in the equilibrated system, as has been described above. Consequently, the curves in Figs. 2a and 2b indicate the "ideal process," though these are probably deformed by a disturbance.

The initial transfer rates at the extrapolated points or the initial state of the "ideal process," are plotted against the thickness of both layers in Figs. 3a and 3b. All the points in each concentration before contact nearly lie on a straight line; the straight lines in the case of carbon tetrachloride are inclined to the horizontal axis, but those in the case of benzene are parallel to the horizontal axis. According to the assumption that the initial state of the

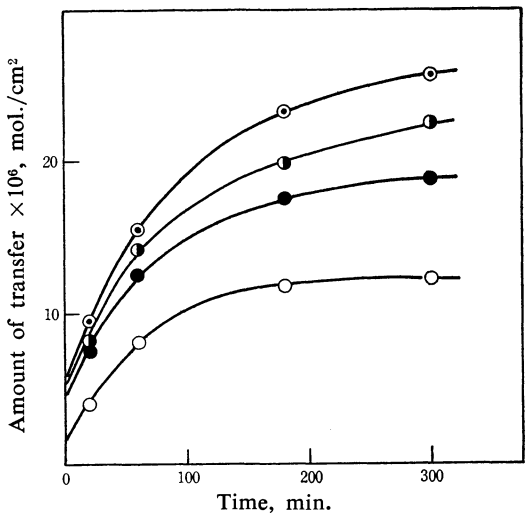



Fig. 2b. Time dependences of the amount of *n*-butyric acid transferred from the aqueous to the benzene phase at 30°C.
Concn. in the aq. soln. = 0.0503 N
Thickness of the layers: ○, 0.78 cm.; ●, 1.56 cm.; ◑, 2.34 cm.; ⊙, 3.12 cm.

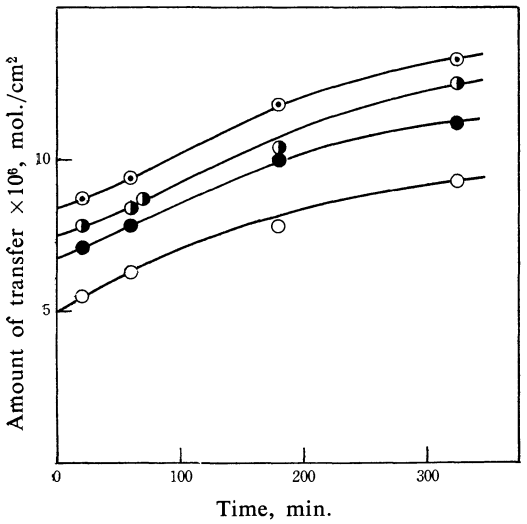



Fig. 2a. Time dependences of the amount of *n*-butyric acid transferred from the aqueous to the carbon tetrachloride phase at 30°C.
Concn. in the aq. soln. ≒ 0.0566 N
Thickness of the layers ○, 0.78 cm.; ●, 1.56 cm.; ◑, 2.34 cm.; ⊙, 3.12 cm.

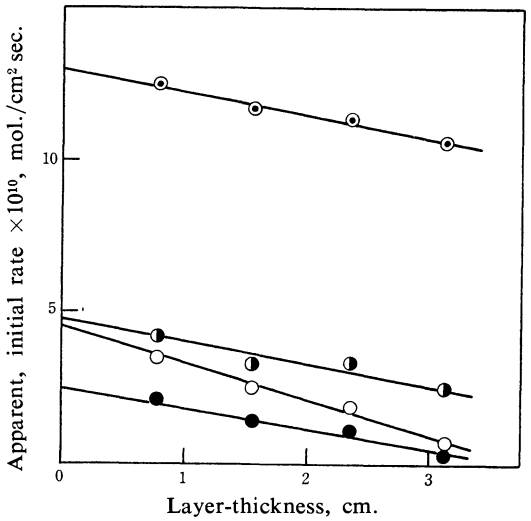



Fig. 3a. Layer-thickness dependence of the apparent, intial transfer-rate of *n*-butyric acid from the aqueous to the carbon tetrachloride phase at 30°C, determined by extrapolation.
Concn. in the aq. soln.: ○, 0.0115 N; ●, 0.0228 N; ◑, 0.0566 N; ⊙, 0.1137 N

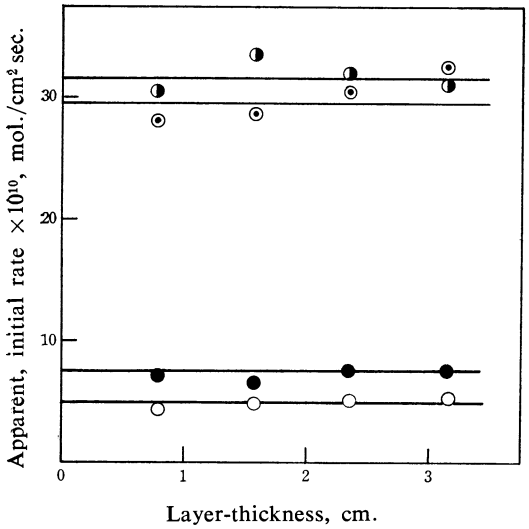



Fig. 3b. Layer-thickness dependences of the apparent, initial transfer-rate of *n*-butyric acid from the aqueous to the benzene phase at 30°C, determined by extrapolation.
Concn. in the aq. soln.: ○, 0.0100 N; ●, 0.0216 N; ◑, 0.0503 N; ⊙, 0.1038 N

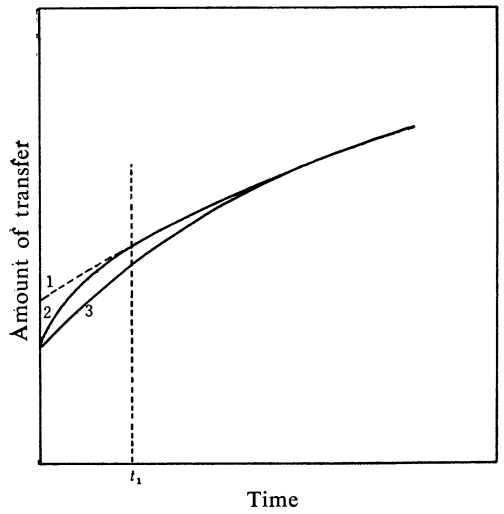



Fig. 4. Scheme of the deformation by the disturbance effect in the "ideal process."
1, Indicating extrapolation; 2, With the disturbance effect; 3, The "ideal process" without the disturbance effect

"ideal process" is independent of the thickness of the layer, all the straight lines in Figs. 3a and 3b should be parallel to the horizontal axis. The present authors attribute the cause of this discrepancy in the case of carbon tetrachloride to a disturbance at the beginning by the injection of carbon tetrachloride beneath the aqueous solution. The larger the thickness of the layer, the longer the time of injection, and therefore the stronger the disturbance. The disturbance deforms the intrinsic curve of the time dependence of the amount of *n*-butyric acid in the carbon tetrachloride phase transferred through the interface, as is shown schematically in Fig. 4. If the determinations are done after $t_1$ in Fig. 4, the initial rate of transfer on the extrapolated line should be less than the intrinsic one, and therefore the

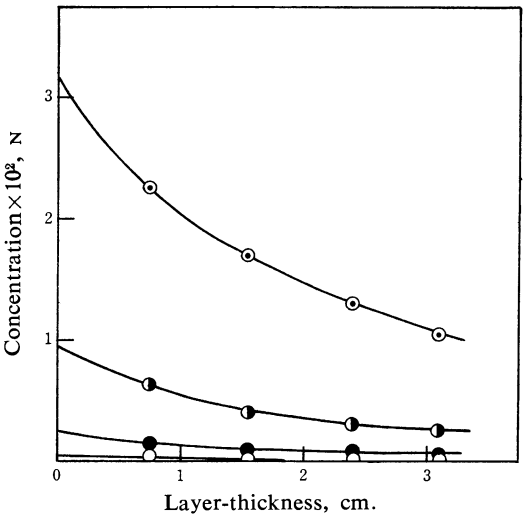



Fig. 5a. Layer-thickness dependences of the initial, average concentration of *n*-butyric acid in the carbon tetrachloride phase, determined by extrapolation, at 30°C.
Concn. in the aq. soln.: ○, 0.0114 N; ●, 0.0228 N; ◑, 0.0566 N; ⊙, 0.1137 N

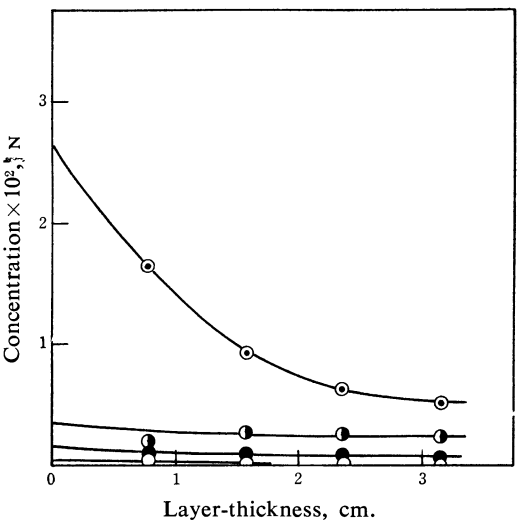



Fig. 5b. Layer-thickness dependences of the initial, average concentration of *n*-butyric acid in the benzene phase, determined by extrapolation, at 30°C.
Concn. in the aq. soln.: ○, 0.0100 N; ●, 0.0216 N; ◑, 0.0503 N; ⊙, 0.1038 N

straight lines should incline to the horizontal axis. Consequently, the correct values of the rate are given by extrapolating the straight lines to zero layer-thickness. On the contrary, the disturbance in the case of benzene is considered to be negligible, since the injection of the aqueous solution of *n*-butyric acid beneath the benzene layer causes much disturbance in the aqueous layer, but scarcely any in the benzene layer, which is sensitive to disturbance because of its low concentration.

The layer-thickness dependence of the average concentrations of *n*-butyric acid transferred into organic solvents at zero time in the apparent "ideal process," which means that it may include the disturbance effect, is shown in Figs. 5a and 5b, which were obtained from the amount of transfer extrapolated to zero time, as in Figs. 2a and 2b, divided by the volume of the layer. However, the values at the points extrapolated to zero thickness of the layer should show no disturbance, as has been described above, while at the same time they indicate the concentrations immediately next to the interface in the organic solvent at zero time in the "ideal process," according to the assumption that the initial state of the "ideal process" is independent of the thickness of the layer.

On the other hand, those for the aqueous phase are given from the following equation:

$$m = c_{10}v - c_{1a}v$$

$$c_{1a} = (c_{10}v - m)/v = c_{10} - c_{2a}$$

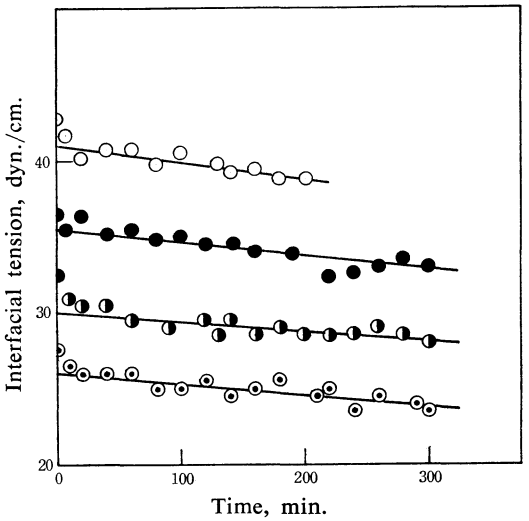



Fig. 6a. Time dependences of the interfacial tension of the pendant drop, when an aqueous solution of *n*-butyric acid and carbon tetrachloride were brought into contact with each other at 30°C.
Concn. in the aq. soln.: ○, zero; ●, 0.0227 N; ◑, 0.0566 N; ⊙, 0.1137 N

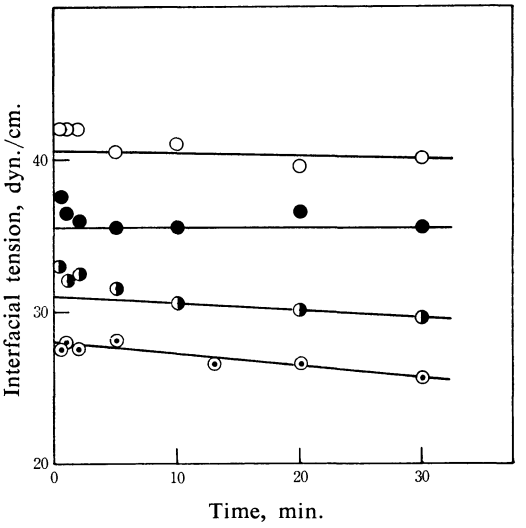



Fig. 6b. Particulars of the variation of the interfacial tension in the early stage of Fig. 6a.

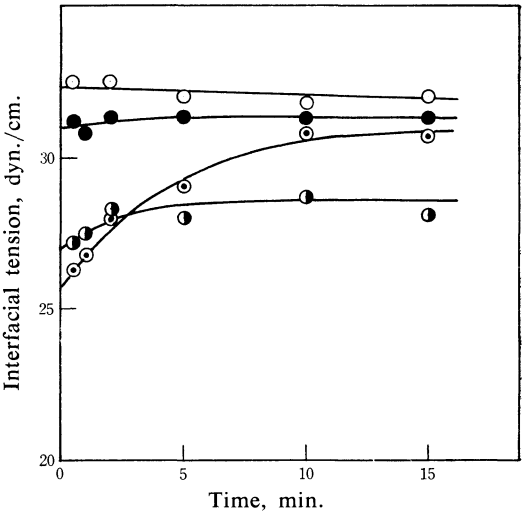



Fig. 6c. Time dependences of the interfacial tension of the pendant drop, when an aqueous solution of *n*-butyric acid and benzene were brought into contact with each other at 30°C.
Concn. in the aq. soln.: ○, zero; ●, 0.0206 N; ◑, 0.0514 N; ⊙, 0.1041 N

where $m$ is the amount of solute transferred at time $t$; $c_{10}$ is the concentration of *n*-butyric acid in the aqueous phase before contact; $c_{1a}$ and $c_{2a}$ are the average concentrations of *n*-butyric acid in an aqueous and an organic solvent respectively at time $t$, and $v$ is volume of the phase.

The results of the pendant drop experiment are shown in Figs. 6a, 6b and 6c. In the case of carbon tetrachloride, all points after about 30 min. are nearly on a straight line in every

run, and the straight lines are nearly parallel with each other. It may be seen that a rapid change of interfacial tension sets in within about 5 min. The first period, within 5 min., is considered to include the "adsorption stage," and the second period, from 5 to 30 min., the "transfer stage," while in the third period, after 30 min., a process is dominant in which carbon tetrachloride in the pendant drop dissolves in the aqueous phase outside the drop.

Therefore, the value obtained by extrapolating the interfacial tensions along the second process to zero time gives an interfacial tension of the "ideal process" at zero time nearly equal to that in the "layer absorption method," because the initial state in the "ideal process" is independent of the thickness and the shape of the layer according to the above assumption, provided that the curvature effect of the drop-surface is assumed to be negligible.

On the other hand, the value by extrapolating it along the third process to zero time gives the interfacial tension at an equilibrium state in the transfer of *n*-butyric acid and water eliminated the effect of transfer for carbon tetrachloride. The concentration in the aqueous phase outside the drop in transfer-equilibrium is approximated as equal to that before contact for a large volume ratio (1000 times) of the aqueous to the carbon tetrachloride phase.

In the case of benzene, the technique to obtain initial interfacial tensions is almost same, but those in transfer-equilibrium at various concentrations in the aqueous phase were obtained with systems previously brought into transfer-equilibrium.

Since the interfacial phases are composed of a mono-layer of *n*-butyric acid,[15] no distribution of the concentration of *n*-butyric acid in the interfacial phases along the transfer coordinate can be defined; therefore, the transfer of *n*-butyric acid in the interfacial phases in the transfer direction is regarded as in equilibrium at every moment, even in the transfer process. Therefore, the equations of state for the interfaces, which exist as a rule in equilibrium systems, must hold even in the rate process. In other words, the amount of adsorption in the rate process is determined by the surface pressure, the difference between the interfacial tension of a certain solution-system and that of the pure solvent-system, at every moment.

Table I shows the results of this experiment. In Table I the fractions of area covered by *n*-butyric acid molecules, $\theta$, are nearly equal to the corresponding fractions, $\theta_1$, calculated by assuming an equilibrium with the concentrations immediately next to the interfaces in the aqueous phase ($c_{1i}$), but the corresponding fractions, $\theta_2$, calculated by assuming an equilibrium with those in the organic phases ($c_{2i}$), are very different from $\theta$ or $\theta_1$ in some cases. ($\theta_1$ and $\theta_2$ are, so to speak, reduced concentrations of $c_{1i}$ and $c_{2i}$ respectively, calculated for comparison with $\theta$.) This indicates that a distinct resistance occurs in the process of desorption into the organic phase required in order to transfer through the interfaces.

TABLE I. THE RESULTS OF EXPERIMENT (30°C)

A) Aq. soln. of *n*-butyric acid - $CCl_4$

| $r_0\times10^{10}$ g. mol./cm² sec. | $c_{1i}\times10^2$ N | $c_{2i}\times10^2$ N | $\theta$ | $\theta_1$ | $\theta_2$ |
|---|---|---|---|---|---|
| 4.50 | 1.10 | 0.04 | 0.30 | 0.26 | 0.05 |
| 2.67 | 2.07 | 0.21 | 0.72 | 0.64 | 0.33 |
| 4.84 | 4.72 | 0.94 | 0.99 | 0.99 | 0.84 |
| 13.00 | 8.20 | 3.20 | 1.00 | 1.00 | 1.00 |

B) Aq. soln. of *n*-butyric acid - benzene

| $r_0\times10^{10}$ g. mol./cm² sec. | $c_{1i}\times10^2$ N | $c_{2i}\times10^2$ N | $\theta$ | $\theta_1$ | $\theta_2$ |
|---|---|---|---|---|---|
| 4.86 | 0.96 | 0.04 | 0.01 | 0.06 | 0.00 |
| 7.23 | 2.02 | 0.14 | 0.10 | 0.11 | 0.02 |
| 31.80 | 4.72 | 0.31 | 0.24 | 0.23 | 0.04 |
| 30.20 | 7.68 | 2.70 | 0.28 | 0.30 | 0.22 |

In comparison with other formula, the following semi-empirical one was fond the best to represent the relation of factors in a simple form:

$$r=k(a_{1i}-K_0a_{2i})A/(1+b\theta) \qquad (1)$$

where $r$ is transfer rate through the interface; $k$ is the apparent rate constant transferring through the interface; $K_0$ is the distribution coefficient for an infinite dilution; $b$ is a constant determined by means of the materials and temperature; $a_{1i}$ and $a_{2i}$ are the activities of the solute immediately next to the interface for bulks 1 and 2 respectively; $\theta$ is the fraction of area covered by adsorbed molecules, and $A$ is the area of the interface. As a process of transferring through the interfaces, an adsorption-desorption mechanism is considered according to the method of Langmuir;[16] when the amount of adsorption is in equilibrium with the concentration in bulk 1 (the aqueous layer) immediately next to the interface, as is indicated in our experiments, and the interaction among adsorbed molecules is negligible, it would seem that an equation replaceing $\theta$ with the $a_{1i}$ in Eq. 1 should be derived.[17] However, a comparison applying

15) R. K. Schofield and E. K. Rideal, *Proc., Roy. Soc.*, **A109**, 57 (1925).

16) I. Langmuir, *J. Am. Chem. Soc.*, **39**, 1858 (1917).

17) S. Glasstone, K. J. Laidler and H. Eyring, "The Theory of Rate Processes," McGraw-Hill, New York (1941), p. 367.

the experimental data prefers Eq. 1. This might be due to interaction among adsorbed molecules.

From Eq. 1:

$$A(a_{1i}-K_0a_{2i})/r=1/k+b\theta/k$$

As in our experiments, $a_{1i}=c_{1i}$ ($f_1=1.000-0.985$); therefore,

$$A(c_{1i}-Kc_{2i})/r=1/k+b\theta/k \qquad (2)$$

where $c_{1i}$ and $c_{2i}$ are the concentrations immediately next to the interface for bulks 1 and 2 respectively; $f_1$ is the activity coefficient in bulk 1, and $K$ is the distribution coefficient. If Eq. 2 holds good, the value on the left-hand side of the equation must be in linear relation to $\theta$, as is shown in Figs. 7a and 7b. The point at $\theta=1.0$ in Fig. 7a is far away from the straight line which indicates the linear relation; the reason for this not distinct. Figures 7a and 7b indicate plainly that the two concentrations immediately next to the respective interfaces, $c_{1i}$ and $c_{2i}$, are not in equilibrium with each other in these cases, because if $c_{1i}=Kc_{2i}$, $A(c_{1i}-Kc_{2i})/r=0$ and all the points should fall on the horizontal axis; the facts are otherwise.

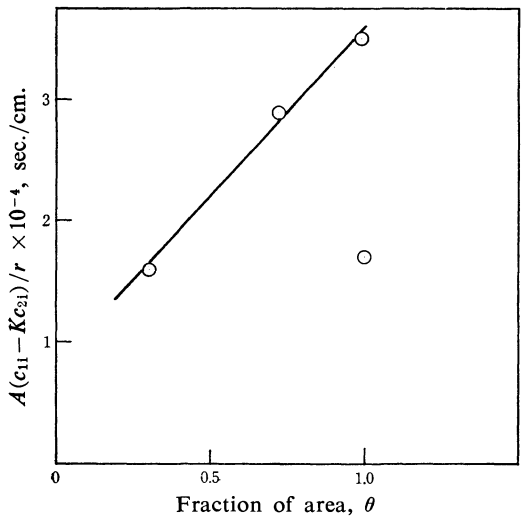



Fig. 7a. Plot of Eq. 2 for the system of an aqueous solution of *n*-butyric acid and carbon tetrachloride at 30°C.

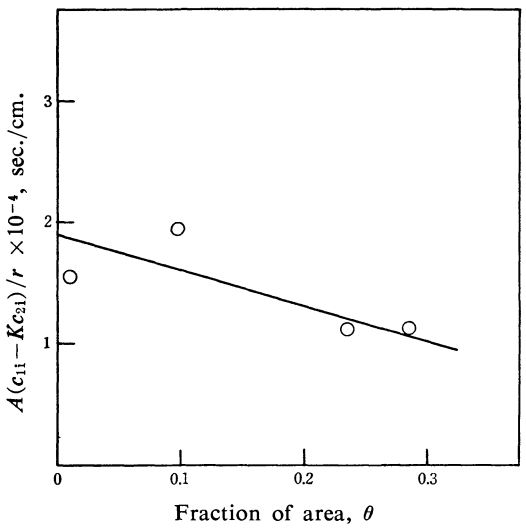



Fig. 7b. Plot of Eq. 2 for the system of an aqueous solution of *n*-butyric acid and benzene at 30°C.

## Discussion

In order to compare it with the theory, Eq. 1 is transformed as follows. If $c_{1i}=\tau'\theta$, $\tau'=\boldsymbol{F}(c_{1i}, T)$, and

$$r_0=r/A=k(\tau'\theta-Kc_{2i})/(1+b\theta)$$
$$=k\tau'\theta/(1+b\theta)-kKc_{2i}/(1+b\theta) \qquad (3)$$

where $\tau'$ is the coefficient representing the equilibrium-relation between $c_{1i}$ and $\theta$; $T$ is the absolute temperature, and $r_0$ is the transfer rate through the interface per unit of area.

A theoretical formula of the adsorption rate,[18] which has exponential factors representing the interaction among adsorbed molecules, is:

$$-r_0=k_{a2}a_{2i}(1-\theta)e^{x\theta}-k_{d2}\theta e^{-y\theta} \qquad (4)$$

where $k_{a2}$ is the rate constant of absorption from bulk 2 to the interface; $k_{d2}$ is the rate constant of desorption from the interface to bulk 2, and $x$ and $y$ are constants representing the effect of interaction among adsorbed molecules.

For an infinite dilution, $\theta\to0$, and $a_{2i}\to c_{2i}$; Eq. 4 then becomes:

$$-r_0=k_{a2}c_{2i}-k_{d2}\theta$$

At the same time, Eq. 3 becomes:

$$r_0=k\tau'_0\theta-kK_0c_{2i}$$

where $\tau'_0$ is the critical value of $\tau'$ for an infinite dilution.

$\theta$ and $c_{2i}$ are mutually independent variables, and therefore

$$k_{a2}=kK_0, \qquad k_{d2}=k\tau'_0 \qquad (5)$$

and

$$-r_0=kK_0a_{2i}/(1+b\theta)-k\tau'\theta/(1+b\theta)$$
$$=kK_0a_{2i}(1-\theta)e^{x\theta}-k\tau'_0\theta e^{-y\theta}$$

Accordingly,

$$\left.\begin{aligned} x&=-(1/\theta)\ln(1+b\theta)-(1/\theta)\ln(1-\theta)\\ y&=(1/\theta)\ln(1+b\theta)-(1/\theta)\ln(\tau'/\tau'_0)\end{aligned}\right\} \qquad (6)$$

The numerical values of $x$ and $y$ obtained from

18) S. Glasstone, K. J. Laidler and H. Eyring, "The Theory of Rate Processes," McGraw-Hill, New York (1941), p. 365.

TABLE II. VALUES OF $x$ AND $y$ (30°C)

A) Aq. soln. of *n*-butyric acid - $CCl_4$

| $\theta$ | $\tau' \times 10^2$ N | $x$ | $y$ |
|---|---|---|---|
| 0.30 | 3.67 | −1.0 | 5.4 |
| 0.72 | 2.87 | 0.1 | 3.3 |
| 0.99 | 4.76 | 3.8 | 2.1 |
| 1.00 | 8.20 | — | 1.6 |
| average | | 1 | 3 |

B) Aq. soln. of *n*-butyric acid - benzene

| $\theta$ | $\tau' \times 10^2$ N | $x$ | $y$ |
|---|---|---|---|
| 0.20 | 4.95 | −1.26 | 6.1 |
| 0.40 | 3.35 | −0.72 | 4.8 |
| 0.60 | 3.12 | −0.20 | 3.8 |
| 0.80 | 3.30 | 0.41 | 3.0 |
| average | | −0.4 | 4.4 |

Eq. 6 are shown in Table II, but actually $x$ and $y$ are rather affected by $\theta$ or $\tau'$.

The free energy of attractive interaction between one adsorbed molecule and its neighbors in a saturated state is calculated as follows:[19]

$$x = psV/\boldsymbol{RT}, \qquad y = (1-p)sV/\boldsymbol{RT}$$
$$\therefore \quad sV = (x+y)\boldsymbol{RT} \tag{7}$$

where $p$ is the fraction of free energy; $s$ is the coordination number of absorbed molecules in a saturated state; $V$ is the free energy of attractive interaction between two adjacent adsorbed molecules; $\boldsymbol{R}$ is the gas constant, and $T$ is the absolute temperature.

According to the activated-complex theory, specific rate constants are given by:

$$k'_{a2} = \kappa_{a2}(\boldsymbol{kT}/\boldsymbol{h})e^{-\Delta F^{\ddagger}_{a2}/\boldsymbol{RT}}$$
$$k'_{d2} = \kappa_{d2}(\boldsymbol{kT}/\boldsymbol{h})e^{-\Delta F^{\ddagger}_{d2}/\boldsymbol{RT}}$$

where $k'_{a2}$ is the specific rate constant of adsorption from bulk 2 to the interface; $k'_{d2}$ is the specific rate constant of desorption from the interface to bulk 2; $\kappa_{a2}$ and $\kappa_{d2}$ are the transmission coefficients; $\boldsymbol{k}$ is the Boltzmann constant; $\boldsymbol{h}$ is the Planck constant; $\Delta F^{\ddagger}_{a2}$ is the free energy of activation to adsorb from bulk 2 to the interface, and $\Delta F^{\ddagger}_{d2}$ is the free energy of activation to desorb from the interface to bulk 2.

From the definitions,

$$k_{a2} = k'_{a2}\lambda \quad \text{or} \quad \lambda = k_{a2}/k'_{a2} \tag{8}$$
$$k_{d2}\theta = (k_{d2}/\Gamma_\infty)\Gamma = k'_{d2}\Gamma \quad \text{or} \quad k'_{d2} = k_{d2}/\Gamma_\infty \tag{9}$$

where $\lambda$ is the length of the adsorption path from the boundary site of bulk 2 to the interface; $\Gamma$ is the amount of adsorption, and $\Gamma_\infty$ is the value of $\Gamma$ in a saturated state.

19) Ibid., pp. 363—366. In the original, $sV$ means the free energy of the repulsive interaction instead of that of the attractive interaction.

If both $\kappa_{a2}$ and $\kappa_{d2}$ are assumed to be unity:

$$k'_{a2} = (\boldsymbol{kT}/\boldsymbol{h})e^{-\Delta F^{\ddagger}_{a2}/\boldsymbol{RT}} \tag{10}$$
$$\Delta F^{\ddagger}_{d2} = \boldsymbol{RT} \ln (\boldsymbol{kT}/\boldsymbol{h}k'_{d2})$$
$$= \boldsymbol{RT} \ln (\boldsymbol{kT}\Gamma_\infty/\boldsymbol{h}k_{d2}) \tag{11}$$
$$\Delta F^{\ddagger}_{a2} = \Delta F^{\ddagger}_{d2} + \Delta F_1 - \Delta\chi \tag{12}$$

where $\Delta F_1$ is the standard free energy of adsorption from bulk 1 to the interface, and $\Delta\chi$ is the standard free energy of transference from bulk 1 to 2.

According to Ward and Tordai,[20]

$$\tau = \delta\boldsymbol{kT}e^{-\Delta F_1/\boldsymbol{RT}}, \text{ or } \Delta F_1 = \boldsymbol{RT} \ln (\delta\boldsymbol{RT}/\tau) \tag{13}$$

where $\tau$ is Traube's constant, and $\delta$ is the thickness of the interfacial phase. Thermodynamically, $\Delta\chi$ is given by:

$$\Delta\chi = \boldsymbol{RT} \ln (a_1/a_2)_e = \boldsymbol{RT} \ln K_0 \tag{14}$$

where $a_1$ and $a_2$ are activities, and e indicates equilibrium.

The values of $\Delta F^{\ddagger}_{d2}$, $\Delta F_1$ and $\Delta\chi$ are calculated according to Eqs. 11, 13 and 14 respectively, with the experimental values, $k_{d2}$, $\Gamma_\infty$, $\tau$ and $K_0$, and $\delta$, which is given as equal to the statistical length of a *n*-butyric acid molecule (9.86Å[20]), because the adsorbed molecules in these cases have been known to form monolayers.[15] Therefore, $\Delta F^{\ddagger}_{a2}$ is given by Eq. 12, considering the continuity of the standard free energy in the transfer process. Then $k'_{a2}$ is calculated by Eq. 10, and finally $\lambda$ is given by Eq. 8.

The results of calculations from the experimental data are given in Table III. The values of both $k_{a2}$ and $k_{d2}$ in one system are very different from those in the other system; nevertheless, the values of $\Delta F^{\ddagger}_{d2}$, the free energy of activation to desorb from the interface into the bulk of organic solvent, in the

TABLE III. RESULTS OF CALCULATION FROM EXPERIMENTAL DATA (30°C)

System: Aq. soln. of *n*-butyric acid - $CCl_4$

| Constants | Unit | S=$CCl_4$ | S=$C_6H_6$ |
|---|---|---|---|
| $k \times 10^4$ | cm./sec. | 1.14 | 0.44 |
| $b$ | — | 3.04 | −1.57 |
| $K_0$ | — | 11.50 | 3.24 |
| $\tau'_0 \times 10^4$ | g. mol./cm³ | 1.05 | 1.56 |
| $k_{a2} \times 10^3$ | cm./sec. | 1.31 | 0.14 |
| $k_{d2} \times 10^8$ | g. mol./cm² sec. | 1.20 | 0.69 |
| $sV$ | kcal./mol. | 2.40 | 0.49 |
| $\Delta F^{\ddagger}_{d2}$ | kcal./mol. | 15.50 | 16.30 |
| $\Delta F_1$ | kcal./mol. | −2.72 | −2.39 |
| $\Delta\chi$ | kcal./mol. | 1.47 | 0.71 |
| $\lambda$ | Å | 7.58 | 7.99 |

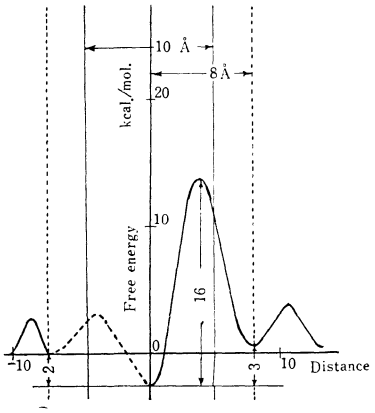
20) A. F. H. Ward and L. Tordai, *Trans. Faraday Soc.*, **42**, 415 (1946).

two systems are nearly equal (16 kcal./mol.), so it may be supposed that the desorptions in the two systems proceed via the same mechanism.

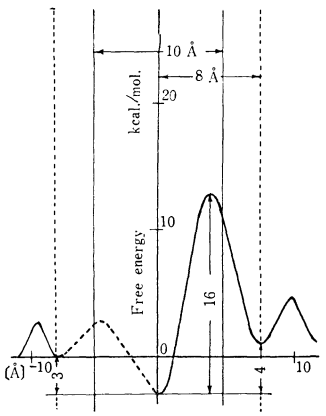
The values of $\lambda$, the length of the adsorption path from the boundary site in an organic bulk to the interface, for the two systems are also nearly equal, 8Å, and are reasonable when compared with the statistical length of an *n*-butyric acid molecule, 9.86Å.

The value of $sV$, the free energy of attraction between an adsorbed molecule and the adjacent one in a saturated state, for the water-benzene system is very small compared with the value for the other system, and both values are positive, indicating that the interactions are both attractive. These results are considered to agree with those given by Schofield and Rideal in a study of surface film.[15]

Figure 8 shows the standard free energy change for our systems in the course of mass transfer through the interface. To interpret the origin of such a potential barrier, the following hypothesis is introduced. As Fig. 9




System : Water - *n*-butyric acid - benzene




System : Water - *n*-butyric acid - $CCl_4$

Fig. 8. Potential barriers near the interfaces.

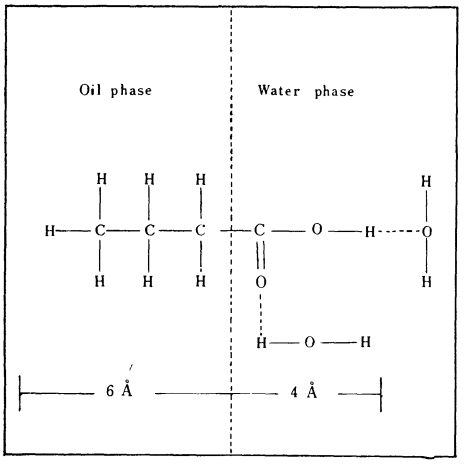



Fig. 9. Model of the adsorption state of a *n*-butyric acid molecule at the oil-water interface.

shows, it is known that two hydrogen bonds exist between two water molecules and a carboxyl radical of the *n*-butyric acid molecule in the state of adsorption at the interface;[21,22] the bonds must be split off when the molecule transfers from the interface into the organic solvent bulk. Therefore, the molecule should have a free energy higher than that required to cut off the hydrogen bonds for the desorption into the organic phase. This may be considered to be the origin of such a high potential barrier, because the energy of that

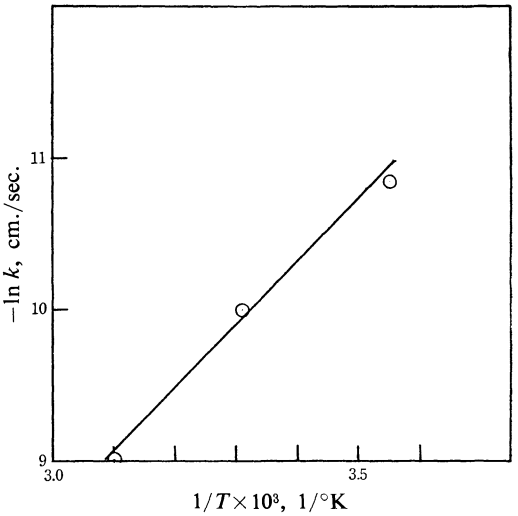



Fig. 10. Arrhenius plot for *n*-butyric acid transfer from the aqueous to the benzene phase.

21) W. J. Moore and H. Eyring, *J. Chem. Phys.*, **6**, 391 (1938).

22) G. C. Pimentel and A. L. McClellan, "The Hydrogen Bond," Freeman, San Francisco (1960), p. 352.

sort of hydrogen bond, O–H–O, is usally about 5—8 kcal./bond.

In order to separate the energy term from the free energy of activation, experiments similar to those which had been made at 30°C were made in the systems of aqueous solutions of *n*-butyric acid and benzene at the temperatures of 10°C and 50°C respectively. The activation energy of mass transfer through the interface from the aqueous to the benzene phase, $\Delta E^*_{12}$, for *n*-butyric acid was determined to be 8.15 kcal./mol. by the Arrhenius plot, as is shown in Fig. 10.

The standard free energy of adsorption from the aqueous phase to the interface, $\Delta F_1$, is determined to be $-2.39$ kcal./mol., as is shown in Table III; if the entropy term is negligible, as in the case of the system composed of an aqueous solution of *n*-butyric acid and air ($\Delta E_1 = -2.83$ kcal./mol., $\Delta F_1 = -2.54$kcal./mol.), the energy of activation for the desorption of *n*-butyric acid from the interface into the benzene bulk, $\Delta E^*_{d2}$, becomes 10.5 kcal./mol. (obtained by subtraction, $\Delta E^*_{12} - \Delta F_1$). If this value is given by the sum of energies for the two hydrogen bonds, the average bond-energy is 5.2 kcal./bond, which agrees well with the literature, 5.1 kcal./bond.[22]

The entropy of activation associated with this process, $\Delta S^*_{d2}$, is calculated as follows:

$$\Delta S^*_{d2} = (\Delta E^*_{d2} - \Delta F^*_{d2})/T = -19.2 \text{ e. u.}$$

Davies observed a large negative entropy of activation ($-20$ e. u.) in the diffusion of potassium iodide from the nitrobenzene phase into the aqueous phase.[1] It is interesting that the present result of the entropy of activation in the desorption of *n*-butyric acid from the water-benzene interface into the benzene phase has the same sign and magnitude as the above datum of Davies.

We should like to express our gratitude to Professor A. F. H. Ward, University of Manchester, for his useful suggestions regarding this work. We also wish to express our indebtedness to Professor Tominaga Keii of this Institute for his helpful discussions of this subject.

*Department of Chemical Engineering*
*Tokyo Institute of Technology*
*Ookayama, Tokyo*

# The Mass Transfer Rate through the Liquid-Liquid Interface. II. The Boundary Condition of the Diffusion Equation at the Interface

By Teruya SHIMBASHI and Tadao SHIBA

(Received April 10, 1964)

When dealing with mass transfer through an interface which consists of either a gas phase and a liquid phase, or two liquid phases, it has been assumed that the concentration for the phase immediately next to the interface is in distribution-equilibrium with that for the other phase. However, this is only an assumption and no distinct theoretical or experimental verification has been given. Therefore, it may be equally probable *a priori* that the equilibrium relation does not hold in the process. In order to verify that the equilibrium relation does exist in the process, it is insufficient to indicate only that the experimental values are in accord with the theoretical values calculated on the basis of this equilibrium; it is also necessary to indicate that the experimental values are not in accord with the theoretical values calculated on the non-equilibrium basis. In other words, when the difference between the experimental and the theoretical values calculated on the basis of this equilibrium is smaller than the experimental error, the experimental values are apparently in accord with the theoretical values, even if the true equilibrium relation does not exist in these concentrations, as has also been described by Ward and Brooks.[1)]

The authors have previously studied a mass transfer through liquid-liquid interface; the results have been described in the preceding paper. In that study the transfer rate of *n*-butyric acid through the water-carbon tetrachloride or the water-benzene interface, both concentrations of *n*-butyric acid immediately next to the respective interfaces, and the

1) A. F. H. Ward and L. H. Brooks, *Trans. Faraday Soc.*, **48**, 1124 (1952).

amounts of adsorption at the respective interfaces were determined under particular conditions; the results of analysis indicate that Nernst's law of distribution, which exists as a rule in equilibrium systems, does not hold in the mass-transfer process between these concentrations immediately next to the interface. This paper will deal with the experimental data as has been described in the first paper, but in the method of analysis these papers differ from each other. This paper will also deal with Fick's differential equation of diffusion.

Some authors have reported mass transfer through liquid-liquid interfaces with Fick's equation of diffusion.[1-8] Crank gave the solution of the one-dimensional semi-infinite composite medium with no interfacial resistance.[9] Scott, Tung, and Drickamer gave a solution of a finite composite medium with finite interfacial resistance phenomenologically in terms of an interfacial transfer coefficient.[3] Auer and Murbach gave some solutions with or without interfacial resistance by means of a three-region model.[5] It seems to us, the present authors, that the boundary and initial conditions have been decided rather conventionally. The properties of the interface have been studied, however, by Gibbs, Langmuir, and others theoretically or experimentally.[10,11] Consequently, the present authors are now concentrating on the interfacial phase, so that a reasonable boundary condition can be derived.

## Theoretical

The nature of a surface, or an interface in general, is very different from a bulk phase, because the state of the aggregation of molecules is converted discontinuously at the interface. Adsorption and desorption, accordingly, are characteristic of the interface. Therefore, in treating a process of mass transfer through an interface, it is rational to distinguish the interfacial phase, in which adsorption and desorption govern mass transfer, from the bulk phases, in which Fick's law of diffusion governs mass transfer.

A model of the neighborhood of the interface is shown in Fig. 1. The positions of the two boundaries of the interfacial phase are appointed on the distance axis as minus-zero and plus-zero, where the activities of the solute in the bulk phase are $a_{1i}$ and $a_{2i}$ respectively; the relation between the two activities, namely, the boundary condition for Fick's law of diffusion at the zero-position, will be derived, so that we can solve the equation of diffusion in the usual manner. The distance between $x=-0$ and $x=+0$, where $x$ is the distance from the interface, has a finite value, about 16 Å, according to our experimental results, as has been indicated in the first paper, but this is to be regarded as zero compared with the thickness of the bulk phase.

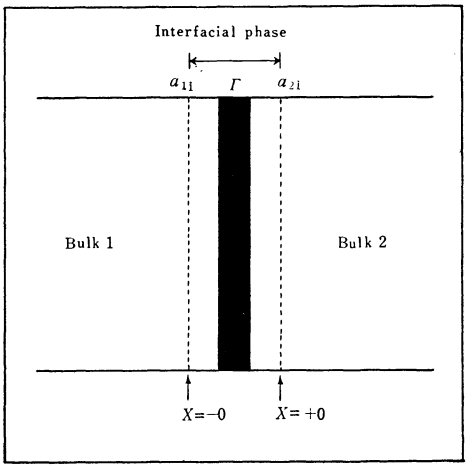



Fig. 1. A model of the neighborhood of the liquid-liquid interface.

Adsorption rate equations, taking the effect of interaction among adsorbed molecules into account,[12] are represented as:

$$\left.\begin{aligned} d\Gamma_1/dt &= k_{a1}a_{1i}(1-\theta)e^{x_1\theta} - k_{d1}\theta e^{-y_1\theta} \\ d\Gamma_2/dt &= k_{a2}a_{2i}(1-\theta)e^{x_2\theta} - k_{d2}\theta e^{-y_2\theta} \end{aligned}\right\} \quad (1)$$

where $\Gamma_1$ and $\Gamma_2$ are the net amounts of the solute adsorbed by the interface per unit of area from bulks 1 and 2 respectively; $t$ is the time; $k_{a1}$ and $k_{a2}$ are the rate constants of the adsorption to the interface from bulks 1 and 2 respectively; $k_{d1}$ and $k_{d2}$ are the rate constants of the desorption from the interface into bulks 1 and 2 respectively; $a_{1i}$ and $a_{2i}$ are the activities of the solute in bulks 1 and

2) J. T. Davies, *J. Phys. and Colloid. Chem.*, **54**, 185 (1950).
3) E. J. Scott, L. H. Tung and H. G. Drickamer, *J. Chem. Phys.*, **19**, 1075 (1951).
4) L. H. Tung and H. G. Drickamer, ibid., **20**, 6, 10 (1952).
5) P. L. Auer and E. W. Murbach, ibid., **22**, 1054 (1954).
6) J. H. Sinfelt and H. G. Drickamer, ibid., **23**, 1095 (1955).
7) J. T. Davies and J. B. Wiggill, *Proc. Roy. Soc.*, **A255**, 277 (1960).
8) J. A. Quinn and P. G. Jeannin, *Chem. Eng. Sci.*, **15**, 243 (1961).
9) J. Crank, "The Mathematics of Diffusion," Oxford University Press, London (1956).
10) J. W. Gibbs, *Scientific Papers*, **1**, 219 (1878).
11) I. Langmuir, *Z. physik. Chem.*, **64**, 385 (1908).
12) S. Glasstone, K. J. Laidler and H. Eyring, "The Theory of Rate Rrocesses," McGraw-Hill, New York (1941), p. 365.

2 respectively immediately next to the interface; $\theta$ is the fraction of area covered by adsorbed molecules, and $x_1$, $y_1$, $x_2$, and $y_2$ are constants representing the effect of interaction among adsorbed molecules.

It is assumed that the amount of adsorption, $\Gamma$, is constant with the lapse of time, as

$$d\Gamma/dt = d\Gamma_1/dt + d\Gamma_2/dt = 0 \tag{2}$$

From Eqs. 1 and 2,

$$a_{2i} = \alpha a_{1i} + \beta \tag{3}$$

$$\alpha \equiv -\left(\frac{k_{a1}}{k_{a2}}\right) e^{(x_1 - x_2)\theta}$$

$$\beta \equiv \left(\frac{k_{d1} e^{-y_1\theta} + k_{d2} e^{-y_2\theta}}{k_{a2} e^{x_2\theta}}\right) \frac{\theta}{1-\theta}$$

where $k_{a1}$, $k_{d1}$, $k_{a2}$ and $k_{d2}$ are positive constants determined by the material system and the temperature, and $\theta$ is a positive constant less than unity due to the definition and the assumption; consequently, in the rate process $\alpha$ is always a negative constant and $\beta$ is always a positive constant.

When a distribution-equilibrium is attained, the net amount of solute adsorbed by the interface from each bulk becomes constant:

$$d\Gamma_1/dt = k_{a1} a_{1i} (1-\theta) e^{x_1\theta} - k_{d1}\theta e^{-y_1\theta} = 0$$

$$\therefore \quad \theta/(1-\theta) = k_{a1} e^{x_1\theta} a_{1i} / k_{d1} e^{-y_1\theta} \tag{4}$$

From Eqs. 3 and 4 the distribution coefficient, $K$, is derived, since $x_1 + y_1 = x_2 + y_2 = sV/\boldsymbol{R}T$:[12]

$$\frac{a_{2i}}{a_{1i}} = \left(\frac{k_{a1}}{k_{d1}}\right) e^{(x_1+y_1)\theta} \Big/ \left(\frac{k_{a2}}{k_{d2}}\right) e^{(x_2+y_2)\theta}$$

$$= \frac{k_{a1}/k_{d1}}{k_{a2}/k_{d2}} = K$$

where $s$ is the coordination number of adsorbed molecules in the saturated state; $V$ is the free energy of attractive interaction between two adjacent adsorbed molecules; $\boldsymbol{R}$ is the gas constant, and $T$ is the absolute temperature.

When $\alpha$ and $\beta$ are defined as only unfixed constants, it becomes possible for the boundary condition derived in the rate process, $a_{2i} = \alpha a_{1i} + \beta$, to represent also the relation in the distribution-equilibrium, for the equilibrium relation is represented by specifying $\alpha = K$, and $\beta = 0$. Consequently, it is possible to distinguish whether or not the equilibrium relation holds between $a_{1i}$ and $a_{2i}$ in the rate process, because $\alpha$ should have a negative and $\beta$, a positive finite value in the case of non-equilibrium on the one hand, and on the other hand, $\alpha$ should be positive, equal to the distribution coefficient, and $\beta$, zero in the case of equilibrium.

As has been described in the first paper, the condition $\theta = \text{const.}$ does not necessarily hold in the initial state of the real process, but it can be assumed that this condition holds even in the initial state of the so-termed "ideal process" obtained by extrapolating the part of the real process where this condition actually holds. The analytical results in the preceding paper, which have been obtained on the basis of this assumption, have not indicated any serious conflict. Consequently, as far as we take the boundary condition to be $a_{2i} = \alpha a_{1i} + \beta$, derived by assuming $\theta = \text{const.}$, the "ideal process" should be studied. The concept of the "ideal process" has been described in detail in the first paper.

Now let us solve the differential equations of diffusion with a suitable initial condition and with the boundary condition obtained for the semi-infinite composite medium in one-dimensional diffusion.

Fick's second law of diffusion is represented by:

$$\left.\begin{aligned} \frac{\partial c_1}{\partial t} &= D_1 \frac{\partial^2 c_1}{\partial x^2}, \quad x<0 \\ \frac{\partial c_2}{\partial t} &= D_2 \frac{\partial^2 c_2}{\partial x^2}, \quad x>0 \end{aligned}\right\} \tag{5}$$

where $c_1$ and $c_2$ are the concentrations of the solute in bulks 1 and 2 respectively, while $D_1$ and $D_2$ are the diffusion coefficients in bulks 1 and 2 respectively.

The initial conditions are, as will be described later, assumed to be:

$$\left.\begin{aligned} c_1 &= c_{10}, \quad x<0, \quad t=0 \\ c_2 &= \xi e^{-\eta x}, \quad x>0, \quad t=0 \end{aligned}\right\} \tag{6}$$

where $c_{10}$ is the initial value of $c_1$, and $\xi$ and $\eta$ are constants independent of $x$.

The boundary conditions are given by:

$$\left.\begin{aligned} c_2 &= \alpha c_1 + \beta, \quad x=0 \\ D_1 \frac{\partial c_1}{\partial x} &= D_2 \frac{\partial c_2}{\partial x}, \quad x=0 \end{aligned}\right\} \tag{7}$$

where $\alpha$ and $\beta$ are defined as unfixed constants independent of time; the second equation represents the mass balance between the positions for the two sides immediately next to the interface, involving that the amount of adsorption is constant.

As the solution of Eqs. 5, 6, and 7, we have

$$c_1 = c_{10} - \left[\frac{\alpha c_{10} + \beta}{\alpha + (D_1/D_2)^{1/2}}\right] \operatorname{erfc}\left\{\frac{|x|}{2(D_1 t)^{1/2}}\right\}$$

$$+ \left[\frac{\xi}{\alpha + (D_1/D_2)^{1/2}}\right] \exp\left\{\eta (D_2/D_1)^{1/2} |x| + D_2 \eta^2 t\right\} \operatorname{erfc}\left\{\frac{|x|}{2(D_1 t)^{1/2}} + \eta (D_2 t)^{1/2}\right\}$$

$$c_2=\left[\frac{(D_1/D_2)^{1/2}(\alpha c_{10}+\beta)}{\alpha+(D_1/D_2)^{1/2}}\right]\mathrm{erfc}\left\{\frac{x}{2(D_2t)^{1/2}}\right\}$$
$$-\left(\frac{\xi}{2}\right)e^{D_2\eta^2t}\left\{e^{-\eta x}\cdot\mathrm{erfc}\left[\frac{x}{2(D_2t)^{1/2}}-\eta(D_2t)^{1/2}\right]+e^{\eta x}\cdot\mathrm{erfc}\left[\frac{x}{2(D_2t)^{1/2}}+\eta(D_2t)^{1/2}\right]\right\}+\xi\cdot\exp\left\{D_2\eta^2t-\eta x\right\}$$
$$+\left[\frac{\alpha\xi}{\alpha+(D_1/D_2)^{1/2}}\right]\exp\left\{\eta x+D_2\eta^2t\right\}\mathrm{erfc}\left\{\frac{x}{2(D_2t)^{1/2}}+\eta(D_2t)^{1/2}\right\} \quad (8)$$

If we assame that $\alpha=K$, $\beta=0$, $\xi=0$, and $\eta$ =finite, we obtain:

$$c_1=\frac{c_{10}}{1+(K(D_2/D_1)^{1/2}}\left[1+K(D_2/D_1)^{1/2}\mathrm{erfc}\left\{\frac{|x|}{2(D_1t)^{1/2}}\right\}\right]$$
$$c_2=\left[\frac{Kc_{10}}{1+K(D_2/D_1)^{1/2}}\right]\mathrm{erfc}\left\{\frac{x}{2(D_2t)^{1/2}}\right\}$$

which is identical with the solution by Crank.[9]

The diffusion rate immediately next to the interface in bulk 1, $r_{1i}$, is given by:

$$r_{1i}=-D_1\left(\frac{\partial c_1}{\partial x}\right)_{x=0}=(D_1/\pi t)^{1/2}[\alpha c_{10}+\beta-\xi+\xi\eta(\pi D_2t)^{1/2}e^{D_2\eta^2t}\mathrm{erfc}\{\eta(D_2t)^{1/2}\}]/[\alpha+(D_1/D_2)^{1/2}]$$

or

$$\alpha+\boldsymbol{F}_1(t)\beta=\boldsymbol{F}_2(t) \quad (9)$$
$$\boldsymbol{F}_1(t)\equiv 1/[c_{10}-r_{1i}(\pi t/D_1)^{1/2}]$$
$$\boldsymbol{F}_2(t)\equiv\{r_{1i}(\pi t/D_2)^{1/2}+\xi[1-\eta(\pi D_2t)^{1/2}\cdot e^{D_2\eta^2t}\mathrm{erfc}\{\eta(D_2t)^{1/2}\}]\}\boldsymbol{F}_1(t)$$

Consequently, it becomes possible to give $\alpha$ and $\beta$ numerically from $D_1$, $D_2$, $c_{10}$, $\xi$, $\eta$, and $r_{1i}(t)$ by means of Eq. 9.

## Results and Discussion

The experimental procedures and the basis of analysis have been described in the first paper. Examples of time dependences of the transfer rate through the interface for *n*-butyric acid from aqueous solutions to carbon tetrachloride layers are shown in Figs. 2a and 2b. The inversion on the early stages in Figs. 2a and 2b is interpreted in terms of a disturbance effect, as has been described in the first paper, resulting from the injection of carbon tetrachloride beneath the aqueous layers of an *n*-butyric acid solution, provided that the initial values are given by extrapolation. Because the two curves representing the time dependences of the transfer rate in 2.34 and 3.12 cm. layer-thicknesses coincide approximately except for the part indicating the inversion by disturbance, they are taken to approximate the case of an infinite layer-thickness. Therefore, the full curve of the

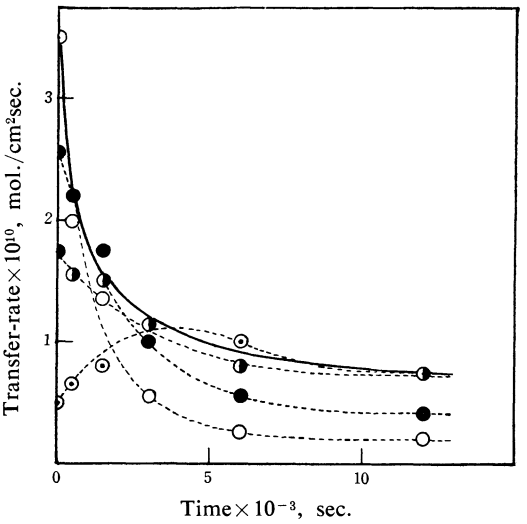



Fig. 2a. Time dependences of the apparent transfer-rate of *n*-butyric acid from the aqueous phase ($c_{10}$=0.0115 N) to the carbon tetrachloride phase in natural, one-dimensional diffusion at 30°C.
Layer-thickness: ○, 0.78 cm.; ●, 1.56 cm.; ◑ 2.34 cm.; ◉, 3.12 cm.

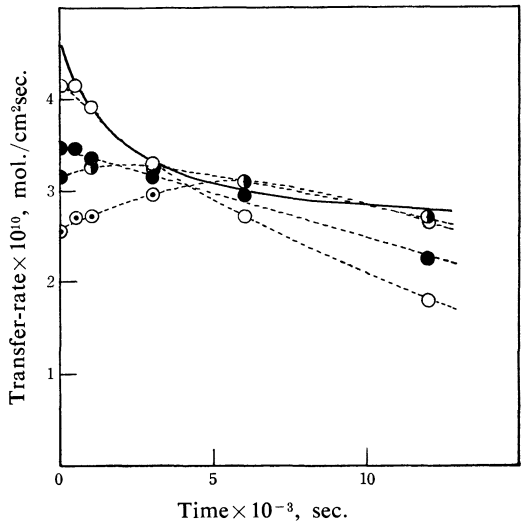



Fig. 2b. Time dependences of the apparent transfer-rate of *n*-butyric acid from the aqueous phase ($c_{10}$=0.566 N) to the carbon tetrachloride phase in natural, one-dimensional diffusion at 30°C.
Layer-thickness: ○, 0.78 cm.; ●, 1.56 cm.; ◑, 2.34 cm.; ◉, 3.12 cm.

envelope in the group of dotted lines is regarded as indicating the case of a semi-infinite composite medium, including no disturbance effect of injection, provided that the initial transfer rates (in the "ideal processes") are obtained by the way described in the first paper.

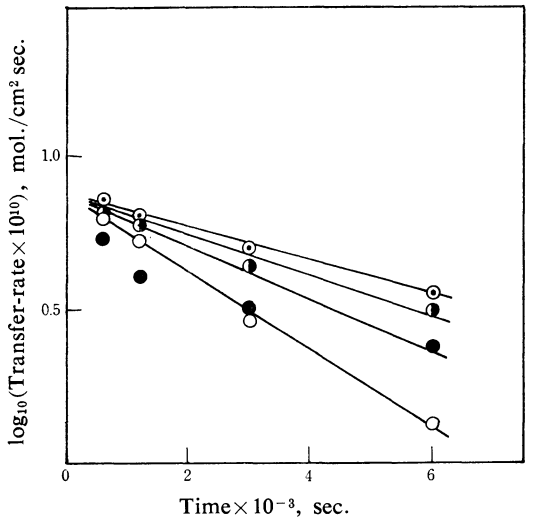



Fig. 3a. Time dependences of the apparent transfer-rate of *n*-butyric acid from the aqueous phase ($c_{10}$=0.0216 N) to the benzene phase in natural, one-dimensional diffusion at 30°C.
Layer-thickness: ○, 0.78 cm.; ●, 1.56 cm.; ◑, 2.34 cm.; ◉, 3.12 cm.

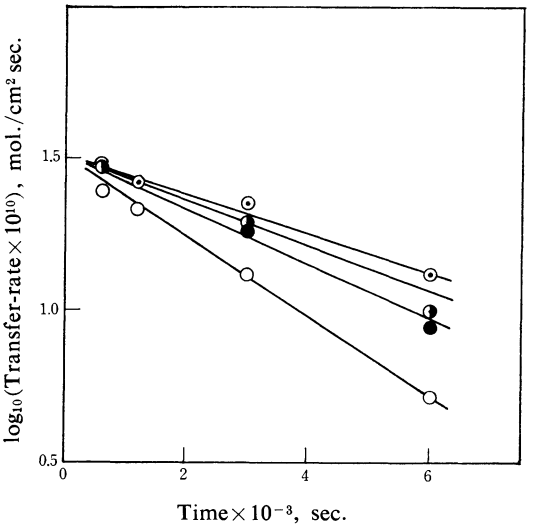



Fig. 3b. Time dependences of the apparent transfer-rate of *n*-butyric acid from the aqueous phase ($c_{10}$=0.0503 N) to the benzene phase in natural, one-dimensional diffusion at 30°C.
Layer-thickness: ○, 0.78 cm.; ●, 1.56 cm.; ◑, 2.34 cm.; ◉, 3.12 cm.

Examples of the time dependences of the apparent transfer rate through the interface for *n*-butyric acid from aqueous solutions to benzene layers are shown in Figs. 3a and 3b. Unlike the case of carbon tetrachloride, Figs.

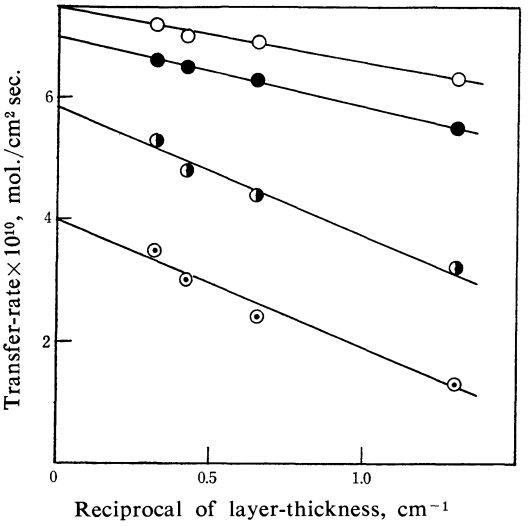



Fig. 4a. Relations between the corrected transfer-rates of *n*-butyric acid and the reciprocals of layer-thickness with the time as a parameter.
System: 0.0216 N aqueous soln. of *n*-butyric acid and benzene (30°C)
Time: ○, 0.60×10³ sec.; ●, 1.20×10³ sec.; ◑, 3.00×10³ sec.; ◉, 600×10³ sec.

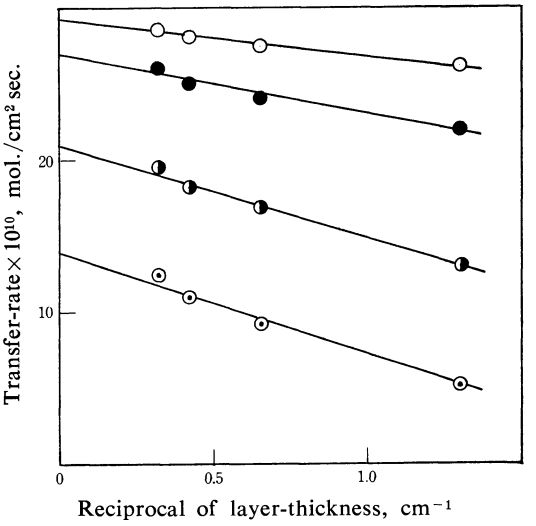



Fig. 4b. Relations between the corrected transfer-rates of *n*-butyric acid and the reciprocals of layer-thickness with the time as a parameter.
System: 0.0503 N aqueous soln. of *n*-butyric acid and benzene (30°C)
Time: ○, 0.60×10³ sec.; ●, 1.20×10³ sec.; ◑, 3.00×10³ sec.; ◉, 6.00×10³ sec.

3a and 3b show no appreciable inversion in the time dependences of the transfer rate, indicating that the disturbance effect is negligible in this case. This agrees with the interpretation of the disturbance effect in this system described in the first paper. Figures 4a and 4b show examples of the relations between the transfer rates and the reciprocals of layer-thickness; the rates extrapolated to zero of the reciprocal of layer-thickness are regarded as indicating one in a semi-infinite composite medium.

The diffusion coefficients of *n*-butyric acid were estimated from the data in the literature.[1,13] They are shown in Table I.

TABLE I. DIFFUSION COEFFICIENTS OF *n*-BUTYRIC ACID AT 30°C

| Solvent | Diffusion coefficient $\times 10^5$, cm²/sec. |
|---|---|
| Water | 1.21 |
| Carbon tetrachloride | 1.60 |
| Benzene | 1.71 |

The initial distributions of concentration in the "ideal process" required in order to obtain $\xi$ and $\eta$ in Eq. 9 were estimated as follows. The time dependences of the amount of solute transferred through the interface in the "ideal process" were obtained from the apparent dependences, correcting the parts deviated by the disturbance, which were easily distinguished in Figs. 2a and 2b, by graphical integration on the curve of the time dependence of transfer rate in the "ideal process," shown as the full curves in these figures. The layer-thicknees dependence of the initial amount of solute transferred in the "ideal process," as defined in the first paper, was obtained from this. The initial distributions of the concentration in an organic solvent in the "ideal process" were finally given from the layer-thickness dependences by graphical differentiation of the initial amount of solute transferred in the "ideal process," assuming that the initial state of the "ideal process" is independent of the layer-thickness. These are approximately represented by the second equation of Eq. 6 in the cases of both carbon tetrachloride and benzene.

The initial condition in the real process is undoubtedly represented as $c_1=c_{10}$, $x<0$ and $t=0$, and $c_2=0$, $x>0$ and $t=0$ instead of Eq. 6. However, the amount of adsorption increases relatively quickly in the early stages after these two bulks are brought into contact with each other if the solute is surface-active; then the boundary condition of Eq. 7 becomes unsuitable, because Eq. 7 holds only when $\theta$ =const. Consequently, if the solute is surface-active and the second equation of Eq. 7 is adopted, the initial condition in the real process, mentioned above, should not be adopted.

The initial distributions of the concentration in the aqueous phase in the "ideal process" could also be obtained in the same way, but the concentrations were estimated to be constant throughout the layer, because the deviation from the values before constact was kept relatively small, even near the interface, for the sake of simplification. This is considered to be the reason why the disturbance effect was negligible in the case of benzene, since the benzene layer was little disturbed, in this case, by the injection of an aqueous solution beneath the benzene layer at the

TABLE II. CONSTANTS SPECIFYING THE INITIAL DISTRIBUTIONS OF CONCENTRATION AND THE TRANSFER RATES AS A FUNCTION OF TIME (30°C)

A) Aqueous solution of *n*-butyric acid - carbon tetrachloride

| $c_{10}\times 10^5$ g. mol./cm³ | $\xi\times 10^6$ g. mol./cm³ | $\eta$ cm$^{-1}$ | $r_{1i}\times 10^{10}$ g. mol./cm² sec. | | | |
|---|---|---|---|---|---|---|
| | | | $t$=20 min. | $t$=1 hr. | $t$=3 hr. | $t$=5 hr. |
| 1.14 | 0.19±0.13* | 1.27±0.14* | 1.95 | 1.16 | 0.85 | 0.72 |
| 5.66 | 3.10±0.19* | 0.74±0.23* | 4.12 | 3.35 | 2.75 | 2.28 |

B) Aqueous solution of *n*-butyric acid - benzene

| $c_{10}\times 10^5$ g. mol./cm³ | $\xi\times 10^6$ g. mol./cm³ | $\eta$ cm$^{-1}$ | $r_{1i}\times 10^{10}$ g. mol./cm² sec. | | | |
|---|---|---|---|---|---|---|
| | | | $t$=10 min. | $t$=20 min. | $t$=50 min. | $t$=100 min. |
| 1.00 | 1.22±0.11* | 1.07±0.11* | 4.30 | 4.04 | 3.19 | 2.01 |
| 2.16 | 1.22±0.08* | 1.07±0.08* | 7.50 | 7.04 | 5.85 | 4.06 |
| 5.03 | 4.30±0.13* | 1.07±0.13* | 29.30 | 27.00 | 21.20 | 14.00 |
| 10.38 | 12.20±0.36* | 1.07±0.36* | 30.00 | 29.60 | 27.70 | 23.50 |

* Estimated standard error

13) C. R. Wilke, *Chem. Eng. Progress*, 45, 218 (1949).

beginning (actually the benzene layer must be more or less disturbed by the so-called "Marangoni effect,"[1,7,14-17] though this effect might be small compared with the disturbance effect of the injection), whereas the aqueous layer was disturbed very much.

The constants specifying the initial distribution of concentration and the transfer rate in the "ideal process" as a function of time are shown in Table II, while the values of $\alpha$ and $\beta$ calculated statistically by the method of least squares from the data in Tables I and II by Eq. 9 are shown in Table III.

Table III. Values of $\alpha$ and $\beta$ calculated from the experimental data (30°C)

| Org. solvent | $c_{10}\times10^5$ g. mol./cm³ | $\alpha$ — | $\beta\times10^5$ g. mol./cm³ |
|---|---|---|---|
| $CCl_4$ | 1.14 | $-0.807\pm0.020$* | $0.964\pm0.014$* |
| $CCl_4$ | 5.66 | $-0.708\pm0.042$* | $4.384\pm0.183$* |
| $C_6H_6$ | 1.00 | $-0.940\pm0.080$* | $0.899\pm0.015$* |
| $C_6H_6$ | 2.16 | $-0.775\pm0.029$* | $1.836\pm0.022$* |
| $C_6H_6$ | 5.03 | $-0.799\pm0.004$* | $4.504\pm0.001$* |
| $C_6H_6$ | 10.38 | $-0.764\pm0.008$* | $9.229\pm0.019$* |

* Estimated standard error

Fairly large errors are estimated in some cases of $\xi$ and $\eta$ parameters of the initial distribution of the concentration in the "ideal process." However, the contribution of such errors in both $\xi$ and $\eta$ to that in $\alpha$ and $\beta$ factors specifying the boundary condition is not very serious. For example, the estimated contributions of the errors in the case of a $c_{10}=1.14\times10^{-5}$ g. mol./cm³ aqueous solution of *n*-butyric acid and carbon tetrachloride, are $\alpha\pm0.073$ and $\beta\pm0.053\times10^{-5}$ g. mol./cm³ (about 9 and 5% $\alpha$ and $\beta$ respectively, against 69 and 11% $\xi$ and $\eta$ respectively).

Moreover, $\alpha<0$ and $\beta>0$ do not come from adopting the initial condition of the "ideal process," since the results of adopting that of the real process, $c_1=c_{10}$ ($x<0$, $t=0$) and $c_2=0$ ($x>0$, $t=0$), are, for example, $\alpha=-0.84$ and $\beta=0.97\times10^{-5}$ g. mol./cm³ and $\alpha=-0.78$ and $\beta=4.51\times10^{-5}$ g. mol./cm³ in $c_{10}=1.14$ and $5.66\times10^{-5}$ g. mol./cm³ aqueous solutions of *n*-butyric acid and carbon tetrachloride respectively.

Table IV shows what the values of $\alpha$ and $\beta$ in Eq. 9 should be when Nernst's law of distribution holds in the two concentrations immediately next to the interface. In order to obtain the theoretical values of $\alpha$ and $\beta$ in Eq. 3 when Nernst's law does not exist generally, it is assumed for the sake of simplification that $k_{a1}=k_{a2}$, $k_{d1}=k_{d2}$, $x_1=x_2$ and $y_1=y_2$; then Eq. 3 becomes

$$\alpha=-(k_{a1}/k_{a2})e^{(x_1-x_2)\theta}=-1$$
$$\beta=[(k_{d1}e^{-y_1\theta}+k_{d2}e^{-y_2\theta})/k_{a2}e^{x_2\theta}]\theta/(1-\theta)$$
$$=2(k_{d2}/k_{a2})e^{-sV\theta/RT}\cdot\theta/(1-\theta) \quad (10)$$

Approximate values of $\alpha$ and $\beta$ obtained by Eq. 10 from the data in the first paper are shown in Table V. It may be clearly seen by comparing Tables III, IV and V with one another that Nernst's law of distribution does not hold in these two concentrations immediately next to the interface in the mass-transfer process for our experimental series.

Table IV. Values of $\alpha$ and $\beta$ in case Nernst's law holds (30°C)

| Org. solvent | $\alpha$ | $\beta$ |
|---|---|---|
| $CCl_3$ | 0.087 | 0 |
| $C_6H_6$ | 0.309 | 0 |

Table V. Approximate values of $\alpha$ and $\beta$ by Eq. 10 (30°C)

| Org. solvent | $c_{10}\times10^5$ g. mol./cm³ | $\alpha$ — | $\beta\times10^5$ g. mol./cm³ |
|---|---|---|---|
| $CCl_4$ | 1.14 | −1 | 0.24 |
| $CCl_4$ | 5.66 | −1 | 3.60 |
| $C_6H_6$ | 1.00 | −1 | 0.61 |
| $C_6H_6$ | 2.16 | −1 | 1.29 |
| $C_6H_6$ | 5.03 | −1 | 2.82 |
| $C_6H_6$ | 10.38 | −1 | 3.70 |

The convection effect resulting from the dependence of the local density on the concentration is, in general, considered to increase the diffusion coefficients obviously. The experiments, however, were made with samples as dilute as possible for the sake of analysis (0.01—0.10 N), so that this effect might be negligible. No such convection effect should take place in the system of an aquous solution of *n*-butyric acid and benzene, considering the variation in density with the concentration. In the case of carbon tetrachloride, however, a little such effect should take place in the aqueous phase. This may be negligible, though, because the convection in the aquenus phase should have little effect on the mass-transfer through the interface, as has been indicated above in discussing the disturbance effect.

Besides the convection arising from the difference in local density, a spontaneous interfacial turbulence resulting from the Marangoni effect, referred to above, must more or less affect the mass transfer. However, the evaluation of this effect is considered to be difficult.

14) C. V. Sternling and L. E. Scriven, *A. I. Ch. E. Journal*, **5**, 514 (1959).
15) A. Orell and J. W. Westwater, ibid., **8**, 350 (1962).
16) J. B. Lewis, *Chem. Eng. Sci.*, **3**, 260 (1954).
17) W. J. McManamey, ibid., **15**, 210 (1961).

We should like to express our gratitude to Professor H. G. Drickamer, University of Illinois, for his useful suggestions on this work. We also wish to express our indebtedness to Professor Tominaga Keii of this Institute for his helpful discussions on this subject.

*Department of Chemical Engineering*
*Tokyo Institute of Technology*
*Ookayama, Tokyo*

# The Mass Transfer Rate through the Liquid-Liquid Interface. III. Factors Specifying Boundary Conditions

By Teruya SHIMBASHI and Tadao SHIBA

(Received April 10, 1964)

In the previous papers of this series, it was found that the resistance to the transfer of *n*-butyric acid through the interfaces of water-benzen and water - carbon tetrachloride systems were appreciably high. In these systems, no equilibrium was established during the transference process for the solute in the two concentrations immediately next to the interface. A rate-determining potential barrier was found on the interfaces of the non-aqueous side, a barrier which was attributed to the breaking of the hydrogen bonds between the carboxyl radicals and water.

In the present paper, the results of studies of carboxylic acids and amines will be summarized. These substances form hydrogen bonds with water and show similar transference resistances. The second paper of this series gave an equation, $c_{11}=\alpha c_{21}+\beta$, which holds when the amount of adsorption on the interface, $\Gamma$, is constant with respect to the time, when, that is, the fraction of coverage, $\theta$, is constant. In this equation, $c_{11}$ and $c_{21}$ are the concentrations (or, more precisely, the activities) of the solute in phases 1 and 2 respectively, next to the interface, and $\alpha$ and $\beta$ are functions of $\theta$, independent of the time at a constant temperature. When the interfacial resistance is not zero, $\alpha<0$ and $\beta>0$; $\alpha=K>0$ and $\beta=0$ otherwise, as has been described in the preceding paper. Here $K$ is Nernst's partition coefficient. It is possible to determine whether the interfacial resistance is zero or not by solving this equation numerically for $\alpha$ and $\beta$. The boundary condition of Fick's diffusion equation is specified by determining the values of $\alpha$ and $\beta$ and the problem of transference through the interface is solved by solving Fick's equation. The numerical evaluation of $\alpha$ and $\beta$ is an important problem from both theoretical and practical points of view.

## Experimental

The apparatus used is shown in Fig. 1. The experimental procedure was given in detail in the first

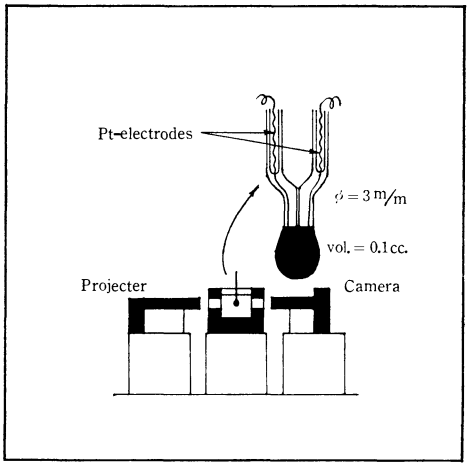



Fig. 1. Apparatus.

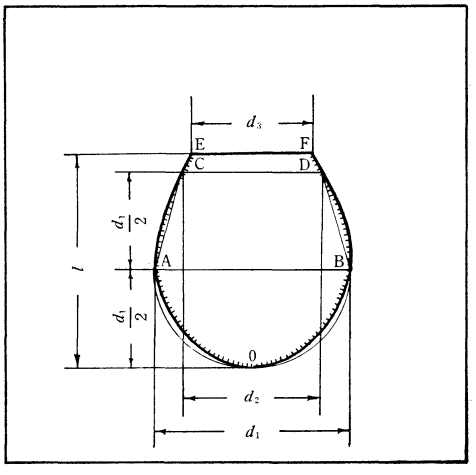



Fig. 2. Scheme of the pendant drop.

paper. As in the pendant-drop method of measuring interfacial tension, a water drop was suspended in an organic solution of a solute, and the change in the average concentration of the solute in the drop was traced conductometrically, with a pair of platinum electrodes coated with platinum black. Every result was recorded automatically. The use of the platinum black increased the sensitivity and improved the response. The average concentration was obtained approximately from the relationship between the equilibrium concentration and the conductivity calibrated beforehand. The actual concentration-distributions in the drop were, however, not uniform, and only approximate values could be estimated by this method. The interfacial tension was determined by the pendant-drop method,[1] in the same time, using photographs of the drop.

The final concentration in the drop was about 0.01—0.10 N. In the calculation of the interfacial tension, the densities of the first and second phases were given to be approximately equal to those of the pure solvents. In order to prevent the communication of the solute from the internal part of the syringe, the tip was made from a capillary tube. No transfer of the solute from the syringe to the drop of pure water hung at the tip of the capillary tube was detected by the conductometry, even when the syringe was filled with a concentrated solution.

The drop was estimated to be a sphere of the same volume. The volume and surface area of the drop were calculated from the OAB hemisphere and from the truncated cones, ABCD and CDEF, shown in Fig. 2, by using these equations:

$$V=\frac{\pi}{24}[2d_1^3+d_1(d_1^2+d_1d_2+d_2^2)+2(l-d_1)(d_2^2+d_2d_3+d_3^2)]$$

$$A=\frac{\pi}{4}[2d_1^2+(d_1+d_2)\{d_1^2+(d_1-d_2)^2\}^{1/2}+(d_2+d_3)\{4(l-d_1)^2+(d_2-d_3)^2\}^{1/2}]$$

where $V$ is the volume of liquid drop, and $A$ is the surface area of the liquid drop. The values obtained by this method were in agreement with those determined by Simpson's method of graphical integration, in which the height was divided into ten sections, with an accuracy of 5%. The radii of spheres with both the same volume and the same interfacial area show a good agreement (within 2%).

All disturbance effects, for example, the disturbance of making the pendant drop, the convection resulting from the difference in local density, and the spontaneous interfacial turbulence, due to the so-called "Marangoni effect," were disregarded.

## Theoretical

Consider a sphere of the first phase suspended in a second phase of infinite dimensions. The three-dimensional diffusion equations[2] are represented as:

$$\frac{\partial U_1}{\partial t}=D_1\frac{\partial^2 U_1}{\partial r^2},\quad 0\leqslant r<R,\ t>0 \tag{1}$$

$$\frac{\partial U_2}{\partial t}=D_2\frac{\partial^2 U_2}{\partial r^2},\quad R<r,\ t>0 \tag{2}$$

$$U_1=\alpha U_2+\beta,\quad r=R,\ t>0 \tag{3}$$

$$D_1\left(\frac{1}{r}\cdot\frac{\partial U_1}{\partial r}-\frac{U_1}{r^2}\right)=D_2\left(\frac{1}{r}\cdot\frac{\partial U_2}{\partial r}-\frac{U_2}{r^2}\right),\quad r=R,\ t>0 \tag{4}$$

$$\left.\begin{aligned}&U_1=rC_{10},\quad 0\leqslant r<R,\ t=0\\&U_2=rC_{20},\quad R<r,\ t=0\end{aligned}\right\} \tag{5}$$

$$C_1:\ \text{finite},\quad r=0 \tag{6}$$

where $U_1$ and $U_2=rC_1$ and $rC_2$ respectively; $r$ is the distance from the center of the sphere; $C_1$ and $C_2$ are the local concentrations of the solute in phases 1 and 2 respectively; $R$ is the radius of the sphere; $D_1$ and $D_2$ are the diffusion coefficients of the solute in both phases; $t$ is the time, and $C_{10}$ and $C_{20}$ are the initial concentrations of the solute in the two phases respectively. Equation 4 expresses the condition of continuity, indicating that the amount of solute flowing into the interface from the first phase in the unit of time is equal to that from the interface into the second.

The initial concentration in the drop of pure water, $C_{10}$, is zero, while $C_{20}$ is the concentration in the solution before their contact. As has been shown in the first paper, however, the amount of adsorption on the interface may be increased very rapidly in the early stage, the "adsorption stage." According to the second paper, Eq. 3 holds only when there is no time-change in the amount of adsorption. In the "adsorption stage," neither Eq. 3 nor 4 is applicable.

As may be seen in Fig. 3, the process in the early stage (in 5 min.) is quite different from that in the later stage. As was described in the second paper, the interfaces of water-benzene and water - carbon tetrachloride systems show a high resistance to the passage of *n*-butyric acid. Putting other resistances in the bulk diffusion of zero as the limiting case, we have:

$$\frac{dm}{dt}=V\frac{dC_1}{dt}=-k(C_1-KC_2)A \tag{7}$$

where $m$ is the amount of solute transferred, and $k$ is the rate constant of transferring through the interface.

Since the concentration-distribution is to be assumed even in each phase, and since the second phase is infinite in volume, we have $C_2=C_{20}$, and

$$\frac{dC_1}{dt}=-k\left(\frac{A}{V}\right)(C_1-KC_{20}) \tag{8}$$

Assuming that the radius of the sphere is

1) J. M. Andreas, E. A. Hauser and W. B. Tucker, *J. Phys. Chem.*, **42**, 1001 (1938).

2) J. Crank, "Mathematics of Diffusion," Clarendon Press, Oxford (1956).

independent of the time, we integrate Eq. 8 as:

$$\ln[(KC_{20}-C_{10})/(KC_{20}-C_1)]=ktA/V \quad (9)$$

An example of the plots of Eq. 9 is shown in Fig 3, where the measured values after about 3 min. fall on a straight line. In some cases no such liner plot was observed. This is probably due to the facts that the interfacial phase is not taken account in Eq. 7, and that the actual situation is not strictly represented by such a limiting equation as Eq. 7.

All the plots obtained consist of two sections, one for the early stage (in 5 min.) and the other for the later stage. The extrapolation of the later section meets the ordinate. The values of $C_{10}$ obtained by this extrapolation are all positive. This result is not contrary to the following interpretation. Let us denote the starting time of the later stage as $t_0$ and then shift the origin to $t_0$. When $t$ is sufficiently large, this transformation produces no error. This situation corresponds to the case where no "adsorption stage" occurs, and $C_{10}>0$. As for $C_{20}$, the values preceding the contact were used. As the magnitude of $C_{20}$ is sufficiently large, the error due to the use of this initial value is considered to be negligible.

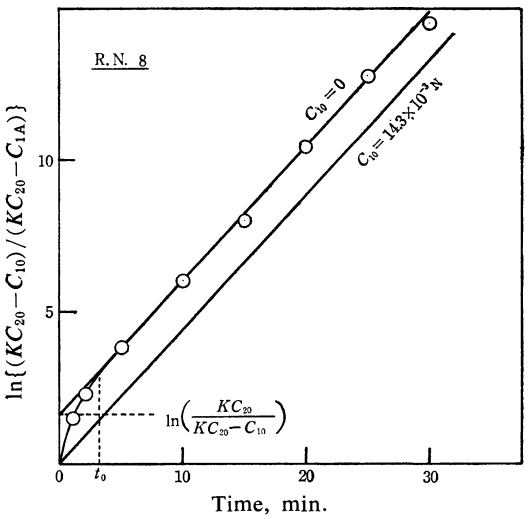



Fig. 3. An example of time dependences of the average concentration in the drop.

Solving Eqs. 1—6 (see Appendix I), we have

$$C_1\fallingdotseq C_{10}+\frac{1}{r}\sum_{n=0}^{\infty}\left\{K_1\left[\mathrm{erfc}\left\{\frac{(2n+1)R-r}{2(D_1t)^{1/2}}\right\}-\mathrm{erfc}\left\{\frac{(2n+1)R+r}{2(D_1t)^{1/2}}\right\}\right]+\frac{K_2}{h}\left[\mathrm{erfc}\left\{\frac{(2n+1)R-r}{2(D_1t)^{1/2}}\right\}-e^{h\{(2n+1)R-r\}+D_1th^2}\,\mathrm{erfc}\left\{\frac{(2n+1)R-r}{2(D_1t)^{1/2}}+h(D_1t)^{1/2}\right\}-\mathrm{erfc}\left\{\frac{(2n+1)R+r}{2(D_1t)^{1/2}}\right\}+e^{h\{(2n+1)R+r\}+D_1th^2}\,\mathrm{erfc}\left\{\frac{(2n+1)R+r}{2(D_1t)^{1/2}}+h(D_1t)^{1/2}\right\}\right]\right\} \quad (10)$$

$$C_2\fallingdotseq C_{20}+\frac{1}{r}\left\{K'_1\left[\mathrm{erfc}\left\{\frac{r-R}{2(D_2t)^{1/2}}\right\}-2\sum_{n=0}^{\infty}\mathrm{erfc}\left\{\frac{2(n+1)(D_2/D_1)^{1/2}R+(r-R)}{2(D_2t)^{1/2}}\right\}\right]+\frac{K'_2}{h'}\left[\mathrm{erfc}\left\{\frac{r-R}{2(D_2t)^{1/2}}\right\}-e^{h'(r-R)+D_2th'^2}\,\mathrm{erfc}\left\{\frac{r-R}{2(D_2t)^{1/2}}+h'(D_2t)^{1/2}\right\}\right]+\frac{K'_3}{h'}\sum_{n=0}^{\infty}\left[\mathrm{erfc}\left\{\frac{2(n+1)(D_2/D_1)^{1/2}R+(r-R)}{2(D_2t)^{1/2}}\right\}-e^{h'\{2(n+1)(D_2/D_1)^{1/2}R+(r-R)+D_2th'^2\}}\,\mathrm{erfc}\left\{\frac{2(n+1)(D_2/D_1)^{1/2}R+(r-R)}{2(D_2t)^{1/2}}+h'(D_2t)^{1/2}\right\}\right]\right\} \quad (11)$$

$$K_1\equiv\frac{R(\alpha C_{20}-C_{10})+\beta}{1+\alpha(D_1/D_2)^{1/2}}$$

$$K_2\equiv\frac{\alpha\{1+(D_1/D_2)^{1/2}\}\{R(\alpha C_{20}-C_{10})+\beta\}}{R\{1+\alpha(D_1/D_2)^{1/2}\}^2}$$

$$h\equiv\frac{1-\alpha D_1/D_2}{R(D_1/D_2)^{1/2}\{1+\alpha(D_1/D_2)^{1/2}\}}$$

$$K'_1\equiv\frac{-(D_1/D_2)^{1/2}\{R(\alpha C_{20}-C_{10})+\beta\}}{1+\alpha(D_1/D_2)^{1/2}}$$

$$K'_2\equiv\frac{(D_1/D_2)^{1/2}\{1+(D_1/D_2)^{1/2}\}\{R(\alpha C_{20}-C_{10})+\beta\}}{R\{1+\alpha(D_1/D_2)^{1/2}\}^2}$$

$$K'_3\equiv\frac{2(D_1/D_2)^{1/2}(1-\alpha D_1/D_2)\{R(\alpha C_{20}-C_{10})+\beta\}}{R\{1+\alpha(D_1/D_2)^{1/2}\}^2}$$

$$h'\equiv\frac{1-\alpha D_1/D_2}{R\{1+\alpha(D_1/D_2)^{1/2}\}}$$

The Concentrations immediately next to the interface, $C_{1i}$ and $C_{2i}$, are given from Eqs. 10 and 11, putting $r=R$, as:

$$C_{1i}\fallingdotseq C_{10}+K_1/R+(K_2/Rh)\times[1-e^{D_1th^2}\,\mathrm{erfc}\{h(D_1t)^{1/2}\}] \quad (12)$$

$$C_{2i}\fallingdotseq C_{20}+K'_1/R\left[1-2\sum_{n=0}^{\infty}\mathrm{erfc}\left\{\frac{(n+1)R}{(D_1t)^{1/2}}\right\}\right]$$

$$+(K'_2/Rh')\,[1-e^{D_2th'^2}\,\mathrm{erfc}\{h'(D_2t)^{1/2}\}]$$
$$+\frac{K'_3}{Rh'}\sum_{n=0}^{\infty}\left[\mathrm{erfc}\left\{\frac{(n+1)R}{(D_1t)^{1/2}}\right\}\right.$$
$$-e^{2(n+1)(D_2/D_1)^{1/2}Rh'+D_2th'^2}\,\mathrm{erfc}$$
$$\left.\left\{\frac{(n+1)R}{(D_1t)^{1/2}}+h'(D_2t)^{1/2}\right\}\right] \qquad (13)$$

Equations 10 and 11 exist strictly at $t\to 0$ (see Appendix I) : $\lim_{t\to 0} C_{11}=C_{10}+K_1/R$, $\lim_{t\to 0} C_{21}=C_{20}+K'_1/R$, and $\lim_{t\to 0} C_{11}=\alpha(\lim_{t\to 0} C_{21})+\beta/R$, that is in accord with Eq. 3.

The average concentration in the drop is represented as:

$$\bar{C}_{1A}=\frac{\iiint_v \bar{C}_1 r^2\sin\theta\,dr\,d\theta\,d\varphi}{\iiint_v r^2\sin\theta\,dr\,d\theta\,d\varphi}=\frac{3}{R^3}\int_0^R \bar{U}_1 r\,dr \qquad (14)$$

where $\theta$ and $\varphi$ are the angles in the solid polar coordinates.

By calculating Eq. 14 by applying Eq. 27 in Appendix I, and by inversion to the original function, we have:

$$C_{1A}\doteqdot C_{10}+[R(\alpha C_{20}-C_{10})+\beta]$$
$$\times\left\{\frac{6(D_1t/\pi)^{1/2}}{R^2}\left[\frac{1+\alpha(D_1/D_2)^{3/2}}{(1-\alpha D_1/D_2)^2}\right]\right.$$
$$-\frac{3D_1t}{R^3(1-\alpha D_1/D_2)}+3\alpha(D_1/D_2)$$
$$\times[1+(D_1/D_2)^{1/2}]^2\,[e^{D_1th^2}\,\mathrm{erfc}\{h(D_1t)^{1/2}\}$$
$$\left.-1]/R(1-\alpha D_1/D_2)^3+S_1+S_2\right\} \qquad (15)$$

$$S_1\equiv\frac{12}{R^2(1+\alpha(D_1/D_2)^{1/2})}\sum_{n=1}^{\infty}[(D_1t/\pi)^{1/2}e^{-n^2R^2/D_1t}$$
$$-nR\,\mathrm{erfc}\{nR/(D_1t)^{1/2}\}]$$
$$S_2\equiv\frac{6\alpha\{1+(D_1/D_2)^{1/2}\}(1-\alpha D_1/D_2)^2}{(D_1/D_2)R^5\{1+\alpha(D_1/D_2)^{1/2}\}^4}$$
$$\times\sum_{n=1}^{\infty}\left[2h\left(\frac{D_1t}{\pi}\right)^{1/2}e^{-n^2R^2/D_1t}\right.$$
$$-(1+2nRh)\,\mathrm{erfc}\left\{\frac{nR}{(D_1t)^{1/2}}\right\}$$
$$\left.+e^{2nRh+D_1th^2}\,\mathrm{erfc}\{nR/(D_1t)^{1/2}+h(D_1t)^{1/2}\}\right]$$

Therefore, our purpose is to determine the numerical values of $\alpha$ and $\beta$ suitable for Eq. 15 from the expermental data, $R$, $C_{10}$, $C_{20}$, $C_{1A}$, $D_1$ and $D_2$. Equation 15 is deformed as:

$$\beta=(C_{1A}-C_{10})/F(\alpha,t)-R(\alpha C_{20}-C_{10}) \qquad (16)$$
$$F(\alpha,t)\equiv\frac{6(D_1t/\pi)^{1/2}}{R^2}\left[\frac{1+\alpha(D_1/D_2)^{3/2}}{(1-\alpha D_1/D_2)^2}\right.$$
$$-\frac{3D_1t}{R^3(1-\alpha D_1D_2)}$$
$$\left.+\frac{3\alpha(D_1/D_2)\,[1+(D_1/D_2)^{1/2}]^2}{R(1-\alpha D_1/D_2)^3}\right.$$
$$\times e^{D_1th^2}\,\mathrm{erfc}\{h(D_1t)^{1/2}\}-1]+S_1+S_2 \qquad (17)$$

As $\beta$ is an explicit function of the time, $t$, it can be evaluated as the function of $t$ by specifying $\alpha$. We denote the values of $\beta$ at $t=t_1, t_2,\cdots\cdots,t_n$ as $\beta=\beta_1, \beta_2,\cdots\cdots,\beta_n$, and define $\tilde{\beta}=(\beta_1+\beta_n)/2$ and $\Delta\beta=|\beta_1-\beta_n|$ (see Appendix II). Therefore, the requisite condition of $\alpha$ and $\beta$ being the solution of Eq. 16 is $\Delta\beta=0$ in a definite value of $\alpha$, because $\alpha$ and $\beta$ are constant with the time-lapse.

An example of plots of $\tilde{\beta}$ and $\Delta\beta$ against $\alpha$ is shown in Fig. 4. In Fig. 4, points A and B satisfy the condition, $\Delta\beta=0$. Point A is,

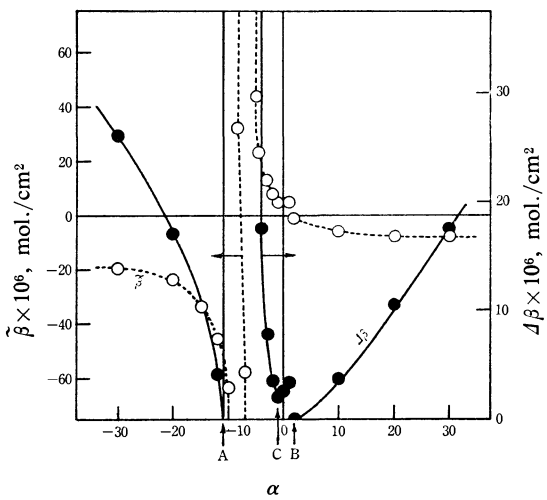



Fig. 4. An example of $\alpha$-dependences of the $\Delta\beta$ and $\tilde{\beta}$.
System: water-benzene solution of *n*-butyric acid ($C_{20}=10.41\times10^{-6}$ mol./cm³) at 30°C.

however, physically meaningless, since $C_1<0$ when $\alpha$ and $\beta<0$ and $C_2>0$ in Eq. 3. Point B has no definite value, because at B, $\alpha=D_2/D_1$, both denominater and numerator in the third term of Eq. 17 become zero; in the limiting value of the indefinite form, $\Delta\beta=0$.

From the physical point of view, one reasonable solution at least should be definitive. If we can assume that the value of point C, where $\Delta\beta$ is at its minimum, must fall on the $\alpha$ axis in spite of its actually taking some finite value because of errors, we can estimate, from the position of the minimum, the approximate value of $\alpha$, or $\alpha_0$, and the corresponding value of $\tilde{\beta}$ (the most probable value of $\beta$), or $\beta_0$, as is shown in Fig. 4. All the experimental plots behave similarly.

$C_{11}$ and $C_{21}$ were estimated by putting the numerical values of $\alpha_0$ and $\beta_0$ obtained by the above graphical method into Eqs. 12 and 13.

TABLE I. EXPERIMENTAL AND CALCULATED RESULTS (30°C)

| No. | System | $C'_{20}\times10^6$ g. mol./cm³ | $\alpha_0$ — | $\beta_0\times10^6$ g. mol./cm² | $C_{1i}\times10^6$ g. mol./cm³ | $C'_{2i}\times10^6$ g. mol./cm³ | $C_S\times10^6$ g. mol./cm³ |
|---|---|---|---|---|---|---|---|
| 1 | PB | 34.5 | −0.6 | 5.0 | 19.0 | −122.0 | 11.3 |
| 2 | PB | 94.5 | −0.8 | 14.0 | 61.7 | −623.0 | 47.0 |
| 3 | PT | 68.0 | −1.0 | 9.6 | 44.7 | −462.0 | 2.5 |
| 4 | PT | 112.5 | −0.7 | 17.0 | 72.9 | −685.0 | 25.5 |
| 5 | PC | 49.0 | −0.6 | 1.8 | 8.7 | −1330.0 | 6.3 |
| 6 | PC | 77.7 | −0.2 | 3.5 | 13.8 | −1730.0 | 2.5 |
| 7 | BuB | 8.7 | −0.7 | 2.0 | 6.6 | 0.1 | 8.4 |
| 8 | BuB | 46.0 | −1.0 | 11.0 | 35.9 | −20.7 | 50.0 |
| 9 | BuT | 36.5 | −0.5 | 12.0 | 44.6 | −43.4 | 31.8 |
| 10 | BuT | 67.3 | −1.2 | 18.0 | 58.5 | 3.9 | 57.5 |
| 11 | BuC | 41.5 | −0.6 | 5.9 | 27.2 | −231.0 | 29.9 |
| 12 | BuC | 57.3 | −1.0 | 8.0 | 41.8 | −574.0 | 39.2 |
| 13 | P'B | 6.2 | −0.6 | 0.8 | 2.1 | 2.4 | 12.0 |
| 14 | P'B | 15.2 | −0.5 | 2.3 | 5.5 | 11.5 | 13.1 |
| 15 | P'C | 68.5 | −0.3 | 6.5 | 24.8 | −40.2 | 30.5 |
| 16 | P'C | 135.1 | −0.1 | 19.0 | 70.1 | −171.0 | 71.0 |
| 17 | Bu'B | 8.2 | −0.5 | 2.4 | 3.7 | 7.0 | 10.0 |
| 18 | Bu'B | 15.7 | −0.6 | 4.6 | 4.6 | 15.7 | 17.0 |
| 19 | Bu'C | 3.8 | −0.9 | 0.9 | 1.8 | 4.0 | 4.5 |
| 20 | Bu'C | 18.2 | −1.0 | 3.7 | 6.1 | 11.8 | 18.5 |

P Propionic acid; B Benzene; Bu *n*-Butyric acid; T Toluene; P' *n*-Propyl amine; C Cyclohexane; Bu' *n*-Butyl amine

## Results

The results obtained are shown in Table I. These were obtained by the aid of an electronic digital computer using Eqs. 12, 13 and 16, assuming that $D_1$ and $D_2$ in these equations can be estimated by Wilke's method.[3] In Table I, no description is given for water, which is a substance common to all the systems. $C_{1i}$ is the concentration of the solute in the first (aqueous) phase immediately next to the interface. $C'_{20}$ and $C'_{2i}$ are the concentrations of the solute in the first phase in equilibrium with those in the second phase, initial ($C_{20}$) and immediately next to the interface ($C_{2i}$). $C_S$ is the concentration of the solute in the first phase in equilibrium with the surface pressure (or the difference between the interfacial tension of the pure solvents and that of the solutions). $C'_{20}$, $C'_{2i}$, and $C_S$ are, so to speak, the reduced concentrations of $C_{20}$, $C_{2i}$ and $\Gamma$ respectively, in comparison with $C_{1i}$. $C_{1i}$, $C'_{2i}$ and $C_S$ are the values at $t=2$ min. In all the results, $\alpha_0<0$ and $\beta_0>0$. No consistent relation is found between $\alpha_0$ and $C'_{20}$, while $\beta_0$ increases with the increase in $C'_{20}$. According to the second report,

$$\alpha = -(k_{a2}/k_{a1})e^{(x_2-x_1)\theta}$$

$$\beta = [(k_{d1}e^{-y_1\theta}+k_{d2}e^{-y_2\theta})/k_{a1}e^{x_1\theta}]\,[\theta/(1-\theta)]\,R$$

where $k_{a1}$ and $k_{a2}$ are the rate constants of the adsorption onto the interface from the two phases respectively; $k_{d1}$ and $k_{d2}$ are the rate constants of desorption from the interface into the two phases respectively; $x_1$, $x_2$, $y$, and $y_2$ are factors defining the mutual interaction of adsorbed molecules, and $\theta$ is the relative amount of adsorption (the fraction of coverage). When $k_{a1}$, $k_{a2}$, $k_{d1}$ and $k_{d2}$ have finite values, $\alpha<0$ and $\beta>0$. If $\theta/(1-\theta)$ has a large effect upon the variation in $\beta$, $\theta$ generally increases with the increase in $C'_{20}$, while $\theta/(1-\theta)$ increases more rapidly, resulting in the increase in $\beta$. The experimental results are not inconsistent with these speculations; this is evidence that a finite interfacial resistance exists in these cases.

In the cases of fatty acids and also in the P'C system (though $C'_{2i}$ shows unreasonable values in these cases), the value of $C_S$ approach those of $C_{1i}$, while others approach those of $C'_{2i}$. These facts may be ascribed to the existence of a rate-determining potential barrier. That is to say, in the former cases the rate-determining stage may be the adsorption from the organic solvent onto the interface, while in the latter it may be the desorption from the interface into the aqueous phase. The reason for the appearance of unreasonable values of $C'_{2i}$ in some cases is not certain, but it may be connected with the long time range, $t_1-t_n$, for the calculation of $\tilde{\beta}$ or $\Delta\beta$, because on a

3) C. R. Wilke, *Chem. Eng. Progress*, **45**, 218 (1949).

longer time range the applicability of the condition, that is, the base of Eqs. 3 and 4, $\theta=$ const., seems poor in these cases; as has been described above, when we put other resistances in a bulk diffusion of zero as a limiting case compared with the interfacial resistance, we have $C_{1i}=C_{1A}$ and $C'_{2i}=C'_{20}$. When $C_S=C_{1i}$, the condition in the cases of fatty acids and in the P'C system, $C_S=C_{1A}$ and $\theta\neq$const.; on the other hand, when $C_S=C'_{2i}$, $C_S=C'_{20}$ and $\theta=$const.

The values of $\alpha$ and $\beta$ recalculated from the data of the reverse, one-dimensional diffusion given in the second paper are as follows: $\alpha=-1.3$; $\beta=2.2\times10^{-6}$ (No. 7) and $13.0\times10^{-6}$ (No. 8) g. mol./cm$^2$. These values are in good agreement with the present results for the Bu-B system shown in Table I, considering rough approximations are included in the present results. The values of the present results, if denoted as $\alpha'$ and $\beta'$, are related to those ($\alpha$ and $\beta$) in the preceding paper as follows: $\alpha'=1/\alpha$, and $\beta'=-R\beta/\alpha$, provided that $R=0.294$ (No. 7), 0.317 (No. 8) cm.; $\alpha=0.779$, that is the average of $\alpha'$ sin $c_{10}=2.16\times10^{-5}$, $5.03\times10^{-5}$ and $10.38\times10^{-5}$ g. mol./cm$^3$ (as shown in Table III of the second paper), and $c_{1i}$, which should fix the value of $\beta$, approximates $c_{10}$. The positions of the potential barriers have been taken to be the same for both sets of results.

The time dependence of the thickness of the diffusion layer in the aqueous drop has also been calculated. As may be seen in Fig. 5,

$$dm/dt=V(dC_{1A}/dt)=D_1(\Delta C_1/l)A$$

or
$$l=D_1\Delta C_1/(V/A)(dC_{1A}/dt) \qquad (18)$$

where $l$ is the thickness of the diffusion layer of phase 1, and $\Delta C_1$ is the difference in the boundary concentrations in the diffusion layer of phase 1.

It is assumed that $C_{1i}$, on which the calculation of $\Delta C_1$ is based, is in equilibrium with the surface pressure. As $C_{1i}=C_S$, we have

$$l=D_1(C_S-C_{1A})/(V/A)(dC_{1A}/dt) \qquad (19)$$

The values of the thicknesses of the diffusion layer, $l$, calculated according to Eq. 19

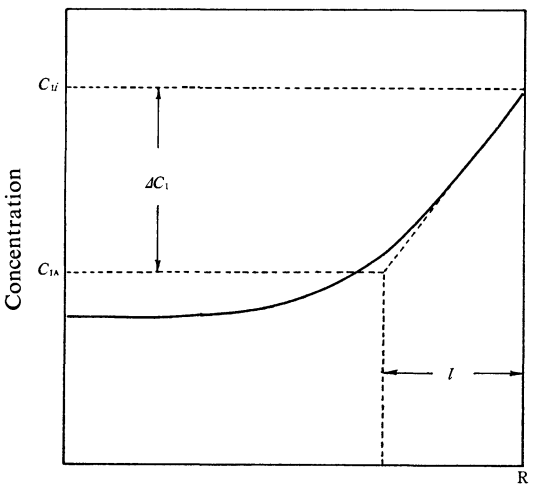



Fig. 5. Scheme of the distribution of concentration in the drop.

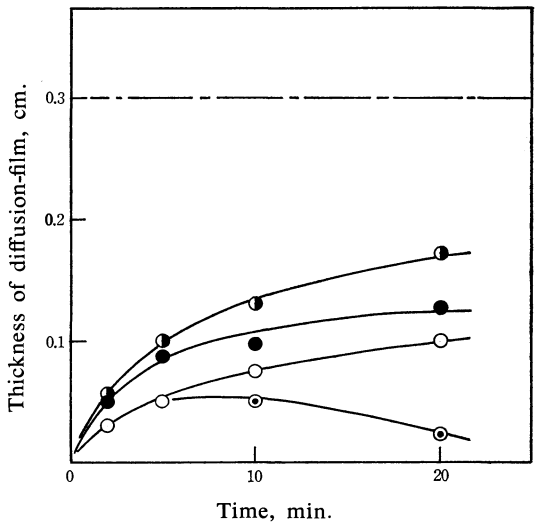



Fig. 6a. Time dependences of the thickness of the diffusion film in fatty acid series of solute (30°C).
System: ○, PB (0.0106 N); ●, BuB (0.0309 N); ◑, PC (0.0053 N); ⊙, BuC (0.0298 N)

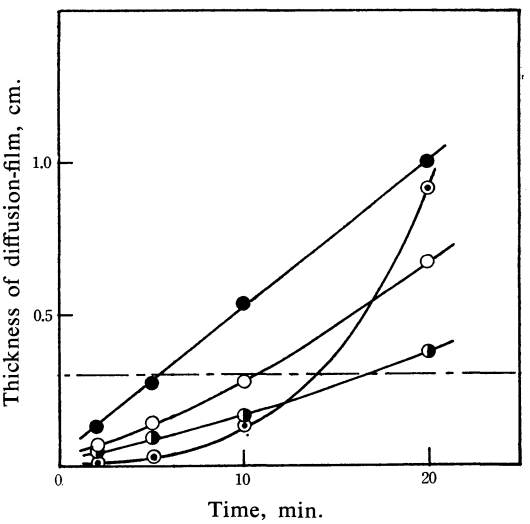



Fig. 6b. Time dependences of the thickness of the diffusion film in fatty amine series of solute (30°C).
System: ○, P'B (0.0201 N); ●, Bu'B (0.0214 N); ◑, P'C (0.0096 N); ⊙, BU'C (0.0200 N)

are shown in Figs. 6a and 6b. As may be seen in these figures, $l$ is smaller than the radius of the aqueous drop for the fatty acids used as solutes, while it becomes much larger than the radius for the fatty amines. When the various theoretical errors included are taken into account, the plots of the fatty acids are quite reasonable, while those of the amines are ununderstandable.

In the cases of fatty acids, the condition, $C_{1i}=C_S$, is satisfied, while in the amine systems except P'C, this condition is not fulfilled in Table I. It should be noted here that Eq. 19 is based on this condition. We put $C_S-C_{1i}=\phi$. Then the error in $l$, $\Delta l$, is represented as $\Delta l=D_1\phi A/V(dC_{1A}/dt)$. For the amine systems except P'C, $\phi\gg 0$. Therefore, $\Delta l>0$, and positive deviations may be anticipated. The unreasonable behavior in the plots of fatty amines is to be ascribed to the error due to the assumption that $C_{1i}=C_S$. The curious results of P'C will be discussed later.

## Discussion

In the first paper, the transference of *n*-butyric acid from the aqueous to the benzene phase was studied. The rate-determining potential barrier which the solute molecules encounter during the passage from the interface into the benzene phase was ascribed to the breaking of the two hydrogen bonds formed per solute molecule between the carboxyl radicals of *n*-butyric acid adsorbed on the interface and water molecules. The energy of the breaking of the hydrogen bonds was assumed to be equal to the activation energy of the desorption process. However, more data must be collected in order to prove the general applicability of this assumption.

In general, it may be assumed that the activation energy of the desorption of a solute from an interface made up of a polar and a non-polar medium to the non-poar sollvent is the sum of the association energies between the polar groups in the adsorbed molecule and the polar solvent (for example, the hydrogen bond), and that the activation energy of the reverse process is the sum of the interaction energies between the non-polar groups in the adsorbed molecule and the non-polar solvent. The entropy associated with the processes is taken to be constant in every case, as in the case of a gas-liquid transition, for which the law of constant entropy is known as Trouton's rule.

If the transfer of *n*-butyric acid from the interface to the benzene phase is the rate-determining step, it may be concluded from the above assumption that the activation energy of the transfer from the interface to the benzene phase is greater than that of the reverse process. Therefore, the association energy between a carboxyl radical and water may be greater than that of a *n*-propyl radical and benzene. The interaction of solute molecules among themselves can be disregarded, because the standard state of the rate process is that of infinite dilution. There is not much difference in the interacticn energies between solute and solvent for the solvents used (benzene, toluene, and cyclohexane), which have similar molecular configurations. Since the interaction energy between a non-polar solvent and the non-polar groups of the solute increases at a rate approximately equal to the increase in the carbon number in the non-polar group of a molecule, the association energy of a carboxyl radical with water may be far greater than the interaction energy between an ethyl radical and benzene. In the present results concerning the fatty acid systems, the assumption given above, on the basis of which the rate-determining step in all these systems is presumed to be the transfer of the solute from the interface into the non-polar solvent, is proved experimentally.

In the case of amine systems besides the system of *n*-propyl amine and cyclohexane, the rate-determining step, on the contrary, is taken to be the transfer from the interface into the aqueous phase. These facts may be explained by assuming that the interaction energy of an amino radical and water is slightly smaller than that of a *n*-propyl radical and benzene. In the *n*-propyl amine and cyclohexane system, if the interaction energy between a *n*-propyl radical and cyclohexane is sufficiently smaller than that with benzene, the situation may be reversed.

As has been shown above, the thickness of the diffusion layer has apparently been found by calculation to become greater than the radius of the water drop in this system. This fact may be explained as follows. The transfer of the solute from the interface into the cyclohexane phase might not be the rate-determining step because of the small difference in interaction energies between an amino radical - water and an *n*-propyl radical - cyclohexane; therefore, no equilibrium may be established between the interfacial tension and the concentration in the aqueous phase immediately next to the interface, whereas the calculation of the thickness of the diffusion layer is based on this equilibrium.

The interaction energies between a non-polar radical and a non-polar solvent are calculated as follows: according to Benson,[4] the interaction energy per mole of a non-polar solvent is represented as:

$$(E_m)_{AA}=\phi_{AA}N\sum_{i=1}^{\infty}n_i/r_i^6$$

were $r_i$ is the distance between $i$-th and the center molecule; $n_i$ is the coordinate number of the $i$-th molecules; $N$ is Avogadro's number, and $\phi_{AA}$ is the force constant between solvent molecules.

Now one solvent molecule (A) is replaced by one solute molecule (B). Hereby it is assumed that the relative positions of the solvent molecules are unchanged. Then the interaction energy between A and B molecules made from the above exchange may be represented as:

$$(E_m)_{AB}=(\phi_{AB}/\phi_{AA})(E_m)_{AA} \qquad (20)$$

Considering that $\phi_{AA}=(3/4)h\nu_A\alpha_A^2$, $\phi_{AB}=(3/2)\alpha_A\alpha_B h\nu_A h\nu_B/(h\nu_A+h\nu_B)$, $\alpha=3[R]/4\pi N$, and $h\nu=P$, the $\phi_{AB}/\phi_{AA}$ factor is represented as:

$$\phi_{AB}/\phi_{AA}=([R]_B/[R]_A)2P_B/(P_A+P_B) \qquad (21)$$

where $\alpha$ is the polarizability: $h$ is Planck's constant; $\nu$ is the intrinsic oscillation number of the electron system; $[R]$ is the molar refraction, and $P$ is the ionization potential. The interaction energy (the dispersion effect) between A and B molecules at an infinite dilution may then be easily calculated according to Eqs. 20 and 21 and the method of Benson.[4]

According to this method, the interaction energies between a propane-molecule and benzene and cyclohexane solvents were calculated for 9.8 and 9.3 kcal./mol. respectively at 30°C, assuming that $(P)_{benzene}=9.6$ eV.,[5] $(P)_{cyclohexane}=9.24$ eV.[6] and $(P)_{propane}=11.3$ eV[7]. If a *n*-propyl radical can be assumed to approximate a propane-molecule (considering that the contribution of a hydrogen-atom is negligible), the interaction energy between an radical and benzene should become more or less higher than that between the radical and cyclohexane; this does not contradict the above discussion.

The relation between the interaction energy of a functional radical of a transfer material with a solvent and the activation energy of the transfer process through the liquid-liquid interface (or the activation free energy) is an important subject both theoretically and experimentally.

The present theory is based on the following crude approximations, and therefore, the conclusion is not precisely quantitative. 1) The pendant drop is taken to be a sphere. 2) The difference between the values of concentration obtained by the conductometric method and the true mean concentrations is neglected. 3) The entropy of activation associated with the desorption of the solute from the interface is assumed to be constant irrespective of the direction of movement and the materials used as solvent and solute. 4) All disturbance effects are disregarded.

We are much indebted to Mr. Setsuo Mimasu of Toyo Koatsu Industries, Inc., Tokyo, for his aid in performing the calculations with an electronic computer.

*Department of Chemical Engineering*
*Tokyo Institute of Technology*
*Ookayama, Tokyo*

## Appendix I

By the Laplace transformation, Eqs. 1—6 are reduced to the ordinary differential equations as:

$$\frac{d^2\overline{U}_2}{dr}-q_1^2\overline{U}_1=-\left(\frac{C_{10}}{D_1}\right)r,\ 0\leqslant r<R \qquad (22)$$

$$\frac{d^2\overline{U}_2}{dr^2}-q_2^2\overline{U}_2=-\left(\frac{C_{20}}{D_2}\right)r,\ R<r \qquad (23)$$

$$\overline{U}_1=\alpha\overline{U}_2+\beta/p \quad r=R \qquad (24)$$

$$D_1\left(R\frac{d\overline{U}_1}{dr}-\overline{U}_1\right)=D_2\left(R\frac{d\overline{U}_2}{dr}-\overline{U}_2\right),\ r=R \qquad (25)$$

$$\overline{C}_1:\ \text{finite},\ r=0 \qquad (26)$$

where $p$ is the conversion parameter in the Laplace transformation, and $q_1$ and $q_2=(p/D_1)^{1/2}$ and $(p/D_2)^{1/2}$ respectively.

Solving Eqs. 22, 23, and 26, we obtain:

$$\overline{U}_1=rC_{10}/D_1q_1^2+A\sinh(rq_1) \qquad (27)$$

$$\overline{U}_2=rC_{20}/D_2q_2^2+B[\cosh(rq_2)-\sinh(rq_2)] \qquad (28)$$

where $A$ and $B$ are integration constants.

Applying the boundary conditions, Eqs. 24 and 25, the constants, $A$ and $B$, in Eqs. 27 and 28 are given as Eqs. 29 and 30.

$$A=\frac{R(\alpha C_{20}-C_{10})+\beta}{p\left[\left\{1-\frac{D_1}{D_2}\left(\frac{\alpha}{1+Rq_2}\right)\right\}\sinh(Rq_1)+\frac{D_1}{D_2}\left(\frac{\alpha Rq_1}{1+Rq_2}\right)\cosh(Rq_1)\right]} \qquad (29)$$

$$B=A\left(\frac{D_1}{D_2}\right)\left\{\frac{Rq_1\cosh(Rq_1)-\sinh(Rq_1)}{(1+Rq_2)[\sinh(Rq_2)-\cosh(Rq_2)]}\right\} \qquad (30)$$

4) S. W. Benson, *J. Chem. Phys.*, **15**, 367 (1947).
5) *Int. Crit. Table*, **6**, p. 72.
6) J. D. Morrison, *J. Chem. Phys.*, **19**, 1305 (1951).
7) D. P. Stevenson and J. A. Hipple, *J. Am. Chem. Soc.*, **64**, 1588 (1942).

$$A=\frac{2[(\alpha C_{20}-C_{10})R+\beta]}{pe^{Rq_1}\left[1-\alpha\left(\frac{D_1}{D_2}\right)\left(\frac{1-Rq_1}{1+Rq_2}\right)\right]\left[1-\left\{\frac{1-\alpha\left(\frac{D_1}{D_2}\right)\left(\frac{1+Rq_1}{1+Rq_2}\right)}{1-\alpha\left(\frac{D_1}{D_2}\right)\left(\frac{1-Rq_1}{1+Rq_2}\right)}\right\}e^{-2Rq_1}\right]} \tag{31}$$

$$A\fallingdotseq\frac{2[(\alpha C_{20}-C_{10})R+\beta]}{pe^{Rq_1}[1-\alpha(D_1/D_2)(1-Rq_1)/(1-Rq_2)](1-e^{-2Rq_1})} \tag{32}$$

Converting Eq. 29 to an exponential function, we have Eq. 31.

If $0<Rq_1\ll 1$, we have Eq. 32.

Then, converted by the binomial theorem into a form in which the inversion is easy, we have:

$$A\fallingdotseq 2\sum_{n=0}^{\infty}\left[K_1\left\{\frac{e^{-(2n+1)Rq_1}}{p}\right\}+K_2\left\{\frac{e^{-(2n+1)Rq_1}}{p(q_1+h)}\right\}\right] \tag{33}$$

$$B\fallingdotseq K'_1\left[\frac{e^{Rq_2}}{p}-2\sum_{n=0}^{\infty}\frac{e^{-Rq_2\{2(n+1)(D_2/D_1)^{1/2}-1\}}}{p}\right]+K'_2\left\{\frac{e^{Rq_2}}{p(q_2+h')}\right\}+K'_3\sum_{n=0}^{\infty}\frac{e^{-Rq_2\{2(n+1)(D_2/D_1)^{1/2}-1\}}}{p(q_2+h')} \tag{34}$$

Even if Eq. 32 does not hold, Eqs. 33 and 34 are approximately true when the time, $t$, is sufficiently small.

Putting Eqs. 33 and 34 into Eqs. 27 and 28, and by inversion to the original functions,[8] we obtain Eqs. 10 and 11.

8) H. S. Carslaw and J. C. Jaeger, "Conduction of Heat in Solids," Clarendon Press, Oxford (1959).

## Appendix II

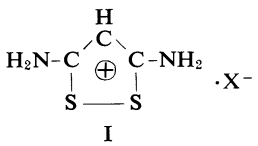
The time range, $t_1$—$t_n$, on the basis of which $\tilde{\beta}$ and $\Delta\beta$ were calculated, was determined to be as follows. As has been described above, Eqs. 3 and 4 do not hold in the "adsorption stage." Therefore, the authors took $t_1$ to be greater than the $t_0$ shown in Fig. 3. Equations 10, 11, 12, 13, and 15 are applicable, on the other hand, in a range where $t$ is sufficiently small (see Apendix I). Precisely speaking, when the true exponential-type solution is composed of an infinite series, these equation hold only approximately in the range where the terms higher than the second of the true solution are negligible. The smaller the value of $t$, the better the approximation obtained generally in such an exponential-type solution. We assume that the terms higher than the second in the true solution and Eq. 17 become negligible at the same time, $t_n$, Therefore, the upper limit of $t_n$ can be estimated from experimental values, specifying $\alpha=-0.01$, $-0.10$, $-1.00$, etc. $S_1$ and $S_2$ in Eq. 17 correspond to the terms higher than the second in the infinite series, and were neglected if their sum was less than 1% of the $F(\alpha, t)$ in Eq. 17.

# Meso-ionic Compounds of the 1, 3-Dithiole Ring System[1]

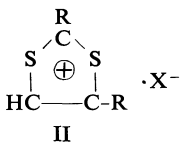
By Masaki OHTA and Masatoshi SUGIYAMA

(Received June 4, 1964)

In connection with the research on the 1, 2- and 1, 3-dithiole ring systems, it has been reported that the oxidation of dithiomalonamide with hydrogen peroxide in the presence of the appropriate acid gives 3, 4-diamino-1, 2-dithiolyl salt (I)[2] and that the dehydration of phenacyl or acetonyl carbodithioate with hydrogen chloride gives 1, 3-dithiolium salts (II).[3]



I



II

In a previous paper,[4] we reported that a new type of meso-ionic compounds containing two sulfur atoms in a ring, which were referred to as dithiolone imine salts, was prepared by the action of hydrogen chloride or acyl chlorides on cyanomethyl dithiobenzoate. The object of this paper is to describe the synthesis of dithiolone, which has an exocyclic oxygen atom instead of a nitrogen atom of dithiolone imine salts, and the properties of dithiolone imine salts.

It has been reported that *N*-thiobenzoylsarcosine under goes ring closure in hot acid anhydrides to give meso-ionic compounds, $\psi$-4-acyl-3-methyl-2-phenylthiazol-5-one.[5] As the

1) This paper is Part XX of Studies on Meso-ionic Compounds.

2) K. A. Jensen, H. R. Baccaro and O. Buchardt, *Acta Chem. Scand.*, **71**, 163 (1963).

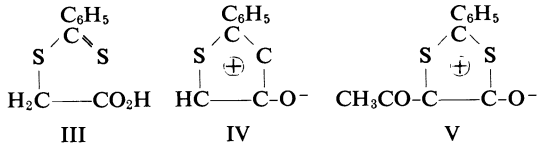
3) D. Leaver and W. A. H. Robertson, *Proc. Chem. Soc.*, **1960**, 252.

4) M. Ohta and M. Sugiyama, This Bulletin, **36**, 1437 (1963).

5) A. Lawson and C. E. Searle, *J. Chem. Soc.*, **1957**, 1556.

formation of a meso-ionic ring occurred between thiocarbonyl and carboxyl groups, a ring closure may be expected with carboxymethyl dithiobenzoate. Carboxymethyl dithiobenzoate was prepared by the action of chloroacetic acid upon potassium dithiobenzoate prepared from benzotrichloride and potassium sulfide by the elimination of potassium chloride.[6]

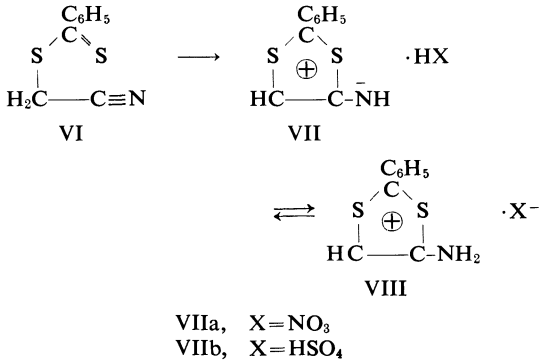
When carboxymethyl dithiobenzoate (III) was heated in acetic anhydride for several hours, a pale red substance which could not be purified was isolated. The treatment of III with acetic anhydride in the presence of triethylamine or pyridine led to tar formation.



III IV V

It is well known that acetic anhydride, in the presence of boron trifluoride, is a strong acetylating agent,[7] but the formation of a meso-ionic ring with this reagent has not been reported.

When carboxymethyl dithiobenzoate (III) was treated with acetic anhydride at 60°C in the presence of a catalytic amount of boron trifluoride etherate, a red substance with an empirical formula, $C_9H_6OS_2$, was isolated. The compound was unchanged on treatment with hot acid or cold alkali, but when treated with hot alkali it decomposed to give a substance of an unknown structure. The analytical results and the infrared spectrum of the compound suggested that it was not acetylated 2-phenyldithiolone (V), but 2-phenyldithiolone (IV). Attempts to prepare the corresponding 2-benzyl derivative were unsuccessful. The treatment of *S*-thiophenacyl thioglycolic acid with acetic anhydride, or with acetic anhydride and boron trifluoride etherate, led to tar formation. It has been expected that an increased charge distribution provided by the phenyl substituent would stabilize the dithiolone ring.



VI VII VIII

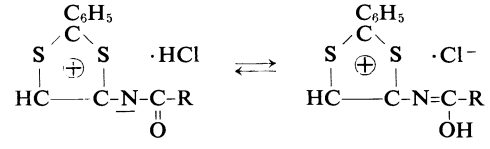
VIIa, X=$NO_3$
VIIb, X=$HSO_4$

The preparations of cyanomethyl dithiobenzoate and of 2-phenyldithiolone imine picrate, *N*-acetyl- and *N*-benzoyl-2-phenyldithiolone imine hydrochlorides were reported in a previous paper.[4]

When a benzene solution of cyanomethyl dithiobenzoate (VI) was treated with an excess of nitric acid and sulfuric acid, the nitrate (VIIa) and the hydrogen sulfate (VIIb) of 2-phenyldithiolone imine crystallized out in 50% and 60% yields respectively. The nitrate is in the form of orange plates and is slightly soluble in water, alcohol and acetone, but insoluble in benzene, ether and chloroform. Dithiolone imine salts are stable towards acids, but a trace amount of even a weak base causes its instant decomposition. An attempt to prepare the corresponding 2-benzyl derivative was unsuccessful owing to the failure to obtain cyanomethyl dithiophenylacetate.

Infrared spectra show that the cation (VII) may be considered to be an amino derivative of the pseudoaromatic ring system isosteric with the dithiolyl cation, it is probable that the phenyl substituent stabilizes the dithiolone imine salts.

By the action of acyl chlorides, e.g., propionyl chloride, (β-carbomethoxy)propionyl chloride and (δ-carbomethoxy)valerianyl chloride, upon VI, the corresponding *N*-acyl derivatives crystallized out, as in the case of benzoyl and acetyl chlorides.[4]

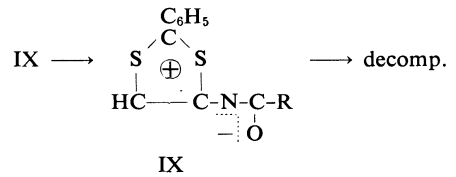


IX X

IXa, R=$CH_2CH_3$
IXb, R=$(CH_2)_2CO_2CH_3$
IXc, R=$(CH_2)_4CO_2CH_3$

The infrared spectrum indicates that they exist, at least in part, in the enolic forms (X).

When the *N*-acyl salts (IX) were treated with a weak base, e.g., sodium hydrogen carbonate or ammonia, free bases (XI) were formed, but when they were treated with a strong base, decomposition occurred.



IX

6) J. C. Crawholl and D. F. Elliott, ibid., **1951**, 2071.
7) V. G. Yashunskii and V. F. Vasil'eva, *Doklady Akad. Nauk. U. S. S. R.*, **130**, 350; *Chem. Abstr.*, **54**, 10999 (1960).

TABLE I. CHARACTERISTIC INFRARED SPECTRA OF DITHIOLONE AND DITHIOLONE IMINE SALTS*

| | |
|---|---|
| 2-Phenyldithiolone | 3050w, 1690s, 1590s, 1570s, 1490m, 1450m, 1135m, 1045m, 755m, 735m, 695m, 685m. |
| 2-Phenyldithiolone imine picrate | 3350s, 3100s, 1635s, 1600m, 1560s, 1515s, 1500s, 1465m, 1360s, 1335s, 1240s, 1080m, 775m, 710m. |
| 2-Phenyldithiolone imine nitrate | 3210s, 3100s, 2920w, 1615s, 1595m, 1520s, 1390s 1295s, 770s, 765s, 750m. |
| 2-Phenyldithiolone imine hydrogen sulfate | 3210s, 3100s, 3050w, 2920w, 1615m, 1595w, 1520s, 1455m, 1295m, 1225s, 1195s, 770s, 765s. |
| *N*-Acetyl-2-phenyldithiolone imine hydrochloride | 3400m br, 3075m, 3050m, 2780s, 2700s, 1670s, 1585m, 1545s, 1475s, 1450s, 1370s, 1285m, 1230m, 1010m, 765s, 680m. |
| *N*-Propionyl-2-phenyldithiolone imine hydrochloride | 3400m br, 3050m, 2780s, 2650s, 1675s 1590w, 1550s, 1470s, 1460s, 1450m, 1370s, 1280s 1195s, 1170s, 760s, 675s. |
| *N*-Benzoyl-2-phenyldithiolone imine hydrochloride | 3400m br, 3050s, 2825s, 2670s, 1645s, 1540s, 1540s, 1507s, 1468s, 1450s, 1305s, 1290s, 1240m, 1190m, 1175m, 835s, 760s, 710s, 670s. |
| *N*-($\beta$-Carbomethoxy) propionyl-2-phenyldithiolone imine hydrochloride | 3400m br, 3050, 2800s, 2675s, 1725s, 1675s, 1585w, 1540s, 1470s, 1280s, 1215s, 1155s, 765m, 680m. |
| *N*-($\delta$-Carbomethoxy) valerianyl-2-phenyldithiolone imine hydrochloride | 3400m br, 3020m, 2900w, 2775m, 2600s, 1715s, 1670s, 1580w, 1435s, 1270s, 1150s, 760m, 670m. |

* Taken on an EPI-S2 Model manufactured by Hitachi Ltd. by KBr tablets and are reported in wave numbers.
s: strong, m: middle, w: weak, br: broad

The frequencies of the infrared absorption bands of the dithiolone imine salts, related compounds and the dithiolone (IV) are shown in Table I. The spectrum of the dithiolone (IV) shows the characteristic strong bands at 1690, 1590 and 1570 $cm^{-1}$ and differs from the spectrum of carboxymethyl dithiobenzoate. The absorptions, ranging between 3000 and 2500 $cm^{-1}$, and 1710 $cm^{-1}$, due to the COOH stretching and deformation, disappear in the spectrum of the dithiolone. Bellamy suggested[8] that the C=O absorption of thiols appeared at 1680 $\pm$ 10 $cm^{-1}$ as a result of the resonance, as is shown below:

$$R\text{-}\overset{O}{\overset{\|}{C}}\text{-}S\text{-}R \longleftrightarrow R\text{-}\overset{O^-}{\overset{|}{C}}\text{=}\overset{+}{S}\text{-}R$$

Accordingly, the absorption of the dithiolone (IV) at 1690 $cm^{-1}$ may, with great certainty, be assigned to the polarized C=O band. The strong band at 1590 $cm^{-1}$ in the spectrum of carboxymethyl dithiobenzoate is assigned to a phenyl absorption. The strong band at 1570 $cm^{-1}$ may be ascribed to a vibration of the aromatic ring system which disappears in the spectrum of the dithiobenzoate (III) and is comparable with the absorption at 1520 $cm^{-1}$ in the spectra of dithiolone imine salts.

The spectra of the picrate, nitrate and hydrogen sulfate are practically identical, they all show a very strong band at ca. 1520 $cm^{-1}$. This band may be ascribed to the vibrations of the aromatic ring system and should be compared with the two strong bands of the dithiolyl cation at 1515 and 1530 $cm^{-1}$. The absorptions at 3210, 3100 and 1615—35 $cm^{-1}$ are assigned to $NH_2$ stretching and deformation frequencies, they are very similar to the absorptions of the dithiolyl salts. A characteristic feature of the spectra of *N*-acyl hydrochlorides is the appearance of broad bands at ca. 3400 $cm^{-1}$ and at 1150—75 $cm^{-1}$. These absorptions are assigned to the OH group and show that acylamino groups are present in part in the enolic form, R-C(OH)=N-. The spectra of *N*-acyl hydrochlorides also show a very strong band due to C=O stretching at 1645—75 $cm^{-1}$. The spectra of the *N*-($\beta$-carbomethoxy)propionyl and *N*-($\delta$-carbomethoxy)valerianyl hydrochlorides, show in addition, strong ester absorptions at 1725 and 1715 $cm^{-1}$ respectively.

8) L. J. Bellamy and P. E. Rogasch, *J. Chem. Soc.*, **1960**, 2218.

## Experimental

**2-Phenyldithiolone (IV).**—In 100 ml. of acetic anhydride, 12.75 g. of carboxymethyl dithiobenzoate (III) was dissolved with heat; then 5 ml. of boron trifluoride etherate was added to the mixture, and the resulting mixture, was stirred for an hour below 60°C. After it had cooled, the mixture was poured onto 500 g. of ice, and the precipitate which separated out was collected, washed with water and dried. Recrystallization of the precipitate from chloroform-ether gave red needles (4.9 g., 42%), m. p. 185—186°C (decomp.).

Found: C, 55.68; H, 3.30; S, 32.73. Calcd. For $C_9H_6OS_2$: C, 55.67: H, 3.09: S, 32.91%.

**2-Phenyldithiolone Imine Nitrate (VIIa).**—The preparation of cyanomethyl dithiobenzoate was described in a previous paper.[4] Forty-eight grams of

crude cyanomethyl dithiobenzoate was dissolved in 100 ml. of benzene to a total volume of 160 ml. (solution A), and the solution was then dried over anhydrous sodium sulfate. A solution of 3.5 g. of nitric acid (65% conc.) in 10 ml. of ethanol was vigorously stirred, drop by drop, into 20 ml. of solution A while the mixture was being cooled with an ice bath, orange plates (3.9 g., 50%) crystallized out. Recrystallization from ethanol-ethyl acetate gave orange plates, m. p. 130.5°C (decomp.).

Found: C, 41.86; H, 3.18; N, 10.75. Calcd. for $C_9H_8N_2O_3S_2$: C, 42.19; H, 3.13; N, 10.94%.

**2-Phenyldithiolone Imine Hydrogen Sulfate (VIIb).**—To 20 ml. of solution A, a solution of 4.5 g. of sulfuric acid in 20 ml. of ethanol was added with vigorous shaking, the temperature of the mixture rose gradually and gave a red oil which, on cooling, gave a red precipitate. The recrystallization of the separated precipitate (5.5 g., 62%) from ethanol gave red-orange needles, m. p. 152—154°C (decomp.).

Found: C, 37.07; H, 3.52; N, 4.81. Calcd. for $C_9H_9NO_4S_3$: C, 37.11; H, 3.19; N, 4.81%.

***N*-Propionyl-2-phenyldithiolone Imine Hydrochloride (IXa).**—To 20 ml. of solution A, 4.6 g. of propionyl chloride was added drop by drop while the solution was cooled and shaken; the mixture was then kept standing for a day. The recrystallization from ethanol of the precipitate (4.7 g., 59%) gave yellow needles, m. p. 215—216°C (decomp.).

Found: C, 50.67; H, 4.28; N, 5.12. Calcd. for $C_{12}H_{12}NOS_2Cl$: C, 50.35; H, 4.20; N, 4.90%.

***N*-(β-Carbomethoxy)propionyl-2-phenyldithiolone Imine Hydrochloride (IXb).**—The treatment of 20 ml. of (β-carbomethoxy)propionyl chloride by a procedure similar to thas described above gave a yellow precipitiate (4.6 g., 49%). The recrystallization of the precipitate from ethanol gave yellow needles, m. p. 186°C (decomp.).

Found: C, 48.83; H, 4.97; N, 3.98. Calcd. for $C_{14}H_{14}NOS_2Cl$: C, 48.84; H, 4.07; N, 4.07%.

***N*-(δ-Carbomethoxy)valerianyl-2-phenyldithiolone Imine Hydrochloride (IXc).**—The recrystallization from ethanol of the yellow precipitate (3.7 g., 36%) obtained from the treatment of 20 ml. of solution A with 6.5 g. of (δ-carbomethoxy)valerianyl chloride in a procedure similar to that used in the experiment with IXa, gave yellow needles, m. p. 196°C (decomp.).

Found: C, 51.27; H, 4.84; N, 4.05. Calcd. for $C_{16}H_{18}NO_3S_2Cl$: C, 51.61; H, 4.84; N, 3.76%.

The preparations of 2-phenyldithiolone imine picrate, *N*-acetyl-2-phenyldithiolone imine and *N*-benzoyl-2-phenyldithiolone imine hydrochlorides were reported in a previous paper.[4]

The authors are indebted to Miss Toshiko Aoyagi for the elementary analysis.

*Laboratory of Organic Chemistry*
*Tokyo Institute of Technology*
*Ookayama, Tokyo*

# The Ionization and Dissociation of Methyl Butyl Ketones under Electron Impact.* I. Methyl *n*-Butyl Ketone and Methyl Isobutyl Ketone

By Motoyoshi HATADA and Kozo HIROTA

(Received June 26, 1964)

The method of equivalent orbitals has been applied by Hall and Lennard-Jones[1,2] to the calculation of the ionization potentials of normal paraffins; Fueki and Hirota[3] applied it to the predictions of the scission probability of each bond of normal paraffin positive ions, calculating the distribution of the positive charge over the molecular ion in the lowest ionized state. However, the order of the secular determinant which has to be solved in this method is too high for larger molecules to be solved without a computer. In the calculation of ionization potentials, Franklin[4] has simplified this problem by assuming that the molecular orbital can be set up from the united atom molecular orbitals, i.e., group orbitals, each of which represents a group of the molecule.

In the present research, calculations have been carried out in an attempt to predict the ionization potentials and the bond scission probabilities of methyl butyl ketones by assuming a wave function for each bond between the groups of the molecule. The results of the calculations have also been compared with those obtained from the mass spectra.

* A part of this paper was presented by M. Hatada and K. Hirota at the 17th Annual Meeting of the Chemical Society of Japan, Tokyo, April, 1964.

1) G. G. Hall, *Proc. Roy. Soc.*, **A205**, 541 (1951).

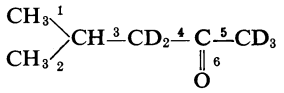
2) J. Lennard-Jones and G. G. Hall, *Trans. Faraday Soc.*, **48**, 581 (1952).

3) K. Fueki and K. Hirota, *J. Chem. Soc. Japan, Pure Chem. Sec.* (*Nippon Kagaku Zasshi*), **81**, 212 (1960).

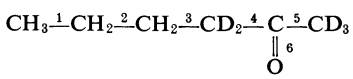
4) J. L. Franklin, *J. Chem. Phys.*, **32**, 1304 (1954).

## Experimental

**Materials.**—Two types of methyl butyl ketone and their deuterated compounds, methyl isobutyl ketone (MIBK-$d_0$) and methyl *n*-butyl ketone (MNBK-$d_0$), were obtained from the Tokyo Kasei Co. and used after drying with drierite. Methyl isobutyl ketone-1,1,1,3,3-$d_5$ (MIBK-$d_5$) and methyl *n*-butyl ketone-1,1,1,3,3-$d_5$ (MNBK-$d_5$) were prepared from the ketones by repeated exchange with deuterium oxide, followed drying with drierite and distillation. Impurities of ca. 5% were found in the samples by gas chromatographic analysis. The isotopic impurities ($d_4$) of MIBK-$d_5$ and MNBK-$d_5$ were ca. 3 and 10% respectively.



(MIBK-$d_5$)



(MNBK-$d_5$)

**The Measurement of Ionization Potentials and Mass Spectra.**—The ionization potentials as well as the mass spectra of these compounds were obtained by the use of a Hitachi RMU-5 type mass spectrometer modified for the present purpose. The mass spectrometer is a 90° sector instrument. The accelerating potential was 1500 V., and magnetic scanning was employed. The ionization potentials were determined by the linear extrapolation method, calibrated with the first ionization potential of argon (15.75 eV.). The mass spectra were obtained using bombarding electrons of 90 eV.

## Calculation

The secular equation for a molecule is:

$$|e_{ij}-\delta_{ij}E|=0$$

where $i$ and $j$ refer to various bonds between groups in the molecule, $e_{ij}$ is the matrix element which shows the interaction between the group bond orbitals, $\phi_i$ and $\phi_j$, and $E$ is the energy of the molecular orbitals, the highest of which corresponds to the lowest ionization potential of the molecule. All interactions except those of adjacent group bonds are assumed to be zero. The secular determinant for methyl-isobutyl ketone is illustrated below:

$$\begin{vmatrix} e-E & b & b & 0 & 0 & 0 \\ b & e-E & b & 0 & 0 & 0 \\ b & b & e-E & b & 0 & 0 \\ 0 & 0 & b & e-E & b & c \\ 0 & 0 & 0 & b & e-E & c \\ 0 & 0 & 0 & c & c & f-E \end{vmatrix} = 0$$

The elements in the determinant are shown in Table I. The $e$ and $b$ elements were taken to be −13.75 eV. and −1.80 eV. respectively from the values obtained by Fueki[5] for saturated hydrocarbons. The elements $c$ and $f$ were calculated from the secular equations for acetone and methyl ethyl ketone using the measured ionization potentials of these two compounds. The values of $c$ and $f$ obtained in this way are −2.626 eV. and −12.37 eV. respectively.

TABLE I

| | $C\overset{i}{-}C$ | $C\overset{i+1}{-}C$ | C-O |
|---|---|---|---|
| $C\overset{i}{-}C$ | $e$ | $b$ | $c$ |
| $C\overset{i+1}{-}C$ | $b$ | $e$ | $c$ |
| C-O | $c$ | $c$ | $f$ |

## Results and Discussion

The calculated ionization potentials of MIBK and MNBK are shown in Table II, along with the measured ones. The square of the coefficient of the group bond orbital in the highest-occupied molecular orbital is shown in Table III as an indication of the distribution of the positive charge when an electron is removed from the molecule.

TABLE II

| | Ionization potential eV. | | |
|---|---|---|---|
| | Calcd. | Obs. | |
| Acetone | (9.92)[a] | 9.73[b] | 9.92[a] |
| Methyl ethyl ketone | (9.76)[a] | — | 9.76[a] |
| Methyl isobutyl ketone-$d_0$ | 9.69[b] | 9.33[b] | |
| Methyl isobutyl ketone-$d_5$ | 9.69[b] | 9.35[b] | |
| Methyl *n*-butyl ketone-$d_0$ | 9.70[b] | 9.77[b] | 9.71[a] |

a) J. D. Morrison and A. J. C. Nicholson, *J. Chem. Phys.*, **20**, 1021 (1952).
b) This work.

The mass spectra of MIBK, MNBK and their deuterated compounds are shown in Fig. 1. The peaks which appear in the mass spectra of MIBK can be classified into ($C_1$), ($C_2$, CO), ($C_2O$, $C_3$), ($C_4$), ($C_3O$), ($C_5O$) and ($C_6O$) groups. The sum of the relative intensities of the peaks in each group in the mass spectra of the $d_0$ compound was nearly equal to the corresponding one, as they were in those of $d_5$.

The peak of $d_0$, at $m/e=43$ which was the highest, shifted to 46 in the mass spectrum of $d_5$. Thus, this ion has been assigned to $\underline{CH_3}CO^+$, which is formed by the scission of bond 4.* Since the peak of $d_0$ at $m/e=57$ shifted to $m/e=59$, this ion is probably $(CH_3)_2CH\text{-}\underline{CH_2}^+$. The peak of $d_0$ at $m/e=58$ shifted to $m/e=63$ upon deuteration. This

5) K. Fueki, *J. Phys., Chem.*, **68**, 2856 (1964).
* The hydrogen atom exchangeable by the exchange reaction with $D_2O$ is shown by $\underline{H}$.

TABLE III

MIBK

| | | 1 | 2 | 3 | 4 | 5 | 6 |
|---|---|---|---|---|---|---|---|
| $c_i^2\%$ | $(\sum_{i=1}^{6} c_i^2=100)$ | 0.89 | 0.89 | 9.45 | 25.45 | 6.88 | 56.44 |
| $c_i^2\%$ | $(\sum_{i=1}^{5} c_i^2=100)$ | 2.3 | 2.3 | 21.7 | 58.4 | 15.8 | — |

MNBK

| | | | | | | | |
|---|---|---|---|---|---|---|---|
| $c_i^2\%$ | $(\sum_{i=1}^{6} c_i^2=100)$ | 0.53 | 2.66 | 8.68 | 26.96 | 6.97 | 56.21 |
| $c_i^2\%$ | $(\sum_{i=1}^{5} c_i^2=100)$ | 1.2 | 6.1 | 19.8 | 57.4 | 15.9 | — |

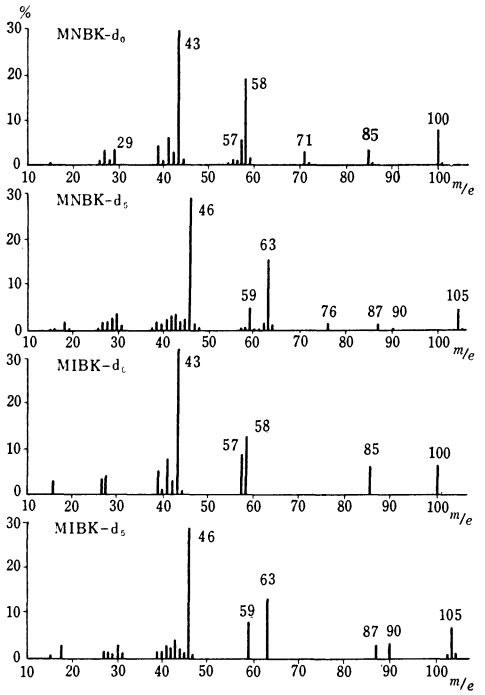



Fig. 1. Mass spectra of MNBK-$d_0$, MNBK-$d_0$, MIBK-$d_5$ and MIBK-$d_5$. Per cent. of total ionization vs. $m/e$.

ion is interpreted as $CH_3COCH_2H^+$ formed by the following hydrogen transfer reaction:

$$CH_3CH(CH_3)-CH_2-COCH_3 \longrightarrow CH_3COCH_2H^+ + CH_3CH=CH_2 + e$$

This reaction was also found by Ausloos[6] in the ionization and dissociation of methyl-*n*-propylketone-1, 1, 1, 3, 3-$d_5$. Since the peak of $d_0$ at $m/e=85$ splits into peaks of $m/e=87$ and 90 upon deuteration, this peak is interpreted as consisting of two ions which have the same mass, $\overset{+}{C}O-CH_2-CH(CH_3)_2$. and $CH_3CO-\overset{+}{C}H_2-CH(CH_3)-CH_3$. Similar results are also obtained in the cases of MNBK-$d_0$ and -$d_5$.

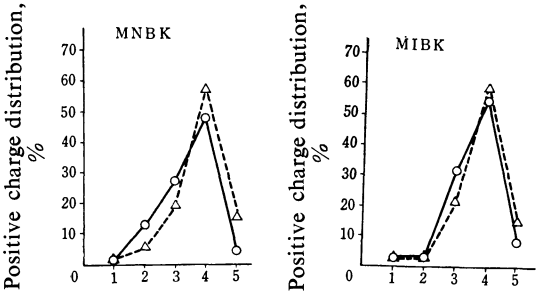



Fig. 2. Bond scission probability and positive charge distribution in MNBK and MIBK.
—○— Experimental: probability of bond scission
--△-- Theoretical: positive charge distribution

Figure 2 shows the relation between the bond scission probability and the position at which the bond scission occurs. The scission at bond 6 was excluded from the calculations, because the removal of an electron from the C=O bond was considered not to cause the scission of this bond and, actually, no scission at this bond was found in the mass spectra. Figure 2 illustrates that a close correlation exists between the measured and calculated values for MIBK and MNBK.

This paper has not described anything about the C-H bond scission, which seems to be related to the $CH_3COCH_2H^+$ formation which involves the hydrogen transfer reaction. This is a problem which will require further study.

Th authors wish to express their deep thanks to Dr. Kenji Fueki of Nagoya University for his helpful discussions concerning this research.

*Japanese Associations*
*for Radiation Research on Polymers*
*Neyagawa, Osaka (M. H. & K. H.)*

*Department of Chemistry*
*Faculty of Science*
*Osaka University*
*Nakanoshima, Osaka (K. H.)*

6) P. Ausloos and E. Murad, *J. Am. Chem. Soc.*, **80**, 5929 (1958).

# A Phase Study of Sodium Soap - Sodium Silicate - Water Systems

By Yasushi KIMURA, Terunosuke SHIMO and Hitoshi SEKIGUCHI

(Received July 22, 1964)

Since it was established by McBain and his collaborators that the ordinary phase rule applies strictly to the phase diagrams of soap, various phase diagrams of soap - water or soap - alkaline electrolyte - water systems have been determined by McBain and by others.[1-3] However, the number of soap systems is so large, and the field to be covered is so extensive, that only minor portions of a few typical systems have as yet received quantitative study.[4] One of the practical industrial applications of these works is to predict the amounts of various builders which will dissolve in soaps at crutching temperatures.[3]

In the soap industry, particularly that concerned with the manufacture of commercial soaps, soap-silicate-water systems are important. However, although the amounts of silicates which can suitably be added to the soap at crutching temperatures have been known empirically for various soaps with different fatty acid compositions, these amounts have been determined incompletely from the phase-rule point of view.

Merrill,[5] using a typical commercial mixed soap and some industrially important silicates or other salts, measured the salting-out power of these salts at the arbitrarily chosen soap concentration of 24%, on the assumption that the relative efficiency is the same for different soap concentrations. However, no one has yet determined the phase behavior of the soap-silicate-water systems using a silicate and soaps with various structures and compositions.

For the purpose of supplying some date on the correlation of the suitable amounts of sodium silicate with the composition of sodium soaps, a phase study of some sodium soap - sodium silicate - water systems has been made using a silicate with a $SiO_2/Na_2O$ weight ratio of 2.1, and six single soaps or their mixtures. This report will describe the $T_c$ temperature in the systems with a 24% soap concentration, at which hydrated crystals or curd fibers change completely to liquid crystals, isotropic solutions, or both upon heating, as determined by the synthetic method.[5] The single sodium soaps used were laurate, palmitate, stearate, oleate, elaidate, and isoöleate (L). The data cover the silicate concentrations to 10 or 15%, and the temperatures to 80°C.

## Experimental

**Materials.**—*Single Soaps.*—Table I gives the properties and compositions of the methyl esters which are the raw materials of these six soaps.

Methyl laurate, palmitate, and stearate were prepared by methanolysis and subsequent fractional distillation from the corresponding reagent grade fatty acids. Methyl oleate was prepared from commercial-grade rice oil by methanolysis and fractional distillation to isolate the C-18 fraction, followed by two low-temperature crystallizations from 15 volumes of acetone at −70°C and one distillation.[6] Methyl elaidate was prepared by the elaidinization[7] of the oleate with potassium nitrite and nitric acid at 30—35°C and four low-temperature crystallizations of the reaction mixture from 10 volumes of acetone at −40°C.

Figure 1 shows the infrared spectra of methyl oleate and methyl elaidate. Methyl elaidate has a strong absorption at 10.36$\mu$, arising from a trans C=C bond ;[8] the melting point of elaidic acid prepared from methyl elaidate was found to be 43.9°C, which is in agreement with the published value of Swern.[9] Therefore, the methyl elaidate used is considered to be pure.

For the purpose of obtaining the position isomers of elaidic acid, which have a double bond in $\Delta^{11:12}$ or $\Delta^{12:13}$ and different melting points,[10] the isoöleates (S) and (L) were prepared from caster oil containing ricinoleic acid by the following procedure: the oil was hydrogenated, using methanol as the solvent and 5% of a Raney nickel catalyst at 57°C and 44 atm. The hydrogenated product, after the solvent and the catalyst, had been removed, was dehydrated with 2% of sodium bisulfate at 200°C and 100 mmHg ; the product was then separated by low-temperature fractional crystallization from the acetone solution into two fractions, one from

1) J. W. McBain, G. C. Brock, R. D. Vold and M. J. Vold, *J. Am. Chem. Soc.*, **60**, 1870 (1938).
2) J. W. McBain, R. D. Vold and W. T. Jameson, ibid., **61**, 30 (1939).
3) J. Davidsohn, E. J. Better and A. Davidsohn, "Soap Manufacture," Coll. Vol. 1, Interscience Publishers, New York (1953), p. 59.
4) J. C. McBain, R. D. Vold and K. Dardiner, *Oil & Soap*, **20**, 221 (1943).
5) R. C. Merrill, *Ind. Eng. Chem.*, **39**, 158 (1947).
6) D. Swern, H. B. Knight and T. W. Findley, *Oil & Soap*, **21**, 133 (1944).
7) G. L. Vandone, *Ind. Vernice*, **4**, 42 (1950); *Chem. Abstr.* **44**, 10354-h (1950).
8) R. T. O'Connor, *J. Am. Oil Chemists' Soc.*, **33**, 1 (1956).
9) D. Swern, H. B. Knight, O. D. Shreve and M. R. Heether, *Oil & Soap*, **27**, 17 (1956).
10) W. F. Huber, *J. Am. Chem. Soc.*, **73**, 2730 (1951).

TABLE I. PROPERTIES AND COMPOSITIONS OF METHYL ESTERS

| Methyl ester | Iodine value* | Saponification value | M.p. °C | $n_D^{40}$ | Composition,**% by wt. $C_{12}$ | $C_{14}$ | $C_{16}$ | $C_{18F_0}$ | $C_{18F_1}$ |
|---|---|---|---|---|---|---|---|---|---|
| Laurate | 0.02 | 261.6 | 7.0 | 1.4242 | 100.0 | | | | |
| Palmitate | 0.02 | 208.0 | 31.4 | 1.4331 | 0.2 | 0.4 | 99.4 | | |
| Stearate | 0.01 | 188.4 | 30.5 | 1.4365 | | | 3.2 | 96.8 | |
| Oleate | 84.7 | 191.2 | | 1.4444 | | | | | 100.0 |
| Elaidate | 85.0 | 189.8 | 12.5 | 1.4432 | | | 0.7 | | 99.3 |
| Isoöleate(L) | 83.7 | 190.6 | | 1.4435 | | | 0.4 | | 99.6 |

* Determined by Wijs method at 15—20°C
** Determined by gas chromatography

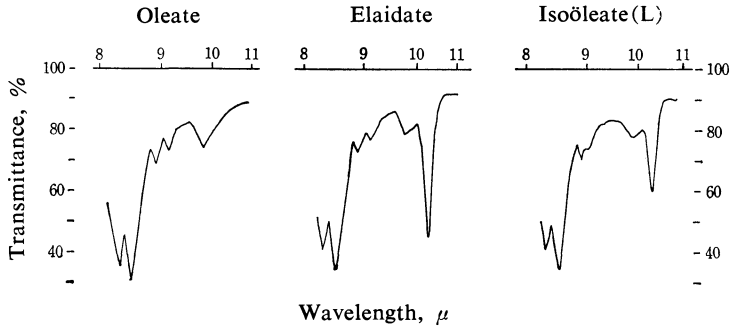



Fig. 1. Infrared absorption spectra of methyl esters of unsaturated fatty acids.

10 volumes of acetone at −30°C and the other from 15 volumes of acetone at −70°C. The solvent was removed, and, by the fractional distillation of the residues, the isoöleates (S) and (L), respectively, were obtained. However, the results of gas chromatography showed that the isoöleate (S) contains about 10% saturated ester. Therefore, this isoöleate was discarded.

Moreover, in the results of the paper chromatography of the mono-basic acids obtained by the periodate-permanganate oxidation of the isoöleate (L), contrary to expectations, it was seen that the isoöleate (L) consists of some position-isomers, $\Delta^{13:14}$ 24.4, $\Delta^{12:13}$ 18.0, $\Delta^{11:12}$ 35.9, $\Delta^{10:11}$ 14.1, and $\Delta^{9:10}$ 5.1, and the saturated 2.5%.

As Fig. 1 shows, furthermore, the isoöleate (L) has a rather weaker absorption intensity at 10.36 μ than that of elaidate; therefore, it is considered that some cis-geometrical isomers are also included.

Partially-hydrogenated commercial oils contain various isoöleates, owing to selective addition or isomerization during the hydrogenation of such elements as the isomers included in the isoöleate (L), and they are used in the manufacture of commercial soaps; therefore, this isoöleate (L) was used as one of raw materials of the soaps for the determination.

All of the single soaps were prepared by the neutralization of the fatty acids obtained from the corresponding methyl esters by saponification and subsequent acidification, and the free alkali of these soaps was adjusted to have a slight excess (less than 0.05%). The isoöleate soap, prepared from the methyl isoöleate (L) by the same procedure, is also described for the sake of convenience as a single soap in spite of its complex composition.

In the following figures, sodium soaps of laurate, palmitate, stearate, oleate, elaidate, and the isoöleate (L) are abbreviated as NaL, NaP, NaOl, NaEl, and Na*i*Ol (L) respectively.

*Two-Single Soaps and Commercial Type Soap.*—Equimolar mixtures of two-single soaps, with such combinations as saturated - saturated soaps and saturated - unsaturated soaps, were prepared from the corresponding single soaps.

A mixed soaps with almost the same composition as that of typical commercial laundry soap was prepared from sodium laurate, palmitate, oleate, and stearate in the ratio of 6.1, 32.6, 42.6, and 18.5% respectively. Hereafter, this mixed soap will simply be described as "commercial soap."

*Sodium Silicate.*—The sodium silicate of the JIS No. 1 grade of the Nihon Chemical Industry, Ltd., was used; the composition as determined by the JIS analytical method (K-1408) was 38.2% $SiO_2$ and 18.2% $Na_2O$; i.e., the $SiO_2/Na_2O$ weight ratio was 2.10.

**Procedure.**—*The Preparation of Materials.*—All date were obtained by the synthetic method,[5] consisting of observing the temperature at which phase changes occur in systems of known compositions. To facilitate the visual observation for the soap phases, the determination was made at the relatively low soap concentration of 24%.

The calculated quantities (total weight 1.65 g.) of soap, silicate, and distilled water were weighed into a 2.35-ml. stainless steel micro-autoclave in the order named. In order to transform the contents into a

single homogeneous solution, the autoclave was then heated in an electric muffle-furnace at about 210°C for a quarter hour and then quenched into ice water to settle the contents in an unseparated state. A part of the solid soap obtained, about 0.5 to 0.6 g., was taken into a 0.75-ml. glass micro-cell (inside diameter, 11 mm.; height, 8 mm.); this cell was covered with a slide glass and then sealed by epoxy adhesives (Bond-E7, Konishi Gisuke Co.).

*The Determination of the $T_c$ Temperature.*—The determination was made by using an electric oven of the hot-plate type, Model MHS-3 (Union Optical Co.), with quartz-glass windows and jackets.

The micro-cell was heated slowly in order to allow adequate time for the soap system to acquire the successive temperature, and then the determination was made of the temperature, $T_c$, at which all traces of the opaque white solid disappeared to complete the formation of an isotropic liquid, an anisotropic liquid crystalline phase, or a mixture of the two. The curve of $T_c$ values is, therefore, a solubility curve.[4] The identification of the phases in a state of equilibrium at the $T_c$ temperature was made by crossed polaroid disks.[11]

The heating rate was rather quick, about 1°C/10 min., until 2—3°C below the $T_c$ temperature; then the system was allowed to reach equilibrium, for which it took more than two hr.[11] Stirring was effected by rotating the oven as a whole slowly and frequently. When the $T_c$ temperature of the materials was lower than 30°C, the cell was dipped in ice-salt solution prior to the determination in order to transform the contents into a completely rigid solid. Moreover, the oven was kept 5°C below the $T_c$ temperature by pumping cold water or a cold salt solution through the jackets, and then the determination was started.

The $T_c$ values are reproducible to within 1°C; the values which were determined in single soap-water binary systems agreed closely with those reported by McBain and Lee,[12] who used the vapor pressure method (Table II). Temperatures were measured with a calibrated thermometer.

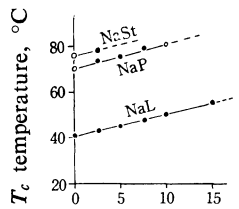
TABLE II. THE $T_c$ TEMPERATURE OF A SINGLE SOAP-WATER BINARY SYSTEM IN °C

| | NaL | NaP | NaSt | NaOl |
|---|---|---|---|---|
| McBain and Lee[12] | 41.5 | 70.0 | 77.5 | 29.0 |
| The present authors | 41.0 | 72.0 | 77.0 | 28.5 |

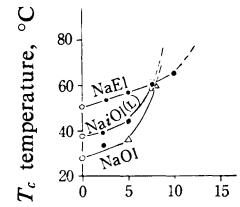
## Results and Discussion

Figure 2 shows the effect of the silicate on the transition temperatures of these six single soaps. The effects on the equimolarly mixed soaps and on the commercial soap are shown in Figs. 3 and 4 respectively.

In the $T_c$ values for single-soap systems, there is a characteristic tendency arising from the structure of the fatty acids of the soaps. Within the range determined, the $T_c$ values for the saturated soaps are raised in proportion to the amounts of the silicate and their $T_c$ value curves are parallel. While the amount of the

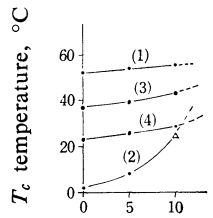



(1) Saturated soaps



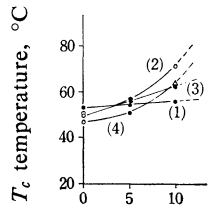

(2) Unsaturated soaps

Fig. 2. The $T_c$ curves of single soap-silicate-water systems. Open circles, filled circles, and open triangles represent the compositions forming liquid crystals, isotropic solutions, and both liquid crystals and isotropic solutions on heating, respectively.




(1) NaL-NaP
(2) NaL-NaOl
(3) NaL-NaEl
(4) NaL-Na*i*Ol

(1) Two-single soaps with sodium laurate




(1) NaP-NaL
(2) NaP-NaOl
(3) NaP-NaEl
(4) NaP-Na*i*Ol

(2) Two-single soaps with sodium palmitate

Fig. 3. The $T_c$ curves of two-single soaps-silicate-water systems.

11) J. W. McBain and W. J. Elford, *J. Chem. Soc.*, **1926**, 421.
12) J. W. McBain and W. W. Lee, *Oil & Soap*, **20**, 17 (1943).

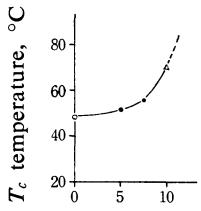



Fig. 4. The $T_c$ curve of commercial soap - silicate - water system.

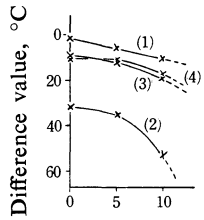
silicate in the system is small, the $T_c$ value of oleate soap is lower than any of the former, but it is elevated steeply when the concentrations of the silicate increase to more than 5%. These results agree with those of McBain et al.,[4] who found that oleate soap is salted out more easily (by sodium chloride) than are saturated fatty acid soaps.

As elaidic acid has a trans structure and its molecular form is similar to that of saturated acid, it may be assumed that the behavior of its soap, which has not yet been determined in any system, resembles that of the saturated soaps.[13] However, the $T_c$ value curve obtained was in the middle of the oleate and palmitate soaps, and that of isoöleate (L) soap, though not pure, resembles that of the oleate. It seems that the influence of the tendency to salt out of cis unsaturated soap present in small amounts is very great.

In the systems of the two-single soaps, also there is a characteristic tendency arising from three main combinations; laurate soap - palmitate soap, the said saturated soap - oleste soap, and the said saturated soap - elaidate soap. The $T_c$ value for the saturated - saturated soap systems is raised in proportion to the amounts of the silicate, as is the case with single-saturated-soap systems. The $T_c$ values for the saturated soap - oleate soap systems are raised rather steeply as the silicate contents become relatively large. In the case of the combination with laurate soap, the $T_c$ shows extremely low values with small amounts of the silicate. The $T_c$ curves for saturated soap - elaidate soap systems are similar to the curves for the saturated - saturated soaps. However, the $T_c$ curves for the saturated soap - isoöleate soap systems do not show any consistent behavior in the combinations with palmitate and with laurate.

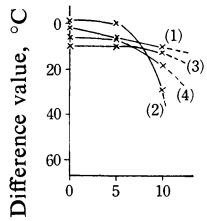
As a rule, the $T_c$ values which have been determined in the present experiment are lower than those estimated on a molecular basis from the $T_c$ values for the ingredient soaps on the assumption that the $T_c$ value has an additive

13) H. Ezaki, K. Ohwada and S. Noguchi, *J. Chem. Soc. Japan, Ind. Chem. Sec.* (*Kogyo Kagaku Zassi*), **62**, 543 (1959).




(1) NaL-NaP
(2) NaL-NaOl
(3) NaL-NaEl
(4) NaL-Na*i*Ol

(1) Two-single soaps with sodium laurate




(1) NaP-NaL
(2) NaP-NaOl
(3) NaP-NaEl
(4) NaP-Na*i*Ol

(2) Two-single soaps with sodium palmitate

Fig. 5. The difference-value curves of two-single soap - silicate - water systems.

property. The same is true also on a weight basis. These differences between determined and estimated values are shown in Fig. 5 as "difference values." It seems likely, as has been suggested previously,[2] that a less soluble soap can be prevented from separating as "curd" simply by adding it to the system of a soap with a shorter chain length. Mixed micelles of a smaller size, less orientation, and greater solubility must be produced by the presence of the shorter laurate molecules among the longer homologs, which is an example of mutual solubilization.[2] In other words, the solubility of sodium palmitate is effectively raised to near that of laurate soap by the addition of laurate soap to the system. The difference in the oleate soap - saturated soap system increases steeply when the silicate contents increase to more than 5%. This phenomenon shows that the tendency of oleate soap to salt out is substantially prevented by the saturated soap. In the commercial soap system, the $T_c$ value determined is also lower than the estimated value. This difference is shown in Fig. 6.

In the manufacture of soap, the temperature at which silicates are mixed into soaps, i.e., the crutching temperature, is about 70—80°C. In this case, for the silicate to be mixed in homogeneously the $T_c$ temperature of these systems must be lower than the crutching temperature.[3] However the $T_c$ temperature increases with the amounts of the silicates added. Therefore, the amounts of the silicates which can be added are restricted. From the findings

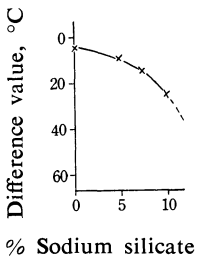



Fig. 6. The difference value curve of the commercial soap - silicate - water system.

concerning two-single soap systems, it may be concluded that, in order to increase the amounts of sodium silicate which can be added to the soap of higher saturated fatty acid, the combination with the lower saturated soap is suitable, because of the effect of lowering the $T_c$ values through the higher concentrations of the silicate (Fig. 3).

Together with the combination of soaps, the mixing ratio of the two-single-soaps also influences the $T_c$ value of two-single-soap systems greatly. This influence was determined for the ternary system of laurate roap - oleate soap - water. As Fig. 7 shows, when the substances are mixed with each other the $T_c$ value is lowered, and at an equimolar ratio the value reaches a minimum, at which it is lower than that of a single-oleate-soap system with a low $T_c$ value. This phenomenon is also due to the multiplicity of mutual effects.

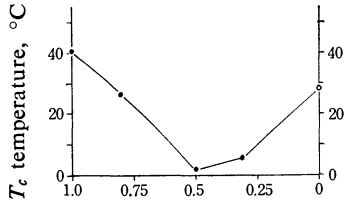



Fig. 7. Molar fraction and the $T_c$ temperature in sodium laurate - sodium oleate - water ternary system.

**Summary**

The $T_c$ temperatures of sodium soap - sodium silicate - water systems, which are important but are usually neglected, have been determined using a silicate with an $SiO_2/Na_2O$ weight ratio of 2.1, and six single soaps or their mixtures.

It has been found that there is a characteristic tendency arising from the structure of the fatty acids of the soaps, saturated (higher or lower) and unsaturated (cis or trans). The $T_c$ values of the saturated - fatty acid soap systems increase linearly in proportion to the silicate in the system. The $T_c$ value curves of the unsaturated soaps are rather complicated. Their $T_c$ values, while the contents of the silicate in the system are small, are relatively lower than those for the former, but when the silicate concentrations increase to relatively large amounts, the $T_c$ values are elevated rapidly. This inclination is more remarkable for cis unsaturated soap than for the trans isomer.

In the system of the mixed soaps, there is a complex mutual effect. By the combination with a lower saturated-soap, the solubility of the higher saturated-soap is increased, and by the combination with a saturated soap, the tendency of unsaturated soap to salt out is substantially prevented. Consequently, the rising of the $T_c$ curve for unsaturated soap becomes mild.

As a rule, the $T_c$ values determined, therefore, are lower than those estimated from the $T_c$ values for the ingredient soaps. It seems that, in order to increase the amount of builder which can be added to the soap of higher saturated-fatty acid, combination with a lower saturated-soap is suitable.

Moreover, in the case of the sodium laurate - sodium oleate - water system, it has been shown that the mixing ratio of the two-single soaps influences the $T_c$ value greatly.

*The Research Laboratory*
*of the Lion Fat and Oil Company*
*Edogawa-ku, Tokyo*

# Über das Waschvermögen und die Hygroskopizität von Natriumdodecylbenzolsulfonat-Natriumsulfat-Systemen

Von Yasushi KIMURA, Syûhei TANIMORI und Terunosuke SHIMO

(Eingegangen am 11. August, 1964)

Natriumdodecylbenzolsulfonat ist als Waschmittel sowohl im Haushalt als auch in der Industrie am weitesten in Gebrauch. Die oberflächenaktiven Eigenschaften von Natriumdodecylbenzolsulfonaten werden zum grossen Teil durch die Zusammenhänge ihrer Strukturen bestimmt. Auch über die Beeinflussung des Waschvermögens durch die verschiedenen Strukturen ist bereits einiges ermittelt worden.

Alle diese Bestimmungen des Vermögens sind jedoch ausnahmslos an Baumwollgeweben mit künstlicher Beschmutzung durch Russ durchgeführt worden. Auch ist als Waschlösung, verschieden von der Praxis, im allgemeinen destilliertes Wasser gebraucht worden. Über den Tellerwaschversuch im harten Wasser durch Natriumdodecylbenzolsulfonate mit verschiedenen Strukturen konnte man noch keine Veröffentlichung finden. Ginn[1] hat von kurzem festgestellt, dass die von dem Waschvermögen stark abhängende Solubilisieraktivität wesentlich von der Wasserhärte und Builder beeinflusst worden ist. Es liess sich also erwarten, dass das Tellerwaschvermögen mit dieser Solubilisieraktivität in besonders engem Zusammenhang stehen.[1,2]

Anderseits sind die Hygroskopizität und Agglomerativität des Waschmittels auf der praktischen Anwendung der Proben sehr wichtig. Die Beeinflussung dieser beiden Eigenschaften durch die verschiedenen Strukturen der Dodecylbenzolsulfonate ist jedoch nur wenig untersucht worden, oder wenn das der Fall war, noch nicht quantitativ versucht worden.[3,4]

So hat man aus praktischen Gesichtspunkten über Natriumdodecylbenzolsulfonate mit verschiedenen Strukturen Solubilisieraktivität und Waschvermögen (im Zusammenhang mit der Härte und Buildereffekt) gearbeitet. Daneben wurden auch die Hygroskopizität und Agglomerativität von Natriumdodecylbenzolsulfonat-Natriumsulfat-Systemen untersucht.

1) M. E. Ginn, F. B. Kinney und J. C. Harris, *J. Am. Oil Chemists' Soc.*, **36**, 332 (1959).
2) J. C. Harris, ebenda, **35**, 428 (1958).
3) R. H. Rovenscroft und M. E. Turney, ebenda, **32**, 418 (1955).
4) H. Stüpel, *Seifen-Öle-Fette-Wachse*, **80**, 170 (1954).
5) F. W. Gray, J. F. Gerecht und I. J. Krems, *J. Org. Chem.*, **20**, 511 (1955).

## Materialien

**Natriumdodecylbenzolsulfonate (DBSNa)**: Es sind folgende sieben Typen davon in Gebrauch genommen;

*n-Dodecylbenzolsulfonate* (*n-DBSNa*), dargestellt vornehmlich nach Gray.[5] Reinheit von mehr als 99.8%.

*Dodecyl-6-benzolsulfonat* (*6-DBSNa*), dargestellt ebenso vornehmlich nach Gray.[5] Reinheit von mehr als 99.8%.

*sek-Dodecylbenzolsulfonat* (*Sek-DBSNa*), dargestellt durch Alkylierung von *n*-Dodecen-1 und Benzol.[6] Die Isomerenzusammensetzung: 2-, 31.9%; 3-, 19.9%; 4-, 16.2%; 5,6-, 31.8% (Die mit dem Bindungsstrich versehene Ziffer stellt die Stellung vom Benzolkern dar.).

*Dobane-JN Sulfonat* (*JN-DBSNa*), Sulfoniertensubstanz des Dodecylbenzols von linearem Typ (Dobane-JN von der Firma Shell Öl Co.).

*Alkane-56 Sulfonat* (*56-DBSNa*), Sulfoniertensubstanz des Dodecylbenzols von tetramerem Typ (Alkane-56 von der Firma Oronite Chem. Co.).

*Die zerlegten DBSNa.*[7] Das Blei Alkane-56 Sulfonat wurde durch fraktionierte Kristallisation in zwei Portionen (löslich und unlöslich) zerlegt, um die reinen Stellungsisomeren zu gewinnen. Diese Zerlegung erfolgte bei 9°C in 10 Teilen von 95%-igem Äthanol. Wobei die bei wiederholten Zerlegungen entstandenen Verhältnisse von löslich und unlöslich DBSNa 0.1 bzw 0.7 gegenüber der ursprünglichen Substanz wurden.

Aber die Bestimmungsergebnisse durch Messung ihrer Dipolmomente* und Infrarot-Spektra zeigen, dass das lösliche DBSNa ein wenig *p*-Stellungsisomer enthält.

Von hier an abbreviiert man die löslichen und unlöslichen DBSNa als FF- bzw CC-DBSNa.

**Natriumsulfat ($Na_2SO_4$).** — Natriumsulfat wurde als Reagenz gebraucht.

**Natriumtripolyphosphat (NaTPP).** — Natriumtripolyphosphat von hoher Reinheit (hergestellt von der Firma Nippon Kagaku Co., $P_2O_5$ im Gehalt von 58%), wurde gebraucht.

**Orange-OT.**—Es wurde durch Rekristallisierung von Orange-OT für spezielles Reagenz, (hergestellt von der Firma Tokyo Kasei Co.), aus 99%igem Äthanol und durch Austrocknung unter vermindertem Druck bei 50°C hergestellt.

6) A. C. Olson, *Ind. Eng. Chem.*, **52**, 833 (1960).
7) Y. Kimura, K. Ōba und M. Tobari, *Yukagaku*, **11**, 36 (1962).
* 5.20 und 5.42 $\mu$ [D] für bzw. löslich und unlöslich DBSNa in Dioxan-Lösung bei 25°C.

## Messergebnisse und Diskussionen

**Solubilisieraktivität.**—Das wurde vornehmlich nach Ginn[1] mit Orange-OT als Solubilizat bestimmt.

*Solubilisieraktivität von DBSNa in dest. Wasser.* —Zusammenhang zwischen den Konzentraten und den solubilisierten Mengen von Orange-OT durch DBSNa in 0.20%igem Natriumsulfatlösungen bei 25°C ist in Abb. 1 aufgetragen. Die solubilisierten Mengen von Orange-OT durch linearen DBSNa waren grösser als jene durch tetrameren. Die Löslichkeit von *n*-DBSNa ist sehr gering (löslich bei 25°C nur unter 0.03%). Dadurch ist die Solubilisieraktivität auch schwach, obwohl es sich um einen linearen Typ handelt.

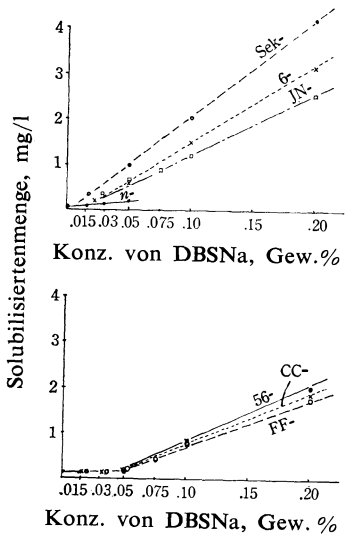



Abb. 1. Solubilisieraktivität der DBSNa für Orange-OT in 0.20%-Natriumsulfatlösung bei 25°C.
Bestimmung durch Extinktionsgrad in 498 mμ

Die kritischen Mizellbildungskonzentrationen (KMK) sind auf der Tabelle I aufgetragen. Die Erniedrigung von KMK durch Natriumsulfat, scheint bei linearem Typ grösser als bei anderen zu sein.

TABELLE I. KRITISCHE MIZELLBILDUNGSKONZENTRATION DER DBSNa
(Konzentration in Gew.%)
Bestimmung durch Solubilisierenverfahren von Orange-OT bei 25°C

| DBSNa | Dest. Wasser | 0.20% $Na_2SO_4$ Lösung |
|---|---|---|
| 6- | 0.06 | 0.01 |
| Sek- | 0.04 | 0.005 |
| JN- | 0.04 | 0.01 |
| 56- | 0.08 | 0.04 |
| CC- | 0.09 | 0.04 |
| FF- | 0.10 | 0.05 |

*Härte und Solubilisieraktivität.* — Die Solubilisieraktivität wurde in einem Bereich von 0 bis 30°dH bestimmt. Die Härte der Lösung wurde durch Kalziumchlorid eingestellt.

Die Menge von solubilisierten Orange-OT in einer Lösung mit dem Gehalt von 0.05% DBSNa und 0.20% $Na_2SO_4$ sind in Abb. 2 dargestellt. Aus diesen Diagrammen ist recht deutlich zu ersehen, dass *n*-DBSNa schwach

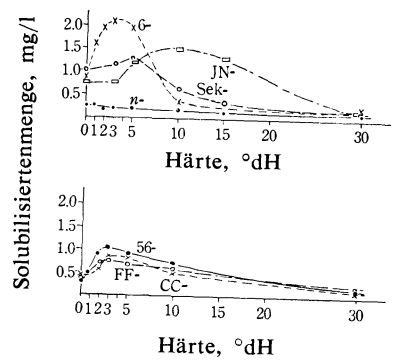



Abb. 2. Solubilisieraktivität der DBSNa bei verschiedener Wasserhärte.
Bestimmung bei 25°C und 0—30°dH in 0.05%-DBSNa Lösungen unter Zusatz von 0.2% $Na_2SO_4$

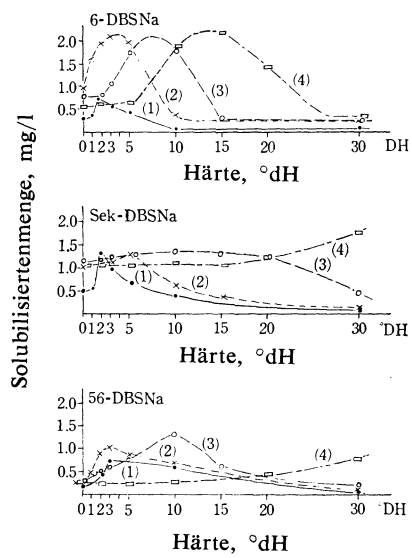
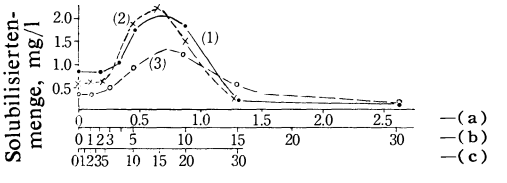



Abb. 3. Effekte von $Na_2SO_4$ und NaTPP auf Solubilisieraktivität von 6-, Sek-, und 56-DBSNa in verschiedener Wasserhärte.
(1) Nicht Builder
(2) 0.20% $Na_2SO_4$
(3) 0.03% NaTPP und 0.19% $Na_2SO_4$
(4) 0.06% NaTPP und 0.16% $Na_2SO_4$
Bestimmung bei 25°C und 0—30°dH in 0.05%-DBSNa Lösungen

löslich ist, die Solubilisieraktivität jedes einzelnen DBSNa stieg höher mit der Zunahme von Härte. Bei einer geeigneten Härte erreicht sie das Maximum und bei weit höherer Härte näherte sie sich dem Nullpunkt.

Abbildung 3 zeigt den Effekt von Natriumsulfat und NaTPP auf die Solubilisieraktivität von 6-, Sek- und 56-DBSNa. Wie aus der Abbildung ersichtlich war, falls kein Builder zugegeben wurde, lag die Solubilisiertenmenge im allgemeinen ganz niedrig. Die Menge erreichte das Maximum bei schwacher Härte und näherte sich bei weiter starker Härte schnell dem Nullpunkt. Wenn Natriumsulfat zugegeben wurde, stieg die Solubilisieraktivität bei relativ schwacher Härte an. Wenn NaTPP, das gegen Kalzium weichmachend wirkt, zugegeben wurde, ging das Maximum nach der höheren Härte über. Diese Tendenz verstärkte sich, wenn noch ein Teil des Natriumsulfat durch NaTPP ersetzt wurde. 6-DBSNa zeigt dieses Übergangsphänomen sehr deutlich. Trägt man in einem Diagramm die Solubilisieraktivität von 6-DBSNa als Ordinate gegen das Äquivalentverhältnis von Ca : NaTPP als Abszisse auf, dann ergibt sich das in Abb. 4 dargestellte Bild. Wie aus der Abb. ersichtlich ist, ist das Maximum der Solubilisieraktivität unabhängig von der Konzentration von NaTPP und DBSNa und liegt bei Äquivalentverhältnis von 0.6 bis 0.7 (Ca/NaTPP).




(a) äqui. Verh. von Ca/NaTPP
(b) °dH (NaTPP 0.03%)
(c) °dH (NaTPP 0.06%)

Abb. 4. Abhängigkeit der Solubilisieraktivität von der Äquivalentverhältnis von Ca : NaTPP, hinsichtlich 6-DBSNa.

| | DBSNa | NaTPP | $Na_2SO_4$ |
|---|---|---|---|
| (1) | 0.05% | 0.03% | 0.19% |
| (2) | 0.05 | 0.06 | 0.16 |
| (3) | 0.03 | 0.03 | 0.19 |

Bestimmung bei 25°C und 0—30°dH

Es lässt sich für diese Phänomene annehmen, dass der Mizellenaufbau sich bei der Umwandlung eines Teils von DBSNa zum Kalziumsalz verändert. Der Solubilisierungstyp von Orange-OT verändert sich auch hierbei und die solubilisierte Menge vermehrt sich.

**Härte und Waschvermögen.**—Der Waschversuch wurde an einer Glasplatte (2.5×7.5 cm) mit künstlicher Anschmutzung eines Gleichmengengemisches von Rindertalg und Sojabohnenöl in der Scrub-O-Meter-Waschmaschine bei 25°C fünf Minuten lang durchgeführt. Aus dem Wegschaffeverhätnis von Schmutz wurde das Waschvermögen bestimmt.

Die Waschlösungen enthielten 0.03% von DBSNa und 0.22% von Builder. Die Härte der Lösungen wurde durch Kalziumchlorid eingestellt. Die Ergebnisse der Bestimmungen zeigt Abb. 5. Abgesehen von *n*-DBSNa mit schwacher Löslichkeit konnte man ersehen, dass das Waschvermögen im allgemeinen in einem bestimmten Härtebereich sich vermehren liess.

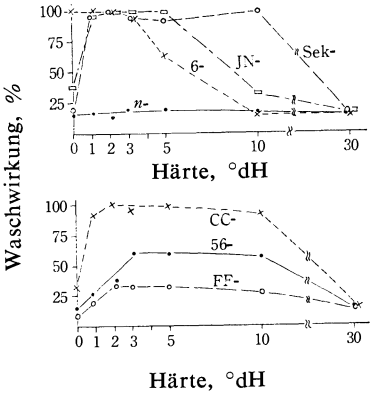



Abb. 5. Waschvermögen der DBSNa bei verschiedener Wasserhärte (I).
Bestimmung durch Glasplattenmethode nach Scrub-O-Meter bei 25°C und 0—30°dH in 0.03%-DBSNa Lösungen unter Zusatz von 0.2% $Na_2SO_4$

Wenn ein Teil von Natriumsulfat durch NaTPP ersetzt wird, so geht der verstärkte Waschvermögensbereich nach der höheren Härte über ; das Waschvermögen aber verringert

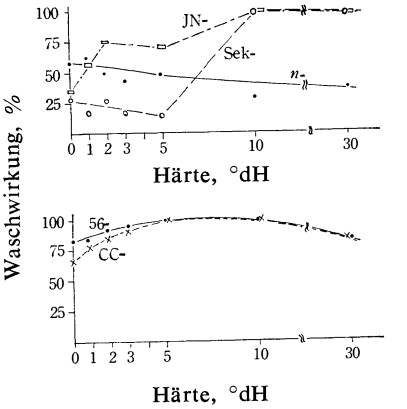



Abb. 6. Waschvermögen der DBSNa bei verschiedener Wasserhärte (II).
Bestimmung bei 25°C und 0—30°dH in 0.03%-DBSNa Lösungen unter Zusatz von 0.03% NaTPP und 0.19% $Na_2SO_4$.

sich auch nicht in der höheren Härte (Abb. 6). Daß das Waschvermögen in jedem Falle in einem bestimmten Härtebereich verbessert wird, beruht auf der Tatsache, dass die mit diesem Vermögen zusammenhängenden Faktoren,[2,8] wie Solubilisieraktivität und Suspendierbarkeit, durch die Bildung der Gemischmizelle von Natrium- und Kalziumsalz stark beeinflusst werden können. In diesem Falle wurde angenommen, dass eine optimale Grenze über die Verhältnisse zwischen diesen beiden Salzen vorhanden ist.[1] So kann man sich vorstellen, dass die Verbesserung des Waschvermögens im höheren Härtebereich durch Zugabe von NaTPP sich auf die Überführung des optimalen Härtebereich nach höherer Seite wegen der weichmachenden Wirkung von NaTPP auf hartes Wasser zurückführen lässt.

**Hygroskopizität und Agglomerativität.** — *Hygroskopizität.*—Ein Teil vom jeder der obengenannten sieben DBSNa wurde mit vier Teilen des Natriumsulfat eingemischt. Dieser wurde in einer Versuchsanlage von Scheibentyp mit Durchmesser von 1.4 m nach parallelströmenden Verfahren bei der Einlassluft-temperatur von 220 bis 230°C sprühgetrocknet.

Die Feuchtigkeit und Freifalldichte der sprühgetrockneten Proben sind auf der Tabelle II und die Teilchenverteilung auf der Tabelle III aufgetragen. In dem folgenden Hygroskopizitätsversuch wurden die Proben während einer Std. bei 110°C getrocknet.

TABELLE II. FEUCHTIGKEIT UND FREIFALLDICHTE DER SPRÜHGETROCKNETEN DBSNa

| DBSNa | Feuchtigkeit | Freifalldichte |
|---|---|---|
| *n*- | 1.6 | 0.19 |
| 6- | 3.7 | 0.24 |
| Sek- | 4.7 | 0.12 |
| JN- | | 0.20 |
| 56- | 7.4 | 0.19 |
| CC- | 3.3 | 0.22 |
| FF- | 1.6 | 0.22 |
| $Na_2SO_4$ (100%ig) | 1.2 | 0.35 |

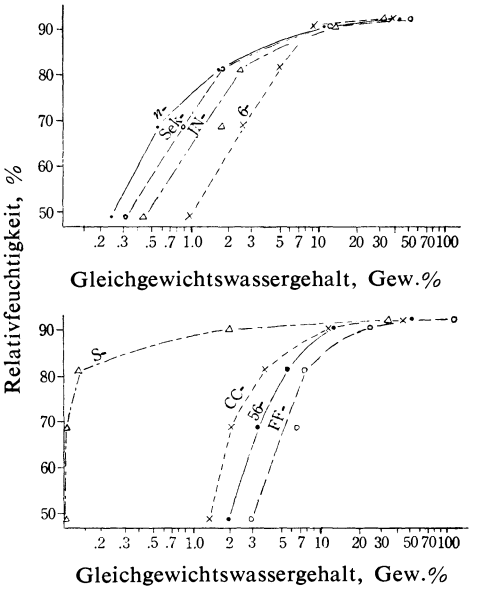
TABELLE III. TEILCHENVERTEILUNG DER SPRÜHGETROCKNETEN DBSNa (Gew.%)

| | "Mesh" | | | | |
|---|---|---|---|---|---|
| DBSNa | <28 | 28—35 | 35—60 | 60—100 | >100 |
| *n*- | 1 | 2 | 83 | 10 | 4 |
| 6- | 50 | 27 | 18 | 3 | 2 |
| Sek- | 1 | 63 | 28 | 6 | 4 |
| JN- | 6 | 39 | 45 | 6 | 4 |
| 56- | 1 | 43 | 47 | 7 | 2 |
| CC- | 7 | 40 | 44 | 6 | 3 |
| FF- | 1 | 1 | 68 | 15 | 15 |
| $Na_2SO_4$ (100%ig) | 1 | 41 | 42 | 7 | 9 |

8) A. M. Mankowich, *Ind. Eng. Chem.*, **44**, 1151 (1952).

In Reagensröhren gleicher Grösse (1.5×10 cm) wurden von jeder Proben 1.0 g eingewogen. Die Röhren wurden in jeden Exsikkatoren gestellt, in dem bei 35°C und 48.5—92% relative Luftfeuchtigkeit vorhanden war (erreicht durch 44.5—15.5 Gew.%iger Schwefelsäure). Die Gewichtszunahme wurde während zweier Monate festgestellt.

Abbildung 7 zeigt die Relativfeuchtigkeit-Gleichgewichtswassergehalt-Diagramm nach zwei Monaten.




Fbb. 7. Abhängigkeit der Relativfeuchtigkeit von der Gleichgewichtswassergehalt von DBSNa - $Na_2SO_4$-Systeme nach 2 Monat. Bestimmung bei 35°C und 48.5—92% relativer Luftfeuchtigkeit.

Es lässt sich feststellen, dass die Hygroskopizität der Proben bei 80% relative Luftfeuchtigkeit von ihren Strukturen stark beeinflusst wird. Je mehr die Alkylkette sich linear gestaltet, je ferner nach dem Kettenende der Benzolkern anhaftet, desto geringer wird das Gleichgewichtswassergehalt; d. h., *n*-DBSNa ist sehr schwach hygroskopisch und die Hygroskopizität vermehrt sich in der Folge von *n*- → Sek- → 6-DBSNa. Ebenso ist die Hygroskopizität von JN-DBSNa von mehr linearem Typ schwächer als die von 56-DBSNa von tetramerem Typ mit mehreren Verzweigästen. Wie es auch aus dem Unterschied von Löslichkeiten verstanden werden kann, ist CC-DBSNa weniger hygroskopisch als 56-DBSNa, dagegen FF-DBSNa mehr hygroskopisch.

*Agglomerativität.* — Diese wurde mit einem neuen Apparat,[9] der die Erniedrigung der Höhe des Fluidiertetbett von Waschmittelteilchen durch Agglomerieren anwendet, bestimmt. Der Apparat ist schematisch auf der Abb. 8 aufgezeichnet. Wenn die Waschmittelteilchen sich mit der feuchten Luft berühren und Wasser aufnehmen, so fangen sie an durch Adhäsion zu agglomerieren. Dadurch wachsen die Korngrössen der Teilchen, ihre Schwimmkraft dagegen verringert sich. So kann die Agglomerativität durch die Zeitabschnitte, die das Fluidierbett von Teilchen braucht bis 25% von der Initialhöhe zuerniedrigen, bestimmt werden.

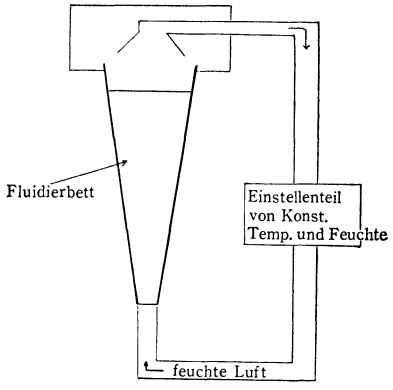



Abb. 8. Der Apparat für Bestimmung von Agglomerativität.

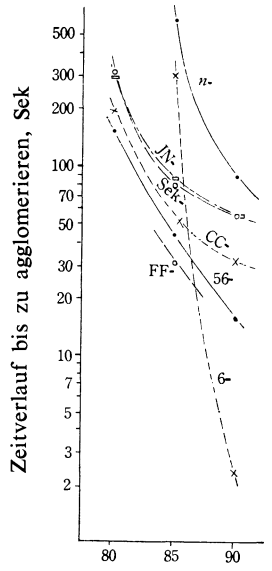



Abb. 9. Agglomerativität der sprühgetrockneten DBSNa.
Bestimmung bei 35°C und 80—90% relativer Luftfeuchtigkeit

Die Ergebnisse der Bestimmung sind in Abb. 9 aufgetragen. Da die Teilchenverteilung und Feuchtigkeit der Proben meist ungleich sind, war ein exakter Vergleich schwer durchzuführen. Da jedoch die Struktur und Zusammensetzung weit grösseren Einfluss ausgeübt haben, konnte man die Unterschiede zwischen einzelnen DBSNa deutlich beobachten.

Wie in Abb. 9 ersichtlich ist, je ferner der Benzolkern nach dem Alkylkettenende liegt, je weniger die Alkylkette einen Verzweigungsgrad hat, desto schwächer ist die Agglomerativität.

Das Bestimmungsergebnis von 6-DBSNa war fraglich, aber wegen des Materialmangels war die Wiederbestimmung nicht durchführbar.

## Zusammenfassung

Es wurde Solubilisieraktivität, Waschvermögen, Hygroskopizität und Agglomerativität von DBSNa-$Na_2SO_4$-Systemen in Abhängigkeit von der Struktur und Zusammensetzung der DBSNa untersucht.

**Solubilisieraktivität und Waschvermögen.**— Linearer Typ hat eine grössere Aktivität für Solubilisierung von Orange-OT in destilliertem Wasser als tetramerer Typ.

Kalzium übt einen starken Einfluss die Solubilisieraktivität und das Waschvermögen von allen DBSNa abgesehen von *n*-DBSNa aus. In einem geeigneten Härtebereich erreichen sie Maxima. Wenn ein Teil von Natriumsulfat durch NaTPP, welches gegen hartes Wasser weichmachend wirkt, ersetzt wird, so wird entweder das Maximum noch weiter nach höherer Härte übergeführt, oder keine Erniedrigung von Solubilisieraktivität und Waschvermögen sogar in weit höherer Härte beobachtet.

**Hygroskopizität und Agglomerativität.**—Diese beide sind ganz verschieden durch die Struktur und Zusammensetzungen des DBSNa.

Je nachdem die Stellung des Benzolkerns von dem Alkylkettenende aus sich nach der Mitte zu bewegt und je nachdem die Alkylkette mehrere Verzweigäste hat, wird die Hygroskopizität verstärkert.

Die mit einem neuen Apparat bestimmte Agglomerativität hat die gleiche Tendenz und zeigt eine deutliche Verschiedenheit durch die Struktur und Zusammensetzung von DBSNa.

Diese Abhandlung wurde aus Beiträgen[9,10] zusammengefasst.

*Untersuchungslaboratorium der Lion Fett u. Öl Gesellschaft AG.*
*Edogawa-ku, Tokyo*

9) Y. Kimura, S. Tanimori, T. Nagai und T. Shimo, *Yukagaku*, **14**, 19 (1965).

10) Y. Kimura, S. Tanimori und T. Shimo, *Yukagaku*, **13**, 656 (1964).

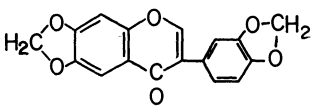
# Synthetic Studies of Sesamol Derivatives. VI.* The Synthesis of 6, 7 : 3′, 4′-Bismethylenedioxyisoflavone, an Isomer of the Maxima Substance A** and Related Compounds

By Kenji FUKUI and Takashi MATSUMOTO

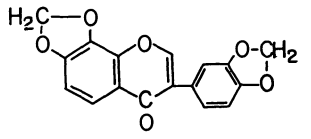
(Received July 24, 1964)

The maxima substance A was isolated from the root of *Tephrosia maxima Aers.* by Rangaswami and Sastry.[1] Their degradative experiments showed it to be 6, 7 : 3′, 4′-bismethylenedioxyisoflavone (I).[2] Up to now it has been the only known naturally-occurring isoflavone containing two methylenedioxy groups in the molecule. On the basis of further experiments, Kukla and Seshadri[3] proposed the revised formula of 7, 8 : 3′, 4′-bismethylenedioxyisoflavone (II) and confirmed its structure by synthesis. However, the isoflavone I has attracted increasing attention as it belongs to the same bismethylenedioxy skeleton. The present report will describe the synthesis of I and some related isoflavones.

The Hoesch condensation of sesamol with 3, 4-methylenedioxybenzyl cyanide (III) yielded 2-hydroxy-4,5-methylenedioxyphenyl 3,4-methylenedioxybenzyl ketone (IV). By a similar Hoesch reaction employing hydroxyhydroquinone, III was converted into 2, 4, 5-trihydroxyphenyl 3, 4-methylenedioxybenzyl ketone (V). The ketone IV was also obtained by the methylenation of V with methylene sulfate. The ketone V was partially methylated with diazomethane to 2, 5-dihydroxy-4-methoxyphenyl 3, 4-methylenedioxybenzyl ketone (VI), and with dimethyl sulfate to 2-hydroxy-4, 5-dimethoxyphenyl 3, 4-methylenedioxybenzyl ketone (VII). On cyclization with ethyl orthoformate, IV afforded 6, 7 : 3′, 4′-bismethylenedioxyisoflavone (I), the melting point, of which 254—255°C, differed from the reported one, 227—229°C,[1,3] of the natural maxima substance A.



I



II

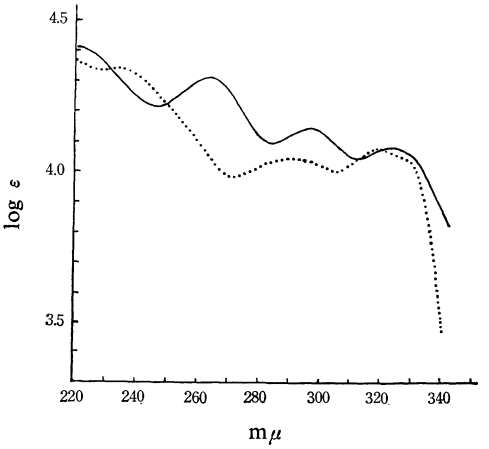



Fig. 1. Ultraviolet spectra of I (—) and XI (···) in ethanol.

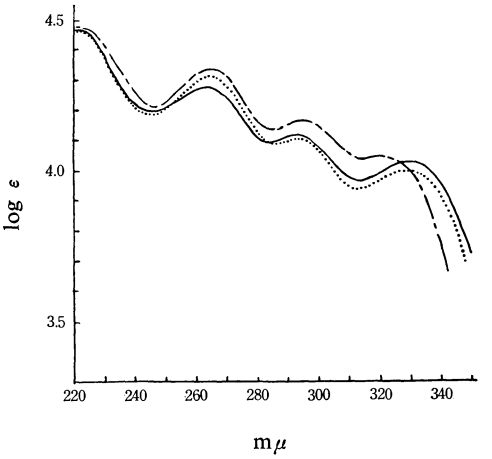



Fig. 2. Ultraviolet spectra of VIII(—), IX (···) and X(-·) in ethanol.

* Part V: K. Fukui and T. Matsumoto, *J. Chem. Soc. Japan, Pure Chem. Sec. (Nippon Kagaku Zasshi)*, **85**, 793 (1964).

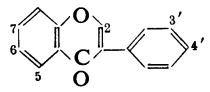
** Recently named maxima isoflavone A by Seshadri et al.[3]

1) S. Rangaswami and B. V. R. Sastry, *Curr. Sci.*, **23**, 397 (1954); *Chem. Abstr.*, **49**, 8568 (1955).

2) S. Rangaswami and B. V. R. Sastry, *Proc. Indian Acad. Sci.*, **44A**, 279 (1956).

3) A. S. Kukla and T. R. Seshadri, *Tetrahedron*, **18**, 1443 (1962).

TABLE I. ULTRAVIOLET SPECTRA OF SOME 3',4'-METHYLENEDIOXYISOFLAVONES IN ETHANOL



| | Substituent | | | | | $\lambda_{max}$, mμ (log ε) | | |
|---|---|---|---|---|---|---|---|---|
| | OH | AcO | MeO | Me | O-$CH_2$-O | | | |
| I | | | | | 3', 4' 6, 7 | 264 (4.31) | 296 (4.14) | 323 (4.08) |
| VIII | 6 7 | | | | 3', 4' | 263.5 (4.28) | 294 (4.12) | 329 (4.03) |
| IX | 6 | | 7 | | 3', 4' | 264.5 (4.31) | 293.5 (4.10) | 329 (4.00) |
| X | | | 6 7 | | 3', 4' | 265 (4.34) | 295 (4.16) | 320 (4.05) |
| XI | | | | 2 | 3', 4' 6, 7 | 235 (4.34) | 291 (4.05) | 319 (4.80) |
| XII | | 6 7 | | 2 | 3', 4' | — | 294 (4.03) | — |
| XIII | 6 7 | | | 2 | 3', 4' | — | 290 (4.80) | 325 (4.03) |
| XIV | | 6 | 7 | 2 | 3', 4' | 248* (4.34) | 296 (4.20) | — |
| XV | 6 | | 7 | 2 | 3', 4, | — | 288 (4.06) | 324 (4.03) |
| XVI | | | 6 7 | 2 | 3', 4' | — | 290 (4.11) | 316 (4.08) |

* Inflexion point

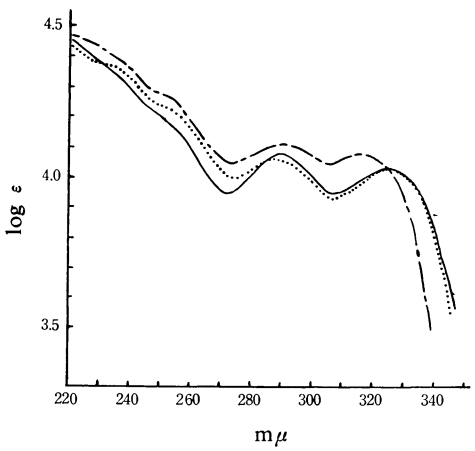
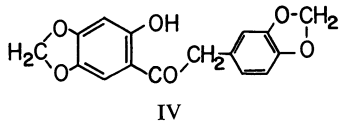



Fig. 3. Ultraviolet spectra of XIII(—), XV(···) and XVI(--) in ethanol.

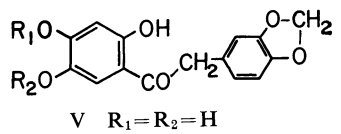
By a similar reaction, the ketones V, VI and VII were converted into 6,7-dihydroxy- (VIII), 6-hydroxy-7-methoxy- (IX) and 6,7-dimethoxy-3',4'-methylenedioxyisoflavone (X) respectively. X was also obtained by the methylation of VIII or IX with dimethyl sulfate.

The reaction of the ketone IV with acetic anhydride in the presence of sodium acetate[4] gave a 2-methyl derivative (XI) of the isoflavone I. 2-Methylisoflavone XI was also obtained from V by the following process. The reaction of V with acetic anhydride gave a cyclized diacetate XII which could easily be

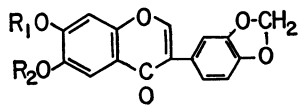
4) W. Baker and R. Robinson, *J. Chem. Soc.*, **127**, 1981 (1925).



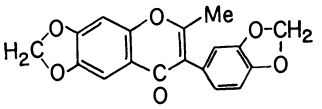
IV



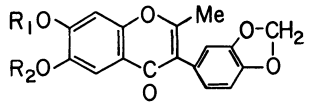
V $R_1=R_2=H$
VI $R_1=Me$ $R_2=H$
VII $R_1=R_2=Me$



VIII $R_1=R_2=H$
IX $R_1=Me$ $R_2=H$
X $R_1=R_2=Me$



XI



XII $R_1=R_2=Ac$
XIII $R_1=R_2=H$
XIV $R_1=Me$ $R_2=Ac$
XV $R_1=Me$ $R_2=H$
XVI $R_1=R_2=Me$

hydrolyzed to 6, 7-dihydroxy-3', 4'-methylenedioxy-2-methylisoflavone (XIII) under mild conditions. The methylenation of XIII with methylene sulfate afforded XI. A similar acetylation of VI gave a cyclized acetate XIV which could be converted into 6-hydroxy-7-methoxy-3', 4'-methylenedioxy-2-methylisoflavone (XV) by alkaline hydrolysis. XIII and XV were methylated with dimethyl sulfate to 6, 7-dimethoxy-3', 4'-methylenedioxy-2-methylisoflavone (XVI), which was then changed to the ketone VII by the alkaline hydrolysis.

The ultraviolet absorption spectra of these synthetic isoflavones are recorded in Figs. 1—3 and Table I.

In most cases there are three characteristic peaks, at ca. 265 (band I), ca. 295 (band II) and ca. 325 m$\mu$ (band III). The methylation of the 6-position (IX—X and XV—XVI) or the and 6-7-positions (VIII—X and XIII—XVI) has little effect on bands I and II, but it causes a hypsochromic shift of 8—9 m$\mu$ in band III, as has been reported previously.[5] A similar shift (6 m$\mu$) in band III is also observed by the methylenation of two vicinal hydroxy groups (VIII—I and XIII—XI). The replacement of the 2-position with a methyl unit causes a displacement (4—5 m$\mu$) of bands II and III towards a shorter wave length.

## Experimental***

**2, 4, 5-Trihydroxyphenyl 3, 4-Methylenedioxybenzyl Ketone (V).**—A mixture of hydroxyhydroquinone (50 g.), 3, 4-methylenedioxybenzyl cyanide (6.5 g.) and anhydrous zinc chloride (3.0 g.) in dry ether (5.0 ml.) was saturated with dried hydrogen chloride in an ice bath and allowed to stand overnight. The ether solution was then decanted from the ketimine hydrochloride which had separated. The residue was heated on a steam bath in water (30 ml.) for 1 hr. The precipitates were collected, washed with water, and recrystallized from aqueous methanol to give V; m. p. 206—208°C (yellow needles); yield, 4.9 g. It gave a dark green color with an alcoholic ferric chloride solution and was soluble in an aqueous potassium carbonate solution. UV $\lambda_{max}^{EtOH}$ m$\mu$ (log $\varepsilon$): 241 (4.13), 287 (4.13), 354 (3.89).

Found: C, 62.29; H, 4.31. Calcd. for $C_{15}H_{12}O_6$: C, 62.50; H, 4.20%.

**2-Hydroxy-4, 5-methylenedioxyphenyl 3, 4-Methylenedioxybenzyl Ketone (IV).**—*From Sesamol.*—A mixture of sesamol (11.0 g.), 3, 4-methylenedioxybenzyl cyanide (13.0 g.) and anhydrous zinc chloride (6.0 g.) in dry ether (150 ml.) was treated with a method similar to that used for V. The product was recrystallized from acetone to give IV; m. p. 172—173°C (yellow needles); yield, 3.0 g. It gave a green color with an alcoholic ferric chloride solution. IR: 1636 (C=O), 1031 (=C-O-C), 916 cm$^{-1}$ (O-$CH_2$-O). UV $\lambda_{max}^{EtOH}$ m$\mu$ (log $\varepsilon$): 240 (4.24), 281 (3.98), 353 (3.96).

Found: C, 64.08; H, 4.15. Calcd. for $C_{16}H_{12}O_6$: C, 64.00; H, 4.03%.

*From V.*—Into a mixture of the ketone V (1.1 g.), ethanol (10 ml.) and potassium hydroxide (1.4 g.) in water (10 ml.), air being excluded by a current of nitrogen, methylene sulfate (0.9 g.) in acetone (15 ml.) was stirred at 45—50°C. After the stirring had been continued another 70 min., the solvent was removed in vacuo. After the residue had been dissolved in water, the solution was saturated with carbon dioxide. The brown precipitates were collected, washed with water, and recrystallized from aqueous acetone to give IV; m. p. 172—173°C (yellow needles); yield, 100 mg. This substance was identified with the above sample by a mixed fusion and a comparison of the infrared spectra.

**6, 7 : 3', 4'-Bismethylenedioxyisoflavone (I).** — A mixture of the ketone IV (1.5 g.), freshly-distilled ethyl orthoformate (5.0 ml.), dry pyridine (6.0 ml.) and piperidine (1.0 ml.) was refluxed for 8 hr. The crystals which separated on cooling were recrystallized from acetic acid to give I; m. p. 254—255°C (colorless needles); yield, 1.1 g. This substance was soluble in concentrated sulfuric acid to a green solution. IR: 1641 (C=O), 1037 (=C-O-C), 931 cm$^{-1}$ (O-$CH_2$-O).

Found: C, 65.90; H, 3.50. Calcd. for $C_{17}H_{10}O_6$: C, 65.81; H, 3.25%.

**2, 5-Dihydroxy-4-methoxyphenyl 3, 4-Methylenedioxybenzyl Ketone (VI).** — To a solution of the ketone V (1.0 g.) in acetone (30 ml.) was added an ethereal diazomethane solution; the mixture was then allowed to stand overnight at room temperature. After the excess diazomethane had been destroyed with acetic acid, the solvent was evaporated and the residue was recrystallized from methanol to give VI; m. p. 194—196°C (pale yellow needles); yield, 0.8 g.. It gave a green color with an alcoholic ferric chloride solution. UV $\lambda_{max}^{EtOH}$ m$\mu$ (log $\varepsilon$): 240 (4.17), 283.5 (4.10), 355 (3.77).

Found: C, 63.39; H, 4.86. Calcd. for $C_{16}H_{14}O_6$: C, 63.57; H, 4.67%.

**2-Hydroxy-4, 5-dimethoxyphenyl 3, 4-Methylenedioxybenzyl Ketone (VII).** — A mixture of the ketone V (230 mg.), anhydrous potassium carbonate (3.0 g.) and dimethyl sulfate (0.2 ml.) in anhydrous acetone (40 ml.) was refluxed for 6 hr. The reaction mixture was then treated in a usual manner. Recrystallization from aqueous acetone give VII in the form of colorless plates; m. p. 153—154°C; yield, 100 mg. It gave a green color with an alcoholic ferric chloride solution. IR: 1625 (C=O), 1033 (=C-O-C), 920 cm$^{-1}$ (O-$CH_2$-O). UV $\lambda_{max}^{EtOH}$ m$\mu$ (log $\varepsilon$): 237.5 (4.24), 280 (4.12), 346 (3.92).

Found: C, 65.41; H, 4.94. Calcd. for $C_{17}H_{16}O_6$: C, 64.55; H, 5.10%.

**6, 7-Dihydroxy-3', 4'-methylenedioxyisoflavone (VIII).** — A mixture of the ketone V (800 mg.), ethyl orthoformate (2.0 ml.), dry pyridine (2.0 ml.) and piperidine (0.3 ml.) was refluxed for 4 hr.

5) K. Fukui and T. Matsumoto, *J. Sci. Hiroshima Univ., Ser. A-II*, **28**, 47 (1964).

*** All melting points are uncorrected. The infrared spectra were measured in Nujol.

The reaction mixture was then poured into dilute hydrochloric acid. The precipitates were collected, washed with water, and recrystallized from aqueous pyridine to give VIII; m. p. 308—310°C (decomp.) (colorless needles); yield, 380 mg. It gave a green color with an alcoholic ferric chloride solution and was soluble in concentrated sulfuric acid to a green solution and in an aqueous sodium carbonate solution to a yellow solution.

Found: C, 64.55; H, 3.55. Calcd. for $C_{16}H_{10}O_6$: C, 64.43; H, 3.38%.

The diacetate was prepared by the pyridine-acetic anhydride method; m. p. 190.5—191.5°C (colorless needles). UV: $\lambda_{max}^{EtOH}$ mμ (log ε): 263 (4.31), 293 (4.14).

Found: C, 63.01; H, 3.88. Calcd. for $C_{20}H_{14}O_8$: C, 62.83; H, 3.69%.

**6-Hydroxy-7-methoxy-3′, 4′-methylenedioxyisoflavone (IX).** — From the ketone VI (1.2 g.), ethyl orthoformate (3.0 ml.), dry pyridine (4.0 ml.) and piperidine (1.0 ml.), synthesis was carried out by a method similar to that used for I. Recrystallization from aqueous pyridine yielded IX; m. p. 250—252°C (colorless needles); yield, 0.5 g. It gave a negative color with an alcoholic ferric chloride solution and was soluble in concentrated sulfuric acid to a green solution.

Found: C, 65.05; H, 3.88. Calcd. for $C_{17}H_{12}O_6$: C, 65.38; H, 3.87%.

**6, 7-Dimethoxy-3′, 4′-methylenedioxyisoflavone (X).**—*From IX.* — A mixture of the isoflavone IX (200 mg.), anhydrous potassium carbonate (5.0 g.) and dimethyl sulfate (0.2 ml.) in dry acetone (100 ml.) was refluxed for 20 hr. The product was recrystallized from aqueous acetic acid to give X; m. p. 237—238°C (colorless needles); yield, 170 mg. It was soluble in concentrated sulfuric acid to a green solution. IR: 1644 (C=O), 1033 (=C-O-C), 926 $cm^{-1}$ (O-$CH_2$-O).

Found: C, 66.34; H, 4.60. Calcd. for $C_{18}H_{14}O_6$: C, 66.25; H, 4.32%.

*From VIII.* — A mixture of the isoflavone VIII (100 mg.), anhydrous potassium carbonate (5.0 g.) and dimethyl sulfate (0.2 ml.) in dry acetone (100 ml.) was treated in a method similar to that used above. Recrystallization from aqueous acetic acid yielded X; m. p. 236—237°C (colorless needles). This substance was identified with the above sample by mixed fusion and a comparison of the infrared spectra.

*From VII.*—A mixture of the ketone VII (0.9 g.), ethyl orthoformate (3.0 ml.), pyridine (4.0 ml.) and piperidine (0.5 ml.) was treated in a method similar to that used for I. Recrystallization from acetone yielded X; m. p. 237—238°C (colorless needles); yield, 0.3 g. This was identical with the above sample.

**6, 7-Diacetoxy-3′, 4′-methylenedioxy-2-methylisoflavone (XII).** — A mixture of the ketone V (4.0 g.) and anhydrous sodium acetate (7.0 g.) in acetic anhydride (70 ml.) was refluxed for 16 hr., and then the excess acetic anhydride was removed in vacuo. The residue was washed with water and recrystallized from methanol to give XII; m. p. 146—147°C (colorless needles); yield, 4.2 g..

Found: C, 63.77; H, 4.27. Calcd. for $C_{21}H_{16}O_8$: C, 63.63; H, 4.07%.

**6,7-Dihydroxy-3′,4′-methylenedioxy-2-methylisoflavone (XIII).**—A mixture of the diacetate XII (3.8 g.), sodium hydroxide (1.2 g.), water (5.0 ml.) and methanol (80 ml.) was refluxed for 30 min.

After the solvent had been distilled off in vacuo, the residue was dissolved into water and the solution was acidified. The precipitates were collected, washed with water, and then recrystallized from ethanol to give XIII; m. p. 293—294°C (colorless needles); yield, 2.8 g. It gave a green color with an alcoholic ferric chloride solution and was soluble in aqueous sodium carbonate to a yellow solution.

Found: C, 65.14; H, 4.07. Calcd. for $C_{17}H_{12}O_6$: C, 65.38; H, 3.87%.

**6,7 : 3′,4′-Bismethylenedioxy-2-methylisoflavone (XI).**—*From IV.*—From a mixture of the ketone IV (600 mg.) and anhydrous sodium acetate (0.8 g.) in acetic anhydride (10 ml.), synthesis was carried out by a method similar to that used for XII. Recrystallization from aqueous acetic acid gave XI; m. p. 219—220°C (colorless needles); yield, 450 mg.. It was soluble in concentrated sulfuric acid to a green solution. IR: 1637(C=O), 1037 (=C-O-C), 934 $cm^{-1}$ (O-$CH_2$-O).

Found: C, 66.59; H, 3.70. Calcd. for $C_{18}H_{12}O_6$: C, 66.67; H, 3.73%.

*From XIII.* — From a mixture of the isoflavone XIII (1.0 g.), potassium hydroxide (680 mg.), ethanol (10 ml.), water (10 ml.) and methylene sulfate (650 mg.) in acetone (15 ml.), synthesis was carried out by a method similar to that used for IV. The product was recrystallized from aqueous acetic acid to give XI; m. p. 218—219°C (colorless needles); yield, 160 mg. It was identified with the above sample by mixed fusion and a comparison of the infrared spectra.

**6-Acetoxy-7-methoxy-3′, 4′-methylenedioxy-2-methylisoflavone (XIV).** — From the ketone VI (1.8 g.), anhydrous sodium acetate (5.0 g.) and acetic anhydride (50 ml.), synthesis was carried out by a method similar to that used for XII. Recrystallization from aqueous acetone gave XIV; m. p. 217—218°C (colorless needles); yield, 1.6 g.

Found: C, 65.17; H, 4.36. Calcd. for $C_{20}H_{16}O_7$: C, 65.21; H, 4.38%.

**6-Hydroxy-7-methoxy-3′,4′-methylenedioxy-2-methylisoflavone (XV).**—From the isoflavone XIV (1.1 g.), sodium hydroxide (0.5 g.), water (5.0 ml.) and ethanol (100 ml.), reaction was carried out by a method similar to that used for XIII. Recrystallization from aqueous pyridine gave XV; m. p. 244—245°C (colorless prisms); yield, 0.9 g. It was soluble in concentrated sulfuric acid to a green solution.

Found: C, 66.10; H, 4.39. Calcd. for $C_{18}H_{14}O_6$: C, 66.25; H, 4.32%.

**6,7-Dimethoxy-3′,4′-methylenedioxy-2-methylisoflavone (XVI).**—*From XIII.*—A mixture of the isoflavone XIII (2.0 g.), anhydrous potassium carbonate (15.0 g.), dimethyl sulfate (4.0 ml.) and dry acetone (190 ml.) was treated by a method similar to that used for VII. Recrystallization from ethanol gave XVI; m. p. 214.5—215°C (colorless microneedles); yield, 2.1 g. IR: 1639

(C=O), 1026 (=C-O-C), 921 $cm^{-1}$ (O-$CH_2$-O).

Found: C, 67.02; H, 4.51. Calcd. for $C_{19}H_{16}O_6$: C, 67.05; H, 4.75%.

*From XV.* — The methylation of isoflavone XV (470 mg.) was carried out by the same procedure; yield, 430 mg.

A mixture of the isoflavone XVI (1.5 g.), sodium hydroxide (1.5 g.), water (10 ml.) and ethanol (150 ml.) was refluxed for 2 hr. under the stream of nitrogen. After the solvent had been removed in vacuo, the residue was dissolved in water and the solution was acidified. The precipitates were collected, washed with water, and recrystallized from aqueous acetone to give colorless plates; m. p. 153—154°C; yield, 1.3 g. This substance was identified with VII by mixed fusion and a comparison of the infrared spectra.

The authors are grateful to the members of the Microanalytical Laboratory, Faculty of Pharmacy, Nagasaki University, for their microanalyses. This work was supported in part by a grant-in-aid from the Ministry of Education.

*Department of Chemistry*
*Faculty of Science*
*Hiroshima University*
*Higashi-sendamachi, Hiroshima*

# Gamma-ray Spectrometry in Radioactivation Analysis with 14 MeV. Neutrons

By Yuzuru KUSAKA, Haruo TSUJI, Isao FUJII, Haruo MUTO and Katsuhiko MIYOSHI

(Received July 25, 1964)

A commercial small-type neutron generator producing 14 MeV. neutrons is becoming popular as a neutron source for the radioactivation analysis of various elements.[1-4] For the practical application of such a neutron generator, however, it is important to determine the analytical sensitivities of various elements under definite experimental conditions. Kusaka et al. reported some experimental results on analytical sensitivities obtained by a gross gamma-ray counting method for the induced radioactivities.[5]

This paper will describe the experimental results concerning the sensitivity obtained by gamma ray spectrometry and will show the gamma ray spectra of 37 elements. All the data are normalized to definite experimental conditions so that they can be compared with each other.

## Experimental

**Neutron Source.** — Monochromatic 14 MeV. neutrons were produced by T-d reaction in a Toshiba Neutron Generator, Model NT-20, in which a thin tritiated titanium target (4 curies; Isotope Div., Harwell, England) was bombarded with a deuteron beam of about 100 $\mu$amp. and 150 to 200 KeV. A target assembly with a sample station for neutron irradiation, similar to that described by Fujii et al.,[3] was used.

The neutron output during the irradiation of a sample was kept constant as far as possible by regulating the accelerating or extraction voltage in the generator. The output was continuously recorded by a plastic neutron scintillator which was set at a definite position below the drift tube of the generator and which was then connected to a counting-rate meter set near the operator. The absolute value of the neutron flux at the irradiation position was determined by the method of activating copper foil, the beta activity of which was measured by a $4\pi$ gas-flow counter using Q gas.

**The Sample Transfer System and Neutron Irradiation.** — Samples were packed tightly in cylindrical polyethylene containers (4.5 cm. long, 1.3 cm. i. d., 0.1 cm. thick). These "bunny" capsules were then transferred through a pneumatic tube system, operated by a vacuum cleaner blower (500 W.), between the irradiation position and the radioactivity detector. At the end of 10.0 min. of irradiation, the sample transfer system was turned on to bring the sample capsule back to the well of the scintillation detector. The average travel time of the capsule was 3.0 sec.

**Radioactivity Measurement.** — The radioactivity of the sample was measured by a shielded well-type sodium iodide scintillation detector (Harshow; 4.45

1) W. W. Meinke and R. W. Shideler, *Nucleonics*, **20**, No. 3, 60 (1962).
2) I. Fujii, H. Muto, K. Ogawa and A. Tani, *J. Atomic Energy Soc. Japan*, **5**, 455 (1963).
3) I. Fujii, H. Muto and K. Miyoshi, *Japan Analyst*, **13**, 249 (1964).
4) J. Wing, *Anal. Chem.*, **36**, 559 (1964).
5) Y. Kusaka, H. Tsuji and T. Adachi, This Bulletin, **36**, 1259 (1963).

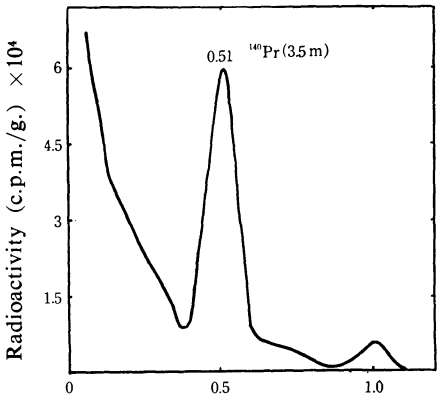



Fig. 1. Praseodymium.

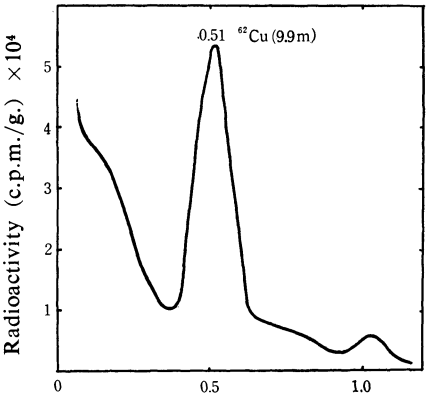



Fig. 2. Copper.

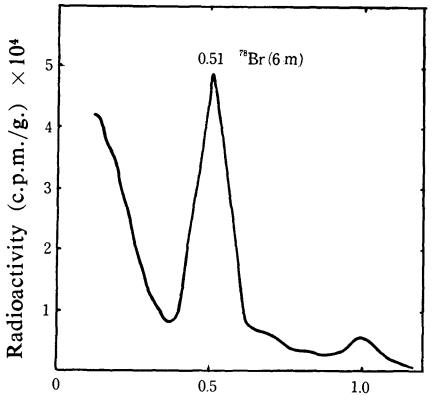



Fig. 3. Bromine.

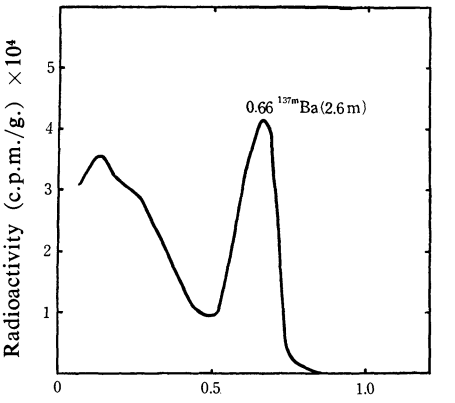



Fig. 4. Barium.

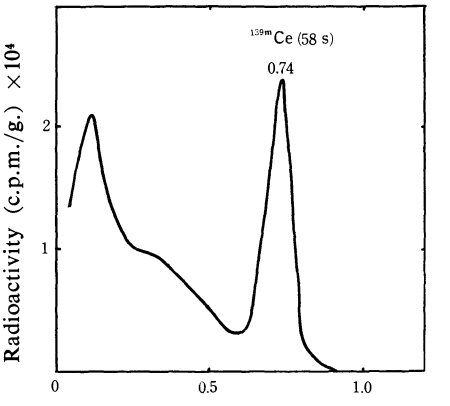



Fig. 5. Cerium.

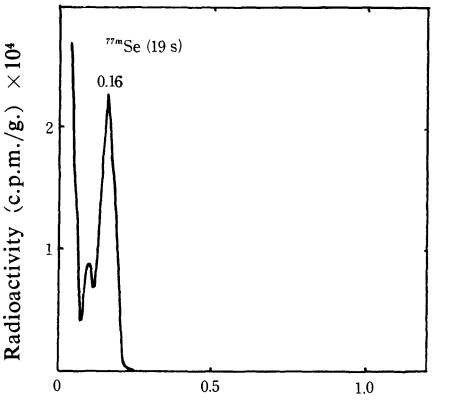
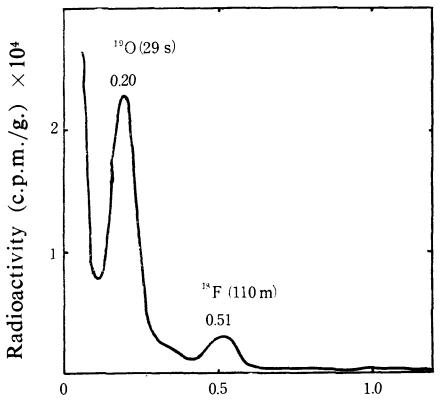
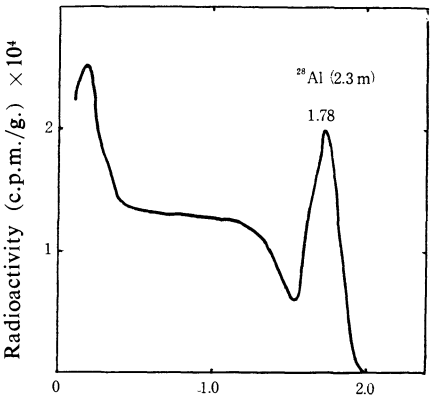



Fig. 6. Selenium.



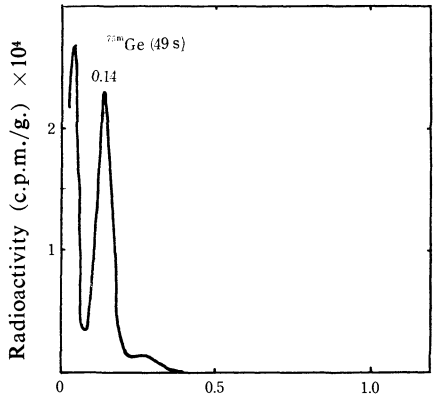

Energy, MeV.

Fig. 7. Fluorine.



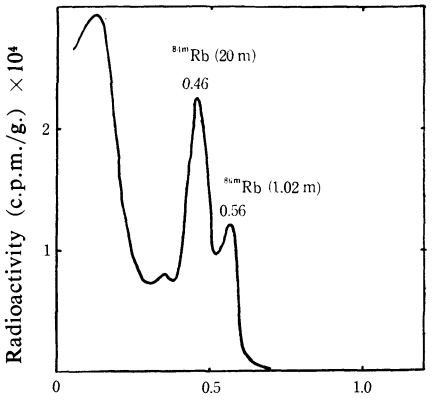

Energy, MeV.

Fig. 8. Silicon.



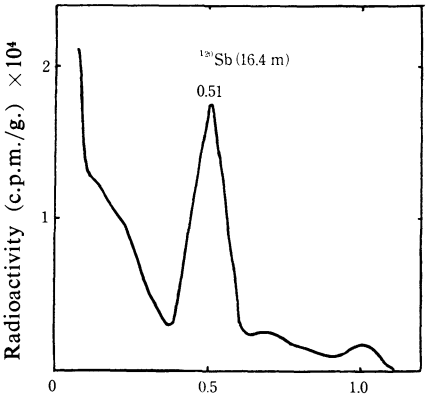

Energy, MeV.

Fig. 9. Germanium.



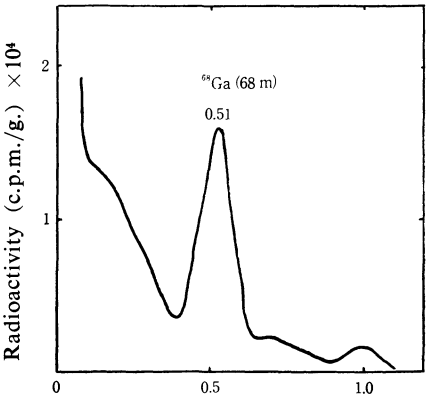

Energy, MeV.

Fig. 10. Rubidium.




Energy, MeV.

Fig. 11. Antimony.




Energy, MeV.

Fig. 12. Gallium.

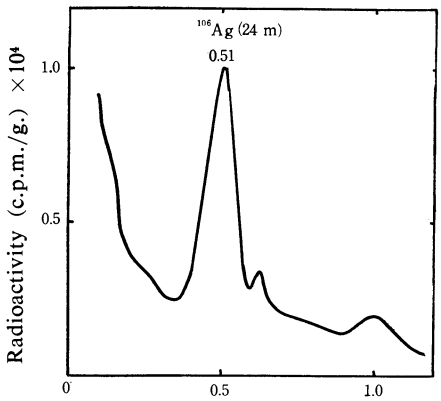



Fig. 13. Silver.

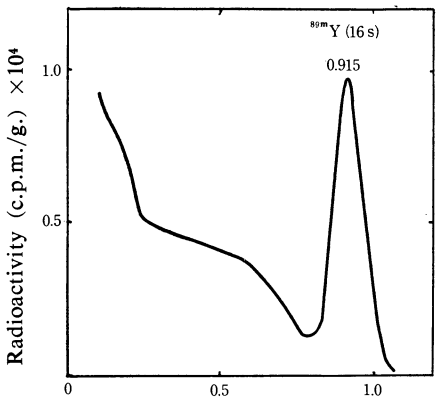



Fig. 14. Yttrium.

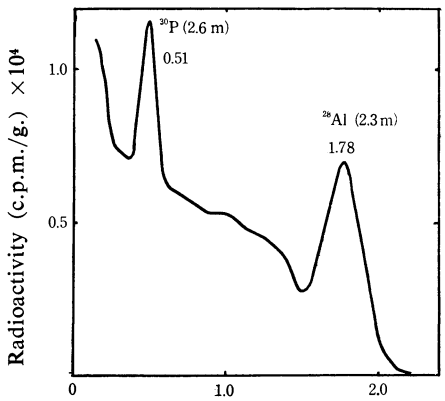



Fig. 15. Phosphorus.

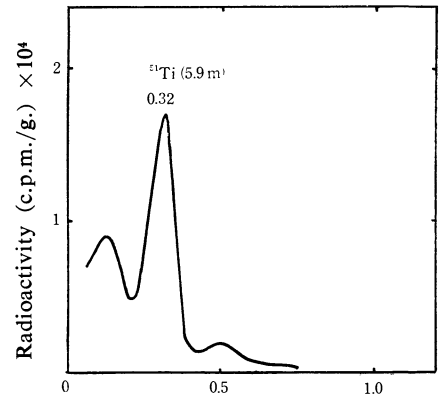



Fig. 16. Vanadium.

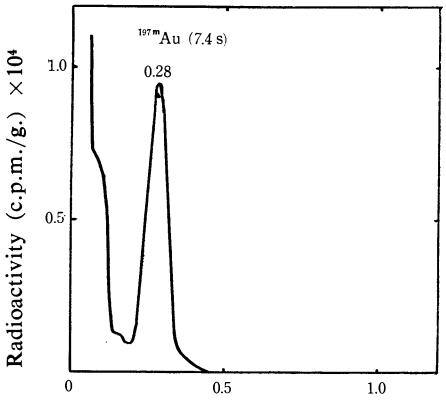



Fig. 17. Gold.

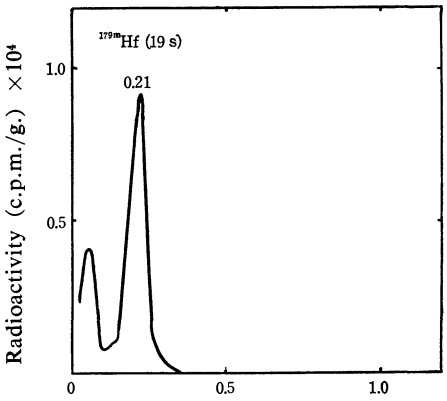



Fig. 18. Hafnium.

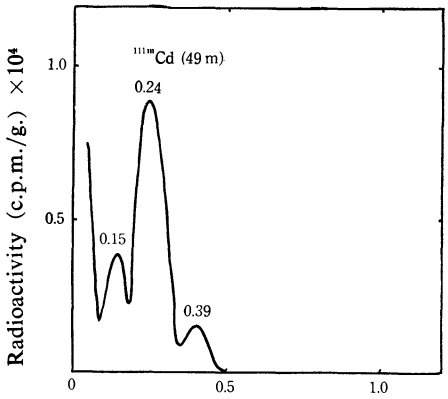



Fig. 19. Cadmium.

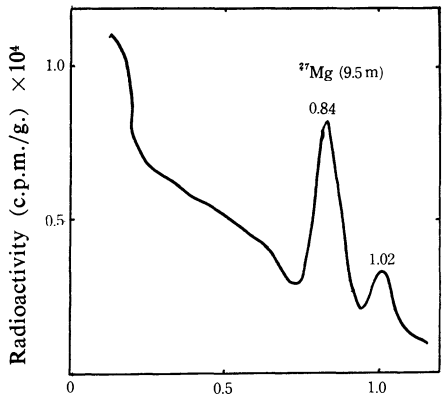



Fig. 20. Aluminum.

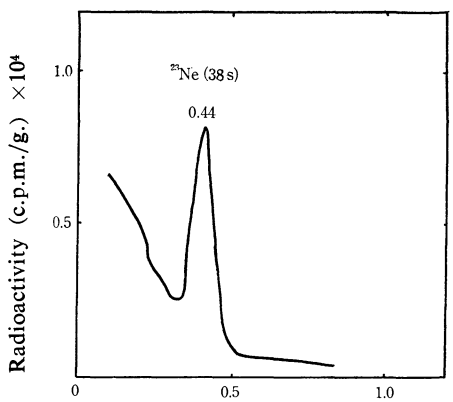



Fig. 21. Sodium.

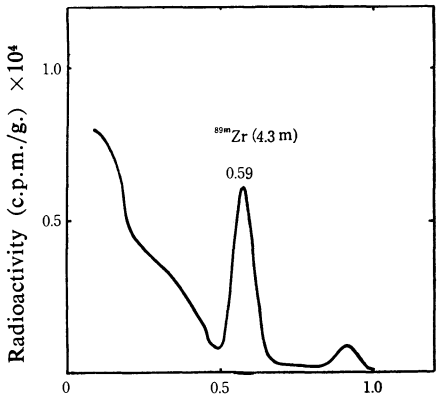



Fig. 22. Zirconium.

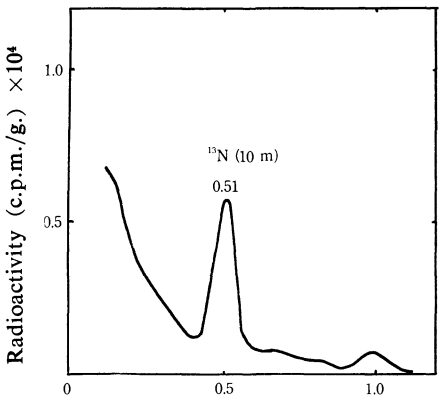



Fig. 23. Nitrogen.

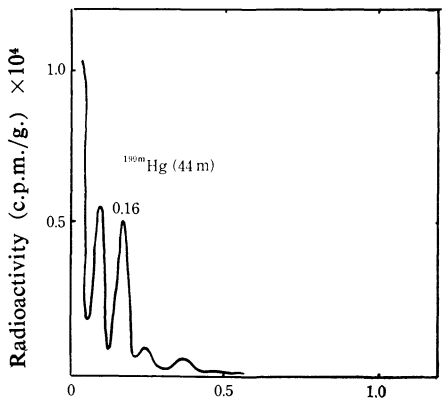



Fig. 24. Mercury

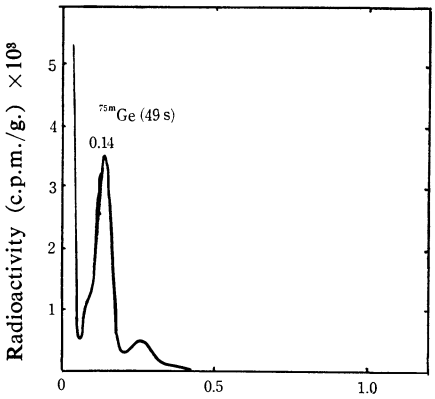



Fig. 25. Arsenic.

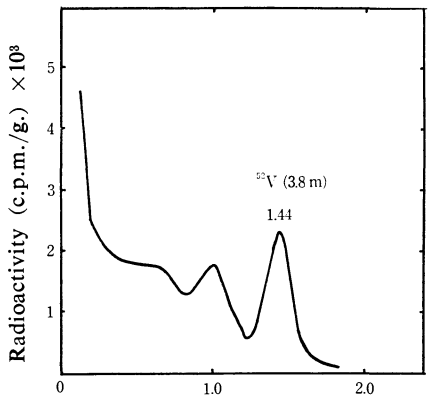



Fig. 26. Chromium.

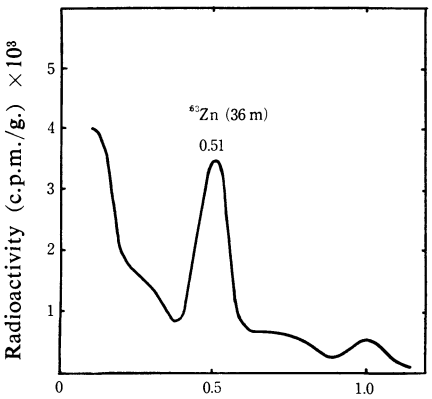



Fig. 27. Zinc.

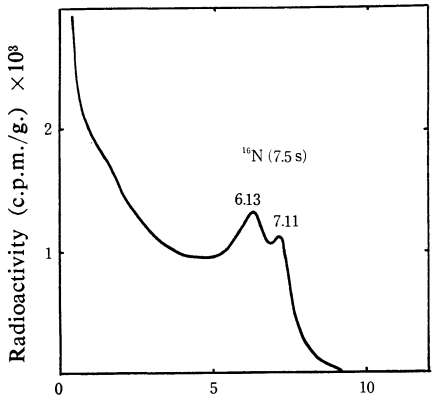



Fig. 28. Oxygen.

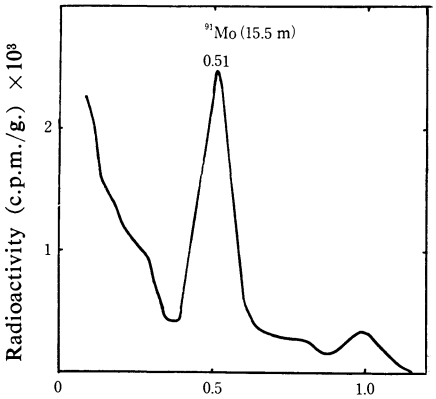



Fig. 29. Molybdenum.

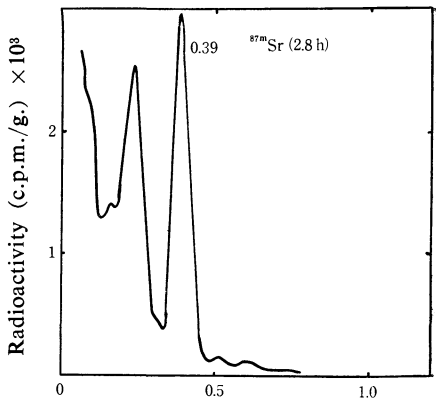



Fig. 30. Strontium.

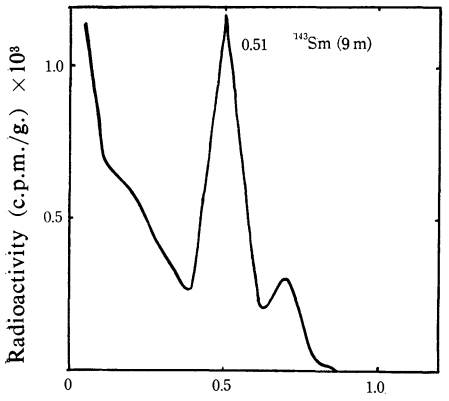



Fig. 31. Samarium.

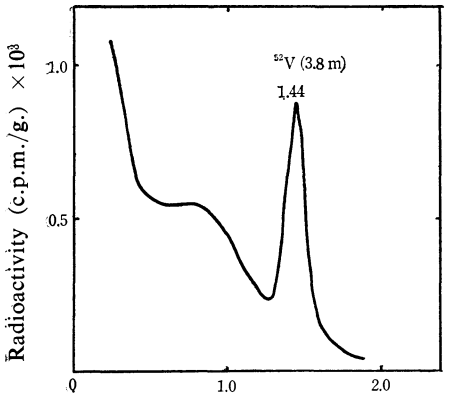



Fig. 32. Manganese.

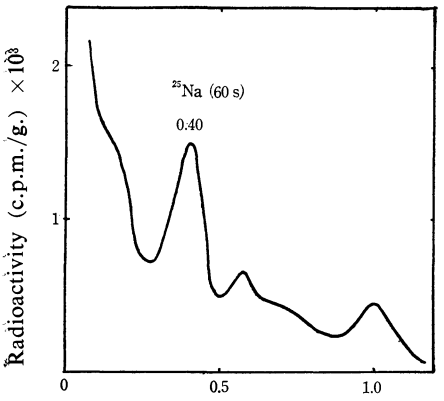



Fig. 33. Magnesium.

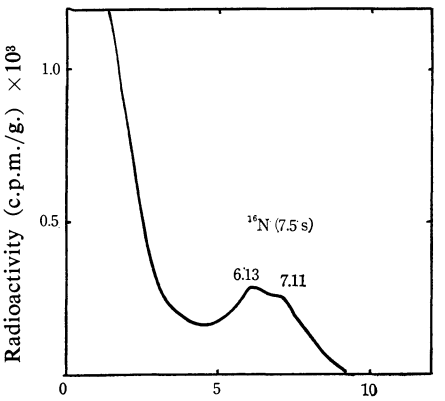



Fig. 34. Fluorine.

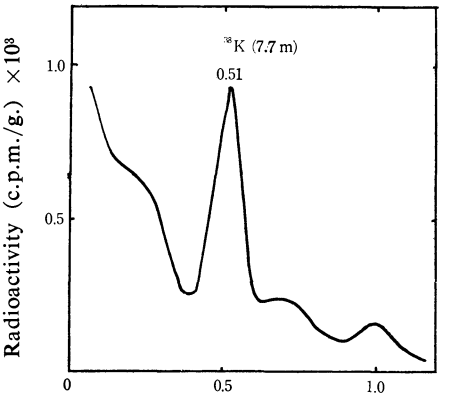



Fig. 35. Potassium.

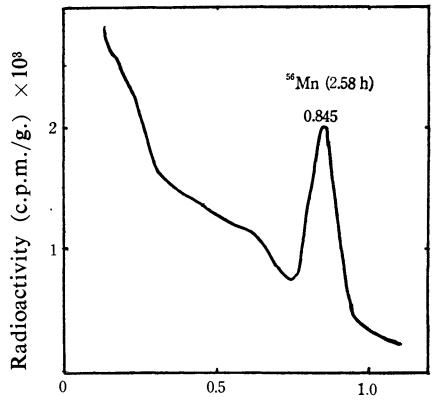



Fig. 36. Iron.

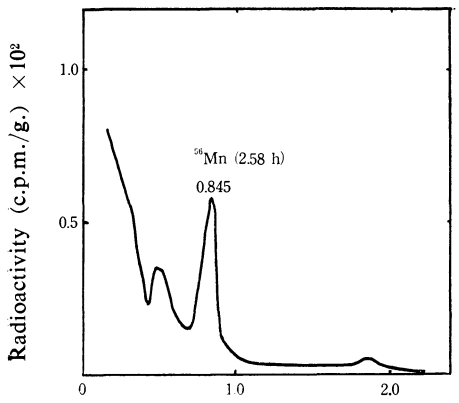



Fig. 37. Cobalt.

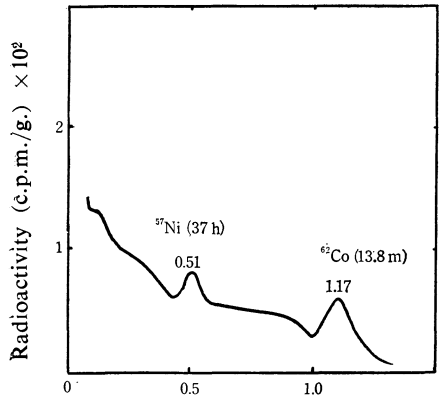



Fig. 38. Nickel.

cm. diameter, 5.08 cm. height, well: 1.91 cm. diameter, 3.81 cm. deep) mounted on a photomultiplier tube (Toshiba-7696) and connected in turn to a Toshiba 128 channel pulse-height analyzer. The resolution of the detector for 0.662 MeV. $^{137}Cs$ gammas was about 12%.

The countings were started 5.0 sec. after irradiation and were stored for 1.0 min. However, the samples containing oxygen were started after 1.0 min., it being necessary to eliminate the influence of the $^{16}N$ produced by the (n, p) reaction on oxygen.

Using the mean value of neutron flux observed during the irradiation, the counting data obtained were normalized to a standard neutron flux of $1.0 \times 10^7$ neutrons per $cm^2$ per sec.

**Irradiation Sample.**—Inside the "bunny" capsule definite amounts of the sample powder mixed with pure carbon powder were packed in a definite volume (1.3 cm. diameter, 2.0 cm. long).

The chemical forms of the samples were as follows: the elements of silver, aluminum, gold, calcium, cadmium, cobalt, chromium, copper, iron, germanium, hafnium, indium, lead, magnesium, manganese, molybdenum, nickel, phosphorus, sulfur, antimony, selenium, silicon, tantalum, tin, titanium, tungsten, zinc and zirconium; the oxides of arsenic, cerium, dysprosium, gallium, gadolinium, erbium, holmium, mercury, lanthanum, praseodymium, samarium, vanadium, yttrium and ytterbium; the carbonates of potassium, sodium and rubidium; the acetates of barium and strontium; fluorine as polytetrafluoroethylene; bromine as dibromobenzene; chlorine as benzene hexachloride; nitrogen as ammonium nitrate, and oxygen as oxalic acid.

## Results

**The Gamma-ray Spectra of the Radioactive Nuclides Produced by 14 MeV. Neutron Reaction.**—The spectra obtained for each element were compared under normalized conditions; weight of sample: 1.0 g. as element; irradiation time: 10.0 min.; neutron flux: $1.0 \times 10^7$ neutrons per $cm^2$ per sec.; counting time: 1.0 min. from the end of irradiation. The results are shown in Figs. 1—38, in which the photopeaks available for the activation analysis are marked with the energies and the nuclides produced. The figures are arranged in the order of the magnitude of the photopeak area, that is, of the sensitivity of the activation analysis.

In the cases of sulfur, chlorine, calcium, titanium, indium, tin, lanthanum, gadolinium, dysprosium, holmium, erbium, ytterbium, and tantalum, no photopeaks usable for the effective activation analysis appeared in the experiments.

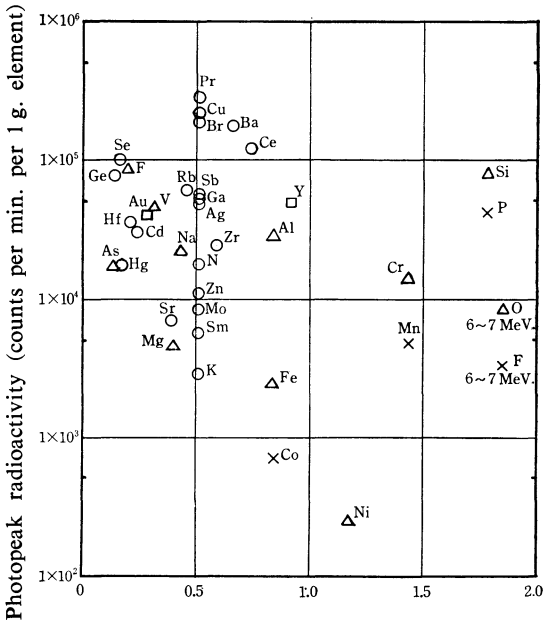



Fig. 39. Sensitivity of gamma-ray spectrometry in 14 MeV. neutron activation analysis.
○: $(n, 2n)$ reaction ×: $(n, \alpha)$ reaction
△: $(n, p)$ reaction □: $(n, n')$ reaction

**The Sensitivity of Gamma-Ray Spectrometry.** —The sensitivity of the analysis can be expressed with the photopeak radioactivity strength, which is obtained by drawing a straight line across the bottom of the peak in the spectrum and by summing up the counts above the line. The values for each element have been summarized in a graphic form and are shown in Fig. 39, in which the photopeak activity is marked with the target element and the kind of the nuclear reaction is plotted against the gamma-ray energy.

It may be possible to improve the sensitivities by using such things as more sensitive detectors, but these plots can give a general impression of the relative sensitivities in the 14 MeV. neutron activation analysis.

The authors wish to thank Dr. Kazunori Yuasa, Mr. Bunzaburo Saeki and Mr. Yoshinao Fujiwara of the Department of Physics, Konan University, for their kind and valuable advice through this study.

*Department of Chemistry*
*Faculty of Science*
*Konan University*
*Higashinada-ku, Kobe*
*(Y. K. & H. T.)*

*Atomic Energy Department*
*Central Research Laboratory*
*Tokyo Shibaura Electric Co., Ltd.*
*Kawasaki*
*(I. F., H. M. & K. M.)*

# The Spectrophotometric Determination of Gallium(III) with Xylenol Orange[1]

By Makoto Otomo*

(Received October 21, 1964)

The color reaction between gallium(III) and xylenol orange [bis-di(carboxymethyl)-aminomethyl-*o*-cresolsulfonephthalein] was first studied by Přibil and Kopanica,[2] who used the reagent for the detection of traces of gallium in the presence of ammonium fluoride and triethanolamine, which served as masking agents for other metal cations. The quantitative determination of gallium based on this reaction has not yet, however, been reported by any workers. It has only been disclosed that, depending on the pH value of the solution, gallium(III) reacts with xylenol orange to form two complexes, with metal-ligand ratios of 1 to 1 and 1 to 2. These reactions are applicable to the spectrophotometric determination of up to 60 $\mu$g. of gallium in 25 ml.

## Experimental

**Reagents.**—*Standard Gallium Solution.*—A standard gallium(III) solution was prepared by dissolving 0.6980 g. of pure gallium metal (99.999% pure) in dilute sulfuric acid and then diluting it with water to 1 l. The concentration of sulfuric acid in this solution was about 0.05 M. Working solutions of gallium were prepared by diluting the standard solution with water.

*Xylenol Orange Solution.*—A $1 \times 10^{-3}$ M xylenol orange solution was prepared by dissolving the Dotite XO reagent (disodium salt), which was used without further purification, in distilled water.

Nitric acid or a mixture of 0.5 M acetic acid and a 0.5 M sodium acetate solution was used for the regulation of the pH value. The former was used for pH values below 2, and the latter for pH values above 2.5. Solutions of diverse ions were prepared by dissolving the respective compounds (all reagent-grade chemicals) in distilled water in appropriate concentrations.

**Apparatus.**—A Hitachi spectrophotometer, model EPV-2, was employed, with 1 cm. cells, for all the absorbance measurements. A Shimadzu glass-electrode pH meter, model GU-1, was employed for all the pH determinations.

**The Standard Procedure for the Determination.**—To a sample solution containing gallium in a 50-ml. Erlenmeyer flask, a desired amount of nitric acid or 5 ml. of the acetate buffer, a given amount of the xylenol orange solution and a small amount of water were added to make the solution about 20 ml. when the sample solution contained aluminum(III), thorium(IV) or zirconium(IV), about 60 $\mu$mol. of potassium fluoride was added before the addition of the xylenol orange solution. The solution was heated in a boiling water bath for a few minutes, cooled with running water, transferred

* Present address: Hachinohe Technical College, Hachinohe, Aomori.

1) This work was presented in part at the 15th Annual Meeting of the Chemical Society of Japan, Kyoto, April, 1962.

2) R. Přibil and M. Kopanica, *Microchim. Acta*, **1962**, 29; *Chem. Abstr.*, **56**, 13530 (1962).

to a 25 ml. volumetric flask and diluted with water to the mark. The resulting solution was kept for about 30 min. in a thermostat at 25 ± 0.5°C. The absorbance of the solution was then measured at the given wavelengths.

## Results and Discussion

**Absorption Curves.**—The visual absorption curves of the gallium - xylenol orange mixture at different pH values are shown in Figs. 1 and 2. These curves were obtained by measuring the absorbance of the colored solutions containing 34.9 μg. of gallium against a reagent blank containing the same amount of xylenol orange. Between pH 0.9 and 1.4, the solutions give identical absorption curves, with one absorption maximum at 530 mμ. Above pH 2, the position of the maximum absorption shifts toward shorter wavelengths with an increase in the pH value. The curves obtained at pH 2.0 and 2.5 have a shoulder at about 545 mμ. Between pH 3.0 and 5.5, however, the solutions again give identical absorption curves, with one absorption maximum at 502 mμ. The slight blue shift in the position of the absorption maximum which was observed at pH 6.1 seems to be caused by the contribution of the absorption by the reagent blank, which absorbs strongly in the wavelength range from 510 to 600 mμ and which decreases its absorbance at shorter wavelengths over pH 6.0. Therefore, it may be concluded that, in the presence of an excess of xylenol orange, two complexes are formed between gallium and xylenol orange.

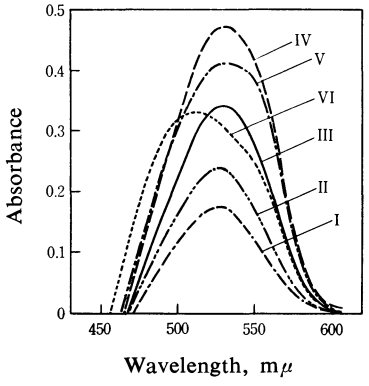



Fig. 1. Absorption curves of Ga-XO in the pH value range from 0.9 to 2.5.
Ga: $2.0\times10^{-5}$ M (34.9 μg.), XO: $1.57\times10^{-4}$ M
Reference: a reagent blank, pH: I, 0.9; II, 1.0; III, 1.1; IV, 1.4; V, 2.0; VI, 2.5

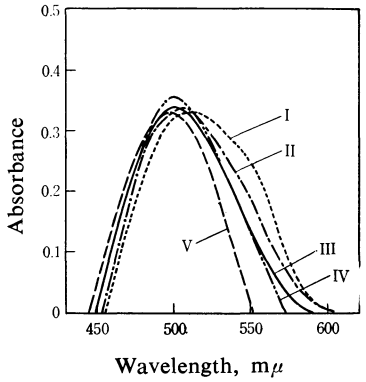



Fig. 2. Absorption curves of Ga-XO in the pH value range from 2.5 to 6.1.
Ga: $2.0\times10^{-5}$ M (34.9 μg.), XO: $1.56\times10^{-4}$ M
Reference: a reagent blank
pH: I, 2.5; II, 3.0; III, 4.5; IV, 5.0—5.5; V, 6.1

**The Effect of pH.**—The effect of pH on the absorbance of the solution was examined by measuring, at two wavelengths, 530 and 502 mμ, the absorbance of a solution containing 34.9 μg. of gallium and 4 ml. of a $1\times10^{-3}$ M solution of xylenol orange. From the curves shown in Fig. 3, it was found that the maximum absorbance is obtained in the pH value range from 1.2 to 1.7 when measured at 530 mμ and from 4.5 to 5.5 when measured at 502 mμ.

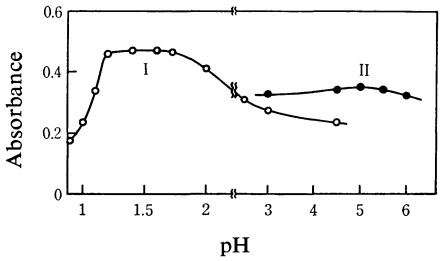



Fig. 3. Effect of pH on absorbance of the complexes at their absorption maxima.
Ga: 34.9 μg., XO: $1.57\times10^{-4}$ M
Reference: a reagent blank
I: at 530 mμ, II: at 502 mμ

**The Effect of the Amount of Xylenol Orange.**—The effect of the reagent concentration was studied with solutions containing a given amount of gallium and varying amounts of a

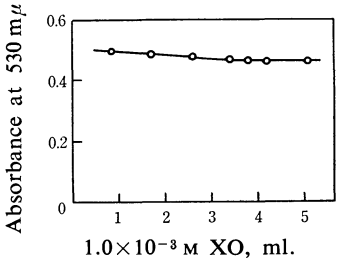



Fig. 4. Effect of amount of XO.
Ga: 34.9 μg., pH: 1.5
Reference: a reagent blank

$1 \times 10^{-3}$ M solution of xylenol orange. The pH values of the solutions were kept constant at 1.5, and the absorbance measurements were carried out at 530 mμ. The results are shown in Fig. 4. A constant absorbance is obtained when 3.5 to 5 ml. of the reagent solution is used. Therefore, 4 ml. of the reagent solution was used in further experiments.

**The Stability of the Color.**—The color formation does not occur instantaneously at room temperature. However, it is greatly accerelated by heating; the maximum color development is attained within only a few minutes when the mixture is heated in a boiling water bath. The absorbance remains almost constant for at least 6 hr. after preparation at pH 1.5 and for about 1.5 hr. when prepared at pH 5.5.

**Calibration Curves for the Gallium Determination.**—The calibration curves for the gallium determination were prepared in the manner described above with solutions containing no fluoride or 60 μmol. of fluoride. In all three curves shown in Fig. 5, linear relationships between absorbance and concentration are found to hold up to 60 μg. of gallium in 25 ml.

The apparent molar extinction coefficients of the two complexes, which were calculated from curves I and III, were found to be 22900 and 16300 respectively. According to Sandell's notation,[3] the sensitivities of the reactions are 0.003 μg. of gallium per $cm^2$ at 530 mμ and 0.004 μg. of gallium per $cm^2$ at 502 mμ.

**The Effect of Diverse Ions.**—The effect of diverse ions on the determination of gallium was then examined with the complex formed at pH 1.5, and the tolerance limit was calculated in each case. The tolerance limit was tentatively defined as the concentration of the foreign ion which affects the absorbance of the system by less than ± 3%. The results are summarized in Table I, from which it may be seen that bismuth(III), iron(III), thorium(IV) and ethylenediaminetetraacetic acid(EDTA)

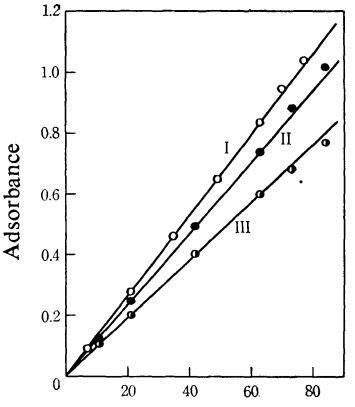



Fig. 5. Calibration curves.

I: in the absence of fluoride; pH: 1.5, 530 mμ
II: in the presence of 60 μmol. of fluoride; pH: 1.5; 530 mμ
III: pH: 5.5; 502 mμ

Table I. Effect of diverse ions
Ga taken: 34.9 μg.

| Diverse ion | μmol. | Relative error % | Tolerance limit μmol. |
|---|---|---|---|
| Al(III) | 0.5 | + 5.7 | 0.25 |
| | 0.5* | − 1.2 | 1.2 |
| Bi(III) | 0.5 | +90.4 | 0 |
| Cd(II) | 0.5 | − 0.4 | large excess |
| Ce(III) | 0.5 | ± 0.0 | large excess |
| Co(II) | 0.5 | + 0.4 | large excess |
| Cr(III) | 0.5 | + 0.9 | 1.1 |
| Cu(II) | 0.5 | + 1.8 | 0.8 |
| Fe(III) | 0.5 | +20.6 | 0.08 |
| | 1.0** | − 0.5 | large excess |
| Hg(II) | 0.5 | − 0.2 | large excess |
| Mn(II) | 0.5 | ± 0.0 | large excess |
| Ni(II) | 0.5 | ± 0.4 | large excess |
| Pb(II) | 0.5 | + 0.7 | 2.1 |
| Pd(II) | 0.5 | + 3.1 | 0.5 |
| | 1.0** | − 1.0 | large excess |
| Th(IV) | 0.5 | +77.6 | 0 |
| | 0.5* | + 0.2 | |
| | 1.0* | +37.7 | |
| Ti(IV) | 0.5 | + 1.3 | 1.2 |
| Tl(III) | 2.0** | − 0.2 | large excess |
| U(VI) | 0.5 | + 0.4 | large excess |
| V(IV) | 0.5 | + 4.6 | 0.3 |
| | 2.0*** | − 0.5 | large excess |
| Zn(II) | 0.5 | ± 0.0 | large excess |
| Zr(IV) | 0.5 | +11.0 | 0.1 |
| | 0.5* | + 5.6 | 0.3 |
| $F^-$ | 10 | − 2.9 | |
| | 25 | − 5.7 | 10 |
| | 100 | −19.3 | |
| $Cl^-$ | 500 | − 0.2 | large excess |
| $SO_4^{2-}$ | 500 | − 7.2 | 200 |
| $C_2O_4^{2-}$ | 0.5 | −12.9 | 0.1 |
| | 2.0 | −36.4 | |
| $C_4H_4O_6^{2-}$ | 50 | − 1.8 | 90 |
| | 100 | − 3.5 | |
| $C_6H_5O_7^{3-}$ | 5 | − 0.2 | >20 |
| | 20 | − 0.4 | |
| $PO_4^{3-}$ | 20 | − 1.5 | 60 |
| | 100 | − 5.0 | |
| NTA | 0.2 | −27.6 | 0 |
| | 0.5 | −56.8 | |
| EDTA | 0.1 | −20.0 | 0 |
| | 0.2 | −37.3 | |

* 60 μmol. of $F^-$ added.
** 60 μmol. of $F^-$ and 1 ml. of 5% ascorbic acid added.
*** 60 μmol. of $F^-$ and 2 drops of 3% $H_2O_2$ added.

3) E. B. Sandell, "Colorimetric Determination of Traces of Metals," 2nd Ed., Interscience Publishers, New York (1950), p. 49.

interfere in even the smallest concentrations examined, but that some interfering cations, including aluminum(III), thorium(IV) and zirconium(IV), are partly masked by adding 60 $\mu$mol. of potassium fluoride. The interference of iron(III), palladium(II) and thallium(III) can be eliminated by the addition of such a reducing agent as ascorbic acid or sodium sulfite.

**Comparison with Other Methods.**—Some sensitive reagents, including rhodamine B,[4] 5,7-dichloro-8-oxine,[5] 2-(2-hydroxy-3-chloro-5-nitrophenylazo)-1-hydroxy-8-aminonaphthalene-3,6-disulfonic acid,[6] rhodamine 6G,[7] 3,4-dihydroxybenzene-4-arsonic acid (stilbazo),[8] 2,2',4'-trihydroxy-5-chloroazobenzene-3-sulfonic acid (luminogallion IREA),[9] quercetin[10] and 1-(2-pyridylazo)-2-naphthol[11] (PAN) have been used for the determination of gallium. These reagents, except stilbazo and PAN, have been used as spectrofluorometric reagents for gallium. Of the reagents which react with gallium to form water-soluble complexes, stilbazo is found to be the most sensitive to gallium. The present method using xylenol orange is very sensitive and is comparable with the stilbazo or the luminogallion IREA method in sensitivity.

**The Compositions of the Complexes.**—The compositions of the two complexes were determined by the following two methods. The method developed by Frank and Oswalt[12] and by Furman and Garner[13] was employed for determining the composition of the complex with an absorption maximum at 530 m$\mu$, and the competing equilibrium method was employed for determining that with an absorption maximum at 502 m$\mu$.

**The Complex with Its Absorption Maximum at 530 m$\mu$.**—An attempt to discover the composition was made with solutions with a given molar concentration of gallium at a given pH value, but with varying xylenol orange concentrations. If only a 1 to 1 complex is formed under certain conditions, and the absorbance, $D$, is measured against a reagent blank, the following relationship may be derived:

$$ab/D=(a+b)/(\varepsilon_C-\varepsilon_{XO})+1/K'_1(\varepsilon_C-\varepsilon_{XO}) \quad (1)$$

where $a$ and $b$ represent the total molar concentrations of gallium and xylenol orang respectively; $\varepsilon_{XO}$ and $\varepsilon_C$, the molar extinction coefficients of xylenol orange and the complex respectively, and $K'_1$, the apparent formation constant of the complex at the given pH value.

In Fig. 6 $ab/D$ is plotted against $(a+b)$ at five wavelengths between 500 and 540 m$\mu$. In these solutions, the concentration of gallium was $2.0\times10^{-5}$ M, while the concentration of xylenol orange varied from $0.8\times10^{-4}$ to $8\times10^{-4}$ M; the pH value of these solutions was held constant at 1.0. The very good linearity of the curves in Fig. 6 supports the assumptions inherent in Eq. 1, indicating that only a 1 to 1 complex is formed under the conditions investigated.

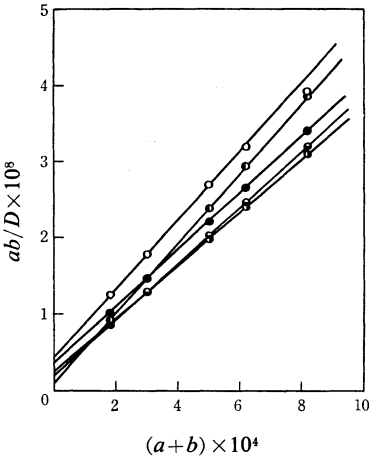



Fig. 6. Plots of $ab/D$ vs. $(a+q)$ at various wavelengths.
—○—: 500 m$\mu$, —●—: 510 m$\mu$,
—◑—: 520 m$\mu$, —◒—: 530 m$\mu$,
—◐—: 540 mu, pH: 1.0

**The Complex with Its Absorption Maximum at 502 m$\mu$.**—A substitution reaction between the complex and EDTA was used to ascertain the result obtained by the mole ratio method, which showed the presence of a 1 to 2 complex in the metal-ligand ratio. This is based on the fact that, at pH 5.5, EDTA can form a far more stable complex with gallium than does xylenol orange, and that, therefore, the xylenol orange in the gallium complex may be replaced by EDTA. A preliminary test showed that nitrilotriacetic acid (NTA) can also form a stable complex with gallium in a slightly acid medium, but it cannot extinguish the color of the gallium-xylenol orange complex at all. Therefore, it may be assumed that, in the presence of an excess of xylenol orange, the

4) H. Onishi, *Anal. Chem.*, **27**, 832 (1955).
5) A. P. Golovina and I. P. Alimarin, *Vestnik Moskov. Univ.* **12**, *Ser. Mat. Mekh., Astron., Fig., Khim.*, No. 3, 211 (1957); *Chem. Abstr.*, **52**, 4391 (1958).
6) A. M. Lukin and G. B. Zavarikhina, *Zhur. Anal. Khim.*, **13**, 66 (1958).
7) D. P. Shcherbov and A. I. Ivankova, *Zavodskaya Lab.*, **24**, 667 (1958); *Chem. Abstr.*, **54**, 10662 (1960).
8) M. Z. Yanpol'skii, *Uchenye Zapiski Kursk. Gosudarst. Pedagog. Inst.*, **1958**, No. 7, 67; *Chem. Abstr.*, **53**, 19692 (1959).
9) A. M. Lukin and E. A. Bozhevol'nov, *Zhur. Anal. Khim.*, **15**, 43 (1960); *Chem. Abstr.*, **54**, 13970 (1960).
10) I. P. Alimarin, A. P. Golovina and V. G. Torgov, *Zavodskaya Lab.*, **26**, 709 (1960); *Chem. Abstr.*, **54**, 19298 (1960).
11) T. Suzuki, *Japan Analyst*, **12**, 655 (1963).
12) H. S. Frank and R. L. Oswalt, *J. Am. Chem. Soc.*, **69**, 1321 (1947).
13) S. C. Furman and C. S. Garner, *J. Am. Chem. Soc.*, **73**, 4528 (1951).

contribution of the absorbance caused by the dissociation of the gallium-xylenol orange complex is almost negligible. When the absorbance is measured against a solution containing the same amounts of gallium and xylenol orange, Eq. 2 may be written for the substitution reaction as:

$$\{(D-D_O)+x\varepsilon_C\}/\varepsilon_{XO}=nx \qquad (2)$$

where

$$D=(a-x)\varepsilon_C+(b-na+nx)\varepsilon_{XO} \qquad (2')$$

$$D_O=a\varepsilon_C+(b-na)\varepsilon_{XO} \qquad (2'')$$

In these solutions, $a$ and $b$ are the initial concentrations of the gallium-xylenol orange complex and xylenol orange respectively, $x$ is the molar concentration of EDTA added, and $\varepsilon_C$ and $\varepsilon_{XO}$ are the molar extinction coefficients of the complex and xylenol orange respectively. If $\{(D-D_O)+x\varepsilon_C\}/\varepsilon_{XO}$ is plotted against $x$, a straight line with the slope $n$ should be yielded.

In this substitution method, the absorbances were measured by adding various amounts of a $1\times10^{-4}$ M EDTA solution to known amounts of gallium ($2.0\times10^{-5}$ M) and xylenol orange ($1.0\times10^{-4}$ M), using a blank solution containing the same amounts of gallium and xylenol orange. The pH value was held constant at 5.5. The absorbances were measured at three wavelengths, 400, 410 and 420 m$\mu$, because the difference in absorbance between xylenol orange and the reference solution was the greatest at about 410 m$\mu$. Figure 7 shows the absorption curves of xylenol orange and its gallium complex at pH 5.5 in the wavelength range from 350 to 570 m$\mu$. Curve IV in Fig. 7 is the absorption curve of the complex which is partly shown by curve IV in Fig. 2. The values of $\varepsilon_C$ were evaluated at the three wavelengths by assuming a 1 to 2 complex, employing the method described by Klotz and LohMing.[14] All the curves are good straight lines with a slope of 2. As a representative result, the values of $\{(D-D_O)+x\varepsilon_C\}/\varepsilon_{XO}$ are plotted in Fig. 8, from which it may be easily understood that a 1 to 2 complex is formed between gallium and xylenol orange.

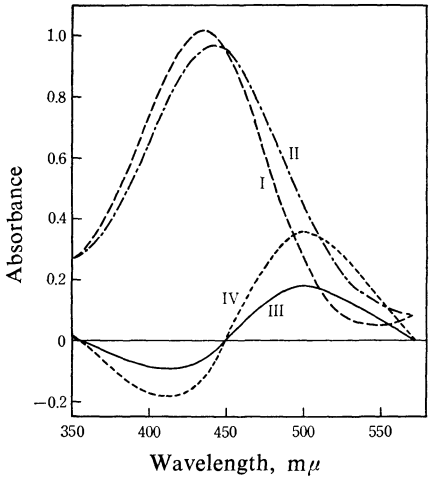



Fig. 7. Absorption curves of XO and its gallium complex at pH 5.5.
I: $0.80\times10^{-4}$ M XO vs. water
II: ($0.80\times10^{-4}$ M XO + $1.0^{-5}$ M (Ga) vs. water
III: ($0.80\times10^{-4}$ M XO + $1.0\times10^{-5}$ M (Ga) vs. reagent blank
IV: ($1.60\times10^{-4}$ M XO + $2.0\times10^{-5}$ M (Ga) vs. reagent blank

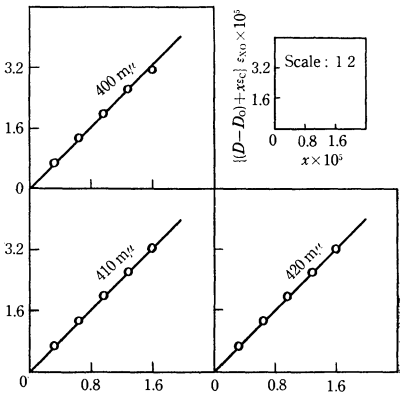



Fig. 8. Plots of $\{(D-D_o)+x\varepsilon_C\}/\varepsilon_{XO}$ vs. $x$ at various wavelengths.
Reference soln: Ga; $2\times10^{-5}$ M, XO; $1\times10^{-4}$ M, pH; 5.5

## Summary

The reaction between gallium(III) and xylenol orange has been studied spectrophotometrically in order to establish the optimum conditions for determining traces of gallium. Depending on the pH value of a solution, gallium(III) reacts with xylenol orange to form two complexes. The 1 to 1 complex which gives a maximum absorbance in the pH range from 1.2 to 1.7 has an absorption maximum at 530 m$\mu$ when measured against a reagent blank. The 1 to 2 complex which gives the maximum absorbance in the pH range from 4.5 to 5.5 has an absorption maximum at 502 m$\mu$. Either with 1 to 1 and 1 to 2 complexes, Beer's law is obeyed up to 60 m$\mu$. of gallium. The apparent molar extinction coefficients of the 1 to 1 and the 1 to 2 complexes have been calculated to be 22900 and 16300 respectively. The present method is comparable in sensitivity with the stilbazo or the luminogallion

14) I. M. Klotz and W.-C. LohMing, ibid., 75, 4159 (1953).

IREA method. The addition of a small amount of fluoride is effective in eliminating some interfering cations, including aluminum(III), thorium(IV) and zirconium(IV).

The author wishes to express his hearty thanks to Professor Kôichi Tonosaki for his kind guidance and encouragement throughout the course of this study.

*Department of Chemistry*
*Faculty of Literature and Science*
*Hirosaki University*
*Hirosaki, Aomori*

# The Behavior of Manganese, Titanium and Phosphorus in Fumarolic Gas at the Mihara Volcano, Japan

By Hiroshi KAMIYA

(Received August 1, 1964)

As was described in a previous paper,[1] the low volatile components present in rocks have really been transported in fumarolic gases, although in small amounts. Because magmatic gas cannot be collected directly, however, the behavior of the low volatile components there must be surmised from observations and analyses of minerals in ore deposits and of gases and sublimates evolved from lava and fumaroles, as well as from laboratory experiments at a high temperature and a high pressure.

From thermodynamic data, Krauskopf[2] showed that magmatic gas at 600°C is, with a few exceptions, capable of transporting the common heavy metals, such as volatile chlorides, to form an ore deposit. Morey[3,4] and Kennedy[5,6] demonstrated the strong solvent action of water vapor on the relatively low volatile components with a sufficient temperature and pressure. As has been suggested by Krauskopf, the low volatile components may be transported mechanically as solid particles in gas as well as vapor.

Matsuo[7] pointed out that many reactions in fumarolic gas are quenched to a certain extent at the orifices of fumaroles. The extent of their quenching, however, will depend on the kinds of reactions and on the temperature and pressure gradients in the fumarole.

Whatever factor plays the most important part in transporting the low volatile components, it is certain that the results stated in the previous paper will correspond to the features of their behavior in the fumarolic gas.

In this paper the writer will describe the behavior in the fumarolic gas of manganese, titanium and phosphorus, which are less familiar but are yet widely distributed in rocks.

## Experimental

The investigation of the behavior of manganese, titanium and phosphorus was made in the same way as that in the previous paper, i. e., by the collection and analysis of the condensed waters from a fumarole at the Mihara Volcano. The components in the condensed water were concentrated by evaporation or separated by coprecipitation, because their contents were too low to be determined directly.

**Sample.**—An equivolume mixture of three condensed waters collected in September, 1959, i. e., in the final period of the sample collection in that year, was used as the sample for 1959. Fifty condensed waters collected in 1961 were divided into five groups according to the iron concentrations. The numbers of the condensed waters included in each group are given in the first column of Table I. The samples in each group were then mixed in the same proportions by volume and used as the samples for 1961.

**Analytical Method.**—First 1000 or 1500 ml. of the combined sample was heated, gently to expel the hydrochloric acid and then strongly until no more sulfuric acid fumes were evolved. The evaporate was then dissolved in 3 ml. of concentrated sulfuric acid and made up to 50 ml. of the final volume by adding distilled water. An aliquot of 25 ml. was used for the determination of manganese, 20 ml., for titanium, and 1 ml., for iron and for aluminum. For the determination of phosphorus, 500 ml. of the raw combined sample was used.

*Manganese.*—Manganese was determined through the photometric measurement of the violet color

* Present address: Department of Chemistry, Nagoya Institute of Technology, Chikusa-ku, Nagoya.

1) H. Kamiya, This Bulletin, **37**, 1477 (1964).
2) K. B. Krauskopf, *Econ. Geol.*, **52**, 786 (1957).
3) G. W. Morey and J. M. Hesselgesser, ibid., **46**, 821 (1951).
4) G. W. Morey, ibid., **52**, 225 (1957).
5) G. C. Kennedy, ibid., **45**, 629 (1950).
6) S. Sourirajan and G. C. Kennedy, *Am. J. Sci.*, **260**, 115 (1962).
7) S. Matsuo, *J. Earth Sci., Nagoya Univ.*, **9**, 80 (1961).

developed by the periodate oxidation of manganese to permanganate, in the presence of orthophosphoric acid to eliminate interference.[8]

*Titanium.* — The determination of titanium was made colorimetrically by comparing the yellow color formed with hydrogen peroxide in a 1 : 9 sulfuric acid solution with the standard color.[9]

*Phosphorus.*—Phosphorus was separated by coprecipitation with aluminum hydroxide and determined by the molybdenum blue method.[10]

*Aluminum and Iron.*—The determination of aluminum and iron was carried out by the method described in the previous paper.

## Results and Discussion

**The Concentrations of Iron, Aluminum Manganese, Titanium and Phosphorus in Condensed Water Collected in 1959 and 1961.**—The average concentrations of iron, aluminum, manganese, titanium and phosphorus in the combined samples in both 1959 and 1961 are given in Table I. The 1959 sample was a mixture of only three condensed waters. The average concentrations in 1961 were calculated from the concentrations of the components in the five classified groups.

The titanium concentration increased and those of manganese and phosphorus decreased in 1961, as compared with their concentrations in 1959. While the increase in titanium and the decrease in phosphorus were in the same order of magnitude, the manganese concentration in 1961 was almost two orders of magnitude lower than that in 1959; i. e., the decrease in the manganese concentration in 1961 was quite remarkable.

In view of the fact that the average concentration of iron, 0.047 mmol./l., in 1959 given in the previous paper differs from that, 0.060 mmol./l., for the same year in Table I, despite the identity in aluminum concentration, it cannot be said that the fumarolic gas in 1959 described in the previous paper had the same quality as the gas from which the three condensed waters in this experiment were obtained.

**The Correlation of Aluminum, Manganese, Titanium and Phosphorus with Iron.**—In order to find the relationship between aluminum, manganese, titanium, phosphorus and iron, the fifty condensed waters collected in 1961 were classified into five groups. As may be seen in Fig. 1, when the concentrations of aluminum, manganese, titanium and phosphorus are plotted against that of iron in the five groups

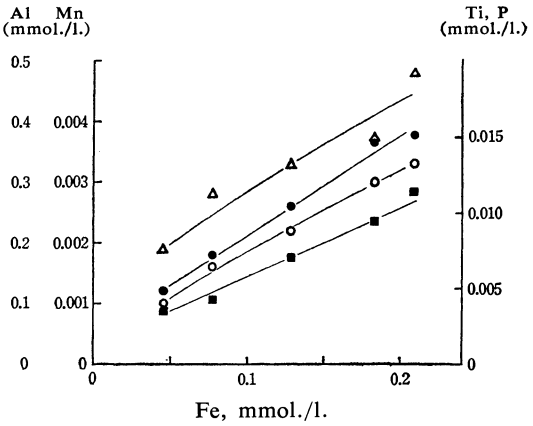



Fig. 1. Correlation of Al, Mn, Ti and P with Fe.

△ Al, ● Ti, ○ Mn, ■ P

of samples in 1961, they tend to increase simultaneously with the iron concentrations. Manganese and titanium show a nearly linear relation with iron, but the same kind of correlation between aluminum and iron is not clear. A linear increase in the concentration of phosphorus with an increasing concentration of iron is noticed.

The behavior of manganese, titanium, phosphorus, etc., in the fumarolic gas of 1959 may not be fully displayed, inasmuch as the concentrations in 1959 given in Table I are the average values from only three condensed waters. However, if the concentrations of aluminum, titanium and phosphorus are plotted against that of iron in 1959, the points fall not so far from the lines in Fig. 1 which represent the relations of aluminum, titanium and phosphorus to iron in 1961. In contrast to the above components, the unusually high concentration of manganese in the combined sample of 1959, when compared with that of iron, is quite noticeable.

**The Transport of Manganese, Titanium and Phosphorus in Gas in Comparison with the Other Major Components.** — The ratios between the mole percentages of the twelve components, including chlorine, sulfur, manganese, titanium and phosphorus, in the condensed water and those in the lava were calculated from the average concentrations of the components in the condensed waters in 1959 and in 1961 and from their contents in the lava (1951) reported by Tsuya et al.[11] and Iwasaki et al.[12] Due to the lack of data on the analysis of sulfur in the lava of 1951, the sulfur content in the lava of

8) F. D. Snell and C. T. Snell, "Colorimetric Methods of Analysis," D. Van Nostrand Co., New York (1954), p. 392.
9) F. D. Snell and C. T. Snell, ibid., p. 438.
10) D. F. Boltz (Editor), "Colorimetric Determination of Nonmetals," Interscience Publisher, New York (1958), p. 29.
11) H. Tsuya, R. Morimoto and J. Ossaka, *Bull. Earthq. Res. Inst.*, **30**, 231 (1952).
12) I. Iwasaki, T. Katsura, N. Sakato and M. Hirayama, *J. Chem. Soc. Japan, Pure Chem. Sec.* (*Nippon Kagaku Zassi*), **78**, 1641 (1951).

Table I. Concentration of Fe, Al, Mn, Ti and P

| | Number of condensed waters combined | Fe | Al | Mn | Ti | P |
|---|---|---|---|---|---|---|
| | | | | (mmol./l.) | | |
| In 1959 | 3 | 0.060 | 0.28 | 0.082 | 0.0063 | 0.0066 |
| In 1961 | 18 | 0.045 | 0.19 | 0.0010 | 0.0048 | 0.0035 |
| | 14 | 0.077 | 0.28 | 0.0016 | 0.0072 | 0.0043 |
| | 10 | 0.128 | 0.33 | 0.0022 | 0.0104 | 0.0070 |
| | 4 | 0.183 | 0.37 | 0.0030 | 0.0147 | 0.0095 |
| | 4 | 0.209 | 0.48 | 0.0033 | 0.0151 | 0.0114 |
| | Average | 0.095 | 0.28 | 0.0018 | 0.0082 | 0.0055 |

Table II. Mole percentage of 12 components in lava and condensed water, and ratio

| | Lava | In 1959 | | In 1961 | |
|---|---|---|---|---|---|
| | | Condensed water | | Condensed water | |
| | $R$, mol. % | $G_1$, mol. % | $G_1/R$ ratio | $G_2$, mol. % | $G_2/R$ ratio |
| Si | 50.4 | 2.9 | 0.058 | 0.22 | 0.0043 |
| Al | 17.5 | 0.32 | 0.018 | 0.13 | 0.0074 |
| Fe | 10.4 | 0.055 | 0.0053 | 0.043 | 0.0042 |
| Mg | 6.7 | 0.019 | 0.0028 | 0.033 | 0.0050 |
| Ca | 10.0 | 0.043 | 0.0043 | 0.10 | 0.010 |
| Na | 3.1 | 1.3 | 0.42 | 0.037 | 0.012 |
| K | 0.41 | 0.13 | 0.32 | 0.0036 | 0.0088 |
| Ti | 1.1 | 0.0074 | 0.0070 | 0.0038 | 0.0036 |
| P | 0.098 | 0.0077 | 0.080 | 0.0025 | 0.026 |
| Mn | 0.081 | 0.096 | 1.2 | 0.00083 | 0.010 |
| S | 0.22 | 16.4 | 76 | 3.24 | 15 |
| Cl | 0.047 | 78.7 | 170 | 96.2 | 2040 |

Table III. Order of ratio for 12 components

| | |
|---|---|
| In 1959 | Cl > S > Mn > Na > K > P > Si > Al > (Ti, Fe) > Ca > Mg |
| In 1961 | Cl > S > P > Na > (Ca, Mn) > K > Al > Mg > (Si, Fe) > Ti |

the central cone as measured by Iwasaki[13] was employed. The results are given in Table II. Moreover, the order of the ratio for the components is shown in Table III. As was stated in the previous paper, it may be considered that the ratio denotes the measure of ease with which the components are transported in gas or the degree of concentration in gas relative to that in lava.

The low volatile components abundant in rocks probably originate from magma and/or wall rock. On the other hand, chlorine may originate from another source, as has been suggested by Matsuo.[7] Wherever they may originate, however, the general tendency of the transport of the components in gas is illustrated by the ratios.

Chlorine and sulfur, excluding the most dominant water vapor in gas, are the largest mobile elements, unless there is the possibility of the secondary addition of these components into gases. In other words, they are concentrated into gas, as they cannot enter the crystal lattice of common rock-forming minerals; in general, chlorine is incorporated in the glassy part rather than in minerals,[12] and the minor sulfur content is due to the sulfur compounds in rocks. As may be seen in Table II, chlorine and sulfur made up over 95% of the whole in 1959 and 99% in 1961.

Manganese was much more mobile than alkali metals, and the component with the largest ratio, except for such highly volatile components as chlorine and sulfur, in 1959. As has been stated previously, although the concentration of manganese became much lower in 1961 than in 1959, still it belongs to the metallic components with a relatively large ratio. Titanium had a ratio comparable to iron in the fumarolic gas of a higher temperature in 1959, but it became less mobile at a lower temperature in 1961. Phosphorus had a smaller ratio than alkali metals in 1959, and it became more mobile than any metals, with a decrease in the ratio of metallic components, in 1961.

As has been stated above, there is a marked difference in the nature of the fumarolic gases between those of 1959 and those of 1961, based

13) I. Iwasaki, ibid., 56, 1518 (1935).

on the chemical analysis of condensed waters. We are led, then, to inquire what factors govern the transport of these components, what kinds of compounds of these components are really transpired and, especially, why the fumarolic gas in 1959 had a particular ability to transport manganese. In order to answer these questions, further experiments at high temperatures and high pressures are needed.

The writer wishes to express his indebtedness to Professor Kimio Noguchi for having been good enough to read this manuscript, and also to Mr. Minoru Yamamoto for help with regard to the analyses.

*Department of Chemistry*
*Faculty of Science*
*Tokyo Metropolitan University*
*Setagaya, Tokyo*

# The Determination of the Heat of Adsorption by the Gas Chromatographic Method. I*

By Kimiko ARITA, Yoshio KUGE and Yozaburo YOSHIKAWA

(Received August 13, 1964)

The determination of the heat of adsorption by the gas chromatographic method has been carried out by Greene and Pust.[1] In our laboratories, the heats of adsorption of some low-boiling-point hydrocarbons and inorganic gases on active charcoal, alumina, silica gel and synthetic zeolite have also been estimated by the gas chromatographic method by using several carrier gases, such as helium, hydrogen and nitrogen.[2-4]

The purpose of this series is to establish the method of the gas chromatographic determination of the heat of adsorption and to compare the results with those obtained by usual static methods.

The heat of adsorption of an eluted gas on an adsorbent is calculated by Eq. 1[5,6]:

$$\frac{R}{R'}=\frac{1}{K_a+1}=\frac{L\cdot A}{F\cdot t_m} \tag{1}$$

where $R$, is the linear velocity of the sample gas; $R'$, the linear velocity of the carrier gas; $K_a$, the equilibrium constant for adsorption; $L$, the packed length of adsorption; $t_m$, the retention time of the sample gas; $A$, the interstitial area of the column, and $F$, the flow rate of the carrier gas.

Then, the equilibrium constant of adsorption ($K_a$) is expressed by Eq. 2, since $\Delta G=\boldsymbol{R}T_c\ln K_a$:

$$K_a=e^{-\Delta G/\boldsymbol{R}T_c}=e^{-\Delta H_a/\boldsymbol{R}T_c}\cdot e^{\Delta S/\boldsymbol{R}} \tag{2}$$

where $T_c$, is the column temperature (the gas-solid equilibrium temperature); $H_a$, the molar differential heat of adsorption; $\Delta G$, the free energy change of adsorption, and $\Delta S$, the entropy change of adsorption.

As $\Delta S$ is assumed to be constant when the temperature range is small and when the adsorbent and the adsorbate are the same substance, Eq. 2 is rewritten as Eq. 3:

$$K_a=Be^{-\Delta H_a/\boldsymbol{R}T_c} \tag{3}$$

where $B$ indicates a constant.

Moreover, the apparent retention time ($t_m'$) is expressed by Eq. 4.[7]

$$t_m'=t_m-\frac{L\cdot A}{F} \tag{4}$$

Then we have Eq. 5 from the relations of 1, 3 and 4.

$$Ft_m'=LABe^{-\Delta H_a/\boldsymbol{R}T_c} \tag{5}$$

When $\log Ft'_m$ is plotted against $T_c$, the heats of adsorption ($\Delta H_a$) can be estimated from the slope of the ($\log Ft'_m$, $1/T_c$) line according to Eq. 5. In practice, however, a slight pressure drop occurs across the column and the velocity of the sample and carrier gases might change slightly through the column. Therefore, the retention volume ($V_m$) is usually corrected in such a way that the pressure drop comes to zero, and the flow rate of the

* Presented in part at the 17th Annual Meeting of the Chemical Society of Japan, Tokyo, April, 1964.

1) S. A. Greene and H. Pust, *J. Phys. Chem.*, **62**, 55 (1958).

2) Y. Kuge, Y. Yoshikawa and K. Yamasaki, *Science Reports (College of General Education, Osaka University)*, **12**, 23 (1963).

3) K. Arita, Y. Kuge, Y. Yoshikawa and K. Yamasaki, ibid., **12**, 131 (1963).

4) K. Arita, Y. Kuge, Y. Yoshikawa and K. Yamasaki, ibid., **13**, 15 (1964).

5) A. J. P. Martin and R. L. M. Synge, *Biochem. J.*, **35**, 1358 (1941).

6) Y. Amenomiya, "Gas Chromatography," Kyoritsu Shuppan, Tokyo (1961), p. 124.

7) "Kiki Gasu Bunsekiho," Kyoritsu Shuppan, Tokyo (1961), p. 182.

carrier gas measured at room temperature is also converted into that at 0°C.

The corrected retention volume ($V_o$) is expressed by Eq. 6.[8,9]

$$V_o = Ft'_m \cdot \frac{273}{T} \cdot \frac{3}{2} \cdot \frac{(P_i/P_o)^2-1}{(P_i/P_o)^3-1} \qquad (6)$$

where $P_i$, is the column inlet pressure; $P_o$, the column outlet pressure, and $T_m$, the room temperature.

Practically, however, $V_m$ is observed as a function of the column temperature only:

$$V_m = Ft'_m \cdot \frac{273}{T_m} \qquad (7)$$

Therefore, we have Eq. 8 by putting Eq. 5 into Eq. 7:

$$V_m = Ce^{-\Delta H_a/RT_c} \qquad (8)$$

where $C$ is a constant.

Therefore, the heat of adsorption may be estimated by plotting $V_m$, in place of $V_o$, against $T_c$ according to Eq. 8.

## Experimental

A Yanagimoto gas chromatograph, GCG-2, was employed.

The column is made of a stainless steel U-shaped tube 5 mm. in inner diameter. The length of the column used is 1 m. in the cases of activated charcoal, molecular sieve 5A and a molecular sieve 13X, and 2 m. in the cases of alumina and silica gel. The adsorbents were supplied mostly by Nishio Industry Co., Ltd., and the size of their particles ranged from 40 to 60 mesh, while alumina was supplied by the Wako Chemical Co., Ltd., in sizes from 28 to 48 mesh.

All the sample gases were synthesized except methane, ethane, acetylene and isobutane, and all the gases used were purified.

After the column had been filled with an adsorbent, the adsorbent was activated by heating it up to 200°C and by sweeping with carrier gas with a flow rate of about 50 cc. per minute, the flow rates of the gases being measured by a soap-film flow meter. To avoid error in the determination of the retention time, the experiments were carried out under conditions which would give a symmetrical shape for any peak.

## Results

In the case of ethane, the corrected retention volume ($V_m$) was estimated for five kinds of adsorbents by using nitrogen as the carrier gas. The logarithmic plots of $V_m$ against $1/T_c$ are found to be quite linear, as Fig. 1 shows.

In the adsorption of other sample gases on active charcoal, hydrogen was employed as the carrier gas. In this case, no hydrogenation of

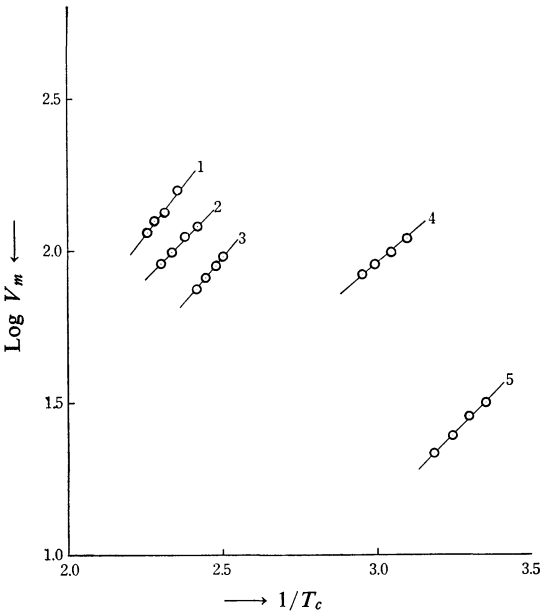



Fig. 1. The retention volume of ethane on five adsorbents. ($N_2$ carrier gas)
1 Charcoal 2 Molecular sieve 5A
3 Molecular sieve 13X 4 Silica gel
5 Alumina

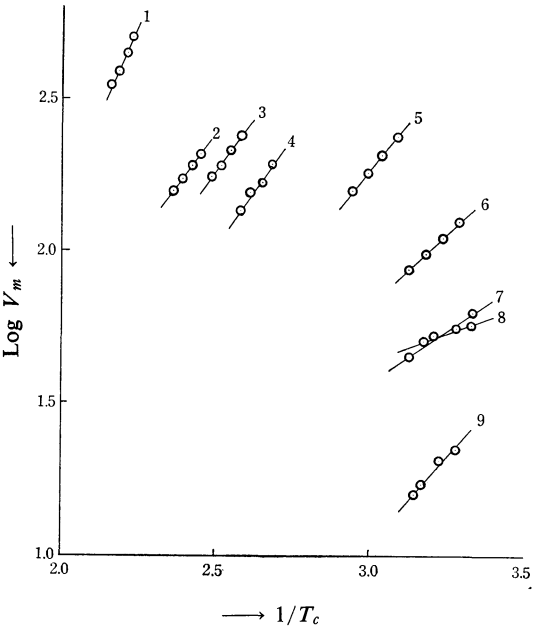



Fig. 2. The retention volume of sample gases on charcoal as a function of temperature. ($H_2$ carrier gas)
1 $C_3H_6$, 2 $C_2H_6$, 3 $C_2H_4$, 4 $C_2H_2$,
5 $CO_2$, 6 $CH_4$, 7 $N_2$, 8 Ar, $O_2$, 9 CO

8) A. B. Littlewood, "Gas Chromatography," Academic Press., New York (1962), p. 31.
9) H. Purnell "Gas Chromatography," John Wiley & Sons, New York (1962), p. 67.

TABLE I. HEATS OF ADSORPTION ON FIVE ADSORBENTS (kcal./mol.)

| Adsorbent | Molecular sieve 5A | | | Molecular sieve 13X | | | Silica gel | | | Charcoal | | | Alumina | | |
|---|---|---|---|---|---|---|---|---|---|---|---|---|---|---|---|
| Carrier gas / Sample | He | $H_2$ | $N_2$ | He | $H_2$ | $N_2$ | He | $H_2$ | $N_2$ | He | $H_2$ | $N_2$ | He | $H_2$ | $N_2$ |
| Ar | ( 25—37 ) 2.5 | ( 26—46 ) 2.4 | ( 20—40 ) 2.7 | ( 7.5—17.5) 2.5 | ( 26—46 ) 2.3 | ( 16—40 ) 2.0 | | | | ( 19—39 ) 2.5 | ( 26—46 ) 2.2 | ( 15—35 ) 2.5 | | | |
| $O_2$ | ( 18—37.5) 2.7 | ( 26—46 ) 2.6 | ( 20—40 ) 2.4 | ( 7—17 ) 2.7 | ( 26—46 ) 2.4 | ( 16—46 ) 2.3 | | | | ( 19—39.5 ) 2.5 | ( 26—46 ) 2.2 | ( 15—35 ) 2.4 | | | |
| $N_2$ | ( 18—36 ) 4.2 | ( 26—46 ) 3.7 | | ( 7—17 ) 4.2 | ( 26—46 ) 2.8 | | | | | ( 19—39.5 ) 2.5 | ( 26—46 ) 2.6 | | | | |
| CO | ( 33—61 ) 3.4 | ( 26—46 ) 5.7 | ( 65—85 ) 4.1 | (12.8—41 ) 4.0 | ( 26—46 ) 3.8 | ( 17—40 ) 3.8 | ( 21—41 ) 4.7 | ( 26—50 ) 4.4 | ( 20—40 ) 2.4 | ( 35—63.5 ) 3.0 | ( 26—46 ) 3.8 | ( 18—35 ) 2.7 | | | |
| $CO_2$ | | | | | | | ( 65—106) 4.7 | (26.5—61 ) 7.1 | ( 50—70 ) 5.4 | ( 143—174.5) 4.4 | ( 46—66 ) 5.8 | ( 91—110) 4.6 | | | |
| $CH_4$ | ( 16—49 ) 3.6 | ( 35—55 ) 3.7 | ( 41—60 ) 3.6 | ( 15—99.5) 3.7 | ( 26—46 ) 3.4 | ( 16—40 ) 3.4 | ( 34—80 ) 3.7 | ( 21—41 ) 3.5 | ( 21—41 ) 2.8 | ( 88.5—173 ) 3.1 | ( 26—46 ) 4.5 | ( 26—45 ) 4.0 | ( 20—70.5) 1.7 | ( 26—46 ) 2.7 | ( 30—50 ) 1.7 |
| $C_2H_6$ | (125—151 ) 5.2 | (130—150) 6.4 | (135—161) 6.0 | ( 43—100 ) 5.9 | ( 71—91 ) 5.1 | (110—140) 5.2 | ( 47—82 ) 4.7 | ( 22—101) 5.4 | ( 50—70 ) 3.9 | (173.5—210 ) 6.2 | (130—150) 6.3 | (150—170) 5.3 | ( 19—69 ) 3.9 | ( 26—46 ) 4.5 | ( 21—40 ) 5.3 |
| $C_3H_8$ | | | | | | | (82.5—116) 6.6 | ( 26—101) 7.1 | (100—120) 6.3 | | | | ( 20—68.5) 6.3 | ( 51—71 ) 6.5 | ( 60—80 ) 7.1 |
| $i$-$C_4H_{10}$ | | | | | | | ( 116—150) 6.4 | ( 100—120) 7.2 | (126—145) 6.6 | | | | (61.5—85 ) 6.9 | ( 70—90 ) 8.3 | ( 90—110) 7.0 |
| $C_4H_{10}$ | | | | | | | ( 98—133) 7.6 | ( 100—125) 8.7 | (120—140) 8.3 | | | | (61.5—85 ) 7.4 | ( 56—76 ) 7.8 | ( 60—80 ) 7.6 |
| $C_2H_4$ | | | | | | | ( 72—99 ) 6.1 | (27.5—61 ) 6.8 | ( 70—90 ) 5.7 | ( 108—173 ) 6.4 | (110—130) 6.1 | (135—154) 5.0 | ( 19—54 ) 5.2 | ( 26—46 ) 3.7 | ( 30—50 ) 4.3 |
| $C_3H_6$ | | | | | | | ( 102—132) 7.8 | ( 100—120) 8.9 | (130—150) 7.7 | ( 170—190 ) 8.8 | (170—190) 8.5 | | (45.5—66.5) 7.6 | ( 40—66 ) 8.7 | ( 60—80 ) 6.6 |
| $C_2H_2$ | | | | | | | | | | ( 108—173.5) 5.4 | (100—120) 6.7 | (110—130) 5.8 | | | |

Figures in parentheses show the temperature range covered experimentally.

TABLE II. ORDERS OF PEAK APPEARANCE AND $\Delta G$ VALUES OF SAMPLE GASES
$\Delta G$ in cal. per deg., per mol., $\Delta S$ in cal. per deg., per mol. at 298.16°K

Charcoal

| | Substance | | | | | | | | |
|---|---|---|---|---|---|---|---|---|---|
| He carrier gas | $Ar(O_2)$ | $\longrightarrow N_2$ | $\longrightarrow CO$ | $\longrightarrow CH_4$ | $\longrightarrow CO_2$ | $\longrightarrow C_2H_2$ | $\longrightarrow C_2H_4$ | $\longrightarrow C_2H_6$ | $\longrightarrow C_3H_6$ |
| $\Delta G$ | 38 | 526 | 402 | 531 | 747 | 539 | 97 | 1283 | |
| $\Delta S$ | 0 | 0 | −1 | 2 | 1 | 1 | −1 | 4 | |
| $H_2$ carrier gas | CO | $\longrightarrow O_2$ | $\longrightarrow N_2$ | $\longrightarrow Ar$ | $\longrightarrow CH_4$ | $\longrightarrow CO_2$ | $\longrightarrow C_2H_2$ | $\longrightarrow C_2H_4$ | $\longrightarrow C_2H_6$ | $\longrightarrow C_3H_6$ |
| $\Delta G$ | 567 | 56 | 0 | 504 | 554 | 774 | 92 | 267 | 1693 | |
| $\Delta S$ | 4 | 1 | 1 | 6 | 3 | 1 | −2 | 0 | 2 | |
| $N_2$ carrier gas | $O_2$ | $\longrightarrow Ar$ | $\longrightarrow CO$ | $\longrightarrow CH_4$ | $\longrightarrow CO_2$ | $\longrightarrow C_2H_4$ | $\longrightarrow C_2H_2$ | $\longrightarrow C_2H_6$ | | |
| $\Delta G$ | 0 | 158 | 522 | 469 | 702 | 49 | 256 | | | |
| $\Delta S$ | 1 | 0 | 3 | 1 | −2 | 3 | −3 | | | |

Silica gel

| | | | | | | | | | |
|---|---|---|---|---|---|---|---|---|---|
| He carrier gas | CO | $\longrightarrow CH_4$ | $\longrightarrow C_2H_6$ | $\longrightarrow CO_2$ | $\longrightarrow C_2H_4$ | $\longrightarrow C_3H_8$ | $\longrightarrow i\text{-}C_4H_{10}$ | $\longrightarrow C_3H_6$ | $\longrightarrow C_4H_{10}$ |
| $\Delta G$ | 571 | 891 | 349 | 83 | 517 | 416 | 266 | 22 | |
| $\Delta S$ | −5 | 1 | −1 | 5 | 0 | −2 | 4 | −1 | |
| $H_2$ carrier gas | CO | $\longrightarrow CH_4$ | $\longrightarrow C_2H_6$ | $\longrightarrow CO_2$ | $\longrightarrow C_2H_4$ | $\longrightarrow C_3H_8$ | $\longrightarrow i\text{-}C_4H_{10}$ | $\longrightarrow C_3H_6$ | $\longrightarrow C_4H_{10}$ |
| $\Delta G$ | 797 | 21 | 1182 | 57 | 823 | 288 | 219 | 210 | |
| $\Delta S$ | −6 | 11 | −9 | 6 | −3 | 4 | 0 | −6 | |
| $N_2$ carrier gas | CO | $\longrightarrow CH_4$ | $\longrightarrow C_2H_6$ | $\longrightarrow CO_2$ | $\longrightarrow C_2H_4$ | $\longrightarrow C_3H_8$ | $\longrightarrow i\text{-}C_4H_{10}$ | $\longrightarrow C_3H_6$ | $\longrightarrow C_4H_{10}$ |
| $\Delta G$ | 183 | 837 | 484 | 91 | 282 | 528 | 319 | 173 | |
| $\Delta S$ | 1 | 1 | 4 | 6 | 1 | −1 | 3 | 1.5 | |

Alumina

| | | | | | | | | |
|---|---|---|---|---|---|---|---|---|
| He carrier gas | $CH_4$ | $\longrightarrow C_2H_6$ | $\longrightarrow C_2H_4$ | $\longrightarrow C_3H_8$ | $\longrightarrow C_3H_6$ | $\longrightarrow i\text{-}C_4H_{10}$ | $\longrightarrow C_4H_{10}$ | |
| $\Delta G$ | 556 | 112 | 723 | 109 | 321 | 184 | | |
| $\Delta S$ | 5 | 4 | 1 | 4 | −3 | 1 | | |
| $H_2$ carrier gas | $CH_4$ | $\longrightarrow C_2H_6$ | $\longrightarrow C_3H_8$ | $\longrightarrow C_2H_4$ | $\longrightarrow C_4H_{10}$ | $\longrightarrow C_3H_6$ | $\longrightarrow i\text{-}C_4H_{10}$ | |
| $\Delta G$ | 1292 | 721 | 160 | 866 | 136 | 128 | | |
| $\Delta S$ | 2 | 5 | 9 | 11 | 2 | −6 | | |
| $N_2$ carrier gas | $CH_4$ | $\longrightarrow C_2H_6$ | $\longrightarrow C_2H_4$ | $\longrightarrow C_3H_8$ | $\longrightarrow C_3H_6$ | $\longrightarrow i\text{-}C_4H_{10}$ | $\longrightarrow C_4H_{10}$ | |
| $\Delta G$ | 170 | 450 | 633 | 326 | 273 | 110 | | |
| $\Delta S$ | 11 | −5 | 7 | −3 | 5 | 3 | | |

unsaturated hydrocarbons was recognized over the temperature range covered experimentally.

The correlation of $V_m$ with $1/T_c$ is shown in Fig. 2.

On the basis of these data, the differential heats of adsorption on sample gases were calculated. The results are listed in Table I.

The values of the heats of adsorption obtained are in almost the same sequence as those found for the van der Waals constant ($a$) of the sample gases.

The difference between the values obtained when helium, hydrogen and nitrogen were used as the carrier gases was found to be rather small. The reason for this will be discussed after the experiments using argon as the carrier gas have been carried out.

Next the relation between the order of peak appearance and the free energy change was investigated.

The relation between the retention time ($t'_m$) and the free energy change ($\Delta G$) has been obtained by Cremer[10] as follows:

$$\Delta G = G_1 - G_2 = \boldsymbol{R}T \ \mathrm{lnt'}_m(1)/t'_m(2) \qquad (9)$$

The numbers in parentheses ((1),(2)) show the kind of adsorbate.

Since the apparent retention volume ($V_m$) can be written as $V_m = Ft'_m$, $\Delta G$ is expressed as Eq. 10:

$$\Delta G = \boldsymbol{R}T \ \ln \frac{V_m(1)}{V_m(2)} \qquad (10)$$

The free energy change of the adsorption of several sample gases on the same adsorbent was calculated according to Eq. 10. The results obtained are listed in Table II, where the values are converted into those at 25°C. As is shown in Table II, the smaller the value of

10) E. Cremer, *Z. anal. Chem.*, **170**, 219 (1959).

the free energy change of adsorption ($-\Delta G$), the greater the velocity of the adsorption of sample gases.

The discussion of the results will appear in the next report.

The authors wish to express their sincere thanks to Dr. Ken-ichiro Yamasaki for his kind guidance throughout the course of this work.

*Institute of Chemistry*
*College of General Education*
*Osaka University*
*Toyonaka, Osaka*

# The Reaction of Carbon Monoxide with Organometallic Compounds.* X. The Reaction of Carbon Monoxide with Phenyl Derivatives of Transition Metals**

By Membo RYANG, Kunihisa YOSHIDA, Hidejiro YOKOO and Shigeru TSUTSUMI

(Received August 22, 1964)

In a previous communication[1] it was reported that the phenylcobalt compound prepared from the reaction between phenylmagnesium bromide and cobalt(II) chloride in diethyl ether reacted with carbon monoxide at a low temperature (−35——10°C) and 1 CO atm., giving benzophenone (22%) and benzoin (12.5%) at −25°C, and benzoin (35%) at −35°C. The formation of benzophenone was explained as resulting from the reaction of carbon monoxide with the phenyl radical which was formed from a homolytic fission of the carbon-cobalt bond in the phenylcobalt compound, while benzoin was assumed to be produced by the dimerization, followed by the hydrolysis, of the benzoylcobalt compound.

This reaction had a few curious and suggestive points for carbon monoxide-insertion reactions. Furthermore, since many transition metal compounds have been used in the synthetic application of carbon monoxide as catalysts and since sometimes the formation of organic derivatives of transition metals as the reaction intermediates were supposed,[2] it was felt desirable to clarify the reaction of carbon monoxide with organic derivatives of transition metals as a unit reaction in some detail, and also to discuss the effects of the variation of transition metals on the reactivities of the organic derivatives of transition metals with carbon monoxide.

This report will deal with the reaction of carbon monoxide with phenyl derivatives of transition metals and also with the relation between various transition metals and their behavior in carbon monoxide-insertion reactions. Moreover, the assumption on benzophenone formation, proposed in the previous communication, will be further discussed. The metals used in this work were divided into two groups: A: chromium, nickel and cobalt, which can form metal carbonyls by the action of carbon monoxide, and B: copper and cadmium, the carbonyls of which have not yet been isolated.

## Results and Discussion

The phenyl derivatives of transition metals were prepared by the reaction between metal halides and phenylmagnesium bromide. Although most transition metal halides react with alkyl and aryl Grignard or organolithium compounds under ordinary conditions, isolable organometallic compounds are frequently not obtained. Moreover, the major successes in the preparation of sigma-bonded transition metal alkyls and aryls have mostly resulted from close attention to experimental conditions (e.g., low temperature reactions) or, more commonly, from the use of the coordination of donor solvents or ligands.[3-5]

Therefore, the preparation of the phenyl

* Part IX: M. Ryang, T. Hashimoto and S. Tsutsumi, This Bulletin, 37, 1704 (1964).

** This work was presented at the 17th Annual Meeting of the Chemical Society of Japan, Tokyo, April, 1964.

1) M. Ryang and S. Tsutsumi, This Bulletin, 34, 1341 (1961).

2) C. W. Bird, *Chem. Revs.*, 62, 283 (1962).

3) G. E. Coats and F. Glockling, "Organometallic Chemistry," A. C. S. Monograph No. 147., Ed. by H. Zeiss, Reinhold Publishing Corp., New York (1961), p. 426.

4) J. Chatt et al., *J. Chem. Soc.*, **1960**, 1718; **1961**, 285.

5) W. Herwig and H. Zeiss, *J. Am. Chem. Soc.*, 81, 4798 (1959).

TABLE I. EXPERIMENTAL RESULTS

| Metal | Reaction condition: Temp. °C | Pres. CO atm. | Solvent | Time hr. | Reaction product,* Yield,** %: Biphenyl | Benzoin | Benzophenone | Triphenylcarbinol |
|---|---|---|---|---|---|---|---|---|
| Co | −35 | 1 | $Et_2O$ | 2 | 30 | 35 | trace | 5 |
| | −25 | 1 | $Et_2O$ | 2 | 44 | 12.5 | 22 | 12 |
| | −10 | 1 | $Et_2O$ | 1 | 80 | trace | 5.5 | trace |
| Cr | −25[a] | 1 | THF | 5 | 15 | | 38 | |
| | −25[b] | 1 | $Et_2O$ | 5 | 20 | | 20 | |
| Ni | 0 | 1 | THF | 5 | 19 | 19 | 11.5 | 5 |
| | 12 | 1 | $Et_2O$ | 3 | 17 | 23 | | 6 |
| | 21 | 1 | $Et_2O$ | 3 | 60 | | | |
| Cu | −5*** | 1 | $Et_2O$ | 5 | 39 | | | |
| | 32 | 1 | $Et_2O$ | 4 | 42 | | | |
| | −20 | 7 | $Et_2O$ | 5 | 29 | | | |
| Cd | 15 | 1 | THF | 3 | 8 | | | |
| | 30 | 7 | THF | 3 | 2 | | | |

* In addition to these products, benzoic acid and other carbonyl compounds were obtained, for example, diphenylbenzoylmethane was obtained in 10% yield from a and in 14% yield from b.
** The calculations of yields are based on the amounts of bromobenzene used to prepare phenylmagnesium bromide.
*** Phenyllithium was used to prepare phenylcopper.

derivatives of transition metals and the reaction with carbon monoxide were carried out at a low temperature in proper solvents (tetrahydrofuran or diethyl ether), and the isolation and identification of the reaction products were carried out by the ordinary methods.[6] The results of the reaction of carbon monoxide with various phenyl derivatives of transition metals are summarized in Table I. Since the reaction of phenylmagnesium bromide with carbon monoxide at −10°C in diethyl ether (for 5 hr.) gave only small amounts of diphenylcarbinol (2%) and triphenylmethane (1%), and since benzene was obtained in about a 90% yield, the carbon monoxide-inserted products in Table I were assumed to be produced from the reaction between carbon monoxide and the phenyl derivatives of transition metals. Also, the hydrolysis of the reaction mixtures obtained from the reaction of phenylmagnesium bromide with transition metal halides in the absence of carbon monoxide gave biphneyl in yields analogous to the yields of biphenyl in the presence of carbon monoxide. (Table II)

TABLE II. THE YIELDS OF BIPHENYL FROM THE REACTION IN THE ABSENCE OF CARBON MONOXIDE

| Metal | Temp. °C | Time hr. | Solvent | Yield % |
|---|---|---|---|---|
| Co | −25 | 4 | $Et_2O$ | 55 |
| Ni | 0 | 4 | THF | 20 |
| Cu | 32 | 4 | $Et_2O$ | 35 |
| Cd | 15 | 4 | THF | 10 |

As may be seen in Table I, the phenyl derivatives of transition metals known to form metal carbonyls, including chromium, nickel and cobalt, reacted with carbon monoxide at a low temperature under 1 CO atm. to give the reaction products derived from carbon monoxide insertion, while diphenylcadmium and phenylcopper were unreactive to carbon monoxide under several reaction conditions and no products derived from carbon monoxide insertion were obtained in isolable amounts. On the basis of the above results, the coordination of carbon monoxide to metals may be considered to be the first step in these reactions; then alkyl-acyl rearrangement[7] occurs to form benzoyl derivatives of transition metals, which decompose to give benzophenone or dimerize to give benzoin.

In the previous communication, the formation of benzophenone was explained as resulting from the reaction of carbon monoxide with the phenyl radical. However, benzophenone was not isolated from the reaction between carbon monoxide and phenylcopper even at a somewhat higher reaction temperature and a more elevated carbon monoxide pressure, although biphenyl was formed in a good yield and the formation of phenyl radical was certain.

On the basis of these results, it may be considered improper to explain the mechanism of benzophenone formation by a simple radical mechanism. Therefore, benzophenone should

6) M. Ryang and S. Tsutsumi, This Bulletin, 35, 1121 (1962); 37, 341 (1964).

7) T. H. Coffield, J. Kozikowski and R. D. Closson, *J. Org. Chem.*, 22, 598 (1957).

be thought to be produced from the decomposition of thermally-unstable benzoyl derivatives of transition metal,[8] which are dimerized and then hydrolyzed, to give benzoin at a lower reaction temperature.

The mechanical aspects of the ketone formation reaction and the studies of the factors which determine the course of benzophenone formation or benzoin formation will be presented in detail in a forthcoming paper.

## Experimental

**Materials.**—*Bromobenzene.*—Commercial bromobenzene was purified by fractional distillation; b. p. 155°C, $n_D^{20}$ 1.5602.

*Metal Halides.*—Commercial anhydrous metal halides (chromium(III) chloride, nickel chloride, cobalt(II) chloride, cuprous iodide and cadmium chloride) were dried by heating under reduced pressure.

**Reactions.**—*The Reaction of Carbon Monoxide with Diphenylnickel.*[9]—The apparatus and procedure employed here were identical with those described in the previous paper.[6] Twenty-six grams (0.2 mol.) of nickel chloride was added to a ethereal solution of phenylmagnesium bromide which had been prepared by using 31.4 g. (0.2 mol.) of bromobenzene, 5.4 g. (0.22 g. atm.) of magnesium and 150 ml. of anhydrous diethyl ether; carbon monoxide was then introduced into the solution at 12°C for 4 hr. The organic layer, separated after the hydrolysis of the reaction mixture, was divided into a neutral part, an acidic part and a phenolic part by means of the ordinary method. The neutral part was distilled under reduced pressure to give the following fractions: (1) b. p. 90—140°C/20 mmHg 2.6 g., (2) b. p. 105—150°C/1 mmHg 4.9 g., (3) b. p. 150—160°C/1 mmHg 1.0 g. and (4) b. p. 190—200°C/1 mmHg 0.4 g. Fraction 1 was identified as biphenyl by its mixed melting point measurement (m. p. 70°C, recrystallized from ethanol). Fraction 2 was recrystallized from ligroin to give white crystals, m. p. 133—134°C, and was identified as benzoin from the results of a mixed melting point measurement, infrared-spectra measurements and an elemental analysis.

Found: C, 79.43; H, 5.56. Calcd. for $C_{14}H_{12}O_2$: C, 79.22; H, 5.70%.

Fraction 3 solidified on standing and was recrystallized from benzene-ligroin to give white crystals, m. p. 161—162°C, which were identified as triphenylcarbinol by a mixed melting point measurement with an authentic sample.

When tetrahydrofuran was used as a solvent, benzophenone (11.5%) was isolated in addition to the above products, and its structure was determined by the results of infrared spectra measurements and a mixed melting point measurement of its oxime (m. p. 140—141°C, recrystallized from ligroin). Furthermore, benzoic acid was obtained from the acidic part and phenol from the phenolic part.

*The Reaction of Carbon Monoxide with Triphenylchromium.*[5]—4.5 g. of chromium trichloride was added at −30°C to a tetrahydrofuran solution of phenylmagnesium bromide which had been prepared by using 15.1 g. of bromobenzene, 2.3 g. of magnesium and 133 ml. of anhydrous tetrahydrofuran, and then the stirring was continued for a further 8 hr. at −25°C. Then dry, pure carbon monoxide was bubbled into the solution at −25°C for 5 hr. The reaction mixture was hydrolized by ethanol-2 N hydrochloric acid and divided into a neutral part, an acidic part and a phenolic part. The neutral part was distilled under reduced pressure to give the following fractions: (1) b. p. ~90°C/12 mmHg 1.1 g., (2) b. p. 105—130°C/1 mmHg 3.3 g. and (3) b. p. 130—190°C/1 mmHg 0.9 g. Fraction 1 was identified as biphenyl by mixed melting point measurements. The infrared spectrum of fraction 2 showed the presence of a carbonyl group (1655 $cm^{-1}$), and fraction 2 was confirmed to be benzophenone from the results of a mixed melting point measurement of its 2,4-dinitrophenylhydrazone (m. p. 236—237°C, recrystallized from ethyl acetate).

Found: C, 62.98; H, 3.96. Calcd. for $C_{19}H_{14}O_4N_4$: C, 62.98; H, 3.89%.

Fraction 3 was recrystallized from ligroin to give white crystals (m. p. 136—138°C); the infrared spectrum of these crystals showed the presence of a carbonyl group (1675 $cm^{-1}$).

Found: C, 87.77; H, 6.16. Calcd. for $C_{20}H_{16}O$: C, 88.20; H, 5.92%.

These crystals were identified as diphenylbenzoylmethane by a mixed melting point measurement with an authentic sample. Small amounts of benzoic acid and phenol were isolated from the acidic part and the phenolic part respectively. When the reaction in diethyl ether was carried out under similar conditions, the products in Table I were isolated.

*The Reaction of Carbon Monoxide with Phenylcopper.*[10]—Phenylcopper was prepared by the reaction of cuprous iodide (19 g., 0.1 mol.) with phenylmagnesium bromide in a diethyl ether solution (0.1 mol.) or with phenyllithium in diethyl ether (0.1 mol.) at −15—−5°C. The reaction with carbon monoxide was carried out under several conditions (Table I). As a reaction product, biphenyl was obtained in a good yield, but no carbonyl compounds were obtained in isolable amounts.

*The Reaction of Carbon Monoxide with Diphenylcadmium.*[11]—To a tetrahydrofuran solution of phenylmagnesium bromide (0.1 mol.), 9.2 g. (0.05 mol.) of anhydrous cadmium chloride was added at −30°C; the reaction mixture was then kept at

8) Re: acetone formation from methylcobalt tetracarbonyl, cf. W. Hieber, O. Vohler and G. Braun, *Z. Naturforsch.*, **13b**, 192 (1958), and Re: the synthesis of tetraphenylcyclopentadienone, cf. G. N. Schrauzer, *J. Am. Chem. Soc.*, **81**, 5307 (1959).

9) E. G. Rochow, D. T. Hurd and R. N. Lewis, "The Chemistry of Organometallic Compounds," John Wiley & Sons, New York (1957), p. 251; M. Tsutsui and H. Zeiss, *J. Am. Chem. Soc.*, **81**, 6090 (1959).

10) H. Gilman, R. G. Jones and L. A. Woods, *J. Org. Chem.*, **17**, 1630 (1952).

11) C. G. Stuckwisch and J. V. Balley, ibid., **28**, 2362 (1963).

15°C for 1 hr. while it was being stirred. The introduction of carbon monoxide was carried out at 15°C or 30°C for 3 hr. After hydrolysis, benzene was obtained in a good yield, but no carbonyl compounds were isolated.

*Department of Chemical Technology*
*Faculty of Engineering*
*Osaka University*
*Miyakojima-ku, Osaka*

# Photolysis of Acetaldehyde in the Presence of Deuterium Sulfide. Deuterium Atom Abstraction from Deuterium Sulfide Molecules by Methyl Radicals

By Naomi IMAI, Takaaki DOHMARU and Osamu TOYAMA

(Received September 3, 1964)

Previous studies of the catalytic effect of hydrogen sulfide on the photolysis[1] and pyrolysis[2] of acetaldehyde, as well as on the pyrolysis of dimethyl ether,[3] have shown that hydrogen atom abstraction from hydrogen sulfide molecules by methyl radicals:

$$CH_3 + H_2S \rightarrow CH_4 + HS \qquad (6')$$

plays an important role in these reactions. The rate constant of this metathetical reaction has been determined by photolyzing acetone[4] and acetaldehyde[1] in the presence of hydrogen sulfide, with the result that the reaction is much faster than ordinary hydrogen abstractions by methyl radicals.

In order to establish further the mechanism of the hydrogen sulfide catalysis, the study of the deuterium sulfide-catalyzed pyrolysis of acetaldehyde is now in progress. Here, in place of reaction 6', the following reaction:

$$CH_3 + D_2S \rightarrow CH_3D + DS \qquad (6)$$

is expected to play a similar role. In this work a mixture of deuterium sulfide and acetaldehyde was photolyzed, and the relative rate of reaction 6 was determined against that of reaction 5:

$$CH_3 + CH_3CHO \rightarrow CH_4 + CH_3CO \qquad (5)$$

which competes with reaction 6.

## Experimental

**Materials.** — Acetaldehyde was supplied commercially, dried by potassium chloride, and purified by repeated bulb-to-bulb distillations. Deuterium sulfide was prepared by dropping deuterium oxide (99.8 mol.%) on aluminum sulfide in an evacuated vessel, dried by passing it through a trap at −78°C, and purified by bulb-to-bulb distillations.

**Apparatus.**—The apparatus used was similar to that described previously.[1] The photolysis was carried out in a cylindrical quartz vessel with a capacity of about 110 cc. A medium-pressure mercury arc was used as the light source, and the light of the wavelength region shorter than 2800 Å was cut off in front of the vessel by a thin glass plate in order to avoid absorption by deuterium sulfide. The light intensity was kept constant by the use of a voltage stabilizer.

**Procedure.** — Required quantities of deuterium sulfide and acetaldehyde were admitted to the reaction vessel. After the gases had been allowed to mix thoroughly for a few minutes, light was admitted into the vessel. After irradiation for a certain time, the reaction mixture was led into a trap at the temperature of liquid air; the non-condensable fraction was then collected and measured by a Toepler gauge. In some runs, this fraction was analyzed by a gas chromatograph and by a mass spectrometer. No peaks at $(m/e)=19$ and 20 corresponding to methane-$d_3$ and -$d_4$ were found by mass spectrometry. The methane-$d_0$ : -$d_1$ : -$d_2$ ratio was determined from the intensities of the peaks at $(m/e)=16$, 17 and 18. Since the three components contribute to these peaks, the quantity of each component was calculated by means of simultaneous equations. The mass spectra of methane-$d_1$ and -$d_2$ were constructed from the measured mass spectrum of pure methane by the method of Schissler, Thompson and Turkevich;[5] the validity of the construction was confirmed by the close agreement between measured and calculated values for the peak at $(m/e)=15$.

## Results and Discussion

It was found by gas chromatographic analysis of the non-condensable products of the photolysis in the presence of deuterium sulfide that

1) N. Imai and O. Toyama, This Bulletin, **33**, 1120 (1960).
2) N. Imai, Y. Yoshida and O. Toyama, ibid., **35**, 752, 758 (1962).
3) N. Imai and O. Toyama, ibid., **34**, 328 (1961).
4) N. Imai and O. Toyama, ibid., **33**, 652 (1960).
5) D. O. Shissler, S. O. Thompson and J. Turkevich, *Discussions Faraday Soc.*, **10**, 46 (1951).

the fraction consists merely of methane and carbon monoxide in equal amounts within the range of experimental error. This fact indicates that acetaldehyde decomposes stoichiometrically to methane and carbon monoxide, as was observed in non-catalyzed[6] and hydrogen sulfide-catalyzed[1] photolyses. Consequently, the rate of decomposition was determined by measuring the amount of the non-condensable fraction of the products.

By analogy with the hydrogen sulfide catalysis, the photolysis of acetaldehyde in the presence of a small amount of deuterium sulfide can be explained by the following mechanism:

$$CH_3CHO + h\nu \rightarrow CH_3 + CHO \quad (1)$$

$$CHO \rightarrow CO + H \quad (2)$$

$$H + CH_3CHO \rightarrow H_2 + CH_3CO \quad (3)$$

$$H + D_2S \rightarrow HD + DS \quad (4)$$

$$CH_3 + CH_3CHO \rightarrow CH_4 + CH_3CO \quad (5)$$

$$CH_3 + D_2S \rightarrow CH_3D + DS \quad (6)$$

$$DS + CH_3CHO \rightarrow HDS + CH_3CO \quad (7)$$

$$CH_3CO \rightarrow CH_3 + CO \quad (8)$$

$$CH_3 + CH_3 \rightarrow C_2H_6[7] \quad (9)$$

Figure 1 shows the progress of decomposition with time. In the photolysis of 300 mm. of acetaldehyde with 10 mm. of deuterium sulfide (run B), the decomposition curve shows, though slightly, autocatalytic behavior in the initial stage. Such behavior is probably to be attributed to the replacement of reaction 6 by the faster reactions 6'' and 6':

$$CH_3 + HDS \rightarrow CH_4 + DS \quad (6'')$$

$$CH_3 + H_2S \rightarrow CH_4 + HS \quad (6')$$

as a result of the conversion of hydrogen sulfide-$d_2$ to -$d_1$ or -$d_0$ by reaction 7 or 7':

$$HS + CH_3CHO \rightarrow H_2S + CH_3CO \quad (7')$$

No autocatalytic behavior can be recognized unless the ratio of deuterium sulfide to acetaldehyde is sufficiently low, as in run B. In the experiments with small amounts of deuterium sulfide, consequently, care was taken to determine the initial decomposition rate by short-time irradiation.

In Fig. 2 the initial decomposition rate is

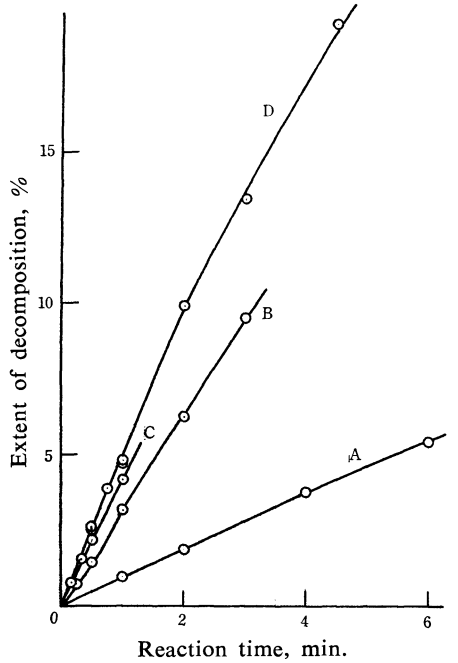



Fig. 1. Photolysis of acetaldehyde in the absence and presence of hydrogen sulfide and deuterium sulfide at 300°C.
A $D_2S$ : 0, $CH_3CHO$ : 100 mmHg
B $D_2S$ : 10 mmHg, $CH_3CHO$ : 300 mmHg
C $D_2S$ : 13.5 mmHg, $CH_3CHO$ : 100 mmHg
D $H_2S$ : 10 mmHg, $CH_3CHO$ : 300 mmHg

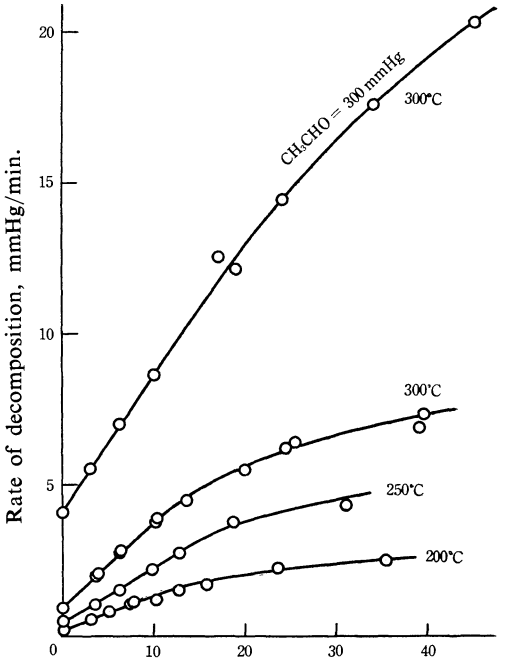



Fig. 2. Dependence of the rate of decomposition in the presence of deuterium sulfide on its pressure.
$CH_3CHO$ : 100 mmHg unless otherwise described.

6) F. E. Blacet and D. Volman, *J. Am. Chem. Soc.*, **60**, 1243 (1938); F. E. Blacet and W. J. Blaedel, ibid., **62**, 3374 (1940); R. E. Dodd and J. D. Waldron, *Nature*, **167**, 655 (1951).

7) In the pyrolysis of acetaldehyde reaction 9 was suggested to be third order (N. Imai, T. Fujii and O. Toyama, This Bulletin, **38**, 410 (1965).) but it is supposed to be second order at lower temperature.

plotted against the deuterium sulfide pressure. At a constant acetaldehyde pressure and light intensity, the rate increases linearly with deuterium sulfide pressure in its low pressure range, but it tends to saturation in its higher pressure range. These phenomena are similar to those found in hydrogen sulfide catalysis and can similarly be explained.

The reaction scheme for the photolysis of acetaldehyde alone[8] (reactions 1, 2, 3, 5, 8 and 9) leads to Rate Eq. I ($I_a$[9] denotes the rate of the absorption of light quanta):

$$-\mathrm{d}[CH_3CHO]/\mathrm{d}t = k_5 k_9^{-1/2} I_a^{1/2} [CH_3CHO] \quad (I)$$

while that in the presence of deuterium sulfide (reactions 1—9) leads to Rate Eq. II:

$$-\mathrm{d}[CH_3CHO]/\mathrm{d}t = k_5 k_9^{-1/2} I_a^{1/2} [CH_3CHO] + k_6 k_9^{-1/2} I_a^{1/2} [D_2S] \quad (II)$$

Equation II explains the linear relation between the rate and deuterium sulfide pressure, while Eqs. I and II explain the coincidence of the intercepts of the linear curves with the rates in the absence of deuterium sulfide, as may be seen in Fig. 2. At higher deuterium sulfide pressures, the concentration of DS radicals increases in relation to that of methyl radicals, and the contribution of DS radicals to chain termination has now to be taken into account. Thus the rate should be lower than that expected from Eq. II, as may be seen in Fig. 2.

From the slopes and intercepts of the linear portions in Fig. 2, the values for $k_6/k_5$ were determined; they are listed in Table I. At 300°C the values for 100 and 300 mm. of acetaldehyde approximately agree with each other.

Table I. Values of $k_6/k_5$ and $k_6'/k_5$

| Temp., °C | $k_6/k_5$ | $k_6'/k_5$ |
|---|---|---|
| 200 | 51[a] | 121 |
| 250 | 35[a] | 80 |
| 300 | 29.2[a] 30.3[b] 28.2[c] | 56 |

a) Obtained from Fig. 2 for 100 mm. acetaldehyde.
b) Obtained from Fig. 2 for 300 mm. acetaldehyde.
c) Obtained from Fig. 3.

The distribution of deuterium in methane was determined mass spectrometrically for the photolysis of 10 mm. deuterium sulfide and 300 mm. acetaldehyde mixtures with varied irradiation times at 300°C. The only methanes detected in appreciable amounts by the mass spectrometer are methane-$d_0$ and -$d_1$. The amount of methane-$d_2$ was negligible. The ratio of methane-$d_1$ to methane-$d_0$ is plotted against the time in Fig. 3, in which the ratio falls off with the progress of the reaction. This falling off in the ratio may, again, be attributed to the conversion of hydrogen sulfide-$d_2$ to -$d_1$ and -$d_0$ by reactions 7 and 7',

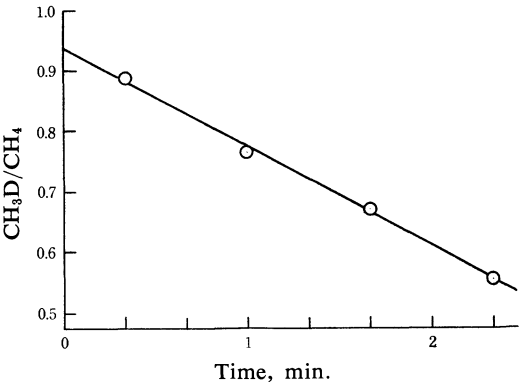



Fig. 3. Dependence of $CH_3D/CH_4$ ratio on reaction time at 300°C.
$CH_3CHO$: 300 mmHg; $D_2S$: 10 mmHg

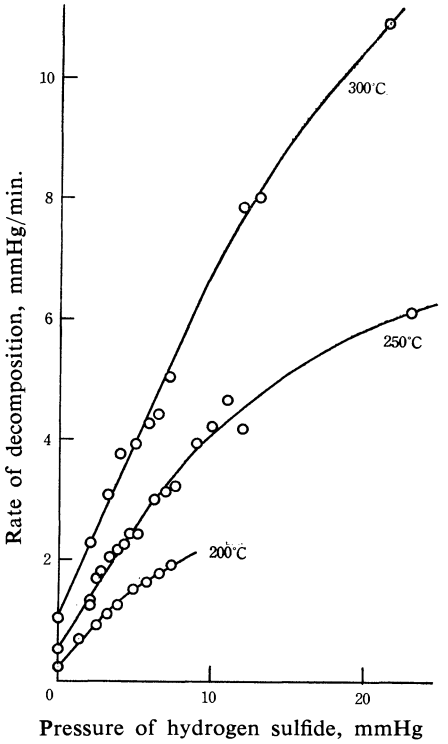



Fig. 4. Dependence of the rate of decomposition in the presence of hydrogen sulfide on its pressure. $CH_3CHO$: 100 mmHg.

8) E. I. Akeroyd and R. G. W. Norrish, *J. Chem. Soc.*, **1936**, 890; J. A. Leermakers, *J. Am. Chem. Soc.*, **56**, 1537 (1934); D. C. Grahame and G. K. Rollefson, *J. Chem. Phys.*, **8**, 98 (1940); C. J. Darby, A. S. Buchanan and I. H. S. Henderson, *J. Chem. Soc.*, **1951**, 1426.
9) $I_a$ was found to be proportional to acetaldehyde pressure in the present experimental condition in Ref. 1.

TABLE II. ISOTOPE EFFECT IN ARRHENIUS PARAMETERS OF HYDROGEN ATOM ABSTRACTION REACTIONS BY METHYL RADICALS

| Reaction | $A_H/A_D$ | $E_D-E_H$ kcal./mol. | $k_H/k_D$ at 200°C | Ref. |
|---|---|---|---|---|
| $CD_3+C_2H_6 \rightarrow CD_3H+C_2H_5$<br>$CD_3+C_2D_6 \rightarrow CD_4+C_2D_5$ | 1 | 1.5 | 5.0 | 10 |
| $CD_3+C_2H_3D_3 \rightarrow CD_3H+C_2H_2D_3$<br>$CD_3+C_2H_3D_3 \rightarrow CD_4+C_2H_3D_2$ | 0.73 | 1.9 | 5.5 | 10 |
| $CH_3+CH_3NH_2 \rightarrow CH_4+CH_3NH$<br>$CH_3+CH_3ND_2 \rightarrow CH_3D+CH_3ND$ | 0.78 | 1.3 | 3.1 | 11 |
| $CH_3+CH_3NH_2 \rightarrow CH_4+CH_2NH_2$<br>$CH_3+CD_3NH_2 \rightarrow CH_3D+CD_2NH_2$ | 1.3 | 1.4 | 5.8 | 11 |
| $CH_3+CH_3OH \rightarrow CH_4+CH_2OH$<br>$CH_3+CD_3OH \rightarrow CH_3D+CD_2OH$ | 1.3 | 1.3 | 5.2 | 11 |
| $CD_3+CH_3COCH_3 \rightarrow CD_3H+CH_3COCH_2$<br>$CD_3+CD_3COCD_3 \rightarrow CD_4+CD_3COCD_2$ | 0.80 | 1.67 | 4.6 | 12 |
| | 0.83 | 1.64 | 4.7 | 13 |
| $CH_3+CH_3CHO \rightarrow CH_4+CH_3CO$<br>$CH_3+CH_3CDO \rightarrow CH_3D+CH_3CO$ | 2.5 | 1.1 | 7.8 | 14 |
| $CH_3+\phi CHDCH_2D \rightarrow CH_4+\phi CDCH_2D$<br>$CH_3+\phi CHDCH_2D \rightarrow CH_3D+\phi CHCH_2D$ | 1.7 | 1.56 | 8.7 | 15 |
| $CH_3+HD \rightarrow CH_4+D$<br>$CH_3+HD \rightarrow CH_3D+H$ | 0.46 | 1.3 | 1.8 | 16 |
| $CD_3+HD \rightarrow CD_3H+D$<br>$CD_3+HD \rightarrow CD_4+H$ | 1.7 | 0 | 1.7 | 16 |
| $CH_3+H_2S \rightarrow CH_4+HS$<br>$CH_3+D_2S \rightarrow CH_3D+DS$ | 0.75 | 1.15 | 2.4 | This work |

if the methane-$d_1$ is not subsequently converted to methane-$d_0$.

Provided that methane-$d_0$ is formed only by reaction 5 and methane-$d_1$, by reaction 6 in the initial stage of the photolysis, the extrapolation of the linear plot in Fig. 3 gives the ratio of the rate of reaction 6 against that of reaction 5 and, consequently, the $k_6/k_5$ ratio shown in Eq. III:

$$\frac{R_{CH_3D}}{R_{CH_4}}=\frac{k_6[CH_3][D_2S]}{k_5[CH_3][CH_3CHO]}=\frac{k_6[D_2S]}{k_5[CH_3CHO]} \quad \text{(III)}$$

The value for $k_6/k_5$ thus obtained shows, as may be seen in Table I, a good agreement with those obtained from Fig. 2.

The values of $k_6/k_5$ in Table I give the Arrhenius expression:

$$k_6/k_5=2.0\exp(3000/\boldsymbol{RT}) \quad \text{(IV)}$$

In this work, the photolysis of acetaldehyde in the presence of hydrogen sulfide was investigated and the results are shown in Fig. 4, which corresponds to Fig. 2. The values of $k_6'/k_5$ obtained from this figure are also listed in Table I. They yield the expression:

$$k_6'/k_5=1.5\exp(4150/\boldsymbol{RT}) \quad \text{(V)}$$

which is in excellent agreement with $k_6'/k_5=1.7\exp(4000/\boldsymbol{RT})$, a value previously obtained by the method of total pressure measurement.[1)]

By dividing Eq. V by Eq. IV, we obtain:

$$k_6'/k_6=0.75\exp(1150/\boldsymbol{RT}) \quad \text{(VI)}$$

The ratio here obtained is fully comparable with that for hydrogen and deuterium atom abstraction from HD molecules by methyl radicals, but it is considerably lower than those for other abstraction reactions by methyl radicals as is shown in Table II.

By combining Eqs. IV and V with the $k_5=10^{11.3}\exp(-6800/\boldsymbol{RT})$ $mol^{-1}$ cc. $sec^{-1}$ reported by Ausloos and Steacie,[14)] we obtain:

$$k_6=10^{11.6}\exp(-3800/\boldsymbol{RT})\ mol^{-1}\ cc.\ sec^{-1} \quad \text{(VII)}$$

and

$$k_6'=10^{11.5}\exp(-2650/\boldsymbol{RT})\ mol^{-1}\ cc.\ sec^{-1} \quad \text{(VIII)}$$

The latter expression is almost identical with

10) J. R. McNesby, *J. Phys. Chem.*, **64**, 1671 (1961).
11) P. Gray and J. C. Thynne, *Trans. Faraday Soc.*, **59**, 2275 (1963).
12) J. R. McNesby, T. W. Davis and A. S. Gordon, *J. Am. Chem. Soc.*, **76**, 823 (1954).
13) J. R. McNesby and A. S. Gordon, ibid., **76**, 1416 (1954).
14) P. Ausloos and E. W. R. Steacie, *Can. J. Chem.*, **33**, 31 (1955).
15) L. Herk and M. Szwarc, *J. Am. Chem. Soc.*, **82**, 3558 (1960).
16) E. Whittle and E. W. R. Steacie, *J. Chem. Phys.*, **21**, 993 (1953).

the $k_6' = 10^{11.4} \exp(-2600/RT)$ $mol^{-1}$ cc. $sec^{-1}$ obtained in the photolysis of acetone in the presence of hydrogen sulfide.[4]

## Summary

The photolysis of acetaldehyde in the presence of deuterium sulfide has been investigated over the temperature range from 200 to 300°C, in order to determine the rate constant for the deuterium atom abstraction from deuterium sulfide molecules by methyl radicals. The effect of deuterium sulfide addition is similar to that of the addition of hydrogen sulfide previously studied. The results obtained with low concentrations of deuterium sulfide can be explained by the following reaction scheme: $CH_3CHO + h\nu \rightarrow CH_3 + CHO$ (1), $CHO \rightarrow CO + H$ (2), $H + CH_3CHO \rightarrow H_2 + CH_3CO$ (3), $H + D_2S \rightarrow HD + DS$ (4), $CH_3 + CH_3CHO \rightarrow CH_4 + CH_3CO$ (5), $CH_3 + D_2S \rightarrow CH_3D + DS$ (6), $DS + CH_3CHO \rightarrow HDS + CH_3CO$ (7), $CH_3CO \rightarrow CH_3 + CO$ (8), and $CH_3 + CH_3 \rightarrow C_2H_6$ (9). The rate equation derived from the scheme, $-d[CH_3CHO]/dt = k_5 k_9^{-1/2} I_a^{1/2} [CH_3CHO] + k_6 k_9^{-1/2} I_a^{1/2} [D_2S]$, is in agreement with the results. The application of this rate equation leads to $k_6/k_5 = 2.0 \exp(3000/RT)$, and to $k_6 = 10^{11.6} \exp(-3800/RT)$ $mol^{-1}$ cc. $sec^{-1}$, if $k_5 = 10^{11.3} \exp(-6800/RT)$ $mol^{-1}$ cc. $sec^{-1}$, as has been reported by Ausloos and Steacie. On reinvestigating the effect of hydrogen sulfide addition, it was found that $k_6'/k_5 = 1.5 \exp(4150/RT)$, where $k_6'$ refers to the $CH_3 + H_2S \rightarrow CH_4 + HS$ (6') reaction. We thus obtain $k'_6/k_6 = = 0.75 \exp(1150/RT)$.

The authors are grateful to Dr. Setsuo Taniguchi of the Radiation Center of Osaka Prefecture for the mass spectrometric analysis.

*Department of Applied Chemistry*
*College of Engineering*
*University of Osaka Prefecture*
*Sakai, Osaka*

# Amylose-Iodine Complex. IV. The Complex in Dimethyl Sulfoxide - Water Mixtures

By Sôzaburo ONO, Takehiko WATANABE, Kozo OGAWA and Nobuhiko OKAZAKI

(Received September 19, 1964)

In a previous report[1] the failure of amylose to form an iodide-free iodine complex in solution has been reported. Judging from the physicochemical properties, Kuge and Ono[2] have suggested a deformed helix conformation, similar to the one proposed by Holló and Szejtli,[3] of amylose in neutral aqueous solutions. However, the dependence of the formation of blue amylose-iodine complex on both the iodide ion and the dissolved state of aqueous uncoupled amylose has not yet been perfectly demonstrated.

In the present work, in order to obtain further knowledge on the conditions of amylose-iodine complex formation, colorimetric, spectrophotometric and viscometric studies have been made of the complex in dimethyl sulfoxide - water mixtures.

1) T. Kuge and S. Ono, This Bulletin, **33**, 1269 (1960).
2) T. Kuge and S. Ono, ibid., **34**, 1264 (1961).
3) J. Holló and J. Szejtli, *Die Stärke*, **10**, 49 (1958).

## Experimental

**Materials.** — Amylose was obtained from potato starch as follows.[4] Potato starch dispersed in a small quantity of water was poured into 1 N sodium hydroxide and dissolved by stirring them with a magnetic stirrer under nitrogen. After the starch had dissolved, the pH of the solution was adjusted to 5.4—5.6 with 2 N hydrochloric acid. The temperature of the solution was then raised to 70—80°C, and the solution was saturated with an excess of *n*-butanol while being stirred constantly, after which it was continually stirred for one day. After centrifugation of the amylose-butanol complex, the complex was recrystallized three times from hot water (about 90°C) in the presence of excess butanol. The recrystallized complex was washed thrice with absolute methanol and then once with absolute ethanol to remove butanol and water, and then dried in a vacuum over anhydrous calcium chloride.

The fractionation of amylose was carried out at

4) H. Azumi and T. Nakajima, *Sci. Rep. Tohoku Univ. Ser. I*, **36**, 278 (1952).

room temperature. The amylose was dissolved in dimethyl sulfoxide (DMSO) and fractionated by the addition of appropriate amounts of absolute ethanol, as described by Everett and Foster.[5] Seven subfractions of amylose were prepared.

The amylose subfraction whose number average molecular weight, as determined by osmotic pressure measurements, was $6\times10^5$ in DMSO at 35°C was principally used in this experiment.

As DMSO, commercially-available DMSO was distilled in a closed system under reduced pressure over Drierite.[6] This procedure gave a distillate whose density and viscosity agreed well with those reported in the literature.[6]

The water used was thrice distilled by using a glass apparatus.

**Sample Solution.**—The amylose DMSO solution was prepared as follows. Amylose was dissolved in DMSO by stirring them with a magnetic stirrer in a glass-stoppered flask for several hours and then allowing the mixture to stand for one night in a desiccator over calcium chloride in order to complete the dissolution.

Iodine purified by sublimation was dissolved in DMSO or potassium iodide aqueous solutions.

Amylose iodine DMSO solutions were prepared by mixing both the amylose and the iodine DMSO solutions.

**Colorimetry.** — The blue-colored amylose-iodine complex DMSO-$H_2O$ solutions were prepared in glass-stoppered test tubes. The test tubes were immersed in a water bath whose temperature was raised at the rate of one degree per minute. Then the colored solution in the test tube changed its color from blue through green to yellow (or red brown*1) with the rising temperature. The temperature at which the greenish color of the solution completely faded ($T_f$) was determined. After the above procedure, the temperature of the bath was reversely allowed to fall slowly and the temperature was determined at which the solution perfectly developed a blue color ($T_d$). Generally, the values of both $T_f$ and $T_d$ obtained were accurate within ±2°C.

**Spectrophotometry.** — The spectrophotometric measurements were carried out by using a Hitachi-type EPU-2A photo-electric spectrophotometer with silica cells 1.00 cm. thick.

**Viscometry.** — Viscosity was determined in suspended-level dilution viscometers modelled after FitzSimons' modification of the Ubbelohde viscometer with one capillary tube. The dimensions were as follows: capillary diameter, 0.6 mm.; capillary length, 110 mm.; volume of efflux bulb, 5 ml.; volume of dilution bulb, 150 ml. The procedure used for determining the change in the viscosity of solutions with dilution by DMSO or by the addition of water to a given amylose DMSO solution, was as follows. Twenty milliliters of a given amylose DMSO solution was pipetted into the dilution bulb of the viscometer in a thermostat at a given temperature and then allowed to stand for 20 min. in order to establish the temperature equilibrium. The efflux time was determined with a stopwatch to the nearest 0.1 sec. The dilution of the solution by DMSO was made up by the repeated dilution of the charged solution in the dilution bulb. The addition of water to the DMSO solution was also made up by the repeated addition of water to the charged solution in the dilution bulb. Dilution by DMSO or the addition of water was done volumetrically. In the case of DMSO-$H_2O$ mixtures, the specific viscosities were obtained by comparing the viscosities of the solutions with those of the corresponding DMSO-$H_2O$ mixtures.

## Results and Discussion

The formation of blue amylose-iodine complex can not be observed in an amylose iodine DMSO solution, but it is sharply observed when the concentration of water in an amylose iodine DMSO-$H_2O$ solution reaches a critical value, as has been reported by Peticolas.[7] Figure 1 shows the dependences of $T_f$ and $T_d$ on the concentration of water in DMSO-$H_2O$ mixtures. The critical concentration of water for the formation of the blue complex could not be reduced below 28 mol./l., irrespective of both the amylose and iodine concentrations. Above the critical water concentration, both $T_f$ and $T_d$ rise with the increase in water concentration. $T_f$ and $T_d$ also rise with the increase in iodine concentration, as is shown in Fig. 2. Figure 3 shows the dependence of $T_f$ on the amylose concentration and also the results with amyloses, whose number average molecular weights were $4\times10^5$ *2 and $4\times10^4$ *3

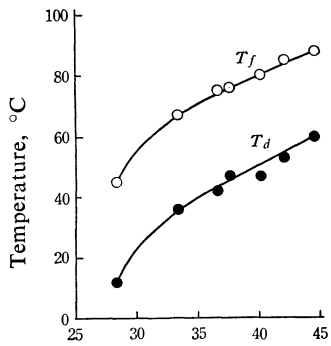



Fig. 1. Plot of $T_f$ and $T_d$ against water concn. in DMSO-$H_2O$ mixture: Concn. of amylose, 2 g./l.; concn. of iodine dissolved, 0.3 g./l.

5) W. W. Everett and J. F. Foster, *J. Am. Chem. Soc.*, **81**, 3459 (1959).

6) R. G. LeBel and D. A. I. Goring, *J. Chem. Eng. Data*, **7**, 100 (1962).

*1 The color of this solution depends on both iodine and water concentrations.

7) W. L. Peticolas, *Nature*, **197**, 898 (1963).

*2 Another subfractionated amylose.

*3 Degraded amylose prepared by treating the amylose (number average molecular weight: $6\times10^5$) iodine DMSO solution at 70°C for 23 hr. (see *4 on the degrading action of iodine).

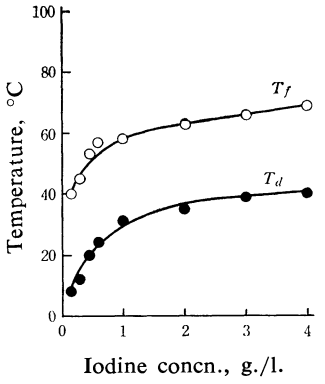



Fig. 2. Plot of $T_f$ and $T_d$ against iodine concn. in DMSO : $H_2O$=1 : 1 (v/v) mixture : Concn. of amylose, 2 g./l.

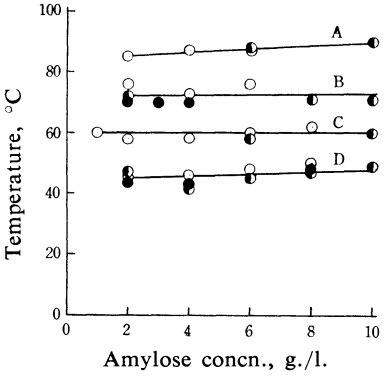



Fig. 3. Plot of $T_f$ against amylose concn. in iodine DMSO-$H_2O$ solution.
Curve A 1 g./l. iodine in DMSO : $H_2O$= 1 : 2 (v/v)
Curve B 0.3 g./l. iodine in DMSO : $H_2O$= 1 : 2 (v/v)
Curve C 1 g./l. iodine in DMSO : $H_2O$= 1 : 1 (v/v)
Curve D 0.3 g./l. iodine in DMSO : $H_2O$= 1 : 1 (v/v)
Molecular weight of amylose: ○, $60\times10^4$; ◐, $40\times10^4$; ●, $4\times10^4$

respectively. The results illustrated in Figs. 1, 2 and 3 show that the influence of amylose concentration and its molecular weight on $T_f$ values is slight compared with that of the water or iodine concentration. This fact, together with the fact that no purple or reddish color was observed at temperatures ranging from $T_d$ to $T_f$, may indicate that in this range of temperature the amylose-iodine complex has a fixed length of iodine chain and that the formation of the complex proceeds in all fashions or in none, irrespective of the concentrations and the molecular weights of amylose.

The dependence of $T_f$ on the composition of potassium iodide-iodine aqueous solutions

Table I. Dependence of $T_f$ on the composition of potassium iodide-iodine solutions

| $T_f$ °C | Equilibrium constant* $K\times10^3$ | Concn., M: Iodine $[I_2]\times10^5$ | Iodide ion $[I^-]\times10^3$ | Triiodide ion $[I_3^-]\times10^5$ |
|---|---|---|---|---|
| 50 | 2.0 | 1.7 | 0.3 | 0.26 |
| 67 | 2.5 | 0.9 | 3.0 | 1.1 |
| 75 | 2.8 | 0.2 | 30 | 1.8 |
| 81 | 2.9 | 6.0 | 3.0 | 6.0 |
| 84 | 3.0 | 0.4 | 30 | 3.6 |
| 90 | 3.1 | 10 | 3.0 | 10 |

* $K=[I_2][I^-][I_3^-]^{-1}$

of a given amylose concentration is shown in Table I. A regular relationship has been found only between $T_f$ values and triiodide ion concentrations (Fig. 4). The iodine, iodide ion and triiodide ion concentrations were calculated with the equilibrium constants[8] of the ($I_3^- \rightleftarrows I_2+I^-$) reaction at the temperature of $T_f$. In these experiments $T_d$ values could not be determined accurately because of the pale blue color development. The results shown in Fig. 4 indicate that the triiodide ion contributes to the thermal stability of the amylose-iodine complex.

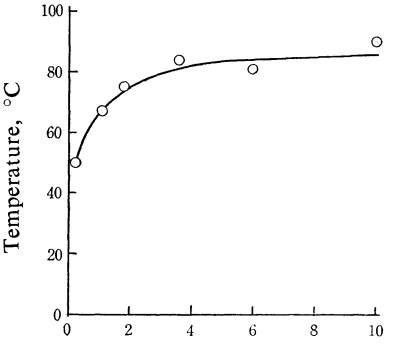



Fig. 4. Plot of $T_f$ against triiodide ion concn. in amylose (0.1 g./l.) potassium iodide-iodine aqueous solution.

The color of the iodine DMSO solution is similar to that of the iodine-iodide aqueous solution. The iodine DMSO solution possesses two absorption peaks (at 295 and 365 mμ), similar to those of the iodine-iodide aqueous solution (at 288 and 350 mμ). When water is added to the iodine DMSO solution, the two peaks shift towards the shorter wavelengths. The addition of amylose to the iodine DMSO solution causes no change in the ultraviolet absorption spectrum of the solution. When

8) M. Davies and E. Gwynne, *J. Am. Chem. Soc.*, **74**, 2748 (1952).

water is added to the amylose iodine DMSO solution, the ultraviolet and visible spectra of this amylose iodine DMSO-$H_2O$ solution show no change in nature compared with those of the corresponding iodine DMSO-$H_2O$ solution, as Fig. 5 shows, unless the blue coloration of the amylose iodine solution has been developed. When the concentration of water has exceeded a critical value, the blue amylose-iodine complex is produced in solution and the suppression of the peak at about 290 m$\mu$ and an increase in the height of the peak at about 355 m$\mu$ are observed, contrasting to the peaks of the corresponding iodine DMSO-$H_2O$ solution (Fig. 6). A similar change in the height of both the peaks in the ultraviolet spectrum

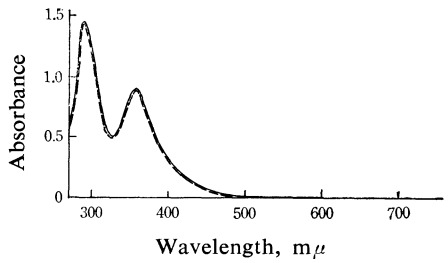



Fig. 5. Absorption spectra of 0.04 g./l. iodine in DMSO : $H_2O$=2 : 3 (v/v) mixture with 0.6 g./l. amylose (solid line) and without amylose (dashed line) at 24°C.

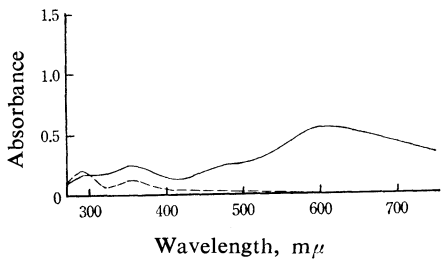



Fig. 6. Absorption spectra of 0.02 g./l. iodine in DMSO : $H_2O$=1 : 4 (v/v) mixture with 0.3 g./l. amylose (solid line) and without amylose (dashed line) at 24°C.

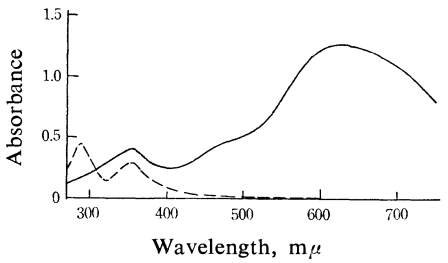



Fig. 7. Absorption spectra of 0.01 g./l. iodine 0.1 g./l. potassium iodide aqueous solution with 0.15 g./l. amylose (solid line) and without amylose (dashed line) at 24°C.

is observed with the amylose iodine-iodide aqueous solution (Fig. 7), as reported by Bebbington et al.[9] and Mould.[10]

These spectrophotometric results show that the nature of the amylose-iodine complex in DMSO-$H_2O$ mixtures is essentially the same as that of the complex in water. Both the peaks observed at the ultraviolet spectrum with a potassium iodide-iodine solution have been attributed to the triiodide ion by Awtrey and Connick.[11] The peaks observed with an iodine DMSO-$H_2O$ solution might also be attributed to the triiodide ion or the chemical species with an electron configuration similar to that of the triiodide ion, i. e., the polyiodide ion. Moreover, the rise in the values of $T_f$ and $T_d$ with the increase in iodine concentration (Fig. 2) seems to be explainable in terms of the increase in the triiodide (polyiodide) ion concentration.

Further spectrophotometric investigation of iodine DMSO-$H_2O$ solutions with or without amylose is in progress.

Figure 8 shows the viscometric results. Curve A shows the relationship between the amounts of water added to the 20 ml. of a 1% amylose DMSO solution and the specific viscosity of

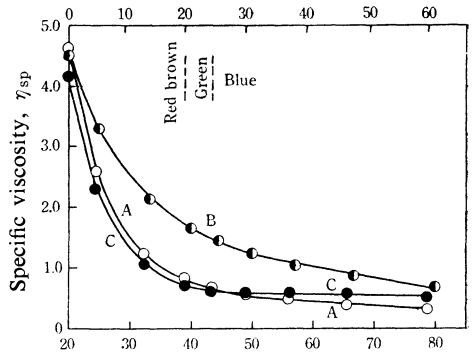



Fig. 8. The change in specific viscosity of the amylose solutions (with and without iodine) observed in the following experiments at 35°C.

Curve A 1% amylose DMSO solution (20 ml.) + water

Curve B 1% amylose DMSO solution (20 ml.) + DMSO

Curve C 1% amylose, 0.15% iodine DMSO solution (20 ml.) + water (in this case blue color development of the solution occurs at the water content shown in figure)

9) A. Bebbington, E. J. Bourne and I. A. Wilkinson, *J. Chem. Soc.*, **1952**, 246.
10) D. L. Mould, *Biochem. J.*, **58**, 593 (1954).
11) A. D. Awtrey and R. E. Connick, *J. Am. Chem. Soc.*, **73**, 1842 (1951).

the solution. Curve B shows the change in the specific viscosity of the amylose DMSO solution in the case of dilution with DMSO. The change in the specific viscosity with the increase in the amount of water (curve A) is very sharp compared to that in the case of simple dilution with DMSO (curve B). Curve C*[4] shows the relationship between the specific viscosity of the amylose iodine solution and the amounts of water added to the 20 ml. of a 1% amylose and 0.15% iodine solution. In this case the color of the solution changes from red brown through green to blue at the water content level where the sharp decrease in the specific viscosity terminates with the addition of water. The viscosity of DMSO-$H_2O$ mixtures shows no appreciable change with the dissolution of iodine. Therefore, the character of curve C may be determined primarily by the dissolved state of amylose in solution. No appreciable discontinuity in the change of the curvature of curve C has been observed at the range of water content where the blue amylose-iodine complex formation proceeds. This fact suggests that the formation of the complex does not accompany any appreciable conformational change of the amylose molecule. With the iodine complex, the molecular chain of amylose takes a helical conformation; therefore, the uncoupled amylose molecule in the corresponding DMSO-$H_2O$ mixture must take a conformation which may easily be transformed into the well-ordered helix accompanying the complex formation, i. e., the deformed helix.[2,3] The critical water concentration for blue amylose-iodine complex formation, as observed by colorimetric studies, agrees with the water content level of the amylose DMSO-$H_2O$ solution at which the sharp decrease in specific viscosity terminates. This fact suggests that the molecular chain of amylose must exist primarily as a deformed helix prior to the formation of the iodine complex.

An experiment similar to that of curve A has been made using 0.05 M iodic acid instead of water. In this case, the production of the triiodide (polyiodide) ion was repressed by the iodic acid,*[5] and no blue-colored complex was formed. The curve obtained was similar to curve A and lay parallel to and somewhat downward from it. This character of the curve shows that the amylose exists as a deformed helix at a high water content, as in the case of curve A. This result suggests that the amylose molecule existing as a deformed helix alone could not form the amylose-iodine complex without the presence of an amount of triiodide (polyiodide) ions sufficient to form the complex in solution.

The fact that the specific viscosity of the amylose-iodine complex solution is higher than that of the amylose solution at a high concentration of water in DMSO-$H_2O$ mixture may be attributed to the rigid nature of the structure of the complex compared to that of the uncoupled amylose.

Everett and Foster[12] have demonstrated that amylose exists as a coil in DMSO. Cowie,[13] on the other hand, has suggested that the existence of a helical structure could be expected of the amylose molecule dissolved in both DMSO and DMSO-$H_2O$ mixtures. Taking these authors' results into account, the present experimental results may be explained as follows. The amylose molecule may exist as a coil in DMSO; however, it can not be expected to exist as a completely extended linear chain because of the $\alpha$-1, 4-glucosidic linkages that impose steric limitations on the molecular chain. When water is added to the amylose DMSO solution, the degree of extension of the molecular chain may decrease, and the chain tends to draw itself into a somewhat helical conformation (the deformed helix[2,3]). This change in molecular chain extension seems to reveal itself as the initial sharp decrease in specific viscosity with the addition of water shown in curve A of Fig. 8. Spectrophotometric studies show that there is no interaction between the amylose and iodine unless the blue complex has been formed. The initial sharp decrease in the specific viscosity observed with curve C of Fig. 8 may be expected to be brought about by the same conformational change in the amylose chain as in the case of curve A.

The deformed helix may be regarded as a chain conformation in which the thermal fluctuations in the conformation of the molecular chain occur between the helically-wound chain conformation and the linear-extended one in a single molecule; the helical conformation is superior to the linear. Probably the

*[4] The amylose DMSO solution shows no change in viscosity after standing for one month after preparation. On the contrary, in the amylose iodine DMSO solution, amylose is degraded by the action of iodine, and the viscosity of the solution slowly decreases. Therefore, the specific viscosity of the amylose DMSO solution (without the addition of water) of curve A (without iodine) does not coincide with that of curve C (with iodine).

*[5] In the present case, the production of the triiodide (polyiodide) ion was not completely repressed. For example, the absorbance at 355 m$\mu$ of the iodine solution in DMSO: 0.05 M iodic acid = 1 : 3 (v/v) decreases by an order of magnitude of $10^{-2}$ compared to that of iodine in DMSO: $H_2O$ = 1 : 3 (v/v); the former solution with amylose could not develop the blue color at 35°C, but it slowly developed a somewhat purple color when the solution was cooled below 20°C.

12) W. W. Everett and J. F. Foster, *J. Am. Chem. Soc.*, **81**, 3464 (1959).

13) J. M. G. Cowie, *Makromol.*, **42**, 230 (1961); **59**, 189 (1963).

formation of the amylose-iodine complex proceeds by holding the iodine molecules inside the helically-wound chain parts of the amylose molecule. Therefore, the number of iodine molecules concerned in the complex formation may be determined by the length of the helically-wound parts of the deformed helical amylose molecule. However, a stable iodine complex may be expected to be formed against the thermal fluctuations of the conformation when the length of the helically-wound parts of the amylose molecule has exceeded a certain value. Therefore, the minimum number of iodine molecules necessary for the stable amylose-iodine complex formation may be determined mainly by the conformation of the amylose molecule. As for the stable iodine complex formation, the concentration of water in a DMSO-$H_2O$ mixture may be the primary factor in determining the amylose conformation, and the concentration of triiodide (polyiodide) ions would be a subsidiary factor contributing to the thermal stability of the iodine molecules in the helix. In these circumstances, the iodine complex with fewer iodine molecules than necessary can not exist stably but will release the combined iodine instantly. This prerequisite to the iodine complex formation reveals itself as an all or nothing feature of the complex formation. The increase in water concentration in the DMSO-$H_2O$ mixture beyond the critical value necessary for the complex formation would cause an increase in the superiority of the helical conformation and also a rise in both $T_a$ and $T_f$ values. With the rise in temperature, the deformed helical amylose molecules would change their conformation to a somewhat extended one as the result of the decrease in the superiority of the helical conformation, and they would become unable to combine with the iodine molecules to form the stable iodine complex because of their deficiency in the conformational prerequisite to the holding of the minimum necessary number of iodine molecules inside the helically-wound parts of the amylose molecule.

Further physicochemical studies of the deformed helical conformation of amylose are in progress.

As for the iodine, its contribution to the formation of the complex may be made through two chemical species, i. e., the iodine molecule and the triiodide (polyiodide) ion. The existence of the triiodide (polyiodide) ion is indispensable for the formation of the complex; the minimum concentration of this ion necessary for complex formation is determined by the water concentration in the DMSO-$H_2O$ mixture at a given temperature and increases with the rise in temperature in a given water concentration. The spectrophotometric results show that no interaction between iodine or the triiodide (polyiodide) ion and the amylose molecule occurs unless the blue complex has been formed in the solution. Therefore, both the chemical species may be said to make a co-operative contribution to the complex formation. In these circumstances, the triiodide (polyiodide) ion may be supposed not only to assist the entrance of the iodine molecules into the helically-wound chain of amylose but also to act as a stabilizer for the fixation of the iodine within the helix. Thus, the resonating iodine chain in the amylose helix may be expected to be stabilized against thermal disturbance by the triiodide (polyiodide) ions adsorbed at both ends of the iodine chain, and the amylose-iodine complex may be expected to become more rigid in nature compared to that of the uncoupled amylose molecule.

## Summary

The temperature at which the blue color due to the formation of amylose-iodine complex fades completely has been determined with a system of amylose and iodine dissolved in dimethyl sulfoxide-water mixtures. This temperature rises with the increase in the concentration of iodine in mixtures, and also with the increasing concentration of water in the mixed solvents.

The spectrophotometric results show that the nature of the amylose-iodine complex in a dimethyl sulfoxide-water mixture is similar to that of one in water, and that the triiodide ion or a chemical species similar to the ion, i. e., the polyiodide ion, contributes to the formation of the complex.

The viscometric studies show that the amylose molecule takes a deformed helix conformation prior to the formation of the blue iodine complex and that this conformational prerequisite to the complex formation is fulfilled when the water concentration in a dimethyl sulfoxide-water mixture exceeds a critical value.

These results stated above may indicate that the triiodide (polyiodide) ion plays the part of "stabilizer" for the fixation of iodine molecules within the helically-wound chain of the amylose molecule when the amylose exists primarily as a deformed helix in solution.

*Laboratory of Biophysical Chemistry*
*College of Agriculture*
*University of Osaka Prefecture*
*Sakai, Osaka*

# The Electrooxidation of Absolute Methanol

By Kazuo SASAKI and Shigeo NAGAURA

(Received September 25, 1964)

Tsutsumi and his collaborators[1] first reported that several hydrocarbons give the corresponding methyl ethers upon the electrolysis of their methanolic solutions. They stated that the reaction proceeds through the formation of a methoxy-free radical.

As is well known,[2] alkoxy-free radicals can generally be produced by neither irradiation nor thermal decomposition from their parent alcohol. Electrolysis, therefore, seems to be a quite specific method for producing alkoxy-free radicals.

In this paper, the electrolytic behavior of absolute methanol containing sodium methylate or certain inorganic salts as supporting electrolytes will be described. The reactions of several hydrocarbons in the methanolic media will be reported on successively.

## Experimental Procedures and Results

**General Description of the Experiment.**— Special grade methanol obtained from the Wako Pure Chemicals company was distilled once and dehydrated by the usual method before use. Smooth or platinized platinum was used for both the anode and the cathode electrode throughout the present investigation. The size of the electrode was changed with each experiment. The electrode potential was measured with reference to a saturated calomel electrode (SCE). Besides sodium methylate, some inorganic salts were examined as supporting electrolytes. Unless otherwise stated, the concentration of the electrolyte was kept at 0.1 mol./l. The solution was deaerated by nitrogen before each experiment.

**The Static Potential of the Platinum Electrode (Fig. 1).**—The electrode potential at a no-current flow was measured as a function of the sodium methylate concentration and of the hydrogen partial pressure, which was varied by mixing hydrogen with dry nitrogen. Both smooth and platinized platinum electrode were examined, but the data concerning the smooth platinum electrode were discarded because of their poor regularity.

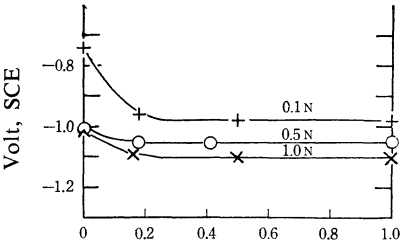



Fig. 1. Static electrode potential of Pt-Pt electrode in absolute methanol.
+ : 0.1 N Sodium methylate
○ : 0.5 N Sodium methylate
× : 1.0 N Sodium methylate

Although no quantitative conclusion can be obtained from this measurement, it is evident that the electrode potential is affected by the methylate concentration. The proportionality coefficient between the potential and the logarithm of concentration can roughly be estimated to be $2RT/F$.

**The Constant-current Polarization in the Stirred Solution.** — The current-potential and potential-time curves under the constant-current conditions were measured for sodium methylate solutions using a smooth platinum electrode with an apparent area of 30 $cm^2$. During the experiment nitrogen was bubbled into the solution.

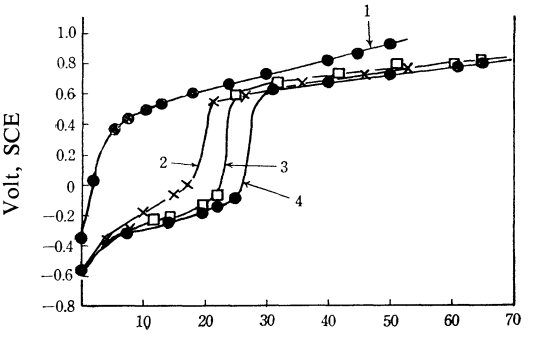



Fig. 2. Current-potential curves for various methylate concentrations.
Curve 1, 0.24 mol./l.; 3, 1.9 mol./l.;
2, 0.96 mol./l.; 4, 2.2 mol./l.

1) T. Inoue, K. Koyama, T. Matsuoka, K. Matsuoka and S. Tsutsumi, *J. Chem. Soc. Japan, Ind. Chem. Sec.* (*Kogyo Kagaku Zasshi*), **66**, 1659 (1963).
2) P. Gray and A. Williams, *Chem. Revs.*, **59**, 239 (1959).

Figure 2 shows the *i-E* curve obtained for solutions with different salt concentrations. It is significant that the *i-E* curves show a sudden rise in potential at a certain current value. The current value at which the potential rises suddenly is shifted regularly to a lower value with a decrease in the methylate concentration. A similar shape of the polarization curve has often been reported in the case of Kolbe electrosynthesis.[3-5]

In the latter case, it has been explained that the accumulation of carboxyl radicals, formed by the discharge of the carboxylate anion, on the electrode surface, causes the potential jump. In any case, it is clear, in the present experiment, that during the discharge of the methylate anion the electrode potential is kept at a lower value.

The potential-time curve obtained by constant current electrolysis is shown in Fig. 3. In this case, the concentration of methylate is kept constant. The figure shows that the time required for the potential rise is lengthened by the decrease in the current applied.

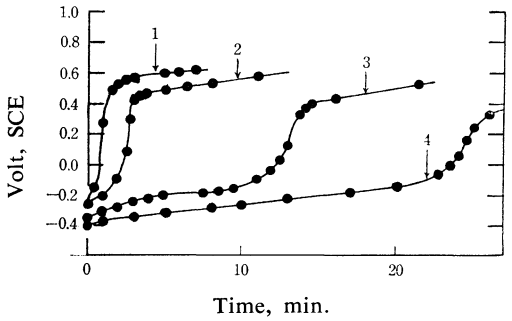



Fig. 3. Potential-time curves in the stirred solution.
Curve 1, 25 mamp.; 3, 12.2 mamp.; 2, 19 mamp.; 4, 8.6 mamp.; 0.1 mol./l. sodium methylate

**Constant-current Polarization under Unstirred Conditions (Chronopotentiometry).** — Another from of potential-time relationship was obtained under unstirred conditions. A schematic diagram of the cell for this measurement is shown in Fig. 4a. The *E-t* curves were obtained by an automatic pen-recorder. Platinized platinum (0.5 mm. in diameter and 5 mm. long) was used as the working electrode.

The most striking feature observed in this experiment is that the shape of the chrono-

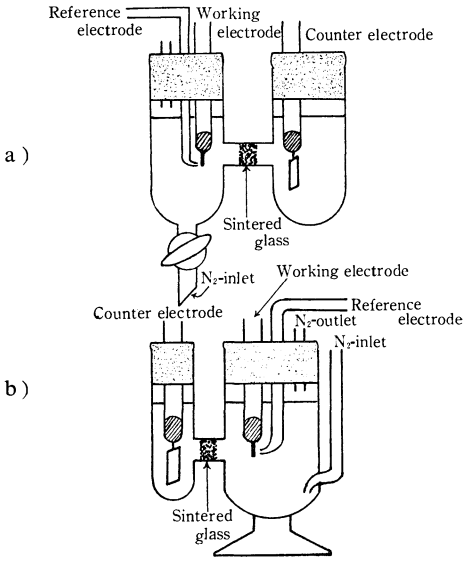



Fig. 4. Electrolysis cells.
a) for chronopotentiometry
b) for potentiostatic voltammetry

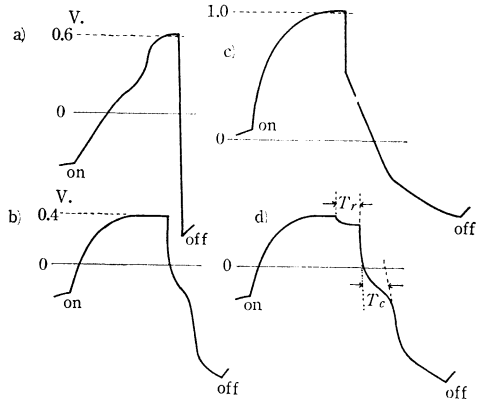



Fig. 5. Chronopotentiograms of current reversal in absolute methanol.
a) Sodium methylate, b) Sodium perchlorate, c) Ammonium chloride
Curve d illustrates the notations used in Fig. 7.

potentiogram is determined solely by the kind of supporting electrolyte used (Figs. 5a—c).

When sodium methylate was examined as a supporting electrolyte, the normal potential arrest (the chronopotentiometric "transition time") was observed in the process of anodic polarization. Upon the immediate reversal of the direction of the current flow, the potential decreased steeply without any characteristic change (Fig. 5a). The potential arrest observed in the anodic process satisfied approximately the requirement of the constancy of $i\tau^{1/2}$. This is illustrated in Fig. 6, which depicts the

3) N. Sato, T. Sekine and K. Sugino, 29th Annual Meeting of the Electrochem. Society of Japan, Sendai, 1962.
4) G. S. Pande and S. N. Schulka, *Electrochem. Acta*, 4, 215 (1961).
5) T. Dickinson and W. F. K. Wynne-Jones, *Trans. Faraday Soc.*, 58, 382, 388, 400 (1962).

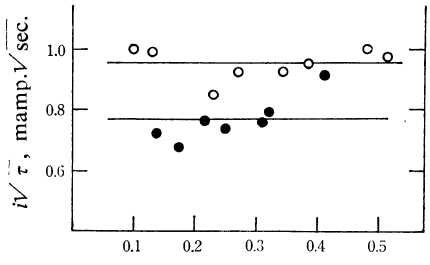



Fig. 6. Relation between $i\tau^{1/2}$ and current for methylate solution obtained from two separate runs; apparent area of Pt-Pt electrode is 0.08 cm$^2$.

results obtained from two separate runs.*

The anodic chronopotentiogram for sodium perchlorate, on the other hand, showed no characteristic potential arrest and reached the final plateau gradually. In this case, however, a definite potential arrest appeared in the cathodic half cycle (Fig. 5b). It is interesting that the potential arrest, $T_c$, is affected by the duration of the current rupture, $T_r$, between the anodic and cathodic half-cycles. Notations are illustrated in Fig. 5d.

As Fig. 7 shows, the cathodic arrest time decreases proportionally with the square root

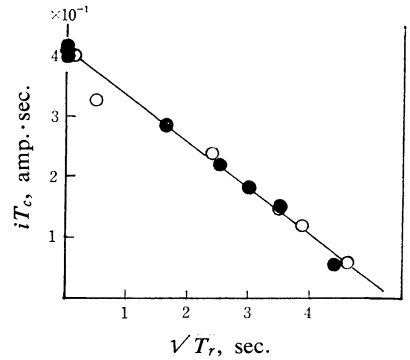



Fig. 7. The effect of the current rupture on the cathodic transition time in the perchlorate system.
Full and empty circles represent the results obtained by polarizing current of 330 and 770 $\mu$amp., respectively.

of the time of the current rupture. Although no active materials in this cathodic potential arrest are known, it is clear that such materials are produced during the anodic half-cycle but disappear from the electrode surface according to some simple kinetic rule.

By EPR measurement, Maki and Geske[8] observed the perchlorate-free radical formed electrolytically in an acetonitrile solution. Their results were confirmed in our laboratory, although no EPR signal was detected in the methanolic media.[9]

Although the shape of the chronopotentiogram of the ammonium chloride solution (Fig. 5c) is not simple enough for us to say more, it is at least clear that no potential arrest is observed in the anodic half-cycle.

The three types of chronopotentiograms obtained above suggest that methanol, as it is, can be oxidized electrochemically only with difficulty. In other works, the primary electroactive species in the electrooxidation of absolute methanol are the supporting electrolytes, not methanol itself or anythingelse which is derived from methanol.

The fact that the final values of the anodic potential for three kinds of electrolytes differ from each other may be a support for this statement.

**Potentiostatic Polarization.** — Potentiostatic measurements were also made using sodium

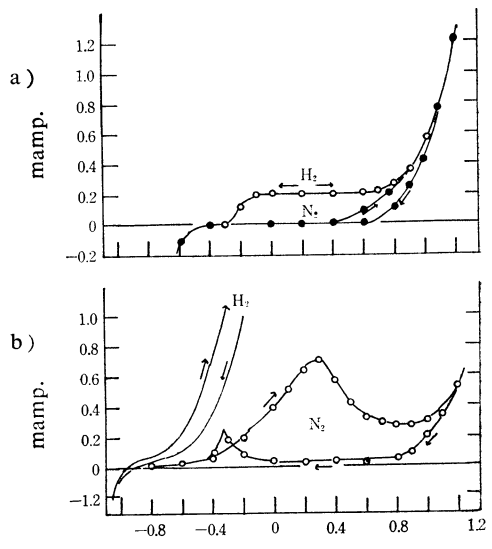



Fig. 8. Potentiostatic $i$-$E$ curves for sodium perchlorate (Fig. 8a) and sodium methylate solution (Fig. 8b).

* By using the mean value of these two experiments, and by evaluating the apparent surface area of the electrode, the concentration of methylate can be estimated as 0.3 mol./cc. If the true area of the platinized platinum electrode is 2000 times greater than the apparent one,[6] the figure calculated above agrees roughly with the real one. This treatment, however, seems to be too arbitrary. In the rigorous sense of the terminology, this case must be treated as the solution containing no supporting (indifferent) electrolyte. Accordingly, the chronopotentiometric transition time will be affected by the electric migration.[7]

6) J. S. Mayell and S. H. Langer, *J. Electroanal. Chem.*, 7, 288 (1964).
7) J. J. Lingane, ibid., 6, 300 (1963).
8) A. H. Maki and D. H. Geske, *J. Chem. Phys.*, 30, 1356 (1959).
9) K. Sasaki and T. Ichikawa, unpublished work.

methylate and sodium perchlorate as the supporting electrolytes. The platinized platinum electrode used in the chronopotentiometry was used again in this experiment. The rate of voltage scanning was 0.05 V./min. The electrolysis cell is shown in Fig. 4b. During the experiment, nitrogen or hydrogen gas was bubbled in order to agitate the solution.

In accordance with the results of the chronopotentiometry, the potentiostatic *i-E* curve was greatly affected by a change in the kind of electrolyte used. Figure 8a represents the results with a perchlorate solution. If the solution was under the nitrogen atmosphere, the *i-E* curve was quite simple and the anodic and cathodic scan curves were on almost the same line. When the solution was saturated with hydrogen, however, a definite diffusion limiting current was observed. The reverse scan curve coincided with the curve of forward scan. The fact that the anodic and cathodic scan curves are on the same line suggests that the complication of the surface change of platinum electrode encountered in the aqueous phase experiment[10] can be ignored in the methanolic media, at least if the scan speed is not exceptionally large.

Figure 8b presents the results concerning the methylate solution. In this case, the shape of the *i-E* curve is quite similar to that obtained in the aqueous solution of methanol. For instance, the anodic current shows a peak in the moderate potential range.

Furthermore, the potential at which the anodic current peak appears in the course of the cathodic scan is shifted to a less positive potential than in the case of the foregoing scan. In addition, the peak value of the anodic current is successively decreased when the scan is multiplicated. In this case the accumulation of electrolytically-inert material may be significant.

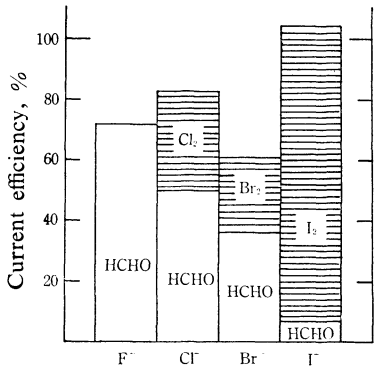



Fig. 9. Current efficiencies for the formation of formaldehyde (empty area) and free halogen (shaded area) with respect to four ammonium halides.

**Product Analysis.**—Methanol in an aqueous solution, especially in an acidic medium, is oxidized anodically to carbon dioxide, but the final product in absolute methanol is carbon monoxide. This was confirmed by mass spectrometric analysis.[11] In the present experiment, the products in the liquid phase was analyzed. One hundred cubic centimeters of absolute methanol containing either one of four ammonium halides or sodium methylate was electrolyzed for two hours at 100 mamp. The electrolysis cell was then cooled by ice-water mixiure in order to minimize the evaporation. The results of the analysis of free halogen and formaldehyde as determined by iodometric titration are shown in Fig. 9. In this figure, the product yield is expressed in terms of current efficiency. It can be seen that the formation of both formaldehyde and free halogen molecules is affected by the change in the supporting electrolyte.

As for ammonium iodide, the current is consumed almost completely in the liberation of the free iodine molecule. No free fluorine was detected, perhaps because of the immediate formation of hydrogen fluoride. It is interesting to notice that the formation of free halogen increased and formaldehyde decreased in the following order of supporting electrolytes: $F^-$, $Cl^-$, $Br^-$ and $I^-$.

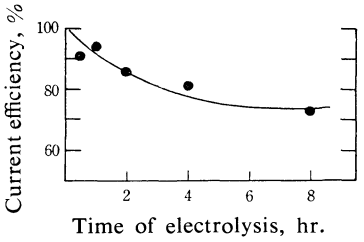



Fig. 10. The current efficiency of the formation of formaldehyde and the duration of the electrolysis. Supporting electrolyte is sodium methylate.

Except the case of iodide, the total current efficiency for the formation of free halogen and formaldehyde differed greatly from 100%. This is also ture when sodium methylate is used as the electrolyte. In the latter case, the current efficiency for the aldehyde formation is reduced by the duration of electrolysis (Fig. 10). The remainder of the current is consumed by the further oxidation of the

10) K. Ohashi, K. Sasaki and S. Nagaura, *J. Electrochem. Soc. Japan*, **32**, 515 (1964).

11) K. Sasaki and S. Nagaura, This Bulletin, **37**, 1086 (1964).

aldehyde, yielding carbon monoxide. In addition, since the present analysis does not cover the vapor phase, the evaporation of the products may be another reason for this discrepancy.

## Summary

From the several experiments described above, it can be concluded that the electroactive species in the anodic reaction of methanol in the moderate potential range is the methylate anion only.

The evidence for this conclusion will be summarized below.

The static potential of the platinized platinum electrode in absolute methanol is affected by the methylate concentration.

It is confirmed that a definite transition time in an anodic chronopotentiogram is observed only for the case of the methylate ion. The results from the potentiostatic experiments also support this conclusion.

Although this is the case, methanol is still electrolyzed to form formaldehyde at a higher potential range. Product analysis shows that the yield of formaldehyde is affected appreciably by the kind of supporting electrolyte. Except fluorine, an appreciable number of free halogen molecules is detected in the solution after electrolysis. Even in the case of an iodine/iodide couple, the thermodynamic potential is far more positive than that of methanol. It may be understood from this fact that the electrooxidation of neutral methanol is strongly irreversible. Furthermore, it seems quite plausible that some part of the methanol is decomposed by the attack of the free radicals (or atoms) formed by the discharge of salt anion. The reaction scheme can be formulated as follows:

$$X^- \rightarrow X + e$$

$$X + CH_3OH \rightarrow HX + CH_3O \text{ (or } CH_2OH)$$

$$2CH_3O \text{ (or } CH_2OH) \rightarrow CH_3OH + HCHO$$

Coinciding with this hypothesis, the current efficiencies of formaldehyde formation are increased in the order of the hydrogen-abstracting power of the four halogen atoms examined, i.e., $I < Br < Cl < F$ (see Fig. 9).

The mechanism of the electrolytic oxidation of methanol in aqueous solution has been studied by many authors, but no mechanism has yet been accepted without any ambiguity.

The static electrode potential observed in an aqueous methanol solution rests near the thermodynamic redox couple:

$$CH_3OH = HCHO + 2H^+ + 2e \quad 0.23 \text{ V. NHE}$$

It is evident, however, that the real process does not proceed through such a simple reversible path.

Another mechanism proposed is the catalytic dehydrogenation:

$$CH_3OH = HCHO + 2H(Ads)$$

$$2H(Ads) \rightarrow 2H^+ + 2e$$

This mechanism seems somewhat plausible, and some indirect evidence for it has been pointed out by the present authors.[12]

Although it is difficult to state a definite conclusion about the reaction mechanism in the aqueous solution, the present conclusion, emphasizing the importance of the methylate ion, seems applicable in the case of the aqueous phase reaction. The fact that the performance of the methanol fuel cell in the alkaline medium is superior to that in the acidic one can thus be understood if the following reaction is taken into account:

$$CH_3OH + OH^- = CH_3O^- + H_2O$$

*Faculty of Engineering*
*Osaka City University*
*Sumiyoshi-ku, Osaka*

12) K. Sasaki and S. Nagaura, 4th Symposium on the primary cell, Kawasaki, October, 1963.

# The Rotatory Dispersion of Cobalt(III) Ammine Complexes Containing Amino Acid as a Unidentate Ligand

By Junnosuke FUJITA*, Takaji YASUI and Yoichi SHIMURA

(Received October 13, 1964)

Although several studies[1-4] have been made of the rotatory dispersion of metallic complexes in which the asymmetric center is not around the metal ion but is only at the atom in the coordinated ligand, most of these studies have been made on planar-type complexes such as copper(II) alaninate. For octahedral complexes, Jaeger[5] has prepared the molecular complex $[Co(NO_2)_3NH_3(d\text{-chxn})]$** and shown that this complex exhibits an anomalous dispersion in the region of the first absorption band. A similar study has been reported by Mathieu[6] on a similar complex, $[Co(NO_2)_3NH_3(d\text{-pn})]$. Recently, Shimura[7] has prepared the complex $[Co(NH_3)_4(\text{L-leuc})]^{2+}$, which has a much simpler structure than those of the above type, and has observed an anomalous dispersion which consists of two inversive dispersions in the vicinity of its first absorption band. Through these experiments, the existence of the so-called "vicinal effect"[1,2] between the central metal ion and the asymmetric atom in the ligand has been proved.

It should be noted, however, that the previous investigations were made with complexes containing an optically active reagent as a chelate ligand. The chelate ligand sometimes takes the gauche form upon coordination, which may result in another optically active structure. In order to study the vicinal effect in more detail, it would be desirable to measure the rotatory dispersion of the complex coordinating with a unidentate optically active ligand. Unfortunately, no complexes of such type are known. It was decided at first, therefore, to prepare cobalt(III) complexes in which amino acid is coordinated as a unidentate ligand.

In the present paper, the preparation and the absorption studies of a large number of pentammine and tetrammine cobalt(III) complexes containing both optically active and inactive amino acids will be described. The rotatory dispersion and the circular dichroism of the optically active complexes will also be measured, and the results will be discussed from the standpoint of the structure of these complexes.

## Experimental

**Preparation.** — *Pentammineglycinecobalt(III) Perchlorate Monohydrate: $[Co(NH_3)_5(glyH)](ClO_4)_3\cdot H_2O$.* — An aqueous solution containing 5 g. of aquopentamminecobalt(III) perchlorate[8] and 2 g. (excess) of glycine in 50 ml. of water was gradually evaporated on a water bath at 75—80°C to a volume of about 20 cc. The dark red solution obtained was kept in a refrigerator overnight. The orange-pink crystals formed were filtered and washed with a water-ethanol (1 : 1) mixture and then with absolute ethanol. This was recrystallized by dissolving it in warm water and then cooling it in a refrigerator. Recrystallization from a cold aqueous solution was also effected by the addition of 30% perchloric acid.

*Pentamminecobalt(III) Perchlorates of β-Alanine, DL-α-Alanine, L-α-Alanine and γ-Aminobutylic Acid: $[Co(NH_3)_5(\beta\text{-alaH})](ClO_4)_3$, $[Co(NH_3)_5(\text{DL-}\alpha\text{-alaH})](ClO_4)_3\cdot H_2O$, $[Co(NH_3)_5(\text{L-}\alpha\text{-alaH})](ClO_4)_3\cdot 2H_2O$ and $[Co(NH_3)_5(\gamma\text{-ambutH})](ClO_4)_3$.* — These complexes were prepared by the same method as the glycine complex described above, using β-alanine, DL-α-alanine, L-α-alanine and γ-aminobutylic acid respectively. These complexes are more soluble in water than is the glycine complex.

*Pentammine-L-phenylalanine-cobalt(III) Perchlorate Monohydrate: $[Co(NH_3)_5(\text{L-phalaH})](ClO_4)_3\cdot H_2O$.* — To 50 ml. of an aqueous solution containing 5 g. of aquopentamminecobalt(III) perchlorate 2 g. (a slight excess) of L-phenylalanine was added. The mixture was warmed on a water bath at 80°C until the amino acid was dissolved. The dark red solution

* Present address; Department of Chemistry, Faculty of Science, Tohoku University, Sendai.

1) I. Lifschitz, *Z. phys. Chem.*, **105**, 27 (1923); **114**, 485 (1925).

2) P. Pfeiffer and W. Christeleit, *Z. physiol. Chem.*, **247**, 262 (1937); **248**, 197 (1937).

3) P. Pfeiffer, W. Christeleit, T. Hesse, H. Pfitzner and H. Thielert, *J. prak. Chem.*, **150**, 261 (1938).

4) I. Lifschitz and F. L. M. Schouteden, *Rec. Trav. Chim.*, **58**, 411 (1939).

5) F. M. Jaeger, *Bull. soc. chim. France*, [5] **4**, 1201 (1937).

** The following abbreviations will be used: chxn = $C_6H_{10}(NH_2)_2$, 1,2-diaminocyclohexane; pn = $NH_2CH(CH_3)CH_2NH_2$; leuc = $NH_2CH(COO^-)CH_2CH(CH_3)_2$; glyH = $NH_3^+CH_2COO^-$; gly = $NH_2CH_2COO^-$; β-alaH = $NH_3^+CH_2CH_2COO^-$; α-alaH = $NH_3^+CH(CH_3)COO^-$; α-ala = $NH_2CH(CH_3)COO^-$; phalaH = $C_6H_5CH_2CH(NH_3^+)COO^-$; γ-ambutH = $NH_3^+CH_2CH_2CH_2COO^-$; bet = $(CH_3)_3N^+CH_2COO^-$.

6) J.-P. Mathieu, *Ann. de Phys.*, [11] **19**, 335 (1944).

7) Y. Shimura, This Bulletin, **31**, 315 (1958).

8) O. Hassel and G. B. Naess, *Z. anorg. Chem.*, **174**, 24 (1928).

obtained was then evaporated on a water bath at 75—80°C to a volume of about 20 cc. and cooled in ice. The red crystals obtained were filtered and washed with a water-ethanol (1 : 1) mixture and then with absolute ethanol. Fine crystalline needles were obtained from a cold aqueous solution by adding 30% perchloric acid.

*Glycinatopentamminecobalt(III) Perchlorate: [Co-gly($NH_3$)$_5$]($ClO_4$)$_2$.* — Three grams of pentammineglycinecobalt(III) perchlorate monohydrate was dissolved in 20 ml. of 30% aqueous ammonia. To the dark red solution obtained ethanol was then added. Upon cooling in ice, the dark red crystals formed were filtered and washed with a water-ethanol (1 : 1) mixture and then with absolute ethanol. This complex was recrystallized from 3% aqueous ammonia by adding ethanol.

*DL-α-Alaninato-pentamminecobalt(III) Perchlorate Monohydrate: [Co(DL-α-ala)($NH_3$)$_5$]($ClO_4$)$_2$·$H_2O$.* — The dark red crystals of this complex were obtained by the method described above for the glycinato complex, but using [Co($NH_3$)$_5$(DL-α-alaH)]($ClO_4$)$_3$·$H_2O$ instead of [Co($NH_3$)$_5$(glyH)]($ClO_4$)$_3$·$H_2O$.

*Tetrammine-bis(glycine)cobalt(III) Perchlorate: [Co($NH_3$)$_4$(glyH)$_2$]($ClO_4$)$_3$.* — To 30 ml. of an aqueous solution containing 5 g. of diaquotetramminecobalt(III) perchlorate[9] a slight excess of glycine (1.8 g.) was added. The resulting solution was gradually evaporated on a water bath at 75—80°C to a volume of about 10 ml. After cooling, the drop-by-drop addition of absolute ethanol to this solution resulted in the formation of purple crude crystals, which were then filtered and washed with ethanol. These crystals were recrystallized by dissolving them in the minimum amount of water and then adding ethanol and a few drops of concentrated perchloric acid. Purple crystals were obtained after the solution had been kept in a refrigerator overnight.

*Tetrammine-bis(DL-α-alanine)-, and Tetrammine-bis(L-α-alanine)cobalt(III) Perchlorates: [Co($NH_3$)$_4$-(DL-α-alaH)$_2$]($ClO_4$)$_3$ and [Co($NH_3$)$_4$(L-α-alaH)$_2$]-($ClO_4$)$_3$·$2H_2O$.*—Purple crystals of these complexes were prepared by the same method as the bis(glycine) complex described above, but using 2 g. of DL-α-alanine and L-α-alanine respectively instead of glycine.

*Aquotetrammineglycinecobalt(III) Perchlorate Monohydrate: [Co($OH_2$)($NH_3$)$_4$(glyH)]($ClO_4$)$_3$·$H_2O$.* — To an aqueous solution of 5 g. of diaquotetramminecobalt(III) perchlorate in 50 ml. of water 1 g. of glycine was added. The purple red solution obtained was warmed on a water bath at 80°C for 15 min. and cooled in ice. Pink-colored crystals were precipitated by adding concentrated perchloric acid; the crystals were then filtered and washed with ethanol. This complex was recrystallized from a cold aqueous solution by adding concentrated perchloric acid.

*Aquotetrammine-DL-α-alanine- and Aquotetrammine-L-α-alaninecobalt(III) Perchlorates: [Co($OH_2$)($NH_3$)$_4$-(DL-α-alaH)]($ClO_4$)$_3$·$H_2O$ and [Co($OH_2$)($NH_3$)$_4$(L-α-alaH)]($ClO_4$)$_3$·$H_2O$.* — These complexes were prepared and recrystallized by the method which has been described above for the aquo-glycine complex, but using 1.2 g. of DL-α-alanine and L-α-alanine respectively instead of glycine. These complexes were more soluble in water than the corresponding

Table I. Chemical analysis of the complexes

| Complex | Co, % | | $H_2O$, % | | C, % | | H, % | |
|---|---|---|---|---|---|---|---|---|
| | Found | Calcd. | Found | Calcd. | Found | Calcd. | Found | Calcd. |
| [Co($NH_3$)$_5$(glyH)]($ClO_4$)$_3$·$H_2O$ | 10.91 | 11.00 | 3.33 | 3.36 | 4.76 | 4.49 | 4.22 | 4.14 |
| [Co($NH_3$)$_5$(β-alaH)]($ClO_4$)$_3$ | 10.70 | 11.09 | — | — | 6.83 | 6.78 | 4.35 | 4.17 |
| [Co($NH_3$)$_5$(DL-α-alaH)]-($ClO_4$)$_3$·$H_2O$ | 10.71 | 10.72 | 3.10 | 3.28 | 6.43 | 6.56 | 4.52 | 4.40 |
| [Co($NH_3$)$_5$(L-α-alaH)]($ClO_4$)$_3$·$2H_2O$ | 10.14 | 10.38 | 6.42 | 6.35 | 6.77 | 6.35 | 4.49 | 4.62 |
| [Co($NH_3$)$_5$(L-phalaH)]($ClO_4$)$_3$·$H_2O$ | 9.24 | 9.42 | 2.97 | 2.88 | 17.66 | 17.28 | 4.58 | 4.51 |
| [Co($NH_3$)$_5$(γ-ambutH)]($ClO_4$)$_3$ | 10.76 | 10.80 | — | — | 9.11 | 8.81 | 4.47 | 4.43 |
| [Co($NH_3$)$_5$bet]($ClO_4$)$_3$ | 10.47 | 10.53 | — | — | 10.91 | 10.73 | 4.68 | 4.68 |
| [Co gly($NH_3$)$_5$]($ClO_4$)$_2$ | 14.27 | 14.13 | — | — | 6.03 | 5.76 | 4.64 | 4.59 |
| [Co(DL-α-ala)($NH_3$)$_5$]($ClO_4$)$_2$·$H_2O$ | 13.26 | 13.12 | 3.91 | 4.01 | 8.44 | 8.02 | 5.20 | 5.16 |
| [Co($OH_2$)($NH_3$)$_4$(glyH)]($ClO_4$)$_3$·$H_2O$ | 11.04 | 10.98 | 3.27 | 3.36 | 4.65 | 4.48 | 3.94 | 3.95 |
| [Co($OH_2$)($NH_3$)$_4$(DL-α-alaH)]-($ClO_4$)$_3$·$H_2O$ | 10.99 | 10.70 | 3.07 | 3.27 | 6.89 | 6.55 | 4.01 | 4.21 |
| [Co($OH_2$)($NH_3$)$_4$(L-α-alaH)]-($ClO_4$)$_3$·$H_2O$ | 10.72 | 10.70 | 2.96 | 3.27 | 6.43 | 6.55 | 4.11 | 4.21 |
| [Co($NH_3$)$_4$(glyH)$_2$]($ClO_4$)$_3$ | 10.19 | 10.24 | — | — | 8.77 | 8.35 | 3.95 | 3.85 |
| [Co($NH_3$)$_4$(DL-α-alaH)$_2$]($ClO_4$)$_3$ | 9.55 | 9.76 | — | — | 12.27 | 11.94 | 4.54 | 4.34 |
| [Co($NH_3$)$_4$(L-α-alaH)$_2$]($ClO_4$)$_3$·$2H_2O$ | 9.25 | 9.21 | 5.62 | 5.63 | 13.70 | 11.27 | 4.89 | 4.73 |
| [Co($NH_3$)$_4$(glyH)(L-α-alaH)]-($ClO_4$)$_3$·$2H_2O$ | 9.42 | 9.42 | 5.74 | 5.76 | 11.66 | 9.60 | 4.60 | 4.51 |
| [Co($NH_3$)$_4$(bet)$_2$]($ClO_4$)$_3$ | 8.81 | 8.93 | — | — | 18.07 | 18.21 | 5.25 | 5.19 |
| [Co(L-α-ala)($NH_3$)$_4$]$SO_4$ | 18.70 | 18.94 | — | — | 11.43 | 11.58 | 5.97 | 5.83 |

9) M. Linhard and M. Weigel, *Z. anorg. Chem.*, **260**, 65 (1949).

glycine complex.

*Tetrammineglycine-L-α-alaninecobalt(III) Perchlorate Dihydrate: $[Co(NH_3)_4(glyH)(L\text{-}\alpha\text{-}alaH)](ClO_4)_3\cdot 2H_2O$.* — To an aqueous solution containing 5 g. of aquotetrammineglycinecobalt(III) perchlorate dissolved in the minimum amount of water 0.9 g. of L-α-alanine was added. The reddish-violet solution obtained was warmed on a water bath at 80°C for 15 min. After it had cooled as a clear, dark violet solution, ethanol was added, resulting in the slow formation of purple crystals. These were filtered and washed with ethanol. Recrystallization from a concentrated aqueous solution was effected by the addition of ethanol and of a few drops of concentrated perchloric acid. Purple crystals were obtained after the solution had been kept in a refrigerator overnight.

*Pentamminebetaine- and Tetrammine-bis(betaine)-cobalt(III) Perchlorates: $[Co(NH_3)_5bet](ClO_4)_3$ and $[Co(NH_3)_4(bet)_2](ClO_4)_3$.*—These betaine complexes were prepared by the method described in the literature[10] and were recrystallized several times from the aqueous solutions.

*L-α-Alaninato-tetramminecobalt(III) Sulfate: $[Co(L\text{-}\alpha\text{-}ala)(NH_3)_4]SO_4$.*—This complex was prepared by the method given by Shimura[11] for the preparation of DL-α-alaninato-tetramminecobalt(III) sulfate. The corresponding D-α-alaninato complex was also prepared by this method.

The results of the chemical analysis for all the complexes prepared are given in Table I.

**Spectral Measurements.**—Visible and ultraviolet absorption spectra were obtained by using a Shimadzu QR-50 spectrophotometer in the 30 to $150\times 10^{13}$ $sec^{-1}$ range. Infrared spectra were obtained with a Hitachi EPI-2G infrared spectrophotometer. The rotatory dispersion measurements were made by a Rudolph photoelectric spectropolarimeter, Model 200S-80. A Roussel-Jouan dichrograph in University of Pittsburgh, U. S. A., was used to obtain the circular dichroism spectra. All the measurements were made in aqueous solutions and at room temperature.

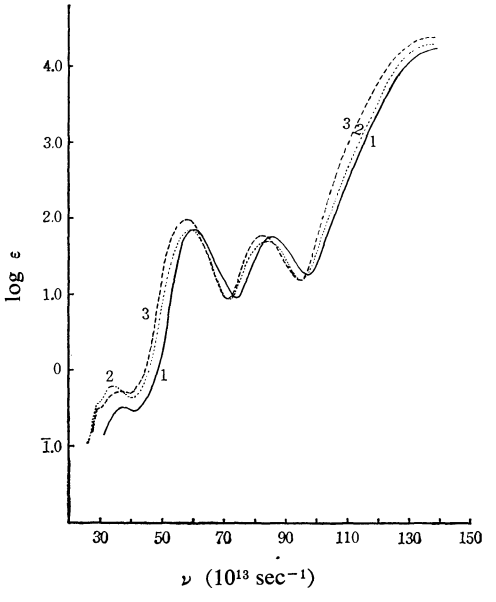



Fig. 1. Absorption spectra of
1, —— $[Co(NH_3)_5(glyH)](ClO_4)_3\cdot H_2O$;
2, ····· *cis*-$[Co(NH_3)_4(OH_2)(glyH)](ClO_4)_3\cdot H_2O$;
3, - - - *cis*-$[Co(NH_3)_4(glyH)_2](ClO_4)_3$.

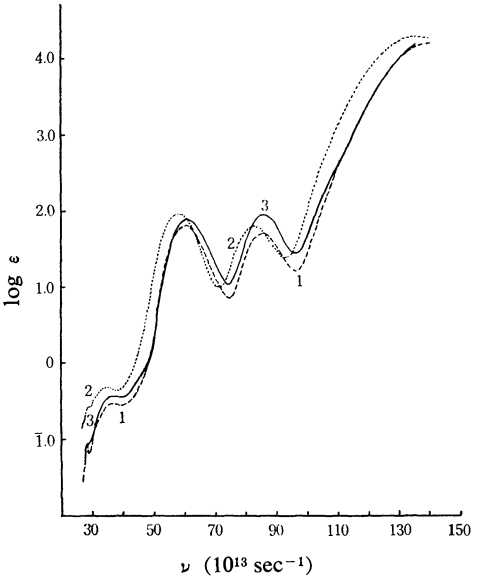



Fig. 2. Absorption spectra of
1, - - - $[Co(NH_3)_5(L\text{-}\alpha\text{-}alaH)](ClO_4)_3\cdot 2H_2O$;
2, ····· *cis*-$[Co(NH_3)_4(L\text{-}\alpha\text{-}alaH)_2](ClO_4)_3\cdot 2H_2O$;
3, —— $[Co(L\text{-}\alpha\text{-}ala)(NH_3)_4]SO_4$.

## Results

Table II lists the numerical data for the A, the first and the second absorption bands obtained in the present measurements. The data for the complexes which contain DL-α-alanine are not listed in this table, because they are exactly identical with those of the corresponding L-α-alanine complexes. Some typical absorption curves of the spectra are shown in Figs. 1 and 2. Figures 3—9 show the rotatory dispersion, the circular dichroism and the absorption curves of different complexes.

## Discussion

**Amino Acid in Unidentate Coordination.** — It has been well known that an amino acid usually coordinates to a metal as a chelate ligand with its amino and carboxyl groups. In some particular complexes, however, the ligand amino acid is considered to act as a

10) J. V. Quagliano, S. Kida and J. Fujita, *J. Am. Chem. Soc.*, **84**, 724 (1962).
11) Y. Shimura, This Bulletin, **31**, 173 (1958).

TABLE II. SUMMARY OF ABSORPTION DATA

The frequencies are given in $10^{13}\,sec^{-1}$, and the intensities by log $\varepsilon$ in parentheses.

| Complex | A | I | II |
|---|---|---|---|
| $[Co(NH_3)_5(glyH)](ClO_4)_3\cdot H_2O$ | 37 ($\bar{1}$.5) | 60.0(1.84) | 85.6(1.74) |
| $[Co(NH_3)_5(\beta\text{-alaH})](ClO_4)_3$ | 37.5($\bar{1}$.5) | 60.2(1.83) | 85.3(1.72) |
| $[Co(NH_3)_5(L\text{-}\alpha\text{-alaH})](ClO_4)_3\cdot 2H_2O$ | 37 ($\bar{1}$.5) | 60.0(1.83) | 85.7(1.73) |
| $[Co(NH_3)_5(L\text{-phalaH})](ClO_4)_3\cdot H_2O$ | 37 ($\bar{1}$.5) | 60.0(1.83) | 85.8(1.74) |
| $[Co(NH_3)_5(\gamma\text{-ambutH})](ClO_4)_3$ | 37.5($\bar{1}$.5) | 60.0(1.89) | 85.2(1.79) |
| $[Co(NH_3)_5bet](ClO_4)_3$ | 38 ($\bar{1}$.5) | 59.8(1.84) | 85.0(1.73) |
| *cis*-$[Co(OH_2)(NH_3)_4(glyH)](ClO_4)_3\cdot H_2O$ | 34.5($\bar{1}$.8) | 58.8(1.84) | 84.0(1.69) |
| *cis*-$[Co(OH_2)(NH_3)_4(L\text{-}\alpha\text{-alaH})](ClO_4)_3\cdot H_2O$ | 35 ($\bar{1}$.9) | 59.3(1.86) | 83.6(1.72) |
| *cis*-$[Co(NH_3)_4(glyH)_2](ClO_4)_3$ | 35 ($\bar{1}$.7) | 58.2(1.98) | 82.8(1.76) |
| *cis*-$[Co(NH_3)_4(L\text{-}\alpha\text{-alaH})_2](ClO_4)_3\cdot 2H_2O$ | 34.5($\bar{1}$.7) | 58.2(1.97) | 82.6(1.82) |
| *cis*-$[Co(NH_3)_4(glyH)(L\text{-}\alpha\text{-alaH})](ClO_4)_3\cdot 2H_2O$ | 35.5($\bar{1}$.7) | 58.3(1.95) | 82.7(1.78) |
| *cis*-$[Co(NH_3)_4(bet)_2](ClO_4)_3$ | 35 ($\bar{1}$.7$_5$) | 58.5(1.97) | 82.7(1.78) |
| $[Co(L\text{-}\alpha\text{-ala})(NH_3)_4]SO_4$ | 36.5($\bar{1}$.5$_5$) | 60.8(1.89) | 86.5(1.94) |

unidentate ligand,[12-15] although no such complexes of cobalt(III) have been isolated. In the present study, the analytical values of the complexes prepared clearly indicate that the amino acids in these complexes coordinate to the cobalt(III) ion as a unidentate ligand. With respect to the amino acids concerned, there are two possible ways of bonding to the cobalt ion as a unidentate ligand. One is to be coordinated to the cobalt with the oxygen atom of the carboxyl group, and the other, with the nitrogen atom of the amino group. In the present case, the results of the absorption measurements suggest that the coordination of amino acid corresponds to the former way. The maximum frequencies and intensities of the first and the second bands of the unidentate amino acid complexes are almost the same as those of the betaine complexes in which the ligand betaine undoubtedly coordinates to the cobalt(III) ion with its carboxyl group (see Table II). Other evidence of the cobalt-oxygen linkage in the unidentate amino acid complexes lies in their infrared spectra. All the unidentate amino acid complexes except for the $[Co\,gly(NH_3)_5](ClO_4)_2$ and $[Co(DL\text{-}\alpha\text{-ala})(NH_3)_5](ClO_4)_2\cdot H_2O$ complexes show the C-O stretching band of the coordinated carboxyl group at about 1650 $cm^{-1}$.[10,16] and the deformation band of $-NH_3^+$ group at about 1500 $cm^{-1}$.[17] The $[Co\,gly(NH_3)_5](ClO_4)_2$ and $[Co(DL\text{-}\alpha\text{-ala})(NH_3)_5](ClO_4)_2\cdot H_2O$ complexes, which are prepared in alkaline media, do not show the $-NH_3^+$ deformation band. This indicates that the structure of the amino group is the $-NH_2$ form caused by the neutralization with alkali. All these facts lead to the conclusion that the carboxyl group is more favored than the amino group in the unidentate coordination to the cobalt(III) ion.

An attempt to prepare a complex in which the unidentate amino acid is coordinated to the cobalt(III) ion with its amino group was not successful. In the reaction of aquopentamminecobalt(III) perchlorate with amino acid, the treatment above 85°C or the addition of activated charcoal always produced complexes containing amino acid as a chelate ligand, with the evolution of ammonia gas.

In the tetrammine-bis(amino-acid)cobalt(III) ion two geometrical isomers, cis and trans, are possible, but only one species for each tetrammine complex has been obtained in the present preparation. As Figs. 1 and 2 show, the first bands of all the tetrammine complexes exhibit no splittings. The tetrammine complex with two oxygen atoms in trans positions may be expected to show distinct splittings of the first absorption band.[18] Thus, it has been concluded that all the tetrammine complexes prepared here correspond to the cis isomers. The first band of the bis(acetato)tetramminecobalt(III) complex, which has a structure similar to that of the unidentate amino acid complexes, shows a remarkable splitting in the trans isomer, but no splitting in the cis isomer.[19]

The first and the second absorption bands of the pentammine(amino-acid)cobalt(III) complexes shifted to a longer wavelength than

12) A. Nakahara, J. Hidaka and R. Tsuchida, This Bulletin, **29**, 925 (1956).
13) R. W. Green and K. P. Ang, *J. Am. Chem. Soc.*, **77**, 5482 (1955).
14) L. M. Volshtein and M. F. Mogilevkina, *Doklady Akad. Nauk S. S. S. R.*, **104**, 418 (1955).
15) L. M. Volshtein and N. S. Velikanova, *Zhur. Neorg. Khim.*, **1**, 48 (1956).
16) K. Nakamoto, J. Fujita, S. Tanaka and M. Kobayashi, *J. Am. Chem. Soc.*, **79**, 4904 (1957).
17) L. J. Bellamy, "The Infrared Spectra of Complex Molecules," 2nd Ed., John Wiley and Sons, New York (1958).
18) H. Yamatera, This Bulletin, **31**, 95 (1958).
19) M. Linhard and M. Weigel, *Z. anorg. Chem.*, **264**, 321 (1951).

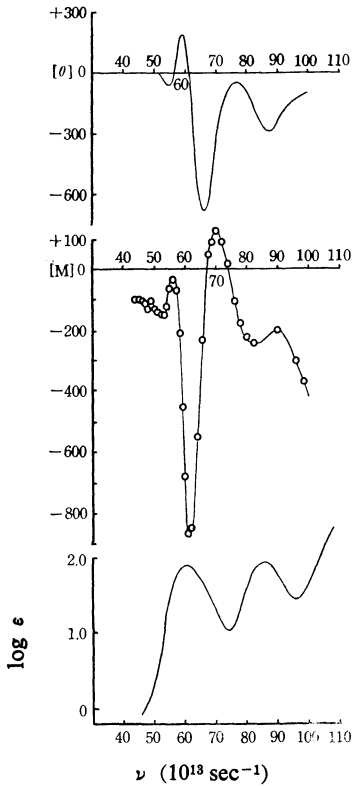



Fig. 3. Circular dichroism, rotatory dispersion and absorption of $[Co(L\text{-}\alpha\text{-ala})(NH_3)_4]SO_4$.

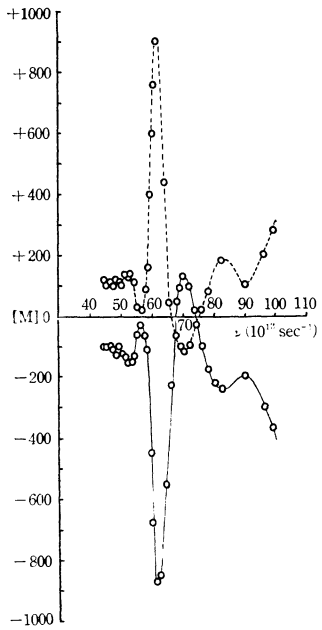



Fig. 4. Rotatory dispersion of:
—— $[Co(L\text{-}\alpha\text{-ala})(NH_3)_4]SO_4$, and - - - $[Co(D\text{-}\alpha\text{-ala})(NH_3)_4]SO_4$.

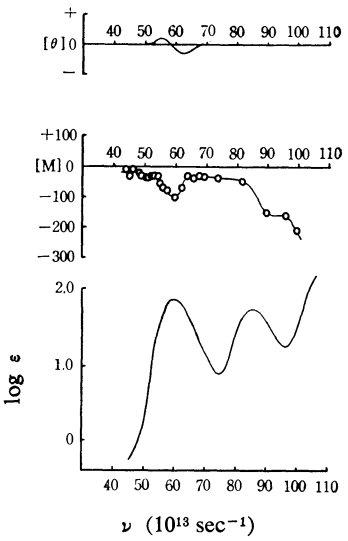



Fig. 5. Circular dichroism, rotatory dispersion and absorption of $[Co(NH_3)_5(L\text{-}\alpha\text{-alaH})](ClO_4)_3 \cdot 2H_2O$.

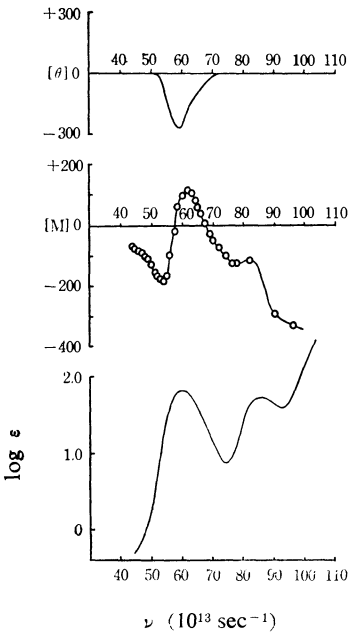



Fig. 6. Circular dichroism, rotatory dispersion and absorption of $[Co(NH_3)_5(L\text{-phalaH}_2)](ClO_4)_3 \cdot H_2O$.

those of the aquopentamminecobalt(III) complex.[20] As Fig. 1 shows, the same relation may be seen to result from the replacement of the water molecule by amino acid in a series of complexes, $[Co(NH_3)_4(glyH)_2]^{3+}$, $[Co(NH_3)_4(OH_2)(glyH)]^{3+}$ and $[Co(NH_3)_4$-

20) Y. Shimura and R. Tsuchida, This Bulletin, 29, 311 (1956).

$(OH_2)_2]^{3+}$. The first and the second bands of the last complex have been observed at 59.4 and $84.6\times10^{13}$ sec$^{-1}$ respectively.[20] From these spectral results, it has been concluded that the position of the unidentate amino acid in the spectrochemical series[20,21] is behind $OH_2$, but higher than $CH_3COO^-$ or $CO_3^{2-}$.

**Rotatory Dispersion and Circular Dichroism.** —As has been mentioned above, Shimura[7] measured the rotatory dispersion of the complex, $[Co(L\text{-leuc})(NH_3)_4]^{2+}$ which contains only one optically active chelate ligand. The shape and the magnitude of the anomalous dispersion of this complex in the region of its first absorption band are very similar to those of $[Co(L\text{-}\alpha\text{-ala})(NH_3)_4]^{2+}$, which has been measured in the present study in order to compare with the dispersion of the unidentate amino acid complexes. Shimura has also shown, by curve analysis, that the first band of $[Co(L\text{-leuc})(NH_3)_4]^{2+}$ exhibits two inversive dispersions, one of which shows a positive Cotton effect and the other, a negative Cotton effect. A similar result is obtained by the analysis of the rotatory dispersion curve of $[Co(L\text{-}\alpha\text{-ala})(NH_3)_4]^{2+}$. The circular dichroism of $[Co(L\text{-}\alpha\text{-ala})(NH_3)_4]^{2+}$, on the other hand, indicates that the first band should have another weak, negative Cotton effect on the longer wavelength side adjacent to the above-mentioned two strong Cotton effects and, moreover, one negative Cotton effect in the region of the second absorption band (see Fig. 3). In the rotatory dispersion curve of $[Co(L\text{-}\alpha\text{-ala})(NH_3)_4]^{2+}$, some indications of the inversive dispersion are seen at 55 and $87\times10^{13}$ sec$^{-1}$. In order to establish these small anomalous dispersions, the rotatory dispersion of $[Co(D\text{-}\alpha\text{-ala})(NH_3)_4]^{2+}$ has been measured. As may be seen in Fig. 4, the dispersion curve of this complex is almost antipodal to that of the corresponding L-$\alpha$-alaninato complex. It may be concluded, therefore, that the first absorption band of the $[Co(L\text{-}\alpha\text{-ala})(NH_3)_4]^{2+}$ complex shows three inversive dispersions and the second band, one or more additional inversive dispersions.

The rotatory dispersion curve of the unidentate amino acid complex $[Co(NH_3)_5(L\text{-}\alpha\text{-alaH})]^{3+}$, on the other hand, shows a very weak anomalous dispersion in its first band compared with that of the chelate complex (see Fig. 5). The magnitude of the partial molar rotation of the former is about 1/10 that of the latter. The circular dichroism of $[Co(NH_3)_5(L\text{-}\alpha\text{-alaH})]^{3+}$ is also so weak that quantitative measurement was impossible. The circular dichroism curve given in Fig. 5 is only qualitative. In the rotatory dispersion curve of $[Co(NH_3)_5(L\text{-phalaH})]^{3+}$ (Fig. 6), a more distinct anomalous dispersion than that of the corresponding L-$\alpha$-alanine complex is observed in the region of the first band, although the magnitude of this dispersion is still very weak compared with those of the chelate amino acid complexes. The difference in the magnitude of anomalous dispersion between the unidentate and the chelate amino acid complexes might be caused by: 1) the difference in the distance from the asymmetric carbon atom to the cobalt ion, Co-O-C-C*- for the unidentate complex, but Co-O-C-C*- and Co-N-C*- for the chelate complex; 2) the conformational difference (that is, the conformation of the amino acid in the chelate complex is fixed by the formation of the chelate ring, but in the unidentate complex the amino acid can rotate about the Co-O bond axis), or 3) the difference in the electronic states of the complex ions caused by the coordination of the different atoms or by the different structures.

In order to study the points above-mentioned in more detail, the rotatory dispersion of three tetrammine complexes of $[Co\,N_4O_2]$ type have been measured. As Fig. 7 shows, the anomalous dispersion of *cis*-$[Co(NH_3)_4(L\text{-}\alpha\text{-alaH})_2]^{3+}$ in its first band is rather remarkable compared with that of $[Co(NH_3)_5(L\text{-}\alpha\text{-alaH})]^{3+}$. The

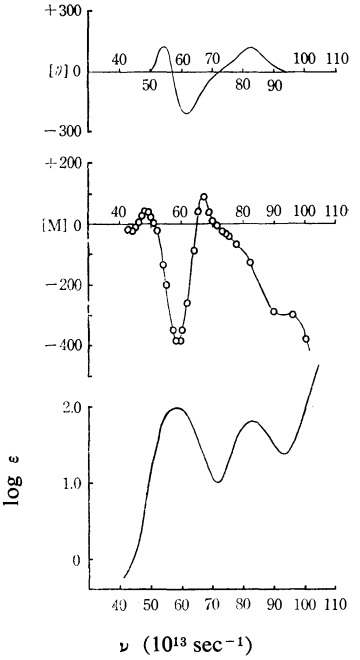



Fig. 7. Circular dichroism, rotatory dispersion and absorption of *cis*-$[Co(NH_3)_4(L\text{-}\alpha\text{-alaH})_2](ClO_4)_3\cdot2H_2O$.

21) R. Tsuchida, ibid., 13, 388, 436 (1938).

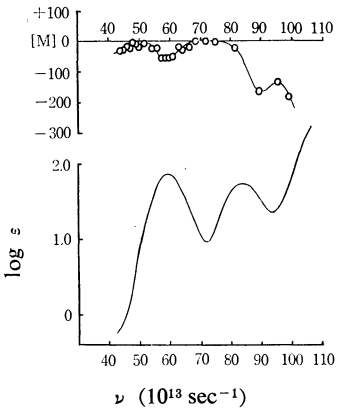



Fig. 8. Rotatory dispersion and absorption of *cis*-$[Co(OH_2)(NH_3)_4(L\text{-}\alpha\text{-alaH})](ClO_4)_3 \cdot H_2O$.

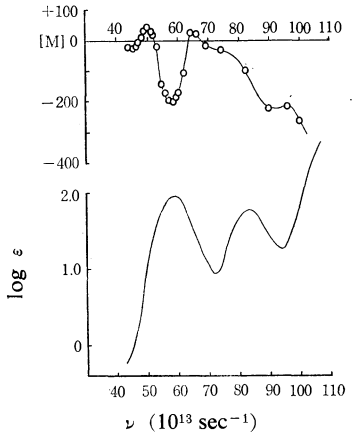



Fig. 9. Rotatory dispersion and absorption of *cis*-$[Co(NH_3)_4(glyH)(L\text{-}\alpha\text{-alaH})](ClO_4)_3 \cdot 2H_2O$.

magnitude of the inversive dispersion in the former is estimated to be almost four times larger than that in the latter. This fact seems to suggest that the magnitude of the anomalous dispersion is not proportional to the number of the optically active ligands. This might be caused by the difference in the conformational mobility of the coordinated amino acid. The difference in the types of the complexes ([Co $N_5O$] and [Co $N_4O_2$]) does not seem to be important in this case. In *cis*-$[Co(NH_3)_4(L\text{-}\alpha\text{-alaH})_2]^{3+}$, two amino acids in the cis positions should take a conformation somewhat restricted by the mutual interaction, in contrast with the fact that the amino acid in $[Co(NH_3)_5(L\text{-}\alpha\text{-alaH})]^{3+}$ should be rather free from the interaction with the coordinated ammonia molecules. The anomalous dispersion of *cis*-$[Co(OH_2)(NH_3)_4(L\text{-}\alpha\text{-alaH})]^{3+}$, in which the conformational mobility of the amino acid is similar to that of $[Co(NH_3)_5(L\text{-}\alpha\text{-alaH})]^{3+}$, is as weak as that of $[Co(NH_3)_5(L\text{-}\alpha\text{-alaH})]^{3+}$. The anomalous dispersion of *cis*-$[Co(NH_3)_4(glyH)(L\text{-}\alpha\text{-alaH})]^{3+}$, on the other hand, shows a shape very similar to that of *cis*-$[Co(NH_3)_4(L\text{-}\alpha\text{-alaH})_2]^{3+}$, but its magnitude is almost half that of the latter (see Figs. 7 and 9). This fact indicates that the L-$\alpha$-alanine *cis*-$[Co(NH_3)_4(glyH)(L\text{-}\alpha\text{-alaH})]^{3+}$ is in the same conformational state as those in *cis*-$[Co(NH_3)_4(L\text{-}\alpha\text{-alaH})_2]^{3+}$ as a result of the effect of the glycine coordinated in the adjacent cis position. Therefore, the proportionality of the magnitudes of the anomalous dispersions to the number of optically active ligands holds in this case.

From all these observations, including the fact that the first band of the chelate complex $[Co(L\text{-}\alpha\text{-ala})(NH_3)_4]^{2+}$ exhibits a strong anomalous dispersion, it may be concluded that the magnitude of the anomalous dispersion of the optically active $\alpha$-amino acid complex in its first absorption band depends mainly on the conformational mobility of the optically active ligand.

As a further investigation, the measurement of the rotatory dispersion for *trans*-$[Co(NH_3)_4(L\text{-}\alpha\text{-alaH})_2]^{3+}$ will be an interesting subject, since the steric condition in the trans complex will be quite different from those in the cis isomers. Several attempts to prepare the trans complex, however, have been unsuccessful.

## Summary

Fifteen new cobalt(III) ammine complexes containing amino acids as unidentate ligands have been prepared. The infrared, visible and ultraviolet absorption spectra of these complexes indicate that the oxygen of the carboxyl group acts as a donor atom. The circular dichroism and the rotatory dispersion of the unidentate complexes of the optically active $\alpha$-amino acids and such chelate amino acid complexes as $[Co(L\text{-}\alpha\text{-ala})(NH_3)_4]^{2+}$ have been measured. The results suggest that the magnitude of the anomalous dispersion of the $\alpha$-amino acid complex in the region of its first absorption band seems to depend mainly on the conformational mobility of the optically active ligand in the coordination sphere.

The authors wish to express their sincere thanks to Professor B. E. Douglas and Dr. J. Hidaka for their aid in obtaining the circular dichroism spectra.

*Department of Chemistry*
*Faculty of Science*
*Osaka University*
*Nakanoshima, Osaka*

# Electrochemical Syntheses. III. The Homolytic Methoxylation of Some Arylated Olefins by the Anodic Oxidation of Methanol

By Tadao Inoue and Shigeru Tsutsumi

(Received July 29, 1964)

A method for the electrochemical methoxylation of furans has been developed.[1-3] Recently, Belleau and Weinberg[4] have reported the anodic methoxylation of dimethoxybenzenes and the ring fission of 1, 2-dimethoxybenzenes.

In the previous papers in this series,[5,6] we have described how the anodic oxidation of methanol in the presence of alkylated aromatic hydrocarbons produces $\alpha$-methoxy derivatives, which are formed by the reaction of the methoxy radical generated by the electrolysis of methanol as an intermediate.

The present investigation was undertaken in order to study the addition of the methoxy radical to olefinic double bonds. Thus, styrene, $\alpha$-methylstyrene and 1, 1-diphenylethylene were chosen as the starting olefins.

## Results and Discussion

**The Addition of the Methoxy Radical to Styrene.**—According to the procedure described earlier,[5-6] the electrolysis of a methanol solution containing sodium methoxide was carried out in the presence of styrene (I) at 34°C; styrene glycol dimethyl ether (II) was obtained as a main proudct (current yield, 16—22%). The formation of $\alpha$-methoxyethylbenzene (III) and $\beta$-methoxyethylbenzene (IV) as by-products was observed; *meso*-1, 4-dimethoxy-2, 3-diphenylbutane (V) was also isolated from the higher boiling fractions, and in addition a small amount of formaldehyde was isolated as its 2, 4-dinitrophenylhydrazone. The results obtained under various conditions are summarized in Table I, where the yield is calculated from the results of gas chromatographic analysis.

Since the methoxy radical may be initially produced as an intermediate in these reaction systems, it was expected that the reaction of methoxy radicals with styrene might take place in the first step of the reaction. The formation of *meso*-1, 4-dimethoxy-2,3-diphenylbutane (V) may be due to the coupling of an unstable intermediate radical (VI), which may be produced by the attack of the methoxy radical, formed by the anodic oxidation of methoxide ion, upon styrene, as is shown below:

$$CH_3O^- \xrightarrow[\text{anode}]{-e} CH_3O\cdot \qquad (1)$$

$$\underset{\text{(I)}}{C_6H_5CH=CH_2} \xrightarrow{\cdot OCH_3} \underset{\text{(VI)}}{C_6H_5CH(\cdot)-CH_2OCH_3} \qquad (2)$$

$$\text{VI} \xrightarrow{\text{dimerization}} \underset{\text{(V)}}{C_6H_5CHCH_2OCH_3 \\ | \\ C_6H_5CHCH_2OCH_3} \ (meso\text{-}) \qquad (3)$$

For the formation of styrene glycol dimethyl ether (II), two reaction paths are possible: In the first, the benzylic intermediate radical (VI) reacts with another methoxy radical to give the dimethyl ether (II), since the environment around the electrode might have a particularly high concentration of the methoxy radical (Eq. 4):

$$\text{VI} \xrightarrow{\cdot OCH_3} \underset{\text{(II)}}{C_6H_5CH(OCH_3)-CH_2OCH_3} \qquad (4)$$

In the second, the intermediate radical (VI) may be oxidized to the carbonium ion (VII) to give the solvolysis product (II) (Eq. 5):

$$\text{VI} \xrightarrow[\text{anode}]{-e} \underset{\text{(VII)}}{C_6H_5\overset{+}{C}H-CH_2OCH_3} \xrightarrow{^-OCH_3} \text{II} \qquad (5)$$

Recently, Bonner and Mango[7] reported that electrolytically-generated benzyl radicals in the Kolbe elctrolysis are oxidized to carbonium ions with greater ease. Such a possibility can not be excluded in the present case.

For the anodic methoxylation of furan-compounds, Clauson-Kaas and his coworkers[1-3]

1) N. Clauson-Kaas, F. Limborg and K. Glens, *Acta Chem. Scand.*, **6**, 531 (1952).
2) N. Clauson-Kaas and Z. Tyle, ibid., **6**, 667 (1952).
3) N. Elming, "Advances in Organic Chemistry," Vol. II, Interscience Publ., New York (1960), p. 67.
4) B. Belleau and N. L. Weinberg, *J. Am. Chem. Soc.*, **85**, 2525 (1963).
5) T. Inoue, K. Koyama, T. Matsuoka, K. Matsuoka and S. Tsutsumi, *J. Chem. Soc. Japan, Ind. Chem. Sec. (Kogyo Kagaku Zasshi)*, **66**, 1659 (1963).
6) T. Inoue, K. Koyama and S. Tsutsumi, This Bulletin, in press.
7) W. A. Bonner and F. D. Mango, *J. Org. Chem.*, **29**, 430 (1964).

TABLE I. ANODIC METHOXYLATION OF STYRENE

| Expt.* No. | $C_6H_5CH=CH_2$ g. (mol.) | $CH_3OH$ g. | Current density amp./dm² | Amp. | Amp.-hr. | hr. | Product II g. (%**) | III g. | IV g. | V g. | Residue g. |
|---|---|---|---|---|---|---|---|---|---|---|---|
| 1 | 50 (0.48) | 75 | 18.8—13.3 | 2.2—1.6 | 24.4 | 12 | 16 (22.1) | 0.9 | trace | 0.7 | 5.4 |
| 2 | 26 (0.25) | 80 | 16.6 | 2.0 | 13.4 | 6.7 | 6.3 (15.1) | 0.5 | trace | 0.4 | 3.2 |
| 3 | 52 (0.5) | 80 | 16.6 | 2.0 | 26.8 | 13.4 | 15.2 (18.3) | 1.2 | trace | 0.8 | 6.0 |
| 4 | 52 (0.5) | 80 | 8.3 | 1.0 | 26.8 | 26.8 | 16.8 (20.0) | 1.3 | trace | 0.8 | 4.5 |

* In these electrolyses, 1.0 g. of metallic sodium was used and the electrodes, 2×3 cm², were used; temperature being kept at 34±1°C.

** The current yields are based on the calculation that two moles of methanol should be oxidized to a one mole of the product II.

TABLE II. ANODIC METHOXYLATION OF ARYLATED OLEFINS

| Expt.* No. | $C_6H_5CR=CH_2$ g. (mol.) | $CH_3OH$ g. | Metallic sodium g. | Current density amp./dm² | Amp. | Amp.-hr. | hr. | Product Dimethyl ether | g. (%)[a] | (%)[b] |
|---|---|---|---|---|---|---|---|---|---|---|
| 1 | R=H 52 (0.5) | 80 | 1.0 | 8.3 | 1.0 | 26.8 | 26.8 | II | 16.8 (20.0) | (32.3) |
| 2 | R=$CH_3$ 59 (0.5) | 80 | 1.0 | 8.3 | 1.0 | 26.5 | 26.6 | VIII | 13.7 (15.0) | (23.2) |
| 3 | R=$C_6H_5$ 45 (0.25) | 40 | 0.5 | 8.3 | 1.0 | 13.6 | 13.6 | IX | 13.8 (23.0) | (30.7) |

a) Current yield. b) Based on the starting olefin.

* The temperature was kept at 34±1°C.

reported that the bromine which is formed during the electrolysis reacts immediately with furan-compounds and methanol to give the methoxylated products and hydrogen bromide. On the other hand, in the present system, the anodic methoxylation of these olefins would proceed in the radical mechanisms, as has been mentioned above. This is also supported by the recent observation that the anodic oxidation of methanol in the presence of 1,2-dimethoxybenzene gives 5,5,6,6-tetramethoxy-1,3-cyclohexadiene under modified conditions.[4]

β-Methoxyethylbenzene (IV) might be produced by the hydrogen abstraction of the intermediate radical (VI) from the solvent:

$$\text{VI} \xrightarrow{CH_3OH} \underset{\text{(IV)}}{C_6H_5CH_2CH_2OCH_3} \quad (6)$$

One possible rationalization for the formation of α-methoxyethylbenzene (III) in this system involves, in the first step, the addition of adsorbed hydrogen, which may be produced by the anodic oxidation of methoxide ions, as has been reported by Buck and Griffith,[8] to styrene; then methanolysis of the subsequent benzylic cation may furnish the methoxylated product (III), as is shown in Eqs. 7—9;

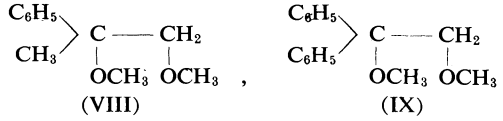
$$CH_3O^- \rightarrow CH_2O^-_{adsorbed} + H_{adsorbed} \quad (7)$$

$$C_6H_5CH=CH_2 + H_{adsorbed} \rightarrow C_6H_5\overset{+}{C}HCH_3 + e \quad (8)$$

$$C_6H_5\overset{+}{C}HCH_3 + CH_3O^- \rightarrow \underset{\text{(III)}}{C_6H_5CH(OCH_3)CH_3} \quad (9)$$

We have little experimental evidence, however, bearing on the validity of this suggestion.

**The Addition of the Methoxy Radical to α-Methylstyrene and 1,1-Diphenylethylene.**—When α-methylstyrene or 1,1-diphenylethylene was used instead of styrene, 1-methyl-1-phenylethylene glycol dimethyl ether (VIII) (current yield, 15%) or 1,1-diphenylethylene glycol dimethyl ether (IX) (current yield, 23%) was obtained as the main product in each case.



(VIII)



(IX)

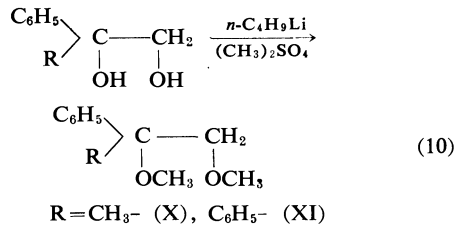
The structure of these products was confirmed by the synthetic route. α-Methylstyrene glycol (X), which had been prepared by hydroxylation with a Milas-reagent,[9] and 1,1-diphenylethylene glycol (XI), prepared by the reaction of benzoylcarbinol with phenylmagnesium bromide,[10] were treated with *n*-butyl lithium and dimethyl sulfate successively in dry benzene to give the corresponding dimethyl ethers, which showed infrared absorptions and melting points identical

8) R. P. Buck and L. R. Griffith, *J. Electro. Chem. Soc.*, **109**, 1005 (1962).

9) N. A. Milas and S. Sussmann, *J. Am. Chem. Soc.*, **58**, 1302 (1936).

10) S. H. Harper, "Chemistry of Carbon Compounds," Coll. Vol. IIIB, Elsevier Publ. Co., New York (1956), p. 1121.

with those of the electrochemical methoxylated products.



(10)

R=$CH_3$- (X), $C_6H_5$- (XI)

The results obtained are summarized in Table II. In these electrolyses, small amounts of the respective mono-ethers were also detected; white crystals which might be formed by the dimerization of an unstable intermediate radical were also isolated, as has been observed above. In the case of α-methylstyrene, in addition, a small amount of acetophenone was isolated as its 2, 4-dinitrophenylhydrazone.[11]

The current yields of these main products increased in the order $CH_3-<H-<C_6H_5-$ in the α-substituent group of styrene, as is shown in Table II.

It is of interest to note that the dimethyl ether derivatives (II, VIII and IX) are easily produced in fairly high yields by the anodic oxidation of methanol in the presence of the respective arylated olefins.

## Experimental

Melting points and boiling points are uncorrected. Electrolyses were carried out by using three platinum-foil electrodes with the apparatus previously described.[5]

**Materials.**—Styrene and α-methylstyrene were commercial materials, carefully purified in the usual manner,[12] distilled before use, and stored in an ice-box. 1, 1-Diphenylethylene was obtained by the dehydration of the alcohol formed by the action of phenylmagnesium bromide and ethyl acetate;[13] b. p. 97—97.5°C/0.5 mmHg, $n_D^{15}=1.6098$. Methanol was purified in a manner described earlier.[5] These materials were confirmed to be pure by gas chromatography.

**The Anodic Oxidation of Methanol in the Presence of Styrene.**—The reaction conditions and the yields of the products are summarized in Table I.

R-4 is exemplified as follows: Metallic sodium (1.0 g., 0.043 mol.) was dissolved in 80 g. of absolute methanol (2.5 mol.), and then 52 g. of freshly-distilled styrene (0.5 mol.) was added to the mixture. After dry nitrogen had been bubbled through the mixture for about 1 hr., the mixture was electrolyzed at 34±1°C for 26.8 hr., during which time a current was maintained at neary 1.0 amp. (current density, 8.3 amp./$dm^2$). The electrolyzed solution turned slightly yellowish-brown. The reaction mixture was then distilled at room temperature under 25—30 mmHg pressure (water-aspirator). From this distillate, trapped by the receiver in a bath containing dry-ice and acetone, a small amount of formaldehyde was identified as its 2, 4-dinitrophenylhydrazone; m. p. 161—162°C; a mixed melting point with an authentic sample showed no depression.

Found: C, 40.22; H, 3.12; N, 26.80. Calcd. for $C_7H_6N_4O_4$: C, 40.00; H, 2.87; N, 26.62%.

The residue was poured into water (50 ml.), neutralized with 3 N hydrochloric acid, and extracted with ether; the extract was dried over magnesium sulfate. After the ether had been removed, the oily residue (49.5 g.) was distilled under diminished pressure to give the following fractions;

| Fraction | B. p. | Weight, g. |
|---|---|---|
| 1 | ~ 51°C/25 mmHg | 18.3 |
| 2 | 30— 90°C/2—3 mmHg | 21.1 |
| 3 | 90—103°C/2—3 mmHg | 3.6 |
| 4 | ~143°C/0.8—0.9 mmHg | 4.0 |
| 5 | Residue | 1.5 |

By gas chromatographic analysis (conditions: column, polyethylene glycol (P. E. G.) 1500, 2 m. and polyester D A (P. E. DA), 3 m.; column temperature, 153°C; carrier gas, $H_2$), it was shown that fractions 1, 2 and 3 were mixtures of unreacted styrene, α-methoxyethylbenzene, β-methoxyethylbenzene and styrene glycol dimethyl ether, and that the total amounts of these products were as follows: unreacted styrene, 23.0 g.; α-methoxyethylbenzen, 1.3 g.; β-methoxyethyl benzene, trace; styrene glycol dimethyl ether, 16.8 g.

Fraction 2 was chromatogroaphed over active alumina (2.5×58 cm.). Elution with benzene led to the isolation of styrene glycol dimethyl ether; b. p. 75—76°C/2 mmHg, $n_D^{20}=1.4948$ (lit.,[14] $n_D^{20}=1.4948$).

Found: C, 72.49; H, 8.79. Calcd. for $C_{10}H_{14}O_2$: C, 72.26; H, 8.49%.

The infrared spectrum of this product showed the characteristic absorption band at 1105 $cm^{-1}$ (C-O-C of aliphatic ether.) and was identical with that of an authentic sample prepared as will be described below.

α-Methoxyethylbenzene and β-methoxyethylbenzene were identified by gas chromatographic analysis.

Fraction 4 was cooled below 0°C to give a white crystal (0.6 g.) of *meso*-1, 4-dimethoxy-2, 3-diphenylbutane (m. p. 128.5-130°C) from methanol; a mixed melting point with the sample prepared as will be described below showed no depression.

Found: C, 80.07; H, 8.19. Calcd. for $C_{18}H_{22}O_2$: C, 79.96; H, 8.20%.

The infrared spectrum of this compound showed the characteristic absorption band at 1112 $cm^{-1}$ (C-O-C). The mother liquid filtered from fraction 4 was chromatographed over active alumina (2.5×30 cm.) and, from the eluate with benzene, 0.2 g. of *meso*-1, 4-dimethoxy-2, 3-diphenylbutane and oily compounds were separated. The latter oily compounds consisted of miscellaneous products, which

11) For the formation of this ketone, further studies are now being undertaken.
12) A. Weissberger, "Technique of Organic Chemistry," Vol. VII, Interscience Publ., New York (1955), p. 331.
13) "Organic Syntheses," Coll. Vol. I, 226 (1956).
14) C. R. Ganellin and R. Pettit, *J. Chem. Soc.*, 1958, 576.

showed the infrared absorption band at 1110 $cm^{-1}$ (C-O-C); b. p. 130—170°C/2—3 mmHg.

**The Synthesis of Styrene Glycol Dimethyl Ether.**—Styrene diacetate was prepared by the reaction of styrene dibromide with fused lead acetate in glacial acetic acid, according to the procedure of Evans and Morgan;[15] b. p. 126—128°C/4—5 mmHg. Styrene glycol was prepared by the hydrolysis of styrene diacetate[14] and was methylated with methyl sulfate as has been described for glucose;[16] b. p. 72—73°C/1.5 mmHg, $n_D^{20}=1.4948$.

**The Synthesis of α- and β-Methoxyethylbenzene.**—α-Methoxyethylbenzene was prepared by the reaction of styrene with methanol according to the procedure of Stanley and was then purified by preparative gas chromatography;[5] b. p. 74—75°C/30—32 mmHg, $n_D^{22}=1.4900$. β-Methoxyethylbenzene was prepared by the reaction of phenethyl alcohol with metallic sodium and methyl iodide; b. p. 46—47°C/3—4 mmHg.

**The Synthesis of *meso*-1, 4-Dimethoxy-2, 3-diphenylbutane.**—*meso*-2, 3-Diphenyl-1, 4-butanediol[17] was prepared by the reduction, with lithium aluminum hydride, of *meso*-diethyl α, α'-diphenylsuccinate,[18] which had been synthesized by the coupling of ethyl phenylacetate[19] with sodium ethoxide and iodine; m. p. 143—144°C (lit., m. p. 143—144°C). *meso*-1, 4-Dimethoxy-2, 3-diphenylbutane was prepared by the following procedure: *meso*-2,3-diphenyl-1, 4-butanediol (1.5 g., 0.006 mol.) was dissolved in 60 ml. of dry benzene, and then the solution was further dried by the distillation of 10 ml. of benzene. To the solution at room temperature, 6 ml. of *n*-butyl lithium in *n*-heptane (21% solution, 0.015 mol.) was added, and then the solution was stirred at 60°C for 1.5 hr. Dimethyl sulfate (3.78 g., 0.03 mol.) in 20 ml. of dry benzene was then added, and the solution was heated at 80°C for 8 hr., cooled in ice, transferred to an amber separatory funnel, and washed successively with a cold solution of 0.5 N sulfuric acid (100 ml.), N ammonium hydroxide (twice) and water (three times). The solution was dried over anhydrous sodium sulfate, filtered, concentrated at 40°C under reduced pressure, and cooled to give crystals (1.4 g., 85% yield) of *meso*-1, 4-dimethoxy-2, 3-diphenylbutane; m. p. 128.5—130°C, from methanol.

**The Anodic Oxidation of Methanol in the Presence of α-Methylstyrene.**—Metallic sodium (1.0 g., 0.043 mol.) was dissolved in 80 g. of absolute methanol (2.5 mol.). and then 59 g. of freshly-distilled α-methylstyrene (0.5 mol.) was added to the mixture. After dry nitrogen had been bubbled through the mixture, the mixture was electrolyzed at 34±1°C, for 26.6 hr. during which time the current was maintained at 1.0 amp. The reaction mixture was then worked up in a manner similar to the procedure described above. After the ether had been removed, the oily residue was distilled under reduced pressure to give the following fractions;

| Fraction | B. p. | Weight, g. |
|---|---|---|
| 1 | ~ 40°C/2—3 mmHg | 20.6 |
| 2 | 40— 55°C/2—3 mmHg | 8.8 |
| 3 | 55—105°C/2—3 mmHg | 22.3 |
| 4 | Residue | 5.3 |

Gas chromatographic analysis (conditions: column, polyester DA, 3 m. and polyethylene glycol 6000, 3 m.; column temperature, 173°C; carrier gas, $H_2$) showed that fractions 1, 2 and 3 were mixtures of unreacted α-methylstyrene, α-methoxyisopropylbenzene, acetophenone, β-methoxyisopropylbenzene and 1-methyl-1-phenylethylene glycol dimethyl ether, and that the total amounts of these products were as follows: unreacted α-methylstyrene, 33.7 g.; α-methoxyisopropylbenzene, 2.2 g.; acetophenone, 3.2 g; β-methoxyisopropylbenzene, trace; 1-methyl-1-phenylethylene glycol dimethyl ether, 13.7 g.

When fraction 3 was distilled through a five-foot vacuum-jacketed column packed with glass helices, 1-methyl-1-phenylethylene glycol dimethyl ether was isolated; b. p. 68—69°C/1.5 mmHg, $n_D^{14}=1.5022$.

Found: C, 73.59; H, 9.20. Calcd. for $C_{11}H_{16}O_2$: C, 73.30; H, 8.95%.

The infrared spectrum of this dimethyl ether showed the characteristic absorption bands at 1110 $cm^{-1}$ and 1128 $cm^{-1}$ (C-O-C) and was identical with that of an authentic sample prepared as will be described below. From the lower boiling fraction, acetophenone was identified as its 2, 4-dinitrophenylhydrazone derivative; m. p. 237—238°C; a mixed melting point with an authentic sample was not depressed.

Found: C, 56.17; H, 3.93. Calcd. for $C_{14}H_{12}N_4O_4$: C, 56.00; H, 4.03%.

α-Methoxyisopropylbenzene and β-methoxyisopropylbenzene were identified by gas chromatographic analysis (conditions; described above). When fraction 4, the residue, was chromatographed over active alumina (2.5×45 cm.) and eluted with benzene, a white crystal (0.1 g. with m. p. 95—96.5°C, from methanol), was isolated from oily miscellaneous products.

Found: C, 80.36; H, 8.89. Calcd. for $C_{20}H_{26}O_2$: C, 80.49; H, 8.78%.

The infrared spectrum of this compound showed the characteristic absorption bands at 1088 $cm^{-1}$ and 1098 $cm^{-1}$ (C-O-C).

**The Synthesis of 1-Methyl-1-phenylethylene Glycol Dimethyl Ether.**—1-Methyl-1-phenylethylene glycol was prepared by the action of Milas reagents on α-methylstyrene[9] and methylated in a good yield with *n*-butyl lithium and dimethyl sulfate in dry benzene in a manner similar to the procedure described above. The product had a b. p. of 66°C/1 mmHg, $n_D^{14}=1.5022$.

**The Synthesis of α- and β-Methoxyisopropylbenzene.**—α-Methoxyisopropylbenzene was synthesized in a manner described earlier;[5] b. p. 77—78°C/12—13 mmHg, $n_D^{20}=1.4911$. β-Methoxyisopropylbenzene was synthesized by the *O*-methylation of β-phenylpropyl alcohol with *n*-butyl lithium and dimethyl sulfate in a manner similar to the

15) W. L. Evans and L. H. Morgan, *J. Am. Chem. Soc.*, **35**, 54 (1913).
16) "Organic Syntheses," Coll. Vol. III, 800 (1955).
17) F. F. Blicke, P. E. Wright and W. A. Gould, *J. Org. Chem.*, **26**, 2114 (1961); D. Fraenkel and P. Bartlett, *J. Am. Chem. Soc.*, **81**, 5582 (1959).
18) H. Wren and C. J. Still, *J. Chem. Soc.*, **1915**, 446.
19) "Organic Syntheses," Coll. Vol. I, 270 (1956).

procedure as described above; b. p. 85—86°C/14 mmHg. β-Phenylpropyl alcohol was prepared by the reduction of β-phenylpropionaldehyde, which was prepared by the dehydration of 1-methyl-1-phenylethylene glycol with 20% sulfuric acid,[20] with zinc and acetic acid[21]; b. p. 99—102°C/7—8 mmHg.

**The Anodic Oxidation of Methanol in the Presence of 1, 1-Diphenylethylene.**—Metallic sodium (0.5 g., 0.022 mol.) was dissolved in 40 g. of methanol (1.25 mol.), and then 45 g. of freshly-distilled 1,1-diphenylethylene (0.25 mol.) was added to the mixture. After dry nitrogen had been bubbled through the cell, the mixture was electrolyzed at 34±1°C, for 13.8 hr., during which time the current was maintained at 1.0 amp. The electrolyzed solution was worked up in a manner similar to the procedure described above, and the oily residue (50.0 g.) was distiiled under reduced pressure to give the following fractions;

| Fraction | B. p. | Weight, g. |
|---|---|---|
| 1 | 90— 99°C/1.0 mmHg | 22.5 |
| 2 | 99—125°C/1.0 mmHg | 23.5 |
| 3 | Residue | 3.0 |

These fractions were chromatographed over active alumina (2.5×26 cm.). Elution with benzene led to the isolation of unreacted 1, 1-diphenylethylene (31.4 g.), 1, 1-diphenylethylene glycol dimethyl ether (13.8 g.), miscellaneous oily products (4.5 g.) and a white crystal (0.4 g.) with a m. p. of 228—230°C, from benzene.

1, 1-Diphenylethylene glycol dimethyl ether was melted at 65.5—66.5°C from ligroin; a mixed melting point with the sample prepared as will be described below showed no depression.

Found: C, 79.06; H, 7.25. Calcd. for $C_{16}H_{18}O_2$: C, 79.31; H, 7.49%.

The infrared spectrum of this dimethyl ether showed the characteristic absorption bands at 1108 $cm^{-1}$ and 1138 $cm^{-1}$ (C-O-C) and was identical with that of the sample prepared as will be described below. The infrared spectrum of a white crystal with a m. p. of 228.5—230°C also showed the characteristic absorption band at 1072 $cm^{-1}$ (C-O-C).

Found: C, 85.53; H, 7.41. Calcd. for $C_{30}H_{30}O_2$: C, 85.27; H, 7.16%.

**The Synthesis of 1, 1-Diphenylethylene Glycol Dimethyl Ether.** — Benzoylcarbinol[22] was prepared by the hydrolysis of benzolycarbinol acetate prepared by the reaction of ω-bromoacetophenone with potassium acetate;[22] m. p. 80—82°C. 1, 1-Diphenylethylene glycol was prepared by the treatment of benzoylcarbinol with phenylmagnesium bromide;[10] m. p. 119—120.5°C (lit.,[10] m. p. 121°C), and methylated in a good yield with *n*-butyl lithium and dimethyl sulfate in dry benzene in a manner similar to the procedure described above. The product was purified by column chromatography (active alumina, 2.5×26 cm.; eluted with benzene); m. p. 65.5—66.5°C, from ligroin.

*Department of Chemical Technology*
*Faculty of Engineering*
*Osaka University*
*Miyakojima-ku, Osaka*

20) S. Danilow and E. Venus-Danilowa, *Ber.*, **60**, 1063 (1927).

21) J. B. Cohen, J. Marshall and H. E. Woodman, *J. Chem. Soc.*, **107**, 887 (1915).

22) W. Madelung and M. E. Oberwegner, *Ber.*, **65**, 931 (1932).

# The Thermal Isomerization of Alkoxycycloheptatrienes and Some Reactions of Its Products[1]

By Tetsuo Nozoe and Kazuko Takahashi

(Received September 3, 1964)

The tropylium ion (I), which is formed from 1, 3, 5-cycloheptatriene by a hydride abstraction, exhibits a highly electrophilic character and can thus readily give rise to compounds (general formula II) in which the cycloheptatriene group is bonded to an oxygen, sulfur, nitrogen, or carbon atom.[2] This cation, in aqueous solutions at a suitable pH, undergoes disproportionation to cycloheptatriene and tropone.[3] Ditropyl ether (III), which is easily obtained by the action of the base on I, also gives rise to cycloheptatriene and tropone in the presence of a trace of tropylium ion or an acid.[4] Thus, the above reactions would

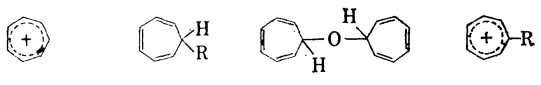
1) A part of the Ph. D. Thesis of Kazuko Takahashi, Tohoku University (1963); partially presented at the 17th Annual Meeting of the Chemical Society of Japan, Tokyo, March, 1964.

2) For a review of tropylium ion, see a) W. von E. Doering and H. Krauch, *Angew. Chem.*, **68**, 661 (1956); b) W. von. E. Doering, "Kekule Synposium" (1958); c) T. Nozoe, *Prog. Org. Chem.*, **5**, 132 (1961).

3) Tropylium ion (I) exhibits a highly electrophilic character and can thus abstract a hydride from tropyl alcohol.

4) a) T. Ikemi, T. Nozoe and H. Sugiyama, *Chem. Ind.*, **1960** 932; b) A. P. ter Borg, R. von Helden, A. F. Bickel, W. Renold and A. S. Dreiding, *Helv. Chim. Acta.*, **43**, 457 (1960); c) M. E. Volpin, Z. N. Parnes and D. N. Kursanov, *Izvest. Akad. Nauk S. S. S. R., Otdel. Khim. Nauk*, 950 (1960).

provide a very convenient route for the synthesis of troponoids and azulenoids, via the corresponding substituted tropones which



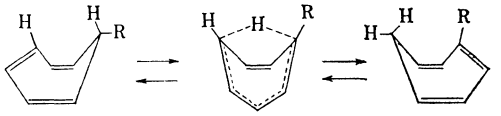
(I) (II) (III) (IV)

should be obtainable from the corresponding tropylium ion (IV) formed from cycloheptatriene derivatives (II), by a similar hydride abstraction.[5] However, *O*-, *S*- and *N*-tropyl compounds are in general labile in acidic media,[2] and some *C*-tropyl compounds undergo fragmentation during treatment with strong acid.[2,6] For this reason, the direct formation of troponoids or azulenoids from cycloheptatriene derivatives is not generally feasible. In the presence of concentrated acids, alkoxycycloheptatrienes (alkyl tropyl ethers) (Va and Vb) and ditropyl ether (III) dissociate quantitatively to the cation (I). Furthermore, these are very effective tropylating reagents since they are quite soluble in most organic solvents and tend to react with phenols, tropolones, and compounds with an active methylene group, giving the corresponding cycloheptatriene derivatives.[7]

During the last few years, the reactions of alkoxycycloheptatrienes and ditropyl ethers have been extensively investigated in our laboratory, with the aim of devising a synthesis of tropones and various derivatives of cycloheptatriene along the lines discussed above. In the course of this study, however, it was noticed that yields varied from time to time and that some reactions led to unexpected products. In order to clarify these ambiguities, we commenced extensive studies of the thermal reactions as well as of the effects of acids and alkalis on these alkoxycycloheptatrienes (Va and Vb).

Ethoxycycloheptatriene, on being mixed with phenols or tropolones, forms 7-substituted cycloheptatrienes, and, as has been previously noted, the heating of these products cases a migration of the double bonds.

The present authors obtained interesting results by following the thermal isomerization of alkoxycycloheptatrienes with the NMR technique. After we had started this work, a detailed study of the thermal isomerization of 7-substituted cycloheptatrienes was published by ter Borg et al.,[8] who examined changes in the NMR and mass spectra of 7-*D*-cycloheptatriene (II; R=D) at 100—140°C and in the NMR and ultraviolet spectra of 7-phenylcycloheptatriene (II; R=ph). They found that successive 1—5 transannular hydrogen shifts were taking place. From the kinetic study of this reaction, they concluded that the transition state had the symmetrical structure A shown below:



(A)

After the completion of our present study, Weth and Dreiding[9] published a short communication on the thermal isomerization of 7-methoxycycloheptatriene (Va); their results seem to be in substantial agreement with ours. The photoisomerization of Va and Vb in the vapor phase has also been noted by Chapman and Borden.[10]

In this paper we will report the results of a study of the thermal isomerization of

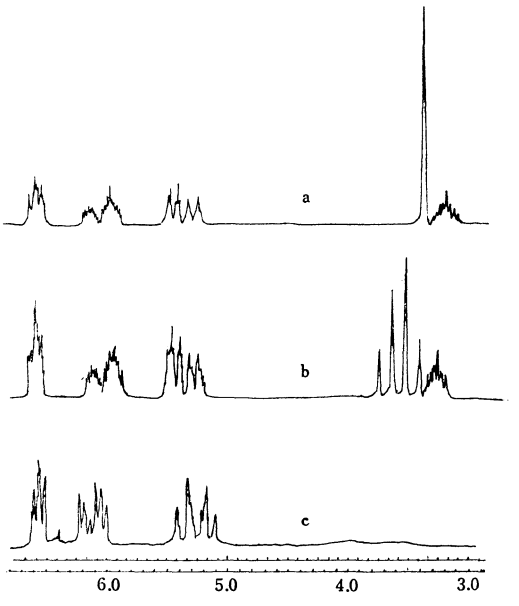



Fig. 1. NMR spectra of 7-methoxycycloheptatriene (a), 7-ethoxycycloheptatriene (b) and cycloheptatriene (c).

5) For reviews of troponoids and azulenoids, see T. Nozoe, "Non-Benzenoid Aromatic Compounds," Ed. by D. Ginsburg, Interscience, New York (1959); T. Nozoe, "Dai Yuki Kagaku" (Comprehensive Organic Chemistry), Vol. 13, Ed. by M. Kotake, Asakura shoten, Tokyo (1960), pp. 1—608.

6) K. Conrow, *J. Am. Chem. Soc.*, **81**, 5461 (1959).

7) a) T. Nozoe and K. Kitahara, *Chem. Ind.*, **1962**, 1192; b) T. Nozoe, K. Takahashi and H. Yamamoto, to be Published; c) T. Nozoe and T. Tezuka, to be published.

8) a) A. P. ter Borg, H. Kloosterziel and N. van Meurs, *Rec. trav. chim.*, **82**, 717 (1963); b) A. P. ter Borg and H. Kloosterziel, ibid., **82**, 741 (1963); c) **82**, 1189 (1963).

9) E. Weth and A. S. Dreiding, *Proc. Chem. Soc.*, **1964**, 59.

10) O. L. Chapman and G. W. Borden, ibid., **1963**, 221.

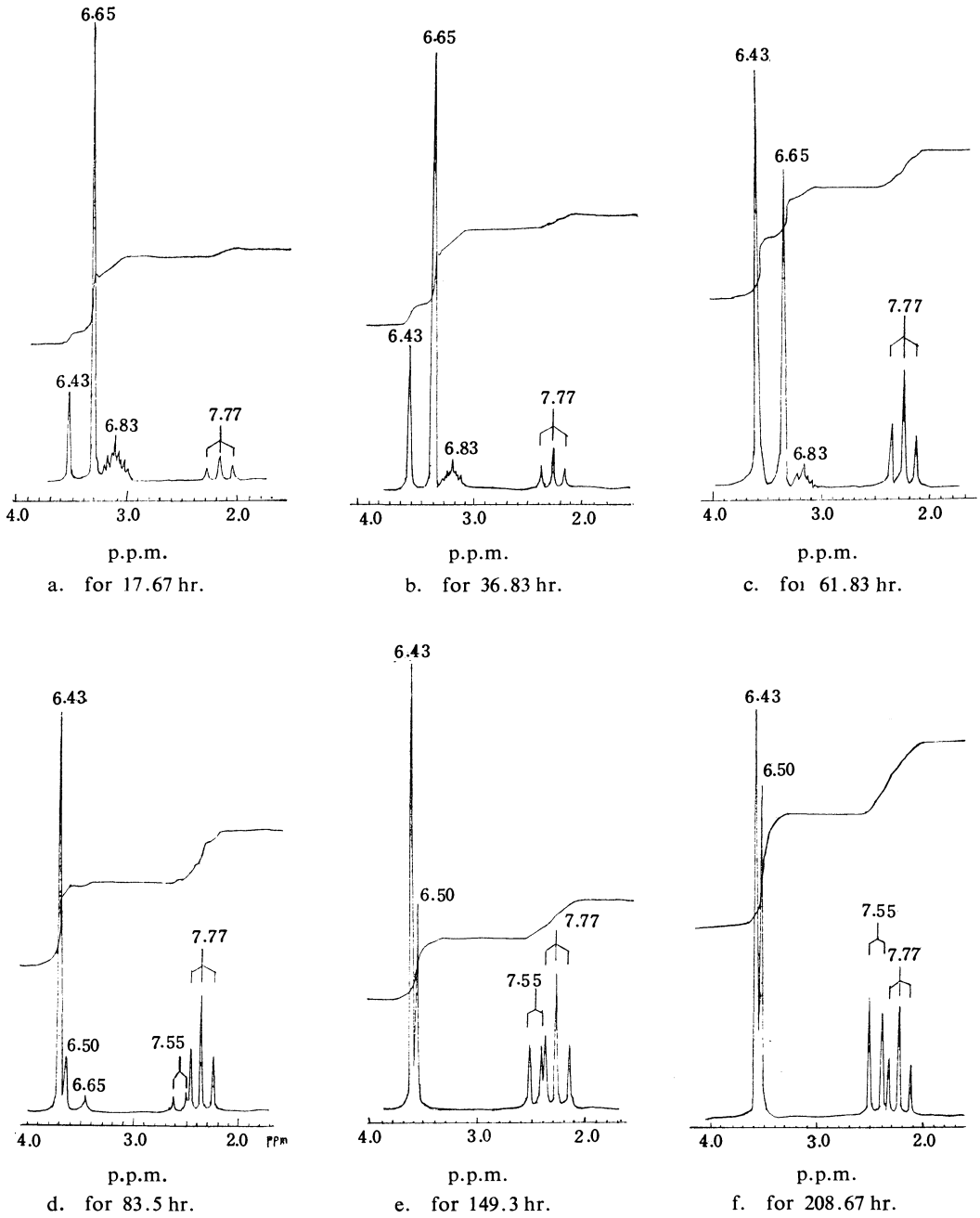



Fig. 2. NMR spectra of 7-methoxycycloheptatriene heated at 103° for various lengths of time.

methoxy- and ethoxy-cycloheptatriene; the reactions of the alkoxycycloheptatriene, obtained as the products of the above isomerization, will also be discussed.

**7-Alkoxycycloheptatriene.**—The 7-substituted cycloheptatrienyl structure can plausibly be assigned to the alkoxycycloheptatrienes (Va and Vb)[11] which are readily obtained by the addition of sodium hydrogen carbonate to a solution of tropylium ions in aqueous alcohols (see Fig. 1). As can be seen from Fig. 1a, the NMR spectrum of Va exhibits methyl signal at 6.65$\tau$ and a signal at 6.83$\tau$ resulting from the methine proton at the 7-position. By analogy with cycloheptatriene,[12] the signals

11) K. Conrow, *J. Am. Chem. Soc.*, **83**, 2347 (1961).

12) a) G. Frankel, R. E. Carter, A. Mc Lachlan and J. H. Richards, ibid., **82**, 5846 (1960); b) R. Barton, L. Pratt and G. Wilkinson, ibid., **83**, 594 (1961).

at 4.46$\tau$, 3.96$\tau$ and 3.59$\tau$ are assigned to the protons at the 1, 6-, 2, 5- and 3, 4-positions respectively. Usually the protons at the 7-position of cycloheptatrienes appears as a triplet. However, this is not the case with 7-methoxycycloheptatriene and 7-ethoxycycloheptatriene (Fig. 1b), as these exhibit symmetrical multiplets, centered at 6.83$\tau$ and 6.76$\tau$ respectively, which are attributed to the existence of a long-range coupling between the 7-proton and the two protons $\beta$ to it (H-2 and H-5), since the signals at 3.96$\tau$ and 3.97$\tau$, due to the protons at positions 2 and 5 in methoxy- and ethoxy-cycloheptatriene, (Va and Vb), are more complicated than the corresponding signals in the spectrum of cycloheptatriene itself (Fig. 1c). The NMR spectrum of 7-ethoxycycloheptatriene (Vb) is quite similar to that of 7-methoxycycloheptatriene, except that in the former additional signals due to the ethyl group appear at 8.79$\tau$ and 6.43$\tau$.

**The Thermal Isomerization of Alkoxycycloheptatrienes.**—The NMR spectrum of neat 7-methoxycycloheptatriene (Va), which had been heated for a short time in a sealed tube was measured in order to obtain information about the process of isomerization occurring in alkoxycycloheptatrienes heated in the 75—220°C temperature range. As an example, the NMR spectrum of a sapmle of 7-methoxycycloheptatriene which had been heated at 103°C for various lengths of time is shown in Fig. 2.

As can be clearly seen in Fig. 2, the signals at 6.65$\tau$ (methyl proton) and 6.83$\tau$ (H-7) decrease with time, and simultaneously two new signals, one a singlet at 6.43$\tau$, 13.1 c./s. lower than the methyl signal of the starting material, and the other a triplet at 7.77$\tau$ ($J$=6.6 c./s.), gradually apppear (curve a) and increase in intensity. Continued heating causes the appearance of two new sets of signals, a singlet at 6.50$\tau$ and a doublet at 7.55$\tau$ ($J$=7.1 c./s.). These results are attributed to the occurrence of consecutive reactions, the second of which occurs after a period of 62 hr. at 103°C, 2.5 hr. at 120°C, or 1.5 hr. at 130°C (curve d). The signal at 6.65$\tau$, due to Va, almost entirely disappears on prolonged heatings, e. g., 100 hr. at 150°C, and does not reappear again. It has, therefore, been concluded that the reverse reaction, VIa or VIb to Va or Vb, does not occur. The doublet signal at 7.55$\tau$ increases with time, and simultaneously the triplet signal at 7.77$\tau$ gradually decreases. At equilibrium new signals appear at 7.83$\tau$ (triplet; $J$=6.0 c./s.) and 6.58$\tau$ as a result of the corresponding methyl group (Fig. 3). It is now clear that the equilibrium mixture is characterized by the appearance of three signals, 6.43$\tau$, 6.50$\tau$ and 6.58$\tau$, in the ratio of 13.6 : 80.5 : 6.0. These signals, appearing on the heating of 7-methoxycycloheptatriene, are summarized in Table I.

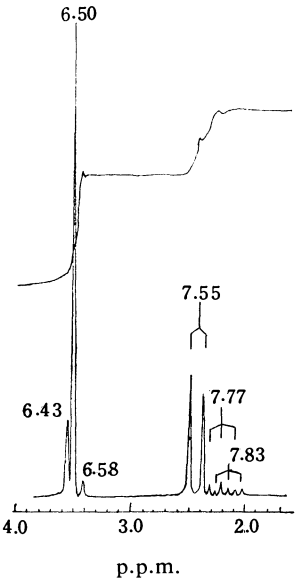



Fig. 3. NMR spectrum of 7-methoxycycloheptatriene which had been heated at 150°C for 100 hr.

Similar results were also obtained for 7-ethoxycycloheptatriene (Vb); these are shown in Table II. The signal due to the hydrogen at the 7-position is observed to undergo changes in the sequence of multiplet → triplet → doublet → triplet. The rate of isomerization seems to be of the same order as that for Va. The same sequence for the appearance of the signals is found at different temperatures for methoxy- and ethoxy-cycloheptatriene. This

TABLE I. THE CHANGES OCCURRING ON HEATING OF 7-METHOXYCYCLOHEPTATRIENE

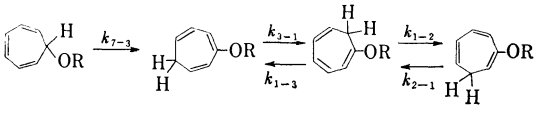
| The sequence of the appearance of the signals | The type of signals | Chemical shift of H-7 $\tau$ | Coupling constant c./s. | Chemical shift of $CH_3$ $\tau$ | Substituted position of $OCH_3$ |
|---|---|---|---|---|---|
| 1 | Multiplet | 6.83 | ca. 4.2 | 6.65 | 7 |
| 2 | Triplet | 7.77 | 6.6 | 6.43 | 3 |
| 3 | Doublet | 7.55 | 7.1 | 6.50 | 1 |
| 4 | Triplet | 7.83 | 6.0 | 6.58 | 2 |

Table II. The changes occurring on heating of 7-ethoxycycloheptatriene

| The sequence for the appearance of the signals | The type of signals | Chemical shit of H-7, $\tau$ | Coupling constant c./s. | Substituted position of OEt |
|---|---|---|---|---|
| 1 | Multiplet | 6.76 | ca. 4.2 | 7 |
| 2 | Triplet | 7.79 | 6.8 | 3 |
| 3 | Doublet | 7.54 | 7.2 | 1 |
| 4 | Triplet | 7.87 | 6.6 | 2 |

means that successive migrations of hydrogen are taking place and that the same 1—5 transannular hydrogen shift observed by ter Borg et al.[8] for 7-*D*- and 7-phenyl-cycloheptatriene is operating in the case of alkoxycycloheptatrienes. As is shown in Tables I and II, all these chemical shifts can be assigned to the revelant isomer from which they originate.

**Kinetic Study.**—The ultraviolet spectrum of 7-methoxycycloheptatriene (Va) exhibits an absorption maximum at 255 m$\mu$ ($\log \varepsilon = 3.61$), and the ultraviolet spectrum of 3-methoxycycloheptatriene (VIa) shows a peaks at 261 m$\mu$ ($\log \varepsilon = 3.60$). Therefore, the ultraviolet spectrophotometric method could not conveniently be applied to a study of the rate of



Va : R=Me Vb : R=Et VIa : R=Me VIb : R=Et VIIa : R=Me VIIb : R=Et VIIIa : R=Me VIIIb : R=Et

thermal isomerization, Va → VIa, as was done in the case of phenylcycloheptatriene. As was mentioned in the preceding section, methyl signals appear at different fields, e.g., at 6.65$\tau$ for Va and 6.43$\tau$ for VIa. The area of these two signals can be separately measured by NMR an integrator technique thus provides a useful method for studying the kinetics.

In Fig. 4, a plot of the area proportion to the total area against time is made for each methyl signal. The straight line indicates that

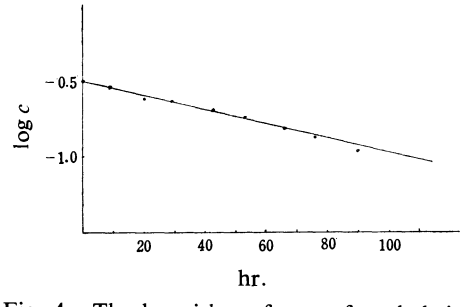



Fig. 4. The logarithm of area of methyl signal proportional to total area ($\log c$) as a function of time at 99.0°C.

Table III. Rate constants of isomerization of 7-methoxycycloheptatriene

| Temp., °C | $K_{7-3}$ |
|---|---|
| 116.3 | $1.76\times10^{-5}$ |
| 99.0 | $3.04\times10^{-6}$ |
| 76.1 | $3.36\times10^{-7}$ |

the isomerization of Va to VIa is of the first order and that the rate constant, $k_{7-3}$, for the conversion of 7-methoxycycloheptatriene (Va) to the first isomer 3-methoxycycloheptatriene (VIa) can be obtained from the slope of the line. This rate constant at different temperatures is given in Table III. These figures were derived from the NMR spectra of aliquots taken at special time intervals. However, it was found necessary to purify the aliquots by vacuum distillation in order to remove a small amount of a high boiling product before measuring the spectra. The yield of a high boiling product became progressively larger as the heating period and temperature were increased, but it did not go beyond 10% under the conditions used.

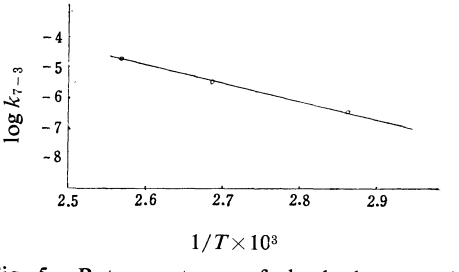



Fig. 5. Rate constants of the hydrogen shifts as a function of temperature.

In Fig. 5, a linear relationship between $\log k_{7-3}$ and $1/T$ is demonstrated. By the method of least squares, Eq. 1 was obtained for the straight line in Fig. 5:

$$\log k_{7-3} = 10.04 - 5.774\times10^3\, T^{-1} \qquad (1)$$

From this relationship, $\log A$ and the experimental activation energy, $\Delta E$, are found to be 10.04 and 26.407 kcal. mol$^{-1}$ respectively. Thus, from the absolute rate theory, the following figures are calculated by assuming the transmission coefficient to be unity: enthalpy

Table IV. Rate constants of the isomerization of cycloheptatriene and 7-methoxycycloheptatriene

| Temp. °C | Cycloheptatriene | 7-Methoxycycloheptatriene |
|---|---|---|
| 98 | $3.8\times10^{-8}$ | $3.07\times10^{-6}$ |
| 121 | $6.0\times10^{-7}$ | $2.48\times10^{-5}$ |
| 140 | $3.2\times10^{-6}$ | $1.17\times10^{-4}$ |

Table V. Rate constants of the isomerization of 7-phenylcycloheptatriene and 7-methoxycycloheptatriene

| Temp. °C | 7-Phenylcycloheptatriene | 7-Methoxycycloheptatriene |
|---|---|---|
| 80.4 | $6.83\times10^{-7}$ | $5.15\times10^{-7}$ |
| 99.9 | $4.76\times10^{-6}$ | $3.68\times10^{-6}$ |
| 120.2 | $3.60\times10^{-5}$ | $2.31\times10^{-5}$ |

of activation: $\Delta H^{\ddagger}=25.7$ kcal. mol$^{-1}$ and entropy of activation: $\Delta S^{\ddagger}=-15.0$ cal. mol$^{-1}$·deg$^{-1}$.

For comparison, Tables IV and V list values of the rate constant, $k_{7-3}$, at different temperatures for the thermal isomerization of cycloheptatriene itself, for that of 7-phenylcycloheptatriene to 3-phenylcycloheptatriene, and for 7-methoxycycloheptatriene, the values for the last compound being calculated from Eq. 1. 7-Methoxycycloheptatriene is seen to undergo isomerization about 100 times faster than cycloheptatriene; $k_{7-3}$ is almost identical in the cases of phenylcycloheptatriene and of methoxycycloheptatriene.

Although a quantitative analysis could not be made of ethoxycycloheptatriene, it seems that its rate of isomerization is not markedly different from that of methoxycycloheptatriene at the initial stage. However, the NMR spectra of the pyrolysates obtained by heating 7-methoxycycloheptatriene and 7-ethoxycycloheptatriene at 195°C for 2 hr., indicate that the former consists of a mixture of 3-methoxy-, 1-methoxy- and 2-methoxy-cycloheptatriene in a ratio of 18.5, 77.0, and 4.63, whereas the latter contains only 3-ethoxy-, and 1-ethoxycycloheptatriene in a ratio of 15.2 and 84.8. It is interesting to note that the formation of 2-ethoxycycloheptatriene is not detected in the isomerization of 7-ethoxycycloheptatriene. This may imply that there is some difference in the ratio of $k_{2-1}$ to $k_{1-2}$ for methoxy- and ethoxycycloheptatriene.

The negative sign of $\Delta S^{\ddagger}$ indicates that this reaction may proceed through a transition state such as that shown by A. The value, $-15.0$ cal. mol$^{-1}$ deg$^{-1}$, seems to be reasonable when compared with the corresponding value, $-8.2$ cal. mol$^{-1}$ deg$^{-1}$, for cycloheptatriene. The fact that this value ($-15.0$ cal. mol$^{-1}$ deg$^{-1}$) is even lower than that ($-11.7$ cal. mol$^{-1}$ deg$^{-1}$) for phenylcycloheptatriene may be ascribed to some contribution of the lone pair of electrons to the rigidity of the transition state. However, before drawing any final conclusion it is necessary to carry out further investigations.

**Chemical Reactions of Alkoxycycloheptatrienes.** — As has been seen above, a simple method is now available for the preparation of cycloheptatriene derivatives in which the alkoxy group is present at positions other than the 7-position. This makes it possible to compare the 7-alkoxycycloheptatrienes with their isomers with regard to their reactivity towards acids, alkalis and dehydrogenating reagents.

When a 7-alkoxycycloheptatriene was shaken with a 6 N hydrochloric acid, tropylium ion (I) was formed in a quantitative yield. The similar treatment of a 7-alkoxycycloheptatriene with a dilute aqueous hydrogen chloride solution at pH 2 for 30 min. gave rise to a 65% yield of the cation I as well as to the formation of some tropone and cycloheptatriene by a disproportionation; however, no traces of the starting material, Va and Vb, were recovered. When a 10% aqueous solution of tropylium bromide (pH=2) was shaken, tropone was slowly formed; this is attributed to a disproportionation of the tropylium ions and tropylalcohol.

On the other hand, the treatment of a mixture of a 3-alkoxycycloheptatriene (VIa and VIb) and a 1-alkoxycycloheptatriene (VIIa and VIIb) with 6 N hydrochloric acid did not result in the formation of tropylium ions to any detectable extent. Similarly, a 95% recovery of the starting materials (as determined by NMR spectral analysis) was obtained when 3-ethoxycycloheptatriene (VIb) and 1-ethoxycycloheptatriene (VIIb) were shaken for 30 min. with 1 N hydrochloric acid at 0°C. When 0.5 N hydrochloric acid was used, 98% of the starting materials was again recovered. These experiments show that, in contrast to 7-alkoxycycloheptatrienes, the isomerization products, 1- and 3-alkoxycycloheptatrienes, are stable in dilute aqueous acid.

When 7-methoxycycloheptatriene was heated at 103°C for 55—60 hr. and when the reaction was then stopped at a point before the doublet signal due to 1-methoxycycloheptatriene (VIIa) appeared in the NMR spectrum, a mixture of Va and VIa was obtained. If this mixture was then shaken with cold 0.5 N hydrochloric acid, Va was transferred to the aqueous phase as tropylium ions, it was thus possible to isolate pure 3-methoxycycloheptatriene (VIa). Pure 3-ethoxycycloheptatriene (VIb) could be obtained by a similar procedure. Fractional distillation could also be used to separate

a mixture of 7-ethoxycycloheptatriene (b. p. 71—76°C/20 mmHg) and 3-ethoxycycloheptatriene (81—82°C/20 mmHg). The NMR spectra of 3-methoxycycloheptatriene and 3-ethoxycycloheptatriene are shown in Figs. 6 and 7.

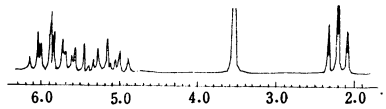



Fig. 6. NMR spectrum of 3-methoxycycloheptatriene and some reaction of its products.

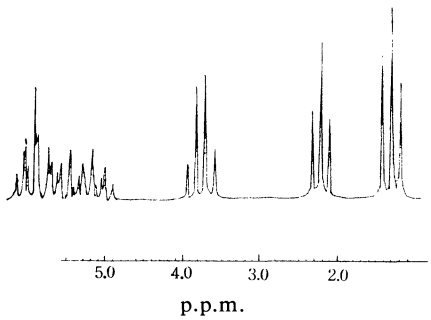
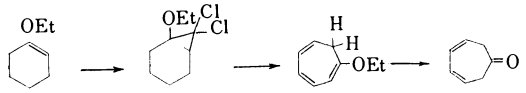



Fig. 7. NMR spectrum of 3-ethoxycycloheptatriene.

Parham et al.[13] have reported that 1-ethoxycycloheptatriene (VIIb) was obtained by heating 1-ethoxy-7, 7-dichlorocarane (X) in quinoline, the X having been prepared from 1-ethoxycyclohexene (IX) and dichlorocarbene.




(IX) (X) (VIIb) (XI)

Parham et al. have also obtained a good yield (95%) of 2, 7-dihydrotropone (XI)[14] through the action of a small amount of acid on a methanol solution of 1-ethoxycycloheptatriene. When 7-ethoxycycloheptatriene was kept at 195°C for 2 hr., it afforded a mixture of 84.8% 1-ethoxycycloheptatriene (VIIb) and 15.19% 3-ethoxycycloheptatriene (VIb), which, after hydrolysis and purification by distillation, afforded a liquid in a 69% yield. The NMR spectrum (see Fig. 8) of this liquid shows a sharp doublet at 7.01$\tau$ ($J$=5.7 c./s.) and the presence of vinylic protons and ethylenic protons whose signals have intensities in the ratio

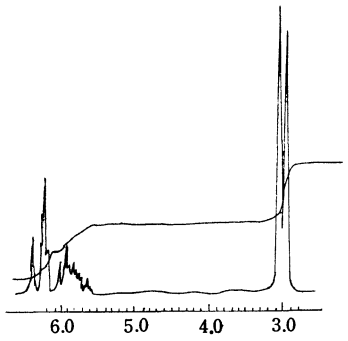



Fig. 8. NMR spectrum of 2,7-dihydrotropone.

of 1 : 1, strongly indicating that the liquid may be 2, 7-dihydrotropone (XI). Since no signals are observed above 7.01$\tau$, the formation of 2, 5-dihydrotropone could not be confirmed.

As has already been noted, the isomerization products, VIa and VIb, VIIa and VIIb, and VIIIa and VIIIb, are stable in dilute aqueous acid. However, the treatment of them with 6 N hydrochloric acid gave cycloheptadienone (XI or its isomer) and also XII as a liquid, b. p. 40—45°C/7 mmHg, and its dimer (XIII) (b. p. 115°C/1 mmHg). The former XII is considered to be hydroxycycloheptenone and the latter XIII, a dimer of XII on the basis of the elementary analyses of their 2, 4-dinitrophenylhydrazones. However, the structure of the latter is not clear.

7-Alkoxycycloheptatriene was found to be stable in alkali at room temperature.

The reaction of 7-alkoxycycloheptatriene with such dehydrogenating reagents as phosphorus pentachloride (Volpin's method[15]) does not give rise to a dehydrogenated product but instead, forms tropylium ions through the elimination of the alkoxy group. However, the treatment of a mixture of 1- and 3-alkoxycycloheptatriene in carbon tetrachloride with 2 molar equivalents of phosphorus pentachloride does not yield tropylium ions but instead produces an alkoxytropylium ions (IV: R= OMe or OEt) in more than a 50% yield. Alkoxytropylium ions separated as a double salt with phosphorous pentachloride from carbon tetrachloride; when this salt was treated with chloroplatinic acid in acetonitrile, the chloroplatinate of IV (R=OMe or OEt) was precipitated as prisms. When the aqueous solution of the double salt was heated, tropone was formed in a quantitative yield.

An unsuccessful attempt was made to prepare

13) W. E. Parham, R. W. Soeder and R. M. Dodson, *J. Am. Chem. Soc.*, **84**, 1756 (1962).
14) J. Meinwald, S. L. Emerman, N. C. Yang and G. Buchi, ibid., **77**, 4401 (1955).
15) a) D. N. Kursanov and M. E. Volpin, *Doklady Akad. Nauk S. S. S. R.*, **113**, 339 (1957); b) M. E. Volpin, I. S. Akhrem and D. N. Kursanov, *Izvest. Akad. Nauk S. S. S. R., Otdel. Khim. Nauk*, **1957**, 760.

ethoxytropopylium bromide by allowing a mixture of 1- and 3-ethoxycycloheptatriene in carbon tetrachloride to react with bromine, and then attempting a dehydrobromination under reduced pressure; however, tropone was obtained. This may be explained by assuming that alkoxytropoylium bromide, a reaction intermediate, was hydrolyzed to tropone during the reaction.

It was hoped that the oxidation of a 3-alkoxycycloheptatriene would yield a 4-alkoxytropone. However, when 3-ethoxycycloheptatriene in dry dioxane was oxidized with selenium dioxide, it unexpectively gave only tropone. Although doubt still remains, this may be attributed to the fact that 3-alkoxycycloheptatrienes (VI) are initially oxidized to an alkoxytropylium salt (IV), which subsequently hydrolyzed to tropone.

The present study has made it clear that 7-alkoxycycloheptatrienes can be converted to alkoxytropylium ions by dehydrogenation after the thermal isomerization. It is also apparent that tropones can be obtained from the dihydrotropones (XI) which are the hydrolysis products of the above isomers of 7-alkoxycycloheptatrienes.

The 7-alkoxycycloheptatrienes gave cation I by the action of acid, and they also reacted with compounds with active hydrogens or with nucleophilic substances,[7] the presence of a trace of acid being sometime necessary. It has thus been established that 7-alkoxycycloheptatrienes may be used effectively as tropylating reagents. As has been mentioned above, one of the advantages of the alkoxycycloheptatrienes (Va and Vb) is that they are readily soluble in organic solvents. In contrast to cation I, alkoxycycloheptatrienes alone do not show any dehydrogenating or oxidizing character. We have also studied the thermal isomerization of alkylmercapto- and amino-cycloheptatrienes, the results of which study will be shortly reported in this Bulletin.

## Experimental

**Reaction Rate Measurements.** — Alkoxycycloheptatrienes (Va and Vb) were sealed in tubes (8 mm. in outer diameter and 40 mm. long) and hung in the vapor of refluxing carbon tetrachloride (76.1°C), water (99.0°C) and acetic acid (116.3°C) respectively. The temperature was uniform over the whole length of the tubes. At regular intervals the tube was taken out and the contents were separated by distillation into alkoxycycloheptatriene and a high boiling product. The NMR spectrum (60 Mc./s. : A-60 Varian spectrometer) was recorded and electrically integrated.

The high-boiling product was found to form more readily from methoxycycloheptatriene than from ethoxycycloheptatriene. When 7-methoxycycloheptatriene (Va) and 7-ethoxycycloheptatriene (Vb) were kept under the same conditions, at 195°C for 2 hr. (these conditions were far more drastic than those applied to the determination of the rate constant $k_{7-3}$), Vb gave a high boiling product in 13.35%, whereas Va gave it in 18.15%.

**7-Ethoxycycloheptatriene (Vb).**—7-Ethoxycycloheptatriene was prepared by a slight modification of the method described by Conrow.[11] A mixture of 6 l. of dry carbon tetrachloride and 1 kg. of phosphorus pentachloride was shaken for 30 min., and then 320 g. of cycloheptatriene was added. The reaction mixture was shaken for 5—6 hr. and allowed to stand overnight. The separated precipitates were collected and poured into 2.6 kg. of ice. After the addition of 260 ml. of ethanol, the solution was neutralized by sodium hydrogencarbonate and extracted by ether (or benzene). The extract was dried over sodium carbonate, and the solvent was evaporated. The residue was then distilled under reduced pressure, giving 173 g. of a colorless liquid, 7-ethoxycycloheptatriene, b. p. 72—73°C/25 mmHg.

**The Action of 6 N Hydrochloric Acid on 7-Alkoxycycloheptatrienes (Va and Vb).**—A mixture of 300 mg. of Vb and 1 ml. of 6 N hydrochloric acid was shaken for 0.5 hr. To the resulting mixture a 30% aqueous solution of $H_2PtCl_6 \cdot 6H_2O$ was added, giving 596 mg. (90.6%) of pale yellow crystals. Its infrared spectrum was identical with that of tropylium chloroplatinate.

Under identical conditions but starting from 300 mg. of Va, 644 mg. (89%) of tropylium chloroplatinate was obtained.

**The Action of 1 N Hydrochloric Acid on 7-Methoxycycloheptatriene (Va).**—A mixture of 3 g. (0.025 mol.) of Va and 23.58 ml. of 1 N hydrochloric acid was adjusted to pH 2 by the addition of some water and shaken for 5 hr. at room temperature. The reaction mixture was then extracted with chloroform. The extract was dried over sodium sulfate, and the solvent was evaporated to give 666 mg. of a liquid. Infrared and ultraviolet spectral analyses showed that the liquid contained 408 mg. (theoretical yield ; 31.4%) of tropone. The aqueous layer was saturated with sodium perchlorate to separate 3.03 g. (64.8%) of colorless needles, the infrared spectrum of which was identical with that of tropylium perchlorate.

**The Action of Water on Tropylium Bromide.**—Tropylium bromide (2.205 g.) was dissolved in about 20 ml. of water, and the pH of the solution was adjusted to ca. 2. by the addition of water. This solution was then shaken vigorously for 5 hr. at room temperature. The reaction mixture was allowed to stand overnight and was extracted with chloroform. After it had dried over sodium sulfate, the solvent was evaporated, giving 212 mg. of a liquid. Ultraviolet spectral analysis showed that the liquid contained 145.5 mg. (theoretical yield ; 21.2%) of tropone. The aqueous layer was saturated with sodium perchlorate to separate 1.92 g. (78.8%) of tropylium perchlorate.

**The Action of 6 N Hydrochloric Acid on Thermally-Isomerized Methoxycycloheptatriene.**—7-Methoxycycloheptatriene (Va) was heated for 2 hr. at 195°C and distilled to remove the high boiling

product. The distillate was a mixture of 3-methoxycycloheptatriene (VIa), 1-methoxycycloheptatriene (VIIa) and 2-methoxycycloheptatriene (VIIIa) in the ratio of 18.5 : 7.70 : 4.63, judging from the analysis of MNR spectrum. The above-obtained mixture (400 mg.) and 1 ml. of 6 N hydrochloric acid were shaken for 30 min. When the reaction mixture was extracted with chloroform, 263 mg. of a brown liquid was afforded by the evaporation of the solvent. Infrared spectrum of the liquid was virtually identical with that of a mixture of XII and the XIII dimer. From the aqueous layer, no precipitates appeared upon the addition of a 30% aqueous solution of $H_2PtCl_6 \cdot 6H_2O$.

**The Action of 1 N Hydrochloric Acid on Thermally-Isomerized Ethoxycycloheptatriene.** — When 7-ethoxycycloheptatriene was heated for 2 hr. at 195°C, it gave a liquid which contained 3-ethoxycycloheptatriene (VIb) and 1-ethoxycycloheptatriene (VIIb) in the ratio of 15.19 : 84.8. To 4 g. of this liquid, 33 ml. (1.1 mol. eq.) of 1 N hydrochloric acid was added. After it had been shaken for 30 min. at 0°C, the reaction mixture was extracted with chloroform. The extract was dried over sodium sulfate, and the solvent was evaporated in vacuo, affording a yellow liquid. Its NMR spectrum showed that this liquid contained 3.87 g. (96.7%) of the starting material.

**The Action of 0.5 N Hydrochloric Acid on Thermally-Isomerized Ethoxycycloheptatriene.**—To 4 g. of the thermally-isomerized ethoxycycloheptatriene, which comprises 15.19% of VIb and 84.8% of VIIb, 66 ml. of 0.5 N hydrochloric acid was added. When this mixture was treated in the same manner as described above, it afforded 3.90 g. (97.5%) of the starting material.

**3-Methoxycycloheptatriene (VIa).** — 7-Methoxycycloheptatriene (Va) was heated for 55—60 hr. at 106°C, affording a liquid which was found to be a mixture of 40% of Va and 60% of VIa by a comparison of its NMR spectrum with those of Va and VIa. To 300 ml. of 0.5 N hydrochloric acid, 34.8 g. of this mixture was added at 0°C. This mixed solution was shaken for 30 min. at 0—5°C and then extracted with chloroform. The extract was washed with a saturated aqueous solution of sodium hydrogen carbonate and dried over sodium sulfate. After the evaporation of the solvent, the residue was distilled under reduced pressure to give 17.10 g. of 3-methoxycycloheptatriene (VIa), b. p. 74—75°C/15 mmHg, 716 mg. of substance A b. p. 60—100°C/0.5 mmHg, and 527 mg. of B b. p. 100—125°C/0.5 mmHg. The NMR spectra showed A to be a mixture of VIa and B, and B to be a mixture of XII and XIII. An undistilled residue (6.76 g.) remained.

**3-Ethoxycycloheptatriene (VIb).**—a) Under the same conditions as with 3-methoxycycloheptatriene, 34.0 g. of a mixture of Vb and VIb afforded 20.29 g. of 3-ethoxycycloheptatriene, b. p. 76 — 80°C/15 mmHg and 294 mg. of a yellow oil, b. p. 125—130°C/0.5 mmHg. The NMR spectrum of the latter is identical with that of above B. An undistilled residue (2.77 g.) remained.

b) After 19 g. of 7-ethoxycycloheptatriene had been heated for 2.5 hr. at 130°C, the thermally-isomerized product was distilled fractionally through a column which was 25 mm. in diameter and 30 cm. long. A colorless liquid, 9.24 g. of A, b. p. 71—76°C/20 mmHg, 3.08 g. of B, b. p. 76—81°C/20 mmHg, and 2.71 g. of C, b. p. 81—82°C/20 mmHg were obtained. From the NMR spectral comparison, it was clarified that A and C were identical with Vb and VIb respectively, and that B was a mixture of the two. An undistilled residue (3.20 g.) remained.

**2, 7-Dihydrotropone (XI).** — 7-Ethoxycycloheptatriene was heated for 2 hr. at 195°C and distilled under reduced pressure to give a liquid which contained 84.8% of VIIb and 15.19% of VIb. A mixture of 80 ml. of methanol, 11 ml. of water and 10 ml. of concentrated hydrochloric acid was then added. After this mixture had been stirred for 2 hr. at 15—20°C, cold water was added to dilute the reaction mixture to a volume of 200 ml. The resulting solution was extracted with 100 ml. of chloroform. After the extract had been washed with a saturated aqueous solution of sodium hydrogen carbonate, the solvent was evaporated to give 4.25 g. of a liquid. By the vacuum distillation of the liquid, 3.28 g. (68.87%) of XI, b. p. 71—74°C/20 mmHg was obtained.

**The Action of 6 N Hydrochloric Acid on Thermally - Isomerized Ethoxycycloheptatriene.** — 7-Ethoxycycloheptatriene (Vb) was heated for 1 hr. at 200°C and distilled to afford a clear liquid which was more than 80% 1-ethoxycycloheptatriene (VIIb). A mixture of 15 g. of this liquid and 51 ml. of 6 N hydrochloric acid was shaken vigorously at room temperature for 5 hr. The reaction mixture was then extracted with 100 ml. of chloroform, and the extract was washed with a saturated aqueous solution of sodium hydrogen carbonate. After the evaporation of the solvent, 13.09 g. of a brown oil was obtained; 4 g. of it was distilled in vacuo to give 314 mg. of a colorless liquid (XII), b. p. 40—55°C/7 mmHg and 1.86 g. of a pale yellow oil (XIII), b. p. 115°C/1 mmHg.

**2, 4-Dinitrophenylhydrazone of XII.**—A mixture of 180 mg. of XII, 10 ml. of ethanol and 825 mg. of 2,4-dinitrophenylhydrazine was refluxed for 1 hr.; then the excess 2,4-dinitrophenylhydrazine was removed by hot filtration. The filtrate was cooled in ice and the resulting crystals recrystallized from ethanol to give red plates, m. p. 175—181°C.

Found: C, 51.67; H, 4.42; N, 17.96. Calcd. for $C_{13}H_{14}O_5N_4$: C, 50.98; H, 4.61; N, 18.29%.

**2, 4-Dinitrophenylhydrazone of XIII.**—A mixture of 300 mg. of XIII, 10 ml. of ethanol and 800 mg. of 2,4-dinitrophenylhydrazine was refluxed for 1 hr.; then the resulting crystals were fractionally recrystallized from ethanol, giving red crystals from the easily soluble part and yellow crystals from the sparingly soluble part. Although the former was difficult to purify, the latter was purified by repeated recrystallization, giving yellow needles, m. p. 161—162°C.

Found: C, 60.64; H, 4.99; N, 13.70. Calcd. for $C_{20}H_{20}O_5N_4$: C, 60.60; H, 5.09; N, 14.14%.

**The Action of Phosphorus Pentachloride on Alkoxycycloheptatriene (Va and Vb).**—A mixture of 3.98 g. (2.6 mol. eq.) of phosphorus pentachloride and 35 ml. of anhydrous carbon tetrachloride

was stirred for 30 min., and then a solution of 1 g. of Vb in 1 ml. of carbon tetrachloride was stirred in. Immediately colorless precipitates were separated out. Stirring was then continued for a further 5 hr. at 15—20°C. The reaction mixture was allowed to stand overnight and poured onto 5 g. of ice. Sodium perchlorate was added to the aqueous layer, giving 1.13 g. (81%) of tropylium perchlorate. Under identical conditions but starting with 1 g. of Va, 1.34 g. (85.8%) of tropylium perchlorate was obtained.

**Methoxytropylium Ions (IV; R=OMe).** — To a mixture of 2.15 g. (2 mol. eq.) of phosphorus pentachloride and 30 ml. of anhydrous carbon tetrachloride, a solution of 1 g. of thermally-isomerized methoxycycloheptatriene (a mixture of 18.5% of VIa, 77.0% of VIIa, and 4.63% of VIIIa) in 1 ml. of carbon tetrachloride was added. After 6 hr. stirring, the reaction mixture was allowed to stand overnight. The resulting colorless precipitates were separated by filtration under dry air; after the precipitates had been dried under the vacuo, they were poured into 2 ml. of anhydrous acetonitrile. The resulting solution was filtered to remove insoluble substances, and then to the filtrate was added, drop by drop, a 30% solution of $H_2PtCl_6 \cdot 6H_2O$ in acetonitrile to give 152 mg. yellow prisms, m. p. 180°C (decomp.)

Found: C, 29.52; H, 2.78; Pt, 29.79. Calcd. for $C_8H_9O_{1/2}PtCl_6$: C, 29.55; H, 2.79; Pt, 30.01%.

The filtrate was then concentrated, giving further 531 mg. of crystals (Total yield: 683 mg.). An infrared spectrum of the crystals differs from that of the chloroplatinate of tropone.

**Ethoxytropylium Ions (IV; R=OEt).** — Under the same conditions with methoxytropylium ions, 600 mg. of thermally-isomerized ethoxycycloheptatriene (a mixture of 15.19% of VIb and 84.81% of VIIb) gave 669 mg. of pale orange prisms, m. p. 164—165°C (decomp.).

Found: C, 32.15; H, 3.25; Pt, 28.55. Calcd. for $C_{18}H_{22}O_2PtCl_6$: C, 31.89; H, 3.27; Pt, 28.76%.

When absolute alcohol was used instead of anhydrous acetonitrile, 1 g. of thermally-isomerized ethoxycycloheptatriene also gave 194 mg. of chloroplatinate of IV; R=EtO.

**The Action of Bromine on Thermally-Isomerized Ethoxycycloheptatriene.**—To a cold solution of 4 g. of thermally-isomerized ethoxycycloheptatriene (a mixture of 15% of VIb and 85% of VIIb) in 35 ml. of carbon tetrachloride, a solution of 4.7 g. of bromine in 13 ml. of carbon tetrachloride was stirred in drop by drop. Stirring was then continued for a further 5 hr. at 15°C, after which the solvent was evaporated at 40—50°C under reduced pressure. The residue was allowed to stand for 3 days at 50°C under 100 mmHg. At the end of this period, 4.68 g. of strongly hydroscopic black precipitates were obtained. These precipitates (1.42 g.) were added to 2 ml. of acetonitrile, and the insoluble substance was removed by filtration. A solution of $H_2PtCl_6 \cdot 6H_2O$ (1 g.) in 2 ml. of acetonitrile was added to the filtrate, giving 139 mg. of orange needles. Their infrared spectrum was identical with that of the chloroplatinate of tropone.

**Tropone from Ethoxytropylium Ions.**—Starting from 3 g. of thermally-isomerized ethoxycycloheptatriene, 11.24 g. of phosphorus pentachloride and 120 ml. of carbon tetrachloride, ethoxytropylium ions were obtained as 7.02 g. of double salt with phosphorus pentachloride. This salt was dissolved in water, and the solution was warmed on a water bath and neutralized by the addition of sodium hydrogen carbonate. The reaction product was extracted with chloroform, giving 1.23 g. of an oil. Its infrared spectrum was identical with that of tropone, and by the action of picric acid, this oil afforded 3.5 g. of topone picrate.

**The Action of Selenium Oxide on 3-Ethoxycycloheptatriene (VIb).**—Into a solution of 5 g. of VIb in 100 ml. of dry dioxane, 8.15 g. (2 mol. eq.) of selenium oxide under a nitrogen atmosphere was stirred. The mixture was heated at 120—125°C for 3 hr. under stirring and allowed to stand overnight. The selenium with separated was removed by filtration, and the solvent was evaporated under reduced pressure. Ether was added to the residue, and 2.15 g. of an oil was obtained by the evaporation of the solvent. Its infrared spectrum was identical with that of tropone, and by the action of hydrazine hydrate, the oil afforded 1.59 g. of 2-aminotropone.[16]

The authors wish to express their sincere gratitude to the Sankyo Co., Ltd., which defrayed a part of the expenses for the present work. Thanks are also due to the Toyo Rayon Co., Ltd., for supplying infrared spectrophotometer which was used for these experiments. The authors are also grateful to Mr. Fujio Masuko for his measurement of the reaction rate.

*Department of Chemistry*
*Faculty of Science*
*Tohoku University*
*Katahira-cho, Sendai*

16) T. Nozoe, T. Mukai, J. Minegishi and T. Fujisawa, *Sci. Repts. Tohoku Univ.*, I, 37, 388 (1953).

# NOTES

## The Thermal Dimerization of 2-Vinylfuran*

By Chuji Aso, Toyoki KUNITAKE and Yoshinari TANAKA

(Received August 31, 1964)

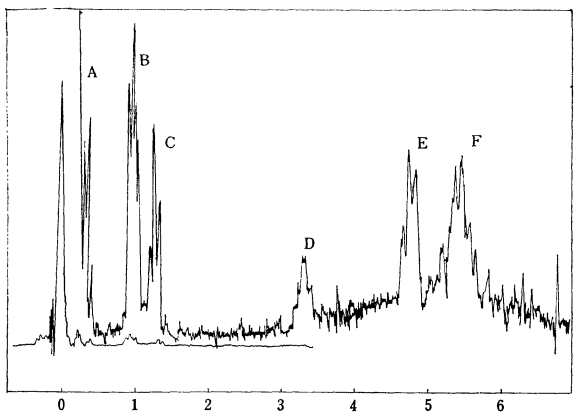
2-Vinylfuran was found to undergo a rather facile thermal polymerization[1] during the course of the study of its free radical polymerization.[2]

Since the thermal dimerization of styrene has been studied in connection with the elucidation of the initiation mechanism of thermal polymerization,[3] similar experiments were carried out for 2-vinylfuran.

### Results

The monomer prepared in a manner described previously[2] was dissolved in purified toluene or bromobenzene (molar ratio 1 : 10) in an ampule. After it had been sealed under reduced nitrogen pressure, the ampule was allowed to stand at 130°C for 300 hr. After the insoluble fraction in methanol had been removed and the solvents had been evaporated at a reduced pressure, viscous oil was obtained. The gas chromatogram of the distillable portion of the oil (ca. 100°C/4 mmHg) consisted of one major peak, and its yield was 10 to 20% with a toluene solvent and 30 to 50% in bromobenzene. Elementary analysis: Found: C, 75.65; H, 6.40. Calcd. for $C_6H_6O$: C, 76.57; H, 6.43%. The molecular weight determination (Vapor Pressure Osmometer, Model 301A, Mechrolab. Inc.) showed the portion to be a dimer (Found: 175, 198. Calcd. for dimer: 188). The residues of the distillation had molecular weights from that of a trimer to that of a hexamer, depending on the solvent used. Thus, the distillate was concluded to be a dimer of 2-vinylfuran. Subsequent measurements of infrared, ultraviolet and NMR spectra gave the following results:

a) IR data. Characteristic bands for furans[4] observed at 3150, 1595, 1500, 1006, 881 and




Up-field shift from benzene, p. p. m.

Fig. 1. NMR spectrum of the dimer.

* Contribution No. 76. from the Department of Organic Synthesis, Faculty of Engineering, Kyushu University.

Part II of "The Polymerization of Vinyl Compounds with Heterocyclic Groups."

1) Y. Tanaka, Master's thesis. Kyushu Univ., 1964.

2) C. Aso and Y. Tanaka, *Chem. High Polymers, Japan*, **27**, 373 (1964).

3) F. Mayo, *J. Am. Chem. Soc.*, **75**, 6133 (1953).

4) Kagaku-no-ryoiki. Special Issue, No. 28. "Infrared Absorption Spectroscopy," Vol. III, Nanko-do, Tokyo (1961), p. 108.

796 $cm^{-1}$. No vinyl absorption. Characteristic bands for aliphatic C-H bonds at 2948, 2866, 1450 and 1380 $cm^{-1}$.

b) UV data. No double bond conjugated with the furan ring present.

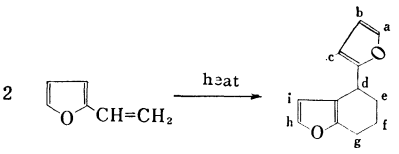
c) NMR data (in benzene, Varian A 60). The NMR assignment shown in the table is consistent with the chemical shifts for other furan derivatives[5] and with the other data obtained for the dimer, although no detailed analysis of spin-spin coupling has yet been carried out.

TABLE I. NMR ASSIGNMENTS

| Peak | A | B | C | D | E | F |
|---|---|---|---|---|---|---|
| Area ratio | 2 | 2 | 1 | 1 | 2 | 4 |
| Assignment | a,h | b,i | c | d | g | e,f |

$J_{de} \fallingdotseq 5$ c. p. s. $J_{fg} \fallingdotseq 5$ c. p. s.

5) R. J. Abraham and H. J. Bernstein, *Can. J. Chem.*, **39**, 905 (1961); G. S. Reddy and J. H. Goldstein, *J. Phys. Chem.*, **65**, 1539 (1961).




The dimer may be formed either by a Diels-Alder type reaction, followed by isomerization, or by a coupling of biradicals. Although it is not clear whether this compound can be related with the thermal initiation of polymerization, the contrast should be interesting between this compound and the cyclobutane derivative obtained thermally from styrene.[3]

We wish to express our thanks to Professor Taku Matsuo of our department for his helpful discussions.

*Department of Organic Synthesis*
*Faculty of Engineering*
*Kyushu University*
*Hakozaki, Fukuoka*

# The Removal of Copper from the Copper Complex of ω-Acylamino Acid with EDTA*

By Shigeru KUWATA and Hiroshi WATANABE

(Received September 14, 1964)

ω-Acyl derivatives of basic amino acids can be synthesized most conveniently by the acylation of the copper complexes of the amino acid, followed by the removal of copper by hydrogen sulfide. This method is, however, rather troublesome for the synthesis of lysine or ornithine derivatives (e. g. ε-carbobenzoxy-lysine or δ-carbobenzoxy-ornithine) when water is used as a solvent, because their final products are only slightly soluble in water or are strongly adsorbed on cupric sulfide. This difficulty can be avoided by using such a solvent as boiling 70—80% acetic acid[1] or dilute hydrochloric acid[2], which dissolves the product. However, it might be desirable to avoid the hydrogen sulfide process for the benefit of subsequent catalytic reduction. For this reason, Zahn[3] has used potassium cyanide in 20% acetic acid to remove copper from the copper complex of ε-lysine peptide. Although we applied this method to the preparation of ε-carbobenzoxy-lysine, we could not obtain any successful results because of the low solubility of the product in this solvent. In principle, a reagent which has a stronger affinity to copper than that of amino acid, may also be useful. Therefore, we intended to use EDTA (ethylenediaminetetraacetic acid), which is well known to form a water-soluble copper chelate, as a copper-removing reagent.

Thus, we were successful in obtaining a ω-acyl derivative, e. g., γ-carbobenzoxy-L-α, γ-diaminobutyric acid or ε-tosyl-L-lysine, from its copper complex by merely boiling it with EDTA in water or aqueous ethanol, from which the product separated as white precipitates in the cold. A ω-acyl derivative, such as ε-carbobenzoxy-L-lysine, which is very slightly soluble even in hot water, was also easily prepared by boiling the aqueous suspension of a copper derivative with EDTA, followed by the recrystallization of the raw product from 50% acetic

* This work was presented at the 17th Annual Meeting of the Chemical Society of Japan, April, 1964.

1) J. Noguchi, T. Hayakawa and M. Hiraoka, *J. Chem. Soc. Japan, Pure Chem. Sec.* (*Nippon Kagaku Zasshi*), **82**, 604 (1961).

2) B. C. Barrass and D. T. Elmore, *J. Chem. Soc.*, **1957**, 3134.

3) H. Zahn and W. Pätzold, *Chem. Ber.*, **96**, 2566 (1963).

Table I. Comparison of EDTA and $H_2S$ methods

| Amino acid | ω-Acyl group† | Method | Copper complex of ω-acyl deriv., g. | EDTA g. | Product g. | % | M. p., °C | $[\alpha]_D^{31}$ |
|---|---|---|---|---|---|---|---|---|
| L-Lysine | Tos | EDTA | 10 | 6 | 8 | 88 | 237—240 | +14.2°(c=3.2, N HCl) |
| | Tos | $H_2S$[4] | 26 | — | 20 | 85 | 238—240 | +14.4°(c=3.2, N HCl) |
| L-Lysine | Z | EDTA | 15 | 9 | 12 | 89 | 251—254 | +14.4°(c=1.6, N HCl) |
| | Z | $H_2S$[5] | 61 | — | 53 | 96 | 253—254 | +14.1°(c=1.6, N HCl) |
| L-α,γ-Diamino-butyric acid | Z | EDTA | 5 | 3.5 | 3.5 | 79 | 237 | |
| | Z | $H_2S$[2] | 5 | — | 3.3 | 75 | 233—235 | |

† Tos=*p*-toluenesulfonyl-; Z=carbobenzoxy-

4) R. Roeske, F. H. C. Stewart, R. J. Stedman and V. duVigneaud, *J. Am. Chem. Soc.*, **78**, 5883 (1956).

5) F. Sanger and A. Neuberger, *Biochem. J.*, **37**, 515 (1943).

acid containing some EDTA, thus removing the trace of copper.

The yields are comparable to those obtained by the hydrogen sulfide method, as is shown in Table I.

## Experimental

The copper complexes of the ω-acyl amino acids were prepared by acylating the copper complexes of the amino acids by the usual method.

EDTA was used as the disodium salt.**

**ε-Tosyl-L-lysine.**—The copper complex of ε-tosyl-L-lysine was suspended in water or 50% ethanol containing EDTA, the mixture was then boiled until the complex had dissolved completely. When the resulting blue colored solution had cooled, colorless needles were separated from it. The crystals were washed with water and recrystallized from 50% ethanol. For further purification, they were dissolved in dilute hydrochloric acid, decolorized, and neutralized with alkali, and the resulting white precipitates were recrystallized from 50% ethanol.

**γ-Carbobenzoxy-L-α,γ-diaminobutyric Acid.** — The copper complex was treated as above.

**ε-Carbobenzoxy-L-lysine.**—The copper complex of ε-carbobenzoxy-L-lysine was suspended in an aqueous EDTA solution and boiled until the violet color of the complex had almost disappeared. After the mixture had cooled, a white product was filtered off, washed thoroughly with water, and recrystallized from 50% acetic acid containing some EDTA in order to remove the trace of unreacted copper. The product was then recrystallized from the same solvent. For further purification, it was treated as above.

The results are summarized in Table I in comparison with those obtained by the hydrogen sulfide method.***

*Laboratory of Chemistry*
*Faculty of Science*
*Kōnan University*
*Okamoto, Higashinada, Kobe*

** Clewat AM (technical grade, kindly supplied by the Teikoku Chem. Ind., Ltd.) or Dotite 2Na (analytical grade, purchased from Wako Pure Chemical Ind., Ltd.) was used. The grade of reagent had no influence on the results.

*** According to the private communication from S. Sakakibara, Institute for Protein Research, Osaka University, this method was also applied successfully in the case of ornithine.

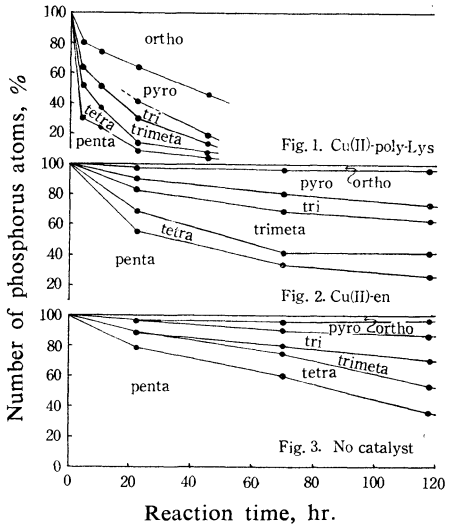
## SHORT COMMUNICATIONS

# The Selective Hydrolysis of Pentaphosphate by Copper Chelate Catalysts*

By Yoshiki MORIGUCHI and Masaji MIURA

(Received December 26, 1964)

Although several studies of the hydrolytic degradation of substances using chelates as the catalyst have recently been made,[1] these have dealt almost exclusively with kinetic problems; little attention has been paid to the selective action of the chelates. We have, therefore, attempted to study the selective hydrolysis of polyphosphates by chelate catalysts and have obtained some interesting results on the hydrolysis of pentaphosphate.




Hydrolytic degradation of pentaphosphate in the presence of copper chelate catalysts at 45°C and pH 8.

Pentaphosphate was prepared by the method which has been reported previously.[2] The decomposition products were identified and determined quantitatively by ion-exchange chromatography, using $^{32}P$ as a tracer.[3]

As may be seen in Table I, the chelates used remarkably accelerate the decomposition rate of pentaphosphate. The main decomposition product is orthophosphate in the presence of copper(II)-polylysine (Fig. 1), while the product is trimetaphosphate in the presence of copper(II)-ethylenediamine (Fig.

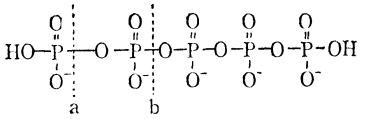



Fig. 4

TABLE I. DATA ON THE HYDROLYTIC DEGRADATION OF PENTAPHOSPHATE BY COPPER CHELATE CATALYSTS AT 45°C AND pH 8

| Metal (M) | Ligand (L) | $M/P_5$*1 mol. ratio | $L/P_5$ | First order rate constant $min^{-1}$ | Half life min. |
|---|---|---|---|---|---|
| — | — | 0 | 0 | $4.92\times10^{-5}$ | $1.41\times10^{4}$ |
| Cu | — | 1 | 0 | $9.23\times10^{-5}$ | $7.51\times10^{3}$ |
| Cu | en*2 | 1 | 1 | $1.86\times10^{-4}$ | $3.73\times10^{3}$ |
| — | Poly-Lys*3 | 0 | $5\times10^{-3}$ | $1.37\times10^{-4}$ | $5.06\times10^{3}$ |
| Cu | Poly-Lys*4 | 1 | $5\times10^{-3}$ | $1.83\times10^{-3}$ | $3.79\times10^{2}$ |

*1 $P_5$: pentaphosphate
*2 Ethylenediamine
*3 Poly-L-lysine (M. W.: 85000)
*4 L/M ratio corresponds to two repeat units per copper.

* Presented at the Annual Japanese Meeting on Coordination Chemistry, Fukuoka, November, 1964.

1) E.g., R. Hofstetter and A. E. Martell, *J. Am. Chem. Soc.*, **81**, 4461 (1959).

2) M. Miura and Y. Moriguchi, This Bulletin, **37**, 1522 (1964).

3) S. Otani, M. Miura and T. Doi, *J. Chem. Soc. Japan, Ind. Chem. Sec.* (*Kogyo Kagaku Zasshi*), **66**, 593 (1963).

2). These results lead us to the conclusion that these two kinds of chelates act in different ways in the hydrolytic degradation of pentaphosphate; that is, the former accelerates the terminal chain attack (Fig. 4a), whereas the latter promotes the intermediate chain attack (Fig. 4b).

Similar studies of various polyphosphates and chelates are in progress.

*Department of Chemistry*
*Faculty of Science*
*Hiroshima University*
*Higashisenda, Hiroshima*

# The Synthesis and Biological Activities of a Hexadecapeptide Corresponding to a Modified Sequence in the Corticotropin Structure

By Hideo OTSUKA, Ken INOUYE, Makoto KANAYAMA and Fusako SHINOZAKI

(Received December 28, 1964)

The syntheses of adrenocorticotropically active peptides, which have chain lengths of less than a half of the 39-amino acid chain in the corticotropin (ACTH) structure, have been reported by several investigators,[1-7] We wish to describe herein the synthesis of a hexadecapeptide with a modified sequence of the first octadecapeptide portion of the ACTH molecule, in which the *N*-terminal serine is replaced by a glycine and the lysyl-lysyl sequence at positions 15—16 is removed; this substance is, namely, glycyl-tyrosyl-seryl-methionyl-glutamyl-histidyl-phenylalanyl-arginyl-tryptophyl-glycyl-lysyl-prolyl-valyl-glycyl-arginyl-arginine (I),*1 which may be designated as $\alpha^{1-14,17-18}$-Gly$^{1}$-ACTH. This synthetic peptide has been shown to have a very low but a consistently reproducible adrenal steroidogenic activity of 0.134 U.S.P. unit per mg., as estimated by the in vitro method;[8] it has also brought about a plasma corticosterone elevation in a hypophysectomized rat.*2 The results may partially validate the finding of Lebovitz and Engel that the hydroxymethyl group of the *N*-terminal serine is not necessary for the ACTH activity.[9] The peptide has been also found to exhibit a high lipolytic potency[10] of the minimal effective doses, 0.00093 $\mu$g. in rabbit adipose tissue and 0.031 $\mu$g. in the rat,*2 values which were of the same order of magnitude as those reported for the heptadecapeptide, $\alpha^{1-17}$-ACTH.[3,10]

$N^{\alpha}$-Cbz-$N^{\varepsilon}$-BOC-lysyl-prolyl-valyl-glycyl-nitroarginyl-nitroarginine benzyl ester (II) (m. p. 114—115°C, $[\alpha]_D^{25}$ −49.4° (*c* 2.0, methanol). Found: C, 52.54; H, 6.49; N, 18.52. Calcd.: C, 52.48; H, 6.78; N, 18.36%) was obtained by the DCCI-mediated condensation of $N^{\alpha}$-Cbz-$N^{\varepsilon}$-BOC-lysyl-prolyl-valyl-glycine[11] with nitroarginyl-nitroarginine benzyl ester, which had been derived by trifluoroacetic acid treatment from the BOC-nitroarginyl-nitroarginine benzyl ester ($[\alpha]_D^{25}$ −18.1° (*c* 2.5, methanol). Found: C, 47.68; H, 6.78; N, 21.42. Calcd.: C, 47.21; H, 6.27; N, 22.94%). Compound II was hydrogenolyzed to give $N^{\varepsilon}$-BOC-lysyl-prolyl-valyl-glycyl-arginyl-arginine diacetate (III) ($[\alpha]_D^{26.5}$ −50.1° (*c* 1.6, 50% acetic acid). Found: N, 19.51; $CH_3CO$, 9.68. Calcd.: N, 19.54; $CH_3CO$, 9.24%), which was then converted into the trihydrochloride (IV) (Found: Cl, 12.05.

1) K. Hofmann, N. Yanaihara, S. Lande and H. Yajima, *J. Am. Chem. Soc.*, **84**, 4470 (1962); "Polyamino Acids, Polypeptides and Proteins," Ed. by M. Stahmann, University of Wisconsin Press (1962), p. 2.
2) R. Schwyzer, W. Rittel and A. Costopanagiotis, *Helv. Chim. Acta*, **45**, 2473 (1962).
3) C. H. Li, D. Chung, J. Ramachandran and B. Gorup, *J. Am. Chem. Soc.*, **86**, 2703 (1964); **84**, 2460 (1962).
4) J. Ramachandran, D. Chung and C. H. Li, *Federation Proc.*, **23**, 369 (1964).
5) C. H. Li, J. Meienhofer, E. Schnabel, D. Chung, T. B. Lo and J. Ramachandran, *J. Am. Chem. Soc.*, **83**, 4449 (1961); **82**, 5760 (1960).
6) R. Schwyzer, W. Rittel, H. Kappeler and B. Iselin, *Angew. Chem.*, **72**, 915 (1960).
7) C. H. Li, J. Ramachandran and D. Chung, *J. Am. Chem. Soc.*, **86**, 2711 (1963); **85**, 1895 (1963).
*1 All amino acid residues are of the L-configuration with the exception of glycine. In this communication the following abbreviations will be used: Cbz, carbobenzoxy; BOC, *t*-butyloxycarbonyl; DCCI, *N*,*N*′-dicyclohexylcarbodiimide; CMC, carboxymethyl cellulose.
8) M. Saffran and A. V. Schally, *Endocrinol.*, **56**, 523 (1955).
*2 The authors are much indebted to Dr. Akira Tanaka for these biological assays.
9) H. E. Lebovitz and F. L. Engel, *Endocrinol.*, **73**, 573 (1963).
10) A. Tanaka, B. T. Pickering and C. H. Li, *Arch. Biochem. Biophys.*, **99**, 294 (1962).
11) H. Otsuka, K. Inouye and Y. Jono, This Bulletin, **37**, 1471 (1964).

Calcd.: Cl, 11.54%).

BOC-glycine was coupled with tyrosine methyl ester (m. p. 134—135°C, $[\alpha]_D^{23.5}$ +26.9° (*c* 2.4, methanol); lit.[12] m. p. 135°C) by DCCI to give the acyldipeptide ester, which was then converted into the BOC-glycyl-tyrosine hydrazide (V) (m. p. 189—190°C, $[\alpha]_D^{26.5}$ +0.5° (*c* 2.0, dimethylformamide). Found: C, 54.56; H, 6.79; N, 15.93. Calcd.: C, 54.53; H, 6.87; N, 15.90%). The BOC-seryl-methionine methyl ester (VI) (m. p. 66—67.5°C, $[\alpha]_D^{25.5}$ −29.5° (*c* 2.0, methanol). Found: C, 48.06; H, 7.61; N, 8.20; S, 9.34. Calcd.: C, 47.98; H, 7.48; N, 7.99; S, 9.15%) was prepared by the DCCI-induced coupling of the methionine methyl ester with the crystalline BOC-serine monohydrate (m. p. 45—47°C, $[\alpha]_D^{25}$ −7.6° (*c* 2.6, water), $[\alpha]_D^{26}$ −3.0° (*c* 2.3, acetic acid). Found: C, 43.25; H, 7.88; N, 6.52; $H_2O$, 7.19. Calcd.: C, 43.04; H, 7.68; N, 6.28; $H_2O$, 8.07%). The azide prepared from V was allowed to react with the dipeptide ester, which had beed derived from VI by HCl/ethyl acetate treatment, to obtain the protected tetrapeptide BOC-glycyl-tyrosyl-seryl-methionine methyl ester (VII) (m. p. 183—185°C, $[\alpha]_D^{24}$ −16.5° (*c* 1.15, methanol). Found: C, 52.44; H, 7.01; N, 9.98; S, 5.70. Calcd.: C, 52.62; H, 6.71; N, 9.82; S, 5.62%). Compound VII was treated with hydrazine to give the corresponding hydrazide hemihydrate (VIII) (m. p. 201—203°C decomp., $[\alpha]_D^{27}$ −19.4° (*c* 1.2, 50% acetic acid). Found: C, 50.07; H, 6.93; N, 14.24; S, 5.48. Calcd.: C, 49.73; H, 6.78; N, 14.50; S, 5.53%).

γ-*t*-Butyl-glutamyl-histidyl-phenylalanyl-arginyl-tryptophyl-glycine[13] and the azide, which had been derived from VIII, were coupled together to give the decapeptide derivative BOC-glycyl-tyrosyl-seryl-methionyl-γ-*t*-butyl-glutamyl-histidyl-phenylalanyl-arginyl-tryptophyl-glycine dihydrate (IX) (m. p. 212—218°C (decomp.), $[\alpha]_D^{26.5}$ −15.5° (*c* 1.7, dimethylformamide). Found: C, 55.17; H, 6.84; N, 15.03; S, 2.14. Calcd.: C, 55.05; H, 6.62; N, 15.33; S, 2.19%). The hydrochloride of IX was then converted into the *N*-hydroxysuccinimide ester,[14] and this active ester was allowed to react with IV in an aqueous pyridine solution to give the hexadecapeptide derivative BOC-glycyl-tyrosyl-seryl-methionyl-γ-*t*-butyl-glutamyl-histidyl-phenylalanyl-arginyl-tryptophyl-glycyl-$N^{\epsilon}$-BOC-lysyl-prolyl-valyl-glycyl-arginyl-arginine (X), which was then partially purified on a CMC column. Compound X was treated with 90% trifluoroacetic acid to yield the free hexadecapeptide I, which was then purified by CMC column chromatography. The purified material was found to be homogeneous in paper electrophoresis and in paper chromatography. $\lambda_{max}^{0.1N\ HCl}$ = 278 mμ (ε = 5990), $\lambda_{shoulder}^{0.1N\ HCl}$ = 288 mμ (ε = 4490); $\lambda_{max}^{0.1N\ NaOH}$ = 281 mμ (ε = 6950), $\lambda_{max}^{0.1N\ NaOH}$ = 288 mμ (ε = 6840). $[\alpha]_D^{52}$ −54.3° (*c* 0.5, 0.1N acetic acid). Amino acid ratios in the acid hydrolysate:[15] Gly 2.84, Tyr 1.01, Ser 1.05, Met 1.05, Glu 1.00, His 1.12, Phe 1.00, Arg 2.89, Lys 0.97, Pro 1.04, Val 0.94 (average recovery 92.5%).*3 The intact hexadecapeptide was determined spectrophotometrically to contain tyrosine and tryptophan in a molar ratio of 1.00 : 0.95.[16]

*Biochemistry Division*
*Shionogi Research Laboratory*
*Shionogi & Co., Ltd.*
*Fukushima-ku, Osaka*

12) J. Ramachandran and C. H. Li, *J. Org. Chem.*, **28**, 173 (1963).

13) K. Inouye, This Bulletin, No.7 (1965), in press.

*3 As calculated for $C_{88}H_{131}N_{29}O_{21}S \cdot 3CH_3COOH \cdot 4H_2O$ (M. W. 2215.542).

14) G. W. Anderson, J. E. Zimmerman and F. M. Callahan, *J. Am. Chem. Soc.*, **86**, 1839 (1964); **85**, 3039 (1963).

15) D. H. Spackman, W. H. Stein and S. Moore, *Anal. Chem.*, **30**, 1191 (1958).

16) T. W. Goodwin and R. A. Morton, *Biochem. J.*, **40**, 628 (1946); G. H. Beavan and E. R. Holiday, *Advances in Protein Chem.*, **7**, 319 (1952).

# A Mössbauer Resonance Absorption Study of the Photolysis and Radiolysis of Ferric Oxalate*1

By Nobufusa SAITO, Hirotoshi SANO, Takeshi TOMINAGA and Fumitoshi AMBE

(Received January 22, 1965)

The technique of the Mössbauer resonance absorption of $\gamma$ rays has recently been applied to the study of the valence state, structure and nature of the chemical bond of various compounds. Because of the favorable properties of $^{57}Fe$ for the observation of the resonance absorption spectra, a number of iron compounds have been investigated. However, the Mössbauer resonance absorption technique has not so far been used to investigate the chemical change induced by ionizing radiation or light in iron compounds.[1] Therefore, the present authors have applied this technique to the study of the photolysis and radiolysis of ferric oxalate.

Ferric oxalate, $Fe_2(C_2O_4)_3 \cdot nH_2O$,*2 was irradiated with $^{60}Co$ $\gamma$ rays at an ambient temperature in the presence of air. The total dose was $2\times10^8$ r. In case of photolysis, the same salt was exposed to the light from a mercury lamp. The resonance absorption of 14.4 KeV. $\gamma$ rays in irradiated and non-irradiated iron oxalates (as absorbers) was measured with a source of $^{57}Co$ diffused into copper foil. The source was moved linearly at a constant velocity by means of a mechanical drive. No remarkable change was observed between the spectra obtained with the same absorber at 22°C and at the temperature of liquid nitrogen. Their Mössbauer spectra are shown in Figs. la-lc.

As may be seen in Fig. la, the spectrum of non-irradiated ferric oxalate consists of two lines, at 0.27 and 0.70 mm./sec. (vs. stainless steel). After irradiation with $\gamma$ rays, the height of both lines is decreased, and new lines appear at about 0.5 and 2.3 mm./sec. (Fig. lb). Since the positions of these new lines nearly correspond to those in the spectrum of non-irradiated ferrous oxalate (Fig. lc), it may be concluded that the electron configuration around the iron atom in ferric oxalate irradiated with $\gamma$ rays

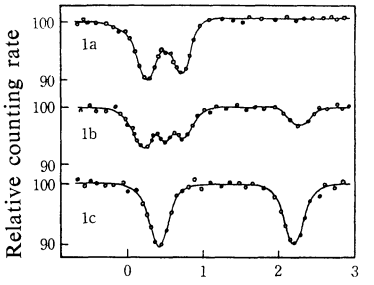



Fig. la-lc. Mössbauer resonance absorption spectra (at 22°C).
la : Non-irradiated ferric oxalate
lb : Irradiated ferric oxalate
lc : Non-irradiated ferrous oxalate

becomes very similar to that in ferrous oxalate (and that, therefore, $Fe^{3+}$ is reduced to $Fe^{2+}$ as the result of radiolysis). The Mössbauer spectrum obtained with ferric oxalate which has undergone photolysis is almost identical in shape with that of $\gamma$ ray-irradiated sample.*3

The above conclusion may be confirmed by the investigation of their infrared spectra shown in Figs. 2a-2c. The infrared spectra of irradiated and non-irradiated iron oxalates were measured as a KBr disk by using a Hitachi EPI-510 spectrophotometer. By examining the 750-850 $cm^{-1}$ (O-C-O bending) and 1250-1350 $cm^{-1}$ (C-O

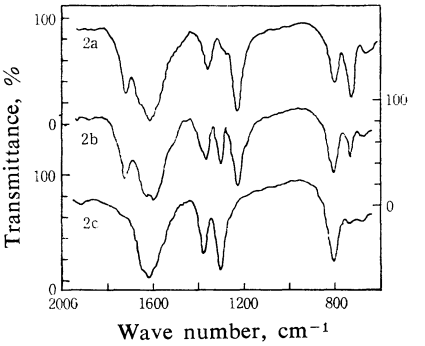



Fig. 2a-2c. Infrared spectra.
2a : Non-irradiated ferric oxalate
2b : Irradiated ferric oxalate
2c : Non-irradiated ferrous oxalate

*1 Presented at the 8th Symposium on Radiochemistry, November, 1964, Osaka.

1) The effect of $\gamma$ rays on the shape of Mössbauer spectra has been reported only on some tin compounds: A. Y. Aleksandrov et al., *Soviet Physics JETP*, **16**, 1467 (1963).

*2 $n$=nearly 5.

*3 It is well known that ferric oxalate is decomposed by light to yield ferrous oxalate.

stretching) regions, it may be concluded that the spectrum of irradiated ferric oxalate (Fig. 2b) is obtainable by the superimposition of the spectrum of non-irradiated ferrous oxalate (Fig. 2c) on that of non-irradiated ferric oxalate (Fig. 2a) in adequate proportions.

Further study is now in progress to investigate the possibility of the semiquantitative determination of the $Fe^{2+}$ formed in ferric oxalate in the course of $\gamma$ radiolysis using the Mössbauer technique.

*Department of Chemistry*
*Faculty of Science*
*The University of Tokyo*
*Hongo, Tokyo* (*N.S., T.T. & F.A.*)

*Faculty of Science*
*Ochanomizu University*
*Otsuka, Tokyo* (*H.S.*)

# The Reactions of Isomeric 1-Chloro-2-methylthio-1, 2-diphenylethanes with the Base

By Michinori Ōki and Atsuko Kimura

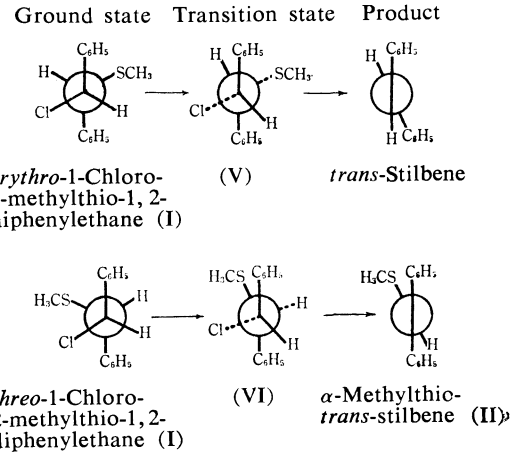
(Received February 8, 1965)

In the course of other study the authors encountered a striking difference in the reactivities of *erythro*- and *threo*-isomers. When isomers of 1-chloro-2-methylthio-1, 2-diphenylethane (I) were treated with potassium *t*-butoxide, the former gave *trans*-stilbene and the other, possibly α-methylthio-*trans*-stilbene (II). The results may be attributed to the different stabilities of the transition states, as will be described below.

*trans*-Stilbene oxide was treated with sodium methylmercaptide in ethanol to produce *erythro*-2-methylthio-1, 2-diphenyl-1-ethanol (III), m. p. 74°C (Found: C, 74.02; H, 6.66. Calcd. for $C_{15}H_{16}OS$: C, 73.75; H, 6.60%), which was converted into *erythro*-I, m. p. 123°C (Found: C, 68.59; H, 5.73. Calcd. for $C_{15}H_{15}ClS$: C, 68.40; H, 5.74%), by treating it with thionyl chloride in chloroform. Similarly, *threo*-III, which was characterized as acetate, m. p. 71.5—72°C (Found: C, 71.49; H, 6.27. Calcd. for $C_{17}H_{18}O_2S$: C, 71.30; H, 6.34%), and *threo*-I, m. p. 52.5°C (Found: C, 68.52; H, 5.76%), were prepared from *cis*-stilbene oxide.

The stereochemistry of these compounds was established by the mode of preparation, since the ring opening of an epoxide proceeds in the trans fashion and the chlorination of an alcohol with thionyl chloride proceeds with the retention of the configuration.[1] The results were further confirmed by the NMR spectra, in which *threo*-I shows a coupling constant of benzylic hydrogens of 7.5 c. p. s., whereas *erythro*-I shows one of 9.5—9.9 c. p. s.

The refluxing of a *t*-butyl alcohol solution of *erythro*-I with ca. 1 N potassium *t*-butoxide for 12 hr. yielded *trans*-stilbene as the sole product. Thus it is apparent that the elimination of methanesulfenyl chloride took place during this treatment. On the other hand, *threo*-I, upon similar treatment, gave II (NMR; $\tau$ 2.3—2.9 (multiplet), $\tau$ 8.05 (singlet), $\tau$ 3.23 (singlet): $\lambda_{max}$ 308 mμ, ε 15000), which was then oxidized with peroxyacetic acid to α-methylsulfonyl-*trans*-stilbene (IV), m. p. 118—119°C (Found: C, 69.48; H, 5.61. Calcd. for $C_{15}H_{14}O_2S$: C, 69.74; H, 5.46%). Thus, the elimination of hydrogen chloride took place wih *threo*-I. The configuration of IV has not been firmly established, but from the mode of elimination, which will be discussed below, the trans configuration seems most probable.




*erythro*-1-Chloro-2-methylthio-1, 2-diphenylethane (I) — *trans*-Stilbene

*threo*-1-Chloro-2-methylthio-1, 2-diphenylethane (I) — α-Methylthio-*trans*-stilbene (II)

1) E. L. Eliel, "Steric Effects in Organic Chemistry," Ed. by M. S. Newman, John Wiley & Sons, Inc., New York (1956), Chap. 2.

One possible explanation* of these results is that an $E_2$-type elimination occurs during this treatment. If so, the results could be interpreted as follows. *threo*-I, taking its most stable conformation, as is shown in the figure, will give II, in accord with expectations, through the transition state VI. *threo*-I must assume a transition state of high energy if it reacts to give *cis*-stilbene. On the other hand, a transition state which gives rise to the elimination of hydrogen chloride from *erythro*-I will be of too high an energy to be a major contribution, because the two bulky phenyl groups are opposed. It may be expected that the transition state V will be formed much more easily. Thus, instead of hydrogen chloride, methanesulfenyl chloride is eliminated from the *erythro* isomer, as is shown in the figure.

In this respect, it is very interesting that Helmkamp and Pettitt reported[2] recently that methanesulfenyl bromide was eliminated when two isomers of 2-bromo-3-methylthiobutane were treated with iodine, irrespective of their configurations.

The isomers of I also behave differently toward pyridine. The effect of the bulkiness of the substituent and/or base on the elimination and the effect of the acidities of $\alpha$-hydrogens are now under investigation.

*Depatment of Chemistry*
*Faculty of Science*
*The University of Tokyo*
*Hongo, Tokyo*

* An alternative explanation will be an anchimeric assistance of a methylthio group to form a bridged cation as a transition state. However, this mechanism is less likely, because no sulfur-containining compound is isolated inspite of an expected competitive abstraction of $CH_3S^+$ or $H^+$.

2) G. K. Helmkamp and D. J. Pettitt, *J. Org. Chem.*, **29**, 3258 (1964).

# A Novel Five-co-ordinate Complex of Cobalt(II)

By Shoichiro YAMADA and Hiroaki NISHIKAWA

(Received February 12, 1965)

Most cobalt(II) complexes are known to be four- or six-co-ordinate; very few five-co-ordinate complexes have so far been characterized.[1] The present communication deals with the successful preparation of a new cobalt(II) complex of a Schiff base, which is now believed to be five-co-ordinate.

The compound prepared (A) is a pyridine adduct of bis-(*N*-*o*, *o*'-xylidyl-salicylideneiminato)cobalt(II), which is abbreviated as Co-(Sal·N·*o*,*o*'-xyl)$_2$·Py. This pyridine adduct has been obtained as green crystals by cooling a hot solution of the red-coloured parent cobalt-(II) complex in pyridine or in pyridine-petroleum ether. Elemental analysis agreed quite well with the above formula with one pyridine molecule, but not with the formula with two pyridine molecules.

The spectrum of compound A in the solid state is quite different from any of the typical spectra[2] of the tetrahedral, the square-planar and the octahedral cobalt(II) complexes, as well as from the spectrum of the parent complex in the solid state or in solution (Fig. 1).

All these findings indicate that the pyridine adduct A in the solid state is most likely to be a five-co-ordinate complex, one in which the pyridine molecule is bound with the cobalt(II) ion.

On the contrary, the use of a similar procedure with the *N*-monosubstituted phenyl complexes of cobalt(II) yielded adducts B, Co-(Sal·N·R)$_2$·2Py, which has been concluded, from electronic spectra and elemental analysis, to be six-co-ordinate. The difference in the structure of the pyridine adduct between the parent complexes of A and B is regarded as due to the much more marked steric hindrance in A, which prevents the complex from taking the otherwise favourable six-co-ordination.[3]

1) G. A. Barclay and R. S. Nyholm, *Chem. & Ind.*, **1953**, 378; R. S. Nyholm and M. L. Tobe, "Essays in Co-ordination Chemistry," Ed. by W. Schneider, G. Anderegg and R. Gut, Birkhäuser Verlag, Basel (1964), p. 112.

2) H. Nishikawa and S. Yamada, This Bulletin, **35**, 1430 (1962); ibid., **37**, 8 (1964); L. Sacconi, M. Ciampolini, F. Maggio and F. P. Cavasino, *J. Am. Chem. Soc.*, **84**, 3246 (1962); L. Sacconi, P. L. Orioli, P. Paoletti and M. Ciampolini, ibid., **85**, 411 (1963), and references therein.

3) Recently Sacconi and Ciampolini (private communication) studied the equilibrium between bis(salicylaldehyde)-*N*, *N*-disubstituted polymethylenediiminato-cobalt-(II) complexes and their pyridine adducts in solution; they concluded the existence in solution of the adduct of the cobalt(II) complex with one pyridine molecule.

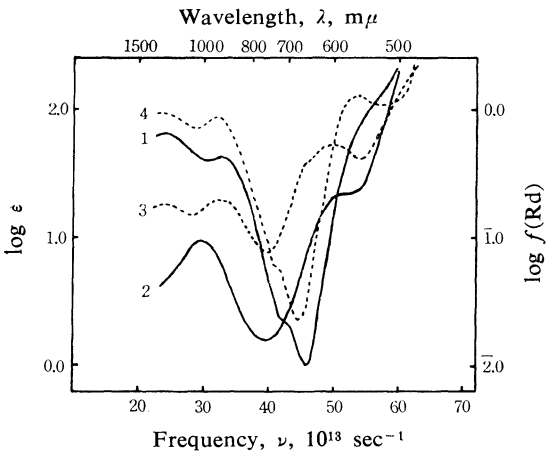



Fig. 1. Electronic spectra of: 1, [Co(Sal·N·*o*,*o*'-xylidyl)$_2$] in chloroform (tetrahedral) ; 2, [Co(Sal·N·*o*-tolyl)$_2$] in pyridine (octahedral); 3, [Co(Sal·N·*o*,*o*'-xylidyl)$_2$·Py] in the solid state by reflectance (five-co-ordinate) ; 4, [Co-(Sal·N·cyclohexyl)$_2$]·lPiperidine in the solid state by reflectance (tetrahedral).

The conclusion of the five-co-ordination in A is also supported by the magnetic moment of A (4.53 B.M.), which is definitely different from the moment of the parent complex (4.35 B. M.). Thus, A is of a high-spin type and differs from the previously-reported five-co-ordinate cobalt(II) complexes, which are of a low-spin type.[1] As has been discussed by Nyholm and others on the basis of the current theory of directed valence,[4] the magnetic moment indicates that, in compound A, $4s4p^34d$ hybridized orditals may most probably be used for bonding, a trigonal-bipyramidal configuration being predicted; a tetragonal pyramid on the basis of $4s4p^24d^2$ hybridization may not be completely eliminated.

It should be noted that the solid spectra of Co(Sal·N·cyclohexyl)$_2$·Py and Co(Sal·N·cyclohexyl)$_2$(Piperidine) are nearly identical with the spectrum of the parent cobalt(II) complex of a tetrahedral configuration.

*Institute of Chemistry*
*College of General Education*
*Osaka University*
*Toyonaka, Osaka*

4) H. Eyring, J. Walter and G. E. Kimball, "Quantum Chemistry," John Wiley & Sons, New York (1949), p. 231.

# The Fe-57 Mössbauer Effect in Ferrocyanide Derivatives

By Hirotoshi SANO and Fukiko HASHIMOTO

(Received February 23, 1964)

The measurement of the nuclear gamma-ray resonance absorption, the so-called Mössbauer effect, has been applied to the study of the electronic environment in various compounds, because the position and structure of resonance lines depend on the state of the chemical bonding of the atom. It has been reported in potassium ferrocyanide that the cyano groups are combined with the central iron atom by $\sigma$ and $\pi$ bonding.[1] The purpose of the present work is to study the effect of outer sphere ions or groups on the Mössbauer spectrum in the ferrocyanide derivatives, and to explain the lower value of the isomer shift of the ferrocyanide ion in Prussian blue and Turnbull's blue than that in potassium ferrocyanide.

Four ferrocyanide derivatives, $H_4[Fe(CN)_6]$,[2] $H_4[Fe(CN)_6](C_2H_5)_2O$,[2] $[Fe(CN)_2(CNCH_3)_4]$[3] and $[Fe(CNCH_3)_6](HSO_4)_2 3H_2O$[4], were prepared by conventional methods. The resonance absorption spectra of 14.4 keV. gamma rays in these compounds and potassium ferrocyanide, Prussian blue and Turnbull's blue were measured at room temperature with a source of cobalt-57 diffused into copper foil. The sample was moved at a constant velocity by means of a mechanical drive. Both the isomer shift and the quadrupole splitting were determined from the gamma ray resonance spectrum. The infrared absorption spectra in the KBr disk of these compounds were also measured.

Table I shows that the isomer shifts of $[Fe(CNCH_3)_6](HSO_4)_2 3H_2O$, $[Fe(CN)_2(CNCH_3)_4]$,

1) L. M. Epstein, *J. Chem. Phys.*, **36**, 2731 (1962); L. R. Walker, G. K. Wertheim and V. Jaccarino, *Phys. Rev. Letters*, **6**, 233 (1961); E. Fluck, W. Kerller and W. Neuwirth, *Angew. Chem.*, **75**, 461 (1963).

2) J. Liebig, *Ann.*, **87**, 127 (1853); K. C. Browning, *J. Chem. Soc.*, **77**, 1233 (1900).

3) J. Meyer, H. Domann, W. Müller, *Z. anorg. u. allgem. Chem.*, **230**, 336 (1937).

4) E. G. I. Hartly, *J. Chem. Soc.*, **97**, 1066, 1725 (1910).

TABLE I. RESULTS FROM THE MÖSSBAUER SPECTRA AND INFRARED SPECTRA

| Compound | Isomer shift relative to stainless steel mm./sec. | Quadrupole splitting mm./sec. | Wave number $cm^{-1}$ |
|---|---|---|---|
| $K_4[Fe(CN)_6]3H_2O$ | $+0.03\pm0.01$ | $0.00\pm0.01$ | 2050 |
| $H_4[Fe(CN)_6]$ | $-0.01\pm0.01$ | $0.00\pm0.01$ | 2090<br>2110 |
| $H_4[Fe(CN)_6](C_2H_5)_2O$ | $-0.01\pm0.01$ | $0.00\pm0.01$ | 2090<br>2110 |
| $[Fe(CN)_2(CNCH_3)_4]$ | $-0.08\pm0.01$ | $0.00\pm0.01$ | 2090<br>2200 |
| $[Fe(CNCH_3)_6[(HSO_4)_23H_2O$ | $-0.08\pm0.01$ | $0.00\pm0.01$ | 2230 |
| Prussian blue and Turnbull's blue | $-0.05\pm0.03$<br>$+0.55\pm0.03$ | $0.00\pm0.02$<br>$0.50\pm0.03$ | 2075 |

$H_4[Fe(CN_6]$ and $H_4[Fe(CN)_6](C_2H_5)_2O$ are lower than that of $K_4[Fe(CN)_6]3H_2O$, and that the wave numbers of the C-N stretching vibration increase in accordance with the decrease in the isomer shift. The results suggest that the $d\varepsilon$ electrons of the iron atom are attracted through the cyano group by the methyl groups, and that then the total $s$ electron density on the iron nucleus increases. The fact that the isomer shifts of the spin-paired iron atom in Prussian blue and Turnbull's blue are lower than that in potassium ferrocyanide may be explained by assuming some co-ordination bonding between nitrogen atoms and spin-free iron(III) ions.

*Department of Chemistry*
*Faculty of Science*
*Ochanomizu University*
*Otsuka, Bunkyo-ku, Tokyo*

# The Mechanism of the Piezochromism of Hexaphenyl-biimidazolyl

By Taro HAYASHI and Koko MAEDA

(Received March 1, 1965)

We have found that 2,2',4,4',5,5'-hexaphenyl-1,1'-biimidazolyl and its derivatives, which exhibit both photochromism and thermochromism,[1] which have been ascribed to a radical dissociation of the N-N bond,[2] exhibit also piezochromism and that the mechanism of this is a radical dissociation of the N-N bond brought about mechanically on grinding or pressing. This piezochromism is probably the first case in which the mechanism has been elucidated.

When pale yellow fine crystals of hexaphenyl-biimidazolyl which had been recrystallized from benzene, m. p. 198—199°C, were ground in an agate mortar or pressed at a pressure of about 10—50 kg./cm$^2$ at room temperature in the dark, they turned reddish-purple. The reddish-purple crystals reverted to the original pale yellow crystals when kept at about 50°C in the dark or when subjected to liquid or to the vapor of ether, ethanol, acetone or benzene.

This piezochromism is not the thermochromism ascribed to a rise in temperature upon grinding or pressing, because the reddish-purple color due to the thermochromism began to appear at about 170°C, which was unlikely to occur upon grinding or pressing, and the piezochromic color hardly faded at room temperatures, whereas the thermochromic color disappeared immediately upon the crystals being cooled to room temperature. The pale yellow solid exhibited no ESR, whereas the reddish-purple solid obtained by grinding or pressing exhibited an ESR of a single peak ($g=2.003$), as in the cases of the photochromism and the thermochromism in a solid state. The spin concentration in the reddish-purple solid which has been obtained by grinding for 5 min. was about $10^{16}$—$10^{17}$ spins/g. This fact indicates the formation of a free radical on grinding or pressing.

The reddish-purple solid, obtained by grinding for 5 min. in the dark or by pressing at a pressure of 30 kg./cm$^2$ for 5 min. at room temperature, showed an absorption maximum at 563 m$\mu$ ; the maximum was measured by the

1) T. Hayashi and K. Maeda, This Bulletin, 33, 566 (1960).
2) T. Hayashi and K. Maeda, ibid., 37, 1564 (1964); 37, 1717 (1964).

opal-glass transmission method and the potassium bromide disk method respectively. A benzene solution of the reddish-purple solid showed an absorption maximum at 554 mμ, a value which agreed with the 554 mμ assigned to the triphenylimidazolyl produced in a benzene solution of hexaphenyl-biimidazolyl on irradiation.

These results indicate that the free radical produced in the piezochromism of hexaphenyl-biimidazolyl is triphenylimidazolyl and that the piezochromism of hexaphenyl-biimidazolyl may be ascribed to the dissociation of the N-N bond to triphenylimidazolyl which is mechanically brought about on grinding or pressing. It seems probable that this conclusion is correct, since the heat of the dissociation of hexaphenyl-biimidazolyl to triphenylimidazolyl by the homolytic rupture of the N-N bond, $\Delta H$, was found to be 26 kcal./mol.[2] in a benzene solution.

2, 2', 4, 4', 5, 5'-Hexa-*p*-tolyl-1, 1'-biimidazolyl, fine, pale greenish-yellow crystals, m. p. 194—195°C, hexa-*p*-chlorophenyl-biimidazolyl, fine, yellow crystals, m. p. 213—214°C and 2, 2'-di-*p*-chlorophenyl-4, 4', 5, 5'-tetraphenyl-1, 1'-biimidazolyl, fine, almost colorless crystals, m. p. 219—220°C which exhibited[2] both photochromism and thermochromism in a solution and in the solid state, were found to exhibit the piezochromism, the color changing from pale greenish-yellow to pale bluish-violet (absorption maximum 589 mμ in the solid state), from yellow to pale bluish-violet (absorption maximum 586 mμ) and from colorless to pale violet (absorption maximum 578 mμ) respectively. The mechanism of the piezochromism in these cases was found to be the same as that of hexaphenyl-biimidazolyl.

The decay rate of ESR due to the piezochromism of hexaphenyl-biimidazolyl was measured by the decrease in the signal intensity $h$ (the vertical distance betweeen two peaks of a signal[2]) and found to obey the following formula; $1/2(1/h^2-1/h_0^2)=kt$, which was obtained by the substitution of $h$ for the concentration in the rate expression of the third order reaction. The values of $k$ were $2.0\times10^{-5}$ at 48.0°C and $8.9\times10^{-5}$($cm^{-2}$, $min^{-1}$) at 51.5°C. Since the line widths of the signals were almost constant during the measurement, $h$ can be assumed to be approximately proportinal to the concentration of triphenylimidazolyl. Hence, the rate of the recombination of triphenylimidazolyl in the fading process of the piezochromism appears to be of the third order, and hence different from the second order of the rate of the recombination of triphenylimidazolyl in the photochromism in a solution.[2] This result seems to suggest that the recombination of triphenylimidazolyl in the piezochromism takes place through a diffusion process which is the rate-determining step of the third order with respect to triphenylimidazolyl.

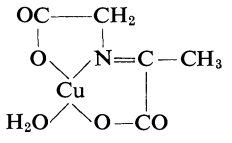
*Department of Chemistry*
*Faculty of Science*
*Ochanomizu University*
*Otsuka, Bunkyo-ku, Tokyo*

# The Copper(II) Complex of the Schiff Base Derived from Glyoxylic Acid and α-Alanine

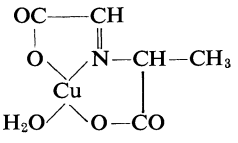
By Yasuo NAKAO, Ken-ichi SAKURAI and Akitsugu NAKAHARA

(Received March 17, 1965)

A number of investigations[1] of non-enzymatic transamination reactions catalyzed by metal ions has resulted in the discovery of the importance of the coordination of metal ions with the Schiff bases produced from aldehydes and amino acids or from keto acids and amines. Comparatively few papers[2] have, however, been published to report on the isolation of metal Schiff-base chelates as the intermediate compounds in the mechanism of these transamination reactions. We have recently prepared a pair of copper(II) Schiff-base complexes, which are considered to be fairly important in any consideration of the mechanism of the transamination reactions in the metal-pyruvate-glycinate and the metal-glyoxylate-alaninate systems; we therefore investigated their properties and correlations. They are the copper(II) complexes of Schiff bases derived from pyruvic acid and glycine,[3] A, and glyoxylic acid and α-alanine. The latter was believed to have the structure B, in the light of many results obtained by other, similar preparations. However, the complex isolated in the crystalline state from the copper-(II)-glyoxylate-alaninate system has been proved to be the pyruvideneglycinatoaquocopper(II) (A) instead of glyoxylidenealaninatoaquocopper(II) (B). This finding is understandable only in connection with some kind of rearrangement—a part of the process of the transamination reaction. Although the transaminations of this kind and of the glyoxylate-pyridoxamine system in the presence of metal ions have already been reported,[4] the previous conclusions were drawn only from the equilibrium studies of solutions; the intermediate complexes were not isolated. The present paper will report on a quite effective transamination based on an investigation of the isolated intermediate complex. It is also of interest to note that only a chelate of glycine with pyruvate and copper(II), not one of alanine with glyoxylate and copper(II), is isolated.



(A)



(B)

The method of the preparation of B employed in this work was the same as that of A which has already been reported in a previous paper.[3] Found: C, 23.03; H, 4.27; N, 5.29; $H_2O$, 20.31. Calcd. for $CuC_5H_5NO_4 \cdot 3H_2O$: C, 23.00; H, 4.21; N, 5.36; $H_2O$, 20.65%.

The complex began to decompose at 192°C, coinciding precisely with the decomposition temperature of A. A microscopic observation of the two crystals, A and B, revealed that there was no difference in their colors, shapes and habits.

No difference was observed either in their solubilities in water, ethanol and dimethylsulfoxide. The infrared studies and the X-ray powder measurements of the two crystals also verified their identity.

However, an additional decisive proof for the identity of the two compounds and the elimination of the possibility of the structure B was given by a cleavage reaction of the Schiff-base >C=N– double bond of the respective complex. The aqueous solutions of the two complexes were separately treated with hydrogen sulfide in order to give the precipitate of copper sulfide from each solution. The two filtrates were then examined for the amino acids they contained by means of paper chromatography. Both solutions exhibited only one spot corresponding to glycine in the presence of pyruvic acid. No other spots, not even that of alanine were detected on the whole strip. If the real structure of the complex produced from copper(II)-glyoxylate-alaninate system were B, alanine would have been detected instead of glycine. This may

1) E. g., D. E. Metzler and E. E. Snell, *J. Am. Chem. Soc.*, **74**, 979 (1952); D. L. Leussing, ibid., **85**, 231 (1963). Many papers other than these have been published.
2) D. E. Metzler, J. B. Longenecker and E. E. Snell, *J. Am. Chem., Soc.*, **76**, 639 (1954); H. N. Christensen, ibid., **79**, 4073 (1957); G. Baddiley, *Nature*, **170**, 711 (1964).
3) A. Nakahara, H. Yamamoto and H. Matsumoto, This Bulletin, **37**, 1137 (1964).
4) D. E. Metzler, J. Olivard and E. E. Snell, *J. Am. Chem. Soc.*, **76**, 644 (1954); H. Mix, *Z. physiol. Chem.*, **325**, 106 (1961).

be one of the most clear-cut examples of effective transamination catalyzed by the copper(II) ion.

*Institute of Chemistry*
*College of General Education*
*Osaka University*
*Toyonaka, Osaka*

# Studies of Ion Exchange Membranes. XXII. Semicontinuous Preparation of Ion Exchange Membranes by the "Paste Method"[1]

By Yukio MIZUTANI, Reiichi YAMANE and Hirozi MOTOMURA

(Rcecived August 10, 1964)

Previous work in this series[2] has presented a method for the preparation of ion exchange membranes called the "paste method," in which paste I, composed of styrene (St), divinylbenzene (DVB), and poly(vinyl chloride) fine powder (PVC), or paste II, composed of St, DVB, 2-methyl-5-vinylpyridine (MVP), and PVC, was coated onto the cloth or the net of the synthetic resin and then heated in order to prepare the polymer film backed with a reinforcing material (Base Membrane), to which the ion exchange group was then introduced by appropriate after-treatments.

The preparative method previously described was excellent in terms of its ease and the mechanical and electrochemical properties of the products, but it was unsuited as a continuous preparative process.

The present investigation was, therefore, undertaken to develop the paste method into a continuous process. In the first stage the continuous preparation of the base membrane was attempted.

The roll coating system being employed, the process of the coating could be carried out continuously, thus obtaining a base membrane 1 m. wide and 50 m. long with a good uniformity. The preparative methods of the base membrane and the ion exchange membrane will be described, and the properties of the products will be discussed in relation to the preparative conditions.

## Experimental

**The Preparation of the Paste.** — Table I shows some typical compositions of the pastes. The components of the paste were mixed to disperse PVC homogeneously, and then the paste was kept for 16 hr. at 20°C (paste I) or 10°C (paste II) in order to stabilize its properties. Prior to coating, the paste was filtered through a 50-mesh polyethylene screen.

**Coating.**—Figure 1 shows the roll coating system. The wind-up roll 3 was the only driven roll; the others were idler rolls. The reinforcing material reserved to roll 1 was tensioned in its length by the application of the brake on roll 1, expanded in its width by the expander roll 5, and then dipped in the paste in the paste reservoir 4. The covering material which was fed from roll 2 was tensioned and expaned in the same ways as the reinforcing material. The reinforcing material coated with the paste was wound up on roll 3 with the covering material in layers. The pressure which was placed on roll 3 by roll 6 adjusted the quantity of the paste coated onto the reinforcing material. The reinforcing material, 1 m. wide and 50 m. long, was coated once.

**Heating.** — After the coating process, roll 3 was dismantled, cramped with iron shackles at the hems of the wound reinforcing material, thus preventing the reinforcing material from shrinking

TABLE I. TYPICAL COMPOSITIONS OF THE PASTES

| Component | Paste I | Paste II |
|---|---|---|
| PVC*1 | 1.00 | 1 |
| St | 2.3 | 0.22 |
| DVB*2 | 0.3 | 0.14 |
| MVP | — | 1.44 |
| Dioctyl phthalate (DOP) | 0.3 | 0.30 |
| Benzoyl peroxide (BPO) | 0.025 | 0.03 |

*1 Sumilit PX-A from the Sumitomo Kagaku Co., Ltd.
*2 Purity of 50% by weight.

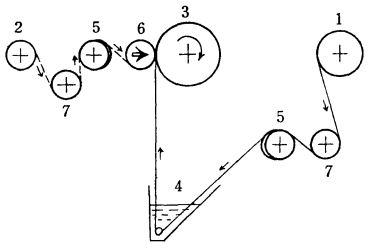



Fig. 1. Coating system.
1 A reserve roll of the reinforcing material, 150 $\phi \times 1250$
2 A reserve roll of the covering material, 50 $\phi \times 1250$
3 A wind-up roll, 215 $\phi \times 1250$
4 A paste reservoir, 28 l.
5 Expander rolls, 115 $\phi \times 1250$
6 A press roll, 95 $\phi \times 1250$
7 Guide rolls, 95 $\phi \times 1250$

1) Presented at the 12th Annual Meeting of the Society of Polymer Science Japan, Tokyo, May, 1963.
2) Y. Mizutani, R. Yamane, H. Ihara and H. Motomura, This Bulletin, 36, 361 (1963).

in width during heating, and then heated at 80—120°C for an hour under high nitrogen pressure (5 kg./cm²) and then at 80°C for 4 hr. The poly(vinyl chloride) was fused to the continuous film, the monomers were polymerized for the first heating, and the polymerization was completed for the second heating. By being unwound from the roll and torn off from the covering material, the base membrane was obtained.

**The Introduction of the Ion Exchange Group to the Base Membrane.**—The ion exchange group was introduced to the base membrane by the after treatments described earlier.[2] Typical conditions of the after-treatments are shown in Table II.

TABLE II. TYPICAL CONDITIONS OF THE AFTER-TREATMENTS

| Active group | Paste | After-treatment |
|---|---|---|
| Cation exchange | I | Sulfonation with sulfuric acid (98%) at 60°C for 12 hr. |
| Anion exchange | II | Quanternization with petroleum ether solution of methyl iodide (methyl iodide/petroleum ether=1/4 by vol.) at 25°C for 24 hr. |

**Measurements.** — *Mechanical Strength.* — Mullen test—burst strength was measured. In the case of the ion exchange membrane, measurement was carried out on a test piece equilibrated with a 0.5 N aqueous solution of sodium chloride.

*Expansion by the After-treatment.* — Expansion was shown as a ratio of the length of the ion exchange membrane, equilibrated with a 0.5 N aqueous solution of sodium chloride, to that of the base membrane before the after-treatment. Measurement was carried out in the direction of the width of reinforcing material.

*Electrochemical Properties.* — The water content, ion exchange capacity, electric resistance, and transport number were measured at 25°C according to the procedures described before.[2] Electric resistance was measured on a membrane dipped in a 0.5 N aqueous solution of sodium chloride. The transport number was calculated by Nernst's equation from the membrane potential of a concentration cell composed of 0.5 N and 2.5 N aqueous solutions of sodium chloride, separated from each other by the ion exchange membrane under consideration.

## Results and Discussion

In relation to the continuous preparation of the base membrane by the roll coating system, the composition of a paste, the choice of a reinforcing material, the choice of a covering material, the conditions of the coating, and the conditions of the heating were investigated.

**The Composition of a Paste.** — The composition of a paste, which was decided mainly on the basis of the electrochemical properties of the ion exchange membrane,[2] also affected its viscosity, which was a main factor in the coating process, and the mechanical properties of the ion exchange membrane.

Table III shows the mechanical and electrochemical properties of the base membrane and the cation exchange membrane in relation to the composition of paste I.

The burst strength of the base membrane did not appreciably change with a weight ratio of either R/PVC or DVB/R, where R was St+DVB or St+DVB+MVP, while that of the ion exchange membrane decreased with an increasing R/PVC. This may be attributed to the brittleness of the sulfonated styrene-divinylbenzene copolymer. The expansion by sulfonation increased with an increasing R/PVC because of the swelling of the styrene-divinylbenzene copolymer through sulfonation.

**Reinforcing Material.** — To provide the ion exchange membrane with mechanical strength and dimensional stability, the following characteristics are required in the reinforcing material: dimensional stability, adhesiveness with the ion exchange resin, and chemical stability in the processes of the preparation and the application.

TABLE III. COMPOSITIONS OF THE PASTES—PROPERTIES OF THE BASE MEMBRANES AND THE ION EXCHANGE MEMBRANES

| Paste | | I | | | | | |
|---|---|---|---|---|---|---|---|
| Reinforcing material | | Teviron-A | | | | | |
| Composition of the paste by weight | R/PVC | 0.8 | 1.7 | 2.5 | 1.7 | 1.7 | 1.7 |
| | DVB/R | 0.04 | 0.04 | 0.04 | 0.025 | 0.07 | 0.10 |
| | DOP/PVC | | | 0.3 | | | |
| | BPO/R | | | 0.01 | | | |
| Temperature of the first heating, °C | | | | 115 | | | |
| Burst strength of the base membrane, kg./cm² | | 6.3 | 6.7 | 6.5 | 6.8 | 6.9 | 6.2 |
| Expansion by the after-treatment*1 | | 1.03 | 1.05 | 1.09 | 1.05 | 1.05 | 1.05 |
| Ion exchange membrane | Burst strength, kg./cm² | 5.3 | 4.6 | 3.6 | 4.5 | 4.5 | 4.4 |
| | Electric resistance, Ω·cm² | 5.0 | 2.6 | 1.8 | 2.3 | 4.1 | 5.3 |
| | Transport number | 0.87 | 0.87 | 0.85 | 0.86 | 0.87 | 0.87 |

*1 Condition of the after-treatment: see Table II.

TABLE IV. PROPERTIES OF THE REINFORCING MATERIALS

| | Dimensional stability | Chemical stability | Adhesiveness with the ion exchange resin | Electrochemical properties of the ion exchange membrane |
|---|---|---|---|---|
| Cation exchange membrane | | | | |
| Vinylchloride-vinyliden chloride copolymer net | ○ | ○ | △ | × |
| Poly(vinyl chloride) net | △ | ○ | ○ | × |
| Polyethylene net | ○ | ○ | △ | × |
| Poly(vinyl chloride) cloth | △ | ○ | ○ | ○ |
| Polypropylene cloth | ○ | ○ | △ | △ |
| Polyacrylonitrile cloth | △ | × | ○ | — |
| Poly(vinyl alcohol) cloth | ○ | × | × | — |
| Poly(ethylene terephthalate) cloth | ○ | × | △ | — |
| Anion exchange membrane | | | | |
| Vinylchloride-vinyliden chloride copolymer net | ○ | × | △ | × |
| Poly(vinyl chloride) net | △ | ○ | ○ | × |
| Polyethylene net | ○ | ○ | △ | × |
| Poly(vinyl chloride) cloth | △ | ○ | ○ | ○ |
| Polypropylene cloth | ○ | ○ | △ | ○ |
| Polyacrylonitrile cloth | × | ○ | ○ | △ |
| Poly(vinyl alcohol) cloth | ○ | ○ | × | △ |
| Poly(ethylene terephthalate) cloth | ○ | ○ | △ | ○ |

○ : good, △ : fair, × : poor, — : could not be judged

TABLE V. THE RESIN RATIOS—ELECTROCHEMICAL PROPERTIES OF THE ION EXCHANGE MEMBRANES

| | Paste | Reinforcing material | Resin ratio g./g. | Ion exchange membrane: Thickness mm. | Electric resistance Ω·cm² | Transport number |
|---|---|---|---|---|---|---|
| Cation exchange membrane | I | Teviron-A | 1.09 | 0.180 | 4.7 | 0.87 |
| | | | 1.26 | 0.190 | 4.6 | 0.87 |
| | | | 1.44 | 0.210 | 4.5 | 0.88 |
| | | | 1.58 | 0.230 | 4.5 | 0.88 |
| | | | 1.79 | 0.235 | 4.7 | 0.87 |
| Anion exchange membrane | II | Teviron-B | 1.46 | 0.190 | 3.0 | 0.91 |
| | | | 1.35 | 0.185 | 3.3 | 0.92 |
| | | | 1.26 | 0.185 | 3.1 | 0.92 |
| | | | 1.17 | 0.180 | 3.4 | 0.91 |
| | | | 1.12 | 0.180 | 3.2 | 0.92 |

Composition of the paste I: R/PVC=2.5, DVB/R=0.10, DOP/PVC=0.15, BPO/R=0.005.
Composition of the paste II: R/PVC=1.8, MVP/R=0.80, DVB/R=0.04, DOP/PVC=0.30, BPO/R=0.01.

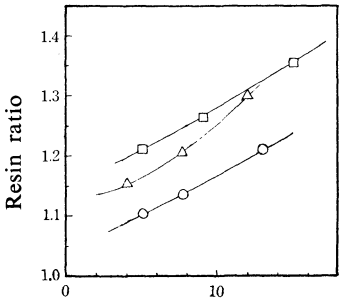
Table IV shows the properties of the reinforcing materials under consideration. It was apparent that the poly(vinyl chlroide) cloth was advisable for a cation exchange membrane, and the poly(vinyl chloride) cloth, the polypropylene cloth, and the poly(ethylene terephthalate) cloth, for an anion exchange membrane. Subsequent experiments were, therefore, carried out with the poly(vinyl chloride) cloth, Teviron-A 0.13 mm. thick and Teviron-B 0.09 mm. thick, from the Teijin Co., Ltd.

**Covering Material.**—With a view of separating the layers of the paste coated onto the reinforcing material, the covering material was wound up simultaneously in layers.

A poly(vinyl alcohol) film (Kurarebiniron film from the Kurashiki Rayon Co., Ltd.) was adopted on the basis of its mechanical strength, flexibility, and lesser adhesiveness with the paste.

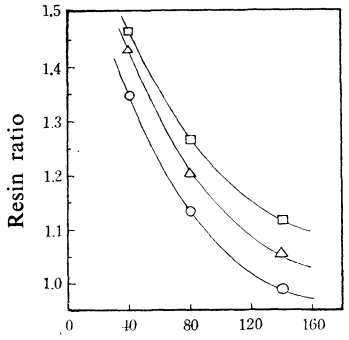
**The Conditions of the Coating.** — It was required that the paste should be coated uniformly in thickness and in composition, without a pinhole. The weight ratio of the paste to the reinforcing material (Resin ratio) was

found to be closely connected with the requirements described above. When the resin ratio was too high (type H), the base membrane was likely to lack uniformity and the ion exchange membrane was apt to be uneven in its plane and the resinous part was apt to come off from the reinforcing material during the after-treatments. When the resin ratio was too low (type L), the ion exchange membrane was likely to have pinholes.



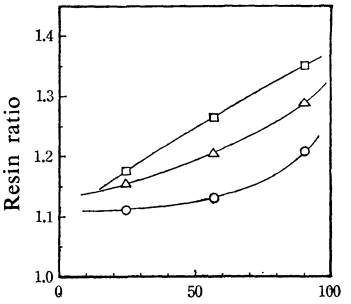

Viscosity of the paste, poise

Fig. 2. Conditions of the coating—viscosity of the paste.
○ Paste I, Teviron-A
△ Paste I, Teviron-B
□ Paste II, Teviron-B
Pressure of the press roll is 80 kg. per a meter of the roll. Tension offered to the reinforcing material in length is 57 kg. per a meter of the reinforcing material in width. Rate of the coating is 1.36 m./min. Viscosity was measured with a viscosimeter from the Rion Co., Ltd.



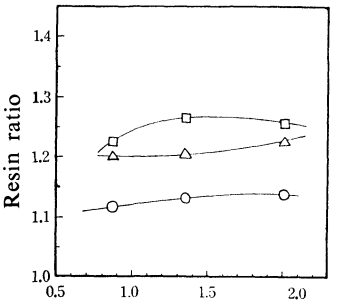

Pressure of the press roll, kg./m. of roll

Fig. 3. Condition of the coating—pressure of the press roll.
○ Paste I, Teviron-A, Viscosity of the paste is 7 poise
△ Paste I, Teviron-B, Viscosity of the paste is 7 poise
□ Paste II, Teviron-B, Viscosity of the paste is 9 poise
Tension offered to the reinforcing material in length is 57 kg. per a meter of the reinforcing material in width. Rate of the coating is 1.36 m./min.




Tension offered to the reinforcing material in length, kg./m. of the reinforcing material in width

Fig. 4. Conditions of the coating—tension offered to the reinforcing material in length.
○ Paste I, Teviron-A, Viscosity of the paste is 7 poise
△ Paste I, Teviron-B, Viscosity of the paste is 7 poise
□ Paste II, Teviron-B, Viscosity of the paste is 9 poise
Pressure of the press roll is 80 kg. per a meter of the roll. Rate of the coating is 1.36 m./min.




Rate of the coating, m./min.

Fig. 5. Conditions of the coating—rate of the coating.
○ Paste I, Teviron-A, Viscosity of the paste is 7 poise
△ Paste I, Teviron-B, Viscosity of the paste is 7 poise
□ Paste II, Teviron-B, Viscosity of the paste is 9 poise
Pressure of the press roll is 80 kg. per a meter of the roll. Tension offered to the reinforcing material in length is 57 kg. per a meter of the reinforcing material in width.

Table V shows, however, that, as far as this study could ascertain, a resin ratio does not affect the electrochemical properties of the ion exchange membrane.

Judging from the mechanical properties and the appearance of the ion exchange membrane, the resin ratios of 1.12—1.17 for Teviron-A and 1.20—1.25 for Teviron-B were found to be most desirable (type M).

Figures 2—5 show the relations between the

resin ratios and the conditions of the coating, i. e., the viscosity of the paste, the pressure of the press roll, the tension of the reinforcing material, and the rate of the coating.

With a paste with a high viscosity, the product is likely to be type H, and vice versa (Fig. 2).

When the pressure of the press roll is too high or low, the base membrane is apt to be type L or H (Fig. 3).

When increasing tension is offered to the reinforcing material, the resin ratio of the base membrane is increased (Fig. 4).

The rate of the coating did not affect the resin ratio, as is shown in Fig. 5, but when it was too high, the base membrane was apt to lack uniformity in its thickness. Considering the balances among the factors described above, the conditions of Table VI are recommended for the coating process.

Table VI. Optimum conditions of the coating process

| Paste | I | II |
|---|---|---|
| Reinforcing material | Teviron-A or B | Teviron-A or B |
| Viscosity of the paste, poise | 8 | 10 |
| Temperature of the paste at the coating, °C | 20 | 20 |
| Pressure of the press roll (kg./m. of roll) | 80 | 80 |
| Tension offered to the reinforcing material in length (kg./m. of the reinforcing material in width) | 50 | 50 |
| Rate of the coating, m./min. | 2 | 2 |

**The Conditions of the Heating.**—When the paste was heated, fine particles of poly(vinyl chloride) were fused to form a continuous film, in which the monomers were polymerized simultaneously, and part of the monomers were immersed and polymerized in the reinforcing material.

Because the fine particles of the poly(vinyl chloride) were swollen with the monomers, its fusion was carried out at comparatively low temperatures; i. e., the heating of paste I at 90°C and of paste II at 70°C were found to be sufficient to obtain a continuous film.

The temperature of the first heating, as well as the concentration of the catalyst in the paste, affected the characteristics of the products.

Table VII shows the effects of the temperature of the first heating. With a rising temperature the strengths of the base membrane and of the ion exchange membrane were decreased, and the expansion by the after-treatment was increased. These effects may be attributed to the fact that the more a monomer is immersed and polymerized in the reinforcing material with a rising temperature, the more the mechanical strength and the dimensional stability of the reinforcing material is decreased because of the polymer composed in it.

The effects of an increasing concentration of the catalyst were the reverse of those of a rising temperature, as Table VIII shows. This is accounted for by the fact that the increasing rate of the polymerization of the monomer, accompanied by the increasing concentration of the catalyst, may exceed the immersion rate of the monomers into the reinforcing material and so lead to a decrease in the polymer content in the reinforcing material; therefore, the strength of the reinforcing material does not decrease very much.

**The Characteristics of Typical Ion Exchange Membranes.**—The characteristics of typical ion exchange membranes obtained by the paste

Table VII. Temperature of the first heating—properties of the base membranes and the ion exchange membranes

| | Cation exchange membrane | | | | | | Anion exchange membrane | | | | | | |
|---|---|---|---|---|---|---|---|---|---|---|---|---|---|
| Paste*1 | I | | | | | | II | | | | | | |
| Reinforcing material | Teviron-A | | | | | | Teviron-B | | | | | | |
| Temperature of the first heating, °C | 102 | 108 | 118 | 132 | 142 | 150 | 64 | 77 | 88 | 102 | 114 | 135 | 149 |
| Burst strength of the base membrane, kg./cm² | 7.1 | 6.5 | 5.5 | 5.0 | 1.8 | 1.8 | 5.0 | 4.8 | 4.7 | 3.4 | 3.2 | 3.0 | 3.1 |
| Expansion by the after-treatment*2 | 1.10 | 1.11 | 1.12 | 1.12 | 1.13 | 1.13 | 1.03 | 1.03 | 1.04 | 1.04 | 1.05 | 1.05 | 1.06 |
| Ion exchange membrane | | | | | | | | | | | | | |
| Burst strength, kg./cm² | 3.9 | 3.7 | 3.3 | 2.8 | 3.0 | 2.8 | 4.9 | 4.4 | 4.0 | 3.4 | 3.6 | 3.0 | 3.4 |
| Electric resistance, Ω·cm² | 2.2 | 2.0 | 1.9 | 2.0 | 2.1 | 2.0 | 3.4 | 3.0 | 3.1 | 3.0 | 3.2 | 3.0 | 3.4 |
| Transport number | 0.87 | 0.87 | 0.86 | 0.86 | 0.85 | 0.86 | 0.86 | 0.90 | 0.91 | 0.91 | 0.92 | 0.92 | 0.90 |

*1 Compositions of the pastes I and II: see Table I.
*2 Conditions of the after-treatment: see Table II.

TABLE VIII. CONCENTRATIONS OF THE CATALYST—PROPERTIES OF THE BASE MEMBRANES AND THE ION EXCHANGE MEMBRANES

| | Cation exchange membrane | | | | | Anion exchage membrane | | |
|---|---|---|---|---|---|---|---|---|
| Paste*1 | I | | | | | II | | |
| Reinforcing material | Teviron-A | | | | | Teviron-B | | |
| BPO/R (by weight) | 0.001 | 0.005 | 0.010 | 0.020 | 0.030 | 0.015 | 0.040 | 0.060 |
| Burst strength of the base membrane, kg./cm² | 2.6 | 5.5 | 6.7 | 7.3 | 7.5 | 4.7 | 5.1 | 5.0 |
| Expansion by the after-treatment*2 | — | 1.12 | 1.11 | 1.10 | 1.09 | 1.04 | 1.02 | 1.01 |
| Ion exchange membrane: Burst strength, kg./cm² | — | 3.3 | 4.0 | 4.0 | 4.2 | 4.0 | 5.0 | 5.1 |
| Ion exchange membrane: Electric resistance, Ω·cm² | 2.6 | 1.9 | 2.1 | 2.0 | 2.0 | 3.1 | 3.7 | 4.4 |
| Ion exchange membrane: Transport number | 0.84 | 0.86 | 0.87 | 0.86 | 0.86 | 0.91 | 0.92 | 0.91 |

*1 Compositions of the pastes I and II: see Table I except BPO.
*2 Conditions of the after-treatment: see Table II. Temperature of the first heating was 120°C for paste I and 90°C for paste II.

TABLE IX. CHARACTERISTICS OF THE ION EXCHANGE MEMBRANES BY THE PASTE METHOD

| Name | Type | Thickness mm. | Water content*1 | Exchange capacity*2 | Electric resistance Ω·cm² | Transport number*3 | Burst strength kg./cm² |
|---|---|---|---|---|---|---|---|
| CL—2.5T | Cation exchange | 0.15—0.17 | 0.30—0.40 | 1.5—2.0 | 2.8—3.3 | 0.98 | 3—4 |
| CH—4 | Cation exchange | 0.20—0.22 | 0.30—0.35 | 2.0—2.5 | 2.3—2.7 | 0.97 | 3—4 |
| AV—4T | Anion exchange | 0.14—0.16 | 0.20—0.30 | 1.5—2.0 | 3.0—4.0 | 0.98 | 6—7 |
| AVS—4T | Anion exchange | 0.15—0.17 | 0.25—0.35 | 1.5—2.0 | 3.7—4.7 | 0.98 | 4—6 |

*1 Equilibrated with 0.5 N sodium chloride aqueous solution, [g. $H_2O$/g. Na-form dry membrane (or Cl-form)].
*2 [meq./g. Na-form dry membrane (or Cl-form)].
*3 Measured by electrophoresis with 0.5 N sodium chloride aqueous solution, current density: 10(mamp./cm²), at 25°C.

method using the roll-coating system are shown in Table IX.

The CL and CH types are cation exchange membranes, and the AV and AVS types are anion exchange membranes; the AVS type especially has much less permselectivity for $SO_4^{2-}$ than $Cl^-$.[3] The transport numbers in the ninth column were measured by the electrophoresis described in a previous paper.[4]

According to the results obtained by the electrophoretic concentration of sea water over a long period,[3] the ion exchange membranes obtained by the paste method were proved to have a good durability.

**Summary**

A method for the preparation of ion exchange membranes called the "paste method" has been developed into a semicontinuous preparation.

The roll-coating system being employed, a base membrane 1 m. wide and 50 m. long is prepared continuously; the ion exchange group is then introduced to it.

The ion exchange membranes thus prepared have been proved to have excellent electrochemical and mechanical properties as well as an excellent appearance.

*Tokuyama Soda Co., Ltd.*
*Tokuyama, Yamaguchi*

3) R. Yamane, Y. Mizutani, H. Motomura and R. Izuo, *J. Electrochem. Soc. Japan (Denki-Kagaku)*, **32**, 277 (1964).
4) R. Yamane, ibid., **31**, 240 (1963).

# The Separation of Rare Earths by Paper Electromigration and Focusing Chromatography

By Yoshiyuki KISO,* Itsuko YAMADA, Yuroku YAMAMOTO and Mutsuaki SHINAGAWA**

(Received February 21, 1964)

Paper electromigration has been used for the separation of rare earths by Maki,[1] Sato et al.,[2] Pučar and Jakovac,[3] Kawamura,[4] and Shvedov and Stepanov.[5] Moreover, Schumacher and Friedli[6] separated rare earths successfully by a new technique, "electorophoretic ion-focusing," i. e., focusing chromatography. However, comparatively little attention has been paid to the theoretical study. In a previous paper[7] one of the present authors has derived a theory of the migration of soluble metal complexes. The present experiment was carried out to examine its applicability to the separation of rare earths by the two procedures of ordinary paper electromigration[7] and focusing chromatography.[8]

## The Theory of Separation by Electromigration

In the paper electromigration, the zone mobility in a complexing agent-background electrolyte solution is given by the following equation[7]:

$$U=1/2\cdot U_M\{(1+(m-n)/m\cdot r_{MA}/r_M)+(1-(m-n)/m\cdot r_{MA}/r_M)\cdot \tanh\,[2.303/2\cdot(pK_{MA}-pC_{H_nA}+p\beta)]\} \quad (1)$$

$$p\beta=1/(1+(H)/K_n+(H)^2/k_nk_{n-1}+\cdots+(H)^n/K_nK_{n-1}\cdots K_1)$$

where $U$ is the zone mobility; $U_{MA}$, the mobility of the complex species MA; $m$, the charge of the single metal ion; $n$, the all over number of hydrogen ions dissociated from the ligand donor, $H_nA$; $r_M$ and $r_{MA}$, the ionic radii of the single and complex species; $K_{MA}$, the stability constant of the complex species; $C_{H_nA}$, the concentration of the complexing agent, and $K_1-K_n$, the consecutive dissociation constants of the complexing agent.

On moist paper, the zone mobility of ions is less than the mobility in a free solution because of the more tortuous path of the ions through the networks of fiber forming the paper or possibly because of other factors related to the affinity of the ion with the medium.[9] This relation is given by:

$$U_Z=\rho U_F \qquad \rho<1 \quad (2)$$

where $U_Z$ is the zone mobility; $\rho$, the obstructive factor and $U_F$, the mobility in a free solution. The zone mobility, $U$, in Eq. 1 corresponds to $U_Z$ in Eq. 2. In the case of EDTA complexes of rare earth elements, Eq. 1 turns into a simpler form, since $m=3$, $n=4$ and $r_{MA}\approx r_M$ for rare earth.[7]

$$U_{RE}\approx U_M\{1/3+2/3\cdot[\tanh\,(2.303/2\cdot(pK_{MA}+pC_{H_4A}+p\beta)]\} \quad (3)$$

with

$$p\beta=1/(1+(H)/K_4+(H)^2/K_4K_3+(H)^3/K_4K_3K_2+(H)^4/K_4K_3K_2K_1) \quad (4)$$

The mobility-pH ($U$-pH) curves in Fig. 1 were obtained by putting the values of $K_{MA}$ for rare earths,[10] the $K_i$ ($i=1$—4) values and $pC_{H_4A}=2.3$ ($C_{H_4A}=5\times10^{-3}$ M) into Eq. 3.

The differences between zone mobilities for two kinds of rare earths reach a maximum at the mean value of their p$S$'s, which represent the pH values at the points of inflection of the $U$-pH curves.

The p$S$ values for EDTA complexes of various rare earths vary with the concentration of EDTA. From the relations in Figs. 1 and 2, it can be predicted that, in one fixed pH of a background solution, one can separate only a few kinds of rare earths. However, all 15 different kinds of rare earths can probably be

* Present address; Research Reactor Institute, Kyoto University, Kumatori, Osaka.
** Department of Nuclear Engineering, Faculty of Engineering, Osaka University, Higashinoda, Miyakojima-ku, Osaka.

1) M. Maki, *Japan Analyst*, 5, 571 (1956).
2) T. R. Sato, H. Diamond, W. P. Norris and H. H. Strain, *J. Am. Chem. Soc.*, 74, 6154 (1952).
3) Z. Pučar and Z. Jakovac, *J. Chromatog.*, 3, 477 (1960).
4) S. Kawamura, Lecture at the Symposium of Radiochemistry of the Chemical Society of Japan, Tokai, October, 1960.
5) V. P. Shvedov and A. V. Stepanov, *Radiokhimya*, 2, 198, 201 (1960).
6) E. Schumacher and W. Friedli, *Helv. Chim. Acta*, 44, 1829 (1960).
7) Y. Kiso, *J. Sci. Hiroshima Univ.*, 27, No. 1, 17 (1963).
8) M. Shinagawa and Y. Kiso, *J. Chem. Soc. Japan, Pure Chem. Sec.* (*Nippon Kagaku Zasshi*), 82, 1019 (1961).
9) R. A. Bailey and L. Yaffe, *Can. J. Chem.*, 38, 1871 (1960).
10) Schwarzenbach, R. Gut and A. Anderegg, *Helv. Chim. Acta*, 37, 937 (1954).

separated by selecting EDTA solutions of several desired pHs as successive background solutions.

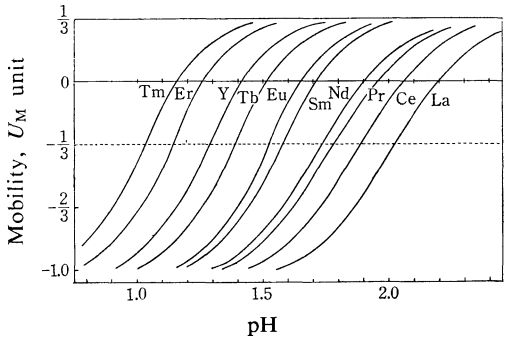



Fig. 1. Theoretical mobility-pH curves of REs-EDTA complexes in $5\times10^{-3}$ M EDTA.

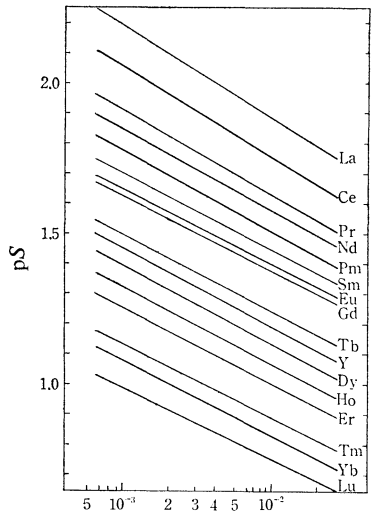



Fig. 2. p$S$ of various RE-EDTA complexes as a function of EDTA concentration.

## Experimental

**Apparatus.**—This apparatus was formed of a high d. c. power supplier, a migration cell, and 20 multi-compartment cells.[7] These were all hand made. The power supplier can give a continuously variable output voltage up to 1000 V. against the multi-compartment cells. By using a large migration cell ($4\times30\times7$ cm$^3$) containing carbon tetrachloride and a water-flowing jacket, the temperature in the migration cell was kept constant; thus the evaporation of water from the paper was also prevented.

**Radioactive Tracers.** — Radioactive isotopes, lanthanum-140, cerium-144 and yttrium-90 were imported, while praseodymium-142 and samarium-135 were produced by the JRR-1 at the Japan Atomic Energy Institute. Each 10-mg. portion of those rare earth oxides was irradiated at a flux of $3\times10^{11}$ n/cm$^2$/sec. for 1—5 hr. The specific activities thus obtained were about 6 mc./g. for samarium-153 and 4 mc./g. for praseodymium-142. Each oxide irradiated was dissolved in hydrochloric acid. The concentration was in the $10^{-3}$—$10^{-4}$ M range. The mixed solution was prepared to have a uniform activity of each species.

**Background Electrolytes.**—The concentration of the EDTA used as the complexing agent was $5\times10^{-3}$—$10^{-4}$ M. In order to keep constant the ionic strength of the solution (mostly $\mu=0.1$), sodium chloride was added supplementarily. The adsorption of migrant rare earth by the paper was minimized at this ionic strength in a manner shown in a previous report.[7] The pH of the background electrolyte was adjusted by the addition of sodium hydroxide or hydrochloric acid.

**Procedure.** — *Ordinary Paper Electromigration.*— First, the paper (Toyo Roshi No. 5, $2\times40$ cm$^2$) was cut in half in the long direction. Each sheet of the paper was then uniformly dipped in the background electrolyte solution, and the excess solution on the paper was removed by using other filter paper. Then about 0.005 ml. of the radioactive migrant solution was placed with a glass capillary on a pencil line on the moist paper. The width of the solution placed on the paper was about 1—2 mm. After twenty sheets of paper had been set into the migration cell, the stabilized voltage ranging from 300 to 500 V. was applied for 20—50 min. The water-cooling jacket and carbon tetrachloride in the migration cell were useful in maintaining the initial temperature of the paper during the migration. Even in the more highly-conducting background electrolytes, such as pH 1.0—1.5, no heating was observed during the migration. After the fixed migration time, all the strips were taken out from the cell and dried as fast as possible by an infrared lamp in order to prevent the diffusion of the separated zone.

*Focusing Chromatography.* — First, a 3-cm.-wide space in the middle of the paper was moistened with the sample solution to be separated; then all the anodic space beside this middle space was moistened with a hydrochloric acid solution adjusted to some selected pH, and finally the rest of the space was moistened with a EDTA solution. In this procedure, particular care was taken to avoid the confusion of the border between the sample and the solution in cathodic or anodic solutions respectively. The other procedure was the same as that used for the ordinary electromigration.

*The Detection and Identification of the Migration Zone.*—The detection of the radioactive migrant on paper was carried out by the autoradiographic or $\beta$-ray counting technique. The identification of radioactive nuclides on paper was carried out by the measurement of the half-life and $\gamma$-ray energy.

## Results and Discussion

**The Effects of the Concentration of the Migrant Ion and the Complexing Agent on the Mobility-pH Curve.**—Figure 3 shows the effect of the EDTA concentration on the $U$-pH curve obtained by a "carrier-free" (yttrium-90)

yttrium-EDTA system. In the concentration of $5\times10^{-3}$—$10^{-3}$ M EDTA, the shift of the *U*-pH curves of yttrium-EDTA toward the higher pH axis was in agreement with the calculated value, as is shown in Fig. 2. In the range below $5\times10^{-4}$ M EDTA, the shift was more pronounced than was the theoretical shift, and the *U*-pH curve in the end was close to that of yttrium-hydroxide complex (Y-OH). Using the EDTA concentration higher than $10^{-3}$ M, the *U*-pH curve for the yttrium-EDTA complex was the same in the concentration range of the carrier-free $\sim10^{-3}$ M of yttrium. Accordingly, in the later experiment, a comparatively high EDTA concentration of $5\times10^{-3}$ M was used in order to make the theoretical analysis and practical use easy.

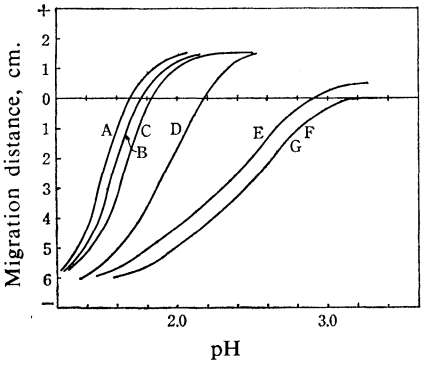



Fig. 3. *U*-pH curve of yttrium at different EDTA concentration.

Intensity of electric field: 300 V./30 cm., migration time: 33 min., temp: 28±1°C, background electrolyte; EDTA concentration A: $5\times10^{-3}$ M, B: $2\times10^{-3}$ M, C: $10^{-3}$ M, D: $5\times10^{-4}$ M, E: $2\times10^{-4}$ M, F: $10^{-4}$ M, G: absent, ionic strength: 0.1 $\mu$, migrant: carrier-free yttrium.

**The Separation of Rare Earths by Ordinary Paper Electromigration.** — From the results shown in Fig. 2, one can evaluate the optimum pH range, 1.7—1.9, for the separation of light rare earths in $5\times10^{-3}$M EDTA. The autoradiogram trace in Fig. 4 shows the separated patterns under the conditions mentioned above and under other pH conditions close to the former. The separation was unsatisfactory in the pH range higher than 2, but the width of each zone was comparatively narrow. Below pH 1.5, the separated zones of lanthanum, cerium and praseodymium were brought close to those of strontium and barium. The separated pattern of each in Fig. 4 was in good agreement with the expected pattern.

**The Separation of Rare Earths by Focusing Chromatography, pH Adjustment in Anodic and Cathodic Sides.**—From the theoretical and experimental results in the ordinary electromigration, one can predict that the pH of a background electrolyte solution mixed with a sample (the rare earth to be separated) will also lie between or be close to the respective p*S* value of rare earths-EDTA in the focusing chromatography process as well as in the ordinary electromigration process. In order to obtain the desired pH condition, one must arrange the initial pHs of the solution on the cathodic and anodic sides. Figure 5 shows the results of the attempt to find a suitable pH arrangement on

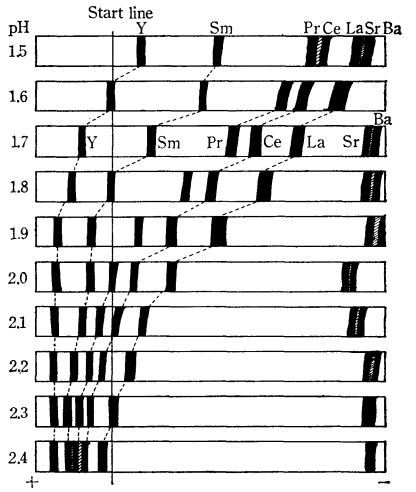



Fig. 4. Separation of RE using ordinary electromigration at different pH for background electrolyte.

Intensity of electric field: 300 V./30 cm., migration time: 50 min., temp.: 25±2°C, background electrolyte: anodic side: pH 1.9—2.1, cathodic side: pH 2.7—4.7 EDTA $5\times10^{-3}$ M, width placed by sample: 3 cm.

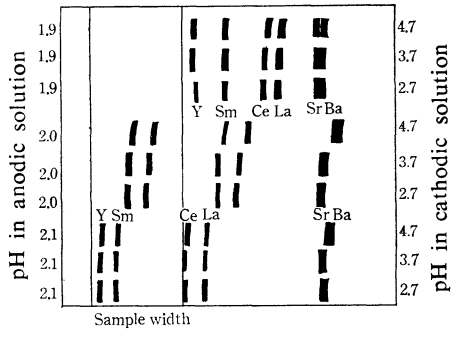



Fig. 5. Focusing chromatographic separation at differant pH gradient.

Intensity of electric field: 800 V./30 cm., migration time: 16 min., temp.: 26±2°C, background electrolyte: anodic side: pH 1.9—2.1, cathodic side: pH 2.7—4.7 ($5\times10^{-3}$ M EDTA, width dipped by sample solution: 3 cm.

each side. In Fig. 5, the selected pHs on the anodic side were 1.9, 2.0 and 2.1. These pH values were the same as the suitable ones of a EDTA background solution for the separation of rare earths by the ordinary electromigration method. On the other hand, the pHs of a EDTA solution on the cathodic side were the same as those on the anodic side (which data are not presented in Fig. 5) and higher than those on the anodic side, i.e., 2.7—4.7.

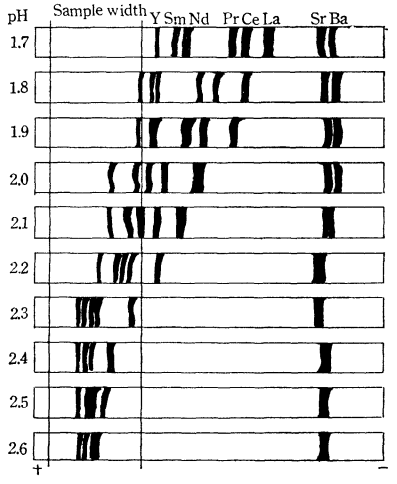



Fig. 6. Focusing chromatogram of RE at different pH in anodic side.

Intensity of electric field: 800 V./30 cm., migration time: 15 min., anodic side: hydrochloric acid, cathodic side: $3\times10^{-3}$ M EDTA, pH 4.7.

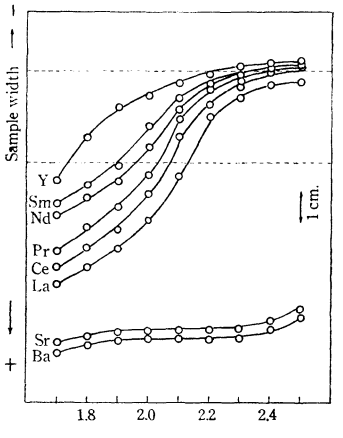



Fig. 7. *U*-pH curves of RE obtained by focusing chromatography.

Intensity of electric field: 800 V./30 cm., migration time: 15 min., temp.: 21—28°C., cathodic side: $3\times10^{-3}$ M EDTA, pH 4.7.

From the results shown in Fig. 5, it may be concluded that one should be careful to adjust the initial pH on the anodic side since the effect of pH on a resolution and the shift of the relative position for the separated bands are much more intensive than those on the cathodic side, and the pH range to be selective on the anodic side is equal to the optimum one obtained by ordinary electromigration. Figure 6 gives autoradiograms showing the separated pattern of rare earths at different pH arrangements between the anodic and cathodic solutions. The pHs in the anodic solution were selected so that they could be compared with the results shown in Fig. 4. The *U*-pH curves shown in Fig. 7 were drawn by plotting the separated bands obtained under the same conditions as that of Fig. 6 except for the pH value of the initial sample solution of rare earths. That is, the pH of the sample solution was about 1.2 in Fig. 6 and 1.5 in Fig. 7. The difference between two separated patterns in both Figs. 6 and 7 was probably caused by the different pH values of the sample solution. If the pH of the sample is the same as that of hydrochloric acid on the anodic side, the separated bands will be close to that obtained by ordinary electromigration.

## Summary

The optimum pH value and concentration of EDTA for separating rare earths (lanthanum, cerium, praseodymium, neodymium, samarium and yttrium) by the technique of paper electromigration have been evaluated on the basis of the migration theory. The validity of the theory has then been justified experimentally. The best condition for separating was at the range of pH 1.7 — 2.1 of $5\times10^{-3}$ M EDTA. Also, the applicability for focusing chromatographic separation has been examined with several pH arrangements between hydrochloric acid on the anodic side and a EDTA complexing agent solution on the cathodic side. Summarizing the above results, it has been concluded that the initial optimum pH of an anodic solution for separation may be obtained by selecting the pH range close to the expected one for the ordinary electromigration, while the effect of pH in a cathodic solution was not as severe as the former.

*Department of Chemistry*
*Faculty of Science*
*Hiroshima University*
*Hiroshima*

# Monolayer Studies of the Interactions between Histidyl Polypeptides and Metal Ions. II. The Effects of Copper, Zinc, Cobalt and Calcium Ions on the Monolayer Properties of Poly-1-benzyl-L-histidine

By Takuya YAMASHITA* and Toshizo ISEMURA

(Received May 19, 1964)

The reactivity of the imidazole group of the histidyl residue in protein has a great importance in the understanding of interactions between proteins and several metal ions.[1] In the preceding paper,[2] the interactions of the cupric ion with poly-1-benzyl-L-histidine and with copoly-2 : 2 : 2 : 1-(glycine, *O*-benzyl-DL-serine, β-benzyl-L-aspartate, 1-benzyl-L-histidine) have been studied by using monolayer techniques at the air/water interface. It was found that the cupric ion has a strong interaction with the poly-1-benzyl-L-histidine monolayer at pH 5.6, while it interacts with the copolypeptide only with difficulty. For the present study, the effects of copper, zinc, cobalt and calcium ions on the film properties of poly-benzyl-1-L-histidine were investigated at the air/water interface when the pH of the subsolution was varied and at the oil/water interface at pH 5.6.

## Experimental

Poly-1-benzyl-L-histidine was spread from a solution in 0.05 N hydrochloric acid containing 20% of isopropyl alcohol, as in the previous study.[2] The desired pH value of the subsolution was obtained with a 0.1 M acetate buffer (acetic acid + sodium acetate) in the range of 4.8—6.2, and with a 0.1 M citrate buffer (sodium citrate + sodium hydroxide) at 6.7. The pH was measured with a Horiba M-3 glass electrode pH-meter.

The surface pressure, the surface viscosity and the surface potential at the air/water interface were measured by the methods described in the preceding paper.[2] The surface moment was calculated from the surface potential by utilizing the Helmholtz formula. The compression of the film was started 20 min. after the polypeptide had been spread.

At the oil/water interface, the interfacial pressure was measured by the ring method. The diameter of the ring used was 2.77 cm. Petroleum ether (boiling point, 85—115°C) was used as an oil phase. The interfacial concentration of the polypeptide was changed by successive injections with an Agla micrometer syringe, and corrected by the Thomas theoretical correction formula.[3-5] The measurement of the interfacial pressure was carried out five minutes after each injection.

All the experiments were performed at room temperature, but the change in temperature never exceeded one degree during the course of an experiment.

## Results

Figures 1, 2, 3 and 4 illustrate, at various pH values, the surface viscosity-area ($\eta_s$-$A$) curves of poly-1-benzyl-L-histidine on subsolutions containing cupric sulfate (0.01 M), zinc sulfate (0.01 M, 0.05 M), cobaltous sulfate (0.01 M, 0.05 M) and calcium chloride (0.05 M) respectively. Figure 5 shows the areas per residue at 0.05 surface poise in the presence and absence of these divalent metal ions against the pH. As can be seen in these figures, the cupric ion has a remarkable effect on the $\eta_s$-$A$ relation of this polypeptide over a wide pH range, while the effects of the zinc, cobaltous and

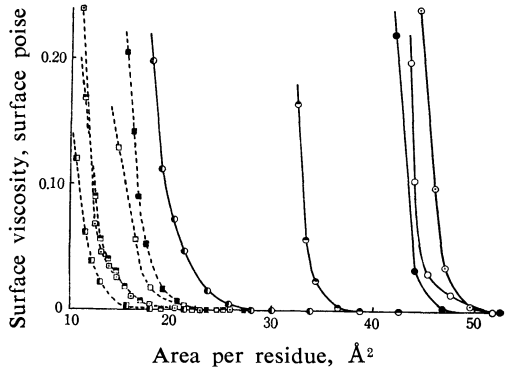



Fig. 1. Effect of the cupric ion on the surface viscosity-area relation of poly-1-benzyl-L-histidine at 24°C. Circles refer to 0.01 M $CuSO_4$ subsolutions; squares refer to control buffer subsolutions: ◓, ◙, pH 4.8; ⊙, ⊡, 5.1; ○, □, 5.6; ●, ■, 6.2; ◐, ◧, 6.7.

* Present address: Department of Chemistry, Faculty of Science, Osaka University, Kita-ku, Osaka.

1) F. R. N. Gurd and P. B. Wilcox, "Advance in Protein Chemistry," Vol. 11, Academic Press, New York (1956), p. 331.

2) T. Yamashita and T. Isemura, This Bulletin, **37**, 742 (1964).

3) A. G. Thomas, *Nature*, **179**, 776 (1957).

4) E. G. Cockbain, K. J. Day and A. I. McMullen, "Proc. 2nd Int. Cong. Surface Activity," Vol. 1. Butterworths Scientific Publications, London (1957), p. 56.

5) T. Yamashita and T. Isemura, This Bulletin, **35**, 929 (1962).

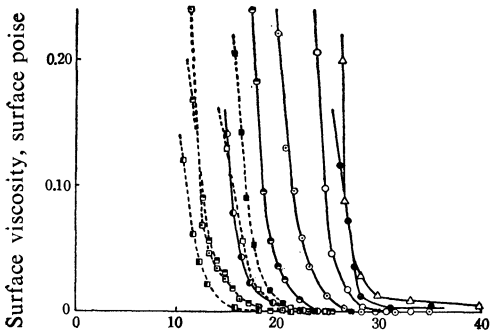



Fig. 2. Effect of the zinc ion on the surface viscosity-area relation of poly-1-benzyl-L-histidine at 24°C. Circles and triangles refer to 0.01 M and 0.05 M $ZnSO_4$ subsolutions, respectively; squares refer to control buffer subsolutions: ◓, ⬒, pH 4.8; ⊙, ⊡, 5.1; ○, △, □, 5.6; ●, ■, 6.2; ◐, ◧, 6.7.

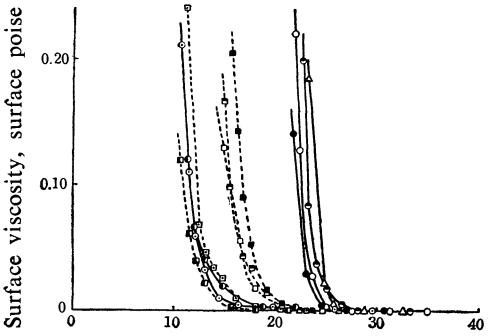



Fig. 3. Effect of the cobaltous ion on the surface viscosity-area relation of poly-1-benzyl-L-histidine at 24°C. Circles and triangles refer to 0.01 M and 0.05 M $CoSO_4$ subsolutions, respectively; squares refer to control buffer subsolutions: ⊙, ⊡, pH 5.1; ○, △, □, 5.6; ◓, ⬒, 5.9; ●, ■, 6.2; ◐, ◧, 6.7.

calcium ions are much less than that of the cupric ion.

The surface pressure-area (*Π-A*) curves of poly-1-benzyl-L-histidine on subsolutions at various concentrations of zinc sulfate are shown in Fig. 6 at pH 5.6. The presence of 0.001 M zinc sulfate does not practically affect the shape of the *Π-A* curve, while the values of 0.01 M and 0.05 M are high enough to cause the disappearance of the plateau of the *Π-A* curve found on the control subsolution.

Figure 7 shows the surface potential-area (*ΔV-A*) and the surface moment-area (*μ-A*) curves of poly-1-benzyl-L-histidine at pH 5.6 in the presence and absence of the zinc ion. In the presence of 0.01 M zinc sulfate, the surface potential and the surface moment are higher by ca. 50 mV. throughout the measured areas, and higher by 52 mD in the linear portion of the *μ-A* curve than on the control subsolution.

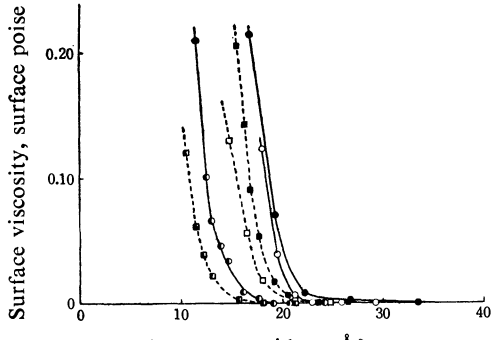



Fig. 4. Effect of the calcium ion on the surface viscosity-area relation of poly-1-benzyl-L-histidine at 24°C. Circles refer to 0.05 M $CaCl_2$ subsolutions; squares refer to control buffer subsolutions: ○, □, pH 5.6; ●, ■, 6.2; ◐, ◧, 6.7.

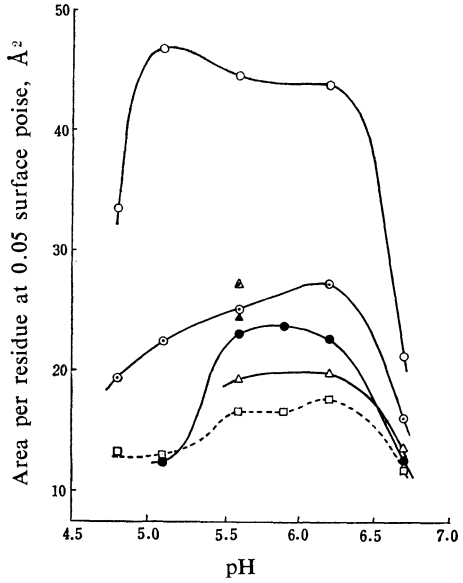



Fig. 5. Areas per residue at 0.05 suface poise against pH at 24°C: ○, 0.01 M $CuSO_4$; ⊙, 0.01 M $ZnSO_4$; ◬, 0.05 M $ZnSO_4$; ●, 0.01 M $CoSO_4$; ▲, 0.05 M $CoSO_4$; △, 0.05 M $CaCl_2$; □, control (without divalent metal ions).

Figure 8 shows the effects of cobaltous sulfate and calcium chloride on the *Π-A* relation of poly-1-benzyl-L-histidine at pH 5.6. In the presence of the cobaltous ion, film expansion was observed. However, even 0.05 M cobaltous sulfate did not cause the disappearance of the plateau of the *Π-A* curve found on the control

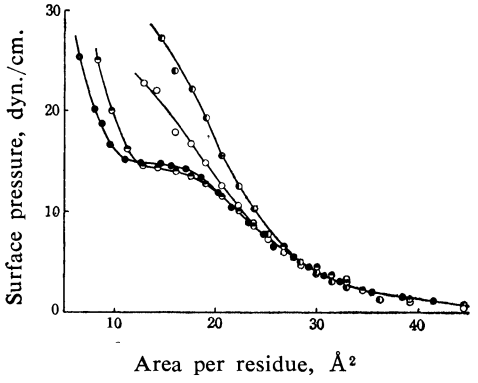



Fig. 6. Effect of the zinc ion on the surface pressure-area relation of poly-1-benzyl-L-histidine at pH 5.6 (0.1 M acetate buffer) : ●, control (20°C) ; ◓, 0.001 M ; ○, 0.01 M ; ◐, 0.05 M ($ZnSO_4$ the last three, at 24°C).

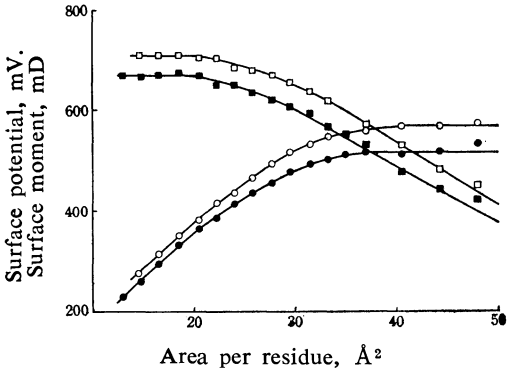



Fig. 7. Surface potential-area and surface moment-area curves of poly-1-benzyl-L-histidine on 0.1 M acetate buffer (pH 5.6 ; ■, ●) and on 0.1 M acetate buffer containing 0.01 M zinc surfate (pH 5.6 ; □, ○) : 12°C.

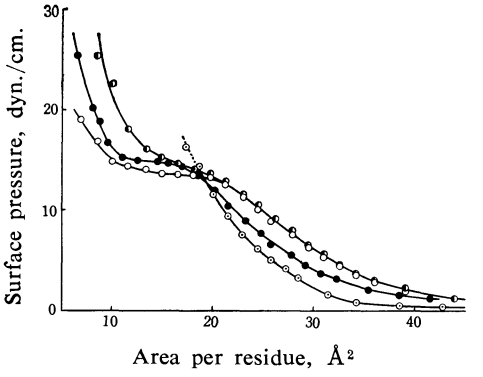



Fig. 8. Effect of the cobaltous and calcium ions on the surface pressure-area relation of poly-1-benzyl-L-histidine at pH 5.6 (0.1 M acetate buffer) : ●, control (20°C) ; ○, 0.01 M $CoSO_4$ ; ◐, 0.05 M $CoSO_4$ ; ⊙, 0.05 M $CaCl_2$ (the last three, at 24°C).

subsolution. On the other hand, 0.05 M calcium chloride resulted in film condensation. The film was unstable over areas smaller than 19 Å² per residue.

The interfacial pressure-area ($\Pi_i$-$A$) curves of poly-1-benzyl-L-histidine at the interfaces between oil and water when various salts were dissolved are shown in Fig. 9. The $\Pi_i$-$A$ curves were nearly identical with one another on the 0.1 M potassium chloride subsolution and on the acetate buffer subsolutions at pH 5.6 with and without 0.01 M zinc or cobaltous sulfate. The cupric ion had a remarkable effect as well as at the air/water interface.[2]

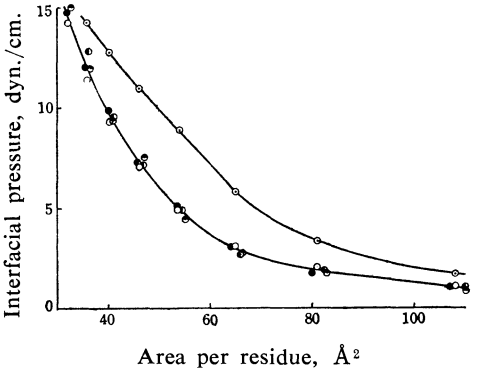



Fig. 9. Monolayers of poly-1-benzyl-L-histidine at the oil/water interface at 21°C : ○, 0.1 M KCl ; ●, 0.1 M Acetate buffer (pH 5.6) ; ⊙, 0.01 M $CuSO_4$ ; ◐, 0.01 M $ZnSO_4$ ; ◓, 0.01 M $CoSO_4$ (the last three salts were dissolved in 0.1 M acetate buffer, pH 5.6).

## Discussion

**Air/Water Interface.** — *The Effect of the Cupric Ion.*—It has been found that the various metal ions form complexes with imidazole,[6,7] 4-methylimidazole,[8] and poly-L-histidine[9] as model substances of the histidyl residue in protein. In the preceding work,[2] a strong interaction of the cupric ion with the poly-1-benzyl-L-histidine monolayer has been found at pH 5.6 at the air/water interface. In the presence of the cupric ion in the subsolution, the surface pressure increased remarkably throughout the measured areas, and the $\eta_s$-$A$ curve shifted to a much larger area than on the control subsolution, the surface pressure being quite low at the area where the surface viscosity began to rise. This finding was interpreted in terms of the cross-linkage formation

6) J. T. Edsall, G. Felsenfeld, D. S. Goodman and F. R. N. Gurd, *J. Am. Chem. Soc.*, **76**, 3054 (1954).
7) R. B. Martin and J. T. Edsall, ibid., **80**, 5033 (1958).
8) Y. Nozaki, F. R. N. Gurd, R. F. Chen and J. T. Edsall, ibid., **79**, 2123 (1957).
9) A. Patchornik, A. Berger and E. Katchalski, ibid., **79**, 5227 (1957).

between molecules at the surface through the complex formation of copper with the side chains of poly-l-benzyl-L-histidine.

In the present study, the effect of the cupric ion on the $\eta_s$-$A$ relation of poly-l-benzyl-L-histidine was investigated in the 4.8—6.7 pH range. As Fig. 1 shows, in the presence of the cupric ion, the $\eta_s$-$A$ curves shift to much larger areas than on the control subsolutions at the pH's studied. The effect of the cupric ion is remarkaly large compared with those of zinc, cobaltous and calcium ions, as Fig. 5 shows. The cross-linked structure should be formed between poly-peptide molecules at the surface in these pH range as a result of complex formation between the cupric ions and the side chains. The optimum pH for the copper-monolayer interaction is in the 5.1—6.2 range.

*The Effect of the Zinc Ion.*—As Figs. 2 and 5 show, the zinc ion interacts considerably with the monolayer of poly-l-benzyl-L-histidine in the pH range of 5.1—6.2, where the areas per residue at the 0.05 surface poise are higher by 8—10 Å$^2$ than on the control subsolutions. This value is much less than in the case of the cupric ion. The cupric ion causes the increment of 26—34 Å$^2$ in the optimum pH range. At pH 5.6, which seems to be an optimum pH for the zinc-monolayer interaction, the plateau of the $\Pi$-$A$ curve found on the control subsolution disappears in the presence of 0.01 M and 0.05 M zinc sulfate. This might be caused by the cross-linkage formation in the monolayer. Such a cross-linked structure has also been found with tanned protein monolayers.[10-12]

The rise in the surface potential or surface moment in the presence of the zinc ion might be caused by the increment in the net positive charge of the film as a result of the combination of zinc ions with the interacting sites of the side chains of polypeptide, as in the case of copper ions,[2] and so may be another evidence of the complex formation. A similar increase in the surface potential has been reported for a gelatin monolayer tanned with basic chromium sulfate.[11]

*The Effect of the Cobaltous Ion.*—The effect of the cobaltous ion on the $\eta_s$-$A$ relation of poly-l-benzyl-L-histidine was investigated in the 5.1—6.7 pH range. The optimum pH for the cobalt-monolayer interaction is found to be in the 5.6—6.2 range, and the cobalt ion does not interact practically at the 5.1 and 6.7 pH's, as Figs. 3 and 5 show. The interaction of the cobalt ion with the monolayer is somewhat weaker than that of the zinc ion in the pH range studied. Such a weaker interaction of the cobalt ion than those of the zinc and copper ions has also been found in bulk with bacterial-$\alpha$-amylase,[13] the interacting sites of which are histidyl groups, and with imidazole.[3]

The effect of the cobaltous ion on the $\Pi$-$A$ relation of poly-l-benzyl-L-histidine was investigated at a pH in the optimum pH range. At pH 5.6, in the presence of the cobaltous ion, the film expanded more than on the control subsolution. However, even 0.05 M cobaltous sulfate does not cause the disappearance of the plateau of the $\Pi$-$A$ curve observed on the control subsolution unlike zinc ion. This fact may indicate that the cross-linked structure caused by the cobalt ion is somewhat looser than that caused by the zinc ion because of its weaker interaction, even though such a structure is formed.

*The Effect of the Calcium Ion.*—The effect of the calcium ion on the $\eta_s$-$A$ relation of poly-l-benzyl-L-histidene is quite small. Even a 0.05 M calcium chloride subsolution causes merely an increase of 2—3 Å$^2$ in areas per residue at a 0.05 surface poise in the 5.6—6.7 pH range. At pH 5.6, the calcium ion reduces the surface pressure more than on the control subsolution, unlike copper,[2] zinc and cobalt ions. This finding resembles the facts found concerning the metal-stearic acid monolayer interactions;[14] it might be caused by the difference in modes of interactions between the alkaline earth metals and the copper, zinc and cobalt ions. The calcium ion might form the cross-linked stucture in the monolayer only with difficulty.

*The Estimation of the Extent of Metal-Monolayer Interactions.*—On the basis of the preceding[2] and the present works, we conclude that the cupric ion interacts especially strongly with the monolayer of poly-l-benzyl-L-histidine, and

Table I. The first association constants for imidazole and 4-methylimidazole with various metal ions at 25°C

| | $Cu^{2+}$ | $Zn^{2+}$ | $Co^{2+}$ | $Ca^{2+}$ |
|---|---|---|---|---|
| Imidazole | 4.33[a] | 2.57[a] | 2.42[b] | 0.08[d] |
| 4-Methylimidazole | 4.13[c] | 2.44[c] | | |

Ionic strength; 0.15—0.16.
a) Ref. 6; b) Ref. 7; c) Ref. 8; d) Ref. 15.

10) J. H. Schulman and M. Z. Dogan, *Discussions Faraday Soc.*, **16**, 158 (1954).
11) S. C. Ellis and K. G. A. Pankhurst, ibid., **16**, 170 (1954).
12) K. G. A. Pankhurst, "Surface Phenomena in Chemistry and Biology," Pergamon Press, London and New York (1958), p. 100.
13) K. Kakiuchi, S. Kato and T. Isemura, unpublished results.
14) T. Sasaki and R. Matuura, This Bulletin, **24**, 274 (1951).
15) J. Schubert, *J. Am. Chem. Soc.*, **76**, 3442 (1954).

Table II. Areas of poly-DL-phenylalanine[5] and poly-1-benzyl-L-histidine under various interfacial pressures

| Polypeptide | Area per residue, Å² | | | |
|---|---|---|---|---|
| | 1 dyn./cm. | 5 dyn./cm. | 10 dyn./cm. | 15 dyn./cm. |
| Poly-DL-phenylalanine* | 47 | 20 | 15 | 13 |
| Poly-1-benzyl-L-histidine** | 100 | 54 | 40 | 32 |

* Oil/distilled water interface (16.5°C).
** Oil/0.1 M acetate buffer interface (pH 5.6, 21°C).

that the decreasing order of the metal-monolayer interactions is $Cu^{2+}$, $Zn^{2+}$, $Co^{2+}$, $Ca^{2+}$. As Table I shows, this order corresponds to the first association constants of imidazole or 4-methylimidazole, which are measures of the extent of interaction.

**The Oil/Water Interface.**—At the oil/water interface, the poly-1-benzyl-L-histidine monolayer expands much more than at the air/water interface as a result of the release of van der Waals force between side chains. The extent of the expansion is considerably larger than the film of poly-DL-phenylalanine which has benzyl groups directly attached to the backbone carbon atoms. The areas occupied by poly-1-benzyl-L-histidine film are compared with those by poly-DL-phenylalanine under various interfacial pressures in Table II. Such a large expansion of the former film suggests that the imidazole groups, which are hydrophilic to some extent because of the effect of nitrogen atoms, lie at the interface.

Unlike at the air/water interface, no appreciable effects of zinc and cobalt ions on the monolayer of poly-1-benzyl-L-histidine are found at the concentrations of 0.01 M at pH 5.6. This fact might be caused by the restriction of the accessibility of these metal ions to the interacting sites by the oil. On the other hand, the effect of the cupric ion is quite large, as at the air/water interface.[2] Accordingly, complexes of cupric ions with poly-1-benzyl-L-histidine should be formed even at the oil/water interface.

Interestingly, the plateau of the *II-A* curve found on the 0.1 M acetate buffer subsolution at pH 5.6 disappears at the oil/water interface. The $\Pi_i$-*A* curve practically agrees with that at the oil/0.1 M potassium chloride interface. At the oil/water interface, the lateral cohesion between side chains is released by the intervening of oil between them. This may be the cause of the lack of a difference between the $\Pi_i$-*A* curves at the interfaces between oil and the 0.1 M potassium chloride solution and between oil and the 0.1 M acetate buffer.

## Summary

The effects of metal ions on the monolayer properties of poly-1-benzyl-L-histidine, a model substance of the histidyl residue in protein, have been investigated at the air/water interface when the subphase pH is varied, and at the oil/water interface at pH 5.6.

At the air/water interface, it was found from the measurements of the surface viscosity that the cupric ion interacts especially strongly with the monolayer of poly-1-benzyl-L-histidine over a wide pH range and that the interaction of the calcium ion is quite weak. The decreasing order of metal-monolayer interactions is $Cu^{2+}$, $Zn^{2+}$, $Co^{2+}$, $Ca^{2+}$. The surface pressure-area isotherms suggest that the cobalt ion forms a somewhat looser cross-linked structure in the monolayer than does the zinc ion because of its weaker interaction.

At the oil/water interface, the film expands remarkably because of the release of van der Waals force between side chains. No appreciable effects on the interfacial pressure-area relation were observed with the zinc and cobaltous ions, because the accessibility of these ions to the interacting sites of side chains would have been restricted by the oil. The cupric ion had a considerable effect here as well as at the air/water interface.

The authors wish to express their hearty thanks to Professor Junzo Noguchi of Hokkaido University for supplying a valuable sample to them.

*Institute for Protein Research*
*Osaka University*
*Kita-ku, Osaka*

# The Syntheses and Properties of 5-Thiazones[1]

By Masaki OHTA and Chung-gi SHIN

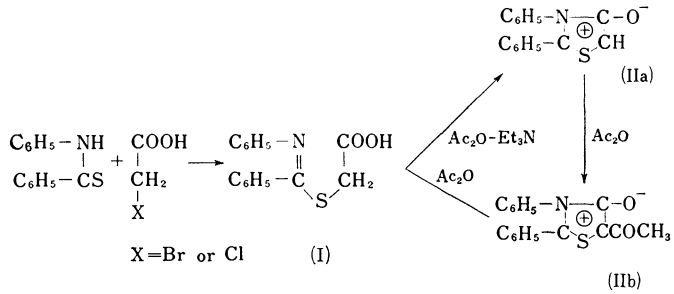
(Received June 10, 1964)

In a previous paper of this series,[2] it was reported that the treatment of *S*-carboxymethylisothiobenzanilide (I) with acetic anhydride in the presence or absence of triethylamine yielded new meso-ionic compounds, which we named 2, 3-diphenyl-4-thiazone (IIa) and 5-acetyl-2, 3-diphenyl-4-thiazone (IIb) respectively:

Syntheses of 5-thiazone derivatives by the ring-closure of *N*-substituted-*N*-thiobenzoylglycine with acetic anhydride or benzoyl chloride have already been reported by Lawson et al., but all of the compounds thus obtained have an acyl substituent in the 4-position which can not be removed by hydrolysis.[3,4]

The present paper will describe the syntheses and properties of 5-thiazones with neither acetyl nor benzoyl group in the 4-position. It has now been found that, as in the case of 4-thiazone, 2, 3-diphenyl- and 3-methyl-2-phenyl-5-thiazone (IV) can be readily obtained by treating *N*-thiobenzoylsarcosine (IIIa) or *N*-thiobenzoyl-*N*-phenylglycine (IIIb) with an acetic anhydride-triethylamine mixture at room temperature. When pyridine is used in place of triethylamine in these cyclization, only a small quantity of 4-acyl derivative (V) is obtained instead of IV. These new meso-ionic compounds, IVa and IVb, are readily soluble in such polar solvents as ethanol, but they are insoluble in such nonpolar solvents as ether. IVa is insoluble in 10% aqueous sodium hydroxide, and IVb is easily hydrolyzed by 10% aqueous hydrochloric acid to the corresponding parent acid. IVb is soluble in hot aqueous sodium hydroxide and insoluble in 10% aqueous hydrochloric acid. The structure of these new meso-ionic compounds is supported by elementary analysis and by their infrared spectra. The infrared spectra of IVa and IVb, in comparison with those of the parent acid, have a strong new absorption at 1620—1630 $cm^{-1}$ and the band near 1700 $cm^{-1}$ disappears as a result of the carbonyl vibration of the carboxy group. This characteristic change of the spectra due to the formation of a meso-ionic ring from III has been observed also in infrared spectra of meso-ionic compounds derived from 2-(carboxymethylmercapto)-pyridine,[5] and from azoles with a carboxymethylmercapto group.[6] Since the 5-thiazone derivatives obtained above should have an aromatic character because their structures are like sydnones, we examined several reactions of IV as in the case of sydnones.

The acetylation of IV with acetic anhydride gave V, which is identical with the *C*-acetyl derivatives prepared directly by the reaction of III with acetic anhydride. On the treatment of IVa with benzoyl chloride in the presence of pyridine, a benzoyl derivative was obtained; it is identical with the *C*-benzoyl derivative obtained by Lawson et al.[3,4] In order to prepare the halogen derivatives substituted at the 4-position, halogenation was carried out under several conditions; the hydrobromide




1) This paper is the part XXI of studies on meso-ionic compounds.

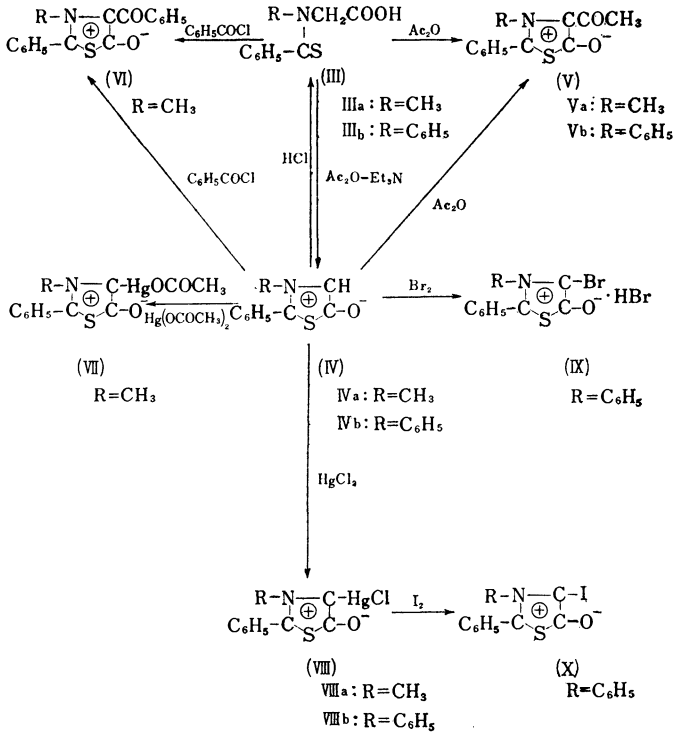
2) M. Ohta, H. Chosho, C. Shin and K. Ichimura, *J. Chem. Soc. Japan, Pure Chem. Sec.* (*Nippon Kagaku Zasshi*), **85**, 440 (1964).

3) A. Lawson and C. E. Searle, *J. Chem. Soc.*, **1957**, 1556.

4) A. Lawson and D. H. Miles, ibid., **1959**, 2865.

5) G. F. Duffin and J. D. Kendall, ibid., **1951**, 734; **1956**, 361.

6) M. Hashimoto and M. Ohta, This Bulletin, **33**, 1394 (1960).




(IX) was obtained in the presence of acetic anhydride. The corresponding free base, however, could not be obtained, even when IX was treated with a weak base, this fact might indicate its instability. Similar properties have been observed also in the case of 4-thiazone.[2] In a procedure similar to that used on sydnones,[7] IV reacted immediately with mercuric chloride in 50% methanol to give chloromercuri derivatives quantitatively, while only IVa reacted with mercuric acetate in methanol to give an acetoxymercuri derivative. These mercuri derivatives are insoluble in almost all organic solvents except ethanol and methanol. Though VIIIa and VIIIb are very stable, VII is unstable in the air and turned into a black material. When the chloromercuri derivative (VIIIb) was treated with iodine in methanol, an iodo derivative was obtained in a good yield ; this derivative was considered from elementary analysis to be X. Attempts to prepare the analogous iodo derivative from VIIIa and bromo derivatives from VIIIa and VIIIb were unsuccessful. These results make it seen likely that the reactivity at the 4-position of 5-thiazone with a phenyl group in the 3-position decreases as a result of the stabilization of the ring and that the halogen at the 4-position becomes reactive, as in the case of usual aromatic compounds.

7) K. Nakahara and M. Ohta, *J. Chem. Soc. Japan, Pure Chem. Sec.* (*Nippon Kagaku Zassi*), **77**, 1306 (1956).

## Experimental

**3-Methyl-2-phenyl-5-thiazone (IVa).** — *N*-Thiobenzoylsarcosine (1 g.) was dissolved in a mixture of acetic anhydride and triethylamine (volume ratio 1 : 2) (3 ml.) at room temperature. The solution immediately turned brown, and after a few minutes yellowish prisms were crystallized out. After 2 hr. in an ice box, the crystals were filtered off and washed with ether. Recrystallization from acetone gave yellow needles, (m. p. 144—145°C (decomp.)). Yield, 0.8 g. $\lambda_{max}^{EtOH}$ 362 m$\mu$ ($\varepsilon$, 10191)

Found: C, 63.91; H, 4.51; N, 7.43. Calcd. for $C_{10}H_9NOS$: C, 62.83; H, 4.71; N, 7.33%.

IVa is easily soluble in methanol and ethanol, soluble in hot benzene, ethyl acetate and acetone, and almost insoluble in ether, petroleum ether and 10% aqueous sodium hydroxide. When treated with 10% aqueous hydrochloric acid at room temperature, IVa was hydrolyzed to give the starting material, *N*-thiobenzoylsarcosine (IIIa).

**2,3-Diphenyl-5-thiazone (IVb).**—*N*-Thiobenzoyl-*N*-phenylglycine (1 g.) was dissolved in a mixture of acetic anhydride and triethylamine (volume ratio 1 : 1) (4 ml.) at room temperature. The solution immediately turned brown, and after a few minutes yellow crystals were crystallized out. After the solution had stood overnight in an ice box, the crystals were filtered off and washed with ether. Recrystallization from ethyl acetate gave yellow needles, (m. p. 130—131°C (decomp.)). Yield, 0.8 g. $\lambda_{max}^{EtOH}$ 382 m$\mu$ ($\varepsilon$, 10170).

Found: C, 70.90; H, 4.38; N, 5.61. Calcd. for $C_{15}H_{11}NOS$: C, 71.15; H, 4.35; N, 5.53%.

IVb is soluble in methanol, ethanol, acetone and hot 10% aqueous sodium hydroxide, and almost insoluble in ether and 10% aqueous hydrochloric acid.

**4-Acetyl-3-methyl-2-phenyl-5-thiazone (Va).**—IVa (0.5 g.) was heated with acetic anhydride at 100°C on a steam bath for 2 hr. The solution slowly darkened, and then the acetic anhydride was removed by evaporation under reduced pressure and by two subsequent evaporations with xylene. The recrystallization of the residual semi-solid from ethyl acetate-petroleum ether gave yellow needles, (m. p. 133—134°C (decomp.)). Yield, 0.6 g.

In the same manner as in the case of Va, the acetyl derivative (Vb) was obtained from IVb (0.5 g.) and recrystallized from benzene-petroleum ether as yellow needles, (m. p. 192—193°C (decomp.)). Yield, 0.4 g. Lawson et al., however, reported the melting point as 170—172°C.

Va and Vb showed no depression on admixture with the compounds by the ring-closure of IIIa and IIIb respectively.

**4-Benzoyl-3-methyl-2-phenyl-5-thiazone (VI).**—Into a solution of IVa (0.8 g.) in pyridine (5 ml.) benzoyl chloride (0.6 g.) was stirred at room temperature. The resultant brown mixture was warmed at 50°C on a water bath for 10 min.; then pyridine was evaporated under reduced pressure, and the green residual oil was washed twice with 10% aqueous hydrochloric acid and water. Recrystallization from benzene gave yellow needles, (m. p. 219—220°C (decomp.)). This compound showed no depression on admixture with an authentic specimen prepared by the ring-closure of IIIa with benzoyl chloride.

**4-Chloromercuri-3-methyl-2-phenyl-5-thiazone (VIIIa).**—A solution of mercuric chloride (1.2 g.) in 50% aqueous methanol (60 ml.) was stirred into a solution of IVa (0.7 g.) and sodium acetate (1.2 g.) in the same solvent at room temperature. Yellow precipitates were immediately separated, collected by filtration, and washed successively with ether, acetone and methanol. This compound did not melt below 300°C. Yield, 1.4 g.

Found: N, 3.41. Calcd. for $C_{10}H_8NOSHgCl$: N, 3.32%.

VIIIa is insoluble in usual organic solvents. In the same manner as in the case of VIIIa, the chloromercuri derivative (VIIIb) was obtained from IVb (0.5 g.) and recrystallized from 50% aqueous ethanol to give yellow needles, (m. p. 187—189°C (decomp.)). Yield, 0.85 g.

Found: N, 2.90. Calcd. for $C_{15}H_8NOSHgCl$: N, 2.89%.

VIIIa is soluble in methanol and ethanol, insoluble in benzene and ether.

**4-Acetomercuri-3-methyl-2-phenyl-5-thiazone (VII).**—A solution of mercuric acetate (0.9 g.) in methanol (30 ml.) was stirred into a solution of IVa (0.5 g) in methanol (10 ml.) at room temperature. The solution immediately turned yellow, and after a few minutes yellow precipitates separated. Recrystallization from ethanol gave small yellow needles, (m. p. 158—159°C (decomp.)). Yield, 1.1 g.

When this compound was kept standing for several days in the air at room temperature, it turned black.

Found: N, 3.12. Calcd. for $C_{12}H_{11}NO_3SHg$: N, 3.11%.

VIIIa is soluble in hot ethanol, and insoluble in methanol, chloroform, ethyl acetate and ether.

**4-Bromo-2, 3-diphenyl-5-thiazone Hydrobromide (IX).**—When a solution of bromine (0.3 g.) in acetic anhydride (3 ml.) was stirred, portion by portion, into a solution of IVb (0.5 g.) in acetic anhydride (5 ml.) below 0°C, orange precipitates were gradually separated. After the solution had stood overnight in an ice box, the precipitates were collected by filtration and washed with ether. Recrystallization from acetone gave pale yellow small needles, (m. p. 163—164°C (decomp.)) Yield, 0.4 g. These crystals are deliquescent.

Found: C, 42.89; H, 3.46; N, 3.24. Calcd. for $C_{15}H_{11}NOSBr$: C, 43.58; H, 2.66; N, 3.39%.

IX is easily soluble in water and methanol, soluble in hot ethanol and acetone, and almost insoluble in ether and benzene.

**2, 3-Diphenyl-4-iodo-5-thiazone (X).**—A solution of iodine (0.42 g.) in methanol (30 ml.) was stirred, portion by portion, into a solution of VIIIb (0.8 g.) in methanol (40 ml.) below 0°C over a 10 min. The color of the iodine immediately disappeared, and yellow precipitates were gradually separated. After the solution had stood overnight in an ice box, the precipitates were collected by filtration and recrystallized from ethanol as yellow needles, (m. p. 168—169°C (decomp.)) Yield, 0.4 g. $\lambda_{max}^{EtOH}$ 405 mμ ($\varepsilon$, 38596).

Found: C, 47.45; H, 2.66; N, 3.72. Calcd. for $C_{15}H_{10}NOSI$: C, 47.49; H, 2.64; N, 3.70%.

X is soluble in hot ethanol, methanol and benzene, but almost insoluble in acetone, ether and ethyl acetate.

The authors are indebted to Miss Toshiko Aoyagi for her elementary analysis and Mr. Eiji Saito for his ultraviolet spectral data.

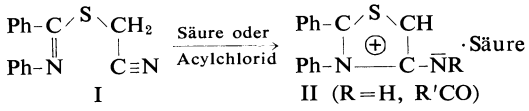
*Laboratory of Organic Chemistry*
*Tokyo Institute of Technology*
*Ookayama, Tokyo*

# Über die Reaktion zwischen *N*-Substituierten Dithiocarbamidsäureestern und α-Chlornitrilen*

Von Kunihiro ICHIMURA und Masaki OHTA

(Eingegangen am 4. September, 1964)

Kürzlich beschrieben wir, dass *S*-Cyanmethyl-isothiobenzanilid (I) durch die Einwirkung von sauren Mitteln oder Acylchloriden unter Ringschluss zum "sydnonimin" ähnlichen Heterocyclus von Formel II überführt wird,[1] das wir bequemlichkeitshalber "2, 3-Diphenyl-thiazonimin-Salz" genannt hatten.[2] In dieser Arbeit haben wir statt Isothioamid Dithiokohlensäure-diesterimid und Isothioharnstoff gewählt, die das analoge Kettensystem $-N{=}C-S-CH_2CN$ wie beim Isothioamid haben.



I II (R=H, R'CO)

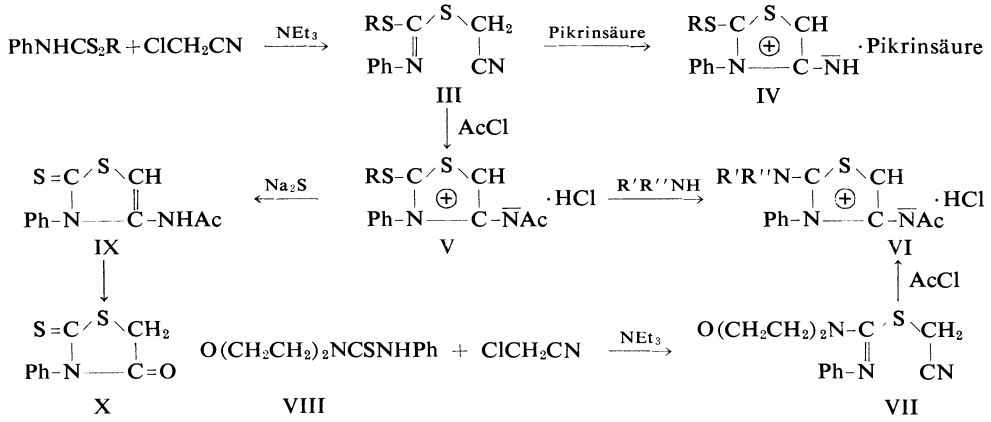
*N*-Phenyldithiocarbamidsäureester wird mit Chloracetonitril in der Gegenwart von Triäthylamin zu *N*-Phenyldithiokohlensäure-diesterimid (III) kondensiert.

Setzt man III mit Pikrinsäure in einer benzolischen Lösung um, so ist unter dem Ringschluss erwartetes 2-Alkylmerkapto-3-phenyl-thiazonimin-pikrat (IV) erhältlich, auf dessen Struktur es aus der Elementaranalyse und dem Infrarot-Spektrum (Abwesenheit des Nitrilbandes) geschlossen wird, während bei der Einwirkung von Chlorwasserstoff auf III eine unbeständige, in reiner Form nicht isolierte Verbindung entsteht.

Bei der Reaktion von III mit Acetylchlorid erfolgt glatt der analoge Ringschluss unter der Bildung von *N*-Acetyl-2-alkylmerkaptothiazonimin-hydrochlorid (V), den Strukturbeweis dafür liefern die Analysenwerte und Infrarot-Spektren.

Die Äthylmerkapto-Gruppe von V wird glatt durch Morpholin substituiert. Die so erhaltene 2-Morpholino-Verbindung (VI; $R'R''N{=}O(CH_2CH_2)_2N$) wird für Vergleichszweck durch ein anderes Verfahren synthesiert; trisubstituierter Thioharnstoff (VIII) liefert mit Chloracetonitril in der Gegenwart von Triäthylamin *S*-Cyanmethylisothioharnstoff (VII). Bei der Einwirkung von Acetylchlorid erlaubt VII in geringer Ausbeute die Darstellung von 2-Morpholino-Verbindung. Diese geringe Ausbeute hat wohl die grössere Basizität des Isothioharnstoffs zur Folge, weshalb es bevorzugter mit Acetylchlorid quarternisiert, als zum Ringschluss gebracht wird.

Mit den anderen aliphatischen Aminen kann 2-Äthylmerkapto-Verbindung gleicherweise in entsprechende 2-Amino-Derivate (VI) überführt werden, aber mit Anilin reagiert sie erst beim Erhitzen unter dem Austritt des Merkaptans zu einer unbekannten Verbindung, deren



* 22. Mitteilung der Untersuchungen über Mesoionische Verbindungen.

1) H. Chosho, K. Ichimura und M. Ohta. Dieses Bulletin, 37, 1670 (1964).

2) Siehe die Fussnote in der 20. Mitteilung (Ref. 1). In dieser Mitteilung nehmen wir auch den Namen "Thiazonimin" für das Ringsystem von II.

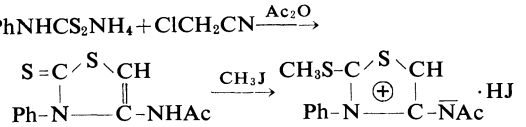
Analysenwert mit dem der 2-Anilino-Verbindung nicht im Einklang steht.

Mit Natriumhydrogencarbonat wird 2-Äthylmerkapto-Verbindung unter Merkaptanentwicklung zu zersetzlichen Kristallen übergeführt.

Bei der Umsetzung mit Natriumsulfid liefert sie 3-Phenyl-4-acetamido-4-thiazolin-2-thion (IX), dessen Strukturbeweis auf dem Analysenwert sowie dem Infrarot-Spektrum, schliesslich auf der Hydrolyse in 3-Phenylrhodanin (X) beruht. Diese Überführung von V in bekanntes X über IX stützt sich intensiv auf die Ringstruktur von V.

3-Phenyl-4-acetamido-4-thiazolin-2-thion (IX) ist auch beim Behandeln des Reaktionsgemisches zwischen dem *N*-phenyl-dithiocarbamidsäuren Ammoniumsalz und Chloracetonitril mit Acetanhydrid erhältlich, wahrscheinlich über 3-Phenyl-4-thiazolin-2-thion, das Davies u. a.[3] bei der Umsetzung der beiden Komponenten jedoch erfolglos zu isolieren versucht hatten.

Methyljodid führt IX in 2-Methylmerkapto-Derivat (XI) über. Seine Struktur wird ausser der Ähnlichkeit seines Infrarot-Spektrums mit denen von 2-Äthyl- und 2-Benzyl-Verdindungen intensiv von dem Austritt des Merkaptans bei der Einwirkung von Benzylamin unterstützt.



## Beschreibung der Versuche

***N*-Phenyldithiokohlensäurediester-imid (II).**—Zur Lösung von 10 g *N*-Phenyldithiocarbamidsäureäthylester und 5.0 g Chloracetonitril in 75 ml Benzol gibt man 21 ml Triäthylamin und erhitzt bei 80°C 2 Std. Nach dem Stehenlassen über Nacht macht man die Lösung von Triäthylamin-hydrochlorid frei, dampft darauf in Vakuum zum Trocknen ein und löst den kristallinen Rückstand aus Methanol um. Man erhält 7.1 g Dithiokohlensäurediester-imid als farblose Kristalle vom Schmp. 59°C.

Gef.: C, 55.85; H, 4.97; N, 11.98. Ber. für $C_{11}H_{12}N_2S_2$: C, 55.93; H, 5.08; N, 11.86%.

**2-Äthylmerkapto-3-phenylthiazonimin-pikrat (IV).**—Man setzt zur Lösung von Dithiokohlensäurediesterimid (III) (0.5 g) in Benzol Pikrinsäure in Äther zu. Beim Stehenlassen scheiden sich gelbe Nadeln aus. Durch Umlösen aus Methanol erhält man 1.25 g reines Pikrat vom Schmp. 158—159°C (Zers.).

Gef.: C, 43.97; H, 3.46; N, 15.10. Ber. für $C_{17}H_{15}N_5S_2O_7$: C, 43.85; H, 3.25; N, 15.04%.

***N*-Acetyl-2-äthylmerkaptothiazonimin-hydrochlorid (V: R=$C_2H_5$).**—Man gibt Acetylchlorid (3.0 ml) zur Lösung von 6.0 g Dithiokohlensäureimid (III) in Benzol zu und lässt das Reaktionsgemisch bei Zimmertemperatur stehen. In einigen Tagen bilden sich farblose Kristalle, und sie werden abgenutscht und getrocknet. Durch Umfällung aus der methanolischen Lösung mit Äther erhält man 5.1 g Hydrochlorid vom Schmp. 170°C (Zers.).

Gef.: C, 49.75; H, 4.81; N, 9.04. Ber. für $C_{13}H_{15}N_2S_2OCl$: C, 49.58; H, 4.80; N, 8.90%.

***N*-Acetyl-2-benzylmerkapto-3-phenylthiazoniminhydrochlorid (V: R=$CH_2Ph$).**—Zur Lösung von 4.80 g Phenyldithiocarbamidsäure-benzylester und 1.50 g Chloracetonitril in 30 ml Benzol versetzt man 8.0 ml Triäthylamin und rührt während einer Stunde bei 60°C. Nach dem Abfiltrieren des Triäthylaminhydrochlorides dampft man das Filtrat im Vakuum zum Trocknen ein, löst den öligen Rückstand wieder in Benzol, setzt darauf 2.0 g Acetylchlorid zu, dabei fällt etwas Harz aus, das durch Filtration entfernt wird. Nach dem Stehenlassen über Nacht nutscht man 2.45 g gebildete Kristalle ab, löst sie in Methanol auf und fällt mit Äther. Farblose Nädelchen vom Schmp. 120°C (Zers.).

Gef.: C, 56.93; H, 4.58; N, 7.69. Ber. für $C_{18}H_{17}N_2S_2OCl$: C, 57.37; H, 4.52; N, 7.44%.

**Überführung von 2-Äthylmerkapto-Verbindung (V: R=$C_2H_5$) in 2-Amino-Verbindung (VI).**—*Mit Morpholin.*—Man löst 0.4 g 2-Äthylmerkapto-Verbindung in 6 ml Äthanol und setzt darauf mit 0.12 g Morpholin um. Unter Merkaptanaustritt lässt man die Lösung bei Raumtemperatur 2 Std. stehen und bei Zusatz von Äther scheiden sich farblose Kristalle aus, die abgenutscht und aus Methanol/Äther umkristallisiert werden; 0.2 g *N*-Acetyl-2-morpholino-3-phenylthiazonimin-hydrochlorid (VI: R'R''N=O($CH_2CH_2CH_2$)$_2$N) als farblose Nädelchen vom Schmp. etwa 260°C (Zers.).

Gef.: C, 53.15; H, 5.66; N, 12.40. Ber. für $C_{15}H_{18}N_3O_2SCl$: C, 53.00; H, 5.32; N, 12.37%.

*Mit Benzylamin.*—Zur Lösung von 0.40 g. 2-Äthylmerkapto-Verbindung in Methanol (2 ml) setzt man 0.14 g Benzylamin zu, wobei es gleich nach Merkaptan riecht, erwärmt um 50°C während einer Stunde und lässt über Nacht stehen. Nach tropfenweisem Zusatz von Äther fällt zuerst etwas von Benzylaminhydrochlorid aus, das sofort abfiltriert wird, dann tropft man in das Filtrat weiter Äther ein und nutscht 0.1 g *N*-Acetyl-2-benzylamino-3-phenylthiazonimin-hydrochlorid (VI: R'=$PhCH_2$, R''=H) als gelbliche Kristalle ab, die aus Methanol/Äther umkristallisiert werden und um 190°C unter Zersetzung schmelzen.

Gef.: C, 60.07; H, 5.23; N, 11.72. Ber. für $C_{13}H_{18}N_3OSCl$: C, 60.08; H, 5.03; N, 11.68%.

*Mit Cyclohexylamin.*—Gleicherweise erhält man aus 0.68 g 2-Äthylmerkapto-Verbindung und 0.22 g Cyclohexylamin in 10 ml Methanol 0.1 g *N*-Acetyl-2-cyclohexylamino-3-phenylthiazonimin-hydrochlorid (VI: R'=H, R''=CH($CH_2$)$_5$) vom Schmp. etwa 218°C (Zers.).

Gef.: C, 58.04; H, 6.35; N, 11.98. Ber. für $C_{17}H_{22}N_3OSCl$: C, 58.05; H, 6.31; N, 11.94%.

**Umsetzung von 2-Äthylmerkapto-Verbindung (V: R=$C_2H_5$) mit Anilin.**—Der Merkaptanaustritt bei der Umsetzung von 0.40 g 2-Äthylmerkapto-Verbindung mit 0.12 g Anilin in Methanol geschieht erst unter Rückfluss und 0.15 g gelbliche, halogen-haltige, in Wasser lösliche Nädelchen vom Schmp. 85°C werden bei Zusatz von Äther niedergeschlagen.

3) W. Davies J. A. Maclaren und L. R. Wilkinson, *J. Chem. Soc.*, **1950**, 3491.

Gef.: C, 45.75; H, 5.60; N, 8.19%.

**Cyanmethyl *N*-Phenylthiolmorpholinimidat (VII).**—In trocknem Dioxan (50 ml) löst man 2.7 g Chloracetonitril und 7.5 g Morpholin-4-thiokohlensäureanilid (VIII), das beim Gemisch von Morpholin und Phenylisothiocyanat in Aceton unter Kühlung glatt hergestellt wird, setzt darauf Triäthylamin (14 ml) zu und erhitzt 3 Std bei 70°C unter Rühren. Nach dem Stehenlassen über Nacht und dem Abfiltrieren von ausgeschiedenem Triäthylamin-hydrochlorid dampft man das Filtrat im Vakuum ein und erhält als Rückstand 5.57 g Kristalle vom Schmp. 78—90°C. Durch dreimaliges Umkristallisieren aus Methanol ergeben sich reiner Isothioharnstoff (VII) vom Schmp. 85—88°C als farblose Säulen, die während langem Stehenlassen in der Luft verbraunt sind.

Gef.: C, 59.64; H, 5.84; N, 16.23. Ber für $C_{13}H_{15}N_3OS$: C, 59.76; H, 5.79; N, 16.08%.

***N*-Acetyl-2-morpholino-3-phenylthiazoniminhydrochlorid (VI: $R'R''N=O(CH_2CH_2)_2N$).**—Wenn man zur Lösung von 1.0 g *S*-Cyanmethylisothioharnstoff (VII) in trocknem Benzol (15 ml) 0.5 g Acetylchlorid zusetzt, wird die Lösung trübe und bald scheiden sich farblose Kristalle aus. Nach dem Stehenlassen über Nacht nutscht man sie ab, versetzt in wenig Methanol, filtriert die in Methanol unlösliche Verbindung ab, setzt dem Filtrat Äther tropfenweise zu und erhält 0.1 g farblose Nädelchen vom Schmp. etwa 260°C (Zers.). So erhaltenes *N*-Acetyl-2-morpholino-3-phenylthiazonimin-hydrochlorid hat keine Schmp.-Depression mit oben erhaltenem ergeben; Infrarot-Spektren sind praktisch identisch.

**Reaktion von 2-Äthylmerkapto-Verbindung (V: $R=C_2H_5$) mit Natriumhydrogencarbonat.**—Man rührt die wässrige Lösung von 0.5 g 2-Äthylmerkapto-Verbindung und 0.20 g Natriumhydrogencarbonat 2 Std bei Raumtemperatur, extrahiert mehrmals mit Chloroform, trocknet die Auszüge und dampft ein. Man erhält 0.35 g kristallinen Rückstand, der in Methanol gelöst und mit Petroläther in reiner Form niedergeschlagen wird. Diese orangen, halogenfreien, strukturunbekannten Kristalle sind in der Luft verfärbt, schmelzen unter Zersetzung bei etwa 140°C und zeigen den folgenden Analysenwert; C, 55.81; H, 6.06; N, 9.94%.

**Reaktion von 2-Äthylmerkapto-Verbindug (V: $R=C_2H_5$) mit Natriumsulfid.**—Zur wässrigen Lösung von 0.45 g 2-Äthylmerkapto-Verbindung setzt man eine Lösung von 0.35 g Natriumsulfidnonahydrat zu, rührt darauf während einer Stunde bei Raumtemperatur (Geruch nach Merkaptan), und filtriert 0.20 g ausgefallene Kristalle. Aus dem Filtrat extrahiert man dieselben (0.1 g) mit Chloroform. Durch Umkristallisieren aus Chloroform/Petroläther wird 3-Phenyl-4-acetamido-4-thiazolin-2-thion (IX) gereinigt, das bei 182—183°C schmilzt.

Gef.: C, 52.82; H, 4.25; N, 11.41. Ber. für $C_{11}H_{10}N_2S_2O$: C, 52.80; H, 4.04; N, 11.20%.

Infrarot-Spektrum: 3220 (NH), 1680 (CO), 1608 (C=C) $cm^{-1}$.

**3-Phenyl-4-acetamido-4-thiazolin-2-thion (IX).**—Setzt man zur Suspension von 5.00 g Ammoniumsalz der *N*-Phenyldithiocarbamidsäure in Chloroform 2.03 g Chloracetonitril unter Kühlung zu, so tritt die Reaktion alsbald unter Erwärmung ein, man lässt darauf eine Stunde stehen, setzt nach dem Freisetzen vom Ammoniumchlorid die dunkel verbraunte Lösung mit Acetanhydrid um und lässt zwei Tage stehen. Nach dem Zusatz von Petroläther nutscht man ausgefallene Kristalle ab: 2.6 g gelbliche Blättchen, die aus Choroform/Petroläther gereinigt werden, bei 182—183°C schmelzen und gemäss Misch-Schmp. und Infrarot-Spektrum mit oben erhaltenem 3-Phenyl-4-acetamido-4-thiazolin-2-thion (IX) identisch sind.

**Säure Hydrolyse von 3-Phenyl-4-acetamido-4-thiazolin-2-thion (IX).**—Eine Suspension von 0.10 g 3-Phenyl-4-acetamid-4-thiazolin-2-thion in 2N Salzsäure kocht man 2 Std unter Rückfluss und nutscht dann ab: 0.07 g gelbliche Kristalle (aus Chloroform/Petroläther), deren Identifizierung mit 3-Phenylrhodanin (X) das Infrarot-Spektrum zugrunde liegt.

**Überführung von 3-Phenyl-4-acetamido-4-thiazolin-2-thion (IX) in 2-Methylmerkapto-3-phenylthiazonimin-hydrojodid (XI).**—Man kocht 0.55 g 3-Phenyl-4-acetamido-4-thiazolin-2-thion und 0.70 g Methyljodid in 5 ml Methanol 15 Minuten unter Rückfluss, setzt Äther nach Kühlung tropfenweise zu und nutscht 0.65 g ausgeschiedene gelbe Nadeln ab, die hygroskopisch sind und bei 100—120°C schmelzen. Durch Umkristallisieren aus Methanol/Äther ergeben sich reines 2-Methylmerkapto-3-phenylthiazonimin-hydrojodid (XI) vom Schmp. 126—128°C (Zers.) als gelbliche Nadeln.

Gef.: C, 36.89; H, 3.61; N, 7.42. Ber. für $C_{12}H_{13}N_2S_2OJ$: C, 36.70; H, 3.32; N, 7.15%.

*Laboratorium für Organische Chemie*
*Tokyo Institut für Technologie*
*Ookayama, Tokyo*

# The Hydroesterification of Propylene with Carbon Monoxide and Methanol in the Presence of Dicobalt Octacarbonyl

By Akio MATSUDA and Hiroshi UCHIDA

(Received June 24, 1964)

The syntheses of esters from olefins, alcohols, and carbon monoxide in the presence of dicobalt octacarbonyl, that is, the hydroesterification of olefins,[1] have been investigated by Natta and his co-workers.[2,3] This reaction is of a considerable interest from the industrial point of view, however, its application to industry has not yet been realized. This may have been due to the fact that this reaction proceeds at a rate much slower than the hydroformylation reaction. Starting with propylene and methanol, the authors of this paper have succeeded in increasing the reaction rate of hydroesterification to such a high level as to be comparable with that of hydroformylation. The details of the rate and the yields of products will be reported in this paper.

## Experimental

The hydroesterification reactions were carried out by using the same 300-cc. stainless-steel autoclave as was used in the hydroformylation reaction of propylene.[4] The procedure was essentially the same as the one previously used except that in most of the runs a small amount of hydrogen was added to the autoclave from a 30-cc. hydrogen-pressure storage before carbon monoxide was introduced from another 500-cc. carbon monoxide pressure storage. The amount of hydrogen introduced was calculated from the pressure drop in the former pressure storage. After the temperature and pressure had been adjusted to definite levels, the stirrer was started. The dicobalt octacarbonyl in a stainless saucer held on a wing of the stirrer was allowed to drop into the liquid phase, and the reaction began. During the reaction period, carbon monoxide was continuously introduced from the pressure storage through a needle valve in order to maintain the autoclave pressure at a constant level of 190 kg./cm$^2$. The pressure in the pressure storage tended to drop as the reaction proceeded, but a simple recording of the pressure drops with time could not always serve as a measurement of the initial rate of hydroesterification, because the hydroesterification and the hydroformylation occurred simultaneously. As it was, the initial rate of the two reactions was determined independently by analyses of the product; samples of a small portion of the liquid product were withdrawn from the autoclave at time intervals during the reaction and were analyzed for methyl butyrate and butyraldehyde dimethylacetal. The former is the product of the hydroesterification of propylene, while the latter is the product formed by the combination of the butyraldehyde formed by the hydroformylation and methanol. The samples were analyzed by means of gas chromatography using a 4 m. column of triethanolamine on cellite at 80°C.[5] Ethylbenzene was used as an internal reference. The gaseous product was analyzed in the same way as has been described previously.[4]

Commercially-available propylene, methanol, and pyridine were used. Propylene was 93% pure and contained 6.5% propane and 0.5% ethane. Methanol and pyridine were distilled before use. The procedure for the preparation of dicobalt octacarbonyl, $Co_2(CO)_8$, was quite the same as has been mentioned previously.[4] Carbon monoxide was prepared by decomposing commercial formic acid with sulfuric acid and was more than 97% pure, containing less than 0.5% hydrogen.

## Results and Discussion

The hydroesterification of propylene using carbon monoxide of a high purity usually proceeds at a much slower rate than the hydroformylation with the $1H_2$-1CO synthesis gas. It has now been found that the addition of even a small amount of hydrogen into the autoclave results in a considerable increase in the rate of propylene conversion, and that some amounts of butyraldehyde dimethylacetal are also produced as a result of the hydroformylation of propylene.

In this connection, attention should be called to the finding of Wender et al.,[6] who stated that the rate of the hydroformylation of cyclohexane is increased by the addition of very small amounts of organic bases and decreased when larger amounts of these bases are present.

1) I. Wender and H. W. Sternberg, "Advances in Catalysis," VII, Academic Press, N. Y. (1955), p. 604.
2) G. Natta, *Brennstoff-Chem.*, **36**, 176 (1955).
3) R. Ercoli, M. Avanzi and G. Moretti, *La Chimica e L'industria*, **37**, 865 (1955).
4) H. Uchida and A. Matsuda, This Bulletin, **37**, 375 (1964).
5) Such standard samples for the gas chromatographic analyses as methylesters of *n*- and isobutyric acids and dimethylacetals of *n*- and isobutyraldehydes were prepared by a reaction of the respective acids and aldehydes with methanol in the presence of *p*-toluenesulfonic acid; they were distilled before use by the aid of a rectifying column of the spinning-band type.
6) I. Wender, H. Greenfield, S. Martin and M. Orchin, "Catalysis," V. Reinhold Publishing, N. Y. (1957), p. 110.

Table I. Preliminary experiments

| Expt. No.[a] | Hydrogen mol. | Pyridine mol. | Propylene conversion mol.% | Products yields per mol. $C_3H_6$ after 1 hr.'s reaction, mol. | | | |
|---|---|---|---|---|---|---|---|
| | | | | *n*-Ester | *i*-Ester | *n*-Acetal | *i*-Acetal[b] |
| 1 | None | None | 45 | 0.32 | 0.09 | 0.01 | 0.004 |
| 2 | 0.1 | None | 69 | 0.46 | 0.12 | 0.07 | 0.03 |
| 3 | 0.1 | 0.03 | 93 | 0.64 | 0.19 | 0.07 | 0.03 |

a) Every run was conducted at the total pressure of 190 kg./cm² at 180°C by use of 0.5±0.01 mol. $C_3H_6$, 2 mol. $CH_3OH$, and 4 mmol. $Co_2(CO)_8$ with or without hydrogen and pyridine.
b) Abbreviations *n*-, *i*-esters and *n*-, *i*-acetals stand for methyl esters of *n*- and isobutyric acids, and dimethylacetals of *n*- and isobutyraldehydes respectively.

Table II. Effects of organic bases on the yields of products

| Expt. No. | Base | Amount of base mol. | Propylene conversion mol. % | Products yields per mol. $C_3H_6$ after 1 hr.'s reaction, mol. | | | |
|---|---|---|---|---|---|---|---|
| | | | | *n*-Ester | *i*-Ester | *n*-Acetal | *i*-Acetal |
| 4 | None | 0 | 41 | 0.26 | 0.08 | 0.02 | 0.01 |
| 5 | Pyridine | 0.02 | 73 | 0.51 | 0.14 | 0.02 | 0.01 |
| 6 | Pyridine | 0.04 | 85 | 0.62 | 0.17 | 0.03 | 0.01 |
| 7 | Pyridine | 0.06 | 92 | 0.67 | 0.19 | 0.02 | 0.01 |
| 8 | *N*,*N*-Dimethylaniline | 0.04 | 42 | 0.28 | 0.08 | 0.02 | 0.01 |
| 9 | Quinoline | 0.04 | 54 | 0.39 | 0.11 | 0.02 | 0.01 |
| 10 | α-Picoline | 0.04 | 45 | 0.32 | 0.09 | 0.02 | 0.01 |
| 11 | Triethylamine | 0.004 | 40 | — | — | — | — |
| 12 | Triethylamine | 0.02 | 0 | 0.26 | 0.08 | 0.02 | 0.01 |
| 13 | Piperidine | 0.004 | 37 | — | — | — | — |
| 14 | Piperidine | 0.02 | 0 | — | — | — | — |
| 15 | Benzylamine | 0.02 | 0 | — | — | — | — |
| (16 | Zinc acetate | 0.008 | 0 | — | — | — | —) |

The raw material consisted of 0.5±0.01 mol. $C_3H_6$, 2 mol. $CH_3OH$, and was added with 4 mmol. $Co_2(CO)_8$. A small amount of hydrogen (0.02 mol.) was introduced before the autoclave was pressured with CO. Every run was conducted at the total pressure of 190 kg./cm² at 160°C.

This finding suggests that the addition of an appropriate amount of organic bases might serve to improve the selectivity for hydroesterification, even though it might retard the rate of propylene conversion to some extent. A few preliminary experiments made along this line have surprisingly proved that the addition of such a large amount of pyridine as 0.03/0.004 in terms of moles of pyridine/moles of $Co_2(CO)_8$ ratio not only improves the selectivity for hydroesterification, but also increases the rate of propylene conversion (cf. Table I). Accordingly, the effect of a variety of organic bases on the yield of the hydroesterification product will have to be examined more closely.

**The Effect of Bases on the Yield of Hydroesterification Product.** — Table II summarizes data obtained on the hydroesterifications in the presence of different amounts of various organic bases. Among the bases studied, pyridine has been found to be most effective in the production of methylbutyrate, and the yield increases with the amount of pyridine in the range under investigation; by the use of 0.06 mol. pyridine, the yield of the reaction for 1 hr. attains as high a level as 0.86 mol. from 1 mol. propylene. In contrast to this base, such strong bases as triethylamine, piperidine, and benzylamine inhibit the hydroesterification completely, even in the relatively small amount of 0.02 mol. The effects of *N*,*N*-dimethylaniline, quinoline, and α-picoline on the yield are very small.[7] Further investigation, therefore, will be directed to the problem of the presence of pyridine.

Figures 1, 2 and 3 illustrate plots of the amounts of methyl butyrate and of butyraldehyde dimethylacetal produced vs. the reaction time at the reaction temperatures of 160, 170 and 180°C respectively. The runs were conducted by using the same amounts of raw materials, of hydrogen, and of $Co_2(CO)_8$, as in the runs of Table II, but pyridine was varied

7) The hydroesterification does not take place at all in the presence of a very small amount of zinc acetate, which reacts readily with $Co_2(CO)_8$ to form the mixed metal carbonyl.

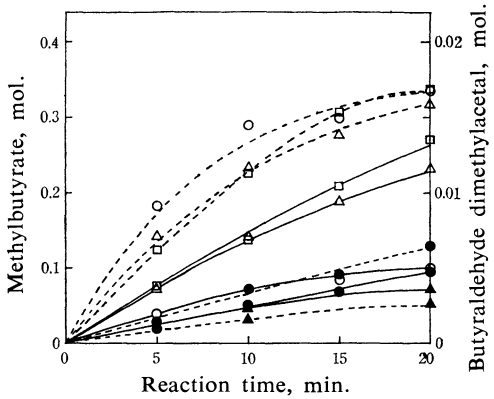



Fig. 1. Products yields from hydroesterification and hydroformylation in the presence of varying amounts of pyridine as function of reaction time.
Full line; methyl butyrate
Dotted line; butyraldehyde dimethylacetal
React. temp., 160°C

| Expt. No. | 17 | 18 | 19 | 20 | 21 |
|---|---|---|---|---|---|
| Pyridine, mol. | 0 | 0.03 | 0.06 | 0.09 | 0.12 |
| Mark | ○ | △ | □ | ● | ▲ |

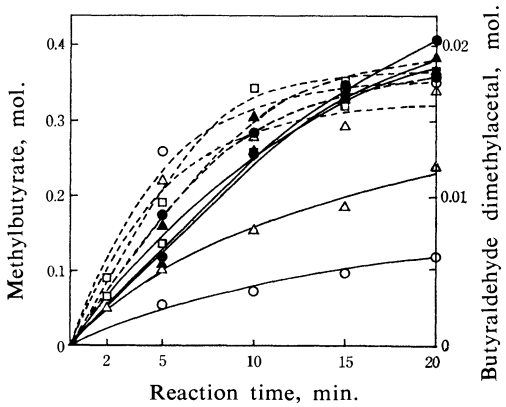



Fig. 2. Products yields from hydroesterification and hydroformylation in the presence of varying amounts of pyridine as function of reaction time.
Full line; methyl butyrate
Dotted line; butyraldehyde dimethylacetal
React. temp., 170°C

| Expt. No. | 22 | 23 | 24 | 25 | 26 |
|---|---|---|---|---|---|
| Pyridine, mol. | 0 | 0.03 | 0.06 | 0.09 | 0.12 |
| Mark | ○ | △ | □ | ● | ▲ |

in amount at 0.03 mol. intervals between 0 and 0.12 mol. The figures show that, throughout every series of runs at the different reaction temperatures, the amount of methyl butyrate produced after a 20 min. reaction increases with the amount of pyridine, reaches a maximum, and then decreases. The optimum amount of pyridine is increased as the reaction temperature is raised.

As is evident from the formula of $C_3H_6+CO+H_2 \rightarrow C_3H_7CHO$ for the hydroformylation, the

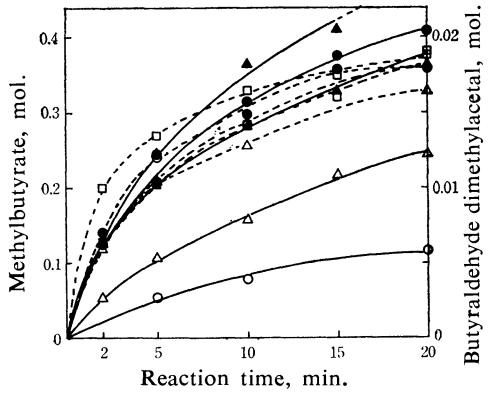



Fig. 3. Products yields from hydroesterification and hydroformylation in the presence of varying amounts of pyridine as function of reaction time.
Full line; methyl butyrate
Dotted line; butyraldehyde dimethylacetal
React. temp., 180°C

| Expt. No. | 27 | 28 | 29 | 30 | 31 |
|---|---|---|---|---|---|
| Pyridine, mol. | 0 | 0.03 | 0.06 | 0.09 | 0.12 |
| Mark | ○ | △ | □ | ● | ▲ |

hydrogen in an autoclave tends to diminish as the hydroformylation proceeds, and the amount of butyraldehyde or its dimethylacetal in the products can not exceed 0.02 mol., which is equivalent to the initial hydrogen content in the autoclave. In fact, the acetal remains about 0.018 mol. at the most. These facts make it difficult to estimate the selectivity for hydroesterification from a simple comparison of the experimental rate of hydroesterification with that of hydroformylation, unless a certain attention is paid to the amount of hydrogen existing in the autoclave. In connection with this, a more reasonable measure of the selectivity may be given by means of the ratio of the initial rate at the zero-conversion of propylene for hydroesterification (hereafter denoted by $r_{oe}$) to the corresponding rate for hydroformylation (hereafter denoted by $r_{of}$); at this stage, the amount of hydrogen is 0.02 mol. The values of $r_{oe}$ and $r_{of}$ are obtained from slopes of the tangents drawn along the plots at the origin.

**The Effect of Pyridine on the Initial Rates of Hydroesterification and Hydroformylation at Zero-conversion.**—Figure 4 illustrates the plots of $r_{oe}$ vs. the amount of pyridine for series of runs at 160, 170, and 180°C. Every plot first rises with the amount of pyridine, and in each the rise at the higher temperature is more rapid than that at the lower temperature. At 160 and 170°C, the maximum of the curve appears at the pyridine amount of 0.06 mol., whereas at 180°C the $r_{oe}$ is maintained essentially constant over the range from 0.06 to 0.12 mol. of pyridine.

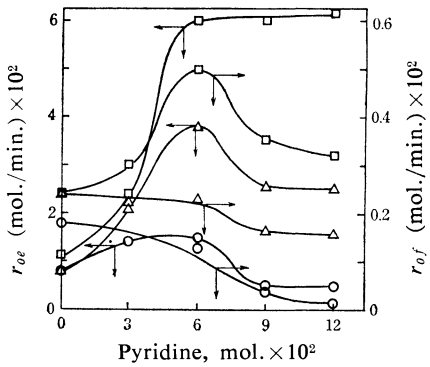



Fig. 4. Initial rates at zero-conversion of propylene for hydroesterification ($r_{oe}$) and hydroformylation ($r_{of}$) as function of pyridine amount.
React. temp.: ○ 160°C, △ 170°C, □ 180°C

Figure 4 includes the same plots with respect to $r_{of}$. The situation is different from that of $r_{oe}$; the plots of $r_{of}$ at 160 and 170°C continue to be lowered slowly with the amount of pyridine, but the plot at 180°C shows a slight maximum at 0.06 mol. The retarding effect of pyridine on the initial hydroformylation rate becomes so remarkable at lower reaction temperatures that the reaction at 160°C is almost completely inhibited by the addition of 0.12 mol. of pyridine.

Figure 5A presents selectivity data for hydroesterification at 160, 170, and 180°C. The curve at 180°C shows an approximately linear increase over the whole range of pyridine amount studied, whereas the curves at 160 and 170°C show the increase only in the range below 0.06 mol. Beyond that amount of pyridine, the ratios stay on the same level, about 12. It should be noted that the molar ratio, $C_3H_7CHO/C_3H_7CH(OCH_3)_2$, after the reaction of 1 hr. is much higher than the $r_{oe}/r_{of}$ ratio; e. g., the former ratio from run No. 7 in Table II is twice as large as the latter ratio of run No. 29. The ratio of $r_{oe}/r_{of}$ thus can not directly relate the yield ratio after a prolonged duration of a batchwise reaction, where the initial hydrogen is allowed to diminish as the reaction proceeds.

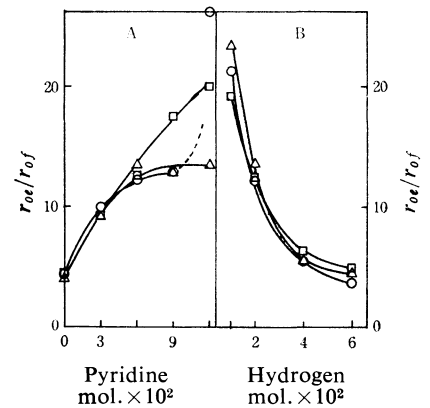



Fig. 5A and 5B. Ratio $r_{oe}/r_{of}$ as function of amount of pyridine (A) and of hydrogen (B).
React. temp.: ○ 160°C, △ 170°C, □ 180°C

**The Effect of Hydrogen on the Initial Rates of Hydroesterification and Hydroformylation at Zero-conversion.**—The $r_{oe}$ and $r_{of}$ values in the presence of various amounts of hydrogen in an initial charge of autoclave were determined by the above-described method. The runs for this purpose were always conducted with the same amounts of raw materials, while the pyridine amount was fixed at 0.06 mol. The hydrogen amount was varied at intervals from 0 to 0.06 mol. Figure 6 illustrates plots of $r_{oe}$ vs. the initial hydrogen amount in the autoclave at 160, 170, and 180°C. Every curve first rises with the amount of hydrogen, reaches a maximum, and then decreases slowly. The rise of the curve at the high temperature is more rapid than that at the lower temperature; at 180°C, the $r_{oe}$ in the presence of 0.02 mol. hydrogen can be five times as fast as the $r_{oe}$ in its absence. It is natural that the $r_{of}$ should increase with the hydrogen amount, as is shown in Fig. 6.[8]

As is shown in Fig. 5B, three plots at 160, 170, and 180°C of $r_{oe}/r_{of}$ vs. the initial amount of hydrogen similarly decrease with the amount of hydrogen. The initial hydrogen amount in an autoclave should be less than 0.01 mol. in order to have such a high selectivity for the hydroesterification as 15 in terms of the $r_{oe}/r_{of}$ ratio. This initial hydrogen content in the

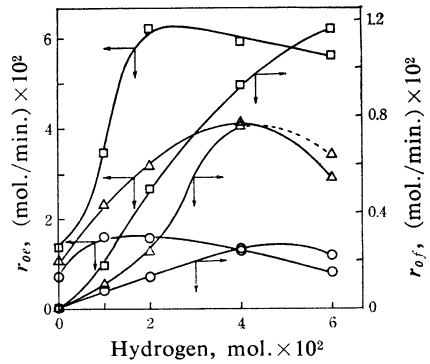



Fig. 6. Dependency of $r_{oe}$ and $r_{of}$ on hydrogen amount.

| | Expt. No. | React. temp. |
|---|---|---|
| -○- | 32—35 | 160°C |
| -△- | 36—39 | 170°C |
| -□- | 40—43 | 180°C |

8) Figure 6 indicates falls in both the $r_{oe}$ and $r_{of}$ by the addition of 0.06 mol. hydrogen at the lower reaction temperatures. There is, as yet, no probable explanation of this finding.

autoclave at the reaction conditions is equivalent to 0.013 in terms of the $H_2/CO$ molar ratio.

**The Initial Rate of Hydroesterification as a Function of the Propylene Concentration.**—Although Ercoli et al.[3] have pointed out the zero-order reaction of the hydroesterification of olefins, such as 1-hexene, cyclohexene, and 2-ethyl-1-hexene, with respect to the olefin concentration, the data presented here on this reaction of propylene, as shown in Figs. 1—3, are rather suggestive of another order, presumably of the first order. However, the experimental runs in the figures were conducted in such a manner that the hydrogen in an initial charge of the autoclave was allowed to decrease with the progress of a simultaneous side-reaction, hydroformylation; hence, the data are not sufficient for us to draw a conclusion from them. An alternative run, therefore, was attempted, in which the hydrogen content was kept at a constant level during the run. The autoclave was charged with the raw material consisting of 0.51 mol. of $C_3H_6$, 2 mol. of $CH_3OH$, 0.06 mol. of pyridine, and 1 mmol. of $Co_2(CO)_8$ placed in a stainless steel saucer; then carbon monoxide containing 2.7% hydrogen was introduced. The initial hydrogen in the gas phase under the reaction conditions amounted to 1.9 mol.%. During the run, the synthesis gas (composed of 91.9% CO, 6.3% $H_2$, and 1.8% $N_2$) was continuously introduced from the pressure storage in order to maintain the total pressure at 190 kg./cm$^2$ at 180°C, and pressure drops in the storage with the reaction time were recorded, from which values the amounts of the gas supplied, $V_s$ (mol.), could be calculated.

When the run was finished, after 1 hr., $V_s$ amounted to 0.526 mol., and propylene was reduced to 0.05 mol. from 0.51 mol., corresponding to a 90% conversion of propylene. The hydrogen was found to be 1.7 mol. %, almost the same as the initial content. The products were 0.32, 0.09, 0.02, and 0.01 mol. for methyl esters of *n*- and isobutyric acids and for dimethylacetals of *n*- and isobutyraldehydes respectively. The sum of products was 0.44 mol. No products other than ethyl acetate[9] (less than 0.005 mol.) were detected. On the basis of these data, the percentage conversion of propylene was calculated to be 86%; this rate is close to, but not identical with, the value obtained from the data of propylene consumption.[11]

In a previous paper[4] dealing with the hydroformylation of propylene, it was described how the amount of synthesis gas supplied stands for the sum of two portions, one consumed by the hydroformylation itself and the other, that necessary to compensate for the fall in partial propylene pressure as the reaction proceed, and that the amount of gas supplied for a hydroformylation run, $V_{sf}$ (mol.), is expressed by:

$$\left.\begin{aligned} & V_{sf}=2(c_0-c)+ap_0(c_0-c)/c_0 \\ \text{or} \quad & V_{sf}=(2+ap_0/c_0)(c_0-c) \end{aligned}\right\} \quad (1)$$

where $c_0$ (mol.) is the initial propylene concentration; $c$ (mol.) is the concentration at the reaction time $t$, $p_0$ is the initial partial propylene pressure, and $a$ is a coefficient whose value is dependent on the reaction temperature. Similarly, the amount of gas supplied for a run of hydroesterification, $V_{se}$ (mol.), is expressed by:

$$V_{se}=(1+ap_0/c_0)(c_0-c) \quad (2)$$

In the present run, in which both of the reactions occur, the amount of gas supplied, $V_s$ (mol.), is, hence, given by Eq. 3, if it may be assumed that the (moles of gas consumed by hydroestrification)/(moles of gas consumed by hydroformylation) ratio remains invariable during the run.

$$V_s=\alpha(c_0-c) \quad (3)$$

where $\alpha$ is a coefficient whose value lies in a range between $(2+ap_0/c_0)$ and $(1+ap_0/c_0)$.

The substitution of the experimental data of $V_s$ at $t=60$ min. (0.526 mol.), $c_0$ (0.51 mol.), and $c$ at $t=60$ min. (0.05 mol.) into Eq. 3 results in the evaluation of $\alpha$ as 1.14.[12] Once $\alpha$ is evaluated, $c$ at any $t$ can, in turn, be calculated by the aid of Eq. 3.

As is shown in Fig. 7, a plot of $(c_0-c)$ vs. $t$ is not linear, whereas a plot of $\ln(c_0/c)$ is linear. This finding leads to the following expression of the over-all initial rate of propylene consumption, $r$ (mol./min.):

$$r=-dc/dt=kc \quad (4)$$

In the present run, the over-all initial rate is the sum of two initial rates, the initial rate of propylene consumption by hydroesterification, $r_e$, and the initial rate by hydroformylation, $r_f$:

$$r=r_e+r_f=kc \quad (5)$$

On the other hand, it has already been shown that the $r_f$ is of the first-order with respect to propylene concentration, namely, $r_f=k'c'$, hence,

9) Ethylacetate can be a product of acetaldehyde, which is produced from methanol under the reaction conditions of oxo synthesis (cf. Ref. 10).

10) G. Natta and R. Ercoli, "Catalysis," II, Reinhold Publishing, N. Y. (1957), p. 171.

11) The disagreement may perhaps be due to an inaccuracy in the determinations of propylene and its products.

12) This value of $\alpha$ is applicable only to the data of the present run.

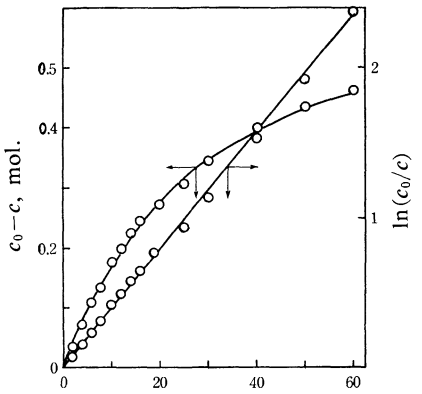



Fig. 7. Amount of propylene consumed under high pressure of carbon monoxide containing hydrogen at 180°C plotted against reaction time (Expt. No. 44).

$$r_e+k'c=kc \quad \text{or} \quad r=(k-k')c \qquad (6)$$

Equation 6 plainly indicates that the initial rate of hydroesterification is first-order with respect to propylene concentration, provided that the run is conducted in the presence of excess pyridine and with carbon monoxide containing a small amount of hydrogen.

Runs (No. 45—47) were conducted with pure carbon monoxide[13] in order to compare them with run No. 44. In these runs, the same amounts of propylene and methanol as in run No. 44 were used with no pyridine, while $Co_2(CO)_8$ was varied in amount over a range from 1 to 4 mmol. The data are presented as plots of $(c_0-c)$ vs. $t$. The plots are linear, showing that the hydroesterification is zero-order with respect to propylene concentration, in accordance with the result of Ercoli et al.[3] Moreover, an approximately linear relationship is found between the initial rate and the amount of $Co_2(CO)_8$. It should also be noted that the initial rate, as conventionally expressed by $(c_0-c)/t$ (mol./min.), where $(c_0-c)=0.1$ mol., of run No. 44 in Fig. 7 is about 30 times as high as the rate of run No. 45 in Fig. 8 with the same amount of $Co_2(CO)_8$ (1 mmol.).

Ercoli et al.[3] stated that cobalt hydrocarbonyl can be the real catalyst for the hydroesterification of olefins. Therefore, it is likely that the addition of hydrogen results in an increase in the initial rate, for the addition considerably facilitates the formation of the hydrocarbonyl. However, in the presence of excess pyridine and methanol, other salts, which contain $[Co(CO)_4]^-$ as an anionic constituent, can be formed. These salts may be, for instance, $[Co(CH_3OH)_6][Co(CO)_4]_2$, $[Co(Pyr)_6][Co(CO)_4]_2$, and $[PyrH][Co(CO)_4]$, and they presumably participate in the reaction as catalysts, either positive or negative. However, no satisfactory interpretation of the effects of hydrogen and pyridine on the initial rate of this reaction can be expected until sufficient knowledge of the catalyst materials and their catalytic behaviors are available.

13) The carbon monoxide contained 0.3% hydrogen.

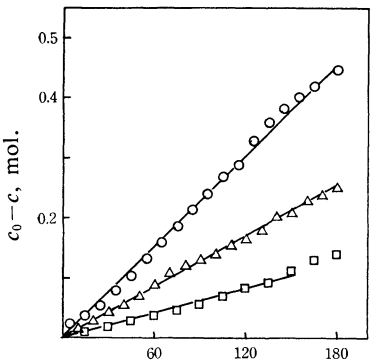



Fig. 8. Amount of propylene consumed under high pressure of pure carbon monoxide at 180°C plotted against reaction time.

| | Expt. No. | $Co_2(CO)_8$, mmol. |
|---|---|---|
| -□- | 45 | 1 |
| -△- | 46 | 2 |
| -○- | 47 | 4 |

## Summary

Propylene can be hydroesterified to methyl butyrate in a good yield and with an initial rate as high as the initial rate of the hydroformylation of propylene, provided a small amount of hydrogen and excess pyridine are present. Detailed data on the initial rates at the zero-conversion of propylene for both the hydroesterification and hydroformylation and the ratio between the two initial rates have been presented as a function of the amount of pyridine and hydrogen, together with data on the products obtained from the respective reactions.

The initial rate of hydroesterification in this study has proved to be first-order with respect to the propylene concentration. This result is different from that of Ercoli et al., who carried out hydroesterification runs of olefins with pure carbon monoxide.

The authors wish to thank Mr. Teiichi Ikeda for his participation in a part of this work.

*Government Chemical Industrial Research Institute, Tokyo*
*Shibuya-ku, Tokyo*

# Effect of Density in the Radiolysis of *n*-Butane

By Tetsuo MIYAZAKI and Shoji SHIDA

(Received June 26, 1964)

The radiolysis of *n*-butane has been studied by several investigators. We reported in a previous paper[1] on the difference between the gas-phase and the condensed-phase radiolyses of *n*-butane and concluded that the fragmentation of the butane ion is important in the gas-phase radiolysis, while that of the butane molecule is predominant in the liquid-phase radiolysis. In order to obtain further information on the different mechanisms involved in the two phases, we have now undertaken a study of the radiolysis of *n*-butane near the critical state. Toi et al.[2] reported on the effect of the density in the radiolysis of ammonia at the critical temperature and found sharp decreases in $G(H_2)$ and $G(N_2)$ in the density region from 0.05 to 0.15 g. $cc^{-1}$. Hotta[3] reported the radiolysis of ethane at high pressures and found a decrease in $G(H_2)$ in the density region from 0.08 to 0.14 g. $cc^{-1}$. Recently Ausloos et al.[4] reported the effect of pressure from 0.05 atm. to 180 atm. in the radiolysis of methane.

In the present work the yields of propane and methane have been found to decrease sharply in the 0—0.1 g. $cc^{-1}$ density region. The results are interpreted in terms of the deactivation of excited ions.

## Experimental

The sample and the analytical procedure are similar to those described before.[1] The critical temperature, pressure and density of *n*-butane are 152°C, 37.5 atm. and 0.228 g. $cc^{-1}$ respectively. The samples were irradiated at 170°C with $\gamma$-rays from cobalt-60 of 16000 c.

Stainless-steel autoclaves have usually been used in high-pressure experiments, but they have some drawbacks, such as the condensation of *n*-butane in the needle valve, contamination by air during the sampling procedure, etc. Therefore, it is useful to use a glass reaction cell, even in a high-pressure experiment. The authors found that a glass cell with a small diameter can bear a pressure of 40 atm. After pure *n*-butane had been sealed off in a glass cell (0.5 cm. external diameter, 0.3 cm. inner diameter and 6 cm. long), the cell was placed in a stainless steel autoclave (30 cc.; 2 cm. inner diameter); the latter was then surrounded by a heated jacket which permitted the temperature to be controlled within ±2°C at 170°C.

The energy absorbed in *n*-butane was calculated from Fricke dosimetry without using any correction factor,[2] on the assumption that the energy input is simply proportional to the electron density. The energy absorbed in the low density is due almost entirely to secondary electrons produced by $\gamma$-ray absorption in the glass vessel wall. If the stopping power per electron in *n*-butane is assumed to be the same as that in the wall, the energy absorbed in *n*-butane of a low density can be determined directly from Fricke dosimetry,[5] as in the liquid. In the intermediate density region, however, it might be necessary to use some correction factor in calculating the energy absorbed.

## Results and Discussion

The variation in the major products of the radiolysis of *n*-butane in the density region from the gas phase of 3.8 atm. to the liquid phase is shown in Table I and Fig. 1. The

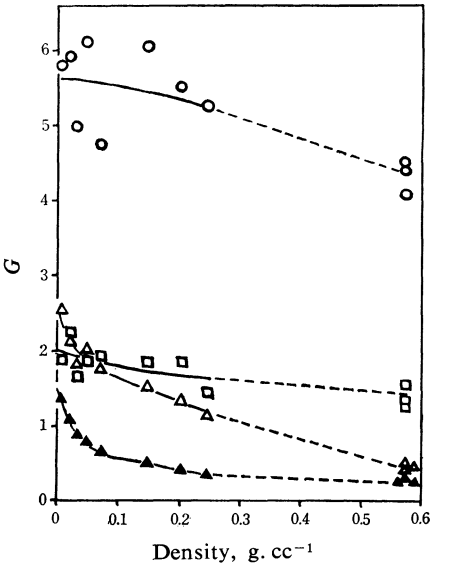



Fig. 1. Variation in $G(H_2)$ (○), $G(C_2H_6)$ (□), $G(CH_4)$ (△) and $G(C_3H_8)$ (▲) with density in the radiolysis of *n*-butane.

1) T. Miyazaki, S. Arai, S. Shida and S. Sunohara, This Bulletin, 37, 1352 (1964).
2) Y. Toi, D. B. Peterson and M. Burton, *Radiation Research*, 17, 399 (1962).
3) H. Hotta, The 14th Annual Meeting of the Chemical Society of Japan, Tokyo, April, 1961.
4) P. Ausloos, R. Gordon, Jr., and S. G. Lias, *J. Chem. Phys.*, 40, 1854 (1964).
5) G. R. A. Johnson, *J. Inorg. Nucl. Chem.*, 24, 461 (1962).

TABLE I. *G*-VALUES OF PRODUCTS IN THE $\gamma$-RADIOLYSIS OF *n*-BUTANE[a)]

| Density g. cc$^{-1}$ | Temp. °C | *G*-Value | | | | | $G(CH_4)-G(C_3H_8)$ |
|---|---|---|---|---|---|---|---|
| | | $H_2$ | $CH_4$ | $C_2H_6$ | $C_3H_8$ | $C_3H_6$ | |
| 0.575[b)] | 20 | 4.50 | 0.49 | 1.55 | 0.30 | 0.15 | 0.19 |
| 0.575[b)] | 20 | 4.41 | 0.47 | 1.31 | 0.25 | 0.11 | 0.22 |
| 0.575[b)] | 20 | 4.05 | 0.42 | 1.25 | 0.27 | 0.09 | 0.15 |
| 0.247 | 170 | 5.25 | 1.16 | 1.43 | 0.36 | trace | 0.80 |
| 0.204 | 170 | 5.52 | 1.31 | 1.83 | 0.41 | trace | 0.90 |
| 0.1479 | 170 | 6.05 | 1.51 | 1.83 | 0.50 | trace | 1.01 |
| 0.0722 | 170 | 4.75 | 1.72 | 1.91 | 0.66 | trace | 1.06 |
| 0.0485 | 170 | 6.12 | 2.00 | 1.85 | 0.79 | trace | 1.21 |
| 0.0309 | 170 | 4.98 | 1.80 | 1.65 | 0.88 | trace | 0.92 |
| 0.0205 | 170 | 5.92 | 2.11 | 2.24 | 1.09 | trace | 1.02 |
| 0.00604[c)] | 170 | 5.80 | 2.56 | 1.89 | 1.37 | trace | 1.19 |

a) Total dose is about $1.9\times10^{21}$ eV. g$^{-1}$ and dose rate is $1.9\times10^{19}$ eV. g$^{-1}$ hr$^{-1}$.
b) Liquid at room temperature.
c) Pressure of the gas is 3.8 atm.

most striking feature of the data is the marked decrease in $G(C_3H_8)$ and $G(CH_4)$ in the density region from 0 to 0.1 g. cc$^{-1}$. $G(H_2)$ and $G(C_2H_6)$ seem, however, to be practically independent of the variation in density. The yields near the critical density except for $G(CH_4)$ are similar to those of the liquid phase.

It seems impossible to explain the marked decrease in $G(C_3H_8)$ in the density region 0—0.1 g. cc$^{-1}$ by means of the cage effect, which has been thought to be one of the most important causes of the difference between the radiolysis of the gas phase and that of the liquid phase.[6)] In the fragmentation of a molecule to radicals, the probability ($\alpha$) of the recombination of fragments was estimated by Franck and Rabinowitsch[7)] as follows:

| Pressure | 1 | 10 | 100 atm. |
|---|---|---|---|
| $\alpha$ | $10^{-9}$ | $10^{-6}$ | $10^{-3}$ |

It is clear that there exists no cage effect in the density of 0.1 g. cc$^{-1}$ (i. e., about 20 atm.). Therefore, the steep decrease must be attributed to some other effects.

It is reasonable, on the basis of a previous study by the present authors[1)] and of a study by Ausloos et al.,[8)] to expect that the butane ion plays an important role in the radiolysis of the gas phase. Since the ion may be formed in highly-excited states, it is probable that the deactivation of an excited ion occurs in the density region from 0 to 0.1 g. cc$^{-1}$; that is,

$$M \xrightarrow{I} M^{+*} + e \qquad (1)$$

$$M^{+*} \begin{cases} \xrightarrow{k_2} P \\ \xrightarrow{k_3} Q \end{cases} \qquad (2), (3)$$

$$M^{+*} + M \xrightarrow{k_4} M^{+} + M \qquad (4)$$

where M: *n*-butane molecule
$M^{+*}$: excited butane ion
$M^{+}$: stable butane ion (or perhaps the ion cluster proposed by Funabashi et al.[9)])
P: product
Q: products except P
*I*: rate of reaction 1
*k*: rate constant

The steady-state treatment leads to Eq. i:

$$G(P)=\frac{Ik_2}{k_2+k_3+k_4[M]} \qquad (i)$$

The decrease in the products with an increase in the density, or an increase in [M], could be explained by Eq. i. However, the constant yield of ethane over the whole density region and that of propane in the high density region cannot be explained by this equation only. Therefore, the production of P by the neutralization of $M^{+}$ should be considered in addition to 1—4.

$$M^{+} + e \xrightarrow{k_5} M^{*} \qquad (5)$$

$$M^{*} \begin{cases} \xrightarrow{k_6} P \\ \xrightarrow{k_7} R \end{cases} \qquad (6), (7)$$

where $M^{*}$: excited butane molecule
R: products except P

Then,

$$G(P)=\frac{Ik_2}{k_2+k_3+k_4[M]}+\frac{Ik_4k_6[M]}{(k_6+k_7)(k_2+k_3+k_4[M])} \qquad (ii)$$

6) L. Kevan and W. F. Libby, *J. Chem. Phys.*, **39**, 1288 (1963).
7) J. Franck and E. Rabinowitsch, *Trans. Faraday Soc.*, **30**, 120 (1934).
8) R. P. Borkowski and P. J. Ausloos, *J. Chem. Phys.*, **39**, 818 (1963).
9) J. L. Magee and K. Funabashi, *Radiation Research*, **10**, 622 (1959).

The first term in Eq. ii represents the production of P by ionic fragmentation, while the second term represents that by neutralization. The constant yield of $C_3H_8$ in the high density region can be explained by Eq. ii. Suppose the yield of P from the excited butane ion to be the same as that from the excited butane molecule; that is, if $k_2/(k_2+k_3)=k_6/(k_6+k_7)$, $G(P)$ is $G(P)=Ik_2/(k_2+k_3)$ and independent of [M]. The constant yield of $C_2H_6$ might be due to this effect.

**The Formation of Propane.**—Since the decomposition of neutral excited *n*-butane produced by electron bombardment in a mass spectrometer[10] yields mainly ethane and ethylene:

$$C_4H_{10}^* \rightarrow C_2H_4 + C_2H_6 \qquad (8)$$

the formation of propane at 0.00604 g. $cc^{-1}$ (i.e., 3.8 atm.) may be due to the ionic process. From the mass spectrometric study, the main fragmentation processes of butane ion are found to be as follows:[11]

$$C_4H_{10}^{+*} \xrightarrow{e_0} \begin{cases} \xrightarrow{k_9} C_2H_5^+ + C_2H_5 & 30 \text{ kcal./mol.} \quad (9) \\ \xrightarrow{k_{10}} C_2H_4^+ + C_2H_6 & 17 \text{ kcal./mol.} \quad (10) \\ \xrightarrow{k_{11}} C_3H_7^+ + CH_3 & 4 \text{ kcal./mol.} \quad (11) \\ \xrightarrow{k_3} Q & (3) \end{cases}$$

where $e_0$ denotes the heat of the reaction of ionic fragmentation. The propyl ion in reaction 11 reacts very rapidly with *n*-butane to produce propane:

$$C_3H_7^+ + n\text{-}C_4H_{10} \rightarrow C_3H_8 + C_4H_9^+ \qquad (12)$$

Propane might also be formed by the combination of the methyl and ethyl radicals produced in reactions 9 and 11, but $G(C_3H_8)=1.37$ at 170°C at 0.00604 g. $cc^{-1}$ is consistent with $G(CH_3\cdot)=1.54$[1] and with the molecular yield, $G_M(C_3H_8)=1.43$,[8] in the gaseous radiolysis of *n*-butane at ordinary pressure. Therefore, it is reasonable to consider that at 0.00604 g. $cc^{-1}$ propane is formed by the ionic process of Reaction 11, followed by 12. Since the constant yield of propane at a high density is relatively low compared with that at 0.00604 g. $cc^{-1}$, Eq. i may be used for an analytically convenient treatment in the low density region, neglecting the formation by the neutralization of butane ion. From reactions 1, 9, 11, 3, 12 and 4, we get:

$$\frac{1}{G(C_3H_8)}=\frac{k_9+k_{10}+k_{11}+k_3}{Ik_{11}}+\frac{k_4}{Ik_{11}}[C_4H_{10}] \qquad (iii)$$

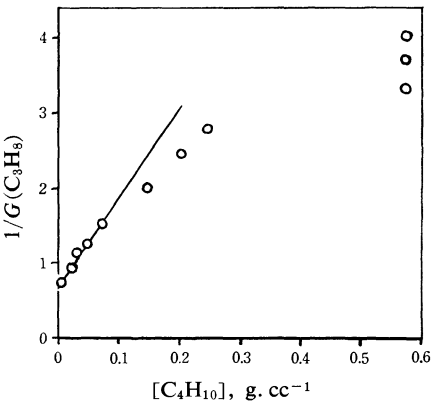



Fig. 2. Relationship between reciprocal of $G(C_3H_8)$ and density of *n*-butane.

Thus, there must be a linear relationship between $1/G(C_3H_8)$ and $[C_4H_{10}]$. As may be seen in Fig. 2, a satisfactory straight line is obtained in the low density region. The discrepancy from the straight line in the high density region may be due to the neglect of the formation by the neutralization of the butane ion. The slope-to-intercept ratio gives: $(k_9+k_{10}+k_{11}+k_3)/k_4=5.7\times10^{20}$ $cc^{-1}$ molecules. Taking $k_4=10^{-9}$ cc. molecules$^{-1}$ $sec^{-1}$ [12], $(k_9+k_{10}+k_{11}+k_3)$ is $5.7\times10^{11}$ $sec^{-1}$. Since this value is the total rate constant of the fragmentation of the excited butane ion, we have tried to estimate $k_{11}$ and $k_9$ separately. From the mass spectral pattern of *n*-butane, the ratios of the processes forming $C_3H_7^+$ and $C_2H_5^+$ to the total ionic fragmentation are 0.48 and 0.28 respectively. Therefore, we get $k_{11}=2.7\times10^{11}$ $sec^{-1}$ and $k_9=1.6\times10^{11}$ $sec^{-1}$.

**The Calculation of the Rate Constant.**—Rosenstock et al.[13] proposed the quasi-equilibrium rate theory for the fragmentation of polyatomic ions. According to the simplified treatment[14] of this theory, the rate constant of the dissociation of the molecule ion of an excitation energy of $e$ is given by $k(e)$:

$$k(e)=P\nu\left(1-\frac{e_0}{e}\right)^{S-1} \qquad (iv)$$

where $P$ is the steric factor in the range from 1 to $10^{-3}$; $\nu$ is the reaction frequency; $S=3N-6$ is the number of degrees of the vibrational freedom of the $N$-atomic molecule ion, and $e_0$ is the dissociation energy of the ion. $P\nu$ is taken as $10^{14}$ $sec^{-1}$ for a simple bond dissociation process and as $10^{12}$ $sec^{-1}$ for a four-center disproportionation process. The molecule ions produced by electron impact have

10) D. Beck and A. Niehaus, *J. Chem. Phys.*, 37, 2705 (1962).
11) F. H. Field and J. L. Franklin, "Electron Impact Phenomena," Academic Press, New York (1957).
12) The rate constant of binary collision for molecules.
13) H. M. Rosenstock, M. B. Wallenstein, A. L. Wahrhaftig and H. Eyring, *Proc. Natl. Acad. Sci., U. S.*, 38, 667 (1952).
14) D. P. Stevenson, *Radiation Research*, 10, 610 (1959).

different excitation energies. If $D(e)$ is the characteristic distribution function of the excitation energy, the total rate constant is as follows:

$$k=\int_0^{e_{max}} D(e)k(e)de \qquad (v)$$

where $D(e)$ is normalized to the range $0\leq e\leq e_{max}$ and where $e_{max}$ is the maximum excitation energy of the molecule ion.

We try to calculate $k_{11}$ and $k_9$ using Eq. v.

$$C_4H_{10}{}^{+*} \xrightarrow{k_{11}} s\text{-}C_3H_7{}^+ + CH_3 \qquad (11)$$

Since the propyl ion produced in reaction 11 is exclusively a secondary ion,[8] this reaction cannot occur by a simple bond dissociation process, but rather only by the dissociation process following rearrangement. Therefore, we take $P\nu=10^{12}$ sec$^{-1}$. The maximum excitation energy is assumed to be:

$$e_{max}=2\bar{e} \qquad (vi)$$

where $e$ is the average excitation energy of the ion. We take the $\bar{e}$ of the propane ion, i.e., 144.3 kcal./mol., as that of the butane ion also. An analytically-convenient distribution function that has been used in the interpretation of the mass spectra of propane[13] is:

$$D(e)=\frac{1}{e_{max}} \qquad (vii)$$

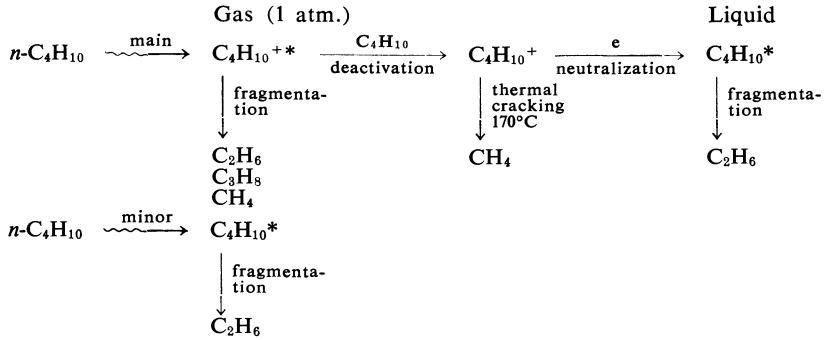
Using $S-1=35$ and $e_0=4$ kcal./mol., we get from Eq. v $k_{11}=3.2\times10^{11}$ sec$^{-1}$. In a similar fashion, we get $k_9=3.3\times10^{11}$ sec$^{-1}$ by using $e_0=30$ kcal./mol. and $P\nu=10^{14}$ sec$^{-1}$ for a simple bond dissociation. The agreement between the observed values and the calculated values is satisfactory in spite of the simplified calculation.

Since the total specific rate of the fragmentation of the ion is $5.7\times10^{11}$ sec$^{-1}$ and since the frequency of successive collisions of a molecule in the liquid phase is of the order of $10^{-13}$ sec$^{-1}$, the excited ion produced in the liquid-phase radiolysis may be exclusively deactivated before its fragmentation, and, therefore, C–C bond rupture from butane ion may be strongly suppressed. This supports the conclusion of the previous paper by the present authors.[1]

**The Formation of Methane.**—The material balance between $CH_4$ and $C_3$-products does not hold in the radiolysis at 170°C (Table I). Methane is partly formed from the methyl radical produced in reaction 11; the yields of methane due to other processes ($G(CH_4)-G(C_3H_8)$) are shown in the last column of Table I. Though $G(CH_4)-G(C_3H_8)$ at 20°C is small, that at 170°C, near the critical state, is about unity, independent of the variation in density. These results seem to be the effect of temperature. No fragmentation products could be observed by the heating of *n*-butane without radiation at 200°C for 80 hr. Since methane is not formed by the thermal cracking of the butyl radical at 170°C,[15] the discrepancy of the material balance might be due to some characteristic reaction near the critical state. The heat of reaction[11] for the formation of methane from the butane ion is very low.

$$C_4H_{10}{}^+ \rightarrow C_3H_6{}^+ + CH_4 \quad e_0=4 \text{ kcal./mol.} \qquad (13)$$

In the fragmentation of the slightly-excited butane ion,[16] a considerable amount of $C_3H_6{}^+$ is formed, though only a small amount is formed in the fragmentation of the highly-excited butane ion. In the radiolysis of neopentane,[17] the inbalance between products has been also observed; i.e., $G(CH_4)\gg G(C_4)$. The abundance of methane might be due to following reactions, as has been suggested by Williams[18]:




Scheme 1

15) A. W. Hay and C. A. Winkler, *Can. J. Res.*, **21B**, 149 (1943).
16) B. Steiner, C. F. Giese and M. G. Inghram, *J. Chem. Phys.*, **34**, 189 (1961).
17) W. H. Taylor, S. Mori and M. Burton, *J. Am. Chem. Soc.*, **82**, 5817 (1960).
18) T. F. Williams, *Trans. Faraday Soc.*, **57**, 755 (1961).

$$neo\text{-}C_5H_{12}^+ \rightarrow \begin{matrix} C_4H_8^+ + CH_4 \quad e_0 = -4 \text{ kcal./mol.} \\ \searrow \\ \text{higher products} \end{matrix} \qquad (14)$$

Therefore, it is probable that in the radiolysis of *n*-butane near the critical state a part of the methane is formed by reaction 13, while $C_3H_6^+$ forms higher products.

From the above results and discussions, the following conclusions may be drawn. It appears difficult to consider the ionic C–C rupture in the liquid-phase radiolysis of *n*-butane at room temperature. It seems proper to consider that the suppression of the ionic C–C rupture in the liquid phase is due to the deactivation of the excited butane ion. The main C–C rupture reactions in the radiolysis of *n*-butane may be depicted as Scheme 1.

## Summary

A study has been made of the effect of density on the radiolysis of *n*-butane at 170°C over the density region 0.006—0.575 g. $cc^{-1}$. While $G(H_2)$ and $G(C_2H_6)$ are not affected by the density change, $G(CH_4)$ and $G(C_3H_8)$ decrease sharply in the density region from 0 to 0.1 g. $cc^{-1}$. The latter facts may be interpreted in terms of the collisional deactivation of the excited ion. The rate constant of the fragmentation of the butane ion has been estimated from the deactivation-fragmentation competition scheme and compared with the rate constant calculated from the quasi-equilibrium theory. Agreement is satisfactory. The formation of methane by ionic fragmentation near the critical state has also been considered.

We wish to express our appreciation to Dr. Shin Sato, Mr. Tomoyoshi Kudo and Mr. Nobuyoshi Sakai for their fruitful discussions. We appreciate also the help of the Japan Atomic Energy Institute in performing the irradiation. This research was supported, in part, by the Watanabe Memorial Foundation for Scientific Research Promotion, to which the authors are grateful.

*Laboratory of Physical Chemistry*
*Tokyo Institute of Technology*
*Ookayama, Tokyo*

# Chelate Formation between Chromate Ions and Disodium-1, 8-dihydroxy Naphthalene-3, 6-disulphonate

By Samir K. BANERJI and Said-ul-Zafar QURESHI*

(Received July 22, 1964)

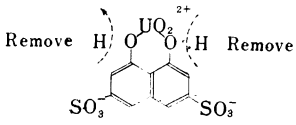
Disodium-1, 8-dihydroxy naphthalene-3, 6-disulphonate, commonly known as chromotropic acid (sodium salt), has found application in colorimetric analysis.[1] It has been reported to yield coloured complexes with vanadium, titanium, mercury, silver, uranium and ferric ions. It has also been found to yield coloured reactions with various other metals.[2,3] More detailed work on the application of this reagent in the estimation of titanium has been done by Sommer and his co-workers. Sommer and Okâć[4] discussed the functional analytical groups for titanium. The spectrophotometric determination of titanium using this reagent has been described by Sommer,[5] and Sommer and Benisêk[6] made a polarographic study of the reaction between titanium and chromotropic acid. Sommer[7,8] then extended the work, working out the details of the reaction and determining the composition and the stability constant. He also discussed the structure. The titanium-chromotropic acid system was also described by Shnaiderman[9] and Babko[10].

Heller and Schwarzenbach[11] studied the chelate formed between trivalent iron and chromotropic acid. They were of the opinion that a six-membered ring is formed and that iron is chelated between the two phenolic oxygens. The formation of manganese(II),

* Present address: Chemistry Department, Aligarh University, Aligarh.

1) The B. D. H. Book of Organic Reagents, Poole, p. 33 (1949).
2) K. C. Mathur and A. K. Dey, *Z. anal. Chem.*, **154**, 347 (1957).
3) L. Sommer, ibid., **163**, 412 (1958).
4) L. Sommer and A. Okâć, *Chem. Listy.*, **50**, 1746 (1956).
5) L. Sommer, ibid., **51**, 875 (1957).
6) L. Sommer and L. Benišek, ibid., **50**, 1215 (1956).
7) L. Sommer, Intl. Conf. Coordination Chem, Rome (1957).
8) L. Sommer, *Chem. Listy.*, **50**, 1729 (1956); Symp. Chem. Coordination Compounds, Agra (1959).
9) S. Ya. Shnaiderman, *Z. neorg. Khim.*, **2**, 2122 (1957).
10) A. K. Babko and O. I. Popva, ibid., **2**, 138 (1957).
11) E. Heller and G. Schwarzenbach, *Helv. Chem. Acta*, **34**, 1869 (1959).

lead and copper chelates has also been described.[12] Mathur and Dey[2] had earlier reported the formation of a red-coloured chelate between uranium and chromotropic acid. Also, Ware[13] had earlier suggested the use of chromotropic acid for the colorimetric determination of uranium, but no details have been recorded. Mukerji and Dey[14,15] have, however, described in detail the colorimetric determination of uranium with this reagent and studied the interference of foreign ions. They also determined the composition of the chelate by conductometric methods and found it to be 1 : 1. Banerji and Dey[16] studied the uranium - chromotropic acid chelate and determined the composition, the stability, the formation constant and the free energy of formation of the chelate. This work confirmed the earlier views that a 1 : 1 chelate is formed; therefore, the following structure for the chelate was proposed:




Uranium - Chromotropic acid chelate

The chelation involved the phenolic oxygens, as had been suggested by the earlier workers.

In the course of these investigations, a detailed study was made of the reaction of chromotropic acid with different metal ions. Details of this are presented in Table I. It may be observed therein that the chromate ion develops a very beautiful red colour with chromotropic acid; this chelate was, therefore, investigated with regard to its composition, stability, formation constant and free energy of formation by the spectrophotometric method. The composition, as investigated by the conductometric method, has also been described.

## Experimental

**Materials.**—Potassium chromate of BDH Analar quality was dissolved in distilled water. A concentrated stock solution of 0.01 M was then prepared. Acid was added to prevent any possible hydrolysis. Standard solutions were prepared from this solution by dilution.

BDH reagent-grade disodium-1, 8-dihydroxy naphthalene-3, 6-disulphonate, commonly known as chromotropic acid (abbreviated as CAD), was used. A 0.01 M stock solution was prepared. Suitable standard solutions were prepared from this solution by dilution.

In all cases freshly-prepared solutions were used. Extremely dilute solutions were used for these studies so that the contraction in volume, if any, would be negligible.

The absorbance measurements were made on a Hilger Uvispek spectrophotometer using glass cells one centimeter thick. The individual solutions and mixtures were kept for 30 min. before absorbance measurements were made in order for them to attain equilibrium. All observations were made in the 2—3 pH range on a Phillips pH meter (GM 4494).

The composition of the chromate - chromotropic acid obtained from absorbance studies has also been investigated by adopting the conductometric method; the results thus obtained support those obtained by spectrophotometric methods. The electrical conductivity studies were made on a Serfass conductivity bridge.

**Optimum Conditions.**—The optimum conditions for the formation of the chelate were determined, and then these conditions were maintained throughout the studies.

**The Order of the Addition of Reagents.**—Studies were made of the addition of the chelating agent to the metal solution and vice versa. It was found that there was no change, whether the metal was added to the reagent and vice versa. To maintain uniformity, however, the chelating agent was added to the metal solution.

**The Effects of Time.**—Time effects were also studied; it was found that the chelate maintained its stability for more than twenty-four hours and, as such, was in keeping with the investigations here.

**Acid Added to Prevent Hydrolysis.**—Acid was added wherever neccessary to prevent hydrolysis.

**Colour Formation with Inorganic Ions.**—For studying the colorimetric reactions with various metal ions, a 0.05 M solution of chromotropic acid was prepared in distilled water. Solutions of various metallic salts using analytical-grade reagents was made of a 0.1 M concentration in distilled water, acid being added in several cases to prevent hydrolysis.

In several test tubes 1 ml. of solutions were placed; then two drops of the reagent solution were added to each and the colour noted visually. This colour was then compared with an equal amount of the reagent diluted to the same extent. The results have been recorded in Table I.

**The Nature of the Complexes Formed.**—The method described by Vosburg and Cooper[17] was employed to determine the nature of the complexes formed in solution. Mixtures containing different proportions of chromium - chromotropic acid (1 : 1, 1 : 2, 1 : 3, and 1 : 4) were prepared, and the absorbances of the solutions at different wavelenghts were measured. The exact compositions have been tabulated in Table II.

12) A. E. Martell and M. Calvin, "Chemistry of Metal chelate compounds," Prentice Hall, N. Y. (1952), p. 503.
13) E. Ware, U. S. Atomic Energy Commission Rep. MDDC (1945).
14) A. K. Mukerji and A. K. Dey, *J. Ind. Chem. Soc.*, **35**, 113 (1958).
15) A. K. Mukerji and A. K. Dey, *J. Inorg. Nucl. Chem.*, **6**, 314 (1958).
16) S. K. Banerji and A. K. Dey, *Nature*, **197**, 1002 (1963).
17) W. C. Vosburg and Cooper, *J. Am. Chem. Soc.*, **63**, 437 (1941); **64**, 1630 (1947).

TABLE I

| | Salt | Coloration | Remark |
|---|---|---|---|
| 1 | Reagent | Light brown | |
| 2 | Li $CH_3COO$ | Light brown | No particular change |
| 3 | $Mg(NO_3)_2$ | Light brown | No particular change |
| 4 | $BaCl_2$ | Light brown | No particular change |
| 5 | $Bi(NO_3)_3$ | Light brown | No particular change |
| 6 | $SrCl_2$ | Light brown | No particular change |
| 7 | $Zr(SO_4)_2$ | Light brown | No particular change |
| 8 | $MnCl_2$ | Light brown | Buff-colored precipitate in an alkaline medium |
| 9 | $PdCl_2$ | Light brown | No particular change |
| 10 | $CoSO_4$ | Light brown | Black precipitate in an alkaline medium |
| 11 | $Na_3AsO_4$ | Light brown | No particular change |
| 12 | $Be(NO_3)_2$ | Light brown | No particular change |
| 13 | $AgNO_3$ | Light brown | No particular change |
| 14 | $CdSO_4$ | Light brown | White precipitate in an alkaline medium |
| 15 | $K_2CrO_4$ | Red | Red colour in an acid medium Very sensitive |
| 16 | $Pb(NO_3)_2$ | Light brown | No particular change |
| 17 | $ZnSO_4$ | Light brown | No particular change |
| 18 | $NiSO_4$ | Light brown | No particular change |
| 19 | $Al(NO_3)_3$ | Light brown | No particular change |
| 20 | $CuSO_4$ | Light brown | No particular change |
| 21 | $Ca(C_2H_3O_2)_2$ | Light brown | No particular change |
| 22 | $K_2WO_4$ | Light brown | No particular change |

TABLE II

| | Final concn. of $K_2CrO_4 \times 10^4$ | Final concn. of CAD $\times 10^4$ | Ratio Cr(VI) : CAD |
|---|---|---|---|
| A | 0.00 | 1.0 | 0 : 1 |
| B | 1.00 | 1.0 | 1 : 1 |
| C | 0.50 | 1.0 | 1 : 2 |
| D | 0.33 | 1.0 | 1 : 3 |
| E | 0.25 | 1.0 | 1 : 4 |

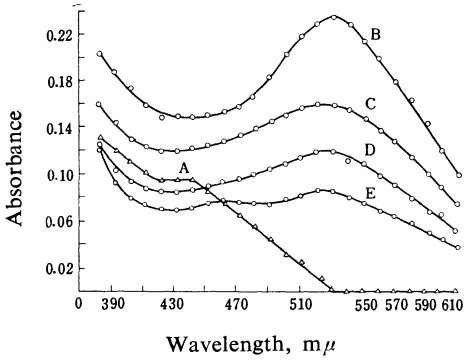



Fig. 1. Absorption spectra studies of mixtures of chromate and disodium-1, 8-dihydroxy naphthalene-3, 6-disulphonate.
Curve A : reagent $1.0 \times 10^{-3}$ M
Curve B : $c = 1.0 \times 10^{-4}$ M, $p = 1$
Curve C : $c = 0.5 \times 10^{-4}$ M, $p = 2$
Curve D : $c = 0.33 \times 10^{-4}$ M, $p = 3$
Curve E : $c = 0.25 \times 10^{-4}$ M, $p = 4$

The results obtained from the absorbance studies have been graphically represented in Fig. 1. It may be seen there that the absorption maxima lies

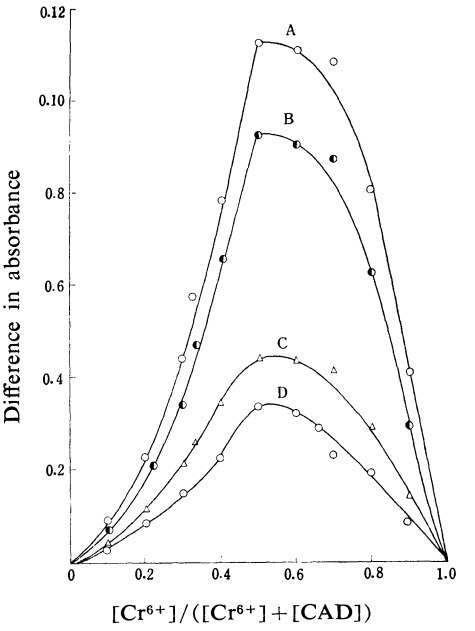



Fig. 2. Determination of the composition from absorption spectra studies at 500 mμ.
Curve A : $c = 13.3 \times 10^{-4}$ M, $p = 1$
Curve B : $c = 10 \times 10^{-4}$ M, $p = 1$
Curve C : $c = 5.0 \times 10^{-4}$ M, $p = 1$
Curve D : $c = 3.3 \times 10^{-4}$ M, $p = 1$

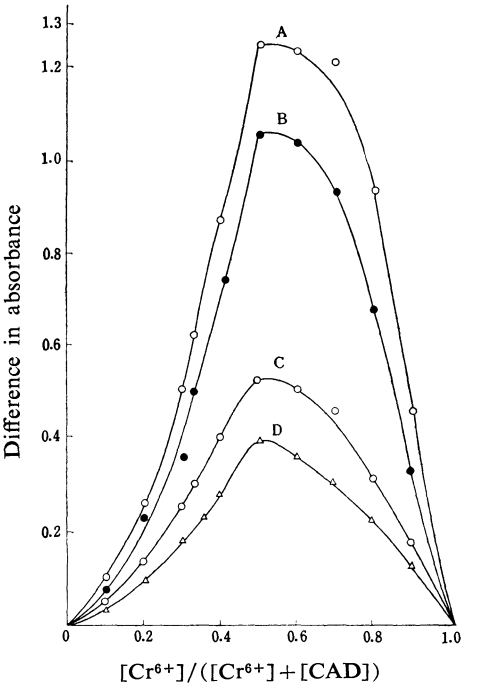



Fig. 3. Determination of the composition from absorption spectra studies at 530 mμ. Concentrations same as Fig. 2.

at 530 mμ, which also indicates that only one complex is formed under the conditions of study.

**The Stoichiometry of the Compounds.**—Job's[18] method of continuous variation has been adopted for the determination of the composition of the coloured complex formed. The total volume in each case was kept at 50 ml. The pH values of the solutions were kept between 2 and 3. The absorption spectra of the $Cr_2O_7$-chelating agent and the mixtures were measured at two different wavelengths, 500 and 530 mμ. Measurements using equimolecular and non-equimolecular solutions, in large numbers, were taken. The results obtained have been represented in Figs. 2—5.

The figures indicate the difference between the absorbance of the mixture and that which would

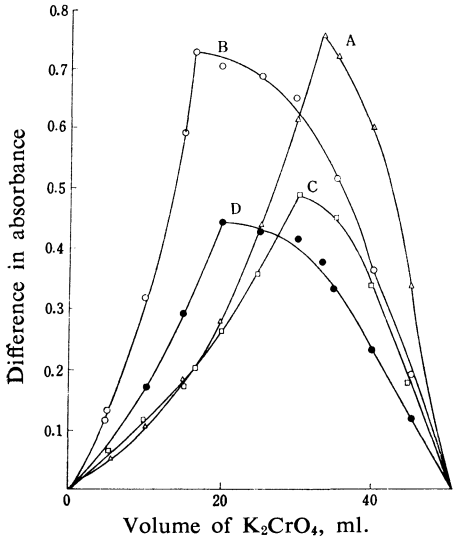



Fig. 4. Determination of the composition from absorption spectra studies at 500 mμ.
Curve A: $c=5.0\times10^{-4}$ M, $p=2$
Curve B: $c=10\times10^{-4}$ M, $p=0.5$
Curve C: $c=3.3\times10^{-4}$ M, $p=1.5$
Curve D: $c=5.0\times10^{-4}$ M, $p=0.66$

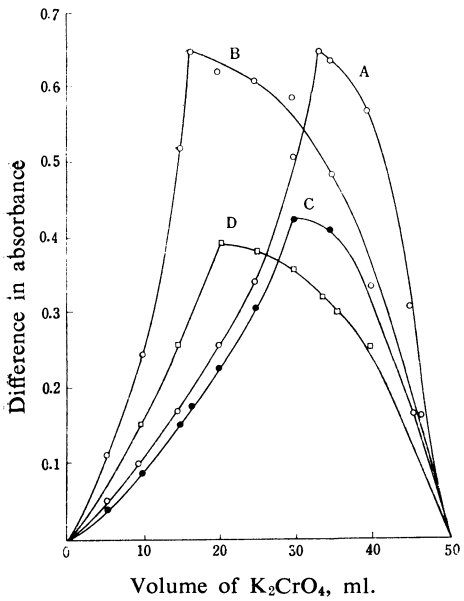



Fig. 5. Determination of the composition from absorption spectra studies at 530 mμ. Concentrations same as Fig. 4.

18) P. Job, *Compt. rend.*, **180**, 928 (1925).

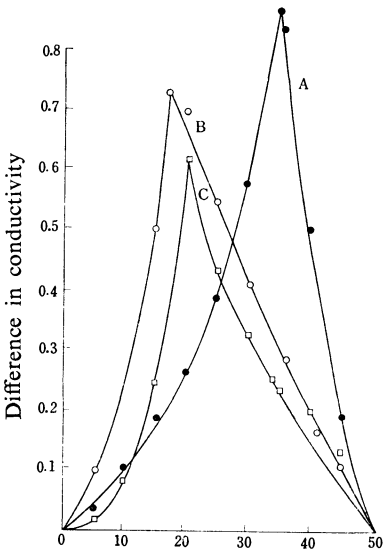



Fig. 6. Determination of the composition from conductivity studies.
Curve A: $c=10\times10^{-4}$ M, $p=1$
Curve B: $c=5.0\times10^{-4}$ M, $p=1$
Curve C: $c=3.3\times10^{-4}$ M, $p=1$

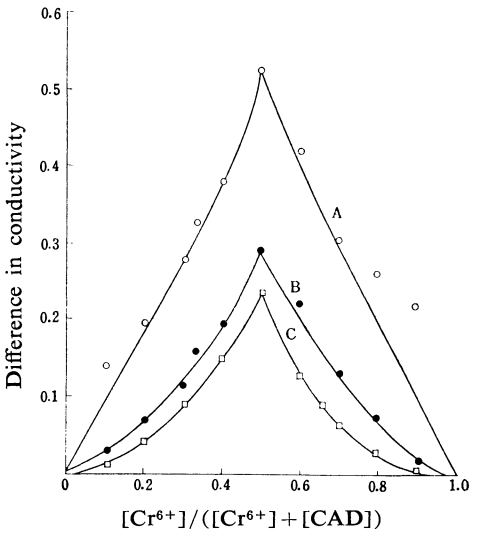



Fig. 7. Determination of the composition from conductivity studies.
Curve A: $c=5.0\times10^{-4}$ M, $p=2$
Curve B: $c=10\times10^{-4}$ M, $p=0.5$
Curve C: $c=5.0\times10^{-4}$ M, $p=0.66$

be shown by the metal and the chelating agent if no chelation took place. This difference is plotted against the composition of the mixtures.

**The Influence of pH on the Stability of the Chelate.**—A detailed study was made of the effect of pH on the absorption maxima of the chelate to find out its stability; it was observed that the chelate is stable in the pH range 1—6. The observations were, therefore, made between pH 2 and 3, in which range the chelate is stable. It was also ascertained beforehand that the reagent did not change colour in this range of pH.

**Conductivity Studies.**—Electric conductivity studies were made at six different equimolecular and non-equimolecular concentrations. The solutions used were always freshly prepared. The results have been graphically represented in Figs. 6 and 7.

## Conclusions

The composition of the chelate has been found to be 1 of the metal and 1 of the chelating agent, as may be seen from Table III, compiled from an examination of Figs. 2—5. The chelate can, therefore, be represented as Cr(CAD).

The results obtained from absorption measurement studies also receive confirmation from conductivity studies, as may be seen from Table IV.

For the purpose of determining the stability, calculations have been made of the formation constant from optical density data according to the method of calculation suggested by Dey[15] and worked out by Banerji and Dey[19-25] in several of their investigations. The method suggested by Dey has an advantage over the earlier method of Anderson et al.[26] wherein one of the reactants may be coloured.

By the above method the value of $\log K$ in the chromate-disodium-1,8-dihydroxy naphthalene-3,6-disulphonate systerm is $8.21 \pm 0.02$ at 25°C.

Table III

| Fig. | Curve | $c \times 10^4$ M | $p$ | Wavelength of the observation mμ | Peak occurs at (vol. of $K_2CrO_4$) ml. | Composition of chelate Cr : CAD |
|---|---|---|---|---|---|---|
| 2 | A | 13.3 | 1.0 | 500 | 25.0 | 1 : 1 |
| 2 | B | 10.0 | 1.0 | 500 | 25.0 | 1 : 1 |
| 2 | C | 5.0 | 1.0 | 500 | 25.0 | 1 : 1 |
| 2 | D | 3.3 | 1.0 | 500 | 25.0 | 1 : 1 |
| 3 | A | 13.3 | 1.0 | 530 | 25.0 | 1 : 1 |
| 3 | B | 10.0 | 1.0 | 530 | 25.0 | 1 : 1 |
| 3 | C | 5.0 | 1.0 | 530 | 25.0 | 1 : 1 |
| 3 | D | 3.3 | 1.0 | 530 | 25.0 | 1 : 1 |
| 4 | A | 5.0 | 2.0 | 500 | 33.5 | 1 : 1 |
| 4 | B | 10.0 | 0.5 | 500 | 16.5 | 1 : 1 |
| 4 | C | 3.3 | 1.5 | 500 | 30.0 | 1 : 1 |
| 4 | D | 5.0 | 0.66 | 500 | 20.0 | 1 : 1 |
| 5 | A | 5.0 | 2.0 | 530 | 33.5 | 1 : 1 |
| 5 | B | 10.0 | 0.5 | 530 | 16.5 | 1 : 1 |
| 5 | C | 3.3 | 1.5 | 530 | 30.0 | 1 : 1 |
| 5 | D | 5.0 | 0.66 | 530 | 20.0 | 1 : 1 |

Table IV

| Fig. | Curve | $c \times 10^4$ M | $p$ | Peak occurs at (Vol. of $K_2CrO_4$) ml. | Composition of the chelate Cr : CAD |
|---|---|---|---|---|---|
| 6 | A | 10.0 | 1.0 | 25.0 | 1 : 1 |
| 6 | B | 5.0 | 1.0 | 25.0 | 1 : 1 |
| 6 | C | 3.3 | 1.0 | 25.0 | 1 : 1 |
| 7 | A | 5.0 | 2.0 | 33.5 | 1 : 1 |
| 7 | B | 10.0 | 0.5 | 16.5 | 1 : 1 |
| 7 | C | 5.0 | 0.66 | 20.0 | 1 : 1 |

19) S. K. Banerji and A. K. Dey, Proc. XVII Intl. Cong. Pure Appl. Chem. Munich., 1072 A (1959).
20) S. K. Banerji and A. K. Dey, *Z. anorg. u. allagem. Chem.*, **309**, 226 (1961).
21) S. K. Banerji and A. K. Dey, *J. Indian Chem. Soc.*, **39**, 3 (1961).
22) S. K. Banerji and A. K. Dey, *Z. anal. Chem.*, **179**, 130 (1961).
23) S. K. Banerji and A. K. Dey, *Z. phys. chem.*, **218**, 173 (1961).
24) S. K. Banerji and A. K. Dey, *J. Indian Chem. Soc.*, **38**, 2 (1961).
25) S. K. Banerji, *Z. anorg. u. allgem. Chem.*, **315**, 229 (1962).
26) R. C. Anderson and S. E. Turner, *J. Am. Chem. Soc.*, **71**, 912 (1949).

The free energy of the formation, $\Delta F^\circ$, of the chelate has been calculated with the help of the relation:

$$\Delta F^\circ = -RT\ln K$$

where $R$ is the gas constant, $T$ is the absolute temperature, and $K$ is the formation constant. The free energy of the chelate investigated here is:

$$-5.42\pm0.11 \text{ kcal. at } 25^\circ\text{C}$$

Judging from the results described here, the composition of the chelate corresponds to Cr(CAD).

## Summary

The formation of a coloured chelate with a $\lambda_{max}$ at 530 m$\mu$ between chromate ion and chromotropic acid (sodium salt)-disodium-1, 8-dihydroxy naphthalene-3, 6-disulphonate has been reported. The composition of the chelate has been studied by the method of continuous variation, using absorption spectra measurements, with a Hilger Uvispek spectrophotometer; it has been found to be Cr(CAD), (Disodium-1, 8-dihydroxy naphthalene-3, 6-disulphonate). The chelate has been found to be stable in the pH range 2—5 and so the investigations have been carried out in this range of pH. The chelate formed is deep red in colour and is very sensitive, being formed even at great dilutions.

The stability has been calculated by a method described earlier; the value of $\log K$ is $8.21\pm0.02$, and the value of the free energy of formation, $\Delta F^\circ$, has been found to be $-5.42\pm0.11$ at 25°C.

*Chemical Laboratories*
*Birla College of Engineering*
*Pilani and Meerut College*
*Meerut, India*

# Absorption Spectra of Dyes. IX.[1] Electronic Spectra of a 1 : 1 and a 1 : 2 Complex, and CT-Bands*

By Toshihiko Hoshi, Yoshié Tanizaki and Noboru Ando

(Received July 27, 1964)

Electronic absorption spectra are generally sensitive to the environment of the sample. In particular, the molecular complex formation brings about remarkable changes in the electronic absorption spectra of the component molecules. By applying the theory of charge transfer as developed by Mulliken[2] to electron donor and acceptor molecules, the authors have found that an intermolecular charge transfer spectrum is obtained from Chlorazol Sky Blue FF and Chrysophenine G in a complex state.[3] Moreover, by analogy with the known theoretical results, they have determined how the molecular orbitals of Chlorazol Sky Blue FF and Chrysophenine G are altered in the formation of a 1 : 1 and a 1 : 2 complex respectively. They have also assigned the actual electronic spectra of these dye complexes to empirical MO patterns, but they have not, however, discussed the relative configurations of the respective MO's in detail.

The purpose of the present investigation is to determine the absorption spectra of 1 : 1 and 1 : 2 complexes and, moreover, to explain the correlation between these electronic bands in terms of the more refined MO pattern derived from the complexes' spectra.

## Experimental and Results

The samples were the same as those used in a previous investigation.[1] The procedure already described[1] was followed in carrying out the experiments. A Shimadzu recording spectrophotometer SV-50A and, when necessary, a Shimadzu QR-50 spectrophotometer were employed in the determination of the absorption spectra at room temperature (about 20°C). The absorption cells used were 10 mm. and 2 mm. long, and the wavelength region observed was 220—700 mμ. Mixed solutions of two different concentrations were prepared, one containing $1\times10^{-5}$ mol./l. of a partner dye

1) Part VIII of this series: Y. Tanizaki, T. Hoshi and N. Ando, This Bulletin, 38, 264 (1965).

* Presented at the 16th Annual Meeting of the Chemical Society of Japan, April, 1963.

2) R. S. Mulliken, *J. Am. Chem. Soc.*, 70, 600 (1950); 74, 811 (1952); *J. Phys. Chem.*, 56, 801 (1952).

3) T. Kobayashi, Y. Tanizaki and N. Ando, This Bulletin, 33, 661 (1960).

(abbreviated as P) with an equal concentration of G (Chrysophenine G), and the other with the same concentration of P, together with from two to nine times the concentration of G.

The absorption spectra of the PG and the $PG_2$ species were determined by calculation, by applying, respectively, the equilibrium constants, $K_1$ and $K_2$ previously obtained[1] at 20°C, to the absorption spectra measured here. The results are illustrated in Figs. 1 and 2 respectively. In Fig. 1, the solid and the dotted

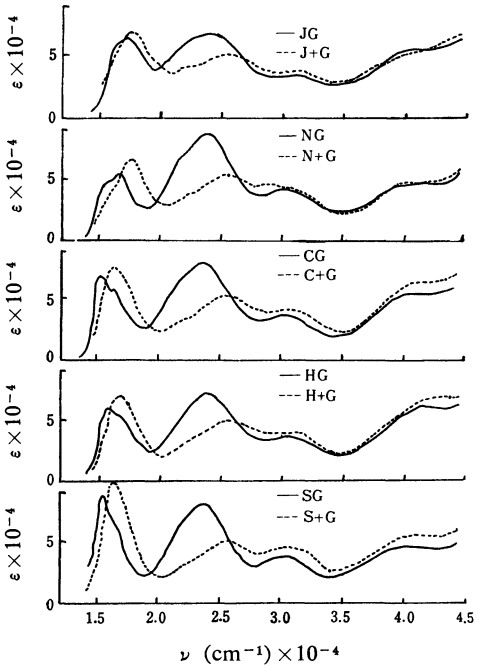



Fig. 1. Absorption spectra of a PG complex (solid lines) and the resultant ones of P and G (dotted lines).

lines indicate, respectively, the absorption curve of a 1 : 1 complex (PG) and the combined absorptions of P and G determined separately at an equimolar concentration. Similarly, the solid line in Fig. 2 indicates the absorption spectrum of a 1 : 2 complex ($PG_2$), while the dotted line represents the additive spectrum of the P curve and two times the height of the G curve.*

First of all, the following points may be noticed in Figs. 1 and 2. In the 16—18 kK (kK = 1000 $cm^{-1}$) region, the first band shifts progressively to the lower wave number,

* The absorption curves concerning $JG_2$ are not illustrated in Fig. 2. This is due to the fact that the quantity of a 1 : 2 complex ($JG_2$) could not be calculated with reliable presision at wave numbers higher than the second band on account of the smaller equilibrium constant ($K_2$).

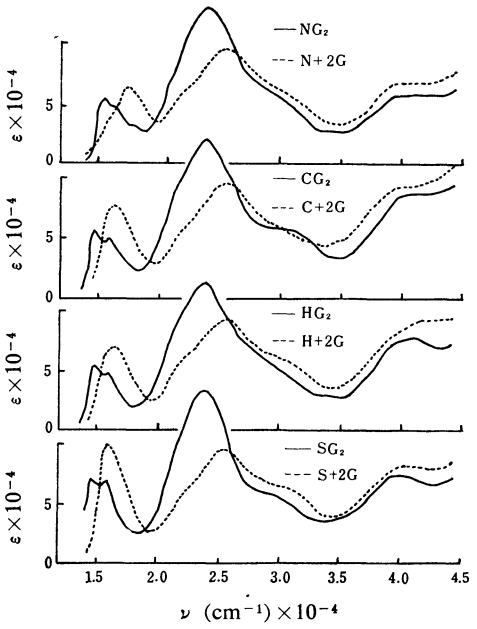



Fig. 2. Absorption spectra of a $PG_2$ complex (solid lines) and resultant ones of P and twice of G (dotted lines).

together with the decrease in intensity, with the formation of a 1 : 1 and a 1 : 2 complex, and, as the case may be, the main band is split into two bands. On the other hand, the second band (22.5 kK) is markedly intensifies by the formation of complexes. Moreover, the maximum point shift toward a much lower side with the 1 : 1 complex formation and then moves in the opposite direction to the higher side with the 1 : 2 complex formation (cf. Fig. 3). In the wave number-region higher than about 30 kK, the complex and the resultant spectrum are nearly the same in shape, but the intensities are somewhat smaller in the former than in the latter in most cases.

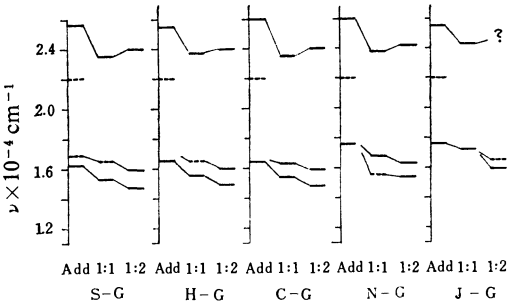



Fig. 3. Correlation of the transition energies (wave number) in the order of the additive (Add.), a PG (1 : 1) and a $PG_2$ complex (1 : 2) spectrum in the P-G system.

The most important fact in the above results is that the first and the second band behave differently. The transition energies (wave numbers) of those parts are illustrated in Fig. 3 in the order of the results of P and G, the PG complex and the $PG_2$ complex spectrum. The figure makes it apparent that in every combination the absorptions at about 16 kK shift down progressively to the low-wave number side as a result of the formation of complexes, while the absorption at about 25 kK shifts up after once falling down. Since the absorption at about 16 kK of the additive spectrum is the first band of P itself and since the 25.5 kK absorption is that of G alone, it may be considered that the variety of complex formations revealed by Fig. 3 has been brought about by interaction between the orbital states of the components in a complex.

## Discussion

The G molecule has two sulfonic groups at positions adjacent to the ethylene bond (see Fig. 4). The groups are so bulky that they may hinder the two monoazo dyes from the conjugation through the ethylene bond.[4] Therefore, the MO pattern which is responsible for the first band of G may be considered to be produced from the interaction (the weak coupling) between the MO's of the half structures (HS in Fig. 4) on the right side and on the left side of the ethylene bond. That is to say, the analogy with Platt's theory[5] leads to the relation shown in Fig. 4. Two pairs of HS levels in the same figure indicate the highest occupied ($\pi$) and the lowest unoccupied molecular orbitals ($\pi^*$). Applying the concept of the simple MO approximation, it can be said that the degenerate orbitals will split as a result of the interaction between two HS's, and that, in consequence the MO levels of FS (full structure) in Fig. 4 will be obtained; FS (i.e. the G molecule) can produce the electronic transitions $(\pi-\pi)\rightarrow(\pi^*+\pi^*)$ and $(\pi-\pi)\rightarrow(\pi^*-\pi^*)$. The actual first band of G is at 25.5 kK and is accompanied by a weak shoulder at about 22 kK.* Therefore, the main band of G may be assigned to the $(\pi-\pi)\rightarrow(\pi^*-\pi^*)$ transition and the shoulder to the $(\pi-\pi)\rightarrow(\pi^*+\pi^*)$. As most of the atoms constituting the conjugate system under consideration are carbon atoms, the location of the individual MO's may be determined without any large error by taking the Coulomb integral, Q, of the $\pi$ electron on the carbon atom as a standardized zero level. In the approximation, the $\pi^*$ and the $\pi$ levels, and also the $(\pi^*+\pi^*)$ and the $(\pi-\pi)$ levels, are arranged at equal distances above and below the Q line, as Fig. 4 shows.

For the sake of convenience, let $\pi_G$ and $\pi_G^*$ stand, respectively, for the $(\pi-\pi)$ and $(\pi^*-\pi^*)$ orbitals of G. The arrangement of $\pi_G$ and $\pi_G^*$ can be determined with respect to the Q line by utilizing the absorption data of G alone, because Q lies at the middle point between $\pi_G$ and $(\pi^*+\pi^*)$.

If the MO's of P could be determined for the Q level, the relative configuration of MO's of P and G could be decided. No such a situation as that in the case of G could, however, be found between the first band of P (disazo dye) and that of its half structure (monoazo dye). That is, for meta-Benzopurpurine, for example, the relation between the absorption specta of the half and the full structure is nearly the same as in the case of G, whereas in the case of ortho-Benzopurpurine, corresponding to P, the situation is quite different; here the first and the second band of the half structure change into an absorption delocalized over the full structure.[6] For that reason, let us suppose that the first

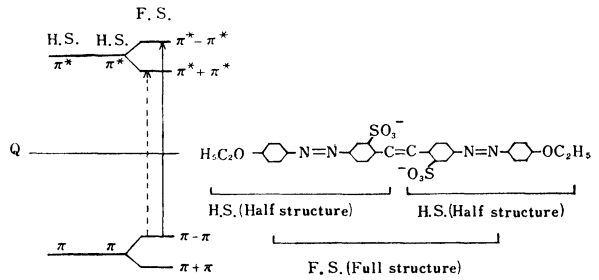



Fig. 4. Schematic MO pattern of the half (HS) and the full structure (FS) of Chrysophenine G.

4) Cf. T. Kobayashi, Y. Tanizaki and N. Ando, This Bulletin, 33, 913 (1960).
5) J. R. Platt, *J. Chem. Phys.*, 19, 101 (1951).

* This shoulder is indicated by the dotted line at 22kK in Fig. 3.
6) H. A. Standing and M. Stein, *J. Textile Inst.*, 44, T224 (1953).

band of P may be attributed to the transition between MO's which are uniformly delocalized, and let us further assume that the occupied and unoccupied MO's of P are arranged symmetrically about the same Q level as G, assuming that P has at least one symmetry species, as is seen in Fig. 1 of Part VIII.[1] Then the relative configuration of MO's concerning the first absorption bands of P and G can be decided by standardizing the Q level. Adopting S for P, the MO pattern labeled by G and S shown in the left part of Fig. 5 is obtained. Here, the Q line of S has been estimated from the maximum point of the first band corresponding to the $\pi_S \rightarrow \pi_S^*$ transition. As will be seen later, the first absorption of S (in general P) consists of two bands. One corresponds to the transition from the $\pi$-type orbital of the functional groups to the $\pi^*$ orbital, while the other corresponds to the $\pi \rightarrow \pi^*$ transition in the usual sense. In Fig. 5 the two MO's responsible for these transitions are both indicated by $\pi_S$.

According to Fig. 3, the wave number of the $\pi_S \rightarrow \pi_S^*$ transition of S (Fig. 5) shifts

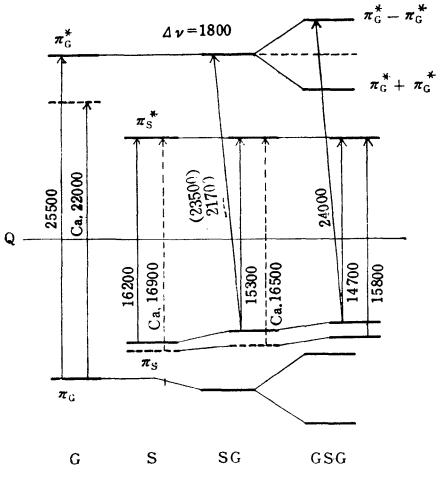



Fig. 5. Change in MO levels of S and G due to complex formations in the S-G system.

downward with the formation of a 1 : 1 complex. This implies that the complex formation has induced some interactions between MO's of G and S. In this case, the interaction should be strongest between $\pi_G$ and $\pi_S$ because the locations of $\pi_G^*$ and $\pi_S^*$ are so far apart that they cannot interact with each other. The interaction between $(\pi^* + \pi^*)$ and $\pi_S^*$ will be also neglected, because it is difficult to suppose any strong interaction between the transition vectors of $\pi_G^* \rightarrow (\pi^* + \pi^*)$ and $\pi_S \rightarrow \pi_S^*$, for the transition intensity of the former is much weaker than that of the latter. Consequently, the main interaction must be considered to be between $\pi_G$ and $\pi_S$, which are the nearest neighbors.

According to the assumption that the repulsive interaction is induced only between $\pi_G$ and $\pi_S$, the SG pattern will be obtained as shown in Fig. 5, in which the upper level of $\pi_S$ is adjusted so as to match the observed and the $\pi_S \rightarrow \pi_S^*$ distance. Figure 3 shows that the second band of the SG complex shifts also to the lower side in the same way as does the first band. However, we could not find any transition distance corresponding to the second band (23.5 kK) from the MO's of G in the SG pattern (Fig. 5). However, the distance between $\pi_S$ and $\pi_G^*$ is 21.7 kK, which corresponds well to the observed one, with a difference of only 1.8 kK. This means that a intermolecular charge transfer occurs from S to G.*

Quite similar correlation diagrams have been obtained for all other P's. The relation of the wave numbers of the $\pi_P \rightarrow \pi_G^*$ transition, as estimated by the same procedure as above, to those of the experiment is summarized in Table I. In all cases, the experimental values are larger than the estimated ones. This may be due to the assumption that the repulsion acts only between $\pi_G$ and $\pi_S$. If, for example, a small interaction between $\pi_G^*$ and $\pi_S^*$ is taken into account, the value to be estimated will become larger in some degree. At any rate, the results shown in Table I support the concept of the charge transfer.

Table I. Comparison of observed and estimated value of the P→G CT-band

| P | Charge transfer band | | |
|---|---|---|---|
| | $\nu_{obs}$ kK | $\nu_{est}$ kK | $\nu_{obs} - \nu_{est}$ |
| S | 23.5 | 21.7 | 1.8 |
| H | 23.7 | 21.7 | 2.0 |
| C | 23.5 | 21.7 | 1.8 |
| N | 23.8 | 21.2 | 2.6 |
| J | 24.3 | 22.9 | 1.4 |

(kK = 1000 $cm^{-1}$)

**Electronic Spectra of the $PG_2$ Complex.**—As may be seen in the explanation of Fig. 3, the first band of a $PG_2$ complex shifts further to the lower side than that of a PG complex, whereas the second band of the former moves in the opposite direction, to the higher wave number than that of the latter. A detailed interpretation of the behavior of the second band will be omitted at this time because the authors' previous explanation[3] can be applied here without any modification.

* According to Ref. 3, the charge transfer takes place from S (electron donor) to G (acceptor).

There is, however, one more subject to be noticed. As has been described in a preceding paper,[1] it is considered that all the partner dyes (P) take a similar sterical configuration in the complex state. If this is true, the degree of interaction between the two G molecules in the GPG (1 : 2) complex state should be constant, regardless of P. That is to say, the distance between the levels of ($\pi_G - \pi_G^*$) and ($\pi_G + \pi_G^*$) in Fig. 5 must be equal in all cases. The estimation* provides 5.8 kK for the cases when P is S, H and C, and 6.2 kK when P is N. The expectation, therefore, may be said to be satisfied.

**First Absorption Bands of Benzidine Disazo Dyes.**—It has been well known as a general tendency that the first band of a benzidine disazo dye reveals one shoulder or other in the dyed state, even when it has a single band with a simple shape in an aqueous solution. A similar tendency appears for the variation in solvent polarity. The constitution of the first absorption band has been described in a preceding paragraph. One is the electronic transition between the molecular orbitals delocalized over the two terminal naphthalene rings, while the other appears on account of the transition of a $\pi$-type lone-paired electron.[7] This is a kind of $n \rightarrow \pi^*$ transition and is called the $l \rightarrow \pi^*$ transition.[8]

The electron which transfers from P to G is the lone-paired electron of the $\pi$-type on the functional groups.[3] Therefore, the transition probability of this electron within the P molecule in the complex state should be decreased, that is, the absorption intensity of the $l \rightarrow \pi_S^*$ transition should be decreased. Indeed, the $l \rightarrow \pi^*$ intensities of C, CG and $CG_2$, for example, decrease in this order (see Figs. 1 and 2). A similar tendency is found in all other cases but the N, NG and $NG_2$ series, which is considered at present to be an exceptional case. In this case, the locations of the two sub-bands to be split may be in a reverse order relative to the other cases. The fact just mentioned makes necessary a consideration of the charge transfer. Consequently, the low wave number band can be assigned to the $l \rightarrow \pi^*$ transition, and the high one, to the $\pi \rightarrow \pi^*$ transition.

## Summary

1) The absorption spectra of binary mixtures of Chrysophenine G (notation: G) and disazo dyes (P), which were the same as those used in a preceding study,[1] have been measured at room temperature (ca. 20°C), and the characteristic spectra of the complexes have been determined by using the equilibrium constants, $K_1$ and $K_2$, previously obtained (at 20°C)[1] for the 1 : 1 (PG) and 1 : 2 ($PG_2$) complex formation.

2) The absorption spectra of the PG and $PG_2$ complex have been compared with the respective corresponding additive spectra (P+G and P+2G), and the correlations among these spectra have been discussed in detail.

3) The MO pattern of the G molecule has been decided empirically by applying Platt's theory; similarly, that of the P molecule has been decided by assuming that there is at least one symmetry species; then the spectral change caused by the complex formation could be explained in relation to the MO's of the component molecules.

4) It has been confirmed that there exists an intermolecular charge transfer from P as an electron donor to G as an acceptor. It has also been shown that the first band of a disazo dye (P) consists of two electronic transitions; one is a $\pi \rightarrow \pi^*$ (shorter wavelength) and the other an $l \rightarrow \pi^*$ transition (longer wavelength).

This work was supported in part by a Scientific Research Grant of the Ministry of Education to which the authors' thanks are due.

*Department of Chemistry*
*Tokyo Institute of Technology*
*Ookayama, Tokyo*

* The estimation was done arithmetically as follows:
$2\{\nu(CT) - [\nu(PG_2) - \nu(P)/2] - [25.5 - 22.0/2]\}$ kK
where CT indicates the charge transfer band; $\nu(PG_2)$ and $\nu(P)$ the first band of the $PG_2$ complex and of the P dye respectively, and 25.5kK and 22.0kK, respectively, the first band and the shoulder of G in Fig. 5.

7) Y. Tanizaki, T. Kobayashi and N. Ando, This Bulletin, 32, 119 (1959).

8) M. Kasha, "The Nature and Significance of $n \rightarrow \pi^*$ Transitions," presented at the Symposium on Light and Life, The McColum-Pratt Institute, The Johns Hopkins University, Baltimore, Maryland, March, 1960.

# A Spectrophotometric Study of Xylenol Orange as a Color Reagent for Beryllium

By Makoto OTOMO*

(Received August 1, 1964)

Xylenol orange reacts with many metal cations in a weakly or a slightly acid medium to form red or reddish-violet complexes, and it has widely been used as a metal indicator in complexometric titrations. This dye also reacts with beryllium ions to give a red coloration. The reaction is applied to the spectrophotometric determination of trace amounts of beryllium. The purpose of this study is to find the optimum conditions under which up to 6 $\mu$g. of beryllium can be determined, to ascertain the effect of diverse ions on the determination, and to determine the composition of the complexes formed. It will also be found that xylenol orange is a better color reagent for beryllium than eriochrome cyanine R[1] and 2-phenoxyquinizarin3, 4-disulfonic acid[2].

## Experimental

**Standard Beryllium Solution.** — A solution of beryllium perchlorate was prepared by dissolving the beryllium hydroxide, freshly precipitated from a beryllium sulfate solution in the presence of ethylenediaminetetraacetic acid (EDTA), which served as a masking agent for contaminating metal ions, in perchlorc acid (0.2 N in excess). The beryllium content was determined gravimetrically as oxide.

**Buffer Solution.**—A hexamethylenetetramine - perchloric acid mixture was prepared by dissolving about 4 g. of hexamethylenetetramine in 100 ml. of water and by adding a perchloric acid solution in order to bring the pH to a desired value.

The other reagents and apparatus used were the same as those reported on previously.[3] All experiments were carried out at 25±0.5°C.

**Standard Procedure for the Beryllium Determination.**—An aliquot of the standard beryllium solution was introduced into a 25 ml. volumetric flask. Ten milliliters of a pH 5.8 buffer, 2.5 ml. of a $1\times10^{-3}$ M xylenol orange solution and then a small amount of water were added to adjust the volume. After having been mixed, the solution was allowed to stand for about 30 min. The absorbance of the solution was measured against a reagent blank treated in a similar manner.

## Results

**Absorption Curves.**—When a buffered, aqueous solution of beryllium is mixed with a xylenol orange solution, a red complex is immediately formed. Figure 1 shows the absorption curves of xylenol orange and its beryllium

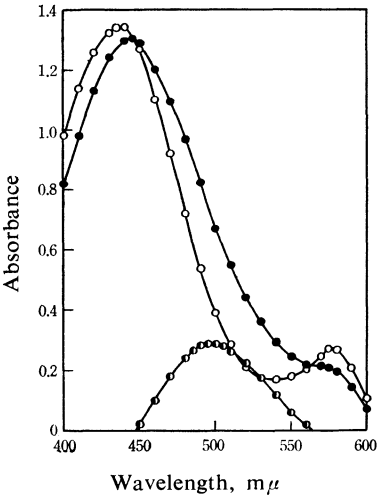



Fig. 1. Absorption curves of xylenol orange and its beryllium complex at pH 5.8.
Be : 4.5 $\mu$g., XO : $1.003\times10^{-4}$ M
—○— XO vs. water
—●— Be-XO + XO vs. water
—◐— Be-XO + XO vs. a reagent blank

complex. The absorption curve of the beryllium complex obtained with a reagent blank as reference has an absorption maximum at about 495 m$\mu$.

**The Effect of pH and Choice of Buffer.** — The pH is very important because the reagent functions as an acid-base indicator. The effect of pH on the color development of the complex was investigated by measuring the absorbance of mixtures containing 4.5 $\mu$g. (0.5 $\mu$mol.) of beryllium and 2.5 $\mu$mol. of the reagent at different pH values; the results are shown in Fig. 2, from which it can be seen that the optimum pH range for analytical purposes lies between 5.6 and 6.2. The buffer system, hexamethylenetetramine - perchloric acid, has a great

* Present address; Hachinohe Technical College, Hachinohe, Aomori.

1) S. Umemoto, This Bulletin, 29, 845 (1956).
2) E. G. Owens, II, and J. H. Yoe, *Anal. Chem.*, 32, 1345 (1960).
3) M. Otomo, This Bulletin, 36, 137 (1963).

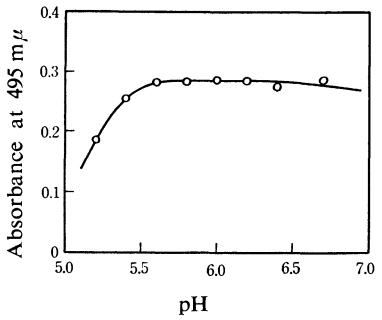



Fig. 2. Effect of pH on color development.
Be: 4.5 μg., XO: $1.003\times10^{-4}$ M

buffering capacity in the pH range from 4 to 7. The amount of the buffer had no effect on the color intensity of the complex provided that more than 3 ml. of the said solution was used. For the sake of comparison, an acetate buffer was also used, but the observed absorbance was always lower than that obtained with the hexamethylenetetramine - perchloric acid buffer.

**The Effect of the Amount of Xylenol Orange.**—Two series of colored solutions were prepared; one contained 4.5 μg. of beryllium, and the other, 9.0 μg. of beryllium. The results are shown in Fig. 3. For both series, about

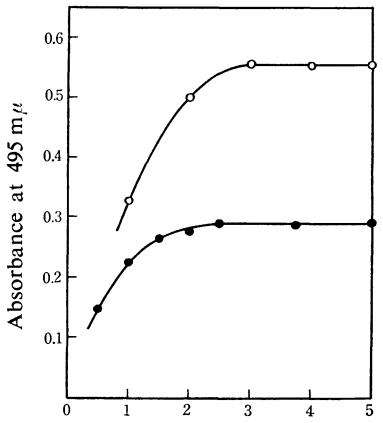



Fig. 3. Effect of amount of xylenol orange.
pH: 5.8, Reference: a reagent blank
—●— Be 4.5 μg.
—○— Be 9.0 μg.

a 4-fold excess of the reagent over the beryllium concentration is necessary in order to obtain the maximum color intensity. As a compromise between sensitivity and absorbance by the blank solution, 2.5 ml. of a $1\times10^{-3}$ M reagent solution was employed.

**The Color Stability.**—The red color of the complex develops immediately at room temperature, and its intensity is independent of the temperature, at least up to 80°C. The complex is very stable, and there was no change in absorbance over a period of 24 hr.

**Adherence to Beer's Law.**—The color system obeys Beer's law over the concentration range up to 0.63 μmol. (about 6 μg.) of beryllium.

**Sensitivity.**—The sensitivity of the reaction as expressed by Sandell's notation[4] is 0.0006 μg. of beryllium per $cm^2$.

**The Effect of Anions and Complexing Agents.**—The influence of various anions and some complexing agents was examined. These materials were added individually to solution containing 4.5 μg. of beryllium. The results are summarized in Table I. Chloride, nitrate and sulfate ions do not interfere, even at a high concentration. Phosphate and oxalate ions at lower concentration have no effect, either; however, these ions give negative errors at higher concentrations. Fluoride and citrate ions bleach the color of the complex, even when less than 1 μmol. is present. Nitrilotriacetic acid (NTA) and EDTA, which form stable complexes with many other metal ions to decompose the corresponding xylenol orange complexes, have almost no influence on the complex formation between beryllium and xylenol orange unless large amounts are added.

Table I. Effect of anions and complexing agents
Be taken: 4.5 μg.

| Anion or complexing agent added, | μmol. | Be found μg. | Deviation μg. |
|---|---|---|---|
| $Cl^-$ | 200 | 4.5 | ±0.0 |
| | 500 | 4.6 | +0.1 |
| $F^-$ | 1 | 4.3 | −0.2 |
| | 5 | 2.8 | −1.7 |
| $NO_3^-$ | 100 | 4.5 | ±0.0 |
| | 200 | 4.5 | ±0.0 |
| $SO_4^{2-}$ | 100 | 4.6 | +0.1 |
| | 250 | 4.5 | ±0.0 |
| $C_2O_4^{2-}$ | 5 | 4.2 | −0.3 |
| | 20 | 3.8 | −0.7 |
| $C_4H_4O_6^{2-}$ | 10 | 4.5 | ±0.0 |
| | 50 | 4.5 | ±0.0 |
| $PO_4^{3-}$ | 5 | 3.9 | −0.6 |
| | 20 | 3.8 | −0.7 |
| $C_6H_5O_7^{3-}$ | 1 | 4.0 | −0.5 |
| | 10 | 1.8 | −2.7 |
| NTA | 1 | 4.5 | ±0.0 |
| | 10 | 4.2 | −0.3 |
| EDTA | 0.1 | 4.5 | ±0.0 |
| | 2 | 4.2 | −0.3 |

4) E. B. Sandell, "The Colorimetric Determination of Traces of Metals," Interscience Publishers, New York (1950), p. 49.

Therefore, NTA and EDTA can serve as excellent masking agents to prevent the interference of other heavy metals. The latter has been used as a masking agent in several methods of beryllium determination,[5-8] and recently Owens and Yoe[2] used the Calcium-EDTA complex as a sequestering agent in the spectrophotometric determination of beryllium.

**The Effect of Cations.**—Xylenol orange is a selective reagent for certain cations when it is used in a relatively strong acid medium. However, in a slightly acid or a neutral medium it reacts with many metal cations to give red or reddish-violet complexes, indicating that a suitable masking agent must be used to increase the selectivity. Disodium salt of EDTA was chosen for this reason. Most common bivalent metal cations except cobalt can be effectively masked by EDTA, as Table II shows. Many ter- and quadrivalent cations, including aluminum, bismuth, thorium and zirconium, however, disturb the estimation.

Table II. Masking effect of EDTA on beryllium determination

Beryllium taken: 4.5 $\mu$g.
Cations added: each 2.0 $\mu$mol.
EDTA added: 2.5 $\mu$mol.

| Cation | Be found, $\mu$g. | Deviation, $\mu$g. |
|---|---|---|
| $Bi^{3+}$ | 4.8 | +0.3 |
| $Cd^{2+}$ | 4.5 | ±0.0 |
| $Co^{2+}$ | 5.4 | +0.9 |
| $Cu^{2+}$ | 4.4 | −0.1 |
| $Fe^{3+}$ | 4.5 | ±0.0 |
| $Hg^{2+}$ | 4.4 | −0.1 |
| $La^{3+}$ | 4.7 | +0.2 |
| $Mg^{2+}$ | 4.4 | −0.1 |
| $Mn^{2+}$ | 4.4 | −0.1 |
| $Pb^{2+}$ | 4.3 | −0.2 |
| $Pd^{2+}$ | 4.4 | −0.1 |
| $Zn^{2+}$ | 4.4 | −0.1 |

## Complex Formation

First, attempts were made to characterize the beryllium - xylenol orange complex by two methods, the method of continuous variations and the mole ratio method. These attempts were performed at various pH values between 5.0 and 7.0, while the absorbance measurements were made at seven wavelengths between 440 and 520 m$\mu$. Both methods revealed that beryllium forms chiefly a 1 to 1 complex with xylenol orange at a pH below 5.0; it gives, however, a mixture of 1 to 1 and 1 to 2 complexes at higher pH values. The results were further supported by the following experiments.

**The Formation of the 1 to 1 Complex.**—A method which had been described by Newman and Hume[9] was applied to the complex formed at relatively lower pH values. If $Be_n(XO)$ is the only beryllium complex in a detectable concentration in solutions containing beryllium and xylenol orange, the apparent formation constant at a given pH value, $(K_1')_H$, may be defined as:

$$(K_1')_H=[Be_n(XO)]/[Be]^n[XO] \quad (1)$$

where [XO] represents the molar concentration of the free xylenol orange at equilibrium. The absorbance of a solution containing the complex and the free xylenol orange is:

$$D=[Be_n(XO)]\varepsilon_{C_1}+([XO]_t-[Be_n(XO)])(\varepsilon_{XO})_H \quad (2)$$

where $\varepsilon_{C_1}$ is the molar extinction coefficient of the complex; $(\varepsilon_{XO})_H$ is the apparent molar extiction coefficient of xylenol orange at a given pH value, and $[XO]_t$ is the total molar concentration of xylenol orange. The concentration of the complex, beryllium and xylenol orange at equilibrium are expressed, respectively, as:

$$[Be_n(XO)]=(D-[XO]_t(\varepsilon_{XO})_H)/(\varepsilon_{C_1}-(\varepsilon_{XO})_H) \quad (3)$$

$$[Be]=[Be]_t-n(D-[XO]_t(\varepsilon_{XO})_H)/(\varepsilon_{C_1}-(\varepsilon_{XO})_H) \quad (4)$$

and

$$[XO]=[XO]_t-(D-[XO]_t(\varepsilon_{XO})_H)/(\varepsilon_{C_1}-(\varepsilon_{XO})_H) \quad (5)$$

By introducing Eqs. 3, 4 and 5 into Eq. 1 and by taking logarithms, Eq. 6 is derived:

$$\log\{(D-D_{XO})/(D_C-D)\}=\log(K_1')_H+n\log\{[Be]_t-n(D-D_{XO})/(\varepsilon_{C_1}-(\varepsilon_{XO})_H)\} \quad (6)$$

where $D_{XO}$ is the absorbance of the total xylenol orange and $D_C$ is the absorbance of a solution containing a large excess of beryllium ions and the given amount of xylenol orange.

The experimental values of $\log\{(D-D_{XO})/(D_C-D)\}$ are plotted against the values of $\log\{[Be]_t-n(D-D_{XO})/(\varepsilon_{C_1}-(\varepsilon_{XO})_H)\}$ at pH 4.5 for five wavelengths between 480 and 510 m$\mu$. When the value of $n$ was assumed to be unity, the plots gave straight lines with a slope of 1.08 (on the average), as may be seen from Fig. 4. When other values, e. g., one-half, two,

5) H. V. Meek and C. V. Banks, *Anal. Chem.*, **22**, 1512 (1950).
6) C. L. Luke and M. E. Campbell, ibid., **24**, 1056 (1952).
7) C. W. Sill and C. P. Willis, ibid., **31**, 598 (1959).
8) P. W. West and P. R. Mohilner, ibid., **34**, 558 (1962).
9) L. Newman and D. N. Hume, *J. Am. Chem. Soc.*, **79**, 4571 (1957).

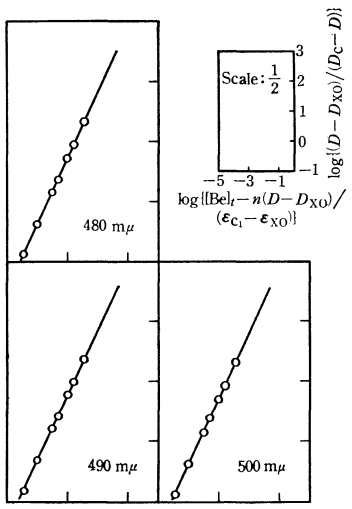



Fig. 4. Plots of $\log\{(D-D_{XO})/(D_C-D)\}$ vs. $\log\{[Be]_t-n(D-D_{XO})/(\varepsilon_{C_1}-\varepsilon_{XO})\}$.
$[XO]_t$: $4.0\times10^{-5}$ M, pH: 4.5
$\mu$: 0.10($NaClO_4$), Reference: water

etc., were assumed for $n$, however, no straight lines with slopes of the assumed values were obtained. Therefore, it may be concluded that the beryllium - xylenol orange complex formed at the investigated pH value has a molar ratio of 1 to 1. As is shown by Eq. 6, the intercept of the straight line should give the value of $\log(K_1')_H$ at pH 4.5. The values of $\varepsilon_{C_1}$, $n$ and $\log(K_1')_H$ obtained are summarized in Table III.

TABLE III. VALUES OF $\varepsilon_{C_1}$, $n$ AND $\log(K_1')_H$ AT pH 4.5

| | Wavelength, mμ | | |
|---|---|---|---|
| | 480 | 490 | 500 |
| $\varepsilon_{C_1}$ | 12550 | 12050 | 11130 |
| $n$ | 1.10 | 1.06 | 1.08 |
| $\log(K_1')_H$ | 4.00 | 3.91 | 3.92 |

**The Formation of a Mixture of 1 to 1 and 1 to 2 Complexes.**—To determine the composition of the complex formed in a higher pH region, the presence of a mixture of 1 to 1 and 1 to 2 complexes was assumed and a method described by McConnell and Davidson[10] was applied. If the total concentration of xylenol orange is high enough compared with that of beryllium and if the pH value of the solution is kept constant, the successive apparent formation constants at given pH values, $(K_1')_H$ and $(K_2')_H$, may be written, respectively, as:

$$(K_1')_H=[Be(XO)]/([Be]_t-[Be(XO)_n])[XO]_t \quad (7)$$

$$(K_2')_H=[Be(XO)_n]/[Be(XO)][XO]_t^{n-1} \quad (8)$$

If the absorbance of the solution is measured against a solution containing the same amount of free xylenol orange as that added to beryllium, it may be given by:

$$D=[Be(XO)](\varepsilon_{C_1}-(\varepsilon_{XO})_H)+[Be(XO)_n](\varepsilon_{C_2}-n(\varepsilon_{XO})_H) \quad (9)$$

where $\varepsilon_{C_1}$ and $\varepsilon_{C_2}$ are the molar extinction coefficient of Be(XO) and $Be(XO)_n$ respectively, and where $(\varepsilon_{XO})_H$ is the apparent molar extinction coefficient of xylenol orange at a given pH value. From Eqs. 7, 8 and 9, the following relationship may be derived:

$$[Be]_t/D=1/(\varepsilon_{C_2}-n(\varepsilon_{XO})_H)+F/(\varepsilon_{C_2}-n(\varepsilon_{XO})_H)(K_1')_H(K_2')_H[XO]_t^n \quad (10)$$

$$F=1+(K_1')_H[XO]_t-(K_1')_H[Be]_t[XO]_t(\varepsilon_{C_1}-(\varepsilon_{XO})_H)/D$$

The experiments were carried out in the concentration range, $[XO]_t=0.89\times10^{-4}$—$3.57\times10^{-4}$ M, the pH value being held constant at 5.30 and the ionic strength being held constant at 0.1. Although the total concentration of xylenol orange was not sufficiently large compared with that of beryllium ($1.996\times10^{-5}$ M), it is assumed, for the first approximation, that the equilibrium concentration of xylenol orange nearly equals the total concentration. The graphical analysis was done at three wavelengths, 480, 490 and 500 mμ, using the value of $(K_1')_H$ at pH 5.30 ($1.60\times10^6$), a value which was obtained according to the method described by Buděšinský,[11] and the calculated values of $(\varepsilon_{C_1}-(\varepsilon_{XO})_H)$. Although good straight lines were not obtained, the values of $(K_2')_H$ at pH 5.30 at the three wavelengths were estimated from the slopes as $7.3\times10^3$, $5.6\times10^3$ and $5.5\times10^3$ respectively. Therefore, for the second approximation to the solution of Eq. 10, the deviation between the total concentration of xylenol orange was calculated using the first approximation for $(K_2')_H$. The correction is small at relatively higher concentrations of xylenol orange, but a large correction (about 30%) was required at the lowest concentration of xylenol orange. The corrected values of the total concentration of xylenol orange were then used, and the linear character of the plots of $[Be]_t/D$ vs. $F/[XO]_t^n$ was examined. Figure 5 shows the results obtained when the value of $n$ equals two, indicating that the plots are good straight lines within the range of experimental error. The third approximation was further applied. However, it was

10) H. McConnell and N. Davidson, ibid., 72, 3164 (1950).

11) B. Buděšinský, *Collection Czechoslov. Chem. Commun.*, 27, 226 (1962).

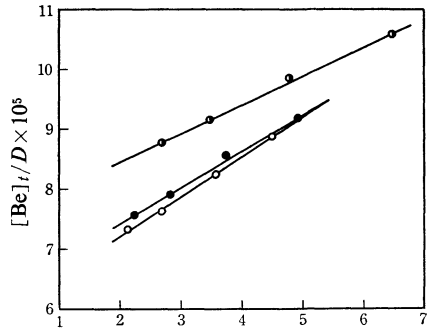



Fig. 5. Plots of $[Be]_t/D$ vs. $F/([XO]_t-[Be(XO)]-2[Be(XO)_2])^2$.

$[Be]_t$: $1.966\times10^{-5}$ M, pH: 5.3
$\mu$: 0.10 ($NaClO_4$), Reference: water
Wavelength: —◑— 480 m$\mu$, —●— 490 m$\mu$
—○— 500 m$\mu$

found that there is little difference between the second and third approximations.

Finally, the concentrations of the 1 to 1 and the 1 to 2 complexes were calculated at pH 5.8 and at varying concentrations of xylenol orange, using the following relationships, which can easily be obtained by solving Eqs. 7 and 8:

$$[Be(XO)]=(K_1')_H[Be]_t[XO]_t/(1+(K_1')_H[XO]_t+(K_1')_H(K_2')_H[XO]_t^2) \quad (11)$$

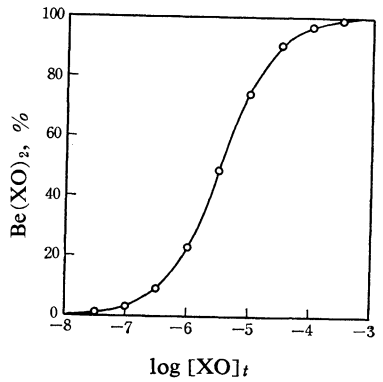



Fig. 6. Percentage occupied by $Be(XO)_2$ in a mixture of Be(XO) and $Be(XO)_2$ at pH 5.8.

Be: $2.0\times10^{-5}$ M

$$[Be(XO)_2]=(K_1')_H(K_2')_H[Be]_t[XO]_t^2/(1+(K_1')_H[XO]_t^2+(K_1')_H(K_2')_H[XO]_t^2) \quad (12)$$

The percentage occupied by the 1 to 2 complex in a mixture of the 1 to 1 and 1 to 2 complexes was calculated as a function of the concentration of xylenol orange. The curve in Fig. 6 was obtained when the total molar concentration of beryllium was constant as $2.0\times10^{-5}$ M. The reciprocal of the value of log $[XO]_t$ at the intercept of the 50% line with the curve should give the value of log $(K_2')_H$ at pH 5.8. The pH value of 5.8 was chosen because the determination of beryllium was performed at this pH value.

## Summary

The red color produced by adding a xylenol orange solution in excess to a beryllium solution has been studied spectrophotometrically in order to ascertain the optimum conditions for the determination of beryllium. The absorption curve of the colored system shows an absorption maximum at 495 m$\mu$ when measured against a reagent solution of pH 5.8. Beer's law is obeyed over the range up to 6 $\mu$g. of beryllium. The composition and the apparent formation constant of the two different complexes have then been obtained by applying some spectrophotometric techniques. Beryllium forms a 1 to 1 complex with xylenol orange below pH 5; it gives, however, mixture of 1 to 1 and 1 to 2 complexes at higher pH values.

The author wishes to thank Professor Kôichi Tonosaki for his kind guidance and encouragement throughout the course of this study and Mr. Hiroshi Osanai for his assistance. Thanks are also due to Professor Yoshinaga Oka of the Faculty of Science, Tohoku University, for his valuable advice.

*Department of Chemistry*
*Faculty of Literature and Science*
*Hirosaki University*
*Hirosaki, Aomori*

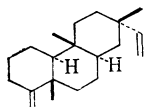
# The Structure of Hibaene[1]

By Yoshio KITAHARA and Akira YOSHIKOSHI

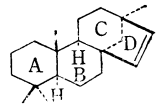
(Received August 3, 1964)

Dolabradiene, a diterpene isolated from the essential oil of the leaves of Hiba (*Thujopsis dolabrata* Sieb. et Zucc.) has been shown[2] by the present authors to have structure I.

A purification by gas liquid chromatography of the fraction of the above oil with a b. p. of 162—167° C/7 mmHg gave a new crystalline diterpene named hibaene. On the basis of the experimental data which will be described below, we could determine the absolute configuration of hibaene to be II.



I



II

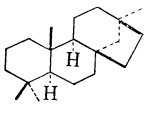
Hibaene is a crystalline compound with a melting point of 30°C; $[\alpha]_D^{23}$ −49.9°; the mass spectrum[3] of hibaene showed a molecular weight of 272. The relative abundance of the parent peak (P) and the (P+1) peak indicated the molecular formula $C_{20}H_{32}$, which was also supported by its elemental analysis.

The infrared absorption spectrum of hibaene indicated the presence of a geminal dimethyl group (1385, 1363 $cm^{-1}$) and *cis*-1,2-disubstituted ethylene (750 $cm^{-1}$). When hibaene was hydrogenated catalytically, it absorbed one molar equivalent of hydrogen, thus yielding a saturated hydrocarbon, dihydrohibaene (III). Oxidation of hibaene by peracid afforded monoepoxide (IV). From these facts, it was assumed that hibaene possesses one double bond; therefore, it must be a tetracyclic diterpene. The nuclear magnetic resonance spectrum of hibaene displays the signals (9.27, 9.19, 9.15, 9.03 $\tau$, all singlet)[4] of four methyl groups bonded on quarternary carbon atoms and the typical AB type signals of olefinic protons (4.39, 4.64 $\tau$, $J$=6 c.p.s., two protons). Accordingly, the double bond was attached to carbon which bears no proton, and the partial sturcture V was deduced.

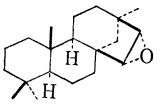
Since these physical constants were different from those of the diterpenes reported hitherto, hibaene was supposed to be a new diterpene.

The dehydrogenation of hibaene by selenium gave pimanthrene (VI), and the oxidation of hibaene using permanganate yielded a dicarboxylic acid (VII) without loss of the carbons. VI was also obtained by the dehydrogenation of VII using selenium. The above facts indicate that three rings out of the four rings of hibaene form a perhydrophenanthrene ring system and that the double bond is contained in the remaining ring (ring D).

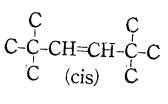
When VII was heated above 220°C or was treated with acetic anhydride, an anhydride (IX) was easily obtained. From the infrared absorption spectrum of IX, this was assumed to be a strainless cyclic anhydride (of the glutaric anhydride type). IX was stable when heated at 300°C and was recovered. The dimethyl ester (VIII) of VII did not undergo hydrolysis with diluted potassium hydroxide; therefore, both of the ester groups are considered to be linked with quarternary carbon. This fact also supports the partial structure V deduced from the nuclear magnetic resonance spectrum of hibaene mentioned before.



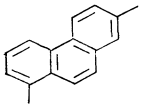
III



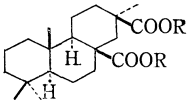
IV



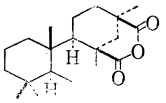
V



VI



VII R=H
VIII R=Me



IX

In view of the experimental facts described so far and from a consideration of the biogenesis[5] of hibaene (Scheme 1), the structure of hibaene is presumed to be II (or its enantiomer).

As was reported earlier, the shifts of methyl group signals observed between II and III in the nuclear magnetic resonance spectra, and those observed between isophyllocladene (X)

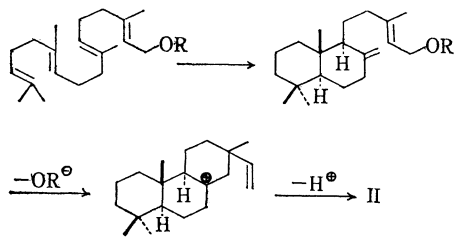
1) This paper was read at the 5th Symposium on the Chemistry of Natural Products, Japan, July, 1962; Y. Kitahara and A. Yoshikoshi, *Tetrahedron Letters*, 1771 (1964).

2) Y. Kitahara and A. Yoshikoshi, ibid., 1755 (1964); A. Yoshikoshi, *J. Chem. Soc. Japan, Pure Chem. Sec.* (*Nippon Kagaku Zasshi*), **85**, 383, 386, 390 (1964).

3) The mass spectrum was measured using Hitachi RMU-6A. The authors wish to express their gratitude to Hitachi, Ltd.

4) The assignments of the signals of the methyl groups were made by Y. Kitahara and A. Yoshikoshi, This Bulletin, **37**, 890 (1964).

5) Cf. L. Ruzicka, *Experientia*, **9**, 357 (1953).




Scheme 1

and phyllocladane (XI), are parallel.[4] This also supports the theory that hibaene has structure II or its enantiomer.

Further proof for the stereochemistry was obtained as follows.

The hydroboration of II, followed by oxidation with dichromate and chromatographical separation on alumina, gave two isomeric ketones. The infrared adsorption spectrum of the polar ketone showed a band (1736 $cm^{-}$) which can be assigned to a five-membered-ring ketone. The ketone reacted with carbonyl reagents to give the corresponding derivatives and underwent oxidation by perbenzoic acid to afford a lactone (XII). On the other hand, the carbonyl band of the less polar ketone shifts to a longer wavelength region (1727 $cm^{-1}$) compared with that of the former ketone. The less polar ketone did not react with carbonyl reagents or perbenzoic acid, and the starting material was recovered.

The abnormality of the carbonyl group of the less polar ketone is considered to be due to the steric interference. Consideration using the molecular model of hibaene gave us the following information. Supposing that hibaene is a *trans-anit-trans* perhydrophenanthrene derivative, the methyl group at C-10 is cis to the D ring. Besides, when the carbonyl group is present at C-15, the carbonyl group is considerably hindered by the methyl group at C-10. Accordingly, it is assumed that the less polar ketone and the polar one are XIII and XIV respectively, or their enantiomers.

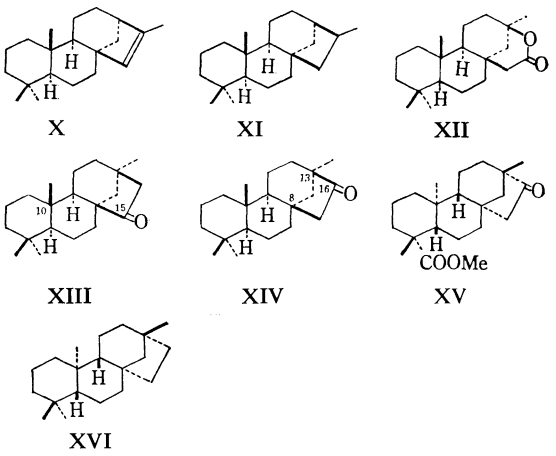
Because the optical rotatory dispersion curve of XIV shows a positive Cotton effect and is antiopodal with that of isosteviol[6] (XV), the absolute configuration of the D ring of XIV is $\beta$ (Fig. 1).

From the afore-mentioned results, out of the five asymmetric centers of hibaene the absolute configurations of C-13 and C-8 became clear; the others were proved as follows.

If the absolute configuration of hibaene is shown by II, dihydrohibaene (III) must be an enantiomer of isostevane[7] (XVI). The infrared absorption spectra of the two compounds, III and XVI, are superimposable, but a mixed melting point determination showed an apparent depression. The optical rotatory dispersion curves of both compounds show plane curves with a value of almost 0°.[8]

On the basis of the various results described hitherto, the absolute configuration of hibaene was definitely proved to be II.

Recently, the fact that hibaene is identical with cupressene[9] and enantiomeric with stachene[10] has been established.[11]



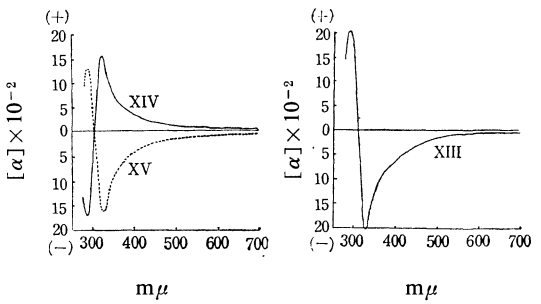




Fig. 1. RD curves of the ketones (XIII, XIV and XV) in methanol.

## Experimental[12]

**The Isolation of Hibaene (II).**—The essential oil obtained from the leaves of Hiba (*Thujopsis*

6) C. Djerassi, R. Riniker and B. Riniker, *J. Am. Chem. Soc.*, **78**, 6362 (1956); C. Djerassi, P. Quitt, E. Mosettig, R. C. Cambie, P. S. Rutledge and L. H. Briggs, ibid., **83**, 3720 (1961).

7) E. Mosettig and W. Nes, *J. Org. Chem.*, **20**, 884 (1955); E. Mosettig, U. Beglinger, F. Dolder, H. Lichti, P. Quitt and J. A. Waters, *J. Am. Chem. Soc.*, **85**, 2305 (1963).

8) The reported specific optical rotation of isostevane (XVI) is $[\alpha]_D+4°$,[6] but $[\alpha]_{300-700\,m\mu}$ by our measurement was 0° within the range of experimental error.

9) L. H. Briggs, B. F. Cain, B. R. Davis and J. K. Wilmshurst, *Tetrahedron Letters*, **No. 8**, 8, 13 (1959).

10) R. D. H. Murray and R. McCrindle, *Chem. & Ind.* **1964**, 500.

11) The direct comparison was made by Professor Briggs (Department of Chemistry, University of Auckland, New Zealand), who kindly informed us (letter dated June 26, 1964).

*dolabrata*) by steam distillation was washed with a diluted sodium hydroxide aqueous solution, dried over anhydrous magnesium sulfate, and fractionally distilled using a spinning band column, the theoretical plate of which was around sixty. The fraction with a b. p. of 162—167°C/7mmHg was obtained in a yield of approximately 5% of the original oil. The gas liquid chromatography (20% DC Silicon oil-Hitachi Carrier. 3 m.; column temperature 235 °C; flowing rate of helium gas 50 ml./min.) of the above fraction indicated that the oil contained a small amount of dolabradiene besides hibaene (retention time 12 min.). By the purification using preparative gas liquid chromatography under the same conditions as the above preliminary chromatography, hibaene was crystallized.

The hibaene fraction obtained from the fractional distillation was cooled to around −50°C; then the crystalline hibaene was added. Most of the liquid hibaene became a crystalline mass, which was then filtered under cooling, recrystallized from ethyl acetate at around −60°C, and further recrystallized from ethanol, thus affording hibaene (II), m. p. 29.5—30.5°C, $[\alpha]_D^{23}$ −49.9° (*c* 0.1, chloroform), molecular weight 272 (mass spectrum).

Found: C, 88.45; H, 11.89. Calcd. for $C_{20}H_{32}$: C, 88.16; H, 11.84%.

IR (KBr disk): 1385, 1363 (*gem.* dimethyl), 750 $cm^{-1}$ (*cis* 1, 2-disubstituted ethylene). NMR (10% carbon tetrachloride solution): 9.27, 9.19, 9.15, 9.03 (singlets, 3 protons each), 4.39, 4.64 $\tau$ (quartet, $J$=6 c.p.s., 2 protons).

**Dihydrohibaene (III).**—When a solution of 0.54 g. of II in 10 ml. of ethyl acetate was submitted to catalytic hydrogenation in the presence of 50 mg. of 10% palladium-charcoal under atomospheric pressure and at room temperature, 0.98 molar equivalent of hydrogen was rapidly absorbed. After the catalyst and the solvent had been removed, the residue was recrystallized from ethanol, yielding colorless plates, m. p. 41.5—42.5°C.

Found: C, 87.83; H, 12.53. Calcd. for $C_{20}H_{34}$: C, 87.51; H, 12.49%.

$[\alpha]_{300-700m\mu}=0°$ (*c* 0.6, dioxane).[13] IR (carbon disulfide solution) was entirely superimposable on that of isostevane, but the melting point of III was depressed below room temperature on admixture with isostevane.

**Monoepoxide (IV) of Hibaene.**—A solution of 0.5 g. of hibaene in 3.6 ml. of chloroform containing 0.28 g. of perbenzoic acid was allowed to stand at 0°C for one day. After ether had been added to the solution, it was washed with a 2% sodium hydroxide aqueous solution and then with water, and dried over anhydrous magnesium sulfate. The removal of the solvent gave a semisolid substance, which was purified by submitting it to alumina column chromatography using 20 g. of alumina and benzene - petroleum ether (1 : 1) as eluting solvent; thus 0.53 g. of crystals, m. p. 63—70°C, were afforded. Recrystallization from acetone gave colorless prisms, m. p. 70—71°C.

12) All melting points are uncorrected. The authors wish to express their thanks to Misses Yoko Endo and Yukiko Endo of this Institute for their microanalyses.

13) Isostevane, m. p. 41.5—43.5°C; $[\alpha]_{300-700m\mu}=0°$ (*c* 0.6, dioxane).

Found: C, 83.46; H, 10.85. Calcd. for $C_{20}H_{32}$: C, 83.27; H, 11.18%.

**The Dehydrogenation of Hibaene by Selenium.**—A mixture of 1.5 g. of hibaene and 3.0 g. of selenium was heated at 320—340°C for 43 hr. The reaction mixture was extracted with ether, and the extract was washed with a 10% potassium hydroxide aqueous solution and then with water, and dried over magnesium sulfate. The removal of the ether yielded 1.38 g. of oil, which was chromatographed on alumina (40 g. of alumina was used). From a petroluem ether - benzene (1 : 1) effluent, 0.45 g. of crystals were obtained; they were recrystallized from ethanol to give colorless leaflets, m. p. 83—84°C. This compound was proved to be pimanthrene[14] by mixed melting point determination and from a comparison of their infrared absorption spectra.

**Dicarboxylic Acid (VII).**—To a solution of 4.9 g. of hibaene in 100 ml. of acetone, 7.5 g. of powdered potassium permanganate was added in portions over a period of 70 min. while the solution was maintained at 30—35°C. After the mixture had been stirred for an additional 90 min. at the same temperature, 30 ml. of water was added. The manganese dioxide formed was reduced by sulfur dioxide gas. The acetone was removed under reduced pressure, and the residue was acidified with diluted hydrochloric acid and extracted with ether. The ether solution was then extracted with a sodium carbonate aqueous solution. The acidification of the sodium carbonate extract yielded 4.17 g. of crystalline dicarboxylic acid, m. p. 240—250°C. Recrystallization from aqueous ethanol gave colorless needles, m. p. 251—253°C (dehydrated around 220°C and thus converted to anhydride).

Found: C, 71.57; H, 9.60. Calcd. for $C_{20}H_{32}O_4$: C, 71.39; H, 9.59%.

IR (KBr disk): ~2600, 1710 $cm^{-1}$ (broad) (carboxyl).

**The Dehydrogenation of Dicarboxylic Acid (VII) by Selenium.**—A mixture of 2.0 g. of dicarboxylic acid and 4.0 g. of selenium was heated at 320—340 °C for 40 hr. The reaction mixture was extracted with ether, and the extract was washed with a 10% potassium hydroxide aqueous solution and water, dried over anhydrous magnesium sulfate, and distilled to yield 1.29 g. of a semisolid sudstance. This was purified by alumina column chromatography using 50 g. of alumina and petroleum ether - benzene (1 : 1) as the solvent, to give 0.41 g. of crystals. Recrystallization from ethanol gave colorless leaflets, m. p. 83—84°C, which were proved to be pimanthrene[14] by a mixed melting point determination and a comparison of their infrared absorption spectra.

**Anhydride (IX).**—After a mixture of 0.56 g. of dicarboxylic acid (VII) and 4 ml. of acetic anhydride had been refluxed for 1 hr., the excess acetic anhydride and acetic acid was distilled off under reduced pressure to yield 0.55 g. of a crystalline compound, m. p. 250—252°C. This was recrystallized from acetone to afford colorless needles, m. p. 253—254°C.

14) R. D. Haworth, B. M. Letsky and C. R. Mavin, *J. Chem. Soc.*, **1932**, 1789.

Found: C, 75.66; H, 9.71. Calcd. for $C_{20}H_{30}O_3$: C, 75.43; H, 9.50%.

IR (KBr disk): 1790, 1758 $cm^{-1}$ (anhydride).

This anhydride was recovered after the mixture had been heated at 300°C for 10 min. without any product being formed.

**Dicarboxylic Dimethyl Ester (VIII).**—A solution of 1.50 g. of dicarboxylic acid (VII) in 40 ml. of ether was methylated with a slight excess of a diazomethane etherial solution. When the reaction mixture was treated by the usual method, 1.58 g. of crude dimethyl ester, m. p. 141.5—143.5°C, was obtained. Recrystallization from aqueous ethanol gave colorless plates, m. p. 144—145°C.

Found: C, 72.42; H, 10.09. Calcd. for $C_{22}H_{36}O_4$: C, 72.49; H, 9.96%.

IR (KBr disk): 1736, 1716 $cm^{-1}$ (ester group).

After a solution of 0.73 g. of the dimethyl ester had been refluxed in 30 ml. of a 0.1 N potassium hydroxide methanolic solution for 2 hr., the reaction mixture was concentrated under reduced pressure, diluted with water, and extracted with ether. The acidification of the water layer with diluted hydrochloric acid did not give any substance. From the ether extract, 0.73 g. of a crystalline compound, m. p. 143—144.5°C, was obtained. Recrystallization from diluted ethanol raised the melting point of the compound to 144—145°C; no depression of melting point was observed on admixture with VIII.

**Ketones (XIII and XIV).**—An excess of diborane was passed to a solution of 7.15 g. of hibaene in 70 ml. of anhydrous tetrahydrofuran under cooling with ice water and under a dry nitrogen atomosphere. After the solution had been allowed to stand at room temperature for 1 hr., the solvent was removed under reduced pressure and the residue was dissolved in 40 ml. of ether. To this solution was added a solution of 11.6 g. of sodium bichromate dissolved in a mixture of 30 ml. of water and 6.0 ml. of sulfuric acid; then the solution was refluxed gently while being stirred at around 40°C for 7 hr. After cooling, the water layer which separated from the ether layer was extracted with ether. The combined ether solution was washed with water and dried over anhydrous magnesium sulfate. The removal of the ether afforded 8.0 g. of a semisolid substance, which was purified by alumina chromatography (200 g. of alumina was used). From the petroleum ether effluent and the successive benzene effluent, 1.98 g. of an oil and 4.75 g. of a crystalline compound respectively were obtained. The crystalline compound was sublimed under reduced pressure (2 mmHg, bath temperature below 120°C) to yield 3.87 g. of crystalline sublimate. This sublimate was further purified using an alumina column containing 200 g. alumina. The results obtained were as follows: i) 0.34 g. of crystals (m. p. 73—84°C) from the petroleum ether - benzene (7 : 3) effluent; ii) 1.66 g. of crystals (m. p. 80—84°C) from the petroleum ether - benzene (5 : 5) effluent; iii) 1.01 g. of crystals (m. p. 66—88°C) from the same solvent as ii; iv) 0.95 g. of crystals (m. p. 95—102°C) from the same solvent as ii, followed by benzene.

Fractions i and ii were combined and recrystallized from methanol to give colorless prisms (XIII), m. p. 88—89°C.

Found: C, 83.19; H, 10.89. Calcd. for $C_{20}H_{32}O$: C, 83.27; H, 11.18%.

IR (KBr disk): 1725 $cm^{-1}$; (carbon tetrachloride solution): 1727 $cm^{-1}$ (carbonyl group). RD (methanol solution $c$ 0.1): $[\alpha]_{700}$ −56°, $[\alpha]_{589}$ −81°, $[\alpha]_{323}$ −2040°, $[\alpha]_{285}$ +2010°.

XIII did not react with 2, 4-dinitrophenylhydrazine or perbenzoic acid under conditions similar to those in the formation of lactone (X), and only the starting material was recovered.

The recrystallization of the crystals from fraction iv from methanol gave colorless prisms (XIV), m. p. 102—103°C.

Found: C, 83.22; H, 10.86. Calcd. for $C_{20}H_{32}O$: C, 83.27; H, 11.18%.

IR (KBr disk): 1733 $cm^{-1}$; (carbon tetrachloride solution): 1736 $cm^{-1}$ (carbonyl group). RD (methanol solution $c$ 0.1): $[\alpha]_{700}$ +30°, $[\alpha]_{589}$ +48°, $[\alpha]_{318}$ +1528°, $[\alpha]_{278}$ −1720°.

2, 4 - Dinitrophenylhydrazone; Recrystallization from ethanol-ethyl acetate gave orange needles, m. p. 231—231.5°C.

Found: N. 12.05. Calcd. for $C_{26}H_{34}O_4N_4$: N, 12.01%.

**Lactone (XII).**—A solution of 3.86 g. of XIV, 39 ml. of chloroform containing 2.42 g. of perbenzoic acid, 40 ml. of acetic acid and 0.45 ml. of sulfuric acid was allowed to stand at 10—20°C for 5 days. The reaction mixture was then poured into water, and the water layer was extracted with ether. The chloroform solution, combined with the ether extract, was washed with a 2% sodium hydroxide aqueous solution and water, and dried over anhydrous magnesium sulfate. The removal of the solvent gave a crystalline residue, which was purified by a neutral alumina column (100 g. of alumina was used). The crystals from the benzene and benzene-ether (1 : 1) effluents, 3.10 g., m. p. 100—110°C, were recrystallized from *n*-hexane, affording colorless needles, m. p. 111—112°C.

Found: C, 78.82; H, 10.49. Calcd. for $C_{20}H_{32}O_2$: C, 78.89; H, 10.59%.

IR (KBr disk): 1713 $cm^{-1}$ (lactone).

## Summary

The structure and absolute configuration of hibaene, a new diterpene isolated from the essential oil of the leaves of hiba (*Thujopsis dolabrata* Sieb. et Zucc.), have been presented.

The authors are indebted to Dr. Yoshio Sato, National Institute of Health, for donating a sample of isostevane and also to the Ogawa Perfumery Co., Ltd., for supplying the original essential oil for this research.

*The Chemical Research Institute of Solutions Non-Aqueous*
*Tohoku University*
*Katahira-cho, Sendai*

# Absorption and Fluorescence Spectra of Anthracene-*s*-Trinitrobenzene Complex Crystal*[1]

By Jiro TANAKA*[2] and Keitaro YOSHIHARA*[3]

(Received August 10, 1964)

The electronic spectra of a crystal of a charge-transfer type molecular complex is of particular interest since the mechanism of the electronic interaction between the electron donor and the acceptor can be elucidated by the aid of polarization measurements. Nakamoto[1] measured the polarized absorption spectra of charge-transfer complexes such as quinhydrone and showed that the charge transfer absorption is stronger along the direction out of the plane of the benzene ring. The absorption spectra of the crystal formed between anthracene and 1, 3, 5-trinitrobenzene (TNB) was also studied by Lawer, Hochstrasser and Reid,[2] and the fluorescence and phosphorescence of this system was investigated by Czekalla et al.[3] and McGlynn and his co-workers.[4] According to these studies, the fluorescence is to be ascribed to a reverse process of charge transfer absorption, since a linear relationship was found between the absorption and the fluorescence for various systems having TNB as an electron acceptor. The theoretical analysis of the charge resonance interaction is facilitated by crystal studies, and the structure of the crystal has been recently determined by Wallwork and his co-workers.[5]

In this paper a polarization measurement of the absorption and fluorescence spectra of the crystal will be reported with the view of obtaining detailed information on the electronic interaction between the electron donor and the acceptor. The electric conductivity of the crystal has already been reported on by Kuroda, Yoshihara and Akamatu.[6]

*1 Presented at the Symposium on the Electronic States of Molecules, Sendai, 1963.

*2 Present address: Department of Chemistry, Faculty of Science, Nagoya University, Chikusa-ku, Nagoya.

*3 Present address: Department of Chemistry, University of California, Riverside, California, U. S. A.

1) K. Nakamoto, *J. Am. Chem. Soc.*, **74**, 1739 (1952); This Bulletin, **26**, 70 (1953).

2) S. K. Lawer, R. M. Hochstrasser and C. Reid, *Mol. Phys.*, **4**, 162 (1961); *J. Chem. Phys.*, to be published.

3) J. Czekalla, A. Schmillen and K. J. Mager, *Z. Eelektrochem.*, **61**, 1053 (1957); **63**, 623 (1959).

4) S. P. McGlynn and J. D. Boggus, *J. Am. Chem. Soc.*, **80**, 5096 (1958); *J. Chem. Phys.*, **32**, 357 (1960); N. Christodouleas and S. P. McGlynn, to be published.

5) D. S. Brown, S. C. Wallwork and A. Wilson, *Acta Cryst.*, **17**, 168 (1964); S. C. Wallwork, ibid., **7**, 648 (1954).

6) H. Kuroda, K. Yoshihara and H. Akamatu, This Bulletin, **35**, 1604 (1962).

## Experimental

Anthracene was purified by recrystallization from a xylene solution, followed by chromatography and sublimation in vacuo. TNB was obtained after recrystallization from an ethanol solution. The crystal for the measurement of the fluorescence of the complex was grown from a carbon tetrachloride solution. The thin flakes of single crystals obtained by sublimation were used for the absorption measurement. The crystal elongates along the c-axis.

The absorption spectrum shown in Fig. 1 was measured by using the light polarized parallel to and perpendicular to the c-axis and by using the ultraviolet microspectrophotometer described in a previous paper.[7] The measurement was made at room temperature.

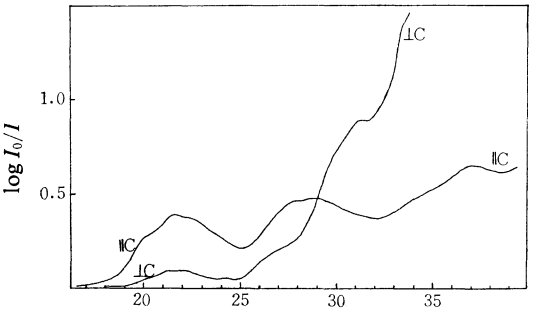



Fig. 1. Absorption spectrum of anthracene-TNB complex.

TABLE I. BAND POSITIONS OF ABSORPTION AND FLUORESCENCE OF CRYSTAL
(Value in wave number)

| Absorption | | Fluorescence | | |
|---|---|---|---|---|
| $C_{\parallel}$ | $C_{\perp}$ | Room temp. | Liq. $N_2$ temp. | Liq. He temp. |
| 20050 | 20260 | 18300 | 18335 | 18350 |
| 21500 | 21200 | 17000 | 17095 | 17040 |
| 22600 | 22200 | 15300 | 15600 | 15748 |
| 27500 | 26200 | | | |
| 28800 | | | | |
| | 29800 | | | |
| | 31300 | | | |
| 37000 | | | | |

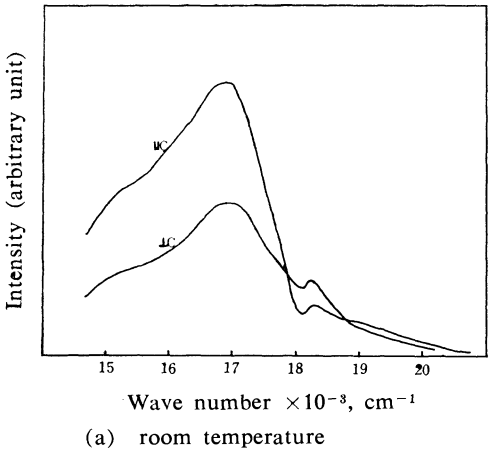
7) J. Tanaka, ibid., **36**, 833 (1963).

TABLE II. LCAO MO

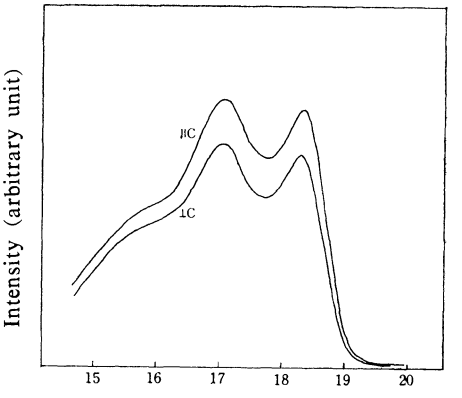
| Symmetry | energy $(-\beta)$ | $C_1$ | $C_2$ | $C_3$ | $C_4$ | $C_5$ | $C_6$ |
|---|---|---|---|---|---|---|---|
| $A_2''$ | 2.52 | 0.2570 | 0.2570 | 0.2570 | 0.1976 | 0.1976 | 0.1976 |
| E''(s) | 2.39 | 0.2102 | −0.1051 | −0.1051 | −0.2096 | 0.1048 | 0.1048 |
| (a) | 2.39 | 0 | 0.1821 | −0.1821 | 0 | 0.0741 | −0.0741 |
| $A_2''$ | 1.75 | −0.3136 | −0.3136 | −0.3136 | −0.3463 | −0.3463 | −0.3463 |
| $A_1''$ | 1.20 | 0 | 0 | 0 | 0 | 0 | 0 |
| E''(s) | 1.14 | 0 | 0 | 0 | 0 | 0 | 0 |
| (a) | 1.14 | 0 | 0 | 0 | 0 | 0 | 0 |
| E''(s) | 0.98 | −0.5158 | 0.2579 | 0.2579 | 0.4946 | −0.2473 | −0.2473 |
| (a) | 0.98 | 0 | −0.4468 | 0.4468 | 0 | 0.4248 | −0.4248 |
| $A_2''$ | 0.25 | 0.0206 | 0.0206 | 0.0206 | 0.135 | 0.135 | 0.135 |
| E''(s) | 0.20 | 0.0968 | −0.0484 | −0.0484 | −0.3722 | 0.1861 | 0.1861 |
| (a) | 0.20 | 0 | 0.0838 | −0.0838 | 0 | −0.3223 | 0.3223 |
| E''(s) | −1.18 | 0.5886 | −0.2943 | −0.2943 | 0.5252 | −0.2626 | −0.2626 |
| (a) | −1.18 | 0 | 0.5099 | −0.5099 | 0 | 0.4549 | −0.4549 |
| $A_2''$ | −2.14 | −0.4104 | −0.4104 | −0.4104 | 0.3951 | 0.3951 | 0.3951 |

The Hückel molecular orbital of trinitrobenzene has been calculated using the parameters as The numbering of atoms is shown in Fig. 4.

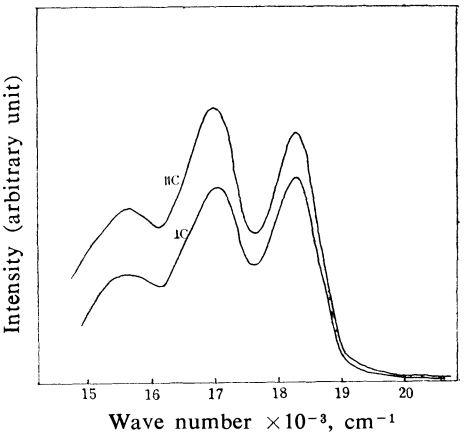
The fluorescence spectrum was measured by a recording spectrofluorometer.* The crystal was excited by a high pressure mercury lamp combined with a Toshiba UVD2 filter in order to obtain the 3650Å radiation. A calcite Glan-Thompson type polarizer of the Olympus Optical Co. was used for the polarization measurement. The spectrofluorometer consists of a Kipp double monochrometer, a RCA 1P22 photomultiplier, and an amplifier in series. The slit width was kept constant at 0.2 mm. during all measurements. The characteristic sensitivity and polarization properties of the instrument were calibrated using a standard light source. The fluorescence spectra at room temperature and at the temperature of liquid helium, and of liquid nitrogen are shown in Fig. 2, and all results are summarized in Table I.




(a) room temperature




(b) liquid nitrogen temperature




(c) liquid helium temperature

Fig. 2. Fluorescence spectrum of anthracene-TNB complex.

* The authors wish to express their sincere thanks to Professor Shoji Makishima and Mr. Masao Hirata for their kind help with the spectrofluorometer.

OF TRINITROBENZENE

Coefficients

| $N_1$ | $N_2$ | $N_3$ | $O_1$ | $O_2$ | $O_3$ | $O_4$ | $O_5$ | $O_6$ |
|---|---|---|---|---|---|---|---|---|
| 0.3901 | 0.3901 | 0.3901 | 0.1949 | 0.1949 | 0.1949 | 0.1949 | 0.1949 | 0.1949 |
| 0.6162 | −0.3081 | −0.3081 | 0.3428 | −0.1714 | −0.1714 | 0.3428 | −0.1714 | −0.1714 |
| 0 | 0.5337 | −0.5337 | 0 | 0.2970 | −0.2970 | 0 | 0.2970 | −0.2970 |
| 0.1781 | 0.1781 | 0.1781 | 0.2040 | 0.2040 | 0.2040 | 0.2040 | 0.2040 | 0.2040 |
| 0 | 0 | 0 | 0.4080 | −0.4080 | 0.4080 | −0.4080 | 0.4080 | −0.4080 |
| 0 | 0 | 0 | 0.5772 | −0.2886 | −0.2886 | 0.5772 | −0.2886 | −0.2886 |
| 0 | 0 | 0 | 0 | 0.500 | −0.500 | 0 | 0.500 | −0.500 |
| −0.0618 | 0.0309 | 0.0309 | 0.2754 | −0.1377 | −0.1377 | 0.2754 | −0.1377 | −0.1377 |
| 0 | −0.0535 | 0.0535 | 0 | 0.2386 | −0.2386 | 0 | 0.2386 | −0.2386 |
| −0.376 | −0.376 | −0.376 | 0.294 | 0.294 | 0.294 | 0.294 | 0.294 | 0.294 |
| −0.4958 | 0.2479 | 0.2479 | 0.3692 | −0.1846 | −0.1846 | 0.3692 | −0.1846 | −0.1846 |
| 0 | −0.4293 | 0.4293 | 0 | 0.3198 | −0.3198 | 0 | 0.3198 | −0.3198 |
| −0.1926 | −0.0963 | −0.0963 | 0.0580 | −0.0290 | −0.0290 | 0.0580 | −0.0290 | −0.0290 |
| 0 | −0.1669 | 0.1669 | 0 | 0.0503 | −0.0503 | 0 | 0.0503 | −0.0503 |
| 0.0893 | 0.0893 | 0.0893 | −0.0191 | −0.0191 | −0.0191 | −0.0191 | −0.0191 | −0.0191 |

follows: $\alpha_O=\alpha_C+1.2\beta_{C-C}$ $\alpha_N=\alpha_C+1.44\beta_{C-C}$ $\beta_{NO}=0.7\beta_{C-C}$ $\beta_{NC}=0.7\beta_{C-C}$ $\alpha_C=4.1\beta_{C-C}$

## Results and Discussion

**(1) Theoretical Consideration.**—The charge transfer resonance interaction between the highest occupied orbital of anthracene and the lower vacant orbitals of TNB is considered. The LCAO MO calculation of TNB has been made, and it has been found that the three lowest vacant orbitals are nearly degenerate. The results of calculation are shown in Table II, where it may be seen that the lower vacant orbitals are composed mainly of nitro groups. The nitro groups have a three-fold symmetry, and the vacant orbitals of these groups are split by mutual interactions into one orbital of the lowest energy of the totally symmetric and two orbitals of a slightly higher energy of E'' symmetry. According to these calculations, the lowest symmetric vacant orbital may have a larger electron affinity than the other two orbitals, about $0.05\beta$, where $\beta$ is the exchange integral ($-2$——$3$ eV.).* However, under the influence of an electron donor or foreign ions on one particular nitro group, the lowest charge transfer state will occur when an electron is transferred into an E'' orbital where the charge density is concentrated on particular nitro groups. For instance, the ESR spectra of the TNB negative ion produced by metallic and photo-reduction shows that the excess electron is accommodated into the E''(s) orbital.[8]

The crystal structure analysis data shows that one nitro group is placed close to anthracene (Fig. 3). The electrostatic energies between partial charges on TNB and positive holes on anthracene have been calculated for molecular separations from 2.8 to 4.0 Å, whereby the geometrical planar configuration is unchanged, as in Fig. 3. The charge density of TNB is taken as those of $A_2''$, E''(s) and E''(a) orbitals, and three different orientations are considered for the calculation with E'' orbitals since the energy is dependent on the local charge densities on particular atoms (cf. Table III). The results are given in Table III, where it is found that E''(s2), E''(a1) and E''(s3) states are most stabilized by an electrostatic force. Other states are higher in energy by about 0.1—0.2 eV.

The theoretical foundation of the charge-transfer type molecular complex was given by Mulliken,[9] and the wave functions for the ground state and the charge transfer state may be given as follows:

$$\Phi_G=\varphi(D\cdot A)+\lambda_1\varphi(D^+\cdot A^-)$$
$$\Phi_C=\varphi(D^+\cdot A^-)+\delta_1\varphi(D\cdot A)+\delta_2\varphi(D^*\cdot A) \quad (1)$$

* Fischer and McDowell (private communication) have made a similar calculation of the Hückel MO of TNB using different parameters. They found a different sequence of energy levels as regards the lowest vacant A and E orbitals, where the $A_2''$ is slightly more unstable than E''. Therefore, these three levels are considered to be nearly degenerate, since the simple Hückel MO result is greatly dependent on the choice of parameters.

8) Although Ward had observed the characteristic of the E'' orbital in accommodating an excess electron, Fischer and McDowell (private communication) have found that by the electrolytic reduction a symmetric anion is formed on which an electron is put in the totally symmetric orbital. See R. L. Ward, *J. Am. Chem. Soc.*, **83**, 1296 (1961); *J. Chem. Phys.*, **38**, 2588 (1963).

9) R. S. Mulliken, *J. Am. Chem. Soc.*, **74**, 811 (1952).

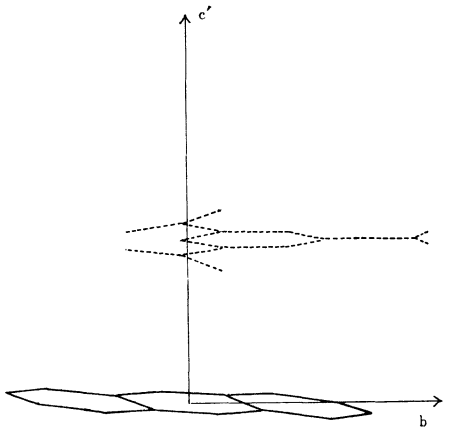



Fig. 3a

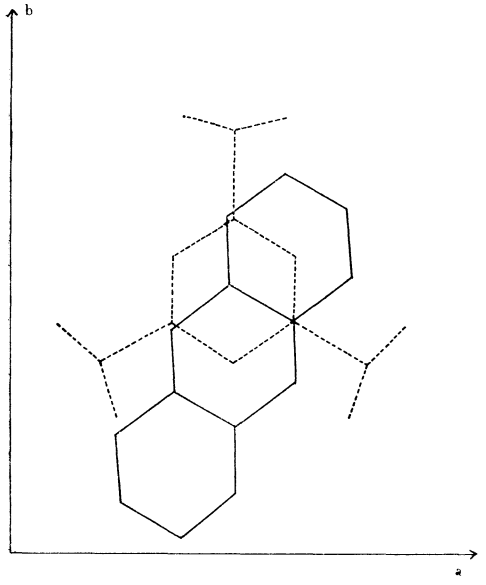



Fig. 3b

Fig. 3. Projections of molecules in the crystal.

where $\varphi(D\cdot A)$, $\varphi(D^+\cdot A^-)$ and $\varphi(D^*\cdot A)$ represent wave functions of a no-bond structure, the charge transfer structure and the local excited state of the donor. The perturbation coefficients are given by:

$$\lambda_1 = \frac{\int \varphi^*(D^+\cdot A^-)\mathbf{H}\varphi(D\cdot A)d\tau}{E_{CT}-E_G} \qquad (2)$$

$$\delta_1 \simeq -\lambda_1$$

$$\delta_2 = \frac{\int \varphi^*(D^*\cdot A)\mathbf{H}\varphi(D^+\cdot A^-)d\tau}{E_{D^*\cdot A}-E_{CT}} \qquad (3)$$

The integrals in Eqs. 2 and 3 might be proportional to the overlap integrals between them, so the overlap integrals have been evaluated

TABLE III. ELECTROSTATIC ENERGY BETWEEN (Anthracene)$^+$(TNB)$^-$, (eV.)

| Molecular separation (Å) | $A_2''$ | $E''$(a1) | $E''$(a2) | $E''$(a3)* |
|---|---|---|---|---|
| 2.8 | 3.055 | 3.227 | 3.027 | 3.052 |
| 3.0 | 2.961 | 3.118 | 2.932 | 2.954 |
| 3.5 | 2.745 | 2.869 | 2.714 | 2.730 |
| 4.0 | 2.554 | 2.652 | 2.521 | 2.533 |
| | | $E''$(s1) | $E''$(s2) | $E''$(s3)* |
| 2.8 | | 3.037 | 3.240 | 3.211 |
| 3.0 | | 2.943 | 3.131 | 3.105 |
| 3.5 | | 2.726 | 2.883 | 2.864 |
| 4.0 | | 2.534 | 2.667 | 2.652 |

* There are three possible orientations of orbitals for the E'' type. We have distinguished them by 1, 2, and 3.

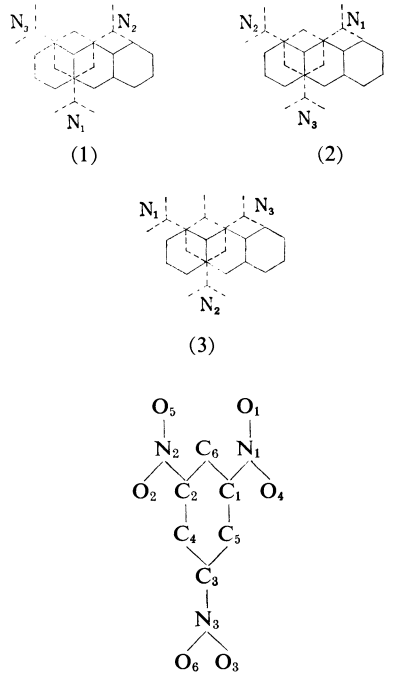



Fig. 4. Numbering of atoms in the TNB molecule.

between the highest occupied and the lowest vacant orbitals of anthracene with the lower vacant orbitals of TNB, using a common orbital exponent for all atoms at $\xi = Z/n = 1.4$[10] and taking into account the overlap between direct-opposite and next-neighbor atoms. The results are shown in Table IV, where it is shown that $E''$(s2) is the most favorable orbital and configuration since the overlap has the same sign for both ground and excited states and since it increases at a shorter molecular separation. This means that both ground and

10) J. N. Murrell and J. Tanaka, *Mol. Phys.*, 7, 363 (1964).

TABLE IV. OVERLAP INTEGRALS BETWEEN THE ORBITALS OF ANTHRACENE AND TNB

| Vacant orbitals of TNB | Orbitals of* anthracene | Overlap integral 2.8 | 3.5 (Å) |
|---|---|---|---|
| $A_2''$ | 1 | 0.0035 | 0.0016 |
| | 2 | −0.0039 | −0.0012 |
| E''(a1) | 1 | 0.0115 | 0.00554 |
| | 2 | 0.0039 | 0.00152 |
| E''(a2) | 1 | −0.00073 | −0.00017 |
| | 2 | −0.00403 | −0.00121 |
| E''(a3) | 1 | 0.01424 | 0.00665 |
| | 2 | 0.00438 | −0.00033 |
| E''(s1) | 1 | −0.0040 | −0.0014 |
| | 2 | −0.0045 | −0.0017 |
| E''(s2) | 1 | −0.01266 | −0.00417 |
| | 2 | −0.05026 | −0.01721 |
| E''(s3) | 1 | 0.02799 | −0.00545 |
| | 2 | 0.0039 | 0.01464 |

* Highest occupied orbital of anthracene is denoted by 1 and the lowest vacant orbital by 2.

excited states are stabilized by charge resonance interaction, particularly at a shorter molecular separation. The molecular separation of 3.28 Å found by X-ray analysis is apparently shorter than the normal van der Waals radii, and the charge transfer resonance force might be responsible for the shortening of the molecular distance. The stabilization of the excited state is demonstrated by a shift of the fluorescence band (loc. cit.).

Since we are concerned with the lowest charge transfer state, we will pay particular attention to a state in which an electron is transferred into the E''(s) orbital. Other states are less convenient from the points of view of electrostatic energy and electron overlap; for instance, the charge transfer state into the E''(a2) orbital is 0.2 eV. higher in electrostatic energy and 1/10 smaller in electron overlap effect.

The energy of the charge transfer state, $E_{CT}$, is estimated by Eq. 4:

$$E_{CT} = I_p - E_A - \sum_{i,j} q_i q_j / R_{ij} \qquad (4)$$

where $I_p$ is the ionization potential of anthracene, $E_A$ is the electron affinity of TNB, and the last term is the electrostatic energy at 3.28 Å separation, where $q_i$ and $q_j$ indicate partial charges on $i$-th and $j$-th atoms. Using values of $I_p = 7.4$ eV.[11] and $E_A = 1.86$ eV.[12] and electrostatic energy for the E''(s2) orbital, $E_{CT}$ is estimated as 2.54 eV. The local excited state of anthracene is the lowest singlet excited state of $^1L_a$ at 3.40 eV. Although it is very difficult to estimate the numerical value of the integrals quantitatively, we will tentatively assign −0.10 eV. for the integral in Eq. 2 and −0.40 eV. for Eq. 3. The perturbation coefficient is estimated as $\lambda_1 = 0.04$.

For the excited state, the perturbation treatment is not accurate enough because the $E_{CT}$ and $E_{D^*\cdot A}$ are close to each other; hence, we have solved a secular equation and found two energies and wave functions as follows:

$$\begin{aligned} &2.39\,\text{eV.}: \ 0.94\,\varphi(D^+\cdot A^-) + 0.33\,\varphi(D^*\cdot A) \\ &3.55\,\text{eV.}: \ 0.33\,\varphi(D^+\cdot A^-) - 0.94\,\varphi(D^*\cdot A) \end{aligned} \qquad (5)$$

The stabilization of the ground state is 0.004 eV. Although this figure is too small to explain the stability of the complex, a much larger energy will arise from charge-transfer interactions of other filled orbitals. Those results will be discussed in a later section.

**(2) Absorption Spectrum.**—The general feature of the spectrum coincides with the findings of Lawer et al.[2] on the longer wavelength side, but the present results show more bands in the shorter ultraviolet region. Three bands are observed along the c-axis, as Fig. 1 shows. This axis is the direction out of the benzene rings, and the charge transfer resonance interaction might occur along this axis since the electron overlap between molecules is larger for this direction (cf. Fig. 3). Three bands, at about 20000 $cm^{-1}$, 28000 $cm^{-1}$ and 37000 $cm^{-1}$, are assigned to the intermolecular charge transfer from anthracene to TNB. The energy of the first band (2.48 eV.) is nearly in agreement with the calculated value (2.39 eV.).

The transitions to $A_2''$ and E''(a2) orbitals might occur in the same energy region, but their intensities will be rather smaller than to E''(s2) since the interaction matrix is smaller. The second and the third charge transfer bands might be ascribed to transitions from the second or third occupied orbital of anthracene to TNB, since the same sort of second and third charge transfer bands were observed in the case of anthracene-tetracyanoethylene complex.[13] The energy difference between the first and second band is 8000 $cm^{-1}$ in both cases. Of course, the possibility cannot be excluded that the second and third bands arise from transitions to higher vacant orbitals of the acceptor. The band at 26500 $cm^{-1}$ observed in the direction perpendicular to the c-axis might be ascribed to the same origin of the transition to the state observed at 27500 $cm^{-1}$ along the c-axis, since the intensity is weaker in the direction perpendicular to the c-axis. It is remarkable that these extra charge transfer bands, which are difficult to see in a

11) G. Briegleb and J. Czekalla, *Z. phys. Chem., N. F.*, **24**, 37 (1960).
12) M. Bertley and L. E. Lyons, *Nature*, **196**, 573 (1962).
13) G. Briegleb, J. Czekalla and G. Reuss, *Z. phys. Chem., N. F.*, **30**, 316 (1961).

solution's spectra, appear distinctly in the crystal spectrum since the polarization is different from the $\pi-\pi^*$ transition of the parent molecules. Three vibrational progressions are observed even at room temperature for the 20000 $cm^{-1}$ system, and they are in perfect agreement with the values of Lawer et al.[2]

The electronic transitions of parent molecules will be weaker in the direction parallel to the c-axis, because the transition moment of the $\pi-\pi^*$ transition is in the plane of the benzene ring. The bands at 29800 $cm^{-1}$ and 31300 $cm^{-1}$ are considered to be the $^1L_a$ bands of anthracene shifted by the interaction with TNB. They appear at 26730 $cm^{-1}$ in a solution and at 25400 $cm^{-1}$ in a crystal. The calculated value mentioned in the previous section is 28500 $cm^{-1}$ (3.55 eV.), so it explains the blue shift of the $^1L_a$ band.

The intensity of the charge transfer transition has been discussed by Murrell[14] in pointing out the important contribution of the donor's local excited configuration. The transition moment integral which is proportional to the coefficients, $\lambda_1$ and $\delta_2$, is given by Eq. 6 by neglecting the electron overlap between A and D and the ground state dipole:

$$\mu=\int \Phi^*_{CT}\mathbf{r}\Phi_G d\tau$$
$$=\lambda_1\langle D^+\cdot A^-|\mathbf{r}|D^+\cdot A^-\rangle+\delta_2\langle D\cdot A|\mathbf{r}|D^*\cdot A\rangle \quad (6)$$

The first bracket is approximately given by a vector connecting the point charge placed on the center of the E''(s2) orbital of TNB and a point-positive charge placed on the center of anthracene. The vector has components about 1 Å along the [110] and 3.3 Å along the [001] directions. The second bracket denotes the transition moment of the $^1L_a$ state of anthracene directed along the short axis of anthracene, in a direction opposite to that of the $\mathbf{r}(D^+A^-)$ vector.

The intensity of the first charge transfer band has been determined by McGlynn et al. as $\varepsilon_{max}=1600$. Using the width of the half-intensity of about 4700 $cm^{-1}$, the oscillator strength, $f$, is obtained as 0.032.* By the use of this value, the magnitude of the transition moment is determined to be 0.36 Å.

The dichroic ratio observed in Fig. 1 is $D_{C\parallel}:D_{C\perp}=5:1$; this value may be related to the vector components in Eq. 6 as follows:

$$\frac{D_{C\parallel}}{D_{C\perp}}=\frac{(\lambda_1\langle D^+\cdot A^-|\mathbf{r}|D^+\cdot A^-\rangle_{C\parallel})^2}{(\delta_2\langle D\cdot A|\mathbf{r}|D^*\cdot A\rangle+\lambda_1\langle D^+\cdot A|\mathbf{r}|D^+\cdot A^-\rangle_{C\perp})^2} \quad (7)$$

If we use values of $\lambda_1=0.09$—$0.10$ and $\lambda_2=0.33$, then the calculated value is in agreement with the observed values. The value of $\lambda_1$ determined from these results is nearly twice as large as the value estimated in the previous section; this discrepancy might be ascribed to uncertainity in the estimation of the integral in Eq. 2, to the point charge approximation for the $\mathbf{r}(D^+\cdot A^-)$ vector, and to the deviation of the intensity from the oriented gas model of the crystal.

**(3) The Fluorescence Spectrum.**—The fluorescence spectrum of the TNB-anthracene system has been ascribed to the reverse process of the charge transfer absorption.[3,4] The shift of the 0-0 band from absorption to emission (Franck-Condon gap) is 1700 $cm^{-1}$ in this experiment, while a value of 7000 $cm^{-1}$ was given by McGlynn et al.[4] The 0-0 emission band may clearly be seen at the temperature of liquid helium.

The fluorescence spectrum shown in Fig. 2 exhibits some unusual characteristics in that the shape of the bands changes markedly with a change in temperature and in that the dichroic ratio is reduced from that of the absorption. The change in the dichroic ratio cannot be understood unless we have assumed a change in the fluorescence state or configuration from that of the absorption. The big change in emission shape caused by the change in temperature will be due to a frequent thermal motion in a shallow potential, which will lead to the reduction of the vibrational overlap integral for the 0-0 transition in the Franck-Condon integral.

The relatively larger shift of the fluorescence of 1700 $cm^{-1}$ will be ascribed to the shortening of the molecular separation after the excitation, since the potential for the excited state is lower in energy at a shorter distance. However, if we ascribe the shift solely to an increase in electrostatic stabilization caused by closing, it will require an unreasonably larger value of the shortening of 0.43 Å to explain the 1700 $cm^{-1}$ shift. Therefore, it is most reasonable that the interaction term in Eq. 3 increases rapidly when the molecular separation is closed. In fact, the overlap integral increases for the excited state from $-0.025$ to $-0.035$ by a shortening of 0.20 Å, and this may correspond to an increase in the integral from $-0.40$ eV. to $-0.56$ eV. by assuming a proportionality of the energy to the overlap

14) J. N. Murrell, *J. Am. Chem. Soc.*, **81**, 5037 (1959).

* This value is smaller than the value suggested by Briegleb. We have used as a formula for oscillator strength:

$$f=4.32\times10^{-9}\int\varepsilon_\nu d_\nu$$

integral. By the use of the electrostatic energy at 3.1 Å of 3.09 eV., the excited state wave functions are given as follows:

$$\begin{aligned} &2.19\,\text{eV.}: \ 0.905\varphi(D^+\cdot A^-)+0.42\varphi(D^*\cdot A) \\ &3.67\,\text{eV.}: \ 0.42\varphi(D^+\cdot A^-)-0.905\varphi(D^*\cdot A) \end{aligned} \quad (8)$$

The excited state is stabilized about 1600 $cm^{-1}$ by this interaction. Of course, the repulsive potential in the ground state might be responsible for some part of the shift of the fluorescence.

Equation 8 involves a larger contribution of the $\varphi(D^*\cdot A)$ state. The dichroic ratio for this emission is calculated, by using Eq. 7 as:

$$D_{C\parallel} : D_{C\perp} = 1.5 : 1.0$$

The observed value is 1.2 : 1.0 at the temperature of liquid nitrogen, and 1.4 : 1.0 at the temperature of liquid helium. The calculated value is nearly in agreement with the observed values.

Therefore, the molecules in the complex are considered to be displaced to a closer position by about 0.2 Å after the excitation, the 0-0 state is stabilized about 1700 $cm^{-1}$, and the dichroic ratio is changed from 5 : 1 in absorption to 1.4 : 1 in fluorescence by an increase of the component of the locally-excited $^1L_a$ state of anthracene. The shallow intermolecular potential for this molecular motion is reflected in the emission spectrum at room temperature, where the 0-0 band decreases in intensity. The vibrational progression of 1300 $cm^{-1}$ might be due to a skeletal vibration of TNB coupled with intermolecular vibration.

**Summary**

The electronic absorption and fluorescence spectra of the single crystal of the anthracene-*s*-trinitrobenzene complex have been measured, and the polarization property of electronic transitions has been discussed in terms of interaction between the no-bond structure, the charge transfer and the locally-excited state of anthracene.

It has been shown that molecules in a pair are displaced to a closer position after the excitation, whereby the mixing of the donor-excited level occurs more than in the ground state (Frank-Condon state), and the fluorescence involves a larger contribution from the in-plane transition of anthracene.

The authors wish to express their sincere thanks to Professors Hideo Akamatu and Saburo Nagakura for their helpful discussions. They would also like to thank Drs. S. C. Wallwork, C. A. McDowell, P. H. H. Fischer and S. K. Lawer for their helpful communications of their unpublished results.

*The Institute for Solid State Physics*
*The University of Tokyo*
*Azabu, Tokyo* (*J. T.*)

*Department of Chemistry*
*Faculty of Science*
*The University of Tokyo*
*Hongo, Tokyo* (*K. Y.*)

# Radiotracer Studies of Metal-Detergent Interaction by Means of a Dip Counter with an Evaporated Metal Film Window*

By Tsutomu SEIMIYA

(Received August 19, 1964)

The properties of metal-solution interfaces under equilibrium state have long been studied from various points of view,[1-5] studies which have offered useful information for the treatment of metals in water. However, for practical systems, the situations are fairly complicated, since several phenomena occur simultaneously and they are often not in equilibrium. Here, the factors affecting the equilibrium are not necessarily important for the kinetic properties of the interface. As for the kinetic nature of metallic interfaces, studies have also been

* The paper was presented at the 14th Colloid Symposium, Shinshû University, Ueda, October, 1961.

1) C. V. King and R. K. Schocket, *J. Phys. Chem.*, **57**, 895 (1953).

2) M. H. Gottlieb, ibid., **64**, 427 (1960).

3) J. H. Schulman, R. B. Waterhouse and J. A. Spink, *Kolloid Z.*, **146**, 77 (1956).

4) F. E. Bartell and P. H. Cardwell, *J. Am. Chem. Soc.*, **64**, 494 (1942).

5) J. E. Brophy and W. A. Zisman, *Annals New York Academy Science*, **53**, 836 (1951).

reported by many authors of, for instance, the coulometric, chronopotentiometric or differential double-layer capacity measurement of surfaces.[6,7] However, the so-called reactive metals usually involve an irreversible process which renders difficult the analysis of the data obtained except for some special cases. Therefore, it may be desirable to trace directly the surface reaction itself, both chemically and electro-chemically, using radioisotopes.

The present paper will describe radiotracer studies upon the interfacial reaction between vacuum-evaporated metal films and an aqueous solution of sodium dodecyl sulfate (SDS). In the usual practice of the measurement of such a reaction or adsorption, solid samples are dipped in a solution containing a radioactive solute and the radioactivity measurements are made for the surface after withdrawing the solid. However, the counting rate due to a merely adhering solution inevitably obscures the counting rate due to the adsorption or chemical reaction, which is generally small compared with that due to the adhering liquid.[8,9] The rinsing of the solid surface often adopted[10] is, therefore, not desirable, since it ensures neither a complete removal of the adhering liquid nor a complete retention of the substance adsorbed. To avoid these difficulties, it is desirable to measure the counting rate directly in the state of immersion, as in the Aniansson's soft beta ray method[11,12] or as in Winkler's hard radiation method[13,14]. Here we adopted the Aniansson's method but somewhat modified it. The rate of the uptake of $^{35}S$-labeled SDS from an aqueous solution by vacuum-deposited metals on a thin Tetoron window of the GM-tube was measured, and the surface nature of several metals was studied under the influence of air.

## Experimental

**Materials and Apparatus.**—Radioactive and non-radioactive SDS were synthesized according to the usual method.[15] The radioisotope $^{35}S$ used in this experiment was obtained from CEA Saclay, France, in the form of a dilute aqueous solution of sulfuric acid. The solution was concentrated, the required amount of non-radioactive sulfuric acid was added, and the mixture was used for the sulfonation of dodecyl alcohol. In the course of the purification of SDS, non-radioactive sodium sulfate was added to remove radioactive sodium sulfate impurities of a high sepecific activity considered to be present and likely to cause an error in the measurement of the counting rate. The radioactive SDS thus prepared had the specific activity of 30 curies per mol. Copper, silver, gold, lead and iron, all of a commercially pure grade, were chosen as the sample metals. These metals were vacuum-deposited on a thin Tetoron film of the Mitsubishi Chemical Industries, Limited (polyethylene terephthalate, Diafoil Type S, No. 12, 1.3 mg./cm$^2$ thick) which had been previously degreased by ether. The apparatus used in this experiment is shown in Fig. 1, where G is the gas flow Geiger-Müller counting tube (Japan Radio Corporation, Aloka FC-16; effective aperture, 34 mm.) equipped with a tambour ring, T, for the exchange of the sample window film and, H, the housing to which the counting tube is fixed. The screw stage, LL', adjusts the height of the adsorption cell, C, containing 8 cc. of a radioactive solution. The microscope, M, equipped with a calibrated scale measures the distance between the solution surface and the window of the GM tube.

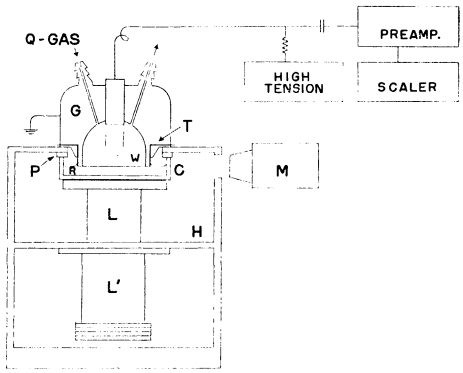



Fig. 1. Diagram of apparatus.

| | |
|---|---|
| G | Gas flow GM-tube |
| W | Sample window |
| T | Tambour ring |
| C | Glass cell |
| R | Radioactive solution |
| M | Microscope |
| P | Rubber packing |
| H | Housing |
| LL' | Screw stage |

**Procedures.**—The sample metal was deposited from vapor on the thin Tetoron film at the pressure of $10^{-6}$ mmHg under the specified conditions of electric current and evaporation time. The rates of deposition for copper, silver, gold, lead and iron samples were 3.83, 1.57, 4.67, 1.83 and 1.30 $\mu$g./cm$^2$sec. respectively. In each case, deposition was made for 30 sec., with the rejection of the initial portion by a magnetically-operated shutter in order

6) O. Gatty and E. C. R. Spooner "Electrode Potential Behaviours of Corroding Metals in Aqueous Solution," Clarenden Press., Oxford (1938).
7) H. A. Latinen, *Anal. Chem.*, **33**, 1458 (1961).
8) T. Seimiya and T. Sasaki, This Bulletin, **35**, 1567 (1962).
9) T. Seimiya and T. Sasaki, *J. Metal Finish. Soc.*, (*in Japanese*) **11**, 230 (1060).
10) M. Green, D. A. J. Swinkels and J. O'M Bockris, *Rev. Sci. Instr.*, 33, 19 (1962).
11) G. Aniansson, *J. Phys. Colloid Chem.*, **55**, 1286 (1951).
12) C. M. Judson, A. A. Argyle, J. K. Dixon and D. J. Salley, *J. Chem. Phys.*, **19**, 378 (1951).
13) A. Baerg C. A. Winkler, *Can. J. Chem.*, **31**, 521 (1953).
14) J. A. Kafalas and H. C. Gatos, *Rev. Sci. Instr.*, **29**, 47 (1958).
15) E. E. Dreger, G. I. Keim, G. D. Miles, L. Shedlovsky and J. Ross, *Ind. Eng. Chem.*, **36**, 610 (1944).

to avoid the contamination of the film by metal oxide. To the opposite side of the window film, copper was deposited; this acted as a part of the cathode of counting tube. The thickness of the vacuum-deposited metal films was directly calculated from their weight, as measured in a special weighing tube in order to avoid errors caused by the electrostatic charge of the film. The measurement of the adsorption was made by directly immersing the window of the counting tube in a radioactive sample solution and by measuring the increase in the counting rate due to the accumulation of the solute on the metal film. This increase in the counting rate was multiplied by the calibration factor $r$ which expresses the ratio of the actual amount of solute on the window to the counting rate resulting from it, which was determined by the separate measurement below. A known amount of radioactive solute was evenly placed in about 100 spots on an Acrylite disk of the same shape and area as those of GM-tube window. (The spots should be small enough to be free from self-absorption.) Then its activity was measured at varying distances, up to 3 mm., between the sample and the window. On the basis of this experiment, the counting rate at the distance zero was calculated by extrapolation. The amount of the sample, divided by this counting rate, gives the factor $r$ in mol./ c. p. m. Since the factor $r$ was determined for each sample film, solute and specific activity, the product of the observed counting rate and $r$ gives the actual amount of solute as corrected for the decay of isotope and the absorption of radiation by the window. The correction for the dead time of 300 $\mu$ sec. of the GM tube was also made.

The counting rate due to the bulk of the solution was measured as follows. The surface count over the aqueous solution of surface-inactive but radioactive sodium sulfate of a known concentration was measured at varying distances in a manner similar to that used in the measurement of $r$. The value thus obtained was extrapolated to the counting rate at zero distance and was used for the evaluation of the counting due to the bulk of each SDS solution. It was also attempted to estimate the radiation from the bulk of the solution by measuring the surface counting rate of an alcoholic solution of radioactive SDS, which showed no surface tension change with concentration and may, therefore, be considered to be free from surface adsorption;[16] however, the measurement was not successful due to the evaporation, creeping and condensation of alcohol on the window of the counting tube.

## Results and Discussion

**Uptakes of Sodium Sulfate and Sodium Dodecyl Sulfate on the Tetoron Surface and Apparent Adsorption on the Aqueous Surface.**—The counting rate before and after the dipping of the Tetoron film in an aqueous solution of sodium sulfate and a SDS solution were measured first as a function of the time; they are shown in Figs. 2 and 3 respectively. In each figure, the points show the total sum of the counting rate (left ordinate) due to the solute taken up by the Tetoron film and the solute in the bulk of the solution. The broken line indicates the counting rate due to the solute in the bulk of the solution. Therefore, the portion of the ordinate above the broken line in Figs. 2 and 3 represents the counting rate proportional to the excess amount of solute (right ordinate) on the Tetoron-solution interface. The points on the vertical axis in these figures indicate, for comparison, a counting rate referring to the counting rate of the aqueous surface. We can see in Fig. 2 that the apparent amount of the adsorption of sodium sulfate at the air-water interface is about the same as the adsorption on Tetoron except for the early period of the contact of Tetoron with water; this anomaly is probably due to the agitation of the surface by the immersion. In the case of SDS, the adsorption on the aqueous surface decreases when the air is replaced by Tetoron.

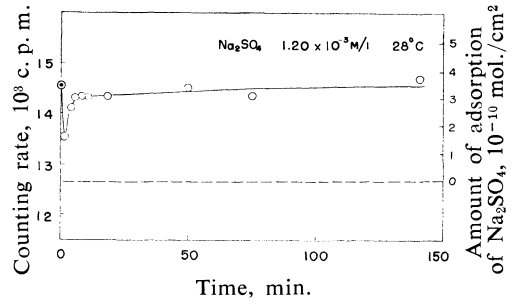



Fig. 2. Adsorption of sodium sulfate on Tetoron surface. Counting rate and amount of adsorption of sodium sulfate on aqueous surface (⊙), Tetoron surface (○), and bulk of the solution (— —).

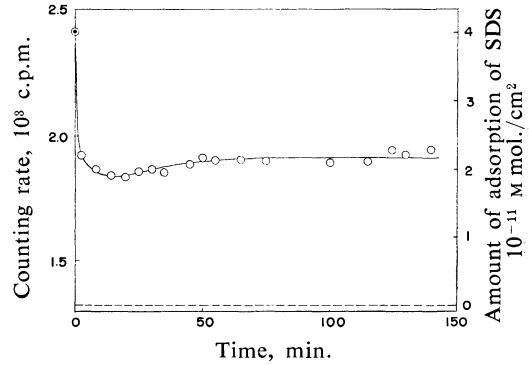



Fig. 3. Adsorption of sodium dodecyl sulfate on Tetoron surface.
Counting rate and amount of adsorption of sodium dodecyl sulfate on Tetoron surface (○), aqueous surface (⊙), and bulk of the solution (— —).

16) T. Seimiya and T. Sasaki, Unpublished data.

Here it should be emphasized that, since we cannot expect any actual adsorption of sodium sulfate on the water surface, the excess counting rate mentioned above is evidently an apparent one exclusively due to the inevitable evaporation of water from the aqueous surface, although the experiment was conducted in a closed vessel. Detailed experiments on an aqueous surface, which will be reported on precisely in a following paper, also revealed that the mere exposure of the aqueous surface to an atmosphere with 40% humidity at 21°C without a special air current resulted in an apparent increase in the 3% surface concentration for a sodium sulfate solution.

Considering this, an evaporation effect may also be responsible to some extent for the apparent adsorption of SDS on an aqueous surface shown in Fig. 3. As will be mentioned in the following paper, this apparent adsorption gradually decreases as the space above the aqueous surface becomes saturated with water vapor. Therefore, it should at least be remarked that such an evaporation effect would introduce in some cases a serious error in the adsorption measurement on the aqueous surface. Throughout the main experiment which follows, we took special care to avoid evaporation, as is illustrated in Figs. 2 and 3, and to confirm the equilibrium count rate of the radiation from the bulk of the solution on he basis of its steady value.

**Uptake of SDS on Various Metals.**—The uptakes of SDS from its aqueous solution onto the surfaces of lead, copper, silver and gold are plotted against the time at pH from 6 to 9 in Fig. 4. From these curves it is possible to classify the metals employed as reactive or non-reactive, as has usually been done. With reactive metals like copper and lead, we can observe the dissolution of metals, as is seen from the change of pH shown in Fig. 4, and the growth of the surface film composed of the reaction product between the metal and SDS, as can be confirmed by the remarkable increase in the counting rate shown in the same figure. In this experiment, iron behaved as a non-reactive metal, like electrochemically-noble gold and silver, instead of as a usual reactive metal. This is probably due to the passivation of iron in the present experimental conditions of exposing its surface to an oxygen atmosphere.

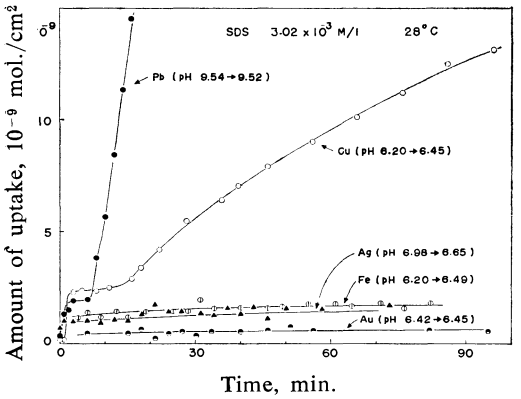



Fig. 4. Uptake of sodium dodecyl sulfate on various metals.

For non-reactive metals, a fluctuation in the counting rate exceeding the statistically probable errors of counting was observed for one and the same surface, whereas the fluctuation was very little for reactive-metal surfaces. It can be observed in Fig. 4 that the plateau appears in an early stage of the uptake curve for lead and copper at the pH listed for each case where the solution does not suffer from the change in pH in the course of SDS uptake, while in other pH regions such a plateau did not appear and the curves of uptake simply and gradually increased, though no diagrams are shown. Such a plateau and succeeding rapid increase in SDS uptake may reasonably be explained by taking account of two processes: rapid physical adsorption, resulting in a monolayer on the metal which is completed in a short time after the immersion of the metal in solution, and the slow formation of a surface film by a certain chemical reaction with the aid of oxygen, such as

$$O+Cu+2RSO_4H \rightarrow Cu(RSO_4)_2+H_2O$$

or $$Cu+O+RSO_4H \rightarrow Cu(OH)SO_4R$$

both processes being independent of the change in pH. Here R indicates the $C_{12}$ hydrocarbon chain.

**The Estimation of the Surface Roughness.**—The roughness factor, namely, the ratio of the actual area to the apparent area of the solid surface, can be obtained by calculating the

Table I. Surface roughness of various metals

| Surface | pH | Uptake of dodecyl sulfate mol./cm² ×10⁻⁹ | Weight of metal film mg./cm² | Roughness factor |
|---|---|---|---|---|
| Cu | 5.60 | 1.68 | 0.290 | 3.64 |
| | 6.20 | 1.53 | 0.071 | 3.32 |
| | 6.55 | 1.76 | 0.102 | 3.82 |
| | 6.65 | 1.71 | 0.116 | 3.71 |
| | 7.40 | 1.86 | 0.127 | 4.04 |
| | 6.20 | 2.40 | 0.497 | 5.21 |
| Pb | 9.54 | 1.92 | 0.055 | 4.17 |
| Fe | 6.20 | 2.00 | 0.039 | 4.34 |
| Ag | 6.98 | 1.70 | 0.047 | 3.69 |
| Au | 6.42 | 0.90 | 0.140 | 1.74 |

actual area, assuming the completion of monolayers at the plateau region in Fig. 4 and an area of 36 Å$^2$ per molecule for SDS.[17] The results for copper, lead, silver, gold and iron are shown in Table I. Table I indicates that copper films of a similar weight show almost the same roughness, independent of the pH used for the measurement.

**The Rate of Surface-film Growth.**—It has already been mentioned that lead and copper reacted with SDS to form a surface film of metallic soap and that these reaction products increased with time beyond the initial plateau region. The rate of uptake is considerably larger for lead than for copper. In both cases, however, the rate tends to decrease gradually with time (Fig. 4). This is considered to be due to the presence of the surface film, which acts to retard further reaction because of the slow diffusion of ions through the film. We can reasonably assume the reaction of surface film formation to take place at the film solution interface[18,19] and consider that, during the film growth, the concentration of metallic ions at a film-solution interface is almost zero, while at a film-metal interface it is large and constant. Since the diffusion rate of metallic ions and, hence, the rate of film growth is proportional to its concentration gradient in the film, the rate of film growth is considered to be proportional to the reciprocal of the film thickness, $m$, as follows:

$$\frac{dm}{dt}=\frac{k}{m} \qquad (1)$$

where $k$ is the proportionality constant. The integration of Eq. 1 gives the following parabolic rate equation, where $c$ is the integration constant:

$$\frac{1}{2}m^2=kt+c \qquad (2)$$

Equation 2 was checked by using the data for copper and lead already shown in Fig. 4. Figure 5 shows the square of the amount of the uptake of dodecyl sulfate plotted against the time for both copper and lead. A linear relation for copper, can be seen 30 min. after the immersion and after 20 min., for lead, which proves the validity of Eq. 2 as a whole. Further, it may be presumed from Fig. 5 that a film of a tight structure grows on copper, whereas a loose film grows on lead.

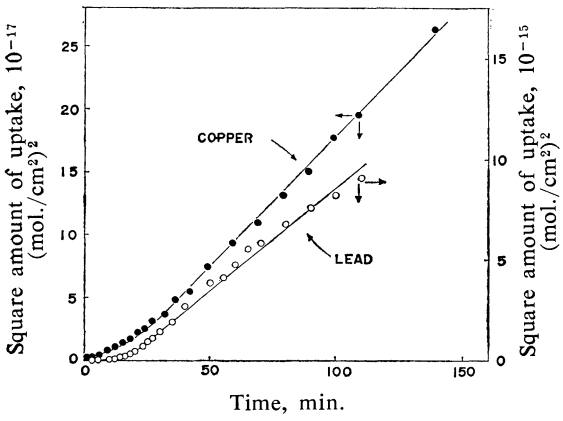



Fig. 5. Film growth on copper and lead in aqueous solution of SDS.

**The Effect of pH on the Rate of Uptake.**—The effect of the initial pH on the uptake of dodecyl sulfate was measured at various pH values for both copper and lead surfaces. The measurement of the final pH of the solution after one hour's immersion of metals was also made. Figures 6 and 7 show the results for copper and lead respectively. The tail of the arrow in these figures shows the initial pH of the solution, while the head shows the final pH measured after one hour's immersion of the metal (abscissa) and the amount of the uptake of dodecyl sulfate (ordinate). The rate of the uptake of dodecyl sulfate shows a maximum at pH 7 and decreases towards both the acid and alkaline sides. The pH increases in the acid region and decreases in the alkaline

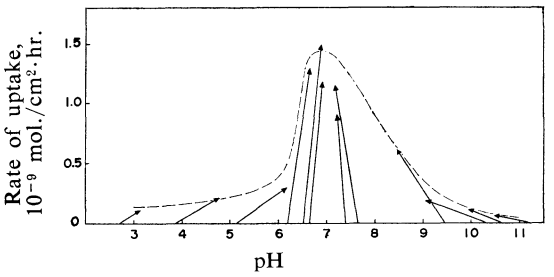



Fig. 6. Effect of pH on the rate of uptake of dodecyl sulfate on copper.

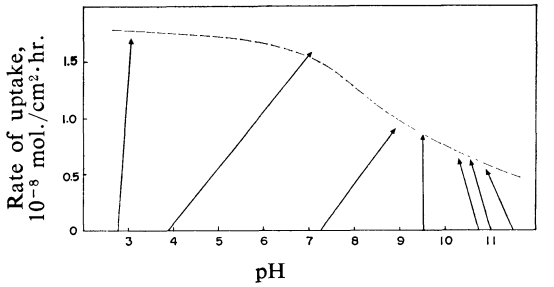



Fig. 7. Effect of pH on the rate of uptake of dodecyl sulfate on lead.

17) H. Lange, Reprint of 2nd International Congress of Surface Activity, 1, 295 (1957).
18) T. P. Hoar and U. R. Evans, *J. Electrochem. Soc.*, 99, 212 (1952).
19) B. D. Cuming and J. H. Schulman, *Australian J. Chem.*, 13, 236 (1960).

region in the course of metal dipping, but it changes little at pH 7, where the rate of uptake is at a maximum. For the lead surface, the rate of uptake is larger in the acid region and it gradually decreases toward the alkaline region. The point of no change in pH appears at pH 9; this point, however, does not correspond to the maximum rate of uptake for copper. Though the exact mechanism of these pH effects is not clear at present, a tentative explanation may be made as follows. Two fundamental types of reactions,

$$\left.\begin{aligned} &RSO_4H \rightleftharpoons RSO_4^- + H^+ \\ &RSO_4^- + H_2O \rightarrow ROH + H^+ + SO_4^{2-} \end{aligned}\right\} \quad (A)$$

$$\left.\begin{aligned} &Cu + O + 2H^+ + 2RSO_4^- \rightleftharpoons \\ &\quad Cu(RSO_4)_2 + 2H_2O \\ &Cu + O + H^+ + RSO_4^- \rightleftharpoons Cu(OH)SO_4R \\ &Cu + O + 2H^+ \rightleftharpoons Cu^{2+} + H_2O \end{aligned}\right\} \quad (B)$$

can be considered to play roles in the change in pH during metal immersion. The hydrolysis reaction of A[20] is slow and $H^+$-producing, while reaction B is $H^+$-consuming. In the acid region reaction B may be dominant, while in the alkaline region reaction A may be considered to affect the pH; in an intermediate pH, the two reactions will be balanced and the pH of the solution is unchanged during the film growth, as has been mentioned above.

However, the matter is not as clear as far as the phenomena in the alkaline region are concerned, since the error introduced during the pH measurement by the inevitable absorption of carbon dioxide obscures the results obtained.

It is interesting to repeat that the characteristic appearance of a plateau in the uptake curves is only observable at the point of no change in pH, that is, pH 7 for copper and pH 9 for lead.

## Summary

The accumulation of solute on metal surfaces has been studied using a radiotracer technique. A dip GM-counter with an end window covered with an evaporated metal film was immersed in an aqueous solution of $^{35}S$-labeled sodium dodecyl sulfate, and the change in counting rate due to the accumulation of solute on the metal surface was traced with time for various metals and pH values of the solution. The accumulation curves obtained turned out to be composed of an initial plateau, representing the region of the physical adsorption of the detergent onto the the metal surface, and/or a rising portion of the accumulation curve, indicative of chemisorption. Assuming the closely packed adsorption of solute, the roughness factors of various metal surfaces have been calculated from these plateau characteristics. The rising portion of the curve corresponds to the formation of a thick metallic soap film. The rate of film growth is controlled by the migration of the detergent or metal ions through the film, and this rate decreases as the thickness of the surface film increases. This leads to the parabolic formula for the surface film growth, which is in good agreement with the experimental results. The effect of the pH of the solution on the rate of the uptake of dodecyl sulfate has also been measured for both copper and lead surfaces. For copper surfaces the rate of the uptake of a detergent shows a maximum at pH 7 and decreases in both acid and alkaline regions. For lead surfaces, the rate is large in the acid region and gradually decreases twoards the alkaline region.

The author wishes to express his hearty thanks to Professor Tsunetaka Sasaki for his helpful guidance throughout this experiment. The cost of this research has been defrayed by a Scientific Research Grant of the Ministry of Education given to Professor Sasaki.

*Department of Chemistry*
*Faculty of Science*
*Tokyo Metropolitan University*
*Setagaya-ku, Tokyo*

20) V. A. Motsavage and H. B. Kostenbauder, *J. Colloid Sci.*, **18**, 603 (1963).

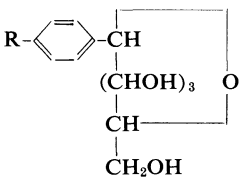
# Surface Chemical Properties in Aqueous Solutions of Glucosyl Alkylbenzenes

By Fumikatsu Tokiwa

(Received August 28, 1964)

For aqueous solutions of fatty acids and alcohols the surface chemical relationships between surface tension and concentration are now well understood.[1-3] However, investigations to extend the concept of the adsorption of solutes at an air/water interface, derived from the above relationships, to surface active non-ionic compounds have scarcely been made, probably because of the difficulties in obtaining pure materials. Thus, in the case of polyoxyethylated non-ionic compounds there is a considerable difficulty either in the synthesis of sharply defined compounds or in the purification of commercial materials.[4]

In the present experiment the author has investigated the surface tension vs. concentration relationship of aqueous solutions of a series of glucosyl alkylbenzenes obtained in a pure state, from which the free energy of adsorption and the attraction between hydrophobic portions in the surface layer were discussed. Glucosyl alkylbenzenes have the structure



where R is an alkyl group. These compounds are also interesting in the sense that they have a benzene ring in the hydrophobic portion. The lower members of glucosyl alkylbenzenes are surface-active but non-micellar in aqueous solution, while higher members are both surface-active and micellar.[5]

## Experimental

**Materials.**—Glucosyl alkylbenzenes were synthesized[6] and purified by Hutchinson et al.[5] The synthesis and purification will be reported in a separate publication. The glucosyl alkylbenzenes studied in this work include *p*-(β-D-glucosyl)methylbenzene, *p*-(β-D-glucosyl)ethylbenzene, *p*-(β-D-glucosyl)propylbenzene and *p*-(β-D-glucosyl)butylbenzene.

**Surface Tension.**—Surface tension measurements on aqueous solutions of these compounds were carried out by the drop-volume method, to which the corrections of Harkins et al.[7] were applied. The drops were formed slowly on a tip 0.408 cm. in diameter, attached to a micrometer syringe, in a thermostat at 25°C. Using drop forming times of five minutes or longer no evidence of aging was found.

## Results and Discussion

Results[5] for the surface tension of aqueous solutions of glucosyl alkylbenzenes at 25°C are shown in Fig. 1* in which the surface tension, $\gamma$, is plotted against the logarithm of the concentration, $c$.

Gibbs' adsorption isotherm for the adsorption of a soluble substance at an interface is written in the following form, if the solution is sufficiently dilute to replace the activity with the concentration.

$$\Gamma = -(c/\boldsymbol{R}T)(\mathrm{d}\gamma/\mathrm{d}c) \qquad (1)$$

where $\Gamma$ is the surface excess of the solute, $T$ is the absolute temperature, and $\boldsymbol{R}$ is the gas constant. On the other hand, the adsorption isotherm developed by Langmuir is written in the form

$$q = k_1 k_2 c/(1+k_2 c) \qquad (2)$$

where $q$ is the amount of the solute adsorbed per unit area of the surface, and $k_1$ and $k_2$ are constants. Here, let us assume that one can put $\Gamma = q$ when the solute molecules are adsorbed in the surface layer.

Combining Eqs. 1 and 2 we obtain

$$\gamma = \gamma_0 - \boldsymbol{R}Tk_1 \ln(1+k_2 c) \qquad (3)$$

1) I. Langmuir, *J. Am. Chem. Soc.*, **39**, 1883 (1917).
2) A. E. Alexander and P. Johnson, "Colloid Science," Oxford University Press, Oxford (1950), p. 513.
3) K. L. Wolf, "Physik und Chemie der Grenzflächen," Springer-Verlag, Berlin (1959), p. 148.
4) T. Nakagawa and K. Shinoda, "Colloidal Surfactants," Academic Press, New York (1963), p. 163.
5) E. Hutchinson, V. E. Sheaffer and F. Tokiwa, *J. Phys. Chem.*, **68**, 2818 (1964)
6) C. D. Hurd and W. A. Bonner, *J. Am. Chem. Soc.*, **67**, 1972 (1945).
7) W. D. Harkins and F. D. Brown, ibid., **41**, 519 (1919).

* Micellization is generally reflected in a fairly abrupt change in the slope of the surface tension vs. logarithm of concentration curve. By this criterion micelle formation is absent in the case of glucosyl methylbenzene and glucosyl ethylbenzene. No evidence for micelle formation with these two compounds was provided by other measurements[5] as well.

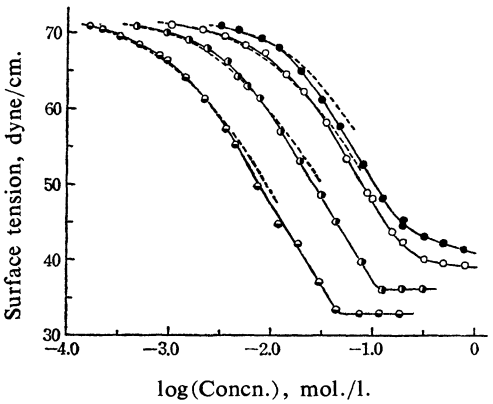



Fig. 1. Surface tension vs. log concentration curves of aqueous solutions of glucosyl alkylbenzenes at 25°C : ●, glucosyl methylbenzene ; ○, glucosyl ethylbenzene ; ◑, glucosyl propylbenzene ; ◒, glucosyl butylbenzene. (Broken lines indicate theoretical curves by Eq. 3, which are in accord with observed curves in the region of relatively low concentrations.)

where $\gamma_0$ is the surface tension of pure water. Equation 3 is consistent with Szyszkowski's empirical equation generally accepted for a series of fatty acids.[1] For concentrated solutions where $k_2c$ is large compared to unity, Eq. 3 reduces to

$$-d\gamma/d\ln c = RTk_1 \quad (4)$$

Thus the value of $k_1$ was estimated from the slope in the region of the $\gamma$-log $c$ curve where $k_2c$ is large compared to unity. The reciprocal of this value gives us the area covered by each molecule, when the surface is saturated. On the other hand, for very dilute solutions where $k_2c$ becomes small compared to unity $-d\gamma/dc$ becomes constant and

$$-d\gamma/dc = RTk_1k_2 \quad (5)$$

Thus the value of $k_2$ was also estimated from the initial slope of the $\gamma$-$c$ curve and $k_1$ according to Eq. 5. The values of $k_1$ and $k_2$ for each glucosyl alkylbenzene are listed in Table I; $k_1$ is nearly independent of the alkyl chain-length. In Fig. 1 the curves thus obtained from Eq. 3 are compared with the observed curves.

TABLE I. VALUES $k_1$ AND $k_2$, AND FREE ENERGY OF ADSORPTION FOR GLUCOSYL ALKYLBENZENES

| Compound | $k_1$ $\times 10^{10}$ | $k_2$ $\times 10^{-2}$ | $-\Delta G^\circ$ kcal./mol. |
|---|---|---|---|
| Glucosyl methylbenzene | 3.65 | 0.52 | 3.53 |
| Glucosyl ethylbenzene | 3.61 | 1.00 | 3.91 |
| Glucosyl propylbenzene | 3.66 | 2.98 | 4.56 |
| Glucosyl butylbenzene | 3.77 | 9.80 | 5.26 |

The standard free energy of adsorption, $\Delta G^\circ$, can be calculated from the equilibrium between surface and solution. Provided that both regions are sufficiently dilute for concentration to replace activity then[2]

$$\Delta G^\circ = -RT\ln(c_s/c) \quad (6)$$

where $c_s$ is the concentration in the surface region. The amount of solute $\Gamma$ adsorbed in the surface layer per square centimeter may be roughly taken to be

$$\Gamma = \tau(c_s - c)/1000 \quad (7)$$

where $\tau$ is the thickness of the surface layer in which adsorption takes place. Combining Gibbs' equation 1 with Eq. 5 we obtain

$$\Gamma = k_1k_2c \quad (8)$$

Eliminating $\Gamma$ from Eqs. 7 and 8 and combining with Eq. 6 gives for dilute solutions

$$\Delta G^\circ = -RT\ln\{1 + (1000k_1k_2/\tau)\} \quad (9)$$

Assuming a reasonable value for $\tau$ (5A), the values of $\Delta G^\circ$ given in Table I were calculated from Eq. 9.

If $\Delta G^\circ_n$ and $\Delta G^\circ_{n-1}$ are the free energies of adsorption for members with $n$ and $n-1$ carbon atoms in the alkyl chain, then

$$\Delta G^\circ_n - \Delta G^\circ_{n-1} = -RT\ln\left\{\frac{1 + (1000k_{1,n}k_{2,n}/\tau)}{1 + (1000k_{1,n-1}k_{2,n-1}/\tau)}\right\} \quad (10)$$

Here $k_{1,n}$ is nearly equal to $k_{1,n-1}$ and $(1000\, k_1k_2/\tau)$ is large compared to unity, therefore Eq. 10 reduces to

$$\Delta G^\circ_n - \Delta G^\circ_{n-1} = -RT\ln(k_{2,n}/k_{2,n-1}) \quad (11)$$

The free energy, $-\Delta G^\circ$, increases by 650—700 cal. for each additional $CH_2$ group, except for the increase in $-\Delta G^\circ$ in going from glucosyl methylbenzene to glucosyl ethylbenzene. (In the above exceptional case the increase in $-\Delta G^\circ$ is 380 cal. Probably, this could be attributed to the effect of the benzene ring on the hydrophobicity of the methyl group attached to the ring.)

The results shown above are comparable with the results obtained by Langmuir for compounds having a straight alkyl chain as a hydrophobic portion, such as fatty acids and alcohols,[1] and also indicate that Traube's rule can be applied to the non-ionic surface active compounds having a benzene ring in their hydrophobic portion.

The surface pressure-area ($\Pi$-$A$) relation for the adsorbed monolayer can be found by the use of Gibbs' equation and identifying the surface excess with an adsorbed monolayer. The result shown in Fig. 2 is plotted in the form $\Pi A/kT$ against $\Pi$, where $k$ is the Boltzmann constant. At low pressures the ideal

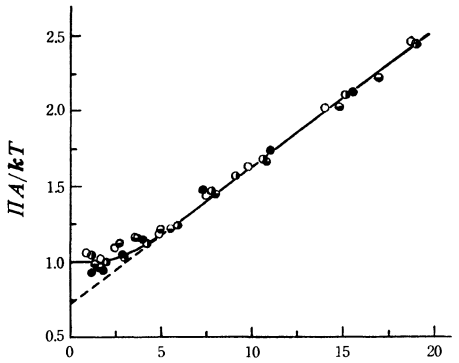



Fig. 2. $\Pi A/kT$-$\Pi$ curves for glucosyl alkylbenzenes: ●, glucosyl methylbenzene; ○, glucosyl ethylbenzene; ◑, glucosyl propylbenzene; ◒, glucosyl butylbenzene.

two-dimensional gas equation $\Pi A = kT$ is approached; at higher pressures an equation of the Amagat type

$$\Pi(A - A_0) = xkT \qquad (12)$$

is followed.

As expected, $A_0$, termed the "co-area," is independent of alkyl chain-length ($A_0 = 37.4$ Å$^2$). It is generally accepted that the deviation of $x$ from unity is a measure of attractive force between hydrophobic portions.[2] Therefore, it was expected, as in the case of a series of fatty acids,[2] that the value of $x$ decreases as the alkyl chain-length increases. However, contrary to expectation, the value of $x$ seems to be nearly independent of the chain-length, as is seen in Fig. 2 ($x = 0.72$). The following explanation may be possible for this. The attraction between the hydrophobic portions, which is responsible for the deviation of $x$ from unity, occurs predominantly between the benzene rings in the hydrophobic portion. This will reduce the effect of the alkyl chain attached to the benzene ring on the attraction, in other words, the attraction between the alkyl chains will be overwhelmed by the attraction between the benzene rings. Thus, the chain-length is not reflected in the change in $x$. The benzene ring seems to play an important role in the attraction between the hydrophobic portions.

## Summary

The surface tension in aqueous solutions of glucosyl alkylbenzenes having various alkyl chain-lengths has been measured. The surface tension vs. concentration relation of these compounds obeys Szyszkowski's equation in a relatively wide range of concentrations. For these compounds the free energy, $\Delta G°$, of adsorption was calculated; $\Delta G°$ changes by 650—700 cal./mol. for each $CH_2$ added to the alkyl chain, except in the case of going from glucosyl methylbenzene to glucosyl ethylbenzene. The adsorbed monolayer obeys an equation of state of the form $\Pi(A - A_0) = xkT$ at relatively high pressures, where $A_0$ is independent of alkyl chain-length in the present experiment. Contrary to expectation, the value of $x$, which is governed by the attractive force between hydrophobic portions, is not influenced by the alkyl chainlengths; the benzene ring in the hydrophobic portion seems to play an important role in this attraction between the hydrophobic portions.

The auther wishes to express his hearty thanks to Professor Eric Hutchinson for his kind guidance and for permission to publish this paper, and to Professor Toshizo Isemura for helpful discussion. He also wishes to express his appreciation to Kao Soap Co., Ltd. for permission to publish this paper.

*Kao-Atlas Laboratory*
*Kao Soap Co., Ltd.*
*Minato-Yakushubata*
*Wakayama*

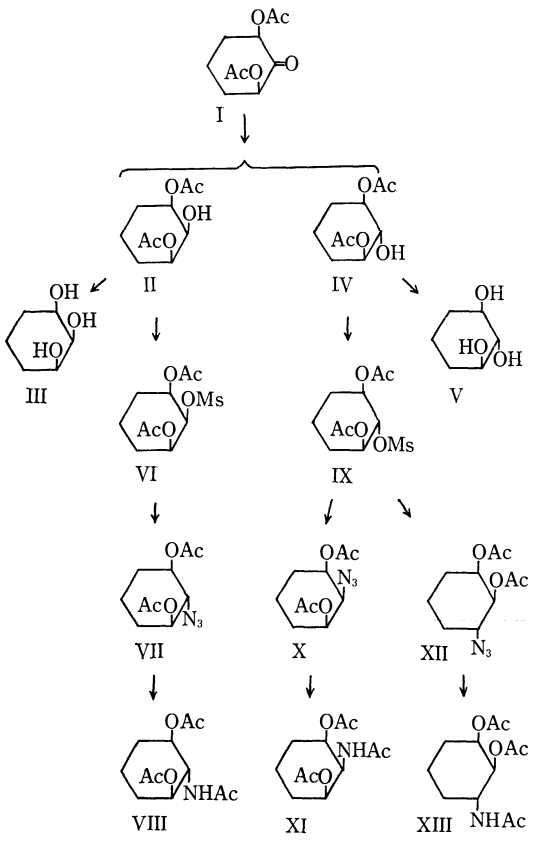
# Aminocyclitols. V. A New Synthesis of 2-Amino-1, 3-cyclohexanediol*

By Tetsuo SUAMI, Frieder W. LICHTENTHALER and Seiichiro OGAWA

(Received September 5, 1964)

In the previous paper,[1] it has been described how the mesyloxy group of di-*O*-mesyl-*trans*-2-acetamido-1, 3-cyclohexanediol can be displaced by an azide group in an anchimeric reaction to DL-2-acetamido-3-azidocyclohexanol. In the present paper, the displacement of the mesyloxy group of 1, 3-di-*O*-acetyl-2-*O*-mesyl-cyclohexanetriol by a highly nucleophilic azide ion is the main subject.

As a starting material, 2, 6-diacetoxycyclohexanone (I)[2] is used, because its configuration has been shown to be cis by Cavill and Solomon.[2] The cis-configuration of I is, furthermore, confirmed by the NMR spectrum, which reveals one sharp signal at 7.79 $\tau$ for the methyl protons of the two acetoxy groups. Subsequently, they must be conformationally equivalent.[3]




When I is hydrogenated in a hydrogen stream with platinum oxide, a mixture of 1, 3-di-*O*-acetyl-*cis*-cyclohexanetriol (II) and 1, 3-di-*O*-acetyl-*trans*-cyclohexanetriol (IV) is obtained. Fractional crystallizations of the mixture from ethanol give only II as crystals in 40% yield. The configuration of II is confirmed by converting it to *cis*-1, 2, 3-cyclohexanetriol.[4] Several attempts have been made to obtain IV as crystals, but no satisfactory result has been achieved.

The deacetylation of the crude oily product of IV gives *trans*-1, 2, 3-cyclohexanetriol[4] (V) in 50% yield; this fact indicates that the oily product consists mainly of the trans-derivative.

Therefore, the above-mentioned, intact mixture is treated with methanesulfonyl chloride and pyridine to yield a mixture of mesyl derivatives VI and IX. When this mixture is then fractionated from ethanol, both VI and IX are obtained in pure crystalline states in 50 and 17% yields respectively. Also, VI is obtained almost quantitatively from II by treating it with methanesulfonyl chloride and pyridine, while IX is prepared from crude IV in 73% yield.

The configurations of VI and IX are substantiated by means of their proton magnetic resonance spectra. The NMR spectrum of VI, as shown in Fig. 1-A, shows signals for the two equatorial acetoxy groups at 7.93 $\tau$, and for the axial mesyloxy group at 6.92 $\tau$. The two axial ring protons show the signal at around 5.20$\tau$, while the equatorial proton (C-2) reveals a 1 : 2 : 1-triplet at 4.90 $\tau$ of $J_{ab}$ 2.5 c.p.s.,[5] proving the cis-configuration. The

* A part of this paper was presented at the 17th Annual Meeting of the Chemical Society of Japan, Tokyo, April, 1964.

1) T. Suami and S. Ogawa, This Bulletin, **37**, 733 (1964).

2) G. W. K. Cavill and D. H. Solomon, *J. Chem. Soc.*, **1955**, 4427.

3) In inositol derivatives, axial acetoxy groups usually absorb within the range of 7.78—7.87 $\tau$ [F. W. Lichtenthaler, *Chem. Ber.*, **96**, 2047 (1963)]. In view of the signal obtained (7.79 $\tau$), this might indicate a diaxial orientation of the acetoxy groups in I. However, there are not sufficient NMR-data available for us to exclude an diequatorial orientation, for the shift to a lower field might also be caused by the neighboring carbonyl group. Thus, the configuration of I can be unequivocally deduced from the NMR spectrum, but not the exact orientation of the acetoxy groups.

4) T. Posternak and F. Ravenna, *Helv. Chim. Acta*, **80** 441 (1947).

5) S. Brownstein and R. Miller, *J. Org. Chem.*, **24**, 1886 (1959).

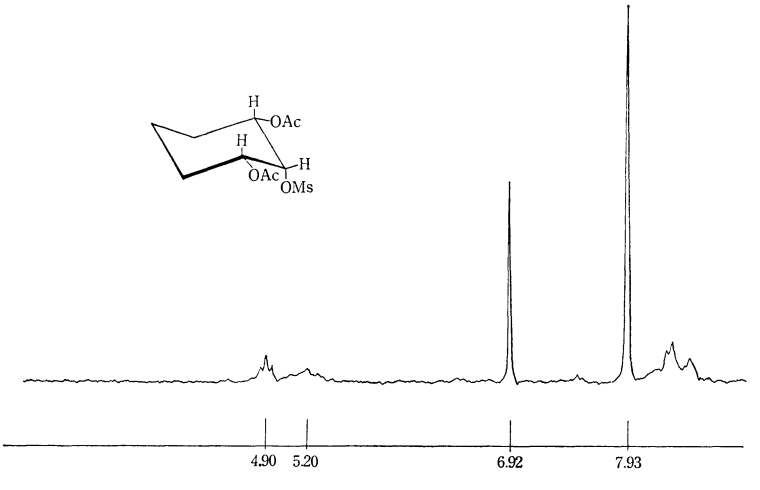



Fig. 1-A

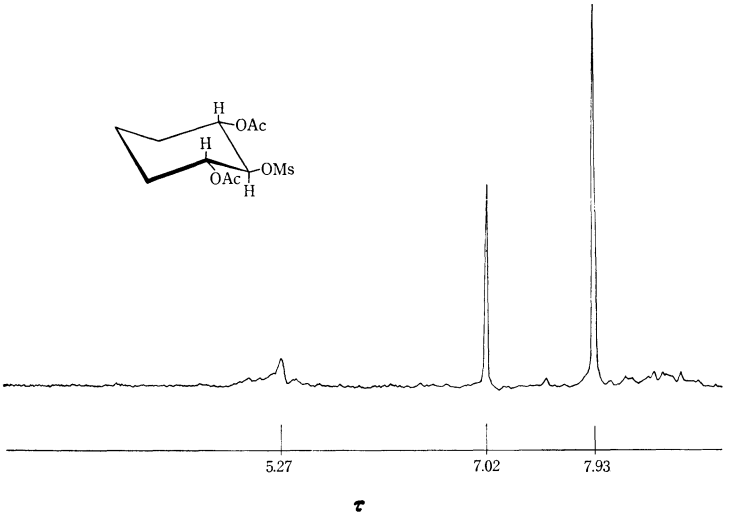



Fig. 1-B

NMR spectrum of IX, as shown in Fig. 1-B, gives signals at 7.93 $\tau$, corresponding to the two equatorial acetoxy groups, and at 7.02 $\tau$, corresponding to the equatorial mesyloxy group. The three axial ring protons are centered around 5.27 $\tau$ as an unresolved broad peaks.

This is the first interesting example of how the protons of mesyloxy groups appear at quite a different field from these of acetoxy groups; and the expected 0.1 p.p.m. difference is obtained between an axial and an equatorial mesyloxy group. Thus, the configuration of VI is established to be 1,3-di-*O*-acetyl-2-*O*-mesyl-*cis*-1,2,3-cyclohexanetriol. The configuration of the other mesylate obtained is probably that of 1,3-di-*O*-acetyl-2-*O*-mesyl-*trans*-1,2,3-cyclohexanetriol (IX). Since no acyl migration has been observed during the course of the reactions in the cis-isomer, there is more certainly no acyl migration[6] in the case of the trans-isomer.

The treatment of VI with sodium azide in boiling aqueous 2-methoxyethanol or in boiling aqueous dimethylformamide yields an oily product (VII), which shows a strong characteristic azide absorption at 2090 $cm^{-1}$.[7] The reduction of VII with a catalyst in a hydrogen stream and subsequent acetylation with acetic anhydride and pyridine give *trans*-2-acetamido-1,3-cyclohexanediol diacetate (VIII)[8,9] in 41% yield.

6) J. M. Sugihara, "Advances in Carbohydrate Chem.," Vol. 8, Academic Press Inc., New York (1953), p. 6.
7) L. J. Bellamy, "The Infrared Spectra of Complex Molecules," John Wiley & Sons, New York (1958), pp. 273—274.
8) F. W. Lichtenthaler, *Chem. Ber.*, **96**, 845 (1963).
9) T. Suami and S. Ogawa, This Bulletin, **37**, 194 (1964).

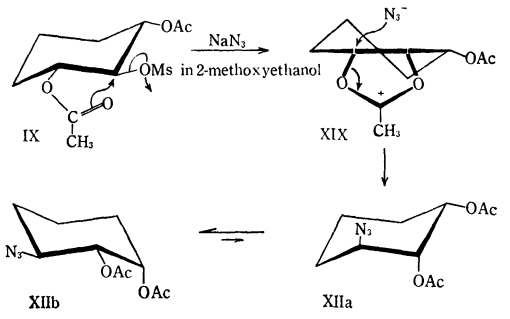
When a cyclohexane ring containing vicinal sulfonyloxy and acetoxy groups in the trans position is treated with sodium acetate in an appropriate solvent, the replacement of the sulfonate group takes place with Walden inversion through an intermediary acetoxonium ion, giving *cis*-acetate alcohol.[10] When they are in the cis position, the replacement occurs at a considerably slower rate,[11] because of an anchimerically-unassisted conformation.[12] A mechanism analogous to that of the reaction with sodium azide has been proposed.[1,13]

In the present experiment, the mesyloxy group of VI is located in the cis orientation to the vicinal acetoxy group; the fact that the *trans*-2-amino-1, 3-cyclohexanediol derivative is obtained as a main product indicates that the introduction of an azide group is operated predominantly by an $S_N2$ mechanism.

The demesylation of the *trans*-mesylate, IX, by an azide ion in boiling aqueous dimethylformamide is also dominated by a direct $S_N2$ reaction, since, upon the catalytic hydrogenation of the azido derivative (X) and the subsequent acetylation, the *cis*-triacetyl derivative (XI)[9] is obtained in 43% yield.

The same reaction, however, proceeds via quite a different stereochemical course when carried out in 2-methoxyethanol. Upon hydrogenation and acetylation *cis*-2-acetamido-1, 3-cyclohexanediol diacetate is obtained in only a 3% yield, whereas DL-3$\beta$-acetamido-1$\alpha$, 2$\alpha$-cyclohexanediol diacetate (XIII)[14,15] can be isolated in 25% yield.

The formation of XIII from IX can only be rationalized by assuming neighboring-group participation from the acetoxy group in the course of the reaction; the mesyloxy group is eliminated with the formation of an acetoxonium ion intermediate (XIX), in which the nucleophilic attack occurs predominantly at the quasi-equatorial C-O bond. Thus the diaxial product (XIIa) is primarily obtained, which product then switches over to the other more stable chair conformation (XIIb). This stereochemical course of the reaction has analogies in the opening of the acetoxonium ring by the acetate ion[12] and also in the nucleophilic oxirane-ring fission.[16,17]




The solvent-dependence of the (IX → XIII) reaction—mainly a direct $S_N2$ reaction in dimethylformamide, and predominantly an anchimeric reaction in 2-methoxyethanol—can be explained by saying that the relative strengths of the two competing nucleophiles—an azide ion and an anchimeric acetoxy group respectively—are different in their solvents. Similar effects have been discussed in the demesylation of hexitol derivatives.[18]

## Experimental

All melting points were measured on a Mitamura-Riken micro hot stage. The NMR spectra were determined at a frequency of 60 Mc.p.s. with Varian Associates A-60 and Japan Electron Optics JNM-C-60 spectrometers in deuteriochloroform. Tetramethylsilane was used as an internal reference. Peak positions were given in $\tau$-values. The infrared spectra were recorded in potassium bromide pellets.

**1, 3-Di-*O*-acetyl-*cis*-1,2,3-cyclohexanetriol (II).**—The starting material, *cis*-2,6-diacetoxycyclohexanone (I), was prepared by the method of Cavill and Solomon.[2] A mixture of 5.0 g. of I and 150 ml. of ethanol was hydrogenated with 0.3 g. of platinum oxide in Parr shaker-type apparatus at 40°C for 23 hr. under 50 p.s.i.g. of an initial pressure of hydrogen. After the catalyst had been removed by filtration, the filtrate was evaporated under reduced pressure to yield 5.0 g. of a colorless semicrystalline residue. The residue was purified by crystallization from ethyl acetate to give 2.2 g. (44%) of needles melting at 103—104°C.

Found: C, 55.71; H, 7.55. Calcd. for $C_{10}H_{16}O_5$: C, 55.54; H, 7.46%.

A solution of 81 mg. of II in 30 ml. of methanol previously saturated with ammonia was allowed to stand at room temperature overnight. The solution was then evaporated in vacuo to yield a crystalline residue, which was recrystallized from ethyl acetate to give 37 mg. of analytically-pure *cis*-1,2,3-cyclohexanetriol (III) melting at 146.5—147.5°C (lit.[3] m. p. 147—148°C). (Found: C, 54.52; H, 8.96%).

10) S. Winstein, H. V. Hess and R. E. Buckles, *J. Am. Chem. Soc.*, **64**, 2796 (1942); S. Winstein, C. Hanson and E. Grundwald, ibid., **70**, 812 (1948).
11) S. Winstein, E. Grunwald, R. E. Buckles and C. Hanson, ibid., **70**, 816 (1948).
12) E. S. Gould, "Mechanism and Structure in Organic Chemistry," Holt, Rinehart and Winston, New York (1962), pp. 565—566.
13) B. R. Baker and A. H. Haines, *J. Org. Chem.*, **28**, 442 (1963).
14) R. A. B. Bannard and L. R. Hawkins, *Can. J. Chem.*, **36**, 1241 (1958).
15) The infrared spectrum of an authentic sample of DL-3$\beta$-acetamido-1$\alpha$, 2$\alpha$-cyclohexanediol diacetate was kindly presented by Dr. R. A. B. Bannard of the Defence Research Chemical Lab., Ottawa, Canada.
16) D. H. R. Barton, *J. Chem. Soc.*, **1953**, 1027; E. Eliel, in M. S. Newman, "Steric Effects in Organic Chemistry," J. Wiley & Sons, New York (1956), pp. 130—134.
17) M. Nakajima, A. Hasegawa and F. W. Lichtenthaler, *Ann. Chem.*, **669**, 75 (1963).
18) B. R. Baker and H. S. Sachdev, *J. Org. Chem.*, **28**, 2132 (1963).

The remaining oily product (450 mg.), obtained by evaporating the mother liquor of II, was treated in the manner which has been described for III to yield 200 mg. of crude *trans*-1,2,3-cyclohexanetriol (V). Recrystallization from ethyl acetate gave 135 mg. of analytically-pure V melting at 107—108°C (lit.[8] m. p. 108°C). (Found: C, 54.67; H, 9.15%).

**1,3-Di-*O*-acetyl-2-*O*-mesyl-*cis*-1,2,3-cyclohexanetriol (VI).**—A 0.6 ml. portion of methanesulfonyl chloride was added to a mixture of 1.0 g. of II and 15 ml. of pyridine under ice cooling, and the mixture was allowed to stand overnight in a refrigerator. Then the mixture was poured into ice-water. The precipitate was collected by filtration, washed with cold water, and dried to yield 1.3 g. (95%) of the crude product melting at 150—151°C. When recrystallized from ethanol, it melted at 152—152.5°C.

Found: C, 45.18; H, 6.23; S, 10.67. Calcd. for $C_{11}H_{18}O_7S$: C, 44.89; H, 6.16; S, 10.90%.

**1,3-Di-*O*-acetyl-2-*O*-mesyl-*trans*-1,2,3-cyclohexanetriol (IX).**—The crude oily product of IV (220 mg.) was treated in the manner described for VI. The reaction mixture was poured into ice water, and the solution was evaporated in vacuo to a half volume to yield the crude product. Recrystallization from ethanol gave 210 mg. (73%) of needles melting at 136—137°C.

Found: C, 45.33; H, 6.12; S, 10.37. Calcd. for $C_{11}H_{18}O_7S$: C, 44.89; H, 6.16; S, 10.90%.

**The Mesylation of the Mixture of II and IV.**—A 3.8 g. portion of the mixture of II and IV obtained by the hydrogenation of 5 g. of I was treated overnight with 3.0 ml. of methanesulfonyl chloride and 50 ml. of pyridine. The mixture was then treated in the manner described for IX to yield 4.2 g. (82%) of a mixture of VI and IX melting at 124—150°C. The mixture was fractionally recrystallized from ethanol to give 2.56 g. (50%) of VI melting at 150—152°C and 0.88 g. (17%) of IX melting at 136—137°C.

***trans*-2-Acetamido-1,3-cyclohexanediol Diacetate (VIII).**—a) A mixture of 0.50 g. of VI, 0.60 g. of sodium azide, and 20 ml. of 85% aqueous 2-methoxyethanol was refluxed for 14 hr. The solvent was then removed by evaporation in vacuo. The residue was repeatedly extracted with hot acetone, and the combined extracts were evaporated to give 480 mg. of a brown oil, showing a strong infrared absorption of an azide group at 2090 $cm^{-1}$. The crude VII dissolved in 8 ml. of ethanol was hydrogenated in an initial hydrogen pressure of 50 p.s.i.g. with Raney nickel. After the catalyst had been removed by filtration, the filtrate was evaporated to yield 415 mg. of an oil. This was acetylated overnight with 10 ml. of acetic anhydride and 10 ml. of pyridine. The mixture was then evaporated in vacuo to dryness, and the residue was triturated with ether to give 180 mg. (41%) of a product which, after recrystallization from ethanol-ether, gave crystals melting at 150—152°C. The melting point showed no depression upon admixture with an authentic sample.[9] b) When the same reaction was carried out in aqueous dimethylformamide, the same results as in a) was obtained.

**DL-3$\beta$-Acetamido-1$\alpha$,2$\alpha$-cyclohexanediol Diacetate (XIII).**—A mixture of 1.4 g. of IX, 1.5 g. of sodium azide, and 60 ml. of 85% aqueous 2-methoxyethanol was refluxed for 30 hr. Then the mixture was treated in a manner similar to that described for VIII to give 0.30 g. (25%) of a product melting at 146.5—147°C. The product was recrystallized from benzene to yield plates melting at 147—148.5°C (lit.[9] m. p. 148—149.5°C). (Found: C, 56.17; H, 7.40; N, 5.48%).

The infrared spectrum was superimposable on that of an authentic sample.[15]

The mother liquor of XIII was kept in a refrigerator for a long time to give 0.04 g. (3%) of crystals melting at 175°C. The crystals were recrystallized from benzene to give needles melting at 175—178°C. The product was identified as *cis*-2-acetamido-1,3-cyclohexanediol diacetate[9] on the basis of a mixed melting point determination and its infrared spectrum.

***cis*-2-Acetamido-1,3-cyclohexanediol Diacetate (XI).**—A mixture of 502 mg. of IX, 550 mg. of sodium azide, and 20 ml. of 85% aqueous dimethylformamide was refluxed for 14 hr. The mixture was treated in a manner similar to that described above to give 190 mg. (43%) of the product melting at 175.5—177°C. The product was recrystallized from ethanol-ether to give needles melting at 175—176°C. A mixed melting point determination with an authentic sample[9] was undepressed.

The authors are indebted to Professor Sumio Umezawa for his helpful advice, to Mr. Saburo Nakada for his microanalysis, to Mr. Masahiko Kitajima and Mr. Yasumasa Ishida for their assistance in the analytical experiments, and to Miss Sunao Ohata for the measurement of the infrared spectra. This research has been supported in part by the Asahi Glass Foundation for Contributions to Industrial Technology and by the Deutsche Forschungs Gemeinschaft.

*Department of Applied Chemistry*
*Faculty of Engineering*
*Keio University*
*Koganei, Tokyo (T. S. & S. O.)*

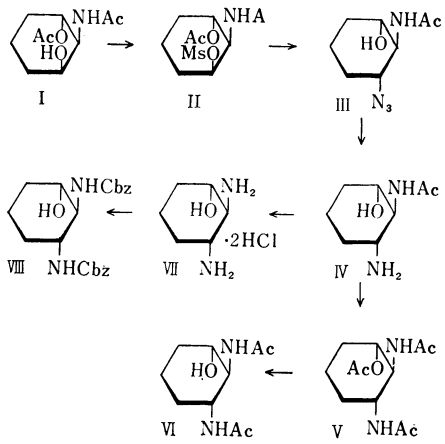
*Institut für Organische Chemie*
*Technische Hochschule*
*61 Darmstadt, Germany (F. W. L.)*

# Aminocyclitols. VI.* The Synthesis and Configurational Analysis of *trans*-2, 3-Diaminocyclohexanol

By Tetsuo SUAMI and Seiichiro OGAWA

(Received September 22, 1964)

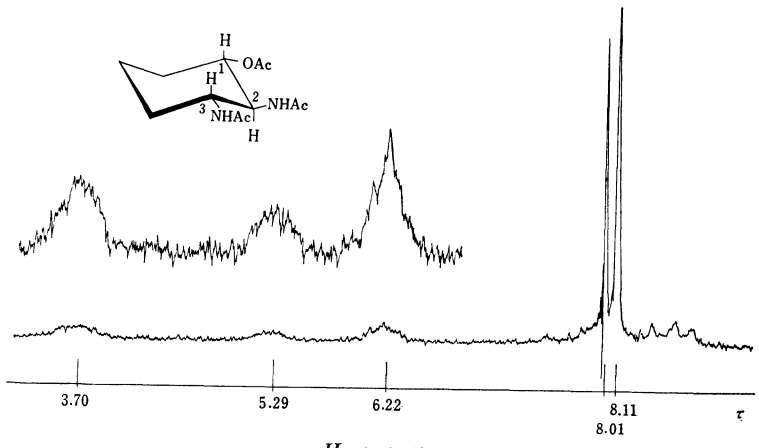
In connection with the previous papers of this series,[1] the synthesis of DL-*trans*-2, 3-diaminocyclohexanol and a study of its structure by means of the proton magnetic resonance spectrum of the acetyl derivative will be described in the present paper.




Starting from 1-*O*-acetyl-DL-2$\alpha$-acetamido-1$\beta$, 3$\alpha$-cyclohexanediol (I),[2] 1-*O*-acetyl-3-*O*-mesyl-DL-2$\alpha$-acetamido-1$\beta$, 3$\alpha$-cyclohexanediol (II) is obtained in 58% yield by treating I with methanesulfonyl chloride in pyridine.

Compound II is treated with sodium azide in boiling 90% aqueous 2-methoxyethanol to give DL-2$\alpha$-acetamido-3$\beta$-azido-1$\beta$-cyclohexanol (III) as colorless crystals in 73% yield. Then III is hydrogenated with a platinum catalyst in a hydrogen stream to give DL-2$\alpha$-acetamido-3$\beta$-amino-1$\beta$-cyclohexanol (IV) in 87% yield. On acetylating IV with acetic anhydride and pyridine, the triacetyl derivative (V) is obtained in 83% yield. When V is refluxed with 6 N hydrochloric acid, deacetylation takes place, giving the dihydrochloride (VII) in 92% yield. By an ordinary method, di-*N*-carbobenzyloxy derivative (VIII) is prepared in 96% yield. By deacetylating V with ammonia in methanol, diacetamidocyclohexanol (VI) is prepared in 89% yield.

The mesyloxy group is located in a cis position to the vicinal acetamido group in II; therefore, the replacement of the mesyloxy group by an azide ion should take place through a direct $S_N2$ mechanism.[3] As a result, the inversion of the configuration at C-3 must occur, and the product should be DL-2$\alpha$-acetamido-3$\beta$-azido-1$\beta$-cyclohexanol. This configuration is also supported by the NMR spectrum of V; as is shown in Fig. 1, the spectrum




*H*, p. p. m.

Fig. 1

1) * Part IV: T. Suami and S. Ogawa, This Bulletin, **37**, 733 (1964).

2) T. Suami and S. Ogawa, ibid., **37**, 194 (1964)

3) T. Suami, F. W. Lichtenthaler and S. Ogawa, ibid., **38**, 754 (1965).

reveals two sharp signals of a 1 : 2 relative intensity, as is to be expected from one equatorial acetoxy group (of 8.01 $\tau$) and two equatorial acetamido groups (of 8.11 $\tau$).[2,4] The two axial ring protons on C-2 and C-3 show the broad signal (peak width : 25 c. p. s.) at 6.22 $\tau$, while the one axial ring proton on C-1 reveals an unresolved broad signal (peak width : 27 c. p. s.) at 5.29 $\tau$. Since the vicinal spin-spin coupling constant is greater between two axial protons than between axial-equatorial protons or two equatorial protons,[5] the broad peak widths of the ring protons correspond to the assigned configuration.

The protons on the nitrogen atoms in amide groups show the signal at 3.70 $\tau$.[6]

## Experimental

All the melting points have been corrected. The NMR spectrum was determined at a frequency of 60 Mc. p. s. with a Japan Electron Optics JNM-C-60 spectrometer in deuteriochloroform. Tetramethylsilane was used as an internal reference in the sample. Peak positions are given in $\tau$-values.

**1-*O*-Acetyl-3-*O*-mesyl-DL-2$\alpha$-acetamido-1$\beta$, 3$\alpha$-cyclohexanediol (II).** — To a mixture of 3.5 g. of 1-*O*-acetyl-DL-2-acetamido-1,3-cyclohexanediol[2,7] and 40 ml. of pyridine, 2.4 g. of methanesulfonyl chloride was added drop by drop under ice cooling with agitation. After it had stood overnight in a refrigerator, the reaction mixture was poured into ice and water. The mixture was then evaporated under reduced pressure until a precipitate appeared; this was collected by filtration and washed with cold water. The crude product (2.75 g.) melted at 159—163°C. The analytical sample was recrystallized from ethanol and melted at 161.5—162°C.

Found: C, 45.00; H, 6.42; N, 4.94; S, 10.70. Calcd. for $C_{11}H_{19}NO_6S$: C, 45.04; H, 6.53; N, 4.78; S, 10.93%.

**DL-2$\alpha$-Acetamido-3$\beta$-azido-1$\beta$-cyclohexanol (III).** —A mixture of 2.2 g. of II, 1.5 g. of sodium azide and 65 ml. of 90% aqueous 2-methoxyethanol was refluxed for 20 hr. The reaction mixture was then evaporated under reduced pressure to dryness, and the residue was extracted repeatedly with boiling acetone. The combined acetone extract was evaporated to yield 1.4 g. of the crystalline residue. The residue was recrystallized from acetone-ether to give 1.09 g. of crystals (73%) melting at 134—137°C. Recrystallization from the same mixed solvent raised the melting point to 137—139°C.

Found: C, 48.57; H, 7.07; N, 28.15. Calcd. for $C_8H_{14}N_4O_2$: C, 48.47; H, 7.12; N, 28.27%.

IR: 3350 (-OH), 2110 ($-N_3$), 3280, 1650, 1628 and 1555 $cm^{-1}$ (amide).

**DL-2$\alpha$-Acetamido-3$\beta$-amino-1$\beta$-cyclohexanol (IV).** —A 1.05 g. portion of III was hydrogenated in 60 ml. of ethanol over 0.2 g. of platinum oxide at room temperature for 10 hr. The catalyst was then removed by filtration, and the filtrate was evaporated to give the crystalline residue. The residue was recrystallized from ethanol-ether to give 0.8 g. of the product (87%) melting at 176—177°C. The analytical sample was recrystallized from ethanol-ether and melted at 180—181°C after having sintered at 178°C.

Found: C, 55.38; H, 9.12; N, 16.02. Calcd. for $C_8H_{16}N_2O_2$: C, 55.79; H, 9.36; N, 16.27%.

**DL-2$\alpha$, 3$\beta$-Diacetamido-1$\beta$-cyclohexanol Acetate (V).**—A mixture of 156 mg. of IV, 5 ml. of acetic anhydride and 5 ml. of pyridine was allowed to stand overnight at room temperature; then it was evaporated under reduced pressure to yield a crystalline residue. The residue was recrystallized from ethanol-ether to give 102 mg. (83%) of needles melting at 223.5—224.5°C. Further recrystallizations did not raise its melting point.

Found: C, 56.38; H, 7.68; N, 10.86. Calcd. for $C_{12}H_{20}N_2O_4$: C, 56.23; H, 7.87; N, 10.93%.

**DL-2$\alpha$, 3$\beta$-Diamino-1$\beta$-cyclohexanol Dihydrochloride (VII).**—A mixture of 455 mg. of IV and 25 ml. of 6 N hydrochloric acid was refluxed for 3 hr. and then evaporated to dryness in vacuo. The residue was recrystallized from ethanol, giving 491 mg. (92%) of crystals which melted at 263°C with decomposition, after having turned brown at 250°C. Further recrystallization from methanol-ether did not raise the melting point.

Found: C, 35.66; H, 8.02; N, 13.40; Cl, 34.65. Calcd. for $C_6H_{14}N_2O \cdot 2HCl$: C, 35.48; H, 7.94; N, 13.79; Cl, 34.91%.

**Paper Chromatography.**—An ethyl acetate - pyridine - acetic acid - water (5 : 5 : 3 : 1) system[12] gave a single spot of $R_f/R_f$glucosamine: 1.14 in ascending development at 24°C with Toyo filter paper No. 51. An upper layer of 1-butanol - acetic acid - water (4 : 1 : 5) gave a single spot of $R_f$ 0.19 at 23°C ($R_f$ of glucosamine hydrochloride: 0.19).

**DL-2$\alpha$, 3$\beta$-Diacetamido-1$\beta$-cyclohexanol (VI).**—A 136 mg. portion of V was added to 20 ml. of methanol which had previously been saturated with ammonia, and the mixture was allowed to stand overnight at room temperature. Then the mixture was evaporated in vacuo. The residue was recrystallized from ethanol-ether to give 101 mg. (89%) of crystals melting at 240—241°C with decomposition.

Found: C, 55.81; H, 8.48; N, 12.72. Calcd. for $C_{10}H_{18}N_2O_3$: C, 56.05; H, 8.47; N, 13.08%.

**Di-*N*-carbobenzyloxy-DL-2$\alpha$,3$\beta$-diamino-1$\beta$-cyclohexanol (VIII).**—To a mixture of 100 mg. of VII, 336 mg. of sodium bicarbonate and 3 ml. of water, 0.3 ml. of carbobenzyloxy chloride (a 85% toluene solution) was added under agitation. After the mixture had been allowed to stand overnight, the precipitate was collected by filtration and washed with cold water and toluene, giving 188 mg. (96%) of the product. The crude product was recrystallized from ethanol to give needles melting at 157—159°C.

Found: C, 66.59; H, 6.45; N, 7.01. Calcd. for $C_{22}H_{26}N_2O_5$: C, 66.31; H, 6.58; N, 7.03%.

4) F. W. Lichtenthaler, *Chem. Ber.*, **96**, 2047 (1963).
5) S. Brownstein and R. Miller, *J. Org. Chem.*, **24**, 1886 (1959).
6) L. M. Jackman, "Applications of Nuclear Magnetic Resonance Spectroscopy in Organic Chemistry," Pergamon Press, London (1962), p. 73.
7) F. W. Lichtenthaler, *Chem. Ber.*, **96**, 845 (1964).

The authors are indebted to Professor Sumio Umezawa for his helpful advice, to Mr. Saburo Nakada for his elemental analyses, and to the Japan Electron Optics Co., Ltd., for the measurement of the NMR spectrum. This research has been supported in part by a grant of the Ministry of Education, to which the authors' thanks are due.

*Department of Applied Chemistry*
*Faculty of Engineering*
*Keio University*
*Koganei, Tokyo*

# Organic Photochemical Reactions. I. The Synthesis of Substituted Oxetanes by the Photoaddition of Aldehydes to Furans[1]

By Susumu TOKI, Kensuke SHIMA and Hiroshi SAKURAI

(Received September 9, 1964)

Photochemical reactions of carbonyl compounds with olefins have been studied by many workers in recent years.[2] On the photoaddition of aldehydes to olefins, acyl addition affording ketones, direct addition yielding oxetanes, and allylic addition giving unsaturated carbinols have been observed. However, little attention has been paid to the addition of aldehydes to conjugated olefins. In the present work, furan and 2-methylfuran were chosen as the conjugated olefins without an activated allylic hydrogen atom. It seemed that it would be interesting to investigate what type of reaction occurs between aldehydes (propionaldehyde and benzaldehyde) and furans on irradiation.

In this experiment, an ultraviolet light from a 350 W. high pressure mercury lamp was used. A mixture of aldehyde and furan (mole ratio: ca. 1 : 4) was irradiated in a nitrogen atmosphere at 5—10°C for 6 hr., and then the reaction product was isolated by distillation under reduced pressure.

The reaction conditions and the yields of the product are summarized in Table I.

The distilled fraction in each case was identified as an oxetane from the following observations. In the photochemical reaction of propionaldehyde and furan, a fraction with a b. p. of 74—75°C (30 mmHg) was obtained. This fraction was decomposed into its starting materials (mole ratio: 1 : 1) when passed through a Dinonyl Phthalate and Silicone DC 550 column at 80°C. This fraction was confirmed to be a 1 : 1 adduct on the basis of the above finding, elementary analysis and molecular weight determination. The infrared spectrum showed the presence of a vinyl ether group[3] and a trimethylene oxide ring,[3] but the absorptions of a carbonyl group and a hydroxy group were not observed. The structure of this photoadduct, therefore, is either Ia or Ib.

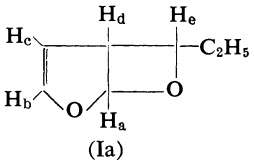
This was determined by means of the NMR spectrum. NMR spectral data are compiled

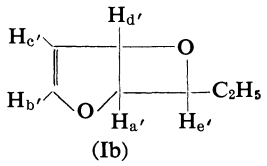
TABLE I. THE REACTION CONDITIONS AND YIELD OF THE PRODUCTS

| Furan g. | Aldehyde g. | Oxetane g. | Residue g. | Yield[a] % | Ultimate yield[b] % |
|---|---|---|---|---|---|
| $C_4H_4O$ 126 | $C_2H_5CHO$ 28 | 10 | 2.5 | 17 | 80 |
| $C_4H_4O$ 112 | $C_6H_5CHO$ 42.5 | 24.5 | 3.5 | 35 | 88 |
| $CH_3$-$C_4H_3O$ 125 | $C_2H_5CHO$ 23.2 | 9.5 | 3.5 | 17 | 73 |
| $CH_3$-$C_4H_3O$ 120 | $C_6H_5CHO$ 38.5 | 22 | 3.4 | 32 | 87 |

a) Yield of products based on aldehyde used.
b) Yield of products based on aldehyde consumed.

1) Reported at the 17th Annual Meeting of the Chemical Society of Japan, Tokyo, April, 1964.
2) M. S. Kharasch, W. H. Urry and B. M. Kuderna, *J. Org. Chem.*, **14**, 248 (1949); G. Büchi, C. G. Inman and E. S. Lipinsky, *J. Am. Chem. Soc.*, **76**, 4327 (1954); P. de Mayo, J. B. Stothers and W. Templeton, *Proc. Chem. Soc.*, **1960**, 72; *Can. J. Chem.*, **39**, 488 (1961).
3) L. J. Bellamy, "The Infra-red Spectra of Complex Molecules," Methuen, London (1958), pp. 117, 119.

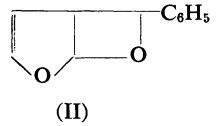

(Ia)

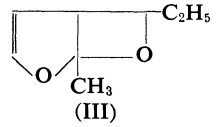

(Ib)

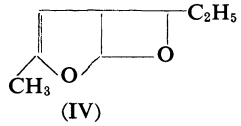
in Table II. Supposing that it is Ib, as all protons except for ethyl protons are adjacent to oxygen or are vinylic, it may be expected that the $\tau$-value of each proton will be less than 5.5. However, a proton with a $\tau$-value of 6.58 was observed. Moreover, although a proton a' would be a triplet and a proton d' would be a sextet or octet in the structure Ib, a doublet and a complex multiplet were actually observed. The structure, therefore, was identified as 6-ethyl-2, 7-dioxa-bicyclo-[3, 2, 0]-$\Delta^3$-heptene (Ia). The infrared spectrum of the residue showed strong bands of the carbonyl and hydroxy groups. The ratio of the residue to Ia increased with the irradiation time. Ia was rather stable in a sealed tube. When Ia was exposed to air, however, its infrared spectrum gradually became similar to that of the residue. The residue, therefore, seems to consist of the products formed from Ia by further reaction by, for instance, light or oxygen.

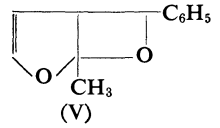
In the photochemical reaction of benzaldehyde and furan, the photoadduct was similarly identified as 6-phenyl-2, 7-dioxa-bicyclo-[3, 2, 0]-$\Delta^3$-heptene (II).

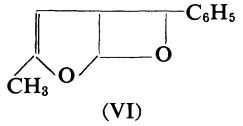
In the case of propionaldehyde (or benzaldehyde) and 2-methylfuran, mixtures of III (or V) and IV (or VI) were obtained.


(II)


(III)


(IV)


(V)


(VI)

The reaction paths for the formation of oxetanes are probably similar in all cases. As a typical example, the reaction of benzaldehyde

$$C_6H_5CHO \xrightarrow[n\text{-}\pi^*\text{transition}]{h\nu} \text{Excited state} \xrightarrow{C_4H_4O}$$

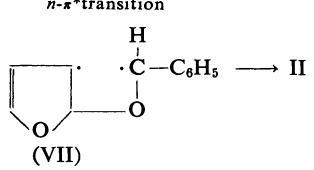
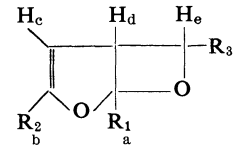

(VII)

TABLE II. NMR SPECTRAL DATA*



| Compound | | $\tau$-Value | Multiplicity | Coupling const., c.p.s. |
|---|---|---|---|---|
| Ia | a | 3.73 | Quartet | $J_{ab}$ 0.9 |
| $R_1$=H | b | 3.40 | Quartet | $J_{ad}$ 4.4 |
| $R_2$=H | c | 4.70 | Triplet | $J_{bc}$ 2.8 |
| $R_3$=$C_2H_5$ | d | 6.58 | Multiplet | $J_{bd}$ 0.9 |
| | e | 5.53 | Sextet | $J_{cd}$ 2.8 |
| | | | | $J_{de}$ 2.8 |
| II | a | 3.53 | Doublet | $J_{ab}$ 0.8 |
| $R_1$=H | b | 3.37 | Quartet | $J_{ad}$ 4.4 |
| $R_2$=H | c | 4.62 | Triplet | $J_{bc}$ 2.9 |
| $R_3$=$C_6H_5$ | d | 6.43 | Multiplet | $J_{bd}$ 0.8 |
| | e | 4.50 | Doublet | $J_{cd}$ 2.9 |
| | | | | $J_{de}$ 2.9 |
| III** | a | 8.38 | Singlet | $J_{bc}$ 3.1 |
| $R_1$=$CH_3$ | b | 3.49 | Quartet | $J_{bd}$ 1.0 |
| $R_2$=H | c | 4.78 | Triplet | $J_{cd}$ 3.1 |
| $R_3$=$C_2H_5$ | d | 6.89 | Sextet | $J_{de}$ 3.1 |
| | e | 5.71 | Sextet | |
| IV** | a | 3.80 | Doublet | $J_{ad}$ 4.0 |
| $R_1$=H | b | 8.10 | Triplet | $J_{bc}$ 1.3 |
| $R_2$=$CH_3$ | c | 5.09 | Sextet | $J_{bd}$ 1.3 |
| $R_3$=$C_2H_5$ | d | 6.63 | Multiplet | $J_{cd}$ 2.7 |
| | e | 5.71 | Sextet | $J_{de}$ 3.2 |
| V** | a | 8.30 | Singlet | $J_{bc}$ 3.1 |
| $R_1$=$CH_3$ | b | 3.38 | Quartet | $J_{bd}$ 0.9 |
| $R_2$=H | c | 4.62 | Triplet | $J_{cd}$ 3.2 |
| $R_3$=$C_6H_5$ | d | 6.60 | Sextet | $J_{de}$ 3.2 |
| | e | 4.48 | Doublet | |
| VI** | a | 3.53 | Doublet | $J_{ad}$ 4.6 |
| $R_1$=H | b | 8.04 | Triplet | $J_{bc}$ 1.2 |
| $R_2$=$CH_3$ | c | 4.93 | Multiplet | $J_{bd}$ 1.2 |
| $R_3$=$C_6H_5$ | d | 6.42 | Multiplet | $J_{cd}$ 3.2 |
| | e | 4.48 | Doublet | $J_{de}$ 3.2 |

* Spectra were obtained on a Varian A-60 spectrometer using chloroform-d as solvent and tetramethylsilane as internal standard.

** Data of III and IV, V and VI were obtained from the spectrum of products mixture, respectively.

with furan probably proceeds by the following path.

The intermediate (VII) has the structure which is to be expected from the principle of the maximum resonance stabilization of the intermediate diradical. VII is also expected from the simple LCAO-MO. Since the excited benzaldehyde has a free radical character[4] at

4) G. S. Hammond and P. A. Leermakers, *J. Am. Chem. Soc.*, **84**, 207 (1962).

the oxygen atom, as is to be expected from an excitation of the $n$-$\pi^*$ type, the oxygen atom with a free radical character will attack the site of higher free valence or a more frontier electron density[5] of the furan ring to yield VII.

## Experimental[6]

**Materials.**—Propionaldehyde was purified by distillation; b. p. 50°C, $n_D^{20}$ 1.3689. Benzaldehyde was also purified by distillation; b. p. 36.5°C (2 mmHg), $n_D^{20}$ 1.5444. Furan[7] was prepared by the decarboxylation of 2-furancarboxylic acid, formed by the Cannizzaro reaction of furfural, and purified by fractional distillation over calcium chloride; b. p. 31.5°C. 2-Methylfuran[8] was prepared by the following method. A mixture of 270 g. of furfural and 300 g. of a 30—40% aqueous hydrazine solution was added drop by drop to 50 g. of potassium hydroxide in a 1-l. Claisen flask, which was then placed in an oil bath heated at 150—160°C. The distillate was collected, and the upper layer was separated, dried over potassium hydroxide and distilled; b. p. 63°C. These materials were gas chromatographically pure and were redistilled before use.

**6-Ethyl-2,7-dioxa-bicyclo-[3,2,0]-$\Delta^3$-heptene (Ia).**—A mixture of 126 g. (1.85 mol.) of furan and 28 g. (0.48 mol.) of propionaldehyde was placed in a 180 ml. reaction vessel and irradiated at 5—10°C in a nitrogen atmosphere for 6 hr.[9] The unreacted materials were then distilled off, and the portion boiling at 70—75°C (30 mmHg) was collected; yield, 10 g. (17%). This fraction was redistilled at 30 mmHg (b. p. 74—75°C); $n_D^{20}$ 1.4567. Principal infrared bands: 3075, 2945, 1605, 1460, 1213, 1198, 1130, 1043, 1013, 985, 950, 887, 850 and 715 $cm^{-1}$.

Found: C, 66.29; H, 8.29; mol. wt., 127. Calcd. for $C_7H_{10}O_2$: C, 66.64; H, 7.99%; mol. wt., 126.

**6-Phenyl-2, 7-dioxa-bicyclo-[3, 2, 0]-$\Delta^3$-heptene (II).**—A mixture of 112 g. (1.65 mol.) of furan and 42.5 g. (0.40 mol.) of benzaldehyde was irradiated at 5—10°C for 6 hr. and then treated in the same manner as has been discribed above. A 100—115°C (2 mmHg) fraction was then collected; yield, 24.5 g. (35%). This fraction was redistilled at 1.2 mmHg (b.p. 104—105°C); m.p. 49—50°C. Principal infrared bands: 3080, 2940, 1608, 1458, 1380, 1198, 1130, 1040, 940 and 708 $cm^{-1}$.

Found: C, 76.12; H, 6.02; mol. wt., 175. Calcd. for $C_{11}H_{10}O_2$: C, 75.84; H, 5.79%; mol. wt., 174.

**1-Methyl-6-ethyl-2, 7-dioxa-bicyclo-[3, 2, 0]-$\Delta^3$-heptene (III) and 3-Methyl-6-ethyl-2, 7-dioxa-bicyclo-[3, 2, 0]-$\Delta^3$-heptene (IV).**—A mixture of 125 g. (1.52 mol.) of 2-methylfuran and 23.2 g. (0.40 mol.) of propionaldehyde was irradiated and then treated in the same manner as has been described above. A 60—90°C (17 mmHg) fraction was collected; yield, 9.5 g. (17%). This fraction was redistilled at 15 mmHg (b. p. 65—68°C), $n_D^{20}$ 1.4473. Principal infrared bands: 3060, 2910, 1668, 1605, 1460, 1382, 1222, 1167, 1125, 1050, 1010, 980, 955, 890, 850 and 720 $cm^{-1}$.

Found: C, 68.45; H, 8.65; mol. wt., 146. Calcd. for $C_8H_{12}O_2$: C, 68.54; H, 8.63%; mol. wt., 140.

This fraction was identified by NMR spectra as being composed of III and IV.

**1-Methyl-6-phenyl-2, 7-dioxa-bicyclo-[3, 2, 0]-$\Delta^3$-heptene (V) and 3-Methyl-6-phenyl-2, 7-dioxa-bicyclo-[3, 2, 0]-$\Delta^3$-heptene (VI).**—A mixture of 120 g. (1.46 mol.) of 2-methylfuran and 38.5 g. (0.36 mol.) of benzaldehyde was irradiated and treated in the same manner as has been described above. A 90—110°C (1 mmHg) fraction was collected; yield, 22 g. (32%). This fraction was redistilled at 1 mmHg (b. p. 100—110°C), $n_D^{20}$ 1.5380. Principal infrared bands: 3000, 2945, 1665, 1605, 1490, 1383, 1350, 1224, 1162, 1103, 1040, 950, 890, 750 and 698 $cm^{-1}$.

Found: C, 76.60; H, 6.63; mol. wt., 186. Calcd. for $C_{12}H_{12}O_2$: C, 76.57; H, 6.43%; mol. wt., 188.

This fraction was identified by NMR spectra as being composed of V and VI.

## Summary

The photochemical reaction of aldehydes (propionaldehyde and benzaldehyde) and furan have been studied in the liquid phase; two new compounds, oxetanes I and II have easily been produced with a high purity by this photo-reaction.

In the case of 2-methylfuran and propionaldehyde (or benzaldehyde), a mixture of oxetanes III and IV (or V and VI) has also been obtained.

The authors are indebted to the Shionogi Research Laboratory (Shionogi & Co., Ltd.) for the measurement of the NMR spectra.

*The Institute of Scientific and Industrial Research*
*Osaka University*
*Sakai, Osaka*

5) S. Nagakura and T. Hosoya, This Bulletin, **25**, 179 (1952).

6) The boiling and melting points are uncorrected. The molecular weights of the samples were determined by the cryoscopic method in benzene.

7) W. C. Wilson, "Organic Syntheses," Coll. Vol. I, 274, 276 (1956).

8) S. Okumura, "Zikken Yūki Kagaku (Experimental Organic Chemistry)", Kyōritsu Shuppan, Tokyo (1953), p. 107.

9) Reaction apparatus: K. Shima, Y. Shigemitsu and S. Tsutsumi, This Bulletin, **35**, 1728 (1962).

# Studies of Chemical Kinetics by Means of the Velocity of Sound. II. The Condensation of Acetaldehyde to Aldol

By Tatsuya YASUNAGA, Nobuhide TATSUMOTO and Masaji MIURA

(Received September 10, 1964)

Bell[1,2] and Matsuyama[3] have investigated the kinetics of the condensation of acetaldehyde to aldol. In his earlier work Bell concluded, from his dilatometric study, that this reaction is of the first order with respect to acetaldehyde concentration and that the reaction velocity is proportional to the concentration of the $OH^-$ catalyst. A major drawback in his experimental setup was that the scale of the dilatometer was not corrected for the increase in temperature in the reaction system at the initial state of this reaction. In his report in 1960, on the other hand, he concluded, from the ultraviolet absorption study, that the reaction is of the second order. With his method it is difficult to measure the time and to control the temperature accurately without disturbing the reaction system, because a part of the solution has to be removed. Matsuyama has also studied the same reaction system with a calorimetric method and has concluded that it is of the second order and that the relation between the velocity constant and the concentration of $OH^-$ is linear. It is objectionable, however, to use, as in his study, a Beckmann thermometer with such a large heat capacity in order to measure the change in temperature in the reaction system. As has been described in a previous paper,[4] we measured the velocity of sound by means of a sing-around velocimeter in order to study the change in the chemical reaction with time. In this work we will attempt to study the condensation of acetaldehyde to aldol by the same method as has been used previously.

## Theoretical

It is highly likely that the change in the velocity of sound is in proportion to the concentration of acetaldehyde, provided that the change in the concentration is comparatively small. Therefore,

$$C_1-C_\infty=\alpha(f_1-f_\infty) \quad (1)$$

$$C_i-C_\infty=\alpha(f_i-f_\infty) \quad (2)$$

where $C_1$, $C_i$, $C_\infty$, $f_1$, $f_i$, and $f_\infty$ are the concentrations of acetaldehyde and the pulse repetition frequencies at times $t_1$, $t_i$ and $t_\infty$, respectively, $t_1$ being the starting time for the measurement, and where $\alpha$ is a proportionality constant. By subtraction,

$$C_1-C_i=\alpha(f_1-f_i) \quad (3)$$

If this reaction is of the second order with respect to the acetaldehyde concentration and if no product reacts consecutively during the measurement, the reaction may be expressed by:

$$1/(a-x)=kt+1/a \quad (4)$$

where $a$ is the initial concentration of acetaldehyde; $x$, the decrease in the concentration of acetaldehyde after the lapse of time, $t$, and $k$, the velocity constant. Equation 4 can be expressed with $C$ in place of $a$ and $x$:

$$1/(C_i-C_\infty)=k\Delta t_i+1/(C_1-C_\infty) \quad (5)$$

Thus:

$$(C_1-C_i)/\{(C_1-C_\infty)(C_i-C_\infty)\Delta t_i\}=k \quad (6)$$

or

$$(C_1-C'_i)/\{(C_1-C_\infty)(C'_i-C_\infty)\Delta t'_i\}=k \quad (7)$$

where $\Delta t_i=t_i-t_1$, $\Delta t'_i=t'_i-t_1$, and $C'_i$ is the concentration of acetaldehyde at $t=t'_i$. From Eqs. 6 and 7,

$$(C_1-C_i)/\{(C_1-C_\infty)(C_i-C_\infty)\Delta t_i\} = (C_1-C'_i)/\{(C_1-C_\infty)(C'_i-C_\infty)\Delta t'_i\} \quad (8)$$

From Eqs. 1, 2, 3 and 8,

$$f_1-f_\infty=\{(f_1-f_i)(f_1-f'_i)(\Delta t'_i-\Delta t_i)\}/\{(f_1-f_i)\Delta t'_i-(f_1-f'_i)\Delta t_i\} \quad (9)$$

where $f'_i$ is the pulse repetition frequency at $t=t'_i$. Equation 5 may also be rewritten as follows:

$$1/(f-f_\infty)=1/\{(f_1-f_\infty)-(f_1-f)\}= \alpha k\Delta t+1/(f_1-f_\infty) \quad (10)$$

Therefore, if a plot of $1/(f-f_\infty)$ obtained from Eqs. 9 and 10 against $\Delta t$ is linear, the reaction must be of the second order. On the other hand, if this reaction is of the first order, the reaction is given as follows:

$$\ln(f-f_\infty)=\ln\{(f_1-f_\infty)-(f_1-f)\}= -k\Delta t+\ln(f_1-f_\infty) \quad (11)$$

1) R. P. Bell, *J. Chem. Soc.*, **1937**, 1636.
2) R. P. Bell and P. T. McTigue, ibid., **1960**, 2983.
3) H. Matsuyama, *Proc. Japan Acad.*, **27**, 552 (1951).
4) T. Yasunaga, N. Tatsumoto and M. Miura, This Bulletin, **37**, 1655 (1964).

Therefore, $f_1-f_\infty$ is given in Eq. 12 under the condition that $2\Delta t_i=\Delta t'_i$:

$$f_1-f_\infty=(f_1-f_i)^2/(f_1+f'_i-2f_i) \qquad (12)$$

If the experimental values of $\ln(f-f_\infty)$ plotted against $\Delta t$ satisfy Eq. 11, giving a linear curve, then the reaction is probably of the first order.

## Experimental

The condensation of acetaldehyde to aldol has been investigated in a dilute aqueous solution of sodium hydroxide (0.0050—0.0145 M). The reagent was extra pure grade acetaldehyde in an ampoule and used without further purification. The acetaldehyde was diluted with air-free water in order to prepare about 0.57 mol./l. of an aqueous solution. The concentration of acetic acid contained in this solution was found to be 0.002 mol./l. by titration.

The sample and the catalyst solution were then mixed in a flask and transferred from it into a cell. Before each measurement, air was replaced with nitrogen. The measurements were carried out in a water bath at 25°C. The temperature was observed in the water bath with a Beckmann thermometer and inside the cell with a thermistor thermometer. (A detailed description of our sing-around velocimeter was given in the previous paper.[4]) As a result of the mixing of the sample solution with the catalyst, the temperature in the reacting system began to rise in seven to ten minutes and reached an equilibrium with the bath temperature, 25°C, in thirty minutes. The correction for the velocity of sound, therefore, should be made for the temperature rise in the initial stage of the reaction. Measurement over a long period is not desirable in this study, for subsequent reactions would probably occur in this system.

## Results

The changes in the velocity of sound, corrected for the temperature change with time, are shown in Fig. 1 for a dilute aqueous solution of sodium hydroxide (0.0050—0.0145 M). The changes in the values for $1/(f-f_\infty)$ and $\ln(f-f_\infty)$ with time are plotted in Figs. 2 and 3 respectively. A comparison of the two curves shows that the results from the former give a better linearity than those from the latter. That is, all of the curves for the former are linear, but those for the latter deviate from the linear line, passing through three points, $\log(f_1-f_\infty)$, $\log(f_i-f_\infty)$ and $\log(f'_i-f_\infty)$. Hence, this reaction is probably of the second order within the period studied here.

## Discussion

The above experimental results can be explained on the basis of a reaction scheme[5] of

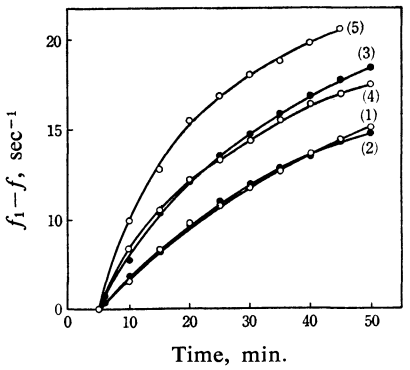



Fig. 1. Change in the repetition frequency with time.

| | $a$, M | Concn. of NaOH M |
|---|---|---|
| (1) | 0.4339 | 0.0015 |
| (2) | 0.4339 | 0.0019 |
| (3) | 0.3978 | 0.0040 |
| (4) | 0.3409 | 0·0080 |
| (5) | 0.4009 | 0.0145 |

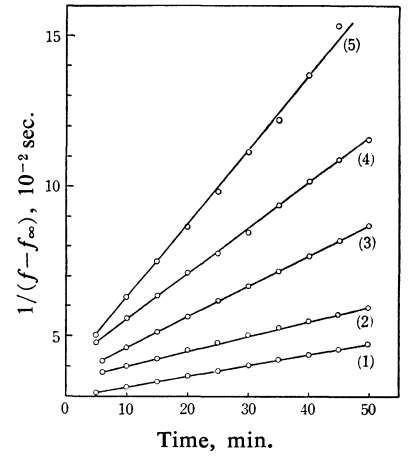



Fig. 2. Change in reciprocal of the difference between $f$ and $f_\infty$ with time.

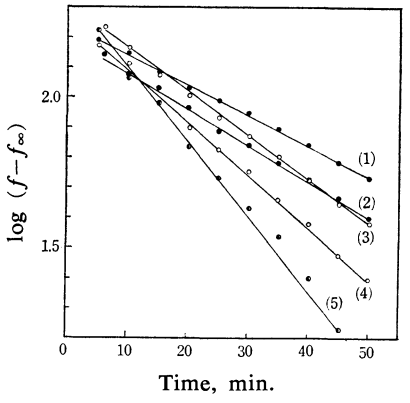



Fig. 3. Change in logarithm of the difference between $f$ and $f_\infty$ with time.

5) A. Frost and R. G. Pearson, "Kinetics and Mechanism," John Wiley & Sons Inc., New York, London (1961), p. 335.

the following condensation of acetaldehyde:

$$HCOCH_3 + B \underset{k_2}{\overset{k_1}{\rightleftarrows}} HCOCH_2^- + BH^+ \quad (13)$$

$$HCOCH_2^- + HCOCH_3 \underset{k_4}{\overset{k_3}{\rightleftarrows}} HCOCH_2\text{-}\underset{CH_3}{\underset{|}{CHO}}^- \quad (14)$$

$$HCOCH_2\text{-}\underset{CH_3}{\underset{|}{CHO}}^- + BH^+ \underset{k_6}{\overset{k_5}{\rightleftarrows}} HCOCH_2\text{-}\underset{CH_3}{\underset{|}{CHOH}} + B \quad (15)$$

where B is a base and $k$ is the velocity constant. The last step being very fast, the above scheme can be reduced to:

$$HCOCH_3 + B \underset{k_2}{\overset{k_1}{\rightleftarrows}} HCOCH_2^- + BH^+ \quad (16)$$

$$HCOCH_2^- + HCOCH_3 \overset{k_3}{\rightarrow} \text{Product} \quad (17)$$

Thus,

$$[HCOCH_2^-] = \{k_1[HCOCH_3][B]\}/\{k_3[HCOCH_3] + k_2[BH^+]\} \quad (18)$$

$$d[\text{product}]/dt = \{k_1k_3[HCOCH_3]^2[B]\}/\{k_3[HCOCH_3] + k_2[BH^+]\} \quad (19)$$

Two limiting cases, in which $k_3[HCOCH_3]$ is much greater or much smaller than $k_2[BH^+]$, are of interest. The first case leads to:

$$\text{rate} = k_1[HCOCH_3][B] \quad (20)$$

and the second to:

$$\text{rate} = k_1k_3[HCOCH_3]^2[B]/k_2[BH^+] = k_1k_3[HCOCH_3]^2[S^-]/k_2K_B \quad (21)$$

where $K_B$ is the ionization constant of the base and $S^-$ is the anion of the solvent, SH. If $k_3[HCOCH_3]$ is greater than $k_2[BH^+]$, the reaction is of the first order. As $[HCOCH_3]$ approaches zero, the rate must become second order with respect to the concentration of acetaldehyde. The concentration of acetaldehyde is so dilute in this study that these reactions would be second order.

The above consideration leads to the conclusion that the measurement of the velocity of sound is a useful method for the study of the chemical kinetics of simple reactions as in our present and previous papers. Further, considering the advantageous characteristics of the sing-around velocimeter, we expect that this method can be extended to the study of the kinetics of the fast reaction, which is difficult to measure with other methods.

*Department of Chemistry*
*Faculty of Science*
*Hiroshima University*
*Higashisenda-machi, Hiroshima*

# Acid and Basic Hydrolyses of *p*-Nitrophenyl Benzenesulfonate*

By Shigeru OAE and Reiko KIRITANI

(Received September 11, 1964)

In previous papers we have reported on studies of both the acid[1] and alkaline[2] hydrolyses of phenyl benzenesulfonate, and have suggested that these reactions proceed through the $S_N2$-type process, in which a nucleophilic attack of either water or the hydroxide ion takes place on the sulfur atom. It was also shown that there was no oxygen exchange in the ester during the hydrolyses, unlike the cases of the esters of carboxylic acid.[3] There was an incorporation of only one equivalent amount of $^{18}O$ in the benzenesulfonic acid isolated from reaction products. In the case of the acid hydrolysis, however, it was found that the phenol isolated from the hydrolysis of the ester with $^{18}O$-enriched water was incorporated with the excess $^{18}O$.

Although the reaction proceeded via the acyl-oxygen cleavage, the phenol formed was found to exchange gradually its oxygen with that of the medium water during the acid hydrolysis.

During the course of our study of the oxygen exchange between phenols and water in both acid and alkaline media, *p*-nitrophenol was found to undergo the oxygen exchange more readily than the other substituted phenols studied.[4] Since the substitution of the nitro group on the benzene ring of an

* Paper IV of Reactions of Phenols and Phenolic Esters.

1) S. Oae, T. Fukumoto and R. Kiritani, This Bulletin, 36, 346 (1963).

2) D. R. Christman and S. Oae, *Chem. & Ind.*, 1959, 1251.

3) M. L. Bender, *J. Am. Chem. Soc.*, 73, 1626 (1951).

4) S. Oae and R. Kiritani, This Bulletin, 37, 770 (1964).

aromatic compound usually causes a strong activation of the ortho- and para-positions of the benzene ring, and hence makes a nucleophilic attack at these positions easier, it is not surprising to expect an aryl-oxygen cleavage, especially in the alkaline hydrolysis of the titled compound. Therefore, one may expect that the substitution of a nitro group at the para-position, namely in the titled compound, will change the course of the hydrolyses.

Recently, Bunnett and Bassett, Jr.[5] have shown through their kinetic study that a number of mono- and dinitro phenol esters of *p*-toluenesulfonic acid are found to undergo both sulfur-oxygen and carbon-oxygen scissions in the reactions with a few such strong nucleophilic reagents as thiophenolate ions, piperidine and methoxide ions.

Meanwhile, Vizgert et al.[6] have also found that the nitro group at either ortho- or para-positions of the phenolic portion of substituted phenyl benzenesulfonates showed a marked accelerating effect in the alkaline hydrolysis of substituted phenyl benzenesulfonates.

The present research was designed to investigate further the mechanisms of both acid and alkaline hydrolyses of the titled compound by means of both the $^{18}O$ tracer technique and a kinetic study of the hydrolyses.

## Results and Discussion

**Acid Hydrolysis.** — The acid hydrolysis of the titled compound was very sluggish and was found to take place only above 160°C in a sealed tube using 10 N hydrochloric acid, much as in the case of phenyl benzenesulfonate. The ester and 10 N hydrochloric acid, made by dissolving hydrogen chloride gas into $^{18}O$-enriched water, were sealed in a tube; the tube was then heated at 180°C for 6 hr. The reaction was stopped before completion in order to see if the hydrolysis reaction proceeds through a reversible addition intermediate; thereby unhydrolyzed ester was recovered, together with the hydrolysis products, i.e., *p*-nitrophenol and benzenesulfonic acid.

Meanwhile, the same reactants were also heated in sealed tubes at 180°C for 24 hr., the ester was completely hydrolyzed, and the products were isolated. In order to see the effects of acid concentration on the hydrolysis, the hydrolysis was also carried out using 3.5 N hydrochloric acid prepared with $^{18}O$-enriched water. When the mixtures of the ester and the 3.5 N hydrochloric acid were also heated at 180°C for 6 hr., 12 hr., and 24 hr. in sealed tubes, it was found that the hydrolysis was half completed after the mixtures had been heated for 24 hr. The reaction products obtained in nearly quantitative yields after the complete hydrolysis were purified in the following ways: *p*-nitrophenol was sublimed, while benzenesulfonic acid was treated with *S*-benzylthiuronium chloride to give the *S*-benzylthiuronium sulfonate. The recovered ester was recrystallized from ethanol, and all these samples were subjected to $^{18}O$ analysis by the usual method.[7] The results are shown in Table I.

In all cases, the $^{18}O$ content of the recovered ester was found to be 0.20 atom% $^{18}O$. As this value represents the natural $^{18}O$ atom%, it illustrates that there is no exchange of $^{18}O$ in the ester during this reaction process, as in the case of phenyl benzenesulfonate. This observation clearly excludes any reversible prior addition of water molecules or hydronium ions during the hydrolysis of the titled compound and suggests that the overall reaction is irreversible. The observation also seems to suggest that the reaction is a $S_N2$-type synchronous one-step process initiated by the attack of water oxygen on the sulfur atom, which bears a formal double-positive charge as in the case of the hydrolysis of phenyl benzenesulfonate. Two alternative mechanistic

TABLE I. DISTRIBUTION OF THE $^{18}O$ LABEL IN ACID HYDROLYSIS PRODUCTS

| Run | Reaction time, hr. | $^{18}O$ Atom% of aq. HCl soln. | $^{18}O$ Atom% of products | | |
|---|---|---|---|---|---|
| | | | *p*-Nitrophenol | Benzenesulfonic acid | Recovered ester |
| 1 | 6 | 1.58 (3.5 N) | — | — | 0.20 |
| 2 | 12 | 1.58 (3.5 N) | 0.20 (0.26)* | — | 0.20 |
| 3 | 24 | 1.58 (3.5 N) | 0.23 (0.29) | 0.62 | 0.20 |
| 4 | 6 | 1.58 (10 N) | 0.22 (0.26) | 0.63 | 0.20 |
| 5 | 24 | 1.58 (10 N) | 0.37 (0.91) | 0.65 | — |

* Numerical values in parentheses represent the $^{18}O$ concentration of phenolic oxygen calculated from the concentration of whole molecule by neglecting the $^{18}O$ exchange nitro group.

5) J. F. Bunnett and J. Y. Bassett, Jr., *J. Am. Chem. Soc.*, **81**, 2104 (1959).
6) a) R. V. Vizgert, *Zhur. Obshchei Khim.*, **28**, 1873 (1958); b) R. V. Vizgert and E. K. Savchuk, ibid., **28**, 2114 (1958); c) R. V. Vizgert, E. K. Savchuk and O. A. Purib, ibid., **31**, 194 (1961).
7) S. Oae, T. Kitao and Y. Kitaoka, *J. Am. Chem. Soc.*, **84**, 3359 (1962).

schemes are also conceivable for this reaction; one involves the nucleophilic attack of water on the aromatic ring carbon para to the nitro group, and the other is a $S_N1$-type process involving a slow cleavage of a sulfur-oxygen or carbon-oxygen bond, followed by rapid solvolysis, to form sulfonic acid and *p*-nitrophenol. However, the aromatic $S_N2$-type mechanism cannot be accepted, since the benzenesulfonic acid isolated was found to be incorporated with one atom equivalent amount of $^{18}O$ of $^{18}O$-enriched water (0.66 atom%); this cannot be reconciled with the aromatic $S_N2$-type mechanism involving the carbon-oxygen cleavage.

The $S_N1$-type mechanism involving the cleavage of the carbon-oxygen linkage is not plausible. The $S_N1$ process of this type did not take place in the acid hydrolysis of phenyl benzenesulfonate. The substitution of a strong electron-withdrawing group, such as a nitro group, at the para-position will suppress even more the $S_N1$-type C–O bond cleavage. On the other hand, the $S_N1$-type cleavage of a S–O bond is also very difficult, since it will leave an additional positive charge on the sulfur atom, which already bears double formal positive charges, and the cleavage would require an enormous energy.

The remaining and the most probable pathway is the $S_N2$-type process initiated by the attack of the water molecule on the sulfur atom. If the reaction proceeds through this process, the benzenesulfonic acid will be incorporated with one equivalent amount of $^{18}O$ and the *p*-nitrophenol will remain natural. While benzenesulfonic acid was incorporated with $^{18}O$ just as much as is required from this process, *p*-nitrophenol was always incorporated with an excess of $^{18}O$ above the natural concentration, and the amount of $^{18}O$ incorporation appeared to increase with prolonged heating, as is shown by Table I.

In separate experiments we have carried out the oxygen exchange reactions of *p*-nitrophenol, phenol, benzenesulfonic acid and

Table II. Oxygen exchange reaction of some compounds in the acidic solution

| Compound | Reaction time, hr. | $^{18}O$ Atom % of aq. HCl soln. | $^{18}O$ Atom % of products |
|---|---|---|---|
| *p*-Nitrophenol | 6 | 1.58 | 0.40 (0.80)* |
| | 24 | 1.58 | 0.37 (0.72) |
| Nitrobenzene | 24 | 1.58 | 0.20 |
| Phenol | 5 | 0.8 | 0.37 |
| | 24 | 0.77 | 0.73 |
| Benzenesulfonic acid | 5 | 0.8 | 0.23 |
| | 24 | 0.8 | 0.24 |

* See footnote in Table I.

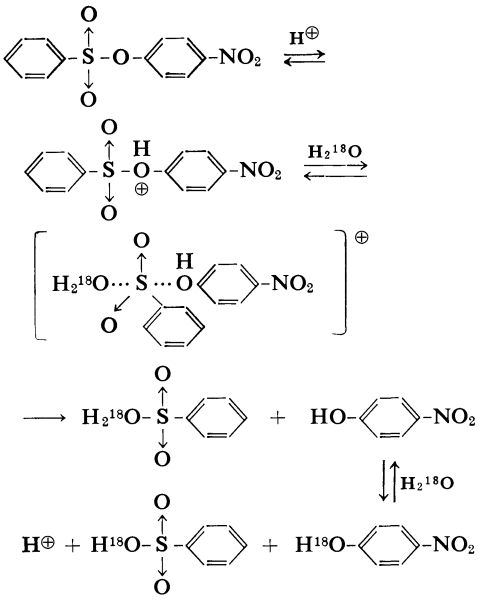


Fig. 1

nitrobenzene in the same acidic (10 N) solutions. The results are shown in Table II.

There was no apparent oxygen exchange in the nitro group; however, *p*-nitrophenol was found to undergo a more facile oxygen exchange than phenol in 6 hours of treatment. This observation also indicates that the *p*-nitrophenol formed during the acid hydrolysis of the ester gradually changed its phenolic oxygen atom with a solvent of $^{18}O$-enriched water. Thus, the overall reaction scheme of this acid-catalyzed hydrolysis of the ester is considered to be the $S_N2$ process, in which the water molecule attacks the sulfur atom, shown by Fig. 1, giving benzenesulfonic acid and *p*-nitrophenol, which then undergoes further phenolic oxygen exchange with the solvent water.

**Alkaline Hydrolysis.**—The titled ester was dissolved in $^{18}O$-enriched water containing 1% potassium hydroxide, and the solution was refluxed for 8 hr. Since the reaction was partially completed, some recovered esters were obtained, together with the reaction products, benzenesulfonic acid and *p*-nitrophenol. Similarly, the ester was hydrolyzed with $^{18}O$-enriched water containing 10% potassium hydroxide and refluxed for 8 hr. In this way the reaction was completed, and benzenesulfonic acid and *p*-nitrophenol were obtained in nearly quantitative yields. All the products and the recovered ester thus obtained were subjected to the usual $^{18}O$ analysis; the results are shown in Table III.

Here again, the $^{18}O$ content of the recovered ester was not increased more than the natural $^{18}O$ content during this partial hydrolysis

TABLE III. DISTRIBUTION OF THE $^{18}O$ LABEL IN ALKALINE HYDROLYSIS PRODUCTS

| Run | Reaction time, hr. | $^{18}O$ Atom% of aq. KOH soln. | $^{18}O$ Atom% of products | | |
|---|---|---|---|---|---|
| | | | *p*-Nitrophenol | Benzenesulfonic acid | Recovered ester |
| 1 | 8 | 1.58 (1%) | 0.26 (0.38)* | 0.54 | 0.20 |
| 2 | 8 | 1.55 (10%) | 0.48 (1.04) | 0.57 | — |

* See footnote in Table I.

TABLE IV. OXYGEN EXCHANGE REACTION OF SOME COMPOUNDS IN THE ALKALINE SOLUTION

| Compound | Reaction time, hr. | $^{18}O$ Atom% of aq. KOH soln. | $^{18}O$ Atom% of products |
|---|---|---|---|
| *p*-Nitrophenol | 8 | 1.58 ( 1% KOH) | 0.21 (0.23)* |
| | 8 | 1.55 (10% KOH) | 0.58 (1.34) |
| Nitrobenzene | 8 | 1.55 (10% KOH) | 0.20 |
| Benzenesulfonic acid | 8 | 1.55 (10% KOH) | 0.22 |
| | 8 | 1.58 ( 1% KOH) | 0.21 |

* See footnote in Table I.

process. The overall reaction was irreversible, and obviously there was no reversible prior addition of hydroxyl ions to the sulfur atom. However, there were a few significant differences between the acid and alkaline hydrolysis of this compound. While the benzenesulfonic acid obtained in the acid hydrolysis was always incorporated with one equivalent amount of the $^{18}O$ (0.66 atom%) resulting from the $^{18}O$-enriched water used, the alkaline hydrolysis yielded benzenesulfonic acid, whose $^{18}O$ incorporation was somewhat lower (0.54, 0.57 atom%) than that of the $^{18}O$-enriched water used. *p*-Nitrophenol was also incorporated with $^{18}O$; its $^{18}O$ incorporation was apparently larger when the potassium hydroxide solution used was more concentrated.

In separate experiments the oxygen exchange reactions were carried out in aqueous potassium hydroxide under the same conditions in order to test the oxygen exchange of these products with solvent water. The results are shown in Table IV.

It is interesting to note that the $^{18}O$ exchange was negligible when the concentration of potassium hydroxide was small (1%), but that it became substantial when the alkaline concentration was increased to 10%. On the other hand, the hydrolysis in the 1% potassium hydroxide solution gave *p*-nitrophenol noticeably enriched with $^{18}O$ and benzenesulfonic acid, the $^{18}O$ concentration of which was apparently lower than what was to be expected from a straight-forward $S_N2$ process involving the nucleophilic attack of the hydroxyl ion on the sulfur atom, as is shown in Fig. 2.

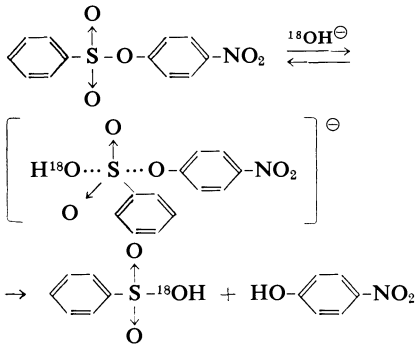


Fig. 2

The small increase in the $^{18}O$ in the *p*-nitrophenol and the decrease in $^{18}O$ in the sulfonic acid can be accounted for if one assumes that a portion of the reaction proceeded via an aromatic $S_N2$ process involving the C–O bond cleavage, as is shown in Fig. 3.

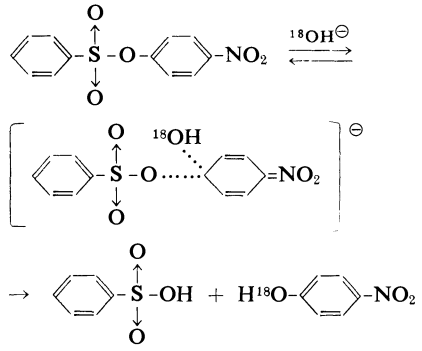


Fig. 3

Therefore, at least in the alkaline hydrolysis with a 1% potassium hydroxide solution, the two reactions appears to compete, though the $S_N2$ process involving the nucleophilic attack on the sulfur atom is by far the predominant path (about 78—80%). In the concentrated alkaline solution (10% potassium hydroxide), the oxygen-exchange was found to take place substantially for *p*-nitrophenol. This somewhat obscures the mechanistic diagnosis with the $^{18}O$ data of the hydrolysis products. One can see, however, that the concentration of

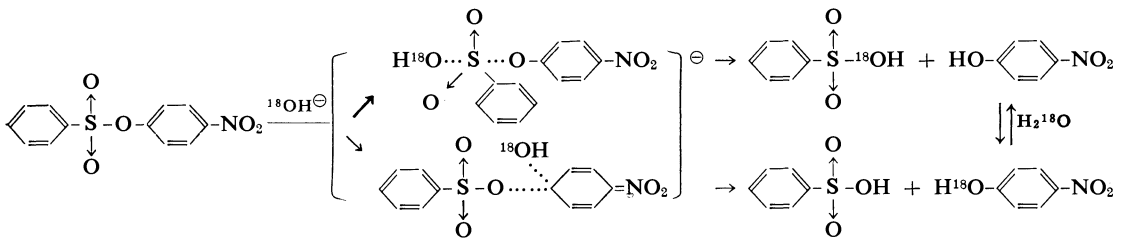
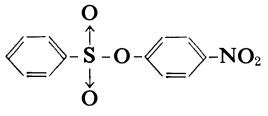


Fig. 4

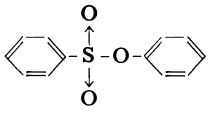
$^{18}O$ in the nitrophenol after 8 hr. of $^{18}O$ exchange was markedly higher (0.58) than that in the same compound obtained in the hydrolysis (0.48). Moreover, the $^{18}O$ concentration of the *p*-nitrophenol obtained by the hydrolysis was far smaller than that of the water used. From these results, it is clear that the major portion of the reaction proceeded via the usual $S_N2$ process involving a nucleophilic attack on the sulfur atom (Fig. 2), much as in the earlier findings with other strong nucleophiles.[5] In contrast to the marked increase in $^{18}O$ in the nitrophenol in the hydrolysis in a 10% alkaline solution, no reduction of $^{18}O$ concentration in benzenesulfonic acid resulted from the change of alkalinity from 1% to 10%. Instead, there was only a slight increase, if any. This may mean that in the concentrated alkaline solution a small portion of the reaction also proceeds via an aromatic $S_N2$ process involving C–O bond cleavage and that the resulting nitrophenol undergoes subsequent $^{18}O$ exchange. Thus, the overall reaction scheme can be represented by the two competing process shown by Figs. 2 and 3; however, the ordinary $S_N2$ process involving the attack of the hydroxyl ion on the sulfur atom is the predominant path. A schematic illustration is shown in Fig. 4.

The rates of the alkaline hydrolyses of two esters, *p*-nitrophenyl benzenesulfonate, and phenyl benzenesulfonate, have been investigated at 49.5±0.05°C in alkaline aqueous 50% dioxane. An inspection of the data reveals that the rate of the former is substantially higher than that of the latter, as Russian workers have shown previously.[7]

$k_2 = 78.6 \times 10^{-3}$ sec$^{-1}$ mol./l. for



$k_2 = 0.416 \times 10^{-3}$ sec$^{-1}$ mol./l. for



This means that the substitution of a nitro group at a para-position markedly facilitates the nucleophilic attack of the hydroxide ion on phenyl benzenesulfonate. At first it was thought that the rate-acceleration due to the *p*-nitro group is related to the facile nucleophilic attack of the hydroxide ion on the aromatic carbon atom via an aromatic $S_N2$ process; however, the $^{18}O$ data do not support this idea. The presence of a *p*-nitro group apparently reduces the electron density around not only the aromatic $C_1$ atom, but also the sulfonyl sulfur atom, thereby causing a large acceleration of the nucleophilic attack of the hydroxide ion on both positions.

## Experimental

***p*-Nitrophenyl Benzenesulfonate.**—*p*-Nitrophenol (28 g., 0.2 mol.) was dissolved in 160 ml. of pyridine. The mixture was cooled in ice water, and an equimolar amount of benzenesulfonyl chloride (35 g.) was stirred into it drop by drop and then allowed to stand at 0°C overnight. The reaction mixture was then poured in ice water. After filtering, the precipitate was repeatedly washed with water and aqueous sodium bicarbonate to remove the pyridinium hydrogen chloride completely and then recrystallized from ethanol. Ninety grams of a colorless plate, *p*-nitrophenyl benzenesulfonate, were obtained (89% purified yield); m. p. 88—89°C.

**Hydrolysis in an Acidic Solution.**—*p*-Nitrophenyl benzenesulfonate (1 g.) was dissolved in 5 ml. of 10 N hydrochloric acid containing 1.58 atom % of $^{18}O$. The mixture was kept for 24 hr. at 180°C in a sealed tube. Then the sealed tube was broken, and all the contents were extracted with ether. The aqueous layer was then evaporated down to 2 ml. To this solution a few drops of hyrochloric acid and *S*-benzylthiuronium chloride (0.7 g.) were added, and 1.3 g. of *S*-benzylthiuronium salt of benzenesulfonic acid (white plate) was obtained, m. p. 148.5°C. This corresponds to 0.55 g. of benzenesulfonic acid (97% yield). The ether extract was dissolved in aqueous sodium carbonate and extracted with ether to remove the unhydrolyzed ester (though none of the ester was extracted). The alkaline layer was then neutralized with weak hydrochloric acid and extracted with ether again. From the combined ether extract, the ether was removed and the residual mass was sublimated

twice to obtain 0.46 g. of pure *p*-nitrophenol, m. p. 113°C (92.4% yield).

**Partial Hydrolysis in an Acidic Solution.**—The same reaction mixture used for the complete acid hydrolysis was made and then heated in a sealed tube for 6 hr. at 180°C. When the products were treated as described above, the unhydrolyzed ester (0.8 g.) and *p*-nitrophenol (0.08 g.) were obtained from the ether layer, while benzenesulfonic acid (0.1 g.) was isolated from the aqueous layer as the *S*-benzylthiuronium sulfonate. Some more experiments on the partial hydrolyses were carried out using the ester and 3.5 N hydrochloric acid containing 1.58 atom% $^{18}O$ at 180°C for 6 hr., 12 hr. and 24 hr. The products were also treated as has been described above.

**Hydrolysis in an Alkaline Solution.** — When potassium hydroxide (1.9 g., 0.034 mol.) was dissolved in 15 ml. of water containing 1.58 atom% $^{18}O$, the $^{18}O$ content of this solution was found to decrease to 1.55 atom% $^{18}O$. The ester (1.2 g., 0.0042 mol.) was dissolved in this solution (10%) and refluxed for 8 hr. The products were extracted with ether (though none of the ether layer was obtained from the ether layer). The alkaline layer was treated as described above, and 0.5 g. of *p*-nitrophenol and 0.6 g. of benzenesulfonic acid were isolated.

**Partial Hydrolysis in an Alkaline Solution.**—The ester (1.2 g.) was dissolved in the solution of 30 ml. of water-$^{18}O$ and 0.38 g. (0.0068 mol.) of potassium hydroxide; this solution, containing 1.58 atom% $^{18}O$, was then refluxed for 8 hr. The recovered ester and the reaction products, *p*-nitrophenol and benzenesulfonic acid, were obtained as has been described above. The ester (1.2 g.) was dissolved in a solution of 60 ml. of 50% dioxane-water-$^{18}O$ containing 0.38 g. of potassium hydroxide, and the solution was kept 50°C for 1 hr. After evaporation, the residue was treated as has been described above. The results were the same as those obtained in a heterogeneous system of aqueous solutions.

**The Kinetic Determination of the Alkaline Hydrolyses of *p*-Nitrophenyl Benzenesulfonate and Phenyl Benzenesulfonate.** — Solutions of *p*-nitrophenyl benzenesulfonate (3.5529 g., 0.0127 mol.) in 100 ml. dioxane and 100 ml. of aqueous potassium hydroxide (0.0382 mol./100 ml.) were separately immersed in a water thermostat set at 49.5±0.05°C for at least 30 min. before mixing. The hydrolyses were then started by mixing the two solutions by means of vigorous shaking. The rates were followed by pippetting out an aliquot portion of the mixture from time to time, then quenching it with an excess of standard hydrochloric acid, and finally back-titrating with standard potassium hydroxide using a pH-meter (the endpoint was PH 4.5).

In a separated experiment, a solution of phenyl benzenesulfonate (2.9769 g., 0.0127 mol.) in 100 ml. dioxane was hydrolyzed in the way which has been described above.

In both hydrolyses, the initial concentrations of the two components, the ester and the hydroxide ion, were made in a 1 : 3 mol. ratio; therefore, one mole equivalent of the hydroxide ion should be left in the solution at the end of the reaction, because every one mole of ester is considered to consume two moles of hydroxide ions in the reaction.

Therefore, the rates were calculated following the second-order rate kinetic equation shown below.

$$kt=\frac{1}{b-2a}\ln\frac{a(b-2x)}{b(a-x)}$$

$a$: Initial hydroxide ion concentration
$b$: Initial ester ion concentration
$x$: Concentration reacted
$t$: Time

A plot of $\ln\frac{a(b-2x)}{b(a-x)}$ versus $t$ gave straight lines in both cases, as is shown by Fig. 5.

**Isotopic Analysis.**—The $^{18}O$ analysis was performed as in a previous experiment.[7]

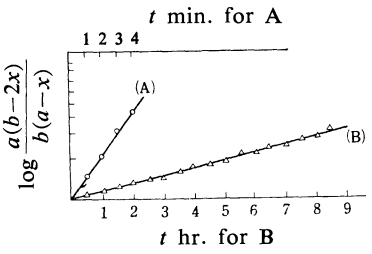



Fig. 5
(A) *p*-Nitrophenyl benzenesulfonate
(B) Phenyl benzenesulfonate

## Summary

The mechanisms of both the acid- and the alkaline-catalyzed hydrolyses of *p*-nitrophenyl benzenesulfonate have been investigated by means of the $^{18}O$-tracer technique. The acid-catalyzed hydrolysis apparently proceeds via a $S_N2$-type process involving the nucleophilic attack of water on the sulfur atom, with a S–O bond cleavage. Much as with the earlier findings concerning other nucleophiles, the major portion of the alkaline hydrolysis was also found to proceed through a $S_N2$ process which involves the nucleophilic attack of the hydroxide ion on the sulfur atom, with a S–O bond fission; only a small portion of the reaction appeared to proceed via an aromatic $S_N2$-type process.

*Department of Applied Chemistry*
*Faculty of Engineering*
*Osaka City University*
*Sumiyoshi-ku, Osaka (S. O.)*

*Department of Chemistry*
*Radiation Center of Osaka Prefecture*
*Sakai, Osaka (R. K.)*

# The Stability Constants of Ethylenediaminetetraacetato, Trimethylenediaminetetraacetato and Propylenediaminetetraacetato Complexes of Some Divalent Metal Ions

By Hiroshi OGINO

(Received September 14, 1964)

The equilibrium constants of substitution reactions involving ethylenediaminetetraacetato[1,2] and propylenediaminetetraacetato complexes[3] have been reported previously. Although Smith has reported the stability constants of propylenediaminetetraacetato complexes,[4] the values seem to be somewhat questionable.[3] Schwarzenbach et al. obtained the stability constants of trimethylenediaminetetraacetato complexes,[5,6] with which the ethylenediaminetetraacetato complexes are closely related. However, their study was restricted to alkaline earth metal, cadmium(II) and mercury(II) ions. Therefore, it seems worthwhile to clarify the relationships between the stability constants of ethylenediaminetetraacetato, trimethylenediaminetetraacetato and propylenediaminetetraacetato complexes of some divalent metal ions containing transition metal ions.

In this paper, these stability constants are determined by two methods. One is a new method which is based on the polarographic measurement of the concentration of an uncomplexed ligand in a solution containing two kinds of ligands and an appropriate metal ion. The other, a modification of the method described in the previous paper,[1] is used for the determination of the relative stability constants of trimethylenediaminetetraacetato complexes.

## Theoretical

**The Determination of the Relative Stability Constants of the Complexes with Different Ligands.**—Let us consider an equilibrated solution which contains a metal ($M^{m+}$) ion and two kinds of ligands (anions of $H_4Y$ and $H_4Z$).*

There exist the following equilibria:

$$MY^{(m-4)+} + Z^{4-} \rightleftarrows MZ^{(m-4)+} + Y^{4-} \quad (1)$$

$$Y^{4-} + nH^+ \rightleftarrows H_nY^{(4-n)-} \quad (2)$$

$$Z^{4-} + n'H^+ \rightleftarrows H_{n'}Z^{(4-n')-} \quad (3)$$

The overall reaction, therefore, may be expressed as:

$$MY^{(m-4)+} + \left\{\begin{array}{c} H_4Z \\ \uparrow\downarrow \\ H_3Z^- \\ \uparrow\downarrow \\ \vdots \\ \uparrow\downarrow \\ Z^{4-} \end{array}\right\} \rightleftarrows MZ^{(m-4)+} + \left\{\begin{array}{c} H_4Y \\ \uparrow\downarrow \\ H_3Y^- \\ \uparrow\downarrow \\ \vdots \\ \uparrow\downarrow \\ Y^{4-} \end{array}\right\} \quad (4)$$

When $[M]_t < [Y]_t + [Z]_t$, the total concentrations of metal and ligands, $[M]_t$, $[Y]_t$ and $[Z]_t$, in the solution are given as,

$$[M]_t = [MY^{(m-4)+}] + [MZ^{(m-4)+}] \quad (5)$$

$$[Y]_t = [MY^{(m-4)+}] + [Y]_f \quad (6)$$

$$[Z]_t = [MZ^{(m-4)+}] + [Z]_f \quad (7)$$

where

$$[Y]_f = \sum_0^4 [H_iY^{(4-i)-}]$$

$$[Z]_f = \sum_0^4 [H_jZ^{(4-j)-}]$$

The equilibrium constant of Eq. 4,

$$K^Y_{Z,app} = \frac{[Z]_f[MY^{(m-4)+}]}{[Y]_f[MZ^{(m-4)+}]} \quad (8)$$

can be calculated by means of the relations given by Eqs. 5 to 7, provided that the value of one term on the right-hand sides of Eqs. 5 to 7 is known. In this study, the values of $K^Y_{Z,app}$ were determined from the polarographic measurements of the concentrations of uncomplexed ethylenediaminetetraacetate or propylenediaminetetraacetate.

Equation 8 is rewritten as,

$$K^Y_{Z,app} = K^Y_Z \frac{\alpha_Z}{\alpha_Y} \quad (9)$$

where

1) N. Tanaka and K. Kato, This Bulletin, **33**, 417 (1960).
2) N. Tanaka, M. Kamada, H. Osawa and G. Satô, ibid., **33**, 1412 (1960).
3) N. Tanaka and H. Ogino, ibid., **38**, 439 (1965).
4) R. L. Smith, "The Sequestration of Metals," Chapman and Hall, London (1959).
5) G. Schwarzenbach and H. Ackermann, *Helv. Chim. Acta*, **31**, 1029 (1948).
6) G. Schwarzenbach, H, Senn and G. Anderegg, ibid., **40**, 1886 (1957).

* Although $H_4Y$ and $H_4Z$ represent alkylenediaminetetraacetic acids, they may be replaced by other appropriate ligands.

$$\alpha_Y = 1 + \frac{[H^+]}{K_{HY}} + \frac{[H^+]^2}{K_{H_2Y}K_{HY}} + \frac{[H^+]^3}{K_{H_3Y}K_{H_2Y}K_{HY}} + \frac{[H^+]^4}{K_{H_4Y}K_{H_3Y}K_{H_2Y}K_{HY}}$$

$$\alpha_Z = 1 + \frac{[H^+]}{K_{HZ}} + \frac{[H^+]^2}{K_{H_2Z}K_{HZ}} + \frac{[H^+]^3}{K_{H_3Z}K_{H_2Z}K_{HZ}} + \frac{[H^+]^4}{K_{H_4Z}K_{H_3Z}K_{H_2Z}K_{HZ}}$$

$$K_Z^Y = \frac{[Z^{4-}][MY^{(m-4)+}]}{[Y^{4-}][MZ^{(m-4)+}]} = \frac{K_{MY}}{K_{MZ}} \qquad (10)$$

$K_{H_4Y}$, $K_{H_3Y}$, $K_{H_2Y}$ and $K_{HY}$ represent, respectively, the first, the second, the third and the fourth dissociation constant of $H_4Y$, and $K_{H_4Z}$, $K_{H_3Z}$, $K_{H_2Z}$ and $K_{HZ}$, those of $H_4Z$, respectively.

Therefore, $K_Z^Y$, which is the ratio of the stability constant of $MY^{(m-4)+}$ to that of $MZ^{(m-4)+}$, can be determined from the value of $K_{Z,app}^Y$ by the use of the dissociation constants of $H_4Y$ and $H_4Z$.

**The Determination of the Relative Stability Constants of Trimethylenediaminetetraacetato Complexes.***—In the course of this study, it was found that the trimethylenediaminetetraacetatocobaltate(II) complex gives a polarographic one-electron oxidation wave.[7] In order to determine the relative stability constants of trimethylenediaminetetraacetato complexes, this anodic wave was utilized.

In an acetate buffer solution which contains cobalt(II) ions, other appropriate metal ions, and trimethylenediaminetetraacetate ions, there exist the following equilibria:**

$$\left\{\begin{matrix} Co^{2+} \\ \downarrow\uparrow \\ CoOAc^+ \end{matrix}\right\} + Mtrdta^{(m-4)+} \rightleftarrows Cotrdta^{2-} + \left\{\begin{matrix} M^{m+} \\ \uparrow\downarrow \\ M(OAc)_n^{(m-n)+} \end{matrix}\right\} \qquad (11)$$

where $trdta^{4-}$ denotes the quadrivalent trimethylenediaminetetraacetate anion.

The total concentrations of metals and TRDTA, $[Co]_t$, $[M]_t$ and $[TRDTA]_t$, in the solution are given as follows:

$$[Co]_t = [Co^{2+}]_{app} + [Cotrdta^{2-}] \qquad (12)$$

$$[M]_t = [M^{m+}]_{app} + [Mtrdta^{(m-4)+}] \qquad (13)$$

$$[TRDTA]_t = [TRDTA]_f + [Cotrdta^{2-}] + [Mtrdta^{(m-4)+}] \qquad (14)$$

where

$$[Co^{2+}]_{app} = [Co^{2+}] + [CoOAc^+]$$

$$[M^{m+}]_{app} = [M^{m+}] + \sum_1^n [M(OAc)_n^{(m-n)+}]$$

When $[Co]_t + [M]_t > [TRDTA]_t$, $[TRDTA]_f$ is negligibly small compared with the concentrations of other species present in the solution.

From the polarographic measurement of $[Cotrdta^{2-}]$, the equilibrium constant of Eq. 11

$$K_{Co,app}^M = \frac{[Co^{2+}]_{app}[Mtrdta^{(m-4)+}]}{[M^{m+}]_{app}[Cotrdta^{2-}]} \qquad (15)$$

is obtained with the relations given by Eqs. 12 to 14.

Equation 15 is rewritten as,

$$K_{Co,app}^M = K_{Co}^M \times \frac{1 + K_{CoOAc}[OAc^-]}{1 + \sum_1^n K_{M(OAc)_n}[OAc^-]^n} \qquad (16)$$

where

$$K_{Co}^M = \frac{[Co^{2+}][Mtrdta^{(m-4)+}]}{[M^{m+}][Cotrdta^{2-}]} \qquad (17)$$

Equation 17 means that $K_{Co}^M$ is equal to the ratio of the stability constant of the $M^{m+}$-TRDTA complex to that of the $Co^{2+}$-TRDTA complex:

$$K_{Co}^M = \frac{K_{MY}}{K_{CoY}} \qquad (18)$$

The values of $K_{Co}^M$ can be calculated from Eq. 16 using the values of $K_{Co,app}^M$ and the formation constants of the acetato complexes.[1,2,8]

## Experimental

**Reagents.** — Standard solutions of metal(II) nitrate, disodium dihydrogen ethylenediaminetetraacetate ($Na_2H_2edta$) and disodium dihydrogen propylenediaminetetraacetate ($Na_2H_2pdta$) were obtained by procedures reported previously.[1-3,9]

Trimethylenediaminetetraacetic acid ($H_4trdta$) was prepared according to the method described in the previous paper.[10] A stock solution of $Na_2H_2trdta$ was prepared from equimolar quantities of $H_4trdta$ and sodium carbonate. The concentration of TRDTA was determined by amperometric titration with standard solutions of copper(II) nitrate, cobalt(II) nitrate and nickel(II) nitrate in acetate buffer solutions of pH 5.4, and that of cadmium(II) nitrate, in ammonia-ammonium nitrate buffer solutions of pH 8.7. The values thus obtained were consistent with each other within the range of experimental error and were in good agreement with the value expected from the weight of $H_4trdta$.

All the other chemicals used were of analytical reagent grade.

**Apparatus and Procedure.** — The polarograph used was the same as that described in the previous paper.[3] The dropping mercury electrode had an $m$ value of $2.13_7$ mg./sec. and a drop time, $t_d$, of

7) The details will be published elsewhere.

* Trimethylenediaminetetraacetate may be replaced by other, appropriate ligands.

** It is known that cobalt(II) forms only a monoacetato complex in a solution containing acetate up to 0.2 M in concentration at ionic strength 0.2.[2]

8) N. Tanaka and K. Kato, This Bulletin, 32, 516 (1959).

9) N. Tanaka and H. Ogino, ibid., 36, 175 (1963).

10) N. Tanaka and H. Ogino, ibid., 37, 877 (1964).

3.96 sec., as measured in an air-free 0.2 M potassium nitrate solution containing 0.01% gelatin at 25°C. The pH of the solution was measured, after the polarographic measurement, with a Hitachi Horiba Model P pH meter.

In order to determine the relative stability constants of ethylenediaminetetraacetatocuprate(II), propylenediaminetetraacetatocuprate(II) and trimethylenediaminetetraacetatocuprate(II) complexes, measurements of the diffusion currents of ethylenediaminetetraacetate or propylenediaminetetraacetate in acetate buffer solutions were carried out with the following two reaction mixtures at 25°C:

(a) copper(II)-EDTA-TRDTA

(b) copper(II)-PDTA-TRDTA

The ionic strength was adjusted to be 0.2 with sodium perchlorate. Gelatin was added as a maximum suppressor by 0.01% in concentration. It was found in the preliminary experiments that the equilibria of systems a and b were attained within 30 min.

In order to determine the relative stability constants of trimethylenediaminetetraacetato complexes, measurements of the diffusion currents of the trimethylenediaminetetraacetatocobaltate(II) complex in the acetate buffer solutions were carried out with the following five reaction mixtures at 25°C:

(c) cobalt(II)-nickel(II)-TRDTA

(d) cobalt(II)-copper(II)-TRDTA

(e) cobalt(II)-zinc(II)-TRDTA

(f) cobalt(II)-cadmium(II)-TRDTA

(g) cobalt(II)-lead(II)-TRDTA

The ionic strength was adjusted to be 0.2 with potassium nitrate. Gelatin was added as a maximum suppressor by 0.005% in concentration. Since it was found that the substitution reactions between cobalt(II) ions and various kinds of metal(II)-TRDTA complexes were attained within 40 hr., measurements were made with solutions which had been kept in a thermostat for 2 days after preparation.

## Results

**The Determination of the Relative Stability Constants of Ethylenediaminetetraacetatocuprate(II), Propylenediaminetetraacetatocuprate(II) and Trimethylenediaminetetraacetatocuprate(II) Complexes.**—It is well known that EDTA gives a polarographic anodic wave[11] as a result of the following electrode reaction:

$$Hg + H_nY^{(4-n)-} \rightleftarrows HgY^{2-} + nH^+ + 2e$$

In the course of this study, it was found that PDTA gave a similar anodic wave and that its half-wave potential was slightly more negative than that of EDTA. TRDTA, on the other hand, was found to produce an ill-defined wave at a more positive potential than EDTA. These facts suggested that the concentrations of free EDTA and PDTA can be determined in systems a and b respectively. In Fig. 1 typical examples are given.

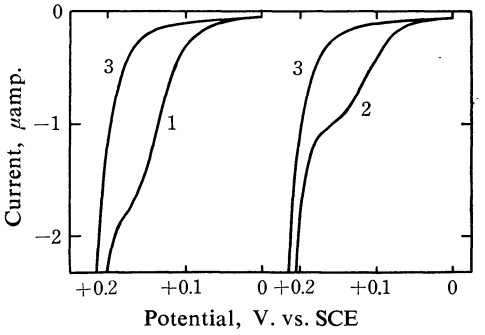



Fig. 1. Polarograms of systems a and b in the acetate buffer solutions of pH 5.38 at 25°C. Total concentrations are: 2.00 mM copper(II), 1.98$_8$ mM EDTA, 4.09$_6$ mM TRDTA (curve 1); 2.00 mM copper(II), 1.98$_8$ mM PDTA, 4.09$_6$ mM TRDTA (curve 2); 4.09$_6$ mM TRDTA (curve 3).

The diffusion current constants of EDTA and PDTA were determined by measuring the diffusion currents at various pH's. The values of $[EDTA]_f$ and $[PDTA]_f$ were calculated, with the aid of these diffusion current constants, from the diffusion currents obtained with the reaction mixtures of systems a and b respectively. Then, the equilibrium constants, $K^Y_{Z,app}$, given by Eq. 8 were calculated. The results obtained for systems a and b are given in Table I.

The reported values of the acid dissociation constants (p$K$) of EDTA, TRDTA and PDTA are summarized in Table II. The relative stability constants of the copper(II)-EDTA complex to the copper(II)-TRDTA complex, $K^{EDTA}_{TRDTA}$, were calculated from the $K^{EDTA}_{TRDTA,app}$ given in Table I and from the p$K$ values of EDTA and TRDTA reported by Schwarzenbach et al.[6] The resulting values at various pH's are presented in Table III.

It seems not appropriate to calculate the values of $K^{PDTA}_{TRDTA}$ from the observed values of $K^{PDTA}_{TRDTA,app}$ with the reported p$K$ values of TRDTA and PDTA, because these p$K$ values have not all been determined under the same conditions. However, a $K^{PDTA}_{TRDTA,app}$ value at a given pH can be converted to a $K^{PDTA}_{EDTA,app}$ value with the aid of a $K^{EDTA}_{TRDTA,app}$ value obtained at the same pH according to the equation,

$$K^{PDTA}_{EDTA,app} = K^{PDTA}_{TRDTA,app} / K^{EDTA}_{TRDTA,app} \quad (19)$$

From the $K^{PDTA}_{EDTA,app}$ thus obtained and the p$K$

11) For instance, J. Goffart, G. Michel and G. Duyckaerts, *Anal. Chim. Acta*, **9**, 184 (1953); C. N. Reilley, W. G. Scribner and C. Temple, *Anal. Chem.*, **28**, 450 (1956).

TABLE I. EQUILIBRIUM CONSTANTS FOR THE SUBSTITUTION REACTION (Eq. 4) AT 25°C AND IONIC STRENGTH 0.2

| System a* | | | System b** | | |
|---|---|---|---|---|---|
| pH | $[EDTA]_{f,mM}$ | $K^{EDTA}_{TRDTA,app}$ | pH | $[PDTA]_{f,mM}$ | $K^{PDTA}_{TRDTA,app}$ |
| 5.39 | 0.201 | $1.6\times10^2$ | 5.36 | 0.099 | $6.9\times10^2$ |
| 5.28 | 0.232 | $1.2\times10^2$ | 5.26 | 0.117 | $4.9\times10^2$ |
| 5.06 | 0.220 | $1.3\times10^2$ | 5.06 | 0.113 | $5.3\times10^2$ |
| 4.84 | 0.211 | $1.5\times10^2$ | 4.88 | 0.113 | $5.3\times10^2$ |

* Total concentrations are: $[Cu]_t=2.00$ mM, $[EDTA]_t=1.98_8$ mM, $[TRDTA]_t=4.09_6$ mM.
** Total concentrations are: $[Cu]_t=2.00$ mM, $[PDTA]_t=1.98_8$ mM, $[TRDTA]_t=4.09_6$ mM.

TABLE II. THE REPORTED VALUES OF THE ACID DISSOCIATION CONSTANTS OF EDTA, TRDTA AND PDTA AT IONIC STRENGTH 0.1

| Chelating agent | Temp., °C | $pK_1$ | $pK_2$ | $pK_3$ | $pK_4$ | Ref. |
|---|---|---|---|---|---|---|
| EDTA | 20 | 2.0 | 2.67 | 6.16 | 10.26 | 6 |
| | 30 | 2.4 | 2.86 | 6.22 | 10.25 | 12 |
| TRDTA | 20 | 2.0 | 2.67 | 7.90 | 10.27 | 6 |
| PDTA | 30 | 2.60 | 3.03 | 6.20 | 10.84 | 12 |

TABLE III. THE DETERMINATION OF THE VALUE OF $K^{EDTA}_{TRDTA}$ OF COPPER(II) COMPLEXES AT 25°C AND IONIC STRENGTH 0.2

| pH | $\alpha_{TRDTA}/\alpha_{EDTA}$ | $K^{EDTA}_{TRDTA}$ |
|---|---|---|
| 5.39 | 50.8 | 3.2 |
| 5.28 | 52.2 | 2.3 |
| 5.06 | 54.2 | 2.5 |
| 4.84 | 55.5 | 2.6 |
| | | 2.7 (av.) |

TABLE IV. THE DETERMINATION OF THE VALUE OF $K^{PDTA}_{EDTA}$ OF COPPER(II) COMPLEXES AT 25°C AND IONIC STRENGTH 0.2

| pH* | $K^{PDTA}_{EDTA,app}$ | $\alpha_{PDTA}/\alpha_{EDTA}$ | $K^{PDTA}_{EDTA}$ |
|---|---|---|---|
| $5.37_5$ | 4.2 | 3.74 | 16 |
| 5.27 | 4.1 | 3.74 | 15 |
| 5.06 | 4.0 | 3.74 | 15 |
| 4.86 | 3.7 | 3.74 | 14 |
| | | | 15 (av.) |

* The pH values of the same line of system a and system b in Table I are averaged.

values of EDTA and PDTA reported by Grimes et al.,[12] the $K^{PDTA}_{EDTA}$ values were determined; they are given in Table IV.

The hydrogen ion concentration used in this calculation was obtained from the observed pH and the activity coefficient of the hydrogen ion, which was assumed to be 0.80 at ionic strength 0.2.

12) J. H. Grimes, A. J. Huggard and S. P. Wilford, *J. Inorg. Nucl. Chem.*, **25**, 1225 (1963).

**The Determination of the Relative Stability Constants of Trimethylenediaminetetraacetato Complexes.**—Cobalt(II)-TRDTA complex gave a reversible anodic wave with the half-wave potential of about +0.05 V. vs. SCE in the acetate media, independent of pH from 4.7 to 5.5. The limiting current of the wave was found to be diffusion-controlled.

The diffusion current constants of the cobalt(II)-TRDTA complex were determined by measuring the diffusion current under various acetate concentrations and pH's. The values of $[Cotrdta^{2-}]$ were calculated, with the aid of these diffusion current constants, from the diffusion currents obtained with systems c to g. Then, the values of $K^{M}_{Co,app}$ given by Eq. 15 and those of $K^{M}_{Co}$ were calculated according to the procedures described above.

The results obtained for systems c to g are summarized in Table V.

Although the measurements were carried out for the cobalt(II)-manganese(II)-TRDTA system, no detectable decrease in the wave height of the cobalt(II)-TRDTA complex was observed. The value of $K^{Mn}_{Co}$, therefore, was calculated to be less than $2\times10^{-4}$ from the experimental errors and from the total concentrations of cobalt(II), manganese(II) and trimethylenediaminetetraacetate ions.

## Discussion

The reported values of the acid dissociation constants of EDTA, TRDTA and PDTA[6,12] ($\mu=0.1$, 20°C or 30°C) were used without correction when $K^{Y}_{Z}$ was calculated from $K^{Y}_{Z,app}$.

TABLE V. THE DETERMINATION OF THE VALUES OF $K^{M}_{Co}$ OF TRDTA COMPLEXES AT 25°C AND IONIC STRENGTH 0.2

| pH | $[OAc^-]_{add}$, M | $[OAc^-]$, M* | $K^{M}_{Co,app}$ | $K^{M}_{Co}$ |
|---|---|---|---|---|
| | | Cobalt(II)-copper(II)-TRDTA system | | |
| 5.29 | 0.100 | $0.099_0$ | $4.59\times10^{2}$ | $3.06\times10^{3}$ |
| 5.22 | 0.100 | $0.098_3$ | $6.08\times10^{2}$ | $4.02\times10^{3}$ |
| 5.19 | 0.0400 | $0.039_3$ | $1.05\times10^{3}$ | $3.26\times10^{3}$ |
| 5.17 | 0.0500 | $0.049_1$ | $1.15\times10^{3}$ | $4.23\times10^{3}$ |
| | | | | $K^{Cu}_{Co}=3.6\times10^{3}$ (av.) |
| | | Cobalt(II)-nickel(II)-TRDTA system | | |
| 5.28 | 0.100 | $0.099_1$ | $5.30\times10^{2}$ | $6.24\times10^{2}$ |
| 5.28 | 0.100 | $0.099_1$ | $5.68\times10^{2}$ | $6.69\times10^{2}$ |
| 5.23 | 0.100 | $0.098_4$ | $5.32\times10^{2}$ | $6.26\times10^{2}$ |
| | | | | $K^{Ni}_{Co}=6.4\times10^{2}$ (av.) |
| | | Cobalt(II)-zinc(II)-TRDTA system | | |
| 5.34 | 0.100 | $0.099_6$ | 0.433 | 0.596 |
| 5.34 | 0.100 | $0.099_6$ | 0.438 | 0.603 |
| | | | | $K^{Zn}_{Co}=0.60$ (av.) |
| | | Cobalt(II)-cadmium(II)-TRDTA system | | |
| 5.22 | 0.100 | $0.097_2$ | $1.49\times10^{-2}$ | $1.63\times10^{-2}$ |
| 5.20 | 0.100 | $0.097_2$ | $1.49\times10^{-2}$ | $1.63\times10^{-2}$ |
| | | | | $K^{Cd}_{Co}=1.6\times10^{-2}$ (av.) |
| | | Cobalt(II)-lead(II)-TRDTA system | | |
| 5.02 | 0.0400 | 0.0205 | $9.33\times10^{-3}$ | $3.52\times10^{-2}$ |
| 4.84 | 0.0200 | 0.0074 | $1.89\times10^{-2}$ | $3.73\times10^{-2}$ |
| | | | | $K^{Pb}_{Co}=3.6\times10^{-2}$ (av.) |

* The concentration of uncomplexed acetate in the solution was calculated by successive approximation.

This procedure, however, does not seem to introduce any appreciable error into the values of $K^{Y}_{Z}$ thus obtained, because the predominant species of uncomplexed ligands are always $H_2Y^{2-}$ for EDTA, TRDTA and PDTA under the present experimental conditions, and their abundances are more than 88%. From this fact, we may approximately express $\alpha_Z/\alpha_Y$ in Eq. 9 by the equation:

$$\frac{\alpha_Z}{\alpha_Y}=\frac{K_{H_2Y}K_{HY}}{K_{H_2Z}K_{HZ}} \qquad (20)$$

indicating that the values of $\alpha_Z/\alpha_Y$ are mainly dependent on the values of the third and fourth dissociation constants of ligands. According to the Debye-Hückel equation, at a given temperature and ionic strength the activity coefficients of the ions with the same charge are determined only by ion-size parameters. Since EDTA, TRDTA and PDTA are closely related compounds, the changes in the activity coefficients of the corresponding ionic species of these compounds with the changes in temperature and ionic strength are considered to be almost identical. Therefore, the values of $\alpha_Z/\alpha_Y$ would not be affected appreciably by the changes in temperature and ionic strength, as long as the acid dissociation constants are determined under the same conditions.

If $MHY^{(m-3)+}$ and $MHZ^{(m-3)+}$ are formed, the equation corresponding to Eq. 9 is given as follows:

$$K^{Y}_{Z,app}=K^{Y}_{Z}\times\frac{\alpha_Z\alpha_{MHY(H)}}{\alpha_Y\alpha_{MHZ(H)}} \qquad (21)$$

where

$$\alpha_{MHY(H)}=1+K^{H}_{MHY}[H^+]$$

$$\alpha_{MHZ(H)}=1+K^{H}_{MHZ}[H^+]$$

$K^{H}_{MHY}$ and $K^{H}_{MHZ}$ represent the formation constants of $MHY^-$ and $MHZ^-$ respectively. Schwarzenbach et al.[13] have reported that $\log K^{H}_{CuHedta}$ was 3.0 at 20°C and ionic strength 0.1. This value indicates that no appreciable amount of $CuHedta^-$ is present in systems a and b. The values of neither $K^{EDTA}_{TRDTA}$ nor $K^{PDTA}_{EDTA}$ are dependent on pH, as is shown in Table III and Table IV respectively. These also suggest that no appreciable amounts of

13) G. Schwarzenbach, R. Gut and G. Anderegg, *Helv. Chim. Acta*, **37**, 937 (1954).

$CuHtrdta^-$ and $CuHpdta^-$ are present under the experimental conditions.

The stability constants of the copper(II)-TRDTA complex and the copper(II)-PDTA complex were calculated by using the $K^{EDTA}_{TRDTA}$ value in Table III, the $K^{PDTA}_{EDTA}$ value in Table IV and the value of $K_{Cuedta}$, which was evaluated with a procedure which has been described previously.[14] The stability constants of the trimethylenediaminetetraacetato complexes of some divalent metal ions were calculated from the $K_{Cutrdta}$ value thus obtained and from the $K^{M}_{Co}$ values of TRDTA in Table V. The $K^{M}_{M'}$ values of EDTA and PDTA complexes determined previously[1-3] were used for the determination of the stability constants of ethylenediaminetetraacetato and propylenediaminetetraacetato complexes. The scheme for the determination of the stability constants is given in Fig. 2. The results obtained are shown in Table VI and Fig. 3.

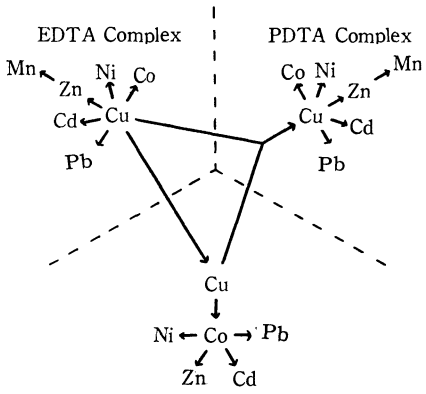



Fig. 2. Scheme for the determination of the stability constants of EDTA, TRDTA and PDTA complexes.

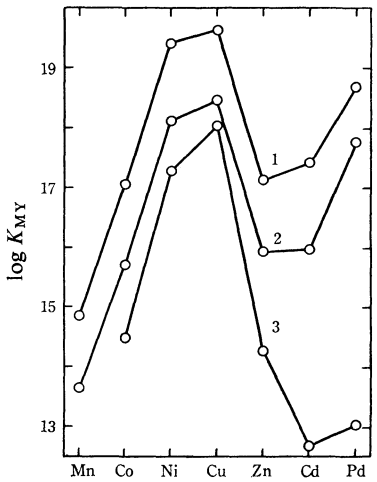



Fig. 3. The logarithmic stability constants of PDTA (1), EDTA (2) and TRDTA (3) complexes at 25°C and ionic strength 0.2.

14) N. Tanaka and K. Kato, This Bulletin, **32**, 1376 (1959).

TABLE VI. THE LOGARITHMIC STABILITY CONSTANTS OF EDTA, PDTA AND TRDTA COMPLEXES AT 25°C AND IONIC STRENGTH 0.2[15]

| Metal ion | EDTA complex | PDTA complex | TRDTA complex |
|---|---|---|---|
| Manganese(II) | 13.64* | 14.85* | <10.8 |
| Cobalt(II) | 15.71 | 17.07 | 14.48 |
| Nickel(II) | 18.12 | 19.42 | 17.29 |
| Copper(II) | 18.46** | 19.64 | 18.04 |
| Zinc(II) | 15.94 | 17.14 | 14.26 |
| Cadmium(II) | 15.98 | 17.43 | 12.69 |
| Lead(II) | 17.76 | 18.69 | 13.04 |

* These values were calculated from unpublished results.

** This value was evaluated with the same procedure as described previously.[14]

The stability constants of EDTA complexes and the cadmium(II)-TRDTA complex obtained in this study seem to be in satisfactory agreement with those reported by Schwarzenbach et al.,[6,13] provided that the differences in temperature and ionic strength between the two sets of results are considered.

For the sake of comparison, the calculations shown in Table VII were carried out. The differences between the logarithmic stability constants of PDTA and EDTA complexes, which are expressed with $\log K^{PDTA}_{EDTA}$ in Table VII, indicate that the stability constants of PDTA complexes are larger than those of

TABLE VII. COMPARISON OF THE STABILITY CONSTANTS OF EDTA, PDTA AND TRDTA COMPLEXES AT 25°C AND IONIC STRENGTH 0.2

| | Mn | Co | Ni | Cu | Zn | Cd | Pb |
|---|---|---|---|---|---|---|---|
| $\log K^{PDTA}_{EDTA}$ | 1.21 | 1.36 | 1.30 | 1.18 | 1.20 | 1.45 | 0.93 |
| $\log K^{EDTA}_{TRDTA}$ | >2.8 | 1.23 | 0.83 | 0.42 | 1.68 | 3.29 | 4.72 |

15) Note added in proof: Recently, stability constants of PDTA complexes[a] and TRDTA complexes[b-d] were reported. They seem to be in good agreement with the values obtained in this study, when the differences in the experimental conditions and in the values of acid dissociation constants used in the calculation are taken into consideration. Irving and Conesa[a] determined $K^{Pb}_{Cu}$ and $K^{Cd}_{Pb}$ of PDTA complexes in acetate media, but they did not consider the effects of acetate ions on the equilibria. The better agreement can be obtained between their values and those obtained in this study by considering the formation of acetato complexes of copper, cadmium and lead.

a) H. M. N. H. Irving and J. P. Conesa, *J. Inorg. Nucl. Chem.*, **26**, 1945 (1964); b) G. Anderegg and F. L'Eplattenier, *Chimia*, **18**, 186 (1964); c) F. L'Eplattenier and G. Anderegg, *Helv. Chim. Acta*, **47**, 1792 (1964); d) G. Anderegg, ibid., **47**, 1801 (1964).

EDTA complexes by about 1.2 $\log K$ unit, without regard to the kind of metal ions. It was found that the fourth dissociation constant of PDTA is higher than that of EDTA, and that the stability constants of alkaline earth chelates of PDTA are larger than those of EDTA.[12] Grimes et al. concluded that these results are attributable to the inductive effect of the methyl group in PDTA.[12] Therefore, the values of $\log K_{EDTA}^{PDTA}$ indicate that the increase in the basicity of the ligand has almost the same effect on the stability constants of the PDTA complexes compared with the EDTA complexes. On the other hand, the values of $\log K_{TRDTA}^{EDTA}$ are considerably dependent on the kind of metal ions. It may be considered that the values of $\log K_{TRDTA}^{EDTA}$ are affected by two factors. The first one is that the increase in basicity due to the third dissociation constant of TRDTA being higher than that of EDTA[5,6] causes the stabilization of TRDTA complexes. The second factor is that the TRDTA complexes are instabilized by the presence of a six-membered chelate ring involving two nitrogen atoms. The first factor may have almost the same effect on the $\log K_{TRDTA}^{EDTA}$ values of various metal ions, as is true in the case of $\log K_{EDTA}^{PDTA}$ values. Therefore, the orders of the instabilization by the presence of a six-membered ring may be given as:

$$Cu < Ni < Co < Zn < Mn\,;\ Zn < Cd < Pb$$

These orders agree with the order of the ionic (crystal) radii[16] of metal ions. This fact indicates that the decrease in the size of metal ions is favorable for the formation of TRDTA complex.

16) T. Moeller, "Inorganic Chemistry," John Wiley & Sons, New York, N. Y. (1952), p. 140.

**Summary**

Two methods are presented for the determination of the stability constants of ethylenediaminetetraacetato, trimethylenediaminetetraacetato and propylenediaminetetraacetato complexes of some divalent metal ions. One is a new method which is based on the polarographic measurement of the concentration of an uncomplexed ligand in a solution containing two kinds of ligands and an appropriate metal ion. The other is a modification of the method described in the previous paper.[1] From the results obtained by these methods and those obtained previously,[1-3] the individual stability constants have been calculated. The values of the logarithmic stability constants of complexes at 25°C and ionic strength 0.2 are: Mn 13.64, Co 15.71, Ni 18.12, Cu 18.46, Zn 15.94, Cd 15.98 and Pb 17.76 for ethylenediaminetetraacetato complexes; Mn <10.8, Co 14.48, Ni 17.29, Cu 18.04, Zn 14.26, Cd 12.69 and Pb 13.04 for trimethylenediaminetetraacetato complexes, and Mn 14.85, Co 17.07, Ni 19.42, Cu 19.64, Zn 17.14, Cd 17.43 and Pb 18.69 for propylenediaminetetraacetato complexes.

The author wishes to thank Professor Nobuyuki Tanaka for his kind guidance and encouragement.

*Department of Chemistry*
*Faculty of Science*
*Tohoku University*
*Katahira-cho, Sendai*

# The Nitration and Sulfonation of 2, 4, 6-Triphenyl-1, 3, 5-triazine[1]

By Yoshiro OGATA, Yasuji IZAWA and Yuji KAWASHIMA

(Received September 15, 1964)

There are many examples of the preparation of cyaphenine, including the trimerization of benzonitrile with acidic,[2,3] basic[4,5] or organometallic catalysts[6,7], or by the high pressure technique.[8,9] It has also been reported that the formation of cyaphenine is possible by way of such condensations as the reaction of benzoyl

1) Contribution No. 67.
2) A. H. Cook and D. G. Jones, *J. Chem. Soc.*, **1941**, 278.
3) A. Pinner and F. Klein, *Ber.*, **11**, 764 (1878).
4) J. J. Ritter and R. D. Anderson, *J. Org. Chem.*, **24**, 208 (1959).
5) F. W. Swamer, G. A. Reynolds and C. R. Hauser, ibid., **16**, 43 (1951).
6) E. Frankland and J. Evans, *J. Chem. Soc.*, **37**, 563 (1880).
7) T. K. Brotherton and J. F. Bunnett, *Chem. & Ind.*, **1957**, 80.
8) T. L. Cairns, A. W. Larchar and B. C. McKusich, *J. Am. Chem. Soc.*, **74**, 5633 (1952).
9) I. S. Bengelsdorf, ibid., **80**, 1442 (1958).

chloride with potassium cyanate,[10] benzaldehyde with tetrasulfur tetranitride,[11] benzonitrile with benzoyl chloride,[12] benzene with cyanogen chloride,[13] ethyl benzimidate with its hydrochloride,[14] 4, 6-diphenyl-1,2,3,5-oxathiodiazine-2-dioxide with benzamidine,[15] and benzamide with phosphorous pentasulfide.[16] It has also been reported that methyl *m*- or *p*-nitrobenzimidate derived from the corresponding nitrobenzonitrile may be converted to 2, 4, 6-tris(*m*- or *p*-nitrophenyl)-1, 3, 5-triazine by an acid catalyst.[17] However, very little information is available on the electrophilic substitutions of cyaphenine.

The present paper will describe our data on the nitration and sulfonation of cyaphenine. The structure of the products was confirmed by infrared spectroscopy and chemical analysis, i. e., by estimations of the nitrogen content in the nitrated cyaphenine and of the sulfonyl group in the cyapheninesulfonic acid.

## Experimental

**Materials.**—Cyaphenine was prepared according to the Cook-Jones procedure.[2] The product was purified by two recrystallizations from toluene (yield, 68.4%), m. p. 233.0—234.0°C (lit.[2] m. p. 232°C). The wave numbers ($cm^{-1}$) of the characteristic infrared absorption bands of cyaphenine (KBr disk) were 1590, 1530, 1450, 1370, 840, 740 and 680 $cm^{-1}$. Cyaphenine had an ultraviolet absorption band ($\lambda_{max}$) at 272 m$\mu$ ($\log \varepsilon = 4.22$) in 95% aqueous ethanol.

**The Nitration of Cyaphenine.**—A mixed acid, that is, a mixture of aqueous nitric acid (sp. wt. of 1.42, 0.09—0.63 mol.) and concentrated sulfuric acid (sp. wt. of 1.84, 0.09 mol.), was added, drop by drop and at 0°C, to a solution of cyaphenine (0.02 mol., 6.18 g.) in 95% sulfuric acid (29 ml.). The reaction mixture was then continuously stirred under the conditions listed in Table I. The crystals separated after the completion of reaction were washed with cold water and recrystallized from nitrobenzene. The number of nitiro groups per molecule of the resulting nitrocyaphenine ($n_{NO_2}$) was determined by infrared spectrophotometry (the concentration of nitrocyaphenine in the KBr disk: 0.25%); it was then calculated by means of the following equation:

$$n_{NO_2} = 0.89 \frac{T_{1350} - T_{1420}}{T_{1370} - T_{1420}}$$

where the $T$'s are the transmittances (%) at the subscripted wave numbers and where the coefficient of "0.89" is a correction factor obtained from standard nitrated cyaphenine, for which the $n_{NO_2}$ value was calculated by the estimation of the nitrogen content according to the Dumas method.

**The Sulfonation of Cyaphenine.**—A mixture of 50% oleum (7 g.) and cyaphenine (1.5 g.) was reacted while being stirred under the conditions listed in Table III. The resulting yellow viscous liquid was then poured into a mixture of ice and water and neutralized with sodium carbonate. The slurry, obtained on the evaporation of water, had 95% ethanol added, until the concentration of ethanol became 50%. The separated sodium sulfate was then filtered off, the filtrate being evaporated to dryness. The residue was extracted with 50% aqueous ethanol. The extract was then evaporated to dryness and extracted again with 70% aqueous ethanol. The extract was condensed, and a considerable amount of 95% aqueous ethanol was added. The precipitate of a colorless crystaline product, sodium cyapheninesulfonate, was collected by filtration, washed with ethanol, and dried. For the determination of sulfonyl groups in the resulting sodium cyapheninesulfonate, the isolated sulfonate was converted into the acid with cation exchange resin, Amberlite IR 120 ($H^+$); the sulfonic acid solution thus obtained was titrated with a standard aqueous solution of sodium hydroxide.

## Results and Discussion

**The Nitration of Cyaphenine.**—Cyaphenine which had been prepared from benzonitrile according to the Cook-Jones method[2] was nitrated with a mixture of sulfuric and nitric acids. The nitrations under various conditions (i. e., reaction time, temperature, and concentrations of reactants) are listed in Table I. It is obvious that the nitration of cyaphenine is rather difficult because of the electron-attracting

Table I. Nitration of cyaphenine with a mixture of nitric and sulfuric acids

| $(HNO_3)$/(Cyaphenine) mol. : mol. | Temp. °C | Time hr. | Yield g. | Number of $NO_2$[a] |
|---|---|---|---|---|
| 4.5 | 0 | 3 | 8.2 | 1.4 |
| 22.5 | 0 | 3 | 8.6 | 1.7 |
| 31.5 | 0 | 3 | 8.6 | 1.8 |
| 4.5 | 20 | 0.5 | 8.2 | 1.1 |
| 4.5 | 20 | 1 | 7.9 | 1.5 |
| 4.5 | 20 | 2 | 8.2 | 1.3 |
| 4.5 | 20 | 5 | 8.5 | 1.5 |
| 4.5 | 20 | 7 | 7.9 | 1.7 |
| 4.5 | 20 | 10 | 8.0 | 1.4 |
| 4.5 | −20 | 3 | 8.4 | 1.1 |
| 4.5 | −10 | 3 | 8.2 | 1.2 |
| 4.5 | 10 | 3 | 8.2 | 1.4 |
| 4.5 | 40 | 3 | 7.8 | 1.7 |
| 4.5 | 60 | 3 | 7.0 | 1.1 |

a) The number of $NO_2$ group per molecule of product.

10) S. Cloez, *Ann.*, **115**, 23 (1860).
11) F. Francis and O. Davis, *J. Chem. Soc.*, **85**, 259 (1904).
12) P. Eitner and F. Kraft, *Ber.*, **25**, 2266 (1892).
13) R. Scholl and W. Norr, *Ber.*, **33**, 1052 (1900).
14) A. Ya Yakubovich, E. L. Zaitseva, G. I. Braz and V. P. Bazov, *Zhur. Obshchei. Khim.*, **32**, 3409 (1962).
15) H. Weidigner and J. Kranz, *Chem. Ber.*, **96**, 2070 (1963).
16) L. Henry, *Ber.*, **2**, 305 (1869).
17) F. C. Schaefer and G. A. Peters, *J. Org. Chem.*, **26**, 2778 (1961).

nature of triazine, yielding a product with no more than two nitro groups. Trinitrocyaphenine is not obtained because of the deactivation of a residual phenyl group by the presence of two nitro groups as well as the triazine ring.

The nitrated cyaphenine shows new infrared absorptions (KBr disk), at 1350 (s), 820 (w), and 800 (s) $cm^{-1}$, not found in the spectrum of original cyaphenine. The absorption bands at 800 and 820 $cm^{-1}$ correspond to meta- and para-substituted benzenes respectively; the band at 1350 $cm^{-1}$ is assigned to the nitro group. Since the band at 820 $cm^{-1}$ (para) is weak, the *p*-nitrocyaphenine content in the product should be much lower than that of the *m*-isomer.

**The Decomposition of Cyaphenine and Nitrocyaphenine with Hydrochloric Acid.**—Frankland and Evans reported, without a detailed description, the conversion of cyaphenine to benzoic acid and ammonia[6] by heating cyaphenine with concentrated hydrochloric acid in a sealed tube to 250°C. Our experiment to confirm this decomposition gave benzoic acid in a 93.2% yield under suitable conditions, as is indicated in Table II. However, cyaphenine was not converted to benzoic acid when heated in an acidic aqueous solution (2.9% sulfuric acid), even in the presence of potassium permanganate at 100°C for 24 hr.

Table II. Decomposition of cyaphenine with aqueous hydrochloric acid in a sealed tube at 250°C for 6 hr.

| Cyaphenine g. | 35%HCl ml. | Yield of $PhCO_2H$ g. | Conversion % |
|---|---|---|---|
| 0.31 | 1 | 0.201 | 55.0 |
| 0.16 | 1 | 0.157 | 85.3 |
| 0.51 | 1 | 0.170 | 93.2 |

In the case of nitrocyaphenine, a similar decomposition was unsuccessful; green or brown solid materials of an unknown structure were obtained, but no nitrobenzoic acid was isolable.

**The Sulfonation of Cyaphenine.**—The sulfonation of cyaphenine with oleum under varying conditions are listed in Table III. Cyaphenine-trisulfonic acid was obtained by heating it at 100°C for 0.5 hr. However, a part of the introduced sulfonyl groups may be eliminated when the reaction mixture is kept standing after the completion of the reaction.

Absorption bands at 790 (s), 1040 (s), and 1100 (s) $cm^{-1}$ in the infrared spectrum (KBr disk) of sodium cyaphenine-trisulfonate may be assigned to the meta-substituted phenyl group. In addition, the lack of absorption at 800—820 $cm^{-1}$ shows the absence of the para-substituted phenyl group. Therefore, the sulfonation of cyaphenine is different from the nitration in that there is no para-substitution.

Table III. Sulfonation of cyaphenine with oleum (50% $SO_3$)

| Temp. °C | Time hr. | Yield g. | Number of $SO_3H$[a] |
|---|---|---|---|
| 40 | 6 | 1.7 | 2.6 |
| 60 | 6 | 2.7 | 2.6 |
| 100 | 6 | 2.4 | 2.3 |
| 100 | 0.35 | 2.0 | 2.7 |
| 100 | 0.5 | 2.0 | 3.0 |
| 100 | 1.2 | 2.2 | 2.8 |
| 100 | 2 | 2.1 | 2.8 |
| 100 | 4 | 2.4 | 2.7 |

a) The number of sulfonyl group per molecule of product.

## Summary

The nitration of cyaphenine (2, 4, 6-triphenyl-1, 3, 5-triazine) with a mixture of nitric and sulfuric acids has been found to give products with mostly meta- and partly para-substituted benzene rings. The composition of products varies with the varying reaction conditions. *m, m'*-Dinitrocyaphenine is the product of the highest number of nitro groups. The sulfonation of cyaphenine with oleum gives trisulfonated cyaphenine at meta-positions of benzene rings; it suffers desulfonation when left standing in the reaction mixture for a long time.

The authors are grateful to Professors T. Takeuchi and K. Fukuzumi for their aid in the measurement of infrared spectra.

*Department of Applied Chemistry*
*Faculty of Engineering*
*Nagoya University*
*Chikusa-ku, Nagoya*

# Nuclear Magnetic Resonance Studies of Fulvenes*1

By Yoshio KITAHARA,*2 Ichiro MURATA,*2 Kunikatsu SHIRAHATA,*2 Shigeyoshi KATAGIRI and Hiroshi AZUMI

(Received September 16, 1964)

Fulvene, a cross-conjugated non-alternant hydrocarbon, is of particular interest because of the relation of its properties to those of its isomer, benzene. Since 1900, when Thiele[1] reported the first synthesis of some simple fulvene derivatives, fulvene has been the subject of much research in both theoretical and experimental organic chemistry.[2,3] Some studies of the nuclear magnetic resonance spectra of fulvene derivatives described in the literature have dealt with 6-ethylfulvene,[4] 6-vinylfulvene,[5] 6-hydroxy-6-methyl-1-phenylazofulvene,[6] methylvinylfulvenes,[7] and fulvene itself.[8] A very recent paper on the nuclear magnetic resonance studies of some fulvene derivatives by Smith and Shoulders[9] has prompted us to report our own independent studies on the same subject.

In this paper, we will describe the proton magnetic resonance spectra of some fulvene derivatives, and we will discuss the magnetic constants, electron density, and especially the theoretical calculation of the ring current effect of the fulvene ring.

## Experimental

The proton magnetic resonance spectra were taken with a Varian A-60 spectrometer on 10% (w./v.) solutions of the samples in carbon disulfide, containing tetramethylsilane as an internal standard at 60 Mc. p. s., and at room temperature. The chemical shifts are expressed as p. p. m. from tetramethylsilane.

All samples were synthesized according to the known procedures[2] and purified by vacuum distillation under a nitrogen atmosphere (6,6-dimethylfulvene, 6-ethyl-6-methylfulvene, 6,6-pentamethylenefulvene) or by recrystallization (6,6-diphenylfulvene, 1,2,3,4-tetraphenylfulvene).

## Results and Discussion

**The Analysis of the NMR Spectrum of 6,6-Diphenylfulvene.**—The protons in the five-membered ring of 6,6-diphenylfulvene appear as a perfectly symmetrical twenty-line AA'BB' type[10-13] spectrum with chemical shifts of $\delta_A=\delta_{A'}=6.390$ and $\delta_B=\delta_{B'}=6.105$ p. p. m. The spectrum calculated from the magnetic parameters $\delta_A-\delta_B=0.285$ p. p. m., $J_{AB}=5.3_7$, $J_{AB'}=1.5_2$, $J_{AA'}=2.0_0$ and $J_{BB'}=2.2_8$ c. p. s., is in quite good agreement with the observed spectrum, as can be seen from Table I and Fig. 1.

TABLE I. A COMPARISON OF THE CALCULATED AND OBSERVED SPECTRA OF 6,6-DIPHENYLFULVENE

| Line | Energy,[a] c. p. s. | | Intensity[b] | |
|---|---|---|---|---|
| | Calcd. | Obs. | Calcd. | Obs. |
| 8 | $4.3_1$ | $4.4_5$ | $0.2_3$ | $0.2_9$ |
| 4 | $5.4_1$ | $5.7_9$ | $1.4_9$ | $2.5_7$ |
| 3 | $5.7_9$ | | $1.3_7$ | |
| 11 | $6.7_1$ | $6.7_0$ | $0.5_6$ | $1.2_2$ |
| 12 | $6.9_9$ | $6.9_9$ | $0.6_5$ | |
| 7 | $8.6_7$ | $8.7_3$ | $0.8_1$ | $0.8_6$ |
| 6 | $9.8_0$ | $9.9_2$ | $0.7_3$ | $0.7_9$ |
| 9 | $10.5_7$ | $10.8_5$ | $0.4_3$ | $0.7_9$ |
| 10 | $10.8_5$ | | $0.3_5$ | |
| 2 | $12.2_1$ | $12.2_8$ | $0.6_7$ | $1.3_7$ |
| 1 | $12.6_8$ | $12.6_8$ | $0.6_3$ | |
| 5 | $14.1_7$ | $14.2_1$ | $0.0_5$ | $0.0_9$ |

a) Relative to the band center.
b) Normalized to the same total intensity as the calculated values.

*1 Presented at the 3rd Symposium on the Nuclear Magnetic Resonance, Osaka, November 11, 1963.
*2 Present address: Department of Chemistry, Faculty of Science, Tohoku University, Sendai, Japan.

1) J. Thiele, *Ber.*, 33, 666 (1900).
2) J. H. Day, *Chem. Revs.*, 53, 167 (1953).
3) J. W. Cook, "Progress in Organic Chemistry," Vol. III, Butterworth Scientific Publications, London (1955), p. 81.
4) G. A. Schönberg, W. v. Philipsborn, L. M. Jackman and H. Schmidt, *Helv. Chim. Acta*, 45, 1406 (1962).
5) M. Neuenschwander, D. Meuche and H. Schaltegger, ibid., 46, 1760 (1963).
6) R. E. Bozak and K. L. Rinehart, Jr., *J. Am. Chem. Soc.*, 84, 1589 (1962).
7) M. Neuenschwander, D. Meuche and H. Schaltegger, *Helv. Chim. Acta*, 47, 1022 (1964).
8) D. Meuche, M. Neuenschwander, H. Schaltegger and H. U. Schlunegger, ibid., 47, 1211 (1964).
9) W. B. Smith and B. A. Shoulders (*J. Am. Chem. Soc.*, 86, 3118 (1964)) reported the analysis of the NMR spectra of 6,6-dimethylfulvene, 6,6-dibenzylfulvene and 6,6-diphenylfulvene; the charge density of the fulvene ring was also discussed briefly. Their results agree essentially with ours described in this paper.
10) J. A. Pople, W. G. Schneider and H. J. Bernstein, "High Resolution Nuclear Magnetic Resonance," McGraw-Hill, New York (1959), p. 142.
11) J. A. Pople, W. G. Schneider and H. J. Bernstein, *Can. J. Chem.*, 35, 1060 (1957).
12) J. A. Martin and B. P. Dailey, *J. Chem. Phys.*, 37, 3594 (1963).
13) D. M. Grant, R. C. Hirst and H. S. Gutowsky, ibid., 38, 470 (1963).

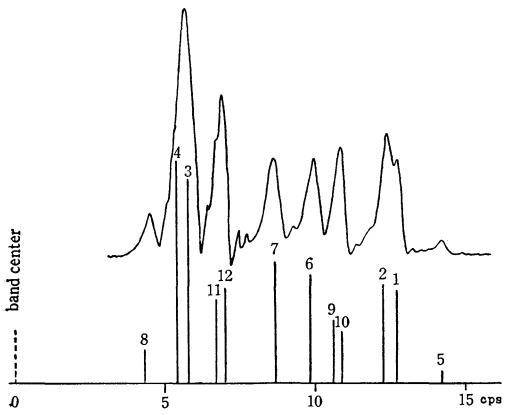
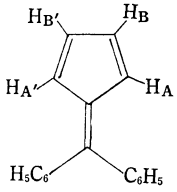



Fig. 1. The observed and calculated spectra of the ring proton of 6,6-diphenylfulvene (upfield portion).




**The Electron Density of Fulvene.**—The signals of the ring protons in 6,6-dimethylfulvene (6.27 p. p. m.), 6-ethyl-6-methylfulvene (6.28 p. p. m.), and 6,6-pentamethylenefulvene (6.31 p. p. m.) are different from those of 6,6-diphenylfulvene, and they are shifted to higher fields where they appear as singlets at almost the same position in each case. The proton at the 6-position of 1,2,3,4-tetraphenylfulvene appears as a singlet at 5.90 p. p. m. The signals arising from the fulvene ring protons show a shift from the olefinic protons of cyclopentadiene, (6.35 p. p. m.), while the 6-proton shows a shift from the olefinic protons of the methylenecycloalkanes [4.68±0.15 p. p. m.[14]]; these shifts are regarded as being due to the increased charge density on the fulvene nucleus and were calculated according to Schneider's equation.[15,16] In the case of the phenyl derivatives, Pople's simple dipole approximation[17] was used to calculate the effect of the diamagnetic shift caused by the ring current of the phenyl group. These diamagnetic shifts of the protons at the 1- or 4-position and at the 2- or 3-position in the 6,6-diphenylfulvene are 0.91 p. p.m. and 0.21 p. p.m. respectively. The shift of the proton at the 6-position of the 1,2,3,4-tetraphenylfulvene is 0.93 p. p. m. However, in the above calculations, the entire molecule was assumed to be coplanar, and the ring current of the fulvene ring was assumed to be small and was neglected. The validity of this assumption about the ring current effect of the fulvene ring was revealed by the theoretical calculations of the LCAO MO method (vide infra). The charge densities obtained were compared with the theoretical values calculated by the MO method and are shown in Table II.

It is clear from Table II that the charge densities obtained from the chemical shifts are in good agreement with those calculated by the MO method. In the case of the diphenylfulvene, however, the observed charge densities are rather high. If the non-planarity of the phenyl groups is allowed for, better results would be obtained. Charge migration from the phenyl group is thought to be responsible for the larger charge density at $C_{(1)}$ than at $C_{(2)}$.

Table II. Electron densities ($\rho$) of fulvene

| | $\rho$ Derived from $\delta_H$ | | | | | $\rho$ Calcd. | |
|---|---|---|---|---|---|---|---|
| | a) | b) | c) | d) | e) | Berthier[f] | Nakajima Katagiri[g] |
| $C_{(1)}$ | 1.009 | 1.008 | 1.005 | 1.083 | | 1.017 | 1.019 |
| $C_{(2)}$ | 1.009 | 1.008 | 1.005 | 1.043 | | 1.016 | 1.018 |
| $C_{(5)}$ | | | | | | 1.038 | 1.016 |
| $C_{(6)}$ | | | | | 0.974 | 0.897 | 0.916 |

a) 6,6-Dimethylfulvene
b) 6-Ethyl-6-methylfulvene
c) 6,6-Pentamethylenefulvene
d) 6,6-Diphenylfulvene
e) 1,2,3,4-Tetraphenylfulvene
f) G. Berthier, *J. chim. phys.*, **50**, 344 (1953).
g) T. Nakajima and S. Katagiri, This Bulletin, **35**, 910 (1962).

14) N. S. Bhacca, L. F. Johnson and J. N. Shoolery, "NMR Spectra Catalog," Vol. 1, No. 109, 132, 180, Varian Associates, Palo Alto, California (1962).
15) H. Spiesecke and W. G. Schneider, *Tetrahedron Letters*, 468 (1961).
16) T. Scheaffer and W. G. Schneider, *Can. J. Chem.*, **41**, 996 (1963).
17) J. A. Pople, *Mol. Phys.*, **1**, 176 (1958); *J. Chem. Phys.*, **24**, 1111 (1956).

TABLE III. RING CURRENT SHIELDING IN FULVENE

| $k$ | Relative to benzene[a] | | | Calculated shielding constants (p. p. m.)[b] | | |
|---|---|---|---|---|---|---|
| | $\bar{\sigma}_{F(1)}/\bar{\sigma}_B$ | $\bar{\sigma}_{F(2)}/\bar{\sigma}_B$ | $\bar{\sigma}_{F(6)}/\bar{\sigma}_B$ | $\bar{\sigma}_{F(1)}$ | $\bar{\sigma}_{F(2)}$ | $\bar{\sigma}_{F(6)}$ |
| 1.0 | 0.118 | 0.116 | 0.041 | 0.206 | 0.202 | 0.072 |
| 0.8 | 0.047 | 0.046 | 0.016 | 0.082 | 0.081 | 0.028 |
| 0.6 | 0.011 | 0.010 | 0.004 | 0.020 | 0.019 | 0.007 |

a) $\bar{\sigma}_B$ and $\bar{\sigma}_F$ are the shielding constants for benzene and fulvene respectively. The position of each proton in fulvene is shown in parentheses.
b) Based on an experimental estimate of 1.75 p. p. m. for the ring current shift in benzene.[20]

**The Ring Current Effect in Fulvene.** — The ring current effect of the fulvene ring was not considered in the previous calculations of the charge density. It is important, however, to decide whether the ring current effect, which depends on the aromaticity of fulvene, can, in fact, be neglected. The chemical shift of each proton in fulvene was calculated by the use of the LCAO MO theory of McWeeny.[18] In this case, electron diffraction data[19] for dimethylfulvene were used to obtain the following dimensions for the fulvene nucleus; $C_{(1)}—C_{(2)}=C_{(3)}—C_{(4)}=C_{(5)}—C_{(6)}=1.382$ Å, $C_{(1)}—C_{(5)}=C_{(4)}—C_{(5)}=C_{(2)}—C_{(3)}=1.496$ Å, $\angle C_{(1)}C_{(2)}C_{(3)}=109°$, $\angle C_{(5)}C_{(1)}C_{(2)}=107°46'$, and $\angle C_{(1)}C_{(5)}C_{(4)}=106°20'$. The fulvene nucleus in diphenylfulvene is non-benzenoid; therefore, one needs to allow for bond alternation by using the bond-alternation parameters $k=\beta_{single}/\beta_{double}$ (no magnetic field) of 1.0, 0.8 and 0.6 respectively. The results are shown in Table III.

The theoretical ratio, $\bar{\sigma}_F/\bar{\sigma}_B$, when $k=1$, is about 0.1; when $k=0.6$, it decreases to a very small value. The chemical shift of each proton in fulvene was calculated by using the estimated ring current shift of benzene. Nakajima and Katagiri[21] have proposed $k=0.57$ as a reasonable value for fulvene. Therefore, as can be seen from Table III, the chemical shift induced by the $\pi$-electron ring current in fulvene is very small and can be neglected. Although the difference is small, the chemical shift of the $C_{(1)}$ proton is larger than that of the $C_{(2)}$ proton. However, the opposite might be expected from a consideration of the charge densities. The fact that the ring protons in 6, 6-dialkylfulvene appear as a singlet may be ascribed to the above opposing effects.

The calculations were made on a NEAC-2230 computer at the Tohoku University Computing Center. Some of the NMR spectra were measured at the Research Institute of the Shionogi Pharmaceutical Company, to which company we express our gratitude.

*The Chemical Research Institute of Non-Aqueous Solutions*
*Tohoku University*
*Katahira-cho, Sendai (Y. K., I. M. & K. S.)*

*Department of Chemistry*
*Faculty of Science*
*Tohoku University*
*Katahira-cho, Sendai (S. K. & H. A.)*

18) I. J. Maddox and R. McWeeny, *J. Chem. Phys.*, **36**, 2353 (1962).
19) M. Rouault and Z. L. Waziutynska, *Acta Cryst.*, **10**, 804 (1957).
20) Ref. 7, p. 182.
21) T. Nakajima and S. Katagiri, *Mol. Phys.*, **7**, 149 (1963).

# Ultraviolet and Visible Absorption Spectra of the Solid States of Aromatic Amine Complexes with Iodine*

By Hideaki KUSAKAWA and Shun-ichiro NISHIZAKI

(Received September 21, 1964)

It is well known that, from the interaction with an iodine molecule, a molecule of an amine forms a charge transfer complex which possesses optical absorption bands in addition to those observed for either component alone. Although many papers have been published on amine-iodine complexes in solution,[1-5] there have been few works on the electronic spectra of amine-iodine complexes in the solid state.

Blomgren and Kommandeur[6] reported that aromatic hydrocarbons become positive ions in aromatic hydrocarbon - antimony pentachloride complexes. If an aromatic amine - iodine complex is a strong charge transfer complex, its ground state is a dative state ($D^+ \cdot A^-$). It has been observed by numerous investigators that the spectrum of the aniline ions is very similar to that of benzene. Recently, Gallagher[7] has shown that the spectra of three mono-protonated isomeric phenylenediamine ions resemble that of aniline, and that the spectra of their divalent ions are similar to that of benzene. Their contention is that the addition of a proton to the lone electron pair on the nitrogen atom quenches the original effect of the amino groups upon the absorption spectrum. As an n-electron of nitrogen atom goes into the $\sigma_u(5P_z)$ antibonding molecular orbit of iodine, it is interesting to see how the electronic state in the aromatic amine changes. We have measured the ultraviolet and visible absorption spectra of the iodine complexes of five aromatic amines: aniline (ANI), *p*-phenylenediamine (*p*-PDA), 1,5-naphthylenediamine (NDA), benzidine (BEN), *o*-tolidine (TOL) and *p,p'*-diaminodiphenylmethane (APM). The spectra of the solid states were measured by means of the KBr disk method.

## Experimental

**Materials.**—The ANI-iodine complex does not precipitate from a non-polar solvent, so this complex was obtained by mixing ANI and iodine at a iodine/ANI mole ratio of 0.50 and 1.00. When the two components are blended, the temperature of the mixture was raised because of the heat of the complex formation. As the mixture is cooled, it becomes a solid which is apparently crystalline. These specimens were used as ANI-iodine complex systems. APM-iodine systems were also prepared in a similar way, and their iodine contents were varied from 0.75 to 1.50.[8]

The preparations of *p*-PDA, NDA, BEN and TOL complexes have been described in previous papers.[8,9]

**The Ultraviolet and Visible Spectra in the Solid State.**—The ultraviolet and visible spectra of these solid complexes were measured by means of the KBr disk method or with a squashed powder between quartz plates in the 222—2000 m$\mu$ wavelength region. The spectra were measured by using a Shimadzu SV50A recording spectrophotometer.

## Results and Discussion

**A. The Ultraviolet Spectra of ANI Complexes and Other Similar Compounds.** — The ultraviolet spectra of ANI hydrochloride and ANI-iodine systems are shown in Fig. 1. The spectrum of the ANI-iodine complex has an extra maximum at 370 m$\mu$ which can not be found in the absorption spectra of either component alone. It seems that this extra band is a charge transfer band. It has been reported that the absorption spectrum of a mixture of ANI and iodine in a chloroform solution has a characteristic charge transfer band at 349 m$\mu$.[5] It seems reasonable to presume that the 349 m$\mu$ band in solution is shifted to 370 m$\mu$ in a solid.

By putting the observed energy of the charge transfer transition of the ANI-iodine complex, $hc/\lambda_{CT}$ ($\lambda_{CT}$=374 m$\mu$), into the following equation,[10] the ionization potential, $I_D$, of ANI is estimated to be 7.9 eV.:

* A part of this paper has been published in *J. Chem. Soc. Japan, Pure Chem. Sec.* (*Nippon Kagaku Zasshi*), **85**, 241 (1964).

1) C. Reid and R. S. Mulliken, *J. Am. Chem. Soc.*, **76**, 3869 (1954).
2) H. Yada, J. Tanaka and S. Nagakura, This Bulletin, **33**, 1660 (1960).
3) H. Tsubomura, *J. Am. Chem. Soc.*, **82**, 40 (1960).
4) D. N. Stamires and D. C. Mukherjee, ibid., **85**, 2557 (1963).
5) A. K. Chandra and D. C. Mukherjee, *Trans. Faraday Soc.*, **60**, 62 (1964).
6) G. E. Blomgren and J. Kommandeur, *J. Chem. Phys.*, **35**, 1636 (1962).
7) P. K. Gallagher, *J. Phys. Chem.*, **68**, 807 (1963).
8) H. Kusakawa and S. Nishizaki, This Bulletin **38**, 313 (1965).
9) S. Nishizaki and H. Kusakawa, ibid., **36**, 1681 (1963).
10) G. Briegleb and J. Czekalla, *Angew. Chem.*, **72**, 401 (1960).

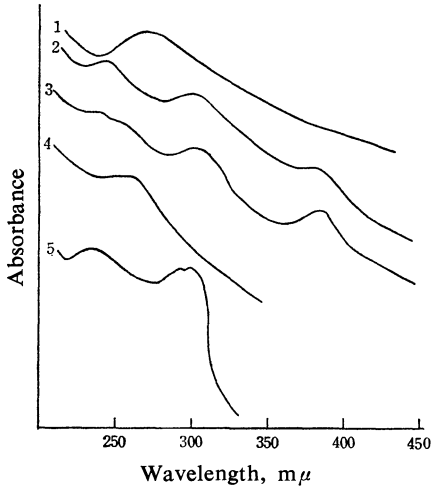



Fig. 1. Ultraviolet spectra of ANI complexes, other similar compounds and iodine in KBr disk.
1 Iodine 2 ANI-$I_2$ (1 : 0.50)
3 ANI-$I_2$ (1 : 100) 4 $C_6H_5NH_3^+Cl^-$
5 ANI (liquid membrane between quartz plates)

$$hc/\lambda_{CT}=I_D-C_1+C_2/(I_D-C_1) \qquad (1)$$

This value is in agreement with the findings of Briegleb and Czekalla,[11] but slightly larger than that of Watanabe's[12] determination with photoionization. In Eq. 1, $C_1$ and $C_2$ are constants; they are 5.20 and 1.5 eV. respectively for iodine complexes.

The 1 : 1 ANI-iodine complex possesses another new absorption band at 255 mμ, which coincides with the position of an absorption band of ANI hydrochloride. Considering this, in the 1 : 1 ANI-iodine complex one part of ANI must be in an electronic state, like the anilinium ion. The following equilibrium may represent standing in a solid state as well as in solution:

$$C_6H_5NH_2\cdot I_2 \rightleftarrows C_6H_5NH_2^+\cdot I_2^- \qquad (2)$$

The lone electron pair of the nitrogen atom is localized on the iodine molecule, and the $n$-$\pi$ resonance within the ANI molecule disappears; therefore, it is reasonable to presume that one part of ANI in the iodine complex shows an absorption spectrum like that of benzene.

**B. The Ultraviolet and Visible Spectra of Aromatic Diamine - Iodine Complexes.** — The ultraviolet spectra of amine crystals and the spectra of iodine complexes are shown in Fig. 2 and Fig. 3 respectively. The wavelength of the spectral maxima of aromatic diamine complexes with iodine in the solid state and other similar compounds are summarized in Tables I to V.

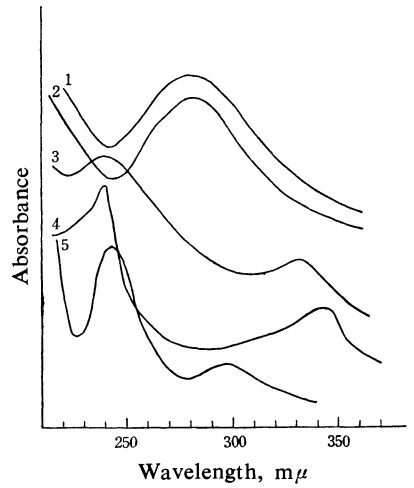



Fig. 2. Ultraviolet spectra of aromatic diamines in KBr disk.
1 BEN, 2 TOL, 3 $p$-PDA, 4 NDA, 5 APM

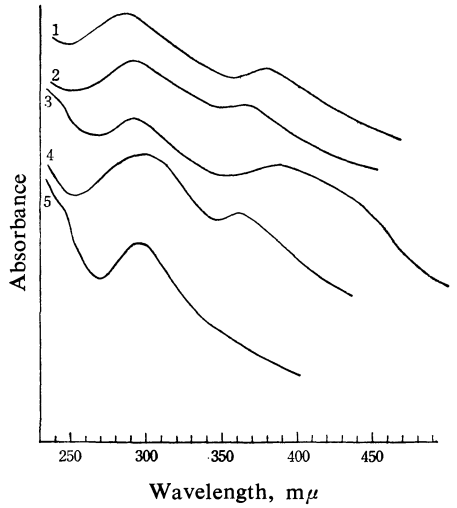



Fig. 3. Ultraviolet spectra of iodine complexes.
1 BEN, 2 TOL, 3 NDA, 4 $p$-PDA, 5 APM

It can be seen from these tables that, in the absorption spectrum of the 0.1 N hydrochloric acid solution, each aromatic diamine, including $p$-PDA,[7] has an absorption band which coincides with that of the aromatic hydrocarbon corresponding to its aromatic skeleton. Judging from those facts, it can be deduced that the spectrum of each mono-protonated diamine is similar to that of the mono-amino substituted derivative of the aromatic hydrocarbons.

In the iodine complexes of $p$-PDA and NDA, the positions of the absorption bands maxima change from 303 mμ to 285 mμ, and from 342 mμ to 296 mμ. From a comparison of these wave-

11) G. Briegleb and J. Czekalla, *Z. Elektro. Chem.*, **63**, 6 (1959).
12) K. Watanabe, *J. Chem. Phys.*, **26**, 542 (1957).

TABLE I. ABSORPTION MAXIMA $\lambda_{max}$ OF *p*-PDA, ITS COMPLEX AND OTHER COMPOUNDS (mμ)

| *p*-PDA | ANI | *p*-PDA in 0.1 N HCl | $C_6H_6$** | Iodine complexes $I_2$/*p*-PDA (mole ratio) | | | | | |
|---|---|---|---|---|---|---|---|---|---|
| | | | | 0.45 | 0.67 | 0.82 | 1.03 | 1.36 | 1.62 |
| 243 | 231 | 255 | 255 | | | | | (237)* | (234) |
| 303 | 294 | | | 283 | 283 | 283 | 288 | 284 | 282 |
| | | | | 350 | 354 | 350 | 348 | 350 | 350 |
| | | | | | | | | 394 | |
| | | | | 830 | 780 | 720 | 750 | 730 | 750 |

* Brackets represent shoulders.
** Quoted from "Organic Electronic Spectral Data," Vol. II, Ed. by H. E. Ungnade, Interscience Publishers Inc., New York (1960).

TABLE II. ABSORPTION MAXIMA $\lambda_{max}$ OF NDA, ITS COMPLEX AND OTHER COMPOUNDS (mμ)

| NDA | α-Naphthyl-amine | NDA in 0.1 N HCl | $C_{10}H_{10}$** | Iodine complexes $I_2$/NDA (mole ratio) | | | |
|---|---|---|---|---|---|---|---|
| | | | | 0.70 | 0.86 | 0.90 | 1.01 |
| 237 | 236 | 221 | 221 | | | | |
| 342 | 303 | 268 | 265 | 300 | 296 | 294 | 292 |
| | | 277 | 275 | | | | |
| | | 286 | 286 | | | | |
| | | | | (370) | (370) | (370) | (370) |
| | | | | 700 | 700 | 700 | 700 |

TABLE III. ABSORPTION MAXIMA $\lambda_{max}$ OF BEN, ITS COMPLEX AND OTHER COMPOUNDS (mμ)

| BEN | *p*-Phenylaniline | BEN in 0.1 N HCl | $C_6H_5 \cdot C_6H_5$** | Iodine complexes $I_2$/BEN (mole ratio) | | | |
|---|---|---|---|---|---|---|---|
| | | | | 0.78 | 0.94 | 1.26 | 1.49 |
| 281 | 278 | 248 | 248 | 294 | 293 | 294 | 292 |
| | | | | 390 | 380 | 379 | 375 |
| | | | | 620 | 610 | 600 | 630 |
| | | | | 1620 | 1650 | 1500 | 1500 |

TABLE IV. ABSORPTION MAXIMA $\lambda_{max}$ OF TOL, ITS COMPLEX AND OTHER COMPOUNDS (mμ)

| TOL | TOL in 0.1 N HCl | Iodine complexes $I_2$/TOL (mole ratio) | | | |
|---|---|---|---|---|---|
| | | 0.94 | 1.02 | 1.29 | 1.53 |
| 283 | 250 | 300 | 298 | 296 | 294 |
| | | 368 | 366 | 358 | 366 |
| | | (470) | (470) | (470) | (470) |
| | | 640 | 640 | 640 | 640 |
| | | (900) | (900) | (900) | (900) |
| | | 1400 | 1400 | 1400 | 1400 |

TABLE V. ABSORPTION MAXIMA $\lambda_{max}$ OF APM, ITS COMPLEX AND OTHER COMPOUNDS (mμ)

| APM | $C_6H_5CH_2C_6H_5$** | APM in 0.1 N HCl | Iodine complexes $I_2$/APM (mole ratio) | | | |
|---|---|---|---|---|---|---|
| | | | 0.75 | 1.00 | 1.25 | 1.50 |
| 246 | | | (255) | (255) | (255) | (255) |
| 299 | 254 | 254 | 299 | 299 | 301 | 301 |
| | 256 | | | | | |
| | 260 | 261 | | | | |
| | 263 | 265 | | | | |
| | 269 | 270 | | | | |
| | | | 384 | 384 | 392 | 386 |
| | | | (450) | (450) | (450) | (450) |
| | | | 585 | 580 | 580 | 580 |

lengths, 285 mμ and 296 mμ, with those of the absorption bands of aniline and α-naphthylamine, it can be presumed that *p*-PDA and NDA become mono-positive ions in solid iodine complexes. The ground states of *p*-PDA-iodine and NDA-iodine complexes are dative states:

$$p\text{-PDA}^+\cdot I_2^- \quad \text{and} \quad \text{NDA}^+\cdot I_2^- \qquad (3)$$

In *p*-PDA-iodine and NDA-iodine complexes, an iodine molecule exists in the visinity of an amino group and localizes the lone electron pair of the nitrogen atom as in the ANI-iodine complex.

On the other hand, in the case of the BEN-iodine complex, a bathochromic shift is found. The maximum of the absorption band at 281 mμ shifts to 294 mμ. Of course, it does not correspond to that of *p*-phenylaniline[13] at 278 mμ. A similar phenomenon is found on the TOL-iodine complex, where the band maximum at 283 mμ shifts to 298 mμ. At the present time we can not explain why the bathochromic shift occurs in the case of a polyphenylene-diamine-iodine complex system.

When APM, a non-conjugated aromatic diamine, is used as the donor, there is no conspicuous change in the ultraviolet spectra of this complex system. The shoulder at 255 mμ probably arises from the reaction of the anilino group with iodine.

Excepting the APM-iodine system, the color of aromatic diamine complexes with iodine is blue at a low iodine content; it becomes black with an increase in the iodine content. As these specimens were dissolved in such polar solvents as alcohols or ketones, the color of the solution was green at first, but it changed brown with the lapse of time.

**C. The Change Transfer Bands of Semiconductive Complexes and the Ionization Potentials of Aromatic Diamines.**—The visible and near infrared absorption bands, which are assumed to be the charge transfer bands of aromatic diamine-iodine complexes, are shown in Fig. 4. In order to estimate the ionization potential of these aromatic diamines, the observed wavelength of the charge transfer band was placed into Eq. 1. However, it was not possible to calculate the ionization potential by this equation because the observed values of the energy of the charge transfer transition are so small that Eq. 1 does not give a real number. Therefore, instead of Eq. 1, the following equation are used[14] to estimate the ionization potential:

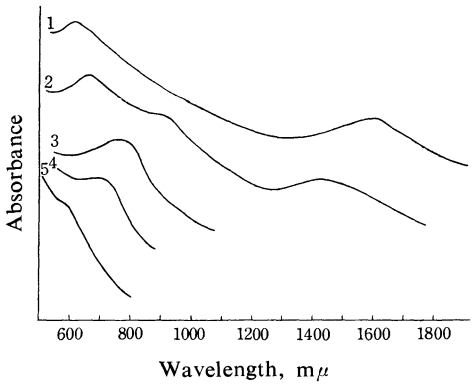



Fig. 4. The spectra of iodine complexes.
1 BEN, 2 TOL, 3 *p*-PDA, 4 NDA, 5 APM

TABLE VI. IONIZATION POTENTIAL ENERGIES ESTIMATED FROM EQS. 4 AND 5 OF AROMATIC AMINES (eV.)

| Donor | From Eq. 4 | From Eq. 5 | Corresponding methyl substituted amine |
|---|---|---|---|
| ANI | 7.9 | 7.9 | 7.2[6] |
| *p*-PDA | 6.1 | 7.2 | 6.7[6] |
| NDA | 6.1 | 7.2 | — |
| BEN | 5.1 | 6.8 | 6.7[7] |
| TOL | 5.2 | 6.8 | — |
| APM | 6.5 | 7.4 | 7.1[6] |

$$hc/\lambda_{CT}=0.87I_D-3.6 \qquad (4)$$

The values obtained are shown in Table VI. In comparison with *N*, *N*, *N'*, *N'*-tetramethyl-*p*-phenylenediamine (TMPD) or *N*, *N*, *N'*, *N'*-tetramethyl-*p*, *p'*-diaminodiphenylmethane,[15] it seems that these values are underestimated. Similar results may be obtained from an emprical linear relation between the ionization potential $I_D$ and the wave number of the charge transfer band, $\tilde{\nu}_{CT}$.[15] Such a relationship have been determined for the complexes of donors of a reliably know ionization potential (namely, 7.9 eV. for ANI[11] and 7.2 eV. for *p*-PDA[11]). This is:

$$I_D=6.5+5.19\times10^{-4}\tilde{\nu}_{CT} \qquad (5)$$

for aromatic amine - iodine complexes in solid states. From measurements of the wave numbers of charge transfer bands of specimens, the ionization potential may be evaluated. The results are quoted in the second column of Table VI. However, Foster and Thomson reported that the *N*, *N*, *N'*, *N'*-tetramethylbenzidine is as strong as TMPD as an electron donor for chloranil.[16]

The results of this investigation imply that

13) E. Sawicki and F. E. Ray, *J. Org. Chem.*, **19**, 1903 (1954).
14) R. S. Mulliken and W. B. Person, *Ann. Rev. Phys. Chem.*, **13**, 107 (1962).
15) R. Foster, *Nature*, **183**, 1253 (1959).
16) R. Foster and T. J. Thomson, *Trans. Faraday Soc.*, **59**, 1059 (1963).

the charge transfer bands of aromatic diamine-iodine complexes, above all, of the polyphenylenediamine-iodine system, unusually appear in the very long wavelength region, and that the order of the energies of the charge transfer transition is in agreement with that of the electrical resistivities of these specimens.[8,9]

## Summary

The ultraviolet and visible spectra of aromatic amine complexes with iodine in the crystalline state have been investigated by means of the KBr disk method or with a squashed powder between quartz plates.

Part of the aniline (ANI) ions in the ANI-iodine system become positive, and the maximum of the spectrum band appears at 255 m$\mu$. *p*-Phenylenediamine (*p*-PDA) and 1,5-naphthylenediamine (NDA) complexes with iodine possess the band maxima at the same position as those of ANI and $\alpha$-naphthylamine. The ground states of these complexes seem to be dative states.

In benzidine (BEN) and *o*-tolidine (TOL) from polyphenylenediamines, and iodine complex systems bathochromic shifts are observed.

By estimating the ionization potential $I_D$ of these aromatic amines from the energies of the charge transfer transition, low values of $I_D$, except for ANI, are obtained.

The electrical resistivities of these specimens are in the order BEN$<$TOL$<$NDA$\approx$*p*-PDA, which is in agreement with that of the energies of the charge transfer transition.

*The Central Research Laboratories*
*Mitsubishi Electric Corporation*
*Amagasaki, Hyogo*

# Studies of the Organic Reactions of Metal Carbonyls. VI.* The Isomerization of Acylcobalt Carbonyls—The Effects of Solvents and of the Structure of the Acyl Group

By Yoshinobu TAKEGAMI, Chikao YOKOKAWA, Yoshihisa WATANABE, Hiromitsu MASADA and Yasukazu OKUDA

(Received September 22, 1964)

The previous works in this laboratory have demonstrated that alkyl- and acylcobalt carbonyls readily isomerize and that this isomerization has a significant effect on the distribution of the products which are given by the reaction of olefin with cobalt hydrocarbonyl.[1,2] Heck and Breslow[3] have also observed that a similar isomerization occurs in the reaction of 1-chlorooctane with sodium cobalt carbonylate. Lately, Wakamatsu[4] has reported that this type of isomerization also occurs in the reduction of acylcobalt carbonyl with synthesis gas under Oxo conditions.

In the present program, the isomerization of acylcobalt carbonyls has been studied in detail by examining the effects of solvent, atmosphere, temperature and the structure of the acyl group on this reaction. The data obtained indicate that the solvents as well as the reaction temperature and the atmosphere have a considerable effect on the isomerization reaction, the rate and the equilibrium, and that the isomerization of $\alpha$-ethylbutyrylcobalt carbonyl to *n*-caproylcobalt carbonyl occurs.

## Experimental

**The Reaction of Acyl Halides with Potassium Cobalt Carbonylate.**—A 100 ml. four-necked flask, fitted with a 50 ml. dropping funnel, a stirrer, and a rubber stopple, was connected with a gas buret and then flushed with carbon monoxide or nitrogen. By the use of a syringe, 50 ml. of 0.09 M cobalt hydrocarbonyl in a toluene solution was put into the flask and then titrated with a 1/2 N ethanol solution of potassium hydroxide in the presence of phenolphthalein. The potassium cobalt carbonylate solution thus obtained was evaporated under a vacuum, and then 50 ml. of various solvents were

* Presented in part at the 17th Annual Meeting of the Chemical Society of Japan, Tokyo, April, 1964. Presented in part at the Symposium of Organometallic Compounds, Osaka, November, 1964.

1) Y. Takegami, C. Yokokawa, Y. Watanabe and Y. Okuda, This Bulletin, 37, 181 (1964).

2) Y. Takegami, C. Yokokawa, Y. Watanabe, H. Masada and Y. Okuda, ibid., 37, 1190 (1964).

3) R. F. Heck and D. S. Breslow, *J. Am. Chem. Soc.*, 85, 2779 (1963).

4) H. Wakamatsu, Abstracts of the 17th Annual Meeting of the Chemical Society of Japan, Tokyo, 1964, p. 151.

added. To the solution of potassium cobalt carbonylate, 4.5 mmol. of acyl halide was added; the mixture was then agitated vigorously for several hours at 0 or 25°C. After a desired reaction time, 30 ml. of a saturated solution of iodine in benzene and 4 ml. of alcohol were stirred into the reaction mixture; the agitation was continued until gas ceased to evolve. By this treatment, acylcobalt carbonyl was converted into the corresponding ester of carboxylic acid.[5] The solution of this ester was concentrated and then gas chromatographed.

**Materials.**—Cobalt hydrocarbonyl was prepared according to the method described in a previous paper.[1] *n*-Butyryl chloride, isobutyryl bromide and *n*-caproyl chloride were obtained commercially. α-Ethylbutyryl chloride was prepared by the chlorination of α-ethylbutyric acid with thionyl chloride.[6] These acyl halides were transformed to the corresponding esters and were proved to be sufficiently pure by gas chromatography. Diethyl ether, ethyl acetate, dioxane, benzene and hexane were dried by the usual methods.

## Results and Discussion

**The Reaction of Butyryl Halides with Potassium Cobalt Carbonylate.** — The results of the reactions of isobutyryl bromide and *n*-butyryl chloride are summarized in Tables I and II respectively. It has been known[1] that the isomerization of butyrylcobalt carbonyls is affected by the reaction conditions (temperature, atmosphere and solvent). In tetrahydrofuran, isobutyrylcobalt carbonyl readily isomerizes to *n*-butyrylcobalt carbonyl, but *n*-butyrylcobalt carbonyl seems to be difficult to isomerize. In isopropyl ether, isobutyrylcobalt carbonyl also isomerizes, but the isomerization proceeds more slowly than in tetrahydrofuran.

In this program, the reactions are carried out in various solvents, such as diethyl ether, ethyl acetate, dioxane, benzene, hexane and some mixtures of two kinds of them, in order to study the effect of the solvent in detail.

All of these reactions were carried out at 25°C, since it is relatively difficult for the isomerization reaction of acylcobalt carbonyl to occur at 0°C.[1] The percentages in the last columns of the tables indicate the degree of the isomerization, the proportion of isomerized iso- or *n*-butyrylcobalt carbonyl.

In diethyl ether under a carbon monoxide atmosphere, isobutyrylcobalt carbonyl isomerized readily to give a large amount of *n*-butyrate (Exps. 1—5). The degrees of the isomerization were 12, 29 and 41% after one

TABLE I. THE REACTION OF ISOBUTYRYL BROMIDE WITH POTASSIUM COBALT CARBONYLATE AT 25°C

| No. | Atmosphere | Solvent* | Time hr. | Yield of esters** [mol./mol. $KCo(CO)_4$] | The degree of isomerization, %*** |
|---|---|---|---|---|---|
| 1 | CO | E | 1 | 0.85 | 12 |
| 2 | CO | E | 3 | 0.86 | 18 |
| 3 | CO | E | 7.5 | 0.93 | 29 |
| 4 | CO | E | 12 | 0.64 | 37 |
| 5 | CO | E | 20 | 0.69 | 41 |
| 6 | $N_2$ | E | 4 | 0.96 | 39 |
| 7 | $N_2$ | E | 10 | 0.48 | 50 |
| 8 | CO | EA | 2 | 0.47 | 13 |
| 9 | CO | EA | 8 | 0.25 | 53 |
| 10 | CO | EA | 14 | 0.49 | 61 |
| 11 | CO | EA | 28 | 0.51 | 69 |
| 12 | CO | D | 1.5 | 0.27 | 77 |
| 13 | CO | D | 2.5 | 0.34 | 100 |
| 14 | CO | B | 3 | 0.31 | 0 |
| 15 | CO | B | 6 | 0.15 | 0 |
| 16 | CO | H | 10.5 | 0.40 | 0 |
| 17 | CO | EA 25+B 25 | 7 | 0.54 | 0 |
| 18 | CO | E 25+B 25 | 5 | 0.76 | 9 |
| 19 | CO | D 40+B 10 | 3.5 | 0.32 | 82 |
| 20 | CO | D 40+B 10 | 10 | 0.25 | 100 |

* E=diethyl ether, EA=ethyl acetate, D=dioxane, B=benzene and H=hexane
EA 25+B 25=a mixed solvent of 25 ml. of ethyl acetate and 25 ml. of benzene
** The reaction products were identified as *n*-propyl *n*-butyrate and *n*-propyl isobutyrate.
*** (*n*-Butyrate/(*n*-Butyrate+Isobutyrate))×100

5) R. F. Heck and D. S. Breslow, *J. Am. Chem. Soc.*, **84**, 2499 (1962).

6) W. H. Miller, A. M. Dessert and G. W. Anderson, ibid., **70**, 502 (1948).

Table II. The reaction of *n*-butyryl chloride with potassium cobalt carbonylate at 25°C

| No. | Atmosphere | Solvent* | Time hr. | Yield of esters** [mol./mol. $KCo(CO)_4$] | The degree of isomerization, %*** |
|---|---|---|---|---|---|
| 21 | CO | E | 2 | 0.58 | 12 |
| 22 | CO | E | 5 | 0.46 | 31 |
| 23 | CO | E | 10 | 0.73 | 41 |
| 24 | CO | E | 15 | 0.65 | 44 |
| 25 | $N_2$ | E | 1.5 | 0.89 | 31 |
| 26 | $N_2$ | E | 4 | 0.73 | 41 |
| 27 | $N_2$ | E | 7 | 0.60 | 44 |
| 28 | $N_2$ | E | 10 | 0.59 | 39 |
| 29 | CO | EA | 2 | 0.54 | 0 |
| 30 | CO | EA | 4 | 0.67 | 0 |
| 31 | CO | EA | 8 | 0.46 | 0 |
| 32 | CO | EA | 14 | 0.52 | 13 |
| 33 | CO | EA | 28 | 0.17 | 17 |
| 34 | CO | D | 9 | 0.13 | 0 |
| 35 | CO | B | 3.5 | 0.36 | 0 |
| 36 | CO | B | 6 | 0.40 | 0 |
| 37 | CO | B | 10 | 0.28 | 0 |
| 38 | CO | H | 10.5 | 0.20 | 0 |

* Abbreviations have the same meanings as in Table I.
** The reaction products were identified as *n*-propyl *n*-butyrate and *n*-propyl isobutyrate.
*** (Isobutyrate/(*n*-Butyrate+Isobutyrate))×100

hour, 7.5 hr. and 20 hr. of reaction time respectively. Thus, the degree of the isomerization increased with an increase in the reaction time. However, with an increase in the reaction time from 12 to 20 hr., the degree of the isomerization increased from 37 to 41% (Exps. 4, 5), suggesting that the velocity of this isomerization is small near this proportion. On the other hand, *n*-butyrylcobalt carbonyl similarly isomerized to give isobutyrate, and the degree of the isomerization increased with an increase in the reaction time (Exps. 21—28); under a carbon monoxide atmosphere, *n*-butyrylcobalt carbonyl gave 12, 31 and 44% of isobutyrate after 2, 5 and 15 hr. of reaction time respectively, but under nitrogen, it gave 31 and 44% of isobutyrate after 1.5 and 7 hr., indicating that the isomerization proceeded faster under nitrogen than under carbon monoxide. Thus, both *n*- and isobutyrylcobalt carbonyls relatively readily isomerized to give an almost equimolar mixture of two isomers. This seems to indicate that there is the following equilibrium between the isomers:

$$\begin{array}{l} \mathrm{C\text{-}C\text{-}C} \\ \quad | \\ \quad \mathrm{COCo(CO)_{3,4}} \end{array} \xrightleftharpoons{\text{in diethyl ether}} \mathrm{C\text{-}C\text{-}C\text{-}COCo(CO)_{3,4}}$$

The equilibrium proportion of two isomers under the conditions used may be about 50 and 50% respectively. The reaction atmosphere had a great effect on the rate of the isomerization, but it seemed to have no effect on the equilibrium.

Similarly, in ethyl acetate the degree of the isomerization increased with a prolonging of the reaction time. Isobutyrylcobalt carbonyl gave 13% of the isomerized product after 2 hr. and about 70% after 28 hr., but *n*-butyrylcobalt carbonyl gave less than 20% of the isomerized product even after 28 hr. This seems to indicate that it is relatively difficult to isomerize *n*-butyrylcobalt carbonyl in this solvent. Thus, in ethyl acetate, the equilibrium proportion of *n*- and isobutyrylcobalt carbonyl seemed to be about 70 and 30% respectively; ethyl acetate evidently removed this equilibrium toward *n*-butyrylcobalt carbonyl more than diethyl ether did. Moreover, in dioxane, isobutyrylcobalt carbonyl easily isomerized (Exps. 15, 16), but *n*-butyrylcobalt carbonyl did not seem to isomerize under the conditions used (Exp. 34), suggesting that this equilibrium is almost completely favorable to *n*-butyrylcobalt carbonyl.

The relation between the reaction time and the proportion of the isobutyrate included in the products is illustrated in Fig. 1. These isomerization curves evidently show that the rate and the equilibrium of the isomerization are remarkably affected by the solvents, as has been described above.

On the other hand, in nonpolar solvents, benzene and hexane, it seemed difficult for the isomerization of both *n*- and isobutyrylcobalt carbonyl to occur (Exps. 12—14, 35—38).

TABLE III. THE REACTION OF α-ETHYLBUTYRYL AND *n*-CAPROYL CHLORIDE WITH POTASSIUM COBALT CARBONYLATE IN DIETHYL ETHER

| No. | Substance | Atmosphere | Temp. °C | Time. hr. | Yield of esters* [mol./mol. $KCo(CO)_4$] | $\frac{n\text{-Ester}\times 100}{\text{Total esters}}$ % |
|---|---|---|---|---|---|---|
| 39 | α-Ethylbutyryl chloride | CO | 0 | 8 | 0.73 | 2 |
| 40 | α-Ethylbutyryl chloride | CO | 25 | 5 | 0.80 | 14 |
| 41 | α-Ethylbutyryl chloride | CO | 25 | 27 | 0.60 | 35 |
| 42 | α-Ethylbutyryl chloride | $N_2$ | 0 | 8 | 0.90 | 2 |
| 43 | α-Ethylbutyryl chloride | $N_2$ | 25 | 3 | 0.75 | 21 |
| 44 | α-Ethylbutyryl chloride | $N_2$ | 25 | 5 | 0.73 | 26 |
| 45 | *n*-Caproyl chloride | CO | 30 | 14 | 0.54 | 58 |

* The reaction products were identified as ethyl α- ethylbutyrate, ethyl α-methylvalerate and *n*-caproate.

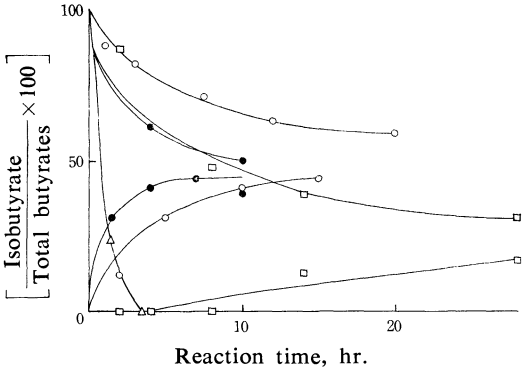



Fig. 1. The proportion of isobutyrate obtained vs. time plots for the reactions of iso- and *n*-butyryl halides with potassium cobalt carbonylate.
- ○ In diethyl ether under carbon monoxide
- ● In diethyl ether under nitrogen
- □ In ethyl acetate under carbon monoxide
- △ In dioxane under carbon monoxide

Potassium cobalt carbonylate relatively readily dissolves in the above-mentioned polar solvents, but it seems difficult for it to dissolve in these nonpolar solvents. However, the expected reaction, the formation of butyrylcobalt carbonyls, was proved to occur even in these solvents.** Thus, the above results with the nonpolar solvents are not due to the insolubility of the potassium cobalt carbonylate in these solvents.

The yields of the expected products, *n*- and isobutyrate, are relatively poor in the reactions in dioxane, benzene and hexane. This may be partly attributed to an instability of intermediates, i. e., *n*- and isobutyrylcobalt carbonyl, in these solvents.

In mixtures of polar and nonpolar solvents, the velocity of the isomerization of isobutyrylcobalt carbonyl was small, as compared with the case using only a polar solvent (Exps. 17—20). Especially in a benzene-dioxane solvent, a relatively small amount of benzene (20%) remarkably decreased the velocity of the isomerization (cf. Exp. 16 and 19).

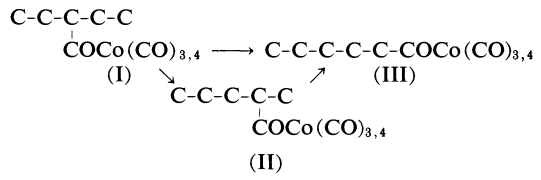
As has been mentioned above, it is evident that solvents have a great effect on the isomerization of butyrylcobalt carbonyls. The reason for these phenomena can not be definitely established, but these effects may be partly attributed to the coordination of solvents with cobalt carbonyl complex, potassium and organocobalt carbonyls. This consideration seems to be supported by the facts that polar solvents have a great effect on the isomerization and that the sodium cobalt carbonylate forms a coordination compound with diethyl ether.[7]

**The Reaction of α-Ethylbutyryl Chloride with Potassium Cobalt Carbonylate.**—The isomerization of α-ethylbutyryl cobalt carbonyl (I) was also investigated. The results of this reaction are summarized in Table III. As is shown in the table, I gave an ester with a straight-chain structure, ethyl *n*-caproate (Exps. 39—44), indicating that I isomerized to *n*-caproylcobalt carbonyl (III); at 0°C, I gave only 2% of the isomerized product after 8 hr. under carbon monoxide and nitrogen atmospheres (Exps. 39, 42), but at 25°C under a carbon monoxide atmosphere, I relatively readily isomerized to give 14 and 35% of the isomerized product after 5 and 27 hr. and, under nitrogen, 21 and 26% after 3 and 5 hr. respectively. Thus, nitrogen atmosphere apparently also accelerated this isomerization. The isomerization of I seemed to proceed more slowly than that of butyrylcobalt carbonyl (cf. Exp. 2, 5 and 40).

As the course of this isomerization, two ways are possible: in the first course, I directly isomerizes to III, while in the second

** In the reactions of butyryl halides with potassium cobalt carbonylate in benzene, butyrylcobalt carbonyls were actually formed, since butyrates were given with the gas evolution when the liquid phase of the reaction mixture was treated with iodine and alcohol. The amount of butyrates increased with an increase in the reaction time, suggesting that insoluble potassium cobalt carbonylate could be transformed into soluble butyrylcobalt carbonyls, even in nonpolar solvents.

7) W. Hieber, O. Vohler and G. Braun, *Z. Naturforsch.*, 13b, 192 (1958).



course I isomerizes to III via $\alpha$-methylvaleryl-cobalt carbonyl (II). In the present case, however, it is impossible to discriminate by gas chromatography between the esters corresponding to I and II. Therefore, it can not be decided which course is taken in this type of isomerization.

The reaction of *n*-caproyl chloride was also carried out in order to check the reverse isomerization from III to I (Exp. 45). The result obtained shows that the isomerization of III to I and/or II occurred. However, it was not decided whether I or II was obtained or whether a mixture of I and II was obtained.

## Summary

The reactions of *n*-butyryl chloride, isobutyryl bromide, $\alpha$-ethylbutyryl chloride and *n*-caproyl chloride with potassium cobalt carbonylate have been studied. The results of this investigation are as follows.

(1) It has been observed that solvents have great effects on the isomerization of butyryl-cobalt carbonyls, as do the reaction temperature and the atmosphere. The rate and the equilibrium of this isomerization are remarkably affected by the solvents; in polar solvents, the equilibrium proportion of products (iso/normal) is almost zero in dioxane, 1/3 in ethyl acetate, and 1 in diethyl ether. This isomerization proceeds more rapidly under nitrogen atmosphere than under carbon monoxide. On the other hand, in nonpolar solvents such as benzene this isomerization apparently does not occur.

(2) $\alpha$-Ethylbutyrylcobalt carbonyl relatively readily isomerizes to *n*-caproylcobalt carbonyl. This isomerization is also accelerated under nitrogen atmosphere.

*Department of Fuel Chemistry*
*Faculty of Engineering*
*Kyoto University*
*Sakyo-ku, Kyoto*

# The Radiolysis of Mono-, Di- and Trimethylamine in the Gas Phase

By Setsuo TAKAMUKU and Hiroshi SAKURAI

(Received September 24, 1964)

The photolysis of methylamine has been extensively studied during the past twenty years.[1-5] Although the mechanism whereby methylamine decomposes is not completely understood, the most recent study[5] has shown that the primary process is the formation of hydrogen atoms; there may also be a small degree of molecular detachment of hydrogen, which is well known in the fields of the vacuum ultraviolet photochemistry and radiation chemistry of hydrocarbons, as well as a dissociation to methyl and amine radicals.

On the other hand, the radiolysis of aliphatic amines in the gas phase has received little attention.[6,7] Hydrogen and *N*, *N'*-tetramethylethylenediamine were observed as the main products in the radiolysis of trimethylamine by Schindler and Krivak.[7] However, much, has been unknown with regard to the primary process.

We, therefore, hoped to clarify the mechanism of the radiolysis of amines and compare the results with those of the photolysis. The present study was undertaken in order to obtain information on the primary process in the radiolysis of methylamines in the gas phase. The methylamines used were mono-, di-, and trimethylamines; the radical scavenger technique was employed to estimate the mechanism of hydrogen formation.

1) W. A. Noyes, Jr., and P. A. Leighton, "The Photochemistry of Gases," Reinhold Publishing Corp., New York (1941), p. 382.
2) C. C. Wetmore and H. A. Taylor, *J. Chem. Phys.*, **12**, 61 (1943).
3) C. I. Johnson and H. A. Taylor, ibid., **19**, 613 (1951).
4) J. S. Watson and B. deB. Darwent, ibid., **20**, 1041 (1952).
5) J. V. Michael and W. A. Noyes, Jr., *J. Am. Chem. Soc.*, **85**, 1228 (1963).
6) J. Collin, *Bull. soc. chim. Belg.*, **67**, 549 (1958).
7) R. N. Schindler and T. G. Krivak "Quarterly Report," Mellon Institute, Radiation Research Laboratories (Jan.—March, 1963), p. 9.

## Experimental

**Materials.** — Methylamine was prepared from hydrochloride which had been purified by recrystallization several times with water and dried in a vacuum desiccator. The hydrochloride was treated with a nearly-saturated solution of potassium hydroxide at atmospheric pressure. The methylamine evolved was dried by passing it through a column of potassium hydroxide and then collected in a trap in liquid nitrogen, attached to a convenient vacuum line. The amine was kept in a storage bulb after trap-to-trap distillation. The infrared analysis of the sample showed that ammonia was not present as an impurity. The preparation of di- and trimethylamine was similar to that of methylamine mentioned above.

Propane was obtained from the Takachiho Chemicals Co., Tokyo, and was purified by treatment with concentrated sulfuric acid in order to remove olefins and by several trap-to-trap distillations.

**Irradiation Procedure.**—$\gamma$-Irradiation was carried out in a 500 ml. cylindrical reaction vessel fitted with graphite-coated electrodes, a guard ring and a breakable seal. This reaction vessel was similar to that described by Back.[8] The vessel was thoroughly baked in a vacuum before each experiment and filled with sample by conventional vacuum techniques. Irradiations were carried out at room temperature with a 1600 curie cobalt-60 source, applying absolute dosimetry.[8] An electric field, up to 2 kV., was applied to the central anode in order to measure the saturation ion current during irradiation. Saturation ion currents were usually measured at the beginning and the end of the irradiation; the time for the measurements was negligible compared to the total time of irradiation. Several runs were also carried out with pure propane in order to compare the results of amines with those of hydrocarbon.

**Analysis.**—After irradiation the reaction vessel was attached to a convenient vacuum line, a breakable seal was broken, and the contents of the cell were transferred to the analytical system, which consisted of the following parts: a mercury cut-off, four liquid nitrogen traps (−196°C), a mercury diffusion pump, and a Toepler pump-gas burette. The non-condensable gas collected contained hydrogen and a small amount of methane, the hydrogen in which was removed by diffusion through a palladium thimble heated at 300°C; the amount of the residual methane was then measured.

Their ion pair yields (M/N) were obtained by relating the product yields to the saturation ion currents measured in the radiolysis

## Results and Discussion

**Saturation Ion Current.**—The ion currents are plotted against the field strength for mono-, di-, and trimethylamine at different pressures in Fig. 1. Good saturation curves were

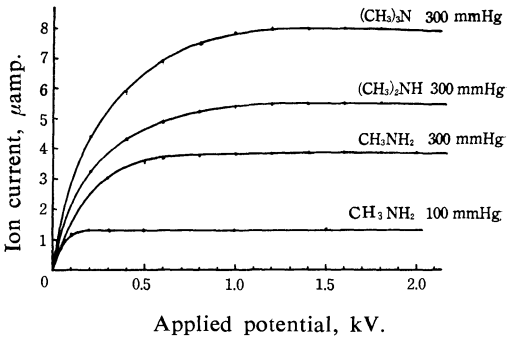



Fig. 1. Ion currents in the $\gamma$-radiolysis of amines.

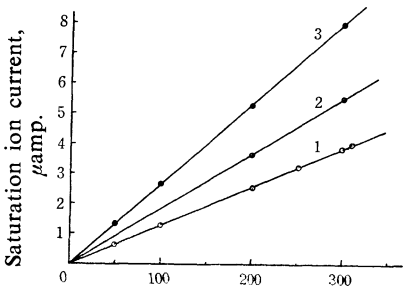



Fig. 2. Saturation ion current as a function of amine pressure.
1: Methylamine, 2: Dimethylamine
3: Trimethylamine

observed with these amines, and the saturation ion currents thus obtained were proportional to the gas pressure, up to 300 mmHg, as is shown in Fig. 2. From these results it is clear that the ions produced by $\gamma$-irradiation were quantitatively collected at the electrode under these experimental conditions and that the saturation ion current were satisfactory for calculating the ion-pair yields of the products. The differences in the saturation ion currents of these amines were due to the difference in their electron densities. After a suitable correction of their electron densities, almost the same saturation ion currents were observed.

**The Radiolysis of Pure Amine.**—The results of the radiolysis of amines at 300 mmHg are shown in Table I. The major volatile products are hydrogen, methane and ammonia. The conversion of amines shown in Table I is based on the yield of hydrogen ($2\times H_2$/amine). Hydrogen was the main product, and the yield was relatively high for methylamine, while it decreased for di- and trimethylamine. On the other hand, the yield of methane was very low for methylamine, and increased about four times for di- and trimethylamine.

On the basis of the mechanism elucidated

8) R. A. Back, T. W. Woodward and K. A. McLauchlan, *Can. J. Chem.*, **40**, 1380 (1962).

TABLE I. γ-RADIOLYSIS OF AMINES AND PROPANE
(Gas pressure, 300 mmHg)

| Compound | $CH_3NH_2$ | $(CH_3)_2NH$ | $(CH_3)_3N$ | $C_3H_8$ |
|---|---|---|---|---|
| Saturation ion current (μamp.) | 3.70 | 5.50 | 7.90 | 6.07 |
| Conversion (%) | 0.09 | 0.14 | 0.13 | 0.08 |
| $(M/N)_{H_2}$ | 3.10 | 2.78 | 1.78 | 1.55 |
| $(M/N)_{CH_4}$ | 0.10 | 0.45 | 0.41 | 0.26 |

for the photolysis of methylamine, the following possible primary dissociations of methylamine may be considered:

$$CH_3NH_2 \xrightarrow{\sim\sim} H + CH_3NH\cdot \quad (1)$$

$$\xrightarrow{\sim\sim} H + \cdot CH_2NH_2 \quad (2)$$

$$\xrightarrow{\sim\sim} \cdot CH_3 + \cdot NH_2 \quad (3)$$

$$\xrightarrow{\sim\sim} CNH_3 + H_2 \quad (4)$$

These primary reactions are followed by the secondary reactions:

$$H + CH_3NH_2 \rightarrow H_2 + CNH_4 \quad (5)$$

$$\cdot CH_3 + CH_3NH_2 \rightarrow CH_4 + CNH_4 \quad (6)$$

$$2\,CNH_4 \rightarrow NH_3 + C_2NH_5 \quad (7)$$

Since methane and ethane formations were very little, reaction 3, which should give methane by secondary reaction 6 and ethane by the recombination of the methyl radicals, seemed to be unimportant. The ammonia formation, therefore, may not be due to the hydrogen abstraction of the $NH_2$ radical produced by reaction 3 but to secondary reaction 7, involving two radicals of the empirical formula $CNH_4$, which was proposed in the photolysis of methylamine.[5]

Hydrogen-forming reactions, for which several mechanisms are possible, must be the principal primary processes. The decision between 1 and 2 must be based on the results with isotopic compounds $CH_3ND_2$ and $CD_3NH_2$, while the processes combining reaction 1 with 2, which are called radical process for hydrogen formation, may be elucidated by a radical scavenger technique, as will be described later. The importance of the amino-hydrogen atom may be pronounced, because the hydrogen yield decreased as the hydrogen atom was replaced with the methyl group, as Table I shows.

Ion-pair yields of hydrogen and methane were measured as a function of the amine pressure, as is shown in Fig. 3. They were independent of the pressure within the range of experimental error, but there was a slight decrease in hydrogen yield at pressures less than 100 mmHg in mono- and trimethylamine. This effect could be due to the wall effect. The neutralization of ions produced by primary processes may occur in the gas phase leading

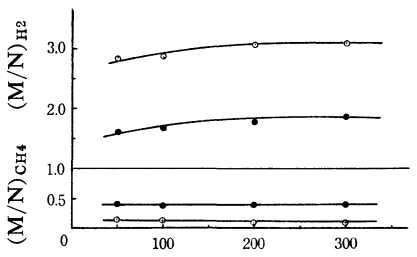



Fig. 3. Ion pair yields of hydrogen and methane as a function of amine pressure.
○ : Methylamine, • : Trimethylamine

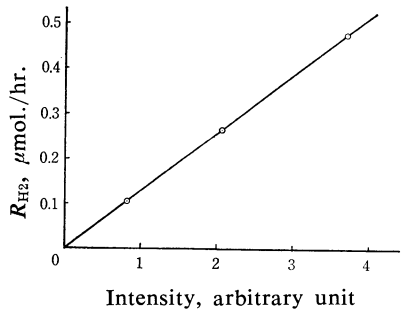



Fig. 4. Hydrogen yields as a function of intensity. (Methylamine 300 mmHg)

to dissociation, or at the surface of the vessel with deactivation. Low pressure should favor the latter and so lower the hydrogen yield.

In Fig. 4, the hydrogen yield is plotted against the irradiation intensity for the radiolysis of methylamine. A linear function was observed. This may be simply interpreted as indicating that the hydrogen atom produced in reactions 1 and 2 reacted with methylamine by reaction 5, and that the back reactions of 1 and 2, and the recombination reaction 8 of the hydrogen atom were not important in these experimental conditions:

$$H + H + M \rightarrow H_2 + M \quad (8)$$

**The Effect of the Radical Scavenger.** — In order to determine the contribution of the

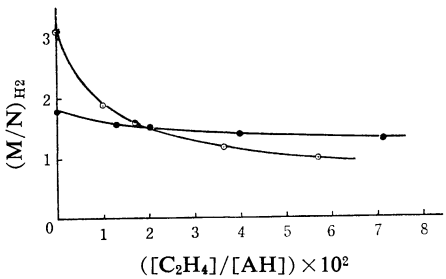



Fig. 5. The effect of added ethylene on the hydrogen yield. (Amine pressure, 300 mmHg)
○ : Methylamine, • : Trimethylamine

radical process to hydrogen formation, a radical scavenger technique, first developed by Back[9] and Hardwick[10] for hydrocarbons, was employed. The presence of a radical scavenger such as ethylene in the radiolysis of amines reduced the hydrogen yield, shown in Fig. 5, by the following reaction:

$$AH \rightsquigarrow H_2 + \text{Residue} \quad (9)$$

$$\rightsquigarrow H + \text{Residue} \quad (10)$$

$$H + AH \rightarrow H_2 + \text{Residue} \quad (11)$$

$$H + C_2H_4 \rightarrow C_2H_5\cdot \quad (12)$$

where AH shows the amine. When AH is methylamine, reaction 9 corresponds to reaction 4; reaction 10, to reactions 1 and/or 2, and reaction 11, to reaction 5. If a steady-state kinetic treatment of hydrogen atom production is made for the amine system with and without ethylene present, the following expression is obtained:

$$\frac{1}{\Delta(M/N)_{H_2}} = \frac{1}{(M/N)_{H_2(10)}} \times \frac{k_{11}[AH]}{k_{12}[C_2H_4]} + \frac{1}{(M/N)_{H_2(10)}} \quad (I)$$

where $\Delta(M/N)_{H_2}$ is the difference in the ion-pair yield of hydrogen, without and with ethylene, and $(M/N)_{H_2(10)}$ is the ion-pair yield of hydrogen by reaction 10. In Fig. 6, the values of the left-hand side of Eq. I are plotted against $[AH]/[C_2H_4]$. From these straight lines, $(M/N)_{H_2(10)}$ and $k_{11}/k_{12}$ were calculated; they are summarized in Table II.

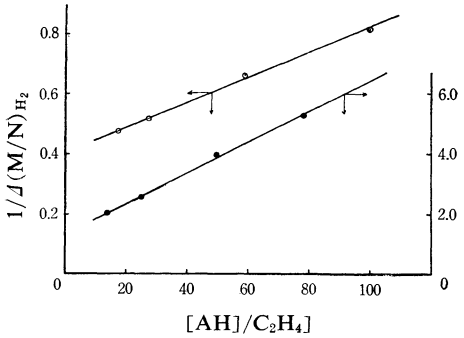



Fig. 6. Kinetic plot of the data from experiments with added ethylene.
○: Methylamine, •: Trimethylamine

TABLE II. HYDROGEN YIELD BY RADICAL PROCESS AND $k_{11}/k_{12}$

| Compound | $CH_3NH_2$ | $(CH_3)_3N$ | $C_3H_8$ |
|---|---|---|---|
| $(M/N)_{H_2(10)}$ | 2.50 | 0.73 | 1.12 |
| Radical (%) | 81 | 41 | 72 (75)[9] |
| Molecular (%) | 19 | 59 | 28 (25)[9] |
| $(k_{11}/k_{12}) \times 10^2$ | 1.05 | 3.56 | 0.13 |

9) R. A. Back, *J. Phys. Chem.*, **64**, 124 (1960).
10) T. J. Hardwick, ibid., **65**, 101 (1961).

These results showed that 81% of the hydrogen produced in the radiolysis of methylamine was scavengable by ethylene, indicating that the non-radical process (19%) were more important than in the photolysis. The hydrogen formed by the latter process was estimated to be less than 10% in the photolysis of methylamine, although the kinetic treatment was not carried out.[5] In the case of trimethylamine, which has no amino-hydrogen atoms, the radical process (41%) became inferior to the non-radical process. Reaction 1. therefore, seemed to be very important for the thermal hydrogen atom formation in the radiolysis, as was pointed out by Michael and Noyes[5] in the photolysis of methylamine. However, it is hoped that, by experiments with the isotopic compounds $CH_3ND_2$ and $CD_3NH_2$, it will be possible to clarify these primary processes with more certainty. At this stage of experiment, it can not be decided whether the non-radical process is a molecular process or a process involving hot hydrogen atoms.

Relatively high $k_{11}/k_{12}$ values were observed with these amines compared with that of propane, showing that the rate of the abstraction of the hydrogen atom from the amine may be estimated to be faster than that from propane.

## Summary

The $\gamma$-radiolysis of methylamines in the gas phase has been investigated, applying the absolute dosimetry involving the measurement of saturation ion currents in the gases during irradiation. The major volatile products are hydrogen, methane and ammonia. Ion-pair yields of hydrogen for mono-, di- and trimethylamine are 3.10, 2.78 and 1.78 respectively. Those of methane are 0.10, 0.45 and 0.41 respectively. The yields of hydrogen and methane are independent of the pressure up to 300 mmHg, but at pressures less than 100 mmHg there are slight decreases in hydrogen yields. The rate of hydrogen formation from methylamine is proportional to the radiation intensity, and the yield decreases in the presence of a small amount of ethylene. By kinetic analyses of the results with an added scavenger, it has been observed that 81% of the hydrogen formed from methylamine is caused by a radical process, while the value is 41% for trimethylamine.

*The Institute of Scientific and Industrial Research*
*Osaka University*
*Sakai-shi, Osaka*

# A Microcell for Differential Thermal Analysis*

By Satohiro TANAKA

(Received August 31, 1964)

In the differential thermal analysis of materials, it is often necessary to use only a small amount of a sample. When the amount of sample is less than 50 mg. in weight, the following methods have been used: (i) The heating rate has been increased in order to obtain a sharper peak. (ii) The sample has been diluted with a large volume of the reference inert material.[1,2] (iii) The sample has been sandwiched between two layers of the reference inert material.[2] (iv) A melting-point capillary tube has been used as a sample cell.[3]

However, each of these methods has some disadvantages. Method i is defective in the drifting of the peak temperature and base line as the heating rate is increased. Methods ii and iii usually involve a troublesome preparation of the sample, such as the homogeneous mixing of sample and reference material. Moreover, relatively large amounts of the sample, more than 10 mg. in weight are needed. In method iv a thermocouple must be inserted directly into the sample, so that the perfect cleaning of the thermocouple before and after measurement is necessary, and care must be taken to position the thermocouple centrally in the tube.

In this work, in order to carry out the differential thermal analysis (DTA) conveniently using a small amount of a sample, simple microcells were used, and the effects on the DTA peak of the amount of sample, the heating rate, the heat capacity of the cell, and the heat transfer coefficient between the cell and the metal block were investigated. The present study has been confined to the melting of benzoic acid.

## Experimental

**Benzoic Acid.** — Benzoic acid, as a standard sample for combustion calorimetry, was obtained from the Resources Research Institute, Japan, and was used without further purification.

**Microcells.**—The microcell body was a 3 mm.$\phi$× 9 mm. platinum rod with two holes, 2 mm.$\phi$×3mm. and 2 mm.$\phi$×5 mm., on the top and the bottom of the body respectively. The top hole was used as a sample hole, and the bottom hole, as a thermocouple hole. The caps, obtained from the Ishifuku Metal Co., were also made of platinum. The microcell body and the cap are shown in Fig. 1.

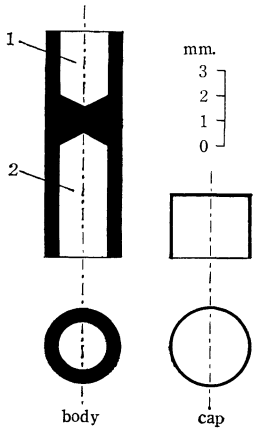



Fig. 1. Microcell.
1, Sample hole; 2, Thermocouple hole

**Metal Block.**—The metal block body and the lid, shown in Fig. 2, were made of aluminum. The body was a 27 mm.$\phi$×27 mm. cylinder with three 6 mm.$\phi$×15 mm. holes, and the lid was a 27 mm.$\phi$ ×5 mm. disk. The microcells and the metal block shown in Fig. 2 were so assembled that the microcells were supported only by the thermocouple and were not in contact with the wall of the metal block.

**Apparatus.**—A Rigakudenki Co. Automatic Recording Differential Thermal Analyzer and Adiabatic Calorimeter was used. The differential temperatures were measured by a two-junction alumel-chromel thermocouple 0.3 mm.$\phi$ in diameter.

**Differential Thermal Analysis.**—Samples, about 1—2 mg. in weight, were placed in the sample hole of a microcell and covered with the cap. The microcells were then laid on the junction of the thermocouple, as is shown in Fig. 2, and heated enough to melt the benzoic acid sample once; after the microcells had then cooled to room temperature, measurements were carried out in air. The weights of the samples were measured before and after every measurement; no appreciable weight loss of sample could be found after such measurements. The reference microcell was used without any reference materials.

* Reported at the 17th Annual Meeting of the Chemical Society of Japan, Tokyo, April, 1964.

1) E. M. Barrall and L. B. Rogers, *Anal. Chem.*, **34**, 1106 (1962).
2) A. Yamamoto, *Japan Analyst (Bunsekikagaku)*, **12**, 26 (1963).
3) D. A. Vassallo and J. C. Harden, *Anal. Chem.*, **34**, 132 (1962).

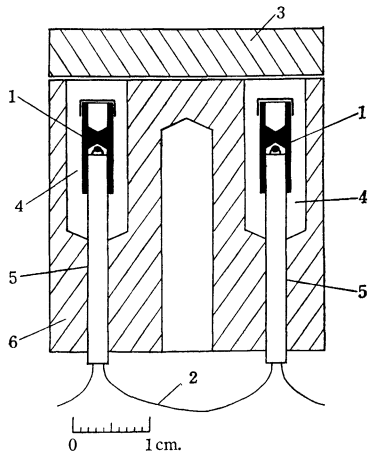



Fig. 2. Metal block and microcell.
1, Microcell
2, Thermocouple lead
3, Lid
4, Hole
5, Insulating tube for thermocouple
6, Metal block

## Results and Discussion

**The Shape of the DTA Curves.**—A typical finding concerning DTA curves for the melting of a benzoic acid sample is shown in Fig. 3. If the amount of sample was less than 1.5 mg. in weight, a normal thermogram (curve a) could be obtained; but when the amount of the sample was more than 1.5 mg. in weight, an abnormal thermogram was obtained (curve b).

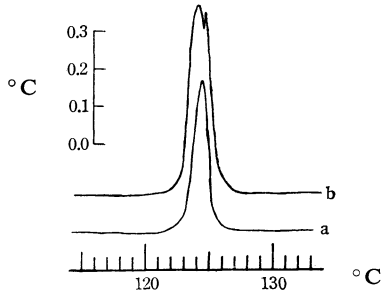



Fig. 3. Differential thermogram of benzoic acid at a heating rate of 1.0°C/min.
a, 1.4 mg. in weight; b, 4.0 mg. in weight

This abnormal curve was probably due to the fact that, as heat is transferred from the bottom to the top of the cylindrical cell, the sample first begins to melt at the bottom; then, a small part of sample stuck on the wall of the cell melts and drops into the molten sample at the bottom.

**Effect of the Sample Amount.**—DTA's were carried out in order to examine the effect of the sample amount on thermograms at a heating rate of 1.0°C/min. As Fig. 4 shows, the peak area is proportional to the sample amount over all the range. However, the peak height is proportional to the sample amount up to 1.5 mg. in weight and is not reproducible above that amount.

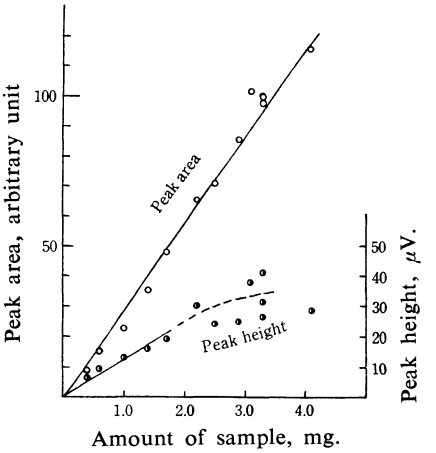



Fig. 4. Effect of sample amount on peak area and peak height at a heating rate of 1.0°C/min.

**Effect of the Heating Rate.**—The effect of the heating rate is shown in Fig. 5 and Fig. 6 using a 1.4 mg. sample. Figure 5 shows that the peak height increases with the heating rate, while the peak area is almost constant with the heating rate. Figure 6 shows that the peak beginning temperature, which is defined on the thermogram as the intersection point of the extrapolated straight-line portion of the low temperature side of the peak and the base line, and the peak temperature, which

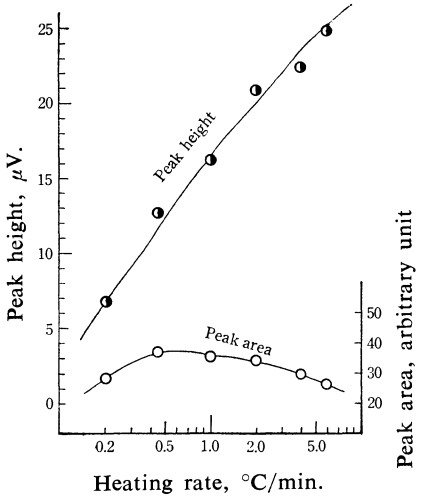



Fig. 5. Effect of heating rate on peak area and peak height using a 1.4 mg. sample.

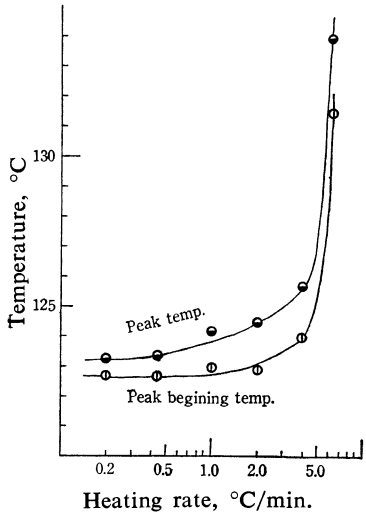



Fig. 6. Effect of heating rate on peak beginning temperature and peak temperature using a 1.4 mg. sample.

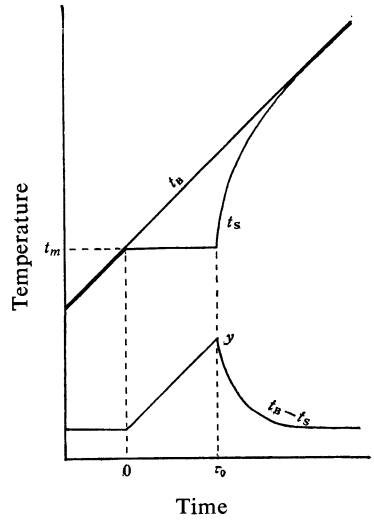



Fig. 7. Illustration of hypothetical thermal process.

is the extrapolated peak temperature, increase with the heating rate; however, if the heating rate is less than 2°C/min., the peak temperature is identical with the melting point within ±1°C.

**A Consideration of the Quality of the Microcell.**—It is necessary to investigate factors which affect the quality of the microcell in order to make further improvements of the microcell. For this purpose, two hypothetical thermal processes which take place in the microcell were considered.

*Process i.* — If the cell may be considered to be thermally isolated, a thermal transformation causes a change in the temperature, $Y$, given by:[4]

$$Y=\frac{Q}{C} \tag{1}$$

where $Q$=the heat of transformation
$C$=the mean specific heat capacity of the cell and sample.

In this work, the cell weighed about 1 g., while the samples weighed about 1—5 mg., therefore, $C$ is almost equal to the specific heat capacity of the microcell.

*Process ii.*—The temperature of the metal block, $t_B$, is equal to that of the reference cell, $t_r$, the sample cell, $t_c$, and the sample, $t_s$, and increases at a constant heating rate, $r$, at first. Then, at time $\tau=0$, the sample begins to melt at a constant temperature, $t_m$, until it finishes melting at time $\tau=\tau_0$. This process is illustrated in Fig. 7; the following equation is obtained:

$$h(t_B-t_s)d\tau=Cdt_s+dQ \tag{2}$$

with the following boundary conditions:

$$\tau=0,\ t_B=t_r=t_c=t_s=t_m$$
$$0\leqq\tau\leqq\tau_0,$$
$$t_c=t_s=t_m=\text{constant melting temperature}$$
$$t_B=t_r=t_m+r\tau$$

where $h$=the heat transfer coefficient between the cell and the wall of the metal block.

The integration of Eq. 2 gives:

$$\int_0^{\tau_0}h(t_B-t_s)d\tau=\int_0^{\tau_0}Cdt_s+\int_0^{\tau_0}dQ$$
$$hr\tau_0^2/2=Q \tag{3}$$

The maximum temperature difference, $Y$, between the temperature of the sample and that of the reference cell or block is:

$$Y=(t_B-t_s)_{\tau=\tau_0}=r\tau_0 \tag{4}$$

From Eqs. 3 and 4, one obtains:

$$Y=\sqrt{2rQ/h} \tag{5}$$

Although Eqs. 1 and 5 represent DTA peak heights in hypothetical thermal processes, some factors relating to the quality of the microcell can be interpreted on the basis of these equations. To increase the peak heights or the sensitivity of microcells, the following methods may be recommended on the basis of Eqs. 1 and 5:

(i) The specific heat of the cell, $C$, should be decreased.

(ii) The heating rate, $r$, should be increased.

4) W. J. Smother and Y. Chiang, "Differential Thermal Analysis," Chem. Publishing Co., N. Y. (1958), p. 79.

(iii) The heat transfer coefficient, $h$, between the microcell and the wall of metal block should be deceased.

Of these, method ii, as has been mentioned earlier, is not useful because of the drifting of base line and peak as the heating rate increases. Methods i and iii have already been applied to the microcells in this work; that is, these microcells are made light in weight [method i] and are supported only by the thermocouple, not coming in contact with the wall of the metal block [method iii]. Therefore, further experiments were made to check upon the efficiency of these methods.

**Experiments to Check on Methods i and iii.** —Three microcells differing in weight were made in order to investigate the effect of the heat capacity of the microcell on peak heights and areas. These microcells differ from each other only in the radius of the sample hole; their surfaces are similar in shape, as is shown in Fig. 8. Therefore, the heat transfer coefficients between each microcell and the wall of the metal block are equal. The results obtained using these cells are shown in Fig. 9 and Fig. 10.

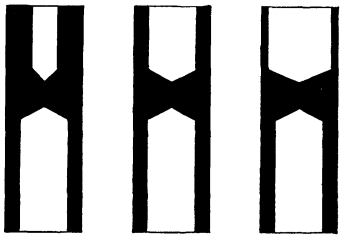



Fig. 8. Three microcells different in weights.

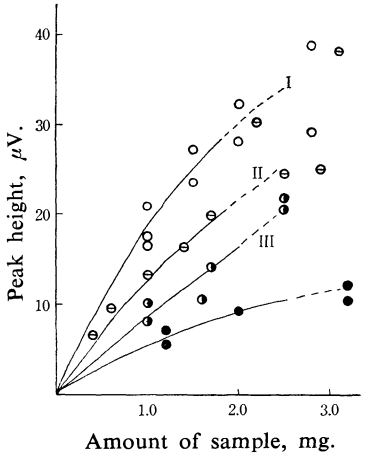



Fig. 9. Comparison of peak heights.
◑, Cell I ○, Cell III
⊖, Cell II ●, in alumina powder

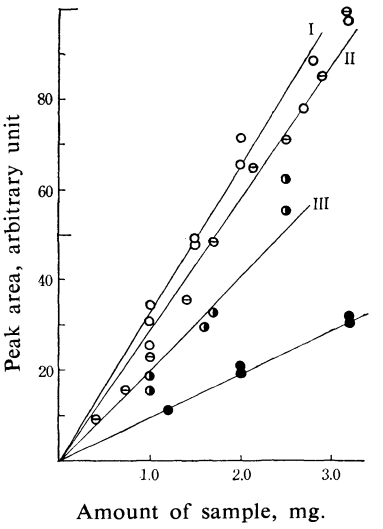



Fig. 10. Comparison of peak area.
◑, Cell I; ○, Cell III;
⊖, Cell II; ●, in alumina pouder.

Further experiments were carried out in order to investigate the effect of the heat transfer between the microcell and the wall of the metal block. The heat transfer coefficient was increased by filling the Hole Space 4 shown in Fig. 2 with alumina powder; that is, air in the space between the microcell and the wall of the metal block was replaced by alumina powder. The results are also shown in Fig. 9 and Fig. 10.

As we anticipated previously from Eqs. 1 and 5, Figs. 9 and 10 show that peak heights or areas increase as the heat capacity of the microcell and the heat transfer coefficient between the microcell and the wall of the metal block decrease. As a conclusion, as a means of improving the quality of the microcell, a smaller cell and finer leads of thermocouple in order to decrease the heat transfer coefficient are recommended.

## Summary

Microcells to carry out differential thermal analysis using a small amount of a sample have been described. The features of these cells are that they are small and light in weight, and are supported only by a thermocouple, not coming in contact with the wall of the metal block. The effects have been described of the variation in heating rate and in sample amount. The peak areas of the benzoic acid melting curve are proportional to the sample amount. The melting temperature can be measured with a precision of ±1°C if the heating rate is less than 2°C/min. The

improvement of the quality of the microcell has also been considered.

The author wishes to express his thanks to Dr. Kazuo Amaya, Dr. Taichi Sato, Mrs. Kazuko Sasaki, Mr. Akira Suzuki, and Mr. Kenjiro Kodama of this Institute for their valuable discussions. He also wishes to thank Dr. Yo-ichiro Mashiko for his kind encouragement.

*The Government Chemical Industrial Research Institute, Tokyo*
*Shibuya-ku, Tokyo*

# Semiconducting Properties of Tetramethylammonium Polyiodides and the Irradiation Effect*

By Shichio KAWAI, Ryôiti KIRIYAMA, Madoka UCHIDA, Shigekazu KUSABAYASHI and Hiroshi MIKAWA

(Received October 2, 1964)

Polyiodides, a remarkable group of salts, are of the $MI_n$ type, in which M is one of the larger alkali metal ions, a substituted ammonium ion or an arsonium ion, and $n=3$, 4, 5, 7 or 9. In triiodide crystals of a kown structure, the triiodide anions exist as separated individuals. In the higher polyiodides, the anion assembly is made up of a number of sub-units ($I^-$, $I_3^-$ and $I_2$ molecules) which are loosely held together to form the more complex $I_n$ system. The triiodide ion has been found to be linear in a number of salts with a large cation.[1] In tetramethylammonium pentaiodide,[2] there are approximately square nets of iodine atoms. An even more complex arrangement is found in tetramethylammonium enneaiodide;[3] five-ninths of the iodine atoms form rather densely-packed layers, while the remaining iodine atoms exist in the form of diatomic iodine pairs, which act as props between those layers. It is to be expected that the electrical behavior of polyiodide crystals will change in parallel with the transition in the nature of the intermolecular or interionic bond in polyiodides; $I_3^-$ ions exist in more or less isolated units, $I_5^-$ ions exist in a layered structure, and $I_9^-$ ions form a three-dimensional network. It was pointed out in a preceding paper that, in organic polyiodides, the electrical resistivity and the activation energy for electronic conduction decreases with the increasing number of iodine atoms in the polyiodide ion, the influence of the cations being of subordinate importance.[4] The present study is concerned with the interrelation between the crystal structure and the electrical behavior in tetramethylammonium polyiodides and especially with the anisotropy of electrical properties in different crystallographic directions.

The effects of irradiation with charged particles or neutrons on semiconducting properties have been studied extensively for many semiconductors; such investigations have provided valuable information above the defects which behave as acceptor levels or as donor levels.[5,6] Studies of the effects of high-energy irradiation on electrical properties are also useful for an understanding of the nature of rather weak bonds in solids. Several examples studied in this line in relation to the dielectric relaxation phenomena of some mineral dielectrics have already been reported.[7,8] In the present investigation, the effects of X- and $\gamma$-irradiations on the electrical conductivity of tetramethylammonium pentaiodide will be studied.

## Experimental

**The preparation of the Compounds.**—Crystals of tetramethylammonium polyiodide were grown by a

* Presented in part at the 16th Annual Meeting of the Chemical Society of Japan, Tokyo, April, 1963, and at the 6th Symposium of Radiation Chemistry, Kyoto, September, 1963.

1) R. C. Mooney and J. S. Slater, *Acta Cryst.*, **12**, 187 (1959).

2) R. J. Hach and R. E. Rundle, *J. Am. Chem. Soc.*, **75**, (1951).

3) W. J. James, R. J. Hach, D. French and R. E. Rundle, *Acta Cryst.*, **8**, 814 (1955).

4) S. Kusabayashi, H. Mikawa, S. Kawai, M. Uchida and R. Kiriyama, This Bulletin, **37**, 811 (1963).

5) J. W. Cleland, J. H. Crawford, Jr., K. Lark-Horovitz, J. C. Pigg and F. W. Yond, Jr., *Phys. Rev.*, **84**, 861 (1951).

6) H. Y. Fan and K. Lark-Horovitz, "Report of the Conference on Defects in Crystalline Solids," Bristol, 232 (1954).

7) R. Kiriyama and S. Kawai, *Mineral. J.*, **3**, 19 (1960).

8) R. Kiriyama and S. Kawai, *Inst. and Ind. Res. Osaka Univ.*, **21**, 111 (1964).

slow cooling of an alcoholic solution of tetramethylammonium iodide from its boiling point with an excess of iodine, as has been described in a previous report.[4] Single crystals, composed of thin flakes 0.5—1 mm. thick and suitable for d. c. measurement, were obtained by cooling a solution with an adequate concentration from 80 to 35°C over a period of several weaks. The melting points agreed with those reported in the literature. Each individual crystalline phase was also identified by X-ray diffraction.

**Measurements.**—The temperature-dependence of anisotropic d. c. conductivity was measured in different crystallographic directions, perpendicular to and parallel to the iodine net in both $(CH_3)_4NI_5$ and $(CH_3)_4NI_9$. In $(CH_3)_4NI_3$, the measurements were carried out in two directions, perpendicular to and parallel to the cleavage plane. Various electrode materials were tested: indium amalgam, copper plate, silver paste and graphite. Graphite powder electrodes were used for the direct current measurement, because it was inert against iodine. The d. c. conductivity of the specimen was measured by a micro-micro ammeter, capable of measuring current down to $10^{-13}$ amp. with an applied potential of 90 V.

Preliminary experiments showed that iodine sublimed from polyiodide crystal on heating. This sublimation of iodine may be a cause of the time-dependent of the d. c. conduction. The time-dependence current could be avoided by enclosing the sample and electrodes in a 3 cc.-capacity glass tube tightly covered with Teflon plates and silicon grease at both openings. On both edges or both sides of a platy single crystal, graphite powder was pressed through platinum plates with wire springs. The electrode assembly was then put in a shield box connected to the ground side of the circuit in order to eliminate any stray field effects. The temperature was measured with a copper-constantan thermocouple located as close as possible to the specimen. The specimen was heated to about 20°C below the melting point, and then the conductivity measurements were made as it was slowly cooled.

The measurement of the thermoelectric power was also attempted for these materials. A test piece 13 mm. in dameter and about 1—2 mm. thick was molded by pressing the crystalline powder of polyiodide under 5 ton/cm$^2$.

**Irradiation.**—The radiation effect on the electric conductivity of $(CH_3)_4NI_5$ was also investigated. The crystal was subjected to about $4.1\times10^6$ r. of X-rays from a copper target tube with a beryllium window operated at 15 kVp and 15 mamp. $\gamma$-Irradiation was performed at about 5°C in order to avoid the annealing effect which appeared at higher temperatures. A brass container with the specimen was immersed into a water pool, at the bottom of which $^{60}Co$ has been placed, and kept there for the required period of time. The total dose attained was from $2\times10^6$ to $10^7$ r.

## Results and Discussion

**The Temperature-dependence of the Conductivity.**—When an external electric field was applied below 0°C, the current decreased with time and reached a steady value after 1 min. This phenomenon, however, could not be observed above 0°C, and the relaxation time of the anomalous current observed below 0°C is in the order of sec.-min.

Sufficient ohmic contact is attained with graphite electrodes below about 200 V./cm. of an applied field. As the thin single crystal was brittle and small, the application of a guard ring in order to eliminate the surface leakage current was abandoned. When a single crystal of $(CH_3)_4NI_5$ was kept in an evacuated condition for 20 min. at room temperature, a little iodine sublimed out from the surface of the crystal and a reddish-brown layer of $(CH_3)_4NI_3$ covered the surface of the crystal. This effect was useful as a means of knowing if the surface leakage current, if any, has any influence on activation energy. No change in the activation energy for d. c. conduction was detected, even when a $(CH_3)_4NI_5$ crystal was used which had been kept for 2 hr. in a vacuum prior to the measurement, until the color of the crystal surface changed sufficiently. The activation energies obtained in the present experiment must, therefore, be reliable values for the real bulk conduction.

The variation in the conductivity with the temperature was found to obey the usual equation of electrical conduction:

$$\sigma=\sigma_0\exp(-\varepsilon/2kT)$$

Figure 1 shows the temperature-dependence of the conductivity with an applied field parallel to and perpendicular to the iodine nets in the cases of $(CH_3)_4NI_5$ and $(CH_3)_4NI_9$ and to the cleavage plane in the case of $(CH_3)_4NI_3$. It is noticeable that the systematic increase in the number of iodine atoms within the polyiodide ion from $(CH_3)_4NI_3$ to $(CH_3)_4NI_9$ is accompanied by a gradual increase in the electronic conductivity.

The activation energies calculated from the conductivity data are given in Table I. As for $(CH_3)_4NI_3$, it may be seen in Fig. 1 that the

Table I. The activation energy for the conductivity of tetramethylammonium polyiodides

| | $\varepsilon_\perp$, eV.* | $\varepsilon_\parallel$, eV.* |
|---|---|---|
| Triiodide** | 2.15 | 2.15 |
| Pentaiodide | 1.36 | 1.39 |
| Enneaiodide | 1.69 | 1.36 |
| Solid iodine | 1.24—1.3[13] | |

* $\varepsilon_\perp$ ($\varepsilon_\parallel$) is the activation energy obtained in the direction perpendicular (parallel) to the nets of iodine atoms.

** Triiodide; normal and parallel to the cleavege plane.

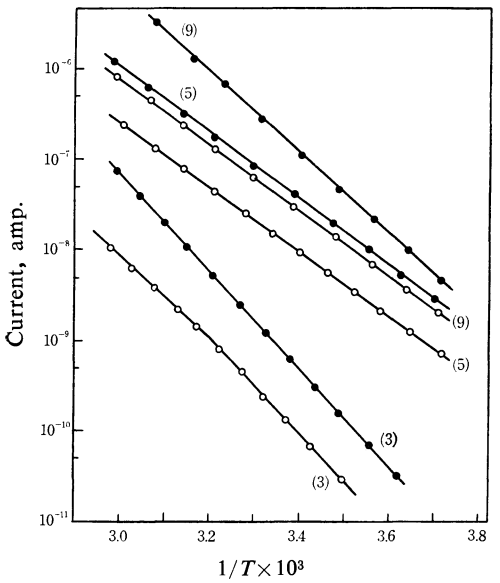



Fig. 1. Temperature-dependence of the electrical conductivity of tetramethylammonium polyiodide. Solid circles indicate the conductivity in the direction perpendicular to the nets of the iodine atoms (pentaiodide and enneaiodide) and to the cleavage planes (triiodide).
Open circles indicate that along the nets (pentaiodide and enneaiodide) and cleavage planes (triiodide). 9) tetramethylammonium enneaiodide, 5) tetramethylammonium pentaiodide, 3) tetramethylammonium triiodide.

plot of the logarithm of the conductivity versus the reciprocal temperature in the direction parallel to the cleavage plane gives two straight lines, with a break around 40°C. The activation energy for the upper part of the break is 1.68 eV., and for the lower part, 2.15 eV. Although a number of runs have been made on several samples, the same results were always obtained, and so, there was a good reproducibility. On the other hand, the temperature-dependence of the conductivity in the direction perpendicular to the cleavage plane gives a single straight line, and the energy of activation is 2.15 eV. It is remarkable that the activation energy in the low temperature range is apparently isotropic. In $(CH_3)_4NI_5$, the activation energy is smaller than that in $(CH_3)_4NI_3$. The values of the activation energy are almost the same both parallel to and perpendicular to the iodine nets. In $(CH_3)_4NI_9$, the values of the activation energy depend on the crystallographic direction; the value perpendicular to the iodine net is larger than that parallel to it, and the latter is the same as that of $(CH_3)_4NI_5$ within the range of experimental error.

**Thermoelectric Power.**—In order to determine the sign of the majority carriers, preliminary measurements of the thermoelectric power were performed on $(CH_3)_4NI_3$, $(CH_3)_4NI_5$ and $(CH_3)_4NI_9$. For all these compounds, the sign of thermo-voltage suggests that a positive-charge carrier is more mobile than a negative one at room temperature. This is quite analogous to the case of solid iodine, where the hole conduction also seems to be predominant judging from a study of space-charge-limited photocurrent.[9]

**The Interrelation between Structure and Conductivity.**—The crystal structures of $(CH_3)_4NI_5$ and $(CH_3)_4NI_9$ are similar to that of solid iodine, all the compounds have a layer structure composed of iodine atoms (Figs. 2, 3). In $(CH_3)_4NI_5$, the I—I distances with in the V-shaped $I_5^-$ ion are 2.93 and 3.14 Å, larger than the I—I distance in the $I_2$ molecule in crystalline iodine (2.68 Å) and considerably smaller than the van der Waals distance. Therefore, the interaction between the iodine atoms within the ions is expected to be strong enough to a partial charge transfer through the resonance of the covalent bond. The shortest distance between neighboring polyiodide ions is shown in Table II, the value for solid iodine being also included for purposes of comparison.[10] The distance between the neighboring polyiodide ions in $(CH_3)_4NI_5$ and also in $(CH_3)_4NI_9$ is shorter than the van der Waals distance, so some direct inter-anionic bonding must be

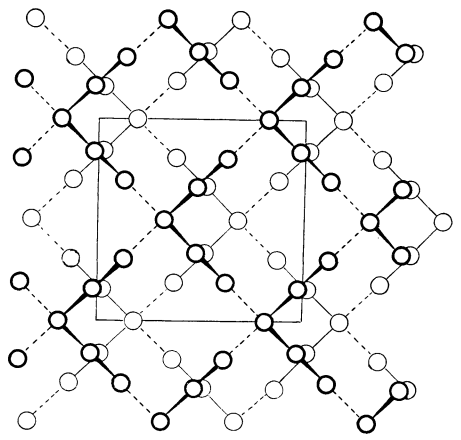


Fig. 2. Projection of the structure of tetramethylammonium pentaiodide on the c-face, showing the nets of iodine atoms in the upper plane and (in fainter line) that in the lower plane.

9) A. Many, M. Simhony, S. Z. Weisz and J. Levinson, *J. Phys. Chem. Solids*, **22**, 285 (1961); A. Many, S. Z. Weisz and M. Simhony, *Phys. Rev.*, **126**, 1989 (1962).
10) A. I. Kitaigorodskii, T. L. Khotsyanova and Yu. T. Struchkov, *Zhur. Fiz. Khim.*, **27**, 780 (1953).

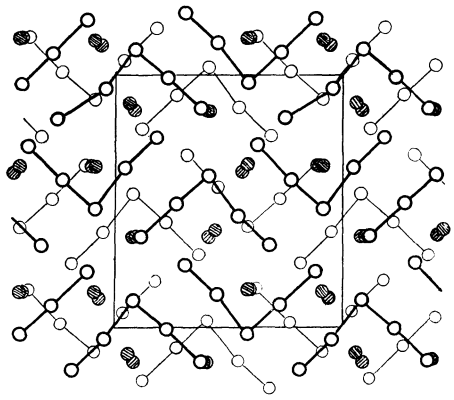


Fig. 3. Projection of the structure of tetramethylammonium enneaiodide on $(10\bar{1})$, showing the nets of iodine atoms in the upper plane and (in fainter line) that in the lower plane.

TABLE II. SHORTEST DISTANCE BETWEEN NEIGHBORING POLYIODIDE IONS

| Anion | Cation | Distance, Å |
|---|---|---|
| Triiodide | Tetraphenylarsonium* | 5.29 |
| Triiodide | Cesium* | 4.03 |
| Pentaiodide | Tetramethylammonium | 3.63 |
| Enneaiodide | Tetramethylammonium | 3.47, 3.67 |
| Solid iodine | | 3.56 |

* Since the value in $(CH_3)_4NI_3$ has not yet been reported, the values in $CsI_3$ and $(C_6H_5)_4AsI_3$ are shown.

involved. The bond angle within and between polyiodide ions, 90° and 180° respectively, is direct evidence for the covalent nature originated by p orbitals of iodine atoms, as in solid iodine.[11,12]

The distance between polyiodide ions in a single net in $(CH_3)_4NI_5$, 3.63 Å, is slightly larger than the $I_2$—$I_2$ distance reported for the $I_2$ crystal, 3.56 Å. It is, therefore, understandable that the activation energy for $(CH_3)_4NI_5$ (1.36—1.39 eV.) is somewhat higher than that for solid iodine (1.24—1.30 eV., the energy separation between $\pi^*$ and $\sigma^*$ bands).[13] It may be expected that the fundamental process of the conduction will be the same in both polyiodide and solid iodine.

When different polyiodides are compared, it is interesting to note that the shorter the shortest distance between polyiodide ions, the smaller the activation energy for hole conduction. The energy band gaps are considered, therefore, to be determined essentially by the shortest distance between polyiodide ions.

11) R. Bersohn, *J. Chem. Phys.*, **36**, 3445 (1962).
12) J. L. Rosenberg, ibid., **40**, 1707 (1964).
13) T. S. Moss, "Photoconductivity in the Elements," Butterworths Scientific Publications, London (1952).

The activation energy in $(CH_3)_4NI_5$ is almost the same both parallel to and perpendicular to the iodine net. The mechanism of electrical transport perpendicular to the layer is difficult to explain in the terms of a hopping mechanism because of the marked anisotropy of the atomic arrangement; that is, the distance between iodine layers is about 0.7 Å longer even than the interatomic distance in the layer. The semiconducting nature across the iodine layer in $(CH_3)_4NI_5$ suggests that the adjacent layers are held not only by the van der Waals force but also by another sort of intermolecular interaction. Although the shorter atomic distance of 4 Å between the layered iodine and the nearest molecular iodine $I_2$ interleaved in the $(CH_3)_4 \cdot NI_9$ lattice is shorter than that of the interlayer spacing of $(CH_3)_4NI_5$, the activation energy perpendicular to the layer of $(CH_3)_4NI_9$ is 0.3 eV. larger than that parallel to the layer. This discrepancy may be attributed to the following causes. The first is the imperfection of the crystal; that is, some sorts of stacking disorder in the direction perpendicular to the sheets should occur, because $I_2$ molecules lying between the layers sublime out rather easily. The second is that the I—I distance within the interleaved $I_2$ molecule is almost equal to that observed in the gaseous $I_2$ molecule. Thus the interatomic interaction within the iodine net through the interleaved $I_2$ molecule in $(CH_3)_4NI_9$ must be relatively weak compared with that between layers in $(CH_3)_4NI_5$.

As has been stated previously, an anomalous current was observed below 0°C, one which was characterized by the relaxation time in the order of sec.-min. Such a time-dependent polarization phenomenon is due to the relative displacement of ionic species rather than to than of electrons or holes.

**Radiation Effects on Semiconducting Properties.**—Since $(CH_3)_4NI_5$ forms a typical layer structure and is more stable than $(CH_3)_4NI_9$, the meaurements were carried out mainly on $(CH_3)_4NI_5$. It is interesting to note that the radiation-induced effect on the electrical conductivity is significantly different between X-rays and $\gamma$-rays; X-rays exert an increasing effect on the conductivity, while $\gamma$-rays exert a decreasing one.

The conductivity and the temperature-dependence of the crystal subjected to about $4.1 \times 10^6$ r. of X-rays are shown in Fig. 4. The X-rays used here are perfectly absorbed at the surface region of the crystalline specimen, because the absorption coefficient of iodine is very large. It seems, therefore, likely that the radiation damage caused by the incident X-rays is concentrated near the surface exposed to X-rays. In Fig. 4, the open circles on a

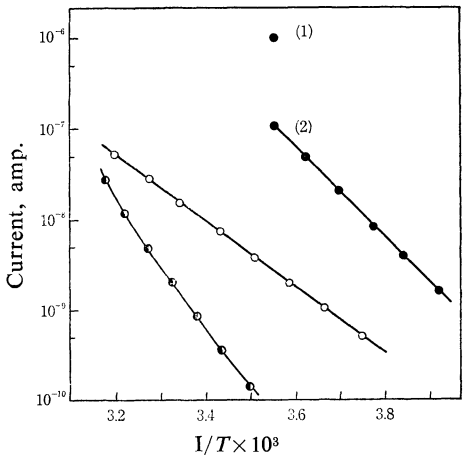



Fig. 4. Irradiation Effects on the temperature-dependence of the conductivity of tetramethylammonium pentaiodide with electric field along the nets of iodine atoms.
Open circles indicate unirradiated specimen. Solid circles indicate X-irradiated specimen 1) just after X-irradiation, 2) after about 24 hr. ◑ indicate $r$-irradiated specimen.

straight line denote the unirradiated specimen and the solid ones, the X-irradiated specimen. It is clear from this figure that the irradiation with X-rays considerably increases the conductivity. If the temperature of the irradiated specimen is raised above room temperature, an appreciable portion of the increment of conductivity will gradually vanish. The activation energy for the conduction of the annealed specimen, however, is greater than that of the unirradiated one (Table III).

Table III. Activation energy for the conductivity of tetramethylammonium pentaiodide irradiated by X- and $\gamma$-rays

| | $\varepsilon_{\parallel}$, eV.* | $\varepsilon_{\perp}$, eV.* |
|---|---|---|
| After the annealing for 24 hr. at room temp., X-irradiation of $4\times10^6$ r. | 2.1 | — |
| $\gamma$-rays, $2\times10^6$ r. | 1.93 | — |
| $\gamma$-rays, $4.8\times10^6$ r. | 1.90 | — |
| $\gamma$-rays, $1.2\times10^7$ r. | 1.87 | 1.96 |
| After annealing at 46°C, $\gamma$-irradiation of $4.8\times10^6$ r. | 1.90 | — |

* $\varepsilon_{\perp}(\varepsilon_{\parallel})$ is the activation energy obtained in the direction perpendicular (parallel) to the nets of iodine atoms.

The temperature-dependence of the conductivity of a $\gamma$-irradiated specimen exposed to about $2\times10^6$ r. is shown in Fig. 4. The conductivity is now actually lowered, and the apparent activation energy for the conduction is larger than that for the original specimen. However, the conductivity of the $\gamma$-irradiated specimen increases gradually with time when kept at room temperature. It happens, therefore, that the apparent activation evergy (3.12 eV.) of the $\gamma$-irradiated sample calculated directly from the $\log_{10} R$ against $T^{-1}$ plot for the heating cycle includes the activation energy for the spontaneous change of the conductivity; the value must be larger than the true one. It has been found that a temperature of measurement of about 0°C or less is required in order to avoid such an annealing effect. Therefore, the true temperature-dependence of the conductivity of the irradiated materials should be measured in a low temperature region, thus avoiding any annealing process. The activation energies obtained for the specimens irradiated up to $1.2\times10^7$ r. are almost the same in both directions, parallel to and perpendicular to the iodine net (Table III).

If an irradiated crystal is stored at particular temperature, an appreciable portion of the radiation-induced change in conductivity is annealed out slowly, at a rate depending on the annealing temperature, and the value reaches a steady value asymptotically (Fig. 5b, 6). The curves of Fig. 6 indicate two types

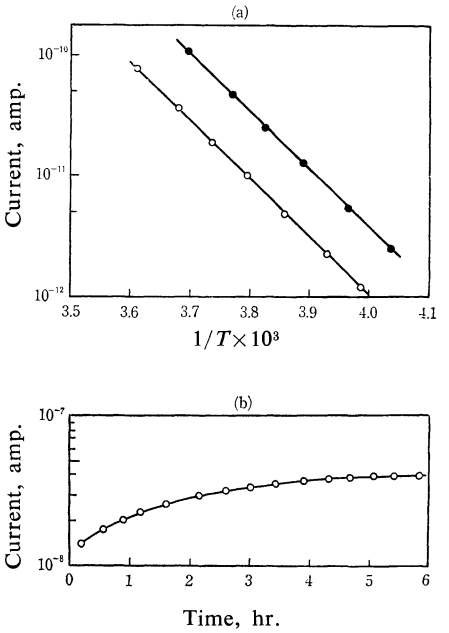



Fig. 5. Effects of annealing on the conductivity of specimen exposed to $\gamma$-rays of $4.8\times10^6$ r.
(a) Open circles indicate the temperature-dependence of the conductivity below 0°C just after $\gamma$-irradiation, solid circles that of specimen annealed out for about 8 hr. at 46°C.
(b) The variation of the conductivity of $\gamma$-irradiated specimen with time at 46°C.

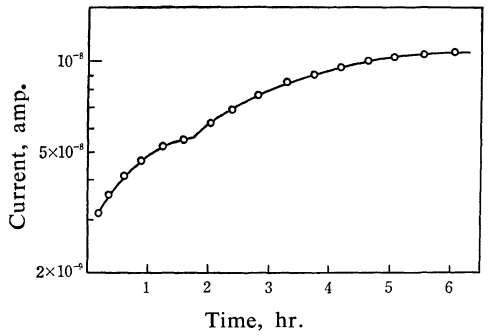



Fig. 6. The variation of the conductivity with time at 40°C for specimen irradiated by $\gamma$-rays of $4.8\times10^{6}$ r.

of annealing process; (i) at a higher annealing temperature, the curve is monotonous, (ii) when the temperature of annealing is decreased, there seems to be a tendency to have an intermediate step. Therefore, it is suggested that there are two separate processes involved in the recovering of the radiation-induced change. Such a long period of time was required for annealing at far lower temperatures that no exact measurements of the rate of annealing could be made. The magnitude of the conductivity at the starting point of annealing can, however, be estimated on the basis of the coductivity data obtained in the temperature region lower than 0°C. The logarithm of time taken to reach half the initial value in the second-stage annealing is plotted as a function of $1/T$. The $\log_{10} T_{1/2}$ versus $T^{-1}$ plot is linear (Fig. 7). The activation energy obtained in the $k=A\exp(-E/kT)$ expression from the slope of the line in Fig. 7 is 1.55 eV.

The true activation energy thus estimated does not change between before and after the annealing, as Fig. 5 shows. It may be concluded that two types of radiation effects exist together, the first being a radiation-induced change which is gradually annealed out, even at room temperature, and the second being an effect which remains unchanged, even up to about 70°C.

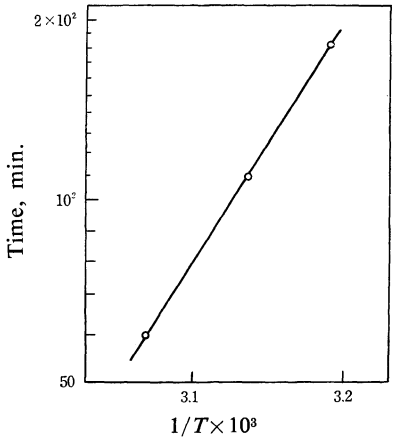



Fig. 7. The time to reach half the initial conductivity plotted as a function of $1/T$ for tetramethylammonium pentaiodide.

**Possible Lattic Imperfections Produced by X- and $\gamma$-Irradiation.**—Upon X-irradiation the conductivity of $(CH_3)_4NI_5$ increased, whereas upon $\gamma$-irradiation the conductivity decreased. Such facts can be understood if one assumes that the number of holes in the valence band is increased or decreased by the respective irradiations. The addition of acceptor levels below the Fermi level will increase the hole concentration in $p$-type semiconductors like $(CH_3)_4NI_5$, while, on the other hand, the addition of donor levels above the Fermi level will reduce the hole concentration in $p$-type semiconductors.

The passing of X-rays or $\gamma$-rays through the specimen must bring about extensive ionization and/or electronic excitation in the crystal lattice, which in turn will lead to bond rupture or bond rearrangement and atomic displacement. Cations, like $I^+$ or $I_2^+$, will be formed easily by the ionization action of moderate X-rays. These charged ions may act as an acceptor level in the crystal. Bond rearrangement will be caused, especially by $\gamma$-irradiation, as a resuls of the slight atomic displacement in the iodine net. Consequently, some anions, like $I_2^-$ or $I_3^-$, may appear in the original polyiodide lattic.

The value of the activation energy of annealing may serve as a clue for the explanation of the conduction mechanism, although the true features of the actual radiation damage will be considerably complicated. The good agreement between the activation energy of annealing, 1.55 eV., and the bond energy in the iodine molecule, 1.57 eV.,[14] suggests that the dissociation of the $I_2$ molecule takes place in the second stage of annealing. If the formation of the iodine molecule, $I_2$, in several sites of the iodine net is a true picture of the $\gamma$-irradiated effect, the electrical conduction in the original pentaiodide crystal, which may be attributed in part to some sort of charge transfer between V-shaped $I_5^-$ ions, will decrease to a certain extent because of the presence of the isolated $I_2$ molecule.

No significant change was observed in the diffraction pattern of the polyiodide crystal between before and after the irradiation. Therefore, the atomic displacement or the damage caused by irradiation must be negligibly

14) L. P. Pauling, "The Nature of the Chemical Bond," 3rd Ed., Cornell University Press, New York, (1960), p. 81.

small within the limits of diffractometer-sensitivity. Thus, it may be concluded that the main effect of the irradiation is the local formation of ions in the matrices of the complex overlapping of the electron clouds of polyiodide ions.

## Summary

Measurements of the temperature-dependence of d.c. conductivity have been made with tetramethylammonium polyiodide in different crystallographic directions, perpendicular to and parallel to the nets of iodine atoms. The systematic increase in the number of iodine atoms from tetramethylammonium triiodide to tetramethylammonium enneaiodide is accompanied by a gradual increase in conductivity. The activation energy for the conductivity along the iodine net is determined mainly by the shortest distance between polyiodide ions. Such as in the case of crystalline iodine, hole conduction is predominant in polyiodide crystals. From the standpoint of structural considerations and the values of the activation energies, the fundamental process in the hole conduction seems essentially be the same in both polyiodides and solid elementary iodine.

The irradiation effects on the electrical conduction may be classified distinctly into two types: (i) the effects of irradiation which can easily be removed by annealing above about 30°C, and (ii) the effects which can not be overcome by heat treatment below 70°C. The conductivity increases on X-irradiation, indicating the production of some acceptor levels, while the conductivity decreases with $\gamma$-irradiation, a phenomenon which may be attributed to some sort of donor level formation.

*The Institute of Scientific and Industrial Research*
*Osaka University*
*Sakai, Osaka*

# Estimation of Anharmonic Potential Constants. I. Linear $XY_2$ Molecules

By Kozo KUCHITSU and Yonezo MORINO

(Received October 10, 1964)

Within the framework of the Born-Oppenheimer approximation, the motions of the nuclei in a molecule can be fully understood if the potential function, *iuclnding the anharmonicity*, of the molecule is known. The fundamental importance of the anharmonic (usually cubic and quartic) potential constants for molecular spectroscopy is, as is well recognized,[1] that they are closely related to the dependence, $\alpha_i$, of the rotational constants on the vibrational quantum numbers; to the vibrational anharmonic constants, $x_{ij}$; to the anharmonic resonance, and to the effects of vibrations on the molecular structure.[2,3]

Potential functions, including anharmonicity, have been the subject of extensive studies concerning diatomic molecules,[4-6] whereas little information has yet been obtained concerning polyatomic molecules; no parameters $\alpha$ and $x$ have been determined by spectroscopic studies under high resolution except for only a few of the simplest molecules. Nor has the physical significance of cubic and quartic potential constants been fully explored, in contrast to the case of the quadratic force constants,[7] which have been studied in relation to the intramolecular force field. In view of the recent development of rotation and rotation-vibration spectroscopy, it seems of practical utility for spectroscopic analyses to investigate the basic relations which exist among the anharmonic potential constants; by means of such relations, one may make quantitative, or at least semiquantitative, estimates of the magnitude of anharmonic constants and those of the $\alpha$ and $x$ parameters for which sufficient experimental data have not been determined.

1) H. H. Nielsen, *Revs. Mod. Phys.*, **23**, 90 (1951).
2) D. R. Herschbach and V. W. Laurie, *J. Chem. Phys.*, **37**, 1668 (1962); V. W. Laurie and D. R. Herschbach, ibid., **37**, 1687 (1962).
3) M. Toyama, T. Oka and Y. Morino, *J. Mol. Spectry.*, **13**, 193 (1964).
4) G. Herzberg "Spectra of Diatomic Molecules," D. Van Nostrand, New York (1950).
5) Y. P. Varshni, *Revs. Mod. Phys.*, **29**, 664 (1957).
6) D. Steele, E. R. Lippincott and J. T. Vanderslice, ibid., **34**, 239 (1962).
7) E. B. Wilson, Jr., J. C. Decius and P. C. Cross, "Molecular Vibrations," McGraw-Hill, New York (1955).

Studies in this direction were originated by Adel and Dennison[8] and by Redlich,[9] and after a long intermission their idea was successfully extended by Pliva.[10] He suggested a potential function of internal coordinates based on the general valence-force field and determined the values of adjustable parameters by using observed spectroscopic constants. The results of the application to $CO_2$, $H_2O$, and HCN show that the function reproduces the vibrational constants very well and may serve for the prediction of the rotation-vibration coupling constants. Kuchitsu and Bartell[11] developed a method by which cubic constants were estimated by using the elements of the $\boldsymbol{L}$ matrix and force constants derivable even in the absence of complete spectroscopic analyses, and they applied their method to $H_2O$ and $D_2O$. Herschbach and Laurie's empirical study[12] of the anharmonic force constants of diatomic molecules led to reasonable predictions of the available cubic constants for bond stretching in polyatomic molecules. Suzuki, Pariseau, and Overend[13] have recently made extensive least-squares calculations for the determination of anharmonic constants from the observed band origins and rotational constants of fundamentals, overtones and combination tones for $CO_2$, $H_2O$, HCN, and $C_2H_2$.

In the present series of papers, a systematic study will be made of the physical significance of the cubic and quartic constants of simple polyatomic molecules in order to set up a simple model for predicting these constants. The linear $XY_2$ molecules may be the most suitable for starting the investigation of this problem. Precise experimental values have been reported for $CO_2$ and $CS_2$, and transformations among the coordinate systems are simple and unique, since the elements of the $L$ matrix depend only on the masses of the component atoms. Accordingly, although $CO_2$[8-10] and $CS_2$[14] have been the subject of previous studies for similar purposes, the anharmonic constants of these molecules will be further examined in the present paper.

The potential function will be expanded in terms of internal coordinates. It has often been pointed out[8-11] that this expansion allows one to use chemical intuition in handling the problem and to correlate the anharmonic constants of isotopic molecules. Even for more complex molecules, it is not difficult, at least in principle, to relate the coefficients of this expansion by appropriate transformation of coordinates to the anharmonic potential constants (in the normal-coordinate system), which are most conveniently applied to theoretical problems.[1]

## Expansion of Internal Coordinates

If the z axis is taken along the equilibrium molecular axis of the $XY_2$ molecule, the displacements of the X-$Y_i$ bond ($i=1, 2$) in the directions parallel and perpendicular to the $z_i$ axis, $\Delta z_i$ and $\Delta\rho$ respectively, are shown to be expanded in terms of the normal coordinates, of which $Q_1$ denotes the totally symmetric stretching vibration; $Q_3$, the antisymmetric stretching, and $Q_{2a}$ and $Q_{2b}$, the degenerate bending vibrations:

$$\left.\begin{aligned}\Delta z_1 &= g_1Q_1+g_2Q_3\\ \Delta z_2 &= g_1Q_1-g_2Q_3\\ \Delta\rho^2 &= g_2^2Q_2^2\end{aligned}\right\} \quad (1)$$

where $g_1=(1/2m_Y)^{1/2}$, $g_2=(1/2m_Y+1/m_X)^{1/2}$

and $Q_2^2=Q_{2a}^2+Q_{2b}^2$

Since the instantaneous changes in the X-$Y_i$ bond length, $\Delta r_i$, and in the $Y_1$-X-$Y_2$ angle, $\Delta\alpha$, are given by:

$$\left.\begin{aligned}\Delta r_i &= \Delta z_i+\Delta\rho^2/2r_e-\Delta z_i\Delta\rho^2/2r_e^2+\cdots\\ r_e\Delta\alpha &= 2\Delta\rho-\Delta\rho(\Delta z_1+\Delta z_2)/r_e\\ &\quad+\Delta\rho(\Delta z_1^2+\Delta z_2^2)/r_e^2-2\Delta\rho^3/3r_e^2+\cdots\end{aligned}\right\} \quad (2)$$

where $r_e=r_e$(X-Y), they may also be expanded in terms of the normal coordinates. The internal symmetry coordinates are shown to be:

$$\left.\begin{aligned}S_1 &= \frac{1}{\sqrt{2}}(\Delta r_1+\Delta r_2)=\sqrt{2}\,g_1Q_1\\ &\quad+\frac{1}{\sqrt{2}\,r_e}g_2^2Q_2^2-\frac{g_1g_2^2}{\sqrt{2}\,r_e^2}Q_1Q_2^2+\cdots\\ S_2^2 &= (r_e\Delta\alpha)^2=4g_2^2Q_2^2-\frac{8}{r_e}g_1g_2^2Q_1Q_2^2\\ &\quad+\frac{1}{r_e^2}(12g_1^2g_2^2Q_1^2Q_2^2\\ &\quad-\frac{8}{3}g_2^4Q_2^4+8g_2^4Q_2^2Q_3^2)+\cdots\\ S_3 &= \frac{1}{\sqrt{2}}(\Delta r_1-\Delta r_2)=\sqrt{2}\,g_2Q_3\\ &\quad-\frac{1}{\sqrt{2}\,r_e^2}g_2^3Q_2^2Q_3+\cdots\end{aligned}\right\} \quad (3)$$

8) A. Adel and D. M. Dennison, *Phys. Rev.*, **44**, 99 (1933).
9) O. Redlich, *J. Chem. Phys.*, **9**, 298 (1941).
10) J. Pliva, *Collection Czechoslow. Chem. Communs.*, **23**, 777 (1958).
11) K. Kuchitsu and L. S. Bartell, *J. Chem. Phys.*, **36**, 2460 (1962).
12) D. R. Herschbach and V. W. Laurie, ibid., **35**, 458 (1961).
13) I. Suzuki, M. A. Pariseau and J. Overend, Symposium on Molecular Structure and Spectroscopy, S7, Columbus, Ohio, June, 1964.
14) J. Pliva, Symposium on Molecular Structure and Spectroscopy, R5, Columbus, Ohio, June, 1960.

It is important to note that higher-order terms of the normal coordinates must be included in the above expressions in order to discuss anharmonic terms.

## Anharmonic Constants

The potential function of the molecule, expanded in terms of the internal coordinates, is given by:

$$V=\frac{1}{2}f_r(\Delta r_1^2+\Delta r_2^2)+f_{r'}\Delta r_1\Delta r_2+\frac{1}{2}f_\alpha r_e^2\Delta\alpha^2 + \frac{1}{r_e}[f_{rrr}(\Delta r_1^3+\Delta r_2^3)+f_{rrr'}(\Delta r_1+\Delta r_2) \times \Delta r_1\Delta r_2+f_{r\alpha\alpha}(\Delta r_1+\Delta r_2)r_e^2\Delta\alpha^2] + \frac{1}{r_e^2}[f_{rrrr}(\Delta r_1^4+\Delta r_2^4)+f_{rrrr'} \times(\Delta r_1^2+\Delta r_2^2)\Delta r_1\Delta r_2+f_{rrr'r'}\Delta r_1^2\Delta r_2^2 +f_{rr\alpha\alpha}(\Delta r_1^2+\Delta r_2^2)r_e^2\Delta\alpha^2 +f_{rr'\alpha\alpha}\Delta r_1\Delta r_2 r_e^2\Delta\alpha^2+f_{\alpha\alpha\alpha\alpha}r_e^4\Delta\alpha^4]+\cdots \quad (4)$$

In terms of the internal symmetry coordinates, on the other hand, it is shown to be:

$$V=\frac{1}{2}(f_1S_1^2+f_2S_2^2+f_3S_3^2) + \frac{1}{r_e}(f_{111}S_1^3+f_{122}S_1S_2^2+f_{133}S_1S_3^2) + \frac{1}{r_e^2}(f_{1111}S_1^4+f_{1122}S_1^2S_2^2+f_{1133}S_1^2S_3^2 +f_{2222}S_2^4+f_{2233}S_2^2S_3^2+f_{3333}S_3^4)+\cdots \quad (5)$$

where the interrelations among the coefficients of Eq. 4 and Eq. 5 are given in Eq. A-1. From Eqs. 3 and 4, it is easy to derive the cubic and quartic potential constants in the expression of the potential function in terms of the dimensionless normal coordinates,[1] $q_i$:

$$V/hc=\frac{1}{2}(\omega_1q_1^2+\omega_2q_2^2+\omega_3q_3^2)+k_{111}q_1^3 +k_{122}q_1q_2^2+k_{133}q_1q_3^2+k_{1111}q_1^4+k_{1122}q_1^2q_2^2 +k_{1133}q_1^2q_3^2+k_{2222}q_2^4+k_{2233}q_2^2q_3^2 +k_{3333}q_3^4+\cdots \quad (6)$$

as is given in the Appendix. These potential constants are related to the $\alpha$ and $x$ in Eq. A-3 of the Appendix, as has been shown by Dennison.[8,15]

Since there are twelve observables and twelve constants, the anharmonic constants, $k$, and the force constants, $f$, can be determined uniquely from the observed values of $\omega$, $\alpha$, and $x$.

The experimental values of $\alpha$ and $x$, reported by Courtoy for $CO_2$,[16] and by Agar et al.[17] and by Stoicheff[18] for $CS_2$, are taken for calculating the anharmonic constants, $k$ (shown in Table I) by using Eq. A-2. The $k$ values for $CO_2$ are in agreement with those calculated by Pliva[10] except for $k_{1122}$ and $k_{2222}$, which are here obtained from $x_{12}+4x_{22}$ and $x_{22}+x_{ll}$ instead of from $x_{12}$ and $x_{22}$ in order to eliminate the effect of the Fermi resonance. The higher-order constants are obtained from the $k$ constants by Eqs. A-1 and A-2; they are listed in Table II. The contributions to $k$ from individual terms in Eq. A-2 are listed in Table III.

It is shown in Eq. A-2 and in Table III that the anharmonic constants which are related to the bending vibration, $\nu_2$, namely, $k_{122}$, $k_{1122}$, $k_{2222}$, and $k_{2233}$, depend on both the quadratic and the higher-order constants. For $k_{122}$ and $k_{2222}$, in particular, the contribution from the quadratic constant, $f_r$, is predominant. The dependence of the $k$ on the quadratic force constants originates from the nonlinear dependence of the internal coordinates, $\Delta r$ and $\Delta\alpha$, on the Cartesian coordinates, $\Delta z$ and $\Delta\rho$, which, on the contrary, transform linearly into the normal coordinates.[10,11] A simple illustration of this situation is given in Fig. 1. Suppose

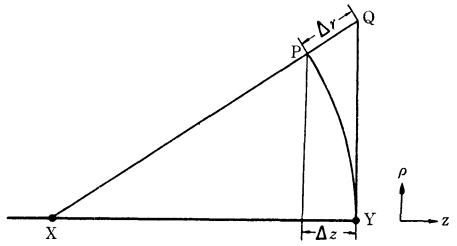



Fig. 1 A model representing the displacement of the Y atom in the X–Y bond relative to the X atom.
Y: Equilibrium position
Y→P: A pure bending displacement
Y→Q: A perpendicular displacement

the atom Y is displaced to the position P by a pure bending displacement. An increase in the total potential energy will not depend on $f_r$, since $\Delta r$ is zero. The quadratic part of the potential energy, however, has a finite term, $(1/2)f_r(\Delta z)^2$, since the projection of the bond on the z axis, $\Delta z$, is finite ($\Delta z<0$). This positive contribution must be compensated for by the negative contributions from the anharmonic

15) D. M. Dennison, *Revs. Mod. Phys.*, **12**, 175 (1940).

16) C. P. Courtoy, *Can. J. Phys.*, **35**, 608 (1957); *Ann. Soc. Sci. Bruxelles*, **I 73**, 5 (1959).

17) D. Agar, E. K. Plyler and E. D. Tidwell, *J. Res. Natl. Bur. Std. (U. S.)*, **66A**, 259 (1962).

18) B. P. Stoicheff, *Can. J. Phys.*, **36**, 218 (1958); his $\omega^0$ and $x$ values have been revised according to his private communication to Y. Morino (1959).

Table I. Anharmonic potential constants derived from observed $\alpha$ and $x$ values (in $cm^{-1}$)

| | $k_{111}$ | $k_{122}$ | $k_{133}$ | $k_{1111}$ | $k_{1122}$ | $k_{1133}$ | $k_{2222}$ | $k_{2233}$ | $k_{3333}$ | Ref. |
|---|---|---|---|---|---|---|---|---|---|---|
| $^{12}C^{16}O_2$ | −45.07 | 73.81 | −252.91 | 1.25 | −9.11 | 20.37 | 2.16 | −27.81 | 6.63 | a |
| $^{13}C^{16}O_2$ | −45.07 | 73.02 | −245.36 | 1.25 | −9.18 | 19.72 | 2.12 | −26.48 | 6.23 | a |
| $^{12}C^{32}S_2$ | −14.89 | 41.55 | −129.97 | 0.11 | −7.48 | 6.45 | 2.06 | −14.93 | 3.80 | b |
| $CS_2$ | −14.71 | 49.40 | −127.84 | 0.16 | 18.36 | 5.93 | −1.89 | −16.39 | 3.55 | c |

a), b), c) Calculated from the $\alpha$ and $x$ values listed in Refs. 16, 17 and 18, respectively, by using Eq. A-3.

Table II. Potential constants in the internal-coordinate system[a] (in md./Å)

| | $f_r$ | $f_{r'}$ | $f_\alpha$ | $f_{rrr}$ | $f_{rrr'}$ | $f_{r\alpha\alpha}$ |
|---|---|---|---|---|---|---|
| $^{12}C^{16}O_2$ | 16.030 | 1.268 | 0.582 | −22.18 | −1.75 | −0.54 |
| $^{13}C^{16}O_2$ | 16.030 | 1.268 | 0.582 | −22.16 | −1.77 | −0.52 |
| $CO_2$(D)[b] | (16.030) | (1.268) | (0.582) | −22.2 | 0 | 0 |
| $^{12}C^{32}S_2$ | 7.880 | 0.648 | 0.236 | −10.98 | 0.51 | −0.26 |
| $CS_2$ | 7.789 | 0.552 | 0.240 | −10.73 | 0.56 | −0.11 |
| $CS_2$(D) | (7.880) | (0.648) | (0.236) | −11.9 | 0 | 0 |
| | $f_{rrrr}$ | $f_{rrrr'}$ | $f_{rrr'r'}$ | $f_{rr\alpha\alpha}$ | $f_{rr'\alpha\alpha}$ | $f_{\alpha\alpha\alpha\alpha}$ |
| $^{12}C^{16}O_2$ | 34.84 | −3.28 | −8.03 | 1.21 | 3.18 | 0.02 |
| $^{13}C^{16}O_2$ | 34.72 | −3.14 | −7.92 | 1.16 | 2.88 | 0.02 |
| $CO_2$(D) | 38.1 | 0 | 0 | 0 | 0 | 0 |
| $^{12}C^{32}S_2$ | 14.53 | −7.80 | −4.89 | −1.28 | −2.52 | 0.04 |
| $CS_2$ | 12.54 | −2.25 | −8.44 | 10.26 | 21.80 | −0.17 |
| $CS_2$(D) | 23.6 | 0 | 0 | 0 | 0 | 0 |

a) Calculated from Table I by using Eqs. A-1 and A-2.
b) Diatomic approximation. See Eq. 9.

terms, $k_{122}$, etc.; these terms must, therefore, depend on $f_r$. If, on the other hand, the atom Y is displaced to the point Q, a part of the increase in the potential energy will come from $(1/2)f_r(\Delta r)^2$, since the X-Y bond is stretched ($\Delta r>0$). Since $\Delta z$ is zero, the quadratic part which depends on $f_r$ is zero. The above increase in the potential energy must, therefore, come from the anharmonic terms, mainly from $k_{2222}$ in this case. The physical significance of this problem in relation to the mean bond displacement has been discussed in more detail by Bartell.[19]

A problem to be explored by the valence theory is presented by the observation that the force constant $f_{r\alpha\alpha}$ is negative in the case of $CO_2$ and $CS_2$. This implies that the X-Y bond is likely to be stretched when the molecule is bent. At the root-mean-square angle of the zero-point bending vibration, $\langle\Delta\alpha^2\rangle^{1/2}$, the average lengthening of the bond for this reason, $-f_{r\alpha\alpha}r_e\langle\Delta\alpha^2\rangle/(f_r+f_{r'})$, is about 0.0003 Å for $CO_2$ and $CS_2$.*1

The potential function for the bending vibration is found to be very nearly harmonic, since the fourth-order constant $f_{\alpha\alpha\alpha\alpha}$ is small. At the angle of $\langle\Delta\alpha^2\rangle^{1/2}$, the quartic part of the potential energy, $f_{\alpha\alpha\alpha\alpha}r_e^2\Delta\alpha^4$, is less than 1% of the quadratic contribution, $(1/2)f_\alpha r_e^2\Delta\alpha^2$.

The constants $k$ which are not related to the $\nu_2$ vibration originate exclusively from the higher-order constants, $f_{rrr}$ or $f_{rrrr}$. As is shown in Table II, the constants $f_{rrr}$ and $f_{rrrr}$ are much larger than the others. This can be understood by a model in which each bond executes a stretching vibration with little interaction (higher than the quadratic) with the other bond. The magnitudes of $f_{rrr}$ and $f_{rrrr}$ are found to be approximately equal to those of the corresponding constants of a diatomic X-Y molecule; this confirms similar statements given in previous papers.[9-12] Since a method for predicting the anharmonic constants based on as simple a potential function as possible is aimed at, an approximate potential function based on the diatomic potential constants will be studied in some detail in the next section.

## An Approximate Potential Function

The potential function of a diatomic molecule is in general expanded around the equilibrium distance as:

19) L. S. Bartell, *J. Chem. Phys.*, **38**, 1827 (1963).

*1 In another expression, the force constant of the bending vibration, $f_\alpha$, is apparently decreased (or increased) as the bonds are symmetrically stretched (or compressed). For the displacement of the root-mean-square amplitude of the bond, ±0.035 Å for $CO_2$ and ±0.039 Å for $CS_2$, the increase in $f_\alpha$ is about 11%.

TABLE III. CONTRIBUTIONS TO THE ANHARMONIC CONSTANTS FROM POTENTIAL CONSTANTS IN THE INTERNAL-COORDINATE SYSTEM[a] (in $cm^{-1}$)

| Molecule | | $f_r$ | $f_{r'}$ | $f_\alpha$ | $f_{rrr}$ | $f_{rrr'}$ | $f_{r\alpha\alpha}$ | $f_{rrrr}$ | $f_{rrrr'}$ | $f_{rrr'r'}$ | $f_{rr\alpha\alpha}$ | $f_{rr'\alpha\alpha}$ | $f_{\alpha\alpha\alpha\alpha}$ | Total |
|---|---|---|---|---|---|---|---|---|---|---|---|---|---|---|
| $^{12}C^{16}O_2$ | $k_{111}$ | 0 | 0 | 0 | −41.78 | −3.29 | 0 | 0 | 0 | 0 | 0 | 0 | 0 | −45.07 |
| | $k_{122}$ | 111.40 | 8.81 | −16.18 | 0 | 0 | −30.22 | 0 | 0 | 0 | 0 | 0 | 0 | 73.81 |
| | $k_{133}$ | 0 | 0 | 0 | −259.74 | 6.83 | 0 | 0 | 0 | 0 | 0 | 0 | 0 | −252.91 |
| | $k_{1111}$ | 0 | 0 | 0 | 0 | 0 | 0 | 1.58 | −0.15 | −0.18 | 0 | 0 | 0 | 1.25 |
| | $k_{1122}$ | −2.68 | −0.21 | 0.58 | −11.11 | −0.88 | 1.45 | 0 | 0 | 0 | 1.61 | 2.13 | 0 | −9.11 |
| | $k_{1133}$ | 0 | 0 | 0 | 0 | 0 | 0 | 19.62 | 0 | 0.75 | 0 | 0 | 0 | 20.37 |
| | $k_{2222}$ | 4.95 | 0.39 | −0.96 | 0 | 0 | −2.68 | 0 | 0 | 0 | 0 | 0 | 0.46 | 2.16 |
| | $k_{2233}$ | −5.55 | 0.44 | 0.81 | −23.05 | 0.61 | 0 | 0 | 0 | 0 | 3.35 | −4.42 | 0 | −27.81 |
| | $k_{3333}$ | 0 | 0 | 0 | 0 | 0 | 0 | 6.78 | 0.63 | −0.78 | 0 | 0 | 0 | 6.63 |
| $^{12}C^{32}S_2$ | $k_{111}$ | 0 | 0 | 0 | −15.62 | 0.73 | 0 | 0 | 0 | 0 | 0 | 0 | 0 | −14.89 |
| | $k_{122}$ | 59.88 | 4.92 | −7.18 | 0 | 0 | −16.07 | 0 | 0 | 0 | 0 | 0 | 0 | 41.55 |
| | $k_{133}$ | 0 | 0 | 0 | −127.98 | −1.99 | 0 | 0 | 0 | 0 | 0 | 0 | 0 | −129.55 |
| | $k_{1111}$ | 0 | 0 | 0 | 0 | 0 | 0 | 0.37 | −0.20 | −0.06 | 0 | 0 | 0 | 0.11 |
| | $k_{1122}$ | −1.08 | −0.09 | 0.19 | −4.51 | 0.21 | 0.58 | 0 | 0 | 0 | −1.40 | −1.38 | 0 | −7.48 |
| | $k_{1133}$ | 0 | 0 | 0 | 0 | 0 | 0 | 6.11 | 0 | 0.34 | 0 | 0 | 0 | 6.45 |
| | $k_{2222}$ | 2.88 | 0.24 | −0.46 | 0 | 0 | −1.55 | 0 | 0 | 0 | 0 | 0 | 0.95 | 2.06 |
| | $k_{2233}$ | −2.95 | 0.24 | 0.36 | −12.33 | −0.19 | 0 | 0 | 0 | 0 | −3.83 | 3.77 | 0 | −14.93 |
| | $k_{3333}$ | 0 | 0 | 0 | 0 | 0 | 0 | 2.78 | 1.49 | −0.47 | 0 | 0 | 0 | 3.80 |

a) Calculated from Table II and Eqs. A-1 and A-2.

TABLE IV. ESTIMATION OF THE ANHARMONIC CONSTANTS OF $CO_2$ AND $CS_2$ BY USE OF THE SIMPLE POTENTIAL FUNCTION (in $cm^{-1}$)

| | | $k_{111}$ | $k_{122}$ | $k_{133}$ | $k_{1111}$ | $k_{1122}$ | $k_{1133}$ | $k_{2222}$ | $k_{2233}$ | $k_{3333}$ | $\alpha_1\times10^3$ | $\alpha_2\times10^3$ | $\alpha_3\times10^3$ | $x_{11}$ | $x_{33}$ | $x_{13}$ | $x_{23}$ | $x_{22}+x_{11}$ | $x_{12}+4x_{22}$ |
|---|---|---|---|---|---|---|---|---|---|---|---|---|---|---|---|---|---|---|---|
| $^{12}C^{16}O_2$ | obs. | −45.1 | 73.8 | −252.9 | 1.25 | −9.11 | 20.37 | 2.16 | −27.81 | 6.63 | 1.20 | −0.72 | 3.09 | −3.75 | −12.63 | −19.37 | −12.53 | 0.15 | 1.13 |
| | est. I[a] | −41.9 | 104.0 | −260.2 | 1.73 | −13.45 | 21.47 | 4.38 | −27.39 | 7.42 | 1.07 | −1.14 | 3.19 | −2.26 | −12.77 | −17.99 | −5.91 | 0.38 | 2.47 |
| | est. II | −41.9 | (73.8) | −260.2 | 1.73 | −11.99 | 21.47 | 1.69 | −27.39 | 7.42 | 1.07 | (−0.72) | 3.19 | −2.26 | −12.77 | −17.99 | −11.71 | −0.32 | −5.05 |
| $^{12}C^{32}S_2$ | obs. | −14.9 | 41.5 | −130.0 | 0.11 | −7.48 | 6.45 | 2.07 | −14.93 | 3.80 | 0.155 | −0.205 | 0.711 | −1.07 | −6.54 | −7.86 | −6.45 | 0.78 | 1.36 |
| | est. I | −16.9 | 57.6 | −138.7 | 0.61 | −5.87 | 9.93 | 2.66 | −15.71 | 4.52 | 0.19 | −0.30 | 0.76 | −0.69 | −7.17 | −7.01 | −3.38 | 0.19 | 2.31 |
| | est. II | −16.9 | (41.5) | −138.7 | 0.61 | −5.29 | 9.93 | 1.11 | −15.71 | 4.52 | 0.19 | (−0.205) | 0.76 | −0.69 | −7.17 | −7.01 | −6.69 | −0.17 | −1.79 |

a) Case I: Estimated by using the constants (D) listed in Table II. Case II: Estimated by using the constants (D) plus $f_{r\alpha\alpha}=-0.544$ md./Å ($CO_2$) and $-0.264$ md./Å ($CS_2$) in order to make $\alpha_2$ agree with the observed values.

$$V(\Delta r)=\frac{1}{2}f_r\Delta r^2-\frac{1}{2}a_3 f_r\Delta r^3+\frac{7}{24}a_4{}^2 f_r\Delta r^4+\cdots \tag{7}$$

An advantage of taking $a_3$ and $a_4$ as independent parameters lies in the approximate equality of $a_3$ and $a_4$; the above expression (Eq. 7) is taken by analogy to the Morse function:[20]

$$V(\Delta r)=D_e[\exp(-2a\Delta r)-2\exp(-a\Delta r)] \tag{8}$$

in which case it follows that $a_3=a_4=a$.

As a natural extension to the $XY_2$ molecule, the following expression of the anharmonic force constants of Eq. 4 are derived by taking the higher-order terms of Eq. 7, other cross-interaction terms simply being ignored:

$$\left.\begin{aligned} &f_{rrr}=-\frac{1}{2}a_3 f_r r_e,\quad f_{rrrr}=\frac{7}{24}a_4{}^2 f_r r_e{}^2\\ &f_{rrr'}\sim 0\quad f_{rrrr'}\sim 0\ \text{and}\ f_{rrr'r'}\sim 0 \end{aligned}\right\} \tag{9}$$

In order to estimate $f_{rrr}$ and $f_{rrrr'}$, $f_r$ and $r_e$ may be taken to be equal to those of the $CO_2(CS_2)$ molecule,*2 and the parameters $a_3$ and $a_4$ may be approximated by those of the CO(CS) molecule, while the parameters $a_3$ and $a_4$ may be approximated by those of the CO (CS) molecule, which are determined by the method to be described in the next section. The constants obtained from Eq. 9 in this way are listed in Table II as a "Diatomic Approximation (D)". The constants $k$, $\alpha$, and $x$ calculated from Eqs. A-2 and A-3 by using the approximate potential constants (D) of Table II are compared in Table IV with the corresponding observed values. The agreement in the order of magnitude is good except for $\alpha_2$ and $x_{23}$. This indicates the practical usefulness of this simple potential function. A better agreement for $x_{23}$ may result, as shown in Table IV, by the introduction of a negative $f_{r\alpha\alpha}$ to make $\alpha_2$ agree with the experimental $\alpha_2$; this adjustment, however, makes the agre ement of $x_{22}+x_{ll}$ and $x_{12}+4x_{22}$ somewhat worse.

There is no analogous principle at present for estimating the constants which are left undetermined in the "diatomic approximation": $f_{rrr'}$, $f_{r\alpha\alpha}$, $f_{rrrr'}$, $f_{rrr'r'}$ $f_{rr\alpha\alpha}$, $f_{rr'\alpha\alpha}$, and $f_{\alpha\alpha\alpha\alpha}$. It is an important problem for future studies to establish a scheme by which plausible estimates may be made for the higher-order terms of the stretching-stretching, stretching-bending, and bending-bending interactions.

20) P. M. Morse, *Phys. Rev.*, **34**, 57 (1929).

*2 An alternative process is to take $f_r$ and $r_e$, as well as the $a_3$ and $a_4$ parameters, to be equal to those of the CO(CS) molecule; the constants, $f_r$ and $r_e$, of CO(CS) are appreciably different from those of the $CO_2(CS_2)$ molecule. There is no definite physical reason for choosing whether we should transfer $a_3$ and $a_4$ or $a_3 f_r r_e$ and $a_4{}^2 f_r r_e{}^2$ from the corresponding diatomic molecule. According to our experience, however, a better agreement is usually obtained by transfering $a_3$ and $a_4$.

### The Parameters $a_3$ and $a_4$

It was shown in the preceding section that the estimation of $a_3$ and $a_4$ is a key step in predicting the anharmonic constants of the stretching vibrations. Some characteristic features of these parameters will, therefore, be discussed in the present section.

The parameters $a_3$ and $a_4$ of a diatomic molecule are readily determined by the following equations, if the constants $\omega_e$, $\alpha_e$, and $\omega_e x_e$ are known by spectroscopic measurements;

$$\left.\begin{aligned} &a_3=\frac{2}{3}\pi\omega_e(c\mu/2hB_e{}^3)^{1/2}(\alpha_e+6B_e{}^2/\omega_e)\\ &a_4=(15a_3{}^2/7-64\pi^2 c\mu\omega_e x_e/7h)^{1/2} \end{aligned}\right\} \tag{10}$$

where $\mu$ is the reduced mass.

From the parameters for various diatomic molecules determined in this way (Tables V and VI), the following general features of $a_3$ and $a_4$ may be observed.

First, the magnitude of $a_3$ is about $2\text{Å}^{-1}$; for most diatomic molecules for which spectroscopic values are available,[4,6,21] $a_3$ is in the range 1.6—2.4$\text{Å}^{-1}$, the largest and the smallest values being 2.55$\text{Å}^{-1}$ (NO) and 1.34$\text{Å}^{-1}$ ($Si_2$) respectively. The only exceptions*3 are those molecules which contain alkali atoms as one or both of their components; their $a_3$ values are much smaller, in many cases less than $1\text{Å}^{-1}$. Second, $a_4$ is equal to, or slightly larger than, $a_3$. For the diatomic molecules studied here, the ratio $a_4/a_3$ is 1.03, with an average deviation of 0.03. Third, an additivity rule, $a_i(\text{X-Y})=(1/2)[a_i(\text{X-X})+a_i(\text{Y-Y})]$ ($i=3$ or 4), is applicable to molecules X-Y, except for alkali hydrides. As for the ratio $[a_i(\text{X-X})+a_i(\text{Y-Y})]/2a_i(\text{X-Y})$, the following average values and average deviations are obtained:

| | $a_3$ | $a_4$ |
|---|---|---|
| Nonhydrides | 1.00±0.04 | 0.98±0.04 |
| Hydrides | 1.05±0.06 | 1.04±0.07 |

These rules may be useful for a simple order-of-magnitude estimation of these parameters.

For estimating the $a_3$ and $a_4$ values of a bond X-Y for which no spectroscopic values of the corresponding diatomic molecules are known, probably a more reliable method than the above additivity rule is the use of an analytical function obtained by a systematic fit to various spectroscopic data of diatomic molecules. For example, for the function proposed by Steele

21) E. R. Lippincott and R. Schroeder, *J. Chem. Phys.*, **23**, 1131 (1955).

*3 Other peculiar exceptions are BrF, SnO, ZrO, and PbS, for which $a_3\sim 3\ \text{Å}^{-1}$ and $a_4\sim 4\ \text{Å}^{-1}$.

TABLE V. PARAMETERS $a_3$ AND $a_4$ OF CO AND CS (in Å$^{-1}$)

| | CO | | CS | |
|---|---|---|---|---|
| | $a_3$ | $a_4$ | $a_3$ | $a_4$ |
| obs.[a] | 2.390 | 2.462 | 1.945 | 2.065 |
| S. L.[b] | 2.40 | 2.48 | 1.89 | 1.96 |
| H. L.[c] | 2.46 | 2.65 | 1.83 | 1.99 |
| Morse[d] | 2.32 | 2.32 | 1.83 | 1.83 |
| Add.[e] | 2.30 | 2.32 | 1.92 | 1.92 |

a) Calculated by using observed values of $\omega_e$, $\alpha_e$, and $\omega_e x_e$.
b) Steele-Lippincott function, Ref. 21.
c) Herschbach-Laurie function, Ref. 12.
d) Morse function, Ref. 20.
e) Additivity rule, $[a(C_2)+a(O_2)]/2$, $[a(C_2)+a(S_2)]/2$.

TABLE VI. PARAMETERS $a_3$ AND $a_4$ FOR DIATOMIC MOLECULES[a] (in Å$^{-1}$)

| | $a_3$ | $a_4$ | | $a_3$ | $a_4$ | | $a_3$ | $a_4$ | | $a_3$ | $a_4$ | | $a_3$ | $a_4$ |
|---|---|---|---|---|---|---|---|---|---|---|---|---|---|---|
| $H_2$ | 2.155 | 2.413 | $K_2$ | 0.528 | 0.359 | NaH | 1.113 | 1.167 | BF | 2.16 | 2.15 | OSi | 1.982 | 2.081 |
| $D_2$ | 2.142 | 2.336 | $Se_2$ | 1.46 | 1.30 | SH[f] | 1.84 | 1.81 | BCl | 1.709 | 1.832 | OP | 2.03 | 2.05 |
| $Li_2$ | 0.715 | 0.692 | $Br_2$[d] | 1.382 | 1.158 | SD[f] | 1.84 | 1.80 | BBr | 1.41 | 1.40 | OS | 2.072 | 2.186 |
| $B_2$ | 1.68 | 1.59 | $I_2$[e] | 1.536 | 1.563 | ClH[g] | 1.855 | 1.966 | CN | 2.268 | 2.294 | OTi | 1.74 | 1.65 |
| $C_2$[b] | 2.131 | 2.074 | LiH | 1.181 | 1.267 | ClD[g] | 1.855 | 1.966 | CO | 2.390 | 2.462 | OGe | 1.91 | 2.00 |
| $N_2$ | 2.443 | 2.461 | LiD | 1.193 | 1.282 | KH | 0.870 | 0.803 | CF[j] | 2.406 | 2.643 | Cl | 1.952 | 2.008 |
| $O_2$ | 2.476 | 2.568 | BH | 1.724 | 1.82 | BrH[h] | 1.719 | 1.806 | CP | 1.878 | 1.881 | OBa | 1.34 | 1.36 |
| $F_2$ | (2.418 | 2.560) | CH | 1.981 | 2.087 | BrD | 1.720 | 1.812 | CS | 1.945 | 2.065 | OPb | 1.78 | 1.75 |
| $Na_2$ | 0.61 | 0.48 | CD | 1.982 | 2.088 | IH[i] | 1.589 | 1.643 | CSe[k] | 1.83 | 1.93 | FP[l] | 1.891 | 2.019 |
| $Si_2$ | 1.344 | 1.413 | OH | 2.305 | 2.464 | ID[i] | 1.589 | 1.643 | NO | 2.549 | 2.618 | FCl | 1.919 | 2.13 |
| $P_2$ | 1.630 | 1.652 | OD | 2.406 | 2.654 | BeO | 2.050 | 2.093 | NSi | 1.932 | 1.961 | AlBr | 1.360 | 1.490 |
| $S_2$ | 1.702 | 1.766 | FH | 2.457 | 2.659 | BeF | 1.914 | 2.017 | NP | 2.018 | 2.039 | SiS | 1.565 | 1.631 |
| $Cl_2$[c] | 1.709 | 1.748 | FD | 2.458 | 2.650 | BO | 2.186 | 2.244 | OMg | 1.71 | 1.69 | ClI | 1.562 | 1.561 |

a) Calculated by Eq. 13 from experimental values of $\omega_e$, $\alpha_e$, and $\omega_e x_e$ listed in Refs. 4 and 22.
b) E. A. Ballik and D. A. Ramsay, *Astrophys. J.*, **137**, 84 (1963).
c) A. E. Douglas, C. K. Møller and B. P. Stoicheff, *Can. J. Phys.*, **41**, 1174 (1963).
d) Y. V. Rao and P. Venkateswarlu, *J. Mol. Spectry.*, **13**, 288 (1964).
e) D. H. Rank and B. S. Rao, ibid., **13**, **34** (1964).
f) D. A. Ramsay, *J. Chem. Phys.*, **20**, 1920 (1952).
g) D. H. Rank, D. P. Eastman, B. S. Rao and T. A. Wiggins, *J. Opt. Soc. Am.*, **52**, 1 (1962).
h) E. K. Plyler, *J. Res. Natl. Bur. Std. (U. S.)*, **64**, 377 (1960).
i) L. H. Jones, *J. Mol. Spectry.*, **1**, 179 (1957).
j) E. B. Andrews and R. F. Barrow, *Proc. Phys. Soc.*, **64A**, 481 (1951).
k) R. K. Laird and R. F. Barrow, ibid., **66A**, 836 (1953).
l) A. E. Douglas and M. Frackowiak, *Can. J. Phys.*, **40**, 832 (1962).

and Lippincott[21,22] (Eq. 5b of their paper[22]), it follows that:

$$\left.\begin{aligned} a_3 &= 1/r_e + ab(n/2r_e)^{1/2} \\ a_4 &= \{(3/7r_e)\,[6a_3 - 2/r_e + n(2ab^2-1)]\}^{1/2} \end{aligned}\right\} \quad (11)$$

where the parameters $a$, $b$, and $n$ for any molecule may be evaluated by the method described in their papers. On the other hand, by the use of the exponential function proposed by Herschbach and Laurie,[12] $a_3$ and $a_4$ (in Å$^{-1}$ units) can be estimated from the $a_{ij}(n)$ and $b_{ij}(n)$ values listed in their Table II:

$$\left.\begin{aligned} \log_{10} a_3 &= [a_{ij}(3) - r_e]/b_{ij}(3) \\ &\quad - [a_{ij}(2) - r_e]/b_{ij}(2) \\ \log_{10} a_4 &= 0.1170 + \frac{1}{2}\{[a_{ij}(4) - r_e]/b_{ij}(4) \\ &\quad - [a_{ij}(2) - r_e]/b_{ij}(2)\} \end{aligned}\right\} \quad (12)$$

The $a_3$ and $a_4$ values of CO and CS estimated by various methods are listed in Table V; they are in substantial agreements with one another.

### Anharmonicity of $NH_2$, $ND_2$, and $BO_2$

Among the linear $XY_2$ radicals which have recently been identified by spectroscopic studies,[23] $NH_2$, $ND_2$ and $BO_2$ have been the

22) D. Steele and E. R. Lippincott, ibid., 35, 2065 (1961).
23) G. Herzberg, *ICSU Review*, 4, 179 (1962).

Table VII. Approximate estimation of the anharmonic costants of $NH_2$, $ND_2$, and $BO_2$ (in $cm^{-1}$)

| | $k_{111}$ | $k_{122}$ | $k_{133}$ | $k_{1111}$ | $k_{1122}$ | $k_{1133}$ | $k_{2222}$ | $k_{2233}$ | $k_{3333}$ |
|---|---|---|---|---|---|---|---|---|---|
| $NH_2$ est.[a] | −264 | 457 | −847 | 25 | −122 | 163 | 39 | −216 | 29 |
| $ND_2$ est. | −157 | 289 | −536 | 13 | −65 | 87 | 22 | −122 | 16 |
| $BO_2$ est. | −45 | 60 | −214 | 2 | −14 | 19 | 2 | −26 | 5 |

| | $\alpha_1$ | $\alpha_2$ | $\alpha_3$ | $x_{11}$ | $x_{22}$ | $x_{33}$ | $x_{12}$ | $x_{13}$ | $x_{23}$ | $x_{ll}$ |
|---|---|---|---|---|---|---|---|---|---|---|
| $NH_2$ est. | 0.15 | (−0.017) | 0.18 | −37 | (11) | −45 | (5) | −153 | −46 | −3 |
| obs.[b] | 0.12 | −0.024 | — | — | 11.4 | — | 5 | — | — | — |
| $ND_2$ est. | 0.05 | (−0.013) | 0.07 | −19 | 6 | −27 | 4 | −80 | −30 | −1 |
| obs. | — | −0.011 | — | — | 8.1 | — | — | — | — | — |

| | $\alpha_1$ | $\alpha_2$ | $\alpha_3$ | $x_{11}$ | $x_{33}$ | $x_{12}$ | $x_{23}$ | $x_{22}+x_{ll}$ | $x_{12}+4x_{22}$ |
|---|---|---|---|---|---|---|---|---|---|
| $BO_2$ est. | 0.0015 | −0.0007 | 0.0031 | −5 | −15 | −20 | −11 | −0.2 | −5 |
| obs.[c] | 0.0002 | −0.0003 | 0.0023 | 0 | — | — | — | — | ∼−12 |

a) Present estimates. Assumed values are enclosed in parentheses.
b) Refs. 24 and 25.
c) Ref. 26.

subject of detailed vibrational analyses. Dressler and Ramsay[24,25] have reported on the $\omega_1^0+x_1^0$, $\omega_2^0$, $x_{12}^0$, $x_{22}^0$, $\alpha_1$, $\alpha_2$, and $B_0$ values of $NH_2$ and $ND_2$ in the $^2A_1\Pi_u$ excited electronic state, while Johns[26] has given $\omega_1$, $\omega_2$, $(1/2)(2\nu_3)$, $\alpha_1$, $\alpha_2$, $\alpha_3$, $x_{22}$, and $x_{12}$ of $BO_2$ in the $A^2\Pi_u$ state. Although exact $\omega_3$ values are unknown, it seems worthwhile to apply the present technique to these molecules in order to make an approximate prediction of the orders of magnitude of the $\alpha$ and $x$ values.

On the basis of a preliminary estimation of $x$ and the product rule of the $NH_2$ and $ND_2$ frequencies, $f_1$ and $f_2$ are estimated to be 7.16 and 0.085 md./Å respectively. With the further assumption that $f_{r'}=0$, $\omega_3$ is found to be $3.7_1\times10^3\,cm^{-1}$ ($NH_2$) and $2.7_9\times10^3\,cm^{-1}$ ($ND_2$). The parameters $a_3$ and $a_4$ are estimated, by the method discussed in the preceding section, to be $2.19\,Å^{-1}$ and $2.28\,Å^{-1}$ respectively. The $f_{rrr}$ and $f_{rrrr}$ constants are, then, 7.64 and 10.32 md./Å respectively. Higher-order potential constants, $f_{r\alpha\alpha}$, $f_{rr\alpha\alpha}$, $f_{rr'\alpha\alpha}$ and $f_{\alpha\alpha\alpha\alpha}$, are adjusted to make the outputs of $\alpha_2$, $x_{12}$, and $x_{22}$ nearly agree with the observed values; they are thus taken to be −0.37, 0.96, 0.41, and 0.03 md./Å respectively.

The estimates of the anharmonic constants resulting from the present crude approximations are given in Table VII.

For $BO_2$, a preliminary estimation based on the vibrational data of Johns suggests that $\omega_3\sim2422\,cm^{-1}$, $f_r\sim11.73$, $f_{r'}\sim-2.42$, and $f_\alpha\sim0.30$ md./Å. With the parameters $a_3$ and $a_4$ transferred from those of the BO radical listed in Table VII, and with $f_{r\alpha\alpha}$ arbitrarily assumed to be $f_{r\alpha\alpha}(CO_2)\cdot f_\alpha(BO_2)/f_\alpha(CO_2)\sim0.28$, the anharmonic constants $\alpha$ and $x$ are predicted (Table VII). The magnitude of $k_{122}(\sim60\,cm^{-1})$ indicates the presence of the strong Fermi resonance observed by Johns, which must influence the observed values of $\alpha_1$ and $\alpha_2$ by intermixing the $\nu_1$ and $2\nu_2$ vibrational states. The agreement of $\alpha_3$ is fair.

## Summary

On the basis of a normal-coordinate analysis of a series expansion of the anharmonic potential field, a set of general expressions has been derived for a linear $XY_2$ molecule for relating the cubic and quartic potential constants ($k$) to the coefficients ($f$) of the potential function expanded in terms of the internal coordinates. The constants $k$ and $f$ for $CO_2$ and $CS_2$ have been calculated by using the observed values of $\alpha$ and $x$ taken from the literature, and the physical significance of the dependence of $k$ on $f$ has been studied.

The anharmonic constants related to the C-O(C-S) bond-stretching vibrations are represented as functions of the parameters of anharmonicity, $a_3$ and $a_4$, which are shown to be transferable from the CO(CS) diatomic molecule. Most of the $k$, $\alpha$, and $x$ values for $CO_2$ and $CS_2$ can be predicted quantitatively by assuming a simple potential function, comprised of ordinary quadratic terms and the anharmonic terms for the bond-stretching vibrations mentioned above, with all other higher-order potential terms ignored.

A number of methods for estimating the parameters $a_3$ and $a_4$, and a general rule regarding their relative magnitudes, have been discussed. The $k$, $\alpha$, and $x$ values of the linear radicals, $NH_2$, $ND_2$, and $BO_2$, may be predicted

24) K. Dressler and D. A. Ramsay, *Phil. Trans. Roy. Soc.*, **A251**, 553 (1959).
25) D. A. Ramsay, *Advances in Spectroscopy*, **1**, 1 (1959).
26) J. W. C. Johns, *Can. J. Phys.*, **39**, 1738 (1961).

in the present scheme by making simple assumptions about their potential constants.

The authors are indebted to Dr. Takao Iijima for his help in the calculations.

*Department of Chemistry*
*Faculty of Science*
*The University of Tokyo*
*Hongo, Tokyo*

## Appendix

The interrelations among the coefficients of the potential function in terms of the internal symmetry and normal coordinates are given by the following sets of equations:

$$\left.\begin{aligned}
&f_r=\frac{1}{2}(f_1+f_3),\quad f_{r'}=\frac{1}{2}(f_1-f_3),\quad f_\alpha=f_2\\
&f_{rrr}=\frac{1}{2\sqrt{2}}(f_{111}+f_{133})\\
&f_{rrr'}=\frac{1}{2\sqrt{2}}(3f_{111}-f_{133}),\quad f_{r\alpha\alpha}=\frac{1}{\sqrt{2}}f_{122}\\
&f_{rrrr}=\frac{1}{4}(f_{1111}+f_{1133}+f_{3333})\\
&f_{rrrr'}=f_{1111}-f_{3333},\\
&f_{rrr'r'}=\frac{1}{2}(3f_{1111}-f_{1133}+3f_{3333})\\
&f_{rr\alpha\alpha}=\frac{1}{2}(f_{1122}+f_{2233}),\quad f_{rr'\alpha\alpha}=f_{1122}-f_{2233}\\
&f_{\alpha\alpha\alpha\alpha}=f_{2222}
\end{aligned}\right\}\quad\text{(A-1)}$$

The cubic and quartic constants in Eq. 6 depend on the force constants of Eq. 5:

$$\left.\begin{aligned}
&k_{111}=\frac{2\sqrt{2}}{r_e}h_{111}g_1^3f_{111}\\
&k_{122}=\frac{1}{r_e}h_{122}g_1g_2^2(f_1-4f_2+4\sqrt{2}f_{122})\\
&k_{133}=\frac{2\sqrt{2}}{r_e}h_{133}g_1g_2^2f_{133}\\
&k_{1111}=\frac{4}{r_e^2}h_{1111}g_1^4f_{1111}\\
&k_{1122}=\frac{1}{r_e^2}h_{1122}g_1^2g_2^2(-f_1+6f_2+3\sqrt{2}f_{111}\\
&\qquad-8\sqrt{2}f_{122}+8f_{1122})\\
&k_{1133}=\frac{4}{r_e^2}h_{1133}g_1^2g_2^2f_{1133}\\
&k_{2222}=\frac{1}{r_e^2}h_{2222}g_2^4\left(\frac{1}{4}f_1-\frac{4}{3}f_2+2\sqrt{2}f_{122}\right.\\
&\qquad\left.+16f_{2222}\right)\\
&k_{2233}=\frac{1}{r_e^2}h_{2233}g_2^4(4f_2-f_3+\sqrt{2}f_{133}+8f_{2233})\\
&k_{3333}=\frac{4}{r_e^2}h_{3333}g_2^4f_{3333}
\end{aligned}\right\}\quad\text{(A-2)}$$

where $h_{ijj}=h^{1/2}/8\pi^3c^{5/2}\omega_i^{1/2}\omega_j$
and $h_{iijj}=h/16\pi^4c^3\omega_i\omega_j$

It has been shown by Dennison[8,15] that these cubic and quartic constants are related to $\alpha$ and $x$ by the following expressions:

$$\left.\begin{aligned}
&\alpha_1=-6B_e^2/\omega_1-3(2B_e/\omega_1)^{3/2}k_{111}\\
&\alpha_2=B_e^2[1/\omega_2-2/(\omega_3+\omega_2)+2/(\omega_3-\omega_2)]\\
&\qquad-(2B_e/\omega_1)^{3/2}k_{122}\\
&\alpha_3=2B_e^2[1/\omega_3-2/(\omega_3+\omega_2)-2/(\omega_3-\omega_2)]\\
&\qquad-(2B_e/\omega_1)^{3/2}k_{133}\\
&x_{11}=\frac{3}{2}k_{1111}-(15/4\omega_1)k_{111}^2\\
&x_{33}=\frac{3}{2}k_{3333}-\frac{1}{8}[4/\omega_1+1/(2\omega_3+\omega_1)\\
&\qquad-1/(2\omega_3-\omega_1)]k_{133}^2\\
&x_{13}=k_{1133}-(3/\omega_1)k_{111}k_{133}-\frac{1}{2}[1/(2\omega_3+\omega_1)\\
&\qquad+1/(2\omega_3-\omega_1)]k_{133}^2\\
&x_{23}=k_{2233}-(1/\omega_1)k_{122}k_{133}\\
&\qquad+[\omega_3/\omega_2+\omega_2/\omega_3]B_e\\
&x_{22}+x_{ll}=k_{2222}-(1/2\omega_1)k_{122}^2\\
&x_{12}+4x_{22}=k_{1122}+6k_{2222}-(3/\omega_1)k_{111}k_{122}\\
&\qquad-[2/\omega_1+1/(2\omega_2+\omega_1)]k_{122}^2
\end{aligned}\right\}\quad\text{(A-3)}$$

The last two equations are adopted in order to eliminate the resonance contribution, $1/(2\omega_2-\omega_1)$, from the expressions.

# Estimation of Anharmonic Potential Constants. II. Bent $XY_2$ Molecules

By Kozo KUCHITSU and Yonezo MORINO

(Received October 10, 1964)

In the preceding paper, Part I,[1] the anharmonic potential constants of the linear $XY_2$ molecules have been estimated on the basis of a simple potential function. That procedure will here be extended to the bent $XY_2$ molecules, for which previous theoretical studies of the anharmonic constants[2-5] have been limited to $H_2O$ and $D_2O$. The purpose of the present study is to set up a convenient method for a quantitative or at least a semi-quantitative prediction of the anharmonic constants in order to achieve a better understanding of the physical significance of these constants. It is also intended to seek for a simple and plausible representation of the anharmonic force field of polyatomic molecules.

The estimation of anharmonic constants is more complicated in this case than in the case of the linear $XY_2$ molecule, because the coordinate transformation depends on the off-diagonal elements of the $L$ matrix (two-dimensional in this case); moreover, the potential constants which depend on the odd power of the angular displacement do not vanish by symmetry requirement, while they do in the case of linear $XY_2$. These circumstances, however, do not seriously disturb the present analysis; in addition, the quadratic force constants for most of the bent $XY_2$ molecules are generally much better known than those for more complex molecules.

The importance of the bent $XY_2$ molecules for the study of anharmonicity is twofold. First, relatively abundant, although far from complete, experimental data have been reported concerning their $\alpha$ and $x$ values, especially for those of $H_2O$, $D_2O$, and $SO_2$, and further information will be obtained in the near future. Secondly, the bent $XY_2$ molecule is one of the few simple systems for which the cubic and most of the quartic potential constants can be determined uniquely, provided all $\alpha$ and $x$ values are known. The following sections will, therefore, present a general formulation necessary for the analysis, a formulation by means of which the "anharmonic constants" of the potential function expressed in the normal-coordinate system can be transformed into the "higher-order constants" in the internal-coordinate system. A simple method for estimating the anharmonic constants will then be presented on the basis of an examination of the physical significance of these higher-order potential constants.

## Expansion of Internal Coordinates

The internal coordinates are expanded in terms of the normal coordinates by the method discussed in Ref. 5. The displacements of the $X\text{-}Y_i$ ($i=1, 2$) bond length, $\Delta r_i$, and that of the $Y_1\text{-}X\text{-}Y_2$ angle, $\Delta\alpha$, from their equilibrium values are first expanded in terms of the Cartesian displacement coordinates shown in Fig. 1; $\Delta z_i$ and $\Delta x_i$ are taken to be the projections of the instantaneous displacement of the $Y_i$ atom with respect to the X atom along and perpendicular to the equilibrium direction of the $X\text{-}Y_i$ bond respectively. The out-of-plane displacements, $\Delta y_i$, are of course zero. It is shown in Eq. 14 of Ref. 5 that:

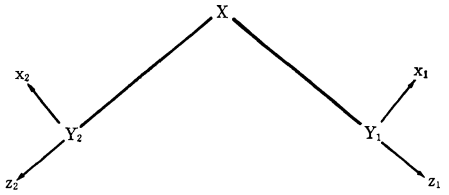



Fig. 1. Cartesian coordinates for the bent $XY_2$ molecule. The $z_i$ axis ($i=1$ or 2) is taken in the direction of the bond $X\text{-}Y_i$ at their equilibrium positions, and the $x_i$ axis is taken on the molecular plane and perpendicular to the $z_i$ axis outwards. The displacement of the $Y_i$ atom relative to the X atom is described in the $x_i$, $z_i$ coordinates.

$$\left.\begin{aligned}
\Delta r_i &= \Delta z_i + \Delta x_i^2/2r_e - \Delta z_i \Delta x_i^2/2r_e^2 + \cdots \\
r_e\Delta\alpha &= \Delta x_1 + \Delta x_2 - (\Delta x_1\Delta z_1 + \Delta x_2\Delta z_2)/r_e \\
&\quad + [\Delta x_1\Delta z_1^2 + \Delta x_2\Delta z_2^2 \\
&\quad - \frac{1}{3}(\Delta x_1^3 + \Delta x_2^3)]/r_e^2 + \cdots
\end{aligned}\right\} \quad (1)$$

1) K. Kuchitsu and Y. Morino, This Bulletin, **38**, 805 (1965).
2) O. Redlich, *J. Chem. Phys.*, **9**, 298 (1941).
3) J. Pliva, *Collection Czechoslov. Chem. Communs.*, **23**, 777 (1958).
4) D. R. Herschbach and V. W. Laurie, *J. Chem. Phys.*, **35**, 458 (1961).
5) K. Kuchitsu and L. S. Bartell, ibid., **36**, 2460 (1962).

TABLE I. MATRIX REPRESENTATION OF CUBIC POTENTIAL CONSTANTS

$$\begin{pmatrix} k_{111}/h_{111} \\ k_{122}/h_{122} \\ k_{133}/h_{133} \\ k_{211}/h_{211} \\ k_{222}/h_{222} \\ k_{233}/h_{233} \end{pmatrix} = \begin{pmatrix} \alpha^2\lambda & \alpha^2\lambda & \alpha(\alpha^2-2\lambda^2) & \alpha^2\lambda \\ \beta(2\alpha\mu+\beta\lambda) & \beta(2\alpha\mu+\beta\lambda) & 3\alpha\beta^2-2\alpha\mu^2-4\beta\lambda\mu & \beta(2\alpha\mu+\beta\lambda) \\ \gamma(\gamma\lambda+2\alpha\nu) & \gamma(\gamma\lambda-2\alpha\nu) & \gamma(\alpha\gamma-2\lambda\nu) & \alpha\gamma\nu \\ \alpha(\alpha\mu+2\beta\lambda) & \alpha(\alpha\mu+2\beta\lambda) & 3\alpha^2\beta-2\beta\lambda^2-4\alpha\lambda\mu & \alpha(\alpha\mu+2\beta\lambda) \\ \beta^2\mu & \beta^2\mu & \beta(\beta^2-2\mu^2) & \beta^2\mu \\ \gamma(\gamma\mu+2\beta\nu) & \gamma(\gamma\mu-2\beta\nu) & \gamma(\beta\gamma-2\mu\nu) & \beta\gamma\nu \end{pmatrix} \begin{pmatrix} f_r/r_e \\ f_{r'}/r_e \\ 2f_{r\alpha}/r_e \\ -4f_\alpha/r_e \end{pmatrix}$$

$$+ \begin{pmatrix} \lambda^3 & \lambda^3 & \alpha\lambda^2 & \alpha\lambda^2 & \alpha^2\lambda & \alpha^3 \\ 3\lambda\mu^2 & 3\lambda\mu^2 & \mu(\alpha\mu+2\beta\lambda) & \mu(\alpha\mu+2\beta\lambda) & \beta(2\alpha\mu+\beta\lambda) & 3\alpha\beta^2 \\ 3\lambda\nu^2 & -\lambda\nu^2 & \alpha\nu^2 & -\alpha\nu^2 & 0 & 0 \\ 3\lambda^2\mu & 3\lambda^2\mu & \lambda(2\alpha\mu+\beta\lambda) & \lambda(2\alpha\mu+\beta\lambda) & \alpha(\alpha\mu+2\beta\lambda) & 3\alpha^2\beta \\ \mu^3 & \mu^3 & \beta\mu^2 & \beta\mu^2 & \beta^2\mu & \beta^3 \\ 3\mu\nu^2 & -\mu\nu^2 & \beta\nu^2 & -\beta\nu^2 & 0 & 0 \end{pmatrix} \begin{pmatrix} 2f_{rrr}/r_e \\ 2f_{rrr'}/r_e \\ 4f_{rr\alpha}/r_e \\ 2f_{rr'\alpha}/r_e \\ 8f_{r\alpha\alpha}/r_e \\ 8f_{\alpha\alpha\alpha}/r_e \end{pmatrix}$$

Units: $k$: $cm^{-1}$; $h_{ijj}=N^{3/2}h^{1/2}/8\pi^3c^{5/2}\omega_i^{1/2}\omega_j$; $\alpha$, $\beta$, $\gamma$, $\lambda$, $\mu$, $\nu$: a. m. u.
$f$: dyne/cm.; $r_e$: cm.

On the other hand, the following linear relations exist between the Cartesian and normal coordinates, $Q$:

$$\left.\begin{aligned} \Delta x_i &= \alpha Q_1+\beta Q_2 \pm \gamma Q_3 \\ \Delta z_i &= \lambda Q_1+\mu Q_2 \pm \nu Q_3 \end{aligned}\right\} \quad (2)$$

where the positive and negative signs of $\gamma$ and $\nu$ apply to $i=1$ and 2 respectively, and where the coefficients are related to the $\boldsymbol{L}$ and the $\boldsymbol{G}$ matrices as follows:

$$\left.\begin{aligned} &\alpha=\frac{1}{2}L_{21}, \quad \beta=\frac{1}{2}L_{22}, \quad \gamma=-G_{12}/2L_{33} \\ &\lambda=\frac{1}{\sqrt{2}}L_{11}, \quad \mu=\frac{1}{\sqrt{2}}L_{12}, \quad \nu=\frac{1}{\sqrt{2}}L_{33} \end{aligned}\right\} \quad (3)$$

The desired expansion of the internal coordinates is, therefore, straightforward.

## Potential Function

The vibrational potential function of the bent $XY_2$ molecule can be expanded in terms of the internal coordinates in the following way:

$$\begin{aligned} V=&\frac{1}{2}f_r(\Delta r_1^2+\Delta r_2^2)+f_{r'}\Delta r_1\Delta r_2 \\ &+f_{r\alpha}(\Delta r_1+\Delta r_2)r_e\Delta\alpha+\frac{1}{2}f_\alpha r_e^2\Delta\alpha^2 \\ &+\frac{1}{r_e}[f_{rrr}(\Delta r_1^3+\Delta r_2^3)+f_{rrr'}(\Delta r_1+\Delta r_2) \\ &\times\Delta r_1\Delta r_2+f_{rr\alpha}(\Delta r_1^2+\Delta r_2^2)r_e\Delta\alpha \\ &+f_{rr'\alpha}\Delta r_1\Delta r_2 r_e\Delta\alpha+f_{r\alpha\alpha}(\Delta r_1+\Delta r_2) \\ &\times r_e^2\Delta\alpha^2+f_{\alpha\alpha\alpha}r_e^3\Delta\alpha^3] \\ &+\frac{1}{r_e^2}[f_{rrrr}(\Delta r_1^4+\Delta r_2^4)+f_{rrrr'} \\ &\times(\Delta r_1^2+\Delta r_2^2)\Delta r_1\Delta r_2+f_{rrr'r'}\Delta r_1^2\Delta r_2^2 \\ &+f_{rrr\alpha}(\Delta r_1^3+\Delta r_2^3)r_e\Delta\alpha \\ &+f_{rrr'\alpha}(\Delta r_1+\Delta r_2)\Delta r_1\Delta r_2 r_e\Delta\alpha \\ &+f_{rr\alpha\alpha}(\Delta r_1^2+\Delta r_2^2)r_e^2\Delta\alpha^2 \\ &+f_{rr'\alpha\alpha}\Delta r_1\Delta r_2 r_e^2\Delta\alpha^2 \\ &+f_{r\alpha\alpha\alpha}(\Delta r_1+\Delta r_2)r_e^3\Delta\alpha^3+f_{\alpha\alpha\alpha\alpha}r_e^4\Delta\alpha^4] \\ &+\cdots \end{aligned} \quad (4)$$

The quadratic force constants, $f_r$, $f_{r'}$, $f_{r\alpha}$, and $f_\alpha$, can be determined uniquely if the elements of the $\boldsymbol{F}$ matrix,

$$\left.\begin{aligned} &f_r=\frac{1}{2}(F_{11}+F_{33}) \qquad f_{r'}=\frac{1}{2}(F_{11}-F_{33}) \\ &f_{r\alpha}=\frac{1}{\sqrt{2}}F_{12} \quad \text{and} \quad f_\alpha=F_{22} \end{aligned}\right\} \quad (5)$$

are known.

Upon replacing $\Delta r_i$ and $r_e\Delta\alpha$ by $\Delta z_i$ and $\Delta x_i$ and the latter by $Q$, by the use of Eqs. 1 and 2, the cubic and quartic constants of the potential function in terms of the dimensionless normal coordinates[6]:

$$\begin{aligned} V/hc=&\frac{1}{2}(\omega_1q_1^2+\omega_2q_2^2+\omega_3q_3^2) \\ &+k_{111}q_1^3+k_{122}q_1q_2^2+k_{133}q_1q_3^2 \\ &+k_{211}q_2q_1^2+k_{222}q_2^3+k_{233}q_2q_3^2 \\ &+k_{1111}q_1^4+k_{1122}q_1^2q_2^2+k_{1133}q_1^2q_3^2 \\ &k_{2222}q_2^4+k_{2233}q_2^2q_3^2+k_{3333}q_3^4 \end{aligned} \quad (6)$$

where

$$q_s=2\pi(c\omega_s/h)^{1/2}Q_s$$

can be expressed in the matrix form shown in Tables I and II.*1 On the other hand, the

*1 Similar expressions for other nonvanishing quartic constants, $k_{1112}$, $k_{1222}$, and $k_{1233}$, are not listed in Table II, since they are not included in $x$ as far as the ordinary second-order perturbation theory is concerned[6-8] and, hence, remain unknown. The orders of magnitude of $k_{1112}$, $k_{1222}$, and $k_{1233}$ may, however, be estimated by an extension of the method given below, if such an estimate is necessary for a discussion of higher-order interactions.

TABLE II. MATRIX REPRESENTATION OF QUARTIC POTENTIAL CONSTANTS

$$
\begin{pmatrix} k_{1111}/h_{1111} \\ k_{1122}/h_{1122} \\ k_{1133}/h_{1133} \\ k_{2222}/h_{2222} \\ k_{2233}/h_{2233} \\ k_{3333}/h_{3333} \end{pmatrix} =
\begin{pmatrix}
\alpha^2(\alpha^2-4\lambda^2) & \alpha^2(\alpha^2-4\lambda^2) & 2\alpha\lambda(\lambda^2-\tfrac{4}{3}\alpha^2) & \alpha^2(3\lambda^2-\tfrac{2}{3}\alpha^2) \\
6\alpha^2\beta^2-4\alpha^2\mu^2 & 6\alpha^2\beta^2-4\alpha^2\mu^2 & & \\
-4\beta^2\lambda^2-16\alpha\beta\lambda\mu & -4\beta^2\lambda^2-16\alpha\beta\lambda\mu & 2(3\lambda\mu-4\alpha\beta)(\alpha\mu+\beta\lambda) & 3\alpha^2\mu^2+3\beta^2\lambda^2 \\
 & & & +12\alpha\beta\lambda\mu-4\alpha^2\beta^2 \\
6\alpha^2\gamma^2-4\alpha^2\nu^2 & 4\alpha^2\nu^2-4\gamma^2\lambda^2 & 2\alpha\lambda\nu^2-3\alpha^2\gamma\nu & 2\alpha^2(\nu^2-\gamma^2) \\
-4\gamma^2\lambda^2-16\alpha\gamma\lambda\nu & -2\alpha^2\gamma^2 & +4\gamma\lambda^2\nu-4\alpha\gamma^2\lambda & +6\alpha\gamma\lambda\nu \\
\beta^2(\beta^2-4\mu^2) & \beta^2(\beta^2-4\mu^2) & 2\beta\mu(\mu^2-\tfrac{4}{3}\beta^2) & \beta^2(3\mu^2-\tfrac{2}{3}\beta^2) \\
6\beta^2\gamma^2-4\beta^2\nu^2 & 4\beta^2\nu^2-4\gamma^2\mu^2 & 2\beta\mu\nu^2-3\beta^2\gamma\nu & 2\beta^2(\nu^2-\gamma^2) \\
-4\gamma^2\mu^2-16\beta\gamma\mu\nu & -2\beta^2\gamma^2 & +4\gamma\mu^2\nu-4\beta\gamma^2\mu & +6\beta\gamma\mu\nu \\
\gamma^2(\gamma^2-4\nu^2) & \gamma^2(\gamma^2+4\nu^2) & -\gamma^3\nu & \gamma^2\nu^2
\end{pmatrix}
\begin{pmatrix} f_r/4r_e^2 \\ f_{r'}/4r_e^2 \\ 2f_{r\alpha}/r_e^2 \\ 2f_\alpha/r_e^2 \end{pmatrix}
$$

$$
+
\begin{pmatrix}
\alpha^2\lambda^2 & 3\alpha^2\lambda^2 & \alpha\lambda(\alpha^2-\lambda^2) & \alpha\lambda(\alpha^2-\lambda^2) & \alpha^2(\alpha^2-4\lambda^2) & \alpha^3\lambda \\
\alpha^2\mu^2+\beta^2\lambda^2+4\alpha\beta\lambda\mu & 3\alpha^2\mu^2+3\beta^2\lambda^2 & 3(\alpha\beta-\lambda\mu) & 3(\alpha\beta-\lambda\mu) & 6\alpha^2\beta^2-4\alpha^2\mu^2 & \\
 & +12\alpha\beta\lambda\mu & (\alpha\mu+\beta\lambda) & (\alpha\mu+\beta\lambda) & -4\beta^2\lambda^2-16\alpha\beta\lambda\mu & 3\alpha\beta(\alpha\mu+\beta\lambda) \\
\alpha^2\nu^2+\gamma^2\lambda^2+4\alpha\gamma\lambda\nu & 3\gamma^2\lambda^2-\alpha^2\nu^2 & \alpha\gamma(\gamma\lambda+2\alpha\nu) & \alpha\gamma(\gamma\lambda-2\alpha\nu) & \alpha^2\gamma^2-4\alpha\gamma\lambda\nu & \alpha^2\gamma\nu \\
 & -4\alpha\gamma\lambda\nu & -\gamma\nu(\gamma\lambda+\alpha\nu) & -\lambda\nu(\gamma\lambda-\alpha\nu) & & \\
\beta^2\mu^2 & 3\beta^2\mu^2 & \beta\mu(\beta^2-\mu^2) & \beta\mu(\beta^2-\mu^2) & \beta^2(\beta^2-4\mu^2) & \beta^3\mu \\
\beta^2\nu^2+\gamma^2\mu^2+4\beta\gamma\mu\nu & 3\gamma^2\mu^2-\beta^2\nu^2 & \beta\gamma(\gamma\mu+2\beta\nu) & \beta\gamma(\gamma\mu-2\beta\nu) & \beta^2\gamma^2-4\beta\gamma\mu\nu & \beta^2\gamma\nu \\
 & -4\beta\gamma\mu\nu & -\mu\nu(\gamma\mu+\beta\nu) & -\mu\nu(\gamma\mu-\beta\nu) & & \\
\gamma^2\nu^2 & -\gamma^2\nu^2 & -\gamma\nu^3 & \gamma\nu^3 & 0 & 0
\end{pmatrix}
\begin{pmatrix} 3f_{rrr}/r_e^2 \\ f_{rrr'}/r_e^2 \\ 4f_{rr\alpha}/r_e^2 \\ 2f_{rr'\alpha}/r_e^2 \\ 4f_{r\alpha\alpha}/r_e^2 \\ -24f_{\alpha\alpha\alpha}/r_e^2 \end{pmatrix}
$$

$$
+
\begin{pmatrix}
\lambda^4 & \lambda^4 & \lambda^4 & \alpha^2\lambda^2 & \alpha^2\lambda^2 & \alpha^4 & \alpha\lambda^3 & \alpha\lambda^3 & \alpha^3\lambda \\
6\lambda^2\mu^2 & 6\lambda^2\mu^2 & 6\lambda^2\mu^2 & \alpha^2\mu^2+\beta^2\lambda^2 & \alpha^2\mu^2+\beta^2\lambda^2 & 6\alpha^2\beta^2 & 3\lambda\mu(\alpha\mu+\beta\lambda) & 3\lambda\mu(\alpha\mu+\beta\lambda) & 3\alpha\beta(\alpha\mu+\beta\lambda) \\
 & & & +4\alpha\beta\lambda\mu & +4\alpha\beta\lambda\mu & & & & \\
6\lambda^2\nu^2 & 0 & -2\lambda^2\nu^2 & \alpha^2\nu^2 & -\alpha^2\nu^2 & 0 & 3\alpha\lambda\nu^2 & -\alpha\lambda\nu^2 & 0 \\
\mu^4 & \mu^4 & \mu^4 & \beta^2\mu^2 & \beta^2\mu^2 & \beta^4 & \beta\mu^3 & \beta\mu^3 & \beta^3\mu \\
6\mu^2\nu^2 & 0 & -2\mu^2\nu^2 & \beta^2\nu^2 & -\beta^2\nu^2 & 0 & 3\beta\mu\nu^2 & -\beta\mu\nu^2 & 0 \\
\nu^4 & -\nu^4 & \nu^4 & 0 & 0 & 0 & 0 & 0 & 0
\end{pmatrix}
\begin{pmatrix} 2f_{rrrr}/r_e^2 \\ 2f_{rrrr'}/r_e^2 \\ 2f_{rrr'r'}/r_e^2 \\ 8f_{rr\alpha\alpha}/r_e^2 \\ 4f_{rr'\alpha\alpha}/r_e^2 \\ 16f_{\alpha\alpha\alpha\alpha}/r_e^2 \\ 4f_{rrr\alpha}/r_e^2 \\ 4f_{rrr'\alpha}/r_e^2 \\ 16f_{r\alpha\alpha\alpha}/r_e^2 \end{pmatrix}
$$

Unit: $k$: cm$^{-1}$; $h_{iijj}=N^2h/16\pi^4c^3\omega_i\omega_j$; $\alpha$, $\beta$, $\gamma$, $\lambda$, $\mu$, $\nu$: a. m. u.; $f$: dyne/cm.; $r_e$: cm.

Table III. Vibrational frequencies of bent $XY_2$ (in $cm^{-1}$)

| | $H_2O$ | $D_2O$ | $H_2S$ | $D_2S$[a] | $H_2Se$[a] | $D_2Se$[a] | $SO_2$ | $ClO_2$ | $^{14}NO_2$ | $^{15}NO_2$ |
|---|---|---|---|---|---|---|---|---|---|---|
| $\omega_1$ | 3832.17 | 2763.80 | 2721.92 | 1950 | 2435 | 1732 | 1167.60 | 962.8 | 1357.8 | 1342.5 |
| $\omega_2$ | 1648.47 | 1206.39 | 1214.51 | 874 | 1054 | 750 | 526.27 | 455.4 | 756.8 | 747.1 |
| $\omega_3$ | 3942.53 | 2888.78 | 2733.36 | 1964 | 2448 | 1743 | 1380.91 | 1128.2 | 1665.5 | 1628.0 |
| Ref. | 9 | 9 | 10 | 11 | 12 | 12 | 13 | 14 | 15 | 15 |

a) Normal frequencies estimated in the present study on the basis of the fundamental frequencies listed in the references.

Table IV. Quadratic force constants (in md./Å) and equilibrium structure of bent $XY_2$

| | $f_r$ | $f_{r'}$ | $f_{r\alpha}$ | $f_\alpha$ | $r_e$ (Å) | $\alpha_e$ | Ref. |
|---|---|---|---|---|---|---|---|
| $H_2O$, $D_2O$ | 8.454 | −0.101 | 0.228 | 0.761 | $0.9572_1$ | 104°31.$_3$′ | 5, 9 |
| $H_2S$[a], $D_2S$ | 4.284 | −0.012 | 0.101 | 0.429 | 1.336[b] | 92°12′ | 10 |
| $H_2Se$[a], $D_2Se$ | 3.493 | −0.020 | 0.055 | 0.327 | $1.460_5$ | 90°55′ | 16 |
| $SO_2$ | 10.332 | 0.081 | 0.227 | 0.815 | 1.4308 | 119°19′ | 8 |
| $ClO_2$ | 7.018 | −0.170 | 0.006 | 0.651 | 1.473 ($r_s$) | 117°36′ ($\alpha_s$) | 17, 18 |
| $NO_2$ | 11.043 | 2.140 | 0.481 | 1.109 | 1.1934 ($r_s$) | 134°4′ ($\alpha_s$) | 19 |

a) Calculated in the present study from the data given in Table III.
b) Calculated from the equilibrium moments of inertia listed in Eq. 14 of Allen and Plyler's paper.[10] The $r_e$ distance of H-S given in their paper, 1.328Å, seems to be in error.

relations between the anharmonic constants and the $\alpha$ and $x$ values have been derived by Darling and Dennison[6-8] as follows:

$$\left.\begin{aligned}
\alpha_1^A &= A_1 + 3a_1k_{111} + a_2k_{211}\\
\alpha_2^A &= A_2 + a_1k_{122} + 3a_2k_{222}\\
\alpha_3^A &= A_3 + a_1k_{133} + a_2k_{233}\\
\alpha_1^B &= B_1 + 3b_1k_{111} + b_2k_{211}\\
\alpha_2^B &= B_2 + b_1k_{122} + 3b_2k_{222}\\
\alpha_3^B &= B_3 + b_1k_{133} + b_2k_{233}\\
\alpha_1^C &= C_1 + 3c_1k_{111} + c_2k_{211}\\
\alpha_2^C &= C_2 + c_1k_{122} + 3c_2k_{222}\\
\alpha_3^C &= C_3 + c_1k_{133} + c_2k_{233}
\end{aligned}\right\} \quad (7)$$

and:

$$\left.\begin{aligned}
x_{11} &= \frac{3}{2}k_{1111} - \frac{15k_{111}^2}{4\omega_1} - \frac{k_{211}^2(8\omega_1^2-3\omega_2^2)}{4\omega_2(4\omega_1^2-\omega_2^2)}\\
x_{22} &= \frac{3}{2}k_{2222} - \frac{15k_{222}^2}{4\omega_2} - \frac{k_{122}^2(8\omega_2^2-3\omega_1^2)}{4\omega_1(4\omega_2^2-\omega_1^2)}\\
x_{33} &= \frac{3}{2}k_{3333} - \frac{k_{133}^2(8\omega_3^2-3\omega_1^2)}{4\omega_1(4\omega_3^2-\omega_1^2)}\\
&\quad - \frac{k_{233}^2(8\omega_3^2-3\omega_2^2)}{4\omega_2(4\omega_3^2-\omega_2^2)}\\
x_{12} &= k_{1122} - \frac{3k_{111}k_{122}}{\omega_1} - \frac{3k_{211}k_{222}}{\omega_2}\\
&\quad - \frac{2k_{211}^2\omega_1}{4\omega_1^2-\omega_2^2} - \frac{2k_{122}^2\omega_2}{4\omega_2^2-\omega_1^2}\\
x_{13} &= k_{1133} - \frac{3k_{111}k_{133}}{\omega_1} - \frac{k_{211}k_{233}}{\omega_2}\\
&\quad - \frac{2k_{133}^2\omega_3}{4\omega_3^2-\omega_1^2} + C_e\zeta_{13}^2\left(\frac{\omega_3}{\omega_1}+\frac{\omega_1}{\omega_3}\right)\\
x_{23} &= k_{2233} - \frac{k_{122}k_{133}}{\omega_1} - \frac{3k_{222}k_{233}}{\omega_2}\\
&\quad - \frac{2k_{233}^2\omega_3}{4\omega_3^2-\omega_2^2} + C_e\zeta_{23}^2\left(\frac{\omega_3}{\omega_2}+\frac{\omega_2}{\omega_3}\right)
\end{aligned}\right\} \quad (8)$$

where*2

$$A_1 = -\frac{6A_e^2}{\omega_1}\sin^2\Gamma, \quad a_1 = -\left(\frac{2A_e}{\omega_1}\right)^{3/2}\sin\Gamma$$

$$A_2 = -\frac{6A_e^2}{\omega_2}\cos^2\Gamma, \quad a_2 = -\left(\frac{2A_e}{\omega_2}\right)^{3/2}\cos\Gamma$$

$$A_3 = -\frac{6A_eC_e}{\omega_3}$$

$$B_1 = -\frac{6B_e^2}{\omega_1}\cos^2\Gamma, \quad b_1 = -\left(\frac{2B_e}{\omega_1}\right)^{3/2}\cos\Gamma$$

6) H. H. Nielsen, *Revs. Mod. Phys.*, 23, 90 (1951).
7) B. T. Darling and D. M. Dennison, *Phys. Rev.*, 57, 128 (1940).
8) Y. Morino, Y. Kikuchi, S. Saito and E. Hirota, *J. Mol. Spectry.*, 13, 95 (1964).

*2 In Refs. 7 and 8, $\sin\Gamma$ is denoted as $\sin\gamma$ and $\cos\Gamma$ as $\cos\gamma$. The symbol $\Gamma$ is used here in order to avoid confusion.

TABLE V. COEFFICIENTS OF THE CARTESIAN DISPLACEMENT COORDINATES[a] (in a.m.u.)

| | $\alpha$ | $\beta$ | $\gamma$ | $\lambda$ | $\mu$ | $\nu$ | $\sin\Gamma$ | $\zeta_{23}^2$ |
|---|---|---|---|---|---|---|---|---|
| $H_2O$ | −0.0019 | 0.7316 | 0.0414 | 0.7197 | −0.0395 | 0.7316 | 0.5913 | 1.0000 |
| $D_2O$ | −0.0348 | 0.5349 | 0.0564 | 0.5207 | −0.0227 | 0.5360 | 0.6210 | 0.9958 |
| $H_2S$ | 0.0149 | 0.7155 | 0.0218 | 0.7139 | −0.0366 | 0.7156 | 0.6670 | 0.9996 |
| $D_2S$ | −0.0077 | 0.5141 | 0.0303 | 0.5125 | −0.0227 | 0.5142 | 0.6828 | 0.9998 |
| $H_2Se$ | 0.0168 | 0.7086 | 0.0089 | 0.7082 | −0.0257 | 0.7088 | 0.6797 | 0.9994 |
| $D_2Se$ | 0.0043 | 0.5046 | 0.0125 | 0.5041 | −0.0169 | 0.5046 | 0.6863 | 0.9999 |
| $SO_2$ | −0.0717 | 0.2228 | 0.0577 | 0.1974 | 0.0030 | 0.2340 | 0.6463 | 0.9061 |
| $ClO_2$ | −0.0824 | 0.2130 | 0.0555 | 0.1966 | 0.0166 | 0.2284 | 0.7046 | 0.8697 |
| $^{14}NO_2$ | −0.1410 | 0.2681 | 0.0847 | 0.2049 | 0.0121 | 0.3029 | 0.6548 | 0.7833 |
| $^{15}NO_2$ | −0.1307 | 0.2658 | 0.0808 | 0.2032 | 0.0098 | 0.2962 | 0.6379 | 0.8054 |

a) See Eqs. 3 and 7.

TABLE VI. ANHARMONIC POTENTIAL CONSTANTS[a] (in $cm^{-1}$)

| cubic[b] | $k_{111}$ | $k_{122}$ | $k_{133}$ | $k_{211}$ | $k_{222}$ | $k_{233}$ |
|---|---|---|---|---|---|---|
| $H_2O$ | −319.4±3.3 | 255.4±31.4 | −921.7± 1.5 | 39.6±2.4 | −61.9±2.5 | 147.3±0.4 |
| $D_2O$ | −193.3±2.1 | 191.1±24.8 | −632.1±18.0 | 7.6±1.6 | −33.4±2.1 | 93.7±2.1 |
| $H_2S$ | −194.9±3.6 | 102.7±13.2 | −587.5± 2.7 | −18.3±3.3 | −1.0±1.4 | 13.9±0.8 |
| $H_2Se$ | −165.4±0.3 | 79.2± 1.5 | −478.4±17.8 | 10.9±0.3 | 1.1±0.2 | 32.5±5.3 |
| $D_2Se$ | −100.8±2.6 | 28.3± 2.7 | −279.2±14.1 | 1.8±2.3 | −4.6±0.3 | 21.5±4.2 |
| $SO_2$ | −44.3±0.4 | 12.0± 0.8 | −159.2± 0.1 | −19.0±0.3 | −6.9±0.1 | 4.6±0.1 |
| quartic[c] | $k_{1111}$ | $k_{1122}$ | $k_{1133}$ | $k_{2222}$ | $k_{2233}$ | $k_{3333}$ |
| $H_2O$ | 38.5±1.4 | −140.4±15.9 | 209.2±2.5 | 11.2±4.1 | −122.2±7.6 | 35.0±0.2 |
| $D_2O$ | 18.8±0.7 | −96.8±13.6 | 135.7±6.5 | 9.9±3.6 | −74.3±5.8 | 26.0±2.3 |
| $H_2S$ | 18.2±1.3 | −58.6± 5.2 | 115.2±2.5 | 0.7±1.2 | −56.3±2.9 | 19.4±0.3 |
| $SO_2$ | 1.77±0.08 | −3.09±0.12 | 15.36±0.17 | −1.62±0.02 | −6.51±0.11 | 3.01±0.01 |

a) Derived from the observed $\alpha$ and $x$ values listed in Tables XII and XIII by using Eqs. 7 and 8.
b) Quoted uncertainties represent the standard errors estimated by a least-squares fit of the observed $\alpha$ values to Eq. 7 (with equal statistical weights for $\alpha^A$, $\alpha^B$, and $\alpha^C$). Because of the inconsistencies among $\alpha^A$, $\alpha^B$, and $\alpha^C$, larger uncertainties have to be assigned to some of the $k_{122}$ and $k_{133}$ constants.
c) The standard errors, which are propagated from those of the cubic constants by the application of Eq. 8, are taken as uncertainties. They are probably somewhat underestimated, because the errors involved in the experimental $x$ values, which are not given in the original references, are left out of consideration.

TABLE VII. HIGHER-ORDER POTENTIAL CONSTANTS[a] (in md./Å)

| | $f_{rrr}$ | $f_{rrr'}$ | $f_{rr\alpha}$ | $f_{rr'\alpha}$ | $f_{r\alpha\alpha}$ | $f_{\alpha\alpha\alpha}$ |
|---|---|---|---|---|---|---|
| $H_2O$ | −9.55±0.06 | −0.32±0.16 | 0.16±0.03 | −0.66±0.01 | 0.15±0.20 | −0.14±0.01 |
| $D_2O$ | −10.18±0.45 | 0.48±0.47 | 0.22±0.06 | −0.46±0.04 | 0.31±0.26 | −0.13±0.02 |
| $H_2S$ | −5.16±0.06 | 0.03±0.15 | −0.40±0.03 | −0.15±0.02 | −0.04±0.08 | −0.01±0.01 |
| $H_2Se$ | −4.04±0.22 | −0.09±0.22 | −0.03±0.05 | −0.13±0.02 | −0.06±0.01 | −0.00±0.01 |
| $D_2Se$ | −3.97±0.30 | −0·23±0.34 | −0.04±0.07 | −0.20±0.03 | −0.14±0.03 | −0.02±0.01 |
| $SO_2$ | −16.95±0.08 | −0.82±0.23 | −0.68±0.05 | −0.76±0.03 | −0.63±0.05 | −0.20±0.01 |
| | $f_{rrrr}$ | $f_{rrrr'}$ | $f_{rrr'r'}$ | $f_{rr\alpha\alpha}$ | $f_{rr'\alpha\alpha}$ | $f_{\alpha\alpha\alpha\alpha}$ |
| $H_2O$ | 15.4±0.3 | 0.8±0.6 | 1.3±1.1 | −1.7±0.8 | −0.5±1.7 | 0.0±0.2 |
| $D_2O$ | 18.5±1.5 | −2.8±2.0 | 0.1±4.0 | −2.7±1.4 | −1.5±2.8 | 0.0±0.2 |
| $H_2S$ | 8.5±0.3 | −0.2±0.6 | −0.3±1.1 | −0.7±0.4 | −0.3±0.8 | −0.0±0.2 |
| $SO_2$ | 33.8±1.2 | −2.2±2.6 | −0.3±4.3 | 0.7±3.2 | 2.8±6.2 | −0.3±0.1 |

a) Calculated from Table VI by the matrix equations given in Tables I and II with the assumption that the contributions from the $f_{rrr\alpha}$, $f_{rrr'\alpha}$, and $f_{r\alpha\alpha\alpha}$ constants to the quartic constants listed in Table VI are zero. The uncertainties are represented somewhat arbitrarily by twice the standard errors estimated from those of the anharmonic constants given in Table VI. The uncertainties introduced by the above assumption are included in the uncertainties of the fourth-order constants.

TABLE VIII. ANALYSIS OF THE CUBIC CONSTANTS INTO COMPONENT TERMS (in $cm^{-1}$)

| $H_2O$ | $k_{111}$ | $k_{122}$ | $k_{133}$ | $k_{211}$ | $k_{222}$ | $k_{233}$ |
|---|---|---|---|---|---|---|
| $f_r$ | 0 | 328.8 | 0.4 | −1.1 | −27.5 | 24.0 |
| $f_{r'}$ | 0 | −3.9 | 0 | 0 | 0.3 | 0.3 |
| $f_{r\alpha}$ | 0 | 3.7 | −0.8 | −22.8 | 27.3 | 0.1 |
| $f_\alpha$ | 0 | −118.3 | 0 | 0 | 9.9 | −4.3 |
| $f_{rrr}$ | −309.2 | −6.5 | −931.5 | 77.6 | 0.2 | 77.9 |
| $f_{rrr'}$ | −10.3 | −0.2 | 10.3 | 2.6 | 0 | −0.9 |
| $f_{rr\alpha}$ | 0 | −2.8 | 0 | 16.5 | 0.1 | 16.6 |
| $f_{rr'\alpha}$ | 0.1 | 5.6 | −0.1 | −33.4 | −0.2 | 33.5 |
| $f_{r\alpha\alpha}$ | 0 | 48.7 | 0 | −0.2 | −4.1 | 0 |
| $f_{\alpha\alpha\alpha}$ | 0 | 0.3 | 0 | 0 | −67.8 | 0 |
| Total | −319.4 | 255.4 | −921.7 | 39.6 | −61.9 | 147.3 |
| $SO_2$ | $k_{111}$ | $k_{122}$ | $k_{133}$ | $k_{211}$ | $k_{222}$ | $k_{233}$ |
| $f_r$ | 1.81 | 38.43 | −1.93 | −16.73 | 0.88 | 13.54 |
| $f_{r'}$ | 0.01 | 0.30 | 0.03 | −0.13 | 0.01 | −0.11 |
| $f_{r\alpha}$ | 0.41 | −1.95 | −0.37 | −1.61 | 2.87 | 0.07 |
| $f_\alpha$ | −0.57 | −12.12 | 0.46 | 5.28 | −0.28 | −2.13 |
| $f_{rrr}$ | −45.07 | −0.07 | −160.64 | −3.05 | 0 | −3.62 |
| $f_{rrr'}$ | −2.17 | 0 | 2.58 | −0.15 | 0 | 0.06 |
| $f_{rr\alpha}$ | 1.31 | −0.27 | 1.56 | −6.02 | 0 | −7.22 |
| $f_{rr'\alpha}$ | 0.73 | −0.15 | −0.87 | −3.36 | 0 | 4.03 |
| $f_{r\alpha\alpha}$ | −0.88 | −18.66 | 0 | 8.13 | −0.42 | 0 |
| $f_{\alpha\alpha\alpha}$ | 0.10 | 6.46 | 0 | −1.40 | −9.96 | 0 |
| Total | −44.31 | 11.96 | −159.18 | −19.04 | −6.92 | 4.62 |

$$B_2=-\frac{6B_e^2}{\omega_2}\sin^2\Gamma,\quad b_2=-\left(\frac{2B_e}{\omega_2}\right)^{3/2}\sin\Gamma$$

$$B_3=-\frac{6B_eC_e}{\omega_3}$$

$$C_1=-\frac{6C_e^2}{\omega_1}+\frac{8C_e^2\omega_3^2}{\omega_1(\omega_3^2-\omega_1^2)}\zeta_{13}^2$$

$$C_2=-\frac{6C_e^2}{\omega_2}+\frac{8C_e^2\omega_3^2}{\omega_2(\omega_3^2-\omega_2^2)}\zeta_{23}^2$$

$$C_3=\frac{2C_e^2}{\omega_3}-8C_e^2\omega_3\left(\frac{\zeta_{13}^2}{\omega_3^2-\omega_1^2}+\frac{\zeta_{23}^2}{\omega_3^2-\omega_2^2}\right)$$

$$c_1=C_e^2(a_1/A_e^2+b_1/B_e^2)$$

$$c_2=C_e^2(a_2/A_e^2+b_2/B_e^2)$$

and $A_e$, $B_e$, $C_e$ are the equilibrium rotational constants. It is easily shown that:

$$\sin\Gamma=(c\lambda-s\alpha)(1/m_X+1/2m_Y)^{1/2}$$

$$\cos\Gamma=(s\beta-c\mu)(1/m_X+1/2m_Y)^{1/2}$$

$$\zeta_{13}^2=(\beta\gamma+\mu\nu)^2/(\beta\lambda-\alpha\mu)^2$$

and

$$\zeta_{23}^2=1-\zeta_{13}^2=(\alpha\gamma+\lambda\nu)^2/(\beta\lambda-\alpha\mu)^2$$

where

$$c=\cos\frac{1}{2}(Y_1\text{-}X\text{-}Y_2)\quad\text{and}\quad s=\sin\frac{1}{2}(Y_1\text{-}X\text{-}Y_2)$$

## Determination of the Higher-Order Potential Constants

The vibrational frequencies, the quadratic force constants, and the coefficients of Eq. 3 used in the following analysis[8-20] are summarized in Tables III—V. Since the normal frequencies for $D_2S$, $H_2Se$, and $D_2Se$ are not available in the literature, they are estimated from the fundamental frequencies by the method described in a previous paper,[21] by

9) W. S. Benedict, N. Gailar and E. K. Plyler, *J. Chem. Phys.*, **24**, 1139 (1956).
10) H. C. Allen, Jr., and E. K. Plyler, ibid., **25**, 1132 (1956).
11) H. C. Allen, Jr., E. K. Plyler and L. R. Blaine, *J. Res. Natl. Bur. Std.* (*U. S.*), **59**, 211 (1957).
12) E. D. Palik, *J. Mol. Spectry.*, **3**, 259 (1959).
13) R. D. Shelton, A. H. Nielsen and W. H. Fletcher, *J. Chem. Phys.*, **21**, 2178 (1953); **22**, 1791 (1954).
14) J. B. Coon and E. Ortiz, *J. Mol. Spectry.*, **1**, 81 (1957).
15) E. T. Arakawa and A. H. Nielsen, ibid., **2**, 413 (1958).
16) T. Oka and Y. Morino, ibid., **8**, 300 (1962).
17) R. F. Curl, Jr., J. L. Kinsey, J. C. Baird, G. R. Bird, R. F. Heidelberg, T. M. Sugden, D. R. Jenkins and C. N. Kenney, *Phys. Rev.*, **121**, 1119 (1961).
18) M. G. K. Pillai and R. F. Curl, *J. Chem. Phys.*, **37**, 2921 (1962).
19) G. R. Bird, J. C. Baird, A. W. Jache, J. A. Hodgeson, R. F. Curl, A. C. Kunkle, J. W. Bransford, J. Rastrup-Andersen and J. Rosenthal, ibid., **40**, 3378 (1964).
20) G. E. Moore, *J. Opt. Soc. Am.*, **43**, 1045 (1953). R. E. Weston, Jr., *J. Chem. Phys.*, **26**, 1248 (1957).
21) K. Kuchitsu, T. Oka and Y. Morino, *J. Mol. Spectry.*, **15**, 51 (1965).

TABLE IX. ANALYSIS OF THE QUARTIC CONSTANTS INTO COMPONENT TERMS[a] (in $cm^{-1}$)

| $H_2O$ | $k_{1111}$ | $k_{1122}$ | $k_{1133}$ | $k_{2222}$ | $k_{2233}$ | $k_{3333}$ |
|---|---|---|---|---|---|---|
| $f_r$ | 0 | −23.2 | 0 | 13.8 | −22.9 | 0 |
| $f_{r'}$ | 0 | 0.3 | 0 | −0.2 | −0.3 | 0 |
| $f_{r\alpha}$ | 0 | −0.4 | 0.1 | 0.4 | −0.3 | 0 |
| $f_\alpha$ | 0 | 12.5 | 0 | −6.6 | 8.3 | 0 |
| $f_{rrr}$ | 0 | −78.6 | −0.1 | −0.6 | −77.9 | −0.1 |
| $f_{rrr'}$ | 0 | −2.6 | 0 | 0 | 0.9 | 0 |
| $f_{rr\alpha}$ | 0 | 0.3 | 0 | −0.2 | 0.3 | 0 |
| $f_{rr'\alpha}$ | 0 | −0.6 | 0.1 | 0.5 | 0.6 | −0.1 |
| $f_{r\alpha\alpha}$ | 0 | −6.9 | 0 | 4.1 | 0 | 0 |
| $f_{\alpha\alpha\alpha}$ | 0 | −0.1 | 0 | −1.2 | 0.5 | 0 |
| $f_{rrrr}$ | 35.2 | 1.5 | 212.2 | 0 | 1.5 | 35.5 |
| $f_{rrrr'}$ | 1.7 | 0.1 | 0 | 0 | 0 | −1.8 |
| $f_{rrr'r'}$ | 1.5 | 0.1 | −3.1 | 0 | 0 | 1.5 |
| $f_{rr\alpha\alpha}$ | 0 | −37.7 | 0 | −0.3 | −37.9 | 0 |
| $f_{rr'\alpha\alpha}$ | 0 | −5.0 | 0 | 0 | 5.0 | 0 |
| $f_{\alpha\alpha\alpha\alpha}$ | 0 | 0 | 0 | 1.5 | 0 | 0 |
| Total | 38.5 | −140.4 | 209.2 | 11.2 | −122.2 | 35.0 |
| $SO_2$ | $k_{1111}$ | $k_{1122}$ | $k_{1133}$ | $k_{2222}$ | $k_{2233}$ | $k_{3333}$ |
| $f_r$ | −0.04 | −0.71 | 0.07 | 0.64 | −1.00 | −0.03 |
| $f_{r'}$ | 0 | −0.01 | 0 | 0.01 | 0.01 | 0 |
| $f_{r\alpha}$ | −0.01 | 0.12 | 0 | 0 | −0.03 | 0 |
| $f_\alpha$ | 0.02 | 0.35 | −0.02 | −0.27 | 0.32 | 0 |
| $f_{rrr}$ | −0.21 | −4.39 | 0.31 | 0 | −5.39 | −0.14 |
| $f_{rrr'}$ | −0.01 | −0.21 | −0.01 | 0 | 0.09 | 0 |
| $f_{rr\alpha}$ | −0.03 | 0.27 | −0.02 | −0.01 | −0.14 | 0.03 |
| $f_{rr'\alpha}$ | −0.01 | 0.15 | 0.04 | −0.01 | 0.08 | −0.02 |
| $f_{r\alpha\alpha}$ | 0.04 | 0.69 | −0.03 | −0.62 | −0.01 | 0 |
| $f_{\alpha\alpha\alpha}$ | −0.01 | −0.45 | 0.01 | 0.02 | 0.12 | 0 |
| $f_{rrrr}$ | 2.11 | 0.01 | 15.02 | 0 | 0.01 | 2.97 |
| $f_{rrrr'}$ | −0.14 | 0 | 0 | 0 | 0 | 0.20 |
| $f_{rrr'r'}$ | −0.01 | 0 | 0.02 | 0 | 0 | −0.01 |
| $f_{rr\alpha\alpha}$ | 0.02 | 0.51 | 0.03 | 0 | 0.62 | 0 |
| $f_{rr'\alpha\alpha}$ | 0.05 | 0.98 | −0.06 | 0 | −1.18 | 0 |
| $f_{\alpha\alpha\alpha\alpha}$ | 0 | −0.38 | 0 | −1.37 | 0 | 0 |
| Total | 1.77 | −3.09 | 15.36 | −1.62 | −6.51 | 3.01 |

a) Contributions from the $f_{rrr\alpha}$, $f_{rrr'\alpha}$, and $f_{r\alpha\alpha\alpha}$ constants are assumed to be zero.

the product rule, and by the $x$ values estimated in the present study. The cubic and the quartic constants listed in Table VI are calculated, by using Eqs. 7 and 8, from the observed $\alpha$ and $x$ values. They are then transformed into the constants in the internal-coordinate system by solving the simultaneous equations based on Tables I and II.*3 The results, with

*3 The solution of the simultaneous equations is unique for the six third-order constants, whereas for the fourth-order constants the number of unknowns (nine) exceeds that of the observed quartic constants (six), since the $k_{1112}$, $k_{1222}$, and $k_{1233}$ constants have not been observed. As Tables II and V indicate, all the matrix elements of Table II related to the $f_{rrr\alpha}$, $f_{rrr'\alpha}$, and $f_{r\alpha\alpha\alpha}$ constants have at least one $\alpha$ or $\mu$ parameter and, hence, are relatively small. The contributions from these constants are, accordingly, assumed to be zero in the course of determining the rest of the fourth-order constants from the simultaneous equations. This assumption, however, does not necessarily mean that these constants are negligibly small; as Table VII shows, the order of magnitude of these constants may be as much as ± 2md./Å. In that case, the three constants may contribute as much as $\pm 10\,cm^{-1}$ to the $k_{1122}$ of $D_2O$ and $H_2S$ and to the $k_{2222}$ of $H_2O$ and $H_2S$, $\pm 5\,cm^{-1}$ to the $k_{1122}$ of $H_2O$ and to the $k_{2222}$ of $D_2O$, and $\pm 3\,cm^{-1}$ to the $k_{1122}$ of $SO_2$. All other contributions are negligible. The effect of this indeterminacy on the determination of the rest of the constants, which is found to be important only in the case of $SO_2$, is, therefore, included in their final uncertainties. The $f_{rrr\alpha}$, $f_{rrr'\alpha}$, and $f_{r\alpha\alpha\alpha}$ constants of $H_2O$ and $D_2O$ can be determined if at least six fourth-order constants of $H_2O$ are assumed to be equal to the corresponding constants of $D_2O$. It is not likely, however, that more definite values of these constants can be obtained by this process because of the smallness of the matrix elements related to these constants and because of the errors involved in the original quartic constants.

TABLE X. COMPARISON OF THE $a_3$ AND $a_4$ PARAMETERS (in Å$^{-1}$)

| | $a_3$ | | $a_4$ | |
|---|---|---|---|---|
| | Diatomic[a] | Bond[b] | Diatomic[a] | Bond[b] |
| O-H | 2.36 | 2.36±0.02 | 2.56 | 2.61±0.03 |
| S-H | 1.84 | 1.80±0.02 | 1.81 | 1.95±0.02 |
| Se-H | (1.65) | 1.58±0.09 | (1.74) | — |
| S-O | 2.072 | 2.29±0.01 | 2.297 | 2.34±0.04 |

a) Taken from Table VI of Ref. 1. The parameters of Se-H are estimated by the Lippincott function, Ref. 24.
b) The parameters pertaining to the bond calculated from the experimental constants given in Table VII by using Eq. 9.

TABLE XI. PARAMETERS OF BOND-STRETCHING ANHARMONICITY (in Å$^{-1}$)

| | | D.[a] | L. S.[b] | H. L.[c] | Add.[d] | Ass.[e] |
|---|---|---|---|---|---|---|
| $H_2O$ | $a_3$ | 2.305(OH)<br>2.406(OD) | 2.33 | 2.44 | 2.31 | $2.35_5$ |
| | $a_4$ | 2.464(OH)<br>2.654(OD) | 2.47 | 2.37 | 2.47 | 2.56 |
| $H_2S$ | $a_3$ | 1.84 | 1.76 | 1.59 | 1.92 | 1.84 |
| | $a_4$ | 1.81 | 1.86 | 1.76 | 2.06 | 1.86 |
| $H_2Se$ | $a_3$ | — | 1.63 | 1.57 | 1.79 | 1.65 |
| | $a_4$ | — | 1.70 | 1.15 | 1.79 | 1.74 |
| $SO_2$ | $a_3$ | 2.072 | 2.16 | 1.92 | 2.07 | 2.07 |
| | $a_4$ | 2.186 | 2.26 | 2.13 | 2.15 | 2.19 |
| $ClO_2$ | $a_3$ | — | 2.19 | 1.88 | 2.06 | 2.13 |
| | $a_4$ | — | 2.30 | 2.07 | 2.14 | 2.23 |
| $NO_2$ | $a_3$ | 2.549 | 2.46 | 2.30 | 2.46 | 2.55 |
| | $a_4$ | 2.618 | 2.56 | 2.52 | 2.51 | 2.62 |

a) Experimental $a_3$ and $a_4$ for the corresponding diatomic radical, Ref. 1.
b) Estimation according to the Lippincott function, Ref. 24.
c) Estimation according to the function of Herschbach and Laurie, Ref. 3.
d) Estimation according to the rule of additivity. See Ref. 1.
e) Values assumed in the present analysis.

TABLE XII. ESTIMATION OF THE CUBIC CONSTANTS OF BENT $XY_2$ (in cm$^{-1}$)

| | | $k_{111}$ | $k_{122}$ | $k_{133}$ | $k_{211}$ | $k_{222}$ | $k_{233}$ |
|---|---|---|---|---|---|---|---|
| $H_2O$ | obs.[a] | −319.4 | 255.4 | −921.7 | 39.6 | −61.9 | 147.3 |
| | calc.[b] | −308.4 | 203.8 | −929.9 | 53.9 | 10.2 | 97.9 |
| $D_2O$ | obs. | −193.3 | 191.1 | −632.1 | 7.6 | −33.4 | 93.7 |
| | calc. | −189.9 | 126.4 | −581.2 | 12.6 | 8.6 | 61.8 |
| $H_2S$ | obs. | −194.9 | 102.7 | −587.5 | −18.3 | −1.0 | 13.9 |
| | calc. | −199.3 | 107.4 | −597.9 | 37.5 | 4.5 | 51.9 |
| $D_2S$ | calc. | −121.4 | 65.5 | −364.4 | 15.8 | 3.4 | 31.1 |
| $H_2Se$ | obs. | −165.4 | 79.2 | −478.4 | 10.9 | 1.1 | 32.5 |
| | calc. | −168.2 | 99.3 | −502.3 | 24.2 | 2.3 | 29.9 |
| $D_2Se$ | obs. | −100.8 | 28.3 | −279.2 | 1.8 | −4.6 | 21.5 |
| | calc. | −101.0 | 59.7 | −301.8 | 12.1 | 1.6 | 17.9 |
| $SO_2$ | obs. | −44.3 | 12.0 | −159.2 | −19.0 | −6.9 | 4.6 |
| | calc. | −39.1 | 24.6 | −147.1 | −16.0 | 3.5 | 8.1 |
| $ClO_2$ | calc. | −36.2 | 15.0 | −131.1 | −23.2 | 2.2 | −7.0 |
| $^{14}NO_2$ | calc. | −40.4 | 25.5 | −260.5 | −41.9 | 10.3 | −3.1 |
| $^{15}NO_2$ | calc. | −40.9 | 26.9 | −253.7 | −38.3 | 9.7 | 0.1 |

a) Taken from Table VI.
b) Calculated by a simple method, which takes into account the quadratic force constants and the principal third-order potential constant $f_{rrr}$ estimated from the $a_3$ parameter given in Table XI.

Table XIII. Estimation of the quartic constants of bent $XY_2$ (in $cm^{-1}$)

| | | $k_{1111}$ | $k_{1122}$ | $k_{1133}$ | $k_{2222}$ | $k_{2233}$ | $k_{3333}$ |
|---|---|---|---|---|---|---|---|
| $H_2O$ | obs.[a] | 38.5 | −140.4 | 209.2 | 11.2 | −122.2 | 35.0 |
| | calc.[b] | 33.8 | −87.8 | 203.6 | 6.9 | −91.6 | 33.9 |
| $D_2O$ | obs. | 18.8 | −96.8 | 135.7 | 9.9 | −74.3 | 26.0 |
| | calc. | 17.7 | −46.9 | 108.6 | 3.8 | −49.0 | 18.1 |
| $H_2S$ | obs. | 18.2 | −58.6 | 115.2 | 0.7 | −56.3 | 19.4 |
| | calc. | 17.4 | −43.7 | 104.2 | 2.7 | −45.7 | 17.4 |
| $D_2S$ | calc. | 9.0 | −22.8 | 53.9 | 1.4 | −23.6 | 8.9 |
| $H_2Se$ | calc. | 15.0 | −37.0 | 89.6 | 2.6 | −38.6 | 14.9 |
| $D_2Se$ | calc. | 7.6 | −18.8 | 45.4 | 1.3 | −19.6 | 7.5 |
| $SO_2$ | obs. | 1.8 | −3.1 | 15.4 | −1.6 | −6.5 | 3.0 |
| | calc. | 1.6 | −4.2 | 13.5 | 0.4 | −5.6 | 2.5 |
| $ClO_2$ | calc. | 1.6 | −3.0 | 13.3 | 0.2 | −4.7 | 2.4 |
| $^{14}NO_2$ | calc. | 1.3 | −4.6 | 26.8 | 0.6 | −12.0 | 7.1 |
| $^{15}NO_2$ | calc. | 1.5 | −4.9 | 26.1 | 0.6 | −11.6 | 6.9 |

a) Taken from Table VI.
b) Calculated by a simple method, which takes into account the quadratic force constants and the principal third- and fourth-order potential constants, $f_{rrr}$ and $f_{rrrr}$, estimated from the $a_3$ and $a_4$ parameters given in Table XI.

Table XIV. Estimation of the $\alpha$ parameters of bent $XY_2$ (in $cm^{-1}$)

| | | $\alpha_1{}^A$ | $\alpha_2{}^A$ | $\alpha_3{}^A$ | $\alpha_1{}^B$ | $\alpha_2{}^B$ | $\alpha_3{}^B$ | $\alpha_1{}^C$ | $\alpha_2{}^C$ | $\alpha_2{}^C$ | Ref. |
|---|---|---|---|---|---|---|---|---|---|---|---|
| $H_2O$ | obs. | 0.750 | −2.941 | 1.253 | 0.238 | −0.160 | 0.078 | 0.2018 | 0.1392 | 0.1445 | 9 |
| | calc. | 0.787 | −1.831 | 1.020 | 0.204 | −0.422 | 0.150 | 0.182 | 0.132 | 0.149 | |
| $D_2O$ | obs. | 0.246 | −1.161 | 0.593 | 0.0958 | −0.0823 | 0.0418 | 0.0768 | 0.0495 | 0.0538 | 9 |
| | calc. | 0.255 | −0.717 | 0.455 | 0.090 | −0.162 | 0.049 | 0.071 | 0.046 | 0.053 | |
| $H_2S$ | obs. | 0.125 | −0.346 | 0.173 | 0.159 | −0.219 | 0.123 | 0.069 | 0.062 | 0.055 | 10 |
| | calc. | 0.222 | −0.319 | 0.241 | 0.095 | −0.238 | 0.082 | 0.079 | 0.054 | 0.056 | |
| $D_2S$ | obs. | (0.066) | (−0.071) | (0.013) | (0.039) | (−0.061) | (0.030) | (0.022) | (0.027) | (0.012) | 11 |
| | calc. | 0.078 | −0.118 | 0.095 | 0.039 | −0.087 | 0.027 | 0.028 | 0.019 | 0.021 | |
| $H_2Se$ | obs. | 0.125 | −0.230 | 0.145 | 0.092 | −0.190 | 0.062 | 0.055 | 0.040 | 0.045 | 12 |
| | calc. | 0.147 | −0.232 | 0.152 | 0.079 | −0.202 | 0.076 | 0.056 | 0.037 | 0.040 | |
| $D_2Se$ | obs. | 0.043 | −0.092 | 0.053 | 0.038 | −0.052 | 0.018 | 0.017 | 0.016 | 0.017 | 12 |
| | calc. | 0.052 | −0.084 | 0.057 | 0.030 | −0.073 | 0.026 | 0.020 | 0.014 | 0.015 | |
| $SO_2$[b] | obs. | −1.036 | −39.224 | 20.682 | 1.673 | −0.073 | 1.163 | 1.429 | 0.534 | 1.097 | 8 |
| | calc. | −1.51 | −24.9 | 20.9 | 1.42 | −1.16 | 0.92 | 1.20 | 0.02 | 0.92 | |
| $ClO_2$[b] | calc. | −3.75 | −19.2 | 14.2 | 1.96 | −1.17 | 1.47 | 1.59 | 0.10 | 1.11 | |
| $^{14}NO_2$[b] | obs. | — | −360 | — | 2.8 | — | 2.4 | — | — | — | 15 |
| | calc. | −117 | −239 | 199 | 2.07 | −1.74 | 2.62 | 2.18 | −0.43 | 2.35 | |
| $^{15}NO_2$[b] | obs.[c] | — | −335 | — | 2.6 | — | 2.1 | — | — | — | 15 |
| | calc. | −97 | −232 | 185 | 2.02 | −1.69 | 2.55 | 2.13 | −0.35 | 2.29 | |

a) Rough estimates from the rotational constants given in Ref. 11.
b) Multiplied by $10^3$.
c) The $\alpha$ values in Table II of Ref. 15 are given in opposite signs. The present revision of the signs is made with reference to the data given in their Table I.

estimated uncertainties, are given in Table VII.

Tables VIII and IX analyze the anharmonic constants into the contributions from various quadratic and higher-order constants on the basis of Tables I and II, expressing which potential constants are the principal contributors to a particular anharmonic constant. For example, $k_{111}$ and $k_{133}$ depend almost exclusively on the $f_{rrr}$ term, and $k_{1111}$, $k_{1133}$, and $k_{3333}$, on the $f_{rrrr}$ term. The rest of the anharmonic constants, on the other hand, are hybrids to a greater or lesser extent. For example, the $k_{122}$ and $k_{1122}$ constants depend strongly on the quadratic force constants. The dependence of $f_r$ on $k_{122}$ originates from the second term of the expansion of $\Delta r^2$ in Eq. 1 and represents the effect of the perpendicular (arc) motion of the X–Y bond. The physical

TABLE XV. ESTIMATION OF THE $x$ PARAMETERS OF BENT $XY_2$ (in $cm^{-1}$)

| | | $x_{11}$ | $x_{22}$ | $x_{33}$ | $x_{12}$ | $x_{13}$ | $x_{23}$ | Ref. |
|---|---|---|---|---|---|---|---|---|
| $H_2O$ | obs. | −42.576 | −16.813 | −47.566 | −15.933 | −165.824 | −20.322 | 9 |
| | calc. | −43.29 | −5.75 | −47.30 | −4.12 | −167.74 | −18.46 | |
| $D_2O$ | obs. | −22.58 | −9.18 | (−26.15) | −7.58 | −87.15 | −10.61 | 9 |
| | calc. | −22.49 | −3.57 | −26.52 | 0.06 | −87.65 | −10.60 | |
| $H_2S$ | obs. | −25.09 | −5.72 | −24.00 | −19.69 | −94.68 | −21.09 | 10 |
| | calc. | −29.23 | −3.29 | −29.88 | −2.28 | −115.71 | −10.24 | |
| $D_2S$ | calc. | −15.00 | −1.76 | −15.60 | −0.93 | −59.59 | −5.32 | |
| $H_2Se$ | calc. | −21.34 | −2.22 | −21.41 | −2.65 | −83.60 | −7.76 | |
| $D_2Se$ | calc. | −10.79 | −1.14 | −10.89 | −1.30 | −42.36 | −3.91 | |
| $SO_2$ | obs. | −3.99 | −3.00 | −5.17 | −2.05 | −13.71 | −3.90 | 13 |
| | calc. | −2.71 | −0.48 | −4.63 | 0.95 | −10.54 | −1.85 | |
| $ClO_2$ | obs. | −4.4 | 0.0 | −2.0 | −3.0 | −14.4 | −13(?) | 14 |
| | calc. | −3.26 | −0.46 | −4.44 | 0.79 | −11.07 | −1.86 | |
| $^{14}NO_2$ | obs. | −9.0 | −0.5 | −16.4 | −9.7 | −28.7 | −2.7 | 15 |
| | obs. | −7.1 | −7.5 | −15.9 | −16.0 | −33.4 | −8.2 | 20 |
| | calc. | −3.59 | 0.59 | −11.80 | −3.46 | −20.88 | −6.10 | |
| $^{15}NO_2$ | obs. | −8.8 | −0.4 | −15.6 | −9.5 | −27.7 | −2.6 | 15 |
| | obs. | −7.0 | −7.3 | −15.1 | −15.6 | −32.3 | −7.9 | 20 |
| | calc. | −3.41 | 0.71 | −11.24 | −4.00 | −20.78 | −5.65 | |

significance of this term has been discussed in Part I in connection with a similar situation involving the $k_{122}$ constant of linear $XY_2$.

Table VII indicates that the $f_{rrr}$ and $f_{rrrr}$ constants are more than ten times as great as the rest of the higher-order constants, and that they are determined with accuracies of about two significant figures. As has been discussed in Part I, these constants originate from the anharmonic stretching vibrations of the $X\text{-}Y_1$ and $X\text{-}Y_2$ bonds, and they may be expressed in terms of the $a_3$ and $a_4$ parameters, introduced in Part I, as follows:

$$f_{rrr} = -\frac{1}{2}a_3 f_r r_e \quad \text{and} \quad f_{rrrr} = \frac{7}{24}a_4^2 f_r r_e^2 \qquad (9)$$

As is shown in Table X, the $a_3$ and $a_4$ parameters of the X-Y bond agree closely (to within 12%) with those of the X-Y diatomic molecule taken from Table VI of Part I. This affords direct support to similar statements presented in previous studies.[1-5]

Table VII further shows that some of the other third-order constants listed in the table are determined significantly. For example, all the $f_{rr'\alpha}$ and $f_{\alpha\alpha\alpha}$ constants are negative, as are all the third-order constants of $SO_2$*4. The third-order constants of $H_2O$ and $H_2Se$ agree with those of the corresponding deuterides within the listed uncertainties (except for the $f_{rr'\alpha}$ constants of $H_2O$ and $D_2O$). The fourth-order constants (except for $f_{rrrr}$), on the other hand, are indeterminate.

It is more difficult to put forward an intuitive model for interpreting the physical significance of the third-order potential constants other than $f_{rrr}$. They are, nevertheless, important, since previous discussions of the molecular potential field have almost always been based on the quadratic part of the potential, and, consequently, an examination of the higher-order constants may give a novel insight into the nature of the potential field. Some discussion of the physical significance of these constants will be given as a separate paper.[23,*5]

## Estimation of Anharmonic Constants

The above findings for the $f_{rrr}$ and $f_{rrrr}$ constants suggest that the simple "diatomic approximation" discussed in Part I may also be used in this case for predicting the anharmonic constants. This method approximates the total potential function (Eq. 4) by the

*4 The same trend has been observed for the $OF_2$ molecule recently studied in our laboratory.[22] All the third-order constants are found to be negative, and they are of an order of magnitude very similar to that of the corresponding constants of the $SO_2$ molecule.[23]

22) Y. Morino and S. Saito, *J. Mol. Spectry*, to be published.

23) K. Kuchitsu and Y. Morino, *Spectrochim. Acta*, to be published.

*5 Note added in proof: The experimental values of $\omega$, $\alpha$ and $x$ of $H_2Se$ have recently been published: R. A. Hill and T. H. Edwards, *J. Chem. Phys.* **42**, 1391 (1965). Some of their $\omega$ and $x$ values of $H_2{}^{80}Se$ ($\omega_1$=2438.66, $\omega_3$=2453.77, $x_{11}$=−21.43, $x_{33}$=−21.71, and $x_{13}$=−84.90 $cm^{-1}$) are in good agreement with the corresponding estimates given in Tables III and XV respectively, while their $x_{12}$(−17.69 $cm^{-1}$) and $x_{23}$(−20.20 $cm^{-1}$) are not, in line with the discussion in the text. Their $\alpha$ values differ from Palik's $\alpha$ values[12]; the third-order constants and the cubic constants based on their $\alpha$ values are accordingly different from those based on Palik's values given in Tables VI, VII and XII by as much as the uncertainties listed in the tables. See Ref. 23.

four quadratic terms plus the $f_{rrr}$ and $f_{rrrr}$ terms and ignores all the other higher-order terms. The constants $f_{rrr}$ and $f_{rrrr}$ are estimated by Eq. 9 with the $a_3$ and $a_4$ parameters transferred from those of the corresponding diatomic radical. The use of the matrices given in Tables I and II then gives approximate values of the cubic and quartic constants and those of $\alpha$ and $x$. It can be expected from Tables VIII and IX that this method will be effective for predicting $k_{111}$, $k_{133}$, $k_{1111}$, $k_{1133}$, and $k_{3333}$ provided the $a_3$ and $a_4$ parameters are estimated properly, while it will give somewhat poorer results for the other constants except when the contributions from the disregarded higher-order constants accidentally cancel one another.

Calculations by means of this method have been made for ten bent $XY_2$ molecules. The estimations of $a_3$ and $a_4$ by the various methods[1,3,24] discussed in Part I are given in Table XI. A comparison of the results with the corresponding observed values in Tables XII–XV verifies the above expectation; the agreement is particularly good for the above five anharmonic constants and for $x_{11}$, $x_{13}$, and $x_{33}$, which almost exclusively depend on these constants. It is shown in the tables that at least the signs and the orders of magnitude are correctly estimated by this method, even for the rest of the constants of all the molecules, except for $k_{222}$, $x_{22}$, and $x_{12}$. It seems that it will be necessary to introduce higher-order cross terms, which are here ignored, in order to make quantitative estimates for these three constants.

This method may be regarded as a primitive but practical representation of the anharmonic potential field. The role of this model may be compared with that of the "valence-force" representation of the quadratic field which prevailed in the early stage of the studies of molecular normal vibrations.

## Application of the Method

The present method for estimating anharmonic constants has been applied in this laboratory to the microwave studies of the $SO_2$ and $OF_2$ molecules in their excited vibrational states. The prediction of the $k_{133}$ and $k_{233}$ constants of the $SO_2$ molecule made it easier to discover and assign the relatively weak absorption lines which belong to the $\nu_3$ state of this molecule, as was reported in a previous paper.[8] In a similar way, the detection and analysis of the lines which belong to the $\nu_1$ and $\nu_3$ states of the $OF_2$ molecule would have been more difficult without the preliminary but approximately correct estimates of the $k_{111}$, $k_{133}$, $k_{211}$, and $k_{233}$ constants obtained by the present method. The details of the analysis will be published as a forthcoming paper.[22]

24) E. R. Lippincott and R. Schroeder, *J. Chem. Phys.*, 23, 1131 (1955); D. Steele and E. R. Lippincott, ibid., 35, 2065 (1961).

## Summary

The vibrational potential function of the bent $XY_2$ molecule has been expanded in terms of the internal coordinates to the fourth order, and a general formulation which relates the coefficients of this expansion (second-, third-, and fourth-order potential constants) to the cubic and quartic constants in the normal-coordinate system has been derived. The third- and fourth-order constants in the internal-coordinate system for $H_2O$, $D_2O$, $H_2Se$, $D_2Se$, and $SO_2$ have been determined by using the experimental $\alpha$ and $x$ values taken from the literature. It has been shown that the third- and fourth-order constants which represent the anharmonic bond-stretching vibration, $f_{rrr}$ and $f_{rrrr}$, are much larger than the other higher-order constants and that they are nearly equal (to within 12 per cent) to the anharmonic potential constants of the corresponding diatomic radicals. The method presented in Part I of this paper, which makes use of the "diatomic approximation" for estimating the anharmonic constants and the $\alpha$ and $x$ values, has been applied to the bent $XY_2$ molecules. A comparison of the results with currently available experimental data has shown that the signs and the orders of magnitude are in most cases correctly predicted by this approximation. This method has been further applied as an aid for the detection and analysis of the microwave absorption lines in the case of the $SO_2$ and $OF_2$ molecules in their excited vibrational states.

*Department of Chemistry*
*Faculty of Science*
*The University of Tokyo*
*Hongo, Tokyo*

# The Electron Spin Resonance and Electronic Absorption Spectra of the 3-Nitropyridine Anion Radical

By Michiya Itoh and Saburo Nagakura

(Received October 23, 1964)

In a previous paper,[1] the present authors and Okamoto studied the ESR and electronic absorption spectra of the 4-nitropyridine anion radical. In the present paper, a similar study has been made of the 3-nitropyridine anion radical.

## Experimental

**Material.**—3-Nitropyridine was prepared by the oxidation of 3-aminopyridine by Caro's acid, and it was purified by repeated recrystallizations. The melting point (41°C) was in good agreement with that reported in the literature.[2]

**The Preparation of the Anion Radical and Measurements.**—The 3-nitropyridine anion radical was prepared at room temperature by the reduction of the parent compound with potassium metal in 1, 2-dimethoxy ethane (DME). The details of the preparation of the anion radical and of the measurements of its ESR and electronic absorption spectra are the same as those reported in the previous paper.[1]

## Experimental Results

The ESR spectrum observed with the DME solution of the 3-nitropyridine anion radical is shown in Fig. 1. From the spectrum, the hyperfine coupling constants associated with the nitrogen and hydrogen atoms were determined to be as shown in Table I.

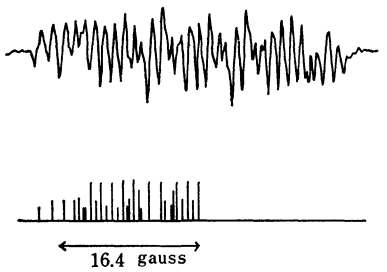



Fig. 1. The ESR spectrum (first derivative) of 3-nitropyridine anion and the reconstruction based on the coupling constants.

The electronic absorption spectrum of the DME solution of the 3-nitropyridine anion has also been measured; the results are shown in Fig. 2. The absorption bands at 304 and 460 mμ can safely be ascribed to the 3-nitropyridine anion, since the intensities of these bands change in parallel with that of the ESR spectrum.

Table I. The coupling constants and spin densities of the 3-nitropyridine anion

| | 3-Nitropyridine anion | | | 4-Nitropyridine anion | |
|---|---|---|---|---|---|
| | | Spin density | | Spin density | |
| Position | Coupling const. | Obs.[a] | Calcd.[b] | Obs.[a] | Calcd.[b] |
| N ($NO_2$) | 10.11 gauss | 0.253 | 0.301 | 0.218 | 0.261 |
| N (ring) | 2.65 | 0.098 | 0.107 | 0.101 | 0.124 |
| 6-H (C) | | | 0.024 | 0.133 | 0.052 |
| 5-H (C) | (4.44)*×2<br>(1.33)*×2 | (0.199)*×2<br>(0.059)*×2 | 0.040 | 0.024 | 0.033 |
| 4-H (C) | | | 0.133 | — | — |
| 2-H (C) | | | 0.024 | 0.133 | 0.052 |

* No attempt was made to assign the observed proton coupling constants to individual hydrogen atoms.

a) Estimated from the ESR coupling constants.

b) Calculated by the molecular orbital method.

1) M. Itoh, T. Okamoto and S. Nagakura, This Bulletin, **36**, 1665 (1963).

2) F. Friedl, *Ber.*, **45**, 429 (1912).

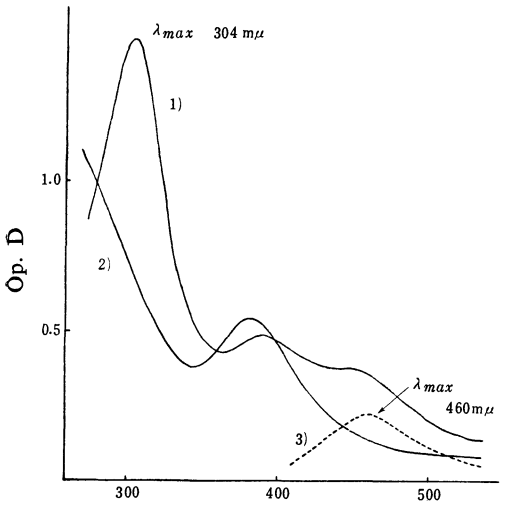



Fig. 2. The electronic absorption spectrum of 3-nitropyridine anion. (The scale factor of vertical axis is arbitrary.)
1) The spectrum of DME solution of the anion.
2) The spectrum of the solution exposed to air.
3) 1)−2).

## Theoretical

Molecular orbital calculation has been carried out with the $\pi$-electron system of the 3-nitropyridine anion radical in order to ascertain the assignment of the observed electronic spectrum and to obtain some knowledge about the electronic structure of this anion. The present calculation of the 3-nitropyridine anion has been performed by a method similar to that employed in the case of the 4-nitropyridine anion.[1] The anion radical was separated into two components, the pyridine anion as an electron donor and the nitro group as an electron acceptor. The interaction between the components was considered by the aid of the configurational interaction among ground, locally excited and charge-transfer configurations. The electron configurations and energies of these configurations are given in Table II. The procedure for evaluating these energies is not described in the present paper, since the details have been mentioned in the previous paper.[1]

The off-diagonal matrix elements, $H_{ij}$'s, of the total electronic Hamiltonian were evaluated by the aid of the method presented by Pople[3] and by Murrell and Longuet-Higgins.[4] The results are shown in Table III. The repulsion integrals necessary for the evaluation of the interaction energies between locally

TABLE II. THE $\pi$-ELECTRON CONFIGURATIONS OF THE 3-NITROPYRIDINE ANION

| Wave function | Energy |
|---|---|
| Ground configuration[a]: | |
| $\psi_1=\Phi_1\lvert\varphi_a\bar{\varphi}_a\varphi_b\bar{\varphi}_b\rvert$ | −0.716 eV. |
| Locally excited configurations within the pyridine ring[a]: | |
| $\psi_2=\Phi_2\lvert\varphi_a\bar{\varphi}_a\varphi_b\bar{\varphi}_b\rvert$ | −0.231 |
| $\psi_3=\Phi_3\lvert\varphi_a\bar{\varphi}_a\varphi_b\bar{\varphi}_b\rvert$ | 2.860[b] |
| $\psi_5=\Phi_5\lvert\varphi_a\bar{\varphi}_a\varphi_b\bar{\varphi}_b\rvert$ | 8.375 |
| $\psi_8=\Phi_8\lvert\varphi_a\bar{\varphi}_a\varphi_b\bar{\varphi}_b\rvert$ | 8.877 |
| $\psi_9=\Phi_9\lvert\varphi_a\bar{\varphi}_a\varphi_b\bar{\varphi}_b\rvert$ | 9.278 |
| Locally excited configurations within the nitro group[c]: | |
| $\psi_{4a}=\frac{1}{\sqrt{2}}(\psi_4{}^1-\psi_4{}^2)$ | 6.303 |
| $\psi_{4b}=\frac{1}{\sqrt{6}}(\psi_4{}^1+\psi_4{}^2-2\psi_4{}^3)$ | |
| $\psi_{6a}=\frac{1}{\sqrt{2}}(\psi_6{}^1-\psi_6{}^2)$ | 5.877 |
| $\psi_{6b}=\frac{1}{\sqrt{6}}(\psi_6{}^1+\psi_6{}^2-2\psi_6{}^3)$ | |
| Charge-transfer configuration: | |
| $\psi_7=\lvert\varphi_1\bar{\varphi}_1\varphi_2\bar{\varphi}_2\varphi_3\bar{\varphi}_3\varphi_a\bar{\varphi}_a\varphi_b\bar{\varphi}_b\varphi_c\rvert$ | $A_P-A_N+\Delta E=-0.885$ |

a) The $\Phi_1$, $\Phi_2$, ····· are the wave functions of locally excited configurations within the pyridine anion which were shown in the previous paper.[1]
b) The energy of this configuration was estimated by combining the experimental value of locally excited energy within the pyridine ring (3, 5-lutidine: 3.54 eV.) with the electrostatic interaction energy.
c) The $\varphi_a$, $\varphi_b$ and $\varphi_c$ are the molecular orbitals of the nitro group (J. Tanaka, *J. Chem. Soc. Japan, Pure Chem. Sec.* (*Nippon Kagaku Zassi*), **78**, 1643 (1957)).
d) The $\psi_4{}^1$, $\psi_4{}^2$, ····· are as follows:

$\psi_4{}^1=\lvert\varphi_1\bar{\varphi}_1\varphi_2\bar{\varphi}_2\varphi_3\bar{\varphi}_3\varphi_4\varphi_a\bar{\varphi}_a\varphi_b\bar{\varphi}_c\rvert$
$\psi_4{}^2=\lvert\varphi_1\bar{\varphi}_1\varphi_2\bar{\varphi}_2\varphi_3\bar{\varphi}_3\varphi_4\varphi_a\bar{\varphi}_a\varphi_b\varphi_c\rvert$
$\psi_4{}^3=\lvert\varphi_1\bar{\varphi}_1\varphi_2\bar{\varphi}_2\varphi_3\bar{\varphi}_3\varphi_4\varphi_a\bar{\varphi}_a\varphi_b\varphi_c\rvert$
$\psi_6{}^1=\lvert\varphi_1\bar{\varphi}_1\varphi_2\bar{\varphi}_2\varphi_3\bar{\varphi}_3\varphi_5\varphi_a\bar{\varphi}_a\varphi_b\bar{\varphi}_c\rvert$
$\psi_6{}^2=\lvert\varphi_1\bar{\varphi}_1\varphi_2\bar{\varphi}_2\varphi_3\bar{\varphi}_3\varphi_5\varphi_a\bar{\varphi}_a\varphi_b\varphi_c\rvert$
$\psi_6{}^3=\lvert\varphi_1\bar{\varphi}_1\varphi_2\bar{\varphi}_2\varphi_3\bar{\varphi}_3\varphi_5\varphi_a\bar{\varphi}_a\varphi_b\varphi_c\rvert$

TABLE III. THE OFF-DIAGONAL MATRIX ELEMENTS (IN UNITS OF eV.) USED IN THE CALCULATION OF THE 3-NITROPYRIDINE ANION

| | |
|---|---|
| $H_{17}=0.573$ | $H_{24a}=-0.002$ |
| $H_{34a}=0.089$ | $H_{26a}=0.078$ |
| $H_{36a}=-0.412$ | $H_{27}=1.044$ |
| $H_{37}=-0.845$ | $H_{54a}=0.234$ |
| $H_{84a}=0.071$ | $H_{56a}=0.009$ |
| $H_{86a}=-0.016$ | $H_{94a}=0.029$ |
| $H_{87}=-0.215$ | $H_{96a}=-0.020$ |

The other off-diagonal elements are zero.

3) J. A. Pople, *Trans. Faraday Soc.*, **49**, 1375 (1953).
4) H. C. Longuet-Higgins and J. N. Murrell, *Proc. Phys. Soc.*, A **68**, 601 (1955).

TABLE IV. THE LOWEST FOUR ENERGY LEVELS AND THEIR WAVE FUNCTIONS OF THE 3-NITROPYRIDINE ANION

| Energy | |
|---|---|
| $W_1=-1.942$ eV. | $\Phi_1=0.367\Psi_1-0.138\Psi_3-0.479\Psi_2+0.785\Psi_7$ |
| $W_2=-0.616$ eV. | $\Phi_2=0.893\Psi_1+0.419\Psi_2-0.155\Psi_7$ |
| $W_3=0.517$ eV. | $\Phi_3=-0.256\Psi_1-0.203\Psi_3+0.767\Psi_2+0.551\Psi_7$ |
| $W_4=3.006$ eV. | $\Phi_4=0.958\Psi_3+0.078\Psi_2+0.135\Psi_{6a}+0.234\Psi_7$ |

TABLE V. THE CALCULATED AND OBSERVED RESULTS FOR THE LOWEST THREE ELECTRONIC TRANSITIONS OF THE 3-NITROPYRIDINE ANION

| Transition | $\lambda_{max}$, eV. calcd. | obs. | Calcd. oscillator strength | Direction of transition moment |
|---|---|---|---|---|
| $W_1 \rightarrow W_2$ | 1.32 | — | $3.60\times10^{-2}$ | $\Theta=30°27'$ |
| $W_1 \rightarrow W_3$ | 2.46 | 2.69 | $4.33\times10^{-1}$ | $\Theta=40°39'$ |
| $W_1 \rightarrow W_4$ | 4.94 | 4.04 | $3.29\times10^{-1}$ | $\Theta=40°17'$ |



excited configurations were obtained in the same way as in the case of the 4-nitropyridine anion studied in the previous paper.[1] The core resonance integral between $2p\pi$ atomic orbitals of the carbon atom on the 3-position and the neighboring nitrogen atom of the nitro group was estimated to be $-3.0$ eV.[1,6]

The energy levels and wave functions can be evaluated by solving the secular equation constructed by the diagonal and off-diagonal matrix elements given in Tables II and III. The actual calculation was made by the aid of a Facom 202 electronic computer in our Institute. The four lowest energy levels and wave functions of the 3-nitropyridine anion are given in Table IV. Oscillator strengths were calculated for the three longest wavelength absorption bands by the method mentioned in the previous paper.[1] The calculated transition energies and oscillator strengths are shown in Table V.

## Discussion

The ESR hyperfine coupling constants associated with the nitrogen atom in the aromatic ring and with that of the nitro group depend not only on the spin densities on the respective atoms, but also on the spin densities on the adjacent atoms via indirect polarization.[7] Fraenkel et al.[8] proposed the following equation for the coupling constant due to the nitrogen nucleus of the nitro group:

$$A_N=Q_N\rho_N+Q_O\rho_O+Q_C\rho_C \qquad (1)$$

where the $\rho_N$, $\rho_O$ and $\rho_C$ are the spin densities of the nitrogen and oxygen atoms of the nitro group, and that of the carbon atom attached to the nitro group, respectively. $Q_N$, $Q_O$ and $Q_C$ are constants; they were determined as follows:

$$Q_N=\pm(99.0\pm10.2)\quad Q_O=\mp(35.8\pm5.9)\quad Q_C\fallingdotseq0$$

from a comparison of the observed nitrogen coupling constants of a the anions of several nitro compounds with the spin densities on the nitro groups calculated by the simple Hückel molecular orbital method.

According to our calculations, the ratio of the $\rho_N$ to $\rho_O$ is always constant, because the molecular orbital wave functions for the nitro group are fixed in the present calculations. Furthermore, we can reasonably assume that the $\rho_C$ term in Eq. 1 may be negligibly small, Thus, Eq. 1 can be reduced to the following equation:

$$A_N=Q_N'\rho_N \qquad (1')$$

where $Q_N'$ is constant. The value of $Q_N'$ was taken to be 40 gauss in the previous paper.[1] The same value has also been adopted in the present paper.

Now let us turn to the coupling constant associated with the nitrogen nucleus of the hetero aromatic ring. Carrington and Santos-Veiga proposed the following equation for the nitrogen-coupling constant, $A_N^{ring}$, and the spin density, $\rho_N^{ring}$, on the nitrogen atom, and estimated the value of $Q_N^{ring}$ to be 25.3 gauss:[9]

$$A_N^{ring}=Q_N^{ring}\rho_N^{ring} \qquad (2)$$

By the aid of Eqs. 1' and 2, the spin densities on the two nitrogen atoms were evaluated from the observed coupling constants; they are shown in Table I. Furthermore, the spin densities on the ring carbon atoms were obtained by the

5) R. Pariser and R. G. Parr, *J. Chem. Phys.*, **21**, 767 (1953).
6) A. Ishitani, K. Kuwata, H, Tsubomura and S. Nagakura, This Bulletin, **36**, 1357 (1963).
7) M. Karplus and G. K. Fraenkel, *J. Chem. Phys.*, **35**, 1312 (1961).
8) P. H. Rieger and G. K. Fraenkel, ibid., **39**, 609 (1963).
9) A. Carrington and J. dos Santos-Veiga, *Mol. Phys.*, **5**, 21 (1962).

use of the following well-known relation for the proton coupling constant: [10] $A_H = Q_H \rho_C$ ($Q_H = -22.5$ gauss). The theoretical values of the spin densities evaluated by the aid of the ground state wave function are also given in Table I for purposes of comparison. It may be said that the spin densities on the two kinds of nitrogen atoms of the 3-nitropyridine anion as estimated from the ESR coupling constants are in good agreement with the calculated values.

As is shown in Table I, the spin density on the nitrogen atom of the nitro group is larger in the 3-nitropyridine anion than in the 4-nitropyridine anion. This result is consistent with the theoretical conclusion that the contribution of the charge-transfer configuration caused by the electron transfer from the pyridine anion ring toward the nitro group increases in the 3-nitropyridine anion in comparison with that in the 4-nitropyridine anion.

The electronic absorption spectrum of the 3-nitropyridine anion shows two absorption bands at 304 and 460 m$\mu$ which can be ascribed to the $W_1 \rightarrow W_4$ and $W_1 \rightarrow W_3$ transitions respectively. Since, in the wave function of the $W_4$ state, the contribution of the locally excited configuration within the pyridine ring amounts to 92%, the 304 m$\mu$ band corresponding to the $W_1 \rightarrow W_4$ transition can be interpreted as the shifted band of the 355 m$\mu$ band of the 3, 5-lutidine (pyridine) anion.[1] This blue shift is caused by the fact that the ground configuration is largely stabilized by resonance interaction with the charge-transfer configuration. Furthermore, from the wave functions, $\Phi_1$ and $\Phi_3$, it can easily be seen that the 460 m$\mu$ band corresponding to the $W_1 \rightarrow W_3$ transition may be regarded as the intramolecular charge-transfer band. The absorption band corresponding to the $W_1 \rightarrow W_2$ transition could not be observed despite careful experimentation. This may be because the $W_1 \rightarrow W_2$ transition band is weak, as is revealed by the calculated oscillator strength value, and is, therefore, covered by other absorption bands due to reaction products.

The authors wish to express their deep thanks to Mr. Koichi Itoh of this Institute for his kind help in measuring the ESR spectra. One of the authors (M. I.) also gratefully acknowledges the encouragement of Professor Toshihiko Okamoto, Faculty of Pharmaceutical Sciences, the University of Tokyo.

*The Institute for Solid State Physics*
*The University of Tokyo*
*Azabu, Tokyo*

10) S. I. Weissman, T. R. Tuttle and E. J. de Boer, *J. Phys. Chem.*, **61**, 28 (1957).

# Stability Order in Metal Chelate Compounds. IV.[1] 2-Pyridylmethanol Complexes*,**

By Yukito MURAKAMI and Makoto TAKAGI

(Received October 26, 1964)

As a part of our investigation of the stability order of the metal chelates formed by the bivalent metals of the first transition series, 2-pyridylmethanol as a chelating agent has been chosen for this study. One of the interesting aspects of this ligand lies in the behavior of the alcoholic hydroxyl group toward metal ions in the process of complex formation. Much work has been done recently on the coördination ability of an alcoholic hydroxyl group present in alkanol-substituted amines. Martell and his coworkers[2] have postulated that the direct coördination of the alkoxy group in its anionic form to the metal ion occurs in a relatively high pH region in aqueous media.

Hall and his associates[3-6] investigated the

* Contribution No. 79 from the Department of Organic Synthesis, Faculty of Engineering, Kyushu University.

** Presented in part at the 17th Annual Meeting of the Chemical Society of Japan, Tokyo, April, 1964.

1) Part III: Y. Murakami and M. Tokunaga, This Bulletin, 37, 1562 (1964).

2) A. E. Martell, S. Chaberek, Jr., R. C. Courtney, S. Westerback and H. Hyytiainen, *J. Am. Chem. Soc.*, 79, 3036 (1957).

3) J. L. Hall, F. R. Jones, C. E. Delchamps and C. W. McWilliams, ibid., 79, 3361 (1957).

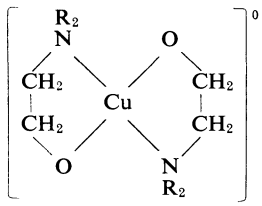
4) J. L. Hall and W. E. Dean, ibid., 80, 4183 (1958).

5) J. L. Hall and W. E. Dean, ibid., 82, 3300 (1960).

6) J. L. Hall, W. E. Dean and E. A. Pacofsky, ibid., 82, 3303 (1960).

reaction between alkanol-substituted ethylenediamines and bivalent metal ions in the presence of a strong base by means of spectrophotometric, conductometric and potentiometric methods. The alcoholic hydroxyl group was found to coördinate to the metal ion on the liberation of its proton, thus forming a new and stable chelate ring which involves an amine-nitrongen and an anionic hydroxyl oxygen as donor atoms. The acid dissociation constants of various metal chelates of such alkanol-substituted ethylenediamines have also been estimated.[6]

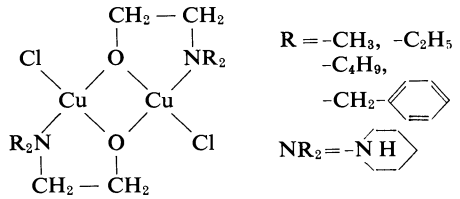
The behavior of *N*-substituted ethanolamine-copper(II) systems upon the addition of a strong base was studied by Ojima and Sone[7] by the spectrophotometric measurement in the visible region and by the paper electrophoresis method. They detected the formation of electrically-neutral chelate species and assigned structure I to them:



R=-H, -$CH_3$ -$C_2H_5$

I

Hall et al.[8,9] have also studied the interaction between copper(II) and ethanolamines, such as monoethanolamine (MEA), diethanolamine (DMA), and triethanolamine (TEA), in the presence of a strong base. The methods employed in their study were polarography, spectrophotometry and electrical migration. The presence of neutral and anionic species of metal complexes was detected in a relatively high pH region, and the corresponding equilibrium constants were evaluated. The metal complexes reported are as follows: $[Cu(MEA)_2(OH)_2]$, $[Cu(DEA)_2(OH)_2]$, $[Cu(TEA)(OH)_2]$ and $[Cu(TEA)(OH)_3]^-$, where OH represents the coordination of either the hydroxide ion or the alkoxide ion. Further information on the behavior of ethanolamines was added by Hein and Beerstecher.[10] Upon the reaction of *N*, *N*-disubstituted ethanolamines with cupric chloride in absolute ethanol, a series of crystalline metal chelates was obtained; the dinuclear structure II was proposed for these materials:



R=-$CH_3$, -$C_2H_5$ -$C_4H_9$, -$CH_2$-⟨⟩, $NR_2$=-NH⟨⟩

II

From the above survey, it is clear that the hydroxyl group of amine-containing ligands is a good donor group and is more likely to undergo coördination in the anionic form under suitable conditions.

Since 2-pyridylmethanol is likely to form a chelate ring similar to those of ethanolamine and other alkanol-substituted amines, there remains a good chance for its hydroxyl group in its anionic form to coördinate with metal ions when experimental conditions are adjusted suitably. So far, two research groups[11,12] have investigated potentiometrically the interaction of 2-pyridylmethanol with one or two bivalent metal ions to a limited extent in an attempt to evaluate the formation constants of the corresponding metal chelates. In the present work, cadmium(II), magnesium(II) and several bivalent first transition metals (manganese, cobalt, nickel, copper and zinc) were employed, and a detailed potentiometric investigation was carried out in order to determine the complexing behavior of 2-pyridylmethanol with these metal ions. In addition, in order to clarify the behavior of the hydroxyl group of the ligand toward metal ions, several copper chelates were isolated and their properties investigated.

## Experimental

**2-Pyridylmethanol.** — 2-Pyridylmethanol (III) was prepared from 2-picoline through the intermediate compounds, 2-picoline-*N*-oxide and 2-pyridylmethanol acetate in this order, by a method described by Boekelheide and Linn;[13] b. p. 88—93°C at 4 mmHg (reported[14] b. p. 111—112°C at 15 mmHg); the picrate, m. p. 160.2—161.5°C (reported[13] m. p. 160.5—161°C); a total yield of 40%. The product is a hygroscopic and colorless liquid, but it gradually turnes yellow in the air. III was, therefore, transformed into the corresponding nitrate salt (IV) by adding concentrated nitric acid to the acetone solution, the salt being isolated as colorless crystals; after repeated recrystallizations

7) H. Ojima and K. Sone, *Z. anorg. u. allgem. Chem.*, **309**, 110 (1961).
8) J. F. Fisher and J. L. Hall, *Anal. Chem.*, **34**, 1094 (1962).
9) J. M. Bolling and J. L. Hall, *J. Am. Chem. Soc.*, **75**, 3953 (1953).
10) F. Hein and W. Beerstecher, *Z. anorg. u. allgem. Chem.*, **282**, 93 (1955).
11) W. D. Luz, S. Fallab and H. Erlenmeyer, *Helv. Chem. Acta*, **38**, 1114 (1951).
12) T. J. Lane, C. S. C., A. J. Kandathil and S. M. Rosalie, O. S. F., *Inorg. Chem.*, **3**, 487 (1964).
13) V. Boekelheide and W. J. Linn, *J. Am. Chem. Soc.*, **76**, 1286 (1954).
14) O. H. Bullitt, Jr., and J. T. Maynard, ibid., **76**, 1370 (1954).

from ethanol, m. p. 116.2—116.7°C; neutralization equivalence, 172.9 (calcd. 172.2).

Found: C, 42.03; H, 4.83; N, 16.16. Calcd. for $C_6H_8O_4N_2$: C, 41.86; H, 4.68; N, 16.27%.

The nitrate IV was dissolved in carbonate-free water in order to prepare a stock solution for potentiometric measurements.

The nitrate was reconverted to its free form for the preparation of the various copper chelates. An aqueous solution of IV was made alkaline with potassium carbonate and extracted with chloroform. After the chloroform solution had been dried over anhydrous potassium carbonate, chloroform was removed from the solution under reduced pressure in order to isolate III. This III was used either in its isolated state or as the chloroform extract mentioned above for the preparation of metal chelates.

**Acetato(2-pyridylmethanolato)copper(II).** — Five grams of copper acetate (monohydrate) was dissolved in concentrated aqueous ammonia and evaporated to dryness under reduced pressure on a water bath at 50°C or lower. The violet crystals of tetraammineacetatocopper(II) thus obtained was mixed with 2-pyridylmethanol isolated from 5 g. of the corresponding nitrate. A homogeneous deep blue solution was prepared by adding 50 cc. of methanol, and then it was evaporated to dryness under reduced pressure below 50°C. The residue was extracted with chloroform (50 cc.), and the volume of the extract was reduced to 5—10 cc. after the insoluble material had been filtered off. A fine blue precipitate separated from the solution as acetone was added (crude yield, 4.3 g.). This crude product was purified by re-precipitation from the chloroform solution with acetone. The intermediate crop obtained in the process of re-precipitation was used for further study. The product (V) is a fine, blue, crystalline material, stable in the air, which decomposes at 180°C. It is soluble in water, alcohols (yellow solution) and chloroform, and slightly soluble in trichloroethylene, but insoluble in acetone, dioxane, ether, benzene, carbon tetrachloride and ligroin.

Found: C, 41.36; H, 4.02; N, 5.98; Cu, 26.68 (as CuO). Calcd. for $C_8H_9O_3NCu$: C, 41.65; H, 3.93; N, 6.07; Cu, 27.54%.

This chelate was also analyzed for 2-pyridylmethanol content by means of spectrophotmetry. The absorption intensity was measured in 0.6 N hydrochloric acid at 262 mμ, where free 2-pyridylmethanol has an absorption maximum of $\varepsilon=6830$; N, 6.10% (converted to nitrogen content). The molecular weight of this chelate was measured by means of a vapor pressure osmometer Model 301A (Mechrolab Inc., Mountain View, Calif., U. S. A.) at 37°C in chloroform; 893 (dibenzoyl as standard); 918 (tris(2,4-pentanedionato)chromium(III) as standard); calcd. for the tetramer, 922.8.

An attempt was made to prepare sodium diacetato(2-pyridylmethanolato)cuprate(II). A concentrated sodium acetate solution and aqueous V were mixed together and allowed to stand for several days. The deep blue crystals which separated from the solution were identified as the hydrated form of V.

**Bis(2-pyridylmethanolato)copper(II).** — Into a chloroform solution of 2-pyridylmethanol freshly isolated from the corresponding nitrate (0.8 g.), sufficient anhydrous potassium carbonate and V (0.5 g.) were added. The blue mixture, when shaken vigorously in a well-stoppered flask, turned violet in a few minutes. After approximately 30 min. of shaking, the reaction mixture was filtered on a glass filter, and the filtrate was condensed to 2 cc. under reduced pressure on a steam bath below 40°C. Bluish-violet needle-like crystals precipitated out as acetone was added to the concentrated solution; the yield was quantitative. The anhydrous product is hygroscopic enough to absorb one mole of water per mole of copper in the air. It decomposes at 150°C, but more slowly below 150°C in the air. This product was recrystallized from water as its hydrated form,* which was then reconverted to the anhydrous form at 56°C in vacuo. The hydrate is insoluble in ordinary organic solvents except for alcohols.

Found: C, 50.96; H, 4.23; N, 9.91; Cu, 22.29 (as CuO). Calcd. for $C_{12}H_{12}O_2N_2Cu$ (anhydrous form): C, 51.52; H, 4.32; N, 10.01; Cu, 22.71%.

**Chloro(2-pyridylmethanolato)copper(II).** — An aqueous solution of V and a concentrated potassium chloride solution were mixed, and the resulted precipitate was washed several times with water; green powder; insoluble in organic solvents.

Found: C, 34.33; H, 3.09; N, 6.73. Calcd. for $C_6H_6ONClCu$: C, 34.79; H, 2.92; N, 6.76%.

**Iodo(2-pyridylmethanolato)copper(II).** — This material was prepared in a manner similar to that used for the corresponding chloro complex; dark yellowish powder; insoluble in water and organic solvents.

Found: C, 24.32; H, 2.21; N, 4.90. Calcd. for $C_6H_6ONICu$: C, 24.14; H, 2.03; N, 4.69%.

**Nitrito(2-pyridylmethanolato)copper(II).** — The procedure for the preparation of this complex was similar to that used for the chloro complex; green powder; slightiy soluble in water and insoluble in organic solvents.

Found: C, 33.22; H, 2.94; N, 13.04. Calcd. for $C_6H_6O_3N_2Cu$: C, 33.11; H, 2.78; N, 12.87%.

**Thiocyanato(2-pyridylmethanolato)copper(II).** — To an aqueous solution of V, a concentrated solution of potassium thiocyanate was added. The bulky precipitate which formed on mixing was repeatedly washed with water by decantation and then allowed to remain in solution for several days. On standing, the precipitate turned to fine deep greenish blue crystals, which were separated by centrifugation; insoluble in water and organic solvents.

Found: C, 36.44; H, 2.81; N, 12.32. Calcd. for $C_7H_6N_2OSCu$: C, 36.59; H, 2.63; N, 12.19%.

**Metal Salts.**—The bivalent metal ions employed in the present work were magnesium, manganese, cobalt, nickel, copper, zinc and cadmium in their salt forms of $Mg(NO_3)_2\cdot 6H_2O$, $MnSO_4\cdot nH_2O$, $Co(NO_3)_2\cdot 6H_2O$, $Ni(NO_3)_2\cdot 6H_2O$, $Cu(NO_3)_2\cdot 3H_2O$, $Zn(NO_3)_2\cdot 6H_2O$ and $Cd(NO_3)_2\cdot 4H_2O$ of analytical

* This hydrate was found to be identical with that isolated from the aqueous mixture of copper salt and 2-pyridinemethanol. The latter procedure was reported by H. Ojima et al. (presented at the 17th Annual Meeting of the Chemical Society of Japan, Tokyo, 1964).

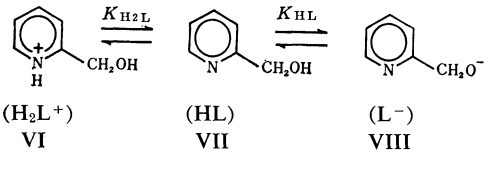
grade obtained from the Wako Pure Chemical Industries, Ltd. These salts were dissolved in carbonate-free water in order to prepare stock solutions which were standardized by the usual methods of chelatometric titration.[15]

**Potentiometric Measurements.** — The apparatus and procedures for potentiometric measurements have been described in a previous paper.[16] All the titrating solutions in this work were maintained at 25.0±0.1°C and at the ionic strength of 0.10 M (by the addition of potassium nitrate) and were kept under a nitrogen atmosphere throughout the titrations. Titrations of the 2-pyridylmethanol chelate systems of various bivalent metals were performed for 1 : 1, 2 : 1 and 5 : 1 molar ratios of ligand to metal ion.

**Spectral Measurements.**—The infrared spectra of various copper chelates were measured in Nujol mull with a Koken model DS-301 spectrophotometer equipped with sodium chloride optics. Ultraviolet and visible spectral measurements were performed in aqueous media with a Hitachi EPS-2-type recording spectrophotometer.

## Results and Discussion

**Acid Dissociation Constant.**—The protonated 2-pyridylmethanol may have two processes of proton dissociation; VI → VII, and VII → VIII. The protonated proton undergoes dissociation in a relatively low pH range, as may be seen in Fig. 1. However, the dissociation of an alcoholic proton was hardly detected at all under the present experimental conditions. Thus the cationic species was treated as a monobasic acid, and its dissociation constant was estimated in a usual manner. The estimated $pK_{H_2L}$ of 2-pyridylmethanol at 25°C is 4.89. This is lower than the $pK$ values for pyridine and $\alpha$-picoline in 0.5 M potassium nitrate which are 5.45 and 6.20 respectively.[17] Although the hydroxymethyl group would change the basicity of a pyridine-nitrogen to a certain limited extent through inductive and resonance interactions,* the lower value of $pK_{H_2L}$ in the present compound seems primarily to be due to strong intramolecular hydrogen bonding between the pyridine-nitrogen and the hydroxyl group.



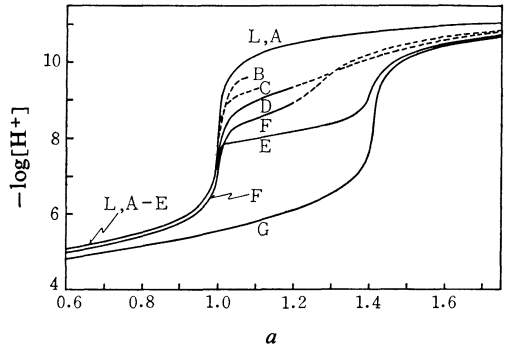
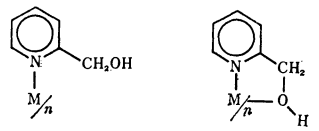




Fig. 1. Potentiometric titration of bivalent metal complexes of 2-pyridylmethanol (nitrate salt) at total ligand concentration of $2.50\times10^{-3}$ M with 5 : 1 molar ratio of ligand to metal ion: A, Mg; B, Mn; C, Cd; D, Co; E, Zn; F, Ni; G, Cu; L, ligand alone; $a$=moles of base added per mole of ligand; $t$=25°C; $\mu$=0.10 M ($KNO_3$).
Dotted curves represent non-equilibrated titrations.

**The Interaction of 2-Pyridylmethanol with Bivalent Metal Ions.**—A family of titration curves are shown in Fig. 1 for the 2-pyridylmethanol chelate systems of magnesium(II), manganese(II), cobalt(II), nickel(II), copper(II), zinc(II), and cadmium(II) for a 5 : 1 molar ratio of ligand to metal ion. In all the metal chelate systems except the copper system, a distinct inflection region was found at $a$=1.0. In the lower buffer regions lying below $a$=1.0, all the potentiometric titrations immediately reached equilibrium and were quite reproducible. Thus, a metal complex either of the ammine type (IX) or of the chelate type, with a hydroxyl group as another donor group (X), is presumably forming in this region.




IX X

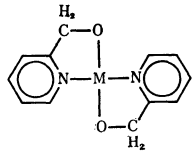
Judging from the extent of the depression of the titration in reference to with that for the free ligand, the stability of the metal chelates with respect to metal ions follows the sequence:

$$Cu(II) > Ni(II) > Co(II) > Zn(II) > Mn(II) > Cd(II)$$

Since titration curves for the free ligand and the magnesium system coincide well with each

15) K. Ueno, "Kireto Tekiteiho (Chelatometric Titration)", (in Japanese), Nankodo, Tokyo (1960).
16) Y. Murakami, *J. Inorg. Nucl. Chem.*, **24**, 679 (1962).
17) J. Bjerrum, G. Schwarzenbach and L. G. Sillén, "Stability Constants, Part I, Organic Ligands," The Chemical Society, London (1957).
* The electron-releasing effect of the hydroxymethyl group described by Lane et al.[12] is not quite convincing to the authors. Further study is needed to clarify this matter.

other over the whole pH range studied, magnesium(II) does not seem to form a chelate with the ligand. Beyond $a=1.0$, where the protonated proton of the conjugate acid is completely neutralized, the downward deviation of the titration curves for manganese and cadmium systems started immediately, followed by the precipitation of the metal hydroxide. For both the cobalt and nickel systems, titration curves demonstrated similar time-dependent behavior. Although no precipitates were observed for these two systems throughout the titrations, equilibrium was not reached in a short period of time beyond $a=1.2$. This sluggish equilibration is considered to be due to the slow formation of the chelates of structure XI and to hydrolytic reactions of the various chelates formed.



XI

In contrast, the titration curve of the zinc chelate system shows another significant inflection around $a=1.4$ in Fig. 1, and it is quite reproducible except in a small region immediately beyond the first inflection ($a>1.0$). Since the hydrolytic tendency of zinc is no greater than those of nickel and cobalt, this second inflection is most probably due to the formation of the 2:1(ligand to metal) chelate of structure XI.

The titration of a solution containing a 5:1 molar ratio of ligand to copper ion resulted in a large pH depression over the whole pH range studied (especially in $1.0<a<1.4$) and in only one steep inflection at $a=1.4$, as is shown in Fig. 1. Since neither pH drifting nor precipitation was observed throughout the titrations, this inflection may be considered to correspond to the formation of the 2:1 chelate, the structure of which may be represented by XI.

From the behavior of titration curves shown in Fig. 1, the interaction of 2-pyridylmethanolate anions with bivalent metal ions can be seen to increase in the following order:

$$\text{Co(II)},\ \text{Ni(II)} < \text{Zn(II)} \ll \text{Cu(II)}$$

Titration curves for all the bivalent metal chelate systems of the present study were also obtained for the first buffer region (and for the whole pH range with the copper system) at a 2:1 molar ratio of ligand to metal ion; they were found to behave in a manner similar to the 5:1 systems. The copper chelate system was also titrated at a 1:1 molar ratio. pH drifting was observed to start beyond $a=1.5$, followed by the precipitation of copper hydroxide.

**Equilibrium Constants.**—In the first buffer region ($a<1.0$) of the chelate systems of manganese, cobalt, nickel, zinc, cadmium and in the early part of the titration curve of the copper chelate system, two types of reactions are considered to compete with each other. One is the acid dissociation of the ligand (VI→VII), and the other is the formation of metal complexes of either structure IX or X. Thus the stability constants were calculated by the usual algebraic method, assuming 2:1 and 1:1 complex formations. The evaluated data are summarized in Table I. The stability constants of these metal complexes are greater than the corresponding pyridine complexes (Table II)[17] by one unit in $\log K$, with the exception of the cadmium complexes. Since the hydroxymethyl group does not seem to increase the basicity of a pyridine-nitrogen to a significant extent, the increased stability of the present complexes may be ascribed to chelate ring formation involving the hydroxyl group. Thus, structure X is prefered to the ammine-type complex, IX.

For the equilibrated region of the copper chelate system at a 1:1 molar ratio, the

TABLE I. STABILITY CONSTANTS OF THE METAL COMPLEXES OF 2-PYRIDYLMETHANOL
25.0±0.1°C, $\mu=0.10$ M ($KNO_3$)

| Metal ion | $\log K_1$ | $\log K_2$ |
|---|---|---|
| Mn(II) | ~1 | — |
| Co(II) | 2.1 | — |
| Ni(II) | 2.79 | 2.60 |
| Cu(II) | 3.41 | 2.81 |
| Zn(II) | 1.9 | — |
| Cd(II) | <1 | — |

$$K_1=\frac{[M(HL)^{2+}]}{[M^{2+}][HL]};\quad K_2=\frac{[M(HL)_2^{2+}]}{[M(HL)^{2+}][HL]}$$

HL stands for the neutral species of 2-pyridylmethanol.

TABLE II. STABILITY CONSTANTS OF THE METAL COMPLEXES OF PYRIDINE[17]
25°C, $\mu=0.5$ M ($C_5H_5N$, $HNO_3$)

| Metal ion | $\log K_1$ | $\log K_2$ |
|---|---|---|
| Co(II) | 1.14 | 0.4 |
| Ni(II) | 1.78 | 1.05 |
| Cu(II) | 2.41 | 1.88 |
| Zn(II) | 0.95 | 0.5 |
| Cd(II) | 1.27 | 0.8 |

$$K_1=\frac{[ML^{2+}]}{[M^{2+}][L]};\quad K_2=\frac{[ML_2^{2+}]}{[ML^{2+}][L]}$$

L stands for the neutral species of pyridine.

following two successive reactions were considered:

$$Cu^{2+} + HL \rightleftarrows Cu(HL)^{2+} \qquad K_1 = \frac{[Cu(HL)^{2+}]}{[Cu^{2+}][HL]}$$

$$Cu(HL)^{2+} \rightleftarrows CuL^{+} + H^{+} \qquad K^{H}_{MHL} = \frac{[CuL^{+}][H^{+}]}{[Cu(HL)^{2+}]}$$

Treating the titration data in the region, $a=0.4$—$1.1$, it was estimated that $pK^{H}_{MHL}=5.5$.

Since the copper ion is known to form rather stable chelates of structure X, the two acid dissociation reactions of the 2:1 chelate were considered to occur in addition to the neutralization of the protonated free ligand in the buffer region lying near the inflection of the 5:1 titration (Fig. 1). These two reactions are:

$$Cu(HL)_2^{2+} \rightleftharpoons CuL(HL)^{+} + H^{+}$$

$$K^{H}_{M(HL)_2} = \frac{[CuL(HL)^{+}][H^{+}]}{[Cu(HL)_2^{2+}]}$$

$$CuL(HL)^{+} \rightleftharpoons CuL_2 + H^{+}$$

$$K^{H}_{ML(HL)} = \frac{[CuL_2][H^{+}]}{[CuL(HL)^{+}]}$$

The estimated dissociation constants are $pK^{H}_{M(HL)_2}=5.55\pm0.01$, and $pK^{H}_{ML(HL)}=6.36\pm0.01$.*

These $pK$ values are slightly lower than those of the alkanol-substituted copper chelates of a 1:1 composition: *N*-hydroxyethylethylenediamine, 7.21,[6] 7.30[18]; *N*, *N'*-dihydroxyethylethylenediamine, 7.18,[6] 7.15[18]; *N*,*N'*-dihydroxypropylethylenediamine, 7.34[6]; *N*, *N*, *N'*, *N'*-tetrahydroxypropylethylenediamine, 6.77.[6] The resonance interaction of the pyridine ring with the chelate ring would produce an additional stabilization of the chelate ring. This stabilization presumably results in an increased labilization of the hydroxyl proton of the chelate.

Although several attempts have been made to analyze the zinc chelate system in its second buffer region (Fig. 1), they have not provided any reasonable results.

**The Coördination Ability of the Alcoholic Hydroxyl Group.**—There have been several discussions of the coördinating behavior of an alcoholic hydroxyl group. As has already been mentioned, several alkanol-substituted amines are likely to chelate with metal ions, involving an alcoholate anion as a donor group. It has been shown in the present work that 2-pyridylmethanol also acts as a bidentate ligand in its anionic form under appropriate conditions. The evidence for this will now be described.

(1) The copper chelate system demonstrated a sharp inflection in its titration curves at the 2:1 and 5:1 molar ratios. This corresponds to the liberation of one proton from each ligand molecule which is already coördinated to the metal ion.

(2) The color of the solutions of the copper chelate system was light blue at the start of titration in the presence of 5 mol. of the ligand per mole of copper ion. As a base was added to the titrating system, the blue color deepened, while a violet coloration was noticed beyond $a=1.2$. The solution finally turned violet at the inflection point, $a=1.4$; the addition of more base did not bring about any further color change. These color changes were followed spectrophotometrically; the $\lambda_{max}$ was nearly 800 m$\mu$ at the beginning and reached 575 m$\mu$ at the end.* The absorption band at 575 m$\mu$ may well correspond to the formation of the 2:1 chelate, which involves the alcoholate anion as a donor group.

(3) The 2-pyridylmethanol-copper(II) chelate of a molar ratio of 2:1 was isolated. This neutral chelate contains only 2-pyridylmethanol and copper(II); other constituents, such as hydroxide ions, do not seem to be involved in this chelate.

(4) Several 1:1 (2-pyridylmethanol: copper) chelates, which also contain inorganic anions, have been prepared. Infrared spectral measurements of these chelates did not provide any supporting evidence for the presence of the OH group.

An abnormally high molecular weight was obtained for acetato(2-pyridylmethanolato)-copper(II) in chloroform. Although this molecular weight corresponds to the tetrameric form of the chelate, a stereochemical structure has not been assigned to this species at the present time.

## Summary

The complexing behavior of 2-pyridylmethanol with magnesium(II), manganese(II), cobalt(II), nickel(II), copper(II), zinc(II) and cadmium(II) has been studied in aqueous media at 25.0±0.1°C and an ionic strength of 0.10 M ($KNO_3$). The stability constants for the 1:1 (ligand to metal) complexes of manganese(II), cobalt(II), nickel(II), copper(II), zinc(II) and cadmium(II) with the

* There may be some uncertainty involved in these values, although good constants were obtained from the data of the 5:1 titration. The above two reactions are simplified versions of the system; some other reactions such as chelate formation would actually be involved in the system. Some further study would clarify this problem.

18) R. C. Courtney, R. L. Gustafson, S. Chaberek, Jr., and A. E. Martell, *J. Am. Chem. Soc.*, **81**, 519 (1959).

* Spectroscopic work, and conductometric and electrophoresis studies of this copper chelate system have also been made by Ojima et al. (presented at the 17th Annual Metting of the Chemical Society of Japan, Tokyo, 1964).

neutral 2-pyridylmethanol and also for the 2:1 complexes of nickel(II) and copper(II) have been evaluated. The resulting stability order with respect to the bivalent metals has been found to follow the sequence:

$$Cd(II) < Mn(II) < Zn(II) < Co(II) < Ni(II) < Cu(II)$$

The higher stability of the present complexes relative to the corresponding pyridine complexes may be ascribed to the formation of a chelate ring which involves the hydroxyl group of the ligand.

After the complex formation between metal ions and the neutral ligand has proceeded to a certain extent, the liberation of a hydroxyl proton from the complex was observed to occur in several metal complex systems. This tendency was greatest for the copper complex, followed by the zinc, nickel and cobalt complexes in this order. Acid dissociation constants for the 1:1 and 2:1 copper complexes have also been evaluated.

Several pieces of evidence have been obtained in support of the coördination ability of the hydroxyl group of the present ligand in its anionic form.

The neutral copper chelate, bis(2-pyridylmethanolato)copper(II), as well as other various copper 2-hyridylmethanolate chelates which involve acetate, chloride, iodide, nitrite and thiocyanate ions as the third component, has been isolated. Acetato(2-pyridylmethanolato)-copper(II) has been found to exist as the tetrameric form in chloroform.

*Department of Organic Synthesis*
*Faculty of Engineering*
*Kyushu University*
*Hakozaki, Fukuoka*

# Direct Preparation of Partially Fluorinated Methane*

By Shunji NAGASE, Kiyoshi TANAKA and Hajime BABA

(Received September 8, 1964)

Numerous methods are available for the preparation of partially fluorinated methane. Some of them[1,2] use the Swarts reaction which consists of the replacement of the original halogens in an organic molecule with fluorine by halides of antimony. Indirect fluorination of halogenated methane with other inorganic fluorides is frequently used.[3-6] Potassium methyl sulfate[7] and methyl tosylate[8] were shown to be a good source of fluoromethane by their reaction with potassium fluoride. Hydrogenolysis,[9] reduction,[10] disproportionation,[11] or pyrolysis[12] of fluorinated compounds has also been reported. Perhaps the most significant method for direct preparation of partially fluorinated methane was described by Bigelow and his co-worker[13] in one of the important papers on fluorination of organic compounds by elementary fluorine. They obtained, besides the expected $C_1$ derivatives, hexafluoroethane and octafluoropropane.

In the present paper, accomplishment of partial fluorination of methane by electrochemical fluorination is described. Mono- and di-fluoromethane were obtained directly from methane in a reasonable conversion and current efficiency, using the electrolytic cell equipped with a specially devised "bubbler," one of the important features of the apparatus.

Little attention has been paid to partial fluorination of organic compounds or to fluorination of slightly soluble gases in hydrogen fluoride by an electrochemical process. Simons observed the formation of partially fluorinated methanes as the cleavage products from acetic acid, acetone, trimethylamine, etc., in his.

* This report will be designated as Part I of a series entitled, "Electrochemical Fluorination of Gases."

1) A. L. Henne, *J. Am. Chem. Soc.*, **59**, 1200, 1400 (1937).
2) W. B. Whalley, *J. Soc. Chem. Ind.* (*London*), **66**, 427 (1947).
3) O. Ruff, O. Bretschneider, W. Luchsinger and G. Miltschitzky, *Chem. Ber.*, **69**, 299 (1936).
4) F. Swarts, *Bull. soc. chim. Belg.*, **46**, 10 (1937); *Chem. Abstr.*, **31**, 7393 (1937).
5) J. H. Simons, R. L. Bond and R. E. McArthur, *J. Am. Chem. Soc.*, **62**, 3477 (1940).
6) C. B. Miller and J. D. Calfee, U. S. Pat. 2676996 (1954).
7) W. H. Bennett, *J. Am. Chem. Soc.*, **51**, 377 (1929).
8) W. F. Edgell and L. Parts, ibid., **77**, 4899 (1955).
9) J. H. Simons, W. H. Pearlson and Wm. R. James, U. S. Pat. 2494064 (1950).
10) A. F. Benning and E. G. Young, U. S. Pat. 2615926 (1952).
11) Wm. S. Murray, U. S. Pat. 2426638 (1947).
12) F. B. Downing, A. F. Benning and R. C. McHarness, U. S. Pat. 2413696 (1947).
13) E. H. Hadley and L. A. Bigelow, *J. Am. Chem. Soc.*, **62**, 3302 (1940).

pioneering work on electrochemical fluorination.[14] Sartori reported a successful attempt at the electrochemical fluorination of gases.[15] Methane, however, was shown to yield tetrafluoromethane and trifluoromethane with very small amounts of di- and mono-fluorinated products.

In the present work, the bubbler type of electrolytic cell afforded as high as 60% (mol.) of monofluoromethane in the fluorinated product, with an anodic current density of 2.2 amp./dm$^2$ and cell temperature of 5—6°C. This result may be regarded as a significant step in the partial fluorination of organic compounds by an electrochemical process.

The metered methane was introduced, with or without diluent helium, into hydrogen fluoride in the cell through the "bubbler" and fluorinated, after which the products were freed from hydrogen fluoride and oxygen difluoride, condensed, and rectified. The bubbling arrangement was found to be very effective for controlling the fluorination reaction, which is frequently explosive in nature, increase both the conversion and current efficiency during the fluorin ation of methane.

## Experimental

**Materials.**—Methane, from a commercial cylinder, was of over 99.5% pure. Hydrogen fluoride, rated better than 99%, was donated by Daikin Industries Co. The diluent employed was Airco helium (grade for gas chromatograhy use). The other, commonly available, reagents used were either of guaranteed or of first grade.

**Apparatus.**—The apparatus used for this fluorination reaction consisted essentially of the electrolytic cell, an iron tube for sodium fluoride pellets, three Ichinose gas washing bottles containing a saturated solution of sodium sulfite in which a small amount of potassium iodide and potassium hydroxide had been added, and glass traps immersed in ice and in liquid air. The size and the kind of the materials composing the electrolytic cell were the same as the one fully described earlier,[16,17] except that the cell body was constructed of Monel Metal, and a bubbling arrangement, termed "bubbler", was provided at the bottom of the cell body. The bubbler was placed just below the end of the nickel electrodes (whose effective surface area was 9.2 dm$^2$) at about 20 mm. distance from them, and standing vertically. The bubbler consisted of $6\phi \times 15$ mm. polyethylene tube, with an internal diameter of 4 mm., whose tip was enlarged to 8 mm. in diameter and capped with a filter paper made of polytetrafluoroethylene (courtesy of Daikin Industries Co.). During operation, the gaseous sample, with or without a metered current of helium, was introduced into hydrogen fluoride, from the bottom of the cell through the drain cock, whose central hole is 4 mm. in diameter, and which is connected directly to this bubbling arrangement. In a preliminary experiment, an attempt was made to produce innumerable minute bubbles in liquid hydrogen fluoride by various methods and materials. Such bubbles should accelerate favorable increase in the concentration of the slightly soluble sample in hydrogen fluoride. Macroscopic observation was made using a semi-transparent polyethylene vessel; the bubbler just described above gave the best results.

Other instruments used in this work were low temperature distillation, gas chromatographic, and infrared spectroscopic apparatus. Rectification unit used was substantially the same as the one described by Calfee, Fukuhara and Bigelow.[18] A Podbielniak low temperature distillation column was the essential part. Analytical chromatographic separation was made with a Hitachi KGL-2A model chromatograph.

Infrared absorption spectra were measured on a Perkin-Elmer model 21 double-beam spectrophotometer.

**Typical Procedure.** — Run 2 is taken as an example. Hydrogen fluoride (1 l.) was placed in the cell and, in order to remove a trace of impurity (mainly water), electrolysis was carried out in a nitrogen atmosphere, prior to the introduction of the sample, with an anodic current density of 2.7 amp./dm$^2$ and at 5—6°C, until the cell voltage rose to 6.0 V. Then 10 g. of sodium fluoride was added, and the metered sample was introduced from the bottom of the cell into the hydrogen fluoride in the cell, maintained at 5—6°C, through the bubbler at an average flow rate of 0.0029 mol./min. In two experiments, metered helium was admitted simultaneously with the sample into the bubbler.

Then the sample was fluorinated at an anodic current density of 2.2 amp./dm$^2$.

When the cell voltage became almost steady at 6—6.5 V., traps were placed in ice and liquid air respectively, and electrolysis was carried out for 71 amp. hr.

Fluorinated gas evolved from the cell was passed through a reflux condenser kept at −20°C, and over sodium fluoride, and then bubbled through an aqueous sodium sulfite solution in an Ichinose gas washer to eliminate a trace of explosive oxygen difluoride, passed through a trap immersed in ice, and finally condensed in two consecutive liquid-air traps. Although fluctuation due to a small explosion was sometimes observed on the flow meter of the sample, performance of this electrofluorination unit was very satisfactory for the fluorination of methane.

The product thus obtained was carefully rectified in the low-temperature rectification unit. The molecular weight of each fraction was often measured to aid in identification of the components. The amounts of the rectified products were measured by volume, and subsequently weighed in

14) J. H. Simons, U. S. Pat. 2519983 (1950).
15) P. Sartori, *Angew. Chem.*, **75**, 417 (1963).
16) S. Nagase and R. Kojima, *J. Chem. Soc. Japan, Ind. Chem. Sec.* (*Kogyo Kagaku Zasshi*), **64**, 1397 (1961).
17) S. Nagase and R. Kojima, This Bulletin, **34**, 1468 (1961).
18) J. D. Calfee, N. Fukuhara and L. A. Bigelow, *J. Am. Chem. Soc.*, **61**, 3552 (1939).

a glass ampule. The mixture was further separated by gas chromatography, using an activated charcoal column, 2 m. long, maintained at 70°C. Activated charcoal was of 30—60 mesh. The carrier gas was helium and the flow rate was at 147 ml./min. Infrared measurements were frequently carried out on components eluted from the column by transferring the highly diluted components into a 5-cm. cell.

## Results and Discussion

The results from the example (run 2) described above and those from a series of similar runs under various operating condition are summarized in the following tabulation.

TABLE I. RECTIFICATION OF FLUORINATED METHANE

| Fraction. No. | B. p., °C | Vol. ml. | Wt. g. | Component |
|---|---|---|---|---|
| 1 | −162—−159 | 13 | 5.6 | $CH_4$ |
| 2 | −128—−126 | 3.8 | 6.7 | $CF_4$[b] |
| 3[a] | −80—−76 | 4.8 | 6.1 | $CH_3F$[c], $CHF_3$[b] |
| 4[a] | −70—hold up | 1.5 | 2.0 | $CH_3F$, $CHF_3$ $CH_2F_2$[b] |

a) This fraction was further resolved chromatographically.

b), c) The infrared spectra of these products agree with those listed in D. G. Weiblen's "Fluorine Chemistry," Ed. by J. H. Simons, Vol. II, Academic Press. Inc., New York (1954), p. 469, and G. Herzberg's "Molecular Spectra and Molecular Structure. II. Infrared and Raman Spectra of Polyatomic Molecules," D. Van Nostrand Inc., New York (1949), p. 315 respectively.

Table I gives the results obtained by rectifying the product of run 2. In Table II, operating conditions for various runs, conversion and current efficiencies, and composition of the products are presented.

Fractions 1 and 2 usually consisted of essentially pure $CH_4$, and $CF_4$, respectively. Fraction 2 in run 6, however, was contaminated with $CH_3F$, and the boiling range was −130 to −90°C. Fractions 3 and 4 came over as a mixture and were further separated chromatographically. Fraction 3 sometimes showed a wider range of boiling point, −80—−51°C, depending on the proportion of the components. Detectable amounts of other components, such as $C_2F_6$ or $C_3F_8$ which are obtained in the reaction of fluorine with methane,[13] were not found in this electrochemical fluorination reaction.

Quantitative analysis of the components separated by chromatography was made on the assumption that the ratio of the peak areas in the chromatogram is a direct measure of the weight per cent of the components.[19,20] The results obtained by this analysis were subsequently converted into mole per cent.

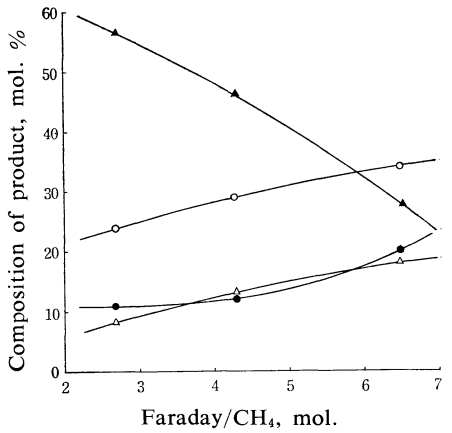



Fig. 1. Relationship between composition of product and Farady/$CH_4$ (mol.).
-○- $CF_4$ mol. %
-●- $CHF_3$ mol. %
-△- $CH_2F_2$ mol. %
-▲- $CH_3F$ mol. %

**Effect of Sample Feed Rate.** — Though a definite mechanism for electrochemical fluorination has not yet been established,[21] the products obtained by the present fluorination reaction appeared to be rather close to those expected from a very mild fluorination of methane with elementary fluorine. It appears, that sufficient agitation and effective dispersion of the heat of reaction takes place in this electrochemical process. An increase in the number of sample bubbles should increase the efficiency of this agitation. It is apparent from Table II that the fluorination reaction becomes milder with an increase in the supply of $CH_4$. This relation is well illustrated in Fig. 1, where the composition of the products obtained in runs 1, 2, and 3 is plotted against the feed factor represented by faraday/$CH_4$(mol.).

It has been reported that agitation has a profound effect on the milder electrochemical fluorination of chloro-olefins.[22]

Electrochemical fluorination is certainly an anodic reaction, therefore the concentration of the sample near the electrode should play an important role in determining the distribution

19) M. J. Root, "Gas Chromatography," Ed, by V. J. Coates, H. J. Noebels and I. S. Fagerson, Academic Press Inc., New York (1958), p. 99.
20) R. Amamiya, "Gasu Kuromatogurafiiy," Kyoritsu Shuppan Co., Ltd., Tokyo, (1958), p. 48.
21) A discussion is presented by J. Burdon and J. C. Tatlow, in "Advances in Fluorine Chemistry," Ed. by M. Stacey, J. C. Tatlow and A. G. Sharpe, Vol. I, Butterworths Scientific Publication Ltd., London (1960), p. 160.
22) General Electric Co., Brit. Pat. 758492 (1956).

Table II. Results of the fluorination of methane operated undfr various conditions

| Run No. | $D_A$ amp./dm² | Total amt. $CH_4$ used mol. | Conversion mol. % | Total current eff., %[e] | Product comp. (mol. %) $CF_4$ | $CHF_3$ | $CH_2F_2$ | $CH_3F$ | Note |
|---|---|---|---|---|---|---|---|---|---|
| 1 | 2.2 | 0.986 | 32.2 | 48.2 | 24.1 | 11.0 | 8.3 | 56.6 | |
| 2 | 2.2 | 0.613 | 42.8 | 44.3 | 29.0 | 12.3 | 12.7 | 46.0 | Effect of feed rate |
| 3 | 2.2 | 0.404 | 47.7 | 38.1 | 34.1 | 20.2 | 18.1 | 27.6 | |
| 4[a] | 2.2 | 0.564 | 46.3 | 37.8 | 17.3 | 10.5 | 18.6 | 53.6 | Effect of temp. |
| 5[b] | 2.2 | 0.635 | 45.7 | 41.7 | 21.9 | 7.0 | 10.8 | 60.3 | Effect of helium |
| 6[b] | 2.2 | 0.479 | 49.6 | 33.8 | 17.2 | 10.9 | 13.5 | 58.4 | |
| 7[c] | 2.2 | 0.536 | 38.1 | 33.6 | 28.9 | 9.9 | 11.9 | 49.3 | Effect of bubbler |
| 8[d] | 2.2 | 0.639 | 45.1 | 45.4 | 13.0 | 26.5 | 14.9 | 45.6 | Effect of NaF |
| 9 | 1.1 | 0.639 | 35.5 | 35.9 | 25.3 | 12.4 | 9.3 | 53.0 | Effect of $D_A$ |

a) Cell temperature was kept at 15—16°C.
b) In runs 5 and 6, diluent helium was used at flow rates of 104 ml./min. ($CH_4$ : He = 1 : 1.6 by vol.) and 150 ml./min. ($CH_4$ : He = 1 : 3 by vol.), respectively.
c) The reaction was carried out without using the "bubbler."
d) NaF (50 g.) was used.
e) Calculation of the current efficiency was based on the amount of electricity assumed to be required to liberate fluorine from a discharging fluoride ion which would substitute hydrogen in $CH_4$ and combine with it to from HF. The total current efficiency shown is the sum of the individual current efficiencies for $CF_4$, $CHF_3$, $CH_2F_2$, and $CH_3F$.

and yield of the products as well as the efficiency of the reaction. Especially for a gaseous sample sparingly soluble in hydrogen fluoride, it is important to consider the effective concentration of the sample in the reaction zone. A higher feeding rate tends to increase the concentration of the sample. On the other hand, it also increases the amount of escaping sample. These consideration could explain the fact that an increased rate of feeding resulted in a decreased conversion and increased current efficiency.

**Effect of Temperature.**—The conductivity of hydrogen fluoride solution increases as the temperature rises. Run 4 proceeded at the lower cell voltage of 5.3—5.5 V. at 15—16°C. A decrease in the voltage would lead to milder fluorination. Furthermore, higher temperatures are expected to decrease the solubility of the gases, and hence the products would probably be liberated from the reaction zone at a less fluorinated stage. An opposing factor to the milder reaction might exist due to an increased reaction temperature. The net result was a milder fluorination reaction with a large amount of partially fluorinated products and a small amount of $CF_4$.

**Effect of Dilution.**—In vapor phase fluorination of organic compounds with elementary fluorine, the sample or fluorine is often diluted with nitrogen or helium to make the reaction milder. The same technique was applied in the present electrochemical fluorination (runs 5 and 6), with the hope that partial fluorination would proceed favorably. Helium should also help the stripping of the product from hydrogen fluoride at a less fluorinated stage, in addition to creating sufficient agitation in the reaction zone. As expected, runs 5 and 6 gave the highest yield of $CH_3F$.

**Effect of the Bubbler.**—Run 7 was carried out without using the bubbler. It was very difficult to control this reaction and frequent explosions were observed.

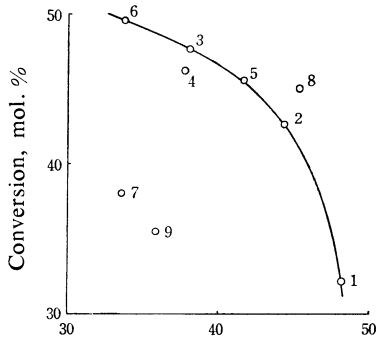



Fig. 2. Relationship between conversion and current efficiency.
The numberals in the diagram indicate run no.

The conversion and current efficiency decreased markedly. Figure 2 is a plot of conversion versus current efficiency and reveals the successful result brought about by the bubbler. It appears that approach of the sample to the electrode is neither steady nor smooth without the bubbler.

**Effect of the Amount of NaF.** — Since hydrogen fluoride which contains hydrocarbons is nonconducting, electrolysis of this solution

is usually carried out by the use of conductivity additives. In the present experiments, NaF (10 g.) was used as the additive, but for run 8, a larger amount of NaF (50 g.) was used with the expectation that the electrolysis could be carried out at a lower voltage for a milder reaction. Run 8, however, proceeded at the same voltage (6—6.5 V.) as that of the others. However, milder fluorination was accomplished and the smallest yield of $CF_4$ obtained. This might be attributed to the decreased solubility of partially fluorinated products in hydrogen fluoride.

**Effect of the Anodic Current Density.** — A smaller current density should make the reaction milder, but run 9, on the contrary, indicates a severe reaction with a smaller conversion and current efficiency.

The lesser degree of agitation may account for this, since the decreased amount of the total gases evolved under this electrolysis condition is not sufficient to cause efficient agitation in the hydrogen fluoride. A similar tendency was observed in the electrochemical fluorination of 2, 2, 3, 3-tetrafluoro-1-propanol.[23]

The overall results seem to demonstrate clearly the usefulness of electrochemical fluorination as a tool for fluorination of gases.

23) S. Nagase, H. Baba and R. Kojima, This Bulletin, **36**, 29 (1963).

**Summary**

Partially fluorinated methanes were obtained directly from methane in a reasonable conversion and current efficiency by electrochemical fluorination, using a cell equipped with a bubbling arrangement. This fluorination unit worked satisfactorily for controlling the fluorination reaction of gases slightly soluble in hydrogen fluoride.

Performance and effect of the bubbler, and the effect of sample feed rate, electrolysis temperature, dilution of the sample with helium, the amount of sodium fluoride, and the anodic current density, on the fluorination reaction are described and discussed in detail.

The authors wish to express their sincere thanks to Daikin Industries Co. for supplying some materials, and Dr. Kan Inukai of this Institute for his interest in this work.

*Government Industrial Research Institute, Nagoya*
*Kita-ku, Nagoya (S. N. & H. B.)*

*Research Laboratories*
*Central Glass Co., Ltd.*
*Ohte-machi, Chiyoda-ku*
*Tokyo (K. T.)*

# The Kinetics of the Acid-catalyzed Transformation of Peroxybenzoic Acids to Acetyl Benzoyl Peroxides in Acetic Acid*

By Yoshiro OGATA, Yoshiaki FURUYA and Keizo AOKI

(Received September 24, 1964)

It is well-known that peroxy acids are obtained by the hydrolysis of the corresponding peroxides.[1-3] However, the reverse reactions of peroxy acids to form peroxides have scarcely been studied at all. The present authors have reported previously on the acid-catalyzed reversible transformation of peroxyacetic acid to acetyl peroxide in acetic acid.[4]

It has been analogously supposed that peroxybenzoic acid in acetic acid may be reversibly transformed to acetyl benzoyl peroxide in the presence of sulfuric acid:

$$C_6H_5CO_3H + CH_3CO_2H \overset{H^+}{\rightleftarrows} C_6H_5COO_2COCH_3 + H_2O \quad (1)$$

As expected, it was observed that the reaction led to acetyl benzoyl peroxide, which was identified by paper chromatography. The reaction rate followed the first-order kinetics if the reversibility of the reaction was taken into account. The present paper will describe the results of a kinetic study of this and related reactions by the iodometric determination of peroxybenzoic acid and acetyl benzoyl peroxide. Thus far, acetyl benzoyl peroxide has been

* Contribution No. 61.

1) A. M. Clover and G. F. Richmond, *Am. Chem. J.*, **29**, 189 (1903).

2) Parke Davis Co., German Pat. 156998.

3) "Organic Syntheses," Coll. Vol. I, 431 (1941).

4) Y. Ogata, Y. Furuya, J. Maekawa and K. Okano, *J. Am. Chem. Soc.*, **85**, 961 (1963).

prepared by the reaction of peroxybenzoic acid with acetic anhydride[5] or by the autoxidation of benzaldehyde in acetic anhydride.[6]

## Experimental

**Materials.**—Peroxybenzoic acid, m. p. 41°C, was prepared by the hydrolysis of benzoyl peroxide.[3] Substituted peroxybenzoic acids were obtained by an analogous procedure from the corresponding benzoyl peroxides, prepared by the reaction of benzoyl chlorides with hydrogen peroxide.[7] Acetyl benzoyl peroxide was prepared by the autoxidation of a mixture of benzaldehyde and acetic anhydride,[6] m. p. 35.5°C. Acetyl peroxide was obtained by the reaction of acetic anhydride with barium peroxide in an ethereal solution at 0°C, the solvent being exchanged with acetic acid for safe storage.[8]

**A Typical Run for the Rate Measurements.**—Peroxybenzoic acid (ca. 0.138 g., 0.001 mol.) was introduced into an acetic acid solution (50 ml.) of 3.6 N sulfuric acid after the solution had been brought to a temperature equilibrium. Aliquots (5 ml. each) were taken out and worked up in a manner reported previously[4] in order to estimate peroxybenzoic acid and acetyl benzoyl peroxide. It was confirmed in a blank test that only 1% of acetyl benzoyl peroxide was hydrolyzed to peroxybenzoic acid under the same conditions after 2 min., although it was completely hydrolyzed after 15 hr. at 20°C.

**Reaction Products Criterion.**—A solution of the reaction products was developed with a mixture of acetic acid and water (2 : 3 in vol.) on acetylated Toyo Filter paper No. 54.[9] When sprayed with a methanolic solution of 3% *p*-dimethylaminoaniline dihydrochloride, the initial reaction mixture gave a single spot corresponding to peroxybenzoic acid ($R_f$: 0.66), while the mixture after 2 hr. gave two spots corresponding to peroxybenzoic acid (0.66) and acetyl benzoyl peroxide (0.45) and no appreciable spots for benzoyl peroxide (0.15), acetyl peroxide (0.92), peroxyacetic acid (0.97) or hydrogen peroxide (0.88). In the reverse reaction, the initial mixture of acetyl benzoyl peroxide in acetic acid gave a spot for acetyl benzoyl peroxide alone (0.45), while the mixture after 2 hr. gave two spots for acetyl benzoyl peroxide (0.45) and peroxybenzoic acid (0.66). Hence, the presence of equilibrium 1 is confirmed. Under these conditions, there was no appreciable interconversion between peroxybenzoic acid and acetyl benzoyl peroxide in the absence of sulfuric acid.

## Results and Discussion

Since there is a large excess of acetic acid and water, the kinetics follow the pseudo first-order equation for reversible reactions, $\ln [z/(z-x)]=kt$, where $z$ is the concentration of consumed peroxybenzoic acid at equilibrium, and $x$ is the concentration of consumed peroxybenzoic acid at time $t$.

Assuming the pseudo first-order rate constants for forward and reverse reactions to be $k_1$ and $k_{-1}$ respectively, the following rate and equilibrium equations are obtained[10]:

$$\ln [z/(z-x)]=(k_1+k_{-1})t=kt$$
$$z/(a-z)=k_1/k_{-1}$$

where $a$ is the initial concentration of peroxybenzoic acid. Therefore, the forward rate constant, $k_1$, is expressed as:

Table I. Typical rate data of the transformation of peroxybenzoic acid to acetyl benzoyl peroxide in acetic acid at 45°C

Initial concn. of $C_6H_5CO_3H$, $2\times10^{-2}$ M; concn. of $H_2SO_4$, 3.6 N ($H_0$, −3.430); concn. of $H_2O$, 0.498 M; concn. of $C_6H_5CO_3H$ in equilibrium, $0.524\times10^{-2}$ M (observed value)

| Time min. | $[C_6H_5CO_3H]$ Remaining $a-x$ $\times10^2$ M | $[C_6H_5CO_3H]$ Consumed $x$ $\times10^2$ M | $[CH_3CO\text{-}O_2\text{-}COC_6H_5]$ $x'$* $\times10^2$ M | $([C_6H_5CO_3H]+[CH_3CO\text{-}O_2\text{-}COC_6H_5])$ $(a-x)+x'$ $\times10^2$ M | $z-x$ $\times10^2$ M | $k_1$ $\times10^4$ sec$^{-1}$ |
|---|---|---|---|---|---|---|
| 0 | 1.846 | | 0.027 | 1.873 | 1.322 | |
| 10 | 1.675 | 0.171 | 0.203 | 1.878 | 1.151 | 1.62 |
| 20 | 1.529 | 0.317 | 0.339 | 1.868 | 1.005 | 1.61 |
| 40 | 1.272 | 0.574 | 0.592 | 1.864 | 0.748 | 1.67 |
| 70 | 1.016 | 0.830 | 0.835 | 1.851 | 0.492 | 1.65 |
| 110 | 0.804 | 1.042 | 1.035 | 1.839 | 0.280 | 1.65 |
| 170 | 0.636 | 1.210 | 1.193 | 1.829 | 0.112 | 1.70 |
| 230 | 0.569 | 1.277 | 1.253 | 1.822 | 0.045 | 1.69 |
| | | | | | | Av. 1.66 |

* $x'$ is the concentration of formed acetyl benzoyl peroxide at time $t$.

5) A. Baeyer and V. Villiger, *Ber.*, **33**, 1569 (1900).
6) J. U. Nef, *Ann.*, **298**, 284 (1897); F. Juračka and R. Chromeček, *Chem. Průmysl*, **6**, 27—30 (1956); *Chem. Abstr.*, **50**, 15458 (1956).
7) H. von Pechmann and L. Vanino, *Ber.*, **27**, 1510 (1894).
8) J. R. Slagle and H. J. Shine, *J. Org. Chem.*, **24**, 107 (1959).
9) J. Janoušek, *Faserforsch. u Textiltech.*, **8**, 339 (1957).
10) L. P. Hammettt, "Physical Organic Chemistry," McGraw-Hill Book Co., New York (1940), p. 102.

TABLE II. THE CONSTANCY OF APPARENT EQUILIBRIUM CONSTANT WITH VARYING CONCENTRATION OF WATER IN THE REACTION MIXTURE WITH 3.6 N SULFURIC ACID AT 45°C

| $H_2O$ added vol. % | $[H_2O]$ M | $[CH_3CO_2H]$[a] M | $\frac{z}{a-z}$[b] | Equilibrium constant[c] $K\times10^2$ |
|---|---|---|---|---|
| 0 | 0.498 | 15.694 | 1.262 | 4.00 |
| 1 | 1.054 | 15.694 | 0.5504 | 3.70 |
| 3 | 2.160 | 15.172 | 0.3193 | 4.55 |
| 5 | 3.272 | 14.822 | 0.1468 | 3.24 |
| 10 | 6.040 | 13.952 | 0.0776 | 3.36 |

a) Concn. of acetic acid was calculated by means of the equation: [volume of $CH_3CO_2H$ (ml.)] × [Sp. gr.]/[Mol. wt. of $CH_3CO_2H$] where sp. gr. is 1.049 at 20°C.

b) The value was calculated from the value of $[CH_3COO_2COC_6H_5]/[C_6H_5CO_3H]$ at equilibrium.

c) The constant was calculated by means of the following equation:

$$K=\frac{[CH_3COO_2COC_6H_5][H_2O]}{[C_6H_5CO_3H][CH_3CO_2H]}=\frac{z}{a-z}\cdot\frac{[H_2O]}{[CH_3CO_2H]}$$

where $[H_2O]$ is the sum of the concentrations of water in original acetic and sulfuric acids and the concentrations of added and formed water.

$$k_1=kz/a$$

As Table I shows, the value of $k_1$ holds constancy.

Moreover, the sum of the concentrations of peroxybenzoic acid and acetyl benzoyl peroxide ($[C_6H_5CO_3H]+[C_6H_5COO_2COCH_3]$) is very nearly constant during the reaction, as is shown in Table I; this means that the reaction is a transformation instead of a decomposition. The rate constant, $k_1$, holds constancy with varying initial concentrations of peroxybenzoic acid ($0.615—1.846\times10^{-2}$ M) with added benzoic acid ($4\times10^{-2}$ M).

As expected, equilibrium 1 moved to the left-hand side when the concentration of water was increased. The constancy of the calculated equilibrium constants in various concentrations of water is apparent from Table II.

The energy and entropy of activation were calculated to be 16.8 kcal. $mol^{-1}$ and −25.7 e. u., respectively, from the following average values of $k_1\times10^4$ $sec^{-1}$: 40°C, 1.01; 45°C, 1.66; 50°C, 2.34; 55°C, 3.42.

The plot of $\log k_1$ vs. $H_0$ gave a straight line, with a slope of −0.96, as is shown in Fig. 1. Therefore, an activated complex with a proton may be suggested for the reaction.

The introduction of an electron-attracting group into the peroxybenzoic acid retarded the reaction, and the Hammett plot (Fig. 2) gave a negative $\rho$-value of −0.37. The introduction of an electron-releasing group, on the other hand, accelerated the reaction. The latter reaction, however, was accompanied by a side reaction, probably such as the cleavage

TABLE III. SUBSTITUENT EFFECT OF THE TRANSFORMATION OF SUBSTITUTED PEROXYBENZOIC ACIDS TO ACETYL BENZOYL PEROXIDES IN ACETIC ACID AT 45°C

Concn. of $H_2SO_4$, 3.6 N ($H_0$, −3.430)

| Substituent | Forward first-order rate const. $k_1\times10^4$ $sec^{-1}$ |
|---|---|
| *p*-$OCH_3$ | (5.20)[a,b] |
| *p*-$CH_3$ | (1.96)[a] |
| *p*-H | 1.66 |
| *p*-Cl | 1.41 |
| *m*-$NO_2$ | 0.92 |
| *p*-$NO_2$ | 0.87 |

a) These data do not seem to express the true substituent effects because of possible side reactions.

b) The reaction for *p*-methoxyperoxybenzoic acid was done at 25°C.

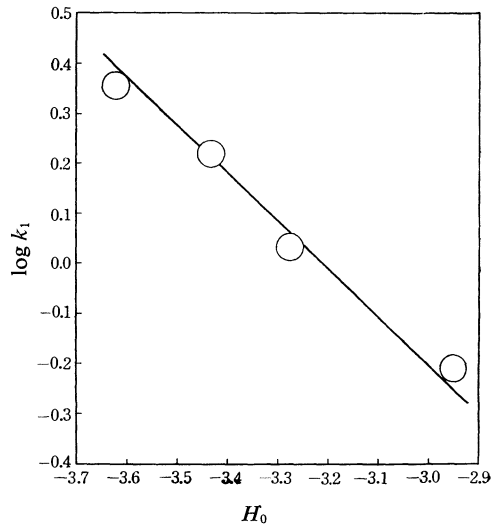



Fig. 1. The plots of $\log k_1$ vs. $H_0$ for the transformation of peroxybenzoic acid to acetyl benzoyl peroxide in acetic acid at 45°C.

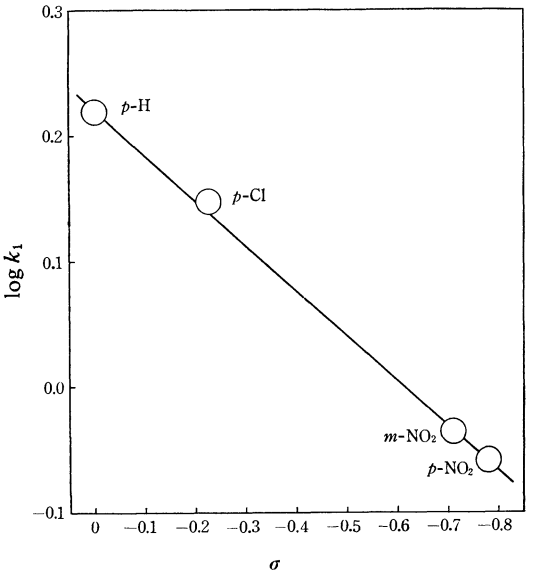



Fig. 2. Hammett plots for the transformation of substituted peroxybenzoic acid to the corresponding acetyl benzoyl peroxide in acetic acid at 45°C. ($H_0$, −3.430)

of the ether linkage of the methoxy group or the oxidation of the methyl group, since the active oxygen content of the system decreased during the reaction.

These facts suggest a mechanism analogous to that postulated for the acid-catalyzed transformation of peroxyacetic acid.[4]

$$CH_3COOH + H^+ \overset{\text{fast}}{\rightleftarrows} CH_3\text{-}\overset{+}{C}(OH)_2 \qquad (2)$$

$$CH_3\text{-}\overset{+}{C}(OH)_2 + Ar\text{-}\overset{O}{\overset{\|}{C}}OOH \rightleftarrows Ar\text{-}\overset{O}{\overset{\|}{C}}\overset{+}{O}OH \quad \underset{\text{(I)}}{CH_3\text{-}C(OH)_2} \qquad (3)$$

$$Ar\text{-}\overset{O}{\overset{\|}{C}}\overset{+}{O}OH \quad \underset{CH_3\text{-}C(OH)_2}{} \rightleftarrows Ar\text{-}\overset{O}{\overset{\|}{C}}\text{-}OO\text{-}\overset{O}{\overset{\|}{C}}\text{-}CH_3 + H_3O^+ \qquad (4)$$

The substituent effect with a negative $\rho$-value is consistent with a rate-determining attack of protonated acetic acid on peroxybenzoic acid (step 3). Moreover, complex I resembles the ortho acid monoester, which is the unstable intermediate in esterification; therefore, step 4 may be much faster than step 3.

The solvent effect was examined with formic, propionic, butyric, isobutyric or isovaleric acid as a solvent. The reactions in these solvents were all faster than that in acetic acid. However, side-reactions such as the oxidation of the solvent seem to occur quite often in these solvents.

## Summary

It has been confirmed by paper chromatography that peroxybenzoic acid in acetic acid is transformed reversibly to acetyl benzoyl peroxide in the presence of a catalytic amount of sulfuric acid. The rate satisfies the first-order equation for reversible reactions. The plot of the logarithm of the forward rate constant vs. the acidity function has given a straight line with a slope of −0.96. The rate decreases upon the introduction of an electron-attracting group to the benzene ring of peroxybenzoic acid, the Hammett's $\rho$-value being −0.37. A mechanism analogous to that postulated previously with peroxyacetic acid, which involves a rate-determining attack of protonated acetic acid on peroxybenzoic acids, is consistent with these facts.

The authors wish to thank the Mitsubishi Chemical Industries, Ltd., and the Dainippon Celluloid Co., Ltd., for their gifts of materials.

*Department of Applied Chemistry*
*Faculty of Engineering*
*Nagoya University*
*Chikusa-ku, Nagoya*

# The Mechanism of the Electrical Conduction in Solid Acetamide*

By Koichi HIRANO

(Received February 25, 1961 ; in revised form November 26, 1964)

The electrical conductivity of ice and solid alcohols has been studied by several investigators;[1-6] it has been concluded that the proton transfer across the hydrogen bonds plays an important role in the conduction mechanism. It would, however, be desirable to obtain further information about the conduction mechanism in crystals with >NH···O< hydrogen bonds, since studies thus far have concerned only the case of OH···O hydrogen bonds.

In the present paper the temperature dependence of solid state acetamide will be described; the conduction mechanism in the >HN···O< hydrogen bond crystal will then be discussed on the basis of the proton transfer model.

## Experimental

After fractional distillation, acetamide was recrystallized thrice from hot benzene by the Lewin and Vance's method[7] and then dried in a Abderhalden drier for five hours. The sample was melted in the cell; it was solidified gradually from its own melt. The cell was then kept at 82°C to remove the strain of the sample which originated from solidification. In comparison with the results reported hitherto by other authors, the a.c. conductivity of molten acetamide at 83.2°C and 87.5°C were measured.

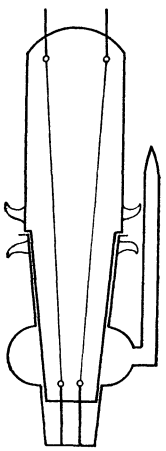


Fig. 1. The conductivity cell.

On the other hand, the temperature dependency of the d.c. conductivity of solid acetamide was measured within the temperature range from 60 to 90°C by the bridge method. The cell, made of pyrex-glass with platinum electrodes,[4,8] is illustrated in Fig. 1.

The cell was calibrated with a potassium chloride solution, and the cell constant was determined to be 0.1408 $\Omega^{-1}cm^{-1}$ at 25°C.

## Results

**The A. C. Conductivity of Molten Acetamide.** —The values of a. c. conductivity at $10^3$ c. p. s. for molten acetamide are presented in Table I, in which are also included the results reported in the literature.

TABLE I. THE SPECIFIC CONDUCTIVITY OF MOLTEN ACETAMIDE

| Specific conductivity at $10^3$ c. p. s. $\sigma\Omega^{-1}cm^{-1}$ | Temp. °C | Author |
|---|---|---|
| $8.8\times10^{-7}$ | 83.2 | Hirano |
| $1.0\times10^{-6}$ | 87.5 | Hirano |
| $3\times10^{-3}$ | 80 | Walden (1903)[9] |
| $4.3\times10^{-5}$ | 100 | Walker (1905)[10] |
| $1.5\times10^{-5}$ | 90 | Belladen (1927)[11] |
| $8.6\times10^{-6}$ | 94 | Grüttner (1952)[12] |
| $2.6\times10^{-6}$ | 94 | Jander and Winkeler (1959)[13] |

From Table I it is obvious that the results here obtained are fairly different from those previously reported by Walden[9] and by others,[10-12] but comparable with the results given by Jander and Winkeler.[13] The wide divergence of Walden's result may, however,

* A part of this paper was presented at the 13th Annual Meeting of the Chemical Society of Japan, Tokyo, April, 1960.

1) J. D. Hoftman and C. P. Smyth, *J. Am. Chem. Soc.*, **71**, 431 (1949).
2) E. J. Murphy, *Phys. Rev.*, **79**, 396 (1950).
3) Y. Kakiuchi, H. Komatsu and S. Kyoya, *J. Phys. Soc. Japan*, **6**, 321 (1951).
4) R. S. Bradley, *Trans. Faraday Soc.*, **53**, 687 (1957).
5) A. Steinemann and H. Grünicher, *Helv. Phys. Acta*, **30**, 553 (1957).
6) J. C. Decorly, C. Jaccard and H. Grünicher, ibid., **30**, 465 (1957).
7) S. Z. Lewin and J. E. Vance, *J. Am. Chem. Soc.*, **74**, 1433 (1952).
8) N. N. Greenwood and R. L. Martin, *Proc. Roy. Soc.*, **A215**, 46 (1952).
9) P. Walden, *Z. physik. Chem.*, **46**, 175 (1903).
10) J. Walker and F. M. G. Jonson, *J. Chem. Soc.*, **87**, 1597 (1905).
11) L. Belladen, *Gazz. Chim. Ital.*, **51**, 407 (1927).
12) B. Grüttner, *Z. anorg. u. allgem. Chem.*, **270**, 223 (1952).
13) G. Jander and G. Winkeler, *J. Inorg. Nucl. Chem.*, **9**, 24 (1959).

be attributed to impure materials, since the conductivity is strongly affected by a small amount of impurities. The very low values obtained by the present author are attributable to the high purity of the specimens used.

**The Temperature Dependency of the D. C. Conductivity of Solid Acetamide.**— In Table II the results of d. c. conductivity for solid acetamide obtained at various temperatures are listed.

Table II. The specific conductivity of solid acetamide

| Specific conductivity D. C. $\kappa\Omega^{-1}cm^{-1}$ | Temp. °C |
|---|---|
| $1.4\times10^{-9}$ | 61.5 |
| $3.5\times10^{-9}$ | 71.0 |
| $5.9\times10^{-9}$ | 73.0 |
| $7.3\times10^{-9}$ | 75.2 |
| $1.2\times10^{-8}$ | 77.4 |
| $3.0\times10^{-8}$ | 79.8 |
| $5.6\times10^{-8}$ | 82.2 |

Judging from the data of a. c. conductivity in the molten state, the purity of specimens is sufficiently high, so the data listed in Table II seem to be rather consistent, though no data which can be compared with have been reported.

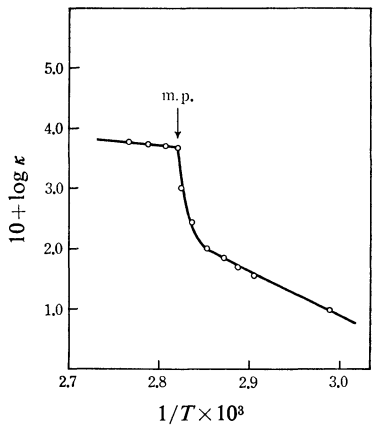



Fig. 2. $10+\log\kappa$ plotted against $1/T$.

In Fig. 2 the plots of $\log\kappa$ against the reciprocal of temperature, $1/T$, are illustrated. In the curve there are lower and upper slopes and a steeper slope just below the melting point, as is general for the solid state. The lower slope corresponds to the molten liquid, and the upper one, to the solid state, while the abrupt change seems to originate from the homophase premelting.[14] This feature is very similar to that with ice. The linear plot of $10+\log\kappa$ vs. $1/T\times10^3$ for the solid state is represented well by the following equation;

$$\kappa=1.7\exp-\{34\times10^3/RT\}\ \Omega^{-1}cm^{-1} \quad (1)$$

where $34\times10^3$ cal./mol. is the activation energy of electrical conduction; $R$, the gas constant, and $T$, the absolute temperature.

## Discussion

In the present paper the author would like to interpret the mechanism of the electrical conduction in solid acetamide from the point of view of proton transfer.

It has been well established by Senti and Harker[15] that the crystal structure of rhombohedral acetamide consists of planar molecules of the keto form arranged in rings of six members, as is shown in Fig. 3. In the rings the adjacent molecules are held together by hydrogen bonds of >NH···O=C<, and along the c-axis of the hexagonal cell the molecules are linked together by the hydrogen bonds in infinite chains. Thereby, the net transfer of protons traveling along the hydrogen bonds in the axis may be expected when the external electrical field is applied. If the proton transfer causes the conduction, however, three kinds of reactions must follow:

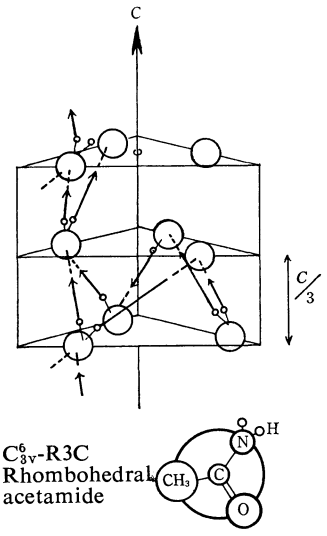



Fig. 3. Crystal structure of acetamide.

**Proton Supply to the Molecular Chains of Hydrogen Bonds.** — The proton supply would be initiated by the ionogenic reaction involving step 2:[16]

14) W. Davis, S. Rogers and A. R. Ubbelohde, *Proc. Roy. Soc.*, **A220**, 14 (1953).

15) F. Senti and D. Harker, *J. Am. Chem. Soc.*, **62**, 2008 (1947).

16) K. Wirtz, *Z. Naturforsch.*, **2b**, 94 (1947).

$$\rangle NH\cdots O{=}C\langle \xrightarrow{\Delta E_1} \rangle \overset{-}{N}: + H\overset{+}{O}C\langle \qquad (2)$$

where $\Delta E_1$ denotes the activation energy, which is identical with the height of the potential barrier between the two positions of equilibrium in the hydrogen bonds in Fig. 4.

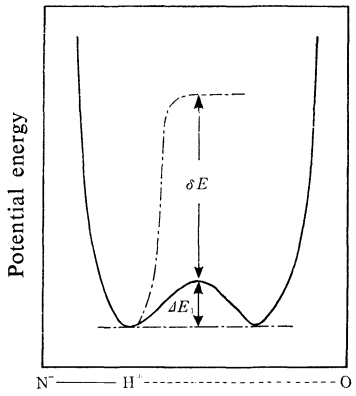



Fig. 4. Potential barrier between the two positions of equilibrium in the hydrogen bonds.
$\Delta E_1 \simeq 20$ kcal./mol.

Consequently, $\Delta E_1$ is represented by:

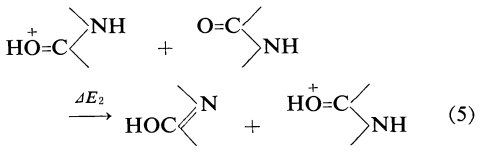
$$\Delta E_1 \simeq (D - \delta E) \qquad (3)$$

where $D$ denotes the energy required to liberate the proton from the restraining negative force field around a given nitrogen atom and $\delta E$, the energy changes associated with the hydrogen bond formation.

Assuming that $D$ would not be so different from the energy of the dissociation of >N-H linkage: hence, $\Delta E_1$ may be estimated from Eq. 4:

$$\Delta E_1 \simeq (104 - \delta E) \text{ kcal./mol.} \qquad (4)$$

**Proton Transfer.** — In the case of ice, the oxonium ion, $H_3O^+$, is intermediate in the proton transfer between the adjacent molecules. In acetamide, however, such ions would not be produced; hence, another scheme must be considered. The following scheme 5, with the protonated amide molecules acting as intermediates, are considered to be the most probable one:

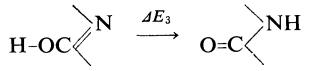



(5)

Here $\Delta E_2$ is the activation energy of proton transfer, and it may be estimated as nearly equal to 3—5 kcal./mol., judging from the quite similar quantity for ice.

**The Recovery of the Hydrogen Bonds.** — According to schemes 2 and 5, it is evident that, after the proton transference, the members of the molecular chain were replaced by molecules of the enol form. It must then be remembered that the further transference of protons does not proceed unless the recovery of the hydrogen bonds has been established in the molecular chain.

In the present paper we assumed keto-enol transformation (6) to be the key reaction in the recovery process; then, the activation energy, $\Delta E_3$, can be estimated to be equal to 5—10 kcal./mol. in analogy with the similar quantity estimated from cis-trans transformation in esters and amines.[17]




(6)

Admitting the above, the activation energy of conduction, $\Delta E$, in the overall reactions 2, 5 and 6, is given in Eq. 7;

$$\Delta E = \Delta E_1 + \Delta E_2 + \Delta E_3 \qquad (7)$$

From the experimental results, 34 kcal./mol. is determined as the value of $\Delta E$. Using the data of $\Delta E$, $\Delta E_2$ and $\Delta E_3$, 20 kcal./mol. is given as the data of $\Delta E_1$; then we immediately determined $\delta E \simeq 80$—85 kcal./mol.

In Table III the activation energies related to the respective processes are summarized.

Table III. Activation energies

| Activation energy | Process | kcal./mol. |
|---|---|---|
| $\Delta E$ | Overall process | 34 |
| $\Delta E_1$ | Liberation of proton | 20 |
| $\Delta E_2$ | Proton transfer | 5 |
| $\Delta E_3$ | Recovery process | 10 |
| $\delta E$ | Changes in the dissociation energy of the >N-H bond associated with hydrogen bond formation | 80—85 |

The value of $\Delta E_1$, the potential barrier in Fig. 4, is consistent with the theoretical estimations of the similar quantities for the N-H···O or O-H···O hydrogen bonds in the liquid state.

Since the height of the potential barrier of this kind does not vary much with the states of the molecular aggregation, $\Delta E_1 \simeq 20$ kcal./mol. is fairly reasonable as the potential barrier between the two positions of equilibrium in the hydrogen bond of solid acetamide.

Accordingly, it may be concluded that the

17) O. Nomoto, *J. Acoust. Soc. Japan*, **13**, 76 (1957).
18) I. Oshida, Y. Ooshika and R. Miyasaka, *J. Phys. Soc. Japan*, **13**, 76 (1957).
19) Y. Sato, *Science of Light*, **6**, 69 (1957).
20) H. Toyoda, *J. Chem. Soc. Japan, Pure Chem. Sec. (Nippon Kagaku Zassi)*, **79**, 1198 (1958).

proton transfer plays an important role in the electrical conduction in solid amide; this conception makes it possible to consider the electrical conduction observed in proteins or related compounds.

## Summary

1) Conductivity measurements of solid acetamide have been carried out over the temperature range of 60—90°C and the specific conductivity, $\kappa = 1.7 \exp -\{34 \times 10^3/\boldsymbol{RT}\}\ \Omega^{-1} \cdot \mathrm{cm}^{-1}$, has been determined.

2) The mechanism of conduction has been discussed in terms of the proton transfer, and the value of the potential barrier between two positions of equilibrium in the NH···O hydrogen bonds has been estimated.

The author is indebted to the Ministry of Education for its financial support.

*Department of Natural Sciences*
*Faculty of Education*
*Tohoku University*
*Kawa-Uchi, Sendai*

# NOTES

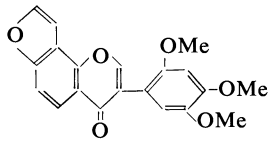
## The Synthesis of Isoelliptol Isoflavone*1

By Kenji FUKUI, Mitsuru NAKAYAMA, Atsushi TANAKA and Shigeo SASATANI

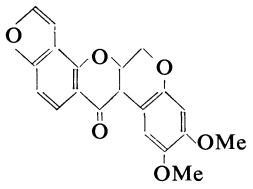
(Received July 27, 1964)

Elliptol isoflavone (furano(2'', 3''; 7, 8)-2', 4', 5'-trimethoxyisoflavone) (I)[1] was prepared from elliptone (II)[2] by Harper. Isoelliptol isoflavone (furano(2'', 3''; 6, 7)-2', 4', 5'-trimethoxyisoflavone) (III) may be obtained similarly from isoelliptone (IV), which was recently isolated by Ollis.[3]

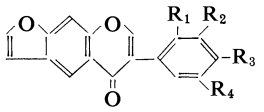
In a previous paper,[4] I was obtained from 7-hydroxy-2', 4', 5'-trimethoxyisoflavone.[5] In the present paper, the synthesis of III will be described. The method used here was virtually identical with that reported for dehydronepseudin (V).[6]



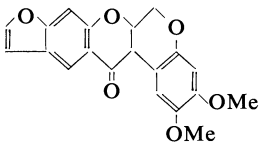
I



II



III $R_1$, $R_3$, $R_4$=OMe; $R_2$=H
V $R_1$, $R_2$, $R_3$=OMe; $R_4$=H

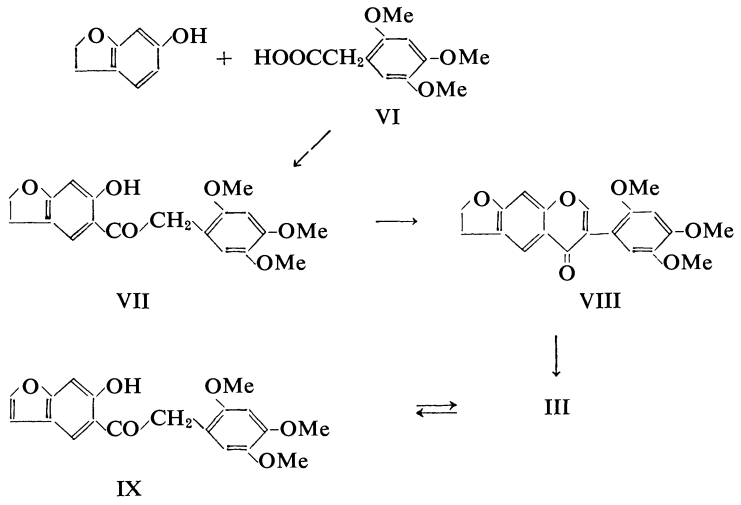


IV

6-Hydroxy-2, 3-dihydrobenzo[b]furan (VI)[7] was condensed with homoasaronic acid (2, 4, 5-trimethoxyphenylacetic acid)[8] in the presence

*1 Presented at the 17th Annual Meeting of the Chemical Society of Japan, Tokyo, April, 1964.

1) S. H. Harper, *J. Chem. Soc.*, **1942**, 595.
2) S. H. Harpar, ibid., **1939**, 1099, 1424.
3) W. D. Ollis, private communication.
4) K. Fukui, M. Nakayama and M. Hatanaka, This Bulletin, **36**, 872 (1963).
5) K. Fukui, M. Nakayama, M. Hatanaka, T. Okamoto and Y. Kawase, ibid., **36**, 397 (1963).
6) K. Fukui and M. Nakayama, *Experientia*, **19**, 621 (1963).
7) J. S. H. Davies, P. A. McCrea, W. L. Norris and G. R. Ramage, *J. Chem. Soc.*, **1950**, 3206.
8) A. Robertson and G. H. Rusty, ibid., **1935**, 1371.




of polyphosphoric acid to give 6-hydroxy-5-(2, 4, 5-trimethoxyphenylacetyl)-2, 3-dihydrobenzo[b]furan (VII) (m. p. 176—177°C). The treatment of VII with ethyl orthoformate-pyridine-piperidine[9] gave the dihydrofurano-isoflavone (VIII) (m. p. 197—198°C). The dehydrogenation of VIII with *N*-bromosuccinimide in carbon tetrachloride gave the furanoisoflavone (III) (m. p. 190—190.5°C) in a 53% yield. The ultraviolet spectra of I, III and VIII are shown in Fig. 1. There are two absorption bands at ca. 230—250 m$\mu$ (band I) and at ca. 300—310 m$\mu$. Band I is due to furano benzenoid and dihydrofurano benzenoid. The dehydrogenation of the dihydrofurano nucleus showed a marked hyperchromic effect. This phenomenon was well exemplified by pachyrrhizin and dihydropachyrrhizin[10] and similar substances[6]. On an alkaline hydrolysis, III gave 6-hydroxy-5-(2, 4, 5-trimethoxyphenylacetyl)benzo[b]furan (IX) (m. p. 169—170°C). The parent isoflavone, III, could be reconstructed from IX by Venkataraman's method.[9] On the basis of this fact, the structure of III was established.

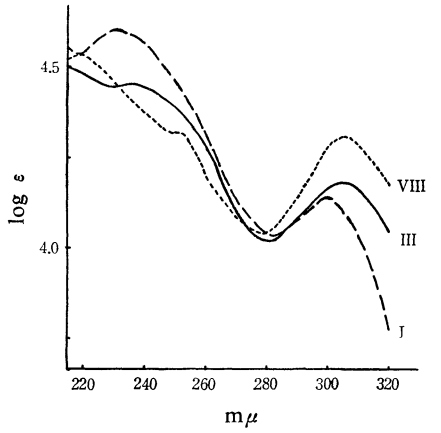



Fig. 1. Ultraviolet Spectra of I, III and VIII.

## Experimental*2

**6-Hydroxy-5-(2, 4, 5-trimethoxyphenylacetyl)-2, 3-dihydrobenzo[b]furan (VII).** — A mixture of VI[7] (1.0 g.), homoasaronic acid[8] (1.6 g.) and polyphosphoric acid ($n$=2.5) (10 g.) was warmed on a steam bath for 15 min. The dark red solution was then poured into ice water, and the resulting product was collected. After being washed with aqueous sodium bicarbonate and then with water, the residue was recrystallized from ethanol to give VII in the form of colorless prisms (m. p. 176—177°C),[11] which were reddish brown in a ferric chloride test in ethanol; yield, 1.1 g. (45%). IR; 1628 (C=O) cm$^{-1}$. UV; $\lambda_{max}$ m$\mu$(log $\varepsilon$); 235 (4.22), 284 (4.18), 332 (4.00).

Found: C, 66.18; H, 5.90. Calcd. for $C_{19}H_{20}O_6$: C, 66.27; H, 5.85%.

**4'', 5''-Dihydrofurano (2'', 3''; 6, 7)-2', 4', 5'-trimethoxyisoflavone (VIII).**—To a solution of VII (2.2 g.) and ethyl orthoformate (8.8 ml.) in pyridine (33 ml.), piperidine (1.1 ml.) was added; the mixture was then refluxed for 24 hr. The cooled reaction mixture was poured into ice-cold dilute hydrochloric acid, and the resulting precipitates were collected. After being washed with water, the residue was recrystallized from ethanol to give VIII in the form of colorless needles (m. p. 197—198°C); yield, 1.7 g. (75%). IR: 1648 ($\gamma$-pyrone) cm$^{-1}$. UV: $\lambda_{max}$ m$\mu$ (log. $\varepsilon$); $250_1$ (4.32), 305 (4.28).

Found; C, 67.95; H, 5.31. Calcd. for $C_{20}H_{18}O_6$: C, 67.79; H, 5.12%.

9) V. R. Sathe and K. Venkataraman, *Current Sci. (India)*, **18**, 373 (1949); *Chem. Abstr.*, **44**, 8916 (1950).

10) E. Simonitsch, H. Frei and H. Schmid, *Monatsh*, **88**, 541 (1957).

*2 All melting points are uncorrected; the infrared spectra were measured in Nujol, while the ultraviolet spectra were measured in an ethanol solution.

11) Y. Kawase, M. Nanbu, M. Uchida and Y. Kugo, 17th Annual Meeting of the Chemical Society of Japan, Tokyo, 1964.

**Isoelliptol Isoflavone (Furano(2'',3'' ; 6,7)-2',4',5'-trimethoxyisoflavone) (III).**—The mixture of VIII (1.7 g.), *N*-bromosuccinimide (0.85 g.) and benzoyl peroxide (0.05 g.) in carbon tetrachloride (130 ml.) was refluxed gently for 2.5 hr. After they had cooled, the precipitates were filtered off, and the filtrate was washed with a sodium bisulfite solution and with water and dried over calcium chloride. The evaporation of the filtrate under reduced pressure left a light yellow solid. After the addition of acetic acid (70 ml.) and potassium acetate (10 g.), the mixture was refluxed for one hour and then poured into water (1000 ml.). The resulting precipitates were collected and recrystallized from ethanol to give III in the form of colorless needles (m. p. 190—190.5°C) ; yield, 0.9 g. (53%). IR : 1634 ($\gamma$-pyrone) $cm^{-1}$. UV $\lambda_{max}$ m$\mu$ (log $\varepsilon$) ; 236 (4.44), 304 (4.18).

Found : C, 67.93 ; H, 4.69. Calcd. for $C_{20}H_{16}O_6$ : C, 68.18, H, 4.58%.

**6-Hydroxy-5-(2, 4, 5-trimethoxyphenylacetyl)-benzo[b]furan (IX).**—A mixture of III (0.6 g.), a 5% aqueous sodium hydroxide solution (40 ml.) and ethanol (60 ml.) was refluxed for 2 hr. on a steam bath. After the solvent had been evaporated, the residue was extracted with ethyl acetate. The resulting precipitates were recrystallized from ethanol to give IX in the form of pale yellow needles (m. p. 169—170°C), which were reddish brown in a ferric chloride test in ethanol ; yield, 0.4 g. (69%). IR : 1639 (C=O) $cm^{-1}$. UV : $\lambda_{max}$ m$\mu$ (log $\varepsilon$) ; 236 (4.41), 283 (4.13), 331 (3.98).

Found : C, 66.49 ; H, 5.58. Calcd. for $C_{19}H_{18}O_6$ : C, 66.66 ; H, 5.30%.

**The Recyclization of IX.**—By a reaction similar to that of VII, III was prepared from IX (0.2 g.), ethyl orthoformate (1 ml.), pyridine (10 ml.) and piperidine (5 drops). Recrystallization from ethanol gave III (m. p. 189—190°C), which was identical with the above sample ; yield, 0.15 g. (71%).

The authors are grateful to Professor Tetsuo Mitsui, Kyoto University, for making the microanalyses. This work was supported in part by a grant-in-aid from the Ministry of Education.

*Department of Chemistry*
*Faculty of Science*
*Hiroshima University*
*Higashi-Sendamachi, Hiroshima*

# Use of the Synergic Solvent Extraction System for the Determination of the Stability Constants of Metal Complexes

By Tatsuya SEKINE, Mitsuo SAKAIRI, Fumitake SHIMADA and Yuko HASEGAWA

(Received August 14, 1964)

The liquid-liquid partition method has been used for the determination of the stability constants of metal complexes.

When a metal ion, $M^{m+}$, is extracted with an organophilic chelating acid, HA, the net distribution ratio, $D=[M]_{total,\,org}/[M]_{total,\,aq}$, and the extraction constant, $K_0$, can be described as:

$$M^{m+}+mHA(org)\rightleftarrows MA_m(org)+mH^+ \quad (1)$$

$$D=[MA_m]_{org}/[M^{m+}] \quad (2)$$

$$K_0=D[H^+]^m[HA]_{org}^{-m} \quad (3)$$

where the suffix "org" denotes the chemical species in the organic phase and "0" denotes no complex formation in the aqueous phase.

Metal complex formation in the aqueous phase with a ligand, $L^{l-}$, decreases the concentration of the free metal ion and:

$$[M]_{total,aq}=[M^{m+}](1+\sum_1^n\beta_n[L^{l-}]^n) \quad (4)$$

$$K=[MA_m]_{org}[H^+]^m[HA]_{org}^{-m}/[M^{m+}](1+\sum_1^n\beta_n[L^{l-}]^n) \quad (5)$$

Here, $\beta_n$ is the over-all stability constant of the $n$th complex:

$$\beta_n=[ML_n^{m-nl}]/[M^{m+}][L^{l-}]^n \quad (6)$$

Therefore, the stability constants can be calculated by the following equation:

$$K_0/K=1+\sum_1^n\beta_n[L^{l-}]^n \quad (7)$$

However, the metal ion in the aqueous phase sometimes forms complexes not only with the ligand to be studied, $L^{l-}$, but also with the extracting chelating acid, HA, which has been distributed from the organic phase into the aqueous phase; the latter complexes, $MA^{m-1}$, $MA_2^{m-2}$, ..., also decrease the concentration of the free metal ion, just as has been shown in Eq. 4:

$$[M]_{total,\ aq}=[M^{m+}](1+\sum_{1}^{n}\beta_n'[A^-]^n) \quad (8)$$

Here, $\beta_n'=[MA_n^{m-n}]/[M^{m+}][A^-]^n$ and the distribution ratio in such systems can be written from Eq. 8, using $K_a=[H^+][A^-]/[HA]$, $K_D=[HA]_{org}/[HA]$, as:

$$D=[MA_m]_{org}/[M^{m+}]\{1+\sum_{1}^{n}\beta_n'(K_a[HA]_{org}/K_D[H^+])^n\} \quad (9)$$

and the distribution constant becomes:

$$K_0'=K_0/\{1+\sum_{1}^{n}\beta_n'(K_a[HA]_{org}/K_D[H^+])^n\} \quad (10)$$

Equation 10 indicates that the extraction constant, $K_0$, calculated by Eq. 3 is decreased by the increase in $[HA]_{org}/[H^+]$ and that thus the aqueous chelate complexes may cause a systematic error in the stability constants calculated by Eq. 7.

This deviation of $K_0$ from the constant value by the aqueous chelate complexes would be decreased by the use of the "synergic" solvent extraction system.*

When a neutral organophilic ligand, N, is added to a chelate extraction system, adduct complexes are sometimes formed:

$$MA_m(org)+nN(org)\rightleftarrows MA_mN_n(org) \quad (11)$$

$$[M]_{total,\ org}=[MA_m]_{org}(1+\sum_{1}^{n}\beta_n''[N]_{org}^n) \quad (12)$$

where $\beta_n''$ is the stability constant of the $n$th adduct complex; that is,

$$\beta_n''=[MA_mN_n]_{org}/[MA_m]_{org}[N]_{org}^n \quad (13)$$

Therefore, the net distribution ratio is:

$$D=[MA_m]_{org}(1+\sum_{1}^{n}\beta_n''[N]_{org}^n)/[M^{m+}] \quad (14)$$

Thus the adduct formation of the chelate complexes in the organic phase makes the metal extraction $(1+\sum_{1}^{n}\beta_n''[N]_{org}^n)$ times higher, and so one can obtain a certain distribution ratio of the metal at a lower $[HA]_{org}/[H^+]$ value.

## Experimental

All the reagents used were of analytical or reagent grade. Europium 152+154 in a tracer concentration was used for the determination of the net distribution ratio. Stoppered glass tubes were added with each 5 ml. of the organic and aqueous solutions and were then agitated mechanically in a thermostatted room at 25°C. Thenoyltrifluoroacetone (TTA) was used as the chelating ligand, and tributylphosphate (TBP) was used as the adduct-forming ligand, the organic solvent being hexane. The aqueous phase was a 0.1 M sodium perchlorate solution buffered with a small amount of sulfanilate or acetate. The hydrogen ion concentration was measured potentiometrically, and the $\gamma$ count-rate was determined with a well-type scintillation counter.

## Results and Discussion

Figure 1-a gives the plot of log $D$ vs. log $[H^+]^{-1}$, while Fig. 1-b gives the corresponding extraction constant calculated by Eq. 3. Figure 2 gives the increase in the extraction constant brought about by the addition of the adduct-forming ligand when the concentration of the chelating ligand is constant.

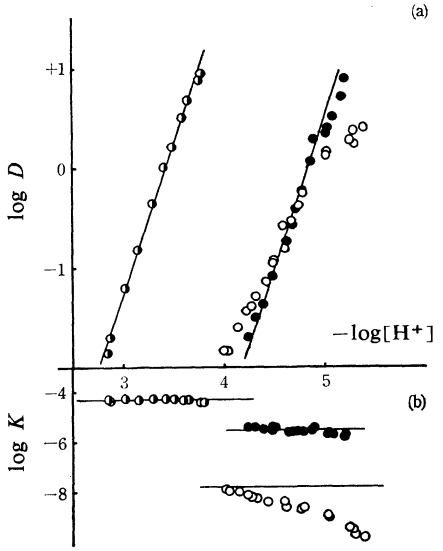



Fig. 1. (a) Distribution ratio of europium(III) as a function of a log $[H^+]^{-1}$. (b) Extraction constant of europium(III) calculated from the data in Fig. 1-a. (cf., Eq. 3).
Aqueous phase: 0.1 M $NaClO_4$
Organic phase: ○, 0.01 M TTA; ●, 0.001 M TTA + $3\times10^{-5}$ M TBP; ◐, 0.01 M TTA + $1\times10^{-4}$ M TBP; in hexane.

Equation 3 shows that $D$ should be proportional to $[H^+]^{-3}$ if $Eu^{3+}$ is the only metal species in the aqueous phase at a constant $[HA]_{org}$ value. However, it may be seen in Fig. 1-a that the plot of log $D$ vs. log $[H^+]^{-1}$ of the extraction with 0.01 M TTA (open circles) deviates somewhat from slope 3, this

* The synergic effect has been reported on the extraction of the actinides in various oxidation states, trivalent lanthanides, $Ca^{2+}$, $Sr^{2+}$, $Cu^{2+}$, $Zn^{2+}$, etc., with several chelating ligands and neutral ligands. A short review of the synergic solvent extraction systems was given in Ref. 1.

1) T. Sekine and D. Dyrssen, *J. Inorg. Nucl. Chem.*, **26**, 1727 (1964).

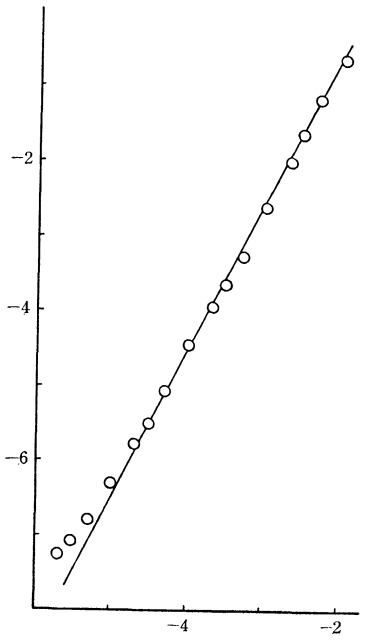



Fig. 2. Variation of the extraction constant (cf., Eq. 3) of europium(III) with 0.01 M TTA in hexane by the addition of TBP.

deviation may be due to the aqueous chelate complex formation. On the other hand, the $D$ is proportional to $[H^+]^{-3}$ in the synergic extraction systems (closed and semiclosed circles); this may be expected from the facts that the $[HA]_{org}/[H^+]$ value for a certain $D$ value is smaller in the synergic extraction systems and that, consequently, the concentration of the aqueous chelate complexes is smaller in these systems.

The extraction constants calculated from these data seem to show this more clearly. In Fig. 1-b, the extraction constant, $K_0$, in the single extraction system deviates very much from the constant value, but those in the synergic systems give nearly constant values (the log $K_0$ value is $-5.52$ for 0.001 M TTA+$3\times10^{-5}$ M TBP and $-4.32$ for 0.01 M TTA+$1\times10^{-4}$ M TBP). Thus, it may be concluded that the determination of $\beta_n$ by Eq. 7 is possible only by the use of the synergic extraction system in the present case.

There is another advantage in the use of the synergic extraction system. As may be seen in Fig. 2, the extraction constant in the metal extraction system can be varied very widely only by changing the concentration of the adduct-forming ligand. For example, one can obtain the 50% extraction of europium(III) with 0.01 M TTA in hexane between log $[H^+]^{-1}$ at 5.0($[TBP]_{org}$ is zero) and at 2.0($[TBP]_{org}$ is about 0.03 M). Thus, the use of one mixed ligand extraction system is worth several single extraction systems with different abilities of metal extraction.

Examples of the determination of stability constants by the synergic extraction system can be seen in Ref. 2.

*Department of Chemistry*
*Tokyo College of Science*
*Kagurazaka, Shinjuku-ku*
*Tokyo*

2) T. Sekine, ibid., 26, 1463 (1964).

# Synthesis of ε-Caprolactam from Cyclohexanecarboxylic Acid by Using Liquid Sulfur Dioxide*

By Niichiro TOKURA, Tetsuyo KAWAHARA and Tadao SATO

(Received September 4, 1964)

Recently two attractive ways of ε-caprolactam syntheses have been disclosed by research groups, one being the synthesis of cyclohexanone oxime via the photonitrosochlorination of cyclohexane,[1] and the other the so-called SNIA process.[2] The latter process consists of the production of ε-caprolactam from cyclohexanecarboxylic acid and a related compound by the action of nitrosylsulfuric acid;

* The Beckmann Rearrangement in Liquid Sulfur Dioxide, Part XII. Part XI: N. Tokura, K. Shiina and T. Terashima, This Bulletin, 35, 1986 (1962).

1) A. E. Müller, *Angew. Chem.*, 71, 229 (1959); *Chem. Ber.*, 90, 1179 (1959); ibid., 92, 63 (1959). B. M. Ito, *J. Soc. Org. Synth. Chem., Japan*, 21, 160 (1963).

2) SNIA Viscosa, Ital. Pat. 603606 (1960); *Chem. Abstr.*, 59, 11273 (1963); Belg. Pat. 582793 ((1960).

the mechanism has also been discussed.[3] Cyclohexane derivatives other than cyclohexanecarboxylic acid, such as cyclohexyl aryl ketones and cyclohexanesulfonic acid, have also been suggested as possible starting materials.[2]

This paper will present a simpler method for converting cyclohexanecarboxylic acid into ε-caprolactam, using liquid sulfur dioxide as the solvent as well as the reagent. When cyclohexanecarboxylic acid was stirred into a mixture of liquid sulfur dioxide, nitric acid and sulfuric acid and the reaction was carried out at a moderate temperature for an appropriate time, ε-caprolactam could be prepared in a fair yield. In the procedure described above, it seems likely that nitrosylsulfuric acid or a reagent which could behave like nitrosylsulfuric acid may be prepared in situ in the reaction mixture from nitric acid and liquid sulfur dioxide.

## Experimental

**Materials.**—Liquid sulfur dioxide was dried with phosphorus pentoxide and distilled. Commercial fuming nitric acid (sp. gr. 15°, 1.50) was used without further purification. Cyclohexanecarboxylic acid was distilled in vacuo; m. p. 31°C, b. p. 232—233°C. Sulfur trioxide was used after one distillation. Sulfuric acid (100% or sulfur trioxide monohydrate) was prepared from 95% sulfuric acid and sulfur trioxide. Chloroform and ether were purified by the ordinary recipes.

**A Typical Procedure.**—Two hundred milliliters of sulfur dioxide was distilled while being stirred into a three-necked flask cooled to −20°C, placed in a dry ice bath and equipped with a deep-freezing cooler. To this solution, 18.9 g. (0.30 mol.) of fuming nitric acid was added slowly; the white crystals which separated in the bottom of the flask dissolved again upon the addition of fuming sulfuric acid. After the dropping of nitric acid was over, fuming sulfuric acid, prepared by mixing 39.2 g. (0.4 mol.) of 100% sulfuric acid and 11.2 g. (0.14 mol.) of sulfur trioxide, was added. To this mixture, 25 g. (0.20 mol.) of cyclohexanecarboxylic acid was added slowly. The temperature was gradually raised to 68—70°C, while the excess sulfur dioxide was purged through the top of the cooler. The mixture was stirred for one more hour, cooled, and poured into ice-water.

The resultant solution was extracted with ether several times to recover the unchanged cyclohexanecarboxylic acid. The aqueous layer was neutralized with a sodium hydroxide solution, and the separated crystal of sodium sulfate was filtered off. Then the solution was repeatedly extracted with chloroform. The chloroform extract was dried over anhydrous sodium sulfate and distilled. ε-Caprolactam distilled under reduced pressure at 120—130°C/5.6 mmHg and solidified to white needles, m. p. (recrystallized from petroleum ether) and mixed m. p. 68—70°C. The infrared spectrum of this sample was superimposable on that of the authentic ε-caprolactam; yield, 12.7 g. (60%, based on the consumed carboxylic acid; 3.7 g. of cyclohexanecarboxylic acid was recovered).

Below 30°C the reaction does not take place. Among the factors which may affect the yield, the reaction temperature seems to be most important.

## Results and Discussion

The process employed here for the synthesis of ε-caprolactam is similar to that employed in the SNIA process except that the former uses liquid sulfur dioxide with fuming nitric acid instead of nitrosylsulfuric acid. It was obvious that, by adding fuming nitric acid to chilled sulfur dioxide, either nitrosylsulfuric acid or a reagent which would behave like nitrosylsulfuric acid was produced in the mixture. A number of methods for preparing nitrosylsulfuric acid have been published.[4] Among them, the introduction of sulfur dioxide gas into nitric acid is the most popular.[4b] However, the present authors believe that the method described in this article is without doubt a simpler method for the conversion of the carboxylic acid to the lactam.

Though the structure of the white crystals formed in the reaction mixture when fuming nitric acid was added to liquid sulfur dioxide have not yet been confirmed, it is believed to be nitrosylsulfuric acid, since the decomposition temperature of the crystal was 68—73°C (literature; [4a] 73.5°C) and the solubility (soluble in sulfuric acid and insoluble in liquid sulfur dioxide) resembled that of nitrosylsulfuric acid. An experiment was carried out using nitrosylsulfuric acid synthesized by the method of Ref. 4b to find out whether the yield was comparable to the above case. In part, a complex formed in situ from sulfur dioxide and nitric acid or a precursor of nitrosylsulfuric acid may also be the effective reagent for the reaction, since the separated crystals were small in amount and since the heat of reaction seemed to be very little.

At the beginning of this project the present authors expected a smooth running of the reaction at below-zero temperatures, since the process is thought to be a combination of nitrosation and the Beckmann rearrangement, which can occur even at −70°C. However, the reaction cannot be carried out below +30°C. This means that the nitrosation needs a somewhat higher energy of activation. A yield of 26% was recorded by the reaction at 30°C. The yield much improves at 68—70°C which

3) Y. Ogata, Y. Furuya and M. Ito, *J. Am. Chem. Soc.*, **85**, 3649 (1963).

4) a) L. Vanino, "Preparative Chem.," Band I, F. Enke, Stuttgart (1923), pp. 99, 106; b) H. S. Booth, "Inorganic Synth.," Vol. I, 55 (1939).

is near the decomposition temperature (73.5°C) of nitrosylsulfuric acid. In such a temperature range the concentration of the effective nitrosonium ion ($NO^+$) may become higher. A search for better conditions and an elucidation of the reaction mechanism is now under way.

The authors wish to acknowledge the gift of liquid sulfur dioxide by the Seitetsu Kagaku Co.

*The Chemical Research Institute of Non-Aqueous Solutions*
*Tohoku University*
*Katahira-cho, Sendai*

*Department of Applied Chemistry*
*Faculty of Engineering*
*Osaka University*
*Higashinoda, Osaka*

# Pulse Radiolysis Applied to Polymerization Reactions: The Intermediate in the Radiation-Induced Polymerization of $\alpha$-Methylstyrene*

By Meiseki KATAYAMA, Motoyoshi HATADA, Kozo HIROTA, Hatsuo YAMAZAKI and Yasutomo OZAWA

(Received September 12, 1964)

A reaction intermediate of radiation-induced polymerization has been observed for the first time in extremely dried $\alpha$-methylstyrene by means of pulse radiolysis. The indication that an anion radical plays an important role in the $\gamma$-ray-induced polymerization arose during the study of sodium-dried $\alpha$-methylstyrene at room temperature,[1] in which a $G$(-monomer) value as high as 36500 was obtained. The main bases on which the intermediate was postulated were; 1) a radical scavenger such as DPPH practically inhibited the reaction, as did an ion scavenger, water, and 2) no copolymer was found in the mixture of $\alpha$-methylstyrene and isobutylene which is known to polymerize through a cationic intermediate, while a copolymer had been found in the mixture of $\alpha$-methylstyrene and methylmethacrylate,[2] which is known to polymerize through a radical intermediate.

There has been a dispute about the reaction mechanism for some time. It seems that much of the discussion has been concerned with the radical and the cationic intermediates; the importance of the anion radical has been overlooked entirely. Although in only a few cases is the anion radical suggested in the radiation-induced polymerization, there are several examples of such an intermediate in such cases as the so-called anionic polymerization initiated by alkali metal.[3] The present investigation has had the purpose of confirming the anion radical mechanism in the radiation-induced polymerization[1] and of obtaining quantitative rate data by the direct observation of the reaction intermediate.

The experimental method is only briefly explained below, because the details will be published elsewhere. The monomer, dried by passing it through a sodium-potassium alloy,** and sealed into a high-purity quartz cell provided with optically-flat windows, was irradiated by a 1.6 $\mu$sec. electron pulse from a Fuji Denki lineac modified to give a single pulse, the energy of which was 4 MeV.; the peak current was $7.5\times10^{-2}$ amp. The electron beam was collimated on the wall of the cell with a diameter of about 1 cm. In the determination of spectra, the cell was irradiated cross-wise. The light source, a quartz tube equipped with tungsten electrodes, containing 75 mmHg xenon, was flashed by discharging a 2 $\mu$f condenser charged to 6 kV. by means of a 2G22P hydrogen thyratron.[4] It was triggered by a signal from the lineac at any delayed time designed by utilizing the delayed trigger circuit of a synchroscope. The duration of the flash was estimated to be 20 $\mu$sec.

* Presented at the 7th Symposium on Radiation Chemistry, Nagoya, July, 1964.

1) K. Hirota and M. Katayama, *Annual Report of JARRP*, 5, 205 (1963—64).

2) K. Hirota and F. Takemura, This Bulletin, 35, 1037 (1962).

3) K. Hirota, K. Kuwata and K. Morigaki, ibid., 31, 538 (1958).

** A novel technique for drying the monomer has been developed in the Chemistry Lab. of Hokkaido University. It was found quite satisfactory for drying styrene; details will be given in a coming publication.

4) J. H. Callomon and D. A. Ramsay, *Can. J. Phys.*, 35, 129 (1957).

The spectra was taken on a spectroscopic process-type Fuji plate by means of a Shimadzu quartz spectrograph. The plate was developed and subsequently fixed according to the recommendations of the manufacturer.

It has been reported[5] that when α-methylstyrene is brought in contact with sodium metal, it turns pale yellow and has an absorption maximum at 3275Å, while after a long time has elapsed or when it is heated it turns red, with the maximum shifting to 5100Å.

In the present investigation, a broad transient absorption below 3500Å was observed in

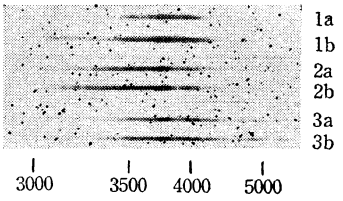



Fig. 1. Absorption spectra of transient species at room temperature.
a: 1.6 μsec. after the pulse and b: without it.
1: extremely dried α-methylstyrene
2: in the presence of trace of water
3: in the presence of DPPH

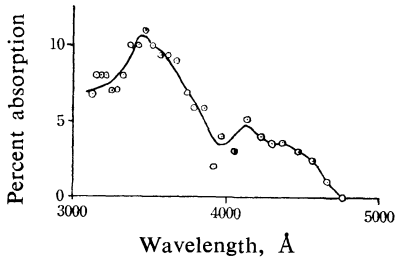



Fig. 2. Absorption spectrum of transient species in extremely dried α-methylstyrene.

the dried α-methylstyrene. 1a and 1b in Fig. 1 show spectra typical of such investigations. The 1a is the spectrum taken 1.6 μsec. after the irradiation of a pulse, while 1b is the spectrum taken without irradiation. The difference in the densitometer reading between 1a and 1b shows (Fig. 2) an absorption maximum at 3500Å, as was visually observed in 1a with a shoulder at about 4200Å. The lower the beam current of the pulse, the weaker became the absorption, and it practically disappeared after a few tenths of a millisecond. We believe that this maximum is in good correspondence with that of 3275Å observed in the sodium-α-methylstyrene system, considering the possible solvent effects, ion pair formation, etc., in the latter system, and that this constitutes a support for the existence of an anion radical in the radiation-induced polymerization of α-methylstyrene.

There still is uncertainty, however, that the absorbing species might not be the one which leads to the polymerization. Since it is known, as has been stated above, that the reaction is practically inhibited by the addition of a small amount of water or DPPH, the transient absorption observed in the dried monomer should diminish upon the addition of these compounds if it is caused by the reaction intermediate. This point has been tested, and this has been found to be the case. 2a and 2b in Fig. 1 show the effect of added water. The spectrum 2a in the figure was obtained 1.6 μsec. after the pulse, and 2b, without it. A visual comparison of these spectra shows that there is hardly any absorption. The densitometer reading also showed only a very weak absorption at the lower wavelength. In the experiment, water was added by the equilibration of the dried monomer with atmospheric moisture. 3a and 3b show the effect of added DPPH in less than $10^{-4}$ M. The notations a and b correspond to those used with the earlier pairs. The densitometer reading revealed that the absorption was greatly diminished, as can be seen by a visual comparison.

In conclusion, new support for the postulated anion radical mechanism in the radiation-induced polymerization of α-methylstyrene has been obtained by the present investigation.

*Department of Chemistry*
*Faculty of Science*
*Hokkaido University, Sapporo (M. K.)*

*Osaka Laboratories*
*Japanese Association for Radiation Research on Polymers*
*Neyagawa, Osaka (M. H.)*

*Department of Chemistry*
*Faculty of Science*
*Osaka University*
*Nakanoshima, Osaka (K. H.)*

*Laboratory for Nuclear Engineering*
*Faculty of Engineering*
*Hokkaido University, Sapporo*
*(H. Y. & Y. O.)*

5) K. Hirota, K. Kuwata, H. Togawa and S. Ishida, *J. Chem. Soc. Japan, Pure Chem. Sec. (Nippon Kagaku Zassi)*, **79**, 602 (1958).

# A Simple Method for Preparing Metallocenes

By Hamao WATANABE, Izumi MOTOYAMA and Kazuo HATA

(Received September 26, 1964)

Many sorts of metallocenes have already been synthesized in various methods by many investigators. However, only a one-step method for the preparation of ferrocene has been proposed;[1] this method consists of a direct reaction between ferric chloride and cyclopentadiene in the presence of an organic base, without the reduction procedure of ferric chloride to ferrous chloride. No simple and convenient method for the direct preparation of metallocenes other than ferrocene has yet been reported.

The present authors wish to report on a simple method for the preparation of such metallocenes as cobaltocene and nickelocene as well as of ferrocene. They can be synthesized in good yields by this convenient procedure.

The reactions of ferric chloride, cobaltous chloride, and nickel chloride with cyclopentadiene were carried out in the presence of an excess of diethylamine. The yields of metallocenes were 84% for ferrocene, 28% for cobaltocene, and 66% for nickelocene. In this procedure the formation of the metallocenes is considered to proceed through the following mechanism: by the reaction of the metal chloride and diethylamine, a corresponding ammine-complex salt of the metal is formed, and the complex salt reacts with cyclopentadiene, which has previously been de-protonated by strongly basic diethylamine.[2]

The infrared spectra of all these metallocenes have essentially identical absorption peaks at 3100 ($\nu_{C-H}$), 1430—1400 ($\nu_{C-C}$ ring), 1110—1100 (ring breathing), 1000 ($\delta_{C-H}$), 820—760 ($\delta_{C-H}$) and 1800—1550 $cm^{-1}$.

**The Synthesis of Ferrocene.**—Anhydrous ferric chloride (210.5 g., 1.30 mol.) was placed in a three-necked flask, equipped with a dropping funnel, a nitrogen inlet tube, a reflux condenser, and a stirrer. A stream of nitrogen was introduced, and dry diethylamine (320.5 g., 4.38 mol.) was added dropwise with stirring and cooling in an ice-water bath. A dark brown suspension was obtained. A mixture of dry cyclopentadiene (320.5 g., 4.85 mol.) and dry diethylamine (420.7 g., 5.76 mol.), previously cooled to 0——15°C with an ice-salt bath, was added with vigorous stirring into the suspension over several minutes. After vigorous stirring for an hour, additional gentle stirring was continued for 3 hr. The entire reaction mixture was then heated so as to evaporate almost to dryness, and then it was submitted to steam distillation in order to collect the ferrocene. During the distillation, a part of separated ferrocene was apt to accumulate in the condenser tube. It was dissolved out by benzene, which was occasionally supplied into the distilling flask. The combination of the steam distillation and the dissolution with benzene was continued until no more ferrocene was distilled out.[3] A mixture of ferrocene and other materials was then collected as a benzene solution. On concentration and cooling, ferrocene was crystallized from the solution, collected on a filter, washed with a small amount of ether, and air-dried. The mixture of the filtrate and the ethereal washing was further concentrated, and a second crop of ferrocene was obtained by a similar treatment. The procedure was repeated several times; the total yield of ferrocene amounted to 210.4 g. (84% based on ferric chloride).

**The Synthesis of Cobaltocene.**—In the same manner as was used with ferrocene, a deep blue mixture was prepared in a stream of nitrogen by the reaction of blue anhydrous chloride[4] obtained from its hydrate ($CoCl_2 \cdot 6H_2O$, 48.2 g., 0.20 mol.) and dry diethylamine (117.0 g., 1.60 mol.). After this mixture had been stirred for half an hour, a cold mixture of dry cyclopentadiene (49.3 g., 0.75 mol.) and dry diethylamine (64.9 g., 0.89 mol.) was added with stirring into the mixture over a 15-min. period. After the reaction mixture had been stirred for an hour, it was refluxed for 15 min. with stirring. The reaction mixture was then cooled to room temperature, and hexane was added in 3 portions (100, 100, and 50 ml.) which

1) R. L. Pruett and E. L. Morehouse, *Advances in Chem. Ser.*, 23, 368 (1959), "The Amine Method for Preparing Ferrocene".

2) F. Ephraim, *Z. physik. Chem.*, **81**, 513 (1913); E. O. Fischer and R. Jira, *Z. Naturforsch.* **8b**, 217, 327, 692 (1953); E. O. Fischer and W. Hafner, ibid., **8b**, 444 (1953); Brit. Pat. 774529 (May 8, 1957); *Chem. Abstr.*, **52**, 2928 (1958); J. F. Cordes, *Chem. Ber.*, **95**, 3084 (1962).

3) The method of removing the clogged ferrocene with benzene was first realized in this laboratory by K. Hata, I. Motoyama, K. Azuma and K. Urushibara.

4) "Inorganic Syntheses," Vol. 5, 153 (1957).

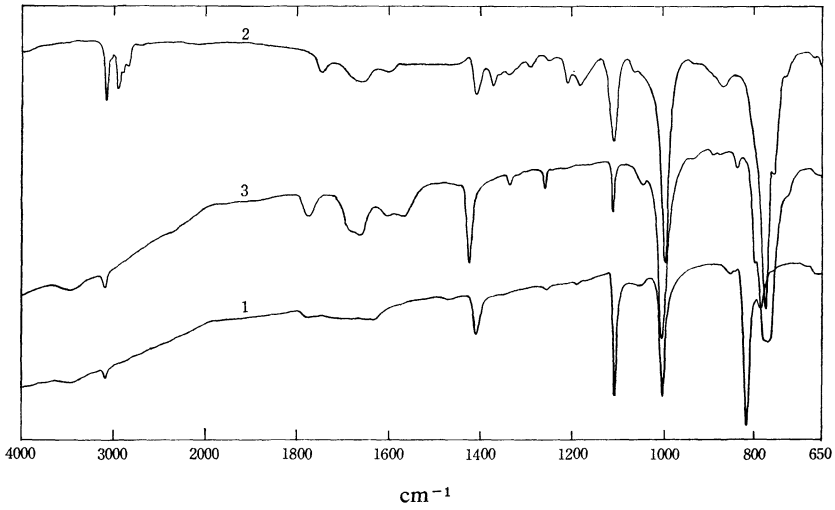



Fig. 1. The infrared spectra of the three metallocenes.
1: Ferrocene in a KBr disk 2: Cobaltocene in a $CS_2$ solution
3: Nickelocene in a KBr disk

has been previously deoxygenated by treatment with nitrogen. After each addition, the combined mixture was agitated thoroughly and left to stand until a violet-brown organic phase was separated as an upper layer. The organic layer was transferred to a round-bottomed flask by means of nitrogen pressure through a siphon, the inlet tube of which was covered with glass wool. The entire violet-brown organic solution was evaporated in a stream of nitrogen to give 12.0 g. of crude cobaltocene, which was then submitted to vacuum sublimation to obtain 10.5 g. (yield, 28%) of the pure substance as large, black-violet, glittering crystals.

**The Synthesis of Nickelocene.**—A deep violet-blue mixture was obtained by the reaction between yellow anhydrous nikel chloride[4] prepared from its hydrate ($NiCl_2 \cdot 6H_2O$, 47.7 g., 0.20 mol.) and dry diethylamine (117.0 g., 1.60 mol.) in the same as manner described above. The following procedure was similar to that used with cobaltocene, except for the addition of 250 ml. deoxygenated petroleum ether in place of hexane. The entire reaction mixture was then filtered, in air, as rapidly as possible. The deep green filtrate thus obtained was evaporated in a stream of nitrogen to give crude nickelocene, which was submitted to vacuum sublimation to obtain 25.1 g. (yield, 66%) of the pure substance as large, deep green, glittering crystals.

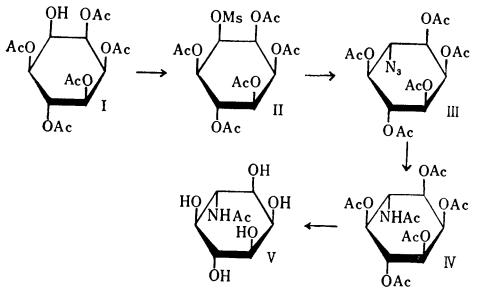
*Department of Chemistry*
*Faculty of Science*
*Tokyo Metropolitan University*
*Setagaya-ku, Tokyo*

# Aminocyclitols. VII. A New Synthetic Route to *myo*-Inosamine-4

By Tetsuo SUAMI and Kenji YABE

(Received October 1, 1964)

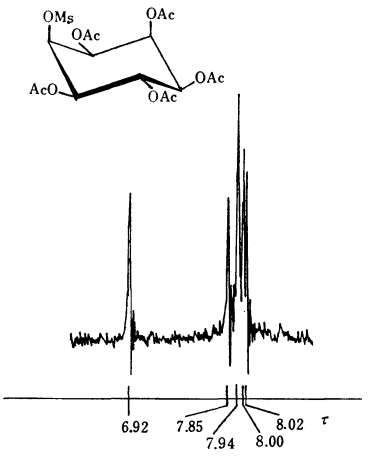
In a previous paper of this series,[1] the replacement of the mesyloxy group of 1-*O*-mesyl-*myo*-inositol pentaacetate by a highly nucleophilic azide ion has been described. In the present paper, the displacement of the mesyloxy group of (±)-2-*O*-mesyl-*epi*-inositol pentaacetate (II) by an azide ion is the main subject. II is prepared in 89% yield from (±)-1, 3, 4, 5, 6-penta-*O*-acetyl-*epi*-inositol (I)[2] by an ordinary procedure of mesylation.




The structure of II is substantiated by the NMR spectrum; as Fig. 1-A shows, the spectrum reveals a sharp signal at 7.85 $\tau$, corresponding to an axial acetoxy group, and sharp signals with a 2 : 1 : 1 relative intensity at 7.94, 8.00 and 8.02 $\tau$, corresponding to four equatorial acetoxy groups.[3] The protons of the mesyloxy group on C-2 reveals a sharp signal at 6.92 $\tau$, as is to be expected from an axial mesyloxy group.[4]

II is then treated with sodium azide in boiling aqueous 2-methoxyethanol for 20 hr. Since the product has been partially deacetylated during the course of the reaction, the product is acetylated with acetic anhydride and pyridine to give the azido derivative (III), m. p. 149—150°C, in 47% yield; this shows an infrared absorption characteristic of an azide group at 2100 $cm^{-1}$.[5] III is reduced with Raney nickel in a hydrogen stream. The reduction product is further acetylated with acetic anhydride and pyridine, giving hexaacetyl-inosamine (IV), m. p. 235—237°C, in 58% yield. *N*-Acetyl-inosamine (V), m. p. 268—269°C (decomp.), is obtained by the selective deacetylation of IV with methanolic ammonia.

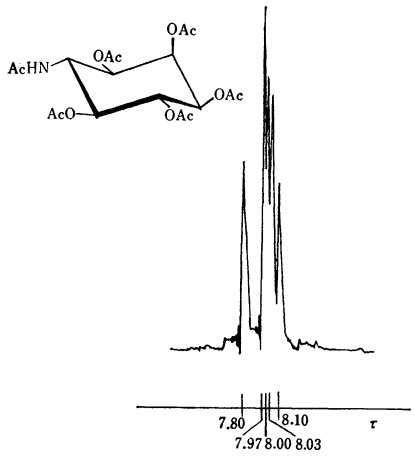
Since both of the vicinal acetoxy groups with respect to the mesyloxy group are located in anchimerically unassisted cis positions in II, the replacement of the mesyloxy group by an azide ion must occur through a direct $S_N2$ mechanism,[6] as has been shown in the case of 1, 3-di-*O*-acetyl-2-*O*-mesyl-*cis*-1, 2, 3-cyclohexanetriol.[4] Therefore, the product, IV, is probably identical with (±)-*myo*-inosamine-4 hexaacetate, which has been described by Anderson et al.[7] The configuration of IV is substantiated by its NMR spectrum. The NMR spectrum of IV, as shown in Fig. 1-B, reveals a sharp signal at 7.80 $\tau$, corresponding to an axial acetoxy group, signals at 7.97 8.00 and 8.03 $\tau$, with a 2 : 1 : 1 relative intensity corresponding to four equatorial acetoxy groups, and one at 8.10 $\tau$, as is to be expected from an equatorial acetamido group.[3]




p. p. m., $H \rightarrow$

Fig. 1-A.

1) T. Suami and S. Ogawa, This Bulletin, **37**, 1238 (1964).
2) T. Posternak, *Helv. Chim. Acta*, **19**, 1333 (1936); *Biochem. Preparations*, **2**, 57 (1952).
3) F. W. Lichtenthaler, *Chem. Ber.*, **96**, 2047 (1963).
4) T. Suami, F. W. Lichtenthaler and S. Ogawa, This Bulletin, **38**, 754 (1965).
5) L. J. Bellamy, "The Infrared Spectra of Complex Molecules," John Wiley & Sons, New York (1958), pp. 273—274.
6) B. R. Baker and A. H. Haines, *J. Org. Chem.*, **28**, 442 (1963).
7) H. Straube-Rieke, H. A. Lardy and L. Anderson, *J. Am. Chem. Soc.*, **73**, 881 (1951).




p. p. m., $H \rightarrow$

Fig. 1-B.

## Experimental

All melting points were measured on a Mitamura Riken micro hot plate. The NMR spectra were determined at a frequency of 60 Mc. p. s. with Japan Electron Optics JNM-C-60 and Hitachi Model H-6013 spectrometers in deuteriochloroform. Tetramethylsilane was used as an internal reference, and peak positions were given in $\tau$-values.

(±)-**2-*O*-Mesyl-*epi*-inositol Pentaacetate (II).**—To a mixture of 2.3 g. of (±)-1,3,4,5,6-penta-*O*-acetyl-*epi*-inositol and 30 ml. of pyridine, 1.0 g. of methanesulfonyl chloride was added under agitation at 0°C. After it had settled overnight in a refrigerator, the mixture was added to 45 ml. of ice cold water. The precipitate was then collected by filtration. The crude product (2.7 g.) was recrystallized from methanol to give 2.4 g. (89%) of needles melting at 196—197°C.

Found: C, 43.52; H, 5.36; S, 6.63. Calcd. for $C_{17}H_{24}O_{13}S$: C, 43.59; H, 5.16; S, 6.85%.

(±)-**4-Deoxy-4-azido-*myo*-inositol Pentaacetate (III).**—A mixture of 2.0 g. of II, 0.9 g. of sodium azide and 50 ml. of 80% aqueous 2-methoxyethanol was refluxed for 20 hr. The mixture was then evaporated to dryness in vacuo. The residue was repeatedly extracted with ethanol. The combined ethanol extract was evaporated, and the residue was added to a mixture of 20 ml. of acetic anhydride and 20 ml. of pyridine. The mixture was then evaporated in vacuo, and the residue was recrystallized twice from ethanol to give 0.84 g. of needles (46.6%) melting at 149.5—150°C.

Found: C, 46.47; H, 5.33; N, 10.07. Calcd. for $C_{16}H_{21}N_3O_{10}$: C, 46.26; H, 5.10; N, 10.12%.

(±)-**Hexaacetyl-*myo*-inosamine-4 (IV).**—A solution of 0.68 g. of III in 100 ml. of ethanol was hydrogenated with Raney nickel T4[8] in hydrogen at an initial pressure of 50 p. s. i. g. for 20 hr. Then the catalyst was removed by filtration, and the filtrate was evaporated in vacuo. The residue was acetylated with a mixture of acetic anhydride and pyridine. The crude product was repeatedly recrystallized from ethanol to give 0.33 g. of needles melting at 235—237°C. (Lit. m. p. 236—239°C).[7] (Found: C, 50.12; H, 5.71; N, 3.25%.)

(±)-***N*-Acetyl-*myo*-inosamine-4 (V).**—A 0.4 g. portion of IV was added to 50 ml. of methanol which had been previously saturated with ammonia. After it had settled overnight at room temperature, the mixture was evaporated under reduced pressure. The residue was washed with ethanol and then recrystallized from a mixture of ethanol and water (2 : 1), giving 0.18 g. (92.7%) of needles melting at 268—269°C (decomp.). [Lit. m. p. 270—271°C (decomp.)].[7] (Found: C, 43.54; H, 7.08; N, 6.40%.)

**Paper Chromatography.**—IV was hydrolyzed with boiling 6 N hydrochloric acid for 6 hr. Then the hydrolyzate was evaporated to dryness in vacuo. The residue was developed in an acetic acid - ethyl acetate - pyridine - water (3 : 5 : 5 : 1) system[9] in ascending paper chromatography. The hydrochloride showed a single spot of $R_f$ 0.24 at 22°C ($R_f$ of D-glucosamine hydrochloride: 0.46). $R_f/R_f$ glucosamine: 0.52 (Lit. $R_f$ DL-*myo*-inosamine-4/$R_f$ glucosamine: 0.53).[10]

The authors wish to thank Professor Sumio Umezawa for his helpful advice, Mr. Saburo Nakada for his elemental analyses, and the Japan Electron Optics Co., Ltd., and Hitachi, Ltd., for the NMR spectra. This research has been supported in part by a grant of the Ministry of Education, to which the authors' thanks are due.

*Department of Applied Chemistry*
*Faculty of Engineering*
*Keio University*
*Koganei-shi, Tokyo*

8) S. Nishimura, This Bulletin, **32**, 61 (1959).
9) F. G. Fischer and H. Dorfel, *Hoppe-Seyler's Z. Physiol. Chem.*, **301**, 224 (1955).
10) F. W. Lichtenthaler, *Chem. Ber.*, **94**, 3071 (1961).

# The Mechanism of the Photochromism and Thermochromism of 2, 2′, 4, 4′, 5, 5′-Hexaphenyl-1, 1′-biimidazolyl in a Solid State

By Taro HAYASHI, Koko MAEDA and Takako KANAJI

(Received October 3, 1964)

Photochromism and thermochromism are exhibited by 2, 2′, 4, 4′, 5, 5′-hexaphenyl-1, 1′-biimidazolyl in the solid state as well as in the solution. The pale yellow substance becomes reddish purple upon irradiation or when heated in a solid state[1], although the color is paler than that in the solution. The mechanism of these phenomena in the solution was previously reported[2] to be the reversible dissociation to the free radical, 2, 4, 5-triphenylimidazolyl.

An electron-spin resonance of hexaphenylbiimidazolyl which became pale reddish purple upon irradiation in a solid state with sunlight at 15°C for 10 min. was observed in a solid state at 15.0°C, the first derivative of a single absorption line where the $g$ value is 2.002 and the line width (from peak to peak) is about 7.8 gauss being measured.[3] Since hexaphenylbiimidazolyl which had been kept in the dark after recrystallization exhibited no ESR signal, this ESR measurement shows that the mechanism of the photochromism of hexaphenylbiimidazolyl in a solid state involves a free radical, probably 2, 4, 5-triphenyl-imidazolyl, as in a solution.

The absorption spectrum of hexaphenylbiimidazolyl in a solid state was measured in the visible region immediately after irradiation with a mercury vapor lamp at 15°C for 10 min. with a Hitachi recording spectrophotometer, the absorption maximum (554 m$\mu$) obtained by the reflection spectroscopic method[4] and the absorption maximum (562 m$\mu$) obtained by the opal glass transmission method[5] and the potassium bromide disk method[6] being shown respectively. The absorption maximum (554 m$\mu$) coincides with the one shown by 2, 4, 5-triphenylimidazolyl in an irradiated benzene solution, whereas the absorption maximum measured with the transmission method, the shift may be attributed to a weak absorption, extending from the ultraviolet region to 620 m$\mu$, by hexaphenyl-biimidazolyl, which exists (562 m$\mu$) shows a red shift of 8 m$\mu$. The species exhibiting the photochromic color in a solid state is most probably 2, 4, 5-triphenylimidazolyl, which shows an absorption maximum of 554 m$\mu$ in benzene. The mechanism of the photochromism of hexaphenyl-biimidazolyl in a solid state can, therefore, be concluded to be the radical dissociation of its N-N bond to triphenylimidazolyl radicals, similar to the mechanism in a solution.

Considering the thermochromic color in a solid state to be similar to the photochromic color, the exhibition of an ESR signal in the thermochromism in a solid state and the mechanism of the thermochromism in a solution,[2] the same mechanism can be applied to the thermochromism in a solid state.

The photochromic color in a solid state hardly faded in the dark at room temperature, whereas it gradually reverted to its original pale yellow color at about 40°C at which temperature the thermochromism is not observed. The decay rate of the intensity of the first derivative ESR spectrum, which is the rate of the recombination of the free radical, 2, 4, 5-triphenylimidazolyl, was measured in the dark at 46.0 and 62.5°C. Unlike the rate in a benzene solution,[2] the rate in a solid state did not obey the rate expression of the second-order reaction.

*Department of Chemistry*
*Faculty of Science*
*Ochanomizu University*
*Bunkyo-ku, Tokyo*

1) The photochromic color appears upon irradiation with sunlight or with a mercury lamp at room temperature, whereas the thermochromic color begins to appear at about 180°C, and the sample becomes intensely reddish purple when fused at 198—200°C. The rate of the disappearance of the color is very slow at room temperature.

2) T. Hayashi, K. Maeda and M. Morinaga, This Bulletin, 37, 1563 (1964); T. Hayashi, K. Maeda and M. Takeuchi, ibid., 37, 1717 (1964).

3) Its spin concentration was about $8\times10^{17}$ spin/g.

4) The mixture of hexaphenyl-biimidazolyl, (0.0149 g.) and magnesium oxide (1 g.) was used.

5) Hexaphenyl-biimidazolyl (1.5 mg.) was used.

6) A mixture of the sample (1.3 mg.) and potassium bromide (200 mg.) was used.

## SHORT COMMUNICATIONS

# The Deoxygenation of Isocyanates by 2-Phenyl-3-methyl-1, 3, 2-oxazaphospholidine. A Convenient Method for the Preparation of Isonitriles

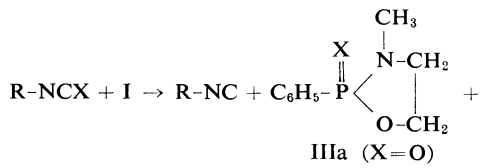
By Teruaki MUKAIYAMA and Yukio YOKOTA

(Received January 25, 1965)

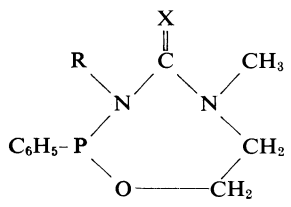
The preparation of 2-phenyl-3-methyl 1, 3, 2-oxazaphospholidine (I) and its application to a synthesis of isonitriles will be described.

The oxazaphospholidine, b. p. 72—75°C/0.3 mmHg (Found: C, 60.21; H, 6.64; N, 7.82. Calcd. for $C_9H_{12}ONP$: C, 59.66; H, 6.68; N, 7.72%), was prepared by treating phenylphosphonous dichloride[1] with 2-methylaminoethanol in the presence of two molecular equivalents of triethylamine (41% yield), or by heating a mixture of phenyl-di-diethylaminophosphine and 2-methylaminoethanol at 120—130°C for two hours (83% yield).

In a previous paper,[2] it was reported that several isonitriles were obtained in 20—57% yields by treating isocyanates with triethyl phosphite above 150°C. In the present study, it was found that I reacted with isocyanates or isothiocyanates at low temperatures (5—36°C) to form the corresponding isonitriles



IIIa (X=O)
IIIb (X=S)



IVa (X=O)
IVb (X=S)

(II) and 2-phenyl-3-methyl-1, 3, 2-oxyzaphospholidine-2-one (IIIa) or 2-phenyl-3-methyl-1,3,2-oxazaphospholidine-2-thione (IIIb) in high yields. IIIa or IIIb was always contaminated with a small amount of 3-substituted-per-2-phenyl-5-methyl-1, 3, 5, 2-oxadiazaphosphepine-4-one (IVa) or -4-thione (IVb). For example, when phenyl isocyanate was added drop-by-drop to a solution of I in petroleum ether (b. p. 34—36°C), the solution began to reflux. After the reaction mixture had been refluxed on a water bath for half an hour under nitrogen, the mixture was fractionated into two fractions. Fraction I was phenylisocyanide (b. p. 70—72°C/31 mmHg), and the yield was 57%. Fraction II consisted mainly of IIIa (b. p. 135—138°C/0.1 mmHg, m. p. 73—75°C) (Found: C, 54.94; H, 6.36; N, 7.26. Calcd. for $C_9H_{12}O_2NP$: C, 54.84; H, 6.11; N, 7.11%), plus a small amount of IVa.

Similarly, phenylisocyanide, *o*-tolylisocyanide, and *p*-chlorophenylisocyanide were obtained in 93, 70 and 51% yields respectively by a reaction of I with phenylisothiocyanate,* *o*-tolylisocyanate, and *p*-chlorophenylisocyanate in refluxing petroleum ether.

On the other hand, a solution of cyclohexylisocyanate and I in ligroin (b. p. 72—80°C) was refluxed on a water bath for two hours under nitrogen; a mixture of cyclohexylisocyanide and cyclohexylisocyanate, and IIIa (82%) were thus obtained, and 5% of I was recovered. The respective yields of cyclohexylisocyanide (74%) (b. p. 76—78°C/27 mmHg) (Found: C, 76.48; H, 10.64; N, 12.60. Calcd. for $C_7H_{11}N$: C, 77.01; H, 10.16; N, 12.83%) and cyclohexylisocyanate (8%) were determined by the addition of cyclohexylamine to the

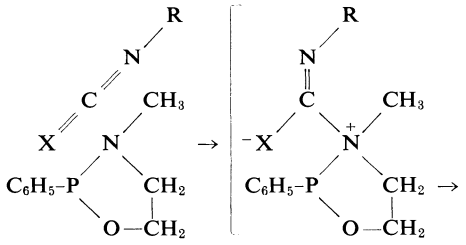
1) B. Buchner and L. B. Lochhart, "Organic Syntheses," **31**, 88 (1951).
2) T. Mukaiyama, H. Nambu and M. Okamoto, *J. Org. Chem.*, **27**, 3651 (1962).

* IIIb (b. p. 148—152°C/0.09 mmHg, m. p. 65—67°C) (Found: C, 50.77; H, 5.82; N, 6.69. Calcd. for $C_9H_{12}ONSP$: C, 50.71; H, 5.63; N, 6.57%).

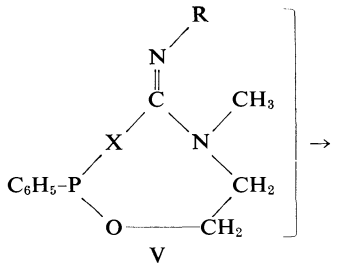
mixture in dry ether and by weighing the amount of *N*, *N'*-dicyclohexylurea produced.

When a mixture of I and ethylisocyanate or ethylisothiocyanate was allowed to stand one day at room temperature (5—10°C) under nitrogen, ethylisocyanide (b. p. 80—82°C) was obtained in a 65 or an 87% yield respectively. The ethylisocyanide was identified by gas chromatography.

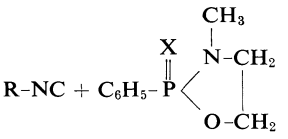
The most probable pathway of the deoxygenation by means of this cyclic oxazaphospholidine (I) may be sketched in the following manner:



(I)



V



(II) (III)

Further study of analogous deoxygenations of the other compounds with a carbonyl group by means of I is now in progress.

*Laboratory of Organic Chemistry*
*Tokyo Institute of Technology*
*Ookayama, Tokyo*

# The Polymerization of Acetylene with Dicyclopentadienyl-titanium

By Kaiji YOKOKAWA and Keiichi AZUMA

(Received February 18, 1965)

It has previously been discovered that ethylene and propylene can easily be polymerized to polymers of a high crystallinity with a catalyst of titanium trichloride, polymethylhydrosiloxane and dicyclopentadienyl-titanium (DCT).[1] It has now been discovered that DCT is a good catalyst for the polymerization of acetylene also. Although a similar finding has been reported on the catalysis of dicyclopentadienyl-vanadium (DCV),[2] it is less reactive than DCT in the polymerization of acetylene under mild conditions.

DCT was prepared by the reduction of dicyclopentadienyl-titanium dichloride with sodium amalgam (the sodium concentration was 0.1 wt. % in mercury) in toluene under an argon atmosphere.[1]

As a typical experiment, 40 ml. of a toluene solution containing 0.24—1.0 mmol. of DCT was added to a 100-ml. three-necked flask equipped with a gas inlet, a gas outlet and a thermometer, under an argon atmosphere. Acetylene was then introduced, with vigorous agitation, through the gas inlet from a gas burette. The polymerization proceeded rapidly but was stopped after 60 min. at 30°C. Black or reddish-black solid polymers were obtained; no liquid products were found. No polymers were obtained with DCV under similar conditions. The results of the experiments are shown in Table I.

In an attempt to ascertain the properties of the polyacetylene obtained, 3.5% of it was extracted by boiling it with benzene for 12 hr. under an argon atmosphere. From infrared examinations it was elucidated that it contained trans-double bonds and that carbonyl groups were formed by exposure to air for a long time. The X-ray diffraction showed a sharp peak at $d=3.8$ Å, indicating the high crystallinity of the polymer. According to the thermal differential analysis, it was gradually oxidized by air, but it was stable in inert gas up to about 300°C. Those properties were the

1) K. Shikata, K. Yokokawa, S. Nakao and K. Azuma, to be published.
2) R. Tsumura and N. Hagihara, This Bulletin, 37, 1889 (1964).

TABLE I. THE POLYMERIZATION OF ACETYLENE

| No. | DCT* mmol. | [DCT]* mmol./l. | $C_2H_2$ mmHg | Temp. °C | Time min. | Solid product g. |
|---|---|---|---|---|---|---|
| 1 | 1.0 | 25 | 760 | 80 | 60 | 1.04 |
| 2 | 1.0 | 25 | 760 | 30 | 60 | 0.84 |
| 3 | 1.0 | 25 | 760 | −15 | 60 | 0.68 |
| 4 | 1.0 | 25 | 760 | −50 | 60 | 0.45 |
| 5 | 1.0 | 25 | 760 | −65 | 60 | 0.32 |
| 6 | 0.5 | 13 | 760 | 30 | 60 | 0.46 |
| 7 | 0.24 | 6 | 760 | 30 | 60 | 0.16 |
| 8 | 0.24 | 6 | 150 | 20 | 60 | 0.1 |
| 9 | 0.24 | 6 | 150 | −70 | 60 | 0.1 |
| 10** | 6.0 | 25 | 760 | 30 | 60 | 3.2 |
| 11*** | 1.0 | 25 | 770 | 27 | 60 | 0.0 |
| 12*** | 1.0 | 25 | 770 | 75 | 180 | 0.0 |

* The amount of DCT in the toluene solution was determined by the concentration of titanium as titanium dioxide. Forty milliliters solution was used in each experiment except No. 10.

** 240 ml. solution was used in a 300-ml. three necked flask.

*** In the experiments of No. 11 and No. 12, DCV was used in place of DCT. It was prepared in the same method as DCT, by the reduction of dicyclopentadienyl-vanadium dichloride with sodium amalgam.

same as those of the conjugated *trans*-polyacetylene obtained by Natta et al.[3] and by Hatano[4]. The polyacetylene obtained with DCT may be assumed to be similar to that obtained with DCV.[2]

In considering the catalytic behavior of metallocene, it is very interesting that acetylene polymerizes more easily with DCT than with DCV.

*Tokuyama Soda Co., Ltd.*
*Tokuyama-shi, Yamaguchi*

3) G. Natta, G. Mazzanti and P. Corradini, *Atti. Accad. naz. Lincei, Rend. Classe Sci. fis. mat. nat.*, 25, 3 (1958); G. Natta, P. Pino and G. Mazzanti, Japanese Pat. 10597 (1957).

4) M. Hatano, *J. Chem. Soc. Japan, Ind. Chem. Sec.* (*Kogyo Kagaku Zasshi*), 65, 723 (1962).

# The Constituents of the Flower Oil of Lily of the Valley[1)]

By Seiji WAKAYAMA and Satoshi NAMBA

(Received March 4, 1965)

The absolute oil of lily of the valley (*Convallaria keisukei Miq.*), which it is known, can not be obtained by steam distillation, has not well been investigated.[2)]

The extraction of the flower (100 kg.) with hexane afforded a yellowish-colored concrete (0.26% of the flower) which was then a digested with methanol.

The methanol-insoluble wax (0.13%) was found to contain palmitone triacontanol, wax with a m. p. of 68—69°C and nonacosane by the comparison of the infrared spectra with those of authentic specimens, by comparing the melting points of the derivatives, and by the elementary analyses.

The methanol-soluble part afforded a pale brown-colored essential oil (0.13%) on the removal of the methanol. About a half weight of the essential oil was a mixture of aliphatic acids; this mixture was collected by the treatment of the oil with sodium carbonate and was found to be composed of acetic, caproic, palmitic, stearic and linoleic acids.

The oil obtained on the removal of the acids had the properties of AV 6.3, EV 90.3, and HV 89.3 and gave no distillate under the diminished pressure of 2 mmHg. The essential oil (5.571 g.)

1) Presented at the 8th Symposium on the Chemistry of Terpenes and Essential Oils, Sendai, September, 1964.

2) E. Guenther, "The Essential Oils," Vol. VI, Van Nostrand Company, New York (1952), p. 75; S. Sabetay, *Chem. Abstr.*, **44**, 5537c (1950).

was subjected to separation by chromatography on alumina* (300 g.). The elutions were made with hexane, hexane-benzene (1 : 1), benzene and benzene-ethanol successively. Some fractions eluted with hexane gave a mixture of esters of aliphatic acids which was one of the major components of the oil (20—25%). It should be noted that these esters have afforded, on saponification, a mixture of fresh, lily-like scented alcohols, although the esters themselves smell faintly like the essence. The chromatography of the mixture of the alcohols on alumina with benzene resulted in the isolation of citronellol, nerol and cinnamyl alcohol. Those alcohols were identified on the basis of both the comparison of the infrared spectra with those of the respective authentic samples and the transformation into the derivatives; citronellol was converted into the silver salt of the acid phthalate[3] (m. p. 124.5—125°C); nerol, into the tetrabromide[4], (m. p. 115—117°C) and the allophanate[4] (m. p. 98.5—99.5°C), and cinnamyl alcohol, into the 3,5-dinitrobenzoate (m. p. 124.2—124.8°C). The acidic constituent consisted mainly of stearic acid.

Some fractions eluted with hexane-benzene afforded a mixture of esters. On saponification, it gave as an acidic component only phthalic acid, which melted at 213°C with decomposition into the anhydride (m. p. 130—131°C). The acid was also identified by derivation into the phenacyl ester (m. p. 152—152.7°C).

Fractions eluted with benzene emitted a lily-like scent, and the infrared spectra suggested that they were a mixture of citronellol and nerol. Rechromatography on alumina with benzene led to the isolation of those alcohols, which were identified as has been mentioned above.

Finally, cinnamyl alcohol was isolated by elution with benzene containing 1% ethanol, followed by rechromatography on alumina with benzene.

In summary citronellol, nerol and cinnamyl alcohol are the principal fragrant constituents of "lily of the valley," and they are present in the plant as both free alcohols and stearates.

Investigations of the other constituents are now in progress.

*Chemical Laboratory*
*Hokkaido Gakugei University*
*Sapporo*

* Brockmann Grade II alumina.

3) E. Funakubo, "Yūki Kagōbutsu Kakuninhō," Vol. I, Yōkendō, Tokyo (1954), p. 147; H. Meyer, "Nachweis und Bestimung organischer Verbindungen," J. Springer, Berlin (1933), s. 39.

4) E. Guenther, "The Essential Oils," Vol. II, Van Nostrand Company, New York (1957), p. 175.

# Acetylene Complexes of Dicyclopentadienyl-vanadium

By Ryuichiro TSUMURA and Nobue HAGIHARA

(Received March 15, 1965)

Previous work has demonstrated a catalytic polymerization[1] of acetylenes with dicyclopentadienyl-vanadium[2] (I) and the preparation[3] of a series of acetylene complexes of vanadium, such as $\pi$-$C_5H_5(HC_2H)V(CO)_2$. The present communication will deal with the preparation of a few acetylene complexes of I as a model substance of an intermediate in the polymerization of acetylene with I. Although a great variety of transition metal-acetylene complexes are known,[4] the acetylene complexes described here may be the first examples of compounds in which the acetylenic bond is directly bonded to the metal coordinated by two $\pi$-cyclopentadienyl rings.

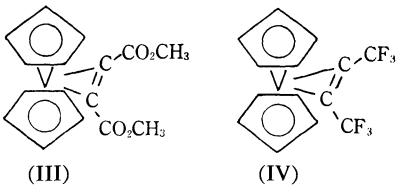
To a stirred, violet solution of 2.79 g. of I in 60 ml. of benzene, 2.40 g. of dimethyl acetylenedicarboxylate (II) was added drop by drop at a room temperature under nitrogen. The reaction solution almost instantaneously turned dark green, with a slight evolution of heat, and some dark-colored crystals precipitated spontaneously. After having been stirred at 50°C for 1 hr., the resulting reaction mixture was evaporated to dryness under reduced pressure. The residue was then recrystallized from toluene to yield 4.20 g. (84.5% yield) of air-sensitive, dark green crystals (III); m. p., 146—147°C (decomp.) (Found: C, 59.33; H, 4.99;

1) R. Tsumura and N. Hagihara, This Bulletin, **37**, 1889 (1964).
2) E. O. Fischer and S. Vigoureux, *Chem. Ber.*, **91**, 2205 (1958).
3) R. Tsumura and N. Hagihara, presented at the 17th Annual Meeting of the Chemical Society of Japan, Tokyo, April, 1964; This Bulletin, to be published.
4) M. A. Bennet, *Chem. Revs.*, **62**, 611 (1962).

mol. wt. (cryoscopic in benzene), 314. Calcd. for $C_{16}H_{16}O_4V$: C, 59.45; H, 4.99%; mol. wt., 323).

The elemental analysis and molecular weight determination indicated a mononuclear vanadium complex with the composition: $(C_5H_5)_2VC_2(CO_2CH_3)_2$. The complex III is paramagnetic, and its electron paramagnetic resonance spectrum showed a *g*-factor of 1.9976 and a hyperfine splitting of 44.0 gauss. The treatment of III with chlorine in carbon tetrachloride gave the original acetylene II and dicyclopentadienyl-vanadium dichloride in 37 and 68% yields respectively. The reduction of III with a large excess of lithium aluminum hydride gave the starting complex I in a 6% yield. These facts suggest that, in the acetylene complex III, both of the $\pi$-cyclopentadienyl rings are left coordinated to vanadium, to which also the acetylene II itself is bonded.

The infrared spectrum of III showed a strong absorption at 1821 $cm^{-1}$; this is probably to be assigned to a carbon-carbon stretching vibration of a multiple bond of the acetylene. This absorption is shifted toward a lower frequency by the coordination of II to vanadium in a cis-type and is increased in intensity through conjugation with two adjacent keto-carbonyls of the esters groups. It may thus reasonably be concluded, in comparison with a proposed structure of the above-mentioned complex $\pi$-$C_5H_5(HC_2H)V(CO)_2$, that the new acetylene complex III has the structure represented in Fig. 1 (III), in which the acetylene is bonded via two $\sigma$-bondings to vanadium, simultaneously having two $\pi$-cyclopentadienyl rings.




(III) (IV)

Fig. 1. Acetylene complexes of dicyclopentadienyl-vanadium.

A similar reaction of I with perfluoro-2-butyne also gave air-sensitive, brown crystals of the corresponding acetylene complex (IV); m. p., 124—126°C (decomp.) (from *n*-hexane and toluene); yield; 87.0% (Found: C, 48.89; H, 3.07; mol. wt. (cryoscopic in benzene), 332. Calcd. for $C_{14}H_{10}F_6V$: C, 49.00; H, 2.94%; mol. wt., 343). The complex IV gave a paramagnetic resonance spectrum with a *g*-factor of 1.9971 and a hyperfine splitting of 46.0 gauss. The infrared spectrum of IV showed a strong absorption near 1800 $cm^{-1}$. This absorption may reasonably be assigned to the stretching vibration of the acetylenic bond, this assignment is consistent with its assignment in the case of the complex III. These facts suggest that the acetylene complex IV also possesses a structure similar to that of III, as is shown in Fig. 1 (IV).

The acetylene complexes III and IV are therefore presumed to reveal a model structure of an initial intermediate in the catalytic polymerization of acetylenes with I.

*The Institute of Scientific and Industrial Research*
*Osaka University*
*Sakai, Osaka*

# Combination of Sulfuric Acid with Cellulose during the Hydrolysis with a Small Amount of Concentrated Sulfuric Acid

By Yoshio SAKAI

(Received August 1, 1963)

In the usual process of wood saccharification with concentrated sulfuric acid, the first stage of the process involves removal of hemicellulose from wood by mild hydrolysis and is called prehydrolysis. Cellulose in the residue of the first process is dissolved and hydrolyzed to a soluble glucose polymer[1] with concentrated sulfuric acid in the second process called mainhydrolysis. Finally, the polymer is hydrolyzed to glucose by dilute acid hydrolysis called posthydrolysis. In the mainhydrolysis a large amount of sulfuric acid is consumed.[2-5] This is a disadvantage of the concentrated sulfuric acid process, although the process has advantages such as large hydrolysis rate[6] and little erosion problem[7].

In order to determine the minimum quantity of sulfuric acid required in the mainhydrolysis, a diagram of the equilibrium relations of the system, soluble glucose polymer - sulfuric acid - water, has been obtained.[8] The dissolving power of sulfuric acid was not so large; for example, 100 parts of 72% sulfuric acid could dissolve and hydrolyze only 49 parts of cellulose to form the soluble glucose polymer, and 100 parts of 84% sulfuric acid was required for 82 parts of cellulose. The formation of a sulfuric acid - cellulose compound was observed in the course of hydrolysis and this compound seemed to play some chemical role in dissolving and hydrolyzing the cellulose, the extent of the combination of sulfuric acid with cellulose being an important factor in determining the yield of the soluble glucose polymer. In order to confirm this point the present work was undertaken. It was also expected to find out the reason why such large amounts of sulfuric acid are consumed during the hydrolysis.

## Material and Method

The experiments were carried out in a manner similar to that in the previous work, using the same material.[8]

Filter paper (Tôyô Roshi, No. 2), after being grated, was used as the cellulose sample. The cellulose flakes dried at 105°C (ca. 5 g.) were immersed in dilute sulfuric acid (20—50% concentration), and then filtered; the content of cellulose and sulfuric acid in the wet material was then calculated. The wet sample (ca. 1 g.) thus obtained was freeze-dried in a test tube for a few hours, until the weight loss reached the desired amount, and the test tube was then sealed under vacuum at low temperature. The weight of cellulose and sulfuric acid was calculated.

The sealed tube was heated in a water bath at 50°C for different periods of time. The tube was immediately cooled, the contents rinsed out with water, and centrifuged, and the insoluble sediment washed with water slightly acidified with hydrochloric acid; the centrifuging and the washing were repeated four times. The combined solution thus obtained was made up to 100 ml. with the requisite amount of hydrochloric acid to give a 2.5% hydrochloric acid concentration (solution I). A portion of solution I was heated at 100°C for 3 hr. to complete the hydrolysis of the soluble glucose polymer.[1]

Reducing sugar in solution I and in hydrolyzed solution I was determined by Somogyi's method.[9] From the amount of reducing sugar in hydrolyzed solution I, the weight of the soluble glucose polymer (as potential reducing sugar) dissolved in concentrated sulfuric acid was estimated. The value obtained by dividing the reducing power of hydrolyzed solution I by that of unhydrolyzed solution I was used as the average degree of polymerization of the soluble glucose polymer. Not only cellulose but also glucose polymer, both soluble and insoluble, are referred to as potential reducing sugars throughout this report.

Four determinations of sulfuric acid were carried out. (1) Sulfate ion in solution I; eqiuvalent to the amount of free sulfuric acid present in the concentrated sulfuric acid saturated with the soluble glucose polymer. (2) Sulfuric acid in the sediment decomposed by nitric acid; sulfuric acid combined with the insoluble glucose polymer.

1) T. Kobayashi and Y. Sakai, *Bull. Agr. Chem. Soc. Japan*, **22**, 117, 277 (1958).
2) J. W. Dunning and E. C. Lathrop, *Ind. Eng. Chem.*, **37**, 24 (1954); Bureau of Mines Report of Investigations 4772, United States Department of Interior, Feb., 1951.
3) T. Kuzuoka, *Mokuzai Tôka Shingikai Hôkoku* (*Report of the Wood Saccharification Discussion Committee*), **No. 2**, 1 (1953).
4) T. Kobayashi and T. Ito, ibid., **No. 4**, 5 (1954).
5) T. Kobayashi, Y. Sakai, K. Mitachi and K. Tsuyuzaki, *Ringyô Shidôsho Kenkyû Hôkoku* (*Report of the Hokkaido Forest Products Research Institute*), **No. 15**, 138 (1959).
6) T. Kobayashi, *Mokuzai Tôka Shingikai Hôkoku* (*Report of the Wood Saccharification Discussion Committee*), **No. 1**, 27 (1952).
7) T. Kuzuoka, *Bôshoku Gijutsu*, **4**, 79, 82 (1955).
8) T. Kobayashi, Y. Sakai and K. Iizuka, *Bull. Agr. Chem. Soc. Japan*, **24**, 443 (1960).
9) M. Somogyi, *J. Biol. Chem.*, **160**, 61 (1945).

(3) Sulfuric acid in solution I after the destruction of organic matter; total sulfuric acid (free acid plus combined acid) in the soluble glucose polymer - sulfuric acid - water system. (4) Sulfuric acid in solution I which had been hydrolyzed in 2.5% hydrochloric acid at 100°C for 3 hr.; values agree with those of (3) (Table I, t-test[10]). The amount of sulfuric acid obtained by (3) or (4) plus sulfuric acid by (2) agreed with the amount of sulfuric acid found by weighing the cellulose - sulfuric acid mixture, although they showed some fluctuations, as shown in Table I (t-test[10]). That the combined sulfuric acid is present as ester sulfate is shown from these results.

The sulfuric acid determinations were carried out by Morgulis and Hemphill's iodometric micro method.[11] Combined sulfuric acid was determined according to Hoffpauir and Guthrie's method[12] involving decomposition of the organic material with nitric acid to which a small amount of perchloric acid had been added.

## Results

The cellulose-concentrated sulfuric acid mixtures prepared by the freeze-drying process described above were heated at 50°C for different periods. Hydrolysis of the cellulose was accompanied by the formation of a cellulose - sulfuric acid compound. When the extent of hydrolysis of cellulose vs. time curve reached a plateau, the extent of sulfuric acid combination vs. time curve also leveled off. An example of the results is shown in Fig. 1. Soluble glucose polymer (SGP), sulfuric acid combined and average degree of polymerization of SGP in the equilibrium state were obtained from the straight lines in the figure. Table II lists the results of the reaction in different sulfuric acid concentrations. A higher extent of sulfuric acid combination was observed with higher concentrations of sulfuric acid. During the hydrolysis and the combination of sulfuric acid, water must have been consumed or formed. Therefore, the sulfuric acid concentration shown here is the initial one.

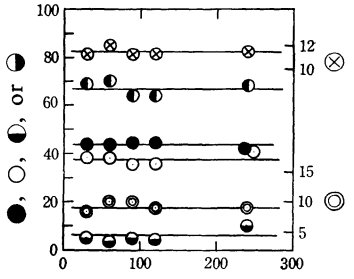



Fig. 1. Sulfuric acid combination during hydrolysis of cellulose in 89% sulfuric acid ($H_2SO_4$/Cellulose=0.5/1.0) at 50°C.
- ● SGP, g./100 g. Cellulose
- ○ Combined $H_2SO_4$, g./100 g. Total $H_2SO_4$
- ⊗ $H_2SO_4$ combined with SGP, g./g. $H_2SO_4$ combined with IGP
- ◐ Combined $H_2SO_4$, mol./100 mol. GU of SGP
- ◒ Combined $H_2SO_4$, mol./100 mol. GU of IGP
- ◎ Av. D. P. of SGP

**Boundary between Concentrated and Dilute Sulfuric Acid in Cellulose Hydrolysis.** — Table III shows that when cellulose was hydrolyzed in 60 or 57% sulfuric acid, no sulfuric acid combines with the soluble glucose polymer and monomer, and only a slight amount is combined with the insoluble glucose polymer. On the other hand, when the concentration was 65% or higher, a significant amount of sulfuric acid combined with the soluble and the insoluble glucose polymers (Table II). Although the hydrolysis product of cellulose in 57% sulfuric acid consisted chiefly of glucose monomer (Table III, Fig. 5), the product in sulfuric acid of 60% or higher concentration had a significantly higher degree of polymerization (Table II). The action of sulfuric acid at about 60% or higher concentrations appears to be different from that at lower concentrations. This is supported by another experiment

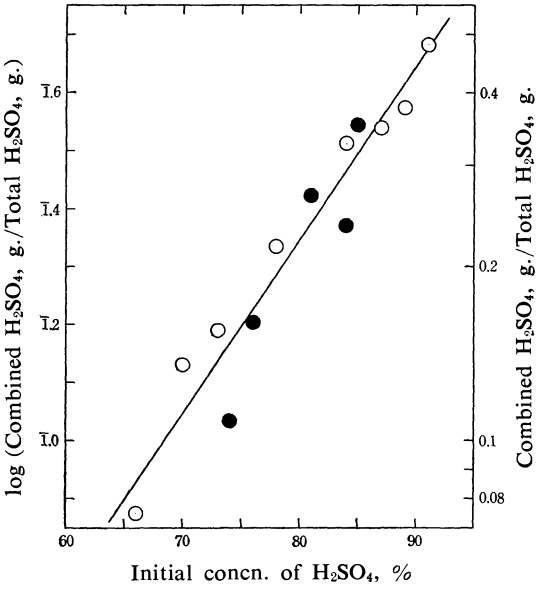



Fig. 2. Relation of the extent of sulfuric acid combination to sulfuric acid concentration in the hydrolysis of cellulose.
$H_2SO_4$/Cellulose: ● 1.0, ○ 0.5

10) O. L. Davies, "Statistical Methods in Research and Production with Special Reference to the Chemical Industry," 2nd ed., London, Oliver and Boyd (1949), p. 51.
11) S. Morgulis and M. Hemphill, *J. Biol. Chem.*, **96**, 573 (1932).
12) C. L. Hoffpauir and J. G. Guthrie, *Ind. Eng. Chem., Anal. Ed.*, **16**, 391 (1944).

Table I. Determination of sulfuric acid

| Initial concn. of $H_2SO_4$ % | $H_2SO_4$ added to 100 mg. of cellulose mg. | $H_2SO_4$ in sol. part: Free $H_2SO_4$ by detn. (1) mg./100 mg. of $H_2SO_4$ added | $H_2SO_4$ in sol. part: Total $H_2SO_4$ by detn. (3) mg./100 mg. of $H_2SO_4$ added | Total $H_2SO_4$ by detn. (4) mg./100 mg. of $H_2SO_4$ added | $H_2SO_4$ in insol. part by detn. (2) mg./100 mg. of $H_2SO_4$ added | $H_2SO_4$ recovery: (3)+(2) mg./100 mg. of $H_2SO_4$ added | $H_2SO_4$ recovery: (4)+(2) mg./100 mg. of $H_2SO_4$ added |
|---|---|---|---|---|---|---|---|
| 56 | 94 | 101 | 101 | 97 | 1 | 102 | 98 |
| 61 | 104 | 95 | 104 | 96 | 1 | 105 | 97 |
| 69 | 51 | 90 | 93 | 93 | 2 | 95 | 95 |
| 74 | 97 | 90 | 95 | 94 | 2 | 97 | 96 |
| 75 | 95 | 83 | 101 | 99 | 1 | 102 | 100 |
| 76 | 95 | 90 | 100 | 103 | 0.3 | 100 | 103 |
| 79 | 48 | 83 | 89 | 94 | 3 | 92 | 97 |
| 85 | 55 | 67 | 103 | 96 | 7 | 110 | 103 |
| 86 | 97 | 70 | 102 | 100 | 0.3 | 102 | 103 |
| 87 | 45 | 67 | 98 | 88 | 6 | 104 | 94 |
| 88 | 49 | 62 | 102 | 98 | 3 | 105 | 101 |
| 90 | 45 | 49 | 93 | 99 | 3 | 96 | 102 |

Table II. Sulfuric acid combination in equilibrium state during hydrolysis of cellulose in sulfuric acid of different concentration at 50°C

| $H_2SO_4$/Cellulose | $H_2SO_4$ concn. | $H_2SO_4$ combined/$H_2SO_4$ total | $H_2SO_4$ combined with SGP/$H_2SO_4$ combined with IGP | $H_2SO_4$ combined/GU of SGP | Av. D P. of SGP |
|---|---|---|---|---|---|
| g./g. | % | g./100 g. | g./g. | M/100 M | |
| 0.5 | 65 | — | — | — | 3.02 |
| | 66 | 7.50 | 4.31 | 20.5 | — |
| | 70 | 13.5 | 3.18 | 29.1 | — |
| | 71 | — | — | — | 5.02 |
| | 73 | 15.5 | 3.65 | 30.0 | 5.02 |
| | 78 | 21.5 | 6.94 | 47.0 | 6.02 |
| | 84 | 32.6 | 5.30 | 55.0 | — |
| | 87 | 34.5 | — | 57.0 | 20.9 |
| | 89 | 37.5 | 11.3 | 67.0 | 8.9* |
| | 91 | 48.4 | 17.2 | 95.2 | 25.1 |
| 1.0 | 54 | — | — | — | 1.10 |
| | 60 | — | — | — | 1.59 |
| | 61 | — | — | — | 1.82 |
| | 74 | 10.8 | 34.7 | — | — |
| | 76 | 16.0 | 26.3 | 28.0 | 6.02 |
| | 81 | 26.5 | — | 47.5 | 8.91 |
| | 84 | 23.5 | 81.0 | — | 15.1 |
| | 85 | 35.0 | 86.4 | 62.0 | 10.0 |

* Fig. 1.

which indicated that the hydrolysis rate constant of pentosan in 60% sulfuric acid deviates from the relationship between rate constant and acid concentration obtained in 50% and lower concentrations.[13]

**Effect of Sulfuric Acid Concentration on the Ratio of Combined Sulfuric Acid to Total Sulfuric Acid.** — When an equilibrium was established in hydrolysis of the cellulose with sulfuric acid of 66% or higher concentration, as shown in Fig. 1 (89% sulfuric acid), the ratio of the combined sulfuric acid to the total sulfuric acid showed a definite value. When the ratios (Table II) are plotted against the "initial" concentration of sulfuric acid, Fig. 2 is obtained. The following empirical equation is obtained from Fig. 2,

$$\log x = -3.047 + 0.0299\,C$$

or

$$x = 0.000897 \times \exp(0.0689\,C) \qquad (1)$$

13) T. Kobayashi, Y. Sakai and S. Mutoh, *Agr. Biol. Chem.*, **26**, 378 (1962).

TABLE III. COMBINATION OF SULFURIC ACID WITH CELLULOSE DURING HYDROLYSIS IN 60°C AND 57% SULFURIC ACID ($H_2SO_4$ : Cellulose=1.0)

| Initial concn. of $H_2SO_4$ | $H_2SO_4$ added to cellulose | $H_2SO_4$ in sol. part | | $H_2SO_4$ in insol. part | | Av. D. P. of sol. glucose polymer | Hydrolysis time at 50°C |
|---|---|---|---|---|---|---|---|
| | | Free $H_2SO_4$ | Combined $H_2SO_4$ | Combined $H_2SO_4$ | Combined $H_2SO_4$ per one glucose unit | | |
| % | mg. | mg. | mg. | mg. | mol./mol. | | hr. |
| 60 | 334 | 333 | 0 | 4 | 0.024 | 1.5 | 18 |
| | 331 | 326 | 2 | 4 | 0.024 | 1.4 | 48 |
| | 332 | 331 | −1 | 4 | 0.024 | 1.8 | 48 |
| 57 | 334 | 332 | −2 | — | — | 1.0 | 63 |
| | 333 | 336 | 7 | 5 | 0.030 | 1.3 | 89 |
| | 360 | 353 | 2 | — | — | 0.9 | 96 |

where $C$ is "initial" concentration of sulfuric acid (%) and $x$, the ratio of combined sulfuric acid to total sulfuric acid. This equation indicates, for example, that when 100 g. of cellulose is hydrolyzed at 50°C in 72% sulfuric acid containing 50 g. of sulfuric acid, $50\times0.128=6.4$ g. of sulfuric acid reacts to form the cellulose - sulfuric acid compound.

**Ratio of Sulfuric Acid Combined with Soluble Glucose Polymer to Sulfuric Acid Combined with Insoluble Glucose Polymer.** — A part of the combined sulfuric acid is in combination with the soluble glucose polymer (SGP) and the other part with the insoluble glucose polymer (IGP). As shown in Fig. 1, the ratio of sulfuric acid combined with the SGP to that combined with the IGP is constant when the hydrolysis of cellulose is at equilibrium. This ratio (Table II) is shown in Fig. 3 against the "initial" concentration of sulfuric acid. The following empirical equation is obtained from the figure.

$$\log y = 0.0354\,C + 1.76\,r - 2.88$$

or
$$y = 0.00132 \exp(0.0815\,C + 4.06\,r) \qquad (2)$$

where $r$ is sulfuric acid : cellulose ratio and $y$, the ratio of sulfuric acid combined with SGP to that with IGP. This equation indicates, for example, that in the hydrolysis of cellulose in 72% sulfuric acid at 50°C, a proportion of $3.5/(3.5+1)$ to one of the combined sulfuric acid is in combination with SGP. So,

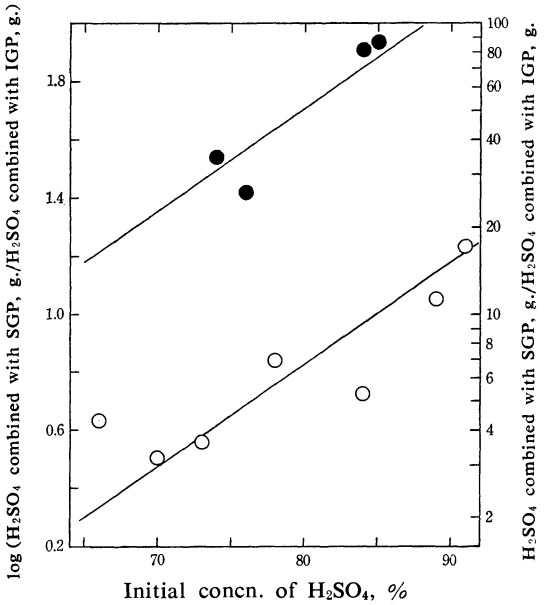



Fig. 3. Ratio of sulfuric acid combined with soluble glucose polymer to sulfuric acid combined with insoluble glucose polymer in different concentration of sulfuric acid.
$H_2SO_4$/Cellulose : ● 1.0, ○ 0.5

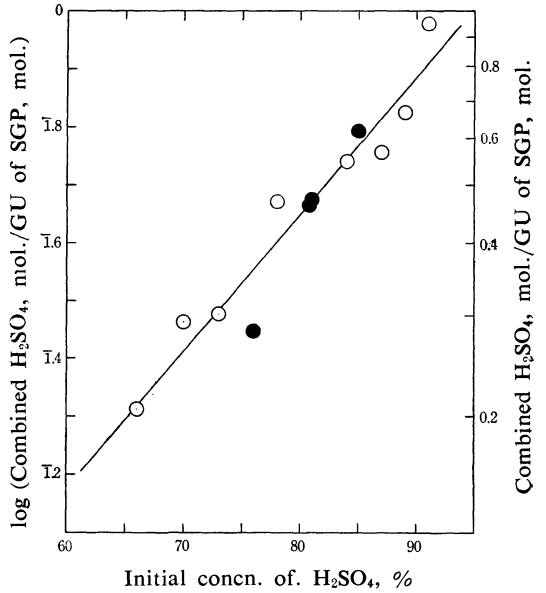



Fig. 4. Ratio of molecules of sulfuric acid combined with soluble glucose polymer (SGP) to glucose units (GU) of soluble glucose polymer.
$H_2SO_4$/Cellulose : ● 1.0, ○ 0.5

when 100 g. of cellulose is hydrolyzed at 55°C in 72% sulfuric acid containing 50 g. of sulfuric acid, $50\times0.128\times3.5/4.5=5.0$ g. of sulfuric acid is in combination with the SGP and $50\times0.128\times1/4.5=1.4$ g. is in combination with IGP.

**Combined Sulfuric Acid Molecules per Glucose Unit of Soluble Glucose Polymer.** — The number of sulfuric acid molecules fixed to one glucose unit (GU) of SGP showed a definite value when the hydrolysis of cellulose was at equilibrium, as shown in Fig. 1. This value depends on the "initial" concentration of sulfuric acid (Table II), as shown in Fig. 4. The following empirical equation is obtained from Fig. 4.

$$\log z = -2.247 + 0.0237C$$
$$z = 0.00566\exp(0.0546C) \qquad (3)$$

where $z$ is the number of sulfuric acid molecules fixed to one GU of the SGP. The equation indicates, for example, that when 100 g. of cellulose is hydrolyzed at 50°C in 72% sulfuric acid containing 50 g. of sulfuric acid, 0.288 mol. of sulfuric acid is fixed to 1 mol. of GU of the SGP. Then, $50\times0.128\times(3.5/4.5)\times(180/98)\times(1/0.288)=32$ g. of cellulose is converted into the SGP.

**Average Degree of Polymerization of Soluble Glucose Polymer.**—When the conversion of cellulose to the SGP reached an equilibrium, the average degree of polymerization (av. D. P.) of the SGP showed a definite value (Fig. 1). Figure 5, a plot of logarithm of av. D. P. of the SGP (Table II) against the "initial" concentration of sulfuric acid, shows a straight line.

$$\log u = -2.218 + 0.0396C$$
$$u = 0.00605\exp(0.0911C) \qquad (4)$$

where $u$ is av. D. P. of the SGP. In a ratio of sulfuric acid to cellulose ranging from 0.5 : 1 to 1.0 : 1, sulfuric acid of higher concentrations yields SGP of larger D. P., for example, 65% sulfuric acid gives SGP having av. D. P. 2.2 and 85% sulfuric acid 13.

**Concentration of Aqueous Sulfuric Acid in the Cellulose - Sulfuric Acid - Water System.** — On the assumption that water is consumed or formed during the hydrolysis according to the following equations,

$$C_6H_{10}O_5 + H_2SO_4 \rightarrow C_6H_9O_5SO_3H + H_2O$$
$$C_6H_{10}O_5 + H_2O \rightarrow C_6H_{12}O_6$$

the "corrected" concentration of sulfuric acid in the cellulose - sulfuric acid mixture was calculated by use of Eqs. 3 and 4. Figure 6 shows this value against the "initial" concentration of sulfuric acid. The "corrected" sulfuric acid concentration in the cellulose-sulfuric acid-water system can not exceed 75%, even when the initial concentration exceeds 85%.

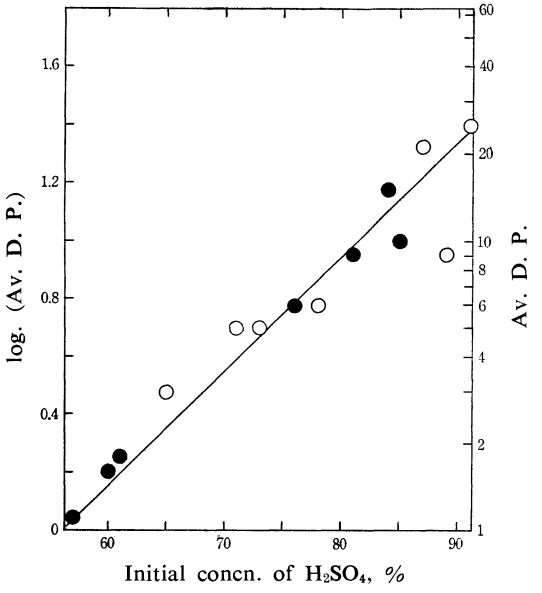



Fig. 5. Relation of average degree of polymerization of soluble glucose polymer to sulfuric acid concentration.
$H_2SO_4$/Cellulose: ● 1.0, ○ 0.5

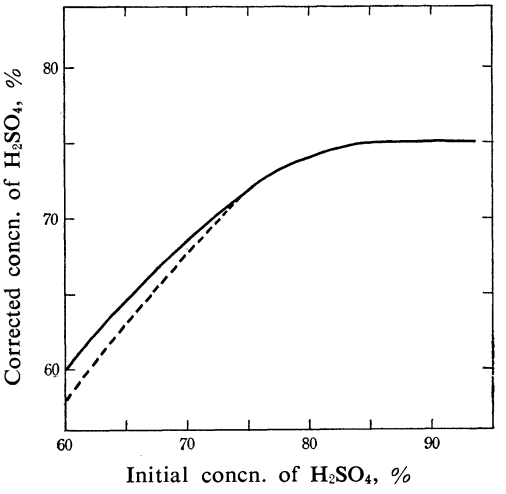



Fig. 6. Corrected concentration of sulfuric acid in cellulose - conc. sulfuric acid system.
$H_2SO_4$/Cellulose: —— 1.0, - - - 0.5

**Yield of Soluble Glucose Polymer and the "Initial" Concentration of Sulfuric Acid and the Sulfuric Acid : Cellulose Ratio.** — The amount of SGP (g.) produced when 100 g. of sulfuric acid is used is:

$$\text{SGP(g.)} = 100\text{(g.)}\left(\frac{\text{combined } H_2SO_4 \text{ (g.)}}{\text{total } H_2SO_4 \text{ (g.)}}\right)$$

$$\times\left(\frac{\text{H}_2\text{SO}_4 \text{ combined with SGP (g.)}}{\text{combined H}_2\text{SO}_4 \text{ (g.)}}\right)$$

$$\times\left(\frac{\text{GU of SGP (mol.)}}{\text{H}_2\text{SO}_4 \text{ combined with SGP (mol.)}}\right)$$

$$\times\left(\frac{180\text{(g./mol.)}}{98\text{(g./mol.)}}\right)$$

$$=100\text{(g.)}\,(x)\left(\frac{y}{1+y}\right)\left(\frac{1}{z}\right)\left(\frac{180}{98}\right)$$

$$=\frac{0.0384 \times \exp(0.0958\,C + 4.06\,r)}{1 + 0.00132 \times \exp(0.0815\,C + 4.06\,r)} \quad (5)$$

The yield of the SGP produced from cellulose in sulfuric acid of various "initial" concentration is shown in Fig. 7 as a function of the sulfuric acid : cellulose ratio.

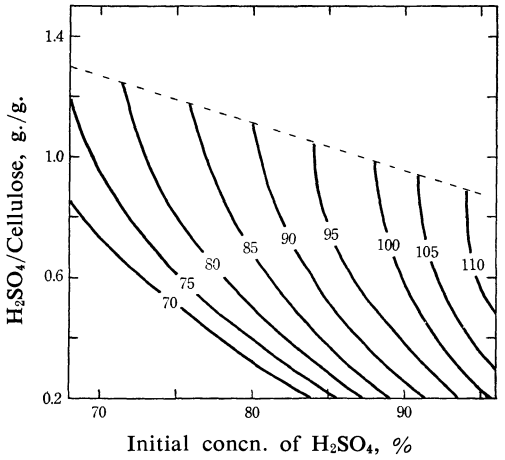



Fig. 7. Soluble glucose polymer yield expressed as a function of sulfuric acid concentration and $H_2SO_4$ : cellulose ratio.

## Discussion

In Table IV the data obtained from some pilot plant tests are compared with the values calculated from Eq. 5. This table shows that, in the ordinary concentrated sulfuric acid process, the reaction did not reach completion. It is considered that this can be attributed to the fact that diffusion of acid into the wood did not reach completion. Kuzuoka[3] has reported that when the mixture of saw dust and concentrated sulfuric acid was treated through the rolls, the larger the number of treatments the higher the yield of reducing sugar (Table IV). On the other hand, in Odincov's experiments,[14] the reducing sugar yield greatly exceeded the equilibrium value calculated from Eq. 5. This suggests that a mechanical force is effective in accelerating the diffusion of sulfuric acid into the wood and the hydrolysis of cellulose.

14) P. N. Odincov, I. I. Beinart and N. F. Murashchenko, *Gidroliz. i Lesokhim. Prom.*, No. 6, 6 (1960).

## Summary

The combination of sulfuric acid with cellulose occurring during the hydrolysis of cellulose in a small amount of concentrated sulfuric acid has been investigated. The amounts of the soluble and the insoluble glucose polymers produced from cellulose, and the amount of sulfuric acid combined with them, have been estimated. To obtain an effective concentration of sulfuric acid on the cellulose, the concentration of the sulfuric acid must be greater than about 60%. The sulfuric acid concentration in the cellulose - sulfuric acid - water system can not exceed 75%, even when the initial concentration exceeds 85%. The amount of soluble glucose polymer (g.) produced by the action of 100 g. of sulfuric acid is given by $0.0384\ \exp(0.0958\,C+4.06\,r)/[1+0.00132\ \exp(0.0815\,C+4.06\,r)]$ ($C$ is "initial" concentration of sulfuric acid (%) and $r$, sulfuric acid - cellulose ratio).

TABLE IV. COMPARISON OF DIFFERENT PROCESSES OF WOOD SACCHARIFICATION WITH CONCENTRATED SULFURIC ACID

$\frac{\text{SGP yield per 100 g. of } H_2SO_4}{\text{Calcd. SGP yield per 100 g. of } H_2SO_4}$, %

| $H_2SO_4$/Cellulose | 0.1 | 0.3 | 0.5 | 1.0 | 1.2 |
|---|---|---|---|---|---|
| Concn. of $H_2SO_4$, % | 75 | 75 | 80 | 80 | 80 |
| Mixing in extruder (Dunning[2]) | | | 97 | 63 | |
| Mixing in extruder (Kobayashi[5]) | | | 91 | 70 | |
| Pressing through rolls (Kuzuoka[3]) | (1 treatment) | | | 87 | 88 |
| | (3 treatments) | | | 97 | 93 |
| Vibration milling (Odincov[14]) | 458 | 144 | (15 min. treatment) | | |
| | 336 | 123 | (120 min. treatment) | | |
| Calcd.* | 40 | 57 | 80 | 90 | 90 |

* Calculated from experimental Eq. 5.

The author thanks Professor Tatsuyoshi Kobayashi for his interest and encouragement and also Mr. Takumichi Kono and Miss Wasako Kumagai for their assistance.

*Faculty of Agriculture*
*Tokyo University of Education*
*Komaba-machi, Meguro-ku, Tokyo*

# Absorption of Carbon Dioxide in a Centrifugal Absorber by Mono- and Diethanolamine Solutions[1]

By Mamoru MATSUDA and Yoshio FUJIOKA

(Received October 21, 1963)

The carbon dioxide concentration in a closed circuit increases upon the respiration of the inhabitants. The rate of carbon dioxide generated by an adult is almost 0.95 mol. per hour, that is, about 25 l. at 30°C under atmospheric pressure.[2]

The effects of the continuous exposure of carbon dioxide on humans have been much investigated. The results may be summarized by saying that the activities of people are considerably reduced when more than three percent of carbon dioxide is present.[3] It is, therefore, indispensable to install a carbon dioxide removal plant and an oxygen generator in a closed circuit when the duration of stay is long.

Solutions of ethanolamines and potassium carbonate are used as regenerative carbon dioxide absorbents, since they absorb carbon dioxide at room temperature and expel the carbon dioxide at a high temperature of about 140°C.[4]

We have constructed new centrifugal absorbers for the removal of carbon dioxide in a closed circuit, using regenerative ethanolamine liquids as absorbents.

The present paper will report on the effects of such variable conditions as the gas flow rate, the liquid flow rate, the composition of the liquid, rotor revolutions per minute, and rotor design on the mass transfer coefficients of the absorbers.

## Experimental

**Apparatus and Procedure.** — On the carbon dioxide absorber, it is advisable to increase the frequency of contacts between carbon dioxide and the liquid. Therefore, a centrifugal-type absorber, which has a large liquid surface,[5] was used with some modifications.

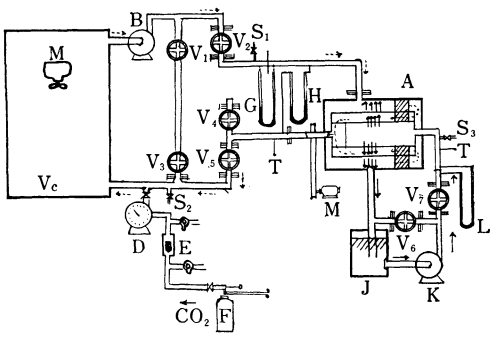



Fig. 1. Experimental arrangement of apparatus.

Figure 1 shows the arrangement of the experimental apparatus. A closed chamber Vc, has a volume of about 3.8 m³. A motor M rotates a perforated rotor of a centrifugal absorber A. The rotating rotor tangentially sprays absorbing liquid, which is introduced by a pump K from a tank J. The liquid flow is controlled by a flowmeter L, and valves, $V_6$ and $V_7$. When the carbon dioxide concentration of the closed chamber becomes 1.5 to 3.0%, the gas is introduced to the liquid-spraying space by a blower B. The gas flow rate and the carbon dioxide concentration are controlled by flowmeters D, E, G, and valves $V_1$, $V_2$, $V_3$, and $V_5$, A cylinder F feeds in carbon dioxide. The gas samples collected from the inlet $S_1$, and the outlet $S_2$ are analyzed for $CO_2$ by a $CO_2$ analyzer.

**The Determination of the Carbon Dioxide Content in a Liquid.**—Carbon dioxide in a liquid was determined according to the method of Reed and Wood,[6] which measures volumetrically the carbon dioxide evolved on the addition of sulfuric acid to the sample.

## Results and Discussion

**Part 1.**—There exist a number of variables which effect the over-all mass transfer coefficient, $K_Ga$, as defined by Eq. 1:

$$K_Ga=\frac{G_M}{VP}\int_{p_2}^{p_1}\frac{dp}{p-p^*} \qquad (1)$$

where

$G_M$ = average rate of gas flow (l./sec.)
$V$ = volume of absorbing space (l.)
$P$ = total pressure of gas flow (atm.)

1) A part of this report was presented at the Autumn Meeting of the Chemical Society of Japan, 1962.
2) R. G. Oliver and F. C. Riesenfeld, Closed Circuit Respiratory Systems Symposium, WADD Technical Report 60—574, 96 (1960).
3) Karl E. Shaefer, *Aerospace Medicine*, 32, 197 (1961).
4) A. L. Kohl and F. C. Riesenfeld, "Gas Purification," McGraw-Hill, N. Y. (1960), p. 8.
5) T. Takamatsu, T. Takahashi, S. Shiga and H. Shoji, *Chemical Engineering of Japan (Kagaku Kogaku)*, 22, 561 (1958).
6) R. M. Reed and W. R. Wood, *Trans. Am. Inst. Chem. Engrs.*, 37, 363 (1941).

TABLE I. CENTRIFUGAL CARBON DIOXIDE ABSORBER

| Type | Dia. of stator | Dia. of rotor | Cross sectional area of absorbing space | Length of absorbing space | Volume of absorbing space | Characteristics of openings | Number of cylinder |
|---|---|---|---|---|---|---|---|
| $D_e$ | $D_S$, cm. | $D_R$, cm. | $S_A$, cm$^2$ | cm. | $V$, l. | | |
| I | 18 | 10 | 176 | 7 | 1.232 | dia. 0.8 mm. $N_h$, 128 | 1 |
| II | 18 | 10 | 176 | 7.5 | 1.320 | dia. 0.8 mm. $N_h$, 960 | 1 |
| III | ca. 28 | $D_{R1}$ 18<br>$D_{R2}$ 10 | 1023.4 | 9.5 | 9.722 | dia. 0.8 mm. $N_h$, 3840 | 2 |
| IV | 55 | $D_{R1}$ 40<br>$D_{R2}$ 18 | 2110 | 30 | 63.300 | #1. Slit<br>#2. Screen<br>#3. Conical perforated plates | 2<br>Packed<br>Packed |
| V | 55 | $D_{R1}$ 43<br>$D_{R2}$ 33<br>$D_{R3}$ 23<br>$D_{R4}$ 10 | 2190 | 57 | 124.800 | perforated aluminum plate dia. 0.5 mm. $N_h$, 90/cm$^2$ plate | 4 |

$p$ = partial pressure of $CO_2$ in absorbing space (atm.)
$p_1$ = partial pressure of $CO_2$ in influent-gas flow (atm.)
$p_2$ = partial pressure of $CO_2$ in effluent-gas flow (atm.)
$p^*$ = partial pressure of $CO_2$ in equilibrium with an amine solution[7] (atm.)

For this report the effects of the following factors on the transfer coefficient were investigated:

Absorbent: monoethanolamine (MEA) and Diethanolamine (DEA) (A)
Solvent: water and glycerol (S)
Concentration of absorbent ($N$, mol./l.)
Concentration of carbon dioxide in the liquid ($M$, mol. $CO_2$/mol. amine)
Liquid flow rate ($L$, l./sec.)
Initial concentration of carbon dioxide in gas stream ($P_1$, atm.)
Revolution rate of rotor ($R_n$, r.p.m.)
Gas flow rate ($G$, l./sec.)
Number of openings of the rotor ($N_h$, —)
Type of rotor ($D_e$, —)

Table I shows the dimensions of the rotors. Tables II and III show the experimental conditions and results.

*The Effect of Revolution.* — The relation between the number of revolutions per minute of a rotor and the transfer coefficients, $K_Ga$, calculated according to Eq. 1, were studied in runs No. 1 to 6. The transfer coefficient dependence on the gas velocity is shown in Fig. 2.

The transfer coefficient, $K_Ga$, increases with the number of revolutions per minutes. When the number of revolutions is less than $1\times10^3$ r.p.m., the increase in gas velocity hardly changes the transfer coefficient, or even decreases it. The decrease may be explained as occuring because the gas stream goes unreacted through the absorbing space near the stator as a result of the insufficient density of liquid, as the revolution rate is small. When the number of revolutions is more than $1\times10^3$ r.p.m., the transfer coefficient rises with the gas velocity.

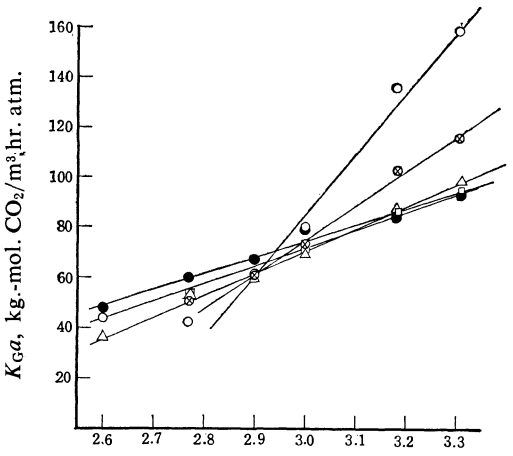



Fig. 2. Relation between coefficient and log $R_n$.
Gas velocity: ● 4.6, □ 7.0, △ 9.5, ⊗ 18.5, ○ 38.0 cm./sec.

*The Concentration of DEA.*—Run No. 10 was carried out under the same conditions as No. 7 except for the normality.

Comparing the transfer coefficients with the normality ($N$) and kinematic viscosity ($\mu$), we obtained:

$$K_Ga \propto \frac{N}{\mu^{0.5}} \qquad (2)$$

7) J. W. Mason and B. F. Dodge, ibid., 32, 27—48 (1936).

Table II. Operation variables and efficiency (Part 1)

| Run | A | S | $N$ mol./l. | $M$ mol. $CO_2$/mol. amine | $L$ l./sec. | Liquid temp. °C | $G$ l./sec. | $P_1$ atm.×100 | Rotor type | $R_n$ r.p.m. | $E$ ×100 | $K_Ga$ kg.-mol. $CO_2$/$m^3$ hr. atm. |
|---|---|---|---|---|---|---|---|---|---|---|---|---|
| 1 | D[a] | W[a] | 1.0 | 0.0 | (39—43)[b] | 20 | (4.6—38)[b] | 0.5 | I | 2000 | 62—16.0 | 94—159 |
| 2 | D | W | 1.0 | 0.0 | (39—43) | 20 | (4.6—38) | 0.5 | I | 1500 | 58—15.5 | 84—136 |
| 3 | D | W | 1.0 | 0.0 | (39—43) | 20 | (4.6—38) | 0.5 | I | 1000 | 54—9.4 | 79—79 |
| 4 | D | W | 1.0 | 0.0 | (39—43) | 20 | (4.6—38) | 0.5 | I | 800 | 50—7.4 | 68—62 |
| 5 | D | W | 1.0 | 0.0 | (39—43) | 20 | (4.6—38) | 0.5 | I | 600 | 46—5.1 | 60—43 |
| 6 | D | W | 1.0 | 0.0 | (39—43) | 20 | (4.6—38) | 0.5 | I | 400 | 39—7.2 | 48—45 |
| 7 | D | W | 1.52 | 0.1105 | 0.35 (73) | 20 | 1.86—4.10 (10.56—23.2) | 3.2—1.71 | II | 2000 | 43.9—25.6 | 122—137 |
| 8 | D | W | 1.25 | 0.0613 | 0.35 | 20 | 6.63—8.39 (37.7—47.7) | 1.375—3.20 | II | 2000 | 18.4—16.95 | 174—177.1 |
| 9 | D | W | 1.24 | 0.020 | 0.100 | 20 | 1.96—7.25 (11.13—41.2) | 1.5—3.5 | II | 2000 | 39.2—12.4 | 116—108 |
| 10 | D | W | 3.25 | 0.0477 | 0.350 | 20 | 2.04—47.34 (11.58—268.5) | 1.73—2.98 | II | 2000 | 56.0—4.5 | 190—214 |
| 11 | D | W | 3.5 | — | 0.550 | 20 | 8.0—30.4 (45.4—172.8) | 2.45—2.83 | II | 960 | 20.1—5.33 | 203—190 |
| 12 | D | W | 3.5 | 0.085 | 0.350 | 20 | 1.74—7.69 (9.89—43.7) | 1.79—2.505 | IIa | 960 | 44.7—18.55 | 117—179 |
| 13 | D | W | 3.5 | 0.094 | 0.350 | 20 | 1.43—8.25 (8.12—46.8) | 1.83—2.58 | IIb | 960 | 49.2—14.45 | 71—86 |
| 14 | D | W | 3.5 | 0.093 | 0.350 | 20 | 2.05—10.51 (11.42—60.2) | 2.05—2.50 | IIc | 960 | 45.2—22.25 | 91—128 |
| 15 | M[a] | W | 7.6 | 0.017 | 0.350 | 20 | 1.75—8.11 (9.93—46.1) | 2.025—2.54 | IId | 960 | 75.2—43.4 | 277—526 |
| 16 | M | W | 7.6 | 0.017 | 0.540 | 20 | 2.05—8.22 (11.65—46.6) | 2.03—2.59 | IId | 960 | 75.8—47.1 | 416—592 |
| 17 | M | W | 7.6 | 0.021 | 0.580 | 20 | 2.05—9.57 (11.63—54.3) | 2.19—2.605 | IIe | 960 | 79.1—48.8 | 363—724 |
| 182 | M | W | 9.80 | 0.00 | 0.200 | 35.0 | 7.18 | 2.80—0.0 | III | 800 | 75.0 | 134 |
| 183 | M | W | 8.36 | 0.00 | 0.212 | 31.5 | 7.20 | 2.98—0.0 | III | 800 | 69.2 | 116 |
| 184 | M | W | 6.24 | 0.00 | 0.200 | 28.4 | 7.15—7.30 | 3.00—0.0 | III | 800 | 60.5 | 92 |
| 185 | M | W | 4.30 | 0.00 | 0.200 | 28.2 | 7.15 | 3.02—0.0 | III | 800 | 55.0 | 79 |
| 186 | M | W | 0.45 | 0.00 | 0.200 | 30.5 | 7.15 | 2.30—0.0 | III | 800 | 35.2 | 64 |

TABLE II. (Continued)

| Run | A | S | $N$ mol./l. | $M$ mol. $CO_2$/mol. amine | $L$ l./sec. | Liquid temp. °C | $G$ l./sec. | $P_1$ atm.×100 | Rotor type | $R_n$ r.p.m. | $E$ ×100 | $K_Ga$ kg.-mol. $CO_2$/$m^3$, hr. atm. |
|---|---|---|---|---|---|---|---|---|---|---|---|---|
| 187 | M | W | 9.80 | 0.095 | 0.200 | 33.0 | 7.15 | 2.83—0.0 | III | 800 | 75.9 | 150 |
| 188 | M | W | 9.75 | 0.197 | 0.212 | 37.5 | 7.20 | 2.80—0.0 | III | 800 | 56.7 | 88 |
| 189 | M | W | 9.76 | 0.279 | 0.205 | 37.0 | 7.15 | 2.65—0.0 | III | 800 | 43.2 | 59 |
| 190 | M | W | 9.77 | 0.330 | 0.212 | 34.5 | 7.15 | 2.70—0.20 | III | 800 | 28.3 | 35 |
| 191 | M | W | 9.67 | 0.375 | 0.200 | 30.4 | 7.10 | 2.85—0.40 | III | 800 | 22.9 | 28 |
| 192 | M | W | 9.69 | 0.425 | 0.210 | 29.3 | 7.20 | 2.85—0.78 | III | 800 | 15.7 | 18 |

a) D=DEA, M=MEA, W=Water, G=Glycerol.
b) Data in parentheses are velocities of liquid or gas flow, cm./sec.
IIa: Type II absorber reduced the number of openings half by taping the opening lines radially arrounded the cylinder on every other line.
IIb: Type II absorber increased both the length of the cylinder to 11.5 cm. and the number of opening rows to 19.
IIc: Type IIb cylinder surrounded with an stainless steel 50-mesh screen.
IId: Type II cylinder surrounded with an 50-mesh screen.
IIe: Type II cylinder, modified with 32 small blades to scatter the sprayed liquid. Blade dimension was 0.8×7×130 mm.

TABLE III. OPERATION VARIABLES AND EFFICINCY (PART 2)

| Run | A | S | $N$ mol./l. | $M$ mol. $CO_2$/mol. amine | $L$ l./sec. | Liquid temp. °C | $G$ l./sec. | $P_1$ atm.×100 | Rotor type | $R_n$ r.p.m. | $E$ ×100 | $K_Ga$ kg.-mol. $CO_2$/$m^3$ hr. atm. |
|---|---|---|---|---|---|---|---|---|---|---|---|---|
| 1 | M[a] | W[a] | (4)[c] 3.72 | $2.19\times10^{-3}$ | (5)[c] 5 | 22.0 | (125)[c] 125 | (1.0)[c] 1.005 | IV3 | (500)[c] 510 | 24.0 | 80 |
| 2 | M | W | (7) 7.08 | $3.16\times10^{-3}$ | (5) 5 | 26.0 | (125) 118 | (2.0) 2.12 | IV3 | (500) 520 | 28.3 | 90 |
| 3 | M | W | (7) 7.07 | | (7) 7 | 23.0 | (90) 94.2 | (1.0) 0.955 | IV3 | (400) 400 | 43.5 | 125 |
| 4 | M | W | (10) 10.4 | $12.1\times10^{-3}$ | (3) 3 | 29.0 | (55) 55 | (1.0) 1.005 | IV3 | (500) 520 | 48.9 | 85 |
| 5 | M | W | (10) 10.4 | $14.5\times10^{-3}$ | (4) 5 | 27.0 | (35) 35.3 | (2.0) 1.98 | IV3 | (400) 400 | 65.1 | 86 |
| 6 | M | W | (13) 13.5 | $9.0\times10^{-3}$ | (3) 3 | 28.5 | (55) 55.8 | (2.8) 2.76 | IV3 | (500) 510 | 62.0 | 123 |

TABLE III. (Continued)

| Run | A | S | $N$ mol./l. | $M$ mol. $CO_2$/mol. amine | $L$ l./sec. | Liquid temp. °C | $G$ l./sec. | $P_1$ atm.×100 | Rotor type | $R_n$ r.p.m. | $E$ ×100 | $K_Ga$ kg.-mol. $CO_2$/$m^3$ hr. atm. |
|---|---|---|---|---|---|---|---|---|---|---|---|---|
| 7 | M | W | (13) 12.8 | $16.3\times10^{-3}$ | (5) 5 | 25.0 | (35) 33.7 | (1.0) 0.99 | IV3 | (400) 400 | 66.6 | 86 |
| 8 | M | W | (4) 4.26 | $6.08\times10^{-3}$ | (7) 7 | 25.0 | (90) 86.5 | (2.8) 2.893 | IV3 | (400) 400 | 45.1 | 119 |
| 9 | M | W | (4) 4.29 | $11.2\times10^{-3}$ | (3) 3 | 22.0 | (35) 34.3 | (1.0) 1.02 | IV1 | (400) 400 | 50.0 | 55 |
| 10 | M | W | (7) 7.30 | $9.0\times10^{-3}$ | (5) 5 | 29.0 | (55) 56 | (1.0) 1.005 | IV1 | (500) 500 | 67.0 | 140 |
| 11 | D[a] | W | (6) 6.05 | $1.62\times10^{-3}$ | (5) 5 | 27.0 | (125) 124 | (2.8) 2.82 | IV1 | (400) 400 | 7.45 | 22 |
| 12 | D | W | (4) 3.97 | $0.97\times10^{-3}$ | (7) 7 | 33.0 | (55) 54.3 | (2.0) 2.04 | IV1 | (400) 400 | 46.5 | 75 |
| 13 | D | W | (3) 3.42 | $0.775\times10^{-3}$ | (5) 5 | 27.0 | (35) 35.6 | (2.8) 2.76 | IV1 | (500) 500 | 44.6 | 48 |
| 14 | D | W | (5) 5.70 | $1.16\times10^{-3}$ | (3) 3 | 25.0 | (90) 90.1 | (2.0) 1.995 | IV1 | (500) 500 | 11.2 | 25 |
| 15 | M | G[a] | (13) 13.0 | 0.0 | (7) 7 | 33.0 | (125) 120.5 | (1.0) 1.035 | IV1 | (500) 510 | 74.6 | 351 |
| 16 | M | G | (10) 10.05 | $4.26\times10^{-3}$ | (5) 5 | 29.5 | (90) 90.8 | (1.0) 0.990 | IV1 | (400) 400 | 34.8 | 89 |
| 17 | M | W | (13) 12.7 | $15.5\times10^{-3}$ | (5) 5 | 24.5 | (90) 88.3 | (2.0) 2.04 | IV2 | (400) 400 | 55.2 | 165 |
| 18 | M | W | (10) 10.45 | $16.1\times10^{-3}$ | (7) 7 | 26.0 | (125) 122.5 | (2.8) 2.85 | IV2 | (500) 510 | 53.6 | 271 |
| 19 | D | W | (6) 6.75 | $7.15\times10^{-3}$ | (3) 5 | 25.0 | (90) 93.1 | (1.0) 0.966 | IV2 | (500) 500 | 19.3 | 46 |
| 20 | D | W | (4) 4.36 | $4.45\times10^{-3}$ | (5) 5 | 25.5 | (35) 34.3 | (1.0) 1.02 | IV2 | (500) 500 | 44.8 | 48 |
| 21 | D | W | (3) 3.54 | $4.06\times10^{-3}$ | (7) 7 | 24.5 | (55) 56.4 | (1.0) 0.975 | IV2 | (400) 400 | 38.5 | 64 |
| 22 | D | W | (5) 5.53 | $3.48\times10^{-3}$ | (5) 5 | 26.0 | (125) 126 | (1.0) 0.99 | IV2 | (400) 400 | 18.2 | 58 |
| 23 | M | G | (7) 6.92 | $2.5\times10^{-3}$ | (3) 3 | 26.0 | (35) 35.4 | (2.8) 2.775 | IV2 | (400) 410 | 31.9 | 31 |

TABLE III. (Continued)

| Run | A | S | $N$ mol./l. | $M$ mol. $CO_2$/mol. amine | $L$ l./sec. | Liquid temp. °C | $G$ l./sec. | $P_1$ atm.×100 | Rotor type | $R_n$ r.p.m. | $E$ ×100 | $K_Ga$ kg.-mol. $CO_2$/$m^3$ hr. atm. |
|---|---|---|---|---|---|---|---|---|---|---|---|---|
| 24 | M | G | (4) 4.65 | $4.75\times10^{-3}$ | (5) 5 | 29.0 | (55) 54.7 | (2.0) 2.010 | IV2 | (500) 510 | 15.65 | 21 |
| 25 | D | W | (3) 3.63 | $6.07\times10^{-3}$ | (3) 3 | 24.0 | (125) 121.4 | (2.0) 2.058 | IV3 | (400) 400 | 14.7 | 45 |
| 26 | D | W | (3) 3.60 | $8.71\times10^{-3}$ | (5) 5 | 24.5 | (90) 91.0 | (1.0) 0.99 | IV3 | (500) 510 | 20.0 | 47 |
| 27 | D | W | (4) 4.08 | $7.08\times10^{-3}$ | (5) 5 | 25.0 | (90) 88.6 | (2.8) 2.82 | IV3 | (500) 510 | 22.5 | 52 |
| 28 | D | W | (4) 4.36 | $10.7\times10^{-3}$ | (3) 3 | 25.0 | (125) 122.2 | (1.0) 1.02 | IV3 | (400) 420 | 26.2 | 86 |
| 29 | D | W | (6) 6.56 | $10.4\times10^{-3}$ | (5) 5 | 30.0 | (55) 54.5 | (1.0) 1.01 | IV2 | (400) 400 | 31.7 | 48 |
| 30 | D | W | (6) 6.52 | $14.3\times10^{-3}$ | (7) 7 | 28.0 | (35) 35.3 | (2.0) 1.986 | IV2 | (500) 510 | 51.4 | 77 |
| 31 | D | W | (5) 5.50 | $7.33\times10^{-3}$ | (7) 7 | 25.0 | (35) 35.9 | (1.0) 0.975 | IV2 | (500) 520 | 54.0 | 64 |
| 32 | D | W | (5) 5.52 | $8.60\times10^{-3}$ | (5) 5 | 26.0 | (55) 54.4 | (2.8) 2.82 | IV2 | (400) 400 | 28.0 | 43 |
| 200 | M | G | 12.65 | $7-280\times10^{-3}$ | 5 | | 125.0 | 2.80 | IV2 | 500 | | 218— |
| 501 | M | W | 9.65 | $39\times10^{-3}$ | 5 | 22.0 | 98 | 0.90—1.02 | V | 500 | 60 | 107 |
| 502 | M | W | 12.5 | $30\times10^{-3}$ | 5 | 24—30 | 98 | 1.03—1.10 | V | 500 | 70 | 139 |
| 503 | M | W | 5 | 0.0 | 5 | 22—25 | 98 | 1.0 | V | 510 | 47 | 74 |

a) D=DEA, M=MEA, W=Water, G=Glycerol
c) Data in parentheses are settled levels of factors.

*The Number of Openings.* — In run No. 7 a type II absorber was used, which had 960 openings, while type I had 128 while it had 960 in run No. 10 and 448 in No. 12.

Figure 3 compares the coefficients of No. 7 and No. 1, and No. 10 and No. 12. If the variation in $K_Ga$ with normality is taken into account, it may be concluded that the increase in the openings does not necessarily increase the transfer coefficient.

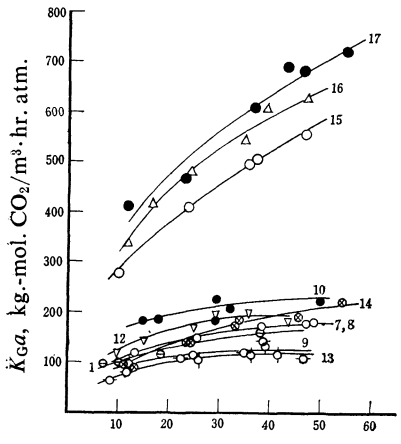



Fig. 3. Relation between gas velocity and coefficient.

*The Type of Rotor.*—Run No. 14 was taken in order to determine the increase in the centrifugal force on a liquid. When it is compared with No. 13 (Fig. 3), the favorable effect of the 50-mesh stainless screen can be observed.

In the runs Nos. 15, 16 and 17, MEA liquid was used. The liquid flow rate effected the transfer coefficient.

The small effect of the gas velocity on the coefficient, $K_Ga\sqrt{S_A/G}$, as shown in Fig. 4, indicates that the rate-determining step is substantially the diffusion of carbon dioxide in the gas stream.

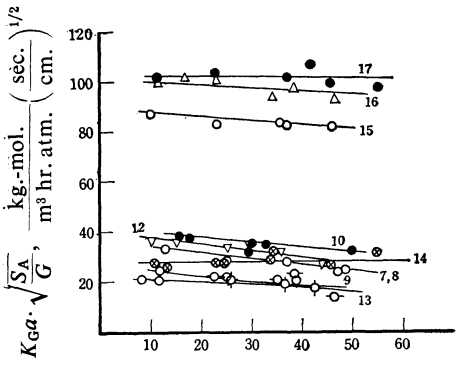



Fig. 4. Relation between $K_Ga\sqrt{S_A/G}$ and coefficient.

*Concentration of MEA.* — In runs No. 182 to No. 186, a closed chamber was used. Assuming that the efficiency, $E$, of the absorber remains constant and that the mixing in the chamber is perfect, the following differential equation can be derived by considering the mass valance in the system:

$$g_A dt - GEp dt = V_C dp \tag{3}$$

When $p=p_0$ at $t=0$, and $p=p_1$ at $t=t$, the solution of Eq. 3 is:

$$p_1 = p_0 \exp\left(-\frac{GE}{V_C}t\right) + \frac{g_A}{GE}\left\{1-\exp\left(-\frac{GE}{V_C}t\right)\right\} \tag{4}$$

$$E=(p_1-p_2)/p_1$$

where $p_0$ is the initial partial pressure (atm.) of carbon dioxide in the closed chamber; $p_1$ is the partial pressure (atm.) of carbon dioxide in the closed chamber at time $t$ (sec.); $p_2$ is the partial pressure of carbon dioxide at the outlet of the absorber; $V_C$ is the volume of the closed chamber (l.); $g_A$ is the rate at which carbon dioxide is added to the closed chamber (l./sec.), and $G$ is the rate of gas flow (l./sec.).

The concentrations of the MEA liquids applied were 9.8, 8.3, 6.2, 4.1 and 0.45 normal. The variation in the carbon dioxide concentration in the chamber with the time is given

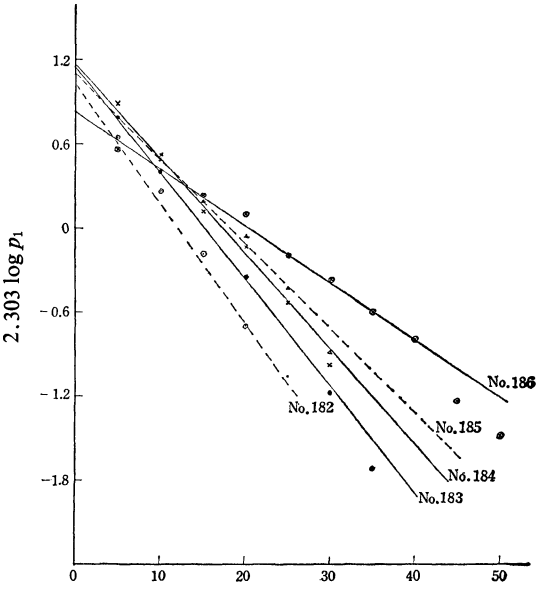



Fig. 5. Variation of $CO_2$ concentration with time in the closed chamber.

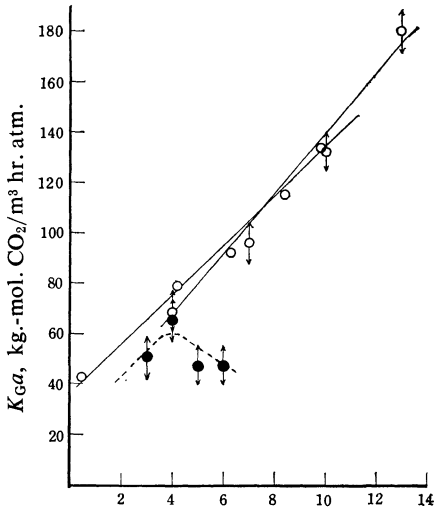



Fig. 6. Relation between liquid concentration and coefficient.
○ Nos. 182—186, MEA
○ Part 2, MEA ● Part 2, DEA

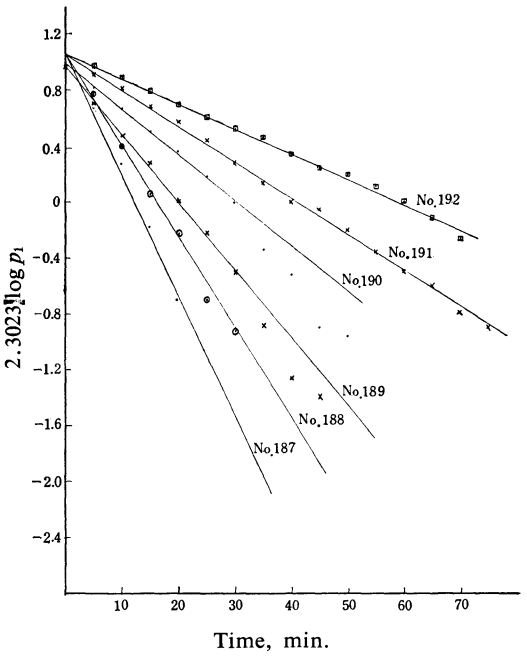



Fig. 7. Variation of $CO_2$ concentration with time in a closed chamber.

in Fig. 5. From Eq. 4, where $g_A$ is zero, the efficiencies of the absorber, $E$, and the transfer coefficients, $K_Ga$, were calculated.

Figure 6 shows that the transfer coefficient increases linearly with the concentration of the MEA solution.

Goodridge[8] described a similar relation between the absorption rate and the concentration.

From the lines of Fig. 5, the efficiency of the absorber can be seen to be independent of the concentration of carbon dioxide in the gas stream. The assumption for Eq. 3 was, therefore, sound.

*The Concentration of Carbon Dioxide in a Liquid.*—In runs No. 187 to No. 192, the closed chamber was used again. The concentrations of carbon dioxide in the liquid were 0.095, 0.197, 0.279, 0.330, 0.375 and 0.425 mol. $CO_2$/mol. MEA.

Figure 7 shows the relation of the carbon dioxide concentration in the chamber to the time. The efficiencies of the absorber and the transfer coefficients were calculated according to Eq. 4. In Fig. 8 the effect of the carbon dioxide concentration in a liquid on the transfer coefficient is plotted. From the slope, the following equation has been obtained:

$$K_Ga \propto e^{-6.56M} \qquad (5)$$

**Part 2.** — In Part 1, carbon dioxide absorption behavior was studied with a small centrifugal absorber (rotor dimensions: ca. 10 cm. in diameter × 7.5 cm.). These investigations into the process of absorption with a chemical reaction have distinguished the effects of several factors on the transfer coefficient. However, effects of these factors on the transfer coefficient were deduced from experiments in which a certain factor was varied while the others were kept constant. We have thus manufactured a centrifugal absorber of a large scale (rotor dimensions: ca. 55 cm. in diameter × 30—57 cm.; Table I, types IV and V).

The experimental design of the orthogonal table[9] is shown in Table III, where settled

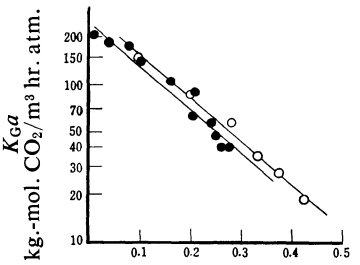



Fig. 8. Relation between $CO_2$ concentration in liquid and coefficient.
○ No. 187—No. 192 ● No. 200

8) F. Goodrige, *Trans. Faraday Soc.*, **51**, 1703 (1955).

9) G. Taguchi, "Method of Experimental Design," Maruzen Book Co., Tokyo (1962).

levels are in parentheses, along with the experimental values and the results. The other experimental procedures were the same as in Part 1.

It was possible to adjust the actual levels of the factors to the settled levels within ±5% deviation. The main effects of each factor are calculated and plotted according to the usual method[9] in Figs. 9 to 12. The arrows shows the range of experimental error.

The dependence of the transfer coefficient on the concentration of the MEA solution is shown in Fig. 6, indicating the same tendency as in Part 1.

Figure 6 shows also the relation between the concentration of DEA and the transfer coefficient.

In both liquids, MEA and DEA, the transfer coefficients show substantially the same magnitude up to a concentration of about four normal. When the normality increases more than 4 N, the transfer coefficient of DEA decreases because the viscosity influences the coefficient, as was stated in Part 1.

Equation 2 is verified by the fact that the $K_G a \mu^{0.5}/N$ for 3, 4, 5 and 6 N DEA solutions with kinematic viscosities of 3.5, 5.6, 10 and 20 c. s., are 31.8, 38.5, 30.0 and 36.0 respectively.

Certainly, the influence of viscosity depends upon the centrifugal force produced by the revolution. The transfer coefficients are plotted against the gas flow rate in Fig. 9. The coefficient increases with the gas flow rate in the MEA system, indicating that the rate-controlling step is still in the gas film, while it changed little in the DEA system, indicating that the step there has been shifted to that in the liquid film.

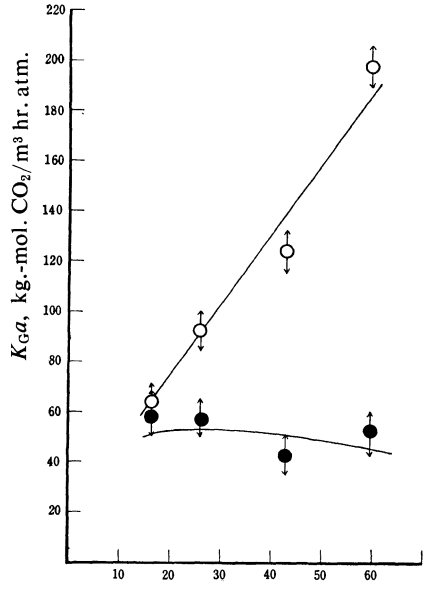



Fig. 9. Relation between gas velocity and coefficient.

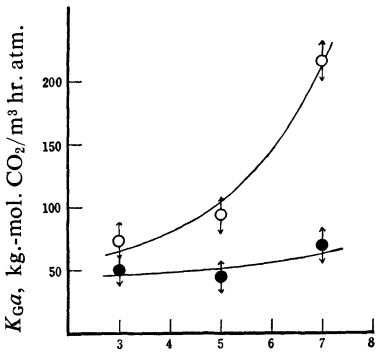



Fig. 10. Relation between liquid flow rate and coefficient.

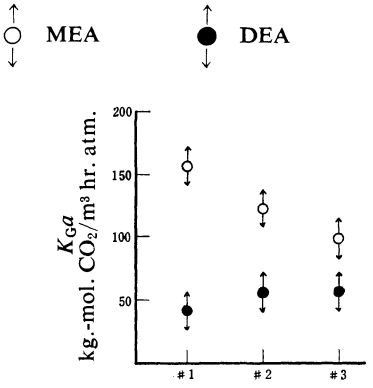



Fig. 11. Relation between type of rotor and coefficient.

#1 Slit, unpacked #2 Screen, packed,
#3 Conical perforated plate, packed

MEA DEA

In Fig. 10 the transfer coefficient increases considerably with the MEA liquid flow rate, but only slightly with the DEA liquid flow rate. Figure 11 shows the effects of the differences of rotors on the transfer coefficient. Generally, it is advantageous to choose a packed rotor when the absorbing liquid is viscous and the liquid flow rate is small.

Figure 12 shows the dependence of the transfer coefficient on the solvent, the revolution rate of the rotor, and the initial concentration of carbon dioxide in the gas stream.

The differences between water and glycerol have hardly any effect on the transfer coefficient. As for the revolution rate and the carbon dioxide concentration, tendencies

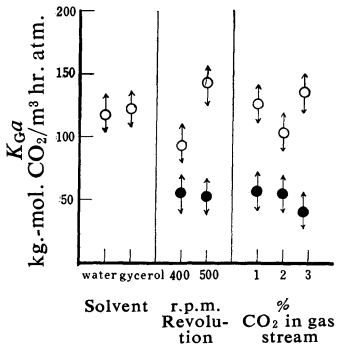



Fig. 12. Effects on coefficients of solvent, revolution rate, and $CO_2$ concentration in gas stream.




similar to those in Part 1 were observed. Additionally, the concentration of carbon dioxide in MEA glycerol solutions affected the transfer coefficient in the same manner as in Part 1 (Fig. 8, Table III, No. 200).

Runs No. 501 to 503 in Table III were obtained with a large, modified centrifugal absorber which had a rotor (55 cm. in diameter $\times$ 57 cm.) comprised of four perforated aluminum cylinders.

The length of the absorbing space, the number of cylinders, and especially the number of openings were increased. From a comparison between No. 501 and Nos. 5 and 16, between No. 502 and Nos. 7 and 17, and between No. 503 and Nos. 8 and 9, it may be concluded that the increase in the number of both openings and cylinders has little effect on the mass transfer coefficient.

## Summary

After a description of a centrifugal carbon dioxide absorber, the effects of variables on the mass transfer coefficient of the absorber have been reported. For the experimental conditions examined, the following conclusions may be arrived at:

(1) When the rate-determining step is gas diffusion, the MEA and DEA liquid of the same concentration have the same mass transfer coefficient as long as the effect of viscosity is negligible.

(2) The transfer coefficient increases linearly as the concentration of an MEA aqueous solution increases.

(3) The relation between the coefficient and the concentration of a viscous DEA aqueous solution is given as:

$$K_Ga \propto N/\mu^{0.5}$$

(4) The relation between the coefficient and the concentration of carbon dioxide in a MEA liquid is given as:

$$K_Ga \propto e^{-6.56M}$$

(5) So long as the gas diffusion is the rate-determining step, the coefficients for two solvents, water and glycerol, differ little.

(6) The coefficient for MEA increases greatly with the liquid flow rate; however, the coefficient for DEA increases only a little.

(7) The coefficient is initially in direct proportion to the square root of the gas flow rate.

(8) The efficiency of the centrifugal absorber remains constant even if the carbon dioxide concentration in the gas stream changes from 3 to 0.2%.

(9) The coefficient is in direct proportion to the logarithm of the rotor revolutions per minute.

(10) Slight modifications, except for packing on the rotor, with the aim of increasing the surface area of a liquid do scarcely anything to improve the absorber.

*2nd R & D Center*
*Technical Research and Development Institute*
*Defense Agency of Japan*
*Setagaya-ku, Tokyo (M. M.)*

*Technical Research Institute*
*Kawasaki Dockyard, Ltd.*
*Ikuta-ku, Kobe (Y. F.)*

# Copolymerization of Propylene with Butene-1 Catalyzed by Triethylaluminum and Vanadium Trichloride or Vanadyl Trichloride

By Wasaburo KAWAI

(Received November 6, 1963)

Natta et al.[1] have studied the copolymerization of ethylene with propylene by using triethylaluminum and vanadium tetrachloride or vanadyl trichloride; Phillips and Carrick[2] have also synthesized the random copolymer of ethylene and propylene by using a hydrocarbon soluble catalyst, $VCl_4$-$(C_6H_5)_4Sn$-$AlBr_3$. Junghanns et al.[3] have reported the copolymerization of ethylene with propylene by using alkylaluminum chloride ($AlRCl_2$ or $1/2Al_2R_3Cl_3$) and vanadyl chloride.

Studies of the copolymerization of other olefins were described by Dunham,[4] who examined the effect of side-chain structure on the properties of poly-$\alpha$-olefin, and by Reding[5] who synthesized the copolymer of 3-methylbutene-1 and 4-methylpentene-1 by using triisobutyl-aluminum and vanadium trichloride. Anderson et al.[6,7] carried out the copolymerization of styrene with 4-methylpentene-1 or 5-methylhexene-1 and determined the monomer reactivity ratio of the monomers. Mark[8] commented on the usefulness of the copolymer of propylene and butene-1.

The present author has been interested in the characterization of the copolymer of propylene and butene-1, whose homopolymers have the same identity period (6.5Å) as the orientated polymers.[9] In the present paper, the copolymerization of propylene with butene-1 by using triethylaluminum combined with vanadium trichloride or vanadyl trichloride will be reported.

1) G. Natta et al., *Chim. e Ind. (Milan)*, **39**, 733 (1057); *Chim. e Ind. (Milan)*, **39**, 743 (1957); *Chim. e Ind. (Milan)*, **39**, 825 (1957).
2) G. W. Phillips and W. L. Carrick, *J. Am. Chem. Soc.*, **84**, 920 (1962).
3) E. Junghanns, A. Gumboldt and G. Bier, *Makromol. Chem.*, **58**, 18 (1962).
4) K. R. Dunhanns, J. Vandenberghe, J. W. H. Faber and L. E. Contois, *J. Polymer Sci.*, **A1**, 751 (1963).
5) F. P. Reding and C. W. McGary, U. S. Pat. 3091601 (1963); *Chem. Abstr.*, **59**, 5282 (1963).
6) I. H. Anderson, G. M. Burnett and J. T. Tait, *Proc. Chem. Soc.*, **1960**, 225.
7) I. H. Anderson, G. M. Burnett and J. T. Tait, *J. Polymer Sci.*, **56**, 391 (1962).
8) H. Mark, Presented at the 15th Annual Meeting of the Chemical Society of Japan, Kyoto, April, 1962.
9) G. Natta, *Makromol. Chem.*, **35**, 94 (1960). For isotactic polybutene-1, the identity period was reported to be 6.85 Å in *Makromol. Chem.*, **21**, 240 (1956).

## Experimental

**Polymerization.**—A given quantity of vanadium trichloride or vanadyl trichloride and a glass ampoule containing triethylaluminum were charged with *n*-hexane (2—5 cc.) in a stainless steel autoclave. After the autoclave had been flushed with a nitrogen stream, liquid propylene and butene-1 were introduced through a steel pipe into the autoclave cooled to −78°C, and the amounts of the monomers were determined by weight. As soon as the glass ampoule in the autoclave had been broken by vigorous shaking, the autoclave was dipped in a thermostatic bath. The polymers obtained were then washed repeatedly by boiling methanolic hydrochloric acid or methanol and dried in a vacuum. As a control, the isotactic polypropylene sample for X-ray diffraction measurement was prepared by the same procedure.

**Samples for Infrared Spectrum and X-Ray Diffraction.**—The polymer dissolved in toluene or xylene was cast on mercury, and the solvent was gradually evaporated by heating. The films thus obtained were used for infrared spectrum and X-ray diffraction measurements. The optical densities at 970 $cm^{-1}$ were determined according to the base line method.

**Intrinsic Viscosity.**—The copolymers were fractionated by solvent extraction with a Soxhlet extractor, and the intrinsic viscosity of each fraction was determined in toluene at 100°C.

## Results and Discussion

The results of copolymerization with various monomer ratios are listed in Tables I and II. In the propylene-butene-1 copolymer, there are two characteristic bands, at 970 $cm^{-1}$ and 760 $cm^{-1}$, in the infrared spectrum which are independent of the crystallinity of the copolymers. The former band, at 970 $cm^{-1}$, has been attributed to the $CH_2$ rocking, C-C stretching, $CH_3$ wagging and rocking modes of polypropylene,[10] while the later band 760 $cm^{-1}$ may be attributed to the $CH_2$ rocking vibration of the ethyl group of polybutene-1.[11] Therefore the optical density ratio, $D(970\ cm^{-1})/D(760\ cm^{-1})$, may be accepted as a measure of the

10) C. Y. Liang and F. G. Pearson, *J. Mol. Spectroscopy*, **5**, 290 (1960).
11) M. C. Harvey and A. D. Ketley, *J. Appl. Polym. Sci.*, **5**, 247 (1961).

TABLE I. COPOLYMERIZATION OF PROPYLENE WITH BUTENE-1 CATALYZED BY TRIETHYLALUMINUM AND VANADIUM TRICHLORIDE[a]

$(AlEt_3) = 8.6 \times 10^{-3}$ mol., $(VCl_3) = 1.27 \times 10^{-3}$ mol.

| Exp. No. | Monomer $10^{-1}$ mol. | | $\frac{\text{Propylene}}{\text{Butene-1}}$ molar ratio | Reaction time, hr. | Conversion % | Optical density ratio[b] $\frac{D(970\,cm^{-1})}{D(760\,cm^{-1})}$ |
|---|---|---|---|---|---|---|
| 1 | Butene-1 | 3.35 | 0 | 3.5 | 24.9 | — |
| 2 | Butene-1 | 2.30 | | | | |
| | Propylene | 1.21 | 0.53 | 3.0 | 37.1 | 1.38 |
| 3 | Butene-1 | 1.45 | | | | |
| | Propylene | 2.21 | 1.54 | 2.5 | 43.0 | 1.87 |
| 4 | Butene-1 | 1.30 | | | | |
| | Propylene | 2.20 | 1.70 | 4.0 | 42.5 | 3.4 |
| 5 | Butene-1 | 1.23 | | | | |
| | Propylene | 2.50 | 2.1 | 2.5 | 62.1 | 2.55 |
| 6 | Butene-1 | 0.08 | | | | |
| | Propylene | 0.285 | 3.65 | 2.0 | 27.3 | 4.15 |
| 7 | Butene-1 | 0.033 | | | | |
| | Propylene | 0.338 | 10.4 | 2.5 | 38.7 | 7.8 |

a) All polymerizations were carried out in a thermostat at 60°C.
b) All samples for optical density measurements were unfractionated. The artificial mixture of polypropylene (30 wt.%) and polybutene-1 (70 wt.%) showed the optical density ratio, $D(974\,cm^{-1})/D(760\,cm^{-1})$, of 0.86.

TABLE II. COPOLYMERIZATION OF PROPYLENE WITH BUTENE-1 CATALYZED BY TRIETHYLALUMINUM AND VANADYL TRICHLORIDE[a]

$(AlEt_3) = 8.6 \times 10^{3}$ mol., $(VOCl_3) = 3.46 \times 10^{-3}$ mol.

| Exp. No. | Monomer $10^{-1}$ mol. | | $\frac{\text{Propylene}}{\text{Butene-1}}$ molar ratio | Reaction time, hr. | Conversion % | Optical density ratio[b] $\frac{D(970\,cm^{-1})}{D(760\,cm^{-1})}$ |
|---|---|---|---|---|---|---|
| 8 | Butene-1 | 3.29 | 0 | 2.0 | 48.1 | — |
| 9 | Butene-1 | 1.81 | | | | |
| | Propylene | 1.26 | 0.715 | 2.0 | 41.5 | 0.86 |
| 10 | Butene-1 | 1.58 | | | | |
| | Propylene | 2.38 | 1.51 | 2.0 | 46.0 | 1.74 |
| 11 | Butene-1 | 1.02 | | | | |
| | Propylene | 2.99 | 3.0 | 2.0 | 60.5 | 4.0 |
| 12 | Butene-1 | 0.8 | | | | |
| | Propylene | 3.26 | 5.9 | 2.0 | 72.1 | 15.0 |

a) All polymerizations were carried out at 30°C.
b) All samples for optical density measurements were not fractionated.

polypropylene content of the copolymers. The infrared spectra of the typical unfractionated copolymers obtained by using triethylaluminum combined with vanadium trichloride or vanadyl trichloride catalysts are shown in Fig. 1.

According to Luongo[12] and Nishioka et al.[13], the determination of the isotactisity of polypropylene and polybutene-1 can be made by the measurement of the optical density ratios, $D(995\,cm^{-1})/D(974\,cm^{-})$ and $D(917\,cm^{-1})/D(1148\,cm^{-1})$ respectively. Both the isotactic sensitive band at $917\,cm^{-1}$ from the butene-1 unit sequence and that at $995\,cm^{-1}$ from the propylene unit sequence are inclined to weaken in the spectra of copolymers obtained by using triethylaluminum and vanadium trichloride catalysts, as may be seen in Fig. 1 (spectrum II). This suggests that a new crystalline copolymer is formed by using the above catalyst, a theory supported by the X-ray diffraction patterns shown in Fig. 2 and Table IV. In the copolymers from triethylaluminum and vanadyl trichloride catalysts, the isotactic-sensitive bands from the butene-1 unit and propylene unit sequences are recognized to be much weakened in optical density. Therefore, these copolymers have scarcely any of the isotactic chains of either monomer unit sequence;

12) J. P. Luongo, *J. Appl. Polym. Sci.*, 3, 302 (1960).
13) A. Nishioka, K. Yanagisawa and T. Naraba, Presented at the 14th Annual Meeting of the Chemical Society of Japan, Tokyo, April, 1961.

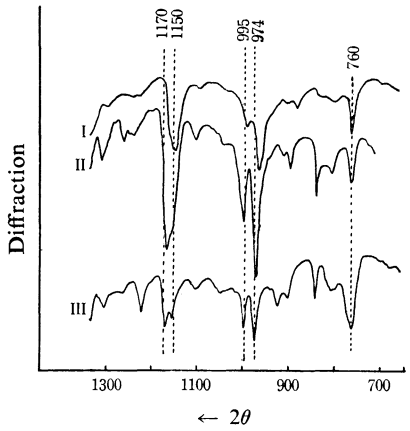



Fig. 1. Comparison of infrared spectra of copolymer and mixed polymer.
I: Copolymer from triethylaluminum and vanadyl trichloride (No. 10)
II: Copolymer from triethylaluminum and vanadium trichloride (No. 4)
III: Mixed polymer (polybutene-1/polypropylene=7/3)

moreover, they are found to be new amorphous copolymers by the X-ray diffraction mearurements. The infrared absorption spectra of the copolymers and mixed homopolymers are compared in Fig. 1. Copolymers lack the absorption at 1170 $cm^{-1}$, whereas the mixed homopolymers show two absorptions, at 1150 $cm^{-1}$ and 1170 $cm^{-1}$, which are due to the component homopolymers. It may be noted also that the copolymers show an absorption at 970 $cm^{-1}$ instead of that at 974 $cm^{-1}$ which is due to the isotactic polypropylene. Consequently, it is clear that the polymers here obtained are not mixtures of polypropylene and

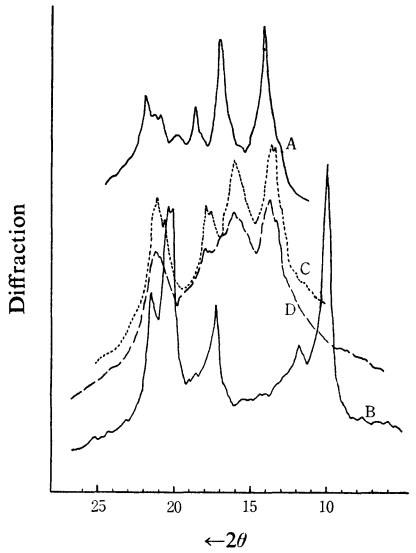



Fig. 2. X-Ray diffraction patterns of polypropylene, polybutene-1 and copolymer obtained by using triethylaluminum and vanadium trichloride catalyst
A: Isotactic polypropylene
B: Polybutene-1 (No. 1)
C: Unfractionated propylene-butene-1 copolymer (No. 3)
D: *n*-Hexane extractable propylene-butene-1 copolymer (No. 3)

polybutene-1 but are copolymers.

The copolymers were fractionated by solvent extraction (diethyl ether, *n*-hexane, isooctane) into four portions, as is shown in Table III. It was found, from the spectrum change between 1150 $cm^{-1}$ and 1170 $cm^{-1}$, that the portion extracted by a lower boiling solvent (diethyl ether) showed the absorption at 1150

Table III. The fractionations and intrinsic viscosities of copolymers[a)]

| No. | Used catalysts | Propylene/Butene-1 molar ratio | Solvent extractions | | | | | | | |
|---|---|---|---|---|---|---|---|---|---|---|
| | | | $Et_2O$ wt.% | $[\eta]$ | *n*-hex. wt.% | $[\eta]$ | iso oct. wt.% | $[\eta]$ | residue wt.% | $[\eta]$ |
| 9 | $AlEt_3$, $VOCl_3$ | 0.715 | 77.4 | 0.22 | 12.9 | 0.51 | 8.1 | 2.25 | 1.6 | — |
| 11 | $AlEt_3$, $VOCl_3$ | 3.0 | 52.0 | 0.31 | 12.2 | 0.95 | 6.3 | 2.1 | 29.5 | 2.5 |
| 3 | $AlEl_3$, $VCl_3$ | 1.54 | 47.5 | 0.82 | 18.0 | 1.8 | 9.8 | 3.8 | 24.7 | 2.1 |

a) The intrinsic viscosities were measured in toluene at 100°C.

Table IV. d-Spacing of copolymer and homopolymer

| Isotactic polypropylene | | Polypropylene ($AlEt_3$, $VOCl_3$) | | Polybutene-1 ($AlEt_3$, $VCl_3$) | | Polybutene-1 ($AlEt_3$, $VOCl_3$) | | Copolymer (No. 6) ($AlEt_3$, $VCl_3$) | |
|---|---|---|---|---|---|---|---|---|---|
| 2θ | d | 2θ | d | 2θ | d | 2θ | d | 2θ | d |
| 14.3 | 6.17 | 14.3 | 6.17 | 10.0 | 8.84 | 10.0 | 8.84 | 13.8 | 7.19 |
| 17.1 | 5.48 | 17.0 | 5.48 | 11.8 | 8.64 | 17.4 | 5.47 | 16.2 | 5.52 |
| 18.7 | 4.90 | 18.7 | 4.90 | 17.4 | 5.47 | 20.4 | 4.42 | 18.0 | 4.93 |
| 21.4 | 4.38 | 21.3 | | 20.4 | 4.42 | 21.4 | 4.38 | 21.3 | 4.39 |
| 21.6 | | 21.7 | | 21.4 | 4.38 | | | | |
| 22.2 | | | | | | | | | |

$cm^{-1}$ of polybutene-1. On the other hand, that extracted by a higher boiling solvent (isooctane) showed the absorption at 1167 $cm^{-1}$, which was near to that at 1168 $cm^{-1}$ ascribed to polypropylene. The polymer extracted by *n*-hexane had the absorption in the middle, between 1168 $cm^{-1}$ and 1150 $cm^{-1}$. It was also ascertained that the polymer extracted by a lower boiling solvent was richer in the butene-1 unit sequence, while that extracted by a higher boiling solvent was richer in the propylene unit sequence. The optical density ratio, $D(970\,cm^{-1})/D(760\,cm^{-1})$ was lower for the portion extracted by a lower boiling solvent than for that extracted by a higher boiling solvent.

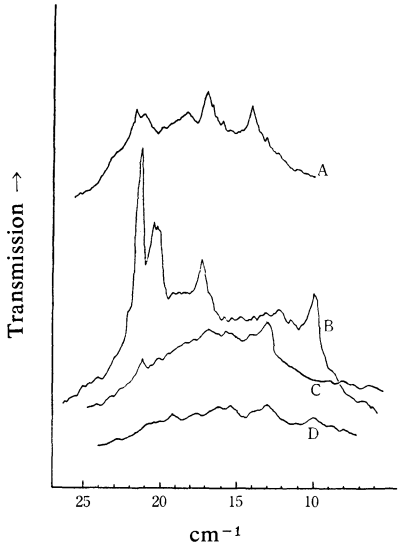



Fig. 3. X-ray diffraction patterns of polypropylene, polybutene-1 and copolymer obtained by using triethylaluminum and vanadyl trichloride catalyst
A: Polypropylene
B: Polybutene-1 (No. 8)
C: Unfractionated propylene-butene-1 copolymer (No. 10)
D: *n*-Hexane extractable propylene-butene-1 copolymer (No. 9)

It was found that the copolymers obtained from propylene and butene-1 had different X-ray diffractions from those of the homopolymers. The copolymer obtained by using triethylaluminum and vanadium trichloride is crystalline; the d-spacing is indicated in Table IV together with that of homopolymers. The X-ray diffraction patterns of crystalline copolymers are shown in Fig. 2. The copolymer prepared with the triethylaluminum-vanadyl trichloride catalyst was amorphous; the X-ray diffraction patterns are shown in Fig. 3.

From the infrared spectra and X-ray diffraction of the copolymers, may it be concluded that the triethylaluminum-vanadium trichloride catalytic system is a stereospecific one, one which produces the crystalline copolymers in the copolymerization of propylene with butene-1, while, on the other hand, the triethylaluminum-vanadyl trichloride catalytic system is a less stereospecific one, one which produces the amorphous copolymers in the copolymerization of the same monomers.

*Government Industrial Research Institute, Osaka*
*Oyodo-ku, Osaka*

# A Kinetic Study of the Redox System Containing Citric Acid and Manganic Acetate

By Gur PRASAD

(Received May 27, 1964)

Waters and his co-workers[1] have studied the oxidation of some carboxylic acids and other organic compounds by using manganese-(III) in the form of pyrophosphate. Manganic acetate has been employed for the oxidation of organic compounds by Zonis and his co-workers.[2] In the present study, manganic acetate has been used as an oxidant for citric acid.

1) W. A. Waters et al., *J. Chem. Soc.*, **1953**, 2836; **1954**, 2456.
2) S. A. Zonis et al., *J. Gen. Chem.* (*U. S. S. R.*), **20**, 1301 (1950); **24**, 815 (1954); *Zhur., Obschei Khim.*, **24**, 814, (1954).

## Experimental

All the chemicals used were of B.D.H., A.R. quality, and fresh solutions of citric acid were prepared in boiled distilled water. Manganic acetate was prepared by the oxidation of manganous nitrate under suitable conditions. It was stored in blackened Pyrex bottles at a low temperature to prevent disproportioning ($2Mn^{3+} \rightleftarrows Mn^{2+} + Mn^{4+}$). Calculated amounts of the reactants (i. e., citric acid

and manganic acetate) were placed separately in a thermostat maintained at ($t\pm0.05$)°C, where $t$ is the desired temperature. Reaction was started by thoroughly mixing the two reactants in a solvent containing 90 per cent glacial acetic acid and 10 per cent water. Five milliliters of the reaction mixture were pipetted out at different intervals, and the concentration of manganese(III) was estimated colorimetrically by using Unicam Photoelectric colorimeter with a Filter No. 303. Lambert-Beer's law was found to hold for the concentration ranges employed in the experiment. The kinetics of the reaction has been followed by varying the concentration of the reactants and the temperature.

## Results and Discussion

It has been found that one molecule of citric acid requires 9.5 equivalents of manganic acetate in order to be oxidized in the temperature range from 20 to 30°C. The rate constants have been determined graphically. $k_1$ and $k_2$ represent the rate constants for the first and second order reactions respectively. Some of the data are reproduced in Tables I, II and III.

TABLE I

| Reactant | Temp. °C | Rate constant | Figure |
|---|---|---|---|
| Citric acid : 0.005 N<br>Mn(III) : 0.005 N | 20 | $k_2=0.08012$ | 1(a) |
| Citric acid : 0.005 N<br>Mn(III) : 0.005 N | 30 | $k_2=0.1354$ | 1(b) |
| Citric acid : 0.005 N<br>Mn(III) : 0.0005 N | 20 | $k_1=0.1497$ | 2(a) |
| Citric acid : 0.02 N<br>Mn(III) : 0.0025 N | 20 | $k_1=0.2917$ | 2(b) |

TABLE II

| Reactant | $t_{1/2}$, min. | $k'$ |
|---|---|---|
| Citric acid : 0.005 N<br>Mn(III) : 0.005 N | 15.2 | 0.07429 |
| Citric acid : 0.005 N<br>Mn(III) : 0.0025 N | 12.1 | 0.07293 |
| Citric acid : 0.005 N<br>Mn(III) : 0.0016 N | 9.4 | 0.07361 |

TABLE III

Temp., : 20°C

| Reactant | | $k_2\times10^{-4}$ |
|---|---|---|
| Citric acid : 0.005 N ; | Mn(III) : 0.005 N | 801 |
| Citric acid : 0.005 N ; | Mn(III) : 0.0016 N | 835 |
| Citric acid : 0.005 N ; | Mn(III) : 0.00125 N | 909 |
| Citric acid : 0.0025 N ; | Mn(III) : 0.0025 N | 674 |
| Citric acid : 0.005 N ; | Mn(III) : 0.0025 N | 752 |
| Citric acid : 0.01 N ; | Mn(III) : 0.0025 N | 806 |

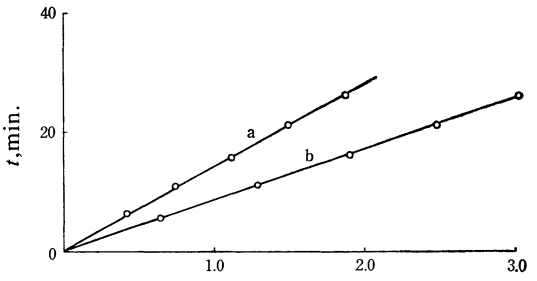



Fig. 1.

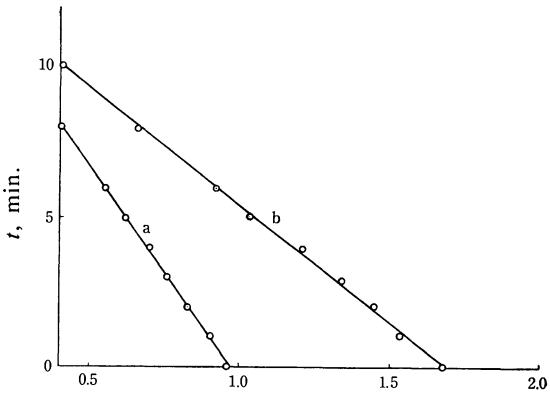



Fig. 2.

It has been noted that if the concentrations of the reactants are approximately equal, the total order of the reaction is two—one with respect to each reactant separately. There is a slight increase in the total value of the rate constant as the concentration of manganese(III) is decreased. It appears that a complex is formed between manganese(III) and citrate which slowly decomposes, giving the reaction product. The temperature coefficient for a 10°C rise in temperature is slightly less than two.

The authors wishes to thank the University Grants Commission, New Delhi, for the award of a Senior Research Fellowship. Thanks are also due to Dr. Y. K. Gupta, Reader, University of Rajasthan, for his helpful suggestions.

*Chemical Laboratories*
*M.N.R. Engineering College*
*Allahabad, India*

# A Simple Method for the Analysis of a Homologous Series of Alcohols using Gas Chromatography

By Mikio SATO, Hiroshi MIYAKE, Mitsuyuki MITOOKA and Koichi ASANO

(Received July 31, 1964)

Gas chromatography has been a useful means for the analysis of complex mixtures of reasonably volatile compounds, and many analyses of lower fatty alcohols are available.

This report will present a study concerning the gas chromatographic analysis of an alcohol mixture which is produced by Ziegler's process.[1-4] This mixture consists of the normal even carbon-numbered alcohols ranging from $C_6$ through $C_{22}$. As the mixture contains components with high boiling points, gas chromatographic separation must be made at quite a high temperature. Therefore, the stationary liquid should be virtually non-volatile at a column temperature of 200—250°C, and, at the same time, the liquid must be stable against thermal decomposition at such a high temperature. From these considerations, acetate-washed grease,[5] Apiezon grease[6,7] or Reoplex[8,9] was expected to be appropriate for this purpose.

On chromatograms, free alcohols usually give rise to asymmetric peaks; they have a drawn-out "trail," a shape obviously unfavorable to their sharp separation and to the quantitative analysis of the components with lower concentrations. The tailing of peaks may be attributed to the polarity of the solid support and to the association of alcohol molecules.[10] Hence, in order to avoid these unfavorable aspects, it was recommended that the alcohols, prior to analysis, be converted to their acetates, which show no tailing and are more stable against the thermal decomposition than the original alcohols. Furthermore, the acetates of $C_6$ and higher alcohols have lower melting points than those of the corresponding alcohols, and a mixture of them is more easily injected into the instrument.

It thus becomes important to convert the individual alcohol in the sample mixture quantitatively to its acetates. However, by the ordinary acetylation method, for example, by the use of acetic anhydride or acetyl chloride, it was found that the distribution of the acetates obtained does not correspond to that of the starting alcohol mixture, mainly because of the difference in the solubility of each acetate into an aqueous solution, which is formed by the washing of the reaction mixture with water after the acetylation process in order to remove the catalysts and excess reagents from the acetates produced.

This paper will report on an attempt to

TABLE I. ANALYTICAL CONDITION AND RETENTION TIMES

| Analytical condition | | Retention time, min. | |
|---|---|---|---|
| Stationary liquid | Silicone greanse (high vacuum) | $n$-$C_6H_{13}OAc$ | 1.4 |
| Solid support | Aqua-regia-treated | $n$-$C_8H_{17}OAc$ | 2.2 |
| | Chromosorb (35—60 mesh) | $n$-$C_{10}H_{21}OAc$ | 3.9 |
| Liquid : Solid | 20 : 80 (wt.) | $n$-$C_{12}H_{25}OAc$ | 7.3 |
| Column length | 225 cm. (I. D. 5 mm.) | $n$-$C_{14}H_{29}OAc$ | 14.9 |
| Column temp. | 220°C | $n$-$C_{16}H_{33}OAc$ | 27.9 |
| Carrier gas | He | $n$-$C_{18}H_{37}OAc$ | 44.7 |
| Flow rate | 66 ml./min. | $n$-$C_{20}H_{41}OAc$ | 100 |
| | | $n$-$C_{22}H_{45}OAc$ | 180 |

1) K. Ziegler, F. Krupp and K. Zosel, *Angew. Chem.*, **67**, 425 (1955).
2) K. Ziegler, French Pat. 1134907 (Apr. 19, 1957).
3) K. Ziegler, British Pat. 804335 (Nov. 12, 1958).
4) K. Ziegler, U. S. Pat. 2892858 (June 30, 1959).
5) F. R. Cropper and A. Heywood, *Nature*, **174**, 1063 (1954).
6) B. Boughton and V. R. Wheatley, *Biochem. J.*, **73**, 144 (1959).
7) A. Ofner, W. Kimel, A. Holmgren and F. Forrester, *Helv. chim. Acta*, **42**, 2577 (1959).
8) M. Hofmann and H. G. Struppe, *Acta chim. Acad. Sci. Hung.*, **27**, 239 (1961).
9) M. E. Link, H. M. Hickman and R. A. Morrissette, *J. Am. Oil Chem. Soc.*, **36**, 300 (1959).
10) Anon, Prices (Bromborough) Ltd., Tech. Publication No. 6; "Gas chromatography Abstracts," Butterworths, London (1960), p. 412.

TABLE II. ANALYTICAL RESULTS (REPEATABILITY OF GAS CHROMATOGRAPHY ITSELF)

| Compt. | Calcd. $X_o$ wt.% | Found, $X_i$ 1 | 2 | 3 | 4 | 5 | Av. $\overline{X}_i$ | Mean error[a] | Dev. from Calcd.[b] | Rel. Dev.[c] |
|---|---|---|---|---|---|---|---|---|---|---|
| $n$-$C_6H_{13}OAc$ | 4.6 | 4.7 | 4.3 | 4.5 | 5.9 | 5.1 | 4.9 | 0.4 | +0.3 | 6.5 |
| $n$-$C_8H_{17}OAc$ | 4.7 | 5.4 | 4.3 | 5.5 | 6.3 | 5.7 | 5.4 | 0.4 | +0.7 | 14.8 |
| $n$-$C_{10}H_{21}OAc$ | 11.2 | 10.9 | 11.7 | 11.3 | 12.4 | 11.8 | 11.5 | 0.4 | +0.3 | 2.7 |
| $n$-$C_{12}H_{25}OAc$ | 11.3 | 11.6 | 11.4 | 12.4 | 12.4 | 12.1 | 12.1 | 0.3 | +0.8 | 7.1 |
| $n$-$C_{14}H_{29}OAc$ | 22.3 | 23.1 | 23.8 | 22.7 | 23.2 | 22.6 | 22.9 | 0.4 | +0.6 | 2.7 |
| $n$-$C_{16}H_{33}OAc$ | 22.6 | 20.5 | 20.5 | 21.0 | 19.8 | 21.1 | 20.6 | 0.4 | −2.0 | 8.9 |
| $n$-$C_{18}H_{37}OAc$ | 23.3 | 23.8 | 24.0 | 22.6 | 20.0 | 21.6 | 22.6 | 1.1 | −0.7 | 3.0 |

a) $\frac{\Sigma|\overline{X}_i - X_i|}{n}$ b) $\overline{X}_i - X_o$ c) $\frac{\overline{X}_i - X_o}{X_o} \times 100$

TABLE III. ANALYTICAL RESULTS (REPEATABILITY OF ACETYLATION-GAS CHROMATOGRAPHY)

| Compt. | Calcd. $X_o$ wt.% | Found, $X_i$ 1 | 2 | 3 | Av. $\overline{X}_i$ | Mean error | Dev. from Calcd. | Rel. Dev. |
|---|---|---|---|---|---|---|---|---|
| $n$-$C_6H_{13}OAc$ | 7.9 | 7.8 | 7.1 | 7.8 | 7.6 | 0.3 | −0.3 | 3.8 |
| $n$-$C_8H_{17}OAc$ | 17.5 | 18.3 | 18.5 | 17.6 | 18.1 | 0.4 | +0.6 | 3.4 |
| $n$-$C_{10}H_{21}OAc$ | 15.0 | 15.4 | 15.7 | 15.5 | 15.5 | 0.1 | +0.5 | 3.3 |
| $n$-$C_{12}H_{25}OAc$ | 20.6 | 21.3 | 21.0 | 20.9 | 21.1 | 0.2 | +0.5 | 2.4 |
| $n$-$C_{14}H_{29}OAc$ | 26.2 | 25.6 | 26.7 | 25.7 | 26.0 | 0.5 | −0.2 | 0.8 |
| $n$-$C_{16}H_{33}OAc$ | 12.8 | 11.6 | 10.9 | 12.4 | 11.6 | 0.5 | −1.2 | 9.4 |

find a quantitative analytical method for a homologous series of alcohols through acetylation by the use of ketene gas. It was generated from acetone, along with methane gas, and was passed through a sample volume of an alcohol mixture for a short time in order to acetylate it. The acetate mixture obtained was, without needing any more treatment, immediately subjected to gas chromatographic analysis.

It was confirmed that, by the ketene-acetylation, alcohols were converted to their acetates quantitatively and yet with the same conversion velocity. Consequently, the operation of the analysis was greatly simplified by this acetylation process. The accuracy of this analytical method was found to be satisfactory, as Tables II and III show.

## Experimental

**Gas Chromatography.** — In this work, silicone grease (Dow Corning High Vacuum Silicone Grease) was used as the stationary substrate, while aqua-regia-treated[11] Chromosorb (Johns-Manville), 35- to 60-mesh size, was used as the solid support. The packing was prepared by adding 80 g. of Chromosorb to 20 g. of silicone grease dissolved in ethyl ether. The solvent was evaporated on a steam-bath, and finally the packing was dried in an air oven at 110°C. The columns were constructed from the packing and stainless steel tubings 0.75, 1.50, 2.25 and 3.00 m. long and 5 mm. in inner diameter, and they were tested at temperatures of 180, 200, 220 and 240°C.

A Shimadzu model GC-1A gas chromatograph equipped with a filament-wire thermal-conductivity cell was used without modification. Helium was used as the carrier gas, and its flow rates were constantly checked with a soap-film flowmeter. In this work the flow rate was controlled at 20, 40 or 66 ml. per minute.

For the standard samples of the higher $n$-alcohols, $C_6$ through $C_{18}$, and of their acetates, commercial alcohols were purchased from the Wako Pure Chemical Co., and purified in our laboratory through their borates and thereafter by the fractional distillation (Podbielniak) of alcohols obtained from the hydrolysis or of their esters acetylated by the ordinary method.

**The Apparatus for and Operation of the Ketene Acetylation of an Alcohol Sample.** — Figure 1 illustrates a ketene generator and acetylation apparatus. At the start, the cock A is opened and the reactor B (5.5 mm.×60 mm., glass), is charged with 1 ml. of an alcohol mixture. Then the acetone in a 3 l.-flask is gently refluxed, and 50-60 V-AC. is supplied to the 300 W.-nichrome wire, hung in the 3 l.-flask, in order to maintain the dark red color of the wire throughout the acetylation. The vapor of the refluxing acetone comes in contact with the hot wire and undergoes cracking. When the evolution of ketene gas mixture becomes stationary, the cock A is closed and the flow rate of the gas is immediately set at an appropriate rate by controlling the by-pass flow rate (level D) by moving the vessel C up and down according to the reading of the scale differences of an orifice meter E, which has been preliminarily graphed against the flow rate of the ketene gas mixture. When the flow rate is 300 ml. and 600 ml. per hour,

11) A. Zlatkis, Su-Yu Ling and H. R. Kaufman, *Anal. Chem.*, **31**, 945 (1959).

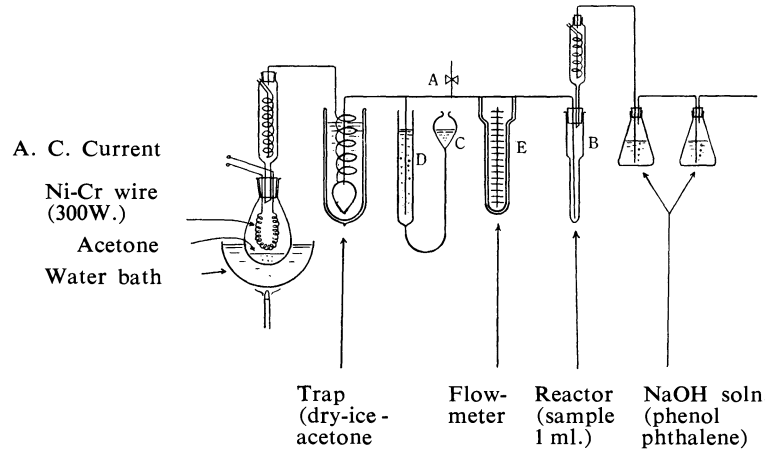



Fig. 1. Keten generator and acetylation apparatus.

it took 2.5 and 1.5 hr. respectively to complete the acetylation of 1 ml. of the alcohol mixture.

## Results and Discussion

**The Accuracy of the Ketene Acetylation Process.**—In order to estimate the loss of the sample during the acetylation process, only the losses of hexyl alcohol and its acetate, which are the most volatile among the compounds under consideration in each series, were investigated. It was found that when flow rate of nitrogen (in place of ketene-metane gas) was 300 ml. per hour, hexylalcohol and its acetate were lost at the rates of 0.7—0.8 mg. and 2.5—3.0 mg. per hour respectively when accompanied by a gas stream. Because, under actual conditions, about 1/4.5 of ketene gas is calculated to be absorbed as a result of the reaction with alcohol, only ca. 0.5 wt.% of the $C_6$-compounds should be lost during the acetylation process. The loss due to the acetylation of $C_8$ and higher alcohols, therefore, should be less than 0.5 wt.% respectively, and there should be essentially no difference in composition between the alcohol mixture and the acetate one during the process.

At times during the acetylation process, portions of the sample were taken out and submitted to gas chromatography in order to check the disappearance of alcohols. At the end of the reaction, each peak of the homologous alcohols disappeared completely and simultaneously, and no peaks other than those due to the acetates were produced. It is obvious, therefore, that the conversion of each alcohol to its acetate is perfectly quantitative, and yet that its conversion velocity is the same in all the alcohols concerned.

**Gas Chromatographic Analysis.** — In the analysis of samples with a very wide boiling range, if complete separation of the lower boiling components is desired the retention times of the higher-boiling components necessarily become too long and, consequently, the peaks of these components become wider. Under such conditions, the limit of detection is undesirably high, and no high accuracy of analysis could be expected. Therefore, the retention time as well as the separation efficiency must be taken into consideration in the determination of analytical conditions. In this work the optimum conditions were selected on the basis of the following evidence; a) analytical time through the retention times of the highest-boiling components, b) separation efficiencies through the height equivalent to a theoretical plate[12] of the components, and c) the stability of the stationary liquid at a high temperature.

As the analytical time is decided by the retention time of the last eluting component, the time of $n$-$C_{22}H_{45}OAc$ must be restricted within definite limitations. The retention times of $n$-$C_6H_{13}OAc$ through $n$-$C_{18}H_{37}OAc$ were measured under various analytical conditions. For a homologous series of organic compounds, it has been shown that a plot of the logarithm of the retention volume or of the time against the number of carbon atoms yields an almost straight line.[13-15] On the basis of the experimental results in this work, it was recognized that a similar relationship is proper for $n$-$C_6H_{13}OAc$ through $n$-$C_{18}H_{37}OAc$. By an extrapolation of the line, the retention times of $n$-$C_{20}H_{41}OAc$ and $n$-$C_{22}H_{45}OAc$ were presumed

12) A. I. M. Keulemans and A. Kwants, "Vapor Phase Chromatography," Butterworths, London (1957), p. 15.
13) A. T. James and A. J. P. Martin, *Analyst*, **77**, 915 (1952).
14) A. T. James and A. J. P. Martin, *Biochem. J.*, **50**, 679 (1952).
15) N. H. Ray, *J. Appl. Chem.*, **4**, 21 (1954).

for each condition. The analytical conditions at which the retention time of $n$-$C_{22}H_{45}OAc$ becomes longer than 180 min. seemed to be unsuitable for a routine analysis.

The relation between the height equivalent to a theoretical plate (HETP) and the gas flow rate ($u$) is given by the following equation.[16]

$$\mathrm{HETP} = A + B/u + Cu$$

where $A$, $B$ and $C$ are constants. Therefore, a plot of the HETP versus $u$ shows a curve with a minimum, at which point the column reaches its highest efficiency. In this work, the values of HETP for 40 and 66 ml. per minute were generally smaller than that for 20 ml. per minute. Therefore, the minimum value seems to be obtained for the flow rate of near 40 or 66 ml. per minute.

At the temperature of 240°C silicone grease was not stable enough for the retention times of the components to decreased in a short time. Therefore, the column temperature should not be maintained at 240°C or over.

In view of these points the analytical conditions shown in Table I were selected for the analysis of $n$-$C_6H_{13}OAc$ through $n$-$C_{22}H_{45}OAc$.

16) J. J. van Deemter, F. J. Zuiderweg and A. Klinkenberg, *Chem. Eng. Sci.*, 5, 271 (1956).

A linear relationship was observed between the weight of each component and its peak area.

**The Accuracy of the Gas Chromatography (Repeatability).**—Table II shows the analytical results of the gas chromatography of a known sample of $n$-$C_6H_{13}OAc$ - $n$-$C_{18}H_{37}OAc$. It is clear from these results that the repeatability of this method is fairly good.

**The Accuracy (Repeatability) of Acetylation by Ketene Gas by Means of Gas Chromatography.**—Table III shows the repeatability of the ketene-acetylation of the known sample of $n$-$C_6H_{13}OH$ - $n$-$C_{16}H_{33}OH$ by the use of gas chromatography. It is clear from these results that the repeatability of this method is also fairly good.

The authors wish to express their appreciation to the Maruzen Oil Co., Ltd., for permission to publish this work, and to Mr. Tsunehide Kozuma and Dr. Hiroshi Hasegawa of the company for their valuable advice and discussions.

*Research Center*
*Maruzen Oil Co., Ltd.*
*Wakayama*

# The Synthesis of Irisolone

By Kenji FUKUI and Takashi MATSUMOTO

(Received August 15, 1964)

Irisolone, a colorless substance, was isolated from the rhizomes of *Iris nepalensis* D. Don by Gopinath et al.[1] They also established its structure as 4'-hydroxy-5-methoxy-6, 7-methylenedioxyisoflavone (I) on the basis of analytical, spectroscopic and degradative studies. It is one of the few isoflavones which contain a methylenedioxy group in the condensed benzene ring, the only others so far known being tlatlancuayin[2] and maxima substance A.[3] Further, it is an unusual type of isoflavone in that the oxygenation pattern is at positions 5, 6 and 7. This class includes irigenin,[4] tectorigenin,[5] muningin,[6] podospicatin,[7] caviunin,[8] and tlatlancuayin as well as irisolone. The present paper will describe the total synthesis of irisolone, its methyl ether and some related compounds.

The methylation of irisolone has yielded the methyl ether (II), which can be converted by dilute alkali hydrolysis into 6-hydroxy-2-methoxy-3, 4-methylenedioxyphenyl 4-methoxybenzyl ketone (III).[1] The ether II has been reformed by the treatment of the deoxybenzoin III with sodium and ethyl

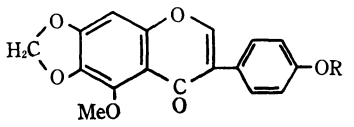
1) K. W. Gopinath, A. R. Kidwai and L. Prakash, *Tetrahedron*, **16**, 201 (1961).
2) P. Crabbe, P. R. Leeming and C. Djerassi, *J. Am. Chem. Soc.*, **80**, 5258 (1958).
3) S. Rangaswami and B. V. R. Sastry, *Curr. Sci.*, **23**, 397 (1954); **24**, 337 (1955); A. S. Kukla and T. R. Seshadri, *Tetrahedron*, **18**, 1443 (1962).
4) W. Baker, *J. Chem. Soc.*, **1928**, 1022.
5) Y. Asahina, B. Shibata and Z. Ogawa, *J. Pharm. Soc. Japan* (*Yakugaku Zasshi*), **48**, 1087 (1928).
6) F. E. King, T. J. King and A. J. Warwick, *J. Chem. Soc.*, **1952**, 96.
7) L. H. Briggs and T. P. Cebalo, *Tetrahedron*, **6**, 143 (1959).
8) O. R. Gottlieb and M. T. Mahalhaes, *J. Org. Chem.*, **26**, 2449 (1961).

formate.[1] The synthesis of the deoxybenzoin III was achieved in two ways. The first method involved the condensation reaction of 3-methoxy - 4, 5 - methylenedioxyphenol (IV). The phenol IV underwent the Hoesch reaction with 4-methoxybenzyl cyanide to give a deoxybenzoin. In previous papers[9] it was demonstrated that the phenol IV was substituted not at the 6-position but at the 2-position in the Hoesch condensation. Therefore, the condensation product was thought to be the ketone III. In order to elucidate the structure of the product, a second, unambigous method of synthesis was explored. 5, 7-Dihydroxy-4'-methoxy - 2 - methylisoflavone (V),[10] when subjected to para hydroxylation, afforded 5, 7, 8-trihydroxy-4'-methoxy-2-methylisoflavone (VI). Subsequent methylenation using the potassium hydroxide - acetone method gave 5-hydroxy-4'-methoxy-7,8-methylenedioxy-2-methylisoflavone (VII). The benzylation of VII with benzyl chloride yielded 5-benzyloxy-4'-methoxy-7, 8 - methylenedioxy - 2 - methylisoflavone (VIII), which was then smoothly converted by boiling dilute alkali into 6-benzyloxy-2-hydroxy-3, 4-methylenedioxyphenyl 4-methoxybenzyl ketone (IX). The ketone IX was first methylated in the 2-position, using the potassium carbonate - acetone method, to a methyl ether (X), and then debenzylated with hydrogen to give the deoxybenzoin III identical with the above ketone. The melting point of the deoxybenzoin was the same as that reported in the literature for the ketone obtained from natural irisolone methyl ether by Gopinath et al.[1] Irisolone methyl ether could be obtained according to the method of Gopinath et al.[1] (Table I).

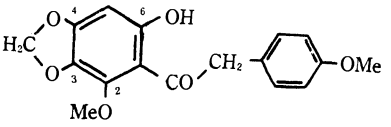
TABLE I. THE MELTING POINTS OF IRISOLONE AND ITS DERIVATIVES (°C)

| | Synthetic compound | Natural compound |
|---|---|---|
| Irisolone (I) | 251—252 | 250—251*1 (269—270)[1] |
| Acetate of I | 162—163 | 156—157[1] |
| Irisolone methyl ether (II) | 182—183 | 179—181*1 (184—185)[1] |
| 5-Demethyl deriv. of II | 211—212 | 214—215[1] |

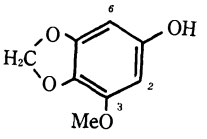
The methylation of VII with dimethyl sulfate yielded 4',5-dimethoxy-7,8-methylenedioxy-2-methylisoflavone (XI), which was then converted into 2-hydroxy-6-methoxy-3,4-methylenedioxyphenyl 4-methoxybenzyl ketone (XII).



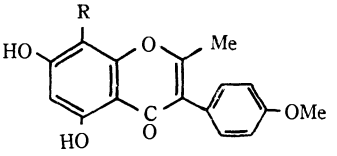
I R=H
II R=Me



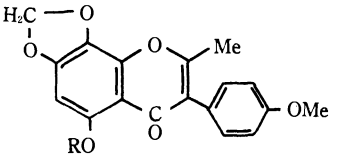
III



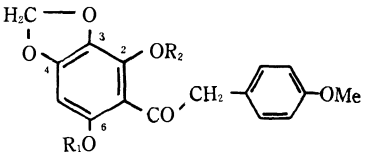
IV



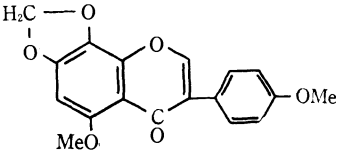
V R=H
VI R=OH



VII R=H
VIII R=$CH_2C_6H_5$
XI R=Me

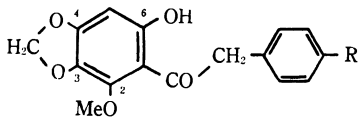


IX $R_1=CH_2C_6H_5$ $R_2=H$
X $R_1=CH_2C_6H_5$ $R_2=Me$
XII $R_1=Me$ $R_2=H$

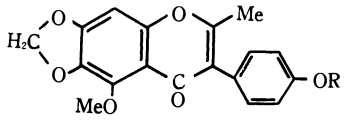


XIII

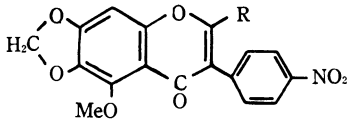
9) K. Fukui and T. Matsumoto, This Bulletin, **36**, 806 (1963); **37**, 266 (1964).
10) W. Baker and R. Robinson, *J. Chem. Soc.*, **1926**, 2713.
*1 Natural irisolone and its methyl ether, kindly supplied by Dr. Gopinath, were measured in this laboratory.



XIV R=OH
XV R=$NH_2$
XVI R=$NO_2$



XVII R=Ac
XVIII R=H



XIX R=H
XX R=Me

The resulting ketone gave the original isoflavone XI with acetic anhydride and was condensed with ethyl formate to give 4', 5-dimethoxy-7, 8-methylenedioxyisoflavone (XIII), an isomer of irisolone methyl ether (II).

The phenol IV underwent the Hoesch reaction with 4-hydroxybenzyl cyanide to give 6-hydroxy-2-methoxy-3, 4-methylenedioxyphenyl 4-hydroxybenzyl ketone (XIV). The same ketone XIV was also obtained from the corresponding amine XV, which was synthesized by the catalytic reduction of a nitroketone XVI; the ketone XVI was derived in turn from 4-nitrobenzyl cyanide by the Hoesch condensation. The ketone XIV was indentical with that obtained from the degradation of natural irisolone by Gopinath et al.[1] The resulting ketone XIV underwent ring closure with ethyl orthoformate or ethyl formate to give 4'-hydroxy-5-methoxy-6, 7-methylenedioxyisoflavone (I), which agreed with natural irisolone (Table I). The identity of the product was established by methylation as well as by demethylation to known products.

The ring closure of the ketone XIV with acetic anhydride gave a monoacetate (XVII), which was then smoothly converted into the 2-methyl derivative (XVIII) of irisolone. By similar methods, 4'-nitroisoflavones (XIX and XX) were also obtained from the ketone XVI.

The ultraviolet absorption spectra of natural and synthetic methylenedioxyisoflavones are shown in Figs. 1 and 2 and Table II. In most

*2 Inflexion point.

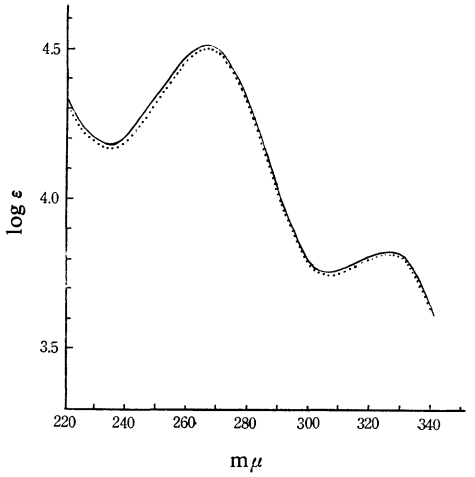



Fig. 1. Ultraviolet spectra of natural (·····) and synthetic irisolone (——) in ethanol.

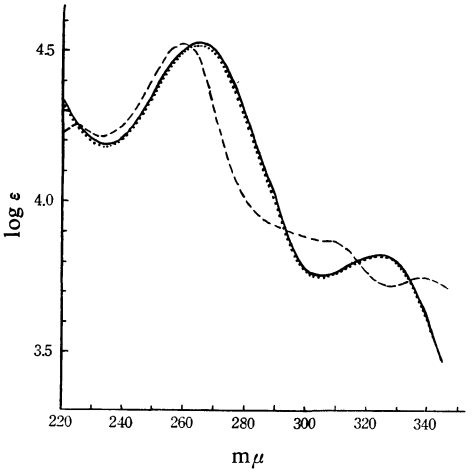



Fig. 2. Ultraviolet spectra of XIII (- - -), natural (·····) and synthetic irisolone methyl ether (——) in ethanol.

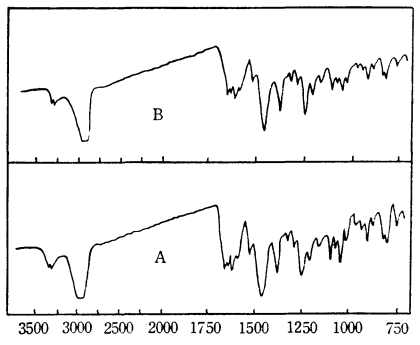
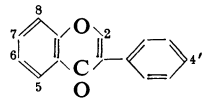



Fig. 3. Infrared spectra of synthetic (A) and natural irisolone (B) in Nujol.

TABLE II. ULTRAVIOLET SPECTRA OF SOME METHYLENEDIOXYISOFLAVONE (in ethanol)



| | Substituent | | | | | $\lambda_{max}$ mμ (log ε) | |
|---|---|---|---|---|---|---|---|
| | OH | OAc | OMe | Me | O-$CH_2$-O | | |
| Irisolone (I) | | | | | | | |
| (synthetic) | 4′ | | 5 | | 6,7 | 266 (4.51) | 325 (3.83) |
| (natural) | 4′ | | 5 | | 6,7 | 266 (4.49) | 325 (3.82) |
| Acetate of I | | 4′ | 5 | | 6,7 | 262 (4·45) | 323 (3.81) |
| Irisolone methyl ether (II) | | | | | | | |
| (synthetic) | | | 4′,5 | | 6,7 | 266 (4.53) | 325 (3.83) |
| (natural) | | | 4′,5 | | 6,7 | 266 (4.52) | 325 (3.83) |
| XIII | | | 4′,5 | | 7,8 | 260 (4.52) | 338 (3.75) |
| 5-Demethyl deriv. of II | 5 | | 4′ | | 6,7 | 274 (4.50) | 336*2 (3.59) |
| XVII | | 4′ | 5 | 2 | 6,7 | 246 (4.43) | 320 (3.83) |
| XVIII | 4′ | | 5 | 2 | 6,7 | 248 (4.42) | 320 (3.85) |
| XI | | | 4′,5 | 2 | 7,8 | 256 (4.51) | 335 (3.83) |
| VII | 5 | | 4′ | 2 | 7,8 | 264 (4.46) | 353 (3.64) |

cases, there are two characteristic peaks, at ca. 260 (band I) and ca. 325 mμ (band II). The displacement effect of the substitution is similar to that reported in previous papers.[11] The absorption curve of XIII (a methylenedioxy group in the 7, 8-positions) is different from that of II (the group in the 6, 7-positions) (Fig. 2).

## Experimental*3

**5, 7, 8-Trihydroxy-4′-methoxy-2-methylisoflavone (VI).**—To a cooled, stirred solution of 5, 7-dihydroxy-4′-methoxy-2-methylisoflavone (V)[10] (4.5 g.) in aqueous sodium hydroxide (4%, 120 ml.), an aqueous solution of potassium persulfate (7.5 g. in 150 ml.) was added drop by drop over a 2 hr. period at 15—20°C. The mixture was allowed to stand at room temperature for 24 hr. and then acidified to litmus with dilute hydrochloric acid. The unchanged compound which had separated out was filtered off, and the filtrate was then heated with concentrated hydrochloric acid (90 ml.) and sodium sulfite (9.0 g.) on a steam bath for 30 min. On cooling, the brown precipitates were collected, washed with water, and then recrystallized from acetone to give VI as yellow needles (or prisms), m. p. 288—289°C (decomp.); yield, 1.2 g. It gave a green ferric chloride reaction in ethanol.

Found: C, 64.87; H, 4.61. Calcd. for $C_{17}H_{14}O_6$: C, 64.96; H, 4.47%.

**5-Hydroxy-4′-methoxy-7, 8-methylenedioxy-2-methylisoflavone (VII).**—Into a mixture of VI (1.6 g.), potassium hydroxide (0.9 g.) and ethanol (15 ml.) in water (15 ml.), air having been excluded by a stream of nitrogen gas, methylene sulfate (1.1 g.) in acetone (20 ml.) was stirred at 45—50°C. The mixture was kept at 45—50°C for another 80 min. and then diluted with aqueous potassium hydroxide. The yellow precipitates were collected, washed with dilute hydrochloric acid, and then water, and recrystallized from aqueous acetone to give VII as yellow needles, m. p. 190—191°C; yield 450 mg. It gave a green ferric chloride reaction in ethanol. IR: 1665 (C=O), 1034 (=C-O-C), 923 $cm^{-1}$ (O-$CH_2$-O).

Found: C, 66.16; H, 4.43. Calcd. for $C_{18}H_{14}O_6$: C, 66.25; H, 4.32%.

**5-Benzyloxy-4′-methoxy-7, 8-methylenedioxy-2-methylisoflavone (VIII).**—The isoflavone VII (1.1 g.) was refluxed with dry acetone (100 ml.), benzyl chloride (450 mg.), sodium iodide (0.1 g.) and anhydrous potassium carbonate (15 g.) for 30 hr. Inorganic salts were filtered off and washed with warm acetone, and the combined acetone solution was distilled off. The residue was washed with water and recrystallized from acetone to give VIII as colorless needles, m. p. 195—196°C; yield 0.7 g. IR: 1646 (C=O), 1028 (=C-O-C), 915 $cm^{-1}$ (O-$CH_2$-O).

Found: C, 72.42; H, 4.99. Calcd. for $C_{25}H_{20}O_6$: C, 72.10; H, 4.84%.

**6-Benzyloxy-2-hydroxy-3,4-methylenedioxyphenyl 4-Methoxybenzyl Ketone (IX).**—A mixture of VIII (600 mg.), aqueous potassium hydroxide (10%, 10 ml.) and ethanol (100 ml.) was refluxed for 2 hr. under a stream of nitrogen gas. The solvent was removed in vacuo, and the residue was acidified with dilute hydrochloric acid. The yellow precipitates were collected, washed with water, and then crystallized from aqueous acetone to give IX as pale yellow needles, m. p. 148—149°C; yield 420 mg. It gave a green ferric chloride reaction in ethanol.

11) K. Fukui and T. Matsumoto, *J. Sci. Hiroshima, Univ., Ser. A-II*, **28**, 47 (1964); *J. Chem. Soc. Japan, Pure Chem. Sec. (Nippon Kagaku Zasshi)*, **85**, 793 (1964); This Bulletin, **38**, 612 (1965).

*3 All melting points are uncorrected; the ultraviolet spectra were measured in ethanol, while the infrared spectra were measured in Nujol.

IR: 1663 (C=O), 1031 (=C-O-C), 915 $cm^{-1}$ (O-$CH_2$-O). UV: $\lambda_{max}^{EtOH}$ m$\mu$ (log $\varepsilon$); 247 (4.12), 296 (4.10), 351 (3.53).

Found: C, 70.70; H, 5.28. Calcd. for $C_{23}H_{20}O_6$: C, 70.40; H, 5.14%.

**6-Hydroxy-2-methoxy-3, 4-methylenedioxyphenyl 4-Methoxybenzyl Ketone (III).**—*From IV.*—3-Methoxy-4, 5-methylenedioxyphenol (IV)[12] (3.7 g.) and 4-methoxybenzyl cyanide (3.7 g.) were dissolved in dry ether (70 ml.), and then fused zinc chloride (1.0 g.) was added. The mixture was saturated with dry hydrogen chloride in an ice bath and allowed to stand overnight. After the ether layer had been decanted, the ketimine hydrochloride was washed with dry ether and then hydrolyzed by heating it with water (40 ml.) on a water bath for 30 min. The solid which had separated on cooling was extracted with ethyl acetate; the extract was washed with aqueous sodium bicarbonate and then with water. After the solvent had been evaporated, the residue was distilled. The distillate (bath temperature 180—240°C/0.01 mm. Hg.) was collected and recrystallized from methanol to give III as yellow needles, m. p. 114—115°C (reported m. p. 113—114°C[1]); yield, 820 mg. It gave a green ferric chloride reaction in ethanol. IR: 1662 (shoulder), 1632 (C=O), 1035 (=C-O-C), 936 $cm^{-1}$ (O-$CH_2$-O). UV: $\lambda_{max}^{EtOH}$ m$\mu$ (log $\varepsilon$); 245.5 (4.08), 286.5 (4.14), 355 (3.72).

Found: C, 64.39; H, 5.10. Calcd. for $C_{17}H_{16}O_6$: C, 64.55; H, 5.10%.

*From IX.*—The ketone IX (360 mg.) was refluxed with dry acetone (40 ml.), dimethyl sulfate (4 drops), and anhydrous potassium carbonate (4.0 g.) for 27 hr. The crude product X, was dissolved into ethyl acetate, and the solution was washed with aqueous potassium hydroxide (5%) and then with water. After the solvent had been evaporated, the residue was dissolved into ethanol (50 ml.) and in the presence of Pd-C (10%, 1.0 g.), the solution was shaken with hydrogen at room temperature for 5 hr. The reaction mixture was filtered, and the filtrate was evaporated. The residue was recrystallized from methanol to give III as yellow needles, m. p. 114—115°C; yield 90 mg. This compound was identical with the above sample.

**4', 5-Dimethoxy-6, 7-methylenedioxyisoflavone (Irisolone Methyl Ether) (II).**—The ketone III (150 mg.) was condensed with ethyl formate (15 ml.) and sodium (0.2 g.) as described by Gopinath et al.[1] Recrystallization from methanol gave II (40 mg.) as colorless plates, m. p. 182—183°C*4 reported m. p. 184—185°C[1]). It was found identical with the natural irisolone methyl ether (m. p. 179—181°C*1,*4)) which had been supplied by Gopinath, by mixed melting point measurement and infrared and ultraviolet spectral comparisons. This substance dissolves into concentrated sulfuric acid to give a yellow solution. IR: 1647 (C=O), 1021 (=C-O-C), 925 $cm^{-1}$ (O-$CH_2$-O).

Found: C, 66.04; H, 4.21. Calcd. for $C_{18}H_{14}O_6$: C, 66.25; H, 4.32%.

12) A. F. Wagner, E. Walton, A. N. Wilson, J. O. Rodin and F. W. Holly, *J. Am. Chem. Soc.*, **81**, 4983 (1959).

*4 The sample was dried in vacuo at 110°C for 2 hr.

**4', 5-Dimethoxy-7, 8-methylenedioxy-2-methylisoflavone (XI).**—A mixture of VII (830 mg.), dimethyl sulfate (2.0 ml.), anhydrous potassium carbonate (10 g.) and dry acetone (80 ml.) was refluxed for 30 hr. The reaction mixture was then filtered, and the inorganic residue was washed with hot acetone. The evaporation of acetone left a solid which was triturated with water, filtered, and crystallized from aqueous acetic acid to give XI as colorless needles, m. p. 214—215°C; yield 750 mg. It dissolves into concentrated sulfuric acid to give a yellow solution. IR: 1668 (C=O), 1029 (=C-O-C), 923 $cm^{-1}$ (O-$CH_2$-O).

Found: C, 67.08; H, 4.94. Calcd. for $C_{19}H_{16}O_6$: C, 67.05; H, 4.75%.

**2-Hydroxy-6-methoxy-3, 4-methylenedioxyphenyl 4-Methoxybenzyl Ketone (XII).**—A mixture of the isoflavone XI (560 mg.), potassium hydroxide (1.0 g.), water (10 ml.) and ethanol (60 ml.) was refluxed for 2 hr. under a stream of nitrogen gas. The reaction mixture was then treated in the usual manner. The product was recrystallized from ethanol to give the ketone XII as yellow plates, m. p. 133—134°C; yield, 460 mg. It gave a green ferric chloride reaction in ethanol. IR: 1671 (C=O), 1033 (=C-O-C), 915 $cm^{-1}$ (O-$CH_2$-O). UV: $\lambda_{max}^{EtOH}$ m$\mu$ (log $\varepsilon$); 246.5 (4.11), 295.5 (4.15), 349 (3.56).

Found: C, 64.49; H, 5.31. Calcd. for $C_{17}H_{16}O_6$: C, 64.55; H, 5.10%.

When the ketone XII (200 mg.) was heated with anhydrous sodium acetate (200 mg.) and acetic anhydride (10 ml.), the parent isoflavone, XI (80 mg., m. p. 214—215°C), was obtained.

**4', 5-Dimethoxy-7, 8-methylenedioxyisoflavone (XIII).**—The ketone XII (600 mg.) in ethyl formate (25 ml.) was added to sodium powder (0.6 g.) at −10°C and left in the refrigerator for 3 days; then the product was worked up. The ether residue gave the isoflavone XIII, which crystallized from aqueous acetone as colorless needles, m. p. 179—181°C; yield 250 mg. It was soluble in concentrated sulfuric acid to give a reddish yellow solution and depressed to 150—152°C on admixture with natural irisolone methyl ether (m. p. 179—181°C*1). IR: 1651 (C=O), 1030 (=C-O-C), 920$cm^{-1}$ (O-$CH_2$-O).

Found: C, 66.47; H, 4.47. Calcd. for $C_{18}H_{14}O_6$: C, 66.25; H, 4.32%.

**6-Hydroxy-2-methoxy-3, 4-methylenedioxyphenyl 4-Nitrobenzyl Ketone (XVI).**—To a solution of 3-methoxy-4, 5-methylenedioxyphenol (IV) (4.4 g.) in dry ether (100 ml.), a mixture of 4-nitrobenzyl cyanide (4.4 g.) and anhydrous zinc chloride (3.0 g.) in dry chloroform (100 ml.) was added. The resulting mixture was saturated with dry hydrogen chloride at 0°C. The reaction mixture was then treated in the usual manner. Recrystallization from aqueous acetone gave the ketone XVI as yellow needles, m. p. 165—167°C; yield, 3.2 g. It gave a green ferric chloride reaction in ethanol. IR: 1623 (C=O), 1515, 1331 ($NO_2$), 1039 (=C-O-C), 923 $cm^{-1}$ (O-$CH_2$-O).

Found: C, 58.04; H, 4.13; N, 4.21. Calcd. for $C_{16}H_{13}O_7N$: C, 58.01; H, 3.96; N, 4.23%.

**6-Hydroxy-2-methoxy-3, 4-methylenedioxyphenyl 4-Aminobenzyl Ketone (XV).**—A solution of the ketone XVI (2.0 g.) in ethyl acetate (120 ml.) was submitted to catalytic reduction at room temperature in the presence of Pd-C (10%, 1.5 g.). After the catalyst had been filtered, the filtrate was evaporated; the residue was then recrystallized from methanol to give XV as yellow plates, m. p. 170—172°C; yield 1.5 g. It gave a green ferric chloride reaction in ethanol. IR: 3453, 3373, 1595, 1340 ($NH_2$), 1623 (C=O), 1044 (=C-O-C), 929 $cm^{-1}$ (O-$CH_2$-O).

Found: C, 63.58; H, 5.35; N, 4.68. Calcd. for $C_{16}H_{15}O_5N$: C, 63.78; H, 5.02; N, 4.65%.

**6-Hydroxy-2-methoxy-3, 4-methylenedioxyphenyl 4-Hydroxybenzyl Ketone (XIV).**—*From IV.*—From the ketone IV (600 mg.), 4-hydroxybenzyl cyanide (700 mg.) and anhydrous zinc chloride (0.3 g.) in dry ether (20 ml.), synthesis was carried out by a method similar to that used for XVI. The product was extracted with ethyl acetate, and the extract was washed with aqueous sodium bicarbonate and then water. After the solvent had been evaporated, the residue was distilled. The distillate (bath temperature 180—240°C/0.04 mmHg) was collected and recrystallized from ether-petroleum ether to give XIV as yellow needles, m. p. 152—153°C (reported m. p. 159—160°C[1]); yield, 70 mg. It gave a ferric green chloride reaction in ethanol. IR: 1630 (C=O), 1051 (=C-O-C), 934 $cm^{-1}$ (O-$CH_2$-O). UV: $\lambda_{max}^{EtOH}$ m$\mu$ (log $\varepsilon$); 245 (4.07), 287 (4.14), 355 (3.72).

Found: C, 63.40; H, 4.89. Calcd. for $C_{16}H_{14}O_6$: C, 63.57; H, 4.67%.

*From XV.*—A solution of sodium nitrite (400 mg.) in water (12 ml.) was added to a suspension of the ketone XV (800 mg.) in dilute sulfuric acid (25%, 55 ml.) at 0°C. After the solution had been stirred at 0—5°C for another hour, the excess nitrous acid was decomposed with urea (350 mg.). The solution was added drop by drop into a boiling solution of cupric sulfate (40 g.) in water (50 ml.). The reaction mixture was cooled and extracted with ether. The ether solution was washed with water, dried, and evaporated, and the residue was distilled. The distillate (bath temperature 180—220°C/0.01 mmHg) was collected and then recrystallized from ether-petroleum ether to give XIV as yellow microneedles, m. p. 152—153°C; yield, 80 mg. This substance was identical with the above sample.

An acetate (m. p. 89—90°C) was obtained by the acetic anhydride-pyridine method. IR: 1762, 1723 (OAc), 1623 (C=O), 1021 (=C-O-C), 915 $cm^{-1}$ (O-$CH_2$-O).

Found: C, 62.14; H, 4.60. Calcd. for $C_{20}H_{18}O_8$: C, 62.17; H, 4.70%.

**4'-Hydroxy-5-methoxy-6, 7-methylenedioxyisoflavone (Irisolone) (I).**—a) The ketone XIV (2.0 g.) in ethyl formate (60 ml.) was added to sodium (2.0 g.) at −10°C, left in a refrigerator for 3 days, and the product worked up. Recrystallization from aqueous pyridine gave I as colorless prisms, m. p. 251—252°C (reported m. p. 269—270°C[1]); yield, 1.1 g. This substance was soluble in aqueous sodium hydroxide (5%) and dissolves into concentrated sulfuric acid to give a yellow solution. It was found identical with the natural irisolone (m. p. 250—251°C*[1]) which was supplied by Gopinath, by mixed melting point measurement and infrared and ultraviolet spectral comparisons. IR: 1645 (C=O), 1028 (=C-O-C), 920 $cm^{-1}$ (O-$CH_2$-O).

Found: C, 65.47; H, 3.85. Calcd. for $C_{17}H_{12}O_6$: C, 65.38; H, 3.87%.

b) A mixture of the ketone XIV (600 mg.), ethyl orthoformate (1.5 ml.), dry pyridine (4.0 ml.) and piperidine (0.3 ml.) was refluxed for 4 hr. under a stream of nitrogen gas. The product which had separated on cooling was recrystallized from aqueous pyridine to give I as colorless prisms, m. p. 251—252°C; yield, 40 mg. It was identical with the above sample.

**The Reaction of Synthetic Irisolone (I).**—An acetate (m. p. 162—163°C) was prepared according to the Gopinath method[1] (reported m. p. 156—157°C[1]). IR: 1767 (OAc), 1649 (C=O), 1026 (=C-O-C), 926 $cm^{-1}$ (O-$CH_2$-O).

Found: C, 64.26; H, 3.92. Calcd. for $C_{19}H_{14}O_7$: C, 64.40; H, 3.98%.

The acetate (310 mg.) was refluxed with aqueous sodium hydroxide (10%, 3.0 ml.) and methanol (40 ml.) for 5 min. The parent isoflavone, I (m. p. 251—252°C, 240 mg.), was thus obtained.

According to the method of Gopinath et al.,[1] the isoflavone I was easily converted into II (m. p. 182—183°C) with dimethyl sulfate. II was demethylated with aluminum chloride in ether to give 5-hydroxy-4'-methoxy-6, 7-methylenedioxyisoflavone (m. p. 211—212°C, pale yellow plates) (reported m. p. 214—215°C[1]) according to the method of Gopinath et al.[1]

Found: C, 65.43; H, 3.84. Calcd. for $C_{17}H_{12}O_6$: C, 65.38; H, 3.87%.

**4'-Acetoxy-5-methoxy-6, 7-methylenedioxy-2-methylisoflavone (XVII).**—A mixture of the ketone XIV (80 mg.), anhydrous sodium acetate (200 mg.) and acetic anhydride (4.0 ml.) was refuxed for 30 hr. The excess acetic anhydride was removed in vacuo. The residue was washed with water and then recrystallized from methanol to give XVII as colorless plates, m. p. 201—202°C; yield 60 mg.

Found: C, 65.27; H, 4.36. Calcd. for $C_{20}H_{16}O_7$: C, 65.21; H, 4.38%.

**4'-Hydroxy-5-methoxy-6, 7-methylenedioxy-2-methylisoflavone (XVIII).**—A mixture of the acetate XVII (420 mg.), ethanol (60 ml.) and an aqueous sodium hydroxide solution (5%, 5.0 ml.) was refluxed for 5 min. After the solvent had been removed in vacuo, the residue was dissolved in water and then acidified. The precipitates were collected, washed with water, and recrystallized from methanol or acetone to give XVIII as colorless prisms, m. p. 284—285°C; yield, 230 mg. It dissolves into concentrated sulfuric acid to give a yellow solution.

Found: C, 66.12; H, 4.15. Calcd. for $C_{18}H_{14}O_6$: C, 66.25; H, 4.32%.

**5-Methoxy-6, 7-methylenedioxy-4'-nitroisoflavone (XIX).**—A mixture of the ketone XVI (1.0 g.), ethyl orthoformate (5.0 ml.), dry pyridine (8.0 ml.) and piperidine (0.5 ml.) was refluxed for 6 hr. The brown precipitates which separated on cooling were

collected, washed with ethanol, and then recrystallized from ethyl acetate to give XIX as pale yellow needles, m. p. 209—211°C; yield, 0.5 g. UV: $\lambda_{max}^{EtOH}$ mμ (log ε); 241*[2] (4.28), 289 (4.36), 315*[2] (4.23).

Found: C, 59.70; H, 3.44; N, 4.20. Calcd. for $C_{17}H_{11}O_7N$: C, 59.82; H, 3.26; N, 4.10%.

**5-Methoxy-6, 7-methylenedioxy-2-methyl-4′-nitroisoflavone (XX).**—A mixture of the ketone XVI (1.0 g.), acetic anhydride (25 ml.) and anhydrous sodium acetate (1.0 g.) was refluxed for 24 hr. The reaction mixture was treated in the usual manner. The product was recrystallized from acetone to give XX as yellow rhombic plates, m. p. 219—220°C; yield, 0.8 g. UV: $\lambda_{max}^{EtOH}$ mμ (log ε); 241.5*[2] (4.35), 284.5 (4.33), 312*[2] (4.11).

Found: C, 60.67; H, 3.80; N, 3.69. Calcd. for $C_{18}H_{13}O_7N$: C, 60.85; H, 3.68; N, 3.94%.

The authors are grateful to Dr. K. W. Gopinath, Muslim University, for his gifts of natural irisolone and its methyl ether. Grateful acknowledgement is also made to the members of the Microanalytical Laboratory, Faculty of Pharmacy, Nagasaki University, for the microanalyses.

*Department of Chemistry*
*Faculty of Science*
*Hiroshima University*
*Higashi-Sendamachi, Hiroshima*

# Oxidation of Alcohols with *t*-Butyl Chromate. I. The Oxidation of Primary Aliphatic Alcohols*[1]

By Takayuki SUGA, Keiichi KIHARA*[2] and Tamon MATSUURA

(Received September 5, 1964)

Oppenauer and Oberrauch[1] have recorded that *t*-butyl chromate[2] in a nonpolar solvent converts primary alcohols, such as cetyl alcohol, geraniol and benzyl alcohol, into the corresponding aldehydes in 80—94% yields, and also that this oxidant in a nonpolar solvent containing such an organic acid as acetic acid oxidizes to a ketone group a methylene group adjacent to a double bond. *t*-Butyl chromate has been employed for the preparation of $\alpha,\beta$-unsaturated ketones.[3] Among primary alcohols, the *t*-butyl chromate oxidation of 2-isopropyl-5-methylhexanol and 3-isopropyl-1-heptenol[4] has been recorded to afford only the corresponding aldehyde in a low yield. However, the action of *t*-butyl chromate on alcohols appears not to have been examined in detail as yet. We have now attempted the oxidation of a variety of aliphatic alcohols with *t*-butyl chromate.

The oxidation was undertaken on a series of aliphatic alcohols, which are shown to have the general formula of $R\cdot CH_2OH$, where R is $CH_3$, $CH_3(CH_2)_2$, $CH_3(CH_2)_3$, $CH_3(CH_2)_4$, $CH_3(CH_2)_{10}$, $CH_3(CH_2)_{14}$ and $CH_3(CH_2)_{16}$. When cetyl alcohol (Exp. 1) was oxidized in benzene for a shorter time (see Table I) than that used by Oppenauer and Oberrauch,*[3] it gave palmitic acid (54%; based on the sample taken) and cetyl palmitate (39%), but not palmitaldehyde. Since Oppenauer et al. have used petroleum ether as a solvent in this oxidation, the oxidation of *n*-lauryl alcohol in petroleum ether (Exp. 2) for a shorter time than that in Exp. 1 was carried out, giving lauraldehyde (3%), lauric acid (52%) and *n*-lauryl laurate (28%); the results resemble those of Exp. 1. Even when *n*-lauryl alcohol was oxidized in benzene with ice-cooling for 6 hr. (Exp. 3), the reaction product consisted of the aldehyde (38%), the

*1 A part of this work has been reported in *J. Chem. Soc. Japan, Pure Chem. Sec.* (*Nippon Kagaku Zasshi*), **80**, 653 (1959). The other part of it was partly presented at the 14th Annual Meeting of the Chemical Society of Japan, Tokyo, April, 1959, and at the 4th Symposium on Perfume, Terpene and Essential Oil Chemistry of the Chemical Society of Japan, Sapporo, July, 1960.

*2 Present address: Tôyô Sôda Manufacturing Company, Ltd., Nanyô-chô Tsuno-gun, Yamaguchi-ken.

1) R. V. Oppenauer and H. Oberrauch, *Anales Asoc. Quim. Argentina*, **37**, 246 (1949).

2) H. Wienhaus, *Ber.*, **47**, 322 (1914); H. Wienhaus and W. Treibs, ibid., **56**, 1648 (1923).

3) D. Ginsberg and R. Pappo, *J. Chem. Soc.*, **1951**, 516; T. Matsuura and K. Fujita, *J. Sci. Hiroshima Univ.*, **A16**, 173 (1952); G. Dupont, R. Dulou and O. Mondou, *Bull. soc. chim. France*, **1953**, 60; K. Fujita and T. Matsuura, *J. Sci. Hiroshima Univ.*, **A18**, 455 (1955); K. Fujita, *J. Chem. Soc. Japan, Pure Chem. Sec.* (*Nippon Kagaku Zassi*), **78**, 1112 (1957); T. Matsuura and T. Suga, ibid., **78**, 1117 (1957); T. Matsuura, T. Suga and K. Suga, ibid., **78**, 1122 (1957); T. Suga, This Bulletin, **31**, 569 (1958); I. Alkony, *Chem. Ber.*, **94**, 2486 (1961); T. Matsuura, T. Suga and T. Sakao, This Bulletin, **35**, 1623 (1963).

4) R. Kitaoka, *J. Chem. Soc. Japan, Pure Chem. Sec.* (*Nippon Kagaku Zassi*), **77**, 630 (1956); **78**, 1597 (1957).

*3 The oxidation recorded by Oppenauer et al. has been carried out at room temperature over a 14-day period, using a petroleum ether solution of *t*-butyl chromate prepared in the 1:2.5 mol. ratio of cetyl alcohol to this chromate and in a 28% concentration, and using a petroleum ether solution of cetyl alcohol in the same concentration as in Exp. 1.

TABLE I. CONDITIONS OF THE OXIDATION

| Exp. | Sample: Alcohol | Sample: Concentration[a] % | Oxidant: Sample to *t*-Bu. chrom.[b] (mol. ratio) | Oxidant: Concentration % | Temp. °C | Time |
|---|---|---|---|---|---|---|
| 1 | Cetyl | 0.9 | 1 : 2.5 | 23 | ca.30 | 5 days |
| 2[c] | *n*-Lauryl | 1.2 | 1 : 2.5 | 28 | ca.25 | 2 days |
| 3 | *n*-Lauryl | 4.5 | 1 : 1 | 36.5 | 1—2 | 6 hr. |
| 4 | *n*-Hexyl | 4.5 | 1 : 1 | 36.5 | 1—2 | 6 hr. |
| 5 | *n*-Butyl | 4.5 | 1 : 1 | 36.5 | 1—2 | 6 hr. |
| 6 | Ethyl | 4.5 | 1 : 1 | 36.5 | 1—2 | 6 hr. |
| 7 | *n*-Amyl | 2.3 | 1 : 1 | 23 | 1—2 | 6 hr. |
| 8 | Isoamyl | 4.5 | 1 : 1 | 36.5 | 1—2 | 6 hr. |
| 9 | Isobutyl | 4.5 | 1 : 1 | 36.5 | 1—2 | 6 hr. |
| 10 | Neopentyl | 4.5 | 1 : 1 | 36.5 | 1—2 | 6 hr. |
| 11 | Geraniol | 4.5 | 1 : 1 | 36.5 | 1—2 | 6 hr. |
| 12 | Isobutyl | 6.8 | 1 : 1.5 | 38 | ca.15 | 66 hr. |

a) Mole in 1000 g. of benzene or petroleum ether.
b) *t*-Bu. chrom.=*t*-Butyl chromate.
c) Petroleum ether was used as a solvent.

carboxylic acid (23%) and the ester (38%). The oxidation of *n*-hexyl alcohol (Exp. 4) under the same conditions as in Exp. 3 gave caproaldehyde (25%), caproic acid (37%) and *n*-hexyl caproate (34%); *n*-butyraldehyde (29%), *n*-butyric acid (32%) and *n*-butyl *n*-butyrate (35%) were also produced in the oxidation of *n*-butyl alcohol (Exp. 5). The oxidation of ethyl alcohol (Exp. 6) afforded acetaldehyde (17%), acetic acid (20%) and ethyl acetate (23%). In all these cases, only a small percentage of unchanged alcohol was recovered. Moreover, *n*-amyl alcohol (Exp. 7), diluted by a double quantity of benzene used in Exp. 3—6, was oxidized under the same conditions as above with a benzene solution of *t*-butyl chromate in a low concentration. The reaction product consisted of *n*-valeraldehyde (43%), *n*-valeric acid (17%) and *n*-amyl *n*-valerate (29%).

The oxidation was tried with alcohols with a variety of $\alpha$- or $\beta$-substituents. The oxidation of isoamyl alcohol (Exp. 8) under the same conditions as in Exp. 3 gave isovaleraldehyde (31%), isovaleric acid (29%) and isoamyl isovalerate (34%). When isobutyl alcohol (Exp. 9) was used, the products were isobutyraldehyde (17%), isobutyric acid (26%), isobutyl isobutyrate (29%) and acetone (4%). The formation of acetone was remarkable in Exp. 12 (17%); it is probably a result of the occurrence of the cleavage reaction. Furthermore, the oxidation of neopentyl alcohol (Exp. 10) yielded trimethylacetaldehyde (36%), trimethylacetic acid (5%) and neopentyl trimethylacetate (13%), and left unchanged the alcohol (38%). This is likely to have been the result of an attack of *t*-butyl chromate on the hydroxymethyl group interrupted by the bulky *t*-butyl group around the hydroxyl group.

Oppenauer et al.[1] have obtained citral in a 80% yield on the *t*-butyl chromate oxidation of geraniol at 28°C for 3 days. A reexamination of the oxidation of geraniol under the same conditions as in Exp. 3 gave citral (77%), geranic acid (2%) and 2-methyl-2-hepten-6-one (3%), but the ester was not obtained. This methylheptenone is presumably produced by an ethylenic bond fission at the allylic position of the sample alcohol.

On oxidation with *t*-butyl chromate, the alcohol with an olefinic double bond on the carbon adjacent to the hydroxymethyl group afforded the corresponding aldehyde in a high yield, but not the ester. On the other hand, saturated primary alcohols with the formula of $X\text{–}CH_2\cdot CH_2OH$ (X: H or alkyl), $\begin{matrix}R\\R\end{matrix}\!\!>\!CH\cdot CH_2OH$ or $\begin{matrix}R\\R\end{matrix}\!\!>\!C\cdot CH_2OH$ were found to produce aldehyde, carboxylic acid and ester corresponding to the alcohol in comparable yields. The formation of an ester was newly recognized in the *t*-butyl chromate oxidation of a saturated aliphatic primary alcohol. The course of the formation of the ester will be discussed in the near future in Part IV of this series.

## Experimental

**Sample Alcohols.**—Neopentyl alcohol was prepared from *t*-butyl chloride and formaldehyde by Grignard reaction;[5] it showed b. p. 110.5—111.5°C

5) S. V. Puntambeker and E. A. Zoellner, "Organic Syntheses," Coll. Vol. I, 510 (1948); A. Courtot, *Bull. soc. chim. France*, **1906**, 985.

TABLE II. THE WEIGHT OF THE SAMPLE ALCOHOL, EACH COMPONENT IN THE OXIDANT AND THE REACTION PRODUCT PRODUCED

| Exp. | Sample | | Oxidant | | | Reaction Product | | | | Unchangd |
|---|---|---|---|---|---|---|---|---|---|---|
| | Alcohol | $C_6H_6$ | $CrO_3$ | *t*-BuOH | $C_6H_6$ | Aldehyde | Acid | Ester | Cleavage product | Alc. |
| | g. | g. | g. | g. | g. | g. | g. | g. | g. | g. |
| 1[a] | Cetyl | 50.0 | 275 | 50.8 | 102.0 | 412 | — | 27.2 | 19.6 | — | 1.9 |
| 2[b] | *n*-Lauryl | 15.0 | 107 | 19.8 | 39.6 | 161 | 0.4 | 7.8 | 4.2 | — | 0.3 |
| 3 | *n*-Lauryl | 30.0 | 36 | 16.1 | 32.2 | 60 | 9.6 | 7.0 | 11.4 | — | 1.5 |
| 4 | *n*-Hexyl | 30.0 | 65 | 29.3 | 59.0 | 110 | 7.6 | 11.0 | 10.1 | — | — |
| 5 | *n*-Butyl | 30.0 | 90 | 40.0 | 80.0 | 150 | 8.8 | 9.5 | 10.5 | — | — |
| 6 | Ethyl | 30.0 | 145 | 65.1 | 130.3 | 244 | 5.1 | 5.9 | 7.0 | — | — |
| 7 | *n*-Amyl | 25.0 | 127 | 28.4 | 56.8 | 214 | 10.7 | 4.2 | 7.2 | — | 2.7 |
| 8 | Isoamyl | 20.0 | 51 | 23.0 | 46.0 | 86 | 6.2 | 5.8 | 6.7 | — | — |
| 9 | Isobutyl | 20.0 | 60 | 27.0 | 54.0 | 100 | 3.4 | 5.2 | 5.8 | 0.7[c] | — |
| 10 | Neopentyl | 30.0 | 76 | 34.0 | 68.0 | 128 | 10.9 | 1.6 | 4.0 | — | 11.3 |
| 11 | Geraniol | 40.0 | 58 | 25.9 | 51.8 | 97 | 30.9 | 0.8 | — | 1.1[d] | 2.0 |
| 12 | Isobutyl | 10.0 | 20 | 20.0 | 44.0 | 60 | 0.5 | 1.8 | 4.3 | 1.7[c] | — |

a) Only benzene is represented by volume (ml.).
b) Petroleum ether (ml.) was used as a solvent.
c) The product is acetone.
d) The product is 2-methyl-2-hepten-6-one.

and m. p. 55—56°C after it had been rectified. Geraniol supplied by the Takasago Perfumery Co., Ltd., was purified following the literature method[6] and showed b. p. 111.8—112°C/11 mmHg, $n_D^{25}$ 1.4714 and $d_4^{25}$ 0.8760. The rest of the sample alcohols were obtained from a commercial source and were purified by distillation or recrystallization.

**Oxidant.**—*t*-Butyl chromate was prepared by adding chromium trioxide in small portions to *t*-butyl alcohol under ice-cooling, diluting the resultant with benzene or petroleum ether, and drying the resultant benzene or petroleum ether solution of *t*-butyl chromate over anhydrous sodium sulfate. The quantity of each component used is shown in Table II. The concentration of *t*-butyl chromate in this solution and the mole ratio of a sample alcohol to this chromate are shown in Table I.

**Oxidation and Treatment of a Reaction Mixture.**—Into the benzene or petroleum ether solution of a sample alcohol (the concentration of the alcohol is shown in Table I), the oxidant prepared as above was stirred over a period of 0.5 hr., keeping the internal temperature at 1—2°C; it was then stirred continuously at the same temperature or at room temperature for a further 5.5 hr. or for a period shown in Table I under an atmosphere of nitrogen. Then the whole reaction mixture was treated with water and oxalic acid, except in Exp. 10 (see below), in order to hydrolyze the residual oxidant. The mixture was separated into a benzene layer and an aqueous one, and the latter was repeatedly extracted with benzene or petroleum ether. The removal of the solvent from the combined benzene or petroleum ether solution, after drying over anhydrous sodium sulfate, left a reaction product. The constituents of the reaction product were examined in a manner shown in each experiment. Each of the constituents was identified by a comparison of its infrared spectrum with that of an authentic sample and by a mixed melting point determination of a constituent or its crystalline derivatives. The yield of the constituents of the reaction product is shown in Table II.

**Oxidation of Cetyl Alcohol (Exp. 1).** — The removal of the solvent from the separated benzene solution gave the reaction product (m. p. 51—54°C), from which palmitic acid (m. p. 61—62°C) was then taken out as the lead salt.[7] The neutral product free from the acid was subjected to liquid-column chromatography on silica gel with a mixture of *n*-hexane and ethyl acetate in order to separate cetyl palmitate (m. p. 51—52°C; $\nu_{max}^{KBr}$ 1735, 1186 $cm^{-1}$) and unchanged cetyl alcohol. No isolated palmitaldehyde could be observed in spite of a careful examination.

**Oxidation of *n*-Lauryl Alcohol (Exp. 2 and 3).** —The distillation of the reaction product gave lauraldehyde (b. p. 103—110°C/3 mmHg), unchanged alcohol (b. p. 115—122°C/3 mmHg) and lauric acid (b. p. 150—151°C/3 mmHg) as the distillate, and *n*-lauryl laurate (m. p. 27—28°C; $\nu_{max}^{KBr}$ 1740, 1161 $cm^{-1}$) as the residue.

**Oxidation of *n*-Hexyl Alcohol (Exp. 4).** — The distillation of the reaction product gave caproaldehyde (120—140°C), caproic acid (b. p. 111—112°C/20 mmHg) and *n*-hexyl caproate (b. p. 129—130.5°C/20 mmHg; $\nu_{max}^{KBr}$ 1736, 1171 $cm^{-1}$). Caproaldehyde was also contained in removed benzene; it was estimated by the hydroxylamine method.[8]

**Oxidation of *n*-Butyl Alcohol (Exp. 5).**—An ether solution of the reaction product (b. p. 99—102°C/81 mmHg) obtained by the removal of the

6) E. Guenther, "The Essential Oils," D. Van Nostrand Company, Inc., New York (1952), p. 171.

7) J. D. Piper, A. G. Fleiger, C. C. Smith and N. A. Kerstein, *Ind. Eng. Chem.*, **31**, 307 (1939); W. F. Whitmore and M. Lauro, ibid., **22**, 646 (1930).

8) W. M. Bryant and D. M. Smith, *J. Am. Chem. Soc.*, **57**, 57 (1935).

solvent from the separated benzene solution was extracted with a 10% sodium carbonate solution. The sodium carbonate extracts gave *n*-butyric acid (b. p. 161—163°C) on acidification, while the removal of the solvent from the neutral ether solution afforded *n*-butyl *n*-butyrate (b. p. 97—99°C/80.5 mmHg; $\nu_{max}^{liq.}$ 1737, 1183 $cm^{-1}$). *n*-Butyraldehyde was separated as the 2,4-dinitrophenylhydrazone[9] from the solvent so removed; it was then estimated.

**Oxidation of Ethyl Alcohol (Exp. 6).**—After the reaction mixture had been treated with oxalic acid and water, acetaldehyde in the separated aqueous solution was estimated by the 2,4-dinitrophenylhydrazine method,[9] while acetic acid was determined by titrating the steam-distillate of the aqueous solution with a standard solution of sodium hydroxide. The separated benzene solution was subjected to gas chromatographic analysis in order to estimate acetaldehyde and ethyl acetate.

**Oxidation of *n*-Amyl Alcohol (Exp. 7).**—The distillation of the reaction product gave *n*-valeraldehyde (b. p. 91—111°C), unchanged alcohol (b. p. 131—145°C), *n*-valeric acid (b. p. 101—103°C/30 mmHg) and *n*-amyl *n*-valerate (b. p. 106—108°C/29 mmHg; $\nu_{max}^{liq.}$ 1735, 1178 $cm^{-1}$).

**Oxidation of Isoamyl Alcohol (Exp. 8).** — The reaction product obtained by the evaporation of the solvent was examined in the same manner as that in Exp. 5; it was seen to consist of isovaleric acid (b. p. 97—99°C/38.5 mmHg) and isoamyl isovalerate (b. p. 100—102°C/39 mmHg; $\nu_{max}^{liq.}$ 1735, 1188 $cm^{-1}$). Isovaleraldehyde contained in the distilled solvent was estimated by the 2, 4-dinitrophenylhydrazine method.

**Oxidation of Isobutyl Alcohol (Exp. 9 and 12).**—The reaction product obtained by the removal of the solvent was found, by the same manner as in Exp. 5, to consist of isobutyric acid (b. p. 152—153°C) and isobutyl isobutyrate (b. p. 146—148°C; $\nu_{max}^{liq.}$ 1156 and 1198 (doublet), 1739 $cm^{-1}$). Acetone and isobutyraldehyde were caught as a mixture of the corresponding 2,4-dinitrophenylhydrazone from the solvent removed, and then the dinitrophenylhydrazone was separated by chromatography on a silica gel column.[10]

**Oxidation of Neopentyl Alcohol (Exp. 10).**—After the oxidation, the reaction mixture was treated with hydrazine sulfate (40 g.) and dilute sulfuric acid in order to hydrolyze the residual oxidant. The distillation of the reaction product gave unchanged alcohol (b. p. 110.5—115°C), trimethylacetic acid (m. p. 34—35°C) and neopentyl trimethylacetate (b. p. 165°C; $\nu_{max}^{liq.}$ 1723, 1154 $cm^{-1}$). The acid and the ester were separated from each other by extracting a fraction (b. p. 161—166°C) of the distillate with a sodium carbonate solution. Trimethylacetaldehyde and also a small amount of unchanged alcohol contained in removed benzene were estimated by gas chromatographic analysis.

**Oxidation of Geraniol (Exp. 11).**— The separated benzene solution was extracted with a 3% sodium bicarbonate solution. Geranic acid was obtained from this alkaline solution on acidification. The distillation of the neutral product obtained from the neutral benzene solution gave 2-methyl-2-hepten-6-one (b. p. 60.2—65°C/11.5 mmHg) and citral (b. p. 107—112°C/11.5 mmHg). No ester could be detected, even by thin layer chromatography and gas chromatography of the distillate and the residue.

9) H. A. Iddles and C. E. Jackson, *Ind. Eng. Chem., Anal. Ed.*, **6**, 454 (1934).
10) Cf., J. Roberts and C. Green, ibid., **18**, 335 (1946).

## Summary

Oxidation with *t*-butyl chromate has been carried out on the straight-chain alcohols with the general formula of $R \cdot CH_2OH$, where R is $CH_3$, $CH_3(CH_2)_2$, $CH_3(CH_2)_3$, $CH_3(CH_2)_4$, $CH_3(CH_2)_{10}$, $CH_3(CH_2)_{14}$ and $CH_3(CH_2)_{16}$, on branched-chain alcohols with a variety of substituents at the carbon alpha or beta to the hydroxymethyl group, and on unsaturated alcohol with an allylic hydroxymethyl group. Thus, a saturated primary alcohol containing the grouping of $-CH_2 \cdot CH_2OH$, $>CH \cdot CH_2OH$ or $>C \cdot CH_2OH$ has been found to produce mixtures of the corresponding aldehyde, acid and ester in comparable yields. On the other hand, an unsaturated primary alcohol with an olefinic double bond on the carbon adjacent to the hydroxymethyl group produces the corresponding aldehyde in a high yield, but not the ester.

The authors wish to express their hearty thanks to the Takasago Perfumery Co., Ltd., for supplying them with a sample of geraniol. This research was aided by a grant from the Ministry of Education.

*Department of Chemistry*
*Faculty of Science*
*Hiroshima University*
*Hiroshima*

# The Synthesis and the Reactions of 2, 4, 6-Tri-(ω-hydroxyalkyl)-1, 3, 5-triazines

By Hiroyuki NOHIRA, Yoshihiro NISHIKAWA, Yoshiaki FURUYA and Teruaki MUKAIYAMA

(Received September 5, 1964)

The present study will deal with the synthesis and the reactions of 2, 4, 6-tri-(ω-hydroxyalkyl)-1, 3, 5-triazines. The formation of the triazines was found in the cours of an experiment to prepare *N*-unsubstituted cyclic iminoethers, which had been expected to afford polyamides by the 1, 4-addition type ring-opening polymerization,[1-4] by treating their hydrochlorides with triethylamine.

The hydrochlorides of cyclic iminoethers (I) were prepared from the corresponding ω-cyanohydrines by the action of hydrogen chloride (Table I). The hydrochlorides decomposed to give the corresponding ring-opening products, ω-chloroalkylamides (II), in high yields when they were heated above their melting points (Table II).

$$N\equiv C-(CH_2)_n-OH + HCl \longrightarrow \underset{HCl}{HN=C}\overset{(CH_2)_n}{\underset{O}{\diagup\diagdown}} \quad n=3,4,5 \qquad (I)$$

$$I \xrightarrow[heat]{} H_2N-\overset{O}{\overset{\|}{C}}-(CH_2)_n-Cl \qquad (II)$$

TABLE I

$$N\equiv C-(CH_2)_n-OH+HCl \rightarrow \underset{HCl}{HN=C}\overset{(CH_2)_n}{\underset{O}{\diagup\diagdown}} \qquad (I)$$

| n | Yield % | M. p. [lit.] °C | Formula | | Analysis, % C | H | N | Cl |
|---|---|---|---|---|---|---|---|---|
| 3 | 95 | 103—105 [95[a]] | $C_4H_8ClNO$ | Found | 38.65 | 6.25 | 11.60 | 29.41 |
| | | | | Calcd. | 39.51 | 6.62 | 11.53 | 29.50 |
| 4 | 90 | 128—129 | $C_5H_{10}ClNO$ | Found | 44.57 | 7.64 | 10.42 | 26.15 |
| | | | | Calcd. | 44.62 | 7.48 | 10.41 | 26.20 |
| 5 | 85 | 143—144 | $C_6H_{12}ClNO$ | Found | 48.11 | 8.25 | 9.55 | |
| | | | | Calcd. | 48.23 | 8.08 | 9.37 | |

a) K. S. Topchiev and M. L. Kirmalova, *Doklady Akad. Nauk S. S. S. R.*, **63**, 281 (1948); *Chem. Abstr.*, **43**, 2579e.

TABLE II

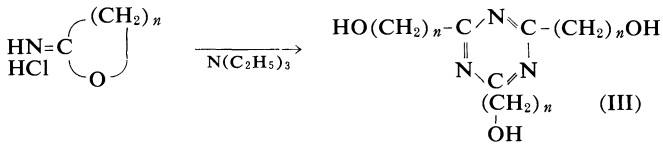
$$\underset{HCl}{HN=C}\overset{(CH_2)_n}{\underset{O}{\diagup\diagdown}} \rightarrow H_2N-\overset{O}{\overset{\|}{C}}-(CH_2)_n-Cl \qquad (II)$$

| n | yield % | M. p. [lit.] °C | Formula | | Analysis, % C | H | N |
|---|---|---|---|---|---|---|---|
| 3 | 95 | 97 [90.4—90.7[a]] | $C_4H_8ClNO$ | Found | 39.25 | 6.50 | 11.65 |
| | | | | Calcd. | 39.51 | 6.62 | 11.53 |
| 4 | 80 | 78 [78—79[b]] | $C_5H_{10}ClNO$ | Found | 44.76 | 7.58 | 10.55 |
| | | | | Calcd. | 44.62 | 7.48 | 10.41 |
| 5 | 95 | 102 | $C_6H_{12}ClNO$ | Found | 48.34 | 7.93 | 9.58 |
| | | | | Calcd. | 48.23 | 8.08 | 9.37 |

a) M. Berthet, *Bull. classe sci. Acad. roy. Belg.*, **27**, 212 (1941); *Chem. Abstr.*, **37**, 3400[7].
b) A. N. Nesmeyanow and L. I. Zakharkin, *Izvest. Akad. Nauk S. S. S. R., Otdel. Kim. Nauk*, **1953**, 988; *Chem. Abstr.*, **49**, 2298c.

1) T. Mukaiyama, T. Fujisawa, H. Nohira and T. Hyugaji, *J. Org. Chem.*, **27**, 3337 (1962).
2) T. Mukaiyama and K. Sato, This Bulletin, **36**, 99 (1963).
3) T. Fujisawa, Y. Tamura and T. Mukaiyama, ibid., **37**, 793 (1964).
4) H. Nohira, Y. Nishikawa and T. Mukaiyama, ibid., **37**, 797 (1964).

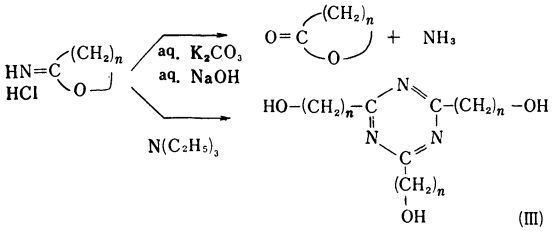
TABLE III



(III)

| $n$ | Yield % | B. p. °C(mmHg) | Formula | | Analysis, % C | H | N | IR absorption $\nu_{max}$, $cm^{-1}$ | UV absorption $\lambda_{max}$, $m\mu(\log \varepsilon)$ |
|---|---|---|---|---|---|---|---|---|---|
| 3 | 53 | 196—198(0.1) | $C_{12}H_{21}N_3O_3$ | Found | 56.65 | 8.08 | 16.62 | 3350(s, broad), 2925(m), 2850(m), 1545(vs), 1060(s) | 259(2.85) |
| | | | | Calcd. | 56.45 | 8.29 | 16.46 | | |
| 4 | 70 | 207—209(0.04) | $C_{15}H_{27}N_3O_3$ | Found | 59.84 | 8.15 | 14.88 | 3340(s, broad), 2925(s), 2855(s), 1543(vs), 1065(s) | 260(2.88) |
| | | | | Calcd. | 60.58 | 9.15 | 14.13 | | |
| 5 | 50 | 218—221(0.01) | $C_{18}H_{33}N_3O_3$ | Found | 63.48 | 9.88 | 12.49 | 3350(s, broad), 2930(s), 2860(s), 1542(vs), 1065(s) | 259(2.82) |
| | | | | Calcd. | 63.68 | 9.80 | 12.39 | | |

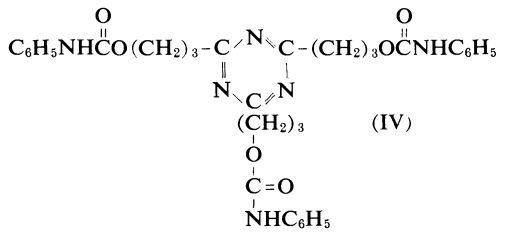
Several attempts to prepare free cyclic iminoethers from the hydrochlorides were made according to the ordinary procedures. When the hydrochlorides were treated with an aqueous solution of potassium carbonate or sodium hydroxide, they were mainly hydrolyzed to give the corresponding lactones and ammonia; free cyclic iminoethers could not be isolated. On the other hand, when the hydrochlorides were treated with anhydrous triethylamine, viscous liquids with a high boiling point resulted. The infrared spectra of these liquids showed strong absorptions at 3350 (OH), 1060 ($CH_2$-OH) and 1545 $cm^{-1}$ (*sym*-triazine ring). Further examinations by means of elementary analyses, ultraviolet spectra and the determination of molecular weight confirmed their structures to be 2, 4, 6-tri-($\omega$-hydroxyalkyl)-1, 3, 5-triazines (III). From the hydrochlorides of the five-, the six- and the seven-membered cyclic iminoethers, the corresponding *sym*-triazines were obtained in fairly good yields, as Table III shows.



(III)

A crystalline derivative (IV) was obtained from the reaction of 2,4,6-tri-($\gamma$-hydroxypropyl)-1, 3, 5-triazine and three equivalent moles of phenylisocyanate:

III + $3C_6H_5$-NCO →
$n=3$



(IV)

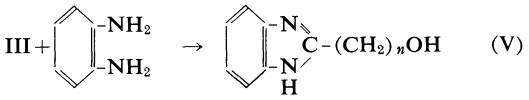
The similar triazine formation reaction of iminoethers reported by Cramer et al.[5] has been developed by Schaefer and Peters[6] into a convenient synthetic method for the preparation of 2, 4, 6-trisubstituted-1, 3, 5-triazines. A possible mechanism of these trimerization reactions of the iminoethers has been proposed by Schaefer and Peters. It does not seem unlikely that the cyclic iminoethers which are formed from their hydrochlorides trimerized by essentially the same mechanism. However, one of the significant features in the trimerization reaction of the cyclic iminoethers is that the cyclic iminoethers trimerize more easily than typical non-cyclic iminoethers. This seems to be attributable to the ring strain of the cyclic systems.

In conclusion, it has now been found that the *N*-unsubstituted cyclic iminoethers tend to trimerize more easily in such a fashion as to give *sym*-triazines, rather than to polymerize so as to give polyamides by the 1, 4-addition-type ring-opening polymerization. As a result, a convenient synthetic method for the preparation of $\omega$-hydroxyalkyl-derivatives of *sym*-triazine has been established.

Next, further study was carried out of the reaction of the 2, 4, 6-tri-($\omega$-hydroxyalkyl)-1, 3, 5-triazines thus obtained.

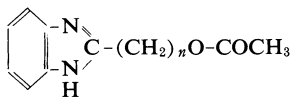
5) F. Cramer, K. Pawelzik and J. Kupper, *Angew. Chem.*, **68**, 649 (1956).
6) F. C. Schaefer and G. A. Peters, *J. Org. Chem.*, **26**, 2778 (1961).

TABLE IV

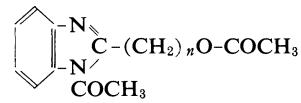


| n | Yield % | M. p. °C | Crystn. Solvent | Formula | | Analysis, % C | H | N |
|---|---|---|---|---|---|---|---|---|
| 3 | 85 | 160—161[163a)] | THF | $C_{10}H_{12}N_2O$ | Found | 67.90 | 7.01 | 16.11 |
| | | | | | Calcd. | 68.16 | 6.86 | 15.90 |
| 4 | 79 | 164—165 | THF | $C_{11}H_{14}N_2O$ | Found | 69.25 | 7.24 | 14.98 |
| | | | | | Calcd. | 69.44 | 7.42 | 14.73 |
| 5 | 55 | 106 | EA | $C_{12}H_{16}N_2O$ | Found | 70.45 | 8.17 | 13.98 |
| | | | | | Calcd. | 70.56 | 7.90 | 13.72 |

THF=tetrahydrofuran, EA=ethyl acetate



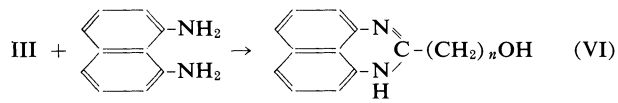
| n | M. p. °C | Formula | | Analysis, % C | H | N |
|---|---|---|---|---|---|---|
| 3 | 88—89 | $C_{12}H_{14}N_2O_2$ | F. | 66.27 | 6.74 | 12.87 |
| | | | C. | 66.03 | 6.47 | 12.84 |
| 4 | 95—97 | $C_{13}H_{16}N_2O_2$ | F. | 66.84 | 7.25 | 12.08 |
| | | | C. | 67.22 | 6.94 | 12.06 |
| 5 | | | | | | |



| M. p. °C | Formula | | Analysis, % C | H | N |
|---|---|---|---|---|---|
| 68—69 | $C_{15}H_{18}N_2O_3$ | F. | 65.71 | 6.70 | 10.20 |
| | | C. | 65.67 | 6.61 | 10.21 |
| 78—79 | $C_{16}H_{20}N_2O_3$ | F. | 66.25 | 6.76 | 9.90 |
| | | C. | 66.64 | 6.99 | 9.72 |

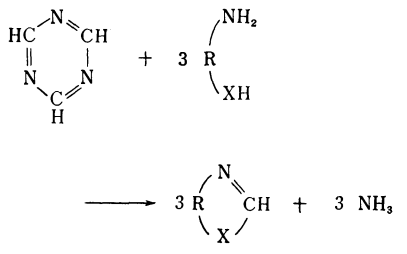
a) W. Reppe, et al., *Ann.*, **596**, 158 (1955).

TABLE V



| n | Yield % | M. p. °C | Crystn. solvent | Formula | | Analysis, % C | H | N |
|---|---|---|---|---|---|---|---|---|
| 3 | 34 | 145—146 | Dioxane | $C_{14}H_{14}N_2O$ | Found | 73.48 | 6.86 | 11.81 |
| | | | | | Calcd. | 74.31 | 6.24 | 12.38 |
| 4 | 45 | 157—158 | THF | $C_{15}H_{16}N_2O$ | Found | 75.17 | 6.90 | 11.71 |
| | | | | | Calcd. | 74.97 | 6.71 | 11.66 |
| 5 | 60 | 185—187 | Dioxane | $C_{16}H_{18}N_2O$ | Found | 75.35 | 7.27 | 10.89 |
| | | | | | Calcd. | 75.56 | 7.13 | 11.02 |

Crundmann[7] has suggested a convenient synthesis of various heterocyclic compounds by the use of unsubstituted *sym*-triazine, as is shown in the following general equation:



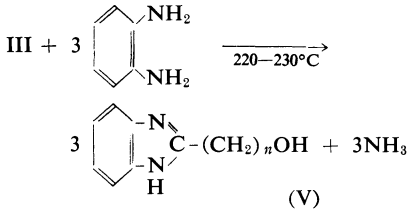
X= -NH-, -O-, -S-

7) C. Grundmann, *Angew. Chem.*, **75**, 393 (1963).

The same investigator and Kreuzberger[8] have reported that this type of ring cleavage is not applicable to 2, 4, 6-trisubstituted-1, 3, 5-triazines; for example, 2, 4, 6-trimethyl-1, 3, 5-triazine does not react with aniline up to 200°C. In the present investigation, however, it has been found that the above-mentioned 2, 4, 6-tri-(ω-hydroxyalkyl)-1, 3, 5-triazines react with diamines when the reactions are carried out above 200°C. That is, when III was heated with three equivalent moles of *o*-phenylenediamine at 220-230°C in a nitrogen atmosphere, the evolution of ammonia was observed, and

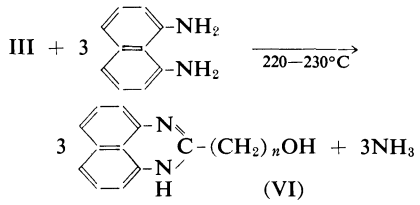
8) C. Grundmann and A. Kreuzberger, *J. Am. Chem. Soc.*, **77**, 6559 (1955).

2-($\omega$-hydroxyalkyl)benzimidazoles (V) were obtained in good yields (Table IV).



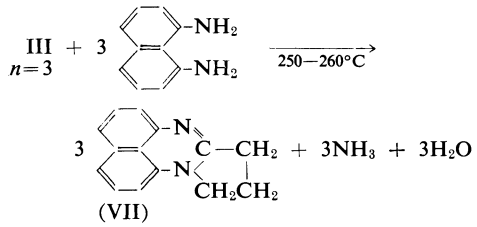
(V)

In a similar fashion, III reacted with 1,8-naphthylenediamine to give 2-($\omega$-hydroxyalkyl)-perimidines (VI) (Table V).



(VI)

At higher temperatures, 250—260°C, however, azolidino[1,2-a]perimidine (VII), a dehydrated product of VI ($n=3$), was obtained by the reaction of 2,4,6-tri-($\gamma$-hydroxypropyl)-1,3,5-triazine (III, $n=3$) with 1,8-naphthylenediamine.



(VII)

## Experimental

**Trimethylen Cyanohydrin.**—This compound was prepared by the reaction of trimethylene chlorohydrin and potassium cyanide in a mixed solvent of ethanol and water;[9] b. p. 107—108°C (11 mmHg); yield, 30%.

**Tetramethylene Cyanohydrin.** — The reported method,[10] which is essentially analogous to the above reaction, gave the cyanohydrin in poor yields only (5—10%). An improved method is given as follows. A mixture of tetramethylene chlorohydrin (22 g., 0.2 mol.), potassium cyanide (33 g., 0.5 mol.), glycerol (50 ml.) and water (25 ml.) was heated while being mechanically stirred at 100—110°C for 15 min. After it had cooled, the mixture was extracted four times with 50 ml. portion of tetrahydrofuran. The extract was then dried over anhydrous magnesium sulfate, and the solvent was subsequently removed. The residue was distilled under reduced pressure; b. p. 86—88°C (0.5 mmHg); yield, 7.0 g. (35%).

When the distillation was carried out without extracting soon after the reaction was complete, another liquid (b. p. 65—66°C) was obtained. This liquid was identified as tetrahydrofuran by comparing its infrared spectrum with that of an authentic specimen. The formation of this liquid can be explained in terms of the cyclization of the chlorohydrin used, with the loss of hydrogen chloride. The yield of this by-product amounted to almost 30%. This seems to be one of the main factors lowering the yield of the tetramethylene cyanohydrin.

**Pentamethylene Cyanohydrin.**—This compound was prepared from pentamethylene chlorohydrin and potassium cyanide by method analogous to that described above; b. p. 97—98°C (3 mmHg); yield, 83%.

**Hydrochloride of 2-Iminotetrahydrofuran (I, $n=3$).**—Dry hydrogen chloride was passed into a solution of 8.5 g. of trimethylene cyanohydrin in 300 ml. of dry ether maintained at 10—15°C with external cooling. The flask was tightly stoppered and allowed to stand at room temperature for 2 days. The crystals were then collected and washed with dry ether; yield, 11.5 g (Table I).

Similarly, hydrochloride of 2-iminotetrahydropyrane (I, $n=4$) was prepared from tetramethylene cyanohydrin and hydrogen chloride. In this case, however, it was necessary to carry the reaction out in a more dilute (1.5—2.0%) ethereal soultion.

**Hydrochloride of 2-Iminooxepan (I, $n=5$).**—Dry hydrogen chloride was passed into a solution of 4.5 g. of pentamethylene cyanohydrin in 150 ml. of dry ether and 80 ml. of dry, glycol acetal-free dioxane with external cooling. The reaction mixture was allowed to stand at room temperature for 4 days, and then refluxed for 3 hr. The solvent was subsequently removed under reduced pressure. The crystals were washed with cold and dry dioxane and successively with dry ether; yield, 5.1 g. (Table I).

**$\omega$-Chloroalkyl Amides (II).**—These compounds were obtained from the corresponding hydrochlorides of cyclic iminoethers (I) by heating them at 150—160°C for about 5 min. or by refluxing them in toluene. They were then recrystallized from ligroin or ligroin-benzene (Table II).

**2,4,6-Tri-($\gamma$-hydroxypropyl)-1,3,5-triazine (III, $n=3$).**—In a 200 ml. flask, 9.6 g. (0.08 mol.) of hydrochloride of 2-iminotetrahydrofuran (II, $n=3$), 16.0 g. of triethylamine and 80 ml. of absolute tetrahydrofuran were placed, and then the flask was tightly closed with a stopper. It was allowed to stand at room temperature with intermittent shaking for 3 days. After the precipitate of the hydrochloride of triethylamine had been filtered off, the solvent and the excess triethylamine were removed by distillation. The residual viscous liquid was distilled under reduced pressure; b. p. 196—198°C (0.1 mmHg), yield, 3.6 g. (53%).

Similarly, 2,4,6-tri-($\delta$-hydroxybutyl)-1,3,5-triazine (III, $n=4$) and 2,4,6-tri-($\varepsilon$-hydroxypentyl)-1,3,5-triazine (III, $n=5$) were obtained from the corresponding hydrochlorides of cyclic iminoethers.

9) G. Aksnes and J. E. Prue, *J. Chem. Soc.*, **1959**, 103.
10) C. C. Price, G. A. Cypher and I. V. Krishnamurti, *J. Am. Chem. Soc.*, **74**, 2987 (1952).

Their yields, boiling points, analyses and infrared and ultraviolet absorptions are summarized in Table III.

**2, 4, 6-Tri-[γ-(phenylaminocarboxy)propyl]-1,3,5-triazine (IV).**—To a solution of 0.5 g. of 2, 4, 6-tri-(γ-hydroxypropyl)-1, 3, 5-triazine in 10 ml. of tetrahydrofuran, 0.7 g. of phenylisocyanate was added. After the mixture had been allowed to stand for 2 days, the solvent was evaporated and the precipitate was recrystallized from 95% ethanol. Yield, 1.1 g. (92%) ; m. p. 124—125°C.

Found : C, 64.00, H, 6.03 ; N, 14.45, Calcd. for $C_{33}H_{36}N_6O_6$ : C, 64.69, H, 5.92 ; N, 13.72%.

**The Reaction of 2, 4, 6-Tri-(ω-hydroxyalkyl)-1, 3, 5-triazine with *o*-Phenylenediamine or 1, 8-Naphthylenediamine.**—A general procedure employed was as follows. A triazine (III) was heated with three equivalent moles of *o*-phenylenediamine or 1, 8-naphthylenediamine in a nitrogen atomsphere in an oil bath maintained at 220—230°C. After a while, the evolution of ammonia gas began ; the heating was continued until the evolution of gas had ceased (15—60 min.). The reaction mixture was then washed with ether, and the precipitate was recrystallized from a suitable solvent, as is shown in Tables IV and V.

*O*-Acetyl-derivatives of V were obtained from the reaction of V and 1.2 equivalent moles of acetic anhydride in pyridine at room temperature.

*O*-, *N*-Diacetyl-derivatives of V were obtained from the reaction of V and 2.5 equivalent moles of acetic anhydride in pyridine at 100°C.

**Azolidino[1, 2-a]perimidine (VII).**—A mixture of 0.5 g. of 2,4,6-tri-(γ-hydroxypropyl)-1,3,5-triazine (III, $n=3$) and 0.7 g. of 1, 8-naphthylenediamine was heated in a nitrogen atmosphere at 250—260°C for one hour. The reaction mixture was then washed with ether, and the precipitate was recrystallized from tetrahydrofuran. Yield, 0.5 g. (34%) ; m. p. 143—144°C.

Found : C, 80.30, H, 6.87; N, 13.71, Calcd. for $C_{14}H_{12}N_2$ : C, 80.74, H, 5.81 ; N, 13.45%.

## Summary

2, 4, 6-Tri-(ω - hydroxyalkyl) - 1, 3, 5 - triazines have been prepared by the reaction of hydrochlorides of cyclic iminoethers, such as 2-iminotetrahydrofuran, 2-iminotetrahydropyrane or 2-iminooxepan, with triethylamine. The reactions of the triazines with *o*-phenylenediamine or 1, 8-naphthylenediamine to give 2-(ω-hydroxyalkyl)benzimidazoles or 2-(ω-hydroxyalkyl)perimidines have also been described.

The authers wish to express their hearty thanks to Miss Toshiko Aoyagi, Miss Setsuko Iimura and Miss Yoko Ota for their microanalyses.

*Laboratory of Organic Chemistry*
*Tokyo Institute of Technology*
*Ookayama Tokyo*

# Detection of the Atomic Oxygen Evolved in the Decomposition of Some Metallic Oxides*

By Kazuo MITANI and Yuji ASAKURA

(Received September 7, 1964)

Atomic oxygen was found to be evolved from the surface of a platinum ribbon, when it is heated to 1400°C in vacuo, if the ribbon has been treated previously with nitrous oxide or discharged oxygen gas.[1-4] It was believed that platinum dioxide is formed on the platinum surface, and that atomic oxygen is given off by the decomposition of platinum dioxide when the ribbon is heated to a high temperature in vacuo. Afterwards, atomic oxygen was found to be evolved when platinum dioxide prepared from ammonium chloroplatinate and sodium nitrate was decomposed in vacuo at a high temperature.[5] This experimental finding was believed to support the above conclusion. Then, various metallic oxides were examined to determine whether they would similarly evolve atomic oxygen when decomposed at a high temperature in vacuo. It was found that some metallic oxides evolve atomic oxygen, while others do not.[6] In order to clarify these phenomena, oxides of chromium, iron, manganese, cobalt and cadmium will be investigated in the present experiment.

## Experimental

**Apparatus.**—The main part of the apparatus is shown in Fig. 1. P is a coil (1 mm.×3.5 mm.×

* Presented at the 16th Annual Meeting of the Chemical Society of Japan, Tokyo, March, 1963.

1) K. Mitani and Y. Haranō, This Bulletin, **33**, 1147 (1960).

2) K. Mitani and Y. Haranō, ibid., **33**, 276 (1960).

3) Y. Haranō, *J. Chem. Soc. Japan, Pure Chem. Sec.* (*Nippon Kagaku Zasshi*), **81**, 1812 (1960).

4) Y. Haranō, ibid., **82**, 22 (1961).

5) Y. Haranō, ibid., **82**, 19 (1961).

6) Y. Haranō, ibid., **82**, 152 (1961).

12 mm.) made of a platinum ribbon (1.3 mm.× 0.10 mm.×62 mm.) which is spot-welded to platinum wires sealed into a glass stem. These platinum wires are subsequently connected to copper wires. A sample of metallic oxide placed on a quartz plate ((0.3—0.4) mm.×2.5 mm.×8 mm.) is inserted into the platinum coil, and then heated by an electric current. The glass tube A can be taken off from the ground joint, and the samples dropping from P can be removed easily.

D is a thin glass plate hung in the side tube of the reaction vessel. Molybdenum trioxide has been deposited on one side of D. Atomic oxygen is detected by the change in the color of molybdenum trioxide from pale yellow to blue.

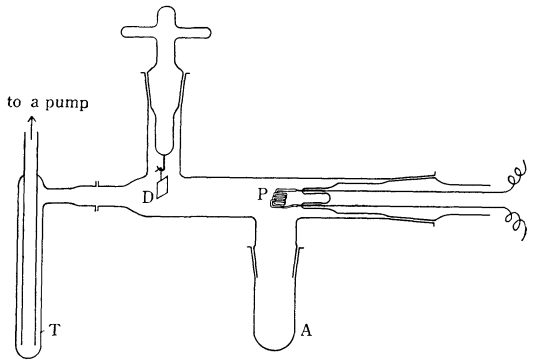



Fig. 1 The main part of the apparatus.

The apparatus can be evacuated by a mercury diffusion pump through a trap cooled by dry ice.

The sensitivity of molybdenum trioxide to atomic oxygen varies with the state of deposition on a glass plate. It seems that the thicker the layer of molybdenum trioxide, the larger its sensitivity. Molybdenum trioxide was deposited uniformly on a thin glass plate in the apparatus shown in Fig. 2. D is a piece of cover-glass for microscopic use, in the middle of one edge of which a small glass hook is attached. When molybdenum wire M is heated by an electric current to red heat, molybdenum is oxidized by air, and the glass bell-jar is filled with the smoke of the molybdenum trioxide thus formed. As tiny lumps of molybdenum trioxide crystals, entangled like cotton, fall to the bottom at first, a glass plate B is placed (as is shown in Fig. 2) in order to catch them. After some time, a uniform smoke is left behind in the bell-jar when the glass plate B is removed. Minute crystals of molybdenum trioxide settle down slowly on pieces of cover-glass, until the required thickness is obtained, whereupon the glass plate B is inserted again to stop further deposition. The molybdenum trioxide deposited on a glass plate by the method mentioned above is white or pale yellow; it changes to blue by atomic oxygen, probably according to the following equation: [7]

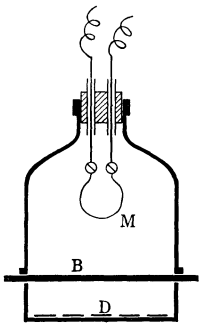



Fig. 2. The device for obtaining a uniform deposit of molybdenum trioxide.

$$3MoO_3+O\rightarrow Mo_3O_8+O_2$$

**Materials.**—Commercial chromic oxide was used at first. Later, chromic oxide was prepared by the following method. Potassium dichromate was heated with sulfur in a porcelain crucible, and the chromic oxide ($Cr_2O_3$) formed was washed free from potassium sulfate and dried.

Ferric oxide ($Fe_2O_3$) was made by heating ferrous sulfate, or by heating ferric hydroxide obtained by the action of excess ammonium hydroxide upon ferric chloride.

Manganese dioxide ($MnO_2$) was prepared by heating manganous nitrate which had been obtained by the action of concentrated nitric acid on manganous carbonate. Manganous nitrate was heated in a porcelain crucible until the evolution of brown gas ceased completely; the residue in the crucible was then boiled with dilute nitric acid, filtered, and washed. The residue was heated again in a crucible to ca. 500°C for an hour. Manganese dioxide was obtained as a black powder.

Cobalt oxide was prepared by heating cobalt nitrate. After being washed with water, the black powder obtained was heated again to 500—600°C in a crucible. The composition of this sample was not definite, but it was supposed to be near $Co_3O_4$.

Cadmium oxide (CdO) was made by heating cadmium carbonate in a platinum crucible until no further change in weight occurred.

Hydrogen was purified by diffusion through a heated palladium tube.

**Procedure.**—Whether atomic oxygen is evolved or not is judged in every case by the change in the color of molybdenum trioxide, when the platinum ribbon is heated to 1400°C for 20 min. in vacuo.

After atomic oxygen is once given off in the thermal decomposition of metallic oxide inserted into the platinum coil, atomic oxygen is found to be evolved from the platinum surface heated in vacuo for a long time.[1,2,8] It is believed that platinum dioxide is formed on the platinum surface, and that atomic oxygen is given off by the decomposition of platinum dioxide when the ribbon is heated to a high temperature in vacuo. Therefore, the following preliminary treatment of the platinum ribbon is necessary before every experiment. After the apparatus is sufficiently evacuated, hydrogen is admitted to a pressure of 3 mmHg and the platinum ribbon is heated to 1400°C for 30 min. Subsequently, the ribbon is degassed at 1400°C for 30 min. in

7) W. H. Rodebush and W. A. Nichols, *J. Am. Chem. Soc.*, **52**, 3864 (1930).

8) K. Mitani and Y. Haranō, This Bulletin, **32**, 1386 (1959).

vacuo. Then, whether or not atomic oxygen is still given off from the platinum surface is determined by the change in the color of molybdenum trioxide, the platinum ribbon being heated to 1400°C for 20 min. If molybdenum trioxide changes its color, the above-mentioned treatment is repeated until no atomic oxygen is given off from the platinum ribbon.

The weight of metallic oxide placed at one time on a quartz plate is about 1 mg. The quartz plate once used reacts with the sample placed on it, and substances difficult to be removed completely by most reagents form. As these substances seem to give off atomic oxygen in some cases, a new quartz plate is used in each experiment. A new one does not give off atomic oxygen when heated to high temperatures.[6]

The sample of metallic oxide placed on a quartz plate is heated in the platinum coil. The temperature of the platinum ribbon is measured with an optical pyrometer. The temperature of the sample, although it can not be determined accurately, is thought to be slightly lower than that of the ribbon.

As the samples appear as powder, it is possible that they adsorb air or water vapor. Therefore, the samples are, in some cases, degassed at 500—700°C for 30 min. in vacuo prior to being heated to 1400°C.

To detect atomic oxygen formed as an intermediate substance of a chemical reaction, a new method has been devised in the authors' laboratory. This method is based upon the fact that a platinum ribbon once in contact with atomic oxygen evolves it for a long time when heated to high temperatures in vacuo. Atomic oxygen has already been confirmed by this method to exist as an intermediate, when nitrous oxide is decomposed at relatively high pressures (10—50 mmHg) on the platinum surface,[1,4] and when carbon monoxide is oxidized by a platinum catalyst.[9] Therefore, in the present investigation, after the experiment of heating a sample of metallic oxide in the platinum coil, the sample and the quartz plate were removed and the platinum ribbon alone was heated to 1400°C for 20 min. in vacuo. If atomic oxygen was evolved in the latter case, it was regarded as further confirmation that atomic oxygen was evolved by the decomposition of metallic oxide.

## Results and Discussion

**Chromic Oxide.**—Chromic oxide was heated several times on a quartz plate, as has been mentioned above, and also to 1400°C directly on the surface of the platinum ribbon. Molybdenum trioxide scarcely changed its color in any case. It is believed that chromic oxide does not give off atomic oxygen. The appearance of a sample remained unchanged even after the experiment, so probably chromic oxide was not decomposed by the heating.

**Ferric Oxide.**—When ferric oxide placed on a quartz plate was heated to 1400°C for 20 min. in the platinum coil, molybdenum trioxide distinctly changed its color from pale yellow to blue. In some cases a sample of ferric oxide was degassed at about 700°C for 30 min. in vacuo before being heated to 1400°C, but the same result was obtained, irrespective of the procedure.

Ferric oxide is red-brown, but a sample after being heated to 1400°C becomes black. It was confirmed that the latter can be attracted by a magnet, while the former can not. From these facts, it is certain that ferric oxide is decomposed by heat, forming ferrosoferric oxide $Fe_3O_4$.

The portion of a quartz plate with which the sample was in contact became somewhat dark during heating.

**Manganese Dioxide.**—Molybdenum trioxide turned blue while manganese dioxide placed on a quartz plate was heated to 1400°C in the platinum coil.

After the experiment, the quartz plate, together with the sample, was removed, and the platinum ribbon alone was heated. Molybdenum trioxide turned blue in this case also.

Manganese dioxide was prepared by the dry method and, moreover, heated to about 500°C in air, so that probably it was not hydrated. Therefore, manganese dioxide was usually heated at once to 1400°C, without a preliminary degassing. To make sure, however, a sample of manganese dioxide was degassed at about 500°C in vacuo, and then heated to 1400°C. In this case, molybdenum trioxide turned blue in the same manner.

A sample of manganese dioxide in the platinum coil was observed through a magnifying glass during heating. When manganese dioxide began to be heated to high temperatures, it was decomposed rapidly, violently evolving gas and jumping about, and in a short time almost all the sample fell from the quartz plate.

The portion of the quartz plate with which the sample was in contact became dark during heating.

**Cobalt Oxide.**—Molybdenum trioxide turned blue in the case of cobalt oxide heated to 1400°C in vacuo.

After the experiment, the quartz plate, together with the sample, was removed, and the platinum ribbon alone was heated. Molybdenum trioxide turned even a deeper blue than when the sample was inserted in the platinum coil.

The sample of cobalt oxide before being heated was black. After the experiment, the surface of the sample was dark brown, while the interior had turned a lighter brown. This

9) Y. Haranō, *J. Chem. Soc. Japan, Pure Chem. Sec.* (*Nippon Kagaku Zasshi*), **82**, 316 (1961).

brown substance is thought to be cobaltous oxide CoO.

As the composition of the cobalt oxide used in this experiment was not definite, samples of cobalt oxide were heated to various temperatures between 500°C and 800°C in air at 1 atm. in order to oxidize them to the higher oxide $Co_3O_4$. The results of the experiments using these samples were the same as the above.

**Cadmium Oxide.**—Molybdenum trioxide turned blue, in the case of cadmium oxide, if the amount of the sample used was very small or if the sample was heated to lower temperatures (700—1100°C). Molybdenum trioxide, however, turned dark gray in a short time if the same amount as the other oxides was heated to 1400°C. Thereafter, the quartz plate was removed, and the platinum ribbon alone was heated. The color of molybdenum trioxide remained unchanged.

Cadmium oxide is easily decomposed by heat. When it is heated to 1400°C in vacuo, it evaporates rapidly and the vapor of the metallic cadmium formed by the decomposition condenses as a metallic mirror with a black tint on the wall of the reaction vessel. Therefore, it appears that the change in the color of molybdenum trioxide is not due to atomic oxygen, but to the vapor of metallic cadmium. Metallic cadmium distilled in vacuo was placed on a quartz plate and inserted into the platinum coil. When the platinum ribbon began to be heated to 1400°C in vacuo, molybdenum trioxide got a bluish tint at first, but in a short time it turned dark gray.

A silver plate was hung up, together with molybdenum trioxide, and cadmium oxide was heated as usual, but the silver plate did not become black.

From the foregoing facts, it is believed that cadmium oxide does not give off atomic oxygen at the time of thermal decomposition, and that the change in the color of molybdenum trioxide is due to the reduction by the vapor of the metallic cadmium produced by the decomposition.

## Conclusion

The results of the present investigation show that chromic oxide and cadmium oxide do not give off atomic oxygen, but that ferric oxide, manganese dioxide, and cobalt oxide do give off atomic oxygen when heated strongly in vacuo.

Previously, Haranō[5,6] investigated whether or not atomic oxygen was evolved when various metallic oxides were heated to high temperatures in vacuo. He concluded that alumina ($Al_2O_3$), silica ($SiO_2$), magnesium oxide (MgO), cuprous oxide ($Cu_2O$), lead monoxide (PbO), lead dioxide ($PbO_2$), silver oxide ($Ag_2O$), and silver peroxide ($Ag_2O_2$) do not evolve atomic oxygen, but that zinc oxide (ZnO), mercuric oxide (HgO), cupric oxide (CuO), and platinum dioxide ($PtO_2$) do evolve atomic oxygen at high temperatures.

When the results of the present investigation are considered together with his results, it is evident that oxides difficult to decompose, i. e., alumina, silica, magnesium oxide, cuprous oxide, and chromic oxide, do not give off atomic oxygen. It can be said at least that atomic oxygen can not be evolved without the decomposition of the sample. This is quite reasonable. On the other hand, atomic oxygen is not found to be given off from lead monoxide, lead dioxide, silver oxide, silver peroxide, and cadmium oxide, though these oxides can be decomposed with ease. After all, atomic oxygen is given off in the thermal decomposition of zinc oxide, mercuric oxide, cupric oxide, platinum dioxide, ferric oxide, manganese dioxide, and cobalt oxide.

Molybdenum trioxide does not turn blue when the platinum ribbon alone is heated to 1400°C in oxygen. Therefore, it is not true that molecular oxygen formed by the decomposition of metallic oxides comes into contact with the platinum ribbon at a high temperature and so is dissociated into atoms.

It is believed that the oxygen given off by the decomposition of metallic oxides at high temperatures is not in equilibrium, and that a part of the oxygen is evolved in the atomic state from the beginning.

As to the detailed mechanism, however, further investigations will be necessary.

A part of the expenses for this investigation have been defrayed by a grant-in-aid from the Ministry of Education.

*Institute of Chemistry*
*Kyoto Prefectural University of Medicine*
*Taishōgun, Kita-ku, Kyoto*

# Synthesis of Some Antituberculars: *N*-Aryl-*N'*-2-(4-arylthiazolyl)-thioureas

By Prithwi Nath BHARGAVA and Suresh Chandra SHARMA

(Received September 7, 1964)

A number of thioureas and their phenyl and sulphanilyl[1] derivatives are found to possess a definite in vitro antitubercular activity and the outstanding tuberculostatic properties of *N*, *N'*-di-(*p*-*n*-butoxyphenyl)-thioureas[2-5] has considerably revived the interest in thioureas derivatives. In view of the findings and the facts that many thiazole derivatives have been found to possess high degree of antitubercular activity,[6-10] the authors have synthesised a series of hitherto thiazolyl thiourea of the formula:

R-NH-CS-NH-R'

where R is 2-(4-arylthiazolylnucleus) and R' is aryl or substituted aryl group.

The compounds of this type have been synthesised by condensing 2-amino-4-phenyl-, -4-*p*-chlorophenyl-, -4-*p*-bromophenyl-, -4-*p*-tolyl-4-*p*-methoxyphenylthiazoles with ten different aryl isothiocyanates in benzene medium. The thiazoles were prepared by the method of Dedson and King[11] from acetophenone and substituted acetophenones.

These synthesised compounds have been tested against Mycobacterium tuberculosis var *hominis* strain $H_{37}Rv$ on Steenken's modification of Proskauer and Beck's medium (one month old growth) at Central Drug Research Institute, Lucknow (India). The in vitro and in vivo (of eight compounds only) antitubercular activities of these compounds were compared with the standard, S.U. 1906 (Ciba): 1-(*p*-*N*, *N'*-dimethylaminophenyl-3-(*p*-*n*-butoxyphenyl)-2-thioureas). A number of compounds have shown sufficiently high degree of activity in vitro (equivalent to that of the standard).

As carbodiimides with a 2-thiazolyl group as substituent do not appear to be known, some of these have been prepared. The procedure followed for the preparation was the usual dehydrosulphurisation[12] of *N*-aryl-*N'*-2-(4-arylthiazolyl)-thioureas with yellow lead oxide in benzene.

## Experimental

2-Amino-4-phenyl-, -4-*p*-chlorophenyl-, -4-*p*-bromophenyl-, -4-*p*-tolyl-, -4-*p*-methoxyphenylthiazoles were prepared from acetophenone, *p*-chloro-, *p*-bromo-, *p*-methyl-, and *p*-methoxy-acetophenones by condensing with simple thiourea and iodine on a water bath for 12 hr.

**Preparation of Aryl Isothiocyanates.**—Phenyl-, *o*-, *m*-, and *p*-tolyl-, *m*-, and *p*-chlorophenyl-, *o*-, *m*-, and *p*-methoxyphenyl-*p*-ethoxyphenyl-isothiocyanates were prepared from the ammonium salt of the corresponding dithiocarbamates by the action of lead nitrate.[13]

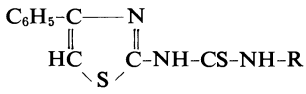
***N*-Phenyl-*N'*-2-(4-phenylthiazolyl)-thiourea.**—In a dry flask 8.8 g. of 2-amino-4-phenylthiazole, 6 ml. of phenylisothiocyanate were taken in 60 ml. of dry benzene and heated on a water bath for 6 hr. The crude product, *N*-phenyl-*N'*-2-(4-phenylthiazolyl)-thiourea, obtained as a precipitate, was filtered and washed well with ether and dilute hydrochloric acid to remove the unreacted phenylisothiocyanate and thiazole respectively. The compound was crystallised from ethanol as slightly yellow crystals, m. p. 255°C.

Similarly, other *N*-aryl-*N'*-2-thiazolylthioureas were prepared by interaction of different 2-amino-4-arylthiazoles and arylisothiocyanates. The results of physical properties and analytical date are mentioned in Tables I—V.

Refluxing time differed for different substituted 2-aminothiazoles and aryl isothiocyanates. The reactivity of aryl isothiocyanates having substituents in different positions lies in order $p>m>o$. In the case of 2-amino-4-*p*-chlorophenyl-, -4-*p*-bromophenylthiazoles the reaction is very slow and it requires sometimes 10—15 hr. heating. In the case of 2-amino-4-*p*-methoxyphenylthiazole this reaction did not take place at all with *o*-tolyl-, *o*-, *m*-, and *p*-methoxyphenyl- and *p*-ethoxyphenyl-isothiocyanates.

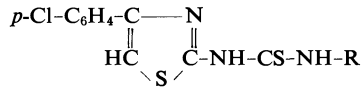
1) R. L. Mayer, *Chem. Abstr.*, **36**, 5199 (1942).
2) R. L. Mayer, P. C. Eisman and E. A. Konopka, *Proc. Soc. Exptl. Biol.*, **82**, 769 (1953).
3) C. F. Huebner, J. L. Marsh, R. H. Mizzoni, R. P. Mull, D. C. Schroeder, H. A. Troxell and C. R. Scholz, *J. Am. Chem. Soc.*, **75**, 2274 (1953).
4) N. P. Hun Hoi and N. D. Xuong, *C. R. Acad. Sci., Paris*, **237**, 498 (1953).
5) N. P. Hun Hoi, N. D. Xuong and V. T. Sun, *J. Chem. Soc.*, **1959**, 2815.
6) F. C. Pennington, W. D. Celmer, W. M. McLamore, V. V. Bogert and I. A. Solomons, *J. Am. Chem. Soc.*, **75**, 109 (1953).
7) B. Prescott and J. M. Webb, *Antibiotic and Chemotherapy*, **18**, 33 (1958).
8) R. L. Mayer, P. C. Eisman, T. A. Gist and E. A. Konopka, *Am. Rev. Tuberc.*, **77**, 694 (1958).
9) P. C. Eisman et al., ibid., **77**, 703 (1958).
10) B. S. Kulkarni, *J. Sci. industr. Res.*, **20C**, 205 (1961).
11) R. M. Dodson and L. C. King, *J. Am. Chem. Soc.*, **67**, 2242 (1945).
12) A. W. Hofmann, *Ber.*, **3**, 266 (1870); ibid., **18**, 3220 (1885).
13) Vogel, A Text Book of Practical Organic Chemistry, p. 615 (1954).

TABLE I. *N*-ARYL-*N'*-2-(4-PHENYLTHIAZOLYL)-THIOUREAS



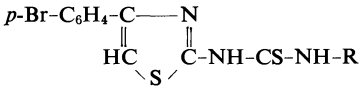
| No. | R | Yield % | M.p. °C | Molecular formula | C, % Found | C, % Calcd. | H, % Found | H, % Calcd. | N, % Found | N, % Calcd. | S, % Found | S, % Calcd. |
|---|---|---|---|---|---|---|---|---|---|---|---|---|
| 1 | Phenyl- | 86 | 225 | $C_{16}H_{13}N_3S_2$ | 61.58 | 61.74 | 4.08 | 4.15 | 13.39 | 13.50 | 20.63 | 20.58 |
| 2 | *m*-Chlorophenyl- | 65 | 208 | $C_{16}H_{12}N_3S_2Cl$ | 55.54 | 55.57 | 3.45 | 3.47 | 12.04 | 12.16 | 18.54 | 18.52 |
| 3 | *p*-Chlorophenyl- | 79 | 215 | $C_{16}H_{12}N_3S_2Cl$ | 55.47 | 55.57 | 3.42 | 3.47 | 12.11 | 12.16 | 18.57 | 18.52 |
| 4 | *p*-Bromophenyl- | 74 | 219 | $C_{16}H_{12}N_3S_2Br$ | 49.16 | 49.23 | 3.06 | 3.08 | 10.68 | 10.77 | 16.38 | 16.41 |
| 5 | *o*-Tolyl- | 63 | 256 | $C_{17}H_{15}N_3S_2$ | 62.72 | 62.77 | 4.59 | 4.62 | 12.83 | 12.93 | 19.60 | 19.69 |
| 6 | *m*-Tolyl- | 60 | 240 | $C_{17}H_{15}N_3S_2$ | 62.68 | 62.77 | 4.54 | 4.62 | 12.85 | 12.93 | 19.73 | 19.69 |
| 7 | *p*-Tolyl- | 73 | 237 | $C_{17}H_{15}N_3S_2$ | 62.70 | 62.77 | 4.60 | 4.62 | 12.89 | 12.93 | 19.68 | 19.69 |
| 8 | *o*-Methoxyphenyl- | 61 | 259 | $C_{17}H_{15}N_3OS_2$ | 59.80 | 59.82 | 4.37 | 4.40 | 12.27 | 12.32 | 18.81 | 18.77 |
| 9 | *m*-Methoxyphenyl- | 66 | 228 | $C_{17}H_{15}N_3OS_2$ | 59.72 | 59.82 | 4.32 | 4.40 | 12.19 | 12.32 | 18.72 | 18.77 |
| 10 | *p*-Methoxyphenyl- | 77 | 212 | $C_{17}H_{15}N_3OS_2$ | 59.69 | 59.82 | 4.35 | 4.40 | 12.23 | 12.32 | 18.69 | 18.77 |
| 11 | *p*-Ethoxyphenyl- | 72 | 213 | $C_{18}H_{17}N_3OS_2$ | 60.81 | 60.85 | 4.73 | 4.79 | 11.75 | 11.83 | 18.05 | 18.03 |

TABLE II. *N*-ARYL-*N'*-2-(4-*p*-CHLOROPHENYLTHIAZOLYL)-THIOUREAS



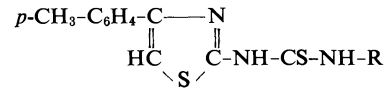
| No. | R | Yield % | M.p. °C | Molecular formula | N, % Found | N, % Calcd. | S, % Found | S, % Calcd. |
|---|---|---|---|---|---|---|---|---|
| 1 | Phenyl- | 78 | 241 | $C_{16}H_{12}N_3S_2Cl$ | 12.11 | 12.16 | 18.57 | 18.52 |
| 2 | *m*-Chlorophenyl- | 73 | 229 | $C_{16}H_{11}N_3S_2Cl_2$ | 11.01 | 11.05 | 16.78 | 16.84 |
| 3 | *p*-Chlorophenyl- | 89 | d. 210 | $C_{16}H_{11}N_3S_2Cl_2$ | 10.98 | 11.05 | 16.87 | 16.84 |
| 4 | *p*-Bromophenyl- | 86 | 228 | $C_{16}H_{11}N_3S_2BrCl$ | 9.84 | 9.89 | 15.11 | 15.08 |
| 5 | *o*-Tolyl- | 74 | 278 | $C_{17}H_{14}N_3S_2Cl$ | 11.61 | 11.68 | 17.75 | 17.80 |
| 6 | *m*-Tolyl- | 71 | 253 | $C_{17}H_{14}N_3S_2Cl$ | 11.59 | 11.68 | 17.81 | 17.80 |
| 7 | *p*-Tolyl- | 82 | 272 | $C_{17}H_{14}N_3S_2Cl$ | 11.63 | 11.68 | 17.84 | 17.80 |
| 8 | *o*-Methoxyphenyl- | 75 | 278 | $C_{17}H_{14}N_3OS_2Cl$ | 11.12 | 11.18 | 17.02 | 17.04 |
| 9 | *p*-Methoxyphenyl- | 85 | 247 | $C_{17}H_{14}N_3OS_2Cl$ | 11.08 | 11.18 | 17.06 | 17.04 |
| 10 | *p*-Ethoxyphenyl- | 86 | 270 | $C_{18}H_{16}N_3OS_2Cl$ | 10.71 | 10.78 | 16.45 | 16.43 |

TABLE III. *N*-ARYL-*N'*-2-(4-*p*-BROMOPHENYLTHIAZOLYL)-THIOUREAS



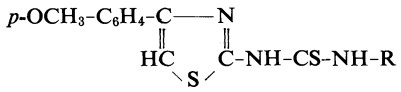
| No. | R | Yield % | M.p. °C | Molecular formula | N, % Found | N, % Calcd. | S, % Found | S, % Calcd. |
|---|---|---|---|---|---|---|---|---|
| 1 | Phenyl- | 76 | 226 | $C_{16}H_{12}N_3S_2Br$ | 10.69 | 10.77 | 16.45 | 16.41 |
| 2 | *m*-Chlorophenyl- | 73 | 240 | $C_{16}H_{11}N_3S_2BrCl$ | 9.82 | 9.89 | 15.03 | 15.08 |
| 3 | *p*-Chlorophenyl- | 80 | 238 | $C_{16}H_{11}N_3S_2BrCl$ | 9.78 | 9.89 | 15.00 | 15.08 |
| 4 | *p*-Bromophenyl | 82 | 236 | $C_{16}H_{11}N_3S_2Br_2$ | 8.91 | 8.96 | 13.69 | 13.65 |
| 5 | *o*-Tolyl- | 63 | 272 | $C_{17}H_{14}N_3S_2Br$ | 10.33 | 10.39 | 15.80 | 15.84 |
| 6 | *m*-Tolyl- | 68 | 239 | $C_{17}H_{14}N_3S_2Br$ | 10.29 | 10.39 | 15.87 | 15.84 |
| 7 | *p*-Tolyl- | 71 | 277 | $C_{17}H_{14}N_3S_2Br$ | 10.35 | 10.39 | 15.79 | 15.84 |
| 8 | *o*-Methoxyphenyl- | 74 | 281 | $C_{17}H_{14}N_3OS_2Br$ | 9.89 | 10.00 | 15.26 | 15.24 |
| 9 | *p*-Methoxyphenyl- | 79 | 237 | $C_{17}H_{14}N_3OS_2Br$ | 9.94 | 10.00 | 15.29 | 15.24 |
| 10 | *p*-Ethoxyphenyl- | 76 | 245 | $C_{18}H_{16}N_3OS_2Br$ | 9.66 | 9.68 | 14.70 | 14.75 |

TABLE IV. *N*-ARYL-*N'*-2-(4-*p*-METHYLPHENYLTHIAZOLYL)-THIOUREAS



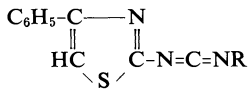
| No. | R | Yield % | M. p. °C | Molecular formula | N, % Found | N, % Calcd. | S, % Found | S, % Calcd. |
|---|---|---|---|---|---|---|---|---|
| 1 | Phenyl- | 88 | 243 | $C_{17}H_{15}N_3S_2$ | 12.83 | 12.92 | 19.75 | 19.69 |
| 2 | *m*-Chlorophenyl- | 79 | 227 | $C_{17}H_{14}N_3S_2Cl$ | 11.59 | 11.68 | 17.67 | 17.80 |
| 3 | *p*-Chlorophenyl- | 90 | 225 | $C_{17}H_{14}N_3S_2Cl$ | 11.64 | 11.68 | 17.84 | 17.80 |
| 4 | *p*-Bromophenyl- | 85 | 222 | $C_{17}H_{14}N_3S_2Br$ | 10.36 | 10.39 | 15.89 | 15.84 |
| 5 | *o*-Tolyl- | 71 | 248 | $C_{18}H_{17}N_3S_2$ | 12.31 | 12.39 | 18.82 | 18.88 |
| 6 | *m*-Tolyl- | 76 | 259 | $C_{18}H_{17}N_3S_2$ | 12.29 | 12.39 | 18.93 | 18.88 |
| 7 | *p*-Tolyl- | 83 | 226 | $C_{18}H_{17}N_3S_2$ | 12.34 | 12.39 | 18.92 | 18.88 |
| 8 | *o*-Methoxyphenyl- | 65 | 273 | $C_{18}H_{17}N_3OS_2$ | 11.81 | 11.83 | 18.00 | 18.03 |
| 9 | *p*-Methoxyphenyl- | 83 | 194 | $C_{18}H_{17}N_3OS_2$ | 11.76 | 11.83 | 18.07 | 18.03 |
| 10 | *p*-Ethoxyphenyl- | 87 | d. 204 | $C_{19}H_{19}N_3OS_2$ | 11.29 | 11.38 | 17.30 | 17.34 |

TABLE V. *N*-ARYL-*N'*-2-(4-*p*-METHOXYPHENYLTHIAZOLYL)-THIOUREAS



| No. | R | Yield % | M. p. °C | Molecular formula | N, % Found | N, % Calcd. | S, % Found | S, % Calcd. |
|---|---|---|---|---|---|---|---|---|
| 1 | Phenyl- | 69 | 239 | $C_{17}H_{15}N_3OS_2$ | 12.30 | 12.32 | 18.73 | 18.77 |
| 2 | *m*-Chlorophenyl- | 60 | 225 | $C_{17}H_{14}N_3OS_2Cl$ | 11.08 | 11.19 | 17.09 | 17.04 |
| 3 | *p*-Chlorophenyl- | 66 | 234 | $C_{17}H_{14}N_3OS_2Cl$ | 11.14 | 11.19 | 17.06 | 17 04 |
| 4 | *p*-Bromophenyl- | 71 | 224 | $C_{17}H_{14}N_3OS_2Br$ | 9.92 | 10.00 | 15.28 | 15.24 |
| 5 | *m*-Tolyl- | 58 | 253 | $C_{18}H_{17}N_3OS_2$ | 11.78 | 11.83 | 18.08 | 18.03 |
| 6 | *p*-Tolyl- | 62 | 233 | $C_{18}H_{17}N_3OS_2$ | 11.81 | 11.83 | 18.07 | 18.03 |

TABLE VI. *N*-ARYL-*N'*-2-(4-PHENYLTHIAZOLYL)-CARBODIIMIDES

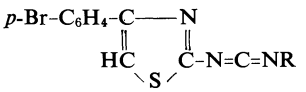


| No. | R | Yield % | M. p. °C | Molecular formula | N, % Found | N, % Calcd. | S, % Found | S, % Calcd. |
|---|---|---|---|---|---|---|---|---|
| 1 | Phenyl- | 55 | 205 | $C_{16}H_{11}N_3S$ | 14.56 | 14.63 | 11.17 | 11.15 |
| 2 | *m*-Chlorophenyl- | 51 | 176 | $C_{16}H_{10}N_3SCl$ | 13.03 | 13.06 | 9.89 | 9.95 |
| 3 | *p*-Chlorophenyl- | 63 | 220 | $C_{16}H_{10}N_3SCl$ | 13.01 | 13.06 | 9.86 | 9.95 |
| 4 | *p*-Bromophenyl- | 64 | 217 | $C_{16}H_{10}N_3SBr$ | 11.45 | 11.48 | 8.76 | 8.74 |
| 5 | *m*-Tolyl- | 50 | 181 | $C_{17}H_{13}N_3S$ | 14.32 | 14.43 | 10.91 | 11.00 |
| 6 | *p*-Tolyl- | 58 | 185 | $C_{17}H_{13}N_3S$ | 14.35 | 14.43 | 10.94 | 11.00 |
| 7 | *o*-Methoxyphenyl- | 53 | 219 | $C_{17}H_{13}N_3OS$ | 13.60 | 13.68 | 10.43 | 10.42 |
| 8 | *m*-Methoxyphenyl- | 56 | 188 | $C_{17}H_{13}N_3OS$ | 13.57 | 13.68 | 10.39 | 10.42 |
| 9 | *p*-Methoxyphenyl- | 64 | 237 | $C_{17}H_{13}N_3OS$ | 13.61 | 13.68 | 10.35 | 10.42 |
| 10 | *p*-Ethoxyphenyl- | 66 | 195 | $C_{18}H_{15}N_3OS$ | 13.03 | 13.08 | 9.95 | 9.97 |

**N-Phenyl-N'-2-(4-phenylthiazolyl)-carbodiimides.** —A mixture of finely powdered 3.1 g. of *N*-phenyl-*N'*-2-(4-phenylthiazolyl)-thiourea and 4.5 g. of yellow lead oxide was suspended in 50 ml. of benzene and heated under reflux on the water bath for about 8 hr. Desulphurisation was complete when no blackening occurred on addition of a further small quantity of lead oxide. The reaction mixture was filtered hot. The filtrate on keeping deposited beautiful colourles crystals of carbodiimide. It was recrystallised from benzene, m. p. 205°C.

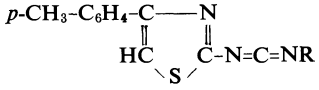
Other *N*-aryl-*N'*-2-(4-arylthiazolyl)-carbodiimides were prepared similarly and their properties and analytical data are recorded in Tables VI—VIII.

TABLE VII. *N*-ARYL-*N'*-2-(4-*p*-BROMOPHENYLTHIAZOLYL)-CARBODIIMIDES



| No. | R | Yield % | M. p. °C | Molecular formula | N, % Found | N, % Calcd. | S, % Found | S, % Calcd. |
|---|---|---|---|---|---|---|---|---|
| 1 | Phenyl- | 63 | 206 | $C_{16}H_{10}N_3SBr$ | 11.41 | 11.48 | 8.78 | 8.74 |
| 2 | *m*-Chlorophenyl- | 58 | 224 | $C_{16}H_9N_3SBrCl$ | 10.45 | 10.49 | 8.02 | 7.99 |
| 3 | *p*-Chlorophenyl- | 73 | 250 | $C_{16}H_9N_3SBrCl$ | 10.39 | 10.49 | 7.96 | 7.99 |
| 4 | *p*-Bromophenyl- | 71 | 258 | $C_{16}H_9N_3SBr_2$ | 9.38 | 9.44 | 7.21 | 7.19 |
| 5 | *o*-Tolyl- | 56 | 314 | $C_{17}H_{12}N_3SBr$ | 11.00 | 11.05 | 8.38 | 8.42 |
| 6 | *m*-Tolyl- | 51 | d. 205 | $C_{17}H_{12}N_3SBr$ | 10.96 | 11.05 | 8.40 | 8.42 |
| 7 | *p*-Tolyl- | 67 | 239 | $C_{17}H_{12}N_3SBr$ | 10.99 | 11.05 | 8.45 | 8.42 |
| 8 | *o*-Methoxyphenyl- | 54 | d. 293 | $C_{17}H_{12}N_3OSBr$ | 10.58 | 10.61 | 8.01 | 8.08 |
| 9 | *p*-Methoxyphenyl- | 60 | 211 | $C_{17}H_{12}N_3OSBr$ | 10.53 | 10.61 | 8.04 | 8.08 |
| 10 | *p*-Ethoxyphenyl- | 65 | 238 | $C_{18}H_{14}N_3OSBr$ | 10.21 | 10.24 | 7.83 | 7.80 |

TABLE VIII. *N*-ARYL-*N'*-2-(4-*p*-METHYLPHENYLTHIAZOLYL)-CARBODIIMIDES



| No. | R | Yield % | M. p. °C | Molecular formula | N, % Found | N, % Calcd. | S, % Found | S, % Calcd. |
|---|---|---|---|---|---|---|---|---|
| 1 | Phenyl- | 59 | d. 228 | $C_{17}H_{13}N_3S$ | 13.87 | 13.95 | 10.65 | 10.63 |
| 2 | *m*-Chlorophenyl- | 43 | 216 | $C_{17}H_{12}N_3SCl$ | 12.46 | 12.52 | 9.50 | 9.54 |
| 3 | *p*-Chlorophenyl- | 60 | 194 | $C_{17}H_{12}N_3SCl$ | 12.49 | 15.52 | 9.48 | 9.54 |
| 4 | *p*-Bromophenyl- | 65 | 235 | $C_{17}H_{12}N_3SBr$ | 11.03 | 11.05 | 8.39 | 8.42 |
| 5 | *m*-Tolyl- | 47 | d. 186 | $C_{18}H_{15}N_3S$ | 13.30 | 13.33 | 10.20 | 10.16 |
| 6 | *p*-Tolyl- | 49 | above 300 | $C_{18}H_{15}N_3S$ | 13.25 | 13.33 | 12.14 | 10.16 |
| 7 | *p*-Methoxyphenyl- | 53 | 211 | $C_{18}H_{15}N_3OS$ | 12.62 | 12.69 | 9.66 | 9.67 |
| 8 | *p*-Ethoxyphenyl- | 61 | 193 | $C_{19}H_{17}N_3OS$ | 12.14 | 12.17 | 9.32 | 9.28 |

**Antitubercular Activity Screening.**—*Standard Thiourea against which Assayed.*—S. U. 1906 (Ciba) : 1-(*p*-*N*,*N'*-dimethylaminophenyl-3-(*p*-*n*-butoxyphenyl)-2-thiourea).

**'In Vitro' Test (Neotetrazolium Test).**—*Medium.*—Modified Sula's medium. Sodium hydrogenphosphate, 0.05% ; Potassium dihydrogenphosphate, 0.075% ; Magnesium sulphate, 0.025% ; Sodium citrate, 0.125% ; Tryptone, 0.5% ; Asparagin, 0.5% ; Sodium glutamate, 0.25% ; Ferri et ammonium citras, 0.0025% ; Glycerine, 1.25% ; Tween 80, 0.05% ; Malachite green, 0.02% ; Distilled water add to 100 ml.

*Inoculum.*—A 3 mm. loopful of Mycobacterium tuberculosis var *Hominis* strain $H_{37}Rv$ on Steenken's Modification of Proskauer and Beck's medium. The growth was a month old.

*Steenken's Modification of Proskauer and Beck's Medium.*—Dipotassium phosphate, 0.5% ; Aspargine, 0.5% ; Magnesium sulphate, 0.06% ; Magnesium citrate, 0.25% ; Glycerol, 2% ; Aqua add to 100.

*Period of Incubation* at 37°C - 4 days.

After incubation 0.25 ml. of 1% 2, 3, 5-triphenyltetrazolium chloride in Sorensen's phosphate buffer pH 7 was added to each dilution of drug and incubated for a further period of 2 hr. 0.25 ml. of tetrazolium was added to 5 ml. of media containing drug.

*End Point.*—Formation of red coloured precipitate (formozan) indicated bacterial growth. In bacterial inhibition the precipitate remained colourless.

Results, reported in Table IX, have been confirmed by the Resazurin Test of Pital.[14]

**'In Vivo' Test.**—*Animal Used.*—White mice.

*Culture Used.*—M. tuberculosis strain $H_{37}Rv$ (human).

*Inoculum.*—$2.2 \times 10^6$ organisms per mouse intravenously.

*Therapy.*—Subcutaneous injections for 28 days.

Only compounds No. 1, 3 (Table I) ; 1 (Table II) ; 1, 3, 4 (Table III) and 1, 4 (Table IV), have been tested for in vivo activity, and the rest are under study. The compound No. 1 in Table I : *N*-phenyl-*N'*-2-(4-phenylthiazolyl)-thiourea has only shown antitubercular activity.

The compounds containing halogens are found to possess pronounced antitubercular activity equal to the standard S. U. 1906 (Ciba) when tested for in vitro using the culture, M. tuberculosis strain

14) A. Pital, R. C. Pital and J. M. Leise, *Am. Rev. Tuberc. and Resp. Disease*, **78**, 111 (1958).

TABLE IX. IN VITRO TESTS OF *N*-ARYL-*N'*-2-(4-ARYLTHIAZOLYL)-THIOUREAS

| No. | Name of the compound | Minimum inhibitory concn. μg./ml. |
|---|---|---|
| 1 | S. U. 1906 (Ciba) Standard | 1 |
| 2 | *N*-*m*-Chlorophenyl-*N'*-2-(4-phenylthiazolyl)-thiourea | 25 |
| 3 | *N*-*m*-Tolyl-*N'*-2-(4-phenylthiazolyl)-thiourea | 25 |
| 4 | *N*-*p*-Tolyl-*N'*-2-(4-phenylthiazolyl)-thiourea | 2.5 |
| 5 | *N*-*o*-Methoxyphenyl-*N'*-2-(4-phenylthiazolyl)-thiourea | 100 |
| 6 | *N*-*p*-Methoxyphenyl-*N'*-2-(4-phenylthiazolyl)-thiourea | 5 |
| 7 | *N*-*o*-Tolyl-*N'*-2-(4-*p*-chlorophenylthiazolyl)-thiourea | 1 |
| 8 | *N*-*m*-Tolyl-*N'*-2-(4-*p*-chlorophenylthiazolyl)-thiourea | 1 |
| 9 | *N*-*p*-Tolyl-*N'*-2-(4-*p*-chlorophenylthiazolyl)-thiourea | 100 |
| 10 | *N*-*p*-Methoxyphenyl-*N'*-2-(4-*p*-chlorophenylthiazolyl)-thiourea | 25 |
| 11 | *N*-*m*-Chlorophenyl-*N'*-2-(4-*p*-methoxyphenylthiazolyl)-thiourea | 1 |
| 12 | *N*-*p*-Chlorophenyl-*N'*-2-(4-*p*-methoxyphenylthiazolyl)-thiourea | 1 |
| 13 | *N*-*p*-Bromophenyl-*N'*-2-(4-*p*-methoxyphenylthiazolyl)-thiourea | 1 |
| | Rest of the compounds | >100 |

$H_{37}Rv$ (human). It will be evident if the values for *N*-*m*-chlorophenyl-, and *N*-*p*-chlorophenyl-*N'*2-(4-phenylthiazolyl)-thioureas ; *N*-*p*-bromophenyl-, *N*-*o*-tolyl, *N*-*m*-tolyl-, and *N*-*p*-methoxyphenyl-*N'*-2-(4-*p*-chlorophenylthiazolyl)-thioureas and *N*-*m*-chlorophenyl-, *N*-*p*-chlorophenyl-, *N*-*p*-bromophenyl-*N'*-2-(4-*p*-methoxyphenylthiazolyl)-thioureas are examined.

A few more compounds namely *N*-phenyl-, *N*-*m*-tolyl, *N*-*p*-tolyl-, and *N*-*p*-methoxyphenyl-*N'*-2-(4-phenylthiazolyl)-thioureas are also found to possess antitubercular activity.

Thanks are due to Dr. S. K. Gupta, C.D.R.I., Lucknow for his kind help extended by assaying the synthesised compounds for antitubercular activity, and to the authorities of Banaras Hindu University, for providing necessary facilities and also to the Council of Scientific and Industrial Research, New Delhi, for an award of a Junior Research Fellowship to one of us (S. C. S.).

*Department of Chemistry*
*College of Science*
*Banaras Hindu University*
*Varanasi, India*

# Some Possible Antihistaminics and Antispasmodics. I. Synthesis of Mannich Bases

By Prithwi Nath BHARGAVA and Suresh Chandra SHARMA

(Received September 7, 1964)

In view of the findings and facts, that all the antihistaminic compounds contain the structural unit $R_2N$–C–C–X in which X is a group beginning with oxygen ($R_2N$–C–C–O), nitrogen ($R_2N$–C–C–N=) or carbon ($R_2N$–C–C–C≡), and the presence of sulphur containing groups like thienyl, thiazolidionyl, thiazolyl, etc., may promote antispasmodic activity as indicated by the observation of Blicke and Tsao,[1] Anderson and Green,[2] Bhargava and Singh[3] and Tripathi et al.[4] and also the musculotropic activity exhibited by thiazoles as described by Chance, Dirnhumber and Robinson,[5] the thiazoles have been taken as the starting material for the synthesis of a number of possible antihistaminics and antispasmodics.

Ketones containing an active methyl or

1) F. F. Blicke and M. U. Tsao, *J. Am. Chem. Soc.*, **66**, 1645 (1944).
2) D. W. Adamson and A. F. Green, *Nature*, **165**, 122 (1950).
3) P. N. Bhargava and P. R. Singh (in this laboratory), Thesis submitted to Banaras Hindu University for Ph. D., March 1962 (unpublished).
4) P. Tripathi, H. K. Pujari and M. K. Rout, *J. Ind. Chem. Soc.*, **35**, 407 (1958).
5) M. R. A. Chance, P. Dirnhuber and F. A. Robinson, *Brit. J. Pharmacol.*, **1**, 153 (1946).

TABLE I. 2-ACETAMIDO-4-ARYL-5-SUBSTITUTED-METHYL-THIAZOLES AND THEIR HYDROCHLORIDES

| Sample No. | Compound | Base | | | | | Hydrochloride | | | | |
|---|---|---|---|---|---|---|---|---|---|---|---|
| | | M. p. °C | Molecular formula | N, % | | S, % (Br., %) | M. p. °C | N, % | | S, % | |
| | | | | Found | Calcd. | Found Calcd. | | Found | Calcd. | Found | Calcd. |
| | 2-Acetamido-4-phenyl | | | | | | | | | | |
| 1 | -5-dimethylaminomethyl-thiazole | 129 | $C_{14}H_{17}N_3OS$ | 15.19 | 15.27 | 11.58 11.64 | — | — | — | — | — |
| 2 | -5-morpholinomethyl-thiazole | 198 | $C_{16}H_{19}N_3O_2S$ | 13.22 | 13.25 | 10.11 10.09 | 201 | 11.82 | 11.88 | 9.06 | 9.05 |
| 3 | -5-piperidinomethyl-thiazole | 158 | $C_{17}H_{21}N_3OS$ | 13.25 | 13.33 | 10.13 10.16 | 196 | 11.89 | 11.95 | 9.01 | 9.10 |
| 4 | -5-methylanilinomethyl-thiazole | 202 | $C_{19}H_{19}N_3OS$ | 12.35 | 12.46 | 9.37 9.49 | 194 | 11.20 | 11.24 | 8.51 | 8.57 |
| 5 | -5-ethylanilinomethyl-thiazole | 205 | $C_{20}H_{21}N_3OS$ | 11.88 | 11.97 | 9.16 9.12 | 180 | 10.76 | 10.84 | 8.19 | 8.26 |
| 6 | -5-*N*-benzylanilinomethyl-thiazole | 196 | $C_{25}H_{23}N_3OS$ | 10.13 | 10.17 | 7.80 7.75 | 198 | 9.28 | 9.34 | 7.03 | 7.12 |
| 7 | -5-*N*-benzimidazolylmethyl-thiazole | 121 | $C_{19}H_{16}N_4OS$ | 16.04 | 16.09 | 9.15 9.19 | — | — | — | — | — |
| 8 | -5-(2'-methyl-*N*-benzimidazolyl-methyl)-thiazole | 123 | $C_{20}H_{18}N_4OS$ | 15.40 | 15.47 | 8.87 8.84 | — | — | — | — | — |
| 9 | Piperazino-1 : 4-bis(2'-acetamido-4'-phenyl-5'-methyl thiazole) | 93 | $C_{28}H_{30}N_6O_2S_2$ | 15.31 | 15.38 | 11.65 11.72 | d.337 | 13.54 | 13.57 | 10.29 | 10.34 |
| | 2-Acetamido-4-*p*-bromophenyl | | | | | | | | | | |
| 10 | -5-dimethylaminomethyl-thiazole | 118 | $C_{14}H_{16}N_3OSBr$ | 11.80 | 11.86 | (22.54) (22.60) | 191 | 11.98 | 12.05 | 9.13 | 9.18 |
| 11 | -5-diethylaminomethyl-thiazole | d.142 | $C_{16}H_{20}N_3OSBr$ | 11.02 | 10.99 | (20.86) (20.94) | d.84 | 10.01 | 10.04 | 7.61 | 7.64 |
| 12 | -5-morpholinomethyl-thiazole | d.115 | $C_{16}H_{18}N_3O_2SBr$ | 10.53 | 10.61 | (20.13) (20.20) | d.197 | 9.62 | 9.71 | 7.41 | 7.40 |
| 13 | -5-piperidinomethyl-thiazole | 129 | $C_{17}H_{20}N_3OSBr$ | 10.62 | 10.66 | (20.24) (20.30) | d.113 | 9.68 | 9.76 | 7.39 | 7.43 |
| 14 | -5-methylanilinomethyl-thiazole | 98 | $C_{19}H_{18}N_3OSBr$ | 10.04 | 10.00 | (19.15) (19.23) | d.125 | 9.21 | 9.29 | 7.03 | 7.07 |
| 15 | -5-*N*-benzylanilinomethyl-thiazole | 130 | $C_{25}H_{22}N_3OSBr$ | 8.52 | 8.54 | (16.20) (16.26) | d.108 | 7.86 | 7.95 | 6.04 | 6.05 |
| 16 | -5-*N*-benzimidazolylmethyl-thiazole | d.136 | $C_{19}H_{15}N_4OSBr$ | 13.06 | 13.11 | (18.64) (18.77) | d.194 | 11.97 | 12.08 | 6.85 | 6.90 |
| 17 | -5-(2'-methyl-*N*-benzimidazolyl-methyl)-thiazole | d.134 | $C_{20}H_{17}N_4OSBr$ | 12.63 | 12.70 | (18.07) (18.14) | 193 | 11.68 | 11.73 | 6.72 | 6.70 |
| 18 | Piperazino-1 : 4-bis(2'-acetamido-4'-*p*-bromophenyl-5'-methyl-thiazole) | d.101 | $C_{28}H_{28}N_6O_2S_2Br_2$ | 11.85 | 11.93 | (22.61) (22.73) | 212 | 10.79 | 10.84 | 8.18 | 8.26 |

| | | | | | | | | | | | | |
|---|---|---|---|---|---|---|---|---|---|---|---|---|
| | 2-Acetamido-4-*p*-tolyl | | | | | | | | | | | |
| 19 | -5-dimethylaminomethyl-thiazole | 107 | $C_{15}H_{19}N_3OS$ | 14.48 | 14.53 | 11.10 | 11.07 | — | — | — | — | — |
| 20 | -5-diethylaminomethyl-thiazole | 205 | $C_{17}H_{23}N_3OS$ | 13.23 | 13.25 | 10.02 | 10.09 | 200 | 11.81 | 11.88 | 8.97 | 9.05 |
| 21 | -5-morpholinomethyl-thiazole | d.186 | $C_{17}H_{21}N_3O_2S$ | 12.61 | 12.69 | 9.55 | 9.67 | d.177 | 11.40 | 11.43 | 8.68 | 8.71 |
| 22 | -5-piperidinomethyl-thiazole | 124 | $C_{18}H_{23}N_3OS$ | 12.68 | 12.77 | 9.65 | 9.73 | 115 | 11.43 | 11.49 | 8.65 | 8.75 |
| 23 | -5-methylanilinomethyl-thiazole | 184 | $C_{20}H_{21}N_3OS$ | 11.93 | 11.97 | 9.13 | 9.12 | 185 | 10.79 | 10.84 | 8.21 | 8.26 |
| 24 | -5-*N*-benzylanilinomethyl-thiazole | 135 | $C_{26}H_{25}N_3OS$ | 9.75 | 9.84 | 7.43 | 7.49 | 117 | 9.02 | 9.06 | 6.87 | 6.90 |
| 25 | -5-*N*-benzimidazolylmethyl-thiazole | 97 | $C_{20}H_{18}N_4OS$ | 15.42 | 15.47 | 8.80 | 8.84 | — | — | — | — | — |
| 26 | Piperazino-1 : 4-bis(2′-acetamido-4′-*p*-tolyl-5′-methyl-thiazole) | 71 | $C_{30}H_{34}N_6O_2S_2$ | 14.51 | 14.63 | 11.18 | 11.15 | d.65 | 12.95 | 13.02 | 9.86 | 9.92 |
| | 2-Acetamido-4-*p*-methoxyphenyl | | | | | | | | | | | |
| 27 | -5-dimethylaminomethyl-thiazole | d. 96 | $C_{15}H_{19}N_3O_2S$ | 13.71 | 13.77 | 10.45 | 10.49 | — | — | — | — | — |
| 28 | -5-diethylaminomethyl-thiazole | 123 | $C_{17}H_{23}N_3O_2S$ | 12.52 | 12.61 | 9.52 | 9.61 | d.146 | 11.37 | 11.37 | 8.59 | 8.66 |
| 29 | -5-morpholinomethyl-thiazole | d. 90 | $C_{17}H_{21}N_3O_3S$ | 12.04 | 12.10 | 9.18 | 9.22 | 196 | 10.86 | 10.95 | 8.30 | 8.34 |
| 30 | -5-piperidinomethyl-thiazole | d. 87 | $C_{18}H_{23}N_3O_2S$ | 12.15 | 12.17 | 9.30 | 9.27 | d. 65 | 10.94 | 11.01 | 8.32 | 8.39 |
| 31 | -5-methylanilinomethyl-thiazole | d.199 | $C_{20}H_{21}N_3O_2S$ | 11.33 | 11.44 | 8.68 | 8.72 | d. 61 | 10.30 | 10.41 | 7.86 | 7.93 |
| 32 | -5-ethylanilinomethyl-thiazole | d. 85 | $C_{21}H_{23}N_3O_2S$ | 10.94 | 11.02 | 8.33 | 8.40 | 199 | 10.01 | 10.06 | 7.70 | 7.66 |
| 33 | -5-*N*-benzylanilinomethyl-thiazole | 203 | $C_{26}H_{25}N_3O_2S$ | 9.39 | 9.48 | 7.25 | 7.22 | d. 73 | 8.68 | 8.76 | 6.63 | 6.67 |
| 34 | -5-*N*-benzimidazolylmethyl-thiazole | d.141 | $C_{20}H_{18}N_4O_2S$ | 14.75 | 14.81 | 8.42 | 8.47 | 203 | 13.47 | 13.51 | 7.69 | 7.72 |
| 35 | -5-(2′-methyl-*N*-benzimidazolyl-methyl)-thiazole | d.107 | $C_{21}H_{20}N_4O_2S$ | 14.21 | 14.29 | 8.19 | 8.16 | d.143 | 12.99 | 13.07 | 7.39 | 7.47 |
| 36 | Piperazino-1 : 4-bis(2′-acetamido-4′-*p*-methoxyphenyl-5′-methylthiazole) | d.214 | $C_{30}H_{34}N_6O_4S_2$ | 13.80 | 13.86 | 10.58 | 10.56 | d.109 | 12.36 | 12.41 | 9.39 | 9.45 |
| | 2-Acetamido-4-$\alpha$-naphthyl | | | | | | | | | | | |
| 37 | -5-diethylaminomethyl-thiazole | 137 | $C_{20}H_{23}N_3OS$ | 11.85 | 11.90 | 9.03 | 9.06 | 202 | 10.72 | 10.78 | 8.20 | 8.22 |
| 38 | -5-morpholinomethyl-thiazole | d. 98 | $C_{20}H_{21}N_3O_2S$ | 11.40 | 11.44 | 8.66 | 8.72 | d. 72 | 10.34 | 10.41 | 7.94 | 7.93 |
| 39 | -5-piperidinomethyl-thiazole | d. 92 | $C_{21}H_{23}N_3OS$ | 11.39 | 11.51 | 8.80 | 8.77 | d.112 | 10.39 | 10.46 | 7.89 | 7.97 |
| | 2-Acetamido-4-$\beta$-naphthyl | | | | | | | | | | | |
| 40 | -5-dimethylaminomethyl-thiazole | d. 91 | $C_{18}H_{19}N_3OS$ | 12.85 | 12.92 | 9.77 | 9.84 | 187 | 11.58 | 11.62 | 8.81 | 8.85 |
| 41 | -5-diethylaminomethyl-thiazole | d. 96 | $C_{20}H_{23}N_3OS$ | 11.87 | 11.90 | 9.01 | 9.06 | 176 | 10.71 | 10.78 | 8.25 | 8.22 |
| 42 | -5-morpholinomethyl-thiazole | 152 | $C_{20}H_{21}N_3O_2S$ | 11.37 | 11.44 | 8.62 | 8.72 | — | — | — | — | — |
| 43 | -5-piperidinomethyl-thiazole | d.121 | $C_{21}H_{23}N_3OS$ | 11.47 | 11.51 | 8.69 | 8.77 | 190 | 10.38 | 10.46 | 10.99 | 7.97 |
| 44 | -5-methylanilinomethyl-thiazole | 123 | $C_{23}H_{21}N_3OS$ | 10.87 | 10.85 | 8.31 | 8.27 | d.105 | 9.84 | 9.92 | 7.48 | 7.56 |
| 45 | -5-*N*-benzylanilinomethyl-thiazole | d.115 | $C_{29}H_{25}N_3OS$ | 9.01 | 9.07 | 6.88 | 6.91 | 180 | 8.36 | 8.41 | 6.39 | 6.41 |
| 46 | -5-*N*-benzimidazolylmethyl-thiazole | d. 93 | $C_{23}H_{18}N_4OS$ | 14.02 | 14.07 | 8.06 | 8.04 | d. 65 | 12.81 | 12.89 | 7.40 | 7.36 |
| 47 | -5-(2′-methyl-*N*-benzimidazolyl-methyl)-thiazole | d. 95 | $C_{24}H_{20}N_4OS$ | 13.50 | 13.59 | 7.68 | 7.76 | 191 | 12.38 | 12.49 | 7.08 | 7.13 |
| 48 | Piperazino-1 : 4-bis(2′-acetamido-4′-$\beta$-naphthyl-5′-methyl-thiazole) | d.130 | $C_{36}H_{34}N_6O_2S_2$ | 12.89 | 13.00 | 9.87 | 9.91 | d.194 | 11.68 | 11.71 | 8.89 | 8.93 |

methylene group have been shown by Mannich[6-8] to condense with formaldehyde and secondary bases. Compounds other than ketones but containing methyl or methylene group, may be induced to go under Mannich reaction.[9] The hydrogen atom at 5-C in thiazole nucleus is very reactive to be a key point for the preparation of Mannich bases from thiazoles.

In the present study 2-acetylamino-4-aryl-thiazoles have been condensed with ten different secondary bases and formalin in absolute ethanol. Mannich base was precipitated out on treatment of the reaction mixture with the saturated solution of potassium carbonate. The bases have been converted into their hydrochlorides by the usual method. The results of the pharmacological tests will be published elsewhere after proper screening.

## Experimental

2-Amino-4-phenyl-, -4-*p*-bromophenyl-, -4-*p*-tolyl, -4-*p*-methoxyphenyl-, -4-$\alpha$-naphthyl-, and -4-$\beta$-naphthyl-thiazoles were prepared by the method of Dodson and King.[10]

2-Acetylamino-4-aryl-thiazoles were prepared by acetylation of 2-amino-4-aryl-thiazoles with acetic anhydride.

**2-Acetamido-4-phenyl-5-diethylaminomethylthiazole.**—In a dry flask 2.2 g. of 2-acetamido-4-phenyl-thiazole was taken and 1 ml. of diethylamine in 5 ml. of acetic acid and 1 ml. of formalin were added into it. The reaction mixture was refluxed for five hours on a water bath. After cooling, 15 ml. of water was added and the reaction mixture was then treated with the saturated solution of potassium carbonate. The precipitate, thus obtained, was filtered, washed well with water and finally recrystallised from ethanol and dried in vacuum desiccator, m. p. 129°C, yield 68% (Found: C, 52.89; H, 5.30; S, 11.58. Calcd. for $C_{14}H_{17}ON_3S$: C, 53.00; H, 5.38; N, 15.27; S, 11.64%).

Similarly other 2-acetamido-4-aryl-thiazoles were condensed with diethylamine, morpholine, piperidine, methylaniline, ethylaniline, *N*-benzylaniline, benzimidazole, 2-methyl-*N*-benzimidazole and piperazine. The bases, obtained on condensation, were converted into their hydrochloride by the usual method. The properties and analytical data of these bases as well as their hydrochlorides are recorded in Table I.

Thanks of the authors are due to the authorities of the Banaras Hindu University for providing facilities and also to the Council of Scientific and Industrial Research, New Delhi, for the award of a Junior Research Fellowship to one of us (S. C. S.).

*Department of Chemistry*
*College of Science*
*Banaras Hindu University*
*Varanasi, India*

6) C. Mannich and B. Kather, *Ber.*, **53**, 1368 (1920).
7) C. Mannich and G. Heilner, ibid., **55**, 356 (1922).
8) C. Mannich, *Arch. Pharm.*, **264**, 741 (1926); **265**, 589 (1927).
9) W. O. Kermack and W. Muir, *J. Chem. Soc.*, **1931**, 3089.
10) R. M. Dodson and L. C. King, *J. Am. Chem. Soc.*, **67**, 2242 (1945).

# Some Possible Antihistaminics and Antispasmodics. II. Synthesis of Mannich Bases

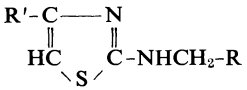
By Prithwi Nath BHARGAVA and Suresh Chandra SHARMA

(Received September 7, 1964)

A definite antispasmodic activity of pyrazolone derivatives,[1,2] certain substituted β-aminoalkylaryl ketones,[3,4] pyridyl and thiazolyl quinoline derivatives[5,6] and quinolyl and pyrazolone derivatives of thiazolidiones,[7] has created an interest in the syntheses of thiazole and thiazolidione derivatives—Mannich bases, and also to study, how the attachment of an additional therapeutically active quinoline and pyrazolone nuclei adds to the importance of thiazole in therapy, particularly their usefulness as antihistaminics and antispasmodics.

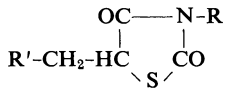
1) L. J. Notkin and D. R. Webster, *Rev. Canadian Biol.*, **1**, 660 (1942).
2) B. Pathak and T. N. Ghosh, *J. Indian Chem. Soc.*, **26**, 371 (1949).
3) F. F. Blicke, *Ann. Rev. Biochem.*, **13**, 549 (1943).
4) J. J. Denton et al., *J. Am. Chem. Soc.*, **71**, 2048, 2050, 2053, 2054 (1949).
5) H. Bader, L. C. Cross, I. Heilbron and E. R. H. Jones, *J. Chem. Soc.*, **1949**, 619.
6) P. Tripathi, H. K. Pujari and M. K. Rout, *J. Ind. Chem. Soc.*, **35**, 407 (1958).
7) P. N. Bhargava and P. R. Singh (in this laboratory), Ph. D. thesis submitted to Banaras Hindu University, March, 1962 (unpublished).

TABLE I. 2-SUBSTITUTED(R)METHYLAMINO-4-ARYL(R')THIAZOLES



| Sample No. | R | Aryl group R' | Yield % | M. p. °C | Molecular formula | N, % Found | N, % Calcd. | S, % Found | S, % Calcd. |
|---|---|---|---|---|---|---|---|---|---|
| 1 | Phenacyl | *p*-Tolyl- | 58 | d. 219 | $C_{19}H_{18}N_2OS$ | 8.65 | 8.70 | 9.85 | 9.94 |
| 2 | 8-Hydroxyquinolinyl- | *p*-Tolyl- | 52 | d. 116 | $C_{20}H_{18}N_3OS$ | 11.95 | 12.06 | 9.21 | 9.19 |
| 3 | *p*-Methylphenacyl- | *p*-Tolyl- | 53 | d. 215 | $C_{20}H_{20}N_2OS$ | 8.31 | 8.33 | 9.55 | 9.52 |
| 4 | 1-Phenyl-3-methyl-5-pyrazolonyl- | *p*-Tolyl- | 48 | d. 178 | $C_{21}H_{20}N_4OS$ | 14.83 | 14.89 | 8.48 | 8.51 |
| 5 | Phenacyl- | *p*-Bromophenyl- | 50 | d. 214 | $C_{18}H_{15}N_2OSBr$ | 7.15 | 7.23 | 8.30 | 8.27 |
| 6 | *p*-Methylphenacyl- | *p*-Bromophenyl- | 58 | 137 | $C_{19}H_{17}N_2OSBr$ | 6.92 | 6.98 | 7.95 | 7.98 |
| 7 | 8-Hydroxyquinolinyl- | *p*-Bromophenyl- | 46 | d. 242 | $C_{19}H_{15}N_3OSBr$ | 10.10 | 10.17 | 7.64 | 7.75 |
| 8 | Phenacyl- | *p*-Methoxyphenyl- | 51 | d. 156 | $C_{19}H_{18}N_2O_2S$ | 8.23 | 8.28 | 9.42 | 9.47 |
| 9 | 8-Hydroxyquinolinyl- | *p*-Methoxyphenyl- | 54 | 212 | $C_{20}H_{18}N_3O_2S$ | 11.46 | 11.54 | 8.75 | 8.79 |

TABLE II. 3-ARYL-5-SUBSTITUTED-METHYL-2 : 4-THIAZOLIDIONES



| Sample No. | Aryl group R | R' | Yield % | M. p. °C | Molecular formula | N, % Found | N, % Calcd. | S, % Found | S, % Calcd. |
|---|---|---|---|---|---|---|---|---|---|
| 1 | Phenyl- | 2'-Methyl-*N*-benzimidazolyl- | 66 | 173 | $C_{18}H_{15}N_3O_2S$ | 12.38 | 12.46 | 9.53 | 9.50 |
| 2 | *p*-Chlorophenyl- | *N*-Benzimidazolyl- | 70 | 196 | $C_{17}H_{12}N_3O_2SCl$ | 11.70 | 11.75 | 8.92 | 8.95 |
| 3 | *p*-Chlorophenyl- | 2'-Methyl-*N*-benzimidazolyl- | 72 | 188—190 | $C_{18}H_{14}N_3O_2SCl$ | 11.24 | 11.31 | 8.62 | 8.61 |
| 4 | *o*-Anisyl- | *N*-Benzimidazolyl- | 63 | 82 | $C_{18}H_{15}N_3O_3S$ | 11.83 | 11.90 | 9.02 | 9.06 |
| 5 | *o*-Anisyl- | 2'-Methyl-*N*-benzimidazolyl- | 65 | 80 | $C_{19}H_{17}N_3O_3S$ | 11.38 | 11.44 | 8.65 | 8.72 |
| 6 | *p*-Phenetyl- | Methylanilino- | 63 | d. 95 | $C_{19}H_{20}N_2O_3S$ | 7.81 | 7.86 | 9.04 | 8.99 |
| 7 | *p*-Phenetyl- | 2'-Methyl-*N*-benzimidazolyl- | 64 | d. 94 | $C_{20}H_{19}N_3O_3S$ | 10.93 | 11.02 | 8.35 | 8.40 |
| 8 | α-Naphthyl- | Methylanilino- | 60 | 81 | $C_{21}H_{18}N_2O_2S$ | 7.70 | 7.73 | 8.85 | 8.84 |
| 9 | α-Naphthyl- | *N*-Benzylanilino- | 65 | 116 | $C_{27}H_{22}N_2O_2S$ | 6.31 | 6.39 | 7.28 | 7.31 |
| 10 | α-Naphthyl- | *N*-Benzimidazolyl- | 68 | d. 73 | $C_{21}H_{15}N_3O_2S$ | 11.19 | 11.26 | 8.53 | 8.58 |
| 11 | α-Naphthyl- | 2'-Methyl-*N*-benzimidazolyl- | 71 | d. 84 | $C_{22}H_{17}N_3O_2S$ | 10.76 | 10.85 | 8.29 | 8.27 |
| 12 | β-Naphthyl- | Methylanilino- | 65 | d. 90 | $C_{21}H_{18}N_2O_2S$ | 7.65 | 7.73 | 8.81 | 8.84 |
| 13 | β-Naphthyl- | *N*-Benzylanilino- | 70 | d. 82 | $C_{27}H_{22}N_2O_2S$ | 6.32 | 6.39 | 7.27 | 7.31 |
| 14 | β-Naphthyl- | *N*-Benzimidazolyl- | 63 | 188 | $C_{21}H_{15}N_3O_2S$ | 11.20 | 11.26 | 8.62 | 8.58 |
| 15 | β-Naphthyl- | 2'-Methyl-*N*-benzimidazolyl- | 60 | 111 | $C_{22}H_{17}N_3O_2S$ | 10.81 | 10.85 | 8.30 | 8.27 |

Table III. Hydrochlorides of 3-aryl-5-substituted-methyl-2 : 4-thiazolidiones

| Sample No. | Aryl group R | R′ | Yield % | M. p. °C | Molecular formula | N, % | | S, % | |
|---|---|---|---|---|---|---|---|---|---|
| | | | | | | Found | Calcd. | Found | Calcd. |
| 1 | Phenyl- | Ethylanilino- | 53 | 134 | $C_{18}H_{18}N_2O_2S\cdot HCl$ | 7.65 | 7.72 | 8.78 | 8.83 |
| 2 | Phenyl- | *N*-Benzylanilino- | 86 | 132 | $C_{23}H_{20}N_2O_2S\cdot HCl$ | 6.52 | 6.60 | 7.58 | 7.54 |
| 3 | Phenyl- | *N*-Benzimidazolyl- | 68 | 136 | $C_{17}H_{13}N_3O_2S\cdot HCl$ | 11.59 | 11.68 | 8.85 | 8.90 |
| 4 | Phenyl- | 2′-Methyl-*N*-benzimidazolyl- | 81 | 135 | $C_{18}H_{15}N_3O_2S\cdot HCl$ | 11.22 | 11.24 | 8.58 | 8.57 |
| 5 | *p*-Chlorophenyl- | *N*-Benzimidazolyl- | 68 | 191 | $C_{17}H_{12}N_3O_2SCl\cdot HCl$ | 10.60 | 10.66 | 8.08 | 8.12 |
| 6 | *o*-Anisyl- | Ethylanilino- | 55 | 83 | $C_{19}H_{20}N_2O_3S\cdot HCl$ | 7.11 | 7.13 | 8.17 | 8.15 |
| 7 | *o*-Anisyl- | *N*-Benzimidazolyl- | 50 | 82 | $C_{18}H_{15}N_3O_3S\cdot HCl$ | 10.71 | 10.78 | 8.22 | 8.21 |
| 8 | *o*-Anisyl- | 2′-Methyl-*N*-benzimidazolyl- | 48 | 79 | $C_{19}H_{17}N_3O_3S\cdot HCl$ | 10.38 | 10.41 | 7.89 | 7.93 |
| 9 | *p*-Phenetyl- | Ethylanilino- | 57 | 104 | $C_{20}H_{22}N_2O_3S\cdot HCl$ | 6.88 | 6.89 | 7.90 | 7.87 |
| 10 | *p*-Phenetyl- | *N*-Benzylanilino- | 61 | 129 | $C_{25}H_{24}N_2O_3S\cdot HCl$ | 5.92 | 5.98 | 6.80 | 6.83 |
| 11 | α-Naphthyl- | Methylanilino- | 54 | above 300 | $C_{21}H_{18}N_2O_2S\cdot HCl$ | 7.01 | 7.03 | 8.06 | 8.03 |
| 12 | α-Naphthyl- | *N*-Benzylanilino- | 48 | d. 201 | $C_{27}H_{22}N_2O_2S\cdot HCl$ | 5.82 | 5.90 | 6.69 | 6.74 |
| 13 | α-Naphthyl- | *N*-Benzimidazolyl- | 60 | d. 209 | $C_{21}H_{15}N_3O_2S\cdot HCl$ | 10.23 | 10.26 | 7.78 | 7.81 |
| 14 | α-Naphthyl- | 2′-Methyl-*N*-benzimidazolyl- | 43 | d. 262 | $C_{22}H_{17}N_3O_2S\cdot HCl$ | 9.81 | 9.92 | 7.49 | 7.56 |
| 15 | β-Naphthyl- | *N*-Benzylanilino- | 50 | d. 87 | $C_{27}H_{22}N_2O_2S\cdot HCl$ | 5.85 | 5.90 | 6.75 | 6.74 |
| 16 | β-Naphthyl- | *N*-Benzimidazolyl- | 55 | 189 | $C_{21}H_{15}N_3O_2S\cdot HCl$ | 10.17 | 10.26 | 7.78 | 7.81 |
| 17 | β-Naphthyl- | 2′-Methyl-*N*-benzimidazolyl- | 41 | d. 128 | $C_{22}H_{17}N_3O_2S\cdot HCl$ | 9.84 | 9.92 | 7.58 | 7.56 |

A few 2-amino-4-aryl thiazoles have been condensed with acetophenone, *p*-methyl-acetophenone, 8-hydroxy-quinoline and 1-phenyl-3-methyl-5-pyrazolone along with paraformaldehyde and hydrochloric acid in absolute ethanol. Another series of derivatives starting from 3-aryl-2 : 4-thiazolidiones has also been synthesised by condensing thiazolidiones with different secondary amine-hydrochlorides and paraformaldehyde. These thiazoles and thiazolidiones were prepared as per procedures laid down by Dodson and King[8] and Bhargava et al.[9-11] respectively. The results of the pharmacological screening of these compounds for antihistaminics and antispasmodic activities will be published elsewhere.

## Experimental

**Condensation of 2-Amino-4-*p*-tolylthiazole with Formaldehyde and Acetophenone.**—In a r. b. flask a mixture of 1.9 g. of 2-amino-4-*p*-tolylthiazole, 1.2 g. of acetophenone and 0.9 g. of paraformaldehyde in 3 ml. of hydrogen chloride and 30 ml. of ethanol was heated on a water bath under reflux for two hours. An addition amount of 0.6 g. of paraformaldehyde was then added and refluxing was continued for three hours more. Ethanol was distilled off and the residue solidified on keeping in contact with ammonia for four hours. It was washed with water and crystallized from ethanol m. p. d. 219°C, yield 58%.

In the case of 1-phenyl-3-methyl-5-pyrazolone, the mixture was heated directly over an asbestos wire gauge for eight hours.

The properties and analytical data of the other products obtained on condensation of acetophenone, *p*-methylacetophenone, 8-hydroxy quinoline and 1-phenyl-3-methyl-5-pyrazolone with different 2-amino-4-arylthiazoles are mentioned in Table I.

**5-(2'-Methyl-*N*-benzimidazolyl-methyl)-3-phenyl-2 : 4-thiazolidione.**—A mixture of 1.9 g. of 3-phenyl-2 ; 4-thiazolidione, 1.3 g. of 2-methyl-*N*-benzimidazolyl, 1.2 g. of paraformaldehyde and 3 ml. of hydrogen chloride in 25 ml. of absolute ethanole was heated under reflux on a water bath for eight hours. The solvent was distilled off and the pasty mass was obtained which on keeping in contact with concentrated ammonia for one to two hours solidified. It was washed well with water and then crystallised from ethanol, m. p. 173°C, yield 66% (Found : C, 63.92; H, 4.43; N, 12.38; S, 9.53. Calcd. for $C_{18}H_{15}O_2N_3S$ : C, 64.09; H, 4.45; N, 12.46; S, 9.50%).

Similarly, other 3-aryl-2 : 4-thiazolidiones were condensed with *N*-benzimidazole, methyl-, ethyl-, and benzyl-anilines. The properties and analytical data of these compounds are reported in Table II.

It is experienced during the course of work that the isolation of the bases sometimes becomes very difficult specially with products obtained on condensation with methyl-, and ethylanilines. A few compounds were obtained as hydrochlorides only because their bases could not be isolated from the reaction product.

**Preparation of the Hydrochlorides of the Above Bases.** — The hydrochlorides of the bases were prepared by the usual procedure of passing dry hydrogen chloride gas into the solution of the base in benzene, or dry ether. These hydrochlorides are recorded in Table III.

Thanks are due to the authorities of the Banaras Hindu University for providing necessary facilities and also to the Council of Scientific and Industrial Research, New Delhi, India for the award of a Junior Research Fellowship to one of us (S. C. S.).

*Department of Chemistry*
*College of Science*
*Banaras Hindu University*
*Varanasi, India*

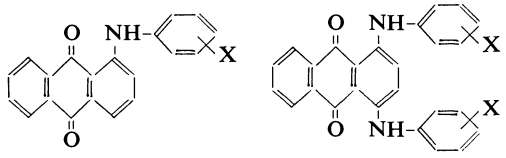
8) R. M. Dodson and L. C. King, *J. Am. Chem. Soc.*, **67**, 2242 (1945).
9) P. N. Bhargava R. P. Rao and M. S. Sastri, *J. Indian Chem. Soc.*, **23**, 596 (1956).
10) P. N. Bhargava, and P. R. Singh, *J. Sci. industr. Res.*, **20C**, 209 (1961).
11) P. N. Bhargava and S. C. Sharma, This Bulletin, **35**, 1926 (1962).

# Spectroscopic Studies of Bis(arylamino)anthraquinones

By Takayuki HAYASHI and Takao TOKUMITSU

(Received September 18, 1964)

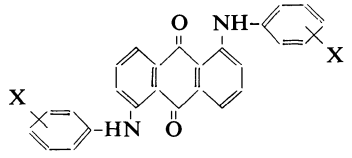
In a previous paper,[1] 1-arylaminoanthraquinones (I) with $NO_2$, Cl, Me, OMe, and $NH_2$ as substituents in the aryl group were prepared, and their visible absorption spectra in solution and infrared spectra in the solid state were measured and discussed. On the basis of these results, the effects of the substituent groups were discussed in view of various properties, such as visible absorption maxima or infrared C=O and N–H frequencies. In this paper, the preparation and spectral characteristics of 1, 4-, 1, 5- and 1, 8-bis(arylamino)anthraquinones (II,



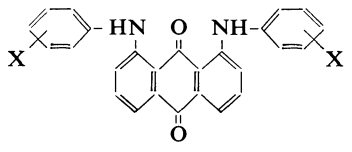
(I)



(II)



(III)



(IV)

III, IV) with the above-mentioned groups as substituents (X) in the aryl group will be reported. These are parent compounds of anthraquinone acid or polyester dyes. As was the case with 1-arylaminoanthraquinones, on the basis of the results of the visible and infrared absorption spectra for bis(arylamino)-anthraquinones, the relations between the shifts of the visible absorption peaks, the C=O or N–H frequencies and their structures will be discussed.

## Results and Discussion

**Visible Absorption Spectra.**—The visible absorption peaks of bis(arylamino)anthraquinones in *o*-dichlorobenzene are shown in Table I. On the basis of these results, relations between the wavelengths or intensities of the absorption maxima and the positions of the arylamino groups have been discussed. Furthermore, for each series of 1, 4-, 1, 5- and 1, 8-bis(arylamino)-anthraquinones, the effects of the substituent (X) upon the wavelength and the intensity of the absorption maximum have been discussed. Compounds I and III give one visible absorption peak, as in the cases of the corresponding amino- and acylamino-anthraquinones.[1-4] The wavelength of the absorption maximum of III (X=H) is somewhat longer than that of I (X=H), but the intensity of the former is approximately twice that of the latter. Such a relation is also seen with other III's. As was shown by Hartmann's results,[5] the absorption maximum of 1, 8-diaminoanthraquinone appeared in the same wavelength region as that of the 1, 5-isomer, and the absorption spectrum was characterized by twin peaks of a lower definition with a shoulder at a lower wavelength, peaks which were similar to those observed for the 1, 4-isomer. The absorption spectral character of 1, 8-diaminoanthraquinone, therefore, appears to be intermediate between those of 1, 4- and 1, 5-isomers. On the contrary, IV (X=H) showed only one absorption band, located at a somewhat longer wavelength than that of the 1, 5-isomer; the intensity of the former absorption is slightly lower than that of the latter, but approximately twice that of I (X=H). II (X=H) gives twin peaks of a similar intensity, unlike those of I (X=H), III (X=H) and IV (X=H). Such a relation is seen with other II's. I, III and IV, each with a strongly electron-attracting $-NMe_3^+$ group as a substituent, gave only one absorption peak in dioxane, but the corresponding II gave a peak at 593 m$\mu$ (12400)* with a shoulder in the region

1) T. Hayashi and M. Matsuo, This Bulletin, **35**, 1500 (1962).
2) R. H. Peters and H. H. Sumner, *J. Chem. Soc.*, **1953**, 2101.
3) G. S. Egerton and A. G. Roach, *J. Soc. Dyers Colorists*, **74**, 401 (1958).
4) T. Hayashi and R. Shibata, This Bulletin, **34**, 1116 (1961); T. Hayashi, *J. Chem. Soc. Japan, Ind. Chem. Sec. (Kogyo Kagaku Zasshi)*, **63**, 1985 (1960).
5) H. Hartmann and E. Lorenz, *Z. Naturforsch.*, **72**, 360 (1952).
* Wavelength, m$\mu$ (molar extinction coefficient).

TABLE I. VISIBLE ABSORPTION PFAKS OF 1-ARYLAMINO-, 1,4-, 1,5- AND 1,8-BIS-(ARYLAMINO)ANTHRAQUINONES

| Substituent of the aryl group (X) | 1,4-Derivative 1st Band $\lambda_{max}$, mμ ($\varepsilon_{max}$) | | 1,4-Derivative 2nd Band $\lambda_{max}$, mμ ($\varepsilon_{max}$) |
|---|---|---|---|
| H[a] | 607 (13000) | | 647 (14300) |
| *p*-$NO_2$[b] | 547* | 615 | 630 |
| *p*-Cl | 550 (5770) | | 605 (12900) 644 (13600) |
| *p*-Me[c] | 551 (6230) | | 617 (14500) 650 (15900) |
| *p*-OMe | 621 (13800) | | 651 (14700) |
| *p*-$NH_2$[b] | 615 | | 629 656 |

| Substituent of the aryl group (X) | 1-Derivative[1] $\lambda_{max}$, mμ ($\varepsilon_{max}$) | 1,5-Derivative $\lambda_{max}$, mμ ($\varepsilon_{max}$) | 1,8-Derivative $\lambda_{max}$, mμ ($\varepsilon_{max}$) |
|---|---|---|---|
| H | 508 (5920) | 538 (13700)[d] | 558 (13500)[d] |
| *m*-$NO_2$ | 489 (6460) | 517 (14900) | |
| *p*-$NO_2$ | 487 (10700) | | 535[b] |
| *m*-Cl | 501 (7220) | 531 (13900) | |
| *p*-Me | 514 (6190) | 544 (14400)[e] | 561 (14100)[f] |
| *p*-OMe | 516 (6000) | 546 (13500) | |
| *p*-$NH_2$ | 525 (5990) | 555[b] | |

* An underlined numerical value denotes a shoulder.

a) 1,4-Bis(phenylamino)anthraquinone gave two peaks at 595 and 632 mμ with a shoulder at 550 mμ in ethanol,[6] two peaks at 602.5 and 640 mμ in chlorobenzene[7] and at about 605 and 645 mμ in 1,2,4-trichlorobenzene.[8]

b) In the saturated solution.

c) 1,4-Bis(*p*-tolylamino)anthraquinone gave two peaks at 600 and 638 mμ with a shoulder at 550 mμ in ethanol,[6] two peaks at 610 and 645 mμ in chlorobenzene,[7] two peaks at 600 and 640 mμ in dioxane,[9] and two peaks at 610 and 645 mμ.[10]

d) Both 1,5- and 1,8-bis(phenylamino)anthraquinones gave a peak at 530 mμ in chlorobenzene.[7]

e) 1,5-Bis(*p*-tolylamino)anthraquinone gave a peak at 540 mμ in chlorobenzene,[7] and a peak at about 530 mμ in dioxane.[9]

f) 1,8-Bis(*p*-tolylamino)anthraquinone gave a peak at 550 mμ in chlorobenzene.[7]

of 610—630 mμ (11600).[11] Hence, this broad shoulder seems to correspond to the two absorption peaks of II (X=*p*-$NO_2$). I, III and IV, with strongly electron-donating $-NMe_2$ substituents, gave a single absorption peak in dioxane.[12] On the other hand, the corresponding II gave a peak at 638 mμ (15300) with a shoulder at 590 mμ (11000) in dioxane, and a peak at 600 mμ (15500) with a shoulder at 590 mμ and a broad peak in the region of 640—655 mμ in ethanol.[11,12] Here, too, these results are similar to the results for II (X=*p*-$NH_2$). Consequently, the relations between the wavelengths or intensities of the absorption maxima and the positions of the arylamino groups agree with those for amino- and acylaminoanthraquinones.[2-4]

In the case of the compound I previously reported,[1] a plot of the wave numbers of the absorption maxima versus the Hammett σ values[13] of the substituents in the aryl group gave a linear relationship, but the plot of the wave numbers varsus the Brown $\sigma^+$ values[14,15] was concave; this was different from the case of acylaminoanthraquinones.[4] Here, too, for the peaks of each series, a plot of the wave numbers versus the former substituent constants gave a linear relationship, as is indicated in Figs. 1 and 2. These results can be explained in the same way as in the case of compound I.[1] It is interesting that the linear

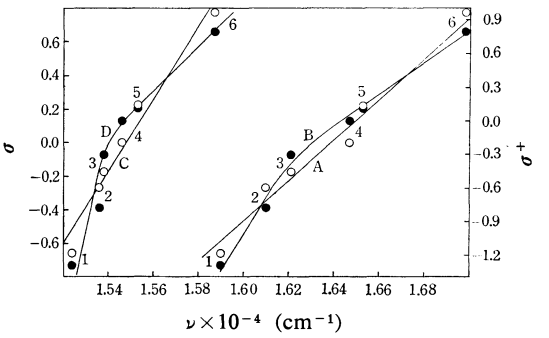



Fig. 1. Plots of wave numbers of the visible absorption maxima versus Hammett σ values and Brown $\sigma^+$ values of the substituents of 1,4-bis(arylamino)anthraquinones.

A : Wave numbers of the first bands versus Hammett σ values

B : Wave numbers of the first bands versus Brown $\sigma^+$ values

C : Wave numbers of the second bands versus Hammett σ values

D : Wave numbers of the second bands versus Brown $\sigma^+$ values

1 *p*-$NH_2$, 2 *p*-OMe, 3 *p*-Me, 4 H, 5 *p*-Cl 6 *p*-$NO_2$

6) K. Naiki, E. Chō and S. Tsuruoka, *J. Soc. Org. Synthet. Chem. Japan* (*Yūki Gōsei Kagaku Kyōkaishi*), **17**, 705 (1959).

7) S. Nakazawa, ibid., **20**, 584 (1962).

8) J. Weinstein and C. Merritt, Jr., *J. Am. Chem. Soc.*, **81**, 3759 (1959).

9) C. F. H. Allen, C. V. Wilson and G. F. Frame, *J. Org. Chem.*, **7**, 169 (1942).

10) N. S. Dokunikhin and T. N. Kurdyumova, *Zhur. Obshchei Khim.*, **25**, 617 (1955); *Chem. Abstr.*, **50**, 3369 (1956).

11) M. Ichikawa and M. Okazaki, *J Chem. Soc. Japan, Ind. Chem. Sec.* (*Koguyo Kagaku Zasshi*), **67**, 138 (1964).

12) M. Ichikawa and M. Okazaki, ibid., **67**, 142 (1964).

13) H. H. Jaffé, *Chem. Revs.*, **53**, 191 (1953).

14) H. C. Brown and Y. Okamoto, *J. Am. Chem. Soc.*, **80**, 4979 (1958).

15) H. C. Brown, "Steric Effects in Conjugated Systems," Ed. by G. W. Gray, Butterworths Scientific Publications, London (1958), p. 100.

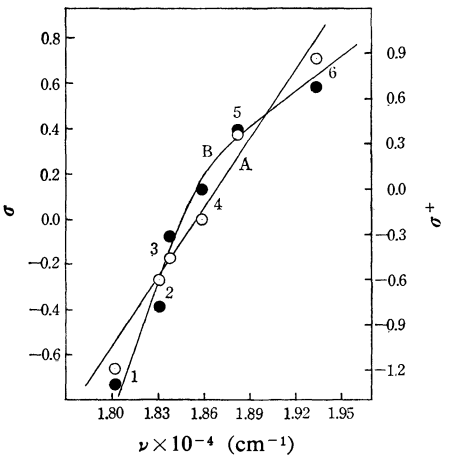



Fig. 2. Plots of wave numbers of the visible absorption maxima versus Hammett $\sigma$ values and Brown $\sigma^+$ values of the substituents of 1,5-bis(arylamino)anthraquinones.
A: Wave numbers versus Hammett $\sigma$ values
B: Wave numbers versus Brown $\sigma^+$ values
1 *p*-$NH_2$, 2 *p*-OMe, 3 *p*-Me, 4 H, 5 *m*-Cl, 6 *m*-$NO_2$

relationship is established for the plots for both the first and the second peaks of II.

**Infrared Absorption Spectra.**—Three $\mu$ bands of the infrared absorption spectra of a few 1,4-bis(arylamino)anthraquinones as Nujol mull have been observed.[16] In this work, the infrared absorption spectra of 1,4-, 1,5- and 1,8-bis(phenylamino)anthraquinones and their related derivatives as Nujol mull were observed, and information about molecular structures in the solid was obtained.

It has been known that 1,4-, 1,5- and 1,8-disubstituted anthraquinones as Nujol mull show characteristic absorption bands at 820—840 and 720—730, 800—820 and 690—710, and 830—850 and 730—750 $cm^{-1}$ respectively, and that these bands have intensities ranging from medium to very strong.[17] Absorption bands in the region of 800—850 and of 690—750 $cm^{-1}$ for II (X=H), III (X=H) and IV (X=H) are shown in Table II. The respective characteristic absorption bands of II (X=H), 829.9 and 728.3 $cm^{-1}$, appeared in the corresponding regions of 1,4-disubstituted anthraquinones, and the same results were obtained for III (X=H) and IV (X=H). The intensities of these absorption bands, except the one of the 829.9 $cm^{-1}$ band, were medium or very strong.

Table II. Absorption bands in the region of 800—850 and of 690—750 $cm^{-1}$ for 1,4-, 1,5- and 1,8-bis(phenylamino)-anthraquinones

| | | | |
|---|---|---|---|
| 1,4-Derivative | 841.8(w), 744.6(m), | 829.9(w), 728.3(vs), | 815.0(w), 695.9(s) |
| 1,5-Derivative | 842.5(s), 695.9(vs) | 806.5(vs), | 714.3(vs), |
| 1,8-Derivative | 844.6(w), 809.7(m), 719.4(w), | 838.9(m), 744.6(vs), 700.8(s), | 819.7(m), 729.9(w), 694.0(vs) |

The absorption bands in the 3 and 6 $\mu$ regions of bis(phenylamino)anthraquinones are shown in Table III, and also in Figs. 3, 4 and 5. Compound III (X=H) gave only one C=O band, this being due to the fact that the strengths of the two C=O bands are equal. For IV (X=H), two C=O bands appeared, and,

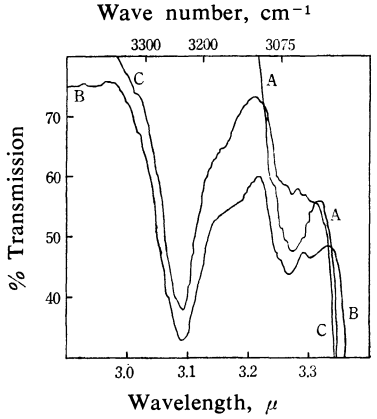



Fig. 3. 3 $\mu$ Bands of 1,4-, 1,5- and 1,8-bis(phenylamino)anthraquinones by Nujol mull technique.
A: 1,4-Derivative, B: 1,5-Derivative, C: 1,8-Derivative

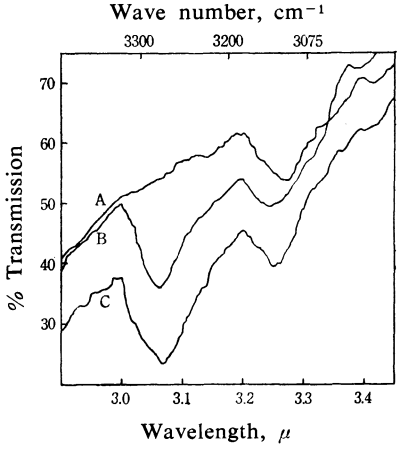



Fig. 4. 3 $\mu$ Bands of 1,4-, 1,5- and 1,8-bis(phenylamino)anthraquinones by potassium bromide disk technique.
A: 1,4-Derivative, B: 1,5-Derivative, C: 1,8-Derivative

16) D. N. Shigorin, "Hydrogen Bonding," Ed. by D. Hadzi, Pergamon Press, London (1959), p. 191.
17) N. Ōi, *Pharm. Bull.* (*Tokyo*), **5**, 153 (1957).

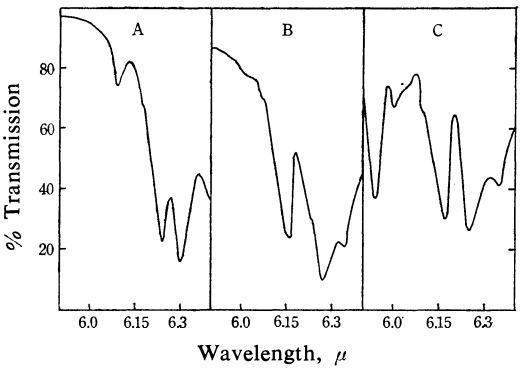


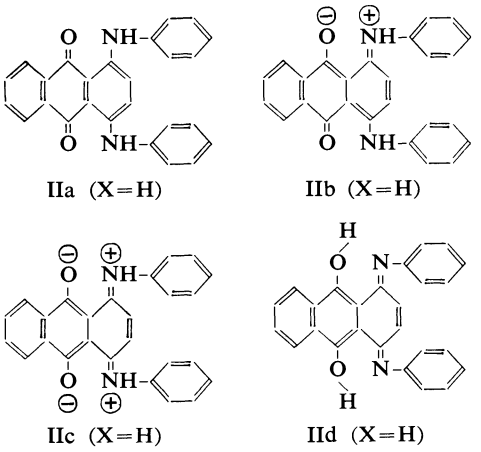

Fig. 5. 6 μ Bands of 1,4-, 1,5- and 1,8-bis-(phenylamino)anthraquinones by Nujol mull technique.
A: 1,4-Derivative, B: 1,5-Derivative,
C: 1,8-Derivative

as was the case with 1-substituted anthraquinones with electron-donating groups as substituents, this splitting of the C=O absorption would appear to be the result of electronic dissymmetry.[18,19] The first C=O band at a higher frequency is assigned to the C=O(a)* vibration, since the frequency is closer to the C=O frequency of anthraquinone, and the second C=O band at a lower frequency is assigned to the C=O(b) vibration in the peri-position of the phenylamino group.

Table III. N-H and C=O Frequencies of Solid Phenylaminoanthraquinones

| | N-H Frequencies $cm^{-1}$ | C=O Frequencies $cm^{-1}$ | |
|---|---|---|---|
| | | (a) | (b) |
| Anthraquinone[18] | | 1676 | |
| 1-Phenylaminoanthraquinone[1] | 3236 | 1672 | 1634 |
| 1,4-Bis(phenylamino)-anthraquinone | 3058 | | 1603 |
| 1,5-Bis(phenylamino)-anthraquinone | 3236 | | 1623 |
| 1,8-Bis(phenylamino)-anthraquinone | 3236 | 1684 | 1621 |

In this connection, it is interesting that the N-H and C-H stretching bands of III (X=H) and IV (X=H) appear at about 3.1 and 3.25 μ respectively, while II (X=H) has only one discrete band at the lower wavelength in this region. If the 3058 $cm^{-1}$ band of II (X=H) is assigned to the C-H vibration, its structure must be indicated by IId (X=H)




instead of IIa (X=H).

Frequencies for the C=N groups[20] are most probably found between 1690 and 1640 $cm^{-1}$, and the influence of conjugation is usually small. For the IId (X=H) structure, therefore, the observed frequency in II (X=H) at 1603 $cm^{-1}$ should be attributed to the C=N vibration. However, this may be too low a frequency to be normally attributed to the C=N vibration. Furthermore, the absorption of 1,4-diamino- and 1,4-bis(methylamino)-anthraquinones,[18] 1,1'-dianthrimide,[21] indanthrone,[8] and 3,4-phthaloylacridone[22] did not show the C=N band. Thus, there is no precedent for assigning the 1603 $cm^{-1}$ band to the C=N vibration; it should probably be assigned to the C=O vibration. Consequently, this band can not be used to support the IId (X=H) structure containing the C=N bond.

Frequencies of the O-H groups are usually found in the frequency range between 3650 and 3450 $cm^{-1}$, and the influence of conjugation is quite large.[23] Many of the frequencies for O-H groups of oxanthrone, anthraquinol and their substituted derivatives in a solid[18] were found in the frequency range from 3500 to 3300 $cm^{-1}$, but the shifts of the frequencies of these O-H groups were not due to conjugation, but mainly to hydrogen bonding. Moreover, the absorptions of 1-arylamino-[1] and 1-benzoylaminoanthraquinones[4], 1,1'-dianthrimide,[21] indanthrone,[8] 1,2- and 3,4-phthaloylacridones,[22] and indigo[24] did not show the O-H band. The 3058 $cm^{-1}$ band

18) M. S. C. Flett, *J. Chem. Soc.*, **1948**, 1441.
19) T. C. Bruice and A. B. Sayigh, *J. Am. Chem. Soc.*, **81**, 3416 (1959).
* The C=O(a) absorptions correspond to the free C=O bands, while the C=O(b) absorptions are assigned to the chelated C=O groups.
20) L. J. Bellamy, "The Infrared Spectra of Complex Molecules," John Wiley & Sons, New York (1958), p. 267.
21) R. A. Durie and J. S. Shannon, *Australian J. Chem.*, **11**, 189 (1958).
22) T. Hayashi and J. Maehara, This Bulletin, **35**, 1690 (1962).
23) L. J. Bellamy, "The Infrared Spectra of Complex Molecules," John Wiley & Sons, New York (1958), p. 96.
24) G. M. Wyman, *J. Am. Chem. Soc.*, **78**, 4599 (1956); W. R. Brode, E. G. Pearson and G. M. Wyman, ibid., **76**, 1034 (1954).

of II (X=H) seems, therefore, to be too low a frequency to be normally assigned to the O–H vibration; thus, this band can not be used to support the structure IId (X=H). Consequently, the 3058 $cm^{-1}$ band should be assigned to the N–H vibration of the arylamino-type structure IIa (X=H). This molecular structure, assigned to its solid state, agrees with that concluded in solution on the basis of the results of visible absorption; moreover, the chemical evidence favors the arylamino-type structure IIa (X=H).

The C=O(b) frequency in the peri-position of the phenylamino group in Table III increases in the order of II (X=H), IV (X=H), III (X=H) and I (X=H); the C=O(b) bond is also strengthened in this order. This result for phenylaminoanthraquinones can be satisfactorily explained by means of the same electronic interpretation as for the shifts of the visible absorption peaks for these derivatives in solutions.

As is indicated in Table IV with 1-(*m*- and *p*-substituted phenyl)aminoanthraquinones, the C=O(b) frequency shifted lower when an arylamino group with electron-donating substituents is placed in the peri-position to the C=O group, while the reverse was found to be true when one with electron-attracting substituents is placed in the same position. A similar result was also obtained for 1-arylamino-5-chloro- and 1,5-bis(arylamino)-anthraquinones. Furthermore, the C=O frequencies of 1-arylamino-5-chloroanthraquinones were much the same as for corresponding 1-arylaminoanthraquinones, this being deduced from the fact that the effects of a chlorine atom on the C=O frequency for 1- and 2-chloroanthraquinones were quite small.[8]

TABLE IV. N–H AND C=O FREQUENCIES OF SOLID 1-ARYLAMINO-, 1-ARYLAMINO-5-CHLORO- AND 1,5-BIS(ARYLAMINO)-ANTHRAQUINONES

| Substituent of the aryl group (X) | 1-Arylamino-[1] | | 1-Arylamino 5-chloro- | | 1,5-Bis-(arylamino)- | |
|---|---|---|---|---|---|---|
| | $\nu_{C=O(a)}$ $cm^{-1}$ | $\nu_{C=O(b)}$ $cm^{-1}$ | $\nu_{C=O(a)}$ $cm^{-1}$ | $\nu_{C=O(b)}$ $cm^{-1}$ | $\nu_{N-H}$ $cm^{-1}$ | $\nu_{C=O}$ $cm^{-1}$ |
| H | 1672 | 1634 | 1675 | 1631 | 3236 | 1623 |
| *p*-$NH_2$ | 1672 | 1639 | 1675 | 1639 | | |
| *m*-$NO_2$ | 1675 | 1637 | | | 3279 | 1634 |
| *p*-Cl | 1678 | 1637 | 1678 | 1634 | | |
| *m*-Cl | 1681 | 1637 | 1681 | 1637 | 3247 | 1629 |
| *p*-Me | 1684 | 1629 | 1678 | 1626 | 3236 | 1621 |
| *p*-OMe | 1678 | 1626 | | | 3226 | 1616 |

For 1-substituted anthraquinones (V, substituents: Y), the wavelengths of the visible absorption maxima in solution and the C=O stretching frequencies increased in the following order:[1]

maximum wavelengths of the visible spectra:

$$V\ (Y=NHCOC_6H_5) < V\ (Y=NH_2) < V\ (Y=NHCH_3) \lesssim V\ (Y=NHC_6H_5)$$

frequencies of the C=O stretching bands:

$$V\ (Y=NH_2) < V\ (Y=NHC_6H_5) \lesssim V\ (Y=NHCH_3) < V\ (Y=NHCOC_6H_5)$$

The fact that the C=O frequencies of V (Y=$NHCH_3$) and V (Y=$NHC_6H_5$) were higher than those of V (Y=$NH_2$) should not be attributable to steric hindrance, but to the reduction by the methyl or the phenyl group of resonance within the chromophoric system of V (Y=$NHCH_3$) and V (Y=$NHC_6H_5$).[1]

TABLE V. N–H AND C=O FREQUENCIES OF SOLID 1,4- AND 1,5-DISUBSTITUTED ANTHRAQUINONES

| Disubstituted anthraquinone | N–H Frequencies $cm^{-1}$ | C=O Frequencies $cm^{-1}$ |
|---|---|---|
| 1,4-Diamino-[18] | 3370, 3250 | 1610 |
| 1,4-Bis(methylamino)-[18] | 3240 | 1610 |
| 1,4-Bis(phenylamino)- | 3058 | 1603 |
| 1,4-Bis(benzoylamino)-[a] | 3125 | 1686 |
| 1,5-Diamino- | 3425, 3311[b] | 1610 |
| 1,5-Bis(methylamino)- | 3333 | 1623 |
| 1,5-Bis(phenylamino)- | 3236 | 1623 |
| 1,5-Bis(benzoylamino)-[a] | 3226 | 1689 |

a) The C=O frequencies of 1-benzoylaminoanthraquinone[4] were observed at 1681, 1669 and 1637 $cm^{-1}$; the highest frequency was assigned to the free C=O group; the middle, to the chelated C=O group, and the lowest, to the benzoyl C=O group.[4,18] On the other hand, the C=O frequencies of 1,4- and 1,5-bis(benzoylamino)anthraquinones[4] were observed at 1686 and 1639, and 1689 and 1639 $cm^{-1}$, respectively. As the free C=O group was absent in them, the respective higher frequencies were assigned to the chelated C=O groups and the respective lower frequencies to the benzoyl C=O groups,[4] as in the case of 1-benzoylaminoanthraquinone.

b) Shigorin[16] gives 3430 and 3310 $cm^{-1}$.

Here, too, for 1,5-disubstituted anthraquinones (VII, substituents: Y), the wavelengths of the visible absorption maxima in solution increased in the following order:

$$VII\ (Y=NHCOC_6H_5) < VII\ (Y=NH_2) < VII\ (Y=NHCH_3) \lesssim VII\ (Y=NHC_6H_5)$$

while, as is indicated in Table V, the C=O stretching frequencies increased in the following order:

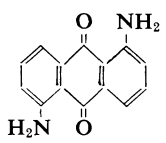
$$\text{VII } (Y=NH_2) < \text{VII } (Y=NHCH_3) = \text{VII } (Y=NHC_6H_5) < \text{VII } (Y=NHCOC_6H_5)$$

As will be clear from the establishment of simple additivity between the two chromophoric systems within VII, the fact that the C=O frequencies of VII ($Y=NHCH_3$) and VII ($Y=NHC_6H_5$) are higher than that of VII ($Y=NH_2$) can be interpreted in the same way as in the case of V.[1]

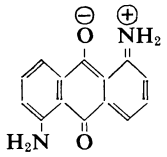
As is indicated in Table V, the N-H frequencies of VII increased in the following order:

$$\text{VII } (Y=NHCOC_6H_5) < \text{VII } (Y=NHC_6H_5) < \text{VII } (Y=NHCH_3) < \text{VII } (Y=NH_2)$$

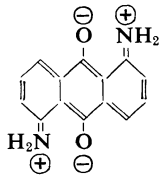
and the reverse was found to be true for their C=O frequencies. This fact can be interpreted in the same way as in the case of V;[1] namely, for VIIa ($Y=NH_2$) it seems that it is impossible to form a powerful hydrogen bonding, as in



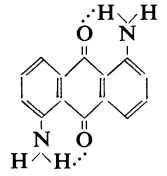
VIIa ($Y=NH_2$)



VIIb ($Y=NH_2$)



VIIc ($Y=NH_2$)



VIId ($Y=NH_2$)

VIId ($Y=NH_2$), between the amino and C=O groups, and that, therefore, a contribution of the ionic structure VIIb ($Y=NH_2$) and VIIc ($Y=NH_2$) to the resonance, rather than the weak hydrogen bonding, is responsible for the considerable lowering of the C=O frequency, the hydrogen bondiag serving only to stabilize the ionic structures. On the other hand, for VII ($Y=NHCH_3$) and VII ($Y=NHC_6H_5$), such resonance within chromophoric systems was reduced by the methyl and phenyl groups respectively. The above-mentioned order of the increase in N-H frequencies, therefore, suggests that the smaller the contribution of the ionic structure to the resonance becomes, the greater the contribution of the hydrogen bonding, as in the case of V.[1]

For monosubstituted anthraquinones, with electron-donating groups as substituents, Peters and Sumner,[2] using a correlation of the Hixon-Johns type,[25] showed the following: An arbitrary straight line was drawn the ordinate scale of which represented the wavelength of the absorption maximum, the abscissa being undefined. The points corresponding to the wavelengths of the visible absorption maxima of 2-substituted anthraquinones were marked on this line, and an arbitrary scale of abscissa was then constructed labelled with the names of the substituents. A plot of the wavelengths of the visible absorption maxima for V versus the scale of the substituents so defined gave a straight line, but a considerable deviation from the linear relation was observed with V with substituents (Y) having internal hydrogen-bonding possibilities. This fact suggests that the latter 1-substituted anthraquinones have wavelengths with absorption maxima greater than would be expected from the electron-donating abilities of their substituents, the excess being attributable to the resonance of the chelate structure.[25] For the latter 1-substituted anthraquinones, the extents of deviation from the straight line were calculated by Hida[26] as follows:

| | kcal./mol. |
|---|---|
| 1-Acetylaminoanthraquinone | 3.3 |
| 1-Methylaminoanthraquinone | 1.5 |
| 1-Phenylaminoanthraquinone* | 1.5 |
| 1-Aminoanthraquinone | 1.3 |

Consequently, it is probable that the magnitude of these values is closely related with the hydrogen-bonding energy between their substituent groups and the C=O groups of the latter 1-substituted anthraquinones.[26] Here, for VII, therefore, it seems that this fact has given other evidence for the above-mentioned interpretation of the extent of the contribution of the ionic structure and of the hydrogen bonding to the increase in N-H frequencies.

For 1,4-disubstituted anthraquinones (VI, substituents: Y), the wavelengths of the visible absorption maxima in solution increased in the following order:

$$\text{VI } (Y=NHCOC_6H_5) < \text{VI } (Y=NH_2) < \text{VI } (Y=NHCH_3) \lesssim \text{VI } (Y=NHC_6H_5)$$

The visible absorption maxima of VI ($Y=NH_2$) and VI ($Y=NHCOC_6H_5$) in solution were, moreover, located at far longer wavelengths than those of the corresponding VII ($Y=NH_2$) and VII ($Y=NHCOC_6H_5$). As is indicated in

25) R. M. Hixon and I. B. Johns, *J. Am. Chem. Soc.*, **49**, 1786 (1927).

26) M. Hida, *Dyestuffs and Chemicals* (*Senryo to Yakuhin*), **8**, 493 (1963).

* Peaks of 1- and 2-phenylaminoanthraquinones appeared at 507 and 465 mμ respectively in methanol. From these results, the extent of the deviation for the former was calculated by the present authors.

Table V, however, the C=O stretching frequencies of VI ($Y=NH_2$) and VII ($Y=NH_2$) are the same, and those of VI ($Y=NHCOC_6H_5$) and VII ($Y=NHCOC_6H_5$) are alike. The C=O stretching frequencies for VI, moreover, increased in the following order:

$$\text{VI } (Y=NHC_6H_5) < \text{VI } (Y=NHCH_3) = \text{VI } (Y=NH_2) < \text{VI } (Y=NHCOC_6H_5)$$

This order was, then, the reverse of the increase in the wavelengths of their visible absorption maxima, these being different from the cases of those for V and VII. Furthermore, the order of the increase of the N-H frequencies for VI is not in the decreasing order of their C=O frequencies, this being different from the case of those for VII. It is interesting, moreover, that both the N-H and C=O frequencies of 1,4-bis(phenylamino)anthraquinone are the lowest among VI's investigated. Because of interaction between their two chromophoric systems, these VI's do not obey the simple additivity rule observed with VII; this interaction is supposed to produce a new chromophore. The above-mentioned results may, therefore, be attributable to the contribution of the ionic structures IIb (X=H) and IIc (X=H), and to the fact that the decreasing effect of the resonance by the phenyl group in the chromophoric system of 1,4-bis(phenylamino)anthraquinone is smaller than in that of 1,5-bis(phenylamino)anthraquinone. By X-ray study, no steric hindrance was estimated in II (X=H), and the coplanarity of the phenyl groups was concluded;[27] it seems that these facts have given support to the above-mentioned interpretation.

## Experimental

**Materials and Apparatus.**—The compounds used in this investigation were purified by repeated crystallization and then by chromatography or hot chromatography on alumina in suitable solvents.

The visible absorption spectra were recorded with a Shimadzu spectrophotometer, type QB-50. The infrared absorption spectra of the solid samples were obtained using a Perkin-Elmer Model 21 double-beam spectrophotometer fitted with a rock-salt prism. *o*-Dichlorobenzene was purified by the method recommended for the purification of chlorobenzene.[28]

The authors wish to express their hearty thanks to Mr. Akira Hara of the Tokuyama Research Laboratory of the Idemitsu Kōsan Co. for the infrared measurements.

*Department of Chemistry*
*Faculty of Literature and Science*
*Yamaguchi University*
*Ushirogawara, Yamaguchi*

27) N. S. Dokunikhin, G. A. Gol'der and G. S. Zhdanov, *Doklady Akad. Nauk S. S. S. R.*, **119**, 87 (1958); *Chem. Abstr.*, **52**, 11512 (1958).

28) A. Weissberger and E. S. Proskauer, "Organic Solvents," Interscience Publishers, New York (1955), p. 407.

# Synthetic Studies starting from β-Cyanopropionaldehyde. II. The Syntheses of Aliphatic Aldehydes and ω-Aldehydic Acids

By Shinichi MOTOKI, Sadayoshi SATSUMABAYASHI and Hajime KUSANO

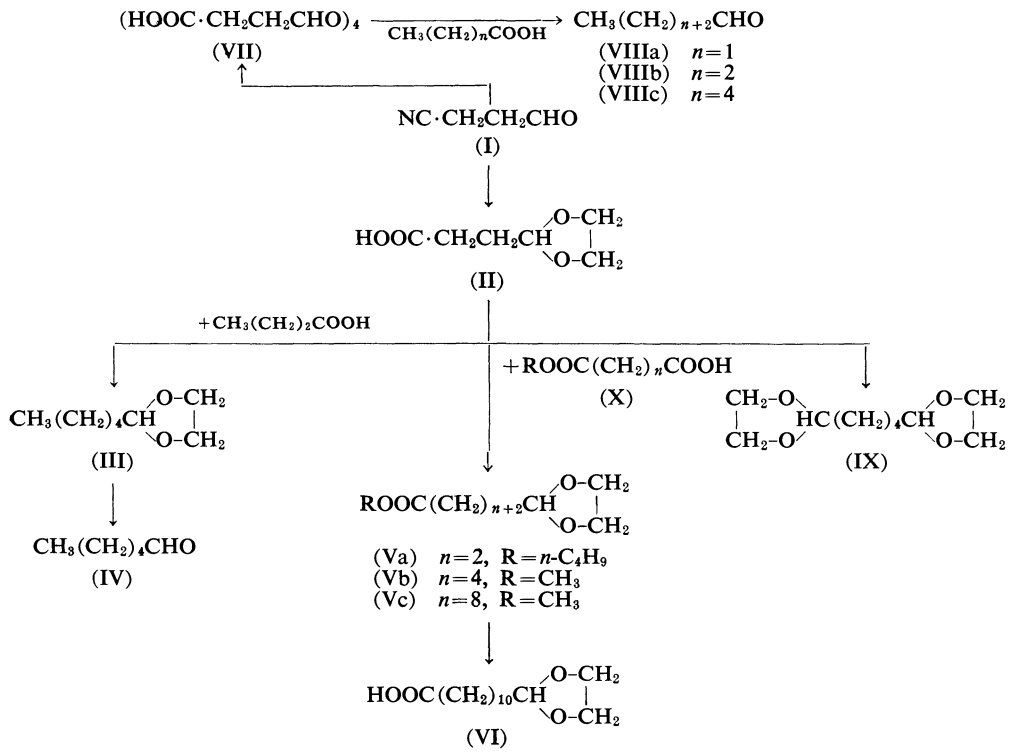
(Received September 22, 1964)

The preceding paper in this series,[1] dealt with the Kolbe electrolysis of the ethylene acetal of β-formylpropionic acid (II) which had been derived from β-cyanopropionaldehyde (I). Electrolysis of this acetal acid gives the diethylene acetal of adipic dialdehyde (IX). Only a few examples of the Kolbe electrolysis of such aldehydic acids have been recorded[2,3] and the crossed electrolysis of aldehydic acids with ordinary carboxylic acids does not appear to have been described. The present paper involves a further extension of the Kolbe reaction as summarized in the accompanying flow sheet.

Electrolysis of the ethylene acetal of β-formylpropionic acid (II) in the presence of butyric acid was found to give the expected product, caproaldehyde ethylene acetal (III), in 25% yield.

The Kolbe electrolysis of the ethylene acetal (II) with succinic acid monobutyl ester

1) S. Motoki, S. Satsumabayashi and I. Tajima, This Bulletin, 37, 646 (1964).
2) M. Stoll and A. Rouvé, *Helv. Chim. Acta*, 20, 525 (1937).
3) A. Wohl and H. Schweizer, *Ber.*, 39, 890 (1906).




gave the ethylene acetal of adipinaldehydic acid butyl ester (Va). When the monomethyl ester of succinic acid was used, the boiling points of the three products (adipinaldehydic acid methyl ester ethylene acetal, dimethyl adipate and adipic dialdehyde diethylene acetal) were too close to isolate the expected aldehydic acid by fractional distillation.

Similar electrolysis of a mixture of adipic acid monomethyl ester and an excess of the acetal (II) gave suberinaldehydic acid methyl ester ethylene acetal (Vb), whereas the compound II and an excess of monomethyl adipate led to a mixture which was difficult to separate. In the latter case, separation of Vb from the large amount of dimethyl sebacate formed was unsuccessful.

Crossed electrolysis of the acetal (II) with sebacic acid monomethyl ester afforded ω-formylundecylic acid methyl ester ethylene acetal (Vc) without any difficulties in separation.

As seen in Table I, the yields of ω-aldehydic acids are better in the presence of II excess of than in the presence of excess of monoesters. ω-Aldehydic acids are generally inaccessible compounds* the properties of which have rarely been described in the literature[4], so these electrolytic reactions starting from β-cyanopropionaldehyde may provide a new convenient synthetic route.

On the other hand, the cyclic tetramer (VII)[5] of β-formylpropionic acid has recently been prepared by the hydrolysis of β-cyanopropionaldehyde tetramer. Since the tetramer (VII) is more easily accessible than the previously reported β-formylpropionic acid ethylene acetal[1] and is inert to oxidation, its possible usefulness in a Kolbe reaction was examined.

Attempted electrolysis of the tetramer itself turned out to be unsuccessful, but the tetramer underwent a normal Kolbe reaction in the presence of fatty acids to give the corresponding aldehydes in relatively good yields; the results are summarized in Table II. In general, it is known that the Kolbe reaction of a polybasic acid results in olefine formation or in evolution of oxygen at the anode, rather than in the formation of a coupling product. As VII can be regarded formally as a polybasic acid, the results obtained here seem to be of much interest.

## Experimental

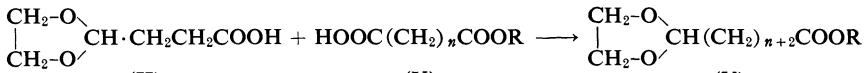
**Materials.** — β-Formylpropionic acid ethylene acetal (II) was obtained by hydrolysis of β-cyanopropionaldehyde ethylene acetal as reported in the

* ω-Formylundecylic acid is a new compound.

4) F. C. Pennington, W. D. Celmer, W. M. McLamore, V. V. Bogert and I. A. Solomons, *J. Am. Chem. Soc.*, **75**, 112 (1953).

5) J. Kato, T. Komatsu, T. Ito, H. Wakamatsu and T. Yoshida, *J. Chem. Soc. Japan, Ind. Chem. Sec.* (*Kogyo Kagaku Zasshi*), **65**, 548 (1962).

Table I



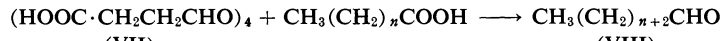
(II) (X) (V)

| | $n$ | R | B. p. | M. p. | Yield, % | Molar ratio II : X |
|---|---|---|---|---|---|---|
| Va | 2 | $n$-$C_4H_9$ | 110—113°C/1 mmHg | Liquid | 26.2 | 1 : 3 |
| Vb | 4 | $CH_3$ | 115—116°C/2 mmHg | Liquid | 40.5 | 3 : 1 |
| Vc | 8 | $CH_3$ | 140—142°C/1 mmHg | 26—27°C | 23.1<br>42.5 | 1 : 3<br>3 : 1 |

| | Molecular formula | Analysis Calcd. | Analysis Found | 2,4-Dinitrophenyl hydrazone* M. p. | Analysis Calcd. | Analysis Found |
|---|---|---|---|---|---|---|
| Va | $C_{12}H_{22}O_4$ | C: 62.58<br>H: 9.63 | C: 62.40<br>H: 9.77 | 78°C<br>orange yellow<br>needles | C: 52.45<br>H: 6.05<br>N: 15.29 | C: 52.27<br>H: 6.29<br>N: 15.50 |
| Vb | $C_{11}H_{20}O_4$ | C: 61.09<br>H: 9.32 | C: 61.08<br>H: 9.48 | 86—87°C<br>orange yellow<br>needles | C: 51.13<br>H: 5.72<br>N: 15.90 | C: 51.19<br>H: 6.18<br>N: 16.12 |
| Vc | $C_{15}H_{28}O_4$ | C: 66.14<br>H: 10.36 | C: 66.42<br>H: 10.57 | 72°C<br>orange yellow<br>needles | C: 55.87<br>H: 6.91<br>N: 13.72 | C: 56.32<br>H: 7.18<br>N: 13.95 |

* Treatment of the acetal ester (V) with ethanolic solution of 2,4-dinitrophenylhydrazine in the usual manner precipitated the 2,4-dinitrophenylhydrazone of the corresponding aldehyde ester gradually.

Table II



(VII) (VIII)

| | $n$ | B. p. | Yield* g. | Yield* % | 2,4-Dinitrophenylhydrazone M. p. °C | Analysis Calcd. | Analysis Found |
|---|---|---|---|---|---|---|---|
| VIIIa | 1 | 101—102°C | 8.2 | 47.5 | 105 | N: 21.04 | N: 21.11 |
| VIIIb | 2 | 131—132°C | 8.3 | 43.8 | 103 | N: 19.99 | N: 19.74 |
| VIIIc | 4 | 58—59°C/9 mmHg | 10.8 | 42.1 | 106 | N: 18.17 | N: 18.31 |

* Based on the β-formylpropionic acid tetramer (VII).

previous paper.[1] Monoesters of succinic, adipic and sebacic acid were prepared by the method given in Org. Syn.[6] Succinic acid monobutyl ester, b. p. 136—137°C/3 mmHg. Adipic acid monomethyl ester, b. p. 162°C/10 mmHg. Sebacic acid monomethyl ester, b. p. 170—174°C/4 mmHg, m. p. 40°C.

**Apparatus.** — Electrolysis was carried out with the apparatus previously described.[1]

***n*-Caproaldehyde Ethylene Acetal (III).**—Twenty grams (0.137 mol.) of II and 35 g. of butyric acid (0.4 mol.) were electrolyzed in 130 ml. of methanol containing 3.1 g. of potassium hydroxide until the electrolyte became slightly alkaline. At the end of the electrolysis the solvent was removed and the residue was washed with water, extracted with ether and dried over anhydrous sodium sulfate. Fractional distillation of the extract gave 5 g. of III, b. p. 78—80°C/34 mmHg, yield 25.4%. Found: C, 66.39; H, 11.41. Calcd. for $C_8H_{16}O_2$: C, 66.63; H, 11.18%.

III was mixed with the same amount of 3% hydrochloric acid and refluxed for one hour. After hydrolysis, the organic layer was extracted with ether and dried over anhydrous sodium sulfate. By distillation caproaldehyde (IV) was obtained. B. p. 130—131°C. 2,4-Dinitrophenylhydrazone, m. p. 106°C.

Found: C, 51.12; H, 6.09; N, 20.03. Calcd. for $C_{12}H_{16}O_4N_4$: C, 51.42; H, 5.75; N, 19.99%.

**Adipinaldehydic Acid Butyl Ester Ethylene Acetal (Va), Suberinaldehydic Acid Methyl Ester Ethylene Acetal (Vb) and ω-Formylundecylic Acid Methyl Ester Ethylene Acetal (Vc).** — A mixture of II and the monoester of the dibasic acid was electrolyzed in methanol, to which sufficient potassium hydroxide had been added to neutralize about 10% of the total acid. At the end of the electrolysis, the solvent was removed and the residue

6) S. Swann, R. Oehler and R. J. Buswell, "Organic Syntheses," Coll. Vol. II, 276 (1943).

was washed with water, extracted with ether and dried. Fractional distillation gave the results shown in Table I.

**ω-Formylundecylic Acid Ethylene Acetal (VI).** — Ten grams of Vc was saponified by refluxing for 3 hr. with 20 ml. of a 50% methanolic solution containing 2 g. of sodium hydroxide. Methanol was then removed by distillation and the aqueous solution was acidified to pH 3 with dilute hydrochloric acid. The crude product which precipitated was recrystallized from 50% aqueous methanol to give 7.7 g. of pure VI, m. p. 73—75°C, yield 81.1%.

Found: C, 65.19; H, 10.28. Calcd. for $C_{14}H_{26}O_4$: C, 65.08; H, 10.14%.

***n*-Valeraldehyde (VIIIa), *n*-Caproaldehyde (VIIIb) and *n*-Caprylaldehyde (VIIIc).** — Twenty grams of β-formylpropionic acid tetramer (VII) and 0.6 mol. of a fatty acid were electrolyzed in 130 ml. of methanol containing 4.5 g. of potassium hydroxide. At the end of the electrolysis, the solvent was removed and the residue was directly hydrolyzed by refluxing with 20 ml. of 5% sulfuric acid for 3 hr. The oily product which separated was taken up in ether and dried over anhydrous sodium sulfate. Distillation of the extract gave the results shown in Table II.

## Summary

Electrolysis of the ethylene acetal of β-formylpropionic acid with butyric acid gave caproaldehyde ethylene acetal as a result of crossed coupling. Crossed electrolysis with monoesters of succinic, adipic and sebacic acid were then studied. The expected products, adipinaldehydic, suberinal dehydic and ω-formylundecylic acid, were obtained as their ethylene acetal ester respectively. As ω-aldehydic acids are usually inaccessible compounds, these electrolytic reactions may provide a new convenient synthetic route.

Furthermore, it has been found that the tetramer of β-formylpropionic acid underwent the normal electrolytic reaction in the presence of fatty acids and the corresponding aliphatic aldehydes were obtained in relatively good yields.

The authors wish the thank Professor Yojiro Tsuzuki for his helpful advice and encouragement. Acknowledgment is also made to the Ajinomoto Co., Ltd. for a grant and for a supply of raw materials.

*Department of Chemistry*
*Faculty of Science*
*Tokyo College of Science*
*Shinjuku-ku, Tokyo*

# Study of Nickel Oxide - Silica - Alumina Catalysts for Ethylene Polymerization. III. The Performance of the Catalysts in Ethylene Polymerization and Butene Isomer Formation and Its Dependence on the Nickel Oxide Content

By Hisao IMAI and Hiroshi UCHIDA

(Received September 26, 1964)

The activity of a particular series of nickel oxide-silica-alumina catalysts for ethylene polymerization and the selectivity in the formation of butene isomers have already been studied.[1,2] The catalysts used differed in aluminum content, though they all had the same nickel content.

To obtain more detailed knowledge about the relation between the catalyst performance and the catalyst composition, the study has recently been extended to another series of catalysts which are the same in aluminum content but different in nickel content. The results of this study will be presented here, and the effects of the addition of aluminum and nickel upon the catalyst performance will be discussed on the basis of these and the previously-obtained results.

Although the performance of nickel-containing catalysts has been studied by some other investigators,[3-7] most of their papers deal with

1) H. Uchida and H. Imai, This Bulletin, 35, 989 (1962).
2) H. Uchida and H. Imai, ibid., 35, 995 (1962).
3) S. Kawaguchi and K. Kihara, *J. Chem. Soc. Japan, Pure Chem. Sec.* (*Nippon Kagaku Zassi*), 75, 15 (1954).
4) A. Ozaki, ibid., 77, 888 (1956).
5) S. Kawaguchi, *J. Phys. Chem.*, 61, 394 (1954).
6) V. C. F. Holm, G. C. Bailey and A. Clark, *Ind. Eng. Chem.*, 49, 250 (1957).
7) A. Takahashi, N. Mogi, H. Takahama and Y. Mita, *J. Chem. Soc. Japan, Ind. Chem. Sec.* (*Kogyo Kagaku Zasshi*), 66, 473 (1963).

the catalytic activity and not with the selectivity. The only exception is the paper recently published by Takahashi et al.,[7] who state that a high selectivity in the 1-butene formation can be obtained by the use of a nickel oxide-silica-alumina catalyst suspended in a medium of cyclohexane.

## Experimental

The catalysts required for this study were prepared in the same way as those designated as "catalysts A" in the previous paper.[1] In other words, they were prepared by mixing a solution of sodium silicate with a solution of aluminum and nickel nitrates and then forming the resulting precipitate into granules 1—2 mm. in size. In this case, the aluminum content of the catalyst, expressed as the Al/(Al+Si) atomic ratio, was fixed at 0.05, and the nickel content, expressed as atom.% nickel (defined by $100\times$Ni/(Ni+Si+Al)), was varied over the range from 0 to 8.

Their catalytic performance was studied by conducting two series of experiments on ethylene polymerization with the catalysts. One series of experiments (Series A) was carried out in order to determine the catalytic activity, while the other series (Series B) was carried out in order to determine the selectivity in the formation of butene isomers. The apparatus used for these experiments, which included a circulatory flow system, was the same as that used in our previous study.[1] In the two series of experiments, the reaction temperature was 40°C and the initial ethylene pressure was 345 mmHg. In the experiments of Series A, 5 ml. of a catalyst was used to form the catalyst bed in the cell (catalyst cell), and the two U-shaped traps, joined, respectively, to the entrance and exit tubes of the cell, were cooled in a dry ice - methanol bath. During each experiment, the pressure drop in the system was recorded at intervals. In the experiments of Series B, 1 ml. of a catalyst was used to form the catalyst bed in the cell, and the traps were cooled in an ice bath so that the butenes formed might be maintained in the circulating gas. A small portion of the circulating gas was withdrawn at intervals from the gas circulation system and analyzed for butene isomers by gas chromatography.

The following physical properties of the catalysts were measured by the methods described in previous papers:[1,2] catalyst acidity, specific surface area, and total pore volume. The total pore volume as measured by the present method represents the sum of the volumes of pores smaller than 300Å in radius. Moreover, in order to see the effects of the addition of nickel on the physical properties of catalysts, samples of the catalysts were depleted of nickel, and then the resultant changes in physical properties were measured. The nickel was removed by the method described in a previous paper,[2] namely, by reducing the original catalyst in a stream of hydrogen and then treating the reduced catalyst at 150°C with carbon monoxide under high pressure until it showed no sign of the presence of nickel.

## Results

**Activity for Ethylene Polymerization.**—From the data obtained in the experiments of Series A, the rate constant for ethylene polymerization at 40°C over a unit quantity of a catalyst, hereafter denoted by $k_g$, is calculated by the aid of the equation proposed by Koizumi et al.[8] (Eq. 1):

$$-dP/dt = k_g wP/\{1+(P_0-P)\} \qquad (1)$$

where $P_0$ (mmHg) is the initial pressure of ethylene; $P$ (mmHg), the ethylene pressure at the reaction time, $t$ (min); $w$, the quantity of catalyst used, and $b$, a constant. The rate constant, $k_g$, thus calculated is plotted against the nickel content of the catalyst in Fig. 1.

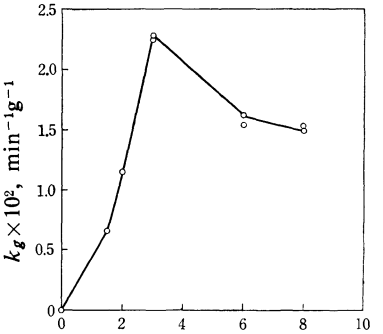



Fig. 1. Dependence of catalyst activity for ethylene polymerization on nickel content.

The plot shows a maximum at about 3 atm.% nickel; this finding is consistent with that of Holm et al.[6]

**Selectivity in the Formation of Butene Isomers.**—From the data obtained in the experiments of Series B, three butene-isomer ratios (concentration ratios), *trans*-2-/1-butene, *cis*-2-/1-butene, and *trans*-2-/*cis*-2-butene, were calculated and plotted against the reaction time, $t$. The plots were then extrapolated to $t=0$ to give the initial butene-isomer ratios.[9] The initial butene-isomere ratios thus obtained are given in Fig. 2 as functions of the nickel content of the catalyst. With the increase in the nickel content, the *cis*-2-/1-butene and *trans*-2-/1-butene ratios both decrease very slowly in nearly the same manner, and then rapidly. In contrast, the *trans*-2-/*cis*-2-butene ratio remains nearly the same (about 1) over the whole range of nickel content studied, though it becomes slightly greater at 3 atm.% nickel, where the highest value of $k_g$ was found.

8) M. Koizumi and S. Taga, *J. Chem. Soc. Japan, Pure Chem. Sec.* (*Nippon Kwagaku Kwaishi*), **64**, 794 (1943).
9) For details of this procedure, see Ref. 1.

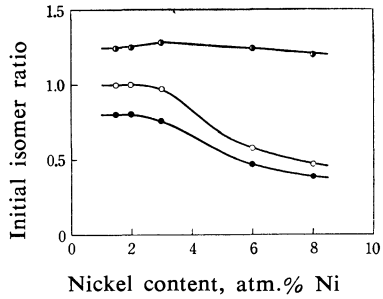



Fig. 2. Dependence of initial butene-isomer ratios on nickel content.
Initial isomer ratio
○ *trans*-2-/1-butene
● *cis*-2-/1-butene
◑ *trans*-2-/*cis*-2-butene

**Catalyst Acidity.**—The catalyst acidity is expressed in millimole equivalents (meq.) of quinoline chemisorbed on a specified quantity of a catalyst sample. In the case of the original catalyst sample containing all three oxides, nickel(II) oxide, silicon oxide, and aluminum oxide, the acidity, $A_g$, is the numerical value determined for 1 g. of the catalyst sample. On the other hand, in the case of the nickel-depleted catalyst sample (which contains only two oxides, silica and alumina), the acidity, $A_g'$, is the numerical value determined for that quantity of the nickel-depleted catalyst sample which has been produced from 1 g. of the original catalyst (i. e., the catalyst containing all three component oxides). In Fig. 3, the acidity values, $A_g$ and $A_g'$, determined for the catalysts used in this study are plotted against the nickel content of the original catalyst. The plot of $A_g$ shows a maximum at 3 atm.% nickel. Whereas the plot of $A_g'$ shows a minimum at the same nickel content. Therefore, it may be seen that the removal of nickel results in a decrease in the catalyst acidity,

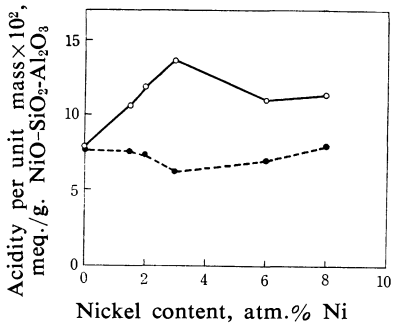



Fig. 3. Acidities per unit mass plotted against nickel content.
—○— Acidity before removal of nickel ($A_g$)
···●··· Acidity after removal of nickel ($A_g'$)

though the extent of the decrease is not directly related to the nickel content of the catalyst.

**Specific Surface Area and Total Pore Volume.**—When the original catalyst contains all three component oxides, the specific surface area, $S$, and the total pore volume, $V$, are the surface area (in $m^2$) and the total pore volume (in ml.) of 1 g. of the catalyst. On the other hand, in the case of a nickel-depleted catalyst sample, the specific surface area, $S'$, and the total pore volume, $V'$, are the surface area (in $m^2$) and the total pore volume (in ml.) of that quantity of the nickel-depleted catalyst sample which has been produced from 1 g. of the original catalyst. In Fig. 4, the four

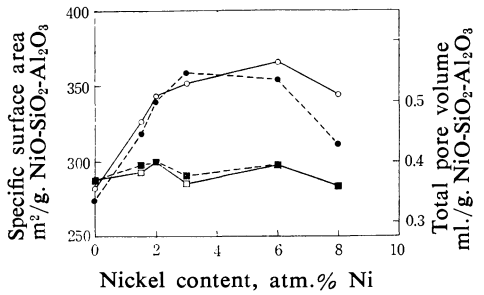



Fig. 4. Specific surface area ($S$) and total pore volume ($V$) of the catalyst samples before and after nickel oxide removal plotted against nickel content.
Circle, $S$ Square, $V$
Empty mark, before the removal
Full mark, after the removal

quantities, $S$, $S'$, $V$, and $V'$, are plotted against the nickel content of the original catalyst. As the nickel content increases, both $S$ and $S'$ first increase, then vary less markedly over the range from 2 to 6 atm.% nickel, and finally decrease. On the other hand, both $V$ and $V'$ remain nearly the same over the whole range of nikel content studied. Except for a pair of catalyst samples—an original catalyst and the nickel-depleted sample produced from this, the specific surface area of a nickel-depleted catalyst ($S'$) is generally smaller than the specific surface area of the original ($S$); on the other hand, the total pore volume of a nickel-depleted catalyst ($V'$) is a little greater than the total pore volume of the original ($V$).

## Discussion

**The Relationship between Activity and Acidity.**—Before considering the relationship between the catalytic activity for ethylene polymerization and the catalyst acidity, let us study, for a moment, the relation between the specific activity, $k_s$, and the specific acidity, $A_s$. The specific activity, i. e., the activity based on the

unit surface area of the catalyst, is obtained by dividing $k_g$ by $S$. Similarly, the specific acidity, i. e. the acidity based on the unit surface area of the catalyst, is obtained by dividing $A_g$ by $S$.

Figure 5 shows a plot of $k_s$ as a function of the nickel content. Since, in the case of

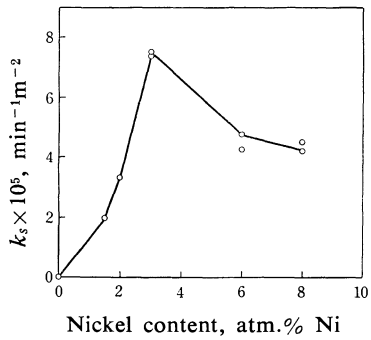



Fig. 5. Specific activity ($k_s$) as a function of nickel content.

acid catalysts,[10-12] $k_s$ is linearly correlated with $A_s$, one may suspect that a similar relationship will be found between the $k_s$ and $A_s$, or more roughly between $k_g$ and $A_g$, for the present catalysts. However, no such correlation can be found in the present case.

On the other hand, we have already found that, for a series of nickel oxide-silica-alumina catalysts with different aluminum contents, $k_s$ is more closely related to the difference between the specific acidity values before and after the removal of nickel, $A_s-A_s'$ (where $A_s'=A_g'/S$) than to $A_g$ or $A_g$ itself, and that

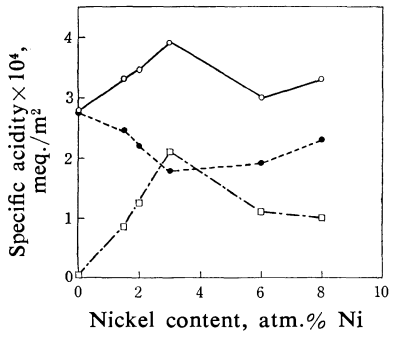



Fig. 6. Specific acidities plotted against nickel content.
—○— Acidity before removal of nickel ($A_s$)
--●-- Acidity after removal of nickel ($A_s'$)
—·□·— Difference between the above two values ($A_s-A_s'$)

10) M. W. Tamelle, *Discussions Faraday Soc.*, **87**, 270 (1950).
11) O. Johnson, *J. Phys. Chem.*, **59**, 827 (1955).
12) E. Echigoya, *J. Chem. Soc. Japan, Pure Chem. Sec.* (*Nippon Kagaku Zassi*), **76**, 1049 (1955).

the relationship between $k_s$ and $A_s-A_s'$ is approximately linear.[2] To see whether such a correlation would hold for the present series of catalysts, we have evaluated the specific acidity difference, $A_s-A_s'$, and plotted the values against the nickel content of the catalyst in Fig. 6.

A comparison of this plot with the plot of $k_s$ in Fig. 5 shows a parallel relationship between them. Moreover, a plot of $k_s$ vs. $A_s-A_s'$ for the present series of catalysts agrees with the straight line obtained for the series of nickel oxide-silica-alumina catalysts with different aluminum contents (see Fig. 7).

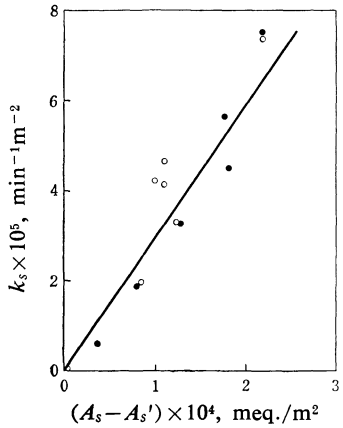



Fig. 7. Specific activity ($k_s$) plotted against the specific acidity difference ($A_s-A_s'$).
● Previously obtained results[2]

These facts indicate that only the acidity produced by the addition of nickel is closely related to the activity of ethylene polymerization, in other words, only the acid sites due to nickel contribute to the ethylene polymerization. However, it must here be noted that the nickel content is not always proportinal to $A_s-A_s'$, and, hence, to $k_s$.

**The Rates of the Formation of Butene Isomers at the Initial Stage of Polymerization and Their Dependence upon the Nickel Content.**—From the data of Figs. 2 and 5, the rates of the formation of three *n*-butene isomers per unit surface area of catalyst at the initial stage of ethylene polymerization can be calculated by the aid of the following equations:

$$r_{02}/r_{01}=[cis\text{-2-}]/[\text{1-butene}] \text{ at } t=0$$

$$r_{03}/r_{01}=[trans\text{-2-}]/[\text{1-butene}] \text{ at } t=0$$

$$r_{03}/r_{02}=[trans\text{-2-}]/[cis\text{-2-butene}] \text{ at } t=0 \quad (2)$$

$$r_0=k_sP_0 \quad (3)$$

$$r_0=r_{01}+r_{02}+r_{03} \quad (4)^{13}$$

13) In the earlier stage of polymerization, where the fraction of ethylene polymerized remained below 0.1, more than 95% of the reaction product was butene.

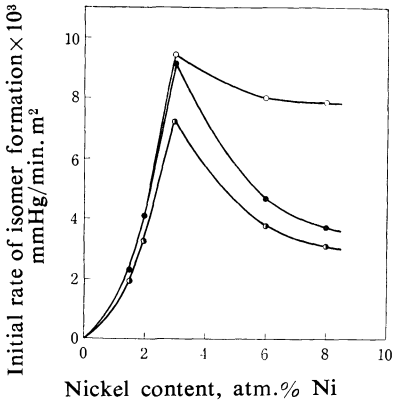



Fig. 8. Dependence of $r_{01}$, $r_{02}$ and $r_{03}$ on nickel content.
○ : $r_{01}$, ◑ : $r_{02}$, ● : $r_{03}$

where $r_{01}$, $r_{02}$, and $r_{03}$ are the rates of the formation of the butene isomers per unit surface area of the catalyst, respectively referring to 1-butene, *cis*-2-butene, and *trans*-2-butene; $r_0$ is the rate of ethylene polymerization per unit surface area of the catalyst, and the brackets indicate the concentration. In Fig. 8, the rates thus calculated, i.e., $r_{01}$, $r_{02}$, and $r_{03}$, are plotted against the nickel content of the catalyst. As the nickel content is increased, all these rates increase up to their respective maxima at 3 atm.% nickel and then decrease. An interesting fact to note here is that, in the range of nickel content above 3 atm.%, the rate $r_{01}$ decreases more slowly than the rates $r_{02}$ and $r_{03}$. This fact seems to indicate the possibility of producing 1-butene selectively by the use of a catalyst containing nickel greatly in excess of a certain amount of aluminum.

**Active Sites for Dimerization and Isomerization.**—For the purpose of explaining the catalytic performance observed in the formation of butene isomers (from ethylene) over nickel oxide-silica-alumina catalysts differing only in aluminum content, it has been postulated in a previous paper[2] that two kinds of active sites, $H^+X^-$ and $H^+Y^-$, as pictured by (≻Si-O-Ni≺) and (≻Si-O-Al≺) respectively, might be present on the catalyst surface, and that the first-named site would participate in the formation of chemisorbed species of 1-butene from ethylene, while the second site would participate in the rearrangement of the chemisorbed species to form the other *n*-butene isomers as the primary products. The concept of the active site $H^+X^-$ serves to explain the straight line relationship observed between the specific activity, $k_s$, and the specific acidity difference, $A_s$—$A_s'$. However, since three *n*-butene isomers were formed as primary products in ethylene dimerization over the catalyst containing no aluminum,[14] it might be necessary to correct this concept as follows: the site $H^+X^-$ contributes not only to the formation of 1-butene but also, in some degree, to the rearrangement of the chemisorbed species of 1-butene which forms the other *n*-butene isomers as the primary products. Nevertheless, we can safely say that only the site $H^+X^-$ contributes to the dimerization of ethylene and that all the sites of this type contribute in equal degree, whatever the aluminum and nickel contents of the catalyst may be.

On the other hand, as the following discussion will show, it has now been found that the data hitherto obtained on the selectivity in the formation of butene isomers are too complicated to allow us to assign the site $H^+Y^-$ simply to the silica-alumina combination, ≻Si-O-Al≺. In the butene-isomer formation over the catalysts described in the previous paper, both *cis*-2-/1-butene and *trans*-2-/1-butene ratios at the initial reaction stage (reaction time: $t=0$) rise rapidly as the aluminum content of the catalyst (expressed as Al/(Al+Si) atomic ratio) increases up to 0.1, while above this value of aluminum content, they remain nearly constant. On the other hand, in the butene-isomer formation over the catalysts described in this paper, these isomer ratios decrease, at first very slowly and then rapidly, as the nickel content of the catalyst increases up to a certain limit. These facts suggest that the selectivity might be related to the Al/Ni ratio rather than to either of the other two factors, aluminum content and nickel content.

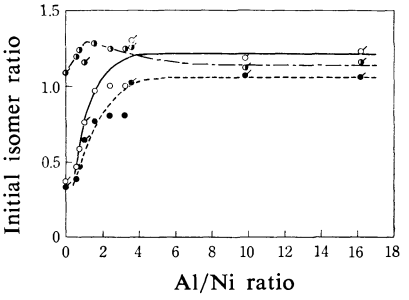



Fig. 9. Dependence of initial isomer ratio on Al/Ni ratio.
○ ♂ *trans*-2-/1-butene
● ♂ *cis*-2-/1-butene
◑ ♂ *trans*-2-/*cis*-2-butene
The marks with dash indicate the previous date with a series of catalysts containing varying amount of aluminum and a fixed amount of nickel.[2]

14) There is a possibility that the catalyst described as containing no aluminum may happen to be contaminated with a minute quantity of aluminum or some other substance, an impurity which might come from the sodium silicate used as a raw material.

In fact, as Fig. 9 shows, both *cis*-2-/1-butene and *trans*-2-/1-butene ratios (at $t=0$) increase as the Al/Ni ratio increases up to 4, but above this Al/Ni ratio they remain nearly constant. On the other hand, the *cis*-2-/*trans*-2-butene ratio is nearly the same throughout the range of the Al/Ni ratio studied, except at an Al/Ni ratio of about 1, where a slight maximum appears in the plot. The trend of the first two plots suggests that all the aluminum in a catalyst can not always be the constituent of the active site capable of accelerating the double-bond shift to form 2-butenes, but that only the aluminum associated in some manner with the nickel, presumably the aluminum joined by an oxygen bond to the nickel as in (≻Si-O-Al-O-Ni≺), can be the constituent.

Moreover, the fact that both *cis*-2-/1-butene and *trans*-2-/1-butene ratios (even their highest values) are much smaller than the corresponding ratios calculated from the thermodynamical data for the chemical equilibrium between butene isomers at 40°C[15] leads us to conclude that the aluminum present in excess of an Al/Ni atomic ratio of 4 cannot accelerate the initial double-bond shift. This conclusion is consistent with the geometry of the aluminum-nickel combination, because, on the basis of the reasonable assumption[16] that one nickel atom is located in the center of a tetrahedron with four oxygen atoms at the corners, it may be considered that four aluminum atoms are joined to one nickel atom by oxygen bridges.

In his study of the selectivity in olefin isomerization over acid catalysts, Brouwer[17] explained the variation in the selectivity with the kind of catalyst by applying the concerted or switch mechanism proposed by Turkevich and Smith[18] and by Horiuchi[19]. Our explanation based on the concept of two active sites is similar to Brouwer's in that two kinds of acid sites, $H^+X^-$ and $H^+Y^-$, are considered. However, the former differs from the latter in that the two acid sites considered in our explanation have different properties, whereas the sites considered by Brouwer are the same. The concerted mechanism alone does not suffice to explain our observation that the activity for ethylene polymerization and the selectivity in the formation of butene isomers change in different ways as the catalyst composition is changed.

The reaction scheme presented in a previous paper[1] can be applied to explain the constancy of the *cis*-2-/*trans*-2-butene ratio observed nearly all over the range of the Al/Ni ratio studied. However, it is not possible to account for the slight maximum appearing in the plot of the isomer ratio at an Al/Ni ratio of about 1.

15) About the equilibrium composition, see Ref. 1.
16) C. L. Thomas, *Ind. Eng. Chem.*, **41**, 7564 (1949).
17) D. M. Brouwer, *J. Catalysis*, **1**, 22 (1962).
18) J. Turkevich and R. K. Smith, *J. Chem. Phys.*, **16**, 446 (1948).
19) J. Horiuchi, *Catalyst (Shokubai)*, **1**, 67 (1948).

## Summary

The activity of nickel oxide - silica - alumina catalysts in ethylene polymerization and the selectivity in the formation of three *n*-butene isomers as the primary products have been studied by employing a series of catalysts with identical aluminum contents but different nickel contents. Also studied have been the changes brought about by nickel removal in the catalyst acidity and in the specific surface area.

In the series of catalysts studied, the specific activity, i.e., the activity per unit surface area of the catalyst, increases with the increasing nickel content of the catalyst, attaining a maximum at 3 atm.% nickel. When the specific activity is plotted against the difference between the specific acidity values observed before and after the removal of nickel, the plot falls approximately on the straight line obtained with a series of catalysts which are the same in nickel content but different in aluminum content. On the other hand, for all the catalysts used in the present and previous studies, the selectivity is more closely related to the Al/Ni ratio than to either aluminum content or nickel content.

Two kinds of active sites have been presented in order to explain the present observations. One kind of active site is the nickel acid site, which contributes to the polymerization of ethylene while facilitating the isomerization to some extent. The other site is the aluminum acid site in contact with the former; it contributes to the initial-bond shift.

*Government Chemical Industrial Research Institute, Tokyo*
*Shibuya-ku, Tokyo*

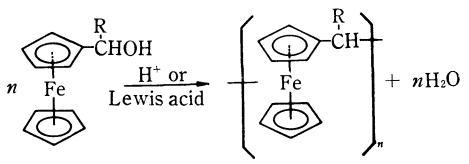
# Ferrocene-containing Polymers. IV. Polymeric Ethers as Intermediates in the Self-condensation of Ferrocenyl Carbinols

By Eberhard W. NEUSE and Edward QUO

(Received September 26, 1964)

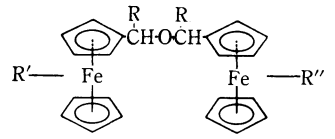
A previous paper[1] described the acid-catalyzed polycondensation of ferrocenyl carbinols of the type I. The reaction, which can be summarized by Eq. 1, was found to lead to polymers II.[2] An ionic mechanism was believed to be operative, with monomeric and polymeric[2] ether structures III occurring as intermediates. Monomers IIIa and IIIb were intercepted; however, under the experimental conditions chosen, no polymeric ethers IIId—f could be isolated.

In the present study, using carbinol Ic,[3]

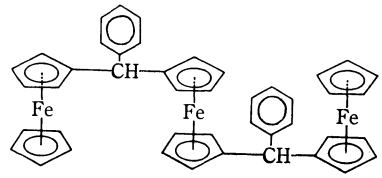



(1)

Ia, R=H IIa, R=H
b, R=$CH_3$ b, R=$CH_3$
c, R=$C_6H_5$ c, R=$C_6H_5$




IIIa, R=H; R', R''=H
b, R=$CH_3$; R', R''=H
c, R=$C_6H_5$; R', R''=H
d, R=H; R', R''=residual polymer chain
e, R=$CH_3$; R', R''=residual polymer chain
f, R=$C_6H_5$; R', R''=residual polymer chain




IV

polycondensation reactions were conducted as before, but under milder experimental conditions, i. e., at lower temperatures and shorter reaction times in the presence of catalytic amounts of mineral acids or, less advantageously, organic acids.[4] The reaction could thus be controlled so as to give the postulated polymeric ether IIIf in addition to the monomeric main product IIIc.

In a typical run, catalyzed by hydrochloric acid, Ic was heated under nitrogen for 15 min. at 95°C. After the catalyst had been removed by water extraction, the melt was separated into a major portion containing monomeric constituents and two small fractions of low-molecular-weight polymeric material. The polymeric fractions, obtained in a total yield of 4.0%, showed number-average molecular weights and analytical data[13] as listed in the first two lines of Table I. The findings are well in accord with the calculated composition of ether IIIf.

From the monomeric portion essentially consisting of ether IIIc, the latter was isolated by chromatography in a 83% yield[5] as a mixture of two diastereomers,[6] which were separated by fractional crystallization from hexane. The analytical data for both isomers are given in the last two lines of Table I. The less soluble species, constituting nearly 75% of the total IIIc, melted at 136—138°C and exhibited proton magnetic resonance signals at $\tau$ 2.72 (ten phenyl protons; singlet, broadening to the high-field side), 5.08 (two methine protons; singlet) and at 6.09 (18 ferrocene protons; singlet, broadening to the low- and high-field sides). The second, slightly

1) E. W. Neuse and D. S. Trifan, *J. Am. Chem. Soc.*, **85**, 1952 (1963).

2) The notation of the left-hand substituent in II (and also of R' and R'' in III) was discussed earlier (Ref. 1).

3) The bulkier R allows for more enhanced manifestation of compositional changes.

4) Strong organic acids such as oxalic and *p*-toluenesulfonic acid, while giving similar results as mineral acids (if applied in somewhat higher concentrations), were frequently found to be partially incorporated into the polymer through esterification.

5) 92% after 5 min. at 85°C. No IIIf isolated in this case.

6) The possibility of polymorphism for the two species is ruled out by the difference in their high-resolution NMR spectra and the absence of heat-of-transition peaks in the differential thermogram. Only heat-of-fusion endotherms were shown at 110—112°C and 134—136°C, respectively. (DTA thermograms recorded by Mr. R. P. Colburn at a heating rate of 10°C/min. in argon, using a du Pont model 900 differential thermal analyzer). See also Ref. 8.

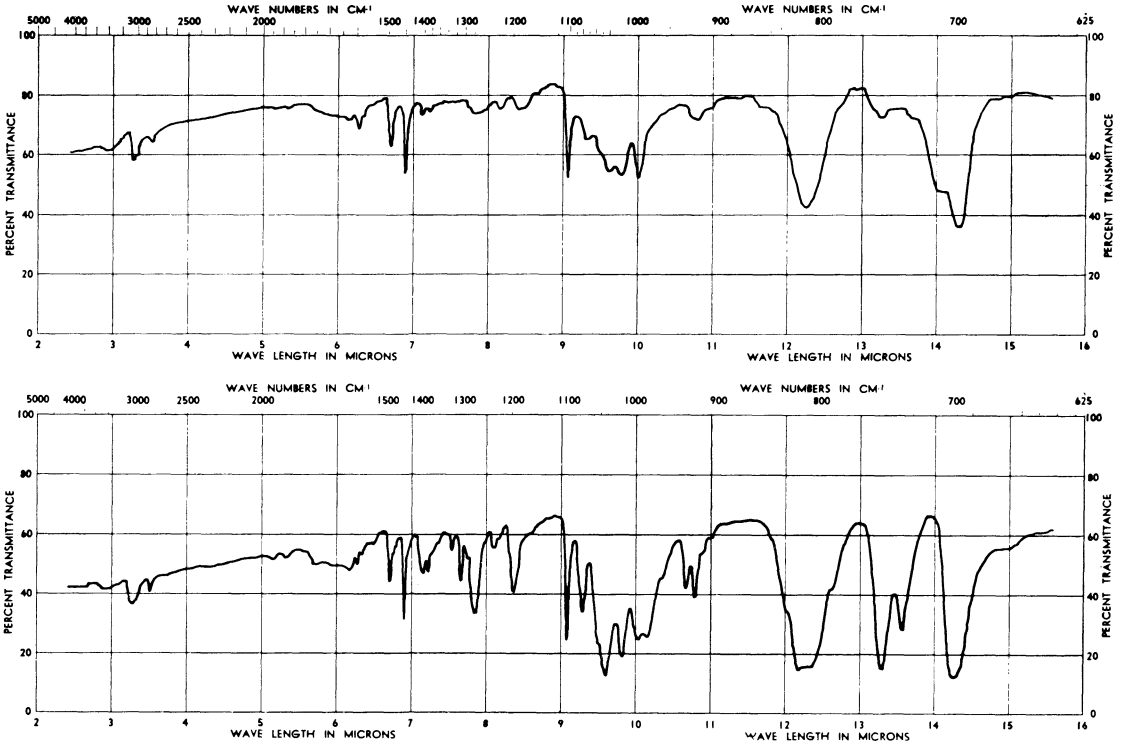



Fig. 1. Infrared spectra (KBr pellet) of:
Monomeric ether IIIc (lower curve)
Polymeric ether IIIf (upper curve)

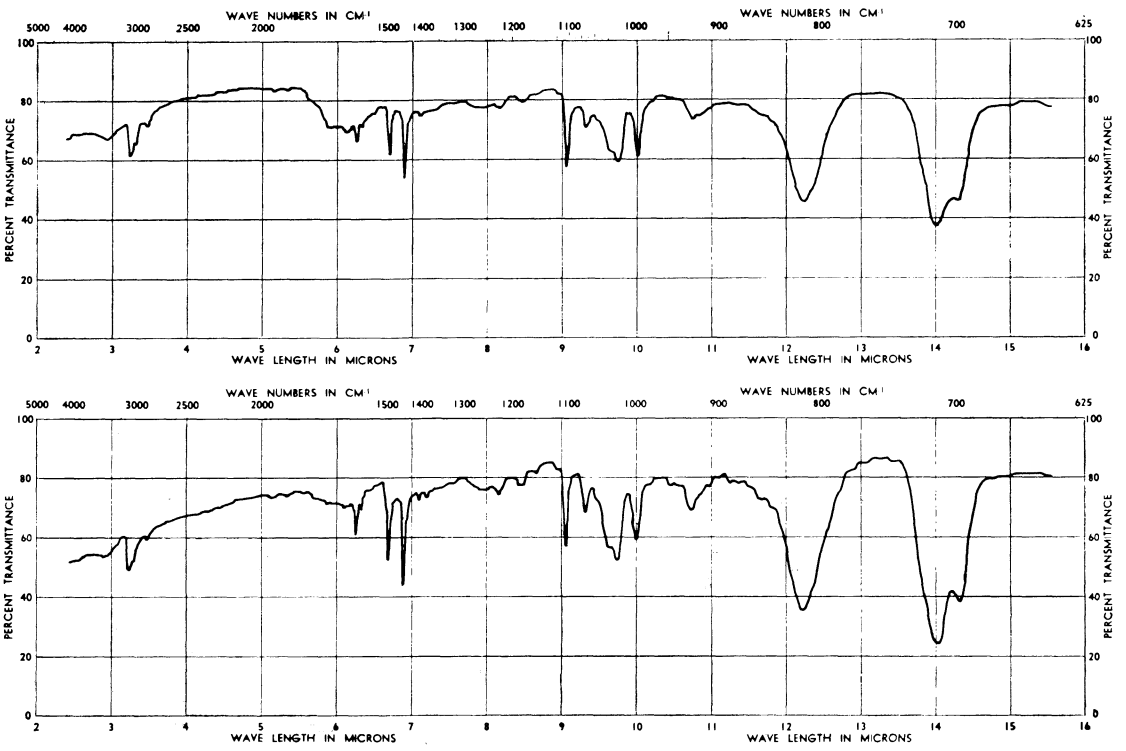



Fig. 2. Infrared spectra (KBr pellet) of:
Polymer IIc obtained by self-condensation of Ic (lower curve)
Polymer IIc obtained by post-condensation of IIIf (upper curve)

more soluble isomer,[7] melting at 111—113°C, gave NMR signals in the region $\tau$ 2.6—2.8 (ten phenyl protons; essentially a doublet structure with peaks at 2.68 and 2.76), at 4.95 and 5.08 (two methine protons; two peaks of an equal intensity), and in the region 5.9—6.2 (18 ferrocene protons; complex multiplet with two predominant peaks at 6.10 and 6.17).[8] The infrared spectra of both diastereomers IIIc, recorded on the solid compounds, were nearly identical. The spectrum of the higher melting isomer[9] is given in the lower curve of Fig. 1. Both species showed strong ether absorption at 7.85 and 9.60 $\mu$ and exhibited the typical intensity enhancement of the methine C–H stretching mode at 3.49 $\mu$. Also strongly enhanced were the phenyl band at 8.40 $\mu$ and the 9.5-$\mu$ ferrocene band. In the skeletal range 10.7—11.0 $\mu$, absorption was noticed at 10.80 $\mu$. A characteristic, strong doublet appeared in the 13.5-$\mu$ region[10]; similarly intense was the phenyl $\delta_{C-H}$ band at 14.25 $\mu$.

These spectroscopic correlations for monomeric IIIc served to corroborate the structural assignment of polymeric IIIf. The infrared spectrum of IIIf (Fig. 1, upper curve), besides showing the essential bands of the oxygen-free polymer IIc[1] presented in Fig. 2 for comparison (lower curve), exhibited low-intensity ether bands at 7.85 and 9.60 $\mu$, the latter partially overlapping the 9.65-$\mu$ ferrocene band. Additional absorption appeared at 10.80 $\mu$ and in the 13.3-$\mu$ region, coupled with enhancement of the aforementioned bands at 3.49, 8.39 and 9.5 $\mu$. The high intensity of the C–H deformation band at 14.25 $\mu$, superimposing upon the analogous absorption shown in the 14.0—14.3-$\mu$ region by IIc, gave rise to a highly characteristic doublet pattern, with the high-wavelength peak dominating in intensity.

Further support of structure IIIf resulted from NMR data. The phenyl proton resonances appeared as a broad, poorly-resolved doublet, with a high-field peak near $\tau$ 2.82 corresponding to the signals of oxygen-free IIc ($\tau$ 2.86) or model compounds phenyldiferrocenylmethane[11] ($\tau$ 2.88) and 1,1′-bis(phenylferrocenylmethyl)-ferrocene[12] (IV, $\tau$ 2.80), and a somewhat stronger low-field signal centered at $\tau$ 2.72 corresponding to the more deshielded signal average of isomers IIIc. Two separate methine resonances were shown; the weak high-field signal near $\tau$ 5.6 corresponds to the broad resonance at 5.5—5.7 in IIc and to the singlets at $\tau$ 5.40 in phenyldiferrocenylmethane and 5.49 in IV, whereas the more intense low-field peak at 5.03 is the counterpart to the average methine proton signal of IIIc. For a more quantitative evaluation of the relative intensities, IIIf was fractionally precipitated so as to give a subfraction with $M_n = 830$, i.e., roughly composed of the trinuclear homologs (analytical data[13] given in third line of Table I). The integrated intensities of the phenyl/methine/ferrocenyl protons for this fraction were in the expected 15 : 3 : 26 ratio. The low-field/high-field phenyl proton ratio was ~1.4. Similarly, the low-field/high-field methine proton ratio was found to be ~1.3. Both ratios are lower than required for IIIf, suggesting contamination by IIc. The presence of IIc is not unexpected in view of the various competing propagation steps[1] operative even under the mild condensation conditions applied. Accordingly, enhanced proportions of IIc, coupled with higher $M_n$ and increased yields

7) N. Weliky and E. J. Gould (*J. Am. Chem. Soc.*, **79**, 2742 (1957)) assigned structure IIIc to a compound with m. p. 52—56°C obtained by treating Ic with $PBr_3$. These workers also mentioned an unidentified by-product melting at 110—112°C. While under present experimental conditions the former substance was not isolated, the latter compound is probably identical with our isomer IIIc, m. p. 111—113°C.

8) Assuming diastereoisomerism for both species IIIc, the three staggered conformations of the *d,l*-form will each give rise to a singlet signal in the methine proton region due to pair-wise equivalence of the two methine protons. At temperatures sufficiently high to ensure rapid interconversion and equal population of the conformers, one may thus expect a single time-average proton signal to occur in the mentioned region. For the meso-form, in contrast, the same temperature conditions will lead to two gauche conformers, each with two non-equivalent methine protons, which, hence, may give a doublet signal due to different shielding, and a trans conformer with two equivalent methine protons, exhibiting a singlet resonance. On this basis, it would appear tempting to assign the meso structure to the lower melting isomer. Such conclusion, however, would rest on the unproven and questionable assumption that the temperatute chosen for measurement (ambient) be high enough to preclude the occurrence of preferred conformations (e.g., trans with respect to methine H), and, hence, would have to be borne out by a study of the temperature function of the methine proton shifts.

9) The isomer with m. p. 111—113°C exhibited additional weak absorption at 11.60 $\mu$, but failed to show the small peak at 7.65 $\mu$. Both compounds gave identical spectra in $CS_2$ solution.

10) Also shown by the corresponding ethers with H or $CH_3$ in lieu of $C_6H_5$.

11) Prepared by condensation of ferrocene with benzaldehyde (E. W. Neuse and D. S. Trifan, Abstr. of papers presented at 148th National Meeting, A. C. S., September 1964, p. 5 S.); identical in infrared spectrum and elemental composition with the compound described by Weliky and Gould (Ref. 7; infrared spectrum kindly furnished by Dr. Weliky).

12) Prepared by Mrs. E. Carter in this laboratory; m. p. 190—193°C (sealed cap.). Found: C, 71.49; H, 5.38; Fe, 22.60, $M_n$, 720. Calcd. for $C_{44}H_{38}Fe_3$ (IV; mol. wt. 734.3): C, 71.97; H, 5.22; Fe, 22.82%. %-Homoannularity, 69.2; X-ray diffractogram, Å: 4.98; 5.57—5.65 (doublet); 6.79; 4.22; 5.37; 3.95.

13) The percent-homoannularity values (for definition and experimental determination see Ref. 1) for fractions IIIf listed in Table I and other fractions of IIIf not mentioned in this paper were consistent with those for fractions of IIc in comparable molecular weight ranges. This identity is to be expected on account of like composition and sequence distribution of the recurring units in polymer chains R′ and R″ of ether IIIf on the one hand and in the backbone of polymer IIc on the other hand.

TABLE I

| Compound | $M_n$[a] | Calcd., % | | | Found, % | | | Percent-homoannularity[b] |
|---|---|---|---|---|---|---|---|---|
| | | C | H | Fe | C | H | Fe | |
| IIIf, First fraction m. p.[e] 125°C | 1070 | 73.28 | 5.24 | 20.04[c] | 73.43 | 5.14 | 19.48 | 73.1 |
| IIIf, Second fraction m. p.[e] 100°C | 680 | 72.46 | 5.31 | 19.85[c] | 72.42 | 5.42 | 19.22 | 75.2 |
| IIIf, Subfraction m. p.[e] 95°C | 830 | 72.88 | 5.28 | 19.93[c] | 73.31 | 5.29 | 19.59 | 76.4 |
| IIIc, Diastereomer with m. p. 136—138°C | 560 | 72.11 | 5.34 | 19.72[d] | 71.90 | 5.46 | 19.55 | — |
| IIIc, Diastereomer with m. p. 111—113°C | 550 | 72.11 | 5.34 | 19.72[d] | 71.92 | 5.54 | 19.68 | — |

a) Mean value from duplicate runs (in benzene).
b) See Ref. 13.
c) Calcd. for IIIf, with mol. wt. 1115 (first fraction), 703 (second fraction), and 840 (subfraction).
d) Calcd. for IIIc, with mol. wt. 566.
e) Upper limit of melting range.

of polymeric products, resulted from extended heating periods under otherwise unchanged experimental conditions. Consistent with this observed trend, it was possible to post-condense IIIf, resulting in the elimination of the internal ether bridge. To this end, in a series of experiments, IIIf was fused for several hours at 100—135°C in the presence of Lewis acids. In all instances, work-up in a manner which has been described[1] gave a polymer identical in composition and spectroscopic behavior with the oxygen-free product IIc prepared earlier.[1] A typical infrared spectrum is presented in the upper curve of Fig. 2.

The described isolation of IIIf and its post-condensation to the polymer IIc devoid of an ether bridge corroborate the mechanistic inferences set forth in an earlier paper[1] regarding the intermediary role of polymeric ethers in polycondensations of ferrocenyl carbinols.

## Experimental[14]

Ferrocenylphenylcarbinol (Ic) was prepared by the sodium borohydride reduction of benzoylferrocene in a manner which has been described earlier[1]; two recrystallizations from hexane gave m.p. 79—81°C. Alcoa-grade F-20 activated alumina was used for chromatography.

**Polycondensation of Ic.**—In an exemplifying experiment, a mixture of 5.0 g. (0.0171 mol.) of carbinol Ic and 0.025 g. of hydrogen chloride (as 1.0 N aqueous hydrochloric acid) was heated for 15 min. at 95°C. A slow stream of nitrogen was passed over the melt during this operation. The vigorously-stirred homogeneous mixture solidified after about 10 min., blocking the stirrer. Extraction of the pulverized melt with water for catalyst removal was followed by fractional extraction with cold hexane. The final residue least soluble in hexane, no longer containing low-molecular ethers or the starting material, was taken up in benzene. Freeze-drying of the concentrated solution furnished a first fraction of IIIf as an orange-brown resin, which was then vacuum-dried for 7 days at 45°C; melting range, 100—125°C. The yield was 0.09 g. (1.9%). A second, lower-molecular fraction of IIIf deposited in a resinous form upon concentration of the combined initial hexane extracts. After the monomer had been removed by hexane trituration, the product, 0.10 g. (2.1%), melted at 80—100°C. For both fractions, $M_n$ and analytical data are collected in Table I.

The supernatant hexane solution, combined with the hexane washings from the trituration of the first fraction IIIf and concentrated to ca. 150 ml., was chromatographed on alumina, using hexane as the eluent. From the lower, major band,[15] 4.02 g. (83.0%) of crude ether IIIc was obtained; melting

14) Melting points uncorrected. Carbon-hydrogen analyses by G. I. Robertson, Jr., Florham Park, N. J. Number-average molecular weights determined by Schwarzkopf Microanalytical Laboratory, Woodside, N. Y., in benzene solution on a Mechrolab model 301A vapor pressure osmometer; values rounded off to nearest 10. X-Ray diffractograms recorded on Norelco X-ray Diffractometer, using vanadium-filtered $K\alpha$ chromium radiation; only six strongest peaks (interplanar spacings d) within $2\theta$ range 10—35° listed in decreasing order of intensity (mean error at $2\theta = 20°, \pm 0.04$ Å). Proton magnetic resonance spectra recorded over a sweep width of 500 c.p.s. in carbon tetrachloride solution on Varian Associates model A-60 NMR spectrometer operating at 60 mc./sec. (tetramethylsilane used as internal standard with $\tau = 10.00$ p. p. m.).

Infrared spectra taken on Baird-Atomic spectrophotometer, model NK-1 equipped with rock salt optics. Quantitative measurements (%-homoannularity. Ref. 1) conducted in spectrograde carbon disulfide, employing a cell-thickness of 0.05 cm. We are indebted to Messrs. W. M. Rade and R. L. Harvey for scanning the X-ray diffractograms and infrared spectra. Dr. S. Manatt, Jet Propulsion Laboratory, Pasadena, Calif., kindly obtained the NMR spectra.

15) Beside trace amounts of IIIf and Ic, benzoylferrocene (0.1%; m. p. 104—106°C) was isolated from the chromatogram, probably formed by oxidation of Ic on the column as repeatedly observed while purifying this carbinol. From an additional, slightly lower band, light yellow and very narrow, 1.9 mg. of an unidentified yellow, infusible crystalline compound were isolated; X-ray diffractogram, Å: 4.87; 5.62; 5.84; 8.49; 4.57; 4.08.

range, 80—125°C; $M_n$, 550.

Found: C, 72.15; H, 5.52; Fe, 19.76. Calcd. for $C_{34}H_{30}Fe_2O$ (IIIc; mol. wt. 566.3): C, 72.11; H, 5.34; Fe, 19.72%.

By fractional crystallization from hexane, the crude isomer mixture was separated into the two diastereomers. This tedious operation was facilitated by the X-ray diffractometric characterization of individual fractions. The less-soluble isomer crystallized as large orange prisms melting at 136—138°C (DTA endotherm,[6] sharp peak at 134—136°C); X-ray diffractogram, Å: 5.70; 6.64; 4.92; 5.43; 4.43; 5.17. The more soluble isomer, melting at 111—113°C (sharp DTA endotherm[6] at 110—112°C), was collected as small, orange-yellow crystal clusters; X-ray diffractogram, Å: 6.05; 4.83; 5.22; 5.34; 5.73; 4.69. The $M_n$ values and elemental analytical findings for both diastereomers are listed in Table I. The two isomers were obtained in a weight ratio of approximately 3:1 (high-melting to low-melting species).

A 70 mg. portion of the second fraction of IIIf listed in Table I was subfractionated from a hexane solution by incremental volume reduction, using a rotating evaporator (environmental water bath maintained at 30±2°C). The four resinous deposits obtained successively were dried in vacuo for 7 days at 45°C. The major cut, 45 mg., showed the melting range of 80—95°C. $M_n$ and analytical data are given in Table I (center line). The iron analyses were performed on material recovered from the $M_n$ determination, which in turn had previously been recovered from NMR and infrared work.

Results similar to those described above, except for lower yields in IIIc, were obtained in condensation reactions catalyzed by 0.5% sulfuric acid (as 1.0 N sulfuric acid; 0.4 hr. heating at 100°C), 2.0% oxalic acid (2 hr. at 110°C) or 1.8% *p*-toluenesulfonic acid (2 hr. at 100°C). In the last-named two cases employing organic acids, these catalysts were partially incorporated into the polymeric reaction products, as is indicated by the elemental analyses and the appearance of ester absorption bands in the infrared spectra. Other experiments were performed in the presence of hydrochloric acid; they were similar to those which have been described but were conducted over extended heating periods. Here, the original polymer fractions isolated exhibited higher $M_n$ values (total yields up to ~30%), and their infrared spectra increasingly resembled, but never became quite superimposable with, those of IIc. For instance, heating for one hour at the started temperature gave a polymer, melting range 100—130°C, $M_n$ 1360, in a total yield of 9.7%.

Found: C, 73.91; H, 5.30; Fe, 20.09. Calcd. for IIIf (for IIc in parentheses): C, 73.51 (74.48); H, 5.23 (5.15); Fe, 20.11% (20.37%).

**Post-Condensation of IIIf.** — A typical fraction of IIIf (0.225 g.) prepared from Ic by sulfuric acid catalysis ($M_n$, 990. Found: C, 73.01; H, 5.28; Fe, 19.88%), was ground together with 0.011 g. of anhydrous zinc chloride[16] and fused for 1.0 hr. at 120°C in a test-tube under a blanket of dry nitrogen. The melt, liquid in the initial stage, finally became highly viscous and "stringy" and solidified on cooling. The mass was ground and extracted with water to remove the catalyst and was then worked up in a manner described in an earlier paper[1] to give two polymer fractions. The major fraction (0.105 g.), a yellow-tan solid, had a melting range of 150—180°C (partial melting); $M_n$, 2020.

Found: C, 74.43; H, 5.22; Fe, 20.20. Calcd. for IIc: C, 74.48; H, 5.15; Fe, 20.37%.

The infrared spectrum is presented in Fig. 2 (upper curve). The somewhat smaller second fraction, 0.070 g., a yellow solid, gave $M_n$ 880. Found: C, 74.16; H, 5.09%. The infrared spectrum, while essentially superimposable with that of the first fraction, showed shoulders at 7.85, 9.60 and near 13.3 $\mu$, indicating the presence of an ether bridge in a very low concentration. When the heating period in this experiment was extended to 2.0 hr., ether absorption vanished completely in both fractions.

## Summary

The acid-catalyzed polycondensation of ferrocenylphenylcarbinol Ic under controlled, mild reaction conditions gives rise to the formation of low-molecular, ferrocene-containing polymeric ethers, to which, on the basis of elemental analysis, infrared and NMR spectroscopic data, the structure IIIf is assigned. Monomeric ether IIIc is isolated in addition under these conditions. In the presence of Lewis acids at elevated temperatures, ethers IIIf continue to react, with the elimination of the ether bridge, to give polymers identical with the previously reported oxygen-free compounds IIc, which were obtained directly from Ic under more rigorous conditions. In the previous work, polymers IIIf containing an ether group were postulated as intermediates but were not isolated. The observed formation of such polymers under the present experimental conditions, coupled with their successful post-condensation to IIc, is thus in accord with the earlier mechanistic implications.

*Polymer Laboratories*
*Missile & Space Systems Division*
*Douglas Aircraft Company, Inc.*
*Santa Monica, California*

16) Comparable results obtained in post-condensation reactions catalyzed by anhydrous aluminum chloride (4% by wt. of IIIf), but large portion (—10% by wt. of IIIf) of insoluble, crosslinked polymer and decomposition products isolated in addition.

# A Shock-Tube Study of the Acetylene-Oxygen Reaction

By Tetsu TAKEYAMA and Hajime MIYAMA

(Received October 2, 1964)

Kistiakowsky and his collaborators have extensively investigated the acetylene-oxygen reaction in shock waves, using a wide variety of techniques to follow reaction processes, i. e., mass spectrometry,[1] X-ray densitometry,[2] vacuum ultraviolet emission spectroscopy,[3] and Langmuir probe technique.[4] They proposed that the rate of the main process operating in the induction period is determined by the reaction, $H+O_2 \rightarrow OH+O$, as in the hydrogen-oxygen reaction.

Observing visible or ultraviolet emission and OH absorption simultaneously, Stubbeman and Gardiner[5] have recently found that OH appears much later than the emission pulse and have explained that the high reactivity of OH is responsible for its delayed appearance. Since both Kistiakowsky's group and Stubbeman and Gardiner studied the reaction at higher temperatures and lower pressures, it now seems worth while to study the reaction under conditions similar to those chosen by us for the hydrogen-oxygen reaction,[6] i. e., at lower temperatures and higher pressures.

In this paper we will report the results obtained from simultaneous measurements of OH absorption, visible emission and pressure over the temperature range 820−1630°K and the pressure range 1.8−5.6 atm.

## Experimental

**Shock Tube and Instrumentation.** — The shock tube used was the same one as that described previously[7] except for a minor change in the observation system : an auxiliary observation station for emission measurement was installed in the lower part of the tube 5.5 mm. from the end plate, the same position as that for OH absorption and pressure measurement. For experiments in incident stock waves, a 1.2 m. tube of the same diameter was connected to the downstream end. A Shimadzu QR-50 monochromator with an R 106 photomultiplier (Hamamatsu TV Company) was used to isolate spectral regions of light transmitted through or emitted from the shock-heated gas at the principal observation station. The width of the exit slit of the monochromator was set at 0.15 mm. for the OH absorption measurement and at 0.50 mm. for the visible emission, the band widths being 7 and 65 Å respectively. The induction period for the onset of visible emission was measured by an 1P28 photomultiplier placed 30 cm. under the tube ; the optical system consisted of a quartz window, a 1 mm. wide slit, an interference filter (Vacuum Optics Corporation of Japan) (peak 4305 Å ; half-band width of 65 Å ; peak transmission 52%), a 1 mm. wide slit, and an 1P28 photomultiplier. A quartz-pressure transducer (Kistler model 603) was used for the pressure measurement 5.5 mm. from the end plate. Two platinum-film resistance thermometers and an electronic counter (Takeda Riken 4247) were used to measure the shock velocities.

**The Calculation of Shock Parameters.**—Temperatures, pressures and other parameters of the gas behind the incident and reflected shock waves were calculated by means of the one-dimensional theory described in a previous paper.[7]

**Materials.**—Matheson acetylene (99.66% min.) was used after being passed through two dry ice traps and having been determined to be free from acetone by a mass spectrometer. Nippon Sanso oxygen (99.5% min.) and argon (99.999% min.) were used without further purification.

## Results

**The Measurement of the Induction Period.**— By using reflected or incident shock waves, the induction periods for the OH appearance, the onset of visible emission and the pressure increase were measured simultaneously at the same location in the tube. The experimental conditions are summarized in Table I.

TABLE I. SUMMARY OF EXPERIMENTAL CONDITIONS

| Mixture | % Ar | $[C_2H_2]/[O_2]$ | Temp. range °K | $[O_2]$ range $10^{-3}$ mol./l. |
|---|---|---|---|---|
| I | 90 | 0.67 | 820—1300 | 1.63—4.08 |
| II | 93 | 0.40 | 970—1630 | 1.13—1.86 |
| III | 95 | 1.5 | 1110—1480 | 0.842—1.21 |
| IV | 94 | 1.0 | 1130—1520 | 1.16—1.76 |

A sample of the oscillograms obtained is shown in Fig. 1. The OH appearance, the onset of visible emission and the increase in

1) J. N. Bradley and G. B. Kistiakowsky, *J. Chem. Phys.*, **35**, 264 (1961).
2) W. C. Gardiner, Jr., ibid., **35**, 2252 (1961).
3) G. B. Kistiakowsky and L. W. Richards, ibid., **36**, 1707 (1962).
4) C. W. Hand and G. B. Kistiakowsky, ibid., **37**, 1239 (1962).
5) R. F. Stubbeman and W. C. Gardiner, Jr., ibid., **40**, 1771 (1964).
6) H. Miyama and T. Takeyama, ibid., **41**, 2287 (1964).
7) H. Miyama and T. Takeyama, This Bulletin, **38**, 37 (1965).

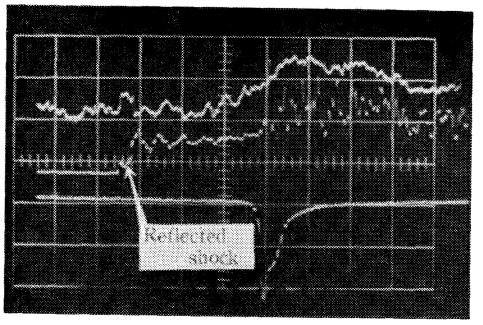



Fig. 1. Sample oscillogram. Mixture I, initial pressure 109.8 mmHg, shock temperature 1060°K, sweep rate 100 $\mu$sec./division. Top trace represents OH absorption, middle trace pressure change and bottom trace emission at 4320Å.

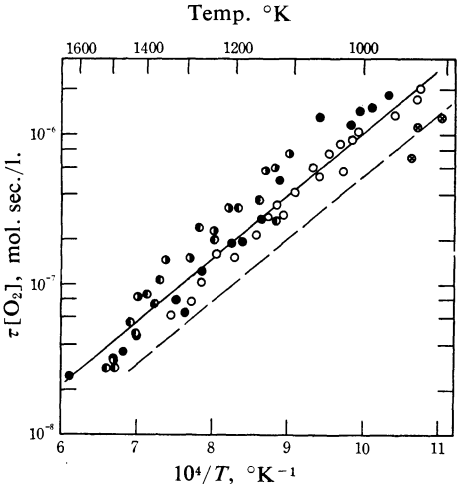



Fig. 2. Induction periods for appearance of OH absorption. Solid line is the least-squares line through the points and dashed line is the one obtained in the hydrogen-oxygen reaction.[6] The points are identified as follows:

| Symbol | Mixture | Type of shock |
|---|---|---|
| ○ | I | reflected |
| ⊗ | I | incident |
| ● | II | reflected |
| ◑ | III | reflected |
| ◐ | IV | reflected |

pressure occurred almost concurrently after an induction period, $\tau$, over the whole temperature range studied. In Fig. 2, the results for $\tau$ measured by OH absorption spectroscopy are shown as a plot of $\log(\tau[O_2])$ vs. $1/T$. The induction periods measured in incident shock experiments were multiplied by the density ratio in order to convert the laboratory time into particle time. Although there are few data from incident shock experiments because of the experimental difficulties encountered, the data we do have fall close to those obtained from reflected shock experiments. It should also be noted that, over the 0.4—1.5 range of acetylene to oxygen ratio there exists a linear relationship between $\log(\tau[O_2])$ and $1/T$; hence, the induction periods are dependent upon the oxygen concentration, as has been reported in the literature.[3,4] The equation of the least-squares line through these points is:

$$\log(\tau[O_2])\ (\text{mol. sec./l.}) = -10.16\pm0.15+(4160\pm140)/T \qquad (1)$$

The dashed line in Fig. 2 is the least-squares line obtained by us in the hydrogen-oxygen reaction.[6]

**The Intensity Distribution of Visible Emission.**—In order to identify the visible emitter, the intensities of emission were measured with the monochromator which had been used for OH absorption spectroscopy; 80 mmHg of gas mixture I (see Table I) was heated by reflected shock waves to 1210±30°K, and the wavelength setting of the monochromator was varied from run to run through the region 4100—4500Å. The intensities measured were corrected with the spectral response of the R106 photomultiplier; they are shown in Fig. 3. There exists a sharp peak at about 4320Å.

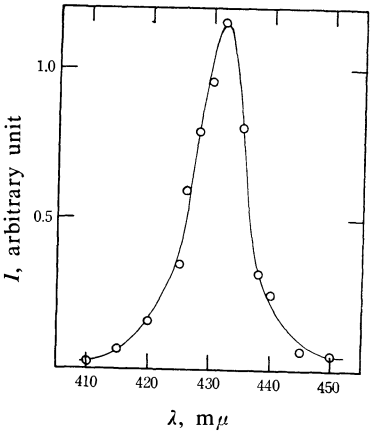



Fig. 3. Emission intensity vs. wavelength.

**The Temperature Dependence of the Intensity of Visible Emission.**—The intensities of visible emission were measured at 4200, 4320 and 4450Å over the temperature range 900—1270°K by using 80 mmHg of gas mixture I (see Table I) as the driven gas and 2.8—3.2 atm. of helium as the driver gas. The results are shown in Fig. 4. Although the intensities observed at 4200 and 4450Å are almost independent of the temperature those at 4320Å show a slight dependence, one which corresponds to an activation energy of about

6 kcal./mol. In these experiments, the concentrations of oxygen were kept nearly constant, ranging from $1.19\times10^{-3}$ to $1.58\times10^{-3}$ mol./l.; hence, it can be considered that no factors other than the temperature are involved in the results shown in Fig. 4.

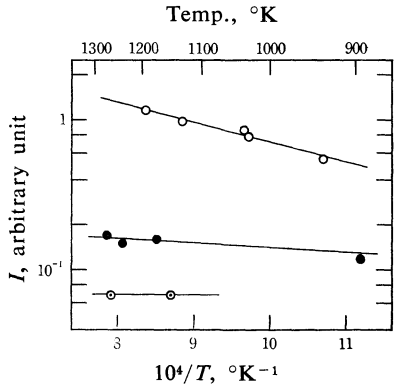



Fig. 4. Emission intensity vs. reciprocal temperature. Intensities measured at 432, 420 and 445 mμ are represented by ○, ●, and ⊙, respectively.

**Ionization.**—In the course of incident shock experiments, the output signals from the thin-film thermometers were found to be unreasonably delayed when the shock Mach number was increased. The oscillogram of these outputs revealed, as Fig. 5 shows, that negative signals occur when the shock front passes the thermometers and that the increase in the resistances of the thermometers due to temperature rise are delayed a few hundred micro seconds. This anomaly is attributable to the ionization of gases surrounding the thermometers ; it was therefore considered necessary to examine the details of ionization.

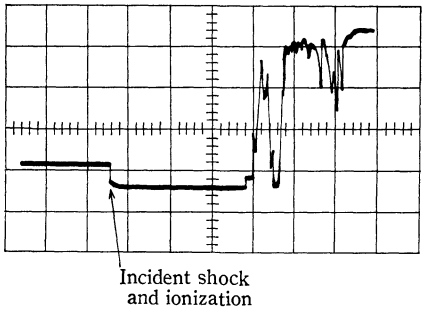



Fig. 5.—Oscillogram of thin-film thermometer showing ionization on arrival of shock. Mixture I, initial pressure 70.7 mmHg, shock temperature 1210°K, sweep rate 200 μsec./division.

A series of experiments was conducted using 100—40 mmHg of mixture I (see Table I) as the driven gas and 5 atm. of helium as the driver. The temperature range thus covered was 850—1200°K. According to the oscillograms obtained at temperatures higher than 1030°K, i. e., $P_1\leq83$ mmHg, the ionization begins as soon as the shock front has arrived.

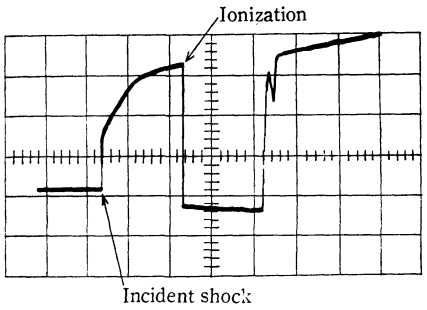



Fig. 6. Oscillogram of thin-film thermometer showing induction period for ionization. Mixture I, initial pressure 87.6 mmHg, shock temperature 920°K, sweep rate 200 μsec./division.

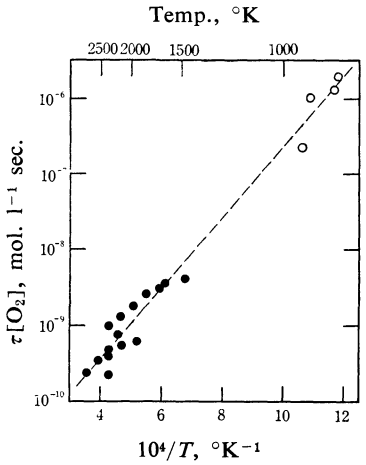



Fig. 7. Induction periods for ionization. Open circles are obtained in the present study with thin-film thermometer and solid circles by Hand and Kistiakowsky with Langmuir probe.

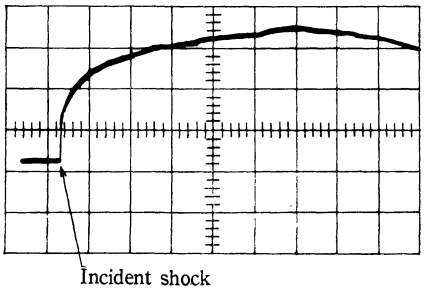



Fig. 8. Oscillogram of thin-film thermometer showing no ionization. Argon, initial pressure 20.0 mmHg, shock temperature 2030°K, sweep rate 100 μsec./division.

However, below this temperature the ionization occurs after an induction period, as Fig. 6 shows. This induction period is of the same order of magnitude as that measured by the pressure transducer at the same time, and it becomes longer as the temperature is lowered. In Fig. 7, the present results are compared with those of Hand and Kistiakowsky (cf. Fig. 4 of their paper[4]). The present data fall just on the line which is an extrapolation of theirs. For purposes of comparison, a strong shock was generated in 20 mmHg of argon or air. No ionization was found in these cases, as is shown in Fig. 8, although the temperatures were much higher than those for the cases where ionization was found in an acetylene-oxygen mixture.

## Discussion

Kistiakowsky and his collaborators[1,3] proposed the following scheme as operating during the induction period of acetylene-oxygen reaction in shock waves:

$$H+O_2 \rightarrow OH+O$$
$$\Delta H=17 \text{ kcal./mol.} \quad \text{(I)}$$
$$O+C_2H_2 \rightarrow C_2H+OH$$
$$\Delta H\leqq 20 \text{ kcal./mol.} \quad \text{(II)}$$
$$OH+C_2H_2 \rightarrow C_2H+H_2O$$
$$\Delta H\leqq 1 \text{ kcal./mol.} \quad \text{(III)}$$
$$C_2H+C_2H_2 \rightarrow C_4H_2+H$$
$$\Delta H=-23 \text{ kcal./mol.} \quad \text{(IV)}$$

Reaction I was considered to be rate-controlling, since the induction period behaves very similarly to that in the hydrogen-oxygen reaction.[8]

The present results shown in Fig. 2 do indicate that, in the range of conditions $820° \leqq T \leqq 1630°K$, $1.8 \leqq P \leqq 5.6$ atm., $8.4\times10^{-4} \leqq [O_2] \leqq 4.1\times10^{-3}$ mol./l., and $0.4 \leqq [C_2H_2]/[O_2] \leqq 1.5$, the induction period depends upon the oxygen concentration and that the activation energy derived from Eq. 1 is $19.0\pm0.6$ kcal./mol. Furthermore, the present data fall close to those obtained by us for a hydrogen-oxygen reaction.[6] Thus, reaction I is also rate-determining under the conditions of the present study.

In the hydrogen-oxygen reaction,[6] it was found that the induction period for an abrupt increase in pressure is much longer than that for OH absorption at temperatures below about 1100°K, and that it depends on the hydrogen rather than on the oxygen concentration. These findings were attributed to the participation of $HO_2$, radicals in the reaction processes at lower temperatures. However, the present study of the acetylene-oxygen reaction revealed no such effects. It is probably due to exothermic side reaction,[9] which prevent the accumulation of $HO_2$ radicals.

Although Stubbeman and Gardiner[5] found that the OH appearance is much later than the emission and ascribed it to the high reactivity of OH radicals, the present study has shown that OH absorption, visible emission and pressure increase occurred simultaneously over the whole temperature range studied. Since OH absorption increases much less rapidly than visible emission, as Fig. 1 shows, the induction period for the appearance of OH absorption is much more dependent upon such experimental conditions as the pressure, temperature, and the detectability of the measuring system. Therefore, we would explain the discrepancy between the present results and those of Stubbeman and Gardiner on the grounds of difference in facilities for detecting OH radicals.

Glass[10] has inferred from experiments with several interference filters that there should be a peak at about 4300Å, and he has suggested that the principal emitter of visible radiation must be the CH radical instead of the reaction $CO+O \rightarrow CO_2+h\nu$ proposed by Stubbeman and Gardiner.[5] The present results obtained with a monochromator give strong evidence, as Fig. 3 shows, that there is a sharp peak at about 4320Å. Accordingly, the visible emission observable in the acetylene-oxygen reaction in shock waves can be assigned to the $^2\Delta \rightarrow {}^2\pi$ transition of CH, as is the case with hydrocarbon-oxygen flames.[11] The probable reactions which cause chemiluminescence are considered to be:

$$C_2H+O_2 \rightarrow CO_2+CH^* \quad \text{(V)}$$

or:

$$C_2H+O \rightarrow CO+CH^* \quad \text{(VI)}$$

However, it is impossible to decide on the basis of the present results which of these is predominant.

The temperature dependence of the maximum intensity in Fig. 4 corresponds to 6 kcal.; it is much smaller than the energy required for placing the CH radical in the $^2\Delta$ state (66.6 kcal.). Therefore, as has been suggested for vacuum ultraviolet emission and ionization,[4] a high collisional yield must be assumed in order to explain the strong visible emission.

The ionization encountered in the course of

8) G. L. Schott and J. L. Kinsey, *J. Chem. Phys.*, **29**, 1177 (1958).

9) W. C. Gardiner, thesis, Harvard University, 1960.

10) G. P. Glass, private communication.

11) A. G. Gaydon, "The Spectroscopy of Flames," Chapman & Hall, London (1957), pp. 113—135, 234—245.

incident shock experiments is apparently chemical in origin, since it was observed only in the case of the acetylene-oxygen mixture and since, moreover, the induction period for ionization was of the same order of magnitude as that for the pressure increase. As is shown in Fig. 7, this chemi-ionization should be essentially the same as that observed by Hand and Kistiakowsky[4] with a Langmuir probe, and the reaction

$$CH^* + O \rightarrow CHO^+ + e^-$$

should be responsible. Thus, it is prospective to use a thin-film resistance thermometer as a detector of chemi-ionization.

## Summary

Acetylene-oxygen reaction in shock waves has been studied over the range of conditions $820° \leq T \leq 1630°K$, $1.8 \leq P \leq 5.6$ atm., $8.4 \times 10^{-4} \leq [O_2] \leq 4.1 \times 10^{-3}$ mol./l. and $0.4 \leq [C_2H_2]/[O_2] \leq 1.5$. Visible emission, OH absorption, and pressure have been measured simultaneously at the same location in the tube. The induction periods obtained from these measurements have been found to be identical with each other and to be dependent upon the oxygen concentration. It has also been found that the activation energy derived from the $\log(\tau[O_2])$ vs. $1/T$ plot is equal to $19.0 \pm 0.6$ kcal./mol. Thus, the reaction $H + O_2 \rightarrow OH + O$ is considered to be rate-determining during the induction period, as in the hydrogen-oxygen reaction.

The visible emission has been found to have a sharp peak at about 4320Å and has been attributed to the $^2\Delta - ^2\pi$ transition of CH radicals.

The authors are grateful to Mr. Akio Sawa for his help in the experiments and to Mr. Daisuke Miura and Mrs. Yukiko Takemura for their computations of shock parameters.

*Basic Research Laboratories*
*Toyo Rayon Company, Ltd.*
*Tebiro, Kamakura*

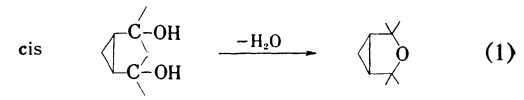
# Small Ring Compounds. VII. The Syntheses of 3-Oxabicyclo-[3. 1. 0]hexane and Its Derivatives

By Tatsuya SHONO, Akira OKU, Takeshi MORIKAWA, Masatoshi KIMURA and Ryohei ODA

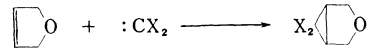
(Received October 6, 1964)

The cyclopropane ring has been reasonably considered to be different from other alicyclic rings in its electronic structure and to show characteristic chemical and physical properties. In order to clarify these points, the authors have reported in the preceding paper[1] of this series on the syntheses of cyclopropane derivatives and on some of their characteristic reactions. In the present paper the syntheses and properties of some cyclic ethers, which include the cyclopropane ring, that is, 3-oxabicyclo-[3. 1. 0] hexane (I) derivatives, will be reported.

Two methods are available for the syntheses of these bicyclic ethers. One of them is the dehydration of *cis*-1, 2-dimethylolcyclopropane and its derivatives (Eq. 1), while the other is the addition of some carbenes to 2, 5-dihydrofuran (Eq. 2):

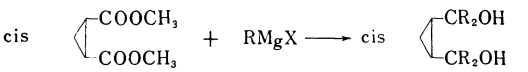



(1)




(2)

The synthesis of *cis*-1, 2-dimethylolcyclopropane was reported in the previous paper,[1] and $\alpha, \alpha, \alpha', \alpha'$-tetrasubstituted homologs were prepared from the corresponding *cis*-diester by Grignard reaction (Eq. 3):

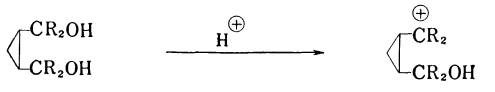



(3)

For the dehydrating ring closure of these glycols, four methods were examined: The use of potassium bisulfate, phosphoric acid and

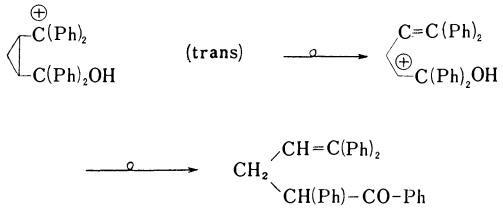
1) Small Ring Compounds. VI. T. Shono, T. Morikawa, R. Okayama and R. Oda, *Makromol. Chem.*, in press.

dimethyl sulfoxide as dehydrating agents, and the alkaline fusion of the tosylate of the glycols. Among these methods, that employing potassium bisulfate gave the best result; by the alkaline fusion of tosylate, the ether was not obtained at all. It is of interest that the dehydration of the glycols in acidic media was affected by the substituents and that sometimes rearranged products were formed. In acidic dehydration, the first-formed cation (see Eq. 4) would be the so-called "cyclopropyl carbinyl"-type cation, which is known to exhibit a complicated behavior in the course of reaction.[2]



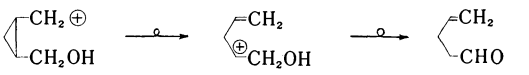
(4)

The cyclopropylcarbinyl cation may be considered to belong to a nonclassical carbonium ion; hence, ring-opening and rearrangement should occur. When the cation has some substituents at appropriate positions, the substituents have a great effect on its character; that is, the substituents determine whether it is a nonclassical or a localized cation. In our results, bicyclic ether was obtained almost quantitatively in the case of $R=CH_3$ (cf. Eq. 4), whereas in the case of $R=H$ or $C_6H_5$, some ring-opened products were obtained besides bicyclic ether. For example, *cis*-1,2-di($\alpha$,$\alpha$-diphenyl)methylolcyclopropane was rearranged through dehydration to give 1,1,4-triphenyl-4-benzoylbutene-1 (80%), which is the same as the product obtained in the acidic dehydration of the trans isomer[3] (Eq. 5):



(5)

The yield of the normally dehydrated product, bicyclic ether, was only 20%. These results show that two competing reactions, i.e., cyclization and rearrangement, occurred. In addition, the dehydrated products from a glycol, where $R=H$, had a very complicated composition. The yield of the expected product, 3-oxabicyclo[3.1.0]hexane, was only 35%, and the formation of an aldehyde (abt. 4%) and a large amount of oligomer containing a carbonyl group was observed. The mechanism of the formation of this aldehyde seems similar to that where $R=C_6H_5$ (Eq. 6):

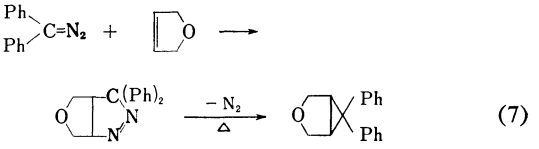


(6)

The 2,4-dinitrophenylhydrazone of this aldehyde gave the same elementary analysis data and melting point as did an authentic sample.

On the other hand, it has been reported that, when methyl group is present at an appropriate position of the cyclopropyl carbinyl cation, this methyl group effects the localization of the cation and diminishes the contribution of the non-classical character.[2] This fact agrees with our finding that no rearrangement was observed in the dehydration of the glycol where $R=CH_3$. The courses of dehydration of these glycols, both cis- and trans-, are now under investigation and will be reported on elsewhere.

The methods of the syntheses of bicyclic ethers through carbene addition to 2,5-dihydrofuran differed according to the character of the carbene. For example, dichlorocarbene was generated by two methods, (1) $CHCl_3$+$t$-$C_4H_9OK$ and (2) $Cl_3CCOOCH_3+CH_3ONa$. Method 2 gave a better result, but in both cases the products were a mixture of two isomeric compounds, which could be separated only by vapor-phase chromatography. One of them was 6,6-dichloro-3-oxabicyclo[3.1.0]-hexane; the structure of the other isomeric product could not be elucidated, though it can be considered to be an insertion product. On the other hand, fluorenyl carbene was generated from the corresponding diazo compound in a solution of 2,5-dihydrofuran with a copper catalyst. Under similar conditions, however, diphenyldiazomethane was directly added to 2,5-dihydrofuran to form a pyrazoline derivative, which lost its nitrogen easily upon heating and afforded the bicyclic ether (Eq. 7):

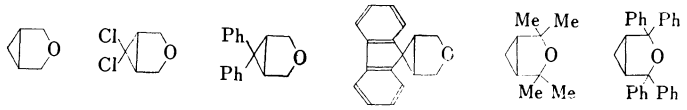


(7)

In addition, the Simmons-Smith[4] method was adopted as a modified procedure for the synthesis of 3-oxabicyclo[3.1.0]hexane, instead of using diazomethane as a carbene source. A zinc-copper couple was prepared by the wet method. The yield was only 5%, though it

2) P. de Mayo, "Molecular Rearrangements," Interscience Publishers, N. Y. (1963), p. 233.
3) R. A. Darby and R. E. Luty, *J. Org. Chem.*, **22**, 1353 (1957).
4) R. D. Smith and H. E. Simmons, "Organic Syntheses," **41**, 72 (1961).

TABLE I. STRUCTURES OF 3-OXABICYCLO[3.1.0]HEXANE DERIVATIVES AND THEIR PREPARATION

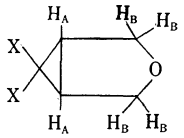


(I) (II) (III) (IV) (V) (VI)

(I) 3-Oxabicyclo[3.1.0]hexane
(II) 6, 6-Dichloro-3-oxabicyclo[3.1.0]hexane
(III) 6, 6-Diphenyl-3-oxabicyclo[3.1.0]hexane
(IV) 3, 4-(9, 9-Fluorenylidene) tetrahydrofuran
(V) 2,2,4,4-Tetramethyl-3-oxabicyclo[3.1.0]hexane
(IV) 2,2,4,4-Tetraphenyl-3-oxabicyclo[3.1.0]hexane

| Compound | Method | Yield, % | M. p. °C (or b. p. °C/mmHg) |
|---|---|---|---|
| I | Dehydration | | |
| | a $KHSO_4$ | 35 | (85—90/760) |
| | b $H_3PO_4$ | 5 | — |
| | c DMSO | 2 | — |
| | Simmons-Smith method | 3—5 | — |
| II | Dichlorocarbene | | |
| | a $CHCl_3$ | 7 | — |
| | b $Cl_3CCOOCH_3$ | 37 | (88—89/35) |
| III | Diazo compd. | 19 | 86.5—87.5 |
| IV | Diazo compd. | 5 | 169—170.5 |
| V | Dehydration ($KHSO_4$) | 77 | (91—91.5/164) |
| VI | Dehydration ($KHSO_4$) | 21 | 166—167 |

TABLE II. CHEMICAL SHIFTS RELATIVE TO TMS AS INTERNAL STANDARD (60 Mc.)



| Compound | X | Solvent | Chemical shift, c. p. s. ($\tau$ value) | | |
|---|---|---|---|---|---|
| | | | $H_A$ | $H_B$ | |
| II | Cl | $CCl_4$ | 137.0(7.55) | 227.6(5.92) | |
| III | $C_6H_5$ | $CCl_4$ | 120.1(7.85) | 215.8(6.13) | |
| IV | $\frac{1}{2}(C_{12}H_8)$ | $CCl_4$ | 130.7(7.65) | 223.4(6.00) | |
| I | H | $CCl_4$ | 78.2(8.60) | $H_B$ | $H_{B'}$ |
| | | | | 199.3(6.46) | 191.7(6.59) |

Coupling constant $J_{BB'}$ (compound I) 8.4 c. p. s.

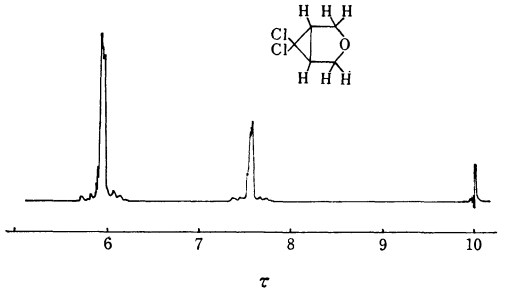



Fig. 1. NMR spectrum of II using TMS as internal standard.

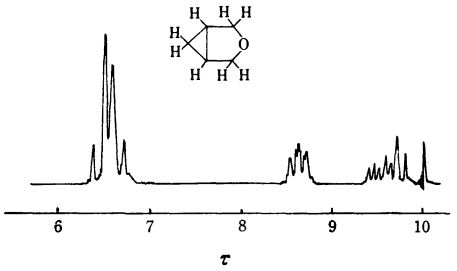
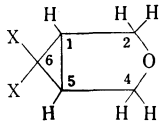



Fig. 2. NMR spectrum of I, using TMS as internal standard.

has been reported that in the case of dihydropyran the yield reached up to 65%.

The NMR spectra of compounds II, III and IV had only two peaks, near $\tau=7.7$ and 6.0 (see Table II) (Fig. 1). These peaks correspond to the bridge-head protons and to the methylene protons adjacent to oxygen respectively. Further, each peak showed a negligibly small fine-structure, indicating that the spin-spin coupling between $H_{(1)}$ and $H_{(2)}$ (or $H_{(5)}$ and $H_{(4)}$) is negligibly small in these bicyclic compounds. In these compounds the three-membered ring and the five-membered ring do not lie on the same plane; hence, the two hydrogens at position 2 or 4 would not be equivalent, and the spectrum of these hydrogens would be of the type AB. In the spectra of 6,6-disubstituted bicyclic ethers, however, the chemical shifts of the two hydrogens of position 2 or 4 were nearly equal, and hence the AB-type spectrum was not confirmed. However, in the case of compound I (X=H), the spectrum of $H_{(2)}$ (or $H_{(4)}$) was clearly of the AB type, and still the coupling between $H_{(1)}$ and $H_{(2)}$ (or $H_{(5)}$ and $H_{(4)}$) (Fig. 2) was negligibly small.




The infrared spectra of these bicyclic ethers showed the presence of a characteristic band near 1090 $cm^{-1}$ (Fig. 3).

Attempts to polymerize these bicyclic ethers (particularly I and II) with phosphorous pentafluoride, antimony pentachloride or a thionyl chloride - ferric chloride complex were unsuccessful. The reason why they could not be polymerized is uncertain. Moreover, neither I nor II copolymerized with 3,3-bischloromethyloxethane in the presence of a modified catalyst of triethyl aluminum ($AlEt_3+H_2O+$ Epichlorohydrin).

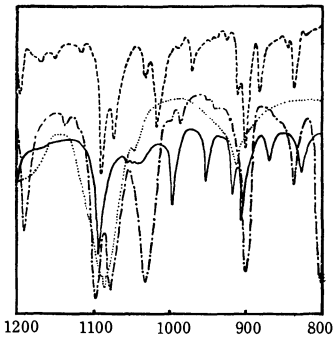



Fig. 3. Infrared spectra of bicyclic ethers.



——: X=H, ------: X=$C_6H_5$
—·—: X=Cl, (·····: THF)

## Experimental

**3-Oxabicyclo[3.1.0]hexane (I).**—*a) By Dehydration using Potassium Bisulfate.*—In a 50 ml. distilling flask 2.6 g. (3/160 mol.) of calcined potassium bisulfate was placed. The flask was then heated at 150—160°C, and 7.6 g. (3/40 mol.) of *cis*-1,2-dimethylolcyclopropane was added drop by drop over a 15-min. period. The distillate separated in two layers, and the organic layer was dried successively over sodium bicarbonate and Drierite (raw yield; 43%). By fractional distillation I was obtained in a 35% yield, b. p. 85—90°C, it contained a slight amount of an aldehyde.

Found (for I): C, 70.78; H, 9.67. Calcd. for $C_5H_8O$: C, 71.39; H, 9.58%.

*b) By Dehydration using Phosphoric Acid.*—Into a flask heated to 260°C, a mixture of 23 g. (0.23 mol.) of *cis*-1,2-dimethylolcyclopropane and 0.25 ml. of 80% phosphoric acid was added drop by drop. The distillate was dried over anhydrous magnesium sulfate and distilled. A fraction with the boiling range of 70—80°C was proved to be pure I by gas chromatography (yield, 5%).

*c) By Dehydration using Dimethyl Sulfoxide (DMSO).*—A mixture of 16 g. (0.16 mol.) of *cis*-1,2-dimethylolcyclopropane and 150 g. of DMSO was heated at 160—170°C under refluxing for 18 hr. Then the mixture was distilled below the boiling point of DMSO, the distillate was extracted with petroleum ether, and the organic layer was dried over anhydrous magnesium sulfate. After fractional distillation, a fraction with the boiling range of 60—106°C was obtained; in this fraction I was detected by gas chromatography and infrared absorption (yield, 2%).

*d) By the Simmons-Smith Reaction.*—The procedure was almost analogous to that of the synthesis of norcarane. The yield was only 3—5% (by gas chromatography).

**6,6-Dichloro-3-oxabicyclo[3.1.0]hexane (II).**—*a) Using Chloroform as the Source of Carbene.*—Dichlorocarbene was generated by the usual method[5] from chloroform and potassium *t*-butoxide in an ether solution of 2,5-dihydrofuran. The reaction mixture was then treated with aqueous phosphoric acid and extracted with ether. The ethereal solution was dried over anhydrous magnesium sulfate and distilled to give a fraction with the boiling range of 80—94°C/60 mmHg; from this fraction II was separated by preparative gas chromatography (yield, 7%).

*b) Using Methyl Trichloroacetate as the Carbene Source.*—The procedure was almost analogous to that of ethyl trichloroacetate.[6] The yield of II was 37% (b. p. 81—85°C/25 mmHg) after it had been purified by gas chromatography.

5) W. von E. Doering and A. K. Hoffmann, *J. Am. Chem. Soc.*, **76**, 6162 (1954).

6) J. C. Anderson and C. B. Reese, *Chem. & Ind.*, **1963**, 575.

**6, 6-Diphenyl-3-oxabicyclo[3. 1. 0]hexane (III).**—Diphenyldiazomethane was prepared according to the usual method.[7] To a solution of 8 g. (0.04 mol.) of diphenyldiazomethane in 27 g. (0.4 mol.) of 2,5-dihydrofuran, a catalytic amount of copper powder was added; then the mixture was heated under refluxing for 10 hr. After the excess dihydrofuran, had been removed, the remaining solid was recrystallized from ligroin and proved to be a pyrazoline derivative. Yield, 2.2 g. (21%). M. p. 119.5 —121°C.

Found: C, 77.12; H, 6.21. Calcd. for $C_{17}H_{16}N_2O$: C, 77.25; H, 6.10%.

When this pyrazoline derivative was heated, a rapid evolution of nitrogen occurred. The recrystallization of the residue gave 1.8 g. (92%) of III. M. p. 86.5—87.5°C.

Found: C, 86.40; H, 6.82. Calcd. for $C_{17}H_{16}O$: C, 86.72; H. 6.83%.

**3, 4-(9, 9-Fluorenylidene)tetrahydrofuran (IV).**—Diazofluorene,[8] prepared from 3 g. of the corresponding hydrazone, was dissolved in 5 g. of dihydrofuran and refluxed for 3 days in the presence of a copper catalyst. After dihydrofuran had been evaporated, the residue was recrystallized from benzene and ether successively to afford 0.2 g. (5%) of IV. M. p. 169—170.5°C.

Found: C, 87.42; H, 5.95. Calcd. for $C_{17}H_{14}O$: C, 87.15; H, 6.02%.

**2, 2, 4, 4-Tetramethyl-3-oxabicyclo[3. 1. 0]hexane (V).**—*cis*-1,2-Di($\alpha$, $\alpha$-dimethyl)methylolcyclopropane (V') was prepared by the usual method from methylmagnesium iodide and *cis*-dimethyl 1,2-cyclopropane dicarboxylate. Yield, 44%. M. p. 85.5—87°C.

Found (for V'): C, 68.33; H, 11.76. Calcd. for $C_9H_{18}O_2$: C, 68.31; H, 11.47%.

A mixture of 11 g. (0.07 mol.) of V' and 5 g. (0.035 mol.) of calcined potassium bisulfate was heated in a distilling flask; then the distillate was collected and dried over calcium chloride. Distillation gave 7.5 g. of V (77%). B. p. 91—91.5°C/164 mmHg.

Found (for V): C, 76.83; H, 11.34. Calcd. for $C_9H_{16}O$: C, 77.09; H, 11.50%.

**2, 2, 4, 4-Tetraphenyl-3-oxabicyclo[3. 1. 0]hexane (VI).**—To a Grignard solution prepared from 24 g. (0.15 mol.) of bromobenzene and 3.7 g. (0.15 mol.) of magnesium, 5.0 g. (0.031 mol.) of *cis*-dimethyl 1,2-cyclopropane dicarboxylate in 10 ml. of ether was added drop by drop while the mixture was being refluxed and stirred. After vigorous stirring for two hours, the reaction mixture was hydrolyzed with a saturated aqueous ammonium chloride solution and extracted with ether. After the ether had been evaporated off, 7.5 g. (61%) of *cis*-1,2-di($\alpha$, $\alpha$-diphenyl)methylolcyclopropane (VI') was obtained. M. p. 198—201°C, recrystallized from ethanol.

Found: C, 86.20; H, 6.64. Calcd. for $C_{29}H_{26}O_2$: C, 85.68; H, 6.45%.

A mixture of 1 g. of VI' and 0.3 g. of calcined potassium bisulfate was melted at 130°C under reduced pressure for 5 min. After the gas evolution had ceased, the reaction mixture was crushed and extracted with petroleum ether. The extract was recrystallized from the same solvent, and two kinds of crystals, white block and fine grain, were obtained. The latter was picked up and recrystallized to give 0.2 g. (21%) of VI. M. p. 166—167°C.

Found (for VI): C, 89.60; H, 6.69. Calcd. for $C_{29}H_{24}O$: C, 89.65; H, 6.23%.

The former was 1,1,4-triphenyl-4-benzoylbutene-1. Yield, 0.75 g. (76%). M. p. 129—131°C. No depression in melting point was observed when it was admixed with an authentic sample.

## Summary

Some bicyclic ethers containing a cyclopropane ring, i. e., 3-oxabicyclo[3. 1. 0]hexane derivatives, have been synthesized. Two methods have been used in the syntheses of these compounds. One of them has been the dehydration of *cis*-1, 2-dimethylolcyclopropane derivatives, and the other, the addition of some carbenes to 2, 5-dihydrofuran. The Simmons-Smith method has also been adopted. The NMR spectra of these bicyclic ethers have been examined. The types of their spectra are fairly simple. The chemical shifts and the coupling constant of some protons have also been measured. Attempts to polymerize these bicyclic ethers, unfortunately, have been unsuccessful.

We are indebted to the Fuji Photo Film Company, Ltd., for its financial support. Thanks are also due to Mr. Tsuneaki Hirazima for his skilled help in the measurement of the nuclear magnetic resonance spectra, and to Mr. Mamoru Narui for his assistance in the experimental work.

*Department of Synthetic Chemistry*
*Faculty of Engineering*
*Kyoto University*
*Sakyo-ku, Kyoto*

7) L. I. Smith and K. L. Howard, "Organic Syntheses," Coll. Vol. III, 351 (1956).
8) C. N. Nenitzescu and E. Solomonica, ibid., Coll. Vol. II, 496 (1948).

# A Nuclear Magnetic Resonance Study of the Water in Calcium Silicate Pastes

By Hiroshi OCHIAI, Hitoshi YAMAMURA, Kenji FUKUNAGA,* Iwao MAKI* and Kozaburo WATANABE*

(Received October 7, 1964)

For a better understanding of the setting and hardening processes of cement, it is very significant to study its hydration mechanism. A number of new techniques have been developed in this field.[1-6] However, the application of thermal techniques, such as the methods of vapor pressure and differential thermal analysis, is severely limited, since a sample is degraded by heating. Furthermore, in such techniques as infrared spectra and the dielectric behavior of hydrated water molecules, it is difficult for the measurements to permit a distinct identification of the individual components contributing to the multi-phase hydration system. The use of the proton magnetic resonance technique may be more directly able to resolve these individual components.

The absorption-line width and shape are profoundly influenced by the magnetic environment of the nuclei. The spin-spin relaxation time, $T_2$, is the line-width parameter associated with the life-time of a given nuclear spin state, and a measure of the interactions between the low frequency component of the local field and the nuclei. Thus, these NMR measurements give us much information about the proton in different states and an important clue to the various hydrated products produced during the hydration process.

The application of this technique to the study of the hydration process of cement has been described by only a few authors.[7-9] Kawachi and his co-workers have reported on the relationship between the absorption line and the mechanical strength of portland cement.[8] Watanabe and Sasaki have observed three absorption lines which can be ascribed to the protons of the free, adsorbed and bounded water respectively, in the order of line width,[9] although they have not confirmed the assignment of these absorption lines satisfactorily.

Under these circumstances, we attempted to shed some light on these problems by making proton magnetic resonance studies of $\beta$-di- and tri-calcium silicates, the main constituents of portland cement. Tricalcium silicate, the first hardening constituent of portland cement, has a high hardening rate. $\beta$-Dicalcium silicate, the second, has a low hardening rate.

It has been supposed that these calcium silicates react with added water, and that then some hydrates contributing to the hardening process are produced as follows.[10]

$$3CaO\cdot SiO_2+(n+2)H_2O = CaO\cdot SiO_2\cdot nH_2O+2Ca(OH)_2$$

$$2CaO\cdot SiO_2+(n+1)H_2O = CaO\cdot SiO_2\cdot nH_2O+Ca(OH)_2$$

$$aCa(OH)_2+bSiO_2\cdot mH_2O = aCaO\cdot bSiO_2\cdot nH_2O$$

In this work, we will measure the spin-spin relaxation time, $T_2$, and the temperature dependence of the line width for the two calcium silicates pastes mentioned above; we will also discuss the hydration process for hardening by comparing its data with the data involving $Ca(OH)_2$ powder, $Ca(OH)_2+H_2O$ paste, $SiO_2+H_2O$ paste, and water.

## Experimental

The $\beta$-di- and tri-calcium silicates used in this investigation were prepared from a mixture of calcium carbonate and silicon dioxide by heating it at 1550°C several times; they were confiremed to be $Ca_3SiO_5$ and $\beta$-$Ca_2SiO_4$, as had been reported by Sasaki, by X-ray analysis.[11] $\beta$-$Ca_2SiO_4$ is stabilized by adding $Na_2O$.

* K. Fukunaga, I. Maki and K. Watanabe, Central Research Laboratories, Ube Industries, Ltd., Ube, Yamaguchi.

1) T. C. Powers and T. L. Brownyard, *Proc. Am. Concrete Inst.*, **43**, 101 (1947).
2) W. Lerch and R. H. Bogue, *Proc. Am. Testing Materials*, **50**, 1235 (1950).
3) H. Woods and H. H. Steinour, *Proc. Am. Concrete Inst.*, **3**, 195 (1931).
4) L. Jesser, *Zement*, **18**, 158 (1929).
5) F. Krauss and G. Jörns, ibid., **20**, 314 (1931).
6) T. Sasaki, K. Watanabe and I. Maki, *Semento Gijutsu Nempo*, **16**, 109 (1962).
7) C. M. French and J. F. Warder, *J. Appl. Chem.*, **9**, 561 (1959).
8) K. Kawachi, M. Murakami and E. Hirahara, *Bull. Faculty of Eng., Hiroshima Univ.*, **4**, 95 (1955).
9) K. Watanabe and T. Sasaki, *Zement-Kalk-Gips*, **50**, 101 (1961).
10) S. Brunauer, J. C. Hayes and W. E. Hass, *J. Phys. Chem.*, **58**, 279 (1954).
11) T. Sasaki, *J. Sci. Hiroshima Univ.*, **A23**, 425 (1960).

The calcium silicate samples employed in the measurements were of a form of paste prepared with a solid-to-water ratio of 0.4 in weight. The calcium hydroxide and silicon dioxide samples were also paste and had the same mixing ratio. Another calcium hydroxide sample was powder which had been dried for several hours in a vacuum at 80°C. All the samples were sealed in glass tubes about 10 mm. in diameter in order to prevent the vaporization of the added water, and then stored in an air-conditioned room at 20°C. Line-width measurements were carried out from room temperature to −160°C by making use of liquid nitrogen, while $T_2$-measurements were made at room temperature.

The apparatuses used were Pound-Watkins- and Bridge-type broad-line NMR spectrometers at 30 Mc./sec., and $T_2$-measurements, a spin-echo NMR spectrometer at 30 Mc./sec., manufactured by the Japan Electron Optics Laboratry Co., Ltd.

## Results

In the NMR absorption spectra of the samples of the β-dicalcium silicate, which have various storage periods at room temperature, a single sharp absorption line, the width of which corresponds to the modulation amplitude, was observed at nearly every room temperature. From the results obtained here, it might be considered that real absorption line width of the samples is very narrow, and that a modulation broadening takes place. As the measuring temperature was lowered, the absorption line became broader due to the superposition of more than two absorption lines in a portion of the wing. The temperature dependence of the maximum slope width ($\Delta H_{m.s}$) of the absorption line for this sample is shown in Fig. 1.

At −70°C, the absorption line became more complex; it had three peaks with widths of about 1, 10 and 17 gauss, hereafter to be referred as the narrow, medium and broad absorption lines respectively. In the lower temperature range, the narrow absorption line, 1 gauss wide, became wider and could not be observed, but the width of the other two remained unchanged down to −160°C. In spite of the different storage periods of the samples, the same temperature dependence was observed. The same result was also obtained in the case of the tricalcium silicate paste.

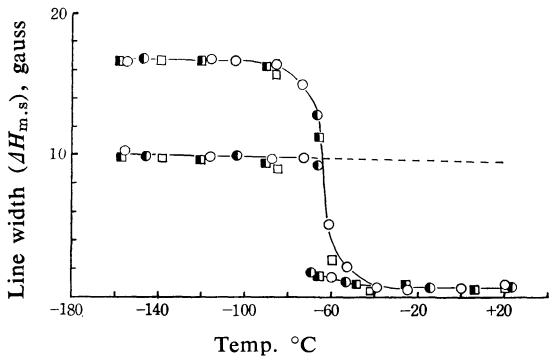



Fig. 1. Line width versus temperature curve for β-di- and tri-calcium silicate.
○ β-$Ca_2SiO_4$ stored 1 day
◑ β-$Ca_2SiO_4$ stored 20 days
□ $Ca_3SiO_5$ stored 1 day
◧ $Ca_3SiO_5$ stored 20 days

In order to clarify the influence of the storage period on the reacted water, we determined the ratio of the areas of the peaks in the decomposed absorption curves, assuming the gaussian curve for absorption line shape and a proportionality between the area of the absorption line and the fraction of protons in the various hydrated states. The narrow line is much affected by modulation broadening and so is not included in Table I, which gives the results for the broad and medium absorption lines, though the decomposition of the absorption line was not simple.

Table I. The ratio of the decomposed absorption lines for β-dicalcium silicate paste at −70°C

| Storage periods | 1 day | 20 days |
|---|---|---|
| The broad line | 23% | 7.8% |
| The medium line | 77% | 92.2% |

Furthermore, in order to clarify the details of the storage effect, the spin-spin relaxation time, $T_2$, was measured at room temperature. The relation of the storage period to $T_2$ in each case of β-di- and tri-calcium silicate pastes is shown in Fig. 2. As this figure shows, the $T_2$-value of β-dicalcium silicate paste decreases very slowly, whereas that of tricalcium silicate decreases very rapidly, as the storage period increases.

To make clear what proton states correspond

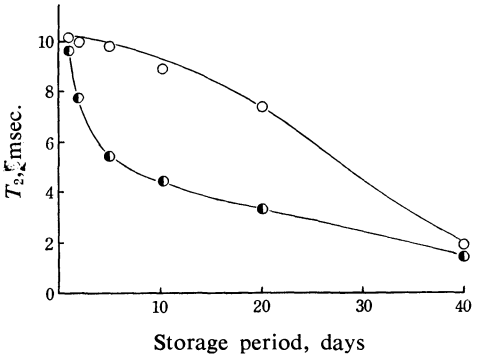



Fig. 2. $T_2$-Value versus storage period at room temperature.
○ β-$Ca_2SiO_4$ ◑ $Ca_3SiO_5$

to the three absorption lines observed in the low temperature region, we carried out broad-line NMR measurements of $Ca(OH)_2$ powder, $Ca(OH)_2+H_2O$, $SiO_2+H_2O$ paste, and water. The results are shown in Fig. 3.

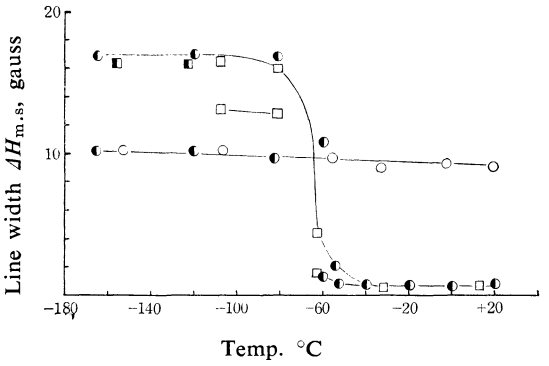



Fig. 3. Line width versus temperature curve for various reference samples.
○ $Ca(OH)_2$ powder ◐ $Ca(OH)_2$ paste
□ $SiO_2$ paste ◧ $H_2O$

The absorption line of water has a width of 16.5 gauss in the low temperature range, a value which is compatible with the results reported by other authors.[12,13]

Calcium hydroxide powder gives an absorption line 9.5 gauss wide, even at room temperature. On the other hand, the paste sample gives the same sharp absorption line as the calcium silicate pastes at room temperature, and also gives the superimposed absorption lines, with widths of 10 and 17 gauss, in the low temperature range.

The absorption line of silicon dioxide paste shows a temperature dependence similar to that of both calcium silicates and calcium hydroxide paste, with line widths of 13 and 17 gauss in the low temperature range.

It is of interest that an absorption line 17 gauss wide is observed in all the paste samples and water studied in this work.

## Discussion

As shown in Fig. 1, the same temperature dependence of the absorption line width was observed for each paste of the two calcium silicates, even when they were stored for different periods. In agreement with the assumption that both silicates form a similar hydrated gel in the hydration process of cement,[10] this result may indicate that the two calcium silicates form similar hydration products.

Table I shows the ratio of the area of the medium absorption line to that of the broad line for storage periods of 1 day and 20 days. The ratio seems to represent the amount of water in the hydrated gel state and in the nonhydrated state, because the area of the medium line increases as the storage period becomes longer. These results show that the hydration process of the samples can be followed from the temperature dependence of the line width. However, it is difficult to investigate their hydration process by the broad line method without setting the samples at a lower temperature, because all the samples give a single sharp absorption line in the room temperature range, regardless of the kinds of silicate and the storage periods of the pastes.

The $T_2$-value obtained at room temperature may be ascribed to some relaxation mechanisms of the protons of the adsorbed or free water.[14] It is a measure of the molecular motion in the corresponding states in which the added water suffers restriction by the ions eluted in the hydration process. Therefore, the change in $T_2$-value may be correlated with the hardening rate of calcium silicates. Namely, $T_2$-value decreases with the progress of hardening. The result in Fig. 2 corresponds to the facts that tricalcium silicate is the first hardening constituent of portland cement and has a high hardening rate, while $\beta$-dicalcium silicate is the second one and has a low hardening rate. The fact that both samples, when stored for forty days, have the same $T_2$-value, 2.5 msec., may be considered, from the viewpoint of nuclear magnetic resonance, to show that the added water is restricted to a similar extent in both the samples.

Let us now consider the three absorption lines observed in the low temperature range. The broad absorption line observed in the calcium silicate pastes is ascribed to the protons in a more immobile state of free water; thus, they do not take part in hydration directly. This absorption line corresponds to the one hitherto ascribed to the protons of the hydrated water in cement paste by some of the present authors.[8] It it reasonable to infer, however, that the broad absorption line is associated with the protons of the free water with an ice structure at the lower temperature, as is shown in the data on ice given by Bloembergen et al.,[12] by Kume[13] and by us.

The medium absorption line, 10 gauss wide at a low temperature, can be ascribed to the protons of a solid chemical structure, such as hydroxyl ion or hydrated water, formed by the reaction between the silicates and added water. This medium absorption line could not

12) N. Bloembergen, E. M. Purcell and R. V. Pound, *Phys. Rev.*, 73, 679 (1948).
13) K. Kume, *J. Phys. Soc. Japan*, 15, 1493 (1960).
14) T. Shaw and R. Elsken, *J. Chem. Phys.*, 21, 565 (1953).

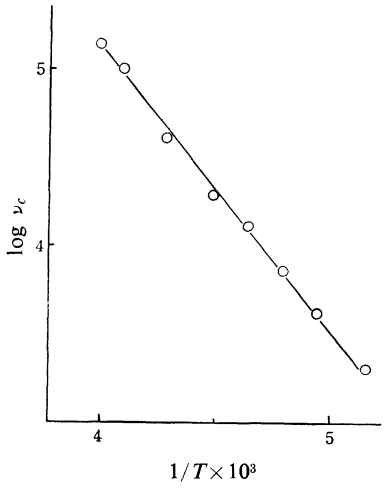



Fig. 4. The temperature dependence of the correlation frequency for the broad absorption line.

be observed at room temperature because the signal of unhydrated water is highyl intense at room temperature. However, this line is considered to appear even in the room temperature range, as is shown in Fig. 1 with an extrapolated broken line.

The narrow absorption line observable at temperatures as low as $-70°C$ may be associated with the freely-moving protons in ice, because the lattice defects in ice crystals produced by various ionic impurities would facilitate the motion of protons, as has been reported by Kume.[13]

An attempt has been made to relate the absorption line width to the motional correlation time of the protons by means of the B.P.P. relaxation theory.[12] The activation energy, $V$, for the motion of the proton is estimated by applying Eyring's theory of rate process as follows;[15]

$$\nu_c = \nu_0 \exp(-V/RT)$$

where $\nu_c$ is the correlation frequency. Figure 4 shows the temperature dependence on $\nu_c$ for the broad absorption line. The slope yields $V=6.53$ kcal./mol. This is in agreement with the activation energy for the proton motion in ice,[13] and supports the abovementioned assignment of the absorption lines.

The authors wish to express their appreciation to Mr. Ichiro Murakami for his valuable guidance and discussions on this work.

*Department of Chemistry*
*Faculty of Science*
*Hiroshima University*
*Hiroshima*

15) S. Glasstone, K. J. Laidler and H. Eyring, "Theory of Rate Processes," McGraw-Hill, New York (1948), p. 548.

# A New Method to Determine Relative Surface Area by Gas Chromatography. I

By Yoshio KUGE and Yozaburo YOSHIKAWA

(Received October 8, 1964)

Two kinds of methods have been employed to determine the surface area of an adsorbent, the common B.E.T. static method, and the B.E.T. flow method* using gas chromatography.

During the investigation of the relation between the sample size and the peak shape, using the same column packing in gas chromatography we found that the displacement point from monolayer- to multilayer-adsorption appeared in the change in peak shape. Therefore, the relative surface area of adsorbent per gram was calculated from the sample size at the displacement point. By this procedure, we determined the relative surface area of a copper complex compound, $Cu(Py)_2(NO_3)_2$.** The results obtained will be discussed.

When this method can be used, the surface area can be more easily determined compared with the results obtained with the methods mentioned above.

## The Estimation of Relative Surface Area

In general, the relation between the sample size and the retention time can be described

* For example, F. M. Nelson and F. T. Eggertsen, *Anal. Chem.*, **30**, 1387 (1958).

** This substance has been found to be a new adsorbent for the analysis of hydrocarbons in gas chromatography by L. B. Rogers and A. G. Altenau (*Anal. Chem.*, **35**, 915 (1953)).

as follows: When a Langmuir-type adsorption isotherm is established, it is observed that the larger the sample size, the shorter the retention time. In the case of an anti-Langmuir-type adsorption isotherm, the larger the sample, the longer the retention time. The shapes of the peak in both cases are shown in Fig. 1.

When the two types of adsorption isotherms are combined, the second type of B.E.T. adsorption isotherm will be obtained, as Fig. 2 shows. This expectation was realized in our experiments. When the sample size is small, the peak shape is symmetrical. As the sample size is increased, however, the peak shape

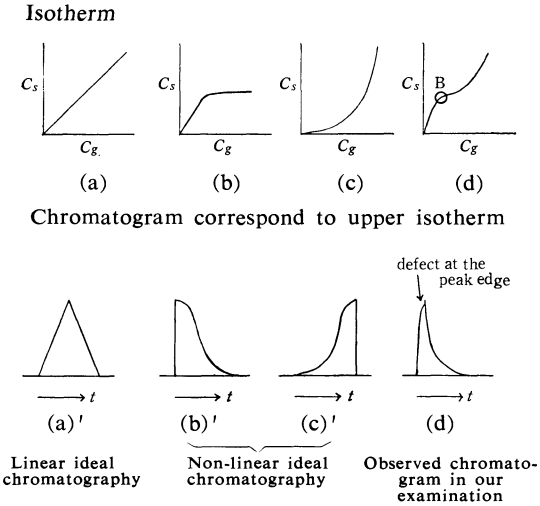



Fig. 1. The relation between peak shapes and the adsorption isotherms.

$C_s$ Concentration in stationary phase
$C_g$ Concentration in moving phase
$t$ Time

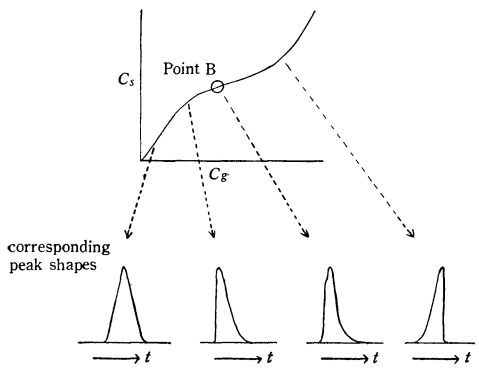



Fig. 2. The second type of B.E.T. adsorption isotherm and corresponding peak shapes.

$C_s$ Concentration in stationary phase
$C_g$ Concentration in moving phase
$t$ Time

acquires a sharp front and a diffuse tail, and a defect at the front side of the peak top; then it obtains a diffuse front and a sharp tail. That the peak begins to have a defect at the front side of the top indicates the point of the displacement from monolayer- to multilayer-adsorption. This point corresponds to the B-point of the B.E.T. II-type adsorption isotherm.

Therefore, the relative surface area of the adsorbent covered with a monolayer of an adsorbate at the displacement point may be calculated by Eq. 1.

$$S=\frac{V}{V_m}\cdot N_A\cdot s \tag{1}$$

where

$S$: the surface area of the adsorbent ($cm^2$)
$V$: the volume of the adsorbate which forms the monolayer (cc.)
$N_A$: Avogadro's number
$s$: the surface area that was occupied by one molecule of the adsorbate ($cm^2$)
$V_m$: the molecular volume (cc.)

Provided the sample is adsorbed in the form of the closest packing of the face-centered cubic lattice on the adsorbent, the surface area ($s$) is expressed as follows:[1]

$$s=\frac{6}{\sqrt{3}}\left(\frac{M}{4\sqrt{2}N_A\cdot D}\right)^{2/3} \tag{2}$$

where

$D$: the density of the adsorbate at the adsorbed temperature
$M$: the molecular weight

The surface area must be reduced to that per gram of the adsorbent, so the authors assumed the next Eq. 3:

$$S_g=\frac{S}{W\cdot\dfrac{w}{\left(\dfrac{a\cdot L}{F}\right)}}=S\left(\frac{1}{W}\cdot\frac{a}{w\cdot F}\cdot L\right) \tag{3}$$

where

$S_g$: the surface area per gram of the adsorbent ($cm^2$/g.)
$W$: the weight of the adsorbent (g.)
$F$: the flow rate of the carrier gas (cc./min.)
$L$: the column length (cm.)
$a$: the cross section area of the column ($cm^2$)
$w$: the peak width

and the term $(aL/F)$ means the time required for the carrier gas to pass through the column.

1) P. H. Emmett and S. Brunauer, *J. Am. Chem. Soc.*, **59**, 1553 (1937).

## Apparatus and Materials

A Yanagimoto gas chromatograph GCG-2 was employed.

The detector used was of the thermal-conductivity type with a tungsten filament. The column was made of U-shaped stainless steel and was 2 m. long and 5 mm. in inside diameter. The flow rate of the carrier gas was measured by a soap-film flow meter.

Di-pyridine-copper nitrate $Cu(Py)_2(NO_3)_2$, used as an adsorbent, was prepared through $Cu(Py)_4(NO_3)_2$ according of Pfeiffer's method.[2] The blue-violet crystals of $Cu(Py)_4(NO_3)_2$ were sorted with a 32—48 mesh and then heated at 100°C for six hours to give a light blue di-pyridine salt.

The change from tetrapyridine salt to di-pyridine salt was observed at 70—83°C by means of the differential thermal analysis of pyridine copper salt, and the identity of the dipyridine salt produced was confirmed by the quantitative analysis of pyridine, that is, by the measurement of the weight change of the sample and by the ultraviolet absorption spectrometric method.*

## Results

Benzene, carbon tetrachloride, cyclohexane and *n*-hexane were used as adsorbates.

The heats of the adsorption of these substances on $Cu(Py)_2(NO_3)_2$ were found to be 8.4, 8.1, 8.4 and 8.0 kcal./mol. respectively, in the temperature range from 30 to 60°C,[3] suggesting the physical adsorption.

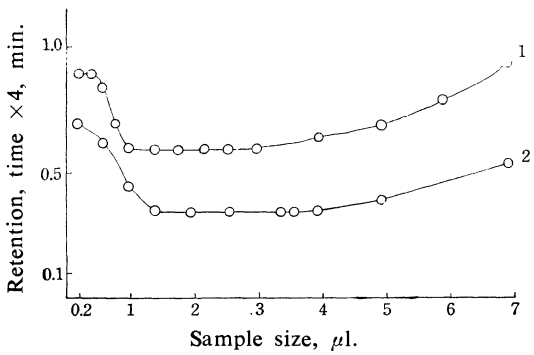



Fig. 3. The change of retention times with increasing sample sizes.

1 Benzene
2 Carbon tetrachloride
cell current 150 mamp, column inlet pressure 0.2 kg./cm², cell temp. 100°C, carrier gas $H_2$, 57.7 cc./min., inlet temp. 118°C, column temp. 50°C, adsorbent $Cu(Py)_2(NO_3)_2$, 32—48 mesh 29.3 g.

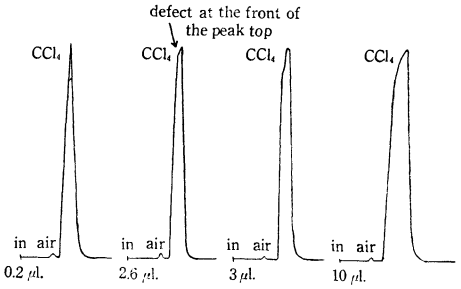



Fig. 4. The change of peak shapes with increasing sample sizes.

cell current 150 mamp., column inlet pressure 0.2 kg./cm², cell temp. 80°C, inlet temp. 118°C, carrier gas $H_2$, 41.7 cc./min. (22.5°C), adsorbent $Cu(Py)_2(NO_3)_2$ 32—48 mesh 29.3 g., column temp. 48°C

The relation between the sample size and the retention time in the cases of benzene and carbon tetrachloride is shown in Fig. 3, while the change in peak shape in the case of carbon tetrachloride is shown in Fig. 4.

The displacement point from monolayer- to multilayer-adsorption may be affected by the flow rate of the carrier gas, the column temperature and the properties of the adsorbate.

First, the relation between the flow rate of the carrier gas and the displacement point was examined.

When the flow rate was increased up to 60 cc./min., the peak width became narrow, but the displacement point of the peak shape showed no change. On the other hand, the flow rate was decreased less than 20 cc./min., the peak changed to a symmetrical shape under the influence of axial dispersion,[4,5] and the displacement point could not be found. Therefore, the experiments were carried out in the flow rate range from 20 to 60 cc./min.

Next, the relation between the sample size at the displacement point and the column temperature was investigated. In the case of cyclohexane, the sample size was found to be 1.4 μl. when the temperature was below 50°C, while the sample size was as large as double that when the temperature rose above 50°C, as is shown in Table I. The results suggest that the relative surface area may be calculated as too large when the temperature rises above 50°C it also calls into question the assumption that the sample molecules are adsorbed in the

2) P. Pfeiffer and V. Pimmer, *Z. anorg. Chem.*, **48**, 98 (1906).
* This method was discovered by Dr. Isao Masuda.

3) Y. Kuge and Y. Yoshikawa, *Sci. Rep. Osaka Univ.*, **12**, 9 (1963).
4) G. Houghton, *J. Phys. Chem.*, **67**, 84 (1963).
5) R. D. Oldenkamp and G. Houghton, ibid., **67**, 597 (1963).

Table I. The correlation of sample size with the temperature at the displcement point

Adsorbate : cyclohexane

| Column temp. °C | Flow rate cc./min. | Sample size $\mu$l. |
|---|---|---|
| 32 | 57.7 | 1.4 |
| 46 | 55.6 | 1.4 |
| 50.5 | 56.6 | 2.4 |

the form of the closest packing of the face-centered cubic lattice at a higher temperature.

At about the boiling points of adsorbates (near 80°C), the peak changed to a symmetrical shape and the displacement point was hardly observed. The range of the temperature applicable for the determination of the relative surface area by this method has not yet been generalized.

With such precautions, the relative surface area of adsorbents was calculated, according to Eq. 3, on the basis of the results obtained when the column temperature was 50°C and the flow rate of the carrier gas was 60 cc./min. The values obtained are listed in Table II.

As Table II shows, the values of the relative surface area were found to be nearly equal for planer and for spherical molecules, such as benzene, carbon tetrachloride and cyclohexane, while a larger value was found for chain molecules such as *n*-hexane. Similar

Tale II. The relative surface area of 29.3 g. of $Cu(Py)_2(NO_3)_2$ for several adsorbates

| Adsorbate | Sample size $\mu$l. | $s \times 10^{16}$ cm$^2$ | Relative surface area m$^2$/g. | Shape of molecule |
|---|---|---|---|---|
| Benzene | 2.7 | 30.6 | 1.75 | Planar |
| Carbon tetrachloride | 2.6 | 33.1 | 1.68 | Spherical |
| Cyclohexane | 2.5 | 34.9 | 1.50 | Planar |
| *n*-Hexane | 5.7 | 38.7 | 3.44 | Chain |

results have been obtained by the ordinary B.E.T. static method.

In this report, we have used the term "relative surface area" instead of "surface area" because the values obtained have not been compared to those obtained by the ordinary B.E.T. method.

The determination of the absolute surface area by static and dynamic B.E.T. methods using gas chromatography is now under way.

The authors wish to express their hearty thanks to Dr. Akitsugu Nakahara and Miss Kimiko Arita for their criticism, and to Dr. Matsuji Takebayashi for his encouragement throughout this work.

*Institute of Chemistry*
*College of General Education*
*Osaka University*
*Toyonaka, Osaka*

# Polyesters Containing Carbazole Rings in the Main Chain. I. Syntheses of Diacylcarbazoles and Carbazoledicarboxylic Acids*

By Yoshio NAGAI and Chin-Chuan HUANG

(Received October 13, 1964)

Despite the numerous heterocyclic compounds such as thiophene-, furan-, and pyridinedicarboxylic acids that have been claimed to be useful in the preparation of high melting polyesters suitable for fibermaking, the carbazole derivatives have never been in much demand as starting materials for such a purpose.

To prepare polyesters containing carbazole rings in the main chains, the authors first synthesized a series of carbazole derivatives and several carbazoledicarboxylic acids by oxidizing the corresponding diacylcarbazoles.

Descriptions appearing in the literature on the synthesis of 3, 6-diacetylcarbazole (I) usually give neither exact yields nor information on 3-acetyl- or 9-acetylcarbazoles which has been shown to be one of the main acylation products. By carefully following the methods of Plant et al.,[1, 2] we have found that under the described conditions, I was obtained only in poor yields, while a large amount of monoacetylcarbazole was isolated. The experimental data also indicated that at higher reaction

* A part of this paper was presented at the 17th Annual Meeting of the Chemical Society of Japan, Tokyo, March, 1964.

1) S. G. P. Plant, K. M. Rogers and S. B. C. Williams, *J. Chem. Soc.*, **1935**, 741.
2) D. R. Mitchell and S. G. P. Plant, ibid., **1936**, 1295.

temperatures, acylation of carbazole tended to give more 9-acetylcarbazole, though carbazole is considered to resemble a secondary aromatic amine in chemical reactivity, with substitution groups preferably entering into para positions to the nitrogen. In the syntheses of 3,6-diacetyl-9-alkylcarbazoles, however, the sole product was the disubstituted 9-alkylcarbazole.

Of the three acylating agents employed, acetyl bromide appeared to be best suited for the preparation of diacetylcarbazoles.

Oxidation of 3,6-diacetyl- and 3,6-diacetyl-9-alkylcarbazoles with an appropriate amount of sodium hypochlorite solution, as shown in Table III, yielded almost quantitatively carbazole-3,6-dicarboxylic and 9-alkylcarbazole-3,6-dicarboxylic acids, previously reported as being obtained only in much lower yields via other reactions.[1-3]

TABLE I. MOLECULAR PROPORTIONS OF CATALYST AND ACETIC ANHYDRIDE PER MOLE OF CARBAZOLE*

| $AlCl_3$* | $(CH_3CO)_2O$* | Yield, % | | |
|---|---|---|---|---|
| | | a | b | c |
| 4.2 | 2.3 | 6.4 | 12.4 | d |
| 5.3 | 2.8 | 14.1 | 4.9 | 11.3 |
| 5.3 | 4.6 | 0.2 | 15.6 | 4.9 |
| 4.2 | 2.3 | — | — | 23.2** |
| 6.3 | 2.3 | 14.8 | 5.2 | 10.5 |

a, 3,6-Diacetylcarbazole; b, 3-Acetylcarbazole; c, 9-Acetylcarbazole; d, Isolation procedure was omitted.; ** Reaction temperature was 5°C.

TABLE II. MOLECULAR PROPORTIONS OF CATALYST AND ACETYL HALIDE PER MOLE OF CARBAZOLE*

| $AlCl_3$* | $CH_3COCl$*1 or $CH_3COBr$*2 | Yield, % | |
|---|---|---|---|
| | | a | b |
| 2.1 | 2.1[1] | 33.5 | 19.1 |
| 2.1 | 2.1[1] | 34.1** | 15.4** |
| 2.1 | 2.0[2] | 6.7 | 4.7 |
| 2.1 | 2.0[2] | 8.4** | c |

a, 3,6-Diacetylcarbazole; b, 9-Acetylcarbazole; c, Isolation procedure was omitted.; ** Reaction time was two hours.

TABLE III. SYNTHESES OF 9-ALKYLCARBAZOLE-3,6-DICARBOXYLIC ACIDS

| a g. | b cc. | Pyridine cc. | Yield % |
|---|---|---|---|
| 2.5* | 22 | 15 | 95 |
| 2.5* | 25 | 15 | 98 |
| 2.5** | 25 | 18 | 91 |
| 2.5** | 30 | 18 | 99 |

a, 3,6-Diacetyl-9-alkylcarbazole (* 9-ethyl; and ** 9-methyl); b, Sodium hypochlorite solution, 6 N.

3) H. Gilman and S. M. Spatz, *J. Am. Chem. Soc.*, **63**, 1553 (1941).

## Experimental

**3,6-Diacetylcarbazole (I).**—A mixture of 6.0 g. of carbazole (m. p. 245°C), 9.0 g. of acetyl bromide, 50 cc. of dry carbon disulfide, and 10 g. of pulverized aluminum chloride was refluxed at the boiling point of the solvent for an hour and then the solvent was distilled off. By treating the residue with ice-dilute hydrochloric acid, I was obtained as a brown solid, which gave almost colorless crystals, 3.0 g.; m. p. 235—237°C, after two recrystallizations from ethanol (decolorizing charcoal added). The reaction of carbazole and acetyl chloride, however, gave I in much poorer yields in the presence of the same catalyst. As shown in Table I, the reaction of 60 g. of carbazole with 105 g. of acetic anhydride at 0 ± 1°C for 6 hr. with stirring also afforded I in 14.1% yield. Use of about two molecular proportions of aluminum chloride per mole of anhydride as a catalyst at 0°C gave 3-acetyl- and 9-acetylcarbazoles besides I, whereas at 5°C the reaction led mainly to 9-acetylcarbazole. An increase in the amount of catalyst, as recommended by Groggins and Nagel,[4] did not increase the yields of I. Prolonging the reaction time also did not cause much improvement of the yield; even the yield from a reaction of 6 hr. compared favorably with that of 8 hr. or longer. Acetylation of carbazole with acetic anhydride in the presence of 3.5 mol. of aluminum chloride gave more 9-acetylcarbazole.

Found: C, 76.46; H, 5.16; N, 5.45. Calcd. for $C_{16}H_{13}O_2N$: C, 76.55; H, 5.17; N, 5.58%.

During crystallization of the crude acylation product from ethanol, 3-acetylcarbazole, m.p. 166—168°C, came out first; concentration of the filtrate afforded I. After removal of the solvent by distillation, the residue, temperature range of m. p. 69—115°C, was recrystallized from methanol to give 9-acetylcarbazole as light yellowish white crystals, m. p. 77—78°C. When a solution of 9-acetylcarbazole in benzene was passed through a column (1.8 cm. inner diameter) packed with alumina (15 cm. in height), and the column successively eluted with benzene, 9-acetylcarbazole was recovered as carbazole.

**Carbazole-3,6-dicarboxylic Acid (II).***—A solution of 5 g. of I in 30 cc. of pyridine was poured into a flask containing 100 cc. of 5% aqueous sodium hydroxide solution. This mixture was kept at 20°C while 44 cc. of 6 N sodium hypochlorite solution was added with stirring. The reaction mixture was stirred for an additional 100 min. and the excess of oxidizing agent decomposed by pouring the product into sodium bisulfite solution, after unaltered I had been removed by filtration. On addition of hydrochloric acid to the filtrate, II came out as a white precipitate, 5.1 g., m. p. above 375°C (decomp.)

Found: C, 65.51; H, 3.63; N, 5.33. Calcd. for $C_{14}H_9O_4N$: C, 65.84; H, 3.55 N, 5.49%.

**Diethyl Carbazole-3,6-dicarboxylate (III).**—A suspension of 10 g. of II in a mixture of 200 cc. of dry ethanol and 30 cc. of concentrated sulfuric acid was refluxed with stirring for 6 hr. and then

4) P. H. Groggins and R. H. Nagel, *Ind. & Eng. Chem.*, **1934**, 26.

* According to the modified method of Uematsu, unpublished paper, this laboratory.

the excess of ethanol removed by distillation. The residue was treated with dilute aqueous sodium carbonate solution to dissolve unchanged acid, and the insoluble residue was recrystallized from ethanol (decolorizing charcoal added) to give III as almost colorless crystals, 8.0 g., m. p. 206—207°C.

Found: C, 69.32; H, 5.49; N, 4.38. $C_{18}H_{17}O_4N$ requires C, 69.47; H, 5.51; N, 4.49%.

**3, 6-Diacetyl-9-methylcarbazole (IV) and 3, 6-Diacetyl-9-ethylcarbazole (V).**—A solution of 1 g. of I in 30 cc. of acetone and aqueous potassium hydroxide (1.5 g. of potassium hydroxide in 1 cc. of water) was refluxed with stirring for 5 min.; then 2.2 g. of dimethyl sulfate was added and the mixture was allowed to react at 35°C for 10 min. The reaction product was poured into 300 cc. water to give a white precipitate, 1.1 g., m. p. 198—200°C.

Found: C, 76.85; H, 5.59; N, 5.23. Calcd. for $C_{17}H_{15}O_2N$: C, 76.98; H, 5.66; N, 5.28%.

IV was also obtained by reaction of 9-methylcarbazole with an acyl halide, such as acetyl chloride or acetyl bromide, in the presence of aluminum chloride. A mixture of 14 g. of I in 280 cc. of acetone with aqueous potassium hydroxide (21 g. of potassium hydroxide in 10 cc. of water) and diethyl sulfate was stirred at room temperature for 10 min.; subsequent dilution of the product with water precipitated V, 15 g., m. p. 181—182°C.

Found: C, 77.16; H, 5.89. Calcd. for $C_{18}H_{17}O_2N$: C, 77.42; H, 6.09%.

V was also synthesized from the reaction of 9-ethylcarbazole with acyl halides, such as acetyl chloride or acetyl bromide, using aluminum chloride as a catalyst. Acetyl bromide reacted with 9-ethylcarbazole and gave V usually in higher yields than did acetyl chloride.

**9-Methylcarbazole-3, 6-dicarboxylic Acid (VI).**—A solution of 1 g. of IV in 10 cc. of pyridine was poured into 20 cc. of 5% aqueous sodium hydroxide solution, and the temperature of the mixture maintained at 20°C while 12 cc. of NaOCl solution (6 N) was added; the reaction mixture was then stirred for one hour and forty minutes at 25°C. Unchanged material was filtered off and the filtrate treated with sodium bisulfite solution. Addition of hydrochloric acid to the filtrate precipitated VI as a white powder, 1.0 g., m. p. above 395°C (decomp.).

Found: C, 66.78; H, 4.21. $C_{15}H_{11}O_4N$ requires C, 66.92; H, 4.09%.

**Diethyl 9-Methylcarbazole-3, 6-dicarboxylate (VII).**—After a suspension of 1.0 g. of VI in a mixture of 25 cc. of ethanol and 2.5 cc. of concentrated sulfuric acid had been refluxed for 6 hr. with stirring, the excess ethanol was removed by distillation. The residue was then treated with 5% aqueous sodium carbonate solution to dissolve unchanged acid and the mixture filtered. The residue after crystallization (decolorizing charcoal added) yielded VII as light yellowish white crystals, 0.7 g., m. p. 163—165°C.

Found: C, 70.18; H, 5.61. Calcd. for $C_{19}H_{19}O_4N$: C, 70.16; H, 5.85%.

**9-Ethylcarbazole-3, 6-dicarboxylic Acid (VIII).**—A mixture of 1.0 g. of V in 7 cc. of pyridine and 200 cc. of 5% sodium hydroxide solution was treated with 14 cc. of 3 N sodium hypochlorite solution at 20°C under stirring for one hour and forty minutes. The resulting reddish orange solution was filtered to remove any unaltered V and discharged into sodium bisulfite solution. VIII was obtained as a white precipitate upon addition of hydrochloric acid. Yield, 1.0 g., m. p. above 380°C (decomp.).

Found: C, 67.22; H, 4.63. $C_{16}H_{13}O_4N$ requires C, 67.56; H, 4.57%.

**Diethyl 9-Ethylcarbazole-3, 6-dicarboxylate (IX).**—The procedure for the preparation of IX was similar to that used in the synthesis of III. Yield, 83%; melting point after crystallization from ethanol (decolorizing charcoal added), 173—174°C.

Found: C, 70.95; H, 6.18. Calcd. for $C_{20}H_{21}O_4N$: C, 70.80; H, 6.19%.

## Summary

Acetylation of carbazole with acetyl halide or acetic anhydride gave both monoacetyl- and diacetylcarbazoles. Several carbazoledicarboxylic acids were prepared in quantative yields by oxidizing the corresponding diacetylcarbazoles.

Acknowledgment is made for the kind cooperation of the Nihon Kayaku Company and the Yahata Kagaku Company in supplying carbazole for this study. The authors also wish to thank Associate Professor Nobuyuki Goto for valuable suggestions and Mr. M. Ishida of this laboratory for experimental help.

*Institute of Industrial Science*
*The University of Tokyo*
*Azabu, Tokyo*

# Reaction of Bis(acetylacetonato)copper(II) with Bromine*

By Yukio NAKAMURA and Shinichi KAWAGUCHI

(Received October 20, 1964)

The halogenation of β-dicarbonyl compounds such as acetylacetone and ethyl acetoacetate proceeds in two steps:[1]

$$R_1COCH_2COR_2 + X_2 = R_1COCHXCOR_2 + HX$$

$$R_1COCHXCOR_2 + X_2 = R_1COCX_2COR_2 + HX$$

These reactions were found to be of first order with respect to the β-dicarbonyl compound, independent of the halogen concentration, and catalyzed by bases in general.[2] Bell and his collaborators analyzed these reactions in aqueous solution and determined the catalytic constants of various bases.[3]

Pedersen investigated the bromination of ethyl acetoacetate in aqueous solution and found that the first of the two consecutive reactions was catalyzed by copper(II)[4] and other divalent metal ions.[5] The intermediate metal chelate of the keto-form of the ester was assumed to transfer a proton to the catalyst base more easily than the substrate itself does. However, details of the succeeding reaction, that is, the bromination of the normal metal enolate ester are not yet clear. Furthermore, the reason why the second bromination step is not catalyzed by these metal ions is not certain at all. The present paper reports reactions of bromine with copper(II) chelates of acetylacetone and 3-bromoacetylacetone which were studied for the purpose of obtaining some information about these points.

## Experimental

**Materials.** — Bis(acetylacetonato)copper(II) was prepared[6] by adding an ammoniacal solution of copper(II) acetate to an ethanolic solution of acetylacetone and was recrystallized from chloroform. (Found: Cu, 23.86; C, 45.90; H, 5.38%)

Bis(3-bromoacetylacetonato)copper(II) can be prepared either by the reaction between 3-bromoacetylacetone and copper(II) ion,[7] or by bromination of bis(acetylacetonato)copper(II) with *N*-bromosuccinimide.[8] We adopted the former route, but prepared 3-bromoacetylacetone in higher purity by the reaction of bis(acetylacetonato)copper(II) with an appropriate quantity of bromine. To a vigorously stirred solution of 33 g. (0.125 mol.) of bis(acetylacetonato)copper(II) in 1.3 l. of chloroform, 250 ml. of a chloroform solution of bromine (0.76 mol./l.; 0.19 mol. bromine) was added dropwise from a burette. The precipitate, copper(I) bromide, was filtered off and most of the solvent was distilled under reduced pressure at room temperature. The residual yellow liquid was then added drop by drop to an acetone solution of copper(II) acetate (0.125 mol. in 400 ml.) under vigorous agitation. The reaction mixture was kept at 0°C for 24 hr. The resulting green powder was filtered off, dried, and then recrystallized twice from benzene. M. p. 180—182°C (decomp.).

Found: Cu, 15.19; C, 28.92; H, 3.30; Br, 37.00. Calcd. for $Cu(C_5H_6O_2Br)_2$: Cu, 15.14; C, 28.39; H, 2.88; Br, 38.09%.

In Fig. 1 the absorption spectrum of bis(3-bromoacetylacetonato)copper(II) in chloroform is compared with that of bis(acetylacetonato)copper(II).

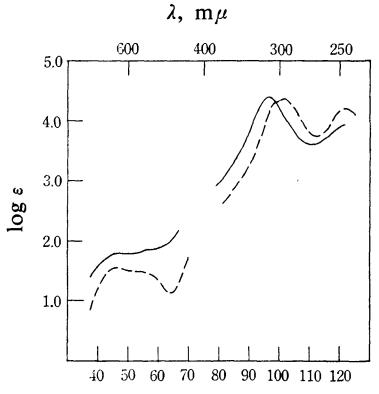



Fig. 1. The absorption spectra of bis(acetylacetonato)copper(II) (dashed curve) and bis(3-bromoacetylacetonato)copper(II) (full curve) in chloroform.

* Presented at the 14th Annual Meeting of the Chemical Society of Japan, Tokyo, April, 1961.

1) K. J. Pedersen, *J. Phys. Chem.*, **37**, 751 (1933); **38**, 581, 601 (1934); *Trans. Faraday Soc.*, **34**, 237 (1938).

2) R. P. Bell and O. M. Lidwell, *Proc. Roy. Soc.*, **A176**, 88 (1940).

3) e. g., R. P. Bell, E. Gelles and E. Möller, ibid., **A198**, 308 (1949).

4) K. J. Pedersen, *Acta Chem. Scand.*, **2**, 252 (1948).

5) K. J. Pedersen, ibid., **2**, 385 (1948).

6) H. F. Holtzclaw, Jr., A. H. Carlson and J. P. Collman, *J. Am. Chem. Soc.*, **78**, 1838 (1956): H. F. Holtzclaw, Jr., K. W. R. Johnson and F. W. Hengeveld, ibid., **74**, 3776 (1952).

7) H. F. Holtzclaw, Jr., and J. P. Collman, ibid., **79**, 3318 (1957).

8) R. W. Kluiber, ibid., **82**, 4839 (1960).

Commercial bromine, after being washed with water more than five times, was dissolved in an aqueous solution of potassium bromide, and then distilled. The distillate was redistilled three times over calcium oxide.

Commercial dichloromethane was washed with concentrated sulfuric acid, then with a dilute solution of sodium hydroxide and finally with pure water. The washed solvent was dried over calcium chloride and distilled in a 60 cm. Widmer column.[9]

**Absorption Spectra.**—Visible and ultraviolet absorption spectra were measured with Beckman Model DU spectrophotometer. Infrared absorption spectra were obtained on an infrared spectrophotometer Model IR-S of the Japan Spectroscopic Co.

**Analysis of the Precipitate.** — The precipitate produced by the reaction between the copper chelate and bromine was dissolved in aqueous ammonia and allowed to stand overnight. The solution was then treated with a small quantity of sodium hydroxide and heated. The precipitate of copper(II) oxide was filtered off, dissolved in nitric acid and submitted to electrolytic analysis. The above filtered solution was acidified and treated with silver nitrate to determine the bromine content gravimetrically.

## Results

**Reaction of Bis(acetylacetonato)copper(II) with Bromine at Room Temperature.** — The reaction was carried out in dichloromethane solution. Bis(acetylacetonato)copper(II) solution was prepared in the same concentration, $3.48\times10^{-2}$ mol./l., as that of bromine. A desired amount of the bromine solution was added from a burette to a given amount of the chelate solution under vigorous agitation. Mole ratios of 1 : 1, 1 : 1.5, and 1 : 2 copper chelate to bromine were examined. When 1 mol. of bromine was added to 1 mol. of the chelate, the solution still showed the light blue color of residual chelate, but after 1.5 mol. or more of bromine had been added the solution was slightly yellow. A white precipitate was produced when the mole ratios were 1 : 1 and 1 : 1.5, but a brownish black precipitate resulted from a 1 : 2 mol. ratio. Analitical results for the precipitate from each experiment are summarized in Table I.

The white precipitate formed in the 1 : 1 and 1 : 1.5 reaction mixtures was copper(I) bromide; the black one formed in the 1 : 2 reaction mixture was found to consist mainly of copper(II) bromide. However, when the latter was allowed to remain in the reaction mixture for a long time, the precipitate gradually turned white and was found to be copper(I) bromide.

After the precipitate had been filtered off from the reaction mixture in Exp. Nos. 3 and 4, most of the solvent was driven off at room temperature under reduced pressure. The residual yellow liquid was submitted to infrared spectroscopy. Frequencies of the main absorption bands are listed in Table II (product A) together with those for acetylacetone. Absorption bands due to the methylene group in acetylacetone are not exhibited by this product. The absorption bands at 1720 and 1701 $cm^{-1}$, which are assigned to the two carbonyl groups in the keto-form of actylacetone, are shifted by 15 and 5 $cm^{-1}$, respectively, to the higher frequency side. This coincides with the shift of the carbonyl stretching frequency of a haloketone, suggesting the liquid product to be 3-bromoacetylacetone. That this is indeed so was unequivocally demonstrated by the preparation and analysis of its copper(II) chelate as descrived in the Experimental.

**Reaction of Bis(3-bromoacetylacetonato)copper(II) with Bromine.**—The reaction between bis(3-bromoacetylacetonato)copper(II) and bromine in dichloromethane solution was carried out in a manner similar to that described in the preceeding section. Bromine was added to the chelate solution in mole ratios of 1 : 1, 1.5 : 1, and 2 : 1. In each case the precipitate was analyzed for copper and bromine, and the filtrate was examined by infrared spectroscopy after evaporation of the solvent.

Bis(3-bromoacetylacetonato)copper(II) reacts with bromine as rapidly as bis(acetylacetonato)copper(II) does and gives quite similar precipitates (Table III). When 2 mol. or more of bromine is used for 1 mol. of the chelate, copper(II) bromide is precipitated, but when 1.5 mol. or less bromine is employed, copper(I) bromide results.

The main infrared absorption bands of the liquid product in Exp. Nos. 10, 11 and 12 are listed in Table II (product B) together with literature data for 3, 3-dichloroacetylacetone.[10] The absorption bands due to the two carbonyl groups appear at 1737 and 1714 $cm^{-1}$, exhibiting shifts of 17 and 13 $cm^{-1}$, respectively, compared with those of acetylacetone. This shift can be ascribed to the effect of halogen substitution in the 3-position; the magnitude of the shift is larger than that observed for product A, suggesting a dibromo substitution product. The strong absorption band around 1600 $cm^{-1}$, which was observed for the enol-form of acetylacetone and the product A, is not observed for the product B indicating the absence of an enol-form. Similar features were also reported for 3, 3-dichloroacetylacetone by Mecke

9) A. Weissberger et al. (ed.), "Organic Solvents," 2nd ed., Interscience Publisher, New York (1955), p. 409.

10) R. Mecke and E. Funck [1], *Z. Elektrochem.*, **60**, 1124 (1956).

TABLE I. ANALYSIS OF THE PRECIPITATE FROM THE REACTION BETWEEN BIS(ACETYLACETONATO)COPPER(II) AND BROMINE

| Exp. No. | Mole ratio of chelate : bromine | Precipitate analyzed, mg. | Copper found, mg. | Bromine found, mg. | Atom ratio Cu : Br |
|---|---|---|---|---|---|
| 1 | 1 : 1 | 77.9 | 32.4 | 45.5 | 1 : 1.12 |
| 2 | 1 : 1 | 83.6 | 35.7 | 44.5 | 1 : 1.00 |
| 3 | 1 : 1.5 | 115.8 | 50.4 | 65.0 | 1 : 1.04 |
| 4 | 1 : 1.5 | 119.4 | 52.2 | 72.2 | 1 : 1.10 |
| 5 | 1 : 2 | 98.1 | 28.1 | 68.2 | 1 : 1.84 |
| 6[a)] | 1 : 2 | 61.4 | 25.0 | 33.4 | 1 : 1.06 |
| 7[a)] | 1 : 2 | 77.2 | 32.0 | 41.8 | 1 : 1.04 |

a) Precipitate allowed to remain in the reaction mixture for two weeks before analysis.

TABLE II. INFRARED ABSORPTION DATA OF REACTION PRODUCTS ($cm^{-1}$)

| Assignment | Acetylacetone | Product A[a)] | Product B[a)] | 3,3-Dichloro-acetylacetone[b)] |
|---|---|---|---|---|
| $\nu$(OH) | ~2800(1) | ~2800(1) | — | — |
| $\nu$(C=O) | 1720(3) | 1735sh(6) | 1737(7) | 1758(9) |
| $\nu$(C=O) | 1701(4) | 1706(6) | 1714(8) | 1740(9) |
| $\nu$(C=O), $\nu$(C=C) | 1610(8) | 1597(8) | — | — |
| $\nu$(C-O), $\delta_a(CH_3)$, $\delta$(OH), $\delta(CH_2)$ | 1445sh, 1408(4) | 1412(5) | 1407(2) | 1422(3) |
| $\delta_s(CH_3)$ | 1359(5) | 1362(6) | 1360(6) | 1361(8) |
| $\gamma(CH_2)$ | 1300(3) | — | — | — |

a) Product A refers to the liquid product from the reaction between bis(acetylacetonato)copper-(II) and bromine in the mole ratio of 1 : 1.5 (Exp. Nos. 3 and 4). Product B refers to the liquid product from the reaction between bis(3-bromoacetylacetonato)copper(II) and bromine in the mole ratio of 1 : 2 (Exp. Nos. 11 and 12).
b) Data from Ref. 10.

TABLE III. ANALYSIS OF THE PRECIPITATE FROM THE REACTION BETWEEN BIS(3-BROMOACETYLACETONATO)COPPER(II) AND BROMINE

| Exp. No. | Mole ratio of chelate : bromine | Precipitate analyzed, mg. | Copper found, mg. | Bromine found, mg. | Atom ratio Cu : Br |
|---|---|---|---|---|---|
| 8 | 1 : 1 | 58.7 | 25.2 | 28.6 | 1 : 0.90 |
| 9 | 1 : 1 | 48.7 | 24.8 | 26.5 | 1 : 0.84 |
| 10 | 1 : 1.5 | 66.7 | 25.9 | 35.1 | 1 : 1.08 |
| 11 | 1 : 2 | 92.4 | 25.7 | 61.2 | 1 : 1.90 |
| 12 | 1 : 2 | 96.6 | 27.0 | 64.2 | 1 : 1.90 |

and Funck.[10)] Product B can thus reasonably be regarded as 3, 3-dibromoacetylacetone.

**Reaction of Bis(acetylacetonato)copper(II) with Bromine at a Low Temperature.** — When the reaction was conducted in chloroform at about −60°C, the color of the solution changed from blue to green, to brown, and eventually to red, but no precipitate was formed after two moles of bromine had been added per mole of the chelate. However, when the solution was warmed to room temperature, a dark precipitate of copper(II) bromide appeared and the solution became colorless.

## Discussion

When bis(acetylacetonato)copper(II) is attacked by bromine in organic solvents, the chelate ring is broken resulting in copper bromides and 3-bromoacetylacetone. When two moles or more of bromine is added to one mole of the chelate, copper(II) bromide is produced (Exp. No. 5). The reaction is represented by the equation,

$$Cu(HA)_2 + 2Br_2 = CuBr_2 + 2HABr \quad (1)$$

where $H_2A$ stands for acetylacetone and

$HA^-$ for the acetylacetonate anion $(CH_3CO\text{-}CHCOCH_3)^-$. Copper(II) bromide thus formed can further react with the other product 3-bromoacetylacetone (HABr) at a much lower rate, and thus is completely converted to copper(I) bromide when allowed to stand for a long period in the reaction mixture (Exp. Nos. 6 and 7).

$$2CuBr_2 + HABr = 2CuBr + ABr_2 + HBr \quad (2)$$

When 1.5 mol. of bromine is employed for 1 mol. of the chelate, the following reaction occurs (Exp. Nos. 3 and 4).

$$Cu(HA)_2 + {}^3/_2Br_2 = CuBr + 2HABr \quad (3)$$

In these cases the copper chelate employed is consumed completely, but when 1 mol. of bromine is added to 1 mol. of the chelate, the excess of the chelate remains unchanged in the solution.

Bis(3-bromoacetylacetonato)copper(II) reacts with bromine in a similar fashion to bis(acetylacetonato)copper(II), producing 3, 3-dibromoacetylacetone and copper bromide. The reaction in the mole ratio of 1 : 1.5 is represented by

$$Cu(ABr)_2 + {}^3/_2Br_2 = CuBr + 2ABr_2 \quad (4)$$

Similarly the reaction in the mole ratio of 1 : 2 is written as

$$Cu(ABr)_2 + 2Br_2 = CuBr_2 + 2ABr_2 \quad (5)$$

In this case the product 3, 3-dibromoacetylacetone has no active hydrogen to react with copper(II) bromide, and thus the latter remains unchanged even after standing a long time in the product solution.

Thus copper(II) chelates, not only of acetylacetone but also of 3-bromoacetylacetone, react instantaneously with bromine in dichloromethane giving 3-bromoacetylacetone and 3, 3-dibromoacetylacetone, respectively. The reason why copper(II) ion does not show any catalytic activity in the second step of the bromination of ethyl acetoacetate in aqueous solution[4] might be due to the instability of the intermediate copper(II) chelate of the ester in these reaction conditions. In fact, crystalline copper(II) chelate of ethyl $\alpha$-bromoacetoacetate could not be isolated[11] in contrast to good stability of the chelate of the nonsubstituted ester. However, the copper(II) chelate of 3-bromoacetylacetone is very stable and can be synthesized in good yield as described in the present paper, and thus the copper(II) ion may be expected to promote the second step of the bromination of acetylacetone.

In the reaction of bis(acetylacetonato)copper-(II) with bromine, copper(I) bromide is formed when less than two moles of bromine is employed for one mole of the chelate. This is very interesting in view of the oxidizing characteristic of bromine. The mechanism of the reactions represented by Eqs. 1 and 2 is not at all clear, but they seem to proceed through a common intermediate. The experiment performed at a low temperature indicates that the intermediate species is quite stable at about $-60°C$. Further investigation of the reaction mixture at a low temperature should shed light on the nature of the intermediate.

## Summary

In the reaction of bis(acetylacetonato)-copper(II) with bromine the chelate ring is broken and 3-bromoacetylacetone and copper-(I) or copper(II) bromide are formed depending on the mole ratio of the reactants.

Bis(3-bromoacetylacetonato)copper(II) also reacts with bromine in a similar fashion resulting in 3, 3-dibromoacetylacetone and copper(I) or copper(II) bromide. The possibility of the copper(II) ion functioning as a catalyst in the second step of the bromination of acetylacetone is suggested.

*Faculty of Science*
*Osaka City University*
*Sumiyoshi-ku, Osaka*

11) T. Ogura, Y. Nakamura and S. Kawaguchi, This Bulletin, to be published.

# Hydroxylation of Olefins with Hydrogen Peroxide in the Presence of Selenium Dioxide Catalyst

By Noboru SONODA and Shigeru TSUTSUMI

(Received October 23, 1964)

Oxidation by hydrogen peroxide in the presence of a metal oxide catalyst is known as one of the simplest procedures for effecting the hydroxylation of olefins.[1]

$$>C{=}C< + H_2O_2 \xrightarrow[\text{catalyst}]{\text{metal oxide}} >\underset{\underset{OH}{|}}{C}-\underset{\underset{OH}{|}}{C}<$$

Although many catalysts for this reaction are known, osmium tetroxide and tungstic acid (or tungsten trioxide) are especially useful for the practical syntheses of *cis*- and *trans*-$\alpha$-diols from the corresponding olefins. Selenium dioxide, which can be used in organic or aqueous solution, has found favor with some investigators,[2-5] but is not so well established a catalyst as osmium tetroxide or tungstic acid. Mugdan and Young[2] have suggested that it may be possible to hydroxylate allyl alcohol with hydrogen peroxide in the presence of selenium dioxide. It has been confirmed that cyclohexene and cyclopentene are hydroxylated to give the corresponding *trans*-$\alpha$-diols[3,4] under similar conditions; recently we also have reported the hydroxylation of some gaseous olefins.[5]

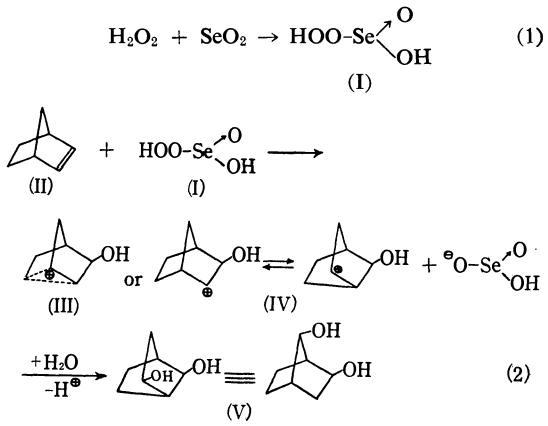
The purpose of the present investigation is to study the use of selenium dioxide as a catalyst in the hydroxylation of olefins with hydrogen peroxide, and also to extend the application of this catalyst.

In order to examine the ionic character of the hydroxylation, oxidation of norbornene was undertaken, because addition of a cation to the double bond of norbornene should cause a Wagner-Meerwein rearrangement via the norbornyl cation.[6,7]

When norbornene (II) was oxidized with 30% hydrogen peroxide in tertiary butyl alcohol in the presence of a catalytic amount of selenium dioxide, the only product was *exo-syn*-norbornane-2, 7-diol (V) which was identified by comparison with an authentic sample. The diol was best isolated as the diacetate (62% yield based on the norbornene used) which was obtained by treatment of the crude product with acetic anhydride. The formation of *exo-syn*-norbornane-2, 7-diol (V) may be due to the hydration of a norbornyl cation (III or IV) produced by the cationic addition of a hydroxyl group to the double bond of norbornene.[6] Although it is still not clear whether rearrangement of the norbornyl cation proceeds via a nonclassical structure (III) or an equilibrium of classical structures (IV),[8] it is evident that the high propensity and stereospecificity of the rearrangement, in this oxidation, indicate the cationic nature of the reaction,[6] since no rearrangement product is known to arise from a radical addition to norbornene[9,10] or in reactions of the norbornyl free radical.[10,11]

On the other hand, the formation of the norbornyl cation (III or IV) suggests that some active oxidizing species having a peroxy acid function may be formed from the selenium dioxide and hydrogen peroxide in the reaction system, and the mechanism of the hydroxylation may be analogous to that proposed for oxidations with organic peracids[12,13] or pertungstic acid.[14] We have assumed[15,16] that peroxyselenious acid (I) is probably the active oxidizing species in the oxidation of ketones under the above reaction conditions. Thus, a likely mechanism for the hydroxylation of norbornene (II) is that shown below.

1) For a review, see F. D. Gunstone, "Advance in Organic Chemistry," Vol. I, Interscience Pub., New York (1960), p. 103.
2) M. Mugdan and D. P. Young, *J. Chem. Soc.*, **1949**, 2988.
3) P. Seguin, *Compt. rend.*, **216**, 667 (1943).
4) A. Stoll, A. Lindenmann and E. Jucker, *Helv. Chim. Acta*, **36**, 268 (1953).
5) N. Sonoda and S. Tsutsumi, *J. Chem. Soc. Japan, Ind. Chem. Sec.* (*Kogyo Kagaku Zasshi*), **63**, 110 (1960).
6) P. de Mayo, "Molecular Rearrangements," Part I, Interscience Pub., New York (1963), p. 111.
7) R. E. Parker and N. S. Isaacs, *Chem. Revs.*, **59**, 737 (1959).
8) For one of the recent discussions of these topics, see P. R. Schleyer, *J. Am. Chem. Soc.*, **86**, 1856 (1964); and earlier papers therein cited.
9) H. Kwart and J. L. Nyce, ibid., **86**, 2601 (1964).
10) S. J. Cristol, G. D. Brindell and J. A. Reeder, ibid., **80**, 635 (1958).
11) S. J. Cristol and R. P. Arganbright, ibid., **79**, 6309 (1957).
12) H. Kwart and W. G. Vosburgh, ibid., **76**, 5400 (1954).
13) H. M. Walborsky and D. F. Loncrini, ibid., **76**, 5396 (1954).
14) K. A. Saegebarth, *J. Org. Chem.*, **24**, 1212 (1959).
15) N. Sonoda and S. Tsutsumi, This Bulletin, **34**, 1006 (1961).
16) N. Sonoda and S. Tsutsumi, *Technol. Repts. Osaka Univ.*, **13**, 223 (1963).



These results suggest that hydroxylation of ordinary olefins, which do not suffer a Wagner-Meerwein rearrangement through attack of a cationic species, may proceed via the corresponding epoxide, a stable intermediate produced by the epoxidation with the active oxidizing species in a similar fashion to the first step of the oxidation of norbornene (II). Oxidation of styrene, with hydrogen peroxide and selenium dioxide in methanol, gave mainly 2-phenyl-2-methoxyethyl alcohol (VIII);[17] this may have been formed by methanolysis of the hydronium ion (VI) which is in equilibrium with styrene oxide (VII) as shown below.

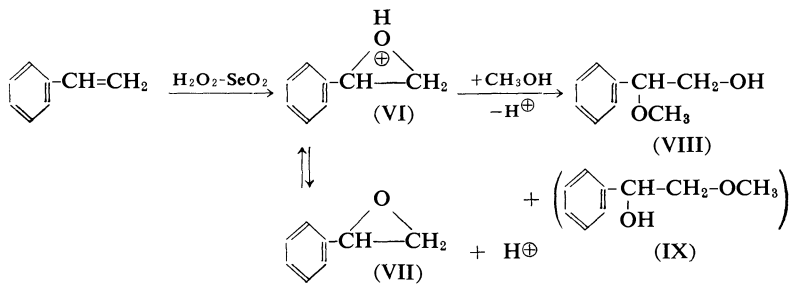
Further evidence for the presence of an epoxide intermediate was obtained by the hydroxylation of cyclohexene in various alcohols. The oxidation of cyclohexene with hydrogen peroxide and selenium dioxide in

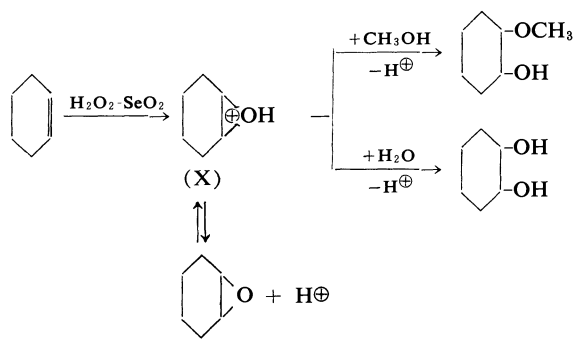
Table I. Hydroxylation of cyclohexene with hydrogen peroxide in the presence of selenium dioxide in various alcohols

| Alcohol | Product: Yield,* % α-Alkoxycyclohexanol | Product: Yield,* % *trans*-Cyclohexane-1, 2-diol |
|---|---|---|
| Methanol | 78 | 10 |
| Ethanol | 56 | 20 |
| *n*-Propanol | 51 | 23 |
| *n*-Butanol | 35 | 27 |
| Isopropanol | 24 | 47 |
| *t*-Butyl alcohol | <1** | 65 |

* Yields are based on the hydrogen peroxide used.

** The pure product was not isolated.





17) Identification of 2-phenyl-2-methoxyethyl alcohol (VIII) was established by elementary analysis, and by the mixed melting point of the α-naphthylurethan derivative with an authentic sample, m. p. 119°C (lit.[18] m. p. 119.5°C). Acid or base catalyzed methanolysis of styrene oxide[7] gave generally a mixture of 2-phenyl-2-methoxyethyl alcohol (VIII) and 1-phenyl-2-methoxyethyl alcohol (IX) (α-naphthylurethan, m. p. 105°C[18]), and it has been reported[18] that the α-naphthylurethan of a sample of 2-phenyl-2-methoxyethyl alcohol (VIII) containing a small amount of the 1-phenyl isomer (IX) also showed a m. p. of 119.5°C, identical with that of the α-naphthylurethan of a pure sample of the 2-phenyl isomer (VIII). Accordingly, it is possible that a small amount of the 1-phenyl isomer may have been formed in this experiment, but no attempt was made to determine the content of the 1-phenyl isomer.

18) W. Reeve and I. Christoffel, *J. Am. Chem. Soc.*, **72**, 1480 (1950).

methanol gave α-methoxycyclohexanol as a main product and *trans*-cyclohexane-1, 2-diol in a small amount. α-Methoxycyclohexanol may be fomed by the methanolysis of the hydronium ion intermediate (X), and the production of *trans*-cyclohexane-1, 2-diol may be attributable to competitive hydrolysis of the same intermediate (X).

The results obtained for the oxidation of cyclohexene with 30% hydrogen peroxide in various alcohols are summarized in Table I.

The yields of α-alkoxycyclohexanol and *trans*-cyclohexane-1, 2-diol shown in Table I are comparable to those obtained by Payne and Smith,[19] and the decrease in the yields of α-alkoxycyclohexanol with the kind of alcohol used can be attributed to the decrease in the polarity of the alcohol.

## Experimental

**Hydroxylation of Norbornene.**—To a solution of hydrogen peroxide in tertiary butyl alcohol, prepared by dilution of 5 ml. (0.05 mol.) of 30% hydrogen peroxide with the alcohol, was added 0.1 g. of selenium dioxide. After the selenium dioxide was dissolved completely, 5 g. (0.04 mol.) of norbornene was added and the solution was heated at 70°C for 13 hr. Most of the solvent and unreacted norbornene was removed by distillation, 50 ml. of ethyl acetate was added to the residue and the ethyl acetate solution was extracted with 10 ml. of 10% sodium hydroxide solution to remove the catalyst. After the ethyl acetate solution had been dried over anhydrous magnesium sulfate, the solvent was removed by distillation under reduced pressure. Sublimation of a small part of the residual crystalline solid gave *exo-syn*-norbornane-2, 7-diol, m. p. 176—177°C (sealed tube) (lit.[20] m. p. 174—176°C), the mixed melting point with an authentic sample (m. p. 176—177°C), synthesized by the procedure described by Kwart,[20] showed no depression, and the infrared spectrum of the product was identical with that of the authentic sample.

Found: C, 65.38; H, 9.32. Calcd. for $C_7H_{12}O_2$: C, 65.59; H, 9.44%.

Since the crude *exo-syn*-norbornane-2, 7-diol was slightly hygroscopic, the diol was acetylated. The residual crystalline solid obtained by the removal of solvent was added to 50 ml. of acetic anhydride containing one drop of sulfuric acid; a slightly exothermic reaction was observed. After the reaction mixture had been allowed to stand overnight at room temperature, a small amount of calcium carbonate was added to neutralize the sulfuric acid, and then filtered off. Removal of the unreacted acetic anhydride by distillation under reduced pressure, gave 5.2 g. of *exo-syn*-2, 7-diacetoxynorbornane in a yield of 62% based on the norbornene used; b. p. 128—132°C (10 mmHg), $n_D^{20}$ 1.4626 (lit.[14] b.p. 130—134°C (11 mmHg), $n_D^{25}$ 1.4620), the infrared spectrum was identical with that of an authentic sample.

**Oxidation of Styrene in Methanol Solution.**—To a solution of 400 ml. of methanol containing 30 ml. (ca. 0.3 mol.) of 30% hydrogen peroxide was dissolved 0.5 g. of selenium dioxide. Then 31.2 g. (0.3 mol.) of styrene was added to the solution and the reaction mixture was gently refluxed for 20 hr. After decantation to remove the polystyrene deposited in the flask, the solvent and unreacted styrene were removed by distillation under reduced pressure, and the residual liquid was distilled; 8.5 g. of a fraction boiling at 108—113°C (6 mmHg) was collected. Purification by redistillation of this fraction gave 7.8 g. of 2-phenyl-2-methoxyethyl alcohol[17] (60% yield based on the unrecovered styrene); the infrared spectrum was practically identical with that of an authentic sample.

Found: C, 70.88; H, 7.72. Calcd. for $C_9H_{12}O_2$: C, 71.02; H, 7.95%.

The α-naphthylurethan melted at 119°C (lit.[18] m. p. 119.5°C), the mixed melting point with an authentic sample (m. p. 119°C) showed no depression and the infrared spectrum was identical with that of an authentic sample.

Found: C, 74.92; H, 5.90. Calcd. for $C_{20}H_{19}NO_3$: C, 74.74; H, 5.96%.

**Hydroxylation of Cyclohexene in Methanol Solution.**—To a solution of 18.4 ml. (0.18 mol.) of 30% hydrogen peroxide in 365 ml. (9.0 mol.) of methanol was added 0.8 g. of selenium dioxide and 29.5 g. (0.36 mol.) of cyclohexene. After the solution had been refluxed for 10.5 hr. (at this stage, hydrogen peroxide was completely consumed), the solvent and unreacted cyclohexene were removed by distillation under reduced pressure. The residual product was separated by distillation into the following three fractions: fraction A, b. p. 106—116°C (65 mmHg); fraction B, b. p. 105—128°C (20 mmHg); fraction C, b. p. 128—133°C (20 mmHg), which crystallized at once. Fraction B, on being allowed to stand overnight at 0°C, deposited a white crystalline solid which was filtered off; the filtrate was combined with fraction A. Redistillation of this mixture gave 18.2 g. of α-methoxycyclohexanol (78% yield based on the hydrogen peroxide used), b. p. 107—111°C (65 mmHg), $n_D^{20}$ 1.4604 (lit.[19] b. p. 122—124°C (100 mmHg), $n_D^{20}$ 1.4595). The infrared spectrum was identical with that of an authentic sample.

Found: C, 64.46; H, 10.78. Calcd. for $C_7H_{14}O_2$: C, 64.58; H, 10.84%.

The crystalline solid collected from fractions A and B was recrystallized from ether to give 2.0 g. (10% yield) of *trans*-cyclohexane-1, 2-diol, m. p. 103—103.5°C (lit.[21] m. p. 103.5—104°C). The mixed melting point with an authentic sample (m. p. 103—103.5°C) was not depressed.

Found: C, 61.85; H, 10.83. Calcd. for $C_6H_{12}O_2$: C, 62.04; H, 10.41%.

**Hydroxylation of Cyclohexene in Ethanol Solution.**—To a solution of 18.4 ml. (0.18 mol.) of 30% hydrogen peroxide in 420 ml. (7.2 mol.) of ethanol

19) G. B. Payne and C. W. Smith, *J. Org. Chem.*, **22**, 1682 (1957).

20) H. Kwart and W. G. Vosburgh, *J. Am. Chem. Soc.*, **76**, 5400 (1954).

21) J. English and J. D. Gregory, *J. Am. Chem. Soc.*, **69**, 2120 (1949).

containing 0.8 g. of selenium dioxide was added 29.5 g. (0.36 mol.) of cyclohexene. The reaction mixture was heated at 55—60°C for 13.5 hr. The reaction products were separated in the same manner as described for the hydroxylation in methanol solution, and 14.5 g. (56% yield based on the hydrogen peroxide used) of α-ethoxycyclohexanol was obtained, b. p. 80—85°C (15 mmHg), $n_D^{20}$ 1.4566 (lit.[19] b. p. 65—67°C(4 mmHg), $n_D^{20}$ 1.4562).

Found: C, 66.78; H, 11.21. Calcd. for $C_8H_{16}O_2$: C, 66.63; H, 11.18%.

*trans*-Cyclohexane-1, 2-diol (4.2 g.) was also isolated in a yield of 20%, m. p. 103—103.5°C. The mixed melting point with an authentic sample showed no depression.

**Hydroxylation of Cyclohexene in *n*-Propanol Solution.**—To a solution of 18.4 ml. (0.18 mol.) of 30% hydrogen peroxide in 540 ml. (7.2 mol.) of *n*-propanol containing 0.8 g. of selenium dioxide was added 29.5 g. (0.36 mol.) of cyclohexene. The reaction mixture was heated at 55—60°C for 16 hr. The reaction products were separated in the same manner as described for the hydroxylation in methanol solution, and 14.4 g. (51% yield based on the hydrogen peroxide used) of α-*n*-propoxycyclohexanol was isolated, b. p. 92—96°C (14 mmHg), $n_D^{20}$ 1.4571 (lit.[22] b. p. 205°C, $n_D^{20}$ 1.4580).

Found: C, 67.89; H, 11.40. Calcd. for $C_9H_{18}O_2$: C, 68.31; H, 11.47%.

*trans*-Cyclohexane-1, 2-diol (4.9 g.) was also isolated in a yield of 23%, m. p. 103—103.5°C. The mixed melting point with an authentic sample was not depressed.

**Hydroxylation of Cyclohexene in *n*-Butanol.**—To a solution of 18.4 ml. (0.18 mol.) of 30% hydrogen peroxide in 660 ml. (7.2 mol.) of *n*-butanol containing 0.8 g. of selenium dioxide was added 29.5 g. (0.36 mol.) of cyclohexene. The reaction mixture was heated at 55—60°C for 17 hr. The reaction products were separated in the same manner as described for the hydroxylation in methanol solution, and 10.8 g. (35% yield based on the hydrogen peroxide used) of α-*n*-butoxycyclohexanol was obtained, b. p. 106—110°C (13 mmHg), $n_D^{20}$ 1.4562 (lit.[23] b. p. 113—115°C (15 mmHg)).

Found: C, 69.49; H, 11.60. Calcd. for $C_{10}H_{20}O_2$: C, 69.72; H, 11.70%.

*trans*-Cyclohexane-1, 2-diol (5.7 g.) was also isolated in a yield of 27%, m. p. 103—103.5°C. The mixed melting point with an authentic sample showed no depression.

**Hydroxylation of Cyclohexene in Isopropanol Solution.**—To a solution of 18.4 ml. (0.18 mol.) of 30% hydrogen peroxide in 550 ml. (7.2 mol.) of isopropanol containing 0.8 g. of selenium dioxide was added 29.5 g. (0.36 mol.) of cyclohexene. The reaction mixture was heated at 55—60°C for 14 hr. The reaction products were separated in the same manner as described for the hydroxylation in methanol solution, and 6.7 g. (24% yield based on the hydrogen peroxide used) of α-isopropoxycyclohexanol was isolated, b. p. 89—93°C (18 mmHg), $n_D^{20}$ 1.4520 (lit.[19] b. p. 94—96°C (20 mmHg), $n_D^{20}$ 1.4506).

Found: C, 68.22; H, 11.36. Calcd. for $C_9H_{18}O_2$: C, 68.31; H, 11.47%.

*trans*-Cyclohexane-1, 2-diol (9.9 g.) was also isolated in a yield of 47%, m. p. 103—103.5°C. The mixed melting point with an authentic sample showed no depression.

**Hydroxylation of Cyclohexene in *t*-Butyl Alcohol Solution.**—To a solution of 18.4 ml. (0.18 mol.) of 30% hydrogen peroxide in 680 ml. (7.2 mol.) of *t*-butyl alcohol containing 0.8 g. of selenium dioxide was added 29.5 g. (0.36 mol.) of cyclohexene. The reaction mixture was heated at 55—60°C for 16 hr. The reaction products were separated in the same manner as described for the hydroxylation in methanol solution, and 0.4 g. of liquid, b. p. 86—91°C (14 mmHg), $n_D^{20}$ 1.4598, was obtained as a first fraction. Although the infrared absorption of this fraction showed strong bands at 3350 $cm^{-1}$ (O-H) and 1250 $cm^{-1}$ (C-O-C), elementary analysis as α-tertiary-butoxy-cyclohexanol gave slightly unsatisfactory result which might be due to the presence of some impurities.

*trans*-Cyclohexane-1, 2-diol (13.5 g.) was also isolated in a yield of 65%, m. p. 103—103.5°C. The mixed melting point with an authentic sample showed no depression.

*Department of Chemical Technology*
*Faculty of Engineering*
*Osaka University*
*Miyakojima-ku, Osaka*

22) M. Mousseron and R. Granger, *Compt. rend.*, **205**, 327 (1937).
23) E. Imoto and K. Azuma, *J. Soc. Org. Synthet. Chem. Japan*, **12**, 405 (1954).

# The Electronic Spectra of Aniline and *N*-Methylaniline Adsorbed on Aluminum Chloride. I

By Hiroyasu SATO,*1 Kozo HIROTA and Saburo NAGAKURA

(Received October 27, 1964)

Recently, the electronic spectra of organic molecules adsorbed on solid catalysts, especially on such cracking catalysts as silica gel and silica-alumina, have been investigated by several authors.[1] The adsorbates studied include benzene derivatives, cata-condensed hydrocarbons, and aromatic amines. On silica gel, these molecules are adsorbed physically or interact with the surface hydroxyl group of the catalysts. On silica-alumina, on the other hand, chemically-adsorbed species are also found. The Lewis-acid nature of silica-alumina is now well known. The molecules chemically adsorbed on silica-alumina either give an electron to the catalyst surface, thus forming cation-radicals, or form a sigma-bond with some electron-accepting center on the catalyst surface by sharing an electron-pair. Such cata-condensed hydrocarbons as anthracene and perylene give cation radicals other than the carbonium ions.[2,3] Aromatic amines form sigma complexes because of the Lewis-base nature of these compounds. In their investigation of aniline adsorbed on silica-alumina, Kotov and Terenin attributed the hypsochromic shift of the 2800Å band of aniline to the interaction of the adsorbed aniline molecule with some electron-accepting center on the catalyst surface.[4] The aim of the present study is to investigate the interaction of the aniline molecule with aluminum chloride, one of the typical Lewis acids, extending the measurement over the vacuum ultraviolet region.*2

## Experimental

**Materials.** — Aluminum chloride was prepared from silver chloride and aluminum foils in vacuo according to Wallace and Willard's procedure.[5] Aniline and *N*-methylaniline of Tokyo-Kasei, G.P. grade, were dried with sodium hydroxide and distilled in vacuo before use. The middle fraction was used for the experiment.

**Procedure.** — Since the system studied here is very sensitive to moisture, all preparations and measurements were carried out in vacuo. The apparatus used in this experiment is shown in Fig. 1. Aluminum chloride was sublimed, via a break-off seal, into a quartz cell by heating it over a free flame.*3 The vapor of aniline (or *N*-methylaniline) was then introduced into the cell by opening the stopcock. After evacuation, the electronic spectrum was recorded.

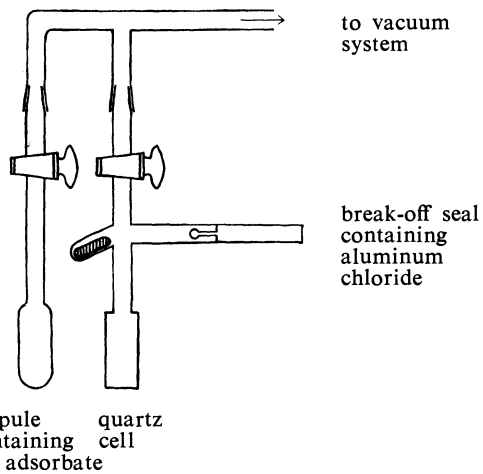



Fig. 1. Apparatus for the absorption study.

The electronic spectra were recorded by a Hitachi recording spectrophotometer model EPS-2 for the 220—340 mμ range; by a Cary recording spectrophotometer model 15 being flushed with dry nitrogen for the 180—300 mμ range, and by a vacuum ultraviolet spectrophotometer constructed in the Institute for Solid State Physics (reported on earlier)[6] for the 150—220 mμ range.

## Experimental Results

The observed electronic spectra of adsorbed aniline and *N*-methylaniline are, in Fig. 2,

*1 Present address: Faculty of Engineering Science, Osaka University, Toyonaka, Osaka.

1) For a survey of the literature, see H. P. Leftin and M. C. Hobson, Jr., *Advances in Catalysis*, **14**, 115 (1963).

2) W. K. Hall, *Journal of Catalysis*, **1**, 53 (1962).

3) D. M. Brouwer, ibid., **1**, 372 (1962).

4) E. I. Kotov and A. N. Terenin, *Doklady Akad. Nauk S. S. S. R.*, **124**, 865 (1959).

*2 Kotov and Terenin in Ref. 4 state that, in the case of a molecular complex of aniline with anhydrous aluminum chloride, a similar hypsochromic shift of the 2800 Å band to the spectrum of aniline adsorbed on silica-alumina can be observed, but no further details are given in that article.

5) C. H. Wallace and J. E. Willard, *J. Am. Chem. Soc.*, **72**, 5275 (1950).

*3 This technique was developed by T. Imanaka; see K. Hirota and T. Imanaka, *J. Chem. Soc. Japan, Pure Chem. Sec.* (*Nippon Kagaku Zasshi*), **84**, 960 (1963).

6) H. Tsubomura, K. Kimura, K. Kaya, J. Tanaka and S. Nagakura, This Bulletin, **37**, 417 (1964).

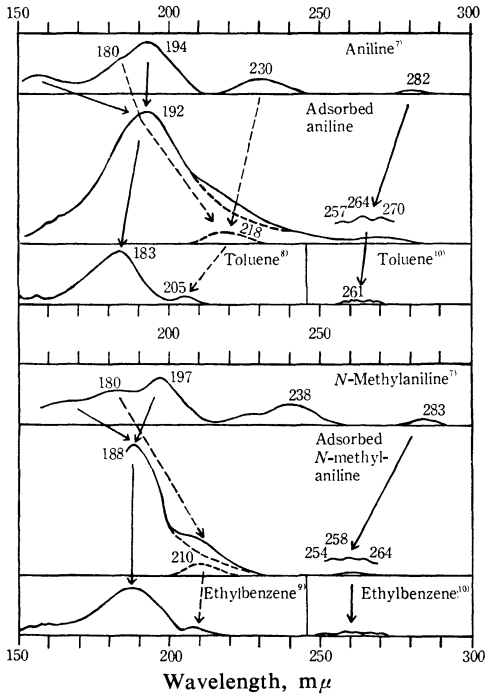



Fig. 2. The electronic spectra of adsorbed aniline and *N*-methylaniline.
Ordinate: optical density (in arbitary units). The enlarged spectra near 260 mμ are also shown. The spectra of aniline, *N*-methylaniline (Kimura et al.[7]), toluene (Kimura et al.[8], Am. Petr. Inst.[10]), and ethylbenzene (Hammond et al.[9]) are shown for purposes of comparison. For ethylbenzene, the spectrum around 260 mμ is drawn according to the data of the isooctane solution (Am. Petr. Inst.[10]). The arrows, → and ⇢, indicate the corresponding bands among these spectra. As to the reference spectra, the ordinates indicate qualitatively the strength of the absorption.

compared with those of vapor aniline, vapor *N*-methylaniline, and vapor alkylbenzenes (cf. Kimura, Tsubomura and Nagakura,[7] Kimura and Nagakura,[8] Hammond, Price, Teegan and Walsh,[9] Am. Petr. Inst.[10]). Because evaporated film was used, no quantitative measurement of the extinction coefficient of the adsorbates could be made. The spectrum of adsorbed aniline consists of a strong band at 192 mμ and a weak band with a vibrational structure around 265 mμ. The former band seems to be accompanied with a band hidden near 218 mμ.

The spectrum of adsorbed *N*-methylaniline consists of a strong band at 188 mμ, with a shoulder near 210 mμ, and a weak band with a vibrational structure around 260 mμ.

## Discussion

The spectrum of aniline has been the subject of many investigations,[7,11-14] and its correlation with the spectra of benzene and alkylbenzenes seems to be well-established. The spectra of adsorbed species can also be interpreted in terms of this correlation (see Fig. 3).

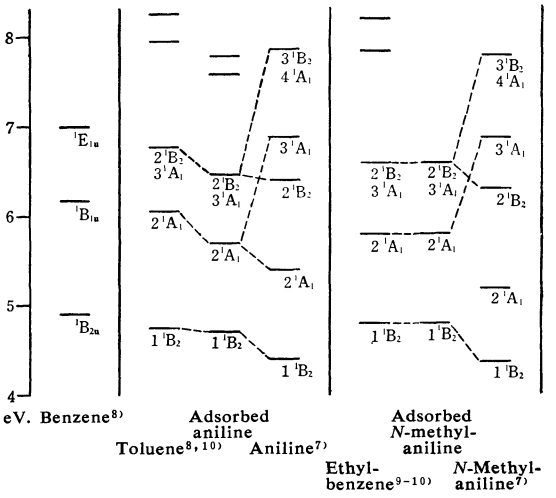



Fig. 3. Correlation diagram of excited states.

The spectrum of adsorbed aniline can be interpreted as follows. The weak band around 265 mμ (with a vibrational structure) is situated just between the 282 mμ band of aniline (broad), and the 261 mμ band of toluene (with a vibrational structure). The strong band at 192 mμ may be correlated with the 194 mμ band of aniline and 183 mμ band of toluene, and the hidden band near 218 mμ, which has something of a charge-transfer character, with the 180 mμ band of aniline and the 205 mμ band of toluene.

The spectrum of adsorbed *N*-methylaniline is nearly the same as that of ethylbenzene.

Another striking feature of these spectra is the disappearance of the 230 mμ band of aniline and the 238 mμ band of *N*-methylaniline, i.e., the intramolecular charge-transfer bands of the two.

These characteristics in the spectra of aniline and *N*-methylaniline can be consistently interpreted in terms of the electron donation from

7) K. Kimura, H. Tsubomura and S. Nagakura, This Bulletin, **37**, 1336 (1964).
8) K. Kimura and S. Nagakura, *Molecular Physics*, to be published.
9) V. J. Hammond, W. C. Price, J. P. Teegan and A. D. Walsh, *Discussions Faraday Soc.*, **9**, 53 (1950).
10) American Petroleum Institute Research Project No. 44, I (1945).
11) J. N. Murrell, *Proc. Phys. Soc.*, **A68**, 969 (1955).
12) T. E. Peacock, *Molecular Physics*, **3**, 453 (1960).
13) I. Fischer-Hjalmars, *Arkiv för Physik*, **21**, 123 (1961).
14) J. E. Bloor and F. Peradejordi, *Theoret. Chim. Acta (Berlin)*, **1**, 83 (1962).

the nitrogen atom in the aniline (or *N*-methylaniline) molecule to some electron accepting center on aluminum chloride-evaporated film. This view is supported by the fact that, in the spectrum of adsorbed aniline, the position of the absorption band draws nearer to that of the anilinium ion, which has peaks at 203 m$\mu$ and 254 m$\mu$.[15] It has been shown by many investigators that, in a sigma complex with Lewis acid, the absorption spectrum is like that of the proton complex, but it generally accompanies some shift.[1,16,17] The electron-accepting center is assumed to be the vacant $sp^3$-orbital of the aluminum atom. This interaction will reduce the electron density on the nitrogen atom, making the intramolecular charge-transfer band vanish and the other part of the spectrum draw nearer to that of alkylbenzenes.

A brief qualitative discussion of the positions of the absorption bands in these spectra will be given here.[18] Attention should be paid to the relative location of the intramolecular charge-transfer (CT) configurations and locally excited (LE) configurations in these molecules. In the case of aniline, two CT configurations ($^1A_1$ and $^1B_2$) lie in the region of 5—6 eV., amidst the LE configurations. These lift the degeneracy of the $^1E_{1u}$ state of benzene and cause hypso- and bathochromic shifts of the absorption bands compared with those of benzene, as Fig. 3 shows. In the case of toluene, however, with the CT configurations beyond the LE configurations, the degeneracy of the $^1E_{1u}$ state of benzene is lifted to a much smaller extent and all the absorption bands shift slightly in the red direction. In the case of adsorbed aniline, just the intermediate case can be expected as to the location of CT configurations; i.e., the CT configurations lie higher than in case of aniline, but lower than in the case of toluene. This will make the spectrum nearer to that of toluene, but with a larger red shift of some absorption bands.

The spectra of *N*-methylaniline, adsorbed *N*-methylaniline and ethylbenzene can be discussed in a similar way. In these cases, however, a larger rise in the energy of the CT configurations of adsorbed *N*-methylaniline reduces its spectrum to almost the same as that of ethylbenzene.

15) H. H. Jaffé and M. Orchin, "Theory and Applications of Ultraviolet Spectroscopy," John Wiley & Sons, New York (1962), p. 257.
16) C. Reid, *J. Am. Chem. Soc.*, **76**, 3264 (1954).
17) W. I. Aalbersberg, G. J. Hoijtink, E. L. Mackor and W. P. Weijland, *J. Chem. Soc.*, **1959**, 3055.
18) A more detailed discussion will be published later in this Bulletin.


## Summary

The electronic spectra of aniline and *N*-methylaniline adsorbed on evaporated film of aluminum chloride have been measured (150—300 m$\mu$ for the former adsorbate and 185—300 m$\mu$ for the latter). In the case of *N*-methylaniline, a spectrum which is nearly the same as that of ethylbenzene has been obtained. In the case of adsorbed aniline, the spectrum shows features intermediate between those of the aniline vapor spectrum and those of the toluene vapor spectrum. These results can be interpreted in terms of the electron donation from the lone-pair electrons on the nitrogen atom of these molecules to some electron-accepting center on aluminum chloride, presumably to the vacant $sp^3$-orbital of the aluminum atom on the surface, resulting in the weakening of the conjugation between the amino- (or *N*-methylamino-) group and the benzene ring. The positions of the absorption bands are interpreted qualitatively in terms of the relative location of charge-transfer and locally-excited configurations in these molecules.


The authors wish to express their gratitude to Dr. Katsumi Kimura*1 and Mr. Koji Kaya, the Institute for Solid State Physics, the University of Tokyo, for their kind measurement in the vacuum ultraviolet region. Dr. Kimura was very kind also in giving valuable, unpublished information on the vacuum ultraviolet spectral data of aniline, *N*-methylaniline and toluene. The authors are also indebted to Professor Hiroshi Tsubomura, Faculty of Engineering Science, Osaka University, by whose kindness measurement by the Cary spectrophotometer was possible. Thanks are also due to Mr. Toshinobu Imanaka,*2 Faculty of Science, Osaka University, for his useful suggestions concerning experimental techniques for preparing the evaporated film of aluminum chloride.

*Department of Chemistry*
*Faculty of Science*
*Osaka University*
*Nakanoshima, Osaka (H. S. & K. H.)*

*The Institute for Solid State Physics*
*The University of Tokyo*
*Azabu, Tokyo (S. N.)*

*1,*2 Present address: Faculty of Engineering Science, Osaka University, Toyonaka, Osaka.

# Near and Vacuum Ultraviolet Absorption Spectra and Electronic Structures of Nitrosobenzene and Its Derivatives

By Katsumi TABEI* and Saburo NAGAKURA

(Received October 29, 1964)

The electronic absorption spectra of nitrosobenzene and its derivatives are interesting subjects from both experimental and theoretical points of view. Nitrosobenzene is colorless in its crystal form but turns green when it is melted or dissolved in some solvents. This phenomenon has been studied spectroscopically and thermochemically by several investigators.[1] It has been found from these studies that the monomer shows a weak $n\rightarrow\pi^*$ transition band at about 750 m$\mu$; this band, which is responsible for the green color, disappears in the colorless dimer.

The $n\rightarrow\pi^*$ transition band of nitrosobenzene has been studied in detail in connection with the above-mentioned color change. Concerning the ultraviolet absorption spectrum of nitrosobenzene, however, only a few experimental and theoretical studies have hitherto been carried out.[2] This might be because nitrosobenzene and some of its derivatives are rather unstable and because, moreover, their ultraviolet absorption spectra are too complicated to be understood by analogy with that of benzene.

Under these circumstances, we have undertaken to study in more detail the absorption spectra of nitrosobenzene and its derivatives from both experimental and theoretical points of view, in order to bring about a better understanding of their electronic structures and clarify the characteristics of the nitroso group as a chromophoric or electron-accepting group.

## Experimental

**Materials.**—Nitrosobenzene and the following *p*-substituted nitrosobenzenes are studied in the present work : nitrosobenzene, *p*-nitrosotoluene, *p*-nitrosochlorobenzene, *p*-nitrosobromobenzene, *p*-nitrosoanisole, *p*-nitrosophenetole, *p*-nitrosophenol, *p*-nitrosoaniline, *p*-nitroso-*N*, *N*-dimethylaniline, *p*-nitroso-*N*, *N*-diethylaniline, *p*-nitroso-*N*-ethyl-*N*-benzylaniline and *p*-nitrosodiphenylamine.

Nitrosobenzene, *p*-nitrosotoluene, *p*-nitrosochlorobenzene, *p*-nitrosobromobenzene, *p*-nitrosoanisole and *p*-nitrosophenetole were derived from the corresponding nitro compounds via. hydroxylamino compounds by the method of Bamberger et al.[3] The products were separated by steam distillation and were purified by repeated recrystallizations from an ethanol-water mixture.

Commercial G.R. grade *p*-nitrosophenol, *p*-nitroso-*N*, *N*-dimethylaniline and *p*-nitrosodiphenylamine were purified by recrystallization with a ligroin-benzene mixture. *p*-Nitrosoaniline was prepared from *p*-nitrosophenol, ammonium acetate and ammonium chloride following the directions of Fischer and Hepp.[4] *p*-Nitroso-*N*, *N*-diethylaniline and *p*-nitroso-*N*-ethyl-*N*-benzylaniline were prepared from the corresponding anilines by a usual nitrosation with sodium nitrite and hydrochloric acid.[5] The products were recrystallized from ligroin. The melting points of the compounds used in the present study are listed in Table I.

*n*-Heptane used as a solvent was shaken with concentrated sulfuric acid and washed with aqueous sodium hydroxide and thereafter with water repeatedly. After being kept standing over calcium chloride for a day or so, it was fractionally distilled over sodium metal.

Commercial ethanol, chloroform, dioxane, ethyl ether and acetonitrile of a G.P. grade were purified by distillation.

**Measurement.**—A Cary recording spectrophotometer model 14-M was used for measuring the visible and near ultraviolet absorption spectra of the solutions with concentrations of the respective nitroso compounds of $10^{-5}$—$10^{-3}$ mol./l. The measurements were made at room temperature by using silica cells with light paths 1 cm. and 0.1 cm. long.

The vacuum ultraviolet absorption spectrum of nitrosobenzene in a *n*-heptane solution was measured by using handmade vacuum ultraviolet spectrophotometer.[6]

* Present address: Tokyo College of Pharmacy, 600, Kashiwagi 4-chome, Shinjiku-ku, Tokyo.

1) E. Bamberger and A. Rising, *Ber.*, **34**, 3878 (1901); C. K. Ingold and H. A. Piggott, *J. Chem. Soc.*, **125**, 173 (1924); D. L. Hammick and W. S. Illingworth, ibid., **1930**, 2358; D. L. Hammick, R. G. A. New and L. E. Sutton, ibid., **1932**, 742; P. Tarte, *Bull. soc. chim. Belges*, **63**, 525 (1954); W. Lüttke, *Z. Electrochem.*, **61**, 302, 976 (1957); **63**, 614 (1959).

2) K. Nakamoto and R. E. Rundle, *J. Am. Chem. Soc.*, **78**, 1113 (1956); Y. Tsuzuki, T. Uemura and N. Hirasawa, *Ber.*, **74**, 616 (1941); H. Labhart and G. Wagnière, *Helv. Chim. Acta*, **46**, 1314 (1963).

3) E. Bamberger, *Ber.*, **28**, 1222 (1895), **42**, 3581 (1909); B. Bennett, "Organic Syntheses," Coll. Vol. III, 668 (1955); Y. Tsuzuki, T. Uemura and N. Hirasawa, *J. Chem. Soc. Japan (Nippon Kwagaku Kwaishi)*, **61**, 1063 (1940); **62**, 85 (1941).

4) O. Fischer and E. Hepp, *Ber.*, **20**, 2475 (1887); **21**, 648 (1888).

5) B. Bennett, "Organic Syntheses," Coll. Vol. II, 223 (1943).

6) H. Tsubomura, K. Kimura, K. Kaya, J. Tanaka and S. Nagakura, This Bulletin, **37**, 417 (1964).

TABLE I. THE MAXIMUM WAVELENGTHS AND MOLAR EXTINCTION COEFFICIENTS OF THE NITROSO COMPOUNDS

| Compound | M. p.,°C | Maximum wavelengths (mμ) and molar extinction coefficients (in parentheses) | Solvent |
|---|---|---|---|
| Nitrosobenzene | 67 | 760(44), 301.4(5200), 280.5(10330), 272*(8200), 222*(5000), 218(6480), 194(11890), 174(~45000) | *n*-Heptane |
| *p*-Nitrosotoluene | 48 | 755(42), 310.8(8825), 285.8(9856), 229*(5877), 224(6769) | *n*-Heptane |
| *p*-Nitrosochlorobenzene | 72 | 750(40), 317*(8000), 310(9230), 288.2(10630), 278*(7500), 231(5910), 226(6810) | *n*-Heptane |
| *p*-Nitrosobromobenzene | 94 | 745(42), 318*(9670), 311.4(10420), 291.8(10860), 232.6(5460), 227(6060), 222*(5400) | *n*-Heptane |
| *p*-Nitrosoanisole | 32 | 738(47), 333(14270), 320(14860), 298*(6920), 242.5(5430), 236(6400), 228*(5360) | *n*-Heptane |
| *p*-Nitrosophenetole | 34.5 | 744(47), 335(15400), 327.5(15870), 298*(6600), 243.5(6380), 237(7300), 231.5*(5000) | *n*-Heptane |
| *p*-Nitrosophenol | 133 | 730(74), 295(16000), 242(2950) | 5% EtOH - *n*-Heptane |
| *p*-Nitrosoaniline | 174 | 690(41), 369(16700), 260(4200) | 5% EtOH - *n*-Heptane |
| *p*-Nitroso-*N*, *N*-dimethylaniline | 92 | 735(62), 393.5(28990), 381.5(26400), 313(1474), 303(1580), 295*(1300), 270.3(5181), 262(5940), 238(4960) | *n*-Heptane |
| *p*-Nitroso-*N*, *N*-diethylaniline | 83 | 730(48), 399(26300), 386(23540), 315(1700), 305(1656), 273(4626), 264(5177), 237(5050) | *n*-Heptane |
| *p*-Nitroso-*N*-ethyl-*N*-benzylaniline | 61 | 742(55), 395.8(33400), 383(29100), 314(1670), 304(1739), 295*(1500), 272(5928), 264(6162), 232(5520) | *n*-Heptane |
| *p*-Nitrosodiphenylamine | 145 | 704(35), 400(11200), 261(5600), 259(4600) | 5% EtOH - *n*-Heptane |

* represents absorption shoulders.

## Experimental Results

A weak absorption band ($\varepsilon=40$—$70$) was observed in the 680—760 mμ wavelength region for all the compounds given in Table I. It has been assigned to the $n\rightarrow\pi^*$ transition band.[7]

The ultraviolet absorption spectra of nitrosobenzene in the gaseous state and in *n*-heptane and ethanol solutions are given in Fig. 1. The peak wavelengths and molar extinction coefficients observed with the *n*-heptane solution are tabulated in Table I. Nitrosobenzene exhibits in the ultraviolet region five absorption maxima, at 301.4 mμ ($\varepsilon=5200$), 280.5 mμ ($\varepsilon=10330$), 218 mμ ($\varepsilon=6480$), 194 mμ ($\varepsilon=11890$), and 174 mμ ($\varepsilon=\sim45000$), and two shoulders at 272 mμ and 222 mμ. The absorption spectra of *p*-nitrosotoluene, *p*-nitrosochlorobenzene and *p*-nitrosobromobenzene shown in Fig. 2 are similar to that of nitrosobenzene.

On the other hand, *p*-nitrosophenol, *p*-nitrosoanisole, *p*-nitrosophenetole, *p*-nitrosoaniline and its *N*-substituted derivatives have more intense absorption bands at a longer wavelength region than nitrosobenzene does. The spectra of some of these compounds are shown in Figs. 2 and 3.

As is revealed by Fig. 1, the 300 mμ band of nitrosobenzene is sensitive to solvents.[8]

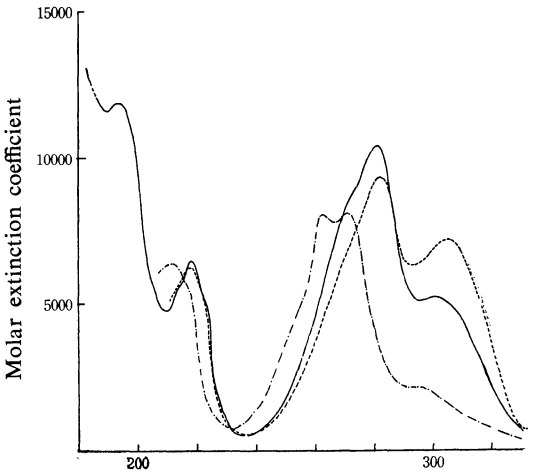



Fig. 1. The ultraviolet absorption spectra of nitrosobenzene in gaseous state, *n*-heptane solution and ethanol solution.
—·—·—·— in gaseous state
———— in *n*-heptane solution
- - - - - - - - - in ethanol solution

The band shows a small red shift and a great increase in intensity with the polarity of the solvent; i. e., the 294 mμ band of nitrosobenzene in the gaseous state shifts to 301.4 mμ

7) K. Nakamoto and R. E. Rundle, *J. Am. Chem. Soc.*, **78**, 1113 (1956).

8) T. Uemura and N. Hirasawa, *Bull. Tokyo Inst. Tech.*, **1943**, 70.

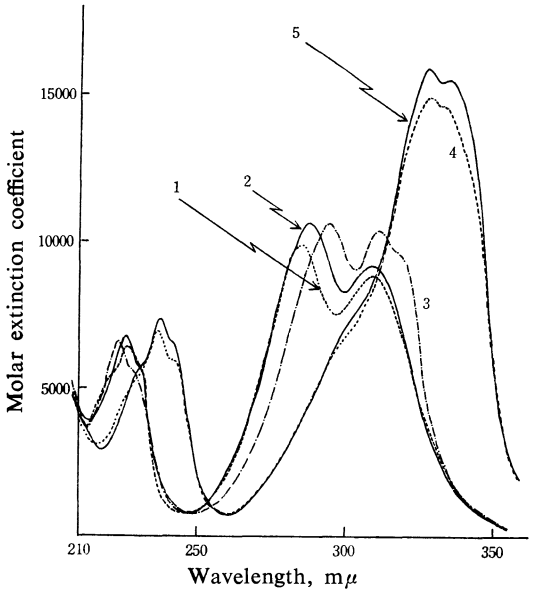
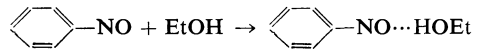



Fig. 2. The ultraviolet absorption spectra of some *p*-substituted nitrosobenzenes in *n*-heptane solution.

(1) ····· *p*-nitrosotoluene
(2) ····· *p*-nitrosochlorobenzene
(3) ····· *p*-nitrosobromobenzene
(4) ····· *p*-nitrosoanisole
(5) ····· *p*-nitrosophenetole

in the *n*-heptane solution and to 304 mμ in the ethanol solution, while the absorption intensity increases from 5200 in the *n*-heptane solution to 7200 in the ethanol solution.

In order to clarify the nature of this solvent effect, we measured the spectrum of nitrosobenzene in ethanol - *n*-heptane mixed solvents. The results are shown in Fig. 4. The 300 mμ and 280 mμ bands respectively increase and decrease in intensity with the concentration of ethanol. This suggests that the following equilibrium might exist between the free nitrosobenzene molecule and the hydrogen-bonded one:




and that the formation of the hydrogen-bonded molecule might be the reason for the change in the above-mentioned absorption spectrum of nitrosobenzene. In order to check this point, we have measured the absorption spectrum of nitrosobenzene in various kinds of solvents with different dielectric constants. The observed maximum wavelengths and molar extinction coefficients are given in Table II.

From the results given in Table II, it is clear that dioxane, chloroform and acetonitrile, in spite of their lack of a proton-donating ability, have an effect on the 300 mμ and 280 mμ bands of nitrosobenzene similar to that of

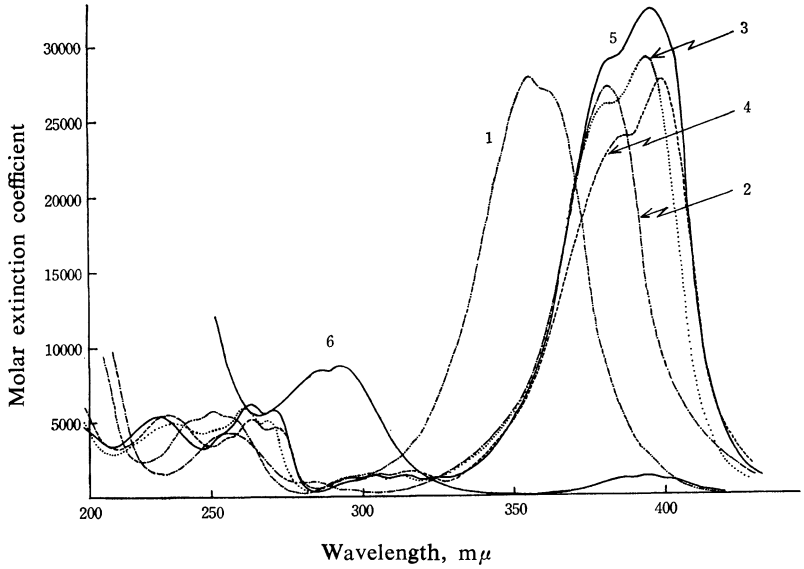



Fig. 3. The ultraviolet absorption spectra of nitrosoaniline and its *N*-substituted derivatives in *n*-heptane solution.

(1) ····· *p*-nitrosoaniline
(2) ····· *p*-nitrosodiphenylamine
(3) ····· *p*-nitroso-*N*, *N*-dimethylaniline
(4) ····· *p*-nitroso-*N*, *N*-diethylaniline
(5) ····· *p*-nitroso-*N*-ethyl-*N*-benzylaniline
(6) ····· *N*-nitrosodiphenylamine

TABLE II. THE SOLVENT EFFECT ON THE 280—300 mμ BAND OF NITROSOBENZENE

| Solvent | Dielectric constant (at 20°C) | Absorption maxima and molar extinction coefficients | |
|---|---|---|---|
| *n*-Heptane | 1.95 | 301.4 mμ (5200) | 280.5 mμ (10330) |
| Ethyl ether | 4.33 | 304 mμ (6070) | 281 mμ ( 9720) |
| Ethanol | 25 | 304 mμ (7200) | 281 mμ ( 9320) |
| Dioxane | 2.21 | 305.5 mμ (7060) | 283 mμ ( 9120) |
| Chloroform | 5.05 | 306 mμ (7890) | 283 mμ ( 9200) |
| Acetonitrile | 38.8 | 306 mμ (7940) | 283.5 mμ ( 9140) |

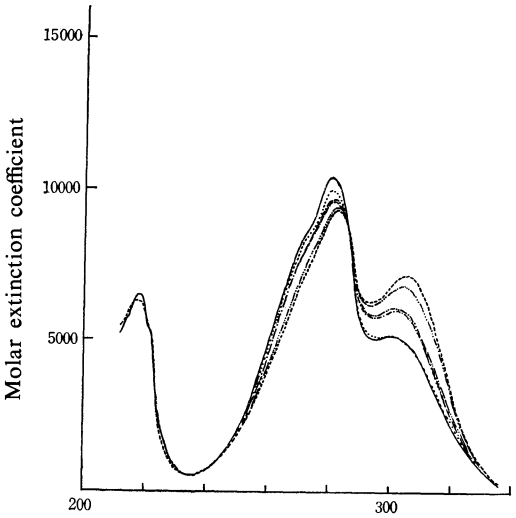



Fig. 4. The dependence of the 300—280 mμ bands of nitrosobenzene upon the ethanol content in the ethanol-*n*-heptane mixed solvents.

EtOH content
0 %
5 %
20 %
40 %
80 %
100 %

ethanol. Therefore, we can safely disregard the possibility that the above-mentioned solvent effect upon the absorption band of nitrosobenzene might be caused by hydrogen bonding. At least, it may be said that hydrogen bonding is not an important factor in the solvent effect. Furthermore, this solvent effect can not be due to the dimer formation because the $n\rightarrow\pi^*$ transition band at 760 mμ does not change in intensity when ethanol is added to the *n*-heptane solution. Therefore, it may be said that the change in the 300 mμ and 280 mμ bands of nitrosobenzene may be regarded as a general solvent effect caused by the polarity of the solvents.*

* In this case the polarity of the solvents has a wide meaning. Besides the average polarity represented by the dielectric constant or refractive index, the local polarity may take part in the solvent effect.

In this connection, it is noteworthy that the electron-donating group at the para position has the same effect upon the intensity of the 300 mμ band of nitrosobenzene. For instance, the corresponding band of *p*-nitrosotoluene, which appears at 310.8 mμ, has the molar extinction coefficient of 8800. This value is apparently larger than that of nitrosobenzene ($\varepsilon=5200$). This means that the methyl substitution brings about the red shift and intensity increment of the 300 mμ band of nitrosobenzene, as the polar solvents do. The above-mentioned solvent and substituent effects may be explained in terms of the stabilization of the charge-transfer structure which is caused by an electron transfer from the benzene ring to the nitroso group. This point will be discussed in detail below.

## Theoretical

The electronic structure of nitrosobenzene has been studied by taking eight π-electrons into account. First, the molecule was divided into two components; the benzene ring and the nitroso group. The molecular orbitals of these components were determined. Then the interaction between the two components was considered by means of the configurational interaction among such electron configurations as the ground, locally excited and charge-transfer configurations.[9] The eight electron configurations taken up in the present study are given in Table III. A similar calculation was made by Tanaka,[10] but he disregarded the locally excited configuration within the nitroso group.

First of all, let us evaluate the energy of each configuration, taking the energy of the ground configuration as the standard; $H_G=0$. The energies of the four locally excited configurations of benzene, $H_{E_{1u}}$, $H_{E_{1u'}}$, $H_{B_{1u}}$, and $H_{B_{2u}}$, were taken from the observed transition energies of the corresponding absorption bands of benzene.[11] Their values are shown in Table

9) H. G. Longuet-Higgins and J. N. Murrell, *Proc. Phys. Soc.*, **A68**, 601 (1955); J. N. Murrell, ibid., **A68**, 969 (1955).
10) J. Tanaka, *J. Chem. Soc. Japan, Pure Chem. Sec. (Nippon Kagaku Zassi)*, **78**, 1647 (1956); **79**, 1114 (1957).
11) K. Kimura and S. Nagakura, *Mol. Phys.*, to be published.

Table III. The energies and wave functions of the eight electron configurations

| Configuration* | Energy, eV. | Wave function |
|---|---|---|
| G ..... | $H_G = 0$ | $\Psi_G = \lvert 1\bar{1}2\bar{2}3\bar{3}s\bar{s}\rvert$** |
| LE* ..... | $H_{E1u} = 6.98$ | $\Psi_{E1u} = 1/2\{\lvert 1\bar{1}2\bar{2}3\bar{5}s\bar{s}\rvert + \lvert 1\bar{1}2\bar{2}5\bar{3}s\bar{s}\rvert - \lvert 1\bar{1}2\bar{4}3\bar{3}s\bar{s}\rvert + \lvert 1\bar{1}4\bar{2}3\bar{3}s\bar{s}\rvert\}$ |
| | $H_{E1u'} = 6.98$ | $\Psi_{E1u'} = -1/2\{\lvert 1\bar{1}2\bar{2}3\bar{4}s\bar{s}\rvert + \lvert 1\bar{1}2\bar{2}4\bar{3}s\bar{s}\rvert + \lvert 1\bar{1}2\bar{5}3\bar{3}s\bar{s}\rvert + \lvert 1\bar{1}5\bar{2}3\bar{3}s\bar{s}\rvert\}$ |
| | $H_{B1u} = 6.17$ | $\Psi_{B1u} = -1/2\{\lvert 1\bar{1}2\bar{2}3\bar{4}s\bar{s}\rvert + \lvert 1\bar{1}2\bar{2}4\bar{3}s\bar{s}\rvert - \lvert 1\bar{1}2\bar{5}3\bar{3}s\bar{s}\rvert - \lvert 1\bar{1}5\bar{2}3\bar{3}s\bar{s}\rvert\}$ |
| | $H_{B2u} = 4.89$ | $\Psi_{B2u} = 1/2\{\lvert 1\bar{1}2\bar{2}3\bar{5}s\bar{s}\rvert + \lvert 1\bar{1}2\bar{2}5\bar{3}s\bar{s}\rvert + \lvert 1\bar{1}2\bar{4}3\bar{3}s\bar{s}\rvert + \lvert 1\bar{1}4\bar{2}3\bar{3}s\bar{s}\rvert\}$ |
| LE ..... | $H_{LE} = 8.00$ | $\Psi_{LE} = (1/2)^{1/2}\{\lvert 1\bar{1}2\bar{2}3\bar{3}s\bar{w}\rvert + \lvert 1\bar{1}2\bar{2}3\bar{3}w\bar{s}\rvert\}$ |
| CT ..... | $H_{CT} = 4.10$ | $\Psi_{CT} = (1/2)^{1/2}\{\lvert 1\bar{1}2\bar{w}3\bar{3}s\bar{s}\rvert + \lvert 1\bar{1}w\bar{2}3\bar{3}s\bar{s}\rvert\}$ |
| | $H_{CT'} = 4.52$ | $\Psi_{CT'} = (1/2)^{1/2}\{\lvert 1\bar{1}2\bar{2}3\bar{w}s\bar{s}\rvert + \lvert 1\bar{1}2\bar{2}w\bar{3}s\bar{s}\rvert\}$ |

* G; ground configuration, LE*; locally (in benzene) excited configurations, LE; locally (in the nitroso group) excited configuration, CT; charge-transfer configurations.

** The precise form is as follows:

$$\Psi_G = (1/8!)^{1/2}\sum(-1)^p P\begin{Bmatrix}\phi_1(1)\phi_1(2)\phi_2(3)\phi_2(4)\phi_3(5)\phi_3(6)\phi_s(7)\phi_s(8)\\ \alpha(1)\ \beta(2)\ \alpha(3)\ \beta(4)\ \alpha(5)\ \beta(6)\ \alpha(7)\ \beta(8)\end{Bmatrix}$$

The molecular orbitals of benzene; $\phi_1$, $\phi_2$, $\phi_3$, $\phi_4$, and $\phi_5$ are given as follows:

$$\phi_1 = (1/6)^{1/2}(\chi_1+\chi_2+\chi_3+\chi_4+\chi_5+\chi_6)$$
$$\phi_2 = (1/12)^{1/2}(2\chi_1+\chi_2-\chi_3-2\chi_4-\chi_5+\chi_6)$$
$$\phi_3 = 1/2(\chi_2+\chi_3-\chi_5-\chi_6)$$
$$\phi_4 = 1/2(\chi_2-\chi_3+\chi_5-\chi_6)$$
$$\phi_5 = (1/12)^{1/2}(2\chi_1-\chi_2-\chi_3+2\chi_4-\chi_5-\chi_6)$$

The molecular orbitals of the nitroso group, $\phi_s$, $\phi_w$ are as follows[10]:

$$\phi_s = 0.6000\chi_N + 0.8000\chi_O$$
$$\phi_w = 0.8000\chi_N - 0.6000\chi_O$$

where $\chi_N$ and $\chi_O$ are the $2p\pi$ atomic orbitals of nitrogen and oxygen of the nitroso group respectively.

III. Furthermore, we assumed the energy of the locally excited configuration of the nitroso group, $H_{LE}$, as 8.00 eV. on the basis of the energy of the $\pi\rightarrow\pi^*$ transition band of chloronitrosocyclohexane. This compound exhibits a $\pi\rightarrow\pi^*$ transition band at about 160 m$\mu$ together with an $n\rightarrow\pi^*$ band at 650 m$\mu$.[12]

The energies of two charge-transfer configurations, $H_{CT}$ and $H_{CT'}$, which are caused by an electron transfer from the benzene ring to the nitroso group, are evaluated by the following equations:

$$H_{CT} = I_B - A_N - \Delta_{CT}$$
$$H_{CT'} = I_B - A_N - \Delta_{CT'}$$

where $I_B$ and $A_N$ are the ionization potential of benzene and the electron affinity of the nitroso group respectively, and where $\Delta_{CT}$ and $\Delta_{CT'}$ are the electrostatic interaction energies between the positive and negative charges caused by the electron transfer. The value of $I_B$ is set at 9.24 eV., a value which was determined by Watanabe[13] from a photoionization experiment. The electron affinity of the nitroso group was assumed to be 0.55 eV. The values of $\Delta_{CT}$ and $\Delta_{CT'}$ were calculated as 4.59 and 4.17 eV. respectively. The two-center

Table IV. The off-diagonal matrix elements*

$$H_{CT\cdot G} = (2/3)^{1/2}\cdot 0.8000\cdot(\beta+\beta') - (1/6)^{1/2}\cdot 0.6000\cdot(\beta''+\beta''')$$
$$H_{CT\cdot LE} = -(1/3)^{1/2}\cdot 0.6000\cdot(\beta+\beta') - (1/12)^{1/2}\cdot 0.8000\cdot(2\beta''+\beta''')$$
$$H_{CT\cdot E1u} = (1/8)^{1/2}\cdot 0.6000\beta'''$$
$$H_{CT\cdot E1u'} = -(1/6)^{1/2}\cdot 0.8000\cdot(\beta-\beta') + (1/24)^{1/2}\cdot 0.6000\cdot(2\beta''-\beta''')$$
$$H_{CT\cdot B1u} = (1/6)^{1/2}\cdot 0.8000\cdot(\beta-\beta') - (1/24)^{1/2}\cdot 0.6000\cdot(2\beta''-\beta''')$$
$$H_{CT\cdot B2u} = -(1/8)^{1/2}\cdot 0.6000\beta'''$$
$$H_{CT'\cdot G} = -(1/2)^{1/2}\cdot 0.6000\beta'''$$
$$H_{CT'\cdot LE} = -(1/2)0.8000\beta'''$$
$$H_{CT'\cdot E1u} = (1/6)^{1/2}\cdot 0.8000(\beta-\beta') - (1/24)^{1/2}\cdot(2\beta''-\beta''')$$
$$H_{CT'\cdot E1u'} = (1/8)^{1/2}\cdot 0.6000\beta'''$$
$$H_{CT'\cdot B1u} = (1/8)^{1/2}\cdot 0.6000\beta'''$$
$$H_{CT'\cdot B2u} = (1/6)^{1/2}\cdot 0.8000\cdot(\beta-\beta') - (1/24)^{1/2}\cdot 0.6000\cdot(2\beta''-\beta''')$$
$$H_{LE\cdot E1u} = (1/2)^{1/2}\{(sw\,|\,35) - (sw\,|\,24)\}$$**
$$H_{LE\cdot E1u'} = -(1/2)^{1/2}\{(sw\,|\,34) + (sw\,|\,25)\}$$**
$$H_{LE\cdot B1u} = -(1/2)^{1/2}\{(sw\,|\,34) - (sw\,|\,25)\}$$**
$$H_{LE\cdot B2u} = (1/2)^{1/2}\{(sw\,|\,35) + (sw\,|\,24)\}$$**

* $\beta$, $\beta'$, $\beta''$, and $\beta'''$ are the core resonance integrals for $C_1$—N, $C_2$—N, $C_1$—O and $C_2$—O bonds (see Fig. 5); they are −2.00 eV., −0.208 eV., −0.208 eV. and −0.062 eV. respectively.

** $(sw\,|\,mn) = \int \phi_s(1)\phi_w(1)\frac{e^2}{r_{12}}\phi_m(2)\phi_n(2)\,d\tau$

12) M. Tanaka and S. Nagakura, unpublished result.
13) K. Watanabe, *J. Chem. Phys.*, **26**, 542 (1957).

TABLE V. ENERGY LEVELS AND WAVE FUNCTIONS OF NITROSOBENZENE

| Energy eV. | Coefficients of electron configurations in the wave function of each level | | | | | | | |
|---|---|---|---|---|---|---|---|---|
| | $\Psi_G$ | $\Psi_{CT}$ | $\Psi_{CT'}$ | $\Psi_{LE}$ | $\Psi_{B_{2u}}$ | $\Psi_{B_{1u}}$ | $\Psi_{E_{1u}}$ | $\Psi_{E_{1u}'}$ |
| $W_0=-0.434$ | 0.9528 | 0.3003 | −0.0023 | −0.0315 | 0.0006 | 0.0239 | 0.0018 | −0.0208 |
| $W_1=4.079$ | −0.1501 | 0.4521 | 0.7120 | −0.1204 | 0.4588 | 0.1228 | 0.1416 | −0.0766 |
| $W_2=4.140$ | 0.2551 | −0.7633 | 0.4271 | 0.1719 | 0.2784 | −0.2005 | 0.0541 | 0.1402 |
| $W_3=5.205$ | −0.0041 | 0.0101 | −0.5164 | 0.0190 | 0.8422 | −0.0044 | −0.1529 | −0.0070 |
| $W_4=6.283$ | 0.0446 | −0.2035 | −0.0017 | 0.0407 | 0.0027 | 0.9653 | −0.0240 | 0.1502 |
| $W_5=6.994$ | −0.0020 | 0.0081 | −0.1852 | −0.2598 | 0.0452 | −0.0397 | 0.8228 | 0.4663 |
| $W_6=7.089$ | −0.0353 | 0.1829 | 0.0939 | −0.0001 | −0.0231 | −0.1038 | −0.4675 | 0.8524 |
| $W_7=8.283$ | −0.0363 | 0.2182 | −0.0276 | 0.9409 | 0.0033 | 0.0005 | 0.2395 | 0.0863 |

TABLE VI. CALCULATED AND OBSERVED TRANSITION ENERGIES AND OSCILLATOR STRENGTHS FOR THE ABSORPTION SPECTRUM OF NITROSOBENZENE

| Transition | Transition energy, eV. | | Oscillator strength | |
|---|---|---|---|---|
| | Calcd. | Obs.[a] | Calcd. | Obs.[a] |
| $W_0 \rightarrow W_1$ | 4.51 | 4.10 (301.4 mμ) | 0.099 | 0.084 |
| $W_0 \rightarrow W_2$ | 4.57 | 4.43 (281 mμ)<br>4.58 (272* mμ) | 0.258 | 0.202 |
| $W_0 \rightarrow W_3$ | 5.64 | 5.57 (222* mμ)<br>5.68 (218 mμ) | 0.002 | 0.087 |
| $W_0 \rightarrow W_4$ | 6.71 | 6.36 (194 mμ) | 0.058 | 0.256 |
| $W_0 \rightarrow W_5$ | 7.43 | 7.09 (174 mμ) | 1.058 | 0.831 |
| $W_0 \rightarrow W_6$ | 7.52 | | 1.115 | |
| $W_0 \rightarrow W_7$ | 8.72 | — | 0.629 | — |

a) The values observed with the *n*-heptane solution. * Vibrational structure

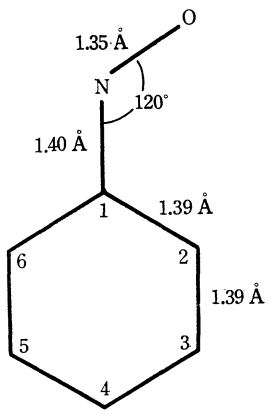



Fig. 5. The geometrical structure of nitrosobenzene.

Coulomb integrals of the (CC|NN) and (CC|OO) types necessary for the evaluation of $\Delta_{CT}$ and $\Delta_{CT'}$ were calculated by the aid of the quadratic equation of an atomic distance derived by Pariser and Parr's method.[14] For the actual calculations, the geometrical structure of nitrosobenzene was reasonably assumed to be as shown in Fig. 5, by making use of the X-ray crystal analysis data of the *p*-bromonitrosobenzene dimer.[15] Thus, the energies of the two charge-transfer configurations, $H_{CT}$ and $H_{CT'}$ were determined to be 4.10 eV. and 4.52 eV. respectively.

The off-diagonal matrix elements of the Hamiltonian of the total electrons were calculated following the procedure developed by Pople[16] and by Longuet-Higgins and Murrell[17]. The results are shown in Table IV, where $\beta$'s are the core resonance integrals; they were estimated on the assumption of the proportionality of the core resonance integrals to the overlap integrals.

The integrals (sw|35) in Table IV can be reduced to two center Coulomb integrals concerning appropriate atomic orbitals, which can be evaluated by the Pariser-Parr method mentioned above.

The energy levels and the wave functions finally evaluated by the aid of a FACOM 202 electronic computer are shown in Table V.

The oscillator strength, *f*, was calculated by means of the usual equation: [18]

$$f_{calc.}=1.085\times10^{-5}\times\nu Q^2$$

where $Q$ and $\nu$ are the transition moment (in

14) R. Pariser and R. G. Parr, ibid., **21**, 466, 767 (1953); **23**, 711 (1955).

15) C. Darwin and D. C. Hodgkin, *Nature*, **166**, 827 (1950).

16) J. A. Pople, *Proc. Phys. Soc.*, **A68**, 81 (1955).

17) H. C. Longuet-Higgins and J. N. Murrell, ibid., **A68**, 601 (1955).

18) R. S. Mulliken, *J. Chem. Phys.*, **7**, 34, (1939); J. R. Platt and H. B. Klevens, *Rev. Modern Phys.*, **16**, 183 (1944).

TABLE VII. DEPENDENCE OF TRANSITION ENERGIES AND OSCILLATOR STRENGTHS UPON THE ENERGIES OF THE CHARGE-TRANSFER CONFIGURATIONS

| | Case | 1 | 2 | 3 | 4 |
|---|---|---|---|---|---|
| | $H_{CT}$ = | 4.30 eV. | 4.10 eV. | 3.90 eV. | 3.70 eV. |
| | $H_{CT'}$ = | 4.72 eV. | 4.52 eV. | 4.32 eV. | 4.12 eV. |
| $W_0 \rightarrow W_1$ | Energy = | 4.63 eV. | 4.51 eV. | 4.38 eV. | 4.25 eV. |
| | $f$ value= | 0.061 | 0.099 | 0.134 | 0.137 |
| $W_0 \rightarrow W_2$ | Energy = | 4.71 eV. | 4.57 eV. | 4.44 eV. | 4.30 eV. |
| | $f$ value= | 0.288 | 0.258 | 0.234 | 0.231 |
| $W_0 \rightarrow W_3$ | Energy = | 5.68 eV. | 5.64 eV. | 5.61 eV. | 5.59 eV. |
| | $f$ value= | 0.003 | 0.002 | 0.002 | 0.001 |

units of Å) and the evaluated transition energy (in units of $cm^{-1}$) respectively. The evaluated oscillator strength values are, in Table VI, compared with the observed ones obtained by the following equation:

$$f_{obs.} = 4.32 \times 10^{-9} \times \int \varepsilon(\nu) d\nu$$

where $\varepsilon$ is the molar extinction coefficient.

### Theoretical Results and Discussion

When the calculated transition energy and the oscillator strength are compared with the observed values, the 174 m$\mu$ band, which was newly found by the present authors, can safely be assigned to the superposed $W_0 \rightarrow W_5$ and $W_0 \rightarrow W_6$ transitions, and the 194 m$\mu$ band, to the $W_0 \rightarrow W_4$ transition. Judging from the wave functions of the $W_4$, $W_5$ and $W_6$ levels, the former may be regarded as the shifted band of the $A_{1g} \rightarrow E_{1u}$ transition band of benzene, and the latter, as that of the $A_{1g} \rightarrow B_{1u}$ transition band of benzene.

The 218 m$\mu$ band corresponding to the $W_0 \rightarrow W_3$ transition may be said to have the nature of the $A_{1g} \rightarrow B_{2u}$ transition band of benzene, but the contribution from one of the charge-transfer configurations ($\phi_3^{-1}\phi_w$) amounts to 25%.

The 280.5 m$\mu$ band can be ascribed to the $W_0 \rightarrow W_2$ transition. The contributions of the charge-transfer configurations to the $W_2$ level amount to 62% (CT) and 17% (CT') respectively. Therefore, the 280.5 m$\mu$ band may safely be regarded as the charge-transfer absorption band, although there are small contributions of such other components as local excitations in the nitroso and benzene groups.

The 301.4 m$\mu$ band corresponding to the $W_0 \rightarrow W_1$ transition may be thought to have a character mixing locally excitation within the benzene ring ($B_{2u}$) and the charge-transfer excitation, since the contributions of the charge-transfer and $B_{2u}$ locally excited configurations are 49% (CT'), 18% (CT) and 20% ($B_{2u}$) respectively.

As was previously stated, the 280 m$\mu$ and 300 m$\mu$ bands are sensitive to the polarity of the solvent. In polar solvents, the absorption bands have a tendency to become similar to those of the *p*-nitrosotoluene and other simple *p*-substituted nitrosobenzene derivatives, as is shown in Fig. 4.

In order to explain the polar solvent effect, we calculated the energy levels and wave functions, changing the energy values of the two charge-transfer configurations, $H_{CT}$ and $H_{CT'}$. The results are tabulated in Table VII. It can be seen that the decrease in the energies of the two charge-transfer configurations brings about a decrease in the transition energies for the $W_0 \rightarrow W_1$ and $W_0 \rightarrow W_2$ and $W_0 \rightarrow W_3$ transitions and causes an increase in the oscillator strength for the $W_0 \rightarrow W_1$ transition. On the other hand, in the $W_0 \rightarrow W_2$ transition which corresponds to the 280 m$\mu$ band of nitrosobenzene, the oscillator strength very slightly decreases in the order of cases 1, 2, 3, and 4.

The above-mentioned theoretical results seem to explain the effects of solvents and of *p*-substituted electron-donating groups. That is to say, the wavelength shifts and intensity changes of the 300 m$\mu$ and 280 m$\mu$ bands may be thought to be caused by the fact that the energies of the charge-transfer configurations change with the polarity of solvents or when an electron-donating group is substituted for the hydrogen atom at the para position.

The authors wish to express their deep thanks to Dr. Katsumi Kimura for the measurement of the vacuum ultraviolet absorption spectrum.

*The Institute for Solid State Physics*
*The University of Tokyo*
*Azabu, Tokyo*

# Effects of Pressure on the Chemical Properties of the Solid Surface. I. Surface Acidities of Some Compressed Sulfates and Bisulfate

By Yoshisada OGINO and Takeshi KAWAKAMI

(Received August 31, 1964)

The effects of pressure on the chemical properties of gases and liquids have been thoroughly investigated. Furthermore, recent advances in high pressure chemistry have revealed an enhanced reactivity of solid substances at high pressures. However, except for some contributions from the Russian researchers,[1] no systematic investigations concerning the effect of pressure on the surface properties of solids have been reported. These circumstances have prompted the authors to investigate the chemical properties of the surface of a compressed solid. In the present paper, which is the first of a series, the effect of pressure on the surface acidity of some sulfates and a bisulfate is investigated.

Some solids have characteristic surface acidities, and it is believed that this acidity plays an important role in some surface catalyses where hydrocarbons or their derivatives are the reactants and products. Thus, it becomes important to increase the acidity to improve the catalytic activity. Attempts have been made to achieve this,[2,3] but application of high pressure to the solid has not yet been tested.

A well known fact[4] that the application of high pressure to an acidic solution makes the solution more acidic suggests that the surface acidity of solids might also be increased by compression. Of course, the detailed mechanism of the compression of solids should be different from that of liquids, and knowledge about a liquid system under high pressure can not always be extended to a solid system under high pressure. Nevertheless, the suggestion seems worth testing experimentally.

In the experimental work in this research, several metal sulfates and potassium bisulfate served as samples. The sample material was pulverized and the powder was compressed in a piston-cylinder apparatus at a pressure of 0—3000 kg./cm$^2$. The surface acidity, the water content, and the X-ray diffraction pattern were obtained for both the compressed sample and the uncompressed one. With some samples, the acidity was increased by the compression, whereas with other samples the acidity remained unchanged. In this paper, details of the experimental results are described and some possible explanations are discussed.

## Experimental

**Apparatus.** — The apparatus used for this study was essentially a piston-cylinder device employing a hardened chromium steel piston and a cylinder assembly of stainless steel. A cross section of the apparatus is given in Fig. 1. The piston consists of a head (20 mm. diam.) and a stem (8 mm. diam.). The cylinder is assembled from a body, a bottom cover, and four sets of nuts and bolts. The body cavity, in which the piston is to be inserted, consists essentially of two concentric vertical holes; the larger hole (20.1 mm. diam.) accomodates the piston head, and the smaller hole (8.1 mm. diam.) houses the piston stem, thus permitting vertical motion of the piston head.

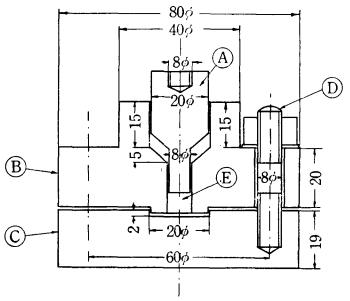



Fig. 1. A cross section of apparatus.
A: Piston B: Body
C: Bottom cover D: Bolt and nut
E: Sample room

The sample is compressed in the space bounded by the upper surface of the bottom cover, the wall of the smaller hole, and the face of the piston stem.

Pressure was applied to the piston by means of a commercial 4 ton scale oil press having two parallel beds, viz. a stationary bed and a moving bed. The load was measured by a Bourdon-gauge which is connected to the oil chamber of the press.

1) M. G. Gonikberg, "Chemical Equilibria and Reaction Rates at High Pressures," Israel Program for Scientific Translations, Jerusalem (1963), p. 92.
2) T. Shiba and E. Echigoya, *J. Chem. Soc. Japan, Pure Chem. Sec.* (*Nippon Kagaku Zasshi*), **76**, 1046 (1955).
3) K. Tanabe and R. Ohnishi, *J. Research Inst. Catalysis, Hokkaido University*, X, 229 (1962).
4) S. D. Hamann, "High Pressure Physics and Chemistry," Vol. 2, Ed. by R. S. Bradley, Academic Press, London and New York (1963), p. 148.

The pressure generated at the sample was estimated by dividing the load by the piston area (0.503 $cm^2$).

**Sapmle.** — The samples used in this study were colorless, commercial, metal sulfates (reagent grade) and potassium bisulfate (reagent grade). The material was gently pulverized in an agate mortar, and about 1 g. of the powder was packed into the sample room of the apparatus. Then, the apparatus was sandwiched between the two beds of the press, and the desired load was applied to the piston during 10 min., at room temperature. After compression, the sample was taken out from the apparatus, pulverized again, weighed and dried in a desiccator for 6 hr. Immediately after the drying,* the sample was submitted to the tests described below.

Uncompressed samples were also prepared by the above procedure but omitting the application of load.

**Surface Acidity.**—The qualitative effect of pressure on the surface acidity was observed by comparing the color of an indicator adsorbed on the sample compressed at 3000 kg./$cm^2$ with that of the same indicator adsorbed on the uncompressed sample. The comparison was carried out in the following way.

A given amount of sample powder was transferred to a 50 ml. conical flask containing 10 ml. of purified benzene. Then, several drops of an 0.1% indicator solution in benzene were added and the surface color of the sample was observed. At the same time, a similar observation was carried out with the uncompressed sample. The difference between the colors of the two samples was recorded. In this comparison, three indicators, i. e. *p*-dimethylaminoazobenzene ($pK_a$=3.3), benzeneazodiphenylamine ($pK_a$=1.5) and dicinnamalacetone ($pK_a$=−3.0) were used.

A quantitative determination of the surface acidity was carried out with four aluminum sulfate samples, compressed at 0, 1000, 2000 and 3000 kg./$cm^2$, respectively. For neutralization of the surface acid, a 1/100 or 1/1000 N solution of *n*-butylamine in benzene was used, and Benesi's method[5] was adopted to determine the quantity of *n*-butylamine required to neutralize the surface acid. In addition to the three indicators described above, phenylazonaphthylamine ($pK_a$=4.0) was also used in each of the determinations.

**Water Content.**—The content of the metal element in the desired sample was determined by a conventional chemical analysis, and on the basis of this result the water content in the sample was calculated. Six aluminum sulfate samples, compressed at 0, 1000, 2000, 3000, 4000 and 5000 kg./$cm^2$ respectively, were analyzed. Samples of magnesium sulfate, zinc sulfate, and potassium bisulfate, each compressed at 3000 kg./$cm^2$, as well as uncompressed samples of the above sulfates were similarly analyzed.

**Identification by X-Rays.**—The X-ray diffraction patterns of the powdered samples were determined with an X-ray diffractometer, employing Cu-$K\alpha$ radiation at 30 kV. and 15 mamp.** All those samples analyzed as above were used in this study.

## Results

**Surface Acidity.**—*Qualitative Results.*—Surface colors of the various samples are given in Table I; the samples are classified into three groups, i. e. I, II and III.

Potassium sulfate, barium sulfate, lead sulfate, and magnesium sulfate fall into group I. Both in the compressed and uncompressed

Table I.* Surface colors of various samples

| Indicator | *p*-Dimethylaminoazobenzene | | Benzeneazodiphenylamine | | |
|---|---|---|---|---|---|
| Pressure kg./$cm^2$ | 0 | 3000 | 0 | 3000 | |
| $BaSO_4$ | No color | No color | No color | No color | I |
| $PbSO_4$ | No color | No color | No color | No color | |
| $K_2SO_4$ | No color | No color | No color | No color | |
| $MgSO_4 \cdot 7H_2O$ | No color | No color | No color | No color | |
| $SrSO_4$ | Pink | Pink ♯ | Red | Red ♯ | II |
| $CaSO_4 \cdot 2H_2O$ | Pink | Pink ♯ | Red | Red ♯ | |
| $MnSO_4 \cdot 4H_2O$ | Pink (faint) | Pink ♯ (faint) | No color | No color | |
| $ZnSO_4 \cdot 7H_2O$ | Red | Red ♯ | Red (faint) | Red ♯(faint) | |
| $CdSO_4 \cdot 8H_2O$ | Red | Red + | Red | Red + | III |
| $Ce_2(SO_4)_3 \cdot 8H_2O$ | Red | Red + | Red (faint) | Red +(deep) | |
| $Fe_2(SO_4)_3 \cdot xH_2O$ | Red | Red + | Red (faint) | Red + | |
| $Al_2(SO_4)_3 \cdot 18H_2O$ | No color | Red + | No color | Red + | |
| $KHSO_4$ | Red | Red + | Red (faint) | Red + | |

* In this table, the mark ♯ indicates a case where the difference between the surface color of the uncompressed sample and the color of the compressed sample is uncertain, and the mark + indicates that the surface color was increased by compression.

* By the use of such a procedure reproducible experimental results were obtained.

5) H. A. Benesi, *J. Phys. Chem.*, **61**, 970 (1957).

** The following experimental conditions were used in the X-ray diffraction study: count full scale 1000 c. p. s., time constant 2 sec., scanning speed 1° 2$\theta$/min., chart speed 1.0 cm./min., divergence slit 0.2 mm., receiving slit 1.0 mm., room temperature 25°C.

states, these sulfates were nonacidic to all the indicators.

Strontium sulfate, calcium sulfate, zinc sulfate and manganese sulfate form group II. Both in the compressed and uncompressed states, all these sulfates were acidic to all the indicators, except for dicinnamalacetone, but the difference in surface color between the two states was hardly recognizable.

The surface acidity of the group III samples, i. e. cadmium sulfate, cerous sulfate, ferric sulfate, aluminum sulfate, and potassium bisulfate, was significantly increased by compression of the samples at 3000 kg./cm$^2$. A typical example of this group is aluminum sulfate. This sulfate in the uncompressed state was nonacidic, whereas in the compressed state it was acidic to all indicators except for dicinnamalacetone.

*Quantitative Results.*—Acid strength distribution curves for the aluminum sulfate samples, compressed at 1000 and 2000 kg./cm$^2$ respectively, are given in Fig. 2. The abscissa is

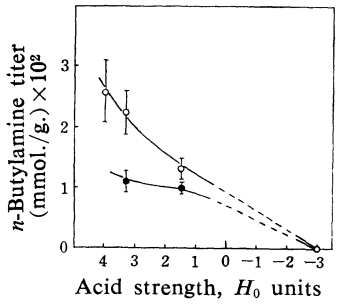



Fig. 2. *n*-Butylamine titers vs. acid strength for two aluminum sulfate samples compressed at 1000 kg./cm$^2$ (●) and 2000 kg./cm$^2$ (○), respectively.

Hammett's $H_0$ function[6] and the ordinate is the *n*-butylamine titer. The figure shows that the acid, which has appeared on the compressed aluminum sulfate, has an $H_0$ value not less than −3.0. This means that the acid on the sample surface is moderately strong. In a separate experiment, it has been shown that even by the compression at 3000 kg./cm$^2$ the $H_0$ value can not be decreased to a value less than −3.0.

The surface acidity of the aluminum sulfate sample at $H_0=3.3$ as a function of the compacting pressure is given in Fig. 3. The figure shows that the acidity is nearly proportional to the compacting pressure up to 2000 kg./cm$^2$, but beyond this pressure the increment of the acidity diminishes with increase of compacting pressure.

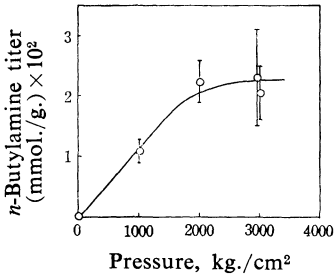



Fig. 3. *n*-Butylamine titers at $H_0=3.3$ vs. compacting pressure for aluminum sulfate.

**Water Content.**—*Aluminum Sulfate.*—The relation between the water content in the aluminum sulfate sample and the compacting pressure is given in Fig. 4 and Table II. In the figure, the water content is expressed as the number of moles of water per two gram atoms of aluminum. This figure shows a nearly proportional decrease of the water content with the compacting pressure in the range of 0—2000 kg./cm$^2$, but beyond 2000 kg./cm$^2$ the decrement of the content becomes smaller with increase of the compacting pressure, and at a pressure of 3000 kg./cm$^2$ or above, the content remains at a constant level.

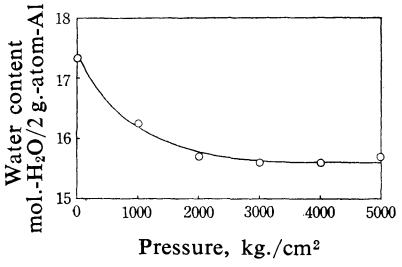



Fig. 4. Water contents of aluminum sulfate samples as a function of compacting pressure.

TABLE II. THE RATIO OF THE WATER CONTENT IN THE COMPRESSED SAMPLE TO THE WATER CONTENT IN THE UNCOMPRESSED SAMPLE

| | Pressure, kg./cm$^2$ | | | | | |
|---|---|---|---|---|---|---|
| Sulfate | 0 | 1000 | 2000 | 3000 | 4000 | 5000 |
| Aluminum sulfate | 1 | 0.94 | 0.91 | 0.90 | 0.90 | 0.91 |
| Magnesium sulfate | 1 | — | — | 0.98 | — | — |
| Zinc sulfate | 1 | — | — | 0.97 | — | — |

6) C. Walling, *J. Am. Chem. Soc.*, **72**, 1164 (1950).

*Potassium Bisulfate.*—A potassium determination showed that the potassium content, $K_0$, in the uncompressed sample is less than the content, $K$, in the compressed sample. Namely, the ratio of $K_0$ to $K$ was 0.96.

*Magnesium Sulfate and Zinc Sulfate.*—The results of the chemical analyses of a magnesium sulfate sample and a zinc sulfate sample given in Table II. For both sulfates, the water content in the compressed sample differed little from the content in the uncompressed sample.

**X-Ray Diffraction Studies.**—*Aluminum Sulfate.*—The X-ray diffraction pattern for an uncompressed aluminum sulfate sample is given in Fig. 5a. A sharp peak at $2\theta=20.1°$ was identified as the most characteristic peak of aluminum sulfate octadecahydrate. Further, each of the other main peaks, except for the peaks at $2\theta=24.8°$, 25.9°, 29°, and 36.8°, had a diffraction angle which corresponds well to the angle of the octadecahydrate, though its relative intensity against the peak height at $2\theta=20.1°$ did not strictly agree with that of the standard value.[7]

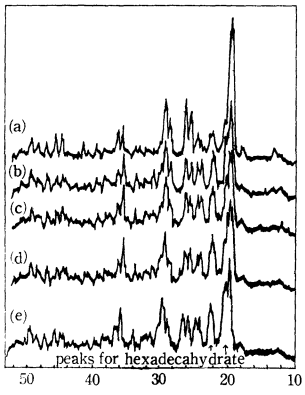



Fig. 5. X-Ray diffraction patterns for aluminum sulfate samples compressed at various pressures.
(a) Uncompressed sample
(b) 1000 kg./cm² (c) 2000 kg./cm²
(d) 3000 kg./cm² (e) 4000 kg./cm²

X-Ray diffraction patterns for aluminum sulfate samples compressed at various pressures are given in Figs. 5b—5e. Almost all the peaks which appear in Fig. 5a are also present in these patterns, though the peak at $2\theta=20.1°$ in Figs. 5b—5e has a low peak height in comparison with the corresponding peak height in Fig. 5a. Further, some peaks, especially peaks at $2\theta=20.3°$ and 22.7°, are more evident in the patterns for the compressed samples than in the pattern for the uncompressed sample. These two peaks were identified as the peaks which belong to the aluminum sulfate hexadecahydrate crystal.[8]

*Potassium Bisulfate.*—The X-ray diffraction pattern for uncompressed potassium bisulfate is given in Fig. 6a. A sharp peak at $2\theta=23°$ was identified as the most characteristic peak of potassium bisulfate. Except for some trivial peaks, e. g. peaks at $2\theta=20.2°$, 20.7°, 21.4°, 25°, and 25.6°, all of the other peaks were identified as the peaks of potassium bisulfate, though the observed diffraction angles and relative intensities against the peak at $2\theta=23°$ were somewhat irregular in comparison with the standard values.[9]

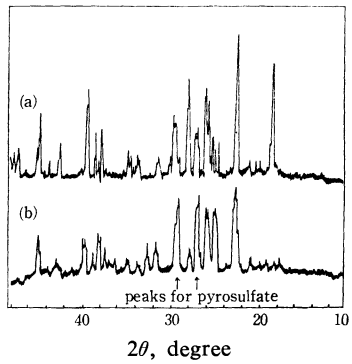



Fig. 6. X-Ray diffraction patterns for potassium bisulfate samples.
(a) Uncompressed sample
(b) Compressed sample (3000 kg./cm²)

The X-ray diffraction pattern for a compressed potassium bisulfate sample is given in Fig. 6b. In comparison with Fig. 6a, a general broadening in peak widths and reductions in peak heights for almost all peaks are seen in this figure. The most remarkable reduction in peak height is seen at $2\theta=23°$. Only a few peaks, e. g. peaks at $2\theta=25.3°$, 27.4° and 29.5°, are more evident in Fig. 6b than the corresponding peaks in Fig. 6a.

*Magnesium Sulfate and Zinc Sulfate.*—X-Ray diffraction patterns for an uncompressed magnesium sulfate sample and a compressed magnesium sulfate sample are given in Figs. 7a and 7b, respectively. In both figures sharp peaks due to magnesium sulfate heptahydrate are present, and small differences in the diffraction angle, in the relative intensity, and in Fig. 7b can be recognized.

X-Ray diffraction patterns of an uncompressed zinc sulfate sample and a compressed zinc sulfate sample are given in Figs. 8a and

7) "Index to the Powder Diffraction File," Ed. by J. V. Smith, ASTM Special Technical Publication 48-M2, Philadelphia (1963), No. 13.

8) H. Basset and T. H. Coodwin, *J. Chem. Soc.*, **1949**, 2239.

9) Ref. 7, No. 132.

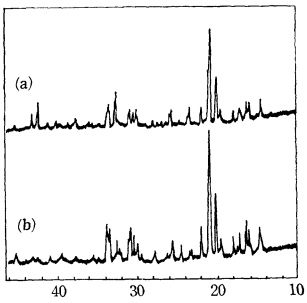



Fig. 7. X-Ray diffraction patterns for magnesium sulfate samples.
(a) Uncompressed sample
(b) Compressed sample (3000 kg./cm²)

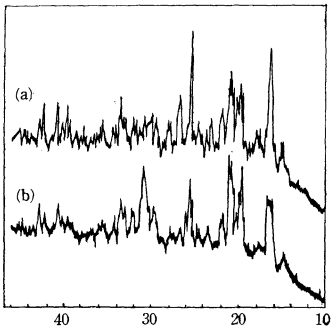



Fig. 8. X-Ray diffraction patterns for zinc sulfate samples.
(a) Uncompressed sample
(b) Compressed sample (3000 kg./cm²)

8b, respectively. There are some differences between these two figures. However, no evidence for the appearance of a new substance in the compressed sample can be seen from an inspection of Fig. 8b.

## Discussion

A brief survey of the experimental results presented in Table I might give the impression that the presence of a large quantity of crystallization water in the original material is the cause of the increase in acidity on compression. However, this impression is incorrect since the surface acidity of potassium bisulfate, which has no crystallization water in its original state, was increased markedly by compression.

Dehydration of the sample on compression seems to correlate with the acidity change on compression. For example, as can be seen from Table II, analysis of the aluminum sulfate samples, which showed a typical increase in acidity on compression, indicates that a considerable amount of water has disappeared from the compressed sample. Further, as is seen in Fig. 3 and Fig. 4, the relation between the water content of the aluminum sulfate sample and the compacting pressure parallels the relation between the acidity at $H_0=3.3$ and the compacting pressure.

The dehydration from the compressed aluminum sulfate samples might also be proved by the results of X-ray diffraction studies. Namely, X-ray diffraction patterns in Figs. 5b—5e show that the compressed aluminum sulfate sample is composed of aluminum sulfate octadecahydrate and aluminum sulfate hexadecahydrate, whereas Fig. 5a shows that the uncompressed aluminum sulfate sample may be regarded as a single phase which is composed of aluminum sulfate octadecahydrate. Irregularities* recognized in Fig. 5a are trivial, and they may be ignored in this discussion. Thus, it seems to be plausible to consider that the hexadecahydrate was formed through compression of the original octadecahydrate by the reaction

$$Al_2(SO_4)_3\cdot 18H_2O \rightarrow Al_2(SO_4)_3\cdot 16H_2O + 2H_2O \qquad (1)$$

It is well known that this sort of reaction can occur under a high pressure.[10]

With the aluminum sulfate sample, an interesting fact was deduced from a comparison of the results of the X-ray diffraction study and chemical analysis. Namely, as is seen in Fig. 4, at about 1300 kg./cm² or above, the water content in the compressed aluminum sulfate sample is less than 16, which corresponds to the number of moles of water in one mole of pure hexadecahydrate, whereas the X-ray diffraction pattern indicated that crystallites of the octadecahydrate and the hexadecahydrate coexist in the compressed sample. This leads to a contradiction, if the compressed sample is regarded as a mixture of these two hydrates with their pure forms. Therefore, a nonstoichiometric water content in either the octadecahydrate or the hexadecahydrate, or in both hydrates, must be assumed in order that the result of the X-ray diffraction study be compatible with the result of the chemical analysis. The surface property of a solid is often attributed to its nonstoichiometric composition, or a defective structure of the surface. Similarly, the deficiency of water in the compressed

10) S. D. Hamann, "Physico-Chemical Effects of Pressure," Butterworths Scientific Publications, London (1957), p. 208.

* Preferred orientations of cleavage planes by compression or structural changes of sample materials by air moisture etc. might be considered as the cause of irregularities of X-ray diffraction patterns of aluminum sulfate sample or other samples.

aluminum sulfate sample is suspected to play an important role in the appearance of acid centers on the surface of this sulfate.

A dehydration from the compressed potassium bisulfate sample is also possible, though this sample has no crystallization water in its original state. For instance, a dehydration through the reaction

$$2KHSO_4 \rightarrow K_2S_2O_7 + H_2O \qquad (2)$$

might occur, because the equivalent volume* of potassium bisulfate is 121.6, and the values for potassium pyrosulfate and water are 112 and 18 respectively, hence, according to Le Chatelier's principle, in a system where liberated water can escape out of the system, a shift of the equilibrium of the reaction 2 towards the right may be expected.

Indirect evidence for the occurrence of reaction 2 can be seen in the results of chemical analysis. Namely, the potassium content of the compressed potassium bisulfate sample is larger than that of the uncompressed sample, indicating that some of the original constituents, presumably water, have disappeared during compression.

The results of the X-ray diffraction study give additional evidence for the dehydration from the compressed potassium bisulfate sample. As is seen in Fig. 6b, the peak at $2\theta=23°$ is broad and low in comparison with the corresponding peak in Fig. 6a. This shows that compression has caused partial destruction of the original crystal structure. Further, the peaks at $2\theta=27.4°$ and 29.5° in Fig. 6b are more evident than the corresponding peaks in Fig. 6a. These two peaks were identified as the peaks of potassium pyrosulfate, though a minor deviation of the diffraction angle from the standard value[11] exists for each peak.

In contrast to the cases where the surface acidity was increased by compression, in cases where the acidity was not altered by compression, only minor dehydration of the compressed sample had occurred and changes in the crystal structure were trivial.

For instance, as is seen in Table II, the difference between the water contents of the compressed and the uncompressed samples of magnesium sulfate is slight. Further, the X-ray diffraction patterns in Figs. 7a and 7b show that little change in the crystal structure has resulted from compression of the magnesium sulfate. These results correspond well with the fact that the surface acidity of this sulfate was not increased by compression. In addition, Figs. 7a and 7b show that well developed crystallites of magnesium sulfate heptahydrate exist in both the compressed and the uncompressed samples, from which it can be concluded that surface defects would be sparse in both samples. This supposition is consistent with the result of the previous discussion in which the surface acidity of the compressed sample was interpreted in terms of a surface defect.

As is seen in Table II, the water content in the compressed zinc sulfate sample is only slightly different from that in the uncompressed sample. Thus, the small effect of pressure on the surface acidity of this sulfate may be attributed to the small extent of dehydration in the compressed sample.

On the other hand, as is seen in Figs. 8a and 8b, there are small differences in the X-ray diffraction patterns of the uncompressed and the compressed zinc sulfate samples; the former pattern has two sharp peaks at $2\theta=16.7°$ and 25.8°, while in the latter pattern these two peaks are broad and low. From this result, some differences in the surface acidities of the two samples might be expected. However, the expected increase in surface acidity could hardly be recognized from a color comparison. This apparent discrepancy may be partly ascribed to the existence of a considerable amount of surface acidity in the original sample, and partly to the small extent of dehydration in the compressed sample. Namely, any small increase in the surface acidity would be insignificant compared to the original high surface acidity of the sample and would not be detected simply by an indicator color change.

The surface acidity of the original zinc sulfate sample may be explained in terms of the X-ray diffraction data. As is seen in Fig. 8a, the peak at $2\theta=21.1°$ is low. If the uncompressed zinc sulfate has a perfect crystal structure, this peak should be the highest.[12] Therefore, it appears that the crystal structure of the uncompressed zinc sulfate is imperfect. As noted previously, imperfect crystal structures may be a cause of surface acidity.

Previously, Kiyama and Yanagimoto[13] reported that neither the chemical composition nor the crystal structure of calcium sulfate dihydrate was altered by compression. As might have been predicted from their results, compression of calcium sulfate dihydrate did not cause any change in its surface acidity (see Table I).

* The equivalent volume is defined by the following formula (Molec. wt./Specific wt.)×(No. of mol. of a reactant or a product in the stoichiometric eq.). (cf. Ref. 10).

11) Ref. 7, No. 134.

12) Ref. 7, No. 190.

13) R. Kiyama and T. Yanagimoto, *Rev. Phys. Chem. Japan*, **22**, 34 (1952).

**Summary**

Compression of potassium bisulfate and certain other metal sulfate has been shown to cause an increase in their surface acidities. This increase in surface acidity has been correlated with dehydration of the compressed sample, and X-ray diffraction studies have revealed that dehydration is accompanied by minor structural changes involving the formation of a less hydrated substance.

In those sulfates where compression produced little or no change in the surface acidity, the extent of the dehydration from the compressed sample was meager, and X-ray diffraction studies proved that neither the formation of a new substance nor a great change in the crystal structure resulted from the compression.

*Department of Chemical Engineering*
*Faculty of Engineering*
*Tohoku University*
*Sakura-Koji, Sendai*

# Initial Stage of the Oxidation Reaction of Polyethylene by Nitrogen Dioxide

By Taeko OGIHARA, Soji TSUCHIYA and Kenji KURATANI

(Received September 24, 1964)

In a previous paper,[1] the oxidation of polyethylene by nitrogen dioxide was investigated by means of infrared absorption spectroscopy, and the production of nitro, nitrite ester, nitrate ester, carbonyl and hydroxyl groups in polyethylene was recognized. The nitro and nitrite ester groups were produced in the early stage of the degradation by the addition of nitrogen dioxide to the reaction site in polyethylene, and then the nitrate ester, carbonyl and hydroxyl groups were formed as the decomposition products of the nitrite ester group. In that paper, however, no explanation was given of the nature of the reaction sites to which nitrogen dioxide reacted. The present report will attempt to clarify the reaction mechanism in the initial stage of the oxidation reaction of polyethylene by nitrogen dioxide. Particularly, an effort has been made to find out what structure in polyethylene is active in reacting with nitrogen diaxide.

## Experimental

The following polyethylenes were used: 1) high pressure polyethylene (HPE), relatively highly-branched polyethylene, called Yukalon, the molecular weight of which as obtained viscosity measurement, was 34000; 2) Phillips-type polyethylene (PhPE), very little-branched polyethylene, called Sholex, the molecular weight of which, as determined by the end group analysis of the infrared spectrum, was 13000; 3) Ziegler-type polyethylene (ZPE), called Hizex, the molecular weight of which as obtained by melt viscosity measurement, was 76000. None of them contained an anti-oxidant. A commercially-available polypropylene called Carlna, was used, from it an anti-oxidant was extractd by propyl alcohol.

The procedure of the reaction of polymers with nitrogen dioxide was the same as that reported in the earlier work.[1] The reaction temperature was 25—120°C, and the partial pressure of nitrogen dioxide in the reaction vessel was 1/3 atm.

Commercial *n*-heptane, decene-1, heptene-2 and 2-ethylhexene-1 were used and purified by fractional distillation. The reaction of the above alkenes with nitrogen dioxide was carried out in the medium of *n*-heptane as follows: the *n*-heptane solution of nitrogen dioxide was added to the *n*-heptane solution of the sample, and the reaction between the sample and nitrogen dioxide was allowed to proceed at 25°C, while the mixture was shaken for an hour. The infrared spectra of the reaction products in the solution of *n*-heptane were measured. Under these conditions, nitrogen dioxide did not react with *n*-heptane. The reaction of *n*-eicosane with nitrogen dioxide was carried out in a sealed tube at 25 and 100°C. The reaction products were dissolved in *n*-octane, washed by an aqueous sodium hydrogen carbonate solution, and water, and dried by sodium sulfate. The products obtained were identified by infrared absorption spectroscopy. Since the infrared spectra of the reaction products of those low molecular hydrocarbons were observed in the solution of *n*-heptane or *n*-octane, the wave number shift of the absorption peak due to the solvent effect was assumed to be similar to that of the reaction products in polyethylene.

1) T. Ogihara, This Bulletin, 36, 58 (1963).

The infrared spectra were measured by Perkin Elmer model 13 and Hitachi EPI-S spectrometers, equipped with NaCl and $CaF_2$ prisms. As the absorption band of the nitro group produced by the reaction was a doublet or had a complex shape, the absorption intensity of the band was of an apparent value. In the present experiment, the absorption intensity of the nitro group produced in polyethylene was the one relative to that of the C-H stretching absorption at 2650 $cm^{-1}$, i.e., $D(\nu_{NO_2})/D(2650\,cm^{-1})$; therefore, this value represented the absorption intensity of the nitro group formed in a polyethylene film of a constant thickness.

## Results and Discussion

Figures 1 and 2 show the absorption band of the N-O anti-symmetric stretching of the nitro group produced by the reaction. The wave number of the band depends on the reaction temperature and on the sample used. It may be seen in Figs. 1 and 2 that the absorption band of the nitro group formed by

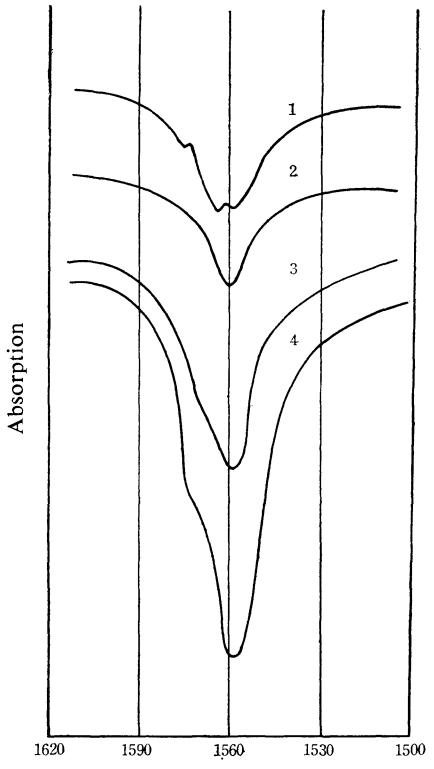



Fig. 1. Absorption band of the anti-symmetric vibration of the nitro group produced in HPE.
The samples are 1: HPE which was heated to 380°C in the atmosphere of nitrogen gas for 1 hr., and 2, 3, 4: untreated HPE. The reaction conditions were 1, 2: 25°C, 0.5 hr., 3: 80°C, 0.5 hr., 4: 109°C, 0.5 hr.

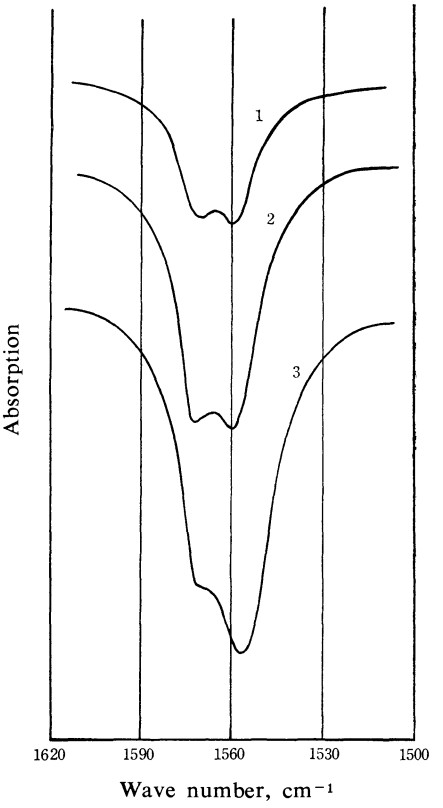



Fig. 2. Absorption band of the anti-symmetric vibration of the nitro group produced in PhPE.
The reaction conditions were 1: 25°C, 0.5 hr., 2: 80°C, 0.5 hr., 3: 120°C, 0.5 hr.

the reaction has two peaks, i.e., in the region A (1555—1560 $cm^{-1}$) and in the region B (1568—1570 $cm^{-1}$). The results are summarized in Table I. All of the polyethylene used, when treated with nitrogen dioxide at various temperatures, showed the absorption peak in the region A. The B absorption band of the nitro group was found in Phillips-type polyethylene (PhPE) oxidized by nitrogen dioxide at both 25 and 120°C. On the contrary, the B band appeared in high-pressure polyethylene (HPE) oxidized above 100°C, while no absorption peak in the region B was observed in HPE treated with nitrogen dioxide at 25°C.

The rate of increase in the absorption intensity of the nitro group formed in PhPE and HPE is given in Fig. 3 as a function of the reciprocal of the reaction temperature. The increment of the rate obtained against the reciprocal of the reaction temperature was not constant in the temperature range of the present experiment; i.e., the negative slope at a high temperature was steeper than that at a low temperature.

TABLE I. WAVE NUMBER OF THE ANTI-SYMMETRIC VIBRATION OF THE NITRO GROUP IN THE REACTION PRODUCTS

| Sample* | Reaction temp. and time | | Wave number of absorption peak | |
|---|---|---|---|---|
| | | | Region A | Region B |
| | °C | hr. | $cm^{-1}$ | $cm^{-1}$ |
| HPE | 25 | 0.5 | 1557 | — |
| | 109 | 0.5 | 1555 | 1568 |
| Degraded HPE | 25 | 0.5 | 1557, 1561 | 1568 |
| PhPE | 25 | 0.5 | 1560 | 1570 |
| | 120 | 0.5 | 1556 | 1568 |
| ZPE | 28 | 0.5 | 1559 | 1569 |
| | 105 | 0.5 | 1555 | 1568 |
| Polypropylene | 30 | 0.5 | — | — |
| | 110 | 0.5 | 1555 | — |
| *n*-Eicosane | 25 | 24 | — | — |
| | 100 | 24 | 1558 | 1570 |
| Heptene-2 | 25 | 1 | 1559 | — |
| 2-Ethylhexene-1 | 25 | 1 | 1561 | — |
| Decene-1 | 25 | 1 | 1562 | 1568 |

* HPE : high pressure polyethylene.
Degraded HPE : HPE which was heated to 380°C in the atmosphere of nitrogen gas for 1 hr.
PhPE : Phillips type polyethylene.
ZPE : Ziegler type polyethylene.

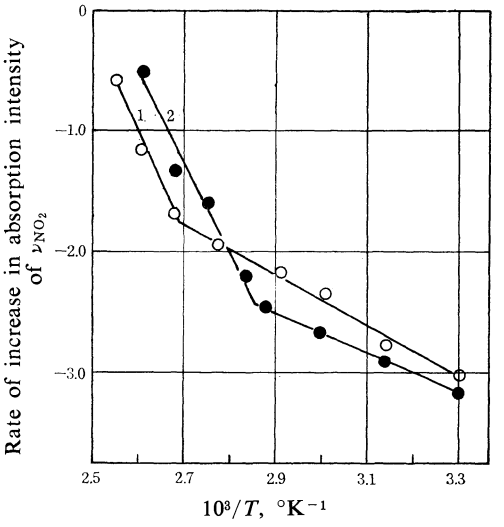



Fig. 3. Rate of increase in the absorption intensity of the nitro group formed in polyethylene. Increasing rate is represented by $\ln d\{D(\nu_{NO_2})/D(2650\,cm^{-1})\}/dt$ $hr^{-1}$.
1 : PhPE, 2 : HPE

The absorption intensity of the nitro groups in PhPE and HPE reached a maximum value in a certain reaction time when the reaction with nitrogen dioxide was carried out at 25°C, as may be seen in Fig. 4. However, the

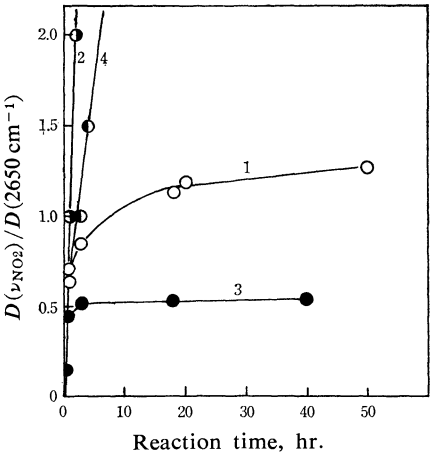



Fig. 4. Rate of formation of the nitro group in polyethylene.
1 : PhPE at 25°C, 2 : PhPE at 100°C, 3 : HPE at 25°C, 4 : HPE at 100°C

absorption intensity of the nitro group increased at an almost constant rate at a high temperature, and the obtained intensity was much larger than that obtained at a low temperature. These results show that the reaction mechanism of polyethylene with nitrogen dioxide at a high temperature differs from that at a low temperature. First, the reaction at low temperature will be discussed.

**The Addition Reaction of Nitrogen Dioxide with a Double Bond in Polyethylene.** — The absorption intensity of the nitro group which was formed by the reaction with nitrogen dioxide at 25°C did not exceed a certain value, even if a specimen of polyethylene was placed in contact with nitrogen dioxide for a long time, as Fig. 4 shows. This indicates that only a limited number of reaction sites which are active in reacting with nitrogen dioxide at 25°C exist in polyethylene.

The nitro group was not formed in *n*-eicosane (*n*-$C_{20}H_{42}$), which was left alone in an atmosphere of nitrogen dioxide at 25°C for 24 hr. or longer. Therefore, nitrogen dioxide did not react with the main methylene chain in polyethylene at 25°C. It is well known that polyethylene contains a small amount of structural irregurarity in the main chain, e. g., branchings and double bonds. Nitrogen dioxide, which has an odd electron, easily undergoes the addition reaction with double bonds in olefin. Decene-1, heptene-2 and 2-ethylhexene-1, all of which had double bonds at various positions, reacted with nitrogen dioxide at 25°C, and the products had an absorption band of the nitro group, while the absorption band due to the out-of-plane vibration of a double bond disappeared in the

infrared absorption spectra of the products. In that case, after all of the double bonds in the olefin solution had disappeared as a result of the addition reaction of nitrogen dioxide, the absorption intensity of the nitro group in the products retained a constant value even if a longer reaction time and a higher concentration of nitrogen dioxide were adopted. That is, there is a linear relationship between the absorption intensity of the nitro group in the products and the initial amount of olefin in the solution. This is illustrated in Fig. 5. Furthermore, polypropylene, in which double bond was not identified by the infrared spectroscopy, did not react with nitrogen dioxide at 25°C, and no formation of the nitro group could be observed.

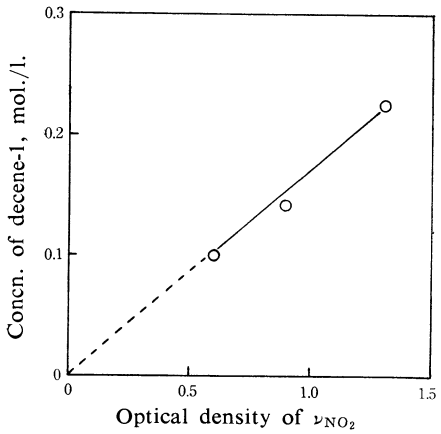
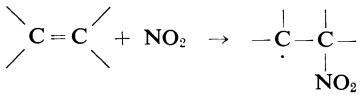
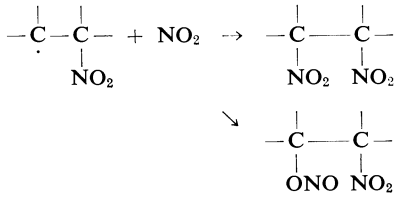



Fig. 5. Relationship between the concentration of decene-1 and the absorption intensity of the nitro group produced. The infrared spectra were measured in *n*-heptane solution and the absorption cell of 0.098 mm. in thickness.

Therefore, it can be concluded that the reaction sites, which react with nitrogen dioxide at 25°C, are double bonds in polyethylene. The nitro group is formed in polyethylene by the addition of nitrogen dioxide to the double bond. Gray and Yoffe have proposed the following mechanism of the addition reaction of nitrogen dioxide with a low molecular olefin[2] first, the nitro group is formed by the reaction:



and the radical produced is subjected to the further addition of nitrogen dioxide:



The products are dinitro and nitro-nitrite compounds in almost equal amounts, and the proportion of the nitro to the nitrite ester group of the products is 3 : 1. This explanation is compatible with the present experimental observation that the absorption intensity of the nitrite ester group is much smaller than that of the nitro group in polyethylene treated with nitrogen dioxide at 25°C. However, a quantitative discussion of the number of the nitro group produced from one double bond in polyethylene is difficult as a result of the complex shape of the absorption band of the nitro group. The nitrite ester group is unstable, and it often changes into a nitrate or carbonyl group, as has already been mentioned.[1]

Figure 6 shows the absorption band of the nitro group which has been produced in decene-1, heptene-2 and 2-ethylhexene-1 by the addition of nitrogen dioxide to their double bonds at 25°C. The absorption band of the nitro group formed in decene-1 had two peaks, at 1562 and 1568 $cm^{-1}$; a similar finding was obtained regarding the absorption band of the nitro group in PhPE, which underwent the addition reaction with nitrogen dioxide at 25°C, as Fig. 2 shows. This can be explained by the fact that most of the double bonds in PhPE are positioned at the terminals of the polymer chains;[3] that is, the double bond in PhPE is of the vinyl type and exactly the same as decene-1. Therefore, the reaction products of PhPE with nitrogen dioxide can be expected to have the same structure as those of decene-1; in other words, it gives the same infrared absorption spectrum. It may be seen in Figs. 1, 2 and 6 that no example of a doublet absorption band of the nitro group, which has been found in the reaction products at 25°C, exists except for the reaction products of PhPE and decene-1. This leads to the conclusion that the absorption band, in which two peaks are observed in the wave number regions A and B is characteristic of the additional reaction product of nitrogen dioxide to the double bond of the terminal vinyl-type in polyethylene. The wave number of the absorption band of the primary nitro compound is slightly larger than that of the secondary or tertiary one.[4] This is probably one of the reasons why the

2) P. Gray and A. D. Yoffe, *Chem. Revs.*, **55**, 1069 (1955).
3) M. Dole, D. C. Milner and T. F. Williams, *J. Am. Chem. Soc.*, **80**, 1580 (1958).
4) J. F. Brown, ibid., **77**, 6341 (1955).

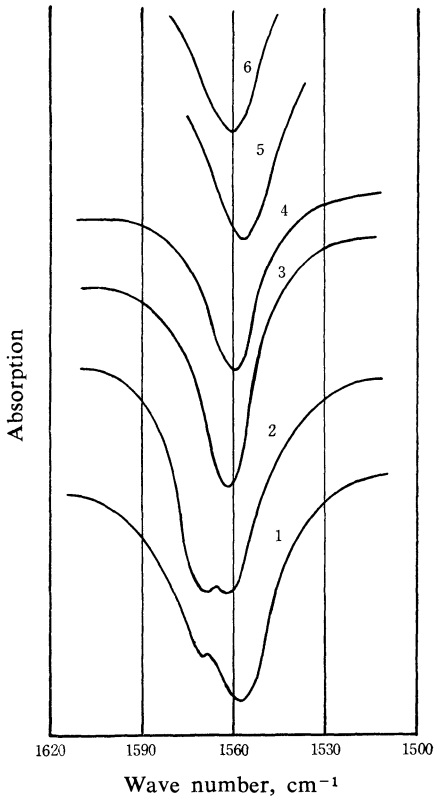



Fig. 6. Absorption band of the anti-symmetric vibration of the nitro group produced in low molecular compounds.
1 : *n*-eicosane, treated with nitrogen dioxide at 100°C for 24 hr., 2 : decene-1, 25°C, 1 hr., 3 : 2-ethylhexene-1, 25°C, 1 hr., 4 : heptene-2, 25°C, 1 hr., 5 : 2-nitropropane, 6 : 1-nitropropane.

nitro group produced in the terminal double bond has two absorption peaks in the regions A and B. Another conceivable reason is the coupling of the $NO_2$ anti-symmetric stretching vibration of the two nitro groups at the chain terminal. This coupling causes the splitting of the two nitro group vibrations.

The absorption band of the nitro group, which was produced in HPE by the reaction at 25°C, had only one peak in the region A. The same result was obtained in the reaction products of heptene-2 and 2-ethylhexene-1, when nitrogen dioxide was added at 25°C. This result is reasonable, since most of the double bonds in HPE are vinylene and vinylidene in type.[3] The dinitro compound obtained from the double bond of the vinylidene type may have primary and tertiary nitro groups, while only one absorption peak in the region A has been observed here. No satisfactory explanation for this fact has been obtained in the present experiment.

Ziegler-type polyethylene (ZPE) has double bonds of the above-mentioned three types,[3] while the absorption band of the nitro group produced in ZPE has two peaks in the regions A and B as Table I shows. However, the absorption intensity of the B band was smaller than that of the A band, since the nitro group produced from double bonds of vinylene and vinylidene types contributed only to the A band.

Though the nitro group produced in HPE at 25°C had no infrared absorption peak in the region B, a specimen of HPE showed a small absorption peak in the region B when heated to 380°C for 1 hr. in an atmosphere of nitrogen gas and reacted with nitrogen dioxide at 25°C after cooling, as is shown in Fig. 1. This result can be interpreted by means of the fact that double bonds of the vinyl-type are formed at the terminal of the polyethylene chain, probably as a result of the scission of the polymer chain.

**Hydrogen Abstraction Reaction by Nitrogen Dioxide.**—At a high reaction temperature, the absorption intensity of the nitro group formed in polyethylene was much stronger than that at a low temperature, and it increased linearly with the reaction time, as may be seen in Fig. 4. This finding shows that the reaction site of polyethylene is not double bond, which exists in a limited amount in polyethylene. Both *n*-eicosane and polypropylene, which did not react with nitrogen dioxide at 25°C, produced the nitro group by the reaction at a high temperature. Therefore, it is evident that the reaction site, which has not existed originally in polyethylene, is formed by nitrogen dioxide at a high temperature. The reaction site cannot be expected to be formed by the thermal decomposition of polyethylene at the present reaction temperature. However, it is probable that the hydrogen atom is abstracted by nitrogen dioxide from polyethylene and that the free radical thus produced becomes the reaction site for the addition reaction of nitrogen dioxide.

In the reaction of PhPE with nitrogen dioxide at a high temperature, both A and B absorption bands of the nitro group were observed, while the intensity of the A absorption band was much stronger than that of the B band. The absorption intensity of the A band increased as the reaction temperature was raised, as may be seen Fig. 2. This means that the hydrogen atom in the methylene chain in the polymer is abstracted and that the radical so produced reacts with nitrogen dioxide to form the secondary nitro group, which has an infrared absorption peak only in the region A. Similarly, the increase in the

absorption intensity of the A band was observed in the reaction of HPE at 110°C, where the absorption shoulder in the region B was found as shown in Fig. 1. This is considered to be due to the formation of the nitro group bonded to the terminal carbon atom of the polymer chain; it can be explained by the assumption that the scission of the polymer chain occurs in the process of the oxidation by nitrogen dioxide.

In the initial stage of the reaction with nitrogen dioxide at a high temperature, the following reactions are conceivable:

$$RH + NO_2 \xrightarrow{k_1} R + HNO_2 \quad (1)$$

$$R + NO_2 \xrightarrow{k_2} RNO_2 \quad (2)$$

$$R + NO_2 \xrightarrow{k_3} RONO \quad (3)$$

where reaction 1 represents the formation of the free radical as the result of the abstraction of the hydrogen atom from polyethylene by nitrogen dioxide. Nitrogen dioxide adds immediately to the radical produced, and the nitro and nitrite ester groups are formed by reactions 2 and 3. In reactions 1—3, the rate-determining step is reaction 1, since the radical recombination rate of reactions 2 and 3 are considered to be fast. The thermal decomposition of the nitro group does not occur in the temperature range of the present experiment, so that the information about the rate of reaction 1 can be obtained by the measurement of the concentration of the nitro group produced in polyethylene. In the present experiment, the increasing rate of the absorption intensity of the nitro group was observed to be independent of the film thickness in the 0.05—0.2 mm. range, where the absorption intensity of the nitro group was relative to that of the 2650 $cm^{-1}$ band and the effect of film thickness was removed. Therefore, it can be assumed that the diffusion of nitrogen dioxide into a polyethylene film has no considerable effect on the rate of the reaction.

The rate of the formation of the nitro group is represented by the following equation:

$$d[RNO_2]/dt = k_1[RH][NO_2]/\{1 + (k_3/k_2)\}$$

where $k_1$, $k_2$ and $k_3$ are the rate constants of reactions 1, 2 and 3 respectively, and a steady condition is assumed. It has been reported in a previous paper[5] that the ratio of the nitro to the nitrite ester group formed in the reaction at 100°C is about 2:1; it is reasonable to consider that this ratio does not vary upon a small change in the reaction temperature. Therefore, $k_3/k_2$ can be assumed to be independent of the reaction temperature. Figure 3 shows the increasing rate of the absorption intensity of the nitro group in the initial stage of the reaction. Here the absorption intensity of the nitro group is approximately proportional to the concentration of the nitro group in polyethylene, and it is further assumed that polyethylene and nitrogen dioxide exist in excess in the reaction system. As has already been mentioned, it may be seen in Fig. 3 that the slope of the straight line in the high temperature region differs from that in the low temperature region. The former slope corresponds to the activation energy of the hydrogen abstraction reaction by nitrogen dioxide, while the latter corresponds to that of the addition reaction of nitrogen dioxide to the double bonds contained in polyethylene.

The apparent activation energy obtained is shown in Table II. The present value of the activation energy is not very accurate, because a number of samples should be used in following the reaction process at a given temperature and so it has been difficult to obtain the complete reproducibility of the reaction. However, the activation energy of the hydrogen abstraction reaction from HPE or ZPE seems smaller than that of PhPE. This is perhaps due to the existence of branching in the polymer chain of HPE or ZPE. Harnsberger[6] obtained the activation energy of the overall reaction, $CH_4 + NO_2 \rightarrow CH_3NO_2$, as 21 kcal./mol. Semenov's empirical formula[7] to obtain the activation energy of the hydrogen abstraction reaction gives a value of 19 kcal./mol. in the $C_3H_8 + NO_2 \rightarrow iso\text{-}C_3H_7 + HNO_2$ reaction. Compared with these values, the present result is considered to be reasonable. Of course, it is

Table II. Apparent activation energy in kcal./mol.*

| Sample** | Hydrogen abstraction reaction | Addition reaction with double bond |
|---|---|---|
| HPE | 14 | 2 |
| PhPE | 17 | 4 |
| ZPE | 14 | 2 |
| Polypropylene | 15 | — |

* The error in activation energy is about ±2 kcal./mol.

** See Table I for abbreviations.

5) T. Ogihara, S. Tsuchiya and K. Kuratani, *Collected Papers of Aero. Res. Inst., Univ. Tokyo (Kôkû Kenkyûsho Shûhô)*, 3. 260 (1963).

6) H. F. Harnsberger, Thesis, Univ. of California, Berkeley (1951), cited in Ref. 2.

7) N. N. Semenov, "Some Problems in Chemical Kinetics and Reactivity," translated by M. Boudart, Princeton Univ. Press, N. J. (1958), p. 29.

unlikely that the present experimental value is the activation energy of the elementary reaction, because the present reaction system is not homogeneous and many assumptions are made.

## Conclusion

The reaction mechanism in the initial stage of the reaction between polyethylene and nitrogen dioxide differs with the reaction temperature. At room temperature, nitrogen dioxide adds to the double bond which exists originally in polyethylene, and dinitro or nitro-nitrite compounds are produced. At a high temperature, above 100°C, in addition to the above reaction, nitrogen dioxide reacts with the methylene chain of polyethylene. That is, the reaction is initiated by the hydrogen abstraction from polyethylene, and the free radicals produced undergo the combination reaction with nitrogen dioxide. The activation energy of hydrogen abstraction reaction by nitrogen dioxide is estimated to be 14—17 kcal./mol. on the basis of the measured data of the absorption intensity of the nitro group.

*The Textile Research Institute of the Japanese Government*
*Kanagawa-ku, Yokohama (T. O.)*

*Institute of Space and Aeronautical Science*
*The University of Tokyo*
*Meguro-ku, Tokyo (S. T. & K. K.)*

# Formation Constants of Sulfato, Acetato and Sulfatoacetato Complexes of Copper(II) at Ionic Strength 1.0

By Nobuyuki TANAKA, Yu SAITO and Hiroshi OGINO

(Received November 6, 1964)

In the previous papers,[1,2] new polarographic methods were presented for the determination of the formation constants of metal acetato complexes. They were based on the quantitative analysis of the effect of acetate ions on the equilibria of the reaction,

$$M + L \rightleftarrows ML$$

or $$M + M'L \rightleftarrows ML + M'$$

where L represents a suitable complex-forming substance such as nitrilotriacetate or ethylenediaminetetraacetate.

The method was extended to the analysis of the effects of acetate ions and co-existing ions Z on the equilibria of the first reaction to determine the formation constants of the complexes with Z ions and those of the mixed ligand complexes with acetate and Z ions.[3,4]

In this study, the method in which the equilibrium of the second reaction is used has been developed and it has been applied to the determination of the formation constants of copper(II) complexes with acetate and/or sulfate ions.

The formation constants of sulfatocopper(II) complexes have been reported by Fronaeus[5,6] and by Näsänen and Lumme[7] and that of sulfatoacetatocuprate(II) by Fronaeus.[5] The values obtained in this study have been compared with those data.

## Theoretical

Let us consider the acetate buffer solution which contains two different metal ions, $M^{m+}$ and $M'^{m'+}$, and ethylenediaminetetraacetate (EDTA) ions and co-existing ions Z. There exist the following equilibria:

$$M^{m+} + M'Y^{(m'-4)+} \rightleftarrows MY^{(m-4)+} + M'^{m'+} \quad (1)$$

$$MY^{(m-4)+} + H^+ \rightleftarrows MHY^{(m-3)+} \quad (2)$$

$$M'Y^{(m'-4)+} + H^+ \rightleftarrows M'HY^{(m'-3)+} \quad (3)$$

$$M^{m+} + i\,OAc^- + j\,Z^{z-} \rightleftarrows M(OAc)_i(Z)_j^{(m-i-zj)+} \quad (4)$$

$$M'^{m'+} + i'OAc^- + j'Z^{z-} \rightleftarrows M'(OAc)_{i'}(Z)_{j'}^{(m'-i'-zj')+} \quad (5)$$

1) N. Tanaka and K. Kato, This Bulletin, **32**, 516 (1959).
2) N. Tanaka and K. Kato, ibid., **33**, 417 (1960).
3) N. Tanaka and H. Ogino, ibid., **34**, 1040 (1961).
4) N. Tanaka, Y. Saito and H. Ogino, ibid., **36**, 794 (1963).
5) S. Fronaeus, Diss. Lund (1948); *Acta Chem. Scand.*, **4**, 72 (1950).
6) S. Fronaeus, ibid., **5**, 859 (1951).
7) R. Näsänen and P. Lumme, ibid., **5**, 13 (1951).

where $Y^{4-}$ means a completely dissociated EDTA anion and $Z^{z-}$, a co-existing ion such as sulfate. As was mentioned previously,[3] the concentrations that can be determined from the polarographic measurement are $[M^{m+}]_{app}$ and $[M'^{m'+}]_{app}$ given by the equations,

$$[M^{m+}]_{app} = \sum_{i=0}^{n}\sum_{j=0}^{p} M(OAc)_i(Z)_j^{(m-i-zj)+} \quad (6)$$

$$[M'^{m'+}]_{app} = \sum_{i'=0}^{n'}\sum_{j'=0}^{p'} M'(OAc)_{i'}(Z)_{j'}^{(m'-i'-zj')+} \quad (7)$$

respectively.

In the present case when the equilibria given by Eqs. 1 to 5 are dealt with, the following equations were obtained by the procedure which is a combination of the procedure for Eq. 14 in Ref. 2 and that for Eq. 13 in Ref. 3 and by replacing $\beta$ and $\beta'$ by $\alpha_{MHY}$ and $\alpha_{M'HY}$ respectively.

$$\frac{1}{K^{M}_{M'app}}\sum_{i'=0}^{n'}\sum_{j'=0}^{p'} K_{M'(OAc)_{i'}(Z)_{j'}}[OAc^-]^{i'}[Z^{z-}]^{j'} = \frac{\alpha_{M'HY}}{\alpha_{MHY}K^{M}_{M'}}\sum_{i=0}^{n}\sum_{j=0}^{p} K_{M(OAc)_i(Z)_j}[OAc^-]^i[Z^{z-}]^j \quad (8)$$

$$K^{M}_{M'app} = \frac{[M'^{m'+}]_{app}\{[MY^{(m-4)+}]+[MHY^{(m-3)+}]\}}{[M^{m+}]_{app}\{[M'Y^{(m'-4)+}]+[M'HY^{(m'-3)+}]\}} \quad (9)$$

$$K^{M}_{M'} = \frac{[M'^{m'+}][MY^{(m-4)+}]}{[M^{m+}][M'Y^{(m'-4)+}]} \quad (10)$$

$$\alpha_{MHY} = 1 + K^{H}_{MHY}[H^+],\ \alpha_{M'HY} = 1 + K^{H}_{M'HY}[H^+] \quad (11)$$

where $K_{M(OAc)_i(Z)_j}$ and $K_{M'(OAc)_{i'}(Z)_{j'}}$ represent the overall formation constants of $M(OAc)_i(Z)_j^{(m-i-zj)+}$ and $M'(OAc)_{i'}(Z)_{j'}^{(m'-i'-zj')+}$, respectively.

Under the condition that $[M]_t + [M']_t > [EDTA]_t$ where subscript t means the total concentration of the species, the concentration of the uncombined EDTA is negligibly small as compared with those of other species in the solution, and consequently $K^{M}_{M'app}$ given by Eq. 9 is obtained by the determination of either $[M^{m+}]_{app}$ or $[M'^{m'+}]_{app}$.

Equation 8 is rewritten as,

$$F_0 = \frac{\alpha_{M'HY}}{\alpha_{MHY}K^{M}_{M'}}\sum_{i=0}^{n}\sum_{j=0}^{p} K_{M(OAc)_i(Z)_j}[OAc^-]^i[Z^{z-}]^j \quad (8')$$

where the left-hand side of Eq. 8 is replaced by $F_0$. The values of $F_0$ are calculated with the known values of $K_{M'(OAc)_{i'}(Z)_{j'}}$ and the $K^{M}_{M'app}$ values which are determined at the given pH, the given ionic strength and various concentrations of acetate and $Z^{z-}$ ions. Equation 8' is essentially the same as the $F_0$ function reported previously.[3] Therefore, all of $K_{M(OAc)_i(Z)_j}$ can, at least theoretically, be determined by means of the same procedure reported previously.[3] On the other hand, when the formation constants of $M(OAc)_i(Z)_j^{(m-i-zj)+}$ are known, similar relations are derived, and the values of $K_{M'(OAc)_{i'}(Z)_{j'}}$ can also be determined by the same procedure as for those of $K_{M(OAc)_i(Z)_j}$.

## Experimental

**Reagents.**—Preparations and standardizations of the solutions of copper(II) nitrate, nickel(II) nitrate and ethylenediaminetetraacetate were made in principle by the same procedures as described in the previous paper.[2] A solution of sodium sulfate was prepared from the guaranteed grade reagent, and the sulfate concentration was determined by the conventional gravimetric method.[8] All other chemicals used were of an analytical reagent grade.

**Apparatus and procedure.**—A Yanagimoto PB-4 pen-recording polarograph was used for the measurement of the current-voltage curves. All measurements were made in the acetate buffer solutions of pH 4.74±0.02 containing sulfate, copper(II), nickel(II) and EDTA at 25°C and ionic strength 1.0. The ionic strength was adjusted with sodium perchlorate. Total concentrations of copper(II), nickel(II) and EDTA were $1.00_6\times10^{-3}$ M, $9.9_0\times10^{-4}$ M and $1.10_8\times10^{-3}$ M respectively. Gelatin was added as maximum suppressor by 0.01% in concentration.

In the preliminary experiments, the rate of the substitution reaction between copper(II) ions and nickel(II)-EDTA complexes was investigated. The result showed that the equilibrium of the reaction was attained within approximately 80 hours after the initiation of the reaction. Therefore, the reaction mixtures were kept standing at the given temperature for nearly four days after the preparation and, then, subjected to the measurement.

## Results and Discussion

The values of $[Cu^{2+}]_{app}$ were obtained at various concentrations of acetate and the given concentrations of sulfate. The left-hand side of Eq. 8 ($F_0$ in Eq. 8') was calculated with the $[Cu^{2+}]_{app}$ obtained and the formation constants of sulfatonickel(II), acetatonickel(II), and sulfatoacetatoniccolate(II) complexes which were previously determined.[4] The $F_0$ values thus calculated were plotted against the acetate concentration.

8) F. P. Treadwell and W. T. Hall, "Analytical Chemistry," Vol. 2, John Wiley and Sons, New York (1951), p. 393.

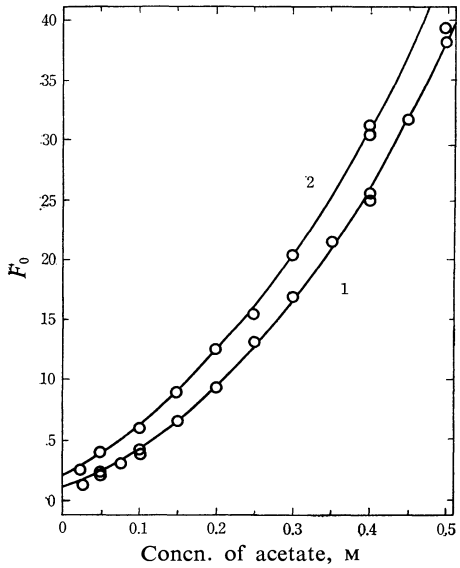



Fig. 1. $F_0$ (Eq. 8') as a function of acetate concentration at 25°C.
Concentrations of sulfate are: 0 (1) and 0.193 M (2).
— indicates the calculated, and ○ the experimental value.

Two typical examples of the $F_0$ plots are shown in Fig. 1. By extrapolating the $F_0$ plots to the zero acetate concentration, the values for

$$\frac{\alpha_{\mathrm{NiHY}}}{\alpha_{\mathrm{CuHY}} K_{\mathrm{Ni}}^{\mathrm{Cu}}}\left(1+\sum_{j=1}^{p} K_{\mathrm{Cu(SO_4)}_j}[\mathrm{SO_4^{2-}}]^j\right)$$

were determined. The $F_1(\mathrm{OAc})$,

$$F_1(\mathrm{OAc}) \equiv \frac{F_0-\dfrac{\alpha_{\mathrm{NiHY}}}{\alpha_{\mathrm{CuHY}} K_{\mathrm{Ni}}^{\mathrm{Cu}}}\left(1+\sum_{j=1}^{p} K_{\mathrm{Cu(SO_4)}_j}[\mathrm{SO_4^{2-}}]^j\right)}{[\mathrm{OAc^-}]}$$

$$=\frac{\alpha_{\mathrm{NiHY}}}{\alpha_{\mathrm{CuHY}} K_{\mathrm{Ni}}^{\mathrm{Cu}}}\sum_{i=1}^{n}\sum_{j=0}^{p} K_{\mathrm{Cu(OAc)}_i(\mathrm{SO_4})_j} \times [\mathrm{OAc^-}]^{i-1}[\mathrm{SO_4^{2-}}]^j \qquad (12)$$

was calculated from the $F_0$ plots and plotted against the acetate concentration, as is given in Fig. 2. Figure 2 shows that the $F_1$ plots are linear. This fact indicates that $n$ is equal to 2 and that no appreciable amount of the complexes with three acetate or more coordinated is present in the solutions investigated. The same result was also obtained with other concentrations of sulfate.

The $F_0$ values were also calculated with the $[\mathrm{Cu^{2+}}]_{\mathrm{app}}$ obtained at various concentrations of sulfate and the given concentrations of acetate. They were plotted against the sulfate concentration, which are given in Fig. 3.

By extrapolating $F_0$ plots to the zero sulfate concentration, the values for

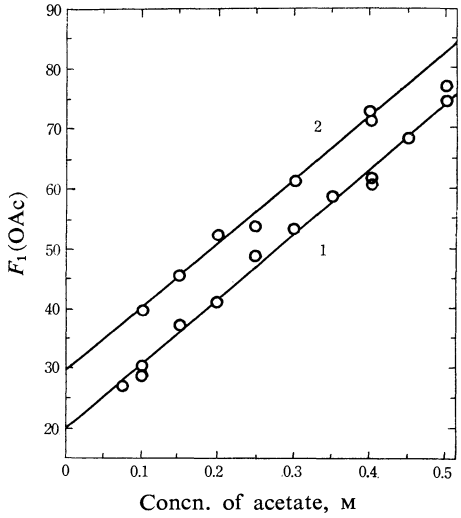



Fig. 2. $F_1$(Eq. 12) as a function of acetate concentration at 25°C.
Concentrations of sulfate are: 0 (1) and 0.193 M (2).

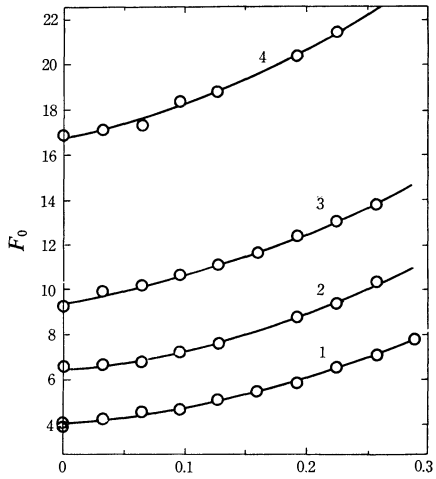



Fig. 3. $F_0$(Eq. 8') as a function of sulfate concentration at 25°C.
Concentrations of acetate are: 0.100 M (1), 0.149 M (2), 0.199 M (3) and 0.299 M (4).
— indicates the calculated, and ○ the experimental value.

$$\frac{\alpha_{\mathrm{NiHY}}}{\alpha_{\mathrm{CuHY}} K_{\mathrm{Ni}}^{\mathrm{Cu}}}\sum_{i=0}^{2} K_{\mathrm{Cu(OAc)}_i}[\mathrm{OAc^-}]^i$$

were obtained. The $F_1(\mathrm{SO_4})$,

$$F_1(\mathrm{SO_4}) \equiv \frac{F_0-\dfrac{\alpha_{\mathrm{NiHY}}}{\alpha_{\mathrm{CuHY}} K_{\mathrm{Ni}}^{\mathrm{Cu}}}\sum_{i=0}^{2} K_{\mathrm{Cu(OAc)}_i}[\mathrm{OAc^-}]^i}{[\mathrm{SO_4^{2-}}]}$$

$$=\frac{\alpha_{\mathrm{NiHY}}}{\alpha_{\mathrm{CuHY}} K_{\mathrm{Ni}}^{\mathrm{Cu}}}\sum_{i=0}^{2}\sum_{j=1}^{p} K_{\mathrm{Cu(OAc)}_i(\mathrm{SO_4})_j} \times [\mathrm{OAc^-}]^i[\mathrm{SO_4^{2-}}]^{j-1} \qquad (13)$$

was calculated from the $F_0$ plots and plotted against the sulfate concentration (Fig. 4). The $F_1$ plots were found to be linear, which indicate that $p$ is equal to 2 and that no appreciable amount of complexes with three sulfates or more coordinated is present in the solutions investigated. These conclusions were confirmed by the direct calculation of $n$ and $p$ of the $F_0$ function with the aid of an electronic computor NEAC 2230 (the Computing Center, Tohoku University).

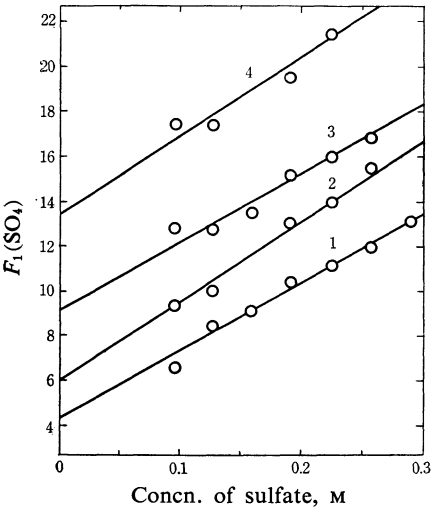



Fig. 4. $F_1$(Eq. 13) as a function of sulfate concentration at 25°C.
Concentrations of acetate are: 0.100 M (1), 0.149 M (2), 0.199 M (3) and 0.299 M (4).

The result that both $n$ and $p$ are equal to 2 suggests that the complex species, $CuOAc^+$, $Cu(OAc)_2$, $CuSO_4$, $Cu(SO_4)_2^{2-}$, $Cu(OAc)(SO_4)^-$, $Cu(OAc)(SO_4)_2^{3-}$, $Cu(OAc)_2(SO_4)^{2-}$ and $Cu(OAc)_2(SO_4)_2^{4-}$, may exist in the solution. However, it was concluded that $Cu(OAc)_2(SO_4)^{2-}$ and $Cu(OAc)_2(SO_4)_2^{4-}$ are not present in appreciable concentrations : The value of $(\alpha_{NiHY}/(\alpha_{CuHY}K_{Ni}^{Cu}))K_{Cu(OAc)_2}$, the coefficient of $[OAc^-]^2$ in the absence of sulfate was found to be identical, within experimental error, with that of $(\alpha_{NiHY}/(\alpha_{CuHY}K_{Ni}^{Cu}))(K_{Cu(OAc)_2} + K_{Cu(OAc)_2(SO_4)}[SO_4^{2-}] + K_{Cu(OAc)_2(SO_4)_2}[SO_4^{2-}]^2)$, the coefficient of $[OAc^-]^2$ in the presence of sulfate, both the coefficients being obtained by a least square method. An agreement of these values indicates that the terms, $K_{Cu(OAc)_2(SO_4)}[SO_4^{2-}]$ and $K_{Cu(OAc)_2(SO_4)_2}[SO_4^{2-}]^2$, are negligible and, consequently, no appreciable amount of $Cu(OAc)_2(SO_4)^{2-}$ and $Cu(OAc)_2(SO_4)_2^{4-}$ is present under the experimental conditions.

The formation constants of other species and the value of $\alpha_{NiHY}/(\alpha_{CuHY}K_{Ni}^{Cu})$ were determined by a least square method with the plots of $F_0$ vs. $[OAc^-]$ and $F_0$ vs. $[SO_4^{2-}]$.

**Determination of the Formation Constants of Acetatocopper(II) Complexes.**—The $F_0$ function obtained in the absence of sulfate is written as

$$F_0=\frac{\alpha_{NiHY}}{\alpha_{C\ HY}K_{Ni}^{Cu}}(1+K_{Cu(OAc)}[OAc^-]+K_{Cu(OAc)_2}[OAc^-]^2) \quad (14)$$

Therefore, the formation constants of $K_{CuOAc}$ and $K_{Cu(OAc)_2}$ and the value of $\alpha_{NiHY}/(\alpha_{CuHY}K_{Ni}^{Cu})$ were determined from curve 1 in Fig. 1 by a least square treatment. Using Eq. 14, the uncertainties of the determined values were examined by a graphical treatment.[9,10]

**Determination of the Formation Constants of Sulfato and Sulfatoacetatocopper(II) Complexes.**—The values of $(K_{CuSO_4}+K_{Cu(OAc)(SO_4)}[OAc^-])$ and $(K_{Cu(SO_4)_2}+K_{Cu(OAc)(SO_4)_2}[OAc^-])$ were determined by a least square method from the coefficients of $[SO_4^{2-}]$ and $[SO_4^{2-}]^2$ in the plots in Fig. 3, respectively. From the value of $(K_{CuSO_4}+K_{Cu(OAc)(SO_4)}[OAc^-])$ obtained for the given concentration of acetate, $K_{CuSO_4}$ and $K_{Cu(OAc)(SO_4)}$ were determined by a graphical treatment.[9,10] $K_{Cu(SO_4)_2}$ and $K_{Cu(OAc)(SO_4)_2}$ were also determined by the same procedure as in the case of the determination of $K_{CuSO_4}$ and $K_{Cu(OAc)(SO_4)}$.

The value of $\alpha_{NiHY}/(\alpha_{CuHY}K_{Ni}^{Cu})$ was obtained to be 1.0 at pH 4.74, and the formation constants obtained are given in Table I. Using

Table I. Formation constants of copper(II) complexes at 25°C and ionic strength 1.0

| | | |
|---|---|---|
| $K_{CuOAc}$ | $2.0\times10$ | $1.\ mol^{-1}$ |
| $K_{Cu(OAc)_2}$ | $1.1\times10^2$ | $1.^2\ mol^{-2}$ |
| $K_{CuSO_4}$ | $<3$ | $1.\ mol^{-1}$ |
| $K_{Cu(SO_4)_2}$ | $\sim3\times10$ | $1.^2\ mol^{-2}$ |
| $K_{Cu(OAc)(SO_4)}$ | $4\times10$ | $1.^2\ mol^{-2}$ |
| $K_{Cu(OAc)(SO_4)_2}$ | $\sim7\times10$ | $1.^3\ mol^{-3}$ |

these values, the values of $F_0$ can be calculated at various concentrations of acetate and/or sulfate. All the solid curves in Figs. 1 and 3 indicate that these calculated values are in satisfactory agreement with the values obtained experimentally.

In the previous study,[2] the formation constants of $K_{CuOAc}$ and $K_{Cu(OAc)_2}$ at 25°C and ionic strength 0.2 were obtained to be 52 and 93, respectively. The value of $K_{CuOAc}$ at ionic strength 1.0 is considerably smaller than that at ionic strength 0.2, while the value of the $K_{Cu(OAc)_2}$ is approximately equal to that at ionic strength 0.2. The value of $\alpha_{NiHY}/\alpha_{CuHY}$

9) A. E. Martell and M. Calvin, "Chemistry of the Metal Chelate Compounds," Prentice-Hall, Inc., N. J. (1959), p. 91.
10) G. Schwarzenbach, A. Willi and R. O. Bach, *Helv. Chim. Acta*, **30**, 1303 (1947).

was calculated with the equilibrium constants, $K^{H}_{CuHY}$ and $K^{H}_{NiHY}$, given by Schwarzenbach, Gut and Anderegg[11] and was found to be approximately unity for this system at pH 4.74. The $K^{Cu}_{Ni}$, the equilibrium constant of the substitution reaction represented by Eq. 1, was obtained to be 1.0 in the present experimental conditions. This value is also smaller than 2.2 which was obtained at 25°C and ionic strength 0.2.[2]

Fronaeus reported the formation constants of copper(II) complexes with acetate and/or sulfate which were determined by the potentiometric method[5] and by the ion-exchange measurements[6] at 20°C and ionic strength 1. The formation constants of sulfatocopper(II) complexes were reported which were obtained by solubility measurements[7] at 20°C and ionic strength 1. These formation constants are given in Table II. It may be seen that the values of $K_{Cu(SO_4)_2}$ given by Fronaeus and Näsänen are considerably smaller than the value obtained in this study.

TABLE II. THE REPORTED VALUES OF FORMATION CONSTANTS OF COPPER(II) COMPLEXES AT 20°C AND IONIC STRENGTH 1

| | Values obtained by Fronaeus [5,6] | | Values obtained by Näsänen et al.[7] |
|---|---|---|---|
| $K_{CuOAc}$ | 45 [c] | | |
| $K_{Cu(OAc)_2}$ | 440 [c] | | |
| $K_{CuSO_4}$ | $9\pm2$ [a] | 10.6 [b] | $\leq 11$ [d] |
| $K_{Cu(SO_4)_2}$ | — | 10—17 [b] | $\sim 3$ [d] |
| $K_{Cu(SO_4)_3}$ | 80 [a] | 200 [b] | $\leq 150$ [d] |
| $K_{Cu(OAc)(SO_4)}$ | $190\pm50$ [a] | | |

a) The e. m. f. method with the quinhydrone electrode.[5]
b) The e. m. f. method with the copper amalgam electrode.[5]
c) The ion exchange method.[6]
d) The solubility method.

11) G. Schwarzenbach, R. Gut and G. Anderegg, *Helv. Chim. Acta*, **37**, 937 (1954).


## Summary

The polarographic method for the determination of the formation constants which is based on the measurement of the effects of acetate and/or other co-existing ions on the equilibrium of the substitution reaction, $M+M'L \rightleftarrows ML+M'$, has been developed, and applied to the study of the copper(II) complexes with acetate and/or sulfate ions. The formation constants obtained at 25°C and ionic strength 1.0 are: $2.0\times10$ for $K_{Cu(OAc)}$, $1.1\times10^2$ for $K_{Cu(OAc)_2}$, $< 3$ for $K_{CuSO_4}$, $\sim3\times10$ for $K_{Cu(SO_4)_2}$, $4\times10$ for $K_{Cu(OAc)(SO_4)}$ and $\sim7\times10$ for $K_{Cu(OAc)(SO_4)_2}$.


The authors wish to thank the Ministry of Education for the financial support granted for this research.

*Department of Chemistry*
*Faculty of Science*
*Tohoku University*
*Katahira-cho, Sendai*

# The Spectrophotometric Determination of Anions by Solvent Extraction with Metal Chelate Cations. VIII.* A New Method for the Determination of Cadmium

By Keiya KOTSUJI

(Received November 7, 1964)

In a previous paper of this series, it has been shown that cadmium iodide complex, as well as mercuric iodide complex, can be extracted into 1,2-dichloroethane with 2,2'-dipyridyl iron(II) chelate.[1] Consequently, a method for the determination of cadmium has been investigated, in which the metal ion in aqueous solution is extracted into dichloroethane with dipyridyl iron(II) chelate in the presence of excess iodide and the absorbance of the resulting chelate in the organic phase is measured.

Many reagents have been used for the

* Presented at the 12th Annual Meeting of the Japan Society for Analytical Chemistry, Kanazawa, October, 1963.

1) Y. Yamamoto and K. Kotsuji, This Bulletin, 37, 594 (1964).

colorimetric determination of cadmium, the most favored being dithizone.[2,3] Other reagents which have been suggested include di-β-naphthylthiocarbazone,[4] 4-hydroxy-3-nitrobenzenearsonic acid,[5] 1-(6-bromobenzothiazol-2-ylazo)-2-naphthol,[6] "Cadion," a triazine dye,[7] glyoxal bis(2-hydroxy-anil),[8] and diethyldithiocarbamate.[9,10] Although a differential ultraviolet spectrophotometric method using 1, 10-phenanthroline has also been devised, numerous interference have been found.[11] However, the proposed method is different from the known methods described above in the mechanism of color reaction.

## Experimental

**Apparatus and Reagents.** — Unless otherwise stated, apparatus and reagents were the same as those described in a previous paper.[12]

*Standard Cadmium Solution.*—Guaranteed cadmium sulfate ($3CdSO_4 \cdot 8H_2O$) was dissolved in distilled water, containing sufficient sulfuric acid to prevent hydrolysis, and diluted with distilled water to a concentration of 1000 p. p. m. of cadmium. The cadmium content was determined by an EDTA titration. This standard solution was diluted to the concentration required for the experiments.

All other reagents of analytical grade were used without further purification.

**Procedure.** — Mix 2,2'-dipyridyl ($8\times10^{-3}$ M), ferrous ammonium sulfate ($2\times10^{-3}$ M), sodium acetate (3 M), potassium iodide (0.3 M), and standard cadmium solution in the proper concentration. Adjust the pH of the solution to the required value with dilute sulfuric acid or dilute sodium hydroxide solution and then dilute it to 25 ml. with distilled water. To this, add 10.0 ml. of dichloroethane and shake the solution for 4 min. After standing the solution for 20 min., transfer the organic layer into a flask containing 1 g. of anhydrous sodium sulfate and shake it vigorously to make the solution transparent. Then transfer it into a 10 mm. cell. Measure the absorbance of the solution at 526 mμ using a reagent blank solution or dichloroethane as a reference. Measure the pH of the aqueous layer after the separation.

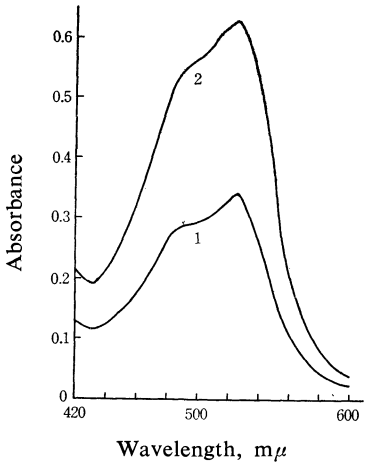



Fig. 1. Absorption spectra.
Reference: Dichloroethane, pH: 6.5
Curve 1: Spectrum of organic phase extracted from the aqueous solution (25 ml.) contained Dip. $6.4\times10^{-4}$ M, Fe(II) $1.6\times10^{-4}$ M, NaAc 0.24 M, KI $8.4\times10^{-2}$ M but Cd is absent.
Curve 2: Spectrum of organic phase extracted from the aqueous solution (25 ml.) containing 1.6 p. p. m. of Cd in addition to the same component as that of curve 1.

## Results and Discussion

**Absorption Spectrum.** — The spectral absorbance curves using dichloroethane as a reference are shown in Fig. 1. Curve 1 is a spectrum of the extract when cadmium ions are absent, while curve 2 is that of the extract with cadmium ions. It is observed that the presence of cadmium ions leads to a considerable increase in the absorbance and that both curves have a maximum absorbance at 526 mμ. The maximum absorbance is shifted from 522 mμ, the value in aqueous solution,[13] to 526 mμ in dichloroethane solution. This slight red shift in the organic layer may be attributed to the effect of the association between the chelate cation and the complex anion in dichloroethane. Feigl[14] has shown that 2,2'-dipyridyl iron(II) chelate can be precipitated as red crystals with a divalent complex anion such as tetra-iodocadmium. From these facts, the chemical formula of the extracted species is assumed to be $Fe(Dip.)_3 \cdot CdI_4$.

The maximum difference in absorbance for curve 1 and curve 2 is found at 526 mμ. Therefore, the absorbance was measured at this wavelength.

**Effect of Reagents.**—*Effect of 2,2'-Dipyridyl*

2) E. B. Sandell, "Colorimetric Determination of Traces of Metals," Interscience Publishers, Inc., New York (1950), p. 228.
3) B. E. Saltzman, *Anal. Chem.*, **25**, 493 (1953).
4) J. Cholak and D. M. Hubbard, *Ind. Eng. Chem., Anal. Ed.*, **16**, 333 (1944).
5) W. Nielsh and G. Boltz, *Chem. Z.*, **79**, 364 (1955).
6) V. G. Brudz, D. A. Drapkina, K. A. Smirnova, N. I. Doroshina, Z. S. Sidenko and G. S. Chizhova, U. S. S. R. 146088, April 6, 1962; *Chem. Abstr.*, **57**, 9219 (1962).
7) P. Chavanne and C. Geronimi, *Anal. Chim. Acta*, **19**, 377 (1958).
8) S. Ôi, *Japan Analyst (Bunseki Kagaku)*, **9**, 770 (1960).
9) E. Sudo, *J. Chem. Soc. Japan, Pure Chem. Sec. (Nippon Kagaku Zassi)*, **73**, 693 (1952).
10) D. F. Boltz and E. J. Havlena, *Anal. Chim. Acta*, **30**, 565 (1964).
11) C. Wadelin and M. G. Mellon, *Anal. Chem.*, **24**, 894 (1952).
12) K. Kotsuji, This Bulletin, **83**, 402 (1965).
13) M. L. Moss and M. C. Mellon, *Ind. Eng. Chem., Anal. Ed.*, **14**, 826 (1942).
14) F. Feigl, "Spot Test, Part I, Inorganic Application," Elsevier Publishing Company, New York (1954), p. 90.

*Iron(II) Chelate and Potassium Iodide Concentration.*—The formation of extractable species may be mainly governed by the concentration of the 2,2'-dipyridyl iron(II) chelate cation as well as the tetraiodo-cadmium complex anion. Moreover, a large excess of potassium iodide is necessary to obtain a quantitative formation of tetraiodo-cadmium complex. The effect of such variables on the extraction was investigated.

To a solution containing a constant amount of cadmium, were added varying amounts of potassium iodide, ferrous ammonium sulfate, and 2,2'-dipyridyl, the mole ratio of dipyridyl to ferrous iron being kept at 4 to 1. In this case, it seems reasonable to assume that the concentration of ferrous iron is approximately equal to that of 2,2'-dipyridyl iron(II) chelate because of the high stability of the chelate.[15] The pH of the solutions was kept at 6.5 and the extraction procedure was carried out for such solutions. The results are shown in

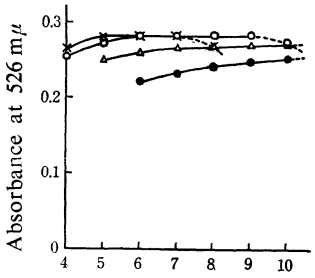



Fig. 2. Effect of 2,2'-dipyridyl iron(II) chelate and potassium iodide concentrations.
The concentration of acetate in the final solutions was 0.24 M.
Concn. of cadmium, 1.6 p. p. m.
pH of aqueous layer, 6.5
Shaking time., 4 mm.
Reference, Reagent blank

| | Concn. of Dip. M | Concn of Fe(II) M |
|---|---|---|
| -×- | $9.6\times10^{-4}$ | $2.4\times10^{-4}$ |
| -○- | $6.4\times10^{-4}$ | $1.6\times10^{-4}$ |
| -△- | $3.2\times10^{-4}$ | $0.8\times10^{-4}$ |
| -●- | $1.6\times10^{-4}$ | $0.4\times10^{-4}$ |

Fig. 2. When the final concentration of the ferrous ammonium sulfate was lower than $8\times10^{-5}$ M, rather low recovery was observed although the recovery increased with rise of potassium iodide concentration. When the concentration of ferrous ammonium sulfate was kept in the range of $1.6\times10^{-4}$—$2.4\times10^{-4}$ M, the recovery reached a maximum provided the iodide concentration was higher than $7.2\times10^{-2}$ M. However, a large excess of iodide or of chelate caused a decrease in the absorbance. Therefore, the concentrations of ferrous ammonium sulfate and potassium iodide were kept at $1.6\times10^{-4}$ M and $8.4\times10^{-2}$ M, respectively, in this work.

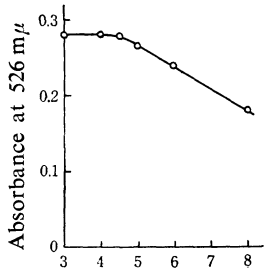



Fig. 3. Effect of mole ratio of Dip. to iron(II).
The concentrations of iron(II), iodide, and acetate in the final solutions were $1.6\times10^{-4}$ M, $8.4\times10^{-2}$ M, and 0.24 M respectively.
Concn. of cadmium, 1.6 p. p. m.
pH of aqueous layer, 6.5
Shaking time, 4 min.
Reference, Reagent blank

*Effect of 2,2'-Dipyridyl Concentration.*—While keeping other variables constant, differing amounts of dipyridyl were added, and the extraction was carried out according to the procedure described above. The results are shown in Fig. 3. When the mole ratio of dipyridyl to iron(II) was higher than 4.5, a decrease in the absorbance was observed. This may be caused by the formation of colorless 2,2'-dipyridyl cadmium chelate, which is more stable than tetraiodo-cadmium complex,[15,16] by the reaction of excess amounts of dipyridyl with tetraiodo-cadmium complex in the presence of excess iodide. On the other hand, a slight excess of dipyridyl is necessary for the stoichiometric formation of the dipyridyl iron(II) chelate cation. Therefore, this mole ratio was kept at 4 in this work.

*Effect of Sodium Acetate Concentration.*—Sodium acetate was effective in keeping the pH of the solution constant. When the acetate concentration was maintained at 0.2 to 0.3 M in the solution to be extracted, no effect on the recovery was observed. The concentration of the acetate was kept at 0.24 M in this work.

**Effect of Shaking Time.**—The shaking time during the extraction was varied from 2 to 20 min., while the other variables were kept constant. Variation in the shaking time did not produce any measurable change in the

15) K. B. Yatsimirskii and V. P. Vasil'ev, "Instability Constants of Complex Compounds," Pergamon Press, Oxford (1960), p. 139.

16) J. Bjerrum, G. Schwarzenbach and L. G. Sillén, "Stability Constants, Part II, Inorganic Ligands," The Chemical Society, London (1958), p. 120.

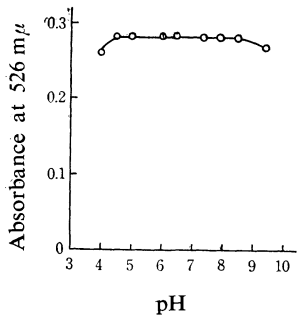



Fig. 4. Effect of pH.
The concentrations of dipyridyl, iron(II), iodide, and acetate in the final solutions were $6.4\times10^{-4}$ M, $1.6\times10^{-4}$ M, $8.4\times10^{-2}$ M, and 0.24 M respectively.
Concn. of cadmium, 1.6 p. p. m.
Shaking time, 4 min.
Reference, Reagent blank

absorbance of the extracts. The shaking time was thus chosen to be 4 min. in this work.

**Effect of pH.**—The effect of the pH of the aqueous layer on the extraction is shown in Fig. 4. Low recoveries were obtained in the pH ranges below 4.5 and above 8.5. The pH of the solution was adjusted to 6.5 in this work.

**Stability of Color.** — Color developed immediately at room temperature and the intensity was not influenced by a temperature at 15—20°C. The color of the extract in the stoppered transmission cell was stable for more than 6 hr.

**Choice of Organic Solvent.** — Besides 1, 2-dichloroethane, various other solvents were tested for the extraction. They were chloroform, carbon tetrachloride, isoamyl alcohol, methylisobutyl ketone, cyclohexanone, benzene, and nitrobenzene. Only 1, 2-dichloroethane proved satisfactory. Although nitrobenzene behaved similarly to dichloroethane in this system, the reagent blank was too high to obtain a satisfactory net absorbance value.

**Percentage of Extraction.** — The degree of extraction of cadmium was checked by stripping cadmium from an aliquot of the dichloroethane extract with 1 N sulfuric acid. The amount of stripped cadmium was determined as follows. The aqueous layer was heated with nitric acid and sulfuric acid until strong fumes were observed. After cooling, the solution was neutralized with sodium hydroxide and diluted to a standard volume. Then an aliquot containing less than 20 μg. of cadmium was taken. The cadmium was determined by the photometric dithizone method, as described by Saltzman.[3]

The degree of the extraction using 10.0 ml. of dichloroethane was about 99%.

**Calibration Curve.** — Two milliliters of the 2, 2′-dipyridyl solution, 2 ml. of the ferrous ammonium sulfate solution, 2 ml. of the sodium acetate solution, 7 ml. of the potassium iodide solution, and varying amounts (1—7 ml.) of the standard cadmium solution (10 p. p. m.) were mixed and diluted to 25 ml. with distilled water. Then 10.0 ml. of dichloroethane was added, and the mixture was treated according

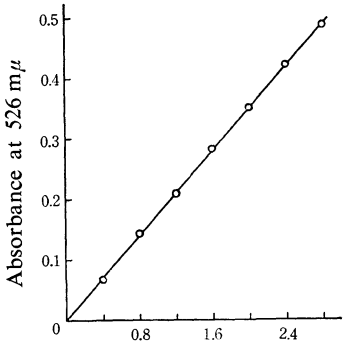



Fig. 5. Calibration curve at 526 mμ.
The concentrations of dipyridyl, iron(II), iodide, and acetate in the final solutions were $6.4\times10^{-4}$ M, $1.6\times10^{-4}$ M, $8.4\times10^{-2}$ M, and 0.24 M respectively.
pH of aqueous layer, 6.5
Shaking time, 4 min.
Reference, Reagent blank

TABLE I. EFFECT OF DIVERSE IONS ON EXTRACTION AND DETERMINATION OF CADMIUM
(0.8 p. p. m. of cadmium taken in each case)

| Ion | Ion concn. p. p. m. | Absorbance at 526 mμ | Relative error % |
|---|---|---|---|
| None | — | 0.141* | |
| $Zn^{2+}$ | 40 | 0.141 | ±0.0 |
| $Pb^{2+}$ | 0.4 | 0.142 | +0.7 |
| $Pb^{2+}$ | 0.8 | 0.144 | +2.1 |
| $Hg^{2+}$ | 0.4 | 0.183 | +29.8 |
| $Hg^{2+}$ | 0.8 | 0.221 | +56.0 |
| $Bi^{3+}$ | 0.4 | 0.160 | +12.9 |
| $Bi^{3+}$ | 0.8 | 0.174 | +23.4 |
| $Cu^{2+}$ | 0.4 | 0.131 | −7.1 |
| $Cu^{2+}$ | 0.8 | 0.124 | −12.1 |
| $SO_4^{2-}$ | 1650 | 0.142 | +0.7 |
| $NO_3^-$ | 1500 | 0.141 | ±0.0 |
| $Cl^-$ | 1700 | 0.140 | −0.7 |
| $Cl^-$ | 3400 | 0.128 | −9.1 |
| $Br^-$ | 1000 | 0.139 | −1.5 |
| $Br^-$ | 2000 | 0.126 | −10.6 |
| Citrate | 400 | 0.138 | −2.1 |
| Tartrate | 1400 | 0.141 | ±0.0 |

pH of aqueous layer: 6.5, other variables were the same as that of the calibration curve.
* The absorbance of 0.8 p. p. m. of cadmium without diverse ions.

to the procedure described above. The absorbance of each of the standard extracts was measured at 526 mμ against the reagent blank. As shown in Fig. 5, Beer's law is followed in the 0.4—2.8 p. p. m. range of cadmium ions.

**Effect of Diverse Ions.**—A study was made on the effects of several cations and anions. Absorbance measurements were made on the dichloroethane extracts obtained from the solutions containing various amounts of diverse ions with 0.8 p. p. m. of cadmium. The results are given in Table I. Nitrate, chloride and sulfate do not interfere even when the concentration is as high as 1500 p. p. m. Zinc ion may be present in the concentration of 40 p. p. m. without interference. Interferences by lead(II), mercury(II), and bismuth(III) ions may be due to the behavior of their iodo-complexes being similar to that of the tetraiodo-cadmium complex anion. Ethylenediaminetetraacetate causes serious interference, even when only a small amount is present, because the cadmium chelate of ethylenediaminetetraacetate[17] is more stable than the tetraiodo-cadmium complex.

**Summary**

A new method for the determination of cadmium has been proposed. The method is based upon solvent extraction of the associated complex formed between 2, 2'-dipyridyl iron(II) chelate cation and tetraiodo-cadmium complex anion and upon estimation of the absorbance due to the chelate cation in the organic phase.

The author wishes to express his sincere thanks to Professor Yuroku Yamamoto of Hiroshima University for his kind guidance and encouragement throughout this work. He is also grateful to Professor Shigehiko Hayashi for his kind advice and to Mr. Toshiyuki Sakurai for his assistance in this work.

*Faculty of Liberal Arts*
*Fukui University*
*Makinoshima, Fukui*

17) J. Bjerrum, G. Schwarzenbach and L. G. Sillén, "Stability Constants, Part I, Organic Ligands," The Chemical Society, London (1957), p. 76.

# The Vertical Distribution of Chlorine in a Lava Flow from the O-sima Volcano in the Izu Islands

By Bunji IWASAKI

(Received November 9, 1964)

The horizontal distribution of chlorine in a lava flow has been reported by Iwasaki and Ozawa.[1] They found that the chlorine content of approximately 120 rock samples was quite homogeneous irrespective of the appearance and locality of the samples.

The vertical distribution of chlorine in a lava flow has also been studied by Kuroda and Sandell,[2] and Yoshida et al.[3] The number of rock samples employed in their studies was too small to permit a detailed study to be made.

Recently, many core holes were drilled in the northwestern part of the O-sima caldera in the Izu Islands. The drill-hole samples were studied by Issiki et al.[4] from standpoints of geology, geophysics, and petrography. As one of the results of their studies, several thick basaltic lava flows were distinguished.

We have determined the chlorine content of two of those lava flows in order to study the vertical distribution of chlorine in such a volcanic body. In addition, the uniformity of major chemical components in the two lava flows is discussed on the basis of the total iron content.

## Experimental

**Selection and Preparation of Rock Samples.**—The rock samples of the two lava flows used in this study originated from two core holes, termed

1) I. Iwasaki and T. Ozawa, read at the Meeting of the Volcanological Society of Japan, May, 1959.

2) P. K. Kuroda and E. B. Sandell, *Bull. Geol. Soc. Am.*, **64**, 879 (1953).

3) M. Yoshida, T. Ozawa and T. Katsura, read at the Meeting of the Volcanological Society of Japan, March, 1963.

4) N. Issiki, K. Nakamura, M. Hayakawa, K. Hirasawa, T. Yukutake, Y. Arai and B. Iwasaki, *Bull. Volcanological Soc. Japan, 2nd Series*, **8**, 61 (1963).

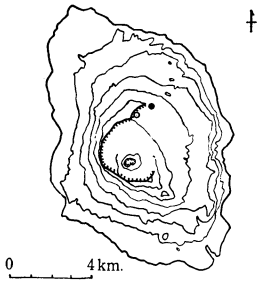



Fig. 1 The locations of the two core holes.
● OH 1 ○ OY 4

OH 1 and OY 4, respectively. The locations of those core holes are given in Fig. 1.

These drill-hole samples, weighing about 1 kg., were taken at about 2 m. intervals through the lava flow. A total of 65 samples, involving 38 samples in one lava flow (OH 1-2) and 27 samples in the other lava flow (OY 4-2), was collected. About 15 g. of each core-hole sample was selected for chemical analysis from the central part of the core to avoid cavities. Then, these rock samples were crushed in a steel mortar and ground to fineness in an agate mortar. In particular, precaution was taken throughout the whole procedure of selection and preparation of rock samples, to avoid any possibility of chlorine contamination.

**Method of Analysis.**—Two or more repeated determinations of the total chlorine content in each rock sample were made by the method of Iwasaki et al.[5] with some improvements, while the water-soluble chlorine in the rock was determined by the thiocyanate method,[6] according to the procedure previously described.[7] By these methods, it is possible to ascertain the chlorine content of the rock within a precision of ±5% for the whole range analyzed.

The total iron in the rock was determined colorimetrically by the $\alpha, \alpha'$-dipyridyl method,[8] within a precision of ±1% in a range of 10.0 to 15.0%.

## Results and Discussion

**The Uniformity of the Two Lava Flows.**—According to the geological observations of Issiki et al.,[4] the two lava flows involved in this study are considered to be uniform, on accunt of the smallness and rareness of phenocrysts such as olivine and augite, and to have formed through ponding into a depression on the caldera floor.

The uniformity of a lava flow can also be determined by the method of Iwasaki et al.,[9] involving chemical analysis. Their results have shown that determination of one of the major chemical components, in a large number of samples from the lava flow, is useful in deciding whether a lava flow containing infrequent and small phenocrysts is uniform in major chemical composition. Accordingly, the total iron contents in each of 14 rock specimens were determined to ascertain the uniformity of the two lava flows. The results obtained are shown in Table I.

Table I. The total iron content in the two lava flows

| Sample | $Fe_2O_3$*, % |
|---|---|
| OH 1-2-1 | 14.1 |
| OH 1-2-3 | 14.4 |
| OH 1-2-9 | 14.3 |
| OH 1-2-14 | 14.3 |
| OH 1-2-17 | 14.4 |
| OH 1-2-20 | 14.4 |
| OH 1-2-23 | 14.4 |
| OH 1-2-25 | 14.2 |
| OH 1-2-31 | 14.1 |
| OH 1-2-34 | 14.4 |
| OH 1-2-38 | 14.3 |
| OH 1-2[4] | 14.4 |
| Mean value | $14.3_1$ |
| Standard deviation | 0.11 |
| OY 4-2-1 | 14.0 |
| OY 4-2-12 | 14.0 |
| OY 4-2-27 | 14.0 |
| OY 4-2[4] | 14.1 |
| Mean value | $14.0_3$ |

$Fe_2O_3$*: Total iron content

In the case of OH 1-2, the total iron content (as $Fe_2O_3$) ranges from 14.1 to 14.4%, and in the case of OY 4-2, from 14.0 to 14.1%. Judging from the total iron content, the two lava flows are considered to be uniform in major chemical composition.

**Chlorine Content.**—The total chlorine content in the rock samples from the two lava flows are shown in Table II.

The rock samples analyzed are presented in order of increasing depth beneath the surface. The water-soluble chlorine in the rock was determined to see whether chlorine is present by contamination in the rock specimens. The results obtained are shown in Table III.

The water-soluble chlorine content in 9 rock samples ranges from 0.001 to 0.003%. As this amount of water-soluble chlorine is normally present in fresh rock specimens,[2,10] it may be said that the chlorine in these rock samples does not come from the cooling water applied

5) I. Iwasaki, T. Katsura and N. Sakato, *J. Chem. Soc. Japan, Pure Chem. Sec. (Nippon Kagaku Zassi)*, **76**, 778 (1955).
6) A. Tomonari ibid., **83**, 693 (1962).
7) B. Iwasaki and T. Katsura, This Bulletin, in press.
8) M. L. Moss and M. G. Mellon, *Ind. Eng. Chem., Anal. Ed.*, **13**, 551 (1941).
9) I. Iwasaki, T. Katsura, T. Ozawa, M. Yoshida, M. Mashima, H. Haramura and B. Iwasaki, *Bull. Volcanological Soc. Japan, 2nd Series*, 5, 9 (1960), etc.
10) I. Iwasaki, T. Katsura, N. Sakato and M. Hirayama, *J. Chem. Soc. Japan, Pure Chem. Sec. (Nippon Kagaku Zassi)*, **76**, 1116 (1955).

TABLE II. THE TOTAL CHLORINE CONTENT IN THE TWO LAVA FLOWS

| Sample | Depth, m. beneath the surface | T-Cl, % | Sample | Depth, m. beneath the surface | T-Cl, % |
|---|---|---|---|---|---|
| OH 1-2-1 | 37.1 | 0.009 | OH 1-2-34 | 105.0 | 0.013 |
| OH 1-2-2 | 39.0 | 0.011 | OH 1-2-35 | 107.2 | 0.012 |
| OH 1-2-3 | 41.0 | 0.017 | OH 1-2-36 | 110.0 | 0.011 |
| OH 1-2-4 | 42.8 | 0.016 | OH 1-2-37 | 111.5 | 0.010 |
| OH 1-2-5 | 46.0 | 0.016 | OH 1-2-38 | 112.2 | 0.012 |
| OH 1-2-6 | 48.0 | 0.017 | OY 4-2-1 | 63.3 | 0.020 |
| OH 1-2-7 | 50.0 | 0.016 | OY 4-2-2 | 65.0 | 0.016 |
| OH 1-2-8 | 52.0 | 0.015 | OY 4-2-3 | 67.0 | 0.014 |
| OH 1-2-9 | 54.0 | 0.015 | OY 4-2-4 | 69.1 | 0.012 |
| OH 1-2-10 | 56.7 | 0.016 | OY 4-2-5 | 71.1 | 0.014 |
| OH 1-2-11 | 58.7 | 0.017 | OY 4-2-6 | 73.0 | 0.012 |
| OH 1-2-12 | 60.0 | 0.015 | OY 4-2-7 | 75.1 | 0.013 |
| OH 1-2-13 | 62.0 | 0.016 | OY 4-2-8 | 77.0 | 0.011 |
| OH 1-2-14 | 64.6 | 0.019 | OY 4-2-9 | 79.0 | 0.013 |
| OH 1-2-15 | 67.5 | 0.016 | OY 4-2-10 | 81.0 | 0.012 |
| OH 1-2-16 | 69.2 | 0.019 S | OY 4-2-11 | 83.0 | 0.012 |
| OH 1-2-17 | 71.0 | 0.020 S | OY 4-2-12 | 85.0 | 0.012 |
| OH 1-2-18 | 73.0 | 0.019 S | OY 4-2-13 | 87.0 | 0.015 |
| OH 1-2-19 | 75.0 | 0.016 | OY 4-2-14 | 89.0 | 0.013 |
| OH 1-2-20 | 77.0 | 0.014 | OY 4-2-15 | 91.0 | 0.014 |
| OH 1-2-21 | 79.0 | 0.017 | OY 4-2-16 | 93.0 | 0.012 |
| OH 1-2-22 | 81.0 | 0.019 | OY 4-2-17 | 95.0 | 0.013 |
| OH 1-2-23 | 83.0 | 0.020 S | OY 4-2-18 | 97.0 | 0.014 |
| OH 1-2-24 | 85.0 | 0.016 | OY 4-2-19 | 99.0 | 0.012 |
| OH 1-2-25 | 87.0 | 0.014 | OY 4-2-20 | 101.0 | 0.012 |
| OH 1-2-26 | 89.1 | 0.014 | OY 4-2-21 | 103.0 | 0.013 |
| OH 1-2-27 | 91.0 | 0.014 | OY 4-2-22 | 105.0 | 0.012 |
| OH 1-2-28 | 93.0 | 0.013 | OY 4-2-23 | 106.9 | 0.013 |
| OH 1-2-29 | 95.0 | 0.012 | OY 4-2-24 | 109.3 | 0.011 |
| OH 1-2-30 | 97.0 | 0.011 | OY 4-2-25 | 111.0 | 0.011 |
| OH 1-2-31 | 99.0 | 0.010 | OY 4-2-26 | 113.0 | 0.013 |
| OH 1-2-32 | 101.0 | 0.012 | OY 4-2-27 | 115.1 | 0.011 |
| OH 1-2-33 | 103.0 | 0.011 | | | |

T-Cl: Total chlorine content S: Spots

TABLE III. THE WATER SOLUBLE CHLORINE CONTENT IN THE TWO LAVA FLOWS

| Sample | W-Cl, % |
|---|---|
| OH 1-2-1 | 0.0007 |
| OH 1-2-9 | 0.0023 |
| OH 1-2-14 | 0.0029 |
| OH 1-2-17 | 0.0028 |
| OH 1-2-20 | 0.0034 |
| OH 1-2-23 | 0.0017 |
| OH 1-2-31 | 0.0014 |
| OH 1-2-38 | 0.0011 |
| OY 4-2-15 | 0.0020 |

W-Cl: Water-soluble chlorine content

to drill holes, etc. Figures 2 and 3 show the relationship between the chlorine content of the rock samples and the depth of the drill core.

The chlorine content of the rock samples from one lava flow (OY 4-2) ranges from

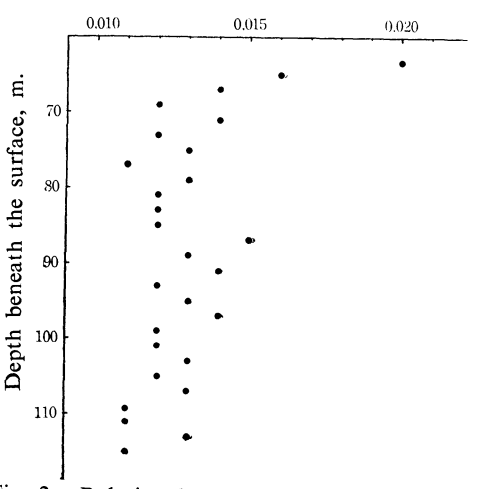



Fig. 2. Relation between the chlorine content of rock samples and the depth of drill core (OY 4-2).

0.011 to 0.020%, and averages 0.012%. It has been reported by Issiki et al.[4] that the base of this lava flow has been intruded by a dike. However, because of the low heat conductivity of rock, it is considered that the effect of this dike intrusion would have introduced no serious change in the vertical distribution of chlorine in the lava flow. Provided that the chlorine content of the basement rock is the same as that of the lower region of the lava flow. With the exception of two rock samples, all the samples would have a nearly uniform chlorine content. The two exceptional samples had been collected from the uppermost parts and are red

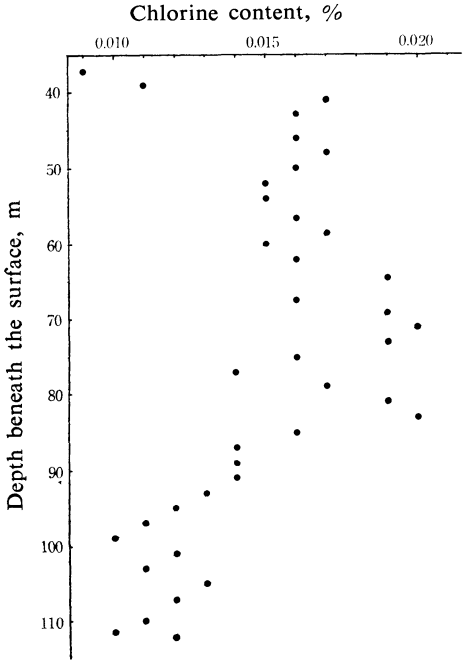



Fig. 3. Relation between the chlorine content of rock samples and the depth of drill core (OH 1-2).

in color. The presence of sublimates containing halogen compounds in these samples might explain the high amount of chlorine present.

On the other hand, the chlorine content of the rock samples from the other lava flow (OH 1-2) ranges from 0.009 to 0.020% and averages 0.014%. As seen from Fig. 3, the variation of chlorine is as follows: the chlorine content increases from the lower part to the middle part, and then, slightly decreases towards the uppermost part, where the chlorine content shows much lower values. The chlorine content in the rock samples from the uppermost parts shows a striking contrast to that found in similar regions of OY 4-2. Some of the rock specimens from the middle parts of the lava flow (OH 1-2) possess many cavities (showing the presence of volatile components) and many spots, which consist of glasses about 0.5 mm. in diameter, according to the microscopic observations of Issiki.* Furthermore, most of the rock specimens possessing these spots show higher amounts of chlorine, as seen in Table II, while the rock samples without the spots show lower amounts of chlorine. Since the former samples are not particularly enriched with apatites, it is considered that a relationship exists between the extent of occurrence of these spots and the chlorine content of the rock samples. Thus, the enriched chlorine content of the middle part is considered to be due to the fixation of chlorine in the glass, rather than the contribution of apatite as a chlorine carrier. A possible explanation for the vertical variation of chlorine content in the lava flow might be as follows: at high temperatures, the lava flow builds up to a thickness of about 76 m. during a short time, and then, begins to cool rapidly from the outside, i. e., the upper part and the lower part. This is supported by the fact that the crystals in the ground masses are very small and phenocrysts have not accumulated at the base. During such a cooling process, chlorine compounds may vaporize and be lost from the surface of the lava to the air; this would encourage diffusion of the chlorine compounds from the lower part to the upper part, and a concentration gradient of chlorine compounds would result in the lower and middle parts of the lava. As the chlorine compounds in the melt are prevented from escaping by the solidified lava surface, they would tend to diffuse downwards to be distributed uniformly in the melt. However, the diffusion rate in the lower part would be decreased by solidification of the lava in this region. Accordingly, the concentration gradient of chlorine compounds in the lower part may remain unchanged during solidificantion of the melt, whereas chlorine compounds in the melt at the upper and middle parts may be distributed uniformly. On the other hand, as the solidifying uppermost lava is heated by the underlying melt, chlorine compounds may be vaporized from the surface of the lava to the air. In this way, the solidification of the lava proceeds. At the final stage of the cooling process, those portions of the lava melt containing a high amount of chlorine compounds solidify as glasses, because chlorine compounds do not enter the rockforming minerals except apatite in this case.

**Frequency Distribution of Chlorine Content.**—Figure 4 shows two cumulative distributions of the chlorine content in the two lava flows

* Personal communications.

(OH 1-2, OY 4-2) and also shows that for the 1950—1951 lava in O-sima for comparison.

They show approximately normal distributions. In other words, a frequency distribution of the chlorine content in a lava flow seems to show a normality. This contrasts exceedingly with the frequency distributions found for the chlorine content in many lava flows in other regions, for example, Hawaiian and Japanese lava flows[7,10] show a lognormality. Perhaps, the difference is due to the much larger variation of the chlorine content in the latter than in the former. As seen from the slope of the lines in Fig. 4, OH 1-2 shows the largest variation, while OY 4-2 shows a variation close to that of the 1950—1951 lava. Judging from the latter fact, the formation of OY 4-2 may have been by a repeated accumulation of thin layers, as in the 1950—1951 lava, rather than by the generation of a lava lake.

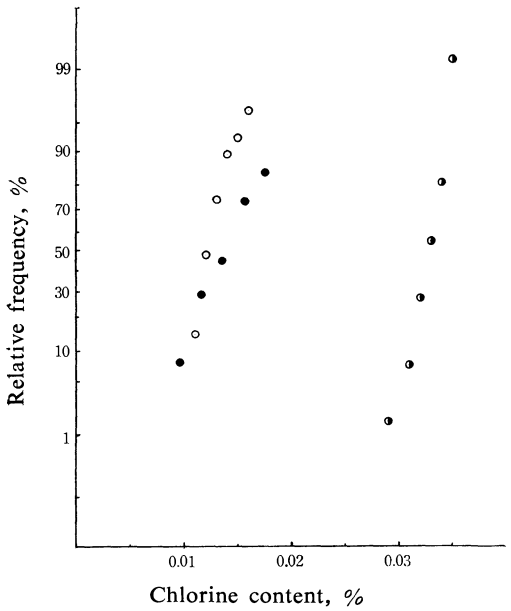



Fig. 4. The frequency curves on normal probability paper.
○ OY 4-2 ● OH 1-2
◑ the 1950—1951 lava

## Conclusion

1) The chlorine content of the first lava flow (OY 4—2) is uniform with some exceptions.

2) The chlorine content of the second lava flow (OH 1—2) shows a vertical variation, increasing from the lower part to the middle part and decreasing towards the uppermost part.

3) The enrichment of chlorine in the middle part of the second lava flow is considered to be due to the fixation of chlorine in the glass.

4) The frequency diagrams of the chlorine content in the two lava flows show approximately normal distributions.

5) The two lava flows are uniform on the basis of total iron content.

The author wishes to express his hearty thanks to Dr. Takashi Katsura, Tokyo Institute of Technology, for his constant guidance throughout this study. He is also much obliged to Dr. Naoki Issiki, Geological Survey of Japan, for his valuable advice and criticism in field and miroscopic observations. His thanks are expressed to Professor Iwaji Iwasaki, Tokyo Institute of Technology, for encouragement throughout this study.

*Department of Chemistry*
*Tokyo Institute of Technology*
*Ookayama, Tokyo*

# Current-Voltage Characteristics in Phenanthrene Single Crystals*1

By Shoichi MATSUMOTO

(Received November 14, 1964)

The nature of semiconduction in organic solids has not been as yet elucidated satisfactorily, though many experiments have been made on aromatic hydrocarbons and related organic compounds. Further experimental studies are needed to establish the mechanism of electrical conduction in these materials. One such study is to find out how much impurity exists in an organic crystal to be measured, whether it is chemical or physical, and, further, what role it plays.

Information about trapping centers in anthracene has been obtained through the conductivity glow-curve method by Bryant, Bree, Fielding and Schneider,[1] the measurement of space-charge-limited currents has been carried out for anthracene by Mark and Helfrich,[2] and the behavior of bulk currents in metal-free phthalocyanine has recently been interpreted as the currents by Heilmeier and Warfield.[3]

In this paper, the current-voltage characteristics of phenanthrene single crystals are studied in detail, and the results are analyzed as space-charge-limited currents phenomena. The information for trapping centers of phenanthrene obtained through the above-mentioned analysis will be discussed in comparison with the related results previously obtained for organic solids.

## Experimental

**Sample Crystals.** — The starting material was Eastman Kodak chemical-purpose-grade phenanthrene, which was purified by recrystallization and sublimation in a manner described previously.[4] As it was desired to obtain rather thin crystals in order to observe current-voltage characteristics up to very high electric fields, the crystals used in these experiments were sublimation flakes grown in the vessel shown in Fig. 1. A small quantity of purified phenanthrene was placed in a glass vessel equipped with conduit pipes for the flow of nitrogen gas,

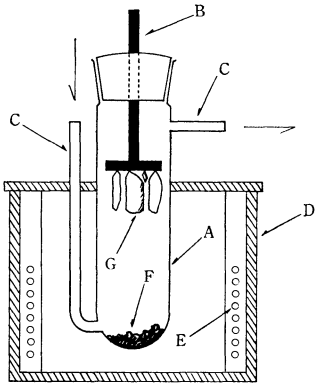



Fig. 1. Apparatus used to grow flaky single crystals of phenanthrene.

A: Glass vessel
B: Copper rod with a round plate
C: Conduit pipe
D: Heating furnace
E: Heating coil
F: Phenanthrene powder
G: Flaky crystals

and the vessel was sealed with a glass stopper bearing a copper rod with a round copper plate. Purified nitrogen was used as the ambient gas in order to prevent the oxidation of phenanthrene. The whole assembly was then placed in a heating furnace. Phenanthrene began to sublime at about 65°C, and flaky crystals grew on the copper plate, which remained nearly at room temperature.

The crystals were approximately 10 $\mu$ thick and had surface areas of 36—100 mm$^2$. About six hours were required to grow these crystals, which were confirmed to be single crystals by examination with a polarizing microscope. It was found that their developed plane coincided with the ab plane of the crystal without exception.

**Specimen Cell and Measuremnts.**—An electrical conductivity cell of the sandwich type was prepared on a teflon block in a manner reported previously.[4] Silver paste (Ecco Bond), which was found to make ohmic contact with these samples, was applied as electrodes, and a guard-ring electrode was grounded in order to prevent an effect of the surface current.

The measuring apparatus consisted of a vibrating-reed electrometer (Takeda TR-88), and a dry-cell power supply. As the bulk current of guard-ringed samples was found to show no difference between the current in air and that in nitrogen gas within the

*1 Presented at the Symposium on Molecular Structure, Sendai, October, 1963.

1) F. J. Bryant, A. Bree, P. E. Fielding and W. G. Schneider, *Discussions Faraday Soc.*, **28**, 48 (1959).
2) P. Mark and W. Helfrich, *J. Appl. Phys.*, **33**, 205 (1962).
3) G. H. Heilmeier and G. Warfield, *J. Chem. Phys.*, **38**, 163 (1963).
4) S. Matsumoto and T. Tsukada, This Bulletin, **37**, 1545 (1964).

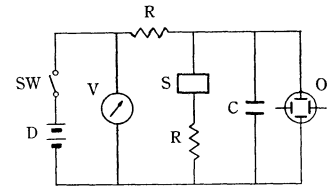



Fig. 2. Circuit used for estimation of the voltage at which a steep increase of current through a sample crystal occurs.

SW: Circuit switch D: Dry cell
V: Voltmeter R: Registor
S: Sample crystal C: Capacitor
O: Oscilloscope

range of experimental error,*2 the measurements were carried out in air.

The circuit shown in Fig. 2 was used to determine more exactly the voltage at which a steep increase of current through a sample crystal occurs; when the circuit is closed by a switch, the effect is merely to charge the capacitor so that a voltage is slowly built up across the capacitor and, at the same time, across a sample crystal. On the other hand, it can be observed that, when the voltage reaches a higher value where the current through a sample crystal rises steeply, the discharge of the capacitor occurs suddenly, and the built-up voltage across the capacitor falls. The above-mentioned phenomena were observed with a oscilloscope.

## Results and Discussion

The current-voltage characteristics obtained can typically be divided into three regions, as is shown in Fig. 3: (1) at low voltages, up to $2\times10^4$ V. per cm., the dependence of the current on the voltage obeyed Ohm's law, (2) at intermediate voltages, the current increased with the square of the voltage, and (3) at higher voltages, over $5\times10^4$ V. per cm., the current rose steeply with the voltage. This behavior is similar to the currnt-voltage relation characteristic of the space-charge-limited currents in solids.

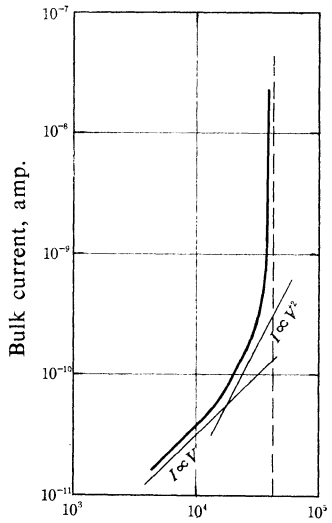



Fig. 3. Typical current-voltage characteristics of phenanthrene single crystal.

The theoretical treatment of space-charge-limited currents has been developed by Rose[5] and Lampert[6]. Smith and Rose also experimentally demonstrated space-charge-limited currents with crystals of cadmium sulfide.[7] Ruppel observed that with zinc sulfide,[8] and so forth.

When a sufficiently large field is applied to an insulator with ohmic contact electrodes, carriers will be injected into the bulk of the material to form a current which is limited by space-charge effects. The following equation can be given for the space-charge-limited current in a solid,

$$I=10^{-12}\,V^2\mu\varepsilon A/4\pi l^3 \qquad (1)$$

where $\mu$ and $\varepsilon$ are the drift mobility and the dielectric constant respectively, $V$ is the applied voltage, $l$ is the electrode spacing, and $A$ is the cross-sectional area. The magnitude of this current in a trap-free material can be quite large, but in practice it is reduced by trapping effects; trapping centers capture the injected carriers, thus reducing the density of free carriers.

As long as the Fermi level, which rises when current injection occurs, is further from the bottom of the conduction band than $E_t$, the trap depth, and moves in a region of the forbidden gap where the level density is much less than $N_t$, the trap density, the ratio of free electrons, $n$, to trapped electrons, $n_t$, is constant and independent of the applied voltage. In this region, the current is given by:

$$I_t=10^{-12}\,V^2\mu\varepsilon Ar/4\pi l^3 \qquad (2)$$

where, if $N_c$ is the effective density of the state in the conduction band, $r$ is approximately given by:

$$r=n/n_t=(N_c/N_t)\exp(-E_t/kT) \qquad (3)$$

Thus, the transition from the ohmic region of current-voltage characteristics to the square-law dependence of the current on the voltage at a higher field is associated with the condition where the space-charge-limited currents become comparable with the intrinsic bulk-current.

*2 The same result for the effect of an ambient atmosphere on the current through the guard-ringed samples of phenanthrene has been explained in a previous paper.[4]

5) A. Rose, *Phys. Rev.*, **97**, 1538 (1955).
6) M. A. Lampert, ibid., **103**, 1648 (1956).
7) R. W. Smith and A. Rose, ibid., **97**, 1531 (1955).
8) W. Ruppel, *Helv. Phys. Acta*, **31**, 311 (1958).

Accordingly, if $V_t$ is the voltage at which the above-mentioned transition occurs, the concentration of bulk-free carriers, $n_o$, which means that of free carriers before injection, is given by:

$$n_o = 10^{-12} V_t \varepsilon r / 4\pi e l^2 \qquad (4)$$

The extremely steep rise of the current at more higher fields corresponds to the condition in which the traps have been essentially filled; the current rises very steeply with the voltage toward the curve characteristic of trap-free behavior. The density of traps which have been filled is calculated from the voltage, $V_{tf}$, where the current rises steeply:

$$eN_t = CV_{tf}/1A = 10^{-12} V_{tf}/4\pi l^2 \qquad (5)$$

where $C$ is the capacity of a sample, and $A$ is the cross-sectional area.

The current-voltage characteristics obtained from sample 63-5 and sample 63-7 are illustrated in Fig. 4. These results were analyzed as space-charge-limited currents phenomena.

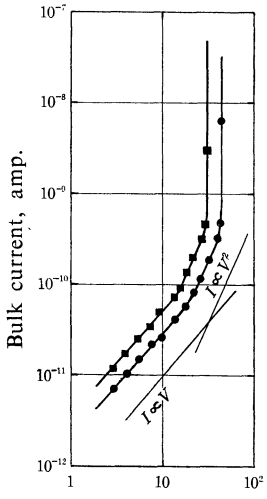



Fig. 4. Current-voltage characteristics of sample 63-5 (■) and sample 63-7 (●).

If the crystal of sample 63-5 is absolutely trap-free, the theoretical space-charge-limited current $I$ at 22 V. is calculated to be $5.89\times10^{-3}$ amp. with Eq. 1, where the values of $\varepsilon=3$ is adopted,[9] and $\mu$ is assumed to be 0.1 $cm^2/V.\cdot sec.$*3 The experimentally-observed current in Fig. 4, that is, $I_t$ for this sample at the same voltage, is $1.15\times10^{-10}$ amp. Therefore, $1.95\times10^{-8}$ is evaluated as the value of $r$.

In Fig. 4, $V_t$, at which point the transition from the ohmic region to square-law behavior occurs, is observed to be about 15 V. Thus, a value of $1.2\times10^6$ $cm^{-3}$ is obtained from Eq. 4 as the concentration of bulk-free carriers. The resistivity $5.2\times10^{13}$ Ω cm., calculated from the formula $\rho=(en_o\mu)^{-1}$ by using $n_o=1.2\times10^6$ $cm^{-3}$ obtained above, is in good agreement with the observed resistivity, $5.4\times10^{13}$ Ω cm., for the ohmic region of current-voltage characteristics of sample 63-5. This self-consistence may support the applicability of space-chage-limited currents analysis for the results of sample 63-5. This consistence is found to exist also for sample 63-7.

The trap density, $N_t$, can be determined from the voltage, $V_{tf}$. $V_{tf}$ was determined by using the circuit of Fig. 2. When the observed value of $V_{tf}$, 30 V., for sample 63-5 is inserted in Eq. 5, the value of $N_t$ can be calculated as $1.24\times10^{14}$ $cm^{-3}$.

Here, the trap-depth, $E_t$, can be evaluated from Eq. 3, if the effective density of the state in the conduction band, $N_c$, is known. If we adopt $N_c=5.76\times10^{15}$ $cm^{-3}$, which is obtained by inserting $n_o=1.2\times10^6$ $cm^{-3}$ and $\Delta\varepsilon=1.14$ eV.[4] into relation, $n_o=N_c\exp(-\Delta\varepsilon/2kt)$, $E_t$ for sample 63-5 is estimated to be 0.55 eV.

Similar results were also obsained for sample 63-7 through analyzing its current-voltage characteristics. The results are summarized in Table I.

Table I

| | $n_o\cdot cm^{-3}$ | $N_t\cdot cm^{-3}$ | $E_t\cdot$eV. |
|---|---|---|---|
| Sample 63-5 | $1.2\times10^6$ | $1.2\times10^{14}$ | 0.55 |
| Sample 63-7 | $1.1\times10^6$ | $1.0\times10^{14}$ | 0.55 |
| Average | $1.2\times10^6$ | $1.1\times10^{14}$ | 0.55 |

The trap density, $N_t=1.1\times10^{14}$ $cm^{-3}$, for phenanthrene obtained here is comparable to the corresponding value for anthracene, $7.6\times10^{13}$ $cm^{-3}$, obtained by Mark and Helfrich,[2] and to that for phthalocyanine, $10^{12}-10^{14}$ $cm^{-3}$, obtained by Heilmeier and Warfield.[3] It is worthy of notice that the value of the trap density is in the order of $10^{12}-10^{14}$ $cm^{-3}$ for all of these organic molecular crystals, and that the trap density of this order seems to be rather low for an organic solid in which some chemical impurity is generally difficult to remove and in which the imperfection of crystal is likely to occur because of the weak binding strength characteristic of molecular crystals. Both facts, their low trap-densities and their agreement, being of the order of $10^{12}-10^{14}$ $cm^{-3}$, might give a key to the establishment of the nature of the trap in organic molecular crystals, although further experimental studies are needed to solve the problem.

9) H. Kronberger and J. Weiss, *J. Chem. Soc.*, Part II, **1944**, 464.

*3 This value of $\mu$ is estimated from the observed mobility of similar aromatic hydrocarbons. Although whether the assumed value is reasonable or not has to be examined by measuring the mobility, the accurate value is not indispensable in the following discussion.

The question of whether electrons or holes are trapped in phenanthrene can not as yet be decided either.

## Summary

The obtained current-voltage characteristics of phenanthrene single crystals exhibited three distinct types of behavior: (1) at low voltages, up to $2\times10^4$ V. per cm., the dependence of the current on the voltage obeyed Ohms' law, (2) at intermediate voltages, the current increased with the square of the voltage, and (3) at higher voltages, over $5\times10^4$ V. per cm., the current rose steeply with the voltage. These results have been analyzed as space-charge-limited currents phenomena, and a value of $1.2\times10^6$ cm$^{-2}$ has been obtained as the concentration of the bulk-free carriers from the transition voltage between the ohmic region and the square-law behavior. The resistivity calculated by applying this value is in good agreement with the resistivity observed for the ohmic region of current-voltage characteristics.

The trap density of $1.1\times10^{14}$ cm$^{-3}$ has been evaluated from the voltage where the current rose steeply. Although this value seems to be rather low for an organic solid, it is comparable to the trap densities for organic molecular crystals ever obtained.

The author wishes to express his thanks to Dr. Haruo Kuroda for his valuable advice, and Dr. Tsutomu Takamura for his encouragement.

*Central Research Laboratory*
*Tokyo Shibaura Electric Co., Ltd.*
*Kawasaki, Kanagawa*

# An Automatic Adiabatic Calorimeter for Low Temperatures. The Heat Capacity of Standard Benzoic Acid[1)]

By Hiroshi SUGA and Syûzô SEKI

(Received November 4, 1964)

In recent years there has been an increasing interest in the heat capacities of crystals at low temperatures as a means to determine, for example, third law entropies, the purity of materials, and the frequency spectra of the lattice modes of vibration. Numerous methods of measuring the low-temperature heat capacity of the crystal have been reported. In the "adiabatic"-type calorimeter, two operators, at least, and tedious labor are required in order to obtain highly accurate results. The development of electronics in recent years has, however, made it possible to replace manual regulation with automatic control and also manual observation with automatic recording, without any general loss of the claimed accuracy. Stull[2)] has, in fact, recently developed such an automatic calorimeter. This report stimulated us to construct such a one-man-operated type low-temperature calorimeter with a high accuracy.

The present paper will report the construction and the operational procedure of this low-temperature calorimeter and will also present the results of our heat-capacity measurement of a standard sample of the benzoic acid crystal, which is used for checking the reliability and accuracy of our results.

1) Reported at the 14th Annual Meeting of the Chemical Society of Japan, Tokyo, April, 1961.
2) D. R. Stull, *Anal. Chim. Acta*, 17, 133 (1957).

## Apparatus

**Calorimeter and Cryostat.**—A schematic cross section of the calorimeter and the cryostat is shown in Fig. 1. The apparatus is of the adiabatic type, consisting of a vacuum-insulated calorimeter surrounded by an adiabatic shield whose temperature is maintained at essentially the same level as that of the calorimeter during heat-capacity measurements. The sample container, A, is made of gold plate, with walls 0.3 mm. thick and with a central re-entrant well into which a combined thermometer-heater is set. In order to obtain good heat conduction between the container and the specimen, six radial fins of platinum 0.1 mm. thick are attached with silver solder to the outside of the well and also to the inside of the container. A brass cap with capillary copper tubing is unsoldered and resoldered in order to change samples.

The calorimeter temperature is measured with a Leeds and Northrup 25-ohm "four

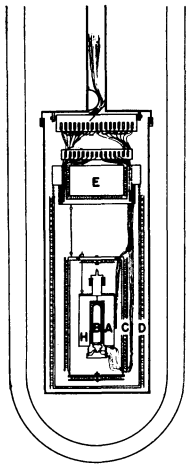



Fig. 1. Schematic diagram of low-temperature adiabatic calorimeter (13—300°K).

lead" platinum-resistance thermometer, 5 mm. in diamerter and 50 mm. long. Around the outside of this thermometer, the calorimeter heater, formed of approximately 100 ohms of #36 B and S constantan wire, for the supply of electrical energy is wound non-inductively and insulated with G. E. adhesive #7031. The surface is coated with gold foil, and the thermometer-heater is set rigidly into the central well of the calorimeter with Wood's metal. Around the protruded bottom of the calorimeter, all the lead wires from the thermometer-heater are wrapped tightly, insulated with the G. E. adhesive, and then soldered to copper lugs. The container is hung from the top of the inner adiabatic shield, C, with three nylon threads, the length of which can be adjusted externally. The empty weight of the container, including the thermometer-heater, is about 100 g.

The inner adiabatic shield is made of brass, 1 mm. thick, and it is chromium-plated on both sides. It consists of three portions, top, sides and bottom. The side portion is fitted with copper lugs to which are connected all the lead wires coming from the container to the outside. All the wires from this connecter are bundled together and wound on the outer surface of the side portion of the shield for four turns and then secured with the adhesive. These wires and the whole of the outer surface of the shield are wrapped with a heater made of #32 B and S constantan wire. The heater is wrapped in three sections. The resistance around the cyrindrical side portion is about 100 ohms, while that of the top and bottom portions is approximately 40 ohms. The entire surface is coated with the adhesive, covered with a heavy grade of aluminum foil.

Difference thermocouples between the container and the inner adiabatic shield are of the Chromel-P constantan type, formed of #38 and #36 B and S wires, and they are placed in seven different positions within the adiabatic shield. The other junctions are gathered together and secured to, but electrically insulated from, the pocket of the sample container.

The inner adiabatic shield is hung with three nylon threads from the upper block, E, which is in turn hung by adjustable nylon cords from the vacuum jacket. This block consists of brass (3 kg.), an embedded constantan heater, copper lugs, and two Chromel-P constantan difference thermocouples whose other junctions are secured to the inner adiabatic shield. Surrounding the inner adiabatic shield, an outer shield, D, is hung with detachable chains from the upper block. The outer shield, 60 mm. in diameter and 250 mm. high, constantan heater and two difference thermocouples whose other junctions are placed on the inner adiabatic shield. In order to obtain good performance in the temperature control of the inner shield, the temperature of the outer shield is kept somewhat below that of the inner shield so as to offer a necessary cold head. All the lead wires from the calorimeter assembly are, after being wrapped to the inner shield, in intimate contact with the upper block and are secured with the adhesive and then passed through a hole to copper lugs attached to the bakelite ring. Hereafter, the wires passed through stainless steel tubing, 25 mm. in diameter and 900 mm. long to the top closure, where they emerge through a vacuum seal made of bees wax.

For the refrigeration, the calorimeter assembly is mounted in the glass dewar, 110 mm. in outer diameter and 1200 mm. long. Liquid nitrogen or liquid hydrogen as a refrigerant is transferred by means of a transfer siphon entering the equipment through the top plate.

**Measuring and Control Circuits.**—A schematic diagram of measuring and control circuits is given in Fig. 2. The resistance of the thermometer could be recorded continuously on a Leeds and Northrup "High-Precision" resistance recorder, by means of which the temperature of the sample could be read to $\pm 0.01$°K at room temperature. When more precision was needed in the temperature measurement, the resistance was measured with a Leeds and Northrup-type G-2 Mueller Bridge in conjunction with a high sensitive galvanometer and lamp scale. At all except the lowest temperatures, the resistance of the thermometer could be read to a precision of one or two parts per ten thousands with this equipment.

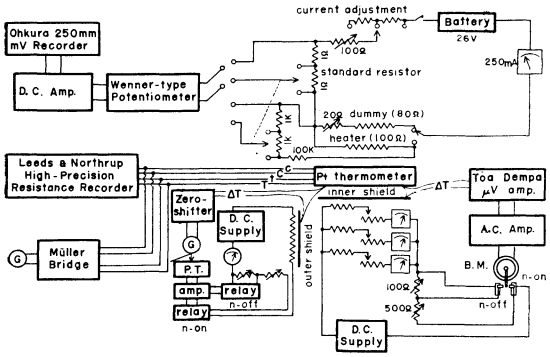



Fig. 2. Circuits diagram for heat capacity measurements.

The electrical energy for heating the calorimeter was supplied by four storage batteries (capacity: 120 amp. hr. at 26 V.). The current was adequately adjusted by means of a six-dial decade resistor and a variable resistor. The current was determined by the potential drop across a 2-ohm (or 1-ohm) series resistor. The potential drop across the calorimeter heater was divided by a 100000-ohm volt box, which had a 100 : 2 (or 100 : 1) ratio certified to 0.01 per cent. These two potential drops were mostly compensated for, respectively, by means of a Leeds and Northrup Wenner potentiometer; the residual differences were, after amplifying by a d.c. amplifier, recorded continuously on a Ōkura 250-mm. voltage recorder. All the necessary standard resistors were contained in a box held at the constant temperature of 32±0.5°C, where the temperature coefficient of the resistance of manganin wire is essentially zero. Since the resistance of the calorimeter heater was not constant over even one heating period, the current and the voltage through and across the heater were recorded alternatively in this period according to Giauque's schedule,[3] i.e., currents at $0.21\,\tau$ and $0.79\,\tau$, and the voltage at $0.50\,\tau$, where $\tau$ means the total heating period. To allow for the small amount of heat generated in the current leads between the calorimeter and the inner adiabatic shield, one of the potential leads was attached to a terminal on the calorimeter, and the other to a terminal on the inner shield. If the resistances of the current leads are similar, this procedure accounts for that part of the heat generated in them which flows to the calorimeter. When the heater was not energized, the current was kept at the same value as that through the heater by connecting the circuit to a dummy heater composed of fixed and variable constantan resistors. The energy input was automatically started and stopped by an electric timer synchronized with a transistor clock, as is shown in Fig. 3. The input interval was held to integral seconds by synchronizing the heater switch with a relay which was closed once each second. The interval was measured by a counter and was found to be accurate to 0.05% or better.

3) W. F. Giauque and C. J. Egan, *J. Chem. Phys.*, 5, 45 (1937).

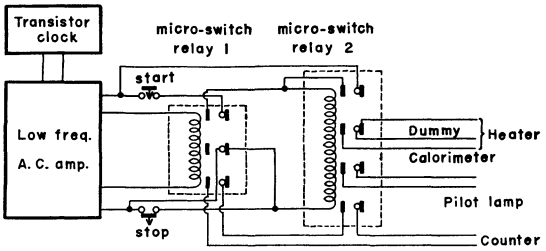



Fig. 3. Circuits of electronic timer.

The precise control of the temperature difference between the calorimeter and the inner shield is essential for accurate measurements in the adiabatic-type calorimeter. For this purpose, a signal from a seven-junction Chromel-P constantan thermocouple which registered any temperature difference between them was fed to a Tôa Dempa AD-4 d.c. amplifier and an a.c. amplifier, the output of the latter amplifier being used to operate a balancing motor (Fig. 4). When the thermocouple thus signaled that the shield was colder than that calorimeter, the balancing motor converted a "normally open" relay to the "closed" state, thus shortening the series resistor in the heater circuit, resulting in an increase in the heater current. In the reverse case, the balancing motor turned off another "normally closed" relay, resulting in zero current. The currents in each step were regulated so as to minimize the "hunting" or temperature swings about the zero point and also to

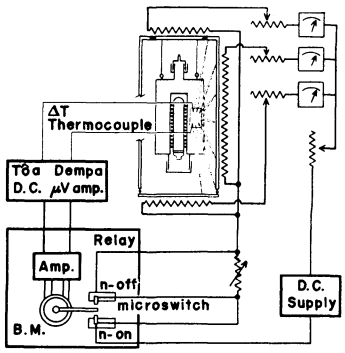



Fig. 4. Control circuits for inner adiabatic shield.

make the length of time spent in the colder state equal to the time spent in the hotter state. The heater current in three parts of the inner shield was separately adjusted to be proportional to the heat capacity of each part. The design of the controller of this type is similar to that of Stull.[2] Manual refinements have been added to permit closer control at the beginning and end of the heating period.

Besides the inner shield, the temperatures of the outer shield and brass block were regulated by another control system. Two-junction Chromel-P constantan thermocouples for detecting any temperature difference between the inner shield and the outer shield and also between the inner shield and the brass block were connected to a highly sensitive galvanometer (the control circuit of the block is not shown in Fig. 2). The light beam from the source was reflected by the mirror of the galvanometer, and then projected on to two photo-transistors, which served to operate two microswitchs attached to heater circuit. By this arrangement, the heater current was adjusted automatically in three steps so as to give no temperature difference between the inner shield and the block. On the other hand, the temperature of the outer shield was adjusted somewhat below that of the inner shield by adding an adjustable bucking potential to the e.m.f. of the difference thermocouple. The temperature of the inner adiabatic shield was kept automatically the same as that of the sample container within $\pm 0.003$°K at room temperature and within $\pm 0.01$°K at 30°K.

## Experimental Procedure

**The Calibration of the Platinum Resistance Thermometer in the Temperature Range from 13 to 300°K.** — It is necessary to calibrate a working platinum resistance thermometer against the international or the thermodynamical temperature scale, since the accuracy of the measurement of the temperature has an important bearing on the precision claimed for the calorimetry. The procedure for calibrating the thermometer is described below.

Above 90°K, the International Temperature Scale (I.T.S.) has been used as a practical scale of temperature in order to give a greater reproducibility and a far simpler realization of the scale than would otherwise be obtained on the gas scale. On the other hand, in only one part of the scale below 90°K has an agreed method of interpolation been adopted internationally, namely, from 0.5 to 5.2°K a scale based on the vapor pressure temperature scale of $He^4$.[4] At the National Bureau of Standards a provisional scale has, however, been established in terms of a gas thermometer with the aim of seeking the uniformity of the temperature scales of the various laboratories doing low-temperature work.

For this purpose a series of Pt resistance thermometers has been made by the Leeds and Northrup Company; they were calibrated at the National Bureau of Stndards,* based on the I.T.S. of 1948 between the boiling points of sulfur and of oxygen, and on the NBS scale of Hoge and Brickwedde[5] below the oxygen boiling point. One of these, No. 1510628, was purchased by our University and served as the standard for the calibration of the working thermometers used in our laboratory. The working thermometer, No. 1526483, was calibrated against the standard thermometer by an intercomparison method at any fixed temperature. For this purpose, two thermometers were fixed with Wood's metal into reentrant wells in a copper block. This copper block was hung in the place of the sample container within the inner adiabatic shield of the calorimeter assembly described above. The measurements of the resistance were carried out by the use of the Mueller Bridge with an accuracy of $\pm 0.00001$ ohm by keeping the temperature difference between the block and the adiabatic shield as small as possible. Practically all the intercomparison experiments were performed with temperature drifts less than $\pm 0.0001$°C/min. of the copper block. The precise $R_0$ value, the resistance at the ice point, was measured in the conventional manner by the use of the apparatus, which is essentially the same as that described by Stimson.[6]

For the smoothing of the intercomparison data, the resistance differences $\Delta R$ between the standard (S) and the working (W) thermometers were plotted against $R_S$. Fortunately, fairly linear relationship was observed between $\Delta R$ and $R_S$ in the measured temperature range, as may be seen in Fig. 5. The scatters of the experimental points from the straight line derived by the method of least squares were nowhere smaller than 0.00007 ohm; they are plotted in Fig. 6. The linear relationship between $\Delta R$ and $R$ is to be expected if the "Z function" method proposed by Cragoe[7] can be

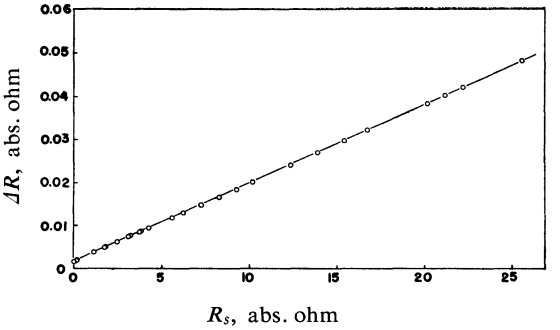



Fig. 5. Plots of $\Delta R(R_x - R_S)$ against $R_S$.

4) H. van Dijk, M. Durieux, J. R. Clement and J. K. Logan, *J. Research Natl. Bur. Standards*, **64A**, 4 (1960).

* We are greatly obliged to Dr. G. T. Furukawa of the N. B. S. for his kindness in making arrangements for the standardization of our thermometer,

5) H. G. Hoge and F. J. Brickwedde, ibid., **22**, 351 (1939).

6) H. F. Stimson, ibid., **24**, 209 (1949).

7) D. R. Stull, *Chem. Eng. News*, **27**, 2772 (1949).

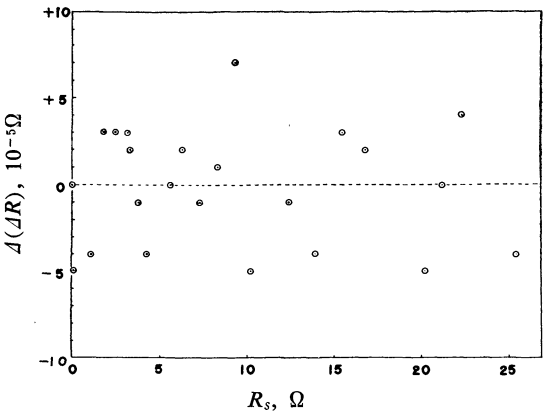



Fig. 6. Deviations of $\Delta R$ from straight line derived by the method of least squares.

exactly applied to these thermometers. That is, if the resistances of the two thermometers obey the Matthiessen rule, and if the temperature dependent components of the resistances can be described with the same function of temperature, the linear relationship follows that between $\Delta R$ and $R$.

It was now possible make a resistance-temperature table directly for the working thermometer through the formula: $R_w = R_s(1+A)+B$, the numerical factors, $A$ and $B$, being determined to be 0.0018325 and 0.001556 respectively. The tabulation was made with intervals of temperature 0.1°K below 90°K and 1°K above 90°K. Also, the temperature variation of the resistance, $dR/dT$, was tabulated by the formula; $dR_w/dT = (1+A)dR_s/dT$. This value served for making a linear interpolation of the resistance at any temperature.

**Measurements of the Heat Capacity.** — After setting the sample in the container, the closure was fastened with soft solder. Then helium gas at the desired pressure was introduced through the copper tubing attached to the closure, and the tubing was pinched off so as to keep helium gas tight. The calorimeter was then assembled, and the insulating vacuum space was pumped for several days at room temperature. The pressure was read on a Phillips gauge with a liquid nitrogen trap.

In order to cool the calorimeter, liquid nitrogen was added to the dewar, and helium gas of about 1 mmHg pressure was introduced into the vacuum space. By pumping off the liquid nitrogen in the dewar vessel, the sample was cooled to about 55°K. In the course of this cooling process, the "High-Precision" resistance recorder was operated in such a manner as to draw a continuous cooling curve of the sample, a curve useful for checking the presence of any thermal anomaly that might be encountered. When the measurements were to be made at lower temperatures, liquid hydrogen was introduced into the dewar vessel through a transfer siphon after the liquid nitrogen had been drawn off and the vacuum space flushed with hydrogen gas. A small amount of helium gas was again introduced into the vacuum space; by pumping on the hydrogen bath, the temperature of the calorimeter could be lowered to about 12°K. The in-

TABLE I. SELECTED VALUES OF THE EXPERIMENTAL HEAT CAPACITY OF THE BENZOIC ACID CRYSTAL

0°C=273.15°K Mol. wt. 122.12

| $T_{av}$ °K | Approx. $\Delta T$ | $\Delta H/\Delta T$ joul./deg. mol. |
|---|---|---|
| | Series I | |
| 15.25 | 2.613 | 6.127 |
| 17.60 | 1.881 | 8.479 |
| 19.66 | 2.027 | 10.781 |
| 21.59 | 1.695 | 12.961 |
| 23.41 | 1.846 | 14.724 |
| 25.56 | 2.375 | 17.380 |
| 28.15 | 2.694 | 20.035 |
| 30.69 | 2.386 | 22.694 |
| | Series II | |
| 15.25 | 2.587 | 6.216 |
| 19.40 | 1.564 | 10.161 |
| 23.11 | 2.262 | 14.498 |
| 32.94 | 2.143 | 25.230 |
| 36.86 | 1.833 | 29.038 |
| 41.35 | 2.861 | 32.515 |
| 46.83 | 2.856 | 37.332 |
| 51.34 | 2.873 | 40.570 |
| 57.04 | 2.793 | 44.178 |
| 60.06 | 2.742 | 45.888 |
| 66.31 | 3.114 | 49.188 |
| 69.14 | 3.050 | 50.717 |
| 72.74 | 2.955 | 52.363 |
| 78.17 | 2.987 | 54.843 |
| 80.83 | 2.930 | 56.243 |
| 86.25 | 2.998 | 58.595 |
| 88.92 | 2.949 | 59.625 |
| 94.55 | 3.151 | 61.828 |
| 100.15 | 3.048 | 63.909 |
| 104.78 | 2.016 | 65.229 |
| 110.17 | 1.956 | 67.637 |
| 118.90 | 1.882 | 70.565 |
| 126.06 | 1.936 | 73.447 |
| 133.10 | 1.880 | 75.965 |
| 145.37 | 3.154 | 80.886 |
| 151.12 | 3.051 | 82.956 |
| 162.52 | 3.055 | 88.376 |
| 173.82 | 2.942 | 91.998 |
| 184.75 | 2.839 | 96.633 |
| 195.96 | 3.145 | 101.46 |
| 207.80 | 3.033 | 106.19 |
| 213.60 | 2.989 | 108.54 |
| 223.67 | 3.227 | 112.89 |
| 235.94 | 3.107 | 118.44 |
| 245.17 | 2.195 | 122.07 |
| 253.63 | 2.144 | 125.82 |
| 257.81 | 2.117 | 127.93 |
| 263.97 | 2.078 | 130.94 |
| 272.05 | 2.032 | 134.74 |
| 281.31 | 3.214 | 139.20 |
| 293.85 | 3.162 | 144.66 |
| 299.99 | 3.070 | 147.14 |
| 303.55 | 3.043 | 148.90 |

sulating vacuum space was then evacuated, and after the sample showed an upward temperature drift a series of measurements were started.

In an individual measurement, the temperature drift was measured before and after the heating period. The rate of energy input was varied from about 0.01 degrees to 0.2 degrees per minute. A series of measurements in the temperature range from 15 to 310°K usually required about 100—150 hr. Additional runs were made on the empty container over the whole temperature range. To obtain the heat capacity of the sample itself, the heat capacity of the filled calorimeter was corrected for the smooth heat capacity of the empty can.

## Experimental Results

In order to verify the performance and the accuracy of this low temperature calorimeter, the heat capacity of the benzoic acid crystal was measured from 15 to 310°K. The sample was obtained through the courtesy of E. J. Prosen of the Chemistry Division of the National Bureau of Standards as a Calorimetry Conference Standard specimen. About 23 g. of this sample was transferred into the sample container.

Figure 7 illustrates an example of heat capacity measurement. In general, the time taken to attain equilibrium after the energy input was between 3 and 5 min. Above 50°K, most of the experiments were carried out with a small thermal leakage, resulting in temperature drifts within ±0.0003—0.0005 deg./min. On the other hand, some experimental difficulties were encountered below 50°K as a result of the decrease in the heat capacities of the specimen and also the increase in the heat exchange between the calorimeter and the surroundings.

The experimental heat capacities, listed in Table I are the ratio of the increment in enthalpy to the increment in temperature, $\Delta H/\Delta T$, and must be corrected for curvature if the differential heat capacities are needed. In the case of the benzoic acid crystal, the correction is for all points less than a change of one in the last figure entered in the table. Also listed in this table are the approximate temperature rise, $\Delta T$, in an individual measurement and $T_{av}$, the arithmetic mean of the initial and final temperatures. The deviation of each measured point from a smooth curve is plotted in Fig. 8 as a function of the temperature; the dotted lines mean a one per cent deviation. An examination of the figure indicates that the greatest divergence is found below 50°K. The reason for this seems to be the difficulties of maintaining the adiabatic conditions of the calorimeter in this temperature range; the equipment becomes insensitive, and the thermal leakages between the assembly and the surroundings increase, while the heat capacities of the constituent materials decrease progressively as the temperature is lowered.

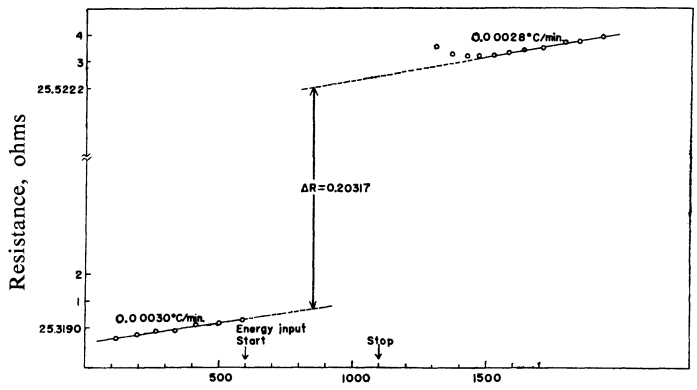



Fig. 7. Typical drift curves before and after an energy input.

| | | | |
|---|---|---|---|
| $I_{av}$ | 35.9495 mamp. | Input energy | 67.084 abs. joul. |
| $V_{av}$ | 3.7321 V. | Lost energy | 0.068 |
| $t$ | 500 sec. | Net input energy ($E$) | 67.016 |
| | | $R_i$ | 25.31904 ohms/ohms |
| | | $R_f$ | 25.52221 |
| | | $\Delta R$ | 0.20317 |
| | | $E/\Delta R$ | 329.85 abs. joul./ohms |
| | | $\frac{\Delta R}{\Delta T}$ at $\frac{R_i+R_f}{2}$ | 0.10729 ohm. |
| | | $C_p=\frac{E}{\Delta T}=\frac{E}{\Delta R}\cdot\frac{\Delta R}{\Delta T}$ | 35.3896 abs. joul./deg. |

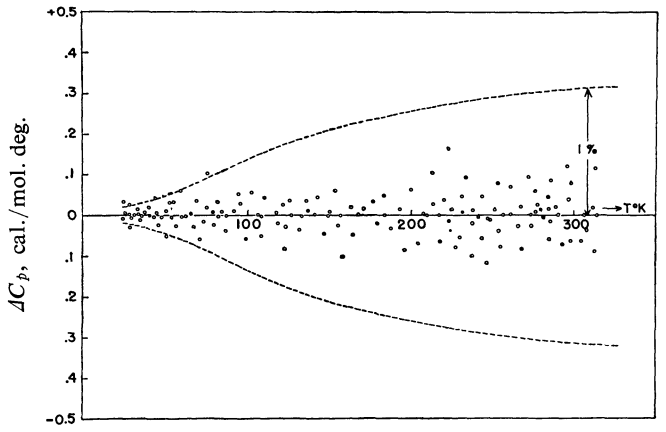



Fig. 8. Deviations of experimental heat capacities of benzoic acid from a smoothed curve.

Above 100°K all the points fall within ±0.5%, and most of them within ±0.3%.

Measurements of the heat capacity of the Calorimetry Conference Standard benzoic acid have hitherto been reported by Furukawa et al.[8], Stout et al.[9], Osborne et al.[10] and by Busey[11]. The smooth curve derived from the present measurements coincides well (within 1%) with their results above 20°K. Remarkable disagreements have been reported among the heat capacity data reported hitherto at temperatures below 20°K. The present data seems to lie between the NBS and Stout data. The increase in the scattering of each measured point, however, makes it impossible to deduce a quantitative conclusion in this temperature range at the present stage.

## Summary

An adiabatic calorimeter for the measurements of the heat capacity of a solid and liquid over the temperature range from 13 to 300°K has been constructed. In order to minimize the operating manpower, all the temperature controls were recorded semiautomatically. The energy input was started and stopped automatically by a timer driven by a signal from a transistor clock. The working platinum resistance thermometer was calibrated against a laboratory standard thermometer which had been calibrated by the National Bureau of Standards. In order to verify the performance and the accuracy of this one-man-operated calorimeter, the heat capacity of a Calorimetry Conference Standard sample of benzoic acid crystal has been measured from 15 to 310°K. The results have compared with the data from the NBS and from other laboratories; this comparison served to establish the reliability of this equipment. The estimated errors are ±2% at 20°K, ±1% below 50°K, and ±0.3% above 50°K.

This work was supported in part by the Scientific Research Expenditure Fund of the Ministry of Education, to which the authors' thanks are due. The authors also wish to express their thanks to Mr. Nobuo Nakamura for his kind help in the numerical calculations.

*Department of Chemistry*
*Faculty of Science*
*Osaka University*
*Toyonaka, Osaka*

8) G. T. Furukawa, R. E. McCosky and G. J. King, *J. Research Natl. Bur. Standards*, **47**, 256 (1951).
9) A. G. Cole, J. O. Huchens, R. A. Robie and J. W. Stout, *J. Am. Chem. Soc.*, **77**, 2737 (1955).
10) D. W. Osborne, E. F. Westrum, Jr., and H. R. Lohr, ibid., **77**, 2737 (1955).
11) R. H. Busey, ibid., **78**, 3263 (1956).

# Heat Capacity and Thermodynamic Functions of $K_2CuCl_4 \cdot 2H_2O$ and $(NH_4)_2CuCl_4 \cdot 2H_2O$ from 13 to 310°K*

By Hiroshi SUGA, Michio SORAI, Tadashi YAMANAKA** and Syûzô SEKI

(Received November 4, 1964)

There have been many investigations of the orientational order-disorder phenomena of ammonium ions in the crystalline state. Among these, the most comprehensive have been those of ammonium halides. In the case of ammonium chloride, it has been revealed from various experimental facts[1-4] and from theoretical considerations[5] that a $\lambda$-type anomaly at $-38$°C in the heat capacity curve can be explained by the co-operative transition from an uniquely defined orientational state to two equally-probable states with respect to the $NH_4^+$ ion.

X-Ray structural study of the $(NH_4)_2CuCl_4 \cdot 2H_2O$ crystal[6] shows that the crystal lattice is, roughly speaking, composed of three units $NH_4^+$, $Cl^-$, and $CuCl_2 \cdot 2H_2O$, with the result that the inter-ammonium distance of ammonium chloride is enlarged two-dimensionally by the introduction of $CuCl_2 \cdot 2H_2O$. It will, therefore, be of some interest to study an orientational ordering process of such a linearly-arranged ammonium ion system and to compare the results with those of an isotropically-arranged one found in ammonium chloride.

The present paper will report on the thermodynamic properties of $(NH_4)_2CuCl_4 \cdot 2H_2O$ and $K_2CuCl_4 \cdot 2H_2O$ crystals from 13 to 310°K. The latter crystal was selected as a reference material because it belongs to the same crystal system ($D_{4h}^{14}$-P4/mnm) as the former and involves a spherical cation, $K^+$, with an ionic radius nearly equal to that of the $NH_4^+$ ion.

## Experimental and Results

**The Preparation of Samples.**—The potassium copper chloride dihydrate, $K_2CuCl_4 \cdot 2H_2O$, is the double salt of KCl and $CuCl_2 \cdot 2H_2O$, while the ammonium copper chloride dihydrate, $(NH_4)_2CuCl_4 \cdot 2H_2O$, is that of $NH_4Cl$ and $CuCl_2 \cdot 2H_2O$. $(NH_4)_2CuCl_4 \cdot 2H_2O$ ($NH_4$-salt) was prepared from a mixed solution of their component substances and was purified by repeated recrystallizations.[7] In the case of $K_2CuCl_4 \cdot 2H_2O$ (K-salt), the crystal was prepared according to the phase diagram[8] of the $KCl$–$CuCl_2$–$H_2O$ system. Commercial analytical reagents of the Wakō Pure Chemical Industry Company were used for the preparation.

**Differential Thermal Analysis.**—The freshly prepared specimens of $NH_4$-salt are reported to exhibit a thermal anomaly at about $-22$°C on cooling.[9] This anomaly is due to the freezing of occluded water, since there is no thermal anomaly in partly-dehydrated samples. In order to eliminate the excess water, the sample was dried over partly-dehydrated $NH_4$-salt in a desiccator for several weeks. In order to determine the temperature of dehydration, differential thermal analysis (DTA) and thermogravimetric analysis (TGA) methods were applied to both crystals; some interesting features due to the process of dehydration were thus found. The results are shown in Fig. 1. As the temperature is raised, K-salt exhibits two apparently separate peaks, at about 93°C and 116°C. In the case of $NH_4$-salt, however, only one peak appears, at about 143.5°C, with a shoulder at 138°C.

Meyerhoffer[10] has found, from dilatometric study, a phase change for K-salt at 92.4°C and has suggested the following decomposition mechanism*:

$$K_2CuCl_4 \cdot 2H_2O \rightleftarrows KCuCl_3 + KCl + 2H_2O$$

* Presented in part at the 15th Annual Meeting of the Chemical Society of Japan, Kyoto, April, 1962.

** Present address: Research Laboratory, Wireless Division, Matsushita Electric Industrial, Co., Ltd., Kadoma, Osaka.

1) F. Simon, *Ann. d. Phys.*, **68**, 241 (1922).

2) H. S. Gutowsky, G. E. Pake and R. Bersohn, *J. Chem. Phys.*, **22**, 634 (1954).

3) E. L. Wagner and D. F. Hornig, ibid., **18**, 296 (1950).

4) H. A. Levy and S. W. Peterson, *Phys. Rev.*, **86**, 766 (1952); G. H. Goldschmidt and D. G. Hurst, ibid., **83**, 88 (1951); **86**, 797 (1952).

5) Y. Nagamiya, *Proc. Phys. Math. Soc. Japan*, **24**, 137 (1942).

6) L. Chrobak, *Z. Krist.*, **88**, 35 (1934); A. Narasimhamurty and D. Premaswarup, *Proc. Phys. Soc.*, **83**, 199 (1964).

7) A. Seidell, "Solubilities of Inorganic and Organic Compounds," Vol. I, 3rd. Ed., Van Nostrand Co., New York (1940).

8) A. Chretien and R. Weil, *Bull. Soc. Chim.*, **2**, 1577 (1935).

9) N. Nakamura, H. Suga and S. Seki, presented at the 14th Annual Meeting of the Chemical Society of Japan, Tokyo, April, 1961.

10) W. Meyerhoffer, *Z. physik. Chem.*, **3**, 336 (1887).

* This decomposition mechanism was recently confirmed by us from Debye-Scherrer photographs taken below and above 93°C. Fairly intensive diffraction lines ascribed to KCl crystal appeared on the photograph taken at about 100°C. We are greatly indebted to Mr. Takemi Yamada of our University for his kind arrangements for taking high-temperature X-ray photographs.

This mechanism was also verified by Vriens[11] from vapor pressure measurements of K-salt and saturated solutions containing K-salt, KCl and $KCuCl_3$. This transition corresponds just to the first peak in the DTA curve. The released water dissolves parts of the crystals and forms a saturated solution, so shat the solution evaporates at a much higher temperature than does the free water. The second peak which appeared on the DTA curve seems to correspond to the evaporation process, because its temperature depends markedly on the pressure of the surroundings. The temperature of the first peak, on the other hand, is almost not influenced at all when the pressure is reduced to 350 mmHg. The thermo-gravimetric analysis of K-salt revealed that the weight of the sample is the same, within the range of experimental error, before and after the first peak I, corresponding to the A- and B-stages in Fig. 1(a) respectively. However, when

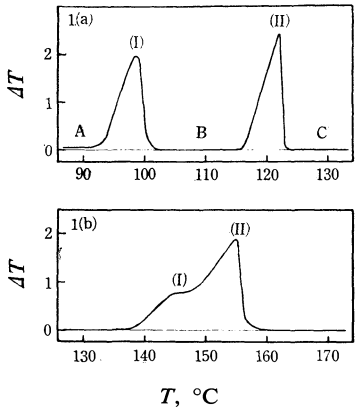



Fig. 1. Curves of the differential thermal analysis: 1(a) for $K_2CuCl_4 \cdot 2H_2O$ and 1(b) for $(NH_4)_2CuCl_4 \cdot 2H_2O$.

passing through the second peak II, at the C-stage in the figure, the sample loses weight nearly equal in amount to the crystalline water involved. From these facts we may regard the phase changes at the I and II peaks to be as follows:

(I) $K_2CuCl_4 \cdot 2H_2O \rightarrow KCuCl_3 + KCl + 2H_2O$ (satd. soln.)

(II) $2H_2O$ (satd. soln.) $\rightarrow 2H_2O$ (vapor)

The occurrence of extra peaks in the DTA curve of hydrates due to the formation of a saturated solution is not uncommon.[12]

In the case of $NH_4$-salt, the first peak appears on a shoulder of the second, so that a similar TGA method can not be applied to this salt. From the fact that the crystal structure of $NH_4$-salt is isomorphous with that of K-salt, we may also assume similar phase changes at the two successive peaks.

**The Heat Capacity of $(NH_4)_2CuCl_4 \cdot 2H_2O$ and $K_2CuCl_4 \cdot 2H_2O$.** — The low temperature calorimeter and the method of measurement are the same as those described in the previous report.[13] The calorimeter contains 26.967 g. (0.09719 mol.) of $(NH_4)_2CuCl_4 \cdot 2H_2O$ and 31.127 g. (0.09740 mol.) of $K_2CuCl_4 \cdot 2H_2O$ with helium exchange gas, respectively, in each experiment.

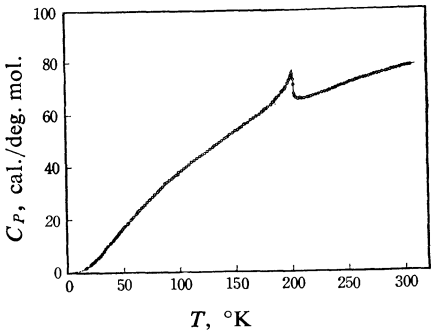



Fig. 2. Heat capacities of $(NH_4)_2CuCl_4 \cdot 2H_2O$ between the temperature range from 13°K to 310°K.

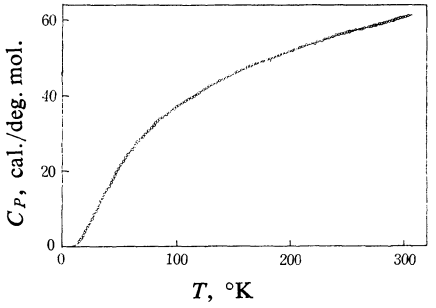



Fig. 3. Heat capacities of $K_2CuCl_4 \cdot 2H_2O$ between the temperature range from 13°K to 310°K.

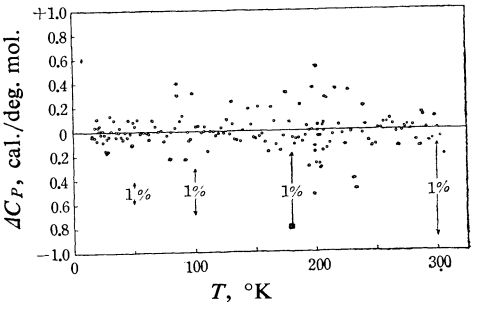



Fig. 4. Deviation of experimental heat capacities of $(NH_4)_2CuCl_4 \cdot 2H_2O$ from a smoothed curve.

11) J. G. C. Vriens, *Z. physik. Chem.*, **7**, 194 (1891).
12) H. J. Borchardt and F. Daniels, *J. Am. Chem. Soc.*, **61**, 917 (1957).
13) H. Suga and S. Seki, This Bulletin, **38**, 1000, (1965).

TABLE I. HEAT CAPACITIES OF $(NH_4)_2CuCl_4 \cdot 2H_2O$

| $T_{av}$ °K | Approx. $\Delta T$ | $\Delta H/\Delta T$ cal./deg.mol. |
|---|---|---|
| | Series I | |
| 155.34 | 2.458 | 55.634 |
| 157.79 | 2.437 | 56.296 |
| 165.38 | 2.605 | 58.679 |
| 167.97 | 2.584 | 59.336 |
| 173.10 | 2.534 | 60.998 |
| 178.23 | 2.550 | 62.867 |
| 180.78 | 2.527 | 63.679 |
| 183.30 | 2.499 | 64.724 |
| 185.79 | 2.471 | 65.796 |
| 189.27 | 2.508 | 67.220 |
| 191.77 | 2.479 | 68.580 |
| 196.71 | 2.401 | 71.949 |
| 199.09 | 2.353 | 74.057 |
| 201.47 | 2.407 | 71.516 |
| 206.55 | 2.528 | 66.219 |
| 211.62 | 2.524 | 66.209 |
| 219.39 | 2.499 | 67.186 |
| 221.89 | 2.492 | 67.424 |
| 229.43 | 2.613 | 68.580 |
| 236.88 | 2.427 | 69.763 |
| 241.78 | 2.547 | 70.638 |
| 246.85 | 2.528 | 71.263 |
| 251.43 | 2.507 | 72.148 |
| 258.91 | 2.479 | 73.135 |
| 268.66 | 2.511 | 74.141 |
| 276.00 | 2.423 | 75.181 |
| 288.03 | 2.390 | 76.401 |
| 291.42 | 2.425 | 76.792 |
| 293.85 | 2.417 | 77.084 |
| 305.86 | 2.390 | 78.102 |
| | Series II | |
| 95.90 | 2.421 | 37.099 |
| 100.66 | 2.342 | 38.739 |
| 102.98 | 2.307 | 39.526 |
| 105.27 | 2.275 | 40.249 |
| 107.52 | 2.243 | 41.026 |
| 121.36 | 2.553 | 45.345 |
| 123.89 | 2.523 | 46.073 |
| 128.88 | 2.464 | 47.592 |
| 130.73 | 1.220 | 48.259 |
| 132.56 | 2.301 | 48.731 |
| 134.85 | 2.278 | 49.410 |
| 139.36 | 2.231 | 50.898 |
| 141.66 | 2.364 | 51.997 |
| 146.34 | 2.326 | 53.114 |
| 150.95 | 2.287 | 54.370 |
| 153.23 | 2.267 | 55.017 |
| | Series III | |
| 192.52 | 2.467 | 69.114 |
| 194.97 | 2.431 | 70.589 |
| 199.15 | 1.174 | 74.175 |
| 200.32 | 1.156 | 75.825 |
| 201.50 | 1.202 | 71.568 |
| 202.72 | 1.253 | 67.151 |
| 203.98 | 1.261 | 66.482 |
| | Series IV | |
| 197.39 | 1.200 | 71.944 |
| 198.59 | 1.186 | 73.194 |
| 199.77 | 1.168 | 74.836 |
| 200.94 | 1.169 | 74.834 |
| 202.14 | 1.242 | 68.118 |
| | Series V | |
| 62.62 | 2.650 | 23.548 |
| 67.74 | 2.455 | 25.857 |
| 72.51 | 2.306 | 27.940 |
| 77.02 | 2.189 | 29.785 |
| 81.92 | 2.078 | 31.818 |
| 87.94 | 1.963 | 34.241 |
| 94.21 | 2.065 | 36.417 |
| 96.26 | 2.037 | 37.067 |
| | Series VI | |
| 15.38 | 2.545 | 1.230 |
| 17.72 | 1.812 | 2.066 |
| 21.78 | 2.571 | 3.691 |
| 22.82 | 2.253 | 4.114 |
| 26.21 | 1.785 | 5.452 |
| 28.31 | 2.247 | 6.392 |
| 30.71 | 2.547 | 7.816 |
| 33.23 | 2.505 | 9.008 |
| 35.64 | 2.243 | 10.159 |
| 38.00 | 2.419 | 11.379 |
| 42.85 | 2.752 | 13.794 |
| 45.48 | 2.528 | 15.240 |
| 48.29 | 2.355 | 16.436 |
| 50.57 | 2.218 | 17.628 |
| 52.96 | 2.588 | 18.853 |
| 55.49 | 2.456 | 20.016 |
| 57.89 | 2.341 | 21.214 |
| 60.18 | 2.245 | 22.313 |
| 62.38 | 2.160 | 23.358 |
| | Series VII | |
| 15.15 | 1.998 | 1.146 |
| 17.34 | 1.825 | 1.857 |
| 19.33 | 1.768 | 2.555 |
| 21.06 | 1.412 | 3.354 |
| 22.79 | 1.774 | 4.058 |
| 24.49 | 1.432 | 4.835 |
| 25.94 | 1.331 | 5.460 |
| 27.57 | 1.846 | 6.168 |
| 29.50 | 1.997 | 7.093 |
| 31.40 | 1.788 | 8.025 |
| 33.24 | 1.904 | 8.917 |
| 35.28 | 2.197 | 9.913 |
| 37.37 | 2.005 | 11.018 |
| 39.57 | 2.412 | 12.102 |
| 41.88 | 2.220 | 13.261 |
| 44.33 | 2.681 | 14.515 |
| 46.91 | 2.488 | 15.843 |

TABLE II. HEAT CAPACITIES OF $K_2CuCl_4 \cdot 2H_2O$

| $T_{av}$ °K | Approx. $\Delta T$ | $\Delta H/\Delta T$ cal./deg.mol. | $T_{av}$ °K | Approx. $\Delta T$ | $\Delta H/\Delta T$ cal./deg.mol. |
|---|---|---|---|---|---|
| | Series I | | 68.39 | 2.281 | 28.551 |
| 90.40 | 2.229 | 35.221 | 70.64 | 2.229 | 29.226 |
| 94.81 | 2.174 | 36.239 | 75.08 | 2.286 | 30.715 |
| 99.11 | 2.126 | 37.159 | 77.35 | 2.240 | 31.385 |
| 105.39 | 2.068 | 38.335 | 79.57 | 2.202 | 31.874 |
| 109.91 | 2.309 | 39.191 | 81.76 | 2.162 | 32.610 |
| 114.47 | 2.269 | 40.023 | 83.91 | 2.128 | 33.157 |
| 121.18 | 2.210 | 41.395 | 86.02 | 2.091 | 33.886 |
| 125.68 | 2.389 | 42.205 | 88.10 | 2.062 | 34.450 |
| 129.30 | 2.357 | 42.902 | | Series III | |
| 136.32 | 2.315 | 43.753 | 21.41 | 1.296 | 4.343 |
| 143.29 | 2.434 | 44.909 | 24.09 | 3.894 | 5.821 |
| 152.94 | 2.374 | 46.357 | 27.50 | 3.000 | 7.769 |
| 157.68 | 2.350 | 46.958 | 30.27 | 2.538 | 9.340 |
| 164.83 | 2.632 | 47.944 | 32.65 | 2.216 | 10.957 |
| 172.67 | 2.539 | 48.879 | 34.76 | 1.998 | 12.255 |
| 177.83 | 2.567 | 49.537 | 36.86 | 2.216 | 13.636 |
| 188.01 | 2.524 | 50.668 | 39.00 | 2.043 | 14.861 |
| 197.02 | 2.493 | 51.571 | 40.98 | 1.910 | 15.958 |
| 204.47 | 2.469 | 52.170 | 43.10 | 2.337 | 17.077 |
| 214.28 | 2.425 | 53.480 | 45.37 | 2.185 | 18.358 |
| 219.14 | 2.415 | 53.740 | 47.51 | 2.056 | 19.619 |
| 223.96 | 2.399 | 54.218 | 49.70 | 2.316 | 20.480 |
| 235.96 | 2.360 | 55.426 | 54.12 | 2.109 | 22.647 |
| 240.88 | 2.565 | 55.870 | 56.31 | 2.242 | 23.557 |
| 248.58 | 2.554 | 56.054 | 58.51 | 2.159 | 24.541 |
| 256.35 | 2.762 | 56.827 | 60.64 | 2.087 | 25.474 |
| 261.81 | 2.729 | 57.807 | 62.70 | 2.028 | 26.227 |
| 267.25 | 2.714 | 58.150 | 64.90 | 2.343 | 27.121 |
| 278.06 | 2.688 | 58.783 | | Series IV | |
| 280.75 | 2.679 | 59.029 | 16.41 | 2.486 | 1.951 |
| 286.11 | 2.657 | 59.706 | 18.62 | 1.806 | 3.060 |
| 288.77 | 2.651 | 59.831 | 20.39 | 1.478 | 3.872 |
| 291.43 | 2.646 | 59.954 | | Series V | |
| 294.08 | 2.637 | 60.219 | 15.15 | 2.985 | 1.502 |
| 296.73 | 2.631 | 60.371 | 17.67 | 2.059 | 2.569 |
| 299.37 | 2.622 | 60.629 | 19.56 | 1.545 | 3.840 |
| 302.00 | 2.614 | 60.852 | 21.49 | 1.833 | 4.385 |
| | Series II | | 23.25 | 1.533 | 5.421 |
| 61.44 | 2.102 | 25.837 | 24.75 | 1.349 | 6.240 |
| 63.69 | 2.424 | 26.622 | 26.07 | 1.212 | 7.050 |
| 66.08 | 2.336 | 27.844 | | | |

The experimental heat capacities listed in Tables I and II are the ratios of the increase in enthalpy, $\Delta H$, to the rise in temperature, $\Delta T$, and are equal to the differential heat capacity, $C_P$, only when the correction for curvature is negligible. Here, a defined calorie equal to 4.1840 absolute joules is used, and the ice point temperature is taken as 273.15°K. Also listed in Tables I and II are $T_{av}$, the arithmetic mean of the initial and final temperatures of each measurement, and the approximate temperature rise, $\Delta T$. The experimental heat capacities and the smoothed curves of both crystals are shown in Figs. 2 and 3.[14] The deviation plot of measured points from the smoothed curve are given in Fig. 4 for the sake of reference.

As is shown in Fig. 2, the $(NH_4)_2CuCl_4 \cdot 2H_2O$ crystal exhibits a heat capacity maximum at 200.50°K. The shape of the heat capacity curve around this temperature is similar to that of

14) The only heat capacity data on K-salt available for comparison is given by Kopp ("Landolt-Börnstein Physikalisch-Chemische Tabellen II," Berlin, 1923), whose value, 63.0 cal./deg. mol. at about 35°C, lies on the extrapolated curve of the present data.

Table III. Thermodynamic properties of $(NH_4)_2CuCl_4 \cdot 2H_2O$ (in cal./deg. mol.)

| $T$, °K | $C_P^0$ | $S^0$ | $\frac{(H^0-H_0^0)}{T}$ | $\frac{-(G_0-H_0^0)}{T}$ |
|---|---|---|---|---|
| 10 | 0.322 | 0.201 | 0.102 | 0.099 |
| 15 | 1.152 | 0.458 | 0.292 | 0.166 |
| 20 | 2.902 | 1.016 | 0.714 | 0.302 |
| 25 | 5.052 | 1.890 | 1.364 | 0.526 |
| 30 | 7.358 | 3.014 | 2.169 | 0.845 |
| 40 | 12.364 | 5.807 | 4.085 | 1.722 |
| 50 | 17.342 | 9.108 | 6.247 | 2.861 |
| 60 | 22.248 | 12.701 | 8.052 | 4.199 |
| 70 | 26.838 | 16.479 | 10.796 | 5.683 |
| 80 | 31.052 | 20.340 | 13.067 | 7.273 |
| 90 | 34.935 | 24.224 | 15.283 | 8.941 |
| 100 | 38.478 | 28.088 | 17.426 | 10.662 |
| 110 | 41.782 | 31.913 | 19.492 | 12.421 |
| 120 | 44.900 | 35.683 | 21.481 | 14.202 |
| 130 | 47.968 | 39.398 | 23.400 | 15.998 |
| 140 | 51.094 | 43.088 | 25.267 | 17.821 |
| 150 | 54.182 | 45.999 | 27.092 | 18.907 |
| 160 | 57.060 | 49.585 | 28.873 | 20.712 |
| 170 | 60.080 | 53.134 | 30.619 | 22.515 |
| 180 | 63.437 | 56.659 | 32.345 | 24.314 |
| 190 | 67.762 | 60.201 | 34.092 | 26.109 |
| 200 | 75.378 | 63.838 | 35.934 | 27.904 |
| 200.50 | 76.290 | Transition point | | |
| 210 | 66.220 | 67.150 | 37.453 | 29.697 |
| 220 | 67.190 | 70.249 | 38.780 | 31.469 |
| 230 | 68.675 | 73.268 | 40.046 | 33.222 |
| 240 | 70.300 | 76.225 | 41.273 | 34.952 |
| 250 | 71.855 | 79.127 | 42.466 | 36.661 |
| 260 | 73.205 | 81.972 | 43.623 | 38.349 |
| 270 | 74.432 | 84.758 | 44.741 | 40.017 |
| 280 | 75.614 | 87.487 | 45.823 | 41.664 |
| 290 | 76.752 | 90.160 | 46.870 | 43.290 |
| 298.15 | 77.588 | 92.302 | 47.701 | 44.601 |

Table IV. Thermodynamic Properties of $K_2CuCl_4 \cdot 2H_2O$ (in cal./deg. mol.)

| $T$, °K | $C_P^0$ | $S^0$ | $\frac{(H^0-H_0^0)}{T}$ | $\frac{-(G^0-H_0^0)}{T}$ |
|---|---|---|---|---|
| 10 | 0.484 | 0.226 | 0.149 | 0.077 |
| 15 | 1.463 | 0.579 | 0.401 | 0.178 |
| 20 | 3.650 | 1.276 | 0.920 | 0.356 |
| 25 | 6.322 | 2.372 | 1.875 | 0.497 |
| 30 | 9.260 | 3.783 | 2.860 | 0.923 |
| 40 | 15.448 | 7.312 | 5.249 | 2.063 |
| 50 | 20.758 | 11.354 | 7.843 | 3.511 |
| 60 | 25.210 | 15.541 | 10.374 | 5.167 |
| 70 | 29.040 | 19.726 | 12.777 | 6.949 |
| 80 | 32.188 | 23.812 | 15.010 | 8.802 |
| 90 | 35.090 | 27.774 | 17.083 | 10.691 |
| 100 | 37.320 | 31.593 | 19.001 | 12.592 |
| 110 | 39.285 | 35.243 | 20.757 | 14.486 |
| 120 | 41.148 | 38.741 | 22.378 | 16.363 |
| 130 | 42.900 | 42.106 | 23.891 | 18.215 |
| 140 | 44.484 | 45.344 | 25.306 | 20.038 |
| 150 | 45.932 | 48.463 | 26.634 | 21.829 |
| 160 | 47.310 | 51.472 | 27.883 | 23.589 |
| 170 | 48.580 | 54.378 | 29.064 | 25.314 |
| 180 | 49.760 | 57.188 | 30.181 | 27.007 |
| 190 | 50.900 | 59.909 | 31.242 | 28.667 |
| 200 | 51.880 | 62.545 | 32.249 | 30.296 |
| 210 | 52.840 | 65.100 | 33.207 | 31.893 |
| 220 | 53.790 | 67.580 | 34.120 | 33.460 |
| 230 | 54.720 | 69.992 | 34.996 | 34.996 |
| 240 | 55.646 | 72.340 | 35.837 | 36.503 |
| 250 | 56.550 | 74.630 | 36.648 | 37.982 |
| 260 | 57.418 | 76.872 | 37.430 | 39.442 |
| 270 | 58.265 | 78.955 | 38.186 | 40.769 |
| 280 | 59.120 | 81.190 | 38.918 | 42.272 |
| 290 | 59.920 | 83.279 | 39.629 | 43.650 |
| 298.15 | 60.524 | 84.950 | 40.194 | 44.756 |

the aniline hydrobromide crystal[15] at the $\lambda$-point, indicating that the phase transition is of a higher order. On the other hand, the $K_2CuCl_4 \cdot 2H_2O$ crystal does not show any thermal anomaly over the entire temperature range investigated.

**Thermodynamic Propertier of $(NH_4)_2CuCl_4 \cdot 2H_2O$ and $K_2CuCl_4 \cdot 2H_2O$.**—The values of the heat capacity, entropy, enthalpy and the free energy function for $NH_4$-salt and K-salt have been derived from the experimental heat capacities with the standard technique; they are summarized in Tables III and IV. The extrapolation to 0°K was made by using the Debye formula. The error of the smoothed heat capacity data is estimated to be ±1% below 60°K and ±0.3% above 60°K. The values of entropy and free energy listed in Tables III and IV do not include the magnetic contributions from copper ions. Haseda[16] has recently reported the magnetic transition of K-salt at about 0.8°K, corresponding to the magnetic transition of the copper ion from the antiferromagnetic to the paramagnetic state. If the magnetic contributions were included in the thermodynamic functions of Tables III and IV, the values of entropy would become greater than the present values by about 1.3 e. u., while the values of free energy would be scarcely changed. On the other hand, the corresponding magnetic transition of $NH_4$-salt has not yet been reported. The $NH_4$-salt has an isomorphous crystal structure with the K-salt, and has lattice constants nearly equal to that of the K-salt, that is, $a_0=7.58$ Å and $c_0=7.96$ Å for the former and $a_0=7.45$ Å and $c_0=7.88$ Å

15) H. Suga, This Bulletin, 34, 426 (1961).

16) T. Haseda, private communication.

for the latter. The corresponding magnetic transition can, accordingly, also be expected for the $NH_4$-salt around 1°K.

**The Anomalous Heat Capacity of $(NH_4)_2CuCl_4 \cdot 2H_2O$.**—As is mentioned above, $NH_4$-salt gives a heat capacity anomaly. The excess heat capacity seems to rise at about 120°K, reaches a maximum value at 200.50°K, and then drops rather rapidly. The anomalous heat capacity, $(\Delta C_p)_{tr}$, at this maximum temperature amounts to 13.24 cal. $deg^{-1}$ $mol^{-1}$. On the other hand, K-salt does not show any such thermal anomaly. Accordingly, the thermal anomaly seems to be associated with a movement of the ammonium group of $NH_4$-salt.

The entropy of transition, $\Delta S_{tr}$, amounts to 1.945 e. u., and the enthalpy of transition, $\Delta H_{tr}$, to 387.7 cal. $mol.^{-1}$ The procedure for calculating these values may be worth mentioning in more detail, so it will be described below.

In order to calculate the entropy and the enthalpy of transition, as well as the heat capacity associated with the ordering phenomena of the ammonium group, it is necessary to subtract the "normal" heat capacity from the experimentally-measured one. An ammonium ion has an excess of twelve internal degrees of freedom compared with a potassium ion. First of all, the contributions from these internal and torsional vibrations must be subtracted from the experimental heat capacity. Infrared or Raman data are, unfortunately, not yet known for this substance. However, it may not be unreasonable to assume that the values of the vibrational frequencies of the ammonium group in $NH_4$-salt will be replaced by those of other ammonium salts, in which the situation of the ammonium ion is similar to that of the present salt; i. e., each of ammonium ions is surrounded by a slightly distorted cube consisting of eight chlorine ions. The present crystal has an N-Cl distance of 3.35 Å and an N-N distance of 3.98 Å, distances which are comparable with those for ammonium chloride, where the N-Cl distance is 3.32 Å and the N-N distance, 3.87 Å. Thus, the values of the vibrational frequencies of the ammonium chloride crystal[3] may be assumed for the present crystal in calculating the contributions arising from the ammonium groups. The adopted values are as follows: $\nu_1=3040\,cm^{-1}$ (1), $\nu_2=1670$ (2), $\nu_3=3100$ (3), $\nu_4=1403$ (3), and $\nu_6$ (torsional) $=310$ (3) (the numbers in parentheses indicate degeneracy).

Now, $C_{int}(NH_4^+)$, the contribution from the internal vibrations and torsional oscillations of the ammonium ions to the heat capacity, can be calculated by using the Einstein function:

$$C_{int}(NH_4^+) = 2R \sum_i d_i \frac{x_i^2 e^{-x_i}}{(1-e^{-x_i})^2} \qquad (1)$$

where $d_i$ is the degeneracy of an $i$-th mode of vibration and $x_i=h\nu_i/kT$. The $\Delta C_P$ (anomal) $= C_P$ ($NH_4$-salt) $- C_{int}(NH^+_4) - C_P$ (normal) quantity should be approximately the extra heat capacity contribution from the orientational motion of the ammonium ion as a whole. Usually the $C_P$ (normal) quantity is estimated graphically rather arbitrarily. In the present case, however, the anomalous heat capacity extends over a considerable temperature range, and there is some latitude in drawing the normal heat capacity of the ammonium salt.

Osborne and Westrum[17,18] have assumed that the lattice contribution to the heat capacities of $UO_2$ and $NpO_2$ equals the heat capacity of the isomorphous diamagnetic, $ThO_2$, in estimating the anomalous magnetic contribution, and also, in another example, that the heat capacity of $ThF_4$ represents the lattice contribution for $UF_4$. This kind of assumption is not tenable for the present case, however, since at a low temperature the observed heat capacity of *K*-salt exceeds that of $NH_4$-salt, and a high temperature the situation is reversed. Stout and Catalano[19] have applied a law of corresponding states in order to estimate the normal heat capacity of antiferromagnetic $MnF_2$, $FeF_2$, $COF_2$ and $NiF_2$ by utilizing the heat capacity data of isomorphous, diamagnetic $ZnF_2$. Although the difference in structural parameters between the present two crystals is not very large,[6] the crystal structure of these salts is too complicated to apply such a simplified treatment in the present case.

In order to carry out a tentative but rather

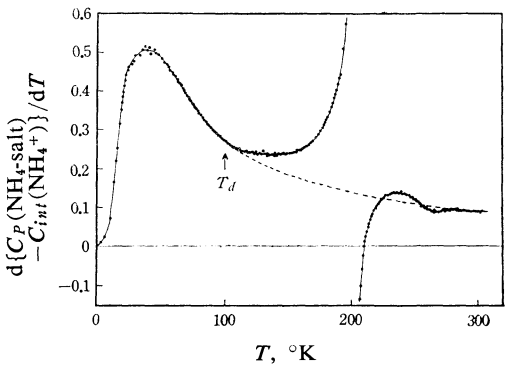



Fig. 5. $d\{C_P(NH_4\text{-salt}) - C_{int}(NH_4^+)\}/dT$ vs. temperature plot for $(NH_4)_2CuCl_4 \cdot 2H_2O$ crystal.

17) D. W. Osborne and E. F. Westrum, Jr., *J. Chem. Phys.*, **21**, 1884 (1953).
18) H. R. Lohr, D. W. Osborne and E. F. Westrum, Jr., *J. Am. Chem. Soc.*, **76**, 3837 (1954).
19) J. W. Stout and E. Catalano, *J. Chem. Phys.*, **23**, 2013 (1955).

agreeable treatment for estimating the normal heat capacity of the $NH_4$-salt, the following procedure was adopted. The differential quantity, $d\{C_P(NH_4\text{-salt}) - C_{int}(NH_4^+)\}/dT$, was plotted against the temperature over the entire temperature range; the results are drawn in Fig. 5. The corresponding value for K-salt, $dC_P(\text{K-salt})/dT$, is given in Fig. 6 for the sake of comparison. This procedure magnifies the effect of the phase transition on the graph. If there is no heat capacity anomaly, the behavior of the $dC_P/dT$ in the $NH_4$-salt should be similar to that of K-salt, which is a monotonous function of the temperature.

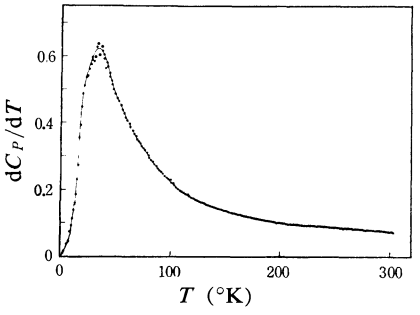



Fig. 6. $dC_P$(K-salt)/$dT$ vs. temperature plot for $K_2CuCl_4 \cdot 2H_2O$ crystal.

There is also some latitude in drawing the dotted curve in Fig. 5, which represents the trend of the normal heat capacity of the $NH_4$-salt. However, there are at least two restrictions to eliminating some of the arbitrariness involved. One is that the curve corresponding to the normal heat capacity, the dotted curve in Fig. 5, must be a monotonously decreasing function; the other is that the normal heat capacity obtained by integrating the differential quantity should not exceed the value, $C_P(NH_4\text{-salt}) - C_{int}(NH_4^+)$, at any temperature. This means that the anomalous heat capacity, $\Delta C_P$(anomal), can not be negative. Consequently, the normal heat capacity at $T$°K was calculated as follows:

$$C_P(\text{normal}) \text{ at } T^\circ\text{K} = \{C_P(NH_4\text{-salt}) - C_{int}(NH_4^+)\} \text{ at } T_d^\circ\text{K} + \int_{T_d}^{T} \frac{dC_P(\text{normal})}{dT}\, dT \qquad (2)$$

where $T_d$ is the temperature at which the $dC_P(\text{normal})/dT$ curve deviates from the $d\{C_P(NH_4\text{-salt}) - C_{int}(NH_4^+)\}/dT$ curve. The anomalous heat capacity, estimated by using Eqs. 1 and 2 and the experimental heat capacity data, is shown in Fig. 7. This curve presumably corresponds to the lower limit of the anomalous heat capacity, in view of the two assumed requirements mentioned above. Above 300°K the dotted curve in Fig. 7 was extrapolated somewhat arbitrarily. The contribution from this part to the entropy of the transition amounts merely to 2.5 per cent of the total. The values of $\Delta S_{tr}$ and $\Delta H_{tr}$ were then calculated from the $\Delta C_P$(anomal) versus temperature curve.

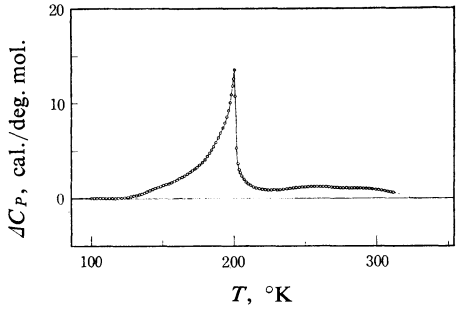



Fig. 7. Anomalous heat capacity of $(NH_4)_2CuCl_4 \cdot 2H_2O$ around 200.50°K.

## Discussion

In order to discuss the nature of the phase transition of $NH_4$-salt, it is desirable to compare with each other the crystal structures of the two crystals.[6] The crystallographic data are summarized in Tables V, while the projections on the (010) and (001) planes of the crystal structure of $NH_4$-salt are depicted in Figs. 8 and 9. As has been mentioned already, each ammonium ion is surrounded by a slightly distorted cube consisting of eight chlorine ions. The N–Cl and N–N distances in the $NH_4$-salt are comparable to those of the ammonium chloride crystal. Therefore, an orientational order-disorder-type phase transition associated with the ammonium ions in ammonium chloride may also be expected for this $NH_4$-salt.

Table V. Crystallographic data of $NH_4$-salt and K-salt[6]

| $(NH_4)_2CuCl_4 \cdot 2H_2O$ | $K_2CuCl_4 \cdot 2H_2O$ |
|---|---|
| $D_{4h}^{14}$ (P4/mnm) | |
| $Z=2$ | |
| $a_0=7.58$ Å | $a_0=7.45$ Å |
| $c_0=7.96$ Å | $c_0=7.88$ Å |
| Cu: 0,0,0; 1/2,1/2,1/2, | |
| $NH_4$ or K: 0,1/2,1/4; 1/2,0,1/4; 0,1/2,3/4, | |
| Cl (1): $\pm(u,u,0; u+1/2,1/2-u,1/2)$ | |
| Cl (2): $\pm(v,v,1/2; v+1/2,1/2-v,0)$ | |
| $H_2O$: $\pm(0,0,w; 1/2,1/2,w+1/2)$ | |
| $u=0.217$ | $u=0.220$ |
| $v=0.221$ | $v=0.220$ |
| $w=0.250$ | $w=0.250$ |

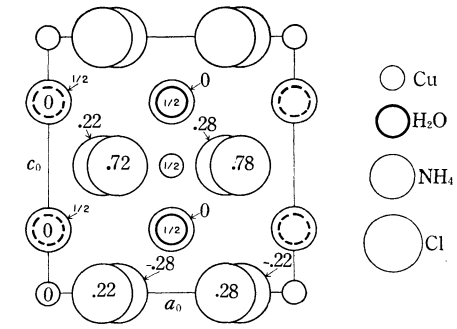



Fig. 8. A projection on the (010) plane of the crystal structure of $(NH_4)_2CuCl_4 \cdot 2H_2O$ (after Wyckoff).

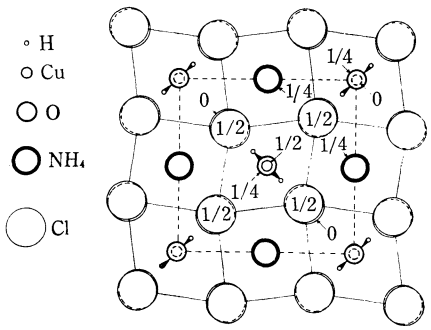



Fig. 9. A projection on the (001) plane of the crystal structure of $(NH_4)_2CuCl_4 \cdot 2H_2O$.

Itoh and Kamiya[20] have recently reported on the temperature variation of the proton nuclear magnetic resonance spectra of the $NH_4$-salt and have observed a motional narrowing associated with the protons of the ammonium group at about 150°K. They found that the situation of the barrier height hindering the flipping motion of the ammonium ion is very similar to that with ammonium chloride. If the nature of the transition of this crystal is very similar to that of the ammonium chloride, the entropy of transition could amount to 2.68 ($2R \ln 2$) e. u. The experimental value is, however, 1.945 e. u., about two thirds of 2.68 e. u.

In the case of ammonium chloride, all chlorine ions are equivalent with respect to the $NH_4^+$ ion, while for the present crystal, Itoh et al.[21] have reported that there are two kinds of chlorine ions; one makes a hydrogen bond with the proton of crystalline water, while the other does not. Other differences from the ammonium chloride are that the present crystal has a tetragonal symmetry and that the N–N distance is quite different in each direction. The N–N distance along the [001] axis is 3.98 Å, while along the [110] axis it is 5.36 Å. Thus, only along the direction of the c-axis is the N–N distance comparable with that of ammonium chloride.

In other words, the principle of the framework of the present crystal is that the $NH_4Cl$ is diluted by $CuCl_2 \cdot 2H_2O$ and the interaction between the ammonium ions is weakened two-dimensionally. In such a pseudo-linear chain of $NH_4^+$ ions, the order parameter describing the randomness with respect to the orientation of ammonium ions is expected to change much less co-operatively than a three-dimensionally-arranged system, as in the case of ammonium chloride. The extraordinary broadness of the anomaly, as well as the much smaller jump of $C_P$ at the transition point, may be ascribed to the weakened interaction between the ammonium ions in this crystal. The maximum anomalous heat capacity of the present crystal amounts merely to 13.24 cal. $deg^{-1}$ $mol^{-1}$, while in the case of ammonium chloride[1] it reaches about 159 cal. $deg^{-1}$ $mol^{-1}$.

It should be mentioned that above the transition point there is a rather broad and small hump in the $\Delta C_P$(anomal) versus temperature curve. It is more magnified in the curve of the derivative of the heat capacity than in the heat capacity curve itself (see Fig. 5). If the residual anomalous part of the heat capacity curve above the phase transition point is exclusively due to the short range order remaining, it may not show such a maximum point. Therefore, we may assume, as one explanation, that the hump arises from the Shottky anomaly, based on the population difference of the individual ammonium ion between the two sites of different energies, associated with the different chlorine ions in the disordered state; in one possible orientation of the ammonium ion, all four protons are directed to the chlorine ions hydrogen-bonded with the crystalline water, while in the other all protons are directed to the free chlorine ions. If the hump is ascribed to the Shottky anomaly, the energy difference between the two possible orientations of the ammonium ions is calculated to be about 1.3 kcal. $mol^{-1}$.

We have not given here the theoretical treatment needed to interpret the transition mechanism of the pseudo one-dimensional ionic array of the present crystal. In order to develop such a treatment, the ordered structure of ammonium ions must be known precisely. Because of the rather small value of the apparent transition entropy ($\fallingdotseq 2/3 \times 2R \ln 2$), however, it is supposed that there still

20) J. Itoh and Y. Kamiya, *J. Phys. Soc. Japan*, **17**, Supplement B-I, 512 (1962).
21) J. Itoh, R. Kusaka, R. Kiriyama and Y. Saito, *Memoirs of the Institute of Scientific and Industrial Research, Osaka Univ.*, **XIV**, 1 (1957).

remains a much larger degree of disorder with respect to the orientation of ammonium groups in the low temperature phase. Further investigations of, for example, neutron diffraction, neutron inelastic scattering, or some other spectroscopic techniques will be useful in understanding more quantitatively the nature of the phase transition.

## Summary

The heat capacity of copper potassium chloride dihydrate and copper ammonium chloride dihydrate crystals have been measured between 13 and 310°K. The latter crystal shows a $\lambda$-type anomaly in the heat capacity curve which seemed to be due to the orientational order-disorder process of ammonium groups. The heat capacity of $(NH_4)_2CuCl_4 \cdot 2H_2O$ exhibits a maximum value of 76.290 cal. deg.$^{-1}$ mol$^{-1}$ at 200.50°K. By plotting the temperature derivative of heat capacities, the normal contribution from the lattice to the heat capacity of $(NH_4)_2CuCl_4 \cdot 2H_2O$ has been estimated. In this case the corresponding values for $K_2CuCl_4 \cdot 2H_2O$ has been taken as a reference. By subtracting the estimated normal heat capacity from the experimentally measured one, approximate values of the entropy change, $\Delta S =$ 1.945 cal. deg.$^{-1}$ mol$^{-1}$, and the heat capacity jump, $\Delta C_P = 13.24$ cal. deg$^{-1}$ mol$^{-1}$, associated with the orientational ordering of the linearly-arranged ammonium ion system have been given.

The values of the heat capacity, entropy, enthalpy, and Gibbs free energy of both crystals have been tabulated at selected temperatures. The standard values of the entropy and enthalpy are: $K_2CuCl_4 \cdot 2H_2O$, $S^0 = 84.95$ cal. deg$^{-1}$ mol$^{-1}$, $H^0 - H_0^0 = 11980$ cal. mol$^{-1}$; $(NH_4)_2 \cdot CuCl_4 \cdot 2H_2O$, $S^0 = 92.30$ cal. deg.$^{-1}$ mol$^{-1}$, $H^0 - H_0^0 = 14220$ cal. mol$^{-1}$.

*Department of Chemistry*
*Faculty of Science*
*Osaka University*
*Toyonaka, Osaka*

# Switch-over of the Mechanism of the Primary Processes in the Photo-oxidation of Xanthene Dyes as Revealed by the Oxygen Consumption Experiments

By Yoshiharu Usui, Keiko Itoh and Masao Koizumi

(Received November 17, 1964)

As early as 1933 Blum and Spealman[1] studied the photo-oxidative bleaching of xanthene dyes by oxygen. Some of their findings on aerated $2.8\times10^{-4}$ M aqueous solutions of eosine were, 1) production of hydrogen peroxide, 2) existence of an induction period in the bleaching course of the dye, 3) decrease of the rate at high concentrations of oxygen. They inferred from the findings 1 and 2, that the reaction may proceed according to the following scheme, $D^*+O_2 \rightarrow D+O_2^*$, $O_2^*+H_2O \rightarrow OH+HO_2$ followed by the decomposition of dye by OH and $HO_2$. Since then no kinetic studies had been made on similar systems until. Imamura and one of the present authors (M. K.) investigated the aerated $1\times10^{-5}$ M solution of dye.[2] They found that all the above phenomena were absent at this concentration, the rate of reaction being simply proportional to the absorbed light and increasing monotonously to a certain constant value as the concentration of oxygen increased. They concluded therefore, that the primary process of the photo-oxidation at this concentration of dye is attack of the oxygen on the triplet dye, resulting in destruction of the dye structure. They did not, however, attempt to interpret the differing results of Blum et al., only attributing them to the experimental conditions, particularly to the different concentration of dye.

Now the flash photolytic investigations made by Lindqvist[3] and Grossweiner et al.[4], the former on fluorescein and the latter on eosine,

1) H. F. Blum and C. R. Spealman, *J. Phys. Chem.*, **37**, 1123 (1933).

2) M. Imamura and M. Koizumi, This Bulletin, **28**, 117 (1955); M. Imamura, *J. Inst. Polytech. Osaka City Univ.*, **5**, 85 (1956).

3) L. Lindqvist, *Arkiv Kemi*, **16**, 79 (1960); V. Kaoshe and L. Lindqvist, *J. Phys. Chem.*, **68**, 817 (1964).

4) E. F. Zwicker and L. I. Grossweiner, ibid., **67**, 549 (1963).

have afforded kinetic data for the various elementary reactions and have revealed much of the details of the photochemical behaviors of these dyes. In particular, Lindqvist proposed an epoch-making view that electron transfer can take place between the triplet dye and the ground state dye of fluorescein. Following this work, Koizumi et al. presented strong evidence for the occurcence of such a process in the actual photochemical reduction of thiazine dyes.[5,6] Further, Ohno and Koizumi[7] found that in the photoreduction of eosine by allyl thiourea, a switch-over of mechanism does take place; the attack of reducing agent on triplet dye (D-R mechanism) predominates at lower concentrations of dye, whereas electron transfer between the triplet and the ground-state dyes (D-D mechanism) becomes the main process at higher concentrations.

The purpose of the present investigation is to provide additional evidence of a switch-over from D-O* to D-D mechanism by studying the photo-oxidative behavior of rather concentrated aqueous solutions of xanthene dye, and further, to give a reasonable correlation between Blum's and Imamura's results.

For this purpose the oxygen up-take of the irradiated aqueous solutions has been investigated by means of Warburg's apparatus and the results are compared with those obtained previously. The results, which are somewhat similar to those of Blum et al., can now be interpreted very satisfactorily and the differences in the results of the two groups of investigators are well interrelated with each other on the basis of the switch-over of the mechanism from a D-O mechanism at low concentrations of dye to a D-D mechanism at higher concentrations. A reinterpretation of Imamura's data is also given.

## Experimental

**Sample.** — *Eosine.* — Merck's G. R. sample was recrystallized twice from ethanol. The maximum molar extinction, $\varepsilon_{max}$ for an aqueous solution is $9.6\times10^4$.

*Erythrosine.*— Merck's G. R. reagent was used without further purification. $\varepsilon_{max}$ was $6.7\times10^4$.

*Fluorescein.*—The Sodium salt of Tokyo Kasei was recrystallized three to four times from ethanol containing a small quantity of sodium hydroxide. $\varepsilon_{max}$ in the phosphate buffer solution was $6.8\times10^4$ (pH 7.65).

**Apparatus and Procedure.**—Warburg's apparatus was the one supplied by Ōtake Co. The light source consisted of three 30W. daylight fluorescent lamps 60 cm. in length placed below the reaction cells with a suitable filter in between. The filters were $30\times100$ cm. plastic plates; the one for eosine and erythrosine cuts off below 480 m$\mu$, and the one for fluorescein cuts off below 340 m$\mu$. Reaction cells, each containing 20.0 ml. of the dye solution $5.0\times10^{-5}$—$8.0\times10^{-3}$ M in concentration, were immersed in a Warburg thermostat at $30.0\pm0.02$°C and after 20—25 min. the illumination was started. The depth of the solutions being about 2 cm., the absorption of light is practically complete in the wavelength region of the visible absorption spectra. The cell constants of all cells are about 2. The quantity of absorbed gas was measured by a push-up method. Correction of atmospheric pressure and temperature was made by means of a thermobarometer. This is necessary, because of the long duration of irradiation and the rather small quantity of absorbed gas. The quantity of bleached dye was measured spectroscopically, after diluting to about $10^{-5}$ M, on a Hitachi EPU-2A spectrophotometer or EPS-3 autorecording spectrophotometer.

The saturated solution of oxygen under 1 atm. was prepared as follows. The sample solution was flushed for fifteen minutes with 1 atm. of oxygen and 20.0 ml. of it was poured into the reaction cell, the operation being done in the current of oxygen.

## Results

**Effect of the Dye Concentration on the Rate of Oxygen Consumption.** — Using the plain aqueous solutions of eosine and erythrosine and the phosphate buffer solutions of fluorescein (pH 7.65), all at various dye concentration, two series of experiments were performed for each dye, one series with the air-saturated solutions ($[O_2]\approx2.5\times10^{-4}$ M) and the other with the solutions saturated with 1 atm. of oxygen ($[O_2]\approx1.2\times10^{-3}$ M).

*Eosine.*—As seen from Fig. 1, oxygen consumption by the air-saturated solution takes place linearly with time. The slope which gives the rate, increases with the dye concentration up until about $\sim5\times10^{-4}$ M is reached but becomes practically constant beyond $10^{-3}$ M of dye.

The results are similar for the oxygen-saturated solutions except for the fact that the limiting rate is attained at a somewhat higher concentration of dye. Figure 2 gives the plots of the rate against the dye concentration. It is worth while to note that the limiting value is practically the same for the air-saturated and the oxygen-saturated solutions.

*Erythrosine.*—Figure 3 shows the results for erythrosine. In this case the limiting value

5) S. Kato, M. Morita and M. Koizumi, This Bulletin, 37, 117 (1964).
6) M. Koizumi, H. Obata and S. Hayashi, ibid., 37, 108 (1964).
7) T. Ohno, Y. Usui and M. Koizumi, ibid., 38, 1022 (1965).
* O denotes oxidant (oxygen). In this case oxygen attacks the triplet dye instead of th reducing agent.

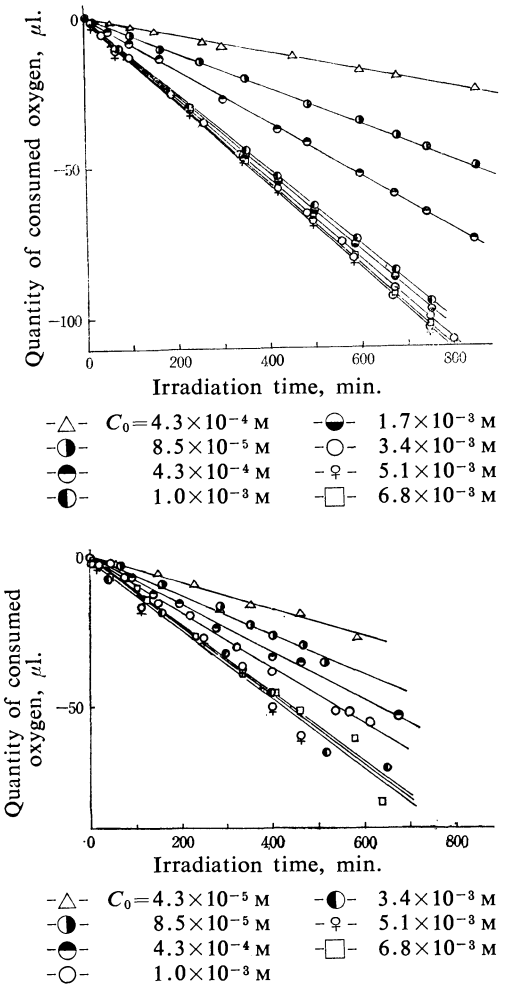
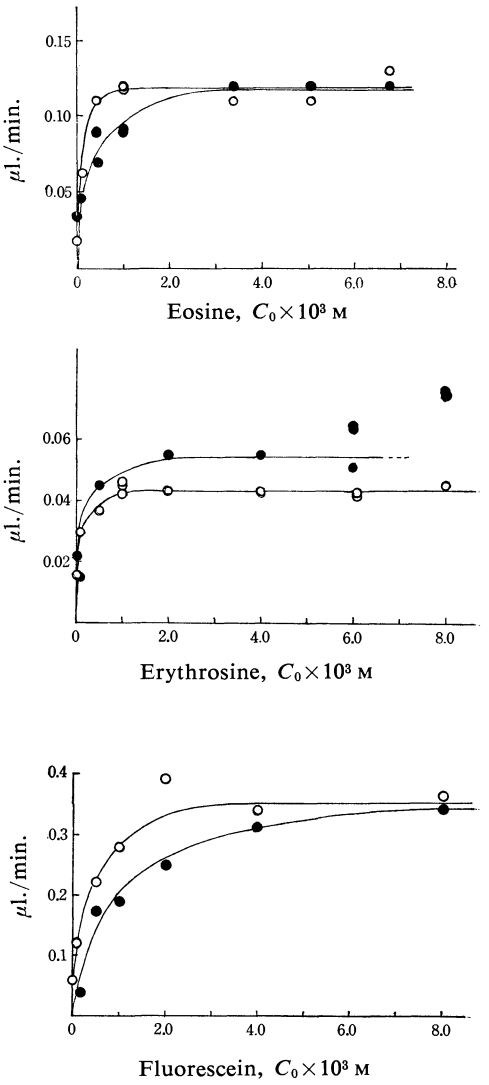



Fig. 1. Examples of oxygen consumption in the air saturated (upper), and oxygen saturated (under) solution of eosine.




Figs. 2, 3 and 4. Dependence of the rate of oxygen consumption on the dye concentration. -●- oxygen saturation, -○- air saturation

for the oxygen-saturated solution seems to be a little higher than that for the air-saturated solution, although its magnitude lies close to the experimental error.

*Fluorescein.*—Figure 4 gives the results for fluorescein at pH 7.65. The main features of the curve are essentially the same as those in the case of eosine except that the attainment of the critical value seems to be realized at a somewhat higher concentration of dye.

Summing up the above results, one can say that all the xanthene dyes behave essentially the same in the neutral region and that the rate of oxygen consumption is constant when the dye concentration is much larger than that of oxygen but begins to fall rather sharply in the region $[D] \approx [O_2]$.

**The Bleaching Rate of the Dye.**—Measurements were made choosing dye concentrations in the region $10^{-5}$ to $10^{-4}$ M, since accurate experiments with more concentrated solutions, which undoubtedly are very desirable, require quite a new technique and, besides, Imamura has pointed out[2] that a simple rate formula ceases to hold near $10^{-4}$ M of dye. A 75V.-500W. tungsten projection lamp was used as a light source and the experiments were made at 30.0°C. A spacer 9.0 mm. in width was used for measuring the optical density of the $10^{-4}$ M solutions. The results are given in Fig. 5 and in Table I. In Fig. 5, the linearity of the curves implies that the rate is simply proportional to the absorption of light. As this figure shows, the linear relation holds as long as $r=[D_0]/[O_2]$ is less than ~0.2. The results at lower $r$-values are in excellent

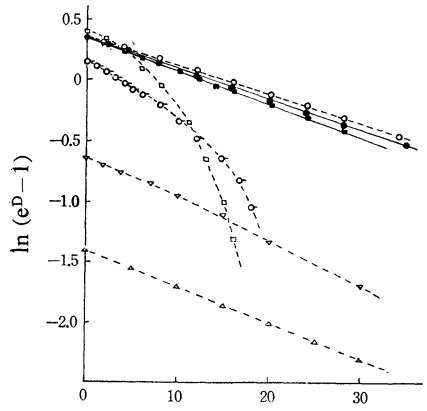



Fig. 5. Photobleaching of eosine at various concentration. ($C_0$)

| | Sign | $C_0$ (M) | $r$ |
|---|---|---|---|
| Air saturation ($2.5\times10^{-4}$ M) | □ | $1.0\times10^{-4}$ | 0.40 |
| | ○- | $8.0\times10^{-5}$ | 0.32 |
| | ▽ | $4.3\times10^{-5}$ | 0.17 |
| | △ | $2.3\times10^{-5}$ | 0.09 |
| Oxygen saturation ($1.2\times10^{-3}$ M) | ● | $1.0\times10^{-4}$ | 0.08 |
| | ■ | $1.0\times10^{-5}$ | 0.008 |

Table I

| Oxygen saturated | $D_0$ (M) | $r$ | Quantum yield |
|---|---|---|---|
| 1 | $1.0\times10^{-4}$ | 0.08 | $3.2\times10^{-4}$ |
| 2 | $1.0\times10^{-5}$ | 0.01 | $3.5\times10^{-4}$ |
| Air-saturated | | | |
| 1 | $1.0\times10^{-5}$ | 0.04 | $3.0\times10^{-4}$* |
| 2 | $2.3\times10^{-5}$ | 0.09 | $3.0\times10^{-4}$ |
| 3 | $4.3\times10^{-5}$ | 0.17 | $3.0\times10^{-4}$ |
| 4 | $8.0\times10^{-5}$ | 0.32 | — |
| 5 | $1.0\times10^{-4}$ | 0.40 | — |

* Koizumi and Imamura[2]

agreement with those of Imamura. In two experiments on the air-saturated solutions for $8.0\times10^{-5}$ and $1.0\times10^{-4}$ M of dye, for which $r$ is respectively 0.32 and 0.40, the initial rate is somewhat larger and, besides, the simple rate formula does not hold, the rate increasing as the reaction progresses. It is estimated that the final rate is several times larger than that at the initial stage. It is remarkable that an oxygen-saturated solution of the same concentration of dye still obeys the simple rate formula with the same slope as the others. There is no doubt, therefore, that the above anomalous behavior is due to the higher value of $r$.

Figure 6 gives the relation between the initial rate and the concentration of oxygen when the dye concentration is fixed at $10^{-4}$ M. It is seen from the figure that the rate increases with the oxygen concentration, reaching a maximum at about $1.5\times10^{-4}$ M of oxygen

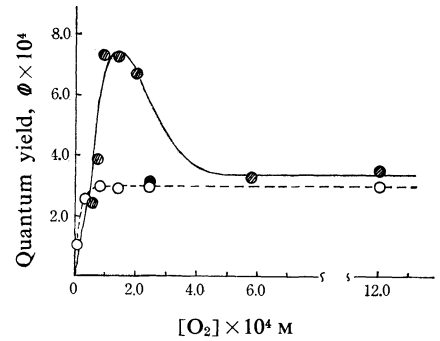



Fig. 6. Oxygen concentration effect on the quantum yield of bleaching.
Eosine concn.:
-●- $1.0\times10^{-4}$ M, -○- $1.0\times10^{-5}$ M

and then falls to a constant value beyond $\sim2.5\times10^{-4}$ M of oxygen.

From the above results one can say that at high concentrations of dye, the rate of the oxydative bleaching of dye decreases when the oxygen concentration exceeds a certain value which is close to the dye concentration.

Such a phenomenon had not been observed in Imamura's experiment on $1\times10^{-5}$ M of dye. This was reconfirmed by the present authors, as shown by a dotted curve in Fig. 6.

**Quantum Yield of the Oxygen Up-take and the Ratio of Oxygen Consumption and the Dye Bleaching.**—The quantity of light absorption in the oxygen consumption experiment was determined by measuring the oxidative photobleaching of dye in the Warburg apparatus under conditions similar to those used in Imamura's experiment and by using the value for the quantum yield reported by Imamura[2] and confirmed by Grossweiner.[4] Then the quantum yields for oxygen consumption are easily calculated from the results given in Figs. 2, 3, 4 and 5. The ratio of the consumed oxygen to the bleached dye was determined by measuring the dye concentration after the oxygen up-take experiment. Table II gives the results.

Although the data for $\Delta[O_2]/\Delta[D]$ scatter to a large extent, it seems that they are from 1 to 2 for eosine and fluorescein, while for erythrosine they are about 1.

There is no doubt from this table, that the value for the photobleaching at $10^{-4}-10^{-3}$ M of dye, as judged from the quantum yield for oxygen consumption and $\Delta[O_2]/\Delta[D]$, is in most cases a few times larger than that at $10^{-5}$ M.

**Production of Hydrogen Peroxide and Its Effect on the Rate.**—The quantity of hydrogen peroxide produced was analyzed by the ordinary iodometry. Some of the results are given in Table III.

Table II. Quantum yields of oxygen-up-take and the values of $\Delta[O_2]/\Delta[D]$

| | Air-saturation | | $O_2$-saturation | |
|---|---|---|---|---|
| $C_0\times10^3$ M | $\gamma_{O_2}\times10^2$ | $\Delta[O_2]/\Delta[D]$ | $\gamma_{O_2}\times10^2$ | $\Delta[O_2]/\Delta[D]$ |
| Eosine | | | | |
| 6.8 | 1.24 | — | 1.14 | — |
| 5.1 | 1.05 | — | 1.14 | — |
| 3.4 | — | — | 1.14 | — |
| 1.0 | 1.14 | 1.4 | 0.85 | 1.9 |
| 0.43 | 1.05 | 1.8 | 0.85 | 2.9 |
| 0.085 | 0.59 | 2.4 | 0.44 | (4.6) |
| 0.043 | 0.17 | 1.9 | 0.32 | — |
| Erythrosine | | | | |
| 8.0 | 0.43 | — | 0.72 | — |
| 6.0 | 0.41 | — | 0.5 | — |
| 4.0 | 0.41 | — | 0.50 | — |
| 2.0 | 0.41 | — | 0.50 | — |
| 1.0 | 0.41 | 1.0 | 0.41 | 1.3 |
| 0.50 | 0.36 | 0.7 | 0.43 | 1 |
| 0.10 | 0.28 | 0.6 | 0.20 | 0.7 |
| 0.050 | 0.14 | 0.4 | 0.18 | — |
| Fluorescein | | | | |
| 8.0 | 1.06 | — | 1.01 | — |
| 4.0 | 1.01 | — | 0.92 | — |
| 2.0 | 1.15 | 2.35 | 0.71 | 1.72 |
| 1.0 | 0.82 | 2.05 | 0.57 | 1.34 |
| 0.50 | 0.65 | 1.88 | 0.50 | 1.49 |
| 0.10 | 0.35 | 2.70 | 0.09 | — |
| 0.050 | 0.19 | (3.4) | — | — |

Table III. Production of hydrogen peroxide

| Dye | Dye-concentration M | Quantity of bleached dye $\mu$M/300 min. | Quantity of produced $H_2O_2$ $\mu$M/300 min. |
|---|---|---|---|
| Fluorescein (phosphate-buffer) | $2.0\times10^{-3}$ | | 2.4 |
| | $1.0\times10^{-3}$ | 2.5 | 2.2, 3.0 |
| | $1.0\times10^{-4}$ | (4.4) | 0 |
| Eosine | $1.0\times10^{-3}$ | 1.4 | 2.6 |
| | $1.0\times10^{-4}$ | 0.5 | 1.4 |
| Erythrosine | $1.0\times10^{-3}$ | 0.7 | 0 |
| | $1.0\times10^{-4}$ | 0.4 | 0 |

It can be said that hydrogen peroxide is really produced when the dye concentration is high, and its quantity is of about the same order as that of the bleached dye. To examine the effect of hydrogen peroxide on the rate, hydrogen peroxide in concentrations as high as $1\times10^{-3}$ M was added to the $1\times10^{-3}$ M solution of eosine. The result was that the rate was the same within the experimental error.

## Discussion

**Reinterpretation of Imamura's Results.**— According to Lindqvist,[3] the triplet state ($D^T$) of fluorescein dianion is deactivated by oxygen or the ground state dye, as follows.

(1) $D^T+O_2\rightarrow D+O_2$ $k_1=1.7\times10^9$ M$^{-1}$ sec$^{-1}$

(2) $D^T+D\rightarrow D+D$ $k_2=1\times10^8$ M$^{-1}$ sec$^{-1}$

Ohno and Koizumi estimated the rate constant of the process 2 for eosine dianion to be $5.5\times10^8$ M$^{-1}$ sec$^{-1}$. These results imply that the lifetimes of the triplet state of these dianions are greatly reduced at $10^{-5}$ M of dye by the bimolecular deactivation process.

In 1955, when nothing was known about the rate constants of various elementary reactions, Imamura and Koizumi supposed that the genuine triplet lifetime is so short that the process 2 need not be taken into account. Hence their data must now be reinterpreted in such a way that, instead of self-deactivation, competitive deactivation is taking place with oxygen and the ground state dye. By slightly modifying the method given by Imamura, one can easily evaluate the ratio $k_1/k_2$ from the previous data for the oxygen concentration effect on the oxidative photobleaching of dye. The results are given in Table IV. These data refer to the solutions with pH near 7. From the above data one can say that the two deactivation processes have in general the same order of magnitude and hence it is very plausible that they are approximately diffusion controlled. A value of $k_1/k_2$ larger than 1 also supports this view.

Table IV

| Dye | Temp, °C | $k_1/k_2$ |
|---|---|---|
| Fluorescein | 30 | 1.8 |
| Eosine | 30 | 1.4* |
| | 40 | 5.3 |
| Erythrosine | 30 | 3.4 |
| (Methylene blue)** | 30 | 1.3 |

* Evaluated from the new data.

** The result for methylene blue is added for comparison.

Lindqvist's result for fluorescein at pH= 0—5.5, $k_1=1.2\times10^9$ M$^{-1}$ sec$^{-1}$ and $k_2=2.5\times10^9$ M$^{-1}$ sec$^{-1}$, as well as the above data for the alkaline region are not inconsistent with the above view. Grossweiner's value for $k_1$ of eosine is rather small, being $2.3\times10^7$ M$^{-1}$ sec$^{-1}$. This was evaluated by analyzing the data on the competitive reaction of $D^T$ with oxygen and phenol and it is suspected that this small value of $k_1$ has resulted from neglections to consider the simple deactivation of $D^T$ by phenol.

**Interpretation of the Oxygen Consuming Reaction.** — Assuming the triplet dye to be simultaneously deactivated by oxygen and the ground state dye, and assuming the occurrence of a genuine reaction between $D^T$ and D such that $D^T+D\rightarrow R+X$ where R and X are the

half-reduced and half-oxidized dyes, respectively, then, during oxidative photobleaching, the D-O mechanism would occur when $[D] \ll [O_2]$ and the D-D mechanism would prevail in the opposite situation.

Now the present experimental conditions are such that the above switch-over of the mechanism should naturally occur. Hence the data will be treated along this line. The reaction scheme for lower concentrations of dye is

$$\text{A}\begin{cases} D \rightarrow D^* & & \text{(i)} \\ D^* \rightarrow D^T & \varphi_{sT} I_{ab} & \text{(ii)} \\ D^T \rightarrow D & k_d & \text{(iii)} \\ D^T + O_2 \rightarrow D^T \cdots O_2 & k_{O_2} \} k^s_{O_2} & \text{(iv)} \\ D^T + O_2 \rightarrow D + O_2 & k_{O_2}^{(d)} \} k^s_{O_2} & \text{(v)} \end{cases}$$

while with higher concentrations of dye, one plausible scheme after the step ii may be written as follows.

$$\text{B}\begin{cases} D^T + D \rightarrow D^+ \cdots D^- & k_D \} k^s_D & \text{(vi)} \\ D^T + D \rightarrow D + D & k_D^{(d)} \} k^s_D & \text{(vii)} \\ D^+ \cdots D^- \rightarrow D + D & k'_d & \text{(viii)} \\ D^+ \cdots D^- + O_2 \rightarrow \text{Prod.} & k'_{O_2} \} k'^s_{O_2} & \text{(ix)} \\ D^+ \cdots D^- + O_2 \rightarrow 2D + O_2 & k'^{(d)}_{O_2} \} k'^s_{O_2} & \text{(x)} \end{cases}$$

In the general case where both A and B are taking place simultaneously, the rate of oxygen consumption (expressed by the concentration dissolved oxygen), $R_{O_2}$, is easily derived as follows,

$$R_{O_2} = \{k_{O_2}[D^T][O_2] + k'_{O_2}[D^+ \cdots D^-][O_2]\}$$
$$= \frac{\varphi_{sT} I_{ab} k_{O_2}[O_2]}{k_d + k^s_{O_2}[O_2] + k^s_D[D]} \times \left\{1 + \frac{k_D k'_{O_2}[D]}{k_{O_2}(k'_d + k'^s_{O_2}[O_2])}\right\} \quad (1)$$

The scheme B is still provisional but it is thought that the resultant expression will not be essentially affected by the details of the scheme. Quantum yield $\gamma_{O_2} = R_{O_2}/I_{ab}$ is given as follows after the neglection of $k_d$ which is very small compared with the competitive terms.

$$\gamma_{O_2} = \frac{\varphi_{sT} k_{O_2}[O_2]}{k^s_{O_2}[O_2] + k^s_D[D]} \left\{1 + \frac{k_D k'_{O_2}[D]}{k_{O_2}(k'_d + k'^s_{O_2}[O_2])}\right\} \quad (2)$$

In an extreme case where $[D] \gg [O_2]$

$$\gamma_{O_2}(\text{D-O}) = \frac{\varphi_{sT} k_{O_2}}{k^s_{O_2}} \quad (2a)$$

and in the other extreme case where $[D] \gg [O_2]$

$$\gamma_{O_2}(\text{D-D}) = \varphi_{sT} \frac{k_D}{k^s_D} \frac{k'_{O_2}[O_2]}{k'_d + k^s_{O_2}[O_2]} \quad (2b)$$

The condition for 2b to hold is fully satisfied when the concentration of dye is large enough, and quite reliable values for $\gamma_{O_2}(\text{D-D})$ can be evaluated directly from Figs. 2, 3 and 4. But this is not so with $\gamma_{O_2}(\text{D-O})$. To estimate this value the following procedure is conventionally adopted. If one puts $\alpha = k^s_{O_2}/k^s_D$, Eq. 2 can rewritten as follows,

$$\{\alpha[O_2] + [D]\} = \frac{\varphi_{sT} k_{O_2}[O_2]}{k^s_D} \times \left\{1 + \frac{k_{O_2}[D] k'_{O_2}}{k_{O_2}(k'_d + k^s_{O_2}[O_2])}\right\} \quad (3)$$

By using the $\alpha$-values given in Table V a plot of the left-hand side of Eq. 3 against [D] can be drawn and this should give a straight line. One can evaluate $\gamma_{O_2}(\text{D-O})$ and $\gamma_{O_2}(\text{D-D})$ from the slope and intercept respectively, although the former is not so reliable as the latter. As Fig. 7 shows, this method is fairly satisfactory and the results are given in Table V. It was checked that moderate change of $\alpha$ does not affect the result so much (cf*). For comparison, Imamura's data on the quantum yield of photobleaching at $[D] = 10^{-5}$ M are added in the last column. It is interesting that $\gamma_{O_2}(\text{D-D})$ for eosine and fluorescein is the same for the air-saturated and oxygen saturated solutions, while this is not so for erythrosine. This may be due to the difference in stability of the D-D redox intermediate.

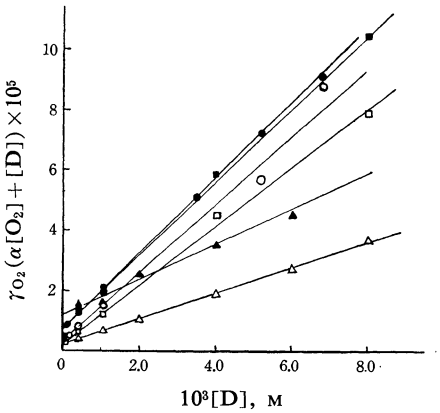



Fig. 7. Estimation of $\gamma_{O_2}(\text{D-O})$ and $\gamma_{O_2}(\text{D-D})$. Dark point is to the case of oxygen saturation and blank point to air saturation.
□■ uranine, ○● eosine, △▲ erythrosine

**Interpretation of the Bleaching Curve.**—As Fig. 5 shows, the rate of bleaching begins to increase when $\gamma = [D_0]/[O_2]$ exceeds about 0.2, and in such cases, the rate increases rapidly with the progress of the reaction. On the basis of the present view that a switch-over from the D-O to the D-D mechanism takes place, the above phenomena are just what is expected, because the D-D mechanism is considered to begin to contribute to the whole

TABLE V. QUANTUM YIELDS OF OXYGEN CONSUMPTION FOR D-O AND D-D MECHANISM

| | $\alpha$ | Air-saturation | | Oxygen saturation | | $\gamma_{dye-bleach}$ |
|---|---|---|---|---|---|---|
| | | $\gamma_{O_2}(D\text{-}O)$ | $\gamma_{O_2}(D\text{-}D)$ | $\gamma_{O_2}(D\text{-}O)$ | $\gamma_{O_2}(D\text{-}D)$ | |
| Eosine | 1.4 | $4\times10^{-3}$ | $1.2\times10^{-2}$ | $6\times10^{-3}$ | $1.3\times10^{-2}$ | $2.7\times10^{-4}$ |
| Erythrosine | 1.5 | $2.8\times10^{-3}$ | $4.3\times10^{-3}$ | $2.2\times10^{-3}$ | $6\times10^{-3}$ | $5.0\times10^{-4}$ |
| | 2.4* | $2.5\times10^{-3}$ | $4.5\times10^{-3}$ | $3.4\times10^{-3}$ | $7\times10^{-3}$ | — |
| Fluorescein (pH 7.65) | 1.8 | $4.4\times10^{-4}$ | $1.1\times10^{-2}$ | $3.7\times10^{-4}$ | $1.2\times10^{-2}$ | $1.3\times10^{-4}$ |

bleaching reaction when $[D_0]$ approaches $[O_2]$, and further, because the oxygen concentration decreases as the reaction proceeds (the experimental condition is static in the bleaching experiment), thus increasing the contribution of the D-D process. Broadly speaking, the bleaching reaction is thought to proceed according to a scheme similar to that of the oxygen consumption reaction, hence it is very plausible that the bleaching rate via the D-D mechanism is several times larger than that via the D-O mechanism, and this is also just what is observed in Fig. 5.

The above view is further supported by the experiments in which the rate of bleaching is measured at a constant dye concentration of $10^{-4}$ M, and at various oxygen concentrations. As Fig. 6 shows, the rate increases with $[O_2]$ in the low $[O_2]$ region, reaches a maximum and finally falls to a constant value which of course corresponds to $\gamma_{O_2}(D\text{-}O)$. The different behavior at $1\times10^{-5}$ M of dye will be considered later.

**Interpretation of Blum's Results and General Discussions.**—Our results reconfirm Blum's observations mentioned at the beginning of this paper and make them more quantitative. Blum in addition, suggested that the formation of hydrogen peroxide is not directly connected with the decomposition of dye. This is clearly understood on the basis of a D-D mechanism. Thus at higher concentrations of dye, the reaction proceeds as follows:

$$D^T + D \rightarrow D^+ \cdots D^-$$

$$D^+ \cdots D^- + O_2 + H^+ \rightarrow HO_2\cdot + D^+ + D$$

Alternatively,

$$D^T + D \rightarrow D^+ + D^-$$

$$D^- + H^+ + O_2 \rightarrow HO_2\cdot + D$$

and hydrogen peroxide is produced from $HO_2\cdot$, while most of $D^+$ is converted into the colorless form. Lindqvist proposed the view that dimerization of $D^+$ occurs. $D^+$ may, however, alternatively lose its dye structure by reacting with oxygen or it may revert to the original dye upon the attack of $HO_2\cdot$ as suggested by Lindqvist. Thus the formation of hydrogen peroxide and the destructive bleaching of dye proceed independently of each other in the later stage. The magnitude of oxidative bleaching and accordingly $\Delta[O_2]/\Delta[D]$ are thought to depend upon the fate of the half-oxidized dye. On the other hand, at low dye concentrations, oxygen directly attacks the triplet state leading to the decomposition of dye without the production of hydrogen peroxide. In this case the kinetic features of the bleaching are very simple.

Lastly, some speculative discussions will be added on the lifetime of the redox intermediate and on the general features of the photooxidative bleaching of the dye. In Imamura's experiments at $[D]=10^{-5}$ M, and as reconfirmed by the present investigation, the rate of the oxidative photobleaching decreases monotonously with the decrease of oxygen concentration below $[O_2]=10^{-5}$ M. But under such circumstances, the D-D mechanism should become appreciable, and if oxygen effectively attacks the D-D redox intermediate, a larger rate than that for the D-O mechanism should be expected. The experimental results thus require the D-D redox intermediate to have such a short lifetime that it has no chance to react with oxygen. Putting $[O_2] \sim 10^{-6}$ M and assuming that the reaction between oxygen and the intermediate is diffusion controlled, the decay constant of the D-D intermediate should be larger than $10^9\times10^{-6}=10^3\,sec^{-1}$. When $[O_2]$ is $10^{-4}$ M, the D-D intermediate of eosine should have enough chance to be attacked by oxygen, because $\gamma_{O_2}(D\text{-}D)$ is independent of the oxygen concentration. Thus the decay constant of the D-D intermediate must be far less than $10^5\,sec^{-1}$. From the above argument, the decay constant of the D-D intermediate for eosine should be of the order of $10^4\,sec^{-1}$. In case of erythrosine this is a little larger since the dependence on $[O_2]$ is really observed. If one assumes that instead of the formation of $D^+\cdots D^-$, the reaction $D^T+D \rightarrow D^+ + D^-$ occurs very effectively, yielding free semiquinone and semi-oxidized dye, then the steady concentration of these species in the present experimental condition is estimated to be of the order of $10^{-9}$ M assuming that the reaction between these species is diffusion-controlled. Hence the lifetime of such species should be of the

order of 1 sec. The present results completely reject this possibility and one can safely conclude that most of the redox intermediate $D^+\cdots D^-$ reverts to the original dye via the reverse reaction without forming separate radical ions.

The lifetime of $D^+\cdots D^-$ and its tendency to form free radical ions will depend sensitively on the experimental conditions as well as on the nature of the dye, and this is perhaps one of the reasons why dyes of the same group show sometimes very different behavior and why the general nature of the reaction is often difficult to understand.

## Summary

The oxygen up-take of irradiated aqueous solutions of xanthene dyes has been investigated by means of Warburg's apparatus, and evidence for a switch-over from a D-O to a D-D mechanism is obtained from the variation of dye-concentration. This view is supported by the photobleaching rate and the oxygen concentration effect at high eosine concentrations ($\sim 10^{-4}$ M).

The quautum yields ($\gamma_{O_2}$) of the consumption are estimated and it is found that $\gamma_{O_2}$ (D-D) is larger than $\gamma_{O_2}$(D-O).

*Department of Chemistry*
*Faculty of Science*
*Tohoku University*
*Katahira-cho, Sendai*

# An Attempt to Determine Eosine's S*→T Transition Probability and Evidence for the Participation of a D–D Redox Mechanism

By Takeshi OHNO, Yoshiharu USUI and Masao KOIZUMI

(Received November 17, 1964)

The primary processes in the photochemical reactions of xanthene dyes have been studied by several workers[1,2] by means of the steady illumination, and the ratios of the rate constants for some elementary reactions have been evaluated. Very few attempts, however, have been made to determine exactly the rate constant of each particular elementary process, and of these attempts the flash photolytic investigations of Lindqvist[3] and Grossweiner[4,5] are the most prominent. The former was concerned with fluorescein while the latter dealt with eosine.

The decay constant of the triplet state and the transition probability of the singlet excited state to the triplet state, i. e., $\varphi_{S\to T}$ are believed to be the most fundamental. If the exact values of these two are known, many of the other rate constants can be evaluated very easily from their ratios.

One method to determine the value of $\varphi_{S\to T}$ is to make use of the kinetic data from a suitable reaction. In principle, the method consists of evaluating the quantum yield under conditions such that all the triplet state dyes react in one definite way. For example, if the photochemical reduction proceeds according to the following scheme,

$$\begin{array}{ccccccc} D & \rightarrow & D^* & \rightarrow & D^t & \xrightarrow{k_r[R]} & \text{Leuco dye} \\ & & \downarrow & & \downarrow k_d & & \\ & & D & & D & & \end{array}$$

where $D^*$, $D^t$ are respectively the singlet excited state and the triplet state of the dye, and R is a reducing agent, then the quantum yield, $\Phi$ is expressed as follows

$$\Phi = \varphi_{S\to T}\frac{k_r[R]}{k_d + k_r[R]} \qquad (1)$$

Hence

$$\frac{1}{\Phi} = \frac{1}{\varphi_{S\to T}} + \frac{1}{\varphi_{S\to T}}\cdot\frac{k_d}{k_r[R]}$$

and the plot of $1/\Phi$ against $1/[R]$ gives $1/\varphi_{S\to T}$ as an intercept. For the above method to be used effectively, certain conditions must be fulfilled. 1) The reducing agent R should

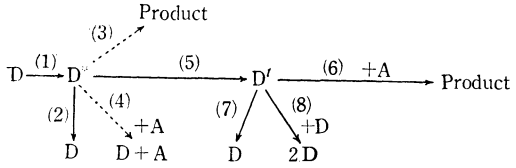
1) M. Imamura and M. Koizumi, This Bulletin, **29**, 899 (1956).
2) G. Oster and A. H. Adelman, *J. Am. Chem. Soc.*, **78**, 913 (1956).
3) L. Lindqvist, *Arkiv Kemi*, **16**, 79 (1960).
4) L. I. Grossweiner and E. F. Zweicker, *J. Chem. Phys.*, **34**, 1411 (1961).
5) E. F. Zwicker and L. I. Grossweiner, *J. Phys. Chem.*, **67**, 549 (1963).

not appreciably affect the ground state or the singlet excited state of the dye. 2) Mere deactivation should not result from the attack of R on $D^t$. 3) The final product must be produced by a one step attack of R on $D^t$ or else the succeeding steps must be known completely.

On the basis of the above principles, Oster obtained the values 0.092 0.020 for $\varphi_{S\to T}$ of eosine and fluorescein, respectively, at pH 7.0.[2] He used allylthiourea (ATU) as a reducing agent and investigated the photoreduction of these dyes in aqueous solution. Oster proposed the following rate formula,

$$\text{rate} = \frac{I_{ab}[A]}{\alpha+\beta[A]} \qquad (2)$$

where $\alpha$, $\beta$ are constants, $I_{ab}$ is the absorbed light per second per liter, and [A] is the concentration of ATU. The scheme for the reaction is




(3)

where dashed arrows indicate processes having negligible rates. The process 8 was added to take into account the fact that the rate decreases with increase of dye concentration. On the basis of the above scheme, he derived the following rate formula,

$$\text{rate} = \frac{I_{ab}k_5k_6[A]}{(k_2+k_5)(k_7+k_6[A]+k_8[D])} \qquad (4)$$

which is the same as the experimental rate formula except for the term $k_8[D]$, and he estimated some of the rate constants.

In view of the importance of $\varphi_{S\to T}$, it seems desirable to repeat this experiment and to ascertain whether in fact the above conditions are fulfilled. In addition, there is a possibility that the reaction scheme is dependent on experimental conditions such as the concentration of dye as well as that of the reducing agent.

It is desirable, therefore, to examine the rate formula for a run and to study the behavior of the intermediate and of the final product before the above method is used.

In this paper we have attempted to determine $\varphi_{S\to T}$ for eosine in aqueous solution at pH= 7.2, paying attention to the above meniioned points. Broadly speaking, we have carried out experiments similar to those of Oster, using ATU and EDTA as reducing agents, and have examined the applicability of 2 and 4. Although we could not get a satisfactory result for $\varphi_{S\to T}$, we have found strong evidence for the participation of a D-D mechanism in this system.

## Experimental

**Materials.**—*Eosine.*—Grübler's product was used. Stock solution ($1\times10^{-4}$ M) which had been kept in the dark was diluted to $4.5\times10^{-6}$ M—$2.4\times10^{-6}$ M for each experiment. Allylthiourea (ATU) was recrystallized from water three times. To avoid degradation of the ATU, it was stored in the ice box. Ethylenediaminetetraacetic acid disodium salt (EDTA) was prepared by dissolving Dotite 2 NA. Disodium hydrogen phosphate ($Na_2HPO_4\cdot12H_2O$) and potassium hydrogen phosphate ($KH_2PO_4$) were recrystallized three times.

**Procedure.**—All the solutions were prepared from 1/25 M phosphate buffer at pH=7.2. Most of the solutions were degassed by use of a mercury diffusion pump, freezing and thawing (in a dry ice bath) being repeated four to six times. The degassed sample in a cell ($1\times1\times4$ cm.) was irradiated with a tungsten projection lamp (50 V. 125 W.) having a yellow glass filter cutting off $<470$ m$\mu$. For solutions with initial dye concentrations in the range $2.4\times10^{-6}$ M—$10^{-5}$ M, the concentration of residual dye was measured colorimetrically without stopping the irradiation. With initial concentrations of dye greater than $10^{-5}$ M, a 7 mm. spacer was inserted into the cell, and the measurements were carried out as above.

A temperature of 25°C was chosen. To determine the quantity of light absorbed by the dye, a calibrated Kipp and Zonen thermopile having a sensitivity of $1.02\times10^{-5}$ V./m$^2$ watt was used, and the output measured with a potentiometer.

## Results

**ATU.**—*Rate Formula for a Run.*—Equation 4 derived from Oster's scheme 3 is not strictly of the same form as Eq. 2 and, moreover, it can not be integrated in a simple way. However, if $k_8[D]\ll k_7+k_6[A]$, then 4 is reduced to 2 and the rate is simply proportinal to the absorption of light. In this case the rate formula for a run can be derived as follows.

Putting

$$I_{ab}=I_o(1-e^{-\alpha cd})$$

where $I_o$ is the number of photons per cm$^2$ and $\alpha$ is the average molar absorbancy, one can write

$$-\frac{dC}{dt}=\Phi\frac{I_o}{d}(1-e^{-\alpha cd})1000 \qquad (2)$$

Integration gives

$$\ln(e^{\alpha cd}-1)=-1000\alpha\Phi\frac{I_o}{d}t+\ln(e^{\alpha c_o d}-1) \qquad (5)$$

Hence the plot $\ln(e^{acd}-1)-t$ should give a straight line with a slope of $1000\,\alpha\Phi I_0$.

Now, as long as the concentration of ATU is in the range $5\times10^{-4}$ M—$2.0\times10^{-2}$ M and the dye concentration is $10^{-5}$ M, the rate formula 5 accommodates the experimental data very satisfactorily until up to 40% of the dye has been bleached. Thus the rate is simply proportional to the absorption of light. When [ATU] becomes less, however, Eq. 5 appears to become less satisfactory and a second order rate formula in regard to dye holds better, although the initial part of the rum can still be expressed by 5. Some examples are shown in Figs. 1 and 2.

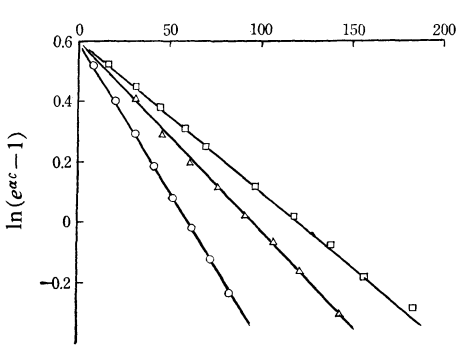



Fig. 1. Fading curves of eosine in vacuo for various concentration of ATU. At 25°C.
○: Eosine, $10^{-5}$ mol./l.
ATU, $2.0\times10^{-2}$ mol./l.
△: Eosine, $10^{-5}$ mol./l.
ATU, $1.1\times10^{-2}$ mol./l.
□: Eosine, $10^{-5}$ mol./l.
ATU, $0.8\times10^{-2}$ mol./l.

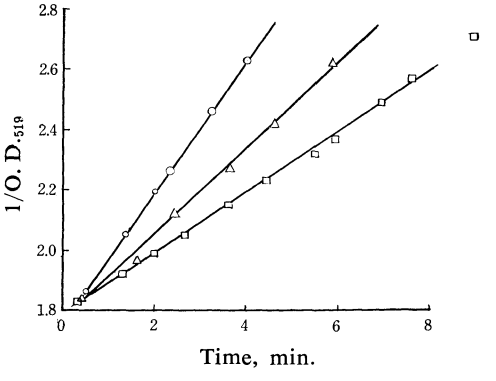



Fig. 2. Fading curves of eosine according to the second order furmula in regard to dye concentration. Dye concentration, $8\times10^{-6}$ mol./l.
○: ATU, $2.5\times10^{-3}$ mol./l.
△: ATU, $1.67\times10^{-3}$ mol./l.
□: ATU, $1.25\times10^{-3}$ mol./l.

Now if $k_8$[D] in the denominator of Eq. 4 is not negligible, then the rate should increase in the later stage and should be larger than that calculated from 5, whereas the actual deviation from 5 in the later stage is always in the opposite direction. This strongly suggests that Eq. 4 needs to be modified in some way. To make this point clear, the effect of various factors upon the quantum yield obtained from the initial slope of the $\ln(e^{acd}-1)-t$ plot was examined.

*The Effect of the Dye Concentration.*—With the concentration of ATU fixed at $5.0\times10^{-3}$ M, $1.0\times10^{-3}$ M and $0.50\times10^{-3}$ M, respectively, the effect of the dye concentration on $\Phi$ was investigated. The dye concentration was varied from $2.6\times10^{-6}$ M to $4.4\times10^{-5}$ M. As Fig. 3 shows, the reciprocal of the quantum yield is in a linear relation to the concentration of the dye when [ATU] is $5\times10^{-3}$ M. But when the concentration of ATU is decreased, this linearity deteriorates. Thus the deviation becomes notable at ca. $2\times10^{-5}$ M of dye for $10^{-3}$ M of ATU and at an even lower dye concentration (ca. $10^{-5}$ M) for $0.5\times10^{-3}$ M of ATU. The initial slopes of the curves for [ATU]$=5\times10^{-4}$M and $10^{-3}$ M agree quite well with that calculated from the slope for [ATU]$=5\times10^{-3}$ M by the use of Eq. 4 (see below). From the slopes in the low concentration region of dye and from the tentative value of $\varphi_{S\to T}$ (0.032, see below), $k_8/k_6$ was evaluated to be $1.8\times10^3$. Table I gives values for the quantum yield under differing conditions. The above deviation in Fig. 3, together with the rather large value of $k_8/k_6$ clearly implies that Eq. 5 does not hold when the concentration of dye becomes large in relation to that of ATU.

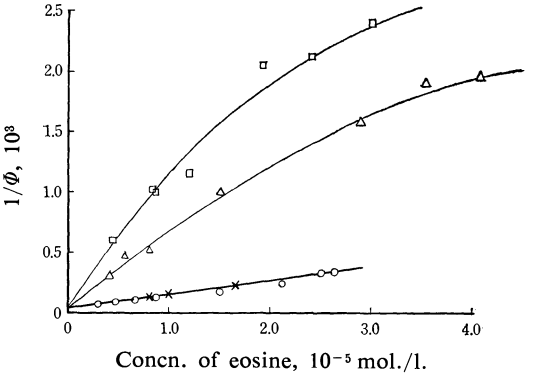



Fig. 3. Effect of eosine concentration on the quantum yield of the photobleaching by ATU.
○: ATU, $5.0\times10^{-3}$ mol./l.
△: ATU, $1.0\times10^{-3}$ mol./l.
□: ATU, $0.5\times10^{-3}$ mol./l.
×: ATU, $5.0\times10^{-3}$ mol./l.
The abscissa is the sum of concentration of eosine and reaction product.

TABLE I. QUANTUM YIELDS AT VARIOUS DYE CONCENTRATIONS

| Concn. of ATU $\times 10^{-3}$ M | Concn. of dye $\times 10^{-6}$ M | $\Phi$ $\times 10^{-3}$ |
|---|---|---|
| 5.0 | 25.4 | 3.1 |
| 5.0 | 4.2 | 13.0 |
| 1.0 | 8.0 | 2.5 |
| 1.0 | 40.0 | 0.52 |
| 0.5 | 12.0 | 0.77 |
| 0.5 | 20.0 | 0.51 |

*The Effect of the Reaction Product on the Rate.*—Because of the rather large value of $k_8/k_6$ and the ratio of the concentration of the dye to that of the reducing agent, Eq. 4 would require that as the reaction proceeds, the rate would deviate and become larger than that given by the plot $\ln(e^{acd}-1)$—$t$.

But contray to this expectation, the experimental data fits quite well in the initial stage and deviates in the opposite direction in the later stages. This suggest the existence of an inhibiting action due to some reaction product. To check this point, the following experiment was performed. A solution of the dye which had been irradiated until about 30% of the dye had bleached, was added to a fresh sample of dye and the rate of bleaching was measured. In Fig. 3 cross notations refer to such experiments for which the sum [Product]+[dye] was taken as abscissa. The points lie close to the line. It is inferred therefore that the term $k_8[D]$ in 4 should be replaced by $k_8[D]+k_9[\text{product}]$. Assuming $k_8 \approx k_9$ and approximating $[\text{product}]=[D]_o-[D]$, this term may be rewritten as $k_8[D]_o$ where $[D]_o$ is the initial concentration of the dye. The rewritten equation will be denoted as 4'.

$$\Phi=\varphi_{S\to T}\times\frac{k_6[A]}{k_7+k_6[A]+k_8[D]_o} \qquad (4')$$

*The Effect of the Concentration of ATU and the Value of $\varphi_{S\to T}$.*—The concentration of ATU was varied from $10^{-3}$ M to $4\times10^{-2}$ M at some fixed dye concentrations. Figure 4 gives the plots of $1/\Phi$ against 1/[ATU], which are satisfactorily linear. This implies that Eq. 4' holds under the present experimental conditions and this is consistent with the results shown in Fig. 3.

From 4'

$$\frac{1}{\Phi}=\frac{k_2+k_5}{k_5}\left(1+\frac{k_7+k_8[D]_o}{k_6[A]}\right)$$

one can evaluate $k_5/(k_2+k_5)$ from the intercept which is $\varphi_{S\to T}$ and $(k_7+k_8[D])_o/k_6$ from the inclination. In Table II, some of the quantum yield are given, and in Table III, the values of $\varphi_{S\to T}$ and $(k_7+k_8[D]_o)/k_6$ are tabulated. The value in parenthesis is Oster's.

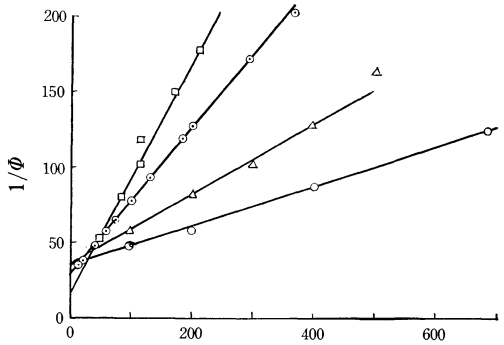



Fig. 4. Effect of ATU concentration on the quantum yield of photoreduction
○: Eosine, $2.4\times10^{-6}$ mol./l.
△: Eosine, $4.0\times10^{-6}$ mol./l.
⊙: Eosine, $8.0\times10^{-6}$ mol./l.
□: Eosine, $11.6\times10^{-6}$ mol./l.

TABLE II

| Concn. of dye, M | Conc. of ATU M | $\Phi$ |
|---|---|---|
| $1.16\times10^{-5}$ | $2.0\times10^{-2}$ | $2.2\times10^{-2}$ |
| $1.16\times10^{-5}$ | $8.0\times10^{-3}$ | $1.1\times10^{-3}$ |
| $8.0\times10^{-6}$ | $1.0\times10^{-2}$ | $1.4\times10^{-3}$ |
| $8.0\times10^{-6}$ | $2.5\times10^{-3}$ | $0.42\times10^{-3}$ |
| $4.0\times10^{-6}$ | $5.0\times10^{-3}$ | $1.4\times10^{-3}$ |
| $2.4\times10^{-6}$ | $1.0\times10^{-3}$ | $0.63\times10^{-3}$ |

TABLE III

| Concn. of dye, M | $\varphi_{S\to T}$ | $\frac{k_7+k_8[D]_o}{k_6}$ |
|---|---|---|
| $1.16\times10^{-5}$ | 0.15 | $29\times10^{-3}$ |
| $1.0\times10^{-5}$ | (0.092) | |
| $8.0\times10^{-6}$ | 0.052 | $16\times10^{-3}$ |
| $4.0\times10^{-6}$ | 0.032 | $7.0\times10^{-3}$ |
| $2.4\times10^{-6}$ | 0.032 | $4.2\times10^{-3}$ |

*The Effect of Temperature.*—As can be seen in Table IV, the effect of temperature on the rate is not large.

TABLE IV

| Temp., °K | $\Phi$ |
|---|---|
| 289 | $10\times10^{-3}$ |
| 298 | $8.1\times10^{-3}$ |
| 308 | $7.9\times10^{-3}$ |
| 320 | $7.3\times10^{-3}$ |

**EDTA.**—*The Rate Formula for a Run.*—It is notable that a certain induction period exists in the case of EDTA. After the induction period, however, the results are satisfactorily reproduced by the plot of Eq. 5, indicating that the rate is simply proportional to the absorption of light. Some typical examples are shown in Fig. 5.

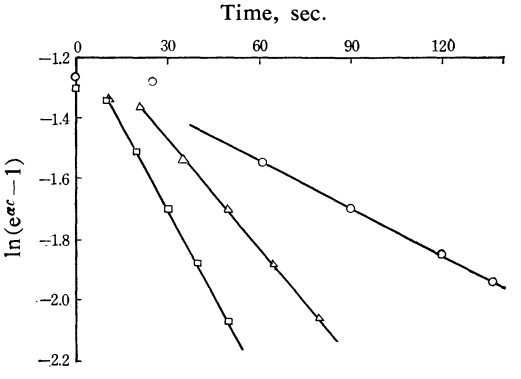
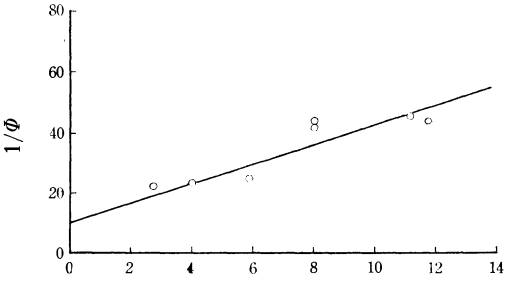


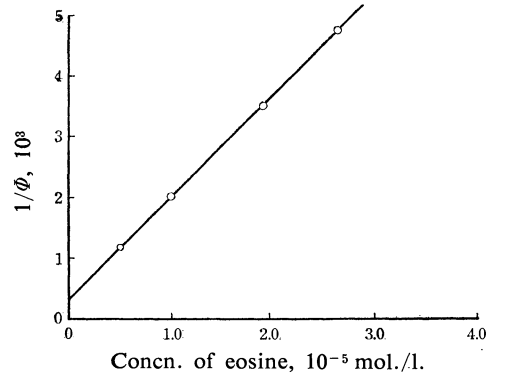

Fig. 5. Fading curves of eosine in vacuo for various concentration of EDTA. Dye concentration, $8\times10^{-6}$ mol./l.
Concn. of EDTA, ○: $2.0\times10^{-3}$ mol./l.
△: $3.3\times10^{-3}$ mol./l.
□: $5.0\times10^{-3}$ mol./l.

*The Effect of the Dye Concentration.*—Figures 6a and 6b give the plot of $1/\Phi$ aginst the dye concentration. Although the data in Fig. 6a show a fair amount of scatter, it is evident that the effect of the dye concentration is much less than in the case of ATU. In Fig. 6b, where a lower concentration of EDTA was used, the linearity is excellent. This result is in sharp contrast with that in the case of ATU for which the deviation from linearity is notable at $[ATU]=0.5\times10^{-3}$ M and $10^{-3}$ M. From the slope and the intercept of the plot in b and from the value (0.080) of $\varphi_{S\to T}$, $k_8/k_6$ was calculated to be $1.3\times10^3$. The result from 6a is $k_8/k_6=1.1\times10^3$, which is in agreements with the above value.




Concn. of eosine, $10^{-6}$ mol./l.

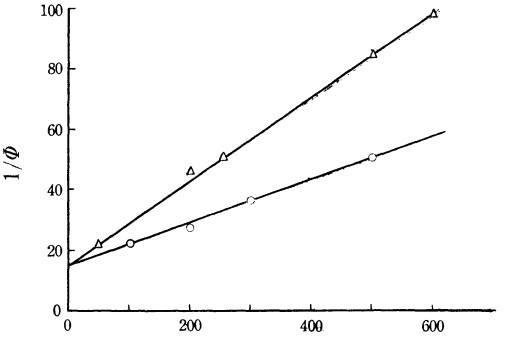
Fig. 6a. Effect of eosine concentration on the quantum yield of photoreduction.
Concn. of EDTA, $5.0\times10^{-3}$ mol./l.




Concn. of eosine, $10^{-5}$ mol./l.

Fig. 6b. Effect of eosine concentration on the quantum yield of photoreduction.
Concn. of EDTA, $10^{-4}$ mol./l.

*The Effect of the Concentration of EDTA.*—The concentration of EDTA was varied from $6.7\times10^{-3}$ M to $2\times10^{-2}$ M at two fixed dye concentrations, $8.0\times10^{-6}$ M and $5.5\times10^{-6}$ M. As Fig. 7 shows, the plots are satisfactorily linear and in this case, the two intercepts are exactly the same. Table V gives the quantum yilds under various conditions and Table VI gives $\varphi_{S\to T}$ and the value of $(k_7+k_8[D]_0)/k_6$.




Reciprocal of concn. of EDTA, l./mol.

Fig. 7. Effect of EDTA concentration on the quantum yield of photoreduction.
○: Eosine, $5.5\times10^{-6}$ mol./l.
△: Eosine, $8.0\times10^{-6}$ mol./l.

TABLE V

| Concn. of dye, M | Concn. of EDTA, M | $\Phi$ |
|---|---|---|
| $8.0\times10^{-6}$ | $1.0\times10^{-2}$ | $1.0\times10^{-2}$ |
| $8.0\times10^{-6}$ | $5.0\times10^{-3}$ | $0.41\times10^{-2}$ |
| $8.0\times10^{-6}$ | $2.0\times10^{-3}$ | $0.12\times10^{-2}$ |
| $5.5\times10^{-6}$ | $3.3\times10^{-3}$ | $0.11\times10^{-2}$ |

TABLE VI

| Concn. of dye, M | $\varphi_{S\to T}$ | $\frac{k_7+k_8[D]_0}{k_6}$ |
|---|---|---|
| $8.0\times10^{-6}$ | 0.080 | $72\times10^{-3}$ |
| $5.5\times10^{-6}$ | 0.080 | $5.8\times10^{-3}$ |

## Supplementary Experiments and Discussion

As will be described later, the finding, that for ATU the linearity between $1/\Phi$ and $[D]_0$ does not hold when $[D]_0$ exceeds a certain value, leads to the conclusion that a switch-over of the mechanism is taking place in this

case. But in most cases Eq. 4′ holds or approximately holds and in such cases, the values of $\varphi_{S\to T}$ can be obtained by formally applying this equation to the experimental data. The rate constants of some elementary reactions can also be estimated in a simple manner. Therefore, we will first discuss these data before entering on a critical discussion of the procedure.

From 4′, the intercept and the inclination of the plots in Fig. 3 and Fig. 6 should be expressed by $\frac{1}{\varphi_{S\to T}}\times\left\{1+\frac{k_7}{k_6[R]}\right\}$ and $\frac{1}{\varphi_{S\to T}}\times\frac{k_8}{k_6[R]}$, respectively. By utilizing the tentative values of $\varphi_{S\to T}$, one can evaluate the ratio $k_8/k_6$ from the inclination. The result, as already stated, is $1.8\times10^3$ M for ATU and $1.3\times10^3$ M for EDTA. Furthermore, it is possible to evaluate $k_6$ by putting[4] $k_7=4.2\times10^2$ in the expression for the intercept. But this procedure is not so reliable, firstly because the value of the intercept is subject to a large error and secondly because this error profoundly affects the value of $k_6$. Hence the following conventional procedure was adopted. The average value of $k_8$ from several determinations for both EDTA and ATU was taken as $5.5\times10^8$ ($\pm1.0\times10^8$) and the value of $k_6$ was calculated from the value of $k_8/k_6$. This results in a value of $k_6=3.1\times10^5$ for ATU, and $4.1\times10^5$ in the case of EDTA.

To check these results, the value of $k_6$ is recalculated from the inclination of the plot $1/\Phi$—$1/[R]$ by inserting the above values of $k_8$ and $k_7$ into the expression $(k_7+k_8[D]_o)/k_6$. The results are as follows.

| Reducing agent | Concn. of dye $\times10^{-6}$ M | The value of $k_6$ |
|---|---|---|
| ATU | 2.4 | $3.8\times10^5$ |
| ATU | 4.0 | $3.4\times10^5$ |
| EDTA | 5.5 | $5.4\times10^5$ |
| EDTA | 8.0 | $4.1\times10^5$ |

In spite of the crudeness of the method, there is no doubt that $k_6$ and $k_8$ are of the order of $10^5$ and $10^8$ respectively, and it seems that the choice of reducing agent makes little difference in these values. But judging from the data given in Table II and Table V, the quantum yield for EDTA is several times larger than that for ATU under otherwise similar conditions. The following data refer to such results. It appears from the above argument that this difference is closely connected with the value of $\varphi_{S\to T}$.

TABLE VII

| $[Dye]\times10^6$ | 4 | 8 | 12 | 16 |
|---|---|---|---|---|
| $\Phi_{EDTA}/\Phi_{ATU}$ | 3.1 | 3.3 | 3.6 | 3.8 |

Next, we will discuss the various conditions necessary for obtaining a reliable value of $\varphi_{S\to T}$ (see the introduction). The first point, which concerns the possibility of the singlet excited state being attacked by R, need not be considered, because neither ATU nor EDTA quenches the fluorescence of eosine appreciably,[2] and also because the $1/\Phi$—$1/[R]$ plots, given in Fig. 4 and Fig. 7, do not show any deviation in the high concentration region of ATU or EDTA.

To investigate the second point which concerns the behavior of the intermediate, a few supplementary experiments were carried out.

In the air-saturated solution, the reaction was found to be completely interrupted in the case of EDTA, but with ATU, for example at $2\times10^{-2}$ M, the reaction proceeds with a quantum yield of 0.005, which is about a quarter of that in the degassed solution under otherwise similar conditions. Such a difference is due, without doubt, to different behaviors of the intermediates in the two cases. In view of the fact that semiquinone produced in ethanol solution is very sensitive to a minute amount of oxygen,[1] the same effect would be expected also in aqueous solution. Therefore, there is a great possibility that semiquinone in a free state is formed in the case of EDTA but not in the case of ATU.* The induction period, which was observed in the case of EDTA, might therefore be due to a small quantity of residual oxygen.

Although the formation of semiquinone in a free state is improbable in the case of ATU, the following experiment strongly suggests the formation of some sort of intermediate with absorption near 360 mμ. Thus when the reaction cell was illuminated from the back with Hg 365 mμ during the reaction, the rate was found to increase by about 20%.

In both cases the behavior of the final product also appears to be quite different. In the case of EDTA, the product had an absorption maximum near 290 mμ and is most probably a leuco dye. But it was found that when the solution was kept in the dark, the oxidized form was regained very slowly. Figure 8 shows that this reversion proceeds as a first order reaction in respect to the photobleached product. This might be due to the formation of a complex composed of molecules of the leuco dye and the oxidized product of EDTA closely held together. The introduction of air increased the rate by about 10%. It is regrettable that in the case of ATU, a spectroscopic investigation could not be carried out due to

* In case of fluorescein, this was really verified by comparing the quantity of semiquinone produced in the two cases. See next paper.

the existing absorption of ATU up to ~290mu. But it was confirmed that the final product is quite stable. All the observations on the intermediate and the final product, although they are still preliminary in nature, suggest that the reaction in question is not so simple and differs from case to case.

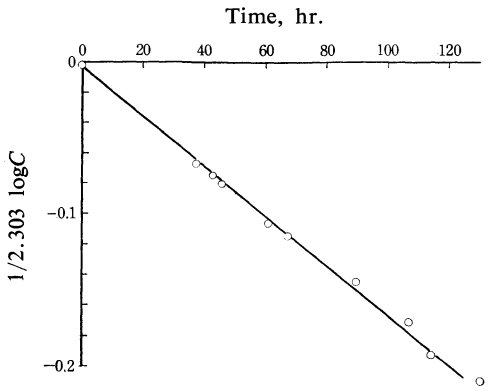



Fig. 8. Reversion curve of eosine according to the first order formula in respect to the photobleached product after eosine was completely photobleached.

As far as the behaviors of the intermediates and final products are concerned, one can not say that the formal procedure of evaluating $\varphi_{S\to T}$ is amply justified. We are at present planning more systematic flash experiments to elucidate the detailed mechanism of the reaction.

Next to be discussed is the switch-over of the mechanism. As has already been clarified by investigations in our laboratory,[6] the photoreduction of methylene blue can proceed by a D-D redox mechanism or a D-R redox mechanism; thus according to the concentration of dye and the type of reducing agent, the primary step of the photoreduction of methylene blue is a) $D^t+D \rightarrow$ semi-reduced dye + semi-oxidized dye (D-D redox mechanism) or b) $D^t+R \rightarrow$ semi-reduced dye + semi-oxidized R (D-R redox mechanism).

Now with the xanthene dyes, photoreduction in the degassed solution does not occur in the absence of a reducing agent.[5] Yet, it was confirmed in the present experiment that deactivation of $D^t$ by the ground state dye occurs, as Oster proposed,[2] and further, it was established that deactivation by leuco dye also occurs, the rate constants for both deactivation processes being close to that controlled by diffusion. This makes us suspect that, with some suitable reducing agents, the photoreduction of this dye may also proceed via a D-D mechanism. This suspicion is further strengthened if one considers Lindqvist's discovery that half-reduced and half-oxidized flurorescein is produced by flash illumination, without addition of any reducing or oxidizing agents.[3]

Now the present results strongly suggest that such a switch-over of the mechanism really exists, in the case of ATU, but not in the case of EDTA, under the present experimental conditions. Thus the findings that the plot of $1/\Phi$—$[D]_o$ begins to deviate at a concentration of $2.4\times10^{-5}$ M of dye when [ATU]$=10^{-3}$, and at $1.2\times10^{-5}$ M dye at $0.5\times10^{-3}$ M ATU, seems to be understandable only on this basis. If the photoreduction in the small concentration region of ATU occurs exclusively by a D-D mechanism, then the rate formula would presumably be given by

$$-\frac{d[D]}{dt}=\frac{\varphi_{S\to T}I_{ab}k_8'[D]}{k_7+k_8[D]_o+k_6[A]}\times\frac{k_r'[A]}{k_d'+k_r^{s'}[A]} \quad (6)$$

where $k_8'$ is the rate constants for $D^t+D\rightarrow D^++D^-$ redox intermediate, and $k_d'$, $k_r'$ are respectively the rate constants for monomolecular deactivation of this intermediate and the rate constants of the reaction with ATU, and $k_r^{s'}$ is the sum of the rate constants for the reaction and deactivation with ATU. According to the following analysis it seems unnecessary to take into account the deactivation of the redox-intermediate by the ground state dye. In the usual condition, $k_8[D]_o \gg k_7$ and $k_8[D]>k_6[A]$, hence one can put approximately

$$\Phi^o{}_{D-D}=\frac{k_r'[A]}{k_d'+k_r^{s'}[A]}\times\frac{k_8'}{k_8}\varphi_{S\to T}$$

In the general case where the D-R and D-D mechanisms occur simultaneously, $\Phi$ is given by

$$\Phi=\Phi_{D-R}+\Phi_{D-D}=\varphi_{S\to T}\times\frac{k_6[A]}{k_7+k_6[A]+k_8[D]_o}+\varphi_{S\to T}\frac{k_8'[D]}{k_7+k_6[A]+k_8[D]_o}\times\frac{k_r'[A]}{k_d'+k_r^{s'}[A]} \quad (7)$$

Since $k_6$ $k_8$ are respectively ~$10^5$ and ~$10^8$, the second term cannot be neglected at $[D]_o \gg 10^{-5}$ M and at [ATU] ~$10^{-3}$ M unless $\Phi_{D-D}{}^o$ is very small, and this view interprets the results given in Fig. 3. Thus the deviation can safely be attributed to the contribution of a D-D process in the entire reaction. Further information about the D-D process can be obtained as follows, although the analysis is still provisional in nature.

From the results shown in Fig. 3, one can easily estimate the dye concentration at which

6) S. Kato, M. Morita and M. Koizumi, This Bulletin, 37, 117 (1964); M. Koizumi, H. Obata and S. Hayashi, ibid., 37, 108 (1964).

$\Phi_{D-D}/\Phi_{D-R}$ attains a value of 0.3 (chosen conventially) for a given concentration of ATU. The results are given in Table VIII.

TABLE VIII

| ATU | Initial slope | $[D]_0$ for $\Phi_{D-D}/\Phi_{D-R}=0.3$ |
|---|---|---|
| $5.0\times10^{-3}$ M | $1.4\times10^{7}$ | — |
| $1.0\times10^{-3}$ | $6.6\times10^{7}$ | $3.5\times10^{-5}$ |
| $0.5\times10^{-3}$ | $14.5\times10^{8}$ | $1.7\times10^{-5}$ |

Now $\Phi_{D-D}/\Phi_{D-R}$ is expressed as follows,

$$\frac{\Phi_{D-D}}{\Phi_{D-R}}=\frac{k'_8[D]}{[A]k_6}\quad\frac{k_r'[A]}{k_d'+k_r^{s'}[A]} \tag{8}$$

By substituting the values of [D], [A], $k_6(=3.8\times10^5)$ and $\Phi_{D-D}/\Phi_{D-R}(=0.3)$ into Eq. 8, one can calculate the value of $k_8'\times k_r'/k_d'+k_r^{s'}[A]$, which is $3.3\times10^9$ for ATU $10^{-3}$ M (9—a) and $7\times10^9$ for ATU $=5\times10^{-4}$ (9—b)
From the ratio of the above two values,

$$\frac{k_d'+k_r^{s'}\times5\times10^{-4}}{k_d'+k_r^{s'}\times10\times10^{-4}}\approx\frac{1}{2}$$

Hence

$$k_r^{s'}\times5\times10^{-4}\gg k_d'$$

This implies that most of the intermediates produced from $D^t$ and D attacked by ATU molecules. The values of $k_8'\times k_r'/k_r^{s'}$, evaluated from (9—a) and (9—b), are respectively $3.3\times10^6$ and $3.5\times10^6$. If this is compared with the value of $k_8'$, the value of $k_8'$ lies in the range $10^8$—$3.3\times10^6$ and the corresponding value of $k_r'/k_r^{s'}$ in the range 1/100—1.

From the above analysis there is scarcely any doubt that in the case of ATU the reaction proceeds via a D-D mechanism, whereas in the case of EDTA no such reaction occurs. The reason for the different behavior is unknown at present, but we have already found a similar result in the photoreduction of methylene blue.[6] It is to be noted that the data in Table VIII are consistent with the result that the rate formula for a run obeys Eq. 5 quite well as long as the concentration of ATU is in the range $10^{-3}$—$2\times10^{-2}$ M and the dye concentration is $\sim10^{-5}$ M.

Finally a brief comment will be given on the value of $\varphi_{S\to T}$. As Fig. 4 and Table III show, the value of $\varphi_{S\to T}$ for ATU appears to depend on the concentration of dye and to increase regularly with it. An interpretation which occurred to us at first was to consider that the higher the dye concentration the greater becomes the contribution of the D-D process, resulting in an apparent increase in the $\varphi_{S\to T}$ value. But the quantitative investigation given above, as well as the values of $k_8$ and $k_6$, completely reject this idea. Although the reason is still unknown, it seems worth metioning that Oster's value at $[D]_0=10^{-5}$ M agrees quite well with ours if one takes the dependence of $\varphi_{S\to T}$ on [D] into consideration. The value $\varphi_{S\to T}=0.032$ for the lowest concentration of dye is close to the value (0.023) that Parker obtained from the phosphorescence experiment using ethanol as solvent[7] and to our own value (0.046) using the same solvent. On the other hand, the value for EDTA (0.080) is about three times larger than the above value for ATU. Since the features of the reaction in the case of EDTA are rather simple, one is tempted to consider the value 0.080 more reliable. But this is not conclusive. The smaller value for ATU might be due to the fact that mere deactivation of $D^t$ is produced much more so by ATU than by EDTA. At present we have no information at all on how the two reducing agents attack $D^t$. Further experiments employing more suitable reducing agents will be necessary to solve this question and to obtain a more reliable $\varphi_{S\to T}$ value.

## Summary

Using ATU and EDTA as a reducing agent, an attempt was made to determine the transition probability of the singlet excited state to the triplet state. The values obtained are 0.032 for ATU and 0.080 for EDTA. The cause of this difference is not known at present.

Deactivation of the triplet state by a leuco dye as well as by the ground state dye was confirmed. In the case of ATU, it was established that a D-D mechanism operates when the concentration of ATU islow and the con centration of dye is high. This conclusion was supported by the fact that at a constant low concentration of ATU the $1/\Phi$—$[D]_0$ plot deviates from linearity, when the dye concentration becomes high.

*Department of Chemistry*
*Faculty of Science*
*Tohoku University*
*Katahira-cho, Sendai*

7) C. A. Parker and C. G. Hatchard, *Trans. Faraday Soc.*, 57, 1894 (1961).

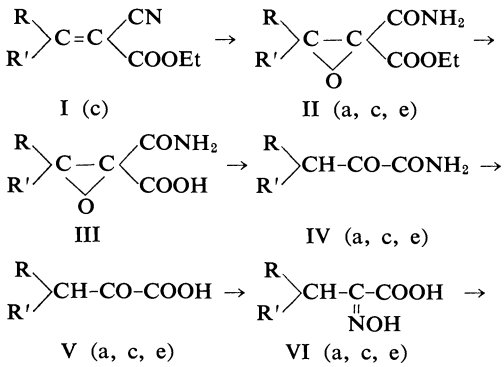
# NOTES

## The Synthesis of α-Amino Acids from Ethyl Alkylidenecyanoacetates

By Akio SAKURAI, Minoru IGARASHI and Hiroshi MIDORIKAWA

(Received June 24, 1964)

The present paper will describe the synthesis of new α-amino acids (2-amino-3, 6-dimethylheptanoic acid (VIIc) and 2-amino-3-isobutyl-5-methylhexanoic acid (VIIe)) through α-keto acids. The α-keto acids were prepared by a method virtually identical with that previously reported by two of the present authors.[1,2]



I (c) II (a, c, e) III IV (a, c, e) V (a, c, e) VI (a, c, e)

VII (a, b, c, d, e)

a $\begin{cases} R=CH_3 \\ R'=iso\text{-}C_3H_7 \end{cases}$ b $\begin{cases} R=CH_3 \\ R'=iso\text{-}C_4H_9 \end{cases}$

c $\begin{cases} R=CH_3 \\ R'=iso\text{-}C_5H_{11} \end{cases}$ d $\begin{cases} R=n\text{-}C_3H_7 \\ R'=n\text{-}C_3H_7 \end{cases}$

e $\begin{cases} R=iso\text{-}C_4H_9 \\ R'=iso\text{-}C_4H_9 \end{cases}$

The reaction sequence is shown in the Chart.

Ethyl alkylidenecyanoacetates (I) were obtained by the condensation of ketones with ethyl cyanoacetate according to the method of Cope and his co-workers.[3] The epoxidation of ethyl alkylidenecyanoacetates with hydrogen peroxide was carried out in the presence of sodium tungstate or trisodium phosphate. In the case of ethyl (1-isobutyl-3-methylbutylidene)cyanoacetate (Ie), the epoxidation could be affected only in the presence of trisodium phosphate. The resulting α-keto acids were converted into the corresponding oximes by the usual method.

The catalytic hydrogenation of the oximes was performed in warm ethanol in the presence of a Raney-nickel as a catalyst. The α-amino acids thus obtained showed a reddish-purple color with ninhydrin and formed the corresponding *N*-benzoyl derivatives.

3, 4-Dimethylnorvaline (VIIa),[4] 3, 5-dimethylnorleucine (VIIb)[4] and 3-*n*-propylnorleucine (VIId)[5] were also prepared by this method (see Tables I—IV).

### Experimental

**Ethyl Alkylidenecyanoacetates** were prepared, according to the method described in the literature[3], from ethyl cyanoacetate and ketones. The cyanoacetate described below is a new compound.

*Ethyl(1,4-dimethylpentylidene)cyanoacetate (Ic)*; b. p. 136—138°C/4 mmHg; yield, 76%.

TABLE I. PREPARATION OF EPOXY AMIDE (II) FROM ETHYL ALKYLIDENECYANOACETATE (I)

| Product | M.p., °C (B.p., °C/mmHg) | Yield % | Formula | Anal., % Calcd. C | Calcd. H | Calcd. N | Found C | Found H | Found N |
|---|---|---|---|---|---|---|---|---|---|
| IIa | 105 | 71 | $C_{10}H_{17}O_4N$ | 55.81 | 7.91 | 6.51 | 55.89 | 7.81 | 6.49 |
| IIc | (186—188/5) | 78 | $C_{12}H_{21}O_4N$ | 59.26 | 8.64 | 5.76 | 58.91 | 8.68 | 5.81 |
| IIe | 97 | 79 | $C_{14}H_{25}O_4N$ | 61.99 | 9.22 | 5.16 | 62.11 | 9.06 | 5.23 |

1) M. Igarashi and H. Midorikawa, This Bulletin, **34**, 1543 (1961).
2) M. Igarashi and H. Midorikawa, *J. Org. Chem.*, **28**, 3088 (1963).
3) A. C. Cope, C. M. Hofmann, C. Wyckoff and E. Hardenbergh, *J. Am. Chem. Soc.*, **63**, 3452 (1941).
4) P. E. Gagnon, P. A. Boivin and H. M. Craig, *Can. J. Chem.*, **29**, 70 (1951).
5) B. J. Meakin, F. R. Mumford and E. R. Ward, *J. Pharm. Pharmacol.*, **12**, 400 (1960).

Table II. Preparation of α-keto amide (IV) from II

| Product | M.p., °C | Yield % | Formula | Anal., % Calcd. C | H | N | Found C | H | N |
|---|---|---|---|---|---|---|---|---|---|
| IVa | 78 | 68 | $C_7H_{13}O_2N$ | 58.74 | 9.09 | 9.79 | 59.21 | 8.92 | 9.73 |
| IVc | 72 | 64 | $C_9H_{17}O_2N$ | 63.15 | 9.94 | 8.19 | 62.97 | 9.71 | 8.07 |
| IVe | 52 | 74 | $C_{11}H_{21}O_2N$ | 66.29 | 10.62 | 7.02 | 65.98 | 10.50 | 6.96 |

Table III. Preparation of α-keto acid (V) and oxime (VI)

| Product | M.p., °C (B.p., °C/mmHg) | Yield % | Formula | Anal., % Calcd. C | H | N | Found C | H | N |
|---|---|---|---|---|---|---|---|---|---|
| Va | 43 (75/5) | 73 | $C_7H_{12}O_3$ | 58.33 | 8.33 | | 58.51 | 8.61 | |
| VIa | 141 (decomp.) | 75 | $C_7H_{13}O_3N$ | 52.83 | 8.18 | 8.80 | 53.08 | 8.16 | 8.73 |
| Vc | (102—104/4) | 85 | $C_9H_{16}O_3$ | 62.79 | 9.30 | | 61.84 | 9.51 | |
| VIc | 103 (decomp.) | 73 | $C_9H_{17}O_3N$ | 57.75 | 9.09 | 7.49 | 57.90 | 8.95 | 7.45 |
| Ve[a] | (108—111/5) | 80 | $C_{11}H_{20}O_3$ | 65.96 | 10.06 | | 65.49 | 10.04 | |
| VIe[b] | 112 (decomp.) | 78 | $C_{11}H_{21}O_3N$ | 61.40 | 9.77 | 6.51 | 61.45 | 9.64 | 6.67 |

a) Lit., b. p. 124—126°C/14 mmHg; G. Freylon, *Ann. Chim. Phys.*, **20**, 101 (1910).
b) Freylon[a] has reported m. p. 159—160°C for this compound.

Table IV. Preparation of α-amino acid (VII) from VI

| α-Amino acid | M.p., °C | Yield % | Formula | Anal., % Calcd. C | H | N | Found C | H | N |
|---|---|---|---|---|---|---|---|---|---|
| VIIa | 268 (decomp.) | 73 | $C_7H_{15}O_2N$ | 57.93 | 10.34 | 9.65 | 57.33 | 10.51 | 9.56 |
| Benzoyl deriv. | 124 | | $C_{14}H_{19}O_3N$ | | | 5.64 | | | 5.64 |
| VIIb[a] | 253 (decomp.) | 72 | $C_8H_{17}O_2N$ | 60.37 | 10.69 | 8.80 | 59.98 | 10.79 | 8.59 |
| Benzoyl deriv. | 177 | | $C_{15}H_{21}O_3N$ | | | 5.32 | | | 5.18 |
| VIIc | 242 (decomp.) | 63 | $C_9H_{19}O_2N$ | 62.43 | 10.98 | 8.09 | 61.94 | 11.01 | 7.96 |
| Benzoyl deriv. | 155 | | $C_{16}H_{23}O_3N$ | | | 5.05 | | | 5.42 |
| VIId[b] | 283[c] (decomp.) | 65 | $C_9H_{19}O_2N$ | 62.43 | 10.98 | 8.09 | 62.17 | 10.91 | 7.95 |
| Benzoyl deriv. | 137 | | $C_{16}H_{23}O_3N$ | | | 5.05 | | | 5.14 |
| VIIe | 257 (decomp.) | 70 | $C_{11}H_{23}O_2N$ | 65.67 | 11.44 | 6.96 | 64.96 | 11.42 | 6.62 |
| Benzoyl deriv. | 151 | | $C_{18}H_{27}O_3N$ | | | 4.59 | | | 4.59 |

a) From 2,4-dimethyl-1-oxohexanoic acid oxime[1,2]
b) From dipropylpyruvic acid oxime[1,2]
c) Lit., m. p. 248—252; Ref. 5

Found: C, 68.66; H, 9.12; N, 6.84. Calcd. for $C_{12}H_{19}O_2N$: C, 68.90; H, 9.09; N, 6.70%.

**The Epoxidation of Ethyl Alkylidenecyanoacetates.** — To a mixed solution of I (0.1 mol.), ethanol (200 g.) and 30% hydrogen peroxide (200 g.), sodium tungstate dihydrate (0.02 mol.) was added. The mixture was then heated on a steam bath for 1—4 hr. to afford II as colorless crystals or as a pale yellow oil.

**The Preparation of α-Keto Amides.**—To a solution of 10% alcoholic potash (50 g.), II (0.05 mol.) was added at room temperature. The resulting potassium salt of III was dissolved in water and then acidified with dilute hydrochloric acid to give III as colorless crystals. III (0.05 mol.) was dissolved in water (40 cc.) and heated for 20—40 min. After it had been cooled, α-keto amide was obtained as colorless crystals.

**The Preparation of α-Keto Acids.**—A mixture of IV (0.03 mol.) and 10% hydrochloric acid (50 cc.) was heated on a water bath for about 3—4 hr. The product was obtained by fractionation.

**The Preparation of Oximes.**—To a mixture of sodium hydroxide (0.03 mol.) in 4 ml. of water and V (0.02 mol.), a solution of hydroxylamine hydrochloride (0.025 mol.) in a mixture of 4 ml. of water and 5 ml. of ethanol was added. The above mixture was then refluxed on a water bath for 1 hr. After cooling, the reaction mixture was acidified with dilute hydrochloric acid to give the product as colorless crystals.

**The Catalytic Hydrogenation of Oximes.** — A solution of VI (0.01 mol.) in ethanol (15 ml.) was shaken with hydrogen in the presence of a Raney nickel as a catalyst (prepared from 1 g. of nickel-aluminum alloy (50 : 50)) at 50°C under an ordinary pressure. The theoretical amount of hydrogen was absorbed within 5—7 hr. After the catalyst had been removed by filtration, the filtrate was concentrated to a small volume and dry ether was added. The reulting precipitate of α-amino acid was collected by filtration. Recrystallization from dilute ethanol gave colorless crystals.

The authors wish to express their hearty thanks to Dr. Taro Hayashi and Dr. Tatsuo Takeshima for their kindly advice. Thanks are also to Dr. Haruo Homma and his staff for microanalyses.

*The Institute of Physical and Chemical Research*
*Komagome, Bunkyo-ku, Tokyo*

# Chlorination by Sulfuryl Chloride. V.[1] Reaction with Benzyl Alcohols

By Mannosuke ARAI

(Received July 18, 1964)

McBee et al.[2] reported that the reaction of fluorine-containing alcohols with elemental chlorine in an inert solvent yielded the corresponding aldehydes or ketones as follows:

$$CF_3CF_2CF_2CH_2OH \xrightarrow[h\nu]{Cl_2} CF_3CF_2CF_2CHO + 2HCl$$

These reactions have been considered to be a radical-chain reaction involving the following steps:

$$Cl\cdot + RCH_2OH \longrightarrow R\dot{C}HOH + HCl$$

$$R\dot{C}HOH + Cl_2 \longrightarrow R\dot{C}H\boxed{O}\boxed{H} + Cl$$

$$\boxed{Cl}$$

$$\downarrow$$

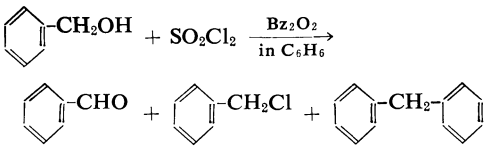
$$RCHO + HCl$$

Lecomte and Defour succeeded in obtaining aldehydes and ketones from primary and secondary aromatic alcohols with the hydroxy group in the $\alpha$-position of the aromatic nucleus, by means of the reaction with *N*-bromoacetoamide in the presence of pyridine.[3]

Similarly it may be expected that the reaction with sulfuryl chloride in the presence of a radical initiator will result in the formation of the corresponding aldehydes or ketones. On the other hand, it is known that sulfuryl chloride reacts with the hydroxyl group of aliphatic alcohols as a chlorosulfonating agent, the products being alkyl chlorosulfonate,[4a] dialkyl sulfate, alkylsulfuric acid and alkyl chloride.[4b] The present paper will study whether or not the reaction of benzyl alcohols with sulfuryl chloride in the presence of benzoyl peroxide yields the corresponding aldehyde.

The reaction of benzyl alcohol with an equivalent amount of sulfuryl chloride in benzene results in the formation of benzaldehyde

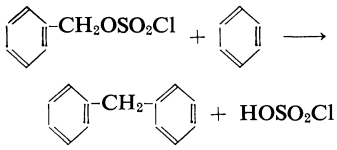
1) Part IV: M. Arai, This Bulletin, **38**, 252 (1965).
2) E. T. McBee, O. R. Pierce and W. F. Marzluff, *J. Am. Chem. Soc.*, **75**, 1609 (1953).
3) J. Lecomte and C. Defour, *Compt. rend.*, **234**, 1887 (1952).
4) a) P. Behrend, *Ber.*, **9**, 1334 (1876); W. W. Binkley and E. F. Degering, *J. Am. Chem. Soc.*, **60**, 2810 (1938); **61** 3250 (1939). b) R. Levaillent and L. Simon, *Compt. rend.*, **169**, 854 (1919).



(10%), diphenylmethane (23%) and benzyl chloride (15%).

However, the reaction in carbon tetrachloride gives only a chlorine-containing viscous substance. The reaction which is carried out without a solvent gives benzaldehyde and benzyl chloride.

The formation of diphenylmethane can be explained as resulting from the reaction of benzyl chlorosulfonate with benzene on the basis of the fact that it takes place only in benzene, and that the reaction between benzyl benzene sulfonate and benzene gives diphenylmethane in a good yield.[5]



These results suggest that sulfuryl chloride probably reacts as a homolytic chlorinating agent as well as a chlorosulfonating agent for benzyl alcohol, under these reaction conditions.

A similar reaction of anisalcohol in benzene gives anisaldehyde (60%) and a small amount of 3-chloroanisaldehyde. The total yield of aldehydes is 70%. Moreover, it might be noted that no product such as *p*-methoxybenzyl chloride was isolated from the reaction with the hydroxyl group. This striking effect of the substituent is interesting and makes this reaction suitable for the oxidation of various benzyl alcohols to the corresponding aldehydes.

Similar reactions with $\alpha$-phenylethyl alcohol, $\alpha$-phenylpropyl alcohol and benzhydrol give acetophenone, propiophenone and benzophenone in yields of 30%, 30% and 40% respectively.

## Experimental

**Materials and Reagents.**—Benzyl alcohol (reagent grade), anisalcohol (reagent grade), $\alpha$-phenylethyl alcohol (first grade) and $\alpha$-phenylpropyl alcohol (first grade) were purifide by vacuum distillation under a nitrogen atomosphere before use. Benzhydrol (reagent grade) was used after recrystallization.

Sulfuryl chloride (first grade) was distilled, stored in a bottle wrapped with aluminum foil, and kept in a desiccator.

5) Z. Foeldi, *Ber.*, **61**, 1609 (1928).

**The Reaction of Benzyl Alcohol and Sulfuryl Chloride.** — *1) Reaction in Benzene.* — 10.8 g. (0.1 mol.) of benzyl alcohol was dissolved in 20 ml. of benzene. After the air in the system had been replaced by dry nitrogen, 50 mg. of benzoyl peroxide was added to the solution. Then the system was heated at 70°C, and an equivalent amount of sulfuryl chloride (8.2 ml.) was dropped through the dropping funnel while the solution was being stirred. After the reaction mixture had stood about 4 hr., when the evolution of gas had ceased, it was cooled and washed with water. The benzene layer, dried with anhydrous sodium sulfate, was then distilled under reduced pressure, yielding 2.80 g. of liquid A (b. p. 45°C/5 mmHg), 3.80 g. of substance B (b. p. 103—105°C/5 mmHg) and a viscous substance which could not be distilled.

The treatment of A with 2,4-dinitrophenylhydrazine sulfate gave a reddish-orange crystalline substance m. p. 237°C, which was identified as benzaldehyde 2,4-dinitrophenylhydrazone by a mixed-melting point test. The yield of benzaldehyde as 2,4-dinitrophenylhydrazone was 10%. The residue of A, from which benzaldehyde had been removed, gave benzyl chloride (yield, 15%); it was identified by the following experiments: benzoic acid formed by oxidation with potassium permanganate, and the reaction with $\beta$-naphtol in the presence of sodium hydroxide in ethanol, yielded a crystalline substance which was further converted into a yellow crystalline when treated with picric acid. The yellow crystalline substance, m. p. 123°C, was identified as the picrate of $\beta$-naphthol benzyl ether by a mixed-melting point test. As for B, it was crystallized out on cooling, its melting point being 26°C. The ultraviolet absorption spectrum and the infrared absorption spectrum indicate that B is diphenyl methane.

Found: C, 92.36; H, 7.25. Calcd. for $C_{13}H_{12}$: C, 92.81; H, 7.19%.

*2) Reaction without the Solvent.*—The same reaction was carried out in the absence of the solvent, using 10.8 g. of benzyl alcohol and 8.2 ml. of sulfuryl chloride. By distillation under reduced pressure, 3.60 g. of a liquid (b. p. 45°C/5 mmHg) was isolated from the remaining viscous substance. This liquid was identified as a mixture of benzaldehyde and benzyl chloride by the same procedure as that performed in 1). The yields were 10% and 20% respectively.

*3) Reaction in Carbon Tetrachloride.* — The same reaction was also carried out in carbon tetrachloride (20 ml.). All attempts to isolate the reaction mixture under reduced pressure failed. Only a dark colored substance was obtained in this procedure, a substance which could not be further purified.

**Reaction with Anisalcohol.**—In an atmosphere of nitrogen, 6.9 g. (0.05 mol.) of anisalcohol, dissolved in 10 ml. of benzene, was treated with 30 mg. of benzoyl peroxide and 4.1 ml. (0.05 mol.) of sulfuryl chloride at 70°C. After the termination of the reaction, the reaction mixture was distilled under reduced pressure, 4.10 g. of substance A (b. p. 86—88°C/3 mmHg) and 0.95 g. of B (b. p. 101—104°C/3 mmHg) being thus obtained. A was identified as anisaldehyde-2,4-dinitrophenylhydrazone.

Found: N, 17.90. Calcd. for $C_{14}H_{12}O_5N_4$: N, 17.72%.

B was crystallized out on cooling; recrystallization from ligroin gave needles, m. p. 52°C. The infrared spectrum shows a strong absorption at 1690 $cm^{-1}$ ($\nu_{C=O}$), and moderate intensity bands at 815, 885 $cm^{-1}$ ($\delta_{CH}$), and at 640 $cm^{-1}$ attributable to the C-Cl bond, suggesting 3-chloroanisaldehyde. It was also identified as 2,4-dinitrophenylhydrazone.

Found: N, 16.21. Calcd. for $C_{14}H_{11}O_4N_4Cl$: 15.98%.

**Reaction with α-Phenylethyl Alcohol.**—2.44 g. of α-phenylethyl alcohol in 15 ml. of benzene was submitted to the reaction described above with an equivalent amount of sulfuryl chloride. After the evaporation of the solvent, treatment with 2,4-dinitrophenylhydrazine sulfate gave 1.72 g. of the 2,4-dinitrophenylhydrazone, m. p. 251—253°C.

**Reaction with α-Phenylpropyl Alcohol.** — In a way similar to that used with α-phenylethyl alcohol, 1.79 g. of the 2,4-dinitrophenylhydrazone, m. p. 190—191°C, was yielded by 2.72 g. of α-phenylpropyl alcohol.

**Reaction with Benzhydrol.**—In a way also similar to that used with α-phenylethyl alcohol, 2.45 g. of the 2,4-dinitrophenylhydrazone, m. p. 239—240°C, was yielded by 2.72 g. of benzhydrol.

The author wishes to express his gratitude to Professor Mamoru Yamaguchi of Tohoku University for his constant guidance in the course of this work.

*College of General Education*
*Tohoku University*
*Kawauchi, Sendai*

# Deviation from Lambert's Law in Measuring the Intensity of 3.5 $\mu$ Bands of Barium Stearate Films

By Shun-ichi IKAWA and Shiro MAEDA

(Received August 31, 1964)

In studying the absolute infrared intensity in pure liquids and solids, it sometimes occurs that a sample has to be chosen considerably less thick than the wavelength. In such a case, the effect of multiple reflections upon the observed absorption coefficients comes to be appreciable, disturbing an accurate application of Lambert's law. It can be inferred from a recent study[1] that the effect of multiple reflections gives rise to a variation in apparent peak intensity depending on the sample thicknesses, in some oscillatory way, and in general converging to a maximum at zero thickness.

In order to examine this phenomenon in practice, it seems appropriate to measure the intensity of a sufficiently intense and well-isolated absorption band in samples of various thicknesses. Films of barium stearate built by the successive deposition of monomolecular layers are fairly suitable for this purpose, as the film has very intense bands at 3.51 and 3.43 $\mu$ and can be easily built up to any thickness.

The films used in the present measurements were built, following Blodgett,[2] by the repeated "dip and lift" of quartz plates across the surface of water covered with a monomolecular layer. The layer was formed by dropping a 0.1% solution of stearic acid in benzene onto the clean surface of water containing minute barium chloride and potassium bicarbonate. It is known that the monomolecular layer of barium stearate formed in this way has a thickness of 24.4Å and contains a molecule in each 20Å$^2$ when deposited on a substrate.[2]

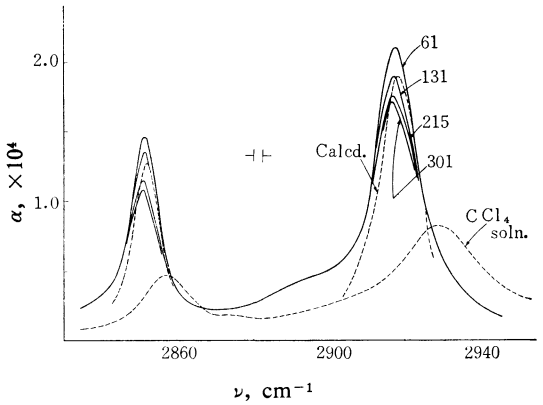



Fig. 1. 61—301: Number of monomolecular layers contained in each film.

The spectra of marked bands were obtained using a Perkin-Elmer model 112 spectrometer

1) S. Maeda, G. Thyagarajan and P. N. Schatz, *J. Chem. Phys.*, **39**, 3474 (1963); S. Maeda, *Bull. Tokyo Inst. Tech.*, **59**, 17 (1964).

2) K. Blodgett, *J. Am. Chem. Soc.*, **57**, 1007 (1935); T. Tachibana, "Jikken Kagaku Kôza," Vol. 7, Maruzen, Tokyo (1950), p. 296.

equipped with a LiF prism; they are given in the figure by apparent absorption coefficients, $\alpha_{app}=(1/d)\ln(I'_0/I)$, where $I'_0$ is the intensity of the light transmitted by the blank substrate. "Apparent" implies the conventional use of Lambert's law without taking the multiple reflection effect into consideration. The upper and lower limits of thickness were chosen so as to give the transmittance at the peak with a reasonable accuracy. A steady increase in apparent peak intensity with diminishing thickness can be seen, indicating the characteristic features of the multiple reflection effect in extremely thin samples.

For a thin sample in which the thickness, $d$, is sufficiently smaller than the wavelength, $\lambda$, the following expression is valid for the reciprocal of transmittance:

$$I'_0/I=1+(2\varepsilon_2/1+\phi)(2\pi d/\lambda)+[1/(1+\phi)^2][(\varepsilon_1-1)(\varepsilon_1-\phi^2)+\varepsilon_2{}^2]\times(2\pi d/\lambda)^2-[2\varepsilon_2(\varepsilon_1-\phi)/3(1+\phi)]\times(2\pi d/\lambda)^3+\cdots\cdots$$

where $\varepsilon_1$ and $\varepsilon_2$ denote the real and the imaginary parts of the dielectric constant of the sample, and $\phi$ is the refractive index of the substrate.[1] For the thinnest film, with 61 layers, the expansion parameter $(2\pi d/\lambda)$ is small enough, so that the fourth and further terms on the right-hand side may be discarded with very little error. Then, if one assumes the function of a damped oscillator model for each band, it is possible to estimate the true absorption coefficients in a good approximation, which is given by a broken-line curve in the figure.

For the sake of comparison, the absorption curve of stearic acid in a dilute carbon tetrachloride solution is given for the same region. It is strikingly different from the "built up" film, while the distinction between the acid and the barium salt is expected to be very little for the spectral features in this region. Such a marked change in an absorption intensity due to a change of state is not unusal, but it has not yet been statisfactorily explained in most cases.

We would like to thank Professor Kunio Kozima, who suggested this work to us, and also Professor Taro Tachibana for his valuable advice on building up the films. Our thanks are also due to Dr. Yoshiko Takeoka for her kind assistance.

*The Research Laboratory of Resources Utilization*
*Tokyo Institute of Technology*
*Ookayama, Tokyo*

# Antioxidant Activity of Glycerylphosphatides* and Their Hydrolysis Products. IV. Reaction of Methyl Oleate Hydroperoxide Concentrate with Phosphoric Acid and β-Glycerylphosphoric Acid and the Isolation of a Phosphorus-containing, Oil-soluble Product from Autoxidized Methyl Oleate in the Presence of β-Glycerylphosphoric Acid

By Chieko URAKAMI, Yoshiko GOTO** and Haru KAMEYAMA**

(Received September 7, 1964)

Phosphate ester as well as phosphatides have tentatively been classified as decomposers of peroxides,[1] but no significant evidence has been presented. Therefore, such a generalization must be subjected to further tests. In connection with this, it has been sugested that a secondary phosphorus-containing, oil-soluble product formed as the result of a reaction of glycerylphosphoric acid with methyl oleate or its oxidation products in the early stages of autoxidatation might be responsible for its antioxidant activity.[2,3]

It was observed that β-glycerylphosphoric acid did not decompose the methyl oleate hydroperoxide concentrate, much as is shown

* The "lecithin" used in the previous papers[2,3] will be changed to this term in future publications.

** Present address: Osaka Furitsu Daigaku, Department of Agricultural Chemistry.

1) K. U. Ingold, *Chem. Revs.*, **61**, 574, 581 (1961).

2) C. Urakami, Y. Kakutani and H. Okura, This Bulletin, **29**, 921 (1956).

3) C. Urakami, H. Kameyama and M. Okada, ibid., **32**, 36 (1959).

Table I. Analysis of the ether-soluble fraction of the reaction products of the methyl oleate hydroperoxide concentrate with phosphoric acid and with β-glycerylphosphoric acid at 45°C in a nitrogen stream

| Reactants | Mol. ratio[a] | Time, hr. | Peroxide value[b] | Iodine value | $R_f$[c] | Phosphorus[d] |
|---|---|---|---|---|---|---|
| P. C. | | 0 | 261 | 61.2 | | |
| P. C. : $H_3PO_4$ | 1 : 1 | 1/3 | 21.8 | 36.2 | 0—0.51 | + |
| | | | | | 0.92 | + |
| P. C. : β-GP[e] | 1 : 0.018 | 1/2 | 234 | 59.8 | | |
| P. C. : β-GP[e] | 1 : 1 | 2 | 245 | 66.5 | 1.00 | − |
| P. C. : β-GP[e] | 1 : 0.7 | 5 | 239 | 67.1 | 1.00 | − |

P. C. stands for the methyl oleate hydroperoxide concentrate[4] and β-GP for β-glycerylphosphoric acid.[2]

a) Based on hydroperoxide oxygen.
b) Expressed in mmol./100 g.
c) Developed with *n*-propanol - water (8 : 1, v/v) and sprayed with bromothymol blue.
d) The sections corresponding to the $R_f$ values were incinerated for phosphorus determination along with a blank, another section of the same size: + indicates the presence of a significant amount, and −, the absence of phosphorus.
e) Glass beads and *n*-heptane were added, and the entire contents were mixed a motor-driven stirrer. For analysis, each of the reaction mixtures was diluted with dry ether, washed with water, dried over anhydrous sodium sulfate, and concentrated.

Table II. The $R_f$ values of the isolated compound and its decomposition and hydrolysis products

| Sample | Days[a] | System | $R_f$ | | | |
|---|---|---|---|---|---|---|
| | | | P | Rh-6G | $(AcO)_2Hg$ | Fuchsine |
| I | 11 | I | 0.49 | 0.51 | 0 | |
| II | 26 | I | 0.48 | −(?) | | |
| III | 45 | I | 0.80 | | | |
| | | | 0.06 | | | |
| IV | 46 | II | 0.92[b] | | 0.86 | 0.91 |
| | | | 0.26[c] | | — | — |
| V=IV+β-GP | 47 | II | 0.91 | | | 0.90 |
| | | | 0.08 | | | — |
| VI=Hyd. prod. of IV | 47 | II | — | | 0.91 | 0.91 |
| | | | 0.26[b] | | — | 0.21 |
| | | | 0.05[c] | | — | — |
| β-GP | | II | 0.07 | | — | |
| $H_3PO_4$ | | II | 0.19 | | | |

System I: Toyo No. 51 paper impregnated with silicic acid with a solvent system of diisobutyl ketone - acetic acid - water (40 : 25 : 5 by vol.). System II: Toyo No. 50 paper with a solvent system of *n*-propanol - acetic acid - water (8 : 1 : 1 by vol.). The $R_f$ values are an average of several runs. β-GP stands for β-glycerylphosphoric acid. The − sign indicates a negative reaction with the reagent for the spot on the corresponding row. (?) For some unknown reason the reaction was negative; it should have been positive, as for sample I. a) A number of days elapsed since the end of autoxidation. The relative intensity of the color of the spots was b>c.

in Table I, in comparison with the hydroperoxide decomposing property of orthophosphoric acid, but it gave rise to a very unstable phosphorus-containing, oil-soluble compound in the early stages of the autoxidation of the methyl oleate containing it. The compound, initially isolated, sample II in Table II, was found to be very readily soluble in a mixture of chloroform and methanol and carbon tetrachloride, somewhat soluble in chloroform and methanol, slightly soluble in acetone, and insoluble in isopropanol. Its ultraviolet spectrum showed a $\lambda_{max\ 1}$ at a wavelength shorter than 240 mμ and a $\lambda_{max\ 2}$ at 276 mμ, with a shoulder at 282 mμ. The infrared absorption bands that appear to be characteristic of the initially-isolated compound (sample II) are as follows: 1730 $cm^{-1}$ for a carbonyl group, the doublet at 1575 and 1595 $cm^{-1}$ for a conjugated double-bond system, 1385 $cm^{-1}$ for the methyl group (presumably the terminal group of a long alkyl

4) J. E. Coleman, H. B. Knight and D. Swern, *J. Am. Chem. Soc.*, 74, 4886 (1952).

chain), and 1285 $cm^{-1}$ for the P=O stretching vibration. All these bands are absent, however, in the spectrum of β-glycerylphosphoric acid. The presence of the P-O-C(alkyl) in the molecule is indicated by the absorption bands at 1170, 1190, and possibly 1040 $cm^{-1}$, and at others in the lower frequencies.

## Experimental

**Isolation of a Phosphorus-containing, Oil-soluble Compound.** — In a reaction tube were placed 16.493 g. of methyl oleate (b. p. 152—156°C/0.9 mmHg., iodine number 89.3, and saponification number 185.3) and an ethanol solution containing 5.207 mg. of β-glycerylphosphoric acid (0.03% in the methyl oleate); the solvent was removed at a temperature not exceeding 50°C. The tube was placed in a bath maintained at 50°C, and the mixture was autoxidized for 192 hr. by passing dry air through a sintered glass gas bubbler; its peroxide value was 50±2.4. After adding a small amount of a 0.05% ethanol solution of hydroquinone, the reaction mixture was dissolved in 200 ml. of freshly-distilled dry ether, and the solution washed successively with 50, 25, and 10 ml. of distilled water to remove unreacted water-soluble β-glycerylphosphoric acid; 1% of the initially-added phosphorus was removed in the combined water washings. After drying the ether solution over anhydrous sodium sulfate, it was diluted further with an equal volume of dry ether and the solution applied to a column (10 mm.×100 mm.) packed with 5.5 g. of a mixture of silicic acid and filter aid (2 : 1 by wt.), followed by elution with fresh dry ether; 10% of the initially added phosphorus was found in the eluate. The adsorbent in the upper half of the column was extracted three times with chloroform-methanol (4 : 1 by vol.). The combined extract (sample I in Table II) was concentrated under mild conditions, and the residue treated with dry carbon tetrachloride. An insoluble fraction was found to be a colored wax and to contain phosphorus. The carbon tetrachloride-soluble fraction was concentrated in the usual manner, and the colored oil thus obtained (sample II in Table II) was subjected to various analyses. A small amount of this oil was hydrolyzed with 5% solution of ethanolic sodium hydroxide, and the reaction mixture deionized with IRC-50 ($H^+$) (sample VI in Table II).

*Faculty of the Science of Living*
*Osaka City University*
*Nishi-ku, Osaka*

# Intramolecular Hydrogen Bonds. II.[1] On the Configuration of Isomeric Methyl 9, 10-Dihydroxyoctadecanoates

By Nobuo Mori, Satoshi Ōmura* and Yojiro Tsuzuki

(Received September 21, 1964)

A high-melting isomer (I: m. p. 131°C) of two 9, 10-dihydroxyoctadecanoic acids was obtained by the oxidation of oleic acid with permanganate and another isomer (II: m. p. 95°C) was obtained similarly from elaidic acid. On the basis of the cis addition of the two hydroxyl groups, the former was assigned to the erythro form and the latter to the threo form.[2]

Further evidence for the configuration was the difference in the rates of the oxidation between the acids with lead tetraacetate[3] and with periodic acid[4], although the relative rates (II/I) were not so high as those of isomeric cycloalkane-1, 2-diols. Also, Swern and his co-workers[5] deduced the above configuration from the strikingly high ability of compound II to form a complex with urea and boric acid.

The present paper provides other support for the assignments through the infrared measurements of their methyl esters III and IV in the O-H stretching region of 3400—3700 $cm^{-1}$, together with those of ethyl $\omega$-hydroxy-pelargonate V and -caprinate VI for the purpose of comparison. The measurements were carried out with a solution in 0.004 mol./l. in carbon tetrachloride at 25°C with a Perkin-Elmer 21 spectrophotometer equipped with a lithium fluoride prism and with a cell 3 cm. long; the observed frequencies

* Present address: The Kitasato Institute, Minato-ku, Tokyo.

1) Part I: N. Mori, S. Ōmura, O, Yamamoto, T. Suzuki and Y. Tsuzuki, This Bulletin, 36, 1401 (1963).

2) D. Swern, *J. Am. Chem. Soc.*, 70, 1235 (1948), and previous papers, as well as references therein cited.

3) T. P. Hilditch and H. Jasperson, *Nature*, 147, 327 (1941).

4) H. W. Wittcoff, O. A. Moe and M. H. Iwen, *J. Am. Chem. Soc.*, 70, 742 (1948).

5) D. Swern, L. P. Witnauer and H. B. Knight, ibid., 74, 1655 (1952).

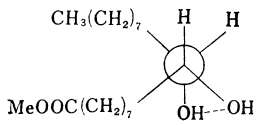
Table I. Data of Hydroxyl bands

| | Compound | M. p., °C (B. p., °C/mmHg) | $\nu_{OH}$, $cm^{-1}$ Free (ε)* | Bonded (ε)* | Lit. |
|---|---|---|---|---|---|
| III | $CH_3(CH_2)_7CH(OH)-CH(OH)(CH_2)_7COOMe$ | 105[8] | 3636 (50) | 3593 (48) | |
| IV | $CH_3(CH_2)_7CH(OH)-CH(OH)(CH_2)_7COOMe$ | 69[8] | 3634 (54) | 3584 (61) | |
| V | $HO(CH_2)_8COOEt$ | (131—132/2)[9] | 3638 (29) | | |
| VI | $HO(CH_2)_9COOEt$ | (146/3)[10] | 3641 (30) | | |
| VII | $CH_3(CH_2)_8CH(OH)(CH_2)_7COOMe$ | | 3629 | | 11 |
| VIII | $C_5H_{11}CH(OH)-CHC_5H_{11}$ (meso) OH | | 3636 | 3593 | 6 |
| IX | $C_5H_{11}CH(OH)-CHC_5H_{11}$ (rac.) OH | | 3636 | 3583 | 6 |

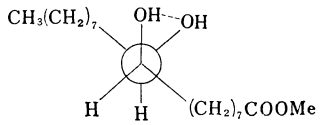
* $\varepsilon = 1/cl \cdot \log I_0/I$ for the apparent OH band.

were calibrated against that of atmospheric vapor. At that concentration, all of the esters were free from intermolecular hydrogen bonding, and only a very weak broad band was observed at 3462 or 3466 $cm^{-1}$; this may be the first overtone of a carbonyl group.

The hydroxyl band of the methyl esters III and IV was a doublet with almost the same intensity, but compounds V and VI had only one sharp band in the region of the free primary alcoholic hydroxyl group. Thus, the esters III and IV had no intramolecular hydrogen bond between the hydroxyl and the methoxycarbonyl group; substantially all of their molecules exist in the conformation containing an intramolecular hydrogen bond between the two hydroxyl groups:




(III)




(IV)

In general, threo 1,2-diols (racemic form) form a stronger hydrogen bond between the hydroxyl groups than do the corresponding erythro diols (meso form)[6,7] because of the conformational preference of the former for intramolecular hydrogen bonding,[6] as is seen in the case of the dodecane-6,7-diols, VIII and IX, in Table I. As the table shows, the separation ($\Delta\nu$) between the two peaks is 43 $cm^{-1}$ for compound III and 50 $cm^{-1}$ for compound IV; this supports the above assignment of the configuration for compounds I and II.

The authors thank Mr. Teruo Kajiura and Mr. Tadao Tamura, Government Chemical Industrial Research Institute Tokyo, for infrared measurements.

*Department of Chemistry*
*Tokyo College of Science*
*Kagurazaka, Tokyo (N.M. & Y.T.)*
*The University of Yamanashi*
*Kōfu-shi, Yamanashi (S.Ō.)*

6) L. P. Kuhn, *J. Am. Chem. Soc.*, **80**, 5950 (1958).
7) G. Chiurdoglu, R. de Groote, W. Masschelein and M. H. van Risseghem, *Bull. soc. chim. Belges*, **70**, 342 (1961).
8) D. Swern and E. F. Jordan, *J. Am. Chem. Soc.*, **67**, 902 (1945). M. p. 105 and 71°C, obtained from compounds I and II, respectively.
9) P. Chuit and J. Hausser, *Helv. Chim. Acta*, **12**, 466 (1929). Me ester: b. p. 147—150°C/13 mmHg.
10) A. Grün and T. Wirth, *Ber.*, **55**, 2206 (1922). Me ester: b. p. 154°C/7 mmHg.
11) J. Grundy and L. J. Morris, *Spectrochim. Acta*, **20**, 695 (1964).

# The Interactions of Some Cations with Deoxyribonucleic Acid Observed by the Use of Toluidine Blue as an Indicator

By Yukiko HUSE, Komei MIYAKI and Masamichi TSUBOI

(Received September 24, 1964)

There have been several studies of the metachromasy of basic dyes induced by deoxyribonucleic acid (DNA)[1,2] and of the effects of inorganic or organic cations on the metachromasy.[3-5]

We have recently observed that toluidine blue shows a marked metachromasy with DNA in solution and that this metachromasy can often be hindered by adding another substance, one which interacts with DNA, to the solution. The degree of hindrance is found to depend upon how strongly the added substance interacts with DNA. This finding suggests a simple and easy method of the semiquantitative analysis of interactions between DNA and other substances of a certain type.

As may be seen in Fig. 1, toluidine blue ($5\times10^{-5}$ mol./l.) in an aqueous soulution at pH 6 shows two absorption peaks, at 600 and 630 m$\mu$ (curve a). When DNA (from salmon sperm) is added, both of these peaks disappear, and a broad and lower peak appears at 570 m$\mu$ (curve b). The maximum metachromatic change is observed with the DNA concentration of $2.5\times10^{-5}$ mol./l. (in *P*), i.e., with the concentration ratio [DNA]/[T. B.]=0.5. When poly-L-lysine is added to the solution, the original features of the toluidine blue spectrum is restored (curves c—e) to an extent depending upon the amount of poly-L-lysine added.

It is very probable that the metachromasy of toluidine blue occurs through its binding to the phosphate group with a negative charge of DNA. When poly-L-lysine is added to the solution, it will be more strongly bound by the DNA molecule through the $N^+$-H$\cdots$$^-$O–P hydrogen bond and polycationic effect than will the toluidine blue molecule, and the latter will be released from DNA. This explains the fact that its original color is restored. It is interesting that the addition of $2.5\times10^{-5}$ mol./l. (in a lysine residue) poly-L-lysine causes a nearly complete restoration of the original spectrum of toluidine blue, because this amount is equal to that of DNA in the solution. This fact suggests that every $NH_3^+$ group of poly-L-lysine added is bound by a $PO_2^-$ group of DNA.

The above simple explanation of what we have observed needs a provisory statement. Toluidine blue seems to interact slightly with poly-L-lysine. This is shown by the fact that the further addition of poly-L-lysine causes a spectrum of toluidine blue somewhat different from the original spectrum (curve a of Fig. 1.). It is quite similar in general features to the original one, but it shows a higher intensity at both peaks, 600 and 630 m$\mu$ (curves f—i in Fig. 1). The spectral change due to the slight interaction of toluidine blue and poly-L-lysine may be more clearly seen by comparing curves a and j in Fig. 1, where curve j is obtained with a mixed solution of toluidine blue and poly-L-lysine without DNA. The fact that no

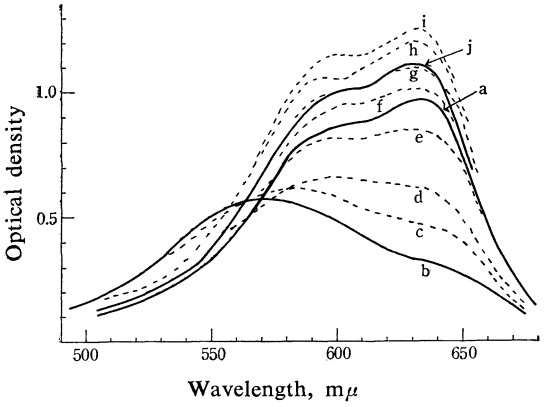



Fig. 1. Absorption curves of toluidine blue ($5\times10^{-5}$ mol./l.) in the following solvents.

a) Distilled water at pH 6
b) $2.5\times10^{-5}$ mol./l. Na-DNA aq. soln.
c) Soln. b plus $8.0\times10^{-6}$ mol./l. poly-L-lysine
d) Soln. b plus $1.6\times10^{-5}$ mol./l. poly-L-lysine
e) Soln. b plus $2.4\times10^{-5}$ mol./l. poly-L-lysine
f) Soln. b plus $3.2\times10^{-5}$ mol./l. poly-L-lysine
g) Soln. b plus $4.0\times10^{-5}$ mol./l. poly-L-lysine
h) Soln. b plus $8.0\times10^{-5}$ mol./l. poly-L-lysine
i) Soln. b plus $1.6\times10^{-4}$ mol./l. poly-L-lysine
j) $8.0\times10^{-5}$ mol./l. poly-L-lysine aq. soln.

1) L. Michaelis and S. Granick, *J. Am. Chem. Soc.*, **67**, 1212 (1945).
2) N. Weissman, W. H. Carnes, P. S. Rubin and J. Fisher, ibid., **74**, 1423 (1952).
3) L. Cavalieri, A. Angelos and M. E. Balis, ibid., **73**, 4902 (1951).
4) A. R. Peacocke and J. N. H. Skerrett, *Trans. Faraday Soc.*, **52**, 261 (1956).
5) P. D. Lawley, *Biochim. Biophys. Acta*, **22**, 451 (1956).

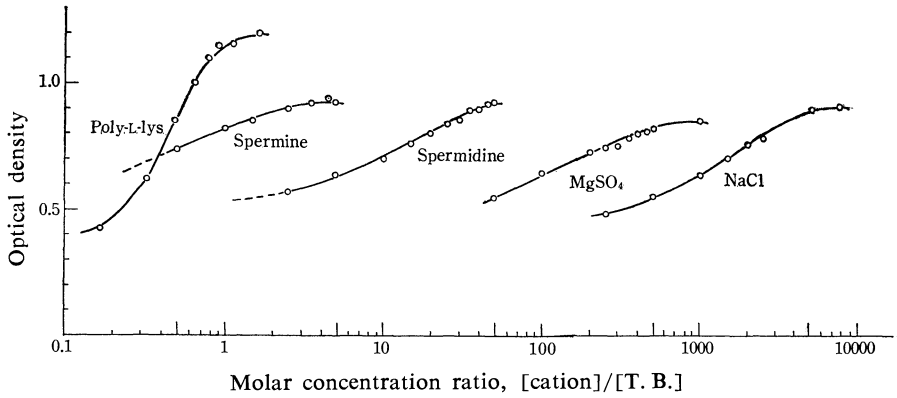



Fig. 2. Optical density of toluidine blue (at 630 mμ or at 600 mμ) in an aqueous solution containing toluidine blue $5\times10^{-5}$ mol./l., Na-DNA $2.5\times10^{-5}$ mol./l. and one of the substances indicated, plotted against the molar concentration ratio [added substance]/[toluidine blue]. The wavelength at which the optical density was observed is 630 mμ for poly-L-lysine, spermine, and spermidine, and is 600 mμ for $MgSO_4$ and NaCl.

distinct isosbestic point is observed in the series of the spectra given in Fig. 1 may be related to this weak interaction between toluidine blue and poly-L-lysine.

We have made similar experiments by adding spermine, spermidine, magnesium sulfate, and sodium chloride to the toluidine blue-plus-DNA system. In every case, a hindrance of the metachromasy of toluidine blue takes place at a certain concentration of the added substance. By adding a sufficient amount, a spectrum is obtained which is very similar to the spectrum of the solution of toluidine blue only. In the case of magnesium sulfate or sodium chloride, however, a slight but appreciable diminution of optical density at 630 mμ compared with the original spectrum is observed; therefore, in these cases, it would be preferable to observe and evaluate the optical densities at 600 mμ instead of at 630 mμ. Thus, the optical density at 630 mμ (or 600 mμ) gives a measure of how much toluidine blue is released from DNA and, therefore, how much the added substance is bound by DNA. This is plotted against the molar concentration of the added substance in Fig. 2. It may readily be seen that spermine is bound by DNA much more strongly than spermidine, and that $Mg^{2+}$ is bound by DNA much more strongly than $Na^+$.

The Na-DNA used in the present experiment was obtained from the California Corporation for Biochemical Research, Los Angeles, and the toluidine blue, from the Merck Co., Inc. The poly-L-lysine hydrobromide, with a molecular weight of 60000, was obtained from Pilot Chemicals, Inc. The spermine tetrahydrochloride was from the Sigma Chemical Company, while the spermidine trihydrochloride was obtained from the Nutritional Biochemicals Corporation.

This work was partly supported by a grant from the U. S. Public Health Service, No. GM-10024-1, and partly by agrant from the Ministry of Education of Japan.

*The Institute of Food Microbiology*
*Chiba University*
*Narashino, Chiba (Y. H. & K. M.)*

*Faculty of Pharmaceutical Sciences*
*The University of Tokyo*
*Hongo, Tokyo (M. T.)*

# PMR Studies of Bromothiophenes*

By Kensuke TAKAHASHI, Tyo SONE, Yasuo MATSUKI and Genjiro HAZATO

(Received October 6, 1964)

At the beginning of the study of thiophene derivatives by PMR, 2, 5- and 3, 4-dibromothiophenes were measured in order to estimate the chemical shift between $\alpha$- and $\beta$-hydrogens in thiophene.[1,2] In this note we will present the experimental results for all bromothiophenes. Tables I and II list the results for the chemical shifts and the coupling constants in cyclohexane solutions at 60 Mc./sec. Chemical shifts for all protons of bromothiophenes occur at a higher applied magnetic field than do those of thiophene itself. Table I shows that the chemical shifts of $\beta$-hydrogens fall into the 5.26—5.43 p. p. m. range with reference to cyclohexane, whereas those of $\alpha$-hydrogens fall at 5.54—5.72 p. p. m., so that the $\alpha$- and $\beta$-hydrogens in bromothiophenes can readily be distinguished from each other by measuring the chemical shifs. The results obtained here are quite useful from the standpoint of the identification of bromothiophenes. The substitution effect of bromine has been discussed in benzene derivatives by many authors and summarized in Smith's paper.[3] Diehl expressed the effect of the X substituent as $S_{o,x}$ or $S_{m,x}$ and stated that the substitution effects in *p*- and *m*-disubstituted benzenes are additive.[4] The $S_o$, $S_m$ and $S_p$ values estimated by Diehl for bromine in some benzene derivatives are 0.22, $-0.11$ and $-0.06$ p. p. m. In thiophene, those effects must be expressed as $S(\mathrm{X})_{ab}$, where *a* and *b* are the positions of the substituent and of the hydrogen in question respectively. By comparing the chemical shifts of the monosubstituted thiophenes with those of the unsubstituted one, $S_{23}$, $S_{24}$, $S_{25}$, $S_{32}$, $S_{34}$ and $S_{35}$ for bromine are estimated as $-0.07$, $-0.28$, $-0.13_5$, $-0.12_5$, $-0.09$ and $-0.11$ p. p. m. respectively, in which the negative values of $S(\mathrm{Br})$ indicate the displacement toward a higher applied magnetic field. The most pronounced effect appears in 4-hydrogen of 2-bromothiophene as about a shift of $-0.28$ p. p. m. The additivity of the substitution effect is also roughly valid in the cases of 2, 4- and 2, 5-dibromothiophenes. In other cases of di- and tribromothiophenes, however, the additional effects on the chemical shift of the proton coming from the interaction between the substituents must be considered.

Now if we only consider the interaction between the *ortho*-positioned substituents, the so-called *ortho*-effect, this additional effect may be expressed as follows: $S(\mathrm{X,Y})_{abc}$, where *a*, *b* and c are the positions of the substituents X and Y and the hydrogen in question. From the shifts of 2, 3- and 3, 4-dibromothiophenes, we can estimate $S_{234}$, $S_{235}$ and $S_{342}$ for the effects of two ortho-positioned bromines, which are 0.16, 0.13 and 0.18 p. p. m. respectively. Using this additional effect, we can estimate the chemical shifts of 2, 3, 4- and 2, 3, 5-tribromothiophenes by additivity in agreement with the experimental values as follows:

$$\delta_5(2,3,4\text{-Br}_3) = 5.73_5 + S_{25} + S_{35} + S_{32} + S_{235} + S_{345}$$
$$= 5.67_5 \quad (\delta_{\mathrm{exp}} = 5.72)$$

$$\delta_4(2,3,5\text{-Br}_3) = 5.54 + S_{24} + S_{34} + S_{23} + S_{234}$$
$$= 5.26 \quad (\delta_{\mathrm{exp}} = 5.32)$$

The observed coupling constants between the ring protons in bromothiophenes have the usual magnitude[1,5] and the values for 3, 4- and 2, 5-dibromothiophenes have been observed in the spectra of the $^{13}$CH satellites in pure liquid.

Another fact of interest is the magnitude of $J(^{13}\mathrm{CH})$. $J(^{13}\mathrm{CH}_\alpha)$ is somewhat larger than $J(^{13}\mathrm{CH}_\beta)$ by about 15 c. p. s., as is shown in Table II. Many more experimental values are needed before we can discuss these results. However, it should be noted that this $J(^{13}\mathrm{CH})$ is concerned with the bond length and s-character of the C-H bond.[6] Therefore, it is assumed that the C-H$_\alpha$ bond has a somewhat larger s-character than the C-H$_\beta$ bond, and also that the latter is somewhat longer than the former in thiophene and its derivatives. Some results for thiophene and its derivatives have been reported by Goldstein and Reddy, and discussed in connection with the magnetic

* Presented partly at the Meeting of Tohoku District of the Chemical Society of Japan, Hirosaki, October, 1962.

1) S. Gronowitz and R. A. Hoffman, *Arkiv Kemi*, **13**, 279 (1958).

2) S. Fujiwara, S. Hayashi, M. Katayama, H. Shimizu and S. Nishimura, This Bulletin, **32**, 201 (1959).

3) G. W. Smith, *J. Mol. Spectr.*, **12**, 146 (1964).

4) P. Diehl, *Helv. Chim. Acta*, **44**, 829 (1961).

5) K. Takahashi, Y. Matsuki, T. Mashiko and G. Hazato, This Bulletin, **32**, 156 (1959).

6) N. Muller and D. E. Prichard, *J. Chem. Phys.*, **31**, 768, 1471 (1959).

TABLE I. CHEMICAL SHIFTS OF THE RING PROTONS IN BROMOTHIOPHENES, REFERRED TO CYCLOHEXANE IN p. p. m. AT 60 Mc./sec.

| Substituent | Concn. in $C_6H_{12}$ mol. % | Assignment | | | |
|---|---|---|---|---|---|
| | | 2-H | 3-H | 4-H | 5-H |
| —* | 0 | $5.73_5$ | 5.54 | 5.54 | $5.73_5$ |
| 2-Br* | 5 | — | 5.47 | 5.26 | 5.60 |
| 3-Br* | 14.5 | 5.61 | — | 5.45 | $5.62_5$ |
| 2,3-$Br_2$ | 7.9 | — | — | 5.33 | 5.62 |
| 2,4-$Br_2$ | 7.4 | — | 5.43 | — | 5.54 |
| 2,5-$Br_2$ | 7.9 | — | 5.26 | 5.26 | — |
| 3,4-$Br_2$ | 10.7 | 5.68 | — | — | 5.68 |
| 2,3,4-$Br_3$ | 4.4 | — | — | — | 5.72 |
| 2,3,5-$Br_3$ | 3.2 | — | — | 5.32 | — |

* K. Takahashi, Unpublished result.

TABLE II. COUPLING CONSTANTS IN BROMOTHIOPHENES IN c. p. s. AT 60 Mc./sec.*1

| Subsequent | $J_{23}$ | $J_{34}$ | $J_{25}$ | $J_{24}$ | $J_{^{13}CH_\alpha}$*2 | $J_{^{13}CH_\beta}$*2 |
|---|---|---|---|---|---|---|
| 2-Br*3 | 5.3 | 3.6 | — | $1.4_5$ | | |
| 3-Br*3 | $4.9_5$ | — | 3.2 | $1.2_5$ | | |
| 2,3-$Br_2$ | $5.7_5$ | — | — | — | $190._5$ | $176._5$ |
| 2,4-$Br_2$ | — | — | — | $1.6_5$ | 195 | $178._5$ |
| 2,5-$Br_2$ | — | 3.7*2 | — | — | — | $174._5$ |
| 3,4-$Br_2$ | — | — | $3.4_5$*2 | — | 194 | — |
| 2,3,4-$Br_3$ | — | — | — | — | $195._5$ | — |
| 2,3,5-$Br_3$ | — | — | — | — | — | 181 |

*1 The measured solutions are the same given in Table I.
*2 The measurement was made in pure liquid.
*3 K. Takahashi, Unpublished result.

anisotropy of the compounds.[7] The difference of about 15 c.p.s. measured in bromothiophenes corresponds to the difference in bond length of about 0.006 Å. The microwave analysis of thiophene suggests about the sameorder of difference in bond length between C-$H_\alpha$ and C-$H_\beta$.[8]

The solvent effects on the chemical shifts for ring protons were also observed. Three typical solvents were used. The measured samples are pure liquid containing 10 wt. % cyclohexane, a 10 wt. % solution in carbon tetrachloride containing 0.5 wt. % cyclohexane, and a 14 wt. % solution in acetone containing 14 wt. % cyclohexane. The results are summarized in Table III. The value in cyclohexane shown in Table I was used as a reference for each compound. The displacements of the chemical shifts in acetone are large and can be divided into two groups. One is that of $\beta$-hydrogen, which falls into the 0.27—0.40 p.p.m. range, while, the other is that of $\alpha$-hydrogen, which falls into the 0.55—0.67 p.p.m. range; the latter shows larger displacement than the former. However, the

TABLE III. DISPLACEMENTS OF THE RING PROTON RESONANCES WHEN THE SAMPLES ARE DILUTED WITH CYCLOHEXANE, CARBON TETRACHLORIDE AND ACETONE, IN p. p. m., REFERRED TO THE VALUES DILUTED WITH CYCLOHEXANE, MINUS SIGN SHOWING THE DISPLACEMENT TOWARD HIGHER FIELD

| Compound | Solvent | | |
|---|---|---|---|
| | Pure | $CCl_4$ | Acetone |
| 2,3-$Br_2$, 4-H | −0.03 | 0.11 | 0.27 |
| 5-H | −0.09 | 0.16 | 0.56 |
| 2,4-$Br_2$, 3-H | −0.03 | $0.09_5$ | 0.27 |
| 5-H | $0.00_5$ | $0.12_5$ | $0.54_5$ |
| 2,5-$Br_2$ | −0.01 | 0.11 | 0.33 |
| 3,4-$Br_2$ | 0.05 | 0.13 | 0.55 |
| 2,3,4-$Br_3$ | | $0.15_5$ | $0.66_5$ |
| 2,3,5-$Br_3$ | $0.04_5$ | 0.13 | 0.40 |

displacements in carbon tetrachloride and in pure liquid are rather small and can not so clearly be divided into groups. These results are similar to those obtained in methylthiophenesulfonylchlorides.[9] The displacement of the chemical shift in acetone is practically dependent on the position of the hydrogen rather than on that of the substituent. It seems that

7) J. H. Goldstein and G. S. Reddy, *J. Chem. Phys.*, 36, 2644 (1962).
8) B. Bak, D. Christensen, L. H-Nygaard and J. R. Andersen, *J. Mol. Spectr.*, 7, 58 (1961).
9) K. Takahashi, Y. Matsuki, Y. Miyake and G. Hazato, This Bulletin, 34, 1599 (1961).

the interaction between thiophenes and acetone occurs usually near the position of the sulfur atom in thiophene. The origin of the displacement of the chemical shifts of these compounds in the polar solvents has not yet been made clear; however, the experimental results concerning the solvent effect, especially in an acetone solution, can be used as criteria for estimating the position of the hydrogen in an unknown thiophene derivative which is $\alpha$ or $\beta$.

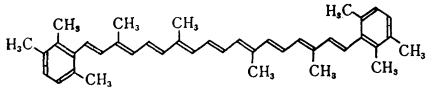
*The Chemical Research Institute of Non-Aqueous Solutions*
*Tohoku University*
*Katahira-cho, Sendai*

# The Identity of Leprotene with Isorenieratene

By Nobuhisa OKUKADO and Masaru YAMAGUCHI

(Received October 23, 1964)

A carotenoid hydrocarbon, leprotene, was first isolated from a strain of the acid-resistant bacteria of a leper in 1937[1]; later it was shown to be a common carotenoid pigment of the *Mycobacterium* genus[2], e. g., *M. phlei*[3] or *M. tuberculosis*[4]. Leprotene has a similar spectral property to that of β-carotene, but it differs in melting point, in chromatographic behavior and in the absence of vitamin A activity.[5] Takeda and Ohta proposed the formula $C_{40}H_{54}$ for leprotene on the basis of their analytical and microhydrogenational results and suggested that leprotene is a dehydrogenated β-carotene.[6] This suggestion has never been established because of a lack of data. Recently, however, one of the present authors, Masaru Yamaguchi, found aromatic carotenoids in a sea sponge[7] and pointed out that one of these aromatic carotenoids, isorenieratene (I), closely resembled leprotene in its properties.[8]



I

In the present study, leprotene was extracted from *M. phlei* and compared with isorenieratene. It was proved that leprotene is completely identical with isorenieratene in mixed melting point determination, ultraviolet- and infrared-spectra, mixed chromatography and CH-analysis.

This result not only clarifies the chemical constitution of leprotene, which has been unknown for a long time, but also establishes the second occurence of an aromatic carotenoid in nature, indicating an even wider distribution of this unique group of carotenoids.

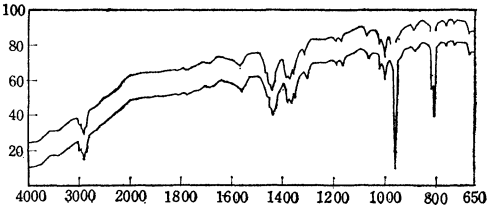



Fig. 1. IR-Spectra of leprotene (upper) and isorenieratene (lower) (KBr disk).

## Experimental

A pure strain of typical *M. Phlei* was cultivated at 35°C for thirteen to fifteen days until the deepest coloration developed on Sauton's medium, which contained sodium glutamate (8 g.), citric acid (2 g.), dipotassium hydrogen phosphate (0.5 g.), magnesium sulfate (0.5 g.), ferrous ammonium citrate (0.05 g.), and glycerol (60 g.) in water (1000 g.). The cells were collected by suction, washed with methanol, and extracted with acetone (the dry weight of the residue of the extraction was 800 g.). Pigments were transferred into petroleum benzine by the addition of water, and the benzine layer was washed with water, dried, and evaporated under a vacuum. The deep red oily concentrate separated a minute quantity of a brown precipitate on standing, this was removed by filtration. The concentrate was then

1) C. Grundmann and Y. Takeda, *Naturwissenschaften*, **25**, 27 (1937).
2) T. W. Goodwin, "Carotenoids," Chemical Publishing Co., New York (1954), pp. 120, 124.
3) Y. Takeda and T. Ohta, *Z. physiol. Chem.*, **262**, 168 (1939); **265**, 233 (1940); T. W. Goodwin and M. Jamikorn, *Biochem. J.*, **62**, 269 (1956).
4) Y. Takeda and T. Ohta, *J. Pharm. Soc. Japan*, **64**, 67 (1944).
5) Y. Takeda and T. Ohta, *Z. physiol. Chem.*, **267**, 171 (1941).
6) Y. Takeda and T. Ohta, ibid., **258**, 6 (1939).
7) M. Yamaguchi, This Bulletin, **30**, 111, 979 (1957); **31**, 51, 739 (1958).
8) M. Yamaguchi, ibid., **30**, 111 (1957).

Table I. Pigments of *M. Phlei*

| The width of the zones mm. | The color of the zones | UV-Max. (mμ) (Petroleum benzine) |
|---|---|---|
| 14(upper) | Dark brown (not homogeneous) | |
| 20 | Colorless | |
| 22 | Reddish orange | 481,451,425 |
| 25 | Red | 481,453,426 |
| 41 | Colorless | |
| 34 | Yellowish orange | 480,451,425 |
| 18(lower) | Yellow | 478,448 |

saponified with ethanolic potassium hydroxide (10%, 100 cc.) in a benzene solution (200 cc.). The mixture was washed with water, dried, and subjected to chromatography (alumina, 23×4.5 cm.; developer, a benzene-benzine mixture). Table I shows the main zones of a typical chromatogram and their ultraviolet-maxima in a petroleum benzine solution. The third reddish orange zone gave leprotene when the concentrate of the elute was treated with ethanol containing benzine. The pigment was recrystallized several times from benzene-methanol and benzene-ethanol mixtures. Copper red needles (6.5 mg.), m. p. 199°C. Abs. max., 481, 451, 425 mμ (petroleum benzine). Found: C, 90.22; H, 9.07. Calcd. for $C_{40}H_{48}$: C, 90.85; H, 9.15%.

The leprotene thus obtained did not show any depression of melting point when admixed with a sample of the isorenieratene obtained from a sponge ($C_{40}H_{48}$; copper red needles; m. p. 199°C; abs. max. 481, 451, 425 mμ)[8] and gave the same absorption curve as that of isorenieratene.[7] Infrared-spectra, Fig. 1. Neither of the pigments separated on an alumina column (25×1.2 cm.).

The authors wish to thank Professor Kenji Takeya and Yutaka Zinnaka, Laboratory of Bacteriology, Faculty of Medicine, Kyushu University, who kindly gave the pure strain of *M. phlei* and afforded many facilities for cultivations. The authors also wish to thank Professor Nobuo Izumiya, Laboratory of Biochemistry of this Department, who also offered conveniences for the cultivation.

*Department of Chemistry*
*Faculty of Science*
*Kyushu University*
*Hakozaki, Fukuoka*

# The Spectrophotometric Determination of Thallium(III) with Xylenol Orange[1]

By Makoto Otomo*

(Received November 6, 1964)

Thallium(III) has been determined spectrophotometrically by extracting the thallium(III)-complexes of *p*-phenetidine,[2] *p*-aminophenol,[3] rhodamine B,[4,5] brilliant green,[6] methylviolet[7] and bis(dimethylaminophenyl)-antipyrylcarbinol[8] into a suitable organic solvent. In the present paper, a very sensitive reagent, xylenol orange, which forms a water-soluble complex with thallium(III), is used for the spectrophotometric determination of trace amounts of thallium.

## Experimental

**Reagents and Apparatus.**—*Standard Thallium(III) Solution.*—An about 0.01 M thallium(III) nitrate solution was prepared by dissolving freshly prepared thallium(III) oxide, which had been precipitated from a thallium(III) chloride solution by adding a diluted aqueous ammonia solution and then carefully washed with water until the filtrate became free from ammonium and chloride ions, in concentrated nitric acid and diluting it with water. The solution was standardized against a standard EDTA solution.[9] The concentration of nitric acid in the solution was about 0.5 M. A working thallium(III) solution was prepared by diluting the above solution with 0.05 M nitric acid.

* Present address: Hachinohe Technical College, Hachinohe, Aomori.

1) This work was partly presented at the 15th Annual Meeting of the Chemical Society of Japan, Kyoto, April, 1962.

2) S. Iijima and Y. Kamemoto, *J. Chem. Soc. Japan, Pure Chem. Sec. (Nippon Kagaku Zassi)*, **75**, 1294 (1954).

3) V. G. Gladyshev and G. A. Tolstikov, *Zavodskaya Lab.*, **22**, 1166 (1956); *Chem. Abstr.*, **51**, 3361 (1957).

4) H. Onishi, This Bulletin, **29**, 945 (1956).

5) C. L. Luke, *Anal. Chem.*, **31**, 1680 (1959).

6) N. T. Voskresenskaya, *Zhur. Anal. Khim.*, **11**, 585 (1956); *Chem. Abstr.*, **51**, 7230 (1957).

7) G. V. Efremov and C. Syui, *Vestnik. Leningrad Univ.*, **13**, No. 16, Ser. Fiz. i Khim. No. 3, 156 (1958).

8) A. I. Busev and V. G. Tiptsova, *Nauk. Dokladyvysshei Shkoly, Khim. i Khim. Tekknol.*, **1959**, No. 1, 105.

9) K. Ueno, "Kireto Tekiteiho (Chelatometric Titration)" (in Japanese), Nankodo, Tokyo (1960), p. 318.

All the other reagents and the apparatus used were the same as those reported on previously.[10]

**Standard Procedure for the Determination.**—To a solution in a 25 ml. volumetric flask which contained 20 to 150 $\mu$g. of thallium, 3 to 8 ml. of a 2 M acetic acid solution and 3 to 5 ml. of a $1\times10^{-3}$ M xylenol orange solution were added. The solution was then diluted to the mark with water and mixed. After 15 min., the absorbance of the solution was measured at 520 m$\mu$, using a reagent blank as the reference.

## Results and Discussion

**Absorption Curve.**—The maximum absorption of the thallium - xylenol orange complex was observed at about 520 m$\mu$, when it was measured against a reagent blank as the reference.

**The Effect of the Concentration of Acetic Acid and the Color Stability.**—The effect of the concentration of acetic acid on the absorbance of the solution was examined; the results are shown in Fig. 1. The maximum absorbance

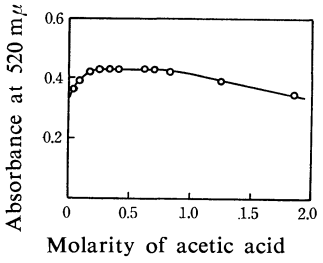



Fig. 1. Effect of concentration of acetic acid
Tl taken: 103 $\mu$g
XO concn.: $1.61\times10^{-4}$ M

is obtained when the acid concentration is adjusted to 0.25 to 0.7 M. In all the concentrations of acetic acid, the color formation was almort instantaneous. However, the intensity of the color of the resulting solution tended to decrease slowly with time; the change in abrorbance with time is indicated in Table I.

TABLE I. EFFECT OF TIME OF STANDING

Thallium taken: 124 $\mu$g.
Xylenol orange concn.: $1.60\times10^{-4}$ M
Acetic acid concn.: 0.41 M

| Time of standing, min. | Absorbance at 520 m$\mu$ |
|---|---|
| 5 | 0.539 |
| 10 | 0.536 |
| 15 | 0.531 |
| 20 | 0.528 |
| 30 | 0.522 |
| 45 | 0.517 |
| 60 | 0.512 |
| 120 | 0.500 |
| 180 | 0.492 |
| 240 | 0.489 |
| 400 | 0.463 |

10) M. Otomo, This Bulletin, 37, 504 (1964).

The effect of the concentration of other acids was also examined. At relatively lower concentrations, nitric acid and perchloric acid gave almost the same absorbance as that obtained with acetic acid. However, the color was unstable; the absorbance decreased by about 10% during the first 15 min. when the concentration of nitric acid was 0.2 M, and by about 4%, at the same concentration, of perchloric acid. Hydrochloric acid, at any concentration, is not adequate as the solvent, because thallium(III) forms stable chloro-complexes with chloride ions.

**The Effect of the Addition of the Reagent.**—Figure 2 shows the effect of the amount of the reagent. A high and almost constant absorbance is obtained when more than 3 ml. of a $1\times10^{-3}$ M xylenol orange solution is added.

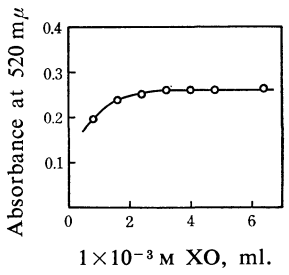



Fig. 2. Effect of addition of xylenol orange.
Tl taken: 62 $\mu$g.
$CH_3CO_2H$ concn.: 0.41 M

**Adherence to Beer's Law.**—As is shown in Fig. 3, Beer's law is oveyed ober the range from 20 to 150 $\mu$g. of thallium in 25 ml.

The apparent molar extinction coefficient of the thallium(III) - xylenol orange complex is 21300 at 520 m$\mu$. The sensitivity of the color reaction at this wavelength is 0.01 $\mu$g. of thallium per cm$^2$.

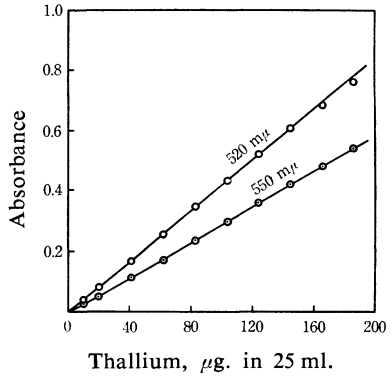



Fig. 3. Calibration curves.
XO concn.: $1.61\times10^{-4}$ M
$CH_3CO_2H$ concn.: 0.41 M

**The Effect of Diverse Ions.**—The effect of diverse ions was examined with solutions containing 103 $\mu$g. of thallium. Of the anions tested, the following did not interfere under the described conditions: fluoride up to 50 $\mu$mol., nitrate up to 500 $\mu$mol., and sulfate up to 100 $\mu$mol. Chloride, bromide, iodide, NTA and EDTA interfere seriously with the determination.

Of the 32 cations, including bi-, ter- and quadrivalent metal cations, bismuth(III), gallium(III), indium(III), iron(III), thorium(IV), vanadium(IV) and zirconium(IV) interfere with the determination by forming colored solutions. The interference of thorium and zirconium can, however, be eliminated by the addition of fluoride ions.

The proposed method, which is rapid and sensitive, seems to be applicable to the determination of traces of thallium in many samples after thallium has been preliminarily separated from the interfering ions by an appropriate method.

**The Composition of the Complex.**—The composition of the thallium(III) - xylenol orange complex was determined by the method of continuous variations as well as by the mole ratio method. Both methods showed that a 1 to 1 complex is formed between thallium(III) and xylenol orange at the acetic acid concentration described above.

The author is indebted to Professor Kôichi Tonosaki for his kind guidance throughout the course of this study.

*Department of Chemistry*
*Faculty of Literature and Science*
*Hirosaki University*
*Hirosaki, Aomori*

# The Dipole Moments of Bromothiophenes

By Takashi SHIMOZAWA

(Received November 21, 1964)

The molecular structures of bromothiophene derivatives were determined by dipole moment measurements. On the basis the results of these values, the bond nature of C-Br bonds can be discussed. The bond moment of the C-Br bond in the $\alpha$-position of the thiophene is 1.08 D., while that of the bond in the $\beta$-position is 1.53 D. The ortho-effect causes the C-Br moment to decrease by about 12%. The bond angle of C-Br bonds in tetrabromothiophene may be increased by steric hindrance.

A number of bromine derivatives of thiophene synthesized by Professor Eiji Imoto of Osaka Prefectural University[1] were used for dipole moment measurements without further purification.

The dipole moments were observed by the solution method at 25.0°C, using benzene as a solvent. The method has been reported previously in detail.[2] The observed and the calculated dipole moments are listed in Table I.

The values listed in column A of Table I were calculated by making the following assumptions: 1) the C-Br bond moment is 1.20 D.; 2) the dipole moment of the thiophene ring is 0.53 D.[3] and has its negative end at the sulfur atom, and 3) the bond angles are the same as in the thiophene ring[4] (Fig. 1). The agreement between the observed and calculated values is fairly good, so that the molecular structures of these molecules may be obtained by the dipole moment measurement. However, it can be expected that the bond moments of the C-Br bonds will change

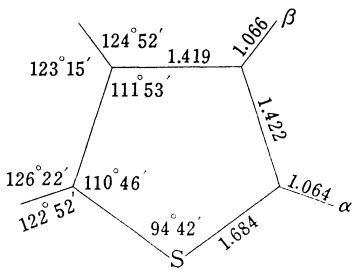



Fig. 1. The molecular structure of thiophene. (Cumper et al., Ref. 4)

1) E. Imoto et al., *J. Chem. Soc. Japan, Pure. Chem. Sec.* (*Nippon Kagaku Zassi*), **78**, 779 950 (1957).
2) T. Shimozawa, Y. Morino and R. Riemschneider, This Bulletin, **58**, 222 (1954).
3) H. de V. Robles, *Rec. Trav. chim.*, **58**, 111 (1939).
4) C. W. N. Cumper et al., *Trans. Faraday Soc.*, **54**, 1266 (1958).

TABLE I. THE DIPOLE MOMENTS OF BROMOTHIOPHENES (BENZENE SOLUTION, 25.0°C)

| Molecules | | | Obs. (D). | Calcd. (D.) | | |
|---|---|---|---|---|---|---|
| | | | | A | B | C |
| α-Bromothiophene | (I) | b. p. 74—75°C/55 mm Hg | 1.33 | 1.44 | | |
| β-Bromothiophene | (II) | b. p. 66—68°C/31 mm Hg | 1.13 | 0.82 | | |
| 3, 4-Dibromothiophene | (III) | b. p. 221—222°C | 1.59 | 1.42 | 1.95 | 1.59 |
| 2, 3-Dibromothiophene | (IV) | b. p. 212—213°C | 1.74 | 1.85 | 1.96 | 1.74 |
| 2, 3, 4, 5-Tetrabromothiophene | (V) | m. p. 115—116°C | 0.12 | 0.80 | | 0.71 |

their values according to their positions. In fact, the observed values of dipole moments are different for the two kinds of monobromothiophenes. These two C-Br bond moments were calculated from the observed values using the second assumption above. The C-Br bond moment of the α-position is 1.08 D., while that of the β-position is 1.53 D. The latter is nearly the same as that of the C-Br bond moment of about 1.5 D. in benzene derivatives. On the other hand, the C-Br bond moment at the α-position is smaller than the usual value. It has been reported[6] that the electron charge density of a carbon atom in the α-position of the thiophene ring is larger than that in the β-position; this would make the bond moment of the C-Br bond at the α-position smaller than that at the β-position.

The values calculated for molecules III and IV by the use of moments described above are listed in Table I (column B). They do not agree with the observed values. As is well known, the value of the dipole moment of ortho di-substituted benzenes is smaller than the values calculated by the vector addition of the dipole moment of mono-substituted compounds; i. e., in the case of ortho-dibromobenzene, for example, the C-Br bond moment calculated from the observed value is 12% smaller than the value for bromobenzene (the so-called the "ortho effect"). It may be assumed that the "ortho-effect" affects the dipole moments of compounds III and IV, too. The dipole moments of these molecules were recalculated using the smaller C-Br bond moments for each pair. These results are also listed in Table I (column C). These values agree with the observed values quite well, except for compound V.

In the case of 2, 3, 4, 5-tetrabromothiophene (V), the observed value of the dipole moment is 0.12 D., which differs greatly from the calculated value. As the experimental error involved in this value of the dipole moment is about ±0.2 D., the difference between the observed and the calculated values is worth further consideration.

If the C-Br bond is assumed to be 1.89 Å, and the valence angles, to be the same as in thiophene, the Br···Br distance is found to be 3.59 Å, which is much smaller than the sum of the van der Waals' radii of two bromine atoms (3.80 Å[7]). Therefore, the steric hindrance between Br···Br atoms would be exerted rather strongly. Thus, in order to avoid this steric hindrance, the C-Br bonds must be bent mutually in-plane or out-of-plane with respect to the thiophene ring. It can easily be shown that the in-plane bending of C-Br bonds strongly affects the value of the dipole moment; on the other hand, the out-of-plane bending does not appreciably change the dipole moment. The bending angles were obtained by a comparison of the observed and the calculated (column C) dipole moments. The results are shown in Fig. 2, where θ is calculated to be

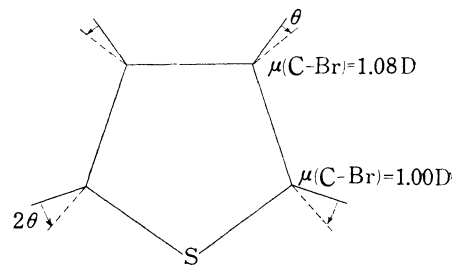



Fig. 2. The C-Br bond moments and in-plane deformations of 2, 3, 4, 5-Tetrabromothiophene.

about 5°. This value of θ seems to be unusually large. However, the Br···Br distance was calculated as 3.83 Å by using this new angle. Since this value is practically the same as the van der Waals value, the steric hindrance mentioned above does not seem to exist under this deformation. Therefore, the discrepancy between the observed and the calculated values (column C) might be due to the deformation. In order to determine the molecular structure of compound V, it is, of course, desirable to investigate its crystal structure by X-ray

5) See McClellan, "Tables of Experimental Dipole Moment," W. H. Freeman and Co., San Francisco and London (1963).

6) H. C. Longuet-Higgins, *Trans. Faraday Soc.*, **45**, 173 (1949).

7) L. Pauing, "The Nature of Chemical Bonds," p. 189.

diffraction and/or by the Zeeman effect of nuclear quadrupole resonance, because these are direct methods for the determination of the bond angles.

The author would like to express his deep appreciation to Professor Eiji Imoto, who kindly provided him with valuable samples, and to Professor Yonezo Morino of the University of Tokyo and Professor Yuzo Kakiuti of Rikkyo University, who gave him very useful advice and participated in many helpful discussions. Also, the author is grateful for a grant for Scientific Research to Private Universities given by the Ministry of Education.

*Department of Chemistry*
*Faculty of Science*
*St. Paul's (Rikkyo) University*
*Ikebukuro, Tokyo*

SHORT COMMUNICATIONS

# The Formation of the Anion Radicals of Pyromeritonitrile and Tetracyanoethylene by Flash Irradiation

By Mitsutaka SOFUE and Saburo NAGAKURA

(Received March 2, 1965)

It is well known that pyromeritonitrile (1, 2, 4, 5-tetracyanobenzene)[1] and tetracyanoethylene[2] are strong electron-acceptors. Furthermore, these electron acceptors are known to give stable anion radicals by reduction with alkalimetals in appropriate solvents.[3,4] In the course of their study of the effect of flash light upon charge-transfer-type complexes, the present authors have found that pyromeritonitrile and tetracyanoethylene can produce anion radicals by the irradiation of flash light, even in the absence of a definife electron donor.

**Pyromeritonitrile.**—Pyromeritonitrile was dissolved in purified acetonitrile in a concentration of $10^{-2}$—$10^{-3}$ M; the resulting solution was thoroughly degassed and used as the sample. As a flash-light source, a flash photolysis apparatus provided with argon flash lamps was utilized. An electric charge of 10—15 kV. in a 10 $\mu$F condenser was discharged through the lamps, and the light pulse generated (500—1200 joule/flash) was irradiated to the degassed sample solution contained in a quartz reaction vessel.

After the irradiation with flash light, the solution showed new absorption bands at 270, 375 and 462 m$\mu$ (see Fig. 1),* and an ESR spectrum with a hyperfine structure of 9 lines.** The electronic absorption spectrum and ESR spectrum observed with the irradiated solution

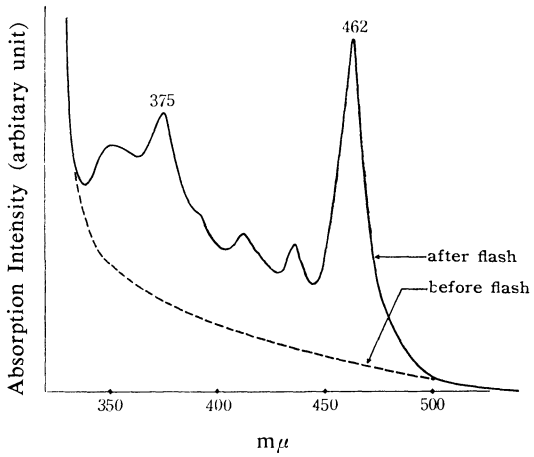



Fig. 1 Ultraviolet absorption spectrum of pyromeritonitrile before and after flash irradiation.

1) S. Iwata and S. Nagakura, to be published.
2) R. E. Merrifield and W. D. Phillips, *J. Am. Chem. Soc.*, **80**, 2778 (1958).
3) A. Ishitani and S. Nagakura, to be published.
4) W. D. Phillips, J. C. Rowell and S. I. Weissman, *J. Chem. Phys.*, **33**, 626 (1960).

* The electronic spectra were measured with a Cary recording spectrophotometer, Model 14 M.

** The ESR spectra were measured with a Hitachi ESR spectrometer, Model MPV-2B (X-band, 100 kc. modulation).

are completely identical with those of the pyromeritonitrile anion produced by the alkali metal reduction method.[3] Thus, it was confirmed that the pyromeritonitrile anion radical was produced by the irradiation of the acetonitrile solution of the parent molecule with an intence flash light.

The electronic absorption spectrum of the anion radical solution slowly decreased in intensity in vacuo and returned to that of the original neutral molecule. The lifetime was estimated to be 5 hr. This anion vanishes quickly if oxygen was introduced into the system.

Similar results were obtained with the ethanol and ethyl ether solutions. The lifetimes of the anions formed in these solvents were estimated to be 40 min. and 3 hr. respectively.

**Tetracyanoethylene.**—A degassed solution of tetracyanoethylene in acetonitrile, when irradiated with an intense flash light, showed a new absorption band at 250—400 m$\mu$ (see Fig. 2), and the sample solution turned pale yellow. The new absorption band was completely identical with that of the tetracyanoethylene anion produced by the alkali metal reduction method; therefore, the formation of the anion was confirmed.

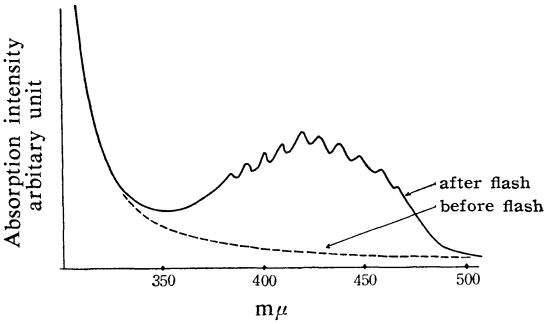



Fig. 2 Ultraviolet absorption spectrum of tetracyanoethylene before and after flash irradiation.

In the cases described above, no counter cations, which may be presumed to be produced simultaneously with the anions, could be detected.

*The Institute for Solid State Physics*
*The University of Tokyo*
*Azabu, Tokyo*

# The Photochemical Transannular Reaction of [2.2]Metacyclophane

By Takeo SATO, Ei-ichi YAMADA, Yoshio OKAMURA, Teruo AMADA and Kazuo HATA

(Received March 27, 1965)

A recent report[1] describing the occurrence of a photochemical equilibrium between *trans*-15, 16-dimethyldihydropyrene and its valence tautomer with a metacyclophane structure has prompted us to submit our findings on the photochemical transannular reaction of [2.2]-metacyclophane (I), which leads to 4, 5, 9, 10-tetrahydropyrene (II), in a preliminary form.

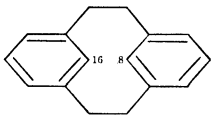
The irradiation of compound I, which had been prepared in a 45% yield by a modification of the method of Müller and Röscheisen[2] using a high dilution condition, was carried out in a quartz vessel placed in a circulating-water jacket housing a 1000 W. mercury arc lamp (Wako Denki Co., HBC-1000). Under a current of nitrogen, a mixture of 53.5 mg. (0.257 mmol.) of compound I, 68.1 mg. (0.268 mmol.) of iodine, and 700 mg. (excess) of sodium bicarbonate in 40 ml. of cyclohexane was irradiated for 44 hr.; it gave 45.5 mg. of colorless plates, m.p. 135—136°C (from methanol-ethanol), the NMR spectra of which in carbon disulfide showed only two singlets at 3.05 (6H) and 7.20 $\tau$ (8H). The disappearance of the characteristic peak of compound I at 5.77 $\tau$ ($C_8$ and $C_{16}$ protons) indicated that the transannular reaction occurred. The compound was shown to be 4, 5, 9, 10-tetrahydropyrene (II) by its identical infrared spectra and by a mixed melting point determination with an authentic specimen, m. p. 137—138°C. The yield reached 85.9%. A series of experiments confirmed that the formation of compound II in a somewhat lower yield was also possible by the irradiation of compound I and iodine in cyclohexane, *n*-hexane or ethanol under nitrogen as well as under oxygen. Compound I itself, however, was shown to be quite stable toward irradiation, and it could be recovered

1) H.-R. Blattmann, D. Menche, E. Heilbronner, R. J. Molyneux and V. Boekelheide, *J. Am. Chem. Soc.*, **87**, 130 (1965).

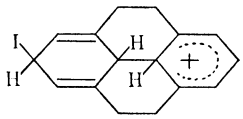
(2 E. Müller and G. Röscheisen, *Chem. Ber.*, **90**, 543 (1957).

in a 56% yield after irradiation for 20 hr. under oxygen.

It is assumed that the mechanism of this reaction is different from that of the related photochemical cyclization,[3] the formation of phenanthrenes from *cis*-stilbenes in the presence of a suitable oxidant (molecular oxygen or iodine), since the mechanism that has been formulated[3] requires the presence of the conjugated system. Further, the fact that the formation of II was best achieved by the reaction with one mole equivalent of iodine in the presence of the base suggested the participation of iodine to give iodinated radicals as the intermediate, followed by transannular reaction and dehydroiodination. Moreover, the driving force of this cyclization step may be sought in the unique features of the metacyclophane structure, namely, the proximity of $C_8$ and $C_{16}$ atoms and the presence of a highly strained ten-membered ring system, which is relieved by going into bicyclic. Thus no reaction occurred when bibenzyl, the open-chain model of compound I, was irradiated under the conditions described above.




(I)




(III)

The attempted iodination reaction of compound I with iodine and silver perchlorate in ether was also shown to give compound II in a 60% yield. Apparently the first step of this reaction is the electrophilic substitution by the iodonium ion, accompanied by the transannular reaction, giving an intermediate III.[4] Compound II is formed by a loss of the proton, followed by dehydroiodination.

*Department of Chemistry*
*Faculty of Science*
*Tokyo Metropolitan University*
*Setagaya-ku, Tokyo*

3) F. B. Mallory, C. S. Wood and J. T. Gordon, *J. Am. Chem. Soc.*, **86**, 3094 (1964), and the literature cited therein.

4) N. L. Allinger, M. A. Da Rooge and R. B. Hermann, ibid., **83**, 1974 (1961).

# Syntheses of 2-, 3- and 4-(1, 8-Dihydroxy-3, 6-disulfo-2-naphthylazo)-mandelic Acids as New Reagents, and the Thorium Complex of the 2-Isomer*

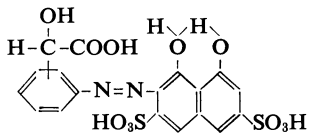
By Kyoji TÔEI, Haruo MIYATA and Tadayasu MITSUMATA**

(Received March 30, 1965)

In a series of phenylazochromotropic acid derivatives, the one with the $-AsO_3H_2$ or $-OCH_2COOH$[1] group is an especially sensitive reagent for thorium ion.

The present paper will describe the preparation of those reagents which have the $-CH(OH)COOH$ group in the ortho-, meta- or para-position to the azo group, and the determination of the acid dissociation constants of the reagents and of the constitution of the thorium complex formed with the 2-isomer.

**The Syntheses of the Reagents.**—The reagents, 2-, 3- and 4-(1, 8-dihydroxy-3, 6-disulfo-2-naphthylazo)mandelic acids, were obtained from the corresponding diazotized amino mandelic acids which were coupled with chromotropic acid respectively; the structures of the reagents were as follows:




**The Determination of the Acid Dissociation Constants of the Reagents.**—The acid dissociation constants of the reagents have been estimated spectrophotometrically; their values are shown in Table I.

The $pK_{a_3}$ value corresponds to the dissociation of the hydrogen ion from the carboxyl group of mandelic acid in the reagents, while

* Read at the Symposium of Analytical Chemistry, Yahata, November, 1964.

** Present address: Matsushita Electric Industrial Co., Ltd., Kadoma-shi, Osaka.

1) K. Tôei, H. Miyata, T. Shibata and S. Miyamura, This Bulletin, 38, 334 (1965).

TABLE I. $pK_{a_3}$ AND $pK_{a_4}$ OF THE REAGENTS AT 7—9°C

| | $pK_{a_3}$ | $pK_{a_4}$ |
|---|---|---|
| 2-Isomer | 3.1 | 9.7 |
| 3-Isomer | 3.4 | 9.7 |
| 4-Isomer | 3.9 | 9.2 |

$pK_{a_4}$ corresponds to one of the hydroxy groups of chromotropic acid.

**Spectral Properties of the Thorium Complex.** —Figure 1 shows the absorption spectra of the 2-isomer solution ($2.5\times10^{-5}$ mol./l.) and its thorium complex.

Figure 2 shows the determination of the mole ratio of thorium to the reagent by the continuous variation method. The result indicates the formation of a 1 : 1 complex.

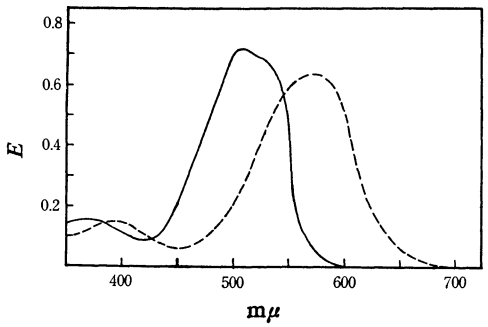



Fig. 1. Absorption spectra of the reagent and its thorium complex (broken line) at pH 2.9.
—— $2.5\times10^{-5}$ mol./l.
---- Thorium concn. to the reagent concn. = 5 : 1

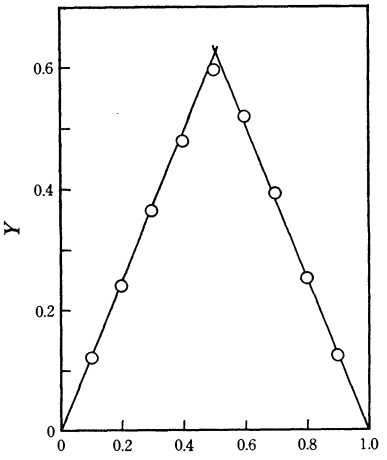



Fig. 2. Continuous variation method.
Thorium concn.+the reagent concn. = $5.0\times10^{-5}$ mol./l.
pH 3.1, 590 mμ

A more detailed study of the properties of the reagents and of the thorium complexes will be reported later.

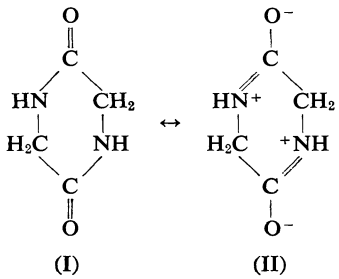
*Department of Chemistry*
*Faculty of Science*
*Okayama University*
*Tsushima, Okayama*

# A Novel Copper(II) Complex of Diketopiperazine

By Akitsugu NAKAHARA, Ken-ichi SAKURAI, Ken-ichi SUZUKI and Yasuo NAKAO

(Received April 12, 1965)

The molecular structure of diketopiperazine has been extensively studied[1-3] and as a result, it is regarded as a resonance hybrid of I and II. X-Ray study has shown that the molecule is nearly planar and has a center of symmetry.[2] Since there are two peptide linkages in the molecule, diketopiperazine is expected to form several types of complexes with metal ions according to the way functional groups are used as donor atoms. No paper has, however, been published to report on the formation of any type of complex, even in solutions.




(I) (II)

1) A. M. Buswell, J. R. Dowing and W. H. Rodebush, *J. Am. Chem. Soc.*, **62**, 2759 (1940); M. Tsuboi, This Bulletin, **22**, 255 (1949). Many papers other than these have also been published.

2) R. B. Corey, *J. Am. Chem. Soc.*, **60**, 1598 (1938); R. Degeilh and E. Marsh, *Acta Cryst.*, **12**, 1007 (1959).

3) F. A. Bovey and G. V. D. Tiers, *J. Am. Chem. Soc.*, **81**, 2870 (1959).

Recently we have succeeded in preparing one of these diketopiperazine complexes in the crystalline state. The new complex is potassium bis(diketopiperazinato)cuprate(II); on the basis of spectroscopic investigations, it is considered to have a very interesting structure. In this paper we will report on the preparation and on the properties of this new compound, and we will also consider its peculiar structure.

A one-to-two mixture of diketopiperazine and potassium hydroxide in an aqueous solution was treated at room temperature with an excess of freshly precipitated copper(II) oxide to give an intense blue solution as a result of the complex formation. The solution was then gently evaporated in a vacuum. The new complex is obtained as beautiful purple prisms, the color of which is fairly sensitive to moisture. In a humid atmosphere, it appears blue-purple, while in a comparatively dry atmosphere it is red-purple.

Judged from this color of the crystal, it is conceivable that all the four donor atoms around copper(II) are nitrogen, as in the bis(ethylenediamine)copper(II) complex. In fact, the wavelength for the maximum absorption in the visible region obtained by the reflection method strongly supports this theory. On the other hand, elemental analyses indicate that the ratio of copper(II) to diketopiperazine is one-to-two. Thus, the structure of the complex has been supposed to be a kind such as is illustrated in Fig. 1, in which two considerably-bent diketopiperazinato ions are coordinated around copper(II) through peptide nitrogens. The validity of this kind of structure is supported not only by the Stuart

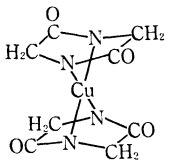


Fig. 1. The sandwich type structure of bis(diketopiperazinato)cuprate(II) ion.

model but also by the infrared study. The spectrum of diketopiperazine in the fingerprint region is very simple, while that of the complex differs in many respects and has a number of additional bands of a weak or medium intensity. These changes are consistent with the change in the conformation of the diketopiperazine molecule from the centrosymmetric to the boat configuration, a change caused by chelation with the copper(II) ion.

This may be a novel type of complex, having a structure of sandwich-type like ferrocene and other so-called $\pi$-complexes. However, the nature of the bondings between nitrogen and copper(II) may be supposed to be, rather, the $\sigma$-type on the basis of spectroscopic and stereochemical considerations. In this respect, the new complex bears a strong resemblance to the palladium(II) and platinum(II) complexes of piperazine reported by Mann and Watson.[4]

*Institute of Chemistry*
*College of General Education*
*Osaka University*
*Toyonaka, Osaka*

4) F. G. Mann and H. R. Watson, *J. Chem. Soc.*, **1958**, 2772.

# The Photochemistry of Hexacyanoferrate(II) Ions in Aqueous Solutions

By Shin-ichi OHNO and Gen-ichi TSUCHIHASHI*

(Received April 15, 1965)

Aqueous hexacyanoferrate(II) solutions decompose in ultraviolet light to give the aquopentacyanoferrate(II) ion.[1] Recently, Matheson et al.[2] observed a transient absorption due to the hydrated electron, $e^-_{aq}$, in the flash photolysis of aqueous hexacyanoferrate(II) solutions. We have studied the photo-induced reaction of aqueous hexacyanoferrate(II) solutions at various pH values, employing two light sources of different wavelengths. We have observed that illumination with a 3660 Å light causes only a ligand substitution reaction:

$$[Fe(CN)_6]^{4-} \xrightarrow[H_2O]{3660\text{Å}} [Fe(CN)_5OH_2]^{3-} + CN^- \quad (1)$$

* Present Adress: Sagami Chemical Research Center, Onuma, Sagamihara-shi, Kanagawa.

1) S. Ašperger, *Trans. Faraday Soc.*, **48**, 617 (1952).

2) M. S. Matheson, W. M. Mulac and J. Rabani, *J. Phys. Chem.*, **67**, 2613 (1963).

As a result of activation with a 2537 Å light, on the other hand, a photo-oxidation reaction was found to take place, giving hexacyanoferrate(III) and "reducing species (r. s.)":

$$[Fe(CN)_6]^{4-} \xrightarrow[H_2O]{2537\ Å} [Fe(CN)_6]^{3-} + \text{"r.s."}(e^-_{aq}) \quad (2)$$

The reducing species thus formed displayed a reactivity similar to that of the hydrated electron produced in water irradiated by fast electrons or $\gamma$-rays.[3]

The pH-buffered solutions of $10^{-2}$ M potassium hexacyanoferrate(II) were irradiated with a 3660 Å light from a high pressure mercury lamp, the solution being stirred by bubbling nitrogen gas. The quantum yield of the initial formation of aquopentacyanoferrate(II) was 0.89 at pH 4.0, the maximum value obtained, and 0.52 at pH 0.65.

Photo-oxidation reaction 2 was studied by using a 2537 Å light from a low pressure mercury lamp. The irradiation of the deaerated solution of $10^{-3}$ M potassium hexacyanoferrate(II) alone caused no significant change in the optical density at 420 m$\mu$. The same solution, however, became colored when irradiated in the presence of nitrous oxide or nitrate ions.[5] The absorption spectra of the solution, as well as the results of thin-layer chromatography, clearly indicate the formation of hexacyanoferrate(III) ions, which may be attributed to reaction 2, followed by:

$$e^-_{aq} + N_2O \longrightarrow N_2 + OH + OH^- \quad (3)$$

$$OH + [Fe(CN)_6]^{4-} \longrightarrow [Fe(CN)_6]^{3-} + OH^- \quad (4)$$

or

$$e^-_{aq} + NO_3^- \longrightarrow NO_2 + 2OH^- \quad (5)$$

$$NO_2 + [Fe(CN)_6]^{4-} \longrightarrow [Fe(CN)_6]^{3-} + NO_2^- \quad (6)$$

The yield of hexacyanoferrate(III) ions increased with the increase in the concentration of nitrous oxide or nitrate ions to reach a limiting value. The quantum yield of the formation of $e^-_{aq}$ was determined to be 0.35. We also noted that no noticeable amount of hexacyanoferrate(III) was produced with a 3660 Å light, regardless of whether an electron scavenger, such as $N_2O$ or $NO_3^-$, was present or not.

Further, acetone appeared to compete with reaction 3 or 5 for $e^-_{aq}$, and ethanol, with reaction 4 for OH. From kinetic data, the rate constant ratios were calculated te be $k(e^-_{ap}+\text{acetone})/k_3=1.5$, $k(e^-_{ap}+\text{acetone})/k_5=0.45$ and $k(OH+\text{ethanol})/k_4=0.16$. Agreements with the reported values are satisfactory.[3]

We may, therefore, conclude that the irradiation of hexacyanoferrate(II) ions with a 2537 Å light (the charge-transfer-to-solvent type of excitation[4]) brings about an electron release to the solvent, while activation by a 3660 Å light (the ligand-field transition type) causes only a ligand substitution reaction. The present photochemical study offers a new method of investigating, in a direct manner, the reactions of hydrated electrons with a variety of inorganic and organic substances: several such studies are now in progress.

*Japan Atomic Energy Research Institute*
*Tokai-mura, Ibaraki*

3) "Radiation Research Supplement" Vol 4, Academic Press, New York and London (1964).
4) A. Treinin, *J. Phys. Chem.*, **68**, 893 (1964).

# Stability Constants of Some Substitution-inert Cobalt(III) Complexes

By Nobuyuki TANAKA and Hiroshi OGINO

(Received May 8, 1965)

Only a few investigations have been made on the stability constants of cobalt(III) complexes.[1] This is because cobalt(III) forms mostly substitution-inert complexes; the formation of such complexes discourages considerably the determination of the stability constant. In this communication, the stability constants of cobalt(III) complexes with ethylenediaminetetraacetate ($edta^{4-}$), propylenediaminetetraacetate ($pdta^{4-}$) and trimethylenediaminetetraacetate ($trdta^{4-}$), which are all substitution-inert, are presented, and compared with the stability constants of some divalent metal ions reported previously.[2]

The equilibrium potentials of the reaction

$$Co^{II}Y^{2-} \rightleftarrows Co^{III}Y^{-} + e \qquad (1)$$

were measured at the dropping mercury electrode with the solutions which contain varied concentrations of $Co^{II}Y^{2-}$ and $Co^{III}Y^{-}$, where $Y^{4-}$ denotes $edta^{4-}$, $pdta^{4-}$ or $trdta^{4-}$ anion. From these values, the standard oxidation-reduction potentials of Eq. 1 ($E^{\circ}_{CoY}$) were calculated. These values agreed to the half-wave potentials of the reduction waves of $Co^{III}Y^{-}$ and the oxidation waves of $Co^{II}Y^{2-}$. The stability constants of $Co^{III}Y^{-}$ ($K_{Co(III)Y}$) were calculated by using the values of $E^{\circ}_{CoY}$, the stability constants of $Co^{II}Y^{2-}$ ($K_{Co(II)Y}$)[2] and the standard oxidation-reduction potential of the $Co(aq.)^{2+}$ - $Co(aq.)^{3+}$ couple (+1.842 V. vs. NHE).[3] The results are given in Table I.

The stability constant of $Co^{III}edta^{-}$ obtained in this study is in satisfactory agreement with that reported by Reilley et al.[4] The stability constant of $Co^{III}pdta^{-}$ is larger than that of $Co^{III}edta^{-}$ by 1.5 in log $K$ unit. This tendency, which agrees essentially with that reported previously,[2] is considered to be attributed to the inductive effect of the methyl group of coordinated $pdta^{4-}$ ion.[2,5] On the other hand, the stability constants of $Co^{III}edta^{-}$ and $Co^{III}trdta^{-}$ are almost the same in maguitude. This supports the previous conclusion that the decrease in the size of metal ion favors the formation of trimethylenediaminetetraacetato complex;[2] the ionic radius of cobalt(III) is smaller than those of manganese(II), cobalt(II), nickel(II), copper(II), zinc(II), cadmium(II), and lead(II). In addition, it should be noted that cobalt(III) gives a stability constant considerably larger than chromium(III),[6] manganese(III)[7] and iron(III)[8] in the case of EDTA complexes and also than iron(III)[9] in the case of TRDTA complexes. This may relate to the fact that EDTA forms a spin-paired complex with cobalt(III),[10] but not with chromium[10]-(III), manganese(III),[11] and iron(III).[10] The details of the study will be reported later.

TABLE I. THE STABILITY CONSTANTS OF COBALT(III) COMPLEXES WITH ETHYLENEDIAMINETETRAACETATE, PROPYLENEDIAMINETETRAACETATE AND TRIMETHYLENEDIAMINETETRAACETATE*

| Couple | $E^{\circ}_{CoY}$ V. vs. SCE | log $K_{Co(II)Y}$[2] | log $K_{Co(III)Y}$ |
|---|---|---|---|
| $Co^{II}edta^{2-}$-$Co^{III}edta^{-}$ | +0.13 | 15.71 | 40.6 |
| $Co^{II}pdta^{2-}$-$Co^{III}pdta^{-}$ | +0.12 | 17.07 | 42.1 |
| $Co^{II}trdta^{2-}$-$Co^{III}trdta^{-}$ | +0.05 | 14.48 | 40.7 |

* The measurements were made with the solution containing 0.05 M acetate buffer (pH 4.6 to 5.4) at ionic strength 0.2 ($KNO_3$) and 25°C.

*Department of Chemistry*
*Faculty of Science*
*Tohoku University*
*Katahira-cho, Sendai*

1) L. G. Sillén and A. E. Martell, "Stability Constants," Chemical Society, London (1964).
2) H. Ogino, This Bulletin, **38**, 771 (1965).
3) A. A. Noyes and T. J. Deahl, *J. Am. Chem. Soc.*, **59**, 1337 (1937).
4) C. N. Reilley, W. G. Scribner and C. Temple, *Anal. Chem.*, **28**, 450 (1956).
5) J. H. Grimes, A. J. Huggard and S. P. Wilford, *J. Inorg. Nucl. Chem.*, **25**, 1225 (1963).
6) R. L. Pecsok, L. D. Shields and W. P. Schaefer, *Inorg. Chem.*, **3**, 114 (1964).
7) N. Tanaka, T. Shirakashi and H. Ogino, This Bulletin, **38** (1965), in press.
8) G. Schwarzenbach and J. Heller, *Helv. Chim. Acta*, **34**, 576 (1951).
9) F. L'Eplattenier and G. Anderegg, ibid., **47**, 1792 (1964).
10) W. Klemm, *Z. anorg. Chem.*, **252**, 225 (1944).
11) Y. Yoshino, A. Ouchi, Y. Tsunoda and M. Kojima, *Can. J. Chem.*, **40**, 775 (1962).

# The Calculation of the State Energies of Benzaldehyde. II. The SCF Molecular Orbital Method

By Kōzō Inuzuka and Toshio Yokota

(Received May 16, 1964)

In the previous paper,[1] we calculated the state energies of benzaldehyde by the Pariser-Parr method[2] and assigned electronic transitions by adopting a model with $C_{2v}$ symmetry for the sake of simplicity. In the actual molecule of benzaldehyde, however, the carbon atom of the carbonyl group is combined with the carbon atom of the benzene ring, where the bond angle of C–C=O is 120°, as is shown in Fig. 1.

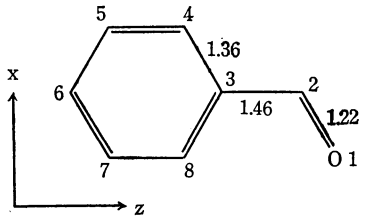



Fig. 1. A model* of benzaldehyde with $C_s$ symmetry.

* Ref. 1

In this paper, therefore, the state energies of benzaldehyde with $C_s$ symmetry are calculated by using the SCF-MO method.[3,4] The bond distances used are the same as those in the previous model.[1]

## Calculation Procedure

The SCF-MO, $\varphi_i$, and its energy, $\varepsilon_i$, are obtained by the following formulas:

$$\varphi_i = \sum_\mu c_{i\mu}\chi_\mu$$

$$\sum_\nu F_{\mu\nu}c_{i\nu} = \varepsilon_i c_{i\mu}$$

$$F_{\mu\mu} = \alpha_\mu + \frac{1}{2}p_{\mu\mu}(\mu\mu/\mu\mu) + \sum_{\nu\neq\mu}(p_{\nu\nu}-1)(\mu\mu/\nu\nu)$$

$$F_{\mu\nu} = \beta_{\mu\nu} - \frac{1}{2}p_{\mu\nu}(\mu\mu/\nu\nu)$$

$$p_{\mu\nu} = 2\sum_i c_{i\mu}c_{i\nu}$$

where $\chi_\mu$ is 2p$\pi$AO of the $\mu$th-atom, $\alpha_\mu$ is the ionization potential of the atom, $\mu$, in the atomic valence state and $\beta_{\mu\nu}$ is the resonance integral over the nearest neighbor atoms, $\mu$ and $\nu$.

The value of the resonance integral, $\beta_{CO}$, over carbon and oxygen atoms is calculated by using Kon's formula,[6] while the value of $\beta_{CC}$ over carbon and carbon atoms is obtained from Pariser and Parr's formula.[2] $(\mu\mu/\nu\nu)$ is the Coulomb repulsion integral; that is,

$$(\mu\mu/\nu\nu) = \int\chi^*_\mu(1)\chi_\mu(1)(e^2/r_{12})\chi^*_\nu(2)\chi_\nu(2)dv$$

It is evaluated from the equations derived by Roothaan[7] and by Anno et al.[5] for $r>2.80$Å and $r\leqq 2.80$Å respectively. The calculations were done using a digital computer. The iteration process in the calculation of SCF-MO's and MO energies started with Hückel MO's and continued until the energies converged.

The excitation energies corresponding to the $i$–$k$ transition are expressed for singlet and triplet states respectively as follows:

$$^1E_{i\text{-}k} = \varepsilon_k - \varepsilon_i - [ii/kk] + 2[ik/ki]$$

$$^3E_{i\text{-}k} = \varepsilon_k - \varepsilon_i - [ii/kk]$$

where

$$[ii/kk] = \int\varphi_i(1)^*\varphi^*_k(2)(e^2/r_{12})\varphi_i(1)\varphi_k(2)dv.$$

Neglecting the differential overlap, the integrals, $[ii/kk]$ and $[ik/ki]$, may be expressed in terms of the Coulomb repulsion integrals over such atomic orbitals as $(\mu\mu/\nu\nu)$.

In addition to the above MO's, the benzaldehyde molecule has a nonbonding orbital which may be represented approximately as follows:

$$\varphi_n = \chi_n$$

where $\chi_n$ is the 2p$\bar{\pi}$ AO of the oxygen atom. Its nodal plane is perpendicular to the molecular plane and contains the CO axis.

The transition moment between the ground state, $\psi_0$, and an excited state, $\psi_i$, is defined by:

1) K. Inuzuka and T. Yokota, This Bulletin, 37, 1224 (1964).
2) R. Pariser and R. G. Parr, *J. Chem. Phys.*, 21, 466, 767 (1953).
3) J. A. Pople, *Trans. Faraday Soc.*, 49, 1375 (1953).
4) N. Mataga and K. Nishimoto, *Z. physik. Chem. N. F.*, 13, 140 (1957).
5) T. Anno, I. Matubara and A. Sadō, This Bulletin, 30, 168 (1957).
6) H. Kon, ibid., 28, 275 (1955).
7) C. C. J. Roothaan, *J. Chem. Phys.*, 19, 116 (1951).

Table I. SCF-MO's and MO energies of benzaldehyde

$\varepsilon_i$ (eV.)

$-15.64805\ \varphi_1 =$
$0.35064\chi_1+0.31879\chi_2+0.45265\chi_3+0.38416\chi_4+0.32816\chi_5+0.30185\chi_6+0.31234\chi_7+0.35580\chi_8$

$-14.57123\ \varphi_2 =$
$0.71105\chi_1+0.45578\chi_2-0.02874\chi_3-0.16431\chi_4-0.26712\chi_5-0.30589\chi_6-0.26170\chi_7-0.15953\chi_8$

$-12.11845\ \varphi_3 =$
$0.13435\chi_1+0.02285\chi_2-0.25176\chi_3-0.56914\chi_4-0.29456\chi_5+0.27578\chi_6+0.57755\chi_7+0.31262\chi_8$

$-12.05362\ \varphi_4 =$
$0.24442\chi_1+0.02381\chi_2-0.49834\chi_3-0.00251\chi_4+0.48448\chi_5+0.47788\chi_6+0.00000\chi_7-0.47776\chi_8$

$-1.43621\ \varphi_5 =$
$-0.36987\chi_1+0.47637\chi_2+0.41637\chi_3-0.34619\chi_4-0.13014\chi_5+0.44474\chi_6-0.21688\chi_7-0.28511\chi_8$

$-0.64024\ \varphi_6 =$
$0.02450\chi_1-0.02847\chi_2-0.02033\chi_3-0.47797\chi_4+0.52382\chi_5-0.04837\chi_6-0.47438\chi_7+0.51764\chi_8$

$0.53306\ \varphi_7 =$
$-0.38261\chi_1+0.64278\chi_2-0.33373\chi_3+0.04843\chi_4+0.266021\chi_5-0.41844\chi_6+0.28216\chi_7+0.03536\chi_8$

$2.72601\ \varphi_8 =$
$0.09939\chi_1-0.22057\chi_2+0.44430\chi_3-0.38839\chi_4+0.37065x_5-0.36833\chi_6+0.38561\chi_7-0.41410\chi_8$

Table II. Calculated lower transition energies of $n$-$\pi$ and $\pi$-$\pi$ transitions of benzaldehyde without configuration interaction

| Electronic transition | Orbital jump | Transition energy, eV. | Electronic transition | Orbital jump | Transition energy, eV. |
|---|---|---|---|---|---|
| $^1A'$-$^3A''$ | $n$-5 | 5.465 | $^1A'$-$^1A''$ | $n$-5 | 5.698 |
| | $n$-6 | 8.696 | | $n$-6 | 8.697 |
| | $n$-7 | 6.860 | | $n$-7 | 7.110 |
| | $n$-8 | 11.498 | | $n$-8 | 11.515 |
| $^1A'$-$^3A'$ | 4-5 | 4.358 | $^1A'$-$^1A'$ | 4-5 | 5.674 |
| | 3-5 | 4.644 | | 3-5 | 5.822 |
| | 4-6 | 4.657 | | 4-6 | 6.124 |
| | 3-6 | 4.395 | | 3-6 | 6.215 |
| | 4-7 | 6.654 | | 4-7 | 7.516 |
| | 3-7 | 7.066 | | 3-7 | 7.649 |
| | 2-5 | 6.674 | | 2-5 | 8.007 |

$$M^r{}_{0i}=\int\psi_0 r\psi_i \mathrm{d}v \quad (r=x,y,z)$$

where $\psi_i$ is expressed approximately by a linear combination of singly-excited configuration functions. The oscillator strength, $f$,[8] is given by:

$$f=1.085\times10^{11}\times\omega_{0i}\sum_r M^r{}_{0i}{}^2,$$

where $\omega_{0i}$ is the frequency of the transition in $cm^{-1}$.

## Results

**State Energies without Configuration Interaction.**—The SCF-MO's and the MO energies so obtained are listed in Table I. The $\pi$-$\pi$ transition energies in singlet and triplet states are calculated from the above equation; the $n$-$\pi$ transition energies are also calculated by the Pariser-Parr method using the above SCF-MO's. In Table II, we show all the energies of $n$-$\pi$ transitions and the lower lying energies of $\pi$-$\pi$ transitions.

**State Energies with Configuration Interaction.**—In large molecules, multiply-excited configurations should make negligibly small contributions to the lower excitation energies. In the present calculation we take account of a singly-excited configurations only. In the $\pi$-$\pi$ transition, all calculations of singly-excited configurations were carried out by solving a 16th-order secular equation for each of the singlet and triplet states. Similarly, in the calculation of the $n$-$\pi$ transition energies, four configurations were taken for each of the singlet and triplet states. The lower-lying state energies and their wave functions as obtained from these four secular equations are listed in Tables III and IV.

The charge densities, bond orders and free valences for the ground state of benzaldehyde

8) R. S. Mulliken and C. A. Rieke, *Rep. Progr. Physics*, **8**, 231 (1941).

TABLE III. WAVE FUNCTIONS FOR LOWER EXCITED STATES OF BENZALDEHYDE

| State | | 1,5 | 1,6 | 1,7 | 1,8 | 2,5 | 2,6 | 2,7 | 2,8 |
|---|---|---|---|---|---|---|---|---|---|
| $^1A'$: | 1 | 0.00984 | 0.02225 | 0.00332 | 0.00722 | −0.00860 | 0.08392 | −0.02236 | 0.00337 |
| | 2 | −0.07075 | 0.00642 | −0.03639 | −0.09112 | 0.00982 | 0.00455 | 0.10966 | 0.04908 |
| | 3 | 0.02130 | −0.03858 | −0.04084 | −0.03677 | −0.32492 | 0.01959 | −0.19221 | 0.07438 |
| | 4 | −0.07474 | −0.04402 | −0.04635 | 0.02088 | −0.06519 | −0.02728 | −0.03255 | −0.01553 |
| $^3A'$: | 1 | 0.00749 | 0.01132 | −0.02712 | 0.18623 | −0.14833 | 0.00827 | −0.25505 | −0.06783 |
| | 2 | −0.21072 | 0.00186 | −0.22530 | −0.04296 | −0.52528 | 0.04140 | −0.40502 | 0.15213 |
| | 3 | 0.05002 | −0.05493 | 0.03981 | 0.00174 | 0.09732 | −0.03173 | 0.07221 | −0.02230 |
| | 4 | −0.13160 | 0.00587 | −0.10258 | 0.02003 | −0.36865 | −0.00203 | −0.18448 | 0.04268 |
| State | | 3,5 | 3,6 | 3,7 | 3,8 | 4,5 | 4,6 | 4,7 | 4,8* |
| $^1A'$: | 1 | 0.56986 | −0.35767 | −0.21659 | −0.02446 | −0.47200 | −0.50474 | 0.11774 | −0.01135 |
| | 2 | 0.45188 | 0.43795 | −0.09676 | 0.00485 | 0.63454 | −0.38581 | −0.11522 | 0.02516 |
| | 3 | −0.02911 | 0.65594 | −0.13755 | 0.01896 | −0.50889 | −0.03055 | −0.36635 | −0.04586 |
| | 4 | 0.66851 | 0.03127 | 0.12750 | 0.06169 | −0.03751 | 0.71660 | 0.02540 | −0.00954 |
| $^3A'$: | 1 | −0.39213 | −0.44564 | 0.09045 | 0.00288 | −0.63530 | 0.29510 | 0.14547 | −0.01665 |
| | 2 | 0.00920 | 0.47292 | −0.17087 | 0.00898 | −0.26416 | −0.23937 | −0.24080 | 0.00953 |
| | 3 | 0.73377 | 0.15715 | −0.23506 | 0.04310 | −0.44048 | 0.33684 | 0.21658 | −0.04559 |
| | 4 | 0.26821 | −0.47089 | −0.21056 | 0.01470 | 0.42672 | 0.42835 | −0.30864 | 0.03004 |
| State | | *n*,5 | *n*,6 | *n*,7 | *n*,8** | | | | |
| $^1A''$: | 1 | 0.78017 | −0.06061 | 0.61279 | −0.11027 | | | | |
| $^3A''$: | 1 | 0.77119 | −0.05880 | 0.62303 | −0.11682 | | | | |

* *i*, *j* represents a state excited from $\varphi_i$ to $\varphi_j$.

** *n*, *j* represents a state excited from nonbonding orbital to $\varphi_j$.

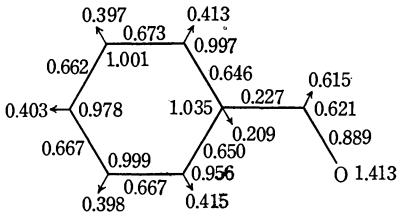



Fig. 2. Molecular diagram of benzaldehyde in the ground state.

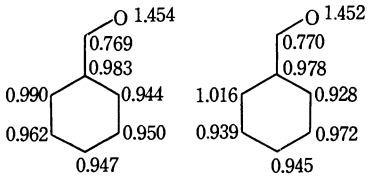



Fig. 3. $\pi$-Electron charge densities of benzaldehyde in excited state.
I: 1st excited state; II: 2nd excited state

are also shown in Fig. 2. The charge densities of the 1st and 2nd excited states are shown in Fig. 3.

## Discussion

Since benzaldehyde has the symmetry $C_s$, all the electronic transitions are symmetry-allowed.

TABLE IV. COMPARISON OF EXPERIMENT AND SCF-MO CALCULATION WITH INTERACTION OF SINGLY EXCITED CONFIGURATIONS

| State | | Calculated | | Experimental | |
|---|---|---|---|---|---|
| | | *E*, eV. | *f* | *E*, eV. | *f* |
| $^1A'$: | | 0 | 0 | 0 | 0 |
| | 1 | 4.771 | 0.017 | 4.50[a] | 0.026[a] |
| | 2 | 5.032 | 0.066 | 5.32[a] | 0.29[a] |
| | 3 | 6.313 | 1.02 | 6.36[b,c] | 0.45[b,c] |
| | 4 | 6.794 | 0.88 | | |
| $^3A'$: | 1 | 3.273 | | | |
| | 2 | 3.937 | | | |
| | 3 | 4.223 | | | |
| | 4 | 4.402 | | | |
| $^1A''$: | 1 | 3.860 | | 3.34[d,e] | 0.55 $\times 10^{-3}$ [d] |
| $^3A''$: | 1 | 3.370 | | 3.22[d] | 1.8 $\times 10^{-7}$ [d] |

a) Ref. 9, b) Ref. 10, c) Ref. 11, d) Ref. 13, e) Ref. 12

The $\pi$-electronic states belong to the irreducible representation, A', of the symmetry group $C_s$, while the $n$–$\pi$ single excitation belongs to the symmetry type A'', since the symmetry of the $n$ orbital is a''. Therefore, the transition moment is perpendicular to the molecular plane, that is, parallel to the $y$ axis.

Benzaldehyde has four absorption bands in the region from 400 to 190 m$\mu$. In a previous

paper,[1] we tried to assign these absorption bands using the $C_{2v}$ model with Hückel MOs. The results for state energies and oscillator strengths in the present calculation are listed in Table IV, along with the observed values. From these results, the band at 285 m$\mu$ (4.50 eV.)[9] corresponds to the calculated energy of 4.771 eV. The bands at 233 m$\mu$ (5.32 eV.)[9] and 195 m$\mu$ (6.36 eV.)[10,11] are correlated with the state energies, 5.032 and 6.313 eV. respectively. On the basis of the above correspondence, they may be assigned to $^1A'$–$^1A'$ transitions. The calculated energy values are in good agreement with the observed values, as compared with the previous values,[1] but the calculated values of the oscillator strengths of the first and second transitions are smaller than the observed values.

The electronic transition at 26929 $cm^{-1}$ (3.34 eV.)[12] corresponds to the calculated energy of 3.860 eV. Therefore, the transition may be assigned to $^1A'$–$^1A''$. This calculated value should be compared with the previous value (3.614 eV.). The calculated state energy, 3.370 eV., is the lowest of the $n, \pi$ state energies and corresponds to $^1A'$–$^3A''$. This value is correlated with the S−T absorption band at 25195 $cm^{-1}$ (3.22 eV.)[13] and should be compared with the previous value (3.124 eV.). On the other hand, the calculated values for the $\pi,\pi$ triplet states are lower than the previous values;[1] however, no experimental data are available.

The reactivity indices for the ground state are shown in Fig. 2. The charge density of the meta position is higher than those of the ortho and para positions. This result indicates a tendency of the carbonyl group to meta orientation for electrophilic reagents, in accordance with the previous calculation.[1] The high-charge densities of ortho positions suggest that they also have a high reactivity for electrophilic reagents. The free valence in carbon atoms is the highest at the carbon atom 2, as is shown in Fig. 2. This suggests that position 2 is reactive in the case of radical reaction, as has been observed in the photo-oxidation reaction of benzaldehyde. The charge densities in two lower excited states are shown in Fig. 3. These results are very different from those of the previous calculations.[1]

9) J. Tanaka, *J. Chem. Soc. Japan, Pure Chem. Sec.* (*Nippon Kagaku Zassi*), **79**, 1114 (1958).
10) W. C. Price and A. D. Walsh, *Proc. Roy. Soc.*, **A191**, 22 (1947).
11) H. B. Klevens and J. R. Platt, Technical Report, Laboratory of Molecular Structure and Spectra, University of Chicago, Chicago (1953—1954).
12) S. Imanishi, K. Semba, M. Ito and T. Anno, This Bulletin, **25**, 150 (1952).
13) Y. Kanda, Private Communication.

## Summary

The state energies, charge densities, bond orders and free valences of benzaldehyde have been elucidated by the use of the SCF-MO method with a model of $C_s$ symmetry, including interactions of all the singly-excited configurations. In the singlet state, the numerical values of state energies are more reliable than the previous results, which were derived from the $C_{2v}$ model by the use of Hückel MO. In the triplet state, however, the numerical values of state energies seem to be lower than the previous results.

The authors wish to express their sincere thanks to Mr. Masuo Suzuki and Dr. Toshinori Munakata for their kind assistance in carrying out the digital computations. The present study was partially financed by the Scientific Research Fund of the Ministry of Education.

*Department of Applied Science*
*Tokyo Electrical Engineering College*
*Chiyoda-ku, Tokyo*

# Formation Constants of Chromium(III)-Oxalato Complexes

By Kyoichi NAGATA,* Akira UMAYAHARA and Ryokichi TSUCHIYA

(Received June 20, 1964)

There have been published a great number of investigations of the syntheses[1] and the properties[2] of oxalato complexes of various metals; the data of the formation constants concerned have been summarized in a review.[3] However, these data concern only the bivalent cations. The formation constants of the oxalato complexes of tervalent metal cations are scarcely known except for a few examples.

In a preceding paper the formation constants of chromium(III) complexes with ethylenediamine were reported;[4] this is the simplest chelating agent which coordinates to the central chromium by means of two nitrogen atoms. In the present study, the formation constants of chromium(III) complexes with oxalate ion, the simplest chelating agent coordinating by two oxygen atoms, have been determined in order to compare them with those published in the previous report.[4] The results found have also been compared with the data of the corresponding complexes of other first-transition metals already known.

## Experimental

**Hexaaquochromium(III) Perchlorate.**—Chromium trioxide was precipitated by adding concentrated sulfuric acid to potassium bichromate. When it was reduced with formic acid[5] in the presence of perchloric acid, the hexaaquochromium(III) perchlorate which was the starting material in the present study was obtained. Since it was very hygroscopic, it was stored in a vacuum desiccator.

The analysis of the chromium in the hexaaquochromium(III) perchlorate prepared as above was carried out by oxidizing the tervalent chromium to bichromate by ammonium persulfate in the presence of a trace of silver nitrate as a catalyst, and by measuring the absorbancy of the solution at 420 mμ with a Hitachi FPW-4 photoelectric photometer after adjusting the pH of the solution to 2. The analysis of the perchlorate ion was made by titrating the elute passed through the cation exchange resin "Amberlite IR-120" with a standard sodium hydroxide solution.

By these analyses it was found that the crystalline hexaaquochromium(III) perchlorate prepared above as the sarting material had the following composition, if the adsorbed water was excluded:

| | |
|---|---|
| $[Cr(H_2O)_6](ClO_4)_3$ | 48.66 mol.% |
| $HClO_4$ | 51.34 mol.% |

**Sodium Oxalate.**—Salt of the highest commercial grade was further purified by recrystallization.

**Procedure.**—The determination of the formation constants was carried out by pH measurement. Mixed solutions of various concentrations of hexaaquochromium(III) perchlorate and sodium oxalate, to which some quantities of sodium hydroxide had been added to make the pH of the solution higher and an appropriate amount of sodium perchlorate, to make the ionic strength of the solution 0.1, were kept at 25°C in a thermostat for one or one-and-a-half months. The pH of the solution was measured with a Toa Denpa pH meter, model HM-8, after the equilibrium in the solution had been attained.

## Results

**Acid Dissociation Constants of Oxalic Acid.**—If the oxalic acid is represented as $H_2ox$, the acid dissociation constants, $K_1$ and $K_2$, may be expressed by:

$$K_1 = [H^+][Hox^-]/[H_2ox] \quad (1)$$

$$K_2 = [H^+][ox^{2-}]/[Hox^-] \quad (2)$$

where [ ] expresses the concentration in moles per liter. If the total concentration of ionizable hydrogen atoms and that of oxalate ions are expressed by $C_H$ and $C_{ox}$ respectively, $\bar{n}_H$, denoted as the average number of hydrogen atoms attached to each oxalate ion, is given by the following equation:

$$\bar{n}_H = \frac{[Hox^-] + 2[H_2ox]}{[ox^{2-}] + [Hox^-] + [H_2ox]} = \frac{C_H - [H^+]}{C_{ox}} \quad (3)$$

On the other hand, $C_H$ is expressed by the equation as:

$$C_H = C_{ox} + C_a - C_{OH} \quad (4)$$

where $C_a$ and $C_{OH}$ are the concentrations of perchloric acid and of sodium hydroxide added respectively.

The determination of the acid dissociation

* Present address: Ishikawa Prefectural Technical High School.

1) J. C. Bailar, Jr., E. M. Jones, H. S. Booth and M. Grennert, "Inorganic Syntheses," Vol. 1, 35 (1939); W. Schramm, *Z. anorg. u. allgem. Chem.*, **180**, 167 (1929).
2) J. Halpern and A. C. Harkness, *J. Chem. Phys.*, **31**, 1147 (1959); D. P. Graddon, *J. Inorg. Nucl. Chem.*, **3**, 308 (1956).
3) K. V. Krishnamurty and G. M. Harris, *Chem. Revs.*, **61**, 213 (1961).
4) M. Ohta, H. Matsukawa and R. Tsuchiya, This Bulletin **37**, 692 (1964).
5) C. Postmus and E. L. King, *J. Phys. Chem.*, **59**, 1208 (1955).

constants was carried out by titrating the mixed solution of oxalic acid and sodium oxalate with perchloric acid or with a sodium hydroxide solution. By inserting the values of $C_H$ calculated from the titre of perchloric acid or sodium hydroxide and the $[H^+]$ values obtained from the pH measurement into Eqs. 3 and 4, the value of $\bar{n}_H$ was obtained. The plot of $\bar{n}_H$ vs. pH is shown in Fig. 1.

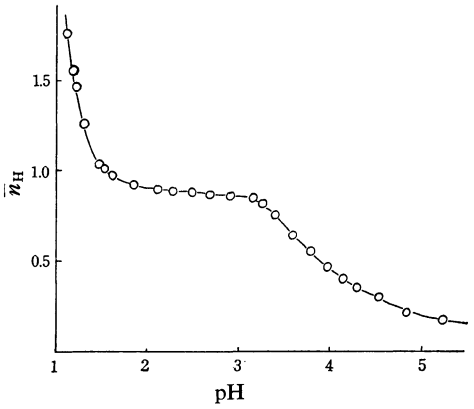



Fig. 1. The relation between $\bar{n}_H$ and pH

The values of the acid dissociation constants of the first and second steps, $pK_1$ and $pK_2$, are obtained from Fig. 1 as 1.13 and 3.85 respectively. These values are in good agreement with the $pK_1=1.14$[6] ($\mu=0.2$, 25°C) and $pK_2=3.85$[6] ($\mu=0.2$, 25°C) already known, although the ionic strength is somewhat different.

**Formation Constants of Oxalato-chromium(III) Complexes.**—When the total concentration of chromium is expressed by $C_M$, that of the oxalate ion as ligand is given by:

$$C_{ox}=[ox^{2-}]+[Hox^-]+[H_2ox]+\bar{n}C_M \quad (5)$$

where $\bar{n}$ is the average number of ligands attached to each chromium. The total concentration of ionizable hydrogen is also given by the following equation:

$$C_H=C_a-C_{OH} \quad (6)$$

On the other hand, $\bar{n}$ is expressed as follows:

$$\bar{n}=\left\{C_{ox}-\frac{C_H-[H^+]}{\bar{n}_H}\right\}\Big/C_M \quad (7)$$

where $\bar{n}_H$ is denoted as the number of ionizable hydrogen atoms attached to oxalate ions against the number of oxalate ions which do not coordinate to chromium. It is calculated by using Eqs. 1, 2 and 3 and by applying the values of the acid dissociation constants of oxalic acid and $[H^+]$.

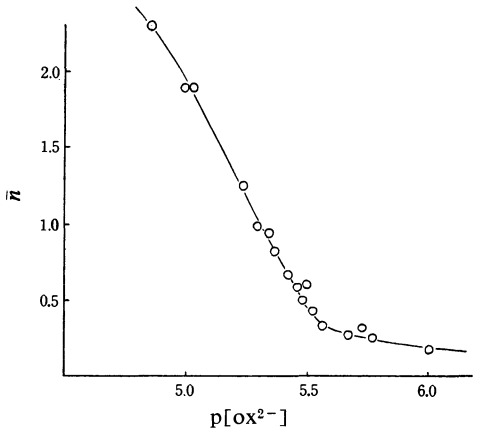



Fig. 2. The formation curve, $\bar{n}$—$p[ox^{2-}]$, concerning with chromium(III) oxalato complexes.

By measuring the pH in mixed solutions of hexaaquochromium(III) perchlorate and sodium oxalate and by applying Eqs. 1, 2, 5, 6 and 7, the values of $\bar{n}$ and $[ox^{2-}]$ were calculated. The formation curve, $\bar{n}-p[ox^{2-}]$, is plotted in Fig. 2. As the slope of this formation curve is relatively steep, the successive oxalato complexes formed seem to have overlapped each other. Since Bjerrum's simplified method cannot be applied in this case, the calculation of the formation constants was carried out in the following way.[7]

In the successive formation of the complexes, there exists the following relationship:

$$\bar{n}=\sum nK_n[ox^{2-}]^n/\{1+\sum K_n[ox^{2-}]^n\} \quad (8)$$

where $K_n=\Pi k_n$, the products of the successive formation constants. Equation 8 can be rearranged to:

$$\bar{n}=(n-\bar{n})[ox^{2-}]^nK_n=\sum J_nK_n \quad (9)$$

where

$$J_n=(n-\bar{n})[ox^{2-}]^n \quad (10)$$

By inserting the values of 0.5, 1.5 and 2.3 into $\bar{n}$ and the corresponding values into $[ox^{2-}]$ in Eqs. 9 and 10, three simultaneous equations are established. By solving these equations, the successive formation constants are obtained as $\log k_1=5.34$, $\log k_2=5.17$ and $\log k_3=4.93$ respectively.

## Discussion

The values of the formation constants of chromium(III) oxalato complexes in the first and second steps are compared with the known values of those of the first transition metals in Table I.

6) R. K. Cannan and A. Kibrick, *J. Am. Chem. Soc.*, **60**, 2314 (1938).

7) B. P. Block and G. H. McIntyre, Jr., *J. Am. Chem. Soc.*, **75**, 5667 (1953).

TABLE I. THE FORMATION CONSTANTS OF THE OXALATO COMPLEXES OF THE FIRST TRANSITION METALS

| | $\log k_1$ | $\log k_2$ | $\log k_3$ | Ionic strength $\mu$ | Temp. °C | Ref. |
|---|---|---|---|---|---|---|
| $TiO^{+}$ | 2.65 | | | — | 23 | 8 |
| $Cr^{3+}$ | 5.34 | 5.17 | 4.93 | 0.1 | 25 | Present study |
| $Mn^{3+}$ | 9.98 | 6.59 | 2.85 | 2 | 25 | 9 |
| $Fe^{3+}$ | 9.4 | 6.8 | 4.0 | — | — | 10 |
| $Co^{3+}$ | | $\log k_1k_2k_3 \cong 20$ | | — | — | 11 |
| $Al^{3+}$ | 7.25 | | | 0 | — | 12 |
| | | $\log k_1k_2$ | | $\mu$ | °C | Ref. |
| $Mn^{2+}$ | | 5.25 | | 0 | 25 | 13 |
| $Fe^{2+}$ | | 4.52 | | 0.5 | 25 | 14 |
| $Co^{2+}$ | | 6.7 | | 0.002 | 25 | 15 |
| $Ni^{2+}$ | | 6.51 | | 0.002 | 25 | 15 |
| $Cu^{2+}$ | | 10.32 | | — | ~20 | 16 |
| $Zn^{2+}$ | | 7.36 | | 0 | 25 | 17 |

It may be found from Table I that the formation constants of oxalato complexes of tervalent metal ions are remarkably larger than those of the corresponding complexes of bivalent metal ions. This is due to the fact that the ionic radii of the former are smaller than those of the latter; this confirms that the covalencies of the former are much stronger than those of the latter. The bivalent metal ions form four coordinated complexes, whereas the tervalent metal ions form six coordinated complexes.

It is found in the second that the formation constants of oxalato complexes become larger in the order of the tervalent titanium, chromium and manganese, iron or cobalt. That is to say, the formation constants of chromium complexes are smaller than those of manganese, iron and cobalt; they are comparable with those of aluminum complexes.

The formation constants of chromium(III) oxalato complexes are remarkably smaller than those of the corresponding ethylenediamine complexes reported in the preceding paper.[4] This suggests that the chelate group with two nitrogen atoms as the donor forms a more stable complex with chromium than does the chelate group with two oxygen atoms as the donor.

## Summary

The formation constants of chromium(III) complexes with the oxalate ion, which is the simplest bidentate ligand coordinating by two oxygen atoms, have been determined by the pH method.

It has been shown that the formation constants of oxalato chromium(III) complexes are larger than those of the corresponding titanium(III) complexes, but smaller than those of the corresponding manganese(III), iron(III) and cobalt(III) complexes in the first transition series.

The formation constants of oxalato chromium(III) complexes have been found to be remarkably smaller than those of the ethylenediamine chromium(III) complexes. This result suggests that two nitrogen atoms form a more stable complex with chromium than do the two oxygen atoms serving as donors in the bidentate chelate.

*Department of Chemistry*
*Faculty of Science*
*Kanazawa University*
*Kanazawa*

8) V. V. Subbanna, G. S. Rao and A. K. Bhattacharya, *J. Sci. Ind. Research (India)*, **18B**, 127 (1959).
9) H. Taube, *J. Am. Chem. Soc.*, **70**, 3928 (1948).
10) J. Lambling, *Bull. soc. chim. France*, **1949**, 495.
11) T. B. Copestake and N. Uri, *Proc. Roy. Soc.*, **A228**, 252 (1955).
12) S. Lacroix, *Bull. soc. chim. France*, **1947**, 408.
13) R. W. Money and C. W. Davies, *J. Chem. Soc.*, **1934**, 400.
14) W. B. Schaap, H. A. Laitinen and J. C. Bailar, Jr., *J. Am. Chem. Soc.*, **76**, 5868 (1954).
15) J. B. Barney, W. J. Argersinger, Jr., and C. A. Reynolds, ibid., **73**, 3785 (1951).
16) L. Meites, Jr., ibid., **72**, 184 (1950).
17) W. C. Vosburgh and F. J. Beckman, ibid., **62**, 1028 (1940).

# Studies of Gas Chromatography with Mixed Stationary Liquids. IV. The Analysis of Aromatic Hydrocarbons from $C_6$ to $C_{10}$ with a Capillary Column*

By Hiroshi MIYAKE, Mitsuyuki MITOOKA and Tadashi MATSUMOTO

(Received July 30, 1964)

The gas chromatographic analysis of aromatic hydrocarbon mixtures through $C_{10}$ needs to be carried out with columns of excellent resolving powers, because these mixtures contain many groups of isomers with similar physical properties. It seems appropriate, for the analysis of such a complex mixture, to use a capillary column. Indeed, it has already been reported that fairly good separation was obtained for many types of hydrocarbon mixtures by the use of such a column,[1-3] but all of the aromatics through $C_{10}$ have not been separated by a single column, although various types of liquids of different polarities have been investigated as stationary phases. Several authors have reported that in these cases the mixed stationary liquid is effective. By changing the composition of the mixed liquid, the selectivities for the solutes were altered widely and continuously, and a column which has a pertinent selectivity may be prepared as an aid in investigating the effects of the composition on the partition coefficients of the solutes in question.[4-6] For all the paraffins, mono-olefins, di-olefins, cycloparafins and acetylenes through $C_4$, an appproximate linearity was observed between the logarithm of the partition coefficient and the composition (wt.%) of the mixed phase. Accordingly, when the retention times on two stationary liquids are known, the retention time of the solute on the mixed liquid of any composition may be presumed.

The presence of similar relationships may be expected from the behaviors of aromatic hydrocarbons on some mixed liquids, and the complex mixtures of aromatic isomers might be efficiently separated by the use of the appropriate mixed liquid.

* Presented at the 17th Annual Meeting of the Chemical Society of Japan, Tokyo, April, 1964.

1) H. Miyake and M. Mitooka, *Bull. Japan Petrol. Inst.*, 5, 58 (1963).

2) R. L. Martin and J. C. Winters, *Anal. Chem.*, 35, 1930 (1963).

3) J. A. Walker and D. L. Ahlberg, ibid., 35, 2023 (1963).

4) H. Miyake and M. Mitooka, *J. Chem. Soc. Japan, Pure Chem. Sec.* (*Nippon Kagaku Zasshi*), 84, 593 (1963).

5) H. Miyake and M. Mitooka, ibid., 84, 923 (1963).

6) H. Miyake and M. Mitooka, ibid., 85, 326 (1964).

## Experimental

**Apparatus.** — A Perkin-Elmer Model 188 vapor fractometer equipped with a flame-ionization detector was used without modification. Helium was used as the carrier, and the pressure was adjusted to a gauge pressure of 30 or 60 p. s. i. at the inlet of the column. A column consists of a 45.7 m. (or 91.4 m.) by 0.254 mm. stainless-steel capillary and is coated with squalane (SQ), dinonyl phthalate (DNP), 7, 8-benzoquinoline (BQ), polyethylene glycol 600 (PEG 600), di-*n*-propyl tetrachlorophthalate (DPTCP), 2, 4-dinitrochlorobenzene (DNCB) or a binary solution composed of these components.

**Coating the Capillary.**—Each of the substrates was coated in the capillary tubing as follows: a weighed amount of the refined liquid was dissolved in ether or methanol to prepare a 10—20% solution, and then this solution was injected into the capillary tubing by the aid of a 5-ml. injection cylinder. After the tubing had been completely filled with the solution, the solvent and the excess substrate were purged out in a stream of helium gas at room temperature. Consequently, the thin substrate was deposited on the inner wall of the capillary tubing. The film thickness obtained was influenced not only by the concentration of the solution, but, contrary to the reported result,[7] strongly by the speed of coating. Namely, as the rate was increased by raising the purging gas, the amount of liquid coated was increased. Therefore, this step is important in the preparation of a column which has an appropriate retention time for the sample component.

## Results and Discussion

**Retention Times on the Single Liquid Phase.** —The relative retention times of aromatic hydrocarbons from $C_6$ to $C_{10}$ and their chromatograms on the six liquid phases with different selectivities are shown in Table I and Fig. 1 respectively. The retention times in Table I have been corrected for the dead volume of the apparatus by substracting the retention time of methane. On all the liquid phases, there are several overlapping peaks: isobutylbenzene - *s*-butylbenzene and 1, 4-diethylbenzene - 1, 2-ethylbenzene on the SQ

7) R. D. Schwartz and D. J. Brasseaux, ACS Preprints-Symposia, Division of Petrol. Chem., 8, (4) C-77 (1963).

TABLE I. RELATIVE RETENTION TIMES ON VARIOUS STATIONARY LIQUIDS
(*n*-PROPYLBENZENE = 1.000)

| No. | Name of compound | Abbreviation | Relative retention time | | | | | |
|---|---|---|---|---|---|---|---|---|
| | | | SQ 90°C | DNP 70°C | BQ 90°C | PEG 600 90°C | DPTCP 90°C | DNCB 70°C |
| 1 | Benzene | B | 0.109 | 0.087 | 0.132 | 0.217 | 0.128 | 0.143 |
| 2 | Toluene | T | 0.248 | 0.221 | 0.269 | 0.382 | 0.296 | 0.337 |
| 3 | Ethylbenzene | EB | 0.500 | 0.484 | 0.533 | 0.630 | 0.534 | 0.566 |
| 4 | *p*-Xylene | *p*-X | 0.559 | 0.536 | 0.582 | 0.658 | 0.666 | 0.863 |
| 5 | *m*-Xylene | *m*-X | 0.567 | 0.553 | 0.608 | 0.681 | 0.642 | 0.834 |
| 6 | *o*-Xylene | *o*-X | 0.664 | 0.683 | 0.759 | 0.816 | 0.859 | 1.120 |
| 7 | Isopropylbenzene | *i*-PB | 0.796 | 0.788 | 0.797 | 0.885 | 0.769 | 0.743 |
| 8 | *n*-Propylbenzene | *n*-PB | 1.000 | 1.000 | 1.000 | 1.000 | 1.000 | 1.000 |
| 9 | 1-Methyl-3-ethylbenzene | 1-M-3-EB | 1.107 | 1.146 | 1.141 | 1.093 | 1.097 | 1.331 |
| 10 | 1-Methyl-4-ethylbenzene | 1-M-4-EB | 1.127 | 1.151 | 1.113 | 1.080 | 1.150 | 1.377 |
| 11 | 1,3,5-Trimethylbenzene | 1,3,5-TMB | 1.290 | 1.351 | 1.370 | 1.209 | 1.289 | 2.097 |
| 12 | 1-Methyl-2-ethylbenzene | 1-M-2-EB | 1.255 | 1.359 | 1.412 | 1.354 | 1.428 | 1.811 |
| 13 | *t*-Butylbenzene | *t*-BuB | 1.340 | 1.357 | 1.221 | 1.171 | 1.234 | 1.234 |
| 14 | 1,2,4-Trimethylbenzene | 1,2,4-TMB | 1.485 | 1.603 | 1.618 | 1.508 | 1.813 | 2.857 |
| 15 | Isobutylbenzene | *i*-BuB | 1.510 | 1.495 | 1.337 | 1.190 | 1.425 | 1.251 |
| 16 | *s*-Butylbenzene | *s*-BuB | 1.523 | 1.540 | 1.464 | 1.251 | 1.374 | 1.206 |
| 17 | 1-Methyl-3-isopropylbenzene | 1-M-3-*i*-PB | 1.690 | 1.772 | 1.599 | 1.374 | 1.483 | 1.646 |
| 18 | 1,2,3-Trimethylbenzene | 1,2,3-TMB | 1.810 | 2.081 | 2.181 | 2.066 | 2.511 | 3.908 |
| 19 | 1-Methyl-4-isopropylbenzene | 1-M-4-*i*-PB | 1.789 | 1.868 | 1.639 | 1.400 | 1.576 | 1.748 |
| 20 | 1-Methyl-2-isopropylbenzene | 1-M-2-*i*-PB | 1.881 | 2.069 | 1.957 | 1.684 | 1.861 | 2.171 |
| 21 | 1,3-Diethylbenzene | 1,3-DEB | 2.071 | 2.239 | 2.058 | 1.672 | 1.859 | 2.320 |
| 22 | 1-Methyl-3-*n*-propylbenzene | 1-M-3-*n*-PB | 2.150 | 2.279 | 2.054 | 1.690 | 1.994 | 2.222 |
| 23 | *n*-Butylbenzene | *n*-BuB | 2.188 | 2.331 | 2.113 | 1.786 | 2.142 | 2.074 |
| 24 | 1-Methyl-4-*n*-propylbenzene | 1-M-4-*n*-PB | 2.244 | 2.352 | 2.059 | 1.714 | 2.126 | 2.314 |
| 25 | 1,2-Diethylbenzene | 1,2-DEB | 2.254 | 2.551 | 2.499 | 1.983 | 2.279 | 2.788 |
| 26 | 1,3-Dimethyl-5-ethylbenzene | 1,3-DM-5-EB | 2.422 | 2.675 | 2.452 | 1.894 | 2.090 | 3.126 |
| 27 | 1,4-Diethylbenzene | 1,4-DEB | 2.258 | 2.432 | 2.167 | 1.761 | 2.032 | 2.251 |
| 28 | 1-Methyl-2-*n*-propylbenzene | 1-M-2-*n*-PB | 2.370 | 2.618 | 2.426 | 2.038 | 2.513 | 2.926 |
| 29 | 1,4-Dimethyl-2-ethylbenzene | 1,4-DM-2-EB | 2.655 | 3.005 | 2.811 | 2.226 | 2.850 | 4.240 |
| 30 | 1,3-Dimethyl-4-ethylbenzene | 1,3-DM-4-EB | 2.784 | 3.179 | 2.964 | 2.311 | 2.868 | 4.343 |
| 31 | 1,2-Dimethyl-4-ethylbenzene | 1,2-DM-4-EB | 2.887 | 3.302 | 3.014 | 2.417 | 2.947 | 4.297 |
| 32 | 1,2-Dimethyl-3-ethylbenzene | 1,2-DM-3-EB | 3.287 | 3.966 | 3.853 | 3.069 | 3.871 | 6.145 |
| 33 | 1,2,4,5-Tetramethylbenzene | 1,2,4,5-TeMB | 3.809 | 4.532 | 4.376 | 3.280 | 4.740 | 9.542 |
| 34 | 1,2,3,5-Tetramethylbenzene | 1,2,3,5-TeMB | 3.976 | 4.806 | 4.612 | 3.477 | 4.830 | 9.811 |
| 35 | 1,2,3,4-Tetramethylbenzene | 1,2,3,4-TeMB | 4.813 | 6.086 | 5.989 | 4.617 | 7.154 | 15.059 |

column; *t*-butylbenzene - 1-methyl-2-ethylbenzene-1, 3, 5-trimethylbenzene and 1-methyl-2-isopropylbenzene - 1, 2, 3-trimethylbenzene on the DNP column; 1, 3-diethylbenzene - 1-methyl-3-*n*-propylbenzene - 1-methyl-4-*n*-propylbenzene, 1, 2, 3-trimethylbenzene - 1, 4-diethylbenzene and 1,3-dimethyl-5-ethylbenzene - 1,2-diethylbenzene on the BQ column; 1-methyl-2-isopropylbenzene - 1-methyl-3-*n*-propylbenzene on the PEG 600 column, and *t*-butylbenzene-isobutylbenzene and others on the DNCB column.

In the case of SQ, which is almost nonpolar and does not have a marked selectivity for solutes, the aromatic hydrocarbons are eluted approximately in order of their boiling points. DNP and PEG have weak polarities and show small selectivities. In the case of BQ, which forms inclusion complexes with aromatic hydrocarbons, the heat of mixing is small and the solute molecules adopt less random configurations.[8] It can be surmised that DPTCP and DNCB form molecular complexes with aromatic hydrocarbons.[9] The heats of the mixing of aromatic hydrocarbons for these two stationary liquids, therefore, must be negative and large; also, the change in the activity coefficients with the temperature must be large. Consequently, it may be expected that the selectivities of these liquids will change considerably with the temperature.

8) D. H. Desty and W. J. Swanton, *J. Phys. Chem.*, **65**, 706 (1961).
9) S. H. Langer, C. Zahn and G. Pantazoplos, *J. Chromotog.*, **3**, 154 (1960).

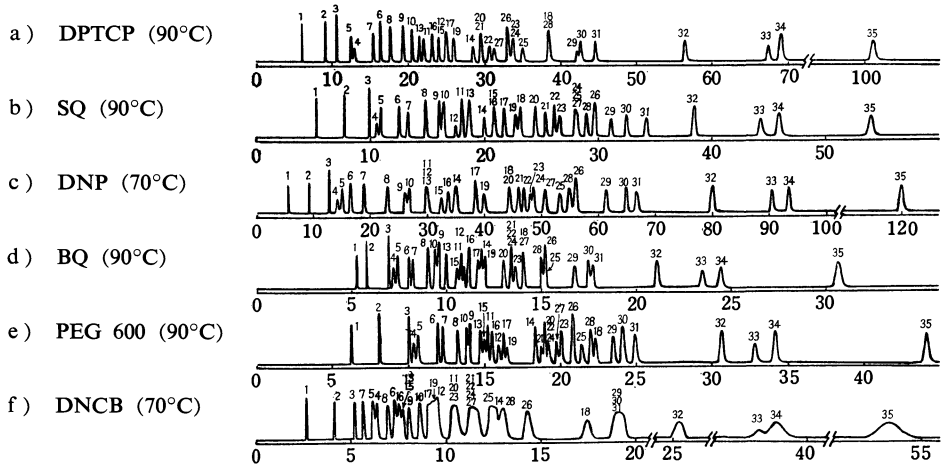



Fig. 1. Chromatograms of $C_6$ through $C_{10}$ aromatic hydrocarbons on the six liquid phases.

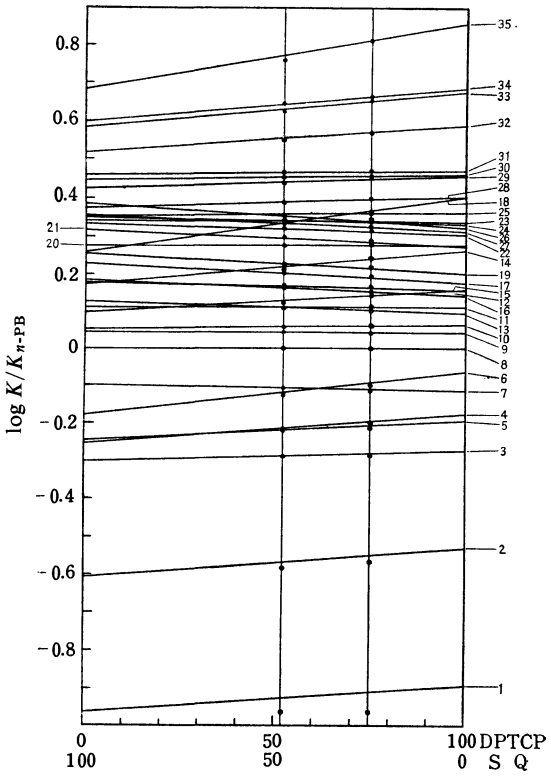



Fig. 2. The relationship between the relative retention time of solute ($\log K/K_{n\text{-PB}}$) and the composition (wt.%) of the mixed stationary liquid SQ-DPTCP at 70°C.

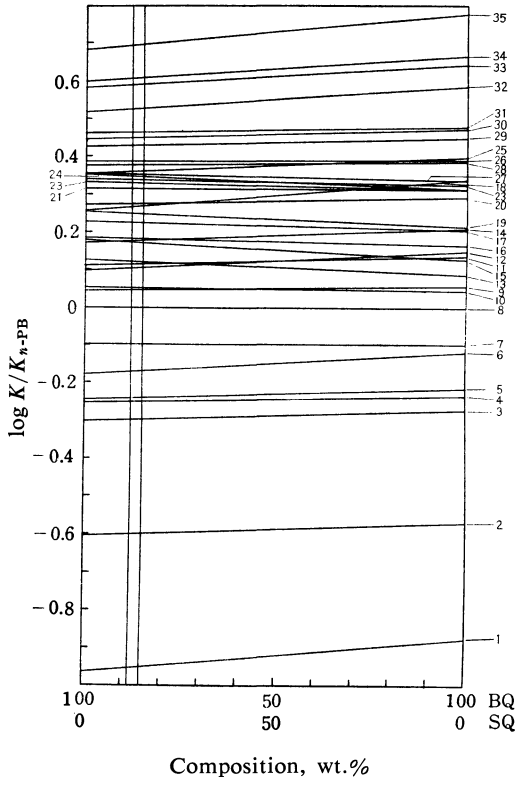



Fig. 3. The relationship between the relative retention time of solute ($\log K/K_{n\text{-PB}}$) and the composition (wt.%) of the mixed stationary liquid SQ-BQ at 70°C.

**The Relationship between the Relative Retention Times and the Composition of Stationary Liquids.**—For each hydrocarbon, the logarithms of the relative partition coefficients on the SQ column and DPTCP column were marked on the left and right ordinates respectively, and a straight line was drawn through them, as Fig. 2 shows.

If a linear relationship of the same kind as

TABLE II. COMPARISON BETWEEN THE PRESUMED AND THE OBSERVED RELATIVE RETENTION TIMES ON THE SQ-DPTCP COLUMNS AT 90°C (*n*-PROPYLBENZENE=1.000)

| No. | Compound | SQ 48%-DPTCP 52% column | | SQ 25%-DPTCP 75% column | |
|---|---|---|---|---|---|
| | | Presumed | Observed | Presumed | Observed |
| 1 | B | 0.118 | 0.108 | 0.121 | 0.108 |
| 2 | T | 0.269 | 0.262 | 0.279 | 0.271 |
| 3 | EB | 0.517 | 0.514 | 0.525 | 0.517 |
| 4 | *p*-X | 0.610 | 0.610 | 0.635 | 0.630 |
| 5 | *m*-X | 0.604 | 0.605 | 0.622 | 0.613 |
| 6 | *o*-X | 0.759 | 0.750 | 0.803 | 0.795 |
| 7 | *i*-PB | 0.785 | 0.782 | 0.778 | 0.770 |
| 8 | *n*-PB | 1.000 | 1.000 | 1.000 | 1.000 |
| 9 | 1-M-3-EB | 1.100 | 1.104 | 1.097 | 1.103 |
| 10 | 1-M-4-EB | 1.140 | 1.139 | 1.148 | 1.145 |
| 11 | 1,3,5-TMB | 1.291 | 1.277 | 1.289 | 1.294 |
| 12 | 1-M-2-EB | 1.340 | 1.320 | 1.385 | 1.386 |
| 13 | *t*-BuB | 1.286 | 1.281 | 1.259 | 1.260 |
| 14 | 1,2,4-TMB | 1.641 | 1.613 | 1.718 | 1.732 |
| 15 | *i*-BuB | 1.462 | 1.476 | 1.449 | 1.464 |
| 16 | *s*-BuB | 1.442 | 1.444 | 1.409 | 1.414 |
| 17 | 1-M-3-*i*-PB | 1.578 | 1.590 | 1.531 | 1.548 |
| 18 | 1,2,3-TMB | 2.143 | 2.165 | 2.312 | 2.303 |
| 19 | 1-M-4-*i*-PB | 1.675 | 1.670 | 1.626 | 1.678 |
| 20 | 1-M-2-*i*-PB | 1.866 | 1.863 | 1.862 | 1.870 |
| 21 | 1,3-DEB | 1.954 | 1.968 | 1.910 | 1.927 |
| 22 | 1-M-3-*n*-PB | 2.089 | 2.085 | 2.033 | 2.059 |
| 23 | *n*-BuB | 2.163 | 2.170 | 2.158 | 2.171 |
| 24 | 1-M-4-*n*-PB | 2.183 | 2.192 | 2.160 | 2.180 |
| 25 | 1,2-DEB | 2.270 | 2.252 | 2.270 | 2.278 |
| 26 | 1,3-DM-5-EB | 2.244 | 2.236 | 2.168 | 2.194 |
| 27 | 1,4-DEB | 2.138 | 2.138 | 2.085 | 2.099 |
| 28 | 1-M-2-*n*-PB | 2.438 | 2.436 | 2.477 | 2.490 |
| 29 | 1,4-DM-2-EB | 2.748 | 2.734 | 2.793 | 2.818 |
| 30 | 1,3-DM-4-EB | 2.825 | 2.809 | 2.851 | 2.861 |
| 31 | 1,2-DM-4-EB | 2.917 | 2.900 | 2.925 | 2.948 |
| 32 | 1,2-DM-3-EB | 3.581 | 3.53 | 3.716 | 3.710 |
| 33 | 1,2,4,5-TeMB | 4.265 | 4.20 | 4.509 | 4.501 |
| 34 | 1,2,3,5-TeMB | 4.406 | 4.42 | 4.592 | 4.601 |
| 35 | 1,2,3,4-TeMB | 5.889 | 5.76 | 6.482 | 6.453 |

that for $C_1$ to $C_4$ hydrocarbons exists for aromatic hydrocarbons, it is possible to deduce the relative retention times on the mixed phases of any composition from Fig. 2. Table II shows the observed values on the mixed phases as compared with the presumed values from the figure. The points in Fig. 2 represent the observed values. These results show that the presumed values are in fair agreement with the observed values. The considerably large differences between the presumed and the observed values of benzene may be due to errors in the measurement of its small retention times. It may be expected that similar linearities also exist in the other sets of liquids.

Table III shows the sets of the six liquids.

To constitute a mixed phase for a capillary column, the two liquids must be soluble in each other. Using the presumed diagrams of

TABLE III. SETS OF STATIONARY LIQUIDS

| | DNCB | DPTCP | PEG 600 | BQ | DNP |
|---|---|---|---|---|---|
| SQ | not miscible | × | not miscible | ● | × |
| DNP | ○ | × | not miscible | × | |
| BQ | × | ● | × | | |
| PEG 600 | × | × | | | |
| DPTCP | × | | | | |
| DNCB | | | | | |

×: There is no possibility of the separation of all hydrocarbons on the presuming diagram.
●: There are same possibilities of the separation on the presuming diagram, however, all hydrocarbons cannot be experimentally separated.
○: All hydrocarbons can be separated.

retention times in Fig. 2 on each set of two liquids, a mixed phase which gives a separation of all the aromatic hydrocarbons from $C_6$ to $C_{10}$ has been sought.

*SQ-BQ System.* — As may be observed in Fig. 3, there are possibilities of the separation of all solutes in the 10—15% range of BQ. Experiments show, however, that isobutylbenzene overlapped with 1, 2, 4-trimethylbenzene on the BQ 12% column. On the BQ 15% column, these components could be separated, but 1, 2, 4-trimethylbenzene overlapped with *s*-butylbenzene. All the other solutes were separated in both cases.

*BQ-DPTCP System.*—As may be observed in Fig. 4, there are possibilities of the separation in the 20—25% range of BQ. However, the mixture of BQ and DPTCP, when allowed to stand, gave a white crystalline material which seems to be a molecular complex of these compounds. In the case of two liquids which constitute a mixed phase interacting strongly with each other, it was doubtful that the linear relationship described above would be present. However, the observed values on the BQ 21% column agreed well with the presumed values. On this column, *n*-butylbenzene and 1-methyl-4-*n*-propylbenzene are unseparated. On a BQ-enriched column, these were separated, while isobutylbenzene and *s*-butylbenzene became inseparable from each other.

*DNP-DNCB System.*—As is described above, the separation on this system might be influenced by the charge transfer interaction between DNCB and the aromatic hydrocarbons to be separated. In these cases, the temperature effect on selectivity seems to be more remarkable. Therefore, retention times were measured at three different temperatures; 70, 80 and 90°C.

Figure 5 is the presumed diagram for retention times at 70°C. In this diagram, there are possibilities of the separation of all the solutes on the mixed phase of DNCB concentration near 10%. As a result of the retention time measurement with three mixed phases, DNCB 9%, 10% and 11%, all the aromatics from $C_6$ to $C_{10}$ (except for 1, 3-dimethyl-2-ethylbenzene) were successfully separated on the DNP 90% - DNCB 10% column. As no standard sample of 1, 3-dimethyl-2-ethylbenzene could be obtained, the retention time of the compound will be presumed afterwards by the use of another relationship. The chromatogram is shown in Fig. 6. The observed

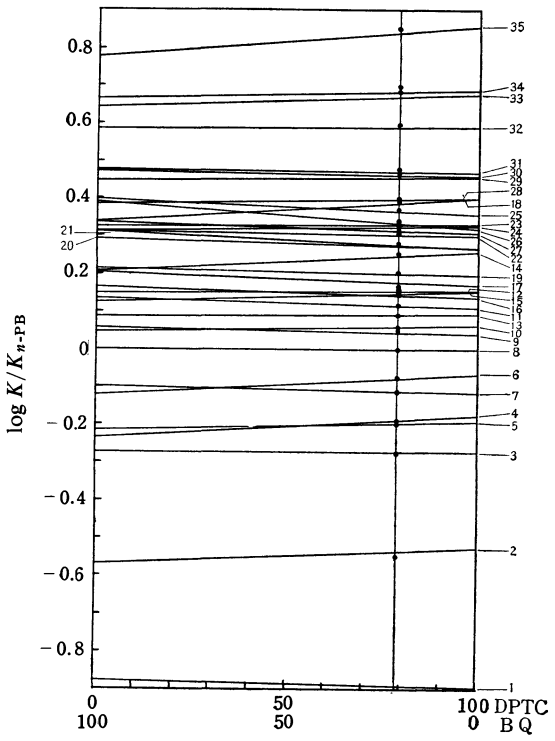



Fig. 4. The relationship between the relative retention time of the solute (log $K/K_{n\text{-PB}}$) and the composition (wt.%) of the mixed stationary liquid DPTCP-BQ at 70°C.

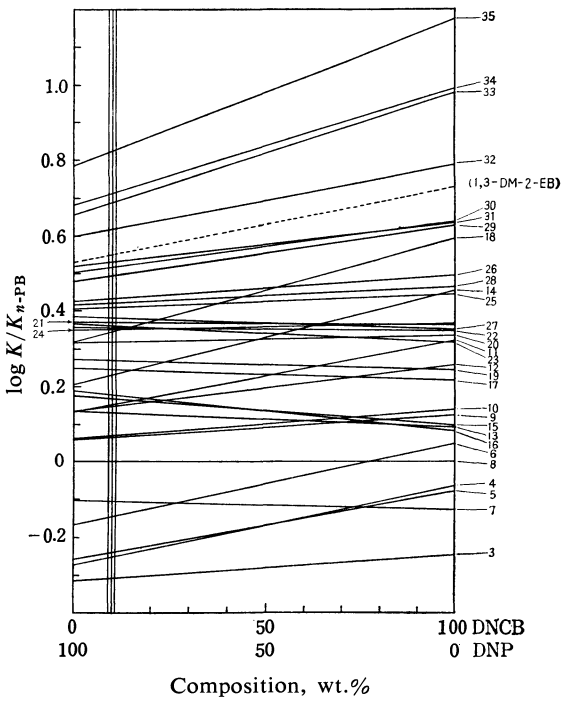
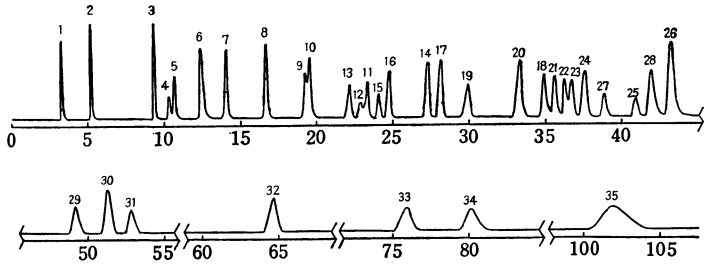



Fig. 5. The relationship between the relative retention time of the solute (log $K/K_{n\text{-PB}}$) and the composition (wt.%) of the mixed stationary liquid DNCB-DNP at 70°C.




Retention time, min.

Fig. 6. The separation of all aromatic hydrocarbons through $C_{10}$ on the DNP 90%-DNCB 10% column.
Column length: 45 m. (I. D. 0.25 mm.), Temp.: 70°C
Carrier gas: He, Inlet pressure 60 p.s.i.g.

Table IV. Relative retention times on DNP 90% - DNCB 10% column (70°C)

| No. | Compound | Presumed | Observed |
|---|---|---|---|
| 1 | B | | 0.093 |
| 2 | T | | 0.229 |
| 3 | EB | 0.491 | 0.488 |
| 4 | *p*-X | 0.559 | 0.553 |
| 5 | *m*-X | 0.576 | 0.570 |
| 6 | *o*-X | 0.708 | 0.708 |
| 7 | *i*-PB | 0.784 | 0.787 |
| 8 | *n*-PB | 1.000 | 1.000 |
| 9 | 1-M-3-EB | 1.159 | 1.159 |
| 10 | 1-M-4-EB | 1.175 | 1.172 |
| 11 | 1,3,5-TMB | 1.413 | 1.410 |
| 12 | 1-M-2-EB | 1.396 | 1.392 |
| 13 | *t*-BuB | 1.346 | 1.352 |
| 14 | 1,2,4-TMB | 1.698 | 1.688 |
| 15 | *i*-BuB | 1.472 | 1.486 |
| 16 | *s*-BuB | 1.500 | 1.522 |
| 17 | 1-M-3-*i*-PB | 1.742 | 1.776 |
| 18 | 1,2,3-TMB | 2.213 | 2.204 |
| 19 | 1-M-4-*i*-PB | 1.854 | 1.874 |
| 20 | 1-M-2-*i*-PB | 2.089 | 2.096 |
| 21 | 1,3-DEB | 2.244 | 2.252 |
| 22 | 1-M-3-*n*-PB | 2.270 | 2.301 |
| 23 | *n*-BuB | 2.302 | 2.330 |
| 24 | 1-M-4-*n*-PB | 2.339 | 2.383 |
| 25 | 1,2-DEB | 2.582 | 2.598 |
| 26 | 1,3-DM-5-EB | 2.717 | 2.757 |
| 27 | 1,4-DEB | 2.404 | 2.446 |
| 28 | 1-M-2-*n*-PB | 2.649 | 2.677 |
| 29 | 1,4-DM-2-EB | 3.098 | 3.138 |
| 30 | 1,3-DM-4-EB | 3.281 | 3.314 |
| 31 | 1,2-DM-4-EB | 3.389 | 3.426 |
| 32 | 1,2-DM-3-EB | 4.131 | 4.163 |
| 33 | 1,2,4,5-TeMB | 4.853 | 4.951 |
| 34 | 1,2,3,5-TeMB | 5.200 | 5.235 |
| 35 | 1,2,3,4-TeMB | 6.669 | 6.697 |

and the presumed values of the relative retention times are shown in Table IV. *t*-Butylbenzene - 1 - methyl - 2 - ethylbenzene - 1, 3, 5-trimethylbenzene and 1-methyl-2-isopropylbenzene - 1, 2, 3-trimethylbenzene, which were unresolved on the DNP column, were separated and eluted in the order of the supposed stabilities of the complexes with DNCB.

Table V shows the gradients of the lines which are calculated from the logarithm of the observed relative retention times of the hydrocarbons on the DNP 100% column and the DNP 90% - DNCB 10% column. These values seem to represent roughly the relative stabilities of the complexes. Hydrocarbons of the same type have close values. Tetramethylbenzenes, the nucleous basicities of which are the highest, have the highest values, while trimethylbenzenes are the next in values. The relatively low values of dimethylethylbenzenes may be due to the steric effects of alkyl groups. It may also stem from the same reason that methylethylbenzenes have higher values than diethylbenzenes, and xylenes have still higher values. Generally, as the alkyl groups of the side chain become longer, the values become higher. In the di-substituted isomers, the values decrease in the order of *o*-(1, 2), *p*-(1, 4) and *m*-(1, 3). These tendencies agree well with that of the interactions of picric acid in chloroform with these aromatic hydrocarbons.[10]

*The Presumption of the Retention Time of 1, 3-Dimethyl-2-ethylbenzene.*—The elution time of 1, 3-dimethyl-2-ethylbenzene on the DNP 90% - DNCB 10% column has been presumed, for its standard sample alone could not be obtained.

For a homologous series of compounds the ratios of the heat of solution and the heat of vaporization of which are constant, a linear relationship between the logarithm of the retention times obtained on the same column and the logarithm of vapor pressures has been

10) H. D. Anderson and O. L. Hammick, *J. Chem. Soc.*, **1950**, 1089.

TABLE VI. RESULTS OF QUANTITATIVE ANALYSES OF AROMATIC HYDROCARBONS IN VARIOUS CRUDE OILS

| No. | | Kuwait | Seria | Khafji | North Sumatra | Bunju |
|---|---|---|---|---|---|---|
| | 45—200°C fraction (vol.%) | 23.1 | 34.5 | 21.6 | 59.2 | 30.7 |
| | Aromatic hydrocarbons (vol.%) | 13.9 | 18.9 | 9.6 | 17.4 | 33.1 |
| 1 | B | 3.6 | 1.4 | 0.8 | 1.2 | 5.2 |
| 2 | T | 12.3 | 12.6 | 7.2 | 19.2 | 15.2 |
| 3 | EB | 6.6 | 2.0 | 6.6 | 3.4 | 5.2 |
| 4 | *p*-X | 3.6 | 4.1 | 4.1 | 5.4 | 4.8 |
| 5 | *m*-X | 12.0 | 36.5 | 10.4 | 21.3 | 19.1 |
| 6 | *o*-X | 7.7 | 6.0 | 7.0 | 10.2 | 8.3 |
| 7 | *i*-PB | 1.1 | 0.4 | 0.8 | 0.8 | 1.7 |
| 8 | *n*-PB | 1.5 | 0.7 | 2.2 | 0.8 | 2.4 |
| 9 | 1-M-3-EB | 3.9 | 2.9 | 3.2 | 2.4 | 3.0 |
| 10 | 1-M-4-EB | 5.6 | 2.3 | 9.5 | 3.6 | 3.9 |
| 11 | 1,3,5-TMB | 4.0 | 6.0 | 3.6 | 7.0 | 3.6 |
| 12 | 1-M-2-EB | 4.3 | 1.0 | 6.1 | 0.6 | 1.6 |
| 13 | *t*-BuB | 0.02 | 0 | 0 | 0 | 0.4 |
| 14 | 1,2,4-TMB | 10.2 | 9.2 | 11.1 | 11.5 | 8.7 |
| 15 | *i*-BuB | 0.3 | 0.2 | 0.2 | 0.4 | 0.3 |
| 16 | *s*-BuB | 0.5 | 0.3 | 0.3 | 0.4 | 1.1 |
| 17 | 1-M-3-*i*-PB | 0.9 | 0.6 | 0.4 | 0.8 | 0.9 |
| 18 | 1,2,3-TMB | 1.9 | 1.9 | 2.1 | 2.3 | 2.4 |
| 19 | 1-M-4-*i*-PB | 0.6 | 0.7 | 0.4 | 0.3 | 0.6 |
| 20 | 1-M-2-*i*-PB | 1.1 | 0.2 | 0.1 | 0.03 | 0.6 |
| 21 | 1,3-DEB | 0.8 | 0.3 | 1.2 | 0.3 | 0.4 |
| 22 | 1-M-3-*n*-PB | 1.4 | 1.1 | 1.5 | 0.1 | 1.5 |
| 23 | *n*-BuB | 0.6 | 0.3 | 1.2 | 0.4 | 0.9 |
| 24 | 1-M-4-*n*-PB | 0.8 | 0.6 | 1.6 | 0.6 | 0.7 |
| 25 | 1,2-DEB | 0.5 | 0 | 1.1 | 0.02 | 0 |
| 26 | 1,3-DM-5-EB | 1.5 | 1.7 | 2.5 | 1.7 | 1.2 |
| 27 | 1,4-DEB | 0.5 | 0.3 | 1.2 | 0.2 | 0.3 |
| 28 | 1-M-2-*n*-PB | 1.6 | 0.2 | 3.2 | 0.4 | 0.5 |
| 29 | 1,4-DM-2-EB | 1.8 | 1.0 | 1.5 | 0.8 | 1.3 |
| 30 | 1,3-DM-4-EB | 2.9 | 1.5 | 4.4 | 1.1 | 1.8 |
| 31 | 1,2-DM-4-EB | 1.6 | 1.2 | 1.9 | 1.2 | 1.1 |
| | 1,3-DM-2-EB (presumed) | 0 | 0.2 | 0.3 | 0 | 0.1 |
| 32 | 1,2-DM-3-EB | 0.7 | 0.2 | 1.2 | 0 | 0.1 |
| 33 | 1,2,4,5-TeMB | 0.6 | 0.6 | 0.2 | 0.9 | 0.3 |
| 34 | 1,2,3,5-TeMB | 0.8 | 1.3 | 0.6 | 0.6 | 0.4 |
| 35 | 1,2,3,4-TeMB | 0.9 | 0.2 | 0.3 | 0 | 0.1 |
| | $C_{11}$ | 1.2 | 0.6 | 0 | 0 | 0.3 |

shown by Hoare and Purnell.[11] This relation is mathematically induced as follows. The gas-liquid partition coefficient ($K$) is given by:

$$K=\frac{\rho RT}{M\gamma^0 P^0} \tag{1}$$

where $\rho$ is the specific gravity of the solvent at the column temperature, $T$ (°C); $M$ is the molecular weight of the solvent; $\gamma^0$ is the activity coefficient of the solute at an infinite dilution, and $P^0$ is the saturation vapor pressure of the solute. If the excess free energy of the mixing of the solute is designated as $\Delta G_m$, the heat of mixing, as $\Delta H_m$, and the entropy of mixing, as $\Delta S_m$, thermodynamics gives the following equations;

$$\Delta G_m=\Delta H_m-T\Delta S_m$$

and

$$\Delta G_m=RT\ln\gamma^0$$

If $\gamma^0=\gamma_t\gamma_a$, it can be written:

$$\ln\gamma_t=\frac{\Delta H_m}{RT},\quad \ln\gamma_a=-\frac{\Delta S_m}{R} \tag{2}$$

where $\gamma_a$ is the athermal activity coefficient. The heat of the vaporization ($\Delta H_v$) of the solute is given by the Clapeyron-Clausius equation as follows:

11) M. R. Hoare and J. H. Purnell, *Trans. Faraday Soc.*, 52, 222 (1956).

$$\ln P^0 = -\frac{\Delta H_v}{RT} + C_1 \quad (3)$$

while the heat of solution ($\Delta H_s$) is:

$$\Delta H_s = \Delta H_m - \Delta H_v \quad (4)$$

From Eq. 1, the logarithm of the relative partition coefficient is given by:

$$\ln K/K_{n\text{-PB}} = \ln \frac{(\gamma_t \gamma_a P^0)_{n\text{-PB}}}{\gamma_t \gamma_a P^0}$$

or $$\ln K/K_{n\text{-PB}} = -\ln \gamma_t - \ln P^0 - \ln \gamma_a + \ln A$$

where $A = (\gamma_t \gamma_a P^0)_{n\text{-PB}}$

The insertion of Eqs. 2 and 3 in this equation then gives:

$$\ln K/K_{n\text{-PB}} = -\frac{\Delta H_s}{RT} - \ln \gamma_a - C_1 + \ln A \quad (5)$$

The rearrangement of Eq. 3 becomes:

$$\Delta H_v = -RT \ln P^0 + C_1 RT \quad (6)$$

and if a constant $a$ is defined as follows:

$$a = -\frac{\Delta H_s}{\Delta H_v}$$

then Eq. 6 will become:

$$-\Delta H_s = -aRT \ln P^0 + C_1 aRT \quad (7)$$

If this is substituted into Eq. 5, the result is:

$$\ln K/K_{n\text{-PB}} = -a \ln P^0 + C_1(a-1) - \ln \gamma_a + \ln A \quad (8)$$

Therefore, it may be recognized from this equation that the plots of $\log K/K_{n\text{-PB}}$ against $\log P^0$ yield a straight line if $\gamma_a$, which is related to the magnitude of the solute and the solvent molecules, changes little and if $a$ is constant for a homologous series of solutes.

Figure 7 illustrates the plots of $\log K/K_{n\text{-PB}}$ obtained on the DNP column against $\log P^0$ for $C_7$ to $C_{10}$ aromatic hydrocarbons. These plots fall on a nearly straight line. It may be considered that the separation of aromatic hydrocarbons on the DNP column does not deviate much from the distillation with an ideal degree of separation because the slope of this straight line is almost unity ($a=0.95$).

For a homologous series of mono-substituted compounds, viz., toluene, ethylbenzene, *n*-propylbenzene and *n*-butylbenzene, a more strict linear relationship is observed. Moreover, since five dimethylethylbenzenes fall on a nearly straight line, it may possibly be thought that 1, 3-dimethyl-2-ethylbenzene will also fall on this line; that is to say, the elution time of 1, 3-dimethyl-2-ethylbenzene on the DNP column may be given by the intersecting point of this line with the dotted line corresponding to $\log P^0$ of 1, 3-dimethyl-2-ethylbenzene, as is shown in Fig. 7.

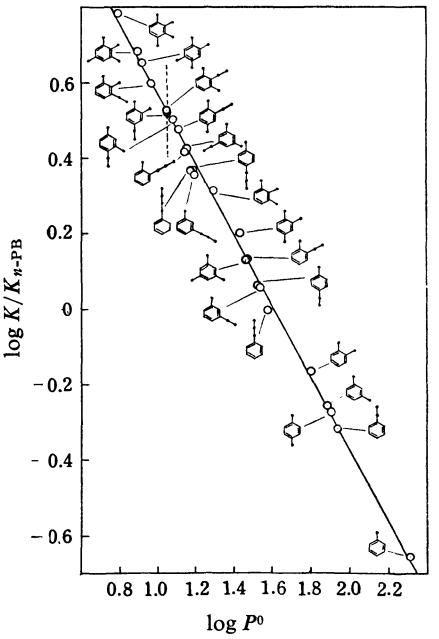



Fig. 7. The relation between the partition coefficient and vapor pressure on the DNP column (70°C).

On the other hand, as is shown clearly in Fig. 8, such plots for the data obtained on the DNCB column do not fall on a straight line. As the number of substituents increases within the compounds of the same carbon number, the plots of the $\log K/K_{n\text{-PB}}$ fall in the upper part of the figure. In $C_9$ aromatic hydrocarbons, for example, the value becomes higher in the order of propylbenzenes, methylethylbenzene and trimethylbenzenes. For xylenes and methylethylbenzenes, it becomes higher in the order of *m*-(1, 3), *p*-(1, 4) and *o*-(1, 2)-substituted.

As Fig. 8 shows, all of the lines connecting the points of a homologous series of compounds are almost linear, and they are parallel to each other.

The elution time of 1, 3-dimethyl-2-ethylbenzene (0.73) was presumed by finding the point corresponding to the vapor pressure ($P^0$) of 1, 3-dimethyl-2-ethylbenzene at the column temperature on the line drawn from the point of 1, 2, 3-trimethylbenzene parallel with the line connecting the points of 1, 2, 4-trimethylbenzene and its homologues. By inserting the presumed values of $\log K_{1,3\text{-DM-2-EB}}/K_{n\text{-PB}}$ on the DNP (0.53) and DNCB (0.73) column into Fig. 5, the presumed relative retention time of 1, 3-dimethyl-2-ethylbenzene on the DNP 90% - DNCB 10% column was found to be 3.55. This shows that 1, 3-dimethyl-2-ethylbenzene will be eluted in the middle

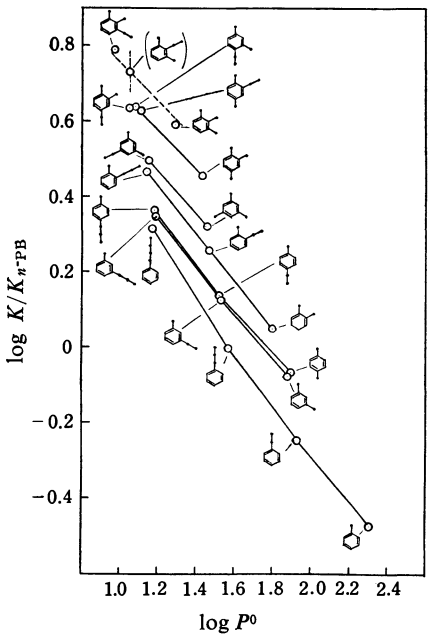



Fig. 8. The relation between the partition coefficient and vapor pressure on the DNCB column (70°C).

of 1,2-dimethyl-4-ethylbenzene and 1,2-dimethyl-3-ethylbenzene and will be overlapped by neither of them.

**The Analysis of Aromatic Hydrocarbons in Crude Oil.**—Aromatic hydrocarbons through $C_{10}$ in several crude oils were analyzed using a capillary column coated with a DNCB 10%-DNP 90% mixed stationary liquid, thus making possible the effective separation of all these compounds. In the beginning, a 45—250°C fraction of each crude oil was collected by distillation, and then aromatic fractions were separated from the distillate by silica-gel chromatography.

On the chromatograms of these samples, several small peaks which do not correspond to any of the components studied in this paper were observed. It might be thought from their relatively longer elution time that all of these peaks except one correspond to the $C_{11}$ aromatic hydrocarbons. Figure 9 shows a part of the chromatogram obtained with the aromatic fraction of Bunju Crude Oil. In this figure, the position corresponding to the presumed retention time of 1,3-dimethyl-2-ethylbenzene is shown by an arrow. It seems that peak A (relative retention time=3.52)

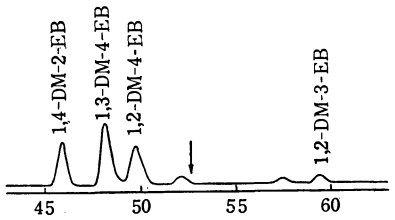



Fig. 9. A part of the chromatogram of the aromatic hydrocarbon fraction in Bunju crude oil.
Stationary liquid: DNP 90%-DNCB 10% mixture.
Column length: 45 m. (I. D. 0.25 mm.)
Temp.: 70°C
Carrier gas: He, Inlet pressure 60 p.s.i.g.

TABLE V. THE GRADIENTS OF LINES CALCULATED FROM THE LOGARITHM OF THE OBSERVED RELATIVE RETENTION TIME ON THE DNP 100% AND DNP 90%-DNCB 10% COLUMNS

| Mono-substituted | | Di-substituted | | Tri-substituted | | Tetra-substituted | |
|---|---|---|---|---|---|---|---|
| EB | 0.03 | *o*-X | 0.16 | 1,2,3-TMB | 0.25 | 1,2,3,4-TeMB | 0.42 |
| | | *m*-X | 0.13 | 1,2,4-TMB | 0.24 | 1,2,3,5-TeMB | 0.37 |
| *i*-PB | −0.01 | *p*-X | 0.14 | 1,3,5-TMB | 0.18 | 1,2,4,5-TeMB | 0.39 |
| *n*-PB | 0.00 | | | | | | |
| | | 1-M-2-EB | 0.11 | 1,2-DM-3-EB | 0.21 | | |
| *n*-BuB | −0.01 | 1-M-3-EB | 0.05 | 1,2-DM-4-EB | 0.16 | | |
| *i*-BuB | −0.03 | 1-M-4-EB | 0.08 | 1,3-DM-2-EB | 0.18 | | |
| *s*-BuB | −0.06 | | | 1,4-DM-2-EB | 0.19 | | |
| *t*-BuB | −0.02 | 1-M-2-*n*-PB | 0.10 | 1,3-DM-5-EB | 0.13 | | |
| | | 1-M-3-*n*-PB | 0.04 | | | | |
| | | 1-M-4-*n*-PB | 0.06 | | | | |
| | | 1-M-2-*i*-PB | 0.05 | | | | |
| | | 1-M-3-*i*-PB | 0.01 | | | | |
| | | 1-M-4-*i*-PB | 0.02 | | | | |
| | | 1,2-DEB | 0.08 | | | | |
| | | 1,3-DEB | 0.03 | | | | |
| | | 1,4-DEB | 0.02 | | | | |

possibly corresponds to 1, 3-dimethyl-2-ethylbenzene and that pear B (4.01) corresponds to any of the $C_{11}$ aromatic hydrocarbon isomers.

The volume fractions of the distillates of several crude oils and the results of the quantitative analyses of aromatic hydrocarbons in these fractions are shown in Table VI. The 1, 3-dimethyl-2-ethylbenzene content is calculated from peak A. In addition to some main components, such as benzene, toluene, xylenes, methylethylbenzenes and trimethylbenzenes, these crude oils contain almost all of the components discussed above, although only small quantities of each.

The authors wish to express their appreciation to the Maruzen Oil Co., Ltd., for permission to publish this work; to Professor Wataru Funasaka and Professor Tsuguo Kojima of Kyoto University for their valuable comments, and to Mr. Tsunehide Kozuma of the Maruzen Oil Co., Ltd., for his valuable advice.

*Research Center*
*Maruzen Oil Co., Ltd.*
*Wakayama*

# Electrometric Studies on the Reaction between Silver and Alkali Metavanadate

By R. S. SAXENA and O. P. SHARMA

(Received August 17, 1964)

In earlier publications[1-4] the authors have studied the reaction between $Ag^+$ and $VO_4^{3-}$, $V_2O_7^{4-}$ ions and some of their analytical applications by electrometric methods. In continuation of previous investigations, the present work has been undertaken with a view to study the formation and composition of silver metavanadate by the interaction of silver nitrate and alkali metavanadate solutions, and to examine the possibility of developing this as an analytical method for the determination of vanadium as silver metavanadate.

## Experimental

Anal. R. (BDH) reagents, vanadium(V) oxide, sodium hydroxide, silver nitrate, and reagent grade nitric acid were used and their solutions prepared in air-free conductivity water. Furthermore a standard solution of sodium orthovanadate was prepared by dissolving the requisite amount of vanadium(V) oxide in a boiling solution of sodium hydroxide of the required strength. Orthovanadate solution thus prepared was treated with a calculated quantity of nitric acid at 100°C to yield standard sodium metavanadate solution.

**Amperometric Titrations.**—A manual polarograph with scalamp galvanometer as a current recorder was used for the amperometric titrations. A dropping mercury electrode having the following characteristics: $m=2.416$ mg./sec., $t=3.58$ sec., and $m^{2/3}t^{1/6}=2.226$ mg$^{2/3}$ sec$^{-1/2}$ at $E_{d.e.}=-1.0$ V. (vs. SCE) was used in conjunction with a SCE connected to the cell by an agar-potassium nitrate bridge. All amperometric titrations were performed in the presence of the base electrolyte sodium nitrate, 0.005% thymol as maximum supressor, and 40% alcoholic media, at $E_{d.e.}=-0.3$ V. (vs. SCE). At this potential under the above conditions, $VO_3^-$ ion does not produce any measurable diffusion current, whereas $Ag^+$ ion yields a diffusion current almost proportional to its concentration. Twenty milliliters of the titer solution was taken in the cell each time and deaerated and stirred by bubbling hydrogen. The diffusion current obtained after each addition of titrant was corrected for the dilution effect and plotted against the volume of titrant in millilitre. The end-point was located graphically. The results of amperometric titrations are summarised in Table I.

TABLE I. SUMMARY OF THE RESULTS OF AMPEROMETRIC TITRATIONS

| Molarity of solutions | | Equivalence points, ml. | |
|---|---|---|---|
| $AgNO_3$ | $Na_2O \cdot V_2O_5$ | Calcd. | Obs. |
| Direct titrations Fig. 1 curve I(D) | | | |
| M/25 | M/250 | 4.00 | 4.00 |
| M/40 | M/500 | 3.20 | 3.20 |
| M/100 | M/1200 | 3.33 | 3.30 |
| M/150 | M/2000 | 3.00 | 3.05 |
| Reverse titrations Fig. 1 curve II(R) | | | |
| M/250 | M/100 | 4.00 | 4.00 |
| M/750 | M/250 | 3.33 | 3.40 |
| M/1500 | M/450 | 3.00 | 3.10 |

1) R. S. Saxena and O. P. Sharma, *Talanta*, **11**, 863 (1964).
2) R. S. Saxena and O. P. Sharma, *Naturwissenschaften*, **51**, 433 (1964).
3) R. S. Saxena and O. P. Sharma, *Indian J. Chem.*, **2**, 502 (1964).
4) R. S. Saxena and O. P. Sharma, *Z. anal. Chem.* (1964) (in press).

TABLE II. RESULTS OF E. M. F. AND GLASS ELECTRODE TITRATIONS

| Molarity of solutions | | Equivalence points, ml. | | |
|---|---|---|---|---|
| | | Calculated for the formation of | Observed from | |
| $AgNO_3$ | $Na_2O \cdot V_2O_5$ | $Ag_2O \cdot V_2O_5$ | Max. $dE/dV$ | Max. $dpH/dV$ |
| Direct titrations Fig. 2 curve I(D) | | | | |
| M/10 | M/100 | 4.00 | 3.98 | |
| M/20 | M/250 | 3.20 | 3.20 | |
| M/50 | M/600 | 3.33 | 3.30 | |
| M/75 | M/1000 | 3.00 | 2.95 | |
| Reverse titrations Fig. 2 curve II(R) and Fig. 3 curves I and II | | | | |
| M/50 | M/20 | 4.00 | 4.02 | 4.00 |
| M/200 | M/75 | 3.75 | 3.74 | 3.78 |
| M/500 | M/150 | 3.00 | 3.00 | 3.02 |
| M/750 | M/250 | 3.33 | 3.30 | 3.30 |

**Potentiometric and Glass Electrode Titrations.** —The E. M. F. and pH of the solutions were measured on a Cambridge (null deflection type) pH meter by means of a bright silver electrode and a glass electrode of the range 0—9 respectively, in conjunction with a saturated calomel electrode connected to the cell by a low resistance salt bridge. After each addition of the titrant, the E. M. F. and pH were measured and plotted against the volume of titrant added, the end point was obtained from the sharp inflection in the titration curves and also from the pronounced maxima in $dE/dV$ and $dpH/dV$ respectively. A series of E. M. F. and pH titrations was performed, using the same concentrations of the reactants for the sake of comparison, both by the direct and inverse methods. Only reverse glass electrode titrations yielded dependable results. The results or the investigations carried out are tabulated below. Only two representative graphs are given for the sake of brevity.

## Discussion

The pH of silver nitrate and $Na_2O \cdot V_2O_5$ was measured with a glass electrode and found to be 6.30 and 7.50 respectively. The titration curves (Fig. 3, curves I and II) illustrate the changes occurring in $H^+$ ion concentration when $Na_2O \cdot V_2O_5$ is added to silver nitrate solution. A sharp change in pH was observed at the stoichiometric end point where the molecular ratio of $Ag^+$ and $VO_3^-$ ions is 1 : 1 corresponding to the formation of silver metavanadate $Ag_2O \cdot V_2O_5$ in the pH-range 6.25—7.0.

An examination of the results of potentiometric titrations (Fig. 2 curves I(D) and II (R)) reveals that the reaction between silver nitrate and $Na_2O \cdot V_2O_5$ can be suitably followed using a bright silver electrode. As the titration proceeds, the E. M. F remains almost constant until in the vicinity of the end point a marked change in E. M. F. occurs; beyond that it remains practically constant.

Conductometric titrations between silver nitrate and $Na_2O \cdot V_2O_5$ were also tried but they failed to provide any conclusion regarding the composition of silver metavanadate.

The same concentrations of reactants were used in potentiometric and pH titrations for the sake of comparison. After each addition of the titrant, it takes a little time for the E. M. F., and pH values to become steady. The results are accurate and reproducible.

The amperometric titration betweens silver nitrate and $Na_2O \cdot V_2O_5$ were performed at an electric tension of $-0.3$ V. vs. SCE. In the direct titrations (Fig. 1, curve I(D)), when $Na_2O \cdot V_2O_5$ is used as the titer, $VO_3^-$ ion does not yield any measurable diffusion current and hence no change in current is observed on the addition of silver nitrate solution untill the stoichiometric end point is reached, after which the diffusion current due to $Ag^+$ ions increases with the addition of silver nitrate. In the case of reverse titrations (Fig. 1, curve II(R)), the diffusion current due to $Ag^+$ ion

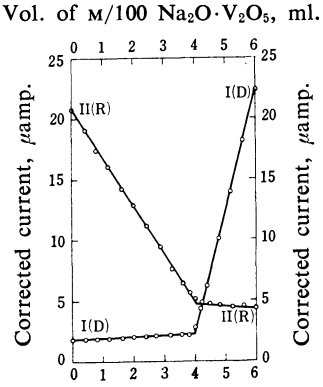



Fig. 1. Direct (I(D)) and reverse (II(R)) amperometric titrations beween $AgNO_3$ and $Na_2O \cdot V_2O_5$.
Curve I(D), M/25 $AgNO_3$ vs. M/250 $Na_2O \cdot V_2O_5$; Curve II(R) M/100 $Na_2O \cdot V_2O_5$ vs. M/250 $AgNO_3$

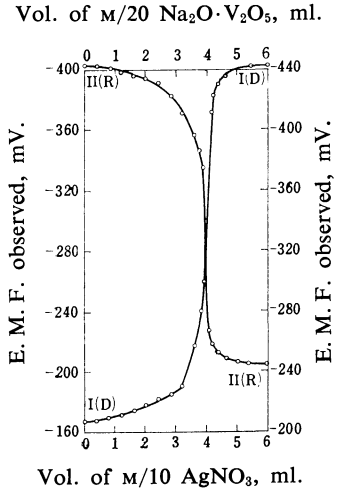



Fig. 2. Direct (I(D)) and reverse (II(R)) potentiometric titrations between $AgNO_3$ and $Na_2O \cdot V_2O_5$.
Curve I(D), M/10 $AgNO_3$ vs. M/100 $Na_2O \cdot V_2O_5$; Curve II(R) M/20 $Na_2O \cdot V_2O_5$ M/50 $AgNO_3$

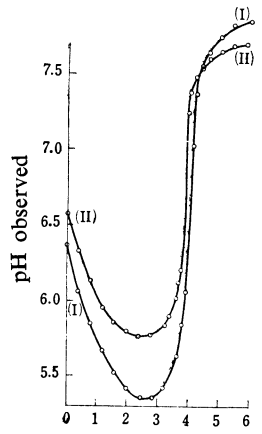



Fig. 3. Reverse pH titrations between $AgNO_3$ and $Na_2O \cdot V_2O_5$.
Curves I M/20 $Na_2O \cdot V_2O_5$ vs. M/50 $AgNO_3$; II M/75 $Na_2O \cdot V_2O_5$ vs. M/200 $AgNO_3$

gradually decreases on the addition of alkali metavanadate solution and reaches a minimum at the end point, beyond which the current almost remains constant. Amperometric titration curves are L shaped; a sharp break is obtained at the end point corresponding to the formation of silver metavanadate $Ag_2O \cdot V_2O_5$ in the pH range 6.25—7.0. The accuracy and reproducibility of these titrations has been found to be excellent even at low concentrations (0.5 mM) [of $Na_2O \cdot V_2O_5$. The presence of 40% ethanol improves the end point as the compound formed is appreciably soluble.

A comparative study of the electrometric experiments clearly suggests that pH and potentiometric titrations yield accurate results only with concentrated solutions of the reactants; at greater dilutions, the breaks and inflections are not strongly defined. Amperometric titrations, however, give very accurate end points even with low concentrations of reactants (Table I). In view of the simplicity, rapidity and accuracy of the titrations, the amperometric method may be recommended for the determination of $V^{5+}$ as silver metavanadate in the pH-range 6.25—7.0.

## Summary

The reaction between $Ag^+$ and $VO_3^-$ ions has been investigated by means of electrometric techniques involving amperometric, potentiometric and glass electrode titrations between silver nitrate and $Na_2O \cdot V_2O_5$ in 40% alcoholic media. The end point obtained from the sharp breaks and inflections in the titration curves, occurs at a stage where the molecular ratio of $Ag^+$ and $VO_3^-$ ions is 1:1 and corresponds to the formation and precipitation of silver metavanadate, $Ag_2O \cdot V_2O_5$, in the pH range 6.25—7.0. Amperometric titrations yield very accurate results and offer a simple and rapid method of determining vanadium(V) as silver metavanadate.

The authors are indebted to the Council of Scientific and Industrial Research, New Delhi, India for the award of fellowship to one of us (O. P. S.) and to Professor Dr. S. S. Dube, Head of the Department of Chemistry for providing Research facilities.

*Department of Chemistry*
*Government College*
*Kota, India*

# The Pectic Acid from the Pulp of Jackfruit (*Artocarpus Integrifolia*). II

By U. K. Sen GUPTA and A. DAS

(Received September 1, 1964)

The constitution of the pectic acid and the associated glucan present in the fleshy pulp of ripe jackfruit has been reported earlier.[1] Additional evidence will be given in the present paper in further confirmation of the proposed structure of the polysaccharide.

When the methylated methyl pectate was subjected to methanolysis, a mixture of methyl glycosides was obtained. Instead of separating the neutral components from the acidic one, we reduced the whole mixture (containing the methyl ester of the acids) with lithium aluminium hydride. The neutral methyl glycosides were then hydrolysed with 1 N hydrochloric acid, and the methyl sugars were repeatedly separated on cellulose columns (vide "Experimental") to give the methyl sugars shown in Table I.

TABLE I. METHYL SUGARS OBTAINED FROM THE METHYLATED PECTIC ACID

| Spot No. | $R_G$ | Name of the component | Yield mg. |
|---|---|---|---|
| 1 | 1.00 | 2,3,4,6-Tetra-*O*-metyl-D-glucose | 19 |
| 2 | 0.82 | 2,3,6-Tri-*O*-methyl-D-glucose | 190.5 |
| 3 | 0.76 | 2,4,6-Tri-*O*-methyl-D-glucose | 178.9 |
| 4 | 0.66 | 2,3,4-Tri-*O*-methyl-D-galactose | 42.2 |
| 5 | 0.56 | 2,3-Di-*O*-methyl-D-glucose | 19.3 |
| 6 | 0.49 | 2,3-Di-*O*-methyl-D-galactose | 3718.8 |

$R_G$ values are with reference to 2,3,4,6-tetra-*O*-methyl-D-glucose in solvent C.

The fact that 2, 3-di-*O*-methyl-D-galactose was obtained in large quantities was in agreement with the structure proposed. The reduction of the methyl ester of galacturonic acid left the $C_6$ position free, and therefore 2, 3-di-*O*-methyl-D-galactose was formed.

Attempts were also made to prepare a neutral polymer from the pectic acid itself. This was achieved through the preparation of ethylene glycol pectate,[2] the pectic acid was treated with ethylene oxide to give the glycol ester, $[\alpha]_D^{29}$ +190° (in water) (anhydrouronic acid 71.6%; equivalent wt. 251).

The ester, on reduction with sodium borohydride, yielded a neutral polysaccharide, mainly a galactan, $[\alpha]_D^{30}$ +240° (in water) (anhydrouronic acid 9.7%). The polysaccharide on hydrolysis yielded 78.3% galactose, 9.75% glucose and a trace of arabinose.

The partially-reduced polysaccharide was methylated, and during methylation the remaining acid portion was reduced with lithium aluminium hydride (vide "Experimental") to yield a methylated galactan, $[\alpha]_D^{29}$ +164° (in chloroform) and $-OCH_3$, 42.1%. The methylated polysaccharide was methanolysed, and the mixture of methyl glycosides was hydrolysed to give a mixture of methyl sugars. This mixture was then separated on a cellulose column in an automatic-fraction collector collecting the 15 ml. in each tube into the following fractions (Table II), from which pure sugars could be isolated and characterised.

The characterisation of tri-*O*-methyl-galactose as 2, 3, 6-tri-*O*-methyl-D-galactose shows that the linkage of the uronic acid units in the original pectic acid is of the 1→4 type. It is evident that the 2, 3, 4, 6-tetra-*O*-methyl-D-galactose originated from the non-reducing end of the galactan and the isolation of a small amount of 2, 3-di-*O*-methyl-D-galactose may be due to the

TABLE II. METHYL SUGARS OBTAINED FROM THE METHYLATED GALACTAN

| Fraction No. | Tube No. | Compound | Yield mg. |
|---|---|---|---|
| 1 | 18—19 | 2,3,4,6-Tetra-*O*-methyl-D-glucose | 7.1 |
| 2 | 20—31 | 2,3,4,6-Tetra-*O*-methyl-D-galactose and 2,3,6-tri-*O*-methyl-D-glucose | 79.7 |
| 3 | 32—49 | 2,3,6-Tri-*O*-methyl-D-glucose, 2,4,6-tri-*O*-metyl-D-glucose and 2,3,6-tri-*O*-methyl-D-galactose | 485.0 |
| 4 | 50—61 | 2,3,6-Tri-*O*-methyl-D-galactose | 905.0 |
| 5 | 63—64 | 2,3-Di-*O*-methyl-D-glucose and 2,3-di-*O*-methyl-D-galactose | 16.1 |

1) U. K. Sen Gupta and C. V. N. Rao, This Bulletin, **36**, 1683 (1963).
2) H. Deuel, *Helv. Chim. Acta*, **30**, 1523 (1947).

incomplete methylation of the reduced polysaccharide. The presence of 2,3,4,6-tetra-, 2,3,6- and 2,4,6-tri-, and 2,3-di-*O*-methyl-D-glucose is in keeping with the structure assigned to the repeating units of the glucan.[1] During the reduction and the methylation, no change in the structure of the methylated polysaccharide takes place.

## Experimental

All specific rotations are equilibrium values. Unless otherwise stated, all evaporations were carried out in vacuo at 30—40°C. Paper partition chromatography was carried out on Whatman No. 1 filter paper with the following solvent systems (v/v) : (A) ethyl acetate : pyridine : water (8 : 2 : 1); (B) ethyl methyl ketone - water azeotrope ; (C) *n*-butanol : ethanol : water (5 : 1 : 4) upper layer. Unless otherwise stated, the $R_G$ values were calculated with reference to 2,3,4,6-tetra-*O*-methyl-D-glucose in solvent C. Demethylation was carried out with hydrobromic acid.[3] The amounts of individual sugars in a mixture were calculated from the specific rotation of that mixture.

**The Methanolysis, Reduction and Hydrolysis of Methylated Methyl Pectate.**—Methylated methyl pectate (5.8 g.) in methanolic hydrogen chloride (4%, 125 ml.) was heated (8 hr.) in a sealed tube on a boiling water bath. The solution was then neutralised with silver carbonate, and the precipitate was removed by a centrifuge. The resulting dry sirup was dissolved in dry tetrahydrofuran (160 ml.), and lithium aluminium hydride (2.5 g.) in dry tetrahydrofuran (60 ml.) was added slowly to the boiling solution over a one-hour period. After the mixture had been refluxed for one hour and kept at room temperature for two hours, the mixture was treated with water. The solvent was then removed, and the residue was shaken with acetone and ethanol. The extracts were dialysed against distilled water, deionised with Amberlite IR-120(H) and IR-45(OH), and evaporated to a sirup. N Hydrochloric acid (200 ml.) was added, and the mixture was heated (6 hr.) on a boilng water bath. After neutrarisation (silver carbonate) and deionisation (Amberlite resins IR-120(H) and IR-45(OH)), the resulting solution was evaporated to a sirup (4.39 g.).

The mixture of methyl sugars (ca. 4.35 g.) was separated through a cellulose column (70×3.5 cm.) using solvent B. It was found that only one pure fraction could be collected in a good quantity; most of the other fractions were mixtures of two or more components. The major pure fraction (3.52 g.), with $[\alpha]_D^{30}$ +78.5° (*c* 1.1, water), $-OCH_3$, 29.7% (calcd. for $C_8H_{10}O_6$: $-OCH_3$, 29.8%), gave only galactose on demethylation. It was characterised as 2,3-di-*O*-methyl-D-galactose through the crystalline *N*-phenyl-2,3-di-*O*-methyl-D-galactosylamine, m. p. and mixed m. p. 152—153°C. The remaining fractions were converted to a combined sirup (790 mg.) and separated through a similar cellulose column into eleven fractions, which were individually evaporated to sirups.

3) L. Hough, J. K. N. Jones and W. H. Wadman, *J. Chem. Soc.*, **1950**, 1702.

**The Examination of the Fractions and Identification of the Methyl Sugars.** — *Fraction 1.*—The chromatographically-pure sirup (17 mg.) had $[\alpha]_D^{30}$ +82° (*c* 0.2, water), $-OCH_3$, 52% (calcd. for tetramethyl hexose : $-OCH_3$, 52.5%), and $R_G$, 1.0, and on demethylation it gave glucose. It was identified as 2,3,4,6-tetra-*O*-methyl-D-glucose by preparing its crystalline *N*-phenyl-2,3,4,6-tetra-*O*-methyl-D-glucosylamine, m. p. and mixed m. p. 136—137°C.

*Fraction 2.*—This fraction (25.5 mg.), with $[\alpha]_D^{30}$ +69° (*c* 0.25, water), produced only glucose on demethylation ; it was chromatographically (solvent B) identified as a mixture of 2,3,4,6-tetra- (2 mg.) and 2,3,6-tri-*O*-methyl-D-glucose (23.5 mg.).

*Fraction 3.*—This chromatographically-pure fraction had $[\alpha]_D^{30}$ +67° (*c* 0.4, water), and $R_G$ 0.82, $-OCH_3$, 41.2% (calcd. for trimethyl hexose : $-OCH_3$, 41.8%), and on demethylation it produced glucose only. It was characterised as 2,3,6-tri-*O*-methyl-D-glucose through its crystalline 2,3,6-tri-*O*-methyl-D-glucose-1,4-di-*p*-nitrobenzoate, m. p. and mixed m. p. 190—191°C.

*Fraction 4.* — This sirup (40.6 mg.), with $[\alpha]_D^{30}$ +70.2° (*c* 0.45, water), furnished only glucose on demethylation ; it was paper chromatographically identified as a mixture of 2,3,6- (21.2 mg.) and 2,4,6-tri-*O*-methyl-D-glucose (19.4 mg.).

*Fraction 5.* — This chromatographically-pure fraction (142.2 mg.), with $[\alpha]_D^{30}$ +72° (*c* 0.5, water), $R_G$ 0.76, $-OCH_3$, 41.1% (calcd. for trimethyl hexose : $-OCH_3$, 41.8%), on demethylation gave only glucose ; it was identified as 2,4,6-tri-*O*-methyl-D-glucose through the crystalline *N*-phenyl-2,4,6-tri-*O*-methyl-D-glucosylamine, m.p. and mixed m.p. 162—163°C.

*Fraction 6.* — The sirup (22.8 mg.), with $[\alpha]_D^{30}$ 82.4° (*c* 0.4, water), produced glucose and galactose on demethylation; it was paper chromatographically identified as a mixture of 2,4,6-tri-*O*-methyl-D-glucose (17.3 mg.) and 2,3,4-tri-*O*-methyl-D-galactose (5.5 mg.).

*Fraction 7.* — The chromatographically-pure sirup (28.5 mg.) had $[\alpha]_D^{30}$ +110° (*c* 0.42, water), $R_G$ 0.66, $-OCH_3$, 41.05%, and furnished galactose only on demethylation. The sugar was characterised as 2,3,4-tri-*O*-methyl-D-galactose by preparing the crystalline *N*-phenyl-2,3,4-tri-*O*-methyl-D-galactosylamine derivative, m. p. and mixed m. p. 163—164°C.

*Fraction 8.*—This fraction (10.3 mg.), with $[\alpha]_D^{30}$ +102° (*c* 0.3, water), produced glucose and galactose on demethylation; it was paper chromatographically identified as a mixture of 2,3,4-tri-*O*-methyl-D-galactose (8.2 mg.) and 2,3-di-*O*-methyl-D-glucose (2.1 mg.).

*Fraction 9.*—The sirup (17.3 mg.) was chromatographically-pure, with $[\alpha]_D^{30}$ +66° (*c* 0.4, water), $R_G$ 0.55, and on demethylation it gave only glucose. The sugar was identified as 2,3-di-*O*-methyl-D-glucose by preparing the crystalline 2,3-di-*O*-methyl-D-gluconophenylhydrazide, m. p. and mixed m. p. 160—161°C.

*Fraction 10.*—This fraction (42.4 mg.) with $[\alpha]_D^{30}$ +76° (*c* 0.5, water), produced glucose and galactose on demethylation ; it was paper chromatographically identified as a mixture of 2,3-di-*O*-methyl-D-glucose (trace) and 2,3-di-*O*-methyl-D-galactose.

*Fraction 11.*—The chromatographically-pure sirup (156.4 mg.), with $[\alpha]_D^{30}$ +78° (*c* 1.0, water), and $R_G$ 0.49, $-OCH_3$, 29.3% (calcd. for dimethyl hexose: $-OCH_3$, 29.8%) gave galactose only on demethylation; it was characterised as 2,3-di-*O*-methyl-D-galactose through the crystalline *N*-phenyl-2,3-di-*O*-methyl-D-galactosylamine derivative, m. p. and mixed m. p. 152—153°C.

**Preparation of Ethylene Glycol Pectate.**[2] — Ethylene oxide (40 ml.) was added to a suspension of pectic acid (sample A,[1] 12.5 g.) in water (250 ml.), and the mixture was shaken (10 days) at room temperature until it became neutral. The resulting glycol ester was precipitated by acetone. The product was redispersed in water and precipitated by ethanol, The glycol ester (9 g.) had $[\alpha]_D^{30}$ +190° (*c* 0.96, water), anhydrouronic acid,[4] 71.6% (≡85.9% anhydrouronic acid in pectic acid), and equivalent wt. 251 (≡70.1% anhydrouronic acid in glycol ester and 84.1% anhydrouronic acid in pectic acid).

**Reduction of Ethylene Glycol Pectate.**—Ethylene glycol pectate (8 g.) in water (250 ml.) containing glycerol (4 g.) was treated with sodium borohydride[5] (2.5 g.) in water (20 ml.); the mixture was then kept overnight at 2°C. The solution was passed through columns of Amberlite IR-120(H) and Amberlite IR-45(OH), and the partially-reduced polysaccharide (6 g.) was isolated by the addition of acetone. This had $[\alpha]_D^{30}$ +236° (*c* 0.9, water), and was 21.32% anhydrouronic acid. The product subjected to four further reductions when the resulting galactan (2.8 g.), with $[\alpha]_D^{30}$ +240° (*c* 0.8, water) and 9.7% anhydrouronic acid, was obtained. The reduced polysaccharide (0.298 mg.) was hydrolysed, and the amounts of individual sugars were estimated by the periodate method,[6] which showed the presence of galactose (78.3%), glucose (9.75%), and arabinose (trace).

**Methylation of Galactan, Hydrolysis and the Separation of Methyl Sugars.** — Partially-reduced pectic acid (anhydrouronic acid, 21.32%; 5g.) was methylated[4,7,8] with methyl sulphate and sodium hydroxide. After dialysis, the solution of the partially-methylated polysaccharide was deionised through Amberlite IR-120(H) and then neutralised with silver carbonate to the silver salt. Silver oxide (30 g.) was added in several lots over a 6-hr. period to a boiling solution of dry silver salt in methyl iodide (100 ml.) containing dry methanol (5 ml.). The mixture was refluxed for 4 hr., and product was extracted with chloroform after distilling off the methyl iodide. The above process was repeated once more to yield a methylated polysaccharide (3.1 g., $-OCH_3$, 40.8%).

The methylated polysaccharide (3 g.) was dissolved in boiling tetrahydrofuran (70 ml.), and lithium aluminium hydride (2 g.) in tetrahydrofuran (100 ml.) was slowly added to it with occasional shaking. The mixture was refluxed for one hour. After the removal of the inorganic salts and deionisation, the reduced methylated polysaccharide was twice subjected to methylation with methyl iodide and silver oxide. The resulting methylated galactan (2.1 g.) had $[\alpha]_D^{29}$ +164° (*c* 1.4, chloroform) and $-OCH_3$, 42.1%. A solution of methylated galactan (2 g.) in 5% methanolic hydrogen chloride (125 ml.) was refluxed for 8 hr. The solution was evaporated to a sirup under reduced pressure. N Hydrochloric acid (100 ml.) was added, and the mixture was heated (6 hr.) on a boiling-water bath. The solution was cooled, neutralised (silver carbonate), and filtered. The filtrate was deionised (Amberlite IR-120(H) and Amberlite IR-45(OH)) and evaporated to give a sirup (1.7 g.), which was then, by using solvent B, separated on a cellulose column (60× 3.5 cm.) into five fractions.

*Fraction 1.*—The sirup (7.1 mg.) had $[\alpha]_D^{30}$ +81° (*c* 0.25, water) and was identified as 2,3,4,6-tetra-*O*-methyl-D-glucose by paper chromatography and its specific rotation.

*Fraction 2.* — The sirup (79.7 mg.), with $[\alpha]_D^{30}$ +72.5° (*c* 0.6, water), on demethylation produced glucose and galactose. Paper chromatography (solvent C) of the sirup separated it into two components ($R_G$ 0.87 and 0.84) corrresponding to 2,3,4,6-tetra-*O*-methyl-D-galactose and 2,3,6-tri-*O*-methyl-D-glucose. The mixture (ca. 50 mg.) was separated on 3MM filter paper with solvent C. Strips corresponding to trimethyl sugar and tetramethyl sugar were eluted with water, and the solutions concentrated. The component which corresponded to 2,3,4,6-tetra-*O*-methyl-D-galactose had $[\alpha]_D^{30}$ +106° (*c* 0.25, water), and the other, which corresponded to 2,3,6-tri-*O*-methyl-D-glucose, had $[\alpha]_D^{30}$ +64° (*c* 0.4, water).

*Fraction 3.* — This fraction (458 mg.), with $[\alpha]_D^{30}$ +77.9° (*c* 0.8, water), was paper chromatographically (solvent C) found to be a mixture of three components ($R_G$ 0.84, 0.77 and 0.70). Demethylation gave galactose and glucose. The mixture (ca. 200 mg.) was separated on 3MM filter paper. The major component (160 mg.) had $[\alpha]_D^{30}$ +79° (*c* 1.05, water) and was identified as 2,3,6-tri-*O*-methyl-D-galactose through the crystalline 2,3,6-tri-*O*-methyl-D-galactonolactone, m. p. and mixed m. p. 96—97°C. The other two components (about 15 mg. each), corresponding to 2,3,6-tri-*O*-methyl-D-glucose and 2,4,6-tri-*O*-methyl-D-glucose, had $[\alpha]_D^{30}$ +65° (*c* 0.32, water) and $[\alpha]_D^{30}$ +73° (*c* 0.37, water) respectively.

*Fraction 4.* — The chromatographically-pure sirup (905 mg.), with $[\alpha]_D^{30}$ +79° (*c* 1.5, water), and $-OCH_3$, 41.6% (calcd. for trimethyl hexose: $-OCH_3$, 41.8%), on demethylation gave galactose only; it was characterised as 2,3,6-tri-*O*-methyl-D-galactose by converting into 2,3,6-tri-*O*-methyl-D-galactonolactone, m. p. and mixed m. p. 96—97°C.

*Fraction 5.*—Paper chromatography of the sirup, which had $[\alpha]_D^{30}$ +70.5° (*c* 0.3, water), showed it to be a mixture of two components ($R_G$ 0.56 and 0.50). Demethylation gave glucose and galactose. The mixture (ca. 10 mg.) was sepapated on 3MM papers, and the components identified as 2,3-di-*O*-methyl-D-glucose (5 mg.), $[\alpha]_D^{30}$ +65° (*c* 0.25, water) and 2,3-di-*O*-methyl-D-galactose (5 mg.), $[\alpha]_D^{30}$ +77° (*c* 0.2, water).

4) C. Doree, "The Methods of Cellulose Chemistry," 2nd ed., Chapman & Hall Ltd., London (1947), p. 381.
5) G. O. Aspinall and A. Cañas Rodriguez, *J. Chem. Soc.*, **1958**, 4020.
6) E. L. Hirst and J. K. N. Jones, ibid., **1949**, 1659.
7) W. N. Haworth, ibid., **107**, 8 (1915).
8) T. Purdie and J. C. Irvine, ibid., **83**, 1021 (1903).

**Summary**

The jackfruit pectic acid has been converted into ethylene glycol ester, which, on reduction with sodium borohydride, gives a galactan. Methylation studies of the original polysaccharide and of the reduced pectic acid suggest the presence of chains of 1→4 linked α-D-galacturonic acid residues in the pectic acid which is associated with a glucan.

The authors are thankful to Dr. P. Bagchi Director of Research, East India Pharmaceutical Works, Ltd., Calcutta, and to Dr. C. V. N. Rao for their kind interest in this paper.

*Department of Macromolecules*
*Indian Association for*
*the Cultivation of Science*
*Calcutta 32, India*

# Structure of the Polysaccharides from Unripe Mango (*Mangifera Indica* LINN). III

By A. Das and U. K. Sen Gupta

(Received September 1, 1964)

Crude polysaccharide was isolated in a 7% yield from the mesocarp of unripe mango (*Mangifera Indica* LINN) by extracting it with hot water and precipitating it with ethanol, as has been described in an earlier communication.[1] The material had a $[\alpha]_D^{30}$ +151.3° in 2% sodium hydroxide (*c* 0.5) and uronic anhydride, 12.3%. On hydrolysis, the neutral portion of the above polysaccharide was found to contain glucose (79.3%) and arabinose (6.98%), while the acidic portion was found to contain galacturonic acid. These results show that the percentages of arabinose and uronic anhydride are greater than those present in the crude polysaccharide isolated from ripe mango.[1]

The polysaccharide did not yield any complex with calcium chloride, cetavlon or Fehling's solution. Hence, the purification of the crude polysaccharide was effected by dissolving it in water and precipitating it with ethanol (70%), which has been reported[2] to dissolve the araban preferentially. After four successive precipitations, the uronic anhydride content decreased to 8.78% and the specific rotation changed to +158.8°. On quantitative hydrolysis and estimation, the percentages of anhydro glucose and anhydro arabinose were found to be 85.9 and 3.5 respectively. Further repetition of the fractionation process could not bring about any appreciable change in the percentage composition of the sugar components or in the specific rotation value of the polysaccharide. It was shown in the case of ripe mango polysaccharide that the trace of arabinose which originally appeared in the crude polysaccharide completely disappeared after purification, and that the uronic acid portion originated from an associated uronan component (pectic acid). In the present case also, since the arabinose and uronic anhydride content gradually decrease during fractionation, it is reasonable to believe that the galacturonic acid and arabinose come from galacturonan and araban components, associated as pectic constituents with the glucan.

The purified polysaccharide gives a violet colour with iodine, but it remains unaffected on diastase treatment. This behaviour is similar to that of the glucan from ripe mango.[1]

The purified polysaccharide was methylated according to the procedure of Falconer and Adams.[3,3a] The fully methylated product, obtained in the form of light yellow flakes, was highly soluble in chloroform; $OCH_3$, 42.3%, $[\alpha]_D^{30}$ +173.5°, in chloroform (*c* 1). The methylated product was methanolised and separated into neutral and acidic components. The neutral sugars were identified as shown in the Table I.

The uronic acid portion was identified as 2, 3-di-*O*-methyl-D-galacturonic acid. The isolation of only 2, 3-di-*O*-methyl-D-galacturonic acid from the hydrolysate of the methylated

1) A. Das and C. V. N. Rao, *Tappi*, **47**, No. 6, 339 (1964).

1a) "The Constitution of the Glucan from Mango," Part II: A. Das and C. V. N. Rao, in press.

2) F. Ehrlich and F. Schuber, *Biochem. Z.*, **203**, 343 (1928).

3) E. L. Falconer and G. A. Adams, *Can. J. Chem.*, **34**, 338 (1956).

3a) G. A. Adams, ibid., **36**, 755 (1958).

TABLE I. NEUTRAL METHYL SUGARS FROM METHYLATED POLYSACCHARIDE

| Spot No. | Component | Derivative | $R_G$* |
|---|---|---|---|
| 1 | 2,3,4,6-Tetra-*O*-methyl-D-glucose | Anilide | 1.0 |
| 2 | 2,3,5-Tri-*O*-methyl-L-arabinose | Amide | 0.94 |
| 3 | 2,3,6-Tri-*O*-methyl-D-glucose | 1,4-Di-*p*-nitrobenzoate | 0.82 |
| 4 | 2,4,6-Tri-*O*-methyl-D-glucose | Anilide | 0.75 |
| 5 | 2,3-Di-*O*-methyl-L-arabinose | 1,4-Di-*p*-nitrobenzoate | 0.62 |
| 6 | 2,3-Di-*O*-methyl-D-glucose | Phenylhydrazide | 0.55 |
| 7 | 2-*O*-Methyl-L-arabinose | Pheylhydrazone | 0.37 |
| 8 | L-Arabinose | | 0.14 |

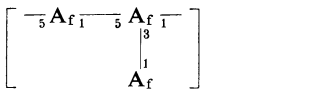
* $R_G$ values are with respect to 2,3,4,6-tetra-*O*-methyl-D-glucose in solvent E.

polysaccharide corroborates the earlier contention that the galacturonic acid originates from the pectic acid component associated with the neutral polysaccharide.

Hence, in view of the above results, it is reasonable to believe that the polysaccharide is a mixture of three components, viz., a glucan, an araban and a galacturonan. On the basis of this, structures for the repeating units of the glucan and araban can be assigned.

The methyl sugars of glucose, viz., 2, 3, 4, 6-tetra-, 2, 3, 6- and 2, 4, 6-tri-, and 2, 3-di-*O*-methyl-D-glucose, occur in the ratio of 1 : 8.84 : 9.0 : 1.14, which is the same as that found in the case of the glucan from ripe mango. Also, the behaviour of this polysaccharide towards diastase and iodine is the same. Hence in view of similar arguments,[1,1a] it is rational to assign the same structure to the repeating unit of the glucan portion.

It has already been mentioned that arabinose occurs from an associated araban; otherwise, it is difficult to account for the isolation of three different methyl sugars of arabinose in sufficient quantities. The mole ratio between the methyl sugars of arabinose (2, 3, 5-tri- : 2, 3-di- : 2-*O*-methyl-L-arabinose) was 1 : 1.15 : 0.94. The characterisation of 2, 3, 5-tri-*O*-methyl-L-arabinose shows that the non-reducing ends of the araban are occupied by arabinofuranose residues. The presence of only one kind of dimethyl sugar, viz., 2, 3-di-*O*-methyl-L-arabinose, indicates that the backbone chain is probably constituted of 1→5 linked arabinofuranose residues. That the araban is highly branched and that the arabinose unit at the branch point is linked through $C_1$, $C_3$ and $C_5$ is proved by the isolation of considerable amounts (about 33% of the total araban) of 2-*O*-methyl-L-arabinose. The isolation of a very small amount of arabinose (from the hydrolysate of the methylated polysaccharide) that might have come from a doubly-branched unit in the araban or might have resulted from incomplete methylation and/or demethylation, seems to have no structural significance. Hence, one of the simplest structures for the repeating unit of the araban, one which satisfactorily fits the above facts, is as follows:



where $A_f$ represents an arabinofuranose unit. From the specific rotation of the polysaccharide (a mixture of three components), it is not logical to draw any conclusion about the type of linkage ($\alpha$ or $\beta$). However, the glucan and the galacturonan in the polysaccharide from ripe mango have been shown to be predominantly $\alpha$-linked; arabans of a similar structure isolated from other sources[4,5] were found to contain $\alpha$-linkage. Hence, in this case also, all the three components of the polysaccharide can be regarded as having predominantly an $\alpha$-type of linkage. From these results, it appears that the pectic constituents gradually decrease with ripening.

## Experimental

Paper chromatography was carried out with Whatman No. 1 filter papers, by the descending method, the solvent being allowed to run against the machine line. The following solvent mixtures (v/v) were used: (A) ethyl acetate : pyridine : water (8 : 2 : 1); (B) *n*-butanol : acetic acid : water (4 : 1 : 5), upper layer; (C) ethyl acetate : acetic acid : water (9 : 2 : 2); (D) ethyl methyl ketone-water azeotrope; (E) *n*-butanol : ethanol : water (4 : 1 : 5), upper layer.

The crude polysaccharide was a white amorphous powder with the following characteristics: moisture, 10.9%; ash, 0.56%, uronic anhydride,[6] 12.3%, methoxyl, 1.3%, nitrogen, traces, lignin,[7] nil, $[\alpha]_D^{30}$ +151.3° in a 2% sodium hydroxide solution (*c* 0.5). A small portion (ca. 0.5 g.) of the above product was hydrolysed (while being followed iodometrically) with N sulphuric acid by heating it (12 hr.) on a boiling water bath. After neutralisation (barium

4) E. L. Hirst and J. K. N. Jones, *J. Chem. Soc.*, **1947**, 1221; **1948**, 2311.
5) E. L. Hirst and J. K. N. Jones, ibid., **1939**, 454.
6) C. Doree, "The Methods of Cellulose Chemistry," 2nd ed., Chapman & Hall Ltd., London (1947), p. 381.
7) C. Doree, ibid., p. 369.

carbonate) and filtration, the solution was concentrated to a small volume (10 ml.). Paper chromatography with solvent A indicated the presence of glucose and arabinose, while that with solvents B and C indicated galacturonic acid in addition to glucose and arabinose.

**Estimation of the Components in the Polysaccharide.**—The polysaccharide (659.5 mg.) was hydrolysed with N sulphuric acid (65 ml.) by heating it (12 hr.) in a sealed tube on a boiling water bath. The hydrolysate was then neutralised (barium carbonate) in the presence of D-ribose (200.8 mg.), filtered, and concentrated (25 ml.). An aliquot portion (0.1 mol.) of the solution was separated on a paper chromatogram (solvent A), and strips corresponding to glucose and arabinose were eluted with water and the sugars therein estimated by the periodate method.[8] Results: anhydro arabinose, 6.98% and anhydro glucose, 79.3%.

**Separation and Identification of the Components.**—The polysaccharide (1 g.) was hydrolysed (N sulphuric acid, 100 ml.) by heating it (12 hr.) on a boiling water bath. The solution was neutralised (barium carbonate) and deionised through Amberlite IR-120(H).* The acidic component from the resulting solution was absorbed on a column of Dowex 1-X4,** and the neutral solution was evaporated to a syrup (0.86 g.). The latter was put on top of a cellulose column (2.5×60 cm.) and resolved (solvent A) into three fractions. Fraction 1 (63.4 mg.), with $[\alpha]_D^{30}$ +104° in water (*c* 1), $R_G$, 1.6 (with reference to D-glucose, solvent A) was chromatographically pure and was identified as L-arabinose through the preparation of crystalline *p*-nitro-*N*-phenyl-L-arabinosylamine; m. p. and mixed m. p. 200—201°C; lit.[9] 202°C. Fraction 2 (35.5 mg.) had $[\alpha]_D^{30}$ +63.5° in water (*c* 0.6) and was paper chromatographically found to be a mixture of glucose and arabinose. Fraction 3 (721 mg.), with $[\alpha]_D^{30}$ +52° in water (*c* 1), $R_G$, 1 (with respect to D-glucose, solvent A), was chromatographically pure and identified as D-glucose through the preparation of crystalline *p*-nitro-*N*-phenyl-D-glucosylamine; m. p. and mixed m. p. 182—183°C, lit.[9] 184°C; $[\alpha]_D^{30}$ −199° in pyridine (*c* 1), lit.[9] −201°.

**Characterisation of the Acidic Component.**—The acidic component was eluted from the Dowex 1-X4 column after thorough washing with water (20 l.), neutralised (barium carbonate), and deionised (Amberlite IR-120(H)). The resulting solution was evaporated to a syrup (105 mg.) with an equivalent weight, 205 (calcd. for monouronic acid, 194). The syrup (ca. 50 mg.) was then converted to its methyl ester methyl glycoside and reduced with lithium aluminium hydride[10] to the corresponding neutral sugar, which was identified as D-galactose through the preparation of crystalline *p*-nitro-*N*-phenyl-D-galactosylamine; m. p. and mixed m. p. 217—218°C, lit.[9] 219°C; $[\alpha]_D^{30}$ −245°C in pyridine (*c* 0.5), lit.[9] −248°.

**Purification of the Polysaccharide.**—The crude polysaccharide (25 g.) was dispersed in water (2 l.) by heating it (4 hr.) on a boiling water bath. The resultant slightly hazy solution was passed through the super centrifuge twice, and the polysaccharide was precipitated by pouring the solution into acidified (pH 4) alcohol whose final volume had been adjusted to 70% with respect to alcohol. The precipitate was collected by centrifugation, followed by the usual process. This product was found to contain uronic anhydride, 9.3%, $[\alpha]_D^{30}$ +152.8° in 2% sodium hydroxide (*c* 0.5). On hydrolysis and quantitative estimation, the material was found to contain anhydro glucose (82.2%) and anhydro arabinose (5.4%). The process of precipitation was repeated three times, after which the final product was found to have the following characteristics: moisture, 11.2%; ash, 0.47%; uronic anhydride, 8.78%; methoxyl, 0.5%; nitrogen, nil; $[\alpha]_D^{30}$ +158.8° in 2% sodium hydroxide (*c* 0.5); anhydro glucose, 85.9%, and anhydro arabinose, 3.5%. Further fractionation could not bring about any substantial change in the relative proportions of the constituent sugars.

**Treatment of the Polysaccharide with Diastase.**[1]—The polysaccharide (112 mg.) was dissolved in an acetate buffer (25 ml., pH 4.6); diastase (98 mg.) was added and incubated at 35°C. It was found that, even after 24 hr., the iodine-staining power remained intact; paper chromatographic examination of the digest failed to detect the presence of any reducing sugars.

**Methylation and Methanolysis of the Polysaccharide.**—The polysaccharide (10 g.) was methylated by the procedure of Falconer and Adams[3,3a] to yield a product (5.3 g.) with $-OCH_3$, 42.3% and $[\alpha]_D^{20}$ +173.5° in chloroform (*c* 1). The methylated product (2 g.) was methanolysed by refluxing it with methanolic hydrogen chloride (200 ml., 2%) for 16 hr., whereupon the optical rotation became constant. The solution was neutralised (silver carbonate) and evaporated to a syrup. The syrup was then heated with a saturated solution of barium hydroxide[11] (50 ml.) on a water bath. Baryta was precipitated out by carbon dioxide and the uronic acid portion was absorbed on a column of Dowex 1-X4 after the usual treatments. The neutral sugar glycosides were hydrolysed to the corresponding methyl sugars by heating them (14 hr.) with N hydrochloric acid on a water bath. The hydrolysate was neutralised (silver carbonate), filtered, and deionised (Amberlite IR-120(H) and IR-45(OH)). The resulting solution was evaporated to a syrup (1.78 g.).

The syrup (1.78 g.) was resolved (solvent D) through a cellulose column (3.5×70 cm.) into fourteen fractions, in which the amounts of methyl sugars of arabinose, in the pure state, were 9.3 mg. of 2,3,5-tri-*O*-methyl-L-arabinose, 10.6 mg. of 2,3-di-*O*-methyl-L-arabinose, and 11.2 mg. of 2-*O*-methyl-L-arabinose, along with 3.4 mg. of arabinose, therefore, another lot of the methylated polysaccharide (2 g.)

8) E. L. Hirst and J. K. N. Jones, *J. Chem. Soc.*, **1949**, 1659.

* A product of the Rohm & Hass Company, Pennsylvania, U. S. A.

** A product of the J. T. Baker Chemical Co. Phillipsburg, N. J., U. S. A.

9) F. Weygand, W. Perkow and P. Kuhner, *Chem. Ber.*, **84**, 594 (1951).

10) M. A. Akher and F. Smith, *Nature*, **166**, 1037 (1950).

11) G. G. S. Dutton and F. Smith, *J. Am. Chem. Soc.*, **78**, 2505, 3744 (1956).

was hydrolysed in the same way, and the neutral fraction of methyl sugars was separated on a similar column. Fractions corresponding to pure methyl sugars of arabinose were combined with the previous pure fractions and used in the characterisations. The ratio between the methyl sugars of glucose and that between the methyl sugars of arabinose were determined from the amounts of each sugar obtained from first column chromatography (the amount of a sugar in a mixture was calculated from the specific rotation of the mixture).

*Fraction 1* (58.5 mg.), with $[\alpha]_D^{30}$ +81° in water (*c* 1) and -$OCH_3$, 51.8%, was chromatographically (solvent D) homogeneous, and the sugar in it was identified as 2,3,4,6-tetra-*O*-methyl-D-glucose through the preparation of a crystalline aniline derivative, m. p. and mixed m. p. 136—138°C; lit.[12] 136—138°C.

*Fraction 2* (28.8 mg.) had $[\alpha]_D^{30}$ +64° in water (*c* 0.4) and was chromatographically (solvent E) identified as a mixture of 2,3,5-tri-*O*-methyl-L-arabinose (4.6 mg.) and 2,3,4,6-tetra-*O*-methyl-D-glucose (24.2 mg.).

*Fraction 3* (9.3 mg.), with $[\alpha]_D^{29}$ −35.5° in water (*c* 0.5), lit.[18] −39.5°, and -$OCH_3$, 48.2% (calcd. for a tri-*O*-methyl pentose: OMe, 48.4%), was chromatographically (solvent D) pure. On demethylation, it produced arabinose, along with some partially demethylated sugars. The fraction was identified as 2,3,5-tri-*O*-methyl-L-arabinose through the preparation of crystalline 2,3,5-tri-*O*-methyl-L-arabonamide, m. p. and mixed m. p. 134—136°C, lit.[4] 138°C.

*Fraction 4* (33.2 mg.), with $[\alpha]_D^{29}$ +58.9° in water (*c* 0.5), gave glucose and arabinose on demethylation; it was identified by paper chromatography as a mixture of 2,3,5-tri-*O*-methyl-L-arabinose (3.2 mg.) and 2,3,6-tri-*O*-methyl-D-glucose (30 mg.).

*Fraction 5* (661.7 mg.), with $[\alpha]_D^{29}$ +67° in water (*c* 1), $OCH_3$, 42% (corresponding to that of a tri-*O*-methyl hexose), was found to be pure 2,3,6-tri-*O*-methyl-D-glucose through the preparation of crystalline 2,3,6-tri-*O*-methyl-D-glucose-1,4-di-*p*-nitrobenzoate, m. p. and mixed m. p. 190°C, lit.[14] 190—192°C; $[\alpha]_D^{27}$ −33° in chloroform (*c* 0.6), lit.[14] −34°.

*Fraction 6* (70 mg.), with $[\alpha]_D^{30}$ +69.1° in water (*c* 0.5), on demethylation yielded glucose; it was paper chromatographically (solvent E) identified as a mixture of 2,3,6- (40 mg.) and 2,4,6-tri-*O*-methyl-D-glucose (30 mg.).

*Fraction 7* (689.2 mg.), with $[\alpha]_D^{30}$ +72° in water (*c* 1), $OCH_3$, 41.5%, was identified as pure 2,4,6-tri-*O*-methyl-D-glucose through the preparation of a crystalline aniline derivative, m. p. and mixed m. p. 161—163°C, lit.[15] 162—166°C; $[\alpha]_D^{28}$ −111° in methanol (*c* 0.6), lit.[15] −113°.

*Fraction 8* (28.7 mg.), with $[\alpha]_D^{30}$ +74° in water (*c* 0.34), on demethylation produced glucose and arabinose; it was identified by paper chromatography (solvent E) as a mixture of 2,4,6-tri-*O*-methyl-D-glucose (25 mg.) and 2,3-di-*O*-methyl-L-arabinose (3.7 mg.).

*Fraction 9* (10.6 mg.), with $[\alpha]_D^{30}$ +88° in water (*c* 0.5), $OCH_3$, 34.2% (calcd. for a di-*O*-methyl pentose: $OCH_3$, 34.8%), was chromatographically pure, and on demethylation it gave arabinose. The sugar in it was identified as 2,3-di-*O*-methyl-L-arabinose through the preparation of a crystalline 1,4-di-*O*-*p*-nitrobenzoate derivative, m. p. and mixed m. p. 150—151°C; lit.[16] 150—153°C.

*Fraction 10* (13.2 mg.), with $[\alpha]_D^{30}$ +75° in water (*c* 0.45), on demethylation furnished glucose and arabinose; it was identified by paper chromatography as a mixture of 2,3-di-*O*-methyl-L-arabinose (5.4 mg.) and 2,3-di-*O*-methyl-D-glucose (7.8 mg.).

*Fraction 11* (78 mg.), had $[\alpha]_D^{29}$ +66.5° in water (*c* 1) and $OCH_3$, 29.8% (calcd. for a di-*O*-methyl hexose: $OCH_3$, 29.8%). The syrup gave glucose on demethylation, and it was identified as 2,3-di-*O*-methyl-D-glucose through a crystalline phenylhydrazide derivative, m. p. and mixed m. p. 159—160°C; lit.[12] 160—162°C.

*Fraction 12* (14.2 mg.) with $[\alpha]_D^{28}$ +85.7° in water (*c* 0.5), produced glucose and arabinose on demethylation; it was identified by paper chromatography (solvent D) as a mixture of 2,3-di-*O*-methyl-D-glucose (9.2 mg.) and 2-*O*-methyl-L-arabinose (5 mg.).

*Fraction 13* (11.2 mg.), with $[\alpha]_D^{29}$ +98° in water (*c* 0.45) and $OCH_3$, 18% (calcd. for a mono-methyl pentose: $OCH_3$, 18.9%), produced arabinose on demethylation. The sugar in it was identified as 2-*O*-methyl-L-arabinose through its crystalline phenylhydrazine derivative, m. p. and mixed m. p. 114—115°C; lit.[4,17] 115—116°C.

*Fraction 14* (3.4 mg.), with $[\alpha]_D^{29}$ +103° in water (*c* 0.25), had the same mobility in the paper chromatogram as that of authentic L-arabinose.

**Characterisation of Methyl Uronic Acid Portion.** —The uronic acid portion was eluted out of the Dowex 1-X4 column with N sulphuric acid (500 ml.) after the column had been thoroughly washed with water. The acid was neutralised (barium carbonate), and the solution after neutralisation (Amberlite IR-120(H)) was evaporated to a syrup (163.8 mg.). This was hxdrolysed with N sulphuric acid and neutralised (barium carbonate), and the resulting solution after deionisation (Amberlite IR-120(H)) was evaporated to a syrup (157 mg.). The syrup ($OCH_3$, 27.3%, equivalent, 230) was found to be paper chromatographically homogeneous.

The acid (ca. 100 mg.) was converted to its methyl ester methyl glycoside by refluxing it with methanolic hydrogen chloride (2%) and reduced[10] with lithium aluminium hydride in an ethereal solution. The corresponding neutral methyl sugar solution, after hydrolysis and usual treatment, was evaporated to a syrup (88 mg.) which was chromatographically homogeneous and which had $[\alpha]_D^{30}$

12) G. O. Aspinall, E. L. Hirst and W. McArthur, *J. Chem. Soc.*, **1955**, 3075.
13) S. Baker and W. N. Haworth, ibid., **127**, 365 (1925).
14) P. A. Rebers and F. Smith, *J. Am. Chem. Soc.*, **76**, 6097 (1954).
15) H. Granichstädten and E. G. V. Percival, *J. Chem. Soc.*, **1943**, 54.
16) H. C. Srivastava and F. Smith, *J. Am. Chem. Soc.*, **79**, 982 (1957).
17) J. K. N. Jones, P. W. Kent and M. Stacey, *J. Chem. Soc.*, **1947**, 1341.
18) G. O. Aspinall and A. Canas-Rodriguez, ibid., **1958**, 4020.

$+80°$ in water (*c* 0.5), $OCH_3$, 29.6%. The demethylation of the syrup produced galactose. The sugar in the syrup was finally identified as 2,3-di-*O*-methyl-D-galactose through its crystalline aniline derivative, m. p. and mixed m. p. 152—153°C; lit.[18] 152—154°C.

## Summary

The polysaccharide isolated from the mesocarp of unripe mango has been found to be a mixture of three component polysaccharides, viz., a glucan, and araban and a galacturonan. By a methylation study, the glucan has been found to have the same structural pattern as that of the glucan isolated from ripe mango. The araban portion yielded 2, 3, 5-, 2, 3- and 2-*O*-methyl-L-arabinose. On the basis of these results, a probable structure has been assigned to the araban. The isolation of only 2, 3-di-*O*-methyl-D-galacturonic acid shows that the galacturonan portion is 1→4 linked.

The authors are thankful to Dr. P. Bagchi Director of Research, East India Pharmaceutical Works, Ltd., Calcutta, for his valuable suggestions and to Dr. C. V. N. Rao for his active cooperation.

*Department of Macromolecules*
*Indian Association for*
*the Cultivation of Science*
*Calcutta 32, India*

# Selective Reduction of Phosphatides with Lithium Aluminum Hydride. II. Reductive Cleavage of the Glycerylphosphorylcholine Linkage

By Haru KAMEYAMA* and Chieko URAKAMI

(Received September 7, 1964)

Reduction of egg yolk lecithin with lithium aluminum hydride under mild conditions, using one-molar excess of the hydride at 10°C for 20 min., gave rise to L, $\alpha$-glycerylphosphorylcholine,[1] the optical purity of which was confirmed later by van Deenen et al.[2] During the course of this study it was observed that the choline moiety of the lecithin and of glycerylphosphorylcholine molecules was released, to an extent of 20% in the case of the latter compound, on either raising the temperature or prolonging the reaction time. It would be of interest, therefore, to investigate this reaction further to see whether optically pure L, $\alpha$-glycerylphosphoric acid is produced under appropriate reaction conditions.

The difficulty of reducing the phosphoryl group with lithium aluminum hydride has been reported by Freeman and Doak.[3] Furthermore, in the literature are found the observations that neither the sulfonyl group of 2-(ethylsulfonyl)ethanol[4] nor the nitro group of methyl 4-nitropentanoate[5] are reduced with this reagent under mild conditions. It may be assumed, therefore, that these phosphorus, sulfur, and nitrogen atoms, which are shielded with oxygen atoms of higher electron densities, form complexes less readily with $AlH_4^-$ or $AlH_3$.[6],* In the lecithin molecule, however, the choline moiety may offer a site for such a coordination with either species, as we have suggested earlier[1] (Fig. 1). This suggestion was based on the fact that at least one extra mole of lithium aluminum hydride, over that required theoretically, had to be used for reductive cleavage of the two fatty acid ester groups of the lecithin molecule; the extra amount of the reagent was assumed to be consumed for complexing with the choline nitrogen. This may be supported in part by the fact that amines form complexes quite readily with aluminum hydride at low temperatures.[7,8]

* Present address: Department of Agriculture Chemistry, Osaka City University, Sakai, Osaka.

1) C. Urakami, H. Okura and M. Okada, This Bulletin, 33, 144 (1960).

2) G. H. De Haas and L. L. M. Van Deenen, *Tetrahedron Letters*, 22, 7 (1960).

3) L. D. Freeman and G. O. Doak, *Chem. Revs.*, 57, 479 (1957).

4) O. Exner, *Chem. Listy*, 47, 869 (1953).

5) H. Feuer and T. J. Kucera, *J. Am. Chem. Soc.*, 77, 5740 (1955).

6) N. L. Paddock, *Nature*, 167, 1070 (1951).

* Paddock suggested the following equilibrium in an ether solution of lithium aluminum hydride: $AlH_4^- \rightleftarrows AlH_3 + H^-$.

7) E. Wiberg and H. Nöth, Z. *Naturforsch.*, 10b, 237 (1955).

8) J. K. Ruff and M. F. Hawthorne, *J. Am. Chem. Soc.*, 83, 535, 1798 (1961).

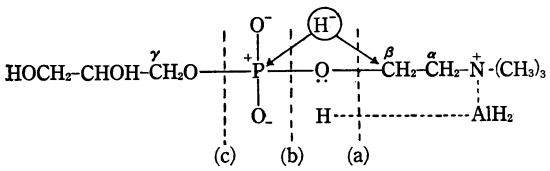



Fig. 1

There are three possible sites for cleavage by the reducing agents; (a), (b) and (c) as shown in Fig. 1. A carbon-oxygen fission (a) has been suggested previously[1] as the most favored one since the hydride ion may readiy attack the $\beta$-carbon which is more electropositive than the $\gamma$-carbon atom of the glyceryl moiety owing to the inductive effects of both the phosphoryl and quaternary ammonium groups. The products of such a cleavage would be ethyltrimethylammonium ion and $\alpha$-glycerylphosphoric acid. A fission at (b), on the other hand, would give choline and a reduced form (or forms) of glycerylphosphoric acid. This cleavage may be brought about either by complexing of the hydride reagent with the ammonium nitrogen as just mentioned, or with the phosphorus atom, followed by attack of hydride ion on the phosphorus atom. The latter mechanism may also bring about a cleavage at (c), giving rise to glycerol and reduced forms of phosphorylcholine. It is less likely, however, that the cleavages proceed through a complex formation with the phosphorus atom under the mild conditions being considered in the present study.

Since this reaction had been found to be quite sensitive to reaction temperature and mole ratios of the reactants, care was taken in controlling these two factors; the temperature was kept in a range of 10—15°C and mole ratios were raised from four to fifteen moles of the reducing reagent per mole of lecithin depending on the extent of cleavage of the choline moiety.

However, the results obtained were contrary to those expected. Instead of a carbon-oxygen fission, a phosphorus-oxygen fission occurred with the formation of choline and reduced forms of the phosphate group.

## Experimental

**Lecithin.**—The sample of hydrogenated egg yolk lecithin was prepared according to Hanahan's method[9] after purifying the crude material through a column of alumina with the solvent system of Rhodes and Lea.[10] The product was recrystallized twice from warm dioxane. This sample showed an $R_f$ value of 0.67 according to the method of Lea,[11] phosphorus: choline=1.0:0.95 (calculated as distearoyllecithin). Another sample without hydrogenation was prepared according to the method described by Nelson.[12]

**DL-$\alpha$-Glycerylphosphorylcholine.**—This compound was synthesized by the method of Baer and Kates.[13] The free base was liberated from its cadmium chloride complex by passing its aqueous solution through columns of Amberlite IRC-50 and Dowex-3.

**Barium $\alpha$-Glycerylphosphate.**—The calcium salt procured from Delta Chemical Works, Inc. (New York) was purified by adsorption chromatography on a small column of alumina and converted to the barium salt.[14] The sample was thoroughly dried for infrared analysis.

**Choline Chloride Reineckate.**—This was prepared for infrared analysis, by a modification of the method used for estimation of choline, and dried over phosphorus pentoxide in a vacuum tube for 24 hr. at the boiling temperture of acetone. The free base released by the reduction was treated similarly.

**Estimation of Choline.**—The base released on reductive cleavage and the choline in glycerylphosphorylcholine were determined according to Schmidt's method,[15] and that in lecithin by Glick's method.[16]

**Determination of Phosphorus.**—Organic samples were digested by the conventional method using 10 N sulfuric acid solution and a few drops of hydrogen peroxide and the inorganic phosphorus released was determined according to the method of Ernester and his co-workers.[17] Phosphorus in the products formed on cleavage was also determined by Burmaster's method.[18]

**$\alpha$-Glycol.** — The periodate oxidation method described by Voris[19] was used.

**Paper Chromatography.**—Paper chromatography for deacylated glycerylphosphatides and the cleaved *phosphorus-containing product(s)* was carried out according to Wheeldon's method,[20] using acid-washed Toyo No. 51 paper and water-saturated phenol containing 1% ammonia as the developing solvent system. The phosphatide samples prepared were examined by both Lea's method[11] and Marinetti's,[21] using Toyo No. 51 paper impregnated with silicic acid in conjunction with the solvent systems of chloroform-methanol (4:1, v/v) and diisobutylketone-acetic acid-water (40:20:3, v/v/v).

9) D. J. Hanahan and M. E. Jayko, ibid., **74**, 5070 (1952).
10) D. N. Rhodes and H. C. Lea, *Biochem. J.*, **65**, 526 (1957).
11) C. H. Lea, D. N. Rhodes and R. D. Stoll, ibid., **60**, 353 (1955).
12) G. J. Nelson, *J. Lipid Research*, **3**, 71 (1962).
13) E. Baer and M. Kates, *J. Am. Chem. Soc.*, **70**, 1394 (1948).
14) C. Urakami, H. Murahashi and Y. Kakutani, This Bulletin, **30**, 379 (1957).
15) G. Schmidt, L. Hecht, P. Fallot, L. Greenbaum and S. J. Thannhauser, *J. Biol. Chem.*, **197**, 601 (1952).
16) D. Glick, "Methods of Biochemical Analysis," Vol. 1, Interscience Publishers, New York (1954), p. 274.
17) L. Ernester, D. Zetterstroem and O. Lidberg, *Acta Chem. Scand.*, **4**, 942 (1950).
18) C. F. Burmaster, *J. Biol. Chem.*, **164**, 233 (1946).
19) L. Voris, G. Ellis and L. A. Maynard, ibid., **133**, 491 (1940).
20) L. W. Wheeldon, *J. Lipid Research*, **1**, 439 (1960).
21) G. V. Marinetti, ibid., **3**, 4 (1962).

TABLE I. RECOVERY OF THE WATER-SOLUBLE PRODUCTS SEPARATED BY AMBERLITE IR-112 (H)

| | Total P | | Free Ch* | | CPC Ch* | | Total Ch* | |
|---|---|---|---|---|---|---|---|---|
| | mg. | % | mg. | % | mg. | % | mg. | % |
| Lecithin | 9.99 | 100 | | | | | 39.06 | 100 |
| Aq. phase | 3.82 | 38 | 20.8 | 53 | 20.7 | 53 | 41.5 | 106 |
| Eluate a | 3.80 | 38 | 0.0 | 0 | 19.0 | 49 | 39.0 | 100 |
| Eluate b | | | 20.0 | 51 | 0.0 | 0 | | |

* Ch stands for choline and GPC for glycerylphosphorylcholine.

**Reaction with Lithium Aluminum Hydride.**—The procedure employed for the reaction was essentially the same as that described previously,[1] except that a small amount of chloroform was used to dissolve the sample of hydrogenated lecithin. The reaction mixture was made acidic with 2—3 ml. of a 10 N sulfuric acid solution, the organic phase separated from the aqueous phase, and each made up to a known volume. The former was analyzed for total phosphorus and the latter for total phosphorus and choline, both in free and ester-bound form. For separation of the individual components of the water-soluble products, the aqueous phase separated without the acid treatment was passed through a column of Amberlite IR-112 (H), and collected eluate a was made up to a known volume for analysis of phosphorus and choline. The column was then washed with a sufficient amount of a normal hydrochloric acid solution to give eluate b, which was made up to a known volume and analyzed for free choline.

Since good separation with a minimum loss of each component was achieved as shown in Table I, this procedure was employed for isolation of the products. The free base in eluate b was converted to the reineckate salt as mentioned earlier. Eluate a (pH 2.4) contaning both glycerylphosphorylcholine and the cleaved *phosphorus-containing product* was passed through a column of Amterlite IR-4B (OH). The glycerylphosphorylcholine which came through was converted to its cadmium chloride complex and recrystallized. The average recovery of glycerylphosphorylcholine, based on analysis for phosphorus, was 95%. The column was then washed with a sufficient amount of a 0.28% solution of ammonia to elute the *phosphorus-containing product*. The last procedure, when tested with the sodium salt of glycerylphosphoric acid, gave an almost quantitative recovery of phosphorus. The eluate was concentrated under mild conditions and the residue treated with barium hydroxide. The barium salt was recrystallized several times from water and alcohol. These isolated products were dried over phosphorus pentoxide in a vacuum desiccator.

## Results

**The Cadmium Chloride Complex of the Isolated Glycerylphosphorylcholine.**—Sample wt. 29 mg. Found: total choline 8.0 mg. (0.066 mmol.); total phosphorus 1.4 mg. (0.045 mmol.); $\alpha$-glycol 0.067 mmol. Calcd.: choline, phosphorus and $\alpha$-glycol 0.063 mmol. $R_f$ value was 0.84 for the isolated sample; 0.84 for the synthetic sample of DL-glycerylphosphorylcholine.

**The Reineckate Salt of the Free Base.**—Found: C, 25.88; H, 4.80; N, 24.57; Cr, 14.60. Calcd. for choline reineckate, $C_5H_{14}N[(NH_3)_2Cr(CNS)_4]$, mol. wt. 422.58: C, 25.60; H, 4.76, N, 23.20; Cr, 14.00%. The infrared absorption spectrum of the salt was found to be identical with that of the reineckate salt of choline, both showing an absorption band at 1080—1075 $cm^{-1}$ for the C–OH stretching vibration of the primary alcohol group.

**The Phosphorus-containing Products.** — See Table III for the analytical results and Table IV for the characteristic infrared absorption bands.

## Discussion

The maximum extent of cleavage of the choline ester linkage appeared to be about 50% as shown in Table II and beyond this extent a loss of the water-soluble phosphorus was observed in separate experiments, perhaps due to further degradation to phosphine.[23] Since it is reasonably certain that this cleavage proceeds via L, $\alpha$-glycerylphosphorylchloline,[1]

TABLE II. ANALYTICAL RESULTS OF THE REACTION PRODUCTS OF EGG YOLK LECITHIN WITH $LiAlH_4$ AT 10°C

| L : Hyd.* mole ratio | Time min. | Aq. phase P, % | Aq. phase Free Ch, % | Org. phase P, % |
|---|---|---|---|---|
| 1 : 4 | 20 | 63 | 32 | 20 |
| 1 : 4 | 40 | 70 | 27 | 22 |
| 1 : 6 | 60 | 76 | 18 | 20 |
| 1 : 8 | 60 | 65 | 43 | — |
| 1 : 10 | 60 | 87 | 56 | 0 |
| 1 : 15 | 120 | 97 | 49 | 0 |
| 1 : 15** | 60 | 89 | 38 | 0 |

* L : Hyd. denotes lecithin : lithium aluminum hydride.
** At 20°C

22) E. Baer and H. O. L. Fischer, *J. Biol. Chem.*, **128**, 491 (1939).
23) P. Karrer and E. Jucker, *Helv. Chim. Acta*, **35**, 1586 (1952).

TABLE III. ANALYSIS OF THE PHOSPHORUS-CONTAINING PRODUCTS ISOLATED FROM THE REACTION MIXTURE

| Product | $R_f$ | mmol. | | | | $[\alpha]_D$ |
|---|---|---|---|---|---|---|
| | | Total P[a] | Total P[b] | α-GP P | Glycol | |
| A | 0.21 | 0.022 | 0.023 | 0.014 | 0.016 | |
| E | | 0.032 | 0.024 | 0.016 | 0.027 | +0.12±0.5 |
| C | 0.28 | | | | | |
| D | 0.53 | | | | | |
| α-GP | 0.25 | | | | | −1.0[c] |

A was prepared under the reaction conditions—lecithin: the hydride reagent 1 : 10, 10°C, 60 min. B 1 : 15, 15°C, 120 min. C and D were separated from B by the paper chromatographic technique of Wheeldon.[20] a) Ernester's method.[17] b) Burmaster's method.[18] c) The reported value for a saturated solution of the silver salt.[22]

The optical activity of B is so small that it is considered to have no optical activity (measured with a Rudolph polarimeter).

TABLE IV. INFRARED ABSORPTION BANDS OF α-GLYCERYLPHOSPHORIC ACID AND THE PHOSPHORUS-CONTAINING PRODUCTS, $cm^{-1}$

| No. | α-GP | A | B | C |
|---|---|---|---|---|
| | 3419—3119 | 3443—3320 | 3430 | 3480 (sh) |
| | | | 3310 | 3340 |
| | | | 3145, 3120 | |
| | | | 3035 | |
| I | 2945 | 2920 | 2910 | 2940 |
| | 2865 (sh) | 2860 (sh) | 2850 (sh) | 2880 (sh) |
| | 2355—2312 (w) | 2320 (br, w) | 2370 (br, w) | |
| | | | 2180 (w) | 2180 (w) |
| | | | 2100 (w) | 2100 (w) |
| II | | 1620 | 1755 (w) | 1643 |
| | | | 1629 (sh) | 1605 |
| | | | 1615 | |
| | | | 1597 (sh) | |
| III | 1463 | 1460—1455 | 1452 | 1460 |
| | 1418 (w) | | 1408 | |
| IV | 1379 | 1375 | 1377 (sh) | 1380 |
| V | 1251 | | | 1255—1260 |
| | 1210 | | | |
| VI | 1120—1104 | 1095 | 1151 | 1099—1090 |
| | 1069 | | 1085 (w) | |
| | | | 1049 (w) | |
| VII | 970, 954 (d) | 956 | | 995 |
| VIII | 957 | 853 (w) | | 875 (w) |
| | | 820 (w) | 822— 813 | 820 (w) |
| | 780 (w) | 710 (w) | 720 (w, br) | 750 (w) |
| | | | | 690 |

α-GP means the barium salt of α-glycerylphosphoric acid.

(d) Stands for doublet, (sh) shoulder, (w) weak, (br) broad. For A, B and C refer to Table III. The absorption bands of D were not very distinct due to some impurities and thus omitted.

its insolubility in anhydrous ether propably prevented the reaction from going to completion.

The isolation of choline evidently indicates that a phosphorus-oxygen fission occurred in this cleavage reaction. Such a fission, therefore, should be accompanied by reduction of the phosphate moiety. This is supported in part by the following observations; the *phosphorus-containing products* isolated differ from α-glycerylphosphoric acid with respect to optical activity, behavior on periodate oxidation (Table III), and infrared absorption bands (Table IV).

Since the interpretations given for the shift in the absorption bands of the P→O and P-O-C groups (pentavalent and trivalent phosphorus) due to modification of the alkyl moiety are still open to discussion, only the absorption bands of interest will be pointed out here to show differences between the spectrum of α-glycerylphosphoric acid and those of the *cleaved products*. In the region indicated by I, Table IV, glycerylphosphorylethanolamine shows an absorption band at 2910—2860 $cm^{-1}$ and glycerylphosphorylcholine at 2865 $cm^{-1}$ [24] but these have not been correlated so far with the groups attached to these molecules. One of the characteristic differences between α-glycerylphosphoric acid and the *products* is shown in the region II. Daasch and Smith[25] have suggested that the absorption band at 1665 $cm^{-1}$ is associate with phosphonic acid and thus the bands in II may indicate the presence of reduced forms of the phosphate group. The absorption bands in the regions III and IV are common to all the compounds under consideration and the former bands have been reported to be associated with the $CH_2$ group.[26] The characteristic P→O stretching vibration in the region V is absent in samples A and B but present in C; its presence in the last sample annot be explained but the P→O group might have been formed on exposure to air during its separation and isolation from the paper chromatogram. Daasch and Smith,[25] however, have pointed out that these bands are so broadened in the case of phosphonic and phosphinic acids that it is difficult to distinguish them from each other, particularly in the spectra of the solid samples. Accordingly, A and B may be considered here again to be reduced forms of the phosphate. The P-O-C (alkyl) group is reported to show absorption bands in the regions 1163 to 1156 $cm^{-1}$ and 1050 to 995 $cm^{-1}$ [26] but the bands (VI and VII) appear to be shifted in α-glycerylphosphoric acid and the *products*. Recently, Chapman and Harper[27] have attributed absorption bands at 990—980 $cm^{-1}$ and 875—855 $cm^{-1}$ to the P-O-C (alkyl) group in phosphites, and Ackerman and his co-workers[28] report that a band near 794 $cm^{-1}$ is due to the same group in acylphosphonates. Since α-glycerylphosphoric acid shows some of these bands (VIII), no comments will be made on the similar band observed in these products.

The fact that the characteristic absorption bands of A differ from those of B and C may indiate that B (or C) is in a more reduced state than A, since the reaction conditions employed for preparation of B were somewhat more drastic than those employed for A (see also Table III). The loss of phosphorus observed on raising the temperature might have resulted from fission at both (b) and (c), Fig. 1, giving rise to phosphine as has been observed by Karrer[23] during the use of drastic conditions.

Brockerhoff[29] attributed the ease of removal of choline in the alkaline hydrolysis of glycerylphosphorylcholine to the following two factors; (1) the influence of the quaternary ammonium group which can balance in part the negative charges on the phosphate oxygens and thus facilitates approach of a nucleophilic reagent, and (2) the initial attack on the phosphorus by the nucleophilic oxygen of the secondary hydroxyl group of the glyceryl moiety. In the present case, however, ionization of the secondary alcohol would be less likely in such a medium as anhydrous ether. Instead, intramolecular hydrogen bonding between the hydroxyl hydrogen of the β-carbon of the glyceryl moiety and the P→O oxygen atom plus an ionic effect of the quarternary ammonium group on the $P-O^-$, or the latter alone, probably distort the normal tetrahedral bond angles of the phosphorus atom[30] in such a manner that the central phosphorus atom, of large radius, might readily be attacked by hydride ion. This may bring about fission at the phosphorus-oxygen linkage, (b) in Fig. 1. The stronger cationic nature of the phosphorus atom, compared with that of the β-carbon of the choline moiety, may also play a role in this cleavage.

24) E. Baer, D. Buchnea and H. C. Stancer, Jr., *J. Am. Chem. Soc.*, **81**, 2169 (1959).
25) L. W. Daasch and D. C. Smith, *Anal. Chem.*, **23**, 853 (1951).
26) R. N. Jones and C. Sandorfy, "Chemical Application of Spectroscopy," Ed. by W. West, Interscience Publishers, New York, (1956), pp. 550—551.
27) A. C. Chapman and R. Harper, *Chem. Ind.*, **1962**, 985.
28) B. Ackerman, T. A. Jordan, G. R. Eddy and D. Swern, *J. Am. Chem. Soc.*, **78**, 4444, 6026 (1956).
29) H. Brockerhoff, *J. Lipid Research*, **4**, 96 (1963).
30) J. R. Van Wazer, "Phosphorus and Its Compounds," Vol. 1, Interscience Publishers, New York (1958), p. 71.

**Summary**

Reduction of egg yolk lecithins with lithium aluminum hydride under the following reaction conditions resulted in release of choline in about 50% based on the total water-soluble phosphorus; mole ratios of lecithin : lithium aluminum hydride of 1 : 10 or 1 : 15 at 10—15°C for 60—120 min. were used. Unexpectedly, the reaction did not give any glycerylphosphoric acid. Instead, the analytical results indicated that a phosphorus-oxygen fission of the cholin-phosphate linkage is accompanied by reduction of the phosphate moiety.

The authors are indebted to Shionogi Research Center for measurement of the optical rotation of the isolated *phosphorus-containing compound.*

*Faculty of the Science of Living*
*Osaka City University*
*Nishi-ku, Osaka*

# 1-Hydroxy-1, 2, 3-benzotriazoles as Analytical Reagents. I. 4-Nitro-1-hydroxy-1, 2, 3-benzotriazole as a Specific Reagent for Silver

By H. L. SHARMA and S. K. MUKERJI

(Received September 16, 1964)

Comparatively few organic reagents afford precipitates with silver which can be directly weighed for estimation of the metal. Only *p*-dimethylaminobenzalrhodamine and some other compounds containing the grouping >NOH have been reported.[1-7] Out of the few hydroxybenzotriazoles, which are under investigation for analytical purposes by one of the authors (H. L. S.), the use of 4-nitro-1-hydroxy-1, 2, 3-benzotriazole (R) in the gravimetric estimation of silver is described in the present communication.

The aqueous-ethanolic (1 : 4 v/v) solution of this reagent R gave a scarlet red precipitate with silver ions. The precipitation was quantitative between pH 2.8—4.3 and the precipitate was stable enough to be dried at 110—125°C to a stoichiometric composition of $AgC_6H_3O_3N_4$.

The chief advantage of the reagent R over existing ones for estimation of silver is that the estimation of silver, when present singly or even in the presence of other metal ions, is fairly rapid and takes only one hour. Filtration of the precipitate is easy and quick and variation of the interval between precipitation and filtration does not affect the results.

The advantages over the recently reported reagent I[7] are that our reagent is specific for silver and that the reagent R is more soluble than I.* Moreover the precipitation of the silver salt could be well effected with reagent R in alcoholic solution, and finally it could also be dried completely whereas the precipitate of silver salt, with the reagent I, cannot be freed from $^1/_2\,C_2H_5OH$ even when dried at 120°C.**

## Experimental

**Preparation and the Solubility of the Reagent R.**—The reagent R, viz. 4-nitro-1-hydroxy-1, 2, 3-benzotriazole was prepared by the method reported earlier.[9] The results in Table I show that the average solubility of reagent R per 100 g. of water at 30°C is 0.21344 g. but an 0.4% solution of R in aqueous ethanol (1 : 4 v/v) was used for all estimations.

1) F. Ephraim, *Ber.*, **63**, 1928 (1930).
2) G. Denigés, *Bull. Soc. Pharm. Bordeaux*, **70**, 101 (1932).
3) D. C. Sen, *J. Indian Chem. Soc.*, **15**, 473 (1938).
4) J. F. Flagg and N. H. Furman, *Ind. Eng. Chem., Anal. Ed.*, **12**, 529 (1940).
5) K. J. Keuning and J. V. Dubský, *Rec. trav. Chim.*, **59**, 978 (1940).
6) P. Wenger, R. Duckert and M. L. Busset, *Helv. Chim. Acta*, **24**, 889 (1941).
7) D. S. Deorha, N. K. Kulshrestha and B. B. Varma, *Indian J. Appl. Chem.*, **27**, 4 (1964).

* The recently reported reagent, 6-chloro-4-nitro-1-hydroxy-1, 2, 3-benzotriazole (I) by Deorha et al.,[7] appears to be more than 0.8—1% soluble as 1% aqueous solution of the reagent I was used by them for all estimation. In comparison to I, we selected R as the reagent with an assumption that it should be more soluble than I. Surprisingly R was found to be only 0.2134% soluble at 30°C, a result under controversy. As such I was also prepared by the method reported earlier[8] and was found to be only 0.0708% soluble at 30°C.

8) S. S. Joshi and D. S. Deorha, *J. Indian Chem. Soc.*, **29**, 548 (1952).

** Deorha et al.,[7] also report that when precipitation was done with an alcoholic solution of the reagent I, the precipitate corresponds to the composition $AgC_6H_2O_3N_4Cl \cdot 1/2C_2H_5OH$, and that the precipitate could not be freed from alcohol even when dried at 120°C. However, such abnormality was not observed in our case.

9) W. Borsehe and D. Rantscheff, *Ann.*, **379**, 152 (1911).

TABLE I

Temp.: 30

| Wt. of the solvent (water) used., g. | Wt. of the solute R after evaporation, g. | Solubility g./100 g. at 30°C |
|---|---|---|
| 10 | 0.02134 | 0.21340 |
| 20 | 0.04271 | 0.21355 |
| 40 | 0.08536 | 0.21340 |
| 60 | 0.12804 | 0.21340 |
| 80 | 0.17074 | 0.21342 |
| 100 | 0.21348 | 0.21348 |

**Silver Nitrate Solution.**—Stock solution of N/20 silver nitrate was prepared and estimated by the usual classical methods. In order to get concordant results, estimations were made in duplicate.

**Composition of the Precipitate.**—The scarlet red precipitate obtained by mixing an excess of the solution of R with a solution of silver nitrate was washed with alcohol to remove excess of the adsorbed reagent R and was analysed after drying at 110°C. It was noted that the precipitate explodes whenever heated in a silica crucible over a flame. So the silver was estimated by obtaining silver as silver chloride from the precipitate by decomposing it with 50% hydrochloric acid. The triazole thus liberated was removed by washing the combined precipitate repeatedly with ethanol until the filtrate gave a negative test for chloride ions.

Found: N, 19.18; Ag, 37.578. Calcd. for $AgC_6H_3N_4O_3$: N, 19.52; Ag, 37.59% (Conversion factor for silver being 0.3759).

**Procedure for Estimation of Silver.**—An aliquot quantity of silver nitrate was diluted to about 100 ml. and the pH was adjusted to about 3—4. Excess of the solution of R was then added with constant stirring. The precipitate was digested on a boiling water bath for about half an hour, filtered through a sintered crucible (No. G3), washed with cold 0.06% solution of the reagent and then with 95% ethanol. It was then dried at 110—120°C to a constant weight. Table II summarizes the results of some experiments.

TABLE II

pH: 3—4 (approx.)

| Ag taken mg. | Wt. of the ppt., mg. | Ag Found mg. | Error mg. |
|---|---|---|---|
| 5.394 | 14.31 | 5.379 | −0.015 |
| 8.091 | 21.60 | 8.119 | +0.028 |
| 10.788 | 28.76 | 10.810 | +0.022 |
| 13.485 | 33.22 | 13.470 | +0.015 |
| 16.182 | 43.10 | 16.201 | +0.019 |
| 18.879 | 50.20 | 18.870 | −0.009 |
| 21.576 | 57.33 | 21.550 | −0.026 |

TABLE III

Ag: Taken 8.091 mg.; pH: 3—4 (approx.)

| Ag: Reagent (mol. ratio) | Wt. of the ppt., mg. | Ag Found mg. | Error mg. |
|---|---|---|---|
| 1 : 1.00 | 20.80 | 7.818 | −0.273 |
| 1 : 1.50 | 21.29 | 8.003 | −0.088 |
| 1 : 2.00 | 21.55 | 8.100 | +0.009 |
| 1 : 2.50 | 21.55 | 8.100 | +0.009 |
| 1 : 3.00 | 21.55 | 8.100 | +0.009 |
| 1 : 3.50 | 21.56 | 8.104 | +0.013 |

TABLE IV

Ag: Taken 8.091 mg.

| pH value | Ag Found mg. | Error mg. |
|---|---|---|
| 2.2 | 7.88 | −0.211 |
| 2.5 | 7.89 | −0.201 |
| 2.8 | 8.06 | −0.031 |
| 3.1 | 8.04 | −0.051 |
| 3.4 | 8.07 | −0.021 |
| 3.7 | 8.08 | −0.011 |
| 4.0 | 8.09 | −0.001 |
| 4.3 | 8.09 | −0.001 |
| 4.6 | 8.03 | −0.061 |
| 4.9 | 7.88 | −0.211 |
| 5.2 | 7.87 | −0.221 |
| 5.5 | 7.86 | −0.231 |

TABLE V

pH: 3—4; Ag: Taken 8.091 mg.

| Ag+Metal present (mg.) | Ag Found mg. | Error mg. |
|---|---|---|
| $Na^+$ Excess | 8.10 | +0.009 |
| $K^+$ Excess | 8.08 | −0.011 |
| $Pb^{2+}$ (8.208) | 8.08 | −0.011 |
| $Pb^{4+}$ (16.416) | 8.09 | −0.001 |
| $Hg^+$ (8.02) | 8.08 | −0.011 |
| $Hg^{2+}$ (8.02) | 8.10 | +0.009 |
| $Bi^{3+}$ (10.45) | 8.11 | +0.019 |
| $Au^{3+}$ (6.573) | 8.08 | −0.011 |
| $Cu^{2+}$ (6.354) | 8.07 | −0.021 |
| $Cd^{2+}$ (11.24) | 8.09 | −0.001 |
| $As^{3+}$ (7.49) | 8.07 | −0.021 |
| $Sb^{3+}$ (6.088) | 8.11 | +0.019 |
| $Sn^{4+}$ (11.87) | 8.08 | −0.011 |
| $Fe^{2+}$ (15.95) | 8.09 | −0.001 |
| $Fe^{3+}$ (31.90) | 8.07 | −0.021 |
| $Cr^{3+}$ (10.40) | 8.09 | −0.001 |
| $Al^{3+}$ (8.99) | 8.06 | −0.031 |
| $Zn^{2+}$ (13.07) | 8.10 | +0.009 |
| $Mn^{2+}$ (9.015) | 8.09 | −0.001 |
| $Ni^{2+}$ (13.04) | 8.12 | +0.029 |
| $Co^{2+}$ (13.09) | 8.12 | +0.029 |
| $Ba^{2+}$ (13.736) | 8.07 | −0.021 |
| $Sr^{2+}$ (8.763) | 8.09 | −0.001 |
| $Ca^{2+}$ (13.36) | 8.06 | −0.031 |
| $Mg^{2+}$ (6.776) | 8.12 | +0.029 |
| $Be^{2+}$ (4.506) | 8.11 | +0.019 |
| $Tl^{3+}$ (10.219) | 8.08 | −0.011 |
| $Ti^{4+}$ (4.79) | 8.09 | −0.001 |
| $Ce^{3+}$ (7.006) | 8.06 | −0.031 |
| $Ce^{4+}$ (7.006) | 8.08 | −0.011 |
| $UO_2^{2+}$ (11.903) | 8.07 | −0.021 |
| $Th^{4+}$ (11.60) | 8.08 | −0.011 |
| $Zr^{4+}$ (9.122) | 8.11 | +0.019 |

**Effect of Reagent Concentration.**—By keeping the amount of silver constant and varying that of the reagent, it was found that the precipitation of silver with the reagent R was not complete unless double the stoichiometrically required amount of the latter was used. Refer Table III.

**Effect of pH.**—Table IV shows that the most suitable pH range for the precipitation is between 2.8—4.3. The negative error increases as we go above pH 4.6 and below pH 2.8. It has been found that the precipitate is soluble in dilute alkalies.

**Effect of Diverse Metal Ions.**—A known amount of a standard solution of silver was taken in a beaker and diluted to 100 ml. with distilled water. Solutions of diverse metal ions were prepared by using nitrates and acetates of the metals. Difinite quantities of these solutions were added to the beaker. Estimation of silver was carried out as described earlier. Hydrolyses of $Bi^{3+}$, $Sb^{3+}$, $Sn^{4+}$ and $Ti^{4+}$ were prevented by using sodium potassium tartarate. In the case of cerium, a small amount of ammonium sulphate was added to keep the cerium salt in solution as the double sulphate.

The results of Table V clearly indicate that there is no interference by other metal ions.

## Summary

4-Nitro-1 - hydroxy - 1, 2, 3 - benzotriazole (R) has been used as a reagent for the gravimetric estimation of silver. The precipitation of the metal by this reagent is complete between pH 2.8—4.3, and after drying at 120°C the composition of the precipitate corresponds to the formula $AgC_6H_3O_3N_4$. The presence of other metal ions does not interfere in the estimation. For complete precipitation of the metal, double the stoichiometrically required amount of R was used and it was found that variation of the interval between the precipitation and filteration does not effect the result. The solubility of R is 0.2134 g./100 g. of water at 30°C.

The authors' sincere thanks are due to Professor Dr. R. C. Mehrotra, Head of the Chemistry Department, University of Rajasthan, Jaipur, Shri B. B. Mathur (H. M.), and Shri P. D. Goswami (S. I.) for providing facilities and to Mrs. Sushama Sharma for carrying out nitrogen estimations.

*Chemistry Laboratories*
*Darbar Multipurpose Higher Secondary School*
*Jaipur (Rajasthan), India*

*Department of Chemistry*
*University of Rajasthan*
*Jaipur (Rajasthan), India*

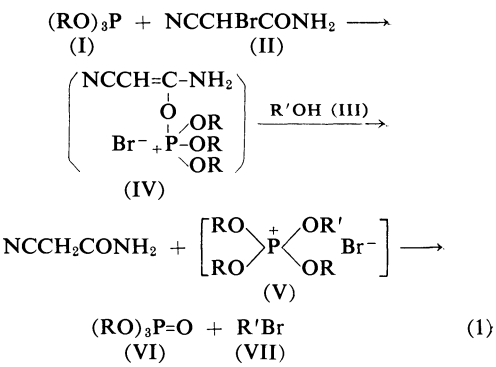
# Phosphorylation of Alcohols by the Use of Benzyldiethyl Phosphite and Monobromocyanoacetamide or *N*-Bromosuccinimide

By Teruaki MUKAIYAMA, Teisuke OBATA and Oyo MITSUNOBU

(Received October 5, 1964)

It has been demonstrated in the previous papers[1,2] that various phosphites (I) and phosphines are easily oxidized by means of monobromocyanoacetamides (II) and allyl or benzyl alcohol (III). The reactions are considered to proceed through the formation of reactive quaternary phosphonium salts (V), which in turn decompose to yield the corresponding phosphates (VI) or phosphine oxides and allyl or benzyl bromide (VII) (Eq. 1).

It is to be noted that allyl or benzyl cation which is considered to be stable might preferentially be split off from the quaternary phosphonium salts (V), resulting in the formation of allyl or benzyl bromide (VII) and oxidized products, pentavalent phosphorus compounds (VI).



(1)

In view of the results, it is expected that the successful phosphorylation of alcohols would

1) T. Mukaiyama, O. Mitsunobu and T. Obata, *J. Org. Chem.*, **30**, 101 (1965).
2) O. Mitsunobu, T. Obata and T. Mukaiyama, *J. Org. Chem.*, **30**, 1071 (1965).

Table I. Reaction of monobromocyanoacetamide with benzyldiethyl phosphite and alcohols

| Alcohol | Charge ml. | Product | | |
|---|---|---|---|---|
| | | Phosphate | Yield, % | B. p., °C/mmHg |
| Ethanol | 2 | $EtOP(O)(OEt)_2$ | 55 | 84—90/7.3 |
| Ethanol* | 2 | $EtOP(O)(OEt)_2$ | 55 | 87—92/7.3 |
| *n*-Propanol | 2 | *n*-$PrOP(O)(OEt)_2$ | 37 | 63—65/0.5 |
| *n*-Butanol | 2 | *n*-$BuOP(O)(OEt)_2$ | 47 | 68—75/0.3 |

* Alcohol was added an hour later to the reaction mixture of monobromocyanoacetamide and benzyldiethyl phosphite at room temperature.

result from the reaction of benzyldiethyl phosphite (VIII) with monobromocyanoacetamide and alcohols through the quaternary phosphonium salts (IX), as is shown in the following Eq. 2.

$$(EtO)_2POCH_2C_6H_5 + NCCHBrCONH_2 + ROH$$
(VIII)

$$\longrightarrow \left[\begin{matrix} EtO \\ EtO \end{matrix}\!\!>\overset{+}{P}<\!\!\begin{matrix} OCH_2C_6H_5 \\ OR \end{matrix}\; Br^-\right] \longrightarrow$$
(IX)

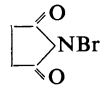
$$(EtO)_2\overset{O}{\overset{\|}{P}}\text{-}OR + C_6H_5CH_2Br \qquad (2)$$

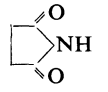
Indeed, when benzyldiethyl phosphite (VIII) was treated with monobromocyanoacetamide in the presence of ethyl alcohol in ether at room temperature, triethyl phosphate was obtained in a 55% yield, and both benzyl bromide (84%) and cyanoacetamide (51%) were also isolated (Eq. 2, R=Et). A similar reaction was observed in the case of the other alcohols (see Table I).

In the above reaction, the initially formed enol quaternary phosphonium salt (IV) is assumed to be rather stable, because there is no noticeable difference in the yield of phosphate even when ethyl alcohol was added an hour later to the reaction mixture of benzyldiethyl phosphite and monobromocyanoacetamide.

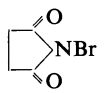
In the second experiment, phosphorylation of alcohols by the use of benzyldiethyl phosphite and *N*-bromosuccinimide was tried under the assumption that the reaction may proceed through an enol phosphonium salt[3] analogous to that of monobromocyanoacetamide (Eq. 3).

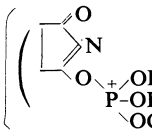
When benzyldiethyl phosphite was added to a suspension of equimolar amounts of *N*-bromosuccinimide and ethyl alcohol in ether, triethyl phosphate (X, R=Et) was obtained in a 61% yield along with benzyl bromide (85%) and succinimide (72%), as expected (Eq. 3); *n*-propyl and *n*-butyl alcohols were also phosphorylated to the corresponding alkyldiethyl phosphates (X, R=$C_3H_7$, $C_4H_9$) in yields of 60% and 31%, respectively (see Table II).

$$\text{  } + (EtO)_2POCH_2C_6H_5 + ROH \longrightarrow$$

$$(EtO)_2\overset{O}{\overset{\|}{P}}\text{-}OR + C_6H_5CH_2Br + \text{  } \qquad (3)$$
(X)

Contrary to the case of monobromocyanoacetamide, when ethyl alcohol was added an hour later to the reaction mixture of *N*-bromosuccinimide and benzyldiethyl phosphite, triethyl phosphate could not be isolated, and diethylphosphorosuccinimidate (XIII) was obtained in a quantitative yield by fractionation. In this case, the unstable quaternary phosphonium salt (XI) may decompose spontaneously, yielding benzyl bromide and imidoyl phosphate

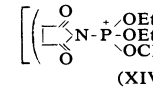
$$\text{  } + (EtO)_2POCH_2C_6H_5 \longrightarrow$$

$$\left[\left(\text{  }\right)^{*}Br^-\right] \xrightarrow{R'OH}$$
(XI)

$$\left[\begin{matrix} EtO \\ EtO \end{matrix}\!\!>\overset{+}{P}<\!\!\begin{matrix} OR' \\ OCH_2C_6H_5 \end{matrix}\; Br^-\right] \longrightarrow$$
(IX)

$$C_6H_5CH_2Br + (EtO)_2\overset{O}{\overset{\|}{P}}\text{-}OR' \qquad (4)$$

* Two alternative structures, the *O*-phosphonium salt (XI) or the *N*-phosphonium salt (XIV), are conceivable for the structure of this quaternary phosphonium salt.

$$\left[\left(\text{  }\right)Br^-\right]$$
(XIV)

The *O*-phosphonium form (XI) is preferred to the *N*-phosphonium form (XIV) in this case, by analogy with the case of the monobromocyanoacetamide. But recent investigation supports the latter structure on the basis of a NMR spectrum (A. K. Tsolis et al., *Tetrahedron Letters*, **1964**, 3217).

3) S. Trippett, *J. Chem. Soc.*, **1962**, 2337.

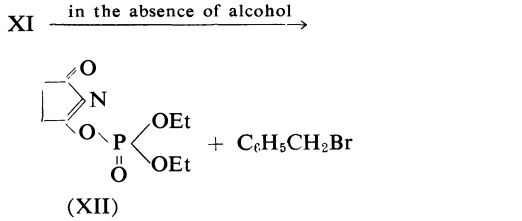
TABLE II. REACTION OF *N*-BROMOSUCCINIMIDE WITH BENZYLDIETHYL PHOSPHITE AND ALCOHOLS

| Alcohol | Charge ml. | Product | | |
|---|---|---|---|---|
| | | Phosphate | Yield, % | B. p., °C/mmHg |
| Ethanol | 2 | $EtOP(O)(OEt)_2$ | 61 | 105—108/27 |
| *n*-Propanol | 1.5 | *n*-$PrOP(O)(OEt)_2$ | 60 | 107—108/7 |
| *n*-Butanol | 1.5 | *n*-$BuOP(O)(OEt)_2$ | 31 | 65—67/0.65 |

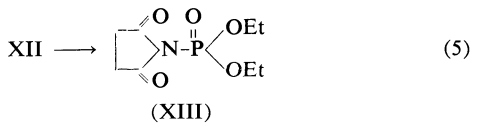
(XII), which is considered to rearrange rapidly to a more stable diethylphosphorosuccinimidate (XIII) (Eq. 5).

Whereas, the diethylphosphorosuccinimidate (XIII) did not react with alcohols at all even when they were refluxed for five hours; the starting materials were recovered.

From these results, it may be stated that imidoyl phosphonium salt (XI) is a necessary intermediate for the reactive quaternary phosphonium salt (IX), from which alkyl-diethyl phosphate may be produced by the elimination of benzyl bromide (Eq. 4).




(XII)




(XIII) (5)

## Experimental

All boiling points are uncorrected.

**Reagents.**—Benzyldiethyl phosphite was prepared by the transesterification of triethyl phosphite with benzyl alcohol.[4] Monobromocyanoacetamide[5] and *N*-bromosuccinimide[6] were prepared by the procedures given in the literature. Alcohols and solvents used were dried and distilled by the ordinary procedures.

**Reaction of Monobromocyanoacetamide with Benzyldiethyl Phosphite and Alcohols.**—To a vigorously stirred suspension of monobromocyanoacetamide (1.63 g., 0.01 mol.) in ethyl alcohol (2 ml.) and ether (20 ml.), an ethereal solution (10 ml.) of benzyldiethyl phosphite (2.28 g., 0.01 mol.) was added drop by drop over a period of 10 min., at room temperature. A white precipitate of cyanoacetamide, soon separated. After the addition was completed, the mixture was stirred at room temperature for 2 hr. and then allowed to stand overnight. Cyanoacetamide (m. p. 110—116°C, 430 mg., 51%) was removed by filtratain. The filtrate was concentrated under reduced pressure, and the resulting oil was treated with dry ether (10 ml.) to remove the residual cyanoacetamide. After concentration, the solution was distilled under reduced pressure, yielding benzyl bromide (b. p. 65—75°C/7.3 mmHg, 1.43 g., 84%) and triethyl phosphate (b. p. 84—90°C/7.3 mmHg, 1.00 g., 55%).

Similarly, *n*-propyldiethyl and *n*-butyldiethyl phosphates were prepared from monobromocyanoacetamide, benzyldiethyl phosphite and the corresponding alcohols. The physical constants of these compounds together with the yields obtained are summarized in Table I.

When ethyl alcohol was added an hour later to the mixture of monobromocyanoacetamide and benzyldiethylphosphite at room temperature, 55% of triethyl phosphate was also obtained via the same procedure as in the above reaction.

**Reaction of *N*-Bromosuccinimide with Benzyldiethyl Phosphite and Alcohols.**—A solution of benzyldiethyl phosphite (2.28 g., 0.01 mol.) in 10 ml. of dry ether was added drop by drop with vigorous stirring to a suspension of *N*-bromosuccinimide (1.78 g., 0.01 mol.) in 1.5 ml. of anhydrous *n*-propyl alcohol and ether (15 ml.). The temperature was controlled at about −40°C by cooling in an ethanol - dry ice bath. After addition was completed, the mixture was stirred for an additional 30 min., and allowed to warm slowly to room temperature. After being stirred for an additional 2 hr., the mixture was concentrated under reduced pressure, and the resulting pale yellow oil was treated with dry ether (2 ml.) at −20°C to separate the succinimide. The white crystalline succinimide (m. p. 124—126°C, 770 mg., 78%) was filtered off and the filtrate was concentrated and distilled. Benzyl bromide (b. p. 75—78°C/7 mmHg, 1.37 g., 80%) and *n*-propyldiethyl phosphate (b. p. 107—108°C/7 mmHg, 1.17 g., 60%) were obtained. The distillation residue was filtered and washed with 5 ml. of ether yielding crude succinimide (m. p. 115—118°C, 180 mg., 18%).

In a similar fashion, ethanol and *n*-butyl alcohol were phosphorylated, yielding triethyl phosphate and *n*-butyldiethyl phosphate. These results are summarized in Table II.

**Reaction of *N*-Bromosuccinimide with Benzyldiethyl Phosphite in the Absence of Alcohol.**—Benzyl diethyl phosphite (25.0 g., 0.11 mol.) was added drop by drop to a suspension of *N*-bromosuccinimide (17.8 g., 0.1 mol.) in dry ether (150 ml.) over a period of 20 min., at room temperature. After refluxing for an additional 3 hr., the solution

4) F. W. Hoffmann, R. J. Ess and R. P. Usinger, Jr., *J. Am. Chem. Soc.*, **78**, 5817 (1956).
5) T. Hata and T. Mukaiyama, This Bulletin, **35**, 1106 (1962).
6) E. Campaingne and B. F. Tullar, "Organic Syntheses," **33**, 96 (1953).

was concentrated and distilled under reduced pressure; benzyl bromide (b. p. 80—83°C/15 mmHg, 5.1 g., 88%) and diethylphosphorosuccinimidate (b. p. 140—155°C/0.03 mmHg, 19.3 g., 82%) were obtained. Redistillation gave white crystalline diethylphosphorosuccinimidate (m. p. 60—62°C, b. p. 145—150°C/0.03 mmHg, 15.3 g., 65%). Found: N, 6.10. Calcd. for $C_8H_{14}O_5NP$: N, 5.96%.

**Summary**

The phosphorylation of alcohols with benzyldiethyl phosphite and monobromocyanoacetamide has been investigated. By this method, the corresponding alkyldiethyl phosphates were obtained in fairly good yields along with benzyl bromide and cyanoacetamide. Similarly, it has been established that *N*-bromosuccinimide can be successfully used in the place of monobromocyanoacetamide in the above phosphorylation.

*Laboratory of Organic Chemistry*
*Tokyo Institute of Technology*
*Ookayama, Tokyo*

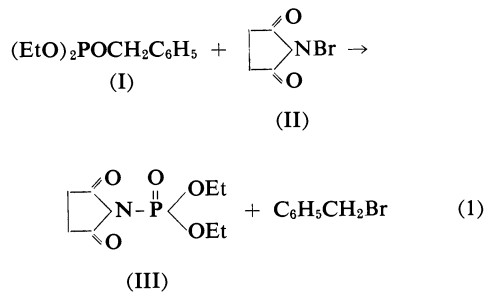
# Phosphorylation by the Use of Diethylphosphorosuccinimidate

By Teruaki MUKAIYAMA, Teisuke OBATA and Oyo MITSUNOBU

(Received October 13, 1964)

In previous papers,[1,2] it has been shown that the oxidation of various phosphines and phosphites by means of monobromocyanoacetamide and allyl or benzyl alcohol gave the corresponding phosphine oxindes and phosphates in good yields.

It was shown[2] that *N*-bromosuccinimide could also be used successfully in the place of monobromocyanoacetamide in the above reactions. During the course of the experiment, it was found that diethylphosphorosuccinimidate (III) was obtained in a good yield when benzyldiethyl phosphite (I) was treated with an equimolar amount of *N*-bromosuccinimide (II) in the absence of the alcohols (Eq. 1).



(I) (II) (III)

$$(EtO)_2POCH_2C_6H_5 + \text{NBr-succinimide} \rightarrow \text{N-P(O)(OEt)}_2\text{-succinimide} + C_6H_5CH_2Br \quad (1)$$

Since diethylphosphorosuccinimidate (III) is a kind of acid anhydride derived from a weak acid and a strong acid, it is expected that its phosphoroimidate bond would be reactive towards active hydrogen compounds, such as alcohols and phenols.

In the present experiment, phosphorylation of alcohols, phenol, and phosphates, by the use of diethylphosphorosuccinimidate was tried.

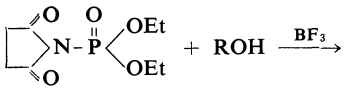
Contrary to expectation, no reaction was observed when diethylphosphorosuccinimidate was refluxed in a large excess of ethyl alcohol for five hours, and the starting materials were recovered. Further, reactions of diethylphosphorosuccinimidate (III) with alcohols in the presence of several catalysts were tried. Firstly, acid catalysts were employed on the consideration that the phosphoroimidate bond might be activated under acidic conditions. Among the catalysts examined, a protonic acid such as *p*-toluene sulfonic acid was found to be ineffective; while Lewis acids such as boron trifluoride and aluminum trichloride were shown to promote the reaction. In the case of aluminum trichloride, succinimide separated quantitatively, although the yield of alkyldiethyl phosphates (IV) was always lower than that in the case of boron trifluoride. Accordingly, the following reactions were tried with boron trifluoride as catalyst.

For example, when diethylphosphorosuccinimidate (III) was treated with a large excess of ethyl alcohol in the presence of a catalytic amount of boron trifluoride etherate under reflux for five hours, triethyl phosphate (IV, R=Et) was obtained in a 72% yield (Eq. 2). The results of phosphorylation of other alcohols by means of diethylphosphorosuccinimidate in the presence of boron trifluoride are summarized in Table I.

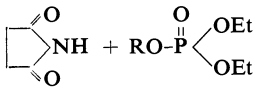
1) T. Mukaiyama, O. Mitsunobu and T. Obata, *J. Org. Chem.*, **30**, 101 (1965).
2) T. Mukaiyama, T. Obata and O. Mitsunobu, This Bulletin, **38**, 1088 (1965).

TABLE I. PHOSPHORYLATION OF ALCOHOLS OR PHENOL BY MEANS OF DIETHYLPHOSPHOROSUCCINIMIDATE IN THE PRESENCE OF BORON TRIFLUORIDE

| Material | Product | | |
|---|---|---|---|
| | Phosphate | Yield, % | B. p., °C/mmHg |
| EtOH | $EtOP(O)(OEt)_2$ | 72 | 98—102/13 |
| *n*-PrOH | *n*-$PrOP(O)(OEt)_2$ | 84 | 104—110/12 |
| *i*-PrOH | *i*-$PrOP(O)(OEt)_2$ | 73 | 98—105/12 |
| *n*-BuOH | *n*-$BuOP(O)(OEt)_2$ | 85 | 120—125/13 |
| $C_6H_5OH$ | $C_6H_5OP(O)(OEt)_2$ | 34 | 80—95/0.3 |



(III)

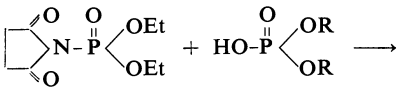


(IV) (2)

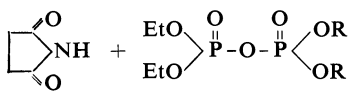
On the other hand, when diethylphosphorosuccinimidate (III) and ethyl alcohol were refluxed in the presence of a catalytic amount of basic catalysts such as sodium or triethyl amine, no reaction was observed and the starting materials were recovered.

In the second place, the reaction of phenol ($pK_a=9.9$) with diethylphosphorosuccinimidate (III) in the presence of a catalytic amount of boron trifluoride was tried. In this case, diethylphenyl phosphate (IV, $R=C_6H_5$) was isolated with some difficulty in only a 37% yield from the viscous greenish-black reaction mixture. But when phenol was treated with an equimolar amount of diethylphosphorosuccinimidate in the absence of catalyst, diethylphenyl phosphate was obtained in a 82% yield.

These results suggest that acidic compounds such as phenol are more readily phosphorylated by diethylphosphorosuccinimidate. This suggestion was confirmed by the fact that diethyl and di-*n*-butyl hydrogen phosphates, with $pK_a$ value about 2.1, were easily phosphorylated with diethylphosphorosuccinimidate (III), yielding tetraethyl pyrophosphate and *unsym.* di-*n*-butyl diethyl pyrophosphate (V, R=Et, *n*-Bu), respectively, in high yields (Eq. 3).



(III)



(V) (3)

In another reaction, preparation of acyl phosphates by the reaction of diethylphosphorosuccinimidate with butyric or valeric acids ($pK_a=4.8$) was tried. Unexpectedly when the carboxylic of acids and diethylphosphorosuccinimidate were refluxed for five hours in benzene, they did not react at all and the starting materials were recovered.

In conclusion, it is noted that phosphorylation alcohols by the use of diethylphosphorosuccinimidate could only be carried out in the presence of certain acid catalysts. On the other hand, more acidic substances such as phenol and dialkyl hydrogen phosphates were readily phosphorylated in quantitative yields even in the absence of catalysts.

## Experimental

The melting points and boiling points are uncorrected.

**Reagents.**—The solvents and alcohols were dried and purified by ordinary procedures. *N*-Bromosuccinimide, and butyric and valeric acids were obtained from a commercial source and purified by recrystallization or distillation. Diethyl hydrogen phosphate[3] and di-*n*-butyl hydrogen phosphate[4] were prepared according to the literature.

**Preparation of Diethylphosphorosuccinimidate by the Reaction of *N*-Bromosuccinimide and Benzyldiethyl Phosphite.**—Benzyldiethyl phosphite (25.0 g., 0.11 mol.) was added drop by drop to a suspension of *N*-bromosuccinimide (17.8 g., 0.1 mol.) in dry ether (150 ml.) over a period of 20 min. at room temperature. After the solution had been refluxed for 3 hr., it was concentrated and distilled under reduced pressure; benzyl bromide (b. p. 80—83°C/15 mmHg, 5.1 g., 88%) and diethylphosphorosuccinimidate (b. p. 140—150°C/0.03 mmHg, 19.3 g., 82%) were obtained. Redistillation gave white crystalline diethylphosphorosuccinimidate (m. p. 60—62°C, b. p. 145—150°C/0.03 mmHg, 15.3 g., 65%).

Found: N, 6.10. Calcd. for $C_8H_{14}O_5NP$: N, 5.96%.

IR-spectrum in Nujol: 1770, 1725, 1300, 1130, 1030 $cm^{-1}$.

Diethylphosphorosuccinimidate decomposes when

3) A. D. F. Toy, *J. Am. Chem. Soc.*, **70**, 3882 (1948).
4) O. Mitsunobu, T. Obata and T. Mukaiyama, *J. Org. Chem.*, **30**, 1071 (1965).

TABLE II. PHOSPHORYLATION OF PHENOL OR DIALKYL HYDROGEN PHOSPHATES BY MEANS OF DIETHYLPHOSPHOROSUCCINIMIDATE IN THE ABSENCE OF BORON TRIFLUORIDE

| Material | Product | | |
|---|---|---|---|
| | Phosphate or Pyrophosphate | Yield, % | B. p., °C/mmHg |
| $C_6H_5OH$ | $C_6H_5OP(O)(OEt)_2$ | 82 | 95—105/0.4—0.6 |
| $(EtO)_2P(O)OH$ | $(EtO)_2P(O)OP(O)(OEt)_2$ | 94 | 115—118/0.3 |
| $(BuO)_2P(O)OH$ | $(BuO)_2P(O)OP(O)(OEt)_2$ | 76 | 124—125/0.03 |

heated above 220°C, but prolonged heating at lower temperature (ca. 180—190°C) may at times have the same effect. For this reason, distillation should be carried out under high vacuum, not more than 50 g. being distilled in one operation; care should also be taken as regards the purity of *N*-bromosuccinimide.

**Reaction of Diethylphosphorosuccinimidate with Alcohols or Phenol in the Presence of Boron Trifluoride.**—To a solution of diethylphosphorosuccinimidate (2.15 g.) in anhydrous *n*-propyl alcohol (2 ml.) was added five drops of boron trifluoride etherate, and the mixture was heated at 100°C for 5 hr. Dry ether (10 ml.) was added to the mixture, which was then allowed to stand at room temperature for some time to permit separation of the resulting succinimide. After separation of the succinimide (1.48 g., 84%), the colorless oil was distilled under reduced pressure and *n*-propyldiethyl phosphate (b. p. 104—110°C/12 mmHg, 1.40 g., 84%) was obtained.

Similarly, triethyl, isopropyldiethyl and *n*-butyldiethyl phosphates were prepared from the reactions of diethylphosphorosuccinimidate with the corresponding alcohols.

In the case of phenol, the reaction mixture turned brown within 30 min. and a small amount of succinimide separated. After heating at 100°C for 5 hr., the resulting viscous greenish-black oil was extracted carefully with several portions of dry ether (20 ml.). The extract was concentrated and diethylphenyl phosphate (b. p. 80—95°C/0.3 mmHg, 0.78 g., 34%) was obtained by distillation. These results are summarized in Table. I

**Reaction of Phenol with Diethylphosphorosuccinimidate.**—Freshly distilled phenol (1.0 g.) was mixed with diethylphosphorosuccinimidate (2.15 g.), and the mixture was heated at 100°C for 5 hr. When dry ether (10 ml.) was added, white crystalline succinimide (0.74 g., 83%) soon separated. The filtrate was concentrated and distilled under reduced pressure. An 82% yield of diethylphenyl phosphate (b. p. 95—105°C/0.4—0.6 mmHg, 1.58 g.) was obtained.

**Reaction of Diethylphosphorosuccinimidate with Diethyl Hydrogen Phosphate, or Di-*n*-butyl Hydrogen Phosphate.**—A mixture of equimolar amounts of diethylphosphorosuccinimidate (2.15 g.) and diethyl hydrogen phosphate (1.40 g.) in dry toluene (5 ml.) was heated at 100°C. The reaction took place rapidly. After heating for 5 hr., a quantitative amount of succinimide (870 mg., 97%) precipitated and was filtered off. From the concentrated filtrate, tetraethyl pyrophosphate (b. p. 115—118°C/0.3 mmHg., 2.43 g., 94%) was obtained by fractionation. This compound was identical with an authentic specimen prepared by the procedure given in the literature.[3]

Similarly, *unsym.* diethyl di-*n*-butyl pyrophosphate (b. p. 124—125°C/0.03 mmHg, 2.26 g., 76%) was obtained from di-*n*-butyl hydrogen phosphate (1.76 g.) and diethylphosphorosuccinimidate (1.97 g.). The results are summarized in Table II.

## Summary

Phosphorylation of alcohols, phenol, and dialkyl hydrogen phosphates by means of diethylphosphorosuccinimidate has been described. Phorphorylation of alcohols with diethylphosphorosuccinimidate could only be carried out in the presence of certain acid catalysts; while more acidic compounds such as phenol and dialkyl hydrogen phosphates were readily phosphorylated to give the corresponding phosphate and *sym.*- or *unsym.*-pyrophosphate in quantitative yields even in the absence of catalysts.

*Laboratory of Organic Chemistry*
*Tokyo Institute of Technology*
*Ookayama, Tokyo*

# The Cationic Copolymerization of Styrene and α-Methylstyrene in Liquid Sulfur Dioxide*

By Masashi IINO and Niichiro TOKURA

(Received October 12, 1964)

When liquid sulfur dioxide has been used as a solvent in the cationic polymerization of styrene, several characteristic features have been observed;[1] (1) the rate of the polymerization is exceedingly fast, (2) the polymer produced is of a high degree of polymerization and of a nearly mono-disperse distribution, and (3) even alkyl, aralkyl or acyl halide can initiate the poymerization in this solvent.[2]

This behavior of liquid sulfur dioxide may adequately be explained by its protophobic nature or by the inertness of this solvent toward the cationic species. In this cationic polymerization, monomer- and solvent-transfer reactions may be considered to be very small and the solvation of this solvent to anionic species may be very strong.

The present article will describe a study of the cationic copolymerization of styrene and α-methylstyrene, since the study of a copolymerization in a solvent can often provide many instructive suggestions on the nature of the solvent used and on the interactions among the cationic polymerizing species and the solvent.

The cationic copolymerizations in liquid sulfur dioxide of some pairs of copolymers, such as styrene-*p*-bromostyrene,[1c] styrene-isobutene,[3] and styrene-methylacrylate,[4] have already been studied, and a number of papers have been published elsewhere.

It has also been recognized that α-methylstyrene polymerizes readily in liquid sulfur dioxide without any catalyst,[5] as do *p*-methyl- and *p*-isopropyl-styrenes.[6]

In the study of the copolymerization of styrene and α-methylstyrene, NMR spectrometry has been adopted for the identification of the monomer units in the copolymer chain, according to the method of Bovey et al.[8a] The copolymerization in liquid sulfur dioxide is compared with that in methylene dichloride.

## Experimental

**Materials.** — Commercially-available styrene was distilled twice in a nitrogen atmosphere under reduced pressure. α-Methylstyrene was washed with a 10 per cent sodium hydroxide solution and water successively, dried with potassium carbonate, and distilled twice under reduced pressure in a nitrogen stream just before use.

Boron trifluoride etherate was used after repeated distillation in vacuo in a dry nitrogen stream and after having been stored in a glass ampule. Liquid sulfur dioxide was dehydrated with phosphorus pentoxide and distilled.

**Polymerization.** — The cationic copolymerization has been carried out at −40°C in liquid sulfur dioxide, since α-methylstyrene polymerizes spontaneously even at −20°C, while it does not undergo such spontaneous polymerization at −40°C. For a comparative study, a similar cationic copolymerization in methylene chloride was also carried out at −20°C, using the same procedure and the same apparatus.

The procedure of the polymerization was the same as in the case of the copolymerization of styrene and *p*-bromostyrene,[1c] using boron trifluoride etherate as a catalyst.

**Analyses of the Copolymer.**—The monomer composition of the copolymer was determined by NMR spectrophotometry, employing a Varian V-4300 B, 60 MC instrument, at 22—23°C. As the solvent for the spectrometry, carbon tetrachloride was used, dioxane being used as an internal reference. Figure 1 presents the NMR spectra in the carbon tetrachloride solutions (0.06 g. polymer in 1 ml. carbon tetrachloride) of polystyrene, poly-α-methyl styrene, a nearly equimolar mixture of the two homopolymers (polystyrene 54.3 mol. %), and a copolymer of styrene and α-methylstyrene (styrene in feed 82.0 mol. %, polymerized in liquid sulfur dioxide) respectively.

The assignment of the proton absorptions in the spectra of polystyrene and poly-α-methylstyrene has already been made.[8] The peak positions of the protons of the respective functional groups of the polymer or the copolymer are tabulated in Table I. As may be seen in Table I, the positions of the respective proton absorptions do not vary, even if

* Polymerization in Liquid Sulfur Dioxide. Part XXIII. Part XXII: M. Matsuda and N. Tokura, *J. Polymer Sci.*, in press.

1) a) R. Asami and N. Tokura, ibid., **42**, 545 (1960); b) N. Tokura, M. Matsuda and I. Shirai, This Bulletin, **35**, 371 (1962); c) N. Tokura, M. Matsuda and M. Iino, ibid., **36**, 278 (1953).

2) a) N. Tokura and T. Kawahara, ibid., **35**, 1902 (1962); b) N. Tokura, T. Kawahara and T. Watanabe, ibid., **36**, 760 (1963).

3) N. Tokura and M. Iino, ibid., **37**, 23 (1964).

4) M. Matsuda, K. Oshima and N. Tokura, *J. Polymer Sci.*, in press.

5) N. Tokura, M. Matsuda, I. Shirai, K. Shiina and Y. Kondo, This Bulletin, **35**, 1043 (1962).

6) a) N. Tokura, M. Matsuda and Y. Ogawa, *J. Polymer Sci.*, **A1**, 2965 (1963); b) N. Tokura, M. Matsuda and K. Arakawa, ibid., **A2**, 3355 (1964).

TABLE I. THE NMR SPECTRA OF HOMOPOLYMERS, COPOLYMER AND A MIXTURES OF POLYSTYRENE AND POLY-α-METHYLSTYRENE

| Polymer | Peak position (τ value) | | | |
|---|---|---|---|---|
| | $-C_6H_5$ | | $CH_2$ and CH | $-CH_3$ |
| Polystyrene (liq. $SO_2$) | 3.01 | 3.50 | 8.49 | — |
| Polystyrene ($CH_2Cl_2$) | 2.92 | 3.37 | 8.27 | — |
| Poly-α-methylstyrene (liq. $SO_2$) | 2.97 | — | 8.51 | 9.87 |
| Poly-α-methylstyrene ($CH_2Cl_2$) | 2.97 | — | 8.46 | 9.81 |
| Mixture of homopolymers (polystyrene 91.5%)* | 3.01 | 3.50 | 8.51 | 9.88 |
| Mixture of homopolymers (polystyrene 33.7%)* | 3.00 | 3.47 | 8.51 | 9.88 |
| Copolymer (styrene feed 53.2%)* | 2.99 | — | 8.51 | 9.89 |
| Copolymer (styrene feed 22.2%)* | 2.99 | — | 8.51 | 9.89 |

* Mole per cent

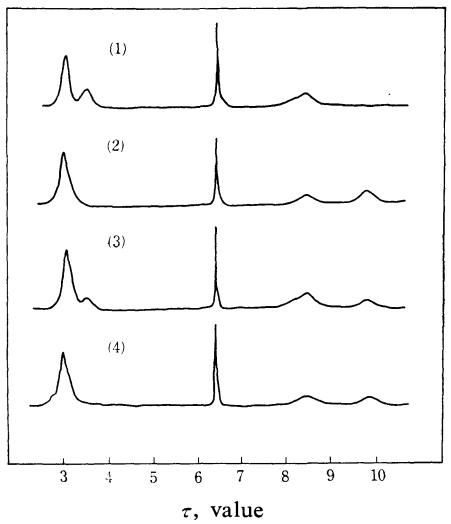



Fig. 1. NMR spectra of polystyrene, poly-α-methylstyrene, a mixture of the homopolymers and a copolymer, in $CCl_4$ (0.06 g. in 1 ml.).

(1) Polystyrene
(2) Poly-α-methylstyrene
(3) Mixture of polystyrene (54.3 mol. %) and poly-α-methylstyrene
(4) Copolymer of styrene (82.0 mol. % in feed) and α-methylstyrene

the polymer is a homopolymer, a mixture of homopolymers or copolymers is not affected by the kind of the solvent (liquid sulfur dioxide or methylene dichloride) used in the polymerization.

Tau (τ) values were calculated from the spectra of the protons, dioxane (τ=6.43) or cyclohexane (τ=8.56 p.p.m.) being used as an internal reference. No specific interaction between the samples and the reference was confirmed in the spectra. The content of each monomer in the copolymer chain of styrene and α-methylstyrene can be estimated either by the dimensional ratio of the proton absorption spectra of the phenyl- to the methyl protons, or by the dimensional ratio of the methyl protons to the methylene and methine protons. The latter method of estimation was chosen, because the estimation was simpler and subject to less error, as will be discussed later.

For the convenience of the experimental performance, a calibration line was prepared (Fig. 2), in which $(A_{CH_3}/A_{CH_2})_{obs}$, (the ratio of methyl- to methylene- and methine-protons) values in various mixtures of polystyrene and poly-α-methylstyrene were examined; the calculated values $(A_{CH_3}/A_{CH_2})_{calcd}$ (from the mixed ratios of the two homopolymers) were then plotted against the observed values $(A_{CH_3}/A_{CH_2})_{obs}$ (from the NMR measurements) on the rectangular coordinates. The fair coincidence between the calculated and the observed values in Fig. 2 may well support the validity of this technique for the estimation of the proportion of the components in the copolymer, as long as the mixture of the homopolymers behaves in a manner similar to that of the copolymer of the same monomers in the NMR phenomena. The NMR measurement was carried out in the concentration range of the polymer, 0.3 to 0.4 g. per 1 ml. of carbon tetrachloride. The dimensions of each proton-absorption area were estimated by weighing the NMR spectrum cut out from the chart of the spectra. Four to six measurements of the spectra of a copolymer were averaged in calculating the value of $(A_{CH_3}/A_{CH_2})_{obs}$.

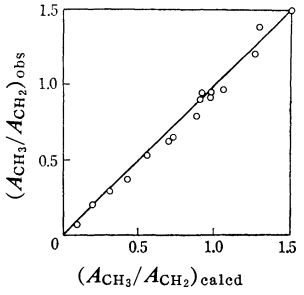



Fig. 2. Calibration line of calculated vs. observed values of $(A_{CH_3}/A_{CH_2})$.

$A_{CH_3}$ NMR absorption area of methyl protons.
$A_{CH_2}$ NMR absorption area of methylene and methine protons.

Harwood's method for the estimation of the comonomer proportion in the styrene-methylmethacrylate copolymer by NMR spectrometry[7] was modified and applied. The relationship between the molar fraction of styrene in the copolymer and the observed or calculated value of $(A_{CH_3}/A_{CH_2})$ is as follous:

$$x=\frac{3-(A_{CH_3}/A_{CH_2})\times 2}{3+(A_{CH_3}/A_{CH_2})}\times 100 \quad (1)$$

or

$$(A_{CH_3}/A_{CH_2})=(100-x)\times 3/(100\times 2+x) \quad (2)$$

where $x$ is the styrene mol.% in the copolymer.

**The Sequences of the Copolymer.** — The mole per cent in the copolymer of the sandwiched styrene ($S$), in the form of the -M-St-M- triad, where St and M are styrene and $\alpha$-methylstyrene units respectively, was estimated by using the following procedure;

$$(b/a)_{calcd}=\frac{2x}{5(100-x)+3x} \quad (3)$$

where $a$ and $b$ are the areas of the meta and para protons, and of ortho protons, respectively.

$$(b/a)_{obs}=2(x-S)/3(x-S)+5S+5(100-x) \quad (4)$$

or

$$S=\frac{x(2-x(b/a)_{obs})-5(b/a)_{obs}(100-x)}{x(2+2(b/a)_{obs})} \quad (5)$$

The derivation and the meaning of these formulae will be discussed later.

## Results and Discussion

**The Reactivity Ratio.**—Figures 3 and 4 show the feed-copolymer composition curves in liquid sulfur dioxide and methylene dichloride respectively. The monomer reactivity ratios, $r_1$ and $r_2$, were estimated by the trial and error method. The results is listed in Table II. In order to suppress the reaction rate, a lower temperature (−40°) was used in liquid sulfur dioxide. On the other hand, in methylene dichloride −20°C was needed to assure good solubility for monomers, though it has been reported that in liquid sulfur dioxide the M.R.R.'s are almost independent of the temperature of the copolymerization.[1c] However, some scattered results in Figs. 3 and 4 are perhaps due to such experimental difficulties as the fast reaction rates, the lesser solubilities of the monomers, and unavoidable error in the NMR determinations.

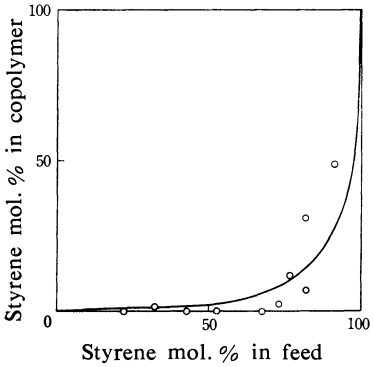



Fig. 3. Copolymer composition curve.
Copolymerization in liquid sulfur dioxide.
$BF_3$ etherate: $7.3\times10^{-5}$ mol./l.
Temperature: −40°C

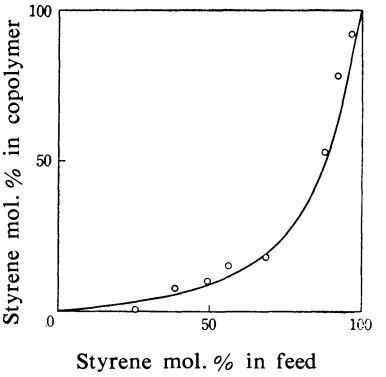



Fig. 4. Copolymer composition curve.
Copolymerization in methylene dichloride.
$BF_3$ etherate: $6.6\times10^{-3}$ mol./l.
Temperature: −20°C

Table II. The monomer reactivity ratios of the copolymerization of styrene and $\alpha$-methylstyrene in two solvents

| Solvent | $r_1$ | $r_2$* |
|---|---|---|
| liq. $SO_2$ (−40°C) | 0—0.1 | over 20 |
| Methylene dichloride (−20°C) | 0.2—0.5 | 12±2 |

* $M_1$: Styrene, $M_2$: $\alpha$-Methylstyrene

It has been confirmed, in spite of the above-discussed defect, that a non-alternating tendency prevails between styrene and $\alpha$-methylstyrene in both the solvents, the tendency being far more conspicuous in liquid sulfur dioxide. In view of the behavior of this solvent hitherto experienced by the present authors, the results are not unexpected.

**The Identification of the Sequence of the Monomer Unit in the Copolymer.**—The NMR spectra of phenyl groups of polystyrene, poly-$\alpha$-methylstyrene, the mixture of homopolymers and the copolymer can be recognized in the lower fields of the respective spectra, 1, 2, 3 and 4, of Fig. 1, where two peaks are observed as these of phenyl protons. These were assigned as the para- and the meta protons (lower field) and the ortho protons (higher field) by Bovey

7) H. J. Harwood and W. M. Ritchey, *A. C. S. Polymer Reprints*, 5, No. 1, Philadelphia Meeting (April, 1964), p. 299.

TABLE III. VALUES OF $b/a$ AND $S$ MOL.% OF STYRENE-α-METHYLSTYRENE-COPOLYMERS

| Styrene in copolymer mol. % | α-Methylstyrene in copolymer mol. % | $(b/a)_{obs}$ | $(b/a)_{calcd}$ | $S_{mol\ \%}$ |
|---|---|---|---|---|
| Liquid sulfur dioxide as solvent | | | | |
| 0.0 | 100 | −0.01 | 0 | 0 |
| 0.0 | 100 | −0.02 | 0 | 0 |
| 1.8 | 98.2 | −0.03 | 0.01 | |
| 11.8 | 98.2 | 0.09 | 0.05 | |
| 30.8 | 69.2 | 0.33 | 0.14 | |
| 49.3 | 50.7 | 0.27 | 0.25 | |
| Methylene dichloride as solvent | | | | |
| 8.3 | 91.7 | 0 | 0.02 | 100 |
| 10.3 | 89.7 | 0 | 0.04 | 100 |
| 15.3 | 84.7 | 0.02 | 0.07 | 68.0 |
| 52.8 | 47.2 | 0.15 | 0.27 | 38.3 |
| 65.5 | 34.5 | 0.20 | 0.36 | 36.3 |
| 78.6 | 21.4 | 0.31 | 0.46 | 24.7 |
| 82.1 | 17.9 | 0.33 | 0.49 | 24.5 |
| 86.6 | 18.4 | 0.31 | 0.53 | 31.6 |
| 92.2 | 7.8 | 0.35 | 0.58 | 29.7 |

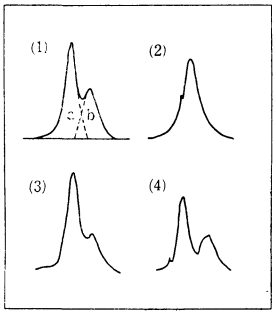



Fig. 5. NMR spectra of phenyl proton in polymers. (Solvent: $CCl_4$)
(1) Polystyrene
(2) Poly-α-methylstyrene
(3) Styrene-α-methylstyrene Copolymer (styrene in feed, 91.1 mol.%)
(4) Styrene polysulfone

et al,[8a] since the ratio of the respective areas is approximately 3 to 2 (Fig. 5).

The phenyl proton spectra afford two peaks because of the difference in the magnetic shielding effected by the adjacent benzene nucleus on the ortho protons and on the para- and meta protons.[8a] However, the spectra of α-methylstyrene do not afford the two peaks, but only one peak, because of the decrease in the interaction of the neighboring phenyl group because of the presence of the α-methyl group.[8a] In the mixture of the two homo-polymers or in the copolymer, the positions of the two peaks due to the phenyl protons are always the same (Table I); such a observation allows us to analyze the monomer sequences in the copolymer.

The dimensional ratios of the two peaks, $b/a$, were calculated (Fig. 5), where $a$ and $b$ are the area of the peak in the lower field and that in the higher one respectively. Therefore, in poly-α-methylstyrene, $b/a$ was 0, while in polystyrene $b/a$ was 2/3. The relation of the styrene mole per cent in the mixed homopolymers or that in the copolymer to the $b/a$ value is presented in Table III.

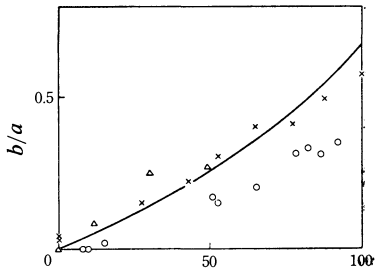



Fig. 6. Relations between styrene content vs. $b/a$ ratio in copolymers.
× Polystyrene, poly-α-methylstyrene-mixture
△ Copolymer in liquid sulfur dioxide
○ Copolymer in methylene dichloride

Figure 6 also demonstrates the relation of the styrene mole per cent in the polymer and the $b/a$ value, where the full line (the calculated plot) agrees well with the crossed dots (the observed values of the mixture of homopolymers). However, the plot of the copolymer (circle dots) is not like this, the points

8) a) F. A. Bovey, G. V. Tiers and G. Fieipovich, *J. Polymer Sci.*, **38**, 73 (1959); ibid., **62**, 197 (1962); b) A. Nishioka, ibid., **62**, 10 (1962); c) S. Brownstein, S. Bywater and D. J. Worsfold, *Makromol. Chem.*, 127 (1961).

here being somewhat below the theoretical curve and this being supposed beyond the range of experimental error.

Such a deviation may be accounted for by the difference in the sequence of the styrene unit in the copolymer, where some styrene units did not demonstrate the two separated peaks in the NMR spectra. The NMR spectrum of the phenyl group in styrene-polysulfone is also shown in Fig. 5 as a reference. Styrene-polysulfone is obtained by a radical polymerization of styrene in liquid sulfur dioxide.[9] The molar ratio of the styrene unit to the sulfur dioxide unit in the copolymer is said to be strictly 2 to 1, the arrangement of the monomer sequence in the chain being believed to be:

$$-SO_2-St-St-SO_2-St-St-$$

where St is the styrene and $SO_2$ is the sulfur dioxide monomer.

From the considerations mentioned above and from the NMR spectrum of the styrene-homopolymer, it may be anticipated that the polymer chain consisting of two and more succssive styrene units will exhibit two separated peaks in the NMR absorption. Therefore, the styrene unit in the copolymer which presents only one peak is likely to have the structure of a styrene unit sandwiched between the two $\alpha$-methylstyrene units, such as:

$$\cdots CH_2-\underset{\underset{C_6H_5}{|}}{\overset{\overset{CH_3}{|}}{C}}-CH_2-\underset{\underset{C_6H_5}{|}}{CH}-CH_2-\underset{\underset{C_6H_5}{|}}{\overset{\overset{CH_3}{|}}{C}}\cdots \qquad (S)$$

If this assumption is reasonable, the proportion of the sandwiched styrene (S) may be calculated by Eq. 5 from the observed curves in Fig. 6. The S value denotes the proportion of the sequences (S). The results are listed in Table III. As may be seen in Table III, the copolymer (equimolarly feed) afforded in methylene dichloride has as much as about 38.3% fragments (S). On the other hand, the copolymer produced in liquid sulfur dioxide seems to be a non-alternate copolymer, where $(b/a)_{obs} \fallingdotseq (b/a)_{calcd}$, and (S) is approximately zero. Such results agree well with the large value of $r_2$. The reaction in liquid sulfur dioxide favors the activity of cationic species remarkably. At a higher temperature, $\alpha$-methylstyrene can be polymerized spontaneously in liquid sulfur dioxide.[5],** This phenomenon is to be attributed to the low $e$ value (of the $Q$, $e$ scheme) of $\alpha$-methylstyrene. Thus, in the mixture of styrene and $\alpha$-methylstyrene, the latter monomer initiates the cationic polymerization faster than does styrene. In addition, styrene in liquid sulfur dioxide may be solvated by sulfur dioxide molecules more strongly than $\alpha$-methylstyrene in the same solvent, whereas the difference in the solvation between the two monomers is supposed to be not as distinguished as in methylene dichloride.

Secondly, in liquid sulfur dioxide, the $\alpha$-methylstyrene would be more reactive toward the growing carbonium ion end than styrene, since the electron density on the vinyl group in the former may be larger than that of styrene due to the $\alpha$-methyl inductive effect and the lesser solvation by a sulfur dioxide solvent on $\alpha$-methylstyrene. The non-alternative nature of such a polymerization is well elucidated by the above discussion.

## Summary

The copolymerizations of styrene and $\alpha$-methylstyrene in liquid sulfur dioxide have been carried out at $-40°C$ using boron trifluoride etherate as a catalyst, and the results compared with the same copolymerizations in methylene dichloride at $-20°C$. The $r_1$ and $r_2$ values have been estimated by NMR spectrometry as 0—0.1 and over 20 in liquid sulfur dioxide, and 0.2—0.3 and $12\pm2$ in methylene chloride. The styrene unit sandwiched between two $\alpha$-methylstyrene units has been calculated by a comparison of the phenyl doublet with phenyl singlet absorptions. The (S) per cent (S is the sandwiched styrene sequence, M-St-M, in the copolymer, where St is the styrene unit and M is the $\alpha$-methylstyrene unit) has been estimated. In liquid sulfur dioxide, S is approximately zero. This fact agrees well with the large $r_2$ value. The reason for such a non-alternative nature of the copolymerization in liquid sulfur dioxide had also been discussed.

The present authors are grateful to the Seitetsu Kagaku K. K. for the donation of liquid sulfur dixide.

*The Chemical Research Institute of Non-Aqueous Solutions*
*Tohoku University*
*Katahira-cho, Sendai*

*Department of Applied Chemistry*
*Faculty of Engineering*
*Osaka University*
*Miyakojima-ku, Osaka*

9) W. G. Barb, *Proc. Roy. Soc.*, **A212**, 66, 177 (1952).

** The present authors are inclined to believe in the initiation of the cationic polymerization without the Lewis acid catalyst, as the $H^+$ is derived from the trace of water in liquid sulfur dioxide as.

$$SO_2 + H_2O = H^+ + HSO_3^-$$

# Studies of Thio Acids. V.[1] The Reaction of Distearoyl Sulfide with Alcohol and Alkali*1

By Yoshio HIRABAYASHI, Masateru MIZUTA and Tetsuro MAZUME*2

(Received October 12, 1964)

In the course of an investigation of the mechanism of the formation of stearic esters from thiostearic acid and alcohols by heating, the formation of distearoyl sulfide as an intermediate in the reaction was confirmed.*3 However, detailed knowledge of the properties of diacyl sulfide was still lacking. Therefore, the present authors synthesized distearoyl sulfide and clarified its properties by investigating the products obtained by heating it in alcohol or by neutralizing it in organic solvents with ethanolic or aqueous potassium hydroxide, thus determining each reaction mechanism. The above mechanisms will be discussed in this paper.

Distearoyl sulfide (m. p. 79.5—80.5°C) was synthesized from potassium thiostearate and stearoyl chloride. Its ultraviolet absorption curve in cyclohexane (Fig. 1) exhibits an absorption maximum at 240 mμ ($\varepsilon=4030$) and an inflection in the 280—320 mμ region; the former is undoubtedly associated with conjugation between the $\pi$ electrons of the carbonyl group and the unshared valency electrons of the sulfur atom, while the latter is probably an R-band due to the carbonyl group. The neutralization value (N. V.) of distearoyl sulfide as determined by neutralization with ethanolic potassium hydroxide in benzene-ether using phenolphthalein as an indicator*4 was 100.4, a value which shows that the reaction between distearoyl sulfide and potassium hydroxide occurs at an equimolar ratio under the above conditions. The sulfur content (in the SH form) of distearoyl sulfide as determined by titration with an iodine solution in ethanol-ether or ethanol-benzene was naught, but that determined by titration with an iodine solution after neutralization with ethanolic potassium hydroxide in the above solvent was 5.70%, in good accord with the sulfur content as determined by Kitamura's method. (The sulfur contents determined by the above methods will be described below as S(J), $S(J)_{NV}$, and S(K) respectively.)

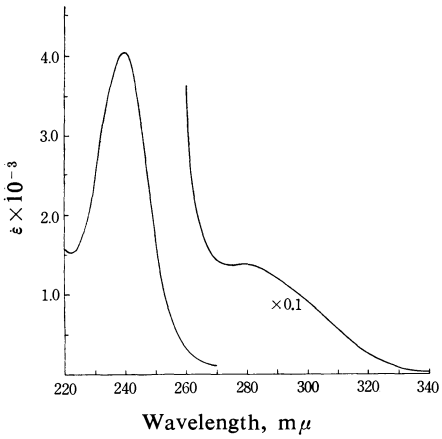



Fig. 1. Ultraviolet absorption spectrum of distearoyl sulfide in cyclohexane.

When distearoyl sulfide (3 g.) had been refluxed with absolute methanol (300 ml.) for 30 hr., the reaction product obtained was found to be composed of distearoyl sulfide (5%), thiostearic acid (35%) and methyl stearate (60%), but methyl thiostearate could not be isolated. This result suggests the following mechanism: When distearoyl sulfide is heated with methanol, methanolysis occurs as shown in Eq. 1, and methyl stearate and thiostearic acid are formed. Starting from the thiostearic acid, distearoyl sulfide is reformed by the elimination of hydrogen sulfide, as is shown in Eq. 2, and then the reaction of Eq. 1 is repeated.*5 It is still unknown whether the reaction of Eq. 3 occurs or not, but the reaction of Eq. 1 is firmly supported by the formation of a large amount of thiostearic acid.

When distearoyl sulfide in benzene or benzene-ether was neutralized with ethanolic potassium hydroxide, it was confirmed that

1) Part IV of this series: Y. Hirabayashi, This Bulletin, 38, 175 (1965).

*1 Most of this study was presented at the 11th Annual Meeting of the Chemical Society of Japan, Tokyo, April, 1958.

*2 Present address: Shimogamo-kishimotocho, Sakyo-ku, Kyoto.

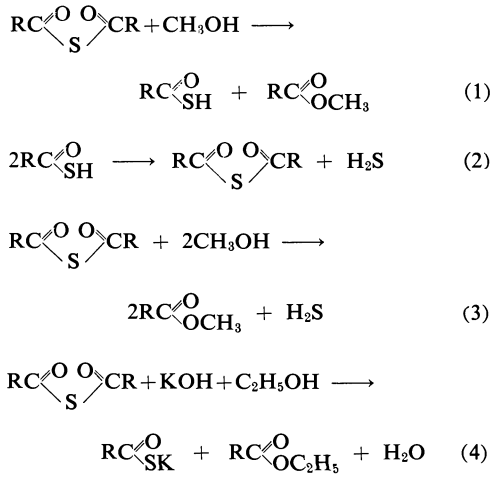
*3 When thiostearic acid is heated with alcohol, first hydrogen sulfide is evolved and distearoyl sulfide is formed as an intermediate, and then the stearic ester and thiostearic acid are formed by the reaction of the intermediate and alcohol. This reaction mechanism will be discussed in the following paper of this series.

*4 In the following experiments, all neutralizations were carried out using phenolphthalein as an indicator.

*5 This will be discussed in the following paper of this series.

potassium thiostearate and ethyl stearate are formed in an equimolar ratio, as in Eq. 4. Therefore, it may be reasonably explained that the observed N. V. of distearoyl sulfide corresponds well with the value calculated by the equimolar ratio described above. It is also confirmed that the difference between the S(J) and the $S(J)_{NV}$ values is caused by the thiostearic acid formed by neutralization with ethanolic potassium hydroxide.

When a small amount (very different from the neutralization equivalent as a 1 : 1 mole ratio) of aqueous potassium hydroxide was added to a solution of distearoyl sulfide in benzene-ethanol, the reaction product was found to be composed of equimolar amounts of ethyl stearate and thiostearic acid (containing potassium thiostearate corresponding to the potassium hydroxide added); that is, alcoholysis occurs between a large amount of alcohol and distearoyl sulfide upon the addition of a small amount of alkali as a catalyzer, and then thiostearic acid and stearic acid ester are formed. This fact shows that when neutralization is carried out in benzene or benzene-ether with ethanolic potassium hydroxide, first alcoholysis occurs upon the addition of alcoholic potassium hydroxide, and then the acid thus formed is neutralized. However, a sufficient amount of alcohol in the solvent or in an alkali solution is needed for alcoholysis. The presence of a large amount of benzene and an equimole of alcohol to distearoyl sulfide does not accelerate the neutralization with aqueous potassium hydroxide. In a benzene - aqueous potassium hydroxide solution, distearoyl sulfide was not changed, even when vigorously stirred while being warmed and the hydrolysis shown in Eq. 5 did not occur. However, it still can not be known whether or not hydrolysis should occur by the regulation of the alkali concentration and the reaction temperature.



$$RC\langle^{O}_{S}\rangle CR + CH_3OH \longrightarrow RC\langle^{O}_{SH} + RC\langle^{O}_{OCH_3} \quad (1)$$

$$2RC\langle^{O}_{SH} \longrightarrow RC\langle^{O}_{S}\rangle CR + H_2S \quad (2)$$

$$RC\langle^{O}_{S}\rangle CR + 2CH_3OH \longrightarrow 2RC\langle^{O}_{OCH_3} + H_2S \quad (3)$$

$$RC\langle^{O}_{S}\rangle CR + KOH + C_2H_5OH \longrightarrow RC\langle^{O}_{SK} + RC\langle^{O}_{OC_2H_5} + H_2O \quad (4)$$

$$RC\langle^{O}_{S}\rangle CR + 2KOH \longrightarrow RC\langle^{O}_{SK} + RC\langle^{O}_{OK} + H_2O \quad (5)$$

$R = C_{17}H_{35}-$

## Experimental*6

**The Synthesis of Distearoyl Sulfide.**—Potassium thiostearate was prepared by the neutralization of thiostearic acid with ethanolic potassium hydroxide in ethanol-ether (1 : 1) and by distilling off the solvent. Stearoyl chloride (9.2 g.) was added drop by drop to a suspension of the potassium thiostearate (10.4 g.) in anhydrous hexane (200 ml.), and then the mixture was refluxed for 7 hr. under a cooler with a calcium chloride tube. After the reaction mixture had been filtered while hot, hexane was distilled off from the filtrate, and the residue was recrystallized from benzene to give distearoyl sulfide (14 g.); m. p. 79.5—80.5°C, colorless plate crystals, N. V. 100.4 (Calcd. by $C_{36}H_{70}O_2S$ : KOH = 1 : 1 mol., 98.95).

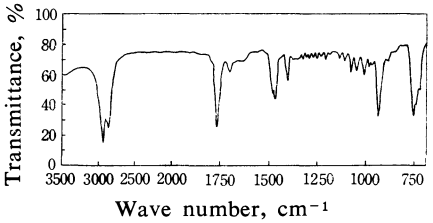



Fig. 2. Infrared absorption spectrum of distearoyl sulfide in KBr disk (1.05 mg./200 mg. KBr).

Found: C, 76.08; H, 12.33; S, 0·S(J), 5.68 $S(J)_{NV}$, 5.70 S(K)%. Calcd. for $C_{36}H_{70}O_2S$: C, 76.26; H, 12.44; S, 5.65%.

UV (cf. Fig. 1): $\lambda_{max}^{cyclohexane}$ 240 mμ (ε=4030); inflection 280—320 mμ. IR (KBr disk, cf. Fig. 2): $\nu_{C=O}$ 1766 $cm^{-1}$.

**The Reaction of Distearoyl Sulfide with Absolute Methanol by Heating.**—A solution of distearoyl sulfide (3 g.) in absolute methanol (300 ml.) was refluxed for 30 hr., and the following product I was obtained by distilling off the methanol under reduced pressure; m. p. 33.5—34.5°C, N. V. 68.3, S(J) 3.33%, $S(J)_{NV}$ 3.58%, S(K) 3.58%.

Its ultraviolet absorption spectrum (curve a, Fig. 3) exhibits a low-intensity absorption maximum at 221 mμ, but the absorption maximum at 240 mμ due to distearoyl sulfide is not seen.

The product I (2.8 g.) was recrystallized several times from hexane and benzene; the properties and the ultraviolet absorption spectrum of each fraction are shown in Table I and Fig. 3 respectively. The composition of each fraction was thus found to be as follows:

*6 All melting points are uncorrected. The ultraviolet absorption spectra were measured with a Shimadzu quartz-spectrophotometer, model QB-50, and silica cells (1 cm.), while the infrared absorption spectrum was measured with a Hilger-H-800 infrared spectrophotometer.

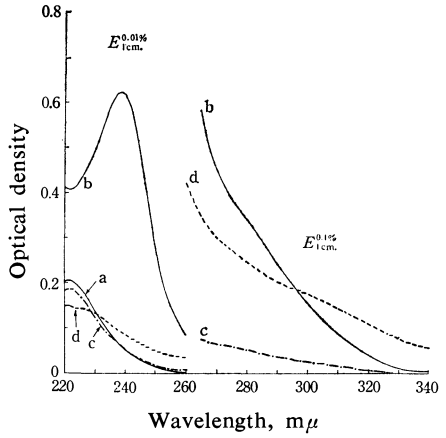



Fig. 3. Ultraviolet absorption spectra in cyclohexane.
a: Product I
b: Fraction 1 in Table I
c: Fraction 3 in Table I
d: Fraction N-2 in Table II

Table I. The properties of fractions obtained from the product I (2.8 g.)

| | Yield g. | M. p. °C | N. V. | $S(J)_{NV}$ | S(K) |
|---|---|---|---|---|---|
| (1) | 0.1 | 79—80 | — | — | 6.02 |
| (2) | 0.05 | 71—77 | — | — | — |
| (3) | 0.8 | 34.5—35.5 | 62.7 | 3.11 | 3.14 |
| (4) | 1.8 | 33—34 | 74.9 | 3.90 | 3.92 |

(1): Unreacted and reformed distearoyl sulfide
(2): Mainly distearoyl sulfide
(3) and (4): Thiostearic acid and ester (RCOOR' or RCOSR')

It was difficult to purify fractions 3 and 4 further by recrystallization. The mixture of 3 and 4 (1.6 g.) was neutralized with ethanolic potassium hydroxide in ethanol*7 and separated into an acidic part A and a neutral part N by the usual method. Each part was then recrystallized; the results of recrystallization are shown in Table II. The fractions A and N-1 were identified as thiostearic acid and methyl stearate respectively. (Neither of them showed any depression of melting point upon admixture with an authentic sample, and the ultraviolet spectrum of A was identical with that of thiostearic acid.) The fraction N-2 was slightly yellow and exhibited the weak absorption in the 260—400 mμ region. This fraction was found to consist mainly of methyl stearate, together with a small amount of an unidentified substance.

Table II. The properties of fractions obtained from the mixture (1.6 g.) of (3) and (4) in Table I

| | Yield g. | M. p. °C | N. V. | $S(J)_{NV}$ | S(K) |
|---|---|---|---|---|---|
| (A) | 0.6 | 39.5—40.5 | 186.4 | 10.54 | 10.57 |
| (N-1) | 0.9 | 38.5—39.0 | 1.5[a] | 0.09 | 0.08 |
| (N-2) | 0.1 | 39.5—40.5 | 41.2[b] | 1.81 | — |

Saponification value (S. V.): a), 185.5; b), 179.5 (calcd. for methyl stearate: 188.0).

*7 Since no difference is found between the S(J) and $S(J)_{NV}$ values, it can be said that no distearoyl sulfide exists in the product, and that no new products are formed by the neutralization of the product.

On the basis of the above results, the compositions of the product I were as follows: unreacted or reformed distearoyl sulfide 5%, methyl stearate 60%, and thiostearic acid 35%.

**The Reaction of Distearoyl Sulfide in Benzene or Benzene-Ether with Ethanolic Potassium Hydroxide.**—A solution of distearoyl sulfide (1.07 g.) in benzene (30 ml.) or benzene (20 ml.) - ether (10 ml.) was neutralized with 0.1 N ethanolic potassium hydroxide; the neutralization value was determined to be 100.5. The reaction mixture was then allowed to stand at room temperature for 2 hr., after which the solvent was distilled off under reduced pressure and water (200 ml.) was added to the residue. The resulting mixture was acidified with dilute hydrochloric acid and extracted with ether. The following product II was obtained by distilling off the ether: m. p. 30.0—31.0°C, N. V. 98.1, S(J) 5.60%, $S(J)_{NV}$ 5.60%.*7

A solution of this product II (0.94 g.) in ether (20 ml.) was neutralized with 0.5 N ethanolic potassium hydroxide (3.25 ml.), and the reaction mixture was allowed to stand at room temperature for 1 hr. Then the deposit part was filtered off. The filtrate (ether solution) was washed with water, and the neutral part N was obtained by distilling off the ether. The above deposit part, combined with washings of the filtrate, was acidified, and the mixture was extracted with ether. The acidic part A was obtained by washing the ether solution with water, followed by distilling off the ether. The same procedures were repeated for three times in each part in order to separate the neutral part from the acidic part as much as possible. The properties of each part are shown in Table III. It was deduced from the above results that almost equal amounts of potassium thiostearate and ethyl stearate are formed by the neutralization reaction of distearoyl sulfide in benzene or benzene-ether with ethanolic potassium hydroxide.

Table III. The properties of fractions obtained from the product II (0.94 g.)

| | Yield g. | M. p. °C | N. V. | $S(J)_{NV}$ |
|---|---|---|---|---|
| (A) | 0.43 | 39.5—40.5 | 184.8 | 10.28 |
| (N) | 0.45 | 34.5—35.5 | 1.0[a] | 0 |

S. V.: a) 180.9 (calcd. for ethyl stearate: 179.5).

**The Neutralization Reaction of Distearoyl Sulfide in Benzene with Aqueous Potassium Hydroxide.**—a) A solution of distearoyl sulfide (1 g.) in methanol (equal mole to distearoyl sulfide) and benzene (50 ml.) was titrated with 0.1 N aqueous potassium hydroxide, using phenolphthalein as an indicator. The titre was less than 0.03 ml.

b) To a solution of distearoyl sulfide (2 g.) in benzene (50 ml.), 36 ml. (calcd. value as 1 : 1 mol. ratio, 35.18 ml.) of 0.1 N ($f$=1.073) aqueous potassium hydroxide was added drop by drop, and then

the mixture was heated while being vigorously stirred at 50°C for 2 hr. Then it was acidified with dilute hydrochloric acid. The benzene layer separated was washed with water and dried, and the benzene was distilled off. The product obtained was distearoyl sulfide.

**The Reaction of Distearoyl Sulfide in Benzene-Ethanol with Aqueous Potassium Hydroxide.**—To a solution of distearoyl sulfide (1 g.) in benzene (80 ml.) and ethanol (20 ml.), 0.15 ml. of 0.5 N aqueous potassium hydroxide was added (distearoyl sulfide : potassium hydroxide = 1 mol.: ca. 0.02mol.). The mixture was heated at 40—50°C for 3 hr. and then allowed to stand overnight at room temperature. It was then acidified with dilute hydrochloric acid. The benzene layer separated was washed with water and dried, and the following product III was obtained by distilling off the benzene; m. p. 29.5—30.5°C, N. V. 97.6, S(J) 5.41%, $S(J)_{NV}$ 5.41%.*[7] A solution of the product III (0.91 g.) in benzene was repeatedly washed with aqueous potassium hydroxide, and the acidic part A and the neutral part N were obtained from the washings and the benzene layer respectively in the usual way. The results are shown in Table IV. It may be deduced from the results that almost equal amounts of thiostearic acid and ethyl stearate were formed by the reaction of distearoyl sulfide in benzene-ethanol with aqueous potassium hydroxide.

Table IV. The properties of fractions obtained from the product III (0.91 g.)

| | Yield g. | M. p. °C | N. V. | $S(J)_{NV}$ | S(K) |
|---|---|---|---|---|---|
| (A) | 0.45 | 39—40 | 186.6 | 10.32 | 10.38 |
| (N) | 0.46 | 34.5—35.5 | 1.3[a)] | 0 | 0 |

S. V.: a) 181.8.

*Faculty of Engineering*
*Gifu University*
*Kagamigahara-shi, Gifu*

# On the Sn–H Bond in Some Organotin Hydrides

By Yoshikane KAWASAKI, Katsuhiko KAWAKAMI and Toshio TANAKA

(Received October 28, 1964)

Many investigations have been carried out with organometallic compounds by the method of nuclear magnetic resonance in order to study the effect of alkyl groups on the shielding of a metal nucleus or of hydrogen bound directly to a metal. The effect of the alkyl group in trialkylsilane or dialkylmercury has been found to be somewhat complicated. In the case of dialkylmercury,[1] the effect of the alkyl group on the shielding of the $^{199}Hg$ nucleus cannot be explained by a simple mechanism, such as the inductive or the hyperconjugation effect. It has been found that the apparent shielding of the $^{199}Hg$ nucleus is a function of the number of the $\beta$ protons of the alkyl group; the shielding increases in the order $CH_3 < n\text{-}C_3H_7 < C_2H_5 < i\text{-}C_3H_7$, and the spin-spin coupling of the $^{199}Hg$ nucleus with the $\beta$ protons was greater than that of the $\alpha$ protons or $\gamma$ protons. The same effect of the alkyl group was found on the shielding of the (Si-)H proton in the trialkylsilane.[2] On the contrary, however, in trialkylphosphines[3] the shielding value of the $^{31}P$ nucleus decreases with an increase in the number of the $\beta$ protons of the alkyl group.

In the case of dialkyltin dichloride, the increasing shielding value of the $^{119}Sn$ nucleus has been reported[4] to be $n\text{-}C_4H_9 < C_2H_5 < CH_3$. This order is different from that of the dialkylmercury or trialkylsilane. In the NMR spectrum of alkyltin compounds, therefore, hyperconjugation seems to be a predominant factor. In order to clarify the effect of the alkyl group in the alkyltin compounds, we studied the proton magnetic resonance and the infrared spectra of the Sn–H bond of some alkyltin hydrides.

## Experimental

**Material.**—All the organotin hydrides were prepared from the corresponding chlorides by reduction with lithium aluminum hydride in ethyl ether or in dioxane. The chlorides were kindly supplied by the Nitto Kasei Co., Ltd. The properties of the alkyltin hydrides used in our experiments are given in Table I.

**Nuclear Magnetic Resonance Spectra.** — The measurements were made at a fixed frequency of 60 Mc./sec. on two spectrometers, a Varian model

1) R. E. Dessy, T. J. Flautt, H. H. Jaffe and G. F. Reynolds, *J. Chem. Phys.*, **30**, 1422 (1959).
2) D. E. Webster, *J. Chem. Soc.*, **1960**, 5132.
3) W. A. Henderson and S. A. Buckler, *J. Am. Chem. Soc.*, **82**, 5794 (1960).
4) J. J. Burke and P. C. Lauterbur, ibid., **83**, 320 (1961).

TABLE I. BOILING POINTS AND ANALYSES

| | Boiling point, °C/mmHg | | Anal. Calcd., % | | | Anal. Found, % | | |
|---|---|---|---|---|---|---|---|---|
| | | | Sn | C | H | Sn | C | H |
| $(CH_3)_3SnH$ | 59—61/760 | (59/760)* | | | | | | |
| $(C_2H_5)_3SnH$ | 73—75/72 | (79—81/92)** | | 34.83 | 7.80 | | 34.87 | 7.10 |
| $(n\text{-}C_3H_7)_3SnH$ | 108—109/37 | (80—81/12)** | | 43.41 | 8.90 | | 44.18 | 9.08 |
| $(n\text{-}C_4H_9)_3SnH$ | 112.5—113.5/8 | (76/0.7 81/0.9)** | 40.78 | 49.52 | 9.69 | 40.25 | 49.44 | 9.41 |
| $(i\text{-}C_3H_7)_3SnH$ | 68—69/16 | | | 43.41 | 8.90 | | 43.23 | 8.90 |
| $(C_6H_5)_3SnH$ | 177.5—178.5/2 | (168—170/0.5)** | 33.81 | 61.59 | 4.60 | 33.87 | 61.25 | 4.69 |
| $(n\text{-}C_3H_7)_2SnH_2$ | 46.5—47.5/35 | (39—40.5/12)** | | | | | | |
| $(n\text{-}C_4H_9)_2SnH_2$ | 61—62/7 | (75—76/12)** | | 40.93 | 8.58 | | 41.01 | 8.53 |
| $n\text{-}C_4H_9SnH_3$ | | (99—101)** | | | | | | |

* A. E. Finholt, A. C. Bond and H. I. Schlesinger, *J. Am. Chem. Soc.*, **69**, 2692 (1947).
** J. G. Noltes and G. J. M. van der Kerk, "Functionally Substituted Organotin Compounds," Tin Research Institute Utrecht (1958).

TABLE II. THE NUCLEAR MAGNETIC RESONANCE SHIELDING VALUE FOR Sn-H PROTON ($\tau$ VALUE) IN ORGANOTIN HYDRIDES

| | $RSnH_3$ | | $R_2SnH_2$ | | $R_3SnH$ | |
|---|---|---|---|---|---|---|
| | $\tau$ Sn-H | Solvent | $\tau$ Sn-H | Solvent | $\tau$ Sn-H | Solvent |
| R=H | 6.11*1 | a | | | | |
| | 6.15[7] | b | | | | |
| $CH_3$ | | | 5.55*2 | c | 5.36 | a |
| | 5.86[7] | c | 5.24[7] | c | 5.27[7] | c |
| $C_2H_5$ | | | | | 5.24 | a |
| | 5.66*2 | b | 5.25*2 | b | 5.00*2 | b |
| $n\text{-}C_3H_7$ | | | 5.42 | a | 5.23 | a |
| $n\text{-}C_4H_9$ | 5.71 | a | 5.43 | a | 5.22 | a |
| | 5.98*1 | a | 5.23*1 | a | 7.93*1 | a |
| $i\text{-}C_3H_7$ | | | | | 4.85 | a |
| | | | 5.07*2 | b | 4.82*1 | b |
| $C_6H_5$ | | | | | 3.03 | a |
| | 4.98*3 | d | 3.98*3 | d | 3.16*3 | d |

*1 P. E. Potter, L. Platt and G. Wilkinson, *J. Chem. Soc.*, **1964**, 524.
*2 N. Flitcroft and H. D. Kaesz, Private Communication.
*3 E. Amberger, H. P. Fritz, C. G. Kreiter and M. Kula, *Chem. Ber.*, **96**, 3270 (1963).
a) Carbon disulfide b) Cyclopentane c) Neopentane d) Diethylether

A-60 and a Japan Electron Optical Laboratory Co., Ltd., model 3H-60. Carbon disulfide was used as the solvent and the tetramethylsilane as the internal standard throughout. Measurements in a cyclohexane solution or in a neat liquid were also carried out in order to check the solvent effect.* The sample with a 2—10% concentration and with 1% tetramethylsilane was mixed in a Pyrex tube 5 mm. in diameter. The temperature was maintained at 20°C. The position of the peak was measured to the nearest 0.1 cycle/sec., the average of at least two determinations being used for each value recorded.

**Infrared Absorption Spectra.**—The infrared spectra were recorded by using a Perkin-Elmer (model 21) double-beam spectrophotometer equipped with sodium chloride optics, or a Hitachi EPI-2G infrared spectrophotometer equipped with gratings. The neat sample was used, and all spectra were calibrated by using known peaks of a polystyrene film.

* Carbon tetrachloride, a usual solvent in the proton magnetic resonance measurement. cannot be used because of its reactivity toward organotinhydrides (D. H. Lorenz and E. I. Becker, *J. Org. Chem.*, **27**, 3370 (1962)).

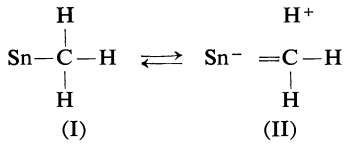
## Results and Discussion

The observed shielding values, in parts per million (p. p. m.), of the resonance of the proton attached directly to the tin atom in various organotin hydrides are shown in Table II together with the values in the literature. The results show that the shielding of the (Sn-)H proton increases in the order of $i\text{-}C_3H_7 < n\text{-}C_4H_9 \simeq n\text{-}C_3H_7 \simeq C_2H_5 < CH_3$ in trialkyltin hydrides. These results may be interpreted by considering such contributions as that of II in the ground state of the molecule, in which a considerable amount of $d_\pi$-$p_\pi$ bonding may take part:

TABLE III. THE INFRARED SPECTRA OF THE Sn-H STRETCHING VIBRATIONS: POSITIONS OF BANDS (in $cm^{-1}$)

| | $RSnH_3$ | | $R_2SnH_2$ | | $R_2SnH$ | |
|---|---|---|---|---|---|---|
| | ν Sn-H | Solvent | ν Sn-H | Solvent | ν Sn-H | Solvent |
| R=H | 1906*1 | a | | | | |
| | 1898*2 | b | | | | |
| $CH_3$ | 1876*4 | | 1858 | | 1830 | |
| | 1870*2 | c | 1845*2 | c | 1833*2 | c |
| $C_2H_5$ | 1869*4 | | | | 1809 | |
| | 1869*4 | c | 1822*3 | c | 1800*3 | c |
| $n$-$C_3H_7$ | | | 1835 | | 1809 | |
| | | | 1835*5 | | 1820*5 | |
| | | | 1842*1 | a | 1795*1 | a |
| $n$-$C_4H_9$ | 1870 | | 1832 | | 1807 | |
| | 1865*1 | a | 1842*1 | a | 1808*1 | a |
| | 1855*3 | c | 1835*3 | c | 1820*5 | |
| $i$-$C_3H_7$ | | | | | 1792 | |
| | | | 1820*2 | c | 1792*2 | c |
| $C_6H_5$ | | | | | 1838 | |
| | 1880*3 | c | 1855*3 | c | 1843*3 | c |

*1 P. E. Potter, L. Platt and G. Wilkinson, *J. Chem. Soc.*, **1964**, 524.
*2 N. Flitcroft and H. D. Kaesz, Private Communication.
*3 E. Amberger, H. P. Fritz, C. G. Kreiter and M. Kula, *Chem. Ber.*, **96**, 3270 (1963).
*4 H. J. Emeleus and S. F. A. Kettle, *J. Chem. Soc.*, **1958**, 2444.
*5 R. Mathis-Noel, M. Lesbre and I. S. de Roche, *Compt. rend.*, **243**, 257 (1956).
a) Di-*n*-butylether b) *n*-Hexane c) Cyclohexane



(I) (II)

Thus, the Sn-C bond would be strengthened, the electron density on the proton bound directly to the tin atom may be increased, and at the same time the Sn-H bond would probably be strengthened. Support for this explanation is found in the recent thermochemical data.[5] The mean dissociation energy, $\bar{D}$(Sn-C), in the tetraalkyltin increases as follows; $C_2H_5 \simeq n\text{-}C_4H_9 \simeq n\text{-}C_3H_7 < CH_3$, which is almost consistent with the above explanation. This order found in organotin hydrides is different from that of the trialkylsilane or dialkylmercury, as has been described already. The low-lying vacant d-orbitals which can accept electrons from the alkyl group through the $d_\pi$-$p_\pi$ bonding are not very different in the tin atom and the silicon atom, although they are a little lower in the former than in the latter. It is not clear why the effect of the hyperconjugation is a predominant factor in the alkyltin hydride but not in the alkylsilane. The $\tau$ value in triphenyltin hydride is smaller than that in trialkyltin hydrides; this may be explained in terms of the electronegativity of the phenyl group.[2] The ring current of the phenyl group may also play a role.

In the shielding of the protons bound directly to the tin atom, the successive replacement of the hydrogen of the $SnH_4$ molecule by an alkyl group results in a progressive decrease in the $\tau$ value, as Table II shows. This tendency is smilar to those in hydrocarbons and might have some correlation with the dissociation energy of the carbon and hydrogen concerned, for some electronic strain may be accumulated on the C-H bond by the replacement of the hydrogen with the alkyl group. The dissociation energies of several kinds of C-H bonds are as follows; $\bar{D}$(C-H) = 101, 96, 94 and 89 kcal./mol. for $CH_3$-H, $CH_3CH_2$-H, $(CH_3)_2CH$-H and $(CH_3)_3C$-H respectively.[6] The result is parallel to the $\tau$ value of the corresponding proton. The same might be true in the alkyltin hydrides. The difference in the $\tau$ value of the (Sn-)H or (C-)H protons cannot be explained by the difference in the electronegativities of the tin atom and the carbon atom; for example, the $\tau$ values in the $(CH_3)_3XH$ molecule decrease independently of the electronegativity of the X atom; (X-)H = 8.46, 6.15, 5.36 and 2.32[7] for

5) J. V. Davies, A. B. Pofe and H. A. Skinner, *Trans. Faraday Soc.*, **59**, 2233 (1963).
6) L. L. Cottrell, "The Strength of Chemical Bonds," Butterworths Scientific Publication London, (1958).
7) N. Flitcroft and H. D. Kaesz, *J. Am. Chem. Soc.*, **85**, 1377 (1963).

X=C, Si, Sn and Pb respectively. One factor which influences these $\tau$ values may be the paramagnetic effect of the central atom X, for the paramagnetic effect seems to increase with an increase in the atomic number.

The frequencies of the Sn-H stretching vibration in the infrared absorption spectra of the alkyltin hydrides are given in Table III, together with the values reported in the literature. In the trialkyltin hydride, the positions of the Sn-H stretching vibration bands are in the order of $i$-$C_3H_7 < n$-$C_4H_9 \simeq n$-$C_3H_7 \simeq C_2H_5 < CH_3$, paralleling the order in the nuclear magnetic resonance spectra. This will support the assumption of the hyperconjugation of the alkyl group, which increases the overlap charge between the tin atom and the hydrogen atom. The position of the Sn-H stretching band in triphenyltin hydride, however, is exceptional, as it is in the case of the silicone analogues. In the dialkyltin or monoalkyltin hydride, only one Sn-H stretching band was found,* although two bands may be predicted from the selection rule. This might be due to the overlapping of the two kinds of Sn-H stretching bands as a result of a relatively small coupling between Sn-H vibrations. The Sn-H stretching band in the dialkyltin or monoalkyltin hydride shifts to a wave number relatively higher than that of the trialkyltin hydride. This tendency is parallel to that of the $\tau$ value.

* H. C. Clark et. al. have reported a doublet, but others do not (see Tables III).

## Summary

The nuclear magnetic resonance spectra of the proton attached directly to the tin atom in several organotin hydrides ($R_nSnH_{4-n}$; $n$= 1, 2, 3) have been measured. The observed shielding values increase in the order of $i$-$C_3H_7 < n$-$C_4H_9 \simeq n$-$C_3H_7 \simeq C_2H_5 < CH_3$ in trialkyltin hydrides. This order is consistent with that of the hyperconjugation effect of the alkyl group. On the other hand, the change in the shielding of the protons bound directly to the tin atom with a step-by-step substitution of $SnH_4$ by an alkyl group is similar to that of hydrocarbons or alkylsilanes. The infrared spectra of organotin hydrides show that there is a close correlation between the $\tau$ values and the Sn-H stretching frequencies.

*Department of Applied Chemistry*
*Osaka University*
*Miyakojima, Osaka*

# Vibrational Assignments and Intramolecular Force Field of Trimethylaluminum*

By Teiichiro OGAWA, Kozo HIROTA and Tatsuo MIYAZAWA

(Received October 30, 1964)

Trimethylaluminum is the simplest member of the trialkylaluminum series, all of which are important components of the Ziegler-type catalyst. Accordingly, this compound has been extensively investigated, although its reactivity is low in olefin polymerization. The reaction and the structure of trimethylaluminum-diphenylamine complex have been reported on previously.[1]

Trimethylaluminum has been found to be in a bridged structure by an X-ray diffraction method.[2] The vibrational spectra and their assignments have been studied by several authors.[3-10] Onishi et al.[7,9] have measured the infrared spectra in the region 700—280 $cm^{-1}$ and have calculated the normal vibrations on the basis of a modified Urey-Bradley field. Ogawa et al.[6,10] have measured the far infrared

* Read at the Symposium on Structual Chemistry, Tokyo, 1964.

1) M. Kawai, T. Ogawa and K. Hirota, This Bulletin, 37, 1302 (1964).

2) P. H. Lewis and R. E. Rundle, *J. Chem. Phys.*, 21, 986 (1953).

3) G. P. van der Kelen and M. A. Herman, *Bull. soc. chim. Belges.*, 65, 362 (1956).

4) E. G. Hoffmann, *Z. Electrochem.*, 64, 616 (1960).

5) K. Hirota, K. Kuwata and T. Imanaka, *J. Chem. Soc. Japan, Pure Chem. Sec.* (*Nippon Kagaku Zasshi*), 83, 1302 (1962).

6) T. Ogawa, K. Hirota, T. Imanaka, K. Fukushima and T. Miyazawa, "Proceedings of the International Symposium on Molecular Structure and Spectroscopy," Science Council of Japan, Tokyo (1962), A309.

7) T. Onishi, I. Nakagawa and T. Shimanouchi, ibid., (1962), A310.

8) A. P. Gray, *Can. J. Chem.*, 41, 1511 (1963).

9) T. Onishi and T. Shimanouchi, *Spectrochim. Acta*, 20, 325 (1964).

10) T. Ogawa, K. Hirota and K. Fukushima, This Bulletin, 37, 1243 (1964).

spectra in the region 700—65 $cm^{-1}$ and have calculated the normal vibrations by the use of the Urey-Bradley potential function as supplemented with a few correction terms. In the present study the treatment of the normal vibrations was refined, and the vibrational spectra were reassigned.

The standard errors of potential constants may be used in discussing the reliability of a potential field and in studying the transferability of the potential terms. The uncertainties in potential constants arise not only from experimental errors, but also from deficiencies in the physical model of the potential field. The standard errors which are due to the latter source have previously been discussed, and a general formula has been derived.[11] This formula was used, in the present study, for the calculation of the standard errors of the potential constants of trimethylaluminum.

## Experimental

In studying the reaction mechanism, it is interesting to measure the infrared spectra of reactive substances or intermediate species. Since unstable organic samples react with or dissolve a vacuum grease, it was not practical to construct a vacuum liquid cell with alkali halide crystals. Therefore, a new device was worked out for the infrared measurement of extremely reactive substances.

This cell was made of polyethylene and could be kept in a vacuum of about $10^{-2}$ mmHg for a few days. The margin of polyethylene films, 10 cm.× 8 cm.×0.5 mm., was heated and pressed by a brass press in order to form an envelope; a glass tube 4 mm. in diameter had been inserted between the films in advance. Polyethylene films were readily melted and adhered to each other and to the glass tube. The cells thus constructed are satisfactorily airtight. In addition, vacuum resin was spread all over the outer surface of the cell, except for the optical path, in order to ensure the vacuum and to prevent the cell from accidentally breaking. The liquid sample was distilled in a side arm near the cell and poured through the glass tube into the cell in a vacuum. When it was necessary to increase the sample thickness, nitrogen gas was introduced in order to help more liquid squeeze into the cell. With this cell, the infrared spectra could be measured in the 4000—3100 $cm^{-1}$, 2500—1500 $cm^{-1}$, 1250—750 $cm^{-1}$, and below 700 $cm^{-1}$ regions.

## Normal Vibration Treatment

The molecular structure of trimethylaluminum (Fig. 1) belongs to the point group $D_{2h}$, and the geometrical parameters are $a=1.99$Å, $b=2.24$Å, $l=2.57$Å, $\angle\alpha=124°$ and $\angle\beta=110°$.[2] This structure of trimethylaluminum is quite similar to that of diborane, and so is the procedure of calculation.[11] The normal vibrations were treated by Wilson's GF matrix method.[12] The methyl group of this molecule was assumed to be a single dynamic unit. This molecule has eight symmetry species. The $B_{1u}$, $B_{2u}$ and $B_{3u}$ vibrations are infrared-active, and the $A_{1g}$, $B_{1g}$, $B_{2g}$ and $B_{3g}$ vibrations are Raman-active, but the $A_{1u}$ vibration is inactive.

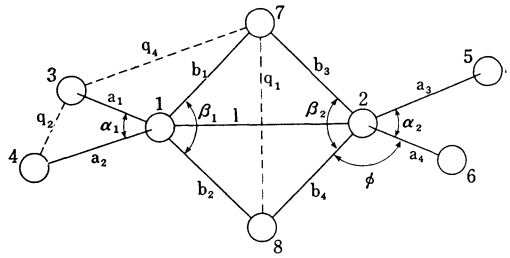



Fig. 1. The structure of the trimethylaluminum molecule, indicating the numbering of the atoms and the internal coordinates.
1, 2, Al; 3, 4, 5, 6, 7, 8, $CH_3$.
$\phi_1$ ∠713, $\phi_2$ ∠714, $\phi_3$ ∠813, $\phi_4$ ∠814, $\phi_5$ ∠826, $\phi_6$ ∠825, $\phi_7$ ∠726, $\phi_8$ ∠725
$\tau_1$ 8172, $\tau_2$ 8271, $\tau_3$ 7182, $\tau_4$ 7281

The internal coordinates are also given in Fig. 1. The symmetry coordinates were constructed as linear combinations of the internal coordinates, $S=UR$. The orthogonal $U$ matrices have been described previously.[11] A modified Urey-Bradley potential function was assumed as follows;

$$\begin{aligned}2V=&\sum_{i=1}^{4}K_a(\Delta a_i)^2+\sum_{i=1}^{4}K_b(\Delta b_i)^2+K_l(\Delta l)^2\\&+\sum_{i=1}^{2}H_\alpha(a\Delta\alpha_i)^2+\sum_{i=1}^{2}H_\beta(b\Delta\beta_i)^2\\&+\sum_{i=1}^{8}H_\phi(b\Delta\phi_i)^2+\sum_{i=1}^{4}H_\tau(b\Delta\tau_i)^2\\&+2tb^2(\Delta\phi_1\Delta\phi_7-\Delta\phi_1\Delta\phi_8+\Delta\phi_2\Delta\phi_3\\&-\Delta\phi_2\Delta\phi_7+\Delta\phi_3\Delta\phi_5-\Delta\phi_3\Delta\phi_6+\Delta\phi_4\Delta\phi_6\\&-\Delta\phi_4\Delta\phi_5)+\sum_{i=1}^{11}F(\Delta q_i)^2\end{aligned}\qquad(1)$$

where $K$, $H$ and $F$ are stretching, bending and repulsive constants respectively, and $t$ is the trans-interaction constant (the cis-interaction constant was set as equal to $-t$). There are three kinds of short $CH_3\cdots CH_3$ distances, as Fig. 1 shows. However, since their intergroup distances are nearly equal, a common repulsion constant, $F$, was used. The linear repulsion term, $F'(=-F/10)$, was omitted. The interaction terms, $k_1$, $f_1$ and $f_2$, in the potential function of diborane[11] were not included in the

11) T. Ogawa and T. Miyazawa, *Spectrochim. Acta*, **20**, 557 (1964).

12) E. B. Wilson, Jr., *J. Chem. Phys.*, **7**, 1047 (1939); **9**, 76 (1941).

present treatment because available experimental data were not sufficient for determining these terms. Although there were apparently nine parameters in the present potential function, $H_\beta$ was set as zero (cf. diborane[11]) and $H_\tau$ was assumed to be 0.02 md./Å. The seven remaining potential parameters were adjusted by the least-squares treatment.[13] A NEAC 2101 computer (Nippon Electric Company, Tokyo) was used for the numerical calculation.

## Results and Discussion

The vibrational assignments made by Hoffmann,[4] Ogawa et al.,[6] Gray[8] and Onishi et al.[9] are shown in Table I, together with the observed spectra and the present assignments.

As was shown in our previous paper,[10] no band was found in the region 400—65 $cm^{-1}$ except for the two at 367 and 175 $cm^{-1}$. All the vibrations except the puckering mode, $\nu_{10}$, are expected to lie in the region above 65 $cm^{-1}$. The rocking mode, $\nu_9$, may well, however, be very weak, since the corresponding band of diborane has not yet been observed.[14] Nevertheless, Hoffmann's assignments need three bands in this region, whereas Gray's assignments need only two. In this respect, Gray's assignments give a one-to-one correspondence between the observed bands and the expected vibrations.

One of the characteristics of Gray's assignments is that the frequencies of the infrared-active vibrations are appreciably higher than those of the corresponding Raman-active vibrations. That makes it very difficult to construct a reasonable potential function and to determine the force constants satisfactorily. A set of Urey-Bradley force constants always predicts higher frequency values for $\nu_1$, $\nu_2$ and $\nu_3$ than those for $\nu_{16}$, $\nu_{17}$ and $\nu_{18}$ respectively, partly because some of the diagonal $G$ matrix elements for the $A_{1g}$ species are larger than the corresponding elements for the $B_{3u}$ species. Therefore, Gray's assignments of Raman lines were tentatively modified; the weak line at 632 $cm^{-1}$ or 725 $cm^{-1}$ was assigned to $\nu_1$, and the lines at 592 $cm^{-1}$, 453 $cm^{-1}$ and 313 $cm^{-1}$ were assigned to $\nu_2$, $\nu_3$ and $\nu_4$ respectively. In some preliminary calculations, however, it was not yet possible to obtain a reasonable potential function in accordance with such assignments.

The isotope shifts of vibrational frequencies have been measured by Gray and used in discriminating the skeletal vibrations from methyl vibrations. Thus, the infrared band at 616 $cm^{-1}$ was assigned to $\nu_{16}$,[8] although in previous studies[4-7,9] the band at 562 $cm^{-1}$ had been assigned to $\nu_{16}$. The infrared band at 772 $cm^{-1}$ had been assigned to $\nu_8$ by Gray.[8] However, this frequency appears to be too high for a skeletal vibration. Accordingly, the band at 697 $cm^{-1}$ was again assigned to $\nu_8$ in the present study.

Onishi and Shimanouchi[9] assigned the infrared band at 367 $cm^{-1}$ to $\nu_{17}$, and the Raman lines at 153 and 185 $cm^{-1}$, to $\nu_4$ and $\nu_{12}$ respectively. They treated the skeletal vibrations on the basis of the Urey-Bradley field modified

TABLE I. THE OBSERVED SPECTRA AND THEIR ASSIGNMENTS

| | | | Hoffmann[4] | Ogawa et al.[6] | Gray[8] | Onishi et al.[9] | Present Study |
|---|---|---|---|---|---|---|---|
| Raman active | $A_{1g}$ | $\nu_1$ (Str.) | 592 | 592 | 592 | 592 | 592 |
| | | $\nu_2$ (Str.) | 453 | 453 | 453 | 453 | 453 |
| | | $\nu_3$ (Ring.) | 313 | 313 | 313 | 313 | 313 |
| | | $\nu_4$ (Bend.) | | | | 153 | 153 |
| | $B_{1g}$ | $\nu_6$ (Str.) | | | 495? | | |
| | | $\nu_7$ (Wag.) | | | | | |
| | $B_{2g}$ | $\nu_{11}$ (Str.) | 683 | 683 | 683 | 683 | 683 |
| | | $\nu_{12}$ (Rock.) | | | | 185 | |
| | $B_{3g}$ | $\nu_{15}$ (Twist.) | | | | | 185? |
| Infrared active | $B_{1u}$ | $\nu_8$ (Str.) | 696 | 697 | 772 | 696 | 697 |
| | | $\nu_9$ (Rock.) | | 171? | | | |
| | | $\nu_{10}$ (Puck.) | | | | | |
| | $B_{2u}$ | $\nu_{13}$ (Str.) | 480 | 487 | 652? | 479 | 480 |
| | | $\nu_{14}$ (Wag.) | | 200?* | | | 175 |
| | $B_{3u}$ | $\nu_{16}$ (Str.) | 564 | 562 | 616 | 565 | 616 |
| | | $\nu_{17}$ (Str.) | | 369 | 480 | 367 | 367 |
| | | $\nu_{18}$ (Bend.) | | 304* | 369 | | 175 |

?: Questionable assignments.
*: These bands were found in the present study to be due to impurities.

13) D. E. Mann, T. Shimanouchi, J. H. Meal and L. Fano, *J. Chem. Phys.*, **27**, 43 (1957).

14) W. L. Smith, I. M. Mills, ibid., **41**, 1479 (1964).

TABLE II. THE OBSERVED AND CALCULATED FREQUENCIES OF TRIMETHYLALUMINUM AND DEUTERATED TRIMETHYLALUMINUM ($cm^{-1}$)

| | | | $Al_2(CH_3)_6$ | | $Al_2(CD_3)_6$ | |
|---|---|---|---|---|---|---|
| | | | Obs.[a] | Calcd. | Obs.[b] | Calcd. |
| Raman active | $A_{1g}$ | $\nu_1$ | 592 | 633 | | 608 |
| | | $\nu_2$ | 453 | 473 | | 436 |
| | | $\nu_3$ | 313 | 305 | | 287 |
| | | $\nu_4$ | 153 | 145 | | 132 |
| | $B_{1g}$ | $\nu_6$ | | 395 | | 378 |
| | | $\nu_7$ | | 210 | | 198 |
| | $B_{2g}$ | $\nu_{11}$ | 683 | 690 | | 659 |
| | | $\nu_{12}$ | | 173 | | 163 |
| | $B_{3g}$ | $\nu_{15}$ | 185 | 186 | | 169 |
| Infrared active | $B_{1u}$ | $\nu_8$ | 697 | 688 | 677 | 657 |
| | | $\nu_9$ | | 257 | | 237 |
| | | $\nu_{10}$ | | 48 | | 44 |
| | $B_{2u}$ | $\nu_{13}$ | 480 | 478 | 435 | 452 |
| | | $\nu_{14}$ | 175 | 173 | | 163 |
| | $B_{3u}$ | $\nu_{16}$ | 616 | 583 | 579 | 544 |
| | | $\nu_{17}$ | 367 | 358 | 315 | 334 |
| | | $\nu_{18}$ | 175 | 183 | | 170 |
| Inactive | $A_{1u}$ | $\nu_5$ | | 151 | | 138 |
| $\lvert\bar{\delta}\rvert$ | (%) | | | 3.0 | | |
| $(\bar{\delta}^2)^{1/2}$ | (%) | | | 3.7 | | |

a) Raman lines: Ref. 4, infrared bands: Refs. 4, 6 and 10.
b) Ref. 8.

TABLE III. THE DIAGONAL ELEMENTS OF POTENTIAL ENERGY DISTRIBUTION ($F_{ii}L^2_{ia}/\lambda_a$)*

| $A_{1g}$ | $S_1{}^a$ | $S_2{}^b$ | $S_3{}^l$ | $S_4{}^\alpha$ | $S_5{}^\phi$ | $B_{1g}$ | $S_8{}^b$ | $S_9{}^\phi$ |
|---|---|---|---|---|---|---|---|---|
| $\nu_1$ | 73 | 14 | 21 | 2 | 0 | $\nu_6$ | 108 | 3 |
| $\nu_2$ | 20 | 67 | 10 | 1 | 1 | $\nu_7$ | 2 | 107 |
| $\nu_3$ | 8 | 24 | 59 | 9 | 0 | | | |
| $\nu_4$ | 0 | 2 | 9 | 61 | 32 | | | |

| $B_{2g}$ | $S_{13}{}^a$ | $S_{14}{}^\phi$ | $B_{1u}$ | $S_{10}{}^a$ | $S_{11}{}^\phi$ | $S_{12}{}^\tau$ |
|---|---|---|---|---|---|---|
| $\nu_{11}$ | 103 | 4 | $\nu_8$ | 103 | 2 | 1 |
| $\nu_{12}$ | 0 | 99 | $\nu_9$ | 0 | 56 | 44 |
| | | | $\nu_{10}$ | 2 | 47 | 55 |

| $B_{2u}$ | $S_{16}{}^b$ | $S_{17}{}^\phi$ | $B_{3u}$ | $S_{20}{}^a$ | $S_{21}{}^b$ | $S_{22}{}^\alpha$ | $S_{23}{}^\phi$ |
|---|---|---|---|---|---|---|---|
| $\nu_{13}$ | 110 | 8 | $\nu_{16}$ | 101 | 3 | 1 | 0 |
| $\nu_{14}$ | 0 | 102 | $\nu_{17}$ | 0 | 88 | 2 | 2 |
| | | | $\nu_{18}$ | 1 | 1 | 73 | 28 |

* The superscripts indicate internal coordinates. See Fig. 1.

with the resonance term. This term mainly affects the $\nu_6$ vibration, which has not been observed experimentally for trimethylaluminum. Accordingly, this term was not included in the present potential function.

In the present study the vibrational assignments were carried out with reference to the results of the frequency calculation. As for the Raman bands at 683, 592, 453 and 313 $cm^{-1}$, Hoffmann's assignments were used. The $\nu_4$ vibration is expected to be very strong, since this vibration belongs to the totally-symmetric species and since the corresponding Raman line of diborane is very strong. In agreement with Onishi's assignment, the strong line at 153 $cm^{-1}$ was thus assigned to $\nu_4$, although it is practically depolarized. As in the case of diborane, the $B_{1g}$ vibrations are not expected to be very strong. Two other Raman-active vibrations, $\nu_{12}$ and $\nu_{15}$, are also expected to lie above 70 $cm^{-1}$. In the case of diborane, the $\nu_{12}$ vibration has not been observed in the Raman effect, whereas the $\nu_{15}$ Raman vibration was of medium intensity. Accordingly, the Raman line of trimethylaluminum at 185 $cm^{-1}$ was tentatively assigned to the $\nu_{15}$ mode.

(This line had been assigned to $\nu_{12}$ by Onishi and Shimanouchi.[7,9]) The infrared bands at 697, 480 and 616 $cm^{-1}$ were assigned to $\nu_8$, $\nu_{13}$ and $\nu_{16}$ respectively, as has been mentioned before. Some of the preliminary assignments[6] were revised in consideration of refined experimental results,[10] and the bands at 367 and 175 $cm^{-1}$ were assigned to $\nu_{17}$ and $\nu_{18}$ respectively.

The results of the normal vibration calculation are shown in Table II, both for trimethylaluminum and for the fully deuterated derivative. The calculated $\nu_{14}$ frequency lies near $\nu_{18}$ with the present potential field. Accordingly, the observed frequencies of the $\nu_{14}$ and $\nu_{18}$ vibrations were both taken to be 175 $cm^{-1}$. The $\nu_{12}$ vibration calculated at 173 $cm^{-1}$ may partly contribute to the broad Raman band at 153—185 $cm^{-1}$. The potential energy distributions ($F_{tt}L_{ta}^2/\lambda_a$)[15] for trimethylaluminum are shown in Table III.

TABLE IV. THE CALCULATED FORCE CONSTANTS AND THEIR STANDARD ERRORS

| | Calculated values md./Å | Standard errors $\sigma_1$ | $\sigma_2$ | $\sigma$(total) |
|---|---|---|---|---|
| $K_a$ | 2.16 | 0.04 | 0.14 | 0.15 |
| $K_b$ | 0.88 | 0.02 | 0.03 | 0.04 |
| $K_l$ | 1.24 | 0.07 | 0.22 | 0.23 |
| $H_\alpha$ | 0.054 | 0.003 | 0.013 | 0.013 |
| $H_\beta$ | 0 | — | — | — |
| $H_\phi$ | 0.040 | 0.006 | 0.016 | 0.017 |
| $H_\tau$ | 0.020 | — | — | — |
| $t$ | 0.013 | 0.001 | 0.000 | 0.001 |
| $F$ | 0.080 | 0.010 | 0.030 | 0.032 |

$\sigma_1$; Standard errors which arise from experimental uncertainties.
$\sigma_2$; Standard errors which arise from deficiencies in the physical model of the potential field.

The force constants adjusted by the least-squares refinements are shown in Table IV, together with their standard errors. As was indicated by preliminary calculations of trimethylaluminum and diborane,[6] the frequency fit was improved by a decrease in the value of the bending constant, $H_\beta$. Therefore, this constant, $H_\beta$, was also set as equal to zero. There are no experimental data on the puckering vibration; accordingly, the value of $H_\tau$ was set arbitrarily at 0.02 md./Å. The trans- and cis-interaction terms were introduced rather arbitrarily and set so as to yield the best agreement between the observed and the calculated $\nu_{15}$ frequencies. Without these interaction terms, the $\nu_5$ and $\nu_{12}$ frequencies would be considerably lower than the calculated values and the $\nu_9$ and $\nu_{15}$ frequencies, higher than the calculated values.

The standard errors of potential constants were calculated by the formula:[11]

$$\sigma^2(K_h) = \frac{n}{n-q} \times \{(\boldsymbol{J}^*\boldsymbol{W}\boldsymbol{J})^{-1}\boldsymbol{J}^*\boldsymbol{W}\rho^2\boldsymbol{W}\boldsymbol{J}(\boldsymbol{J}^*\boldsymbol{W}\boldsymbol{J})^{-1}\}_{hh} \quad (2)$$

where $n$ and $q$ are the numbers of the observed frequencies and adjustable force constants respectively. $\boldsymbol{J}$ is the Jacobian matrix, and $\rho$ is the diagonal matrix of the residuals between the calculated and the observed data. In the calculation of standard errors of potential constants, the standard errors of the observed frequencies were assumed to be one per cent.

The similarity of the molecular structure of trimethylaluminum to that of diborane was repeatedly used in the vibrational assignments or normal vibration treatments. The formula of the potential function and also the relation of the magnitude of the potential constants are similar in the two molecules. However, the methyl group of trimethylaluminum is larger than the hydrogen atom of diborane, and the mutual repulsion terms among methyl groups were taken into account.

In the present potential function, there were several characteristics which were similar to those of diborane. The first was that the terminal-bond stretching constant ($K_a$) was more than twice as great as the bridge-bond stretching constant ($K_b$). This shows that the bridge half-bond was considerably weaker than the terminal single bond. The second was that in-plane angle-deformation potential terms ($H_\beta$) of the bridge may be neglected in the potential function of this molecule. The bridge bond was not expected to have much directional property, and the infinitesimal change in the bridge angle was not expected to be confronted by a strong restoring force. The third was that the stretching constant ($K_l$) between two aluminum atoms was large enough for us to confirm the existence of a bond between them. In fact, the interatomic distance, 2.57Å, is approximately equal to the sum (2.52Å) of Pauling's tetrahedral covalent radii.[2,16]

Because of the lack of enough observed data for deuterated species, the values of the standard errors of the potential constants were greater than those in the case of diborane, but they were nevertheless satisfactory since all constants were essentially determined.

15) Y. Morino and K. Kuchitsu, *J. Chem. Phys.*, 20, 1809 (1952): I. Nakagawa, *J. Chem. Soc. Japan, Pure Chem. Sec.* (*Nippon Kagaku Zassi*), 74, 243 (1953).

16) L. Pauling, "The Nature of the Chemical Bond," Cornell University Press, Ithaca, New York, U. S. A. (1960), p. 246.

The present assignments were finally set on the basis of Hoffmann's assignments, taking Gray's data on isotope shift into consideration.

## Summary

A vacuum infrared cell for reactive or intermediate species has been devised by the use of polyethylene sheets as optical windows. The infrared spectra in the 4000—3100 $cm^{-1}$, 2500—1500 $cm^{-1}$, 1250—750 $cm^{-1}$ and 700—65 $cm^{-1}$ regions can be measured with this liquid cell.

The vibrational assignments of the observed spectra have been carried out. The band at 367 $cm^{-1}$ has been assigned to $\nu_{17}$, and the band at 175 $cm^{-1}$, to $\nu_{18}$ and $\nu_{14}$.

The normal vibrations have been calculated, and the potential function of this molecule has been studied. A bond has been concluded to lie between two aluminum atoms. The characteristics of the potential function and the bond structure of trimethylaluminum have also been discussed.

The authors are indebted to Miss Yoshiko Ideguchi for her assistance in the numerical calculations.

*Department of Chemistry*
*Faculty of Science*
*Osaka University*
*Nakanoshima, Osaka* (*T. O. & K. H.*)

*Institute for Protein Research*
*Osaka University*
*Kita-ku, Osaka* (*T. M.*)

# Studies of the Liquid-Liquid Partition Systems. I. The Distribution of Radon(0) between Various Organic Solvents and Aqueous Solutions

By Tatsuya SEKINE* and Akira YAMASAKI**

(Received October 31, 1964)

The partition of a chemical species between two equilibrated immiscible liquid phases has been studied for a long time, and the constants have been determined for various distribution, association, or dissociation equilibria. At the same time, the partition method has been applied in many different fields, and the "solvent extraction method" has been recognized as one of the most rapid and effective methods for the separation or the purification of various materials.

The present series will present the results of our study of the liquid-liquid partition systems. In them chemical species are distributed between two phases; usually one is an aqueous solution which contains non-electrolytes, complex-forming ligands, or electrolytes, while the other is an organic solvent with various extractants.

The first paper of this series will report on the distribution of radon(0) between aqueous solutions and pure organic solvents. Inert gases were chosen as one of the simplest molecules, and radon was chosen because it may be most easily polarized or most easily interacted with other molecules among the inert gas elements.

**The Previous Work.**—Even though the inert gases show a very poor interaction with other atoms or molecules, it has been established that they have some solubility in water. The distribution ratio of radon between the air and water was determined at different temperatures,[1-5] and it was reported to be affected by solutes in the water.[6] It was also found that radon is distributed from air to various solvents better than to water.[7] These findings were reviewed by Bonner and Kahn.[8]

Recently, some authors have studied the behavior of inert gases in solutions. Lawrence

* Department of Chemistry, Tokyo College of Science, Kagurazaka, Shinjuku-ku; and Laboratory of Nuclear Chemistry, Institute of Physical and Chemical Research, Komagome, Bunkyo-ku, Tokyo.

** Guest Scientist; Permanent Address: Department of Chemistry, Faculty of Science, The University of Tokyo, Hongo, Tokyo.

1) J. J. Thomson, *Phil. Mag.*, (6) 4, 352 (1902).
2) H. F. Rausch von Traubenberg. *Phys. Z.*, 5, 130 (1904).
3) R. Hofmann, ibid., 6, 337 (1905).
4) H. Mache and S. Meyer, ibid., 6, 696 (1905).
5) R. M. Boyle, *Phil. Mag.*, (6), 22, 840 (1911).
6) M. Kofler, *Phys. Z.*, 9, 6 (1908).
7) E. Ramstedt, *le Radium*, 8, 253 (1911).
8) N. A. Bonner and M. Kahn, "Radioactivity applied to Chemistry," Ed. by A. C. Wahl and N. A. Bonner, John Wiley & Sons, Inc., New York (1951), p. 157.

and his co-workers[9] described how xenon is twice as soluble in water and fat as nitrogen, while helium shows a lower solubility. They reviewed the solubilities of hydrogen, oxygen, carbon dioxide, nitrogen, helium, argon, krypton, xenon and radon in water and oil. Semenchenko[10] described a theory for the solubility of gases and discussed that of radon. Morrison and Billet[11,12] described the salting-out of non-electrolytes and discussed the solubility of gases. Friedman[13] determined the solubility of rare gases, sulfur hexafluoride and osmium tetroxide in nitromethane and gave an equation which, in his opinion, correlated the solubility with two terms that depend on the solvents and gases. Diamond and Tuck[14] gave an indirect estimation of the distriribution of helium, neon, argon, krypton and xenon between water and nitromethane on the basis of Friedman's data. Clever and his co-workers[15] reported on the solubility of helium, neon, argon, krypton and xenon in methylcyclohexane and perfluorocyclohexane, and Nussbaum and Hursh[16] reported on the solubility of radon in fatty acids and triglycerides. Namiot[17] discussed the solubility of nonpolar gases in water.

The formation of inert gas hydrates or deuterates[18-21] has been observed and explained in terms of the dipole-induced dipole attraction. The hydration numbers of these compounds, $G \cdot xH_2O$ and $G \cdot yD_2O$, $x$ and $y$, were reported to be approaching six, but becoming so only with the heaviest inert gases. The crystals of these compounds are obtained only when water and inert gases are cooled at a low temperature under pressure. Other examples of such solvates have been also reported, for instance, phenol derivatives, $Kr \cdot 2C_6H_5OH$, $Xe \cdot 2C_6H_5OH$, and $Rn \cdot 2C_6H_5OH$.[22] Among other examples of the interaction between the inert gas atom and other atoms or molecules, the most remarkable are the xenon compounds with fluorine or oxygen, or krypton with fluorine.[23]

**The Present Work.**—The present work will first describe the distribution of radon between various organic solvents and water; next, it will describe the distribution of radon between carbon tetrachloride and calcium chloride solutions of various concentrations at 25°C. Finally, it will suggest the use of solvent extraction as a convenient separation or concentration technique for radon in various aqueous solutions where radium and its daughter nuclides coexist.

## Experimental

**Reagents and Solutions.**—All of the reagents used in this study were of reagent grade. The calcium content in the stock calcium chloride solution was determined by complexametry using a murexide indicator, while the chloride ion was titrated by argentometry using a fluorescein indicator. The calcium and chloride ion contents thus determined agreed with each other very well. Calcium chloride solutions of various concentrations were made by the addition of a weighed portion of water to a weighed portion of a calcium chloride stock solution.

The organic radon stock solution was prepared as follows: A pure radium nitrate solution in a bottle with a stopper had been left standing for a few days after the chemical separation from the daughter nuclides; then an organic solvent was added, and the whole was shaken for a few minutes. Then the organic phase was pipetted out and transferred into a stoppered centrifuging tube. Water was then added, and the tube was shaken again and centrifuged. The organic phase was pipetted off and used as the radon organic stock solution. In the earlier stage of the work, radon was emanated from a radium sulfate-barium sulfate precipitate into pure water. Radon was extracted from the supernatant solution with the various solvents to be studied.

**Procedures.**—All of the experiments were carried out in a thermostated room at 25°C. Ten milliliters of one of the organic radon solutions and 10 ml. of water were added to a glass stoppered centrifuging tube. The volume of the tube was about 21—22 ml. The two phases in the tube were equilibrated by mechanical agitation for about one hour and they separated by centrifugation. An 8 ml. portion was pipetted off from each phase and transferred into a small glass-stoppered 10 ml. test tube. Then 2 ml. of a non-radioactive organic solvent or water was added into the test tube to expel the air left at the top in order to avoid any changes in the geometrical efficiency of the radioactivity measurement which could be caused by the escape of radon into the gas phase.

The distribution ratio of radon between carbon tetrachloride and calcium chloride solutions of various concentrations was determined in just the

9) J. H. Lawrence, W. F. Loomis, C. A. Tobias and F. H. Turpin. *J. Physiol. (London)*, **106**, 197 (1946); *Chem. Abstr.*, **41**, 6991 (1947).
10) V. K. Semenchenko, *Vestnik. Moskov. Univ.*, **1947**, No. 5, 49.
11) T. J. Morrison, *J. Chem. Soc.*, **1952**, 3814.
12) T. J. Morrison and F. Billet, ibid., **1952**, 3819.
13) H. L. Friedman, *J. Am. Chem. Soc.*, **76**, 3294 (1954).
14) R. M. Diamond and D. G. Tuck, *Progr. Inorg. Chem.*, **2**, 109 (1961).
15) H. L. Clever, J. H. Saylor and P. M. Gross, *J. Phys. Chem.*, **62**, 89 (1958).
16) E. Nussbaum and J. B. Hursh, ibid., **62**, 81 (1958).
17) A. Yu. Namiot, *Zhur. Strukt. Khim.*, **2**, 408 (1961); *Chem. Abstr.*, **57**, 4053 (1962).
18) P. Villard, *Compt. rend.*, **123**, 377 (1896).
19) R. de Forcrand, ibid., **135**, 959 (1902); **176**, 355 (1923); **181**, 15 (1925).
20) M. Godchot, G. Cauquil and R. Calas, ibid., **202**, 795 (1936).
21) B. A. Nikitin, *Z. anorg. u. allgem. Chem.*, **227**, 81 (1936).
22) B. A. Nikitin, *Compt. rend. acad. sci. U. S. S. R.*, **24**, 562 (1939).
23) H. H. Hyman, *J. Chem. Educ.*, **41**, 174 (1964).

same way as has been described above, except that the calcium chloride solutions were used as the aqueous phase instead of pure water.

**The Measurement of Radioactivity.**—After the samples in the small glass-stoppered test tubes for radioactivity measurements had been left stand more than six hours, the $\gamma$-radioactivity was measured with a well-type scintillation counter with a sodium iodide(Tl) scintillator.

## Results

**The Decay of the $\gamma$-Radioactivity.**—Figure 1 gives an example of the decay curves of the $\gamma$-radioactivity. The half-life of the $\gamma$-radioactivity in all samples properly prepared agreed with the literature value (3.825 days for $^{222}Rn$) after the radioactive equilibrium was reached. Six hours' standing after the phase separation was enough for both phases to reach the radioactive equilibrium.

**The Distribution Constant for Radon between Water and Various Solvents.**—The distribution constants, $K_D$, was defined as follows:

$$K_D=[Rn]_{org}/[Rn]_{aq} = \frac{\gamma\text{-count rate per ml. of org. soln.}}{\gamma\text{-count rate per ml. of aq. soln.}} \quad (1)$$

Table I gives the distribution constants of radon between water and various organic solvents.

**The Distribution of Radon between Carbon Tetrachloride and Calcium Chloride Solutions of Different Concentrations.**—Table II gives the results of the distribution ratio of radon between carbon tetrachloride and aqueous solutions of calcium chloride at various concentrations. Figure 2 gives the plot of the distribution ratio against the calcium chloride concentration.

Table I. Distribution constants of radon between water and various organic solvents at 25°C

$K_D=[Rn]_{org}/[Rn]_{aq}$

| | Solvent | $K_D$* |
|---|---|---|
| 1 | Carbon tetrachloride | 59 |
| 2 | Chloroform | 56 |
| 3 | Bromoform | 39 |
| 4 | Hexane | 80 |
| 5 | Methyl isobutyl ketone (Hexone) | 37 |
| 6 | Methyl isobutyl carbinol (Hexol) | 33 |
| 7 | Chlorobenzene | 56 |
| 8 | Bromobenzene | 39 |
| 9 | Nitrobenzene | 21 |
| 10 | *o*-Dichlorobenzene | 50 |

* The values of $K_D$ gives the average. The original data are follows: 1 (52, 53, 57, 61, 62, 62, 63); 2 (47, 51, 59, 60, 61); 3 (39, 39, 40); 4 (71,81, 89); 5 (32, 36, 44); 6 (27, 35, 36); 7 (53, 54, 61); 8 (39, 39, 40); 9 (20, 21, 22, 22); 10 (41, 47, 52, 53, 53, 55). The results for benzene, toluene and xylene are not reproducible. The values are as follows: benzene (88, 88, 92, 113, 114, 119); toluene (72, 72, 82, 116, 118, 137); xylene (56, 65, 73, 84, 95, 107).

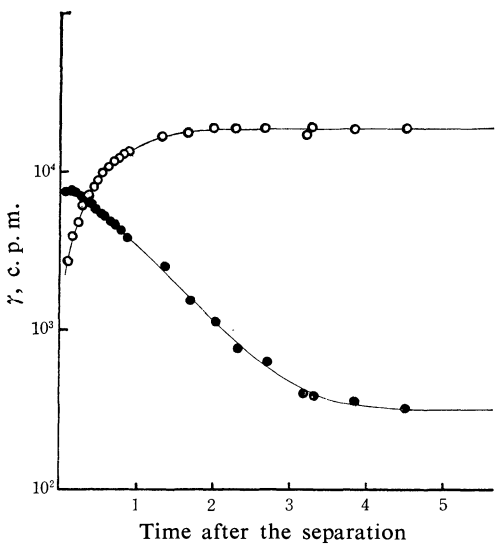



Fig. 1. Change of the $\gamma$-radioactivity in the organic and aqueous samples
Open circles; carbon tetrachloride
Closed circles; pure water

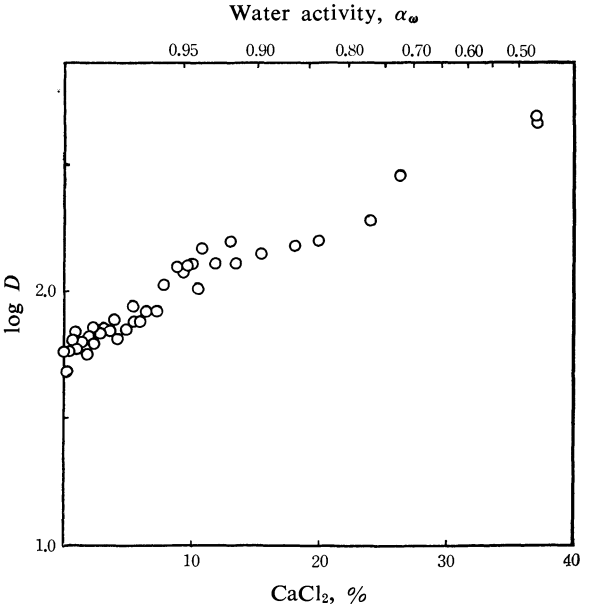



Fig. 2. Distribution of radon between calcium chloride solutions and carbon tetrachloride at 25°C.

Table II. Distribution ratio of radon between calcium chloride solutions and carbon tetrachloride at 25°C

$D=[Rn]_{org}/[Rn]_{aq}$

| $CaCl_2$ % | log$D$ | $CaCl_2$ % | log $D$ | $CaCl_2$ % | log $D$ |
|---|---|---|---|---|---|
| 0.28 | 1.674 | 2.92 | 1.840 | 9.71 | 2.100 |
| 0.45 | 1.766 | 3.10 | 1.863 | 9.97 | 2.104 |
| 0.65 | 1.811 | 3.60 | 1.842 | 10.36 | 2.017 |
| 0.81 | 1.833 | 3.92 | 1.899 | 10.70 | 2.176 |
| 0.83 | 1.849 | 4.14 | 1.810 | 11.81 | 2.114 |
| 1.17 | 1.772 | 4.81 | 1.859 | 12.91 | 2.201 |
| 1.39 | 1.792 | 4.89 | 1.859 | 13.37 | 2.114 |
| 1.77 | 1.743 | 5.36 | 1.941 | 15.38 | 2.146 |
| 1.93 | 1.818 | 5.43 | 1.877 | 17.93 | 2.179 |
| 2.20 | 1.852 | 5.95 | 1.880 | 19.73 | 2.201 |
| 2.24 | 1.780 | 6.49 | 1.920 | 23.84 | 2.277 |
| 2.42 | 1.851 | 7.18 | 1.915 | 25.04 | 2.431 |
| 2.56 | 1.840 | 7.75 | 2.025 | 26.10 | 2.460 |
| 2.65 | 1.847 | 8.84 | 2.109 | 36.94 | 2.664 |
| 2.91 | 1.869 | 9.41 | 2.084 | 36.94 | 2.682 |

## Discussion

**The Measurement of $\gamma$-Radioactivity.**—The decay chain of $(4n+2)$ series after $^{226}Ra$ has been well established. As the radium stock solution was purified from $^{210}Pb$ (half-life is 22 years.) before use, the radioactivity of the daughter nuclides after $^{210}Pb$, $^{210}Bi$, $^{210}Po$ and $^{206}Tl$ can be neglected in this experiment.

Figure 1 seems to show the following; (i) the distribution of radon into the organic phase is very high, but that of its $\gamma$-radioactive daughter nuclides is low. (ii) The $\gamma$-radioactive daughter nuclides in the decay products of $^{222}Rn$, $^{214}Pb$ (RaB, 26.8 min.) and $^{214}Bi$ (RaC, 19.7 min.) grow in the organic phase during the radon decays to $^{218}Po$ (RaA, 3.05 min.). On the other hand, these nuclides in the aqueous phase decrease, until finally the radioactive equilibrium is reached between the $^{222}Rn$ and these nuclides. (iii) The radioactive equilibrium between $^{222}Rn$ and these $\gamma$-radioactive daughter nuclides is first reached in the organic phase, but it takes longer in the aqueous phase because a large amount of $^{214}Pb$ and $^{214}Bi$ are back-extracted from the organic phase, which contains a much larger amount of $^{222}Rn$ than does the aqueous phase.

From these results, it may be concluded that the distribution ratio of $^{222}Rn$ in a liquid sample in an air-tight container can be determined by the direct measurement of the $\gamma$-radioactivity with a welltype scintillation counter if the samples are left standing until the radioactive equilibrium between the $^{222}Rn$ and its $\gamma$-radioactive daughter nuclides, $^{214}Pb$ and $^{214}Bi$, is reached.

**The Distribution of Radon between Water and Varous Organic Solvents.**—In a liquid-liquid partition system, the $K_D$ value generally gives the ratio of the relative solubility of radon in the two phases when they are mutually saturated; that is,

$$K_D=\frac{\text{the solubility of Rn in the organic solvent satd. with water}}{\text{the solubility of Rn in the water satd. with the organic solvent}} \quad (2)$$

and when the distribution constant of radon between air and a liquid, $K$, is defind as follows:

$$K=\frac{\text{the concn. of Rn in the liquid}}{\text{the concn. of Rn in air } (\sim 1 \text{ atm.})} \quad (3)$$

Therefore, one may calculate $K_D'$ as follows:

$$K_D'=\frac{\text{the solubility of Rn in a pure organic solvent}}{\text{the solubility of Rn in pure water}}=\frac{K_{org}}{K_{aq}} \quad (4)$$

The difference between $K_D$ in Eq. 2 and $K_D'$ in Eq. 4 depends on whether or not the two phases are mutually saturated. Table III gives $K_D'$ values calculated from previous data by Eq. 4.

Table III. Calculated distribution constants of radon between water and various organic solvents at 18°C from previous work

$K_D'=K_{org}/K_{aq}$

$K=\dfrac{\text{(concn. of Rn in liq. phase)}}{\text{(concn. of Rn in air (ca. 1 atm.))}}$

| Solvent | $K_{org}$ | $K_D'$ | Ref. |
|---|---|---|---|
| Chloroform | 15.1 | 53.0 | 7 |
| Chloroform | 15.08 | 52.9 | 1 |
| Carbon disulfide | 23.1 | 81.1 | 7 |
| Hexane | 16.56 | 58.1 | 7 |
| Benzene | 12.82 | 45.0 | 7 |
| Toluene | 13.24 | 46.5 | 1 |
| Toluene | 13.2 | 46.3 | 7 |
| Xylene | 12.75 | 44.7 | 1 |
| Xylene | 15.4 | 54.0 | 7 |
| Cyclohexane | 18.04 | 65.3 | 7 |
| Ethyl acetate | 7.35 | 25.8 | 7 |
| Ethyl acetate | 7.35 | 25.8 | 1 |
| Ethyl ether | 15.1 | 53.0 | 7 |

The $K_D$ values in Table I (present work) and the $K_D'$ values in Table III do not agree well, except for chloroform. Until now it has not been possible to ascertain whether these differences were caused by the mutual saturation or by some other reasons.

The total recovery of radon was found to be nearly quantitative; that is, the escape of radon from the two phases was small. However, if some part of the aqueous phases escapes into the air during the operation, it

causes a large error in $K_D$ even though it causes only a small loss in the total recovery because the aqueous phase contains an only small part of the total radon.

The results for benzene, toluene, and xylene were scattered, and so no values are given for these solvents in Table I, but the data obtained are shown at the foot of the table.

The results in Table I can be summarized as follows: (i) The distribution constant of radon is generally smaller when the solvent is more soluble in the water (methyl isobutyl carbinol $\sim$ methyl isobutyl ketone $<$ hexane). (ii) Bromine-containing solvents give smaller distribution constants than their chlorine homologues (bromoform $<$ chloroform, bromobenzene $<$ chlorobenzene). (iii) The distribution constants are much larger than unity; that is, the relative solubility of radon in the organic solvents is much higher than that in water.

The interaction between radon and water has been explained by the dipole-induced dipole interaction.[21] However, radon interacts with the organic solvents better than with water, although the solvents show smaller dipole moments than the water. Further information seems to be necessary in order to explain these results.

**The Distribution of Radon between Calcium Chloride Solutions and Carbon Tetrachloride.**—It was observed in the present work that the addition of calcium chloride to the water increases the extraction of radon even when the concentration is less than 10%. This agrees with the observation of Kofler.[24] He described how the solubility of radon in water is decreased by the addition of even a very small amount of salts. For example, he reported that the addition of 1% sodium chloride decreases the relative solubility of radon, $K$ in Eq. 3, to 88.5% of that in pure water (0.270 at 18°C).

Radon in the aqueous phase may be hydrated (cf. Refs. 18—21), whereupon some or all of the water molecules combined with radon will be dissociated when the radon is distributed from the aqueous phase to the organic phase. It may also happen that the hydration number of radon changes with the change in the water activity. Thus the change in the water activity may be one of the reasons for this strong salting-out. Figure 2 also shows the water activity in the solution described in the literature.[25]

**A Solvent Extraction Method for the Separation and the Concentration of Radon from Aqueous Radium Solution.**—From the results of the present work, the following solvent extraction procedure can be suggested for the separation and the concentration of radon in aqueous solutions of radium(II).

*Solvents.*—Any of the organic solvents in Table I can be used. However, those which are not very soluble in water are more useful, and the use of carbon tetrachloride or hexane, for example, is recommended.

*Aqueous Solution.*—Any radium(II) aqueous solution can be used. The addition of a small amount of acid or a complexing agent (such as disodium ethylenediaminetetraacetate) will prevent the radiocolloid formation which sometimes causes the loss of radium or the contamination of the organic phase. The addition of electrolytes may improve the recovery of radon into the organic phase.

*Recommended Procedure.*—The aqueous radium solution and the organic solvent are placed in a small, stoppered tube. The space occupied by air should be minimized for a good recovery. The tube is then rotated mechanically to agitate the phases, and centrifuged. The organic phase is taken as a radon solution and, if necessary, the organic solution is washed with an aqueous solution containing acid or some complexing reagent in order to make further purification from radium and the daughter nuclides. When no quantitative recovery of radon is necessary, radon can be extracted only by shaking an aqueous solution of radium with an organic solvent in a glass-stoppered bottle or a separatory funnel.

## Summary

(1) The distribution of radon between various organic solvents and water has been determined at 25°C. Radon is always distributed better into the organic phase. The distribution constants of radon in these liquid-liquid partition systems are in the range from 25 to 80.

(2) The distribution of radon between aqueous calcium chloride solution of various concentrations and carbon tetrachloride has been determined at 25°C. A remarkable salting-out effect for radon has been observed.

(3) A solvent extraction method for the separation of radon from radium(II) and the decay products in aqueous solutions has been suggested.

The authors are very grateful to Professor Nobufusa Saito, the chief of the Laboratory of Nuclear Chemistry, Institute of Physical and

24) M. Kofler, *Monatshefte*, **34**, 389 (1913).
25) R. H. Stokes and R. A. Robinson, *Ind. Eng. Chem.*, **41**, 2013 (1949). Cf. B. E. Conway, "Electrochemical Data," Elsevier, Amsterdam (1952).

Chemical Research, where part of this work was carried out. They are also grateful to Drs. Tadashi Nozaki and Mariko Inarida of the same laboratory for their invaluable discussions and technical help.

*Department of Chemistry*
*Tokyo College of Science*
*Kagurazaka, Shinjuku-ku, Tokyo*

# Thermodynamic Properties and Order-Disorder Phase Transitions of the Potassium Cyanide Crystal

By Hiroshi SUGA, Takasuke MATSUO and Syûzô SEKI

(Received November 4, 1964)

Potassium cyanide, though it consists of spherical $K^+$ and spheroidal $CN^-$ ions, has a cubic symmetry[1] ($O_h^5$; NaCl-type) at room temperature. When the crystal is cooled, it undergoes a phase transition[2] at 168.3°K, with an entropy change approximately equal to $R \ln 4$. According to Bijvoet and his collaborators,[1] the cyanide ions either rotate freely or are orientated randomly in eight body-diagonal directions in the cubic phase, while they are all parallel to the b-axis of the orthorhombic lattice of the low temperature phase. Matsubara and Nagamiya[3] have calculated the lattice energies for both phases and have determined the transition point between them from the theoretical point of view. They have also calculated the potential barrier hindering the rotation of cyanide ions in both phases and concluded that the cyanide ions are subjected to hindered rotation with a barrier height of approximately 1.4 kcal. $mol^{-1}$ in the cubic phase. These results imply that the cyanide ions have an orientational entropy of $R \ln 8$ in the cubic phase. If one takes the difference between the carbon and the nitrogen atoms of the cyanide ion into consideration also, it may be expected that, when the crystal is cooled further, it will undergo another phase transition, one which corresponds to the orientational order-disorder rearrangement of the cyanide ion with respect to its head and tail. Otherwise, the crystal would have a residual entropy of $R \ln 2$ at the lowest temperature, as in the case of carbon monoxide[4] and nitrogen suboxide[5] crystals.

On the other hand, in the course of the X-ray structural analysis of the potassium cyanide crystal at the transition temperature range, Ubbelohde and his collaborators[6] have recently observed the occurrence of an intermediate phase which appears when the crystal is subjected to a composite temperature cycle around 168°K. The new phase has been reported to belong to the monoclinic system, which was eventually transformed into the stable orthorhombic system at about 158°K when the crystal was cooled and to the stable cubic system at 166°K when it was heated. They also found the co-existence of various domains of the low temperature form in "hybrid" single crystals, as well as of domains of the low and high temperature forms over a range of temperatures.

The object of the present research was to study the thermal properties of the stable potassium cyanide crystal at lower temperatures and also those of the above-mentioned new phase around the transition region.

## Experimental

"Pro analysi" potassium cyanide (Merck reagent) was recrystallized twice from an absolute methyl alcohol solution by evaporating it under a stream of nitrogen gas.[7] The purity of the sample was assured by the method of purification.[7] The specimen was dried in a vacuum ($10^{-5}$ mmHg) at 110—130°C for several hours. In a spectrochemical analysis of the specimen, the only metallic impurities found were traces of silicon, manganese and iron, all less than 0.05 per cent. The predominant impurity was the $CO_3^{2-}$ ion, since a fairly intensive C=O stretching vibration appeared on the infrared absorption spectra. The amount was analyzed by a comparison

1) J. M. Bijvoet and J. A. Lery, *Rec. trav. chim.*, **59**, 908 (1940); Structure Reports 1942—44, 9, Utrecht: N. V. A. Oosthoek's Vitgevers Mij.
2) C. E. Messer and W. T. Ziegler, *J. Am. Chem. Soc.*, **63**, 2610 (1941).
3) T. Matsubara and T. Nagamiya, *Sci. Papers Osaka Univ.*, **No. 14** (1949).
4) J. O. Clayton and W. F. Giauque, *J. Am. Chem. Soc.*, **54**, 2610 (1932).
5) R. W. Blue and W. F. Giauque, ibid., **57**, 991 (1935).
6) A. Cimino, G. S. Parry and A. R. Ubbelohde, *Proc. Roy. Soc.*, **A252**, 445 (1959); G. S. Parry, *Acta Cryst.*, **15**, 596 (1962).
7) M. R. Thompson, *J. Research Natl. Bur. Standards*, **6**, 1051 (1931).

of the intensity of the spectra with those involving a given amount of carbonate ions; it was thus revealed that the specimen used for heat capacity measurement contained 0.3 per cent of $CO_3^{2-}$ ions. In order to avoid possible contamination by humidity and carbon dioxide in the air, the procedure of transferring the sample was carried out in a vacuum-type dry-box under an atmosphere of nitrogen gas.

All measurements were made on a single loading of 20.5785 g. or 0.31596 mol., taking 65.120 as the molecular weight of potassium cyanide. The heat capacity was measured in the temperature range from 15 to 310°K by means of a low-temperature adiabatic calorimeter, the details of which have been reported previously.[8]

The occurrence of the intermediate, monoclinic phase was re-examined by a differential thermal analysis (DTA) apparatus[9] that operates automatically at low temperatures.

In order to follow the appearance and disappearance of the domains around the transition temperature, the intensity of natural light with a wavelength in the neighborhood of 5000Å transmitted through the crystal was measured by means of a photo-tube. A schematic diagram of the apparatus is given in Fig. 1. Specimen B in the disk

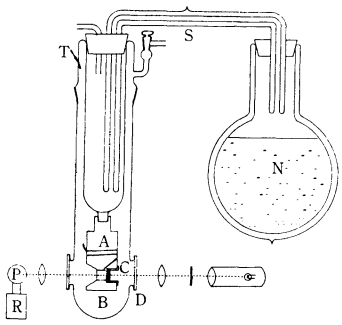



Fig. 1. Schematic diagram of apparatus for investigating transmission of natural light.

form is placed inside the hole fitted in a copper block, A, which is connected with the inside of a modified Dewar vessel by means of a "Housekeeper" seal so as to make vacuum tight. A fairly transparent disk specimen is obtained by compressing the powdered specimen, as in making infrared measurements of the KBr disk. In order to obtain better thermal contact, a thin film of "silicon" grease is coated over the edge of the specimen and the cap, C. In order to cool the crystal, cold gas from the storage vessel, N, containing liquid nitrogen was run through the transfer siphon, S. The temperature of the specimen was measured with a Chromel-P constantan thermocouple; it could be maintained for a long period of time within ±0.1°C at any temperature by adjusting the flow rate of cold gas. The photocurrent from a PL 50 V phototube was recorded on a voltage recorder.

8) H. Suga and S. Seki, This Bulletin, **38**, 1000 (1965).
9) H. Suga, H. Chihara and S. Seki, *J. Chem. Soc. Japan, Pure Chem. Sec.* (*Nippon Kagaku Zasshi*), **82**, 24 (1961).

## Experimental Results

**Heat Capacity.**—The observed heat capacity data are listed in Table I in chronological order. These values are expressed in terms of the defined thermochemical calorie, equal to 4.1840 absolute joules. The ice point is taken to be 273.15°K. The heat capacities listed in the table are the ratios of the increase in enthalpy, $\Delta H$, to the rise in temperature, $\Delta T$. Also listed in Table I are the values of the approximate temperature rise in each measurement. The temperature given for each point is the arithmetic mean of the initial and the final temperatures. These results are plotted graphically in Fig. 2.

Series I comprises several exploratory measurements after the initial cooling of the calorimeter to liquid nitrogen temperatures. The calorimeter was then cooled to 12°K and the data of series II taken. In this measurement a new heat capacity anomaly was found at about 83°K. In order to define more closely the shape and the reproducibility of the curve in the anomalous region, measurements of series III were made. No evidence was found from the measurements for checking the dependence of the observed heat capacity on the thermal history of the sample, and the points obtained from all the series coincide with each other within the expected range of error. In the neighborhood of the maximum heat capacity, there was no evidence of sluggishness in the attainment of thermal equilibrium.

Series III also involves the upper thermal anomaly, corresponding to the orthorhombic-cubic phase transition reported previously by Bijvoet et al.[1] and Ziegler et al.[2]

Parallel to the heat capacity measurements, the occurrence of the intermediate, monoclinic phase around the upper transition temperature was re-examined by the DTA method. The results are reproduced in Fig. 3. Run 1 shows a heating curve up to about 30°C higher than the transition temperature, and run 2 is for the subsequent cooling curve. Runs 3, 4 and 5 all give heating curves which follow just after runs 2, 3 and 4 respectively are over. In this process, a new upheaval appears a few degrees below the orthorhombic-cubic transition temperature. As the temperature cycles are repeated further, this lower component of thermal anomaly increases with the consumption of the upper component, which eventually disappears (see run 5). Run 6 corresponds to the cooling curve just after the repeated temperature cycles; this is same procedure as that adopted by Ubbelohde et al.[6] Accordingly, the broad thermal anomaly located at about

TABLE I. SELECTED VALUES FOR HEAT CAPACITY OF KCN

| $T_{av}$ °K | $\Delta H/\Delta T$ cal. mol$^{-1}$ deg$^{-1}$ | Approx. $\Delta T$ |
|---|---|---|
| | Series I | |
| 89.02 | 12.84 | 2.123 |
| 91.16 | 12.71 | 2.127 |
| 94.43 | 12.96 | 2.088 |
| 98.57 | 13.17 | 2.054 |
| 103.09 | 13.46 | 2.306 |
| 107.43 | 13.76 | 2.266 |
| 116.33 | 14.43 | 2.178 |
| 120.78 | 14.62 | 2.155 |
| 125.06 | 14.85 | 2.126 |
| 129.28 | 15.11 | 2.096 |
| 135.57 | 15.58 | 2.237 |
| | Series II | |
| 14.23 | 0.579 | 2.510 |
| 15.63 | 0.661 | 2.935 |
| 17.42 | 0.837 | 2.533 |
| 18.13 | 0.928 | 2.103 |
| 20.04 | 1.197 | 1.683 |
| 21.61 | 1.424 | 1.438 |
| 24.02 | 1.806 | 3.041 |
| 26.93 | 2.274 | 2.841 |
| 29.53 | 2.713 | 2.123 |
| 32.66 | 3.250 | 2.014 |
| 35.78 | 3.879 | 1.982 |
| 37.70 | 4.241 | 1.827 |
| 39.63 | 4.649 | 1.986 |
| 42.03 | 5.187 | 2.043 |
| 44.53 | 5.901 | 1.965 |
| 46.95 | 6.513 | 1.887 |
| 49.21 | 7.078 | 2.311 |
| 51.76 | 7.662 | 2.474 |
| 54.35 | 8.258 | 2.670 |
| 56.95 | 8.874 | 1.984 |
| 59.39 | 9.474 | 1.970 |
| 61.94 | 10.12 | 1.894 |
| 64.61 | 10.82 | 2.580 |
| 67.89 | 11.65 | 2.204 |
| 70.05 | 12.22 | 2.121 |
| 72.18 | 12.83 | 2.119 |
| 74.35 | 13.49 | 2.145 |
| 76.45 | 14.28 | 2.058 |
| 78.46 | 15.16 | 1.968 |
| 80.39 | 16.16 | 1.878 |
| 82.32 | 17.15 | 1.977 |
| 84.37 | 15.42 | 2.112 |
| 86.49 | 13.05 | 2.123 |
| | Series III | |
| 77.29 | 14.63 | 2.015 |
| 79.26 | 15.56 | 1.925 |
| 80.69 | 16.32 | 1.814 |
| 81.61 | 16.86 | 2.145 |
| 82.51 | 17.25 | 2.063 |
| 83.40 | 17.20 | 1.982 |
| 84.32 | 15.47 | 1.908 |
| 85.32 | 13.58 | 2.069 |
| 86.90 | 13.00 | 2.117 |
| 92.23 | 12.87 | 2.106 |
| 96.51 | 13.05 | 2.071 |
| 100.77 | 13.31 | 2.330 |
| 105.39 | 13.59 | 2.285 |
| 137.32 | 15.65 | 2.228 |
| 143.93 | 16.08 | 2.160 |
| 148.26 | 16.46 | 2.142 |
| 152.51 | 16.84 | 2.121 |
| 156.66 | 17.45 | 2.056 |
| 160.72 | 18.25 | 1.995 |
| 164.56 | 21.20 | 1.806 |
| 166.74 | 49.23 | 0.962 |
| 167.48 | 87.79 | 0.585 |
| 168.41 | 119.86 | 0.468 |
| 168.88 | 103.42 | 0.568 |
| 169.51 | 60.17 | 0.816 |
| 172.31 | 17.04 | 2.078 |
| 176.56 | 16.11 | 2.141 |
| 182.97 | 16.03 | 3.221 |
| 187.89 | 16.09 | 3.198 |
| 191.07 | 16.30 | 3.170 |
| 194.25 | 15.99 | 3.203 |
| 200.65 | 15.97 | 3.199 |
| 205.79 | 15.95 | 3.104 |
| 210.04 | 15.95 | 3.051 |
| 214.28 | 15.93 | 3.004 |
| 227.30 | 15.94 | 2.122 |
| 236.81 | 15.94 | 4.239 |
| 241.04 | 15.89 | 4.233 |
| 249.31 | 15.90 | 4.634 |
| 253.95 | 15.93 | 4.622 |
| 258.60 | 15.93 | 4.615 |
| 263.18 | 15.91 | 4.603 |
| 272.38 | 15.91 | 4.598 |
| 276.54 | 15.85 | 4.594 |
| 285.73 | 15.82 | 4.591 |
| 290.30 | 15.87 | 4.571 |
| 303.94 | 15.86 | 4.566 |
| 308.50 | 15.85 | 4.556 |
| | Series IV | |
| 160.05 | 19.24 | 0.966 |
| 161.01 | 19.65 | 0.953 |
| 162.41 | 20.39 | 1.858 |
| 164.19 | 23.11 | 1.707 |
| 165.48 | 55.29 | 0.872 |
| 166.50 | 189.99 | 0.287 |
| 166.29 | 248.01 | 0.222 |
| 166.50 | 265.12 | 0.208 |
| 167.07 | 51.01 | 2.022 |
| 168.53 | 17.82 | 2.311 |
| 170.60 | 16.48 | 2.120 |
| 172.72 | 16.16 | 2.143 |
| 177.02 | 16.11 | 2.143 |
| 179.16 | 16.08 | 2.144 |

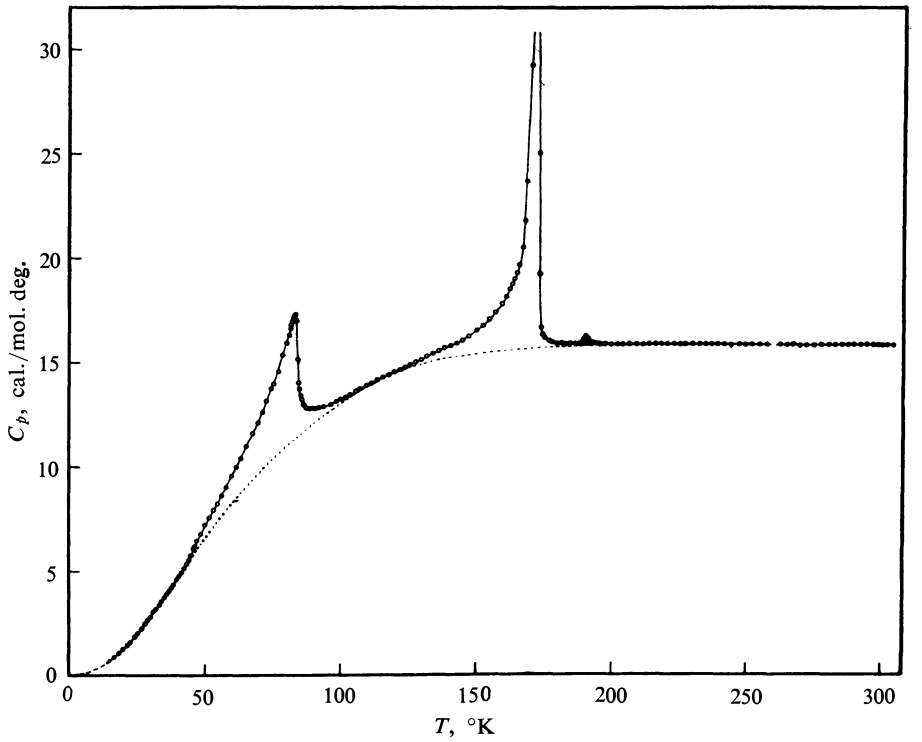



Fig. 2. Heat capacity versus temperature curve of KCN crystal.

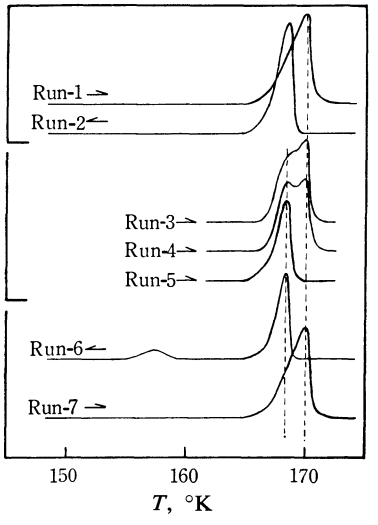



Fig. 3. DTA curves of KCN crystal undergoing various temperature cycles.

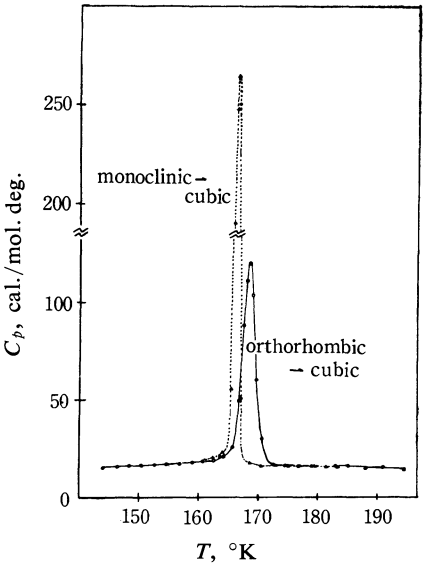



Fig. 4. Heat capacity versus temperature curves of KCN crystal around upper transition regions.

158°K corresponds to the monoclinic-orthorhombic transformation. These results agree well with the X-ray findings by Ubbelohde et al.

The monoclinic-cubic transformation was then studied more precisely by the calorimetric method. The results are grouped as series IV. The heat capacity anomaly corresponding to this transformation is plotted in Fig. 4, together with those for the orthorhombic-cubic transformation. In the neighborhood of both heat capacity maxima, the rate of attainment to the equilibrium was too slow for the final

TABLE II. TEMPERATURES, ENTHALPIES AND ENTROPIES OF TRANSITIONS OF KCN CRYSTAL

| | $T$ °K | $\Delta H$ cal. mol$^{-1}$ | $\Delta S$ cal. mol$^{-1}$ deg$^{-1}$ |
|---|---|---|---|
| Lower transition | 82.9±0.2 | 95.1±1.0 | 1.32±0.01 |
| Upper transition | 168.3±0.1 | 339 ±5 | 2.01±0.03 |
| Monoclinic-cubic transition | 166.5±0.1 | 291 ±5 | |

state to be reached in a reasonable period of time. The heat capacity values in these regions are, therefore, inferior in accuracy to the other results.

The heat capacity in the cubic phase keeps essentially a constant value. Such temperature-independent behavior of the heat capacity in the cubic phase has also been found by us in other alkali cyanides;[10] for example, sodium cyanide, rubidium cyanide, cesium cyanide and thallium cyanide. These results will be reported in the near future.

The only data available for comparison with these results are the measurements by Ziegler and Messer[2] on potassium cyanide from 100 to 340°K. Their data deviate 1.5 per cent at 100°K and are 2 per cent lower at 300°K than ours.

The lower anomaly in heat capacity, which has not been observed hitherto, has the lambda shape characteristic of processes where a co-operative ordering is taking place. The question as to whether the curve near the maximum is continuous, or cusped, can not be unambiguously decided on the basis of the present data. Because of the finite temperature increment in an individual measurement, it appears that a cusped curve would be smoothed out. It appears from a magnified scale plot of the data in the immediate neighborhood of the maximum that the data are better represented by a smooth curve, taking into account the finite resolution and precision of the measurement. The heat capacity reaches a maximum value of 17.25 cal. mol$^{-1}$ deg$^{-1}$ at 82.9±0.2°K.

The temperatures, enthalpies, and entropies of the phase transition are summarized in Table II. The transition temperature was taken as the one where the heat capacity reached a maximum value. The enthalpy of the transition was evaluated by integrating the excess heat capacity over the normal heat capacity, represented by the dotted line in Fig. 2. The method of estimating the normal heat capacity will be described later. The enthalpy of the transition, corresponding to the monoclinic-cubic transformation, was evaluated by assuming that the heat capacity of the monoclinic crystal had the same value as that of the orthorhombic crystal. It follows immediately that the enthalpy of the intermediate, monoclinic form is higher than that of the orthorhombic form by 53.9±0.5 cal. mol$^{-1}$ at 159.6°K.

A short comment should be added here about the small hump in the heat capacity observed around 190°K. This anomaly is very broad and so small as to make it almost invisible in Fig. 2. Six series of heat capacity measurements were made to ascertain its reality on specimens having different thermal history. These results are omitted from Table I, since they are reproduced in Fig. 5 on a magnified scale. It is of interest to point out that this thermal anomaly appears only for the cubic crystal which has been brought into the orthorhombic or the monoclinic phase prior to the measurement. This endothermic anomaly is presumable associated with some higher-order structural defect created by the phase transition.

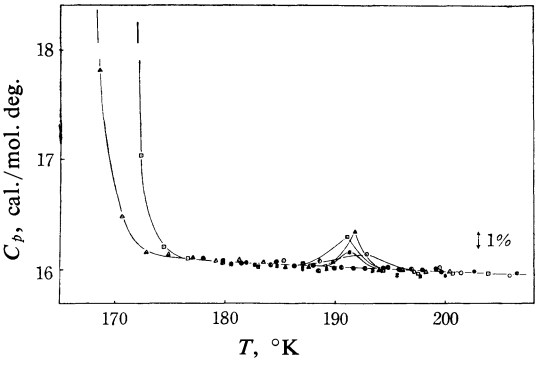



Fig. 5. Heat capacity versus temperature curves of KCN around 190°K.
-⊡- Series II -△- Series III
-✳- Series IV -⊗- Series V
-⊙- Series VI -●- Series VII

**The Thermal Transition of the Transparency around 168°K.**—Successive temperature cycles for the transmission of the disk specimen are recorded in Fig. 6. The transmission is plotted on an arbitrary scale, taking the room temperature form value as 100. The curve also affords a sensitive way of following the progress of the transformation. By taking readings at intervals and at a constant temperature, it was found that an equilibrium was attained for a considerably long time in the neighborhood of the transition point. There is a wide

10) H. Suga, T. Matsuo, M. Sugizaki and S. Seki, to be published.

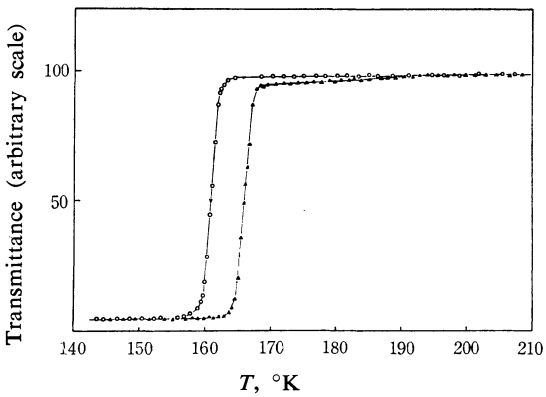



Fig. 6. Thermal transition of transparency in KCN crystal.
○ Temp. falling △ Temp. rising

hysteresis loop in the thermal transition of the transparency. Similar results were also obtained for the monoclinic-cubic transformation. The transition point on heating, taken as the maximum slope temperature of the transmission curve, does not agree exactly with the results of heat capacity measurement. The difference seems to be due to the less accurate temperature measurement resulting from the poorer thermal contact in this apparatus. The difference seems also to be due to the disk specimen employed, which may presumably not be free from the strain sustained when it is pressurized to form the disk. The width of this hysteresis loop is, however, consistent with those of the X-ray results obtained by Ubbelohde et al. and of the thermal findings by DTA.

## Thermodynamic Properties of Potassium Cyanide

The values of the heat capacity, the entropy and the enthalpy and Gibbs energy functions of the potassium cyanide crystal at selected temperatures are listed in Table III. The values of $C_p^\circ$ were determined at round temperatures on the smoothed curve drawn through the measured heat capacity data. These values may well be regarded as the true differential heat capacity, except for the anomalous regions, where they change very rapidly and require correction for curvature. In order to make the extrapolation to the absolute zero of temperature, plots were made of $C_p/T^3$ against the temperature in the range from 13 to 40°K. The extrapolated contribution to the entropy below 15°K is merely 0.307 cal. $mol^{-1}$ $deg^{-1}$.

The error of the smoothed heat capacity data is estimated as 2 per cent at 20°K and 0.3 per cent above 50°K. Although the in-

TABLE III. THERMODYNAMIC PROPERTIES OF KCN CRYSTAL
(in cal./deg. mol.)

| $T$, °K | $C_p^\circ$ | $S^\circ$ | $\frac{(H^\circ-H_0^\circ)}{T}$ | $-\frac{(G^\circ-H_0^\circ)}{T}$ |
|---|---|---|---|---|
| 5 | (0.074) | (0.037) | (0.002) | (0.035) |
| 10 | (0.266) | (0.140) | (0.092) | (0.048) |
| 15 | 0.609 | 0.307 | 0.202 | 0.104 |
| 20 | 1.182 | 0.554 | 0.370 | 0.185 |
| 30 | 2.794 | 1.324 | 0.898 | 0.426 |
| 40 | 4.794 | 2.366 | 1.593 | 0.772 |
| 50 | 7.266 | 3.695 | 2.475 | 1.219 |
| 60 | 9.639 | 5.228 | 3.470 | 1.757 |
| 70 | 12.190 | 6.902 | 4.531 | 2.372 |
| 80 | 15.956 | 8.745 | 5.695 | 3.051 |
| 82.9±0.2 | Lower transition | | | |
| 90 | 12.795 | 10.487 | 6.699 | 3.778 |
| 110 | 13.934 | 13.144 | 7.894 | 5.249 |
| 130 | 15.169 | 15.574 | 8.921 | 6.654 |
| 150 | 16.624 | 17.840 | 9.844 | 7.995 |
| 168.3±0.1 | Upper transition | | | |
| 190 | 16.186 | 23.545 | 12.817 | 10.728 |
| 210 | 15.949 | 25.139 | 13.121 | 12.018 |
| 230 | 15.930 | 26.590 | 13.366 | 13.224 |
| 250 | 15.910 | 27.916 | 13.570 | 14.346 |
| 270 | 15.887 | 29.141 | 13.743 | 15.398 |
| 290 | 15.844 | 30.283 | 13.887 | 16.396 |
| 298.15 | 15.843 | 30.712 | 13.942 | 16.770 |
| 310 | 15.850 | 31.330 | 14.015 | 17.315 |

accuracy of the functions $S^\circ$, $(H^\circ-H_0^\circ)/T$ and $-(G^\circ-H_0^\circ)/T$ is about 0.3 per cent above 50°K, the numbers in Table III are given to a higher precision than this so that they will be internally consistent.

## Discussion

**Thermal Anomaly around 190°K.** —Concerning the nature of the upper phase transition at 168.3°K, Matsubara and Nagamiya[3] have proposed a suitable model, one upon which they calculated its transition point and obtained fairly satisfactory results. On this topic, therefore, there is further comment to be added. Here, however, a brief account may be given of the nature of the heat capacity anomaly around 190°K.

Ubbelohde and his collaborators[6] have found that the intermediate, monoclinic form was always produced by applying a particular, composite temperature cycle. This involved the direct cooling of a crystal from room temperature to below the transition temperature, then warming it to about 3°C above the transition onset temperature, and subsequently recooling it through the transition range. The intermediate form was never observed during any direct cooling. They also found that various

domains of the orthorhombic form co-exist when the crystal is directly cooled through the transition point. These observations led them to the conclusion that "scars," resulting from the effects of strain within the domains, exist in the cubic phase just above the transition point.

The "critical temperature," 3°C higher than the transition onset temperature, seems to depend markedly on the physical states of the crystal, as well as on the heating rate employed and on the period of time spent at that temperature. In fact, we have found from another series of DTA measurements that in the specimen raised even above 25°C higher than the transition temperature, followed by immediate recooling, the monoclinic form was formed, though the heating rate employed in this case, 0.5—0.8°C $min^{-1}$, is much higher than that of the heat capacity measurement, 0.03—0.1°C $min^{-1}$.

The heat capacity anomaly around 190°K seems to correspond exactly to the "critical temperature." The reasons are as follows. In the first place, this thermal anomaly appears only for the cubic crystal brought into the orthorhombic or the monoclinic crystal prior to the measurement. Two series of measurements made on a specimen cooled to just above the transition temperature showed no sign of heat capacity anomaly. Additional evidence is offered by the experimental findings on the thermal transition of the transparency. The transparency of the scarred cubic crystal is somewhat lower than one directly cooled from room temperature. The scarred cubic crystal seems, therefore, to be a state in which the inter-domain walls produced by the formation of the orthorhombic form are not perfectly recovered. This state persists to higher temperature but ultimately changes into the cubic crystal, losing its scars around the "critical temperature."

The free energy of a crystal can by no means be expressed fully by only its volume, temperature and pressure. It may be also a functions of the strain and of the internal surface energy[11] when the crystal is composed of "sub-structure" or domains. The excess free energy assumed in the scarred cubic crystal seems to be responsible for the preferential formation of the intermediate phase on subsequent recooling.

A simple calculation was made on the average size of domains, based on the assumption that the cyanide ion located at the domain surfaces had less configurational entropy by the amount of $k \ln 2$ than that of the bulk phase, and also on the assumption that the entropy increment at the "critical temperature" was caused by a gain in the entropy of such ionic groups. The total entropy change around 190°K, merely about 0.005 cal. $mol^{-1}$ $deg^{-1}$, combined with the above assumption, leads to the value of 4000Å for the average domain size. Although this rough estimation, neglecting entirely the contribution from vibrational aspects of the ions, has no significance other than as an order of magnitude, the derived value is well in the range estimated by the X-ray method.[6] In order to obtain more quantitative knowledge on the average size as well as on its distribution, single crystal and monochromatized light should be used.[12] Such an experiment is being planned in our laboratory.

**The Nature of the Phase Transition at 83°K.** —The heat capacity anomaly takes place over a wide temperature range, with a maximum at 82.9°K, and has the lambda shape characteristic of processes where co-operative ordering is taking place. This phase transition resembles in thermal properties the lower phase transition at 172°K in the sodium cyanide crystal.[2] In the orthorhombic phase ($D_{2h}^{25}$ Immm) of both crystal,[1,13] all the C-N bonds in cyanide ions are arrayed along the b-axis of the unit cell. The orientations of the cyanide ions with respect to its head and tail have not, however, been clarified in the present stage of X-ray structural analysis. Preliminary Debye-Scherrer photographs* taken below and above the lambda point of the potassium cyanide crystal indicate only that there is no appreciable change in the atomic arrangement of either phase. Similar results have been reported also for the sodium cyanide crystal.[14]

Such a minor change in structure may be explained by assuming that the co-operative rearrangement with respect to the head and tail of the cyanide ion takes place over the anomalous heat capacity region, since there is no appreciable difference in the atomic scattering factor between the carbon and nitrogen atoms. Thus, we may picture the temperature effect as follows. At the lowest temperatures, all the cyanide ions are arranged along the b-axis with a uniquely defined orientation (a completely ordered state), and as the temperature is raised, the flipping motion between the two orientations with respect to the head and tail of the cyanide ion is excited progressively;

11) A. R. Ubbelohde, *Brit. J. Appl. Phys.*, **7**, 313 (1956); *Quart. Rev.*, **11**, 246 (1957).

12) T. Horie, K. Kawabe and T. Iwai, *Ann. Rep. Scient. Works, Fac. Sci. Osaka Univ.*, **4**, 45 (1956).

13) H. J. Verweel and J. M. Bijvoet, *Z. Krist.*, **100**, 201 (1939); Structure Reports, loc. cit.

* We are greatly indebted to Mr. Yasuo Yamaguchi of our University for his kind arrangements for taking the X-ray photographs.

at the transition point these two orientations of the cyanide ion become exactly equal energetically (a completely disordered state). The magnitude of the entropy change associated with this phase transition, which is nearly equal to $R \ln 2$ ($=1.38$ cal. mol$^{-1}$ deg$^{-1}$), affords strong support for such an explanation of the mechanism of the phase transition.

The mode of the relative arrangement of cyanide ions in the completely ordered state is, however, not exactly clear at the present stage. Preliminary calculations involving the dipole-dipole interaction among the cyanide ions of the potassium cyanide crystal suggest strongly that the polar structure of the cyanide ions along the b-axis (space group; $C_{2v}^{20}$ Imm2) seems to be the most stable.** This polar structure was also suggested by Siegel[14] for the lowest modification of the sodium cyanide crystal.

**The Torsion-Rotational Motion of Cyanide Ions.**—In order to get more detailed knowldge about the thermal motion of cyanide ions in the crystalline state, the Eucken-Morrison type of analysis was applied to the present case. In the first place, the heat capacity at a constant volume, $C_v$, was computed from the observed $C_p$ value by the usual procedure. Here, the correction was made by use of the relation $C_p - C_v = 1.1 \times 10^{-5} C_p T^2$, the numerical factor being estimated rather arbitrarily.[2] It may easily be seen that this crystal has $6N$ degrees of the translational freedom, $2N$ degrees of the torsional or the rotational freedom, and $N$ degrees of the internal-vibrational freedom of cyanide ions. The contribution from the last freedom to the heat capacity was evaluated by the Einstein function, using the wave number of 2085 cm$^{-1}$, obtained by the infrared spectroscopic method.[15] This vibrational heat capacity does not contribute in any significant degree within the temperature range measured. After subtracting this contribution from the total, the apparent Debye temperature $\Theta_D$ was calculated on the assumption that the other $8N$ degrees of freedom could be represented by a single Debye temperature. The $\Theta_D$ value thus obtained is given in Fig. 7 as a function of the temperature. The influence of the phase transition on this $\Theta_D$ - $T$ curve is much more sensitive than that on the heat capacity curve itself, so the ambiguities in the estimation of the "normal" lattice part of the heat capacity are considerably reduced when we utilize

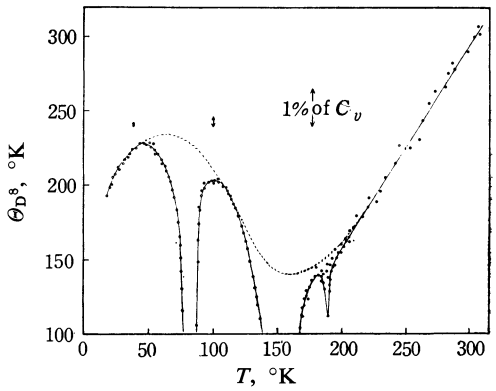



Fig. 7. Debye temperature versus temperature curve of KCN crystal, taking degree of freedom as 8.

$\Theta_D$ - $T$ relationship for this purpose. The assumed dotted line in this figure is for the temperature variation of the normal heat capacity. The procedure adopted above for estimating the normal heat capacity is, of course, not severely rigorous, but it may be nevertheless looked upon as a convenient method for determining the effect of phase transitions on the total heat capacity.

Having excluded the effect of the phase transition, we shall now try to separate the torsion-rotational heat capacity. The principal difficulty encountered in an analysis of a heat capacity curve in an effort to determine frequencies other than those of the lattice vibration arises from the necessity for an accurate representation of the heat capacity of the lattice itself. This difficulty is minimized by assuming that the contribution from the translational degree of freedom to the heat capacity of the present crystal is well represented by the heat capacity of a suitable alkali halide crystal. The $\Theta_D$-$T$ curves of potassium chloride and potassium bromide[16] were selected as references since they are crystals of a similar nature with no torsional degree of freedom. Figure 8 summarized the variations of the Debye temperatures for potassium chloride, potassium bromide and potassium cyanide crystals. In this figure, the wide temperature variations of $\Theta_D$ for potassium chloride and potassium bromide crystals are a consequence of the procedure in which the heat capacity of the alkali halide crystal, with $6N$ degrees of freedom, is expressed by a single Debye temperature. It is presumably possible to describe the total heat capacity by a combination of the Einstein function with a single value of the Einstein temperature for the $3N$ degrees

** The results of our calculations will be given in a later paper. At any rate, it is desirable to determine the ordered arrangement of cyanide ions by an experimental method such as the neutron diffraction technique.

14) L. A. Siegel, *J. Chem. Phys.*, **11**, 1146 (1949).

15) A. Maki and J. C. Decius, ibid., **31**, 772 (1959); F. A. Miller and C. H. Wilkens, *Anal. Chem.*, **24**, 1253 (1952).

16) W. T. Berg and J. A. Morrison, *Proc. Roy. Soc.*, **A242**, 467, 478 (1957).

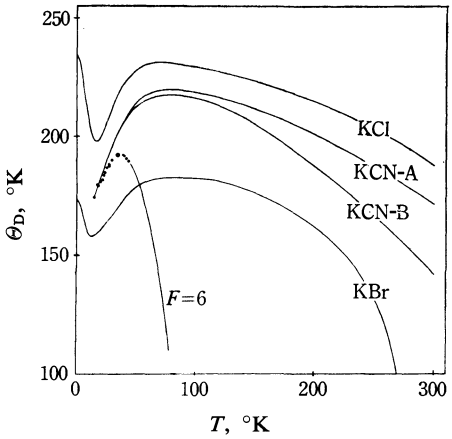



Fig. 8. Debye temperatures of KCl, KBr and KCN crystals as functions of temperature, A and B indicating the assumed upper and lower limits for KCN.

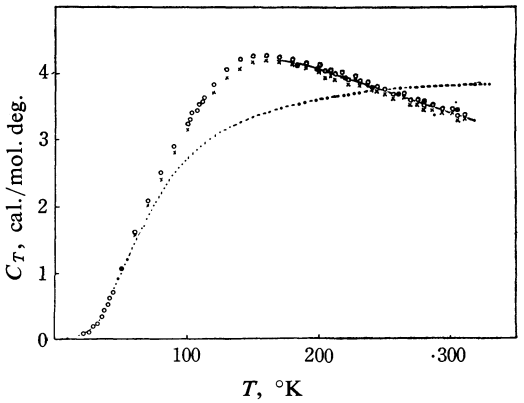



Fig. 9. Torsion-rotational heat capacity of cyanide ions in KCN crystal.
○ Observed values (case A)
× Observed values (case B)
---- $\omega=160\,cm^{-1}$ two simple harmonic oscillators
—— $V=1300$ cal./mol. two-dimensional
● $V=1350$ cal./mol. hindered rotator

of freedom (optical modes), and the Debye function with a single value of the Debye temperature for the other $3N$ degrees of freedom (accoustic modes), both characteristic temperatures being temperature-insensitive. If one assumes only $6N$ translational degrees of freedom in the computation of the $\Theta_D$ of the potassium cyanide crystal, one obtains a steeply declining curve (the $F=6$ curve in Fig. 8). This decrease can be regarded as the result of a progressively-increasing torsional contribution of the cyanide ions. The hypothetical $\Theta_D$ curve of potssium cyanide, if there were no torsional modes, would go somewhere between the $\Theta_D$ curves of potassium chloride and potassium bromide. Two curves (KCN-A and KCN-B) in Fig. 8 are such hypothetical extrapolations from the low temperature region; this seemed to be a reasonable spread. Actually, the choice of either of the two does not make any significant difference in the evaluation of the torsion-rotational contribution, since $\Theta_D$ is far more sensitive than the heat capacity itself.

In Fig. 9 we compare the calculated and the observed torsion-rotational heat capacities. In the low temperature region, the observed torsional heat capacity values lie well on the calculated curve based on the model of two independent harmonic oscillators with the wave number of $160\,cm^{-1}$. For the harmonic oscillator approximation, this torsional frequency corresponds to 7.5 kcal. $mol^{-1}$ of barrier height if we employ the usual cosine-type hindering potential. As the temperature is raised, the difference between them becomes progressively more conspicuous; there can never be any model which explains the difference as long as we retain a simple harmonic oscillator model. One satisfactory explanation of the torsion-rotational heat capacity may, however, be given by a hindered rotator model. It is well known by Pitzer's treatment[17] that the heat capacity of a hindered rotator can rise to a maximum value greater than $R$ cal. $deg^{-1}$ per rotational degree of freedom and then falls off with an increase in the temperature, approaching the $1/2\,R$ cal. $deg^{-1}$ per degree of freedom, the value for a classical free rotator.

This treatment was recently extended to the two-dimensional hindered rotator by Stepakoff and Coulter[18] with adequate approximations. The application of their results to the present case shows that the rotational heat capacity in the cubic phase may be well represented by the contribution from the two-dimensional hindered rotator with a barrier height of 1.30—1.35 cal. $mol^{-1}$ over a wide temperature range. This barrier height agrees well with the theoretical calculation by Matsubara and Nagamiya.[3] (In passing, we should like to point out that a recent study of the potassium cyanide crystal by Elliott and Hastings,[19] using neutron diffraction techniques, led them to the conclusion that the free rotational model is satisfactory for the cubic phase. Their analysis, however, has entirely neglected the Debye-Waller temperature factor in calculating the intensity data. Accordingly, we may say that their model may not be looked upon as conclusive.)

17) K. S. Pitzer and W. D. Gwinn, *J. Chem. Phys.*, **10**, 428 (1942).
18) G. L. Stepakoff and L. V. Coulter, *J. Phys. Chem. Solids*, 1435 (1963).
19) N. Elliott and J. Hastings, *Acta Cryst.*, **14**, 1018 (1961).

The rotational heat capacity data in the intermediate temperature region, however, can never be represented by a single value of barrier height, even with the two-dimensional hindered rotator model. It varies continuously from 7.5 kcal. $mol^{-1}$ at 60°K to 1.40 kcal.$mol^{-1}$ at 168°K. This continuous variation in barrier height merely reflects the continuously varying estimated "normal" heat capacity. Actually, the barrier height would change abruptly with the phase transition phenomenon accompanying an abrupt volume change. Although such variation in the barrier height can not be clarified quantitatively and in detail by an analysis of the heat capacity data alone, and although the present model is merely a very simple one, a variation in barrier height with the temperature does not seem to be at all improbable. Actually, the crystal is subject to thermal expansion in a single phase, and the lattice parameter changes abruptly at the transition point. A simple calculation of the hindering potential demonstrates easily that a slight decrease in the lattice constant causes a marked change in the barrier height, since the repulsive part of the hindering potential varies with the inter-atomic distance, $r$, in the $r^{-9}$ form.[20] Such situations differ distinctly from the case of the internal hindered rotation of methyl groups in ethane, for example, where the hindering potential arises from its intramolecular interaction and is, therefore, very insensitive to the temperature variation.

These results may be summarized as follows. In the lowest temperature region, the cyanide ions undergo torsional oscillation with the wave number of 160 $cm^{-1}$. As the temperature is raised, this torsional motion is gradually excited, the barrier height diminishing gradually in a single phase or abruptly via the transition points; the torsional motion changes into a hindered rotational motion with a barrier height of approximately 1.35 kcal. $mol^{-1}$ in the cubic phase, and eventually into the state of free rotation at much higher temperatures.

## Summary

The heat capacities of the potassium cyanide crystal have been measured over the temperature range from 13 to 310°K by using a low temperature adiabatic calorimeter. It has been found that there are two regions of anomalous heat capacity, with maxima at 82.9±0.2°K and 168.3±0.1°K respectively. The heats and entropies of transition have been evaluated by utilizing a $\Theta_D$-versus-temperature plot. The entropy of the lower transition amounts to about $R \ln 2$, which means that the transition is due to the orientational order-disorder rearrangement of the cyanide ion with respect to its head and tail. A perfectly-ordered structure for the orientation of the cyanide ions has been suggested. A certain small anomaly in heat capacity has been found around 190°K, one which seems to be associated with some change in higher-order structural defects created by the upper transition phenomenon.

The torsion-rotational heat capacity of the cyanide ions has been separated from the total on some reasonable assumptions. The results show that the cyanide ions below the lower transition point are subjected to torsional oscillation with the wave number of about 160 $cm^{-1}$, a value which corresponds to the barrier height of 7.5 kcal. $mol^{-1}$ based on a simple harmonic oscillator model. On the other hand, they are in a hindered rotational state with a barrier height of approximately 1.35 kcal. $mol^{-1}$ in the cubic phase, the barrier height diminishing from 7.5 kcal. $mol^{-1}$, gradually in a single phase or abruptly via the transition points.

The thermodynamic functions for this crystal have been evaluated by integrating the heat capacity data. The values at 298.15°K are, in units of cal. $mol^{-1}$ $deg^{-1}$: $C_p^\circ = 15.84$, $S^\circ = 30.71$, $(H^\circ - H_0^\circ)/T = 13.94$ and $-(G^\circ - H_0^\circ)/T = 16.77$ respectively.

The authors wish to express their deep thanks to Mr. Nobukatsu Fuzino of the Sumitomo Metal Manufacturing Co., Ltd., for taking care of the spectrochemical analysis.

*Department of Chemistry*
*Faculty of Science*
*Osaka University*
*Toyonaka, Osaka*

20) L. Pauling "The Nature of the Chemical Bond," Cornell University Press, Ithaca, New York (1940), p. 355.

# Phase Transition in the Ammonium Bromide Crystal: The Thermal Motion of the Ammonium Ion*

By Michio SORAI, Hiroshi SUGA and Syûzô SEKI

(Received November 4, 1964)

Ammonium halide crystals are well-known as typical substances which exhibit various kinds of polymorphism in the solid state. Among them, it has been established that in bromides[1-6] the following transformations occur:

$NH_4Br$: Phase I (NaCl) $\xrightarrow{411°K}$ Phase II (CsCl) $\xrightarrow{235°K}$ Phase III (tetragonal) $\xrightarrow{108°K}$ Phase IV (CsCl ?)

$ND_4Br$: Phase I (NaCl) $\xrightarrow{398°K}$ Phase II (CsCl) $\xrightarrow{215°K}$ Phase III (tetragonal) $\xrightarrow{169°K}$ Phase IV (CsCl)

It is noticeable that $ND_4Br$ again takes the cesium chloride modification when it is cooled down through the tetragonal phase to a lower temperature. Stephenson and Adams[5] reported a new transition in ammonium bromide also at about 78°K on cooling and at about 108°K on warming. This seems to correspond to the transformation at 169°K in $ND_4Br$.[6] The possibility of the occurrence of this transition was also confirmed by Stevenson[7] through high-pressure experiments. Concerning the present material, Simon et al.[1] measured the heat capacity in the temperature range from −70°C to room temperature. Although Stephenson and Adams[5] reported briefly on the discovery of the new transition, as has been mentioned above, they have not yet published any detailed data on the heat capacities.

The purpose of our present investigation is to obtain detailed thermal data on ammonium bromide in the temperature range from 13°K to 305°K, and, in particular, to study the rotational motion or the torsional vibration of ammonium ions in crystals by analyzing our thermal and infrared data.

## Experimental

**Material.** — A chemically pure-grade reagent ammonium bromide (Wakō Pure Chemical Industries, Ltd.) was recrystallized twice from distilled water and then sublimed under a vacuum of $10^{-4}$ mmHg at about 240°C. The specimen obtained was further recrystallized from distilled water and dried under a vacuum at about 50°C for several hours. About 30 g. of the specimen was then packed into the calorimeter cell.

For the measurement of the infrared absorption spectra, thin films of ammonium bromide on a rocksalt plate were used. The film was prepared by subliming the purified ammonium bromide through a loose glass wool plug onto a polished rocksalt plate under a pressure of about $10^{-2}$ mmHg at 110—130°C.[8]

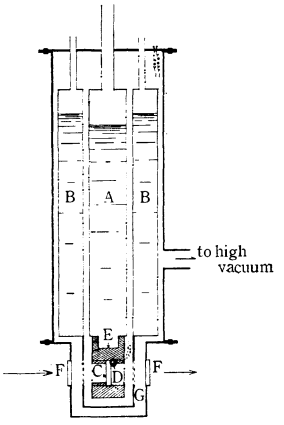



Fig. 1. Infrared absorption cell for use at low temperatures.
A, coolant reservoir (liquid He or $H_2$)
B, liquid $N_2$
C, rocksalt film-support
D, carbon resistance thermometer
E, copper cooling block
F, rocksalt window
G, radiation shield (liquid nitrogen temperature)

* Presented at the 17th Annual Meeting of the Chemical Society of Japan, Tokyo, April, 1964.

1) F. Simon, Cl. von Simson and M. Ruhemann, *Z. physik. Chem.*, **129**, 339 (1927).
2) H. A. Levy and S. W. Peterson, *J. Am. Chem. Soc.*, **75**, 1536 (1953).
3) J. A. A. Ketelaar, *Nature*, **134**, 250 (1934).
4) J. Weigle and H. Saini, *Helv. Phys. Acta*, **9**, 515 (1936).
5) C. C. Stephenson and H. E. Adams, *J. Chem. Phys.*, **20**, 1658 (1952).
6) K. Clusius, A. Kruis and W. Schanzer, *Z. anorg. u. allgem. Chem.*, **236**, 24 (1938).
7) R. Stevenson, *J. Chem. Phys.*, **34**, 1757 (1961).
8) E. L. Wagner and D. F. Hornig, ibid., **18**, 305 (1950).

TABLE I. THE HEAT CAPACITY OF AMMONIUM BROMIDE

| $T_{av}$ °K | Approx. $\Delta T$ | $\Delta H/\Delta T$ cal./deg. mol. | $T_{av}$ °K | Approx. $\Delta T$ | $\Delta H/\Delta T$ cal./deg. mol. |
|---|---|---|---|---|---|
| | Series I | | 212.29 | 2.389 | 20.294 |
| 21.89 | 3.010 | 1.329 | 217.01 | 2.335 | 20.989 |
| 24.57 | 2.360 | 1.744 | 221.93 | 2.485 | 21.801 |
| 26.76 | 2.015 | 2.039 | 226.81 | 2.398 | 22.961 |
| 28.99 | 2.485 | 2.381 | 229.28 | 2.534 | 23.811 |
| 31.57 | 2.715 | 2.786 | 231.66 | 2.260 | 25.058 |
| 34.55 | 3.281 | 3.137 | 233.82 | 2.064 | 28.555 |
| 37.84 | 3.368 | 3.714 | 235.96 | 2.211 | 25.826 |
| 41.01 | 3.013 | 4.165 | 240.93 | 2.627 | 19.755 |
| 53.05 | 2.879 | 5.751 | 243.56 | 2.636 | 19.621 |
| 55.85 | 2.734 | 6.068 | | Series II | |
| 58.81 | 3.217 | 6.395 | 246.46 | 2.632 | 19.589 |
| 61.87 | 2.943 | 6.795 | 249.07 | 2.625 | 19.641 |
| 64.95 | 3.256 | 7.148 | 251.79 | 2.829 | 19.771 |
| 68.12 | 3.125 | 7.487 | 257.08 | 2.593 | 19.936 |
| 71.40 | 3.468 | 7.830 | 259.66 | 2.585 | 20.009 |
| 74.78 | 3.342 | 8.169 | 262.23 | 2.575 | 20.107 |
| 78.27 | 3.685 | 8.528 | 264.79 | 2.569 | 20.157 |
| 81.88 | 3.591 | 8.912 | 267.07 | 2.567 | 20.173 |
| 86.67 | 3.407 | 9.348 | 272.17 | 2.542 | 20.448 |
| 90.04 | 3.337 | 9.666 | 274.71 | 2.538 | 20.479 |
| 93.32 | 3.242 | 9.968 | 277.33 | 2.724 | 20.563 |
| 96.52 | 3.176 | 10.241 | 280.05 | 2.715 | 20.636 |
| 99.65 | 3.115 | 10.505 | 282.74 | 2.705 | 20.740 |
| 102.22 | 2.043 | 10.817 | 285.43 | 2.701 | 20.757 |
| 104.24 | 2.014 | 10.959 | 288.11 | 2.685 | 20.932 |
| 106.07 | 1.692 | 14.862 | 290.78 | 2.683 | 20.932 |
| 107.53 | 1.428 | 19.433 | 296.08 | 2.667 | 21.071 |
| 109.04 | 1.693 | 14.762 | 298.72 | 2.655 | 21.191 |
| 110.80 | 1.876 | 12.263 | 301.40 | 2.747 | 21.392 |
| 112.66 | 1.888 | 12.063 | | Series III | |
| 114.53 | 1.883 | 12.069 | 98.53 | 1.599 | 10.561 |
| 116.85 | 2.800 | 12.193 | 100.12 | 1.587 | 10.652 |
| 119.61 | 2.770 | 12.351 | 102.08 | 2.352 | 10.819 |
| 122.52 | 3.084 | 12.540 | 104.40 | 2.321 | 11.012 |
| 125.56 | 3.046 | 12.740 | 106.30 | 1.529 | 11.181 |
| 128.71 | 3.294 | 12.956 | 107.80 | 1.516 | 11.322 |
| 131.95 | 3.248 | 13.203 | 109.29 | 1.503 | 11.442 |
| 135.31 | 3.513 | 13.461 | 110.76 | 1.491 | 11.578 |
| 138.78 | 3.464 | 13.722 | 112.21 | 1.479 | 11.708 |
| 142.17 | 3.419 | 13.970 | 113.65 | 1.465 | 11.865 |
| 145.55 | 3.380 | 14.177 | 115.08 | 1.447 | 12.094 |
| 148.89 | 3.335 | 14.450 | | Series IV | |
| 152.18 | 3.294 | 14.705 | 100.75 | 2.346 | 10.665 |
| 157.87 | 2.122 | 15.053 | 103.04 | 2.313 | 10.863 |
| 160.05 | 2.272 | 15.249 | 104.93 | 1.522 | 11.062 |
| 164.55 | 2.236 | 15.619 | 106.38 | 1.455 | 11.965 |
| 168.97 | 2.198 | 16.024 | 107.54 | 1.045 | 20.548 |
| 173.70 | 2.475 | 16.373 | 108.58 | 1.229 | 15.931 |
| 178.46 | 2.338 | 16.768 | 109.84 | 1.406 | 12.605 |
| 183.10 | 2.301 | 17.183 | 111.23 | 1.435 | 12.101 |
| 187.77 | 2.487 | 17.615 | 112.98 | 2.152 | 12.051 |
| 192.71 | 2.476 | 18.086 | 115.10 | 2.143 | 12.075 |
| 197.57 | 2.401 | 18.548 | | Series V | |
| 202.53 | 2.490 | 19.090 | 223.64 | 1.555 | 22.140 |
| 207.46 | 2.440 | 19.662 | 225.16 | 1.536 | 22.526 |

TABLE I (continued)

| $T_{av}$ °K | Approx. $\Delta T$ | $\Delta H/\Delta T$ cal./deg. mol. | $T_{av}$ °K | Approx. $\Delta T$ | $\Delta H/\Delta T$ cal./deg. mol. |
|---|---|---|---|---|---|
| 229.65 | 1.472 | 23.987 | | Series VII | |
| 230.75 | 0.722 | 24.677 | 15.72 | 2.132 | 0.550 |
| 231.46 | 0.714 | 25.093 | 18.25 | 2.724 | 0.813 |
| 232.16 | 0.699 | 25.841 | 20.97 | 2.816 | 1.146 |
| 232.85 | 0.683 | 26.770 | 23.54 | 2.556 | 1.570 |
| 233.51 | 0.654 | 28.448 | 27.31 | 1.898 | 2.167 |
| 234.14 | 0.593 | 32.588 | 29.54 | 2.471 | 2.476 |
| 234.70 | 0.536 | 37.404 | 31.87 | 2.184 | 2.816 |
| 235.30 | 0.675 | 27.187 | 34.22 | 2.569 | 3.158 |
| 236.02 | 0.769 | 22.341 | 36.69 | 2.439 | 3.475 |
| 236.80 | 0.807 | 20.707 | | Series VIII | |
| 237.61 | 0.821 | 20.134 | 40.75 | 3.378 | 4.132 |
| 238.43 | 0.825 | 19.969 | 43.94 | 3.067 | 4.538 |
| | Series VI | | 46.85 | 2.833 | 4.932 |
| 15.82 | 3.357 | 0.529 | 49.43 | 2.392 | 5.282 |
| 18.52 | 2.296 | 0.840 | 51.94 | 2.708 | 5.601 |
| | | | 54.53 | 2.569 | 5.935 |

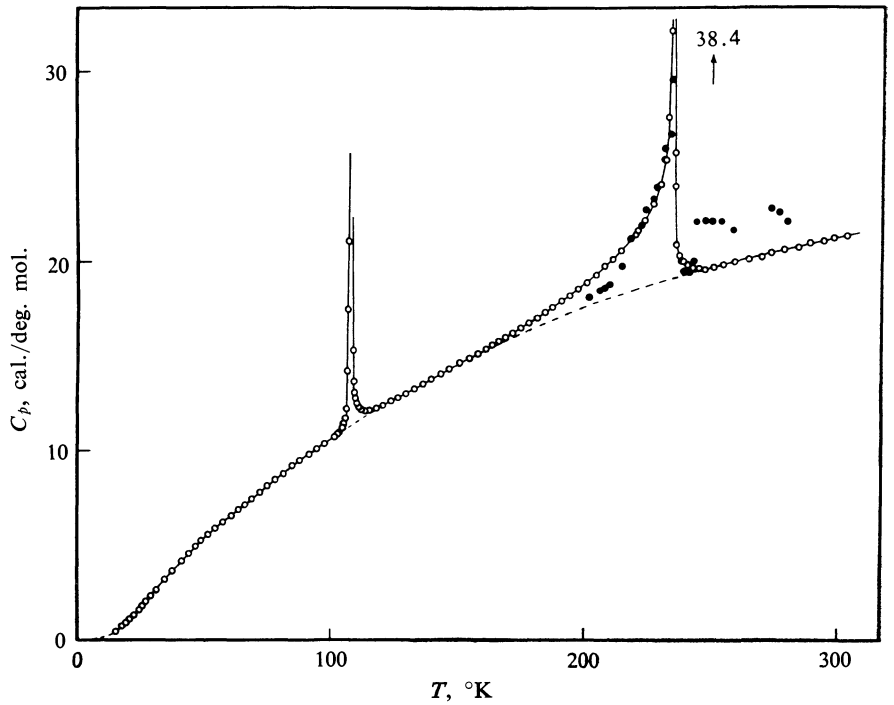



Fig. 2. Heat capacities of $NH_4Br$ between the temperature range from 13°K to 305°K.
Broken lines represent "normal" heat capacity.
○ This work, ● Simon et al. (1927)

**Apparatus.**—The heat capacity measurements were carried out by the low-temperature automatic and adiabatic calorimetry techniques. A detailed description of them has already been given in the previous paper.[9]

The infrared spectra were recorded on a Nihon Bunkō Co. Double-beam spectrometer (model DS-402G). The cryostat for a low temperature measurement is illustrated in Fig. 1.

## Results

**The Heat Capacities of Ammonium Bromide.**—The heat capacities of ammonium bromide were measured in the temperature range from

9) H. Suga and S. Seki, This Bulletin, 38, 1000 (1965).

13 to 305°K. The calorie defined as equal to 4.1840 absolute joules was used. The ice-point temperature was taken as 273.15°K. The calorimeter contained 28.5387 g. (0.29136 mol.) of ammonium bromide and helium gas for heat exchange. The experimental heat capacities, listed in Table I, are the ratios of the increase in enthalpy, $\Delta H$, to the rise in temperature, $\Delta T$, and are equal to the differential heat capacity, $C_p$, only when the correction for curvature is negligible. Also listed in Table I are $T_{av}$, the arithmetic mean of the initial and the final temperatures of each measurement, and the approximate temperature rise, $\Delta T$. Our values for the heat capacities of ammonium bromide, together with those of Simon, von Simson, and Ruhemann,[1] are plotted in Fig. 2. We thus reconfirmed the new transition phenomenon reported by Stephenson, and also an unusually wide hysteresis effect associated with it. Here the broken lines are drawn as the "normal" heat capacity. The method of estimating these broken lines will be described later. We can see that the values given by Simon et al. are considerably scattered, so we are convinced that our values are much more accurate.

Anomalous heat capacities arising from the gradual phase transition at 235°K are reproducible in the repeated measurements. In the temperature region of normal heat capacity, including the anomalous region around 235°K, the calorimeter attained thermal equilibrium within a few minutes after an individual energy input. In the transition region at 108°K, however, the calorimeter established the thermal equilibrium only with difficulty, even after several hours. The approach to the thermal equilibrium in this region is compared with

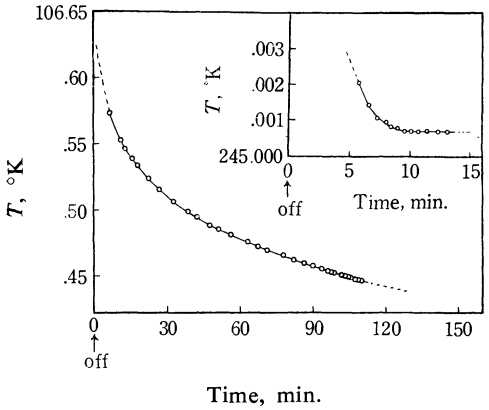



Fig. 3. Typical temperature drift curves showing behavior approaching to thermal equilibrium after an energy input. Upper one; ordinary temperature region. Lower one; transition region at 107.5°K.

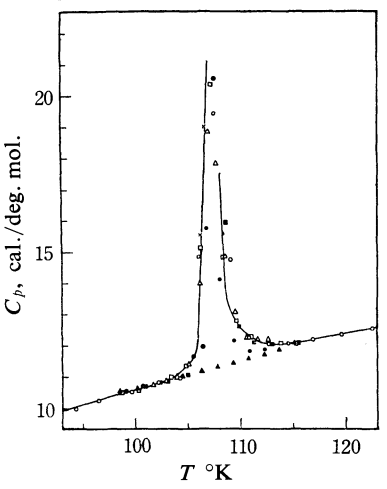



Fig. 4. Heat capacity of $NH_4Br$ around the phase transition at 107.5°K.
○, the specimen was cooled down to 20°K; ●, to 75°K; △, to 69°K; ▲, to 97°K; □, to 70°K; ■, to 74°K; ×, to 63°K

that of a normal case in Fig. 3 for the sake of reference. The measurements of the heat capacity of ammonium bromide in the anomalous region around 108°K are plotted in Fig. 4. In this region the heat capacity values are not as accurate as in normal temperature regions.

**The Thermodynamic Properties of Ammonium Bromide.**—Smoothed values of the heat capacity, entropy, enthalpy, and Gibbs energy functions, and also of the standard thermodynamic values at 298.15°K, are listed in Table II. The differential heat capacity, $C_p^\circ$, listed in the table, which is obtained from the observed values of $\Delta H/\Delta T$, was not corrected for curvature because of the small rise in temperature, $\Delta T$.

**The Anomalous Heat Capacities of Ammonium Bromide at 235°K and 108°K.** — As is shown in Fig. 2, the heat capacity anomaly around 235°K covers a considerable temperature range, so there is some latitude in drawing a broken curve to obtain the normal heat capacity. To subtract the anomalous part, it is often useful to describe the heat capacity of a solid in terms of the Debye function. For this purpose, the experimentally-observed heat capacities, $C_p$, were represented by the apparent Debye characteristic temperature, $\Theta_D$, with arbitrary degrees of freedom. The Debye characteristic temperature is known to be more sensitive than the heat capacity itself for the same amount of uncertainty in the heat capacity. Figure 5 shows the temperature dependence of the apparent Debye characteristic temperature, ${}_{12}\Theta_D$, the degrees of freedom

Table II. Thermodynamic properties of $NH_4Br$ crystal (in cal./deg. mol.)

| $T$ °K | $C_p^\circ$ | $S^\circ$ | $\frac{(H^\circ-H_0^\circ)}{T}$ | $-\frac{(G^\circ-H_0^\circ)}{T}$ |
|---|---|---|---|---|
| 10 | (0.188)* | (0.1052)* | (0.0665)* | (0.0387)* |
| 15 | 0.474 | 0.2273 | 0.1478 | 0.0795 |
| 20 | 1.027 | 0.4344 | 0.2940 | 0.1404 |
| 30 | 2.533 | 1.134 | 0.7881 | 0.3454 |
| 40 | 4.000 | 2.064 | 1.408 | 0.6557 |
| 50 | 5.353 | 3.103 | 2.063 | 1.040 |
| 60 | 6.582 | 4.190 | 2.716 | 1.474 |
| 70 | 7.686 | 5.289 | 3.378 | 1.911 |
| 80 | 8.705 | 6.382 | 3.955 | 2.428 |
| 90 | 9.665 | 7.464 | 4.537 | 2.927 |
| 100 | 10.584 | 8.530 | 5.096 | 3.434 |
| 107.5 | 27.5 | Transition point | | |
| 110 | 12.535 | 9.831 | 5.880 | 3.951 |
| 120 | 12.382 | 10.89 | 6.405 | 4.486 |
| 130 | 13.061 | 11.91 | 6.890 | 5.018 |
| 140 | 13.813 | 12.90 | 7.358 | 5.546 |
| 150 | 14.546 | 13.88 | 7.812 | 6.069 |
| 160 | 15.234 | 14.84 | 8.255 | 6.587 |
| 170 | 16.069 | 15.79 | 8.689 | 7.101 |
| 180 | 16.908 | 16.73 | 9.123 | 7.610 |
| 190 | 17.814 | 17.67 | 9.556 | 8.115 |
| 200 | 18.805 | 18.61 | 9.993 | 8.616 |
| 210 | 19.980 | 19.55 | 10.44 | 9.114 |
| 220 | 21.482 | 20.52 | 10.91 | 9.611 |
| 230 | 24.165 | 21.52 | 11.41 | 10.11 |
| 235.0 | 38.4 | Transition point | | |
| 240 | 19.799 | 22.52 | 11.96 | 10.61 |
| 250 | 19.690 | 23.37 | 12.27 | 11.10 |
| 260 | 20.020 | 24.15 | 12.56 | 11.59 |
| 270 | 20.338 | 24.91 | 12.85 | 12.07 |
| 280 | 20.647 | 25.66 | 13.12 | 12.54 |
| 290 | 20.947 | 26.39 | 13.38 | 13.00 |
| 300 | 21.246 | 27.10 | 13.64 | 13.46 |
| 298.15 | 21.194 | 26.97 | 13.59 | 13.38 |

* They were calculated from graphically extrapolated $C_p$ values.

being assumed to be twelve. The broken lines in Fig. 5 are assumed to represent reasonably the course of the normal Debye characteristic temperature corresponding to the normal heat capacity. The enthalpy and entropy of transition, $\Delta H_{tr}$ and $\Delta S_{tr}$ respectively, the transition temperature, $T_{tr}$, and the transition range are given in Table III. The heat of transition was evaluated from the combined method of total heat input analysis and graphical integration.

**Infrared Spectra at Low Temperatures.**—The infrared spectra of thin, non-scattering films of ammonium bromide were obtained at 298°K (phase II), 100°K and 88°K (phase III), and

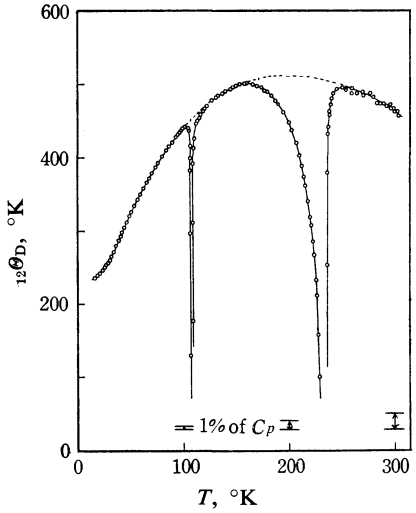



Fig. 5. The temperature dependence of the apparent Debye characteristic temperature, $_{12}\Theta_D$, where the degrees of freedom is arbitrarily chosen to be twelve.

40°K and 18°K (phase IV) respectively. The temperature of the specimen in the low temperature region was measured with an Allen-Bradley carbon resistance thermometer (nominal 47Ω, 1/10W.) which had been calibrated previously by using Clement-Quinell's equation. The two constants in this equation were determined by means of the resistance values at fixed temperatures, the boiling points of liquid helium and nitrogen. A copper: constantan thermo-couple, calibrated with a standard platinum resistance thermometer,[9] was used in the temperature region above the boiling point of liquid nitrogen.

The Wagner-Hornig assignments were employed for the analysis of the torsional frequency of the ammonium ion. The observed and inferred frequencies are summarized in Table IV. The spectrum of ammonium bromide in phase IV at 18°K is illustrated in Fig. 6 as an example. The combination band,

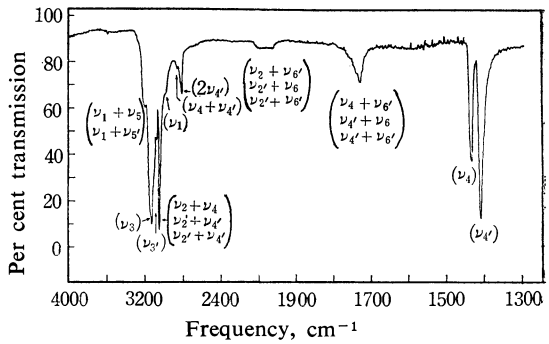



Fig. 6. Infrared spectrum of $NH_4Br$ in phase IV at 18°K.

TABLE III. TEMPERATURES, ENTHALPIES AND ENTROPIES OF TRANSITIONS, AND TRANSITION RANGES OF $NH_4Br$ CRYSTAL

| | $T_{av}$ °K | $\Delta H_{tr}$ cal./mol. | $\Delta S_{tr}$ e. u. | Transition range |
|---|---|---|---|---|
| Lower transition | 107.5±0.5 | 29.29 | 0.271 | 102—125°K |
| Upper transition | 235.0±0.2 | 156.1 | 0.714 | 158—248°K |

TABLE IV. OBSERVED FREQUENCIES, ASSIGNMENTS (AFTER WAGNER AND HORNIG), AND INFERRED FREQUENCIES FOR $NH_4Br$, CONCERNING TORSIONAL OSCILLATION OF AMMONIUM ION

| $T$, °K | 298 | 100 | 88 | 40 | 18 |
|---|---|---|---|---|---|
| Phase | II | III[a] | III[a] | IV | IV |
| | | Observed frequencies ($cm^{-1}$) | | | |
| $\nu_4'$ | 1402 | 1411 | 1409 | 1411 | 1411 |
| $\nu_4$ | 1428 | 1436 | 1432 | 1435 | 1434 |
| $\nu_4+\nu_6'$ | | 1754(w) | | 1757(w) | 1756(w) |
| $\nu_4'+\nu_6$ | 1742 | 1731 | 1732 | 1731 | 1734 |
| $\nu_4'+\nu_6'$ | | | | | |
| $2\nu_4'$ | 2804 | 2804 | 2810 | 2806 | 2815 |
| $\nu_4+\nu_4'$ | | 2851 | 2854 | 2852 | 2855 |
| | | Inferred frequencies ($cm^{-1}$) | | | |
| $\nu_6$ or $\nu_6'$ | (313) | (319) | (323) | (321) | (323) |

(a) In these cases the specimen was cooled from room temperature down to these temperatures and did not experience the phase transition at about 78°K.
(w) Very weak shoulder.

($\nu_4'$ or $\nu_4$) + ($\nu_6'$ or $\nu_6$), gets sharper gradually and the fine structures appear progressively as the sample is cooled.

## Discussion

The degrees of freedom contributing to the heat capacity at a constant pressure, $C_p$, for the ammonium halide crystal may be the following: $6N$ degrees for translational freedom (lattice vibrations ($C_v^L$)); $9N$ degrees for internal vibrations ($C_v^I$); $3N$ degrees for torsional vibrations of ammonium ions ($C_v^t$); and $C_p-C_v$ correction. The heat capacity, $C_p$, is then given by:

$$C_p=C_v^L+C_v^I+C_v^t+(C_p-C_v) \quad (1)$$

We should like to discuss each term on the right hand side of Eq. 1 separately.

**$C_p-C_v$ Correction.**—The quantity measured is the heat capacity at a constant pressure; this is the basic result from which other quantities may be derived. The heat capacity at a constant volume, which is the quantity most suitable for comparisons with available theory, may be computed from the well-known thermodynamic relation:

$$C_p-C_v=\alpha^2VT/\chi \quad (2)$$

where $\alpha$ is the cubical coefficient of thermal expansion; $V$, the molar volume, and $\chi$, the isothermal compressibility. Unfortunately, thermal expansion and compressibility data are incomplete in the present temperature region. Therefore, it is necessary to have recourse to the quasi-thermodynamic relation:

$$C_p-C_v\simeq AC_p^2T \quad (3)$$

where $A$ is a constant. From Eqs. 2 and 3, the constant $A$ is determined:

$$A\simeq\alpha^2V/\chi C_p^2 \quad (4)$$

The numerical value of the constant, $A=9.547\times10^{-6}$ mol./cal., was computed from the following values at 0°C:

$$\alpha^{10,11)}=16.20\times10^{-5}\ deg^{-1}$$

$$\chi^{12)}=6.188\times10^{-6}\ cm^2/kg.$$

$$V^{10,13)}=40.107\ cm^3/mol.$$

$$C_p=20.435\ cal./deg.\ mol.$$

The differences between $C_p$ and $C_v$ were calculated from Eq. 3.

**Internal Vibrations in Ammonium Ions ($C_v^I$).**—The contributions of the internal vibrations in ammonium ions to the heat capacity are usually best represented by the summation of the Einstein functions corresponding to the normal vibrational modes. That is:

$$C_v^I=\sum g_iE(\Theta_{E_i}/T) \quad (5)$$

where the summation is extended over the

10) V. T. Deshpande and D. B. Sirdeshmukh, *Acta Cryst.*, **14**, 353 (1961).
11) F. Simon and R. Bergmann, *Z. physik. Chem.*, **8**, 255 (1930).
12) P. W. Bridgman, *Phys. Rev.*, **38**, 182 (1931).
13) H. E. Swanson and R. K. Fuyat, NBS Circular 539, Vol. I, 353 (1953).

nine normal vibrational modes, the degeneracy, $g_i$, being taken from Wagner-Hornig's data[8] and $\Theta_{E_i}=h\nu_i/kT$. Their values are:

$\nu_1=3040\,cm^{-1}$ (degeneracy 1); $\nu_2=1640$ (2); $\nu_3=3130$ (3), and $\nu_4=1410$ (3).

**Correction for Thermal Expansion.** — The quantity, $C_v$, mentioned above corresponds to the heat capacity at a constant volume at each temperature. For comparisons with available theory, this quantity, $C_v$, must be reduced to a fixed volume at 0°K. The heat capacity at a constant volume less the contribution from internal vibrations is $C_v^L+C_v^t$. The quantity $C_v^L+C_v^t$ is represented by the apparent Debye characteristic temperatures, ${}_9\Theta_D(V_T)$, for nine degrees of freedom, as a function of the temperature. In order to reduce the ${}_9\Theta_D(V_T)$ values to the volume at 0°K, the following approximate formula is used:

$$ {}_9\Theta_D(V_O)/{}_9\Theta_D(V_T)=(\rho_O/\rho_T)^\gamma=(V_T/V_O)^\gamma \fallingdotseq 1+\gamma\Delta V/V_O \qquad (6) $$

where $V_O$ and $\rho_O$ are, respectively, the volume and density at 0°K, and $\gamma$ is the Grüneisen parameter defined by Kittel[14] as follows:

$$ \gamma=\alpha V/\chi C_v \qquad (7) $$

For lack of data on the temperature dependence of the molar volume and the Grüneisen parameter for ammonium bromide, we assumed that the behavior of the temperature dependence for ammonium bromide would be similar to that for potassium bromide.[15] The absolute values of $V_T$ and $\gamma$ for ammonium bromide, which, of course, are different from those for potassium bromide, are calculated by multiplying the factors determined at 0°C. The magnitude of the correction for ammonium bromide is illustrated in Fig. 7.

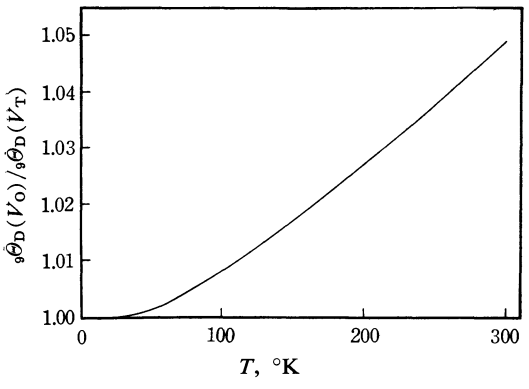



Fig. 7. The change of ${}_9\Theta_D$ with volume for ammonium bromide between 0°K and 300°K.

14) C. Kittel, "Introduction to Solid State Physics," Wiley, New York (1953).
15) B. Yates and C. H. Panter, *Proc. Phys. Soc.*, **80**, 373 (1962).

**The Torsional Frequency of the Ammonium Ion and the Potential Barrier.**—As has already been mentioned, the bromide in phase IV (below 107.5°K) may be regarded as of the CsCl-type on analogy with the neutron diffraction study[2] of deuterated ammonium bromide. In contrast to the same modification at room temperature, here the orientation of tetrahedral ammonium ions which are located at the center of a cube determined by eight halogen ions will be regularly ordered, and each ammonium ion will undergo torsional vibration about the two-fold symmetry axis of the ion in this modification.[2,16]

Recently Wulff[17] determined the barrier heights for the rotation of the methyl groups in some organic crystal by using the heat capacity data. Suga, Matsuo, and Seki[18] in our laboratory also estimated the torsional frequency of the $CN^-$ ions in the potassium cyanide crystal and discussed the contribution of the rotational vibration to the heat capacity. In both these cases, however, no direct comparison of the frequency determined from the thermal data with that determined from the spectroscopic data has been made. In the present case the pure torsional vibration of ammonium ions is spectroscopically inactive, but fortunately the quite sharp bands arising from the combination band can be observed. Therefore, there is a distinct possibility of a comparison of the torsional vibration frequency of $NH_4^+$ ions derived from the analysis of the thermal data with those obtained from the infrared and Raman data. Moreover, the potential barrier height hindering the internal rotation of the ammonium ion about the two-fold symmetry axis obtained from the thermal data for the solid phase may also be compared with the NMR data of Gutowsky, Pake and Bersohn,[16] and Sachs.[19]

For these purposes, we have tried the following analysis for phase IV, working below 107.5°K, because of the complicated effects due to the phase transitions and the anharmonicity of vibrations at higher temperatures. The heat capacity, $C_v(V_O)$, calculated from the Debye temperature, ${}_9\Theta_D(V_O)$, in Eq. 6 consists of the "translational" effect for six degrees of freedom and the "torsional vibration" for three degrees of freedom, with the fixed volume at 0°K. As we have no "a priori" methods for separating the contribution arising from the

16) H. S. Gutowsky, G. E. Pake and R. Bersohn, *J. Chem. Phys.*, **22**, 643 (1954).
17) C. A. Wulff, ibid., **39**, 1227 (1963).
18) H. Suga, T. Matsuo and S. Seki, Preprint of the Symposium on Thermodynamics and Thermochemistry, Lund, Sweden, July, 1963; This Bulletin, **38**, 1115 (1965).
19) A. M. Sachs, Ph. D. Thesis, Harvard University, 1949.

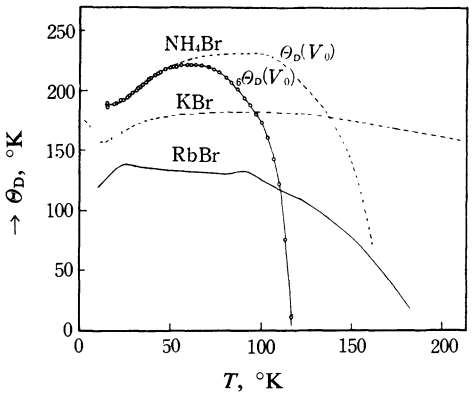



Fig. 8. Debye temperature of $NH_4Br$, KBr, and RbBr. Two curves for $NH_4Br$ are explained in text.

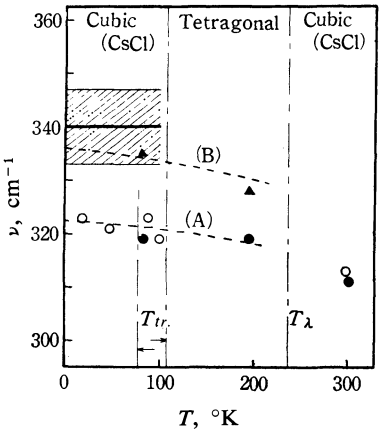



Fig. 9. Temperature dependence of the torsional frequency of ammonium ion.
○ ; The result from the analysis of infrared combination bands measured by us. ● ; Infrared absorption data by Wagner and Hornig. ▲ ; Fundamental vibration frequency observed by the method of Raman spectroscopy by Krishnan. The shaded area represents the result from the analysis of thermal data.

torsional vibration and that from the translational motion, empirical assumptions are needed to calculate the torsional frequency and the potential barrier heights from the analysis of the thermal data. The first assumption is that the behavior of the temperature dependence of the Debye characteristic temperature, $\Theta_D$, which corresponds to the "translational heat capacity" of ammonium bromide, may be similar to those of alkali halides, the crystal structure of which is of the CsCl-type at low temperatures, as in the case of ammonium bromide. Cesium bromide and chloride presumably satisfy this condition. As we have no suitable thermal data, however, about cesium bromide and cesium chloride in hand, the data for potassium bromide[20] and rubidium bromide[21] are used for the sake of comparison, although the crystal structure of both compounds is of the NaCl-type. The temperature dependences of the Debye characteristic temperatures of potassium bromide and rubidium bromide are reproduced in Fig. 8. The curves for both compounds are almost flat in the temperature range between 50 and 140°K for potassium bromide, and from 40 to 90°K for rubidium bromide, which means that the Debye model is applicable to these substances in these temperature ranges. The contribution to the heat capacity arising from the torsional vibration of the $NH_4^+$ ion may be approximately represented by an Einstein function, $E(\Theta_E/T)$, for three degrees of freedom with an empirically-chosen $\Theta_E$. The "translational" or "lattice" heat capacity is then given by:

$$C_v^L = C_v(V_0) - E(\Theta_E/T) \qquad (8)$$

By trial and error, an adequate Einstein characteristic temperature, $\Theta_E$, was determined, so that the curve of the temperature dependence of the apparent Debye temperature, $\Theta_D$, corresponding to the heat capacity, $C_v^L$, might be flat in some temperature regions. The value of $\Theta_E$ determined in such a way is 490 ±10°K, which corresponds to the torsional oscillation of the $NH_4^+$ ion about its two-fold symmetry axes with the wave number of 340 ±7 cm$^{-1}$. The value of 340±7 cm$^{-1}$ is consistent with the infrared data obtained by us and by Hornig et al.[8] and also with Raman data[22] extrapolated to the lowest temperature (see Fig. 9). One can see that in Fig. 9 there are rather small but significant differences between the infrared frequencies and those of Raman data. According to the discussion by Wagner and Hornig,[8] the torsional vibration of the ammonium ion, the $\nu_6$ mode (triply degenerated in phases II and IV), splits into two components, $\nu_6(A_2)$ and $\nu_{6'}(E)$, in the tetragonal modification with the point group $V_d$ (phase III), the latter mode ($\nu_{6'}$) being active in both the infrared and Raman spectra. The Raman frequencies[22] shown in Fig. 9 are the fundamental vibrations ($\nu_{6'}$ mode). The infrared data, however, are the results of the analysis of the complicated combination bands, whose assignments have not yet been fully established. In fact, the combination band gets sharper gradually, and

20) W. T. Berg and J. A. Morrison, *Proc. Roy. Soc.*, **A242**, 467 (1957).
21) K. Clusius, J. Goldmann and A. Perlick, *Z. Naturforsch.*, **4a**, 424 (1949).
22) R. S. Krishnan, *Proc. Ind. Acad. Sci.*, **A27**, 321 (1948).

the fine structures appear progressively when the specimen is cooled down to a lower temperature. This band has a width of about 50 $cm^{-1}$ even at the lowest temperatures, so there is some uncertainty involved in resolving the combination bands into their component frequencies. In addition, the two spectra (infrared and Raman) should not be expected to coincide unless the coupling between ammonium ions is very weak.[8] Thus, one can not compare the absolute values of the two spectra directly until the complete assignment is established. Curve A in Fig. 9 represents approximately the temperature dependence of the torsional frequency as determined by an analysis of the combination bands. We can find that the frequency of the torsional oscillation shows almost no temperature dependence in the low temperature region. This fact justifies our treatment of the thermal data with a harmonic Einstein function. Curve B in the figure was drawn for the fundamental torsional oscillation by assuming the same temperature dependence as that of curve A in phase IV. The extrapolated fundamental values of the Raman data to the lowest temperatures compare quite well with those determined by the analysis of the thermal data. To check the results, it is also very desirable to measure the fundamental vibration in phase III (tetragonal modification) by the method of infrared absorption.

Now, we should like to proceed to the problem of the potential barrier. We have adopted the following potential function,[23] which is usually taken for such internal rotation or torsional oscillations as $CH_3$–, OH–, or $C_2H_5$– groups:

$$U(\phi)=\frac{1}{2}U_0(1-\cos n\phi) \tag{9}$$

where $\phi$ is the angle of rotation; $n$, the symmetry number; and $U_0$, the potential barrier height.

In the case of ammonium bromide, the symmetry number, "$n$," is approximately four, judging from the crystal structure. In phase II, the crystal structure of the ammonium bromide is of the CsCl-type. The orientations of the ammonium ions in this phase are found to be disordered. In the temperature region of phase III, the structure of the bromide is tetragonal[3,4] and the orientations are still in the ordered state. Below 107.5°K, the structure (phase IV) is of the CsCl-type and of the ordered orientations, analogous with the results of the neutron diffraction study[2] of deuterated ammonium bromide.

23) K. S. Pitzer, "Quantum Chemistry," Prentice-Hall, New York (1953).

As to the possible orientations of the tetrahedral ammonium ion which is located at the center of a cube determined by eight halogen ions, there are two possibilities. In the disordered phase II, these two orientations are equally probable and are distributed statistically at random over the whole lattice. On the other hand, in the ordered phase IV, all the ammonium ions have one and the same orientation.

In the disordered phase the symmetry number is exactly four, and the potential function is well represented by Eq. 9. In the ordered phase, however, the potential energy between two orientations is slightly different. The potential function, then, is better represented by:

$$U(\phi)=\frac{1}{2}U_0(1-\cos n\phi)+\frac{1}{2}U_1S\left(1-\cos\frac{1}{2}n\phi\right) \tag{10}$$

where $S$ is an order parameter concerning the orientations of ammonium ions, and $U_1$ is the potential energy difference between the two orientations at 0°K.

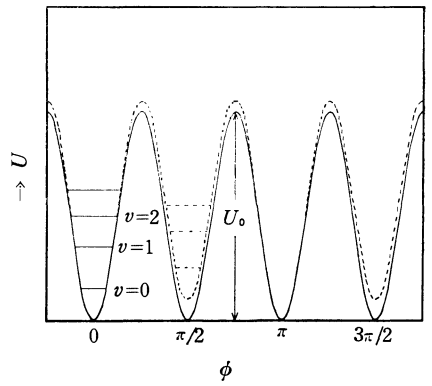



Fig. 10. Potential curves hindering rotation of ammonium ion about its two-fold symmetry axis.
——: $U(\phi)=(1/2)U_0(1-\cos 4\phi)$
----: $U(\phi)=(1/2)U_0(1-\cos 4\phi)+(1/2)U_1S(1-\cos 2\phi)$

The potential curves given by Eqs. 9 and 10 are illustrated in Fig. 10. Equation 10 requires knowledge about the temperature dependence of the $S$ parameter. We assumed also the periodic function, with $n=4$, even in the ordered phases (phases III and IV). When the ions undergo torsional oscillation at a low temperature, the angle of rotation, $\phi$, may be small. Then one can expand the potential function in a power series in $\phi$ as follows:

Table V. Potential barriers to rotation of the $NH_4^+$ ion in the ammonium halides (CsCl modification), in kcal./mol.

| Compound | $U_0$(Eq. 14) | $U_0$(elec.)[a] | $U_0(\nu)$[b] | $U_0(T_1)$[c] |
|---|---|---|---|---|
| $NH_4Br$ | 4.00±0.16 | 3.73 | 4.18 | 4.65 |
| $NH_4Cl$ | 6.24±0.26[d] | 5.40 | 5.25 | 6.41 |

a) These values are entirely from an electrostatic calculation; Refs. 15 and 17.
b) These results obtained from the observed torsional frequencies; Ref. 15.
c) $U_0(T_1)=E$(activation energy from $T_1$)$+(3/2)h\nu_{obs.}$; Refs. 15 and 16.
d) This value is calculated by using Eq. 14 and the smoothed $C_p$-curve determined by Simon.[1]

$$U(\phi)=\frac{1}{2}U_0\left(\frac{n^2\phi^2}{2!}-\frac{n^4\phi^4}{4!}+\frac{n^6\phi^6}{6!}-\cdots\right) \quad (11)$$

By using the first-order perturbation theory, the energy levels of this anharmonic oscillator are calculated to be:

$$E_v=h\nu_0\left(v+\frac{1}{2}\right)-\frac{1}{2U_0}\frac{1}{4!}(h\nu_0)^2(6v^2+6v+3)+\frac{1}{2U_0^2}\frac{1}{6!}(h\nu_0)^3(20v^3+30v^2+40v+15) \quad (12)$$

and

$$\nu_0=\frac{n}{2\pi}\sqrt{\frac{U_0}{2I}} \quad (13)$$

where $\nu_0$ is the frequency corresponding to the simple harmonic oscillator approximation; $I$ is the moment of inertia of the ammonium ion, and $v$ is the quantum number of the vibration.

If the torsional wave number $\nu=340\pm7\ cm^{-1}$, as determined from thermal data, is assumed to be the difference between $v=1$ and $v=0$, i.e., $h\nu=E_{v=1}-E_{v=0}$, then we have:

$$h\nu=h\left(\frac{n}{2\pi}\sqrt{\frac{U_0}{2I}}\right)-\frac{6h^2}{4!U_0}\left(\frac{n}{2\pi}\sqrt{\frac{U_0}{2I}}\right)^2+\frac{45h^3}{6!U_0^2}\left(\frac{n}{2\pi}\sqrt{\frac{U_0}{2I}}\right)^3 \quad (14)$$

and the potential barrier height, $U_0$, is 4.00± 0.16 kcal./mol. On the other hand, a simple harmonic oscillator approximation using Eq. 13 gives the value of $U_0=3.52\pm0.16$ kcal./mol., and the potential function given by Eq. 10 gives a value of several per cent[24] smaller than 4.00±0.16 kcal./mol.

In calculating the potential barrier height, the numerical values of $I=4.778\times10^{-40}$ g. cm$^2$, the N-H distance=1.035Å,[16] and $U_1=kT_C$ ($T_C=235$°K) were used.

Gutowsky, Pake, and Bersohn[16] and Sachs[19] calculated the potential barriers to rotation of the $NH_4^+$ ions in the ammonium halides (CsCl modification) by measuring the spin-lattice relaxation time, $T_1$, by means of NMR studies. They also estimated the potential barrier by electrostatic calculation. The values of the potential barrier obtained are all summarized in Table V. We ourselves determined the value of $U_0$ for ammonium chloride with the above-mentioned technique by using the heat capacity data of Simon[25] and Eq. 14.

**The Contribution of the Torsional Oscillation to the Heat Capacity.**—If the periodic potential function given by Eq. 9 is assumed, the heat capacity, $C_v^t$, arising from the torsional vibration is a function of the temperature, $T$, of the symmetry number, $n$, and of the potential barrier $U_0$; i.e., $C_v^t=f(n, U_0, T)$.

Pitzer and Gwinn[23] have tabulated the thermodynamic functions for the contribution of the rotation. By using their table instead of the Einstein function, $E(\Theta_E/T)$, we have computed $C_v^t$. Figure 11 shows two cases of the temperature dependence of the "torsional" heat capacities, $f(n, U_0, T)$ and $E(\Theta_E/T)$.

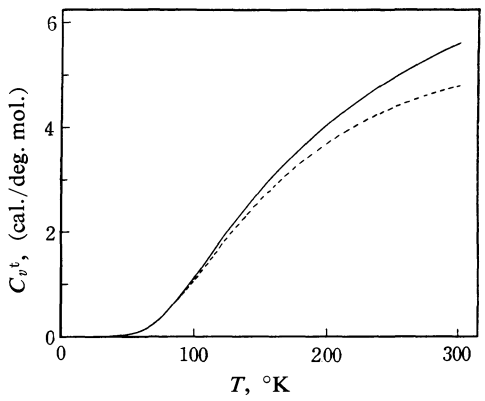



Fig. 11. Contribution from torsional oscillation to heat capacity.
——: $f(n, U_0, T)$, $n=4$, $U_0=4.00$ kcal./mol.
----: $E(\Theta_E/T)$, $\Theta_E=490$°K, $\nu=340\ cm^{-1}$

Finally, the "translational" or "lattice" heat capacity is computed by using this equation:

$$C_v^L=C_v(V_0)-f(n, U_0, T) \quad (15)$$

24) For instance, assuming $S=1$ and $U_1=kT_C$ for phase IV, we get a value of $U_0$ several per cent smaller than 4.00 ±0.16 kcal./mol.

25) F. Simon, *Ann. Phys.*, **68**, 241 (1922).

Figure 8 shows the temperature dependence of the Debye characteristic temperatures, $\Theta_D(V_O)$ and ${}_6\Theta_D(V_O)$, which correspond to the heat capacities $C_v^L$ and $C_v^L+C_v^t$ respectively.

**Phase Transition.**—As is well known, neutron diffraction studies,[2] and theoretical consideration[26] of the anomalous changes of the heat capacities, and also of various other physical quantities at the gradual phase transition point ($\lambda$-point) (235°K for the bromide and 243°K for the chloride), have confirmed that the transitions are of the order-disorder type with relation to the orientations of the $NH_4^+$ ions in the crystalline lattice. If the orientations of the $NH_4^+$ ions are fully disordered above the $\lambda$-point and are completely ordered below it, the treatment of the Bragg-Williams type by Nagamiya[26] requires $R\ln 2$ e. u. as the entropy of transition.

In the case of ammonium chloride, the crystal structure in phase III is of the ordered CsCl-type and that of phase II, of the disordered CsCl-type. Moreover, the volume change at the transition point is very small. Thus the observed transition entropy may be only the contribution from a co-operative phenomenon arising from the order-disorder nature. The observed value, $\Delta S_{tr}=1.2$ e. u.,[27] is nearly equal to $R\ln 2$, which thus confirming the validity of the interpretation.

In the case of ammonium bromide, however, the crystal structures below and above the $\lambda$-transition point are slightly different from each other. The observed entropy change consists of the contributions from the order-disorder phenomenon and from the difference between the lattice energies of the two modifications. Staveley[28] estimated the entropy change of 0.34 e. u. for ammonium bromide by using Simon's heat capacity data.[1] However, as has already been mentioned, this value is not very reliable. The entropy change obtained in our measurements is 0.714 e. u., which is still much less than $R\ln 2$. To interpret this feature in ammonium bromide, we may take into account the fact that the orientations of $NH_4^+$ ions in phase III are already disordered by a considerable amount far below the $\lambda$-point; we also have a lower temperature modification (phase IV) in the case of this substance, while in ammonium chloride there is no such intermediate state.

On the other hand, the phase transition at 107.5°K is very likely of the first-order type, in view of the wide hysteresis[29] phenomenon and the slow establishment of thermal equilibrium near the transition point.

## Summary

We have measured the heat capacities of the ammonium bromide crystal from 13°K to 305°K and have found two phase transitions in this temperature region. From the results, the heat and entropy of transitions at the transition points, 107.5°K and 235.0°K, have been derived: for the lower transition, $\Delta H_{tr}=29.29$ cal. mol.$^{-1}$ and $\Delta S_{tr}=0.271$ cal. deg$^{-1}$ mol$^{-1}$; for the upper one, $\Delta H_{tr}=156.1$ cal. mol$^{-1}$ and $\Delta S_{tr}=0.714$ cal. deg$^{-1}$ mol$^{-1}$. The values of the entropy and enthalpy function at 298.15°K are: $S^\circ=26.97$ cal. deg$^{-1}$ mol$^{-1}$ and $(H^\circ-H_0^\circ)/T=13.56$ cal. deg$^{-1}$ mol$^{-1}$. The torsional motions of the ammonium ions may well be represented in terms of a periodic potential function at the lowest temperature modification. The torsional frequency, $340\pm 7$ cm$^{-1}$, and the potential barrier height, $4.00\pm 0.16$ kcal. mol$^{-1}$, as determined on the basis of the thermal data, agree well with the values obtained in other experiments.

The infrared spectra of thin, non-scattering films of ammonium bromide have been obtained at 298°K, 100°K, 88°K, 40°K and 18°K. The torsional frequencies determined from the spectra by adopting Wagner-Hornig's assignments have been found to be almost independent of the temperature in the lowest modification.

The authors would like to express their sincere thanks to Dr. Takeshi Okuno of the Institute of Scientific and Industrial Research, Osaka University, who kindly permitted them to use and modify his cryostat for their spectroscopic measurement. The authors are also grateful to the members of their laboratory for their useful discussions.

*Department of Chemistry*
*Faculty of Science*
*Osaka University*
*Toyonaka, Osaka*

## Note Added in Proof

(i) In order to interpret the small but significant difference between the torsional frequencies determined from infrared and Raman spectra, we measured the far-infrared spectra of ammonium bromide at about 100°K (phase III) and at room temperature (phase II) after the completion of

26) T. Nagamiya, *Proc. Phys. Math. Soc. Japan*, **24**, 137 (1942); **25**, 540 (1943).
27) C. C. Stephenson, R. W. Blue and J. W. Stout, *J. Chem. Phys.*, **20**, 1046 (1952).
28) L. A. K. Staveley, *Quart. Rev.*, **3**, 65 (1949).
29) Stephenson et al. found that this transition takes place at 108.5°K on heating and 78°K on cooling. We also reconfirmed the fact by differential thermal analysis.

this work. For the measurement a film of ammonium bromide on polyethylene plate was used. The spectra at 100°K show two peaks reproducibly; one is a considerably intensive peak at 345 $cm^{-1}$ and the other is a weak one at 335 $cm^{-1}$. These two peaks, however, vanish at room temperature. From these facts, two peaks might be concerned with the active fundamental torsional frequency predicted by Wagner and Hornig.[8]

The authors would like to express their grateful acknowledgment to Dr. Tatsuo Miyazawa of the Institute for Protein Research, Osaka University, who permitted them to use Perkin Elmer Spectrometer (model 201 C) in his laboratory and gave them helpful advice.

(ii) Stephenson, Wulff and Lundell[30] reported quite recently the torsional frequencies of ammonium halide crystals determined from thermal analysis. For the torsional frequency in ammonium bromide they have quoted the Ph.D. thesis by A. G. Cole.[31] The heat capacity of ammonium bromide by Dr. Cole is about one per cent smaller than ours in the whole temperature region. With respect to the torsional frequency, however, the value, $335\pm5$ $cm^{-1}$, reported in Dr. Cole's thesis agrees rather well the result by us, $340+7$ $cm^{-1}$, within their experimental errors. In passing, we should like to remark that his value of the entropy of transition at 234.5°K is overestimated due to the no subtraction of the normal heat capacities from the total observed values. The authors are indebted to Microreproduction Laboratory of Massachusetts Institute of Technology for sending them the microfilm of Dr. Cole's thesis.

30) C. C. Stephenson, C. A. Wulff and O. R. Lundell, *J. Chem. Phys.*, 40, 967 (1964).

31) A. G. Cole, Ph. D. Thesis, M. I. T. (1952).

# Polyesters Containing Carbazole Rings in the Main Chain. II. The Syntheses of Polyesters from Carbazole Keto Acids*

By Yoshio NAGAI and Chin-Chuan HUANG

(Received November 4, 1964)

As has been described previously,[1] to prepare polyesters containing carbazole rings in the main chain, the authors first synthesized several carbazole- and *N*-alkylcarbazole-dicarboxylic acids. Carbazole-dibasic acids of the general formula X-R-X, where X is $-COC_2H_4CO_2H$ or $-(CH_2)_3CO_2H$ and R is carbazole or a 9-methylcarbazole ring, were also synthesized in better yields by a modification of the method of Mitchell and Plant.[2]

New polyesters were derived from diethyl carbazole- and diethyl 9-methylcarbazole-3, 6-$\gamma,\gamma'$-diketobutanoates in the presence of various catalysts.

## Experimental

**The Preparation of Monomers.** — *Carbazole-3,6-$\gamma,\gamma'$-diketobutanoic Acid (I).*—The succinoylation of carbazole according to the method of Mitchell and Plant[2] gave I in yields lower than 40 per cent. These results indicated that the use of at least 2.5 molecular proportions of aluminum chloride per mole of succinic anhydride is a requisite and that the extension of the reaction time up to 16 hr. is preferable in increasing the yield of I. Table I shows the molecular proportions of aluminum chloride per mole of succinic anhydride and the relative per cent yields of keto acid.

Found: C, 65.71; H, 4.65. Calcd. for $C_{20}H_{17}O_6N$: C, 65.32; H, 4.64%.

*Carbazole-3,6-dibutanoic Acid (II).*[7] — Reducing I also by the Clemmensen method, Mitchell and Plant[2] prepared II in a 50 per cent yield. As Table II shows that, when I was reduced in an aqueous acetic acid, II was obtained in a more than 80 per cent yield. II can be alternatively synthesized from the ethyl ester of I by the Clemmensen method. A zinc amalgam was prepared by mixing 300 g. of zinc powder, 300 cc. of a 10% aqueous mercuric chloride solution, and 10 cc. of concentrated hydrochloric acid. The mixture was stirred for 5 min., and then the residue which remained after the decantation of the aqueous solution was covered with 300 cc. of water. To this mixture was added 30 g. of I and 300 cc. of glacial acetic acid; then the

* A part of this paper was presented at the 17th Annual Meeting of the Chemical Society of Japan, Tokyo, March, 1964.

1) Y. Nagai and C.-C. Huang, This Bulletin, **38**, 951 (1965).

2) D. R. Mitchell and G. P. Plant, *J. Chem. Soc.*, **1936**, 1295.

3) U. S. Pat. 2534028 (1948).

4) U. S. Pat. 2647885 (1951).

5) U. S. Pat. 2578660 (1949).

6) British Pat. 727790 (1952).

7) Syntheses of polyesters from II and V will be described in the succeeding paper, "III. Syntheses of Polyesters from Carbazoledicarboxylic and Carbazoledibutanoic Acid."

TABLE I. SYNTHESIS OF CARBAZOLE-3,6-$\gamma,\gamma'$-DIKETOBUTANOIC ACID

| Carbazole g. | Nitrobenzene cc. | $AlCl_3$ g. | Succinic anhydride g. | Reaction Time hr. | Reaction Temp. °C | Yield g. | Yield % |
|---|---|---|---|---|---|---|---|
| 30.0 | 420 | 102.0 (4.3) | 36.0 (2.0) | 6 | 0±2 | 24.0 | 36.4 |
| 30.0 | 420 | 102.0 | 36.0 | 7 | 0±2 | 25.2 | 38.2 |
| 30.0 | 420 | 102.0 | 36.0 | 8 | 0±2 | 24.8 | 37.5 |
| 30.0 | 420 | 102.0 | 36.0 | 8 | 0±2 | 25.1 | 38.0 |
| 30.0 | 420 | 128.0 (5.3) | 36.0 (2.0) | 6 | 0±2 | 32.2 | 48.8 |
| 30.0 | 420 | 144.0 (6.0) | 36.0 (2.0) | 6 | 0±2 | 33.6 | 50.9 |
| 30.0 | 420 | 192.0 (8.0) | 36.0 (2.0) | 6 | 0±2 | 34.5 | 52.3 |
| 30.0 | 420 | 216.0 (9.0) | 36.0 (2.0) | 6 | 0±2 | 33.8 | 51.8 |
| 30.0 | 420 | 128.0 | 36.0 | 12 | 0±2 | 35.8 | 54.3 |
| 30.0 | 420 | 128.0 | 36.0 | 16 | 0±2 | 41.6 | 63.2 |

Numbers in the parentheses are molecular proportions of aluminum chloride or succinic anhydride per mole of carbazole.

TABLE II. SYNTHESIS OF CARBAZOLE-3,6-DIBUTANOIC ACID

| I g. | Zinc amalgam g. | Glacial AcOH cc. | Other solvent cc. | Concd. HCl[a] cc. | Reaction Time hr. | Reaction Temp. °C | Yield g. | Yield % |
|---|---|---|---|---|---|---|---|---|
| 30.0 | 300 | 300 | 40[b] | 300 | 4 | 90—95 | 13.2 | 47.6 |
| 30.0 | 300 | 300 | 25[b] | 300 | 4 | 90—95 | 12.0 | 43.3 |
| 30.0 | 300 | 300 | 75[b] | 300 | 4 | 90—95 | 9.0 | 32.5 |
| 30.0 | 300 | 300 | 40[c] | 300 | 4 | 90—95 | 12.8 | 46.0 |
| 30.0 | 300 | 300 | 60[c] | 300 | 4 | 90—95 | 12.9 | 46.2 |
| 30.0 | 300 | 300 | 300[d] | 300 | 4 | 90—95 | 22.4 | 80.7 |
| 30.0 | 300 | 300 | 300[d] | 300 | 4 | 90—95 | 22.6 | 81.3 |
| 30.0 | 300 | 300 | — | 300 | 4 | 90—95 | 14.5 | 52.3 |
| 30.0[e] | 300 | 300 | — | 300 | 4 | 90—95 | 15.0 | 62.5 |

a) $d$=1.175 g./cc. b) Toluene c) Xylene d) Water e) Diethyl ester of I.
I, Carbazole-3,6-$\gamma,\gamma'$-diketobutanoic acid.

whole was refluxed and stirred while 300 cc. of concentrated hydrochloric acid was added, drop by drop, over a 4-hr. period. After the completion of the reaction, the upper layer of the product was decanted and the residual amalgamated zinc was refluxed with glacial acetic acid to take up any product remaining on the top of the amalgam or on the wall of the flask. On cooling, the combined solution of the filtrate and the decanted layer yielded II as white flakes; 22.5 g., m. p. 198—200°C.

Found: C, 70.59; H, 6.20; N, 5.73. Calcd. for $C_{20}H_{21}O_4N$: C, 70.80; H, 6.19; N, 5.81%.

*Diethyl Carbazole-3,6-$\gamma,\gamma'$-diketobutanoate (III).*—The reaction of I with a mixture of ethanol and concentrated sulfuric acid for 6 hr. gave III as white plates; m. p. 175—176°C after crystallization from ethanol (decolorizing charcoal added).

Found: C, 68.12; H, 5.92. Calcd. for $C_{24}H_{25}O_6N$: C, 68.10; H, 5.92%.

*Diethyl 9-Methylcarbazole-3,6-$\gamma,\gamma'$-diketobutanoate (IV).*—A solution of 1.5 g. of III in 300 cc. of acetone was poured into a flask containing 1.5 g. of an aqueous potassium hydroxide in 1.0 cc. of water, and to this mixture was added 2.0 cc. of dimethyl sulfate. The mixture was then stirred for 12 min. at 25°C, and the product was poured into 2 l. of water to give white precipitates which yielded IV as white crystals (1.5 g.; m. p. 145—146°C after recrystallization from ethanol).

Found: C, 67.37; H, 6.11. Calcd. for $C_{25}H_{27}O_6N$: C, 67.09; H, 6.04%.

*9-Methylcarbazole-3,6-dibutanoic Acid (V).*[7]—For this synthesis, a zinc amalgam was prepared as has been described in the preparation of II. The procedure was also essentially the same except that IV was reduced instead of I. The melting point of V is 227—229°C.

Found: C, 71.06; H, 6.58. Calcd. for $C_{21}H_{17}O_4N$: C, 71.35; H, 6.52%.

**Polycondensation.** — *General Procedure.* — Polyesters were obtained by heating a mixture of ethylene glycol and III or IV in a glass flask. The

ester exchange reaction in the presence or in the absence of a catalyst was effected under such condition that the displaced alcohol could be removed by distillation; this involved the use of a reaction temperature below the boiling point of ethylene glycol, but well above that of the alcohol to be displaced. In carrying out the reaction, at least two molecular proportions of ethylene glycol per molecular proportion of III or IV were used, and the heating in a stream of nitrogen was continued until the distillation of the displaced alcohol ceased. The resulting low polymeric products could be converted to polyesters by heating them, at a temperature above the boiling point of ethylene glycol, under reduced pressure (below 1 mmHg). The polyesters thus prepared were reprecipitated several times in order to increase the homogeneity.

For the following polycondensations, ethylene glycol was first dried over anhydrous sodium sulfate and then purified by dissolving metallic sodium in it (1.0 g. per 100 cc.) and refluxing it in an atmosphere of nitrogen for 1 hr. and then distilling it (b. p. 99—100°C/15 mmHg).

In syntheses of the polyesters PX-1 to PX-18, 10 g. of III and 3 g. of ethylene glycol were used. Various catalysts and the corresponding weights for each preparation are shown in Table III. Two preparations will be described as examples; the rest are essentially the same.

*PX-4.*—The following ingredients were introduced into a hard glass flask: III, 10.0 g.; ethylene glycol, 3.0 g.; calcium acetate, 0.041 g. and antimony trioxide, 0.01 g. The mixture was then heated in a stream of oxygen-free nitrogen in a vapor bath of 195°C for 2 hr., until most of the ethanol distilled off. The low polymeric product was then heated further at an elevated temperature, 210°C at the early stage and finally at 280°C, over a period of 5 hr. in the full vacuum used at the last phase of the reaction. The resulting condensation product exhibited an intrinsic viscosity of 0.18 in *m*-cresol at 30°C.

*PX'-1.* — A mixture of 10.5 g. of IV, 3.0 g. of ethylene glycol, and 0.005 g. of lead acetate was allowed to react in a stream of oxygen-free nitrogen for 2 hr., while the ethanol was being continuously removed; then it was polycondensed under the same conditions as in the previous example and over the same period to give, in *m*-cresol at 30°C a polyester with the intrinsic viscosity of 0.23.

Table III. Polyesters based on diethyl carbazole-3,6-$\gamma,\gamma'$-diketobutanoate

| Polyester code | Catalyst | Weight g. | $[\eta]$[a] | PMT[b] °C |
|---|---|---|---|---|
| PX-1 | Na | 0.0014 | 0.12[p] | 160(9) |
| PX-2 | $Na_2CO_3$ | 0.0150 | 0.09[p] | 115(5) |
| PX-3 | PbO | 0.0600 | 0.14[p] | 166(9) |
| PX-4 | $Ca(CH_3CO_2)_2 \cdot H_2O$ | 0.0410 | 0.18[c] | 170(9) |
| | $Sb_2O_3$ | 0.0100 | | |
| PX-5 | $Ca(CH_3CO_2)_2 \cdot H_2O$ | 0.0120 | 0.11[p] | 160(8) |
| | $Sb_2O_3$ | 0.0031 | | |
| PX-6 | $Ca(CH_3CO_2)_2 \cdot H_2O$ | 0.0500 | 0.18[c] | 172(8) |
| | $Sb_2O_3$ | 0.0120 | | |
| PX-7 | $Ca(CH_3CO_2)_2 \cdot H_2O$ | 0.0210 | 0.15[c] | |
| | $Sb_2O_3$ | 0.0050 | | |
| PX-8 | $Ca(CH_3CO_2)_2 \cdot H_2O$ | 0.0250 | 0.16[c] | 170(7) |
| | $Sb_2O_3$ | 0.0062 | | |
| PX-9 | $Ca(CH_3CO_2)_2 \cdot H_2O$ | 0.0330 | 0.18[c] | |
| | $Sb_2O_3$ | 0.0076 | | |
| PX-10 | $Co(CH_3CO_2)_2 \cdot 4H_2O$ | 0.0047 | 0.21[c] | 175(7) |
| PX-11 | $Co(CH_3CO_2)_2 \cdot 4H_2O$ | 0.0063 | 0.21[c] | |
| PX-12 | $Co(CH_3CO_2)_2 \cdot 4H_2O$ | 0.0018 | 0.19[c] | 172(9) |
| PX-13 | $Pb(C_2H_3O_2)_2 \cdot 3H_2O$ | 0.0050 | 0.23[c] | 180(10) |
| PX-14 | $Pb(C_2H_3O_2)_2 \cdot 3H_2O$ | 0.0060 | 0.24[c] | 183(10) |
| PX-15 | $Pb(C_2H_3O_2)_2 \cdot 3H_2O$ | 0.0092 | 0.24[c] | |
| PX-16 | $GeO_2$ | 0.0040 | 0.18[c] | 171(7) |
| PX-17 | $GeO_2$ | 0.0020 | 0.16[c] | 168(8) |
| PX-18 | $GeO_2$ | 0.0083 | 0.23[c] | 178(8) |
| PX-19 | $GeO_2$ | 0.0061 | 0.23[c] | |
| PX-20 | $GeO_2$ | 0.0102 | 0.23[c] | |
| PX-21 | Control | — | 0.08[p] | 106(5) |

a) The intrinsic viscosity, $[\eta]$, was obtained from plotting inherent viscosity numbers versus concentration and extrapolating to zero concentration.
b) PMT, polymer melting temperature; Numbers in the parentheses are PMT temperature range.
c) Measured in *m*-cresol at 30°C.
p) Measured in pyridine at 30°C.

## Results and Discussion

Since I and 9-methylcarbazole-3,6-$\gamma,\gamma'$-diketobutanoic acid dissolve sparingly in most organic

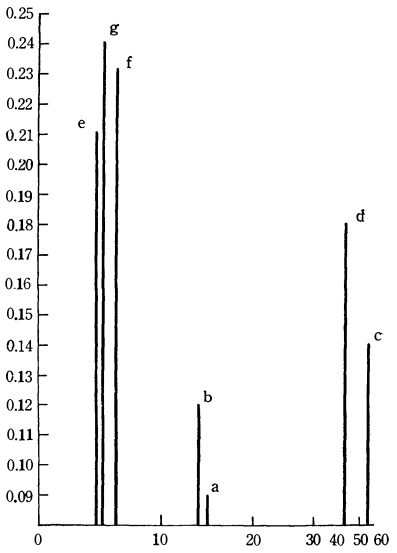



Fig. 1. Maximum intrinsic viscosity attained with various catalysts.
a Sodium carbonate b Sodium
c Lead monoxide d Calcium acetate
e Cobaltous acetate f Germanium-dioxide
g Lead acetate

TABLE IV. SOLUBILITY OF POLY(ETHYLENE CARBAZOLE-3,6-$\gamma,\gamma'$-DIKETOBUTANOATE) IN VARIOUS SOLVENTS

| Solvent | Polymer | | | | | |
|---|---|---|---|---|---|---|
| | PX-1 | PX-3 | PX-6 | PX-10 | PX-14 | PX-18 |
| Acetone | 4 | 4 | 4 | 4 | 4 | 4 |
| Chloroform | 4 | 4 | 4 | 4 | 4 | 4 |
| *cis*-1,2-Dichloroethylene | 4 | 4 | 4 | 4 | 4 | 4 |
| Methanol | 4 | 4 | 4 | 4 | 4 | 4 |
| Carbon tetrachloride | 4 | 4 | 4 | 4 | 4 | 4 |
| Benzene | 4 | 4 | 4 | 4 | 4 | 4 |
| Cyclohexane | 4 | 4 | 4 | 4 | 4 | 4 |
| Toluene | 4 | 4 | 4 | 4 | 4 | 4 |
| Pyridine | 1 | 1 | 2 | 4 | 4 | 4 |
| Phenol | 1 | 1 | 1 | 1 | 1 | 1 |
| *o*-Cresol | 1 | 1 | 1 | 1 | 1 | 1 |
| *m*-Cresol | 1 | 1 | 1 | 1 | 1 | 1 |
| Nitrobenzene | 6 | 6 | 6 | 6 | 6 | 6 |
| DMF | 1 | 1 | 1 | 2 | 2 | 2 |
| Dichlorobenzene | 3 | 3 | 3 | 6 | 6 | 6 |
| Concd. $H_2SO_4$ | 7 | 7 | 7 | 7 | 7 | 7 |

1: Soluble in hot solvent and remains soluble cold.
2: Very low solubility, or little solvent action on solute.
3: Inbives hot solvent and swells.
4: No effect of solvent on solute.
5: Soluble in hot solvent, precipitated cold.
6: Melted or sticky in hot solvent.
7: Soluble in cold solvent.

TABLE V. ELEMENTARY ANALYSES OF PECKB AND 9-MePECKB

| Polymer code | C, % | H, % | O, % |
|---|---|---|---|
| PX-4 | 66.18 | 5.03 | 25.49 |
| PX-6 | 66.44 | 4.99 | 24.28 |
| PX-10 | 66.72 | 5.01 | 24.65 |
| PX-15 | 66.65 | 5.01 | 25.43 |
| PX-18 | 66.72 | 5.03 | 24.54 |
| PX'-1 | 67.03 | 5.22 | 23.81 |
| Calcd. for $-(C_{22}H_{19}O_6N)-$ | 67.18 | 4.84 | 24.43 |
| Calcd. for $-(C_{23}H_{21}O_6N)-$ | 67.82 | 5.16 | 23.59 |

solvents, III and IV were used in the practical polycondensation.

In the absence of a catalyst, merely a low polymeric condensation product was obtained. Among several catalysts, e.g., lead monoxide,[3] calcium acetate,[4] germanium dioxide,[5] and antimony trioxide,[3] which have been proclaimed as excellent catalysts for preparing white aromatic polyesters when applied either singly or in combination, lead monoxide has proved to be inadequate in the synthesis of poly(ethylene carbazole-3,6-$\gamma,\gamma'$-diketobutanoate) (PECKB) from the viewpoint of the color of the product. The use of lead monoxide less than 0.6% by weight of III yielded only a low polymeric product, and an attempt to synthesize high polymeric PECKB by adding more lead monoxide resulted in a product the color of which was usually very dark amber. In preparations of PECKB and 9-MePECKB, the catalytic effect of germanium dioxide compared favorably with that of cobaltous acetate or lead acetate, which is generally considered to be a good accelerator in polycondensation. In the presence of about 0.6% by weight of lead acetate, a relatively high polymeric PECKB was obtained, as is illustrated in Fig. 2, though

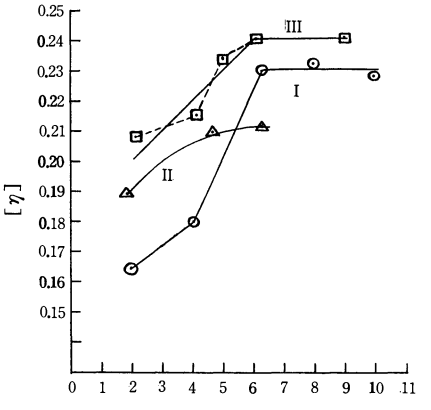



Fig. 2. Relation between the weight of catalyst and the intrinsic viscosity.
I Germanium dioxide II Cobaltous acetate
III Lead acetate

a rather irregular increase in viscosity in accordance with the increment of the catalyst was observed. The color of PECKB or 9-MePECKB tends to become darker upon the addition of more than 0.1% by weight of lead acetate or germanium dioxide; the addition of more than 0.06% by weight of cobaltous acetate to the reaction mixture also is apt to give a polyester of a very dark amber color. The use of more than 5 times by weight of calcium acetate in comparison with other catalysts was necessary, as is clearly shown in Figs. 1 and 3; otherwise, the viscosity increased steadily up to 0.18 with the increase in the weight of the catalyst.

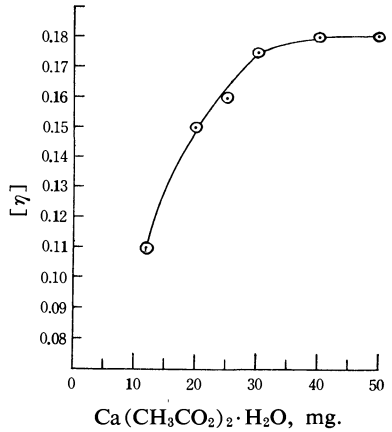



Fig. 3. Relation between the weight of catalyst and the intrinsic viscosity.

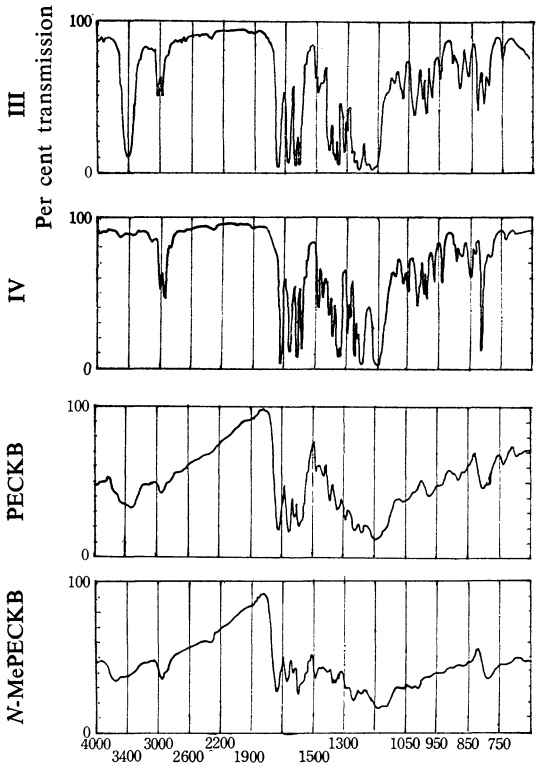



Fig. 4. Infrared spectra of III, IV, PECKB, *N*-MePECKB.

Infrared spectrum of III was obtained on the pressed disk of 3.8 mg. of III/700 mg. KBr; and that of IV on the pressed disk of 3.9 mg. of IV/700 mg. KBr.

Infrared spectra of PECKB and 9-MePECKB were obtained on the pressed disks of 4.5 mg. of PECKB/700 mg. KBr and 5.5 mg. of 9-MePECKB/700 mg. KBr respectively.

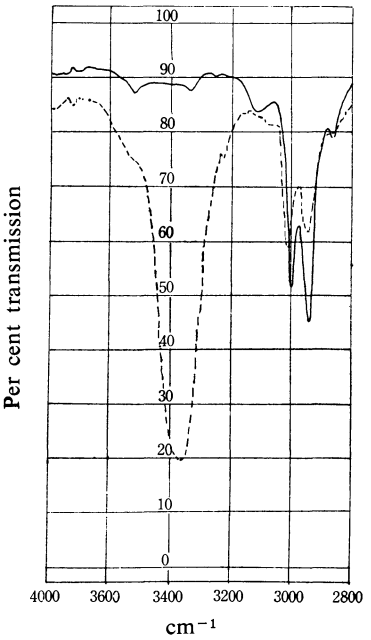



Fig. 5. Infrared spectra of III* and IV**.
* On pressed disk of 3.5 mg. III/700 mg. KBr.
** On pressed disk of 3.5 mg. IV/700 mg. KBr.

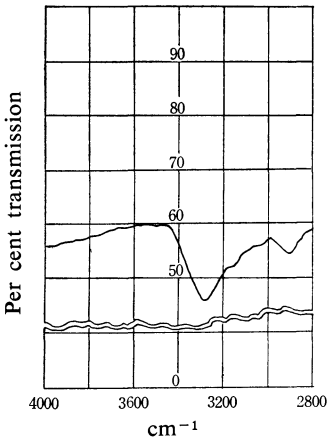



Fig. 6. Infrared spectrum of poly(ethylene carbazole-3,6-$\gamma,\gamma'$-diketobutanoate)*, PECKB.
* On pressed disk of 3.5 mg. PECKB/700 mg. KBr.

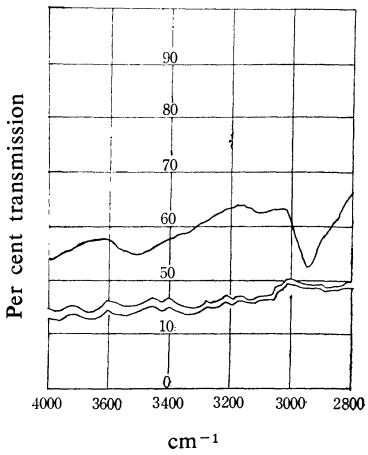



Fig. 7. Infrared spectrum of poly(ethylene 9-methylcarbazole-3,6-$\gamma,\gamma'$-diketobutanoate)*, 9-MePECKB.

* On pressed disk of 3.5 mg. 9-MePECKB/700 mg. KBr.

PECKB and 9-MePECKB have, in general, good resistance to many organic solvents, though not to pyridine, phenol and cresol. Condensation products exhibiting an intrinsic viscosity lower than 0.14 dissolve in pyridine at the boiling point of the solvent, whereas PECKB and 9-MePECKB, which show an intrinsic viscosity of 0.15 or higher, dissolve in only phenol or cresol at the boiling point of the solvent; all the polyesters synthesized dissolve slowly in concentrated sulfuric acid.

The wide temperature range of polymer melting points shown in Table III seems to indicate that polyesters based on III or IV are largely amorphous. Figures 4, 5, 6, and 7 show the infrared spectra of III, IV, PECKB, and 9-MePECKB. The data from elementary analyses of the polycondensation product and the characteristic absorption bands shown in these figures indicate that synthesized PECKB and 9-MePECKB are linear plyesters with the following recurring units:

PECKB,

$$-(OCC_2H_4CO-C_{12}H_7N-COC_2H_4CO_2C_2H_4O)-$$

9-MePECKB,

$$-(OCC_2H_4CO-C_{13}H_9N-COC_2H_4CO_2C_2H_4O)-$$

The authors wish to thank the kind cooperation of Nihon Jōriu Company, Nihon Kayaku Company, and Yahata Kagaku Company in supplying carbazole for this study. We are also grateful for the experimental help, in preparation of monomers, of Messrs. Y. Yoshida, S. Fujinami and Y. Ikeda of the Nagai Laboratory, Institute of Industrial Science, the University of Tokyo.

*Institute of Industrial Science*
*The University of Tokyo*
*Azabu, Tokyo*

# Oxidation of Alcohols with *t*-Butyl Chromate. II. The Oxidation of Primary Aromatic Alcohols*1

By Takayuki SUGA, Keiichi KIHARA*2 and Tamon MATSUURA

(Received November 10, 1964)

The oxidation of benzyl alcohol with *t*-butyl chromate has been reported to give benzaldehyde in a quantitative yield[1] and to be accelerated by pyridine.[2] In the preceding paper of this series,[3] the *t*-butyl chromate oxidation of the primary aliphatic alcohols with the $-CH_2 \cdot CH_2OH$, $>CH \cdot CH_2OH$, or $\equiv C \cdot CH_2OH$ groups was found to yield a mixture of the corresponding aldehyde, acid and ester in a comparable yield. On the other hand, the oxidation of the primary allylic alcohol was established as giving the corresponding aldehyde in a high yield, but not the ester. We have now tried the oxidation of benzyl alcohol and its *p*-substituted derivatives, β-phenylethyl alcohol, and *trans*-cinnamyl alcohol with *t*-butyl chromate.

*1 The oxidation of benzyl alcohol has been recorded in *J. Chem. Soc. Japan, Pure Chem. Sec.* (*Nippon Kagaku Zasshi*), **80**, 653 (1959), by one of the present authors. An other part of this work was presented at the 3rd Symposium on Perfume, Terpene and Essential Oil Chemistry of the Chemical Society of Japan, Tokyo, October, 1959.

*2 Present address: The Tôyô Sôda Manufacturing Company, Ltd., Nanyô-chô, Tsuno-gun, Yamaguchi-ken.

1) R. V. Oppenauer and H. Oberrauch, *Anales asoc. quim. arg.*, **37**, 246 (1949).

2) A. Leo and F. H. Westheimer, *J. Am. Chem. Soc.*, **74**, 4383 (1952).

3) Part I: T. Suga, K. Kihara and T. Matsuura, This Bulletin, **38**, 893 (1965).

The re-examination of the oxidation of benzyl alcohol (Exp. 1) under conditions similar to those reported by Oppenauer et al.[1],*3 gave benzaldehyde (81% yield based on the alcohol) and benzoic acid (17%). When this alcohol was oxidized (Exp. 2) at 1—2°C for 6 hr. with the oxidant solution prepared in the 1 : 1 mol. ratio of the alcohol to *t*-butyl chromate, as employed in many cases of a primary aliphatic alcohol,[3] the yield of benzaldehyde increased to 90% and the formation of benzoic acid was suppressed to 7%. No such ester as produced in the case of a saturated primary aliphatic alcohol[3] was formed in Exps. 1 and 2.

The effect of the para substituent on the formation of the aldehyde and the ester was checked with *p*-chlorobenzyl alcohol and *p*-isopropylbenzyl alcohol. The oxidation of *p*-chlorobenzyl alcohol (Exp. 3) under the same conditions as in Exp. 2 gave *p*-chlorobenzaldehyde (83%) and *p*-chlorobenzoic acid (10%), but it did not yield the ester. When this oxidation was repeated using a benzene solution with a lower concentration of the oxidant and the sample alcohol (Exp. 4), the yield of *p*-chlorobenzoic acid decreased to 5%, and *p*-chlorobenzaldehyde was obtained in a 91% yield. The oxidation of *p*-isopropylbenzyl alcohol (Exp. 5) under the same conditions as in Exp. 4 afforded *p*-isopropylbenzaldehyde (79%) and *p*-isopropylbenzoic acid (10%), but no ester was obtained. Thus, the electron-attractive or the electron-repulsive group in the para position was found neither to affect remarkably the yield of the aldehyde nor to cause the formation of the ester.

The oxidation of β-phenylethyl alcohol (Exp. 6) gave the corresponding ester, i. e., β-phenylethyl β-phenylacetate (46%), β-phenylacetaldehyde (3%) and β-phenylacetic acid (3%), accompanied by anomalous oxidation products, such as benzaldehyde (2%) and benzoic acid (7%). The formation of the anomalous products is probably due to the cleavage of the side chain. Besides, a resinous substance, probably a polymer of β-phenylacetaldehyde, was obtained in ca. 10% yield. The different oxidation mode between benzyl alcohol and β-phenylethyl alcohol will be discussed, together with the course of the formation of the ester, in Part IV of this series.

The oxidation of *trans*-cinnamyl alcohol (Exp. 7) under the same conditions as in Exp. 2 produced *trans*-cinnamaldehyde (61%) and *trans*-cinnamic acid (1%). In addition, benzaldehyde (6%) and benzoic acid (2%), presumably formed by the allylic double-bond fission, were obtained. Oxidation (Exp. 8) similar to that of Exp. 7, with a reaction time of 2 hr., gave the corresponding aldehyde (49%), the corresponding acid (1%), benzaldehyde (5%) and benzoic acid (3%). When *t*-butyl chromate dissolved in benzene containing glacial acetic acid and acetic anhydride was used as an oxidant (Exp. 9), *trans*-cinnamaldehyde was obtained in a 59% yield, even with a short oxidation time similar to that of Exp. 8, and the original alcohol was almost entirely exhausted. In this case, the yields of cinnamic acid, benzaldehyde and benzoic acid were 8, 10 and 1%. The oxidation (Exp. 10) with a neutral benzene solution of the oxidant under the same conditions as in Exp. 1 afforded cinnamaldehyde (52%), cinnamic acid (6%), benzaldehyde (6%) and benzoic acid (2%), but no original alcohol. The formation of the ester was not observed with cinnamyl alcohol (Exps. 7—10).

Therefore, when a primary aromatic alcohol with a phenyl group or an ethylenic double bond adjacent to the hydroxymethyl group was oxidized with *t*-butyl chromate, the aldehyde corresponding to the sample alcohol was obtained as the main reaction product, but the corresponding ester was not formed. On the other hand, the oxidation of an aromatic alcohol with a methylene between the phenyl group and the hydroxymethyl group produced the aldehyde, the acid and the ester corresponding to the sample alcohol, as in the oxidation of a saturated primary aliphatic alcohol.[3]

## Experimental

**Sample Alcohols.** — Benzyl alcohol and β-phenylethyl alcohol were obtained from a commercial source. Cinnamyl alcohol (m. p. 33—34°C; $\lambda_{infl.}^{EtOH}$ 249 and $\lambda_{max}$ 251 mμ, log ε 4.272 and 4.274) was supplied by the Takasago Perfumery Co., Ltd. Its melting point and ultraviolet absorption spectrum indicated this alcohol to be a trans-form.[4] *p*-Chlorobenzyl alcohol (m. p. 70.5—71°C) and *p*-isopropylbenzyl alcohol (b. p. 124—125°C/13 mmHg) were prepared from the corresponding benzoic acids by reduction with lithium aluminum hydride in ether.[5,6] All the sample alcohols were purified by distillation or recrystallization just before use.

*3 The oxidation recorded by them has been carried out at room temperature over a 7-day period, using a benzene solution of *t*-butyl chromate prepared in the 1 : 1.3 mol. ratio of benzyl alcohol to this chromate.

4) E. A. Braude, E. R. H. Jones and E. S. Stern, *J. Chem. Soc.*, **1946**, 396; E. B. Bates, E. R. H. Jones and M. C. Whiting, ibid., **1954**, 1854.

5) Cf. R. F. Nystrom and W. G. Brown, *J. Am. Chem. Soc.*, **69**, 2548 (1947).

6) Cf. C. C. Price and S.-T. Voong, *J. Org. Chem.*, **14**, 115 (1949).

TABLE I. THE WEIGHTS OF THE ALCOHOL USED AND EACH COMPONENT IN THE OXIDANT, AND CONDITIONS OF THE OXIDATION

| Exp. | Sample | | | | Oxidant | | | | |
|---|---|---|---|---|---|---|---|---|---|
| | Alcohol | | $C_6H_6$ | Concn.[a] | $CrO_3$ | *t*-BuOH | $C_6H_6$ | Concn. | Time |
| | | g. | g. | % | g. | g. | g. | % | |
| 1[b] | Benzyl | 16.2 | 70 | 2.4 | 20.0 | 44.0 | 70 | 37 | 7 days |
| 2 | Benzyl | 30.0 | 90 | 4.5 | 28.0 | 56.0 | 110 | 35 | 6 hr. |
| 3 | *p*-Chlorobenzyl | 40.0 | 63 | 4.5 | 28.1 | 55.9 | 100 | 35 | 6 hr. |
| 4 | *p*-Chlorobenzyl | 40.0 | 280 | 1.0 | 28.1 | 55.9 | 339 | 15 | 6 hr. |
| 5 | *p*-Isopropyl-benzyl | 13.0 | 86.5 | 1.0 | 8.7 | 17.3 | 107 | 15 | 6 hr. |
| 6 | β-Phenylethyl | 30.0 | 54.6 | 4.5 | 24.6 | 49.1 | 92 | 35 | 6 hr. |
| 7 | *trans*-Cinnamyl | 30.0 | 49.8 | 4.5 | 22.4 | 44.8 | 84 | 35 | 6 hr. |
| 8 | *trans*-Cinnamyl | 30.0 | 49.8 | 4.5 | 22.4 | 44.8 | 84 | 35 | 2 hr. |
| 9[c] | *trans*-Cinnamyl | 30.0 | 49.8 | 4.5 | 22.4 | 44.8 | 84 | 30[d] | 2 hr. |
| 10 | *trans*-Cinnamyl | 30.0 | 90 | 2.5 | 29.8 | 66.3 | 91 | 38 | 7 days |

a) Mol. in 1000 g. of benzene.
b) The mol. ratio of the sample alcohol to *t*-butyl chromate was 1 : 1.3 and the oxidation was carried out at 22—25°C. Only benzene is represented by volume (ml.).
c) To the benzene solution of *t*-butyl chromate, 15 g. of glacial acetic acid and 10 g. of acetic anhydride were added.
d) The cocentration in the acidified benzene solution is shown.

**Oxidation, and the Treatment of a Reaction Mixture.**—A benzene solution of *t*-butyl chromate was prepared in the same manner as that in the preceding paper.[3] The quantity of each component and the concentration of *t*-butyl chromate in this solution are shown in Table I, which also lists the quantities of the sample alcohol and its solvent. The oxidation was carried out under the conditions described above in a manner similar to that described in Ref. 3. After the oxidation, the reaction mixture was treated with oxalic acid and water, except in Exp. 1, and then separated into a benzene solution and an aqueous one (see Ref. 3). The separated benzene solution containing a reaction product was subjected to the examinations described in each experiment. Each of the constituents of the reaction product was identified by the same method as used in the preceding study;[3] the yield of the constituents has been shown above.

**The Oxidation of Benzyl Alcohol (Exp. 1).**—After the oxidation, the reaction mixture was treated with hydrazine sulfate and 20% sulfuric acid instead of oxalic acid and water. An ether solution of the reaction product, obtained by the removal of the solvent from the separated benzene solution, was extracted with a 5% sodium carbonate solution, which gave benzoic acid on acidification. The removal of the solvent from the ether solution gave a neutral reaction product, which consisted of benzaldehyde (15%) and dibenzalhydrazine (85%). The steam distillation of this dibenzalhydrazine in the presence of dilute sulfuric acid gave benzaldehyde quantitatively. The formation of dibenzalhydrazine is considered to result from the reaction of hydrazine sulfate with benzaldehyde while the residual oxidant was hydrolyzed with this reagent.

**(Exp. 2).**—The reaction mixture was treated with oxalic acid and water, and then the separated benzene solution was repeatedly extracted with a 5% sodium carbonate solution, which gave benzoic acid on acidification. The neutral reaction product was obtained from the neutral benzene solution by the removal of the solvent. Thin-layer chromatographic analysis (silica gel) as well as infrared and ultraviolet spectroscopic analyses indicated the neutral product to be only benzaldehyde.

**The Oxidation of *p*-Chlorobenzyl Alcohol (Exps. 3 and 4).**—The separated benzene solution was treated in the same manner as in Exp. 2. *p*-Chlorobenzoic acid (m. p. 234—235°C) was obtained from the sodium carbonate extracts. Thin-layer chromatography (silica gel) indicated that the neutral product consisted of *p*-chlorobenzaldehyde (m. p. 45—46°C) and unchanged alcohol (0.2 and 4% in Exps. 3 and 4 respectively). The aldehyde was estimated by the 2,4-dinitrophenylhydrazine method.[7]

**The Oxidation of *p*-Isopropylbenzyl Alcohol (Exp. 5).**—The reaction product was examined in a manner similar to that used in Exps. 2—4. The boiling point of *p*-isopropylbenzaldehyde isolated was 98—100°C/8 mmHg, and *p*-isopropylbenzoic acid melted at 115—116°C. The unchanged alcohol amounted to 8.5%.

**The Oxidation of β-Phenylethyl Alcohol (Exp. 6).**—The distillation of a reaction product obtained from the separated benzene solution gave benzaldehyde (b. p. 73—78°C/22 mmHg), β-phenylacetaldehyde (b. p. 90—95°C/22 mmHg), unchanged alcohol (21% yield; b. p. 110—113°C/22 mmHg) and a residue (20.5 g.). Liquid-column chromatography on silica gel with a mixture of ethyl ether and

7) H. A. Iddles, A. W. Low, B. D. Rosen and R. T. Hart, *Ind. Eng. Chem., Anal. Ed.*, **11**, 102 (1939).

*n*-hexane indicated that this residue contained benzoic acid (m. p. 120—121°C), β-phenylacetic acid (m. p. 76—76.5°C), β-phenylethyl β-phenylacetate (b. p. 180—182°C/5 mmHg; $\nu_{max}^{liq.}$ 1730, 1150 $cm^{-1}$), and a resinous substance, probably a polymer of β-phenylacetaldehyde.

**The Oxidation of *trans*-Cinnamyl Alcohol (Exps. 7—10).**—The reaction product was distilled to separate as five fractions, and then some fractions and the residue were individually subjected to liquid-column chromatography on silica gel with a mixture of ethyl acetate and *n*-hexane. The reaction product consisted of *trans*-cinnamaldehyde[8] (b. p. 96—100°C/3.5 mmHg; $\lambda_{max}^{EtOH}$ 287 mμ, log ε 4.36), *trans*-cinnamic acid (m. p. 132—132.5°C), benzaldehyde, benzoic acid and unchanged alcohol (2, 19 and 2% in Exps. 7, 8 and 9 respectively).

## Summary

The oxidation with *t*-butyl chromate has been carried out with benzyl alcohol, its *p*-substituted derivatives and *trans*-cinnamyl alcohol, and also with β-phenylethyl alcohol. In the former alcohols, the corresponding aldehyde was obtained as the main product, but the corresponding ester was not formed. On the other hand, the latter alcohol, containing a methylene group adjacent to the hydroxymethyl group, produced the corresponding ester, aldehyde and acid, as in the case of a saturated primary aliphatic alcohol.

The authors wish to express their hearty thanks to Messrs. Tadahisa Yanagihara and Yoshinobu Nakamura, who assisted in a part of this research, and to the Takasago Perfumery Co., Ltd., for supplying a sample of cinnamyl alcohol. This research was aided by a grant from the Ministry of Education.

*Department of Chemistry*
*Faculty of Science*
*Hiroshima University*
*Hiroshima*

8) G. Gamboni, V. Theus and H. Schinz, *Helv. Chim. Acta*, **38**, 255 (1955).

# The Dimerization of Benzoic Acid in Carbon Tetrachloride and Chloroform

By Yasumasa I'HAYA and Tai-ichi SHIBUYA*

(Received November 10, 1964)

Although the dimerization equilibria of benzoic acid in various solvents have been spectroscopically studied by many authors,[1-6] the equilibrium constants obtained so far extend over a wide range. In the very dilute solutions which are often used for ultraviolet spectroscopy, the interaction of the carboxylic group of the acid with a small amount of water present in the solvents might have a considerable effect on the dimerization equilibrium.

We have studied the dimerization of benzoic acid in the concentration range from 0.0001 mol. to 0.1 mol. in carbon tetrachloride and chloroform by infrared spectroscopy, and have calculated the dimerization constant from the integrated intensities of the carbonyl-stretching vibration bands corresponding to the monomer and the dimer forms of benzoic acid. Barrow and Yerger[7] used the same infrared technique to obtain the dimerization constant of acetic acid in carbon tetrachloride and chloroform from the optical densities at the absorption maxima of the respective carbonyl absorption bands. Davies and Sutherland[1] obtained the dimerization constant of benzoic acid from the integrated intensity of the hydroxyl-stretching vibration band.

The purpose of the present paper is two-fold: to apply the integrated intensity technique for the determination of the monomer and dimer concentrations to the carbonyl-stretching band, using a high resolution infrared spectrometer, and to compare the effect of carbon tetrachloride upon acid dimerization with that of

* Present address: Department of Physics, University of the Pacific, Stockton, Calif.

1) M. M. Davies and G. B. B. M. Sutherland, *J. Chem. Phys.*, **6**, 767 (1938).

2) J. T. Harris, Jr., and M. E. Hobbs, *J. Am. Chem. Soc.*, **76**, 1419 (1954).

3) J. W. Wenograd and R. A. Spurr, ibid., **79**, 5844 (1957).

4) J. T. Lindberg, *Soc. Scientiarium Fennica*, **20**, 5 (1957).

5) M. Ito, *J. Mol. Spectry.*, **4**, 144 (1960).

6) H. Hosoya, J. Tanaka and S. Nagakura, ibid., **8**, 257 (1962).

7) G. M. Barrow and E. A. Yerger, *J. Am. Chem. Soc.*, **76**, 5248 (1954).

chloroform. Barrow and Yerger[7] assumed that a weak association of acetic acid with chloroform occurs through hydrogen bonding to the monomer carbonyl. The present paper will examine whether a like association exists in the benzoic acid - chloroform system.

## Experimental

**The Measurement of Dimerization Constants.**—The basic equation from which infrared intensity measurements proceed is:

$$A=(Cl)^{-1}\int \ln(I_0/I)_\nu d\nu \qquad (1)$$

where $A$ is the *true* integrated intensity; $C$, the molar concentration of an absorbing species; $l$, the optical path length, and $I_0$ and $I$, the incident and transmitted intensity of the monochromatic radiation of the frequency, $\nu$, respectively. In practice, because of the use of a finite slit width, the radiation is not monochromatic and the intensity measured experimentally is not $I$ but the apparent intensity, $T$. Therefore, Eq. 1 should be replaced by:

$$B=S/Cl, \text{ with } S=\int \ln(T_0/T)_\nu d\nu \qquad (2)$$

where $B$ is the *apparent* integrated intensity. As Ramsay has shown,[8] the apparent band intensity, $B$, determined in this way is not the true physical constant of the absorbing species but depends upon the instrumental conditions employed. However, if one assumes that the $(T_0/T)_\nu/(I_0/I)_\nu$ ratio does not significantly depend upon the ratio of the apparent half-intensity band width to the slit width, one can reasonably determine the concentration of the absorbing species from Eq. 2 by putting an appropriate value into $B$. In fact, when this was checked by measuring the carbonyl band of ethyl methyl ketone, the deviation of the apparent integrated intensity from the true integrated intensity was found not to be significant, the decrease in peak intensity produced by the finite slit width being approximately compensated for by an increase in the half-intensity band width.

All measurements were made with a Koken DG 201 infrared spectrophotometer equipped with a grating or a rock-salt prism. Dry air was led into the instrument after it had passed through a column packed with a molecular sieve in order to remove the carbon dioxide and water present in the air. A set of rock salt cells was used; the cell thickness was 0.190 mm., as determined by interference patterns, and 1.20, 3.10, 9.9, and 20.0 mm., as determined by direct measurement with a micrometer.

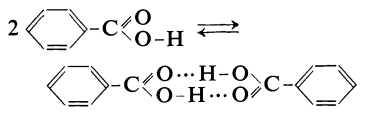
The acetic acid concentrations used were in the range from $7.35\times10^{-2}$ to $3.03\times10^{-4}$ mol. in carbon tetrachloride and $7.64\times10^{-2}$ to $1.31\times10^{-4}$ mol. in chloroform. The temperature of the samples was not specifically controlled but was between room temperature, 23°C, and that of the instrument, 25°C.

**Materials.**—Wako special-grade benzoic acid was recrystallized from water, dried under a vacuum, and sublimated in a flask. The carbon tetrachloride was Kanto Kagaku reagent grade, washed several times with concentrated sulfuric acid, a sodium hydroxide aqueous solution and water, dried over calcium chloride and then over phosphorus pentoxide, and finally passed through a column packed with aluminum oxide. It was stored in a brown desiccator placed in a dark and cool place and used within two day.

The chloroform was of the same grade and was purified in the same manner as carbon tetrachloride.

## Results and Discussion

The dimerization equilibrium of benzoic acid in non-dissociating solvents is assumed to be:



(3)

The infrared absorption spectrum of benzoic acid has been fairly well established.[9] The O–H stretching vibration band was found at 3525 $cm^{-1}$, which corresponds to that of monomer benzoic acid, and the out-of-plane O–H deformation, at 945 $cm^{-1}$. The C=O stretching vibration bands used to determine the monomer and dimer concentrations were found at 1737 $cm^{-1}$ for the monomer and at 1692 $cm^{-1}$ for the dimer in carbon tetrachloride, and at 1725 and 1690 $cm^{-1}$ for the

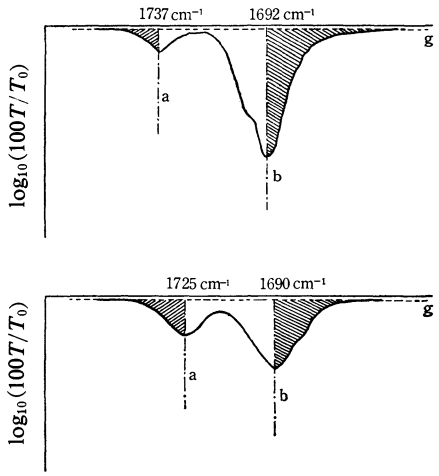



Fig. 1. $Log_{10}(T/T_0)_\nu$ versus $\nu$ plot of the C=O stretching vibration bands of benzoic acid.
Above: 0.0073 M benzoic acid in $CCl_4$;
Below: 0.0076 M benzoic acid in $CHCl_3$
The cell length is 1.20 mm.

8) D. A. Ramsay, ibid., 74, 72 (1952).

9) L. J. Bellamy, "The Infrared Spectra of Complex Molecules," Methuen, London (1957), p. 139ff.

TABLE I. THE EQULIBRIUM CONSTANT FOR THE DIMERIZATION OF BENZOIC ACID IN CARBON TETRACHLORIDE

| M mol. $l^{-1}$ | $l$ mm. | $S_m$ $cm^{-1}$ | $S_d$ $cm^{-1}$ | $C_m$ mol. $l^{-1}$ | $C_d$ mol. $l^{-1}$ | $K\times10^{-3}$ $l.mol^{-1}$ |
|---|---|---|---|---|---|---|
| 0.07349 | 0.190 | 0.907 | 37.240 | $3.33\times10^{-3}$ | $3.08\times10^{-2}$ | 2.78 |
| 0.05060 | | 0.898 | 28.483 | 3.29 | 2.36 | 2.18 |
| 0.02530 | | 0.584 | 13.454 | 2.14 | 1.11 | 2.42 |
| 0.01012 | 1.20 | 2.131 | 32.374 | 1.24 | $4.24\times10^{-3}$ | 2.76 |
| 0.007349 | | 1.975 | 23.209 | 1.15 | 3.04 | 2.30 |
| 0.005060 | 3.10 | 4.211 | 38.853 | $9.46\times10^{-4}$ | 1.97 | 2.20 |
| 0.004048 | | 3.780 | 32.960 | 8.49 | 1.67 | 2.32 |
| 0·003036 | | 3.198 | 24.483 | 7.19 | 1.24 | 2.40 |
| 0.002024 | | 2.685 | 15.790 | 6.03 | $8.01\times10^{-4}$ | 2.20 |
| 0.001515 | | 2.103 | 10.301 | 4.73 | 5.22 | 2.33 |
| 0.001012 | 9.9 | 5.499 | 21.110 | 3.87 | 3.35 | 2.24 |
| 0.0007349 | | 4.417 | 13.165 | 3.11 | 2.09 | 2.16 |
| 0.0005060 | 20.0 | 6.805 | 15.108 | 2.37 | 1.19 | 2.12 |
| 0.0003036 | | 5.070 | 8.808 | 1.77 | $6.92\times10^{-5}$ | 2.21 |
| | | | | | (average | 2.33) |

TABLE II. THE EQUILIBRIUM CONSTANT FOR THE DIMERIZATION OF BENZOIC ACID IN CHLOROFORM

| M mol. $l^{-1}$ | $l$ mm. | $S_m$ $cm^{-1}$ | $S_d$ $cm^{-1}$ | $C_m$ mol. $l^{-1}$ | $C_d$ mol. $l^{-1}$ | $K\times10^{-3}$ $l.mol^{-1}$ |
|---|---|---|---|---|---|---|
| 0.07644 | 0.190 | 6.314 | 34.912 | $9.36\times10^{-3}$ | $3.11\times10^{-2}$ | 3.55 |
| 0.04375 | | 4.408 | 21.743 | 6.54 | 1.94 | 4.53 |
| 0.02188 | | 3.263 | 9.270 | 4.84 | $8.26\times10^{-3}$ | 3.53 |
| 0.008750 | 1.20 | 11.424 | 21.660 | 2.68 | 3.05 | 4.25 |
| 0.007644 | | 10.820 | 17.880 | 2.54 | 2.52 | 3.91 |
| 0.004375 | 3.10 | 20.386 | 25.234 | 1.85 | 1.38 | 4.03 |
| 0.003500 | | 16.748 | 17.775 | 1.52 | $9.70\times10^{-4}$ | 4.20 |
| 0.002625 | | 14.723 | 12.290 | 1.34 | 6.71 | 3.74 |
| 0.001750 | | 10.920 | 6.759 | $9.92\times10^{-4}$ | 3.69 | 3.75 |
| 0.001313 | 9.9 | 26.930 | 13.206 | 7.66 | 2.26 | 3.85 |
| 0.000875 | | 19.310 | 7.281 | 5.50 | 1.24 | 4.10 |
| 0.0007644 | | 18.790 | 6.583 | 5.35 | 1.13 | 3.95 |
| 0.0004375 | 20.0 | 21.706 | 4.147 | 3.06 | $3.51\times10^{-5}$ | 3.75 |
| 0.0002625 | | 12.028 | 1.778 | 2.19 | 2.02 | 4.20 |
| 0.0001313 | | 6.351 | 0.587 | 1.29 | $6.65\times10^{-6}$ | 4.02 |
| | | | | | (average | 3.96) |

monomer and dimer, respectively, in chloroform. These assignments are consistent with those already reported.

In Fig. 1 plots of $\log_{10}(T_0/T)_\nu$ versus the frequency, $\nu$, are shown for the C=O stretching vibration bands of benzoic acid in carbon tetrachloride and chloroform. In this frequency region, benzoic acid does not show any absorption except for the two C=O stretching bands of the free and associated species, so one may regard the $g$ shown in the figure as the base line. The broken lines, a and b, show the position of the absorption maxima corresponding to the monomer and dimer forms. The area intensity, $S_m$, is taken to be twice the shaded area to the left of line a in Fig. 1; similarly, $S_d$ is taken to be twice the shaded area to the right of line b. This procedure was utilized because the two absorption bands overlapped in the region between lines a and b in Fig. 1. (Hereafter the suffixes m and d will be used to specify quantities concerning the monomer and dimer respectively). The shaded parts of the figure were then cut off and weighed. The area intensities thus obtained for a set of experiments are shown in Table

TABLE III. THE APPARENT INTEGRATED INTENSITIES OF THE CARBONYL STRETCHING BANDS OF THE BENZOIC ACID MONOMER AND DIMER (1. $mol.^{-1}$)

| | in $CCl_4$ | in $CHCl_3$ |
|---|---|---|
| $B_m\times10^{-4}$ | 1.44 | 3.55 |
| $B_d\times10^{-4}$ | 6.36 | 5.91 |

I for the carbon tetrachloride solution and in Table II for the chloroform solution.

To obtain the apparent integrated intensity, $B_m$ (or $B_d$), it is necessary to make an extrapolation of the ($S_m/lM$ or $2S_d/lM$) measured for a series of different concentrations to a zero (or finite) concentration, $M$ being the total concentration of benzoic acid in carbon tetrachloride and chloroform. A difficulty lies in the fact that these extrapolations are very sensitive to measurements of the area intensities at small concentrations, where the experimental errors in determining band areas are quite large. In fact, the approximate values of the extrapolated ($S_m/lM$) and ($2S_d/lM$) as obtained for the carbon tetrachloride solution, for example, range from 0.9 to $1.5\times10^4$ and from 5.8 to $6.5\times10^4$ $1.\,mol^{-1}\,cm^{-2}$ respectively. These uncertainties can not be eliminated by even the inclusion of more experimental data gathered at small concentrations.

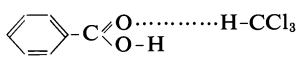
Therefore, it is advisable to determine the apparent integrated intensities, $B_m$ and $B_d$, by the method of least squares so as to satisfy the stoichiometrical relations:

$$S_m/lB_m + 2S_d/lB_d = M \qquad (4)$$

for a set of different concentrations. The values of $B_m$ and $B_d$ thus obtained are listed in Table III. With these values of $B_m$ and $B_d$ and with the observed area intensities listed in the third and fourth columns of Table I and Table II, the monomer and dimer concentrations of benzoic acid are calculated from Eq. 1 for a set of benzoic acid concentrations. The equilibrium constants, $K$, for the dimerization of benzoic acid are then obtained. The results are shown in the fifth, sixth, and the last columns of Tables I and II.

The equilibrium constants for both carbon tetrachloride and chloroform solutions are satisfactorily constant; the value as averaged over a set of benzoic acid concentrations is 2300 $1.\,mol^{-1}$ for the former and 400 $1.\,mol^{-1}$ for the latter. These values of $K$ seem to be more reliable than those obtained by Harris and Hobbs[2] or even by Barrow and Yerger,[7] who showed the concentration dependence of the equilibrium constant, in particular, at high dilutions. For instance, Barrow and Yerger gave, for the dimerization equilibrium of acetic acid in carbon tetrachloride, values between 1000 and 2650 $1.\,mol^{-1}$ for concentrations in the range from 0.17 mol. to 0.000112 mol. (Note that they treated not the integrated intensity but the optical density of the carbonyl stretching band maxima.) The values of the equilibrium constant obtained in the present paper are smaller than those previously reported by several authors; for example, Davies and Sutherland[1] gave the values of 13700 $1.\,mol^{-1}$ at 19.5°C and 220 $1.\,mol^{-1}$ at 76.5°C for the carbon tetrachloride solution, while Harris and Hobbs obtained a value of about 7000 $1.\,mol^{-1}$ at room temperature for the same solution.

The equilibrium constant in chloroform is smaller than that in carbon tetrachloride by a factor of about ten. This trend is parallel with the results obtained by Barrow and Yerger for acetic acid. As is shown in Fig. 1, the position of the carbonyl-stretching vibration band of the monomer in carbon tetrachloride is considerably different from that in chloroform. Moreover, the band width of the monomer band is broader in chloroform than in carbon tetrachloride, while the dimer bands have almost the same width in the two solvents. This agrees with the general observations that the position of a stretching vibration band of a hydrogen-bonded chromophore tends to shift to the lower frequency side and that the band width becomes broader than that of a free species. Therefore, one might expect a weak association in the chloroform solution. The values of the apparent integrated intensity give further support to this conclusion; as Table III shows, $B_d$ is about the same in magnitude in both solvents, while the $B_m$ in chloroform is larger than that in carbon tetrachloride by a factor of 2.5.



## Summary

The dimerization equilibrium of benzoic acid has been studied by high resolution infrared spectroscopy over a wide range of acid concentrations. The concentrations of the monomer and the dimer fractions have been determined from the integrated intensities of the respective carbonyl-stretching vibration bands. The calculated equilibrium constant is 2300 $1.\,mol^{-1}$ for carbon tetrachloride and 400 $1.\,mol^{-1}$ for chloroform, both values being considered more reliable than that determined by peak intensity measurements. A weak association of chloroform with benzoic acid has been suggested as occurring through hydrogen bonding to the monomer carbonyl.

*Laboratory of Physical Chemistry*
*The University of Electro-Communications*
*Chofu-shi, Tokyo* (*Y. I.*)

*Department of Chemistry*
*Tokyo University of Education*
*Otsuka, Tokyo* (*T. S.*)

# Syntheses of Peptides Related to the *N*-Terminal Structure of Corticotropin. V. Synthesis of the Peptide Fragments, His-Phe-Arg-Try, His-Phe-Arg-Try-Gly and Glu-His-Phe-Arg-Try-Gly

By Ken INOUYE

(Received November 11, 1964)

It has been shown in our previous communications that the tetrapeptide sequence His-Phe-Arg-Try, which occupies the positions 6 to 9 in the molecules of corticotropin and the $\alpha$-type of melanocyte-stimulating hormone ($\alpha$-MSH), provides an essential core for eliciting the MSH and the lipolytic activities with these hormones.[1] In connection with the synthesis of the tetrapeptide L-histidyl-L-phenylalanyl-L-arginyl-L-tryptophan (I), we have next achieved the synthesis of a pentapeptide L-histidyl-L-phenylalanyl-L-arginyl-L-tryptophyl-glycine (II) and a hexapeptide L-glutamyl-L-histidyl-L-phenylalanyl-L-arginyl-L-tryptophyl-glycine (III), which corresponds to the amino acid sequences of positions 6—10, and 5—10, respectively, of the corticotropin and $\alpha$-MSH molecules, together with a new synthesis of the tetrapeptide I, in order to try the comparative tests of the biological properties among these three peptides. An intermediate product to the hexapeptide III, namely $\gamma$-*t*-butyl-L-glutamyl-L-histidyl-L-phenylalanyl-L-arginyl-L-tryptophyl-glycine (XVII), is a key fragment for the synthesis of adrenocorticotropically active peptides.[2,3] The present synthesis has improved the procedure to obtain this key material.

The tetrapeptide and the pentapeptide were built up stepwise from their carboxyl terminal residues, where *t*-butyloxycarbonyl-nitro-L-arginine (IV) was utilized to incorporate the arginine residue and the *N*,*N'*-dicyclohexylcarbodiimide (DCCI) method[4] was employed except for the last coupling step. In the last step to introduce the histidine, a crystalline active ester $N^{\alpha}$, $N^{Im}$-dicarbobenzoxy-L-histidine *p*-nitrophenyl ester (V), gave excellent results. The protected hexapeptide was synthesized by coupling of the phenylalanyl tetrapeptide ester (X) with carbobenzoxy-$\gamma$-*t*-butyl-L-glutamyl-L-histidine azide which was derived from a new crystalline compound carbobenzoxy-$\gamma$-*t*-butyl-L-glutamyl-$N^{Im}$-carbobenzoxy-L-histidine methyl ester (XIII).

Figure 1 outlines the synthetic steps for the

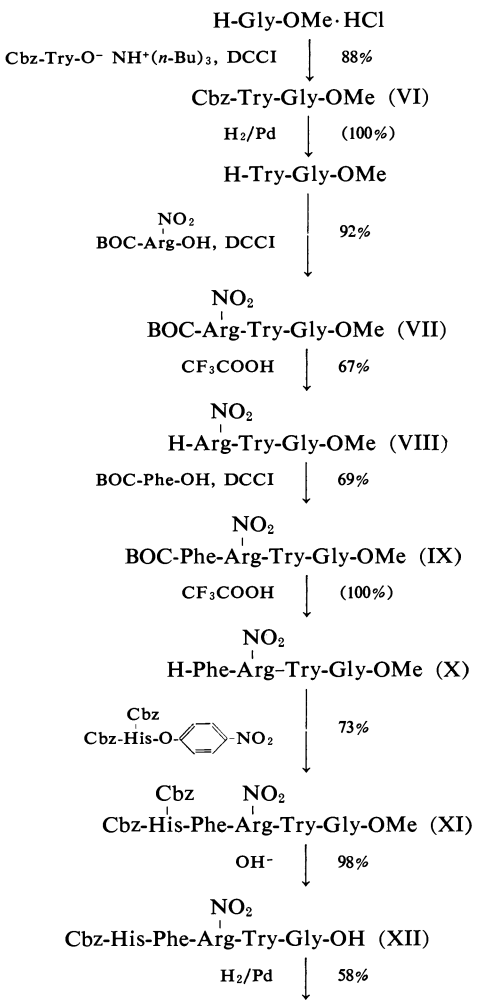



Fig. 1. Scheme for the synthesis of L-histidyl-L-phenylalanyl-L-arginyl-L-tryptophyl-glycine. Cbz, carbobenzoxy; BOC, *t*-butyloxycarbonyl; Me, methyl; Bu, butyl; DCCI, *N*,*N'*-dicyclohexylcarbodiimide

1) H. Otsuka and K. Inouye, This Bulletin, **37**, 289 (1964); **37**, 1465 (1964).
2) R. Schwyzer and H. Kappeler, *Helv. Chim. Acta*, **46**, 1550 (1963).
3) R. Geiger, K. Sturm and W. Siedel, *Chem. Ber.*, **97**, 1207 (1964).
4) J. C. Sheehan and G. P. Hess, *J. Am. Chem. Soc.*, **77**, 1067 (1955).

pentapeptide II. Carbobenzoxy-L-tryptophylglycine methyl ester (VI) was obtained in an excellent yield (88%) by coupling of the hydrochloride of glycine methyl ester with the soluble tri-*n*-butylamine salt of carbobenzoxy-L-tryptophan, which was formed in a methylene chloride solution. *t*-Butyloxycarbonyl-nitro-L-arginine (IV), which crystallized from an ethyl acetate solution, was found to combine a half mole of the solvent molecule. Compound IV was linked with the dipeptide ester, which was prepared from the hydrogenolysis product of compound VI, to obtain *t*-butyloxycarbonyl-nitro-L-arginyl-L-tryptophyl-glycine methyl ester (VII). Compound VII failed to crystallize, but it could easily be purified by reprecipitation from ethyl acetate. The trifluoroacetic acid treatment[5] of VII afforded the tripeptide trifluoroacetate (VIII). A small amount of a colored by-product, which gave an anomalous color reaction with the Ehrlich reagent and which ran a little faster than the desired product VIII on paper in the system of 1-butanol - acetic acid - water (4 : 1 : 2), was removed by simple extraction of the aqueous solution with ethyl acetate. The purified tripeptide ester was then condensed with *t*-butyloxycarbonyl-L-phenylalanine to obtain the crystalline protected tetrapeptide *t*-butyloxycarbonyl-L-phenylalanyl-nitro-L-arginyl-L-tryptophyl-glycine methyl ester (IX). The diacyl-L-histidine *p*-nitrophenyl ester V was prepared in the form of fine needles by two different methods. One of these was the ordinary DCCI method, by which $N^{\alpha}$,$N^{Im}$-dicarbobenzoxy-L-histidine[6] was condensed with *p*-nitrophenol in an excellent yield. Another procedure involved transesterification between the diacyl-L-histidine and *p*-nitrophenyl trifluoroacetate, which was very recently utilized by Sakakibara and Inukai for the preparation of carboxylic acid *p*-nirophenyl esters.[7] The latter method also gave the desired compound in a moderate yield, especially with high purity. This active ester was allowed to react in an acetonitrile solution with the phenylalanyl tetrapeptide ester (X), which was derived from the protected peptide IX by the trifluoroacetic acid treatment, affording in a yield of 72.3% the pentapeptide $N^{\alpha}$,$N^{Im}$-dicarbobenzoxy-L-histidy-L-phenylalanyl-nitro-L-arginyl-L-tryptophyl-glycine methyl ester (XI), which crystallized as the monohydrate upon treating with hot 90% methanol. Saponification of the methyl ester XI yielded carbobenzoxy-L-histidyl-L-phenylalanyl-nitro-L-arginyl-L-tryptophyl-glycine (XII), accompanied by splitting of the $N^{Im}$-carbobenzoxy group.

The procedure for synthesis of the hexapeptide III is shown in Fig. 2. Carbobenzoxy-$\gamma$-*t*-buty-L-glutamyl-$N^{Im}$-carbobenzoxy-L-histidine methyl ester (XIII) was synthesized by the coupling of carbobenzoxy-$\gamma$-*t*-butyl-L-glutamic acid[8] with $N^{Im}$-carbobenzoxy-L-histidine methyl ester, the preparation of which has already been described.[6] The yield amounted to 90 per cent after recrystallization. Hydrazinolysis in the next step brought about an immediate cleavage at the $N^{Im}$-carbobenzoxy bonding to result in the formation of benzyl carbazate which was isolated subsequent to the desired carbobenzoxy-$\gamma$-*t*-butyl-L-glutamyl-L-histidine hydrazide (XIV). Compound XIV

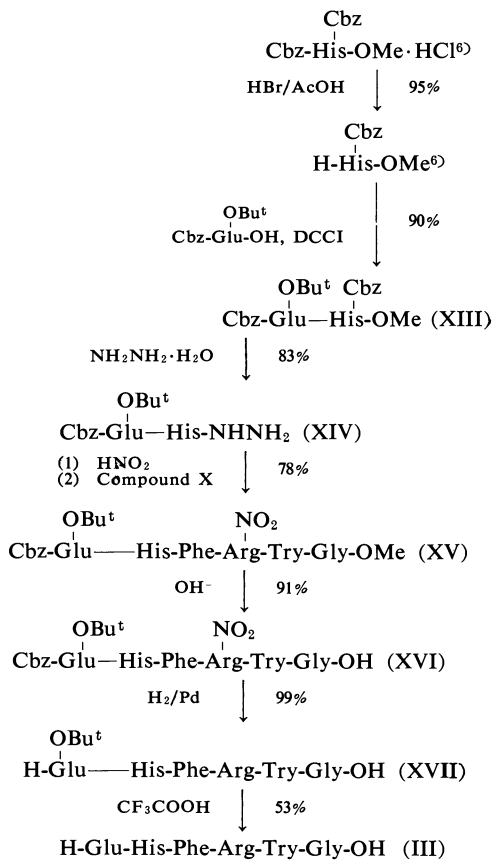



Fig. 2. Scheme for the synthesis of L-glutamyl-L-histidyl-L-phenylalanyl-L-arginyl-L-tryptophyl-glycine.
Cbz, carbobenzoxy; Me, methyl; Bu$^t$, *t*-butyl; DCCI, *N*, *N'*-dicyclohexylcarbodiimide

5) H. Kappeler and R. Schwyzer, *Helv. Chim. Acta*, **43**, 1453 (1960).
6) K. Inouye and H. Otsuka, *J. Org. Chem.*, **27**, 4236 (1962); **26**, 2613 (1961).
7) S. Sakakibara and N. Inukai, This Bulletin, **37**, 1231 (1964).
8) R. Schwyzer and H. Kappeler, *Helv. Chim. Acta*, **44**, 1991 (1961); H. Kappeler and R. Schwyzer, ibid., **44**, 1136 (1961).

was obtained in an 83 per cent yield as the monohydrate which melted first at 85—95°C, resolidified at 105—115°C and melted again at 144—146°C. The hydrazide XIV and the phenylalanyl tetrapeptide ester trifluoroacetate X (1.1 : 1.2 molar ratio) were converted into the corresponding azide and the free base, respectively, and these were allowed to react in an acetonitrile-ethyl acetate (2 : 5 by volume) mixture to obtain the protected hexapeptide carbobenzoxy-$\gamma$-*t*-butyl-L-glutamyl-L-histidyl-L-phenylalanyl-nitro-L-arginyl-L-tryptophyl-glycine methyl ester (XV) in an excellent yield (80%). The methyl ester of compound XV was preferentially saponified to give carbobenzoxy-$\gamma$-*t*-butyl-L-glutamyl-L-histidyl-L-phenylalanyl-nitro-L-arginyl-L-tryptophyl-glycine (XVI), which was purified by reprecipitation from dimethylformamide-methanol to remove the unreacted diester XV. The monoacid monoester XVI gave a single round spot ($R_f$=0.68) on silica gel in the system of dimethylformamide-ethyl acetate (1 : 1 by volume), whereas the diester XV had an $R_f$ value of 0.92 in the same solvent system.

Figure 3 summarizes the present synthesis of the tetrapeptide I, an outline of which has

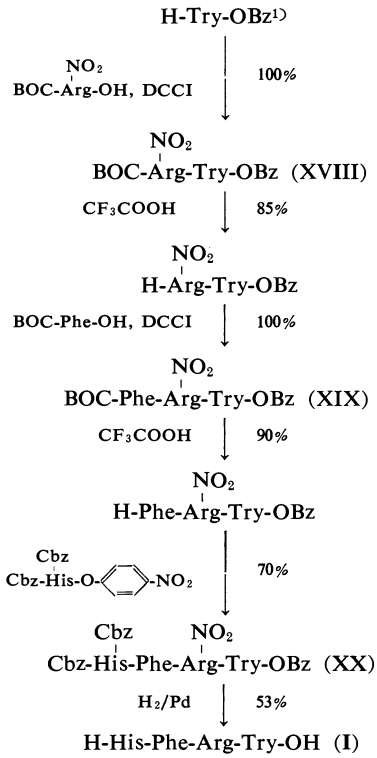



Fig. 3. Scheme for the synthesis of L-histidyl-L-phenylalanyl-L-arginyl-L-tryptophan.
Cbz, carbobenzoxy; BOC, *t*-butyloxycarbonyl, Bz, benzyl; DCCI, *N*, *N'*-dicyclohexylcarbodiimide.

already been cited in the previous paper dealing with the first synthesis of I.[1] The synthetic steps for each intermediate product are substantially identical with those employed in the course of the synthesis of compound XI. The carbodiimide coupling reactions afforded the protected dipeptide *t*-butyloxycarbonyl-nitro-L-arginyl-L-tryptophan benzyl ester (XVIII) and the tripeptide *t*-butyloxycarbonyl-L-phenylalanyl-nitro-L-arginyl-L-tryptophan benzyl ester (XIX) in quantitative yields; the occurrence of unfavorable side reactions seemed to be slight since they were not detectable by thin-layer chromatography on silica gel. Both of these products, however, resisted all attempts at crystallization. The protected tripeptide XIX was found to be contaminated with a small amount of an impurity which gave an anomalous yellow color reaction with the Ehrlich reagent and which had chromatographic behaviors very similar to the desired product. It appeared most likely that the impurity was derived from a side product which had formed through the trifluoroacetic acid treatment prior to the coupling reaction. Compound XIX was then used in the subsequent reaction without further purification. The reaction of $N^{\alpha}$ $N^{\mathrm{Im}}$-dicarbobenzoxy-L-histidine *p*-nitrophenyl ester (V) with the tripeptide ester, which was derived form XIX in the usual way, was carried out in an acetonitrile solution to obtain the protected tetrapeptide $N^{\alpha}$, $N^{\mathrm{Im}}$-dicarbobenzoxy-L-histidyl-L-phenylalanyl-nitro-L-arginyl-L-tryptophan benzyl ester (XX), the greater part of which separated in a pure form from the reaction medium. In contrast to the tosylated tetrapeptide derivative $N^{\alpha}$, $N^{\mathrm{Im}}$-dicarbobenzoxy-L-histidyl-L-phenylalanyl-$N^{\mathrm{G}}$-*tosyl*-L-arginyl-L-tryptophan benzyl ester,[1] which was freely soluble even in ethyl acetate, compound XX had very low solubilities in most of the ordinary solvents.

The carbobenzoxy, nitro, and benzyl ester groups were removed by subsequent catalytic hydrogenolysis to liberate the free tetrapeptide (I) and the free pentapeptide (II) from compounds XX and XII, respectively, and the partially protected hexapeptide (XVII) was obtained from compound XVI in the same way. The free hexapeptide (III) was obtained from XVII by the treatment with trifluoroacetic acid.

Each of these fully deblocked peptide preparations was purified on a carboxymethyl cellulose (CMC) column by means of step-by-step elution with ammonium acetate buffers, where it was found especially in case of the tetrapeptide that a clear-cut separation of the pure material by the CMC column chromatography could be easily performed when the crude sample had previously been purified by partitioning on a

Sephadex column with a solvent system such as 1-butanol - acetic acid - water (4 : 1 : 2 by volume). The results typical of the chromatographic experiments with the tetrapeptide are presented in Figs. 4 and 5. The purified peptides I, II and III gave in each case a single ninhydrin, Pauly, Ehrlich, and Sakaguchi reactive spot on paper chromatography in the different solvent systems and on paper electrophoresis at different pH values. These peptide preparations were also found to be completely digestible by leucine aminopeptidase to give the amino acids in molar ratios consistent with the theoretical values. The biological investigations of these synthetic peptides will be presented in a separate communication in the near future.

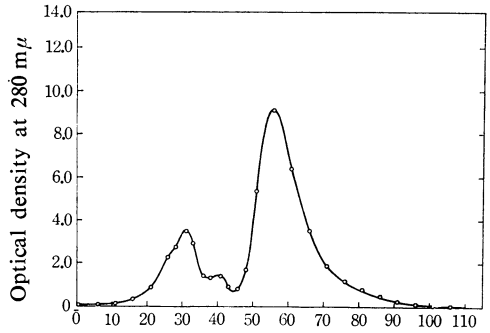



Fig. 4. Partition chromatography of crude L-histidyl-L-phenylalanyl-L-arginyl-L-tryptophan on a Sephadex G-25 column.
Material: Synthetic tetrapeptide, 0.350 g.
Column: Sephadex G-25 (coarse), 2.8×105 cm.
Solvent system: 1-Butanol - acetic acid - water (4 : 1 : 2 by vol.)
Flow rate: 0.8 ml./min.

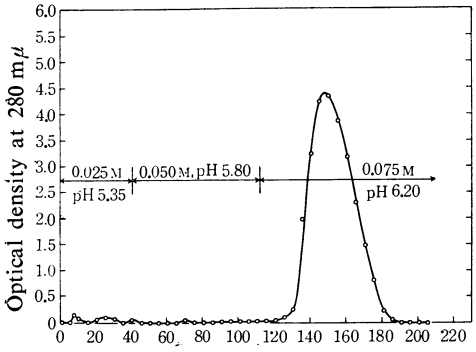



Fig. 5. Rechromatography of purified L-histidyl-L-phenylalanyl-L-arginyl-L-tryptophan on a carboxymethyl cellulose column.
Material: Synthetic tetrapeptide, 0.430 g.
Column: CM-cellulose (Serva, 0.44 meq./g.), 1.7×40 cm.
Buffer: Ammonium acetate
Flow rate: 2 ml./min.

## Experimental

All melting points were uncorrected.

***t*-Butyloxycarbonyl-nitro-L-arginine (IV).**—Nitro-L-arginine (32.9 g., 0.15 mol.) and 19.1 g. (0.18 mol.) of sodium carbonate were dissolved in 300 ml. of water at 60—70°C and dioxane (300 ml.) was introduced. To this solution was added - dropwise 25.8g. (0.18 mol.) of *t*-butyl azidoformate[9,10] at a bath temperature of 45°C and the mixture was stirred for 18 hr. at the same temperature. The reaction mixture was then cooled in an ice-bath and neutralized with 90.0 ml. of ice-cold 4 N hydrochloric acid (pH 4). After the fine precipitates of unreacted nitro-L-arginine had been removed by filtration (6.0 g., 0.028 mol.) the filtrate was concentrated to about 200 ml. at 40—45°C in vacuo. The concentrated solution was acidified to below pH 2 with ice-cold 4 N hydrochloric acid in the presence of ethyl acetate (300 ml.) at 0°C. The aqueous phase was extracted three times with 150 ml.-portions of cold ethyl acetate. The ethyl acetate extracts were pooled, dried over anhydrous sodium sulfate, and evaporated at 35°C in vacuo. The resultant sirupy residue crystallized upon treatment with 150 ml. of ethyl acetate. After storage in a refrigerator overnight the crystals were filtered off, washed with cold ethyl aetate and ether, and dried at room temperature in vacuo to give the product, which combined about a half mole of ethyl acetate; yield 30.20 g. (68.2% as calculated for 0.122 mol.), m. p. 98—102°C (resolidified at 165—166°C followed by decomposition at 237—238°C). A methanolic solution of the 0.50 g. sample was evaporated in vacuo and the sirupy residue was crystallized from ethyl acetate and air-dried to give a sample for analyses; m. p. 98—100°C, $[\alpha]_D^{25.5}$ +2.8±1° (*c* 2.296, methanol), $[\alpha]_D^{23.5}$ −3.0±1° (*c* 1.614, water), $[\alpha]_D^{23.5}$ −0.7±0.5° (*c* 1.597, acetic acid).

Found: C, 42.67; H, 7.03; N, 19.69; $CH_3CO$, 5.21. Calcd. for $C_{11}H_{21}N_5O_6 \cdot 1/2CH_3COOC_2H_5$: C, 42.97; H, 6.93; N, 19.27; $CH_3CO$, 5.92%.

A sample was treated with trifluoroacetic acid followed by neutralization with ammonia to give, in a 93% yield, nitro-L-arginine which had $[\alpha]_D^{25.5}$ +23.9±0.5° (*c* 4.031, 2 N hydrochloric acid); lit.[11] $[\alpha]_D^{25}$ +24.5° (*c* 4.12, 2 N hydrochloric acid).

***N*$^{\alpha}$, *N*$^{\mathrm{Im}}$-Dicarbobenzoxy - L - histidine *p* - Nitrophenyl Ester (V).**—*By the DCCI Method.*—*N*$^{\alpha}$, *N*$^{\mathrm{Im}}$-Dicarbobenzoxy-L-histidine[6] (12.70 g., 0.03 mol.) and 4.18 g. (0.03 mol.) of *p*-nitrophenol were dissolved in 60 ml. of warm ethyl acetate and to this mixture was added an ethyl acetate solution of 6.20 g. (0.03 mol.) of *N*, *N'*-dicyclohexylcarbodiimide (DCCI) at 0°C. The reaction mixture was then

9) L. A. Carpino, *J. Am. Chem. Soc.*, **79**, 98 (1957); L. A. Carpino, C. A. Giza and B. A. Carpino, ibid., **81**, 955 (1959).
10) K. Inouye, M. Kanayama and H. Otsuka, *J. Chem. Soc. Japan, Pure Chem. Sec.* (*Nippon Kagaku Zasshi*), **85**, 599 (1964).
11) K. Hofmann, W. D. Reckham and A. Rheiner, *J. Am. Chem. Soc.*, **78**, 238 (1956).

allowed to stand in a refrigerator overnight. After the separated *N,N'*-dicyclohexylurea had been removed (6.65 g., 98.8%), the filtrate was evaporated in vacuo to afford an amorphous solid mass. The solid residue was dissolved in 90 ml. of hot anhydrous ethanol and the solution was allowed to cool to separate the crystalline *p*-nitrophenyl ester. After storage in a refrigerator overnight the crystals were filtered off, washed with cold ethanol, and dried in vacuo; yield 13.68 g. (84.0%), m. p. 111—112.5°C. Recrystallization from anhydrous ethanol gave fine needles with m. p. 112—113°C, $[\alpha]_D^{24.5}$ −15.0±0.7° (*c* 3.097, ethyl acetate), $[\alpha]_D^{25}$ −13.8±1° (*c* 2.523, chloroform). Lit. amorphous, m. p. 86—90°C;[12] m. p. 109—110°C.[13]

Found: C, 62.04; H, 4.66; N, 10.02. Calcd. for $C_{28}H_{24}N_4O_8$: C, 61.76; H, 4.44; N, 10.29%.

*By the Use of Sakakibara's Reagent.*[7]—To a solution of 2.117 g. (5 mmol.) of $N^{\alpha}$, $N^{Im}$-dicarbobenzoxy-L-histidine[6] in 5 ml. of pyridine was added 1.176 g. (5 mmol.) of *p*-nitrophenyl trifluoroacetate[7] at 0°C, and the mixture was allowed to stand at room temperature for 30 min. Most of the solvent was removed in vacuo at a bath temperature of 40°C; the oily residue was then treated with 15 ml. of anhydrous ethanol. The Amorphous precipitates which formed crystallized slowly. After storage in a refrigerator overnight the crystals were filtered off, washed with anhydrous ethanol, and dried in vacuo; yield 1.904 g. (70.0%), m. p. 104—106°C. Recrystallization from anhydrous ethanol gave, in a recovery of 85%, a sample with a m. p. of 110—111°C; $[\alpha]_D^{24.5}$ −15.9±1° (*c* 2.018, ethyl acetate), $[\alpha]_D^{24.5}$ −13.3±1° (*c* 1.948, chloroform).

Found: C, 61.72; H, 4.55; N, 10.30. Calcd. for $C_{28}H_{24}N_4O_8$: C, 61.76; H, 4.44; N, 10.29%.

**Carbobenzoxy-L-tryptophyl-glycine Methyl Ester (VI).**—To a suspension of 4.06 g. (0.012 mol.) of carbobenzoxy-L-tryptophan in 40 ml. of methylene chloride was added 2.86 ml. (0.012 mol.) of tri-*n*-butylamine. The resultant clear solution was kept in an ice-bath and to this were added 1.51 g. (0.012 mol.) of glycine methyl ester hydrochloride and a methylene chloride solution of 2.48 g. (0.012 mol.) of DCCI with stirring. The reaction mixture was then allowed to stand at 0°C overnight.*1 The separated dicyclohexylurea was removed by filtration (2.55 g., 94.8%) and the filtrate was evaporated in vacuo to afford a foamy residue, which was redissolved in ethyl acetate. The solution was washed with ice-cold N hydrochloric acid, water, 5% sodium bicarbonate, and finally with water, and dried over anhydrous sodium sulfate. The crystalline precipitate, which separated during concentration of the ethyl acetate solution, was collected to give a yield of 4.69 g. (95.5%); m. p. 153—157°C. Recrystallization from ethyl acetate-ether gave, in a recovery of 92.5%, crystals with m. p. 156—158°C, $[\alpha]_D^{24}$ −12.1±0.7° (*c* 3.058, glacial acetic acid). Lit. m. p. 158—159°C, $[\alpha]_D^{27}$ −11.0° (*c* 2, glacial acetic acid);[14] m. p. 156—158°C, $[\alpha]_D^{22}$ −11.0±0.5° (*c* 3, glacial acetic acid).[15]

Found: C, 64.47; H, 5.84; N, 10.34. Calcd. for $C_{22}H_{23}N_3O_5$: C, 64.54; H, 5.66; N, 10.26%.

***t*-Butyloxycarbonyl-nitro-L-arginyl-L-tryptophyl-glycine Methyl Ester (VII).**—A suspension of 11.25 g. (0.0275 mol.) of compound VI in 180 ml. of methanol containing 3 ml. of acetic acid was hydrogenated over palladium black catalyst for 2.5 hr. After the catalyst had been removed by filtration the filtrate was evaporated in vacuo at 35°C. The resultant foamy residue was dissolved in 50 ml. of water and the aqueous solution was washed with 15 ml. portions of ethyl acetate. A mixture of this aqueous solution and 80 ml. of methylene chloride was shaken with 40 ml. of ice-cold 50% (w/v) potassium carbonate at 0°C. The aqueous phase was extracted again with methylene chloride. The organic extracts were combined, dried over anhydrous sodium sulfate and concentrated to about 60 ml. at 20°C in vacuo to give a solution of the dipeptide ester. To this was then added a solution of 9.32 g. (0.025 mol.) of compound IV in 25 ml. of dimethylformamide and a methylene chloride solution of 5.68 g. (0.0275 mol.) of DCCI at 0°C. The reaction mixture (total volume ca. 120 ml.) was kept in a refrigerator for 34 hr. The gelatinous precipitate which formed was collected by filtration and washed with cold methylene chloride; the mother liquor and washings were pooled. The precipitate was redissolved in 150 ml. of hot ethyl acetate and the solution was carefully filtered to remove the insoluble urea (5.32 g., 95.0%). The mother liquor was washed successively with ice-cold N hydrochloric acid, water, 5% sodium bicarbonate, and water. The gelatinous precipitate which separated during these washes was collected, washed with water and redissolved in 100 ml. of hot ethyl acetate, and this solution, after being dried quickly over anhydrous sodium sulfate, was combined with the ethyl acetate solution obtained above. The combined solution (total volume 300 ml.) was allowed to stand in a refrigerator overnight and the separated precipitate was filtered off, washed with cold ethyl acetate and with ether, and dried over phosphorus pentoxide at 60°C in vacuo to constant weight; yield 13.21 g. (91.7%), hygroscopic powder, m. p. 111—114°C. Thin-layer chromatography on silica gel in a solvent system of chloroform-methanol (85:15) gave a single round spot ($R_f$=0.7). A sample was reprecipitated from ethyl acetate, dried as above and stabilized in the air for analyses; m. p. 112—114°C, $[\alpha]_D^{24.5}$ −21.7±0.7° (*c* 3.022, methanol).

Found: C, 51.93; H, 6.68; N, 19.00. Calcd. for $C_{25}H_{36}N_8O_8 \cdot 1/2H_2O$: C, 51.27; H, 6.37; N, 19.14%.

**Nitro-L-arginyl-L-tryptophyl-glycine Methyl Ester Trifluoroacetate (VIII).**—To a solution of 7.22 g. of the anhydrous compound VII in 7 ml. of glacial acetic acid was added 40 ml. of anhydrous trifluoroacetic acid and the mixture was allowed to

12) F. Sakiyama, This Bulletin, **35**, 1943 (1962).
13) J. Meienhofer, *Chimia*, **16**, 385 (1962).
*1 At this stage the crystalline dipeptide often separated together with *N,N'*-dicyclohexylurea.
14) K. Hofmann, H. Yajima and E. T. Schwartz, *J. Am. Chem. Soc.*, **80**, 1486 (1958).
15) R. Geiger, K. Sturm and W. Siedel, *Chem. Ber.*, **96**, 1080 (1963).

stand under nitrogen at room temperature for 45 min., after which time 500 ml. of ether was introduced under ice-cooling. The resultant precipitate was collected by filtration, washed thoroughly with ether, and dried to give the crude tripeptide ester trifluoroacetate; yield 6.79 g. (92.0%). This crude preparation was dissolved in 80 ml. of water and the aqueous solution was washed three times with 20 ml. portions of ethyl acetate and then lyophilized, affording a pale yellow fluffy powder (4.93 g.) which gave a single ninhydrin and Ehrlich reactive spot on paper [$R_f$=0.74 (BAW)]*2; m. p. 122—126°C, $[\alpha]_D^{23.5}$ +16.1±1° (*c* 1.918, methanol).

Found: C, 44.13; H, 5.12; N, 18.78. Calcd. for $C_{20}H_{28}N_8O_6 \cdot CF_3COOH$: C, 44.75; H, 4.95; N, 18.98%.

The ethyl acetate washings were combined and evaporated in vacuo to afford a light brown solid, which gave a minor spot ($R_f$=0.85) in addition to a major one ($R_f$=0.74) on paper in the same solvent system as above. The minor component was positive to ninhydrin but it gave an anomalous bluish color reaction with the Ehrlich reagent.

***t*-Butyloxycarbonyl-L-phenylalanyl-nitro-L-arginyl-L-tryptophyl-glycine Methyl Ester (IX).**—A solution of 5.02 g. (8.5 mmol.) of compound VIII in 10 ml. of water was mixed with 8 ml. of 1-butanol and 40 ml. of ethyl acetate. The mixture was shaken with 20 ml. of ice-cold 50% (w/v) potassium carbonate at 0°C. The aqueous phase was extracted again with 1-butanol-ethyl acetate (1:5). The organic extracts were combined, dried over anhydrous sodium sulfate, and evaporated in vacuo. The oily residue was triturated with ether and the resulting white solid was dried over sodium hydroxide pellets in vacuo. The tripeptide ester so obtained was dissolved in acetonitrile together with *t*-butyloxycarbonyl-L-phenylalanine (prepared from 3.795 g. (8.5 mmol.) of the dicyclohexylamine salt)[1] and to this solution was added an acetonitrile solution of 1.75 g. (8.5 mmol.) of DCCI at 0°C. The reaction mixture (total volume ca. 50 ml.) was kept in a refrigerator overnight. The urea which formed was removed (1.73 g., 91.2%) and the solution was evaporated in vacuo. The residue was redissolved in 60 ml. of ethyl acetate and the solution was washed successively with ice-cold N hydrochloric acid, water, M sodium bicarbonate, and water, dried briefly over anhydrous sodium sulfate, and then allowed to stand in a refrigerator overnight. The gelatinous precipitate was filtered off, washed with cold ethyl acetate and ether, and dried in vacuo to afford 5.28 g. (85.9%) of the tetrapeptide, which crystallized readily from hot acetonitrile. Recrystallization from acetonitrile was repeated twice to give colorless needles in a recovery of 80%; m. p. 172—173°C, $[\alpha]_D^{25}$ −20.1±1° (*c* 2.054, methanol).

Found: C, 56.24; H, 6.57; N, 17.35. Calcd. for $C_{34}H_{45}N_9O_9$: C, 56.42; H, 6.27; N, 17.42%.

**L-Phenylalanyl-nitro-L-arginyl-L-tryptophyl-glycine Methyl Ester Trifluoroacetate (X).**—To a solution of 1.810 g. of IX in 2 ml. of acetic acid was added 8 ml. of anhydrous trifluoroacetic acid at 0°C and the mixture was kept under nitrogen at room temperature for 45 min., after which time 100 ml. of ether was introduced. The resultant precipitate was filtered off, washed thoroughly with ether, and dried in vacuo to give the tetrapeptide trifluoroacetate as a slightly cream-colored powder; yield 1.765 g. (96.0%). An aqueous solution of a small amount of this crude material was twice washed with ethyl acetate and then lyophilized to give an almost colorless fluffy powder; $[\alpha]_D^{27}$ −1.5 ±1° (*c* 1.384, methanol).

Found: C, 49.27; H, 5.34; N, 16.68. Calcd. for $C_{29}H_{37}N_9O_7 \cdot CF_3COOH \cdot H_2O$: C, 49.79; H, 5.52; N, 16.50%.

***N*$^{\alpha}$, *N*$^{\mathrm{Im}}$-Dicarbobenzoxy-L-histidyl-L-phenylalanyl-nitro-L-arginyl-L-tryptophyl-glycine Methyl Ester (XI).**—A 1.476 g. sample (2.0 mmol.) of the crude trifluoroacetate X obtained just above was dissolved in 4 ml. of 1-butanol and 20 ml. of ethyl acetate, and this solution was shaken vigorously with 5 ml. of ice-cold 50% (w/v) potassium carbonate at 0°C. The separated organic phase was dried over anhydrous sodium sulfate and evaporated in vacuo at 30°C. The oily residue, which solidified upon addition of ether, was dried in vacuo. The ensuing free ester was dissolved in acetonitrile and this was mixed with an acetonitrile solution of 1.090 g. (2.0 mmol.) of *N*$^{\alpha}$, *N*$^{\mathrm{Im}}$-dicarbobenzoxy-L-histidine *p*-nitrophenyl ester (V). The reaction mixture (total volume 22 ml.) was kept in a refrigerator for 56 hr. The precipitate, which had separated during the storage, was filtered off, washed with cold acetonitrile and ether, and dried in vacuo; wt. 0.800 g., m. p. 145—147C (decomp.) (sintering at 131°C). The filtrate and washings were combined and evaporated in vacuo to give a foamy residue, which was dissolved in ethyl acetate and washed with 12 ml. portions of ice-cold N ammonia (4 times). The precipitate, which separated during these washes, was collected, washed with ethyl acetate and water, and dried over phosphorus pentoxide in vacuo; wt. 0.960 g., m. p. 145—146°C decomp. (sintering at 132°C). Total yield amounted to 1.760 g. (85.9%). A suspension of the product (1.760 g.) in 15 ml. of acetone was stirred for several minutes at the boiling point of the solvent and then refrigerated overnight. The precipitate was treated again with hot acetone to obtain the pure pentapeptide; wt. 1.487 g. (recovery 84.5%), m. p. 157—159°C (decomp.) (sintering at 150°C), $[\alpha]_D^{25.5}$ −22.7±0.5° (*c* 3.179, dimethylformamide).

Found: C, 59.25; H, 5.75; N, 16.20. Calcd. for $C_{51}H_{56}N_{12}O_{12}$: C, 59.52; H, 5.49; N, 16.33%.

An additional treatment with hot 90% methanol caused the compound to crystallize as the monohydrate; recovery 97%, m. p. 158—159°C (decomp.) (sintering at 136°C), $[\alpha]_D^{25.5}$ −21.5±0.5° (*c* 2.429, dimethylformamide).

Found: C, 58.27; H, 6.06; N, 16.00. Calcd. for $C_{51}H_{56}N_{12}O_{12} \cdot H_2O$: C, 58.50; H, 5.58; N, 16.05%.

**Carbobenzoxy-L-histidyl-L-phenylalanyl-nitro-L-arginyl-L-tryptophyl-glycine (XII).**—To a suspension of 0.515 g. (0.5 mmol.) of compound XI in 6 ml. of 90% dioxane was added 1.5 ml. of N sodium

*2 Abbreviation for the solvent systems employed in paper chromatography is as follows: BAW=1-butanol-acetic acid-water (4:1:2 by vol.). BAPW=1-butanol-acetic acid-pyridine-water (30:6:20:24 by vol.).

hydroxide and the mixture was shaken at room temperature for 30 min., after which time ice-cold water (25 ml.) was introduced and the resultant solution was neutralized (pH 4) with 1.5 ml. of N hydrochloric acid. The gelatinous precipitate was filtered off, washed with water, and then reprecipitated from hot acetic acid - water; yield 0.453 g. (98.0%), m. p. 212—213°C (decomp.). A sample for analyses was reprecipitated again from acetic acid - water, dried over phosphorus pentoxide at 80°C and 2—3 mmHg pressure for several hours, and then equilibrated in the air overnight; m. p. 222—227°C (decomp.), $[\alpha]_D^{25.5}$ $-26.0\pm2°$ (*c* 1.065, dimethylformamide). Lit. m. p. 246—249°C, $[\alpha]_D^{26}$ $-29.2°$ (*c* 1.2, dimethylformamide);[16] m. p. 226—228°C (decomp.), $[\alpha]_D^{22}$ $-26.8\pm0.5°$ (*c* 3, dimethylformamide).[15]

Found: C, 54.79; H, 5.71; N, 18.75; $H_2O$, 4.60; $CH_3CO$, 0.00. Calcd. for $C_{42}H_{48}N_{12}O_{10}\cdot2.5H_2O$: C, 54.48; H, 5.77; N, 18.15; $H_2O$, 4.86; $CH_3CO$, 0.00%.

**Carbobenzoxy-γ-*t*-butyl-L-glutamyl-$N^{1m}$-carbobenzoxy-L-histidine Methyl Ester (XIII).**—To a solution of 4.74 g. (0.01 mol.) of $N^{\alpha}$, $N^{1m}$-dicarbobenzoxy-L-histidine methyl ester hydrochloride[6,17] in 10 ml. of glacial acetic acid was added 30 ml. of 33% (w/w) hydrogen bromide in acetic acid and the mixture was kept at room temperature for 15 min. with occasional shaking. At the end of this period anhydrous ether (200 ml.) was introduced and the resultant precipitate was filtered off, washed with methylene chloride and with ether, and dried in vacuo to give the dihydrobromide of $N^{1m}$-carbobenzoxy-L-histidine methyl ester;[6] wt. 4.40 g. (94.7%). To an aqueous solution of this product in 30 ml. of water were added 60 ml. of methylene chloride and 4 ml. of ice-cold 28% aqueous ammonia, and the mixture was shaken vigorously at 0°C. The aqueous phase was extracted again with cold methylene chloride. The organic extracts were pooled, dried over anhydrous sodium sulfate at 0°C and evaporated in vacuo at a bath temperature of 25°C. The resultant sirupy residue was dissolved in methylene chloride together with carbobenzoxy-γ-*t*-butyl-L-glutamic acid (prepared from 4.15 g. (0.008 mol.) of the dicyclohexylamine salt by treatment with Dowex-50)[8] and to this was added a methylene chloride solution of 1.65 g. (0.008 mol.) of DCCI at 0°C. The reaction mixture was then allowed to stand in a refrigerator overnight. After removal of the separated urea (1.73 g., 96.6%) the solvent was evaporated in vacuo. The sirupy residue was dissolved in ethyl acetate and the solution was washed successively with ice-cold N hydrochloric acid, water, ice-cold 5% sodium bicarbonate, and with water, dried over anhydrous sodium sulfate, and evaporated to afford a sirupy residue, which crystallized from ethyl acetate - petroleum ether; yield 4.57 g. (91.8%), m. p. 100—102°C. Recrystallization from the same solvent gave 4.48 g. (90.0%); m. p. 101—102°C, $[\alpha]_D^{24}$ $-6.1\pm1°$ (*c* 2.475, methanol).

Found: C, 61.87; H, 6.30; N, 9.38. Calcd. for $C_{32}H_{38}N_4O_9$: C, 61.75; H, 6.15; N, 9.00%.

**Carbobenzoxy-γ-*t*-butyl-L-glutamyl-L-histidine Hydrazide (XIV).**—Compound XIII (12.45 g., 0.02 mol.) was suspended in 60 ml. of anhydrous ethanol and to this was added 6.0 ml. of hydrazine hydrate at 0°C. The reaction mixture was stirred at 0°C until the solid disappeared within several minutes. After the mixture had been allowed to stand in a refrigerator for 68 hr., water (240 ml.) was introduced. The ensuing sirupy precipitate soon crystallized and the crystals were filtered off, washed with cold water and dried; wt. 8.51 g. Concentration of the mother liquor gave an additional 0.735 g. of crystals; total yield amounted to 9.245 g. (91.3%). These crystals were recrystallized from ethanol-water (1 : 4) to give a yield of 8.425 g. (83.2%). The pure sample melted first at 85—95°C, resolidified at 105—115°C, and melted again at 144—146°C, $[\alpha]_D^{23}$ $-41.0\pm1°$ (*c* 2.075, N hydrochloric acid). Lit.[8] m. p. 140—142°C (sintering at 75°C), $[\alpha]_D^{26}$ $-40.5\pm0.5°$ (*c* 1.91, N hydrochloric acid).

Found: C, 54.40; H, 6.98; N, 16.71. Calcd. for $C_{23}H_{32}N_6O_6\cdot H_2O$: C, 54.53; H, 6.77; N, 16.59%.

Refrigeration of the mother liquor, from which the second crop of the compound XIV had been separated, afforded thin needles of *benzyl carbazate*; wt. 1.40 g., m. p. 62—66°C.

Found: C, 57.71; H, 6.21; N, 16.95. Calcd. for $C_8H_{10}N_2O_2$: C, 57.82; H, 6.07; N, 16.86%.

**Carbobenzoxy-γ-*t*-butyl-L-glutamyl-L-histidyl-L-phenylalanyl-nitro-L-arginyl-L-tryptophyl-glycine Methyl Ester (XV).**—To a solution of 5.57 g. (0.011 mol.) of the hydrazide XIV in ca. 10 ml. of dimethylformamide, which had been previously cooled in an ice-salt bath, were added 45 ml. of ice-cold N hydrochloric acid and 6.05 ml. (0.012 mol.) of ice-cold 2 M sodium nitrite, and the mixture was stirred for 4 min., after which time 45 ml. of ice-cold M sodium carbonate and 30 ml. of ice-cold saturated sodium chloride were added. The ensuing precipitate of the azide was taken up into ice-cold ethyl acetate. The ethyl acetate extracts were pooled, dried over anhydrous sodium sulfate, and mixed with a solution of L-phenylalanyl-nitro-L-arginyl-L-tryptophyl-glycine methyl ester (prepared from 8.87 g. (0.012 mol.) of the tritfluoroacetate X in the same manner as described in the synthesis of XI) in 95ml. of acetonitrile. The reaction mixture (total volume 350 ml.) was then kept at 0—4°C for 48 hr. The gelatinous precipitate, which formed, was filtered off, washed with ethyl acetate and with ether, and dried; yeild 9.52 g. (80.1%), m. p. 183—186°C (sintering at 173°C). The crude product (9.42 g.) was suspended in 110 ml. of acetonitrile and this was stirred for several minutes at the boiling point of the solvent to afford a homogeneous mixture, which was allowed to stand in a refrigerator overnight. The precipitate was filtered off, washed with acetonitrile and with ether, and dried to give the pure hexapeptide derivative; wt. 9.21 g. (recovery 97.8%), $R_f$=0.92 in thin-layer chromatography on silica gel in the system of dimethylformamide - ethyl acetate (1 : 1 by vol.), m. p. 185—186°C (sintering at 180°C), $[\alpha]_D^{27.5}$ $-33.0\pm1°$ (*c* 1.999, dimethyl-

16) K. Hofmann and S. Lande, *J. Am. Chem. Soc.*, **83**, 2286 (1961).
17) A. Patchornik, A. Berger and E. Katchalski, ibid., **79**, 6416 (1957).

formamide), $[\alpha]_D^{27.5}$ $-33.1\pm4°$ (*c* 0.592, methanol). Lit.[8] m. p. 176—178°C (sintering at 170°C), $[\alpha]_D$ $-30.9\pm0.5°$ (*c* 2.01, methanol).

Found: C, 56.83; H, 6.24; N, 16.83. Calcd. for $C_{52}H_{65}N_{13}O_{13}\cdot H_2O$: C, 56.87; H, 6.15; N, 16.58%.

**Carbobenzoxy-γ-*t*-butyl-L-glutamyl-L-histidyl-L-phenylalanyl-nitro-L-arginyl-L-tryptophyl-glycine (XVI).**—Compound XV (3.85 g., 3.5 mmol.) was dissolved in 50 ml. of 75% dioxane and to this was added 4.0 ml. of N sodium hydroxide. The mxiture was shaken at room temperature for 30 min., after which time ice-cold water (300 ml.) was introduced. The solution was then neutralized with 4.15 ml. of N hydrochloric acid to separate the desired product as a gelatinous precipitate. After refrigeration for a few hours the precipitate was filtered off, washed with water and dried to give 3.76 g. (99.2%), m. p. 215—216.5°C (decomp). (sintering at 190°C). The precipitate was reprecipitated from 15 ml. of dimethylformamide and 105 ml. of methanol; yield 3.44 g. (90.8%), m. p. 217—218°C (decomp.). A small sample was reprecipitated from a large volume of 90% methanol resulting in partial crystallization as needles; $R_f$= 0.68 in thin-layer chromatography on silica gel in the system of dimethylformamide-ethyl acetate (1 : 1 by vol.), m. p. 217°C (decomp.), $[\alpha]_D^{26.5}$ $-26.8\pm1°$ (*c* 2.141, dimethylformamide), lit.[8] m. p. 210°C, $[\alpha]_D$ $-22.2\pm1°$ (*c* 1.056, dimethylformamide).

Found: C, 56.12; H, 6.46; N, 16.46; $H_2O$, 2.89. Calcd. for $C_{51}H_{63}N_{13}O_{13}\cdot1.5H_2O$: C, 56.03; H, 6.09; N, 16.66; $H_2O$, 2.47%.

**γ-*t*-Butyl-L-glutamyl-L-histidyl-L-phenylalanyl-L-arginyl-L-tryptophyl-glycine Monoacetate (XVII).**—A solution of 1.084 g. (1.0 mmol.) of XVI in 40 ml. of 90% acetic acid was stirred under hydrogen in the presence of palladium-black catalyst for 17 hr. Fresh catalyst was added after 6 hr. of hydrogenolysis. The catalyst was removed from the clear solution which was then evaporated at a bath temperature of 40—45°C, and the resultant oily residue was dissolved in a small volume of methanol. The peptide was precipitated by the addition of ether, lyophilized, and dried over phosphorus pentoxide and sodium hydroxide pellets at room temperature in vacuo; yield 0.977 g. (99.4%). A sample for analyses was dried over phosphorus pentoxide at 60°C and 2—3 mmHg pressure for 8 hr. and then equilibrated in the air overnight. Paper chromatography: $R_f$=0.60 (BAPW); 0.375 (BAPW) after the trifluoroacetic acid treatment. $[\alpha]_D^{27}$ $-10.3\pm4°$ (*c* 0.624, dimethylformamide); lit.[15] $[\alpha]_D^{20}$ $-13.5\pm1°$ (*c* 1, dimethylformamide).

Found: C, 54.26; H, 7.30; N, 17.13; $CH_3CO$, 4.16. Calcd. for $C_{43}H_{58}N_{12}O_9\cdot CH_3COOH\cdot2.5H_2O$: C, 54.48; H, 6.81; N, 16.94; $CH_3CO$, 4.34%.

***t*-Butyloxycarbonyl-nitro-L-arginyl-L-tryptophan Benzyl Ester (XVIII).**—A 4.00 g. sample (0.011 mol.) of *t*-butyloxycarbonyl-nitro-L-arginine (IV) was dissolved in 30 ml. of hot acetonitrile and the solution was cooled in an ice-bath. To this were added 3.24 g. (0.011 mol.) of L-tryptophan benzyl ester[1] and an acetonitrile solution of 2.27 g. (0.011 mol.) of DCCI, and the mixture was kept in a refrigerator overnight. The urea which formed was removed by filtration (2.28 g., 92.7%) and the filtrate was evaporated in vacuo. The resultant foamy residue was dissolved in ethyl acetate and this was washed successively with ice-cold N hydrochloric acid, water, M sodium bicarbonate and water, dried over anhydrous sodium sulfate and evaporated in vacuo. The residue was redissolved in a small volume of acetonitrile and a small amount of urea, which separated upon chilling, was filtered off. Evaporation of the solvent gave a foamy residue, which was dried over phosphorus pentoxide in vacuo to give an amorphous powder; yield 6.77 g. (100%), homogeneous to the Ehrlich reagent in thin-layer chromatography on silica gel in ethyl acetate, $[\alpha]_D^{22}$ $-4.2\pm1°$ (*c* 2.565, methanol).

Found: C, 59.16; H, 6.61; N, 15.61. Calcd. for $C_{29}H_{37}N_7O_7$: C, 58.48; H, 6.26; N, 16.46%.

The above analysis suggests that the product is contaminated with a small amount of urea, but it was utilized in the subsequent reaction without further purifiaction.

***t*-Butyloxycarbonyl-L-phenylalanyl-nitro-L-arginyl-L-tryptophan Benzyl Ester (XIX).**—Compound XVIII (4.47 g., 7.5 mmol.) was dissolved in 4 ml. of acetic acid and to this solution was added 25 g. of anhydrous trifluoroacetic acid. The mixture was allowed to stand at room temperature for 60 min. under dry nitrogen. The dipeptide ester trifluoroacetate was then precipitated by the addition of 200 ml. of ether. The precipitate was filtered off, washed with cold methylene chloride and ether, and dried in vacuo; wt. 3.89 g. (85.2%), $[\alpha]_D^{25}$ $+11.6\pm1.5°$ (*c* 1.409, methanol).

Found: N, 15.91. Calcd. for $C_{24}H_{29}N_7O_5\cdot CF_3COOH$: N, 16.09%.

A solution of 3.74 g. (6.14 mmol.) of the trifluoroacetate in 50 ml. of 1-butanol-methylene chloride (1 : 3 by vol.) was cooled in an ice-bath and shaken with 10 ml. of 50% (w/v) potassium carbonate. The organic phase was dried over sodium sulfate and evaporated in vacuo to afford a sirupy residue, which was triturated and washed thoroughly with ether, and then dried in vacuo to give nitro-L-arginyl-L-tryptophan benzyl ester (3.19 g.). This free ester was then dissolved in 20 ml. of acetonitrile containing *t*-butyloxycarbonyl-L-phenylalanine (prepared from 2.90 g. (6.5 mmol.) of the dicyclohexylamine salt)[1] and to this was added an acetonitrile solution of 1.34 g. (6.5 mmol.) of DCCI at 0°C. The reaction mixture was allowed to stand in a refrigerator overnight. The dicyclohexylurea, which formed, was removed by filtration (1.34 g., 92.1%) and the filtrate was evaporated in vacuo to give an amorphous solid residue; the subsequent treatment was carried out in the same manner as for XVIII. Yield 4.78 g. (100%), $[\alpha]_D^{25}$ $-11.8\pm1°$ (*c* 2.272, methanol). Thin-layer chromatography on silica gel in ethyl acetate revealed the presence of a small amount of an impurity which moved ahead of and overlapped the desired tripeptide, and which gave a yellow color reaction with the Ehrlich reagent.

Found: C, 62.06; H, 6.73; N, 14.11. Calcd. for $C_{38}H_{46}N_8O_8$: C, 61.44; H, 6.24; N, 15.09%.

**$N^{\alpha}$, $N^{Im}$-Dicarbobenzoxy-L-histidyl-L-phenylalanyl-nitro-L-arginyl-L-tryptophan Benzyl Ester**

(**XX**).—To a solution of 1.860 g. (2.5 mmol.) of XIX in 2 ml. of acetic acid was added 8 ml. of anhydrous trifluoroacetic acid and the mixture was allowed to stand at room temperature for 45 min. under nitrogen. To this was then added 80 ml. of ether with ice-cooling; the resultant precipitate was collected, washed thoroughly with ether, and dried in vacuo to give 1.695 g. (89.8%) of the tripeptide ester trifluoroacetate. A suspension of the trifluoroacetate (1.695 g., 2.24 mmol.) in 20 ml. of ethyl acetate was shaken with 5 ml. of ice-cold 50% (w/v) potassium carbonate at 0°C. The organic phase was separated, dried over sodium sulfate and evaporated in vacuo. The resultant foamy residue was dissolved in 10 ml. of acetonitrile and this solution was combined with a solution of 1.220 g. (2.24 mmol.) of $N^{\alpha}$, $N^{\mathrm{Im}}$-dicarbobenzoxy-L-histidine *p*-nitrophenyl ester (V) in 15 ml. of acetonitrile and the mixture was then kept in a refrigerator for 44 hr. The precipitate which formed was filtered off, washed with cold ethyl acetate and with ether, and dried in vacuo; wt. 1.244 g. Evaporation of the filtrate gave a foamy residue, which was washed in an ethyl acetate solution with 12 ml. portions of ice-cold N ammonia (6 times), ice-cold N hydrochloric acid and with water, dried quickly over anhydrous sodium sulfate, and concentrated to about 15 ml. in vacuo. The precipitate, which separated during storage in a refrigerator, was collected and amounted to 0.699 g.; total yield 1.943 g. (82.7%), m. p. 161—163°C (decomp.). A suspension of the product in 20 ml. of ethyl acetate was stirred for several minutes at the boiling point of the solvent and then kept in a refrigerator overnight. The precipitates (1.686 g., m. p. 164—165°C (decomp.)) were treated again with hot ethyl acetate to afford the pure protected tetrapeptide; wt. 1.650 g. (recovery 85.0%), m. p. 167—168°C (decomp.), $[\alpha]_{\mathrm{D}}^{24\cdot5}$ $-12.3\pm1°$ (*c* 2.080, dimethylformamide).

Found: C, 63.25; H, 5.59; N, 14.78. Calcd. for $C_{55}H_{57}N_{11}O_{11}$: C, 63.03; H, 5.48; N, 14.70%.

**L-Histidyl-L-phenylalanyl-L-arginyl-L-tryptophan Monoacetate (I).**—The protected tetrapeptide XX (0.500 g.) was dissolved in 20 ml. of 90% acetic acid and the solution was stirred under hydrogen in the presence of palladium black for 18 hr. After the catalyst had been removed the solvent was evaporated at a bath temperature of 45°C and the residue was lyophilized twice to give 0.375 g. of fluffy powder. This crude tetrapeptide (0.350 g.) was dissolved in 5 ml. of a mixture 1-butanol - acetic acid - water (4 : 1 : 2 by vol.) and the solution was applied onto a column (2.8×105 cm.) of Sephadex G-25 (coarse, dry wt. 180 g.), which had been equilibrated with the BAW mixture. The column was then eluted with the same solvent system at a flow rate of 0.8 ml. per min.; 10 ml. fractions were collected. The chromatogram is shown in Fig. 4. The fractions in Tubes No. 51—95 were pooled and evaporated at 50°C in vacuo. The residue was then lyophilized twice to afford 0.430 g. (recovery 57% as calculated from the absorbance at 280 mμ) of fluffy powder. This purified peptide was next submitted to ion-exchange chromatography for further purification. The partially purified material (0.43 g.) was dissolved in 10 ml. of 0.025 M ammonium acetate (pH 5.35) and the solution was applied onto a column (1.7×40 cm.) of carboxymethyl cellulose (Serva, 0.44 meq./g.) which had been equilibrated with the same buffer solution. The column was then eluted successively with the following ammonium actate buffers: 0.025 M (pH 5.35), 400 ml.; 0.050 M (pH 5.80), 700 ml. (0.075 M (pH 6.20), 1000 ml. Individual fractions (10 ml. each) were collected at a flow rate of approximately 2 ml. per min. The chromatographic pattern is illustrated in Fig. 5. The fractions in Tubes No. 131—185 corresponding to the major peak were pooled and the bulk of water was removed at 50—55°C using a rotatory evaporator. The rest was then lyophilized three times affording a colorless fluffy powder; yield 0.188 g. (53% as based on XX used). The purified peptide behaved as a single ninhydrin, Pauly, Ehrlich, and Sakaguchi reactive spot in paper chromatography [$R_f$=0.48 (BAW), 0.49 (BAPW)], and in paper electrophoresis at pH 3.8, 6.6 and 11.1. A sample for analyses was dried over phosphorus pentoxide at 60°C and 2—3 mmHg pressure for 8 hr. and then equilibrated in the air overnight. $\lambda_{max}^{0.1\mathrm{N\ HCl}}$=280 mμ (ε=5450), 288 mμ (ε=4600); $\lambda_{max}^{0.1\mathrm{N\ NaOH}}$=280 mμ (ε=5500), 288 mμ (ε=4700). $[\alpha]_{\mathrm{D}}^{25}$ $-7.8\pm1.5°$ (*c* 1.484, N hydrochloric acid).*3 Amino acid ratios in acid hydrolyzate: His 1.00, Phe 0.91, Arg 0.95, Try 0.71 (decomposed partially with acid); amino acid ratios in leucine aminopeptidase*4 digest: His 1.00, Phe 0.94, Arg 0.94, Try 0.95.[18]

Found: C, 52.30; H, 6.56; N, 18.46. Calcd. for $C_{32}H_{40}N_{10}O_5\cdot CH_3COOH\cdot 4H_2O$: C, 52.57; H, 6.75; N, 18.03%.

**L-Histidyl-L-phenylalanyl-L-arginyl-L-tryptophylglycine Monoacetate (II).**—A suspension of 0.250 g. of XII in 20 ml. of 90% acetic acid was stirred under hydrogen in the presence of palladium-black catalyst for 14 hr. The catalyst was removed by filtration and the filtrate was evaporated at a bath temperature of 40—45°C in vacuo. The resultant oily residue was lyophilized and dried over phosphorus pentoxide and sodium hydroxide pellets affording 0.220 g. of fluffy powder. This crude pentapeptide was dissolved in 25 ml. of 0.025 M ammonium acetate (pH 5.35) and the solution was aplied to a column (1.2×50 cm.) of carboxymethyl cellulose (Serva, 0.6 meq./g.) which had been equilibrated with the same buffer solution. The column was then eluted successively with the following ammonium acetate buffers: 0.025 M (pH 5.35), 300 ml.: 0.05 M (pH 5.80), 600 ml.; 0.075 M (pH 6.20), 1600 ml. Individual fractions (10 ml. each) were collected at a flow rate of 2 ml. per min. Absorbancy measurements at 280 mμ revealed the presence of one major peak in Tubes No. 201—235 in the chromatogram. These fractions

*3 In our preceding papers the value, $[\alpha]_{\mathrm{D}}^{24\cdot5}$ $-5.4\pm2°$ (*c* 0.947, N hydrochloric acid), was given for this peptide as a result of a single measurement.[1] The present result appeared more reliable than the former, because the value was reproducible in repeated measurements.

*4 LAP Lot No. 5930, Worthington Biochemical Corporation, Freehold, New Jersey, U. S. A.

18) D. H. Spackman, W. H. Stein and S. Moore, *Anal. Chem.*, 30, 1191 (1958).

corresponding to the major peak were pooled and the bulk of water was removed at a bath temperature of 50—55°C in vacuo resulting in the separation of a gelatinous precipitate of the peptide. The rest was lyophilized three times to give a colorless fluffy powder; yield 0.125 g. (58% as based on XII used). The purified material behaved as a single nihydrin, Pauly, Ehrlich, and Sakaguchi reactive spot in paper chromatography [$R_f$=0.38 (BAW), 0.41 (BAPW)], and in paper electrophoresis at pH 3.8, 6.6 and 11.1. A sample for analyses was dried over phosphorus pentoxide at 60°C and 2—3 mmHg. pressure for 8 hr. and equilibrated in the air overnight. $\lambda_{max}^{0.1N\ HCl}$=280 mμ (ε=5500), 288 mμ (ε=4650); $\lambda_{max}^{0.1N\ NaOH}$=280 mμ (ε=5650), 288 mμ (ε=4800). $[\alpha]_D^{26.5}$ −11.9±3° (*c* 0.606, N hydrochloric acid); lit. $[\alpha]_D^{26}$ −11.8° (*c* 0.9, N hydrochloric acid),[16] $[\alpha]_D^{22}$ −11.7±0.5° (*c* 1, N hydrochloric acid).[15] Amino acid ratios in acid hydrolyzate: His 1.00, Phe 0.90, Arg 0.97, Try 0.73 (decomposed patially with acid), Gly 0.98; amino acid ratios in leucine aminopeptidase*4 digest: His 1.00, Phe 0.92. Arg 0.91, Try 0.92, Gly 0.93.[18]

Found: C, 51.71; H, 6.88; N, 18.12; $CH_3CO$, 6.81; $H_2O$, 8.62. Calcd. for $C_{34}H_{43}N_{11}O_6 \cdot CH_3COOH \cdot 4H_2O$: C, 51.85; H, 6.65; N, 18.48; $CH_3CO$, 5.61; $H_2O$, 8.64%. Calcd. for $C_{34}H_{43}N_{11}O_6 \cdot 1.5CH_3COOH \cdot 4H_2O$: C, 51.44; H, 6.65; N, 17.84; $CH_3CO$, 7.47; $H_2O$, 8.34%.

**L-Glutamyl-L-histidyl-L-phenylalanyl-L-arginyl-L-tryptophyl-glycine (III).**—An 0.250 g. sample of XVII was dissolved in 4 ml. of anhydrous trifluoroacetic acid and the solution was allowed to stand at room temperature for 30 min., after which time, ether was introduced to precipitate the hexapeptide trifluoroacetate. The precipitate was dissolved in a few milliliters of water and the solution was passed through a small Amberlite IR-45 column (acetate form). The column was washed with water and the eluate were pooled and lyophilized, affording the hexapeptide; wt. 0.234 g. This crude peptide was dissolved in 20 ml. of 0.025 M ammonium acetate (pH 5.35) and the solution was added to a column (1.2×50 cm.) of carboxymethyl cellulose (Serva, 0.6 meq./g.) which had been equilibrated with the same buffer solution. The column was then eluted successively with the following ammonium acetate buffers: 0.025 M (pH 5.35), 450 ml.; 0.0375 M (pH 5.35), 1600 ml.; 0.050 M (pH 6.45), 600 ml. Individual fractions (10 ml. each) were collected at a flow rate of approximately 2 ml. per min. Absorbancy measurements at 280 mμ revealed the presence of one major peak in Tubes No. 146—190 in the chromatogram. These fractions corresponding to the major peak were pooled and the bulk of water was removed at a bath temperature of 50—55°C in vacuo. The rest was lyophilized three times affording a colorless fluffy powder; yield 0.199 g. (86% as based on XVII used). This material was twice reprecipitated from water-ethanol to give 0.123 g. (recovery 62%). The purified peptide behaved as a single ninhydrin, Pauly, Ehrlich, and Sakaguchi reactive spot in paper chromatography [$R_f$=0.30 (BAW), 0.25 (BAPW)], and in paper electrophoresis at pH 3.8, 6.6 and 11.1. A sample for analyses was dried over phosphorus pentoxide at 60°C and 2—3 mmHg pressure for 8 hr. and then equilibrated in the air overnight. $\lambda_{max}^{0.1N\ HCl}$=280.5 mμ (ε=5500), 288 mμ (ε=4700); $\lambda_{max}^{0.1N NaOH}$=280.5 mμ (ε=5600), 288 mμ (ε=4800). $[\alpha]_D^{26.5}$ −18.0±3° (*c* 0.621, N acetic acid); lit. $[\alpha]_D$ −15.1±1° (*c* 0.1042, N acetic acid),[8] $[\alpha]_D^{25}$ −17.3° (*c* 1, acetic acid).[19]

Amino acid ratios in acid hydrolyzate: Glu 1.00, His 1.04, Phe 0.97, Arg 1.07, Try 0.71 (decomposed partially with acid), Gly 1.00; amino acid ratios in leucine aminopeptidase*4 digest: Glu 1.00, His 1.11, Phe 1.03, Arg 1.03, Try 1.02, Gly 0.96.

Found: C, 51.15; H, 6.92; N, 18.13; $H_2O$, 9.66. Calcd. for $C_{39}H_{50}N_{12}O_9 \cdot 5H_2O$: C, 50.86; H, 6.57; N, 18.25; $H_2O$, 9.78%.

## Summary

1) Synthesis of the peptides L-histidyl-L-phenylalanyl-L-arginyl-L-tryptophan, L-histidyl-L-phenylalanyl-L-arginyl-L-tryptophyl-glycine and L-glutamyl-L-histidyl-L-phenylalanyl-L-arginyl-L-tryptophyl-glycine, which corresponded to the amino acid sequences of positions 6—9, 6—10 and 5—10, respectively, of the corticotropin and α-MSH molecules, has been described.

2) The synthetic procedure for γ-*t*-butyl-L-glutamyl-L-histidyl-L-phenylalanlyl-L-arginyl-L-tryptophyl-glycine, a key intermediate to the higher peptides eliciting the adrenocorticotropic activity, has been improved.

3) An active ester $N^{\alpha}$, $N^{Im}$-dicarbobenzoxy-L-histidine *p*-nitrophenyl ester has been found to be of value for the synthesis of histidyl peptides.

4) An effective use of partition chromatography on a Sephadex column for purification of peptides has been cited.

The author expresses his deep gratitude to Dr. Hideo Otsuka for unfailing guidance throughout the course of this work. Thanks are also due to Dr. Mitsuo Ebata for amino acid analyses, Dr. Kaoru Kuriyama and staff for optical rotation measurements, Dr. Satoshi Mizukami and staff for elemental microanalyses, and Mr. Makoto Kanayama, Miss Fusako Shinozaki and Miss Yoshiko Jono for valuable technical assistance.

*Biochemistry Division*
*Shionogi Research Laboratory*
*Shionogi & Co., Ltd.*
*Fukushima-ku, Osaka*

19) C. H. Li, B. Gorup, D. Chung and J. Ramachandran, *J. Org. Chem.*, **28**, 178 (1963).

# A Note on the Stereospecific Formation of α-Aminoalcohols*

By Akitami ICHIHARA, Haruki MAEKAWA, Reiko KANDA, Haruhisa SHIRAHAMA and Takeshi MATSUMOTO

(Received November 16, 1964)

In previous papers[1a] the present authors have reported on the synthesis of *dl*-muscarine and its stereoisomers. In connection with synthetic studies in this field,[1b] the synthesis of a compound described as Ia, which probably possesses an erythro configuration, was performed. The structure Ib was erroneously proposed for muscarine by Kögl[2] in 1931.

First, attempts were made to prepare bromoacetal (III) through bromoaldehyde (II), which was obtained by the bromination of the sodium salt of acetoacetaldehyde.[3] The latter salt was conveniently prepared by the alkaline hydrolysis of commercially-available 1, 1-dimethoxybutanone-3.[4] However, since the overall yield of the sequence of reactions was quite poor, another method for obtaining bromoacetal (III) from butanonal acetal directly by means of a suitable brominating agent was next attempted. For this purpose we examined pyridine perbromide, which is expected to keep the reaction medium nearly neutral, thus minimizing undesirable side reactions. Although the resultant products consisted of various substances, the products were separable through fractional distillation into the desired bromoacetal (16%), methylmethoxybromovinyl ketone ($\lambda_{max}^{EtOH}=237$) and bromoaldehyde (II). The formation of these products indicates that the reaction was accompanied by elimination and hydrolysis reactions, and suggested that the addition of methanol to the reaction system would be favorable for the formation of the desired product. In fact, by the addition of methanol, the yield was raised to 37%.

Dimethylaminoketoacetal (IV) was readily

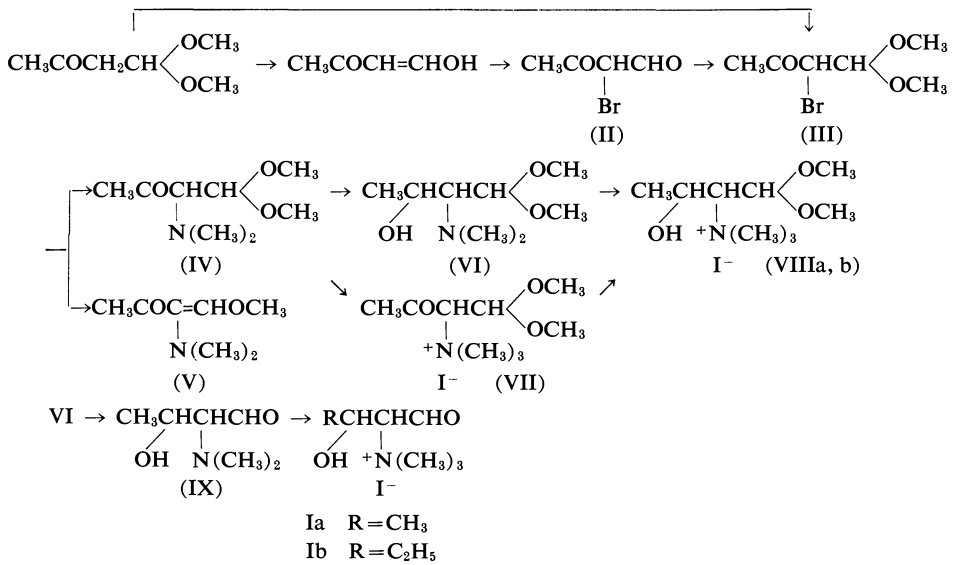



Fig. 1

* Presented at the Local Meeting of the Chemical Society of Japan, Hokkaido, July, 1960.

1) a) T. Matsumoto and H. Maekawa, *Angew. Chem.*, **70**, 507 (1958); T. Matsumoto and A. Ichihara, *Biochem. Z.*, **331**, 580 (1959); H. Maekawa, A. Ichihara and T. Matsumoto, This Bulletin, **38**, 1161 (1965). b) T. Matsumoto and A. Ichihara, This Bulletin, **33**, 1015 (1960); A. Ichihara, T. Yamanaka and T. Matsumoto, ibid., **38**, 1165 (1965).

2) F. Kögl, H. Duisberg and H. Erxleben, *Ann.*, **489**, 156 (1931).

3) The compound has been obtained by N. K. Kochetkov and E. E. Nifant'ev through the following sequence. *Doklady Akad. Nauk U. S. S. R.*, **121**, 462 (1958):

$$CH_3COCH_2CH(OCH_3)_2 \xrightarrow[BaCO_3\text{-}H_2O]{Br_2} II$$

4) In general, β-ketoaldehyde dimethylacetal affords β-hydroxyvinyl ketone by alkaline hydrolysis (H. Shirahama and T. Matsumoto, in preparation).

obtained by the treatment of bromoacetal (III) with dimethylamine in benzene. Besides the expected product (IV) (b. p. 34—36°C/0.2 mmHg), a small amount of a fraction (b. p. 67—72°C/4 mmHg) was obtained through distillation. Since the latter compound showed in the infrared spectrum strong bands at 1640, 1605 ($\alpha,\beta$-unsaturated carbonyl system), 1050 $cm^{-1}$ (ether), and a positive test to sodium tetraphenylboronate, indicating the presence of the dimethylamino group, the structure V was tentatively assigned. The structure of this compound will be studied in the near future.

The dimethylaminoketone (IV) was next converted to a dimethylaminoalcohol (VI) by means of sodium borohydride in methanol. In this reaction, the formation of a mixture of two diastereoisomers is to be expected. However, gas chromatography of the product indicated only one peak. Moreover, the methiodide (VIIIa) derived from VI showed a melting point of 123.5—125°C, which did not change after repeated recrystallizations.

Therefore, the reduction proceeded in a stereospecific manner, producing only one stereoisomer. A similar stereoselective reduction of aminoketone hydrochloride to erythro-aminoalcohol by sodium borohydride has been observed and explained as the attack on the least-hindered site with the participation of a lone pair of nitrogen atom, as is expressed by the following formula[5] (Fig. 2):

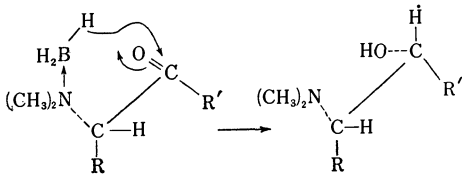
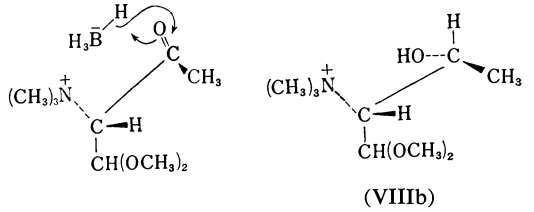



Fig. 2

Since a similar steric course can be assumed for the case of dimethylaminoketone (IV), the product VI most probably possesses the erythro configuration.

On the other hand, the reduction of trimethylammonium ketone (VII), derived from IV by means of methyl iodide under the same conditions gave a hydroxy compound (VIIIb), whose infrared spectra in the solid state and in solution and whose melting point (122—124°) were identical with those of trimethylammonium iodide (VIIIa) derived from the dimethylaminoalcohol (VI) obtained above. These results suggest that the product from VII is also an erythro isomer. The preferential formation of the erythro isomer may be accounted for by the mechanism involving an ion pair (Fig. 3):



(VIIIb)

Fig. 3

All attempts to hydrolyze the methiodide (VIIIa, b) of dimethyl aminoalcohol (VI) to the desired aldehyde (Ia) were unsuccessful. Even when it was refluxed for several hours, the formation of the aldehyde group could not be detected with tetrazolium chloride. This may be explained in terms of the presence of a charged quarternary nitrogen atom.[6] On the other hand, tertiary aminoalcohol (VI) was slowly but gradually hydrolyzed with 6 N hydrochloric acid to the aldehyde (IX).

Finally, the desired Ia was obtained by the treatment of IX with methyl iodide.

Although the methiodide Ia of 2-dimethylamino-3-hydroxybutanal was not obtained in a crystalline state, reineckate was crystallized and gave the correct analytical values.

## Experimental

**2-Bromo-3-keto-*n*-butyraldehyde (II).**—*By Claisen Condensation.*—The sodium salt of 3-keto-*n*-butyraldehyde was prepared in the usual manner from 27 g. of sodium methoxide, 29 g. of acetone and 38 g. of ethyl formate in 300 ml. of absolute ether. After the completion of the reaction, the ether was removed and the residue was dried in a vacuum desiccator. To a suspended solution of 20 g. of the sodium salt in 150 ml. of carbon tetrachloride, 29.6 g. of bromine in 50 ml. of carbon tetrachloride was added slowly under ice cooling. The precipitate was then filtered off, and the filtrate was poured into an equal volume of petroleum ether. After the precipitate had been removed, the filtrate was concentrated in vacuo. The solidified residue was crystallized from carbon tetrachloride to afford 1.2 g. of II; m. p. 108—109°C (decomp.), $\lambda_{max}^{EtOH}$ 228 mμ (ε 9570), (lit.[3] m. p. 109—110°C (decomp.)).

Found: C, 29.40; H, 3.15, mol. wt. (Rast) 161. Calcd. for $C_4H_5O_2Br$: C, 29.12; H, 3.05%, mol. wt. 164.

*From 3-Keto-n-butyraldehyde Dimethylacetal.* — A mixture of 1.6 g. of acetal, 0.48 g. of sodium hydroxide and 4 ml. of water was shaken for 10 hr. at room temperature. The solution was then evaporated

5) D. J. Cram and K. R. Kopecky, *J. Am. Chem. Soc.*, **81**, 2748 (1959); T. Matsumoto, T. Nishida and H. Shirahama, *J. Org. Chem.*, **27**, 79 (1962).

6) R. B. Woodward, *Angew. Chem.*, **69**, 50 (1957).

in vacuo and dried in a vacuum desiccator. The sodium salt thus obtained (1.1 g.) was treated in the manner described above to give 0.2 g. of a crystalline bromide, m. p. 108—109°C (decomp.), which was identical with the II prepared by the Claisen condensation.

**2-Bromo-3-keto-*n*-butyraldehyde Dimethylacetal (III).**—*From 2-Bromo-3-keto-n-butyraldehyde (II).*—A mixture of 2.1 g. of bromoaldehyde (II) and 24 ml. of 6.6% methanolic hydrogen bromide was gently refluxed for 8 hr. on a water bath. The reaction mixture was then concentrated in vacuo and the residue extracted several times with petroleum ether. The combined petroleum solution was dried over magnesium sulfate and distilled to give 0.7 g. of III, b. p. 73—75°C (6 mmHg).

*From 1,1-Dimethoxybutanone-3.*—Pyridine perbromide was prepared by the procedure of McElvain and Morris.[7] A mixture of 21 g. of powdered dry pyridine perbromide, 10 g. of 1,1-dimethoxybutanone-3 and 1 ml. of absolute methanol was shaken for 10 min., and the orange-colored solution was allowed to stand for 2 hr. under ice-cooling. The reaction mixture was extracted with several portions of warm petroleum ether. The turbid petroleum solution was clarified with celite. After the solvent had been removed, the residue was distilled under reduced pressure to give 5.9 g. (yield 37%) of bromoacetal, b. p. 70—74°C (7 mmHg).

Found: C, 33.67; H, 5.22. Calcd. for $C_6H_{11}O_3Br$: C, 34.14; H, 5.25%.

**2-Dimethylamino-3-keto-*n*-butyraldehyde Dimethylacetal (IV).**—To a solution of dimethylamine (ca. 30%, 50 ml.) in benzene was added, drop by drop, 2 g. of bromoacetal (III) in 5 ml. of benzene; the mixture was then allowed to stand for 24 hr. at room temperature. The resulting precipitates of dimethylamine hydrobromide were filtered off, and the filtrate was concentrated in vacuo. The residue was extracted with several portions of benzene, and the combined extracts were dried over anhydrous potassium carbonate. After the solvent had been removed, the crude product was distilled, yielding 1.1 g. of the desired aminoketone, b. p. 34—36°C (0.2 mmHg) and a small amount of a fraction with a b. p. of 67—72°C (0.4 mmHg). The infrared spectrum of the former compound exhibited absorption bands at 2820, 2660, 1704, and 1073 $cm^{-1}$, while the latter compound did at 1640, 1605, and 1060 $cm^{-1}$, suggesting the presence of a COC=C system.

**Tetraphenylboronate of IV.**—A small amount of IV was dissolved in 1 ml. of water and slightly acidified with acetic acid. To this solution a 50% aqueous solution of sodium tetraphenylboronate was added to give white precipitate which, on being recrystallized from water-ethanol, gave pure tetraphenylboronate of IV, m. p. 123—124°C (decomp.).

Found: N, 2.83. Calcd. for $C_{32}H_{38}O_3NB$: N, 3.03%.

**The Reduction of Dimethylaminoketone (IV).**—A mixture of 0.6 g. of dimethylaminoketone in 4 ml. of methanol and a few drops of a 10% aqueous solution of sodium hydroxide was added to a solution of 0.6 g. of sodium borohydride in 6 ml. of methanol. The solution was then allowed to stand overnight at room temperature. After the solvent had been removed, the residue was repeatedly extracted with ethyl acetate, and the combined solutions were dried over anhydrous sodium carbonate and distilled to give 0.48 g. of hydroxyaminoacetal (VI), b. p. 68—71°C (4 mmHg). Vapor phase chromatography showed only one peak with the retention time of 15 min. on a PEG 1000 column at 152°C (carrier gas, $H_2$). The Reinecke salt of VI was recrystallized from ethanol; m. p. 135—136°C (decomp.).

Found: C, 28.99; H, 4.92; N, 19.56. Calcd. for $C_{12}H_{26}O_3N_7S_4Cr$: C, 29.02; H, 4.87; N, 19.74%.

**The Methiodide (VII) of Dimethylaminoketone.**—An excess of methyl iodide was added to a solution of 1 g. of dimethylaminoketone (IV) in 3 ml. of absolute methanol. The resulting mixture was then allowed to stand for 3 hr. at room temperature. After the solvent had been evaporated to dryness, the red-colored residue was solidified by rubbing it with a glass rod. The recrystallization of the crude product from absolute ethanol yielded 1.5 g. of plates, m. p. 152—153°C (decomp.).

Found: C, 34.30; H, 6.48; N, 4.09. Calcd. for $C_9H_{20}O_3NI$: C, 34.08; H, 6.36; N, 4.42%.

**The Methiodide (VIIIa) of VI.**—A small amount of hydroxydimethylaminoacetal (VI) was dissolved in methanol, and to this solution an excess of methyl iodide was added. The reaction mixture was then allowed to stand at room temperature for 3 hr. After the solvent had been removed, the residue was dried in a vacuum desiccator for several hours to give an amorphous solid, which, on being recrystallized from ethanol, afforded white crystals, m. p. 120—124°C. Further purification of this compound with chloroform-ethylacetate raised the m. p. to 123.5—125°C (decomp.).

Found: C, 33.70; H, 6.68; N, 4.65. Calcd. for $C_9H_{22}O_3NI$: C, 33.86; H, 6.95; N, 4.45%.

**The Reduction of VII to VIIIb.**—The compound VII (0.6 g.) in 6 ml. of methanol was added, drop by drop, to 9 ml. of methanol containing 500 mg. of sodium borohydride. The reaction mixture was then allowed to stand overnight at room temperature. After the solvent had been removed, the reduction product was extracted with several portions of warm chloroform. The recrystallization of the crude product with absolute ethanol gave hydroxytrimethylammonium iodide, m. p. 122—124°C, undepressed upon the admixture of VIIIa.

Found: C, 34.34; H, 7.40; N, 4.51. Calcd. for $C_9H_{22}O_3NI$: C, 33.86; H, 6.95; N, 4.45%.

**The Hydrolysis of Hydroxydimethylaminoacetal (VI).**—Hydroxydimethylaminoacetal (0.26 g.) was dissolved in 2 ml. of 6 N hydrochloric acid and allowed to hydrolyze at room temperature for 5 hr. After the reaction mixture had then been concentrated in a vacuum desiccator, the residue was dissolved in 1 ml. of methanol, and to this solution 31 mg. of sodium in 1 ml. of methanol was added. The separated layer was extracted with several portion of chloroform. The combined chloroform solutions were dried over anhydrous potassium carbonate and concentrated under reduced pressure

7) S. M. McElvain and Leo R. Morris, *J. Am. Chem. Soc.*, **73**, 206 (1951).

to leave IX as an oil. The reineckate of IX was purified by recrystallization from water-ethanol; m. p. 232—233°C (decomp.).

Found: C, 26.54; H, 4.57; N, 21.23. Calcd. for $C_{10}H_{20}O_2N_7S_4Cr$: C, 26.64; H, 4.43; N, 21.35%.

**The Methiodide of IX.**—To an ethanolic solution of the aldehyde (IX), excess methyl iodide was added and the mixture was allowed to stand overnight. The removal of the solvent left a red-colored residue which exhibited, in the infrared spectrum, bands for aldehyde at 2740 and 1717 $cm^{-1}$. The reineckate of Ia was obtained in a crystalline state and showed a m. p. of 221—222°C after recrystallization from water-ethanol.

Found: C, 28.04; H, 5.11. Calcd. for $C_{11}H_{22}O_2N_7S_4Cr$: C, 28.43; H, 4.77%.

## Summary

The synthesis of the compound which was erroneously proposed for muscarin by Kögl in 1931 has been described.

*Department of Chemistry*
*Faculty of Science*
*Hokkaido University*
*Sapporo*

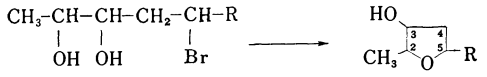
# The Synthesis of *dl*-Muscarine and *dl*-Allomuscarine[1,2]

By Haruki MAEKAWA, Akitami ICHIHARA and Takeshi MATSUMOTO

(Received November 16, 1964)

Since the structure and stereochemistry of muscarine (I) have been determined by X-ray analysis,[3] extensive studies of the synthesis of muscarine and its stereoisomers have been made by European workers.[4] However, none of them have completed the synthesis in a stereospecific manner. In the present paper, the authors would like to describe a new synthetic method in which hydroxyl and methyl groups are introduced in trans orientation by a stereospecific method.

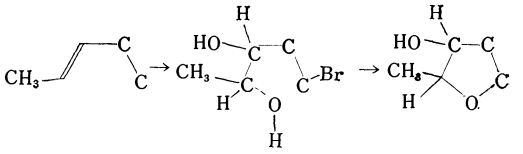
The principle underlying the present synthesis is as follows:



(A) (B)

Fig. 1

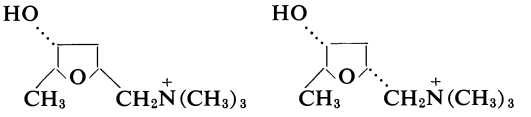
In the cyclization of A to form B (Fig. 1), the relative configuration of the methyl group at $C_2$ and of the hydroxyl group at $C_3$ in the tetrahydrofurane derivative, B, is determined by the stereochemistry of its precursors, the butane derivatives A. As is shown in Fig. 2,



(C) (D) (E)

Fig. 2

a trans compound, E, should be produced from an erythro compound, D, which, in turn, should be obtained by the dihydroxylation of a trans olefinic compound, C, with peracid. From the above considerations, ethyl crotylmalonate (III) was used as the starting material.



(I) (II)

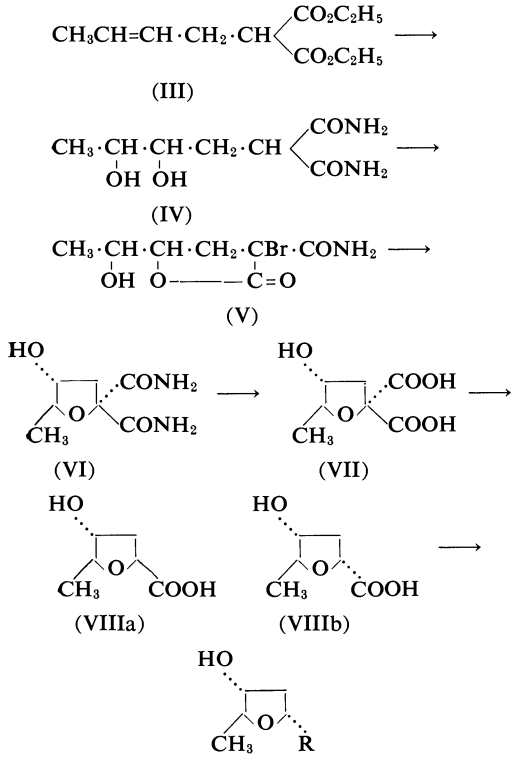
The oxidation of III with performic acid and the subsequent treatment of the product with alcoholic ammonia gave the dihydroxydiamide IV, m.p. 164—165.5°C, which is expected to be an erythro compound. On treatment with bromine in acetic acid, IV was converted to the bromolactone V, m.p. 110—111°C. Although two stereoisomers are possible for V, the relative configuration of methyl and hydroxyl groups in V should be independent of the stereochemistry of the $\alpha$ carbon atom of the bromolactone V and remain unchanged during the recyclization of V to VI. Therefore, no attempt was made to examine the configuration of the $\alpha$ carbon atom of V.

1) Preliminary communication: T. Matsumoto and H. Maekawa, *Angew. Chem.*, **70**, 507 (1958).

2) Nomenclature of muscarine isomers was assigned according to the convention of Hardegger, Eugster and Kögl. Cf. Ref. 4a.

3) F. Jellink, *Acta Cryst.*, **10**, 277 (1957); F. Kögl, C. A. Salemink, H. Schouten and F. Jellink, *Rec. trav. chim.*, **76**, 109 (1957).

4) a) H. Corrodi, E. Hardegger and F. Kögl, *Helv. Chim. Acta*, **40**, 2454 (1957); b) E. Hardegger, F. Lohse, ibid., **40**, 2383 (1957); c) C. H. Eugster, F. Häfliger, R. Denss and E. Girod, ibid., **41**, 205 (1958).



IXa R = $-COOCH_3$
IXb R = $\cdots COOCH_3$
Xa R = $-CON(CH_3)_2$
Xb R = $\cdots CON(CH_3)_2$
XIa R = $-CH_2N(CH_3)_2$
XIb R = $\cdots CH_2N(CH_3)_2$
XIIa R = $-CH_2N^+(CH_3)_3I^-$
XIIb R = $\cdots CH_2N^+(CH_3)_3I^-$
XIIIa R = $-CH_2N^+(CH_3)_3(C_6H_5)_4B^-$
XIIIb R = $\cdots CH_2N^+(CH_3)_3(C_6H_5)_4B^-$
XIVa R = $-CH_2N^+(CH_3)_3Cl^-$
XIVb R = $\cdots CH_2N^+(CH_3)_3Cl^-$

Fig. 3

The ammonolysis of V in alcoholic ammonia proceeded smoothly to give the tetrahydrofurandiamide VI, m. p. 204—205°C. The hydrolysis of VI was carried out in a 10% sodium hydroxide solution to afford the acid VII, which was purified through the lead salt or by ion exchange chromatography.

The acid VII, m. p. 170—176°C, was then decarboxylated by heating it 15 min. at 175—180°C in a sealed tube to give an amorphous solid. The careful recrystallization of the solid from a large volume of dichloroethane gave a monocarboxylic acid VIIIa as needles, m. p. 145°C, after the concentration of the filtrate, an isomeric monocarboxylic acid VIIIb, m. p. 109—111°C, was obtained as granular crystals from the mother liquor. Since these two acids have the same molecular formula, $C_6H_{10}O_4$, and show similar infrared spectra (Fig. 4, VIIIa and VIIIb), they are clearly the expected two stereoisomers, VIIIa and VIIIb. However, no reliable evidence of their stereochemistry was obtained at this stage.

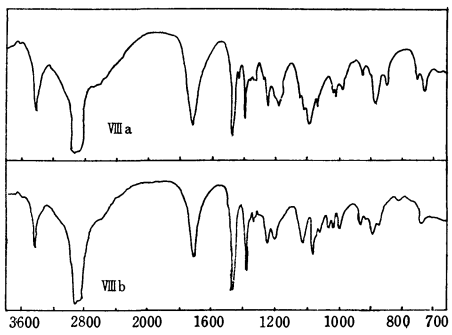



Fig. 4. Infrared absorption spectra of VIIIa and VIIIb (Nujol).

The esterification of these two acids with diazomethane afforded extremely hygroscopic methyl esters, IXa and IXb respectively. The NMR spectra of these esters were different from each other, but no decisive information about the stereochemistry could be derived therefrom. On the other hand, the inspection of the infrared spectra of IXa and IXb in a high dilute condition showed that IXa has an absorption band at 3617 $cm^{-1}$ (0.0024 mol. in carbon tetrachloride) due to a free hydroxyl group, while IXb has a rather broad absorption band at 3480 $cm^{-1}$ (0.0024 mol. in carbon tetrachloride) attributable to an intramolecularly hydrogen-bonded hydroxyl group, as is shown in Fig. 5. Therefore, it may be concluded that

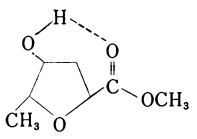


Fig. 5

the 145°C and 111°C compounds should be represented by VIIIa and VIIIb respectively.

By means of dimethylamine, IXa and IXb were converted to dimethylamides, Xa and Xb. In this reaction, the ester IXb, in which hydroxyl and methyl ester groups have the cis orientation, was converted to Xb about four times faster than the IXa isomer. At first, the slow reaction of IXa was attributed to the steric hindrance exerted by the bulky methyl group on the same side as the ester group. However, since the same phenomenon was also

observed in dimethyl ester series,[5] it is more reasonable to ascribe the acceleration to the neighboring participation of the hydroxyl group.[6,7]

The reduction of the dimethylamides Xa and Xb with lithium aluminum hydride gave normuscarine (XIa) and allonormuscarine (XIb). Finally *dl*-muscarine iodide (XIIa) and *dl*-allomuscarine iodide (XIIb) were prepared by the treatment of the noramines XIa and XIb with methyl iodide. Further, *dl*-muscarine chloride (XIVa) (m. p. 148—149°C) and *dl*-allomuscarine chloride (XIVb) (m. p. 143—144°C) were derived from the tetraphenylboronates (XIIIa and XIIIb) of the quarternery amines, and the chloride XIVa was shown to be identical with a sample prepared from natural material in infrared spectrum.[4c] *dl*-Muscarine chloride XIVa showed a marked physiological activity in the isolated heart of a frog, while that of *dl*-allomuscarine chloride was about one-half physiologically active as *dl*-muscarine.[1]

## Experimental

**Ethyl Crotylmalonate (III).**—This was prepared by the method of Linstead.[8]

**3, 4-Dihydroxypentane-1, 1-dicarbonamide (IV).**—To a solution of 32 g. of III in 135 ml. of formic acid (80% solution), 73 g. of hydrogen peroxide (28% solution) was added slowly under ice-cooling. The mixture was stirred for 20 min. and then allowed to stand for 12 hr. at room temperature. After the solvent had been removed, the residue was mixed with 100 ml. of dry benzene and the solvent was slowly removed under reduced pressure. The residue was dissolved in 50 ml. of absolute ethanol, and the solution was added to 500 ml. of an ethanol solution saturated with ammonia at 0°C. The mixture was then swirled gently and allowed to stand overnight at room temperature. The resultant precipitates were recrystallized from ethanol (95%) to give 20 g. of IV, m. p. 164—165.5°C. Infrared spectrum: $\nu_{max}^{Nujol}$ 3430, 3420, 1665, 1040 $cm^{-1}$.

Found: C, 44.55; H, 7.43; N, 14.59. Calcd. for $C_7H_{14}O_4N_2$: C, 44.20; H, 7.42; N, 14.73%.

**2-Bromo-2-carbamoyl-3, 4-dihydroxypentanoic Acid Lactone (1→4).**—A solution of 20 g. of diamide (IV) in 100 ml. of glacial acetic acid was refluxed gently on an oil bath, and then 17 g. of bromine in 10 ml. of glacial acetic acid was added drop by drop. After the mixture had been cooled, the separated ammonium bromide was removed and the filtrate was concentrated under reduced pressure. The oily residue was washed several times with a small amount of benzene and allowed to stand overnight, thus giving an amorphous solid which was recrystallized from chloroform to give 25 g. of V, m. p. 110—111°C. Infrared spectrum: $\nu_{max}^{Nujol}$ 3430, 1788, 1758, 1683, 1599, 1206, 1003 $cm^{-1}$.

Found: C, 33.45; H, 3.86; N, 5.95. Calcd. for $C_7H_{10}O_4NBr$: C, 33.35; H, 4.00; N, 5.95%.

**2-Methyl-3-hydroxy-5, 5-tetrahydrofurandicarbonamide (VI).**—To a solution of 500 ml. of ethanol saturated with ammonia at 0°C, 25 g. of V in 50 ml. of ethanol was added; the mixture was then allowed to stand for 12 hr. at room temperature. After the solution had been cooled, the precipitated crystals were collected by means of a funnel and recrystallized from ethanol (95%) to give 16 g. of VI, m. p. 204—205°C. Infrared spectrum: $\nu_{max}^{Nujol}$ 3380, 3200, 1680, 1585, 1140, 1009 $cm^{-1}$.

Found: C, 45.05; H, 6.60; N, 14.87. Calcd. for $C_7H_{12}O_4N_2$: C, 44.68; H, 6.43; N, 14.88%.

**2-Methyl-3-hydroxy-5, 5-tetrahydrofurandicarboxylic Acid (VII).**—In 80 ml. of an aqueous solution (10%) of sodium hydroxide, 10 g. of VI was hydrolyzed on a water bath for 4 hr. After the reaction mixture had been cooled, the solution was acidified with acetic acid added to 25 g. of lead acetate dissolved in a small amount of water, and then allowed to stand for 10 hr. at −5°C. The resultant precipitates were collected and washed with a small amount of water. After the hydrogen sulfide was led into the suspension of the lead salts, the filtrate was concentrated to leave plates which were recrystallized from glacial acetic acid to give 7 g. of VII. Another purification was carried out by eluting the reaction mixture through an ion exchange resin IR-120 column. The removal of water from the eluted solution gave pure acid (VII), m. p. 175—176°C. Infrared spectrum: $\nu_{max}^{Nujol}$ 3385, 2650, 1702, 1202, 1087 $cm^{-1}$.

Found: C, 44.39; H, 5.33. Calcd. for $C_7H_{10}O_6$: C, 44.21; H, 5.30%.

**2-Methyl-3-hydroxy-5-tetrahydrofurancarboxylic Acids (VIIIa) and (VIIIb).**—A solution of 5 g. of VII in 50 ml. of water was heated at 175—180°C for 15 min. in a sealed tube, and then the solution was concentrated to leave an amorphous solid which was recrystallized from 100 ml. of ethylene dichloride to give needles of VIIIa, (m. p. 143—145°C, yield, 1.0 g.

Found: C, 49.12; H, 6.81. Calcd. for $C_6H_{10}O_4$: C, 48.97; H, 6.90%.

The further concentration of the solution yielded VIIIb as granules, m. p. 109—111°C, yield 0.9 g.

Found: C, 49.16; H, 7.00. Calcd. for $C_6H_{10}O_4$: C, 48.97; H, 6.90%.

**Methyl 2-Methyl-3-hydroxy-5-tetrahydrofurancarboxylate (IXa).**—One gram of VIIIa in 10 ml. of methanol was added to 36 ml. of an ethereal solution of diazomethane (ca. 4%), and then the mixture was allowed to stand for 2 hr. at room temperature. The solution was concentrated to leave a residue which was distilled under reduced pressure to yield 1.0 g. of IXa (hygroscopic; b. p. 113—115°C/3.5 mmHg). The infrared spectrum of IXa in carbon tetrachloride (0.0021 mol.) showed an absorption

5) A. Ichihara, T. Yamanaka and T. Matsumoto, This Bulletin, **38** 1165 (1965).

6) a) H. B. Henbest and B. J. Lovell, *J. Chem. Soc.*, **1957**, 1965; b) S. M. Kupchan, P. Slade, R. J. Youg and G. W. A. Milne, *Tetrahedron*, **18**, 499 (1962); c) T. C. Bruice and T. H. Fife, *J. Am. Chem. Soc.*, **84**, 1973 (1962).

7) The kinetic study will be published in another paper. T. Yamanaka, A. Ichihara, K. Tanabe and T. Matsumoto, in preparation.

8) E. N. Eccott and R. P. Linstead, *J. Chem. Soc.*, **1929**, 2153.

band at 3717 $cm^{-1}$ due to a free secondary hydroxyl group; NMR spectrum: $\tau$ 8.80d ($CH_3$), 7.8q ($CH_2$), 6.27s ($CO_2CH_3$), 6.02s (OH), 5.48t (proton $\alpha$ to the ester group).

**Methyl 2-Methyl-3-hydroxy-5-tetrahydrofurancarboxylate (IXb).**—This was prepared in the same way as the cis acid VIIIb described above. The reaction of 0.9 g. of VIIIa with diazomethane gave 0.8 g. of ester (IXb), b. p. 109—111°C/3.5mmHg. IXb showed absorption bands at 3617 $cm^{-1}$ (free OH) and 3480 $cm^{-1}$ (broad, bonded OH) in carbon tetrachloride (0.0024 mol.); NMR spectrum: $\tau$ 8.82d ($CH_3$), 7.25—8.22 m ($CH_2$), 6.25s ($-CO_2CH_3$), 6.10s (OH), 5.53q (proton $\alpha$ to the ester group).

**2-Methyl-3-hydroxy-5-tetrahydrofurancarboxylic Acid Dimethylamide (Xa).**—One gram of IXa dissolved in 10 ml. of dry benzene was added to 50 ml. of a benzene solution of dimethylamine (ca. 30%) and allowed to stand for 25 hr. at 100°C in a sealed tube. The solvent was then evaporated to leave a residue which was washed with a small amount of ether to give Xa. Infrared spectrum: $\nu_{max}^{film}$ 3370, 1638, 1079 $cm^{-1}$.

**2-Methyl-3-hydroxy-5-tetrahydrofuran Carboxylic Acid Dimethylamide (Xb).**—To 40 ml. of a benzene solution of dimethylamine was added 0.8 g. of IXb in 10 ml. of benzene. The mixture was heated for 6 hr. at 100°C in a sealed tube. After the evaporation of the solvent, the resulting residue was washed with ether to give 0.7 g. of Xb. Infrared spectrum: $\nu_{max}^{film}$ 3360, 1640, 1071 $cm^{-1}$.

***dl*-Normuscarine (XIa).**—A solution of Xa (0.8 g.) in 5 ml. of tetrahydrofurane was added drop by drop to a solution of lithium aluminum hydride (1 g.) in 80 ml. of tetrahydrofurane and refluxed for 6 hr. on a water bath. After the excess lithium aluminum hydride had been decomposed by adding ethyl acetate, the reaction mixture was concentrated and the residue was dissolved in an aqueous solution of sodium hydroxide (20%). After several extractions with ether, the combined solution was dried over anhydrous potassium carbonate and evaporated to give Xa, b. p. 88—92°C/4 mmHg. Infrared spectrum: $\nu_{max}^{CCl_4}$ 3390, 1456, 1085, 1035 $cm^{-1}$. Reineckate of XIa: recrystallized from ethanol-water; m. p. 161—162°C (decomp.).

Found: C, 30.07; H, 5.23; N, 20.49. Calcd. for $C_{12}H_{24}O_2N_7S_4Cr$: C, 30.11; H, 5.54; N, 20.49%.

***dl*-Allonormuscarine (XIb).**—XIb was prepared in the same manner as XIa from 0.7 g. of Xb, b. p. 65—66°C/4 mmHg. Yield, 0.5 g. Infrared spectrum: $\nu_{max}^{CCl_4}$ 3200, 1460, 1158, 1105, 1063, 1033, 1015, 910, 858 $cm^{-1}$. Reineckate of XIb: recrystallized from ethanol-water, m. p. 164—165°C (decomp.).

Found: C, 29.99; H, 5.51; N, 19.70. Calcd. for $C_{12}H_{24}O_2N_7S_4Cr$: C, 30.11; H, 5.54; N, 20.49%.

***dl*-Muscarine Iodide (XIIa).**—To 0.1 g. of XIa in 1 ml. of ethanol, 0.3 g. of methyl iodide was added; the resultant solution was allowed to stand for 1 hr. at room temperature. After the excess methyl iodide and the solvent had been evaporated an oily residue was obtained. The rubbing of the residue with a glass rod gave crystals which were recrystallized from ether-isopropanol to yield 50 mg. of *dl*-muscarine iodide (XIIa), m. p. 116—118°C (the lit.[4c] has reported an m. p. of 107—108°C). Infrared spectrum: $\nu_{max}^{KBr}$ 3400, 1085, 1001, 970, 920 $cm^{-1}$.

Found: C, 36.14; H, 6.74; N, 4.64. Calcd. for $C_9H_{20}O_2NI$: C, 35.89; H, 6.69; N, 4.69%.

***dl*-Allomuscarine Iodide (XIIb.)**—By treating 0.3g. of XIb the same as XIa we obtained 0.2 g. of *dl*-allomuscarine iodide (XIIb), m. p. 131—132°C (Ref. 9 reported an m. p. of 131—132°C). Infrared spectrum: $\nu_{max}^{KBr}$ 3400, 1095, 1062, 995, 964, 910 $cm^{-1}$.

Found: C, 36.01; H, 6.66; N, 4.47. Calcd. for $C_9H_{20}O_2NI$: C, 35.89; H, 6.69; N, 4.65%.

***dl*-Muscarine Tetraphenylboronate (XIIIa).**—Recrystallized from acetone-ethanol; m. p. 174—175°C (lit.[4c] 173—174°C).

Found: N, 3.11. Calcd. for $C_{33}H_{40}O_2NB$: N, 2.84%.

***dl*-Allomuscarine Tetraphenylboronate (XIIIb).**—Recrystallized from acetone-ethanol; m. p. 176—177°C (lit.[9] 175—176°C).

Found: N, 3.04. Calcd. for $C_{33}H_{40}O_2NB$: N, 2.84%.

***dl*-Muscarine Chloride (XIVa).**—Upon treatment with cesium chloride, 0.3 g. of XIIIa was converted to muscarine chloride which was then recrystallized by ether-isopropanol; m. p. 148—149°C (lit.[4c] m. p. 147—148°C). The infrared spectrum was identical with those of a natural sample and of a synthetic specimen of Eugster. Infrared spectrum: $\nu_{max}^{KBr}$ 3250, 1485, 1105, 1075, 1056, 918 $cm^{-1}$.

Found: C, 51.29; H, 9.68; N, 6.72. Calcd. for $C_9H_{20}O_2NCl$: C, 51.54; H, 9.62; N, 6.68%.

***dl*-Allomuscarine Chloride (XIVb).**—XIIIa (0.4 g.) was converted to allomuscarine chloride. The recrystallization of the product from ether-isopropanol gave 0.2 g. of XIVb, m. p. 152.5—153.5°C (lit.[9] 153—154°C). Infrared spectrum: $\nu_{max}^{Nujol}$ 3300, 1090, 1065, 977, 959, 928 $cm^{-1}$.

Found: C, 51.33; H, 9.60; N, 6.47. Calcd. for $C_9H_{20}O_2NCl$: C, 51.54; H, 9.62; N, 6.68%.

## Summary

The synthesis of *dl*-muscarine (I) and *dl*-allomuscarine (II) starting from ethyl crotylmalonate has been described. Trans oriented methyl and hydroxyl groups in these compounds have been introduced stereospecifically into the tetrahydrofurane ring.

We wish to thank Professor Akira Ooga, Hokkaido University, for the pharmacological proof of our samples. Thanks are also due to Mr. Tsutomu Yamanaka and Mr. Noriki Ito for their assistance in the experimental work.

*Department of Chemistry*
*Faculty of Science*
*Hokkaido University*
*Sapporo*

9) C. H. Eugster, F. Häflinger, R. Denss and E. Girod, *Helv. Chim. Acta*, **41**, 583 (1958).

# The Synthesis of *cis*- and *trans*-Demethylmuscarines[1]

By Akitami ICHIHARA, Tsutomu YAMANAKA and Takeshi MATSUMOTO

(Received November 16, 1964)

In previous papers[2,3] we reported the synthesis and pharmacological activities of *dl*-muscarine and its stereoisomers. Since the activities were found to depend sensitively upon the structure, it appeared of interest to synthesize *dl*-demethylmuscarines and investigate their physiological activities.

The route previously described for the synthesis of *dl*-muscarine and *dl*-allomuscarine was applied to the preparation of *dl*-demethylmuscarine, starting with ethyl allylmalonate (I).

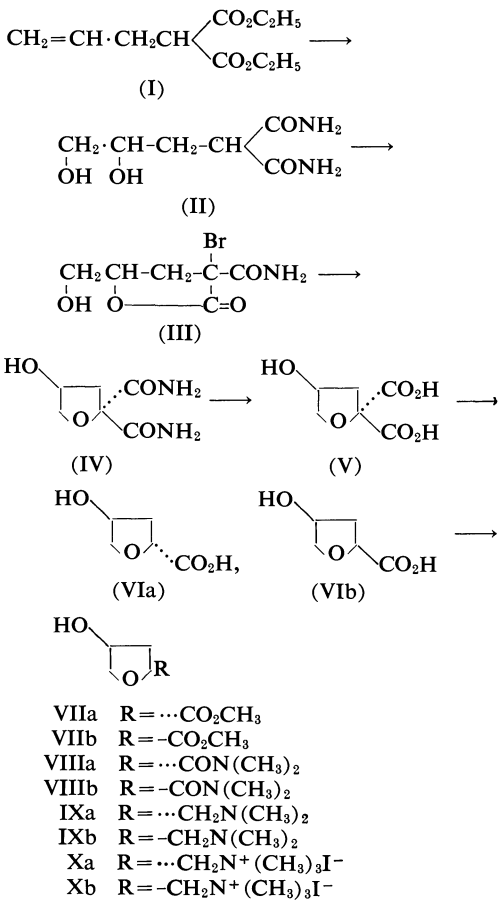



Fig. 1

The oxidation of ethyl allylmalonate (I) with performic acid gave an oily product which was without purification, allowed to react with ammonia in ethanol to form dihydroxydiamide II. Bromolactonamide III, prepared by the reaction of dihydroxydiamide with bromine,[4] was then subjected to ammonolysis in order to give tetrahydrofurandicarboxylic acid diamide IV, which was subsequently hydrolyzed to dicarboxylic acid V.

The decarboxylation of this acid, V, by heating it at 150—160°C in a sealed tube gave an amorphous solid, from which two acids were isolated in the ratio 1 : 1; one of these acids was crystallized from ethyl acetate as rhombic crystals, m. p. 127—129°C, while the other acid was obtained as a granular crystals, m. p. 142—143°C, by further concentration of the filtrate. These two compounds have the same molecular formula, $C_5H_8O_4$, and similar absorption bands in infrared spectra (Fig, 2, VIa and VIb). Therefore, these are the

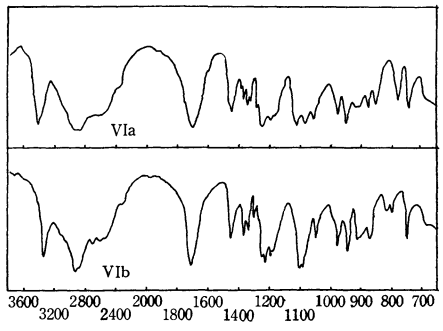



Fig. 2. Infrared absorption spectra of VIa and VIb (Nujol).

expected stereoisomers VIa and VIb. The treatment of these acids, VIa and VIb, with ethereal diazomethane gave the corresponding methyl esters, VIIa and VIIb respectively. The infrared spectrum of VIIb exhibited a broad absorption band at 3482 $cm^{-1}$ (0.077 mol. in carbon tetrachloride) attributable to the presence of an intramolecular hydrogen bond between the carbonyl group and the secondary hydroxyl group. On the other hand, the compound VIIa showed two absorption bands at

1) Short communication: T. Matsumoto and A. Ichihara, This Bulletin, 33, 1015 (1960).
2) a) T. Matsumoto and H. Maekawa, *Angew. Chem.*, 70, 507 (1958); b) H. Maekawa, A. Ichihara and T. Matsumoto, This Bulletin, 38, 1161 (1965).
3) T. Matsumoto and A. Ichihara, *Biochem. Z.*, 331, 589 (1959).
4) W. Traube, *Ber.*, 37, 4540 (1904).

3620 $cm^{-1}$ (sharp, free OH) and 3485 $cm^{-1}$ (broad, bonded OH, 0.068 mol. in carbon tetrachloride); the intensity of the band at 3620 $cm^{-1}$ relative to the band at 3485 $cm^{-1}$ is increased with further dilution. Therefore, VIa is a trans compound and VIb is cis compound. The tetrahydrofurancarboxylic acid esters, VIIa and VIIb, were then converted with dimethylamine to tetrahydrofurancarboxylic acid dimethylamides, VIIIa and VIIIb. In these reactions an interesting difference in the rate of reaction was observed; the cis ester was converted to VIIIb about three or four times faster than the trans isomer. The effect of acceleration in cis-ester should be ascribed to the presence of an hydroxyl group near the ester group.[5] A similar facilitation by hydroxyl groups has been reported in other compounds.[6]

The reduction of the dimethylamides VIIIa and VIIIb with lithium aluminum hydride gave the dimethylamines IXa and IXb respectively. A stereoisomeric mixture of cis and trans amines, IXa and IXb, resulting from the sequence of reactions VIa and VIb to IXa and IXb, is also easily separable by chromatography on alumina.

Since the infrared spectrum of the cis isomer IXb also exhibits a broad absorption band at 3194 $cm^{-1}$ (0.0072 mol. in carbon tetrachloride) ascribed to the intramolecular hydrogen bond between dimethylamino and hydroxyl groups, it has been ascertained that the reactions in the sequence VI to IX proceeded without any configurational changes.

Finally, by means of methyl iodide, the IXa and IXb amines were converted to *trans-dl*-demethylmuscarine (Xa) (m. p. 119—120°C) and *cis-dl*-demethylmuscarine (Xb) (m. p. 117—118°C) respectively, whose infrared spectra were identical with those of Eugster's specimens.[7] In physiological activity for an isolated heart of a frog, *trans*-demethylmuscarine is slightly stronger than the cis-isomer, but rather weaker than *dl*-muscarine itself.

## Experimental.[8]

**Ethyl Allylmalonate (I).**—This was prepared by the procedure of Linstead.[9]

**3, 4-Dihydroxybutane-1, 1-dicarbonamide (II).** — To a solution of 120 g. of ethyl allylmalonate in 540 ml. of formic acid (80% solution), 73 g. of hydrogen peroxide (28% solution) was added slowly under ice cooling. The mixture was stirred for 20 min. and allowed to stand for 12 hr. at room temperature. After removal of the solvent, the residue was mixed with 200 ml. of dry benzene, and the benzene was slowly removed under reduced pressure. The residue was then added to 2 l. of ethanol saturated with ammonia at 0°C, and the mixture was swirled gently and allowed to stand overnight at room temperature. The precipitated crystals were recrystallized from ethanol (95%) to give 72 g. of II, m. p. 157—158°C; infrared spectrum: $\nu_{max}^{Nujol}$ 3330, 1765, 1664, 1593, 1178, 1070 $cm^{-1}$.

Found: C, 40.76; H, 6.84; N, 15.66. Calcd. for $C_{16}H_{12}O_4N_2$: C, 40.90; H, 6.78; N, 15.90%.

The compounds III, IV and V were prepared by the method of Traube.[4] 3-Hydroxy-5, 5-tetrahydrofurandicarboxylic acid (V) recrystallized from glacial acetic acid showed a m. p. of 138—140°C.

Found: C, 41.13; H, 4.67. Calcd. for $C_6H_8O_5$: C, 40.91; H, 4.58%. (Ref. 3 described an m. p. of the hydrate but not of the anhydrous compound).

***trans*- and *cis*-4-Hydroxy-2-tetrahydrofurancarboxylic Acid (VIa and VIb).** — A solution of 10 g. of tetrahydrofurandicarboxylic acid V in 100 ml. of water was heated for 1 hr. in a sealed tube at 150—160°C. The removal of water under reduced pressure left a residue which was solidified by rubbing it with glass rod to give 6.8 g. of an amorphous solid, m. p. 108—111°C. The solid was carefully recrystallized from 50 ml. of ethyl acetate to afford 2.6 g. of VIb as rhombic crystals, m. p. 127—129°C, infrared spectrum: Fig. 2, VIa.

Found: C, 45.59; H, 5.99. Calcd. for $C_5H_8O_4$: C, 45.45; H, 6.10%.

The trans acid VIa, m. p. 142—143°C, was obtained as granular crystals by concentrating the above filtrate. Infrared spectrum: Fig. 2, VIb.

Found: C, 45.50; H, 6.10. Calcd. for $C_5H_8O_4$: C, 45.45; H, 6.10%. (Ref. 4 reports a mixture of VIa and VIb, m. p. 110°C).

***trans*-Methyl-4-hydroxy-2-tetrahydrofurancarboxylate (VIIa).** — A solution of 0.9 g. of *trans* acid (VIa) in 10 ml. of methanol was added slowly to 100 ml. of ethereal solution (ca. 8%) of diazomethane at room temperature. A reaction took place, smoothly evolving nitrogen. After the mixture had been allowed to stand for 1 hr., the solvent was evaporated and the residue was distilled under reduced pressure to give 0.8 g. of *trans*-methyl ester (VIIa), b. p. 110—115°C/7 mmHg.

The infrared spectrum of VIIa in carbon tetrachloride (0.068 mol.) showed absorption maxima at 3620 and 3485 $cm^{-1}$ attributable to free hydroxyl and intermolecularly-associated hydroxyl groups respectively. With further dilution (0.0024 mol.), the intensity of the former band relative to the latter one was increased.

Found: C, 49.27; H, 7.15. Calcd. for $C_6H_{10}O_4$: C, 49.31; H, 7.15%.

***cis*-Methyl-4-hydroxytetrahydrofuran-2-carboxylate (VIIb).** — This was prepared, in the way described above, from 0.6 g. of *cis*-tetrahydrofurancarboxylic acid, VIb. The distillation of the crude

5) T. Yamanaka, A. Ichihara, K. Tanabe and T. Matsumoto, *Shokubai* (*Catalyst*), **6**, 304 (1964); *Tetrahedron*, in press.

6) For further examples see Ref. 2b.

7) Guido Zwicky, P. G. Waser and C. H. Eugster, *Helv. Chim. Acta*, **42**, 1177 (1959).

8) Melting points are uncorrected. The infrared spectra in high dilution condition were measured on a Nippon Bunko grating infrared spectrometer model DS-401G, using 50 mm. KBS cell under high resolution condition.

9) E. N. Eccott and R. P. Linstead, *J. Chem. Soc.*, **1929**, 2153.

product gave 0.5 g. of the *cis*-ester VIIb, b. p. 105—110°C/7 mmHg, whose infrared spectrum showed an absorption band at 3482 $cm^{-1}$ due to an intramolecularly-hydrogen-bonded hydroxyl group in carbon tetrachloride (0.077 mol.).

Found: C, 49.22; H, 6.87. Calcd. for $C_6H_{10}O_4$: C, 49.31; H, 6.90%.

***trans*-4-Hydroxy-2-tetrahydrofurancarboxylic Acid Dimethylamide (VIIIa).** — The *trans*-methyl ester (0.5 g.) was added to 35 ml. of a solution (30%) of dimethylamine in absolute ethanol, and the mixture was heated for 25 hr. in a sealed tube at 80—90°C. The cooled reaction mixture was then concentrated to leave an oily residue, whose infrared absorption showed bands at 3350, 1638, 1105, 1077 $cm^{-1}$ for amide VIIIa and a rather weak absorption at 1730 $cm^{-1}$ for the unchanged ester (VIIa), which was removed by extracting it with ether.

***cis*-4-Hydroxy-2-tetrahydrofurancarboxylic Acid Dimethylamide (VIIIb).** — *cis*-Amide (VIIIb) was prepared in a way similar to that used for the trans-isomer described above. *cis*-Methyl ester (0.47 g.) was added to 30 ml. of an ethanolic solution (30%) of dimethylamine, and the mixture was heated for 8 hr. in a sealed tube at 80—90°C. The oily residue obtained by the evaporation of the solvent exhibited the following bands in the infrared spectrum: $\nu_{max}^{film}$ 3370, 1640, 1092, 1075 $cm^{-1}$. No absorption bands attributable to the ester VIIb were observed.

***trans*-(4-Hydroxy-2-tetrahydrofurfuryl)methyldimethylamine (IXa).** — To a solution of 0.6 g. of lithium aluminum hydride in 21 ml. of dried tetrahydrofuran, *trans*-dimethylamide (0.7 g.) in 5 ml. of tetrahydrofurane was added drop by drop under ice cooling; the mixture was then refluxed for 4 hr. on a steam bath. After the excess lithium aluminum hydride had been decomposed by adding 20 ml. of ethyl acetate to the cooled reaction mixture, the solvent was evaporated and the residue was treated with a solution (20%) of sodium hydroxide. The undissolved material was extracted several times with ethyl acetate. The extracts were combined, dried over anhydrous potassium carbonate, and evaporated to leave an oily residue. The residue was then chromatographed on 40 g. of deactivated alumina, using a mixture of benzene and methanol (0.5—10%) as a developer. Elution with benzene-methanol (5%) gave 0.45 g. of the *trans*-dimethylamine IXa. Infrared spectrum: $\nu_{max}^{CCl_4}$ 3400, 1103, 1070, 1035, 976 $cm^{-1}$. Reineckate of IXa: m. p. 167—187°C (decomp.)

Found: C, 28.55; H, 5.01; N, 20.91. Calcd. for $C_{12}H_{25}O_2N_7S_4Cr$: C, 28.44; H, 4.77; N, 21.10%.

***cis*-(4-Hydroxy-2-tetrahydrofurfuryl)methyldimethylamine (IXb).** — The cis-isomer IXb was prepared by exactly the same procedure as was the trans-isomer. The *cis*-dimethylamide VIIIb (0.7 g.) gave 0.42 g. of the *cis*-dimethylamine IXb, b. p. 75—80°C/4 mmHg, the infrared spectrum of which in high diluted conditions exhibited a broad band at 3194 $cm^{-1}$ ascribed to the intramolecularly-hydrogen-bonded hydroxyl group in carbon tetrachloride (0.0072 mol.). Infrared spectrum: $\nu_{max}^{CCl_4}$ 3220, 1110, 1086, 1062, 1037, 1027 $cm^{-1}$. Reineckate of IXb: m. p. 183—184°C (decomp.).

Found: C, 28.40; H, 5.05; N, 20.94. Calcd. for $C_{12}H_{25}O_2N_7S_4Cr$: C, 28.44; H, 4.77; N, 21.10%.

***trans*-Demethylmuscarine (Xa).** — To a solution of 0.2 g. of *trans*-amine IXa in ethanol an excess of methyl iodide was added, and the mixture was allowed to stand for 1 hr. at room temperature. The reaction mixture was then evaporated under reduced pressure to leave a solid which was recrystallized twice from ethanol-water to give 0.2 g. *trans*-demethylmuscarine (Xa), m. p. 119—120°C; infrared spectrum: $\nu_{max}^{Nujol}$ 3345, 1103, 1072, 992, 953, 918 $cm^{-1}$. (Ref. 7 reported an m. p. of 119.5—120°C.)

Found: C, 33.63; H, 6.24; N, 4.70. Calcd. for $C_8H_{18}O_2NI$: C, 33.47; H, 6.32; N, 4.88%,

The reineckate of *trans*-demethylmuscarine was recrystallized from water-enthanol; m. p. 175.5—177°C (decomp.).

Found: N, 20.32. Calcd. for $C_{12}H_{24}O_2N_7S_4Cr$: N, 20.49%.

***cis*-Demethylmuscarine (Xb).** — The same treatment of IXb as that of the trans-isomer Xa gave a crude product which was recrystallized from water-ethanol to yield *cis*-demethylmuscarine (Xb), m. p. 117—118°C; infrared spectrum: $\nu_{max}^{Nujol}$ 3395, 1103, 1067, 1015, 995, 968, 962, 940 $cm^{-1}$. (Ref. 7 reported an m. p. of 119.5—120.5°C)

Found: C, 33.33; H, 6.36; N, 4.71. Calcd. for $C_8H_{18}O_2NI$: C, 33.47; H, 6.32; N, 4.88%.

The reineckate of *cis*-demethylmuscarine showed an m. p. of 169—171°C (decomp.) after recrystallization from water-ethanol.

Found: N, 20.04. Calcd. for $C_{12}H_{24}O_2N_7S_4Cr$: N, 20.49%.

## Summary

Two stereoisomeric *dl*-demethylmuscarines have been prepared by the procedure described for the synthesis of *dl*-muscarine, starting from ethyl allylmalonate.

We are indebted to Professor Hiroshi Ooga, Veterinary Department, Hokkaido University, for performing pharmacological tests.

*Department of Chemistry*
*Faculty of Science*
*Hokkaido University*
*Sapporo*

# The Synthesis of Tlatlancuayin and Some Related Compounds

By Kenji FUKUI, Takashi MATSUMOTO and Shigehiro NAKAMURA

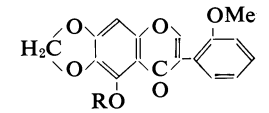
(Received November 19, 1964)

Tlatlancuayin was isolated from *Iresine celosioides L.* (*fam. Amarantaceae*) by Crabbé et al.[1] They established its structure as 2', 5-dimethoxy-6, 7-methylenedioxyisoflavone (I) from analytical, spectroscopic and degradative studies. As an isoflavone it is a unique compound which has a fully-alkylated system, with a lone 2'-methoxyl in the side phenyl and a methylenedioxy group in the chromone nucleus. Two methods for the synthesis of the compound have been reported by Arora et al.[2] In previous papers the present authors have reported the synthesis of irisolone (4'-hydroxy-5-methoxy-6, 7-methylenedioxyisoflavone) (II),[3] one of the few naturally-occurring isoflavones containing a methylenedioxy substituent, and some 6, 7-methylenedioxyisoflavones.[4,5]

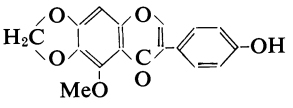
The present paper will describe the synthesis of tlatlancuayin and some related compounds.

In previous papers,[3,6] the authors have shown that, in the Hoesch reaction, 3-methoxy-4, 5-methylenedioxyphenol (III)[7] was condensed with some acetonitriles at the 2-position (not at the 6-position). By a similar reaction with 2-methoxybenzyl cyanide, III yielded 2-hydroxy-4, 5-methylenedioxy-6-methoxyphenyl 2-methoxybenzyl ketone (IV) which had been obtained by the degradation[1] of natural tlatlancuayin with alkali. According to the method of Crabbé et al.,[1] IV was cyclized with ethyl formate to tlatlancuayin (I), whose identity with the natural substance was confirmed by mixed melting point determination and by ultraviolet and infrared spectral comparisons (Figs. 1 and 2). The synthetic substance, I, was converted into the known product, V, by demethylation.

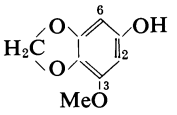
By a similar reaction with benzyl cyanide, 3, 4-methylenedioxybenzyl cyanide and 3, 4-dimethoxybenzyl cyanide, III was derived to the



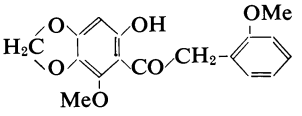

(I) R=Me (V) R=H




(II)




(III)




(IV)

respective ketones, VI, VII and VIII. These ketones were also cyclized with ethyl formate to the corresponding isoflavones (IX, X and XI). The treatment of IX and X with aluminum chloride in boiling ether gave the 5-demethyl derivatives (XII and XIII), which could also be methylated back into the parent isoflavones (IX and X), indicating that no

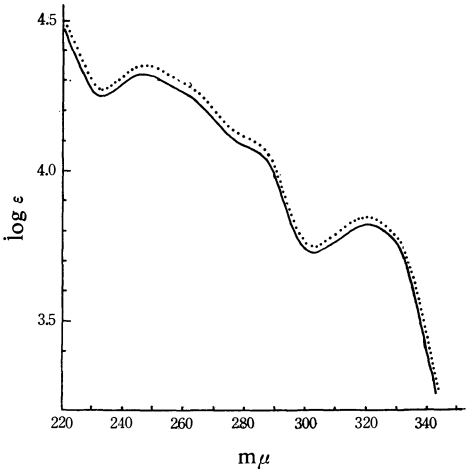



Fig. 1. Ultraviolet spectra of natural (·····) and synthetic tlatlancuayin (——) in ethanol.

1) P. Crabbé, P. R. Leeming and C. Djerassi, *J. Am. Chem. Soc.*, **80**, 5258 (1958).
2) S. K. Arora, A. C. Jain and T. R. Seshadri, *Tetrahedron*, **18**, 559 (1962).
3) K. Fukui and T. Matsumoto, This Bulletin, **38**, 887 (1965).
4) K. Fukui and T. Matsumoto, *J. Chem. Soc. Japan, Pure Chem. Sec.* (*Nippon Kagaku Zasshi*), **85**, 793 (1964). to be published.
5) K. Fukui and T. Matsumoto, This Bulletin, **38**, 612 (1965)
6) K. Fukui and T. Matsumoto, ibid., **36**, 806 (1963).
7) A. F. Wagner, E. Walton, A. N. Wilson, J. O. Rodin and F. W. Holly, *J. Am. Chem. Soc.*, **81**, 4983 (1959).

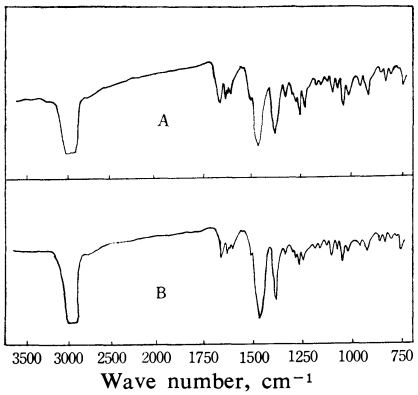
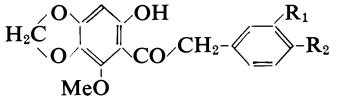
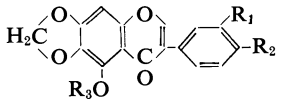



Fig. 2. Infrared spectra of natural (A) and synthetic tlatlancuayin (B) in Nujol.

isomerization occurs during the treatment with aluminum chloride.



(VI) $R_1=R_2=H$
(VII) $R_1$, $R_2$=O-$CH_2$-O
(VIII) $R_1=R_2=OMe$



(IX) $R_1=R_2=H$ $R_3=Me$
(X) $R_1$, $R_2$=O-$CH_2$-O $R_3=Me$
(XI) $R_1=R_2=OMe$ $R_3=Me$
(XII) $R_1=R_2=R_3=H$
(XIII) $R_1$, $R_2$=O-$CH_2$-O $R_3=H$

## Experimental*1

**2-Hydroxy-4, 5-methylenedioxy-6-methoxyphenyl 2-Methoxybenzyl Ketone (IV).** — 3-Methoxy-4, 5-methylenedioxyphenol (III)[7] (5.0 g.) and 2-methoxybenzyl cyanide[8] (5.0 g.) were dissolved in dry ether (120 ml.), and then fused zinc chloride (1.5 g.) was added. The mixture was saturated with dry hydrogen chloride in an ice-bath and allowed to stand overnight. The ether solution was decanted from the ketimine hydrochloride-zinc chloride complex which had separated. The residue was washed with dry ether and heated on a steam bath with water (100 ml.) for 75 min. The oil which had separated on cooling was extracted with ethyl acetate. The organic layer was washed with aqueous sodium bicarbonate and then with water. After the solvent had evaporated, the residue was distilled. The distillate (bath temperature 230—280°C/0.1 mmHg) was collected and crystallized from ether-petroleum ether to give IV as yellow needles; m. p. 115—116°C (reported m. p. 115—116°C[1]); yield, 0.6 g. This gave a green ferric chloride reaction in ethanol. UV: $\lambda_{max}^{EtOH}$ mμ (log ε); 243.5 (4.08), 284 (4.13), 351 (3.70). In all these properties it agreed with that substance obtained by Crabbé et al.[1]

Found: C, 64.26; H, 5.07. Calcd. for $C_{17}H_{16}O_6$; C, 64.55; H, 5.10%.

**Tlatlancuayin (2', 5-Dimethoxy-6, 7-methylenedioxyisoflavone) (I).**—According to the method of Crabbé et al.,[1] the ketone IV (1.44 g.) by cyclization with sodium (3.0 g.) in ethyl formate (200 ml.) gave I (480 mg.) as colorless prisms, m. p. 147—148°C (reported m. p. 145—147°C,[1] 147—148°C[2]). This gave no ferric chloride reaction. This substance was found to be identical with the natural substance by mixed melting point measurement and by infrared and ultraviolet spectral comparisons. IR; 1645, 1614, 1603, 1589, 1016, 938 $cm^{-1}$. UV: $\lambda_{max}^{EtOH}$ mμ (log ε); 246 (4.32), 281*2 (4.08), 321 (3.82).

Found: C, 66.28; H, 4.37. Calcd. for $C_{18}H_{14}O_6$: C, 66.25; H, 4.32%.

**The Partial Demethylation of Tlatlancuayin (I).**—According to the method of Crabbé et al.,[1] I was demethylated with aluminum chloride to give 5-hydroxy-2'-methoxy-6, 7-methylenedioxyisoflavone (V) as yellow needles, m. p. 191—192°C (reported m. p. 192—193°C[1]). This gave a green ferric chloride reaction in ethanol. UV: $\lambda_{max}^{EtOH}$ mμ (log ε); 243.5 (4.25), 271.5 (4.27), 332*2 (3.58).

Found: C, 65.21; H, 3.89. Calcd. for $C_{17}H_{12}O_6$; C, 65.38; H, 3.87%.

**2-Hydroxy-4, 5-methylenedioxy-6-methoxyphenyl Benzyl Ketone (VI).**—From the phenol III (5.0 g.), benzyl cyanide (4.0 g.), fused zinc chloride (1.5 g.) and dry ether (120 ml.), synthesis was carried out by a method similar to that used for IV. The product was recrystallized from methanol to give VI as yellow needles, m. p. 162—164°C, which gave a green ferric chloride reaction in ethanol; yield 2.0 g. UV: $\lambda_{max}^{EtOH}$ mμ (log ε); 245.5 (4.06), 289 (4.12), 357 (3.68).

Found: C, 67.21: H, 4.69. Calcd. for $C_{16}H_{14}O_5$: C, 67.12; H, 4.93%.

**2-Hydroxy-4, 5-methylenedioxy-6-methoxyphenyl 3, 4-Methylenedioxybenzyl Ketone (VII).** — From the phenol III (19.8 g.), 3, 4-methylenedioxybenzyl cyanide (21.0 g.), fused zinc chloride (6.0 g.) and dry ether (350 ml.), synthesis was carried out by a method similar to that used for IV. The product was recrystallized from chloroform-methanol to give VII as yellow needles, m. p. 153—154°C, which gave a green ferric chloride reaction in ethanol; yield 4.3 g. UV: $\lambda_{max}^{EtOH}$ mμ (log ε); 241.5 (4.12), 289 (4.21), 355 (3.70).

Found: C, 61.58; H, 4.17. Calcd. for $C_{17}H_{14}O_7$: C, 61.82; H, 4.27%.

**2-Hydroxy-4, 5-methylenedioxy-6-methoxyphenyl 3, 4-Dimethoxybenzyl Ketone (VIII).** — From the phenol III (15.0 g.), 3, 4-dimethoxybenzyl cyanide (17.5 g.), fused zinc chloride (4.5 g.) and dry ether (1000 ml.), synthesis was carried out by a method

*1 All melting points are uncorrected; the infrared spectra were measured in Nujol, while the ultraviolet spectra were measured in an ethanol solution.

8) J. B. Niederl and R. T. Roth, *J. Am. Chem. Soc.*, **60**, 2140 (1938); Z. Horii, *J. Pharm. Soc. Japan* (*Yakugaku Zasshi*), **77**, 252 (1957).

*2 Inflection point.

similar to that used for IV. The product was distilled, and the distillate (bath temperature 300—330°C/0.05 mmHg) was collected and then crystallized from chloroform-methanol to give VIII as yellow needles, m. p. 121.5—122°C, which gave a green ferric chloride reaction in ethanol; yield 450 mg. UV: $\lambda_{max}^{EtOH}$ mμ (log ε); 287.5 (4.18), 355 (3.72).

Found: C, 62.23; H, 5.23. Calcd. for $C_{18}H_{18}O_7$: C, 62.42; H, 5.24%.

**5-Methoxy-6, 7-methylenedioxyisoflavone (IX).**—The ketone VI (1.0 g.) in freshly-distilled ethyl formate (60 ml.) was added slowly to sodium powder (2.0 g.) at −10°C. The reaction mixture was allowed to stand for 24 hr. at 0°C and then for 48 hr. at room temperature. Ice water containing hydrochloric acid was added, and the solution was extracted with ether. The ether solution was washed with aqueous sodium bicarbonate and then with water, and dried. The recrystallization of the residue from ethanol gave IX as colorless needles; m. p. 145—147°C; yield 330 mg. UV: $\lambda_{max}^{EtOH}$ mμ (log ε); 260 (4.41), 324 (3.82).

Found: C, 68.99; H, 3.95. Calcd. for $C_{17}H_{12}O_5$: C, 68.91; H, 4.08%.

**5-Methoxy-6, 7; 3', 4'-bismethylenedioxyisoflavone (X).**—From the ketone VII (3.9 g.), freshly-distilled ethyl formate (320 ml.) and sodium powder (7.0 g), synthesis was carried out by a method similar to that used for IX. The product was recrystallized from chloroform-methanol to give X as yellow needles; m. p. 223—224°C; yield 1.5 g. UV: $\lambda_{max}^{EtOH}$ mμ (log ε); 267 (4.41), 290*[2] (4.18), 320*[2] (3.84).

Found: C, 63.36; H, 3.67. Calcd. for $C_{18}H_{12}O_7$: C, 63.53; H, 3.55%.

**3', 4', 5-Trimethoxy-6, 7-methylenedioxyisoflavone (XI).**—From the ketone VIII (450 mg.), freshly-distilled ethyl formate (60 ml.) and sodium powder (1.0 g.), synthesis was carried out by a method similar to that used for IX. The product was recrystallized from ethanol to give XI as colorless needles; m. p. 178—178.5°C; yield 110 mg. UV: $\lambda_{max}^{EtOH}$ mμ (log ε); 266.5 (4.45), 324 (3.82).

Found: C, 63.99; H, 4.61. Calcd. for $C_{19}H_{16}O_7$: C, 64.04; H, 4.53%.

**5-Hydroxy-6, 7-methylenedioxyisoflavone (XII).**—A mixture of IX (1.3 g.) and anhydrous aluminum chloride (13.0 g.) in dry ether (130 ml.) was refluxed for 10 hr. The reaction mixture was then poured into ice water and kept for 14 hr. at room temperature. The resulting yellow precipitate was collected and refluxed with a solution of acetic acid (45 ml.) and concentrated hydrochloric acid (45 ml.) for 30 min. The reaction mixture was then diluted with water. The precipitate was collected, washed with water, and recrystallized from acetone to give XII as yellow prisms, m. p. 198—199°C, which gave a green ferric chloride reaction in ethanol; yield 0.9 g. UV: $\lambda_{max}^{EtOH}$ mμ (log ε); 244 (4.32), 270.5 (4.38), 332*[2] (3.58).

Found: C, 68.03; H, 3.53. Calcd. for $C_{16}H_{10}O_5$: C, 68.08; H, 3.57%.

The acetate of XII: acetic anhydride-pyridine method; m. p. 178—179°C (colorless needles from ethanol). UV: $\lambda_{max}^{EtOH}$ mμ (log ε); 251 (4.40), 321 (3.95).

Found: C, 66.42; H, 3.80. Calcd. for $C_{18}H_{12}O_6$: C, 66.67; H, 3.73%.

XII was methylated, by the usual dimethyl sulfate-potassium carbonate method, to IX, which was undepressed on admixture with the above sample.

**5-Hydroxy-6, 7; 3', 4'-bismethylenedioxyisoflavone (XIII).**—A mixture of X (1.47 g.), anhydrous aluminum chloride (12.0 g.) and dry ether (100 ml.) was treated by a method similar to that used for XII. The product was recrystallized from acetone to give XIII as yellow needles, m. p. 232.5—233.5°C, which gave a green ferric chloride reaction in ethanol; yield 780 mg. UV: $\lambda_{max}^{EtOH}$ mμ (log ε); 274 (4.39), 294*[2] (4.29), 336*[2] (3.59).

Found: C, 62.87; H, 2.98. Calcd. for $C_{17}H_{10}O_7$: C, 62.58; H, 3.09%.

The acetate of XIII: acetic anhydride-pyridine method; m. p. 216—217°C (colorless needles from aqueous methanol). UV: $\lambda_{max}^{EtOH}$ mμ (log ε); 265 (4.29), 293.5 (4.11), 317*[2] (3.94).

Found: C, 61.71; H, 3.24. Calcd. for $C_{19}H_{12}O_8$: C, 61.96; H, 3.29%.

XIII was methylated, by the usual dimethyl sulfate-potassium carbonate method, to X, which was undepressed on admixture with the above sample.

The authors are grateful to Professor Carl Djerassi, Stanford University, for a gift of natural tlatlancuayin. Grateful acknowledgement is also made to the members of the Microanalytical Laboratory, Faculty of Pharmacy, Nagasaki University, for the microanalyses.

*Department of Chemistry*
*Faculty of Science*
*Hiroshima University*
*Higashi-Sendamachi, Hiroshima*

# Szilard-Chalmers Reaction of Trioxalatochromium Ion on Ion Exchange Resin—Static Irradiation and Its Kinetic Analysis

By Yoshihiro SENSUI and Tatsuo MATSUURA

(Received November 21, 1964)

The Szilard-Chalmers process can generally be divided into the following four consecutive processes.[1,2]

1) First process. This is purely a physical disruption of the bond due to the nuclear recoil. The yields in this process should be almost independent of the chemical constitution of the target material.

2) Second process. The hot atoms are thermalized in this epithermal process. In the case of a liquid phase, the hot atoms will be incorporated into some familiar stable chemical species at the end of this step.[3] Thus the yields may be more or less dependent on the chemical environment of the system.

3) Third process. During irradiation, the products of the second process undergo the radiation-induced thermal reactions. The yields are usually much influenced by various factors, such as irradiation time, chemical enviroment, and absorbed radiation dose of the system.[4]

4) Fourth process. This is the ordinary thermal annealing process. In addition, separation-induced processes may sometimes occur. The yields depend further on many factors, such as standing time and temperature[4].

It should be noted that the concomitant radiations other than the thermal neutrons in a reactor, i. e., the fast and the epithermal neutrons and the gamma rays, always produce the very same degraded species through processes similar to those mentioned above.[5] They usually decrease the separable yield through enhancement of the recombinations in the third process, and thus are the main factors complicating the true results of the recoil phenomena.

One of the authors has recently developed a flow method, using a complex-ion-loaded ion-exchanger in which an appropriate eluent continuously leaches out the recoil products from the target material immediately after their production.[6] Since this method can almost eliminate the third process, it may shed light on the immediate results at the end of the second process. Trioxalatochromium ion on an anion exchange resin is one of the most suitable samples for this purpose, considering its chemical constitution and the ionic stability in water. This paper deals with the results of the batch-wise experiments and their kinetic analysis, which have been done as an introductory approach to the flow method in this system.

## Experimental

**Material.**—Trioxalatochromium complex ion was adsorbed on the acetate form of the anion exchange resin,[7] Dowex 1X8 (100—200 mesh), from an aqueous solution of $K_3Cr(C_2O_4)_3 \cdot 3H_2O$ prepared by the usual method.[8] At about 15 hr. prior to irradiation, the resin was freed from aquated impurities with 0.01 N nitric acid and washed with water. As an irradiation sample, about 4 ml. of the resin was pipetted into a polyethylene vial with 3 ml. of the digesting solution, which was adjusted to pH 2.0 with nitric acid, pH 3.15 with acetic acid or pH 3.85 with acetic acid. The sample was stored in a frozen state until just before the irradiation.

**Pile Irradiation.**—Most of the samples were irradiated in a position of the reactor having minimum concomitant radiations, i. e., behind a leadblock (6.5 cm. thick) inserted in the thermal column of the TRIGA Mark II reactor, for 1.5—12 hr. at 100 kW. The thermal and the fast neutron fluxes here are about $3\times10^{10}$ and $1\times10^{8}$ n./cm$^2$/sec., respectively, and the external gamma exposure rate is about $7\times10^{3}$ r./hr. The internal radiation dose rate, i. e., the radiation energy absorbed by the sample per unit time due to the (n, $\gamma$) and the $N$(n, p) reactions and the collision of fast neutrons in the sample irradiated at this condition, was estimated to be about the same order of magnitude as the external exposure rate.

Some exploratory experiments were made using different positions, i. e., in the rotary specimen

1) A. G. Maddock and J. I. Vargas, *Trans. Faraday Soc.*, **57**, 992 (1961).
2) K. Svoboda, IA-666-tr. (1962).
3) G. Harbottle and N. Sutin, "Advances in Inorganic Chemistry and Radiochemistry," Vol. I, Academic Press Inc., New York (1959).
4) J. H. Green, G. Harbottle and A. G. Maddock, *Trans. Faraday Soc.*, **49**, 1413 (1953).
5) R. R. Williams, *J. Phys. & Colloid Chem.*, **52**, 603 (1948).
6) T. Matsuura, Proc. 5th Japan Conference on Radioisotope, 4-27 (1963): T. Matsuura, *J. Inorg. & Nucl. Chem.*, to be published.
7) Y. Inoue, A. Kawamura, K. Wada and H. Okamura, *Japan Analyst*, **2**, 121 (1953).
8) H. S. Booth, "Inorganic Syntheses," Vol. I, 37 McGraw-Hill Book Co., Inc., New York (1939).

rack, in which the thermal and the fast neutron fluxes are about $6\times10^{11}$ and $5\times10^{10}$ n./sec./cm$^2$ respectively and the gamma exposure rate is about $1.4\times10^6$ r./hr., or in the thermal column without the lead shield, in which the gamma exposure rate is about $2\times10^4$ r./hr. However, with the samples which were irradiated in the rotary specimen rack, the yields of $^{51}$Cr in the cationic species were found to be negligibly small, and even with those which had received only threefold increased gamma ray exposures by omitting the lead shield in the thermal column, the yield decreased as much as 17% on the average compared with the samples with the lead shield. In view of these results, further experiments were always carried out with the lead shield in the thermal column of the reactor.

**Chemical Separation.**—Although it has been reported that some part of the chromium can change its initial oxidation state by recoil[9-13] most of the chromium in this liquid system seems to maintain its lower oxidation state,[14] because the oxalate ion and the strong basic type anion exchanger form a highly reductive environment. Thus the main products from the parent complex ion were assumed to be hexaquo-, monoxalatotetraquo- and dioxalatodiaquo-chromium ions. Within 5—30 min. after the irradiation, the resin was transferred into a column (1 cm. i. d.) containing about 0.5 ml. of the acetate form of Dowex 1X8; the cationic species [$Cr(H_2O)_6^{3+}$ and $Cr(OX)(H_2O)_4^+$] were firstly eluted from the resin with about 100 ml. of water, and the dioxalato species was separated from it with 300 ml. of 0.01 N nitric acid. The parent ion was finally eluted from the resin with 100 ml. of 1 N ammonium nitrate which had been adjusted to pH 1.0 with nitric acid. Though the dioxalato species was not so clearly separated from the parent one, they were distinguished by the steep change in the enrichment factors in the effluents. The cationic species were further separated by using 0.5 M perchloric acid and 6 N hydrochloric acid as eluents on a column of a cation exchange resin[15] in a few earlier runs, however this procedure was omitted in later runs and these portions were treated together as "cationic species," because the reported high rate of the equilibration reaction between them[16] was evidenced from about the same values of enrichment factors found in these fractions.

**Determination of $^{51}$Cr Activity and Total Chromium.**—The activities of aliquots of the effluents were measured by counting the 0.32 MeV. photon emission of the $^{51}$Cr with a well-type NaI(Tl) scintillation counter and a single channel analyzer. The amounts of total chromium (active and non-active chromium) were determined colorimetrically by the chromate method (using a filter of 372 m$\mu$).[17]

## Results

**The Percentage Yield of $^{51}$Cr.** — The $^{51}$Cr yields in the cationic, dioxalato and trioxalato chromium species are plotted against the irradiation time, for immersing solutions of varying pH values in Figs. 1, 2 and 3, respectively. They show that the yields of $^{51}$Cr in

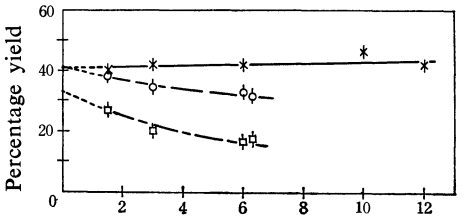



Fig. 1. Percentage yields of $^{51}$Cr in the cationic species (hexaquo and monoxalatotetraquo) species against irradiation time.
—*— pH 2.0; ——○—— pH 3.15; - -□- - pH 3.85
The lines are the calculated values.

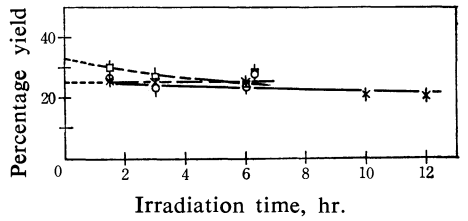



Fig. 2. Percentage yields of $^{51}$Cr in dioxalato species against irradiation time.
—*— pH 2.0; ——○—— pH 3.15; - -□- - pH 3.85
The lines are the calculated values.

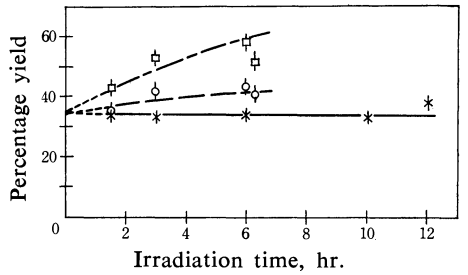



Fig. 3. Percentage yields of $^{51}$Cr in trioxalato species against irradiation time.
—*— pH 2.0; ——○—— pH 3.15; - -□- - pH 3.85
The lines are the calculated values.

9) G. Harbottle, *J. Chem. Phys.*, **22**, 1083 (1954).
10) L. M. Fishman and G. Harbottle, ibid., **22**, 1088 (1954).
11) N. Shibata and K. Yoshihara, This Bulletin, **32**, 422 (1959).
12) N. Matsuura, Y. Kurimura and Y. Tsunoda., ibid., **35**, 1679 (1962).
13) N. Saito, H. Sano and T. Tominaga, *Chem. & Ind.*, **1961**, 1796.
14) W. H. Burgus and J. W. Kennedy, *J. Chem. Phys.*, **18**, 97 (1950).
15) E. L. King and E. B. Dismukes, *J. Am. Chem. Soc.*, **74**, 1674 (1952).
16) K. V. Krishnamurty and G. M. Harris, *Chem. Revs.*, **61**, 213 (1961).
17) E. B. Sandell, "Colorimetric Determination of Traces of Metals," Interscience Pubs., New York (1950).

the cationic species decrease with the pH value of the digesting solution, whereas the yields of the parent species increase with it. It should be noted that while the yields of all species at pH 2.0 are almost unchanged with the irradiation time, the dependence of the yields on the irradiation time becomes noticeable as the pH value increases.

It follows from these figures, that the recombination rate is small at pH 2.0 but becomes noticeable with increasing pH value. The figures also show that the yields at zero irradiation time, i. e. the initial distribution of $^{51}Cr$ in each species in the epithermal process, is influenced by the pH value.

**The Percentage Yield of Total Chromium and Enrichment Factor.**—The yields of total chromium in the cationic, dioxalato and trioxalato species are plotted against irradiation time in Figs. 4, 5 and 6, respectively. Dividing the yields of $^{51}Cr$ in each species, by the yields of total chromium in the corresponding species, gives the enrichment factors shown in Fig. 7. The enrichment factors of the enriched species decrease with the irradiation time according

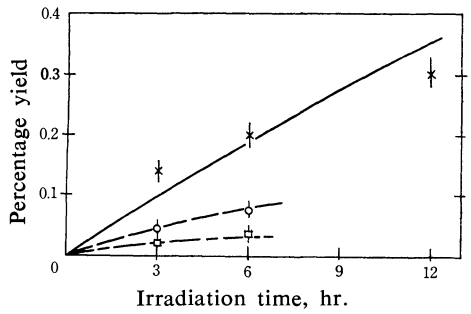



Fig. 4. Percentage yields of total chromium in the cationic species against irradiation time.
—*— pH 2.0; ——○—— pH 3.15;
——□—— pH 3.85
The lines are the calculated values.

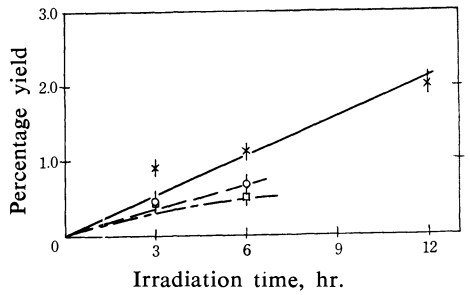



Fig. 5. Percentage yields of total chromium in dioxalato species against irradiation time.
—*— pH 2.0; ——○—— pH 3.15;
——□—— pH 3.85
The lines are the calculated values.

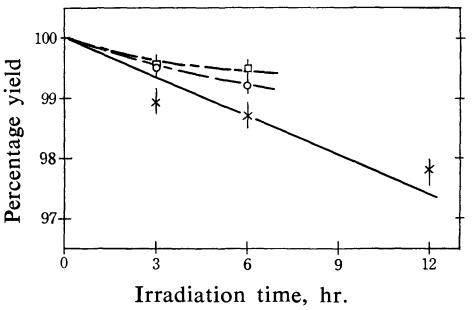



Fig. 6. Percentage yields of total chromium in trioxalato species against irradiation time.
—*— pH 2.0; ——○—— pH 3.15;
——□—— pH 3.85
The lines are the calculated values.

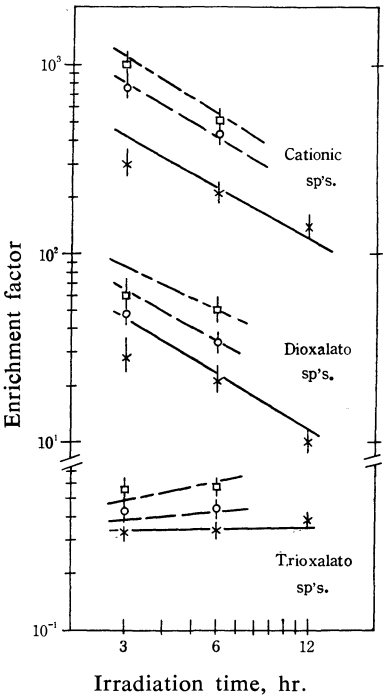



Fig. 7. Enrichment factor in each species against irradiation time.
—*— pH 2.0; ——○—— pH 3.15;
——□—— pH 3.85
The lines are the calculated values.

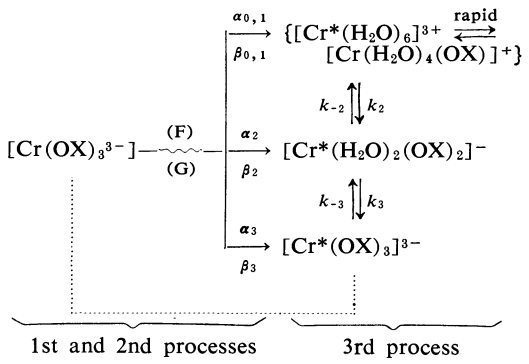
to the general law.[18] Figure 7 also shows that the enrichment factor increased with the pH value of the digesting solution.

## Discussion

The overall reaction including the epithermal process accompanied by both recoil and gross radiolysis, and the subsequent thermal process

18) G. E. Boyd, J. W. Cobble and S. Wexler, *J. Am. Chem. Soc.*, 74, 237 (1952).

of interconversion among the main products during irradiation, can be represented by the following scheme:




Here, it should be noted that although the first and the second processes can be distinguished in the case of the labeled species, this can not be so with the total chromium species, i. e., the rate constant of the actual degradation of $Cr(OX)_3^{3-}$ species is expressed as $\{G(\beta_2+\beta_{0,1})+k_{-3}\}$.

Then the labeled and the total chromium species can be followed simultaneously by the following rate equations, the radioactive decay terms for this nuclide being neglected:

$$\left.\begin{aligned}
\frac{d(X_{0,1}^*+X_{0,1})}{dt} &= \alpha_{0,1}FN_{cr} \\
&+k_{-2}(X_2^*+X_2)+\beta_{0,1}G(X_3^*+X_3) \\
&-k_2(X_{0,1}^*+X_{0,1}) \\
\frac{d(X_2^*+X_2)}{dt} &= \alpha_2FN_{cr}+k_2(X_{0,1}^*+X_{0,1}) \\
&+(\beta_{0,1}G+K_{-3})(X_3^*+X_3) \\
&-(k_{-2}+k_3)(X_2^*+X_2) \\
\frac{d(X_3^*+X_3)}{dt} &= \alpha_3FN_{cr}+k_3(X_2^*+X_2) \\
&-\{(\beta_{0,1}+\beta_2)G+k_{-3}\}(X_3^*+X_3)
\end{aligned}\right\} \quad (1)$$

where

$F$=rate constant of formation of $^{51}Cr$, $a\cdot\phi_{th}\cdot\sigma_{act}$,*

$G$=rate constant of initial decomposition of parent ion by radiolysis,**

$\alpha_i$=initial fraction of distribution of $^{51}Cr$ in each species by recoil,

$\beta_i$=initial fraction of distribution of total chromium in each species by radiolysis,

$k_{-i}$=apparent rate constants of the aquation under irradiation condition, with respect to the complex ion,

$k_i$=apparent rate constants for complex formation under irradiation condition, with respect to the complex ion,

$X_i^*$=number of $^{51}Cr$ in each species,

$X_i$=total number of chromium atoms in each species,

$N_{cr}$=total number of chromium atoms in the whole system.

We obtain the equations for the active chromium by eliminating the nonactive terms in Eq. 1, and those for the total chromium by neglecting the first and the labeled terms. We assume that not only the aquation rate but also the complexing rate are first order with respect to the complex ion for each pH value as is reported in the cold condition.[19,20]

Judging from the data for the yields of $^{51}Cr$ and the total chromium at pH 2.0, we can assume that the complexing rates are small compared with the respective aquation rates for both the labeled and total chromium at pH 2.0. Thus by disregarding the complexing terms in Eq. 1, the following solutions are obtained for active and total chromium at pH 2.0:

$$\left.\begin{aligned}
X_{0,1}^* &= \frac{x_{0,1}^*N_{cr}^*}{100} = (\alpha_{0,1}+\alpha_2)FN_{cr}t \\
&-\frac{\alpha_2FN_{cr}}{k_{-2}}\{1-\exp[-k_{-2}t]\} \\
X_2^* &= \frac{x_2^*N_{cr}^*}{100} \\
&= \frac{\alpha_2FN_{cr}}{k_{-2}}\{1-\exp[-k_{-2}t]\} \\
X_3^* &= \frac{x_3^*N_{cr}^*}{100} = \alpha_3FN_{cr}t
\end{aligned}\right\} \quad (2\text{-a})$$

$$\left.\begin{aligned}
X_{0,1} &= \frac{x_{0,1}N_{cr}}{100} = \frac{\beta_{0,1}GN_{cr}}{(\beta_{0,1}+\beta_2)G+k_{-3}} \\
&\times\{1-\exp[-\{(\beta_{0,1}+\beta_2)G \\
&+k_{-3}\}t]\} \\
X_2 &= \frac{x_2N_{cr}}{100} = \frac{(\beta_2G+k_{-3})N_{cr}}{k_{-2}-(\beta_{0,1}+\beta_2)G+k_{-3}} \\
&\times\{\exp[-\{(\beta_{0,1}+\beta_2)G \\
&+k_{-3}\}t]-\exp[-k_{-2}t]\} \\
X_3 &= \frac{x_3N_{cr}}{100} \\
&= N_{cr}\exp[-\{(\beta_{0,1}+\beta_2)G+k_{-3}\}t]
\end{aligned}\right\} \quad (2\text{-b})$$

where $x_i^*$ and $x_i$ are the percentage yields of $^{51}Cr$ and total chromium in the species $i$, respectively, and $N_{cr}^*$ is the number of $^{51}Cr$ atoms produced after $t$ hr. of irradiation.

* $a$=abundance of $^{50}Cr$,
$\phi_{th}$=thermal neutron flux,
$\sigma_{act}$=thermal neutron cross section for the reaction $^{50}Cr(n,\gamma)^{51}Cr$.

** This is not the rate constant of the apparent radiolytic decomposition but includes the immediate recombination into the parent form in the epithermal reaction, and thus is defined as pH-independent.

19) R. E. Hamm and R. E. Davis, ibid., 75, 3085 (1953).
20) R. E. Hamm and R. H. Perkins, ibid., 77, 2083 (1955).

At pH 3.15 and pH 3.85 it can safely be assumed that the complexing rate constants are much greater than the respective aquation ones, from the results in Figs. 1—7 and the data from the cold condition.[19-21] Thus by neglecting all the aquation terms for the $^{51}Cr$ and the total chromium in Eq. 1 except that for the aquation of the total parent ions, the following relationships are obtained for pH 3.15 and 3.85:

$$\left.\begin{aligned} X_{0,1}^* &= \frac{x_{0,1}^* N_{cr}^*}{100} \\ &= \frac{\alpha_{0,1} F N_{cr}}{k_2}\{1-\exp[-k_2 t]\} \\ X_2^* &= \frac{x_2^* N_{cr}^*}{100} = \frac{(\alpha_{0,1}+\alpha_2) F N_{cr}}{k_3} \\ &\times\{1-\exp[-k_3 t]\} - \frac{\alpha_{0,1} F N_{cr}}{k_3-k_2} \\ &\times\{\exp[-k_2 t]-\exp[-k_3 t]\} \\ X_3^* &= \frac{x_3^* N_{cr}^*}{100} = F N_{cr} t - (X_{0,1}^* + X_2^*) \end{aligned}\right\} \quad (3\text{-a})$$

$$\left.\begin{aligned} X_{0,1} &= \frac{x_{0,1} N_{cr}}{100} \\ &= \frac{\beta_{0,1} G N_{cr}}{k_2}\{1-\exp[-k_2 t]\} \\ X_2 &= \frac{x_2 N_{cr}}{100} = \frac{\{(\beta_{0,1}+\beta_2)G + k_{-3}\} N_{cr}}{k_3} \\ &\times\{1-\exp[-k_3 t]\} - \frac{\beta_{0,1} G N_{cr}}{k_3-k_2} \\ &\times\{\exp[-k_2 t]-\exp[-k_3 t]\} \\ X_3 &= \frac{x_3 N_{cr}}{100} = N_{cr} - (X_{0,1}+X_2) \end{aligned}\right\} \quad (3\text{-b})$$

From the experimental plots in Figs. 1—3, the initial fractions of distribution of $^{51}Cr$ at the end of the second process are read as $\alpha_{0,1}=0.41$, $\alpha_2=0.25$ and $\alpha_3=0.34$ for pH 2.0 and 3.15 and $\alpha_{0,1}=0.33$, $\alpha_2=0.32$ and $\alpha_3=0.35$ for pH 3.85, respectively. After these values were put into the Eqs. 2-a, 2-b, 3-a and 3-b, the other parameters $\beta_{0,1}G$, $\beta_2 G$, $k_{-i}$ and $k_i$ which may also be pH-dependent were estimated by trial and error method for each pH value, to give calculated yields of $^{51}Cr$ and total chromium which best fit the experimental ones, as is shown in Figs. 1—6. The agreement between the calculated curves and the observed plots implies that the assumptions made are reasonable. The rate constants thus determined are shown in Fig. 8.

As can be seen in Fig. 8 the gross decomposition rate constant of the parent ion under irradiation, $\{(\beta_{0,1}+\beta_2)G+k_{-3}\}$, and the rate constant of the initial direct formation of cationic species from the parent ion by radiolysis, $\beta_{0,1}G$, are only slightly dependent on the pH value, while the corresponding aquation rate constants under the cold condition have been reported to be much more dependent on the pH value.[21,22] However, the fact that the numerical values observed under irradiation condition were found to be much larger than those of the corresponding aquation rate constant of the parent ion under cold condition* may imply that the pH-independent radiation-induced term is predominant over the pH-dependent cold term even in low radiation fields as in this irradiation condition.

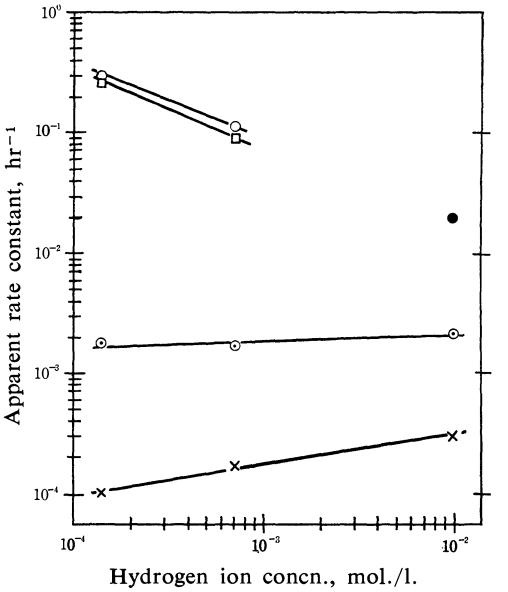



Fig. 8. The best-fit apparent rate constants against the hydrogen ion concentration.
○ $k_3$; □ $k_2$; ⊙ $(\beta_{0,1}+\beta_2)G+k_{-3}$; × $\beta_{0,1}G$; ● $k_{-2}$

On the other hand, Fig. 8 shows that the apparent rate constants of the complex-forming reaction, $k_i$'s, are nearly inversely proportional to the hydrogen ion concentration, in accord with the corresponding ones under the cold condition both in tendency and in magnitude.[19,20] This suggests that the radiation-induced term does not seriously contribute to the apparent complexing rate constant at least in the low radiation fields. However, as can be seen from the exploratory experiment, higher radiation fields may increase the recombination rate.

21) K. V. Krishnamurty and G. N. Harris, *J. Phys. Chem.*, **64**, 346 (1960).

22) N. K. Dutt and B. Sur, *Z. anorg. u. allgem. Chem.*, **293**, 195 (1957).

* These values are calculated to be $2.2\times10^{-4}$ and $5\times10^{-6}$ $hr^{-1}$ for pH 2.0 and 3.85 respectively according to Krishnamurty's data.[21]

We believe that the dependence on pH value, of the initial fraction of distribution of $^{51}Cr$ among each species, $\alpha_i$, is reasonable, because in the epithermal reaction, an immediate recombination of the degraded ion should have occured, and its extent will depend on the pH value. The lowest value of $\alpha_3$ obtained, 0.34 can be referred to as the "initial retention" in this system. However, as this is the value after the completion of the epithermal reaction in this chemical environment, it seems difficult to relate it with the nuclear inefficiency of the bond rupture due to the $^{51}Cr$ recoil in the first process. The authors believe this value for chromium should be almost zero, as was evidenced by the reported almost zero value of retention in the $Cr(SCN)_6^{3-}$ system.[23] The same author[23] reports that the most aquated species is the most enriched one, and this is just what we found in our system, as is shown in Fig. 7.

## Summary

Trioxalatochromium ion, on Dowex 1X18 immersed in a solution of pH 2.0—3.85, was irradiated batch-wise in the thermal column of a reactor for various irradiation times. With decreasing pH, the $^{51}Cr$ yield of the most enriched species (hexaquo- and monoxalatotetraquo-chromium ion) increased, but the enrichment factor decreased. With increasing irradiation time, while the changes in the $^{51}Cr$ yield of each chemical form are small at pH 2.0, the recombination reaction becomes noticeable at pH 3.15 and 3.85. These results were analyzed kinetically, and the rate constants of the aquation and the complex formation under irradiation condition as well as the initial fractions of distribution of $^{51}Cr$ and the total chromium among each chemical species were determined for the respective pH values.

The authors wish to express their hearty thanks to the IAEA, in whose research project (Contract No. 221/RB, "the use of an ion-exchanger to increase the specific activity of radioisotopes in Szilard-Chalmers reactions") this work is included. The authors' thanks are also to be extended to Professor Tetsuo Takaishi of our Institute for his helpful discussions on the kinetic analysis, and to the reactor operating staff of our Institute for their cooperation.

*Institute for Atomic Energy*
*Rikkyo (St. Paul's) University*
*Sajima, Yokosuka*

23) S. Kaufman, *J. Am. Chem. Soc.*, **82**, 2963 (1960).

# The Determination of the Water Content in Acetaldehyde by Means of the Karl Fischer Reagent

By Kaname MUROI, Kunihiko OGAWA and Yaeko ISHII

(Received November 21, 1964)

Carbonyl compounds generally interfere with the Fischer titration. This is due to their tendency to form acetals or ketals by the reaction with methanol contained in Karl Fischer reagent, a process accompanied by the production of additional water:[1]

$$RCHO + 2CH_3OH \rightarrow RCH(OCH_3)_2 + H_2O \quad (1)$$

$$R_2CO + 2CH_3OH \rightarrow R_2C(OCH_3)_2 + H_2O \quad (2)$$

Mitchell et al.[2] have suggested, therefore, the use of Fischer reagent after converting carbonyl compounds to cyanohydrin with hydrogen cyanide. However, considerable difficulty is encountered in preparing a dried solution of toxic hydrogen cyanide and dioxane or pyridine; moreover, a complicated treatment is required prior to the titration.

Other methods have been proposed for the direct titration of water with modified Fischer reagents containing a great excess of pyridine[3] or containing methyl Cellosolve;[4] these methods are applicable to ketones, but not to aldehydes, in which the precise titration of water cannot be expected because reaction 1 accompanies the reaction 3 of absorbing water from the sample;[5]

1) K. Fischer, *Angew. Chem.*, **48**, 394 (1935).
2) W. M. D. Bryant, J. Mitchell, Jr., and D. M. Smith, *J. Am. Chem. Soc.*, **62**, 3504 (1940).
3) G. Wernimont, F. J. Hopkinson, *Ind. Eng. Chem., Anal. Ed.*, **15**, 272 (1943).
4) E. D. Peters, J. L. Tungnickel, *Anal. Chem.*, **27**, 450, (1955).
5) J. Mitchell, Jr., and D. M. Smith, "Aquametry," Interscience, New York (1948), p. 149.

$$RCHO + C_5H_5N \cdot SO_2 + H_2O \rightarrow C_5H_5N\langle_{H}^{SO_3CH(OH)R} \quad (3)$$

In previous papers, the present authors reported methods for the direct titration of water in low polymers[6,7] of formaldehyde and in ketones[8] by using the alcohol-free Karl Fischer reagent SS (Mitsubishi) and by keeping the interfering reactions under control. On the basis of these methods, the authors have now established the present method for the quantitative determination of water in acetaldehyde.

## Experimental

**Materials.**—Special-class reagents of acetaldehyde were used without further purification. Dried acetaldehyde was obtained by the distillation of para-aldehyde. Pyridine was obtained commercially. Propylene glycol was dried by boiling it. The Karl Fischer reagent SS (Mitsubishi), supplied by Mitsubishi Chemical Industries, was used (titer: 3.0 mg. $H_2O$/ml.)

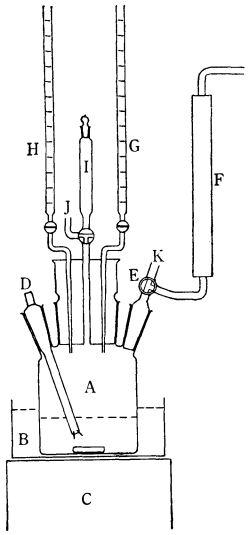



Fig. 1. Apparatus for electrometric titration.
A : Titration flask, 50 ml.
B : Water bath
C : Magnetic stirrer
D : Platinum electrode
E : Three way stop cock
F : Drying tube for nitrogen
G : Buret for Karl Fischer reagent
H : Buret for standard water-methanol
I : Outlet (with drying tube)
J : Outlet for nitrogen
K : Inlet for sample

6) K. Muroi and K. Ogawa, This Bulletin, **36**, 965 (1963).
7) K. Muroi and K. Ogawa, ibid, **36**, 1278 (1963).
8) K. Muroi, K. Ogawa and Y. Ishii, *Japan Analyst*, **12**, 963 (1963).

**Apparatus.**—The Karl Fischer electrometric titration apparatus, operating by the dead-stop method, was manufactured by the Tsutsui Chemical Instrument Co. The apparatus is illustrated in Fig. 1.

**Procedure.**—*Sampling Method.*—A carefully-dried injector (volume, 5 ml.; length of injection needle, about 10 cm.), with a small piece of silicone rubber stuck on the needle tip, was inserted in a polyethylene bag and then placed in an electric refrigerator. The injector thereby cooled and a vessel, which had been similarly stored and which contained the acetaldehyde sample and with a three-way cock for drawing the liquid, were taken out of the refrigerator. The injector was then inserted into the three-way cock in order to draw acetaldehyde from the vessel. The inside of the injector was rinsed twice with the sample, and then, the third time, 5 ml. of cold acetaldehyde was collected in the injector. (Each time after the drawing, the needle tip was wrapped with dry gauze so that the traces of moisture and of the sample which adhered to it were removed.)

*Titrating Method.*—Five milliliters of a solvent mixture of pyridine-propylene glycol (3 to 1, by volume) was added to a titration flask, which was then subjected to a water bath at 25 to 30°C. While passing dry nitrogen through the three-way cock, E, illustrated in Fig. 1, into this flask at the flow rate of 0.9 l./min., drops of the Karl Fischer reagent SS were added in order to bring it to the dead stop end point. The introduction of nitrogen was then stopped, and the injector was inserted through the three-way cock, E, into the titration flask until the needle tip was soaked in the liquid surface. Then the acetaldehyde was released into the pyridine - propylene glycol mixture as rapidly as possible. Now, while the solution was stirred, nitrogen was again introduced into the flask, and the titration was simultaneously carried out until the end point was obtained, where a drop of the SS (Mitsubishi) reagent kept the magic eye open as long as 50 to 60 sec.

## Results and Discussion

Acetaldehyde, among carbonyl compounds, showed the greatest velocity in the interfering reaction 1. Accordingly, an investigation with a view of avoiding this interference was carried out. Because of the difference in the boiling points of acetaldehyde and water, it was possible, after adding an exactly-weighed sample to a titration flask containing the pyridine - propylene glycol mixture solvent which was effective in controlling reaction 1, to evaporate almost all the interfering acetaldehyde with dry nitrogen directed toward the surface of the solution, and to titrate the remaining water in the solvent with the SS reagent. When acetaldehyde was evaporated with nitrogen, a small quantity of the liquid dissolved and remained in the solvent. In order to study any effect of the remaining acetaldehyde on the titration, 0.1, to 0.5 ml.

Table I. Effects of acetaldehyde in terms of its amounts employed

| Amount of sample ml. | Titration temp., °C | Titration value ml. | Interfering reaction | Nature of end point |
|---|---|---|---|---|
| 0.1 | 25 | 0.18 | Not occur | Distinct |
| 0.2 | 25 | 0.37 | Not occur | Distinct |
| 0.3 | 25 | 0.55 | Occurs | Distinct |
| 0.4 | 25 | 0.80 | Occurs | Indistinct |
| 0.5 | 25 | 0.87 | Occurs | Indistinct |

Table II. Effects of titration temperatures

| Titration temp., °C | Amount of sample ml. | Titration value ml. | Interfering reaction | Nature of end point |
|---|---|---|---|---|
| 10 | 0.2 | 0.38 | Not occur | Distinct |
| 15 | 0.2 | 0.37 | Not occur | Distinct |
| 20 | 0.2 | 0.39 | Not occur | Distinct |
| 25 | 0.2 | 0.38 | Not occur | Distinct |
| 30 | 0.2 | 0.39 | Not occur | Distinct |

Table III. Effects of the mixing ratios of pyridine-propyene glycol in the solvent

| Mixing ratio in the solvent pyridine : propylene glycol | Titration temp., °C | Amount of sample ml. | Titration value ml. | Interfering reaction | Nature of end point |
|---|---|---|---|---|---|
| 1 : 1 | 25 | 0.2 | — | Occurs | Indistinct |
| 2 : 1 | 25 | 0.2 | 0.35 | Occurs | Indistinct |
| 3 : 1 | 25 | 0.2 | 0.38 | Not occur | Distinct |
| 4 : 1 | 25 | 0.2 | 0.39 | Not occur | Distinct |
| 5 : 1 | 25 | 0.2 | 0.34 | Not occur | Indistinct |

of purified acetaldehyde was added to 5 ml. of the 3 : 1 solvent mixture of pyridine - propylene glycol in a flask. The water content in the solution was then titrated with the reagent SS. Tables I, II and III show the results obtained in the investigation of how the interfering reactions were affected by the amounts of acetaldehyde employed, the titration temperatures and the mixing ratios of the solvent components. These tables confirmed that the interference from acetaldehyde was not observed at room temperatures when less than 0.2 ml. of acetaldehyde was contained in 5 ml. of the pyridine - propylene glycol. On the other hand, when a 5 : 1 mixture of pyridine-propylene glycol was employed as the titration solvent for the sample, the end point titration became indistinct because of the pyridine-inhibiting reaction between water and the reagent described. Therefore, the 3 : 1 mixture of pyridine-propylene glycol proved to be the most suitable solvent for the direct titration of water in acetaldehyde.

In determining the amount of the solvent to be employed, 0.1 to 0.5 ml. (both inclusive), of the sample (as in Table I) was added to 20 ml. of the mixture solvent, and then the water content in the solution was titrated. The results obtained show that the sample solvent had not much effect on the attempt to avoid interfering reactions, because acetaldehyde began to interfere when the amount of acetaldehyde present in the mixture exceeded 0.4 ml.

Next, 2 ml. of acetaldehyde was added to 5 ml. of the pyridine - propylene glycol solvent kept at 25°C in a titration flask. While dry nitrogen, adjusted to various velocities of 0.3 to 1.5 l./min., was passed into the flask, the water content in the solution was titrated with the reagent SS. Table IV shows the results obtained. Although acetaldehyde interfered with the titration because of its insufficient evaporation when nitrogen gas was added at a velocity of less than 0.6 l./min., it no longer interfered, because of its good evaporation when nitrogen was passed at a flow rate of

Table IV. Effects of the velocities of nitrogen gas

| Velocity of nitrogen l./min. | Titration values ml. | Interfering reaction | Nature of end point |
|---|---|---|---|
| 0.3 | — | Occurs | Indistinct |
| 0.6 | 4.68 | Occurs | Indistinct |
| 0.9 | 4.67 | Not occur | Distinct |
| 1.2 | 4.57 | Not occur | Distinct |
| 1.5 | 4.45 | Not occur | Distinct |

more than 0.6 l./min. However, a velocity of more than 1.2 l./min. was found to be undesirable because then the nitrogen tended to drive water from the solvent. Moreover, the amount of acetaldehyde remaining in 5 ml. of the solvent after nitrogen had been passed through at a velocity of more than 0.6 l./min. measured less than 0.1 ml. From this fact, as well as from the afore-mentioned results, it was concluded that a process which involved evaporating the sample by means of nitrogen could have a considerable effect on the elimination of interfering reactions in direct titration.

To 5 ml. of the pyridine-propylene glycol maintained at 25°C 0.2 to 5.0 ml. of acetaldehyde was added. The water content in the solution was then titrated, while nitrogen gas was passed through at a constant velocity of 0.9 l./min. The results, committed to a line graph in Fig. 2, show the rectilinearity and the stable nature of the end point in the titration when 0.2 to 2.50 ml. of acetaldehyde was present in the solvent. However, when more than 3 ml. of acetaldehyde was present, minus errors increased as the titration values increased. On a conjecture that these minus errors might be introduced by the interfering

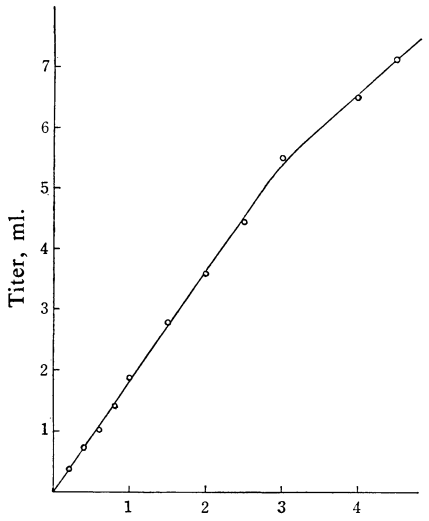



Fig. 2. Effects of amounts of acetaldehyde.

reaction 3, three kinds of reagents, in which molar ratios of $I_2$ to $SO_2$ to $C_5H_5N$ were maintained at 1 : 1.5 : 5, 1 : 3 : 10 and 1 : 6 : 20, were then prepared with the reagent SS. After 0.5 to 2.5 ml. of the sample had been added to 5 ml. of the solvent mixture, the water content in the solution was titrated with these modified reagents by directing nitrogen toward the surface of the solution. The results, shown in Fig. 3, indicate that minus errors tended to increase as the molar ratio between $SO_2$ and $C_5H_5N$ departed further from 1.5 : 5 ; these results confirmed the early conclusion that these minus errors might result from the interfering reaction 3.

Accordingly, it may be suggested that a restriction should be imposed upon titration values in order to eliminate the interference thoroughly. Moreover, a restriction on the titration value (i. e. $C_5H_5N \cdot SO_2$ concentration

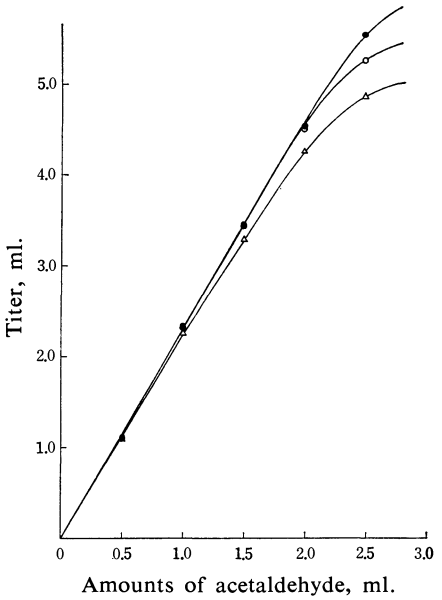



Fig. 3. Effects of molor ratios of $I_2$ to $SO_2$ to $C_5H_5N$ in the reagent.
△, 1 : 6 : 20 ○, 1 : 3 : 10 ●, 1 : 1.5 : 5

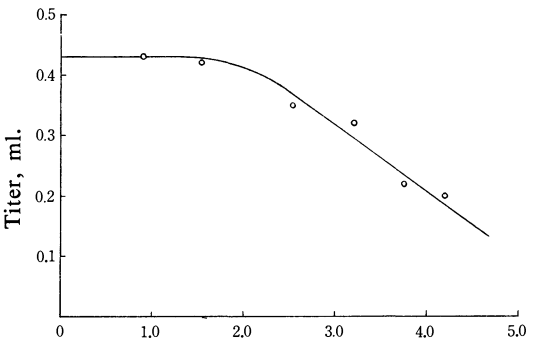



Fig. 4. Effects of water contents in the solvent.

in the reagent) involves a restriction of water content in the solvent employed. Therefore, for our present purposes, the effects of water content on the interfering reaction were studied. To 5 ml. of the 3 : 1 mixture of pyridine and propylene glycol containing various quantities of water, 0.2 ml. of the

TABLE V. RESULTS OF THE TOTAL ANALYSIS

| Sample | Acetaldehyde % | Water % | Impurities % | Total % |
|---|---|---|---|---|
| Commercial grade reagent | 88.7 | 10.1 | 1.0 | 99.8 |
| Acetaldehyde purified and distilled from the reagent | 99.5 | 0.67 | 0.08> | 100.2 |

sample was added. The results of the titrations, suggest that more than about 1.5 mg. (about 0.03%) of water in 5 ml. of the solvent caused minus errors (Fig. 4). Morever, the use of a large quantity of the solvent necessitated an increase in the amount of the reagent consumed for it, so it was found profitable to carry out the titration with the least possible amount of the solvent mixture.

In order to further develop the results shown in Table IV that water content, as well as acetaldehyde, tended to be evaporated when nitrogen was passed through at a velocity of more than 1.2 l./min., we attempted to determine the most suitable time for passing through nitrogen and for beginning the titration after acetaldehyde was added to the pyridine-propylene glycol. The results obtained show that the vaporizasion of water was not observed when nitrogen was introduced shortly after the beginning of titration, whereas it was obviously observed when nitrogen was passed through for more than about 30 sec. prior to the titration, and the resulting titration values were found to involve minus errors. When nitrogen was introduced almost at the end of the titration, interference from the acetaldehyde was observed because the acetaldehyde dissolved in about 4 ml. of the reagent was consumed, increasing the amount of it present in the solvent. Accordingly, in order to avoid evaporating the water, it was necessary to pass nitrogen through simultaneously with the titration, and to titrate the water content while the acetaldehyde was being evaporated.

The optimum conditions for the determination of the water content in acetaldehyde were established as follows:

*Solvent*: Five milliliters of 3:1 mixture (by volume) of pyridine-propylene glycol (water content, less than 0.03 per cent).

*Titration Temperature*: 25 to 30°C.

*Velocity of the Nitrogen Passed*: 0.8 to 1.0 l./min.

(Pass nitrogen into a titration flask simultaneously with the beginning of titration.).

*Sample*: Sample so that the titration value with the reagent (3 mg. $H_2O$/ml. titer) is approximately 4 ml. (equivalent to 12 mg. of water); for example, about 0.1 g. of the sample when it contains 10 per cent water; about 1 g. of the sample, when it contains 1 per cent water, and less than about 10 g. of the sample when it contains less than 0.1 per cent water.

In order to confirm the accuracy of the present method, quantitative determinations of acetaldehyde and the other impurities were made by means of the acid sodium sulfite method and by chromatography, and the values calculated were added to those of the water content. The results shown in Table V suggest the adequacy of the present method for the determination of the water content of acetaldehyde.

TABLE VI. RESULTS OF THE DETERMINATION OF A SMALL AMOUNT OF WATER IN REFINED ACETALDEHYDE

| Sample ml. | Titration value ml. | Water content mg. | Water content % |
|---|---|---|---|
| 1 | 0.14 | 0.42 | 0.053 |
| 3 | 0.41 | 1.23 | 0.052 |
| 5 | 0.65 | 1.95 | 0.050 |
| 7 | 1.06 | 3.17 | 0.057 |
| 10 | 1.32 | 3.95 | 0.050 |

TABLE VII. RESULTS OF THE DETERMINATION OF WATER IN REFINED ACETALDEHYDE CONTAINING A KNOWN AMOUNT OF WATER ADDED

| Sample ml. | Pyridine added ml. | Theoretical amount of water mg. | Water content value measured mg. | Difference from theoretical value mg. |
|---|---|---|---|---|
| 5 | — | — | 1.95 | — |
| 5 | 0.1 | 2.07 | 2.10 | +0.03 |
| 5 | 0.2 | 2.18 | 2.16 | −0.02 |
| 5 | 0.4 | 2.41 | 2.40 | −0.01 |
| 5 | 0.6 | 2.64 | 2.67 | +0.03 |
| 5 | 0.8 | 2.87 | 2.88 | +0.01 |
| 5 | 1.0 | 3.10 | 3.05 | −0.05 |

A small quantity of water in pure acetaldehyde prepared with para-aldehyde was determined by the present method. The water content values indicated in Table VI show a reproducibility. Moreover, from the water content values indicated in Table VII for 5 ml. of purified acetaldehyde determined in the presence of a fixed amount of pyridine containing a known quantity of water, it was reaffirmed that the determination of a minimal amount of water in acetaldehyde was carried out with accuracy by the present method.

## Summary

Approximately 5 ml. of the sample has been added to 5 ml. of a 3 : 1 solvent mixture of of pyridine - propylene glycol in a titration flask. The difference in boiling point between acetaldehyde and water made it possible to evaporate almost all the interfering acetaldehyde from the solution with nitrogen gas passed into the flask at a velocity of about 0.9 l./min. The water remaining in the solution was titrated with the Karl Fischer reagent SS (Mitsubishi).

Because this reagent is free from alcohol, which would show an interfering reaction in Eq. 1, and because it is somewhat lower than the general Karl Fischer reagent in its concentration of $C_5H_5N \cdot SO_2$, which is the main component responsible for the interfering reaction in Eq. 3, it proves to be the most satisfactory for the present titration method.

A small quantity of water in purified acetaldehyde was determined by the present method, and subsequent anlysis of water content values showed an excellent reproducibility.

*Central Reserch Laboratory*
*Mitsubishi Chemical Ind. Ltd.*
*Kawasaki, Kanagawa*

# Studies of Antibiotics and Related Substances. XXI. The Synthesis of Deoxy and Chlorodeoxy Derivatives[1] of Kanamycin

By Tsutomu TSUCHIYA and Sumio UMEZAWA

(Received November 26, 1964)

In the course of our investigation into the effects of structural changes in kanamycin on its antibacterial activity, the syntheses of some aminosugar glucosides of deoxystreptamine and related compounds were previously reported.[2] The present report is concerned with the extension of this work.

Since kanamycin[3] contains two aminosugar moieties in the sequence 3-amino-3-deoxy-D-glucose—deoxystreptamine—6-amino-6-deoxy-D-glucose, an interesting type of structural variant would be the exchange of the aminosugars for another sugar by a partial synthesis from the antibiotic. Modifications of the primary alcoholic group in the 3-amino-3-deoxy-D-glucose moiety will be described in this paper.

As has previously been reported,[4] 4-*O*-(6-amino-6-deoxy-α-D-glucopyranosyl)-deoxystreptamine and 6-*O*-(3-amino-3-deoxy-α-D-glucopyranosyl)-deoxystreptamine were isolated from the acid-hydrolyzate of kanamycin by controlled hydrolysis; it was thus found that the former showed considerable antibacterial activity, whereas the latter did not show any activity against microorganisms tested. This suggested that (6-amino-6-deoxyglucosyl)-deoxystreptamine moiety may take the leading role in exhibiting the antibacterial activity of kanamycin. Accordingly, the synthetic variation of the 3-amino-3-deoxyglucose part of kanamycin was undertaken.

Kanamycin (I) contains seven alcoholic hydroxyl groups, one of which is primary; the others are all secondary. The difference[5]

1) Presented at the 17th Annual Meeting of the Chemical Society of Japan, Tokyo, March, 31, 1964. A brief communication has already been given of the synthesis of deoxykanamycin: T. Tsuchiya, S. Iriyama and S. Umezawa, *J. Antibiotics*, **A16**, 173 (1963).

2) a) S. Umezawa and Y. Ito, This Bulletin, **34**, 1540 (1961); b) T. Suami, S. Ogawa and S. Umezawa, ibid., **36**, 460 (1963); T. Suami, S. Ogawa, T. Yoshizawa and S. Umezawa, ibid., **37**, 1538 (1964); c) T. Tsuchiya, H. Fujita and S. Umezawa, *J. Antibiotics*, **A17**, 181 (1964); d) S. Umezawa and S. Koto, ibid., **A17**, 186 (1964).

3) S. Umezawa, Y. Ito and S. Fukatsu, ibid., **A11**, 120, 162 (1958); This Bulletin, **32**, 81 (1959).

4) S. Umezawa and T. Tsuchiya, *J. Antibiotics*, **A15**, 51 (1962).

5) See, e. g., R. S. Tipson, "Advances in Carbohydrate Chem.," Vol. 8, Academic Press. Inc., New York, N. Y. (1953), p. 127.

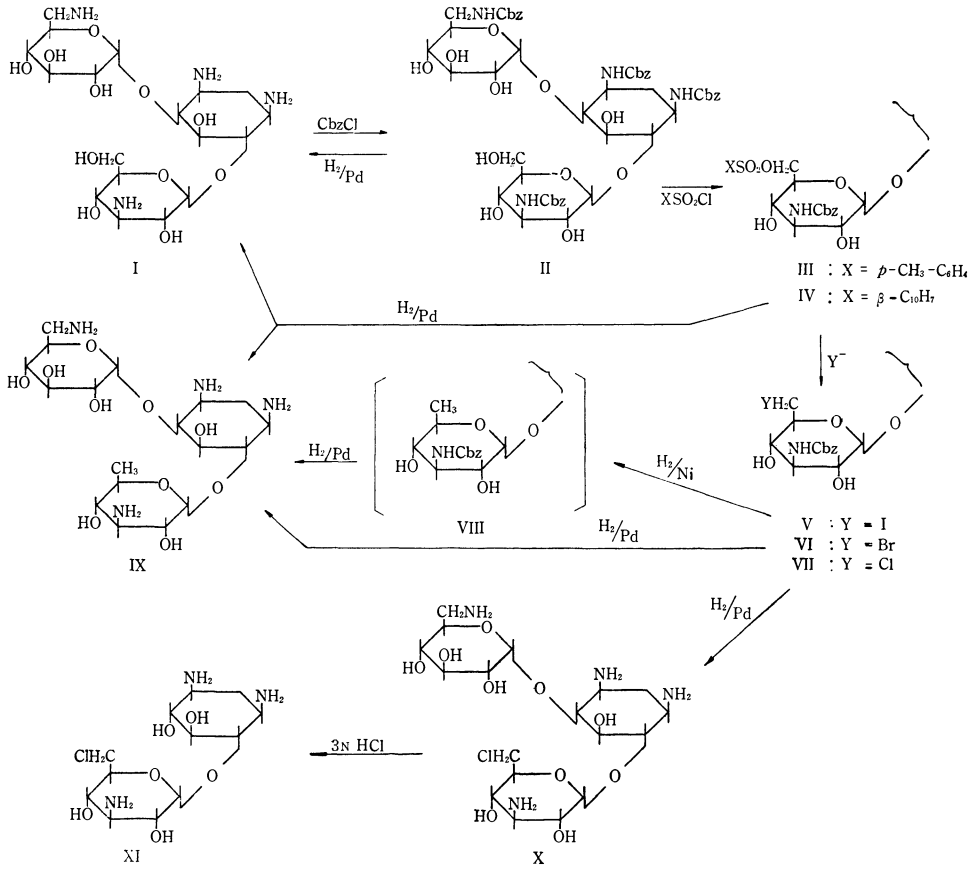



Chart 1

in the ease of the arylsulfonylation of primary and secondary alcoholic groups—the primary hydroxyl can be more easily esterified than the secondary ones—has been used for the present synthesis.

The treatment of an aqueous acetone suspension of kanamycin and sodium carbonate with carbobenzoxy chloride in toluene afforded tetra-*N*-carbobenzoxykanamycin (II). Since difficulty was experienced in avoiding contamination by the formation of an *O*-carbobenzoxylated product, the crude product was treated with dilute ethanolic hydrogen chloride at room temperature to afford an analytically pure sample of II (Chart 1).

The arylsulfonylation of the primary hydroxyl group of II was effected by *p*-toluenesulfonyl chloride, followed by fractional precipitation and silica gel column chromatography; by this method, a mono-*O*-tosylated product (III) was obtained in about a 20% yield. Alternatively, β-naphthalenesulfonyl chloride was used to convert II to a mono-*O*-nasylated product (IV). However, the yield of arylsulfonylation was only slightly improved.

The replacement of the tosyloxy group of III or the nasyloxy group of IV by an iodine atom was readily brought about by heating the ester (III or IV) with sodium iodide in an acetone-dioxane solution, thus affording the deoxyiodo derivative (V) of tetra-*N*-carbobenzoxykanamycin (II) in a 94% yield (from III). On the basis of the extensive studies by Oldham and Rutherford[6] and other workers[7], it can be said that the facility of the replacement reaction indicates that the tosyl group in III was joined to the primary hydroxyl group. The corresponding chlorodeoxy and bromodeoxy derivatives (VII and VI) were also obtained from IV by the use of lithium chloride and bromide in similar reactions. The well-known order of nucleophilic reactivity, $I^- > Br^- > Cl^-$, has been again observed in the fact that sodium iodide reacted faster than lithium bromide, which in turn reacted faster than lithium chloride, to precipitate the corresponding alkaline salt of β-naphthalenesulfonic acid. The

6) J. W. H. Oldham and J. K. Rutherford, *J. Am. Chem. Soc.*, **54**, 366 (1932).

7) W. T. Haskins, R. M. Mann and C. S. Hudson, ibid., **64**, 132 (1942); G. R. Barker and R. W. Goodrich, *J. Chem. Soc.*, **1949**, *Supplm.*, 233; H. Schmid and P. Karrer, *Helv. Chim. Acta*, **32**, 1371 (1949).

crude product of VII, which could not be readily obtained in a pure form, was used for the next step without further purification.

The deoxyiodo derivative (V) was converted, by hydrogenolysis with a Raney nickel catalyst, to the corresponding deoxy derivative (VIII) of tetra-*N*-carbobenzoxykanamycin, and thence, by repeated hydrogenolysis with palladium black in a dioxane - water - acetic acid solution, to deoxykanamycin. Attempts to effect direct hydrogenolysis by the palladium catalyst to deoxykanamycin without the prior use of a Raney nickel catalyst were unsuccessful.

The hydrogenolysis of the bromodeoxy derivative (VI) with palladium black by a similar procedure also gave the deoxykanamycin.

A similar hydrogenolysis of the chlorodeoxy derivative (VII) with a palladium catalyst, followed by column chromatography on Dowex 1 X2 resin, led to chlorodeoxy-kanamycin (X).

The hydrogenolysis of the nasyl derivative (IV) by the palladium catalyst in aqueous dioxane containing a small amount of acetic acid proceeded smoothly, and the formation of the expected kanamycin, accompanied by deoxykanamycin, was confirmed by paper chromatography.

Paper chromatography of the deoxykanamycin (IX) and chlorodeoxy-kanamycin (X) by ninhydrin coloration, using a *t*-amylalcohol - pyridine - water - acetic acid (6 : 4 : 3 : 1) solvent system and Toyo filter paper No. 50, showed $R_f$ 1.3 and 2.2 respectively, the $R_f$-value of kanamycin being taken as 1.0.

Structural evidence for chlorodeoxy-kanamycin (X) and deoxykanamycin (IX) was further obtained from the results of the controlled hydrolysis of X. (3-Amino-6-chloro-3, 6-dideoxy-D-glucosyl)-deoxystreptamine (XI) has been isolated from the hydrolyzate of X by a paper chromatographic technique.

We[2c] have previously reported that the $R_{fD}$-value*1 of a di-glucoside of deoxystreptamine is approximately given by the product of the two $R_{fD}$-values of the constituent mono-glucosides. The application of the $R_{fD}$-values of XI ($R_{fD}$ 1.33) and 4-*O*-(6-amino-6-deoxyglucosyl)-deoxystreptamine ($R_{fD}$ 0.39) to the multiplication rule showed a good accordance with the experimental value of $R_{fD}$ (0.52) of X: $1.33 \times 0.39 = 0.52$.*2

Deoxykanamycin (IX) was hydrolyzed by refluxing it in 3 N hydrochloric acid, and the hydrolyzate was submitted to paper chromatography. Detection by ninhydrin-coloration showed a spot of $R_f$ (1.67) relative to the $R_f$-value of 3-amino-3-deoxy-D-glucose taken as 1.0, in addition to the spots corresponding to deoxystreptamine and 6-amino-6-deoxy-D-glucose. Evidently, the new spot indicated the presence of 3-amino-3, 6-dideoxy-D-glucose in the deoxykanamycin. The paper chromatography of the hydrolyzate obtained by mild hydrolysis of chlorodeoxy-kanamycin showed the spot of (3-amino-6-chloro-3, 6-dideoxy-D-glucosyl)-deoxystreptamine (XI), in addition to the spots of deoxystreptamine, 6-amino-6-deoxy-D-glucose, 4-*O*-(6-amino-6-deoxy-D-glucosyl)-deoxystreptamine[4] and unchanged chlorodeoxy-kanamycin.

Both deoxykanamycin and chlorodeoxy-kanamycin showed strongly antibacterial activity, and their antibiotic spectra*3 were essentially similar to that of kanamycin as shown in Table I. XI had no antibacterial activity against organisms tested.

## Experimental

**Paper Chromatography and Bioautography.**— Paper chromatography was performed by the descending technique, using Toyo filter paper No. 50. The solvent system used was *t*-amylalcohol - pyridine - water - acetic acid (6 : 4 : 3 : 1). Aminosugars and their glucosides were detected by ninhydrin-coloration, using a general procedure. Spots corresponding to the antibacterial components were also detected on the bioautograms by a general procedure[8] using *Bacillus subtilis* as the test organism.

**Tetra-*N*-carbobenzoxykanamycin (II).**— A mixture of a kanamycin base (1.5 g. 3.1 mmol.) and sodium carbonate decahydrate (4.1 g.) in 75% aqueous acetone (60 ml.) was cooled to about −5°C, and into the mixture was then vigorously stirred a solution of carbobenzoxy chloride (2.15 g. 12.6 mmol.) in toluene (7 ml.) in portions over a 5 min. period. After the addition was complete, stirring was continued at about 5°C for 3 hr. The reaction mixture became almost clear once, and then the resulting product began to separate. The reaction mixture was placed in a refrigerator overnight. The mixture was poured into a large volume of a mixture of water and ether, and then vigorously agitated. The flocculent product which had been precipitated between two layers was collected and pressed between filter papers to remove the solvents.

The product was added to a solution of ethanol and concentrated hydrochloric acid (10 : 1), and the mixture was stirred at room temperature for 1.5 hr.

*1 $R_{fD}$ is an $R_f$-value relative to the $R_f$-value of deoxystreptamine, taken as 1.0.

*2 In this experiment, by the general procedure described in the beginning of the "Experimental" section and analogous to that described in the report of Ref. 2c) The $R_{fD}$-values of (3-amino-3-deoxy-D-glucosyl)-deoxystreptamine and kanamycin were 0.60 and 0.23 respectively. The experimental value for kanamycin also showed a good accordance with the calculated value: $0.60 \times 0.39 = 0.23$.

*3 The antibiotic spectrum of deoxykanamycin was previously presented in a short communication by T. Tsuchiya, S. Iriyama and S. Umezawa; see Ref. 1.

8) The method first used for the analysis of penicillins: R. R. Goodall and A. A. Levi, *Nature*, **158**, 675 (1946); *Analyst*, **72**, 277 (1947).

The product was filtered and washed with water; yield 3.09 g. (96%), m. p. 259—261°C (decomp.). A sample (1.0 g.) was recrystallized from dioxane-water to give an analytically pure sample (0.76 g.) of the title compound (II); m. p. 259—261°C, $[\alpha]_D^{18}$ +68.2° (*c* 2.038, in dimethyl formamide).

Found: C, 58.89; H, 6.18; N, 5.41. Calcd. for $C_{50}H_{60}O_{19}N_4$: C, 58.81; H, 5.92; N, 5.49%.

It was confirmed by van Slyke determination that the pure sample did not contain the free $NH_2$ group.

**The Hydrogenolysis of II to Kanamycin.** — A sample (400 mg.) of II was dissolved in 15 ml. of aqueous dioxane (1 : 1) containing a drop of acetic acid and hydrogenated over palladium black (100 mg.) under atmospheric pressure at 45°C for 13 hr. The reaction mixture was filtered, and the filtrate was evaporated to dryness. An aqueous solution of the residue (270 mg.) was passed through a column of Amberlite IRA-400 resin (OH form) (4 ml.). Ninhydrin-positive, strongly-alkaline fractions were collected and concentrated to a small volume by evaporation. The addition of ethanol to the concentrate caused crystallization; yield 120 mg. The product was proved to be identical with intact kanamycin by elementary analysis and biological assay.

Found: C, 44.63; H, 7.26; N, 11.46; 11.2 (van Slyke). Calcd. for $C_{18}H_{36}O_{11}N_4$: C, 44.62; H, 7.49; N, 11.56%.

**Tetra-*N*-carbobenzoxy-mono-*O*-tosylkanamycin (III).**—A sample (10.2 g. 10 mmol.) of II was dissolved in dry pyridine (60 ml.) and cooled to −18°C, and then to it was added *p*-toluenesulfonyl chloride (2.10 g.) in one portion. The mixture was vigorously shaken and then allowed to stand at about the same temperature for 4 hr., at 0°C for 20 hr., and additionally at room temperature for 24 hr. After a small volume of water had been added and after it had stood for 1 hr., the reaction mixture was poured into a large volume of ice water. The precipitate was collected by centrifuge and washed with water; yield 10.5 g. The crude product was extracted with three 30-ml. portions of hot ethyl acetate in order to remove the higher tosylated product (1.05 g.; S, 5.28%). The insoluble residue was pressed between filter papers and dried in a desiccator; yield 7.8 g. The product was powdered and extracted with three 300-ml. portions of hot dry acetone to separate the unchanged II, which is almost insoluble in acetone. The resulting acetone extract was filtered and concentrated to a volume of about 65 ml. After the concentrate had been allowed to stand at room temperature for a while, the resulting solid was filtered; yield 1.9 g., S, 1.83%.

A sample (450 mg.) of the product was dissolved in a solvent of *n*-butanol - acetic acid - water (3 : 2 : 1) and was chromatographed through a silica gel column (17×310 mm.) using the same solvent system. After 30 ml. of the eluate had been collected, the desired product emerged in the next 13 ml. This fraction, after evaporation to dryness, weighed 370 mg. (13.3%). Additional material (770 mg.) was obtained by the concentration of the above acetone mother-liquor to 20 ml.; the total yield was 20%; m. p. 200—202°C (decomp.), $[\alpha]_D^{14}$ +67° (*c* 1.96, in dimethyl formamide).

Found: C, 58.29; H, 5.88; S, 2.41. Calcd. for $C_{57}H_{66}O_{21}N_4S$: C, 58.25; H, 5.66; S, 2.73%.

**Tetra-*N*-carbobenzoxy-mono-*O*-nasylkanamycin (IV).**—A sample (7.0 g.) of II was dissolved in dry pyridine (40 ml.) and cooled to about −18°C, and to it was added β-naphthalenesulfonyl chloride (1.95 g.). The reaction mixture was then submitted to a procedure similar to that described above for III, giving crude IV (8.4 g.). The crude product (720 mg.) was extracted with acetone (35 ml.) by refluxing it for a while, and, after it had cooled to room temperature, the acetone extract was filtered and evaporated to dryness (510 mg.). This was again extracted with ethyl methyl ketone (75 ml.) by refluxing it for a while; the extract was filtered and evaporated to dryness to give a residue (390 mg.) with a sulfur content of 3.03%. The product was further treated with hot ethyl acetate (20 ml.), and the insoluble residue was collected and dried in a desiccator; yield 230 mg. (32%); m. p. 186—187°C (decomp.).

Found: S, 2.69%. Calcd. for $C_{60}H_{66}O_{21}N_4S$: S, 2.53%.

**Tetra-*N*-carbobenzoxy-deoxyiodo-kanamycin (V).**—A solution of III (1.0 g.) and sodium iodide (0.38 g.) in anhydrous dioxane - acetone (1 : 1) was heated in a sealed tube in a boiling water bath for about 50 min. After the mixture had been heated for 5 min., sodium *p*-toluenesulfonate began to precipitate. After cooling, the reaction mixture was filtered and evaporated to dryness; the residue was washed with water and dried in a desiccator. A mixture of the product and anhydrous acetone was refluxed for a while and then allowed to stand overnight. The precipitate was collected by filtration to give the title compound; yield 900 mg. (94%); m. p. 220—223°C (decomp.).

Found: C, 53.32; H, 5.14; I, 11.30. Calcd. for $C_{50}H_{59}O_{18}N_4I$: C, 53.20; H, 5.26; I, 11.20%.

The infrared spectrum of the product showed the absence of the absorption at 1170 $cm^{-1}$ ($\nu_s$ $SO_2$) which was found in the spectrum of III.

This compound was also prepared from IV and sodium iodide by a procedure similar to that described above. In this reaction, the precipitation of sodium β-naphthalenesulfonate began after the reaction mixture had been heated for 10 min.

**Deoxykanamycin (IX).**—A sample of V (200 mg.) in 80% aqueous dioxane (6.0 ml.) was refluxed, hydrogen being passed through in the presence of Raney nickel (W-4) (0.2 ml.) for 10 min. After cooling, the mixture was filtered, and the filtrate was repeatedly treated with fresh Raney nickel and hydrogen. The concentration of the filtrate, followed by the addition of water, afforded a crude product of tetra-*N*-carbobenzoxy-deoxykanamycin (VIII); yield 150 mg.

The product was dissolved in a mixed solvent dioxane - water - acetic acid (4 : 1 : 0.04) (10 ml.) and hydrogenated with palladium black (40 mg.) under hydrogen-pressure of 3.0 atm. at 35°C for 1 hr. A small quantity of water was added to the mixture, and again the hydrogenation was continued for about 2 hr. The repetition of this procedure,

followed by filtration and evaporation, gave a crude product, which was washed with hot acetone. The resulting solid was dissolved in 95% ethanol, treated with a small quantity of active charcoal, and evaporated to give deoxykanamycin tetraacetate; yield 82 mg., $[\alpha]_D^{15}$ +99.6° (*c* 0.88, in water).

Found: C, 44.24; H, 7.13; N, 8.08. Calcd. for $C_{18}H_{36}O_{10}N_4 \cdot 4CH_3CO_2H$: C, 44.06; H, 7.39; N, 7.91%.

By the general procedure of paper chromatography, the product showed an $R_f$-value of 1.3 relative to an $R_f$-value of kanamycin of 1.0.

The acetate (70 mg.) was dissolved in a small quantity of water, placed on the top of a column of Amberlite IRA-400 resin (OH form) (1 ml.), and developed with water. Ninhydrin-positive fractions were collected, filtered, and evaporated to dryness. The residue was dissolved in a small quantity of hot 90% ethanol and filtered; concentration, followed by the addition of ethanol to turbidity, afforded the free base of deoxykanamycin; yield 25 mg.

Found: C, 46.36; H, 7.51; N, 11.81. Calcd. for $C_{18}H_{36}O_{10}N_4$: C, 46.15; H, 7.75; N, 11.96%.

A small quantity of IX was heated with 3 N hydrochloric acid for 2 hr. in a boiling water bath, and the hydrolyzate was submitted to paper chromatography by the general procedure. Detection by ninhydrin coloration showed the spot of 3-amino-3,6-dideoxy-D-glucose ($R_f$ 1.67, relative to an $R_f$-value of 3-amino-3-deoxy-D-glucose of 1.0), in addition to the spots corresponding to deoxystreptamine and 6-amino-6-deoxy-D-glucose.

**Chlorodeoxy-kanamycin (X).** — A mixture of a crude sample (400 mg.) of IV and dry lithium chloride in 14 ml. of anhydrous dioxane-acetone (1 : 1) was heated in a sealed tube for 5 hr. in a boiling water bath. No precipitation of lithium β-naphthalenesulfonate occurred until the heating of the mixture had been continued for 2 hr. After cooling, the resulting mixture was filtered and worked up by a procedure similar to that described above for V; the yield of the crude product of VII was 360 mg. (Cl, 2.83%).

A crude sample (1.74 g.) of VII was dissolved in a mixture of dioxane (40 ml.), water (25 ml.) and acetic acid (0.4 ml.) and hydrogenated with palladium black (250 mg.) under a hydrogen-pressure of 3.0 atm. at 35°C for 15 hr. When water (20 ml.) was added, the reaction mixture became turbid; this indicated that the hydrogenation was not completed. Hydrogenation was therefore continued for a further 3 hr. Water (15 ml.) was added to the reaction mixture, and the hydrogenation was again continued for about 10 hr., after which the reaction mixture was filtered and the filtrate was concentrated to about 50 ml. Since the paper chromatography of the concentrate still showed three, strongly ninhydrin-positive spots ($R_f$ 4.3, 8.7 and 14, relative to an $R_f$-value of X of 1.0) other than X, the concentrate was again treated with a fresh palladium catalyst (250 mg.) and hydrogen for 20 hr. and filtered. The filtrate was concentrated to about 10 ml., placed on a column (27×280 mm.) of Dowex 1 X2 (OH form), and developed with water at the rate of 0.5 ml./min.; the eluates were submitted to paper chromatography and bioautography. After 350 ml. of eluate had been collected, kanamycin emerged in the next 130 ml., and then chlorodeoxykanamycin emerged from 590 ml. to 710 ml. The former fractions (fraction A) were collected, neutralized with hydrochloric acid to pH 3.0, and concentrated, and acetone was added to give kanamycin tetrahydrochloride; yield 90 mg. By a similar procedure, the latter fractions (fraction B) gave a syrup, which was dissolved in a small quantity of methanol and treated with active charcoal, and acetone was added to afford chlorodeoxy-kanamycin tetrahydrochloride; yield 170 mg., $[\alpha]_D^{15}$ +95° (*c* 0.8, in water).

Found: C, 32.31; H, 6.19; N, 8.60; Cl, 26.20. Calcd. for $C_{18}H_{35}O_{10}N_4Cl \cdot 4HCl \cdot H_2O$: C, 32.42; H, 6.20; N, 8.40; Cl, 26.59%.

In another experiment, fraction B was neutralized

Table I. Minimal inhibitory concentration of chlorodeoxy-kanamycin tetraacetate, mcg./ml.

| Test organism | Chlorodeoxy-kanamycin tetraacetate | Kanamycin tetraacetate |
|---|---|---|
| *Staphylococcus aureus* 209p | 3.12 | 3.12 |
| *Staphylococcus aureus* Terashima | 1.56 | 3.12 |
| *Streptococcus faecalis* ATCC 8043 | 50 | 50 |
| *Streptococcus haemolyticus* Cook | 50 | 50 |
| *Sarcina lutea* | 12.5 | 25 |
| *Diplococcus pneumoniae* Type I | 1.56 | 3.12 |
| *Escherichia coli* var. *communis* | 12.5 | 12.5 |
| *Salmonella typhi* O-901-W | 3.12 | 3.12 |
| *Salmonella typhi* T-58 | 3.12 | 6.25 |
| *Shigella dysenteriae shigae* | 1.56 | 3.12 |
| *Proteus vulgaris* OX 19 | 25 | 50 |
| *Pseudomonas aeruginosa* | 100 | 100 |
| *Bacillus subtilis* PCI 219 | 3.12 | 3.12 |
| *Mycobacterium phlei* No. 56 | 1.56 | 3.12 |
| *Mycobacterium* 607 | 1.56 | 1.56 |
| *Mycobacterium tuberculosis* H37Rv | 3.12 | 3.12 |

with acetic acid to pH 4 and worked up by a procedure similar to that used for the above hydrochloride to give chlorodeoxy-kanamycin tetraacetate; $[\alpha]_D^{15}$ +90° (*c* 0.9, in water).

Found: C, 39.42; H, 7.66; Cl, 4.54. Calcd. for $C_{18}H_{35}O_{10}N_4Cl \cdot 4CH_3CO_2H \cdot 2H_2O$: C, 40.08; H, 7.11; Cl, 4.55%.

A small quantity of X was heated with 3 N hydrochloric acid in a boiling water bath for 20 min., and the hydrolyzate was submitted to paper chromatography by the general procedure. Detection by ninhydrin coloration showed the spot ($R_{fD}$ 1.33) of XI, in addition to the spots of deoxystreptamine ($R_{fD}$ 1.00), 6-amino-6-deoxy-D-glucose ($R_{fD}$ 1.72), 4-*O*-(6-amino-6-deoxy-D-glucosyl)-deoxystreptamine ($R_{fD}$ 0.39) and unchanged chlorodeoxy-kanamycin ($R_{fD}$ 0.52).

**6-*O*-(3-Amino-6-chloro-3, 6-dideoxy-α-D-glucopyranosyl)-deoxystreptamine Hydrochloride (XI).*** — A sample (108 mg.) of chlorodeoxy-kanamycin tetrahydrochloride was dissolved in 3 N hydrochloric acid and heated for 20 min. in a boiling water bath. The reaction was quenched by cooling the mixture with tap water, and then the resulting solution was evaporated to dryness under reduced pressure and the residue dried in a desiccator to give a solid (109 mg.). This was dissolved in a small quantity of water, paper chromatographed on 3 sheets of Toyo filter paper No. 50 (40×40 cm.), and developed with the *t*-amylalcohol - pyridine - water - acetic acid (6 : 4 : 3 : 1) solvent system by the descending method for 40 hr. A zone corresponding to the compound of $R_{fD}$ 1.33 was clipped from each paper and extracted with water, and the aqueous extract was evaporated to dryness. The residue (28 mg.) dissolved in a small quantity of water was placed on a column (4×110 mm.) of Dowex 1 X2 resin (OH form) and developed with water. After a small amount of deoxystreptamine has been eluted, the desired compound emerged from 1.7 to 3.5 ml. of the eluate. The fraction, which was strongly alkaline and positive in the Beilstein test for halogen, was neutralized with hydrochloric acid to pH 3.0 and evaporated to dryness. The residue was dissolved in a small quantity of methanol, and acetone was added to precipitate the title compound; yield 11 mg.; $[\alpha]_D^{20}$ +73° (*c* 0.7, in water).

Found: C, 32.33; H, 6.25. Calcd. for $C_{12}H_{24}O_6N_3Cl \cdot 3HCl$: C, 31.94; H, 6.03%.

The product showed no reducing property.

**Tetra-*N*-carbobenzoxy-bromodeoxy-kanamycin (VI) and Hydrogenolysis.**—A mixture of a sample (30 mg.) of IV and dried lithium bromide (10 mg.) in 0.5 ml. of anhydrous dioxane - acetone (1 : 1) was heated in a sealed tube for 2 hr. in a boiling water bath. When the mixture was heated for 30 min., lithium β-naphthalenesulfonate was precipitated. The resulting mixture was worked up by a procedure similar to that described above for V to give 26 mg. of VI.

Found: Br, 7.7. Calcd. for $C_{50}H_{59}O_{18}N_4Br$: Br, 7.4%.

A small quantity of the above sample was hydrogenated with palladium black by a procedure similar to that used for the hydrogenolysis of VII to afford deoxykanamycin, which was detected by both paper chromatography and bioautography.

* According to Rinehart and Hichens, 3-amino-3-deoxy-D-glucose is linked to the C-6 of deoxystreptamine; see K. L. Rinehart and M. Hichens, *J. Am. Chem. Soc.*, **85**, 1547 (1963).

## Summary

1) Deoxykanamycin has been synthesized in a four-stage sequence beginning with kanamycin. Kanamycin has been converted to tetra-*N*-carbobenzoxykanamycin, and this transformed in turn to tetra-*N*-carbobenzoxy-mono-*O*-tosylkanamycin (or the corresponding nasyl derivative), to tetra-*N*-carbobenzoxy-deoxyiodokanamycin, and finally to deoxykanamycin.

2) The above nasyl derivative has been transformed via tetra-*N*-carbobenzoxy-chlorodeoxy-kanamycin to chlorodeoxy-kanamycin.

3) 6-*O*-(3-Amino-6-chloro-3, 6-dideoxy-α-D-glucosyl)-deoxystreptamine hydrochloride has been obtained by the controlled acid-hydrolysis of chlorodeoxy-kanamycin.

4) The hydrogenolysis of tetra-*N*-carbobenzoxy-bromodeoxy-kanamycin has given deoxykanamycin.

5) It has been found that deoxykanamycin and chlorodeoxy-kanamycin are strongly antibacterial and that their antibiotic spectra are essentially similar to that of kanamycin.

Part of the expenses for this work were defrayed by a grant-in-aid for Scientific Research from the Ministry of Education, a grant which is gratefully acknowledged. The authors are indebted to Mr. Saburo Nakada for his micro-analyses and to Mrs. Setsuko Iriyama of this Laboratory and to the Central Laboratories of the Meiji Seika Co. for their bioassays. The authors are also grateful to Mr. Kuniaki Tatsuta and Mr. Tadashi Takeshiro for their assistance in the experimental work.

*Department of Applied Chemistry*
*Faculty of Engineering*
*Keio University*
*Koganei-shi, Tokyo*

# The Phosphorescence Spectra of 2, 2'- and 4, 4'-Bipyridyls

By Yasuhiko GONDO and Yoshiya KANDA

(Received December 11, 1964)

The blue-green phosphorescence spectra of 2, 2'-bipyridyl, and the blue phosphorescence spectra of 4, 4'-bipyridyl, in ethanol, carbon tetrachloride, and cyclohexane at 90°K, have been studied and the results are reported here. The phosphorescence spectra of 2, 2'- and 4, 4'-bipyridyls had not been observed previously. Kanda, Shimada, and Sakai[1] studied in detail the green-blue phosphorescence of biphenyl in EPA, petroleum ether, cyclohexane, and carbon tetrachloride at 90°K. Since the molecular structures of 2, 2'- and 4, 4'-bipyridyls are closely related to that of biphenyl, it was assumed that the phosphorescence spectra of the bipyridyls must be very similar to the spectrum of biphenyl. The vibrational analyses are discussed.

## Experimental

2, 2'-Bipyridyl, from Tokyo Kasei Co., was recrystallized twice from ethanol. The melting point was 69.5°C. 4, 4'-Bipyridyl-dihydrochloride was obtained from K & K Laboratories.[2] Three grams of 4, 4'-bipyridyl-dihydrochloride was treated with 1.2 g. of caustic soda in water, and the 4, 4'-bipyridyl which precipitated was recrystallized twice from hot water; the product was 4, 4'-bipyridyl-dihydrate which was dried in air for 2 days and then in a desiccator over sulfuric acid for 20 days until a theoretical loss in weight corresponding to two molecules of water resulted. The melting point was 110.2—110.5°C. Solvent used in this study were ethanol, cyclohexane, and carbon tetrachloride which were purified as described previously.[1,3] The optical setup was the same as described previously.[3]

## Results and Discussion

The triplet-singlet emission spectra of 2, 2'- and 4, 4'-bipyridyls in ethanol, carbon tetrachloride, and cyclohexane at 90°K have been observed, and the microphotometer tracing curves are shown in Figs. 1 and 2. Spectral data and the analyses are given in Tables I and III. The spectrum of 2, 2'-bipyridyl will be discussed first. This compound emitted blue-green phosphorescence with a lifetime of about 2 to 3 sec. by visual estimation. Exposure time ranged from 1 to 7 hr. with slit width of 100 $\mu$ and Kodak Tri-X film. The phosphorescence bands were broad in ethanol, somewhat resolved in carbon tetrachloride and very sharp and well resolved in cyclohexane. Therefore, the vibrational analyses ware made first with the spectrum in cyclohexane. The highest wave number band at 23545 $cm^{-1}$ was taken as the 0, 0-band of the system and vibrational frequencies of 235, 325, 460, 605, 755, 815, 895, 995, 1155, 1235, 1310, 1460, and 1570 $cm^{-1}$ were found; and the 1570 $cm^{-1}$ frequency was seen to form the main progression of the system. These frequencies seem to correspond to the Raman frequencies of 615, 995, 1150, 1239, 1302, 1475, and 1574 $cm^{-1}$. The Raman data were obtained by us but unfortunately the frequencies corresponding to the phosphorescence bands of 235, 325, 755, 815, and 895 $cm^{-1}$ have not yet been found. The phosphorescence band of 460 $cm^{-1}$ may be explained as $2\times235$ $cm^{-1}$. For comparison, the infrared spectrum was also studied. The vibrational frequencies are listed in Table II.

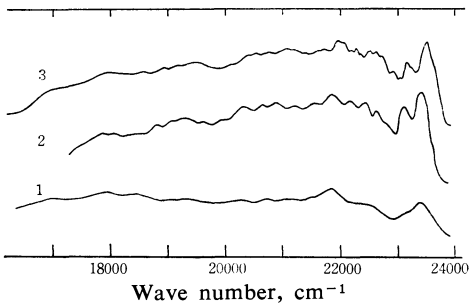



Fig. 1. Phosphorescence spectra of 2, 2'-bipyridyl at 90°K.
Concn.: $1\times10^{-2}$ M, in ethanol (1), carbon tetrachloride (2) and cyclohexane (3)

4, 4'-Bipyridyl emitted blue phosphorescence and the lifetime was about 2 sec. by visual estimation. Exposure time ranged from 5 to 10 hr. with slit width of 100 $\mu$ and Kodak Tri-X film. The phosphorescence bands were broad in ethanol, somewhat resolved in carbon tetrachloride and very sharp and well resolved in cyclohexane as shown in Fig. 2. This behavior is very similar to that of 2, 2'-bipyridyl.

1) Y. Kanda, R. Shimada and Y. Sakai, *Spectrochim. Acta*, **17**, 1 (1961).
2) K & K Laboratories, Inc. 177—10 93rd Avenue, Jamaica 33, N. Y., U. S. A.
3) Y. Kanda and R. Shimada, *Spectrochim. Acta*, **15**, 211 (1959).

TABLE I. PHOSPHORESCENCE SPECTRUM OF 2, 2′-BIPYRIDYL
$\nu$: Wave number in $cm^{-1}$

| In cyclohexane | | | In $CCl_4$ | | | In ethanol | | | Analysis |
|---|---|---|---|---|---|---|---|---|---|
| $\nu$ | Rel. int. | $\Delta\nu$ | $\nu$ | Rel. int. | $\Delta\nu$ | $\nu$ | Rel. int. | $\Delta\nu$ | |
| 23545 | 10 | 0 | 23450 | 10 | 0 | 23420 | 8 | 0 | 0,0 |
| 23310 | 6.5 | 235 | | | | | | | 0-235 |
| 23220 | 7 | 325 | 23130 | 8.5 | 320 | | | | 0-325 |
| 23085 | 5.5 | 460 | | | | | | | 0-235×2 |
| 22940 | 6.5 | 605 | 23860 | 6.5 | 590 | | | | 0-615 |
| 22790 | 8.5 | 755 | 22685 | 8 | 765 | | | | 0-760 |
| 22730 | 8.5 | 815 | | | | | | | |
| 22650 | 8.5 | 895 | | | | 22525 | 7 | 895 | 0-895 |
| 22550 | 9 | 995 | 22465 | 9 | 985 | | | | 0-995 |
| 22390 | 9 | 1155 | | | | | | | 0-1150 |
| 22310 | 9 | 1235 | 22205 | 9 | 1245 | | | | 0-1239 |
| 22235 | 9 | 1310 | | | | | | | 0-1302 |
| 22085 | 10 | 1460 | | | | | | | 0-1460 |
| 21975 | 10 | 1570 | 21880 | 10 | 1570 | 21865 | 10 | 1555 | 0-1574 |
| 21740 | 9 | 1805 | | | | | | | 0-1574-235 |
| 21640 | 9 | 1905 | 21555 | 9 | 1895 | 21495 | 9 | 1925 | 0-1574-325 |
| 21405 | 9 | 2140 | 21240 | 8.5 | 2210 | | | | |
| 21215 | 9 | 2330 | 21125 | 8.5 | 2325 | 21120 | 9 | 2300 | 0-1574-760 |
| 21075 | 9.5 | 2470 | | | | | | | 0-1574-895 |
| 20980 | 9 | 2565 | 20875 | 9 | 2575 | 20790 | 9 | 2630 | 0-1574-995 |
| 20830 | 8.5 | 2715 | | | | | | | 0-1574-1150 |
| 20745 | 9 | 2800 | 20655 | 8.5 | 2795 | | | | 0-1574-1239 |
| 20650 | 8.5 | 2895 | | | | | | | 0-1574-1302 |
| 20515 | 8.5 | 3030 | | | | | | | 0-1574-1460 |
| 20405 | 8.5 | 3140 | 20310 | 8.5 | 3140 | 20330 | 9 | 3090 | 0-1574×2 |
| 20130 | 7 | 3415 | 19980 | 7 | 3470 | | | | |
| 19500 | 7 | 4045 | 19645 | 7 | 3805 | | | | |
| 19220 | 7 | 4325 | 19315 | 7.5 | 4135 | 19450 | 9 | 3970 | |
| 18950 | 6.5 | 4595 | 19070 | 7 | 4380 | 19040 | 9 | 4380 | |
| 18555 | 6.5 | 4990 | 18830 | 6.5 | 4620 | | | | |
| 17940 | 6.5 | 5605 | 18430 | 6 | 5020 | 18530 | 9 | 4890 | |
| | | | 18070 | 6 | 5380 | | | | |
| | | | 17880 | 6 | 5570 | 17930 | 9 | 5490 | |
| 16935 | 7 | 6610 | | | | 17045 | 9 | 6375 | |

TABLE II. VIBRATIONAL FREQUENCIES OF 2, 2′-BIPYRIDYL ($cm^{-1}$)

| Raman | | Infrared | Raman | | Infrared |
|---|---|---|---|---|---|
| In $CS_2$ | In $CCl_4$ | KBr disk | In $CS_2$ | In $CCl_4$ | KBr disk |
| | | 405 m | 1190(1) | 1187(2) | |
| | | 428 w | | | 1210 w |
| | 615(3) | 621 s | 1240(3) | 1239(4) | 1250 s |
| | | 655 m | | | 1268 vw |
| | | 741 w | 1307(2) | 1302(3) | |
| | | 757 vs | | | 1397 w |
| | | 894 w | | | 1418 vs |
| | | 975 vw | 1455(3) | 1475(3) | 1454 vs |
| 1003(3) | 995(5) | 993 s | 1490(3) | 1490(3) | 1507 w |
| 1050(1) | 1045(2) | 1040 s | | | 1529 w |
| | | 1065 m | | | 1559 s |
| | | 1084 s | 1575(3) | 1574(3) | |
| | | 1089 s | 1595(3) | 1595(3) | 1582 vs |
| | 1150(2) | 1140 m | | | 3051 vw |

TABLE III. PHOSPHORESCENCE SPECTRUM OF 4, 4'-BIPYRIDYL

$\nu$: Wave number in $cm^{-1}$

| In cyclohexane | | | In $CCl_4$ | | | In ethanol | | | Analysis |
|---|---|---|---|---|---|---|---|---|---|
| $\nu$ | Rel. int. | $\Delta\nu$ | $\nu$ | Rel. int. | $\Delta\nu$ | $\nu$ | Rel. int. | $\Delta\nu$ | |
| 24530 | 10 | 0 | 24530 | 10 | 0 | 24585 | 8 | 0 | 0,0 |
| 24385 | 9 | 145 | | | | | | | 0-145 |
| 24240 | 5 | 290 | 24240 | 7 | 290 | | | | 0-290 |
| 24055 | 4 | 475 | | | | | | | 0-475 |
| 23955 | 5 | 575 | 23960 | 6 | 570 | | | | 0-575 |
| 23775 | 8 | 755 | 23775 | 7 | 755 | 23750? | 7 | 835 | 0-755 |
| 23635 | 8 | 895 | | | | | | | 0-755-145 |
| 23525 | 9 | 1005 | 23530 | 8.5 | 1000 | 23500? | 8 | 1085 | 0-1005 |
| 23380 | 8.5 | 1150 | | | | | | | 0-1005-145 |
| 23260 | 9.5 | 1270 | 23260 | 9.5 | 1270 | 23275 | 9.5 | 1310 | 0-1270 |
| 23110 | 9 | 1420 | | | | | | | 0-1270-145 |
| 22920 | 10 | 1610 | 22925 | 9.5 | 1605 | 22975 | 10 | 1610 | 0-1610 |
| 22780 | 9 | 1750 | | | | | | | 0-1610-145 |
| 22525 | 8.5 | 2005 | 22575 | 8 | 1955 | | | | 0-1610-475 |
| 22265 | 8.5 | 2265 | 22250 | 8 | 2280 | 22290 | 7 | 2295 | 0-1610-755 |
| 21955 | 9 | 2575 | 21985 | 8.5 | 2545 | 21980 | 7.5 | 2605 | 0-1610-1005 |
| 21790 | 8 | 2740 | | | | | | | 0-1610-1005-145 |
| 21660 | 9 | 2870 | 21660 | 8.5 | 2870 | 21685 | 7 | 2900 | 0-1610-1270 |
| 21500 | 8 | 3030 | | | | | | | 0-1610-1270-145 |
| 21330 | 8 | 3200 | 21340 | 7 | 3190 | 21350 | 5 | 3235 | 0-1610×2 |
| 21180 | 6 | 3350 | | | | | | | 0-1610×2-145 |
| 20960 | 4 | 3570 | 21030 | 2.5 | 3500 | | | | 0-1610×2-475 |
| 20710 | 3 | 3820 | 20705 | 1 | 3825 | 20715 | 1 | 3870 | 0-1610×2-755 |
| 20395 | 1 | 4135 | 20390 | 0.5 | 4140 | 20380 | 0.5 | 4205 | 0-1610×2-1005 |
| 20070 | 0.5 | 4460 | 20080 | 0.2 | 4450 | 20060 | 0.3 | 4525 | 0-1610×2-1270 |

The vibrational analysis was made with the spectrum in cyclohexane. Each strong band was accompanied by a weak satellite band with a separation of 145 $cm^{-1}$. The highest wave number band at 24530 $cm^{-1}$ was taken as the 0, 0-band of the system and the vibrational frequencies of 290, 475, 575, 755, 1005, 1270, and 1610 $cm^{-1}$ were found. The frequency of 1610 $cm^{-1}$ was seen to form the main progression of the system. These frequencies seem to correspond to the Raman frequencies of 575, 755, 1002, 1295, and 1595 $cm^{-1}$. The Raman data were obtained by us but unfortunately the frequencies corresponding to the phosphorescence bands of 145, 290, and 475 $cm^{-1}$ have not yet been found. For comparison, the infrared spectrum was also studied. The vibrational frequencies are listed in Table IV. Because of symmetry relations the infrared data may sometimes be useless. However, we can not neglect them, if the presence of any anomalous vibrational band structures in the spectrum is to be checked. Incidentally, anomalous band structures had been found in the phosphorescence spectra of aromatic compounds, such as benzoic acid and aniline.[4] It seems that both the spectra of 2, 2'- and 4, 4'-bipyridyls show no anomalous vibrational structure. The overall spectral features of the bipyridyls are very similar to those of biphenyl.[1]

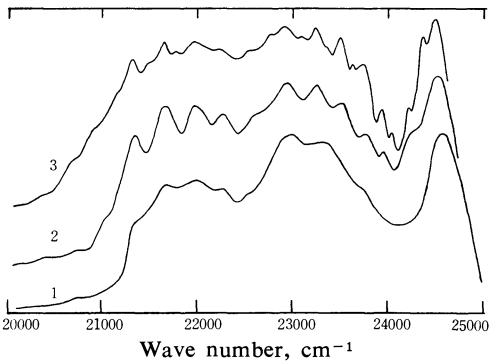



Fig. 2. Phosphorescence spectra of 4, 4'-bipyridyl at 90°K.
Concn.: $1\times10^{-2}$ M, in ethanol (1), carbon tetrachloride (2) and cyclohexane (3)

We also studied the near ultraviolet absorption spectrum of 2, 2'-bipyridyl in cyclohexane and observed the change of the spectrum

4) Y. Kanda, R. Shimada, Y. Gondo, M. Nakamizo, K. Hanada, M. Koyanagi and Y. Takenoshita, *Proc. Intern. Symp. Mol. Struct. Spectry., Tokyo*, **1962** (B303); Y. Kanda, R. Shimada and Y. Takenoshita, *Spectrochim. Acta*, **19**, 1249 (1963).

TABLE IV. VIBRATIONAL FREQUENCIES OF 4, 4'-BIPYRIDYL ($cm^{-1}$)

| Raman | | Infrared |
|---|---|---|
| In $CHCl_3$ | In $C_6H_6$ | KBr disk |
| | 575(0) | |
| | 660(3) | |
| | | 733 m |
| 755(1) | | 745 w |
| | | 760 w |
| | | 806 vs |
| | | 850 m |
| | | 879 m |
| | | 968 m |
| | | 976 w |
| | | 988 s |
| 1002(2) | | 1006 w |
| | | 1037 w |
| | | 1075 m |
| | | 1097 w |
| | | 1127 w |
| 1155(2) | | |
| 1217(3) | | 1217 s |
| 1295(2) | 1297(3) | |
| | | 1325 w |
| | 1357(1) | |
| | | 1409 vs |
| | | 1493 m |
| 1530(1) | 1535(1) | 1535 s |
| 1595(1) | | 1592 vs |
| | | 1943 w |
| | | 2780 w |
| | | 3015 s |

through addition of trichloroacetic acid. The spectrum showed a remarkable red shift as can be seen in Fig. 3. This shows that the broad band with maximum at 284 m$\mu$ belongs to a $\pi$-$\pi^*$ type transition.[5] The compound can be assumed to consist of two pyridine rings. The lowest excited level of pyridine is of an $n$-$\pi^*$ type and its second one is of a $\pi$-$\pi^*$ type. Now, because of the interaction of $\pi$-electron systems the lowest excited state of 2, 2'-bipyridyl is not of an $n$-$\pi^*$ type but a $\pi$-$\pi^*$ type. The spectral features of 2, 2'-bipyridyl do not resemble those of biphenyl. This has been clearly explained in a theoretical work by

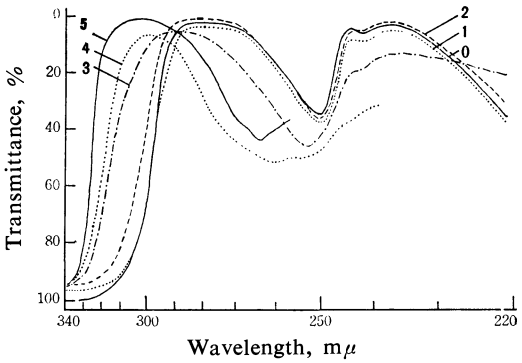



Fig. 3. Ultraviolet absorption spectra of 2, 2'-bipyridyl with trichloroacetic acid in cyclohexane.
2, 2'-Bipyridyl: $1\times10^{-4}$ M,
$CCl_3COOH$: 0; without acid, 1; $1\times10^{-5}$ M, 2; $1\times10^{-4}$ M, 3; $1\times10^{-3}$ M, 4; $1\times10^{-2}$ M, 5; $1\times10^{-1}$ M

Gondo.[6] If the 2, 2'-bipyridyl molecule is assumed to be trans-coplanar,[7,8] the lowest excited singlet state is a $^1B_u$, and the lowest triplet state is a $^3B_u$ state. Thus, a $\pi$-$\pi^*$ type excited triplet state is believed to be responsible for the phosphorescence of 2, 2'-bipyridyl, and may also be the case with 4, 4'-bipyridyl. The similarity found between the phosphorescence spectra of biphenyl,[1] 2, 2'- and 4, 4'-bipyridyl seems to support this interpretation. The rather long lifetimes of 2, 2'- and 4, 4'-bipyridyls are also compatible with the above interpretation.[5]

The authors wish to express their thanks to the Ministry of Education for grants-in-aid out of the Scientific Research Expenditure.

*Department of Chemistry*
*Faculty of Science*
*Kyushu University*
*Hakozaki, Fukuoka*

5) M. Kasha, *Discussions Faraday Soc.*, **9**, 14 (1950).

6) Y. Gondo, Dissertation submitted to the Graduate School, Kyushu University, 1964, and *J. Chem. Phys.*, in press.

7) P. E. Fielding and R. J. W. Le Fèvre, *J. Chem. Soc.*, **1951**, 1811.

8) L. L. Merritt, Jr., and E. D. Schroeder, *Acta Cryst.*, **9**, 801 (1956).

# Chemical Studies on the Black Rot Disease of Sweet Potatoes. XVII.*1,*2 Abnormal Semicarbazone of Ipomeanine and of Related Compounds

By Takashi KUBOTA, Teruo MATSUURA and Yasuzo KAKUNO

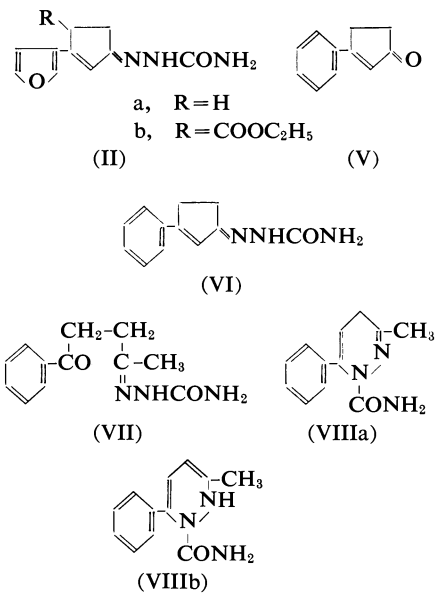
(Received December 11, 1965)

An abnormal semicarbazone, $C_{10}H_{11}O_2N_3$, was formed by the elimination of two molecules of water, when ipomeanine (I), one of the constituents of black-rotted sweet potatoes, was treated with semicarbazide by the usual procedure.[1] Kubota and Ichikawa[1] suggested, on the basis of an analogous finding by Borsche and his collaborators,[2] the formula IIa for the semicarbazone and the formula IIb for the abnormal semicarbazone of the ester III, an intermediate in the course of the synthesis of ipomeanine (I). The latter investigators gave the structure VI, the semicarbazone of 3-phenylcyclopentenone (V), for the abnormal semicarbazone of phenacylacetone (IV).

Recently, several questions have arisen about the structure II. First, the abnormal semicarbazone of ipomeanine is not regenerated to I by mild acid treatment but rather resinifies,[1] while the semicarbazone VI is easily regenerated to V under the same conditions. Secondly, the infrared spectrum of the abnormal semicarbazones is quite different from that of normal ones.[3] Thirdly, the ultraviolet maximum (265 m$\mu$) of the semicarbazone of ipomeanine is not consistent with the structure II, since the maximum of the structure II should be more bathochromically shifted than that (263—264 m$\mu$) of the semicarbazone of $\beta$-furylketone.[4] A reinvestigation of the structure of these semicarbazones has led us to the conclusion that the abnormal semicarbazones of ipomeanine and of the ester III possess the structures XIV and XV, respectively.

Finzi isolated a monosemicarbazone, m. p. 191°C, in the reaction of phenacylacetone (IV) and semicarbazide.[5],*3 The monosemicarbazone was easily obtained under mild conditions. It showed an infrared band of a benzoyl carbonyl at 1690 $cm^{-1}$ and a broad ultraviolet maximum at 231.5 m$\mu$, which is assigned as an overlapping absorption of a benzoyl group and of a semicarbazone of an aliphatic ketone.[6] The structure of the monosemicarbazone must be represented as VII.

When the semicarbazone VII was allowed to stand at pH 4.7 for ten days, two kinds of crystalline products were obtained, A, $C_{12}H_{13}ON_3$, m. p. 218—219°C as the main product and B,*4 m. p. 208—210°C, as the minor product. The product A was also obtained in a good yield by the treatment of an aqueous alcoholic solution of phenacylacetone (IV) with semicarbazide at room temperature for a long period of time, as has been described by Borsche et al.,[2] or at the refluxing temperature. They described the formation of the semicarbazone VI from phenacylacetone under




*1 Part XVI, T. Kubota and T. Matsuura, *J. Chem. Soc. Japan, Pure Chem. Sec.* (*Nippon Kagaku Zassi*), **79**, 490 (1958).

*2 This work was presented at the 16th Annual Meeting of the Chemical Society of Japan, April, 1963.

1) T. Kubota and N. Ichikawa, *J. Chem. Soc. Japan, Pure Chem. Sec.* (*Nippon Kagaku Zassi*), **75**, 450 (1954).

2) W. Borsche, W. Menz and A. Fels, *Ber.*, **41**, 199 (1908).

3) W. H. T. Davison and P. E. Christie, *J. Chem. Soc.*, **1955**, 3389.

4) T. Matsuura, K. Naya, N. Ichikawa and T. Kubota, This Bulletin, **35**, 1695 (1962).

5) C. Finzi, *Gazz. chim. ital.*, **42**, II, 356 (1912); *Chem. Zentr.*, **1912**, II, 2082.

*3 Finzi reported that the nitrogen analysis of a by-product, m. p. 210°C, was consistent with a monosemicarbazone.

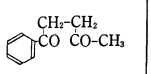
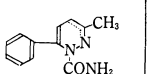
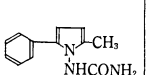
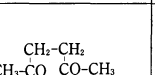
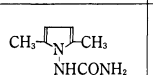
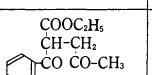
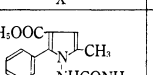
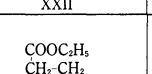
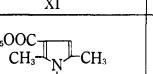
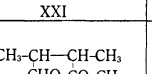
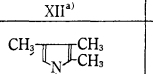
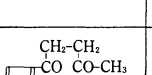
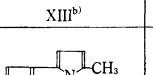
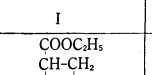
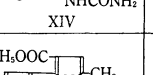
6) K. Hirayama, in "Jikken Kagaku Koza," Vol. 1, Ed. by the Chemical Society of Japan, Maruzen Co., Tokyo (1957), pp. 63, 166.

*4 The product B could not be isolated in several other runs.

such conditions. However VI could not be detected in our experiments. The infrared spectrum of the compound A showed no bands assigned to normal semicarbazones,[3] and elemental analyses showed that the compound A is formed by the intramolecular dehydration of the monosemicarbazone (VII) of phenacylacetone. It follows that the dihydropyridazine structure, VIIIa or VIIIb, or the pyrrylurea structure, IX, should be suggested to the compound A.

Several examples of the formation of abnormal semicarbazones, such as XI,[7] XII,[8] and XIII,[9],*5 from 1, 4-dicarbonyl compounds have been reported, as is shown in Table I. However there is no clear evidence for the pyrrylurea structure of these substances, and it still remains questionable whether the pyrrylurea structure or an alternative dihydropyridazine structure is to be chosen. On the other hand, acetonylacetone gives a normal bis-semicarbazone.[10] The treatment of the bis-semicarbazone with formic acid yields *N*-(2, 5-dimethylpyrryl)-urea (X), whose structure was established by conversion to urea and 2, 5-dimethylpyrrolidine.[10] The infrared spectrum of *N*-(dimethylpyrryl)urea (X) showed characteristic bands, at 3480, 3320, 3200, 1675, 1585 and 1525 $cm^{-1}$, which differ from the bands[3] of the usual semicarbazones in shape and position. The infrared spectrum (Table I) of the abnormal semicarbazones XI, XII, XIII, XIV (from ipomeanine (I)), and XV (from the ester III) also showed bands at 3450±30, 3300±20, 3225 ±25 (νNH), 1670±10, 1595±10, and 1535±15 $cm^{-1}$ (νC=O and νC=C). These bands are characteristic of the pyrrylurea X. The pyrrylurea structures, XI, XII, XIII, XIV, and XV, may, therefore, be given to these abnormal semicarbazones.

TABLE I. STRUCTURES AND INFRARED BANDS OF ABNORMAL SEMICARBAZONES

| 1,4-Dicarbonyl compounds | Abnormal semicarbazone | Infrared bands: νNH | Amide I | νC=C or Amide II |
|---|---|---|---|---|
|  IV |  VIII | | | |
| IV |  IX | | | |
|  X |  | | | |
|  XXII |  XI | | | |
|  XXI |  XII[a] | | | |
|  |  XIII[b] | | | |
|  I |  XIV | | | |
|  III |  XV | | | |

a) Bands at 3300 $cm^{-1}$ and 3200 $cm^{-1}$ are overlapped.
b) Cf. Ref. 9.

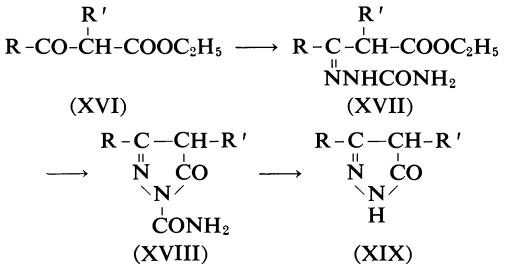
Of the two abnormal semicarbazones, A and B, obtained from phenacylacetone (IV), the infrared spectrum (Table I) of the minor product (B) showed bands assigned to the pyrrylurea structure, as has been discussed above. Therefore, the product B can be formulated as IX. Since the infrared spectrum of the major product A differs considerably from the spectrum of the pyrrylurea type of compounds, it seems that the product A may possess a dihydropyridazine structure, VIIIa or VIIIb. In spite of the similarity in structure of 1, 4-dicarbonyl compounds, phenacylacetone (IV) cyclizes to give mainly the dihydropyridazine derivative under usual conditions, but ipomeanine (I) to the pyrrol derivative.

Furthermore, in the case of ethyl acetonylacetoacetate (XXI), the initial product is a normal bis-semicarbazone, which easily cyclizes to the pyrrol derivatives XII upon recrystallization from hot water. In conclusion, it is difficult to predict at present how the structural factor of the parent 1, 4-dicarbonyl compounds will be affected in the formation of a normal semicarbazone or an abnormal semicarbazone, such as VIII and IX.

It is known that, in the reaction of a β-ketoester (XVI) with semicarbazide, a normal semicarbazone (XVII) is initially formed and that it in turn is converted to a 3-pyrazolone, XVIII or XIX, depending on the conditions

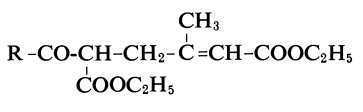
7) W. Borsche and A. Fels, *Ber.*, **39**, 1922 (1906).
8) G. Korschun and C. Roll, *Bull. soc. chim. France*, (4), **33**, 59 (1923).
9) W. Keller-Schierlein, M. Lj. Mihailovic and V. Prelog, *Helv. Chim. Acta*, **41**, 221 (1958).
*5 The formations of such abnormal semicarbazones from ethyl phenacylacetoacetate, ethyl phenacylbenzoylacetate (W. Borsche and M. Spannagel, *Ann.*, **331**, 298 (1904)), and 6-methyl-2, 5-heptadione (O. Wallach and F. Meister, *Ann.*, **362**, 261 (1908) and Ref. 20) were reported.
10) E. E. Blaise, *Compt. rend.*, **172**, 221 (1921); *Chem. Zentr.*, **1921**, I, 674.

employed.[11-15] In previous reports[16,17] of this series, it was reported that the intermediate compounds XX of the syntheses of ipomeamarone and of its phenyl analog yielded abnormal semicarbazones whose structures were unknown. We can now formulate these compounds as XIX (R=β-furyl, R'=H and R=phenyl, R'=H) from the results of the elemental analyses and from the results of a comparison of the infrared spectrum with that of 5-phenyl-3-pyrazolone obtained from ethyl benzoylacetate.



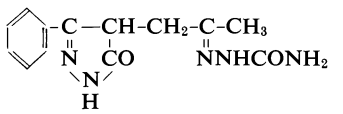
(XVI) (XVII) (XVIII) (XIX)

Ethyl acetonylacetoacetate (XXI), ethyl acetonylbenzoylacetate (XXII), and the ester III, all of which have a β-ketoester group in addition to a 1,4-dicarbonyl function in the molecule, can form pyrazolone derivatives, such as XVIII and XIX, by the action of semicarbazide. In fact, ethyl acetonylbenzoylacetate (XXII) yields a pyrazolone derivative, XXIII, in addition to the abnormal semicarbazone, XI, at an elevated temperature.



a, R= $C_6H_5$- b, R= 

(XX)



(XXIII)

## Experimental[*6]

**The Regeneration of the Semicarbazone (VI) of 3-Phenylcyclopent-2-en-1-one (V).** — The semicarbazone VI was prepared according to the procedure of Borsche et al.[2] m. p. 232°C. A mixture of 96 mg. of the semicarbazone and 30 ml. of 5% aqueous sulfuric acid was heated at 100°C for 1.5 hr. with occasional shaking until the mixture became clear. On cooling, 3-phenylcyclopent-2-en-1-one (V) was deposited as needles, m. p. 81—82°C,[*7] whose infrared spectrum was identical with that of an authentic sample. Yield, 74%. $\lambda_{max}^{EtOH}$ 284 mμ (ε 23300).

**The Monosemicarbazone (VII) of Phenacylacetone (IV).**—Into an ice-cooled solution of 1.0 g. of phenacylacetone[18] in 10 ml. of ethanol, a solution of 0.7 g. semicarbazide hydrochloride and 0.7 g. of anhydrous potassium acetate in 2 ml. of water was added with stirring. Precipitates were collected by filtration and recrystallized from ethanol to give 1.4 g. (48%) of the semicarbazone VII as needles, m. p. 191°C, lit. m. p. 191°C.[5] $\lambda_{max}^{EtOH}$ 231.5 mμ (ε 9400).

**The Formation of VIII and IX from the Monosemicarbazone (VII) of Phenacylacetone at pH 4.7** — A mixture of 72 mg. of the monosemicarbazone (VII), 72 mg. of anhydrous potassium acetate, 1.6 ml. of acetic acid. 1 m.l of water and 20 ml. of ethanol (PH 4.7) was allowed to stand at room temperature for 10 days. When the mixture was concentrated to about 10 ml. and cooled, 30 mg. (45%) of the crude VIII ("the product A" in the text) was obtained as crystals, m. p. 216—217°C. Recrystallization from ethanol yielded crystals, m. p. 218—219°C. $\lambda_{max}^{EtOH}$ 285 mμ (ε 16000) and $\lambda_{Infl.}$ 220 mμ (ε 9600).

Found: C, 67.26; H, 6.06; N, 19.14. Calcd. for $C_{12}H_{13}ON_3$: C, 66.95; H, 6.09; N, 19.52%.

The mother liquor from VIII deposited a few milligrams of IX ("the product B" in the text), m. p. 208—210°C, which could be sublimed. $\lambda_{max}^{EtOH}$ 205.5 mμ (ε 13800) and 285.5 mμ (ε 14000).

**The Formation of VIII from Phenacylacetone (IV).**—A mixture of 389 mg. of phenacylacetone, 390 mg. of semicarbazide hydrochloride, 390 mg. of potassium acetate, 2 ml. of water and 20 ml. of pyridine was allowed to stand at room temperature for 10 days. After concentrating, the mixture was diluted with 10 ml. of water and 285 mg. (57%) of the crude VIII, m. p. 218—219°C, which was identical with the VIII obtained above (as determined by mixed melting point and infrared spectrum determination).

When a solution of phenacylacetone, an excess of semicarbazide hydrochloride and potassium acetate in aqueous ethanol was refluxed for 5 hr., VIII was obtained in a 78% yield. In both cases, the semicarbazone (VI) of 3-phenylcyclopentenone could not be isolated.

11) J. Thiele and O. Stange, *Ann.*, **283**, 30 (1894).
12) A. Sonn and W. Litten, *Ber.*, **66**, 1512 (1933).
13) A. Michael, *J. Am. Chem. Soc.*, **41**, 424 (1919).
14) H. C. House, J. W. Blaker and D. A. Madden, ibid., **80**, 6386 (1958).
15) W. Borche and M. Spannagel, *Ann.*, **331**, 98 (1904).
16) T. Matsuura, *J. Chem. Soc. Japan, Pure Chem. Sec.* (*Nippon Kagaku Zassi*), **77**, 248 (1956).
17) T. Matsuura, ibid., **78**, 389 (1957); T. Kubota and T. Matsuura, *J. Chem. Soc.*, **1958**, 735.

*6 Melting points were uncorrected. The infrared spectra were measured in Nujol mull with a Nippon Bunko recording spectrophotometer, Model IR-S. The ultraviolet spectra were measured with a Hitachi recording spectrophotometer, Model EPS-2. The microanalyses were made by Mr. J. Goda and his associates of this Faculty.

*7 Lit. m. p. 83—84°C. Recrystallization from ethanol gave crystals, m. p. 63—64°C, whose infrared and ultraviolet spectra were identical with those of the sample, m. p. 83—84°C. Recrystallization from water or aqueous ethanol gave crystals, m. p. 83—84°C.

18) J. H. Helberger, *Ann.*, **522**, 269 (1963).

**The Bis-semicarbazone of Acetonylacetone.**—When a solution of 1.90 g. of acetonylacetone[19] in 10 ml. of ethanol was treated with a solution of 3.81 g. of semicarbazide hydrochloride and anhydrous potassium acetate in 3 ml. of water, white precipitates deposited immediately. After standing overnight, the precipitates (2.60 g., 71%) were collected and recrystallized from hot water to give the bis-semicarbazone as crystals, m. p. 225—226°C, lit. m. p. 223—224°C.[20] $\lambda_{max}^{EtOH}$ 224.5 mμ (ε 21800).

The mother liquor from the bis-semicarbazone deposited crystals (20 mg.) after standing several weeks. Recrystallization from aqueous ethanol yielded crystals, m. p. 215—217°C. $\lambda_{max}^{EtOH}$ 264 mμ (ε 21800). $\nu_{max}^{Nujol}$ 3460, 3200, 1680 and 1568 $cm^{-1}$.

Found: C, 54.83; H, 7.39. Calcd. for $C_7H_{11}ON_3$: C, 54.88; H, 7.24%.

This compound was considered to be a dimethyldihydropyridazine but it was not further investigated.

**1-(2, 5-Dimethylpyrryl) urea (X).**—According to the method of Blaise,[10] 100 mg. of the bis-semicarbazone of acetylacetone was mixed with 2 ml. of 50% aqueous formic acid, and then the mixture was heated at 70°C for 3 min. On cooling 27 mg. (40%) of crystals deposited; they were recrystallized from ethanol as crystals, m. p. 235—236°C, lit. m. p. 245°C.[10] $\lambda_{max}^{EtOH}$ 216 mμ (ε 6710).

Found: C, 55.13; H, 7.39; N, 27.76. Calcd. for $C_7H_{11}ON_3$: C, 54.88; H, 7.24; N, 27.43%.

**The Formation of XI and XXIII from Ethyl Acetonylbenzoylacetate (XXII).**—a) To a solution of 1.16 g. (4.5 mmol.) of ethyl acetonylbenzoylacetate (XXII)[7] in 10 ml. of ethanol, a solution of 0.56 g. (5 mmol.) of semicarbazide hydrochloride and 0.60 g. of anhydrous potassium acetate in 3 ml. of water was added. After standing for 1 hr., precipitates (0.51 g., 39%) deposited were collected and recrystallized from water to give XI as needles, m. p. 219—221.5°C, lit. m. p. 224—226°C.[7] $\lambda_{max}^{EtOH}$ 207 mμ (ε 13700) and 285 mμ (ε 4500).

Found: C, 62.78; H, 5.98; N, 14.64. Calcd. for $C_{15}H_{17}O_3N_3$: C, 62.70; H, 5.96; N, 14.63%.

b) A mixture of 1.54 g. of the ester XXII, 2.67 g. (a large excess) of semicarbazide hydrochloride, 2.7 g. of anhydrous potassium acetate, 5 ml. of water and 30 ml. of ethanol was heated under reflux for 5 hr. and then filtered while still hot in order to remove insoluble materials. After standing overnight, the filtrate deposited 0.22 g. (13%) of XI as needles, m. p. 218—220°C, which were identical with the compound obtained above (as ascertained by mixed melting point and infrared spectrum determination).

From the above mother liquor, crystals deposited after spontaneous evaporation. Recrystallization from aqueous ethanol yielded 40 mg. of XXIII as crystals, m. p. 230—231°C (decomp.). $\lambda_{max}^{EtOH}$ 230 mμ (ε 16400) and $\lambda_{infl.}$ 255 mμ (ε 12300). $\nu_{max}^{Nujol}$ 3520, 3380, 3280, 2800—2300, 1680, 1650, 1570 and 1520 $cm^{-1}$.

Found: C, 56.38; H, 5.73; N, 25.64. Calcd. for $C_{13}H_{15}O_2N_5$: C, 57.13; H, 5.53; N, 25.63%.

**The Reaction of Ethyl Acetonylacetoacetate (XXI) with Semicarbazide.**—To a solution of 500 mg. of ethyl acetonylacetoacetate[19] in 30 ml. of ethanol, a solution of 275 mg. (an equimolar amount) of semicarbazide hydrochloride and 360 mg. of anhydrous potassium acetate in 5 ml. of water was gradually added. The crystals deposited were collected by filtration, washed with water and dried. The yield of the bis-semicarbazone, m. p. 186—187°C, was 285 mg. (34%). The infrared spectrum and ultraviolet spectrum ($\lambda_{max}^{EtOH}$ 226 mμ (ε 17200)) showed bands characteristic of a normal semicarbazone.[3,6]

Found: C, 43.77; H, 6.90; N, 27.12. Calcd. for $C_{11}H_{20}O_4N_6$: C, 43.99; H, 6.71; N, 27.99%.

When the mother liquor from the bis-semicarbazone was allowed to stand for 1 week, 165 mg. (13%) of XII deposited as plates, m. p. 222—223°C, the melting point and infrared spectrum of which did not change after recrystallization from ethanol. $\lambda_{max}^{EtOH}$ 228.5 mμ (ε 6200) and 264 mμ (ε 6300). Lit. m. p. 230°C.[8]

Found: C, 53.60; H, 6.78; N, 18.56. Calcd. for $C_{10}H_{15}O_3N_3$: C, 53.32; H, 6.71; N, 18.66%.

**The Formation of XII from the Bis-semicarbazone of Ethyl Acetonylacetoacetate (XXI).**—The recrystallization of the bis-semicarbazone from water or ethanol gave needles, m. p. 233—234°C. The infrared and ultraviolet spectra were identical with those of XII, m. p. 222—223°C, obtained above. The mixed melting point was 233—234°C.

Found: N, 18.68. Calcd. for $C_{10}H_{15}O_3N_3$: N, 18.66%.

**5-Phenyl-3-pyrazolone (XIX; R=$C_6H_5$, R'=H).**—This compound was prepared according to the method of House et al.,[14] m. p. 239—240°C (decomp.), lit. m. p. 242—243°C (decomp.). $\lambda_{max}^{EtOH}$ 208 mμ (ε 16000), and 255 mμ (ε 16200), lit. $\lambda_{max}$ 274 mμ (ε 17000). $\nu_{max}^{Nujol}$ 2800—2300, 1630, 1600 and 1550 $cm^{-1}$.

**The Abnormal Semicarbazone (XIX; R=$C_6H_5$, R'=$-CH_2-C(CH_3)=CH-COOC_2H_5$)[16] of Diethyl 2-Methyl-4-benzoyl-1-butene-1, 4-dicarboxylate (XXa).**—$\lambda_{max}^{EtOH}$ 207 mμ (ε 19000) and 248 mμ (ε 10800). $\nu_{max}^{Nujol}$ 3400, 2800—2300, 1697, 1650, 1600 and 1550—1525 $cm^{-1}$.

**The Abnormal Semicarbazone (XIX; R=β-furyl, R'=$-CH_2-C(CH_3)=COOC_2H_5$)[17] of Diethyl 2-Methyl-4-(β-furyl)-1-butene-1, 4-dicarboxylate (XXb).**—$\nu_{max}^{Nujol}$ 3400, 2800—2300, 1695, 1645, 1590 and 1550 $cm^{-1}$. $\lambda_{max}^{EtOH}$ 207 mμ (ε 19000) and 248 mμ (ε 10800).

*Faculty of Science*
*Osaka City University*
*Sumiyoshi-ku, Osaka*

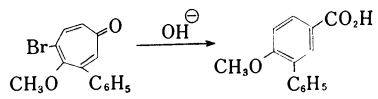
19) V. M. Rodionom and E. F. Polumna, *Doklady Akad. Nauk. U. S. S. R.*, **68**, 535 (1949); *Chem. Abstr.*, **43**, 535 (1949).
20) T. Posner, *Ber.*, **34**, 3973 (1901).

# The Mechanism of the Rearrangement Reaction of 3-Phenyl-4-methoxy-5-bromotropone to 3-Phenyl-4-methoxybenzoic Acid[1]

By Yoshio KITAHARA,*1 Ichiro MURATA*1 and Tadashi MUROI*2

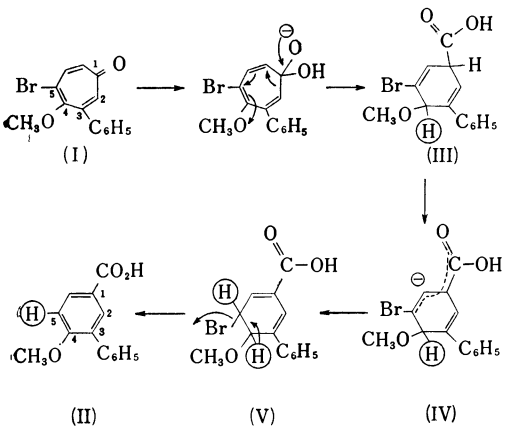
(Received December 19, 1964)

An examination of the reaction mechanism of the rearrangement of 2-phenyl-4-bromotropone to 2-phenylbenzoic acid by using heavy water was described in a preceding paper.[2] A similar reaction has recently been found by one of the present authors (T. M.)[3] in the rearrangement of 3-phenyl-4-methoxy-5-bromotropone (I) to 3-phenyl-4-methoxybenzoic acid (II), a reaction which cannot be explained by the known mechanism of the rearrangement reaction of tropoids.



(I) (II)

The reaction mechanism depicted below has been assumed for the rearrangement of I to II; this hypothesis was examined, using deuterium as the tracer element.



As is shown in this chart, the reaction begins with the attack on the carbonyl carbon in I by a hydroxyl ion, which causes a ring contraction, and then the carbon atom carrying the methoxyl group undergoes protonization to form III. III forms the anion IV by the action of a base and, through the formation of V by protonization to the carbon atom in the 5-position or by an intramolecular proton 1, 3-transfer,[4] forms II by dehydrobromination.

If this rearrangement is carried out in a system containing deuterium, the position marked with Ⓗ in the above chart will be occupied by deuterium atoms. If, on the other hand, the formation of the intermediate V is due to protonization, the deuterium content at the 5-position in the rearrangement product should be close to the theoretical value (8.33 atom.%), while the value will be far smaller than the theoretical if the 1, 3-transfer of the proton has occurred. In any case, if the foregoing reaction mechanism is correct, the position of the deuterium ion in II should be 5 and not any other position.

A solution of I dissolved in a system of deuterium oxide,[5] sodium hydroxide-*d*, and methanol-O-*d*[6] was refluxed for 30 min.; the rearrangement product so obtained was converted to the methyl ester with diazomethane, and the ester was hydrolyzed with alkali,[2] thus affording deuterated 3-phenyl-4-methoxybonzoic acid (II) with a m. p. of 214—215°C.[7]

*1 Present address: Department of Chemistry, Faculty of Science, Tohoku University, Sendai.

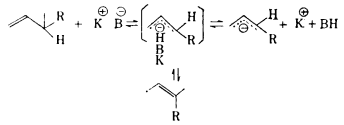
*2 Present address: Hitachi Central Research Laboratory, Hitachi, Ltd., Kuji-machi, Ibaraki.

1) Paper read at the 13th Annual Meeting of the Chemical Society of Japan, Tokyo, April, 1960.

2) Y. Kitahara, I. Murata and T. Muroi, This Bulletin, 34, 1359 (1961).

3) T. Muroi, This Bulletin, 34, 178 (1961).

4) The relative rates of the double-bond migration and of deuterium exchange of perdeuterio-1-pentene with unlabeled 2-methyl-1-pentene and solvent have been determined at 55°C in the system of potassium *t*-butoxide in dimethyl sulfoxide by S. Bank, C. A. Rowe, Jr., and A. Schriesheim, *J. Am. Chem. Soc.*, 85, 2115 (1963). They found that the isomerization is 16 times faster than the exchange. Thus they concluded that the isomerization reaction involves an intramolecular proton transfer. A reasonable mechanism can be developed on the basis of a tightly-bound ion pair.



5) Product of the Asahi Kasei Ind., Ltd. Purity, 99.80%, $d_4^{25}$ 1.1043.

6) D. H. Hill, B. Stewart, S. W. Kantor, W. A. Judge and C. R. Hauser, *J. Am. Chem. Soc.*, 76, 5129 (1954).

7) It was confirmed through infrared spectral identification that 3-phenyl-4-methoxybenzoic acid does not undergo secondary deuteration under these rearrangement reaction conditions.

The infrared absorption spectrum of II (cf. Table I) was somewhat different from that of the 3-phenyl-4-methoxybenzoic acid[8] (II') prepared from anisic acid from the out-of-plane to the finger-print region and indicated the presence of deuterium. The deuterium content was found to be 0.28 atom.% by mass analysis; this is far smaller than the theoretical value. This result shows that the base-catalysed protropic migration is intramolecular.

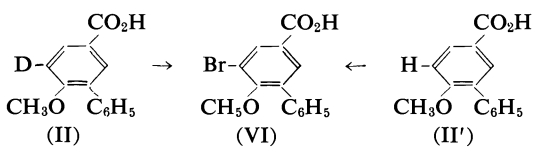
TABLE I. INFRARED ABSORPTION MAXIMA OF II AND II'*

| II | II' |
|---|---|
| 665 (w) | 665 (w) |
| 695 (s) | 694 (s) |
| 700 (s) | — |
| 728 (s) | 723 (s) |
| 772 (s) | 772 (s) |
| 824 (m) | 824 (m) |
| 832 (m) | — |
| 870 (w) | 870 (w) |
| 907 (w) | 907 (w) |
| 920 (m) | — |
| — | 930 (m) |
| 957 (w) | — |
| 1023 (s) | 1023 (s) |
| 1043 (s) | 1044 (s) |
| 1078 (w) | 1077 (w) |
| 1120 (m) | 1121 (m) |
| 1139 (s) | 1139 (s) |
| 1146 (m) | — |
| — | 1177 (m) |
| 1185 (w) | 1186 (w) |
| 1245 (s) | — |
| 1260 (s) | 1260 (s) |
| 1270 (s) | — |
| 1312 (s) | 1307 (s) |
| 1400 (m) | 1404 (m) |
| 1440 (s) | 1440 (s) |
| — | 1450 (s) |

* IR spectra are measured using a Perkin-Elmer Model 21 double beam spectrophotometer in KBr pellet.

The position of the deuterium atom in II should be 5 (the position meta to the carboxyl carbon), according to the hypothetical mechanism, and this atom should be replaced by the bromine atom upon the bromination of II. The bromination of II with 1 mol. of bromine in glacial acetic acid afforded a monobrominated compound (VI) with a m. p. of 231—232°C, the infrared absorption spectrum of which was identical with that of the brominated product of II'.

It follows, therefore, that the deuterium atom in II is at the 5-position and that there are none in other positions. This fact supports the mechanism described above.




## Experimental[9]

**The Rearrangement Reaction of 3-Phenyl-4-methoxy-5-bromotropone (I) in a Heavy Water System.**—Sodium (0.11 g.) was dissolved in methanol-O-*d* (8 ml.); deuterium oxide (8 ml.) and I (0.4 g.) were added to it, and the mixture was refluxed on a water bath for 25 minutes, protected with a calcium chloride tube. Methanol was evaporated under reduced pressure, and the residue was diluted with 10 ml. of water and extracted with chloroform in order to remove a neutral portion. The aqueous layer was acidified to Congo red with hydrochloric acid; the crystals that separated out were collected, and the filtrate was extracted with chloroform. The crystals obtained were combined and suspended in ether, and an ether solution of diazomethane was added to it in order to effect esterification. The crystal obtained by the evaporation of ether were dissolved in a mixture of methanol (4 ml.) and 2 N sodium hydroxide (1.5 ml.), and the mixture was refluxed for 4 hr. Methanol was evaporated under reduced pressure, and the residue was diluted with water and acidified. The crystals that separated out were collected by filtration to crude crystals (0.25 g.) of II, m. p. 202—206°C. This was purified by sublimation under reduced pressure, and the sublimate was recrystallized from methanol to II as colorless prisms, m. p. 214—215°C.

Found: C, 73.48; H, 5.49; D, 8.33. Calcd. for $C_{14}H_{14}DO_3$: C, 73.67; H, 5.30%; D, 0.23 atom.%.

**3-Phenyl-4-methoxy-5-bromobenzoic Acid (VI).**—Bromine (70 mg.) was added to a solution of II (80 mg.) dissolved in glacial acetic acid (0.5 ml.) by heating, and then the mixture was heated on a water bath at 45—55°C for 4 more hours. The crystals that separated out were collected by filtration to 70 mg. of crude crystals with a m. p. of 217—222°C. Recrystallization from ethanol gave VI melting at 231—232°C.

VI was similarly obtained from II'.

Found: C, 54.55; H, 3.37. Calcd. for $C_{14}H_{11}O_3Br$: C, 54.74; H, 3.61%.

The determination of deuterium by mass analysis was carried out by Dr. Sumio Horibe, Faculty of Science, Tokyo Metropolitan University, while the infrared spectral measurement was made by Mr. Hideji Aono of this Institute, to both of whom the authors wish

8) K. H. Slotta and A. E. Nold, *Ber.*, **68**, 2226 (1935).

9) All melting points are uncorrected.

to express their deep gratitude. This work was supported in part by a grant-in-aid for Scientific Research from the Ministry of Education.

*The Chemical Research Institute*
*of Non-Aqueous Solutions*
*Tohoku University*
*Katahira-cho, Sendai*

# Structure of Three-coordinated Copper(II) Complexes. Salicylalsalicylaminecopper(II) and Related Compounds

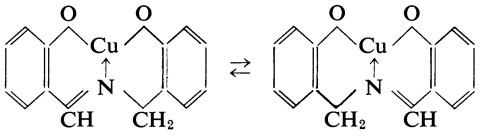
By Yoko INAGAKI, Osamu OHASHI, Michihiko KISHITA and Masaji KUBO

(Received December 21, 1964)

A majority of the so-called three-coordinated copper(II) complexes show magnetic moments per copper atom smaller than the theoretical spin moment, 1.73 Bohr magnetons, for one unpaired electron.[1] On the basis of this fact, the present writers predicted that the crystals of these compounds are made up of dimeric molecules having a pair of contiguous copper atoms close enough to permit spin interaction between them. The prediction was varified by an X-ray crystal analysis carried out by Barclay and collaborators[2] on a single crystal of acetylacetonemono(*o*-hydroxyanil)copper(II). It is noteworthy that the three-coordinated copper(II) complexes of this type were presumed to have monomeric units with a planar structure because they involve highly conjugated systems. In fact, the X-ray crystal analysis mentioned above confirmed this presumption. Therefore, one might suspect that the planar structure of ligands is an important factor leading to the subnormal magnetic moments of these copper(II) complexes. This generalization seems to be plausible because subnormal magnetic moments found for various copper-(II) complexes[2,3] are a result of close proximity of two copper atoms in a dimeric molecule and the geometric configuration of ligands is surely responsible for the approach of the two copper atoms.

There is another group of three-coordinated copper(II) complexes, which show normal magnetic moments of 1.8—1.9 B. M.[4] Complexes belonging to this group are characterized by the presence of a six-membered chelate ring having a nonplanar structure in a monomeric molecule. Arguments based on infrared spectroscopy have led to a conclusion that complexes of this type also form dimeric molecules in crystals, in which copper atoms are bridged in pairs by two Cu-O-C-O-Cu links rather than by two oxygen atoms as in the copper(II) complexes of the first group. Thus, one is led to an important conclusion that "three-coordinated copper(II) complexes" in the literal sense of the word do not exist.[5]

Salicylalsalicylaminecopper(II) or salicylal-*o*-hydroxybenzylaminecopper(II) presents a single exception to this rule. It shows a subnormal magnetic moment of 0.87 B. M. at room temperature notwithstanding that a copper atom of this complex takes part in the formation of a six-membered ring having only one aromatic bond. However, the chemical formula as given to this molecule is based on the synthesis of the corresponding Schiff base. When the copper(II) complex is formed, one half of the monomeric unit might become equivalent to the other half, leading to a symmetric planar structure. It is because prototropic rearrangement involving slight displacements of three hydrogen atoms might take place.

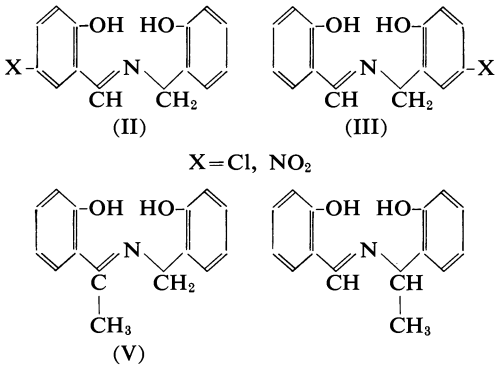



(I-Cu)

For this reason, the problem of possible prototropy in this compound is important in discussing the structure of three-coordinated

1) M. Kishita, Y. Muto and M. Kubo, *Australian J. Chem.*, **10**, 386 (1957).
2) G. A. Barclay, C. M. Harris, B. F. Hoskins and E. Kokot, *Proc. Chem. Soc.*, **1961**, 264.
3) J. N. van Niekerk and F. R. L. Schoening, *Acta Cryst.*, **6**, 227 (1953).
4) M. Kishita, Y. Muto and M. Kubo, *Australian J. Chem.*, **11**, 309 (1958).
5) M. Kubo, Y. Kuroda, M. Kishita and Y. Muto, ibid., **16**, 7 (1963).
6) M. Yamaguchi, *J. Chem. Soc. Japan, Pure Chem. Sect.* (*Nippon Kagaku Zasshi*), **74**, 261 (1953).

copper(II) complexes. The question can be answered by examining two derivatives of salicylalsalicylaminecopper(II), one having a substituent in the aldehyde portion of the Schiff base and the other having the same substituent at the corresponding position of the amine portion of the Schiff base. Yamaguchi[6] has already examined three isomeric pairs of Schiff bases which can form three-coordinated




copper(II) complexes on replacing two hydrogen atoms with a copper atom. It is reported that no appreciable difference was found between the isomers in their ability to form coordination compounds but that those Schiff bases having a substituent on the aldehyde side show slightly lower melting points than those of the corresponding isomers having the same substituent on the amine side. (The three-coordinated copper(II) complexes have no sharp melting points, because they readily decompose before they melt.) Since the measurement of melting points alone is not very conclusive in deciding whether or not prototropy takes place in the molecules of this type, the present writers have undertaken to determine the infrared absorption spectra, the X-ray powder patterns, and the nuclear magnetic resonance spectra of salicylalsalicylamine and related compounds as well as their copper(II) salts.

## Experimental

The following Schiff bases and the corresponding three-coordinated copper(II) complexes were prepared by essentially the same method as that employed by Yamaguchi.[6]

**Salicylalsalicylamine (I).**—This compound was prepared by the method described in a previous paper.[1] It forms yellow needle crystals, m.p. 182°C. This and the following Schiff bases were transformed into their copper(II) salts by means of copper(II) acetate dissolved in ethanol. Recrystallization from pyridine yielded monopyridine adducts, which lost pyridine completely on boiling in ethanol.

Found: N, 5.0; Cu, 22.0. Calcd. for $C_{14}H_{11}O_2NCu$: N, 4.9; Cu, 22.0%.

**5-Chlorosalicylalsalicylamine (II).**—Salicylaldehyde was chlorinated with sulfuryl chloride in the presence of aluminum trichloride. 5-Chlorosalicylaldehyde separated as white crystals and was recrystallized from ethanol, m. p. 100°C. It was subjected to condensation with salicylamine in an ethanol solution. Recrystallization from ethanol yielded yellow needle crystals, m. p. 200°C.

Found: C, 63.8; H, 4.6; N, 5.3. Calcd. for $C_{14}H_{12}O_2NCl$: C, 64.2; H, 4.6; N, 5.3%.

Found: C, 52.5; H, 3.3; N, 4.4. Calcd. for $C_{14}H_{10}O_2NClCu$: C, 52.0; H, 3.1; N, 4.3%.

**Salicylal-5-chlorosalicylamine (III).**—*N*-(Hydroxymethyl)phthalimide was prepared by the reaction of phthalimide and formalin, m. p. 142°C. It was allowed to react with hydrochloric acid to obtain *N*-(chloromethyl)phthalimide, which was recrystallized from benzene, m. p. 132°C. On heating a mixture of this compound, *p*-chlorophenol, and zinc chloride, the reaction product solidified. Extraction with hot ethanol yielded white needle crystals of 2-hydroxy-5-chlorobenzylphthalimide, m. p. 171°C.[7] This compound was heated with hydrochloric acid in a sealed tube. On cooling, phthalic acid separated. When the filtrate was concentrated, 5-chlorosalicylamine hydrochloride precipitated. The precipitates were dissolved in water and neutralized with ammonia. The crystals of 5-chlorosalicylamine separated and were crystallized from ethanol, m. p. 204°C. This compound was allowed to condense with salicylaldehyde in an ethanol solution to form a Schiff base. Recrystallization from ethanol yielded yellow hexagonal plate crystals, m. p. 214°C.

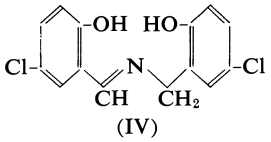
Found: C, 64.4; H, 4.5; N, 5.3. Calcd. for $C_{14}H_{12}O_2NCl$: C, 64.2; H, 4.6; N, 5.3%.

Found: C, 52.2; H, 3.2; N, 4.5. Calcd. for $C_{14}H_{10}O_2NClCu$: C, 52.0; H, 3.1; N, 4.3%.

**5-Chlorosalicylal-5-chlorosalicylamine (IV).**—This compound was obtained by the condensation of 5-chlorosalicylaldehyde and 5-chlorosalicylamine in an ethanol solution as yellow needle crystals, m. p. 203°C.

***o*-Hydroxyacetophenonesalicylamine (V).**—A solution of *o*-hydroxyacetophenone and salicylamine in ethanol was refluxed for 3 hr. The resulting condensation product was recrystallized from ethanol. Pale yellow crystals were obtained, m. p. 193°C (lit.[6] 188°C).

**Benzalbenzylamine (VI).**—Benzaldehyde and benzylamine were allowed to condense in an ether solution. After drying, ether was removed and the residue was fractionated under reduced pressure to obtain a colorless liquid, b. p. 140—145°C/5 mmHg (lit.[8] 200—202°C/10—20 mmHg).




Infrared absorpiton spectra were obtained of potassium bromide disks and Nujol mulls with a Model DS-402G grating spectrometer equipped with

7) M. Yamaguchi, ibid., 73, 393 (1952).
8) A. T. Mason and G. R. Winder, *J. Chem. Soc.*, 65, 191 (1894).

potassium bromide optics from Japan Spectroscopic Company, Ltd. The wave number range covered 400—4000 $cm^{-1}$.

The X-ray powder patterns were taken by use of a Norelco X-ray diffractometer at room temperature with the copper K$\alpha$ line filtered through nickel.

Nuclear magnetic resonance spectra were recorded at room temperature by means of a JNM-3 NMR spectrometer from the Japan Electron Optics Laboratory Company operating at 60 Mc. Materials were dissolved in dimethyl sulfoxide to 8—9% by weight unless otherwise specified. Cyclohexane was employed as an external standard.

## Results and Discussion

A crucial test in this study is to see whether or not 5-chlorosalicylalsalicylamine (II) and its copper(II) salt (II-Cu) are identical with salicylal-5-chlorosalicylamine (III) and its copper(II) salt (III-Cu), respectively. If the prototropic rearrangement of hydrogen atoms takes place in the molecules of compound I and its derivatives, tautomeric equilibrium would be established between compounds II and III as well as between the salts, II-Cu and III-Cu. As a result, one would obtain one and the same Schiff base and its copper(II) salt regardless of whether chlorine is introduced in the aldehyde portion or the amine portion of compound I. For this reason, experimental results on related compounds are consulted below only when they are pertinent to the solution of the problem.

The infrared spectrum of compound II bears fairly close resemblance to that of III. However, there are certain features indicative of the nonidentity of the two compounds as shown in Fig. 1. The same conclusion can be derived from the spectra of three-coordinated copper(II) complexes, II-Cu and III-Cu, shown in Fig. 2. The assignments of observed bands are feasible to some extent on the basis of analysis carried out by Ueno and Martell[9] on a variety of metal chelates and free ligand molecules. However, the results are trivial for the present purpose and need not be discussed here.

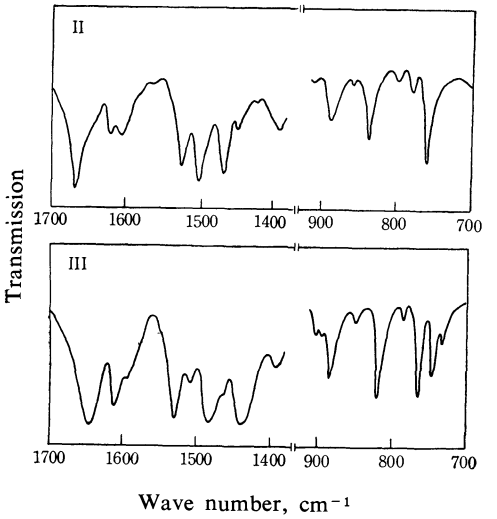



Fig. 1. Infrared spectra of 5-chlorosalicylalsalicylamine (II) and salicylal-5-chlorosalicylamine (III).

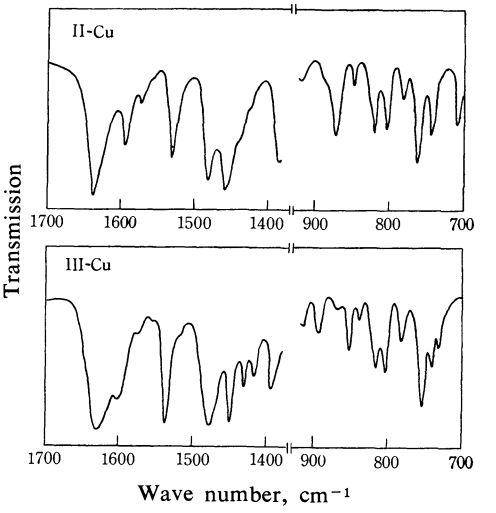



Fig. 2. Infrared spectra of 5-chlorosalicylalsalicylaminecopper(II) (II-Cu) and salicylal-5-chlorosalicylaminecopper(II) (III-Cu).

The X-ray powder patterns of free ligands, II and III, are quite different from each other (Fig. 3). The copper(II) salts of I, II, III, and IV also show powder patterns differing from one another as shown in Fig. 4.

It was not feasible to observe the nuclear magnetic reasonance spectra of the three-coordinated copper(II) complexes, because they are

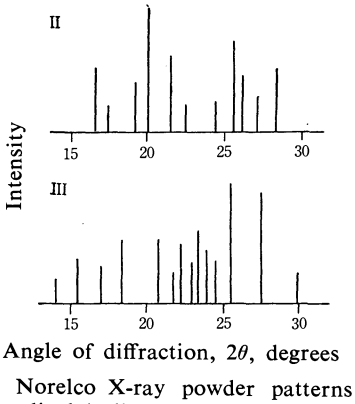



Fig. 3. Norelco X-ray powder patterns of 5-chlorosalicylalsalicylamine (II) and salicylal-5-chlorosalicylamine (III).

9) K. Ueno and A. E. Martell, *J. Phys. Chem.*, **59**, 998 (1955); **60**, 1270 (1956).

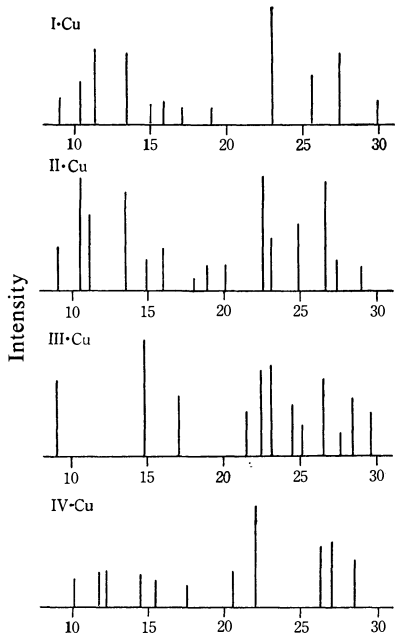



Fig. 4. Norelco X-ray powder patterns of the copper(II) complexes of salicylalsalicylamine (I-Cu), 5-chlorosalicylalsalicylamine (II-Cu), salicylal-5-chlorosalicylamine (III-Cu), and 5-chlorosalicylal-5-chlorosalicylamine (IV-Cu).

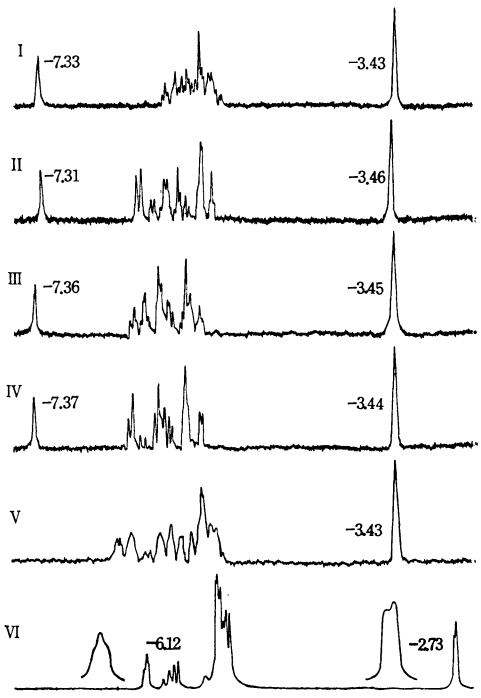



Fig. 5. Proton magnetic resonance spectra of salicylalsalicylamine (I) and related compounds (II—VI). The two peaks of compound VI as recorded in the pure liquid state show multiplet structure under a low sweep rate. They shift to low field when examined in solutions.

insoluble in almost all common solvents except pyridine, aniline, quinoline, etc. It is known that three-coordinated copper(II) complexes readily form monopyridine derivatives,[1,4] which show normal magnetic moments even when the corresponding pyridine-free complexes show subnormal magnetic moments. Accordingly, one is led to conclude that the dissolution of three-coordinated copper(II) complexes in pyridine involves the rearrangement of ligands and that the binuclear complex molecules dissociate into monomeric molecules each having a pyridine molecule as an additional ligand.[5] Undoubtedly, pyridine and other nitrogen-containing solvents are not suitable for the study of the structure of three-coordinated copper(II) complexes.

Therefore, proton magnetic resonance studies were made on free ligands, which also are sparingly soluble in a majority of common solvents. Internal standards were not employed, solely because it was desired to maintain the samples free from admixtures. No correction was made for the bulk magnetic susceptibility, because comparison between the NMR spectra of various compounds rather than the exact data of chemical shifts was the present writers' immediate concern.

The proton magnetic resonance spectra of compounds I—VI are shown in Fig. 5. The spectra of compounds I—IV look very much alike. Each consists of a sharp peak on the low-field side, a more intense sharp peak on the high-field side, and a group of closely spaced lines located between them. The intensity ratio of the two single lines is 1 : 2. Accordingly, the weak line is attributable to -CH= protons while the strong line is due to $-CH_2-$ protons. The group of lines can be assigned to protons attached to aromatic rings. The signal of -CH= protons is missing in the spectrum of compound V, which has $-C(CH_3)=$ in place of -CH=. The methyl signal of this compound was unobservable, because it overlaps the strong peak of dimethyl sulfoxide used as a solvent. The spectrum of compound VI also is comprised of a -CH= proton signal, a $-CH_2-$ signal, and a group of peaks due to protons in phenyl groups. Since this compound could be examined in the pure liquid state, it was feasible to detect the multiplet structure of the -CH= and $-CH_2-$ signals. The former signal has a line contour of a partly resolved 1 : 2 : 1 triplet while the latter shows a doublet structure. This indicates the existence of weak coupling between the -CH=

proton and $-CH_2-$ protons. The signals of OH protons could not be observed, except for compound V for which a barely detectable flat peak was observed at −15.16—15.36 p.p.m. Probably, they are broadened by the intermolecular exchange of protons involving solvent molecules to escape detection. The results of assignments are summarized in Table I.

Table I. Chemical shifts (in p.p.m.) of salicylalsalicylamine (I) and related compounds (II—VI) in dimethyl sulfoxide solutions with cyclohexane as a standard

| Compound | $-CH=$ | $C_6H_3$, $C_6H_4$, $C_6H_5$ | $-CH_2-$ |
|---|---|---|---|
| I | −7.33 | −5.34—6.25 | −3.43 |
| II | −7.31 | −5.39—6.30 | −3.46 |
| III | −7.36 | −5.47—6.28 | −3.45 |
| IV | −7.37 | −5.54—6.26 | −3.44 |
| V | | −5.33—6.45 | −3.43 |
| VI (pure liq.) | −6.12 | −5.23—5.96 | −2.73 |

The appearance of two separate peaks for $-CH=$ and $-CH_2-$ protons provides a conclusive evidence for discarding possible prototropy in these molecules. As pointed out by Katritzky and Waring,[10,11] fast exchange can render two or more protons equivalent in a tautomeric compound and therefore the molecules simulate a more symmetric structure. In other words, if prototropy takes place in the molecules of salicylalsalicylamine and related compounds, one would have a single line for the $-CH=$ and $-CH_2-$ protons in contradiction with the present observations.

## Conclusion

The experimental results described above indicate unequivocally that prototropy does not take place in the $-CH=N-CH_2-$ portion of molecules of salicylalsalicylamine (I) and its derivatives as well as of the copper(II) salts derived from them. This fact has an interesting bearing on the structure of three-coordinated copper(II) complexes.

The so-called three-coordinated copper(II) complexes can be classified into two main groups. Those belonging to group I show subnormal magnetic moments, whereas group II complexes show normal magnetic moments. The latter differ from the former in two respects. First, a six-membered chelate ring having only one aromatic bond is present in a molecule (condition 1). The resulting nonplanar structure of the chelate ring might hinder the approach of two copper atoms. Secondly, complexes belonging to group II have a carbonyl group separated from a copper atom by two chemical bonds (condition 2), whereas a carbonyl oxygen capable of being coordinated on a copper atom of another monomeric molecule is missing in complexes classified as group I.

If one could prepare complexes having a three-dimensional configuration without any carbonyl oxygen and also those of a planar structure involving a carbonyl group at an appropriate position, it would be possible to decide which of the aforementioned two conditions is the main factor leading to normal magnetic moments. Quite recently, the present writers have succeeded in preparing salicylaldehydeglycinecopper(II), which satisfies condition 2 but not condition 1 and found that it shows a subnormal magnetic moment.[12] Salicylalsalicylaminecopper(II) studied in the present investigation satisfies condition 1 but not condition 2, since the double bond in the $-CH=N-CH_2-$ portion of the molecule is localized. It shows a subnormal magnetic moment.[1] Thus, it is concluded that both of the aforementioned two conditions are necessary for three-coordinated copper(II) complexes to form a binuclear structure in which two copper atoms are bridged in a pair by two Cu-O-C-O-Cu links, whereas when either one or both of the two conditions are dissatisfied, dimeric complex molecules are formed, in which two copper atoms are bridged in a pair by two oxygen atoms.

## Summary

On the basis of infrared spectroscopy and X-ray powder patterns, it is shown that 5-chlorosalicylalsalicylamine and its copper(II) salt are different from salicylal-5-chlorosalicylamine and its copper(II) salt, respectively, in the crystalline state. The nuclear magnetic resonance studies on salicylalsalicylamine and related compounds in solutions show that the double bond in the $-CH=N-CH_2-$ portion of these molecules is localized, i. e., the prototropic rearrangement of hydrogen atoms does not take place. Therefore, salicylalsalicylaminecopper(II) presents an example of a new type of three-coordinated copper(II) complexes showing a subnormal magnetic moment in spite of having ligands of a three-dimensional structure. This provides an additional evidence in favor of a presumption made by the present writers on the structure of three-coordinated copper(II) complexes showing a normal magnetic moment.

10) A. R. Katritzky and A. J. Waring, *Chem. & Ind.*, **1962**, 695.

11) W. G. Schneider, "Hydrogen Bonding," Ed. by D. Hadži, Pergamon Press, London (1959), p. 67.

12) M. Kishita, A. Nakahara and M. Kubo, *Australian J. Chem.*, **17**, 810 (1964).

We express our deep appreciation to Dr. Yoko Kuroda for technical assistance in infrared spectroscopy and to Dr. Daiyu Nakamura for taking X-ray diffraction patterns.

*Department of Chemistry*
*Nagoya University*
*Chikusa, Nagoya*

# Studies of Peptide Antibiotics. II. Cyclo-L-valyl-L-ornithyl-L-leucyl-D-phenylalanyl-L-prolylglycyl

By Tetsuo KATO, Michio KONDO, Motonori OHNO and Nobuo IZUMIYA

(Received December 21, 1964; in revised form April 10, 1965)

A number of polypeptide antibiotics[1] such as gramicidin S, tyrocidine A and polymyxin B have several characteristic features in common. These features are, namely, the occurrence of D-amino acids, basic amino acids, and a cyclic structure in the molecule. For a study of the relationship between chemical structure and biological activities of antibacterial cyclic peptides, some dipeptide anhydrides, which are the simplest compounds possessing the characteristics mentioned above, were prepared and their biological activities were tested as described in a previous paper.[2] However, they were found to be devoid of antibacterial activity. Although the reason for the inactivity of the dipeptide anhydrides is not yet clear, it appears that in addition to the characteristics mentioned above, other structural features such as a certain minimum ring size and/or a specific amino acid sequence, are necessary in this type of molecule for the exhibition of antibacterial activity. Therefore, it became of interest to determine whether or not a larger cyclic peptide with an appropriate amino acid sequence would exhibit the antibacterial properties.

It appears that difficulties have been encountered in the synthesis of cyclic tripeptides. It has been found, for example, that a linear tripeptide active ester or azide yields a cyclic hexapeptide through cyclization by the dimerization reaction.[3,4] Furthermore, cyclization of a linear tetra or pentapeptide gave a cyclic tetrapeptide in very poor yield[3] or was accompanied with the dimerization reaction to yield a cyclic decapeptide.[5] On the other hand, it has been found that several cyclic hexapeptides can be synthesized without any difficulty.[3,6] Therefore, we have decided to attempt the synthesis of a cyclic hexapeptide with the appropriate amino acid sequence.

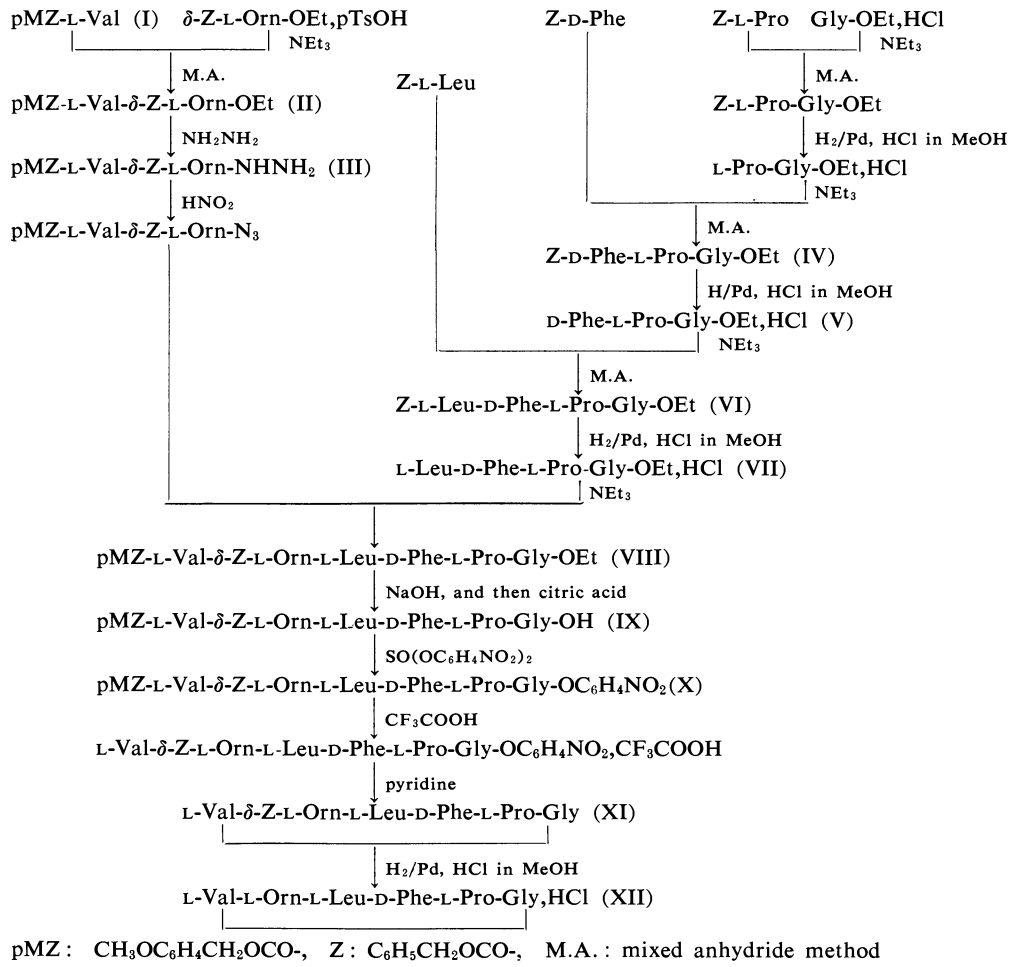
This paper is concerned with the synthesis and an antibacterial assay of the cyclic hexapeptide, cyclo-L-valyl-L-ornithyl-L-leucyl-D-phenylalanyl-L-prolylglycyl, which contains the partial sequence -L-Val-L-Orn-L-Leu-D-Phe-L-Pro- found in gramicidin S and tyrocidines.[1]

The sequence of reactions employed in the synthesis of the cyclic hexapeptide (XII) is indicated in the following scheme (p. 1203). The final product XII was obtained as colorless crystals containing five moles of water of crystallization; its homogeneity was demonstrated by paper and thin layer chromatographies.

In order to ascertain whether or not the cyclic peptide XII described herein possesses antibacterial activity, the effect of various levels of XII on the growth of *Escherichia coli*, *Bacillus subtilis*, and several other microorganisms was examined. It was found that there was no retardation of growth of any of these microorganisms.

Hence, it appears that even the presence of six amino acid residues in a cyclic peptide does not satisfy the requirements for antibacterial activity. Experiments on the preparation and studies on the properties of several other cyclic hexapetides are in progress in this laboratory in order to extend this study further.

1) R. O. Studer and K. Vogler, *Helv. Chim. Acta*, **45**, 819 (1962).
2) N. Izumiya, T. Kato, Y. Fujita, M. Ohno and M. Kondo, This Bulletin, **37**, 1809 (1964).
3) R. Schwyzer, B. Iselin, W. Rittel and P. Sieber, *Helv. Chim. Acta*, **39**, 872 (1956).
4) J. C. Sheehan and W. L. Richardson. *J. Am. Chem. Soc.*, **77**, 6391 (1955); G. W. Kenner, P. J. Thompson and J. M. Turner, *J. Chem. Soc.*, **1958**, 4148; R. Schwyzer and P. Sieber, *Helv. Chim. Acta*, **41**, 2190 (1958); M. Rothe, K. D. Steffen and I. Rothe, *Angew. Chem.*, **75**, 1207 (1963).
5) R. Schwyzer and P. Sieber, *Helv. Chim. Acta*, **41**, 2186 (1958); German Patent, *Chem. Abstr.*, **57**, 949 (1962).
6) T. Wieland and K. W. Ohly, *Ann.*, **605**, 179 (1957); R. Schwyzer and B. Gorup, *Helv. Chim. Acta*, **41**, 2199 (1958); K. D. Kopple and D. E. Nitecki, *J. Am. Chem. Soc.*, **84**, 4457 (1962); J. C. Sheehan and D. N. McGregor, ibid., **84**, 3000 (1962).




pMZ: $CH_3OC_6H_4CH_2OCO$-, Z: $C_6H_5CH_2OCO$-, M.A.: mixed anhydride method

In this connection, it should be noted that it was recently reported that gramicidin $J_2$, previously described as a cyclic hexapeptide, is identical with gramicidin S,[7] a cyclic decapeptide.

## Experimental

All melting points are uncorrected.

***p*-Methoxybenzyloxycarbonyl-L-valine (I).**—To a solution of L-valine (1.172 g., 10 mmol.) and sodium bicarbonate (1.64 g., 20 mmol.) in water (20 ml.) was added a solution of *p*-methoxybenzyloxycarbonyl azide[8] (2.486 g., 12 mmol.) in dioxane (20 ml.), and the reaction mixture stirred for 48 hr. at room temperature. After removal of dioxane in vacuo, water (20 ml.) was added to the residue. The aqueous solution was extracted with ethyl acetate (20 ml.). The combined aqueous layer was acidified with 0.5 M citric acid to pH 5 in an ice bath, and then thrice extracted with ethyl acetate (30 ml. each). The extract was dried over anhydrous sodium sulfate, and after removal of the salt by filtration, evaporated in vacuo. The residual oil weighed 2.036 g. (72%).

***p*-Methoxybenzyloxycarbonyl-L-valyl-δ-benzyloxycarbonyl-L-ornithine Ethyl Ester (II).**—To a solution of I (2.036 g.) and triethylamine (1.0 ml.) in absolute tetrahydrofuran (20 ml.) at −5°C, was added isobutyl chloroformate (0.94 ml.). After 15 min., a cold mixture of δ-benzyloxycarbonyl-L ornithine ethyl ester *p*-toluenesulfonate (3.359 g.)[2] and triethylamine (1.0 ml.) in chloroform (20 ml.) was added, and the mixture was allowed to stand overnight at room temperature. After removal of the solvent by evaporation in vacuo, the resultant oily residue solidified. The solidified product was treated with water and the mixture was filtered; the residue was washed successively with 4% sodium bicarbonate, water, 10% citric acid, and water; yield, 3.379 g. This solid was recrystallized from methanol-ether-petroleum ether to give 3.126 g. (76%); m. p. 140—144°C; $[\alpha]_D^{23}$ −7.8° (*c* 1, acetic acid).

Found: C, 62.22; H, 6.96; N, 7.61. Calcd. for $C_{29}H_{39}O_8N_3$: C, 62.46; H, 7.05; N, 7.54%.

***p*-Methoxybenzyloxycarbonyl-L-valyl-δ-benzyloxycarbonyl-L-ornithine Hydrazide (III).**—To a solution of II (1.115 g., 2 mmol.) in dimethylformamide (4 ml.) was added hydrazine hydrate (1 ml.)

7) K. Kurahashi, *J. Biochem.*, **56**, 101 (1964).
8) F. Weygand and K. Hunger, *Chem. Ber.*, **95**, 1 (1962).

and the solution was stored for 48 hr. at room temperature. The reaction mixture was evaporated in vacuo below 50°C. The hydrazide which precipitated upon the addition of water (20 ml.) was filtered off, washed with water and dried in a desiccator; 991 mg. (91%); m. p. 211—212°C (decomp.); $[\alpha]_D^{23}$ −4.2° (*c* 1, dimethylformamide).

Found: C, 59.53; H, 6.87; N, 12.77. Calcd. for $C_{27}H_{37}O_7N_5$: C, 59.65; H, 6.86; N, 12.88%.

**Benzyloxycarbonyl-D-phenylalanyl-L-prolylglycine Ethyl Ester (IV).**—To a chilled solution of benzyloxycarbonyl-D-phenylalanine (2.155 g., 7.2 mmol.) and triethylamine (1.01 ml.) in tetrahydrofuran (15 ml.) was added isobutyl chloroformate (0.94 ml.). After 15 min. a mixture of L-prolylglycine ethyl ester hydrochloride (1.805 g.),[9] triethylamine (1.01 ml.) and chloroform (20 ml.) was added. The mixture was left overnight at room temperature and then evaporated in vacuo. The residual oil was dissolved in ethyl acetate (50 ml.), and the solution was washed successively with 2% hydrochloric acid, 4% sodium bicarbonate and water, and then dried over anhydrous sodium sulfate. The filtered solution was evaporated in vacuo. The residual oil solidified after the addition of ether and petroleum ether. The product was filtered off, dried in air and weighed; 2.588 g. (75%); m. p. 105—106°C; $[\alpha]_D^{23}$ −52.6° (*c* 2, dimethylformamide).

Found: C, 63.85; H, 6.51; N, 8.25. Calcd. for $C_{26}H_{31}O_6N_3 \cdot 1/2H_2O$: C, 63.66; H, 6.57; N, 8.56%.

When dried at 100°C in vacuo, the crystals lost 1.5% of their weight. Calcd. for $1/2H_2O$: 1.8%.

**D-Phenylalanyl-L-prolylglycine Ethyl Ester Hydrochloride (V).**—To a solution of IV (2.407 g., 5 mmol.) in methanol (20 ml.) was added 0.494 N methanolic hydrogen chloride (10.7 ml.). The solution was then subjected to hydrogenolysis in the presence of palladium black. After being filtered from the catalyst, the solution was evaporated to dryness in vacuo; yield, 1.944 g. (100%).

**Benzyloxycarbonyl-L-leucyl-D-phenylalanyl-L-prolylglycine Ethyl Ester (VI).**—To a chilled solution of benzyloxycarbonyl-L-leucine (1.327 g., 5 mmol.) and triethylamine (0.70 ml.) in tetrahydrofuran (15 ml.) was added isobutyl chloroformate (0.66 ml.). After 15 min., a solution of V (1.944 g., 5 mmol.) and triethylamine (0.70 ml.) in chloroform (20 ml.) was added at −10°C. The mixture was left overnight at room temperature and evaporated in vacuo. The residual oil was treated in the manner described above. The oily residue weighed 2.910 g. (97%).

**L-Leucyl-D-phenylalanyl-L-prolylglycine Ethyl Ester Hydrochloride (VII).**—VI (1.189 g., 2 mmol.) was subjected to hydrogenolysis in the presence of palladium black and 0.48 N methanolic hydrogen chloride (4.5 ml.), and then treated as mentioned above. The resulting oil gradually solidified to form an amorphous powder; yield, 961 mg. (97%).

***p*-Methoxybenzyloxycarbonyl-L-valyl-δ-benzyloxycarbonyl-L-ornithyl-L-leucyl-D-phenylalanyl-L-prolylglycine Ethyl Ester (VIII).**—The following operations were carried out in a cold room. To a chilled solution of III (544 mg., 1 mmol.) in glacial acetic acid (12 ml.) were added successively with stirring 1.09 N hydrochloric acid (1 ml.), 76 mg. of sodium nitrite in 1 ml. of water, and additional 1.09 N hydrochloric acid (1 ml.). After 6 min., cold water (50 ml.) was added. The azide which precipitated as a white mass was filtered off and washed successively with cold water, saturated sodium bicarbonate solution, and water, and then dried under vaccum in a desiccator. The azide was added to a solution of VII (497 mg., 1 mmol.) and triethylamine (0.14 ml.) in dimethylformamide (4 ml.), and the mixture was stirred for 3 days at 0°C. The insoluble substance was removed by filtration. The precipitate which formed upon addition of water (50 ml.) to the filtrate was collected, washed with 0.5 M citric acid, 4% sodium bicarbonate solution and water, and dried. Recrystallization from dioxane and ether gave 696 mg. (72%) of VIII; m. p. 125—129°C; $[\alpha]_D^{23}$ −33.5° (*c* 2, dimethylformamide).

Found: C, 62.15; H, 7.01; N, 9.93. Calcd. for $C_{51}H_{69}O_{12}N_7 \cdot 1/2H_2O$: C, 62.42; H, 7.19; N, 9.99%.

***p*-Methoxybenzyloxycarbonyl-L-valyl-δ-benzyloxycarbonyl-L-ornithyl-L-leucyl-D-phenylalanyl-L-prolylglycine (IX).**—To a solution of VIII (990 mg., 1 mmol.) in methanol (15 ml.) was added 0.52 N sodium hydroxide (3 ml.), and the solution was allowed to stand for 4 hr. at 40°C. After the addition of water (15 ml.), the solution was concentrated in vacuo, extracted with ether and acidified with 0.5 M citric acid in an ice-cold bath. After storing in a refrigerator, the crystals were collected by filtration, washed with water and dried. Recrystallization from acetone and ether did not raise the melting point. The yield was 736 mg. (79%); m. p. 154—158°C; $[\alpha]_D^{23}$ −39.4° (*c* 2, dimethylformamide).

Found: C, 62.09; H, 6.83; N, 10.20. Calcd. for $C_{49}H_{65}O_{12}N_7$: C, 62.34, H, 6.94; N, 10.39%.

***p*-Methoxybenzyloxycarbonyl-L-valyl-δ-benzyloxycarbonyl-L-ornithyl-L-leucyl-D-phenylalanyl-L-prolylglycine *p*-Nitrophenyl Ester (X).**—To a solution of IX (472 mg., 0.5 mmol.) in pyridine (4 ml.) was added di-*p*-nitrophenyl sulfite[10] (648 mg., 2 mmol.), and the reaction mixture was allowed to stand for 24 hr. at room temperature. After evaporation of the solvent, the oily product was triturated in petroleum ether and washed repeatedly with a mixture of ether and petroleum ether (1 : 1) by decantation. When the reaction mixture had been washed completely, the washings did not give the yellow color of *p*-nitrophenol on addition of sodium hydroxide solution. The residual solid was filtered off, washed with a mixture of ether and petroleum ether (1 : 1) and dried. It weighed 509 mg. (95%). A *p*-nitrophenyl group estimation was carried out spectrophotometrically by measuring the optical density of the compound at 412 mμ. The purity of the product was estimated to be 101%.

**Cyclo-L-valyl-δ-benzyloxycarbonyl-L-ornithyl-L-leucyl-D-phenylalanyl-L-prolyglycyl (XI).**—To X (788 mg., 0.74 mmol.), were added successively

9) H. N. Rydon and P. W. G. Smith, *J. Chem. Soc.*, 1956, 3642.

10) B. Iselin and R. Schwyzer, *Helv. Chim. Acta* 3, 1760 (1960).

Table I. Inhibitory activity of peptide XII and gramicidin S on microorganisms*
Minimum inhibitory concentrations, μg./ml.

| Compound | Synthetic medium[a] | | Bouillon agar medium[b] | |
|---|---|---|---|---|
| | *E. coli*[c] | *B. subtilis*[d] | *E. coli*[c] | *B. subtilis*[d] |
| XII | >100 | >100 | >100 | >100 |
| Gramicidin S[e] | >100 | 10 | >100 | 10 |

a) Stephenson-Whetham's medium (modified); $KH_2PO_4$ lg., NaCl lg., $FeSO_4 \cdot 7H_2O$ 0.03 g., $MgSO_4 \cdot 7H_2O$ 0.7 g., Na-glutamate 4 g., glucose 5 g./1000 ml. and agar 20 g.
b) Usual bouillon agar medium, pH 7.0.
c) *Escherichia coli IRO 3044.*
d) *Bacillus subtilis PCI 219.*
e) A product of Astra Co, U.S.A.

* In addition to *E. coli* and *B. subtilis*, microbiological assays were also performed against *Proteus vulgaris*, *Staphylococcus aureus*, *Bacillus cereus*, *Mycobacterium avium*, *Mycobacterium avium* (Streptomycin resistant St.), *Mycobacterium SP 607*, *Mycobacterium semegmatis*, *Candida albicans*, *Saccharomyces cerevisiae* and *Piricularia oryzae* in bouillon agar medium. Peptide XII was inactive at 50 μg./ml. against any of microorganisms tested here. Gramicidin S inhibits the growth of *Proteus vulgaris* in 10 μg./ml., *Staphylococcus aureus* in 5 μg./ml. and *Mycobacterium semegmatis* in 10 μg./ml. in bouillon agar medium.

anisole (0.4 ml.) and trifluoroacetic acid (3 ml.) at a temperature below 0°C. The solution was evaporated in vacuo at 0°C, and the residue was triturated with ether (10 ml.). The crude hexapeptide *p*-nitrophenyl ester trifluoroacetate was collected in the cold room, washed with ether - petroleum ether mixture and dried in vacuo over phosphorous pentoxide.

The dried trifluoroacetate was dissolved in dimethylformamide (5 ml.) containing 0.1 ml. of glacial acetic acid, and the solution was added dropwise to pyridine (200 ml.) at 62°C over a period of 3 hr. under continuous stirring; stirring was then continued for an additional 2 hr. at the same temperature. After removal of the solvent, the residual oil was dissolved in a mixture of methanol (40 ml.) and water (10 ml.), the insoluble substance was removed by filtration, and the filtrate was passed successively through columns of Dowex 1 ($OH^-$ form) and Dowex 50 ($H^+$ form). The columns were eluted with the same solvent (150 ml.), the collected effluent was evaporated to dryness in vacuo. The residual amorphous product (455 mg.) was dissolved in a mixture of ethyl acetate (20 ml.) and methanol (5 ml.). After removal of insoluble substances by filtration, the solution was evaporated, and the residue was triturated with ethyl acetate (4 ml.) and ether (1 ml.). The product which solidified as needles was filtered off, and recrystallized by the same procedure mentioned above. The yield was 139 mg. (32%); m. p. 224—226°C; $[\alpha]_D^{16}$ −22.9°(*c* 1.95, dimethylformamide); $R_f$=0.66 on thin layer chromatography.[11]

Found: C, 62.28; H, 7.18; N, 12.66. Calcd. for $C_{40}H_{55}O_8N_7 \cdot 1/3H_2O$: C, 62.56; H, 7.30; N, 12.77%. Mol. wt. Found: 652, 598.[12] Calcd. 762.

The air-dried compound lost 0.75% of its weight after drying over phosphorus pentoxide for 3 hr. at 120°C, 2 mmHg. Calcd. for $1/3H_2O$: 0.78%.

**Cyclo-L-valyl-L-ornithyl-L-leucyl-D-phenylalanyl-L-prolylglycyl Hydrochloride (XII).**—XI (38 mg., 0.05 mmol.), dissolved in methanol (2 ml.) containing 0.0455 N methanolic hydrogen chloride (1.22 ml.), was subjected to hydrogenolysis in the presence of palladium black. The solution after being filtered from the catalyst was evaporated to dryness in vacuo. The residue was dissolved in ethanol (0.2 ml.), then acetone (4 ml.) and ether (1 ml.) were added dropwise to the solution which was then stored overnight at 0°C. The crystals of XII which formed were filtered off, washed with acetone-ether (1 : 1) and dried in air. The yield was 24 mg. (72%); m. p. 283°C (decomp.); $[\alpha]_D^{24}$ −125° (*c* 1.01, 50% methanol, v/v); $R_f$=0.88 on paper,[11] 0.61 on silica gel.[11]

Found: C, 50.77; H, 7.70; N, 12.83. Calcd. for $C_{32}H_{50}N_7O_6Cl \cdot 5H_2O$: C, 50.95; H, 8.02; N, 12.89%.

The compound lost 10.4% of its weight after drying over phosphorus pentoxide for 3 hr. at 120°C, 2 mmHg. Calcd. for $5H_2O$: 11.9%.

XII, after hydrolysis with 6 N hydrochloric acid at 110°C for 16 hr., gave six distinctly separated spots when chromatographed on paper. $R_f$ values were 0.69, 0.65, 0.53, 0.38, 0.23 and 0.17. The $R_f$ values of authentic L-Leu, D-Phe, L-Val, L-Pro, Gly and L-Orn are 0.68, 0.63, 0.51, 0.36, 0.22 and 0.16, respectively.[11]

**Microbiological Assays.***—The microorganisms employed are shown in Table I. The minimum amount of compound necessary for complete inhibition of growth was determined by a dilution

11) Toyo Roshi No. 52 paper was used for paper chromatography, and Merck silica gel G for thin layer chromatography. Solvent system used in both cases was a mixture of *n*-butanol: acetic acid: pyridine: water, 4:1:1:2 in v/v.

12) Micro Rast method. The solvent used was hexahydro-*p*-amino benzoic acid lactam (G. Wendt, *Chem. Ber.*, 75, 425 (1962)).

* The authors are indebted to Research Laboratories, Takeda Chemical Industries, Ltd., Osaka, for the microbiological assays.

method with bouillon agar medium and with synthetic medium. As shown in Table I, cyclohexapeptide XII exhibited no antibacterial activity against any of the microorganisms tested, even at high concentration of the test compound, whereas gramicidin S, a cyclic decapeptide, exhibited considerable activity against some of the microorganisms at comparable concentration.

## Summary

A cyclic hexapeptide, cyclo-L-valyl-L-ornithyl-L-leucyl-D-phenylalanyl-L-prolylglycyl, was synthesized for the purpose of comparing its antibacterial action, if any, with the cyclopeptide antibiotics, such as gramicidin S, with which it shares several common structural features.

Synthesis was achieved by condensation of *p*-methoxybenzyloxycarbonyl-L-valyl-*δ*-benzyloxycarbonyl-L-ornithine azide with L-leucyl-D-phenylalanyl-L-prolylglycine ethyl ester, followed by treatment of the resulting diacyl hexapeptide ester with alkali to remove the ethyl ester group. The diacyl hexapeptide so derived was converted to the *p*-nitrophenyl ester by the action of di-*p*-nitrophenyl sulfite, and after removal of the *p*-methoxybenzyloxycarbonyl group with trifluoroactetic acid, the hexapeptide *p*-nitrophenyl ester was transformed to the cyclic benzyloxycarbonyl-substituted hexapeptide by treatment with a large excess of pyridine. The cyclic benzyloxycarbonyl-substituted peptide was hydrogenated in the presence of palladium black to yield the desired cyclic hexapeptide hydrochloride.

The effects of the synthesized cyclic peptide on bacterial growth were examined. No antibacterial activities were observed against the microorganisms utilized here.

*Laboratory of Biochemistry*
*Faculty of Science*
*Kyushu University*
*Fukuoka*

# Asymmetric Hydrogenation with Modified Raney Nickel. V. Studies on the Modified Hydrogenation Catalyst. VI

By Yoshiharu IZUMI, Susumu TATSUMI, Masami IMAIDA, Yoshio FUKUDA and Shiro AKABORI

(Received December 24, 1964)

In previous papers of this series, the asymmetric hydrogenation of methyl acetoacetate to methyl 3-hydroxybutyrate using Raney nickel catalysts modified with various optically active compounds, such as amino acids and hydroxy acids, has been reported.[1-4]

In the present work, the asymmetric activity of Raney nickel catalysts modified with (+)-2-methylglutamic acid* or (+)-2-benzylglutamic acid* was tested to study the role of a substituent at the asymmetric $\alpha$-carbon atom in an $\alpha$-amino acid. The asymmetric activities of these catalysts were compared with that of the catalyst modified with L-glutamic acid.

2-Methyl- and 2-benzylglutamic acid are characterized by the lack of a hydrogen atom on the asymmetric $\alpha$-carbon atom, and thus have the structure, $HOOCCH_2CH_2(R)C(NH_2)$-COOH, where R is a methyl or a benzyl group. L-Glutamic acid however has an $\alpha$-hydrogen atom on the $\alpha$-carbon. It is interesting to find out whether a methyl or a benzyl group on the asymmetric $\alpha$-carbon in an amino acid takes part in the mechanism of the asymmetric hydrogenation.

## Results

**The Effect of the pH of the Modifying Solution.** — Measurements were made of the asymmetric activities of the catalysts modified at 0°C with solutions of (+)-2-methylglutamic acid, (+)-2-benzylglutamic acid or L-glutamic acid,[1)] the pH's of which had been adjusted to specified values. The results are shown in Fig. 1.

As shown in Fig. 1, the catalyst modified with (+)-2-methylglutamic acid produced

1) Y. Izumi, M. Imaida, H. Fukawa and S. Akabori, This Bulletin, 36, 21 (1963).
2) Y. Izumi, M. Imaida, H. Fukawa and S. Akabori, ibid., 36, 155 (1963).
3) S. Tatsumi, M. Imaida, Y. Fukuda, Y. Izumi and S. Akabori, ibid., 37, 846 (1964).
4) Presented at the 3rd International Congress on Catalysis, Amsterdam, July, 1964.
* The preparation of this amino acid was reported recently by the present authors, This Bulletin, in press.

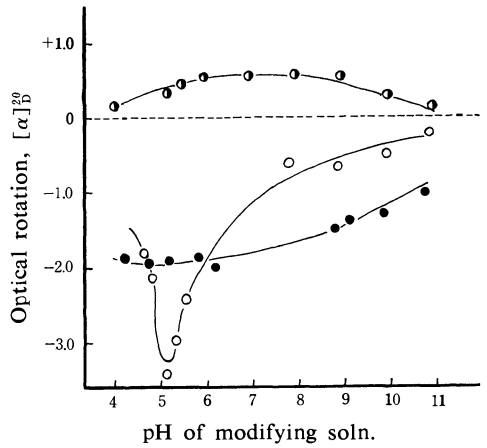



Fig. 1. Effect of modifying pH (modifying temp. at 0°C).
-○- L-Glutamic acid
-●- (+)-2-Methylglutamic acid
-◑- (+)-2-Benzylglutamic acid

levorotatory methyl 3-hydroxybutyrate and that modified with (+)-2-benzylglutamic acid produced the dextrorotatory form. With these amino acids, the asymmetric activities of both modifications of the catalyst were less influenced by the pH of the modifying solution than that of the catalyst modified with L-glutamic acid, and the optimum pH range for asymmetric activity was pH 5—8. This pH range approximately corresponds to the pH jumping region of the neutralization curves of these *α-C*-substituted glutamic acids. Thus, the two activity curves were alike in character except for the direction of their optical rotation. However, the asymmetric activity of the catalyst modified with L-glutamic acid was much influenced by the pH of the modifying solution. The greatest asymmetric activity was observed at pH 5.1 and there was considerable diminution in activity at both higher and lower pH values.

The effects of the pH values of modifying solutions at 100°C on the asymmetric activities of the modified catalysts are shown in Fig. 2.

Optimum asymmetric activities were observed when catalysts were modified with solutions of the three amino acids at pH 7—9.5. On modifications with (+)-2-methyl- and (+)-2-benzylglutamic acid, the asymmetric activity curves showed tendencies similar to those shown on modification at 0°C. In the case of modification with L-glutamic acid, however, the dextrorotatory product was obtained below pH 5.4 or above pH 11 and the levorotatory product in the intermediate range.

**The Effect of the Modifying Temperature.**— The effect of the temperature of the modifying solution was studied at pH 5.2; the results are shown in Fig. 3.

As shown in Fig. 3, the asymmetric activity of the catalyst modified with (+)-2-methylglutamic acid was greater than that of the catalyst modified with (+)-2-benzylglutamic acid and both activities increased with elevation of the modifying temperature. On modification with L-glutamic acid, however, the activity was characteristically different from those obtained on modification with the other two amino acids; the highest activity was obtained by modification at 0°C and the asymmetric

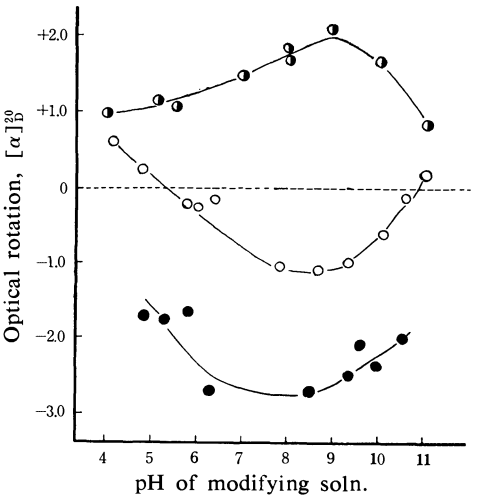



Fig. 2. Effect of modifying pH (modifying temp. at 100°C).
-○- L-Glutamic acid
-●- (+)-2-Methylglutamic acid
-◑- (+)-2-Benzylglutamic acid

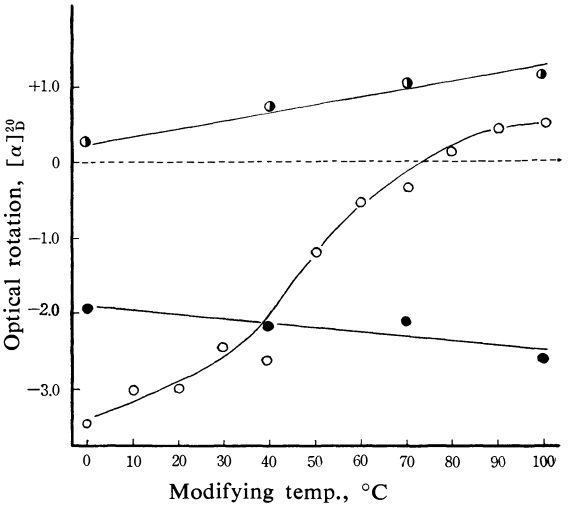



Fig. 3. Effect of modifying temperature.
-○- L-Glutamic acid (pH 5.2)
-●- (+)-2-Methylglutamic acid (pH 5.2)
-◑- (+)-2-Benzylglutamic acid (pH 5.2)

activity decreased at higher temperatures. If the catalyst was treated with the same modifying solution at temperatures higher than 80°C, the hydrogenation products showed reverse optical rotations.

## Discussion

Two kinds of asymmetric hydrogenation catalyst are obtained by modification with L-glutamic acid. One has the asymmetric capacity to hydrogenate methyl acetoacetate predominantly to levorotatory methyl 3-hydroxybutyrate and the other has the capacity to produce the dextrorotatory product. On the other hand, only one asymmetric catalyst is obtained by modification with (+)-2-methylglutamic acid or (+)-2-benzylglutamic acid under a variety of modifying conditions as shown in Figs. 1, 2 and 3.

These results show that on modification with L-glutamic acid, at least two types of asymmetric center are produced on the surface of the modified catalyst; but only one type is formed, or this type is in excess on modification with $\alpha$-*C*-substituted glutamic acid under all modifying conditions.

The difference between glutamic acid and $\alpha$-*C*-substituted glutamic acid is caused by the substituent on the asymmetric $\alpha$-carbon atom. The steric hindrance of the substituent on the $\alpha$-carbon atom regulates the adsorption of $\alpha$-*C*-substituted glutamic acid on Raney nickel catalyst and permits the formation of only one or mainly one type of asymmetric center. The relationship between the bulk of the substituent on the $\alpha$-carbon atom of the modifying reagent and the optical direction of the asymmetric activity of the modified catalyst will be discussed after the absolute configuration of (+)-2-methylglutamic acid and (+)-2-benzylglutamic acid have been confirmed.

## Experimental

The preparation and modification of the Raney nickel catalyst, the hydrogenation of methyl acetoacetate and the measurement of the asymmetric activity of the catalyst were performed as described in a previous paper.[1]

## Summary

1) The asymmetric activities of Raney nickel catalysts modified with (+)-2-methylglutamic acid or (+)-2-benzylglutamic acid have been formed to be quite different from that of the catalyst modified with L-glutamic acid.

2) Levorotatory methyl 3-hydroxybutyrate is obtained by the catalyst modified with (+)-2-methylglutamic acid, and the dextrorotatory product by the catalyst modified with (+)-2-benzylglutamic acid. With the catalyst modified with L-glutamic acid, however, the direction of optical rotation of the hydrogenation product is much influenced by the pH and by the temperature of the modifying solution.

This research was made possible through the support of the Kawaken Fine Chemicals Co., Ltd., Tokyo and Ajinomoto Co., Inc., Tokyo.

*Division of Organic Chemistry*
*Institute for Protein Research*
*Osaka University*
*Kita-ku, Osaka*

# NOTES

## The Synthesis of New Silicon-functional Silanols*

By Shigemi KOHAMA

(Received March 4, 1964)

Some years ago a new method[1] for the preparation of diphenylsilanediol was applied to the synthesis of various organosilanols[2] and named as the "Silanolate method."[3] This procedure involves neutralization of sodium silanolate in an aqueous solution with hydrochloric acid to give silanol. Now it has been found that the above method can be extended to the preparation of silicon-functional silanols possessing both hydroxyl and alkoxyl groups on the silicon atom. The present paper describes the synthesis of such new silanols and their properties, reactions, and infrared absorptions. The synthetic route attempted to prepare various alkoxysilanols is indicated in the following scheme:

$$R_nSiCl_{4-n} + mR'OH + mC_5H_5N \rightarrow R_nSi(OR')_mCl_{4-n-m} + mC_5H_5N\cdot HCl$$

$$R_nSi(OR')_mCl_{4-n-m} + \text{excess } 5\%\ NaOH_{aq} \rightarrow R_nSi(OR')_m(ONa)_{4-n-m}$$

$$R_nSi(OR')_m(ONa)_{4-n-m} + (4-n-m)HCl_{aq} \rightarrow R_nSi(OR')_m(OH)_{4-n-m}$$

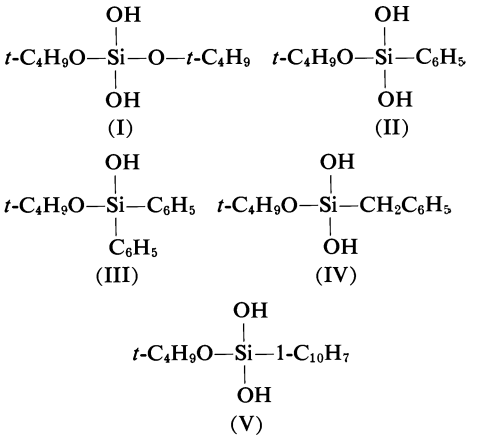
R: $CH_3$, $i$-$C_3H_7$, $C_6H_{11}$, $CH_2CH_2C_6H_5$, $CH_2C_6H_5$, $C_6H_5$, 1-$C_{10}H_7$

R': $CH_3$, $C_2H_5$, $n$-$C_3H_7$, $i$-$C_3H_7$, $n$-$C_4H_9$, $t$-$C_4H_9$, $C_6H_{11}$, $C_6H_5$, $CH_2CH_2NH_2$

$n$: 0—2, $m$: 1—2

Thus, five new silicon-functional silanols containing a $t$-butoxyl group were obtained, these being di-$t$-butoxysilanediol (I), phenyl-$t$-butoxysilanediol (II), diphenyl-$t$-butoxysilanol (III), benzyl-$t$-butoxysilanediol (IV) and 1-naphthyl-$t$-butoxysilanediol (V).

I, in particular, derived from tetrachlorosilane is a unique silanol containing no silicon-bond; other similar organoalkoxysilanols could not be so obtained. In these cases, the corresponding siloxanes and alcohols were afforded by further condensation and hydrolysis. Grubb[4] suggested that base-catalyzed silanol condensation-reactions are sensitive to steric factors. The fact that only alkoxysilanols surrounded with bulky groups were isolated might support this suggestion. In spite of the fact that di-$t$-butoxysilanediol (I) was isolated in a good yield, isolation of di-$t$-butoxyorganosilanols was not successful, because the reaction products were all liquids and decomposed during distillation even at low pressure. Details of the synthesis of $t$-butoxysilanols, and their analyses, melting points, and crystal forms are shown in Table I.




The infrared spectra for all of the silanols obtained show a band at 1385—1395 $cm^{-1}$ and a strong one at 1365 $cm^{-1}$; these are assigned to the $t$-butyl group.[5] Evidence for the presence of an OH group is provided by the existence of a band at 3350—3400 $cm^{-1}$, and for the Si-O grouping by a band at 1000—1100 $cm^{-1}$. In general, almost all organosilanols in the solid state have an OH absorption band

* Presented at The Symposium on Organometallic Compound, Nagoya, Oct., 1963.

1) S. Kohama, *J. Chem. Soc., Japan, Ind. Chem. Sec.* (*Kogyo Kagaku Zasshi*), **63**, 1439 (1960).

2) S. Kohama, *J. Chem. Soc. Japan, Pure Chem. Sec.* (*Nippon Kagaku Zasshi*), **81**, 1760 (1960); ibid., **81**, 1874 (1960); ibid., **81**, 1889 (1960); ibid., **83**, 188 (1962).

3) S. Kohama, ibid. **82**, 69 (1961).

4) W. T. Grubb, *J. Am. Chem. Soc.*, **76**, 3408 (1954).

5) L. J. Bellamy, "The Infrared Spectra of Complex Molecules," Methuen and Co. Ltd., London (1958), p. 13.

TABLE I. TERTIARY

| Chlorosilane | Reaction: *t*-BuOH | Pyridine | 5% NaOH | Ice | Silanol |
|---|---|---|---|---|---|
| | g. | g. | ml. | g. | |
| $SiCl_4$ | 11 | 9.0 | 9.5 | 250 | 100 | $(t\text{-}C_4H_9O)_2Si(OH)_2$ |
| $C_6H_5SiCl_3$ | 10 | 7.5 | 8.0 | 200 | 100 | $C_6H_5(t\text{-}C_4H_9O)Si(OH)_2$ |
| $(C_6H_5)_2SiCl_2$ | 10 | 2.8 | 3.2 | 80 | 50 | $(C_6H_5)_2(t\text{-}C_4H_9O)SiOH$ |
| $C_6H_5CH_2SiCl_3$ | 12 | 4.0 | 4.2 | 200 | 100 | $C_6H_5CH_2(t\text{-}C_4H_9O)Si(OH)_2$ |
| $1\text{-}C_{10}H_7SiCl_3$ | 13 | 3.4 | 3.9 | 200 | 100 | $1\text{-}C_{10}H_7(t\text{-}C_4H_9O)Si(OH)_2$ |

* All the melting points are uncorrected.
W : Water, B : Benzene, P : Petroleum ether. s : Soluble, p : Partially soluble, i : Insoluble.

near 3250 $cm^{-1}$.[1,2,6-8] It is of interest that *t*-butoxysilanols show OH bands at frequences higher by about 100 $cm^{-1}$ than those for ordinary organosilanols. The OH stretching absorption bands of *t*-butoxysilanols are listed in Table II, together with those of various organosilanols for comparison. The butoxysilanols obtained were stable in a desiccator but, on standing in the air, turned greasy.

TABLE II. STRETCHING FREQUENCY OF O-H BOND IN VARIOUS SILANOLS (in Nujol)

| Compound | (O-H) $cm^{-1}$ | Literature |
|---|---|---|
| $(t\text{-}C_4H_9O)_2Si(OH)_2$ | 3400 | |
| $C_6H_5(t\text{-}C_4H_9O)Si(OH)_2$ | 3350 | |
| $(C_6H_5)_2(t\text{-}C_4H_9O)SiOH$ | 3400 | |
| $C_6H_5CH_2(t\text{-}C_4H_9O)Si(OH)_2$ | 3350 | |
| $1\text{-}C_{10}H_7(t\text{-}C_4H_9O)Si(OH)_2$ | 3300 | |
| $(CH_3)_3SiOH$ | 3257 | *1 |
| $(CH_3)_2Si(OH)_2$ | 3125 | *1 |
| $HOSi(CH_3)_2OSi(CH_3)_2OH$ | 3247 | *1 |
| $(C_2H_5)_2Si(OH)_2$ | 3220 | *2 |
| $(C_6H_5)_3SiOH$ | 3260 | *3 |
| $(C_6H_5)_2Si(OH)_2$ | 3260 | *3 |
| $HO[Si(C_6H_5)_2O]_2H$ | 3260 | *3 |
| $HO[Si(C_6H_5)_2O]_3H$ | 3260 | *3 |
| $CH_3C_6H_5CH_2Si(OH)_2$ | 3250 | *4 |
| $CH_3(1\text{-}C_{10}H_7)Si(OH)_2$ | 3250 | *4 |
| $C_6H_5C_6H_5CH_2Si(OH)_2$ | 3250 | *4 |
| $C_6H_5(p\text{-}CH_3C_6H_4CH_2)Si(OH)_2$ | 3250 | *4 |
| $CH_3(p\text{-}CH_3C_6H_4)Si(OH)_2$ | 3250 | *5 |
| $CH_3(p\text{-}CH_3OC_6H_4)Si(OH)_2$ | 3200 | *5 |
| $CH_3(p\text{-}ClC_6H_4)Si(OH)_2$ | 3150 | *5 |
| $CH_3(p\text{-}BrC_6H_4)Si(OH)_2$ | 3150 | *5 |
| $CH_3(p\text{-}(CH_3)_2NC_6H_4)Si(OH)_2$ | 3250 | *5 |
| $CH_3(p\text{-}CH_2BrCHBrC_6H_4)Si(OH)_2$ | 3200 | *6 |
| $CH_3(p\text{-}CH_2{=}CHCH_2C_6H_4)Si(OH)_2$ | 3200 | *6 |
| $CH_3(p\text{-}CH_2{=}CHC_6H_4)Si(OH)_2$ | 3200 | *6 |

*1 S. W. Kantor, *J. Am. Chem. Soc.*, **75**, 2712 (1953).
*2 M. Kakudo, *J. Chem. Phys.*, **21**, 1894 (1953).
*3 R. E. Richards, H. E. Thompson, *J. Chem. Soc.*, **1949**, 125.
*4 S. Kohama, *J. Chem. Soc. Japan, Pure Chem. Sec. (Nippon Kagaku Zasshi)*, **81**, 1760 (1960).
*5 S. Kohama, ibid., **82**, 69 (1961).
*6 S. Kohama, ibid., **81**, 1889 (1960).

Treatment of these silanols with dilute sodium hydroxide solution gave a clear aqueous solution, from which the starting materials were recovered, together with a small quantity of oily matter, by neutralization. Diphenyl-*t*-butoxysilanol (III) in 90% aqueous acetone when hydrolyzed with a drop of aqueous hydrochloric acid at room temperature gave quantitatively diphenylsilanediol, in spite of the possibility of a silanol condensation taking place also.

$$(C_6H_5)_2Si(O\text{-}t\text{-}C_4H_9)OH \xrightarrow{H^+} (C_6H_5)_2Si(OH)_2 + t\text{-}C_4H_9OH$$

Under the same conditions, phenyl-*t*-butoxysilanediol (II) was converted into an oil which was soluble in almost all organic solvents but insoluble in dilute sodium hydroxide solution, and which exhibited a weak infrared band at 1365 $cm^{-1}$. Such a behavior of II towards acids is in accord with those of the previously reported silanols.[2,3]

## Experimental

**Materials.** — Methyltrichlorosilane, phenyltrichlorosilane, diphenyldichlorosilane and tetrachlorosilane were all commercial products and were purified by redistillation, b. p. 65—66°C, 200—202°C, 160°C/10 mmHg, 57—58°C, respectively. Isopropyltrichlorosilane, cyclohexyltrichlorosilane, benzyltrichlorosilane, 2-phenylethyltrichlorosilane and 1-naphthyltrichlorosilane were prepared by the usual methods ; b. p. 118—200°C, 195—199°C, 213—215°C 239—240°C and 181°C/30 mmHg, respectively. All alcohols used were purified by the ordinary way and redistilled before use.

**General Procedure for the Synthesis of *t*-Butoxysilanols.** — An organochlorosilane (about 10 g.) and 50 ml. of dry ether were placed in a 300 ml. three-necked flask. A solution of the appropriate amounts (equivalent in moles to chlorosilanes) of *t*-butanol and pyridine in 20 ml. of dry ether was added dropwise to the stirred contents

6) S. W. Kantor, *J. Am. Chem. Soc.*, **75**, 2712 (1953).
7) M. Kakudo, *J. Chem. Phys.*, **21**, 1894 (1953).
8) R. E. Richards, H. E. Thompson, *J. Chem. Soc.*, **1949**, 125.

BUTOXYSILANOLS

| Yield g. (%) | M. p.* °C | Solubility W | B | P | Crystal from | Analysis Si, % Calcd. | Si, % Obs. | OH, % Calcd. | OH, % Obs. |
|---|---|---|---|---|---|---|---|---|---|
| 8.1 (60) | 105—106 | s | p | i | Needles | 13.40 | 13.38 | 16.26 | 16.40 |
| 9.5 (75) | 112—113 | s | s | p | Needles | 13.19 | 13.16 | 15.94 | 15.88 |
| 2.9 (27) | 55— 56 | p | s | s | Leaflets | 10.29 | 10.31 | 6.23 | 6.12 |
| 9.1 (76) | 79— 80 | p | s | p | Needles | 12.41 | 12.40 | 15.03 | 15.22 |
| 6.6 (51) | 84— 86 | p | p | i | Small leaflets | 10.70 | 11.01 | 12.96 | 12.25 |

at room temperature over a period of 10 min. After the addition, the solution was warmed slightly to complete the reaction. Then the mixture was cooled in an ice bath and filtered from salts; the filter cake on a glass filter was washed with dry ether. The combined filtrate was poured cautiously with stirring into a mixture of excess 5% aqueous sodium hydroxide solution, ice and ether. The ether layer was separated and the aqueous layer was repeatedly extracted with small portions of ether totaling 50 ml. To the aqueous portion was added a small amount of ice so as to avoid further condensation of the silanol. Then the alkaline mixture was neutralized with aqueous hydrochloric acid (ca. 6%) using Brom-thymol Blue as an indicator. The solution was extracted with ether and the ethereal solution was dried over sodium sulfate. After the solvent had been removed in vacuo, the crude silanols obtained were recrystallized from hot benzene. Since diphenyl-*t*-butoxysilanol (III) is very soluble in petroleum ether, the extraction of III is conveniently carried out using this solvent. Analytical results and yields for the above *t*-butoxysilanols are given in Table I. All attempts to prepare other organoalkoxysilanols gave only tacky oils, which were insoluble in 5% aqueous sodium hydroxide solution and gradually changed into resins. These oils were assumed to be the corresponding siloxanes, from their silicon contents and infrared spectra.

**The Hydrolysis of III.**—Into a solution of III (5 g.) in 30 ml. of 90% aqueous acetone, a drop of concentrated hydrochloric acid (ca. 12 N) was added with stirring at room temperature; the mixture was further stirred for 10 min. and then allowed to stand for 1 hr. The precipitated crystals were filtered off. After the mother liquor had been repeatedly treated in the same manner as above, the aqueous acetone solution was evaporated to dryness. Recrystallization of the combined crystals from hot benzene afforded colorless needles (3.9 g.) melting at 165—167°C. This substance was identified as diphenylsilanediol by comparison of its infrared spectrum with that of an authentic sample[1] and by mixed melting point determination.

**The Condensation of II with Hydrochloric Acid.**—In the same treatment as described above, II (5 g.) gave only an oil. By removal of the solvent in vacuo, the oil was collected (3.9 g.). This was insoluble in 5% sodium hydroxide aqueous solution and, by heating in an electric heater at 150°C, 5 hr., gave a resin melting at 130°C.

**Absorption Spectra.** — Spectral measurements (Nujol mull) were performed with a Reiz infrared spectrophotometer at room temperature.

**Analysis.** — Silicon contents were determined gravimetrically by a simple digestion method,[9] and for active hydrogen the Zerewitinoff method[10] was used.

The author would like to express his hearty thanks to Professor Hiromu Murata of Hiroshima University for his helpful discussion and guidance, and to Dr. Keiji Oshima, Director of this Institute for his continuous encouragement throughout the course of this work.

*The Osaka Municipal Technical Research Institute*
*Kita-ku, Osaka*

9) S. Kohama, This Bulletin, **36**, 830 (1963).
10) S. Siggia (Translated by Tsutomu Kuwata), "Quantitative Analysis via Functional Group," John Wiley and Sons, Inc., New York; Japanese Edition, Maruzen Co., Tokyo (1954), p. 74.

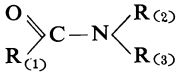
# Double Resonance Proton Spectra of Amides

By Hirotake KAMEI

(Received October 27, 1964)

Several groups of workers have used a double resonance technique in NMR spectroscopy to eliminate the effect of the $^{14}N$ nucleus, which causes quadrupole broadening of the resonance signals from amide protons.[1,2] The structure of the amine proton spectrum, however, has not been completely resolved and a full analysis of the spectrum could not be performed. This presumably can be attributed to incomplete decoupling of the $^{14}N$ nucleus from the protons. The completely decoupled spectra of formamide (pure, in water, and in acetone solution), acetamide (in water solution), and *N*-methyl acetamide, have now been observed and are analyzed in this work.

Proton resonance spectra were recorded at 40 Mc./s. using a JEOL JNM-3 spectrometer equipped with a double resonance system.[3] The groups in the various amides are labeled as follows:



The decoupled spectra of formamide in different conditions are shown in Fig. 1. The signal due to the formyl proton, $H_{(1)}$, appears as a quartet at low field. In the spectrum of the neat liquid, the signal due to the amine protons, $H_{(2)}$ and $H_{(3)}$, contains six lines, whereas with the same sample in aqueous solution, the $H_{(3)}$ signal shifts to lower field and appears as a triplet, as shown in Fig. 1(b). In the case of the pure liquid, therefore, the $H_{(2)}$ signal

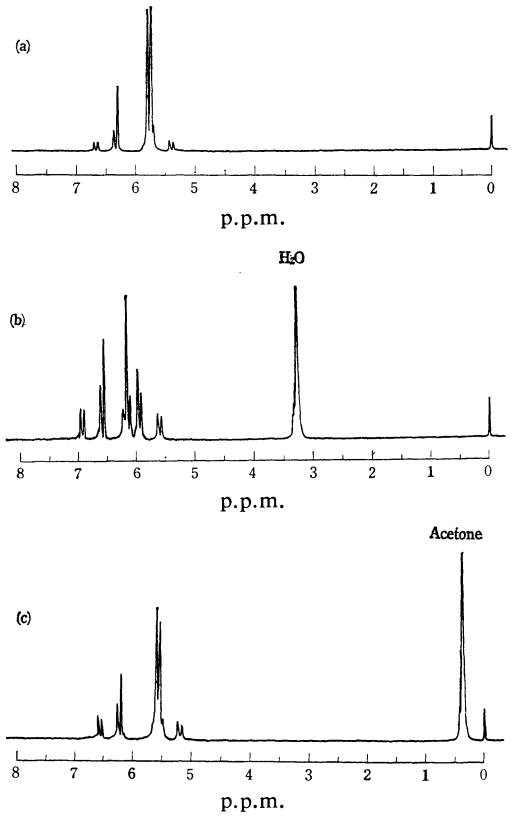



Fig. 1. Proton resonance spectra of $^{14}N$ decoupled formamide measured relative to cyclo hexane as external reference at 40 Mc./s. (a) pure liquid, (b) 18 mol.% in water, (c) 48 mol.% in acetone. The solvent resonances were recorded at lower amplifications.

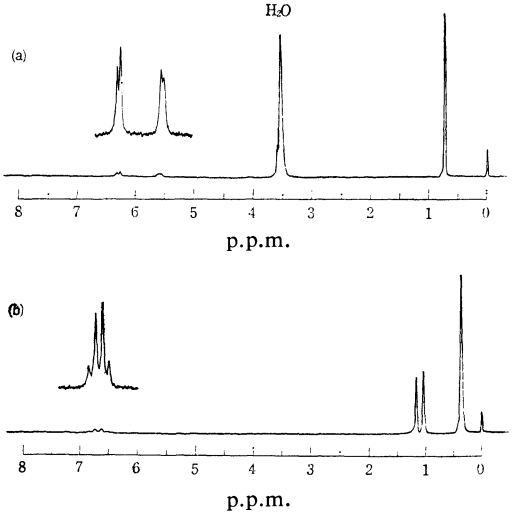
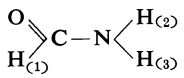
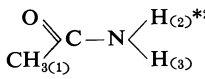
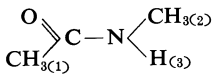



Fig. 2. Proton resonance spectra of $^{14}N$ decoupled (a) acetamide in 13 mol.% aqueous solution relative to external cyclohexane reference, and (b) *N*-methyl acetamide relative to internal cyclohexane reference at 40 Mc./s. The water resonance was recorded at a lower gain.

1) L. H. Piette, J. D. Ray and R. A. Ogg, *J. Mol. Spectroscopy*, **2**, 66 (1958).
2) E. W. Randall and J. D. Baldeschwieler, ibid., **8**, 365 (1962).
3) H. Kamei, *Bull. Electrotechnical Lab.*, **28**, 591 (1964) H. Kamei, *Japanese J. Appl. Phys.*, **4**, 212 (1965).

TABLE I. CHEMICAL SHIFTS (in p.p.m., relative to cyclohexane)*1 AND COUPLING CONSTANTS (in c./s.) OF SOME AMIDES

| |  | 18 mol.% $HCONH_2$ in water | 48 mol.% $HCONH_2$ in acetone |  |  |
|---|---|---|---|---|---|
| $\delta_1$ | −6.71 | −6.63 | −6.70 | −0.61 | −0.55*3 |
| $\delta_2$ | −5.78 | −5.70 | −5.67 | −5.36 | −1.29*3 |
| $\delta_3$ | −6.01 | −6.05 | −5.90 | −6.14 | −6.74*3 |
| $J_{12}$ | 13.4 | 13.4 | 13.8 | | |
| $J_{13}$ | 2.2 | 2.1 | 2.0 | | |
| $J_{23}$ | 2.4 | 2.2 | 2.5 | 2.4 | 4.7 |

*1 Corrected for bulk diamagnetic susceptibility, $\chi_v$. The values of $\chi_v(\times 10^6)$ for formamide, acetamide, water, acetone, and cyclohexane are taken to be −0.551, −0.618, −0.721, −0.460, and −0.631, respectively (Fujiwara et al., "Kōbunkainō Kakujikikyōmei, Kagaku eno Ōyō," Maruzen, Tokyo (1962); Hodgman et al., "Handbook of Chemistry and Physics," The Chemical Rubber Publishing, Cleveland (1963)).

*2 In 13 mol.% aqueous solution.

*3 Relative to cyclohexane as internal reference.

apparently consists of a quartet whose line at lowest field overlaps the highest field component of the $H_{(3)}$ triplet. The assignment of the lines is indicated in Fig. 1. Analysis of the spectra has been carried out on the basis of an ABX system and the estimated values of the chemical shifts and the coupling constants are shown in Table I. The values of these NMR parameters are in good agreement with those obtained for $^{15}N$-substituted formamide.[4] The variation in the chemical shifts and the coupling constants which occurs with change of solvent, may arise from the different natures of the hydrogen bonding interactions in the three systems.

Figure 2(a) shows the spectrum of acetamide in 13 mol.% aqueous solution, and Fig. 2(b) shows the spectrum of *N*-methyl acetamide at 30°C. The signal of the amine protons of acetamide appears as an AB type quartet which must be due to nonequivalence of the two protons, $H_{(2)}$ and $H_{(3)}$. By analogy with formamide the low-field doublet is assigned to the proton, $H_{(3)}$, which is in the cis position relative to the methyl group. Broadening of the line width may be caused by spin coupling with the protons of the methyl group. The amine proton of *N*-methyl acetamide appears as a quartet due to spin coupling with the *N*-methyl protons. The results of the analysis of the spectra are shown in Table I. The internal chemical shift between $R_{(1)}$ and $R_{(3)}$, $\delta_{13}$, in *N*-methyl acetamide is 0.66 p.p.m. greater than that observed in the case of acetamide. Substitution of an *N*-methyl group in formamide was observed to cause $\delta_{13}$ to decrease by 0.48 p.p.m.

The $^{14}N$ resonance frequency for the amides considered above has been found to be 2889500 ±25 c./s.

4) B. Sunners, L. H. Piette and W. G. Schneider, *Can. J. Chem.*, **38**, 681 (1960).

*Electrotechnical Laboratory*
*Tanashi-machi, Kitatama-gun, Tokyo*

# Ultraviolet Spectrophotometric Determination of Lead using Thiomalic Acid*

By Yasuhisa HAYASHI, Shigeo HARA and Isao MURAKI

(Received November 9, 1964)

As has been reported,[1] thiomalic acid (henceforth abbreviated TMA) and lead form a stable, colorless complex in acidic and alkaline solutions. As can be seen from the absorption spectra of lead-TMA solutions at various pH values ranging from 5.8 to 10.5 (Fig. 1), the lead-TMA complex has a maximum absorption at 265 m$\mu$ in acidic, and at 305 m$\mu$ in alkaline solutions. As the absorption spectrum of a TMA solution is not affected by pH change,[1] the wavelength of 305 m$\mu$ is adopted for the spectrophotometric determination of small amounts of lead. Here are presented conditions for the ultraviolet spectrophotometric determination of lead; the composition of the complex is also discussed.

* Presented at the 13th Annual Meeting of the Japan Society for Analytical Chemistry, Sendai, Sept,, 1964.

1) I. Muraki, S. Hara and Y. Hayashi, *Japan Analyst*, in press.

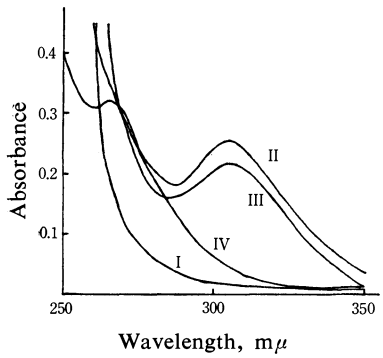



Fig. 1. Absorption spectra of lead-TMA solutions at various pH values.
Curve I 0.1% TMA soln. only, pH 10.5
Curve II Pb-TMA soln., 10 p.p.m. Pb, pH 10.5
Curve III Pb-TMA soln., 10 p.p.m. Pb, pH 9.2
Curve IV Pb-TMA soln., 10 p.p.m. Pb, pH 5.8
Buffer: 0.1 M $NaOH-Na_2B_4O_7$ system., 20 ml./100 ml.
Reference: Water Temp.: 18°C

Standard lead solution was prepared as follows: 1.0000 g. of 99.999% pure lead was dissolved in nitric acid, and the solution was evaporated to dryness; the residue was dissolved in water and diluted to 1000 ml. with water. An aliquot of this solution was then diluted with water to prepare a standard solution containing 100 p.p.m. of lead. Other materials and apparatus were the same as reported in the preceeding paper.[1] The procedure for making the calibration curve is as follows: Pipet an aliquot of the standard lead solution into a 100 ml. measuring flask, and add 20 ml. of 0.1% TMA solution and 20 ml. of buffer solution and dilute to the mark with water and then measure the absorbance of the solution at 305 mμ against water.

To obtain optimum conditions for the determination of lead, various factors were studied: In order to find an optimum pH range, the absorbances at 305 mμ were plotted against pH values. Maximum absorption was found in the pH range of 10.0—11.0. The absorbances of two series of solutions containing 5.0 and 10.0 p.p.m. of lead, respectively, and various amounts of the reagent were measured. It was found that the optimum amount of TMA was 15.0—25.0 ml. of a 0.1% solution in 100 ml.; a larger excess of TMA caused a slight increase in absorbance. The absorbance of the solutions of lead-TMA complex showed no appreciable change within about 20 hr. In order to confirm the mole ratio of the lead-TMA complex, the continuous variation method and the mole ratio method were used. In the first method,

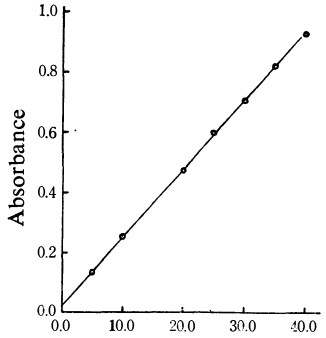



Fig. 2. Calibration curve.
TMA: 0.1% soln. 20 ml./100 ml.
Buffer: 0.1 M $NaOH-Na_2B_4O_7$ system, 20 ml./100 ml., pH 10.5
Wavelength: 305 mμ.
Reference: Water Temp.: 19°C

Table I. Effect of diverse ions added to the 10.0 p.p.m. solutions of lead

| Ion | Added p.p.m. | Added as | Absorbance at 305 mμ |
|---|---|---|---|
| — | — | — | 0.253 |
| Cd(II) | 50 | Sulfate | 0.247 |
| Cd(II) | 25 | Sulfate | 0.254 |
| Zn(II) | 30 | Sulfate | 0.245 |
| Zn(II) | 15 | Sulfate | 0.252 |
| Al(III) | 50 | Chloride | 0.252 |
| As(III) | 20 | Chloride | 0.245 |
| As(III) | 10 | Chloride | 0.252 |
| Sb(III) | 30 | Chloride | 0.485 |
| Sn(IV) | 20 | Chloride | Ppt. |
| Cu(II) | 20 | Sulfate | 1.08 |
| Cu(II) | 5 | Sulfate | 0.266 |
| Cu(II) | 2 | Sulfate | 0.254 |
| NaCl | 10 ml. | 1 M Soln. | 0.252 |
| $Na_2SO_4$ | 10 ml. | 1 M Soln. | 0.332 |
| $NH_4Cl$ | 10 ml. | 1 M Soln. | 0.250 |
| $NaNO_3$ | 10 ml. | 1 M Soln. | 0.252 |

absorbances of a series of solutions containing various amounts of $5\times10^{-3}$ M TMA were measured against the reagent blank. When the mole ratio of lead to TMA was 1 to 3, maximum absorbance resulted. The results of the second method also confirmed that the mole ratio corresponds to 1 to 3. The calibration curve (Fig. 2) shows that Beer's law is obeyed over the concentration range from 0.5 to 40.0 p.p.m. of lead. The molar absorptivity of the method is $5.2\times10^3$, and the sensitivity is 0.04 μg. Pb/cm$^2$ for $\log I_0/I=0.001$. As is shown in Table I, it is found that colored ions such as copper(II), cobalt(II), nickel(II), iron(II, III), etc., and metal ions forming precipitates in alkaline solutions such as tin interfere. The proposed method is much inferior to the

dithizone method[2] in sensitivity, but the procedure is simpler. As the procedure is operated in alkaline solution (pH 10.5), interferences from diverse ions must be considered.

2) E. B. Sandell, "Colorimetric Determination of Traces of Metals," 3rd. Ed., Interscience Pub., New York (1959), p. 563.

*Faculty of Science and Technology*
*Kinki University*
*Fuse, Osaka (Y. H. & I. M.)*

*Government Industrial Research Institute, Osaka*
*Ikeda, Osaka (S. H.)*

# Concerning the Structure of Trimethyltin Fluoride

By Kiyoshi YASUDA, Yoshikane KAWASAKI, Nobutami KASAI and Toshio TANAKA

(Received November 12, 1964)

Recently there has been much interest in the structure of organotin compounds. Among the trimethyltin halides, trimethyltin fluoride is markedly different in physical and chemical properties from the remaining halides; the fluoride has a high melting point (>360°C) and does not sublime, while the other halides melt and sublime at lower temperatures. The former is soluble in hot alcohol, slightly soluble in water, and almost insoluble in non-polar organic solvents, while the latter are soluble in common organic solvents.

The structures of trimethyltin chloride, bromide, and iodide have been determined[1] by electron diffraction to be nearly tetrahedral in the vapor state, but no structural determination had been made on the fluoride until recently. In 1960, one of the present authors reported[2] on the basis of infrared spectral evidence that the fluoride contains a planar trimethyltin group. However, the X-ray analysis by Clark et al.[3] showed that the electron-density distribution could be equally well interpreted either in terms of a planar or pyramidal trimethyltin group. To clear up this ambiguity concerning the structure of the trimethyltin group and the nature of the bond represented by Clark et al.[3] as Sn–F···Sn (the bond distance; Sn–F 2.1 Å, Sn···F 2.2—2.6 Å) in this compound, it is necessary to consider the most probable structure of this compound with reference to some findings from the infrared and Raman spectra, as well as a few additional X-ray data obtained from this compound and from related trimethyltin compounds which have been studied in our laboratory.

In the infrared spectrum of this compound only one band* is observed at 556 $cm^{-1}$, which is assigned to the Sn–C stretching vibration, and we can assume the following two possible structures for the trimethyltin group. One is the planar equilateral triangular structure with the tin atom at the center and three carbon atoms at the corners, which gives infrared active degenerate and inactive symmetric stretching vibrations associated with the Sn–C bonds. Another possible structure is a pyramidal one. If we assume a point group of $C_{3v}$ for this molecule, this structure would give two Sn–C stretching vibrations of $A_1$ and E species in the infrared spectrum according to the selection rule. Our infrared studies seem to rule out this structure, but it is also possible** that the frequency associated with the Sn–F stretching vibration might be close enough to that of the Sn–C symmetric stretching vibration to cause coupling. We may then expect that one would be higher and the other lower than either of the original ones by this coupling; one of these two bands could fall near 550 $cm^{-1}$, overlapping with the Sn–C stretching vibration of E species. However, the Raman spectrum of solid trimethyltin fluoride showed that the assumed coupling does not take place, and hence the second structure is not probable, since two bands which are associated with the Sn–C stretching vibrations.

1) H. A. Skinner, L. E. Sutton, *Trans. Faraday Soc.*, **40**, 164 (1944).
2) R. Okawara, D. E. Webster and E. G. Rochow, *J. Am. Chem. Soc.*, **82**, 3287 (1960).
3) H. C. Clark, R. J. O'Brien and J. Trotter, *Proc. Chem. Soc.*, **1964**, 85,; *J. Chem. Soc.*, **1964**, 2332.

* Although it is reported in Ref. 3. that another band was observed at 515 $cm^{-1}$ in the infrared spectrum of very concentrated Nujol mulls of trimethyltin fluoride, no band was observed in this region in our repeated experiments.

** This was tentatively suggested by Dr. Ichiro Nakagawa of the The Universiuy of Tokyo.

at 517 $cm^{-1}$ (s) and 556 $cm^{-1}$ (w) were observed in the Raman spectrum.

Clark et al.[3] reported that the structure of this compound has trimethyltin groups and fluorine atoms arranged alternately in a chain-like manner along the a axis, and they offered two interpretations of the three dimensional electron-density distribution. One is that the non-planar trimethyltin group is ordered in any chain. The bond angles calculated by us from the electron-density distribution map given by them are about 111° and 117° for $C_2$-Sn-$C_3$ and $C_1$-Sn-$C_2$, respectively. This distortion of the trimethyltin group from the normally trigonal coplanar structure should give a fairly intense infrared absorption band due to the Sn-C symmetric stretching vibration. Their second structure, in which the planar trimethyltin groups are tilted alternately with respect to the a axis, should give a repeat distance of twice the cell length. Though we repeated their X-ray diffraction measurements with a larger crystal, we could not observe any reflection which corresponds to twice their reported cell length along the needle axis even with long exposures, and this suggests that their second structure also is not suitable.

If we assume that the space group given by Clark et al. is reasonable, the peculiarities in the electron-density distribution can be interpreted in terms of disorder in the crystal structure. Clark et al. proposed that the chains could be disordered with respect to each other. This kind of disorder was observed in trimethyltin hydroxide[4] and formate[5], which are now being studied in our laboratory. Besides, in the hydroxide, we found that the trimethyltin groups are disordered also in a chain, forming a helix-like structure. A structure having random chains has been found also in polyvinyl alcohol.[6] In the structure of trimethyltin fluoride, the disorder in one chain should also be taken into account.

Determination of the precise structure of any compound containing a heavy metal atom, such as tin, by X-ray diffraction is usually difficult, for there is often some ambiguity in the position of the light atoms. In the analysis of the fluoride, Clark et al. were not able to use the ($h$00) reflections, and the determination of the positions of carbon and fluorine atoms seems to be difficult, especially in the $x$-coordinates. We would like to propose a reasonable structure which is consistent with

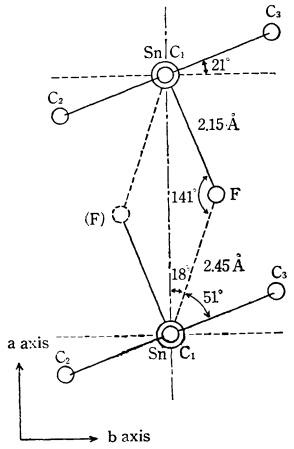



Fig. 1. A projection of the probable crystal structure of trimethyltin fluoride down to the (001) plane.
F and (F) indicates the two possible positions of fluorine atom of the same potential energy.

the results of the X-ray diffraction study by Clark et al., and takes into account the results from infrared and Raman spectra. We assume that the trimethyltin group forms a planar equilateral triangular structure and is inclined to the plane perpendicular to the a axis, and that one of the Sn-C bonds, Sn-$C_1$, lies along the c axis, and further that the trimethyltin groups and the fluorine atoms are arranged alternately along the a axis as shown in Fig. 1. Concerning the Sn-F bond, we observed a broad strong band at 350 $cm^{-1}$ in the infrared spectrum and assign this to the Sn-F stretching vibration. We could not observe any Raman line due to the Sn-F symmetric stretching in the region down to about 150 $cm^{-1}$, where the Raman lines due to the $SnC_3$ deformations are usually observed. It can be concluded, therefore, that one of the two Sn-F bonds is fairly strong and the other is weak, and this is consistent with the results of the X-ray study by Clark et al. The angle formed by the covalent Sn-F bond and the Sn-$C_1$ bond is shown to be almost 90° by the electron-density distribution map of Clark et al., but the angle between the covalent Sn-F bond and the plane of trimethyltin group can not be determined from their work. Taking for this angle a value of 90° and an Sn-F bond distance of 2.15 Å, the calculated distance between the fluorine atom and the carbon atoms in other chains is larger than the sum of the van der Waals radii of the atoms; this is consistent with the compound's crystal habit, i. e., bundles of very fine needles. As the repeat distance along the a axis has been determined[3] to be

4) N. Kasai, K. Yasuda and R. Okawara, *J. Organometal.*, 3, 172 (1965).
5) N. Kasai, H. Matsumoto, N. Tanaka and R. Okawara, presented at the 17th Annual Meeting of the Chemical Society of Japan, Tokyo, 1964.
6) J. Kakinoki, *The Annual Reports of the Textile Research Institute of Osaka Univ.*, 5, 19 (1950) (in Japanese).

4.32 Å, the planes of the trimethyltin groups should be parallel to each other in the chain. The weak Sn···F bond is in the opposite direction to the strong Sn-F bond with respect to the plane, and the angle between the weak Sn···F bond and the plane of trimethyltin is calculated to be about 51°, so that the F-Sn···F bond is not linear and should have a bond angle of about 141°. This is consistent with the results of Clark et al. that the integrated electron-density of the Sn peak in the a axis projection was 50.08 electrons, indicating that the fluorine atom is not situated on the axis connecting the tin atoms, which is parallel to the a axis. This value for the Sn-F···Sn angle is reasonable if we take into account the fact that in solid hydrogen fluoride the angle H···F-H is about 134° [7] and that this bond angle is explained[8] in terms of participation of the lone pair orbital of the fluorine atom. This distorted bipyramidal configuration around the tin atom could be explained by assuming that the d-orbitals are involved in the hybridization of the orbitals in the tin atom; this is also expected to be the case in trimethyltin hydroxide. In the structure of trimethyltin fluoride proposed above, we can expect two positions of minimum potential energy for the fluorine atom, F and (F) given in Fig. 1. The potential barrier between them is considered to be small, and this can explain the anomaly in the electron-density distribution of the fluorine atom.

7) R. Gunther, K. Holm and H. Strunz, *Z. phys. Chem.*, B33, 229 (1939).
8) W. G. Schneider, *J. Chem. Phys.*, **23**, 26 (1955).

## Experimental

The infrared spectrum of trimethyltin fluoride as a Nujol mull was recorded in the 4000—270 $cm^{-1}$ region on a Perkin-Elmer double beam spectrometer model 221 equipped with NaCl or KBr optics, and on a Koken double beam spectrometer model DS-401 G equipped with a grating and CsBr optics. The Raman spectrum for the solid state was recorded on a Nippon Yuki-gosei Raman Spectrograph.

The needle crystal with average width 0.3 mm., used for the $CuK_\alpha$ oscillation photograph, was obtained by recrystallization of trimethyltin fluoride from ethyl alcohol.

## Summary

The structure and the nature of the bonds in trimethyltin fluoride are discussed on the basis of the infrared and the Raman spectra with reference to the results of the X-ray diffraction study by Clark et al. and a few additional X-ray data obtained on the fluoride and related trimethyltin compounds. The most reasonable structure is one in which the planar trimethyltin group is bridged by the fluorine atom forming a non-linear unsymmetrical Sn-F···Sn bond. The distorted bipyramidal configuration around the tin atom can be explained in terms of involvement of the d-orbitals of the tin atom in the bonding.

*Department of Applied Chemistry*
*Osaka University*
*Miyakojima-ku, Osaka*

# Determination of the Purity of 2, 2-Diphenyl-1-picrylhydrazyl and 2, 2-Di-(*p*-tolyl)-1-picrylhydrazyl by Iodometry

By Shigeo TAZUKE, Koji UNO and Seizo OKAMURA

(Received November 16, 1964)

2, 2-Diphenyl-1-picrylhydrazyl (DPPH) has been often employed as a radical scavenger and as a standard substance for ESR measurements. In each case the purity of the hydrazyl free radicals was assumed to be 100% and a satisfactory method of determining the purity was not established.

Elemental analysis may be a measure of purity, but it is a rather insensitive way to determine the purity. It has been reported that DPPH reacts quantitatively with hydroquinone to yield 1, 1-diphenyl-2-picrylhydrazine and benzoquinone,[1] but no experimental results were presented. The extent of conversion of various hydrazines to the corresponding hydrazyl free radicals, has been estimated by the reaction of the hydrazyl free radicals with ascorbic acid.[2]

1) S. Goldschmidt and K. Renn, *Ber.*, 55, 628 (1922).
2) D. Braun, I. Löflund and H. Fischer, *J. Polymer Sci.*, 58, 667 (1962).

TABLE I. IODOMETRIC TITRATION OF DPPH AND DTPH

| Sample | Weight | 1/100 N $Na_2S_2O_3$ ($f$=0.9908) calcd. volume* ml. | Volume consumed ml. | $\frac{\text{Volume consumed}}{\text{Calcd. volume}} \times 100$ | |
|---|---|---|---|---|---|
| Crude DPPH before recrystallization | 37.7 | 10.02 | 8.67 | 86.3 | Average 87.1 |
| | 24.1 | 6.39 | 5.56 | 87.1 | |
| | 29.5 | 7.51 | 6.60 | 87.8 | |
| DPPH after once recrystallization | 28.7 | 7.35 | 7.11 | 96.8 | 97.0 |
| | 28.3 | 7.23 | 7.03 | 97.1 | |
| DTPH freshly prepared in benzene** | 60.36 | 14.42 | 14.17 | 98.3 | 98.6 |
| | 60.36 | 14.42 | 14.24 | 98.8 | |

* Based on one equivalent for reduction of the hydrazyl free radicals.
** The concentration of DTPH was calculated from the weight of the hydrazine used in its preparation.

The authors have found that DPPH and analogous hydrazyl free radicals can be satisfactorily determined by iodometry. The technique is almost the same as that used in the determination of organic peroxides.[3]

The iodometric determination of relatively stable phenoxy radicals has been reported by Müller and Ley.[4] They reduced the phenoxy radical to the corresponding phenol with sodium iodide using glacial acetic acid as a solvent and carrying out the determination under an atmosphere of carbon dioxide.

DPPH, prepared by the method of Goldschmidt and Renn,[1] was recrystallized from benzene-ligroin, then dried under reduced pressure at 77°C for 50 hr.

Found: C, 54.7; H, 3.08; N, 18.0. Calcd. for $C_{18}H_{12}O_6N_5$: C, 54.8, H, 3.07; N, 17.8%.

1, 1-Di-(*p*-tolyl)-2-picrylhydrazine was prepared by the method of Poirier and Benington.[5] M. p. 159.0°C (uncorrected), lit. 161°C.[5]

Found: C, 56.4; H, 4.16; N, 16.3. Calcd. for $C_{20}H_{17}O_6N_5$: C, 56.7; H, 4.05; N, 16.5%.

The hydrazine was oxidized to 2, 2-di-(*p*-tolyl)-1-picrylhydrazyl (DTPH) with a freshly prepared suspension of lead dioxide in benzene. DTPH is as stable as DPPH in solution. However, an attempt to separate pure DTPH in solid form failed. Gradual evaporation of a concentrated solution of DTPH in benzene under reduced pressure gave a dark violet solid which turned brown on standing. The solid DTPH reported in the literature[6] also seems to be contaminated since its analytical data do not agree with the calculated values, and N–H absorption occurs in its infrared spectra.

All other reagents were commercial materials.

Ten milliliters of redistilled acetic anhydride and an excess of sodium iodide (ca. 1 g. of sodium iodide for 0.1 g. of hydrazyl) were added to the hydrazyl in a glass stoppered flask. After being allowed to stand in the dark for 10 min., 50 ml. of water and 15 ml. of benzene were poured into the flask; the mixture was then saturated with sodium sulfate to clear the aqueous layer. The liberated iodine was titrated with 1/100 N sodium thiosulfate solution with vigorous shaking and using 0.5% starch solution as an indicator. Benzene was added to take up colored organic products so that the end point of titration was clearly detectable.

The results are shown in Table I.

The products from the titration were studied spectrophotometrically. The spectrum of DPPH after reduction with sodium iodide was exactly the same as that of 1, 1-diphenyl-2-picrylhydrazine, showing a maximum absorption at 320 mμ. The DPPH which had been formed in the reduction and extracted into benzene, was quantitatively reoxidized to DPPH on treatment with lead dioxide.

The origin of the hydrogen transferred to the hydrazyls is not clear. The violet color of the hydrazyl was observed to disappear after addition of sodium iodide to the acetic anhydride solution of the hydrazyl. This indicates that the reduction of the hydrazyl is completed in acetic anhydride before addition of water. Small amounts of acetic acid in the acetic anhydride may be the source of the proton transferred to the hydrazyl. Under the present experimental conditions, less than 0.1% of acetic acid in the acetic anhydride would be sufficient to complete the reaction. Reduction of the hydrazyl by sodium iodide also proceeds rapidly in acetic acid. However, the use of acetic acid as solvent brings about spontaneous oxidation of the sodium iodide unless the reaction is carried out under an

3) K. Nozaki, *Ind. Eng. Chem., Anal. Ed.*, **18**, 583 (1946).
4) E. Müller and K. Ley, *Chem. Ber.*, **87**, 922 (1954).
5) R. H. Poirier and F. Benington, *J. Org. Chem.*, **19**, 1157 (1954).
6) M. M. Chen, A. F. D'Adamo and R. I. Walter, ibid., **26**, 2721 (1961).

atmosphere of inert gas. The following reaction scheme may be proposed from these observations.

$$2\,\text{Hydrazyl} + 2\text{NaI} + 2\text{CH}_3\text{COOH} \rightarrow 2\,\text{Hydrazine} + 2\text{CH}_3\text{COONa} + \text{I}_2 \quad (1)$$

The ratio of the volume consumed to the calculated volume of 1/100 N sodium thiosulfate will then express the purity of the reducible nitrogen radicals in the sample. The purity of DPPH is quite high. Although DTPH is not a stable solid, conversion of the hydrazine to the hydrazyl is almost complete in solution.

*Department of Polymer Chemistry*
*Faculty of Engineering*
*Kyoto University*
*Sakyo-ku, Kyoto*

# Neutron Activation Analysis for Traces of Sodium in Polycarbonate

By Hitoshi KAMADA, Yûsuke UJIHARA, Katsuaki FUKUDA, Shôtaro KEIMATSU and Yoshihiro TSURUMI

(Received November 19, 1964)

The determination of microgram quantities of sodium in polycarbonate has received particular attention, because of its importance in an investigation of the properties, as well as in the development of an improved process for the production of this polymer.

Although the p.p.m. level of sodium in the polymer may be detemined by a combination of preliminary chemical concentration and subsequent flame-photometry, acid-base titration or polarography, these analytical methods are either difficult or troublesome, time-consuming, and apt to be inaccurate, therefore reliable results are rarely expected.

The authors have applied neutron activation and $\gamma$-ray spectrometry to the determination of sodium in bisphenol A-Polycarbonate, following the successfull use of this method in the determination of traces of sodium in aluminum,[1,2] diamond,[3] polyethylene[4] and polypropylene[5].

## Experimental and Results

A half to two grams of the accurately weighed polycarbonate sample was sealed in a polyethylene pouch and, together with standard sample, irradiated for 2 hr. in the JRR-1 which produces neutron flux of about $10^{11}$ n./cm$^2$·sec. The irradiated sample was washed with nitric acid and water, and transferred to a test tube. No activity was found in the washings. The standard sample was prepared by impregnating a filter paper (Toyo Roshi, No. 5B, diam. 5.5 cm.) with 1 mg. of sodium (1 mg.-Na/ml. sodium oxalate solution), then drying the paper under an infrared lamp, and sealing it in a polyethylene pouch. After irradiation, the sodium was extracted with water, diluted to a suitable volume, and an aliquot of the resulting solution was transferred to a test tube.

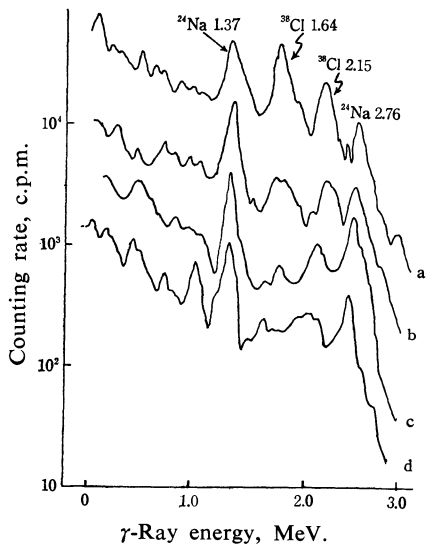



Fig. 1. $\gamma$-Ray spectra of irradiated polycarbonate.
(Sample II) (Na 25 p.p.m., Cl 700 p.p.m.)
Cooling a: 2.5, b: 4.5, c: 22.0, d: 46.0 hr.

1) H. A. Das, *Nucl. Sci. Abstr.*, **17**, 14171 (1963).
2) R. Chauvin and P. Leveque, *Int. J. Appl. Rad. Isot.*, **1**, 115 (1956).
3) E. C. Lightowlers, *Anal. Chem.*, **34**, 1285 (1963).
4) Y. Suzuki, O. Saito, N. Sairenji and N. Saito, "Kiki Ni Yoru Kobunshi-Bunseki II," (Instrumental Methods in High Polymer Analysis, II) Hirokawa Publ. Co., Tokyo (1964), p. 172.
5) T. Takeuchi and D. Ishii, ibid., p. 180.

The $\gamma$-ray spectra of the polycarbonate and of the standard samples were obtained intermittently using a $3\times3$ inch$^2$ NaI(Tl) crystal attached to the TMC*1-256 channel pulse height analyzer, the spectral imformation being recorded on an electric paper printer.

A representative $\gamma$-ray spectrum of the irradiated polycarbonate is shown in Fig. 1. The activity of chlorine-38 (half-life 37 min.) was dominant shortly after the irradiation. This activity would have come from a $^{37}Cl$ (n, $\gamma$) $^{38}Cl$ reaction, since methylene chloride had been employed as solvent in the production of the polycarbonate. After the chlorine-38 activity had decayed away, only the activity of sodium-24 remained and this was counted at convenient intervals.

The sodium contents were calculated from the 1.37 MeV photopeak height (above broken line) of sodium-24, which decayed with a half-life of about 15 hr.

As spectrochemical studies had already established the absence of magnesium and aluminum,*2 interference by $^{24}Mg$ (n, p) $^{24}Na$ or $^{27}Al$ (n, $\alpha$) $^{24}Na$ reactions would be negligible.

No appreciable self-shielding effect was observed in this experiment. The purity of the 1.37 MeV. photopeaks was verified by measurements of the half-life.

Typical results of the analyses are shown in Table I, where the samples shown in column B were obtained by treating the samples indicated in column A in order to decrease sodium content.

The proposed analytical method was applied to an investigation of the efficiency with which sodium is extracted into water from a methylene chloride solution of the polycarbonate.

The extraction procedure was as follows: 100 g. of the polycarbonate sample was dissolved in 500 ml. of methylene chloride, and this solution was shaken for 1 min. with 500 ml. of water in a separating funnel.

A repetition of the above procedure with additional amounts of water gave the samples which had been repeatedly washed. After separation of the water layer, isopropyl alcohol was added to the organic layer with stirring until polycarbonate powder precipitated; the precipitate was then dried in vacuo.

The results are shown in Fig. 2 and indicate that the repeated washing of the polymer solution with water does not effectively remove the sodium.

Table I. Results of analyses for sodium in various polycarbonate samples

(I—III pellet, IV—VI powder, sample taken ~1 g.)

| Sample | Sodium content p.p.m. A | Sodium content p.p.m. B | Chloride content p.p.m. |
|---|---|---|---|
| I | 30 | — | 113 |
| II | 25 | — | 700 |
| III | 0.7 | — | 147 |
| IV | 11 | 1.8 | — |
| V | 4.5 | 0.8 | — |
| VI | 5.1 | 1.0 | — |

*1 Technical Measurement Company.

*2 800 $\mu$g. of magnesium or 10 mg. of aluminum is equivalent to 1 $\mu$g. of sodium.

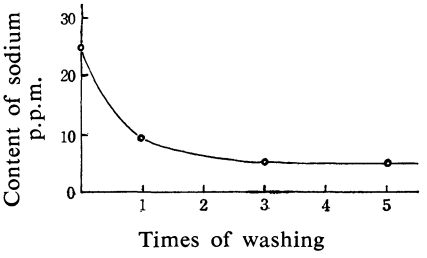



Fig. 2. Washing of the polymer with water.

*Department of Industrial Chemistry*
*Faculty of Engineering*
*The University of Tokyo*
*Hongo, Tokyo*

SHORT COMMUNICATIONS

# The Polymerization of Tetrahydrofuran Catalyzed by Tungsten(VI) Chloride

By Yoshinobu TAKEGAMI, Toru UENO and Ryuichi HIRAI

(Received March 15, 1965)

Tetrahydrofuran (THF) has been known to be polymerized by such catalysts as Lewis acid - cocatalyst systems,[1,2] triethyl aluminum - cocatalyst systems,[3-5] the triethyl aluminum - water(1 : 1) -cocatalyst,[3] ferric chloride - triphenyl phosphite,[6] phosphorous(V) fluoride,[7] and antimony(V) chloride.[7] Of these catalysts, phosphorous(V) fluoride and antimony(V) chloride appear highly active. We will now report on the utility of tungsten(VI) chloride, whose activity nearly corresponds with those of the above two catalysts.

Tetrahydrofuran was dried over sodium and distilled immediately before use. Polymerization was carried out in a sealed tube which had been allowed to stand at a desired temperature while being occasionally shaken. The initiation of the polymerization was shown by a change in the color of the polymerization mixture from a black suspension to a reddish brown solution. The mixture was washed with acetone-water (20 : 1), and the crude polymer was isolated by cooling. The polymer was then purified by pouring a THF solution of the crude polymer into a large amount of water, followed by washing it with methanol and drying it in vacuo at room temperature.

In all the experiments presented, 0.5 g. of tungsten(VI) chloride was used for 20 ml. of THF. This catalyst level of 0.5 mol. % was found to be the optimum. A further increase in the amount of the catalyst resulted in a decrease in the yield of the polymer.

A summary of the results is presented in Table I. The first six runs indicate that the yield and the reduced viscosity maxima occur at 0°C. At 20—40°C, the color of the polymerization mixture turns blue after about 3 hr. It appears that in the blue-colored mixture no polymerization but, rather, a rather slow depolymerization occurs. At 0°C, the yield of the polymer is 80% at a reaction time of 8 hr. and is slightly affected by a further increase in the reaction time.

TABLE I. THE YIELD AND THE REDUCED VISCOSITY OF THE POLYMER

| Time hr. | Temp. °C | Yield % | $\eta_{sp}$* |
|---|---|---|---|
| 8 | −20 | 1.5 | — |
| 8 | −10 | 54.5 | 0.80 |
| 8 | 0 | 81.1 | 1.15 |
| 8 | 10 | 74.4 | 0.75 |
| 8 | 20 | 41.4 | 0.55 |
| 8 | 30 | 6.2 | 0.20 |
| 2 | 0 | 29.8 | 0.80 |
| 4 | 0 | 64.0 | 1.30 |
| 24 | 0 | 79.8 | 0.75 |
| 48 | 0 | 85.5 | 0.60 |

* Measured on a solution of 0.2 g. polymer in 100 ml. of benzene at 30°C.

The infrared spectra of the polymer are very similar to that of polytetrahydrofuran prepared by the use of the other catalyst.[3]

A further investigation of this polymerization is in progress and will be reported on later.

*Department of Fuel Chemistry*
*Faculty of Engineering*
*Kyoto University*
*Sakyo-ku, Kyoto*

1) H. Meerwein, D. Delfs and H. Morschel, *Angew. Chem.*, **72**, 927 (1960).
2) T. Saegusa, H. Imai, S. Hirai and J. Furukawa, *Makromol. Chem.*, **54**, 218 (1962).
3) T. Saegusa, H. Imai and J. Furukawa, ibid., **65**, 60 (1963).
4) K. Weissermel and E. Nölken, ibid., **68**, 140 (1963).
5) I. Yamashita, M. Serizawa and T. Miyakawa, This Bulletin, **36**, 1368 (1963).
6) I. Yamashita and M. Serizawa, ibid., **37**, 1721 (1964).
7) E. L. Muetterties, U. S. Pat. 2856370 (1958). In this patent Muetterties compared two polymers, prepared with phosphorous(V) fluoride and with antimony(V) chloride.

# Reactive Monomers Derived from *p*-Vinylbenzoic Acid

By Yoshio IWAKURA, Keikichi UNO, Nobuo NAKABAYASHI and Takakazu KOJIMA

(Received March 16, 1965)

The preparation and the application of reactive polymers have been studied in our laboratory.[1,2] Generally, reactive polymers can be obtained by the polymerization of so-called reactive monomers, which have a carbon-carbon double bond, and another functional group, such as epoxide, aziridine or isocyanate.

The present paper will describe the preparation of new reactive monomers derived from *p*-vinylbenzoic acid.[3,4] Jäger's method was adopted for preparing the acid in this report.

**Glycidyl *p*-Vinylbenzoate.**—*p*-$\beta$-Bromoethylbenzoic acid (I) was prepared by the procedure of Foreman.[5] I was treated with potassium hydroxide in ethanol in order to obtain potassium *p*-vinylbenzoate (II). The reaction of II and epichlorohydrin using triethylbenzylammonium chloride as a catalyst produced glycidyl *p*-vinylbenzoate (III), which was then distilled at 115.5—116.5°C/0.1 mmHg. The yield was 71%.

Found: C, 70.63; H, 6.01. Calcd. for $C_{12}H_{12}O_3$: C, 70.57; H, 5.92%.

The infrared absorption spectrum showed carbon-carbon double-bond bands at 1629, 987 and 918 $cm^{-1}$, epoxide at 907 and 839 $cm^{-1}$, carbonyl at 1720 $cm^{-1}$ and *p*-phenylene at 856 $cm^{-1}$. The epoxide content was 98.0%.

When the radical polymerization of III was carried out, linear poly-III was obtained; it had a $\eta_{sp}/c$ value of 0.20 (0.2 g./100 ml. dioxane at 30.0°C), and the epoxide content of the polymer was 96.0%. The copolymerization of III ($M_2$) with styrene ($M_1$) was also studied. The monomer reactivity ratios were as follows: $r_1=0.40\pm0.02$, and $r_2=0.95\pm0.10$ (at 70.0±0.1°C). Alfrey-Price's $Q$ and $e$ values were 1.18 and 0.18 respectively. Nucleophilic reagents such as hydrogenchloride and alkyl amine, could easily be added to epoxy groups in the poly-III and the copolymer.

***p*-Vinylphenylisocyanate.** — This compound[6] (b. p. 40.5—41.5°C/0.1 mmHg) was obtained through the acid chloride and the acid azide. The isocyanate gave a homopolymer with a vinyl group by means of the anionic polymerization of the isocyanate group at a low temperature. The radical polymerization, on the other hand, brought about one with a isocyanate group.

The details will be pulished in a short time.

*Department of Synthetic Chemistry*
*Faculty of Engineering*
*The University of Tokyo*
*Hongo, Tokyo*
*(Y. I., K. U. & T. K.)*

*Research Institute of Dental Materials*
*Tokyo Medical and Dental University*
*Yushima, Bunkyo-ku*
*Tokyo (N. N.)*

1) Y. Iwakura, T. Kurosaki and N. Nakabayashi, *Makromol. Chem.*, **44/46**, 570 (1961).
2) Y. Iwakura, N. Nakabayashi and H. Suzuki, ibid., **78**, 168 (1964).
3) S. Merill, *J. Org. Chem.*, **26**, 1301 (1961).
4) P. Jäger and E. S. Waight, *J. Chem. Soc.*, **1963**, 1339.
5) E. L. Foreman and S. M. McElvain, *J. Am. Chem. Soc.*, **62**, 1435 (1940).
6) U. S. Pat. 2468713 (1949).

# A Molecular Orbital Treatment of $^{13}C$–H Spin-Spin Coupling Constant

By Teijiro YONEZAWA, Isao MORISHIMA, Mutsuo FUJII and Kenichi FUKUI

(Received March 26, 1965)

The correlation between the $^{13}C$-H spin-spin coupling constant, $J_{C-H}$, and the degree of hybridization of the carbon atom has been investigated both experimentally and theoretically by several authors.[1-7]

Here we will present a semi-quantitative approach to an interpretation of the values of the coupling constant, $J_{C-H}$, for some saturated and unsaturated compounds; the approach uses an extended Hückel treatment which has recently been proposed by Hoffmann.[8] In this method, a molecular orbital is expressed by a linear combination of valency atomic orbitals, that is, the 1s orbitals of a hydrogen atom, the 2s, 2px, 2py and 2pz orbitals of a carbon atom, and so on. The orbital energy is then given by solving the secular equation:

$$det\,|H_{ij}-S_{ij}\varepsilon\,|=0 \qquad (1)$$

where $H_{ij}$ is a matrix element and $S_{ij}$ is the overlap integral between the $i$th and $j$th atomic orbitals. These are evaluated by a procedure similar to those previously reported.[8,9]

When we assume that $J_{C-H}$ is exclusively determined by the contact term, it is expressed by the equation:[10]

$$J_{C-H}=(1/h)(2\beta\hbar)^2\gamma_C\gamma_H(1/\Delta E)\times[(2\pi^2/3)P^2(2s_C\,|\,\delta\,|\,2s_C)(1s_H\,|\,\delta\,|\,1s_H)] \qquad (2)$$

where $P=2\sum_{i}^{occ} a^i_{1s_H}b^i_{2s_C}$, and where $a^i_{1s_H}$ and $b^i_{2s_C}$ are coefficients of the hydrogen 1s and carbon 2s orbitals in the $i$th molecular orbital respectively. $\Delta E$ is the mean excitation energy, which is assumed to be a constant throughout this treatment. Equation 2 is then simply written as:

$$J_{C-H}=AP^2 \qquad (3)$$

It may be seen that $J_{C-H}$ is proportional to the square of the bond order, $P^2$. The values of the calculated $P^2$ and the observed $J_{C-H}$ are cited in Table I. Since cyclobutane is nonplanar and has two groups of a nonequivalent C-H bond, their mean value is indicated in the table. For the sake of simplicity, the calculation of $J_{C-H}$ is carried out with respect to only one configuration, the chair form for cyclohexane, and the staggered form for ethane.

TABLE I. CALCULATED VALUES OF $P^2$ AND OBSERVED $J_{C-H}$

| Compound | $P^2$ | $J_{C-H}$, c. p. s. |
|---|---|---|
| Group a Cycloalkanes and epoxide | | |
| $C_2H_4O$ | 0.324 | 175 |
| $C_3H_6$ | 0.270 | 161 |
| $C_4H_8$ | 0.240 | 134 |
| $C_5H_{10}$ | 0.209 | 128 |
| $C_6H_{12}$ | 0.206 | 124 |
| Group b Halomethanes and ethane | | |
| $CHCl_3$ | 0.240 | 209 |
| $CH_2Cl_2$ | 0.206 | 178 |
| $CH_3Cl$ | 0.178 | 150 |
| $C_2H_6$ | 0.176 | 126 |
| $CH_4$ | 0.152 | 125 |
| Group c Unsaturated compounds | | |
| $HC\equiv CH$ | 0.377 | 248 |
| $C_6H_5{}^{13}CHO$ | 0.336 | 174 |
| Benzene | 0.268 | 159 |
| $CH_2=CH_2$ | 0.248 | 157 |

In each group, a, b and c, one can find a linear relationship between the values of $P^2$ and $J_{C-H}$, with a few discrepancies. These discrepacies may partly be attributed to the parametrization of the matrix element in an extended Hückel method, and partly also to the fact that only the contact term is taken into account as contributing to the coupling constant.

*Faculty of Engineering*
*Kyoto University*
*Sakyo-ku, Kyoto*

1) N. Muller and D. E. Pritchard, *J. Chem. Phys.*, **31**, 768, 1471 (1959).
2) J. N. Shoolery, ibid., **31**, 1427 (1959).
3) C. Juan and H. S. Gutowsky, ibid., **37**, 2198 (1962).
4) S. S. Foote, *Tetrahedron Letters*, No. 9, 579 (1963).
5) J. H. Goldstein and R. T. Hobgood, Jr., *J. Chem. Phys.*, **40**, 3592 (1964).
6) A. Veillard and G. Del Re, *Theoret. Chem. Acta*, **2**, 55 (1964).
7) P. R. Certain, V. S. Watts and J. H. Goldstein, ibid., **2**, 324 (1964).
8) R. Hoffmann, *J. Chem. Phys.*, **39**, 1397 (1963); ibid., **40**, 2474, 2480, 2745 (1964).
9) H. Kato, T. Yonezawa, K. Morokuma and K. Fukui, This Bulletin, **37**, 1710 (1964); K. Morokuma, H. Kato, T. Yonezawa and K. Fukui, This Bulletin, to be published.
10) H. M. McConnell, *J. Chem. Phys.*, **24**, 460 (1956); J. A. Pople and D. P. Santory, *Mol. Phys.*, **8**, 1 (1964).

# The Photochemical Oxidation Reaction of Benzylic Alcohols in Dimethyl Sulfoxide

By Takeo SATO, Ei-ichi YAMADA, Takeo AKIYAMA, Hiroshi INOUE and Kazuo HATA

(Received March 27, 1965)

Of the numerous reactions using dimethyl sulfoxide (DMSO), the oxidation reaction of alcohols to aldehydes and ketones has been reported from several laboratories.[1-3] This paper will record a new approach, the use of DMSO as a solvent for the photochemical oxidation reaction of benzylic alcohols under neutral conditions at room temperature.

On irradiation,[4] a solution of 9-hydroxyfluorene in DMSO absorbed oxygen smoothly, and after 9 hr. 9-fluorenone was isolated in a 71% yield (conversion). 1-Phenylethanol was also converted to acetophenone in a 53% yield (as 2, 4-dinitrophenylhydrazone), whereas benzhydrol afforded 61.5% of benzophenone, together with 21% of bis(diphenylmethyl) ether.[5]

Since this oxidation reaction seemed to be rather general, several varieties of benzyl alcohols were also subjected to the reaction conditions in the hope of obtaining the corresponding aldehydes. A mixture of benzyl alcohol (0.5 mol.) and DMSO (2.5 mol.) absorbed 0.27 mol. of oxygen during 13.5 hr. to form 38% of benzaldehyde (as 2, 4-dinitrophenylhydrazone), the yield of benzoic acid being 13.6%. In one experiment, in which a 1 : 2 solution of benzyl alcohol and DMSO was used, the reaction mixture was analyzed by the vapor phase chromatography of the aliquots removed at one-hour intervals for over 20 hr. using 30% Carbowax-1500 on a celite column at 190°C.[6] It was found that the yield of benzaldehyde reached a maximum (48%) in 14 hr. It was well established that the otherwise very slow uptake of oxygen was much facilitated by the use of DMSO as a solvent. Although the formation of a small amount of dimethyl sulfone was shown to accompany this reaction, the rest of the DMSO could be recovered by distillation. Other solvents, including dimethylformamide, acetonitrile and ligroin, were shown to be not effective. The fact that the aldehyde group was protected in DMSO from further oxidation into the carboxyl group was confirmed by comparing the irradiation reaction of benzaldehyde in DMSO and in other solvents, for example ligroin, in which photo-oxygenation occurred quite rapidly. In the DMSO solution 83.7% of benzaldehyde could be recovered, even after irradiation for 9 hr. under vigorous shaking in oxygen.

*p*-Methyl- and *p*-methoxybenzyl alcohols gave the corresponding benzaldehydes in 46.5 and 37.5% yields respectively, the uptake of oxygen being much faster in these compounds than in benzyl alcohol. *m*-Methyl- and *p*-isopropylbenzaldehydes (35.1 and 37.7% yields respectively) were also prepared by this method. On the other hand, *p*-chloro-, *m*- and *p*-nitrobenzyl alcohols were recovered unchanged. *p*-Bromobenzyl alcohol, however, gave 15% of the aldehyde upon irradiation in a quartz vessel.

Finally, mention should be made of the photochemical stability of sulfoxides. DMSO itself resisted the photochemical oxygenation reacion, and only 1.4% of dimethyl sulfone was formed after 12.5 hr. In a quartz vessel it was irradiated for 20.5 hr. under nitrogen to give a small amount of dimethyl sulfide and dimethyl sulfone (both less than 1%), 92% of DMSO being recovered.[7] Likewise, diphenyl sulfoxide was found to be quite stable toward benzene light. In contrast, a benzene solution of dibenzyl sulfoxide, when irradiated under nitrogen in a quartz cell, was shown to be decomposed into benzyl mercaptan (isolated as dibenzyl disulfide) and benzaldehyde.

*Department of Chemistry*
*Faculty of Science*
*Tokyo Metropolitan University*
*Setagaya-ku, Tokyo*

1) K. E. Pfitzner and J. G. Moffat, *J. Am. Chem. Soc.*, **85**, 3027 (1963).

2) V. J. Traynelis and W. L. Hergenrother, ibid., **86**, 298 (1964).

3) T. Sato, A. Takatsu and K. Hata, This Bulletin, **37**, 902 (1964), and the literature cited therein.

4) Unless otherwise stated, in all the photochemical reactions described here a solution of alcohol and DMSO (1 : 5) was placed in a Pyrex vessel connected with a buret for the measurement of the oxygen uptake; then, under vigorous shaking, it was irradiated with a 1000 W. mercury arc lamp (Wako Denki Co., HBC-1000) mounted in a water-cooled Pyrex jacket. The yield is based on the starting materials used, except for 9-fluorenone.

5) The irradiation of benzhydrol in a quartz cell led to the formation of benzopinacol.

6) V. E. Cates and C. E. Meloan, *Anal. Chem.*, **35**, 658 (1963).

7) Cf. G. O. Schenk and C. H. Krauch, *Chem. Ber.*, **96**, 517 (1963).

# Three New Synthetic Minerals with Tohdite-like Structures

By Goro YAMAGUCHI, Hiroaki YANAGIDA, Shuichiro ONO
Takehisa MIKI and Akira SETO

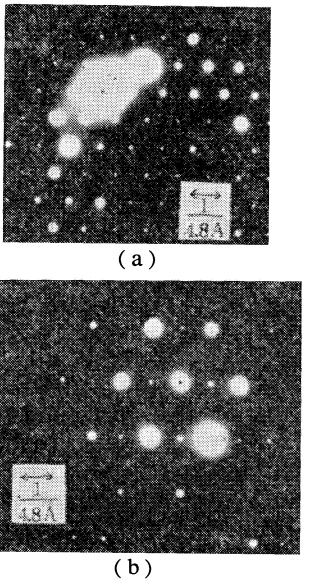
(Received March 31, 1965)

A new mineral, tohdite $5Al_2O_3 \cdot H_2O$, has been reported in previous papers.[1,2] The present authors have synthesized three more new minerals with tohdite-like structures, they have been named deuterium tohdite, rhombic tohdite and lithium tohdite.

**Deuterium Tohdite, $5Al_2O_3 \cdot D_2O$.**—Deuterium boehmite AlOOD was obtained from eta-alumina when it was treated with $D_2O$ in a Morey-type autoclave at 350°C under 150 atm. Then the deuterium boehmite was again treated hydrothermally with $D_2O$ and a small amount of $AlF_3$ as a mineralizer at 480°C under 1000 atm. for 20 hr. In this process deuterium boehmite was converted into deuterium tohdite.

Deuterium tohdite is distinguished from normal tohdite by its infrared absorption spectra. Absorption bands are found at 2440 $cm^{-1}$ for the OD-stretching mode and at 1080 $cm^{-1}$ for the OH-deformation mode (for normal tohdite, the locations are at 3260 $cm^{-1}$ and 1140 $cm^{-1}$ for the OH stretching and deformation modes respectively).

**Rhombic Tohdite, the Orthorhombic Form of $5Al_2O_3 \cdot H_2O$.**—Boehmite AlOOH was treated hydrothermally with a small amount of $AlF_3$ at 480°C under 300 atm. for 40 hr. In the product rhombic tohdite was found. Rhombic tohdite is characterized by an electron diffraction pattern which shows an orthorhombic symmetry (Fig. 1).




(a)

(b)

Fig. 1. *N*-Patterns of normal tohdite (a) and rhombic tohdite (b) (electron beam ∥ c-axis).

**Lithium Tohdite, $5Al_2O_3 \cdot LiHO$.** — Lithium aluminate gel was precipitated by ammonium hydroxide from an aqueous solution of lithium chloride and aluminum chloride (1 : 5). The precipitate was then washed, dried, and treated hydrothermally at 400°C under 200 atm. for 20 hr. Lithium tohdite was formed in this treatment.

Chemical analysis showed that the lithium tohdite was 1.69% water and 2.78% lithium oxide, and NMR measurement did not detect the existence of any fluorine. Therefore, the chemical formula was determined to be $5Al_2O_3 \cdot LiHO$.

The refractive index and the density were 1.726—1.730 and 3.73 respectively.

The infrared absorption bands are found at 3310 $cm^{-1}$ for the OH-stretching mode and at 1130 $cm^{-1}$ for the OH-deformation mode.

The X-ray powder diffraction pattern is similar to that of normal tohdite except for slight differences in the *d*-values. The electron diffraction pattern shows a pseudo-hexagonal orthorhombic symmetry, as is shown in Fig. 2. The pseudo-hexagonal lattice dimensions were determined to be $a=5.57$ Å and $c=8.87$ Å. (For normal tohdite, they are $a=5.576$ and $c=8.768$.)

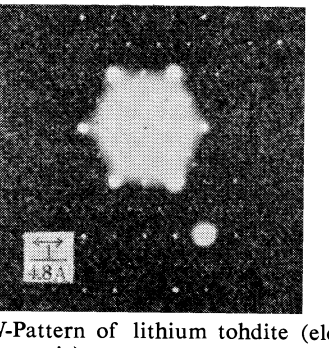



Fig. 2. *N*-Pattern of lithium tohdite (electron beam ∥ c-axis).

1) G. Yamaguchi, H. Yanagida and S. Ono, This Bulletin, 37, 752 (1964).
2) G. Yamaguchi, H. Yanagida and S. Ono, ibid., 37, 1555 (1964).

*Department of Industrial Chemistry*
*Faculty of Engineering*
*The University of Tokyo*
*Hongo, Tokyo*

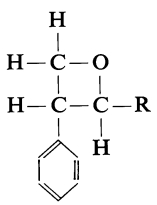
# The Synthesis of Oxetanes by the Photochemical Reaction of Aliphatic Aldehydes and Styrene*

By Hiroshi SAKURAI, Kensuke SHIMA and Isao AONO

(Received April 9, 1965)

We wish to report on the synthesis of oxetanes by the photoaddition of acetaldehyde and propionaldehyde to styrene.

An equimolar mixture of acetaldehyde and styrene was irradiated under nitrogen at 10—15°C for 8 hr. using a 350 W. high-pressure mercury lamp.[1] After the irradiation, the unreacted materials were distilled off and a fraction with a b. p. of 69—70°C/2 mmHg ($n_D^{20}$ 1.5202) was obtained. Found: C, 80.80; H, 8.23; mol. wt., 150.[2] Calcd. for $C_{10}H_{12}O$: C, 81.04; H, 8.16%; mol. wt., 148. $\lambda_{max}^{EtOH}$, 249, 253.5, 259, 262, 265.3 and 269 mμ (log ε, 2.94, 3.04, 3.12, 3.08, 2.97 and 2.93). The infrared spectrum of this product showed the presence of an oxetane[3] (980 $cm^{-1}$), but the absorption bands characteristic of hydroxy and carbonyl groups were not observed. The orientation of the addition was established by means of a study of the NMR spectrum. The NMR spectrum[4] showed a sextet (1 H) at τ 6.38 (hydrogen β to oxygen on the ring) and a complex multiplet (3 H) centered at τ 5.4 (hydrogens α to oxygen). It was assigned the structure Ia on the basis of these data.



Ia R=$CH_3$

Ib R=$C_2H_5$

From propionaldehyde and styrene, a fraction with a b. p. of 70—71°C/2 mmHg ($n_D^{20}$ 1.5144) was obtained. Found: C, 81.40; H, 8.96; mol. wt., 162. Calcd. for $C_{11}H_{14}O$: C, 81.44; H, 8.70%; mol. wt., 162. $\lambda_{max}^{EtOH}$, 249, 254, 259.5, 262.5, 265.5 and 269.3 mμ (log ε, 2.92, 3.02, 3.09, 3.05, 2.95 and 2.91). It was proposed that the product was Ib.

The reaction conditions and the yield of products are summarized in Table I.

Table I. The reaction conditions and the yields of products

| Aldehyde | Acetaldehyde | Propionaldehyde |
|---|---|---|
| Aldehyde used, g. | 42 | 58 |
| Styrene used, g. | 104 | 104 |
| Aldehyde consumed, g. | 6 | 4 |
| Styrene consumed, g. | 16.3 | 13.3 |
| Oxetane, g. | 8 | 4.3 |
| High boiling residue, g. | 13 | 10.5 |
| Wt.% of oxetane in the products | 38 | 29 |
| Ultimated yield of oxetane based on aldehyde consumed, mol. % | 49.4 | 38.5 |
| Ultimated yield of oxetane based on styrene consumed, mol.% | 31.5 | 20.7 |

It is of interest to note that the photoaddition of aliphatic aldehydes to styrene gives only oxetanes, while the addition of the aldehydes to 1-olefins generally gives ketones, which are formed by the addition of the acyl radical to olefins.[5]

These oxetanes will be stereochemically considered and the mechanistic implications will be discussed elsewhere.

*The Institute of Scientific and Industrial Research*
*Osaka University*
*Sakai, Osaka*

* Organic Photochemical Reactions. Part II. Part I; This Bulletin, in press.

Presented at the 18th Annual Meeting of the Chemical Society of Japan, Osaka, April, 1965.

1) For reaction apparatus, cf. K. Shima, Y. Shigemitsu and S. Tsutsumi, This Bulletin, 35, 1728 (1962).

2) The molecular weight was determined by the cryoscopic method in benzene.

3) L. J. Bellamy, "The Infra-red Spectra of Complex Molecules," Methuen, London (1958), p. 119.

4) The NMR spectra of oxetanes show the α hydrogens to oxygen at 5.0—6.0 τ, while the β hydrogen to oxygen on the ring occurs at 6.4—7.4 τ. D. R. Arnold, R. L. Hinman and A. H. Glick, *Tetrahedron Letters*, 1425 (1964).

5) M. S. Kharasch, W. H. Urry and B. M. Kuderna, *J. Org. Chem.*, 14, 248 (1949).

# A Nuclear Gamma-ray Resonance Study of Several [$FeX_6$]-type Ferrous Complexes

By Hirotoshi SANO and Hiroko KONO

(Received April 12, 1965)

The study of the nuclear $\gamma$-ray resonance (the Mössbauer effect) has recently been extended to metal compounds, especially those of iron and tin.[1] A number of iron compounds have so far been investigated. However, there have been few studies of the effect of the nature of the ligand on the spectrum of various [$FeX_6$]-type ferrous complexes. The purpose of the present work is to clarify the features of the chemical bond between the central iron atom and the ligand in the complexes.

The potassium calcium hexanitroferrate(II)[2] and potassium hexathiocyanatoferrate(II)[3] used as absorbers were synthesized by conventional methods. Commercial analytical-grade potassium hexacyanoferrate(II) and hexaquoferrous ammonium sulfate (Mohr's salt) were also used as absorbers without further purification. The resonance absorption spectra of 14.4 keV. $\gamma$-rays in these compounds were measured at room temperature with a source of $^{57}Co$ diffused into copper foil. The sample was moved at a constant velocity by means of a mechanical drive.

Figures 1 and 2 illustrate the nuclear $\gamma$-ray resonance spectra of potassium hexacyanoferrate(II) and Mohr's salt, and of potassium calcium hexanitroferrate(II) and potassium hexathiocyanatoferrate(II), respectively. The latter two compounds show the same spectra as those reported by previous investigators.[4] The results suggest that the isomer shifts of the hexa-coordinated ferrous complexes increas in positive value when the $\pi$ bonding character between the ligands and the iron atoms decreases in the sequence of:

$$CNCH_3{}^* > CN^- > NO_2^- > SCN^- > OH_2$$

The little larger value of the isomer shift in hexanitroferrate(II) than that in hexacyanoferrate(II) suggests that the bond between the nitro ligands and the iron atoms still has a considerable $\pi$ bonding character, whereas the much larger isomer shift in hexathiocyanatoferrate(II) shows a poor $\pi$ bonding character, probably because of lesser availability of d orbitals in sulfur atoms.

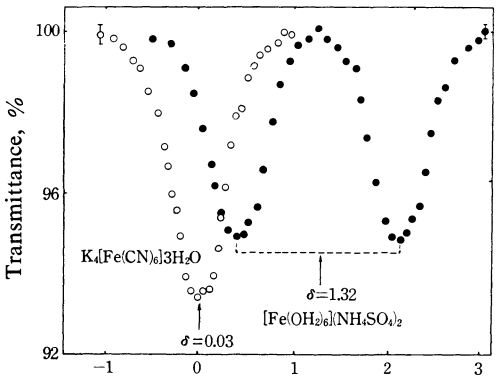



Fig. 1. Nuclear $\gamma$-ray resonance absorption spectra of $K_4[Fe(CN)_6]3H_2O$ and $[Fe(OH_2)_6](NH_4SO_4)_2$.

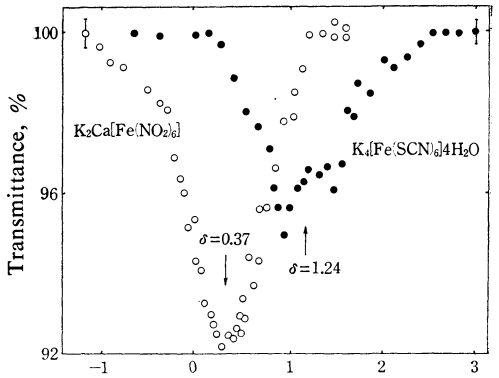



Fig. 2. Nuclear $\gamma$-ray resonance absorption spectra of $K_2Ca[Fe(NO_2)_6]$ and $K_4[Fe(SCN)_6]\cdot 4H_2O$.

*Department of Chemistry*
*Faculty of Science*
*Ochanomizu University*
*Otsuka, Bunkyo-ku, Tokyo*

1) H. Sano, *Radioisotopes*, **14**, 52 (1965).
2) L. Cambi, A. Ferrri, C. Colla, *Gazz. Chim. ital.*, **65**, 1162 (1936).
3) A. Rosenheim, E. Rochrich, L. Trewendt, *Z. anorg. u. allgem. Chem.*, **207**, 97 (1932).
4) S. DeBenedetti, G. Land, R. Ingalls, *Phys. Rev. Letters*, **6**, 60 (1961); L. M. Epstein, *J. Chem. Phys.*, **36**, 2731 (1962); E. Fluck, W. Kerler, W. Neuwirth, *Angew. Chem.*, **75**, 461 (1963).
* The Mössbauer spectrum of $[Fe^{II}(CNCH_3)_6](HSO_4)_2$ was reported previously.[5] The value of the isomer shift was −0.08 mm./sec. relative to stainless steel at room temperature.
5) H. Sano, This Bulletin, **38**, 684 (1965).

# The Effect of Nitrous Oxide on the $\gamma$-Radiolysis of Liquid Methanol

By Hiroshi SEKI and Masashi IMAMURA

(Received May 7, 1965)

The formation of a solvated electron in irradiated liquid methanol has been generally assumed.[1,2] Evidence has also been given for methanol as well as for other alcohols.[3-5] Nitrous oxide has frequently been employed in determining the yield of the hydrated electron in aqueous solutions, for hydrated electrons react rapidly with nitrous oxide to produce nitrogen;

$$N_2O + e_{aq}^- \rightarrow N_2 + O^- \qquad (1)$$

while hydrogen atoms react relatively slowly. This communication will report our preliminary findings regarding the effect of nitrous oxide on the $\gamma$-radiolysis of liquid methanol.

Extra-pure methanol (Wako Pure Chemicals) was rectified after it had been refluxed with sodium borohydride. The middle third of the distillate was dried over magnesium turnings by refluxing. Pure nitrous oxide (Takachiho Chemicals, 99.9%) was further purified by distillation. The solutions were irradiated with $^{60}$Co-$\gamma$ rays at a dose rate of $(1.4—1.5)\times10^{17}$ eV./ml./min. for about 150 min. The determination of the products was carried out by methods similar to those described elsewhere.[6]

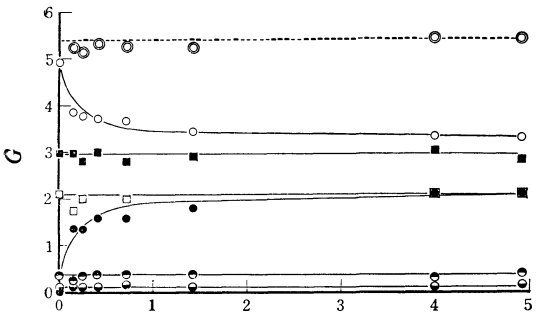



Fig. 1. Effect of $N_2O$ on the product yields of methanol.
○, $H_2$; ●, $N_2$; ■, $(CH_2OH)_2$; □, $CH_2O$; ◓, $CH_4$; ◒, CO; ◎, $H_2+N_2$

The results are shown in Fig. 1. The addition of nitrous oxide decreases the $G(H_2)$ and leads to the formation of nitrogen. It should be noted, however, that, in spite of the considerable effect of nitrous oxide on $G(H_2)$, the yields of all the other products remain unaffected, and that the limiting $G(H_2)+G(N_2)$ value is 5.4, which is the same as the $G(H_2)$ values for pure methanol ascertained by Meshitsuka and Burton,[7] and by Baxendale and Mellows.[2] It would appear, therefore, that no nitrogen-formation reactions other than reaction 1 take place. It is also reasonable to assume that the reaction of nitrous oxide with hydrogen atoms is negligible under the present experimental conditions.*

Thus, insofar as nitrous oxide is assumed to react solely with the solvated electrons in the irradiated methanol, the yield of the solvated electron should be equal to the limiting $G(N_2)=2.1$. This value is substantially higher than those obtained from kinetic study (1.2)[2] and from pulse radiolysis study (1.1).[5] The reason for this disagreement is not obvious at present. Further studies are therefore in progress into the effects of the pH value and of higher nitrous oxide concentrations; our results will be published in the future.

*The Institute of Physical and Chemical Research*
*Bunkyo-ku, Tokyo*

1) E. Hayon and J. J. Weiss, *J. Chem. Soc.*, **1961**, 3970.
2) J. H. Baxendale and F. W. Mellows, *J. Am. Chem. Soc.*, **83**, 4720 (1961).
3) I. A. Taub, D. A. Harter, M. C. Sauer, Jr., and L. M. Dorfman, *J. Chem. Phys.*, **41**, 979 (1964).
4) G. E. Adams, J. H. Baxendale and J. W. Boag, *Proc. Roy. Soc.*, **A277**, 549 (1964).
5) M. C. Sauer, Jr., S. Arai and L. M. Dorfman, *J. Chem. Phys.*, **42**, 708 (1965).
6) N. N. Lichtin, *J. Phys. Chem.*, **63**, 1449 (1959).
7) G. Meshitsuka and M. Burton, *Radiation Res.*, **8**, 285 (1958).

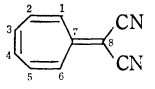
* The fact that the $G(N_2)$ value at a low pH value is negligibly small (unpublished results) would support this assumption.

# The Crystal Structure of 8, 8-Dicyanoheptafulvene

By Hirotaka SHIMANOUCHI,* Tamaichi ASHIDA, Yoshio SASADA, Masao KAKUDO, Ichiro MURATA and Yoshio KITAHARA

(Received May 15, 1965)

8, 8-Dicyanoheptafulvene (I) is a stable derivative of heptafulvene, which is a sort of the non-alternant hydrocarbon. This compound has been studied by several groups of workers in recent years.[1-5]




(I)

The present investigation was undertaken in order to reveal its molecular parameters by X-ray analysis.

This compound crystallizes in a monoclinic unit cell with dimensions: $a=7.84$ Å, $b=13.14$ Å, $c=3.99$ Å, and $\beta=97.9°$. The space group is $P2_1$ or $P2_1/m$. Since intensity statistics showed the existence of a center of symmetry, it was decided that the space group was the latter. There are two molecules in the unit cell, and the molecule should have a mirror plane in it.

Multiple-film equi-inclination Weissenberg photographs were taken for layers 0 to 3 about the c axis with Cu-$K\alpha$ radiation, and the integrated intensities were estimated visually against a standard scale.

The structure was solved by the interpretation of Patterson projections along the c and b axes and Harker section $P(u, 1/2, w)$. The positional and thermal parameters of each atom so obtained were refined by the least-squares method. The final electron density projection along the c axis is shown in Fig. 1. The molecule is planar and lies approximately parallel to the (101) plane; the interplanar spacing is 3.4 Å. A crystallographic mirror plane normal to the b axis passes through the atoms $C_7$ and $C_8$ and is perpendicular to the molecular plane.

A detailed account of this work will be presented in the near future.

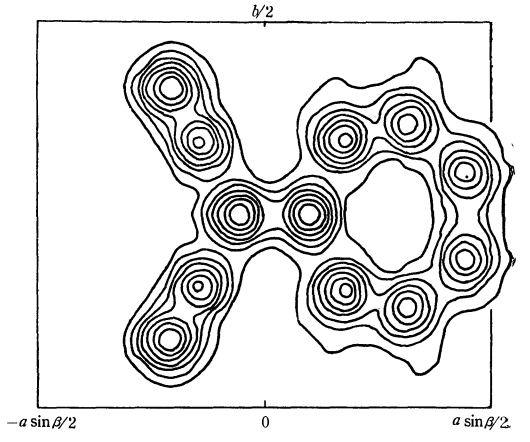



Fig. 1. The final electron density projection on the (001). Contours at intervals of 1.0 e. Å$^{-2}$, the lowest being at 1.0 e. Å$^{-2}$.

*Institute for Protein Research*
*Osaka University*
*Kita-ku, Osaka*
*(H. S., T. A., Y. S. & M. K.)*

*Department of Chemistry*
*Faculty of Science*
*Tohoku University*
*Ka'ahira-cho, Sendai*
*(I. M. & Y. K.)*

* On leave from Department of Chemistry, Faculty of Science, Tohoku University.

1) T. Nozoe, T. Mukai, K. Osaka and N. Shishido, This Bulletin, **34**, 1384 (1961).
2) M. Yamakawa, H. Watanabe, T. Mukai, T. Nozoe and M. Kubo, *J. Am. Chem. Soc.*, **82**, 5665 (1960).
3) K. Hafner, H. W. Riedel and M. Danielisz, *Angew. Chem.*, **75**, 344 (1963); *Angew. Chem. Internat. Edit.*, **2**, 215 (1963).
4) C. Jutz, *Chem. Ber.*, **97**, 2050 (1964).
5) D. J. Bertelli, C. Golino and D. L. Dreyer, *J. Am. Chem. Soc.*, **86**, 3329 (1964).

# The Thermal Condensation of Formaldehyde with Cycloolefins

By Shoji WATANABE

(Received April 14, 1964)

In a previous paper,[1] observations of the behavior of representative aliphatic olefins in their thermal condensation with formaldehyde were reported. It seemed desirable to extend this research by examining also the thermal condensation of some cycloolefins with formaldehyde. The present paper will describe the products obtained from β-pinene, camphene, thujopsene, dihydrothujopsene, 3-*p*-menthene, cyclohexene, 1-butyl-2, 6, 6-trimethyl-1-cyclohexene and 1-(2'-buten-1'-yl)-2, 6, 6-trimethyl-1-cyclohexene in their respective condensations with formaldehyde.

In this study all condensations with paraformaldehyde were carried out in acetic anhydride and at temperatures varying from 180 to 220°C, the products obtained being mainly acetates of olefinic, primary alcohols, in which the double bond, except those in the condensation products from camphene,[2] was located at a position adjacent to its original site in the starting olefins. The various condensation products are given in Table I.

β-Pinene (I) and camphene (III), which have an end methylene group, react readily with paraformaldehyde to give predominantly 2-acetoxyethyl-6, 6-dimethyl-bicyclo[3, 1, 1]-hept-2-ene (II) (nopyl acetate) and 8-acetoxymethylcamphene (V) respectively. From camphene, however, 8-hydroxymethylcamphene, isoborneol and isobornyl acetate were also obtained in fairly good yields under the experimental conditions shown in Table I.

The thermal condensations of thujopsene (V),[3] dihydrothujopsene (VIII) and 3-*p*-menthene (XI), which have a trisubstituted double bond, afforded rather complicated results. From the crude condensation product of thujopsene (V), an unsaturated acetate and an ether were separated successfully by means of column chromatography using a silica gel column. The acetate was saponified to give an alcohol, $C_{16}H_{27}OH$, which absorbed 95% of one equivalent amount of hydrogen over an Adams catalyst. The infrared spectrum showed primary hydroxyl absorption bands at 3300 and 1045 $cm^{-1}$, and a characteristic band of the trisubstituted double bond at 820 $cm^{-1}$. Therefore, this compound must be 1, 2, 3, 4, $4_a$, 5, 6, $8_a$-octahydro-6-(hydroxymethyl)-1, 1, $4_a$, 7, $8_a$-pentamethylnaphthalene (VI). The structural assignment was further supported by the nuclear magnetic resonance spectrum, as will be shown in the "Experimental" section (Fig. 1). On the other hand, the ether, $C_{17}H_{26}O$, $F_1$, was considered to be a cyclic ether, since the infrared spectrum showed a strong absorption band at 1100 $cm^{-1}$. The nuclear magnetic resonance spectrum indicated the signal of the allyl proton at 7.8 τ. The signal at 6.3 τ is presumably due to protons on the cyclic ether ($-CH_2-O-CH_2-$), while the signal at 9.3 τ was presumably due to the protons of the cyclopropane ring (Fig. 2). From this spectral evidence and from comparison with a similar case recently reported,[4] it was considered that this cyclic ether was 3, 4, 5, 6, 7, 8, $8_a$, 9, 10, $10_a$-decahydro-5, 5, $8_a$-trimethyl-10, $10_a$-methylene-1*H*-2-oxa-anthracene (VII).

Although dihydrothujopsene (VIII) scarcely reacted at all with paraformaldehyde in acetic

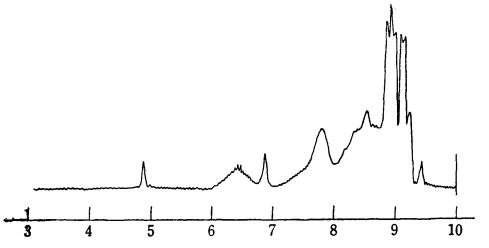



Fig. 1. The nuclear magnetic resonance spectrum of VI.

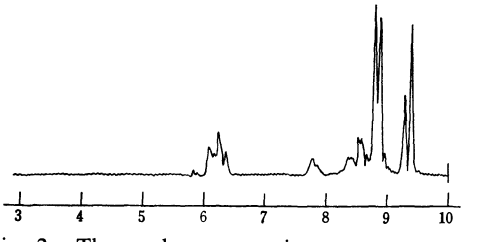
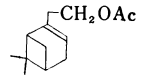
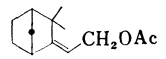
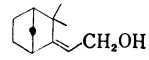
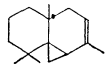
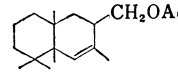
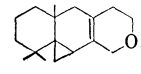
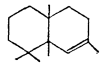
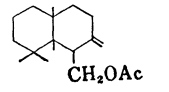
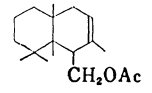
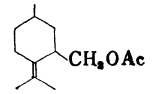
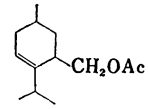
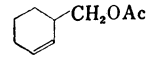
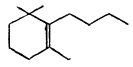
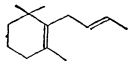
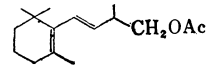



Fig. 2. The nuclear magnetic resonance spectrum of VII.

1) S. Watanabe and K. Suga, This Bulletin, **36**, 1495 (1963).
2) Y. Watanabe, *J. Chem. Soc. Japan, Pure Chem. Sec.* (*Nippon Kagaku Zasshi*), **81**, 827 (1960).
3) S. Watanabe and K. Suga, ibid., **84**, 993 (1963).
4) A. Arai, *Kobayashi Rigaku Kenkyusho Hokoku*, **10**, 29 (1960).

TABLE I. CONDENSATION OF OLEFIN WITH FORMALDEHYDE IN ACETIC ANHYDRIDE

| Olefin: Name | Olefin: Structure | Reaction temp. °C | Reaction time hr. | Recovered olefin % | Product (yield, %) |
|---|---|---|---|---|---|
| β-Pinene (I) |  | 200—205*1 | 5 | 31 |  (II) (60) |
| Camphene (III) |  | 180 | 5 | 53 |  (IV) (20) and  (4), Isobornyl acetate*3 (17) and Isoborneol*3 (10) |
| Thujopsene (V) |  | 185 | 3 | 38 |  (10) and  (10) Acetate of VI (VII) |
| Dihydrothujopsene (VIII) |  | 200—210*2 | 10 | 85 |  and  (5) Acetate of IX Acetate of X |
| 3-*p*-Menthene (XI) |  | 200 | 3 | 57 |  and  (22) Acetate of $XII_B$ Acetate of $XII_A$ |
| Cyclohexene (XV) |  | 220 | 9 | 50 |  (XVI) (12) |
| 2,6,6-Trimethyl-1-butyl-1-cyclohexene (XVII) |  | 200—210*2 | 10 | 75 | A primary alcohol, $C_{14}H_{26}O$ (XVIII) (6) |
| 2,6,6-Trimethyl-1-[2'-butyl-1'-yl]-1-cyclohexene (XIX) |  | 220 | 10 | 60 |  (10) Acetate of XX |

*1 Under 100 kg./cm² of hydrogen pressure.
*2 Acetic acid and a trace of $H_2SO_4$ added.
*3 Identified with authentic samples.

anhydride, it did react in a mixture of acetic anhydride, acetic acid and a trace of concentrated sulfuric acid to give an inhomogeneous acetate, which was then saponified to an inseparable mixture of unsaturated isomeric alcohols, $C_{16}H_{27}O$. The infrared bands at 810, 860 and 1040 $cm^{-1}$ indicated the presence of a trisubstituted double bond, a terminal methylene, and a primary hydroxyl group. Thus, the mixture presumably consisted of 1, 2, 3, 4, $4_a$, 5, 6, 7, 8, $8_a$-decahydro-7-methylene-8-(hydroxymethyl)-1, 1, $4_a$, $8_a$-tetramethylnaphthalene (IX) and 1, 2, 3, 4, $4_a$, 5, 8, $8_a$-octahydro-8-(hydroxymethyl)-1, 1, $4_a$, 7, $8_a$-pentamethylnaphthalene (X). The saponification of the condensation product from 3-*p*-menthene (XI) gave a mixture of unsaturated alcohols. The direct separation of the isomeric components by fractional distillation and gas chromatography was unsuccessful. The infrared absorption spectrum showed an absorption band at 810 $cm^{-1}$, indicating the presence of a trisubstituted ethylenic bond. Reduction gave 3-hydroxymethyl-*p*-menthane (XIV). Oxidation with potassium permanganate gave acetone, indicating the presence of an isopropylidene group, while oxidation with chromic anhydride gave an α, β-unsaturated aldehyde which was thought to be 3-formyl-3(4)-*p*-menthene (XIII). These results suggested that 3-hydroxymethyl-4(5)-*p*-menthene (XIIA) and 3-hydroxymethyl-4(8)-*p*-menthene (XIIB) were the main components of the mixture.

Cyclohexene (XV) reacted with paraformaldehyde to give (2-cyclohexenyl)methyl acetate (XVI) as the main product.

From the condensation product of 2, 6, 6-trimethyl-1-butyl-1-cyclohexene (XVII), which has a tetrasubstituted olefinic bond, an unsaturated alcohol, $C_{14}H_{26}O$, $F_1$ (XVIII) was obtained in a very poor yield. The infrared absorption spectrum indicated, however, that it was a primary alcohol, the structure of which has not yet been determined.

From the condensation of 2, 6, 6-trimethyl-1-[2′-buten-1′-yl]-1-cyclohexene (XIX) and paraformaldehyde, an unsaturated alcohol, $C_{14}H_{24}O$, $F_2$ (XX) was obtained in a poor yield. Its ultraviolet absorption spectrum ($\lambda_{max}$ 242 m$\mu$) indicated that it contained a dienic group. The infrared absorption spectrum showed the characteristic absorption bands of a trans-olefinic bond and a primary hydroxyl group. Therefore, 2-methyl-4-[2′, 6′, 6′-trimethyl-1′-cyclohexen-1′-yl]-3-buten-1-ol (XX) is a reasonable assignment for the alcohol.

The foregoing observations indicate that the thermal condensation of formaldehyde with cycloolefins in the presence of acetic anhydride occurs most readily with end methylene-type olefins, $CH_2=CR_1R_2$, and that trisubstituted olefins ($R_1CH=CR_2R_3$) and disubstituted olefins ($R_1CH=CHR_2$) are less reactive. Tetrasubstituted olefins of the $R_1R_2C=CR_3R_4$ type are least reactive.

## Experimental

**Materials.** — $\beta$-Pinene, camphene, thujopsene, 3-*p*-menthene and cyclohexene were obtained from the Takasago Perfumary Co., Ltd.

*Dihydrothujopsene (VIII)*[5] was prepared by the hydrogenation of thujopsene over palladised charcoal; b. p. 129—130°C/13 mmHg; $d_D^{20}$ 0.9252; $n_D^{20}$ 1.5039. The gas chromatogram showed one peak.

The preparation of *1-(2′-butenyl)-2, 2, 6-trimethyl-1-cyclohexene (XIX)*[6] was carried out as follows. A mixture of 450 g. of $\beta$-ionone, 280 cc. of absolute ethanol, and 250 g. of hydrazine hydrate was refluxed for 4 hr. To this mixture, 800 g. of diethylene glycol, 180 g. of potassium hydroxide and 70 cc. of benzene were added, and the new mixture was refluxed for 2 hr. Fractional distillation gave 200 g. of crude 1-(2′-butenyl)-2, 6, 6-trimethyl-1-cyclohexene (XIX) (b. p. 75—135°C/45—50 mmHg), which was then fractionally redistilled to give 100 g. of an oil, b. p. 81.5°C/5 mmHg; $d_D^{20}$ 0.8469; $n_D^{21}$ 1.4836 (reported[6] b. p. 91—93°C/11 mmg; $d_4^{18}$ 0.8580; $n_D^{18}$ 1.4795); molecular refraction: 60.18 (calcd. for $C_{13}H_{22}$, $F_2$, 59.10). IR (liq. film): $\nu_{max}$ 970 cm$^{-1}$ (trans-olefinic bond). The gas chromatogram showed one peak.

*1-Butyl-2, 6, 6-trimethyl-1-cyclohexene (XVII)* was obtained by the hydrogenation of 1-(2′-butenyl)-2, 6, 6-trimethyl-1-cyclohexene (XIX) at 20 kg./cm$^2$ hydrogen pressure and room temperature, using a Pd-C catalyst. Distillation gave an oil (b. p. 73—78°C/3 mmHg; $d_4^{20}$ 0.8460; $n_D^{20}$ 1.4700). Bromine value: 100 (calcd. for $C_{13}H_{24}$, $F_1$, 89). NMR: 8.4 $\tau$ ($=\overset{|}{C}-CH_3$), 9.05 $\tau$ (*gem*-dimethyl group), 9.1 $\tau$ ($-CH_3$).

**Condensation Procedure.** — A mixture of 1 mol. of an olefin, 1 mol. of paraformaldehyde, and 0.5 mol. of acetic anhydride was heated at 180—220°C in a stainless autoclave for several hours. After it had been cooled, the reaction mixture was extracted with ether. The ethereal solution was washed with water, dried over anhydrous sodium sulfate, and then treated in ordor to separate the components. For the respective condensations, the main conditions are given in Table I.

**The Condensation of $\beta$-Pinene (I) with Formaldehyde.** — From a mixture of 45 g. of I, 17 g. of acetic anhydride and 10 g. of paraformaldehyde, 14 g. of I and 41 g. of an oily product boiling at 98—168°C/10 mmHg were obtained. This product was proved by means of gas liquid chromatography to consist of 90% of 2-acetoxyethyl-6, 6-dimethyl-bicyclo[3, 1, 1]-hept-2-ene (II), and 8% of a high boiling fraction. Fractional distillation gave pure II (b. p. 98—100°C/10 mmHg). The saponification of II gave 6, 6-dimethyl-bicyclo[3, 1, 1]-hept-2-enyl ethanol (nopol), since the gas chromatogram and the infrared spectrum were identical with those of an authentic sample, b. p. 98—102°C/8 mmHg; $d_4^{11}$ 0.9716; $n_D^{13}$ 1.4945; bromine value, 99.51 (calcd. for $C_{11}H_{18}O$, $F_1$, 90.12); hydroxyl group, 8.62% (calcd. for monohydric alcohol, 10.2%).

**The Condensation of Camphene (III) with Formaldehyde.** — From a mixture of 340 g. (2.46 mol.) of III, 66.5 g. (2.2 mol.) of paraformaldehyde and 107 g. of acetic anhydride, 180 g. of III and 150 g. of a crude product (b. p. 100—130°C/7 mmHg) were obtained. This product consisted of 34% isobornyl acetate, 21% isoborneol, 40% 8-acetoxymethylcamphene (IV) and 5% 8-hydroxymethylcamphene, according to the gas liquid chromatographic analysis. The mixture (65 g.) was distilled to give the following fractions: (a) 20 g., b. p. 97—98°C/4 mmHg, (b) 25 g., b. p. 114—114.5°C/4 mmHg. The saponification of fraction b (24 g.) gave 18 g. of 8-hydroxymethylcamphene, b. p. 110—115°C/5 mmHg; $d_4^{25}$ 0.9810; $n_D^{25}$ 1.5016; molecular refraction, 50.20 (calcd. for $C_{11}H_{18}O$, $F_1$, 49.66); phthalic acid monoester, m. p. 127°C (reported[2] m. p. 127—127.5°C); 3, 5-dinitrobenzoate, m. p. 89°C. The saponification of the fraction a gave isoborneol (m. p. 130°C).

**The Condensation of Thujopsene (V) with Formaldehyde.** — From a mixture of 50 g. of thujopsene (V), 9 g. of paraformaldehyde and 13 g. of acetic anhydride, 19 g. of an unsaturated hydrocarbon and 12 g. of a crude product (b. p. 120—140°C/5 mmHg; $d_4^{18}$ 1.0196; $n_D^{22}$ 1.5193) were obtained. The saponification of the crude product (50 g.) gave an oil (37 g.), b. p. 135—140°C/5 mmHg; $d_4^{22}$ 1.0097; $n_D^{22}$ 1.5216; hydroxyl group, 4.45% (calcd. for monohydric alcohol, 7.23%). The liquid chromatography of 10 g. of the oil with silica gel (70 g.) gave 4 g. of a viscous oil (A) from the

5) S. Forsen and N. T. Norin, *Acta Chem. Scand.*, **15**, 592 (1961).

6) R. Fischer, G. Lardelli and O. Jeger, *Helv. Chim. Acta*, **34**, 1577 (1951).

elute with benzene and 4 g. of a viscous oil (B) from the elute with methanol.

The redistillation of A gave 3,4,5,6,7,8,8a,9,10,-10a-decahydro-5,5,8a-trimethyl-10,10a-methylene-2*H*-2-oxa-anthracene (VII), b. p. 136°C/5 mmHg; bromine value, 139.2 (calcd. for $C_{17}H_{26}O$, $F_1$, 115.6). IR (liq. film): $\nu_{max}$ 1100 $cm^{-1}$ (a cyclic ether). NMR:[7] 7.8 $\tau$ (allyl proton), 8.85, 8.87, 9.37 $\tau$ (three methyl groups), 6.3 $\tau$ ($-CH_2-O-CH_2-$), 9.3 $\tau$ (cyclopropane ring).

Found: C, 81.37; H, 10.28. Calcd. for $C_{17}H_{26}O$ (VII): C, 82.34; H, 11.36%.

Similarly, 1,2,3,4,4a,5,6,8a-octahydro-6-(hydroxymethyl)-1,1,4a,7,8a-pentamethylnaphthalene (VI) was obtained from B, b. p. 139°C/5 mmHg; $d_4^{15}$ 0.9907; $n_D^{15}$ 1.5194; bromine value, 68.3 (calcd. for $C_{16}H_{26}O$, $F_1$, 74.6); hydroxyl group, 6.00% (calcd. for $C_{16}H_{25}(OH)$, 7.23%). IR: $\nu_{max}$ 3300, 1045 $cm^{-1}$ (primary alcohol), $\nu_{max}$ 820 $cm^{-1}$ (trisubstituted double bond). NMR: 4.93 $\tau$ (singlet, $-\overset{|}{C}-CH=\overset{|}{C}-$), 6.4 $\tau$ ($-\overset{|}{C}H-CH_2OH$).

Found: C, 81.18; H, 11.10. Calcd. for $C_{16}H_{28}O$ (VI): C, 81.29; H, 11.97%.

**The Condensation of Dihydrothujopsene (VIII) with Formaldehyde.** — From 124 g. of VIII, 21.6 g. of paraformaldehyde, 30.6 g. of acetic anhydride, 18 g. of acetic acid and one drop of concentrated sulfuric acid, 7 g. of a pale yellow oil (135—150°C/3 mmHg; $n_D^{20}$ 1.5040; $d_4^{20}$ 0.9920) was obtained. The saponification of this product gave an alcoholic compound. Liquid chromatography with silica gel gave a crude alcohol from the elute with methanol. The molecular distillation of this alcohol with a pot still gave 3 g. of 1,2,3,4,4a,5,6,7,8,8a-decahydro-7-methylene-8-(hydroxymethyl)-1,1,4a,8a-tetramethylnaphthalene (IX) and 1,2,3,4,4a,5,8,8a-octahydro-8-(hydroxymethyl)-1,1,4a,7,8a-pentamethylnaphthalene (X). Bath temperature, 70°C/$10^{-3}$ mmHg; $d_4^{20}$ 0.9918; $n_D^{20}$ 1.5193. IR: $\nu_{max}$ 810 $cm^{-1}$ (a trisubstituted olefinic bond), $\nu_{max}$ 860 $cm^{-1}$ (an end methylene group) and $\nu_{max}$ 1040 $cm^{-1}$ (a primary hydroxy group). NMR: 5.3 $\tau$ ($-\overset{|}{C}=CH_2$), 4.6 $\tau$ ($CH_2-CH=\overset{|}{C}-$), 6.4 $\tau$ ($-\overset{|}{C}H-CH_2OH$).

Found: C, 79.72; H, 11.39. Calcd. for $C_{16}H_{28}O$: C, 81.29; H, 11.97%.

**The Condensation of 3-*p*-Menthene (XI) with Formaldehyde.** — From a mixture of 180 g. of XI, 60 g. of paraformaldehyde and 75 g. of acetic anhydride, 102 g. of XI and 60 g. of a crude acetate (b. p. 90—110°C/5 mmHg) were obtained. The saponification of the product gave 25 g. of a mixture of 3-hydroxymethyl-*p*-menthene; b. p. 100—104°C/5 mmHg; $n_D^{30}$ 1.4815; $d_4^{30}$ 0.9160; molecular refraction, 52.21 (calcd. for $C_{11}H_{20}O$, $F_1$, 51.85); hydroxyl group, 10.81% (calcd. for monohydric alcohol, 10.11%); bromine value, 107 (calcd. for $C_{11}H_{20}O$, $F_1$, 95); IR (liquid film): $\nu_{max}$ 1050 $cm^{-1}$ (a primary alcohol), 810 $cm^{-1}$ (a trisubstituted double bond).

*3,5-Dinitrobenzoate* was recrystallized from methanol; m. p. 79—80°C.

Found: N, 7.88. Calcd. for $C_{18}H_{22}O_6N_2$: N, 7.73%.

**3-Hydroxymethyl-*p*-menthane (XIV).**—3-Hydroxymethyl-*p*-menthene (XII) was hydrogenated over a nickel catalyst in a methanol solution at 150°C under 50 kg./$cm^2$ of initial hydrogen pressure to give 3-hydroxymethyl-*p*-menthane (XIV); b. p. 91—94°C/5 mmHg; $n_D^{20}$ 1.4738. The gas chromatogram showed one peak.

**3-Formyl-3-*p*-menthene (XIII).**—To a mixture of 8 g. of XII and 50 cc. of glacial acetic acid, a mixture of 8 g. of chromic anhydride and 50 cc. of glacial acetic acid was added over an hour's period with vigorous agitation at 25°C; the mixture was then stirred for 2 hr., after which it was treated as usual. By fractional distillation, 3 g. of XIII (b. p. 70—80°C/5 mmHg) was obtained.

This gave a positive reaction with Schiff's reagent and reduced an ammoniacal silver nitrate solution.

*2,4-Dinitrophenylhydrazone* was recrystallized from a mixture of pyridine and methanol in the form of red needles; m. p. 141—142°C; UV: $\lambda_{max}$ 380 m$\mu$, $\varepsilon$ 24000.

Found: N, 16.14. Calcd. for $C_{17}H_{22}O_4N_4$: N, 16.18%.

**The Oxidation of XII with Potassium Permanganate.** — A mixture of 7 g. of potassium permanganate and 50 cc. of water was added to 4 g. of XII and 20 cc. of water with vigorous agitation over a 30 min. period, the mixture was then left at room temperature for two days. After the unreacted potassium permanganate had been decomposed with hydrogen peroxide, the solution was filtered and extracted with ether. The ethereal solution (A) was washed with water and dried over anhydrous sodium sulfate. The aqueous solution and the washings were then combined (B). The solution A was distilled to give a small amount of a carbonyl compound, the structure of which was not determined. From the solution B, a carbonyl compound was separated as crude 2,4-dinitrophenylhydrazone. Liquid chromatography with a silica gel column gave yellow needles (m. p. 121°C), which was identical with that of an authentic sample of acetone 2,4-dinitrophenylhydrazone.

**The Condensation of Cyclohexene (XV) with Formaldehyde.**—From a mixture of 82.1 g. (1 mol.) of cyclohexene (XV), 30 g. (1 mol.) of paraformaldehyde and 51 g. (0.5 mol.) of acetic anhydride, 40 g. of a crude product was obtained. Distillation gave 10 g. of 1-hydroxymethyl-2-cyclohexene and 5 g. of a high-boiling fraction. 1-Hydroxymethyl-2-cyclohexene has the following properties: b. p. 74°C/11 mmHg; $d_4^6$ 0.9816; $d_4^{25}$ 0.9697; $n_D^{15}$ 1.4914; $n_D^{25}$ 1.4825; molecular refraction, 33.2 (calcd. for $C_7H_{12}O$, $F_1$, 33.2); bromine value, 127.5 (calcd. for $C_7H_{12}O$, $F_1$, 142). $\alpha$-Naphthylurethan, m. p. 87°C (reported 87°C[8]).

Found: C, 76.66; H, 6.82. Calcd. for $C_{18}H_{19}O_2N$: C, 76.48; H, 6.81%.

1-Hydroxymethyl-2-cyclohexene (2 g.) was hydrogenated at 20 kg./$cm^2$ pressure in a stainless autoclave with Adam's catalyst. The usual workup

7) L. M. Jackman, "Application of NMR Spectroscopy in Organic Chemistry," Pergamon Press, London (1959), p. 85.

8) A. T. Blomquist, J. Verdol, C. L. Adami, J. Wolinsky and D. D. Phillips, *J. Am. Chem. Soc.*, 79, 4978 (1957).

gave 1.0 g. of cyclohexylmethanol; b. p. 176—177°C; $n_D^{25}$ 1.4617[6].

The high boiling fraction was found by gas liquid chromatography to be composed of various components, the structures of which were not determined.

**The Condensation of 1-Butyl-2, 6, 6-trimethyl-1-cyclohexene (XVII) with Formaldehyde.**—From a mixture of 25 g. of XVII, 7.2 g. of paraformaldehyde, 10.2 g. of acetic anhydride, 6 g. of glacial acetic acid and a trace of sulfuric acid, 3 g. of a crude product were obtained. The saponification of this product gave 1.5 g. of a crude alcohol (b. p. 100—115°C/3 mmHg). The chromatographic purification with activated silica gel gave 1 g. of an alcohol ($n_D^{20}$ 1.4898) from the elution of methanol. The gas chromatogram showed one peak. IR: $\nu_{max}$ 1050 $cm^{-1}$ (a primary alcohol).

Found: C, 78.91; H, 12.08. Calcd. for $C_{14}H_{26}O$: C, 79.52; H, 12.87%.

**The Condensation of 1-[2'-Butenyl]-2, 6, 6-trimethyl-1-cyclohexene (XIX) with Formaldehyde.**—From a mixture of 100 g. of XIX, 16.6 g. of paraformaldehyde and 24 g. of acetic anhydride, the following main fraction (10 g.) was obtained; b. p. 115—130°C/3 mmHg; UV: $\lambda_{max}^{C_2H_5OH}$ 240 m$\mu$, $\varepsilon$ 2162; IR: 1760 $cm^{-1}$ (acetate), 1240 $cm^{-1}$ (acetate), 970 $cm^{-1}$ (trans olefinic bond). The saponification of this product gave 5 g. of 2-methyl-4-[2', 6', 6'-trimethyl-1'-cyclohexene-1'-yl]-3-butene-1-ol (XX), b. p. 110—120°C/3 mmHg; $d_4^{15}$ 0.9164; $n_D^{15}$ 1.5012; molecular refraction, 66.89 (calcd. for $C_{14}H_{24}O$, 66.24); UV: $\lambda_{max}^{C_2H_5OH}$ 242 m$\mu$, $\varepsilon$ 3213; IR: 1045 $cm^{-1}$ (a primary alcohol), 970 $cm^{-1}$ (trans-olefinic bond). The gas chromatogram showed one peak.

Found: C, 81.43; H, 11.62. Calcd. for $C_{14}H_{24}O$: C, 80.69; H, 11.63%.

**Absorption Spectra.** — The infrared absorption spectra were measured by using a Koken IRS spectrophotometer, while the ultraviolet absorption spectra were measured with a "Shimadzu" photometric spectrophotometer type QB-50.

**Gas Liquid Chromatography.** — The gas liquid chromatography was measured under the following conditions:

I, III, XI and XV: Column, LAC-2R-446 (20%) on Celite 545, 2 m.; temperature, 120°C; carrier gas, He 45 ml./min.

V, VIII, XVII, XIX, II, IV, XII and XVI: Temperature, 180°C; other conditions, the same as above.

VI, VII, IX, X, XVIII and XX: Column; silicone DC 200 (20%) on Celite 545, 2 m.; temperature, 230°C; carrier gas, He 45 ml./min.

The author is indebted to the Takasago Perfumary Co., Ltd., for providing materials; to Professor Sho Ito of Tohoku University for the magnetic resonance spectroscopy, and to Professor Kyoichi Suga of Chiba University for his cordial guidance throughout this work.

*Department of Applied Chemistry*
*Faculty of Engineering*
*Chiba University*
*Yayoicho, Chiba*

# The Formation Constants of Chromium(III)-Glycinato and α-Alaninato Complexes*

By Hiroharu MATSUKAWA, Mitsuo OHTA, Shichiro TAKATA and Ryokichi TSUCHIYA

(Received June 20, 1964)

Few reports on the formation constants of chromium(III) complexes have been published. In their own preceding papers the present authors have discussed the formation constants of chromium(III) complexes with ethylenediamine, the simplest chelating agent coordinating by two nitrogen atoms,[1] and those with oxalate ion, the simplest chelating agent coordinating by two oxygen atoms.[2]

Glycine, the simplest α-amino acid, is the intermediate chelating agent between ethylenediamine and oxalate ions from the structural point of view. In the present study the formation constants of chromium(III) complexes with glycine and α-alanine will be determined.

## Experimental

**Hexaaquochromium(III) Perchlorate.**—The preparation of this salt and the method of the analyses of chromium and free perchloric acid were the same as those described in a preceding paper.[2] The compositions of the crystalline salts used for chromium(III) glycinato and α-alaninato complexes respectively were as follows:

* Read at the 13th Symposium on Coordination Compounds of the Chemical Society of Japan, Nagoya, October, 1963.

1) M. Ohta, H. Matsukawa and R. Tsuchiya, This Bulletin, 37, 692 (1964).

2) K. Nagata, A. Umayahara and R. Tsuchiya, ibid., 38, 1059 (1965).

$[Cr(H_2O)_6](ClO_4)_3$, 45.61 mol.%;
$HClO_4$, 54.39 mol.%
$[Cr(H_2O)_6](ClO_4)_3$, 55.37 mol.%;
$HClO_4$, 44.63 mol.%

**Glycine and α-Alanine.**—The glycine used was a guaranteed reagent, and α-alanine was a reagent of the highest commercial grade.

**Procedure.**—The formation constants were determined by a pH method similar to that used in a preceding paper.[2] A mixed solution of hexaaquochromium(III) perchlorate and glycine or α-alanine, the ionic strength of which was adjusted to 0.1 by adding sodium perchlorate, was kept in a thermostat at 25°C, and the pH of the solution was measured with a Toa Denpa pH meter, model HM-8, after the equilibrium had been established.

## Results

**The Determination of the Acid Dissociation Constants of Glycine and α-Alanine.**—It is reasonable to presume that α-amino acids are present in an aqueous solution in the three species as $H_3N^+$—CHR—COOH, $H_3N^+$—CHR—$COO^-$ and $H_2N$—CHR—$COO^-$, where R is H for glycine and R is $CH_3$ for α-alanine.

When these three species are expressed by $H_2A^+$, HA and $A^-$ respectively, the acid dissociation constants of the amino acid are defined as follows:

$$H_2A^+ \rightleftarrows H^+ + HA \quad K_1=[H^+][HA]/[H_2A^+] \quad (1)$$

$$HA \rightleftarrows H^+ + A^- \quad K_2=[H^+][A^-]/[HA] \quad (2)$$

where [ ] expresses the concentration of each species in mole per liter.

The acid dissociation constants of glycine at 0.1 of ionic strength and at 25°C were taken from a preceding work[3] to be $pK_1=2.43$ and $pK_2=9.62$, but those of α-alanine have never been known. They were determined by titrating the aqueous solution at an ionic strength of 0.1 and at 25°C with hydrochloric acid or sodium hydroxide and by applying the following equation[3]:

$$pK_1=pH-\log\left(\frac{C}{A-[H^+]}-1\right)$$

or

$$pK_2=pH-\log\left(\frac{C}{B-[OH^-]}-1\right)$$

where $C$ is the total concentration of amino acid, and $A$ and $B$ are the concentrations of hydrochloric acid and sodium hydroxide solution as calculated from their titres. The values of $[H^+]$ and $[OH^-]$ were calculated by applying the activity coefficient of hydrogen ion at an ionic strength of 0.1 to the activity of the hydrogen ion obtained by pH measurement. The results of titration with hydrochloric acid are listed in Table I, those with sodium hydroxide being, however, omitted. The acid dissociation constants of α-alanine have been found to be $pK_1=2.53$ and $pK_2=9.59$ respectively.

3) F. Basolo and Y. T. Chen, *J. Am. Chem. Soc.*, **76**, 953 (1954).

Table I. Determination of acid dissociation constants, $pK_1$

Concentration of HCl: 0.10403 N
Initial concentration of α-alanine: 0.01 mol./l.
$\mu=0.1$, 25°C

| Titre of HCl, ml. | pH | $[H^+]\times10^4$ | $A\times10^4$ | $pK_1$ |
|---|---|---|---|---|
| 0.1 | 4.37 | 0.5139 | 2.076 | 2.49 |
| 0.2 | 4.04 | 1.099 | 4.351 | 2.49 |
| 0.3 | 3.88 | 1.588 | 6.205 | 2.49 |
| 0.4 | 3.76 | 2.094 | 8.256 | 2.50 |
| 0.5 | 3.66 | 2.636 | 10.30 | 2.50 |
| 0.6 | 3.58 | 3.169 | 12.34 | 2.51 |
| 0.7 | 3.51 | 3.724 | 14.36 | 2.51 |
| 0.8 | 3.45 | 4.275 | 16.38 | 2.51 |
| 0.9 | 3.39 | 4.908 | 18.39 | 2.51 |
| 1.0 | 3.35 | 5.381 | 20.40 | 2.53 |
| 1.1 | 3.31 | 5.900 | 22.39 | 2.54 |
| 1.2 | 3.27 | 6.470 | 24.38 | 2.54 |
| 1.3 | 3.23 | 7.095 | 26.36 | 2.54 |
| 1.4 | 3.19 | 7.779 | 28.34 | 2.54 |
| 1.5 | 3.16 | 8.335 | 30.30 | 2.54 |
| 1.6 | 3.13 | 8.930 | 32.26 | 2.55 |
| 1.7 | 3.10 | 9.570 | 34.21 | 2.55 |
| 1.8 | 3.07 | 10.26 | 36.15 | 2.55 |
| 1.9 | 3.05 | 10.74 | 38.08 | 2.57 |
| 2.0 | 3.02 | 11.51 | 40.01 | 2.56 |
| | | | mean | 2.53 |

**The Determination of the Formation Constants of Glycinato and α-Alaninato Chromium(III) Complexes.**—When the total concentrations of chromium, of amino acid as a ligand and of the total ionizable hydrogen, including $HClO_4$, are expressed by $C_M$, $C_A$ and $C_H$ respectively, the following relationships exist:

$$C_A = [A^-] + [HA] + [H_2A^+] + \bar{n}C_M \quad (3)$$

$$C_H = [H^+] + [HA] + 2[H_2A^+] \quad (4)$$

where $\bar{n}$ is the average number of ligands attached to each chromium ion.

The value of $\bar{n}$ is calculated by the following equation, on the basis of Eqs. 3 and 4:

$$\bar{n}=\left\{C_A-\frac{C_H-[H^+]}{\bar{n}_H}\right\}/C_M \quad (5)$$

where $\bar{n}_H$ denotes the number of hydrogen atoms attached to amino acid against the number of the amino acid which does not coordinate to chromium. $\bar{n}_H$ is expressed by using the values of the acid dissociation constants, 1 and 2, such as:

$$\bar{n}_H=\{K_1+2[H^+]\}/\{K_1K_2/[H^+]+K_1+[H^+]\} \quad (6)$$

On the other hand, if the concentrations of

the free perchloric acid contained in the hexaaquochromium(III) perchlorate used as the starting material and of the sodium hydroxide added to the solution are expressed by $C_a$ and $C_{OH}$ respectively, the concentration of the total ionizable hydrogen is given as;

$$C_H = C_a - C_{OH} + C_A \quad (7)$$

By introducing the measured values of the acid dissociation constants and $[H^+]$ values into Eqs. 5, 6 and 7, the values of $\bar{n}$ and $p[A^-]$ were calculated; Table II lists them only for the glycinato chromium(III) complex, those for the α-alaninato complex being omitted. The plots of $\bar{n}$ vs. $p[A^-]$ with relation to glycinato and α-alaninato chromium(III) complexes are shown in Fig. 1. The approximate values of the formation constants of glycinato and α-alaninato chromium(III) complexes were found from the values of the abscissa at $\bar{n}=0.5$ and 1.5 in the formation curves in Fig. 1. The slope of the formation curves was not so steep that the correct values of the formation constants were obtained as $\log K_1 = 8.62$ and $\log K_2 = 7.65$ for the glycinato chromium(III) complexes and as $\log K_1 = 8.53$ and $\log K_2 = 7.44$ for the α-alaninato chromium(III) complexes by applying the method of successive approximation to the approximate values obtained above.

TABLE II. THE VALUES OF $\bar{n}$ AND $p[A^-]$ CALCULATED FOR GLYCINATO CHROMIUM(III) COMPLEX AT $\mu=0.1$ AND 25°C

| $C_M \times 10^3$ | $C_A \times 10^2$ | pH | $\bar{n}$ | $p[A^-]$ |
|---|---|---|---|---|
| 2.469 | 0.25 | 3.89 | 2.065 | 6.440 |
| 2.469 | 0.20 | 3.80 | 1.995 | 6.632 |
| 2.469 | 0.15 | 3.68 | 1.854 | 6.887 |
| 1.975 | 0.10 | 3.72 | 1.810 | 7.020 |
| 2.469 | 0.10 | 3.51 | 1.715 | 7.251 |
| 1.967 | 7.50 | 3.50 | 1.626 | 7.387 |
| 1.317 | 0.05 | 3.63 | 1.607 | 7.420 |
| 1.967 | 6.25 | 3.43 | 1.511 | 7.545 |
| 1.967 | 5.00 | 3.38 | 1.380 | 7.685 |
| 1.975 | 0.05 | 3.45 | 1.360 | 7.630 |
| 1.967 | 4.50 | 3.32 | 1.230 | 7.814 |
| 1.967 | 4.00 | 3.29 | 1.134 | 7.901 |
| 1.967 | 3.50 | 3.25 | 0.969 | 8.004 |
| 1.967 | 3.04 | 3.20 | 0.860 | 8.125 |
| 0.983 | 1.20 | 3.21 | 0.651 | 8.510 |
| 3.950 | 0.025 | 3.00 | 0.527 | 8.780 |
| 0.983 | 0.80 | 3.11 | 0.513 | 8.810 |
| 0.983 | 0.60 | 3.06 | 0.359 | 9.010 |
| 0.983 | 0.40 | 2.98 | 0.278 | 9.260 |
| 0.983 | 0.20 | 2.90 | 0.125 | 9.720 |

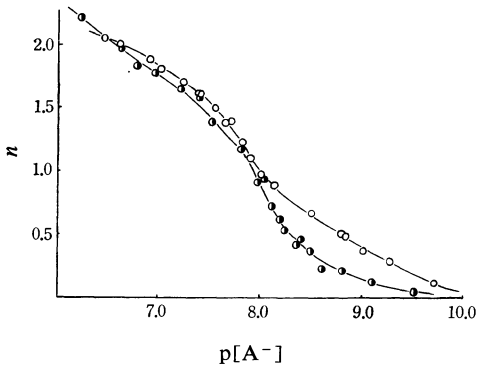



Fig. 1. The formation curve, $\bar{n}$-$p[A^-]$.
○ Chromium(III) glycinato complexes
◑ Chromium(III) α-alaninato complexes

## Discussion

The values of the formation constants of chromium(III) glycinato and α-alaninato complexes obtained in the present study are summarized in Table III, together with those of chromium(III) ethylenediamine and oxalato complexes reported by the present authors in preceding papers.[1,2]

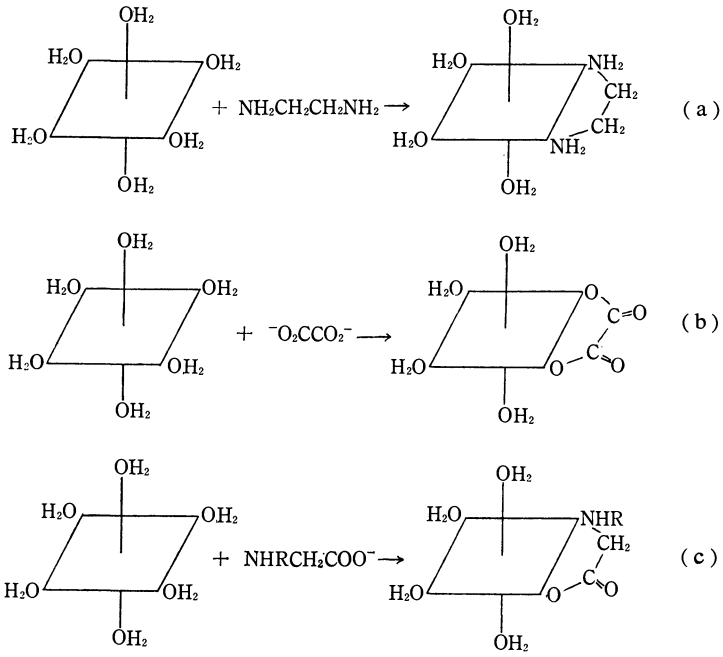
This table indicates, first, that the formation constants of glycinato and α-alaninato complexs are nearly all the same. This may be due to the fact that these two amino acids form the same five-membered chelate ring with chromium ions except that α-alanine has a methyl group, whereas glycine has none. It may also be suggested that the presence of a methyl group in the side chain of α-amino acids has little influence upon the ability to form chromium(III) complexes.

Table III also shows that the values of the formation constants of glycinato and α-alaninato complexes are between those of ethylenediamine and oxalato complexes. This is to be expected from the fact that glycine and α-alanine are N, O-type ligands, whereas ethylenediamine is an N, N-type ligand and the oxalate ion is an O, O-type ligand.

TABLE III. THE FORMATION CONSTANTS OF ETHYLENEDIAMINE-, GLYCINATO-, α-ALANINATO-, AND OXALATO-CHROMIUM(III) COMPLEXES IN AQUEOUS SOLUTION OF IONIC STRENGTH 0.1 AT 25°C

| | $\log k_1$ | $\log k_2$ |
|---|---|---|
| Ethylenediamine complex | 16.5 | <14 |
| Glycinato complex | 8.62 | 7.65 |
| α-Alaninato complex | 8.53 | 7.44 |
| Oxalato complex | 5.34 | 5.17 |

When the values in Table III are compared with each other in more detail, it is found that the values of the formation constants of glycinato and α-alaninato complexes are closer to those of oxalato complexes rather than to those of ethylenediamine complexes. Although




it is impossible to account this fact completely satisfactorily, it may be roughly understood in terms of speculation concerning the entropy effect.

Let us take into account the processes by which mono-ethylenediamine, mono-oxalato and mono-$\alpha$-amino acid complexes are formed from the hexaaquo complex by the following processes, a, b and c:

The free energies of formation in the processes, a, b and c, are expressed by the enthalpy and entropy terms as follows:

$$\Delta G_{en} = \Delta H_{en} - T\Delta S_{en} \quad (8)$$

$$\Delta G_{ox} = \Delta H_{ox} - T\Delta S_{ox} \quad (9)$$

$$\Delta G_{a} = \Delta H_{a} - T\Delta S_{a} \quad (10)$$

where the suffixes en, ox and a designate the processes a, b and c. If it is crudely assumed that the bond energy of chromium with $\alpha$-amino acid as the N, O-type ligand is approximately equal to the mean value of the bond energy of chromium with ethylenediamine as an N, N-type ligand and that of the chromium with the oxalate ion as an O, O-type ligand, then the following equation may be roughly presented:

$$\Delta H_{a} \fallingdotseq 1/2\ (\Delta H_{en} + \Delta H_{ox}) \quad (11)$$

By substracting Eq. 10 from half of the sum of Eqs. 8 and 9 and by taking Eq. 11 into account, the following equation is obtained:

$$\Delta G_{a} - 1/2(G_{en} + \Delta G_{ox}) = T\left(\frac{\Delta S_{en} + \Delta S_{ox}}{2} - \Delta S_{a}\right) \quad (12)$$

As the rough values of the free energies of the formation of ethylenediamine, oxalato and glycinato complexes in the processes a, b and c, $\Delta G_{en} = -27$ kcal., $\Delta G_{ox} = -9$ kcal. and $\Delta G_{a} = -14$ kcal. are, respectively, obtained from the formation constants in Table III. When we insert those values into Eq. 12, we can obtain the difference between the mean values of the entropy changes of the formation of ethylenediamine in the process a and of oxalato complexes in b and the value of the entropy change of the formation of the glycinato complex in c. If the entropy changes of the formation of ethylenediamine and oxalato complexes are assumed to be approximately equal because of the resemblance between their changes in atomic configuration, the rough relation below is obtained:

$$(-\Delta S_{a}) - (-\Delta S_{en} \text{ or } -S_{ox}) = 14 \text{ e. u.}$$

This shows that the entropy decrease in the formation of the glycinato complex is larger by about 14 entropy units than the entropy decrease in the formation of the ethylenediamine or oxalato complex; this can be roughly understood by considering that mono-ethylenediamine and mono-oxalato complexes have roughly a symmetry such as $C_{2v}$, whereas the mono-$\alpha$-amino acid complexes have a lower symmetry such as $C_s$.

## Summary

The formation constants of chromium(III) glycinato and $\alpha$-alaninato complexes have been

determined by the pH method. The values connected with these two complexes are so close to each other that no effect of the presence of a methyl group could be found.

The values of the first formation constants of these complexes are smaller than the mean value of those of ethylenediamine and oxalato complexes. These facts have been explained in terms of the finding that the decrease in the entropies of the formation of $\alpha$-amino acid complexes is larger than that of ethylenediamine or oxalato complexes because the symmetry of the amino acid complexes is lower than that of the ethylenediamine or oxalato complexes.

The authors wish to thank the Ministry of Education for the financial support granted for this research.

*Department of Chemistry*
*Faculty of Science*
*Kanazawa University*
*Kanazawa*

# A Theoretical Treatment of the Kinetics of the Oxidation of Metals

By Hiroshi YOSHISAKI and Toyojiro ISANO

(Received July 14, 1964)

It is generally believed that the progression of the isothermal oxidation of metals is governed by the so-called parabolic law which can be represented by the following equation:

$$y^2 = Gt \qquad (1)$$

where $y$ represents the total quantity of oxide produced during the time lapse, $t$, both measured from the initiation of the progression, and where $G$ is a constant.[1,3]

Actually, the above law holds with moderate accuracy as long as the observations are restricted within sufficiently short periods and are made after sufficiently long lapses of time from the initiations. However, when the above conditions are not satisfied we can never use Eq. 1 with success, especially for early periods. According to the parabolic law, the initial rate of oxidation should be infinite, whereas no facts have ever been found to suggest the existence of an infinite rate; moreover, such a rate is, indeed, erroneous in principle also. In fact, we can see as much when we look at the example of our recent observations, still unpublished, shown in Fig. 1. It can clearly be seen from this figure that the process begins with a finite rate, not an infinite one.

Under these circumstances, we have undertaken this investigation with the purpose of looking into the discrepancies of the parabolic law and of deduction of a more reasonable law, one which can agree with the actual functions controlling the process of the oxidation of metals.

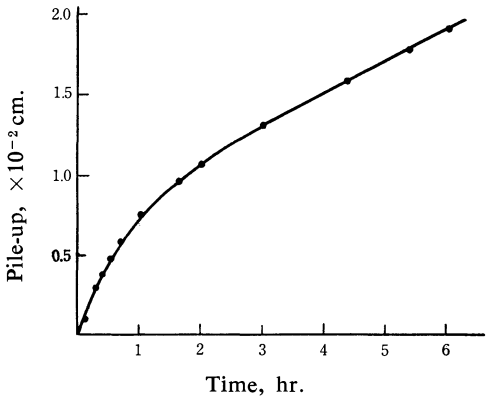



Fig. 1. Oxidation isotherm of copper in the air at 825°C.

## The Mechanism of the Progression

When a metal regulus is held at a high temperature under an oxidizing atmosphere, it becomes covered by an oxide film, which gradually grows thicker and thicker as time elapses. If the coverage is assumed to be perfect, then the oxidation must continue its progression by means of one of two processes; in one, oxygen molecules from the atmosphere pass by diffusion through the oxide layer towards the oxide-metal boundary surface, where they combine with the metal atoms upon arrival; in the other, metal atoms from the regulus diffuse through the layer towards the surface exposed to the atmosphere, where they combine with oxygen upon arrival. Several papers recently published suggest that in reality the latter is

1) P. V. Geld and A. K. Krasovskaya, *Zhur. Fiz. Khim.*, **34**, 1585 (1960).

the case, for in major cases the oxide scale produced shows evidence that the growth of the scale is due to the accumulation of oxide on the exposed surface.[2,3] This opinion, therefore, seems reasonable.

As to the time rate of the oxidation of metals, it is clear that it is determined by the slowest of the consecutive processes of which the whole change consists. According to our point of view, as the rate of the combination of metal with oxygen should greatly surpass that of its diffusion through the oxide layer, the rate of oxidation should be determined by the diffusion of metal.

However, there is a difficulty. If the oxidation progresses in the above-mentioned manner then the metal surface should of itself retire from the initial place into the interior of the regulus due to the surrendering of the metal material to the oxide layer, while, on the other hand, the inside surface of the oxide layer should stay unmoved, so that a vacant space or interstice grows up between them; nevertheless, in reality this is not the case. Probably this problem may be answered in terms of the heterogeneity in the structure of the scale, so as Mrowec states.[2,3]

## The Deduction of an Equation Isotherm

It is well known that the parabolic law comes from the assumption that the concentration of diffusing matter is distributed at a uniform gradient all through the medium, so that;

$$\nabla c = \text{constant}$$

where $c$ represents the concentration at any point. However, this condition can never be satisfied in reality since the medium can not be perfectly homogeneous nor can the surface of the regulus be ideally even, regardless of how it is made. Thus the diffusion must unavoidably be a turbulent one. For this reason we should refer to the general condition to begin with:

$$\nabla^2 c = k^2 c \qquad (2)$$

where $k$ represents a constant. If we now restrict ourselves to one dimention, the general solution of Eq. 2 is obtained as follows:

$$c = (K/k)\sinh(-kx+\kappa) \qquad (3)$$

where $x$ is the coordinate of the point at which the concentration, $c$, is measured, and $K$ and $\kappa$ are two constants. If we assume for the boundary condition that the concentration of the reactant metal on the surface of the scale in contact with the oxidizing atmosphere is zero, then Eq. 3 becoms:

$$c = (K/k)\sinh\{k(\xi-x)\} \qquad (4)$$

where $\xi$ represents the coordinate of a point on the exposed surface.

Now we will take up a small portion, $\sigma$, of the exposed surface, localized at will, so small that it can be taken as a part of a spherical surface with the center of curvature at O. Moreover, we will set up an x axis with O as the origin, and crossing $\sigma$ at a point, P, in its interior, as is shown in Fig. 2. The coordinate

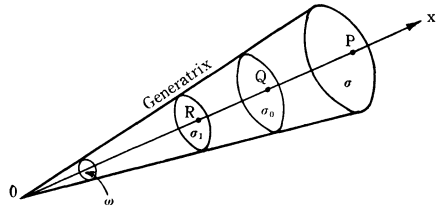



Fig. 2. Scheme of the space under consideration.

at P is $\xi$, of course. The solid segment based on $\sigma$ and with O as its vertex, cuts the surface elements, $\sigma_0$ and $\sigma_1$, from the initial metal surface and the oxide-metal boundary surface respectively, both of which can be taken as spherical and concentric with $\sigma$. The intersections of these surfaces with the x axis are Q and R, the coordinates at which being $x_0$ and $x_1$ respectively.

Now, if we assume, at time $t$, that the amount of metal which was initially contained in the disk-like space enclosed by $\sigma_0$, $\sigma_1$ and the generatrices has turned as a whole into the oxide scale contained in the disk-like space enclosed by $\sigma$, $\sigma_1$ and the generatrices, then the following equation should hold:

$$\frac{\omega}{4\pi}\cdot\frac{4}{3}\pi(x_0^3-x_1^3)c_r = \frac{\omega}{4\pi}\cdot\frac{4}{3}\pi(\xi^3-x_1^3)c_p \qquad (5)$$

where $c_r$ and $c_p$ represent the total concentrations of metal in the reactant regulus and in the resultant scale respectively, and $\omega$, the solid angle enclosed by the generatrices. Differentiating Eq. 5 with respect to $\xi$, we obtain:

$$\frac{dx_1}{d\xi} = -\frac{\xi^2}{x_1^2}\cdot\frac{c_p}{c_r-c_p} \qquad (6)$$

Assuming that the rate of the loss of metal in the regulus is equal to the rate of its transfer across any fixed surface section enclosed by the generatrices, we can write:

$$\omega x^2 cu = -c_0\omega x_1^2\frac{dx_1}{dt} \qquad (7)$$

2) S. Mrowec, *Zeit. f. pfys. Chem. Neue Folge*, **29**, 48 (1961).
3) L. Czerski, S. Mrowec and T. Werber, *J. Electrochem. Soc.*, **109**, 273 (1962).

where $u$ represents the average value of the $x$-components of the atomic velocities on the surface apart from O as far as x, and $c_0$ represents the concentration on the boundary surface, which can be taken as a constant. Combining this relation with the fundamental equation:

$$cu = -D\frac{dc}{dx}$$

we obtain the following equation:

$$Dx^2\frac{dc}{dx} = c_0 x_1^2\frac{dx_1}{dt} \tag{8}$$

where $D$ represents the diffusion constant of the metal in the scale. Substituting $dc/dx$ in the left hand side according to Eq. 4, we obtain:

$$\int_{x_0}^{\xi}\frac{\xi^2 d\xi}{\cosh\{k(\xi-x)\}} = \frac{KD}{c_0}\left(\frac{c_r}{c_p}-1\right)\int_0^t x^2 dt + L \tag{9}$$

where $L$ is the integration constant which must vanish for the initial condition, $\xi=x_0$, for $t=0$.

If we define $X$ as $X=\xi-x_0$, where the initial surface, $\sigma_0$, on which $x$ takes a value $x_0$, is prefered as a fixed reference surface, then $X$ represents in practice the pile-up of the exposed surface of the resultant oxide scale due to the progress, and is a measurable quantity. Then Eq. 9 becomes:

$$\int_0^X\frac{(X+x_0)^2}{\cosh(kX)}dX = Ax_0^2 t \tag{10}$$

where

$$A = \frac{KD}{c_0}\left(\frac{c_r}{c_p}-1\right)$$

As Eq. 10 has been derived for a convex portion of the metal surface, it can also be obtained for a concave portion with the identical terms. Thus this equation can be taken as a general equation isotherm at a point, either convex or concave, $x_o$ being the radius of the curvature. We can reasonably assume that, if the observation is done on a well-finished sound regulus, Eq. 10 may be satisfied in a macroscopic extent by substituting a function, $\bar{x}_0$, for $x_0$, $\bar{x}_0$ being characteristic of the evenness of the surface in a macroscopic scale. Moreover, if we define $\gamma$ as the reciprocal of $\bar{x}_0$, then Eq. 10 becomes:

$$\int_0^X\frac{\left(X+\frac{1}{\gamma}\right)^2}{\cosh(kX)}dX = \frac{1}{\gamma^2}At \tag{11}$$

where $\gamma$ represents a parameter indicating the coarseness of the surface. This is the general equation isotherm for the oxidation of metals holding in measurable scales.

For a small value of $X$, that is, unless too long a time has elapsed since the initiation, we can expand the integrand in Eq. 11 into a power series of $X$ and integrate it, writing it as follows:

$$X + \gamma X^2 + \frac{1}{3}\left(\gamma^2-\frac{k^2}{2}\right)X^3 - \frac{1}{4}\gamma k^2 X^4 - \frac{1}{2}k^2\left(\frac{1}{5}\gamma^2-\frac{1}{12}k^2\right)X^5 + \frac{5}{72}\gamma k^4 X^6 + \cdots = At \tag{12}$$

where $A$ represents a constant proportional to the diffusion constant of the metal in the oxide layer.

## Discussion

As has been established in the preceding section, the progression of isothermal oxidation is governed by a somewhat more complicated law than the parabolic law. That Eq. 12 begins with a linear term shows that, for a short initial period, the oxidation process begins with a finite velocity instead of an infinite one; a theory supported by the experimental facts.

Now, we find that the left hand side of Eq. 12 consists of three groups of terms: first, those independent of $\gamma$; second, those each containing a factor $\gamma$; and third, those each containing a factor $\gamma^2$. Thus we can rewrite Eq. 12 as follows:

$$\left[X - \frac{1}{6}k^2X^3 + \frac{1}{24}k^4X^5 - \cdots\right] + \gamma\left[X^2 - \frac{1}{4}k^2X^4 + \frac{5}{72}k^4X^6 - \cdots\right] + \gamma^2\left[\frac{1}{3}X^3 - \frac{1}{10}k^2X^5 + \cdots\right] = At \tag{13}$$

As $\gamma$ can vary from zero to infinity, it may be seen that the progression of oxidation may have considerably different aspects, even for the same reactant species, because of the fluctuation of the coarseness of the surface. If the surface is ideally flat, the progression of the oxidation will be governed by the following equation:

$$X - \frac{1}{6}k^2X^3 + \frac{1}{24}k^4X^5 - \cdots = At$$

since the second and third terms on the left hand side of Eq. 13 vanish for $\gamma\to 0$. On the other hand, for very coarse surfaces, for instance, with finely pulverized metals, it will be governed by:

$$\frac{1}{3}X^3 - \frac{1}{10}k^2X^5 + \cdots = \frac{1}{\gamma^2}At$$

the third term in Eq. 13 assuming prominent values because of the large value of factor $\gamma^2$, except in the early stages. In major cases, however, all terms in Eq. 13 will contribute equally. Thus we may suggest the following equation as a rough approximation for sufficiently small values of $X$:

$$X + \gamma X^2 + \frac{1}{3}\left(\gamma^2 - \frac{k^2}{2}\right)X^3 = At \qquad (14)$$

## Summary

We have attributed the deficiency of the parabolic law to its original assumption of a uniform gradient of the concentration of the reactant, and, beginning with a general assumption of a turbulent gradient, we have deduced an alternative equation, one somewhat more complicated than the parabolic one. In discussing the behavior of the new equation, it was found that the mode of progression largely changes its profile as a result of the fluctuation of the coarseness of the surface to be oxidized.

We are indebted to Messrs. Yutaka Sakuma and Tsutomu Itô for their honest assistance.

*Department of Chemistry*
*Faculty of Liberal Arts and Science*
*Yamagata University*
*Koshirakawa-cho, Yamagata*

## Appendix

**Deduction of Equation 2.**—This equation was deduced as follows: Take arbitrarily, in the field of the turbulent stationary diffusion, a space element shaped like a rectangular cylinder; the axis thereof may be taken as a coordinate axis, $x$, as is shown in Fig. 3. We will designate the area of both base planes and the height of the cylinder as $\sigma$ and $\delta x$ respectively. When the coordinate of one base plane, $S_1$, on which the concentration of the diffusing substance may be designated as $c$, is taken as $x$, then the coordinate and the concentration at the other base plane, $S_2$, should be $x+\delta x$ and $c+(\partial c/\partial x)\delta x$ respectively. As is well known, the rate of the passage of a diffusing substance through a plane perpendicular to the x axis is proportional to

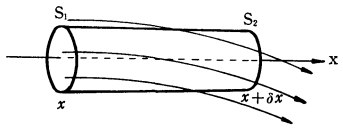



Fig. 3

$-\partial c/\partial x$. Thus, the rate of flow in the left-to-right direction through $S_1$ and $S_2$ in Fig. 3 should amount to $-D_1\sigma(\partial c/\partial x)$ and $-D_1\sigma[\partial c/\partial x+(\partial^2 c/\partial x^2)\delta x]$ respectively, where $D_1$ is a constant. On the other hand, the rate of the flow out through the generating surface of the cylinder can be taken as proportinal to the mean concentration in the cylinder, multiplied by a constant, $s$ for instance, chracteristic of the structure of the medium, which can be represented as $sl\delta x\cdot c$, where $l$ represents the length of the border-line of a rectangular cross-section of the cylinder. Consequently, the rate of the total flow out of the cylinder should be $D_1\sigma(\partial c/\partial x)-D_1\sigma[\partial c/\partial x+(\partial^2 c/\partial x^2)\delta x]+sl\delta x\cdot c$. For a stationary or quasi-stationary diffusion, the above quantity must vanish, so that

$$D_1\sigma\frac{\partial^2 c}{\partial x^2} = slc$$

namely:

$$\frac{\partial^2 c}{\partial x^2} = k^2{}_1 c$$

where

$$k^2{}_1 = \frac{sl}{\sigma D_1}$$

In three-dimentional treatments:

$$\nabla^2 c = k^2 c$$

where $k$ is a constant.

**Comparison with the Hatta Theory.**—The above equation takes the same form as that of the well-known Hatta theory, which treats diffusion phenomena accompanied with the consumption of diffusing substances due, for instance, to a chemical reaction of the first order, to absorption or to capillary phenomena. This coincidence seems to us very interesting, for these results, obtained by a different method of computation, may not yet be taken as utterly different in physical meaning. This theory is all the more convincing because we notice that the irregular turn-asides of stationary flow lines can reasonably be replaced with a definite distribution of wells and sinks in dynamical treatments of a turbulent flow of a fluid. For this reason, the present case can be taken as closely analogous to Hatta's case, and so it is not strange that the same hydrodynamic equation is applicable in both cases.

# The Oligomerization of Butadiene with an Iron Complex Catalyst

By Masanobu HIDAI, Yasuzo UCHIDA and Akira MISONO

(Received August 11, 1964)

Several complex catalyst systems for the selective dimerization and trimerization of butadiene have been reported,[1] most of them are composed of first-row transition metal complexes and organometallic compounds. Attempts have also been made to elucidate the relationship between the sorts of transition metals and electron-donating additives as catalyst components, on the one hand, and the structure of the oligomers formed therewith on the other.

In a previous paper[2] the authors reported that butadiene dimerizes selectively to 3-methylhepta-1, 4, 6-triene with the catalyst prepared by the reaction of cobalt(III) acetylacetonate and triethylaluminum in the presence of butadiene. It has now been found that *n*-dodeca-1, 3, 6, 10-tetraene is formed selectively with the catalyst prepared by the reaction of iron(III) acetylacetonate instead of the cobalt complex.

This paper will be concerned, in particular, with the structural determination of the trimers and of the factors affecting the reaction. Measurements of the visible light absorption spectra and of the magnetic susceptibility of the reaction solution for the elucidation of the transition complex of the oligomerization will also be described.

## Experimental

**Reagents.**—Benzene was purified by washing it with concentrated sulfuric acid and then distilling it over metallic sodium under nitrogen.

Triethylaluminum (Ethyl Corporation, U. S. A.) was used without further purification.

Butadiene (Nihon Petrochemical Company) was dried by passing it through columns of calcium chloride and silica gel.

Iron(III) acetylacetonate was prepared according to the method described by Steinbach et al.[3]

**Procedure.**—A 30 ml. Schlenk tube or a 200 ml. glass autoclave was used as a reactor. Calculated amounts of iron(III) acetylacetonate, benzene, butadiene and triethylaluminum were introduced in that order into the reactor, which had previously been swept with nitrogen. During the procedure, the reactor was cooled below −10°C to prevent the evaporation of butadiene. Then the reactor was sealed or stoppered and kept at 50°C during the reaction. Products were analyzed by gas chromatography immediately or after hydrogenation with palladium black.

**Analysis.**—*Gas Chromatography.*—For the analysis of the dimers, a copper tube (4 mm. in diameter and 2.5 m. long) packed with tricresylphosphate on Simalite (Shimadzu Seisakusho Ltd.) was used. The temperatures of the thermostat and the inlet were 90°C and 140°C respectively; the helium gas speed was 30 ml./min. For the trimers, a copper tube (4 mm. in diameter and 7 m. long) packed with polydiethylene glycol-succinate on Diasolid (Shimadzu Seisakusho Ltd.) was used. The temperatures of the thermostat and the inlet were 130°C and 220°C respectively, and the helium gas speed was 22 ml./min. For the determination of the molecular distribution of the products, hydrogenated products were used. Hydrogenation was carried out with 5% of palladium black under atmospheric pressure at room temperature. $C_{16}$- and $C_{20}$-products were determined by gas chromatography with a copper tube (4 mm. in diameter and 7 m. long) packed with polydiethylene glycol-succinate on Diasolid. The conditions were as follows; temperature of thermostat, 190°C: that of inlet, 270°C, and helium gas speed, 22 ml./min.

*Distillation.*—For the determination of the molecular weight distribution of the reaction products, hydrogenated products were fractionated by vacuum distillation and molecular distillation ($10^{-3}$ mmHg) into 7 parts. The average molecular weight of each fraction was determined by vapor pressure osmometry.

*Infrared Spectra.*—The spectra of the samples were taken with a Nihon-bunko double-beam spectrometer model 401 G.

*NMR Spectra.*—The spectra were recorded on a Nihon-Denshi model 3H-60.

*Ultraviolet and Visible Light Spectra.*—The spectra were recorded on a Hitachi model EPS spectrometer, using a 10 mm.-path-length quartz cell for the ultraviolet measurements and a 0.1 mm.-path-length quartz cell for the visible light spectra measurements. Magnetic susceptibilities were measured with a Gouy balance in the field of 10000 gauss at room temperature.

1) Studiengesellschaft Kohl, *Austrian.*, 219580 (1962); G. Wilke, *Angew. Chem.*, **75**, 10 (1963); S. Ohtsuka, T. Taketomi and T. Kikuchi, *J. Chem. Soc. Japan, Ind. Chem. Sec.* (*Kogyo Kagaku Zasshi*), **66**, 1094 (1963); *J. Am. Chem. Soc.*, **85**, 3709 (1963); H. Takahashi, *J. Org. Chem.*, **28**, 1409 (1963); S. Tanaka, K. Mabuchi and N. Shimazaki, ibid., **29**, 1636 (1964).

2) T. Saito, T. Ohno, Y. Uchida and A. Misono, *J. Chem. Soc. Japan, Ind. Chem. Sec.* (*Kogyo Kagaku Zasshi*), **66**, 1099 (1963).

3) J. F. Steinbach and J. H. Burns, *J. Am. Chem. Soc.*, **80**, 1839 (1958).

## Results and Discussion

**The Identification Oligomers.** — Liquid polymer, trimers and dimers were obtained by the reaction. The conversion of butadiene versus the reaction time is shown in Fig. 1, while the

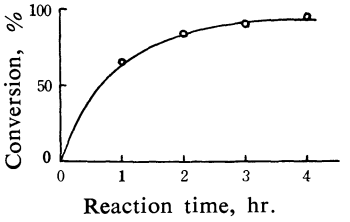



Fig. 1. Conversion of butadiene.

Benzene: 7.4 g. Butadiene: 3.7 g.
$Fe(acac)_3/BD$: $4\times10^{-3}$ $AlEt_3/Fe(acac)_3$: 3
Reaction temp.: 50°C

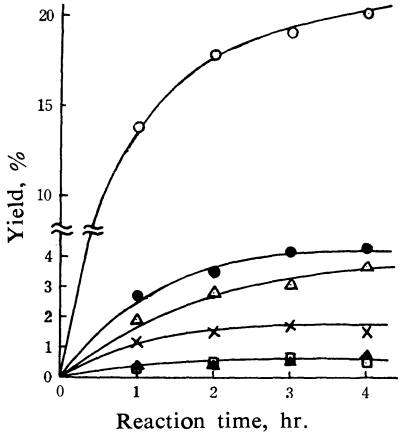



Fig. 2. Relation between reaction time and yields of products.

- ○ *n*-Dodeca-1,3,6,10-tetraene
- ● A trimer
- △ Cycloocta-1,5-diene
- × 3-Methylhepta-1,4,6-triene
- ■ *n*-Octa-1,3,6-triene
- ▲ 4-Vinylcyclohexene

yields of each oligomer is given in Fig. 2. The yield of the dimers was only a small percentage of the products. The dimers were identified as 3-methylhepta-1,4,6-triene, *n*-octa-1,3,6-triene, 4-vinylcyclohexene and cycloocta-1,5-diene by gas chromatography. Trimers consisted of two kinds of isomers. One of the main products was separated and purified with preparative gas chromatography, and then the structure was determined. The results of elemental analysis (C, 87.5%; H, 11.2%) and molecular weight determination (M.W.=162) indicate that this compound is a trimer of butadiene. From the iodine value and the infrared spectra, it was confirmed that the trimer has two isolated double bonds and a pair of conjugated double bonds in its structure. In the infrared spectra (shown in Fig. 4) the absorption of the C=C conjugated stretching vibration (1650, 1600 $cm^{-1}$), the C-H out of plane deformation vibration of the conjugated vinyl group (895, 1000 $cm^{-1}$), that of the trans double bond (970 $cm^{-1}$), that of the conjugated trans double bond (955 $cm^{-1}$), and that of the cis double bond (700 $cm^{-1}$) were observed. In the ultraviolet spectra, the absorption of the conjugated double bond was observed at 228 m$\mu$, the molecular absorption coefficient being $3\times10^4$. In the NMR spectra (shown in Fig. 5) the absorption of the protons of the methylene group between two double bonds, those of the methylene group adjacent to a double bond and those of the methyl group adjacent to a double bond were found at 7.1, 7.8 and 8.3 $\tau$ respectively. The ratio of the peak areas was 2:4:3. Moreover, the hydrogenated product of this trimer was identified as *n*-dodecane by gas chromatography. Judging from these results the structure of the trimer is *n*-dodeca-1,3,6,10-tetraene.

$$CH_2=CH-CH=CH-CH_2-CH=$$
$$CH-CH_2-CH_2-CH=CH-CH_3$$

Another trimer, which was formed in an amount about one-fourth of *n*-dodecatetraene, was a branched-chain isomer, judging from infrared and NMR observations.

**Molecular Weight Distribution of the Product.** —To solve the question of whether these trimers are the lower parts of liquid polybutadiene or those formed by a process different from polymerization, the molecular weight distribution was determined with the hydrogenated products. The hydrogenated products were fractionated into 7 fractions by vacuum distillation (trimers) followed by molecular distillation (5 fractions and the residue). The amounts and the average molecular weight of the fractions are given in Table I. For the fraction with the average polymerization degree of 4.5, the $C_{12}$, $C_{16}$ and $C_{20}$ contents were measured by gas chromatography. From these results and from the amount and average polymerization degree of the fraction, the $C_{24}$ content was calculated. In the same way, for the fraction with the average polymerization degree of 5.5, the $C_{12}$ (which could not be found), $C_{16}$ and $C_{20}$ contents were determined by gas chromatography. Then the $C_{24}$ and $C_{28}$ contents were calculated on the assumption that the fraction with an average polymerization degree between $n$ and $n+1$, obtained by molecular distillation, consists of $C_{4(n-1)}$, $C_{4n}$, $C_{4(n+1)}$ and $C_{4(n+2)}$. From the results concerning both fractions, the mole ratio of components was

TABLE I. $\overline{P}$ OF FRACTIONATED PRODUCT

| Fraction | B. p. °C/mmHg | $\overline{P}$ | Weight, g.* |
|---|---|---|---|
| 1 | | 2 | 0.6 |
| 2 | 90/8 | 3 | 3.3 |
| 3 | 90—100/$10^{-3}$ | 4.5 | 1.1 |
| 4 | 100—120/$10^{-3}$ | 5.5 | 1.4 |
| 5 | 120—130/$10^{-3}$ | 6.5 | 1.2 |
| 6 | 130—160/$10^{-3}$ | 7.5 | 1.6 |
| 7 | 160—210/$10^{-3}$ | 8.5 | 2.4 |
| 8 | Dist. residue | 9.5 | 1.1 |

* The amount of dimers were determined by gas chromatography.

estimated to be nearly $C_{4(n-1)} : C_{4n} : C_{4(n+1)} : C_{4(n+2)} = 1 : 3 : 3 : 1$. On the assumption that the fractions with an average polymerization degree larger than 5.5 consisted of components in the same 1 : 3 : 3 : 1 ratio, the amounts of all the component in the fractions were estimated. By obtaining the sum of the components of each fraction, the molecular weight distribution of products was estimated (Fig. 3). The result shows that the products evidently consist of two parts, one of which is dimers and trimers and the other is liquid polybutadiene, with an average polymerization degree of seven. It was,

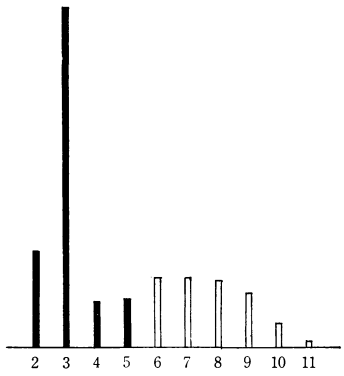



Fig. 3. Molecular weight distribution of products.

▬: The molecular weight distribution of these components was also determined by gas chromatography.

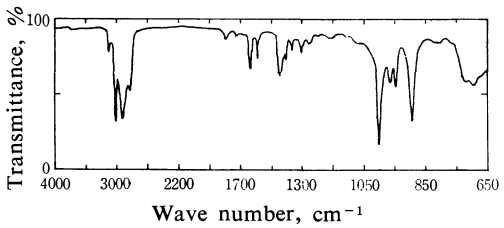



Fig. 4. Infrared spectra of *n*-dodeca-1,3,6,10-tetraene.

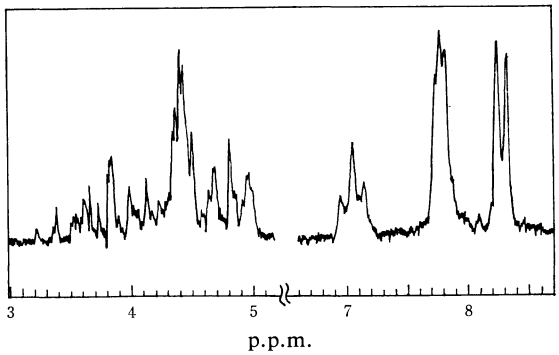



Fig. 5. NMR spectrum of *n*-dodeca-1,3,6,10-tetraene.

therefore, concluded that trimers were formed by a mechanism different from that of polymerization.

**The Effect of the Ratio of $AlEt_3$ to $Fe(acac)_3$.** —Figure 6 shows the relation between the selectivity of linear trimer formation and the mole ratio of catalyst components. When more than 3 times the amount of the iron(III) acetylacetonate of triethylaluminum was used, the selectivity of the formation of trimers was lowered and polymer formation became predominant. However, the *n*-dodecatetraene ratio in linear trimers was not affected. Figure 7 gives the effect of the ratio of catalyst components on the apparent reaction rates of the formation of the linear trimers and liquid polybutadiene. It indicates that the rate of the formation of liquid polybutadiene is nearly proportional to the ratio of triethylaluminum to the iron(III) acetylacetonate used. When

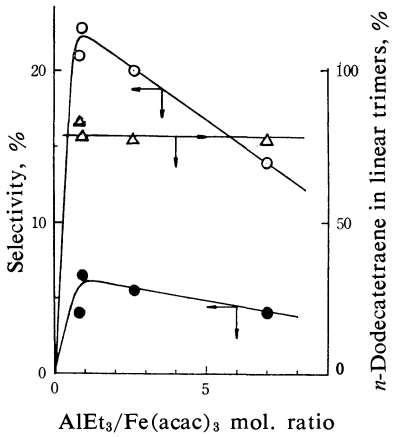



Fig. 6. Relation between selectivity of linear trimers and $AlEt_3/Fe(acac)_3$ mol. ratio.

○ *n*-Dodeca-1,3,6,10-tetraene
● A branched trimer
△ *n*-Dodecatetraene in linear trimers
Benzene: 7.3 g. Butadiene: 2.1 g.
$Fe(acac)_3/BD$: $5 \times 10^{-3}$ Reaction temp.: 50°C

TABLE II. MIXING ORDER OF CATALYST COMPONENTS

| Mixing order | Conversion of BD, % | Composition of product, % | | |
|---|---|---|---|---|
| | | Dimer | Linear trimer | Poly-BD |
| Fe+Bz+BD+Al | 82 | 6 | 31 | 62 |
| Fe+Bz+Al+BD | 40 | 5 | 27 | 68 |

$Fe(acac)_3$: 0.100 g. Benzene: 8.1 g. Butadiene: 3.8 g.
Al/Fe mol. ratio: 3 Reaction temp.: 46°C Reaction time: 3 hr.

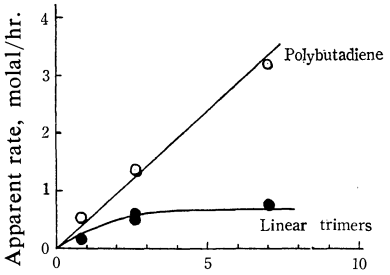



Fig. 7. Effect of $AlEt_3/Fe(acac)_3$ mol. ratio on apparent rate.

only triethylaluminum was applied as a catalyst, butadiene did not react. This phenomenon suggests that both iron and aluminum compounds take part in the formation of the active transition state of the catalyst for polymerization, while only the iron reduced, perhaps to the zero-valent state, by a definite amount of triethylaluminum is involved in the trimerization of butadiene.

**The Effect of Catalyst Concentration.**—The effect of the catalyst concentration on the apparent reaction rate is shown in Fig. 8. The apparent rates of the formation of both trimers and liquid polybutadiene were nearly proportional to the catalyst concentration.

**The Effect of the Mixing Order of the Catalyst Components.**—As has been mentioned in previous papers,[2,4] in the linear dimerization of butadiene with a catalyst composed of cobalt(III) acetylacetonate and triethylaluminum, the order of mixing the catalyst components and butadiene has a great effect on the rate of the formation of the dimer. The same phenomenon was expected in the present reaction. The effect of the order of mixing the catalyst components and butadiene is given in Table II. The apparent rate of the oligomerization of butadiene was greater when iron(III) acetylacetonate, butadiene and triethylaluminum were mixed in that order than when triethylaluminum was allowed to react with iron(III) acetylacetonate in the absence of butadiene. These results suggest that the coordination of butadiene to reduced iron prevents the coagulation of reduced iron and plays an important role in the formation of the oligomers.

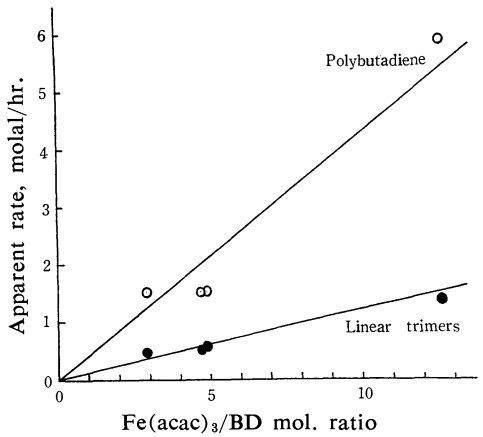



Fig. 8. Effect of concentration of catalyst.

Benzene: 7.3 g. Butadiene: 2.1 g.
$AlEt_3/Fe(acac)_3$: 2.5 Reaction temp.: 50°C

**The Observation of the Reaction Solution.**—When triethylaluminum was added to a benzene solution of iron(III) acetylacetonate ($Fe^{3+}$ was reduced to $Fe^{2+}$ and then to the zero-valent state.), the solution became unstable and immediately gave rise to a black precipitate. The system showed a ferromagnetism probably caused by the coagulated reduced iron. In the presence of butadiene, the solution became reddish brown and showed paramagnetism, while a shoulder absorption was found at about 400—420 m$\mu$ in the visible light absorption spectrum. This absorption has also been observed in $\pi$-[BD $Co(CO)_2]_2$ and $\pi$-BD $Fe(CO)_3$.[5] On the basis of these results and on the assumption that the active complex for polymerization is diamagnetic,[6] *n*-dodecatetraene is considered to be formed through a paramagnetic intermediate complex in which three molecules of butadiene coordinate to a zero-valent iron atom.

## Summary

The oligomerization of butadiene with the catalyst system of iron(III) acetylacetonate and triethylaluminum has been studied. The

4) T. Saito, Y. Uchida and A. Misono, This Bulletin, 37, 105 (1964).
5) S. Ohtsuka, *Kagaku-Zokan*, No. 13, 87, (1964).
6) K. Tamai, M. Hidai, Y. Uchida and A. Misono, This Bulletin, to be published.

products obtained by the use of this catalyst consist of two types, one of which is dimers and trimers, and the other is polybutadiene, with an average polymerization degree of seven. The dimers are 3-methylhepta-1, 4, 6-triene and cycloocta-1, 5-diene. The trimers have been confirmed to be *n*-dodeca-1, 3, 6, 10-tetraene and a branched isomer.

The effects of the ratio of the catalyst components to the concentration of the catalyst have been also studied.

From these results, it has been concluded that oligomerization proceeds by a mechanism different from that of polymerization.

To elucidate a transition state for oligomerization, the visible light spectra and the magnetic susceptibility of the reaction solution have been measured and a complex in which butadiene coordinates to reduced iron atom has been assumed as the transition state.

*Department of Industrial Chemistry*
*Faculty of Engineering*
*The University of Tokyo*
*Hongo, Tokyo*

# A Study of the Acid Dissociation of Furan- and Thiophenedicarboxylic Acids and of the Alkaline Hydrolysis of Their Methyl Esters

By Shigeru OAE, Naomichi FURUKAWA, Takao WATANABE
Yoshio OTSUJI and Masayuki HAMADA

(Received August 15, 1964)

The physical and chemical behavior of furan- and thiophenemonocarboxylic acids and their derivatives has been investigated extensively and shown to be considerably different from that of benzoic acid.[1] Cocker et al. have suggested the formation of an intramolecular hydrogen bond in their study of the acid dissociations of four carboxylic groups and the infrared spectrum of furantetracarboxylic acid.[2] Meanwhile, a few dicarboxylic acids, such as succinic acid[3] and maleic acid,[4] have been known to form intra- or intermolecular hydrogen bondings that create substantial differences between their first and second dissociation constants.

Meanwhile, although there have been many reports on the alkaline hydrolysis of the monocarboxylic esters and the reaction mechanism of the saponification has been well elucidated,[5] only a few investigations of the hydrolyses of dicarboxylic esters have been carried out. This is perhaps due to the extreme difficulty of following the kinetics of the hydrolyses of these diesters, because they do not obey the simple second-order kinetic equation. However, a few noteworthy treatments have been made. Namely, one of the earliest treatments of the competitive consecutive second-order reaction for the alkaline saponification of diesters has been carried out by Ingold.[6] However, this graphic approximation gives by no means an accurate estimation. Meanwhile, other investigators have made many efforts to get accurate kinetic data for those dicarboxylic esters.[7] Frost and Schwemer have presented what appears to be the first legitimate method for the calculation of the consecutive competitive second-order kinetic equation of the alkaline hydrolysis of dicarboxylic esters.[8]

The present work was initiated in order to investigate the nature of the interaction between the two carboxyl groups attached to the furan and thiophene rings and the alkaline hydrolyses of the diesters of these carboxylic

* Preliminary results have been reported previously in *Ann. Rept. of Radiation Center Osaka Pref.*, **2**, 106 (1961).

1) a) C. C. Price and E. A. Dudley, *J. Am. Chem. Soc.*, **78**, 68 (1956); b) S. Oae and C. C. Price, ibid., **79**, 2547 (1957); c) E. Imoto, Y. Otsuji, T. Hirai and H. Inoue, *J. Chem. Soc. Japan, Pure Chem. Sec.* (*Nippon Kagaku Zassi*), **77**, 804, 809 (1959).

2) W. Cocker, W. J. Oavis, T. B. H. McMurry and P. A. Start, *Tetrahedron*, **7**, 299 (1959).

3) L. Eberson, *Acta Chem. Scand.*, **2**, 13 (1959).

4) a) M. Shahat, *Acta Cryst.*, **5**, 763 (1962); b) H. M. E. Cardwell, J. D. Danitz and L. E. Orgel, *J. Chem. Soc.*, **1953**, 3740.

5) a) J. Hine "Physical Organic Chemistry," McGraw-Hill Book Company, New York (1962), pp. 275—301; b) C. K. Ingold, "Organic Chemistry," Cornell University Press, Ithaca, New York (1953); c) M. L. Bender, *Chem. Revs.*, **60**, 53 (1960).

6) C. K. Ingold, *J. Chem. Soc.*, **1931**, 2170.

7) a) M. Ritchie, ibid., **1931**, 3112; b) F. H. Westheimer, W. A. Jones and R. A. Lad, *J. Chem. Phys.*, **10**, 478 (1942); c) D. French, *J. Am. Chem. Soc.*, **72**, 4806 (1950); **73**, 4541 (1951).

8) A. A. Frost and W. C. Schwemer, ibid., **74**, 1268 (1952).

acids in comparison with the dissociations of phthalic acids and maleic acid and the saponification of their esters.

## Experimental

**Materials.** — *2, 3-Furandicarboxylic Acid.*[9] — 4,4-Diethoxybutyronitrile, obtained from acrolein, was condensed with diethyl oxalate, giving 2-ethoxalyl-4,4-diethoxybutyronitrile. Ethyl 3-carbamyl-2-furancarboxylate, prepared by the cyclization of the above nitrile, was hydrolyzed to 2,3-furandicarboxylic acid. Colorless crystals of the acid melted at 221—222°C, and the yield was 20% on the basis of the 2-ethoxalyl-4,4-diethoxybutyronitrile used.

*The 2-Monomethyl Ester of 2,3-Furandicarboxylic Acid.*—The above acid was converted to its monosilver salt by adding 1.2 mol. of silver nitrate to one mole of the monosodium salt in water. To a solution of one mole of the dried monosilver salt obtained above in benzene, one mole of methyl iodide was added, and then the mixture was refluxed for two hours and filtered to remove the silver iodide. The benzene solution was evaporated to dryness, and recrystallization from water gave the monoester in a 70% yield. M. p. 118°C.

Found: C, 49.28; H, 3.97. Calcd. for $C_7H_6O_7$: C, 49.44; H, 3.56%.

Since in 2,3-furandicarboxylic acid the 2-carboxylic group is much more acidic than the 3-carboxylic group, it is reasonable to assume that 2,3-furandicarboxylic acid is esterified first at the 2-position by the method used in this investigation. Thus the monoester obtained would have to be 2-monomethylester of 2,3-furandicarboxylic acid.

*3, 4-Furandicarboxylic Acid.*[10]—Diethyl α-formylsuccinate was converted to its acetal, which was again formylated to diethyl 1-formyl-2-diethoxymethylsuccinate. 3, 4-Furandicarboxylic acid was prepared by the cyclization of the above compound. Recrystallization from water gave colorless crystals (m. p. 214°C), and the yield was 50% on the basis of the diethyl succinate used.

*The 3-Monomethyl Ester of 3, 4-Furandicarboxylic Acid.*—This ester was obtained in a 76% yield by the method used for the esterification of 2,3-furandicarboxylic acid (m. p. 135—137°C).

Found: C, 49.06; H, 3.76. Calcd. for $C_7H_6O_5$: C, 49.44; H, 3.56%.

*2, 5-Furandicarboxylic Acid.*[11] — This acid was obtained first by chloromethylating ethyl 2-furancarboxylate and then by oxidizing the resulting compound (m. p. 365°C) in a 70% yield.

*2,4-Furandicarboxylic Acid.*[12]—This acid was prepared by the rearrangement of the methyl 6-bromocoumalin 5-carboxylate obtained from coumalin 5-carboxylic acid (m. p. 268-269°C) in a 48% yield.

*3,4-Thiophenedicarboxylic Acid.*[10]—This acid was prepared from diethyl 1-formyl-2-diethoxymethylsuccinate, the method of synthesis which has been reported earlier. The cyclization of diethyl 1-formyl-2-diethoxymethylsuccinate was carried out using phosphorous pentasulfide. The diethyl 3,4-thiophenedicarboxylate thus obtained was hydrolyzed with aqueous sodium hydroxide to the acid (m. p. 225.5—226.5°C) in 20% yield.

*The 3-Monomethyl Ester of 3,4-Thiophenedicarboxylic Acid.*—The monoester of 3,4-thiophenedicarboxylic acid was prepared by the same method as was used for the synthesis of the 3-monomethyl ester of 3,4-furandicarboxylic acid (m. p. 115.5—116.5°C).

*2, 5-Thiophenedicarboxylic Acid.*[13]—Thiophene was chloromethylated with paraformaldehyde as usual to give 2,5-dichloromethylthiophene, which was further treated with sodium acetate and subsequent hydrolysis to yield 2,5-dihydroxymethylthiophene. This alcohol was oxidized with potassium permanganate to obtain the dicarboxylic acid (m. p. 358.5°C) in a 75% yield.

**p*K*-Measurements.**—p*K* measurements of the acids were made by potentiometric titrations using a Horiba model P pH meter (glass and calomel electrodes). The acids were dissolved in an aliquot amount of carbon dioxide-free distilled water, and then carbon dioxide-free nitrogen gas was added to the solution, while the temperature was maintained constant during the measurements. The titration was carried out using a 0.100 N standard potassium hydroxide solution, and the p*K*'s of the acids were calculated by the method described in the literature.[14] The graphical method using titration curves shown in Figs. 1 and 2 was also applied to the acids for which the $\Delta pK$ was small (the difference between $pK_1$ and $pK_2$).

**Infrared Spectrum.**—The infrared spectra of the acids were taken in their potassium bromide disks. In the case of 3,4-furandicarboxylic acid, carboxylic hydrogen was exchanged with deuterium by repeated recrystallization from $D_2O$, and this deuterated dicarboxylic acid was examined similarly.

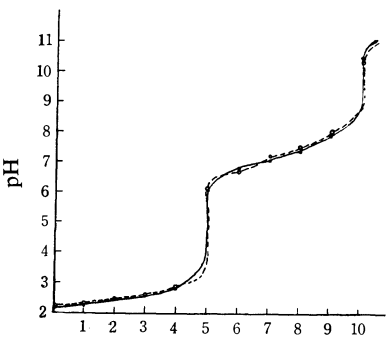



Fig. 1

—— 2,3-Furandicarboxylic acid
---- 3,4-Furandicarboxylic acid

9) R. G. Jones, ibid., **77**, 4069 (1955).
10) E. C. Kornfeld and R. G. Jones, *J. Org. Chem.*, **19**, 1617 (1954).
11) Y. Shono and Y. Hachihama, *J. Chem. Soc. Japan, Ind. Chem. Sec.* (*Kogyo Kagaku Zassi*), **57**, 836 (1954).
12) H. Gilman and R. Burther, *J. Am. Chem. Soc.*, **55**, 2903 (1933).
13) J. M. Griffing and L. F. Salisburg, ibid., **70**, 3416 (1948).
14) A. Albert and E. P. Serjeant, "Ionization Constants of Acids and Bases," John Wiley & Sons, New York (1962).

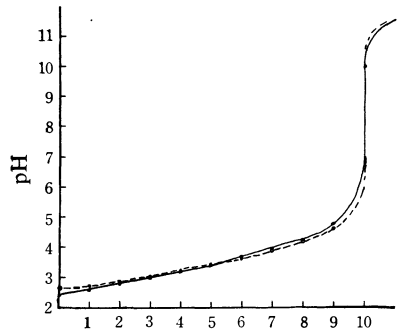



Fig. 2

—— 2,4-Furandicarboxylic acid
---- 2,5-Furandicarboxylic acid

**X-Ray Diffraction.** — The X-ray diffraction of 3,4-furandicarboxylic acid and its analysis[15] were carried out by Williams and Rundle at Iowa State University.

**Kinetics.**—*Dimethyl Esters.* — All the dimethyl esters except dimethyl terephthalate were synthesized in the following manner (dimethyl terephthalate was a commercially-available product which was purified just before use). Dicarboxylic acid (0.064 mol.) was refluxed with 10 ml. of anhydrous methanol in a benzene solution with one or two drops of concentrated sulfuric acid for several hours. After the removal of the excess methanol, the residual dimethyl ester was recrystallized from a suitable solvent several times to give the correct melting point.

By this method the following compounds were obtained:

| Ester | Solvent for recryst. | M. p. °C | Yield % |
|---|---|---|---|
| Dimethyl 2,5-furan-dicarboxylate | $H_2O$ - MeOH | 112 | 68.7 |
| Dimethyl 3,4-furan-dicarboxylate | Ether - *n*-Hexane | 47.5 | 77.2 |
| Dimethyl 2,5-thiophene-dicarboxylate | Benzene | 150—150.5 | 74.3 |
| Diemthyl 3,4-thiophene-dicarboxylate | Ether - *n*-Hexane | 60—61 | 81.5 |

*Monomethyl Terephthalate.*—Dimethyl terephthalate (20 g.) was dissolved in 50 ml. of an alcoholic aqueous solution containing 5.6 g. of potassium hydroxide and refluxed for several hours; then the unreacted dimethyl ester was filtered off. The aqueous alcoholic solution was acidified with concentrated hydrochloric acid. The precipitated monoester was recrystallized several times from water. The yield was 5.0 g. (25%), (m. p. 216.5—217°C).

*Kinetic Procedure.* — A detailed procedure for kinetic determination is described in the literature.[1a,b,8] The solvent used was 70% aqueous dioxane, which was made by diluting 30 ml. of carbon dioxide-free water with dioxane to 100 ml. of the solution. The rate measurements were carried out by mixing equal volumes of sodium hydroxide and ester solutions of the same concentration at the desired temperature, and then pippeting an aliquot into an excess of standard hydrochloric acid from time to time, it was then back titrated with a standard sodium hydroxide solution, using phenolphthalein as the indicator.

**The Calculation of Consecutive Competitive Rate Constants.**—The calculation of the consecutive competitive rate constants for the saponification of the diesters was carried out using the following Frost equation[8]:

$$A + B \xrightarrow{k_1} C + E, \qquad A + C \xrightarrow{k_2} D + E$$

$$dA/dt = -k_1AB - k_2AC, \qquad dB/dt = -k_1AB,$$

$$dC/dt = k_1AB - k_2AC$$

where A, B and C represent the molar concentrations of the corresponding chemical species. Then the above equations were expressed as follws, by

Table I. The saponification rate of dimethyl 3,4-furandicarboxylate with sodium hydroxide in a 70% dioxane - water - 0.200 N potassium chloride solution

| Time sec. | NaOH ml. in titration | $OH^-$, N | $\alpha = [OH^-]/[OH^-]_0$ |
|---|---|---|---|
| 0 | 0 | 0.009738 | 1.000 |
| 98 | 5.55 | 0.00881 | 0.905 |
| 439 | 6.06 | 0.00778 | 0.799 |
| 797 | 6.48 | 0.00694 | 0.713 |
| 1079 | 6.79 | 0.00633 | 0.650 |
| 1458 | 7.04 | 0.00581 | 0.597 |
| 1833 | 7.19 | 0.00551 | 0.566 |
| 2411 | 7.55 | 0.00478 | 0.491 |
| 2762 | 7.67 | 0.00454 | 0.466 |
| 3194 | 7.78 | 0.00432 | 0.433 |
| 3789 | 7.97 | 0.00393 | 0.403 |
| 4139 | 8.04 | 0.00379 | 0.389 |

Run: Initial concentration of reactants, 0.00974 N; normality of sodium hydroxide for titration, 0.02016 N; normality of hydrochloric acid, 0.0200 N; temperature at 20±0.01°C.

Table II. Calculations of rate constants for dimethyl 3,4-furandicarboxylate

| % Rx. | $t$, sec. | Percentages compared | $t$, ratio | $1/\kappa$ |
|---|---|---|---|---|
| 20 | 436 | 60/20 | 8.862 | 5.779 |
| 30 | 855 | 60/30 | 4.519 | 4.789 |
| 40 | 1437 | 60/40 | 2.689 | 4.578 |
| 50 | 2342 | 60/50 | 1.650 | 4.446 |
| 60 | 3864 | 50/20 | 5.371 | 7.010 |
| | | 50/30 | 2.739 | 5.101 |
| | | | Aver. | 4.728 |

| % Rx. | $\tau$ | $k_1$ | |
|---|---|---|---|
| 20 | 0.2684 | 0.126 | |
| 30 | 0.4835 | 0.116 | $k_1 = 0.115$ l.mol$^{-1}$sec$^{-1}$ |
| 40 | 0.8014 | 0.114 | $k_2 = 0.115 \times (1/4.728)$ |
| 50 | 1.305 | 0.114 | $= 0.0243$ l.mol$^{-1}$sec$^{-1}$ |
| 60 | 2.175 | 0.115 | |
| | Aver. | 0.115 | |

15) D. Williams and R. E. Rundle, *J. Am. Chem. Soc.*, **86**, 1660 (1964).

introducing the dimensionless variables, $\alpha$, $\beta$, $\tau$ and $\kappa$:

$$\alpha=A/A_0,\quad \beta=B/B_0,\quad \tau=B_0k_1t,\quad \kappa=k_2/k_1$$

$A_0$, $B_0$; initial concentrations of $A$ and $B$.

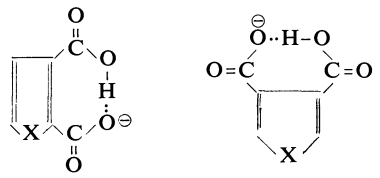
A typical run is shown in Tables I and II.

The rate constants of the monomethyl esters were calculated as usual.

## Results and Discussion

The titration curves of the acids are shown in Figs. 1 and 2. The p$K$'s of the acids are summarized in Table III. The rate constants of the esters are also tabulated in Table IV.

The p$K$'s for the furan- and thiophene-dicarboxylic acids change considerably with the change in the location of two carboxyl groups in the furan or thiophene ring. The acids in which two carboxyl groups are at adjacent carbon atom, e.g., 2,3- and 3,4-furan- or thiophene-dicarboxylic acids, have large $\Delta$p$K$ values, while the other acids (2,4- and 2,5-acids) have relatively small $\Delta$p$K$ values. The relatively large $\Delta$p$K$ values found for the former acids are undoubtedly caused by the formation of strong intramolecular hydrogen bonds in the resulting acid ions, as is shown below:



X; O or S

Therefore, the acids which would from a strong intramolecular hydrogen bond increase the first dissociation of a dicarboxylic acid and decrease the second one, eventually giving rise to a large $\Delta$p$K$ value.

In contrast, those acids in which the two carboxyl groups are separated by extra CH groups in the furan or thiophene ring and cannot form intramolecular hydrogen bonding,

Table III. The dissociation constants of acids

| | p$K_1$ | p$K_2$ | $\Delta$p$K$ | p$K_e$ | $\Delta$p$K_e$ |
|---|---|---|---|---|---|
| 2,3-Furan | 2.45 | 7.25 | 4.80 | 3.09 | 0.64 |
| 3,4-Furan | 2.51 | 7.43 | 4.92 | 3.75 | 1.24 |
| 2,4-Furan | 2.63 | 3.77 | 1.14 | | |
| 2,5-Furan | 2.60 (2.95*) | 3.55 (4.13*) | 0.95 | | |
| 2-Furan[1c] | 3.12 | | | | |
| 3-Furan[14] | 3.95 | | | | |
| 3,4-Thiophene | 2.81 | 6.93 | 4.02 | 3.57* | (0.76) |
| 2,5-Thiophene | (3.18*) | (4.28*) | 1.10 | | |
| Phthalic[a] | 2.98 | 5.28 | 2.30 | 3.32 | 0.34 |
| Isophthalic[a] | 3.46 | 4.46 | 1.00 | | |
| Terephthalic[a] | 3.51 | 4.82 | 1.31 | | |
| Benzoic[a] | 4.20 | | | | |
| Maleic[a] | 1.92 | 6.23 | 4.31 | | 1.03 |

* 30 wt.% of EtOH-$H_2O$

a) The p$K$'s of these compounds are taken from H. C. Brown, D. H. McDaniel and O. Hafligen, "Dissociation Constants," Chapter 14, "Determination of Organic Structure by Physical Method," Academic Press, New York (1955).

p$K_1$, p$K_2$: first and second dissociation constants respectively.

$\Delta$p$K$: the difference between p$K_1$ and p$K_2$.

p$K_e$: the dissociation constants of monoesters.

$\Delta$p$K_e$: the difference between p$K_1$ and p$K_e$.

Table IV. The rate constants of the esters at 20±0.01°C in 70% dioxane solutions

| Ester | $K_1$ l. mol$^{-1}$ sec$^{-1}$ | $K_2$ l. mol$^{-1}$ sec$^{-1}$ | $1/\kappa = K_1/K_2$ |
|---|---|---|---|
| Dimethyl 2,5-furandicarboxylate | 1.48 | 0.553 | 2.67 |
| Dimethyl 3,4-furandicarboxylate | 0.115 | 0.0243 | 4.73 |
| Dimethyl 2,5-thiophenedicarboxylate | 0.228 | 0.03 | 7.36 |
| Dimethyl 3,4-thiophenedicarboxylate | 0.0260 | 0.005 | 5.17 |
| Dimethyl terephthalate | 0.0886 | 0.0113 | 7.84 |
| Monomethyl 3,4-furandicarboxylate | 0.0469 | | |
| Monomethyl 3,4-thiophenedicarboxylate | 0.0134 | | |
| Monomethyl terephthalate | 0.0208 | | |

have small $\Delta pK$ values. Symmetrical dicarboxylic acids usually have a small statistical $\Delta pK$ value (ca. 0.1).

A substantially larger value of $\Delta pK$ than the statistical value must result from a specific interaction between the functional groups in a dicarboxylic acid. In the case of furan and thiophene dicarboxylic acids, small deviations from the statistical $\Delta$pK value are considered to be due to the polar interaction between the two carboxyl groups.

2, 3- and 3, 4-Furan- or thiophenedicarboxylic acids were found to give large $\Delta pK$ values. A similar large $\Delta pK$ value has also been observed for maleic acid (Table III), where the difference has been explained in terms of the formation of an intramolecular hydrogen bond of the resulted acid anion. Recently evidence for the existence of hydrogen bonding in maleic acid in the crystalline state has been given by Schahat and by others from their investigations of the acid by X-ray and infrarred analyses.[4a)] Phthalic acid is also considered to form a fairly strong intramolecular hydrogen bond, but the $\Delta pK$ value is found to be much smaller than those of 2, 3- and 3, 4-furan or thiophene-dicarboxylic acids. Hydrogen bonding is obviously involved as one of the important factors in determining these $\Delta pK$ values, and a heterocyclic aromatic ring such as furan or thiophene must also play a significant role in favoring the formation of a relatively stable acid ion from the furan- or thiophene-dicarboxylic acids than that from phthalic acid. One conceivable reason for this differences is the difference in geometry between the monohydrogen phthalate ion and the monohydrogen furan or thiophene dicarboxylate ion. The

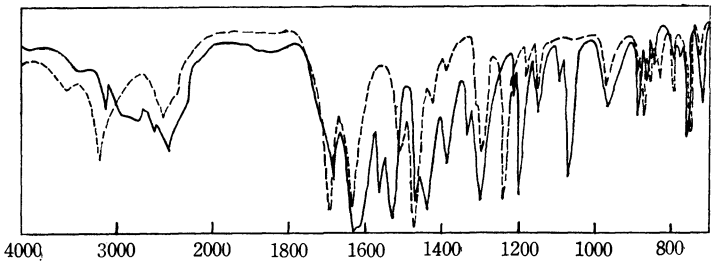



Fig. 3

—— 3,4-Furandicarboxylic acid
---- 3,4-Thiophenedicarboxylic acid

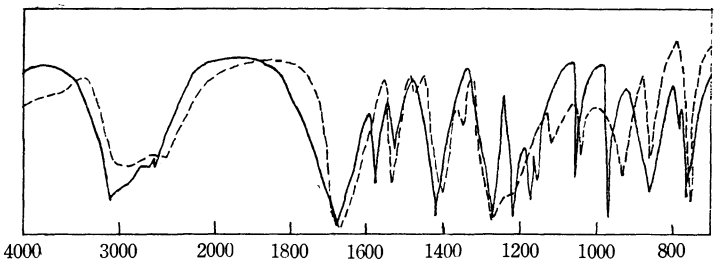



Fig. 4

—— 2,5-Furandicarboxylic acid
---- 2,5-Thiophenedicarboxylic acid

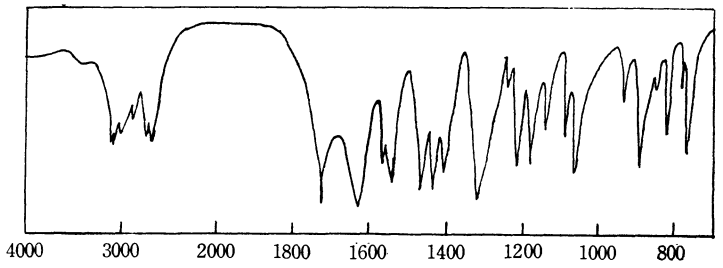



Fig. 5

Monomethyl ester of 3,4-furandicarboxylic acid

latter hydrogen-bonded ions are of 5- and 7-membered binuclear condensed rings, like an azulene ring, which are known to be quite stable. In the case of the monohydrogen phthalate ion, the structure is composed of 6- and 7-membered rings, which may not provide a very stable arrangement for an intramolecular hydrogen bond formation. It is also interesting to note that the $\Delta pK_a$ value for 3, 4-furandicarboxylic acid is larger than that for the corresponding thiophene counterpart. It may be that the furan ring is geometrically more favored for the hydrogen bond formation because of the smaller size of the oxygen atom than that of the sulfur atom of the thiophene ring.

A comparison of the strengths of the half esters of the dicarboxylic acids with these of the corresponding free acids, gives further support to the postulate that the internal hydrogen bonding in the carboxylate acid ions is an important factor. There is considerable evidence that the polar effect of carboalkoxyl group is similar to that of a carboxyl group. Consequently, in the absence of specific interactions, such as hydrogen bonding between the two functional groups, it may be expected that $\Delta pK_e$ (the difference between $pK_1$ and $pK_e$ for the monoester of the dicarboxylic acid) would have the value of 0.3, corresponding to the statistical value for the dicarboxylic acids. Phthalic acid has a value close to 0.3. Other acids for which a strong intramolecular hydrogen bonding is proposed exhibit considerably larger values: 2, 3-furandicarboxylic acid, 0.64; 3, 4-furandicarboxylic acid, 1.24; 3, 4-thiophenedicarboxylic acid, 0.76; maleic acid, 1.03. These values are consistent with the discussion above.

Other support for the existence of an intramolecular hydrogen bonding in 2, 3- and 3, 4-furan- or thiophene-dicarboxylic acids is given by the infrared data for the acids (Figs. 3, 4, and 5) and by the X-ray analysis for 3, 4-furandicarboxylic acid (Figs. 6 and 7).

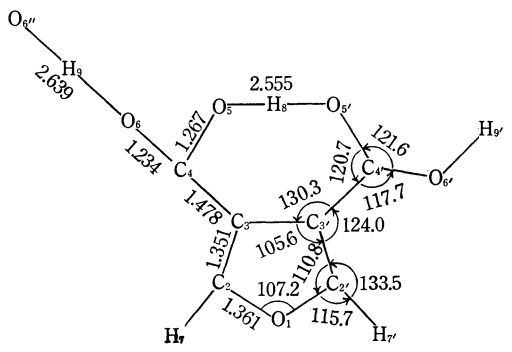



Fig. 6. Intramolecular distances and angles.

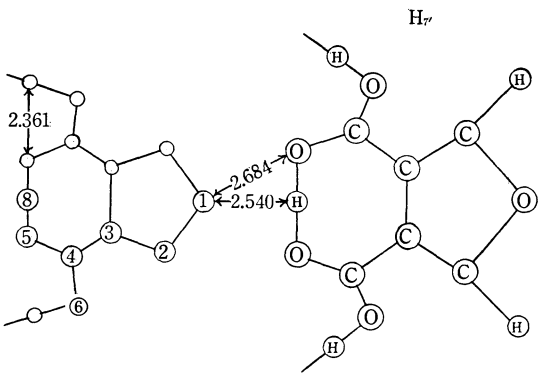


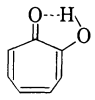

Fig. 7. The structure projected onto the ring square plane.

From the infrared spectra taken as KBr disks, the hydroxyl bands for all the acids investigated appear as broad absorption bands with many submaxima between 3000 $cm^{-1}$ and 2000 $cm^{-1}$ instead of the normal hydroxyl band near 3500 $cm^{-1}$. This fact is consistent with the existence of the intramolecular hydrogen bonding. Also, it has been proposed that the acids which are capable of forming an intramolecular hydrogen bonding give the carbonyl absorption between 1670 $cm^{-1}$ and 1650 $cm^{-1}$ [16] (the normal carboxylic acid C=O band appears near 1700 $cm^{-1}$) when examined in the solid or liquid state, while the normal aromatic acids absorb at 1700 $cm^{-1}$. Phthalic acid is normal in this regard, showing a simple C=O band at 1690 $cm^{-1}$, 2, 4- and 2, 5-furan- or thiophenedicarboxylic acids were also found to give a single intense carbonyl band between 1680 $cm^{-1}$ and 1700 $cm^{-1}$, indicating that these acids are normal. On the other hand, 2, 3- and 3, 4-furan- or thiophenedicarboxylic acids have double carbonyl bands (Fig. 3), one of which is near 1700 $cm^{-1}$ and the other between 1650 $cm^{-1}$ and 1620 $cm^{-1}$. The latter bands are fairly intense as compared to the normal carbonyl absorption band. All these observation are consistent with the assumption that these acids are intramolecularly hydrogen-bonded, even in undissociated forms. When hydroxyl hydrogen was replaced by deuterium, the absorption bands due to the -OH stretching shifted towards longer wavelengths. However, no remarkable effect appeared in the C=O stretching region. For example, acetic acid, which generally forms a dimer which absorbs at 3125 $cm^{-1}$ due to OH stretching, changes its band to 2299 $cm^{-1}$ upon deuterium substitution.[16] A better example would be tropolone, which forms a strong intramolecular

16) See, for example, L. J. Bellamy, "The Infra-red Spectra of Complex Molecules," John Wiley & Sons, New York (1958), pp. 161—176.

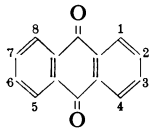
hydrogen bond[17] and the hydrogen-bonding structure of which is somewhat similar to that of 3, 4-furan- or thiophenedicarboxylic acid.

The -OH band is also shifted to a longer wavelength when -OH is changed to -OD, but no effect is observed in C=O stretching. Hadzi and Sheppard[18] have reported that the substituted anthraquinones show a remarkable shift of -OH upon deuterium substitution, as is shown in Table V.



Tropolone

TABLE V

| | | (OH) or (OD) $cm^{-1}$ | (C=O) $cm^{-1}$ |
|---|---|---|---|
|  Anthraquinone | 1,4-diOH | 2860 | 1626 |
| | 1,4-diOD | 2260 | 1626 |
| | 1,5-diOH | 2950 | 1637 |
| | 1,5-diOD | 2280 | 1637 |

In the case of 3, 4-furandicarboxylic acid, in which carboxyl -OH was exchanged with -OD, a similar effect was observed; the band due to the -O···H stretching at 2500—2800 $cm^{-1}$ disappeared and a new broad band was observed near 1980 $cm^{-1}$, a band which is assumed to be that of the intramolecular hydrogen-bonded -OD.

The X-ray analysis of 3, 4-furandicarboxylic acid in Figs. 6 and 7 gives fairly good proof for our suggestion of the existence of a strong intramolecular hydrogen bonding in 2, 3- and 3, 4-furan or thiophenedicarboxylic acids. The analysis of 3, 4-furandicarboxylic acid shows that because of the intramolecular hydrogen bonding hydrogen atom lies just in the middle of the two adjacent carboxyl oxygens. The distance of the O-H-O hydrogen bond reveals a marked shortening of O-H-O linkage as compared to the acetic acid dimer or other hydrogen-bonded acids.[19]

17) V. von Keussler and G. Rosomy, *Z. Electrochem.*, **60**, 136 (1956).
18) D. Hadzi and N. Sheppard, *Trans. Faraday Soc.*, **50**, 911 (1956).
19) R. Hofstadter, *J. Chem. Phys.*, **6**, 540 (1938).

In Table II one can see substantial fluctuations in the rate constants obtained. The main reason for the deviations is that the determination of the end point with phenolphthalein is not sharp because of the facile hydrolysis of the second ester groups in the diesters during the hydrolysis. Therefore, each of the rates, actually observed and summarized in Table III, may contain a substantial margin of inherent error. However, even at its greatest the error is not so large as to lead to a wrong conclusion.

Despite the inherent errors, one can draw a few interesting conclusions from the data. First, the order of reactivity in the hydrolysis of the diesters is furan>thiophene>benzene. This is in accord with that of the alkaline hydrolysis of the ethyl esters of monocarboxylic acids in the same solvent[1] and also is to be expected from the magnitudes of the acidity constants of these mono or dicarboxylic acids. Here again, it was confirmed that the thiophene ring is more electron-attracting than the benzene ring, but less so than the furan ring. The fact that the first hydrolysis rate constant, $k_1$, for dimethyl 2, 5-furandicarboxylate is of an especially high value, is to be expected from the calculation by the Hammett equation using the data for the hydrolysis rate constants of furoic acid.[1]

Another interesting fact is that the rates of the hydrolyses of the diesters in which the two ester groups are attached to adjacent carbon atoms are substantially lower than those of the esters in which the carboxyl groups are separated by CH groups. One reason for this may be that the nucleophilic attack with the hydroxyl ion on the first carbonyl carbon is retarded by the charge repulsion with the adjacent carboxyl oxygen.

*Department of Applied Chemistry*
*Faculty of Engineering*
*Osaka City University*
*(S. O., N. F. & T. W.)*

*Department of Applied Chemistry*
*College of Engineering*
*The University of Osaka Prefecture*
*Sakai, Osaka (Y. O.)*

*Department of Chemistry*
*Radiation Center of Osaka Prefecture*
*Sakai, Osaka (M. H.)*

# A Study of Monolayer Penetration by the Radiotracer Method

By Akira MATSUBARA

(Received August 25, 1964)

The phenomenon of the penetration of insoluble monolayers of cholesterol, hexadecyl alcohol, etc., by long-chain water-soluble compounds such as sodium salts of long-chain alkyl sulfates was first discovered by Schulman and Hughes.[1] Since then, this phenomenon has been extensively investigated by Schulman and his co-workers, and it has been concluded that stoichiometric complexes between insoluble and soluble species are formed.[1]

Harkins, however, has questioned this idea of complex formation, because the surface tension data observed by Schulman et al. were not those of the true equilibrium.[2] Hutchinson has also shown that the surface tension of aqueous solutions containing octyl alcohol and sodium dodecyl sulfate in various mole ratios does not exhibit the obvious variation which would suggest the stoichiometric complex formation.[3]

Opposing these papers, Matalon[4] and Goddard and Schulman[5] have published experimental evidence for their own views as follows: "By injecting sodium hexadecyl sulfate (SHS) below cholesterol monolayer at constant surface pressure the occupied area of cholesterol molecule increases and its rapid initial increase is from 20 to 27 Å$^2$. Since this increase approximately corresponds to a cross-sectional area of SHS, a 1 : 1 complex is formed. For hexadecyl alcohol monolayer this rapid initial increase does not correspond to a 1 : 1 complex, but a considerable quantity of SHS is held and stabilized in the surface by hexadecyl alcohol. These complexes are stable up to the collapse points of the mixed monolayers." [5]

Dervichian has considered the monolayer penetration as a partition of soluble species between the surface phase containing the monolayer and the substrate phase. On the basis of this idea he has suggested that certain particular patterns in the mutual arrangement of the molecules appear and that, in the case of the penetration of the hexadecyl alcohol monolayer by SHS, 1 : 1, 1 : 2 and 1 : 3 associations exist.[6]

The thermodynamics of monolayer penetration has been studied by Pethica and Anderson[7] and by Fowkes.[8,9] Especially, Fowkes has asserted that the mixed film resulting from the penetration may be regarded as an ideal mixture rather than as a stoichiometric complex.

The above-mentioned arguments have been based on the data obtained by the measurement of the surface pressure, potential and viscosity. However, data decisive enough to persuade us have not been reported yet on either side of the question. If detergent molecules penetrate into monolayers to form 1 : 1 complexes, the penetrated amount should be of the order of $10^{-10}$ mol./cm$^2$, which is enough to be detectable by means of the radiotracer method. Hence, the direct measurements of the amount of some long-chain alkyl sulfates penetrating cholesterol and hexadecyl alcohol monolayers were carried out by the radiotracer method, using $^{35}$S-labeled detergents. In addition, octadecyl amine, which is known to form a 1 : 1 salt with these anionic detergents in a bulk solution, was used as a reference monolayer.

A short communication has already come from our laboratory on this subject.[10]

## Experimental

**Materials.**—The $^{35}$S-labeled sodium dodecyl sulfate (SDS), sodium tetradecyl sulfate (STS) and sodium hexadecyl sulfate (SHS) used were synthesized from the corresponding fatty alcohols and $^{35}$S-labeled sulfuric acid according to the published method.[11]

Pure fatty alcohols were obtained from commercial alcohols by fractional distillation through a

1) J. H. Schulman and A. H. Hughes, *Biochem. J.*, **29**, 1243 (1935); J. H. Schulman, *Trans. Faraday Soc.*, **33**, 1116 (1937); J. H. Schulman and E. K. Rideal, *Proc. Roy. Soc.*, **B122**, 29, 46 (1937); J. H. Schulman and E. Stenhagen, ibid., **B126**, 356 (1938); J. M. Marsden and J. H. Schulman, *Trans. Faraday Soc.*, **34**, 748 (1938).

2) W. D. Harkins, "Physical Chemistry of Surface Films," Reinhold Publ. Corp., New York, N. Y. (1952).

3) E. Hutchinson, *J. Colloid Sci.*, **3**, 413 (1948).

4) R. Matalon, ibid., **8**, 53 (1953).

5) E. D. Goddard and J. H. Schulman, ibid., **8**, 309, 329 (1953).

6) D. G. Dervichian, "Surface Phenomena in Biology and Chemistry," Ed. by J. F. Danielli, K. G. A. Pankhurst and A. C. Riddiford, Pergamon Press, New York, N. Y. (1958), pp. 80—87.

7) B. A. Pethica, *Trans. Faraday Soc.*, **51**, 1402 (1955); P. J. Anderson and B. A. Pethica, ibid., **52**, 1080 (1956).

8) F. M. Fowkes, *J. Phys. Chem.*, **65**, 355 (1961).

9) F. M. Fowkes, ibid., **67**, 1982 (1963).

10) R. Shimozawa and R. Matuura, This Bulletin, **34**, 457 (1961).

11) R. Matuura, H. Kimizuka, S. Miyamoto and R. Shimozawa, ibid., **31**, 532 (1958).

rectifying column of 65 plates at a reflux ratio of 15. Fractions which distilled at 130—131°C/8.0 mmHg, 168°C/13.8 mmHg and 181.5—181.7°C/10.0 mmHg for dodecyl, tetradecyl and hexadecyl alcohols respectively were collected. The melting points of these alcohols showed normal values.

The $^{35}S$-labeled sulfuric acid was obtained from the Radiochemical Center, England, in a carrier-free state and was isotopically diluted with a small amount of sulfuric acid before use. The specific radioactivity of the $^{35}S$-labeled sodium alkyl sulfates thus prepared were ca. 10 mc./mmol.

Octadecyl amine was distilled in the same way as were fatty alcohols, and a fraction which distilled at 198.5—198.8°C/9.2 mmHg was collected. Distilled hexadecyl alcohol and octadecyl amine and the cholesterol of Merck's reagent were all recrystallized from their ethanol solutions and dried in a vacuum. These monolayer substances were spread from benzene solutions.

The water used was redistilled from a quartz still.

**Method.**—The procedure of measuring the surface excess by the radiotracer method was the same as that in the preceding paper.[12] The surface excess of a detergent at the free surface of its solution, $\Gamma_d$ (in mol./cm$^2$), and that at the surface with a monolayer, $\Gamma_m$, were calculated according to the following equations:

$$\Gamma_d=\frac{I_d-I}{SA},\quad \Gamma_m=\frac{I_m-I}{SA} \qquad (1)$$

where $I_d$ and $I_m$ are the intensities, in count/min., of the radiation from the detergent solution in the absence and in the presence of a monolayer respectively, and where $I$ is the intensity of the radiation from a sulfuric acid solution, used as a reference, which has the same specific activity and concentration as the detergent solution. $S$, the specific activity of the detergent in count/min./mol., and $A$, the surface area of the solution in cm$^2$, were determined by using a point source, as has been reported previously.[12]

The measurement of the surface pressure was simultaneously carried out by a modified Wilhelmy-type balance.[13]

All experiments were carried out at 35°C.

## Results and Discussion

So far various insoluble and soluble substances have been used in the study of the monolayer penetration. The aim of this study was, however, to obtain more exact information on the phenomenon of the monolayer penetration itself. Hence, cholesterol and hexadecyl alcohol as insoluble species and sodium alkyl sulfates as soluble species were used as typical examples.

Three kinds of experimental procedures were applied in order to obtain exact information on the mechanism of the monolayer penetration. Namely, the surface pressure and the surface excess of the detergent as a function of the surface area or of time were measured with (1) the monolayer spread on the detergent solution; (2) the monolayer under which the detergent solution was injected, and (3) the monolayer formed by the spreading of a film substance-detergent mixture on water.

Since the results obtained for three sodium alkyl sulfates are qualitatively similar, the results for SHS only will be described in detail.

**The Monolayers Spread on the Surface of the Detergent Solution.**—In order to minimize the effect of adventitious ionic contamination, the experiments were carried out on the SHS solution with $10^{-3}$ mol./l. sodium chloride for cholesterol and hexadecyl alcohol monolayers, and on that with $10^{-3}$ mol./l. hydrochloric acid for the octadecyl amine monolayer, as was done by Goddard and Schulman.[5] On the other hand, the experiment with the octadecyl amine nonolayer was also carried out on the SHS solution without an added electrolyte.

Prior to the penetration experiment, the measurements were carried out on the free surface of the SHS solution. After sweeping the surface of the SHS solution, the surface excess of SHS at the free surface, $\Gamma_d$, and the surface pressure, $\Pi$, were measured simultaneously. It was found that both values increase with time and that the former reaches equilibrium within an hour, while the latter still increases very slowly. Two hours after the sweeping, the $\Gamma_d$ and the change in $\Pi$ with compression, $\Delta\Pi$, were measured by compressing the free surface of the SHS solution. The

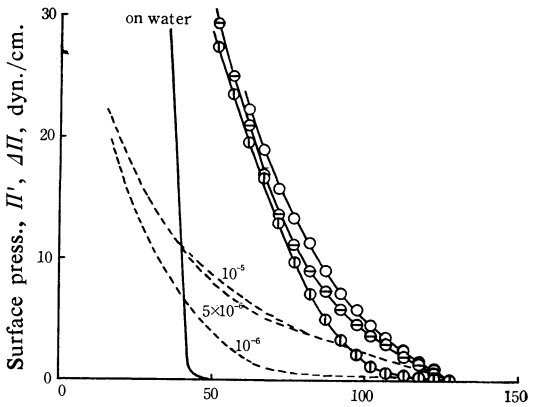



Fig. 1. $\Pi'$-$A$ curves for cholesterol monolayers on $10^{-6}$, ①; $5\times10^{-6}$, ⊖; and $10^{-5}$, ○, mol./l. SHS solutions with $10^{-3}$ mol./l. NaCl. Broken lines represent the increase in the surface pressure due to the compression of the free surface of each substrate solution.

12) A. Matsubara, R. Matuura and H. Kimizuka, ibid., 38, 369 (1965).
13) R. Matuura and I. Hayashi, *Memoirs Fac. Sci., Kyushu Univ. C*, 1 (1948).

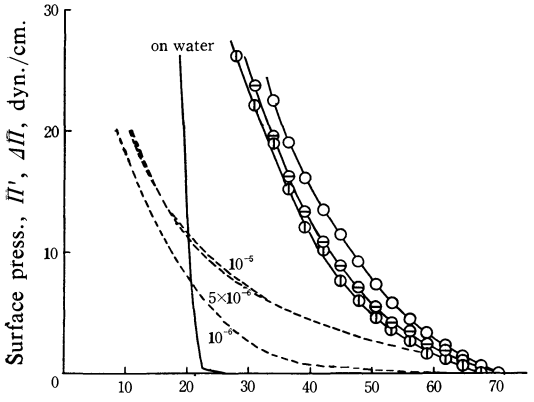



Fig. 2. $\Pi'$-$A$ curves for hexadecyl alcohol monolayers on $10^{-6}$, ⊕; $5\times10^{-6}$, ⊖; and $10^{-5}$, ○, mol./l. SHS solutions with $10^{-3}$ mol./l. NaCl. Broken lines represent the increase in the surface pressure due to the compression of the free surface of each substrate solution.

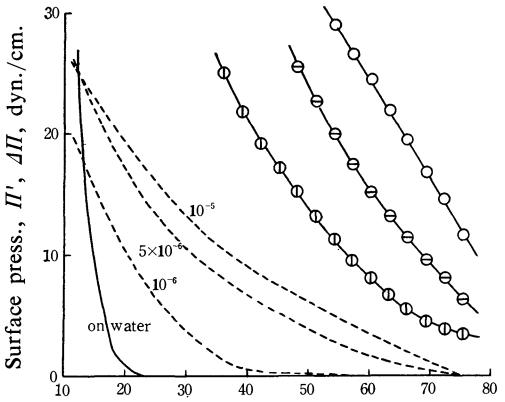



Fig. 4. $\Pi'$-$A$ curves for octadecyl amine monolayers on $10^{-6}$, ⊕; $5\times10^{-6}$, ⊖; and $10^{-5}$, ○, mol./l. SHS solutions without added electrolyte. Broken lines represent the increase in the surface pressure due to the compression of the free surface of each substrate solution.

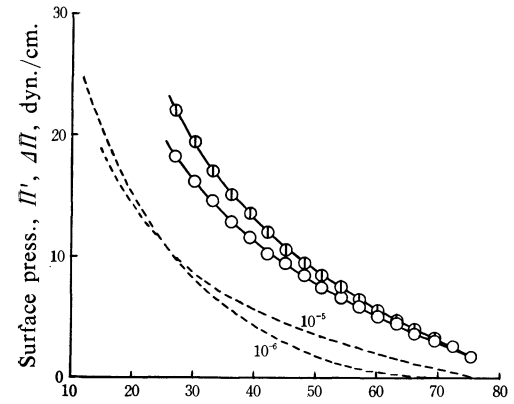



Fig. 3. $\Pi'$-$A$ curves for octadecyl amine monolayers on $10^{-6}$, ⊕; and $10^{-5}$, ○, mol./l. SHS solutions with $10^{-3}$ mol./l. HCl. Broken lines represent the increase in the surface pressure due to the compression of the free surface of each substrate solution.

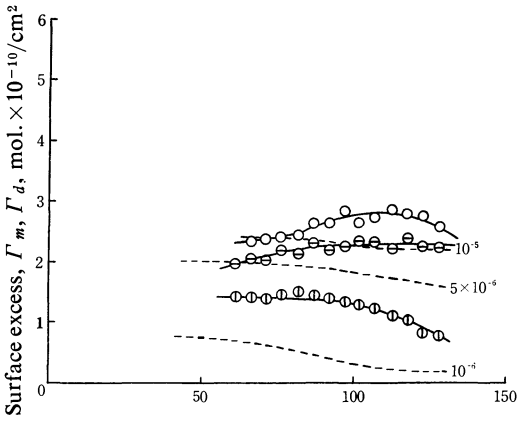



Fig. 5. $\Gamma_m$-$A$ curves for cholesterol monolayers on $10^{-6}$, ⊕; $5\times10^{-6}$, ⊖; and $10^{-5}$, ○, mol./l. SHS solutions with $10^{-3}$ mol./l. NaCl. Broken lines represent the change in the surface excess due to the compression of the free surface of each substrate solution.

compression was carried out at the rate of 1 cm. of the trough scale a minute (trough: $15\times30$ cm$^2$) and at three-minute intervals.

At the end of the measurements on the free surface of the SHS solution, the surface was again swept and the monolayer was spread as quickly as possible. Two hours after the spreading, the values of $\Gamma_m$ and the surface pressures referred to each substrate solution, $\Pi'$, were measured as a function of the occupied area of the insoluble molecule by compressing the monolayer at the same rate and interval as in the measurement with the free surface. The results are shown in Figs. 1—4 (for $\Delta\Pi$ and $\Pi'$) and in Figs. 5—8 (for $\Gamma_d$ and $\Gamma_m$).

It should be noticed in these figures that, with the compression of the free surface of the SHS solution, the surface pressure increased with a considerable stability, as is shown by the broken lines in Figs. 1—4, while there was little change in the surface excess, as Figs. 5—8 show. It may also be seen in these figures that cholesterol and hexadecyl alcohol monolayers spread on the SHS solutions expanded two or three times in comparison with those on water, while the surface excess of SHS did

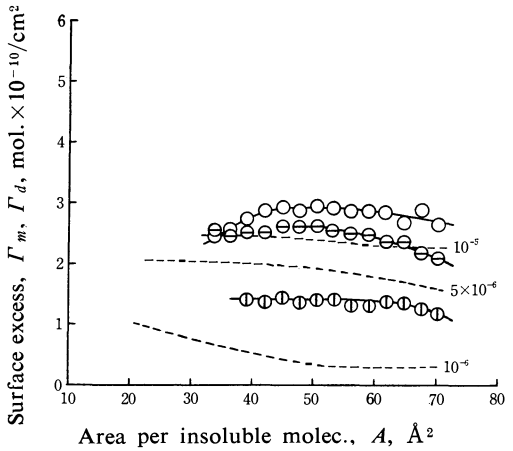



Fig. 6. $\Gamma_m$-$A$ curves for hexadecyl alcohol monolayers on $10^{-6}$, ⏀; $5\times10^{-6}$, ⊖; and $10^{-5}$, ○, mol./l. SHS solutions with $10^{-3}$ mol./l. NaCl. Broken lines represent the change in the surface excess due to the compression of the free surface of each substrate solution.

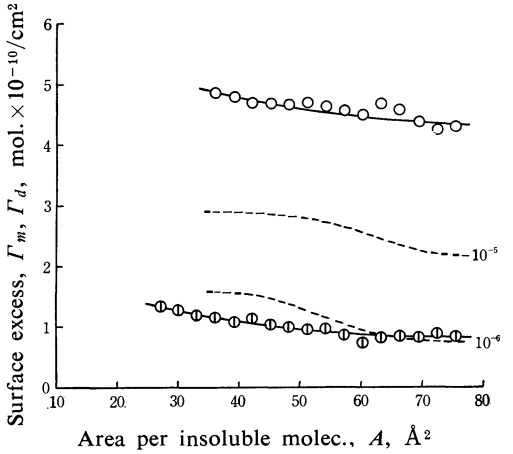



Fig. 7. $\Gamma_m$-$A$ curves for octadecyl amine monolayers on $10^{-6}$, ⏀; and $10^{-5}$, ○, mol./l. SHS solutions with $10^{-3}$ mol./l. HCl. Broken lines represent the change in the surface excess due to the compression of the free surface of each substrate solution.

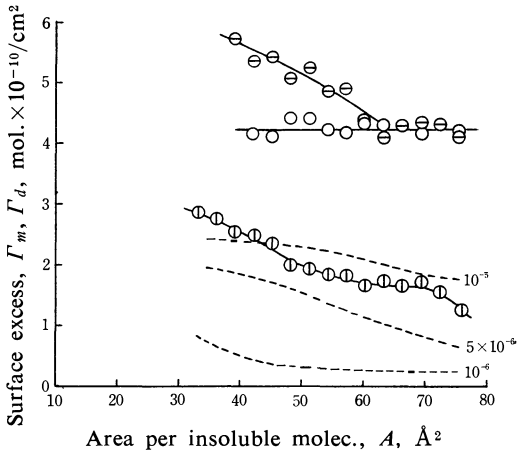



Fig. 8. $\Gamma_m$-$A$ curves for octadecyl amine monolayers on $10^{-6}$, ⏀; $5\times10^{-6}$, ⊖; and $10^{-5}$, ○, mol./l. SHS solutions without added electrolyte. Broken lines represent the change in the surface excess due to the compression of the free surface of each substrate solution.

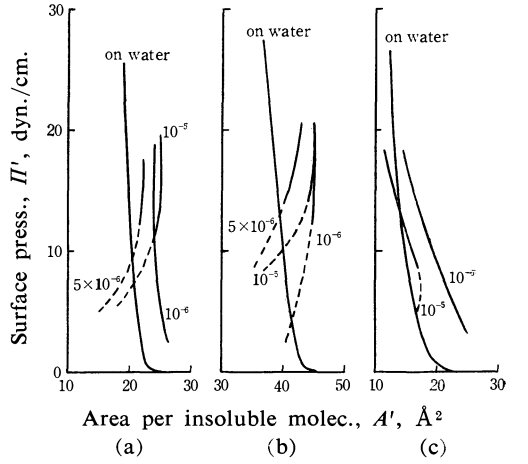



Fig. 9. (a) and (b) represent $\Pi'$-$A'$ curves for hexadecyl alcohol and cholesterol monolayers on SHS solutions with $10^{-3}$ mol./l. NaCl, respectively and (c) represents that for octadecyl amine monolayer on SHS solutions with $10^{-3}$ mol./l. HCl.

not increase so much as to explain this large expansion and was insufficient to form the 1 : 1 complex, as is shown by solid lines in Figs. 1—8. Especially at higher concentrations of SHS, the $\Gamma_m$'s were almost the same as the corresponding $\Gamma_d$'s, indicating that no extra detergent ion was taken up by the insoluble monolayer.

Since in the surface the adsorbed detergent ions are present in addition to the cholesterol or hexadecyl alcohol molecules, it is quite natural that these monolayers expand remarkably. In addition, it should be noted that the abnormally large expansion of the $\Pi'$-$A$ curves, as seen in Figs. 1—4 and in previous papers,[1,5] involves the effect of the compression of the free surface. In fact, subtracting the area of the free surface from that of the penetrated film at the same surface pressure, we obtain the surface pressure - area curve ($\Pi'$-$A'$ curve), as is shown in Figs. 9(a) and (b). These curves indicate only small expansions of the limiting areas of monolayers. The presence of this free surface effect is characterized by the features of the $\Pi'$-$A$ curves,

indicating an increase in the surface pressure from just the area at which the spreading solution has been dropped, as Figs. 1—4 show. This feature is observed also in the $\Pi$-$A$ curves reported by Schulman et al.[1,5] It has been stated[5] that the complex produced by the penetration of the detergent is stable up to the collapse point. This statement is inconsistent with the present findings that the apparent increase in the surface area is mainly due to the compression of the free surface and that the $\Gamma_m$ is almost constant with the compression of the monolayer and never reaches the amount corresponding to the 1 : 1 complex. Further, the $\Pi'$-$A$ curves of the monolayers on the SHS solution are strongly time-dependent. From these reasons it should be concluded that the $\Pi'$-$A$ curves obtained by compressing the insoluble monolayer on the SHS solution can not be used for the thermodynamic consideration.

In the experiments with the octadecyl amine monolayer spread on the SHS solution without hydrochloric acid, the $\Pi'$-$A$ curves showed a much more remarkable expansion than those of cholesterol and hexadecyl alcohol monolayers, and the surface excess of SHS also increased pronouncedly in comparison with that in the case of the free surface. The differences between $\Gamma_m$ and $\Gamma_d$ nearly corresponded to the 1 : 1 salt formation at the $5\times10^{-6}$ and $10^{-5}$ mol./l. concentrations of SHS and over a larger area. However, these differences are almost constant, independent of the compression of the monolayer.

In the experiments with the octadecyl amine monolayer spread on the SHS solution containing $10^{-3}$ mol./l. hydrochloric acid, the $\Pi'$-$A$ curves are quite similar to those of cholesterol and hexadecyl alcohol monolayers in spite of the fact that the surface excess of SHS corresponds to the 1 : 1 salt formation at the SHS concentration of $10^{-5}$ mol./l. and over a larger area. In Fig. 10, $\Pi'$-$A'$ curves for the octadecyl amine monolayers on SHS solutions, in the absence of hydrochloric acid, are given. As may be seen in this figure, the curves still indicate a remarkable expansion as compared with the monolayer on water. This seems to be a characteristic feature, one which provides us with evidence for the complex formation. However, $\Pi'$-$A'$ curves obtained in the presence of $10^{-3}$ mol./l. hydrochloric acid show only a small expansion, as is shown in Fig. 9(c). These findings suggest that the expansion of the $\Pi'$-$A'$ or $\Pi'$-$A$ curve cannot be an indication of the complex formation.

**The Injection of Detergents below Monolayers.**—Insoluble monolayers were spread on the surface of water and compressed up to a surface pressure of 15 dyn./cm. Then the solution of detergents was injected below the monolayer by means of a wide-mouth pipette and the substrate solution was rendered uniform by gentle sucking and blowing for five minutes. The concentration of the injecting solution was twenty-five times as high as the equilibrium concentration of the substrate solution, and its volume was 10 cc. The $\Gamma_m$'s at a constant area were measured as a function of the time. The results are shown in Figs. 11—13 for combinations of three kinds of monolayers and three detergents. It may be seen from these figures that, after the injection of the detergents, the surface excesses of detergents increase with the time. In the case of cholesterol and hexadecyl alcohol monolayers, their equilibrium values are approximately the same as

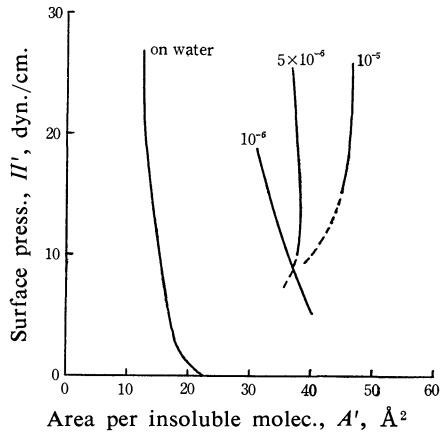



Fig. 10. $\Pi'$-$A'$ curve for octadecyl amine monolayer on SHS solutions without added electrolyte.

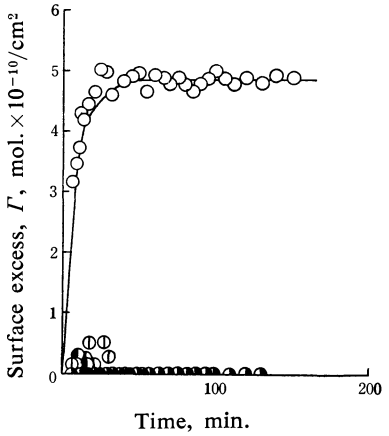



Fig. 11. Injection of SDS below the free surface, ⓘ; and cholesterol, ◑; hexadecyl alcohol, ◐; and octadecyl amine, ○, monolayers. The equilibrium concentration of the substrate solution is $10^{-5}$ mol./l.

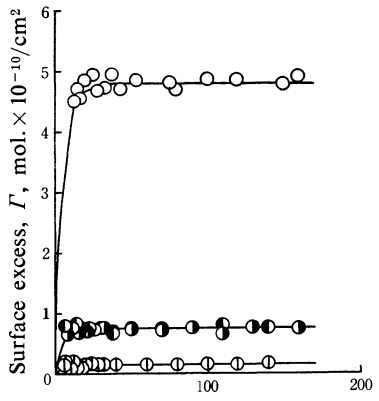



Fig. 12. Injection of STS below the free surface, ⓘ; and cholesterol, ◑; hexadecyl alcohol, ◐; and octadecyl amine, ○, monolayers. The equilibrium concentration of the substrate solution is $10^{-5}$ mol./l.

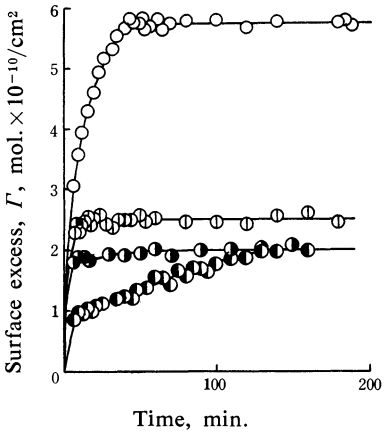



Fig. 13. Injection of SHS below the free surface, ⓘ; and cholesterol, ◑; hexadecyl alcohol, ◐; and octadecyl amine, ○, monolayers. The equilibrium concentration of the substrate solution is $10^{-5}$ mol./l.

that at the surface without a monolayer. On the other hand, in the case of the octadecyl amine monolayer the surface excess increases remarkably beyond that of the free surface. This is incontrovertible evidence that cholesterol and hexadecyl alcohol monolayers do not interact with SHS in such a way as to form the 1 : 1 complex, as has been observed with the octadecyl amine monolayer. It has been suggested[4,5] that, in the experiment with the injection of SHS below the cholesterol monolayer at a constant surface pressure, the rapid initial change in the surface area is due to the 1 : 1 complex formation and that the subsequent slow increase is due to the "solution" of SHS in excess of a 1 : 1 ratio into the monolayer. This interpretation is clearly a misunderstanding. Our suggestion is that the rapid initial change is due to the formation of the adsorbed film of detergents at the surface in the presence of the monolayer, and that the subsequent slow change is to be attributed to the so-called surface ageing which is frequently observed in the surface tension measurement of detergent solutions. Incidentally, the surface potential vs. time curves obtained by Goddard and Schulman[5] are similar to our surface excess vs. time curves; i. e., both curves show a rapid initial change, followed by no slow change.

**The Mixed Monolayers of Insoluble and Soluble Species Spread on the Surface of Water.** —A mixture of insoluble substances and soluble detergents in the ratio of 1 : 1 was spread on the surface of water by using a mixed solvent composed of benzene, isopropanol and water (25 : 23 : 2 in volume). Thirty minutes after the spreading of the mixture, the surface film was compressed at the same rate and interval as those used previously and the surface concentration, $\Gamma$, of the detergent was measured as a function of the occupied area of the insoluble molecule. In these experiments, even if all the molecules of the detergents have dissolved into the substrate, the radiation from the bulk of the substrate is negligibly small, because only a minute amount of detergent has been spread.

The $\Pi$-$A$ and $\Gamma$-$A$ curves for the mixed monolayers of insoluble species and SHS molecules in the ratio of 1 : 1 are shown in Figs. 14—16. In the case of cholesterol- and hexadecyl alcohol - SHS mixed films, the surface concentrations of SHS are very low, approximately the same as that obtained by spreading SHS only; in addition, there is no appreciable increase in the surface count with the compression of the mixed films. On the contrary, the surface concentration of SHS in the octadecyl amine - SHS mixed film is much higher

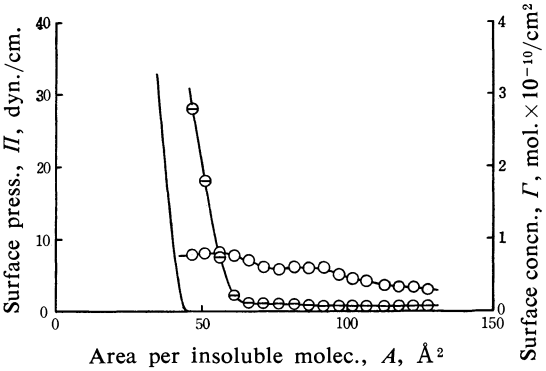



Fig. 14. $\Pi$-$A$, ⊖; and $\Gamma$-$A$, ○; curves for cholesterol-SHS (1 : 1) mixed film. Solid line represents $\Pi$-$A$ curve for cholesterol monolayer.

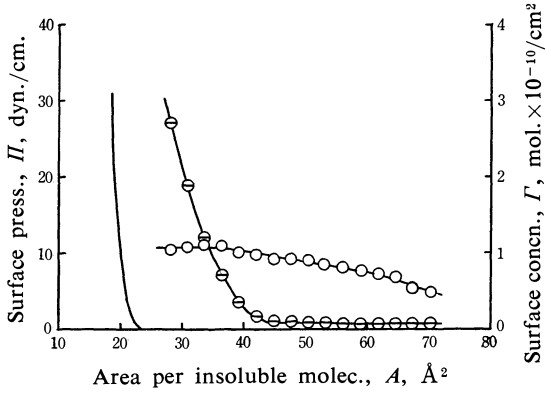



Fig. 15. $\Pi$-$A$, ⊖; and $\Gamma$-$A$, ○; curves for hexadecyl alcohol - SHS (1 : 1) mixed film. Solid line represents $\Pi$-$A$ curve for hexadecyl alcohol monolayer.

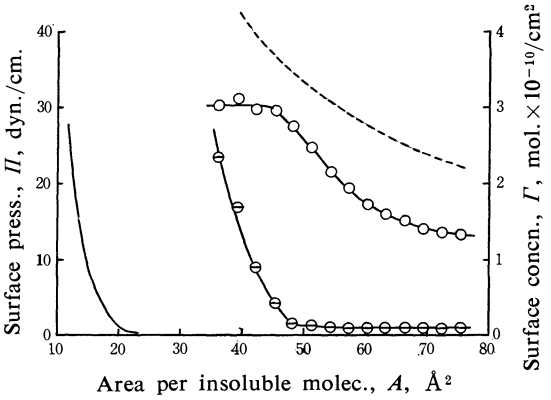



Fig. 16. $\Pi$-$A$, ◑; and $\Gamma$-$A$, ○; curves for octadecyl amine - SHS (1 : 1) mixed film. Broken line represents an ideal $\Gamma$-$A$ curve for 1 : 1 mixed film. Solid line represents $\Pi$-$A$ curve for octadecyl amine monolayer.

than those in the case of cholesterol and hexadecyl alcohol and increases in accordance with the increase in the surface concentrations with the compression of the mixed film at a low surface pressure. The mole ratio of SHS to octadecyl amine at the surface is ca. 0.8 at the limiting area. In conformity to this fact, the $\Pi$-$A$ curve for the octadecyl amine - SHS mixed film shows a remarkable expansion. It should, however, be pointed out that the increase in the limiting area in the cholesterol- and hexadecyl alcohol - SHS mixed films are ca. 20 Å² per insoluble molecule, although the surface concentrations of SHS in these films are much lower than that corresponding to the 1 : 1 complex. This situation is similar to that which holds for the monolayers spread on the SHS solution.

It has been reported by Goddard and Schulman[5] that the result obtained by injecting SHS below the spread cholesterol-SHS mixed film also shows a rapid initial change. This has been considered to be an unexpected result, one inconsistent with the concept they themselves had proposed, that the rapid initial change was due to the 1 : 1 complex formation. This, however, seems quite natural in terms of our interpretation that it is due to the formation of the adsorbed film of SHS. Namely, most of SHS molecules in the spread mixed film have dissolved into the substrate, and only a very low surface concentration of SHS molecules in equilibrium with the bulk concentration remains at the surface. Therefore, if SHS is again injected below such a film, the surface excess of SHS may increase as a result of the increase in the bulk concentration. Hence, a rapid initial change occurs again to form the adsorbed film of SHS.

It may be seen in Fig. 16 that the surface concentration of SHS in the spread octadecyl amine - SHS mixed film does not increase with the compression of the film over areas smaller than the limiting area of the mixed fiilm. As has been mentioned already, in the case of the octadecyl amine monolayer spread on the SHS solution, the surface excess of SHS also shows no increase with the compression of the monolayer. This seems to be due to the collapse of the octadecyl amine - SHS film at a relatively low surface pressure.

When cholesterol- and hexadecyl alcohol - STS mixed films are spread, molecules of STS dissolve almost completely into the substrate. On the other hand, for the octadecyl amine - STS mixed film, molecules of STS corresponding to the ratio of 1 : 1 remain at the surface, as Fig. 17 shows.

All the results obtained in the present experiments clearly indicate that the mode of interaction of sodium alkyl sulfates with the

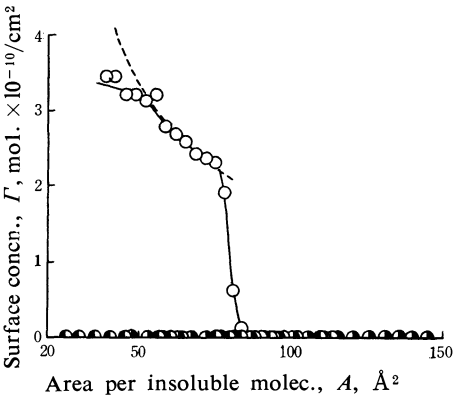



Fig. 17. $\Gamma$-$A$ curves for cholesterol -, ◑; hexadecyl alcohol -, ◐; and octadecyl amine - STS (1 : 1), ○, mixed films. Broken line represents an ideal $\Gamma$-$A$ curve for octadecyl amine - STS (1 : 1) mixed film.

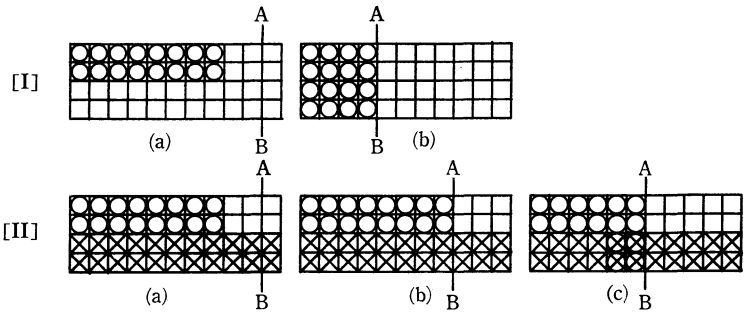



Fig. 18. Compression processes for monolayers [I] on water and [II] on detergent solution, respectively.
(b) represents the closely packed state.
AB, barrier; ○, insoluble molecule; ×, detergent molecule

monolayer of cholesterol or hexadecyl alcohol is quite different from that with the monolayer of octadecyl amine. In the latter case the evidence is ample for the formation of the 1 : 1 salt, but we can not obtain any direct evidence for the 1 : 1 complex formation in the former case. Although the true nature of the interaction between sodium alkyl sulfates and cholesterol or hexadecyl alcohol monolayer is as yet obscure, we may suppose that a very weak interaction, such as the van der Waals force, may play a role between two species. But in any way, we can completely deny the well-defined 1 : 1 complex formation.

As Figs. 1—8 show, the surface pressure of the SHS solution, both with and without an insoluble monolayer, increases with compression, while the surface excess does not change appreciably. This phenomenon has not yet been explained completely, but it may be supposed that such a mechanism as, for example, the rearrangement of the adsorbed detergent molecules may influence the kinetic surface pressure, while it has nothing to do with the surface excess. (The disagreement between the surface pressure and the surface potential as regards the time effect had already been noticed by Addison.[14])

On the basis of the experimental results obtained with a cholesterol or hexadecyl alcohol monolayer on detergent solutions in the present study, we may show the change occurring in the monolayer on compression schematically as in Fig. 18. In this figure the II-b state corresponds to the limiting area of the resulting mixed film. This limiting area is larger than that, the I-b state, for the monolayer on water. Therefore, even if the surface excess of SHS at the surface with a monolayer is the same as that at the free surface, the resulting mixed film must expand. This expansion of the monolayer by SHS molecules adsorbed at the surface will be discussed quantitatively.

The *Π-A* curves of the monolayers on the detergent solutions previously obtained by many workers involve the effect resulting from the compression of the free surface. The reason why the surface pressure increases, while the surface excess of detergent does not, with the compression of the free surface, has not yet been made clear. It is important here that the increase in the surface pressure is not due to the increase in the surface density of SHS. In order to avoid this effect, Harkins et al. have measured the surface pressure by injecting SHS below the hexadecyl alcohol monolayer at each area.[2] These *Π-A* curves are very different from those obtained by Schulman et al.[1] Therefore, by assuming that the expansions of *Π-A* curves are due to the presence of SHS molecules adsorbed at the surface, the surface excess of SHS can be estimated from the increase in the limiting area and can be compared with that obtained directly by the radiotracer method.

According to Harkins et al., the limiting areas obtained by extrapolating the linear portions of each curve to the surface pressure of each substrate solution are larger than that for the monolayer on water by ca. 13.5, 24.5 and 25 Å$^2$ per hexadecyl alcohol molecule for the SHS concentrations of $3\times10^{-6}$, $10^{-5}$ and $3\times10^{-5}$ mol./l. respectively. These values represent the difference in the area between the I-b and II-b states in Fig. 18 in Å$^2$ per hexadecyl alcohol molecule.

In the hexadecyl alcohol monolayer, which is in the closely packed state, there are $5\times10^{14}$ molecules per cm$^2$. Therefore, the increase in the total surface area of the mixed film per unit area of hexadecyl alcohol molecules is

14) C. C. Addison and D. Litherland, *Nature*, **171**, 393 (1953).

$24.5\times5\times10^{-2}$ cm$^2$ for the SHS concentration of $10^{-5}$ mol./l. This increase is regarded as being due to the SHS molecules adsorbed at the surface. If it is assumed that the molecular area of SHS is 40 Å$^2$,[8] this increase in the surface area corresponds to $(24.5\times5\times10^{14})/(40\times6\times10^{23})$ mol. of SHS. Since this quantity of SHS exists within the surface area of $(1+24.5\times5\times10^{-2})$ cm$^2$, $\Gamma_m$ is $2.3\times10^{-10}$ mol./cm$^2$. This value is in excellent agreement with that obtained by our direct measurements, as is shown in Table I. The estimated results for other concentrations of SHS are also shown in Table I.

TABLE I. THE SURFACE EXCESS OF SHS CALCULATED FROM THE DATA OF HARKINS ET AL.

| Concn. of SHS mol./l. | $\Delta A$ Å$^2$ | $\Gamma_m$ (Calcd.) mol. $\times10^{-10}$/cm$^2$ | $\Gamma_m$ (Obs.) mol. $\times10^{-10}$/cm$^2$ |
|---|---|---|---|
| $3\times10^{-6}$ | 12.5 | 1.6 | 1.0 |
| $10^{-5}$ | 24.5 | 2.3 | 2.0 |
| $3\times10^{-5}$ | 25 | 2.3 | 2.0 |

These results show that the expansion of the monolayer can be interpreted as being due to SHS molecules adsorbed at the surface, without assuming the 1 : 1 complex formation. Accordingly, it may be expected that the monolayer will expand as the surface concentration of detergent becomes higher because then the surface concentration of species, including both soluble and insoluble species, becomes higher.

By injecting the identical detergent below various monolayers, the increase in the surface pressure has been measured and has been considered as a measure of the interaction of insoluble with soluble species.[1] However, even if the same adsorption of SHS takes place at the surface with different monolayers, the increases in the surface pressure are not necessarily the same. For the monolayers in the closely-packed state especially, the stability of the monolayer and the change in the chemical potential of the monolayer substance due to the adsorption of SHS, etc., which are also responsible for the increase in the surface pressure, should be taken into consideration.

It can be concluded from the foregoing discussion that the so-called reactivity for penetration is nothing but the surface activity of the detergent. In other words, although Schulman et al. have considered the complex formation to be the principal factor in the phenomenon of the monolayer penetration, we consider it to be the surface activity of soluble species. This concept is consistent with these previous experimental data:

(1) The soluble species which are known to cause the monolayer penetration are all surface active substances.

(2) Therefore, the order of the penetration reactivity of detergents for the identical monolayer should be that of the surface activity of soluble species.

a) It has been shown that, for the detergents with a $C_{12}$-alkyl chain, the order of the penetration reactivity of polar heads is as follows;[15]

$$-SO_4^{2-} > -SO_3^{2-} > -NH_3^+ > -COO^- > -N(CH_3)_3^+$$

By regarding the CMC of detergents as a measure of the surface activity, the order of the penetration reactivity is the same as that for the surface activity of soluble species.

b) For long-chain alkyl sulfates, the longer the alkyl chain, the stronger the penetration reactivity of the detergents.[1] The surface activities of detergents are, of course, in the same order.

c) It has been shown that the penetration reactivity of detergents increases with the addition of salt.[7] This should be attributed to the well-known fact that the addition of salt increases the surface adsorption of detergents.[16]

In the present paper we have pointed out the misinterpretation of the monolayer penetration and have verified that the difference between the properties of the monolayers on the detergent solution and those on water is to be attributed merely to the presence of the detergent molecules adsorbed at the surface.

Finally, it is important to note here that the change in the surface pressure alone in the course of the penetration experiment provides no exact information as to whether the complex is formed or not.

## Summary

The surface pressure - area isotherms of monolayers of cholesterol, hexadecyl alcohol and octadecyl amine on sodium alkyl sulfate solutions and the surface excess of alkyl sulfate have been measured by the film balance and the radiotracer methods respectively. These measurements were carried out with (1) the monolayers spread on the alkyl sulfate solutions, (2) those below which the detergent solutions were injected, and (3) those formed by the spreading of the insoluble species - detergent mixtures on water.

All the surface pressure - area curves showed

15) B. A. Pethica and J. H. Schulman, *Biochem. J.*, **53**, 177 (1953).

16) R. Matuura, H. Kimizuka and A. Matsubara, This Bulletin, **34**, 1512 (1961).

remarkable expansions; the results were essentially the same as those observed by Schulman et al. and by others.

On the other hand, the surface excess of alkyl sulfates showed no appreciable increase in the case of cholesterol and hexadecyl alcohol, and it was too low to form a stoichiometric complex between the insoluble species and the alkyl sulfate; only in the presence of the octadecyl amine did it increase to an amount sufficient to form the 1 : 1 stoichiometric salt.

Thus it has been concluded that the expansion of the surface pressure - area curve can not be an indication of the stoichiometric complex formation. It has been pointed out that the surface pressure of the detergent solution increases with the compression, even in the absence of a monolayer; this is the main cause for the expansion of the surface pressure - area curve of the penetrated monolayer. The phenomenon of monolayer penetration has been explained in terms of the formation of the adsorbed layer of alkyl sulfate, and the reactivity for penetration has been related to the surface activity of detergents.

The author wishes to express his thanks to Professor Ryohei Matuura and Dr. Hideo Kimizuka of our laboratory for their valuable advice and constant encouragement.

*Department of Chemistry*
*Faculty of Science*
*Kyushu University*
*Hakozaki, Fukuoka*

# A Molecular Orbital Treatment of Hydrogen Bonds. I. Preliminary Results

By Keiji MOROKUMA, Hiroshi KATO, Teijiro YONEZAWA and Kenichi FUKUI

(Received September 2, 1964)

The hydrogen bond, a weak bonding between a hydrogen donor, such as hydroxyl and amino groups, and an acceptor, such as oxygen and nitrogen atoms, has long attracted the attention and interest of many researchers, in both the experimental and theoretical fields.[1,2]

As to the theoretical study, Coulson and Dannielsson[3] calculated semiempirically the delocalization energy of the hydrogen bond in a fictitious O—H···O fragment. Tsubomura's nonempirical study was carried out on water.[4] Arranging existing theoretical treatments, Coulson[5] tabulated the contribution of various kinds of energy to the hydrogen-bond stabilization of water, thus emphasizing that the delocalization energy plays an important role in the stabilization.

This series of papers will attempt to discuss the stabilization energy and other changes in electronic structures by the hydrogen-bond formation from the point of view not of the fictitious fragment but of the whole molecule.

In the present paper, as a preliminary discussion, we will calculate the changes in the electronic energy and the charge distribution upon the hydrogen-bond formation, by using the simple LCAO MO method extended by Hoffmann,[6] in which all valence atomic orbitals (AO) are taken into account. The Coulomb integral, $H_{rr}$, of an atomic orbital is the negative value of the ionization potential of the valence state of the neutral atom,[7] which is tabulated in Table I. The resonance integral,

Table I. Coulomb integral of various atomic orbitals (eV.)

| Atom | Orbital | | |
|---|---|---|---|
| | 1s | 2s | 2p |
| Hydrogen | −13.60 | — | — |
| Carbon | — | −21.43 | −11.42 |
| Oxygen | — | −35.30 | −17.76 |

$H_{rs}$, between the $r$th and the $s$th AO's is given by the following equation:

1) "Hydrogen Bonding," Ed. by D. Hadzi, Pergamon Press, London (1959).
2) G. Pimentel and A. L. McClellan, "The Hydrogen Bond," W. H. Freeman & Co., San Francisco (1960).
3) C. A. Coulson and V. Dannielsson, *Arkiv Fysik*, **8**, 239, 245 (1954).
4) H. Tsubomura, This Bulletin, **21**, 415 (1954).
5) C. A. Coulson, *Research*, **10**, 149 (1957).
6) R. Hoffmann, *J. Chem. Phys.*, **39**, 1397 (1963).
7) H. O. Pritchard and H. A. Skinner, *Chem. Revs.*, **55**, 745 (1955).

$$H_{rs}=\frac{1}{2}KS_{rs}(H_{rr}+H_{ss})$$

where $K=1.75$ and $S_{rs}$ is the overlap integral between the AO's. Calculation is carried out on formic acid and its dimer, acetylacetone and salicylaldehyde (with a hydroxyl group as a proton donor and with a carbonyl group as an acceptor), and also on benzyl alcohol and allyl alcohol (with a hydroxyl group as a proton donor and a $\pi$ electron system as an acceptor).

The program was coded so that, on giving tables of the Coulomb integrals of every kind of atom included, of the three-dimensional coordinates of atoms, and of the effective nuclear charges of atomic orbitals, the overlap integrals can be calculated with Slater AO's by means of the formulae of Mulliken et al.,[8] the resonance integrals can also be calculated, and the secular equation can be diagonalized to give the eigen-values and eigenvectors, the total energy, the atomic orbital populations, and the atomic populations. The effective nuclear charges employed were $Z_H=1.0$, $Z_C=3.25$ and $Z_O=4.55$.

In all compounds, except for those noted, the atomic distances were taken as follows:[9] C-H: 1.09Å, C-C: 1.54Å, C=C: 1.34Å, C-C (aromatic): 1.40Å, C-O: 1.23Å, C-O (alcohol): 1.43Å, C-O (carboxylic acid): 1.36Å, O-H: 0.96Å. The bond angles are assumed to be 120° for an unsaturated carbon atom, the tetrahedral angle for a saturated carbon atom.

## The Electronic Structure of Non-Hydrogen-Bonded Molecules

Prior to discussing the hydrogen bond, a brief review of the calculated electronic structures of some carboxylic acid, of ketone, of aldehyde and of alcohol will be given in this section, since the extended LCAO MO method has not previously been applied to such polar compounds.

Figure 1 shows the net charge on each atom of formic acid and salicylaldehyde. One can see in the figure that, though the general tendency of the polarization is well visualized, the net negative charge on each oxygen atom seems to be too large, whereas the population on the hydroxyl hydrogen atom is unexpectedly small. In this approximation the polarity of a polar bond seems to be overestimated. This is because the Coulomb integral of an atomic orbital was kept constant although it might really be more positive when the population on the atom increases. It is indispensable for this extended LCAO MO method to decide the Coulomb integral of an atomic orbital in a polar group not merely by the ionization potential of the neutral atom but also by the population on the atom. On this point we will give a detailed discussion is a following paper.

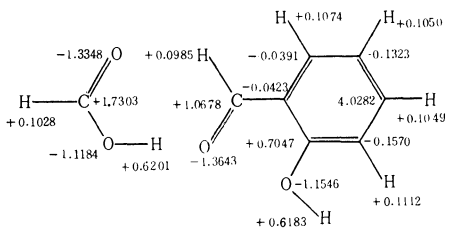



Fig. 1. Net charge of formic acid and salicylaldehyde.

The total energy of methyl alcohol is calculated for various configurations in Table II. As to the rotational isomers, the configuration I, in which the OH bond takes the trans conformation to the CH bond in the C-O-H plane*, is predicted to be a configuration of local minimum energy.

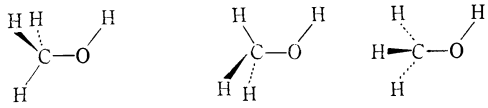
TABLE II. TOTAL ENERGY OF METHYL ALCOHOL AND ACETYLACETONE

A) Methyl alcohol

| Configuration | ∠COH | Total energy, eV. |
|---|---|---|
| III | 110° | −287.4014 |
| II | 110° | −287.3941 |
| I | 110° | −287.4087 |
| I | 105° | −287.3293 |
| I | 100° | −287.2362 |

B) Acetylacetone

| Configuration | Total energy, eV. |
|---|---|
| Keto | −789.4969 |
| Enol | −788.3440 |



(I) (II) (III)

Keto and enol forms of acetylacetone are also compared in Table II. The keto form is more stable than the enol form, contrary to experience. This is either due to the inappropriate parametrization in this method, mentioned in the previous section, or to a substantial defect involved in the present method,

8) R. S. Mulliken, C. A. Rieke, D. Orloff and H. Orloff, *J. Chem. Phys.*, **17**, 1248 (1949).

9) Tables of Interatomic Distances and Configuration in Molecules and Ions, Special Publication No. 11, The Chemical Society, London (1958).

* In the figure, the bonds drawn with full lines denote those lying in the C-O-H plane, the atoms indicated by wadges being above the same plane and those by dotted lines, below that plane.

where electronic and nuclear repulsion energies are not explicitly taken into account.

## Energy and Electron-distribution Changes Caused by Hydrogen-bond Formation

In this section will be calculated the energy and electron distribution changes caused by the hydrogen-bond formation. The configurations on which the calculations were carried out are shown in Fig. 2, as are the coordinates and the numbering of the atomic orbitals. They include some configurations in which the hydroxyl hydrogen is located near the carbonyl group (IV, V and VIII) or near the conjugated system (XI and XIII).

**Overlap Integral.**—Table III shows some values of the overlap integral between the hydroxyl hydrogen or the hydroxyl oxygen of a formic acid monomer and the carbonyl oxygen of the other monomer at various $O_3$-$O_7$ and $O_7$-$H_6$ distances. One can see from the table that a considerable amount of overlapping exists between the hydrogen, $H_6$ and the oxygen, $O_3$. (Compare the 1s—2s overlap integral in a normal O-H bond, 0.5076.) The overlap between $O_3$ and $O_7$ is very small.

**Delocalization Energy.**—Tables IV, V and VI give the total electronic energy of each configuration of the formic acid dimer, of salicylaldehyde and of acetylacetone respectively. In the tables "tetra" means the tetrahedral angle, 109°28′.

Table III. Overlap integrals between proton acceptors and donors in formic acid dimer

| | | | | | | |
|---|---|---|---|---|---|---|
| $O_3$-$O_7$ | distance, Å | 2.8 | 2.7 | 2.6 | 2.7 | 2.6 |
| $O_4$-$H_5$ | distance, Å | 0.96 | 0.96 | 0.96 | 1.06 | 1.06 |
| $O_3$-$H_6$ | 2s-1s | 0.1365 | 0.1593 | 0.1853 | 0.1853 | 0.2148 |
| | 2px-1s | 0.1151 | 0.1323 | 0.1513 | 0.1513 | 0.1719 |
| | 2py-1s | 0.0258 | 0.0314 | 0.0381 | 0.0381 | 0.0461 |
| | 2pz-1s | 0 | 0 | 0 | 0 | 0 |
| $O_3$-$O_7$ | 2pz-2pz | 0.0010 | 0.0014 | 0.0019 | 0.0014 | 0.0019 |

Table IV. Delocalization energy of hydrogen bond in formic acid dimer[a)]

| Model | $O_3 \cdots O_7$ distance Å | $O_7 \cdots H_6$ distance Å | $O_3 \cdots H_6$ distance Å | Total energy eV. | Delocalization energy eV. |
|---|---|---|---|---|---|
| Monomer | — | 0.96 | — | −402.9270 | — |
| 1 | 2.8 | 0.96 | 1.89 | −806.0106 | +0.1566 |
| 2 | 2.7 | 0.96 | 1.79 | −806.0181 | +0.1641 |
| 3 | 2.6 | 0.96 | 1.69 | −806.0031 | +0.1491 |
| 4 | 2.7 | 1.06 | 1.69 | −805.6966 | −0.1574 |
| 5 | 2.6 | 1.06 | 1.60 | −805.7198 | −0.1342 |

a) ∠COH was assumed to be tetrahedral.

Table V. Delocalization energy of hydrogen bond in salcylaldehyde

| Model | Configuration | $\angle C_5O_{11}H_{12}$ | O···H distance, Å | Total energy, eV. | Delocalization energy, eV. |
|---|---|---|---|---|---|
| 1 | V | tetra | 1.7 | −895.9422 | +0.0697 |
| 2 | VI | tetra | — | −895.8623 | −0.0102 |
| 3 | VII | tetra | — | −895.8725 | 0 |
| 4 | V | 100° | 1.63 | −895.7905 | +0.0918 |
| 5 | VI | 100° | — | −895.6987 | 0 |

Table VI. Delocalization energy of hydrogen bond in acetylacetone

| Model | Configuration | $\angle C_8O_{14}H_{15}$ | O···H distance, Å | Total energy, eV. | Delocalization energy, eV. |
|---|---|---|---|---|---|
| 1 | VIII | tetra | 1.64 | −788.3440 | +0.0813 |
| 2 | IX | tetra | — | −788.2627 | 0 |
| 3 | X | tetra | — | −787.9316 | −0.3311 |
| 4 | VIII | 100° | 1.57 | −788.1908 | +0.0901 |
| 5 | IX | 100° | — | −788.1007 | 0 |

TABLE VII. ORBITAL ENERGIES AND ATOMIC ORBITAL COEFFICIENTS

| No. | | | 1 | 2 | 3 | 4 | 5 | 6 |
|---|---|---|---|---|---|---|---|---|
| Orbital energy | | | −37.6982 | −35.4224 | −21.5491 | −18.6819 | −18.5219 | −18.3101 |
| Orbital energy of dimer | | | −37.8687 | −35.6519 | −21.9509 | −19.1322 | −18.6206 | −18.3317 |
| | | | −37.5304 | −35.2149 | −21.1862 | −18.2247 | −18.4591 | −18.2884 |
| Atomic orbital coefficient | $H_1$ | 1s | −0.0172 | 0.0067 | −0.2234 | −0.0208 | −0.1474 | 0.0 |
| | $C_2$ | 2s | 0.2744 | 0.0413 | −0.4266 | 0.0428 | −0.0289 | 0.0 |
| | | 2px | 0.0221 | 0.0331 | 0.1392 | 0.0385 | 0.1907 | 0.0 |
| | | 2py | 0.0107 | 0.0949 | 0.0812 | 0.1471 | −0.1546 | 0·0 |
| | | 2pz | 0.0 | 0.0 | 0.0 | 0.0 | 0.0 | 0.2403 |
| | $O_3$ | 2s | 0.6186 | 0.6017 | 0.2515 | −0.1266 | 0.0224 | 0.0 |
| | | 2px | 0.0090 | 0.0168 | 0.3015 | −0.3297 | 0.5778 | 0.0 |
| | | 2py | 0.0097 | 0.0191 | 0.2871 | −0.4246 | −0.3640 | 0.0 |
| | | 2pz | 0.0 | 0.0 | 0.0 | 0.0 | 0.0 | 0.7348 |
| | $O_4$ | 2s | 0.5347 | −0.6885 | 0.1373 | −0.1023 | −0.0532 | 0.0 |
| | | 2px | −0.0066 | 0.0092 | 0.2658 | 0.6977 | 0.0434 | 0.0 |
| | | 2py | −0.0034 | 0.0194 | −0.3382 | 0.0669 | 0.5258 | 0.0 |
| | | 2pz | 0.0 | 0.0 | 0.0 | 0.0 | 0.0 | 0.5363 |
| | $H_5$ | 1s | 0.0496 | −0.1031 | 0.1848 | 0.1747 | −0.0374 | 0.0 |

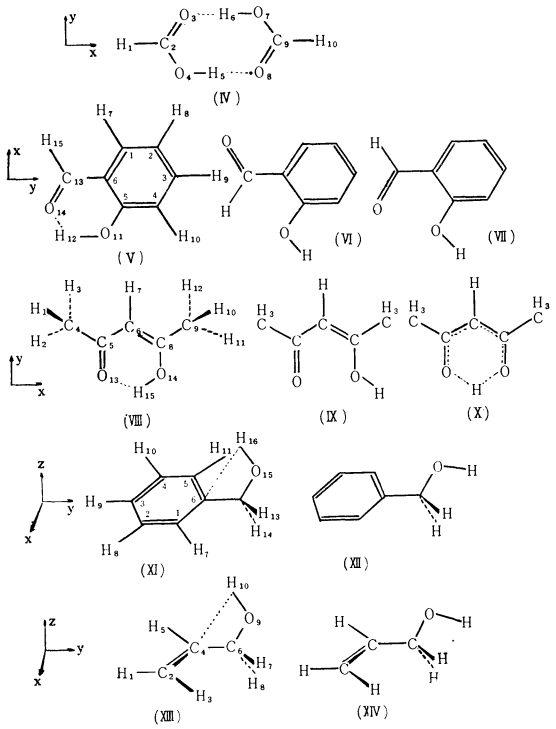


Fig. 2. Configurations compared.

In the present treatment, the delocalization energy due to hydrogen bonding, $E_d$, is given by the difference in the total electronic energies between a configuration with a hydrogen bond and a configuration without it.

For the formic acid dimer, the delocalization energy is calculated in Table IV as the difference between the total electronic energy of two monomers and that of a dimer. Model 2 (O···O distance 2.7Å and O-H distance 0.96Å) is the most stable from the viewpoint of the delocalization energy. It is interesting that the approach from 2.7Å to 2.6Å makes the dimer more unstable, though the O···H overlap gets larger. As was discussed in the preceding section, factors other than the delocalization will participate in deciding the most stable configuration of the hydrogen-bonded species. However, it is noteworthy that, in this example, the observed O···O distance in the gaseous dimer, 2.72—2.73Å,[10] corresponds well with the prediction. Model 3 shows that a also shortened O···O distance decreases the stabilization, though it also causes an increase of the oxygen-hydrogen overlap (Table III). The delocalization energy of model 2 is 0.164 eV., 3.77 kcal./mol., whereas the observed stabilization energy, $\Delta H$, of two hydrogen bonds in the gaseous dimer is ca. 7.1 kcal./mol.[11] Coulson estimated the contribution of the delocalization energy to the stabilization energy of the hydrogen bond of water to be 8 ± 4 kcal./mol.[4,5] The value obtained in this approximation might be somewhat too small. There may be two reasons for this in addition to the one stated in the preceding chapter: 1) As was stated in the previous section, since in this approximation the polarity of a bond is emphasized too much, the delocalization of electrons on the proton acceptor to the proton donor seems to be hindered. 2) In this approximation the delocalization energy is exclusively attributed to the $\sigma$ electrons (including so-called lone pairs), and not at all to the $\pi$ electrons. Since a hydrogen atom has no

10) J. Karle and L. O. Brockway, *J. Am. Chem. Soc.*, **66**, 574 (1944); O. Bastiansen, *Tids. Kjemi. Bergvesen Met.*, **4**, 81 (1944), cited in Ref. 2.

11) Average value of data collected in Ref. 2.

OF FORMIC ACID AND ORBITAL ENERGIES OF ITS DIMER (MODEL 2)

| 7 | 8 | 9 | 10 | 11 | 12 | 13 | 14 |
|---|---|---|---|---|---|---|---|
| −17.6885 | −17.5253 | −16.0660 | −9.4663 | 0.9907 | 10.6161 | 15.1478 | 29.3562 |
| −17.7038 | −17.5484 | −16.1880 | −9.4673 | 1.7635 | 12.1657 | 15.2001 | 29.3304 |
| −17.6733 | −17.4925 | −15.9437 | −9.4654 | 2.0067 | 13.3014 | 15.8455 | 29.4173 |
| 0.0 | −0.0700 | 0.4509 | 0.0 | −0.1640 | −0.1405 | −1.1468 | 0.7473 |
| 0.0 | −0.0232 | 0.1655 | 0.0 | −0.3620 | −0.2192 | 0.4499 | −1.3246 |
| 0.0 | 0.1012 | −0.3639 | 0.0 | −0.4428 | −0.3450 | −1.1393 | −0.2156 |
| 0.0 | 0.0808 | 0.0287 | 0.0 | 0.8258 | 0.5366 | −0.4383 | −0.6898 |
| −0.0123 | 0.0 | 0.0 | 1.0048 | 0.0 | 0.0 | 0.0 | 0.0 |
| 0.0 | −0.0190 | −0.0438 | 0.0 | −0.0455 | 0.0611 | 0.4732 | 0.8183 |
| 0.0 | 0.0899 | 0.6149 | 0.0 | 0.1285 | 0.1111 | −0.1545 | −0.4784 |
| 0.0 | −0.6853 | −0.0687 | 0.0 | −0.1297 | −0.1409 | −0.3055 | −0.5019 |
| −0.5852 | 0.0 | 0.0 | −0.4056 | 0.0 | 0.0 | 0.0 | 0.0 |
| 0.0 | 0.0548 | −0.1053 | 0.0 | 0.0437 | 0.9007 | −0.1422 | 0.0638 |
| 0.0 | −0.3507 | 0.2913 | 0.0 | −0.5895 | 0.3556 | 0.1301 | −0.0062 |
| 0.0 | −0.5977 | −0.2301 | 0.0 | 0.5290 | 0.3020 | −0.0599 | 0.1478 |
| 0.8140 | 0.0 | 0.0 | −0.2649 | 0.0 | 0.0 | 0.0 | 0.0 |
| 0.0 | −0.0596 | 0.0648 | 0.0 | 0.7980 | −0.9594 | 0.0992 | 0.0754 |

$\pi$ orbital, the direct overlap between oxygen atoms is very small, as is shown in Table III. This small overlap contributes almost nothing to the stabilization energy.

The contribution of the vacant $2p\pi$ orbital on the intervening hydrogen atom, which might play the role of a stepping stone between two oxygen orbitals, will be discussed below.

There is another possibility of the $\pi$-electron stabilization. The transfer of the $\sigma$ electron on the carbonyl oxygen to the O-H bond (see the next section) will actually change the Coulomb integral of their $\pi$ orbitals. This effect may cause a variation in the total $\pi$ electron energy of the system. As was shown in the previous section, this effect was not taken into account in the approximation employed here.

For salicylaldehyde the energy of the hydrogen-bonded configuration (V) is lower than those of other configurations (VI and VII). The delocalization energy is of the order of 0.07 eV. When the COH angle, i.e., the distance between the hydroxyl hydrogen and the carbonyl oxygen, is decreased, the delocalization energy seems to increase with the formation of a stronger hydrogen bond, though the total energy decreases. For the enol form of acetylacetone, the delocalization energy of model 1 referred to that of model 2 is 0.081 eV. Model 3 is the configuration in which the hydrogen atom, $H_{15}$, is situated between two oxygen atoms, with the COH angle tetrahedral, and in which the molecule has a normal plane of symmetry, with the C-O bond length of 1.33Å and the C-C bond length of 1.44Å. The calculation shows this configuration to be very unstable.

**Orbital Energy.**—Table VII shows the energy levels and their atomic orbital coefficients of the formic acid monomer, with the corresponding energy levels of its dimer. In the extended LCAO approximation every atomic orbital can conjugate with other atomic orbitals; therefore, no completely localized molecular orbital (lone-pair orbital) remains. In the present calculation, the highest occupied orbital is a sigma-type bond, and the next highest orbital seems to correspond to the lone-pair orbital. This point seems to be a difficulty which might be overcome by an SCF technique.

In the present calculation, each level of the monomer splits into two levels upon the dimer formation, one being higher and the other lower than the initial level, as may be seen in Table VII, which may cause a red shift for both $\pi$-$\pi^*$ and $n$-$\pi^*$ types of transitions in contradiction to the experimental finding by Barnes and Simpson (*J. Chem. Phys.*, **39**, 670 (1963)). They observed that the spectrum undergoes a blue shift upon dimerization. As to salicylaldehyde, the calculated sequence of the lone pair, the $\pi$ and the $\sigma$ orbitals does not agree with the order expected from the references.[12] Hence, the present result is unsuccessful in predicting the shift of their transition.

This discrepancy probably stems from an inappropriate parametrization of the lone-pair atomic orbitals. The Coulomb integral of the 2p lone pair atomic orbital of oxygen remains at −17.76 eV., too low to be compared with the experimental results.

**Population Analysis.**—The atomic orbital population, $N_r$; the atomic population, $M_x$; the atomic orbital bond population, $N_{rs}$, and the

12) E. g., J. W. Sidman, *Chem. Revs.*, **58**, 689 (1958).

bond population $M_{xy}$, are defined as follows:[13]

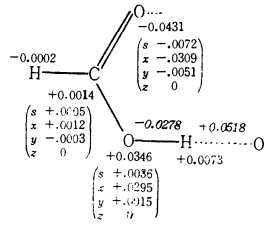
$$N_r = 2 \sum_{l}^{occ} \sum_{s} C_r^l C_s^l S_{rs}$$

$$M_x = \sum_{r}^{onX} N_r$$

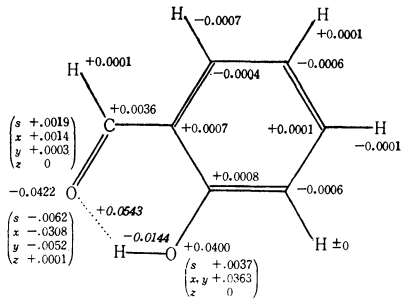
$$N_{rs} = 4 \sum_{l}^{occ} C_r^l C_s^l S_{rs}$$

$$M_{xy} = \sum_{r}^{onX} \sum_{s}^{onY} N_{rs}$$

where $C_r^i$ is the coefficient of the $r$th AO in the $i$th molecular orbital. Figure 3 shows the increase in the AO population and in the atomic population caused by the hydrogen bonding. The population on the carbonyl oxygen decreases, while, on the other hand, the population on the hydroxyl group increases. This is what one may expect. One can see in Fig. 3, in the case of formic acid, that the population on the 2px orbital, the orbital directing to the hydrogen atom of the partner molecule, plays a dominant role. An inspection of the orbital coefficients of the formic acid dimer makes it clear that the population transfers not within a monomer but from the carbonyl group of one monomer to the hydroxyl bond of the other. It is interesting that the increase in the population takes




a) Formic acid (difference between the model 2 and monomer)




b) Salicylaldehyde (difference between the models 1 and 3)

Fig. 3. Increase of population by hydrogen bond.

13) R. S. Mulliken, *J. Chem. Phys.*, **23**, 1833, 1841, 2338, 2343 (1955). The notation is a little different from that of Mulliken's paper.

place at the oxygen atom, not at the hydrogen atom. The population on the hydrogen atom increases in some cases (e. g., formic acid) and decreases in other cases (e. g., salicylaldehyde).

The bond populations of several interesting bonds are also given in Fig. 3 in italic letters. The bond population, $N_{O\cdots H}$, between the carbonyl oxygen and the hydroxyl hydrogen is positive, showing that there is a weak "bond" between them. The ratio of the AO population of the 2s atomic orbital of the oxygen to the sum of those of the 2px and 2py orbitals is approximately 1 to 2.2. On the other hand, the bond population, $N_{OH}$, of the hydroxyl group decreases. In the case of formic acid, for instance, the $N_{OH}$ of the monomer, 0.458, decreases by (0.028) about 5% of the initial value.

These results qualitatively correspond to the lowering of the O-H stretching frequency in the infrared spectrum.[1]

**The Contribution of the 2p$\pi$ Orbital on the Hydrogen Atom.**—As has been stated previously, the vacant 2p$\pi$ orbital on the hydroxyl hydrogen was taken into consideration in order to see the effect of the direct conjugation of $\pi$ electrons through the hydrogen atom.[14] The Coulomb integral of the orbital is taken to be −3.4 eV. on the basis of the spectroscopic date,[15] with the effective nuclear charge being $Z=1.0$. The energy levels thus calculated are shown in Table VIII. (The 2p$\pi$ orbital is considered only on the hydroxyl hydrogen.)

The $\pi$ delocalization energy, which was −0.0002 eV. without the orbital, rises to 0.002 eV. when the 2p$\pi$ orbital is included ; the amount is still negligible, however. Thus, we can hardly expect the delocalization energy due to the 2p$\pi$ conjugation through the hydrogen atom.

Paoloni[16] discussed the contribution of the 2p$\sigma$ orbital on the hydrogen atom to the delocalization energy. In this paper this effect is not considered.

**The $\pi$ Hydrogen Bond.**—It has been recognized that $\pi$ electron systems, such as the phenyl group or the olefinic group, can be proton acceptors when they interact with proton donors. Benzyl alcohol and allyl alcohol, for instance, are known to have a $\pi$ hydrogen bond. The stabilization energy, $\Delta H$, due to a $\pi$ hydrogen bond has been estimated to be 1 to 2 kcal./mol.,[2] smaller than that of usual hydrogen bonds.

With respect to benzyl alcohol and allyl alcohol, we made the same calculation as was

14) D. N. Shigorin, Ref. 1, p. 191 (1959).
15) L. C. Moore, "Atomic Energy Levels," National Bureau of Standards.
16) L. Paoloni, *J. Chem. Phys.*, **30**. 1045 (1959).

TABLE VIII. $\pi$ ENERGY LEVELS OF FORMIC ACID AND ITS DIMER WITH 2p ORBITAL ON THE HYDROGEN ATOM

| | | Monomer | Dimer (model 2) |
|---|---|---|---|
| $\pi$ Energy level | Occupied | −18.3131 eV. | −18.3365 eV. |
| | | | −18.2897 |
| | | −17.6894 | −17.7060 |
| | | | −17.6736 |
| | Unoccupied | −9.4668 | − 9.4696 |
| | | | − 9.4686 |
| | | −2.5463 | − 3.2799 |
| | | | + 0.7923 |
| Total energy | | −72.0049 | −144.0117 |
| Total energy (without hydrogen $2p\pi$ orbital) | | −71.9972 | −143.9942 |

TABLE IX. ENERGY OF $\pi$ HYDROGEN BOND IN BENZYL ALCOHOL AND ALLYL ALCOHOL

Benzyl alcohol

| Model | Configuration | ∠COH | $C_6\cdots H_{16}$ distance, Å | Total energy, eV. | Delocalization energy, eV. |
|---|---|---|---|---|---|
| 1 | XI | tetra | 2.33 | −780.0563 | −0.0129 |
| 2 | XII | tetra | — | −780.0692 | 0 |
| 3 | XI | 90° | 2.01 | −779.6947 | +0.0284 |
| 4 | XII | 90° | — | −779.6663 | 0 |

Allyl alcohol

| Model | Configuration | ∠CCO | ∠COH | $C_4\cdots H_{10}$ distance, Å | Total energy, eV. | Delocalization energy, eV. |
|---|---|---|---|---|---|---|
| 1 | XIII | 110° | 110° | 2.35 | −463.0088 | −0.0141 |
| 2 | XIV | 110° | 110° | — | −463.0229 | 0 |
| 3 | XIII | 110° | 100° | 2.18 | −462.8460 | +0.0005 |
| 4 | XIV | 110° | 100° | — | −462.8455 | 0 |
| 5 | XIII | 105° | 110° | 2.24 | −463.0052 | +0.0078 |
| 6 | XIV | 105° | 110° | — | −462.9974 | 0 |
| 7 | XIII | 105° | 100° | 2.07 | −462.8414 | +0.0200 |
| 8 | XIV | 105° | 100° | — | −462.8214 | 0 |
| 9 | XIII | 100° | 110° | 2.12 | −462.9125 | +0.0271 |
| 10 | XIV | 100° | 110° | — | −462.8854 | 0 |
| 11 | XIII | 100° | 100° | 1.95 | −462.7471 | +0.0365 |
| 12 | XIV | 100° | 100° | — | −462.7106 | 0 |

carried out in the previous sections. The geometrical data of the molecules calculated are collected in Table IX. The overlap integrals between the hydroxyl hydrogen, $H_{10}$, and the nearest $sp^2$ carbon, $C_4$, for instance, in model 3 (with the hydrogen bond) and model 4 (without the hydrogen bond) of allyl alcohol are as follows:

| | Model 3 | Model 4 |
|---|---|---|
| Hls-C2s | 0.1519 | 0.0321 |
| Hls-C2py | 0.0898 | 0.0350 |
| Hls-C2pz ($\pi$) | 0.1368 | 0.0138 |

The magnitude of these overlap integrals for model 3 is of the same order as for the dimer of formic acid (Table III).

In spite of this large overlap, the delocalization energy calculated is extremely small. For the most stable CCO and COH angles (models 1 and 2) of allyl alcohol, the hydrogen-bonded configurations, XIII, is a little more unstable than the nonbonded configuration, XIV. There are two factors affecting the delocalization energy. One is the energetic contribution of the methylol group to the total electronic energy. Referring to Table II, in which the total energy of methyl alcohol is given with respect to three configurations, it may be considered that the methylol group in the configuration XIII of Fig. 2 makes a smaller contribution to the total energy than that in the configuration XIV of the same figure. The other factor is the stabilization due to the formation of a $\pi$ hydrogen bond. On comparing models 1 and 2, since the $C_4\cdots H_{10}$ distance is rather large and since, therefore, the delocalization energy is small, and is, furthermore, in this approximation estimated

to be too small, the former factor overcomes the latter. If we shorten the $C_4 \cdots H_{10}$ distance by reducing the CCO or/and the COH angles, the energy of the configuration XIII referred to that of XIV becomes more stable, as is shown in Table IX.

Thus, the small stabilization energy of a $\pi$ hydrogen bond seems partly due to the compensation with the energy difference between the configurations, such as I and II.

The change in atomic and bond population upon the hydrogen bonding, that is, the population difference between models 3 and 4 of allyl alcohol, is shown in Fig. 4. One can notice that the population transfers from the allyl group to the hydroxyl group. However, the change amounts to only 10% of that in a usual hydrogen bond (Fig. 3).

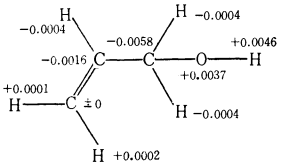



Fig. 4. Increase of population by $\pi$ hydrogen bond (difference between the models 3 and 4).

## Discussion

In discussing the changes in electronic structures by the hydrogen-bond formation, some defects of the extended LCAO MO method were revealed: 1) The absolute value of the Coulomb integral of the so-called lone-pair atomic orbital is too large. 2) A change in the population on a orbital does not affect the Coulomb integral of the orbital. Accordingly, the stabilization energy is very small.

These two defects may be overcome if the Coulomb integral is varied according to the AO population on the atomic orbital and according to those on the other atomic orbitals on the same atom. This correction may mean considering the electronic interaction implicitly.

Finally, a certain apparent parallelism between the delocalization energy and the experiments is observed; the electronic and nuclear repulsion energies are, however, not taken into account explicitly, as has been pointed out above, in the present treament. The agreement should be checked by further investigation. These improvements, together with the problems of the parametrization of the resonance integral, will be reported on in the near future.

## Summary

1) The changes caused by hydrogen bonds in the electronic structure of several molecules have been discussed by the use of the extended LCAO MO method.

2) The delocalization energy have been calculated to be 3.8 kcal./mol.

3) The frequency shifts in the ultraviolet spectrum cannot be explained.

4) In the formic acid dimer it has clearly been shown that the population transfers from the carbonyl group to the hydroxyl group and that a small bond population arises between them.

5) The $2p\pi$ orbital on the hydrogen atom contributes almost nothing to the $\pi$ delocalization energy.

6) The $\pi$ hydrogen bond has also been discussed.

7) The defects in the extended LCAO MO method in treating molecules with polar groups or lone pairs have been pointed out, a method for improvement suggested, and some critical discussion of the present treatment added.

The calculation was carried out on the IBM 7090 at the Japan IBM Co., with the permission of the UNICON Committee, whose kindnees we hereby acknowledge.

*Faculty of Engineering*
*Kyoto University*
*Sakyo-ku, Kyoto*

# The Nuclear Magnetic Resonance Spectra of Some 4, 6-Disubstituted *o*-Cresols*

By Michio KONDO

(Received September 12, 1964)

In the application of the NMR technique to the organic structure determination, it is a useful principle that chemical shifts of aromatic ring protons can be estimated by using several substituent parameters. Many studies have been carried out in order to obtain such substituent parameters. Spiesecke and Schneider[1] determined the shielding parameters of substituents from their study of a series of partially-deuterated monosubstituted benzenes. Diehl[2] also evaluated these parameters by an indirect method, in which he assumed that two equal or different substituents in the meta or the para position behave additively with respect to the chemical shift of a ring proton. The discrepancies between the two results, which probably reflect the approximate validity of the additivity rule, are less than 0.1 p. p. m. The utility of these substituent parameters has been demonstrated for several *m*- and *p*-disubstituted benzenes.[3] Martin and Dailey[4] showed that the ring-proton chemical shifts of a number of polysubstituted benzenes can be represented by simple sums of substituent-shielding constants with an accuracy of about 0.1 p. p. m., except for ring protons adjacent to substituents which are ortho to each other. In these positions, the large deviations observed presumably arise from strong interaction between the neighboring substituents separated approximately by the sum of van der Waals radii. They discussed the shielding mechanism and concluded that the proton chemical shifts in the disubstituted benzenes appear to arise primarily from changes in the $\pi$-electron density in the ring due to substituent perturbation. Other factors, for example, electric field and magnetic anisotropy of substituents, have minor effects upon ring proton chemical shifts.

Since it is not obvious whether or not the shielding parameters remain unchanged in the case of tetrasubstituted benzenes, it is of interest to test the additivity of shielding parameters in some 4, 6-disubstituted *o*-cresols. In addition, these compounds are suitable for studying the correlation between ring proton-coupling constants and the electronegativities of substituents, because there are only meta proton couplings.

On the other hand, the broadening of the NMR signals of methyl-substituted benzenes has been ascribed to the spin-spin coupling between methyl and ring protons (hereafter referred to as "benzylic coupling"). Quite recently, Nair and Gopakumar[5] studied the correlation between the variation in the benzylic coupling and changes in the $\pi$-electron distribution in some methyl-substituted aromatic compounds. They reported that the values of benzylic couplings in 2-methylnaphthalene and 2-methylanthracene are 0.7 and 0.8 c. p. s. respectively, and that the well-known difference in the bond order for the 1–2 bonds in naphthalene and anthracene is reflected in the observed splittings. The coupling to the 3-protons was reported to be weak. The following conclusion was drawn regarding the possibility of the splitting of the NMR signal of a methyl group attached to an aromatic ring with protons in both ortho positions. When the bond order values of the two bonds adjacent to a C–$CH_3$ bond are comparatively small and not very different from each other, no splitting can be expected for its resonance peak. On the other hand, when there is a considerable difference between the bond-order values or when the bond order values are both quite large, clear splittings should be observable. Shoolery[6] presented a good example, showing a close relation between the benzylic coupling and the bond-order values of the ring. Whereas a benzenoid thymol system shows no resolvable benzylic coupling, a thymoquinone system shows clear splittings in the signals. Regarding this point, it is suggestive that the coupling between methyl and ring protons is observed in heteroaromatic compounds, such

* Presented partly at the 17th Annual Meeting of the Chemical Society of Japan, Tokyo, April, 1964.

1) H. Spiesecke and W. G. Schneider, *J. Chem. Phys.*, **35**, 731 (1961).

2) P. Diehl, *Helv. Chim. Acta*, **44**, 829 (1961).

3) B. Bak, J. B. Jensen, A. L. Larsen and J. Rastrup-Andersen, *Acta Chem. Scand.*, **16**, 1031 (1962).

4) J. S. Martin and B. P. Dailey, *J. Chem. Phys.*, **39**, 1722 (1963).

5) P. M. Nair and G. Gopakumar, *Tetrahedron Letters*, No. **13**, 709 (1964).

6) J. N. Shoolery, *Varian Associates, Tech. Bull.*, **2**, 8 (1957); J. D. Roberts, "Nuclear Magnetic Resonance—Applications to Organic Chemistry," McGraw-Hill Inc., New York (1959), p. 54.

as 2-methylthiophenes[7], methylfurans,[8] and methyl-substituted *N*-heteroaromatic compounds.[9,10] These facts seem to indicate that the benzylic coupling might be observed when a ring system is less aromatic, i.e., when $\pi$-electrons are much localized in a C–C bond involving a carbon atom to which a methyl group is bonded.

## Experimental

**Materials.**—Commercial products were available for 4,6-dinitro-, 4,6-dichloro-, $\alpha$, 4,6-tribromo-, and 4,6-dimethyl-*o*-cresol. The bromination in acetic acid[11a] of 4-nitro-*o*-cresol, derived from 2-amino-5-nitrotoluene by boiling it in 30% aqueous sodium hydroxide for 20 hr.,[11b] yielded 4-nitro-6-bromo-*o*-cresol. Two halogenated compounds, 4,6-dibromo-*o*-cresol and 4,6-diiodo-*o*-cresol,* were prepared by the bromination and by the iodination of *o*-cresol respectively.[11c,11d] All the materials used were purified by recrystallization from appropriate solvents.

**Measurements of NMR Spectra.** — The NMR spectra were obtained with a Varian A-60 spectrometer in dilute deuterochloroform solutions (ca. 8 mol. %) containing a small amount of tetramethylsilane as an internal standard. Chemical shifts were read on standardized charts calibrated with the signal of chloroform. The resolution was checked with acetaldehyde. The accuracies of the chemical shifts and of the coupling constants are within about $\pm 0.02$ p. p. m. and $\pm 0.2$ c. p. s. respectively.

## Results and Discussion

All the spectra of the examined compounds show simple first-order patterns. As an example, the spectrum of 4,6-dichloro-*o*-cresol is illustrated in Fig. 1. Each of the ring proton signals A and B consists of a pair of quartets. The methyl signal is composed of three peaks with a relative intensity of about 1 : 2 : 1. The middle component is somewhat broader than the outer components, suggesting the superposition of two signals. These features of the spectrum reveal the spin-spin coupling between the two ring protons and the methyl protons. Of the two signals A and B, the signal B, indicating a stronger coupling with the methyl protons, was assigned to the proton 3, while the signal A was assigned to the proton 5.

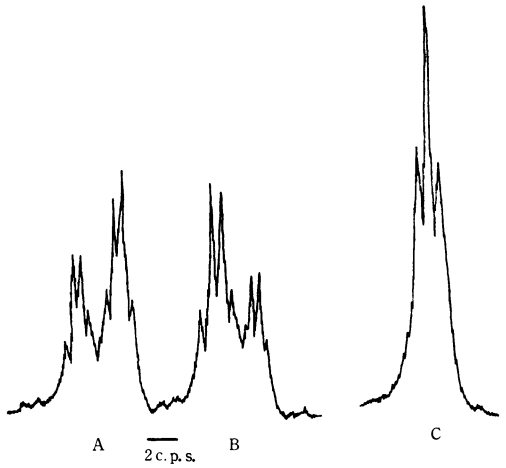



Fig. 1. The NMR spectrum of 4,6-dichloro-*o*-cresol.
A: ring proton 5, B: ring proton 3, C: methyl protons

The positions of the signals of various kinds of protons are given in Table I in p. p. m. relative to the internal standard.

**Chemical Shifts.** — The signals of the ring protons 5 are always observed at lower fields than are those of the protons 3, except for 4,6-dimethyl-*o*-cresol (2,4,6-trimethyl phenol), in which the two ring protons are magnetically equivalent. It appears reasonable that the proton 5, which is ortho to both of the electronegative substituents, 4 and 6, is more deshielded than is the proton 3, which is ortho to 4 and para to 6, because the deshielding effects of the substituents in question are strongest on the ortho proton (see Table II).

If the effects of substituents on the chemical shift of a ring proton are simply additive, the shift should be equal to the algebraic sum of substituent constants. In the present case, the chemical shifts of protons 3 and 5 should be:

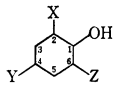
$$\delta(3) = d_o(CH_3) + d_m(OH) + d_o(Y) + d_p(Z) + \delta(\text{benzene})$$

$$\delta(5) = d_p(CH_3) + d_m(OH) + d_o(Y) + d_o(Z) + \delta(\text{benzene})$$

Therefore, the proportional relationship between these chemical shifts should be observed, provided that the proportional relationship is observed between substituent parameters, $d_o(R)$

7) R. A. Hoffman and S. Gronowitz, *Arkiv Kemi*, **16**, 563 (1960); *Chem. Abstr.*, **55**, 26682 (1961).
8) G. S. Reddy and J. H. Goldstein, *J. Phys. Chem.*, **65**, 1539 (1961).
9) B. D. N. Rao and J. D. Baldeschwieler, *J. Chem. Phys.*, **37**, 2473 (1962).
10) K. Tori, M. Ogata and H. Kano, *Chem. Pharm. Bull.*, **11**, 235 (1963).
* The magnitude of the spin-spin coupling constant, 2.2 c.p.s., between two ring protons of the diiodo-*o*-cresol indicates that the two ring protons are in meta positions to each other. The infrared spectrum reveals that one of the two iodine atoms exists at the position 6; the observed OH stretching vibration frequency coincides with the value reported by Baker[12] for the cis (hydrogen bonded) form of *o*-iodophenol.
11) a) *Beilstein* **6**, 367; b) ibid., 366; c) ibid., 360; d) ibid., 364.
12) A. W. Baker, *J. Am. Chem. Soc.*, **80**, 3598 (1958).

TABLE I. CHEMICAL SHIFT (IN P. P. M. FROM TMS) OF PROTONS OF SOME *o*-CRESOLS




| | X | Y | Z | $CH_3$ | H(3) | H(5) | OH |
|---|---|---|---|---|---|---|---|
| I | $CH_3$ | $NO_2$ | $NO_2$ | 2.48 | 8.38 | 8.95 | 11.4 |
| II | $CH_3$ | $NO_2$ | Br | 2.38 | 8.05 | 8.30 | 6.25 |
| III | $CH_3$ | Cl | Cl | 2.27 | 7.03 | 7.18 | 5.57 |
| IV | $CH_3$ | Br | Br | 2.27 | 7.25 | 7.45 | 5.57 |
| V | $CH_3$ | I | I | 2.23 | 7.38 | 7.78 | 5.32 |
| VI | $CH_3$ | $CH_3$ | $CH_3$ | 2.22 | 6.83 | 6.83 | 4.55 |
| VII | $CH_2Br$ | Br | Br | 4.53 | 7.45 | 7.60 | 5.83 |

TABLE II. COMPARISON BETWEEN THE OBSERVED AND CALCULATED CHEMICAL SHIFTS OF RING PROTONS

| | | Proton 3 | | | Proton 5 | | |
|---|---|---|---|---|---|---|---|
| Y | Z | Obs. | Calcd.* | Obs.-Calcd. | Obs. | Calcd.* | Obs.-Calcd. |
| $NO_2$ | $NO_2$ | −1.00 | −0.96 | −0.04 | −1.57 | −1.69 | +0.12 |
| $NO_2$ | Br | −0.67 | −0.60 | −0.07 | −0.92 | −0.85 | −0.07 |
| Cl | Cl | +0.35 | +0.48 | −0.13 | +0.20 | +0.30 | −0.10 |
| Br | Br | +0.13 | +0.23 | −0.10 | −0.07 | −0.02 | −0.05 |
| I | I | 0.00 | +0.03 | −0.03 | −0.40 | −0.43 | +0.03 |
| $CH_3$ | $CH_3$ | +0.55 | +0.67 | −0.12 | +0.55 | +0.67 | −0.12 |

* Martin and Dailey's parameters[4] were used except for $d_m$(OH).

$d_o(NO_2) = -0.995$ $d_o(Cl) = 0.000$ $d_o(Br) = -0.159$
$d_p(NO_2) = -0.29$ $d_p(Cl) = +0.16$ $d_p(Br) = +0.07$
$d_o(I) = -0.363$ $d_o(CH_3) = +0.183$ $d_m(OH) = +0.14$**
$d_p(I) = +0.07$ $d_p(CH_3) = +0.16$

** F. Langenbucher, E. D. Schmid and R. Mecke, *J. Chem. Phys.*, **39**, 1901 (1963).

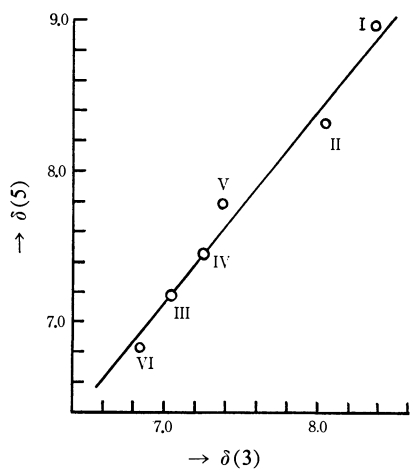



Fig. 2a. Correlation of $\delta(3)$ with $\delta(5)$.

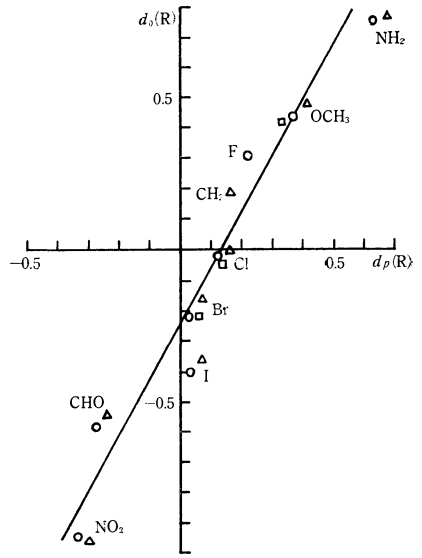



Fig. 2b. Correlation of $d_o$(R) with $d_p$(R).
○: Spiesecke and Schneider;[1] △: Martin and Dailey;[4] □: Diehl[2]

and $d_p$(R). This is the case, as Fig. 2 shows. Comparisons of the observed and calculated chemical shifts were made in order to ascertain the validity of the additivity rule. Table II gives the values relative to the chemical shift of benzene in deuterochloroform. The agreement among them is good in view of the rough approximation used. This fact indicates that

the additivity rule holds in the case of tetrasubstituted benzenes. A good agreement is again observed in the case of durene. The observed chemical shift of the ring protons in durene[13] (6.741 p. p. m.) agrees well with that estimated from the assumed additivity rule (6.716 p. p. m.).

The OH proton signal of 4, 6-dinitro-*o*-cresol was observed at an extraordinarily low field. This observation can be ascribed to the formation of an intramolecular hydrogen bond between OH and $NO_2$ groups. It has been pointed out that the OH proton signal of 2, 4-dinitrophenol appears at a field lower than that of 2, 4-dichlorophenol by about 5.6 p. p. m. because of the formation of strong intramolecular hydrogen bonds.[14] The OH proton signal of $\alpha$, 4, 6-tribromo-*o*-cresol was observed at a field lower than that of 4, 6-dibromo-*o*-cresol. This downfield shift results from the formation of intramolecular hydrogen bonds between $CH_2Br$ and OH groups, in addition to that between OH and Br groups.*

Methyl signals are shifted to lower fields with the increasing electronegativities of substituents. In the case of 4, 6-dinitro-*o*-cresol, it appears at a field lower than that of the parent compound by 0.21 p. p. m. Yamaguchi[15] studied the shielding effect of nitro groups and observed that a nitro group deshields methyl protons at the meta position of *m*-nitrotoluene by 0.12 p. p. m. The chemical shift of the methyl protons described above on 4, 6-dinitro-*o*-cresol is in good agreement with the calculated value, $2\times0.12=0.24$ p. p. m.

**Spin-Spin Coupling.**—The spin-spin coupling constants obtained are summarized in Table III.

TABLE III. SPIN-SPIN COUPLING CONSTANTS

| | $J$(3-5) c. p. s. | $J$(3-$CH_3$) c. p. s. | $J$(5-$CH_3$) c. p. s. |
|---|---|---|---|
| I | 2.9 | 0.9 | 0.6 |
| II | 2.7 | 0.8 | 0.5 |
| III | 2.5 | 0.7 | 0.5 |
| IV | 2.4 | 0.7 | 0.5 |
| V | 2.2 | 0.8 | 0.6 |
| VI | — | — | — |
| VII | 2.4 | — | — |

The coupling constants between two ring protons are in the 2.2—2.9 c. p. s. range. The coupling constant is larger when substituents at the positions 4 and 6 are more electronegative. Figure 3 shows the correlation between the meta coupling and the sum of the electronegativities of substituents 4 and 6. This proportional relationship indicates the additive effect of substituents on the ring proton coupling. A similar situation of meta coupling was reported for some *m*-[16] and

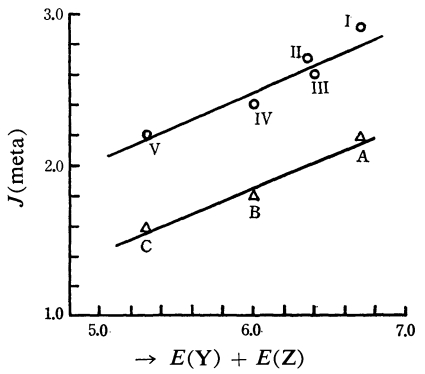



Fig. 3. Correlation between the meta coupling and the sum of electronegativities of the substituents 4 and 6.
-○-: $J$(3-5) for 4,6-disubstituted *o*-cresols
-△-: $J$(2-6) for *m*-disubstituted benzenes[16]
A: *m*-dinitrobenzene; B: *m*-dibromobenzene; C: *m*-diiodobenzene

*p*-disubstituted benzenes.[17] It was reported[17] that proportionality exists between the proton-proton coupling and the electronegativity of substituents, although no detailed discussion of coupling mechanism has yet been undertaken.

Proton-proton coupling constants are, in general, affected by two contributing factors, $\sigma$- and $\pi$-electrons. The dependence of the vicinal coupling constant on the electronegativities of substituents has been studied in some ethane[18] and ethylene derivatives.[19] For ethane and ethylene derivatives, the vicinal coupling constants are expressed as:[20]

$$J(CH_3CH_2X)=7.9(1-0.09\Delta E)$$

$$J_{trans}=19(1-0.17\Delta E);$$

$$J_{cis}=11.7(1-0.34\Delta E)$$

where $\Delta E$ is the difference in electronegativity

13) G. V. D. Tiers "Tables of $\tau$-Values for a Variety of Organic Compounds," Central Research Lab., Minnesota Mining and Manufacturing Company, Minnesota (1958), p. 5.
14) L. W. Reeves, W. A. Allan and K. O. Strømme, *Can. J. Chem.*, **38**, 1249 (1960).
* Whereas two OH stretching vibrations, at 3600 and 3526 $cm^{-1}$, were found for 4, 6-dibromo-*o*-cresol, a single band was observed, at 3520 $cm^{-1}$, for $\alpha$, 4, 6-tribromo-*o*-cresol in the OH-stretching region. Baker[12] observed two peaks, at 3598 and 3524 $cm^{-1}$, for *o*-bromophenol and assigned them to the trans (free) and cis (hydrogen bonded) forms respectively.
15) I. Yamaguchi, *Mol. Phys.*, **6**, 105 (1963).
16) J. Martin and B. P. Dailey, *J. Chem. Phys.*, **37**, 2594 (1962).
17) P. F. Cox, *J. Am. Chem. Soc.*, **85**, 380 (1963).
18) R. E. Glick and A. A. Bothner-By, *J. Chem. Phys.*, **25**, 362 (1956).
19) J. S. Waugh and S. Castellano, ibid., **35**, 1900 (1961); S. Castellano and J. S. Waugh, ibid., **34**, 295 (1961); T. Schaefer, *Can. J. Chem.*, **40**, 1 (1962).
20) C. N. Banwell and N. Sheppard, *Discussions Faraday Soc.*, **34**, 115 (1962).

between X and the hydrogen atom. In ethylene derivatives, the variation in coupling constants with the electronegativity is much greater than that in substituted ethanes. From this fact, it may be concluded that the contributions of both $\sigma$- and $\pi$-electrons are reduced by the introduction of an electronegative group. In other words, a decrease in the charge density in the double bond caused by the introduction of an electronegative groups is reflected in a decrease in the coupling constant of vicinal protons.

In the case of 4, 6-disubstituted *o*-cresols, however, the meta coupling intensifies the proportionality with an increase in the electronegativity of substituents. This discrepancy indicates the participation of another mechanism, which probably arises from the presence of a benzene ring contributing to the coupling. Since the angle between two C–H bonds can be assumed to be fixed, the change in the meta coupling is attributable to that in electron distribution, but it is not possible to give a clear interpretation immediately, because it is not clear whether the changes in the proton-coupling constants in these compounds are due to changes in the $\sigma$-electronic system or to changes in the $\pi$-orbitals.

**Long-range Coupling.** — The coupling constants, $J(3\text{–}CH_3)$ and $J(5\text{–}CH_3)$, are less than 1 c. p. s. It is reasonable that $J(3\text{–}CH_3)$ is slightly larger than $J(5\text{–}CH_3)$. However, it is noteworthy that an unexpectedly large value was observed for the spin-spin coupling constant between the methyl group and the ring proton at the para position across six bonds. Whereas the value of $J(5\text{–}CH_3)$ is quite similar within the range of the accuracy of this experiment, the value of $J(3\text{–}CH_3)$ seems proportional to the electronegativity of the substituents 4 and 6.

It is to be expected that a larger contribution from the methyl-hyperconjugation and the resulting shift of the NMR signal of methyl protons to a lower field will be observed for compounds with more powerful electron-withdrawing substituents. Therefore, there should be a proportional relationship between the chemical shift of the methyl protons and the benzylic coupling constant, $J(3\text{–}CH_3)$, provided that the hyperconjugation of the methyl group contributes considerably to the benzylic coupling. In Fig. 4, the plots for compounds I, II, III, and IV fall well on a straight line, but the plot for compound V deviates from the line, probably because of the effect of the large volume of iodine atoms at the ortho position.

It can also be expected that the replacement of a methyl group with a bromomethyl group

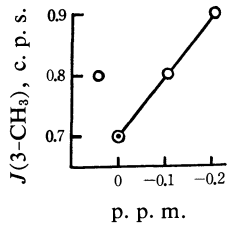



Fig. 4. Difference between methyl proton chemical shifts of 4, 6-disubstituted *o*-cresols and that of 4, 6-dichloro-*o*-cresol vs. $J(3\text{–}CH_3)$.

decreases the extent of hyperconjugation because of the fixation of the bromomethyl group in a conformation inadequate for hyperconjugation by an intramolecular hydrogen bond. As expected, no benzylic coupling was observed in the case of $\alpha$, 4, 6-tribromo-*o*-cresol. This fact indicates a significant contribution by the hyperconjugation to the benzylic coupling. In other words, the hyperconjugation of a methyl group with the benzene ring is due to the partial transfer of charges from the methyl group to the ring system. The introduction of bromine into the methyl group reduces the charge transfer from the substituent to the ring system and makes the benzylic coupling very weak. In short, a resolvable benzylic coupling indicates an appreciable migration of charges from the methyl group to the ring system. From this point of view, it seems possible to give an interpretation of the facts described in the introduction.

Although there are two kinds of methyl groups in 4, 6-dimethyl-*o*-cresol, only a single signal was observed for the methyl protons. It is not possible to estimate the benzylic coupling constants directly from the spectrum, but a considerable magnitude of benzylic coupling may be inferred from the appreciable broadening of the signals of both the methyl and ring protons.

Freeman et al.[21] have reported the presence of a weak long-range coupling between the OH proton and the ring proton 4 at the meta position in methyl salicylate. In the present case, however, it may be concluded that the OH proton couples with neither of the two ring protons at the meta positions since no changes in the fine structure of signals were observed in methanol, acetone, or NaOD-$D_2O$.

## Summary

The nuclear magnetic resonance spectra of seven 4, 6-disubstituted *o*-cresols (4, 6-dinitro-, 4-nitro-6-bromo-, 4, 6-dichloro-, 4, 6-dibromo-, 4, 6-diiodo-, 4, 6-dimethyl-, and $\alpha$, 4, 6-tribromo-*o*-cresol) have been examined in dilute

21) R. F. Freeman, N. S. Bhacca and C. A. Reilly, *J. Chem. Phys.*, 38, 293 (1963).

deuterochloroform solutions at 60 Mc./sec.

The observed chemical shifts of the ring protons 3 and 5 of 4, 6-disubstituted *o*-cresols are in good agreement with the values calculated from the shielding parameters of substituents by assuming the additivity rule.

The spin-spin coupling constant between two ring protons is proportional to the sum of the electronegativities of the substituents 4 and 6.

There are weak long-range couplings between the methyl and ring protons. It has been suggested that hyperconjugation contributes to these couplings.

The author wishes to thank Dr. Munetoshi Matsui and Dr. Akira Itō for their encouragement throughout this investigation.

*Research Laboratories*
*Sankyo Co., Ltd.*
*Shinagawa-ku, Tokyo*

# The Magnetic Susceptibilities of Mononuclear and Binuclear Chromium(III) Complexes*

By Toshiyuki MORISHITA, Kuniko HORI, Eishin Kyuno and Ryokichi TSUCHIYA

(Received September 19, 1964)

A chromium(III) ion under the ligand field in an octahedral environment has three unpaired electrons in the three-fold degenerated $t_{2g}$ orbitals, irrespective of whether the field is strong or weak. Since the degree of the covalency of the bonding in a chromium(III) complex cannot, in general, be estimated by measuring only the magnetic susceptibility, the measurement has so far been of little interest to investigators of chromium(III) complexes.

In spite of this, however, there have been found almost diamagnetic binuclear complexes, such as $[Cr_2(NH_3)_{10}O](ClO_4)_4$,[1] and nitrosyl complexes of abnormal valency, such as $K_4 \cdot [Cr(CN)_5NO] \cdot H_2O$,[2] whose magnetic moment, 0.7 B. M., is smaller than the spin-only value for three unpaired electrons.

In addition, there have been several reports[3-5] with respect to the magnetic susceptibility of mono- and bi-nuclear chromium(III) complexes, but most of them have not described the magnetic moment and have not even mentioned the relation between the presence of the exchange interaction between two chromium atoms and the color of the binuclear complexes. In order to establish the relation in detail, the magnetic susceptibility of several mono- and bi-nuclear chromium(III) complexes and of the salts consisting of complex cations and anions was measured.

## Experimental

The samples used for the measurement of the magnetic susceptibility are those listed in Table I. The methods of preparing several of them will be described below; otherwise they were prepared as in the foot notes in the table.

***cis*-Potassium Hydroxobis(oxalato)aquochromate(III) Hydrate, $K_2[Cr(OH)ox_2(H_2O)] \cdot H_2O$.**—This was prepared by adding pyridine to the *cis*-potassium bis(oxalato)diaquochromate(III) (6) in Table I.

Found: Cr, 14.78. Calcd.: 15.24%.

**Hydroxooxalatoaquoethylenediaminechromium(III), [Cr(OH)ox($H_2O$)en].**—This was prepared by adding pyridine to the oxalatodiaquoethylenediaminechromium(III) bromide (8) in Table I.

Found: Cr, 22.43; N, 11.95. Calcd.: Cr, 22.11; N, 11.91%.

**Di-$\mu$-hydroxobis(bisethylenediaminechromium(III)) Bromide Dihydrate, $[en_2Cr(OH)_2Cr\,en_2]Br_4 \cdot 2H_2O$.**—This was prepared by the reaction of ammonium bromide with the binuclear complex (9) in Table I.

Found: Cr, 13.95; N, 13.18. Calcd.: Cr, 13.99; N, 15.26%.

The molecular conductivity, $\Lambda_{10000}$, was 480.9 mho·cm²/mol. at the concentration of $10^{-4}$ mol./1. at 25°C.

**Sodium Di-$\mu$-hydroxobis(bisoxalatochromate(III)) Tetrahydrate, $Na_4[ox_2Cr(OH)_2Crox_2] \cdot 4H_2O$.**—This was prepared by the reaction of sodium

* Read at the 13th Symposium on Coordination Compounds of the Chemical Society of Japan, Nagoya, October, 1963.

1) H. Kobayashi, T. Haseda, E. Kanda and M. Mori, *J. Phys. Soc. Japan*, **15**, 1646 (1960).
2) W. P. Griffith, *J. Chem. Soc.*, **1963**, 3286.
3) E. Rosenbohm, *Z. phys. Chem.*, **93**, 693 (1919).
4) D. M. Bose, *Phil. Mag.*, **5**, 1048 (1928).
5) D. M. Bose, *Z. Physik.*, **65**, 677 (1930).

bromide with ammonium di-$\mu$-hydroxobis(bisoxalatochromate(III)).

Found: Cr, 14.94. Calcd.: Cr, 15.07%.

$\Lambda_{10000}=504.3$.

**Di-$\mu$-hydroxobis(bis-$\alpha$-alaninatochromium (III)), [$\alpha$-ala$_2$Cr(OH)$_2$Cr $\alpha$-ala$_2$]·H$_2$O.**—This was prepared from a mixed solution of chromic chloride hexahydrate and $\alpha$-alanine in a way similar to that used for the binuclear glycinato complex (16) in Table I.

Found: Cr, 20.72; N, 11.92. Calcd.: Cr, 21.65; N, 11.66%.

Samples 18, 19 and 20 in Table I were precipitated by mixing the saturated solutions of the two complex salts containing a corresponding cation or anion.

The magnetic susceptibility was measured by a Gouy balance at room temperature. The effective magnetic moment per chromium atom was evaluated from the value of the magnetic susceptibility on the assumption that the magnetic susceptibility is inversely proportionate to the absolute temperature, as $\chi=C/T$, where $\chi$, $C$ and $T$ are the magnetic susceptibility, a Curie constant, and the absolute temperature respectively.

## Results

The values of the magnetic susceptibility and of the calculated magnetic moment of mono- and bi-nuclear complexes and salts consisting of the complex cation and anion are listed in Table I. The table shows that the magnetic moment of the mononuclear complexes, except for sample 9, is close to the spin-only value for three unpaired electrons.

The values of the magnetic moment of binuclear complexes are remarkably lower than the value of the magnetic moment for the spin-only value except for sample 11. This fact makes us expect the exchange interaction between two chromium atoms in the binuclear complexes.

However, when we compare the values in detail, it is found that even if the binuclear complex ions contained are the same, the magnetic moment of sample 11 is larger than that of sample 12, and that that of 13 is larger than that of 14, where the former two samples have the same binuclear cation and the latter two have the same binuclear anion. Since the ionic radius of the anti-ion of the binuclear complex cation in 11, the dithionate ion, is larger than that of the bromide ion in 12, and since that of the potassium ion in 13 is larger than that of the sodium ion in 14, we may

Table I. The magnetic susceptibility per gram $\chi_g$ and the effective magnetic moment, $\mu_{eff}$ per a chromium of atom mononuclear and binuclear complexes and salts consisting of the complex cation and anion

| | | Temp., °K | $\chi_g\times10^6$ | $\mu_{eff}$(B. M.) |
|---|---|---|---|---|
| (1) | KCr(SO$_4$)$_2$·12H$_2$O | 291.2 | 12.6 | 3.95 |
| (2) | [Cren$_3$]Cl$_3$·3·5H$_2$O[6] | 298.2 | 14.9 | 3.89 |
| (3) | [Croxen$_2$]Br[6] | 297.5 | 17.2 | 3.81 |
| (4) | K[Crox$_2$en]·H$_2$O[6] | 286.5 | 17.1 | 3.75 |
| (5) | K$_3$[Crox$_3$]·3H$_2$O[7] | 294.2 | 12.3 | 3.85 |
| (6) | *cis*-K[Crox$_2$(H$_2$O)$_2$]·2H$_2$O[8] | 289.2 | 18.3 | 3.87 |
| (7) | K$_2$[Cr(OH)ox$_2$(H$_2$O)]·H$_2$O | 288.3 | 17.3 | 3.95 |
| (8) | [Crox(H$_2$O)$_2$en]Br[6] | 289.6 | 18.9 | 3.80 |
| (9) | [Cr(OH)ox(H$_2$O)en] | 287.2 | 23.6 | 3.65 |
| (10) | [Crgly$_3$]·H$_2$O[9] | 289.2 | 21.5 | 3.89 |
| (11) | [en$_2$Cr(OH)$_2$Cren$_2$](S$_2$O$_6$)$_2$[10] | 296.2 | 16.5 | 3.81 |
| (12) | [en$_2$Cr(OH)$_2$Cren$_2$]Br$_4$·2H$_2$O | 289.2 | 14.0 | 3.55 |
| (13) | K$_4$[ox$_2$Cr(OH)$_2$Crox$_2$]·6H$_2$O[10] | 301.2 | 13.7 | 3.63 |
| (14) | Na$_4$[ox$_2$Cr(OH)$_2$Crox$_2$]·4H$_2$O | 298.7 | 14.4 | 3.43 |
| (15) | [oxenCr(OH)$_2$Croxen][10] | 289.2 | 23.8 | 3.53 |
| (16) | [gly$_2$Cr(OH)$_2$Crgly$_2$]·H$_2$O[9] | 298.2 | 20.3 | 3.37 |
| (17) | [$\alpha$-ala$_2$Cr(OH)$_2$Cr$\alpha$-ala$_2$]·H$_2$O | 290.2 | 20.3 | 3.43 |
| (18) | [Cren$_3$][Crox$_3$] | 298.2 | 18.4 | 3.55 |
| (19) | [Croxen$_2$][Crox$_2$en] | 297.7 | 21.0 | 3.74 |
| (20) | [Cr(OH)(H$_2$O)en$_2$][Cr(OH)ox$_2$(H$_2$O)] | 300.7 | 25.4 | 3.88 |

6) E. Kyuno, N. Tanaka and M. Kamada, Read at the 12th Symposium on Coordination Compounds of the Chemical Society of Japan, Tokyo, November, 1962.
7) J. C. Bailar, Jr., E. M. Jones, H. S. Booth and M. Grennert, "Inorganic Syntheses," Vol. 1, 35 (1939).
8) A. Werner, W. J. Bowis, A. Hoblik, H. Schwarz and H. Surber, *Ann.*, **406**, 261 (1914).
9) H. Ley, *Ber.*, **45** 380 (1912).
10) E. Kyuno, R. Honjo and R. Tsuchiya, Read at the 16th Annual Meeting of the Chemical Society of Japan, Tokyo, April, 1963.

suppose that, as the radius of the anti-ion becomes smaller, the exchange interaction between the chromium atoms through the hydroxy group becomes stronger.

The magnetic moments of samples, 15, 16 and 17 are especially small. This fact can be understood by considering that the exchange interaction between two chromium atoms in a binuclear complex is very large, though the reason for this can not be exactly determined. In addition, there may be some exchange interaction between chromium atoms in the neighboring complex molecules in these cases, since they do not contain the anti-ions.

The values of the magnetic moments of 18 and 19 are obviously lower than the spin-only value, which suggests the presence of an exchange interaction between chromium atoms in the neighboring complex cation and anion.

The magnetic moments of mono- and bi-nuclear complexes in relation to their color and the position in their synthetic course are summarized in Fig. 1. The qualitative information is deduced from Fig. 1 that the complexes which have a normal magnetic moment (close to 3.87 B. M.) exhibit a reddish color in general, except for a few fundamental complexes used as starting materials, whereas the complexes

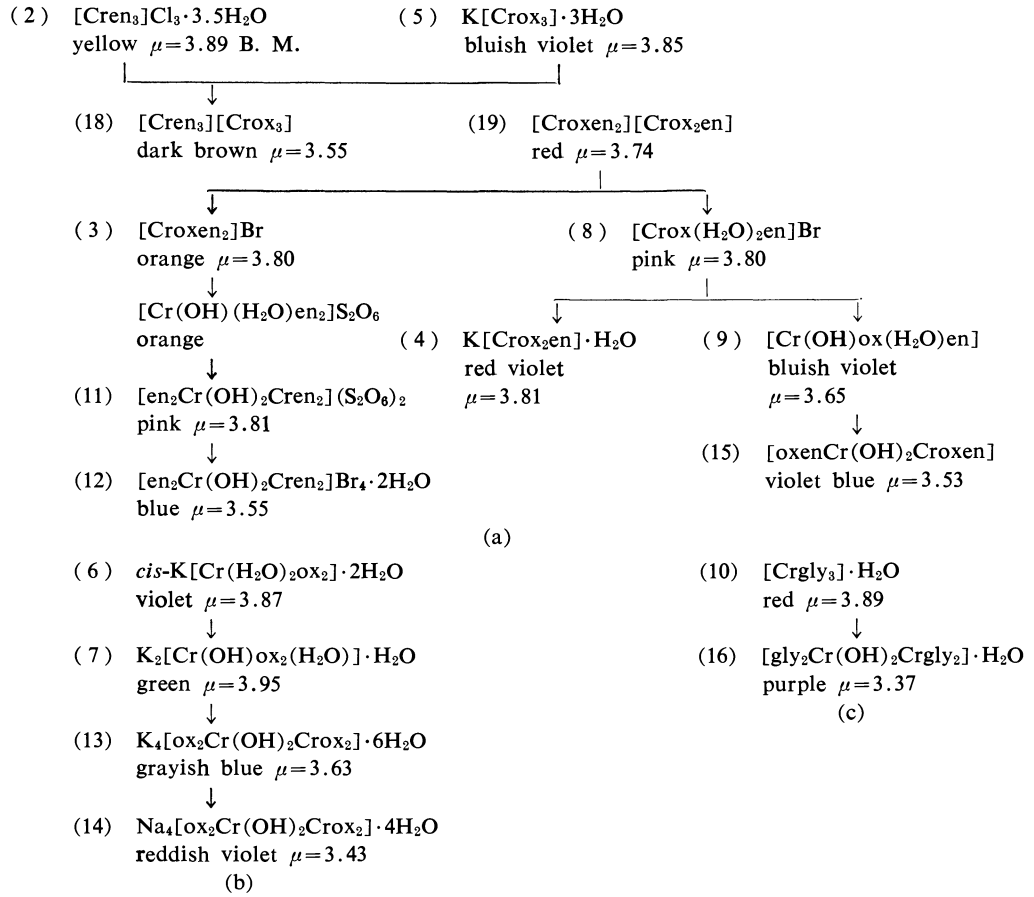



Fig. 1. The magnetic moment and the color of the complexes in the diagrams of the synthesis course of (a) ethylenediaminechromium(III) series, (b) oxalatochromium(III) series and (c) glycinatochromium(III) series.

TABLE II. THE WAVELENGTH AT A PEAK IN THE FIRST ABSORPTION BAND, $\lambda_{max}$, OF THE BINUCLEAR COMPLEXES AND THE MONONUCLEAR ONES WHICH ARE THE MOTHER MATERIALS FOR THE SYNTHESES OF THE FORMERS

| Mother material | $\lambda_{max}$, mμ | Binuclear complex | $\lambda_{max}$, mμ |
|---|---|---|---|
| $[Cr(H_2O)_2en_2]^{3+}$ | 515[6] | $[en_2Cr(OH)_2Cren_2]^{4+}$ | 530[10] |
| $[Crox_2(H_2O)_2]^-$ | 570[6] | $[ox_2Cr(OH)_2Crox_2]^{4-}$ | 580[10] |
| $[Crox(H_2O)_2en]^+$ | 524[6] | [oxenCr(OH)2Croxen] | 550[10] |

which have a subnormal magnetic moment (lower than the spin-only value) show a bluish color such as samples 9, 12, 13, 14 and 15 or, at least, show purple, as does 16.

The wavelengths at the maximum absorption peak in the first absorption band of the binuclear chromium(III) complexes, $\lambda_{max}$, are compared with those of the mononuclear complexes which are the mother materials for the syntheses of the former in Table II. It may be concluded from Fig. 1 and Table II that, as the exchange interaction between the chromium atoms appears, the first absorption band is shifted to red and that, as a result, the color of the compounds changes from reddish to bluish.

The authors wish to thank the Ministry of Education for the financial support granted for this research.

*Department of Chemistry*
*Faculty of Science*
*Kanazawa University*
*Kanazawa*

# The Preparation of Heavy Metal Hydride and Its Catalytic Activity. VII. The Hydrogenation of Various Olefins with a Ferric Chloride-Lithium Aluminum Hydride or a Cobaltous Chloride-Lithium Aluminum Hydride Catalyst*

By Yoshinobu TAKEGAMI, Toru UENO and Takao FUJII

(Received October 26, 1964)

In preceding publications[1,2] we reported our observation that certain heavy metal halides react readily with a solution of lithium aluminum hydride in tetrahydrofuran to give a new catalyst system for the hydrogenation of styrene and cyclohexene. A typical catalyst is composed of ferric chloride plus lithium aluminum hydride (the iron catalyst) in an $LiAlH_4/FeCl_3$ ratio of 1:1. In the course of investigating this catalyst system, we were led to the conclusion that iron hydride, present in appreciable concentrations in the catalyst system, might be responsible for the hydrogenation reaction.

We will now report on an extension of the scope of this iron catalyst. The hydrogenations of various compounds containing olefinic linkages have been studied. In addition, a cobaltous chloride plus lithium aluminum hydride (the cobalt catalyst) system has been included in this study in order to compare the two catalysts.

## Experimental

**Materials.**—Lithium aluminum hydride was obtained from Metal Hydride, Inc. A lithium aluminum hydride solution in tetrahydrofuran was prepared and used as a clear solution. The concentration of the stock solution (0.2–0.3 mol./l.) was determined by analysis using active hydrogen prior to use (by hydrolysis). The anhydrous heavy metal halides and olefins used were the purest among the available commercial materials. Tetrahydrofuran was dried over sodium and freshly distilled just before use.

**Procedure.**—Since in all cases the catalysts were sensitive to air and moisture, all operations were carried out in a nitrogen or a hydrogen atmosphere. The apparatus for the preparation of catalysts and the hydrogenation of olefins consisted of a four-necked flask equipped with a stirrer, a dropping funnel (60 ml.), and a thermometer, and was jointed to a gas burrete through a silica gel tube. Before the reaction, the apparatus was flushed with hydrogen. A solution of 70 ml. of tetrahydrofuran containing about 0.005 mol. of the heavy metal halide was stirred at 0°C for 40 min. To this solution a desired amount of a lithium aluminum hydride solution was then added through the dropping funnel. The time of addition varied from 2 to 10 min. The color of the solution immediately changed black or brown-black, and there was an accompanying hydrogen evolution. The mixture was stirred for an additional several hours until the hydrogen evolution ceased.

The hydrogenation of the olefin was carried out by introducing 5 ml. of the olefin into the catalyst solution described above. The speed of stirring was kept at 900 r.p.m. during the hydrogenation reaction. After the hydrogenation, the catalyst was destroyed

* Presented at the 17th Annual Meeting of the Chemical Society of Japan, Tokyo, March, 1964.

1) Y. Takegami and T. Ueno, *J. Chem. Soc. Japan, Ind. Chem. Sec.* (*Kogyo Kagaku Zasshi*), **67**, 246 (1964).

2) Y. Takegami, T. Ueno and T. Fujii, ibid., **67**, 1009 (1964).

by the addition of 20 ml. of 15% aqueous hydrochloric acid; the amount of hydrogen thus evolved was measured. The hydrogenation product was extracted with diethyl ether, washed with water, concentrated by the evaporation of ether, and analyzed by gas chromatography.

The amounts of hydrogen evolved on the hydrolysis of the catalysts at several $LiAlH_4/FeCl_3$ ratios are given in Table I. For purposes of comparison, the amounts of hydrogen evolved during the preparation of the catalysts, reported in a preceding paper,[2] are also included in Table I.

TABLE I. THE AMOUNTS OF HYDROGEN EVOLVED

| Catalyst | $LiAlH_4/MX_n$ ratio | On hydrolysis | During the preparation |
|---|---|---|---|
| | | mol./mol. $MX_n$ | |
| Iron | 0.8 | 1.22 | 1.46 |
| | 1.0 | 1.58 | 1.79 |
| | 1.2 | 2.04 | 2.22 |
| | 1.5 | 2.88 | 2.41 |
| Cobalt | 0.8 | 1.28 | 1.78 |
| | 1.0 | 1.76 | 1.92 |

## Results

**Hydrogenation with Iron Catalysts.** — The hydrogenation reaction was carried out under hydrogen at an atmospheric pressure and at 0°C. Among the solvents tested, diethyl ether, pyridine and tetrahydrofuran, the last was the best for this catalyst system. For most of the experiments, 5 ml. of olefin was used, the ratio of olefin to the iron catalyst being about 10 : 1. In order to establish a general relationship between the activity and the composition (the $LiAlH_4/FeCl_3$ ratio) of the iron catalyst, the amounts of absorbed hydrogen are plotted in Fig. 1 against the reaction times for the hydrogenation reaction of cyclohexene with the iron catalyst at various $LiAlH_4/FeCl_3$ ratios. No attempt has been made to estimate the rate constants of the hydrogenation reaction. The first reaction was carried out with the iron catalyst at an $LiAlH_4/FeCl_3$ ratio of 0.71 : 1. No hydrogen absorption was observed with this catalyst. Then several aliquots of a lithium aluminum hydride solution were added to the system at intervals. An appreciable activity appeared when the $LiAlH_4/FeCl_3$ ratio reached 0.89 : 1. Then the catalytic activity of the iron catalyst was found to rise steadily as the $LiAlH_4/FeCl_3$ ratio rose from 0.89 : 1 to 1.00 : 1, but thereafter to decrease as the ratio increased further. These successive procedures, in which the $LiAlH_4/FeCl_3$ ratio is raised step by step, will be described as "the step-by-step procedures" in a further discussion. In addition to the step-by-step procedures, the hydrogenation was also carried out with an iron catalyst freshly prepared in the $LiAlH_4/FeCl_3$ ratio of 1.00 : 1, the most active of the step-by-step procedures. The rate of this single hydrogenation, shown by a dotted line in Fig. 1, nearly corresponds to that observed in the hydrogenation at an $LiAlH_4/FeCl_3$ ratio of 1.00 : 1 in the step-by-step procedures.

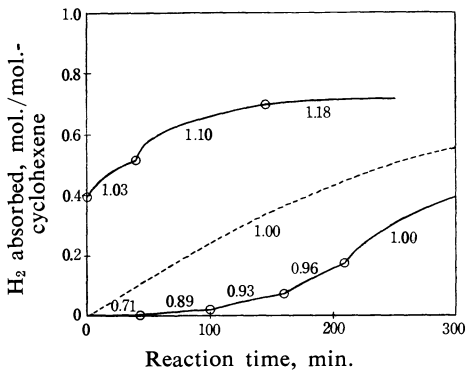



Fig. 1. Hydrogenation of cyclohexene with the iron catalyst.

Conditions; $FeCl_3$: 4.92 mmol., THF: 100 ml., cyclohexene: 5 ml. (49.6 mmol.), reaction temp.: 0°C

The thick or dotted line represents the step-by-step or single hydrogenation, respectively. Figures represent the $LiAlH_4/FeCl_3$ ratios.

○ represents the point where lithium aluminum hydride solution was added.

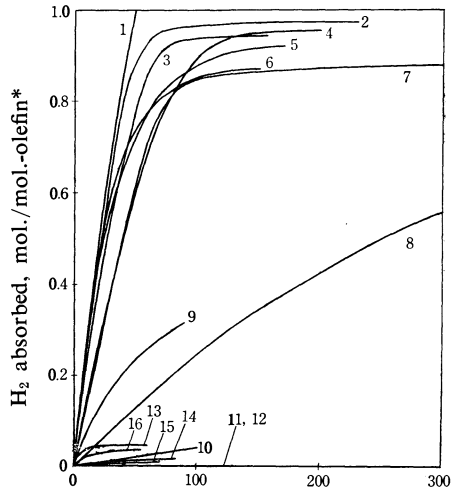



Fig. 2. Hydrogenation of various olefins with the iron catalyst.

Names of the compounds, the $LiAlH_4/FeCl_3$ ratio for the catalyst used and the amounts of hydrogen evolved during the hydrolysis subsequent to the hydrogenation are given in Table II.

* It changes to 1/2 (mol./mol.-olefin), in the cases of isoprene(7) and *d*-limonene(9).

Table II. Hydrogenation with the iron catalyst*1

| Curve No. in Fig. 2 | Olefin | $LiAlH_4/FeCl_3$ ratio | Ratio of hydrogen evolution*2 |
|---|---|---|---|
| 1 | Styrene | 1.00 | — |
| 2 | α-Methylstylene | 1.02 | 0.88 |
| 3 | Safrole | 1.02 | 0.76 |
| 4 | Indene | 1.01 | 0.74 |
| 5 | Isosafrole | 1.12 | 0.59 |
| 6 | Anethole | 1.21 | 0.59 |
| 7 | Isoprene | 1.00 | 0.89 |
| 8 | Cyclohexene | 1.00 | — |
| 9 | *d*-Limonene*3 | 1.08 | 0.78 |
| 10 | α-Pinene | 0.80—1.20 | 0.83 |
| 11 | Furan | 0.82—1.54 | 0.80 |
| 12 | Squalene | 0.79—1.19 | 0.74 |
| 13 | Ethyl acrylate | 0.88—1.20 | 0.08 |
| 14 | Vinyl acetate | 0.80—1.70 | 0.09 |
| 15 | Acrylonitrile | 1.00—1.36 | 0.04 |
| 16 | Allyl chloride | 0.79—1.43 | 0.18 |

*1 $FeCl_3$ : 0.005 mol., THF : ca. 100 ml., olefin : 5 ml., reaction temp. : 0°C. Hydrogen absorption curves are given in Fig. 2.

*2 The amounts of hydrogen evolved are represented by the ratio $R/R_0$, where $R$ is the amount of hydrogen evolved during hydrolysis subsequent to the hydrogenation (mol./mol. $FeCl_3$) and $R_0$ is the amount of hydrogen evolved during the hydrolysis of the catalyst with same $LiAlH_4/FeCl_3$ ratio without hydrogenation.

*3 A mixture of cis- and trans-isomers.

In order to determine how the olefin structure influences the rate of hydrogenation, the iron catalyst was tested with various olefinic compounds. The bulk of the experiments were performed according to the step-by-step procedures, and the value of the $LiAlH_4/FeCl_3$ ratio of the most active catalyst was determined in each case. The hydrogen absorption curves obtained with the most active catalysts are shown in Fig. 2. The values of the $LiAlH_4/FeCl_3$ ratios of the catalysts employed and the amounts of hydrogen evolved on the hydrolysis subsequent to the hydrogenation are given in Table II.

On the basis of the information given in Fig. 2, the olefins and unsaturated compounds employed in this work can be divided into three groups according to the ease of hydrogenation : (I) styrene, α-methylstyrene, safrole, isosafrole, indene, anethole and isoprene ; (II) cyclohexene and *d*-limonene, and (III) α-pinene, squalene, furan, vinyl acetate, ethyl acrylate, allyl chloride and acrylonitrile.

*The Hydrogenation of the Olefins in the First Group.*—When compared at the most active composition of the catalysts, the rates of the hydrogenation of the olefins of this group were almost the same, as Fig. 2 shows. However, the ranges of the $LiAlH_4/FeCl_3$ ratios of the active catalysts and the values of the ratios of the most active catalysts varied to some extent ; the ranges of the $LiAlH_4/FeCl_3$ ratios of the active catalysts for the hydrogenation of styrene, isosafrole, anethole and isoprene, for instance, were 0.78—1.45 : 1, 0.99—1.43 : 1, 1.21—1.41 : 1 and 0.78—1.23 : 1 respectively.

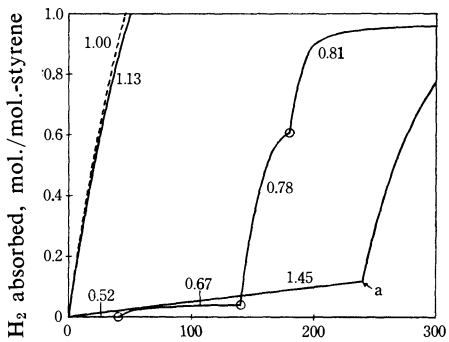



Fig. 3. Hydrogenation of styrene with the iron catalyst.

$FeCl_3$ : 4.94 mmol., THF : 100 ml., styrene : 5 ml. (43.5 mol.), reaction temp. : 0°C
5 mmol. of water was added at "a."
Others are same to in Fig. 1.

The results of a representative run for styrene are shown in Fig. 3. At low $LiAlH_4/FeCl_3$ ratios, the initial rates were high, but either instantaneously or gradually the rates decreased, as may be seen from the curves corresponding to the (0.67) and (0.78) ratios in Fig. 3. For the run carried out with the optimum ratio, the plots of the amounts of hydrogen absorbed vs. the reaction time were linear up to almost 100% conversion. The slope, however, became gentle with a further increase in the $LiAlH_4/FeCl_3$ ratio, as may be seen from the curve representing the (1.45) ratio in Fig. 3. Similar trends were observed in the runs carried out with the other olefins.

If a small amount (0.005 mol.) of water was added to the less active catalyst with a larger $LiAlH_4/FeCl_3$ ratio, the catalyst became highly active, as may be seen in Fig. 3. A similar phenomenon was observed for the hydrogenation of indene with the iron catalyst with the $LiAlH_4/FeCl_3$ ratio of 1.69 : 1. We previously reported[1] that the iron catalyst has catalytic activity when its hydrogen content is limited in a certain region and that the hydrogen content rises with an increase in the $LiAlH_4/FeCl_3$ ratio. From these facts, it is evident that the iron catalyst with a high $LiAlH_4/FeCl_3$ ratio

is less active because of its large hydrogen content. Therefore, the activation of the catalyst when a small amount of water is added is conceivably due to the diminution of the hydrogen content of the catalyst.

On the other hand, in the hydrogenation of anethole with the iron catalyst with the $LiAlH_4/FeCl_3$ ratio of 1.61 : 1, which had no activity at the initial stage of the hydrogenation, an appreciable activity gradually appeared after a long induction period (about 12 hr.) with no addition of water.

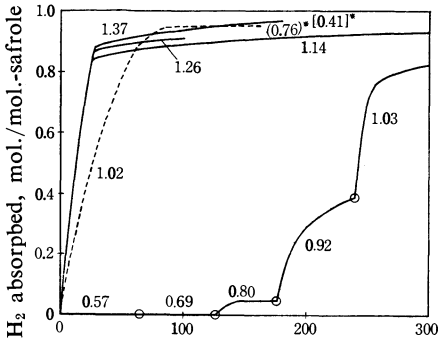



Fig. 4. Hydrogenation of safrole with the iron catalyst.

$FeCl_3$ : 4.60 mmol., THF : 100 ml., safrole : 5 ml. (33.9 mmol.), reaction temp. : 0°C

* Amount of hydrogen evolved during the hydrolysis subsequent to the hydrogenation (see footnote of Table II). The amount of hydrogen evolved during the hydrolysis subsequent to the single hydrogenation is given in parenthesis and that subsequent to the stepwise hydrogenation is given in brackets. Others are same to in Fig. 1.

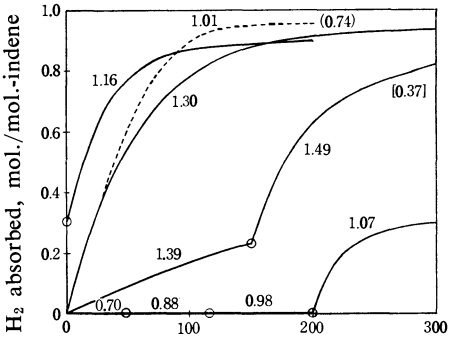



Fig. 5. Hydrogenation of indene with the iron catalyst.

$FeCl_3$ : 4.26 mmol., THF : 100 ml., indene : 5 ml. (42.7 mmol.), reaction temp. : 0°C
Others are same to in Figs. 1 and 4.

The ranges of the $LiAlH_4/FeCl_3$ ratios of the active catalysts for the hydrogenation of safrole, indene and ethyl vinyl ether were somewhat different from those of styrene. The results of the hydrogenation of safrole and indene are shown in Figs. 4 and 5 respectively. As may be seen in Fig. 4, the iron catalysts with the $LiAlH_4/FeCl_3$ ratios of 1.26 : 1, 1.37 : 1 and 1.41 : 1 had almost the same activities in the hydrogenation of safrole. If the catalyst was hydrolyzed after the step-by-step hydrogenation, the amount of hydrogen evolved* was relatively small (0.41), whereas it was relatively large (0.76) after the single hydrogenation. As may be seen in Fig. 5, the range of the $LiAlH_4/FeCl_3$ ratio of the active catalyst for the hydrogenation of indene was also different from that for styrene, and the amount of hydrogen evolved on hydrolysis subsequent to the step-by-step hydrogenation was again relatively small.

On the other hand, as may be seen in Fig. 5, the iron catalyst freshly prepared in the $LiAlH_4/FeCl_3$ ratio of 1.01 : 1 was more active than the catalyst with the $LiAlH_4/FeCl_3$ ratio of 1.07 : 1 in the step-by-step procedures. A similar phenomenon was observed in the hydrogenation of isoprene; the iron catalyst freshly prepared in the $LiAlH_4/FeCl_3$ ratio of 1.04 : 1 was more active than the catalyst with the ratio of 1.01 : 1 in the step-by-step procedures, as may be seen in Fig. 6. Thus, the catalytic activity of the catalyst with the same $LiAlH_4/FeCl_3$ ratio can be greatly altered by the method of preparation chosen (that is, it depends on whether the step-by-step or the single procedure is used).

The relationship between the $LiAlH_4/FeCl_3$

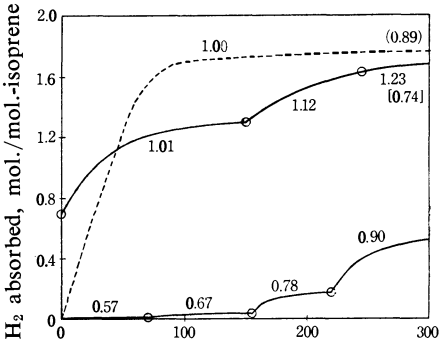



Fig. 6. Hydrogenation of isoprene with the iron catalyst.

$FeCl_3$ : 4.71 mmol., THF : 80 ml., isoprene : 5 ml. (50.0 mmol.), reaction temp. : 0°C
Others are same to in Figs. 1 and 4.

* See footnote of Table II.

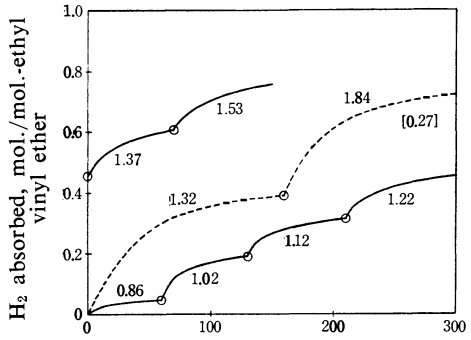



Fig. 7. Hydrogenation of ethyl vinyl ether with the iron catalyst.
$FeCl_3$: 4.68 mmol., THF: 110 ml., ether: 5 ml. (52.9 mmol.), reaction temp.: 0°C
Others are same to in Figs. 1 and 4.

ratio and the catalytic activity was much more complicated in the hydrogenation of ethyl vinyl ether; as may be seen in Fig. 7, when the $LiAlH_4/FeCl_3$ ratio was raised step-by-step, $0.86 \rightarrow 1.02 \rightarrow 1.12 \rightarrow \cdots$, the rate of hydrogen absorption decreased after about 0.15 (mol./mol.-ether) of hydrogen had been absorbed at each ratio. With the iron catalyst prepared in the $LiAlH_4/FeCl_3$ ratio of 1.32:1, the rate decreased after about 0.4 (mol./mol.-ether) of hydrogen had been absorbed, as the dotted line in Fig. 7 shows. A similar phenomenon was observed when the ratio was raised from 1.32:1 to 1.84:1. That is, the amount of hydrogen absorbed seems to correspond to the amount of lithium aluminum hydride added to raise the $LiAlH_4/FeCl_3$ ratio. The amount of hydrogen evolved on the hydrolysis subsequent to the hydrogenation was quite small.

*The Hydrogenation of d-Limonene (Olefins in the Second Group).*—The range of the $LiAlH_4/FeCl_3$ ratio for the active catalyst for the hydrogenation of *d*-limonene was almost the same as that for the hydrogenation of cyclohexene described above, whereas the value of the $LiAlH_4/FeCl_3$ ratio for the most active catalyst was somewhat different—1.00:1 and 1.08:1 for the hydrogenation of cyclohexene and *d*-limonene respectively. *d*-Limonene did not absorb more than 1.0 (mol./mol.-limonene) of hydrogen.

*The Hydrogenation of Unsaturated Compounds in the Third Group.*—Squalene, α-pinene, furan, vinyl acetate, ethyl acrylate, allyl chloride and acrylonitrile did not appreciably absorb hydrogen in the presence of the iron catalyst at any $LiAlH_4/FeCl_3$ ratio. The amounts of hydrogen evolved on the hydrolysis subsequent to the hydrogenation seem to indicate that these compounds can be divided into two groups. In the cases of squalene, α-pinene and furan, the amounts of hydrogen evolved were relatively large, whereas they were quite small or practically zero in the cases of vinyl acetate, ethyl acrylate, allyl chloride and acrylonitrile. For the latter compounds, the color of the reaction mixture changed during the course of the hydrogenation, from black to blackish brown for ethyl acrylate and acrylonitrile, and to ocher for allyl chloride.

**Hydrogenation with Cobalt Catalysts.**—Since the iron catalyst was less active in the hydrogenation of cyclohexene, *d*-limonene, squalene, α-pinene, ethyl vinyl ether, vinyl acetate, ethyl acrylate, allyl chloride and acrylonitrile, the hydrogenation of these compounds was performed with the cobalt catalyst with a view to exploring the more active catalyst. The results obtained with the cobalt catalyst are shown in Fig. 8 and Table III. As may be seen in Fig. 8, cyclohexene and *d*-limonene were rapidly hydrogenated with this catalyst. *d*-Limonene probably did not absorb more than 1.0 (mol./mol.-limonene) of hydrogen in spite of the very rapid hydrogenation because only the terminal bouble bond of *d*-limonene was hydrogenated. The hydrogenation of ethyl vinyl ether, which was achieved with only a limited success with the iron catalyst (Fig. 7),

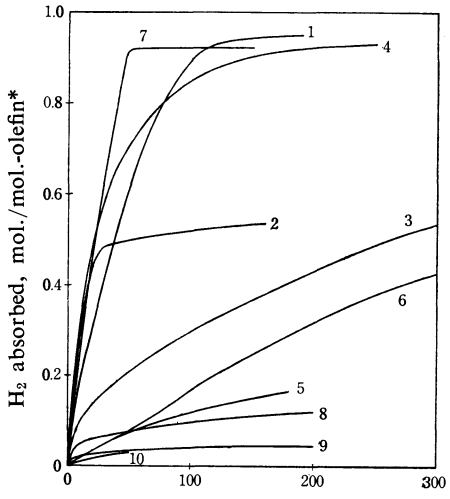



Fig. 8. Hydrogenation of various olefins with the cobalt catalyst.
Names of the compounds, the $LiAlH_4/CoCl_2$ ratio for the catalyst used and the amounts of hydrogen evolved during the hydrolysis subsequent to the hydrogenation are given in Table III.
* It changes to 1/2 (mol./mol.-olefin) in the cases of *d*-limonene(2) and furan(5), and to 1/6 (mol./mol.-olefin) in the case of squalene(6).

TABLE III. HYDROGENATION WITH THE COBALT CATALYST*1

| Curve No. in Fig. 8 | Olefin | $LiAlH_4/CoCl_2$ ratio | Ratio of hydrogen evolution*2 |
|---|---|---|---|
| 1 | Cyclohexene | 0.82 | — |
| 2 | *d*-Limonene*3 | 0.98*4 | 0.58 |
| 3 | $\alpha$-Pinene | 1.00*4 | 0.63 |
| 4 | Ethyl vinyl ether | 0.81 | 0.71 |
| 5 | Furan | 0.79 | 0.62 |
| 6 | Squalene | 0.98*4 | 0.60 |
| 7 | Ethyl acrylate | 0.80 | 0.66 |
| 8 | Vinyl acetate | 0.80 | 0.36 |
| 9 | Acrylonitrile | 0.82 | 0.00 |
| 10 | Allyl chloride | 0.81 | 0.06 |

*1 $CoCl_2$: ca. 0.005 mol., THF: ca. 100 ml., olefin: 5 ml., reaction temp.: 0°C. Hydrogen absorption curves are given in Fig. 8.
*2 See footnote of Table II.
*3 A mixture of cis- and trans-isomers.
*4 When the $LiAlH_4/CoCl_2$ ratio was 0.78—0.80, no appreciable hydrogen absorption was observed.

was performed successfully with the cobalt catalyst. It is noteworthy that a very large variation in catalytic activity for the hydrogenation of ethyl acrylate exists among the iron and cobalt catalysts. Furthermore, squalene and $\alpha$-pinene were found to undergo a relatively fast hydrogenation, while furan was found to undergo a slow hydrogenation with the cobalt catalyst, although these compounds did not undergo any hydrogenation at all with the iron catalyst. Only a small amount of hydrogen was evolved on the hydrolysis subsequent to the hydrogenation of vinyl acetate, acrylonitrile and allyl chloride. However, a relatively large amount of hydrogen was evolved on the hydrolysis subsequent to the hydrogenation of ethyl acrylate. This hydrogen evolution seems to be related to the fast hydrogenation of ethyl acrylate with the cobalt catalyst.

## Discussion

The effect of the nature of the olefin on the hydrogenation rate with the iron catalyst is illustrated in Fig. 2. The relative order of the hydrogenation rate expressed by the half-periods is: styrene > $\alpha$-methylstyrene $\simeq$ safrole $\simeq$ isosafrole $\simeq$ anethole > isoprene $\simeq$ indene > cyclohexene $\simeq$ *d*-limonene $\gg$ squalene $\simeq$ $\alpha$-pinene. Evidently, terminal olefins are hydrogenated more rapidly than internal olefins.

*d*-Limonene absorbed only 1.0 (mol./mol.-limonene) of hydrogen, and $\alpha$-pinene did not absorb any appreciable amount of hydrogen at all. These facts suggest that only the terminal double bond of *d*-limonene was hydrogenated. Comparisons of the rate for $\alpha$-methylstyrene with that of *d*-limonene and of indene with cyclohexene show that the conjugated olefins were hydrogenated more rapidly than the nonconjugated ones.

The $LiAlH_4/FeCl_3$ ratios corresponding to the active catalysts vary with the nature of the olefins, such as styrene, safrole, indene and ethyl vinyl ether. We shall discuss this variation in the $LiAlH_4/FeCl_3$ ratios below.

We have previously studied[2,3] the amount of ethylbenzene produced during the reaction of the iron catalyst with styrene under a nitrogen atmosphere; the results may be summarized thus: (a) the hydrogen which migrates from the catalyst (iron hydride) to the styrene amounts to 1.0 g. atom/mol. $FeCl_3$ when the $LiAlH_4/FeCl_3$ ratio is 1:1; (b) after the hydrogen migration, a part of the iron hydride is regenerated rapidly when the reaction atmosphere is changed from nitrogen to hydrogen, but the remaining part is regenerated very slowly; (c) this rapidly-regenerated hydride is considered to be responsible for the catalytic activity, and (d) the rapidly-regenerated hydride amounts to 0.3—0.4 g. atom/mol. $FeCl_3$ when the $LiAlH_4/FeCl_3$ ratio is 1:1 and decreases with the increase in the ratio, although the total hydrogen content of the catalyst increases steadily with the increase in the ratio. The variation in the ranges of the $LiAlH_4/FeCl_3$ ratio for the active catalysts and the values of the ratios for the most active catalyst may be explained in terms of the diminution of the hydrogen content of the catalyst through the hydrogen migration from the catalyst to olefins, followed by a very slow hydrogen absorption. The fact that the iron catalysts with the relatively high $LiAlH_4/FeCl_3$ ratios of 1.3—1.4:1 were active in the hydrogenation of safrole and indene in the step-by-step procedures, whereas the iron catalyst with the $LiAlH_4/FeCl_3$ ratio of 1.41:1 was less active in the hydrogenation of styrene, is due to the diminution in the hydrogen content of the catalyst through the hydrogen migration from the catalyst to the safrole or indene. This hydrogen migration may occur more rapidly in the hydrogenation of ethyl vinyl ether, in which the successive addition of a lithium aluminum hydride solution is necessary to continue the hydrogen absorption (Fig. 7). The facts that the amounts of hydrogen evolved during the hydrolysis subsequent to the step-by-step procedure were smaller than those subsequent to the single hydrogenation, and that a long induction period appeared in the

3) Y. Takegami, T. Ueno and T. Fujii, *Catalyst (Shokubai)*, **6**, 339 (1964).

hydrogenation of anethole with the iron catalyst with the relatively high $LiAlH_4/FeCl_3$ ratio of 1.61 : 1, can be taken as further support of the diminution of hydrogen content through the hydrogen migration from the catalyst to the olefins.

In the hydrogenation of vinyl acetate, ethyl acrylate, acrylonitrile and allyl chloride, no hydrogen absorption was observed, and the amounts of hydrogen evolved during the hydrolysis subsequent to the hydrogenation were quite small. In these cases, not hydrogenation but, rather, the reaction of these compounds with the iron catalyst occurred.* When vinyl acetate was added to the active catalyst with the $LiAlH_4/FeCl_3$ ratio of 1 : 1, the catalyst was "killed" and became quite inactive in the hydrogenation of styrene.

* For example, 3-pentanol and ethyl acetate were obtained by the reaction of the iron catalyst with diethyl ketone and vinyl acetate respectively.

As has been mentioned above, the iron catalyst is selective in its hydrogenating ability. On the other hand, it can be seen from a comparison of Figs. 2 and 8 that the cobalt catalyst is highly active in its hydrogenating ability; internal olefins can be hydrogenated successfully with the cobalt catalyst.

For practical purposes, perhaps only the slow addition of a lithium aluminum hydride solution to a mixture of olefin and heavy metal salt, before the occurrence of hydrogen absorption, can provide a simple and convenient procedure for the hydrogenation of various olefins.

We are grateful to Dr. Kunio Okamoto for his helpful advice and discussions.

*Department of Fuel Chemisty*
*Faculty of Engineering*
*Kyoto University*
*Sakyo-ku, Kyoto*

# Complex Compounds of Gallium with Mandelic Acid

By T. N. Srivastava and D. C. Rupainwar

(Received October 26, 1964)

In a previous communication from this laboratory[1] it has been reported that aluminium hydroxide and mandelic acid form two compounds, an insoluble basic salt and a water-soluble chelate, both possessing a metal-to-ligand ratio of 1 : 2. Gallium, indium and thallium, other metals of the same group, are known to show a close resemblance to aluminium in their tendency to form coordination complexes. A study of the gallium chloride - mandelic acid - water system has been undertaken with a view of establishing the nature of the complex species. The results are communicated in this paper.

## Experimental

**pH and Conductivity Studies.**—A stock solution of gallium chloride was prepared by dissolving freshly-precipitated gallium hydroxide in a minimum quantity of dilute hydrochloric acid. The metal content was determined gravimetrically by the use of 8-quinolinol. The gallium chloride solution was adjusted to an initial pH of 2.95 in each case by adding a requisite quantity of a standard sodium hydroxide solution prior to the preparation of a particular set of mixtures.

Mandelic acid (British Drug House, extra pure quality) was dissolved in conductivity water and used as such.

Using 0.004 M solutions of gallium chloride and mandelic acid, three sets of mixtures, with metal-to-ligand ratios of 1 : 1, 1 : 2 and 1 : 3, were prepared. To these solutions varying quantities of a standard alkali solution were added and the volumes made up to the same mark in each case. The mixtures were then shaken well and left overnight to attain equilibrium. The pH values and conductances of these solutions were measured at a constant temperature. For purposes of comparison, solutions of gallium chloride and mandelic acid of the same concentration were also separately titrated with the standard alkali under identical conditions.

The pH determinations were carried out with the help of a sensitive pH meter (made by Leeds and Northrup Co ; Philadelphia, U. S. A. Cat. No. 7667) equipped with a glass and a saturated calomal electrode. The pH values of all the sets are plotted against the amount of alkali added, and the curves obtained are shown in Fig. 1.

Conductivity experiments were performed with a dip-type conductivity cell (cell constant, 1.46 ml.)

1) T. N. Srivastava and D. C. Rupainwar, *J. prakt. Chem.*, to be published.

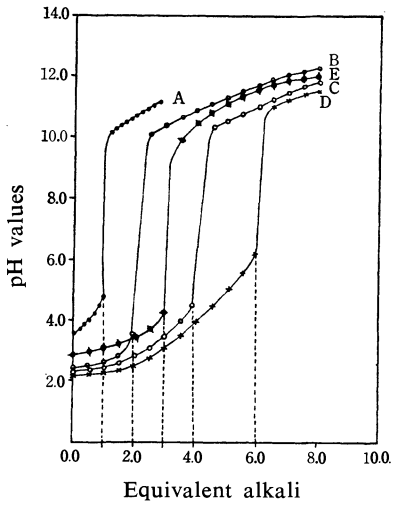



Fig. 1. Electrometric titration of mixtures of 0.004 M gallium chloride and 0.004 M mandelic acid at 30±1°C.
$GaCl_3$ : Mandelic acid
A, 0 : 1 B, 1 : 1 C, 1 : 2 D, 1 : 3 E, 1 : 0

using an electrical Mullard Conductivity Bridge, the null point being detected by the use of a magic eye. The results are shown in Fig. 2, where the specific conductance is directly plotted against the equivalents of alkali added.

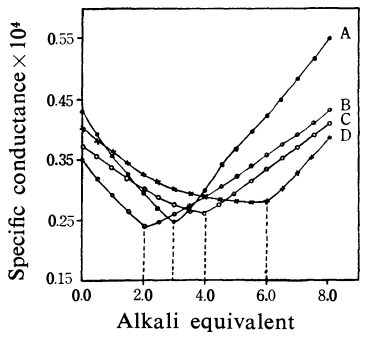



Fig. 2. Conductometric titrations of mixtures of 0.004 M gallium chloride and 0.004 M mandelic acid at 30±1°C.
$GaCl_3$ : Mandelic acid
A, 1 : 0 B, 1 : 1 C, 1 : 2 D, 1 : 3

**Solubility Measurements.**—A set of ten samples containing almost the same weight of freshly-precipitated gallium hydroxide and a 100 ml. aqueous solution of mandelic acid of the different concentrations ranging from 0.005 M to 0.05 M, was prepared in 250 ml. Erlenmeyer flasks. The amount of the hydroxide was so chosen that in a few of the later samples the gallium-to-mandelic acid ratio exceeded 1 : 3, while in several sets in the beginning the amount of the hydroxide was always larger than that required for a 1 : 3 ratio. All the flasks were shaken in a mechanical shaker at room temperature for 24 hr. Known aliquots were taken out with cotton-plugged pipettes, and their metal and mandelic acid contents were analysed, the former gravimetrically by 8-quinolinol and the latter volumetrically with cerium(IV) sulphate.[2] The observations are represented graphically in Fig. 3.

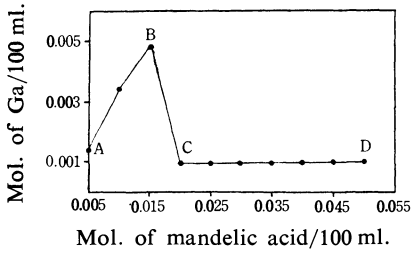
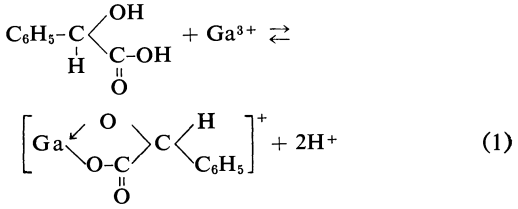



Fig. 3 Solubility of gallium hydroxide in aqueous mandelic acid solution (0.005—0.05 M) at 31±1°C.
Portion AB=Excess of gallium hydroxide
Portion CD=Excess of mandelic acid

## Results and Discussion

**pH and Conductivity Measurements.**—Curve A (Fig. 1) represents the titration of mandelic acid alone; as is to be expected for a monobasic acid, it shows a sudden rise in pH when nearly one equivalent of alkali has been added. Curve B for a 1 : 1 mixture of gallium chloride and mandelic acid gives an inflection at 2 equivalents of alkali, indicating the formation of a 1 : 1 chelate. The chelation takes place by the donation of a lone pair of electrons from the hydroxyl oxygen atom, making the hydrogen atom attached to it more labile and causing a lowering of the pH value. Consequently, two equivalents of alkali are consumed in the titration. The overall equation may, then, be represented as follows:




(1)

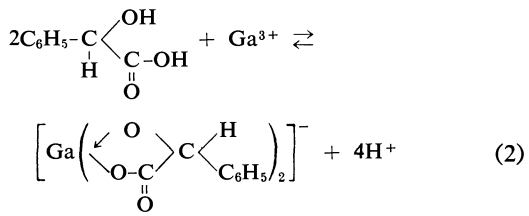
This is supported by the lower pH value of the mixture (2.40) as compared to that of individual gallium(III) chloride (2.95) and mandelic acid (3.60) solutions.

The further addition of alkali brings about a sudden increase in the hydroxide ion concentration, and the curve registers an abrupt rise in pH value.

Titrations of the 1 : 2 and 1 : 3 mixtures represented by curves C and D respectively

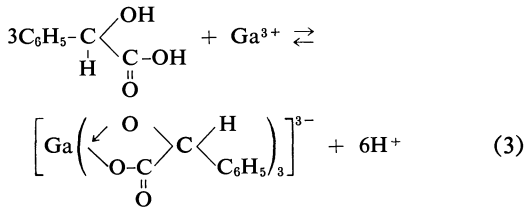
2) M. R. Varma and S. D. Paul, *J. Sci. Ind. Res.*, **13B**, 347 (1954).

(Fig. 1) show inflection points at four and six equivalents of alkali. This corresponds to the formation of complexes with 1 : 2 and 1 : 3 metal-to-ligand ratios respectively; the complexes may be represented by the following equations:



(2)

and



(3)

Curve A (Fig. 2), representing the conductometric titration of a 0.004 M gallium chloride solution with sodium hydroxide, shows a well-defined inflection at 3 equivalents of alkali corresponding to the precipitation of the hydroxide. Curves B, C and D, obtained for 1 : 1, 1 : 2 and 1 : 3 mixtures respectively, show minimum conductances at two, four and six equivalents of alkali. The decrease in conductivity with the addition of an alkali solution in the beginning may be due to the replacement of the fast-moving $H^+$ by the slow-moving $Na^+$. When all the $H^+$ is removed, the conductance rises abruptly on account of the excess $Na^+$ and $OH^-$ present in the solution, which cause a break in the curve. The formation of the three chelates may be explained by the same three equations given above for pH titrations.

**Solubility.**—The straight line marked AB in Fig. 3 represents a consistent ratio of 1 : 3 between the metal and the ligand, indicating the nature of the soluble species formed in this region. The curve registers an abrupt fall at point B, showing that almost all the gallium has gone out of the solution, forming an insoluble compound which separates as a white granular solid in the flasks. The CD portion of the curve may represent the solubility of this species in a solution with an excess of mandelic acid. The experiment thus shows the formation of two compounds, a soluble 1 : 3 chelate (compound I) when the hydroxide is present in excess and an almost insoluble white crystalline solid (compound II) when mandelic acid is present in excess.

**The Isolation and Characterisation of the Compounds.**—*Compound I.*—The combined filtrate obtained from the samples in the region AB of the solubility curve (Fig. 3) was concentrated by slow evaporation on a water bath, and then left for crystallisation when a white crystalline solid separated. This was washed with an ethanol-water mixture and with ether, and air-dried.

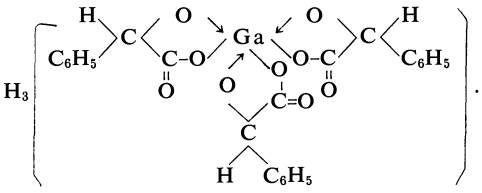
*Compounds II.*—Compound II obtained as a white insoluble granular solid from samples after the point B on the solubility curve was collected, washed with an ethanol-water mixture and with ether, and air-dried.

The gallium and mandelic acid contents of both the compounds were analysed. The water molecules were also examined by heating a known weight of the air-dried sample in an oven at 110°C and then ascertaining the loss in weight. The results of the analysis, along with the formulae tentatively assigned, are given below:

| Tentative formula for the compound | | % Gallium | % Mandelate | % Water |
|---|---|---|---|---|
| $C_{24}H_{27}O_{12}Ga$ (I) | Found | 12.10 | 79.3 | 9.15 |
| | Calcd. | 12.07 | 79.1 | 8.89 |
| $C_{16}H_{19}O_8Ga$ (II) | Found | 16.80 | 71.92 | 8.68 |
| | Calcd. | 17.12 | 73.96 | 8.87 |

The good agreement between the calculated and the experimental values observed above indicates that the molecular formulae tentatively assigned are correct.

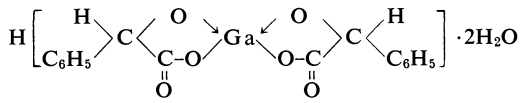
Compound I, with a metal-to-ligand ratio of 1 : 3, is soluble in water and ethanol, but insoluble in other common organic solvents. It is acidic to litmus and needs 3 equivalents of alkali for complete neutralisation. Taking three molecules of water as the water of crystallisation, its structure, in analogy with several other such chelates of tervalent metals,[3-6] may be given as:



Compound II, possessing a metal-to-ligand ratio of 1 : 2, is sparingly soluble in water, the solubility being 0.025 g./100 cc. at room temperature (30.5°C). It is insoluble in ethanol, ether and other common organic solvents. It is acidic to litmus and requires for complete

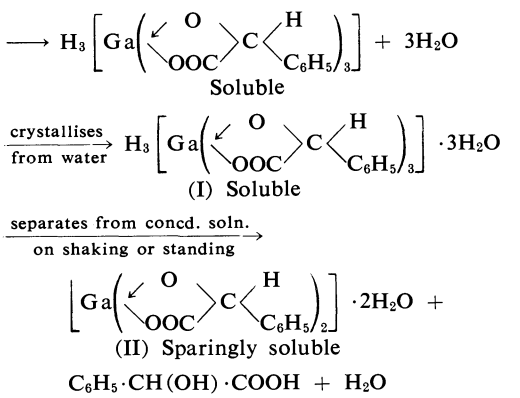
3) T. Moellor, *J. Am. Chem. Soc.*, **62**, 2444 (1940).
4) N. K. Dutta and P. Bose, *J. Indian Chem. Soc.*, **30**, 431 (1953).
5) K. Peters, *Chem. Abstr.*, **53**, 13525 (1959).
6) E. N. Deichman and G. V. Rodicheva, *Zhur. Neorg. Khim.*, **9**(4), 807 (1964).

neutralisation three equivalents of alkali, two of which are consumed by the released mandelic acid formed by the ready hydrolysis of the compound, and the remaining one, by the cationic hydrogen. The complex thus behaves as a monobasic acid. On being heated at 110°C, it loses two molecules of water. The structure of compound II may be written as:



The structures assigned to the two complexes support Eqs. 2 and 3, which represent the physico-chemical investigations. Attempts to isolate the 1 : 1 complex shown by Eq. 1 were, however, unsuccessful.

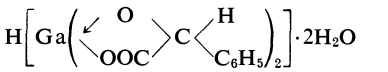
The reaction between gallium hydroxide and mandelic acid solutions represented by the portion CD of the solubility curve (Fig. 3) may now be reconsidered. It appears that when the concentration of the 1 : 3 chelate is relatively large in the solution and when it is vigorously shaken to induce precipitation, the more stable and less soluble 1 : 2 complex separates out. This was supported by separately taking a concentrated solution of the 1 : 3 chelate and shaking it vigorously for a few hours, a compound thereupon separated which, on analysis, was found to be identical with compound II. The change was found to be irreversible; no former species could be identified in solution when the latter was shaken with an excess of mandelic acid. The changes taking place may be represented by the following equation:



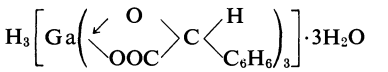
The metal-to-ligand ratio obtained for compound II is similar to that of aluminomandelic acid reported previously.[1] The compound differs from the aluminium complex in being more insoluble and thus is not converted into the corresponding basic salt. Further, unlike the $Al^{3+}$ - mandelic acid - water system, the treatment of the mixture containing concentrated solutions of gallium chloride and mandelic acid with ammonia did not result in the precipitation of a basic salt. On the other hand, the above solution, when shaken and left overnight, gave a white crystalline compound, the analysis of which agreed with that of compound II.

## Summary

pH and conductometric studies of the gallium chloride - mandelic acid - water system show the existence of three chelates in solution with a metal-to-ligand ratio of 1 : 1, 1 : 2 and 1 : 3. The solubility of freshly-precipitated gallium hydroxide in aqueous solutions of mandelic acid of varying concentrations, however, indicates the presence of only, 1 : 2- and 1 : 3-type species. These two complexes have here been isolated in the crystalline state. Their structures may be represented by



and



respectively. The 1 : 1 complex indicated by electrometric titrations appears to be fairly unstable, as it could neither be inferred from solubility experiments nor isolated in the crystalline state.

The authors are thankful to Professor S. N. Shukla, Head of the Chemistry Department, for providing laboratory facilities, and to the Director, Indian Sugar Cane Research Institute, Lucknow, for permission to use their instruments for physico-chemical studies. One of us (D. C. R.) is also thankful to the C. S. I. R., New Delhi, for the award of a junior research fellowship.

*Chemistry Department*
*Lucknow University*
*Lucknow, India*

# The Synthesis of 1-Phenylpropane Derivatives. IV*

By Takeshi MATSUMOTO and Haruhisa SHIRAHAMA

(Received November 2, 1964)

In previous papers[1,2] the syntheses of several *threo* and *erythro* 1-phenyl-2-amino-1, 3-propanediol derivatives, starting from benzoyl chloride and ethylene, have been described. The steric courses which led to these stereoisomeric products have also been discussed. In this paper, the preparation of *threo* and *erythro* 1-phenyl-2-acetamido-1, 3-propanediol and related compounds starting from benzoly chloride and vinyl chloride will be reported. The synthetic processes are outlined in Fig. 1.

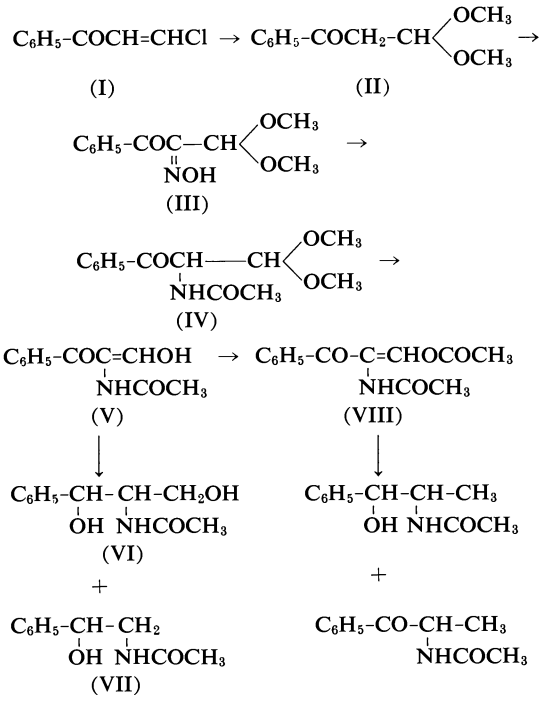


Fig. 1

The starting material, phenyl β-chlorovinyl ketone, was obtained in a 70—90% yield by a modification of Klinko's method.[3] After this compound had been converted to benzoylacetaldehyde dimethy acetal (II)[4] by methanolic sodium hydroxide, the product was treated with amyl nitrite in methanolic sodium methoxide.[5] The isolation of the desired oximinoketone (III), which is present in the reaction mixture as a sodium salt, offered considerable difficulty, however.[6] The compound III appears to be sensitive to acidic substances; neutralization with even such weak acids as acetic, phosphoric, and boric acids resulted in the formation of only an intractable mixture. After many unsuccessful attempts, the difficulty was overcome by the use of ammonium chloride as a neutralizing agent. By this procedure, the pure oximinoketone was obtained in a 76% yield. In the hope of preparing 1-phenyl-2-amino-1, 3-propanediol derivatives by the routes shown in Fig. 2, attempts were made to convert oximinoketone (III), acetoximinoketone (III′) and their reduction products IX and IX′ to the alcohols X, X′, XI, and XI′ respectively. However, the hydrolysis of the acetal group of III, III′, IX and IX′ with a variety of acids, including boric, phosphoric, and acetic acids, did not afford pure crystalline materials.

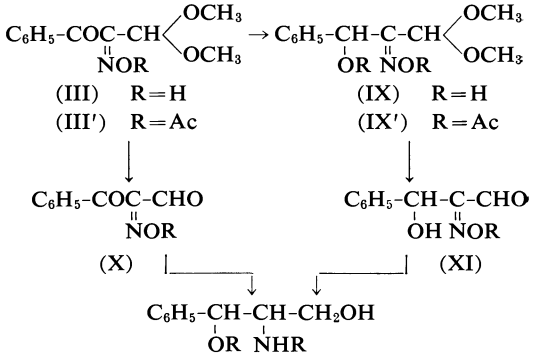


Fig. 2

* Part III: Ref. 10b.

1) T. Matsumoto and K. Hata, *J. Am. Chem. Soc.*, **79**, 5506 (1957).

2) T. Matsumoto, H. Shirahama and T. Nishida, *J. Org. Chem.*, **27**, 79 (1962).

3) V. T. Klinko, V. A. Mikhalv and A. P. Sklodinov, *Zhur. Opschei Khim.*, **27**, 370 (1957); *Chem. Abstr.*, **51**, 15499 (1957).

4) C. C. Price and J. A. Pappalardo, *J. Am. Chem. Soc.*, **72**, 2613 (1950).

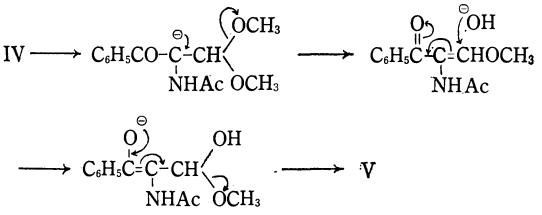
5) L. Claisen and O. Manasse, *Ber.*, **20**, 2194 (1887).

6) The reaction mixture in which oximinoketone (III) is present exhibits deep blue coloration upon the addition of an aqueous ferrous sulfate solution. On the contrary, the ferrous sulfate test for oximinoketones according to Feigl's procedure, which is performed in the presence of ammonia (F. Feigl, "Tüpfelreaktionen," Akademishe Verlagsgesellshaft, Leibzig (1938), p. 87) was negative for pure III. However, the addition of dilute ethanolic sodium ethoxide seems to provide a more sensitive method, at least for this case.

Syntheses along these lines were, therefore, abandoned.

The catalytic hydrogenation of oximinoketone (III) in 3 N methanolic hydrogen chloride in the presence of palladium was examined next. The stereospecific formation of norephedrine from α-oximinopropiophenone under similar conditions has been reported.[7] The removal of the solvent left, however, an intractable tarry material, probably formed by the hydrolysis of the acetal group by hydrogen chloride and by subsequent condensation between the aldehyde group and the newly-formed amino group. Therefore, the reaction mixture was, in the next attempt, at first neutralized by passing through ammonia. The removal of ammonium chloride by the addition of ether, the evaporation of the solvent, and the subsequent benzoylation of the residue afforded a small amount of crystals. Elemental analysis indicates that the product is dibenzoyl-1-phenyl-2-amino-3, 3-dimethoxy-1-propanol (the configuration was not examined). In a separate attempt, after the absorption of three moles of hydrogen, a small amount of water was added to effect the hydrolysis of the acetal group. The catalyst was then replaced by platinum oxide, and the hydrogenation was continued until one further mole of hydrogen had been absorbed. The benzoylation of the product afforded a compound with an elemental composition corresponding to that of a tribenzoyl derivative (m. p. 204—207°C) of 1-phenyl-2-amino-1, 3-propanediol, which is probably a mixture of threo and erythro diastereoisomers judging by a comparison of its melting point with those of pure isomers.[8] However, the yield of this route was, again, not satisfactory.

The hydrogenation of α-oximino-β-ethoxypropiophenone by palladium in a mixture of acetic anhydride and acetic acid has been shown to afford α-acetamido-β-ethoxypropiophenone in a good yield.[2] Under similar conditions, parallel to this result, the reduction of oximinoketon (III) give a 90% yield of α-acetamido-β, β-dimethoxypropiophenone (IV). The hydrolysis of the acetal group of the latter compound IV by hydrochloric acid, did not, however, produce V in a good yield, the starting material being recovered. On the other hand, the treatment of IV with an aqueous alkaline solution afforded the desired hydroxymethylene compound, V, in an excellent yield. It is well known that the acetal group resists base-catalyzed hydrolysis. In this particular case, however, the seemingly anomalous hydrolysis by the base probably proceeds through a vinyl ether, which is a vinylog of ester, as is shown below:



The attempted hydrogenation of the hydroxymethylene ketone thus obtained resulted in the recovery of the starting meterial. The inertness to hydrogenation of the carbonyl group in V is probably due to the carboxylic group-like character of the -COCH=CHOH system.

Several examples of the successful hydrogenation of hydroxymethylene ketone to the corresponding diol by means of a Raney nickel catalyst have been reported.[9]

The reduction of V by this method afforded an excellent yield (90%) of the desired 1-phenyl-2-acetamido-1, 3-propanediol (VI). That the product was a mixture of approximately equal amounts of threo and erythro compounds was inferred from a comparison of its infrared spectrum with those of pure stereoisomers. From the product, the threo isomer was isolated through recrystallization, while the erythro isomer was separated as a triacetyl compound (47% based on the hydroxymethylene compound) after the treatment of the reaction product with acetic anhydride and pyridine.

A minor product of catalytic hydrogenation with Raney nickel was isolated in the course of separation; it had an elemental composition of $C_{10}H_{13}NO_2$ and was identified as 1-phenyl-2-acetamido-1-ethanol (VII) by comparison with an authentic specimen prepared by treating acetamidoacetophenone with sodium borohydride. The course which led to this product is obscure; it might involve the deformylation of the hydroxymethylene ketone by alkaline substances on the surface of Raney nickel.

Lastly, the reduction of enolacetate (VIII) was attempted. The enolacetate (m. p. 117°C) was readily obtained by treating the sodium salt of the hydroxymethylene ketone (V) with acetic anhydride under cooling. The acetate is very susceptible to alkaline hydrolysis, regenerating V. Acetylation without cooling gave a product, $C_{13}H_{13}NO_4$ with a m. p. of 130°C, this also regenerates V on alkaline

7) W. H. Hartung and Y. C. Chang, *J. Am. Chem. Soc.*, 75, 89 (1953).
8) T. Taguchi, T. Tomoeda and T. Ishida, *Yakugaku Zasshi*, 75, 666 (1955).
9) H. Rupe and O. Klemm, *Helv. Chim. Acta*, 21, 1538 (1938); B. D. Astill and V. Boekelheide, *J. Am. Chem. Soc.*, 77, 4079 (1955).

hydrolysis and exhibits an infrared spectrum consistent with an enolacetate structure. The compounds with m. p. of 117 and 130°C may, therefore, be cis and trans isomers of the enolacetate. The catalytic hydrogenation of the enolacetate with Raney nickel gave a 50% yield of an erythro compound *N*-acethylnorephedrine and 14% of acetamidopropiophenone. *N*-acethylpseudonorephedrine was not present in an isolable amount.

## Experimental

**Phenyl β-Chlorovinyl Ketone (I).**—This compound was prepared by a modification of the method of Klinko et al. A mixture of 100 g. of benzoyl chloride and 100 g. of aluminum chloride was heated gently to give an adduct. The adduct was then dissolved in 200 ml. of tetrachloroethane. Dry vinyl chloride was introduced into the solution through an inlet tube reaching to the bottom of the vessel. A large test tube was employed as a reaction vessel in order to keep the gas in good contact with the solution. The vinyl chloride was then generated by the decomposition of 120 g. of dichloroethane with 150 g. of sodium hydroxide in 500 ml. of 60% ethanol. The temperature of the generating flask was adjusted so that the gas produced was effectively absorbed in the reaction mixture. It took 10 hr. for the reaction to be completed. After it had been set aside for several hours, the resultant solution was poured into a mixture of ice and dilute hydrochloric acid. The product was extracted with ether, and the extract was washed successively with dilute hydrochloric acid, twice with a 10% sodium hydroxide solution, and with water, then it was dried over sodium sulfate. After the removal of the solvent, the residue was distilled in vacuo. A pale-yellow viscous oil boiling at 124°C (12 mmHg) was collected; yield 93 g. (78.5%).

**Benzoylacetaldehyde Dimethyl Acetal (II).**—The general procedure described by Nelles[10] was used.

**α-Oximino-β, β-dimethoxypropiophenone (III).**—A solution of 5.8 g. sodium in 180 ml. of methanol was cooled in an ice-water bath and stirred. To this solution, 29.5 g. of isoamyl nitrite (or an equivalent amount of isopropyl nitrite) and 49 g. of acetal II was added successively. After it had stood for three days in a refrigerator, the light orange reaction mixture was poured onto ice water. The solution was then washed with ether three times. From this ethereal solution, 9 g. of unchanged acetal was recovered. The aqueous solution of the product was saturated with ammonium chloride and extracted with ether. The extract was dried over sodium sulfate, and the solvent was removed. The residual yellow paste was crystallized after being set aside for several hours. The crystalline cake was washed with a small amount of benzene and recrystallized from the same solvent; yield 20 g. From the benzene used for washing and recrystallization, a further 15 g. of the product was obtained by extraction with an adequate quantity of 5% aqueous sodium hydroxide, followed by saturation with ammonium chloride and subsequent extraction with ether (76%). The purified product melted at 86—87°C.

Found: C, 59.92; H, 5.37; N, 6.34. Calcd. for $C_{11}H_{13}NO_4$: C, 59.19; H, 5.87, N, 6.28%.

The acetoxyimino compound was obtained as follows. A yellow solution of 500 mg. of the isonitroso ketone III in 4 ml. of 5% aqueous sodium hydroxide was shaken with a solution of few drops of acetic anhydride in 4 ml. of ether. The mixture was decolorized immediately. From the ether extract the product was obtained in a crystalline condition, m. p. 90—92°C. Yield 600 mg. (quantitative).

Found: C, 59.22; H, 5.97; N, 5.68. Calcd. for $C_{13}H_{15}NO_5$: C, 58.86; H, 5.70; N, 5.28%.

The treatment of the oximino compound with benzoyl chloride gave the corresponding benzoyl oximino derivative; m. p. 63—65°C. Yield 95%.

Found: C, 66.15; H, 5.20. Calcd. for $C_{18}H_{17}NO_5$: C, 66.05; H, 5.24%.

Both acetoximino and benzoximino compounds were dissolved in 5% aqueous sodium hydroxide to give a yellow solution. The original oximino ketone III was regenerated by saturation with ammonium chloride and by extraction with ether.

**The Catalytic Hydrogenation of α-Oximino-β, β-dimethoxypropiophenone (III).**—a) Oximino ketone III (2 g.) was dissolved in a 3 N methanolic hydrogen chloride solution and hydrogenated in the presence of 400 mg. of palladium charcoal. After 3 mol. of hydrogen had been absorbed, an equal amount of water was added to the solution. The catalyst was then replaced by platinum oxide, and the hydrogenation was continued until 1 mol. of hydrogen had been further absorbed. The catalyst was then removed, the solution was washed with ether, and the aqueous solution was made alkaline with concentrated sodium hydroxide. The product was next taken up in ethyl acetate, and the extract was dried and evaporated to leave an yellow oil. The benzoylation of this oil by the Schotten-Baumann method gave a small amount of white crystals. The benzoate, recrystallized from ethyl acetate, melted at 204—207°C. The comparison of the melting point of this crystal with those described in the literature[8] indicates the product to be a mixture consisting of two diastereoisomers of 1-phenyl-2-amino-1, 3-propanediol tribenzoate.

Found: C, 75.09; H, 5.71; N, 3.33. Calcd. for $C_{30}H_{25}NO_5$: C, 75.14; H, 5.26; N, 2.92%.

b) Two grams of oximino ketone III in a 3 N methanolic hydrogen chloride solution were hydrogenated in the presence of 400 mg. of palladium-charcoal. After 3 mol. of hydrogen had been absorbed, the catalyst was removed and the solution was made alkaline by passing through gaseous ammonia. Ether was then added to the solution, and the precipitated ammonium chloride was removed by filtration. The evaporation of the solvent under reduced pressure at room temperature left a brown past which was treated with benzoyl

10) a) J. Nelles, Brit. Pat. 466890 (1937); *Chem. Abstr.*, 31, 7886 (1937); b) T. Matsumoto, R. Ishida and H. Shirahama, *J. Chem. Soc. Japan, Pure Chem. Sec.* (*Nippon Kagaku Zasshi*), 83, 147 (1962).

chloride under Schotten-Baumann conditions to give white crystals. The benzoate, recrystallized from methanol, melted at 155—157°C. The analysis indicated that the product was 1-phenyl-2-amido-3, 3-dimethoxy-1-propanol dibenzoate.

Found: C, 71.54; H, 6.20. Calcd. for $C_{25}H_{25}NO_5$: C, 71.58; H, 6.01%.

**α-Acetamidohydroxymethyleneacetophenone (V).**—a) A solution of 9 g. of the oximino ketone III in a mixture of 40 ml. of acetic acid and 40 ml. of acetic anhydride was shaken with hydrogen in the presence of 1.5 g. of 10% palladium on charcoal until 2 equivalents of hydrogen had been absorbed. After the catalyst had been removed by filtration and the solvent had been evaporated, the residue was vigorously shaken with 160 ml. of 0.5 N aqueous sodium hydroxide. The solution was washed with benzene, made acidic with 2 N hydrochloric acid, and extracted with benzene. The extract was dried and the solvent removed to leave the crystalline hydroxymethylene ketone V. The product, washed with ethanol and recrystallized from benzene, melted at 113—115°C. Yield 6.7 g. (81%).

Found: C, 64.58; H, 5.62; N, 6.88. Calcd. for $C_{11}H_{11}NO_3$: C, 64.38; H, 5.40; N, 6.83%.

b) The hydrogenation of 3 g. of oximino ketone was carried out in the manner described in a). The paste obtained after the removal of acetic acid - acetic anhydride, crude α-acetamido-β, β-dimethoxy propiophenone, was dissolved to a homogeneous solution by shaking it with 190 ml. of 2 N hydrochloric acid for 2 hr. The ultraviolet spectra of the resultant solution showed $\lambda_{max}$ 251 mμ (ε 1030), whereas a solution of pure V in 2 N hydrochloric acid showed $\lambda_{max}$ 251 mμ (ε 11400). Thus, in the reaction mixture only 10% of the original acetal was estimated to be converted to the hydroxymethylene compound. Since further treatment of the solution for 6 hr. did not produce any increment in the extinction coefficient, the solution was extracted with ethyl acetate. The extract afforded 0.3 g. of the desired V.

**α-Acetamidoacetoxymethyleneacetophenone (VIII).**—A solution of V in an equivalent amount of 0.5 N aqueous sodium hydroxide was overlayered by ether, and an equivalent amount of acetic anhydride was added portion by portion with continuous shaking and cooling. When the yellow color of the alkaline solution had disappeared, the ethereal layer was separated and dried. After the solvent had been removed, the crystalline acetate VIII was obtained in a good yield; m. p. 116—117°C.

Found: C, 63.47; H, 5.47; N, 5.60. Calcd. for $C_{13}H_{13}NO_4$: C, 63.15; H, 5.30; N, 5.67.

An isomeric acetate was obtained as a colorless crystal which melted at 128—130°C when acetylation was carried out without cooling. Both acetates gaves red coloration with ferric chloride and were converted to the original aldehyde (m. p. 113—115°C) when treated with aqueous alkali.

Found: C, 63.35; H, 5.35; N, 5.52. Calcd. for $C_{13}H_{13}NO_4$: C, 63.15; H, 5.30; N, 5.67%.

**The Hydrogenation of V with a Raney Nickel Catalyst.**—To a solution of 1 g. of the hydroxymethylene compound in 10 ml. of tetrahydrofuran, 1 ml. of Raney nickel was added. Hydrogenation at 100 atm. was carried out at room temperature. After the catalyst and solvent had been removed, the residue was dissolved in a small amount of ethyl acetate. Upon scratching the wall of vessel, a mixture of two diastereoisomers of 1-phenyl-2-acetamido-1,3-propanediol (m.p. 92—117°C, 310 mg.) was crystallized out. Recrystallization from ethyl acetate and then from ethanol gave the threo isomer (m. p. 134°C), whose melting point and infrared spectra were identical with those of the literature.

Found: C, 63.09; H, 7.53; N, 6.36. Calcd. for $C_{11}H_{15}NO_3$: C, 63.14; H, 7.23; N, 6.69%.

The paste obtained from the mother liquor was chromatographed on a column of aluminum oxide by ethyl acetate. Fractions eluted at earlier stages contained 101 mg. (10%) of 1-phenyl-2-acetamido-1-ethanol, which was identified with a sample prepared by the sodium-borohydride reduction of acetamidoacetophenone.

Found: C, 67.98; H, 7.57; N, 7.78. Calcd. for $C_{10}H_{13}NO_2$: C, 67.02; H, 7.31; N, 7.82%.

The fraction eluted later contained 595 mg. of a mixture of the isomeric propanediols VI, bringing the total yield to 88.5%. For the separation of each diastereoisomer, the mixture was converted to a triacetly compound by treating it with acetic anhydride and pyridine. The *erythro* triacethyl-1-phenyl-2-amino-1, 3-propanediol (595 mg.; 47% yield based on aldehyde) thus obtained melted at 115—118°C. Both the melting point and the infrared spectrum were consistent with those of the literature.

Found: C, 61.07; H, 6.61. Calcd. for $C_{15}H_{19}NO_5$: C, 61.42; H, 6.53%.

**The Hydrogenation of α-Acetamidoacetoxymethyleneacetophenone (VIII).**—One gram of α-acetamidoacetoxymethyleneacetophenone (VIII) in 5 ml. of ethanol was hydrogenated with 0.5 ml. of a Raney nikel catalyst at room temperature under a pressure of 50 atm. After 4 hr. shaking, the catalyst and solvent were removed to leave a pasty mass containing crystalline *N*-acetyl-norephedrine. The product (320 mg.), recrystallized from ethyl acetate, melted at 134—135°C. The mixed melting point determination with an authentic specimen prepared by a known process showed no depression. The noncrystalline portion of the product was dissolved in ether and chromatographed on aluminum oxide. A further quantity (75 mg.) of *N*-acetyl-norephedrine was obtained (total yield, 46.7%). Besides, 165 mg. (14%) of α-acetamidopropiophenone and 105 mg. of a paste, the infrared spectrum of which was consistent with 1-phenyl-2-acetamido-1, 3-propanediol monoacetate, were obtained. In the reaction mixture *N*-acetylnorpseudoephedrine could not be detected.

**1-Phyenyl-2-oximino-3, 3-dimethoxy-1-propanol (IX).**—To a solution of oximinoketone (III) in methanol an excess of sodium borohydride was added. The reaction mixture foamed vigorously and became yellow. After 24 hr., the foaming ceased and the solution became colorless. The methanolic solution was evaporated to dryness, and the residue was dissolved in dilute aqueous sodium hydroxide and the product taken up by extraction with ethyl acetate. The extract was then dried. The removal of the solvent left a crude product

which was recrystallized from ethyl acetate to give a pure sample (m. p. 83—85°C). The treatment of the product obtained above with acetic anhydride and pyridine gave an acetoxyimino alcohol (m. p. 83—85°C). A mixed melting point determination with the original isonitroso alcohol showed a distinct depression.

Found: C, 58.04; H, 6.14; N, 4.92. Calcd. for $C_{15}H_{19}NO_6$: C, 58.24; H, 6.19; N, 4.53%.

*Department of Chemistry*
*Faculty of Science*
*Hokkaido University*
*Sapporo*

# Some Unexpected Reactions in the Synthesis of 1-Phenyl-2-aminopropane-1, 3-diol Starting from Phenyl β-Chlorovinyl Ketone*

By Haruhisa SHIRAHAMA and Takeshi MATSUMOTO

(Received November 24, 1964)

In a previous paper[1] the synthesis of 1-phenyl-2-aminopropane-1, 3-diol (VI) from phenyl β-chlorovinyl ketone (I) was described. The reactions to be recorded below were examined in an attempt to find other routes to prepare VI from I. However, in each process, unexpected results were obtained. These new findings obtained in the course of this work will be reported here.

**Route. 1.**—The synthetic process described in the preceding paper involved two hydrogenation steps starting from α-oximino-β, β-dimethoxypropiophenone (V), derived from I. It was felt that the replacement of V by α-oximino-β, β-dibenzyloxypropiophenone (IV) might directly give the diol VI by a single hydrogenation through the hydrogenolysis of the benzyl group. Although the synthesis along this line was not successful, as will be described below, some interesting information about the reactivity of β, β-dibenzyloxypropiophenone (II) was obtained. Some chemical properties of II will therefore be reported on here.

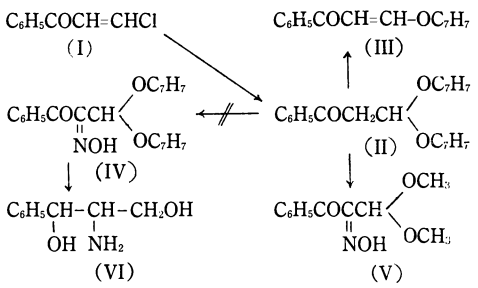



Fig. 1

The acetal (II) was prepared from I following the method for the preparation of VII.[1] A benzyl alcoholic solution of sodium benzyloxide was used as the alkaline reagent. Since the solution was very viscous and since a 5% solution gradually solidified at room temperature, a specially-designed separatory funnel was needed to add it portion by portion to the reaction vessel. The reaction proceeded as in the case of dimethyl acetal.[1] The product II looses benzyl alcohol upon prolonged heating and gives phenyl β-benzyloxyvinyl ketone (III). The elimination of alcohol from the β-keto acetal by heat was also observed in the case of the dimethyl acetal (VII). The oximation of II in methanol following Claisen's method[2] unexpectedly yielded V instead of IV. A possible explanation for the exchange of the alkoxy group of II may be that described in Fig. 2. In fact, V could be derived from II, III, VII and VII' by the same treatment.

In order to prepare IV, therefore, it was anticipated that the oximation of II in benzyl

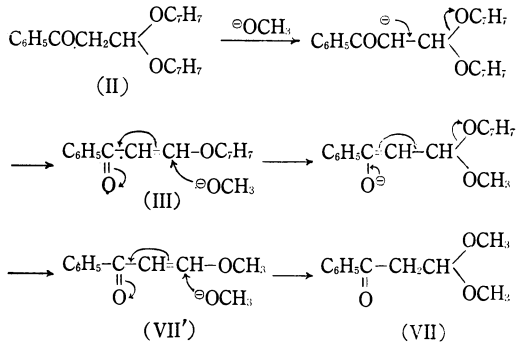



Fig. 2

* The Synthesis of 1-Phenylpropane Derivatives. V. Part IV: Ref. 1.

1) H. Shirahama and T. Matsumoto, This Bulletin, **38**, 1289 (1965).

2) C. Claisen and O. Mannasse, *Ber.*, 20, 2194 (1887).

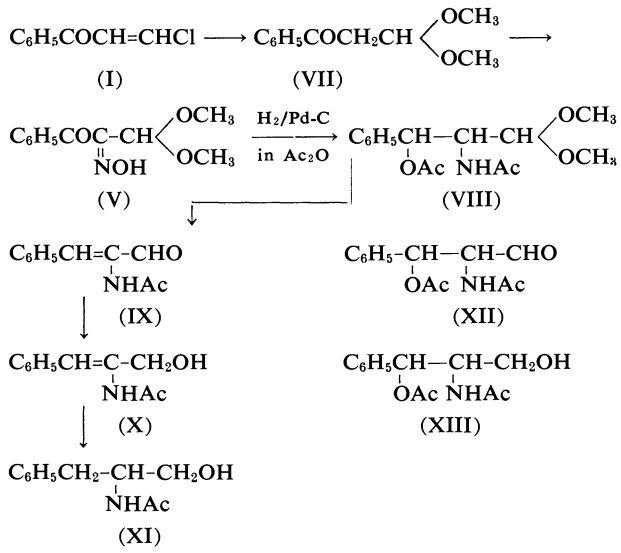


Fig. 3

alcohol would give favorable results. However, the reaction did not proceed in benzyl alcohol, and the original material was recovered after a few days treatment.[3] The inertness of II in a benzyl alcoholic solution may be due to the steric hindrance exerted by the benzyloxy group and/or to the polarity of the solvent.

**Route 2.**—The experiments outlined in Fig. 3 were originally attempted in order to convert VII to α-acetamido-β-acetoxyhydrocinnamaldehyed (XII), a possible intermediate for the synthesis of 1-phenyl-2-aminopropane-1, 3-diol. However, the hydrolysis of the α-acetamido-β-acetoxyhydrocinnamaldehyde dimethyl acetal under a variety of conditions was found to yield the α, β-unsaturated aldehyde (IX) invariably. Although the attempt along the original lines was thus unsuccessful, *N*-acetyl phenylalaninol was obtained for the first time in the crystalline state through the aldehyde (IX).

The hydrogenation of V with palladium charcoal in a mixture of acetic acid and acetic anhydride afforded a mixture of *threo* and *erythro* α-acetamido-β-acetoxyhydrocinnamaldehyde dimethyl acetals (VIII) in a ratio of 1 to 1. Although the separation of these isomers by recrystallization was difficult, it was achieved by forming large crystals and collecting the crystals of each component by hand. According to infrared studies of chloramphenicol and allied compounds by Suzuki and Shindo,[4] *threo O, N*-diacyl 1-phenyl-2-aminopropane-1-ol in its crystalline state invariably exhibits the amide I band at a higher wave number and the amide II band at a lower wave number than does the *erythro* isomer, and a strong absorption band always appears in the 950—1000 $cm^{-1}$ region in the *threo* series and in the 900—950 $cm^{-1}$ region in the *erythro* series. Of the two diacetyl compounds VIII, one absorbs at 1640, 1570 and 940 $cm^{-1}$ and the other, at 1650, 1555 and 995 $cm^{-1}$. These results indicate that the former, which is in the form of needles and which melts at 132—133°C, belongs to the *erythro* series and that the latter, which is cubic and which melts at 137—138°C, belongs to the *threo* series. A solution of either *threo* or *erythro* VIII in acetic acid diluted with a small amount of water was boiled for a short time in order to hydrolyze the acetal group. The products (m. p. 125—126°C) reduced Fehling's solution, and the analytical data as well as its infrared spectrum suggested that the product was α-acetamidocinnamaldehyde (IX). The reduction of IX with sodium borohydride afforded the known[5] α-acetamidocinnamyl alcohol (X). The hydrogenation of X yielded crystalline *N*-acetylphenylalaninol (XI) (m. p. 90—95°C), which was hitherto known[6] only in the form of an oil.

The action of aqueous calcium chloride upon the acetal (VIII) was next examined for the purpose of preparing α-acetamido-β-acetoxyhydrocinnamaldehyde (XII). This treatment,

3) During the oximation reaction, the presence of oximino ketone was determined by means of ferrous sulfate.[1]

4) M. Suzuki and H. Shindo, *J. Pharm. Soc. Japan*, **76**, 927 (1956). An explanation of their results will be given in this paper.

5) T. A. Girard and R. J. Moshy, *J. Org. Chem.*, **23**, 1942 (1958).

6) L. Berlinguet, *Can. J. Chem.*, **32**, 1931 (1954).

however, also resulted in the formation of IX, with a loss of acetic acid. The treatment of finely-powdered VIII with dilute sulfuric acid at room temperature gave a small amount of IX, most of the starting material also being recovered.

**Route 3.**—The experiments were initially started in order to prepare 1-phenyl-2-phthalimidopropane-1, 3-diol from the same starting material (Fig. 4). However, the treatment of $\alpha$-bromo-$\beta$, $\beta$-dimethoxypropiophenone (XIV), derived from I, with potassium phthalimide unexpectedly yielded the phenyl $\alpha$-methoxy-$\beta$-phthalimidovinyl ketone (XVI) rather than the desired $\alpha$-phthalimido-$\beta$, $\beta$-dimethoxypropiophenone (XVII). Moreover, the methoxyl group of XVI located at the $\alpha$ position to the carbonyl group was readily hydrogenolysed to afford 1-phenyl-3-phthalimidopropane-1-ol (XXX).

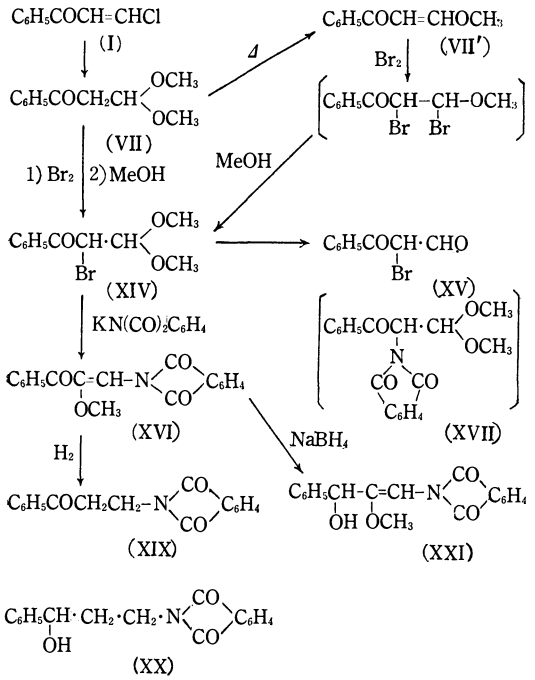


Fig. 4

The bromination of $\beta$, $\beta$-dimethoxypropiophenone[1] with bromine in carbon tetrachloride was attempted at first to prepare the bromo compound XIV. However, the reaction was accompanied by the hydrolysis of the acetal group by the hydrogen bromide generated during the reaction and yielded benzoyl-$\alpha$-bromoacetaldehyde (XV). The product was identified by comparing it with an authentic sample prepared by a known method.[7] The desired bromoacetal was obtained by first adding bromine to the phenyl $\beta$-methoxyvinyl ketone (VII) formed from VII upon distillation at 20 mmHg in a carbon tetrachloride solution and subsequently treating the product with methanol. The bromoacetal was also obtained by treating VII in the same manner.

The reaction of the bromoacetal XIV and potassium phthalimide was carried out first in dimethylformamide.[8] However, only an intractable tar was obtained even though the reaction conditions were carefully controlled. When methanol was employed as the solvent, a crystalline product (m. p. 81.5—82.5°C $\lambda_{max}$ 298 m$\mu$ ($\varepsilon$ 22600), $\nu_{max}$ 1730, 1645, 1600 and 1585 cm$^{-1}$) was produced. The analytical and spectral data of the product first suggested that it was phenyl $\alpha$-phthalimido-$\beta$-methoxyvinyl ketone (XVIII). The attempt to obtain the corresponding aldehyde by the hydrolysis of the vinyl ether group[9] was not successful, and the product (m. p. 82.5°C) was shown to be stable against cold aqueous sodium hydroxide and hydrochloric acid.

The hydrogenation of the product (m. p. 82.5°C) eventually revealed that the compound was not an $\alpha$-, but a $\beta$-phthalimide derivative. Namely, by hydrogenation over platinum oxide in acetic acid, the compound yielded $\beta$-phthalimido propiophenone (XIX) (m. p. 128—129°C) and 1-phenyl-3-phthalimidopropane-1-ol (XXV) (m. p. 76.5—78°C), both of which are known in the literature.[10,11] Therefore, the compound with a m. p. of 82.5°C must be either the

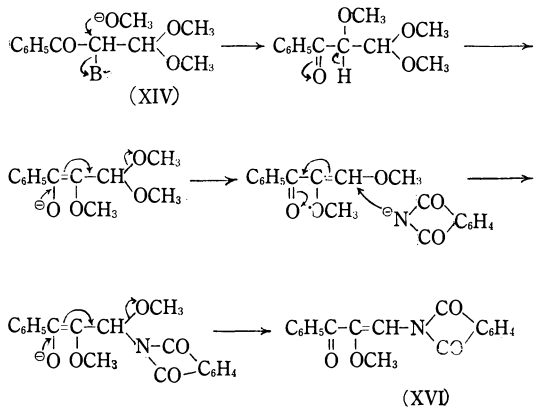


Fig. 5

7) M. S. Matta, R. Kaushal and S. S. Deshapande, *J. Indian Chem. Soc.*, 23, 454 (1946).

8) J. C. Sheehan and W. A. Bolhofer, *J. Am. Chem. Soc.*, 72, 2786 (1950).

9) It is known that, in alkaline conditions, $\beta$-methoxyvinyl ketone undergoes readily hydrolysis to give $\beta$-ketoaldehyde, which then further decomposes into methyl ketone.[1]

10) R. E. Davis and G. Powell, *J. Am. Chem. Soc.*, 67, 1466 (1945).

11) R. E. Lutz, J. W. Wilson, A. J. Deinet, G. H. Harnest, H. A. Martin and J. A. Freek, *J. Org. Chem.*, 12, 103 (1947).

phenyl α-methoxy-β-phthalimidovinyl ketone or the phenyl β-methoxy-β-phthalimidovinyl ketone. For the purpose of differentiating between these two alternatives, the compound was reduced by sodium borohydride to an unsaturated alcohol. The NMR spectrum of the product exhibited, in addition to aromatic proton signals, four singlets at τ 6.5 ($CH_3O$-), 5.7 (-CH-OH), 4.3 (OH) and 3.26 (-C=CH-). These results clearly indicate that the alcohol produced is phenyl α-methoxy-β-phthalimidovinyl carbinol (XXI) and that hence, the ketone is the α-methoxy-β-phthalimidovinyl ketone (XVI). The formation of XVI may be explained as follows (Fig. 5).

## Experimental

**β, β-Dibenzyloxypropiophenone (II).**—Into a mixture of 10 g. of the phenyl chlorovinyl ketone (I) and 10 g. of benzyl alcohol, a solution of 1.4 g. of sodium in 23 g. of benzyl alcohol was gradually added and stirred. During the reaction period, the vessel was kept in an ice-salt bath and the temperature was adjusted so as not to rise over −5°C. Since the solution of sodium benzylate solidified at lower temperatures, the addition was carried out by the use of a specially-designed separatory funnel. After being set aside overnight, the reaction mixture was poured into ice water and extracted with ether. The extract was then dried and distilled. β, β-Dibenzyloxypropiophenone (II) was distilled out at 186°C (1.5 mmHg) as a sticky yellow oil; yield 5 g. (24%).

Found: C, 79.89; H, 6.19. Calcd. for $C_{23}H_{22}O_3$: C, 79.74; H, 6.40%.

**Phenyl β-Benzyloxyvinyl Ketone (III).**—On the slow redistillation of the benzyl acetal (II), an appreciable amount of benzyl alcohol ran out first, and phenyl β-benzyloxyvinyl ketone distilled out as a deep yellow oil (b. p. 185°C (2 mmHg) $\nu_{max}$ 1655, 1600, 1585, 1570, 1491, 1185 and 1170 $cm^{-1}$). The vinyl ketone readily decolorized the permanganate solution, was unstable, and was used without purification for the oximation. The treatment of this ketone with alkyl nitrite and sodium methoxide in methanol, as described in the next section, yielded α-oximino-β, β-dimethoxypropiophenone.

**The Oximation of II.**—a) To a solution of 0.2 g. of sodium in 5 ml. of methanol, 1.2 ml. of isoamyl nitrite and 2 g. of β, β-dibenzyloxypropiophenone (II) were gradually added under cooling in an ice bath. After it had then been set aside for 2 or 3 days in a cool place, the reaction mixture was poured into ice water and washed three times with ether in order to remove the isoamyl alcohol and the unchanged ketone. The product was then taken up in ether after the addition of excessive ammonium chloride. The removal of the ether left white crystals (m. p. 83—85°C) which showed no depression on admixture with authentic α-oximino-β, β-dimethoxypropiophenone. The identity was confirmed by a comparison of the infrared spectra.

b) The same procedure was used as in a) except that 5 ml. of benzyl alcohol was used instead of 5 ml. of methanol. Even after 3 days the reaction mixture gave only a faint coloration in the ferrous complex test. After it had been set aside for 4 days, the reaction mixture was treated with ice water and ether. The working up of the ether extract afforded original β, β-dibenzyloxypropiophenone.

**α-Acetamido-β-acetoxyhydrocinnamaldehyde Dimethyl Acetal (VIII).**—A solution of 500 mg. of α-oximino-β, β-dimethoxypropiophenone (V) in a mixture of 10 ml. of acetic acid and 10 ml. of acetic anhydride was hydrogenated in the presence of 150 mg. of 10% palladium-on-charcoal[12] for 3 hr. The absorption ceased when 3.5 equivalents of hydrogen were taken up. The catalyst was then filtered off, and the solution was allowed to stand overnight with four drops of pyridine. After the removal of the solvent, the crystalline residue was recrystallized from ethyl acetate to afford colorless crystals of α-acetamido-β-acetoxyhydrocinnamaldehyde dimethyl acetal (m. p. 135—137°C).

Found: C, 60.77; H, 7.50; N, 4.75. Calcd. for $C_{15}H_{21}NO_5$: C, 61.00; H, 7.17; N, 4.74%.

A sample of the acetal was recrystallized slowly to afford a mixture of two kinds of large crystals. Both the crystals, which were obtained in almost the same amounts, were separated by a pincette and recrystallized respectively to yield white needles, VIIIa (m. p. 132—132.5°C) and cubic crystals, VIIIb.

VIIIa: $\nu_{max}^{Nujol}$ 3300 (-NH-); 1735 (OAc); 1640, 1570 (-NHAc); 1120, 1090, 1060 (acetal); 940 $cm^{-1}$.

Found: C, 61.05; H, 7.24. Calcd. for $C_{15}H_{21}NO_5$: C, 61.00; H, 7.17%.

VIIIb: $\nu_{max}^{Nujol}$ 3350 (-NH-); 1730 (-OAc); 1650, 1555 (-NHAc); 1180, 1100, 1065 (acetal); 995 $cm^{-1}$.

Found: C, 60.96; H, 7.16. Calcd. for $C_{15}H_{21}NO_5$ C, 61.00; H, 7.17%.

**The Hydrolysis of α-Acetamido-β-acetoxyhydrocinnamaldehyde Dimethyl Acetal (VIII).**—*a) The Production of α-Acetamidocinnamaldehyde.* 1) To a solution of 100 mg. of the acetal (VIIIa or VIIIb) in 1 ml. of acetic acid, a few drops of water were added, and then the solution was boiled for a short time, until a light brown coloration was obtained. The removal of the solvent and recrystallization of the residue from ethyl acetate or benzene yielded white needles (m. p. 125—126°C); it reduced the Fehling solution and the Nessler reagent.

Found: C, 69.25; H, 5.93; N, 7.03. Calcd. for $C_{11}H_{11}NO_2$: C, 69.82; H, 5.86; N, 7.40%.

2) To a 10% aqueous solution of calcium chloride the acetal (VIII) was added; the solution was then refluxed for 3 hr. and extracted with ethyl acetate. After drying, the removal of the solvent left crystalline aldehyde (IX).

*b) An Attempt to Obtain α-Acetamido-β-acetoxyhydrocinnamaldehyde (XII).*—A sample of 20 mg. of the crystalline acetal (VIII) was well ground into fine powder and dissolved in 4 ml. of 1 N sulfuric acid. After an hour, the solution was extracted with ethyl acetate. The working-up of a extract yielded the original acetate (VIII) and a small amount of the cinnamaldehyde (IX).

12) R. Mozingo, "Organic Syntheses," Vol. 26, 77 (1948).

**α-Acetamidocinnamyl Alcohol.** (X).—A solution of a sample (about 20 mg.) of α-acetamidocinnamaldehyde in ethanol was allowed to stand overnight with an excess of sodium borohydride. After the removal of the solvent, the residue was dissolved in dilute alkali and extracted with benzene. The evaporation of the benzene left a crystalline cake which was then recrystallized from benzene to yield the cinnamyl alcohol (X) quantitatively (m. p. 101—103°C). The melting point corresponded to that which appeared in the literature.[5]

***N*-Acetyl Phenylalaninol (XI).**—A solution of a sample (20 mg.) of cinnamyl alcohol (X) in ethanol was hydrogenated in the presence of 10% palladium charcoal. One mole of hydrogen was readily absorbed, and fine crystals (m. p. 90—95°C) were obtained. Though repeated recrystallizations from ethyl acetate - benzene had no effect in narrowing the melting point range, the analysis of the crystals gave good values for *N*-acetyl phenylalaninol.

Found: C, 68.39; H, 7.70. Calcd. for $C_{11}H_{15}NO_2$: C, 68.37; H, 7.82%.

**The Bromination of β, β-Dimethoxypropiophenone (VII).**—a) To a solution of the ketone VII in twice the volume of carbon tetrachloride, an equivalent amount of bromine was added slowly. The resulting mixture was distilled under reduced pressure to give a yellow oil (b. p. 110°C ($10^{-2}$ mmHg)), which soon crystallized. Recrystallization from benzene gave a pure sample (m. p. 110—111°C) which shows no depression on admixture with authentic benzoylbromoacetaldehyde.

b) To a solution of the ketone VII in twice the volume of carbon tetrachloride, an equivalent mole of bromine was added drop by drop. The resulting mixture was diluted with an equal volume of methanol and allowed to stand overnight. The solution was then concentrated to a quarter and extracted with petroleum benzine, and the extract was dried and distilled to remove the volatile solvent. The residue, crude α-bromo β, β-dimethoxypropiophenone (XIV), exhibited in the infrared spectrum bands at 2800 ($OCH_3$), 1690, 1600 (COPh); 1115, 1160 (acetal) $cm^{-1}$. Although the compound was unstable and was not purified, it afforded benzoylbromoacetaldehyde in a very good yield upon hydrolysis and was pure enough for use in the next reaction. Yield, 70%.

**Phenyl β-Methoxyvinyl Ketone (VII').**—A sample of VII was distilled at reduced pressure with a small amount of potassium bisulfate. The β-methoxyvinyl ketone (VII') distilled off with methanol at 140°C. The distillate was redistilled, and the fraction boiling at 135°C (5—6 mmHg) was collected; $\nu_{max}$ 1660, 1600, 1590, 1578, 1200 $cm^{-1}$; yield 20%. Although it was difficult to remove completely the unchanged acetal VII ($\nu_{max}$ 2800, 1675, 1590, 1580, 1115, 1075, 1050 $cm^{-1}$), the distillate was pure enough for the next reaction. Treatment with semicarbazide yielded benzoylacetaldehyde monosemicarbazone.

Found: C, 58.39; H, 5.17; N, 20.40. Calcd. for $C_{10}H_{11}N_3O_2$: C, 58.50; H, 5.37; N, 20.50%.

**The Bromination of the Phenyl β-Methoxyvinyl Ketone (VII').**—In the same way as has been described in the bromination of VII—b), this yielded α-bromo-β, β-dimethoxypropiophenone.

**Phenyl α-Methoxy-β-phthalimidovinyl Ketone (XVI).**—The bromoacetal XVI (35.5 g.) and potassium phthalimide (23.9 g.) were added to methanol (40 g.), and the whole was refluxed for 6 hr. After the solvent had been removed, the residue was extracted with benzene. The extract was washed with 1 N sodium hydroxide and then with water, and dried over sodium sulfate. The evaporation of the benzene left a crystalline cake which was recrystallized from ethanol. The purified product, which melted at 81.5—82.5°C, weighed 14.6 g. and exhibited an ultraviolet absorption maximum at 298 mμ (ε 22600) in an ethanol solution and infrared bands at 1730, 1645, 1600 and 1585 $cm^{-1}$.

Found: C, 70.16; H, 4.07; N, 4.58. Calcd. for $C_{18}H_{13}NO_4$: C, 70.35; H, 4.26; N, 4.56%.

**The Hydrogenation of the Phenyl α-Methoxy-β-phthalimidovinyl Ketone (XVI).**—A sample of XVI was dissolved in acetic acid and hydrogenated in the presence of platinum oxide. After the absorption of hydrogen had ceased, the catalyst and the solvent were removed. The residue, a colorless paste, was chromatographed to afford two kinds of crystals. They were recrystallized separately from a mixed solvent of benzene-petroleum. The one melting at 128—129°C was β-phthalimidopropiophenone.[11]

Found: C, 72.97; H, 4.71; N, 5.31. Calcd. for $C_{17}H_{13}NO_3$: C, 73.11: H, 4.69; N, 5.02.

The other product melted at 76.5—78°C and was phenyl β-phthalimidoethyl carbinol (XX').

Found: C, 72.59; H, 5.32; N, 4.77. Calcd. for $C_{17}H_{15}NO_3$: C, 72.58; H, 5.37; N, 4.98%.

**The Reduction of the Phenyl α-Methoxy-β-phthalimidovinyl Ketone (XVI) with Sodium Borohydride.**—A sample of XVI was treated with sodium borohydride in dioxane. After it had been set aside overnight, the reaction mixture was worked up in the usual way. The product was obtained as a colorless paste which was difficult to crystallize. The NMR spectrum of the product was measured at 56.4 Mc. in carbon tetrachloride. Four singlets at τ 6.5 ($CH_3O$-), 5.7 (C<u>H</u>-OH), 4.3 (OH), 3.26 (>C=C<u>H</u>), and an aromatic multiplet signal were observed. When the ethereal solution of the pasty alcohol was oxidized[13] with chromic acid and a few drops of sulfuric acid, the original ketone XVI was obtained.

*Department of Chemistry*
*Faculty of Science*
*Hokkaido University*
*Sapporo*

13) H. C. Brown and C. P. Gary, *J. Am. Chem. Soc.*, **83**, 2952 (1961).

# The Electronic Structures of the Benzenium Ion and Its Methyl Derivatives

By Ichiro HANAZAKI and Saburo NAGAKURA

(Received November 7, 1964)

It is well known that methylbenzenes are protonated in acidic media (HF, $HF+BF_3$, etc.) to give benzenium-type ions. They are considered to be a typical model of the intermediates of aromatic substitution reactions.[1]

Mackor et al.[2] studied the electronic absorption spectra of the methyl-substituted benzenium ions in $HF+BF_3$. According to them, the 2, 4, 6-trimethylbenzenium, 2, 3, 4, 6-tetramethylbenzenium and pentamethylbenzenium ions show two bands in the wavelength region longer than 200 m$\mu$. One of them appears at 350—400 m$\mu$, the other, at $\sim$250 m$\mu$.

Reid[3] also studied the ultraviolet absorption spectra of the benzenium ion and its methyl derivatives under low temperatures ($\sim$70°C); he found that the benzenium ion itself shows a band at 410 m$\mu$. Mackor et al.,[4] however, reported that, at least at room temperature, they could not detect the formation of the benzenium ion in the benzene-HF-$BF_3$ system.

Kilpatrick and Hyman[5] also observed the absorption spectra of benzene, mesitylene and hexamethylbenzene in various solvents. In the case of benzene, no new band appears in the visible and ultraviolet regions, even in strong acid (HF). On the other hand, in the case of mesitylene and hexamethylbenzene in strong acid, a new band appears in the 350—400 m$\mu$ region.

Recently Olah et al.[6] succeeded in isolating the salts of the methyl-substituted benzenium ions with $BF_4^-$ in the solid form. They were prepared at a low temperature and were gradually decomposed at room temperature even in a sealed capsule. They showed a rather high electric conductance in the solid state. This fact seems to support the existence of ionic species.

Mulliken et al.[7] calculated the $\pi$-electron structure of the benzenium ion, including the hyperconjugation effect of the methylene group, by the $\omega$-technique. They evaluated the stabilization energy (hyperconjugation energy) to be 14.5 kcal./mol. This work was restricted to the Hückel approximation, so it may not give reliable predictions to the excitation energies.

The SCFMO calculations were performed by Mackor et al.[2,8] Although their calculation considered no hyperconjugation effect, they succeeded in predicting the excitation energies qualitatively.

Recently Morita[9] studied the $\pi$-electronic structure of the benzenium ion by the SCFMO method including the hyperconjugation of the methylene group and obtained a reasonable agreement with the experimental results. There remain some ambiguities, however, in his determination of the parameters belonging to the methylene group.

In the present work, we have undertaken to improve the calculation of the $\pi$-electron structure of the benzenium ion by evaluating the molecular integrals belonging to the methylene group as rigorously as possible and by considering the effect of the electronic charge and of the configurational interaction with doubly excited electron configurations. Moreover, the effect of the substituted methyl groups has been studied in the following manner. The methyl-substituted ion is divided into its components, the benzenium ion and the methyl groups. Then the interaction among them is taken into account in terms of the configurational interaction among several electron configurations constructed by putting the electrons in the orbitals of the components.

## The Benzenium Ion

**The Simple SCFMO Calculation (Method I).**—The geometrical structure of the benzenium

1) V. Gold and F. L. Tye, *J. Chem. Soc.*, **1952**, 2172, 2181, 2184.
2) G. Dallinga, E. L. Mackor and A. A. Verrijn Stuart, *Mol. Phys.*, **1**, 123 (1958).
3) C. Ried, *J. Am. Chem. Soc.*, **76**, 3264 (1954).
4) a) C. MacLean, J. H. van der Waals and E. L. Mackor, ibid., **1**, 247 (1958); b) E. L. Mackor, A. Hofstra and J. H. van der Waals, *Trans. Faraday Soc.*, **54**, 66, 186 (1958).
5) M. Kilpatrick and H. H. Hyman, *J. Am. Chem. Soc.*, **80**, 77 (1958).
6) G. A. Olah and S. J. Kuhn, ibid., **80**, 6535 (1958).
7) N. Muller, L. W. Pickett and R. S. Mulliken, ibid., **76**, 4770 (1954); L. W. Pickett, N. Muller and R. S. Mulliken, *J. Chem. Phys.*, **21**, 1400 (1953).
8) J. P. Colpa, C. MacLean and E. L. Mackor, *Tetrahedron*, **19**, 65 (1963).
9) T. Morita, This Bulletin, **33**, 1486 (1960).

ion was confirmed by the NMR measurements[4a,10,11] as follows: $H^+$ attacks an appropriate carbon atom of the benzene ring, and two hydrogen atoms are both bonded to the atom symmetrically with respect to the ring plane. The hybridization of the carbon atom changes from $sp^2$ of the benzene to $sp^3$ of the benzenium ion* (Fig. 1).

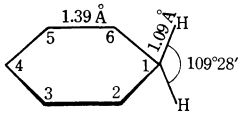



Fig. 1. The geometrical configuration of the benzenium ion.
(The conformation of the ring is assumed to be identical with benzene.)

First of all, let us consider the linear combination of the two hydrogen 1s orbitals, $\chi_1$ and $\chi_2$, of the methylene group:

$$\left.\begin{aligned}\chi_\sigma &= [2(1+S)]^{-1/2}(\chi_1+\chi_2)\\ \chi_\pi &= [2(1-S)]^{-1/2}(\chi_1-\chi_2)\end{aligned}\right\} \quad (1)$$

where $S$ denotes the overlap integral between the two hydrogen 1s AO's. Of these, $\chi_\sigma$ corresponds to the $\sigma$-type orbital and $\chi_\pi$ corresponds to the $\pi$-type orbital. The $sp^3$ hybridized orbitals of the carbon, to which the two hydrogen atoms are attached, can be reduced into three nonequivalent $sp^2$ hybrid orbitals and the one $2p\pi$ AO by taking linear combinations of them. One of the nonequivalent $sp^2$ hybrid orbitals can make a bond with the $\chi_\sigma$ orbital, and the $2p\pi$ one can interact with the $\chi_\pi$ orbital and the conjugated system of the cyclopentadienyl ring. (See Appendix for the justification of this procedure.)

We have performed the SCF calculation taking the six $2p\pi$ AO's of the ring and the $\chi_\pi$ orbital into account. The calculation has been made by the method combining Pariser-Parr's method[12] with Roothaan's SCF method[13,14]. The orbital energy of the AO is replaced by the minus of the valence state ionization potential of the atom, and the one-center repulsion integrals (pp|pp) are replaced by the ionization potentials minus electron affinities.

To perform the above-mentioned calculation procedure, we must evaluate the ionization potential and the electron affinity of the pseudo $\chi_\pi$ orbital. Using the Slater 1s AO, the valence state energy of the pseudo atom $H_2$ is found to be:

$$E = I_\sigma + I_\pi + J_{\sigma\pi} - 1/2\, K_{\sigma\pi} \quad (2)$$

where

$$\left.\begin{aligned} I_1 &= \int \chi_1(1)\mathbf{H}^{\mathrm{core}}(1)\chi_1(1)\,dv_1\\ J_{\sigma\pi} &= \int \chi_\sigma(1)\chi_\sigma(1)e^2/r_{12}\chi_\pi(2)\chi_\pi(2)\\ &\quad \times dv_1 dv_2\\ K_{\sigma\pi} &= \int \chi_\sigma(1)\chi_\pi(1)e^2/r_{12}\chi_\sigma(2)\chi_\pi(2)\\ &\quad \times dv_1 dv_2\end{aligned}\right\} \quad (3)$$

The valence state energy of the $H_2^+$ ion, in which an electron in $\chi_\pi$ is removed, is;

$$^+E = I_\sigma \quad (4)$$

Therefore, the valence state ionization potential is:

$$^+E - E = -I_\pi - J_{\sigma\pi} + \frac{1}{2}K_{\sigma\pi} \quad (5)$$

If we reduce these molecular integrals into integrals over the Slater-type 1s AO's with $Z=1$, we can evaluate them non-empirically.*

Similarly, the electron affinity can be evaluated from the relation:

$$E - E^- = -I_\pi - J_{\sigma\pi} - J_{\pi\pi} + \frac{1}{2}K_{\sigma\pi} \quad (6)$$

where $E^-$ is the valence state energy of $H_2^-$ in which two electrons occupy $\chi_\pi$:

$$E^- = I_\sigma + 2I_\pi + J_{\pi\pi} + 2J_{\sigma\pi} - K_{\sigma\pi} \quad (7)$$

Using the Slater AO's for hydrogen 1s:

$$\left.\begin{aligned} I_p(H_2) &= {}^+E - E = 9.4219\ \mathrm{eV.}\\ A_p(H_2) &= E - E^- = -0.7007\ \mathrm{eV.}\end{aligned}\right\} \quad (8)$$

10) C. MacLean and E. L. Mackor, *Mol. Phys.*, **4**, 241 (1961).
11) C. MacLean and E. L. Mackor, *J. Chem. Phys.*, **34**, 2208 (1961).
* If $sp^3$ hybrid orbitals are formed completely, the carbon skeleton of the benzene ring may be deformed to a considerable extent. In fact, the hybridization may be in some intermediate state between $sp^2$ and $sp^3$. In the present work, however, the two hydrogen atoms are assumed to take the same geometrical configuration as in the case of methane, and the deformation of the ring skeleton is not considered explicitly.
12) R. Pariser and R. G. Parr *J. Chem. Phys.*, ibid., **21**, 466, 767 (1953).
13) C. C. J. Roothaan, *Revs. Mod. Phys.*, **23**, 69 (1951).
14) a) A. Brickstock and J. A. Pople, *Trans. Faraday Soc.*, **50**, 901 (1954); b) J. A. Pople, *Proc. Phys. Soc.*, **A68**, 81 (1955); c) H. Kon, This Bulletin, **28**, 275 (1955).

* Strictly speaking, the values of the same type of molecular integrals are different when they appear in $E$ and in $E^+$:

$$E^+ - E = -I_\pi - J_{\sigma\pi} + \frac{1}{2}K_{\sigma\pi} + (I_\sigma^+ - I_\sigma)$$

the difference, $I_\sigma^+ - I_\sigma$, being attributed to the difference in the electron distribution. (if we consider the Slater AO's, it is reduced to the difference in the effective charge.) Fortunately, $I_\sigma^+ - I_\sigma$ may be canceled out with other types of errors (for example, the error coming from the atomic orbitals), so that we may still expect a good result when $I_\sigma^+ - I_\sigma$ are disregarded. This is the reason why Koopmans' theorem holds generally with considerable exactness. (Cf. W. Moffitt, *Proc. Roy. Soc.*, **A202**, 534 (1950); R. G. Parr and R. S. Mulliken, *J. Chem. Phys.*, **18**, 1338 (1950).).

TABLE I. THE RESULT OF SCF CALCULATION FOR THE BENZENIUM ION (METHOD I)

| $\varepsilon$*, eV. | MO wave function** | | | | | | |
|---|---|---|---|---|---|---|---|
| | 0 | 1 | 2 | 3 | 4 | 5 | 6 |
| −23.0586 | 0.5132 | 0.7081 | 0.2946 | 0.1550 | 0.1172 | 0.1550 | 0.2946 |
| −19.3204 | −0.2687 | −0.2593 | 0.1772 | 0.4827 | 0.5759 | 0.4827 | 0.1772 |
| −17.7571 | 0 | 0 | −0.5038 | −0.4962 | 0 | 0.4962 | 0.5038 |
| − 8.9572 | −0.3706 | −0.0805 | 0.5218 | 0.0164 | −0.5578 | 0.0164 | 0.5218 |
| − 6.2615 | 0 | 0 | −0.4962 | 0.5038 | 0 | −0.5038 | 0.4962 |
| − 4.1381 | −0.2716 | 0.1123 | 0.2384 | −0.4802 | 0.5821 | −0.4802 | 0.2384 |
| − 0.5573 | 0.6733 | −0.6421 | 0.2296 | −0.1101 | 0.0684 | −0.1101 | 0.2296 |

* Orbital energy.
** Coefficients of AO's in MO $\phi_i$ are shown in the $i$-th row. Numbering of carbon atoms are shown in Fig. 1. 0 means $\chi_\pi$ orbital constructed by the linear combination of the two hydrogen 1s orbital of the methylene group.

TABLE II. THE RESULT OF SCF CALCULATION FOR THE BENZENIUM ION (METHOD II)*

| $\varepsilon$, eV. | MO wave function | | | | | | |
|---|---|---|---|---|---|---|---|
| | 0 | 1 | 2 | 3 | 4 | 5 | 6 |
| −23.3453 | 0.5197 | 0.6733 | 0.3138 | 0.1719 | 0.1435 | 0.1719 | 0.3138 |
| −19.9319 | −0.2992 | −0.2771 | 0.1559 | 0.4585 | 0.6039 | 0.4585 | 0.1559 |
| −18.3641 | 0 | 0 | −0.5263 | −0.4722 | 0 | 0.4722 | 0.5263 |
| − 9.8833 | −0.3853 | −0.0874 | 0.5207 | 0.0314 | −0.5475 | 0.0314 | 0.5207 |
| − 6.8657 | 0 | 0 | −0.4722 | 0.5263 | 0 | −0.5263 | 0.4722 |
| − 4.7863 | −0.2565 | 0.1116 | 0.2380 | −0.4985 | 0.5581 | −0.4985 | 0.2380 |
| − 0.9909 | 0.6529 | −0.6706 | 0.2224 | −0.1040 | 0.0587 | −0.1040 | 0.2224 |

* See Table I for the notation.

On the basis of these results and of the valence state ionization potential (11.24 eV.) and electron affinity (0.62 eV.) of the carbon 2p$\pi$ AO, which have been derived from spectroscopic data,[15] two center repulsion integrals (pp|qq) over $\pi$-type AO's have been evaluated by using the Pariser-Parr method.[12]

The resonance integral, $\beta_{CC}$, between the adjacent carbon 2p$\pi$ AO's of the ring is taken to be −2.39 eV. which is the value determined by Pariser and Parr for benzene.[12] The resonance integral, $\beta_{C-\chi_\pi}$, between $\chi_\pi$ and the adjacent carbon 2p$\pi$ AO is determined from the equation:

$$\beta_{C-\chi_\pi} = (S_{C-\chi_\pi}/S_{C-C})\beta_{C-C}$$

where $S_{C-\chi_\pi}$ is the overlap integral between $\chi_\pi$ and the adjacent carbon 2p$\pi$ AO and $S_{C-C}$ is the overlap integral between the adjacent carbon 2p$\pi$ AO's of benzene ($S_{C-C}=0.248$). Assuming the geometrical configuration shown in Fig. 1, $S_{C-\chi_\pi}$ has been evaluated as 0.613. Thus, $\beta_{C-\chi_\pi}$ is determined to be −5.90 eV.

The numerical calculation was performed using a FACOM 202 electronic computer at our Institute.* The result of the SCF calculation is shown in Table I. Of seven MO's, the lower three are occupied in the ground configuration.

**The Effect of Changing the Effective Charge (Method II).**—The above-mentioned calculation is based on the parameters which are determined from the ionization potentials and the electron affinities of neutral atoms.

In the present case, however, the molecule as a whole possesses a +1 charge in the conjugate system. For this reason, the appropriate $Z$ values may differ to some extent from those of neutral atoms. In this connection, we have performed the 'SCE' calculation[16] in which the effective nuclear charge, $Z$, of an atom is changed proportionally to the change in the charge density of the atom; that is, for the carbon atom,

$$Z_p = 3.25 + 0.35\, q_p \qquad (9)$$

where $q_p$ is the formal charge on atom p. For $H_2$ pseudo AO, $\chi_\pi$, the relation is;

$$Z_H = 1.00 + 0.39\, q_H \qquad (10)$$

according to the Slater rule.

15) G. Pilcher and H. A. Skinner, *J. Inorg. Nucl. Chem.*, 24, 937 (1962).

* The computer programs for SCF and transition moment calculations were written by one of the present authors, while the program for secular equations was written by Mr. Hidechika Takahashi and revised by Mr. Suehiro Iwata.

16) R. D. Brown and A. Penfold, *Trans. Faraday Soc.*, 53, 397 (1957); R. D. Brown and M. L. Heffernan, ibid., 54, 757 (1958).

TABLE III. MATRIX ELEMENTS FOR CONFIGURATION INTERACTION*

A. Method I

Symmetric:

| | 0 | 3→5** | 2→4 | 2→6 | 1→4 |
|---|---|---|---|---|---|
| 0 | 0 | | | | |
| 3→5 | 0 | 6.3861 | | | |
| 2→4 | 0 | 0.6199 | 5.4679 | | |
| 2→6 | 0 | −0.4250 | 0.1901 | 9.1331 | |
| 1→4 | 0 | −0.2087 | 0.0227 | 0.2047 | 8.1417 |

Antisymmetric:

| | 3→4 | 3→6 | 2→5 |
|---|---|---|---|
| 3→4 | 3.6539 | | |
| 3→6 | −0.0562 | 7.8571 | |
| 2→5 | −0.6841 | −0.0136 | 7.3598 |

B. Method II

Symmetric:

| | 0 | 3→5 | 2→4 | 2→6 | 1→4 |
|---|---|---|---|---|---|
| 0 | 0 | | | | |
| 3→5 | 0 | 6.4477 | | | |
| 2→4 | 0 | 0.7031 | 5.3051 | | |
| 2→6 | 0 | −0.3907 | 0.0987 | 9.1872 | |
| 1→4 | 0 | −0.1556 | 0.0549 | 0.1972 | 7.5910 |

Antisymmetric:

| | 3→4 | 3→6 | 2→5 |
|---|---|---|---|
| 3→4 | 3.5366 | | |
| 3→6 | −0.0625 | 7.8501 | |
| 2→5 | −0.6877 | 0.0301 | 7.3989 |

* All results are shown in eV.

** $i \rightarrow j$ denotes the configuration in which an electron in $\phi_i$ is excited to $\phi_j$. The wave function is, for example,

$$\Psi_{3\rightarrow4}=\frac{1}{\sqrt{2}}\{|1\bar{1}2\bar{2}3\bar{4}|+|1\bar{1}2\bar{2}4\bar{3}|\}$$

TABLE IV. THE LOWER EXCITED STATES OF THE BENZENIUM ION

A. Method I

| State | $E$, eV. | $f$* | Wave function |
|---|---|---|---|
| G | 0 | | $1.000\,\Psi_0$ |
| $A_1$ | 3.5309 | 0.202 | $0.9843\,\Psi_{3\rightarrow4}+0.0133\,\Psi_{3\rightarrow6}+0.1759\,\Psi_{2\rightarrow5}$ |
| $S_1$ | 5.1195 | 0.128 | $-0.4659\,\Psi_{3\rightarrow5}+0.8797\,\Psi_{2\rightarrow4}-0.0893\,\Psi_{2\rightarrow6}-0.0327\,\Psi_{1\rightarrow4}$ |
| $S_2$ | 6.6496 | 1.081 | $0.8685\,\Psi_{3\rightarrow5}+0.4742\,\Psi_{2\rightarrow4}+0.1041\,\Psi_{2\rightarrow6}+0.1000\,\Psi_{1\rightarrow4}$ |

B. Method II

| State | $E$, eV. | $f$ | Wave function |
|---|---|---|---|
| G | 0 | | $1.000\,\Psi_0$ |
| $A_1$ | 3.4171 | 0.224 | $0.9853\,\Psi_{3\rightarrow4}+0.0127\,\Psi_{3\rightarrow6}+0.1701\,\Psi_{2\rightarrow5}$ |
| $S_1$ | 4.9504 | 0.163 | $-0.4400\,\Psi_{3\rightarrow5}+0.8951\,\Psi_{2\rightarrow4}-0.0596\,\Psi_{2\rightarrow6}-0.0401\,\Psi_{1\rightarrow4}$ |
| $S_2$ | 6.7341 | 1.079 | $0.8816\,\Psi_{3\rightarrow5}+0.4457\,\Psi_{2\rightarrow4}+0.1140\,\Psi_{2\rightarrow6}+0.1053\,\Psi_{1\rightarrow4}$ |

* Oscillator strength

We then take the valence state ionization potential and the electron affinity[15] of the isoelectronic series of the carbon ($B^-$, C, $N^+$, $O^{2+}$) and hydrogen (H, $He^+$, $Li^{2+}$) atoms, and plot them against the $Z$ values obtained by means of the Slater rule. Thus approximate quadratic equations are obtained between $I_p$ or $A_p$ and $Z_p$:

$$\left.\begin{aligned}
&\left.\begin{aligned}
&I_p=3.69\,Z_p^2-10.04\,Z_p+4.89\\
&A_p=3.75\,Z_p^2-16.50\,Z_p+14.64
\end{aligned}\right\}\text{(carbon)}\\
&\left.\begin{aligned}
&I_p=13.6064\,Z_p^2-4.2579\,Z_p+0.0734\\
&A_p=13.6051\,Z_p^2-12.7417\,Z_p-1.5641
\end{aligned}\right\}\text{(hydrogen)}
\end{aligned}\right\}\quad(11)$$

These relations, together with Eqs. 9 and 10, allow us to determine the appropriate $I_p$'s and $A_p$'s as the functions of the charge densities. We calculate $I_p$ and $A_p$ by the use of the $q_p$, the formal charge of atom p, obtained by method I. The SCF procedure is then performed again by using the newly-evaluated $I_p$ and $A_p$ values. This procedure is repeated until the charge distribution becomes self-consistent.* The results are shown in Table II.

**Configuration Interaction.** — The above-mentioned two kinds of SCF calculations have

* In the present calculation, the one-center integrals,

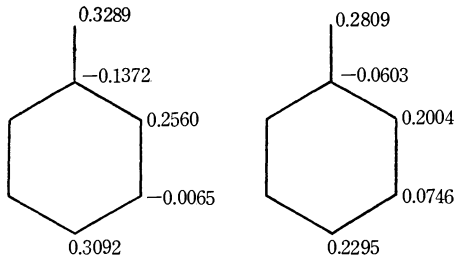
$$W_p=-I_p$$

and

$$(pp\mid pp)=I_p-A_p$$

are adjusted by the SCE procedure. However, the two-center integrals ($\beta$ and $(pp\mid qq)$) are not adjusted because the change in these integrals caused by the change in the charge distribution is small.

been improved by considering the configuration interaction. Singly excited configurations, the excitation energies of which are below 10 eV., are taken into account. The selected configurations and matrix elements are shown in Table III. The resultant energies and wave functions for the ground and lower-excited states are shown in Table IV. The charge distributions of the ground state are shown in Fig. 2.



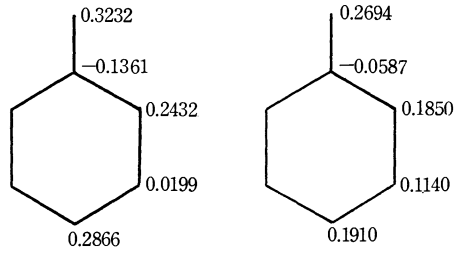




Fig. 2. The charge distribution in the ground state of the benzenium ion.
(The charge distributions calculated by SCF without CI and by SCF with CI among singly excited configurations are identical because the singly excited configurations do not mix with the ground configuration)

### The Methyl-Substituted Benzenium Ions

In order to evaluate the hyperconjugation effect of the methyl group, the charge-transfer configuration, $A \rightarrow \phi_4$, where A denotes the occupied pseudo $\pi$ MO of the methyl group A and $\phi_4$ denotes the lowest vacant MO of the benzenium ion, was taken into account, in addition to the singly excited configurations mentioned above.

The ionization potential for removing an electron from the pseudo $\pi$ MO of the methyl group had been evaluated in the case of the *t*-butyl cation: the pseudo $\pi$ AO which can be constructed from the three 1s AO's of the $H_3$ group can form a pseudo $\pi$ MO by means of interaction with the $2p\pi$ AO of the carbon atom of the methyl group. The calculations on this system were performed by the SCFMO method and gave the following results[17]:

$$\left.\begin{aligned} &\varepsilon_1 = -13.245 \text{ eV.} \\ &\phi_1 = 0.5505\chi_H + 0.8348\chi_C \\ &\varepsilon_2 = +0.708 \text{ eV.} \\ &\phi_2 = 0.8348\chi_H - 0.5505\chi_C \end{aligned}\right\} \quad (12)$$

where $\chi_C$ is the carbon $2p\pi$ AO and where the pseudo $\pi$ AO $\chi_H$ is defined as:

$$\chi_H = \frac{1}{\sqrt{6(1-S)}}(2\chi_1 - \chi_2 - \chi_3) \quad (13)$$

$\chi_1$, $\chi_2$ and $\chi_3$ being the 1s AO's of the three hydrogen atoms. The ionization potential for removing an electron from $\phi_1$ is a minus of the orbital energy of $\phi_1$:

$$I_p(\text{methyl}) = -\varepsilon_1 = 13.245 \text{ eV.} \quad (14)$$

The electron affinity of the benzenium ion has never been measured; therefore, the minus of the calculated orbital energy of the lowest vacant MO was adopted. In the present calculation, however, we make use of the zero-differential overlap approximation, so there is probably some error. Hush and Pople[18] calculated the ionization potentials of alternant hydrocarbons and of odd alternant radicals with the approximation of neglecting the overlap integrals. They found that it is necessary to take the orbital energy of the carbon $2p\pi$ AO to be about −9.50 eV. in order to obtain a good agreement with the experimental data. The valence state ionization potential of carbon $2p\pi$ AO is 11.24 eV., so a correction of about 1.7 eV. is necessary. Therefore, in the present case, the electron affinity of the benzenium ion is corrected by about 1.7 eV. The calculated electron affinity by method I (neutral parameters) is 8.957 eV.; after the correction of 1.7 eV., it is reduced to 7.257 eV.

The diagonal element for the charge-transfer (hereafter abbreviated as 'CT') configuration is

$$E_{CT} = I_p(\text{methyl}) - A_p(\text{benzenium}) \quad (15)$$

where the small correction resulting from the electrostatic interaction between the methyl and benzenium groups has been disregarded. Putting the above-mentioned values into Eq. 15, the diagonal element is

$$E_{CT} = 13.245 - 7.257 = 5.988 \text{ eV.} \quad (16)$$

(Taking the energy of the ground configuration as the standard)

The off-diagonal elements can also easily be obtained. When, for example, a methyl group

17) I. Hanazaki, H. Hosoya and S. Nagakura, This Bulletim, **36**, 1673 (1963).
18) N. S. Hush and J. A. Pople, *Trans. Faraday Soc.*, **51**, 600 (1955).

is substituted at the 2 position,* the CT configuration, $CT_{A\to4}$, must be considered in addition to the configurations included in the case of the configuration interaction of the benzenium ion:

$$(G|\mathbf{H}|CT_{A\to4}) = \int |1\bar{1}2\bar{2}3\bar{3}A\bar{A}| \times \mathbf{H}\frac{1}{\sqrt{2}}\{|1\bar{1}2\bar{2}3\bar{3}A\bar{4}| + |1\bar{1}2\bar{2}3\bar{3}4\bar{A}|\}\,d\tau = \sqrt{2}\,(A|\mathbf{H}^{core}|4)^{**} \quad (17)$$

where the zero-differential overlap approximation is invoked. If we neglect resonance integrals between the non-adjacent atoms,

$$(A|\mathbf{H}^{core}|4) = \int (c_1\chi_H + c_2\chi_C)\mathbf{H}^{core} \times (\sum_p c_{4p}\chi_p)\,d\tau = c_2c_{42}\beta \quad (18)$$

where $c_2$ denotes the coefficient of the carbon AO $\chi_C$ in the methyl group; $c_{42}$ denotes the coefficient of the AO $\chi_2$ in the MO $\phi_4$ of the benzenium ion, and $\beta$ is the resonance integral between ring carbon 2 and the carbon atom in the methyl group.

Next, the electronic structure of the 2,4,6-trimethylbenzenium ion was calculated. The wave functions of the CT configurations in this case are as follows:

$$\left.\begin{aligned} \Psi_{CT_1} &= \frac{1}{\sqrt{2}}[\Psi_{CT_A} + \Psi_{CT_E}]^{***} \\ \Psi_{CT_2} &= \Psi_{CT_C} \\ \Psi_{CT_3} &= \frac{1}{\sqrt{2}}[\Psi_{CT_A} - \Psi_{CT_E}] \end{aligned}\right\} \quad (19)$$

the first two wave functions being symmetric and the last antisymmetric. The matrix elements between the ground and locally excited configurations and those within the locally excited configurations are the same as in the case of the non-substituted benzenium ion. The matrix elements including the CT configurations are as follows:

$$\left.\begin{aligned} \langle G|\mathbf{H}|CT_1\rangle &= \frac{1}{\sqrt{2}}\{\langle G|\mathbf{H}|CT_A\rangle + \langle G|\mathbf{H}|CT_E\rangle\} = 2\langle\phi_4|\mathbf{H}|A\rangle \\ \langle G|\mathbf{H}|CT_2\rangle &= \langle G|\mathbf{H}|CT_C\rangle = \sqrt{2}\langle\phi_4|\mathbf{H}|C\rangle \end{aligned}\right.$$

* See the footnote of Table I for the numbering. Hereafter, the methyl groups substituted at the 2, 3, 4, 5 and 6 positions are denoted as A, B, C, D and E respectively.

** Here A denotes the $\pi$-type MO ($\phi_1$ of Eq. 12) of the methyl group A.

* $CT_A$ and $CT_E$ denote the CT configurations $CT_{A\to E}$ and $CT_{E\to4}$ respectively.

Table V. The lower excited states of the methyl-substituted benzenium ions (method I)

2,4,6-Trimethylbenzenium ion ($\Delta$=0.4299 eV.*)

| | Calcd. eV. | Calcd. ($f$)** | Calcd. CT%*** | Obs. eV. | Obs. ($\varepsilon$) |
|---|---|---|---|---|---|
| G | 0 | | 6.3 | | |
| $A_1$ | 3.673 | (0.268) | 9.5 | 3.493 | (11100) |
| $S_1$ | 5.147 | (0.321) | 25.2 | 4.844 | (8800) |
| $S_2$ | 6.480 | (0.247) | 56.1 | | |
| $A_2$ | 6.698 | (0.067) | 89.1 | | |

2,3,4,6-Tetramethylbenzenium ion ($\Delta$=0.4300 eV.)

| | Calcd. eV. | Calcd. ($f$) | Calcd. CT% | Obs. eV. | Obs. ($\varepsilon$) |
|---|---|---|---|---|---|
| G | 0 | | 6.3 | | |
| 1 | 3.543 | (0.247) | 12.9 | 3.397 | (7500) |
| 2 | 4.992 | (0.301) | 28.6 | 4.751 | (5350) |
| 3 | 6.417 | (0.126) | 95.8 | | |
| 4 | 6.514 | | 55.4 | | |

Pentamethylbenzenium ion ($\Delta$=0.4301 eV.)

| | Calcd. eV. | Calcd. ($f$) | Calcd. CT% | Obs. eV. | Obs. ($\varepsilon$) |
|---|---|---|---|---|---|
| G | 0 | | 6.3 | | |
| $A_1$ | 3.438 | (0.234) | 17.6 | 3.289 | (9800) |
| $S_1$ | 4.813 | (0.273) | 33.3 | 4.559 | (4300) |
| $S_2$ | 6.411 | (0.143) | 95.5 | | |
| $A_2$ | 6.430 | (0.012) | 100 | | |

* Ground state depression by the methyl substitution.

** Oscillator strength.

*** Percentage of the charge-transfer configurations in the wave function of the state.

Table VI. The lower excited states of some methyl-substituted benzenium ions*

| | $E$, eV.** | | $\Delta$, eV.*** |
|---|---|---|---|
| *o*-Toluenium | 3.536 | 5.238 | 0.146 |
| *m*-Toluenium | 3.373 | 4.903 | 0.000 |
| *p*-Toluenium | 3.696 | 4.976 | 0.165 |
| 2,5-Dimethylbenzenium | 3.400 | 4.994 | 0.146 |
| 2,4-Dimethylbenzenium | 3.689 | 5.070 | 0.302 |
| 3,5-Dimethylbenzenium | 3.251 | 4.658 | 0.000 |
| 2,3-Dimethylbenzenium | 3.387 | 5.045 | 0.146 |
| 3,4-Dimethylbenzenium | 3.536 | 4.817 | 0.165 |
| 2,3,4,5-Tetramethylbenzenium | 3.434 | 4.721 | 0.302 |
| 2,3,5,6-Tetramethylbenzenium | 3.290 | 4.899 | 0.282 |

* Calculated by method I.

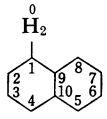
** The energies of the lower two excited states are shown (the ground state energy is taken to be zero in each case).

*** The ground state energy depression caused by the methyl substitution.

TABLE VII. THE RESULT OF THE SCF CALCULATION

| | MO Wave | | | | |
|---|---|---|---|---|---|
| ε, eV. | 0 | 1 | 2 | 3 | 4 |
| −22.3064 | 0.4834 | 0.6691 | 0.2871 | 0.1661 | 0.1433 |
| −19.7560 | −0.2832 | −0.3020 | −0.0669 | 0.1437 | 0.3425 |
| −18.3811 | −0.1025 | −0.1019 | 0.3675 | 0.5770 | 0.4239 |
| −16.4698 | 0.0004 | 0.0015 | −0.3345 | −0.3018 | 0.0985 |
| −16.1632 | −0.2015 | −0.1308 | 0.1219 | 0.2257 | 0.0553 |
| − 8.4763 | −0.2949 | −0.0667 | 0.5461 | 0.0042 | −0.5924 |
| − 5.5295 | 0.0315 | 0.0046 | −0.4691 | 0.4624 | −0.0429 |
| − 5.0915 | −0.2019 | 0.0354 | 0.1198 | −0.1257 | 0.4302 |
| − 3.7692 | −0.1548 | 0.0602 | 0.2678 | −0.4815 | 0.5231 |
| − 1.9361 | −0.2310 | 0.1422 | −0.0203 | −0.0735 | 0.1928 |
| 4.2848 | −0.6549 | −0.6357 | 0.2159 | −0.0994 | 0.0659 |

* Atoms are numbered in the following way;




$$
\begin{aligned}
&\langle 2\to 4\,|\mathbf{H}|\,CT_1\rangle \\
&\quad=\frac{1}{\sqrt{2}}\{\langle 2\to 4\,|\mathbf{H}|\,CT_A\rangle \\
&\qquad+\langle 2\to 4\,|\mathbf{H}|\,CT_E\rangle\} \\
&\quad=-\sqrt{2}\langle\phi_2\,|\mathbf{H}|\,A\rangle \\
&\langle 2\to 4\,|\mathbf{H}|\,CT_2\rangle=-\sqrt{2}\langle\phi_2\,|\mathbf{H}|\,C\rangle \\
&\langle 1\to 4\,|\mathbf{H}|\,CT_1\rangle=-\sqrt{2}\langle\phi_1\,|\mathbf{H}|\,A\rangle \\
&\langle 1\to 4\,|\mathbf{H}|\,CT_2\rangle=-\sqrt{2}\langle\phi_1\,|\mathbf{H}|\,C\rangle \\
&\langle 3\to 4\,|\mathbf{H}|\,CT_3\rangle \\
&\quad=\sqrt{2}\langle 3\to 4\,|\mathbf{H}|\,CT_A\rangle \\
&\quad=-\sqrt{2}\langle\phi_3\,|\mathbf{H}|\,A\rangle
\end{aligned}
\qquad (20)
$$

All other elements including the CT configurations vanish.

The pentamethyl- and 2, 3, 4, 6-tetramethylbenzenium ions are treated in a similar manner. The results are shown in Table V, together with the experimental data. Some other methyl-substituted benzenium ions are also calculated in the same manner. The results are shown in Table VI.

### The Effect of Doubly Excited Configurations

In the last part of this work, we shall examine the effect of doubly excited configurations. Let us take the naphthalenium ion as an example.* There are two possibilities of protonation when naphthalene is dissolved in a $HF+BF_3$ solution; protonation at the $\alpha$- or at the $\beta$-position.[2] The SCF calculation was carried out for the two ions by method I to give $\pi$-electron energies of −427.2 eV. and −422.8 eV. for the $\alpha$- and $\beta$-ions respectively. Therefore, the $\alpha$-ion probably predominates in the $HF-BF_3$ solution.**

TABLE VIII. THE RESULTS OF CONFIGURATION INTERACTION FOR α-NAPHTHALENIUM ION

| Calcd. | | | | Obs. | |
|---|---|---|---|---|---|
| I[a] | | II[b] | | | |
| eV. | (f) | eV. | (f) | eV. | (ε) |
| 3.172 | (0.053) | 2.887 | (0.043) | 3.024 | (shoulder) |
| 3.459 | (0.211) | 3.277 | (0.323) | 3.179 | (10900) |
| 5.175 | (0.139) | 4.811 | (0.059) | 4.430 | (14800?) |
| 5.406 | (0.048) | 5.228 | (0.024) | 4.880 | (13000?) |

a) Singly excited configurations alone.
b) Singly and doubly excited configurations included.

The result of the SCF calculation (method I) for the $\alpha$-naphthalenium ion is given in Table VII. The results improved by considering the configuration interaction with and without doubly excited configurations are shown in Table VIII.

The 2, 4, 6-trimethyl-, 2, 3, 4, 6-tetramethyl- and pentamethylbenzenium ions are also calculated by means of the configuration interaction, including the doubly excited configurations (Table IX).

### Discussion

It can be seen from the results summarized in Tables V, VIII and IX that the calculated

* The methyl-substituted benzenium ions are not adequate for examining the effect of the doubly excited configurations because of some arbitrariness in the choice of parameters belonging to the CT configurations. The absorption spectrum of the benzenium ion itself has not been observed, so it is necessary to examine the effect in the case of the non-substituted naphthalenium ion.

** The energy of the σ-electron system is approximately the same for both ions, so it is reasonable to compare the total stabilities in terms of the π-electron energies.

FOR $\alpha$-NAPHTHALENIUM ION (METHOD I)

function*

| 5 | 6 | 7 | 8 | 9 | 10 |
|---|---|---|---|---|---|
| 0.0821 | 0.0440 | 0.0614 | 0.1358 | 0.3384 | 0.2067 |
| 0.3848 | 0.2946 | 0.2432 | 0.2404 | 0.2531 | 0.5198 |
| −0.0643 | −0.2139 | −0.3172 | −0.3400 | −0.2410 | 0.0852 |
| −0.0968 | −0.4815 | −0.4750 | −0.1225 | 0.3439 | 0.4236 |
| −0.5271 | −0.3397 | 0.1729 | 0.5442 | 0.3453 | −0.1869 |
| 0.2939 | −0.0245 | −0.2908 | 0.0037 | 0.2925 | 0.0481 |
| 0.1437 | 0.2825 | −0.3712 | −0.0271 | 0.3933 | −0.4118 |
| −0.5185 | 0.4257 | 0.1587 | −0.5492 | 0.3797 | 0.0698 |
| 0.0801 | 0.2268 | −0.3852 | 0.2382 | 0.0361 | −0.3618 |
| 0.4093 | −0.4510 | 0.4261 | −0.3526 | 0.2683 | −0.3669 |
| 0.0626 | −0.0417 | 0.0587 | −0.1165 | 0.2610 | −0.1241 |

TABLE IX. THE LOWER EXCITED STATES OF THE METHYL-SUBSTITUTED BENZENIUM IONS BY THE CONFIGURATION INTERACTION INCLUDING THE DOUBLY EXCITED CONFIGURATION[a)]

2,4,6-Trimethylbenzenium ion

| $E$, eV. | $f$[b)] |
|---|---|
| 3.603 | 0.231 |
| 4.580 | 0.095 |
| 6.317 | 0.595 |

2,3,4,6-Tetramethylbenzenium ion

| $E$, eV. | $f$ |
|---|---|
| 3.481 | 0.218 |
| 4.494 | 0.102 |
| 6.265 | 0.556 |

Pentamethylbenzenium ion

| $E$, eV. | $f$ |
|---|---|
| 3.384 | 0.205 |
| 4.380 | 0.106 |
| 6.209 | 0.465 |

a) The ground state energy is taken to be zero in each case.
b) Oscillator strength.

transition energies for the methyl-substituted benzenium ions and for the $\alpha$-naphthalenium ion are in good agreement with the experimental results. Although the calculated absorption intensities can not be expected to be satisfactorily coincident with the observed values in this type of calculation, the results obtained by considering the configuration interaction including the doubly excited configurations seem to be rather good (The $\varepsilon$ values for the 280 m$\mu$ and 254 m$\mu$ bands of the $\alpha$-naphthalenium ion do not represent true intensities, since these two bands are superposed with the very intense band with a peak probably below 200 m$\mu$; the true intensities are far less than that of the second transition).

The shift of the 350 m$\mu$ and 250 m$\mu$ bands upon the methyl substitution is well explained by the present calculation. It has been observed that the substitution of a methyl group for one of the ring hydrogen atoms of the 2, 4, 6-trimethylbenzenium ion causes these two bands to shift toward a longer wavelength by 0.1 eV. The corresponding calculated values are 0.13 (0.12) and 0.16 (0.09) eV. respectively (the results with doubly excited configurations are shown in parentheses). When a methyl group is substituted for the ring hydrogen atom of the 2, 3, 4, 6-tetramethylbenzenium ion, the first and second bands shift toward longer wavelengths by 0.1 and 0.2 eV. respectively. The corresponding calculated values are 0.11 (0.10) and 0.18 (0.11) eV. respectively.

As has been pointed out earlier, the SCE treatment does not have any significant effect on the excitation energy or on the transition intensity of the benzenium ion* (see Table IV).

The results of the NMR absorption measurement, however, show that the charge distribution (0.22, 0.16 and 0.25 for the ortho-, meta- and para-positions respectively[8)]) is more even than that calculated by the usual SCF procedure. In this connection, the charge distribution calculated by method II seems to be more adequate than that calculated by method I (see Fig. 2). However, too much importance should not be attached to this comparison, because there is some ambiguity in determining the charge distributions from the NMR data.

* The same is true for the methyl-substituted benzenium ions, although the calculated results are not shown in the present paper.

TABLE X. THE LOWER EXCITED STATES OF THE BENZENIUM ION BY SEVERAL METHODS*1,*2

| Method I | | |
|---|---|---|
| Without CI | With CI(SE)*3 | With CI(DE)*4 |
| 3.65 (0.271) | 3.53 (0.202) | 3.54 (0.172) |
| 5.47 (0.601) | 5.12 (0.128) | 4.36 (0.026) |
| 6.39 (0.537) | 6.65 (1.081) | 6.76 |
| **Method II** | | |
| Without CI | With CI(SE) | With CI(DE) |
| 3.54 (0.298) | 3.42 (0.224) | 3.37 (0.181) |
| 5.31 (0.620) | 4.95 (0.163) | 4.07 (0.038) |
| 6.45 (0.536) | 6.73 (1.079) | 6.34 (0.549) |

*1 Energies are shown in eV. (the ground state is taken to be zero.)
*2 Oscillator strengths are shown in parenthesis in each case.
*3 Configuration interaction with the singly excited configurations alone.
*4 Configuration interaction with the singly and doubly excited configurations.

The inclusion of the doubly excited configurations changes the energies and the wave functions to some extent. The effect is negligible on the first excitation energies and on the intensities of the benzenium, methyl-substituted benzenium and $\alpha$-naphthalenium ions. However, the effect seems to be significant on the second excited states of the benzenium and methyl-substituted benzenium ions (see Table X for a comparison in the case of the benzenium ion), while there is no significant effect on the four excited states of the $\alpha$-naphthalenium ion. When we compare the calculated intensity ratio of the methyl-substituted benzenium ions with the experimental results, the calculation with the doubly excited configurations seems to be better.

The results of the semi-empirical calculation of this type always depend on the choice of the parameter $\beta$ (the resonance integral). The value selected in the present work, $-2.39$ eV., was originally evaluated to fit to the lowest excitation energy of benzene in the configuration-interaction calculation with singly excited configurations alone.[12] Anno et al.[19] examined the effect of the doubly excited configurations in the case of benzene and found the $\beta$ value of $-2.72$ eV. to be adequate. If we also take $\beta=-2.72$ eV. in our calculation of the configuration interaction including the doubly excited configurations, the lower excitation energies may become closer to the values evaluated by the configuration-interaction calculation without the doubly excited configuration.

As is shown in Table VI, the methyl substitution at ortho- and para-positions stabilizes the ground state of the benzenium ion by $\delta_o=0.146$ eV. (3.45 kcal./mol.) and $\delta_p=0.165$ eV. (3.89 kcal./mol.) respectively, while the meta-substitution causes little stabilization. An approximate additivity is satisfied for the stabilization due to the methyl-substitution. Thus the following equation can be obtained assuming that the stabilization energy due to the methyl substitution at the meta-position is zero:

$$\Delta=n_o\delta_0+n_p\delta_p$$

where $\Delta$ is the total stabilization energy of the methyl-substituted ion, and where $n_o$ and $n_p$ are the numbers of the methyl groups substituted at the ortho- and para-positions respectively. For example, the stabilization in the 2, 4-dimethylbenzenium ion is evaluated at 0.302 eV., while the sum of the stabilization energies of the ortho- and para-methylbenzenium ions is $0.146+0.165=0.311$ eV.

*The Institute for Solid State Physics*
*The University of Tokyo*
*Azabu, Tokyo*

## Appendix

**The Valence State Energy of the Carbon Atom.** —The carbon atom to which $H^+$ is attached may be considered to be nearly in the $sp^3$ hybrid valence state. In the present calculations, a pure $2p\pi$ AO was extracted by taking a linear combination of the $sp^3$ hybrid AO's, and the valence state ionization potential of the 2p AO of the non-hybridized carbon was used for the orbital energy of the extracted $2p\pi$ AO. In order to examine the validity of this choice, we shall consider here the valence state of the carbon atom in the methane molecule.

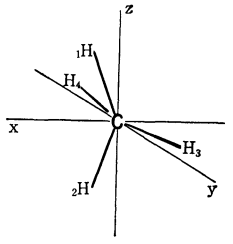



Fig. 3. Location and numbering of the four hydrogen atoms in the methane molecule.

If two hydrogen atoms, $H_1$ and $H_2$, are located in the xz plane and $H_3$ and $H_4$, in the xy plane (Fig. 3), the electronic states can generaly be represented by the following four bonding MO's:

$$\left.\begin{aligned}
\phi_1&=\frac{1}{\sqrt{1+\lambda_1^2}}\left[s+\frac{\lambda_1}{2}(h_1+h_2+h_3+h_4)\right]\\
\phi_2&=\frac{1}{\sqrt{1+\lambda_2^2}}\left[x+\frac{\lambda_2}{2}(h_1+h_2-h_3-h_4)\right]\\
\phi_3&=\frac{1}{\sqrt{1+\lambda_3^2}}\left[y+\frac{\lambda_3}{\sqrt{2}}(h_3-h_4)\right]\\
\phi_4&=\frac{1}{\sqrt{1+\lambda_4^2}}\left[z+\frac{\lambda_4}{\sqrt{2}}(h_1-h_2)\right]
\end{aligned}\right\}\quad(21)$$

19) T. Anno and A. Sado, *J. Chem. Phys.*, **39**, 2293 (1963).

and the corresponding antibonding MO's. (Here s, x, y and z denote the 2s, 2px, 2py and 2pz AO's of carbon respectively, and $h_1$ denotes the 1s AO of hydrogen $H_1$.) If the ideal $sp^3$ hybridization is achieved, the relation:

$$\lambda_1=\lambda_2=\lambda_3=\lambda_4=1$$

must hold. In this case the ground state energy is;

$$E=2\sum_{i=1}^{4}I_i+\sum_{i=1}^{4}J_{ii}+4\sum_{i<j}J_{ij}-2\sum_{i<j}K_{ij} \qquad (22)$$

The orbital energy of the MO $\phi_4$ is:

$$\begin{aligned}\varepsilon_4&=I_4+\sum_{j=1}^{4}(2J_{4j}-K_{4j})\\&=\frac{1}{2}\alpha_z+\frac{1}{4}J_{zz}+\frac{1}{2}(J_{yz}+J_{xz}+J_{sz})\\&\quad-\frac{1}{4}(K_{yz}+J_{xz}+J_{sz})\\&\quad+\{\text{Integrals belonging to the hydrogen 1s AO's}\}\\&\quad+\{\text{Integrals representing the interaction between the carbon and hydrogens}\}\end{aligned} \qquad (23)$$

If we define:

$$W_z=\alpha_z+(J_{yz}+J_{xz}+J_{sz})-\frac{1}{2}(K_{yz}+K_{xz}+K_{sz}) \qquad (24)$$

then

$$\varepsilon_4=\frac{1}{2}W_z+\frac{1}{4}J_{zz}+\cdots\cdots \qquad (25)$$

In the conventional $\pi$-electron treatment, $W_z$ is taken to be the minus of the valence state ionization potential of the carbon 2p AO.

The valence state ionization potential is determined from the atomic spectroscopy data as follows. For example, we consider first the ionization potential for removing an electron from the 2p AO in the non-hybridized carbon (in $(2s)(2p)^3$ configuration). The valence state energies of C and $C^+$ are;

$$E=\alpha_s+3\alpha_p+3(J_{sp}+J_{pp'})-\frac{3}{2}(K_{sp}+K_{pp'})$$

$$E^+=\alpha_s^+ +2\alpha_p^+ +2J_{sp}^+ +J_{pp'}^+ -K_{sp}^+ -\frac{1}{2}K_{pp'}^+,$$

and the ionization potential in question is:

$$-I_p(sxyz\rightarrow sxy)=\alpha_p+J_{sp}+2J_{pp'}-\frac{1}{2}K_{sp}-K_{pp'}+\Delta$$

where $\Delta$ is the sum of the differences in the corresponding integrals in C and $C^+$ caused by the change in the distribution of the electron cloud (the change in the effective charge, $Z$, if we consider the Slater atomic orbitals).

We will consider next the ionization of the electron in the $2p\pi$ AO in sp-hybridized carbon:

$$\begin{aligned}E&=\alpha_{d_1}+\alpha_{d_2}+\alpha_y+\alpha_z+J_{d_1y}+J_{d_1z}+J_{d_2y}+J_{d_2z}\\&\quad+J_{d_1d_2}+J_{yz}-\frac{1}{2}(K_{d_1y}+K_{d_1z}+K_{d_2y}+K_{d_2z}\\&\quad+K_{d_1d_2}+K_{yz})\\&=\alpha_s+3\alpha_p+\frac{1}{8}(J_{ss}+J_{pp})+\frac{11}{4}J_{sp}+3J_{pp'}\\&\quad-2K_{sp}-\frac{3}{2}K_{pp'},\end{aligned}$$

$$\begin{aligned}E^+&=\alpha_{d_1}^+ +\alpha_{d_2}^+ +\alpha_y^+ +J_{d_1y}^+ +J_{d_2y}^+ +J_{d_1d_2}^+\\&\quad-\frac{1}{2}(K_{d_1y}^+ +K_{d_2y}^+ +K_{d_1d_2}^+)\\&=\alpha_s^+ +2\alpha_p^+ +\frac{1}{8}(J_{ss}^+ +J_{pp}^+)+\frac{7}{4}J_{sp}^+ +J_{pp'}^+\\&\quad-\frac{3}{2}K_{sp}^+ -\frac{1}{2}K_{pp'}^+,\end{aligned}$$

$$\therefore\quad -I_p(d_1d_2yz\rightarrow d_1d_2y)=E-E^+=\alpha_p+J_{sp}+2J_{pp'}-\frac{1}{2}K_{sp}-K_{pp'}+\Delta$$

Here $d_1$ and $d_2$ are the digonal orbitals:

$$d_1=\frac{1}{\sqrt{2}}(s+x)$$

$$d_2=\frac{1}{\sqrt{2}}(s-x)$$

Therefore, if we neglect $\Delta$, $-I_p(d_1d_2yz\rightarrow d_1d_2y)$, $-I_p(sxyz\rightarrow sxy)$ and $W_z$ should be equal. The same equality can be proved for $-I_p(t_1t_2t_3z\rightarrow t_1t_2t_3)$.

There is a little difference between the ionization potentials of the various hybridization states tabulated in the references:[15]

| | $I_p$, eV. |
|---|---|
| $sxyz\rightarrow sxy$ | 11.31 |
| $d_1d_2yz\rightarrow d_1d_2y$ | 11.24 |
| $t_1t_2t_3z\rightarrow t_1t_2t_3$ | 11.22 |

It is possible to calculate the total $\pi$-electron state of the $CH_4$ molecule starting from several sets of orbitals; that is, non-hybridized (s, $p_x$, $p_y$ and $p_z$), digonally-hybridized ($d_1$, $d_2$, y and z), trigonally-hybridized ($t_1$, $t_2$, $t_3$ and z) or tetragonally-hybridized ($T_1$, $T_2$, $T_3$ and $T_4$) AO's. There are some differences in the orbital energies (the ionization potentials) of these orbitals depending on whether we choose one set of orbitals or another. For example, the ionization potential of the $2p_z$ orbital differs to some extent (see the data tabulated above) according to the choice of the set of $\sigma$-orbitals. This difference, however, may be canceled by the difference in $\sigma$-$\pi$ interaction caused by the difference in the type of $\sigma$-orbitals; if we adopt an approximation or a set of parameters in common, the calculations based on different hybridization states give the exactly same result.

In the present case, however, we adopt the $\pi$-electron approximation, so the above-mentioned cancellation does not appear exactly. Fortunately, the difference, caused by the choice of the $\sigma$-orbitals (caused by the difference in $\Delta$) is very small, and no significant effect may be expected even if we chose any value of the ionization potentials tabulated above.

# Electron Paramagnetic Resonance Study of $\gamma$-Ray Irradiated Phosphate Glasses*

By Yasuo NAKAI

(Received November 26, 1964)

In the last few years considerable progress has been made in acquiring knowledge about network defects in the glassy state by using paramagnetic resonance measurements.

Paramagnetism due both to defects produced in the lattice and to the presence of impurity atoms has been observed in irradiated quartz,[1] some silicate glasses[2] and alkali borate glasses.[3] Typical paramagnetic centers ascribed hitherto in silicate or borate glasses are an electron trapped at an oxygen vacancy, an electron trapped in the alkali ion, and a hole trapped at an oxygen ion. The paramagnetic centers described as impurity centers are a hole trapped on a bridging oxygen which is bonded to a substitutional $Al^-$ ion for silica in the silicon oxide, and an electron trapped in an interstitial hydrogen atom in a glass network.

The phosphate glasses become strongly colored under $\gamma$-ray irradiation. The most sensitive glass for irradiation is silver-activated phosphate glass. The phosphate glasses offer a simple and precise method of measuring gamma-ray doses with a commercial densitometer or a spectrophotometer.

The EPR study of the defect centers in irradiated glass containing phosphorus was first reported by Karapetyan and Yudin.[4] They observed an EPR spectra consisting of a two-line structure at $g=2.0038$. This two-line structure was attributed to hyperfine interaction with a $^{31}P$ nucleus.

In the present investigation, it has been found that there are three distinct types of defect centers in irradiated phosphate glasses. These paramagnetic centers seem to be connected with the peculiar structure of phosphate glass.

The basic structure of phosphate glass, which consists of $sp^3$ orbitals with an unsymmetric $PO_4$ tetrahedron, shows a considerable $\pi$-bond character.[5] The structure of such multiply-bonded glass is different from that of the silicate or borate glasses. Moreover, the compositions of the phosphate glasses have ratios of "modifier" oxide to phosphorus(V) oxide between one and three. In contrast, the silicate or borate glasses usually investigated have such compositions that this ratio is less than one.

In the present study, the relation between defect centers and the composition of phosphate glass will be discussed.

## Experimental

The EPR spectra were obtained by using a Varian Model 4501 EPR spectrometer at a microwave frequency of 9.4 kMc./sec. operating with a 100 kc./sec. field modulation. The EPR data presented in this study were obtained at room temperature.

The hyperfine structure of an alcoholic dilute solution of manganese(II) chloride was used as a standard for the magnetic field, and DPPH, for the $g$-value. Powder or glassy samples were enclosed in evacuated glass tubes during the $\gamma$-ray irradiation and the measurements.

The composition of alkaline phosphate glasses was $x\%M_2O(100-x)\%P_2O_5$ [M=Li, Na, K], where M/P=1.5 and 2.0, while that of alkaline earth phosphate glasses was $x\%RO(100-x)\%P_2O$ [R=Ca, Ba], where R/P=0.5 and 1.0 (in this paper weight percentages are used). These samples were melted in a platinum crucible at about 1100—1400°C. Metaalkaline phosphate glass was made from $(MPO_3)$, where M=Li, Na. The composition of the alumino alkaline phosphate glasses used in this investigation was $50\%LiPO_3 - 50\%AlPO_3$ and $80\%LiPO_3 - 20\%AlPO_3$.

Samples of condensed phosphate were prepared by the dehydration of $(RH_{1-2}PO_4)$ [R=Li, Na, K, Ca or Ba] at an elevated temperature, usually in the 500—800°C range.

The samples were irradiated at room temperature with $^{60}Co$ rays ($5—6\times10^6$ r.).

* Preliminary communication,: This Bulletin, 37, 1087 (1964).

1) R. A. Weeks, *J. Appl. Phys.*, 27, 1376 (1956); J. H. E. Griffith, J. Owen and I. M. Ward, Report of the Conference on Defects in Crystalline Solids, p. 81 (1955), London, Physical Society; M. C. M. O'Brien, *Proc. Roy. Soc.*, A231, 404 (1955).

2) J. S. van Wieringen andA. Kats, *Philips Res. Rep.*, 12, 432 (1957); C. M. Nelson and R. A. Weeks, *J. Am. Ceram. Soc.*, 43, 399 (1960); S. Lee and P. J. Bray, *Phys. Chem. Glass*, 3, 37 (1962).

3) Y. Nakai, *J. Chem. Soc. Japan, Pure Chem. Sec. (Nippon Kagaku Zasshi)*, 82, 1629 (1961); Y. Nakai, *Zeits, f. Phyik. Chem.*, in press; S. Lee and P. J. Bray, *J. Chem. Phys.*, 39, 2863 (1963).

4) G. O. Karapetyan, D. M. Yudin, *Soviet Phys. Solid State*, 3, 2063 (1963).

5) J. R. van Vazer, "Phosphorus and its Compounds," Interscience Publishers, Inc., New York (1958).

## Results

Before irradiation no paramagnetic resonance was found on any sample, but after irradiation all of them showed resonance and were purple or pink rose.

Figures 1 and 2 shows the EPR spectra of irradiated alkaline or alkaline-earth phosphate glasses. In the case of a sodium or potassium phosphate glass, the peaks of $P_a$ and $P_b$ disappear, leaving only two central peaks, $P_{c1}$ and $P_{c2}$. No spectra were observed from the sample of $(KPO)_3$-condensed phosphate irradiated with γ-rays ($5\times10^6$ r.).

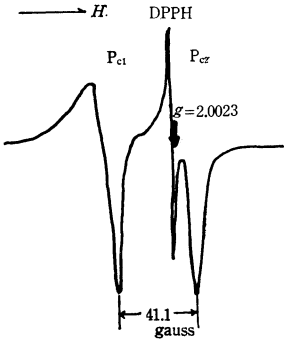



Fig. 1. The EPR spectrum obtained for γ-ray irradiated alkaline or alkaline earth phosphate glass.

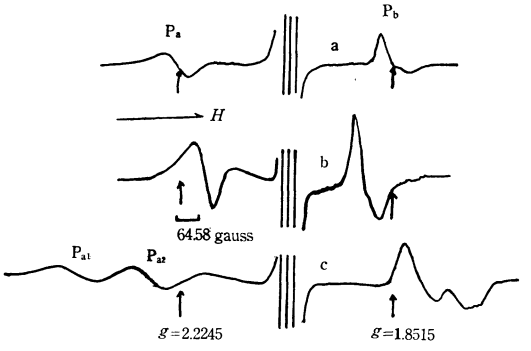



Fig. 2. The EPR spectra in low and high magnetic fields obtained for γ-ray irradiated phosphate glasses. The central lines are the spectra due to the phosphorus center shown in Fig. 1.
a) $LiPO_3$ glass
b) 10% $BaCO_3$ - 90% $LiPO_3$ glass
c) 41.3% $CaCO_3$ - 49.7% $P_2O_5$ glass

The $g$-values of the derivative peaks denoted $P_{c1}$ and $P_{c2}$ are independent of the kind of alkaline or alkaline earth modifier incorporated. These correspond to those reported by Karapetyan and Yudin.[4] The $g$-value at the center of these two peaks is measured as 2.0058. The distance between the derivative peaks, $P_{c1}$ and $P_{c2}$, is 41.1 gauss.

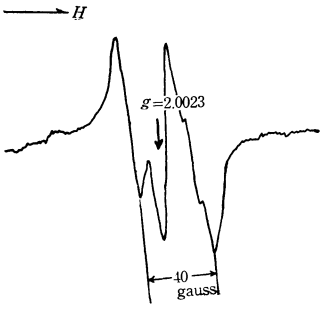



Fig. 3. The EPR spectrum obtained for γ-ray irradiated $(LiPO_3)_n$ condensed phosphate.

Figure 3 shows the EPR spectrum obtained from the irradiated condensed phosphate from which $LiPO_3$ glass was made. As a result, the difference between $LiPO_3$ glass and $LiPO_3$ condensed phosphate was found.

The intensity of the two-line structure, $P_{c1}$ and $P_{c2}$, can easily be reduced by heating it at 130—160°C. The fading speed by the thermal treatment is dependent on the kind of alkaline or alkalin-earth modifiers. The resistance to thermal bleaching increases in the order $Ca\approx Ba<Li<Na<K$. Moreover, the fading speed is dependent on the $R=M/P$ ratio. As the ratio ranges from three to one, the fading speed shows a tendency gradually to become slower. The two-line structure has the same response to both thermal annealing and optical annealing.

In addition to the two-line structure, the observed spectra appear to display other two weak absorption lines, $P_a$ and $P_b$, on the low and high magnetic field sides. Figure 2 shows that the position and the width of the anisotropic resonances, $P_a$ and $P_b$, depend greatly upon the type of alkaline or alkaline-earth ions.

The position and the width of two weak resonances in lithium phosphate glasses contaminated with calcium or barium are different from those exhibited in pure lithium phosphate glass, but the shape may be substantially the same, as Figs. 2a and 2b show.

It appears that the relative intensity of the two weak peaks increases in the order $Li<Ba\approx Ca$. Moreover, a relation exists between the radiation-induced paramagnetic intensity and the constitution of glass. As the proportion of the network-modifying atom increases in glasses, the relative intensity greatly increases. We have found that the two weak peaks are completely removed by annealing them at 380—450°C for 30 min.

It is remarkable that the derivative curve on the low magnetic field side obtained from alkaline-earth phosphate glasses consists of

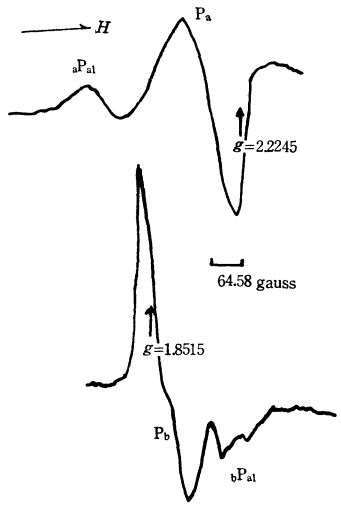



Fig. 4. The EPR spectrum obtained for $\gamma$-ray irradiated alumino phosphate glass of composition 50% $Al(PO_3)_3$ - 50% $LiPO_3$.

two peaks, as is shown in Fig. 2c. The fading speed of $P_{a1}$ to the thermal annealing may be a little more rapid than that of $P_{a2}$.

In phosphate glasses modified with such an ion as calcium, barium or lithium, the two weak resonances, $P_a$ and $P_b$, seem to appear easily.

Alumino alkaline phosphate glasses irradiated with $\gamma$-rays exhibit the same two-line structure, $P_{c1}$ and $P_{c2}$ as that displayed in $LiPO_3$ glass. The EPR intensity of the outer side peaks, ${}_aP_{a1}$ and ${}_bP_{a1}$, increases in proportion to the $Al_2O_3$ content of the $LiPO_3$ glass. However, as Fig. 4 shows, the shapes of the $P_a$ and $P_b$ centers are independent of the $Al_2O_3$ content.

## Discussion

**Alkali or Alkaline-earth Phosphate Glasses.**—The irradiated phosphate glasses exhibit the EPR spectra of two strong lines ($P_{c1}$ and $P_{c2}$) and of the other two weak absorption lines. One of the weak absorption lines appears to display a broad derivative peak on the low magnetic field side ($g=2.2245$), and the other, a broad asymmetric derivative peak on the high magnetic field side ($g=1.8575$). The former is denoted by $P_a$, and the latter, by $P_b$.

***$P_c$ Center.***—Two peaks ($P_{c1}$ and $P_{c2}$) in the derivative curve have the same response in the thermal annealing and optical bleaching, and this structure is independent of the kind of alkaline modifier and of the isotopic substitution of hydrogen. These facts suggest that the two lines arise from only one type of paramagnetic center, and so the magnetic hyperfine structure of two peaks may be ascribed to $^{31}P$ with $I=1/2$.

The observed $g$-value of the two-line structure shown in Fig. 1, which is larger than that of a free electron, suggests that the paramagnetic center is a trapped hole produced in the glass network by irradiation.

In order to analyze the observed two-line structure in terms of the hyperfine interaction of an unpaired spin, $S=1/2$, with a $^{31}P$ nucleus, it is assumed that the phosphorus center experiences a crystalline field whose symmetry is axial. If the crystalline electric field experienced by the phosphorus center were spherically symmetric or lower than axial, the shape of the derivative curve would be symmetrical or more complicated.

The spin resonance of the $(PO_4)$ defect can be described in terms of the following spin Hamiltonian:[6]

$$\mathscr{H}=\beta[g_{\parallel}S_zH_z+g_{\perp}(S_xH_x+S_yH_y)]+AS_zI_z+B(S_xI_x+S_yI_y) \quad (1)$$

where $g_{\parallel}$ and $g_{\perp}$ are the $g$ factors along and at right angles to the z direction, while A and B are the hyperfine interaction parameters of the $^{31}P$ nuclei. The $^{31}P$ nuclei ($I=1/2$) have no quadrupole moment, and the dipole-dipole interaction of neighboring centers is neglected in order to simplify the analysis of the observed hyperfine structure.

In the case of a glassy or powdered substance, $\theta$ takes random values, and the hyperfine structure is the envelope of the properly-weighted spectra obtained in simple crystals at all possible orientations.

According to the theoretical calculation,[7] the shape of the glassy spectrum, $g(H)$, is the sum of the line shape functions of $2I+1$ components as follows:

$$g(H)=\sum_{M=-I}^{I} g_M(H)$$

where $$g_M(H)=\frac{No}{2}\sin\theta\frac{d\theta}{dH}$$

The first-order hyperfine resonance condition given by the spin Hamiltonian is shown as follows:[6]

$$H=\frac{h\nu_0}{\beta}(g^2_{\parallel}\cos^2\theta+g^2_{\perp}\sin^2\theta)^{-1/2}-\frac{M}{\beta}(A^2g^2_{\parallel}\cos^2\theta+B^2g^2_{\perp}\sin^2\theta)^{1/2}\times(g^2_{\parallel}\cos^2\theta+g^2_{\perp}\sin^2\theta)^{-1} \quad (3)$$

6) B. Bleaney, *Phil. Mag.*, **42**, 441 (1951).
7) R. H. Sands, *Phys. Rev.*, **99**, 1222 (1955); S. M. Blinder, *J. Chem. Phys.*, **33**, 748 (1960); R. Neiman and D. Kivelson, ibid., **35**, 156 (1961).

Differentiating 3 with respect to $\theta$, and substituting $d\theta/dH$ in 3, we find the glassy spectrum, $g(H)$.

From the present measurements of the phosphorus center, $P_c$, which gives rise to the two-line hyperfine structure observed at the X-band frequency, we find

$$S=\frac{1}{2}, \qquad I=\frac{1}{2}$$

$$g_{\parallel}=2.0243, \quad g_{\perp}=2.0058$$

$$|A|=3.81\times10^{-3}\,\mathrm{cm}^{-1}, \quad |B|=3.75\times10^{-3}\,\mathrm{cm}^{-1}$$

This result is consistent with the two-line hyperfine structure observed in the irradiated phosphate glasses and shown in Fig. 5.

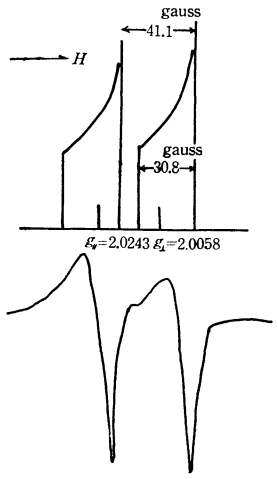



Fig. 5. Comparison between the hyperfine structure contructed from the spin Hamiltonian of Eq. 1 for the case of X-band frequency and the first derivative obtained for γ-ray irradiated phosphate glass.

As models for this resonance, two possibilities were considered: (1) a hole trapped on a singly-bonded oxygen, and (2) a hole trapped on the phosphorus atom in the $PO_4$ unit.

The wave function of the hole is assumed to occupy an orbital:

$$\Psi=\eta_P\phi_P+\eta_O\phi_O \qquad (4)$$

where $\phi_O$ and $\phi_P$ are hybrid orbitals on singly-bonded oxygen and phosphorus respectively. The coefficients are subjected to the normalizing requirements:

$$\eta^2_P+\eta^2_O+2\eta_O\eta_P S=1$$

where $S$ is the overlap, $\int\phi_P\phi_O d\tau$.

The hybrid orbital on phosphorus, $\phi_P$, is considered to consist mainly of a tetrahedral bonding orbital of the form $[(1/2)(|3s>+\sqrt{3}\,|3p>)]$, where $|3s>$ and $|3p>$ are the 3s and 3p orbitals of the phosphous that are used in the P—O covalent bonding. After γ-ray irradiation, the configuration of the $PO_4$ structure assumed to remain tetrahedral.

The hyperfine interaction parameters, $A$ and $B$, of the molecular orbital 4 with the phosphorus nucleus are related to the contact and the dipolar interaction by:[8]

$$A=\frac{1}{4}g\beta\left(\frac{\mu}{I}\right)\left[\frac{8\pi}{3}|\varphi_{3s}(0)|^2_P+\frac{12}{5}\langle r^{-3}\rangle_{3p,P}\right]\eta^2_P$$

$$B=\frac{1}{4}g\beta\left(\frac{\mu}{I}\right)\left[\frac{8\pi}{3}|\varphi_{3s}(0)|^2_P-\frac{6}{5}\langle r^{-3}\rangle_{3p,P}\right]\eta^2_P$$

where $\varphi_{3s}(0)$ denotes the wave function of the unpaired electron evaluated at the phosphorus, and $\langle r^{-3}\rangle$ is the average for the 3p orbital about the phosphorus atom.

Mayers[9] has performed a SCF treatment of the ground state phosphorus atom, and for his wave function the 3s orbital has $(8\pi/3)\times|\varphi_{3s}(0)|^2=46.93$ a. u. Similarly, Mayer's wave function gives, for the 3p orbital, $\langle r^{-3}\rangle=3.34$ a. u.

Therefore, it is possible to evaluate the hyperfine parameters of the ground-state phosphorus atom. We find that the isotropic part, $(8\pi/3)g\beta(\mu/I)|\varphi_{3s}(0)|^2$, is $0.33\,\mathrm{cm}^{-1}$; the anisotropic part, $(6/5)g\beta\times(\mu/I)\langle r^{-3}\rangle_{3p,P}$, is $2.86\times10^{-2}\,\mathrm{cm}^{-1}$, and the calculated values of the hyperfine interaction parameter, $A/\eta^2_P$ and $B/\eta^2_P$, are $96.8\times10^{-3}\,\mathrm{cm}^{-1}$ and $75.3\times10^{-3}\,\mathrm{cm}^{-1}$ respectively.

By comparing the experimental data and the calculated values of the hyperfine interaction parameters, we find $\eta_P=0.2$.

It can be seen, thus, that the experimental data obtained for the phosphorus center suggest that the hole interacting with a P nucleus is only weakly associated with the phosphorus atom. Perhaps the phosphorus center consists mainly of a hole trapped at a singly-bonded oxygen atom in the $PO_4$ unit, and the hole would spend 95—96% of its time on the oxygen and 4—5% of its time on the phosphorus atom.

The material from which $LiPO_3$ glass was made was subjected to γ-ray irradiation at room temperature. After irradiation, the spectrum shown in Fig. 3 was observed. In spite of its having the same composition, however, the position and also the shape of the EPR spectrum in the glassy state are different from those of the condensed phosphate. However, the EPR spectrum of the phosphorus center obtained at room temperature from the irradiated $(NaPO_3)_3$ of a ring structure was the same as those obtained from irradiated phosphate glasses. In the

8) See, for example, A. R. Reinberg, *J. Phys. Chem.*, **41**, 850 (1964).

9) See, J. R. Morton, *Mol. Phys.*, **6**, 193 (1963).

irradiated $(KPO_3)_n$ condensed phosphate, no paramagnetic resonance could be observed at room temperature. This point is difficults to explain.

*$P_a$ and $P_b$ Center.*—The compositions of the phosphate glasses lie between one and three in the M/P ratio. Therefore, the quantity of alkali or alkaline-earth modifier in the phosphate glasses is much larger than that in silicate or borate glasses. As the proportion of the network-modifying atom is increased, the breakdown of the phosphorus-oxygen network occurs, and the average molecular weight of the phosphate anions is found to decrease quite rapidly with time toward a moderately low limiting value. The alkaline-metal or alkaline-earth metal occasionally associates with the chain anions by attaching oxygen atoms of the "End" groups.[5]

The EPR intensity of $P_a$ and $P_b$ peaks increases in proportion to the alkaline or alkaline earth content under conditions of the same dosage. The line width, the position and the shape of resonance are dependent on the kind of alkaline or alkaline-earth incorporated. The formation of these centers becomes easier in the order $K<Na<Li<Ba\approx Ca$, and, according as the samples change from the vitreous state to the crystalline state, the formation of these centers seems to become more difficult. In the irradiated phosphate glasses of $Na/P=1$, these peaks disappear.

In the case of the alkaline-earth and alkaline-metal ions, it would be logical to expect that the tendency toward coordinate formation would increase with an increase in the charge/radius$^2$ ratio.[10] The charge/radius$^2$ ratios for $Ca^{2+}$, $Ba^{2+}$, $Li^{1+}$ and $Na^{1+}$ are 3.4, 2.6, 1.7 and 1.0 respectively. Therefore, the stability of the coordinate formation may increase in the order $Na<Li<Ba<Ca$. As has been shown by Takahashi[11] in studying the effect of network modifiers on the expansion coefficients of binary phosphate glasses, the expansion coefficient decreases in the order $K<Na<Li<Ba<Ca$, and decreases as the cation behaves as a network former rather than as a modifiers.

These facts suggest that, in phosphate glass modified with such ions as calcium, barium or lithium, which can coordinate with the tetrahedral oxygen atom in "End" groups, the weak resonance lines of two distinct types seem to appear easily; this is probably connected with the ability of coordinate formation.

In the region of the "End" group $(-PO_3)$, two, four or six nonbridging anions and some alkali cations as counter ions may be accidentally adjacent to each other, giving a localized region of excess negative charge. This configuration can trap holes.

The observed *g*-value of the $P_a$ center which is larger than that of a free electron, as is shown in Fig. 2, suggests that the paramagnetic center is a trapped hole produced in the glass network by irradiation, as in the above discussion.

In the case of irradiated alkaline-earth phosphate glass, it appears that the $P_a$ center consists of two different peaks which show a different fading speed to thermal annealing. However, the author believes that these two peaks may be the same type of center, while the electric coulombic field near these centers is different.

The *g*-value of the $P_b$ center which is smaller than that of a free electron, as is shown in Fig. 2, suggests that the paramagnetic center is the trapped electron in the vicinity of alkaline or alkaline-earth ions. The difference between the *g*-value of the $P_b$ center and the free electron value, $g=2.0023$, is contributed by the orbital magnetic moment. An electron in a paramagnetic ion is influenced not only by the applied magnetic field but also by the field due to its own orbital motion. It follows that the $P_b$ center has an appreciable amount of orbital angular momentum: a 1s hydrogen atom-like model would give a poor approximation for the wave function of the center.

The change of the line width in proportion to the measuring frequency has not been observed. However, the author believes that the *g*-value and the width depend upon the electric coulombic field near the center and on its orientation in the diamagnetic field. The shape of the resonance in lithium phosphate glass exhibited a very high symmetry. The coordination number of the $Li^+$ ion is high in the glass. Therefore, the electric field around the lithium atom in the glass network would be of a considerably high symmetry. In contrast, the coordination number of the alkaline-earth ion is low. The electric field would be of a low symmetry. The shape of barium or calcium phosphate glass was observed to be of low symmetry.

In lithium phosphate glass containing a small quantity of an alkaline-earth modifier as an impurity, the position and the width of the resonance are different from that displayed in pure lithium phosphate glass, but the shape is substantially the same, as Figs. 2a and 2b

10) A. E. Martell and M. Calvin, "Chemistry of the Metal Chalate Compounds," Prentics-Hall, Inc., New Jersey (1952).

11) K. Takahashi, "Binary Phosphate, Silicophosphate, Borophosphate and Aluminophosphate Glasses, their Properties and Structure," a report presented at the 6th International Congress on Glass, Washington, D. C., July, 1962.

show. If the resonances of the lithium center and the barium center are observed independently, these types of resonances would appear. Therefore, the electric field created by the oxygen atoms that are in the sphere around the lithium atom would be changed by the addition of an alkaline-earth impurity.

In short, the defect center in glass should be discussed from the viewpoint of the dynamic state of the glass structure and the stability of the glass structure.

**Alumino Phosphate Glasses.** — The network in aluminophosphate glasses is said to be formed by the interlinking of $(AlO_4)^{5-}$ and $(PO_4)^{3-}$ groups via bridging oxygens.[5]

A paramagnetic center due to hyperfine interaction with the nucleus of a four-co-ordinated aluminum ion has been observed in irradiated alumino silicate glasses and a single crystal of qurtz contaminated with aluminum ions, and the aluminum center has exhibited a spectrum consisting of a six-line structure in the vicinity of $g=2.010$.[1,2]

In the present investigation, thus, it was to be expected that a broad resonance caused by such a hyperfine interaction with a phosphorus and an aluminum nucleus would appear in the vicinity of $g=2.01$. However, samples of alumino alkaline phosphate glasses irradiated with γ-rays were not found to exhibit a six-line structure with a $g$-value of ca. 2.01. The formation of a paramagnetic center due to a four-co-ordinated aluminum atom in phosphate glasses would be protected against γ-ray irradiation.

In contrast, the EPR intensity of the outer side, ${}_aP_{a1}$ and ${}_bP_{a1}$, increases in proportion to the aluminum oxide content of the glass. The EPR spectra of these outer sides may arise from the defect centers due to the interstitial aluminum.

## Summary

The EPR spectrum, consisting of a two-line structure and two other distinct types of weak resonances, obtained from irradiated phosphate glasses suggests that these paramagnetic centers are connected with the peculiar structure of phosphate glasses.

The two-line structure arises from an axially-symmetric hyperfine interaction of a hole with a $^{31}P$ nucleus. Two distinct types have been demonstrated: one is a trapped hole produced in the glass network, and the other is the trapped electron in the alkaline or alkaline-earth ion. In phosphate glasses modified with such ions as calcium, barium or lithium that can coordinate with the tetrahedral oxygen atom in "End" groups ($-PO_3$), the weak resonances seem to appear easily.

The author wishes to express his thanks to Professor Kozo Hirota and Associate Professor Keiji Kuwata of Osaka University for their helpful advice and kind encouragement throughout this work. The author would also like to express his deep thanks to Dr. A. R. Weeks of the Oak Ridge National Laboratory and to Professor P. J. Bray of Brown University for reading the manuscript.

*Central Research Laboratory*
*Tokyo Shibaura Electric Co., Ltd.*
*Toshiba-cho, Kawasaki*

# Theory of Solvent Effects on Molecular Electronic Spectra. Frequency Shifts

By Takehiko ABE

(Received November 26, 1964)

Several quantitative theories[1-9] have been presented for solvent effects on electronic spectra. These theories give good theoretical interpretations for observed frequency shifts, but they can be used only with difficulty to calculate general frequency shifts, since their expressions are either very complicated or only applicable to non-polar solvents.

In the present work, by the application of the van der Waals interaction, an attempt has been made to derive a general theoretical expression for the frequency shifts, from which expression the frequency shifts can be calculated by the use of other observed values.

Among the solvent effects on the electronic spectra, there is the important effect of hydrogen bonding between a solute and solvent molecules found by Nagakura and Baba.[10] In the present theory, however, this effect has not been considered.

## Theoretical

The method of treatment consists of the application of the van der Waals interaction to the calculation of the electronic interactions among molecules of a solution containing N identical solvent molecules and one solute molecule. The spectra of solutions are usually measured at very low concentrations in the longer wavelength regions in which no solvents absorb. We will, therefore, consider the $i$th excited electronic state of the solution in which the solute molecule is in its $i$th excited electronic state and all the solvent molecules are in their ground states. We will suppose that all the spherical molecules have fixed positions. In view of the Franck-Condon principle, the same positions are appropriate to the ground and excited states of the solution.

In the zeroth order of approximation, we consider that all the spherical isotropic molecules do not interact. The zeroth-order electronic state energies are sums of the electronic state energies of the unperturbed component molecules; the energies corresponding to the ground and excited states of the solution are given, respectively, by:

$$E_0^0 = w_0^{\mathrm{u}} + Nw_0^{\mathrm{v}}$$
$$E_i^0 = w_i^{\mathrm{u}} + Nw_0^{\mathrm{v}}$$

where $w$ denotes the electronic state energy of an unperturbed molecule. Throughout this paper the notations u and v($p$) will refer to the solute and the $p$th solvent molecule, while the subscript zero will indicate the ground electronic state, and $i$, the $i$th excited electronic state. Thus, the energy difference in $cm^{-1}$ between the zeroth and $i$th states of the solute in gas will be expressed by:

$$\nu_{i0}^0 = (w_i^{\mathrm{u}} - w_0^{\mathrm{u}})/\boldsymbol{hc} \qquad (1)$$

where $\boldsymbol{h}$ is the Planck constant and $\boldsymbol{c}$, the velocity of light.

Assuming that there are no strong dipole orientations among the molecules, we represent the energy of the interaction of all the molecules in solution by the energy of the van der Waals interaction,[11] which is given by:

$$\begin{aligned} E_i' = &-\sum_{p=1}^{N} \frac{1}{R_{\mathrm{u}\mathrm{v}(p)}^6} \left\{ \frac{2}{3} \cdot \frac{(\mu_i^{\mathrm{u}})^2 (\mu_0^{\mathrm{v}(p)})^2}{\boldsymbol{kT}} \right. \\ &+ (\alpha_i^{\mathrm{u}})(\mu_0^{\mathrm{v}(p)})^2 + (\alpha_0^{\mathrm{v}(p)})(\mu_i^{\mathrm{u}})^2 \\ &\left. + \frac{3}{2} \cdot \frac{I_i^{\mathrm{u}} \cdot I_0^{\mathrm{v}(p)}}{I_i^{\mathrm{u}} + I_0^{\mathrm{v}(p)}} \cdot (\alpha_i^{\mathrm{u}})(\alpha_0^{\mathrm{v}(p)}) \right\} \\ &- \frac{1}{2} \sum_{p=1}^{N} \sum_{q=1}^{N} \frac{1}{R_{\mathrm{v}(p)\mathrm{v}(q)}^6} \left\{ \frac{2}{3} \cdot \frac{(\mu_0^{\mathrm{v}(p)})^2 (\mu_0^{\mathrm{v}(q)})^2}{\boldsymbol{kT}} \right. \\ &+ (\alpha_0^{\mathrm{v}(p)})(\mu_0^{\mathrm{v}(q)})^2 + (\alpha_0^{\mathrm{v}(q)})(\mu_0^{\mathrm{v}(p)})^2 \\ &\left. + \frac{3}{2} \cdot \frac{I_0^{\mathrm{v}(p)} \cdot I_0^{\mathrm{v}(q)}}{I_0^{\mathrm{v}(p)} + I_0^{\mathrm{v}(q)}} \cdot (\alpha_0^{\mathrm{v}(p)})(\alpha_0^{\mathrm{v}(q)}) \right\} \qquad (2) \end{aligned}$$

where $R$ denotes the distance between two molecules in solution, and $I$, the ionization potential of an unperturbed molecule in gas.

1) N. S. Bayliss, *J. Chem. Phys.*, **18**, 292 (1950).
2) Y. Ooshika, *J. Phys. Soc. Japan*, **9**, 594 (1954).
3) H. C. Longuet-Higgins and J. A. Pople, *J. Chem. Phys.*, **27**, 192 (1957).
4) W. W. Robertson. O. E. Weigang, Jr., and F. A. Matsen, *J. Mol. Spectry*, **1**, 1 (1957).
5) E. G. McRae, *J. Phys. Chem.*, **61**, 562 (1957).
6) A. Julg, *J. chim. phys.*, **54**, 493 (1957).
7) T. Abe, *Sci. Reports. Tohoku Univ., Ser. I*, **40**, 141 (1957).
8) C. A. Coulson, *Proc. Roy. Soc.*, **A255**, 69 (1960).
9) O. E. Weigang, Jr., *J. Chem. Phys.*, **33**, 892 (1960).
10) S. Nagakura and H. Baba, *J. Am. Chem. Soc.*, **74**, 5693 (1952).
11) H. Margenau, *Rev. Mod. Phys.*, **11**, 1 (1939).

Here $k$ is the Boltzmann constant, and $T$ is the absolute temperature.

The energy of the perturbed $i$th excited state of the solution, corresponding in the zeroth order of approximation to the unperturbed $i$th excited state, is given by:

$$E_i = E_i^0 + E_i' \tag{3}$$

A similar expression for the ground state of the solution is obtained by replacing $i$ by 0. The frequency shift, $\Delta\nu_{i0}$, is given by:

$$hc\cdot\Delta\nu_{i0} = (E_i - E_0) - (E_i^0 - E_0^0) \tag{4}$$

With the aid of Eq. 3, Eq. 4 can be written:

$$hc\cdot\Delta\nu_{i0} = E_i' - E_0' \tag{5}$$

The ionization potential of the $i$th excited state of the solute molecule is approximated as smaller than that for the ground state by $hc\nu_{i0}^0$ erg. We then obtain for $I_i^u$ (in erg):

$$I_i^u = I_0^u - hc\nu_{i0}^0 \tag{6}$$

From the assumption that all the spherical solvent molecules are identical, it follows that they have identical dipole moments of $\mu_0^v$ (gas) and identical ionization potentials of $I_0^v$. From Eqs. 2, 5 and 6, we find:

$$hc\cdot\Delta\nu_{i0} = -\left(\sum_{p=1}^{N} 1/R_{uv(p)}^6\right)\left[\frac{2}{3}\cdot\frac{(\mu_0^v)^2}{kT}\{(\mu_i^u)^2 - (\mu_0^u)^2\} + (\mu_0^v)^2\{(\alpha_i^u) - (\alpha_0^u)\} + (\alpha_0^v)\{(\mu_i^u)^2 - (\mu_0^u)^2\} + \frac{3}{2}\cdot(\alpha_0^v)\cdot I_0^v\left\{\frac{I_0^u - hc\nu_{i0}^0}{I_0^v + I_0^u - hc\nu_{i0}^0}\cdot(\alpha_i^u) - \frac{I_0^u}{I_0^v + I_0^u}\cdot(\alpha_0^u)\right\}\right] \tag{7}$$

**The Reduction of** $\left(\sum_{p=1}^{N} 1/R_{uv(p)}^6\right)$. — If the solute and the solvent molecules are spherical, their radii can be written, respectively, as:

$$r^u = (3M^u/4\pi A_0 d^u)^{1/3} \tag{8}$$

$$r^v = (3M^v/4\pi A_0 d^v)^{1/3} \tag{9}$$

Here $A_0$ is the Avogadro number; $M$, a molecular weight, and $d$, a liquid density. We then have for the values of $R_{uv(p)}$:

$$(r^u + r^v),\ (r^u + 3r^v),\ (r^u + 5r^v), \cdots$$

The numbers of the solvent molecules at the distances corresponding to the above values of $R_{uv(p)}$ may be approximated as, respectively:

$$\frac{4\pi(r^u + r^v)^2}{(2r^v)^2},\ \frac{4\pi(r^u + 3r^v)^2}{(2r^v)^2},\ \frac{4\pi(r^u + 5r^v)^2}{(2r^v)^2}, \cdots$$

We then write:

$$\sum_{p=1}^{N}\frac{1}{R_{uv(p)}^6} = \frac{4\pi(r^u + r^v)^2/(2r^v)^2}{(r^u + r^v)^6} + \frac{4\pi(r^u + 3r^v)^2/(2r^v)^2}{(r^u + 3r^v)^6} + \frac{4\pi(r^u + 5r^v)^2/(2r^v)^2}{(r^u + 5r^v)^6} + \cdots \tag{10}$$

where we can neglect terms higher than the third, so that we derive, approximately:

$$\sum_{p=1}^{N} 1/R_{uv(p)}^6 = \frac{\pi}{(r^v)^2}\{(r^u + r^v)^{-4} + (r^u + 3r^v)^{-4} + (r^u + 5r^v)^{-4}\} \tag{11}$$

**General Formula.**—From Eqs. 7, 8, 9 and 11, we obtain, for the frequency shift in an absorption transition from the ground state to the $i$th excited state of an isotropic molecule:

$$\Delta\nu_{i0} = -\frac{16\pi^3 A_0^2}{9hc}\cdot\left(\frac{d^v}{M^v}\right)^{2/3}\times\left[\left\{\left(\frac{M^u}{d^u}\right)^{1/3} + \left(\frac{M^v}{d^v}\right)^{1/3}\right\}^{-4} + \left\{\left(\frac{M^u}{d^u}\right)^{1/3} + 3\left(\frac{M^v}{d^v}\right)^{1/3}\right\}^{-4} + \left\{\left(\frac{M^u}{d^u}\right)^{1/3} + 5\left(\frac{M^v}{d^v}\right)^{1/3}\right\}^{-4}\right]\times\left[\frac{2}{3}\cdot\frac{(\mu_0^v)^2}{kT}\{(\mu_i^u)^2 - (\mu_0^u)^2\} + (\mu_0^v)^2\{(\alpha_i^u) - (\alpha_0^u)\} + (\alpha_0^v)\{(\mu_i^u)^2 - (\mu_0^u)^2\} + \frac{3}{2}\cdot(\alpha_0^v)\cdot I_0^v\left\{\frac{I_0^u - hc\nu_{i0}^0}{I_0^v + I_0^u - hc\nu_{i0}^0}\cdot(\alpha_i^u) - \frac{I_0^u}{I_0^v + I_0^u}\cdot(\alpha_0^u)\right\}\right] \tag{12}$$

where $16\pi^3 A_0^2/9hc = 1.007\times10^{65}$ erg$^{-1}$ cm$^{-1}$ and $2/3kT = 1.647\times10^{13}$ erg$^{-1}$ at 20°C.

**Approximate Formula.** — It is well-known that a molecular deformation polarization is approximately equal to a molecular refraction. We, therefore, have:

$$\alpha_0^v = \frac{3}{4\pi A_0}\cdot[R]^v \tag{13}$$

where $[R]^v$ denotes the molecular refraction of the solvent, which can be calculated as a sum of the atomic refractions from a table.

The values of $\alpha_i^u$ and $\mu_i^u$ are for the solute molecule in gas. According to the Clausius-Debye equation, we have:

$$\alpha_0^u = \frac{3}{4\pi A_0}\cdot\frac{M^u}{d_0^{u(g)}}\cdot\frac{\varepsilon_0^u - 1}{\varepsilon_0^u + 2} - \frac{(\mu_0^u)^2}{3kT} \tag{14}$$

$$\alpha_i^u = \frac{3}{4\pi A_0}\cdot\frac{M^u}{d_i^{u(g)}}\cdot\frac{\varepsilon_i^u - 1}{\varepsilon_i^u + 2} - \frac{(\mu_i^u)^2}{3kT} \tag{15}$$

where $d^{u(g)}$ and $\varepsilon^u$ denote the density and the dielectric constant of the solute in gas respectively.

On the assumption that all the molecules have the same positions in the ground and excited states of the solution, we may write:

$$d_0^{u(g)} = d_i^{u(g)} \tag{16}$$

From $I_0^u - h c \nu_{i0}^0 < I_0^u$, we may suppose the following inequality, since $I_0^v + I_0^u - h c \nu_{i0}^0 > I_0^u - h c \nu_{i0}^0$, although $I_0^v + I_0^u - h c \nu_{i0}^0 < I_0^v + I_0^u$:

$$\frac{I_0^u - h c \nu_{i0}^0}{I_0^v + I_0^u - h c \nu_{i0}^0} < \frac{I_0^u}{I_0^v + I_0^u} \tag{17}$$

It may be assumed that the dielectric constant of the excited state of the solute is greater than that for the ground state; that is:

$$\varepsilon_i^u > \varepsilon_0^u$$

From Eqs. 17 and 18, we may assume the following approximation:

$$\frac{I_0^u - h c \nu_{i0}^0}{I_0^v + I_0^u - h c \nu_{i0}^0} \cdot \frac{\varepsilon_i^u - 1}{\varepsilon_i^u + 2} = \frac{I_0^u}{I_0^v + I_0^u} \cdot \frac{\varepsilon_0^u - 1}{\varepsilon_0^u + 2} \tag{19}$$

Using Eqs. 13, 14, 15, 16 and 19, we may reduce Eq. 12 approximately to:

$$\begin{aligned} \Delta\nu_{i0} = & -\frac{4\pi^2 A_0}{3hc} \cdot \left(\frac{d^v}{M^v}\right)^{2/3} \times \left[ \left\{ \left(\frac{M^u}{d^u}\right)^{1/3} + \left(\frac{M^v}{d^v}\right)^{1/3} \right\}^{-4} + \left\{ \left(\frac{M^u}{d^u}\right)^{1/3} + 3\left(\frac{M^v}{d^u}\right)^{1/3} \right\}^{-4} \right. \\ & \left. + \left\{ \left(\frac{M^u}{d^u}\right)^{1/3} + 5\left(\frac{M^v}{d^v}\right)^{1/3} \right\}^{-4} \right] \times \left[ \frac{4\pi A_0}{9kT} \cdot \right. \\ & (\mu_0^v)^2 \{(\mu_i^u)^2 - (\mu_0^u)^2\} + [R]^v \{(\mu_i^u)^2 - (\mu_0^u)^2\} \\ & - \frac{1}{2kT} \cdot I_0^v \cdot [R]^v \cdot \left\{ \frac{I_0^u - h c \nu_{i0}^0}{I_0^v + I_0^u - h c \nu_{i0}^0} \cdot (\mu_i^u)^2 \right. \\ & \left. \left. - \frac{I_0^u}{I_0^v + I_0^u} \cdot (\mu_0^u)^2 \right\} \right] \end{aligned} \tag{20}$$

where $4\pi^2 A_0/3hc = 3.992 \times 10^{40}\ \mathrm{erg^{-1}\,cm^{-1}}$, $4\pi A_0/9kT = 2.078 \times 10^{37}\ \mathrm{erg^{-1}}$, and $1/2kT = 1.236 \times 10^{13}\ \mathrm{erg^{-1}}$ at 20°C.

## Discussion

Assuming that all the molecules in the solution are spherical, we have derived Eqs. 12 and 20. Accordingly, these equations are not applicable to rod-like molecules. For the rod-like molecules, the values of $\sum_{p=1}^{N} 1/R_{uv(p)}^6$ must be otherwise estimated.

Equations 12 and 20 are limited for use to solutions in which no complete dipole orientations occur between solutes and solvent molecules, because Eq. 2 includes the isotropic polarizabilities. These equation, however, hold for the solutions in which there are strong dipole orientations among the solvent molecules, because Eq. 5 excludes this effect. When there is a complete dipole orientation between a solute and the solvent molecules, anisotropic polarizabilities must be used instead of the isotropic ones and Eq. 11 can not be applied.

When the frequency shifts are small, Eqs. 12 and 20 cannot be applied quantitatively, since the above assumptions do not hold.

When there is a small orientation effect between a solute and the solvent molecules, $\Delta\nu_{i0}^0$ is chiefly governed by the third term of the dispersion effect in the second bracket in Eq. 12. Accordingly, in order to calculate $\mu_i^u$, it is better to apply Eq. 12 to the polar solvents, since the first term of the orientation effect in the second bracket is included.

As has been mentioned above, Nagakura and Baba[10] have found that the hydrogen bonding causes the frequency shifts. Since Eqs. 12 and 20 do not include this effect, they will give the deviated $\Delta\nu_{i0}$ from the observed frequency shift for a polar solvent forming a hydrogen bond with a solute. This deviation may be due to the hydrogen bonding.

**The Relationship Between $\Delta\nu_{i0}$ and the Refractive Index and the Dielectric Constant of the Solvent.** — Considering that all the molecules do not interact in the zeroth order approximation, we have derived Eqs. 12 and 20. When we consider an unperturbed solute molecule and the solvent molecules already interacting with one another in the zeroth order approximation, we must write:

$$\begin{aligned} E_i' = -\sum_{p=1}^{N} \frac{1}{R_{uv(p)}^6} \left\{ \frac{2}{3} \cdot \frac{(\mu_i^u)^2 (\mu_0^{v(p)})^2}{kT} \right. \\ + (\alpha_i^u)(\mu_0^{v(p)})^2 + (\alpha_0^{v(p)})(\mu_i^u)^2 \\ \left. + \frac{3}{2} \cdot \frac{I_i^u \cdot I_0^{v(p)}}{I_i^u + I_0^{v(p)}} \cdot (\alpha_i^u)(\alpha_0^{u(p)}) \right\} \end{aligned} \tag{21}$$

where $\mu_0^{v(p)}$ is the dipole moment, $\mu_0^{v(l)}$, of the liquid solvent. By the same procedure we obtain the same final formulae as Eqs. 12 and 20. According to Onsager,[12] the dipole moment of the liquid solvent is given approximately by:

$$(\mu_0^{v(l)})^2 = \frac{9kT}{4\pi A_0} \cdot \frac{M_v}{d^v} \cdot \frac{\{\varepsilon^v - (n^v)^2\}\{2\varepsilon^v + (n^v)^2\}}{\varepsilon^v \{(n^v)^2 + 2\}^2} \tag{22}$$

Here $\varepsilon^v$ and $n^v$ denote the static dielectric constant of the solvent, and its refractive index extrapolated to zero frequency, respectively.

It is well-known that the molecular refraction can be expressed by:

$$[R]^v = \frac{(n^v)^2 - 1}{(n^v)^2 + 2} \cdot \frac{M^v}{d^v} \tag{23}$$

For example, by putting Eqs. 22 and 23 into the same form as Eq. 20, we obtain:

12) L. Onsager, *J. Am. Chem. Soc.*, **58**, 1486 (1936).

TABLE I. THE $\pi$-$\pi^*$ TRANSITION (240 m$\mu$) IN NITROBENZENE

| No. | Solvent | $\nu_{max}$(cm$^{-1}$) | $\mu_0$(D, gas)[15] | $\alpha_0\times10^{25}$(cm$^3$)[15] | $I_0$(eV.) |
|---|---|---|---|---|---|
| | Nitrobenzene (gas) | 41680[13] | 4.23 | 129.2 | 10.15[16] |
| 1 | *n*-Heptane | 39700[13] | 0 | 136.1 | 10.35[15] |
| 2 | Cycohexane | 39540[13] | 0 | 108.7 | 9.24[17] |
| 3 | Carbon tetrachloride | 39170[14] | 0 | 105 | 11.0[15] |
| 4 | Dioxane | 38650[13] | 0 | 94.4 | 9.52[17] |
| 5 | Chloroform | 38150[14] | 1.05 | 82.3 | 11.5[15] |

$$\Delta\nu_{i0}=-\frac{4\pi^2A_0}{3hc}\cdot\left(\frac{M^v}{d^v}\right)^{1/3}\times\left[\left\{\left(\frac{M^u}{d^u}\right)^{1/3}+\left(\frac{M^v}{d^v}\right)^{1/3}\right\}^{-4}+\left\{\left(\frac{M^u}{d^u}\right)^{1/3}+3\left(\frac{M^v}{d^v}\right)^{1/3}\right\}^{-4}+\left\{\left(\frac{M^u}{d^u}\right)^{1/3}+5\left(\frac{M^v}{d^v}\right)^{1/3}\right\}^{-4}\right]\times\left[\frac{\{\varepsilon^v-(n^v)^2\}\{2\varepsilon^v+(n^v)^2\}}{\varepsilon^v\{(n^v)^2+2\}^2}\cdot\{(\mu_i^u)^2-(\mu_0^u)^2\}+\frac{(n^v)^2-1}{(n^v)^2+2}\{(\mu_i^u)^2-(\mu_0^u)^2\}-\frac{1}{2kT}\cdot\frac{(n^v)^2-1}{(n^v)^2+2}\cdot I_0^v\left\{\frac{I_0^u+hc\nu_{i0}^0}{I_0^v+I_0^u-hc\nu_{i0}^0}\cdot(\mu_i^u)^2-\frac{I_0^u}{I_0^v+I_0^u}\cdot(\mu_0^u)^2\right\}\right] \quad (24)$$

where the refractive index may be replaced approximately by the value appropriate to the sodium-D line.

## Application

**The Application of Eq. 12 to Nitrobenzene.** —The frequency shifts of the 239.9 m$\mu$ band of nitrobenzene in solvents and the other observed values to be used are listed in Table I. The values of $d$ from Lange's table[18] and other sources were used for 20°C. Assuming that the temperature is 20°C, the author can apply Eq. 12 to nitrobenzene. By means of the least square method, $\alpha_i^u$ and $\mu_i^u$ are estimated as $580.7\times10^{-25}$ cm$^3$ and 8.18 D respectively. Putting the above values into Eq. 12, the author obtained a good agreement in the frequency shifts between the theoretical and the experimental results, as is indicated in Fig. 1. The finding that the dipole moment of the excited state caused by the 240 m$\mu$ transition in nitrobenzene is greater than that for the ground state is consistent with Nagakura and Tanaka's theory.[19] They have interpreted the band of nitrobenzene in terms of the intramolecular charge-transfer involving an excitation of a bonding electron of the highest-occupied orbital of benzene to the vacant orbital of the nitro group. Bayliss and McRae[15,20] have also mentioned that there is a greater dipole moment in the excited state of nitrobenzene.

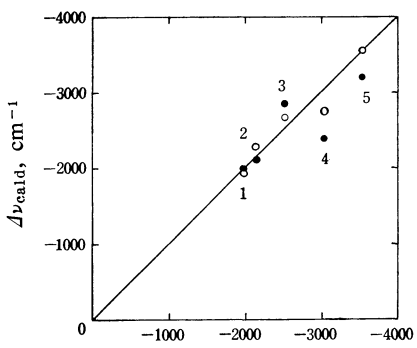



Fig. 1. Calculated vs. observed frequency shifts in the 240 m$\mu$ band of nitrobenzene.
○ calculated from Eq. 12
● calculated from Eq. 20

**The Application of Eq. 20 to Nitrobenzene.**— Equation 20 is applied to the frequency shift of the 240 m$\mu$ band of nitrobenzene at 20°C. The values of $[R]^v$ were calculated from a table. By putting the observed shift for *n*-heptane into Eq. 20, the author estimated $\mu_i^u$ to be 4.67 D, and then, using that value, he calculated the frequency shifts for other solvents, as Fig. 1 indicates. The $\mu_i^u$ value of 4.67 D is considerably smaller than that obtained from Eq. 12. The points calculated from Eq. 20 are also worse fitted to the full straight line than those calculated from Eq. 12, as is shown in Fig. 1.

**The Application of Eq. 20 to Acetophenone.** —The frequency shifts of the 231.3 m$\mu$ band of acetophenone in non-polar solvents are listed in Table II.

13) W. M. Schubert, J. Robins and J. L. Haun, ibid., 79, 910 (1957).
14) N. S. Bayliss and E. G. McRae, *J. Phys. Chem.*, 58, 1006 (1954).
15) Landolt-Börnstein, "Physikalisch-chemische Tabellen," 6th Ed., Springer, Berlin (1951), pp. 395, 386, 509.
16) S. Nagakura and J. Tanaka, This Bulletin, 32, 734 (1959).
17) J. D. Morrison and A. J. C. Nicholson, *J. Chem. Phys.*, 20, 1021 (1952).
18) N. A. Lange, "Handbook of Chemistry," 10th Ed., McGraw-Hill, London (1961), p. 382.
19) S. Nagakura and J. Tanaka, *J. Chem. Phys.*, 22, 236 (1954).
20) N. S. Bayliss and E. G. McRae, *J. Phys. Chem.*, 58, 1002 (1954).

TABLE II. THE $\pi$-$\pi^*$ TRANSITIONE IN ACETOPHENONE

| Solvent | $\nu_{max}$ ($cm^{-1}$)[13] |
|---|---|
| Acetophenone (gas) | 43230 |
| *n*-Heptane | 41980 |
| Cyclohexane | 41940 |

The ionization potential of acetophenone is 9.77 eV.[15] Putting the observed shifts into Eq. 20 at 20°C, the author has estimated $\mu_0^u$ and $\mu_i^u$ to be 3.81 and 4.42 D respectively. The value of 3.81 D accords fairly with the experimental value of 3.00 D (gas).[15] The result of $\mu_i^u > \mu_0^u$ is consistent with the intramolecular charge-transfer band[19,21,22] and with Bayliss and McRae's interpretation.[20]

The author is particularly indebted to Professor Hiroshi Azumi and Professor Yoshito Amako for their discussions with him.

*The College of General Education*
*Tohoku University*
*Kawauchi, Sendai*

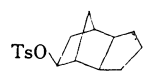
21) S. Nagakura, *J. Chem. Phys.*, **23**, 1441 (1955).
22) J. Tanaka, S. Nagakura and M. Kobayashi, ibid., **24**, 311 (1956).

# The Solvolysis of 5, 6-Trimethylene-2-norbornyl *p*-Toluenesulfonates. Evidence for the Formation of Classical Carbonium Ion Intermediates in the Solvolysis

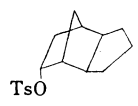
By Ken'ichi TAKEUCHI, Takao OSHIKA and Yuzo KOGA

(Received November 27, 1964)

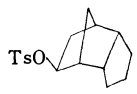
Kinetic studies of the solvolysis of four isomeric 5, 6-trimethylene-2-norbornyl *p*-toluenesulfonates (I, II, III and IV) were carried out by Bartlett and Barnes.[2] These authors observed that these isomers obeyed good first-order kinetics in glacial acetic acid, absolute ethanol, and 80% ethanol, and that the first-order rate constants were different with each isomer.



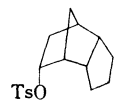

I




II

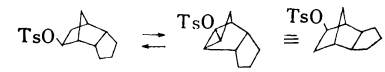



III




IV

These results have been interpreted as indicating that the isomers are not interchanged during solvolysis.[2b,3] However, Winstein and Trifan observed that the rate of the racemization of optically-active *exo*-2-norbornyl *p*-bromobenzenesulfonate exceeds the rate of the formation of *p*-bromobenzenesulfonic acid.[4] This was explained by the mechanism involving internal return. Accordingly, when we consider the solvolyses of I and III, it is conceivable that isomerization between I and III would occur.




(III) (I)

On the other hand, Cristol and his coworkers[3] reported that the addition of methanol to *endo*- and *exo*-5, 6-trimethylenenorbornene, in the presence of sulfuric acid, yielded products with different compositions. This seems to suggest that two different precursors exist in these systems.

The purposes of this study were to test the previous work[2] and to clarify the behavior of I and III during solvolysis. We also hoped to examine the propriety of explaining the solvolysis of these systems by the non-classical carbonium ion mechanism which has been proposed by Bartlett and Barnes.[2]

1) Presented at the 17th Annual Meeting of the Chemical Society of Japan, Tokyo, April, 1964.

2) a) R. S. Barnes, Ph. D. Thesis, Harvard University, 1951; b) P. D. Bartlett, Abstracts of Papers, 12th National Organic Chemistry Symposium, June, 1951, p. 1.

3) S. J. Cristol, W. K. Seifert, D. W. Johnson and J. B. Jurale, *J. Am. Chem. Soc.*, **84**, 3918 (1962).

4) S. Winstein and D. Trifan, ibid., **74**, 1154 (1952).

## Results and Discussion

**The Preparation and Characterization of *endo*-5, 6-Trimethylene-*exo*-2-norbornyl *p*-Toluenesulfonate (III).**—The *p*-toluenesulfonate III was prepared by the usual method of treating the corresponding alcohol with *p*-toluenesulfonyl chloride in pyridine at 0°C overnight.

Surprisingly enough, the III synthesized by us exhibited a melting point of 76.5—77.0°C instead of 48—49°C or 49—50.5°C, as Bartlett and Barnes[2] or Cristol et al.[3] respectively had reported. The analytical data agreed well with the calculated values, and NMR and infrared spectra also showed that our III should have the assigned structure.[5] A detailed investigation of the melting-points diagram of the mixtures of I and III, as shown in Fig. 1, indicated that an eutectic mixture has a melting point of ca. 50°C.

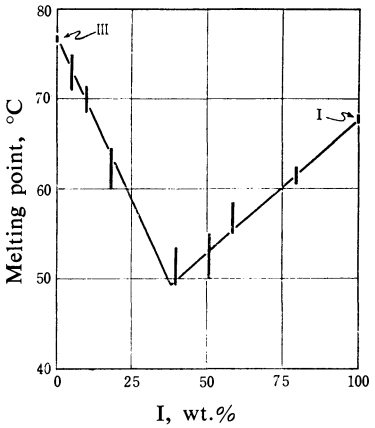



Fig. 1. Melting point diagram for mixtures of I and III.

These results suggested that the III prepared by the authors was pure, while those described in previous articles[2,3] were mixtures of I and III.

**The Kinetics of the Solvolyses of I and III in Methanol.**—The solvolyses of I and III were followed titrimetrically to approximately 90% completion in methanol at 59.7°C. The plots of $\log a/(a-x)$ vs. the reaction time for the methanolyses of I and III are shown in Fig. 2.

In the case of I, the first-order plot was almost linear to about 53% reaction, but afterwards a slight upward drift was observed.[6] On the other hand, the first-order plot for III showed a considerable downward drift to 44% reaction,[7] and then it became linear, which was nearly parallel to what had been calculated

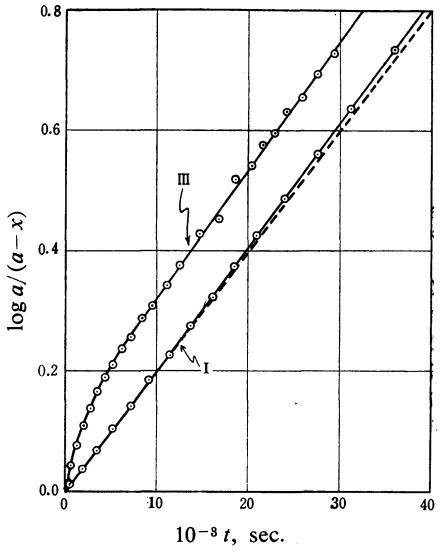
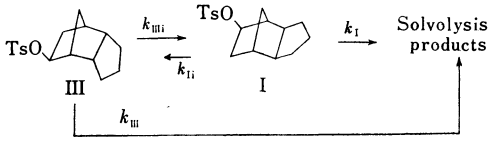



Fig. 2. Solvolysis rates of I and III in absolute methanol at 59.7°C.
[Tosylate]$_0$=0.1000 M

for I between 50 and 90% reaction. These observations suggested that III solvolyzed and isomerized simultaneously in methanol and that isomerization was essentially complete by approximately 44% reaction. This was verified by isolating unsolvolyzed *p*-toluenesulfonate and by observing its melting point and infrared spectrum

The solvolytic behavior of the isomeric *p*-toluenesulfonates I and III are summarized by the following scheme:




Scheme 1

That the first-order plot for the solvolysis of I showed a slight upward drift after 53% reaction indicates that a small portion of I also isomerized to III.

This behavior is very analogous to the solvolysis of $\alpha,\alpha$-dimethylallyl chloride, which proceeds with a concurrent intramolecular isomerization to primary chloride $\gamma,\gamma$-dimethylallyl chloride;[8] thus, the same kinetic procedure was used in this work to calculate the

5) See "Experimental" section.

6) Similar trends were observed for the solvolyses in acetic acid and ethanol.

7) In acetolysis, the first-order plot became linear after about 23% reaction, and in ethanolysis, after about 29% reaction.

8) W. G. Young, S. Winstein and H. L. Goering, *J. Am. Chem. Soc.*, **73**, 1958 (1951). Similar behavior was found in the solvolysis of bicyclo(2.2.2)octan-2-yl *p*-toluenesulfonate (H. L. Goering and M. F. Sloan, *J. Am. Chem. Soc.*, **83**, 1992 (1961)) and of *exo*-4-*syn*-8-dichlorodibenzobicyclo(3.2.1)octadiene (S. J. Cristol and D. D. Tanner, *J. Am. Chem. Soc.*, **86**, 3122 (1964)).

specific rate of the solvolysis of III and that of the isomerization of III to I. Table I gives the data for a representative kinetic run for III.

TABLE I. SOLVOLYSIS RATE OF III IN ABSOLUTE METHANOL AT 59.7°C

| Time sec. | Tosylate $10^2$M | $10^5 k$ $sec^{-1}$ a) | $10^5 k_{IIIe}$ $sec^{-1}$ b) |
|---|---|---|---|
| 0 | 10.00 | (16.9) c) | |
| 240 | 9.62 | 15.9 | |
| 480 | 9.27 | 15.0 | |
| 720 | 8.96 | 13.7 | |
| 960 | 8.69 | 12.7 | |
| 1200 | 8.44 | 11.8 | |
| 1440 | 8.21 | 11.3 | |
| 1680 | 8.00 | 10.8 | |
| 1920 | 7.80 | 10.1 | |
| 2160 | 7.62 | 9.72 | |
| 2400 | 7.45 | 9.09 | |
| 6000 | 5.84 | 5.49 | |
| 11040 | 4.55 | | 4.80 |
| 12600 | 4.20 | | 4.93 |
| 14820 | 3.73 | | 5.05 |
| 20400 | 2.87 | | 4.87 |
| 21600 | 2.66 | | 5.02 |
| 22800 | 2.53 | | 4.94 |
| 24300 | 2.34 | | 4.97 |
| 25800 | 2.21 | | 4.87 |
| 29400 | 1.87 | | 4.84 |
| | | Mean: | $4.92\pm0.08$ |

a) Instantaneous first-order rate constant.
b) Values obtained from integrated equation for a first-order reaction, using a starting point after equilibration is attained: $t=8400$ sec.; [Tosylate]$=0.0515$ M.
c) Extrapolated value.

By extrapolating the instantaneous rate constants to 0% reaction, the first-order rate constant for solvolysis ($k_{III}$) was estimated to be approximately $16.9\times10^{-5}$ $sec^{-1}$. The rate constant after equilibration was calculated from the integrated equation ($k_{IIIe}=(1/t)\ln a/(a-x)$), using a starting point after equilibration had been attained. The estimated value was $(4.92\pm0.08)\times10^{-5}$ $sec^{-1}$. On the other hand, the first-order rate constant for isomerization ($k_{IIIi}$) was found to be approximately $37\times10^{-5}$ $sec^{-1}$ by calculating ($k_{III}+k_{IIIi}$) (the procedure is shown in Fig. 3).

For the methanolysis of I, the rate constants before 50% ($k_I$) and after 55% reaction ($k_{Ie}$) were calculated to be $(4.59\pm0.03)\times10^{-5}$ and $(4.81\pm0.04)\times10^{-5}$ $sec^{-1}$ respectively. From these rate constants, the mole fraction of III, $F$, after equilibration was calculated from Eq. 1[8] to be 2—3%;

$$F=(k-k_I)/(k_{III}-k_I) \quad (1)$$

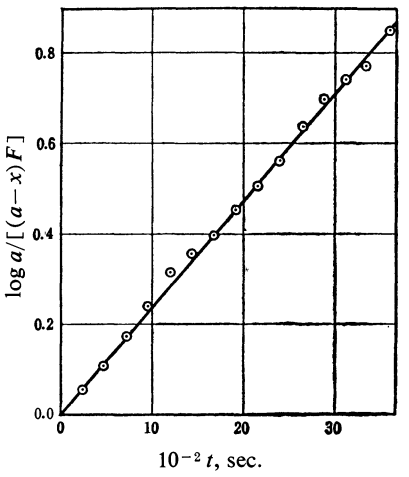



Fig. 3. Calculation of ($k_{III}+k_{IIIi}$) for the methanolysis of III at 59.7°C.
$F=(k-k_I)/(k_{III}-k_I)$ : cf. Ref. 8
$k_{III}+k_{IIIi}=54\times10^{-5}$ $sec^{-1}$

where $k$ is $k_{Ie}$ or $k_{IIIe}$.

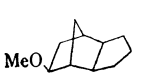
The first-order rate constants of the solvolyses and isomerizations of I and III are summarized in Table II.

TABLE II. SUMMARY OF THE FIRST-ORDER RATE CONSTANTS FOR METHANOLYSES OF I AND III AT 59.7°C

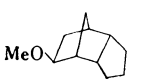
[Tosylate]$_0=0.1000$ M

| $10^5 k$, $sec^{-1}$ | Remark |
|---|---|
| $k_{IIIi}=37$ | Isomerization |
| $k_{Ii}=0$ | Isomerization |
| $k_I=4.59\pm0.03$ | Solvolysis (Initial rate) |
| $k_{III}=16.9$ | Solvolysis (Initial rate) |
| $k_{Ie}=4.81\pm0.04$ | Solvolysis (After equilibration) |
| $k_{IIIe}=4.92\pm0.08$ | Solvolysis (After equilibration) |

**The Distributions of Products from Methanolyses of *exo*- and *endo*-5, 6-Trimethylene-*exo*-2-norbornyl *p*-Toluenesulfonates (I and III).**— The distributions of products from methanolyses of I and III at an infinite reaction time have been investigated by Cristol et al.[3,9] by means of the v. p. c. technique; it has thus been revealed that the products are composed of a large portion of V and a small portion of VI, and that no other product is yielded. These authors reported that I and III yielded VI in essentially identical amounts.




V




VI

In the present study, the distributions of products from the methanolyses of I and III

Table III. Percentages of VI in the products from methanolyses of I and III at 59.7°C

$[Tosylate]_0=0.1000$ M

| Titrimetric conv., % | Tosylate I | Tosylate III |
|---|---|---|
| 5 | — | 7.3 |
| 10 | — | 7.1 |
| 20 | — | 6.4 |
| 30 | 3.2 | 6.3 |
| 50 | 3.3 | 6.3[a] |
| | | 5.9[a] |
| 100 | 3.2 | 4.4 |
| | | 4.6[a] |
| | | 4.3[a] |

a) Methanolysis in the presence of 0.101 M NaOMe.

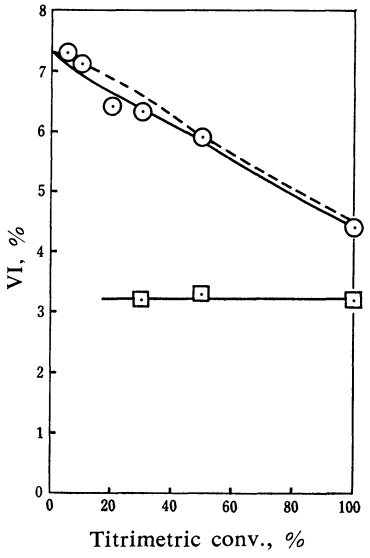


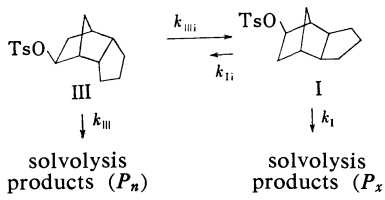

Fig. 4. Percentages of VI in the products from methanolyses of I and III at 59.7°C.
⊙, from III; ⊡, from I;
Dotted line, calculated by Eq. 5

at various percentages of reaction were also determined by the v.p.c. technique. The products were composed of a large portion of V and a small portion of VI; no other product was detected. The results are shown in Table III and Fig. 4.

The distributions of products at an infinite reaction time differed between isomeric *p*-toluenesulfonates I and III; moreover, in the case of III, the percentage of VI in the solvolysis products decreased from 7.3% at 5% reaction to 4.4% at completion (100%). On the other hand, VI in the products from the methanolysis of I was approximately constant (ca. 3.2%) throughout the reaction.

These results show that the distribution of the direct products from III is different than in the case of I. The decrease in the percentage of VI obtained from the methanolysis of III may be attributed to the occurrence of the solvolysis of I which was formed from III through isomerization.

These results were further confirmed by being duplicated with those of isomerization as follows. The solvolytic behavior of III may be described by the following scheme:




Scheme 2

Since it is reasonable to assume $k_{I_i}$ to be negligibly small, the sum ($x$) of isomerized and solvolyzed III may be obtained by Eq. 2, where $a$ is the initial concentration of III:

$$x=a(1-e^{-(k_{III_i}+k_{III})t}) \quad (2)$$

Then the concentration of $P_n$ is defined by Eq. 3:

$$P_n=a(k_{III}/(k_{III_i}+k_{III}))(1-e^{-(k_{III_i}+k_{III})t}) \quad (3)$$

By dividing $P_n$ by the titrimetric conversion, it is possible to derive the fraction of product which is produced from III itself, which is given by Eq. 4:

$$P_n/(P_n+P_x)=\frac{(k_{III}/(k_{III_i}+k_{III}))(1-e^{-(k_{III_i}+k_{III})t})\times 10^2}{\text{Titrimetric conversion (\%) at time } t} \quad (4)$$

When we estimate that the VI values in $P_n$ and $P_x$ are 7.3 and 3.2% respectively, by means of extrapolation in Fig. 4, it is possible to estimate the percentage of VI in the products at any reaction time by Eq. 5:

$$\text{VI in the solvolysis products (\%)}=7.3(P_n/(P_n+P_x))+3.2(1-(P_n/(P_n+P_x))) \quad (5)$$

These values were calculated and are plotted with a dotted line in Fig. 4, a line which is in good agreement with the observed values.

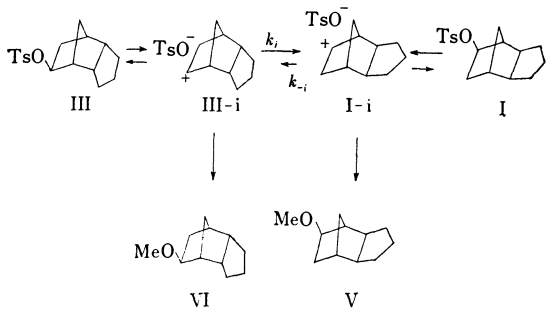
**The Mechanism of the Solvolyses of *exo*- and *endo*-5, 6-Trimethylene-2-norbornyl *p*-Toluenesulfonates (I and III).**—The results of the distributions of products suggest that the intermediates are classical carbonium ions. A reasonable reaction mechanism would be as follows:

9) The melting point of III used by these authous was 49—50.5°C.

TABLE IV. FIRST-ORDER RATE CONSTANTS FOR SOLVOLYSES OF FOUR ISOMERIC *p*-TOLUENESULFONATES

| *p*-Toluene-sulfonate | Solvent | Temp. °C | $k$ $10^5$ sec$^{-1}$ | $\Delta H^{\neq}$ kcal./mol. | $\Delta S^{\neq}$ e. u. | Relative rates for methanolysis at 74.8°C | | |
|---|---|---|---|---|---|---|---|---|
| I | AcOH | 74.8 | 21.9 | | | | | |
| | | 50.1 | 1.11 | 26.3 | 0.0 | | | |
| | MeOH | 74.8 | 25.3 | | | 1.00 | 10.4 | 40.6 |
| | | 59.7 | 4.59 | | | | | |
| | | 50.1 | 1.35 | 25.8 | −1.1 | | | |
| | EtOH | 99.5 | 45.1 | | | | | |
| | | 74.8 | 3.65 | 25.5 | −5.7 | | | |
| II | AcOH | 99.5 | 30.9 | | | | | |
| | | 74.8 | 2.32 | 26.3 | −4.4 | | | |
| | MeOH | 99.5 | 30.8 | | | | | |
| | | 74.8 | 2.44 | 25.8 | −5.9 | 0.0965 | 1.00 | 3.92 |
| | EtOH | 99.5 | 8.46 | | | | | |
| | | 74.8 | 0.694 | 25.4 | −9.4 | | | |
| III | MeOH | 59.7 | 16.9[a] | | | | | |
| | | 39.8 | 1.30[a] | 26.0 | −2.2 | | | |
| | | (74.8) | (97.3)[b] | | | 3.84 | 39.9 | 156 |
| IV | AcOH | 99.5 | 12.1 | | | | | |
| | | 74.8 | 0.803 | 27.6 | −2.8 | | | |
| | MeOH | 99.5 | 8.63 | | | | | |
| | | 74.8 | 0.623 | 26.7 | −5.8 | 0.0246 | 0.255 | 1.00 |
| | EtOH | 124.8 | 24.6 | | | | | |
| | | 99.5 | 2.19 | 27.5 | −6.7 | | | |

a) Initial rate. b) Extrapolated from the values at other temperatures.




Scheme 3

The fact that the isomerization of III to I is much faster than the reverse may be explained by assuming that III-i isomerizes to I-i faster than the reverse; i. e., $k_i \gg k_{-i}$. This is supported by the fact that *exo*-trimethylenenorbornanes are more stable than their *endo*-counterparts to the extent of 2—3 kcal./mol.[10] A common non-classical carbonium ion VII cannot account for the quite different distribution observed in the products from I and III. In addition, it appears difficult to account for the very large amount of V in the product (97% V, 3% VI) on the basis of a highly selective opening of the non-classical ion, VII. On the other hand, the marked difference in the stabilities of the two classical ions (or ion-pairs), III-i and I-i, provides a simple, plausible explanation for the observed



VII

distribution.

**The Solvolysis Rates of Four Isomeric 5, 6-Trimethylene-2-norbornyl *p*-Toluenesulfonates (I, II, III and IV).**—Although the kinetics of the solvolysis of these four isomers had been extensively studied by Bartlett and Barnes,[2] it seemed necessary to investigate them again, this time using the *p*-toluenesulfonates prepared by us. The results are summarized in Table IV. The solvolyses of II and IV obeyed good first-order kinetics, no trend of isomerization being observed.

In the last column of Table IV, the relative rates of the methanolysis of the four isomers at 74.8°C are given. A comparison of the rate ratio of 10.4 for I to II with that of 156 for III to IV suggests that the trimethylene group in III assists ionization, while that in IV retards it. This is also verified by the finding that $k_{III}/k_I$ is 3.84, while $k_{IV}/k_{II}$ is only 0.255. Apparently the retarding effect by the trimethylene group in IV should be attributed to a steric hindrance toward the leaving TsO-group.[11]

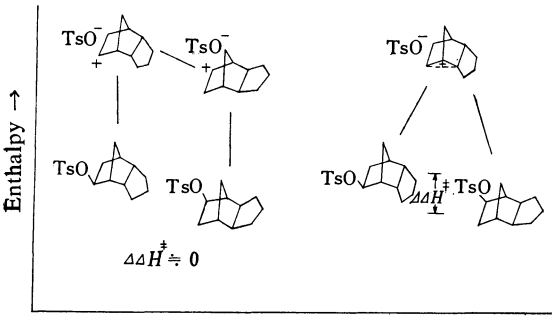
10) L. Kaplan, H. Kwart and P. von R. Schleyer, *J. Am. Chem. Soc.*, **82**, 2341 (1960), footnote 15.

11) A similar interpretation has been made for the solvolysis of the *endo*-2-norbornyl system, in which the steric hindrance by the hydrogen atoms at the 5- and 6-carbons toward the leaving group was considered. H. C. Brown, F. J. Chloupek and Min-Hon Rei, *J. Am. Chem. Soc.*, **86**, 1248 (1964).

With respect to the activation enthalpy $\Delta H^{\neq}$, I has about the same value as III. This fact supports the theory that the intermediate is different with each isomer; that is, if the intermediate is common to two isomers, some higher $\Delta H^{\neq}$ for I may be expected. As the schemes show, the approximately identical values of $\Delta H^{\neq}$ for I and III can be explained only by assuming two classical carbonium ions. It has also been reported that anchimeric assistance is but slight in the case of I.[12]

Scheme 4. Classical ions

Scheme 5. Non-classical ions




**The Distributions of Products from Methanolyses of *endo*- and *exo*-5,6-Trimethylene-*endo*-2-norbornyl *p*-Toluenesulfonates (II and IV).**— The finding that the solvolyses of II and IV obeyed good first-order kinetics shows that these *p*-toluenesulfonates do not isomerize to any other isomers, which is in accord with the solvolysis of *endo*-2-norbornyl *p*-bromobenzenesulfonate, in which no internal return was observed.[13] Accordingly, the products of the solvolysis of II and IV at completion (100%) give exactly the distribution of products from II and IV respectively.

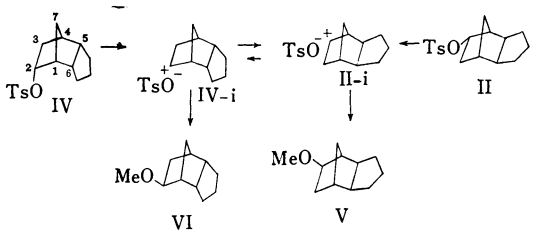
TABLE V. PERCENTAGES OF VI IN THE PRODUCTS FROM METHANOLYSES OF FOUR ISOMERIC *p*-TOLUENESULFONATES

$[\text{Tosylate}]_0 = 0.1000$ M

| | *p*-Toluenesulfonates | | | |
|---|---|---|---|---|
| | I | II | III | IV |
| Reaction temp., °C | 59.7 | 74.8 | 59.7 | 74.8 |
| % Reaction | 100 | 100 | 0[a] | 100 |
| VI in products, % | 3.2 | 1.6 | 7.3[a] | 23.4 |

a) Extrapolated to 0% reaction in Fig. 4.

The results are shown in Table V, where they are compared with those from I and III. In all cases, the products were composed of V and VI. The finding that IV yielded 23% of VI may be explained by the mechanism by which the reaction proceeds through ion pairs with classical structures. The finding that the percentage of VI from IV was greater than that from III may be explained by assuming that the $C_1-C_6$ bond migration is hindered by the departing $TsO^-$ and also that the attack by the solvent molecule from the *exo*-direction is more favored for IV-i than for III-i.




## Experimental[14]

**Materials.**—Four isomeric 5,6-trimethylene-2-norborneols (VIII, IX, X and XI) were prepared by the methods described in early articles. *exo*-5,6-Trimethylene-*exo*-2-norborneol (VIII) was prepared by adding water to *endo*-dicyclopentadiene in the presence of sulfuric acid,[15] followed by hydrogenation in the presence of platinum(IV) oxide in ethanol at room temperature; m. p. 51.5—53.5°C (reported,[3] 53—54°C).

*exo*-5,6-Trimethylene-*endo*-2-norborneol (IX) was prepared by the oxidation of VIII to ketone with Chromium(VI) oxide in acetic acid, b. p. 105—106°C/12 mmHg (reported,[2a] 113.5—116.5°C/19 mmHg), $n_D^{20}$ 1.5024[16] (reported,[2a] $n_D^{24}$ 1.5152), followed by reduction with lithium aluminum hydride, b. p. 113—114°C/11.5 mmHg (reported,[2a] 129°C/24 mmHg), $n_D^{20}$ 1.5136, *p*-nitrobenzoate, m. p. 107.5—108.5°C (reported,[2b] 108—109°C). *endo*-5,6-Trimethylene-*exo*-2-norborneol (X) was prepared by the method described by Cristol et al.,[17] via the reaction of NBS with *exo*-5,6-trimethylenenorbornene derived from VIII, m. p. 80.0—80.8°C (reported,[17] 80.5—81.5°C), *p*-nitrobenzoate, m. p. 128—128.5°C (reported, 123—124°C,[2b] 129.5°C[17]). *endo*-5,6-Trimethylene-*endo*-2-norborneol (XI) was prepared by the oxidation of X to ketone with chromium trioxide in acetic acid, followed by reduction with lithium aluminum hydride; m. p. 113.5—115.0°C (reported, 89—90°C,[2a] 120—121°C[18]). The alcohols VIII, IX and X were proved not to be contaminated with other isomeric alcohols on v. p. c. analyses. Analyses were carried out with a Perkin-Elmer vapor phase fractometer, model 154-D, on a 1/4″×2 m. (4 m. in the case of X)

12) P. von R. Schleyer, ibid., **86**, 1856 (1964).
13) S. Winstein and D. Trifan, ibid., **74**, 1147 (1952).
14) All melting points were observed in capillary tubse by heating them in a sulfuric acid bath and were then corrected.
15) H. A. Bruson and T. W. Riener, *J. Am. Chem. Soc.*, **67**, 723 (1945).
16) In repeated oxidation experiments, the authors observed a $n_D^{21}$ value of 1.5018.
17) S. J. Cristol, W. K. Seifert and S. B. Soloway, *J. Am. Chem. Soc.*, **82**, 2351 (1960).
18) Although Bruson and Riener did not confirm the structure, the compound they synthesized was probably XI. See Ref. 14.

stainless steel column packed with "R" Ucon oil LB-550-X. The alcohols showed the following retention times under the respective corresponding conditions; VIII, 81.2 min.; X, 92.0 min. at 150°C with a helium flow of 72 cc./min.; and IX, 79.9 min. at 190°C with a helium flow of 40 cc./min. The analysis of XI has not been carried out.

Four isomeric *p*-toluenesulfonates (I, II, III and IV) were prepared by treating the above alcohols with *p*-toluenesulfonyl chloride in pyridine at 0°C overnight. All the *p*-toluenesulfonates, with the exception of II, were recrystallized three times from *n*-hexane: m. p.: I, 67.5—67.8°C (reported, 60—61°C,[2] 65.3—67.5°C[3]); II, liq. (reported,[2] liq.); III, 76.5—77.0°C (reported, 48—49°C,[2] 49—50.5 °C[3]); IV, 54.0—55.0°C (reported,[2] 59.5—60°C). Anal. for III, calcd. for $C_{17}H_{22}O_3S$; C, 66.63; H, 7.24; S, 10.46; solvolysis equiv., 306.42; molecular weight, 306.42. Found; C, 67.11; H, 7.71; S, 10.29; solvolysis equiv., 301; molecular weight, 310 (determined by vapor pressure osmometer model 301 A, Mechrolab Inc.). II was used without any purification.

Methanol and ethanol were dried by refluxing them over the corresponding magnesium alkoxide for 10 hr. and then distilled carefully. Anhydrous acetic acid was prepated by refluxing reagent-grade acetic acid with the calculated amount of acetic anhydride for 10 hr. and by subsequent distillation. They were stored under an argon atmosphere.

**The Mixed Melting Points of I with III.**—About 50-mg. portions of mixtures of I and III were prepared. The melting points were observed in capillary tubes by heating these portions in a sulfuric acid bath.

**Infrared Spectra Measurements.**—The infrared spectra of the *p*-toluenesulfonates (I, II, III and IV), corresponding alcohols (VIII, IX, X and XI), corresponding methyl ethers and tetrahydro-*endo*-dicyclopentadiene were taken in 0.1 M carbon disulfide; it was thus revealed that the compounds posessing an *endo*-trimethylene group exhibited a characteristic peak at 1250 $cm^{-1}$.

**NMR Spectra Measurements.**[19]—Proton NMR spectra of I, III and tetrahydro-*endo*-dicyclopentadiene were run at 20±2°C on a Japan Electron Optics Lab., model JNM-C-60, high-resolution spectrometer at 60 Mc. in carbon tetrachloride solutions, using tetramethylsilane as an internal standard. The spectra of III and tetrahydro-*endo*-dicyclopentadiene exhibited characteristic peaks between $\tau$=8.7 and 8.3, whereas I exhibited a broad peak between $\tau$=9.5 and 8.8 which was not observed in either III or tetrahydro-*endo*-dicyclopentadiene. The complete analysis of the NMR spectra has not been carried out.

**Kinetic Measurements.** — The sealed ampoule technique was emloyed. Methanolysis and ethanolysis were followed by titrating produced *p*-toluenesulfonic acid with standard sodium ethylate in ethanol, using bromocresol purple as an indicator. Acetolysis was followed by titrating with standard sodium acetate in acetic acid, using crystal violet as an indicator. Several infinity titers showed the purities of the *p*-toluenesulfonates to be; I, 99.2%; II, 96.2%; III, 99.0%; IV, 99.2%.

**The Isolation of the Unsolvolyzed *p*-Toluenesulfonate in the Methanolysis of III.**—A solution of 733 mg. (2.5 mmol.) of III in 25 ml. of absolute methanol was heated in an ampoule at 59.7°C in a constant temperature bath. After 184 min. (55% reaction), the reaction mixture was cooled at 0°C and poured into 100 ml. of ice-water. Unsolvolyzed *p*-toluenesulfonate, separated as fine crystals, was isolated by filtration and washed with two 5-ml. portions of water and dried in a vacuum desiccator. The yield was 198 mg. (60% of theor.); m. p. 66—67°C. The infrared spectrum (0.1 M in carbon disulfide) agreed exactly with that of an authentic sample (I) in the 650—4000 $cm^{-1}$ range.

**The Analysis of the Products from the Methanolyses of Four Isomeric *p*-Toluenesulfonates (I, II, III and IV).**—A solution (50 ml.) of the *p*-toluenesulfonates in anhydrous methanol (0.1000 M) was divided into several portions (5—25 ml.), placed in ampoules, and heated in a constant temperature bath. The reaction was stopped by cooling at various percentages of reaction, and the reaction mixture was poured into ice-water and extracted with two 5-ml. portions of *n*-pentane. The pentane extracts were combined, washed with a 10% sodium carbonate solution and water, and dried over sodium sulfate. After concentration to about half volume, the pentane solution was cooled to −50°C in order to crystallize the unsolvolyzed *p*-toluenesulfonate. After the solution had stood overnight at that temperature, the pentane layer was decanted and concentrated to about 0.5 ml. The v. p. c. analyses of the products, methyl ethers, were carried out with a Perkin-Elmer vapor phase fractometer, model 154-D, on a 1/4"×4 m. stainless steel column packed with "R" Ucon oil LB-550-X at 190°C and with a helium flow of 40 cc./min. The ethers V and VI showed retention times of 37.2 and 40.1 min. respectively. The percentage compositions of a mixture were determined by measuring the peak areas of the chromatogram by the triangularization method. Analytical data were reproducible to about ±0.3%.

The authors wish to thank Professor Herbert C. Brown for his many helpful suggestions, Dr. Kunio Okamoto for his valuable discussions, and Mr. Hiroshi Wakida for his measurements of the solvolysis rates.

*The Central Research Laboratory*
*Toa Nenryo Kogyo Co.*
*Ohi-mura, Iruma-gun, Saitama*

19) We are indebted to Mr. Kato for measuring the spectra.

# Studies on Amino-hexoses. VIII. The Fischer Synthesis of Methyl D-Glucosaminides

By Yoshio MATSUSHIMA and Tsuyoshi MIYAZAKI

(Received December 4, 1964)

The Fischer synthesis of methyl glycosides using methanolic hydrogen chloride[1] seems to have failed in the case of glucosamine[2] because the positive charge on the amino-sugar repels the catalyst proton. Some of the known ways of glucosaminide synthesis detour to *N*-benzyloxycarbonyl- or *N*-acetylglucosamine, which do not have a cationic nature. The fission of the benzyloxycarbonyl group by catalytic hydrogenation[2] or by reduction with sodium in liquid ammonia[3] after the Fischer glycosidation regenerates the free amino group. *N*-Deacetylation by hydrazinolysis of methyl *N*-acethylglucosaminide also provides a way to methyl glucosaminide.[4]

As has been mentioned above, the glycosidation reaction of the amino-sugar may be slow under the usual conditions of the Fischer method, but the reaction will be appreciably accelerated when the reactants and the catalyst are brought to a satisfactorily high concentration. As one of way of realizing the idea, the authors treated glucosamine and excess methanol with an excess amount of a strong cation exchanger, which combines glucosamine through the salt linkage and limits the site of the reaction to the surface of the resin only, thus bringing the reactants and the catalyst close to one another. As will be shown in the Experimental section below, D-glucosamine hydrochloride was converted, in a considerably high yield, into a methyl glucosaminide mixture, of the components of which methyl 2-amino-2-deoxy-$\alpha$- and $\beta$-D-glucopyranoside were unambiguously identified after separation by the recently-developed column chromatography using Dowex-1 X 4 free base resin.[5] The probable formation of the two furanosides was inferred from paper chromatographic and other physical data.

## Experimental

**Glycosidation.**—A mixture of 15 g. D-glucosamine hydrochloride, 150 g. of dried Amberlite IR-120 ($H^+$-form, 200—400 mesh) and 1500 ml. of absolute methanol was refluxed while being mechanically stirred for 10 hr. The reaction mixture was then poured into a glass tube 5.5 cm. in diameter, and the methanol was sucked off. After the resin had been washed with absolute methanol, the glycoside mixture was eluted with methanolic ammonia. The evaporation in vacuo of the eluted solution (1600 ml.) gave 13.1 g. of a brown syrup. It was found by the Somogyi method[6] that the syrup contained reducing sugar, corresponding to 2.3 g. of glucosamine hydrochloride, which had escaped the glycosidation.

**The Separation of the Glycoside Mixture by Column Chromatography.**—Thirteen grams of the above-mentioned syrup in 30 ml. of water was placed in a Dowex-1 X 4 column ($OH^-$-form, 200—400 mesh) 55 cm. high by 3.7 cm. in diameter and was eluted with water. Each 10 ml. of the fraction was then collected, and the elution was traced by optical rotation measurements. After the elution pattern had been established, the appropriate fractions were combined and evaporated in vacuo, and the specific rotation of each combined fraction, A to I (as shown in Fig. 1), was measured. The recovery of the glycosides was 7.8 g. This corresponded to about 70% of the total non-reducing material obtained. The reducing sugar which escaped the

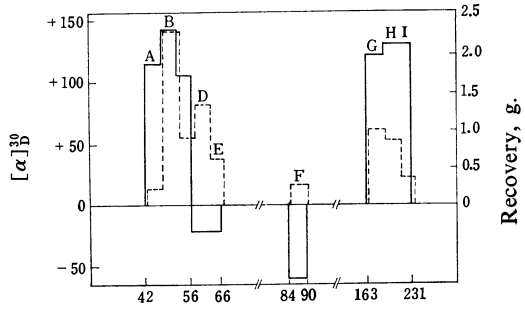



Fig. 1. The separation of the glycosidation products by the column chromatography using Dowex-1 X 4 ($OH^-$-form) resin.
Solid line: specific rotation; broken line: recovery in grams

1) E. Fischer, *Ber.*, **26**, 2400 (1893).
2) A. Neuberger and R. P. Rivers, *J. Chem. Soc.*, **1939**, 122.
3) A. B. Foster, D. Horton and M. Stacey, ibid., **1957**. 81.
4) M. Fujinaga and Y. Matsushima, This Bulletin, **37**, 468 (1964).
5) Y. Matsushima, T. Miyazaki and J. T. Park, *J. Biochem.*, **54**, 109 (1963); P. W. Austin, F. E. Hardy, J. G. Buchanan and J. Baddiley, *J. Chem. Soc.*, **1963**, 5350; Y. Matsushima and T. Miyazaki, *J. Biochem.*, **55**, 464 (1964).
6) M. Somogyi, *J. Biol. Chem.*, **195**, 19 (1952).

glycosidation was supposed to have changed to some acidic substance during contact with the strong base resin[7] and to have been retained in the column. Of fractions A to I, only fraction B was obtained as a crystalline material; the others were all a brown syrup.

**Methyl 2-Amino-2-deoxy-α-D-glucopyranoside.**—The raw crystalline material (2.1 g) obtained from fraction B was recrystallized using absolute ethanol. The colorless crystals obtained weighed 1.6 g. and melted at 155—159°C alone or at 154—159°C on admixture with an authentic specimen[4]. $[\alpha]_D^{30}$ +159.8 (*c* 1.01, water).

Found: C, 43.65; H, 7.92; N, 7.32. Calcd. for $C_7H_{15}O_5N$: C, 43.51; H, 7.82; N, 7.25%.

**Methyl 2-Benzyloxycarbonylamino-2-deoxy-α-D-glucopyranoside.**—A solution of 0.4 g. of methyl 2-amino-2-deoxy-α-D-glucopyranoside in 15 ml. of water was mixed with 0.4 g. of sodium bicarbonate and 0.4 g. of benzyloxycarbonyl chloride. The reaction was continued for 2.5 hr. at room temperature while the mixture was being mechanically stirred. The crystals thus obtained were washed with chloroform. The specimen melted at 158—160°C alone or at 153—158°C on admixture with a sample prepared by the literature method.[2,4] $[\alpha]_D^{30}$ +100.2[5] (*c* 1.04, pyridine)

Found: C, 54.72; H, 6.50; N, 4.25. Calcd. for $C_{16}H_{21}O_7N$: C, 55.04; H, 6.47; N, 4.28%.

Another crop, with essentially the same physical constants, was obtained from the mother solution. The total yield was 0.57 g.

**Methyl 2-Amino-2-deoxy-β-D-glucopyranoside.**—An absolute ethanol solution of 0.45 g. of a syrup from fraction E gave a crystalline material when left standing for a long time in a refrigerator. The specimen melted at 130—132°C. $[\alpha]_D^{18}$ −40.7 (*c* 1.57, water)

Found: C, 43.31; H, 7.87; N, 7.29. Calcd. for $C_7H_{15}O_5N$: C, 43.51; H, 7.82; N, 7.25%.

The compound, on paper chromatography using two solvent systems, behaved in the exactly same way as the standard specimen[9] which was prepared by the deacetylation of methyl 2-acetamido-2-deoxy-β-D-glucopyranoside.

**Methyl 2-Benzyloxycarbonylamino-β-D-glucopyranoside.**—The syrup from fraction D was *N*-benzyloxycarbonylated by a method similar to that used for the corresponding α-isomer, and 1.2 g. of the syrup gave 1.3 g. of a crystalline material which melted at 165—167°C after recrystallization from ethanol. $[\alpha]_D^{30}$ −34.6 (*c* 1.00, pyridine) The melting point and the optical activity data are in good agreement with those in the literature.[2,3]

Found: C, 54.32; H, 6.49; N, 4.24. Calcd. for $C_{16}H_{21}O_7N$: C, 55.04; H, 6.47; N, 4.28%.

**Methyl 2-(2′, 4′-Dinitrophenyl)amino-2-deoxy-α-D-glucofuranoside.**—Ten milliliters of an aqueous solution of 0.3 g. of the syrup from fraction I was mixed with 0.2 g. of sodium carbonate and 0.3 g. of 2, 4-dinitrofluorobenzene in 3 ml. of acetone, and then the mixture was shaken overnight at room temperature. The reaction mixture was dried in vacuo, and the crystalline residue was successively washed with water and petroleum ether. Recrystallization from ethanol gave 0.12 g. of yellow crystals melting at 113—167°C. $[\alpha]_D^{27}$ +36.5 (*c* 0.96, acetone)

Found: C, 42.96; H, 4.11; N, 12.44. Calcd. for $C_{13}H_{17}O_9N_3$: C, 43.46; H, 4.78; N, 11.69%.

As the broad range of the melting points shows, the purification of the compound was unsatisfactory. Paper chromatography with *n*-butanol: ethanol: water (4: 1: 5) gave two spots, with $R_f$ values of 0.89 and 0.92 respectively. The literature[10] gave the following physical constants: m. p. 166—167°C; $[\alpha]_D^{18}$ +30.6 (*c* 1.0, acetone); $R_f$ 0.88 in the same solvent system.

**Methyl 2-Acetamido-2-deoxy-β-D-glucofuranoside.**—The syrup (0.22 g.) from fraction F was mixed with 20 ml. of acetic anhydride, 50 ml. of water and Dowex-1 X 4 ($OH^-$-form), and then the mixture was stirred at room temperature overnight. The resin was removed by filtration and washed with water. The filtrate and washing were combined and evaporated in vacuo. The syrup thus obtained was decolorized with a small amount of active charcoal and dried over phosphorus pentoxide. The syrup (0.18 g.) obtained failed to crystallize. $[\alpha]_D^{30}$ −20.9 (*c* 1.24, water). This syrup showed the same $R_f$ value (0.45) in the ascending paper chromatographic system (*n*-butanol: ethanol: water =4: 1: 5) as did the specimen obtained by the literature method.[11]

## Summary

The direct synthesis of methyl D-glucosaminides by proton catalysis using a strong cation exchanger has been investigated. The formation of the two anomeric pyranosides has been proved unambiguously. Also, the two anomeric furanosides, which have been obtained in an unsatisfactory purity, have been inferred, according to their physical constants, to have formed in the glycosidation reaction.

This investigation was supported by U. S. Public Health Service Grant No. AI-04586-03.

*Department of Chemistry*
*Osaka University*
*College of Science*
*Nakanoshima, Osaka*

7) J. D. Phillips and A. Pollard, *Nature*, **171**, 41 (1953); A. C. Hulme, ibid., **171**, 610 (1953).
8) M. L. Wolfrom, R. A. Gibbons and A. J. Huggard, *J. Am. Chem. Soc.*, **79**, 5043 (1957).
9) M. Fujinaga and Y. Matsushima, to be published.
10) P. F. Lloyd and M. Stacey, *Tetrahedron*, **9**, 116 (1960).
11) M. W. Whitehouse and P. W. Kent, ibid., **4**, 425 (1958).

# The Addition Reaction of Dinitrogen Trioxide with Cinnamyl Acetate

By Yoshie KURIHARA* and Kazuo YAMAGISHI**

(Received December 5, 1964)

A number of investigations[1-4] have been carried out into the reaction between dinitrogen trioxide and unsaturated compounds, and it is well known that the dimer of the nitro-nitroso compound is the main product in those reactions. In an earlier paper[5] from our laboratory, it was demonstrated, however, that not the nitro-nitroso compound but nitro-alcohol and nitro-olefin were formed in the reaction between methyl crotonate and dinitrogen trioxide. The present study was undertaken, firstly, to examine whether or not only the nitro-nitroso compound is obtained in the addition reaction of dinitrogen trioxide to cinnamyl acetate (I) and, secondly, to synthesize from the reaction products 2-amino-1-phenyl-1, 3-propanediol, which is an important intermediate for synthesizing chloramphenicol.

Fodor et al.[6] examined the reaction of dinitrogen trioxide with compound I according to the technique presented by Bruckner[3] and obtained the dimer of the nitro-nitroso compound, from which chloramphenicol could be derived. In the present study, however, through a close examination of this reaction under Bruckners condition, two reaction products were isolated; they are white and relatively stable crystals and unstable yellow oil. The crystalline substance was found, through its elemental analysis and through the fact that it becomes blue when dissolved in benzene, to be the dimer of the nitro-nitroso compound (IIa). Although the purification of the oily substance by vacuum distillation was unsuccessuful, it was purified chromatographically by the use of silica gel as the adsorbent. We assigned the structure IIb to the second oily product on the basis of the elemental analysis, its infrared spectrum and Liebermann's nitroso reaction, which indicated the presence of -NO and/or -ONO groups. The infrared spectrum of the oil indicated the presence of both -ONO (1659 $cm^{-1}$) and $-NO_2$ groups (1561 and 1367 $cm^{-1}$).[7] Compound IIb gradually lost nitrous acid at room temperature, forming $\beta$-nitro cinnamyl acetate (III). When the benzene solution of IIb was passed through a alumina column or warmed with sodium acetate for one or two hours, compound III, was quantitatively obtained. For the purpose of synthesizing 2-amino-1-phenyl-1, 3-propanediol, it is recommended that the crude product be directly transformed into compound III without isolation.

The ratio of IIa to IIb formed by the addition of nitrogen trioxide to cinnamyl acetate was greatly influenced by the solvent used and by the other experimental conditions. Toluene was the best among the solvents tried (i.e. toluene, ether and cyclohexane) for minimizing the product, IIb. The IIa/IIb ratio decreased progressively when the solvent was changed in the following order: toluene—cyclohexane—ether. With 20 mol. of toluene to cinnamyl acetate, the main product was IIa. The decrease in the amount of toluene greatly affected the relative amounts of IIa and IIb formed. For example, the use of less than 10 mol. of toluene yielded IIb in a greater quantity than IIa. When the reaction temperature was raised higher than 0°C, the formation of IIb also increased.

Compound IIa and compound III obtained from IIb underwent substitution or addition reaction to yield, finally, 2-amino-1-phenyl-1, 3-propanediol. Figure 1 illustrates the entire process adopted in this research. When IIa was treated with sodium methylate at 0°C, the nitroso group of IIa was converted into the methoxy group and compound IV was obtained in a 76% yield.

As an analogous reaction of this type, it was found in our laboratory that 1-methoxy-2-nitro-1-phenylethane (XI) was obtained directly

* Present address: Yokohama National University, Faculty of Engineering, Minami-ku, Yokohama.

** Present address: Dainippon Celluloid Co., Ltd., Central Research Laboratory, Oi-mura, Iruma-gun, Saitama-ken.

1) H. Wieland, *Ber.*, **36**, 2558 (1903).

2) H. Wieland, *Ann.*, **328**, 154 (1903); **329**, 239 (1903); **424**, 71 (1921).

3) V. Bruckner, ibid., **518**, 226 (1935).

4) V. Bruckner, G. Fodor, J. Kiss and J. Kovacs, *J. Chem. Soc.*, **1948**, 885; G. Fodor, J. Kiss and M. Szekerke, *J. Org. Chem.*, **15**, 227 (1950). The reaction between nitrogen oxide and unsaturated compounds was reviewed by J. L. Riebsomer, *Chem. Revs.*, **36**, 157 (1954).

5) K. Yamagishi and Y. Ishibiki, *J. Chem. Soc. Japan, Pure Chem. Sec. (Nippon Kagaku Zasshi)*, **81**, 971 (1960).

6) G. Fodor, I. Toth, E. Kovacs and J. Kiss, *Izvest. Akad. Nauk., U. S. S. R.*, 441 (1955).

7) L. J. Bellamy, "The Infrared Spectra of Complex Molecules," 2nd Ed., John Wiley & Sons, Inc., New York, N. Y. (1958), p. 298.

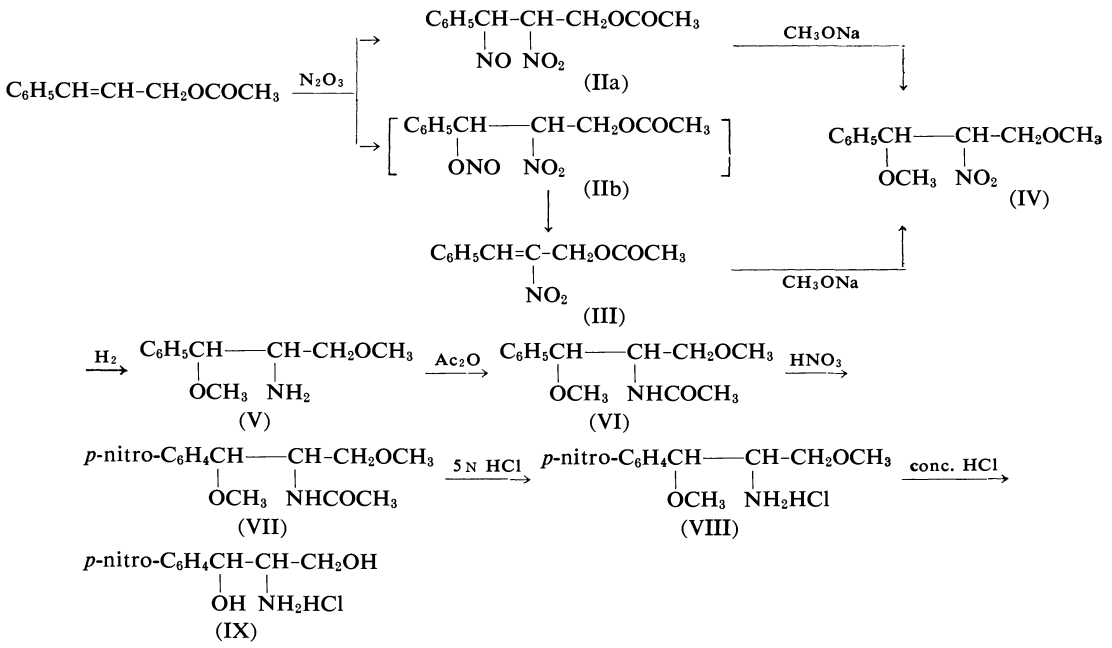
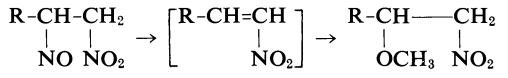


Fig. 1

in a good yield by the reaction of 1-nitroso-2-nitro-1-phenylethane (X) with sodium methylate. Meisenheimer[8] and Rosenmund[9] reported that ω-nitrostyrene (X′) reacted with sodium alcoholate to afford 1-alkoxy-2-nitro-1-phenylethane. Moreover, Wieland[1] described how compound X was transformed into compound X′ through treatment with sodium methylate. Therefore, it may be supporsed that the reaction between X and sodium methylate would proceed via ω-nitrostyrene, as is described below (1) :

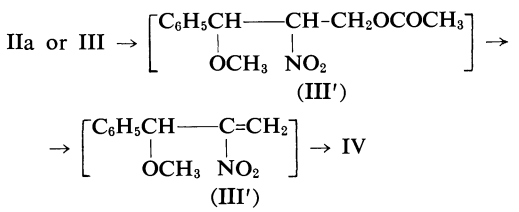


(X) (X′) (XI)

$R = C_6H_5$ (1)

When sodium methylate was added to compound III, the same reaction product IV was obtained. A new finding in this reaction was that the acetyl group of compound IIa or III was transformed into the methoxy group. Probably, with one mole of sodium methylate, IIa or III may be changed into compound III′ which then may be transformed into compound III″ by losing acetic acid,[10] and finally compound IV may be formed with the excess sodium methylate.

Compound IV was reduced to V in the presence of a Raney nickel catalyst in methyl



(III′)

alcohol at 40°C under the pressure of 110 atm. of hydrogen. Glittering white crystals (VI) were obtained by the acetylation of V. After the introduction of the nitro group at the para position of the benzene ring by the known method,[11] VII (m. p. 109—110°C) was obtained. Compound VII seems to be *dl-erythro*-2-acetoamido-1, 3-dimethoxy-1-(*p*-nitrophenyl)-propane, because Gabor et al.[11] reported that the melting point of the threo form of VII was 129—130°C. Compound VII was hydrolyzed into compound VIII with 5 N hydrochloric acid; then, after the hydrolysis of VIII with concentrated hydrochloric acid, white crystals were obtained. The melting point of this end product was 209°C, which agreed with the melting point of *dl-erythro*-2-amino-1-(*p*-nitrophenyl)-1, 3-propanediol hydrochloride.[12] As has been described above (reaction 1), the nitroso group was converted into the methoxy group, probably via nitro-olefin (trans form) through the action of sodium methylate. Therefore, it seems likely that compound IIa

8) J. Meisenheimer and F. Heim, *Ber.*, **38**, 466 (1905).
9) K. W. Rosenmund, ibid., **46**, 1034 (1913).
10) G. D. Buckley and J. L. Charlich, *J. Chem. Soc.*, 1947, 1473.
11) V. Gabor, J. Kollonitsch and A. Hajos, *Acta Chim. Acad. Sci.*, **10**, 239 (1956).
12) Sueo Tatsuoka (Takeda Pharmaceutical Industries Co.), Japanese Pat. 1524 (1952).

reacts with sodium methylate to afford IV via an intermediate, III. This is the reason why the erythro form was obtained in the reaction of IIa with sodium methylate.

## Experimental[13]

**3-Acetoxy-1-nitroso-2-nitro-1-phenylpropane (IIa).**—To a mixture of 30 g. (0.17 mol.) of cinnamyl acetate (b. p. 102—103°C/0.2 mmHg, $n_D^{25}$ 1.5391) in 430 ml. of toluene and 94 g. (1.4 mol.) of sodium nitrite in 100 ml. of water, 370 ml. of 20% sulfuric acid (0.85 mol.) was stirred in drop by drop at 0°C for 6—7 hr. The stirring was then continued for thirty minutes after the addition had been completed. The precipitate in the toluene layer was filtered and washed with cold water, and then with ether. A white powder of IIa, 21 g. (49%), was obtained; m. p. 116—117°C (decomp.) (lit.[6] 124°C).

Found: N, 11.01. Calcd. for $C_{11}H_{12}O_5N_2$: N, 11.11%.

**3-Acetoxy-2-nitro-1-phenyl-1-propyl-nitrite (IIb).**—The filtrate of the toluene layer, which is free from IIa, contained unreacted cinnamyl acetate and compound IIb. It was neutralized with a 5% sodium dicarbonate solution and dried over magnesium sulfate. By removing toluene under reduced pressure, 9 g. of a crude red oil was obtained. The crude oil was dissolved in anhydrous benzene, passed through a silica gel column, and eluted with benzene. First, the unreacted cinnamyl acetate (2.5 g.) was eluted, and then the second fraction was collected. When the solvent was removed, 5.4 g. of IIb was obtained as a pale yellow oil. The infrared spectrum showed bands at 1561, 1367 $cm^{-1}$ ($NO_2$) and 1659 $cm^{-1}$ (ONO).

Found: C, 49.55; H, 4.71; N, 10.22. Cacld. for $C_{11}H_{12}O_6N_2$: C, 49.25; H, 4.51; N, 10.45%.

When the reaction was carried out at 7—10°C, no IIa was obtained; the only reaction product was IIb (22 g.). When the reaction was carried out at 0°C, however, using 200 ml. of toluene and the other experimental conditions were not varied, 4.5 g. of IIa and 23 g. of IIb were obtained. When 450 ml. of ether was employed instead of toluene and the other experimental conditions were not varied, a small amount of IIa (1.8 g.) was obtained, while most of the reaction product was IIb (20 g.). When 450 ml. of cyclohexane was used as the solvent, 8 g. of IIa and 18 g. of IIb were formed from 30 g. of cinnamyl acetate.

Compound IIb, if desired, could be isolated as has been mentioned above. However, IIb was highly unstable. It is, therefore, recommended that, after neutralizing it with a sodium bicarbonate solution and removing the solvent, the crude product be directly transformed into compound III without the isolation of IIb.

**β-Nitro Cinnamyl Acetate (III).**—A mixture of 3 g. of the crude product of IIb and 1.5 g. of sodium acetate in 100 ml. of benzene was warmed at 60—80°C for 5 hr. When the mixture was poured into cold water, yellow needle crystals were formed. 1.8 g. of III was obtained; m. p. 81.5—82°C (recrystallized from alcohol and water (15 : 5)). Compound III was also obtained by passing the benzene solution of the crude product of IIb through an alumina column.

Found: C, 59.76; H, 4.95; N, 6.57. Calcd. for $C_{11}H_{11}O_4N$: C, 59.72; H, 5.01; N, 6.33%.

**1-Nitroso-2-nitro-1-phenylethane (X).**—To a mixture of 160 g. (1.53 mol.) of styrene in 900 ml. of ether and 570 g. (8.3 mol.) of sodium nitrite in 570 ml. of water, 1500 g. of 20% sulfuric acid was added drop by drop in the course of four or five hours at about 0°C. When the addition of sulfuric acid was complete, the precipitate present in the ether layer was filtered off and washed thoroughly with cold water in order to remove the inorganic salt; then it was washed with ether. One hundred and sixty-eight grams (61%) of X was obtained; m. p. 130°C (lit.[3] m. p. 129°C).

Found: N, 15.63. Calcd. for $C_8H_8O_3N_2$: N, 15.56%.

**1-Methoxy-2-nitro-1-phenylethane (XI).**—To a suspension of 9 g. (0.025 mol.) of compound X in 50 ml. of anhydrous methyl alcohol, sodium methylate prepared from 2.3 g. of sodium and 50 ml. of methyl alcohol was added with a rapid agitation at −5°C. The temperature immediately rose from −5°C to 7°C, and the reaction was completed within one or two minutes. A clear red solution was obtained. After it had been neutralized with carbon dioxide, the mixture was poured into a large amount of water and extracted with three 30-ml. portions of ether. The ether solution was dried over anhydrous magnesium sulfate, and the ether was removed. The nitro ether was distilled at 0.3 mmHg; b. p. 90—91°C (lit.[9] 140—141°C at 15 mmHg), $n_D^{20}$ 1.5190. Yield: 4.9 g. (55%).

Found: C, 59.71; H, 6.11; N, 7.85. Calcd. for $C_9H_{11}O_3N$: C, 59.66; H, 6.08; N, 7.74%.

***dl-erythro*-1, 3-Dimethoxy-2-nitro-1-phenylpropane (IV).**—*Procedure from IIa.*—Sodium methylate which had been prepared from 4.6 g. (0.2 g.-atom) of sodium and 118 ml. of methyl alcohol was added quickly at −5°C to a suspension of 25.2 g. (0.1 mol.) of IIa in 100 ml. of anhydrous methyl alcohol. The reaction proceeded spontaneously, and the mixture became transparent. After it had been neutralized with carbon dioxide, the mixture was poured into a large amount of water and extracted three times with 50 ml. of ether. Anhydrous magnesium sulfate was then added to the ether extract. Compound IV was purified by distillation at 118°C/0.08 mmHg, m. p. 58—59°C (recrystallized from water and methyl alcohol (1 : 1)). Yield: 17 g. (76%).

Found: C, 58.48; H, 6.63; 6.18. Calcd. for $C_{11}H_{15}O_4N$: C, 58.65; H, 6.71; N, 6.22%.

*Procedure from III.*—The same procedure as above was employed in the preparation of IV from III. Thus, 16.5 g. (70%) of IV was obtained from 22.1 g. of III in 100 ml. of methyl alcohol.

***dl-erythro*-2-Acetoamido-1,3-dimethoxy-1-phenylpropane (VI).**—Compound IV (13.7 g.) in 30 ml. of methyl alcohol was hydrogenated in an autoclave with 4 g. of Raney nickel at 40°C under an initial

13) Boiling points and melting points are uncorrected. infrared spectra were measured with a Perkin-Elmer Model 321 double-beam spectrophotometer.

pressure of 110 atm. Three molecular equivalents of hydrogen were absorved over a five-hour period. The solvent, methyl alcohol was removed under reduced pressure. The residue (7.5 g.) was mixed with 22.5 g. of acetic anhydride and warmed at 50°C. After the mixture had cooled, 5.0 g. of white crystals were obtained; m. p. 106°C (recrystallized from *n*-hexane and ethyl acetate (4 : 14)).

Found: C, 66.05; H, 8.10; N, 6.00. Calcd. for $C_{13}H_{19}O_3N$: C, 65.80; H, 8.07; N, 5.90%.

***dl-erythro*-2-Acetoamido-1, 3-dimethoxy-1-(*p*-nitrophenyl)-propane (VII).**—According to the method of Gabor,[11] from 2 g. of VI, 3.4 ml. of acetic anhydride and 10 ml. of fuming nitric acid, 1.1 g. of VII was obtained as pale-yellow-needle crystals, m. p. 109—110°C (from benzene).

Found: C, 55.98; H, 6.77; N, 9.69. Calcd. for $C_{13}H_{18}O_5N_2$: C, 55.31; H, 6.43; N, 9.92%.

***dl-erythro*-2-Amino-1, 3-dimethoxy-1-(*p*-nitrophenyl)-propane Hydrochloride (VIII).**—A 1.5 g. of sample of VII was mixed with 5 ml. of 5 N hydrochloric acid, and then the mixture was heated at 100°C for 4 hr. After the mixture had cooled, white crystals of VII (0.9 g.) were obtained; m. p. 216°C (from ethyl alcohol).

Found: C, 47.23; H, 6.27; N, 10.24. Calcd. for $C_{11}H_{16}O_4N_2 \cdot HCl$: C, 47.70; H, 6.15; N, 10.11%.

***dl-erythro*-2-Amino-1-(*p*-nitrophenyl)-1, 3-propanediol Hydrochloride (IX).**—The mixture of 0.8 g. of VIII and 15 ml. of concentrated hydrochloric acid was heated at 120—125°C for 2 hr. in the sealed tube. Then the solution was concentrated in a vacuum, and the residue was recrystallized from methyl alcohol. White crystals were obtained; m. p. 209°C (lit.[12] 206—208°C).

Found: C, 43.60; H, 5.12; N, 11.66. Calcd. for $C_9H_{12}O_4N_2 \cdot HCl$: C, 43.42; H, 5.22; N, 11.26%.

## Summary

This study of the reaction between dinitrogen trioxide and cinnamyl acetate has indicated that the 3-acetoxy-2-nitro-1-phenyl-1-propyl-nitrite (IIb) is formed, in addition to 3-acetoxy-1-nitroso-2-nitro-1-phenylpropane (IIa), in yield depending on the experimental conditions. Those products have been transformed in good yields into 1, 3-dimethoxy-2-nitro-1-phenylpropane, from which *dl*-erythro-2-amino-1-(*p*-nitrophenyl)-1, 3-propanediol has been synthesized.

The authors wish to express their heartfelt gratitude to Professor Toshio Hoshino for his guidance and constant encouragement throughout this study. The authors also are grateful to Dr. Asaji Kondo for his help in the elemental analyses of the products and to Dr. Yoichiro Mashiko for his advice for interpreting the infrared spectra.

*Laboratory of Organic Chemistry*
*Tokyo Institute of Technology*
*Ookayama, Tokyo*

# The Electrolytic Formation and Dissolution of the Oxide Layer on Rhodium in an Acid Solution

By Shigeo SHIBATA

(Received December 8, 1964)

The surface oxidation of rhodium has been studied in parallel with that of platinum by means of chronopotentiometry,[1] the triangular voltage sweep[2,3] and rest-potential measurement[4]. However, there has as yet been very little study aimed at giving a coherent mechanism of the formation and dissolution of the surface oxide under the conditions of controlled current electrolysis.

The present paper will describe the results obtained with rhodium electrodes using techniques similar to those applied to the platinum electrode in this laboratory.[5]

## Experimental

The electrical circuit and the electrolytic cell used were fundamentally similar to those previously described.[4] The electrode was a smooth rhodium wire 0.5 mm. in diameter and 10.3 mm. long. The electrode was stored in 10 N nitric acid when not in use. The counter electrode was a platinum cylinder placed concentrically around the test electrode. The electrolytic solution was 2 N sulfuric

1) M. Breiter, C. A. Knorr and W. Völkl, *Z. Elektrochem.*, **59**, 681 (1955).
2) F. G. Will and C. A. Knorr, ibid., **64**, 270 (1960).
3) W. Böld and M. Breiter, *Electrochim. Acta*, **5**, 169 (1961).
4) J. P. Hoare, *J. Electrochem. Soc.*, **111**, 232 (1964).
5) S. Shibata, This Bulletin, **37**, 410 (1964).

acid, which had been freed from dissolved oxygen by passing purified nitrogen gas through, unless otherwise stated.

The experiments were made in an all-glass, double-wall cell which allowed the electrolyte to be thermostated and also permitted the bubbling of nitrogen gas. All experiments were made at 25 ±0.1°C.

The reference electrode was a mercury-mercurous sulfate electrode in 2 N sulfuric acid. The values of the potential described in this paper are on the standard hydrogen scale.

## Results and Discussion

**Charging Curves.**—Typical charging curves for oxygen- and hydrogen-free solutions are shown in Figs. 1A and 2A.

A constant current is passed through, and the potential of the electrode is followed as a function of the time. The potential rises slowly (the $\alpha_a$ region) until all the hydrogen adsorbed on the electrode has been oxidized. The potential then rises rapidly through the region, $\beta_a$, where the only process is the charging of the electrical double layer. At 0.6 V. an anodic process begins, and the potential increases more gradually through the $\gamma_a$ region. Eventually the oxygen evolution potential is reached, causing a leveling off of the potential (the $\delta_a$ region). If the current is reversed and the electrode thus anodized is made the cathode, the cathodic charging curve

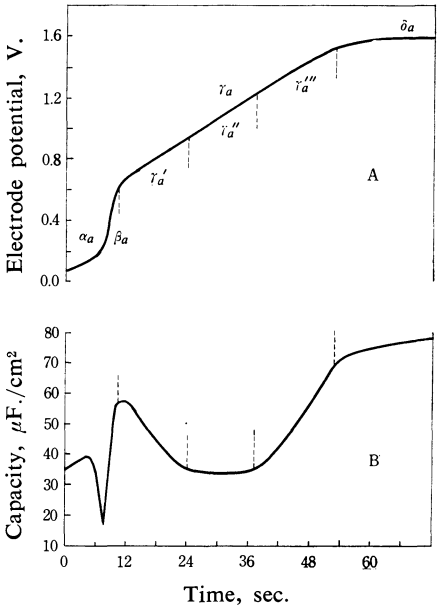



Fig. 1. Comparison of charging and capacity curves.
A Anodic charging curve. $i_a$=46 μamp./cm²
B Differential capacity curve recorded simultaneously with curve A.

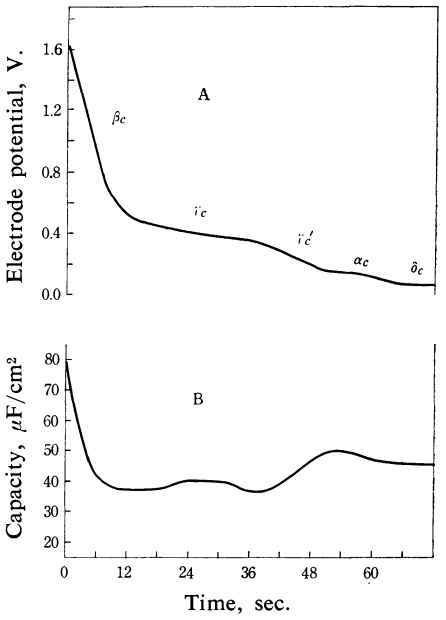



Fig. 2. Comparison of charging and capacity curves.
A Cathodic charging curve of the oxidized electrode. $i_c$=46 μamp/cm²
B Differential capacity curve recorded simultaneously with curve A.

of Fig. 2A is observed. The potential drops very rapidly to about 0.5 V., where there is a plateau (the $\gamma_c$ region) due to the reduction of the oxide layer formed in the $\gamma_a$ region of the anodization. The potential drop is slow in both the $\gamma_c$ and $\gamma_c'$ regions, and the difference in the slopes of these curves is so small that the starting potential of $\alpha_c$ is not satisfactory determined. The $\delta_c$ region is attributed to the evolution of hydrogen.

The anodic and cathodic charging curves do not have the same shape. If the difference in their shapes were due to the effect of the polarization as the result of a slow reaction, the curves would become more similar as the current density is decreased. However, a very low current density study showed that the hysteresis is not decreased significantly by a decrease in the current density. Such an intrinsic hysteresis suggests a reaction which is so irreversible that the oxidation and reduction occur by different mechanisms.

A comparison of the anodic and cathodic curves shows that the $\gamma_a$ region is always larger than the $\gamma_c+\gamma_c'$ region, indicating that more electricity is used to form the oxide than is required to remove it. (The $\gamma_c$ region is also the reduction stage of the oxide layer. Its experimental evidence will be given later.) This inequality in electricity can be explained without inconsistency if, in the course of

cathodization, the reduction of the oxide to hydrogen peroxide is assumed.[6] However, it was shown in a previous paper[5] that this hypothesis is not applicable to platinum. It is necessary to examine whether or not the hydrogen peroxide theory is true for rhodium.

**The Variation in Double Layer Capacity during the Anodic and Cathodic Polarizations.**— The differential double layer capacity of the rhodium electrode was measured by the galvanostatic pulse method previously described.[5] The pulse-rise time was 0.2 $\mu$sec., and the duration was 5 $\mu$sec. The ratio of the current to the slope of the potential-time curve, $\Delta E/\Delta t$, gives the double layer capacity. In practice, the pulse current was so adjusted that $\Delta E$ was 1—4 mV. at a $\Delta t$ of 5 $\mu$sec. To prevent the lowering of the double layer capacity by the traces of surface-active impurities adsorbed on the electrode, the electrode was first anodized in order to eject the impurity.[7] The clean electrode was then reduced before measurements made.

The value of the double layer capacity thus observed showed an interesting mode of time change during the constant current anodic and cathodic polarizations, as may be seen in Figs. 1B and 2B respectively. These results suggest that the $\gamma_a$ region of the anodic charging curve can be divided into three regions, $\gamma_a'$, $\gamma_a''$ and $\gamma_a'''$, in spite of its simple tone. Starting with the oxygen deposition potential of 0.6 V., the first stage, $\gamma_a'$, is characterized by a fall of the double layer capacity with an increase in the potential until 0.9 V. The second stage, $\gamma_a''$, is marked by a constant minimum value of 34 $\mu$F./cm$^2$ in the potential from 0.9 to 1.2 V., and the final stage, $\gamma_a'''$, by an increase in the value until the potential of 1.5 V., at which the evolution of oxygen begins.

It has been suggested by Llopis and Colum[8] that the cause of the increase in the electrode capacity at the anodization is the presence of such dipoles as M···O or M···OH at the electrode-solution interface. These dipoles would replace the water molecules and the ions which form the electrical double layer at the reduced electrode surface. The behavior of the electrode capacity due to the anodization seems to give us some information about the mechanism of the surface oxidation. In the first stage, $\gamma_a'$, with the high capacity value, highly polar groups may be expected to exist at the metal-solution interface of the electrode, which may be represented as Rh···OH. In the $\gamma_a''$ stage, these polar groups of the hydroxyl radical may be converted into non-polar groups or into the definite oxide, and in the final stage, $\gamma_a'''$, the polar groups may be adsorbed on this oxidized surface.

The capacity change during the cathodization of the oxidized electrode is monotonic compared with that during the anodization.

**The Electrode Reaction in the $\gamma_c'$ Region.**— For the platinum electrode, the oxide layer is reduced exhaustively at the one stage of 0.8 V. which corresponds to the plateau, $\gamma_c$, of 0.5 V. for the rhodium electrode. When all of the oxide on the platinum has been reduced, the potential drops rapidly to about 0.3 V., where the deposition of hydrogen begins. However, for the rhodium electrode, following the $\gamma_c$ plateau a slow linear fall of the

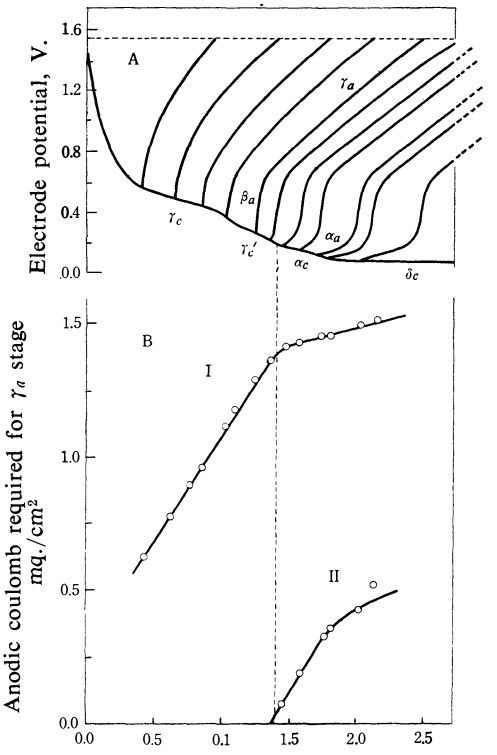



Fig. 3. A. Anodic charging curves from various initial potentials. $i_a$=94 $\mu$amp./cm$^2$.

B. Plot of anodic coulombs required for the stages of $\gamma_a$ (curve I) and $\alpha_a$ (curve II) of the anodic charging curves for the electrode which was polarized from various initial potentials vs. cathodic coulombs used to polarise the oxidized electrode to these initial potentials.

6) K. J. Vetter and D. Berndt, *Z. Elektrochem.*, **62**, 378 (1958).

7) H. A. Latinen and C. G. Enke, *J. Electrochem. Soc.*, **107**, 773 (1960).

8) J. Llopis and F. Colum, "Proceedings of the International Committee on Electrochemical Thermodynamics, Eighth Meeting, 1958," Butterworths, London, pp. 414—427.

potential, $\gamma_c'$, is observed. In order to look into the reaction taking place in this region, the following measurements were carried out.

The electrodes oxidized by a constant current anodization up to the potential of 1.55 V., which is the end potential of the $\gamma_a$ region, were polarized cathodically with a constant current up to various potentials, and then the current was reversed immediately. The charging curves obtained by these procedures are shown in Fig. 3. In general, following the initial steep ascent of the potential ($\beta_a$), the potential curves turn to a slow linear rise, $\gamma_a$. However, when the cathodic current was reversed at the potential below 0.2 V., the $\alpha_a$ plateau, the ionization stage of the adsorbed hydrogen, appears on the anodic curves. As long as the quantity of electricity, which has been passed through the oxidized electrode at the cathodization, $q_c$, does not suffice to reduce the oxide layer exhaustively, the quantity of electricity, $q_a$, which is required to restore the thus-cathodized electrode to the oxidized state will increase as $q_c$ is increased. The number of coulombs required to oxidize a given electrode from the completely reduced state into the completely oxidized state would be constant. Consequently, it may be seen from the comparison of the potential curve in Fig. 3A with the coulombic curve I in Fig. 3B that the $\gamma_c'$ region, together with the $\gamma_c$ of the cathodic charging curve corresponding to the steeper branch of the curve I, can be attributed to the reduction of the oxide layer. The $\alpha_c$ region, corresponding to the less sloped branch of curve I and to curve II, can be ascribed to the adsorption of hydrogen on the electrode after the completion of the reduction of the surface oxide.

The fact that the oxide layer is reduced in two regions by the consecutive cathodization suggests that the oxide layer consists of two different species of oxide or that it is removed subsequently through two-stage reactions.

**The Anodic and Cathodic Coulombs.** — The applied anodic current is immediately reversed at various potentials, $E_\gamma$'s, in the $\gamma_a$ region. The charging curves thus obtained are shown in Fig. 4. The ratio of $q_a$, the quantity of electricity used in the region from the initial potential of $\gamma_a$ to the potential, $E_\gamma$, on the anodic curve, to $q_c$, that used from $E_\gamma$, to the end potential of $\gamma_c'$ on the cathodic curve, was traced against $E_\gamma$; the results are represented by curve A in Fig. 5. Furthermore, the anodic and cathodic charging curves were taken in the same manner as above except that the circuit was let stand open for one minute after the anodic polarization up to $E_\gamma$ till the outset of the cathodic one. The results thus obtained

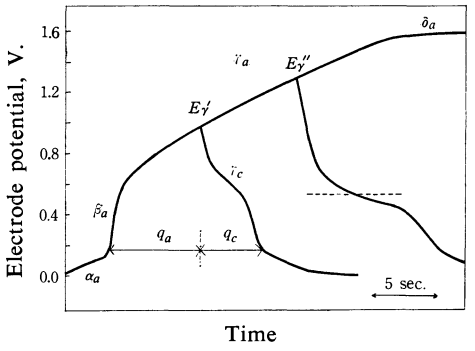



Fig. 4. Alternating anodic-cathodic charging curves when the current was reversed at potentials, $E_\gamma'$ and $E_\gamma''$. $i_a=i_c=94$ $\mu$amp./cm$^2$

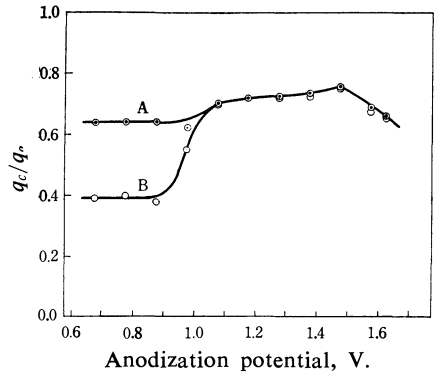



Fig. 5. Plots of the anodic and cathodic coulomb ratio vs. the potential at which the current was reversed or turned off. $i_a=i_c=$ 94 $\mu$amp./cm$^2$
Curve A, immediately reversed.
Curve B, allowed to remain at open circuit for 1 min. in stationary solution before the cathodic polarization starts.

are represented as curve B in Fig. 5. The spontaneous decrease in the $q_c/q_a$ ratio for the electrode anodized up to potentials in the $\gamma_a'$ region indicates that the oxygen deposited in this potential region is unstable and less tightly bound with the metal than the oxygen in higher potential regions, $\gamma_a''$ and $\gamma_a'''$.

**The Reduction Potential of the Oxide Layer, the Open Circuit Potential and the Quantity of Electricity Required for the $\gamma_c'$ Stage as a Function of the Pre-anodization Potential.** — The potential of the $\gamma_c$ plateau, i. e., the reduction potential of the oxide layer on the electrode, varies with the potential at which the electrode is pre-anodized, as is shown in Fig. 6. This curve can be divided into three linear sections corresponding to three potential regions, $\gamma_a'$, $\gamma_a''$ and $\gamma_a'''$, of the anodic charging curve.

When the pre-anodization potential was taken in the $\gamma_a'$ region, the slope of the

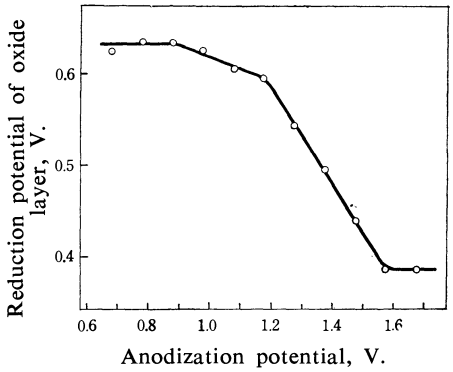



Fig. 6. Plot of the reduction potential of oxide layer at the stage $\gamma_c$ vs. the pre-anodization potential.

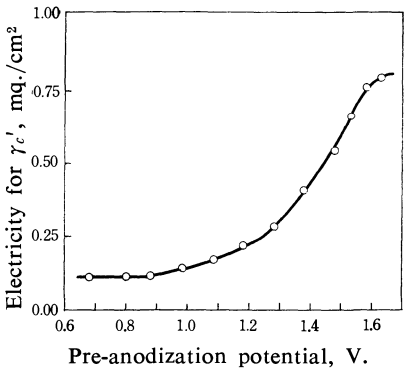



Fig. 7. Plot of the quantity of electricity required for the region $\gamma_c'$ vs. the pre-anodization potential.

curve $\gamma_c'$, for this electrode was almost equal to that of the curve, $\beta_a$, which is attributed only to the charging of the double layer. Consequently, under this pre-anodization the current passing through the electrode in the $\gamma_c'$ region should be nonfaradaic. However, the slope of $\gamma_c'$ decreases and the electricity required for this stage increases with an increase in the pre-anodization potential in the region of $\gamma_a'''$, as may be seen in Fig. 7. This plot indicates that only when the electrode is polarized at potential above 1.2 V. is the stable oxide which is reduced at a more negative potential formed.

When the current is turned off after the anodic polarization, the electrode potential drops rapidly at first, but more slowly as time elapses. The open circuit potential of the electrode was measured 1 and 5 min. after the circuit was broken. The open-circuit potential increases linearly with an increase in the pre-anodization potential up to about 1.2 V., and then it remains approximately constant in the region of the pre-anodization potential from

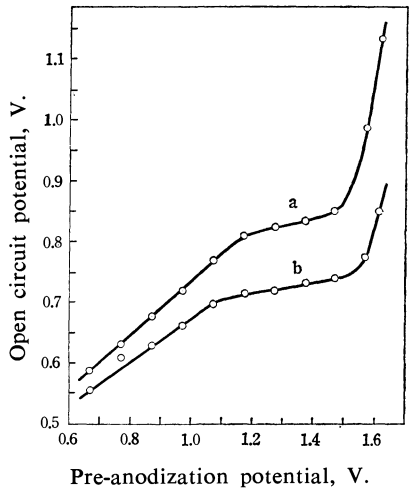



Fig. 8. Plots of the open circuit potential vs. the pre-anodization potential.
Curve a, 1 min. after the pre-anodization current was turned off.
Curve b, 5 min. after the pre-anodization current was turned off.

1.2 to 1.5 V. corresponding to the $\gamma_a'''$ (Fig. 8).

**The Cathodic Behavior of the Electrode in the Solution Containing Hydrogen Peroxide.**— If the hydrogen peroxide theory[6] is correct as to the cause of the inequality between the quantity of electricity required for the $\gamma_a$ stage and that for $\gamma_c+\gamma_c'$, the hydrogen peroxide formed during the cathodization of the oxidized electrode and also the oxygen which may be produced by the decomposition of hydrogen peroxide would diffuse away from the surface of the electrode into the solution, without being further reduced cathodically to water at the reduction potential of the oxide layer. In other words, the reduction potential of hydrogen peroxide or oxygen molecules on the electrode should be sufficiently less positive than that of the oxide layer.

To find the reduction potential of hydrogen peroxide and oxygen on the rhodium electrode, the cathodic charging curves were measured with a smooth rhodium wire in a 2 N sulfuric acid solution containing each of these substances. The mesurements were started one minute after the electrode had been introduced into the solution in order to keep the solution quiescent.

Curve a in Fig. 9 is the cathodic curve obtained with a reduced electrode in the solution containing hydrogen peroxide of $3.7\times10^{-4}$ mol./l. The potential was confined at a constant value of 0.65 V. during the electrolysis. Curve b is for the oxidized electrode. From a comparison of curve d, which is the reduction curve of the oxidized electrode in the

solution freed from both hydrogen peroxide and oxygen, with curves a and b, it is evident that the remaining of constant potentials on curves a and b can be attributed to the reduction of the hydrogen peroxide. The chronopotentiometric reduction potentials of hydrogen peroxide on the reduced and oxidized electrodes are 0.65 and 0.45 V., while those of oxygen on the reduced and oxidized electrodes are 0.62 and 0.41 V. respectively. All of these potentials are more positive than the reduction potential of the oxide layer. When electrodes are polarized with a larger current density, the potential falls after a definite time, $\tau$ (the transition time), as may be seen in curves c and c' of Fig. 9.

For chronopotentiograms with a wire electrode, Eq. 1 has been derived theoretically:[9]

$$\frac{i\tau^{1/2}}{C}=\frac{\pi^{1/2}nFAD^{1/2}/2}{1-\pi^{1/2}D^{1/2}\tau^{1/2}/4r+D\tau/4r^2-3\pi^{1/2}D^{3/2}\tau^{3/2}/32r^3} \quad (1)$$

where $i$ is the constant current; $C$, the concentration of the electroactive substance in the bulk solution; $D$, the diffusion coefficient; $n$, the number of electrons per molecular unit of reaction; $F$, the Faraday constant; $A$, the area of the electrode, and $r$, the radius of the electrode.

If a completely-reduced electrode is used, the oxide will be formed by the direct reaction between the metal and the hydrogen peroxide included in the solution while the electrode is let stand in the cell before the measurement starts. When the oxide thus formed is reduced at the same time as the hydrogen peroxide, it is necessary to make a correction for the value of the observed current, $i_{obs}$, in the chronopotentiometry. The value of the current, $i$, used to reduce the hydrogen peroxide during the transition time can be estimated by substracting the current for the reduction of the oxide from $i_{obs}$. The values of $i$ were calculated by assuming that the amount of the oxide formed during the standing time of the electrode is constant and that the current resulting from the reduction of the oxide remains constant during the entire time of transition.

$$i=i_{obs}-q/\tau \quad (2)$$

where $q$ is the quantity of electricity used to reduce the oxide. The value of $q$ was selected by trial and error.

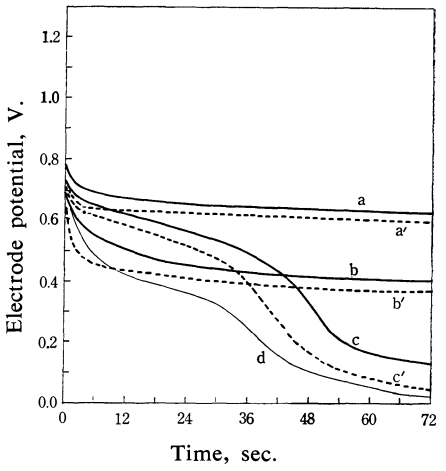



Fig. 9. Cathodic curves.
Solid lines: in the solution containing hydrogen peroxide
Curve a, for the reduced electrode $i_c=47$ $\mu$amp./cm$^2$
Curve b, for the oxidized electrode $i_c=47$ $\mu$amp./cm$^2$
Curve c, for the reduced electrode $i_c=73$ $\mu$amp./cm$^2$
Broken lines: in the air saturated solution
Curve a', for the reduced electrode $i_c=47$ $\mu$amp./cm$^2$
Curve b', for the oxidized electrode $i_c=47$ $\mu$amp./cm$^2$
Curve c', for the reduced electrode $i_c=83$ $\mu$amp./cm$^2$
Fine line: curve d, for the oxidized electrode in the solution freed from hydrogen peroxid and oxygen. $i_c=47$ $\mu$amp./cm$^2$

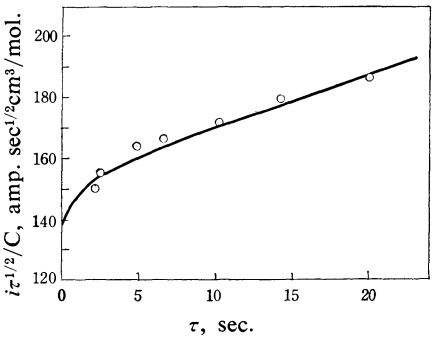



Fig. 10. Variation of $i\tau^{1/2}/C$ with transition time $\tau$ for the reduction of hydrogen peroxide in 2 N sulfuric acid; $C=3.76\times10^{-4}$ mol./l., $r=0.025$ cm., $A=0.195$ cm$^2$, $i=i_{obs}-11.3/\tau$. The solid line is the theoretical curve according to Eq. 1.

The corrected values of $i\tau^{1/2}/C$ were plotted against $\tau$ and are represented as tiny circles in Fig. 10. The solid line in the same figure is the theoretical curve according to Eq. 1 using the

9) J. J. Lingane, *J. Electroanal. Chem.*, 1, 379 (1960); 2, 1, 46 (1961).

diffusion coefficient of hydrogen peroxide ($1.71 \times 10^{-5}$ cm./sec.) reported by Kern.[10] The agreement of the observed values with those predicted by the theoretical equation shows that, in chronopotentiometry, hydrogen peroxide on the electrode is quantitatively reduced to water at a potential which is not less positive than the reduction potential of the oxide layer. Consequently, even if the oxide might be reduced to hydrogen peroxide during the cathodization, or even if this peroxide might be decomposed on the surface, these products should be further immediately reduced to water. Thus the hydrogen peroxide theory described above is not applicable to the rhodium electrode.

The fact that more electricity is used for the $\gamma_a$ stage than is required to remove the oxide may be caused by a mixed anodic process where a reaction of oxygen evolution occurs simultaneously with the oxide formation reaction and so consumes some of the electricity.

**The Corrosion by Square-wave Alternating-current Electrolysis.**—The test electrodes for these experiments were rhodium wires 0.5 mm. in diameter and 4—6 mm. long; a new one was used for every run of measurement. The frequency of the square-wave alternating current was 78 c. p. s., the rise time was 1 $\mu$sec., and the output voltage of the generator was 100 V. The square-wave alternating current from the generator was passed through a current-limiting resistor in order to obtain the constant current.

The electrolysis was carried out in a hydrogen-saturated solution. The amplitude of the oscillating-electrode potential during the alternating-current electrolysis increased with the increase in the current density. The minimum value of the potential which appears during negative semicycle of alternating current electrolysis was slightly increased by the hydrogen overpotential when the current density was increased, whereas the maximum potential during a positive semicycle increased rapidly with the increase in the current. The current was so adjusted that this maximum potential was the desired value, $E_s$, during the electrolysis.

The degree of the corrosion of the surface by alternating current electrolysis may be estimated by measuring the increase in the true area per apparent unit area, i. e., the increase in the roughness factor, because the surface is coarsened by the electrolytic attack. Since the value of the electricity, $Q_a$ (coulombs/apparent unit area), required to form the oxide layer is proportionate to the true area of the electrode, the degree of the corrosion is estimated by the ratio of the $Q_a'$ for the electrode already electrolyzed for one hour to the $Q_a^0$ for that not yet electrolyzed. The values of the $Q_a'$ and $Q_a^0$ were obtained from anodic charging curves, which were measured by means of the cathode-ray oscilloscopic technique.

The dependence of the degree of the corrosion on the maximum potential, $E_s$, was traced; the results are shown in Fig. 11. It can be seen from this curve that the surface does not suffer from the corrosion until the $E_s$ potential reaches a critical value, $E_s^0 = 0.88$ V., but after the potential has exceeded this value, the $Q_a'/Q_a^0$ ratio rises very rapidly and the bright surface becomes cloudy.

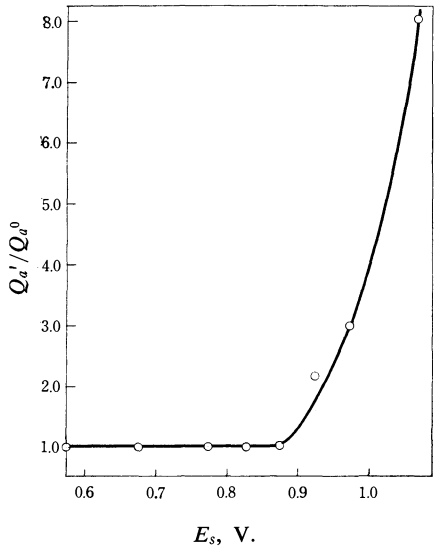



Fig. 11. Plot of the extent of corrosion vs. the maximum value, $E_s$, of oscillating potential in square wave alternating current electrolysis.
Frequency, 78 c.p.s. Etectrolyzing time, 1 hr.

The corrosion by the alternating-current electrolysis may be attributed to the repetition of the alternate formation and reduction of the "oxide" layer, as has been suggested previously for the platinum electrode.[5] The rearrangement of the rhodium atoms on the surface due to the repeated formation and dissolution of oxide lattices should cause a recrystallization on the surface. The fact that the surface did not suffer from any attack at all until the $E_s^0$ potential was reached indicates that the oxygen atoms deposited on the surface in the potential region, $\gamma_a'$, are only in a state of adsorption or are attached to the surface by relaxed bonds so that they

10) D. M. Kern, *J. Am. Chem. Soc.*, **78**, 4207 (1954).

are not able to effect a serious change in the Rh-Rh bonds.

On the basis of the observed data for the rhodium electrode, the mechanism of the surface oxidation can be considered. The oxidation is completed through three steps taking place at the different potential regions. The number of coulombs required for each of these regions, $\gamma_a'$, $\gamma_a''$ and $\gamma_a'''$, are equal to one other.

The first step of the $\gamma_a'$ region can be attributed to the formation of an intermediate which is adsorbed on the electrode surface. The intermediate may be hydroxyl redicals which come from water with one electron per molecular unit change:

$$Rh + H_2O \rightarrow Rh\cdots OH + H^+ + e^- \quad (3)$$

The highly polar group, Rh···OH, thus formed is unstable and may be converted to a less polar group which is close to the oxide, Rh-OH or $Rh_2O$, as the electrode potential increases.

The second stage, $\gamma_a''$, is the reaction in which the "oxide" is formed;

$$Rh\text{-}OH \rightarrow Rh\text{-}O + H^+ + e^- \quad (4)$$

Sidgwick[11] stated that the only stable oxide formed by rhodium is $Rh_2O_3$, while Hoare[4] found that the end product formed by the anodic polarization is $Rh_2O_3$. From the polarization data and the coulombic studies of Butler and Drever,[12] and Böld and Breiter,[3] it seems true that the oxide layers on the rhodium do not grow much beyond a monolayer. Therefore, in the third stage, $\gamma_a'''$, the following reaction may take place, with an intermediate of a polar group:

$$Rh\text{-}O + H_2O \rightarrow Rh\text{-}O\cdots OH + H^+ + e \quad (5)$$

where Rh-O···OH has the same empirical formula as hydrated $Rh_2O_3$.

At the cathodization, the oxide layer is reduced in two stages of different potentials. As the quantity of electricity required for the first reduction stage, $\gamma_c$, is almost twice as much as that required for the second stage, $\gamma_c'$, which is equal to that for the hydrogen deposition stage, $\alpha_c$, the first stage seems to be a reducing reaction using two electrons per molecular unit of reaction, and the second stage, one using one electron.

## Summary

Surface oxides on the smooth rhodium electrode have been characterized by anodic oxidation and by cathodic stripping with a constant current under various conditions.

The oxidation reaction of the surface should consist of three stages with a characteristic potential region; the adsorption of OH, the formation of an oxide, Rh-O, and, finally, the formation of a higher oxide, $Rh_2O_3$. The oxide thus formed is cathodically reduced step-by-step in two different potential regions. These mechanisms are supported by the experimental data of the charging curves taken under various conditions, the corrosion by the square-wave alternating-current electrolysis, and the variation in the electrode capacity during the electrolysis.

The author is indebted to N. Yamamoto and T. Sugimoto for their assistance in the experimental work.

*Department of Chemistry*
*Faculty of Liberal Arts and Science*
*Yamagata University*
*Koshirakawa-cho, Yamagata*

11) N. V. Sidgwick, "Chemical Elements and Their Compounds," Oxford Press (1950), p. 1533.
12) J. A. V. Butler and G. Drever, *Trans. Faraday Soc.*, 32, 427 (1936).

# The Preparation of Optically Active α-C-Substituted Glutamic Acid

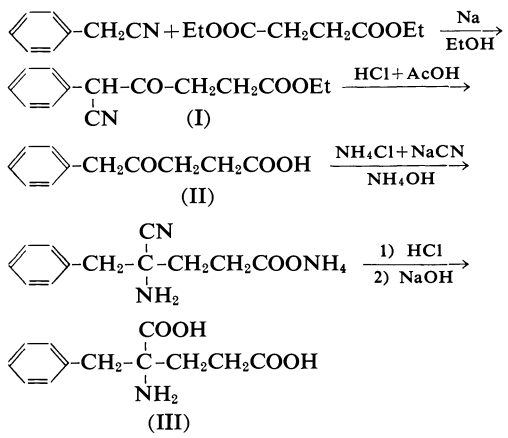
By Yoshiharu IZUMI, Susumu TATSUMI, Masami IMAIDA, Yoshio FUKUDA and Shiro AKABORI

(Received December 10, 1964)

α-C-Dialkyl-substituted glycine is an interesting substance from the biochemical point of view, with regard to α-amino acid and also with ragard to the relation between its optical rotation and its absolute configuration. However, although several α-C-dialkyl-substituted glycines have been synthesized, only two have been resolved into the optically active isomers.[1,2]

In the present work, two optically active α-C-dialkyl-substituted glycines, 2-methyl and 2-benzylglutamic acid, were prepared. DL-2-Methylglutamic acid was synthesized from levulinic acid by Takenishi's procedure,[3] and then its optical resolution was performed. *N*-Benzoylated DL-2-methylglutamic acid was resolved with brucine by the method of the differential solubility of the isomers in water. The optical rotation values of the isomers were as follows; (+) isomer, $[\alpha]_D^{20}$ +12.1° (*c* 4, 6 N HCl); (−) isomer, $[\alpha]_D^{20}$ −12.1° (*c* 4, 6 N HCl).

DL-2-Benzylglutamic acid was prepared from benzyl cyanide and diethyl succinate by the following process:




The optical resolution of this amino acid was performed by means of a methanolic solution with strychinine. The optical rotation values of two optically active isomers of this amino acid were as follows:

(+) isomer, $[\alpha]_D^{20}$ +1.65° (*c* 10, 4 N HCl);
(−) isomer, $[\alpha]_D^{20}$ −1.60° (*c* 10, 4 N HCl).

## Experimental

**The Preparation of DL-2-Methylglutamic Acid.**—DL-2-Methylglutamic acid was prepared from levulinic acid by Takenishi's procedure.[3]

**The Preparation of *N*-Benzoyl-2-methylglutamic Acid.**—One hundred and fifty milliliters of 2 N sodium hydroxide and 42.5 g. of benzoyl chloride in 100 ml. of dioxane were simultaneously stirred, drop by drop, into a solution of 48.3 g. of DL-2-methylglutamic acid in 600 ml. of N sodium hydroxide at 5—10°C; the addition took about 2 hr. Stirring was then continued for one more hour at the same temperature. The reaction mixture was washed with two 100 ml. portions of ethyl ether and concentrated to about 500 ml. in vacuo. This solution was then acidified with 100 ml. of concentrated hydrochloric acid, and stored for two days in an ice box. The crude material obtained was washed several times with boiling ligroin. The resulting crystals were dissolved in 230 ml. of methyl alcohol and filtered. The filtrate was stirred into 500 ml. of water, and the mixture was allowed to stand overnight in an ice box. White crystalline *N*-benzoyl-2-methylglutamic acid was collected, washed with cold water, and dried in air. m. p. 198°C. Yield, 50 g.

Found: C, 58.48; H, 5.66; N, 5.15. Calcd. for $C_{13}H_{15}NO_5$: C, 58.86; H, 5.70; N, 5.28%.

**The Optical Resolution of *N*-Benzoyl-2-methylglutamic Acid.**—After 69 g. of *N*-benzoyl-2-methylglutamic acid and 255 g. of brucine had been dissolved in 3.4 l. of boiling water, the solution was left to stand overnight in a refrigerator. The crystals were then collected, washed with cold water, and dried in air at room temperature. Two recrystallizations of this crude product from 1.4 parts of water gave 125 g. of pure *N*-benzoyl-2-methylglutamic acid brucine salt. One hundred and ten grams of the brucine salt were decomposed with 150 ml. of 2 N sodium hydroxide solution, and the brucine was removed by filtration. The alkaline solution was neutralized with hydrochloric acid and then evaporated to about 100 ml. in vacuo. This solution was boiled with 100 ml. of concentrated hydrochloric acid for 4 hr. and then left to stand overnight in a refrigerator. Benzoic acid was removed by filtration and extraction with 100 ml. of

1) T. Kaneko, *J. Chem. Soc. Japan (Nippon Kwagaku Kwaishi)*, **60**, 531 (1939).
2) C. G. Baker, S. C. J. Fu, S. M. Birnbaum, H. A. Sober and J. P. Greenstein, *J. Am. Chem. Soc.*, **74**, 4701 (1952).
3) T. Takenishi and O. Shimamura, This Bulletin, **27**, 207 (1954).

ethyl ether. The aqueous layer was evaporated to dryness in vacuo. To the residue a small amount of water was added, and the solution was evaporated to dryness in order to remove the free hydrochloric acid. Then the residue was taken up in 30 ml. of water, decolorized with charcoal, and adjusted to pH 3.2 with 20% sodium hydroxide. The mixture was stored overnight in a refrigerator, and the resulting crude crystals were collected, washed with 5 ml. of 50% methanol, and dried in air, yielding 7.1 g. of (+)-2-methylglutamic acid. On recrystallization from 10 ml. of boiling water, pure (+)-2-methylglutamic acid was obtained as fine needles. Yield, 6.3 g. $[\alpha]_D^{20}$ +12.1° (*c* 4, 6 N HCl).

Found: C, 44.99; H, 6.80; N, 8.60. Calcd. for $C_6H_{11}NO_4$: C, 44.71; H, 6.88; N, 8.69%.

The mother liquor of the *N*-benzoyl-(+)-2-methylglutamic acid brucine salt was concentrated to a paste. After it had stood for a week in a refrigerator, the brucine salt was collected. (−)-2-Methylglutamic acid was similarly obtained from the brucine salt by the procedure described above. Yield, 1.8 g. $[\alpha]_D^{20}$ −12.1° (*c* 4, 6 N HCl).

Found: C, 43.39; H, 6.77; N, 8.44%.

**The Preparation of DL-2-Benzylglutamic Acid (III).**—*Ethyl 5-Phenyl-5-cyanolevulinate (I).*—A mixture of 37.2 g. of freshly-distilled benzyl cyanide and 26.1 g. of diethyl succinate was added, with vigorous shaking, to 120 ml. of a sodium ethoxide solution containing 8.4 g. of sodium. The mixture was then refluxed for 2 hr., stored overnight at room temperature, poured into 350 ml. of cold water, and neutralized slowly with glacial acetic acid. An oily brown ester was separated, and the aqueous layer was extracted with ethyl ether. The ether layer was combined with the oily ester, washed twice with water, and dried over magnesium sulfate. Then the ether was evaporated off, and unreacted benzyl cyanide and diethyl succinate were removed by distillation in vacuo. The residual oily substance was allowed to stand for a few hours at −20°C. Brown crystals were thus obtained. Recrystallization from benzene - petroleum ether (1 : 1) gave white crystals. Yield, 54.8 g. M. p. 154°C. Betts and Davey[4] reported a m. p. of 152°C for this material.

Found: C, 68.05; H, 6.15; N, 5.69. Calcd. for $C_{14}H_{15}NO_3$: C, 68.55; H, 6.16; N, 5.71%.

*5-Phenyllevulinic Acid (II).*—Crude I (44 g.) was added to a mixture of glacial acetic acid (300 ml.), concentrated hydrochloric acid (100 ml.) and water (90 ml.), and the mixture was refluxed for 14.5 hr. Then it was evaporated to dryness in vacuo, and the residue was taken up in ether. The ether layer was washed twice with water and repeatedly extracted with a 5% potassium carbonate solution. The alkaline solution was then washed with ether and adjusted to pH 3—4 with 3 N hydrochloric acid. II was obtained as a brown oil. For the purification of crude II, this oil was dissolved in a small amount of water containing equimolar potassium hydroxide, and then a large quantity of acetone was added to the solution. After the mixture had stood in an ice box for 4 hr., the colorless crystalline potassium salt of II was collected. Recrystallization from water-acetone (1 : 4) gave 32 g. of the pure salt. This was dissolved in water, adjusted to pH 3—2 with concentrated hydrochloric acid, and extracted with ether. The ether layer was washed with water and dried over magnesium sulfate. When the ether was evaporated off, II was obtained as white crystals. Yield, 25 g. M. p. 57°C.

Found: C, 68.89; H, 6.29. Calcd. for $C_{11}H_{12}O_3$: C, 68.73; H, 6.29%.

**DL-2-Benzylglutamic Acid (III).**—After a solution containing 23 g. of II and 34 ml. of 12% aqueous ammonia had been cooled to 0—5°C in an ice water bath, 7.4 g. of sodium cyanide in 27 ml. of water and 8 g. of ammonium chloride in 27 ml. of water were added. The flask was tightly stoppered, and the mixture was shaken vigorously in a water bath at 50—70°C for 6 hr. Then the reaction mixture was cooled in an ice water bath and poured into 1.5 l. of concentrated hydrochloric acid; the mixture was allowed to stand overnight at room temperature before it was refluxed for 2 hr. The hydrolyzate was concentrated in vacuo, and during this procedure inorganic salts were removed by filtration. The residue was dissolved in a small amount of water and redried in vacuo in order to remove the free hydrochloric acid. It was taken up in a small amount of water, and the solution was decolorized, adjusted to pH 3.2 with dilute sodium hydroxide, and allowed to stand in a refrigerator. White crystals of III were collected, washed with cold water, and dried in air. Yield, 21 g. M. p. 214—215°C (decomp.).

Found: C, 60.71; H, 6.35; N, 5.88. Calcd. for $C_{12}H_{15}NO_4$: C, 60.75; H, 6.37; N, 5.90%.

**The Preparation of *N*-Benzoyl-DL-2-benzylglutamic Acid.**—*N*-Benzoyl-DL-2-benzylglutamic acid was prepared from 47.4 g. of III and 91 g. of benzoyl chloride using a procedure similar to that described for the preparation of *N*-benzoyl-DL-2-methylglutamic acid. Yield, 50 g. M. p. 193°C.

Found: C, 66.80; H, 5.61; N, 4.08. Calcd. for $C_{19}H_{19}NO_5$: C, 66.85; H, 5.61; N, 4.10%.

**The Optical Resolution of *N*-Benzoyl-DL-2-benzylglutamic Acid.**—Seventy-three grams of strychinine and 37 g. of *N*-benzoyl-DL-2-benzylglutamic acid were dissolved in 600 ml. of boiling methanol. The solution was then cooled to room temperature, 20 ml. of water was added with vigorous shaking, and the mixture was allowed to stand overnight in a refrigerator. The crystalline precipitate was collected and recrystallized twice from methanol. An optically pure *N*-benzoyl-2-benzylglutamic acid distrychinine salt was obtained. Yield, 44 g. M. p. 173—175°C, $[\alpha]_D^{20}$ +11.9° (*c* 1.2, methanol).

Forty-four grams of the distrychinine salt were decomposed with 270 ml. of 0.5 N sodium hydroxide at 5°C, and crystallized strychinine was removed. The alkaline solution was washed twice with 50 ml. of chloroform, and the aqueous layer was concentrated to half its volume and then acidified with 15 ml. of concentrated hydrochloric acid. The acidic solution was then left to stand overnight in an ice box, and 15 g. of *N*-benzoyl-(+)-2-benzylglutamic acid was obtained. $[\alpha]_D^{20}$ +52.6° (*c* 2.5, methanol). *N*-Benzoyl-(+)-2-benzylglutamic acid

4) B. E. Betts and W. Davey, *J. Chem. Soc.*, **1961**, 3336.

(14.7 g.) were hydrolyzed with 90 ml. of 20% hydrochloric acid for 4 hr. After standing overnight in a refrigerator, the crystallized benzoic acid was removed from the hydrolyzate and the filtrate was washed twice with ether. The solution was evaporated to drynesss in vacuo. The residue was dissolved in a small amount of water, and the solution was evaporated to dryness again in order to remove the free hydrochloric acid. To the residual syrup, 20 ml. of water was added. The resulting solution was decolorized with charcoal, neutralized with alkali, and allowed to stand in an ice box. The crude product was collected, and for purification it was converted to the hydrochloride and neutralized with sodium hydroxide. Crystals of optically pure (+)-2-benzylglutamic acid were collected, washed with methanol-water, and dried. Yield, 6.0 g. M. p. 209°C, $[\alpha]_D^{20}$ +1.65° (*c* 10, 4 N HCl).

Found: C, 60.67; H, 6.28; N, 5.86. Calcd. for $C_{12}H_{15}NO_4$: C, 60.75; H, 6.37; N, 5.90%.

When the mother liquor of the *N*-benzoyl-(+)-2-benzylglutamic acid distrychinine salt was treated in the manner described above, crystals of (−)-2-benzylglutamic acid were obtained. Yield, 3.2 g. M. p. 208°C, $[\alpha]_D^{20}$ +1.60° (*c* 10, 4 N HCl).

Found: C, 60.70; H, 6.33; N, 5.83. Calcd. for $C_{12}H_{15}NO_4$: C, 60.75; H, 6.37; N, 5.90%.

**Summary**

1) The optical resolution of DL-2-methylglutamic acid has been performed using brucine as a resolving reagent; the two optically active isomers have been obtained.

2) DL-2-Benzylglutamic acid has been synthesized using benzyl cyanide and diethyl succinate as the starting materials. Moreover, the optical resolution of this amino acid has been performed using strychinine as a resolving reagent. The two optically active isomers were obtained.

This research was made possible by support by the Kawaken Fine Chemicals Ltd. Co., Tokyo, and the Ajinomoto Co., Inc., Tokyo. The authors wish also to express their sincere thanks to Miss Kiku Koike and Miss Masako Kawakita of this Institute for their elemental analysis.

*Division of Organic Chemistry*
*Institute for Protein Research*
*Osaka University*
*Kita-ku, Osaka*

# Chemical Effects Associated with $\beta$-Decay Process. I. The Chemical Behavior of a Decayed Product, $^{144}Pr$, in the EDTA Complex System

By Takanobu SHIOKAWA, Hiroshi KUDO and Takashi OMORI

(Received December 11, 1964)

Many papers on the chemical effects of $\beta$-decay processes have appeared in current literature, with especial emphasis laid on the change in the oxidation state of radioactive daughter atoms. It has been widely accepted that the unusual behavior of radioactive daughter atoms is to be attributed, in the main, to an electronic excitation resulting from the abrupt change in the nuclear charge. On the other hand, the probability of a bond rupture resulting from the recoil only is fairly small, because in many cases the effective recoil energy and the chemical bond energy are of the same order of magnitude.

The lanthanides provide an opportunity to study the chemical behavior of the radioactive daughter atoms formed by the $\beta$-decay process, especially the effects of the electronic excitation; that is, their chemical properties are similar to each other, and the daughter atoms are in an excited state or are thermodynamically unstable, even in the simple $\beta$-decay.

Cerium-praseodymium-144 possesses several advantages in its nuclear and chemical properties for this purpose. The present investigation will study the chemical behavior of $^{144}Pr$ atoms formed by the $\beta^-$-decay of the $^{144}Ce$-labeled cerium(III) ethylenediaminetetraacetate (Ce(III)-EDTA) complex in aqueous and aqueous-alcohol solutions. Previously, the chemical behavior of $^{144}Pr$ in the $^{144}Ce$(III) acetylacetonate system was investigated by Edwards and Coryell[1] and was found to be considerably different from that of the parent $^{144}Ce$. In the lanthanide system it was also reported that 59 per cent of the $^{177}Lu$ atoms formed by the

1) R. R. Edwards and C. D. Coryell, TID-13363 (1961).

$\beta^-$-decay of the $^{177}Yb(III)$-EDTA complex escape from the complex, and appear in solution in the cationic form, $^{177}Lu^{3+}$.[2]

## Experimental

**Reagents.**—Carrier-free Ce-Pr-144 in a hydrochloric acid solution was imported from the Oak Ridge National Laboratory. The solution of disodium ethylenediaminetetraacetate (EDTA) was standardized against a standard zinc(II) solution by volumetric titration, using Eriochrome Black T as an indicator. A stock solution of cerium(III) was prepared by dissolving guaranteed-reagent-grade $Ce(NO_3)_3 \cdot 6H_2O$ in hydrochloric acid, and it was standardized volumetrically against the standard EDTA solution with Eriochrome Black T. All the other chemicals used were of guaranteed-reagent grade.

**Apparatus and Procedure.**—An aliquot of the cerium(III) chloride solution labeled with $^{144}Ce$ was evaporated to dryness in the presence of hydrogen peroxide. To the solid cerium(III) chloride, a known amount of a EDTA solution was added, less in amount than the equivalent ([EDTA]/[Ce(III)]=0.766), and then the Ce(III)-EDTA complex solution was prepared by passing it through a Dowex 50W-X8 column at pH 6.5 in order to remove the excess cerium. The separate experiments ensured that the separation was quantitative, indicating the presence of no excess EDTA. The final concentration of cerium(III) was $1.2 \times 10^{-3}$ M. The pH was adjusted by the addition of an ammonium acetate buffer. Aliquots of the solution were allowed to stand in a bath of the desired temperature for 4 hr. The samples were then withdrawn through a Dowex 50W-X8 column (8 mm.×20 mm.), and the free-ion fraction was separated from the complex fraction. The resin used had been treated previously with an appropriate buffer.

The yield of the free-ion fraction was obtained by counting the $\gamma$-activities of both the resin phase and the combined effluents. The cerium-144 was assayed by counting only the hard $\gamma$-activities of $^{144}Pr$ in secular equilibrium with $^{144}Ce$ 3 hr. later. The yield of $^{144}Pr$ ions was obtained by extrapolating the $^{144}Pr$ decay (or growth) curve to the time of chemical separation, using the half-life of 17.5 min.[3] The pH of the solution was measured with a glass-electrode pH meter, with an accuracy of 0.02 pH.

## Results

The experiments have shown that the apparent yield of the $^{144}Pr$ ion, which is defined as the extent of the free-ion fraction absorbed on the resin, depends on the pH, the concentration of ethyl alcohol, and the temperature.

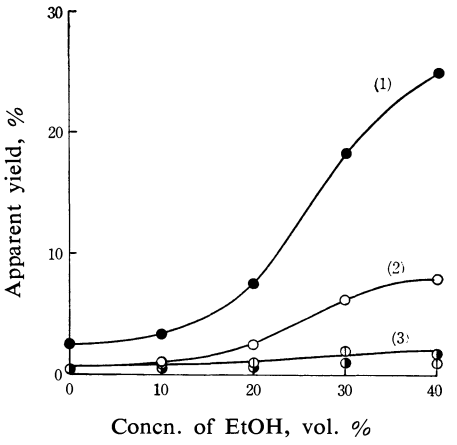



Fig. 1. Effect of concentration of ethyl alcohol on apparent yields of $^{144}Pr^{3+}$ and $^{144}Ce^{3+}$ at pH 6.7.
(1) and (2) : $^{144}Pr$ ; (3) : $^{144}Ce$
○ and ⓘ : 28°C ; ● and ◑ : 3°C

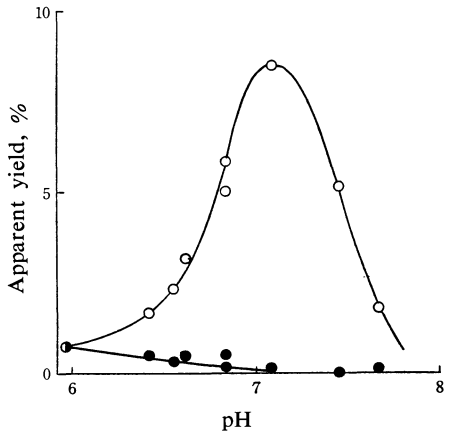



Fig. 2. Apparent yields of $^{144}Pr^{3+}$ and $^{144}Ce^{3+}$ in aqueous solution at 3°C.
○ : $^{144}Pr$ ; ● : $^{144}Ce$

As Fig. 1 shows, the apparent yield of $^{144}Pr$ ions increases slightly up to 20 per cent ethyl alcohol, while above this point the yield increases abruptly. The maximum concentration of ethyl alcohol used in the experiments was 40 per cent because of the small solubility of the Ce(III)-EDTA complex.

The distribution of the apparent yields of $^{144}Pr$ ion and $^{144}Ce$ ion as a function of the pH at a constant temperature is shown in Figs. 2 and 3. These figures show that there is a remarkable difference between the distribution curves of $^{144}Pr$ and $^{144}Ce$. For instance, the yield of free cerium ions decreases gradually as the pH increases, whereas the distribution curves of praseodymium have a maximum.

According to the formation constant of the

2) P. Glentworth and R. H. Betts, *Can. J. Chem.*, **39**, 1049 (1961).
3) B. S. Dzhelepov and L. K. Peker, "Decay Schemes Radioactive Nuclei," Pergamon Press, New York (1961), p. 422.

Ce(III)-EDTA complex,[4] cerium(III) forms completely the complex with EDTA under these experimental conditions. Because of the absence of excess EDTA, however, it should be noted that the cerium absorbs to some extent on the resin as the apparent formation constant decreases. These facts are clearly shown by the distribution behavior of $^{144}Ce$ in Figs. 2 and 3.

The distribution curves of $^{144}Pr$ may be influenced by both the normal distribution and the so-called "hot-atom" effect. To obtain the net "hot-atom" effect of $^{144}Pr$, we subtracted the extent of normal distribution from the apparent distribution curve, on the assumptions that the normal distribution curve of praseodymium is similar to that of cerium, and that the distribution constants of cerium and praseodymium are equal. The results are shown in Fig. 4.

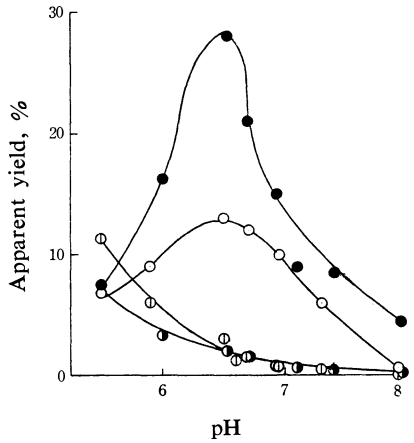



Fig. 3. Apparent yields of $^{144}Pr^{3+}$ and $^{144}Ce^{3+}$ in 40 % alcohol solution.
○ and ●: $^{144}Pr$; ⦶ and ◑: $^{144}Ce$
○ and ⦶: 25°C; ● and ◑: 3°C

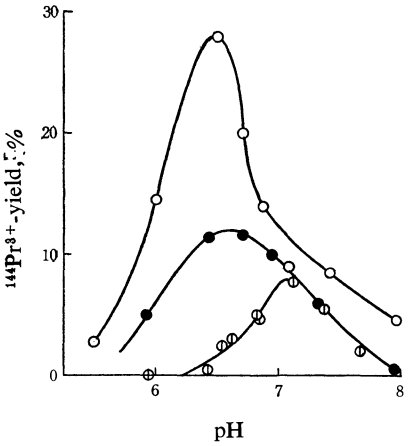



Fig. 4. $^{144}Pr^{3+}$-yield as a function of pH.
⦶: Aqueous solution at 3°C
●: 40 % alcohol solution at 25°C
○: 40 % alcohol solution at 3°C

## Discussion

The maximum yield of the $^{144}Pr$ ion is 28 per cent in a 40 per cent alcohol solution at 3°C, suggesting that in at least 28 per cent of the events the cerium(III)-EDTA bonds were ruptured as a result of the $\beta^-$-decay of $^{144}Ce$. Since the nuclear event itself is insensitive to the surrounding conditions, the extent of the bond rupture should also be independent of the pH. The results shown in Fig. 4, therefore, suggest that, after nuclear events, the de-excited $^{144}Pr$ atom causes a chemical reaction with environmental substances during its lifetime.

It has been found that the rate of isotopic exchange reaction in the La(III)(Nd(III))-EDTA systems is fairly rapid.[5] In these systems, the rate of the exchange reaction, $R$, is expressed as:

$$R=k[\mathrm{LnY^-}]\ [\mathrm{H^+}] \qquad (1)$$

where $k$ is a rate constant of about $10^5$ l.·mol$^{-1}$min$^{-1}$ and where $\mathrm{LnY^-}$ designates the EDTA complex. Although the mechanism of the exchange reaction in the alkaline region has not been investigated, the mechanism seems to be similar to that in the In(III)-EDTA system:[6]

$$R=k[\mathrm{InY^-}]\ [\mathrm{OH^-}]^2 \qquad (2)$$

in which the rate of exchange is expressed as in Eq. 1 in the acid region. These values of the rate constants cannot be directly applied to the present system. On the basis of kinetics, however, the distribution curves of $^{144}Pr$ ion can be qualitatively explained. In the neutral region, the exchange rate has a minimum value, producing a maximum point in the distribution curve. The pH at which the yield of $^{144}Pr$ ions is at a maximum shifts to a lower value with an increase in the concentration of ethyl alcohol. These results suggest that the reaction expressed in Eq. 1 is depressed as compared with the reaction expressed in Eq. 2 in the alcoholic solution. As the temperature rises, the re-chelation of $^{144}Pr$ with EDTA

4) J. Bjerrum, G. Schwarzenbach and L. G. Sillén, "Stability Constants of Metal Ion Complexes, Part I. Organic Ligands," The Chemical Society, London (1958), p. 76.

5) R. H. Betts, O. F. Dahlinger and D. M. Munro, "Radioisotopes in Scientific Research. Proceedings of the First UNESCO International Conference, Paris, 1957," Vol. II, Pergamon Press, New York (1958), p. 326.

6) K. Saito and M. Tuchimoto, *J. Inorg. Nucl. Chem.*, **25**, 1245 (1963).

will be promoted; therefore, the yield of $^{144}Pr$ ion decreases with the temperature. These considerations lead to the conclusion that, in the $^{144}Ce(^{144}Pr)$-EDTA system, the very extensive disruption of the EDTA complex takes place as a result of the $\beta^-$-decay of $^{144}Ce$.

The cerium-144 is transformed to $^{144}Pr$ by $\beta^-$-decay with energies of 0.320 (60 per cent) and 0.184 (30 per cent) MeV.[3] The recoil energy is low, ranging from 0 to 1.6 eV. according to the partition of energy between the $\beta^-$-particle and neutrino. This means that the probability of bond rupture as a result of the recoil only is much less than 1. Consequently, the fairly complete disruption of the complex may arise from the abrupt change in the atomic number of the metal ion.

Positively-charged species result from the increase in the nuclear charge in the $\beta^-$-decay, even in the absence of orbital electron ionization. At the instant of the simple $\beta^-$-decay of the $^{144}Ce$(III)-EDTA complex, $^{144}Pr$ exists in the tetravalent state, and the instability of tetravalent praseodymium in solution is favorable for an instantaneous stabilization reaction. For this stabilization reaction, it was suggested that, in the $\beta^-$-decay of $^{144}Ce$(III) acetylacetonate, the electron transfer of tetravalent $^{144}Pr$ with parent cerium(III) acetylacetonate might reduce the excited complex to stable $^{144}Pr$(III) acetylacetonate.[1] In the present system, however, considering that the EDTA is a reducing agent,[7] it is most probable that the electron transfer between the tetravalent $^{144}Pr$ and EDTA is predominant and that it, via an intermediate complex, results in the extensive bond rupture needed to liberate the $^{144}Pr$ ion. Moreover, it has been confirmed that such an intramolecular electron-transfer is often followed by a bond-rupture process.[8] (In order to treat the results strictly, however, it should be borne in mind that the presence of higher-charged $^{144}Pr$ in consequence of internal conversion cannot be ignored.)

Although the explanation offered here is not rigorous, it will be recognized that the most important factor in determining the fate of $^{144}Pr$ atoms is an increase in the nuclear charge of $^{144}Pr$ as a result of the $\beta^-$-decay of $^{144}Ce$. Furthermore, it is evident that the exchange reaction plays an important part in determining the $^{144}Pr^{3+}$-yield, even if the question remains unresolved of whether the intermediate complex has a finite lifetime, or whether it decomposes instantaneously.

## Summary

The chemical behavior of $^{144}Pr$ formed by the $\beta^-$-decay of the $^{144}Ce$(III)-EDTA complex has been investigated. The chemical behavior of $^{144}Pr$ is remarkably different from that of $^{144}Ce$. The results suggest that an increase in the nuclear charge of $^{144}Pr$ plays the most important role in determining the yield of $^{144}Pr$ ions and leads to the extensive disruption of the complex molecule by intramolecular electron-transfer. The liberated $^{144}Pr$ ion reforms the complex according to its kinetic law. The recoil as a result of $\beta^-$-decay seems not to be the cause of the formation of the free $^{144}Pr$ ions.

*Department of Chemistry*
*Faculty of Science*
*Tohoku University*
*Katahira-cho, Sendai*

7) T. Moeller, F. A. J. Moss and R. H. Marshall, *J. Am. Chem. Soc.*, **77**, 3182 (1955).

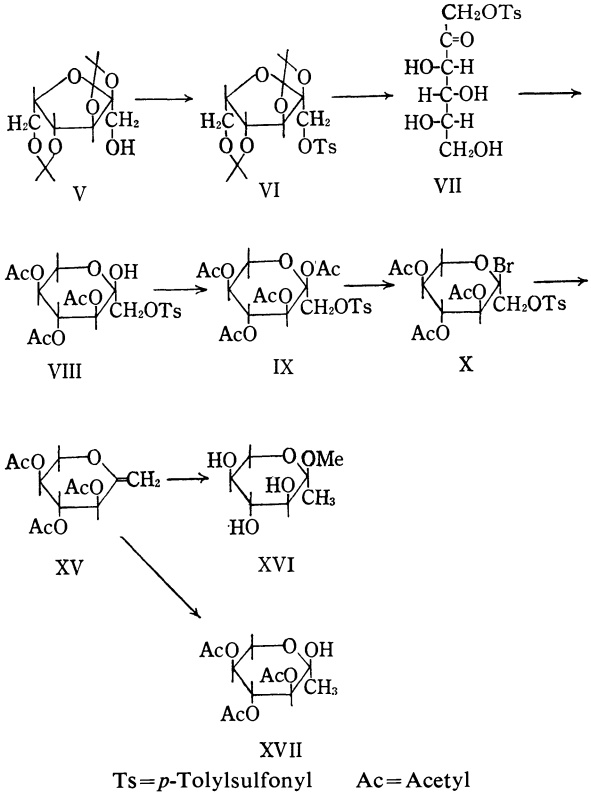
8) D. R. Stranks, "Modern Coordination Chemistry," Ed. by J. Lewis and R. G. Wilkins, Interscience Pub. Inc., New York (1960), p. 160.

# Sorboses. VI. 1, 2-Unsaturated-L-sorboses[1]

By Kanji TOKUYAMA, Etsuko TSUJINO (née HONDA) and Masumi KIYOKAWA

(Received December 14, 1964)

Although the 1, 2-unsaturated aldoses (glycals), which were first synthesized by Fischer,[2] have become important intermediates in the synthesis of a variety of carbohydrates,[3] no information about the synthesis of 2, 3-unsaturated ketoses, corresponding to glycals, has yet been reported. Our attempt to synthesize the 2, 3-unsaturated derivative of L-sorbose (I), a glycal homologue of ketohexose, was also unsuccessful. That is, by Fischer's method,[2] 1, 3, 4, 5-tetra-*O*-acetyl-α-L-sorbopyranosyl chloride (II),[4,5] which had been derived from 1, 2, 3, 4, 5-penta-*O*-acetyl-α-L-sorbopyranose (III),[4] was not converted into the compound with a double bond, but into 1, 3, 4, 5-tetra-*O*-acetyl-α-L-sorbopyranose (IV).[4] Under the reaction conditions employed, only solvolyses were always observed. These results prompted us to synthesize 1, 2-unsaturated L-sorbose.




Ts=*p*-Tolylsulfonyl Ac=Acetyl

Chart 1

The synthesis of 1, 2-dideoxy-1, 2-ene-L-sorbopyranose was achieved by the schemes outlined in Chart 1. For the introduction of a double bond into the C-1, 2 position, the synthesis of 1-*O*-tosyl-2-bromo derivatives of I was desired. At the outset, 1-*O*-tosyl-L-sorbose (VII),[6] which was obtainable from 2, 3 : 4, 6-di-*O*-isopropylidene-α-L-sorbofuranose (V)[7] via 1-*O*-tosyl-2, 3 : 4, 6-di-*O*-isopropylidene-α-L-sorbofuranose (VI),[8] was prepared as the starting material.

The acetylation of VII with acetic anhydride in pyridine gave triacetate (VIII), whose infrared spectrum showed the characteristic bands due to a pyranose ring[9,10] and whose optical rotation suggested that it was an α-anomer. Therefore, the structure VIII was confirmed to be 1-*O*-tosyl-3, 4, 5-tri-*O*-acetyl-α-L-sorbopyranose. The further acetylation of VIII with acetic anhydride in the presence of sodium acetate at room temperature gave 1-*O*-tosyl-2, 3, 4, 5-tetra-*O*-acetyl-α-L-sorbopyranose (IX), whose configuration was supported by the optical rotation and the infrared spectrum.[9,10] This compound is not very stable, but it can be kept well under cold conditions. The treatment of IX with dry hydrogen bromide in acetic acid gave a crystalline bromo-derivative, 1-*O*-tosyl-2-deoxy-2-bromo-3, 4, 5-tri-*O*-acetyl-α-L-sorbopyranose (X), which was very sensitive to moisture. The configuration of this compound was confirmed as follows (see Chart 2). The methanolysis of X in the presence of silver

1) Part V of this series: K. Tokuyama, This Bulletin, **37**, 1133 (1964).

2) E. Fischer, *Ber.*, **47**, 196 (1914).

3) a) For review see B. Helferich, *Advan. Carbohydrate Chem.*, **7**, 209 (1952). b) R. J. Ferrier, W. G. Overend and A. E. Pyan, *J. Chem. Soc.*, **1962**, 1488; P. T. Manolopoulous, M. Mednich and N. N. Lichtin, *J. Am. Chem. Soc.*, **84**, 2203 (1962).

4) H. H. Schlubach and G. Graefe, *Ann.*, **532**, 211 (1937); Y. Khounine and G. Arragon, *Bull. soc. chim. France*, **1938**, 1404.

5) W. Korytnyk and J. A. Mills, *J. Chem. Soc.*, **1959**, 636.

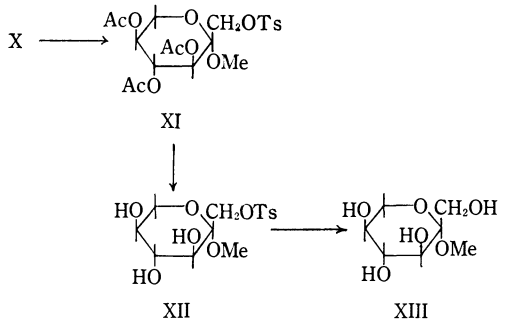
6) T. S. Gardner and J. Lee, *J. Org. Chem.*, **12**, 73 3 (1947).

7) T. Reichstein, *Helv. Chim. Acta*, **17**, 3111 (1934).

8) W. R. Sullivan, *J. Am. Chem. Soc.*, **67**, 837 (1945).

9) K. Tokuyama, M. Kiyokawa and N. Hōki, This Bulletin, **36**, 1392 (1963).

10) S. A. Barker and R. Stephens, *J. Chem. Soc.*, **1954**. 4550; S. A. Barker, E. G. Bourne, M. Stacy and D. H. Wiffen, ibid., **1954**, 171.



Me=Methyl

Chart 2

carbonate gave methyl 1-*O*-tosyl-3,4,5-tri-*O*-acetyl-β-L-sorbopyranoside (XI), whose optical rotation become much more positive than that of X. The deacetylation of XI with lithium aluminum hydride in tetrahydrofuran to form methyl 1-*O*-tosyl-β-L-sorbopyranoside (XII), followed by reduction with sodium in liquid ammonia, gave methyl β-L-sorbopyranoside (XIII). A comparison of the optical rotation of XIII obtained here with that of methyl α-L-sorbopyranoside (XIV)[11] indicated that the former was a β-anomer. Therefore, X was confirmed to be an α-anomer, and XI and XII to be β-anomers.

The treatment of X with sodium iodide in acetone under absolutely anhydrous conditions gave unstabl crystals (XV) with no bromine atom. Its infrared spectrum showed no band of a *p*-tolyl group, but that of a double bond at 1660 $cm^{-1}$. Some chemical investigations were carried out to decide whether or not the double bond is of an exo-methylene type because the out-of-plane deformation band at 1800—1750 $cm^{-1}$, which is characteristic of an exo-methylene type, was not observed because of overlapping with bands of the acetate groups around 1760 $cm^{-1}$. The deacetylation of XV with sodium methylate in methanol gave a deacetylated compound (XVI), which had no band of a double bond in the infrared spectrum, but two singlet peaks of a methyl ($\tau$ 8.66) and a methoxyl group ($\tau$ 6.81) in the NMR. Therefore, the structure of XVI was determined to be methyl 1-deoxy-L-sorbopyranoside formed by the addition of methanol to XV. When a benzene and ether solution of XV was passed through a silica gel column, another product, XVII, was obtained; it also had no double bond in the infrared spectrum and a methyl group in the NMR ($\tau$ 8.60). This compound reduced the Fehling solution. On the basis of these facts, the structure of XVII was determined to be 1-deoxy-3,4,5-tri-*O*-acetyl-L-sorbopyranose, which is an addition product of water to XV. The sugars obtained here seem to be α-anomers, judging from their optical rotations. The conversion of XV into XVI and XVII gave positive support to the assignment of the double bond, which should be an exo-methylene type. Thus, the structure of XV was established as 1,2-dideoxy-1,2-ene-3,4,5-tri-*O*-acetyl-L-sorbopyranose. A similar attempt to add ammonia or hydrogen sulfide to XV did not yield crystalline products.

Further studies of the addition reactions of XV were carried out (see Chart 3). The treatment of XV with bromine in a carbon tetrachloride solution at room temperature gave unstable 1,2-dideoxy-1,2-dibromo-3,4,5-tri-*O*-acetyl-α-L-sorbopyranose (XVIII). The methanolysis of XVIII in the presence of silver carbonate gave methyl 1-deoxy-1-bromo-3,4,5-tri-*O*-acetyl-β-L-sorbopyranoside (XIX). On the other hand, the reaction of XV with methanolic mercuric acetate yielded a sirup mixture containing mercury. The purification

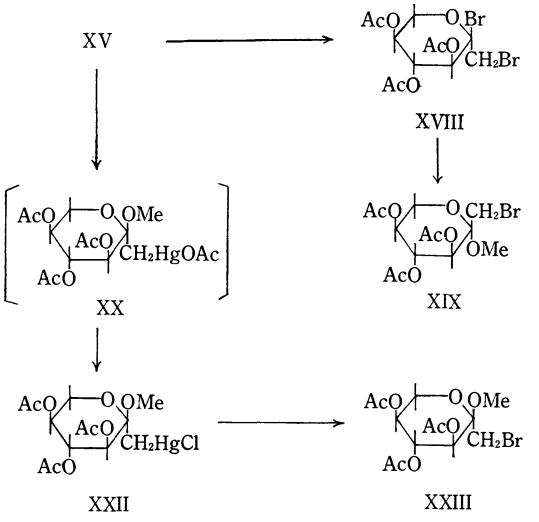


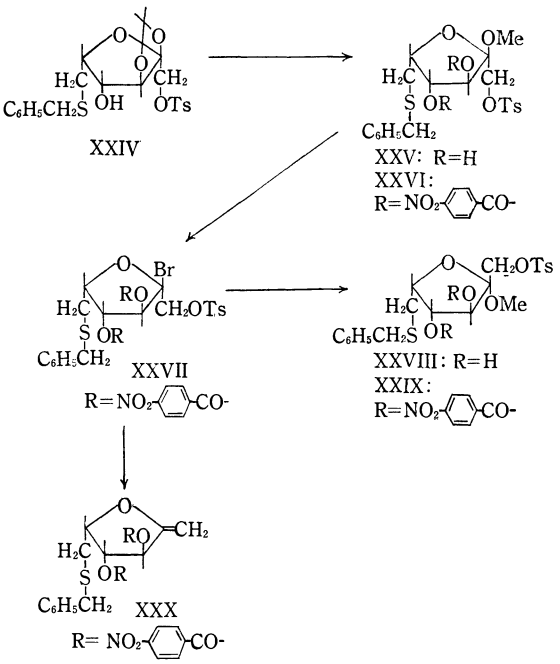
Chart 3

of the sirup was unsuccessful, but it was, on the basis of the evidence presented below, composed mainly of methyl 1-deoxy-1-acetoxymercuri-3,4,5-tri-*O*-acetyl-α-L-sorbopyranoside (XX), plus its β-anomer (XXI). When the sirup was shaken with a saturated solution of sodium chloride, a crystalline chloromercuric compound (XXII) was separated in a pure state. The optical rotation of the mother liquor shifted to a positive side than that of XXII. After the mother liquor had been evaporated, the residual solid gave satisfactory analytical data for the structure of XXII. Therefore, the structure of XXII was confirmed

11) E. Fischer, *Ber.*, **28**, 1145 (1895).

to be methyl 1-deoxy-1-chloromercuri-3, 4, 5-tri-*O*-acetyl-α-L-sorbopyranoside, while the mother liquor was composed of XXII and its β-anomer. These results suggest that the major component (XX) in the former sirup is probably methyl 1-deoxy-1-acetoxymercuri-3, 4, 5-tri-*O*-acetyl-α-L-sorbopyranoside, while the minor component (XXI) is a β-anomer of XX. The displacement reaction of mercury of XXII with bromine in a chloroform solution at room temperature gave methyl 1-deoxy-1-bromo-3,4,5-tri-*O*-acetyl-α-L-sorbopyranoside (XXIII). The conclusion that XXIII is an α-anomer and XIX, a β-anomer was obtained from the comparison of their optical rotations. Consequently, the configurations of XVIII, XX and XXII were confirmed as α-anomers.

The preparation of 1, 2-unsaturated sorbofuranose is also shown in Chart 4; it is almost identical with that used for 1, 2-unsaturated sorbopyranose (XV). In order to obtain an acylated sorbofuranose, we used 1-*O*-tosyl-2, 3-*O*-isopropylidene-6-*S*-benzyl-6-thio-α-L-sorbofuranose (XXIV)[12] as the starting material.




Chatr 4

The deacetonation of XXIV in a methanol solution with 1% of hydrogen chloride yielded methyl 1-*O*-tosyl-6-*S*-benzyl-6-thio-α-L-sorbofuranoside (XXV), which, under the standard conditions of *p*-nitrobenzoylation, formed a crystalline di-*p*-nitrobenzoate, methyl 1-*O*-tosyl-3, 4-di-*O*-*p*-nitrobenzoyl-6-*S*-benzyl-6-thio-α-L-sorbofuranoside (XXVI). The di-*p*-nitrobenzoate (XXVI) reacted with dry hydrogen bromide in acetic acid to yield 1-*O*-tosyl-2-deoxy-2-bromo-3, 4-di-*O*-*p*-nitrobenzoyl-6-*S*-benzyl-6-thio-α-L-sorbofuranose (XXVII), which was not obtainable in a pure state because of its instability. The glycosidation of XXVII with methanol in the presence of silver carbonate gave methyl 1-*O*-tosyl-6-*S*-benzyl-6-thio-β-L-sorbofuranoside (XXVIII), which was then converted into crystalline 1-*O*-tosyl-3, 4-di-*O*-*p*-nitrobenzoyl-6-*S*-benzyl-6-thio-β-L-sorbofuranoside (XXIX) A comparison of the optical rotations of two anomers, XXVI and XXIX, indicated that the former was an α-anomer and the latter, a β-anomer. Therefore, XXVII was determined to be an α-anomer. The treatment of XXVII with sodium iodide in acetone under absolutely anhydrous conditions gave 1, 2-dideoxy-1, 2-ene-3, 4-di-*O*-*p*-nitrobenzoyl-6-*S*-benzyl-6-thio-L-sorbofuranose (XXX), which has a band characteristic of a double bond at 1660 $cm^{-1}$ in the infrared spectrum. However, further studies of XXX failed because of its instability to moisture.

## Experimental[13]

**1-*O*-Tosyl-3, 4, 5-tri-*O*-acetyl-α-L-sorbopyranose (VIII).**—Into a cooled solution of 1-*O*-tosyl-L-sorbose (VII) (10 g.) in dry pyridine (100 ml.), acetic anhydride (100 ml.) was stirred in portions. After having been stirred at 0—5°C for 3 hr., the reaction mixture was poured onto ice, made alkaline with sodium carbonate, and extracted with benzene. The extract was washed with 5% sulfuric acid and then with water, and dried, after which the solvent was removed under reduced pressure. The recrystallization of the residue from ether and acetone or from alcohol gave colorless needles (10.7 g.); m. p. 141—144°C (decomp.), $[\alpha]_D^{24.5}$ +4.3 (*c* 0.997, chlororform).

Found: C, 49.79; H, 5.40; S, 6.94. Calcd. for $C_{19}H_{24}O_{11}S$ (460): C, 49.57; H, 5.22; S, 6.96%.

**1-*O*-Tosyl-2, 3, 4, 5-tetra-*O*-acetyl-α-L-sorbopyranose (IX).**—A solution of VIII (9 g.) and sodium acetate (9 g.) in acetic anhydride (90 ml.) was stirred at room temperature for 10 hr. The reaction mixture was then poured into chilled water. Neutralizing the solution with sodium carbonate separated a sirup which became crystalline on cooling. The solution was then filtered, and the residue washed with water. Recrystallization from ether gave colorles needles (9 g.); m. p. 118°C (decomp.), $[\alpha]_D^{26}$ −20.8 (*c* 1.097, chloroform).

Found: C, 50.28; H, 5.42; S, 6.38. Calcd. for $C_{21}H_{26}O_{12}S$ (502): C, 50.20; H, 5.18; S, 6.37%.

12) K. Tokuyama and M. Kiyokawa, *J. Org. Chem.*, **29**, 1475 (1964).

13) All melting points were measured by a Kofler block and are corrected. The NMR spectra were determined on a Varian A-60 spectrometer at 60 Mc. in deuteriochloroform at room temperature, using tetramethylsilane as an internal standard.

**1-*O*-Tosyl-2-deoxy-2-bromo-3, 4, 5-tri-*O*-acetyl-α-L-sorbopyranose (X).**—A solution of IX (5 g.) in acetic acid (20 ml.) was saturated with dry hydrogen bromide at 5—10°C. After it had stood at this temperature for 1 hr., the reaction mixture was extracted with chloroform, washed with a cooled sodium bicarbonate solution and then cold water, and dried, and the chloroform was removed. The recrystallization of the residue from ether and petroleum ether (b. p. 40—60°C) gave colorless needles (4 g.); m. p. 105—107°C (decomp.), $[\alpha]_D^{25.5}$ −69.7 (*c* 1.031, chloroform).

Found: C, 43.43; H, 4.42; S, 6.59; Br, 15.08. Calcd. for $C_{19}H_{23}O_{10}SBr$ (523): C, 43.59; H, 4.40; S, 6.12; Br, 15.11%.

**Methyl 1-*O*-Tosyl-3, 4, 5-tri-*O*-acetyl-β-L-sorbopyranoside (XI).**—A solution of X (0.8 g.) and silver carbonate (1.6 g.) in methanol (24 ml.) was stirred at room temperature for 1.5 hr. The solution was then filtered, the filtrate was evaporated to dryness under reduced pressure, and the residue was extracted with ether. After the removal of the ether, XI was obtained as a powder (0.6 g.); $[\alpha]_D^{23.5}$ +59.6 (*c* 1.094, chloroform).

Found; C, 50.40; H, 5.55; S, 6.67. Calcd. for $C_{20}H_{26}O_{11}S$ (504): C, 50.63; H, 5.48; S, 6.75%.

**Methyl 1-*O*-Tosyl-β-L-sorbopyranoside (XII).**—A solution of XI (0.95 g.) in tetrahydrofuran (10 ml.) was cooled at 0°C, and lithium aluminum hydride (0.126 g.) was added. After it had stood overnight at room temperature, the solution was refluxed for 8 hr. and then extracted with chloroform. The chloroform solution was washed with diluted hydrochloric acid and then water, and dried. The evaporation of the chloroform gave a sirup (0.2 g.), $[\alpha]_D^{23.5}$ +37.5 (*c* 0.62 methanol).

Found: C, 48.03; H, 5.96; S, 8.92. Calcd. for $C_{14}H_{20}O_8S$ (348): C, 48.26; H, 5.78; S, 9.20%.

**Methyl β-L-Sorbopyranoside (XIII).**—With constant stirring at −40°C, enough small pieces of sodium metal were added to a solution of XII (0.57 g.) in liquid ammonia (20 ml.) for the blue color to persist for 20 min. Then water was added to discharge the blue color. The ammonia was allowed to evaporate, and the residue was diluted with water. The aqueous solution was passed through an Amberlite XE 100 column, neutralized with silver carbonate, and evaporated to dryness under reduced pressure. The residue was extracted with methanol, and the solvent was removed. The residue was purified by silica gel thin-layer chromatography with chloroform and methanol (4:1, v/v). XIII was obtained as a colorless sirup (0.08 g.); $[\alpha]_D^{23.5}$ −13.3 (*c* 0.817, methanol).

Found: C, 42.70; H, 6.82. Calcd. for $C_7H_{14}O_6$ (194): C, 43.29; H, 7.27%.

**1, 2-Dideoxy-1, 2-ene-3, 4, 5-tri-*O*-acetyl-L-sorbopyranose (XV).**—Sodium iodide (12 g., freshly dried at 180°C and 3 mmHg pressure) was dissolved in acetone (60 ml.) which had been dried over potassium carbonate. The solution was then chilled to 5°C and stirred while X (3.9 g.) was added. The bromide was dissolved promptly, and the brown color of free iodine became apparent almost immediately. After the reaction mixture had stood overnight at room temperature, it was filtered and the residue was washed with acetone (15 ml.). The combined filtrate and washings were concentrated to dryness at room temperature under reduced pressure. Benzene was added, and the resulting solution was washed with cooled aqueous sodium bicarbonate containing a little sodium thiosulfate. After drying, the halogen-free solution was evaporated under reduced pressure. The recrystallization of the residue from ether and *n*-hexane gave colorless needles (1.35 g.); m. p. 80—82°C, $[\alpha]_D^{26.5}$ −9.3 (*c* 1.135, chloroform).

Found: C, 52.88; H, 6.09. Calcd. for $C_{12}H_{16}O_7$ (272): C, 53.06; H, 5.92%.

**Methyl 1-Deoxy-L-sorboside (XVI).**—XV (480 mg.) was dissolved in methanol (120 ml.) containing 2% of sodium. After standing overnight at room temperature, the reaction mixture was passed through the cation exchange resin column (Amberlite IR 120, 20 ml.) and then through the anion exchange column (Dowex 1, 20 ml.), and evaporated to dryness under reduced pressure. The recrystallization of the residue from acetone gave colorless needles (120 mg.); m. p. 149—150°C, $[\alpha]_D^{27.5}$ −103.4 (*c* 1.016, water).

Found: C, 46.94; H, 8.05. Calcd. for $C_7H_{14}O_5$ (178): C, 47.19; H, 7.87%.

**1-Deoxy-3, 4, 5-tri-*O*-acetyl-L-sorbopyranose (XVII).**—A solution of XV (100 mg.) in benzene and ether (1:1, v/v) was passed through the silica gel column (5 g.). After the solvent had been removed, colorless needles were obtained which were then recrystallized from acetone; m. p. 156—158°C, $[\alpha]_D^{27.6}$ −28.4 (*c* 1.055, chloroform).

Found: C, 49.56; H, 6.32. Calcd. for $C_{12}H_{18}O_8$ (290): C, 49.65; H, 6.25%.

**1, 2-Dideoxy-1, 2-dibromo-3, 4, 5-tri-*O*-acetyl-α-L-sorbopyranose (XVIII).**—To a solution of XV (0.4 g.) in carbon tetrachloride (2 ml.), bromine in carbon tetrachloride was added until the color persisted. After the mixture had been stirred at room temperature for 10 min., the solvent was removed and the residue was recrystallized from ether. Colorless needles were obtained (0.25 g.); m. p. 130°C (decomp.), $[\alpha]_D^{24}$ −3.5 (*c* 0.116, methanol).

Found: C, 33.54; H, 3.90; Br, 36.30. Calcd. for $C_{12}H_{16}O_7Br_2$ (432): C, 33.55; H, 3.73; Br, 36.99%.

**Methyl 1-Deoxy-1-bromo-3, 4, 5-tri-*O*-acetyl-β-L-sorbopyranoside (XIX).**—To a solution of XVIII (0.25 g.) in methanol (10 ml.), silver carbonate (0.5 g.) was added. After it had been stirred at room temperature for 2 hr., the solution was filtered and the residue was washed with methanol. The combined filtrate and washings were concentrated to dryness under reduced pressure. The residue was purified by thin layer chromatography (silica gel, chloroform-acetone, 9:1, v/v). XIX was obtained as a sirup (45 mg.); $[\alpha]_D^{24}$ +57.6 (*c* 0.184, methanol).

Found: C, 41.12; H, 5.14; Br, 20.33. Calcd. for $C_{13}H_{19}O_8Br$ (383): C, 40.74; H, 5.00; Br, 20.85%.

**Methyl 1-Deoxy-1-chloromercuri-3, 4, 5-tri-*O*-acetyl-α-L-sorbopyranoside (XXII).**—To a solution of mercuric acetate (1.54 g.) in absolute methanol

(25 ml.), XV (1.4 g.) was added. After the mixture had stood overnight at room temperature, the solvent was removed and extracted with ether, and then the ether was removed. The residue, which was a mixture of XX as the major component and XXI as the minor component, was dissolved in chloroform, shaken with a saturated aqueous sodium chloride solution for 20 min., washed with sodium bicarbonate and then with water, dried, and the solvent removed. The recrystallization of the residue from ethanol gave colorless crystals (0.48 g.); m. p. 150—152°C, $[\alpha]_D^{25}$ −8.9 (*c* 1.025, methanol).

Found: C, 29.42; H, 3.61; Hg, 37.86. Calcd. for $C_{13}H_{19}O_8HgCl$ (539): C, 29.09; H, 3.84; Hg, 37.14%.

**Methyl 1-Deoxy-1-bromo-3, 4, 5-tri-*O*-acetyl-α-L-sorbopyranoside (XXIII).**—Bromine in chloroform was stirred at room temperature into a solution of XXII (0.2 g.) in chloroform (4 ml.) until the color persisted. The solution was then filtered and evaporated to dryness under reduced pressure. The recrystallization of the residue from methanol gave needles (80 mg.); m. p. 106—107°C, $[\alpha]_D^{24}$ −28.6 (*c* 1.040, methanol).

Found: C, 40.62; H, 5.03; Br, 21.16. Calcd. for $C_{13}H_{19}O_8Br$ (383): C, 40.70; H, 5.00; Br, 20.85%.

**Methyl 1-*O*-Tosyl-3, 4-di-*O*-*p*-nitrobenzoyl-6-*S*-benzyl-6-thio-α-L-sorbofuranoside (XXVI).**—A solution of XXIV (1.1 g.) in methanol (120 ml.) containing 1% of hydrogen chloride was refluxed for 3 hr. After it had cooled, the solution was neutralized with silver carbonate and filtered, and then the solvent was removed under reduced pressure. A solution of the residue (crude XXV) and *p*-nitrobenzoyl chloride (1.4 g.) in dry pyridine (8 ml.) was stirred at room temperature for 3 hr. After standing overnight at room temperature, the reaction mixture was poured onto ice, neutralized with sodium carbonate, and extracted with chloroform. The chloroform was washed with diluted sulfuric acid and then water, and the chloroform was removed. The recrystallization of the residue from ethanol gave colorless crystals (0.8 g.); m. p. 55—57°C, $[\alpha]_D^{23}$ −50.8 (*c* 0.748, chloroform).

Found: C, 55.32; H, 4.37; N, 3.92; S, 8.33. Calcd. for $C_{35}H_{32}N_2O_{13}S_2$ (752): C, 55.85; H, 4.25; N, 3.72; S, 8.51%.

**1-*O*-Tosyl-2-deoxy-2-bromo-3, 4-di-*O*-*p*-nitrobenzoyl-6-*S*-benzyl-6-thio-α-L-sorbofuranose (XXVII).**—A solution of XXVI (1 g.) in acetic acid (5 ml.) was saturated with dry hydrogen bromide at 0—5°C. After standing at this temperature for 30 min., the reaction mixture was extracted with chloroform, washed with cooled aqueous sodium bicarbonate, dried, and evaporated under reduced pressure to give XXVII as an unstable sirup (1.17 g.); $[\alpha]_D^{24}$ −110.7 (*c* 1.073, chloroform).

Found: Br, 11.77. Calcd. for $C_{34}H_{29}N_2O_{12}S_2Br$ (801): Br, 9.99%. (The attempt to purify the sirup obtained here failed because of its instability.)

**Methyl 1-*O*-Tosyl-3, 4-di-*O*-*p*-nitrobenzoyl-6-*S*-benzyl-6-thio-β-L-sorbofuranoside (XXIX).**—To a solution of XXVII (500 mg.) in methanol (100 ml.), silver carbonate (7 g.) was added. After it had been stirred at room temperature for 9 hr., the reaction mixture was filtered and the residue washed with methanol. The filtrate and washings were concentrated under reduced pressure to give a colorless sirup (162 mg.). To a solution of the sirup in dry pyridine (5 ml.), *p*-nitrobenzoyl chloride (300 mg.) was added. After it had been stirred at room temperature for 11 hr. the reaction mixture was poured into ice water, neutralized with sodium carbonate, and extracted with chlorofrom. The chloroform solution was then washed with cooled dilute sulfuric acid and then water, and the solvent was removed. The recrystallization of the residue gave colorless needles (236 mg.); m. p. 46—50°C, $[\alpha]_D^{23.5}$ −8.3 (*c* 1.058, chloroform).

Found: C, 55.86; H, 4.36; N, 3.88; S, 8.15. Calcd. for $C_{35}H_{22}O_{13}N_2S_2$ (752): C, 55.85; H, 4.25; N, 3.72; S, 8.51%.

**1, 2-Dideoxy-1, 2-ene-3, 4-di-*O*-*p*-nitrobenzoyl-6-*S*-benzyl-6-thio-L-sorbofuranose (XXX).**—To a solution of XXVII (300 mg.) in dry acetone (8 ml.) freshly-dried sodium iodide (600 mg.) was added. After the reaction mixture had stood at room temperature for 68 hr., it was filtered and the residue was washed with acetone (15 ml.). The combined filtrate and washings were concentrated to dryness at room temperature under reduced pressure. Benzene was added to the residue, and the resulting solution was washed with cooled aqueous sodium bicarbonate containing a little sodium thiosulfate. After it had been dried, the halogen-free solution was evaporated under reduced pressure. The recrystallization of the residue from alcohol gave unstable crystals (240 mg.); m. p. 55—57°C, $[\alpha]_D^{23}$ −58.7 (*c* 0.732, chloroform).

Found: C, 58.64; H, 4.08; N, 4.86; S, 5.93. Calcd. for $C_{27}H_{22}O_9N_2S$ (550): C, 58.91; H, 4.00; N, 5.09; S, 5.82%.

The authors wish to express their deep gratitude to Dr. Ken'ichi Takeda, Director of this Laboratory, and to Dr. Kaname Hamamoto for their encouragement. They are also indebted to Dr. Kazuo Tori of this Laboratory for his valuable discussion of the NMR spectra.

*Shionogi Research Laboratory*
*Shionogi & Co., Ltd.*
*Fukushima-ku, Osaka*

# Reactive Fiber. IV. The Graft Copolymerization of Glycidyl Methacrylate onto Polypropylene and Polyvinyl Chloride Fibers

By Yoshio IWAKURA, Toshikazu KUROSAKI, Kuniharu NAGAKUBO
Kenji TAKEDA and Masatoshi MIURA

(Received December 14, 1964)

In a series of studies of reactive fibers, the epoxide group containing fibers[1] from acrylonitrile-glycidyl methacrylate (GMA), the acrylonitrile-glycidyl acrylate copolymer, the GMA-grafted cellulose fiber[2] and fibers[3] from *N-p-*(*N'-β*-chloroethylaminosulfamoyl)phenylacrylamide and *N-p-*(*N'-β*-chloroethylaminosulfamoyl)phenylmethacrylamide copolymers were synthesized and their chemical reactivities investigated.

In this paper, the graft copolymer of GMA onto polypropylene (PP) and polyvinyl chloride (PVC) fiber were prepared by the $\gamma$-ray pre-irradiation technique in vacuo. The present method avoided the homopolymerization of GMA and the oxidative degradation of PVC fiber, and introduced epoxide groups into the fibers under mild conditions.

The grafted fibers obtained had high chemical reactivities with amines and hydroxyamines.

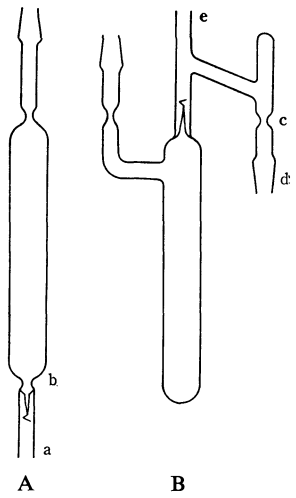



Fig. 1. Ampoules for grafting.

## Experimental

**Materials.** — Polypropylene fiber, the product of Avisun (3—4 deniers), extracted with acetone for six hours in a Soxhlet apparatus.

Polyvinyl chloride fiber, the product of the Teijin Co. (3—4 deniers), was wound on an aluminum plate and extracted with benzene for an hour, and then with acetonitrile for an additional hour in a Soxlet apparatus.

Glycidyl methacrylate (GMA) was purified by distillation under reduced pressure through a column with copper McMahon packing.

Tetrahydrofuran was washed with a mixture of ferrous sulfate and concentrated sulfuric acid in order to remove peroxides, and then distilled.

The other solvents were purified by the usual methods.

**Graft Copolymerization.**—Graft copolymerization was carried out in the sealed-glass apparatus[4] shown in Fig. 1. Tube A, which contained the fiber, was evacuated at $10^{-3}$ mmHg for eitht hours, sealed, and then irradiated by $\gamma$-ray from 4000 curie $^{60}$Co at room temperature. Tube B, which contained a monomer solution, was degassed and sealed. The irradiated tube A was connected to B through a and e, evacuated to $10^{-3}$ mmHg through d, and sealed at f. The monomer in B was transferred into A by breaking two breakable joints, and then the system was sealed at b and placed in a constant temperature bath for a definite time. The grafted fiber was separated from the system, washed with acetone (in the case of polypropylene) or with acetonitrile (polyvinyl chloride) by means of a Soxhlet apparatus, and dried in vacuo. The grafting ratio was expressed by the ratio of the weight gain to the initial weight.

**The Measurement of the Dye Exhaustion.**—The fiber was treated in a dyeing bath at 90°C for 60 min. (in the case of polypropylene) or at 60°C for 100 min. (polyvinyl chloride). The extent of dye exhaustion was measured by a spectrophotometer. The dyes used were Direct Sky Blue FF and Benzopurprine 4B (direct dyes), and Acid Orange II, and Acid Brilliant Scarlet 3R (acid dyes). The composition of the dyeing bath was as follows:

For direct dye: 0.02 parts of dye, 0.02 parts of sulfuric acid, 0.04 parts of anhydrous sodium sulfate and 50 parts of water.

For acid dye: 0.02 parts of acid dye, 0.02 parts of acetic acid and 50 parts of water.

One part of the grafted fiber was used for the dyeing bath prepared above.

1) Y. Iwakura, T. Kurosaki and N. Nakabayashi, *Makromol, Chem.*, **44/46**, 570 (1961).
2) Y. Iwakura, T. Kurosaki, K. Uno and Y. Imai, *J. Polymer Sci.*, **4C**, 673 (1961).
3) Y. Iwakura and N. Nakabayashi, *Makromol. Chem.*, will be published.
4) M. Miura and S. Kawamatsu, *Kobunshi Kagaku*, **19**, 175 (1962).

**The Determination of the Epoxy Value.**—The epoxide value of the grafted fiber was determined by the HCl-Dioxane method.[5] A portion of approximately 100 mg. of grafted PVC fiber was immersed in a solution of 25 ml. of dioxane and 20 ml. of 0.1 N hydrochloric acid-dioxane. The mixture was then allowed to stand overnight, and the excess hydrochloric acid was treated with 0.1 N sodium hydroxide aqueous solution, using phenolphtalein as an indicator.

## Results and Discussion

**The Graft Copolymerization of Glycidyl Methacrylate to Polypropylene.** — When the polypropylene fiber irradiated at dose of 5 Mr. was immersed in undiluted GMA at 30°C, the monomer polymerized into a jelly state. The homopolymer producted was insoluble in acetone and dioxane, which are good solvents for polyglycidyl methacrylate. The cross linking of the homopolymer was prevented by adding a solvent, such as acetone, ethyl acetate, tetrahydrofuran or benzene, in the graft polymerization. The Influence of the solvent on the grafting ratio is given Fig. 2. A solvent such

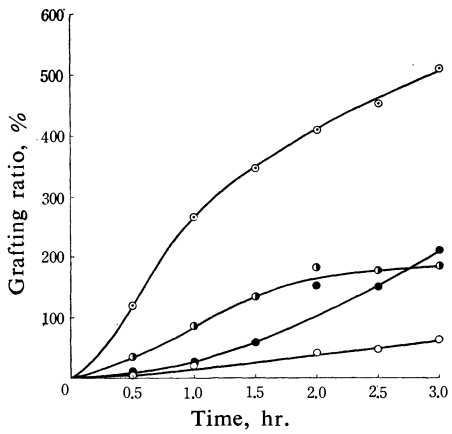



Fig. 2. Influence of solvent on the grafting ratio at the graft polymerization of GMA to polypropylene at 30°C.
Irradiation dose 5 Mr., dose rate $2.7\times10^5$ r./hr., monomer concentration 20 wt. %

○ Acetone ● Ethylacetate
◑ Tetrahydrofuran ⊙ Benzene

as ethyl acetate or acetone gave a slow initial grafting rate, while benzene gave a higher one. The former two solvents cannot swell as polypropylene fiber, but the latter one can swell the fiber. Figures 3 and 4 show the relation between the grafting ratio and the monomer concentration in benzene or tetrahydrofuran. On all occasions, the addition of a small amount of solvent to GMA increased the

5) G. P. King, *Nature*, **164**, 706 (1964).

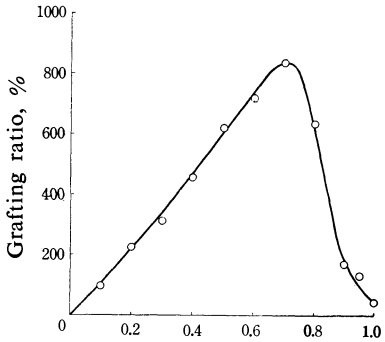



Fig. 3. Influence of monomer concentration on the grafting ratio at the graft polymerization of GMA to polypropylene in benzene.
Irradiation dose 5 Mr., dose rate $2.7\times10^5$ r./hr., grafting temperature 30°C, reaction time 1 hr.

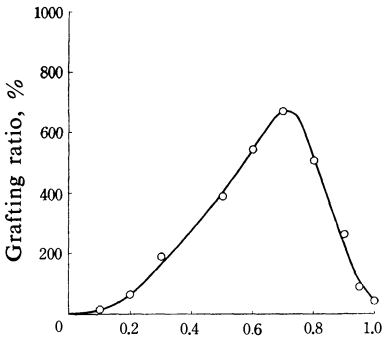



Fig. 4. Influence of monomer concentration on the grafting ratio at the graft polymerization of GMA to polypropylene in tetrahydrofuran.
Irradiation dose 5 Mr., dose rate $2.7\times10^5$ r./hr., grafting temperature 30°C, reaction time 1 hr.

grafting ratio. The effect of the solvent can be explained by assuming that the monomer molecules could diffuse into the polymer swelled by the solvent.

**The Graft Copolymerization of Glycidyl Methacrylate to Polyvinyl Chloride.**—The graft copolymerization was carried out at 16°C in a 20 wt. % monomer solution, using benzene, acetone, *n*-hexane, carbon tetrachloride or ethanol as the solvent. It was found that no graft polymerization proceeded in a solvent, such as *n*-hexane, carbon tetrachloride or ethanol, which did not swell the polyvinyl chloride. On the other hand, the graft polymerization did proceed in benzene or acetonitrile. The influence of the temperature on the grafting in benzene is shown in Fig. 6.

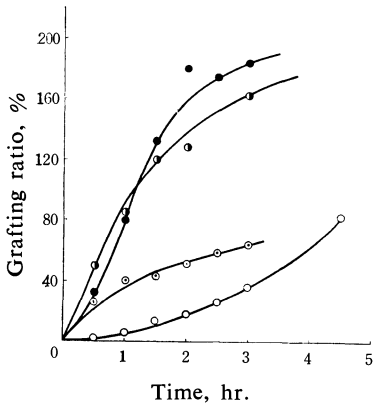



Fig. 5. Influence of temperature on the grafting ratio at the graft polymerization of GMA to polypropylene.
Irradiation dose 5 Mr., dose rate $2.7\times10^5$ r./hr., solvent tetrahydrofuran, monomer concentration 20 wt. %
○ 15.5°C ● 30°C ◑ 45°C ⊙ 60°C

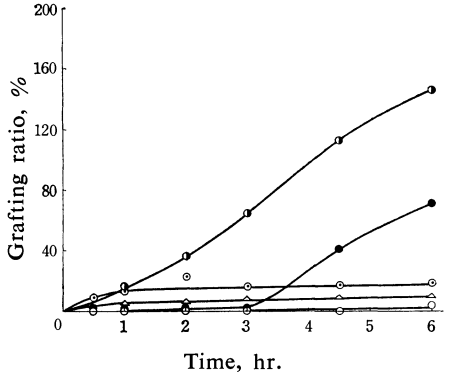



Fig. 6. Influence of temperature on the grafting ratio at the graft polymerization of GMA to polyvinyl chloride in benzene.
Irradiation dose 1.5 Mr., dose rate $7.8\times10^4$ r./hr, monomer concentration 20 wt. %
○ 5°C ● 8.5°C ◑ 16°C ⊙ 26°C △ 35°C

The optimum temperature for grafting is in a range from 10 to 20°C. Figure 5 shows the influence of the grafting temperature on the grafting ratio when tetrahydrofuran was used as solvent. The preferred temperature range for grafting was 30—45°C. At a temperature lower than 30—45°C, the initial grafting rate decreased because of the slow diffusion of the monomer molecules into the polymer. At a temperature higher than 30—45°C, the termination and the recombination of the trapped free radicals predominated the propagation and the grafting ratio was saturated, as is shown in Fig. 5.

Comparing polypropylene with polyvinyl chloride, the difference in the optimum temperature range for grafting may be explained as follows. In the case of polypropylene, the intermolecular forces in the crystalline regions are strong enough to keep the crystalline state up to a comparatively high temperature, even in the presence of a solvent. In the case of polyvinyl chroride, however, the intermolecular forces at the crystallline region become weak when the monomers diffuse into the amorphous region and the trapped free radicals recombine easily.

The temperature dependency on the grafting rate in acetonitrile is shown in Fig. 7. The grafting rate decreased in a temperature range from 8.5 to 52°C. Figure 8 shows the influence of the monomer concentration on the

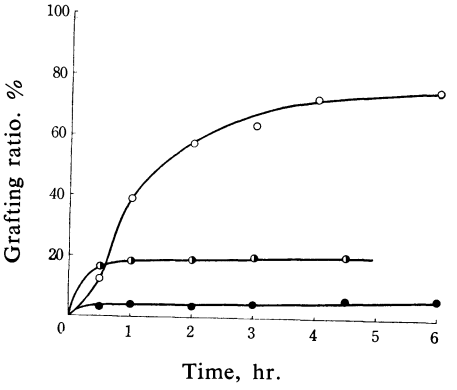



Fig. 7. Influence of temperature on the grafting ratio at the graft polymerization of GMA to polyvinyl chloride in acetonitrile.
Irradiation dose 1.9 Mr., dose rate $7.8\times10^4$ r./hr., monomer concentration 20 wt. %
○ 8.5°C ◑ 16°C ● 25°C

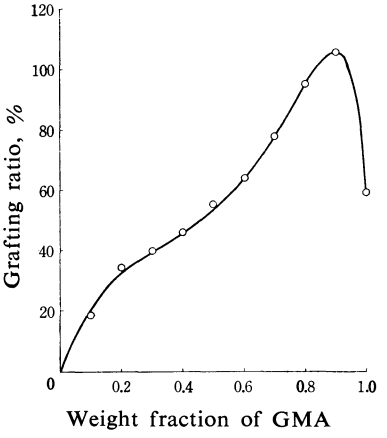
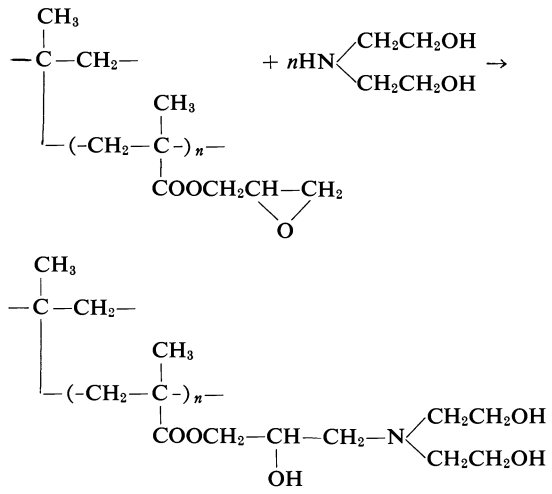



Fig. 8. Influence of monomer concentration on the grafting ratio at the graft polymerization of GMA to polyvinyl chloride at 16°C in benzene.
Irradiation dose 1.9 Mr., dose rate $7.8\times10^4$ r./hr., reaction time 2 hr.

grafting in benzene. The addition of a small amount of solvent to the monomer increased the grafting ratio, as in the case of polypropylene.

**The Reaction of Grafted Polypropylene with Polyhydroxyamines and the Dyeability of the Resultant Polymer.** — The epoxide groups are reactive with various reagents, such as amines,[6] acids,[7] phenols,[8] etc. Here, the reaction was investigated with polyhydroxyamine. The polypropylene fibers with a grafting ratio of 40.1% or 76.1% were refluxed in an acetone solution containing a 20 wt. % of diethanolamine.



The extent of the reaction of amine with the epoxide group in the grafted polymer was calculated from the nitrogen values by the Kjeldahl method. As can be seen from Fig. 9, the reaction of the epoxide group with the amine proceeds quantitatively, regardless of the grafting ratio. It has been known that such bases as pyridine catalyze the reaction of epoxide and amine. In this paper, 2.5 mol. % of pyridine was added to the solution of diethanolamine. However, the effect of pyridine was not noticeable, as Fig. 9 shows. Figure 10 shows the infrared absorption spectra of the GMA grafted polypropylene film and of the grafted film treated with diethanolamine.

The grafted polypropylene showed the absorption characteristic of epoxide group at 910 $cm^{-1}$, but not the absorption around 3500 $cm^{-1}$ characteristic of the hydroxyl group. After it had been treated with diethanolamine, a hydroxyl absorption appeared at 3300 $cm^{-1}$ and the absorption at 910 $cm^{-1}$ disappeared. This indicates the ring opening of the epoxide group.

6) L. Smith, *Kgl. Frusiograf Lund Handl.*, **42**, 1 (1946).
7) M. Imoto, T. Kishida and K. Kho, *J. Chem. Soc. Japan, Ind. Chem. Sec. (Kogyo Kagaku Zassi)* **56**, 807 (1953).
8) V. Bradley, *J. Chem. Soc.*, **1951**, 1589.

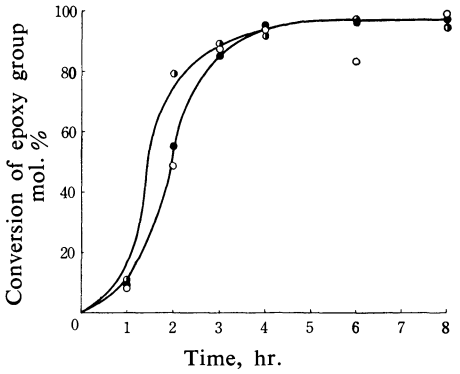



Fig. 9. Reaction of GMA-grafted polypropylene and diethanolamine at 62°C in acetone. Amine concentration 20 wt. %

○ Grafting ratio 40.1%
● Grafting ratio 76.1%
◑ 2.5 mol. % of pyridine was added to amine, grafting ratio 76.1%

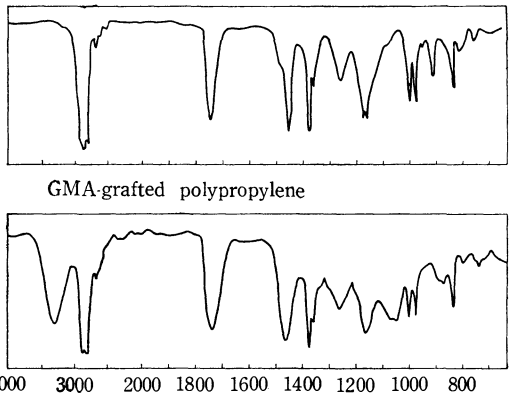



Fig. 10. Infrared absorption spectra of GMA-grafted polypropylene, grafting ratio 25%.

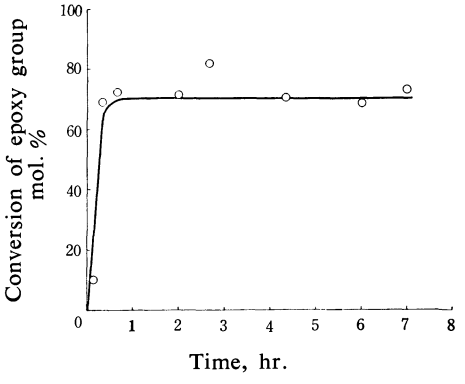



Fig. 11. Reaction of GMA-grafted polypropylene and methylglucamine in dioxane at 100°C.
Grafting ratio 64.7%, methylglucamine concentration 4 wt. %

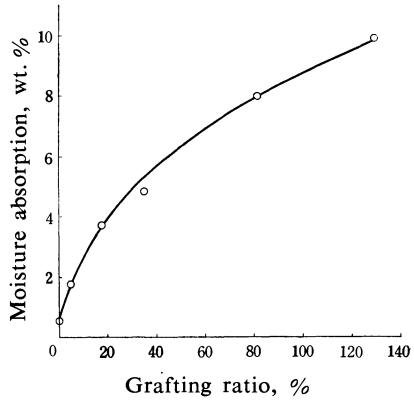



Fig. 12. Moisture absorption of GMA-grafted polypropylene treated with diethanolamine. Amine treatment was carried out for 5 hr. at the same condition as in Fig. 9, relative humidity 60%.

The reaction of methyl gulcamine with the grafted polypropylene fiber was also examined. The grafted polymer was treated with 4 wt. % of methyl glucamine in dioxane at 100°C. The conversion of epoxide groups was 70%, as is shown in Fig. 11.

The moisture absorption of the grafted fiber treated with diethanolamine is given in Fig. 12. The moisture absorption of the polypropylene fiber was increased by grafting. The dyeability of the polypropylene fiber was improved remarkably by treating the grafted fiber with polyhydroxyamine. The results are summarized in Table I.

Table I. Dyeability of GMA-grafted polypropylene fiber treated with polyoxyamines

| Grafting ratio, % | Amine | Dyeability: Direct dye | Dyeability: Acidic dye |
|---|---|---|---|
| 12 | Methyl glucamine | +++ | ++ |
| 12 | Diethanolamine | ++ | ++ |
| 23 | Diethanolamine | ++ | +++ |
| 100 | Diethanolamine | +++ | +++ |

+++ 100% of dye was absorbed in fiber.
++ More than 50% was absorbed.
+ Less than 50% was absorbed.
Conentration of dye 0.04%, weight ratio of dyestuff to fiber grafted.

The fiber of grafting ratio of 12% had a good dyeability by direct dyes after treatment with methyl glucamine. The diethanolamine-treated fiber of 23% grafted polypropylene showed encough dyeability to acid dyes.

**The Reaction of the Grafted Polyvinyl Chloride with Amines.** — The epoxide values of GMA-grafted polyvinyl chloride were determined by the HCl-dioxane method. The results are shown in Table II. The epoxide values obtained were more than 90% of the epoxide values calculated from the grafting ratio.

The amine treatment was carried out in a mixture of water and acetone (water 60, acetone 40). The results of the diethanolamine treatment are shown in Fig. 13. The extent of the reaction was 60% for epoxide groups. The addition of pyridine increased the initial grafting rate, but it had no influence on the ultimate conversion. Figure 14 shows the reaction of aniline with the grafted polymer.

Both the reaction rate and the ultimate conversion were lower in the case of aniline than in the case of diethanolamine.

The polyvinyl chloride fiber grafted with GMA were gradually discolored from yellow to brown during treatment with an aliphatic amine such as diethylamine or diethanolamine. Table III shows the nitrogen and chlorine values of the ungrafted PVC fiber treated with

Table II. Amount of epoxy group in GMA-grafted polyvinyl chloride

| Grafting ratio | Amount of epoxy group $\times 10^3$ mol./g.: from grafting ratio | Amount of epoxy group $\times 10^3$ mol./g.: from analysis* |
|---|---|---|
| 20.2 | 0.7 | 0.6 |
| 50.1 | 1.5 | 1.3 |
| 68.3 | 2.0 | 1.9 |
| 105.7 | 3.1 | 2.9 |

* Analysis for epoxy groups were performed by the HCl-dioxane method.

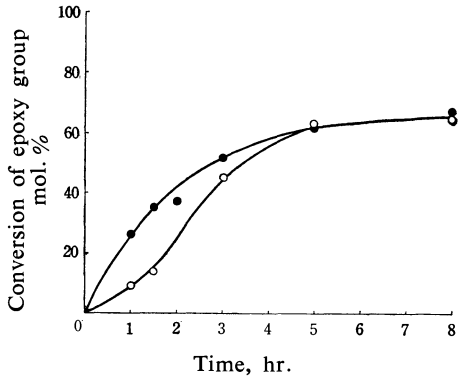



Fig. 13. Reaction of GMA-grafted polyvinyl chloride and diethanolamine at 50°C.
Grafting ratio 58.2%, solvent (water 40: acetone 60, wt. ratio), amine concentration 2 mol./l.
○ Without pyridine
● With 0.4 mol./l. pyridine

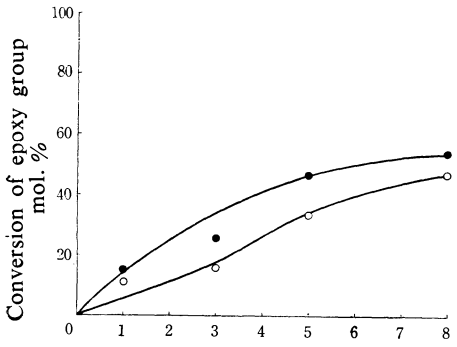



Fig. 14. Reaction of GMA-grafted polyvinyl chloride and aniline at 50°C.
Grafting ratio 64.7%, solvent (water 40: acetone 60, wt. ratio), amine concentration 2 mol./l.

○ Without pyridine
● With 0.4 mol./l. pyridine

Table III. Chlorine and nitrogen percent of polyvinyl chloride (ungrafted) after the treatment with amines

| Amine | Cl, % | N, % |
|---|---|---|
| No treatment | 56.43 | 0 |
| Diethanolamine | 53.31 | 0.27 |
| Diethylamine | 53.09 | 0.31 |

diethylamine or diethanolamine at 50°C. The chlorine values decreased with the treatment, while the nitrogen values increased. Therefore, the substitution of chlorine in polyvinyl chloride with amines seems to occur.

The extent of dye exhaustion was measured using 10% grafted fiber which had been treated with diethanolamine for five hours. The dyes were almost 100% exhausted into the fiber.

## Summary

The graft polymerization of glycidyl methacrylate onto polypropylene or polyvinyl chloride fiber has been carried out by the technique of $\gamma$-ray pre-irradiation in vacuo, and the reactions of the grafted fiber with amines have been investigated. In the case of polypropylene, the addition of benzene or tetrahydrofuran to the monomer remarkably increases the grafting rate.

The initial grafting rate is slow in acetone or ethylacetate. The epoxide groups of the grafted polypropylene react with diethanolamine quantitatively, but with methyl glucamine partially, with a yield of 70%. In the case of polyvinyl chloride, benzene or acetonitrile is suitable as a grafting solvent. Graft polymerization proceeds in a narrow range of temperature from 10 to 20°C. Diethanolamine or aniline reacts with yields of 50—60% with the epoxide groups of the grafted polyvinyl chloride. Polyhydroxyamine-treated graft fibers have a good dyeability to both direct and acid dyes.

*The Department of Synthetic Chemistry*
*Faculty of Engineering*
*The University of Tokyo*
*Hongo, Tokyo (Y. I. & K. T.)*

*Research Laboratory of Resources Utilization*
*Tokyo Institute of Technology*
*Ookayama, Tokyo (T. K. & K. N.)*

*Hitachi Central Research Laboratory*
*Kokubunji-shi, Tokyo (M. M.)*

# The Synthesis of α-Amino Acid Menthyl Esters. II[1]

By Tadao HAYAKAWA* and Kaoru HARADA

(Received December 15, 1964)

In the previous study,[2] menthyl esters of α-amino acids have been synthesized from amino acids and menthol by the use of the azeotropic distillation method. However, the reaction conditions of this method were so strong as to decompose serine during the reaction. Some amino acids, such as optically active α-phenylglycine, one of the most racemizable amino acids, may also lose their optical activity during the reaction. In order to use these menthyl esters of α-amino acids as stereochemical standard compounds, it is necessary to compare them with α-amino acid menthyl esters which have been synthesized under milder reaction conditions.

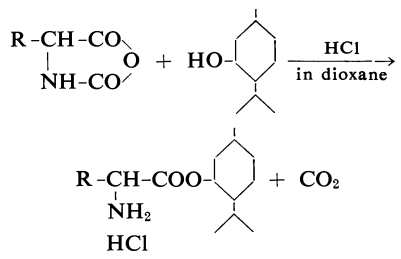
1) Contribution No. 43 of the Institute of Molecular Evolution, University of Miami.

* Department of Chemistry, Faculty of Science, Kanazawa University, Kanazawa.

2) K. Harada and T. Hayakawa, This Bulletin, 37, 191 (1964).

α-Amino acid *N*-carboxy anhydride (α-amino acid NCA) has been used in the synthesis of amino acid benzyl esters by Bergmann et al.[3] and later by Erlanger and Brand[4].

In this report, the synthesis of α-amino acid *l*-menthyl esters, under mild conditions, by the use of α-amino acid NCA and *l*-menthol will be described. α-Amino acid NCA prepared by the phosgene method[5] was dissolved in dry dioxane or in a dioxane-ether mixture




containing *l*-menthol ($[\alpha]_D$ −50.0° (*c* 3.50, abs. EtOH), m. p. 42—44°C) and hydrogen chloride. The reaction mixtures were then allowed to stand for one to four days at room temperature. The α-amino acid menthyl esters were isolated as the hydrochlorides; their names will be abbreviated as amino acid M·HCl. The fact that the amino acid M·HCl synthesized under these milder reaction conditions exhibited physical properties almost identical to those observed in the earlier study[2] suggests that the racemization of the amino acid M·HCl prepared by the earlier azeotropic distillation method[2] is small. In this method and also in the earlier method,[2] higher yields of D-amino acid M·HCl than of L-amino acid M·HCl were observed. The fractionation of two diastereomers of the racemic amino acid M·HCl was also observed. The specific rotations of the isolated DL-phenylalanine M·HCl before and after recrystallization were −56.0° and −65.0° respectively, whereas the calculated value is −47.8.°

One advantage of this method is that it can be used for the synthesis of L- and DL-serine M·HCl from *O*-benzyl L- and DL-serine NCA and menthol. *O*-Benzyl-L-serine[6] and *O*-benzyl-DL-serine[7] were treated with phosgene to convert them to the corresponding *O*-benzyl L-serine NCA and *O*-benzyl DL-serine NCA. These NCAs were reacted with *l*-menthol in dry dioxane and ether in the presence of hydrogen chloride at room temperature for four days. *O*-Benzyl L-serine and DL-serine menthyl-esters were thus isolated as hydrochlorides. The attempted debenzylation of these *O*-benzyl L- and DL-serine menthyl-esters by acid hydrolysis (5 N hydrochloric acid, boiling for one hour) was not successful, whereas *O*-benzyl serine was easily debenzylated by acid hydrolysis.[6,7] The debenzylation of α-amino acid M·HCl was carried out under relatively strong hydrogenolysis conditions through the use of 5% palladium on charcoal.

The specific rotations of *O*-benzyl L-ser M·HCl and *O*-benzyl DL-ser M·HCl were found to be −47.5° and −46.5° respectively. However, after debenzylation, L-ser M·HCl and DL-ser M·HCl showed specific rotations of −69.8° and −56.6° respectively. The fractionation of *O*-benzyl DL-ser M·HCl by the recrystallization procedure (ethyl acetate - ether) was also observed. Three fractions of *O*-benzyl DL-ser M·HCl were isolated (see Experimental section): Fractions I (m. p. 179—180°C), II (m. p. 135—150°C) and III (m. p. 128—130°C). The melting point of fraction I (the least soluble fraction) rose to 181—182°C after recrystallization. Fraction III (the most soluble fraction) has the same melting point and optical rotation as *O*-benzyl-L-ser M·HCl. The mixed melting point test of fraction III with *O*-benzyl-L-ser M·HCl showed no depression of the melting point. The hydrogenolysis of fraction III gave serine M·HCl, which showed $[\alpha]_D^{17}$ −67.8° and a m. p. of 218—219°C. The mixed melting point test of serine M·HCl obtained from fraction III and L-serine M·HCl indicated that the two compounds were identical. These results show that *O*-benzyl DL-serine M·HCl is considerably fractionated by the recrystallization procedure to the least soluble fraction (*O*-benzyl-D-ser M·HCl rich) and the most soluble fraction (*O*-benzyl-L-ser M·HCl rich). DL-Serine M·HCl was also prepared from *O*-acetyl DL-ser NCA and *l*-menthol under similar reaction conditions. The *O*-acetyl group was removed during the reaction. The specific rotation of the isolated DL-serine M·HCl was −56.9° before recrystallization. After recrystallization, two fractions of DL-serine M·HCl, I and II, were isolated. Fraction I decomposed at 213—220°C and showed a specific rotation of $[\alpha]_D^{26}$ −61.6°. Fraction II, which was less alcohol-soluble, decomposed at 209—214°C and showed a specific rotation of $[\alpha]_D^{26}$ −68.7°. Elemental analyses of both I and II agreed with the theoretical value of serine M·HCl. Fractions I and II are both supposed to be L-rich fractions, while fraction II might be an almost pure L-ser M·HCl.

3) M. Bergmann, L. Zervas and W. F. Ross, *J. Biol. Chem.*, **111**, 245 (1933).
4) B. F. Erlanger and E. Brand, *J. Am. Chem. Soc.*, **73**, 3508, 4025 (1951).
5) A. C. Farthying and R. J. W. Reynolds, *Nature*, **165**, 647 (1950); A. C. Farthying, *J. Chem. Soc.*, **1951**, 2294.
6) K. Okawa, This Bulletin, **29**, 486 (1956).
7) K. Okawa and H. Tani, *J. Chem. Soc. Japan, Pure Chem. Sec.* (*Nippon Kagaku Zassi*), **75**, 1199 (1954).

TABLE I. α-AMINO ACID MENTHYL ESTER HYDROCHLORIDES, R-CH-COOM
NH$_2$ HCl

| α-Amino acid M·HCl | Yield % | Recryst. solvent[a] | After recryst. m. p. °C[b] | After recryst. $-[\alpha]_D^{25-26}$ [d] | c | Molecular formula | Elemental analysis Calcd., % C | H | N | Found, % C | H | N |
|---|---|---|---|---|---|---|---|---|---|---|---|---|
| D-Ala | 75 | Et | 188—189 | 72.0 | 1.74 | $C_{13}H_{26}O_2NCl$ | 59.18 | 9.93 | 5.31 | 59.25 | 10.10 | 5.21 |
| L-Ala | 74 | Et | 219—220 | 66.7 | 1.89 | $C_{13}H_{26}O_2NCl$ | 59.18 | 9.93 | 5.31 | 59.14 | 9.83 | 5.20 |
| D-Phe | 63 | Et | 187—188 | 77.8 | 1.57 | $C_{19}H_{30}O_2NCl$ | 67.14 | 8.90 | 4.12 | 67.19 | 8.98 | 4.05 |
| L-Phe | 49 | Et | 162—163 | 13.8 | 3.23 | $C_{19}H_{30}O_2NCl$ | 67.14 | 8.90 | 4.12 | 67.22 | 9.09 | 3.94 |
| DL-Phe | 73 | Et | 145—169[c] | 65.0 | 1.77 | $C_{19}H_{30}O_2NCl$ | 67.14 | 8.90 | 4.12 | 66.96 | 8.91 | 4.27 |
| D-Val | 73 | Et | 207—208 | 74.4 | 1.69 | $C_{15}H_{30}O_2NCl$ | 61.71 | 10.36 | 4.80 | 61.85 | 10.60 | 4.85 |
| L-Val | 47 | Et | 225—226 | 49.8 | 2.64 | $C_{15}H_{30}O_2NCl$ | 61.71 | 10.36 | 4.80 | 61.66 | 10.37 | 4.77 |
| D-Phenylgly | 84 | A | 253—254 | 127.0 | 1.03 | $C_{18}H_{28}O_2NCl$ | 66.34 | 8.66 | 4.30 | 66.41 | 8.68 | 4.38 |
| L-Phenylgly | 82 | A | 253—254 | − 9.6 | 0.98 | $C_{18}H_{28}O_2NCl$ | 66.34 | 8.66 | 4.30 | 66.42 | 8.63 | 4.57 |
| DL-Phenylgly | 86 | A | 252—253 | 65.7 | 1.10 | $C_{18}H_{28}O_2NCl$ | 66.34 | 8.66 | 4.30 | 66.35 | 8.57 | 4.39 |
| DL-Ser[e] | 68 | A | (I) 213—220 decomp.[c]<br>(II) 209—214 decomp.[c] | (I) 61.6<br>(II) 68.7 | 1.65<br>1.16 | $C_{13}H_{26}O_3NCl$ | 55.80 | 9.37 | 5.01 | (I) 55.83<br>(II) 55.85 | 9.42<br>9.56 | 5.00<br>5.13 |
| *O*-Benzyl L-Ser | 68 | EP | 132—133 | 47.5[h] | 1.11 | $C_{20}H_{32}O_3NCl$ | 64.94 | 8.72 | 3.73 | 64.75 | 8.68 | 3.68 |
| *O*-Benzyl DL-Ser | 68 | Et | (I) 181—182 | 46.0[h] | 1.13 | $C_{20}H_{32}O_3NCl$ | 64.94 | 8.72 | 3.73 | 65.18 | 8.67 | 3.65 |
| L-Ser[f] | 66 | A | 216—219 decomp. | 69.8[h] | 0.702 | $C_{13}H_{26}O_3NCl$ | 55.80 | 9.37 | 5.01 | 55.75 | 9.29 | 5.08 |
| DL-Ser[g] | 90<br>53 | A<br>A | (I) 164—166<br>(II) 218—219 decomp. | 56.6[h]<br>67.8[h] | 1.08<br>0.640 | $C_{13}H_{26}O_3NCl$ | 55.80 | 9.37 | 5.01 | 55.87<br>55.85 | 9.33<br>9.40 | 5.12<br>4.99 |

a) Recrystallization solvent: Et=ethyl acetate and ether; EP=ethyl acetate and petroleum ether; A=alcohol and ether.
b) All melting points are uncorrected.
c) Melting point and decomposition points are not sharp.
d) All samples were measured in abs. ethanol at 25—26°C.
All samples exhibited negative rotations except L-phenylgly M·HCl.
e) Prepared from *O*-acetyl DL-serine.
f) Prepared from *O*-benzyl L-serine.
g) Prepared from *O*-benzyl DL-serine.
h) Measured at 17°C.

## Experimental

**L-α-Phenylglycine *N*-Carboxy Anhydride.**—Phosgene was bubbled through a stirred suspension of finely pulverized L-α-phenylglycine[8] (1.51 g. (0.01 mol.) ($[\alpha]_D^{20}$ +156.4°, 1 N HCl)) in 50 ml. of dry dioxane in a water bath at 50°C until a clear solution was obtained. The reaction mixture was then treated with a stream of dry nitrogen for one hour at room temperature in order to expel the unreacted phosgene. The solvent was distilled off in vacuo at 40°C. The residual oily product was crystallized by treating it with petroleum ether. The crystals were filtered, washed with petroleum ether, and dried. The product was recrystallized from ethyl acetate and petroleum ether. A yield of 1.45 g. (82%) of L-phenylglycine NCA was obtained; m. p. 114°C. Titration: calcd. for $C_9H_7O_3N$, neut. equiv. 177.2. Found: neut. equiv. 177.5. The neutral equivalent values were determined by titration in methanol with N/50 sodium methoxide, using thymol blue as an indicator.

The NCAs of D-α-phenylglycine and DL-α-phenylglycine were prepared in the same way as has been described above. The specific rotation of the original D-α-phenylglycine[8] was $[\alpha]_D^{20}$ −155.4° (*c* 0.49, 1 N HCl). The yields, melting points, and neutral equivalents of D- and DL-α-phenylglycine NCA[9] are as follows:

| | D | DL |
|---|---|---|
| Yield, % | 84 | 85 |
| M. p., °C | 112 | 100 |
| Neut. equiv. | 175.8 | 176.5 |

**L-α-Phenylglycine Menthyl Ester Hydrochloride.**—To a solution of 1.42 g. (0.008 mol.) of L-α-phenylglycine NCA in 40 ml. of dry dioxane, 6.0 g. of *l*-menthol and 25 ml. of dioxane previously saturated with hydrogen chloride were added at 0°C. After the reaction mixture had been stirred magnetically for 24 hr. at room temperature, the solvent was distilled off in vacuo at 50°C. The residual crystals were treated with petroleum ether, filtered, and dried. The crystals thus obtained were mixed with an 8% sodium hydrogen carbonate solution, and the resulting oil was extracted with ether to obtain the free menthyl ester. The ethereal layer was washed once with water and dried with anhydrous sodium sulfate. To this dried solution, dry hydrogen chloride gas was introduced in order to precipitate the L-α-phenylglycine M·HCl, which was then kept in a refrigerator overnight. The ester hydrochloride crystals were filtered and washed with petroleum ether. L-α-Phenylglycine M·HCl (2.0 g., 77%) was obtained. This was recrystallized from abs. ethanol and ether; m. p. 253—254°C $[\alpha]_D^{25}$ +9.6° (*c* 0.98, ethanol). The analytical data are shown in Table I.

Menthyl ester hydrochlorides of D- and DL-α-phenylglycine were prepared in the way which has been described earlier. The physical and analytical data are shown in Table I.

***O*-Benzyl L-Serine *N*-Carboxy Anhydride.**[10]—*O*-Benzyl L-ser NCA was synthesized by the phosgene method in the same way as α-phenylglycine NCA. Yield 81%, m. p. 71—72°C.

Found: neut. equiv., 222.5; N, 6.43. Calcd. for $C_{11}H_{11}O_4N$: neut. equiv., 221.2; N, 6.33%.

***O*-Benzyl-L-serine Menthyl Ester Hydrochloride.**—A mixture of *O*-benzyl-L-ser NCA[10] (4.4 g. (0.02 mol.) in 10 ml. of dry dioxane) and *l*-menthol (10.0 g. in 15 ml. of dry dioxane) was mixed with 80 ml. of ether which had been saturated with hydrogen chloride at 0°C. This mixture was then stirred at room temperature for four days. After the evaporation of the solvent under reduced pressure, the residual syrup was dissolved in 200 ml. of petroleum ether, and the resulting *O*-benzyl-L-ser M·HCl was extracted with water three times. The aqueous layers were combined, and sodium hydrogen carbonate was added in order to precipitate the oily free ester. The free ester was extracted with ether twice, and the ether solution was dried with anhydrous sodium sulfate and filtered. To the filtrate, dry hydrogen chloride gas was introduced, and the ether was evaporated. After the crystallization of *O*-benzyl-L-ser M·HCl, petroleum ether was added. The crystals were filtered and dried. *O*-Benzyl L-ser M·HCl (5.0 g.) was obtained (68%); m. p. 125—130°C. This was recrystallized from ethyl acetate and petroleum ether; m. p. 132—133°C, $[\alpha]_D^{17}$ −47.5° (*c* 1.11, ethanol). The analytical data are shown in Table I.

***O*-Benzyl-DL-serine Menthyl Ester Hydrochloride.**—A mixture of *O*-benzyl-DL-ser NCA[7] (5.1 g. (0.023 mol.) in 10 ml. of dioxane) and menthol (12.0 g. in 15 ml. of dioxane) was mixed with 80 ml. of ether which had been saturated with hydrogen chloride at 0°C. The reaction mixture was treated in the same way as that of the L-serine derivative.

*O*-Benzyl-DL-ser M·HCl (5.8 g.) was obtained (68%); m. p. 135—151°C, $[\alpha]_D^{17}$ −46.5° (*c* 1.01, ethanol). This was recrystallized from ethylacetate and ether. Three fractions were isolated by the recrystallization procedure: fraction I, 2.0 g., m. p. 181—182°C, $[\alpha]_D^{17}$ −46.0° (*c* 1.13, ethanol), fraction II, 1.80 g., $[\alpha]_D^{17}$ −47.0° (*c* 0.962, ethanol) m. p. 135—150°C, and fraction III, 1.50 g., $[\alpha]_D^{17}$ −46.8° (*c* 0.960, ethanol), m. p. 128—130°C. No melting point depression was observed in the mixed melting point test of fraction III with *O*-benzyl L-ser M·HCl. Elemental analyses of carbon, hydrogen, and nitrogen of fractions II and III also agreed with the theoretical values.

**L-Serine Menthyl Ester Hydrochloride.**—The hydrogenolysis of *O*-benzyl-L-ser M·HCl (1.0 g. in 100 ml. of 80% ethanol) was carried out with 2.0 g. of 5% palladium on charcoal for 12 hr. After the reaction had been completed, the catalyst was removed by filtration. The filtrate was then evaporated in order to crystallize the ester hydrochloride. The crystals were dissolved in water containing excess sodium hydrogen carbonate. The liberated free ester was extracted with ether. The ether solution was washed once with water, dried with anhydrous sodium sulfate, and filtered. Dry hydrogen chloride gas was introduced into the ether

8) E. Fischer and O. Weichhold, *Ber.*, **41**, 1292 (1908).
9) H. Leuchs and W. Geiger, ibid., **41**, 1721 (1908).
10) Zvi Bohak and E. Katchalski *Biochemistry*, **2**, 228 (1963).

solution in order to crystallize L-serine M·HCl. The crystals were filtered, washed with ether, and dried. L-Serine M·HCl (0.50 g.) was obtained (66%); m. p. 216—219°C (decomp.), $[\alpha]_D^{17}$ −69.8° (*c* 0.702, ethanol). The analytical data are shown in Table I.

**DL-Serine Menthyl Ester Hydrochloride I.**—*O*-Benzyl-DL-serine M·HCl (fraction I; m. p. 181—182°C, 0.5 g.) was dissolved in 50 ml. of 80% ethanol. In order to remove the benzyl group, hydrogenolysis was carried out with 1.0 g. of 5% palladium on charcoal for 12 hr. The reaction product was treated in the same way as that of the L-serine derivative; 0.34 g. (90%) of DL-serine M·HCl was thus obtained, m. p. 164—166°C, $[\alpha]_D^{17}$ −56.6° (*c* 1.08, ethanol). The analytical data are shown in Table I.

**DL-Serine Menthyl Ester Hydrochloride II.**—*O*-Benzyl-DL-ser M·HCl (fraction III: m. p. 128—130°C, 0.50 g.) was treated in the manner which has been described above. When debenzylated serine M·HCl was recrystallized from ethanol and ether, 0.20 g. of the product was obtained; m. p. 217—219°C (decomp.), $[\alpha]_D^{17}$ −67.8° (*c* 0.640, ethanol). The mixed melting point test with L-ser M·HCl did not show any melting point depression. The analytical data are shown in Table I.

A part of this work was supported by Grants NsG-173-62 and NsG-689 from the National Aeronautics and Space Administration. The authors wish to express their thanks to Professor Sidney W. Fox for his encouragement. Thanks are extended to Mr. Charles R. Windsor for reading the manuscript.

*Institute of Molecular Evolution and*
*Department of Chemistry*
*University of Miami*
*Florida, U. S. A.*

# Photo-induced Reaction. II.[1),*1] The Photo-sensitized Oxidation of Hindered Phenols

By Teruo MATSUURA, Kanji OMURA and Ruka NAKASHIMA

(Received December 25, 1964)

It is well known that a phenol produces a phenoxy radical by oxidation with so-called "one electron transfer oxidizing agents" and that the radical couples to form various types of products.[2)] Since the type of the product largely depends upon the oxidant and the starting phenol employed, it is rather difficult to predict the structures of such products. It has been suggested that a large number of natural products may be formed by the oxidative coupling of their phenol precursors in vivo.[2,3)] It may also be supposed that such phenol precursors can be oxidized photochemically in the presence of natural pigments serving as sensitizers, particularly in plants. We expected that the photo-sensitized oxidation of phenols might give some specific products, and so we investigated the photo-oxidation of several hindered phenols.

In general, phenols are destructively oxidized under the influence of ultrasonic radiation.[4)] Arnow has reported that when an aqueous solution of tyrosine is irradiated with an ultraviolet light 3,4-dihydroxyphenylalanine is formed.[5)] Several investigators have reported that the primary reaction in the irradiation of phenols with an ultraviolet light or a visible light in the presence of a photo-sensitizer is the formation of phenoxy radicals,[6-8)] but they did not describe the subsequent behavior of the radicals in detail. Very recently Johnson and Tam have reported that some simple phenols dimerize on ultraviolet irradiation under bubbling oxygen.[9)]

As a preliminary experiment, we examined the photochemical oxidation of 2,6-di-*t*-butylphenol (I) using various photo-sensitizers: eosin Y, erythrosin, methylene blue, chlorophyllin, methyl orange, riboflavin tetraacetate, and 2,5-di-*t*-butyl-*p*-benzoquinone. Eosin Y and

1) Part I. T. Matsuura, This Bulletin, **37**, 564 (1964).

*1 This work was supported in part by U. S. Public Health Service Research Grant AM 07955, from the National Institute of Arthritis and Metabolic Diseases.

2) H. Musso, *Angew. Chem.*, **75**, 965 (1963).

3) a) D. H. R. Barton and T. Cohen, "Festschrift Arthur Stoll," Birkhäuser, Basel (1957), p. 117; b) H. Erdtman and C. A. Wachtmeister, ibid., p. 144.

4) B. Robert, R. O. Prudhomme and P. Grabar, *Bull. soc. chim. biol.*, **37**, 897 (1955).

5) L. E. Arnow, *J. Biol. Chem.*, **120**, 151 (1937).

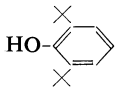
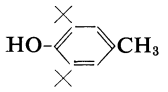
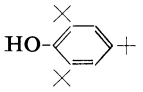
6) L. I. Grossweiner and E. F. Zwicker, *J. Phys. Chem.*, **67**, 549 (1963).

7) E. J. Land and G. Porter, *Trans. Faraday Soc.*, **59**, 2061 (1963).

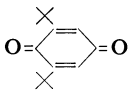
8) J. O. Roebber, *J. Chem. Phys.*, **37**, 1974 (1962).

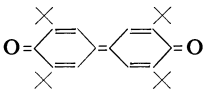
9) A. W. Johnson and S. W. Tam, *Chem. & Ind.*, **1964**, 1425.

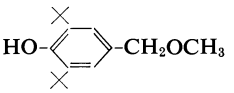
TABLE I. PHOTOSENSITIZED OXIDATION OF HINDERED PHENOLS[a]

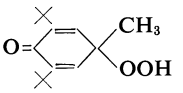
| Phenol | Sensitizer | Tungsten lamp, W. | Irradiation period, hr. | Recovered phenol, % | Non-volatile products, g. | Peoduct isolated or identified (yield[b]) |
|---|---|---|---|---|---|---|
| 2, 6-Di-*t*-butylphenol | Eosin Y | 200 | 50 | 41 | 1.02 | IV (11%) V (18%) |
|  | Erythrosin | 500 | 30 | 23 | 1.01 | IV (12%) V (33%) |
| | Erythrosin[c] | 500 | 30 | 16 | 0.86 | IV (11%) V (42%) |
| (I) | Methylene blue | 500 | 32 | 64 | 0.32 | IV (12%) V (15%) |
| 2, 6-Di-*t*-butyl-*p*-cresol | | | | | | |
|  | Eosin Y | 200 | 20 | 16 | — | VI (4.2%) VII (2.8%) |
| (II) | | | | | | |
| 2, 4, 6-Tri-*t*-butylphenol | | | | | | |
|  | Eosin Y | 500 | 30 | 53 | — | IV (13%) VIII (1.1%) |
| (III) | | | | | | |

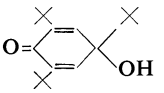
a) A solution of 3.00 g. of the starting phenol and 0.30 g. of the sensitizer in 100 ml. of methanol was irradiated under bubbling oxygen.
b) Yields were based on consumed starting phenol.
c) Crystals of 3, 5, 3′, 5′-tetra-*t*-butyl-4, 4′-diphenoquinone deposited in the course of the reaction were collected time to time.


(IV)


(V)


(VI)


(VII)


(VIII)

erythrosin were found to be most effective (see Experimental). A solution of a hindered phenol and a sensitizer in methanol was irradiated with a tungsten lamp under bubbling oxygen. The products were either isolated by column chromatography or analyzed by infrared and ultraviolet spectra and vapor phase chromatography. Three hindered phenols, 2, 6-di-*t*-butylphenol (I), 2, 6-di-*t*-butyl-*p*-cresol (II) and 2, 4, 6-tri-*t*-butylphenol (III), were oxidized under these conditions. The results are shown in Table I.

The photo-sensitized oxidation of 2, 6-di-*t*-butylphenol (I) with eosin Y yielded 2, 6-di-*t*-butyl-*p*-benzoquinone (IV) and 3, 5, 3′, 5′-tetra-*t*-butyl-4, 4′-diphenoquinone (V).[10] When erythrosin wasused as the sensitizer, the yield of the diphenoquinone V was considerably increased, but the yield of the benzoquinone IV was not altered. In both cases, some of the starting phenol I was recovered, and non-volatile products, probably several polymerized substances, were formed.

10) C. D. Cook, E. S. English and B. J. Wilson, *J. Org. Chem.*, **23**, 755 (1958).

The reaction with 2, 6-di-*t*-butyl-*p*-cresol (II) seems to be rather complicated, giving many products. Among them, two crystalline products, a phenol and a hydroperoxide, were isolated in low yields. The NMR spectrum*2 of the former phenol showed five singlets, at $\tau$ 8.57, 6.73, 5.75, 4.99, and 3.03, which were assigned to two *t*-butyl, a methoxyl, a hydroxyl, a benzyl, and two aromatic protons respectively. The structure VI was suggested for the compound; this was confirmed by comparing it with an authentic sample of VI.[11,12] The hydroperoxide was shown to have the structure VII by comparing it with an authentic sample.[13]

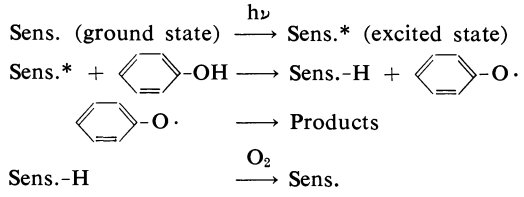
2, 4, 6-Tri-*t*-butylphenol was somewhat resistant to the photo-oxidation under these conditions. 2, 6-Di-*t*-butyl-*p*-benzoquinone (IV) was isolated as the main product, and 2, 4, 6-tri-*t*-butyl-4-hydroxy-2, 5-cyclohexadien-1-one (VIII),

*2 The NMR spectrum was kindly measured at the Faculty of Pharmaceutical Science of this University.
11) D. H. Kim and F. A. Kummerow, *J. Am. Oil Chem. Soc.*, **39**, 150 (1962).
12) T. Fujisaki, *J. Chem. Soc. Japan, Pure Chem. Sec. (Nippon Kagaku Zassi)*, **77**, 727 (1956).
13) M. S. Kharasch and B. S. Joshi, *J. Org. Chem.*, **22**, 1439 (1957).

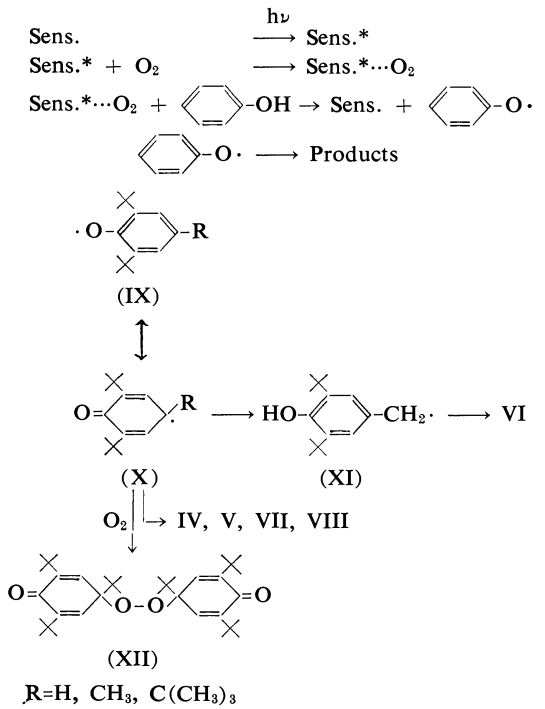
as the minor product. The formation of IV can be explained in terms of the thermal[14] or photochemical[1] conversion of the peroxide, XII, which is formed from the tri-*t*-butylphenoxy radical X (R=*t*-butyl) and oxygen.

When the photo-oxidation reaction was carried out without irradiation or in the absence of the sensitizer, all the startiug phenols, I, II and III, were recovered unchanged. It appears, therefore, that the formation of a phenoxy radical in the primary process of this reaction requires both the irradiation and the presence of the sensitizer. The radical may be formed by hydrogen abstraction from the phenolic hydroxyl group by the excited photosensitizer molecule (Scheme 1), as has been suggested by Grossweiner and Zwicker.[6] Another possible mechanism, that the excited sensitizer-oxygen complex, proprosed by Schenck[15] in connection with the photosensitized addition of oxygen to olefins, can remove a hydrogen atom from the phenolic hydroxyl group, may also be taken into consideration (Scheme 2). In any case, the phenoxy radical, IX, can give various products via either its mesomeric form X or its tautomeric form XI.

Scheme 1




Scheme 2




A large number of reports on the oxidation of these three phenols, I, II, and III, with one electron-transfer oxidizing agents have recently been published. The oxidation of 2,6-di-*t*-butylphenol gives mainly 2,6-di-*t*-butyl-*p*-benzoquinone (IV) and the diphenoquinone V,[10,13,16-18] in accordance with the results we obtained in the photo-sensitized oxidation. Because of the capability of the formation of the benzyl radical XI the oxidation of 2,6-di-*t*-butyl-*p*-cresol (II) with various oxidants is complicated and the products are obtained usually in low yields.[13,16,19-22] The oxidation of 2,4,6-tri-*t*-butylphenol (III) gives the stable free radical IX (R=*t*-butyl), under a nitrogen atmosphere, while it forms the peroxide XII and other products in the presence of oxygen.[16,20,23,24]

An unhindered phenol, *p*-cresol, was submitted to photosensitized oxidation using erythrosin under the same conditions. From the reaction mixture, some non-volatile products were also obtained besides volatile products, including the starting material. The analysis of the volatile products by vapor phase chromatography showed a pattern similar to that[25] of the products obtained from *p*-cresol by the oxidation with alkaline ferricyanide, except for the appearance of a new peak in the former case. Further studies of the photosensitized oxidation of *p*-cresol and of other unhindered phenols are in progress.

## Experimental

**The Photo-sensitized Oxidation of 2,6-Di-*t*-butylphenol (I).**—A typical procedure using eosin Y as the sensitizer will be described below. A solution of 3.00 g. (15 mmol.) of 2,6-di-*t*-butylphenol and 0.30 g. (0.43 mmol.) of eosin Y in 100 ml. of methanol was placed in a 300-ml. flask and irradiated with a 200 W. tungsten lamp under bubbling oxygen at the reflux temperature. After it had been irradiated for 50 hr., the mixture was concentrated

14) C. D. Cook, R. C. Woodworth and P. Fianu, *J. Am. Chem. Soc.*, **78**, 4159 (1956).
15) G. O. Schenck, *Angew. Chemie*, **69**, 579 (1957).
16) H. R. Gersman and A. F. Bickel, *J. Chem. Soc.*, **1959**, 2711.
17) A. S. Hay, H. S. Blanchard, G. F. Endres and J. W. Eustance, *J. Am. Chem. Soc.*, **81**, 6335 (1959).
18) H. Hart and F. A. Cassis, ibid., **73**, 3179 (1951).
19) G. R. Yohe et al., ibid., **75**, 2688 (1953); *J. Org. Chem.*, **21**, 1829 (1956); ibid., **24**, 1251 (1959).
20) C. D. Cook, ibid., **18**, 261 (1953).
21) J. I. Wasson and W. M. Smith, *Ind. Eng. Chem.*, **45**, 197 (1953).
22) C. D. Cook, N. G. Nash and H. R. Flanagan, *J. Am. Chem. Soc.*, **77**, 1783 (1955).
23) C. D. Cook and R. C. Woodworth, ibid., **75**, 6242 (1953).
24) E. Müller and K. Ley, *Chem. Ber.*, **87**, 922 (1954).
25) Unpublished data from this laboratory.

to a small volume. The crystals (0.29 g.) which formed were collected by filtration and recrystallized from methanol and ethanol to give reddish brown crystals, m. p. 235—237°C. The infrared spectrum was identical with that of an authentic sample (m. p. 238°C) of 3, 5, 3', 5'-tetra-*t*-butyl-4,4'-diphenoquinone (V),[10] lit. m. p. 240—241°C.

The filtrate was then evaporated to dryness, and the residue was treated with petroleum ether to remove the eosin Y. The insoluble eosin Y (quantitatively recovered) was filtered off. The evaporation of the filtrate left a reddish-orange liquid which, on distillation, yielded 1.43 g. of a yellow liquid, b. p. 100—140°C/1 mmHg. The residue weighed 1.04 g. The distillate consisted of 2, 6-di-*t*-butylphenol (I) and 2, 6-di-*t*-butyl-*p*-benzoquinone (IV). The two components in the distillate were measured i) by vapor phase chromatographic analysis (conditions: stationary phase, silicone D. C. 550 on celite; carrier gas, helium; gas pressure, 0.8 kg./cm$^2$; temperature, 178°C), ii) by analysis of the intensity of the infrared bands, 750 cm$^{-1}$ of I and 1660 cm$^{-1}$ of IV, and iii) by analysis of the ultraviolet maxima, 255.5 m$\mu$ (log $\varepsilon$ 4.25) of IV and 278.5 m$\mu$ (log $\varepsilon$ 3.29) of I in cyclohexane, as 85.3% of I and 14.7% of IV. The amount (0.07 g.) of the diphenoquinone V in the residue was estimated from the intensity of its ultraviolet maximum, 403 m$\mu$ (log $\varepsilon$ 4.74) in cyclohexane. Therefore, the amounts of IV, V, and I were found to be 0.21 g., 0.35 g., and 1.22 g. respectively.

Photo-sensitized oxidation reactions of I with erythrosin, and methylene blue were carried out in a similar manner; the results are summarized in Table I.

A solution of 3.00 g. of 2, 6-di-*t*-butylphenol (I) in 150 ml. of methanol was heated under reflux and bubbled with oxygen for 55 hr. The reaction mixture was evaporated to dryness and then treated with petroleum ether and filtered. The evaporation of the filtrate gave a residue whose infrared spectrum was identical with that of the starting phenol I, except for very small bands at 1600 and 1660 cm$^{-1}$.

**The Photo-sensitized Oxidation of 2, 6-Di-*t*-butyl-*p*-cresol (II).**—A solution of 3.00 g. (14 mmol.) of the phenol II and 0.30 g. of eosin Y in 100 ml. of methanol was irradiated for 20 hr., as has been described above. The residual liquid (2.46 g.), which was obtained by the removal of the sensitizer, was dissolved in petroleum ether and passed through a column containing 80 g. of silica gel. Elution with petroleum ether yielded 0.48 g. of the starting phenol II, which was identified by infrared spectrum and vapor phase chromatography. Elution with benzene yield 0.12 g. of crystals. Recrystallization from petroleum ether gave colorless crystals, m. p. 98—100°C, which were identical with 3, 5-di-*t*-butyl-4-hydroxybenzyl methyl ether (VI)[11,12] (infrared spectrum and mixed melting point).

Elution with benzene-ether (9 : 1) yielded 80 mg. of yellow crystals, m. p. 106—111°C. The infrared spectrum was identical with that of an authentic sample (m. p. 112—114°C) of 2, 6-di-*t*-butyl-4-methyl-4-hydroperoxy-2, 5-cyclohexadien-1-one (VII).[13]

Elution with methanol yielded 0.87 g. of a yellow liquid which showed several peaks in vapor phase chromatography but which was not further investigated.

A solution of the phenol II (3.00 g.) and eosin Y (0.30 g.) in methanol (100 ml.) was placed in a brown flask and heated under reflux with bubbling oxygen for 50 hr. The product 2.60 g. was obtained as colorless crystals, m. p. 64—65°C. The infrared spectrum was identical with that of the starting phenol II, m. p. 66—68°C.

**The Photosensitized Oxidation of 2, 4, 6-Tri-*t*-butylphenol (III).**—A solution of 3.00 g. (11 mmol.) of 2, 4, 6-tri-*t*-butylphenol*3 and 0.30 g. of eosin Y in 100 ml. of methanol was irradiated with a 500 W. tungsten lamp for 50 hr., as has been described above. The mixture was then treated in the same manner. The residual liquid (2.90 g.) was dissolved in petroleum ether and passed through a column containing 110 g. of neutralized alumina (grade I). Elution with petroleum ether yielded 1.76 g. of pale yellow crystals which were found, by vapor phase chromatographic analysis, to be a mixture of the starting phenol III, 2, 6-di-*t*-butyl-*p*-benzoquinone (IV) and a minor product (ratio, 91 : 7 : 2). The analysis was carried out under the following conditions: stationary phase, silicon D.C. 550 on celite; carrier gas, helium; gas pressure, 0.8 kg./cm$^2$; temperature, 240°C. Elution with petroleum ether-benzene (1 : 1) yielded 145 mg. of a semi-solid, from which 16 mg. of colorless crystals, m. p. 102—123°C, were obtained. The infrared spectrum was identical with that of 2, 4, 6-tri-*t*-butyl-4-hydroxy-2, 5-cyclohexadien-1-one (VIII),[26] m. p. 133—134°C.

A solution of the phenol III (3.00 g.) in methanol (1.00 ml.) was irradiated with a 500 W. tungsten lamp under bubbling oxygen for 31 hr. The evaporation of the mixture left colorless crystals, which were identified as pure 2, 4, 6-tri-*t*-butylphenol by infrared and vapor phase chromatographic analyses.

**The Photo-sensitized Oxidation of *p*-Cresol.**—A solution of 1.20 g. (11 mmol.) of *p*-cresol and 0.20 g. of erythrosine in 100 ml. of methanol was irradiated with a 500 W. tungsten lamp, as has been described above. The distillation of the products gave 0.40 g. of a distillate, b. p. 120—180°C/$10^{-1}$ mmHg, and 0.35 g. of a residue. The pattern of the vapor phase chromatographic analysis of the distillate was almost identical with that of the products obtained from *p*-cresol by oxidation with alkaline ferricyanide,[25] except for one unknown peak.

On irradiation without a sensitizer, *p*-cresol was recovered unchanged.

**A Comparison of the Effect of Sensitizers in the Oxidation of 2, 6-Di-*t*-butylphenol (I).**—Solutions of the phenol I and 0.05 mmol. of each of the following sensitizers in 10 ml. of methanol were irradiated with a 200 W. tungsten lamp under bubbling oxygen for 6.5 hr.: eosin Y (35 mg.) erythrosin (44 mg.), methylene blue (19 mg.), riboflavin tetraacetate (29 mg.), chlorophyllin (36 mg.), methyl orange (16 mg.), and 2, 5-di-*t*-butyl-*p*-benzoquinone (11 mg.). After the removal of the sensitizer, the intensities of the infrared bands, 1660 cm$^{-1}$ (characteristic of

*3 Kindly supplied by the Koppers Co., Inc.

26) E. Müller and K. Ley, *Chem. Ber.*, **88**, 601 (1955).

2, 6-di-*t*-butyl-*p*-benzoquinone (IV)) and 1600 $cm^{-1}$ (characteristic of V), of the products in each case were compared. This comparison showed that eosin Y and erythrosin are most effective.

*Department of Synthetic Chemistry*
*Faculty of Engineering*
*Kyoto University*
*Sakyo-ku, Kyoto.*

# Studies of Halogenoacetato Cobalt(III) Complexes.* I. The Preparation and Some Properties of Bromoacetato Cobalt(III) Complexes

By Kashiro KURODA and Philip S. GENTILE

(Received December 28, 1964)

Although several species of fluoroacetato and chloroacetato ammine cobalt(III) complexes have been prepared and their chemical and physical properties studied,[1-6] bromoacetato and iodoacetato ammine cobalt(III) complexes have not yet been isolated. Riolo and Soldi[4] attempted to prepare $[Co(CH_2BrCO_2)(NH_3)_5]X_2$ and $[Co(CH_2ICO_2)(NH_3)_5]X_2$ by the reaction between $[CoCO_3(NH_3)_5]NO_3$ and $CH_2BrCO_2H$ or $CH_2ICO_2H$ in carbon tetrachloride, but they could not isolate the desired compounds. The difficulty in making such a preparation has been attributed to the instability of the bromoacetate and iodoacetate ions at high temperatures, which must be maintained during the reaction period since halogenoacetate ions do not coordinate rapidly enough with cobalt at room temperature. However, the higher the temperature, the larger the danger of the decomposition and/or the hydrolysis of the halogenoacetate ions. Despite the possibility of many side reactions occurring, bromoacetate ions are not so unstable[7,8] as to deter entirely the formation of their complexes. It was, therefore, considered that the desired compound must be present in the reaction products of a carbonato-complex with bromoacetic acids, and that by regulating the reaction temperature, time, and concentration of the reactants and by applying fractional extraction and precipitation, the complexes could be isolated with a high level of purity. Accordingly, after many attempts, several new species of monobromoacetato- and dibromoacetato-complexes were isolated.

The group of halogenoacetato complexes is of especial interest because, since the atomic and/or electronic configuration around the coordination bond is the same in all of the complexes, and since the basicity and the volume of the ligands change regularly with the increase in the number of halogen atoms in the halogenoacetato ligands, one is able to examine the influence of these factors on the physical and chemical properties of the complexes. This standpoint will be maintained throughout this series of studies.

## Experimental

**Materials.**—Monochloroacetic acid, dichloroacetic acid and trichloroacetic acid (Fisher Scientific Co.), monobromoacetic acid (Eastman Organic Chemicals), dibromoacetic acid, tribromoacetic acid (K & K Laboratories, Inc.), and all other reagent-grade chemicals were used without further purification.

**Analysis.**—Cobalt was analyzed by a direct EDTA titration, using murexide as an indicator,[9] after the decomposition of a complex with hot concentrated sulfuric and nitric acid. The other elements were analyzed microquantitatively by the Schwarzkopf Microanalytical Laboratory.** An indication of the degree of purity of the complexes was also

* The most part of this research was done in the laboratory of Department of Chemistry, Fordham University, New York 58, N. Y., U. S. A., during the period in which the former of the authors was a visiting chemist to the University.

1) M. Linhard and M. Weigel, *Z. anorg. Chem.*, **260**, 65 (1949); **264**, 321 (1951).
2) M. Linhard and G. Stirn, ibid., **268**, 105 (1952).
3) M. Linhard and B. Rau, ibid., **271**, 121 (1953).
4) C. B. Riolo and T. Soldi, *Gazz. chim. ital.*, **86**, 282 (1956).
5) F. Basolo, J. G. Bergmann and R. G. Pearson, *J. Phys. Chem.*, **56**, 22 (1952).
6) K. Kuroda, *J. Chem. Soc. Japan, Pure Chem. Sec. (Nippon Kagaku Zasshi)*, **82**, 572 (1961).
7) H. Brooke and H. M. Dawson, *J. Chem. Soc.*, **1936**, 497.
8) F. Kunze and H. Merkader, *Z. physik. Chem.*, **A187**, 285 (1940).

** Schwarzkopf Microanalytical Laboratory, Woodside, New York, U. S. A.
9) H. Flaschka, *Mikrochemie ver. Mikrochim. Acta*, **39**, 38 (1952).

TABLE I. ABSORPTION SPECTRA OF $[Co(halac)(NH_3)_5](ClO_4)_2$, *cis*-$[Co(halac)_2(NH_3)_4]ClO_4$ AND *cis*-$[Co(halac)_2(en)_2]ClO_4$

| | 1st band | | 2nd band | | 3rd band | |
|---|---|---|---|---|---|---|
| | $\nu(10^{13}/sec.)$ | $\log\varepsilon$ | $\nu(10^{13}/sec.)$ | $\log\varepsilon$ | $\nu(10^{13}/sec.)$ | $\log\varepsilon$ |
| $[Co(halac)(NH_3)_5](ClO_4)_2$ | | | | | | |
| $CH_3CO_2$ | 59.7 | 1.877 | 85.2 | 1.774 | — | — |
| $CH_2ClCO_2$ | 59.7 | 1.869 | 85.5 | 1.766 | — | — |
| $CHCl_2CO_2$ | 59.8 | 1.850 | 85.8 | 1.750 | — | — |
| $CCl_3CO_2$ | 59.8 | 1.857 | 85.9 | 1.756 | — | — |
| $CH_2BrCO_2$ | 59.7 | 1.875 | 85.5 | 1.778 | — | — |
| $CHBr_2CO_2$ | 59.7 | 1.860 | 85.7 | 1.751 | — | — |
| *cis*-$[Co(halac)_2(NH_3)_4]ClO_4$ | | | | | | |
| $CH_3CO_2$ | 57.3 | 2.050 | 82.2 | 1.808 | 133 | 4.27 |
| $CH_2ClCO_2$ | 57.4 | 2.003 | 82.6 | 1.794 | 133 | 4.24 |
| $CHCl_2CO_2$ | 57.9 | 1.985 | 82.8 | 1.791 | 134.5 | 4.28 |
| $CCl_3CO_2$ | 58.4 | 1.929 | 83.1 | 1.775 | 135 | 4.28 |
| $CH_2BrCO_2$ | 57.5 | 2.018 | 82.6 | 1.802 | 134.5 | 4.16 |
| $CHBr_2CO_2$ | 57.8 | 2.003 | 82.9 | 1.814 | 136 | 4.31 |
| *cis*-$[Co(halac)_2(en)_2]ClO_4$ | | | | | | |
| $CH_3CO_2$ | 59.3 | 2.175 | 82.9 | 1.980 | 132 | 4.29 |
| $CH_2ClCO_2$ | 59.8 | 2.134 | 83.0 | 1.955 | 131.5 | 4.30 |
| $CHCl_2CO_2$ | 60.2 | 2.090 | 83.1 | 1.935 | 133 | 4.32 |
| $CCl_3CO_2$ | 60.3 | 2.101 | 83.1 | 1.944 | 132.5 | 4.34 |
| $CH_2BrCO_2$ | (not obtained) | | | | | |
| $CHBr_2CO_2$ | 60.1 | 2.147 | 83.1 | 1.984 | 133 | 4.37 |

Ionization constants of the halogenoacetic acids:

| | | | |
|---|---|---|---|
| $CH_3CO_2H$ | $CH_2ClCO_2H$ | $CHCl_2CO_2H$ | $CCl_3CO_2H$ |
| $1.75\times10^{-5}$ | $1.4\times10^{-3}$ | $5\times10^{-2}$ | $2\times10^{-1}$ |
| | $CH_2BrCO_2H$ | $CHBr_2CO_2H$ | |
| | $1.38\times10^{-3}$ | ? | |

obtained by converting the perchlorate to other salts, and by using equivalent weights, comparing the molar extinction coefficients at their maxima in the visible region.

**Apparatus and Spectral Measurements.**—The visible and ultraviolet absorption spectra of the complexes were measured with a Cary 15 spectrophotometer using a pair of 1 cm. quartz cells; in some cases the maxima in the absorption bands were confirmed using a Beckman DU spectrophotometer. The concentrations were 0.005 mol./l., except in the case of *cis*-$[Co(CHBr_2CO_2)_2(en)_2]ClO_4$, where a 0.0025 mol./l. solution was used because of the solubility limitation. The complexes were dissolved in 0.01 N and 0.04 N perchloric acid in order to avoid the possibility of a rapid base hydrolysis; it was confirmed that a difference in the acid concentration does not change the spectra in most cases. However, where the acidity accelerates the aquation of the complexes, i.e., in *cis*-$[Co(CH_3CO_2)_2(NH_3)_4]^+$ and *cis*-$[Co(CH_3CO_2)_2(en)_2]^+$, the spectra of aqueous solutions were measused. Infrared spectra were also taken with a Perkin-Elmer Infracord in order to verify the composition of the compounds. All of them showed absorptions characteristic of $NH_3$, CO, and $ClO_4$ groups. The results are shown in Table I and in Figs. 1 and 2.

**The Assignment of the Configuration.** — For complexes of the $Coa_4b_2$ type it has been established,

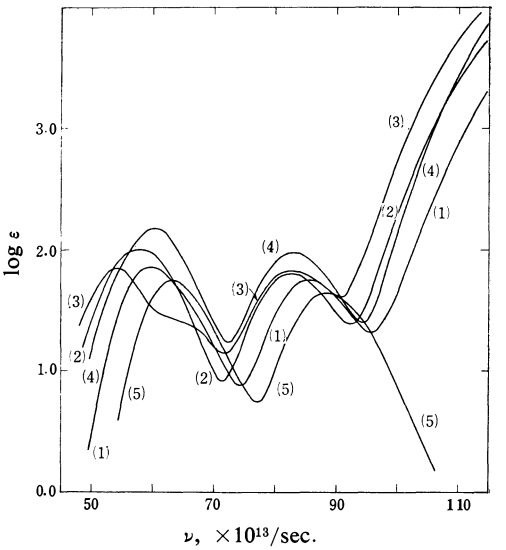



Fig. 1. Absorption spectra of dibromoacetatocobalt(III) complexes.
(1) $[Co(CHBr_2CO_2)(NH_3)_5](ClO_4)_2$
(2) *cis*-$[Co(CHBr_2CO_2)_2(NH_3)_4]ClO_4$
(3) *trans*-$[Co(CHBr_2CO_2)_2(NH_3)_4]ClO_4$
(4) *cis*-$[Co(CHBr_2CO_2)_2(en)_2]ClO_4$
(5) $[Co(NH_3)_6](ClO_4)_3$

TABLE II. SOLUBILITIES AND PRECIPITATION REACTIONS OF THE PERCHLORATES OF HALOGENOACETATO COBALT(III) COMPLEXES

| Complex | HCl 6 N | $NH_4Cl$ 2 N | $HNO_3$ 6 N | $NH_4NO_3$ 2 N | $HClO_4$ 6 N | $NaClO_4$ 2 N | NaBr 2 N | KI 2 N | $Na_2S_2O_3$ N | KSCN N | $Na_2C_2O_4$ sat. | $K_2CrO_4$ N | $K_2Cr_2O_7$ sat. | Solubility ml. $H_2O$/g. |
|---|---|---|---|---|---|---|---|---|---|---|---|---|---|---|
| $[Co(CH_3CO_2)(NH_3)_5]^{2+}$ | — | — | 4 | 4 | 4 | 4 | — | 3 | — | — | — | — | 4 | 65 |
| $[Co(CH_2ClCO_2)(NH_3)_5]^{2+}$ | — | — | 4 | 3 | 4 | 3 | — | 1 | — | — | — | 2 | 4 | 55 |
| $[Co(CHCl_2CO_2)(NH_3)_5]^{2+}$ | — | — | 2 | — | 4 | 4 | — | — | — | — | — | 4 | 2 | 70 |
| $[Co(CCl_3CO_2)(NH_3)_5]^{2+}$ | — | — | — | — | 3 | 2 | — | — | — | — | — | — | 2 | 120 |
| $[Co(CH_2BrCO_2)(NH_3)_5]^{2+}$ | — | — | 2 | 2 | 4 | 4 | — | — | — | — | — | 4 | 4 | 63 |
| $[Co(CHBr_2CO_2)(NH_3)_5]^{2+}$ | — | — | — | — | 4 | 4 | — | 4 | 3 | 3 | — | 4 | — | 26 |
| *cis*-$[Co(CH_3CO_2)_2(NH_3)_4]^+$ | — | — | — | — | — | — | — | — | — | — | — | — | — | vs |
| *cis*-$[Co(CH_2ClCO_2)_2(NH_3)_4]^+$ | — | — | 1 | — | 3 | 1 | — | — | — | — | — | — | — | 24 |
| *cis*-$Co(CHCl_2CO_2)_2(NH_3)_4]^+$ | — | — | — | — | 2 | 4 | 2 | 3 | — | — | — | — | — | 25 |
| *cis*-$[Co(CCl_3CO_2)_2(NH_3)_4]^+$ | 1 | 1 | — | 1 | 3 | 4 | — | — | — | — | — | — | 1 | 56 |
| *cis*-$[Co(CH_2BrCO_2)_2(NH_3)_4]^+$ | — | — | — | — | 3 | 2 | — | — | — | — | — | — | — | 10 |
| *cis*-$[Co(CHBr_2CO_2)_2(NH_3)_4]^+$ | 1 | 1 | 1 | 1 | 4 | 4 | 4 | 4 | — | 1 | — | — | 4 | 50 |
| *cis*-$[Co(CH_3CO_2)_2(en)_2]^+$ | — | — | — | — | — | — | — | — | — | — | — | — | — | vs |
| *cis*-$[Co(CH_2ClCO_2)_2(en)_2]^+$ | — | — | — | — | — | 2 | — | 1 | — | — | — | — | — | 62 |
| *cis*-$[Co(CHCl_2CO_2)_2(en)_2]^+$ | — | — | — | — | 2 | 3 | — | — | — | — | — | — | — | 89 |
| *cis*-$[Co(CCl_3CO_2)_2(en)_2]^+$ | 1 | — | 1 | 1 | 3 | 4 | 1 | — | — | 2 | 2 | — | — | 280 |
| *cis*-$[Co(CHBr_2CO_2)_2(en)_2]^+$ | — | — | — | — | 3 | 4 | 3 | 3 | — | 1 | 1 | — | — | 160 |

—: No precipitation
1: A small amount of deposit observable on the surface of the test tube
2: A small amount of precipitate
3: A large amount of precipitate (the liquid phase still has the color of the complex)
4: Almost complete precipitation (the liquid phase is almost colorless)
vs: Very soluble

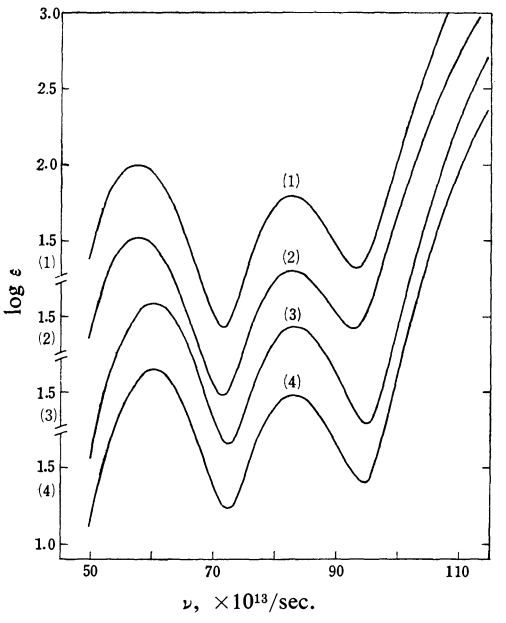



Fig. 2. Absorption spectra of some *cis*-bis-(halogenoacetato)-cobalt(III) complexes.
(1) *cis*-$[Co(CH_2ClCO_2)_2(NH_3)_4]ClO_4$
(2) *cis*-$[Co(CH_2BrCO_2)_2(NH_3)_4]ClO_4$
(3) *cis*-$[Co(CHCl_2CO_2)_2(en)_2]ClO_4$
(4) *cis*-$[Co(CHBr_2CO_2)_2(en)_2]ClO_4$

experimentally[1,10] and theoretically[11,12], that the first band of the trans-isomer splits significantly into two parts, whereas that of the cis-isomer does not. In addition, the third band (the charge-transfer band) of the trans-isomer appears at a low frequency than that of the cis-isomer.[13-15] In all the cases studied here, the corresponding isomers showed these spectral characteristics, as the figures show.

**Some Physical and Chemical Properties.**—Solubilities were measured semiquantitatively by the following method: A definite amount (0.1—1.0 g.) of a complex was placed in a 50 ml. flask; water was then added in 1 ml. increments until the solid was completely dissolved. The temperature was maintained at 20±1°C. The solubility data are, therefore, not equilibrium values; however, because all complexes were powdery or fine crystalline, the data are fairly accurate.

In the precipitation tests, 1 ml. of a reagent was added to 1 ml. of a saturated solution of the complex which had been obtained from the solubility test and cooled to 0°C. In several cases, where the complexes were very soluble, 0.05 molar solutions were tested. The results are summarized in Table II.

10) Y. Shimura, This Bulletin, **25**, 49 (1952).
11) C. J. Ballhausen and C. K. Jörgensen, *Kgl. Danske Videnskab. Selskab. Mat. Fys. Medd.*, **29** (14) (1955).
12) L. E. Orgel, *J. Chem. Phys.*, **23**, 1004 (1955).
13) H. Kuroya and R. Tsuchida, This Bulletin, **15**, 427 (1940).
14) F. Basolo, *J. Am. Chem. Soc.*, **72**, 4393 (1950).
15) Y. Shimura, ibid., **73**, 5079 (1951).

**Preparations.**—*1) Monobromoacetato-pentammine-cobalt(III) Perchlorate, $[Co(CH_2BrCO_2)(NH_3)_5](ClO_4)_2$.*—Ten grams of $[CoCO_3(NH_3)_5]NO_3$ was suspended in 20 ml. of water, and a solution was added which contained 30 g. of $CH_2BrCO_2H$ in 30 ml. of water. The solution was heated for one hour at 70°C, and then cooled to 0°C. After the violet residue which had formed had been removed, 10 ml. of a 25 per cent ammonium nitrate solution was added to the filtrate, and the resulting reddish-orange precipitate was also filtered off. Then 30 ml. of ethanol was added to the cold filtrate with continuous stirring. After the mixture had stood in an ice-water bath for an hour, a reddish-white precipitate formed; this was collected and washed with ethanol and ether. The nitrate, the bromine content of which was a little low, was purified by transformation to the perchlorate. To a saturated solution of the nitrate (one gram of it dissolves in 100 ml. of water at room temperature), concentrated perchloric acid was added. After the mixture had stood at 0°C, the pinkish-orange precipitate was collected, washed with ethanol and ether, and then dried in a desiccator. Yield, ca. 2 g.

Found: Co, 12.15; C, 5.13; H, 3.77; N, 14.67; Br, 16.91. Calcd. for $[Co(CH_2BrCO_2)(NH_3)_5](ClO_4)_2$: Co, 12.25; C, 4.99; H, 3.56; N, 14.56; Br, 16.62%.

*2) Dibromoacetato-pentammine-cobalt(III) Perchlorate, $[Co(CHBr_2CO_2)(NH_3)_5](ClO_4)_2$.*—Seven grams of $[CoCO_3(NH_3)_5]NO_3$ was suspended in 10 ml. of water, and then a solution of $CHBr_2CO_2H$ (20 g.) in 30 ml. of water was added. The solution was heated for one hour and then cooled in an ice bath. The residue which formed was collected on a glass-filter, and an extract was obtained by washing the residue with 100 ml. of a 50 per cent ethanol-water mixture, A 25 per cent ammonium nitrate solution was added to the extract until precipitation was almost complete. The reddish-white nitrate was isolated and washed with ethanol and ether. The nitrate, the bromine content of which was a little low, was transformed to the perchlorate. The nitrate (ca. 5 g.) was dissolved in 125 ml. of water, and 15 ml. of concentrated perchloric acid was added. The precipitate formed was washed with ethanol and ether. Yield, 5 g.

Found: Co, 10.38; C, 4.38; H, 2.77; N, 12.77; Br, 28.80. Calcd. for $[Co(CHBr_2CO_2)(NH_3)_5](ClO_4)_2$: Co, 10.53; C, 4.29; H, 2.88; N, 12.51; Br, 28.55%.

*3) cis-Bis(acetato)-tetrammine-cobalt(III) Perchlorate, $cis$-$[Co(CH_3CO_2)_2(NH_3)_4]ClO_4$.*—Although this compound was originally prepared by Linhard and Weigel,[1] the following procedure was found to be much simpler. To 3 g. of $[CoCO_3(NH_3)_4)ClO_4$, a 30 per cent perchloric acid at 50°C was added until the evolution of $CO_2$ ceased. Sodium acetate (1.7 g.) was added to the solution, which was then evaporated to almost complete dryness at ca. 60°C. Ten milliliters of absolute alcohol was stirred into the product, and the residue which had collected on a filter was washed with absolute alcohol and ether. This perchlorate (3 g.) was dissolved in 60 ml. of an 85 per cent alcohol-water mixture, and, after filtration, 90 ml. of ether was added. The

reddish-purple crystals formed were washed with a 50 per cent ethanol - ether mixture and ether. Yield, 2 g.

Found: Co, 17.08. Calcd. for *cis*-$[Co(CH_3CO_2)(NH_3)_4]ClO_4$: Co, 17.10%.

*4) cis - Bis(monobromoacetato) - tetrammine - cobalt(III) Perchlorate, cis-*$[Co(CH_2BrCO_2)_2(NH_3)_4]ClO_4$.—A mixture of $[CoCO_3(NH_3)_4]ClO_4$ (3 g.), $CH_2BrCO_2H$ (3.2 g.), and water (4 ml.) was evaporated to almost complete dryness at 50—55°C. The product was then dissolved in 20 ml. of a very dilute perchloric acid solution at 40°C and filtered. Five milliliters of concentrated perchloric acid was added to the filtrate, which was then cooled to 0°C. The resulting reddish-purple crystals were washed with ethanol and ether. The crude perchlorate, the yield of which was ca. 3 g., was recrystallized from 20 ml. of a slightly acidified water with perchloric acid at 40°C. Yield, 2.0 g.

Found: Co, 11.61; C, 9.79; H, 3.23; N, 11.46; Br, 32.02. Calcd. for *cis*-$[Co(CH_2BrCO_2)_2(NH_3)_4]ClO_4$: Co, 11.73; C, 9.56; H, 3.21; N, 11.15; Br, 31.81%.

*5) cis-Bis(dibromoacetato)-tetrammine - cobalt(III) Perchlorate, cis-*$[Co(CHBr_2CO_2)_2(NH_3)_4]ClO_4$. — A solution of $CHBr_2CO_2H$ (4.8 g.) and $[CoCO_3(NH_3)_4]ClO_4$ (3 g.) in 4 ml. of water was evaporated to dryness at 50—55°C. After the addition of a dilute perchloric acid and filtration, the residue on the filter was extracted with 50 ml. of warm water. The extract was cooled, and several drops of perchloric acid were added. The resulting reddish-purple crystals were recrystallized in the same way as 4). Yield, 3.5 g.

Found: Co, 8.95; C, 7.49; H, 2.22; N, 8.67; Br, 48.50. Calcd. for *cis*-$[Co(CHBr_2CO_2)_2(NH_3)_4]ClO_4$: Co, 8.93; C, 7.28; H, 2.14; N, 8.49; Br, 48.41%.

*6) cis - Bis(dibromoacetato) - bis(ethylenediamine) - cobalt(III) Perchlorate, cis-*$[Co(CHBr_2CO_2)_2(en)_2]ClO_4$.—A mixture of $[CoCO_3(en)_2]ClO_4$ (2 g.), $CHBr_2CO_2H$ (2.7 g.) and water (3 ml.) was evaporated at ca. 60°C until the mixture nearly solidified. The product was then mixed with 20 ml. of dilute perchloric acid; the reddish precipitate which formed was washed with alcohol and ether. The crude perchlorate, the yield of which was 1.5 g., was dissolved in 40 ml. of warm water and recrystallized in a way similar to that used in 4). Yield, 1.5 g.

Found: Co, 8.12; C, 13.58; H, 2.71; N, 8.05. Calcd. for *cis*-$[Co(CHBr_2CO_2)_2(en)_2]ClO_4$: Co, 8.27; C, 13.49; H, 2.55; N, 7.87%.

*7) cis-Bis(acetato)-bis(ethylenediamine)-cobalt(III) Perchlorate, cis-*$[Co(CH_3CO_2)_2(en)_2]ClO_4$.—This compound has already been prepared,[2] but it was found that the following procedure was simpler and gave a high yield. To 3 g. of $[CoCO_3(en)_2]ClO_4$, a 30 per cent solution of perchloric acid at 50°C was added until the evolution of carbon dioxide ceased. Sodium acetate (1.5 g.) was then added to the mixture, and it was evaporated to almost complete dryness at 60—65°C. The product was thoroughly mixed with 10 ml. of alcohol, and the resulting precicipitate was washed several times with alcohol and finally with ether. The bright red crystals thus obtained were the double salt, *cis*-$[Co(CH_3CO_2)_2(en)_2]ClO_4 \cdot NaClO_4$, judging from the analytical results and the spectra of its solution. Yield, 3.5 g. The neutral perchlorate is very soluble in water and unobtainable by usual methods. It was isolated as follows: To a mixture of 30 ml. of alcohol and the double salt, water was slowly added, drop by drop, by continuous stirring, until the color suddenly changed to violet. At this point a few extra drops of water were added, and the precipitate was collected and washed with alcohol several times and finally with ether. The filtrate also contained a large amount of the complex, and upon the addition of ether, additional perchlorate was obtained in a pure state. Yield, 3 g. Although the perchlorate and the double salt are different colors in the solid state, the absorption spectra of their solutions were exactly identical.

Found: Co, 14.73. Calcd. for *cis*-$[Co(CH_3CO_2)_2(en)_2]ClO_4$: Co, 14.86%.

*8) cis - Bis(chloroacetato) - tetrammine - cobalt(III) Perchlorate, cis-*$[Co(clac)_2(NH_3)_4]ClO_4$ *and cis-Bis(chloroacetato)-bis(ethylenediamine)-cobalt(III) Perchlorate, cis-*$[Co(clac)_2(en)_2]ClO_4$, where clac= $CH_2ClCO_2$, $CHCl_2CO_2$, $CCl_3CO_2$. These complexes were prepared by the method of Linhard and Weigel.[1]

## Results and Discussion

**Preparations.**—The usual procedure for the preparation of $[Co(X)(NH_3)_5]^{n+}$-type complexes[16] requires that the mixture of $[Co(H_2O)(NH_3)_5]^{3+}$ and X be kept at a temperature (usually higher than room temperature) for a suitable period in an acidic solution. This approach was used for the preparation of $[Co(CH_2BrCO_2)(NH_3)_5]^{2+}$ and $[Co(CHBr_2CO_2)(NH_3)_5]^{2+}$. However, unlike many other ligands, the bromoacetate ions are relatively unstable at high temperatures and yet do not rapidly coordinate at low temperatures. It was, therefore, observed, from the color and absorption spectra of the by-products, that at higher temperatures and for longer periods than those described in the Experimental section, the yield of the desired complexes became lower as a result of the decomposition and/or hydrolysis of the ligands, whereas at lower temperatures the main product was the unreacted aquo-complex.

The preparation of $[Co(CBr_3CO_2)(NH_3)_5]X$ was also attempted in a similar way. In this case, however, the tribromoacetate of the aquo-complex, $[Co(H_2O)(NH_3)_5](CBr_3CO_2)_3$, precipitates immediately after the starting materials are mixed. When the temperature is elevated, the tribromoacetate ion decomposes to an oily material, and the desired complex is not obtained.

16) J. C. Bailar, Jr., "Inorganic Syntheses," Vol. IV, 171 (1953).

Linhard and his co-workers[1-3] studied the $[Co(clac)_2(NH_3)_4]X$ complexes and found that cis-isomers were obtained when $[CoCO_3(NH_3)_4]ClO_4$ and an equivalent amount of chloroacetic acid were evaporated at a relatively low temperature, whereas trans-isomers were obtained when a large excess of acids was used and the evaporation occurred at a higher temperature. This principle was used for the preparation of the cis-isomers of the bromoacetato complexes, and the desired complexes, except for *cis*-$[Co(CH_2BrCO_2)_2(en)_2]ClO_4$, were obtained with comparative ease. The preparation of *cis*-$[Co(CH_2BrCO_2)_2(en)_2]ClO_4$ was attempted, with varying temperatures, solvents and starting materials. However, the resulting reaction products were always extremely hygroscopic and no definite solid material was obtained, although the spectra of solutions of some products showed fairly satisfactory features.

**Solubilities.**—Although several reversed cases may be noted, there are definite trends in the solubilities of the complexes. That is, the larger the halogen content of the ligands, the less soluble they are in water and the more soluble they are in ethanol, especially when the compound is slightly moist.

**Precipitation Reactions.**—In addition to the anions shown in Table II, it was observed that a 1 N solution of sodium carbonate, sodium acetate, sodium nitrite and sodium sulfite, and a saturated solution of sodium hydrogen phosphate, 6 N sulfuric acid and 2 N ammonium sulfate did not precipitate any of the complexes. This table may prove useful for the transformation of the anion of the complexes, and it suggests the possibility of utilizing the complexes for the analysis of anions. For example, $[Co(CHBr_2CO_2)(NH_3)_5]^{2+}$ precipitates with iodide but not with bromide and chloride. Therefore, the complex presents the possibility of detecting the $I^-$ ion in the presence of $Br^-$ and $Cl^-$ ions.

**Visible and Ultraviolet Absorption Spectra.**—As may be seen in Table I, in the case of pentammine complexes the maxima of the first band appear at almost identical frequencies, and those of the second band are also very close to each other. However, in the tetrammine series, obvious differences in the maxima are observable; that is, the larger the halogen content in the halogenoacetato ligand, the larger the frequencies of both the first and the second bands. The same order exists in the bis-(ethylenediamine) series. It has been pointed out[17] that if the ligand "a" is replaced in a complex $Ma_6$ by a ligand "b", the shift of the maxima is approximately as represented by the following equation:

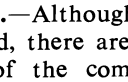
$$\nu(Ma_{6-n}b_n)=\frac{6-n}{6}\nu(Ma_6)+\frac{n}{6}\nu(Mb_6)$$

Therefore, the difference in $\nu$ between $Ma_4b_2$ and $Ma_4b'_2$ should be twice as large as that between $Ma_5b$ and $Ma_5b'$. This relation holds in the present complexes. Thus, the relative position of the ligands in the spectrochemical series is determined to be:

$$I<\cdots<CH_3CO_2<\left\{\begin{matrix}CH_2ClCO_2<CHCl_2CO_2<CCl_3CO_2\\ \wr\qquad\qquad\wr\\ CH_2BrCO_2<CHBr_2CO_2<(CBr_3CO_2)\end{matrix}\right\}<\cdots<CN$$

from the data of bis-(halogenoacetato) as well as mono-(halogenoacetato) series.

Now, since all the complexes have the



atomic arrangement, it may be said that the factors which may influence the spectra are: (1) the polarity of the cobalt-halogenoacetato bond, (2) the volume of the ligands, and (3) the chemical (especially the oxidation-reduction) property of halogens. We shall now consider these factors.

Previously, Linhard and his co-workers[1-3] measured the absorption spectra of $[Co(RCO_2)(NH_3)_5]^{2+}$ and *cis*-$[Co(RCO_2)_2(NH_3)_4]^+$ where R=alkyl, and found that in each case the absorption maxima of both the first and the second bands appear at almost identical frequencies, with a variety of R. This indicates that the volume of a ligand is a minor factor in the spectral characteristics of complexes. The same situation exists in the present case, since there is little shift in the absorption maxima with the variety of halogen species, and chlorine and bromine have fairly different atomic radii.

It is well-known that, when halogens coordinate to the central atom directly, the corresponding halogeno-complexes (e.g., $[CoCl(NH_3)_5]^{2+}$ and $[CoBr(NH_3)_5]^{2+}$) have greatly different spectral features. This phenomena have been attributed to the different oxidation-reduction properties of halogens. On the contrary, corresponding chloroacetato- and bromoacetato-complexes show identical features, as may be seen in Figs. 1 and 2. Furthermore, the halogen-carbon bondings have no absorption in the visible and near ultraviolet region. Thus, it is clear that the differences in the chemical property of halogens in the ligands are also a minor factor in affecting the positions of the first and the second absorptions.

17) Y. Shimura and R. Tsuchida, This Bulletin, **28**, 572 (1955).

(Since carbon-halogen bondings have a slight absorption in far ultraviolet region, the third band may be influenced by the variety of halogen.)

The first factor, the polarity of Co–O bonds, is not known exactly, but it may be assumed that it parallels the polarity of the H–O bonds of the halogenoacetic acids, which can be placed in a qualitative order by the dissociation constant of each acid, or by the basicity of each halogenoacetate ion. The experimental results show that the smaller the basicity of the halogenoacetato ligand, the larger the frequencies of the absorption maxima, as may be seen in Table I. That the polarity of central atom - ligand bonding is the predominant factor in the energy splitting of the d-electrons in a complex is a fundamental assumption of the recent ligand field theory of complex compounds; this assumption has been experimentally verified by the present results.

The authors are grateful for the support provided for this research by the Atomic Energy Commission of the U. S. A. under Contract No. AT(30-1)-906.

*Department of Chemistry*
*Kyoto Gakugei University*
*Fushimi-ku, Kyoto (K. K.)*

*Department of Chemistry*
*Fordham University*
*New York 58, N. Y. (P.S.G.)*

# Studies of Halogenoacetato Cobalt(III) Complexes. II.[1],* The Preparation and Some Properties of *trans*-Bis(halogenoacetato)-tetrammine-cobalt(III) and *trans*-Bis(halogenoacetato)-bis(ethylenediamine)-cobalt(III) Complexes

By Kashiro KURODA and Philip S. GENTILE

(Received December 28, 1964)

In the preceding communication,[1] the authors have reported on the *cis*-isomers of bis(halogenoacetato)-tetrammine and bis(halogenoacetate)-bis(ethylenediamine) cobalt(III) complexes, *cis*-$[Co(halac)_2(NH_3)_4]^+$ and *cis*-$[Co(halac)_2(en)_2]^+$, where halac=$CH_3CO_2$, $CH_2ClCO_2$, $CHCl_2CO_2$, $CCl_3CO_2$, $CH_2BrCO_2$ and $CHBr_2CO_2$. There should be a geometrical isomer (trans-isomer) for each of the cis-isomers. Previously, Linhard and his co-workers[2,3] studied the complexes, $[Co(clac)_2(NH_3)_4]X$ and $[Co(clac)_2(en)_2]X$ (clac=acetato and three chloroacetato ligands); although they isolated many of the cis-isomers, only a few trans-isomers were obtained. The difficulties in the preparation of trans-isomers are to be attributed to the fact that the fraction of trans-isomer is small in a reaction product of a carbonato complex ($[CoCO_3(NH_3)_4]X$ or $[CoCO_3(en)_2]X$) and a halogenoacetic acid, and that no suitable reagent is known for the separation of geometrical isomers. As will be described in the following sections, the authors have found that trichloroacetic acid is an excellent precipitant for trans-isomers; it can separate them from mixtures which contain a large fraction of cis-isomers. As a result, many new species of the trans-isomers of bromoacetato-complexes as well as of chloroacetato-complexes have been isolated as trichloroacetates, and they have been converted to the perchlorates. Some of their physical and chemical properties have been studied, and interesting phenomena have been observed, especially in their absorption spectra.

## Experimental

**Materials.**—Monochloroacetic, dichloroacetic and trichloroacetic acid (Fisher Scientific Co.), monobromoacetic acid (Eastman Organic Chemicals) and dibromoacetic acid (K & K Laboratories, Inc.), and all the other reagent-grade chemicals were used without further purification.

**Analysis.** — Cobalt was analyzed by a direct

* The most part of this research was done in the laboratory of Department of Chemistry, Fordham University, New York 58, N. Y., U. S. A., during the period in which the former of the authors was a visiting chemist to the University.

1) Part I of this series: K. Kuroda and P. S. Gentile, This Bulletin, **38**, 1362 (1965).

2) M. Linhard and M. Weigel, *Z. anorg. Chem.*, **260**, 65 (1969); **264**, 321 (1951).

3) M. Linhard and G. Stirn, ibid., **268**, 105 (1952).

TABLE I. ABSORPTION SPECTRA OF *trans*-$[Co(halac)_2(NH_3)_4]ClO_4$ AND *trans*-$[Co(halac)_2(en)_2]ClO_4$

| | 1st band | | | | 2nd band | | 3rd band | |
|---|---|---|---|---|---|---|---|---|
| | Ia | | Ib | | | | | |
| | $\nu(10^{13}/sec.)$ | log $\varepsilon$ | $\nu(10^{13}/sec.)$ | log $\varepsilon$ | $\nu(10^{13}/sec.)$ | log $\varepsilon$ | $\nu(10^{13}/sec.)$ | log $\varepsilon$ |
| *trans*-$[Co(halac)_2(NH_3)_4]ClO_4$ | | | | | | | | |
| $CH_3CO_2$ | 54.5 | 1.806 | shoulder | | 82.4 | 1.839 | 126 | 4.18 |
| $CH_2ClCO_2$ | 54.0 | 1.818 | shoulder | | 82.9 | 1.827 | 126 | 4.22 |
| $CHCl_2CO_2$ | 53.8 | 1.795 | shoulder | | 83.6 | 1.801 | 127* | 4.20 |
| $CCl_3CO_2$ | 53.3 | 1.798 | 65.7 | 1.38 | 84.0 | 1.778 | 128* | 4.25 |
| $CH_2BrCO_2$ | 54.1 | 1.835 | shoulder | | 82.9 | 1.848 | 124.5 | 4.20 |
| $CHBr_2CO_2$ | 53.9 | 1.846 | shoulder | | 83.3 | 1.839 | 133.5* | 4.26 |
| *trans*-$[Co(halac)_2(en)_2]ClO_4$ | | | | | | | | |
| $CH_3CO_2$ | 55.8 | 1.778 | 66.7 | 1.462 | 84.0 | 1.863 | 128 | 4.25 |
| $CH_2ClCO_2$ | 55.2 | 1.782 | 67.3 | 1.468 | 84.2 | 1.849 | 129 | 4.28 |
| $CHCl_2CO_2$ | 54.8 | 1.771 | 67.9 | 1.471 | 84.5 | 1.831 | —* | — |
| $CCl_3CO_2$ | 53.9 | 1.756 | 68.5 | 1.456 | 85.2 | 1.784 | 132* | 4.33 |
| $CH_2BrCO_2$ | (not obtained in purity) | | | | | | | |
| $CHBr_2CO_2$ | 54.8 | 1.798 | 67.7 | 1.441 | 84.5 | 1.855 | 131* | 4.33 |

Ionization constants of the halogenoacetic acids:

| | | | |
|---|---|---|---|
| $CH_3CO_2H$ | $CH_2ClCO_2H$ | $CHCl_2CO_2H$ | $CCl_3CO_2H$ |
| $1.75\times10^{-5}$ | $1.4\times10^{-3}$ | $5\times10^{-2}$ | $2\times10^{-1}$ |
| | $CH_2BrCO_2H$ | $CHBr_2CO_2H$ | |
| | $1.38\times10^{-3}$ | ? | |

* Obvious deformation around max. is observed.

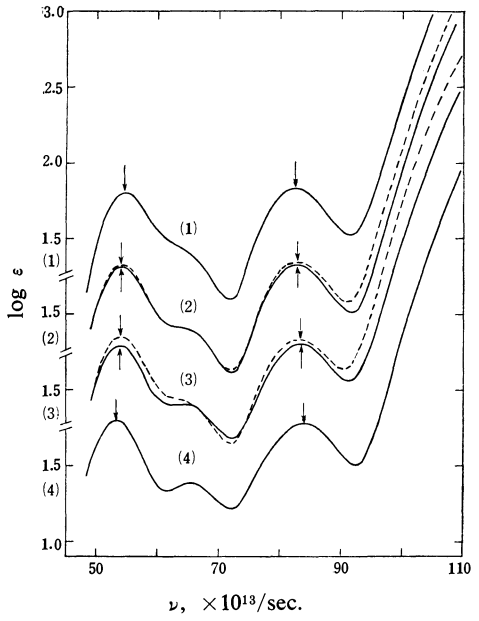



Fig. 1. Absorption spectra of *trans*-bis-(halogenoacetato)-tetrammine-cobalt(III) complexes.
(1) *trans*-$[Co(CH_3CO_2)_2(NH_3)_4]ClO_4$
(2) —— *trans*-$[Co(CH_2ClCO_2)_2(NH_3)_4]ClO_4$
--- *trans*-$[Co(CH_2BrCO_2)_2(NH_3)_4]ClO_4$
(3) —— *trans*-$[Co(CHCl_2CO_2)_2(NH_3)_4]ClO_4$
--- *trans*-$[Co(CHBr_2CO_2)_2(NH_3)_4]ClO_4$
(4) *trans*-$[Co(CCl_3CO_2)_2(NH_3)_4]ClO_4$

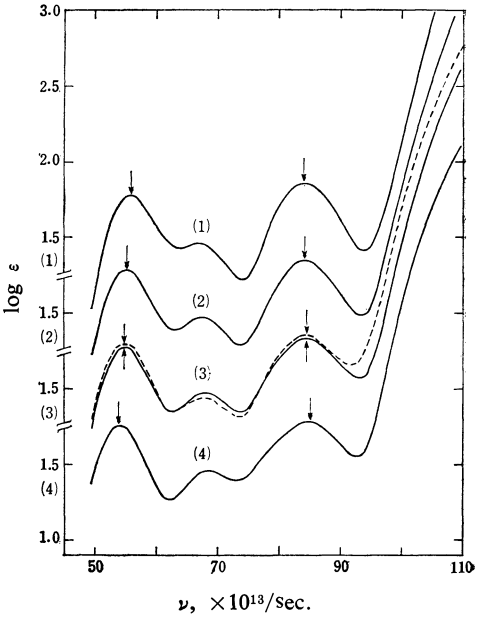



Fig. 2. Absorption spectra of *trans*-bis-(halogenoacetato)-bis(ethylenediamine)-cobalt-(III) complexes.
(1) *trans*-$[Co(CH_3CO_2)_2(en)_2]ClO_4$
(2) *trans*-$[Co(CH_2ClCO_2)_2(en)_2]ClO_4$
(3) —— *trans*-$[Co(CHCl_2CO_2)_2(en)_2]ClO_4$
--- *trans*-$[Co(CHBr_2CO_2)_2(en)_2]ClO_4$
(4) *trans*-$[Co(CCl_3CO_2)_2(en)_2]ClO_4$

TABLE II. SOLUBILITIES AND PRECIPITATION REACTIONS OF THE PERCHLORATE OF *trans*-BIS(HALOGENOACETATO)-COBALT(III) COMPLEXES

| Complex | HCl 6 N | $NH_4Cl$ 2 N | $HNO_3$ 6 N | $NH_4NO_3$ 2 N | $HClO_4$ 6 N | $NaClO_4$ 2 N | NaBr 2 N | KI 2 N | $Na_2S_2O_3$ N | KSCN N | $K_2Cr_2O_7$ sat. | $CCl_3CO_2H$* 2 N | Solubility ml.$H_2O$/g. |
|---|---|---|---|---|---|---|---|---|---|---|---|---|---|
| *trans*-$[Co(CH_3CO_2)_2(NH_3)_4]^+$ | 4 | — | — | — | 3 | — | — | 1 | — | — | — | 2 | 17 |
| *trans*-$[Co(CH_2ClCO_2)_2(NH_3)_4]^+$ | — | — | — | — | 2 | 2 | — | 1 | — | — | — | 4 | 108 |
| *trans*-$[Co(CHCl_2CO_2)_2(NH_3)_4]^+$ | — | — | — | — | 2 | 2 | — | 1 | — | — | 2 | 4 | 20 |
| *trans*-$[Co(CCl_3CO_2)_2(NH_3)_4]^+$ | — | — | 1 | 3 | 2 | 3 | — | — | — | — | — | 4 | vs |
| *trans*-$[Co(CH_2BrCO_2)_2(NH_3)_4]^+$ | — | — | — | — | 2 | 3 | — | 1 | — | — | — | 4 | 77 |
| *trans*-$[Co(CHBr_2CO_2)_2(NH_3)_4]^+$ | — | — | — | — | 3 | 3 | 1 | 4 | — | 1 | 3 | 4 | 54 |
| *trans*-$[Co(CH_3CO_2)_2(en)_2]^+$ | — | — | — | — | 4 | 1 | — | — | 4 | — | — | 2 | vs |
| *trans*-$[Co(CH_2ClCO_2)_2(en)_2]^+$ | — | — | — | — | 1 | 1 | — | — | — | — | — | 4 | 57 |
| *trans*-$[Co(CHCl_2CO_2)_2(en)_2]^+$ | — | — | — | — | 1 | 2 | — | — | — | — | — | 4 | 260 |
| *trans*-$[Co(CCl_3CO_2)_2(en)_2]^+$ | — | — | — | — | 4 | 4 | — | 3 | — | 2 | — | 4 | 370 |
| *trans*-$[Co(CH_2BrCO_2)_2(en)_2]^+$ | (not obtained in purity) | | | | | | | | | | | | |
| *trans*-$[Co(CHBr_2CO_2)_2(en)_2]^+$ | — | — | — | — | 3 | 3 | 1 | 3 | — | 2 | — | 4 | 280 |

—: No precipitation
1: A small amount of deposit observable on the surface of the test tube
2: A small amount of precipitate
3: A large amount of precipitate (the liquid phase has still the color of the complex)
4: Almost complete precipitation (the liquid phase is almost colorless)
vs: Very soluble
* All cis-isomers of these complexes do not precipitate with trichloroacetic acid.

EDTA titration, using murexide as an indicator,[4] after the decomposition of a complex with hot concentrated sulfuric and nitric acid. The other elements were analyzed microquantitatively by the Schwarzkoph Microanalytical Laboratory (Woodside, New York, U. S. A.).

**Apparatus and Measurments.** — The absorption spectra of the complexes were measured with a Cary 15 spectrophotometer using a pair of 1 cm. quartz cells. The concentration of the complexes was 0.005 mol./l. (for *trans*-$[Co(CH_3CO_2)_2(en)_2]^+$, a 0.01 mol./l. solution was used) for the measurments in the visible and near ultraviolet region, whereas the original solutions were diluted to 0.0005 and 0.00005 mol./l. for the far ultraviolet region. In most cases, the complexes were dissolved in a 0.01 N and 0.04 N perchloric acid solution in order to avoid the possibility of a rapid base hydrolysis. It was found that a different concentration of the acid does not change the spectra. The spectra of the trichloroacetates of the complexes were also measured; it was found that the absorption curve was identical within the range of experimental error with that of the corresponding perchlorate in the visible and near ultraviolet region. The results are shown in Figs. 1 and 2 and Table I.

The solubility of the complexes was measured semiquantitatively in the same way as has been described in the previous report.[1] The precipitation reactions with various anions were also tested by a previously-reported[1] method. These experimental results are summarized in Table II.

**Preparations.** — *1) trans-Bis(acetato)-tetrammine-cobalt(III) Perchlorate, trans-*$[Co(CH_3CO_2)_2(NH_3)_4]ClO_4$*, and trans-Bis(monochloroacetato)-tetrammine-cobalt(III) Perchlorate, trans-*$[Co(CH_2ClCO_2)_2(NH_3)_4]ClO_4$. — These complexes were prepared by the method of Linhard and Weigel.[2]

*2) trans-Bis(dichloroacetato)-tetrammine-cobalt(III) Perchlorate, trans-*$[Co(CHCl_2CO_2)_2(NH_3)_4]ClO_4$. — A mixture of $[CoCO_3(NH_3)_4]ClO_4$ (5 g.), $CHCl_2CO_2H$ (10 g.) and water (10 ml.) was evaporated to almost complete dryness at 70—75°C. The cooled reaction product was mixed with 30 ml. of dilute perchloric acid and filtered with a glass-filter, then the residue on the filter was extracted with 10 ml. of alcohol. After the addition of 50 ml. of water to the extract, 3 g. of trichloroacetic acid was added and the solution was cooled to 0°C. The violet crystals formed were collected and washed with alcohol(10%)-ether mixture and ether. (If concentrated perchloric acid is added to the alcoholic extract, the perchlorate is obtained, but it is always contaminated with the cis-isomer, which is difficult to remove.) The yield of the trichloroacetate is ca. one gram. The trichloroacetate was dissolved in 60 ml. of a alcohol(90%)-water mixture and, after filtration, 20 ml. of concentrated perchloric acid was added. After the mixture had stood at 0°C, the resulting light violet crystals, the acidic salt, were collected on a filter and washed with ether in order to remove the aqueous phase mechanically as completely as possible, and then with absolute alcohol and ether. During the treatment with alcohol, the acidic salt changes to the neutral salt. Since the acidic salt is very soluble in alcohol when it is wet, it should be dry when it is treated with alcohol, as has been described above. Yield, 0.7 g.

Found: Co, 12.18; C, 10.06; H, 3.02; N, 11.80. Calcd. for *trans*-$[Co(CHCl_2CO_2)_2(NH_3)_4]ClO_4$: Co, 12.22; C, 9.96; H, 2.92; N, 11.62%.

*3) trans-Bis(trichloroacetato)-tetrammine-cobalt(III) Perchlorate, trans-*$[Co(CCl_3CO_2)_2(NH_3)_4]ClO_4$. —A solution of $[CoCO_3(NH_3)_4]ClO_4$ (3 g.) and $CCl_3CO_2H$ (15 g.) in 10 ml. of water was evaporated to dryness at 70—75°C. The product was washed four times with 25 ml. portions of very dilute perchloric acid to remove the cis-isomer, and then extracted with 50 ml. of warm (~40°C) water. After three grams of $CCl_3CO_2H$ had been added to the extract, the resulting light violet precipitate was collected and washed in the way described in 2). Yield of the trichloroacetate, 1.5 g. To convert it to the perchlorate, 1 g. of the trichloroacetate was dissolved in 30 ml. of water. and 15 ml. of a 50 per cent sodium perchlorate solution was added. The precipitate formed was washed as in 2). Yield, 0.6 g. Even if perchloric acid is used for the precipitation, the acidic perchlorate is obtained.

Found: Co, 10.43; C, 9.17; H, 2.46; N, 10.40. Calcd. for *trans*-$[Co(CCl_3CO_2)_2(NH_3)_4]ClO_4$: Co, 10.69; C, 8.71; H, 2.19; N, 10.16%.

*4) trans-Bis(monobromoacetato)-tetrammine-cobalt(III) Perchlorate, trans-*$[Co(CH_2BrCO_2)_2(NH_3)_4]ClO_4$. — A mixture of $[CoCO_3(NH_3)_4]ClO_4$ (5 g.), $CH_2BrCO_2H$ (12.5 g.) and water (10 ml.) was evaporated to a small, tarry, volume at 60—65°C. The product was mixed with 20 ml. of a very dilute perchloric acid and the precipitate formed, after having been washed with a small amount of cold water, was extracted with 40 ml. of warm water. Two milliliters of concentrated perchloric acid was added to the extract, which was then cooled, and the violet precipitate formed was washed with a small amount of cold water, alcohol and ether. For further purification, the complex was converted once to the trichloroacetate and then to the perchlorate, as in 2). Yield, 0.7 g.

Found: Co, 11.66; C, 9.86; H, 3.32; N, 11.60. Calcd. for *trans*-$[Co(CH_2BrCO_2)_2(NH_3)_4]ClO_4$: Co, 11.73; C, 9.56; H, 3.21; N, 11.15%.

*5) trans-Bis(dibromoacetato)-tetrammine-cobalt(III) Perchlorate, trans-*$[Co(CHBr_2CO_2)_2(NH_3)_4]ClO_4$. — A mixture of $[CoCO_3(NH_3)_4]ClO_4$ (2 g.), $CHBr_2CO_2H$ (7 g.) and water (7 ml.) was evaporated at 70—75°C until crystals appeared. The product was mixed with 20 ml. of dilute perchloric acid, and the resulting precipitate was washed with 60 ml. of warm water. This treatment washed out the cis-isomer almost completely. (From the extract, the cis-isomer can be obtained by cooling.) The violet residue was dissolved in 100 ml. of warm water, and the solution was cooled to 0°C after the addition of several drops of perchloric acid. The violet crystals formed were washed with a small amount of cold water, an ethanol(10%)-ether mixture and ether. Yield, 0.7 g. The complex in the final filtrate is recoverable as the

4) H. Flaschka, *Mikrochemie ver. Mikrochim. Acta*, **39**, 38 (1952).

trichloroacetate by the addition of trichloroacetic acid. Yield of the trichloroacetate, 0.5 g.

Found: Co, 8.98; C, 7.40; H, 2.37; N, 8.60. Calcd. for *trans*-$[Co(CHBr_2CO_2)_2(NH_3)_4]ClO_4$: Co, 8.93; C, 7.28; H, 2.14; N, 8.49%.

*6) trans-Bis(acetato)-bis(ethylenediamine)-cobalt(III) Perchlorate, trans-*$[Co(CH_3CO_2)_2(en)_2]ClO_4$.— Although this compound had already been prepared by Linhard and Stirn,[3] it was found that the following procedure was simpler and gave a high yield. A mixture of $[CoCO_3(en)_2]ClO_4$ (3 g.), $CH_3CO_2H$ (4.5 g.) and water (5 ml.) was evaporated, using a small free flame, until solidification occurred. The product was mixed with 30 ml. of water, and, after filtration, 3 ml. of concentrated perchloric acid was added. The reddish crystals which formed were the acidic perchlorate, *trans*-$[Co(CH_3CO_2)_2(en)_2]ClO_4 \cdot HClO_4$; they were washed with dilute perchloric acid, ethanol and ether. Yield, 4.0 g. In order to obtain the neutral complex, 3 g. of the acidic salt was covered with ether in a flask, and anhydrous gaseous ammonia was bubbled through the mixture for ten minutes. The complex should be slightly wet; otherwise neutralization does not occur. The crystalline salt gained in volume by this treatment. After filtration, the residue on a filter was extracted with a small amount (<5 ml.) of warm (~40°C) water, and the filtrate was cooled sufficiently at 0°C. The red precipitate formed was washed with ethanol and ether. Yield, 0.5 g. After the dilution of the final filtrate to 50 ml. and the addition of perchloric acid, the complex can be recovered as the acidic perchlorate almost quantitatively.

Found: Co, 14.81; C, 24.32; H, 5.62; N, 14.20. Calcd. for *trans*-$[Co(CH_3CO_2)_2(en)_2]ClO_4$: Co, 14.86; C, 24.22; H, 5.59; N, 14.12%.

*7) trans-Bis(monochloroacetato)-bis(ethylenediamine)-cobalt(III) Perchlorate, trans-*$[Co(CH_2ClCO_2)_2(en)_2]ClO_4$. — A reaction product was obtained by the evaporation of a mixture of $[CoCO_3(en)_2]ClO_4$ (3 g.), $CH_2ClCO_2H$ (7 g.) and water (10 ml.) at ~70°C. It was mixed with 20 ml. of dilute perchloric acid, and the resulting precipitate was washed with ethanol and ether. The perchlorate thus obtained was dissolved in 180 ml. of warm water containing several drops of perchloric acid, and recrystallized. The violet crystals formed were washed with ethanol and ether. Yield, 2.0 g.

Found: Co, 12.63; C, 21.03; H, 4.56; N, 11.70. Calcd. for *trans*-$[Co(CH_2ClCO_2)_2(en)_2]ClO_4$: Co, 12.66; C, 20.64; H, 4.33; N, 12.03%.

*8) trans-Bis(dichloroacetato)-bis(ethylenediamine)-cobalt(III) Perchlorate, trans-*$[Co(CHCl_2CO_2)_2(en)_2]ClO_4$.—A product was obtained by the evaporation of a mixture of $[CoCO_3(en)_2]ClO_4$ (3 g.), $CHCl_2CO_2H$ (10 g.) and water at ~70°C. The precipitate which was formed by the addition of dilute perchloric acid was extracted, with 100 ml. of warm water; then the extract was set aside. (This extract contains the cis-isomer.) A second separate extract was made with another 300 ml. of warm water; It was cooled after the addition of several drops of perchloric acid. The reddish purple crystals which formed were washed with cold dilute perchloric acid, ethanol and ether. Yield, 2.0 g.

Found: Co, 10.97; C, 18.14; H, 3.64; N, 10.40. Calcd. for *trans*-$[Co(CHCl_2CO_2)_2(en)_2]ClO_4$: Co, 11.03; C, 17.98; H, 3.40; N, 10.48%.

*9) trans-Bis(trichloroacetato)-bis(ethylenediamine)-cobalt(III) Perchlorate, trans-*$[Co(CCl_3CO_2)_2(en)_2]ClO_4$. — A mixture of $[CoCO_3(en)_2]ClO_4$ (2 g.), $CCl_3CO_2H$ (8.5 g.) and water (6 ml.) was evaporated at ~70°C to a small volume; then it was heated on a small flame until the color changed from dark red to deep violet. As soon as the color change was finished, the mixture was quickly cooled. The product was mixed with 20 ml. of dilute perchloric acid, and the resulting precipitate, after having been washed with a perchloric acid solution, was extracted with 100 ml. of an ethanol (50%)-water mixture. The last 80 ml. portion was separated from the first 20 ml., which was contaminated with the cis-isomer. After the addition of several drops of perchloric acid, the extract was cooled. The violet crystals which formed were washed in the way described in 2).

Found: Co, 9.54; C, 16.02; H, 2.86; N, 9.70. Calcd. for *trans*-$[Co(CCl_3CO_2)_2(en)_2]ClO_4$: Co, 9.77; C, 15.92; H, 2.67; N, 9.29%.

*10) trans-Bis(monobromoacetato)-bis(ethylenediamine)-cobalt(III) Perchlorate, trans-*$[Co(CH_2BrCO_2)_2(en)_2]ClO_4$.—This complex was not isolated in a highly pure state. Many procedures similar to those used for the others were tried, but the reaction products were always very hygroscopic, as in the case of *cis*-$[Co(CH_2BrCO_2)_2(en)_2]ClO_4$. Trichloroacetic acid could form a precipitate with some of the reaction products, and although the spectra showed a fairly satisfactory feature (a large splitting of the first band), it was also hygroscopic.

*11) trans-Bis(dibromoacetato)-bis(ethylenediamine)-cobalt(III) Perchlorate, trans-*$[Co(CHBr_2CO_2)_2(en)_2]ClO_4$. — A mixture of $[CoCO_3(en)_2]ClO_4$ (2 g.), $CHBr_2CO_2H$ (7 g.) and water (5 ml.) was evaporated at 65—70°C and then heated and boiled carefully on a small flame for a few minutes. When the color suddenly changed from dark red to reddish-violet, the mixture was quickly cooled. The precipitate, which was formed by the addition of dilute perchloric acid, was washed with a dilute perchloric acid and then extracted with 150 ml. of an ethanol(75%)-water mixture. The last 120 ml. protion, which was kept separate from the first 30 ml., was cooled after the addition of several drops of perchloric acid. The dark purple crystals which formed were washed with ethanol and ether. Yield, 1.5 g.

Found: Co, 8.22; C, 13.78; H, 2.77; N, 7.94. Calcd. for *trans*-$[Co(CHBr_2CO_2(en))_2]ClO_4$: Co, 8.27; C, 13.49; H, 2.55; N, 7.87%.

## Discussion

**Preparation.** — Linhard and his co-workers[2] studied the $[Co(clac)_2(NH_3)_4]X$ complexes and found that the cis-isomer was obtained when an aqueous solution of $[CoCO_3(NH_3)_4]ClO_4$ and an equivalent amount of a chloroacetic acid was evaporated at a relatively low temperature, whereas the *trans*-isomer was

obtained when a large excess of chloroacetic acid was used and the evaporation occurred at a higher temperature. With dichloroacetato- and trichloroacetato-complexes, however, they could not isolate the trans-isomers.

The same principle was applied in the preparation of all the complexes which were studied in this report, (the preparations of cis-isomers have been reported already);[1] it was observed again that it was easier to isolate cis-isomers than trans-isomers, except for acetato-complexes. It was also noted that the yield of trans-isomers was small, especially for ligands with a high halogen content. Therefore, along with the known procedures, two new techniques were applied whereby the trans-isomer can be separated from a large amount of cis-isomer and/or the yield of trans-isomer can be raised. First, as has been described in the Experimental section and as may be seen in Table II, it was found that trichloroacetic acid selectively precipitated trans-isomers and that, therefore, a small quantity of trans-isomer could be isolated from a mixture containing a large quantity of cis-isomer. This method was applied in the isolation of *trans*-$[Co(CHCl_2CO_2)_2(NH_3)_4]^+$ and *trans*-$[Co(CCl_3CO_2)_2(NH_3)_4]^+$, and in the purification of the others.

Second, after the evaporation of the solution of the starting materials had nearly been completed, the product was boiled for a short time. In the bis(ethylenediamine)- series, the coordination of ethylenediamine is still stable at a high temperature; therefore, boiling the reaction mixture causes a rapid rearrangement of the cis- to the trans-configuration, resulting in a higher yield of the trans-isomer. This technique was used for the preparation of *trans*-$[Co(CCl_3CO_2)_2(en)_2]ClO_4$ and *trans*-$[Co(CHBr_2CO_2)_2(en)_2]ClO_4$. In the tetrammine-series, however, there is a possibility of the decomposition of the complexes themselves.

**Solubilities and Precipitation Reactions.**—Similarly to the case of cis-isomers,[1] it was noted that complexes with a large halogen content are soluble in alcohol or even in an alcohol-ether mixture, especially when they are slightly moist. One should therefore be careful in the washing of the complexes in their preparations.

In addition to the anions listed in Table II, it was observed that 1 N solution of sodium carbonate, sodium nitrite, sodium acetate, potasium chromate, sodium sulfite or sodium oxalate, and a saturated solution of sodium hydrogen phosphate, 6 N sulfuric acid and 2 N ammonium sulfate did not precipitate with any of the complexes. As has been described in the Experimental section, most of the *trans*-isomers form acidic salts with perchloric acid. In the cases of two acetato-complexes, acidic salts are relatively insoluble compared with the neutral salts; therefore, precipitation occurs upon the addition of perchloric acid but not upon that of sodium perchlorate. Similar phenomena take place in *trans*-$[Co(CH_3CO_2)_2(NH_3)_4]^+$ with hydrogen chloride and ammonium chloride.

**Absorption Spectra.**—The visible and ultraviolet absorption spectra of the *trans*-$[Coa_4b_2]$ complexes are of especial interest because of a large splitting which occurs in the first band. All of the present complexes showed the splitting, as can be seen in Figs. 1 and 2, by which the assignment of the geometrical configuration has been made.

Shimura[5] proposed an empirical rule regarding the relative positions between the maxima of cis- and trans-isomers of $Coa_4b_2$:

$$\nu_{cis} - \nu_{trans} \gtrless 0$$

if "a" is to the $\left\{\begin{array}{l}\text{left (I side)}\\ \text{identical}\\ \text{right (CN side)}\end{array}\right\}$ of "b" in

the spectrochemical series; this rule has been supported theoretically.[6] Concerning the present complexes, $NH_3$ or en (a) is to the right of the halogenoacetato ligands (b), and the $\nu_{cis}$'s are larger than the corresponding $\nu_{trans}$'s thereby confirming Shimura's rule.

The order of the ligands in the spectrochemical series has already been determined to be:[1]

$$\mathrm{I} < \cdots < CH_3CO_2 < \left\{\begin{array}{l}CH_2ClCO_2 < CHCl_2CO_2 < CCl_3CO_2\\ CH_2BrCO_2 < CHBr_2CO_2 (< CBr_3CO_2)\end{array}\right\} < \cdots < NH_3 < en < \cdots < CN$$

(increasing ligand field)

and it has been verified that the basicity of the ligands is the main factor in determining the spectral characteristic of each series of halogenoacetato-complexes. Therefore, it may be said that the degree of splitting increases with an increase in the halogen content in the halogenoacetato-ligands, or with a decrease in the basicity of the ligands, as may be seen in Table I and the figures.

Since the spectrochemical series represents the order of the strengths of the ligand fields, the tetragonality (tetragonal deviation from a cubic symmetry) of a $Coa_4b_2$ complex increases with the increase in the distance between "a" and "b" in the series. According to the ligand field theory, the

5) Y. Shimura, This Bulletin, **25**, 49 (1952).
6) L. E. Orgel, *J. Chem. Phys.*, **23**, 1004 (1955).
7) C. J. Ballhausen and C. K. Jörgensen, *Kgl. Danske Videnskab. Selskab. Mat. Fys. Medd.*, **29**, (14) (1955).

magnitude of the band splitting depends on the degree of tetragonality.[7] Therefore, it may be predicted that the splitting in the acetato-complex will be the largest and that in the trichloroacetato-complex the smallest. However, this predicted order seems to be entirely the reverse of the observed order. This reversal is considered to be of interest; further examination of the spectral curves is needed for an interpretation. After an analysis of the curves separating into single bands, a quantitative consideration of the band splitting will be reported.

The authors are grateful for the support provided for this research by the Atomic Energy Commission of U. S. A. under Contract No. AT(30-1)-906.

*Department of Chemistry*
*Kyoto Gakugei University*
*Fushimi-ku, Kyoto(K.K.)*

*Department of Chemistry*
*Fordham University*
*New York 58, N. Y. (P. S. G.)*

# 11-Deoxojervine, A New Alkaloid from *Veratrum* Species[1]

By Tadashi MASAMUNE, Yoichi MORI, Mitsuo TAKASUGI, Akio MURAI
Shigehiro OHUCHI, Norio SATO and Nobukatsu KATSUI

(Received January 9, 1965)

*Veratrum* species have been extensively investigated, and a large number of alkaloids have been isolated.[2] In connection with a study aimed at the synthesis of C-nor-D-homosteroid hormones, we have searched for alkaloids from a kind of *Veratrum* species and have found a new alkaloid to be a principal component. In a preliminary communication,[3] we reported that this alkaloid was 11-deoxojervine; the present paper will describe the details.

Benzene extracts of the alkalized, ground roots of *V. album L. var. glandiflorum Maxima. (V. glandiflorum Loesen. fil.)* which had been collected in May in the Tokachi district, Hokkaido, were subjected to separation according to a modified Jacobs' procedure.[4] The new alkaloid was isolated in a 0.30% yield, along with veratramine, rubijervine and solanidine,[5] from the basic fraction, and β-sitosterol, from the neutral fraction. While Saito and Suginome had obtained jervine,[6] together with veratramine,[7] as a major alkaloid from the plant collected in October at Nopporo, Hokkaido, no jervine was isolated in the present investigation. On the other hand, Takaoka[8] has reported the isolation of a sterol from the same plant; judging from a comparison of their melting points, the sterol seems to be the same compound as that obtained in the present research.

The new alkaloid (I) (m. p. 237—238°C, $[\alpha]_D^{23}$ −44.2°) was analyzed for $C_{27}H_{41}O_2N$; both the infrared and ultraviolet spectra indicated the absence of a carbonyl group and a conjugated diene. The acetylation of I with acetic anhydride and pyridine on a steam bath afforded the *O,N*-diacetyl derivative (Ia), which melted at 163—165°C, resolidified, and again melted at 195—197°C. The infrared spectrum showed no absorption due to a hydroxyl group in the region of 3 μ; therefore, the remaining oxygen must be an ether function. An attempted reduction of I with lithium aluminum hydride or with lithium in liquid ammonia led to a quantitative recovery of the starting material and ruled out the possibility of an epoxide group. Absorptions near 1050 $cm^{-1}$ in the infrared spectra of I and Ia (1062 and 1037 $cm^{-1}$ respectively) suggested[9] the

1) Part IV of "C-Nor-D-homosteroids and Related Alkaloids"; Part III; Ref. 17.

2) For reviews, see; C. R. Narayanan, "Progress in the Chemistry of Organic Natural Products," Vol. XX, Springer-Verlag, Wien (1962), p. 298; K. J. Morgan and J. A. Bartrop, *Quart. Rev.*, **12**, 34 (1958).

3) T. Masamune, Y. Mori, M. Takasugi and A. Murai, *Tetrahedron Letters*, **1964**, 913.

4) W. A. Jacobs and L. C. Craig, *J. Biol. Chem.*, **155**, 565 (1944); ibid., **160**, 555 (1945); A. Stoll, D. Stauffacher and E. Seebeck, *Helv. Chim. Acta*, **38**, 1964 (1955).

5) It appears that no paper has yet been published showing the isolation of solanidine from *Veratrum* species. Cf. H. G. Boit, "Ergebnisse der Alkaloid-Chemie bis 1960," Akademie-Verlag, Berlin (1961), p. 758.

6) K. Saito, H. Suginome and M. Takaoka, This Bulletin, **9**, 15 (1934).

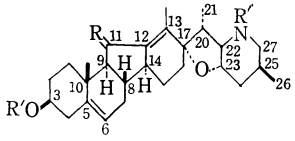
7) K. Saito, ibid., **15**, 22 (1940).

8) M. Takaoka, *J. Chem. Soc. Japan (Nippon Kwagaku Kwaishi)*, **60**, 1090 (1939).

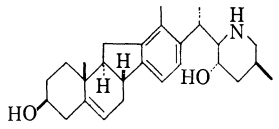
9) A. R. H. Cole, R. N. Jones and K. Dobroner, *J. Am. Chem. Soc.*, **74**, 5571 (1952).

presence of a $\Delta^5$-3$\beta$-hydroxyl group, a probability of which was supported by the NMR spectrum. The NMR spectrum of Ia closely resembled that of diacetyljervine[10] (IIa), but two new sharp peaks appeared at $\tau$ 8.29 and 9.06; these were comparable to the signals due to C-18 methyl ($\tau$ 7.81) and C-19 methyl groups ($\tau$ 8.99) of IIa. Furthermore, the treatment of I with sulfuric acid in the presence of ferric sulfate yielded veratramine (III), although the yield was low. All these results strongly suggested that I was 11-deoxojervine.

The structure was confirmed by the removal of the oxygen on C-11 of jervine (II).

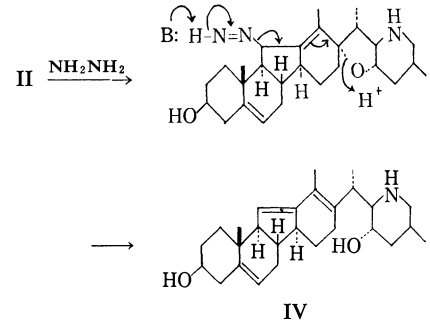


(I) R=H$_2$, R′=H
(Ia) R=H$_2$, R′=Ac
(II) R=O, R′=H
(IIa) R=O, R′=Ac



(III)

The carbonyl group of II is sterically hindered[11] and formed no oxime, even under severe conditions.[12] The Clemmensen reduction of 12, 13-dihydrojervine[13] gave rise to no crystalline substances beside the starting material. However, the Wolff-Kishner reduction of II according to the procedure by Barton[14] resulted in the formation of two crystalline compounds IV, m. p. 211—213°C, and V, m. p. 236—238°C. The former, IV, had a molecular formula of $C_{27}H_{41}O_2N$, and its infrared (1615 cm$^{-1}$) and ultraviolet spectra ($\lambda_{max}$ 245 m$\mu$, $\varepsilon$ 25500) showed that it was a conjugated diene. The diene was converted to the corresponding *O*, *O*, *N*-triacetyl derivative (IVa), m. p. 116—118°C. The NMR spectrum of IVa had a broad peak centered at $\tau$ 4.53 (2H), a broad multiplet which consisted of three peaks centered at $\tau$ 4.93, 5.25 and 5.36 (3H),[15] and a singlet at $\tau$ 8.29, indicating that two olefinic protons were present, that a methyl group was attached to olefinic carbon, and also that the cleavage of the ether linkage of II was taking place. On the basis of these facts, the formula IV seems to be the most favorable structure for the compound with a m. p. of 211°C, as the reaction has been considered to proceed through the following sequence:[16]



IV

This diene was also obtained by the treatment of jervine-11$\beta$-ol with sodium and butanol. On the other hand, the compound V has been shown to be identical with the compound I by a mixed melting point determination and by a comparison of the infrared spectra; thus, the new alkaloid is 11-deoxojervine. While the configuration of the B/C juncture has been established to be *trans* in the previous communication,[17] the direct transformation of the deoxojervine into veratramine also supports the $\alpha$-configuration of the hydrogen on C-9.

## Experimental

The melting points are uncorrected. The optical rotations and the ultraviolet spectra were measured in 95% ethanol and 99% ethanol, and the infrared spectra in Nujol unless otherwise stated. The NMR spectra were taken in deuterochloroform at 60 Mc., using tetramethylsilane as an internal standard.

**The Extraction and Fractionation of the Roots.**[4] —The ground, dried roots of *V. grandiflorum Loesen. fil.* (29 kg.), collected in May at Toyoni, Tokachi, Hokkaido, were moistened with about 1 N aqueous ammonia (16 l.) and extracted with benzene (116 l.) at room temperature for 5 days. During the extraction, the entire mixture was shaken several times a day. The extracts were drained through filter pads and found to amount to 60 l.

The extraction was repeated nine times; each time 40 l. of benzene was added anew, and 45 l. of the extracts were percolated every 4 days. The roots, after extraction with benzene, were finally treated with 95% ethanol (40 l.) for 1 week; the

10) T. Masamune, M. Takasugi, M. Gohda, H. Suzuki, S. Kawahara and T. Irie, *J. Org. Chem.*, **29**, 2282 (1964).
11) L. F. Fieser and M. Fieser, "Steroids," Reinhold Publishing Corporation, New York, N. Y. (1959), p. 871.
12) Cf. N. L. Hosansky and O. Wintersteiner, *J. Am. Chem. Soc.*, **78**, 3126 (1956).
13) Cf. J. Fried and A. Klingsberg, ibid., **75**, 4929 (1953).
14) D. H. R. Barton, D. A. J. Ives and B. Thomas, *J. Chem. Soc.*, **1955**, 2056.
15) Cf. Ref. 10, footnote 33a.
16) Cf. H. H. Szmant and C. M. Harmuth, *J. Am. Chem. Soc.*, **86**, 2909 (1964), and the references cited there.
17) T. Masamune, M. Takasugi and Y. Mori, *Tetrahedron Letters*, **1965**, 489.

alcoholic extracts were designated fraction A.

The benzene extracts were shaken seven times (15 min. each time) with 5% aqueous tartaric acid (500 ml. per 10 l. of the benzene extracts). The tartaric acid solutions were made alkaline to pH 9 with 20% aqueous sodium carbonate below 12°C, and an amorphous mixture of the bases thus separated was collected by filtration. The basic mixtures were then combined and dried, yielding 650 g. The aqueous filtrate was shaken with chloroform (3 l. per 10 l. of the aqueous filtrate), and the chloroform extracts were washed with water, dried, evaporated to dryness and combined (fraction B).

The entire alkaloidal mixture was divided, by treatment with seven portions of 9 l. of benzene, into benzene-soluble and benzene-insoluble fractions. These fractions were worked up as will be described in parts a and b below. During the fractionation of the mixture of alkaloids, the content and homogeneity of each fraction were always checked by paper chromatography.[18]

a) The benzene-soluble fraction (65 l.) was shaken twice with equal volumes of a 0.1 M aqueous citrate buffer solution (pH 6.0). The buffered solutions were extracted with chloroform after having been made alkaline to pH 9 with 20% aqueous sodium carbonate; the chloroform extracts left 155 g. of a tarry material (fraction C) when the solvent was removed.

The benzene solution which was separated from the buffered solutions was washed, dried, and evaporated to dryness. The residue was dissolved in 10% aqueous acetic acid (5 l.) and filtered to remove intractable tarry matters. To the acidic solution was added a saturated aqueous solution of ammonium sulfate (1.1 l.), yielding gelatinous precipitates which were collected by filtration. The aqueous filtrate was made alkaline with ammonia and extracted with chloroform. The chloroform extracts were washed with water, dried over sodium sulfate, and evaporated to dryness, leaving 50 g. of tarry substances (fraction D).

The precipitates of the sulfates were suspended in 10% aqueous sodium hydroxide and then shaken with chloroform (total 4.7 l.) vigorously and repeatedly, until the precipitates disappeared completely. The combined chloroform extracts were washed with water, dried, and evaporated to dryness, leaving 178 g. of an amorphous solid. The solid was dissolved in ethanol (1 l.) and concentrated hydrochloric acid (35 ml.) was added, yielding crystalline hydrochlorides, which were then collected by filtration. The filtrate was designated as fraction E. When the crystalline hydrochlorides were dissolved in boiling 65% aqueous ethanol (350 ml.), made alkaline with concentrated aqueous ammonia and then allowed to stand overnight, crude 11-deoxojervine (m. p. 224—227°C) was regenerated and collected by filtration (yield 15 g.).

b) The benzene-insoluble fraction left after the removal of the benzene-soluble part was fractionated in a way similar to that used for the benzene-soluble part; it was dissolved in 10% aqueous acetic acid (7.5 l.) and treated with a saturated solution of ammonium sulfate (800 ml.) to yield 225 g. of the precipitates of sulfates, which were then filtered. Regeneration from the filtrate with concentrated aqueous ammonia and extraction with chloroform gave 33 g. of a crystalline solid (fraction F).

The precipitates of sulfates suspended in 10% aqueous sodium hydroxide were repeatedly shaken with chloroform (total 6.9 l.); the chloroform extracts gave an amorphous solid after the solvent had been removed. The amorphous solid was dissolved in ethanol (700 ml.) and afforded, on the addition of cocentrated hydrochloric acid (40 ml.), crystalline hydrochlorides; these were then collected by filtration and found to amount to 103 g. The filtrate gave, when made alkaline with concentrated aqueous ammonia (200 ml.), 59 g. of an amorphous solid (fraction G). The regeneration of the free base from the crystalline hydrochlorides dissolved in boiling 65% aqueous ethanol (3.6 l.) with concentrated ammonia (190 ml.), cooling and filtration, afforded 80 g. of crude deoxojervine, m. p. 225—227°C.

**The Isolation of Veratramine from Fraction G.**—Fraction G consisted mainly of veratramine (III) and 11-deoxojervine (I); it was fractionated on the basis of the following facts; (1) the hydrochloride of I was less soluble in ethanol than that of III, and (2) I decomposed readily upon treatment with sulfuric acid in refluxing ethanol, whereas III was stable under those conditions. A part (50 g.) of fraction G was dissolved in boiling ethanol (130 ml.), cooled, and filtered. The crystalline precipitates (10.6 g.) were converted into the hydrochlorides and recrystallized three times. Each of the filtrates left after recrystallization was made alkaline to yield a mixture of bases; this mixture was collected by filtration and combined. The combined mixtures contained more III than I; they amounted to 5.8 g. after having been dried. On the other hand, water (100 ml.) was added to the filtrate after the removal of the first crystalline precipitates, separating 26.6 g. of an amorphous solid which contained more III than I. These veratramine-rich fractions (total 32.4 g.) were combined and worked up in a way similar to that mentioned above, yielding 20.2 g. of crude veratramine. To the crude veratramine dissolved in ethanol (500 ml.), concentrated sulfuric acid (20 ml.) was added under cooling; the mixture was then refluxed for 1 hr. The alkalification of the solution with ammonia (60 ml. of concentrated ammonia and 1 l. of water), followed by cooling and filtration, afforded veratramine, which was recrystallized from aqueous ethanol (200 ml. of ethanol and 140 ml. of water) and found to have a m. p. of 204—205°C. The yield was 14.3 g. Identification was made by a mixed melting point determination with an authentic sample and by a comparison of the infrared spectra and of the paper chromatograms.

**The Isolation of Rubijervine from Fraction F.**—Fraction F was dissolved in acetone; the concentration of the solution led to the separation of

18) The following three systems were used for paper chromatography; A) *n*-butyl acetate - *n*-butanol - formic acid - water (10 : 25 : 10 v. v.); B) ethylene chloride - Cellosolve acetate - pyridine (15 : 10 : 1), and c) *n*-butyl acetate - *n*-butanol - formic acid - water (100 : 1 : 1.5 : 0.5).

crude rubijervine (11.9 g.), m. p. 241—243°C. Recrystallization from acetone gave pure rubijervine, m. p. 246—246.5°C, which was identified by a mixed melting point determination with an authentic sample and by a comparison of the infrared spectra and of the paper chromatograms.

**The Isolation of Solanidine and Veratramine from Fraction E.**—One-third (350 ml.) of fraction E was evaporated in vacuo, and the residue was dissolved in water (240 ml.), made alkaline with 2 N aqueous ammonia, and extracted with chloroform (230 ml.). The chloroform solution was washed with water (300 ml.), dried over sodium sulfate, and then evaporated to dryness, leaving 45 g. of a tarry material. This was refluxed in 1 N methanolic sulfuric acid (300 ml.) for 2 hr. to remove 11-deoxojervine and cooled, and then water (400 ml.) was added. The whole mixture was made alkaline with 10% aqueous sodium carbonate and extracted with chlorom (200 ml.). The chloroform solution gave, on the removal of the solvent, 36.4 g. of a tarry material, which was then dissolved in benzene (200 ml.) and chromatographed on alumina (Merck neutral, 900 g.) in a column (diameter 50 mm.). All those fractions eluted with mixtures of benzene and ether, and all those eluted with mixtures of ether and chloroform (20 : 1 and 17 : 1) were crystallized, on the removal of the solvent and trituration with acetone, and were combined; they amounted to 350 mg. On recrystallization from acetone, pure solanidine (100 mg.), m. p. 217—219°C, was obtained.

Found: C, 81.70; H, 11.18; N, 3.70. Calcd. for $C_{27}H_{43}ON$: C, 81.55; H, 10.90; N, 3.52%.

On treatment with acetic anhydride and pyridine at room temperature overnight, this was converted to the acetate, m. p. 205—206°C.

Found: C, 79.00; H, 10.51; mol. wt. 439 by the mass spectrum. Calcd. for $C_{29}H_{45}O_2N$: C 79.22; H, 10.32%; mol. wt. 439.66.

Identification was made by means of a comparison of the infrared spectrum with that described in Ref. 19 and by an analysis of the NMR spectra.

Fractions eluted with mixtures of ether and chloroform (4 : 1 to 1 : 8) crystallized on the removal of the solvents, which contained veratramine as a major component. Recrystallizations from acetone afforded 4.0 g. of veratramine, m. p. 202—204°C.

**The Isolation of β-Sitosterol from Fraction A.**—Fraction A was concentrated to 2 l., and a part (500 ml.) of the concentrate thus obtained was shaken with three poritions of 500 ml. of petroleum ether (b. p. 30—60°C) to remove any resinous substances. The concentrate separated from the petroleum ether solution was shaken with 1 N aqueous acetic acid (1 l.), centrifuged, and divided into fractions soluble and insoluble in the acidic solution. The insoluble material (35 g.) was continuously treated with ether in a Soxhlet extractor for 6 hr. The resulting ether-insoluble solid (29 g.) was further refluxed with 2 N hydrochloric acid in 95% ethanol on a water bath for 2 hr., and then cooled. After the removal of the ethanol in vacuo, the residue was extracted with ether to yield a brown oil, which was then chromatographed on alumina (Merck neutral, 30 g.). Fractions eluted with mixtures of petroleum ether and benzene (5 : 5 to 3 : 8) and those eluted with benzene crystallized on the removal of the solvent and were combined; yield 200 mg. On recrystallization from ethanol, 60 mg. of β-sitosterol, m. p. 134—136°C and $[\alpha]_D^{23}$ −32°, was obtained. The alcohol gave, when treated with acetic anhydride and pyridine at room temperature overnight, the corresponding acetate, which had a m. p. of 118—119°C and $[\alpha]_D^{23}$ −33° on recrystallization from ethanol. Identification was made by a mixed melting determination with an authentic sample and by a comparison of the infrared spectra and the NMR spectra.[20] The sterol isolated by Takaoka[8] had a m. p. of 135—136°C.

**11-Deoxojervine and 3-*N*-Diacetyl-11-deoxojervine.**—The recrystallization of crude deoxojervine from methanol gave a pure sample, m. p. 236—238°C, which contained the solvent and which showed an infrared spectrum different from that of the sample after drying. For analysis, this was recrystallized from methanol and dried at the temperature of boiling xylene; it thus had a m. p. of 237—238°C and $[\alpha]_D^{23}$ −44.2°; UV only end absorption; IR $\nu_{max}$ 3270, 1067, 1060 and 809 $cm^{-1}$.

Found: C, 78.78, 78.87; H, 10.12, 9.91; N, 3.59, 3.53. Calcd. for $C_{27}H_{41}O_2N$: C, 78.78; H, 10.04; N, 3.40%.

11-Deoxojervine (101 mg.) was treated with acetic anhydride (1 ml.) and pyridine (1 ml.) on a water bath for 2 hr., and then worked up as usual to yield the crude diacetyl derivative. On recrystallization from aqueous ethanol, 84 mg. of diacetyl-11-deoxojervine was obtained; this contained the solvent and melted at 163—164°C, resolidified, and then melted again at 195—197°C; IR: $\nu_{max}$ 3550, (solvent), 3460 (solvent), 1722, 1655 (shoulder), 1640, 1254 and 817 $cm^{-1}$.

Found: C, 72.97; H, 8.93; N, 2.90. Calcd. for $C_{31}H_{45}O_4N \cdot H_2O$: C, 72.48; H, 9.22; N, 2.73%.

On being dried at the temperature of boiling xylene, this had a m. p. of 195—197°C and $[\alpha]_D^{23}$ +1.1°; IR: $\nu_{max}$ 1733, 1640, 1231 and 812 $cm^{-1}$; NMR: a broad peak centered at $\tau$ 4.56 (1H, olefinic proton on C-6), a broad multiplet centered at $\tau$ 5.40 (1H, proton on C-3), two singlets at $\tau$ 7.90 and 7.97 (each 3H, *N*- and *O*-acetyl groups), a singlet at $\tau$ 8.29 (3H, 18-methyl group), two doublets ($J$=7 and 6 c. p. s.) centered at $\tau$ 8.99 and 9.06 (each 3H, two secondary methyl groups), and a singlet at $\tau$ 9.06 (3H, 19-methyl group).

Found: C, 75.26; H, 8.93; N, 2.89. Calcd. for $C_{31}H_{45}O_4N$: C, 75.11; H, 9.15; N, 2.83%.

**The Treatment of 11-Deoxojervine with Sulfuric Acid.**—To a solution of 11-deoxojervine (220 mg.) in methanol (50 ml.) concentrated sulfuric acid (3.1 ml.) and ferric sulfate (55 mg.) were added under cooling. The solution was then stirred for 5 hr. at room temperature. After the addition of water (100 ml.), the solution was made alkaline with 2 N aqueous ammonia and extracted with three portions of 30 ml. of chloroform. The chloroform extracts were then washed with water, dried over sodium sulfate, and evaporated to dryness,

19) S. W. Pelletier and W. A. Jacobs, *J. Am. Chem. Soc.*, **75**, 4444 (1953).

20) G. Slomp and F. A. MacKellar, ibid., **84**, 204 (1962).

leaving 205 mg. of an amorphous solid which showed 5 spots on the paper chromatogram. The residue was dissolved in 5% aqueous acetic acid (10 ml.) and filtered. The addition of a saturated solution of ammonium sulfate yielded resinous precipitates, which were collected by decantation and then washed with water. A suspension of the precipitates in aqueous ammonia was shaken with three portions of 10 ml. of chloroform. The chloroform extract gave, after drying and the removal of the solvent, 53 mg. of an amorphous solid, which crystallized on trituration with acetone. Recrystallization from acetone afforded veratramine (10 mg.), m. p. 201—203°C.

**The Wolff-Kishner Reduction of Jervine.**[14]—To freshly-distilled diethylene glycol (325 ml.) sodium (7.5 g.) was added; the mixture was then heated to 180°C and cooled. To this solution anhydrous hydrazine (45 ml.)[21] was added, and the mixture was refluxed for a while and then cooled. After the addition of jervine (5.0 g.), the entire mixture was heated at 180±5°C for 60 hr., further heated to 210°C to remove the excess hydrazine, and again refluxed for another 24 hr. To the cooled solution water (250 ml.) was added, and the whole mixture was extracted with three 250 ml. portions of chloroform. The chloroform extracts were washed with water, dried over sodium sulfate, and evaporated to dryness, yielding 5.0 g. of an amorphous solid, which was then crystallized on trituration with acetone. Fractional recrystallizations from acetone, purity of each fraction being checked by paper chromatography, led to the successful separation of two crystalline compounds. One (1.1 g.) had a m. p. of 236—238°C on recrystallization from a mixture of methanol and acetone; it was identical with 11-deoxojervine in all respects.

Another compound, conjugated diene (IV), had a m. p. of 211—213°C and $[\alpha]_D^{23}$ +3.5° when recrystallaized from acetone or methanol, and it amounted to 0.45 g.; UV: $\lambda_{max}$ 245 mμ (ε 25500); IR: $\nu_{max}$ 3420, 1615, 1058, 878 and 815 $cm^{-1}$.

Found: C, 78.74; H, 10.24; N, 3.78. Calcd. for $C_{27}H_{41}O_2N$: C, 78.78; H, 10.04; N, 3.40%.

The acetylation of the conjugated diene (77 mg.) with acetic anhydride (1 ml.) and pyridine (1 ml.) on a water bath for 3 hr. afforded 48 mg. of the triacetyl derivative with a m. p. of 116—118°C and $[\alpha]_D^{23}$ +46° after recrystallization from a mixture of methanol and ethanol; UV: $\lambda_{max}$ 243 mμ (ε 23800); IR: $\nu_{max}$ 1733, 1637, 1615, 1242, 1022 and 811 $cm^{-1}$; NMR: a broad peak centered at τ 4.53 (2H, protons on C-6 and C-11), a broad multiplet which consisted of three peaks centered at τ 4.93, 5.25 and 5.36 (3H, protons on C-3, C-22 and C-23),[15] a singlet at τ 7.98 (9H, *N*- and two *O*-acetyl groups), a singlet at τ 8.29 (3H, 18-methyl group), a doublet ($J$=6 c. p. s.) centered at τ 8.86 (6H, two secondary methyl groups), and a singlet at τ 8.99 (3H, 19-methyl group).

Found: C, 71.27; H, 8.58; N, 2.59. Calcd. for $C_{33}H_{47}O_5N \cdot H_2O$: C, 71.32; H, 8.89; N, 2.52%.

**The Treatment of Jervine-11β-ol with Sodium and Butanol.** — To a solution of jervine-11β-ol (507 mg.)[22] in boiling *n*-butanol (500 ml.), 36 g. of sodium was added over a period of 5 hr.; the mixture was then refluxed for another 1.5 hr. while being stirred and cooled. After the removal of the butanol by steam distillation, the residue was extracted with three portions of 70 ml. of chloroform, and the chloroform extracts were dried over sodium sulfate and evaporated to dryness, leaving 501 mg. of an amorphous solid. The solid was dissolved in *n*-butanol (350 ml.) and treated with sodium (29 g.) for 6.5 hr. When the reaction mixture was worked up in a way similar to that mentioned above, it left 478 mg. of the residue. Crystallization and recrystallization from a mixture of acetone and ether afforded 83 mg. of the conjugated diene (IV), m. p. 213—214°C. The paper chromatogram of the filtrate showed that it consisted of IV and the starting material, which prevented IV from further isolation because of its lower solubility in the solvent.

Found: C, 78.36; H, 10.24; N, 3.78. Calcd. for $C_{27}H_{41}O_2N$: C, 78.78; H, 10.04; N, 3.40%.

The acetylation of the diene obtained above gave the corresponding triacetyl derivative, m. p. 120—121°C. For analysis it was dried at the temperature of boiling methanol for a long time.

Found: C, 73.86, 73.56; H, 9.02, 9.08; N, 2.88, 3.06. Calcd. for $C_{33}H_{47}O_5N$: C, 73.71; H, 8.81; N, 2.61%.

The conjugated diene and the acetyl derivative were identical with the corresponding compounds obtained by the Wolff-Kishner reduction of jervine.

The authors wish to express their thanks to Professor Toshi Irie for his encouragement and also to Mr. Shigezo Shimokawa and Mr. Seiichiro Ohnishi, the Toyo Rayon Company, Ltd., for their measurement of the NMR spectra. They are also indebted to Mr. Naoyuki Sakamoto and Mr. Shoji Ueno for collecting the plants.

*Department of Chemistry*
*Faculty of Science*
*Hokkaido University*
*Sapporo*

21) L. I. Smith and K. L. Howard, *Org. Synth.*, **24**, 53 (1944).

22) B. M. Iselin, M. Moore and O. Wintersteiner, *J. Am. Chem. Soc.*, **78**, 403 (1956).

# The Reaction of Dimethyltin Dichloride with Carboxylic Acids and Phenols in an Aqueous Solution

By Mitsuaki O'HARA, Rokuro OKAWARA and Yoshiaki NAKAMURA

(Received Junuary 12, 1965)

The reaction of dimethyltin dichloride in an aqueous solution with various inorganic and organic compounds has previously been reported by Rochow, Seyferth and Smith,[1] and the reaction with acetic acid anhydride or glacial acetic acid has also been studied by Okawara and Rochow.[1,2]

In this paper the reaction of dimethyltin dichloride with carboxylic acids and phenols in an aqueous solution will be described. In reactions with the acids and phenols shown in Table I, precipitation occurs only when deprotonating reagents such as concentrated aqueous ammonia are added. The precipitates are recrystallized from methanol containing a small amount of the corresponding acid or phenol in order to prevent decomposition, thus yielding tetramethyl-1, 3-di(substituted)-distannoxanes. These products all have a strong, and characteristic absorption near 600 $cm^{-1}$, as is shown in Table I, an absorption which has previously been assigned to the Sn-O-Sn stretching vibration in polymeric[4] or dimeric[3,5] compounds.

In the reaction with benzoic acid, the initial precipitate seems to be tetramethyl-1, 3-dibenzoyloxydistannoxane. However, recrystallization from methanol containing a small amount of benzoic acid gives large colorless crystals of $(CH_3)_2Sn(C_6H_5CO_2)_2$, which melts at 162—164°C. Reaction with catechol, mercaptoacetic acid or oxalic acid gives a precipitate without deprotonating reagents. The products are $(CH_3)_2Sn(C_6H_4O_2)$, $(CH_3)_2Sn(SCH_2CO_2)$ and $(CH_3)_2Sn(C_2O_4)\cdot H_2O$ respectively. Because of their poor solubility in non-polar solvents, the molecular weight of these three compounds, as well as those of the other distannoxanes shown in Table I, were not determined.

In the case of resorcinol, hydroquinone or malonic acid, precipitation does not occur by mixing in an aqueous solution of the reagents, but a precipitate can be obtained by adding concentrated aqueous ammonia. However, the products are not simple and, therefore, can not be characterized.

## Experimental

**Starting Materials.** — Crude dimethyltin dichloride was purified by recrystallization from benzene[1] or by sublimation.[2] Carboxylic acids and phenols commercially obtained were used without further treatment.

**Infrared Spectra*.**—The infrared spectra in the 5000—400 $cm^{-1}$ region were recorded in Nujol mull using a Hitachi-EPI-2G spectrophotometer with gratings. The positions of the bands associated with the Sn-O-Sn stretching vibration are listed in Table I.

**Tetramethyl-1, 3-diformoxy-distannoxane.**—To a solution of dimethyltin dichloride (5 g. 0.023 mol.) and formic acid (4 g. 0.087 mol.) in 100 ml. of water, concentrated aqueous ammonia was stirred in drop by drop until no additional precipitate was formed. The precipitate was then washed with dilute aqueous formic acid, and then by a small amount of methanol, and dried in vacuo. Recrystallization from methanol containing a small amount of formic acid gave large colorless crystals which melted at 185°C, as is shown in Table I. The analysis for tin content was carried out in a manner already described elsewhere.[2]

The other compounds shown in Table I were prepared by a similar procedure in a good yield (70—80%). However, the *o*-methoxyphenoxy compound could be recrystallized from methanol or benzene without adding guaiacol.

**Dimethyltin Dibenzoate.**—To a 500 ml. of a hot aqueous solution containing 4 g. (0.018 mol.) of dimethyltin dichloride and 6 g. (0.049 mol.) of benzoic acid, concentrated aqueous ammonia was added carefully until no additional precipitate formed. The white precipitate, which was washed with hot water and methanol and dried in vacuo, seemed to be a distannoxane derivative.[1]

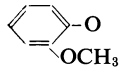
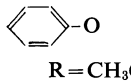
Found: Sn, 42.25. Calcd. for $C_{18}H_{22}O_5Sn_2$: Sn, 42.71%.

Recrystallization from methanol containing a small amount of benzoic acid gave large colorless crystals of dimethyltin dibenzoate. M. p. 162—164°C. (Reported[7]: m. p. 160—162°C). Yield:

1) E. G. Rochow, D. Seyferth and A. C. Smith, Jr., *J. Am. Chem. Soc.*, **75**, 3099 (1953).
2) R. Okawara and E. G. Rochow, ibid., **82**, 3285 (1960).
3) R. Okawara and M. Wada, *J. Organometal. Chem.*, **1**, 81 (1963).
4) M. P. Brown, R. Okawara and E. G. Rochow, *Spectrochim. Acta*, **16**, 595 (1960).
5) M. Wada and R. Okawara, to be published in *J. Organometal. Chem.*

* A discussion of the infrared spectra of these compounds will be published later.
6) W. J. Considine, J. J. Ventura, A. J. Gibbons, Jr., and A. Ross, *Can. J. Chem.*, **41**, 1239 (1963).
7) G. A. Razuvaev, O. A. Schepetkova and N. S. Vyazankin, *Zhur. Obs. Khim.*, **32**, 2152 (1962).

TABLE I. TETRAMETHYL-1,3-DI(SUBSTITUTED)DISTANNOXANES: $R(CH_3)_2SnOSn(CH_3)_2R$

| R | M. p. °C | % Sn Found (Calcd.) | % C Found (Calcd.) | % H Found (Calcd.) | Sn-O-Sn Str. Vib. ($cm^{-1}$) |
|---|---|---|---|---|---|
| HCOO | 185 (decomp.) | 58.79 (58.82) | 17.76 (17.86) | 3.60 (3.50) | 612 |
| $C_2H_5COO$ | 185 | 51.77 (51.64) | 26.23 (26.13) | 4.82 (4.82) | 639 |
| *n*-$C_3H_7COO$ | 161—162 | 48.77 (48.67) | 29.29 (29.55) | 5.22 (5.37) | 639 |
| $CH_2ClCOO$ | 226—227 | 47.64 (47.43) | 19.42 (19.20) | 3.25 (3.22) | 636 |
| $CHCl_2COO$ | 232—233 | 41.81 (41.69) | 16.72 (16.87) | 2.81 (2.48) | 625 |
| $CCl_3COO$ | 221—222 | 37.11 (37.19) | 14.52 (15.05) | 2.10 (1.90) | 631 |
| $CH_2(CN)COO$ | 300 | 49.37 (49.29) | 24.86 (24.94) | 3.44 (3.35) | 637 |
| $CH_2BrCOO$ | 172—174 | 40.32 (40.27) | 16.29 (16.30) | 2.92 (2.74) | 636 |
|  | 235—236 | 42.00 (42.41) | 38.64 (38.62) | 4.67 (4.68) | 639 |
|  | 202* | 47.42 (47.50) | 38.40 (38.45) | 4.35 (4.44) | 625 |

R=$CH_3COO$; m. p. 237°C (Reported[2] m. p. 240°C)
* Reported[6] m. p. 190—197°C with a crude product.

40—50%.

Found: C, 48.99; H, 3.90; Sn, 30.33. Calcd. $C_{16}H_{16}O_4Sn$: C, 49.15; H, 4.13; Sn, 30.36%.

**(*o*-Phenylenedioxy)dimethyltin.** — A white precipitate was obtained immediately by stirring in, drop by drop, 35 ml. of 10% aqueous catechol to a solution of 1.4 g. (0.0064 mol.) of dimethyltin dichloride in 50 ml. of water. After the reaction mixture had been digested on a water bath for several hours, the precipitate was filtered, repeatedly washed with hot water until the filtrate was free from chlorine, and dried at 120°C. Yield: 60%. It was purified by sublimation at 260—220°C in vacuo as has been reported.[8] The results of the analysis and of the infrared spectra in the 5000—400 $cm^{-1}$ region of the precipitate and the sublimate were quite identical. Neither compound showed any infrared absorption bands due to O-H stretching vibrations.

Found: C, 37.42; H, 3.92; Sn, 46.20. Calcd. for $C_8H_{10}O_2Sn$: C, 37.41; H, 3.92; Sn, 46.21%.

In the methanol solution, dimethyltin dichloride and catechol produced no precipitate in spite of the insolubility of $(C_6H_4O_2)Sn(CH_3)_2$ in methanol. On the other hand, dimethyltin dichlororide produced no precipitate with resorcinol or hydroquinone in an aqueous solution.

**The Reaction of Dimethyltin Dichloride with Marcaptoacetic Acid.**—To a solution of dimethyltin dichloride (5.5 g. 0.025 mol.) in 50 ml. of water, 50 ml. of 15% aqueous mercaptoacetic acid was added slowly. The filtrate was then washed thoroughly with water and then by a small amount of methanol, and dried in vacuo. Yield: 75—80%. This compound could be recrystallized from a large amount of boiling water without decomposition. The infrared spectra of the precipitate and the recrystallized product could be superimposed in the 5000—400 $cm^{-1}$ region and showed no absorption band due to the S-H or the O-H stretching vibration. The recrystalized product gradually became brown near 200°C and melted at 257—259°C.

Found: C, 20.03; H, 3.62; Sn, 49.80. Calcd. for $C_4H_8O_2SnS$: C, 20.11; H, 3.38; Sn, 49.69%.

**Dimethyltin Oxalate Monohydrate.**[1]—To 100 ml. of a 4% hot aqueous solution of dimethyltin dichloride, 100 ml. of 3% hot aqueous oxalic acid was added. The white precipitate thus obtained was digested on a steam bath for several hours, filtered, washed with hot water, and dried at 120°C. It could be recrystallized from a large amount of boiling water, but complete dehydration could not be accomplished without decomposition.

Found: C, 18.67; H, 3.12. Calcd. for $C_4H_8O_5Sn$: C, 18.85; H, 3.16%.

On the other hand, dimethyltin dichloride produced no precipitate with malonic acid in an aqueous solution.

## Summary

The reactions of dimethyltin dichloride with carboxylic acids and phenols in aqueous solution have been described, and ten new compounds reported. In many cases tetramethyl-1,3-di(substituted)distannoxanes are formed in good yields by adding such deprotonating reagents as concentrated aqueous ammonia. In other cases, simple dimethyltin derivatives can be obtained without deprotonating reagents.

*Department of Applied Chemistry*
*Osaka University*
*Miyakojima-ku, Osaka*

8) H. J. Emeleus and J. J. Zuckerman, *J. Organometal. Chem.*, 1, 328 (1964).

# The Nucleophilic Replacement of the Phenolic Hydroxy Group by the Mercapto Group in Acidic Media*

By Shigeru OAE and Reiko KIRITANI

(Received January 18, 1965)

During our study of the acid-catalyzed hydrolysis of phenyl benzenesulfonate with concentrated hydrochloric acid in $^{18}O$-enriched water, we have found that the phenol recovered is always incorporated with an excess of $^{18}O$ when the hydrolysis is carried out at 180°C in a sealed tube, and also that the amount of $^{18}O$ incorporation increases as the heating prolonged.[1] Even in the case of *p*-nitrophenyl benzenesulfonate, it has been shown that the *p*-nitrophenol recovered is incorporated with an excess of $^{18}O$ only at the phenolic oxygen.[2]

We have suggested that, in a strong acidic medium, phenol readily accepts a proton at either the ortho- or para-position, thus forming a quasi-stable incipient carbonium ion intermediate in which the original hydroxyl function acquires more of a carbonyl character and, hence, facilitates the oxygen exchange with $^{18}O$-enriched water.[1,3]

Meanwhile, it has been known that carbonyl group of either ketone or aldehyde undergoes a very facile oxygen isotopic exchange in both acidic and alkaline aqueous media.[4] Therefore, it is not very surprising that a phenolic hydroxy group undergoes a nucleophilic replacement with $^{18}O$-enriched water, when the phenolic hydroxy group acquires a rather carbonyl character. In fact, β-naphthol, which is known to have some carbonyl character, has been known to react with nucleophilic reagents, such as sulfurous acid[5] and thioglycolic acid,[6] to replace the phenolic hydroxyl group and form β-naphthyl sulfonic acid and thioglycolic acid respectively.

If the oxygen isotopic exchange of the phenolic hydroxy group in acidic media takes place by means of the nucleophilic attack of the water molecule, phenols in general would react better with other nucleophiles, such as alcohols and mercaptans, under the same conditions as those in which the oxygen exchange takes place. Indeed, we have isolated the corresponding ethers or sulfides by adding alcohols or mercaptans to the reaction mixture of phenol with hydrochloric acid and heating the mixtures at 180°C for a few days in a sealed tube.

The present work was designed to investigate in detail the nature of the reaction by which sulfides are formed from mercaptans and phenols in the presence of a strong acid.

## Results and Discussion

We have proposed that the acid-catalyzed oxygen exchange reaction of phenol above 180°C in a sealed tube proceeds through the "quasi-stable quinoid intermediate"[1] with a proton attached to either the ortho- or para-position, and that the quinoid intermediate, which has a substantially long life, is attacked by water molecule on the quasi-carbonyl carbon in the succeeding step, thus causing the remarkable oxygen isotopic exchange. The essential feature of this mechanism is identical to that of any of the known nucleophilic replacements involving a carbonyl carbon. Therefore, one would expect that other nucleophiles would also undergo similar nucleophilic replacements.

Our first choice of nucleophilic reagents were mercaptans, since the thiol group has been known to be strong nucleophiles and quite stable in strong acidic media. Accordingly, under the conditions in which the oxygen isotopic exchange takes place, thiol may be expected to replace the phenolic hydroxy group. The results of rough kinetic experiments of the phenolic oxygen exchange carried out in strong acidic media enriched with $^{18}O$-water are shown in Table I.

Phenol was then heated in sealed tubes at 180°C and 110°C with various mercaptans for a long time in the presence of hydrochloric acid. Indeed, when heated at 180°C for some hours, at which the oxygen exchange occurs, and the mercaptans, i.e., *n*-butylmercaptan,

* Reactions of Phenols and Phenolic Esters. VI., previous papers, D. R. Christman and S. Oae, *Chem. & Ind.*, 1959, 1251 and Refs. 1, 2 and 3.

1) S. Oae, T. Fukumoto and R. Kiritani, This Bulletin, **36**, 346 (1963).

2) S. Oae and R. Kiritani, ibid., **38**, 765 (1965).

3) S. Oae and R. Kiritani, ibid., **37**, 770 (1964).

4) a) M. Cohn and H. C. Urey, *J. Am. Chem. Soc.*, **60**, 679 (1938); b) J. N. E. Day, *Science Progress*, **34**, 47 (1939).

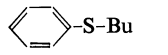
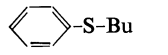
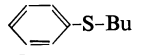
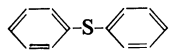
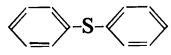
5) See Bucherer Reaction in "Organic Reaction," Vol. I, John Wiley & Sons, New York (1942), p. 105.

6) F. M. Furman, J. H. Thelin, D. W. Hein and W. B. Hardy, *J. Am. Chem. Soc.*, **82**, 1450 (1960).

TABLE I. OXYGEN EXCHANGE REACTION OF PHENOL IN 10 N HYDROCHLORIC ACID

| Reaction condition | | $^{18}O$ Atom. % of | | Exchange |
|---|---|---|---|---|
| Time, hr. | Temp., °C | aq. HCl soln. | Product | % |
| 5 | 180 in a sealed tube | 0.8 | 0.37 | 28.3 |
| 12 | 180 in a sealed tube | 0.77 | 0.55 | 61.4 |
| 24 | 180 in a sealed tube | 0.77 | 0.73 | 93.0 |
| 24 | 110 in a sealed tube | 0.77 | 0.21 | 0 |
| 6 | Reflux | 0.77 | 0.20 | 0 |

TABLE II. THE REACTION OF PHENOL WITH MERCAPTAN

| Reactant | Reaction condition | | | Product | |
|---|---|---|---|---|---|
| Mercaptan | Mole ratio* | Time, hr. | Temp., °C | Sulfide | Yield, % |
| *n*-Butylmercaptan | a | 48 | 180 |  | 31 |
| | b | 48 | 180 |  | 22.0 |
| | b | 24 | 180 |  | Trace |
| | a | 48 | 110 | None | None |
| | a | 48 | Reflux | None | None |
| Benzylmercaptan | a | 48 | 180 |  | 43.4 |
| Thiophenol | a | 72 | 180 |  | 26.7 |
| | a | 119 | 180 |  | 32.2 |

* Mole ratio; phenol: mercaptan, a; 1:5, b; 1:1.

benzylmercaptan and thiophenol, were all found to react with phenol and to give the corresponding sulfides; on the other hand, no reaction took place under milder conditions, such as heating at 110°C, at which no oxygen exchange occurs. The phenyl sulfides obtained are shown in Table II, together with the yields.

When the three marcaptans were allowed to react with phenol at 180°C, the corresponding sulfides were obtained in considerable yields. The yields of sulfides increased with prolonged heating. It appears that the ease of sulfide formation is also related to the nucleophilicity of the mercaptan used. The *n*-butyl phenyl sulfide was identified by comparing it with an authentic sample, while the other sulfides were identified on the basis of their elemental analyses and their infrared spectra. The reaction appears to involve the attack of the thiol group on the 1-carbon of phenol, which is presumably protonated at either the ortho- or the para-position. This is analogous to the mechanism suggested for the acid-catalyzed phenolic oxygen exchange reaction involving nucleophilic substitution at the C-1 position, as is shown in Fig. 1.

Meanwhile, one may postulate another alternative pathway, i.e., one that involves the nucleophilic addition of the thiol group at one of the ortho-positions or at the para-position

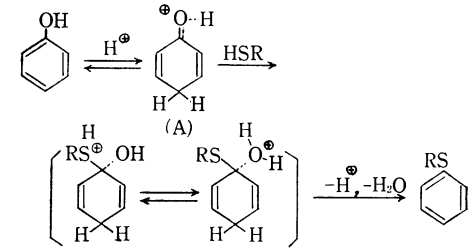


Fig. 1.

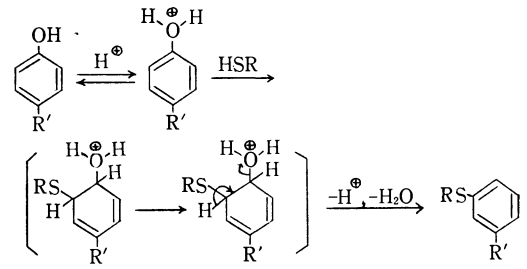


Fig. 2.

of phenol, followed by the elimination of water, as is shown below (in Fig. 2).

Recently Mc. Arnett and Wu,[7] in their study of the p$K_a$'s of the oxonium ions of phenol

7) E. Mc. Arnett and C. Y. Wu, *J. Am. Chem. Soc.*, **82**, 5660 (1960).

Table III. Oxygen exchange reaction of cresols

| Compound | Reaction time hr. | $^{18}O$ Atom. % of aq. HCl soln. | $^{18}O$ Atom. % of Product | Exchange % |
|---|---|---|---|---|
| *o*-Cresol | 24 | 0.77 | 0.37 | 31.6 |
| *m*-Cresol | 24 | 0.77 | 0.45 | 43.9 |
| *p*-Cresol | 24 | 0.77 | 0.45 | 43.9 |

and various phenyl ethers under normal conditions, have suggested that the primary site of protonation in the phenolic compound is the oxygen. If this is the case, even at a higher temperature, the oxonium group would induce the nucleophilic attack at either the ortho- or para-position, as in the case of the Bamberger reaction.[8] In this case, one would expect to get a rearranged product. This mechanism was, however, contradicted by the reaction with *p*-substituted phenol. Namely, when *p*-cresol was allowed to react with *n*-butyl mercaptan in the presence of hydrochloric acid at 180°C for 48 hr. in a sealed tube, *p*-tolyl *n*-butyl sulfide was obtained in a 14% yield, while no *m*-tolyl *n*-butyl sulfide was obtained, as Table IV shows. The identification was made by comparing the infrared absorption spectrum with that of an authentic sample of *p*-tolyl *n*-butyl sulfide.

In separate experiments, *o*-, *m*- and *p*-cresols were subjected to the oxygen exchange reaction at 180°C in the same acidic medium, they were found to exchange their respective phenolic oxygen with $^{18}O$ of the medium, as is shown in Table III.

Here, one finds that the same amount of $^{18}O$ exchange occurred in both *m*- and *p*-cresols, whereas the amount of $^{18}O$ exchange of *o*-isomer was a little less, probably due to a small steric hindrance by the *o*-methyl group. These results, together with the formation of the sulfide, strongly suggest that the reaction involves the nucleophilic attack at the phenolic carbon rather than at the ortho-position of phenol.

Another possible path would be the aromatic $S_N2$-type reaction involving the nucleophilic replacement of the hydroxy group by thiol, as is shown in Fig. 3.

In this case, when the bond-forming is the controlling stage, electron-withdrawing substituents will enhance the reactivity, whereas if the reaction is controlled by the bond-fission stage, electron-releasing substituents will accelerate the reaction. However, in both oxygen exchange reaction and sulfide formation, the substitution of any group at the ring carbon usually retards the reactions. Furthermore, one would anticipate that the reaction would

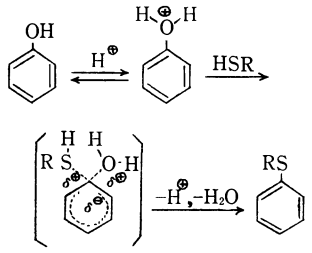



Fig. 3.

be more facile with a better leaving group, such as benzenesulfonate, instead of the hydroxy group. However, neither phenyl benzenesulfonate nor *p*-nitrophenyl benzenesulfonate undergoes any facile hydrolyses, nor do their hydrolyses proceed via Ar-oxygen cleavage, while there was no formation of the sulfides between these compounds and *n*-butyl mercaptan under similar reaction conditions. These results clearly disfavor the aromatic $S_N2$-type mechanism and favor the first one, since any substituent would destroy the symmetry of the protonated species and decrease the lifetime of the intermediate incipient carbonium ion (A),* thus effecting less change in the nucleophilic attack at the phenolic carbon, which will presumably assume a quasi-carbonyl character; moreover, the replacement of phenolic hydrogen by the benzenesulfonyl group will destroy the phenolic hydroxyl group, which is essential for the nucleophilic replacement via the incipient carbonium ion (A). As a corollary deduction from this mechanism, one may expect a more facile nucleophilic replacement with phenols with a more carbonyl character. In fact, naphthols were found to give naphthyl *n*-butyl sulfides in better yields in the acid-catalyzed reaction with *n*-butyl mercaptan, as Table IV shows.

The formation of β-naphthyl sulfide was noticed earlier by Furman et al.,[6] when β-naphthol was heated at 110—120°C with various mercaptans for 16 hr. in the presence of and also without any solvent. They have also proposed a similar reaction mechanism analogous to the Bucherer reaction involving the

8) C. K. Ingold, "Structure and Mechanism in Organic Chemistry," Cornell University Press, London (1953).

* Carbonium ion (A):

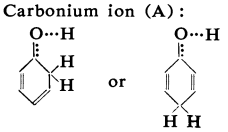
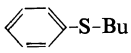
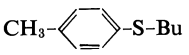
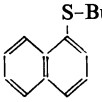
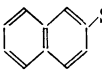


TABLE IV. THE REACTION OF *n*-BUTYLMERCAPTAN WITH *p*-CRESOL, *α*-, *β*-NAPHTHOLS

| Reactant Phenol | Reaction condition | | | Product | |
|---|---|---|---|---|---|
| | Mole ratio* | Time, hr. | Temp., °C | Sulfide | Yield, % |
| Phenol | b | 48 | 180 |  | 22.0 |
| *p*-Cresol | b | 48 | 180 |  | 14.0 |
| *α*-Naphthol | a | 52 | 180 |  | 69.5 |
| *β*-Naphthol | b | 48 | 180 |  | 55.4 |

* Mole ratio; phenol : mercaptan, a; 1 : 5, b; 1 : 1.

attack of the mercaptan on the carbonium ion derived from *β*-naphthol by the protonation of the hydroxy group.

## Experimental

**Phenyl *n*-Butyl Sulfide.** — A mixture of phenol (0.94 g., 0.01 mol.), *n*-butyl mercaptan (4.5 g., 0.05 mol.) and 12 N hydrochloric acid (1 ml.) was sealed in a tube and then heated at 180°C for 48 hr. The sealed tube was then broken, the unreacted *n*-butyl mercaptan was distilled off under reduced pressure, and the residue was extracted with ether. The ether layer was treated with an aqueous sodium hydroxide solution to remove the unchanged phenol, and the two layers were separated. The ether layer was washed with dilute hydrochloric acid, and then with water, and dried. Distillation gave 0.52 g. of phenyl *n*-butyl sulfide in a 31% yield. The infrared spectra is completely in agreement with that of an authentic sample. Found: C, 72.35; H, 8.43%, $n_D^{20}$ 1.5426, b. p. 75°C/1 mmHg. Meanwhile, when the same reaction mixture was heated in a sealed tube at 110°C for 48 hr. and treated as above, no sulfide was obtained.

In a separated experiment, a mixture of phenol (0.94 g., 0.01 mol.), *n*-butyl mercaptan (0.9 g., 0.01 mol.) and 12 N hydrochloric acid (1 ml.) was heated at 180°C for 48 hr. in a sealed tube; 0.37 g. of phenyl *n*-butyl sulfide was thereby obtained (yield 22%). However, when the same mixture was heated at 180°C for 24 hr. in a sealed tube, only a trace amount of phenyl *n*-butyl sulfide was obtained. The sulfide was found to be identical with an authentic sample in infrared spectra. Meanwhile, an authenthic sample of phenyl *n*-butyl sulfide was prepared by reacting diazotized aniline with sodium *n*-butyl mercaptide in over a 90% yield; b. p. 83°C/2 mmHg.

**Phenyl Benzyl Sulfide.** — A mixture of phenol (0.94 g., 0.01 mol.), benzyl mercaptan (6.2 g., 0.05 mol.) and 12 N hydrochloric acid (1 ml.) was sealed in a tube and heated at 180°C for 48 hr. The sealed tube was then broken, and two layers were separated. The upper, yellow layer neutralized with an aqueous sodium hydroxide solution, dried, and then distilled under reduced pressure. Two and six-tenths grams of phenyl benzyl sulfide was obtained (yield 43.4%); b. p. 118°C/3.5 mmHg. Found: C, 77.92; H, 6.00%, $n_D^{20}$ 1.6083. From the lower layer 2 g. of dibenzyl disulfide was obtained; m. p. 71°C.

**Diphenyl Sulfide.**—A mixture of phenol (0.94 g., 0.01 mol.), thiophenol (5.5 g., 0.05 mol.) and 12 N hydrochloric acid (1 ml.) was sealed in a tube and heated at 180°C for 72 hr. The sealed tube was then treated as has been described in the case of phenyl *n*-butyl sulfide. Diphenyl sulfide (0.5 g., 26.7% yield) was obtained, together with 0.3 g. of diphenyl disulfide. Found: C, 77.18; H, 5.38%, $n_D^{20}$ 1.6298, b. p. 113°C/1 mmHg.

In a separate experiment, the same mixture was heated at 180°C for 119 hr., 0.6 g. of diphenyl sulfide was thereby obtained (yield 32.2%).

***p*-Tolyl *n*-Butyl Sulfide.**—A mixture of *p*-cresol (1.08 g., 0.01 mol.), *n*-butyl mercaptan (1 g., 0.011 mol.) and 12 N hydrochloric acid (2 ml.) was sealed in a tube and heated at 180°C for 48 hr. The sealed tube was then broken, and two layers were separated. The lower layer consisted of hydrochloric acid and was discarded. The upper layer was treated as has been described above, thereby removing the unreacted *p*-cresol and *n*-butyl mercaptan. Then the product was collected by distillation in vacuo. *p*-Tolyl *n*-butyl sulfide (0.7 g.) was obtained in a yield of 14%. The product was identified with that of the authentic sample by comparing their infrared spectra. Found: C, 73.19; H, 8.85%, $n_D^{20}$ 1.5397, b. p. 92—94°C/2 mmHg. An authentic sample of *p*-tolyl *n*-butyl sulfide was prepared by reacting diazotized *p*-toluidine with *n*-butyl mercaptan; 95% yield; b. p. 90°C/2 mmHg.

***β*-Naphthyl *n*-Butyl Sulfide.** — A mixture of *β*-naphthol (4.3 g., 0.03 mol.), *n*-butyl mercaptan (2.7 g., 0.03 mol.) and 12 N hydrochloric acid (2 ml.) was sealed in a tube and heated at 180°C for 48 hr. The sealed tube was then broken, and the entire contents were treated as has been described in the case of phenyl *n*-butyl sulfide. When the ether extract was distilled, 3.6 g. of *β*-naphthyl *n*-butyl sulfide was obtained (yield 55.4%). Found: C, 77.57; H, 7.40%, $n_D^{20}$ 1.6229, b. p. 130—135°C/2 mmHg.

***α*-Naphthyl *n*-Butyl Sulfide.** — A mixture of *α*-naphthol (1.44 g., 0.01 mol.), *n*-butyl mercaptan (4.5 g., 0.05 mol.) and 12 N hydrochloric acid (1

ml.) was sealed in a tube and heated at 180°C for 52 hr. The entire contents in the sealed tube were then treated as has been described above. When the ether extract was distilled, 1.9 g. of α-naphthyl *n*-butyl sulfide was obtained (yield 69.5%). Found: C, 77.77; H, 7.19%, $n_D^{20}$ 1.6190, b. p. 140—142°C/2.5 mmHg.

**Benzenesulfonate.**—Phenyl benzenesulfonate (2.34 g., 0.01 mol.) was sealed in a tube with *n*-butyl mercaptan (4.5 g., 0.05 mol.) and 12 N hydrochloric acid (1 ml.). The mixture was then kept at 180°C for 48 hr. The entire contents in the sealed tube were treated as has been described above. The reactants, phenyl benzenesulfonate and *n*-butyl mercaptan, were recovered quantitatively. Also when *p*-nitrophenyl benzenesulfonate (2.79 g., 0.01 mol.) was treated by a procedure similar to that used for phenyl benzenesulfonate, no reaction products were obtained.

*Department of Applied Chemistry*
*Faculty of Engineering*
*Osaka City University*
*Sumiyoshi-ku, Osaka (S. O.)*

*Department of Chemistry*
*Radiation Center of Osaka Prefecture*
*Sakai, Osaka (R. K.)*

# The Solvent Extraction and Spectrophotometric Determination of Vanadium(V) with Thenoyltrifluoroacetone[1]

By Akira IKEHATA and Tamako SHIMIZU

(Received January 27, 1965)

In 1963, De and Rahaman[2] reported a method for the rapid extraction of the vanadium(V)-thenoyltrifluoroacetone (TTA) complex using *n*-butyl alcohol. Except for this short communication, however, little work has been reported on this subject.[3-5] However, in the above method, the complex can not be extracted completely because *n*-butyl alcohol has a relatively large solubility in water. In this paper, a detailed study of the extraction of the vanadium(V)-TTA complex will be made, with special reference to the effect of solvents, the absorption spectra, and the composition of the extracted species.

## Experimental

**Reagents.**—All the reagents used were guaranteed reagents.

The standard vanadium(V) solution was prepared by the fusion of 0.9094 g. of vanadium pentoxide with five times as much sodium carbonate for about one hour at about 900°C. This was dissolved in diluted sulfuric acid and diluted to 1 l. The final sulfuric acid concentration was about 6 N. This solution contains $10^{-2}$ mol./l. of vanadium. A diluted vanadium(V) solution was prepared daily. The organic solvents used for extraction were isoamyl acetate, *n*-butyl acetate, methyl isobutyl ketone, chloroform, benzine, ethyl acetate, carbon tetrachloride, ethylbenzene, toluene, chlorobenzene, cyclohexane, kerosene, xylene, benzene and isopropyl ether.

TTA: Solutions in the above solvents (up to 0.3 M).

**Apparatus.**—A Hitachi model EPU-2A spectrophotometer, a Hitachi-Horiba model M-3 pH meter (accuracy ±0.05 pH unit), a Toadempa HM-8 pH meter (accuracy ±0.005 pH unit), and an Iwaki KM shaker were used.

Experiments were performed by extracting 50 ml. of an aqueous solution of vanadic acid with 10 ml. of organic solvents containing TTA at 25°C.

## Results and Discussion

**The Absorption Spectra of the Vanadium(V)-TTA Complex and of the Chelating Agent.**—As Fig. 1 shows, TTA is a typical diketone which is in keto-enol equilibrium in an aqueous solution.[6,7] It is the enol form that reacts with numerous metals.[8] Figures 2 and 3 show the various absorption spectra of the chelate extracted in various organic solvents.

1) This work was presented at the 11th General Meeting of the Hokkaido District of the Japan Society for Analytical Chemistry, Sapporo, January, 1964.
2) A. K. De and M. S. Rahaman, *Anal. Chem.*, 35, 1095 (1963).
3) G. H. Morrison and H. Freiser, "Solvent Extraction in Analytical Chemistry," Wiley, New York (1957), p. 159.
4) T. Takeuchi and M. Suzuki, *Japan Analyst*, 9, 901, 965 (1960).
5) E. B. Sandel, "Colorimetric Determination of Traces of Metals," Interscience Publishers, Inc., New York (1950), p. 605.
6) E. L. King and W. H. Reas, *J. Am. Chem. Soc.*, 73, 1806 (1951).
7) E. H. Cook and E. W. Taft, ibid., 74, 6103 (1952).
8) R. W. Taft and E. H. Cook, ibid., 81, 46 (1959).

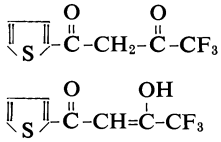


Fig. 1

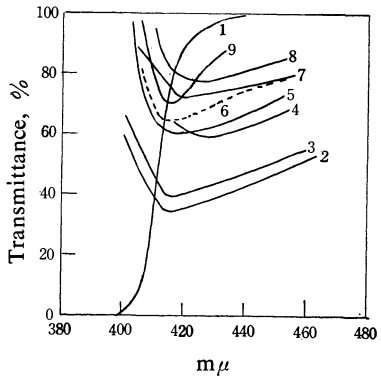



Fig. 2. Absorption spectra of vanadium(V)-TTA complex extracted in aliphatic solvents.
1) 0.1 M TTA isoamyl acetate soln.
2) Isoamyl acetate
3) *n*-Butyl acetate
4) Methyl isobutyl ketone
5) Benzine
6) Ethyl acetate
7) Chloroform
8) Carbon tetrachloride
9) Isopropyl ether

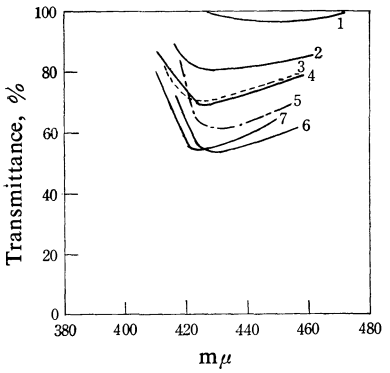



Fig. 3. Absorption spectra of vanadium(V)-TTA complex extracted in aromatic solvents.
1) Xylene, 2) Toluene, 3) Cycrohexane, 4) Chlorobenzene, 5) Benzene, 6) Kerosene, 7) Ethylbenzene

In these experiments, vanadium(V) was extracted for about one hour at pH 3. It was apparent that this complex was extracted more easily in aliphatic solvents, especially isoamyl acetate and *n*-butyl acetate, than in aromatic solvents.

As is shown in Table I, the blue shifts of $\lambda_{max}$ and the increment of the absorbance of these chelates were observed in accordance with a decrease in the refractive indices and with an increase in the dielectric constants of organic solvents, with the exception of a few solvents. Within the range of experimental error, the shifts of these chelate bands in organic solvents seem to obey the equation set forth by McRae, which predicts a linear relationship between the frequency shifts in absorption spectra and the expression $(n^2-1)/(2n^2+1)$, and $(D-1)/(D-2)$, where $n$ is the refractive index and $D$ is the dielectric constant of the solvent.[9-12]

Table I. Shifts of the absorption maximum of the complex

| | Dielectric constant | Reflactive index | $\lambda_{max}$ mμ |
|---|---|---|---|
| *n*-Butyl alcohol | 17.1 | 1.39[a] | 410 |
| Isoamyl acetate | 6.05[a] | 1.40[b] | 414.5 |
| Ethyl acetate | 6.02 | 1.37[a] | 416 |
| Chlorobenzene | 5.62 | 1.52[a] | 426 |
| Buthyl acetate | 5.01[a] | 1.39[a] | 416 |
| Chloroform | 4.80[a] | 1.44[a] | 420 |
| Isopropyl ether | 3.88 | 1.36[c] | 416 |
| Toluene | 2.37 | 1.48[c] | 422 |
| Benzene | 2.27 | 1.50[d] | 430 |
| Ethyl benzene | | 1.49 | 424 |
| Carbon tetrachloride | 2.22[a] | 1.46[a] | 423 |
| Cyclohexane | 2.01 | 1.42[a] | 424 |

a) 20°C, b) 21°C, c) 23°C, d) 29°C, other datas are at 25°C.

**The Effect of the Concentration of the Chelating Agent.**—The effect of the concentration of the chelating agent on the extraction of the complex was determined by varying the concentration of the chelating agent at a constant vanadium(V) concentration. The changes in the absorbance of the organic phase were measured at 420 mμ since the absorption of the chelating agent was negligible at this point.

As Fig. 4 shows, the absorbance increased up to a maximum value of 0.1 M TTA, beyond which the increase in the chelating agent had no significant effect. Thus, in this experiment, the 0.2 M TTA concentration was used.

**The Effect of the Extracting Time.**—The effect of the extracting time was determined. About 30 min. were required for the attainment of the extraction equilibrium (Fig. 5).

**The Effect of pH.**—The effect of pH was determined by controlling the pH with sulfuric acid and sodium hydroxide. The results are as shown in Fig. 6. The chelate was completely extracted over the pH range from 2 to 3.

9) H. McConnel, *J. Chem. Phys.*, **20**, 700 (1952).
10) J. W. Sidman, *Chem. Revs.*, **58**, 689 (1958).
11) O. Popovych and L. B. Dogers, *J. Am. Chem. Soc.*, **81**, 4469 (1959).
12) E. G. McRae, *J. Phys. Chem.*, **61**, 562 (1957).

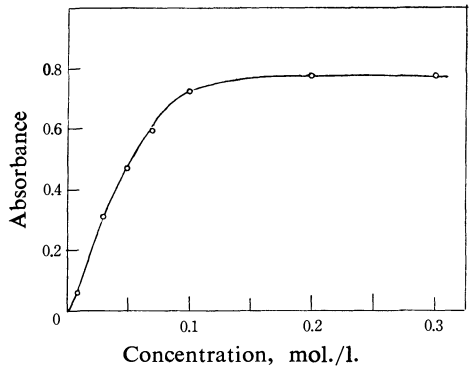



Fig. 4. Effect of the concentration of the chelating agent at pH 2.5 using isoamyl acetate.

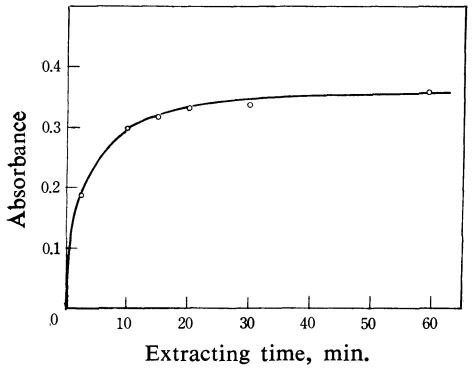



Fig. 5. Effect of the extracting time.

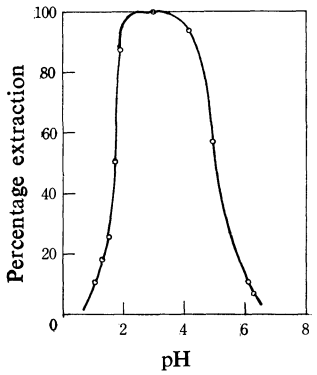



Fig. 6. Effect of pH.

**The Determination of the Mole Ratio of Vanadium(V)-TTA Complex.**—The determination of the mole ratio of vanadium(V) and TTA of this complex extracted in isoamyl acetate was made by the following two methods.

*The Continuous Variation Method.*[13]—The sum total of the concentrations of the metal ion and of the chelating agent was held at $10^{-2}$ mol./l., and the absorbance was plotted against the $[M^{n+}]/([M^{n+}]+[HR])$.

$[M^{n+}]$ and [HR] are the initial concentrations of the vanadium(V) and of the chelating agent respectively. In this method $n=2$ (Fig. 7).

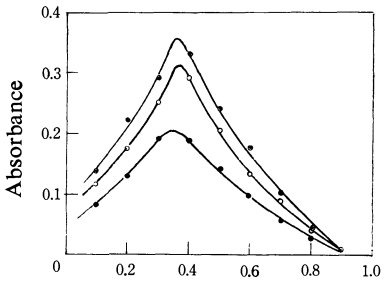



Fig. 7. Cotinueous variation method.
- ⊙ Determined at 410 mμ
- ○ Determined at 420 mμ
- ● Determined at 450 mμ

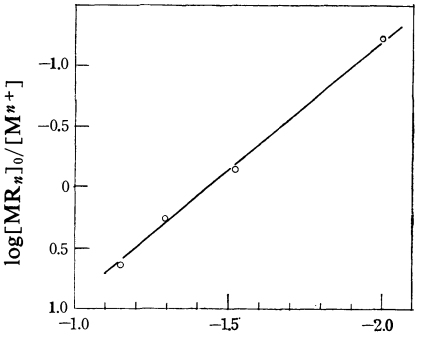



Fig. 8. Slope ratio method.

*The Slope Ratio Method.*[14]—Provided all intermediate complexes can be neglected,

$$M^{n+}+nR^- \rightleftharpoons MR_n$$

$$K_f=[MR_n]/[M^{n+}][R^-]^n$$

If the complexation of $M^{n+}$ with a ligand other than $R^-$ is not appreciable, we have:

$$K_f=K_{DR}^n[MR_n]_0[H^+]^n/K_{DX}K_A^n[M^{n+}][HR]_0^n$$

Then, at a constant pH:

$$n\log[HR]_0=C+\log D$$

where $C=-\log K_{DX}K_A^nK_f/K_{DR}^n[H^+]^n$ and $D$ refers to the distribution ratio of M between the aqueous and organic solvent.

From the plots of $\log[HR]_0$ vs. $\log[MR_n]_0/[M^{n+}]$, $n$ was obtained. As Fig. 8 shows, we obtain a slope of $n=2$.

**The Calibration Curve and the Effect of Foreign Ions.**—Under these conditions, the

13) Y. Niimura and N. Itoh, "Chemistry of Complex" (Vol. 11 in the "Zikken Kagaku Kohza" series), Maruzen, Tokyo (1963), p. 311.

14) H. E. Bent and C. L. French, *J. Am. Chem. Soc.*, **63**, 568 (1941).

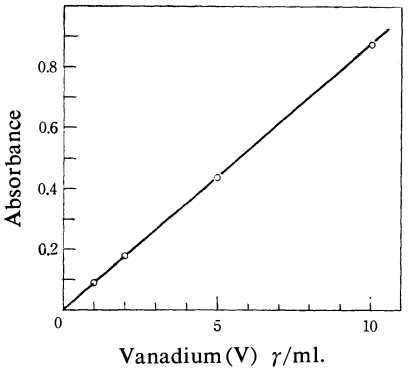



Fig. 9. Calibration curve.
TTA=0.2 mol./l., dissolved in isoamyl acetate, pH 2.5, at 420 mμ.

TABLE II. TOLERANCE LIMIT FOR DIVERSE IONS

| Foreign ion | Added as | Tolerance limit p. p. m. |
|---|---|---|
| $Ti^{4+}$ | Sulfate | 50 |
| $Fe^{3+}$ | $FeSO_4(NH_4)_2SO_46H_2O$ | 10 |
| $Al^{3+}$ | Sulfate | 500 |
| $Mn^{2+}$ | Sulfate | 500 |
| $Zn^{2+}$ | Sulfate | 500 |
| $Cu^{2+}$ | Sulfate | 50 |
| $Ca^{2+}$ | Chloride | 500 |
| $Mg^{2+}$ | Sulfate | 500 |
| $Mo^{6+}$ | $(NH_4)_2MoO_4$ | 500 |
| $Pb^{2+}$ | $Pb(NO_3)_2$ | 500 |

relation between the absorbance and the vanadium(V) concentration was linear up to 10γ/ml. of vanadium(V) in an aqueous solution (Fig. 9). The fading was almost negligible.

Table II shows the effect of several metal ions on this method. Experiments were made in the presence and in the absence of $2\times10^{-2}$ mol./l. of vanadium(V). The tolerance limit indicates the maximum concentration of diverse ions which affects the absorbance of the system by less than ±2%.

Because comparable amounts of $Ti^{4+}$, $Fe^{3+}$, $Cu^{2+}$ interfere with the method, these ions should be removed from the sample by the usual methods.

## Summary

The extraction of the vanadium(V)-TTA complex has been studied using various organic solvents. The complex has been extracted quantitatively in isoamyl acetate and *n*-butyl acetate. The quantitative extraction has been realized within a range from pH 2 to 3, with the absorption maximum at 410 mμ. The mole ratio of the complex is vanadium(V)-1 : 2-TTA, and Beer's law is applicable in the range from 0 to 10γ/ml. of vanadium(V) at 420 mμ. The solvent effects on the absorption spectra of this complex have also been studied.

*The Government Industrial Development Laboratory, Hokkaido*
*Sapporo, Hokkaido*

# The Exchange Reaction of Oxygen Atoms between Inorganic Anions and Water

By Toshizo TITANI, Kaoru DATE and Mitsuko AMBE

(Received November 26, 1964)

About 25 years ago Titani and Goto[1] investigated the exchange reaction of O-atoms between some inorganic oxyanions and water, and found that the oxyanions of strong acids, such as $SO_4^{2-}$, $NO_3^-$, and $ClO_3^-$, exchanged their O-atoms with those of water in acid solutions, but not in neutral solutions. They found, further, that the same exchange reaction took place in the solutions of the neutral salts of such weak acids as potassium carbonate without any catalytic additives, although in this case the solutions turned alkaline as a result of the hydrolytic dissociation of the salts. The same result was obtained by Blumenthal and Herbert[2] with potassium phosphate. At almost the same time, it was reported by Ingold and his collaborators[3] that sodium sulfate rapidly exchanged its O-atoms with those of water in the presence of alkali. Since all these results suggested that

1) T. Titani and K. Goto, This Bulletin, **14**, 77 (1939).

2) E. Blumenthal and J. B. M. Herbert, *Trans. Faraday Soc.*, **33**, 849 (1937).

3) S. C. Datta, J. N. E. Day and C. K. Ingold, *J. Chem. Soc.*, **1937**. 1968,

the reaction was catalyzed by both acid and alkali, we assumed the conventional acid-base catalysis as a primary mechanism of the reaction. At the same time, however, we proposed as an alternative mechanism a reversible dissociation of the neutral acid molecules, such as:

$$H_2SO_4 \rightleftarrows H_2O + SO_3 \quad (1)$$

Neutral acid molecules can be formed either by the addition of hydrogen ions to the oxyanions:

$$2H^+ + SO_4^{2-} \leftrightarrows H_2SO_4 \quad (2)$$

as in the case of the acid solutions of strong acid salts, or by hydrolytic dissociation:

$$CO_3^{2-} + 2H_2O \rightleftarrows H_2CO_3 + 2OH^- \quad (3)$$

as in the case of weak acid salts. With this alternative mechanism, we can explain the results of Titani and Goto as well as those of Blumenthal and Herbert. The only exceptions were the results of the experiment of Ingold and his collaborators, who found the exchange of O-atoms between the oxyanions of such strong acids as $SO_4^{2-}$ and water in an alkaline solution, as has been described above. Therefore, we attempted first to repeat the experiment of Ingold and his collaborators. Unfortunately, however, it was very difficult to carry out such an experiment because the glass surface of the reaction vessel was seriously attacked by the aqueous alkaline solutions at elevated temperatures.

Since the publication of the papers mentioned above, several similar studies have appeared,[4-9] and the reversible anhydride formation has also been assumed by several workers[6,8,9] as the mechanism of the reaction. Furthermore, Winter, Carlton and Briscoe[4] could not observe the catalytic action of the hydroxyl ion on the exchange reaction of the sulfate ion and they suggested that, in view of the rapid exchange of sodium metasilicate, the reaction between the glass wall of the reaction vessel and the strongly alkaline solution might account for the observed exchange in such cases. The same finding and opinion were presented by Hall and Alexander.[7] Mill[6] observed, however, no exchange reaction between Pyrex glass and a strongly alkaline solution at a high temperature, even though the glass was markedly etched, and suggested that different kinds of glass react differently.

Such problems can now easily be solved by the use of a stainless steel vessel. In this way we have studied the reaction in a strongly alkaline solutions. As a result we have come to the conclusion that no exchange reactions take place betwen $SO_4^{2-}$ and water in an alkaline solution; the decrease in the heavy oxygen content of the water which is observed in the case of alkaline solutions in glass reaction vessels must be ascribed to the exchange of O-atoms between the water and the surface of the glass reaction vessel.

## Experimental and Results

The experiments were carried out using both ordinary glass ampoules and a stainless steel reaction vessel which will be described below. The stainless steel vessel consists of four parts, A, B, C and D, which are shown on the left hand side of Fig. 1. A is a stainless steel guard ring. B is a strainless steel plate, at the center of which a short Kovar tube K is welded. This Kovar tube is then welded to an ordinary glass tube, G, by means of Kovar glass, KG. C is a packing ring made of Teflon. D is a stainless steel cylinder which is 3 cm. in inner diameter and 20 cm. long. This lower end of the cylinder is sealed by welding, while the upper end of the cylinder is welded to a guard ring which has the same form and size as the guard ring A mentioned above. These four parts are tightly screwed together by six sets of bolts and nuts, as is shown on the

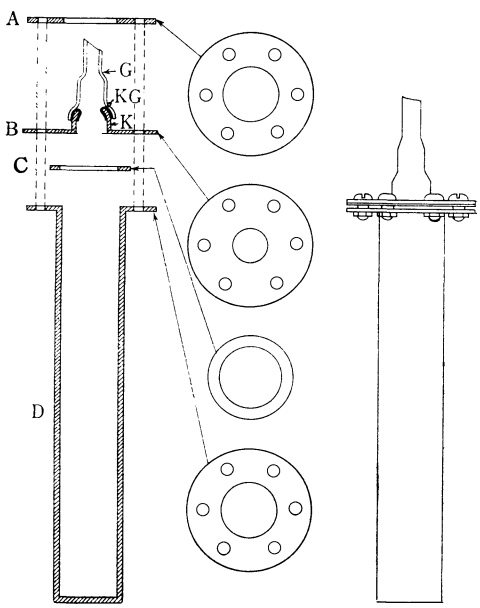



Fig. 1. Stainless steel reaction vessel.

4) E. R. S. Winter, M. Carlton and H. V. A. Briscoe, ibid., **1940**, 131.
5) G. A. Mills and H. C. Urey, *J. Am. Chem. Soc.*, **62**, 1019 (1940).
6) G. A. Mills, ibid., **62**, 2833 (1940).
7) N. F. Hall and O. R. Alexander, ibid., **62**, 3455 (1940).
8) E. R. S. Winter and H. V. A. Briscoe, *J. Chem. Soc.*, **1942**, 631.
9) T. C. Hoering and J. W. Kennedy, *J. Am. Chem. Soc.*, **79**, 56 (1957).

TABLE I. EXPERIMENTS WITH GLASS AMPOULES

| No. | $H_2{}^{18}O$ g. | $Na_2SO_4$ g. | Na g. | Time hr. | $^{18}O$ % $C_B$ | $^{18}O$ % $C_A$ |
|---|---|---|---|---|---|---|
| 1 | 3.424 | 6.804 | 0 | 24 | 0.302 | 0.301 |
| 2 | 3.940 | 1.776 | conc. HCl 0.051* | 24 | 0.332 | 0.317 |
| 3 | 3.970 | 1.843 | 0.03 | 24 | 0.332 | 0.329 |
| 4 | 3.789 | 1.510 | 0.10 | 26 | 0.329 | 0.326 |
| 5 | 2.861 | 4.204 | 0.08 | 24 | 0.315 | 0.302 |
| 6 | 3.235 | 4.901 | 0.09 | 70 | 0.332 | 0.315 |
| 7 | 2.538 | 0 | 0.13 | 24 | 0.291 | 0.280 |
| 8 | 3.130 | 0 | 0.08 | 70 | 0.284 | 0.280 |

* Instead of sodium, 0.051 g. of concentrated hydrochloric acid was added.

TABLE II. EXPERIMENTS WITH A STAINLESS STEEL VESSEL

| No. | $H_2{}^{18}O$ g. | $Na_2SO_4$ g. | Na g. | Time hr. | $^{18}O$ % $C_B$ | $^{18}O$ % $C_A$ |
|---|---|---|---|---|---|---|
| 9 | 3.535 | 1.359 | 0.10 | 70 | 0.332 | 0.333 |
| 10 | 3.560 | 5.150 | 0.09 | 70 | 0.292 | 0.288 |

right hand side of Fig. 1. In this way this stainless steel vessel can be welded to a glass vacuum line just as an ordinary glass ampoule.

All the experiments were carried out in the same way, either with glass ampoules or with the stainless steel vessel. First, a weighed amount of purified anhydrous sodium sulfate and metallic sodium were placed in the reaction vessel. After this vessel had been welded to a vacuum line, a weighed amount of $^{18}O$-enriched water was distilled into the vessel. Then the vessel was evacuated, sealed off from the vacuum line, and heated at 100°C for more than 24 hr. in an air thermostat. After the heating, the vessel was again connected to the vacuum line and the water was distilled off into the other glass ampoule. The concentration of $^{18}O$ in the separated water was measured by the conventional method; the water was brought into equilibrium with the $CO_2$, and the $^{18}O$ content of the latter was measured by a mass spectrometer.

The experimental results are shown in Tables I and II, where $C_B$ and $C_A$ represent the atomic percentage of $^{18}O$ in the water before and after the experiment respectively.

Among the results of the experiments with glass ampoules which are shown in Table I, the results of Nos. 1 and 2 are in accord with the previous results of Titani and Goto; the exchange reaction of O-atoms does not take place between $SO_4^{2-}$ and water in neutral solutions, but it does in acid solution. On the contrary, the results of the experiments from Nos. 3 to 6, which were carried out with the addition of sodium, i. e., alkali, conflict somewhat with one other. Although a small decrease in the $^{18}O$-content of the water was observed in all experiments, as was expected from the experimental results of Ingold and his collaborators, the amount of the decrease is very irregular; it is not always proportional to the amount of sodium sulfate and sodium and to the time of the reaction, as may be seen, for example, by a comparison of the results of Nos. 4 and 5 and Nos. 5 and 6. These results suggest that the cause or the mechanism of the decrease in the $^{18}O$-content in water is too complicated to be explained solely by the exchange reaction between $SO_4^{2-}$ and water. From this point of view, we carried out experiments Nos. 7 and 8, where only sodium, but no sulfate, was added to the solutions. Here we have found also the same degree of decrease in the $^{18}O$-content of the water as in those experiments with the addition of sulfate, i. e., experiments from No. 3 to 6. We, therefore, assumed that the decrease in the $^{18}O$-content of the alkaline solution might be entirely due to the exchange reaction of O-atoms between the water and the surface of the glass reaction vessels.

This assumption was actually confirmed by the experiments with the stainless steel reaction vessel, the results of which are shown in Table II. From Table II, we can safely conclude that no exchange of O-atoms take place within the limits of experimental error when there is no glass surface in the reaction system; the decreases in the $^{18}O$-content of the water which is observed with alkaline solutions in glass reaction vessels are entirely due

to the exchange reaction of O-atoms between water and the glass surface of the reaction vessels.

## Discussion

From the present experiments it can be concluded that the exchange reaction of O-atoms between oxyanions of strong acids and water takes place only in acid solutions, but in neither neutral nor alkaline solutions. This result excludes the acid-base catalyzed mechanism, at least in its general form,[10] from the two alternative mechanisms which we have previously presented; the exchange reaction must be explained either by the reversible anhydride formation or by some other appropriate mechanism. The decreas in $^{18}O$-content in the alkaline solutions of oxyanions of strong acids is entirely due to the exchange of O-atoms between water and the glass surface of the reaction vessels. Recently it has been repoted by Maass[11] that the exchange of O-atoms between water vapor and the glass surface takes place above 100°C without the addition of alkali. If this result is taken into account, the exchange of the O-atoms observed in the present experiments at 100°C between alkaline solutions and the glass surface may be said to be due to the corrosion of the glass surface by alkali. At any rate, we must be very careful of the exchange reaction between water and the glass surface in the experiments with $^{18}O$-enriched water using glass reation vessels, as has already been pointed out by Maass.

*Department of Chemistry*
*Faculty of Science*
*Tokyo Metropolitan University*
*Setagaya-ku, Tokyo*

10) The reaction proceeds by the ternary collison between the reactant molecule, Brönsted's acid and base.

11) I. Maass, *Kernenergie*, 3, 843 (1960).

# The Diamagnetic Study of the Nature of the Association of Acetic Acid. II. The Binary Systems of Acetic Acid with Triethylamine, Pyridine and Aniline

By S. Sriraman, V. Shanmugasundaram and R. Sabesan

(Received August 6, 1964)

The interpretation of the observed magnetic susceptibility of carboxylic acids in different solvents is complicated by the fact that they are mostly in polymeric forms in the pure state and tend to associate in some solvents but to ionize in others. In an earlier communication,[1] the authors investigated the nature of the association of acetic acid in solvents like benzene, carbon tetrachloride, toluene, and cyclohexane, all of the non-interacting type, and also with dioxan and ethyl acetate, which have powerful anionoid centres. The reaction of protonic acids with bases leads to the formation of ion-pair salts associated through a hydrogen bond, or if the solvent base is weak, the proton may remain covalently bonded to the acid itself and the base will be associated with the hydrogen through an electrostatic attraction. Various physico-chemical studies of liquid mixtures of acetic acid with bases like aniline, pyridine and triethylamine[2-6] have indicated many singularities in the property-concentration relationship. The intermolecular complex formation between the acetic acid and bases employed has been held responsible for such singularities by different workers.[7-10] However, Suriyanarayana and Venkatesan[11] have shown that the equivalent conductivity, viscosity, volume contraction and refractive index

1) S. Sriraman and V. Shanmugasundaram, This Bulletin, 37, 395 (1964).

2) M. G. Andre, *Compt. rend.*, 125, 1187 (1897); 126, 1105 (1898).
3) A. E. Dunstan and F. B. Thole, *J. Chem. Soc.*, 95, 1556 (1934).
4) C. G. Balachandran, *J. Indian Inst. Sci.*, 36, 10 (1954).
5) Laxmanan, ibid., 36, 97 (1954).
6) L. Swearingen and R. F. Ross, *J. Phys. Chem.*, 38, 395 (1934).
7) S. Venkataraman, *J. Indian Chem. Soc.*, 17, 297 (1940).
8) A. S. Naumova, *Zhur. Obshchei Khim.*, 19, 1216 (1964); 19, 1222 (1949).
9) M. Bokhovkin, ibid., 27, 856 (1957).
10) R. Mierzecki, *Acta Phys. Polon.*, 12, 26 (1953).
11) C. V. Suryanarayana and V. K. Venkatesan, *J. Phys. Chem.*, 60, 777 (1956).

TABLE I

| Solvent | Mol.% of acetic acid | Wt. fraction of acetic acid $W$ | Density $\rho$ | $\chi_{obs.}$ | $\chi_{additive}$ | $\Delta\chi$ | $\frac{\Delta\chi}{W}$ |
|---|---|---|---|---|---|---|---|
| | 100 | 1.00 | 1.042 | 0.533 | — | — | — |
| | 90 | 0.8576 | 1.039 | 0.582 | 0.573 | +0.009 | +0.0105 |
| Triethylamine | 80 | 0.7134 | 1.020 | 0.625 | 0.614 | +0.011 | +0.0154 |
| | 70 | 0.5856 | 0.9915 | 0.654 | 0.650 | +0.004 | +0.0068 |
| | 66.66 | 0.5381 | 0.9757 | 0.666 | 0.663 | +0.003 | +0.0056 |
| | 60 | 0.4721 | 0.9430 | 0.683 | 0.682 | +0.001 | +0.0021 |
| | Triethylamine | — | 0.721 | 0.815 | — | — | — |
| | 80 | 0.8074 | 1.068 | 0.562 | 0.553 | +0.009 | +0.0111 |
| | 66.66 | 0.6984 | 1.054 | 0.575 | 0.563 | +0.012 | +0.0171 |
| Pyridine | 50 | 0.4859 | 1.021 | 0.587 | 0.581 | +0.006 | +0.0123 |
| | 40 | 0.3839 | 1.007 | 0.596 | 0.589 | +0.007 | +0.0182 |
| | 33.33 | 0.3265 | 1.001 | 0.599 | 0.593 | +0.006 | +0.0183 |
| | 20 | 0.1682 | 0.9845 | 0.607 | 0.605 | +0.002 | +0.0119 |
| | Pyridine | — | 0.9757 | 0.616 | — | — | — |
| | 80 | 0.7202 | 1.079 | 0.577 | 0.573 | +0.004 | +0.0056 |
| | 66.66 | 0.5676 | 1.076 | 0.598 | 0.594 | +0.004 | +0.0071 |
| Aniline | 50 | 0.3718 | 1.054 | 0.628 | 0.622 | +0.006 | +0.0162 |
| | 30 | 0.2210 | 1.037 | 0.640 | 0.644 | −0.005 | −0.0181 |
| | 20 | 0.1266 | 1.025 | 0.653 | 0.658 | −0.005 | −0.0395 |
| | Aniline | — | 1.015 | 0.675 | — | — | — |

of the acetic acid - pyridine system exhibit maxima at 83 mol.% of the acid and pointed out the possibility of the ionisation of the acetic acid molecule. A similar conclusion was obtained by Isobe et al.[12] on the basis of proton magnetic resonance studies of the acetic acid - aniline system. The present investigation was undertaken with a view of elucidating the nature of the association of acetic acid with sufficiently strong bases, such as triethylamine, pyridine and aniline.

## Experimental

All the solvents and the acid were of B.D.H.A.R. quality and were distilled in an all-glass apparatus before use. The acid and the solvents gave physical constants in good agreement with the previously-recorded values.

The magnetic susceptibilities of the pure liquids and the mixtures were determined by the Gouy method described in the earlier paper.[1] Benzene was used as the standard, its susceptibility being taken as 0.702.*

## Results

The specific susceptibility values of the pure liquids and mixtures studied at different concentrations are given in Table I with an experimental accuracy of ±0.5%. For mixtures, the $\chi$ values, calculated on the basis of the additive law, are also given in that table. If $W$ is the weight percentage of the acid and $\Delta\chi = \chi_{(observed)} - \chi_{(additive)}$, the values of $\Delta\chi/W$ are as given in the last column of Table I.

## Discussion

From Table I it can be seen that, for acetic acid - pyridine and acetic acid - triethylamine, the $\Delta\chi/W$ value is positive at all concentrations. In the case of acetic acid - pyrridine, Desphande and Pathki[13] have explained these positive exaltations as arising from the stabilization of monomers, neglecting the effect of hydrogen bonding on magnetic susceptibilty. Our results also confirm such positive deviation from additivity. However, the question arises of whether the effect of the hydrogen bond on magnetic susceptibility can be completely neglected. The recent precision magnetic measurements by Jatkar et al.[14] of several binary systems capable of forming intermolecular hydrogen bonding showed considerable deviations from linearity. Also, it has been shown by other physico-chemical studies that the species resulting from the reaction of acetic acid with pyridine and triethylamine is not completely an electrostatic complex but,

12) I. Isobe, T. Ikenoue, and G. Hazato, *J. Chem. Phys.*, **30**, 1371 (1959).

* All susceptibility values in this paper are diamagnetic values and are expressed in $10^{-6}$ c. g. s. units.

13) V. T. Deshpande and K. G. Pathki, *Trans. Faraday Soc.*, **58**, 2134 (1962).

14) S. K. K. Jatkar, V. S. Jatkar and A. J. Mukhedekar, *Indian J. Chem.*, **1**, 465 (1963).

rather, is partially ionic, resulting in the formation of pyridinium and triethyl ammonium ions respectively. Barrow's infrared measurements[15] indicated the formation of such ions in at least the case of triethylamine. The maximum value of the equivalent conductivity observed by Suryanarayana and Venkatesan[11] at 83 mol.% of acid in the acetic acid - pyridine system has been explained as arising from the maximum ionisation at that concentration. According to them, the progressive fall of conductivity beyond 83% represents only the extent of ionisation. The degree of such deprotonation of acid will depend upon the energy required to break the bond, the stabilisation of the anion, and the strength of the base employed. The mixtures of acetic acid with triethylamine, pyridine and aniline are typical systems in which the bases are strong enough to produce ion-pair salts. The formation of such ion pairs results in an increased diamagnetism as a result of the release of constraints. Accordingly, it may be presumed that the positive exaltations of magnetic susceptibility observed in these cases only indicate the extent of ionisation, and that the maximum deviations observed at different concentrations in these three systems may be taken as indications of the maximum ionisation at these concentrations.

The behaviour of the acetic acid - aniline mixture is quite interesting. When acetic acid is diluted with aniline, there is a marked increase in $\Delta\chi/W$ at the initial dilutions, but the value decreases on further dilutions. In the free aniline molecule, the trivalent nitrogen can resonate with the phenyl group, and such resonance is held responsible for the negative exaltation of the magnetic susceptibility observed[16] in pure aniline. From the proton magnetic resonance study[12] of this system, it is found that such resonance is more pronounced in very dilute concentrations of the acid. This may be responsible for the negative exaltation at low acid concentrations. As more acid is added to the base, the aniline molecule is slowly converted into the anilinium ion, accompanied by a fast proton exchange reaction which gives rise to a positive exaltation.

15) G. Barrow, *J. Am. Chem. Soc.*, **76**, 5211 (1954).

16) S. Sriraman and R. Sabesan, *Trans. Faraday Soc.*, **58**, 1080 (1962).

## Summary

The diamagnetic susceptibilities of three binary systems have been studied using the Gouy method. Deviations of the observed diamagnetic susceptibility values from Wiedemann's additive law have been discussed in the light of the partial ionisation of acetic acid with the solvent bases.

One of the authors (R. S.) is thankful to the Council of Scientific and Industrial Research, Government of India, for the award of a research fellowship.

*Department of Physics*
*Annamalai University*
*Annamalainagar, S. India*

# Studies in the Two Phase System : Sodium Formate - Pyridine. VII. Extraction of Mercury

By G. S. Deshmukh and A. L. J. Rao*

(Received September 17, 1964)

While ethyl ether[1-3] has been widely used for the extraction of mercury and its separation from many elements, carbon tetrachloride[4,5] and chloroform[6] are employed by few workers. Recent results from these laboratories initiated work on the distribution of metal ions in the

* Present address : Department of Chemistry, Punjabi University, Patiala, India.

1) R. Bock, H. Kusche and E. Bock, *Z. anal. Chem.*, **167**, 138 (1953).
2) W. F. Wischer and W. Chalybaens, *Z. anorg. Chem.*, **277**, 255 (1948).
3) H. M. Irving and F. J. C. Rossoti, *Analyst.*, **80**, 77 (1952).
4) E. A. Hakkila and G. R. Waterbury, *Anal. Chem.*, **32**, 1340 (1960).
5) H. Bode, *Z. anal. Chem.*, **142**, 414 (1954).
6) E. Sudo, *Sci. Reports. Res. Inst., Tohoku Univ.*, **8**, 363 (1956).

two phase system, sodium formate - pyridine.[7] The present paper deals with the extraction of mercury by pyridine from sodium formate.

## Experimental

**Reagents.**—Reidel de Haen's recrystallized sodium formate, Baker's analytical grade pyridine and Merck's analytical grade mercuric nitrate were used.

**Extraction Procedure.**—To an aliquot of 5 ml. of 4 M sodium formate, mercuric nitrate is added, followed by 5 ml. of pyridine and the whole mixture is equilibrated for 2 min. After settling, both layers are separated. The mercury extracted into the pyridine layer is determined volumetrically using diphenyl carbazone as an internal indicator.[8]

**Effect of Formate Concentration.** — Mercuric nitrate solution is added to formate solutions of various molarities and in each case it is extracted with 5 ml. of pyridine and the amount extracted is determined. The results showed that the concentration of formate need not be kept rigorously constant but it should be in the range of 3—6 M.

**Effect of pH.**—Maximum extraction of mercury into the pyridine is obtained at a pH range of 7—7.5. Above pH 7.5, the whole of the mercury was precipitated and retained in the formate layer and therefore studies at higher pH's were not possible. (Table I)

**Effect of Volume of Pyridine.**—The effect of volume of pyridine on the extraction of mercury is studied by adding various volumes of pyridine to 5 ml. of 4 M sodium formate containing an aliquot of mercuric nitrate and the amount extracted in each case is determined. The % $E$ increased upto 5 ml. of pyridine and remained the same with further increase in volume of pyridine. (Table II)

Table I. Effect of pH on the extraction of mercury

| pH | %$E$ |
|---|---|
| 7.0 | 99 |
| 7.5 | 99 |
| 8.0 | 50 |
| 8.5 | 20 |
| 9.0 | 3 |

Table II. Effect of volume of pyridine

| Vol. of pyridine, ml. | %$E$ |
|---|---|
| 2 | 62 |
| 3 | 73 |
| 4 | 84 |
| 5 | 99 |
| 6 | 99 |

Table III. Extraction of mercury

Volume of pyridine, 5 ml.
Sodium formate, 5 ml. (4 M)
Temperature, 25°C

| Amount of mercury added, mg. | Amount of mercury extracted, mg. |
|---|---|
| 0.540 | 0.535 |
| 1.080 | 1.072 |
| 1.620 | 1.618 |
| 2.700 | 2.697 |
| 3.780 | 3.778 |

Almost complete extraction of mercury is obtained with 5 ml. of pyridine from 5 ml. of 4 M sodium formate at a pH range of 7—7.5. (Table III)

Elements like iron, aluminium, chromium, lead, and uranium do not interfere with this extraction procedure.

## Summary

The distribution of mercuric mercury in the two phase system sodium formate - pyridine is studied. Almost quantitative extraction of mercury into pyridine is obtained from sodium formate (4 M) at a pH range of 7—7.5 with 5 ml. of pyridine and the extracted mercury is determined volumetrically using diphenylcarbazone as an internal indicator.

Sincere thanks of the authors are due to Professor G.B. Singh for providing the necessary facilities and to the University Grants Commission for the award of a Research Fellowship to one of them (A. L. J. R.).

*Department of Chemistry*
*Banaras Hindu University*
*Patilana, India*

7) G. S. Deshmukh and A. L. J. Rao, *J. Sci. Ind. Res. (India)*, **21B**, 141 (1962); This Bulletin, **36**, 941 (1963); *Z. anorg. u. allgem. Chem.*, **324**, 308 (1963); *Indian J. Chem.*, **1**, 469 (1963); *Chemist-Analyst*, in press; *Z. anal. Chem.*, in press.

8) G. S. Deshmukh and A. L. J. Rao, This Bulletin, **35**, 900 (1962).

# NOTES

## Measurements of the Self-diffusion Coefficients of Carbon Dioxide, Hydrogen Carbonate Ions and Carbonate Ions in an Aqueous Solution

By Takusei HASHITANI* and Kunihiko KIGOSHI

(Received June 13, 1964)

The diffusion coefficients of carbon dioxide in water have been reported by several workers,[1] but the observed values do not agree well with each other.[2] The present authors, therefore, desired to make a contribution to solving the problems of the measurement of the diffusion coefficients of carbon dioxide in water. This paper will report on the diaphragm cell technique as applied to an aqueous carbon dioxide solution and on the details of measurements of the self-diffusion coefficients of carbon dioxide, hydrogen carbonate ions and carbonate ions. The results obtained have been reported in a previous paper[3] except for the value obtained by one additional experiment.

### Apparatus and Procedures

The measurements of the self-diffusion coefficients were carried out by a diaphragm cell[4] of a modified Northrop-McBain type, as is shown in Fig. 1. The upper and lower compartments, each containing 20 ml., were filled with solutions of the same chemical composition, containing sodium ions, carbonate ions, hydrogen carbonate ions and carbon dioxide; these solutions were adjusted to pH 4.0, 8.0 and 12.5 at 25°C. These pH values were selected as best for solutions containing almost pure (at least 99%) carbon dioxide, hydrogen carbonate and carbonate ions respectively, as is shown by the calculations using $K_1=4.45\times 10^{-7}$ [5] and $K_2=4.69\times 10^{-11}$ [6] for the dissociation constants of carbonic acid. The concentration of the latter two ions in the solution was held at ca. 0.1 M, while that of carbon dioxide was ca. 0.06 M. The carbon tracer, C-14, of a $2.3\times 10^{-2}$ $\mu$c./ml. concentration was contained in the lower compartment.

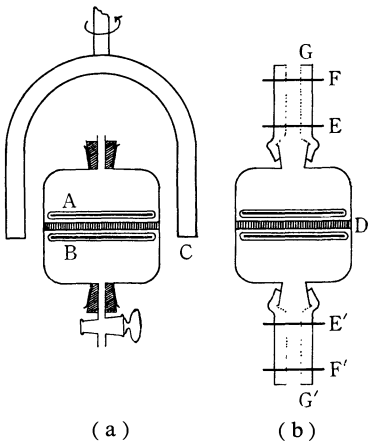



Fig. 1. Diaphragm cells.
a: Used for the solutions with pH>4
b: Used for the solution with pH=4
A and B: Stirrers
C: Magnet (60 r.p.m.)
D: Sintered-glass disk
E, E', F and F': Screw clamps
G and G': Rubber tubes

Before each run, except for the case of the solution with a pH of 4.0, the upper compartment and the diaphragm of the sintered glass disk were filled with a degassed solution and preliminary diffusion was allowed to take place for a few hours in order that a stationary concentration gradient in the diaphragm

* Present address: The Institute of Physical and Chemical Research, Komagome, Bunkyo-ku, Tokyo.

1) G. Hüfner, *Z. phys. Chem.*, **27**, 227 (1898); T. Carlson, *J. Am. Chem. Soc.*, **33**, 1027 (1911); G. Tammann and V. Jessen, *Z. anorg. u. allgem. Chem.*, **179**, 125 (1929); A. Ringbom, ibid., **238**, 94 (1938); K. H. Gertz and H. H. Loeschcke, *Z. Naturforschg.*, **11b**, 61 (1956).

2) As is shown in Gertz and Loeschcke's paper.

3) K. Kigoshi and T. Hashitani, This Bulletin, **36**, 1372 (1963).

4) R. H. Stokes, *J. Am. Chem. Soc.*, **72**, 763 (1950).

5) H. S. Harned and R. Davis, Jr., ibid., **65**, 2030 (1943).

6) H. S. Harned and S. R. Scholes, Jr., ibid., **63**, 1706 (1941).

might be attained. Then the cell was taken out of the bath and the upper compartment was refilled with a non-active solution. In the case of the solution with a pH of 4.0, no preliminary diffusion was allowed because it was difficult to prepare solutions with carbon dioxide of a constant concentration. In this case the results obtained were corrected on the basis of similar diffusion experiments on a potassium chloride solution, which showed that the diffusion coefficient measured without preliminary diffusion was 1.9% less than that measured with preliminary diffussion.

After the diffusion had been allowed to take place for one or two days, the solution in each compartment was taken out and barium carbonate was precipitated by adding barium hydroxide. In the case of pH 4, the escape of carbon dioxide after the diffusion process was prevented by the use of a sodium hydroxide solution. After the run with a solution of pH 4, the rubber tubes shown in Fig. 1(b) were filled with the sodium hydroxide solution and the screw clamps, E and E′, were loosened in order to mix the sodium hydroxide solution with the solution in the cell.

The barium carbonate samples for radioactivity measurements were mounted on dishes of stainless steel. The amounts of barium carbonate were adjusted in order to attain the condition of infinite thickness for $\beta$-rays of C-14. A proportional gas flow counter and a G-M counter were used for $\beta$ countings.

The self-diffusion coefficients were calculated by the formula originally developed by Northrop and Anson:

$$D = (1/Kt) \log (\Delta C_0/\Delta C)$$

where $K$ is a cell constant, and $\Delta C_0$ and $\Delta C$ are the differences between the concentration of C-14 in the two compartments of a cell at times zero and $t$ respectively. The cell constant was obtained by diffusion measurements for solutions of potassium chloride and hydrogen chloride of known diffusion coefficients. The diffusion coefficient of potassium chloride from a 0.1 M solution into water of $1.873\times10^{-5}$ $cm^2/sec$.[7] at 25°C and that of 0.43 M hydrogen chloride of $1.61\times10^{-5}$ $cm^2/sec$.[8] at 0°C were used. The measurements were conducted in a thermostat held at 0, 25, and 30±0.01°C.

## Results

Over-all self-diffusion coefficients of a given solution containing carbon dioxide, hydrogen carbonate ions, and carbonate ions can be estimated as a weighted mean of the self-diffusion coefficients of these species. For instance, in the solution of pH 10.0[9] at 30°C, the concentration ratio, $(HCO_3^-)$ : $(CO_3^{2-})$, is 66 : 34[10] and a calculated self-diffusion coefficient of carbon compounds becomes $(1.18\pm0.01)\times10^{-5}$, showing good agreement with the observed value in this measurement $(1.21\pm0.013)\times10^{-5}$.

*Department of Physics and Chemistry*
*Gakushuin University*
*Mejiro, Tokyo*

7) R. H. Stokes, *J. Am. Chem. Soc.*, 73, 3527 (1951).
8) J. D. R. Scheffer, *Z. phys. Chem.*, 2, 390 (1888).
9) Buffer solution containing 0.025 M $Na_2CO_3$ and $NaHCO_3$ respectively per liter.
10) This concentration ratio is calculated on the basis of the dissociation constant: $K_2 = 5.13\times10^{-11}$ (30°C).[6]

# Transition Metal Complex Catalysts for the Oligomerization of Butadiene. III. The Behavior of Evolved Ethylene from Triethylaluminum in the Catalyst-forming Reaction

By Taro SAITO, Yasuzo UCHIDA and Akira MISONO

(Received August 11, 1964)

The reaction of the ethyl radical formed by the decomposition of such organoaluminum compounds as triethylaluminum and diethylaluminum chloride in the polymerization of butadiene with cobalt complex catalysts has aroused much interest and discussion in connection with the polymerization mechanism.[1-3]

In the course of our studies of the reaction of triethylaluminum and cobalt(III) acetylacetonate, which are used for the linear dimerization of butadiene,[4,5] we found that the gas evolution in the reaction was much less than the theoretical value (about 60% of the calculated volume) and that it was composed mostly of ethane.[6] However, when butadiene was present in the system, a product other than butadiene dimers was detected by gas chromatography. We supposed that this is a $C_6$ hydrocarbon formed by the reaction of butadiene and ethylene from triethylaluminum. In order to prove this hypothesis, we carried out the reaction of butadiene and ethylene with the same catalyst system, thus obtaining a product. On the basis of chemical analysis, infrared and NMR spectra, this product was determined to be *n*-hexa-1, 3-diene.

$$CH_3CH_2CH{=}CHCH{=}CH_2$$

The gas chromatographic retention time of the unknown product described above exactly coincided with that of *n*-hexa-1, 3-diene, and the amount of it nearly corresponded to the amount calculated for ethylene.

These findings can be explained by assuming that, in the reaction, the ethylation of the reduced cobalt takes place as the first step, followed by the rapid disproportionation of the ethyl radical to give equimolecular ethane and ethylene, while the ethylene remains complexed with the cobalt. The ethylene does not come out of the system because of the complexing, but it is active enough to react with butadiene to form *n*-hexa-1, 3-diene, which is also obtained in a large quantity by the reaction of ethylene and butadiene with the same catalyst as is used for methyl-heptatriene synthesis. At the present time, however, we do not know whether or not ethylene interacts with cobalt as a $\pi$-bonding ligand. If it did, it would prevent cobalt from coagulation even when butadiene is absent in the system. This is not the case, however, and so we tentatively propose that ethylene combines with cobalt as a ligand with a weak $\pi$-bonding nature.

## Experimental

1) $1\times10^{-3}$ mol. of cobalt(III) acetylacetonate, and $3.5\times10^{-3}$ mol. of butadiene were dissolved in

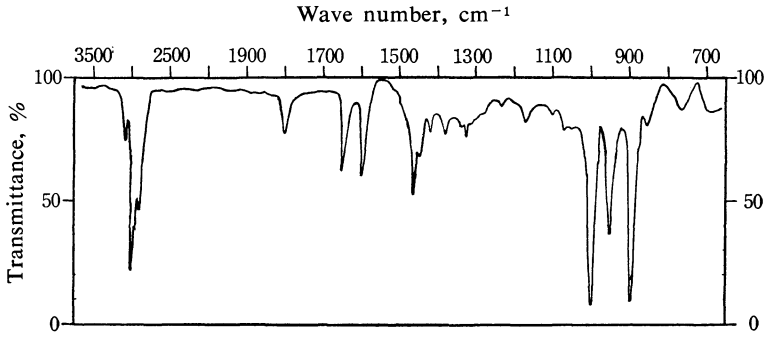



Fig. 1

1) C. W. Childers, *J. Am. Chem. Soc.*, **85**, 229 (1963).
2) W. Cooper, D. E. Evans and G. Vaughan, *Makromol. Chem.*, **67**, 229 (1963).
3) G. Natta, L. Porri, A. Carbonaro and A. Greco, ibid., **71**, 207 (1964).
4) T. Saito, T. Ohno, Y. Uchida and A. Misono, *J. Chem. Soc. Japan, Ind. Chem. Sec.* (*Kogyo Kagaku Zasshi*), **66**, 1094 (1963).
5) T. Saito, Y. Uchida and A. Misono, This Bulletin, **37**, 105 (1964).
6) K. Tamai, T. Saito, Y. Uchida and A. Misono, ibid., to be published.

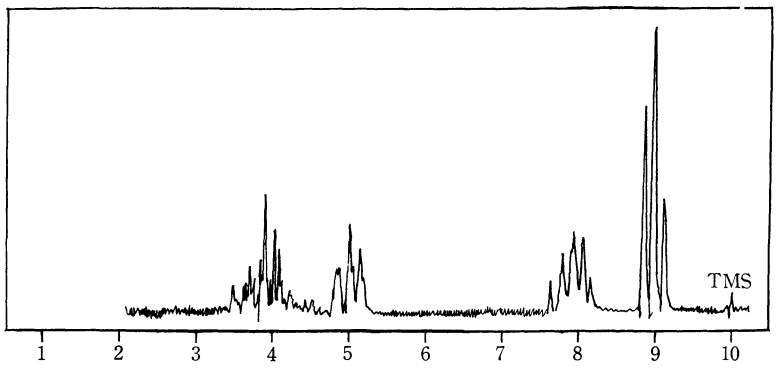


Fig. 2

10 g. of benzene, and then $1\times10^{-3}$ mol. of triethylaluminum was added to the solution under nitrogen. The reaction was carried out at 20°C, and the products were identified and quantitatively analyzed by a gas chromatograph. *n*-Hexa-1, 3-diene was formed in about 70% of the calculated value ($1.5\times10^{-3}$ mol., if the ethylene reacted completely with butadiene), in 100 hr.

2) 0.37 g. of cobalt(III) acetylacetonate and 10 g. of butadiene were dissolved in 50 ml. of toluene, and then 2 ml. of triethylaluminum in toluene (14.5 wt.% solution) was added to the solution at a low temperature under nitrogen. The whole solution was then transferred to a 300-ml. stainless autoclave and 6 g. of ethylene was pressured in. The reaction was carried out at 30°C overnight. (The initial pressure was ca. 8 atm.) The reaction mixture was washed with dilute hydrochloric acid and distilled. The yields of *n*-hexa-1, 3-diene and butadiene dimers were 10 mol.% and 25 mol.% respectively, based on the charged butadiene, and the rest were unreacted monomers and low molecular-weight polymers. The hexadiene part was further purified by a preparative gas chromatograph. The elemental analysis, the molecular weight measurement, and the infrared (Fig. 1) and NMR (Fig. 2) spectra indicated that it was *n*-hexa-1, 3-diene.

*Department of Industrial Chemistry*
*Faculty of Engineering*
*The University of Tokyo*
*Hongo, Tokyo*

# The Formation of $Al^{3+}$–$SO_4^{2-}$ Ion-pair in an Aqueous Solution of Potassium Aluminum Alum*

By Takashi NISHIDE** and Ryokichi TSUCHIYA

(Received August 22, 1964)

In a previous paper[1] the formation constant of the $Cr^{3+}$–$SO_4^{2-}$ ion-pair in an aqueous solution of violet hexaaquochromium(III) sulfate or potassium chromium alum was reported by one of the present authors. Aluminum and iron have similar properties in an aqueous solution with chromium, as is shown by the fact that these three elements belong to the same group in qualitative analysis. In order to investigate the ionic state in an aqueous solution of potassium aluminum alum, the formation constant of the $Al^{3+}$–$SO_4^{2-}$ ion-pair was measured.

## Experimental

Potassium aluminum alum was purified by the recrystallization of the highest grade commercial reagent. The measurement of the electrical conductivity of the solution was carried out with a Yokokawa Universal Bridge BV-Z-13A; that of the pH, with a Toa Denpa pH meter HM-8, and that of the viscosity, with an Ostwald viscosimeter.

* Read at the 17th Annual Meeting of the Chemical Society of Japan, Tokyo, April, 1964.

** Present address: Kanazawa Hisui High School, Kanazawa.

1) R. Tsuchiya and A. Umayahara, This Bulletin, **36**, 554 (1963).

### Method of Calculation and Results

In an aqueous solution of potassium aluminum alum, the following equilibria are thought to be established:

$$[Al(H_2O)_6]^{3+} + SO_4^{2-} \overset{K}{\rightleftarrows} [Al(H_2O)_6]SO_4^{+} \quad (1)$$

$$[Al(H_2O)_6]^{3+} \overset{K_a}{\rightleftarrows} [Al(OH)(H_2O)_5]^{2+} + H^{+} \quad (2)$$

$$[Al(OH)(H_2O)_5]^{2+} + SO_4^{2-} \overset{K}{\rightleftarrows} [Al(OH)(H_2O)_5]SO_4 \quad (3)$$

$$K^{+} + SO_4^{2-} \overset{K'}{\rightleftarrows} K\text{-}SO_4^{-} \quad (4)$$

where the formation constants of reactions 1, 2 and 4 are expressed by $K$, $K_a$ and $K'$ respectively. It is reasonable to assume that the formation constant of reaction 3 is approximately equal to that of reaction 1. This assumption is justified by the two reasons described below.

By using the formation constant calculated below, we ascertained that the concentration of $[Al(OH)(H_2O)_5]SO_4$ is in the order of $10^{-6}$ if the initial concentration of $[Al(H_2O)_6]^{3+}$ is $10^{-4}$. Aluthogh the exact value of the formation constant of Eq. 3 is not known, it is thought to be at least not larger than that of Eq. 1. Therefore, the ratio of the variation of the concentration of $[Al(OH)(H_2O)_5]SO_4$ against the concentration of $[Al(H_2O)_6]^{3+}$ with the value used as the formation constant of Eq. 3, is in the range of a few per cent. The error of the formation constant of $K$ is very small, even where it is assumed to be equal to that of Eq. 3. The other reason, which will also be shown below, is based on the finding that the value of the acid dissociation constant, $pK_a = 4.9$, calculated by the assumption is in good agreement with the value, 5.036, in the literature.[2]

When the total concentration of aluminum contained in an aqueous solution of potassium aluminum alum is expressed by $a$; the concentration of sulfate ions spent for the formation of an $Al\text{-}SO_4^{+}$ ion-pair, by $x$, and that of sulfate ions spent for the formation of a $K\text{-}SO_4^{-}$ ion-pair, by $x'$, and when the molecular conductivities of $[Al(H_2O)_6]^{3+}$, $SO_4^{2-}$, $K^{+}$, and hydrogen ions are expressed by $\Lambda_1$, $\Lambda_2$, $\Lambda_5$, and $\Lambda_H$ respectively, we have, in a manner similar to that used in obtaining Eqs. 12 and 13 in the previous paper,[1] determined that:

$$K = x/(a-x)(2a-x-x') \quad (5)$$

$$(5a\Lambda_1 + C_H\Lambda_1 + 6a\Lambda_2)x + (6a\Lambda_5 + 4a\Lambda_2)x' = 6a^2(\Lambda_5 + \Lambda_1 + 2\Lambda_2) - 2aC_H\Lambda_1 + 6aC_H\Lambda_H - 3a^2\Lambda_0\eta \quad (6)$$

where $\Lambda_0$ is the observed conductivity of potassium aluminum alum in the aqueous solution and $\eta$ is the specific viscosity of the solution.

The plot of the molecular conductivity of a potassium aluminum alum solution, $\Lambda_0$, measured at 25°C against the square root of the concentration, $a$, is shown in Fig. 1.

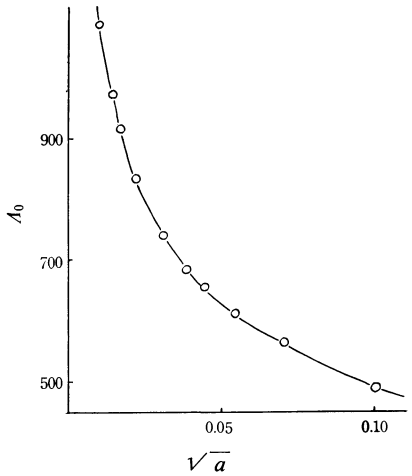



Fig. 1. The plottings of the molecular conductivities at 25°C vs. the square root of the concentrations of the potassium aluminum-(III) alum solution.

By using the value of the conductivity of the potassium sulfate solution and by applying an assumption similar to that used in obtaining Eqs. 9, 13 and 15 in the previous paper[1] to Eqs. 5 and 6, the formation constant of the ion-pair, $[Al(H_2O)_6]SO_4^{+}$, and the acid dissociation constant of $[Al(H_2O)_6]^{3+}$ were computed, were $\Lambda_1 = 189$[3] was employed as the molecular conductivity of $[Al(H_2O)_6]^{3+}$ instead of that of $[Cr(H_2O)_6]^{3+}$ as in the previous paper.[1]

The values of the formation constant of the ion-pair and the corresponding ionic strength are given in Table I, as are the values of the conductivity and the pH of the potassium aluminum alum solution. The logarithm of the formation constant is plotted against the square root of the corresponding ionic strength in Fig. 2. By extrapolation of the plottings up to $\mu \to 0$, the thermodynamic formation constant of the ion-pair at 25°C was obtained as $K = 5.4 \times 10^3$.

2) T. Ito and N. Yui, *Sci. Rep. Tohoku Univ. Ser. I*, 37, 185 (1953).

3) Landolt-Börnstein, "Phys. Chem. Tabellen," Ergänzungsband III, Teil III, Verlag von Julius Springer, (1936), p. 2059.

Table I. The observed values of conductivity and pH of the solution of potassium aluminum alum and the calculated values of the formation constant of ion-pair $Al^{3+}$-$SO_4^{2-}$ and the acid dissociation constant of hexaaquoaluminum(III) ion at the various ionic strengths of the solution at 25°C

| $a$ | $\Lambda_{obs}$ | pH | $\eta$ | $K\times10^{-3}$ | log $K$ | $K_a\times10^6$ | log $K_a$ | $\sqrt{\mu}$ |
|---|---|---|---|---|---|---|---|---|
| 0.0001 | 1093.6 | 4.66 | 1.000 | 4.038 | 3.606 | 6.433 | $\bar{6}$.8084 | 0.02294 |
| 0.0002 | 977.11 | 4.47 | 1.000 | 3.872 | 3.588 | 7.434 | $\bar{6}$.8712 | 0.03038 |
| 0.0003 | 923.03 | 4.39 | 1.000 | 3.332 | 3.523 | 7.004 | $\bar{6}$.8454 | 0.03616 |
| 0.0005 | 837.15 | 4.26 | 1.000 | 3.430 | 3.535 | 7.586 | 6.8800 | 0.04345 |
| 0.0010 | 745.51 | 4.12 | 1.000 | 3.045 | 3.484 | 7.193 | $\bar{6}$.8569 | 0.05665 |
| 0.0015 | 690.59 | 4.01 | 1.000 | 3.148 | 3.498 | 7.974 | $\bar{6}$.9017 | 0.06508 |
| 0.0020 | 663.70 | 3.97 | 1.001 | 2.778 | 3.444 | 7.184 | $\bar{6}$.8564 | 0.07346 |
| 0.0030 | 613.68 | 3.84 | 1.001 | 2.876 | 3.458 | 5.467 | 6.7378 | 0.08475 |
| 0.0050 | 568.71 | 3.75 | 1.003 | 2.786 | 3.445 | 3.524 | 6.5470 | 0.1032 |
| 0.0100 | 493.95 | 3.62 | 1.011 | 4.159 | 3.618 | 2.023 | 6.3060 | 0.1324 |

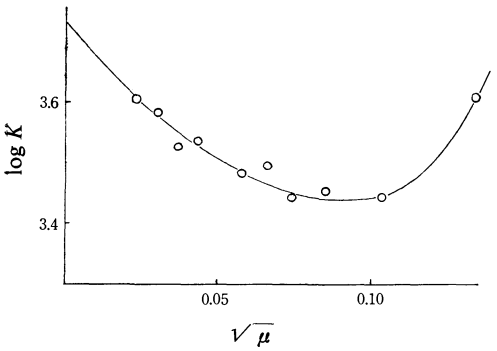



Fig. 2. The plottings of the formation constants of the ion-pair, $[Al(H_2O)_6]$-$SO_4^+$, in the potassium aluminum(III) alum solution vs. the square root of the ionic strength at 25°C.

In addition, the thermodynamic acid dissociation constant at 25°C was evaluated as $pK_a = 4.9$ in the same manner as in the previous paper.[1]

## Discussion

The values of the formation constant of the ion-pair, $[Al(H_2O)_6]SO_4^+$, and of the acid dissociation constant of $[Al(H_2O)_6]^{3+}$ obtained in the present study are summarized in Table II, together with the corresponding values concerning $[Cr(H_2O)_6]SO_4^+$ and $[Cr(H_2O)_6]^{3+}$ obtained in the preceding paper.[1]

Table II. The formation constants of the ion-pairs, $[Cr(H_2O)_6]SO_4^+$, and $[Al(H_2O)_6]SO_4^+$ and the acid dissociation constants of $[Cr(H_2O)_6]^{3+}$, and $[Al(H_2O)_6]^{3+}$ ions at $\mu=0$ and 25°C

| | $K$ | $pK_a$ |
|---|---|---|
| $[Cr(H_2O)_6]^{3+}$ | $6.3\times10^4$ | 3.95 |
| $[Al(H_2O)_6]^{3+}$ | $5.4\times10^3$ | 4.9 |

As Table II shows, both the formation constant of the ion-pair and the acid dissociation constant are a little larger in a chromium(III) aquo complex than in an aluminum(III) aquo complex. This can be explained as follows: in a chromium(III) aquo complex, the hydrogen atom in an aquo ligand is made more positive because the stronger inductive effect of chromium attracts the electron cloud from the ligand; consequently, the acid dissociation becomes easier, and the hydrogen bonding of an aquo ligand with a sulfate ion becomes a little stronger than in an aluminum(III) aquo complex.

*Department of Chemistry*
*Faculty of Science*
*Kanazawa University*
*Kanazawa*

# Studies in Rare Metal Tungstates—Amperometric Titrations of Lanthanum(III) with Alkali Tungstate

By C. M. Gupta

(Received September 8, 1964)

In view of the interesting results reported in the amperometric studies of certain isopoly acid salts,[1] it was considered of interest to study the similar rare isopoly tungstate. As no amperometric study on the composition of lanthanum tungstate, appears to have been carried out so far, the present investigation was initiated. Amperometric titrations have been performed between $La(NO_3)_3$ and $Na_2WO_4$ with a view of studying the possibility of developing the reaction as an analytical method for the determination of lanthanum at a definite pH value. Amperometric methods of analysis possess attributes which extend their value far beyond the direct determination of chemical elements.

AnalR (BDH) reagents sodium tungstate and lanthanum nitrate were used; their solutions were prepared in conductivity water. Lanthanum was estimated as an oxalate[2] by potentiometry, while the tungsten in $Na_2WO_4$ was determined as its oxinate.[3] A manual polarograph, with a scalamp galvanometer as a current recorder, was used for amperometric titrations. A capillary ($m=2.416$ mg./sec., $t=3.58$ sec. and $m^{2/3}t^{1/6}=2.226\ mg^{2/3}\ sec^{-1/2}$) was used in conjunction with a saturated calomel electrode connected to the cell by a low-resistance salt bridge. A series of polarograms of solutions containing lanthanum nitrate in the presence of 0.1 M potassium chloride and 0.01% gelatin were drawn, and the almost limiting current plateau potential was determined to be $-1.5$ V. (vs. SCE). This potential was applied to the electrodes of the cell throughout the investigations. All the amperometric titrations were carried out in the absence of a supporting electrolyte and in the presence of of 0.01% gelatin. Twenty millilitres of the titre solution was placed in the cell each time, and the cell solution was deaerated by bubbling in hydrogen. The observed current was corrected for the dilution effect, and the end-points were located graphically. The addition of alcohol has often been recommended in these titations, especially because of its favourable influence on the solubility of the precipitate. Therefore, investigations have also been undertaken in this direction. In 50% ethanol, the equivalence point was found to have been much improved.

The precipitation of $La_2O_3 \cdot 3WO_3$ is quantitative over the pH range from 5 to 6.5; the results are accurate within an error range of 1% at $10^{-3}$ M concentrations of the reactants studied. The only product formed at this pH is the normal tungstate of lanthanum, probably due to the fact that normal $WO_4^{2-}$ is predominant over the other species. The present method has limitations, although it is rapid, simple and accurate for the determination of small amounts of $La^{3+}$. Anions like molybdate, chromate, and vanadate, and such cations as cerium, thorium and silver interfere and hence must remain absent. The work at different pH values did not give satisfactory results.

The above results have been substantiated by pH titrations between alkali tungstate and lanthanum nitrate using glass electrode, both by direct and reverse methods. The electrometric curves reveal a sharp maxima in $dpH/dV$ at the stoichiometric end point corresponding to the formation of normal tungstate. The sharp inflexion in the curve when $Na_2WO_4$ is added to lanthanum nitrate in the presence of 40% ethanol suggests the possibility of using methyl red for the visual detection of the end point in the 5.0—6.8 pH range.

Grateful thanks are due to Professor Dr. R. C. Mehrotra, D. Phil, Ph. D., F.R.I.C., F.N.A.Sc., F.N.I., Professor of Chemistry, University of Rajasthan, Jaipur (India), for providing the necessary facilities and also encouragement.

*Department of Chemistry*
*University of Rajasthan*
*Jaipur, India*

1) C. M. Gupta and R. S. Saxena, *J. Inorg. & Nucl. Chem.*, **14**, 297 (1960); *Indian J. Chem.*, 1964 (in press); C. M. Gupta, *Naturwissenschaften*, **50**, 545 (1963); *Z. anal. Chem.*, **204** (3), 181 (1964).
2) I. A. Atanasiu, *Z. anal. Chem.*, **112**, 19 (1938).
3) R. Nierickerand W. D. Treadwell, *Helv. Chim. Acta*, **29**, 1472 (1946).

# The Polymerization and Polymers of Itaconic Acid Derivatives. VIII. A Cation Exchange Resin from Itaconic Anhydride[1,2]

By Susumu NAGAI and Keinosuke YOSHIDA

(Received September 25, 1964)

A cation exchange resin prepared from itaconic acid may be expected to have a large ion exchange capacity. The resins obtained by Akashi[3] and Sugihara[4], however, showed relatively low ion exchange capacities. The resins prepared by the solution copolymerization of itaconic acid and divinylbenzene in methyl alcohol, ethyl alcohol and acetone showed exchange capacities of 4.3—7.6, 7.86 and 9.57 meq./g. respectively. The resin obtained by the bulk copolymerization of the two materials at 160°C showed 7.35 meq./g. The pearl copolymerization in a sodium chloride solution resulted in a low-capacity resin, and an attempt to saponify the dimethyl itaconate-divinylbenzene copolymer did not succeed.

It might be due to the poor homopropagation reactivity of itaconic acid that a high-capacity resin was not obtained under these preparation conditions.

The authers have succeeded in the synthesis of a high-capacity ion exchange resin by using itaconic anhydride as the monomer and diallyl itaconate as the cross-linking agent.

## Results and Discussion

In order to prepare a copolymer rich in itaconic acid, the copolymerization system must be considered to be preferable to the homopropagation of itaconic acid. First, it is recognized that itaconic acid homopolymerizes only in an aqueous solution.[5] However, the application of the aqueous system seems unsuitable, for it requires a water-soluble cross-linking agent. Second, it is of interest to apply the finding reported by Higuchi that itaconic acid shows different copolymerization reactivities against styrene in such different solvents as methyl alcohol, pyridine and aniline.[6] Pyridine and aniline seem to promote the homopropagation of itaconic acid. However, these solvents are not only expensive, but they are also capable of some side reactions with itaconic acid. Third, it should be noticed that, when copolymerized with styrene, itaconic anhydride shows a larger reactivity ratio than that of styrene.[7] The author has also reported that itaconic anhydride readily homopolymerizes in bulk and that the polymer is rapidly hydrolyzed as soon as it is dissolved in water.[8] These facts suggest the probability of preparing the ion exchange resins with large capacity. The results obtained by means of the third method are described below.

The polymerization of itaconic anhydride was carried out in tetrahydrofuran, using divinylbenzene as the cross-linking agent. When the charged composition of divinylbenzene was 20 per cent, the polymerization product consisted exclusively of itaconic anhydride, showing much solubility to an alkaline solution as well as to acetone. Both runs, charged with 40 and 60 % divinylbenzene, on the contrary, yielded cross-linked polymers containing no carboxylic group.

These results suggest that cross-linking agents with an almost "ideal"[9] copolymerization reactivity against itaconic anhyride should be used instead of divinylbenzene. Therefore, we tried to use diallyl itaconate as the cross-linking agent.

The results of the copolymerization of itaconic anhydride and diallyl itaconate are shown in Table I.

The ion exchange resins thus obtained showed a satisfactorily large ion exchange capacity, though their swelling ratios (R-COONa/R-COOH) were relatively high.

There is a question of whether or not this type of resin, consisting of ester cross-linkage, is resistant to alkali and acid for a long time. The resin, afterward immersed both in alkali and acid (1 N) for one month, did not show as much decrease in weight as the commercial resin of the weak-acid type (Duolite CS 101).

1) Part VII of this series: S. Nagai, *Sci. and Ind. (Kagaku to Kogyo)*, **38**, 565 (1964).
2) Presented at the 13th Annual Meeting of the Society of Polymer Science, Japan, Kyoto, June, 1964.
3) H. Akashi, *J. Chem. Soc. Japan, Ind. Chem. Sec. (Kogyo Kagaku Zasshi)*, **60**, 505 (1957).
4) M. Sugihara and N. Yoden, *Sci. and Ind. (Kagaku to Kogyo)*, **33**, 144 (1959).
5) S. Nagai and K. Yoshida, *Kobunshi Kagaku*, **17**, 748 (1960).
6) T. Higuchi, *Bull. Gov. Ind. Res. Inst., Osaka*, **13**, 78 (1962).
7) J. Drougas and R. L. Guile, *J. Polymer Sci.*, **55**, 297 (1961).
8) S. Nagai, This Bulletin, **37**, 369 (1964).
9) F. T. Wall, *J. Am. Chem. Soc.*, **66**, 2050 (1944).

TABLE I. THE COPOLYMERIZATION OF ITACONIC ANHYDRIDE AND DIALLYL ITACONATE IN AN ATTEMPT TO PREPARE THE CATION EXCHANGE RESIN

| No. | ItAnh | DAI | BPO | DAI / ItAnh+DAI | Yield* | Ion exchange capacity meq./g. | | | Swelling ratio |
|---|---|---|---|---|---|---|---|---|---|
| | g. | g. | g. | mol. % | g. | Found | Theor. | % | |
| I | 3.628 | 0.258 | 0.080 | 3.65 | 2.5 | 12.9 | 14.5 | 89 | ~1.8 |
| II | 3.804 | 0.515 | 0.077 | 6.73 | 2.5 | 12.2 | 13.8 | 88 | ~1.6 |
| III | 3.246 | 0.787 | 0.080 | 11.45 | 2.5 | 11.7 | 12.8 | 92 | ~1.7 |
| IV | 3.034 | 1.006 | 0.079 | 15.0 | 2.2 | 11.2 | 12.0 | 93 | ~1.8 |

ItAnh: Itaconic anhydride; DAI: diallyl itaconate; BPO: benzoyl peroxide

* After they had been copolymerized for 1 hr. at 75°C, followed by an after cure for 3 hr. at 110°C, the copolymers were treated by the routine method of conditioning. The yield indicates the weight of the dry ion exchange resin obtained in this way, including no unreacted monomers or water-soluble polymers.

## Experimental

**Materials.** — Itaconic anhydride was synthesized by the reaction of itaconic acid and acetyl chloride. It was recrystallized twice from anhydrous ethyl ether. M. p. 67—68°C. Commercial divinylbenzene was used as supplied, composed of 50 per cent divinylbenzene and 50 per cent ethylstyrene. Diallyl itaconate was prepared by the esterification of itaconic acid with allyl alcohol in the presence of a catalytic amount of sulfuric acid. B. p. 130—132°C (~7 mmHg).

**The Copolymerization with Divinylbenzene.**— When the charged amount of divinylbenzene (net) was 20 mol. %, a mixture of 4.481 g. of itaconic anhydride, 2.853 g. of 50% divinylbenzene, 20 ml. of tetrahydrofuran, and 0.269 g. of benzoyl peroxide was copolymerized in a glass tube at 60°C. After 44 hr., the homogeneous solution was poured into water in order to precipitate the powdery polymer. The polymer precipitated in the water, however, expanded and dissolved when alkali was added to the system, though it reprecipitated when hydrochloric acid was added. The polymer was also soluble in acetone, though it was insoluble in ethyl ether. The yield was 2.9 g. The alkaline solution of the polymer sample indicated no sign of the existence of benzene derivatives in the ultraviolet spectrum. When charged with 40 and 60 mol. % of net divinylbenzene, the cross-linked, alkali-insoluble polymers were obtained. However, their ion exchange capacities were almost zero.

**The Copolymerization with Diallyl Itaconate.**— The four runs of the bulk copolymerization, in which the charged compositions of diallyl itaconate ranged from 3.65 to 15.0 mol. %, were carried out in glass tubes at 75°C. After 15—20 min., the reaction mixtures of all four runs solidified and then small cracks occurred in them. After one hour the solid products were discharged from the reaction tubes and were postcured for 3 hr. at 110°C. The products were crushed, poured into water, and then immersed in 1 N sodium hydroxide for about 24 hr. Then they were washed with water and immersed in 1 N hydrochloric acid. After the alternative immersions in alkali and acid had been repeated two more times, they were dried for 4 hr. at 105—110°C. The swelling ratio of the wet volume of the resin in the form of R-COONa against that of R-COOH was measured roughly by means of a graduated cylinder.

**The Determination of the Ion Exchange Capacity.**—About 0.5 g. of the resin was exactly weighed in a beaker. Then 30 ml. of 0.1 N sodium hydroxide and 40 ml. of 0.1 N sodium chloride were pipetted into the beaker. After about 20 hr., 10 ml. of the upper solution in the beaker was pipetted out and back-titrated with 0.1 N hydrochloric acid.

The authors wish to express their gratitude to Dr. Taizo Uno and Dr. Tadashi Kimura for their encouragement, and to Dr. Mizuho Sugihara, Dr. Toshio Yoshino and Mr. Masato Nishimura for their kind suggestions. They also wish to express their thanks to the Taito Pfizer Co. for supplying materials.

*The Osaka Municipal Technical Research Institute*
*Kita-ku, Osaka (S. N.)*

*Fukui Vinyl Co.*
*38 Sha-machi, Fukui (K. Y.)*

# Crystallographic Data on Ammonium Dioxovanadium(V) Bisoxalate Dihydrate by the X-Ray Powder Method

By D. N. SATHYANARAYANA and C. C. PATEL

(Received November 19, 1964)

Recently, we reported a new method for the preparation of ammonium dioxovanadium(V) bisoxalate dihydrate, $(NH_4)_3[VO_2(C_2O_4)_2]\cdot 2H_2O$, its physico-chemical properties and its structure.[1] X-Ray diffraction studies have now been carried out on the powdered crystals, and the crystal system and the unit cell parameters have been determined. The crystals of the complex were prepared in the manner reported earlier.[1] The crystals were then powdered to nearly a 300-mesh size and filled in a 0.5 mm. (inner diameter) Lindemann glass capillary. The X-ray diffraction pattern of the powdered substance was taken with a 114.6 mm. Philips Powder Camera using nickel-filtered Cu$K_\alpha$ radiation (1.5418 Å) at 34 kV. and 18 mamp. at 25°C. The exposure time was six hours.

The complex crystallized from aqueous solutions on a microscopic slide at the laboratory temperature, when viewed under a polarising microscope, gave straight extinctions, and the optic axis figure showed the biaxial nature of the crystals. The crystal growth also clearly demonstrated that the lengths of the edges were unequal. These observations point to the possibility of an orthorhombic system for the compound. Microscopic examination further showed a prismatic type of crystals with domed faces. Five faces, (100), (010), (001), (110), and (101), appeared to be present. The powder pattern was indexed for an orthorhombic system using Hesse-Lipson's procedure;[2] the observed and calculated $\sin^2\theta$ values, together with the visually-assigned relative intensities of the lines, are given in Table I. The results show that the observed and computed $\sin^2\theta$ values for the orthorhombic system compare well. The values for the unit cell parameters are: $a=15.75$ Å, $b=11.09$ Å, and $c=8.015$ Å, as calculated from the observed $\sin^2\theta$ values of the first three lines, the volume of the unit cell being 1400 Å$^3$. The density of the crystals was found to be 1.665 g. ml$^{-1}$ at 25°C, using carbon tetrachloride. Using this density, the

Table I. X-Ray powder data of $(NH_4)_3[VO_2(C_2O_4)_2]\cdot 2H_2O$

| Line No. | $\sin^2\theta$ obs. | $\sin^2\theta$ calcd. | $hkl$ | Relative intensity |
|---|---|---|---|---|
| 1 | 0.00959 | 0.00961 | 2 0 0 | 75 |
| 2 | 0.01166 | 0.01165 | 1 0 1 | 100 |
| 3 | 0.01442 | 0.01445 | 2 1 0 | 35 |
| 4 | 0.01660 | 0.01650 | 1 1 1 | 35 |
| 5 | 0.01900 | 0.01937 | 0 2 0 | 25 |
| 6 | 0.02393 | 0.02373 | 2 1 1 | 40 |
| 7 | 0.02896 | 0.02899 | 2 2 0 | 40 |
| 8 | 0.03105 | 0.03093 | 1 2 1 | 55 |
| 9 | 0.03568 | 0.03573 | 3 1 1 | 15 |
| 10 | 0.03837 | 0.03845 | 4 0 0 | 15 |
| 11 | 0.04113 | 0.04100 | 3 2 0 | 15 |
| 12 | 0.04422 | 0.04424 | 1 1 2 | 25 |
| 13 | 0.05030 | 0.05025 | 3 2 1 | 55 |
| 14 | 0.05267 | 0.05254 | 4 1 1 | 15 |
| 15 | 0.05620 | 0.05636 | 0 2 2 | 65 |
| 16 | 0.06686 | 0.06707 | 4 2 1 | 55 |
| 17 | 0.07461 | 0.07417 | 5 1 1 | 45 |
| 18 | 0.07969 | 0.07990 | 1 4 0 | 20 |
| 19 | 0.08314 | 0.08299 | 1 3 2 | 25 |
| 20 | 0.08642 | 0.08651 | 6 0 0 | 15 |
| 21 | 0.09090 | 0.09047 | 1 1 3 | 25 |
| 22 | 0.09656 | 0.09636 | 2 4 1 | 20 |
| 23 | 0.1047<br>0.1047 | 0.1048<br>0.1050 | 3 0 3<br>1 2 3 | 10 |
| 24 | 0.1100 | 0.1097 | 3 1 3 | 20 |
| 25 | 0.1169 | 0.1169 | 1 4 2 | 15 |
| 26 | 0.1261 | 0.1265 | 4 1 3 | 20 |
| 27 | 0.1369<br>0.1369 | 0.1373<br>0.1364 | 0 7 0<br>2 2 3 | 45 |
| 28 | 0.1410 | 0.1411 | 4 2 3 | 20 |
| 29 | 0.1733 | 0.1732 | 8 2 0 | 20 |
| 30 | 0.1829 | 0.1824 | 3 4 3 | 20 |
| 31 | 0.1916 | 0.1913 | 4 1 4 | 20 |
| 32 | 0.2068 | 0.2067 | 1 5 3 | 15 |
| 33 | 0.2141 | 0.2139 | 2 5 3 | 15 |
| 34 | 0.2218 | 0.2221 | 4 6 1 | 15 |
| 35 | 0.2425<br>0.2425 | 0.2428<br>0.2422 | 4 5 3<br>3 7 3 | 15 |
| 36 | 0.2473 | 0.2471 | 3 4 4 | 15 |
| 37 | 0.2794 | 0.2792 | 3 6 3 | 15 |
| 38 | 0.2961 | 0.2961 | 5 1 5 | 15 |
| 39 | 0.3073 | 0.3069 | 3 7 4 | 15 |
| 40 | 0.3251 | 0.3249 | 1 6 4 | 15 |

$a=15.75$ Å, $b=11.09$ Å, $c=8.015$ Å;
$\alpha=\beta=\gamma=90°$

1) D. N. Sathyanarayana and C. C. Patel, This Bulletin, 37, 1736 (1964).

2) R. W. M. D'Eye and E. Wait, "X-ray Powder Photography," Butterworths Scientific Publications, London (1960), pp. 88—92.

number of formula units of the complex per unit cell was found to be $4.02 \doteq 4$.

The authors thank Drs. J. Shanker and M. D. Kharkhanwala for providing facilities for the X-ray work.

*Department of Inorganic and Physical Chemistry*
*Indian Institute of Science*
*Bangalore-12, India*

# The Thermal Decomposition of Zinc Oxide in an Oxygen and a Nitrogen Stream

By Tatsuya IMOTO, Yoshio HARANO and Yasuhide NISHI

(Received December 14, 1964)

In a previous paper[1] on the thermal decomposition of zinc oxide in vacuo, it was reported that oxygen and zinc are not evolved equally with stoichiometric composition, but that more oxygen is released than zinc. If zinc oxide decomposes by such a process, the rate of the decomposition of zinc oxide will be affected by the oxygen pressure. As far as we know, very few investigations of the rate of the decomposition of zinc oxide in an oxygen or a nitrogen stream have been made except for Moore and Williams's.[2] Their report, however, shows neither the initial amount of zinc oxide nor the pressures of the flowing gases, i.e., oxygen and nitrogen. Therefore, it is very difficult to gather enough quantitative information concerning the effect of oxygen on the rate of decomposition.

Meanwhile, we[3] have studied the kinetics of the reduction of zinc oxide by hydrogen over the range of temperature, 617—762°C, with a hydrogen pressure of 10—95 mmHg, and have deduced that the reduction proceeds via the following two processes: the decomposition of zinc oxide into oxygen and zinc vapor, and the reaction of the evolved oxygen with hydrogen. When the amount of zinc oxide is smaller than that of hydrogen, the decomposition process of zinc oxide controls the overall reaction.[4] In this case, the effect of nitrogen gas on the decomposition of zinc oxide is found to be represented by the following relation:

$$\frac{\text{Reduction rate by mixed gas}}{\text{Reduction rate by hydrogen}} = 1-\theta_{N_2}$$

where $\theta_{N_2}$ is expressed by a form similar to the Langmuir-type adsorption isotherm. Here, the rate of the decomposition of zinc oxide is expected to be affected by the nitrogen pressure. In this expectation the present work was carried out.

## Experimental

The apparatus is the same as that used in a previous work[6] on the reduction of zinc oxide by hydrogen by a flow method at low pressures. In this work, oxygen or nitrogen was used as the flowing gas instead of hydrogen. The samples used in this work are that used in our previous papers[1,3-6] and a sintered one. The former is a commercial product supplied by the Sakai Chemicals Co., Ltd., while the latter is prepared from the former by sintering it at 900°C for several hours and then sieving it (−40+60 mesh). The decomposition time was 200 min. In this period, the amount of decomposed zinc oxide was very small compared with its initial amount, and the change of its surface area by decomposition was negligibly small. Hence, the rate of decomposition can be expressed as $\Delta w/w_0 t$, where $\Delta w$ is the total weight loss for the decomposition time, $w_0$ is the initial amount, and $t$ is the decomposition time.

1) T. Imoto, Y. Harano and Y. Nishi, This Bulletin, 37, 1181 (1964).
2) W. J. Moore and E. L. Williams, *J. Phys. Chem.*, 63, 1516 (1959).
3) T. Imoto, Y. Harano and Y. Nishi, *J. Chem. Soc. Japan, Pure Chem. Sec.* (*Nippon Kagaku Zasshi*), 84, 115 (1963).
4) T. Imoto, Y. Harano, Y. Nishi and S. Masuda, ibid., 85, 106 (1964).
5) T. Imoto, Y. Harano, Y. Nishi and S. Masuda, This Bulletin, 37, 441 (1964).
6) T. Imoto, Y. Harano and Y. Nishi, *J. Chem. Soc. Japan, Pure Chem. Sec.* (*Nippon Kagaku Zasshi*), 86, 485 (1965).

## Results and Discussion

Experimental results at 740°C are shown in Fig. 1. The ordinate is the rate of decomposition, and the abscissa is the pressures of oxygen or nitrogen.

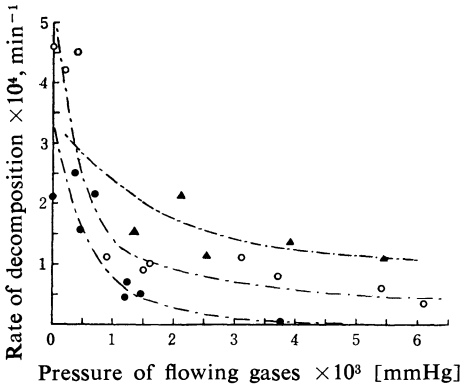



Fig. 1.
○·····unsintered ZnO
● ▲···sintered ZnO
$O_2$ $N_2$

**The Effect of Oxygen.**—Figure 1 shows that the rate of decomposition decreases with the increase in oxygen pressure, while the effect of oxygen is much greater than that of nitrogen. No sintered zinc oxide decomposed at about $10^{-2}$ mmHg of oxygen pressure, a level which is nearly equal to the decomposition equilibrium pressure at 740°C. These observations clealy reveal that oxygen in the gas phase retards the evolution of oxygen from the surface of zinc oxide. This is quite reasonable, since the higher oxygen pressure means a higher oxygen concentration in the vicinity of the zinc oxide surface.

**The Effect of Nitrogen.**—Figure 1 shows that the rate of decomposition also decreases with the increase in nitrogen pressure. The results obtained are applied to Eq. 1. From Eq. 1, one gets:

$$\theta_{N_2}=1-\frac{r_{N_2}}{r_{N_2=0}} \tag{2}$$

were $r_{N_2=0}$ is the rate of decomposition in vacuo, and $r_{N_2}$ is that in the nitrogen stream. Now, $\theta_{N_2}$ will be expressed by Eq. 3:[4]

$$\theta_{N_2}=\frac{K_{N_2}P_{N_2}}{1+K_{N_2}P_{N_2}}=1-\frac{1}{1+K_{N_2}P_{N_2}} \tag{3}$$

The combination of Eqs. 2 and 3 gives:

$$\frac{r_{N_2}}{r_{N_2=0}}=\frac{1}{1+K_{N2}P_{N_2}} \quad \text{or} \quad \frac{r_{N_2=0}}{r_{N_2}}=1+K_{N_2}P_{N_2} \tag{4}$$

When we substitute experimental values into Ep. 4, $K_{N_2}$ is calculated to be 533 $mmHg^{-1}$. This value is in fairly good areement with that of a previous paper[4] ($K_{N_2}=657$ $mmHg^{-1}$). In both cases the same sintered samples were used. The reactivity of zinc oxide depends very much on the nature of the surface state of the samples. It seems that the fluctuation in the experimental values and the difference between the two values for $K_{N_2}$ may originate in the variation in the surface state of zinc oxide. These results seem to verify our previous deduction that nitrogen interacts with the surface of zinc oxide to produce a retarding substance. At present, we have very little information about the nature of this retarding substance.

*Department of Applied Chemistry*
*Faculty of Engineering*
*Osaka City University*
*Sumiyoshi-ku, Osaka*

# Recoil Reactions in the Irradiated Tris-(ethylenediamine)-cobalt(III) Complexes

By Nobufusa SAITO, Takeshi TOMINAGA and Hirotoshi SANO*

(Received December 25, 1964)

It was previously reported[1] that the outer anions might play an important role in the radiocobalt recoil reactions in the neutron-irradiated hexammine- and aquopentammine cobalt(III) complexes. For the purpose of confirming such effects of outer anions, the present authors have investigated a similar system, a group of tris-(ethylenediamine)-cobalt(III) complexes containing various outer anions, of which only the nitrate and bromide have been studied before.[2-4]

The five kinds of complex compounds listed in Table I were irradiated with slow neutrons in JRR-1 reactor for 1 hr. at pile temperature in the presence of air. The neutron flux was estimated to be approximately $3\times10^{11}$ n/cm$^2$·sec. After it had been stored in dry ice for one to three days, the irradiated salt was dissolved in distilled water and the $^{60}$Co-labeled species present in the aqueous solutions were separated by means of paper electrophoresis, ion-exchange, precipitation, or recrystallization. The results are summarized in Table I. The dependence of the retention value and of the *S*-value** of the tris-(ethylenediamine)-cobalt complexes upon the stability as ligands of the outer anions are shown in Figs. 1 and 2 respectively. For convenience of discussion, the retention value and the *S*-value for hexammine- and aquopentammine-cobalt(III) complexes[1] are also shown together.

As may be seen in Fig. 1, the retention in the three systems generally tends to increase with a decrease in the stability of the outer anion as a ligand. Namely, the restoration of parent chemical forms may be more favored in the salt containing less stable outer anions. Figure 2 indicates that the *S*-value in the three systems increases in almost the same

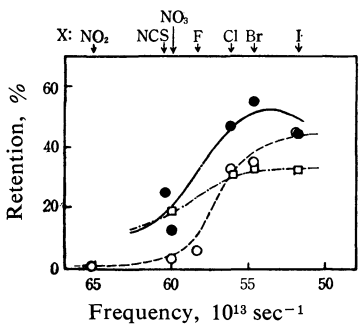



Fig. 1. The relationship between retention and frequency of the maximum in the first absorption band of $Co(NH_3)_5X$.
—●— $[Co(en)_3]X_3$
--○-- $[Co(NH_3)_6]X_3$
-·□-· $[Co(NH_3)_5H_2O]X_3$

TABLE I. PERCENTAGE DISTRIBUTION OF $^{60}$Co-LABELED SPECIES IN THE IRRADIATED TRIS-(ETHYLENEDIAMINE)-COBALT(III) COMPLEXES

| Target | $^{60}$Co-labeled species, %*1 | | | | | | |
|---|---|---|---|---|---|---|---|
| | $Co\,en_3^{3+}$ *2 | $Co\,en_2a_2^{3+}$ | $Co\,en_2aX^{2+}$ | $Co\,en_2X_2^{+}$ | $Co^{2+}$ | Neutral species | Anionic species |
| $[Co(en)_3](NCS)_3$ | 24.8 | 2.5 | 2.9 | 1.4 | 53.9 | 3.8 | 13.0*3 |
| $[Co(en)_3](NO_3)_3$ | 12.2 | 6.0 | 7.0 | 1.4 | 69.4 | 1.8 | 1.4 |
| $[Co(en)_3]Cl_3\cdot3H_2O$ | 47.3 | 13.8 | 10.7 | 1.8 | 23.7 | 1.3 | 0.1 |
| $[Co(en)_3]Br_3\cdot3H_2O$ | 55.0 | 10.0 | 4.5 | 0.9 | 28.8 | 1.3 | 0.5 |
| $[Co(en)_3]I_3\cdot H_2O$ | 44.0 | 4.0 | 7.7 | 1.1 | 41.1 | 0.3 | — |

*1 a=$H_2O$
*2 Retention, or labeled chemical species (%) identical with the target.
*3 Attributed to some unidentified $^{60}$Co-labeled anionic species.

* Present address: Ochanomizu University, Bunkyo-ku, Tokyo.

1) N. Saito, T. Tominaga and H. Sano, This Bulletin, **35**, 365 (1962); ibid., **36**, 230 (1963).
2) A. Zuber, USAEC Document NYO-6142 BNL (1954).
3) L. L. Williams, N. Sutin and J. M. Miller, *J. Inorg. & Nucl. Chem.*, **19**, 175 (1961).
4) T. Costea and I. Dema, *Nature*, **189**, 479 (1961).

** $S=\frac{\text{[Sum of percentages of } ^{60}\text{Co-labeled complexes containing more anionic ligands than the target]}}{\text{[Sum of percentages of all } ^{60}\text{Co-labeled complexes]}}$

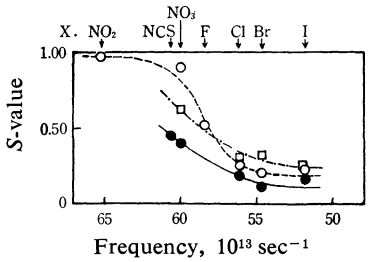



Fig. 2. The relationship between *S*-value and frequency of the maximum in the first absorption band of $Co(NH_3)_5X$.
—●— $[Co(en)_3]X_3$
--○-- $[Co(NH_3)_6]X_3$
-·□-· $[Co(NH_3)_5H_2O]X_3$

manner with the increasing stability of the outer anion as ligand, and thus the incorporation of outer anions into ligands seems to be more favored in the salt containing more stable outer anions. This dependence of the retention value and the *S*-value on the stability of the outer anion may be generally explained by assuming that the outer anions and ligand groups ($NH_3$, ethylenediamine, or $H_2O$ molecules), more or less ruptured as a result of recoil, compete with each other in the subsequent reactions, during which various $^{60}Co$-labeled complexes are formed through the reactions of recoil cobalt atoms with neighboring entities according to their concentrations and stabilities as complexed with cobalt.

*Department of Chemistry*
*Faculty of Science*
*The University of Tokyo*
*Hongo, Tokyo*

# The Oxidation of Red Phosphorus with Hydrogen Peroxide and the Isolation of Disodium Dihydrogen Hypophosphate

By Norimasa YOZA and Shigeru OHASHI

(Received January 16, 1965)

Hypophosphate has been prepared by the wet oxidation of elementary phosphorus with various oxidizing agents, i. e., hypochlorite,[1] chlorite,[2-5] bleaching powder,[6] copper nitrate,[7,8] permanganate,[9] iodine,[10] and hydrogen peroxide.[9,11]

Remy and Falius[4] pointed out that hypophosphate prepared by Vogel's method,[9] i. e., by oxidizing red phosphorus with hydrogen peroxide in a solution of sodium hydroxide, contained several oxo acids of phosphorus as impurities and that the further purification of it was very difficult. On the other hand, Dragulescu et al.[11] reported a method for the preparation of hypophosphate by the oxidation of red phosphorus with hydrogen peroxide in aqueous ammonia. In this case ammonium ions must be removed by passing the reaction products through ion exchange resin in order to isolate sodium hypophosphate.

The present work was undertaken in order to examine the oxidation products of red phosphorus with hydrogen peroxide in a solution of sodium carbonate or in a solution free from other electrolytes, and to isolate disodium dihydrogen hypophosphate by crystallization from a mixture of ethyl alcohol and water.

## Experimental

**The Preparation of Disodium Dihydrogen Hypophosphate.** — Ten grams of red phosphorus is suspended in 200 ml. of water (in a 1 l.-beaker), and then 30 ml. of a solution of hydrogen peroxide is added. After an hour 120 ml. more of the solution of hydrogen peroxide is added. (If 150 ml. of hydrogen peroxide is added at one time, a drastic reaction will occur.) The mixture is allowed to stand for 3 days at room temperature, after which

1) J. Probst, *Z. anorg. u. allgem. Chem.*, **179**, 155 (1929).
2) E. Leininger and T. Chuluski, *J. Am. Chem. Soc.*, **71**, 2385 (1949).
3) H. Remy and H. Falius, *Naturwissenschaften*, **43**, 177 (1956).
4) H. Remy and H. Falius, *Z. anorg. u. allgem. Chem.*, **306**, 211 (1960).
5) J. A. R. Genge, B. A. Nevette and J. E. Salmon, *Chem. & Ind.*, **1960**, 1079.
6) W. G. Palmer, *J. Chem. Soc.*, **1961**, 1079.
7) W. Jung, *Anales asoc. quim. argentina*, **30**, 99 (1942).
8) A. Rosenheim and J. Pinsker, *Ber.*, **43**, 2003 (1910).
9) F. Vogel, *Z. angew. Chem.*, **42**, 263 (1929).
10) T. Milobedzki, J. H. Kolitowska and J. Berkan, *Roczniki Chem.*, **17**, 620 (1937).
11) C. Dragulescu, M. Enache, and T. Simonescu, *Acad. Rep. Populare Romine, Baza Cercetari Stiint. Timisoara, Studdi Cercetari, Stinnte Chim.*, **10**, 23 (1963); *Chem. Abstr.*, **61**, 331 (1964).

time the small, unreacted portion of red phosphorus is filtered off with Toyo No. 5B filter paper. After the pH of the filtrate is adjusted to 4.5 with a solution of sodium hydroxide, a half volume of ethyl alcohol is added. The precipitate, almost free from other oxo acids of phosphorus, is recrystallized by the same procedure and dissolved in 400 ml. of water. (It may be warmed to accelerate the dissolution of the precipitate.) The solution is adjusted to pH 5.2 and filtered off, if necessary, to remove such insoluble hypophosphates as alkaline earth hypophosphates. Finally, disodium dihydrogen hypophosphate hexahydrate, $Na_2H_2P_2O_6 \cdot 6H_2O$, is recrystallized from 1 : 2 ethyl alcohol. The crystals are filtered off, washed with 1 : 2 ethyl alcohol, and air dried. The yield is about 23% on the basis of the weight of the red phosphorus used.

Large crystals are obtained by dissolving the salt in hot water (60°C) with subsequent cooling in a refrigerator overnight.

The chemical composition of the final product was confirmed to be $Na_2H_2P_2O_6 \cdot 6H_2O$ by the following methods: I) the qualitative identification by paper chromatography[12] and spectrophotometry (hypophosphoric heteropoly blue[13]); II) the release of hydrated water at 110°C; III) the determination of the hydrogen ions released by precipitation reaction with silver nitrate ($Ag_4P_2O_6$) and IV) the determination of the total phosphorus by gravimetry as $Mg_2P_2O_7$.

## Discussion

The known method of preparing hypophosphate from red phosphorus and hydrogen peroxide in a solution of sodium hydroxide is complicated because of the necessity of suppressing the rise in temperature due to the heat of the reaction. The present work was undertaken to overcome this disadvantage. The new method for the preparation of hypophosphate described in the Experimental section does not need any special cooling apparatus. As will be mentioned below, the reaction of red phosphorus with hydrogen peroxide in a solution of sodium carbonate has some disadvantages, i. e., the violent evolution of heat and the difficulty of the complete removal of by-products.

**The Reaction in a Solution of Sodium Carbonate.**—Hydrogen peroxide reacts with red phosphorus in a solution of sodium carbonate with the evolution of the heat of the reaction. The products obtained by the oxidation of 10 g. of red phosphorus with 150 ml. of 30% hydrogen peroxide in a solution of sodium carbonate (10 g. of $Na_2CO_3$ in 200 ml. of water) include at least six oxo acids of phosphrus. The $R_f$ values of the species on paper chromatogram correspond to phosphite, phosphate, diphoshate, hypophosphate, $\overset{5}{P}\text{-O-}\overset{4}{P}\text{-}\overset{4}{P}\text{-}$, and $\overset{4}{P}\text{-}\overset{3}{P}\text{-}\overset{4}{P}$-anions in the order of decreasing $R_f$. Some of them can be removed from hypophosphate by crystallization from 1 : 2 ethyl alcohol at pH 4.5. However, this procedure is not satisfactory in eliminating the phosphorus compounds with lower $R_f$ values than that of hypophosphate.

**The Reaction in a Neutral or Acid Solution.**—As has been described in the Experimental section, red phosporus is also oxidized with hydrogen peroxide in the absence of other electrolytes to form hypophosphate. The solution is neutral at the start of the reaction, while the acidity of the solution increases with the formation of oxo acids of phosphorus. The hypophosphate thus produced contains two components as impurities, i. e., phosphite and phosphate, which are easily removed from the hypophosphate by treatment with 1 : 2 ethyl alcohol at pH 4.5. The reaction under the conditions described in the Experimental section proceeds so slowly that it is not necessary to cool the reaction vessel.

*Department of Chemistry*
*Faculty of Science*
*Kyushu University*
*Hakozaki, Fukuoka*

12) E. Thilo and D. Heinz, *Z. anorg. u. allgem. Chem.*, **281**, 303 (1955).
13) N. Yoza and S. Ohashi, This Bulletin, **37**, 33 (1964).

# The Electrical Conduction of 10-Methylacridinium Polyiodides

By Shigekazu KUSABAYASHI and Hiroshi MIKAWA

(Received January 28, 1965)

In a previous paper,[1] it was indicated that the specific resistivities at 20°C and the band gap energies of organic polyiodides decrease with the number of iodine atoms in the polyiodide anion, not very much difference in these values being observed with different kinds of cations. It was also established that the iodine framework in the crystal structure is of primary importance in determining the electrical conductivity.

The present investigation has been made to find what influences, if any the size and shape of the cation has on the conduction.

**Preparation.**—*10-Methylacridinium Monoiodide.*—Monoiodide was prepared by the action of methyl iodide on acridine. The melting point agreed with the compound reported in the literature.[2]

*10-Methylacridinium Polyiodides.*—A hot solution of the required amount of iodine and 1.00 g. of monoiodide in 145 ml. of 99% alcohol was cooled to yield the product.

*10-Methylacridinium Triiodide.*—From 1.03 g. of iodine, 1.75 g. of triiodide was obtained. It was then recrystallized from the alcohol-tetrahydrofuran mixture. Dark brown crystals; m. p. 170°C.

Found: C, 28.35; H, 2.40; N, 3.07; I, 65.58. Calcd. for $C_{14}H_{12}NI_3$: C, 29.25; H, 2.10; N, 2.44; I, 66.21%.

*10-Methylacridinium Pentaiodide.*—The reaction of 2.85 g. of iodine gave 2.20 g. of pentaiodide. It was then recrystallized from the iodine-alcohol-tetrahydrofuran solution. Dark purple crystals, m. p. 94.5°C.

Found: C, 21.48; H, 1.92; N, 2.29; I, 74.40. Calcd. for $C_{14}H_{12}NI_5$. C, 20.29; H, 1.46; N, 1.69; I, 76.56%.

*10-Methylacridinium Heptaiodide.*—4.74 g. of iodine yielded 2.32 g. of heptaiodide. It was then recrystallized in the same way as pentaiodide. Dark green crystals; m. p. 86°C.

Found: C, 17.84; H, 1.51; N, 1.36; I, 79.51. Calcd. for $C_{14}H_{12}NI_7$: C, 15.53; H, 1.12; N, 1.29; I, 82.06%.

A drying of the crystal for analyses inevitably causes some loss of iodine, thus decreasing slightly the analytical iodine content.

**Absorption Spectra.**—The absorption spectra of 10-methylacridinium polyiodides are shown in Fig. 1. In a tetrahydrofuran solution all three spectra were nearly identical, except that

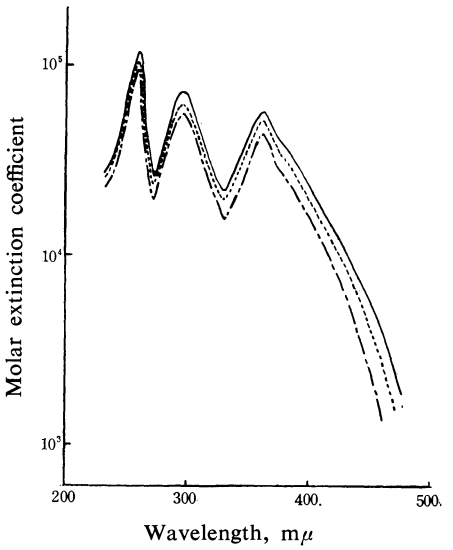



Fig. 1. Absorption spectra of 10-methylacridinium poyiodides in tetrahydrofuran.
— — — Triiodide ····· Pentaiodide
——— Heptaiodide

the molar extinction coefficicients were slighly different. The main peaks are at 259, 295 and 360 mμ. Subtracting from this absorption curve the absorption due to acridinium ion, which has main absorption peaks at 259 and 360 mμ, one obtains a curve with peaks at 295 and 360 mμ, peaks which conform fairly well with the absorption curves reported for the tetramethylammonium polyiodides in ethylene chloride[3] and several triiodides in various solvents.[4] Therefore, in the 10-methylacridinium polyiodides as well as in the tetramethylammonium polyiodides, these facts are consistent with the interpretation that the triiodide is the only polyiodide stable in a dilute solution.

The absorption spectra of the solid were also measured. However, the absorption band was very broad, extending over about a 500 mμ region from the ultraviolet region.

1) S. Kusabayashi, H. Mikawa, S. Kawai, M. Uchida and R. Kiriyama, This Bulletin, 37, 811 (1964).

2) A. I. Vogel, "A Text-Book of Practical Organic Chemistry," Longmans, Green and Co., London (1951), p. 634.

3) R. E. Buckles, J. P. Yuk and A. I. Popov, *J. Am. Chem. Soc.*, 74, 4379 (1952).

4) C. K. Tinkler, *J. Chem. Soc.*, 1908, 1611; F. L. Gilbert, R. R. Goldstein and T. M. Lowry, ibid., 1931, 1092; A. D. Awtrey and R. E. Connick, *J. Am. Chem. Soc.*, 73, 1842 (1951); A. I. Popov and R. E. Swensen, ibid., 77, 3724 (1955).

**Electrical Conduction.**—The electrical resistivity was measured on a compressed disk of crystalline powder by the DC method. The apparatus and method were the same as have been described previously.

The relation between the current and the applied voltage obeyed Ohm's law up to 2000 V./cm. at least.

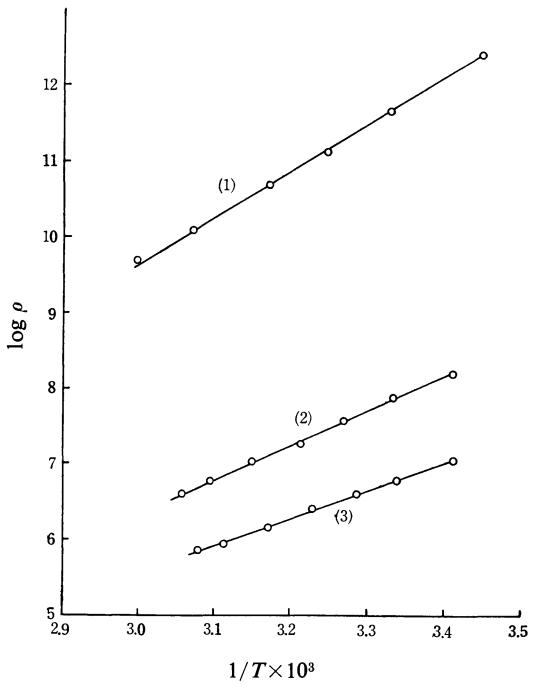



Fig. 2. Temperature dependence of the resistivity of 10-methylacridinium polyiodides.
(1) Triiodide (2) Pentaiodide
(3) Heptaiodide

The relationship between the logarithm of resistivity and the reciprocal of temperature is shown in Fig. 2. The specific resistivity at 20°C ($\rho_{20}$) and the band-gap energy ($\varepsilon$), as calculated from the temperature dependence of the resistivity by the equation $\rho = \rho_0 \exp(\varepsilon/2kT)$, are tabulated in Table I.

The values of $\rho_{20}$ and $\varepsilon$ decrease with an increase in the number of iodine atoms. This is similar to the previous finding. However, generally the present values of $\rho_{20}$ and $\varepsilon$ are larger than those reported for other polyiodides.

Table I. Electrical properties of 10-methylacridinium polyiodides

| Substance | $\rho_{20}$ Ω cm. | $\varepsilon$ eV. | Temp. range °C |
|---|---|---|---|
| Triiodide | $1.6\times10^{12}$ | 2.49 | 17—60 |
| Pentaiodide | $1.5\times10^{8}$ | 1.72 | 20—55 |
| Heptaiodide | $1.2\times10^{7}$ | 1.47 | 20—52 |

The size of the acridinium cation is the largest of all the polyiodides investigated. Therefore, it is possible that the iodine framework is deformed by the size and shape of the cation and that the shortest distance between anions is larger than those of other polyiodides. As has been shown in the previous paper, the shortest distances between neighboring polyiodide anions of the known crystal structures decrease with an increase in the number of the iodine atoms of polyiodide anions. In so far as the electrical conduction is effected through the overlap of the molecular orbitals of polyiodide anions, it is understandable that the values of $\rho_{20}$ and $\varepsilon$ are larger than those reported for other polyiodides.

On the basis of the present and previous papers, it is certain that the iodine framework in the crystal structure is of primary importance in determining the electrical conductivity; the theory has obtained an additional confirmation in the present paper's finding that the size of the cation increases the deformation of the iodine framework and, as expected, influences the electrical properties.

The authors wish to express their thanks to Professor Ryôiti Kiriyama and Dr. Shichio Kawai for their helpful advice, and to Mr. Takuzo Fujino and Mr. Tsuneyo Shishido for their elementary analyses.

*The Institute of Scientific and Industrial Research*
*Osaka University*
*Sakai, Osaka*

SHORT COMMUNICATIONS

# A New Method for Releasing Oxytocin from Fully-protected Nona-peptides Using Anhydrous Hydrogen Fluoride

By Shumpei SAKAKIBARA and Yasutsugu SHIMONISHI

(Received April 23, 1965)

Methods of the synthesis of oxytocin[1] are generally based on the principle that the *S*-benzyl group is stable against hydrogen bromide or trifluoroacetic acid and can only be removed by treatment with sodium in liquid ammonia. This procedure, however, has several defects; for instance, the product is inevitably contaminated with sodium salts, and it may be partially decomposed by the strong alkali used during the procedure. The *S*-*p*-methoxybenzyl group is also stable against hydrogen bromide, but it can be removed by boiling trifluoroacetic acid in contrast with the *S*-benzyl group.[2] However, it has been shown[3] that it is more difficult to remove, with trifluoroacetic acid, the *S*-methoxybenzyl group in a large peptide such as oxytocin than that in a small peptide. Therefore, a more effective method for the removal of these protecting groups is required. Katz[4] first showed that anhydrous hydrogen fluoride (HF) is a good solvent for proteins, and that the biological activity of proteins is not irreversibly affected by this solvent. Moreover, anhydrous HF is known to be a very strong acid, although it becomes a weak acid in the presence of water.[5] These facts were effectively utilized by Hess et al.[6] in an *N*, *O*-acyl migration reaction with serine or threonine peptides. The above-mentioned facts also suggested that this solvent might be an effective reagent for the acidolysis of various protecting groups. The boiling point of the solvent (19.5°C) was also considered to give it an additional advantage. The basic idea of the present project arose from these considerations.

First, cysteine formation from *S*-benzylcysteine and from *S*-*p*-methoxybenzylcysteine in anhydrous HF was tested by iodometry, and the quantitative removal of the protecting groups was observed during one-hour reactions at room temperature in both cases. These experiments indicated clearly, as expected, that anhydrous HF is the first effective reagent for the acidolysis of *S*-benzyl groups. Then, the pre-oxytocin nona-peptides, *N*-carbobenzyloxy-*S*-benzyl-L-cysteinyl-L-tyrosyl-L-isoleucyl-L-glutaminyl-L-asparaginyl-*S*-benzyl-L-cysteinyl-L-prolyl-L-leucylglycine amide (I)[1] and the *N*-carbobenzyloxy-*S*-*p*-methoxybenzylpeptide of the same sequence (II),[3] were each subjected to the HF reaction under the same conditions. The addition of anisole to the reaction mixture effectively prevented the succeeding polymerization of the benzyl fluoride which may be formed in the solution; it also protected the tyrosyl residue from possible modification by benzyl fluoride. After the peptides had been oxidized by air to cystinyl peptides, the hormonal activities of the resulting products were determined by the rat-uterine contraction test; 133 units per mg. of I and 148 units per mg. of II were observed (about 370 units per mg. would correspond to quantitative recovery),[7] whereas the acidolysis of II with trifluoroacetic acid gave only 33 units per mg.[3]

Further possibilities for the use of HF in general peptide synthesis are being studied.

**Experimental.**—*Reaction in Anhydrous HF.*—The procedure was, in principle, the same as that for the *N*, *O*-acyl migration reaction in HF.[6] Compound I or II was dried over phosphorous pentoxide in vacuo at 80°C for 3 hr. before the reaction. The dried material (50

1) Of. M. Bodanszky and V. du Vigneaud, *J. Am. Chem. Soc.*, **81**, 5688 (1959).
2) S. Akabori, S. Sakakibara, Y. Shimonishi and Y. Nobuhara, This Bulletin, **37**, 433 (1964).
3) S. Sakakibara, Y. Nobuhara, Y. Shimonishi and R. Kiyoi, ibid., **38**, 120 (1965).
4) J. J. Katz, *Arch. Biochem. Biophys.*, **51**, 293 (1954).
5) J. H. Simons, "Fluorine Chemistry," Vol. I, Academic Press, New York (1950), p. 225.
6) S. Sakakibara, K. H. Shin and G. P. Hess, *J. Am. Chem. Soc.*, **84**, 4921 (1962); J. Lenard and G. P. Hess, *J. Biol. Chem.*, **239**, 3275 (1964).

7) The authors wish to express their thanks to Dr. Keiji Nakamura of the Dai Nippon Pharmaceutical Co. for determining the oxytocic activities.

mg.) was placed in the reaction vessel, together with anisole (0.1 ml.); anhydrous HF (ca. 2 ml.) was then distilled into the mixture, which was then kept for one hr. at room temperature before the solvent was removed by distillation. The remaining HF was completely removed by letting the material stand over sodium hydroxide in vacuo, and the residue was dissolved in water (50 ml.). The solution was adjusted to pH 6.5 by adding dilute ammonia, and then carbon dioxide-free air was bubbled through the solution for about 2 hr. until the nitroprusside test became negative. Then the oxidized solution was brought to pH 4 with acetic acid, and the insoluble materials formed were removed by filtration. An aliquot of this filtrate was subjected to the biological test.

*Peptide Center*
*Institute for Protein Research*
*Osaka University*
*Kita-ku, Osaka*

# Fluorescence Properties of Europium-trisbenzoylacetonate in a Chloroform Solution

By Takeshi MATSUO

(Received May 13, 1965)

There has been much interest in the fluorescence properties of europium chelates from the standpoint of the use of these compounds as laser devices.[1-3] However, it is very difficult to obtain a laser action by using these compounds in the form of a liquid or a fluid solution, because such organic laser materials as europium-trisbenzoylacetonate ($EuB_3$) have poor spectroscopic properties in organic solvents; in such cases the half-width of their fluorescence line becomes broader, the intensity of the fluorsesecence line becomes weaker, and the fluorescence decay time becomes shorter than the corresponding values of $EuB_3$ in the crystalline state.

Recently we found that the fluorescence decay time of $EuB_3$ in a chloroform solution was about twice as strong, and its fluorescence intensity stronger than those of $EuB_3$ in a methanol solution.

The chelate compound used here was prepared by adding an equivalent base and then an alcohol solution of $EuCl_3 \cdot 6H_2O$ to a solution of the benzoylacetone. The white-yellow precipitation was collected with suction, washed several times with alcohol, and then dried under 1 mmHg pressure for 20 hr. Found: C, 57.40; H, 4.16. Calcd. C, 56.60; H, 4.25%. The measurement of the fluorescence decay time constant was performed as follows. A xenon flash lamp with a 10 $\mu$ sec. pulse duration was used to excite the sample, and the decay curve was recorded with an oscilloscope. The spectral properties of the fluorescence of the $EuB_3$ solid and of the solutions were

TABLE I. OBSERVED FLUORESCENCE PROPERTIES OF $EuB_3$ IN VARIOUS STATES

| Matrix or state | Decay time in $\mu$sec. at 300°K | Spectral region in m$\mu$ | Relative fluorescent intensity | Half-value width Å |
|---|---|---|---|---|
| Chloroform | 314±10 | total* | strong | 44 |
| Methanol | 164±10 | total | moderate | 60 |
| PMMA | 250±10 | total | strong | 65 |
| Microcrystalline | 440±10 | 613 | strong | 20 |

* Measured spectral region for the decay time constant.

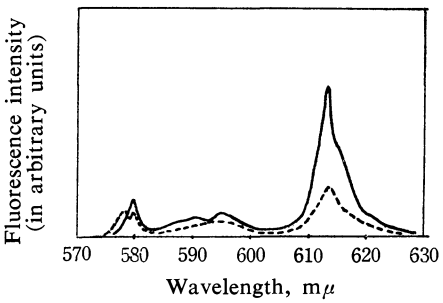



Fig. 1. Fluorescence spectra of $EuB_3$ at 300°K in chloroform solution (perfect line) and in methanol solution (dotted line)

1) A. Lempicki and H. Samelson, *Phys. Letters*, 4, 133 (1963).
2) E. J. Schimitscek, *Appl. Phys. Letters*, 3, 117 (1963).
3) A. Lempicki, H. Samelson and C. Brecher, *J. Chem. Phys.*, 41, 1214 (1964).

measured with a Cary model 14 spectrophotometer.

The observed spectroscopic properties of $EuB_3$ in a chloroform solution are, in Table I and Fig. 1, compared with those of various other matrices.

It is highly probable, judging from the results of the investigation of these spectroscopic properties, that chloroform interacts with $EuB_3$, perhaps through something like hydrogen bonding, and that the co-ordinated $Eu^{3+}$ ion in the complex is protected from external perturbation.

The details of this study will be reported in a later paper.

*Department of Chemistry*
*Central Research Laboratory*
*Tokyo Shibaura Electric Co., Ltd.*
*Kawasaki-shi, Kanagawa*

# The Adsorbed State of Oxygen on Zinc Oxide as Revealed by the Electron Spin Resonance Method

By Morio SEDAKA and Takao KWAN

(Received May 18, 1965)

The asymmetrical doublet ESR signal around $g=2.0$ obtained when a small amount of oxygen is introduced on zinc oxide has been ascribed to the adsorbed peroxy radical or to the molecular oxygen ion by several workers.[1] None of them has, however, dealt with the dynamical characteristic of this signal. It is known from the simple temperature rising method that adsorbed oxygen on zinc oxide at room temperature is transformed into at least two types, near 200 and 370°C, when subjected to gradual heating up to 500°C.[2] Such changes in the adsorbed type has now been investigated by the ESR method. It has been found that the doublet signal is transformed into a singlet one above 170°C and that it decays at much higher temperatures.

The sample tube for the ESR measurement was connected, by means of several flexible joints, to a high vacuum apparatus. The Pirani gauge was affixed close to the tube so that the pressure of the oxygen inside could be measured during the ESR measurement. A sample of zinc oxide placed in the tube was outgassed at 500°C for one hour, and then oxygen ($10^{-1}$ mmHg) was introduced onto the adsorbent kept at room temperature. After having been shortly pumped off, the sample was heated at a rate of about 10°C per min.; changes in the doublet signal due to heating were followed in situ, while the pressure inside

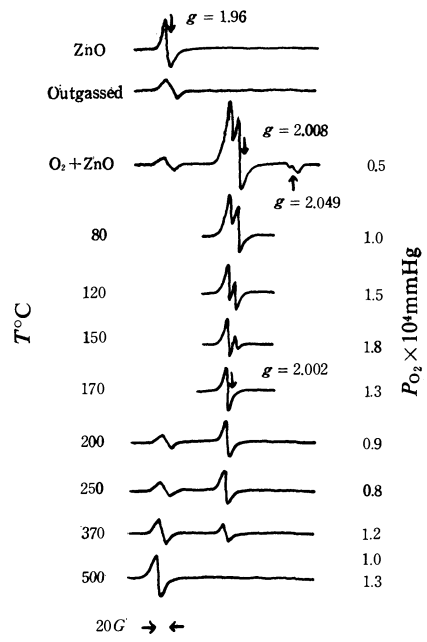



Fig. 1. ESR Spectra for $O_2$ on ZnO. The spectra were observed at the temperature shown by the respective figure on the left, except for those of the upper three and the last three, which were determined at room temperature. The pressure of oxygen inside the tube, as shown by the figure on the right, ranges from $0.5\times10^{-4}$ to $2\times10^{-4}$ mmHg.

1) E. V. Baranov, V. E. Kholmagorov and A. N. Terenin, *Dokl. Acad. Nauk SSSR*, **146**, 125 (1962); Y. Fujita and T. Kwan, *Shokubai (Catalyst)*, **5**, 206 (1963); R. J. Kokes, *Proceedings of The Third International Congress on Catalysis*, North-Holland Pub. Co., Amsterdam (1965), p. 484.

2) M. Sedaka, N. Dokoshi, Y. Fujita and T. Kwan, presented at the 18th Annual Meeting of the Chemical Seciety of Japan, April, 1965. Cf. T. Kwan, "Hikari-kagaku to sono Oyo" Kagaku-Dojin, Kyoto (1965), p. 109.

the tube was being measured simultaneously. The ESR measuement was made with a JEOL-type P-10 spectrometer at the X band. The signals obtained, along with the heat treatment, are shown in Fig. 1.

Here we shall confine ourselves only to the change in the doublet signal at $g=2.008$, 2.002. The transition of the doublet to a singlet at $g=2.002$ is apparent. It took place near 170°C when the second type of adsorption* set in, as judged from the pressure change. This singlet was stable for a time beyond 250°C, but it appeared to decay near 370°C. The decay seemed to be associated with the appearance of the third type of adsorption.**

A singlet signal of the same $g$-value and of the same shape as that mentioned above was found to appear even when $N_2O$ was introduced onto the outgassed zinc oxide sample at room temperature. Thus, it seems very likely that the transition of the doublet to the singlet is due to the dissociation of the molecular oxygen ion into atomic species as $O^-$.

*Devision of Physicochemical Technology*
*Faculty of Pharmaceutical Sciences*
*The University of Tokyo*
*Hongo, Tokyo*

* By the first type will be meant the oxygen adsorbed at room temperature.

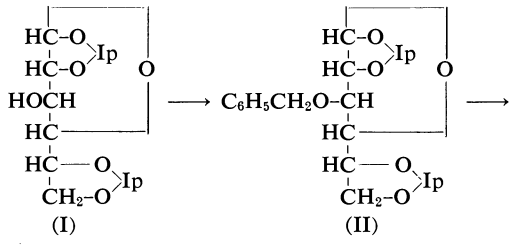
** The third type is most probably $O^{2-}$, which is non-paramagnetic. Thus, the appearance of this type may mean the recovery of the original zinc oxide; this suggestion agrees with the resemblance of the ESR spectra between the initial and the final state.

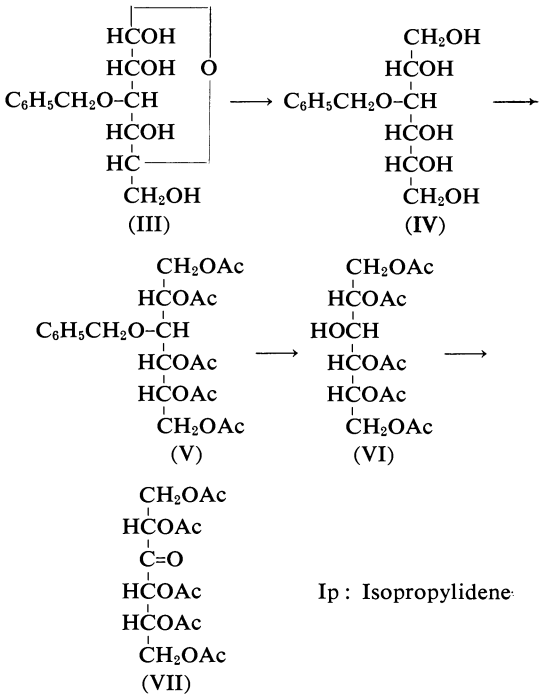
# Studies on the Chemical Decomposition of Simple Sugars. XVIII. The Synthesis of D-*ribo*-3-Hexulose Pentaacetate*

By Akira SERA and Ryozo GOTO

(Received May 20, 1965)

Although some 3-hexuloses have been synthesized,[1-3] their chemical properties have been received only limited attention. In the mechanism posturated by Hayami[4] for the acetol formation from monosaccharides in a concentrated phosphate buffer solution, 3-hexulose might play an important role as an intermediate. However, there has been no unequivocal experimental evidence. In the present paper, a synthesis of D-*ribo*-3-hexulose pentaacetate, a new 3-hexulose derivative, and its rapid conversion to acetol in a phosphate buffer solution will be described.




The treatment of diacetone-D-glucose (I) with sodium hydride and benzyl bromide in

* Presented at the 18th Annual Meeting of the Chemical Society of Japan, Osaka, April, 1965.

1) J. K. N. Jones, *J. Am. Chem. Soc.*, **78**, 2855 (1956).
2) J. M. Sugihara and G. U. Yuen, ibid., **79**, 5780 (1957).
3) G. U. Yuen and J. M. Sugihara, *J. Org. Chem.*, **26**, 1598 (1961).
4) J. Hayami, This Bulletin, **34**, 927 (1961).

ether gave 3-*O*-benzyl-1,2; 5,6-di-*O*-isopropylidene-D-glucofuranose (II).[5,6] The hydrolysis of II with sulfuric acid in aqueous methanol yielded 3-*O*-benzyl-D-glucopyranose (III),[6] 38%, m. p. 141.5—142.5°C. Compound III consumed 1.01 mol. of sodium metaperiodate per mole of substrate. The sodium borohydride reduction of III in water gave a thick syrup of 3-*O*-benzyl-D-sorbitol (IV) which, on acetylation with acetic anhydride and pyridine, gave a syrupy 3-*O*-benzyl-D-sorbitol pentaacetate (V) in a 83% yield. The removal of the benzyl group of V by catalytic hydrogenolysis with palladium black in acetic acid gave 1,2,4,5,6-penta-*O*-acetyl-D-sorbitol (VI) quantitatively as a slightly yellow syrup, b. p. 164—167°C/0.1 mmHg, $[\alpha]_D^{10}+8.2°$ (ethanol), $\nu_{OH}$ 3550 $cm^{-1}$. Found: C, 49.01; H, 6.10. Calcd. for $C_{16}H_{24}O_{11}$: C, 48.98, H, 6.17%. D-*ribo*-3-Hexulose 1,2,4,5,6-pentaacetate (VII) was obtained by the chromium trioxide oxidation of VI in acetic acid, 54%; pale yellow syrup, b. p. 138—139°C/0.05 mmHg, $[\alpha]_D^{10}-18.2°$ (ethanol), $\nu_{C=O}$ 1756 $cm^{-1}$, $\lambda_{max}$ 273 m$\mu$, $\varepsilon_{max}$ 109 (ethanol). Found: C, 49.11; H, 5.91. Calcd. for $C_{16}H_{22}O_{11}$: C, 49.23; H, 5.68%.

The treatment of VII with a concentrated phosphate buffer solution (pH 9.0) gave an acetol more quickly than when D-glucose or $\beta$-D-glucose pentaacetate was used. This behavior of the 3-hexulose derivative might prove that 3-hexulose or its ene-diolate ion is an intermediate in an acetol formation from monosaccharides; it might also support the mechanism proposed by Hayami.[4] Further investigations are in progress, and additional details will be published later.

*Department of Chemistry*
*Faculty of Science*
*Kyoto University*
*Sakyo-ku, Kyoto*

5) A. S. Meyer and T. Reichstein, *Helv. Chim. Acta*, **29**, 152 (1946).
6) K. Freudenberg et al., *Chem. Ber.*, **58**, 666 (1925).

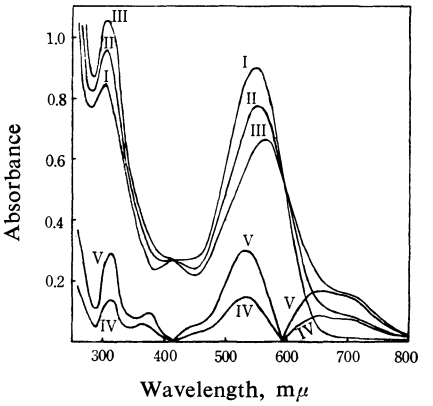
# A New Spectrophotometric Method for the Determination of Copper(II) with Calcichrome

By Hajime Ishii and Hisahiko Einaga

(Received June 8, 1965)

A new spectrophotometric method for the determination of trace of copper(II) has been developed. It is based upon the formation of a stable bluish-violet copper(II) complex of Calcichrome, which had been reported by some investigators[1-5] to be a reagent for the determination of calcium.

The absorption spectra of the complex are shown in Fig. 1. The complex spectrum has three absorption maxima with reference to the reagent blank in the visible ($\lambda_{max}$ 535 and 650 m$\mu$) and ultraviolet regions ($\lambda_{max}$ 310 m$\mu$), and also two isosbestic points, at 415 and 595 m$\mu$, in the pH range from 3 to 10. As may




Absorption spectra of Cu(II)-Calcichrome complex.

Calcichrome: $4\times10^{-5}$ mol./l., pH: 5. I; Cu 0, II; Cu : $C_{ch}$ 1 : 2, III; Cu : $C_{ch}$ 1 : 1, IV; Difference between I and II, V; Difference between I and III.

1) R. A. Close and T. S. West, *Talanta*, **5**, 221 (1960).
2) A. M. Lukin, K. A. Smirnova and G. B. Zavarikhina, *J. Anal. Chem. (USSR)*, **18**, 389 (1963).
3) M. H.-Lancina and T. S. West, *Anal. Chem.*, **35**, 2131 (1963).
4) P. Pakalns and T. M. Florence, *Anal. Chim. Acta*, **30**, 353 (1964).
5) H. Ishii and H. Einaga, *Japan Analyst (Bunseki Kagaku)*, **14**, 162 (1965).

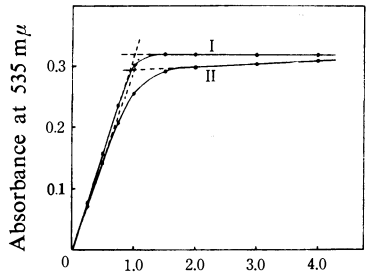



Fig. 2. Determination of mole ratio of Cu(II)-Calcichrome complex by the method of molar ratio.
Calcichrome: $4\times10^{-5}$ mol./1.
I; pH 5, II: pH 4

be seen in Fig. 2, the composition of the complex is 1 to 1. At 535 mμ, the concentration range in which copper(II) obeyed Beer's law is dependent upon the concentration of Calcichrome; for instance, up to 3.5 p. p. m. of copper(II), the law is obeyed when the concentration of Calcichrome is $6\times10^{-5}$ mol. The molar extinction coefficient is about $8\times10^{3}$, and the sensitivity is 0.008 μg. Cu/cm$^2$, which corresponds to $\log I_0/I=0.001$. At 310 mμ, similar results were obtained. The proposed procedure for the determination is as follows. To a sample solution containing copper(II) in a 50 ml. volumetric flask, 5.0 ml. of a Calcichrome solution ($6\times10^{-4}$ mol./1.) and 5 mol. of a sodium acetate - acetic acid buffer solution (pH 5) are added. After the solution has been diluted to the mark with distilled water, the absorbance of the solution is measured at 535 or 310 mμ with reference to a reagent blank solution. The full color develops instantaneously and is very stable. Copper(I) is also found to behave as copper-(II). Some metals, such as vanadium, nickel, and hydroxy group metals, interfere under the conditions proposed.

Further, detailed studies are now in progress.

*Central Research Laboratory*
*Onoda Cement Co., Ltd.*
*Koto-ku, Tokyo*

# Faraday Rotation for the Hydrogen Molecule

By Yasumasa I'HAYA

(Received June 11, 1965; in revised form July 17, 1965)

Quantum mechanical theories of the magneto-optical rotation in polyatomic molecules have been developed by Kronig,[1] Serber,[2] Carroll,[3] and Groenewege.[4] Recently we included the contribution of the induced magnetic moment and of the perturbed Boltzmann factors and, using a time-dependent second-order perturbation theory, derived a general formula for the Faraday effect of diamagnetic molecules.[5] The Verdet constant, which is the rotation per gauss per cm., is shown to be temperature-dependent for polyatomic molecules of any symmetry, but temperature-independent for diamagnetic diatomic molecules (no paramagnetic rotation).

If we consider states of up to 3d, the molecular wave function in the hydrogen molecule is $(1s\sigma)^2$ for the ground state and $(1s\sigma)(2p\pi)$, $(1s\sigma)(3p\pi)$, $(1s\sigma)(4p\sigma)$ for the excited state. These are:

$$(1s\sigma)^2 : N=N_1[s_a(1)+s_b(1)]\ [s_a(2)+s_b(2)]$$

$$(1s\sigma)(2p\pi) : \Pi=N_2[s_a(1)+s_b(1)]\ [\pi_a(2)+\pi_b(2)]$$

$$(1s\sigma)(3p\pi) : \Pi'=N_3[s_a(1)+s_b(1)]\ [\pi'_a(2)+\pi'_b(2)]$$

$$(1s\sigma)(4p\sigma) : \Sigma=N_4[s_a(1)+s_b(1)]\ [\sigma_a(2)+\sigma_b(2)]$$

where $N_i$ is the normalization constant and where $s_i$, $\sigma_i$, $\pi_i$, and $\pi'_i$ are the complex normalized hydrogenic atomic orbitals of 1s, $2p_0$, $2p_+$, and $3p_+$ respectively. The other elements do not contribute to the theoretical expression for the Verdet constant because of their symmetry.

With these molecular orbitals, the Verdet constant may be expressed as:

1) R. de L. Kronig, *Z. Physik*, **45**, 458, 508 (1927).
2) R. Serber, *Phys. Rev.*, **41**, 489 (1932).
3) T. Carroll, ibid., **52**, 822 (1937).
4) M. P. Groenewege, *Mol. Phys.*, **5**, 541 (1962).
5) Y. I'Haya, to be published.

$$V=\frac{4\pi e^3 N\nu^2}{3hmc^2 i}\left[\frac{1}{\nu_4}\left(\frac{1}{\nu_1^2-\nu^2}-\frac{1}{\nu_3^2-\nu^2}\right)\times i\langle N|x|\Pi\rangle\langle\Pi\left|z\frac{\partial}{\partial x}-x\frac{\partial}{\partial z}\right|\Sigma\rangle\langle\Sigma|z|N\rangle+\frac{\nu_1^2}{(\nu_1^2-\nu^2)^2}\langle\Pi\left|x\frac{\partial}{\partial y}-y\frac{\partial}{\partial x}\right|\Pi\rangle\left|\langle N|x|\Pi\rangle\right|^2+\frac{2\nu_2^2}{(\nu_2^2-\nu^2)^2}\langle\Pi'\left|x\frac{\partial}{\partial y}-y\frac{\partial}{\partial x}\right|\Pi'\rangle\left|\langle N|x|\Pi'\rangle\right|^2\right] \quad (1)$$

$e$, $m$, $h$, and $c$ being the usual notations and $N$, the number of molecules per unit volume ($N=0.2686\times10^{20}\,\mathrm{cm}^{-3}$ at 0°C, 1 atm.). Here $\nu_i$ is the energy difference between the states measured in units of reciprocal seconds, as is shown in Fig. 1. Their observed values are[6]: $\nu_1=2.999249$, $\nu_2=3.414317$, $\nu_3=3.447654$ (estimated), and $\nu_4=0.448405$, all expressed in units of $10^{15}\,\mathrm{sec}^{-1}$. The matrix elements which appear in Eq. 1 are calculated using elliptical coordinates, the internuclear distance in $H_2$ being assumed to be 1.40 a.u. When the frequency of the incident light, $\nu$, is $0.519027\times10^{15}\,\mathrm{sec}^{-1}$ (5780A), the Verdet constant is calculated to be 3.140 $\mu$min. (microminutes) per oe.-cm.-atm.

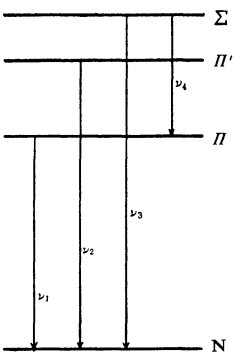



Fig. 1. Molecular electronic states in $H_2$, which contribute to the Faraday rotation.

The corresponding experimental value reported by Ingersoll and Liebenberg is 6.269 $\mu$min. per oe.-cm.-atm.[7] We cannot judge at this stage whether the many other excited states, $4p\pi$, $5p\pi$, and so on, contribute strongly. Further studies are, therefore, now in progress with more elaborate excited-state wave functions; the results will be published elsewhere.

*Department of Materials Science*
*The University of Electro-Communications*
*Chofu-shi, Tokyo*

6) G. Herzberg, "Spectra of Diatomic Molecules," Van Nostrand, New York (1950), p. 531.

7) L. R. Ingersoll and D. H. Libenberg, *J. Opt. Soc. Am.*, **46**, 538 (1956).

# The Absorption Spectra of Naphthalene Sulfonic Acid Derivatives*

By Yoshié TANIZAKI, Hiroyasu INOUÉ and Noboru ANDO

(Received July 27, 1964)

The purpose of the present investigation is to explain the electronic spectra of some naphthalene sulfonic acid derivatives which have the amino and/or the hydroxyl groups as the functional. The samples used here show a marked spectral change with the pH variation of the solution. In view of the fact that an intense effect as a proton acceptor or donor of the groups must be responsible for the spectral change, we attempted to explain this by considering the relative position between the functional and the sulfonic group, the intramolecular hydrogen bonding effect, and, moreover, the resonance effect of the functional groups. Further, the assignment of the electronic bands of the derivatives could be made experimentally from the band shift, taking into account the band assignment of naphthalene, which is already known.

## Experimental

The chemical structures of the samples used here are shown in Table I. Naphthionic acid (Sample No. 2), γ-acid (No. 5), J-acid (No. 6) and H-acid (No. 9) were purified by repeated precipitations by hydrochloric acid, and the rest, by repeated recrystallizations from water.

The concentrations of the sample solutions were about $10^{-5}$ mol./l. The pH value of the solution was adjusted by hydrochloric acid or sodium hydroxide. The absorption measurement was made immediately after the determination of pH. When the pH of a solution becomes higher than 10, the absorption of the solvent can not be neglected. In such cases, a sodium hydroxide solution with the same pH value is used as the reference.

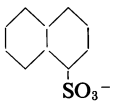
The absorption measurement was carried out by a Shimadzu QR-50 spectrophotometer and also by a Hitachi EPSO22 spectrophotometer. The pH value was determined by a Tōa Denpa Kōgyo pH meter HM-5A.

## Results

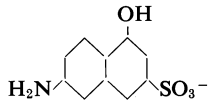
Figure 1 illustrates the absorption spectra of the naphthalene sulfonic acid ions (Nos. 1, 4 and 7 in Table I). None of them shows any appreciable spectral change within the limits of pH 2 to 11.

TABLE I. NAMES AND STRUCTURES OF SAMPLES

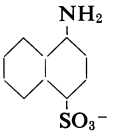
α-Naphthalene sulfonic acid

1 

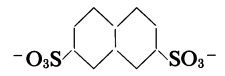
J-acid

6 

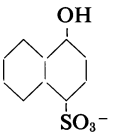
Naphthionic acid

2 

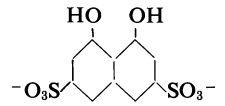
2, 7-Naphthalene disulfonic acid

7 

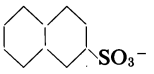
NW-acid

3 

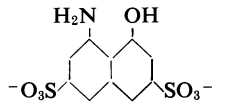
Chromotropic acid

8 

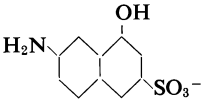
β-Naphthalene sulfonic acid

4 

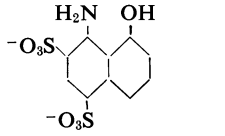
H-acid

9 

γ-acid

5 

SS-acid

10 

The spectra of the naphthionic acid ion (No. 2) are illustrated in Fig. 2. In this case, the spectral change was not observed above pH 4.4, and the spectra were in accord with curve I, while for pH values below 4.4 the spectra changed, while, however, keeping the isosbestic points. The absorption curve (V) for the smallest pH value closely resembles that of α-naphthalene sulfonic acid, which is shown in Fig. 1.

The absorption spectra of NW-acid (No. 3) are shown in Fig. 3. The isosbestic points appeared in the 6.3—10.8 pH range, and the curve did not change in shape below pH 6.3.

According to the above data, naphthionic acid and NW-acid show the two isosbestic

* Presented at the Local Meeting of the Chemical Society of Japan, Kōriyama, October, 1963.

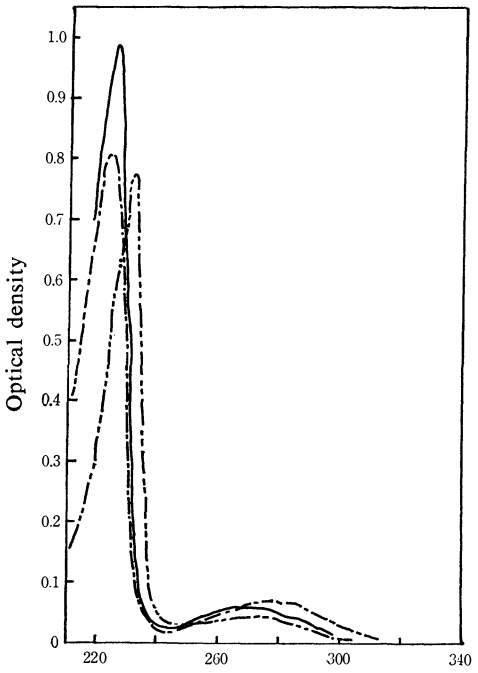



Fig. 1. Absorption spectra of naphthalene sulfonic acids, pH 2—11.
— — — α-Naphthalene sulfonic acid
——— β-Naphthalene sulfonic acid
— — — — 2,7-Naphthalene disulfonic acid

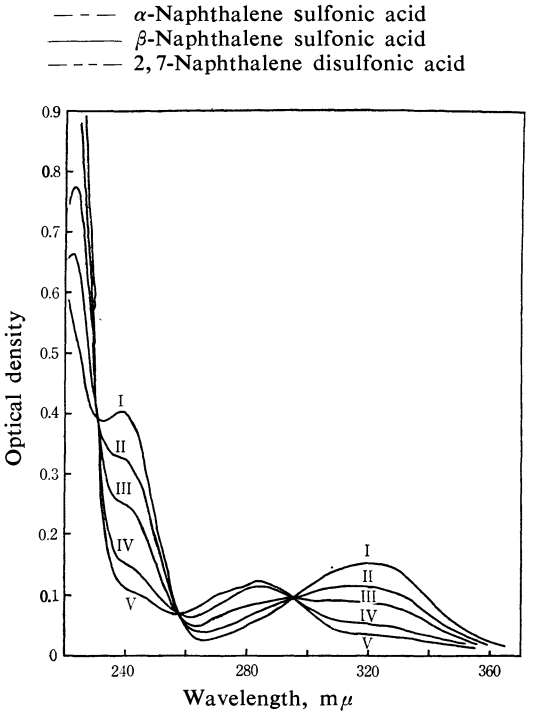



Fig. 2. Spectral change of naphthionic acid with pH.

| | | |
|---|---|---|
| I | pH | 11.1 |
| II | | 3.2 |
| III | | 2.7 |
| IV | | 2.0 |
| V | | 1.5 |

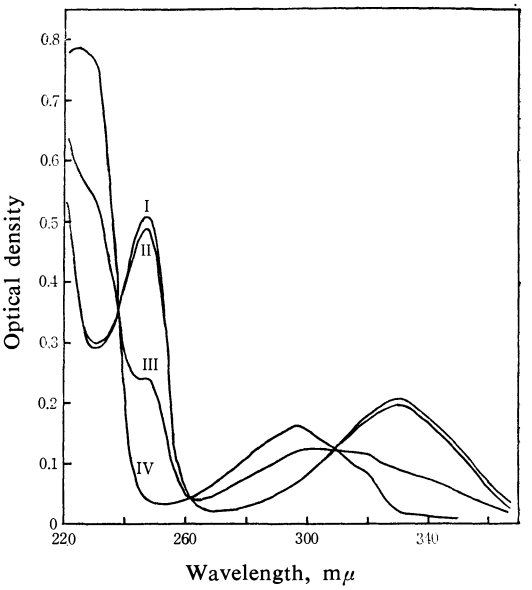



Fig. 3. Spectral change of NW-acid with pH.

| | | |
|---|---|---|
| I | pH | 10.8 |
| II | | 10.0 |
| III | | 9.2 |
| IV | | 6.3 |

points in different pH regions, namely the acid and alkali regions respectively. Because this is apparently due to the different properties of the amino and the hydroxyl groups, samples with two such kinds of groups are expected to show the isosbestic points in the two corresponding pH ranges. In truth γ-acid (No. 5), J-acid (No. 6) and H-acid (No. 9) behaved as expected. The case of γ-acid is shown as an example in Figs. 4a and 4b; there are well defined isosbestic points in the respective pH regions of 2.55—6.5 and of 9.2—10.6. In the pH range of about 5—8, of course, the absorption spectra did not change.

The pH regions in which the isosbestic points appear are illustrated schematically in Fig. 5 for all samples. In the figure, the shadings indicate the pH range with the isosbestic points, and the blank spaces, that with no spectral change. According to Fig. 5, the shading of naphthionic acid (with only one amino group) and that of NW-acid (one hydroxyl group) exist in quite separated pH regions. The two shaded regions of J-acid (with amino and hydroxyl group) nearly correspond in situation to those of naphthionic acid and NW-acid, whereas, in the case of γ-acid or H-acid, the two shaded regions do not coincide with those of naphthionic acid and NW-acid, and shift together toward the higher pH side. Further, the following facts are noticed: SS-acid indicates no spectral change in the acid region

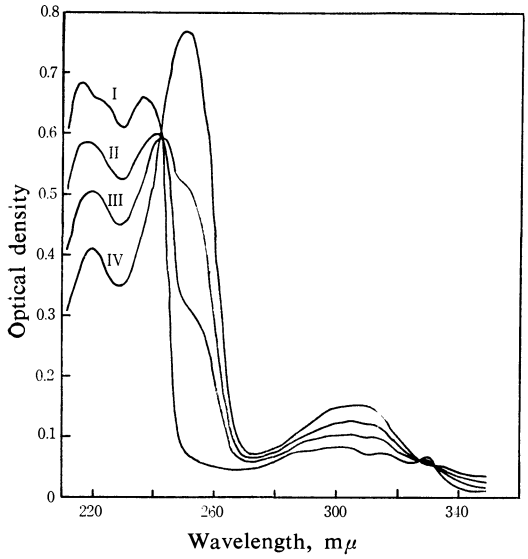



Fig. 4a. Spectral change of γ-acid with pH in acidic solution.
I pH 2.6
II 3.6
III 4.1
IV 6.5

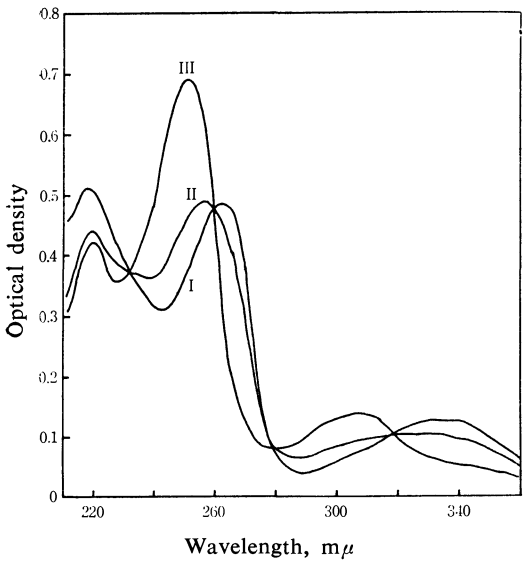


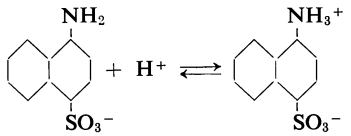

Fig. 4b. Spectral change of γ-acid with pH in basic solution.
I pH 10.6
II 9.8
III 9.2

despite the presence of an amino group, the shading region of chromotropic acid corresponding to that of NW-acid shifts to a much lower pH side, and so on. In the following section these problems will be discussed.

## Discussion

The existence of the isosbestic points implies that there are two kinds of molecular species with different characters in absorption, with an equilibrium kept between them. The equilibrium depends on the change in pH. There will be, therefore, an equilibrium in the addition and dissociation of the hydrogen ion. Since the naphthalene sulfonic acid ion did not show any spectral change in the pH range measured here, the amino and hydroxyl groups must be responsible for the spectral change in connection with the hydrogen ion.*

For that reason, the following equilibrium can be considered for the case of naphthionic acid;




If we use the notation, for instance, of $(-NH_2)_N$, etc. standing for naphthionic acid, etc., the above equilibrium can be written as follows;

$$(-NH_2)_N + H^+ \rightleftarrows (-NH_3^+)_N \qquad (1)$$

The lone pair electrons on the nitrogen atom ($2p\pi$ type) can not conjugate with the naphthalene link when a proton is attached to the amino group. Thus, the above-mentioned fact that the absorption spectrum of naphthionic acid in the solution of pH 1.45 (Fig. 2) is almost identical with that of α-naphthalene sulfonic acid (Fig. 1) can be explained as the result of the complete shift of the equilibrium 1 to the right side.

For NW-acid, similarly, the following equation may be considered as the dissociation equilibrium of the hydroxyl groups;

$$(-OH)_{NW} \rightleftarrows (-O^-)_{NW} + H^+ \qquad (2)$$

This equilibrium should move toward the right side with a lowering of the concentration of the hydrogen ion. Therefore, it can be said that curves I and IV in Fig. 3 indicate the electronic spectra of $(-O^-)_{NW}$ and $(-OH)_{NW}$ respectively.

Similarly, all the spectral changes of the other samples should be explained by a proton addition or dissociation process like that of Eq. 1 or 2. According to Fig. 5, however, the

* From a different standpoint from that of the present discussion, an equilibrium may be plausibly considered between the monomer and the dimer (e.g., an ion pair). This would, however, be unreasonable for the following reason: the spectrum of naphthionic acid in the acid solution, for instance, did not reveal the Davydov splitting, even in the most concentrated hydrogen ion employed here, but, on the contrary, approached the simple spectrum of α-naphthalene sulfonic acid.

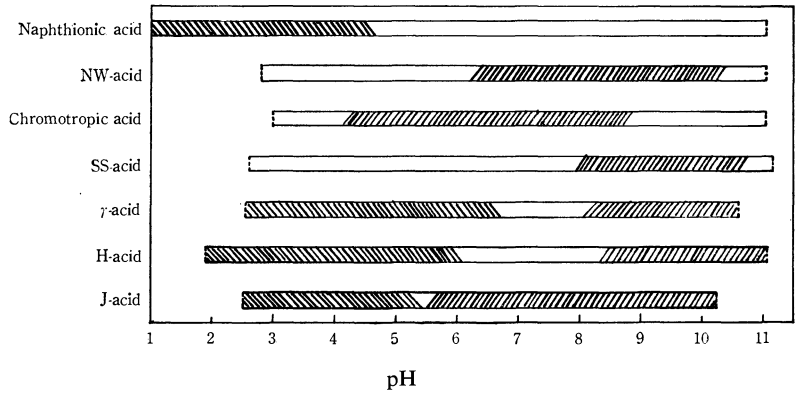



Fig. 5. Schematical diagram of the pH ranges with the spectral change; The shading indicates the pH ranges with the isosbestic points and the blank space that with no spectral change.

TABLE II. THE ORDER OF THE STARTING pH VALUES OF THE ADDITION AND THE DISSOCIATION PROCESS

| Sample[1] | Effects by[2] (A) sulfonic group and (B) hydrogen bond | The order of the starting pH values of the process of addition or dissociation | | |
|---|---|---|---|---|
| | | To be estimated by factor A and B[2] | Taking account of factor C | Observed |
| N-acid | $\sigma_p$ ($-NH_2$) | | | |
| NW-acid | $\sigma_p$ ($-OH$) | Addition | Addition | Addition |
| Ch-acid | $\sigma_m-\delta$ ($-OH$), $\sigma_m+\delta$ ($-OH$) | $N<\binom{\gamma}{J}<H$ | $\begin{cases} N<J<H \\ J<\gamma \end{cases}$ | $N<J<H<\gamma$ |
| SS-acid | $\sigma_{o,p}+\delta$ ($-NH_2$), $-\delta$ ($-OH$) | | | |
| γ-acid | $\sigma_m$ ($-NH_2$), $\sigma_m$ ($-OH$) | Dissociation | Dissociation | Dissociation |
| H-acid | $\sigma_m-\delta$ ($-NH_2$), $\sigma_m+\delta$ ($-OH$) | | | |
| J-acid | $\sigma_m$ ($-NH_2$), $\sigma_m$ ($-OH$) | $\binom{Ch}{H}<\binom{\gamma}{J}<NW<SS$ | $\begin{cases} Ch<J<NW<SS \\ Ch<H \\ J<\gamma \end{cases}$ | $Ch<J<NW<\binom{SS}{\gamma}{H}$ |

Note. 1) N-acid and Ch-acid mean naphthionic acid and chromotropic acid, respectively.
2) The electric charge induced by the sulfonic group or by the hydrogen bond formation is indicated by $\sigma$ or $\delta$, respectively, and is assumed that $\delta>\sigma$.

starting values of the pH of the corresponding processes do not always coincide with one another; the orders of the pH value are $N<J<H<\gamma$ for the addition process and $Ch<J<NW<SS\leq\gamma\leq H$ for the dissociation (see Table II). The possible reasons for this may be a change in the electron density of the functional group as a result of (A) the displacement of the $\sigma$ electron by the sulfonic group as the electron-accepting group, (B) the formation of an intramolecular hydrogen bond between the functional groups, and (C) the resonance effect of the functional group.

First let us consider the A factor. The electron density on a substituent will be reduced by the inductive effect of the sulfonic group. If the effect from the sulfonic group in the other link is disregarded, the positive charge on each functional group will be represented by the notation $\sigma$, as is shown in the second column of Table II, where the suffix of $\sigma$ used with, for example, *o*, *m* or *p* indicates the position of the sulfonic group with respect to the functional group. Since the magnitude of $\sigma$ will be in the order $\sigma_o>\sigma_m>\sigma_p$, the amino and the hydroxyl groups of H-acid, for instance, become more positive than the corresponding groups of naphthionic acid and NW-acid. Therefore, the following processes, 3 and 4, for H-acid

$$(-NH_2, -OH)_H + H^+ \rightleftarrows (-NH_3^+, -OH)_H \quad (3)$$

$$(-NH_2, -OH)_H \rightleftarrows -(NH_2, -O^-)_H + H^+ \quad (4)$$

will take place at a lower pH than Eqs. 1 and 2 respectively. Thus the orders of the pH values starting the processes of addition and dissociation because of only the A factor will become SS<H<N<$\gamma$=J and Ch=$\gamma$=H=J<NW<SS respectively.

Next let us consider the B factor. The formation of the intramolecular hydrogen bond between the two functional groups will occur in chromotropic acid, SS-acid and H-acid. The relative displacement of charge due to this effect will be described by the notation $-\delta$ or $+\delta$, as is shown in Table II. Here, as for H-acid, the hydrogen atom of the amino group is employed in the hydrogen bond in order to make both of the groups conjugate to the naphthalene link.* On the other hand, in the case of SS-acid, hydrogen of the hydroxyl group may be used, because the N–C bond is largely twisted from the plane of the link due to the steric hindrance of the sulfonic group adjacent to the amino group[1] (see Table I). Therefore, the spectral change corresponding to the proton addition to the amino group of SS-acid should not appear. This is indeed true, as is indicated in Fig. 5. For only the B factor, therefore, the starting points in the pH value of the addition or the dissociation process to be estimated will become the order N=$\gamma$=J<H or Ch=H<NW=$\gamma$=J<SS respectively.

As for the A and B factors in connection with the $\sigma$-electron, if we assume that the effect of A is smaller than that of B, the correlations of the starting pH values of the proton addition and the dissociation process will be obtained as shown in the third column of Table II.

Finally, let us take into consideration the effect of the C factor; the resonance effect of the functional groups in connection with the $\pi$-electron system. In only $\gamma$-acid is the direct conjugation through the link between the functional groups allowed. In such a particular case, the positive charge on the groups to be produced by the migration of $\pi$-electron to the link should be much decreased compared to the case without such direct conjugation or lacking in either functional groups. For that reason, the negative net charge on the two groups of $\gamma$-acid may be the largest. According to the experimental results (the last column of Table II), $\gamma$-acid is ranked in the highest orders of the pH values of the addition and the dissociation process. This indicates that the resonance effect by the direct conjugation is quite large.

For the other samples, the two functional groups will indirectly affect each other by means of repulsive interaction between the negative charges on the link induced by the resonance effect of the individual group. As will be seen later, the order of the magnitude of the resonance effect of the groups on the naphthalene link is $-NH_3^+ < -OH < -NH_2 < -O^-$. From this relation, it may be accepted that $-OH^{-\delta} < -NH_2^{-\delta}$. The $-OH^{+\delta}$ group of H-acid to be dissociated, therefore, should become more negative than that of chromotropic acid as a result of the resonance effect of $-NH_2^{-\delta}$ being larger than that of $-OH^{-\delta}$. For that reason, the dissociation process of H-acid becomes more difficult than that of chromotropic acid, namely, Ch<H. Unfortunately, at present the relative position of H-acid in the order can not be decided.

At any rate, most of the experimental results have been explained, as is shown in the fourth column of Table II, though the order in each case does not always coincide in detail with that observed; for example, the expected and the observed order of NW-acid and J-acid are just the converse of one another.

**The Direction of the Transition Moment of the Absorption Bands.**—With the introduction of the amino and/or the hydroxyl group, the absorption spectra of the original naphthalene sulfonic acid ion are changed markedly by the resonance effect of the group. According to the clarified findings concerning such a substitution effect,[2,3] in $\alpha$-substitution the band with the transition vector in the a direction (short axis) is subjected to a larger effect than when the vector is in the b direction (long axis). Here, in order to obtain some information about the transition direction of each band, the spectral change will be discussed from this standpoint.

Figure 6 illustrates the substitution effect on the absorption spectra of $\alpha$-naphthalene sulfonic acid. The intense band in the higher wave number region (to be called the second band) of $\alpha$-naphthalene sulfonic acid is shifted

* Though it is generally accepted that the proton-donating power is stronger in the hydroxyl group than in the amino group, in the case of H-acid the hydrogen bond of the N-H···O type must be considered, because H-acid shows the typical spectral change for the proton addition process. This indicates that the lone-pair electrons on the amino group can migrate to the naphthalene link in the neutral state.

1) T. Kobayashi, Y. Tanizaki and N. Ando, This Bulletin, 33, 913 (1960).

2) N. Jones, *J. Am. Chem. Soc.*, 67, 2127 (1945).

3) S. Suzuki and H. Baba, This Bulletin, 37, 519 (1964).

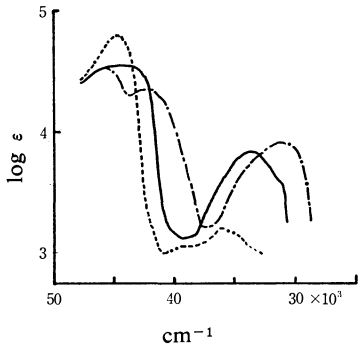



Fig. 6. Substitution effect on the absorption spectra of α-naphthalene sulfonic acid.
- - - - α-Naphthalene sulfonic acid
——— NW acid; [−OH]
— - — Naphthionic acid; [$-NH_2$]

merely 350 $cm^{-1}$ lower when the hydroxyl group is introduced to the α-position (NW-acid), while the weak band in the lower region (the first band) is shifted lower by as much as 2190 $cm^{-1}$. Moreover, the $\varepsilon_{max}$ of the first band increases from 5340 to 7050, whereas that of the second band decreased nearly one half, from 61600 to 35100. In the case of naphthionic acid, nearly the same relation as that above may be seen. Figure 7 also indicates that a similar tendency appears for the cases of chromotropic acid and H-acid with two substituents at α-positions. This time, however, in the first band there appeared a fine structure which was not obvious for 2, 7-naphthalene disulfonic acid, the parent molecule of the samples (cf. Fig. 1). Such a fine structure appears at about 285 mμ of the naphthalene spectrum; according to Platt,[4] this can be assigned to the $^1L_a$ transition. Therefore, it seems plausible that the transition

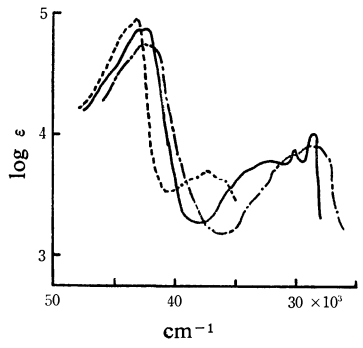



Fig. 7. Substitution effect on the absorption spectra of 2, 7-naphthalene disulfonic acid.
- - - - 2, 7-Naphthalene disulfonic acid
——— Chromotropic acid; [−OH, −OH]
— - — H-acid; [$-NH_2$, −OH]

4) J. R. Platt, *J. Chem. Phys.*, **17**, 487 (1949).

vector of the first band of the naphthalene sulfonic acid derivatives is in the a direction on the naphthalene skeleton as a result of the shifting of the $^1L_a$ transition. On the other hand, the second band is in the b direction. It is not possible, however, to assign the intense second band to the $^1L_b$ transition, because the $^1L_b$ of naphthalene appears at about 310 mμ and is very weak. The second band under consideration, therefore, must be the $^1B_b$ transition, which is the next b direction. In this case, the bands shift to the longer wavelength side without changing the order.

As γ-acid has the hydroxyl group at the α-position and the amino group at the β, it is interesting to compare the band position in the acidic, the neutral and the basic solutions (Fig. 8). When we compare the spectra in the neutral solution of γ-acid with that of β-naphthalene sulfonic acid, which is the parent molecule, it is found that both the first and the second band shift to the lower wave number in the same order (about 4000 $cm^{-1}$). Since the hydroxyl group at the α-position shifts the band with the transition moment of the a direction (the first band), the displacement of the second band must be brought about mainly by the amino group at the β-position. However, it may be noticed that the first band of γ-acid shifts by 4080 $cm^{-1}$ in contrast with the shift of 2190 $cm^{-1}$ of NW-acid. This means that the effect of the amino group at the β-position is largely responsible for the first band, too. On the other hand, in the acidic solution, only the hydroxyl group at the α-position is left as a group able to resonate with the link, since the substitution effect of the amino group is very much reduced. In such a situation, the first band is

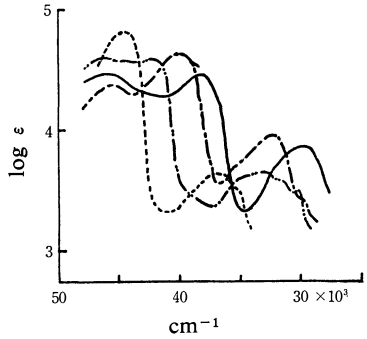



Fig. 8. Substitution effect on the absorption spectra of β-naphthalene sulfonic acid.
- - - - β-Naphthalene sulfonic acid
——— γ-Acid in alkaline solution; [$-NH_2$, $-O^-$]
— - — γ-Acid in neutral solution; [$-NH_2$, −OH]
— - - — γ-Acid in acidic solution; [$-NH_3^+$, −OH]

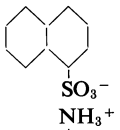
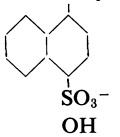
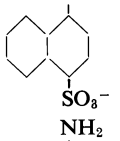
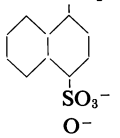
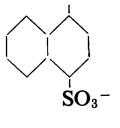
expected to be affected more largely than the second band; this expectation is in agreement with the results of NW-acid and others described above. In the basic solution, the shifts of both bands become the same order again, because the $-O^-$ group is at the $\alpha$- and the $-NH_2$ group at the $\beta$-position. As may be seen from Fig. 8, the shifts are, even though very slight, relatively large for the second band in the neutral solution and for the first band in the basic solution. This must be due to the magnitude of the resonance effect of the substituent groups; judging from the present deta, it seems that $-NH_2 < -O^-$.

Taking into account the band shifts of $\gamma$-acid in the neutral and the acid solutions, the order of the effect of the amino group at the $\beta$-position on the a and b directions can be estimated approximately.* Because the amino group of $\gamma$-acid loses its resonance effect in the acid solution, the contribution by the amino group must be estimated by subtracting the change of the wave number in the acid solution from that in the neutral one. The results indicate that the contribution is 420 $cm^{-1}$ for the first band (a direction) and 2350 $cm^{-1}$ for the second (b direction). Consequently, it is established that the substituent at the $\beta$-position is more effective in the b direction (five to sixfold) not in the same order in both the directions, a and b.

In order to decide the order of magnitude of the substitution effect, the positions of the first bands for the $\alpha$-substituent were compared. The results are shown in Table III. It is apparent from the table that the order of the substitution effect is as follows;

$$-NH_3^+ < -OH < -NH_2 < -O^-$$

TABLE III. SUBSTITUTION EFFECT ON THE FIRST BAND

| Sample (nature of solution) | Structure | First band mμ |
|---|---|---|
| α-Naphthalene sulfonic acid |  | 280 |
| Naphthionic acid (acidic) |  | 285 |
| NW-acid (acidic) |  | 295 |
| Naphthionic acid (alkaline) |  | 318 |
| NW-acid (alkaline) |  | 330 |

* When the amino and the hydroxyl group coexist, the respective resonance effects will have an influence upon each other. However, the order of the magnitude will roughly be obtained.

## Summary

1) The absorption spectra of some naphthalene sulfonic acid derivatives have been determined in various pH solutions.

2) The remarkable spectral change revealed by the variation in pH value can be interpreted in terms of the process of the proton association and dissociation of the functional groups.

3) The pH region in which the process takes place is characteristic of the kinds, $-NH_2$, $-OH$, and the number of the functional groups and their locations on the naphthalene skeleton.

4) The relative pH regions have been explained in outline by taking into account the effects of the sulfonic group, the intramolecular hydrogen bond formed between the functional groups, and the resonance of the functional group to the link.

5) The band assignment concerning the transition direction of the derivatives has been decided; the first and the second band correspond, respectively, to the $^1L_a$ and $^1B_b$ of naphthalene.

6) The order of the magnitude of the substitution effect has been clarified as $-NH_3^+ < -OH < -NH_2 < -O^-$.

The authors wish to thank Professor Saburo Nagakura of the University of Tokyo, the Institute for Solid State Physics, for his helpful advice, and to Sankyō Co., Ltd. for permission to use a Hitachi EPSO22 spectrophotometer.

*Laboratory of Physical Chemistry*
*Tokyo Institute of Technology*
*Ookayama, Tokyo*

# Studies of the Stability of Cobalt Ferrocyanide Sol in Ultrasonic Field. The Ultrasonic Dispersion of Cobalt Ferrocyanide

By Satya PRAKASH, Om PRAKASH and Sheo PRAKASH

(Received August 8, 1964)

High frequency, inaudible sound waves can bring about various dispersion effects, such as the mutual emulsification of the liquid phase, the disintegration of certain solids, the peptization and liquefaction of gels, and the depolymerization of high molecular substances. Polotoskii[1] prepared hydrosol of camphor and iodine in water, and Sata and his co-workers[2] dispersed metallic hydroxide in water by means of ultrasonic waves. Prakash and Pandey[3] successfully utilized ultrasonic energy in the preparation of a colloidal cobalt hydroxide solution. The present authors have been able to obtain a very stable sol of cobalt ferrocyanide by using the ultrasonic dispersion method. The sol obtained was then stabilized by further irradiation. Our findings on the influence of ultrasonic waves on this sol in presence as well as in absence of oxygen and in presence of non-electrolytes, such as methanol, ethanol and acetone, will be reported in this paper.

## Experimental

**Materials.**—B. D. H. (Analar) samples of potassium ferrocyanide, cobalt chloride, barium chloride, potassium chloride and hydrochloric acid and distilled methanol, ethanol and acetone (B. D. H., L. R.) were used.

**Instruments, Procedures and Calculation.**—*Electrical Conductance Measurements.*—The measurements of electrical conductance were carried out with a Leeds and Northrup Kohlrausch slidewire, with an audio-frequency oscillator. A dip-type cell was used. The temperature was kept constant (30±0.2°C).

*pH Measurements.*—The hydrogen ion concentration of the solution was measured with a Leeds and Northrup direct-reading pH indicator with a glass calomel electrode system. The instrument was standardised from time to time with a standard buffer of pH 6.8.

*Transmission Measurements.*—The transmission in percentage was determined with a Unicam SP 1400 prism absorptiometer, and the optical density was calculated by the equation:

$$\text{Optical density} = \log (1/T)$$

where $T$ is the transmission.

*Ultrasonic Generator.*—The source of ultrasonic power was a Mullard high frequency ultrasonic generator, type E-7562, with a barium titanate transducer. The principal diagram of the electrical circuit is shown in Fig. 1. The frequency of the transducer was 1 Mc./sec.

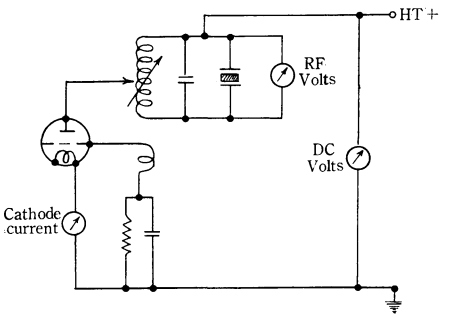



Fig. 1

Decinormal solutions of cobalt chloride and potassium ferrocyanide were mixed together, with more of the latter. The precipitate of cobalt ferrocyanide was filtered and washed. The precipitate was put into distilled water in a Jena glass bottle and exposed to ultrasonic waves. A cobalt ferrocyanide sol of a dirty brown colour was obtained within thirty minutes. In this way a sufficient amount of the sol was prepared and stored in a Jena bottle for detailed study. The sol was then purified by dialysis for three days. The concentration of the sol was determined by evaporating a known volume of the sol to dryness on a water bath. The sol concentration was found to be 19.3526 g./l.

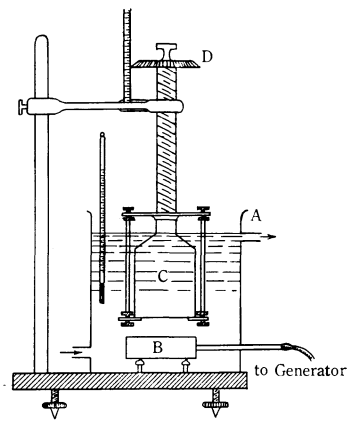



Fig. 2

1) G. G. Polotoskii, *Colloid. J. (U. S. S. R.)*, **6**, 779 (1940).
2) N. Sata and S. Watanabe, *Kolloid-Z.*, **73**, 50 (1935).
3) S. Prakash and A. D. Pandey, ibid., **181**, 46 (1962).

The above sol, 30 ml., was then placed in a 250 ml. flat-bottomed Jena glass vessel with a ground glass stopper and exposed to the action of ultrasonic waves for various intervals of time. The ultrasonic bath (Fig. 2) was kept at a constant temperature (30±0.2°C) by circulating water into it. The Jena vessel was held vertically above the transducer, and the distance between the vessel and the crystal was so adjusted as to produce a maximum fountain inside the vessel. The distance was kept unchanged as much as possible during the course of the experiments.

The stability of the sol was determined after each exposure by noting the amount of potassium chloride and barium chloride required to coagulate the negatively-charged sol of cobalt ferrocyanide in a fixed time (30 min.). The variation in specific conductivity and hydrogen-ion concentration of the sol was also recorded every time. The change in optical density was thus observed.

The experiments were carried out in the absence of oxygen. The air was replaced with nitrogen by bubbling for thirty minutes. Nitrogen from a cylinder had previously been passed through solutions of vanadous sulphate and alkaline pyrogallol in order to remove the oxygen.

The influence of ultrasonic waves on this sol in the presence of methanol, ethanol and acetone was also studied. Measurements similar to those mentioned above were carried out after each exposure, and the results were compared with those when no non-electrolyte was present.

## Results and Discussion

Figure 3 shows the amount of the dispersion of cobalt ferrocyanide when it is subjected to ultrasonic waves. As may be seen in the figure, the amount increases rapidly in the beginning. When the exposure time is further increased, the increment is slowed down and attains a maximum value.

The coagulation values of the sols under various conditions are shown in Tables I and II.

A perusal of these tables will show that, with the increase in the time of exposure to

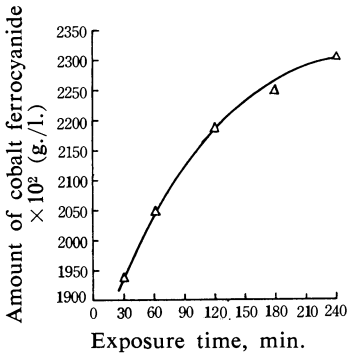



Fig. 3. Ultrasonic dispersion of cobalt ferrocyanide.

TABLE I. SOL A

Volume of sol taken, 2 ml.
Total volume, 8 ml.
Time allowed for coagulation, 30 min.
Temperature, 30±0.2°C
R. F. output voltage, 2.4 kV. (approx.)

| Time of exposure min. | Coagulation values | | | |
|---|---|---|---|---|
| | In presence of air | | In absence of oxygen | |
| | (M/100) $BaCl_2$ | (M/10) KCl | (M/100) $BaCl_2$ | (M/10) KCl |
| 0 | 0.95 | 2.45 | 0.95 | 2.45 |
| 60 | 1.10 | 2.60 | 1.05 | 2.55 |
| 120 | 1.20 | 2.70 | 1.15 | 2.65 |
| 180 | 1.25 | 2.80 | 1.15 | 2.70 |
| 240 | 1.30 | 2.85 | 1.25 | 2.85 |
| 300 | 1.40 | 3.00 | 1.35 | 2.05 |

TABLE II. SOL A/2

| Time of exposure min. | Coagulation values | | | |
|---|---|---|---|---|
| | In presence of air | | In absence of oxygen | |
| | (M/100) $BaCl_2$ | (M/10) KCl | (M/100) $BaCl_2$ | (M/10) KCl |
| 0 | 0.65 | 2.00 | 0.65 | 2.00 |
| 60 | 0.75 | 2.15 | 0.75 | 2.20 |
| 120 | 0.80 | 2.20 | 0.80 | 2.25 |
| 180 | 0.90 | 2.30 | 0.90 | 2.30 |
| 240 | 1.00 | 2.40 | 0.95 | 2.45 |
| 300 | 1.15 | 2.55 | 1.10 | 2055 |

TABLE III

| Time of exposure min. | Coagulation values with M/5 HCl | | | |
|---|---|---|---|---|
| | 25 ml. sol + 5 ml. water | 25 ml. sol + 3 ml. water + 2 ml. methanol | 25 ml. sol + 3 ml. water + 2 ml. ethanol | 25 ml. sol + 3 ml. water + 2 ml. acetone |
| 0 | 1.30 | 1.20 | 1.20 | 1.20 |
| 60 | 1.45 | 1.30 | 1.30 | 1.20 |
| 120 | 1.60 | 1.35 | 1.30 | 1.30 |
| 180 | 1.70 | 1.35 | 1.30 | 1.30 |
| 240 | 1.85 | 1.45 | 1.35 | 1.30 |

TABLE IV

| Time of exposure min. | Coagulation values with M/5 HCl | | | |
|---|---|---|---|---|
| | 25 ml. sol + 5 ml. water | 25 ml. sol + 5 ml. methanol | 25 ml. sol + 5 ml. ethanol | 25 ml. sol + 5 ml. acetone |
| 0 | 1.30 | 1.10 | 1.10 | 1.15 |
| 60 | 1.45 | 1.25 | 1.20 | 1.20 |
| 120 | 1.60 | 1.25 | 1.20 | 1.20 |
| 180 | 1.70 | 1.25 | 1.20 | 1.20 |
| 240 | 1.85 | 1.30 | 1.20 | 1.20 |

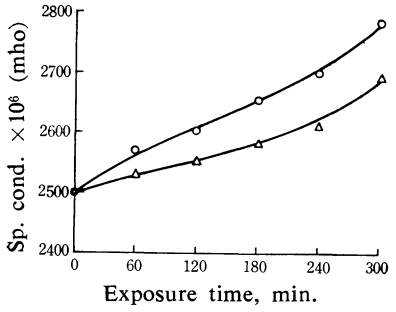



Fig. 4. Variation in sp. cond. in sol A.
○—○ In presence of air
△—△ In absence of oxygen

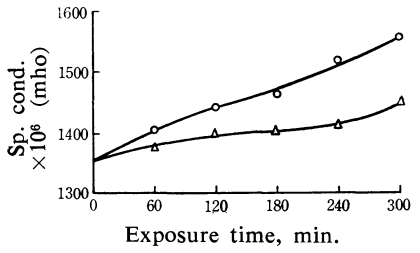



Fig. 5. Variation in sp. cond. in sol A/2.
○—○ In presence of air
△—△ In absence of oxygen

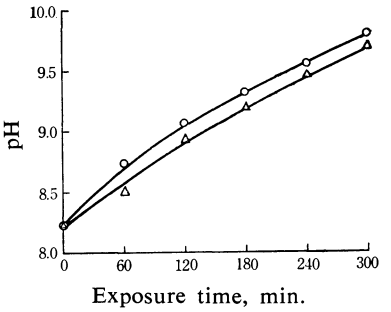



Fig. 6. pH variation in sol A.
○—○ In presence of air
△—△ In absence of oxygen

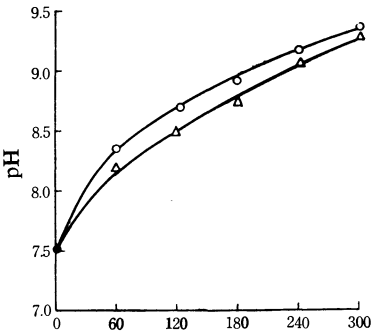



Fig. 7. pH variation in sol A/2.
○—○ In presence of air
△—△ In absence of oxygen

the ultrasonic waves, the stability of the sol increases in the presence as well as in the absence of oxygen. The small difference in the extent of stabilization under the two conditions shows that the presence or absence of oxygen in no way affects the ultrasonic action on this sol, as had previously been observed by the present authors in the case of the manganese dioxide sol.[4] As the sol is negatively charged, the enhanced stability may be attributed to the decrease in hydrogen ion concentration. The hydroxyl ions are increased in the system; they are adsorbed on the double layer, with the result that the sol attains more stability.

4) S. Prakash and O. Prakash, *Kolloid-Z.*, **188**, 136 (1963).

Dhar and his collaborator[5] have shown that ferrocyanide sols are appreciably hydrolysed in aqueous solutions and that this hydrolysis makes the sol more stable towards electrolytes. It is possible that, under the influence of ultrasonic waves, the sol of cobalt ferrocyanide becomes more hydrolysed and hence more stable to electrolytes. As Figs. 4 and 5 show, the specific conductivity of the sol also increases as the time of exposure is increased. A number of investigators[6-9] have found $H_2O_2$, $HNO_2$ and $HNO_3$ present in the sonolysis of water exposed to ultrasonic waves. The acid nature of these substances would increase the specific conductivity.

In spectroscopic studies (Figs. 8 and 9) of the unexposed and exposed sol, it is observed that an absorption maximum occurs at the same wavelength in both cases suggesting that no change in the basic characters of the substance has taken place. It seems that the ultrasonic waves have brought about a change in the physical character of the particles by their own cavitating action on larger aggregates, thus making them smaller. This theory is confirmed by the observation that, as the time of exposure increases, the turbidity in the unexposed sol continues to vanish and the sol becomes transparent.

The stability, specific conductivity and hydrogen ion concentration of the sol are very little affected by ultrasonic waves in the presence of methanol, ethanol and acetone, as Tables III and IV, and Figs. 10, 11 and 12 show. The great majority of the disruptive actions and the chemical reactions caused by ultrasonic

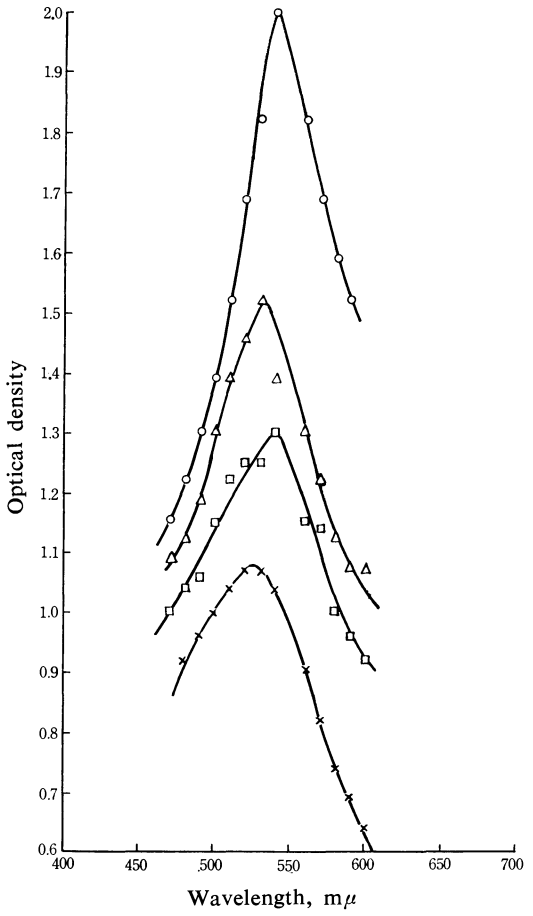



Fig. 8. Cobalt ferrocyanide sol A/4.
○ Unexposed
△ Exposed for 1/2 hr.
□ Exposed for 1 hr.
× Exposed for 2 hr.

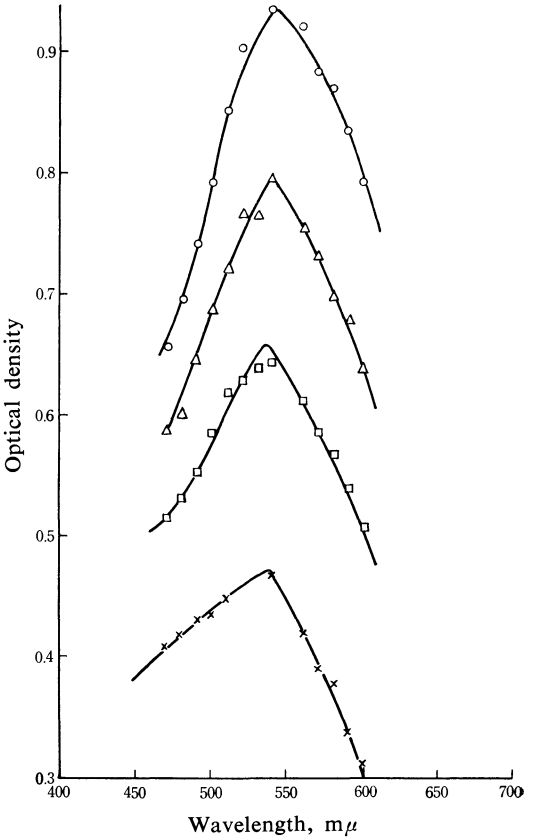



Fig. 9. Cobalt ferrocyanide sol A/8.
○ Unexposed
△ Exposed for 1/2 hr.
□ Exposed for 1 hr.
× Exposed for 2 hr.

5) S. Ghosh and N. R. Dhar, *J. Phys. Chem.*, **29**, 659 (1925); *Kolloid-Z.*, **39**, 349 (1926).
6) I. G. Polotskii, *J. Gen. Chem.* (*U. S. S. R.*), **17**, 649 (1947).
7) H. Beuthe, *Z. Phys. Chem. Abt.*, **A163**, 161 (1933).
8) S. Akiya and S. Okui, *J. Pharm. Soc. Japan*, **67**, 232 (1947).
9) O. Nomoto and S. Okui, *J. Phys. Soc. Japan*, **3**, 47 (1948).

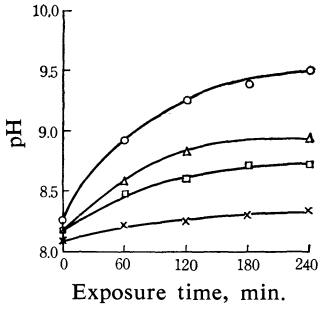



Fig. 10. pH variation in presence of non-electrolytes in sol A.

○—○ Without non-electrolyte
△—△ In presence of 2 ml. methanol
□—□ In presence of 2 ml. ethanol
×—× In presence of 2 ml. acetone

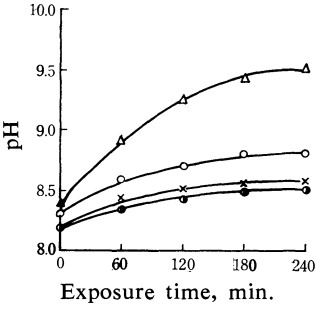



Fig. 11. pH variation in presence of non-electrolyte in sol A.

△—△ Without non-electrolyte
○—○ In presence of 5 ml. methanol
×—× In presence of 5 ml. ethanol
◑—◑ In presence of 5 ml. acetone

waves have been attributed to the phenomenon of cavitation. Because of a high dielectric constant, high surface tension and low vapour pressure values of water, the aqueous medium greatly favours the formation of cavitation bubbles, with the result that the ultrasonic activity observed in such a medium will be at a maximum. Thus, the inhibitive effect of non-electrolytes, e. g., methanol, ethanol and acetone, may be due to the suppression of this cavitation, because the presence of substances of a high vapour pressure[10] suppresses the breakdown of cavitation bubbles. Consequently, ultrasonic activity is very much lessened. Secondly, the energy released upon the collapse of the cavitation bubble is comparatively much less if the surface tension[11] and the internal

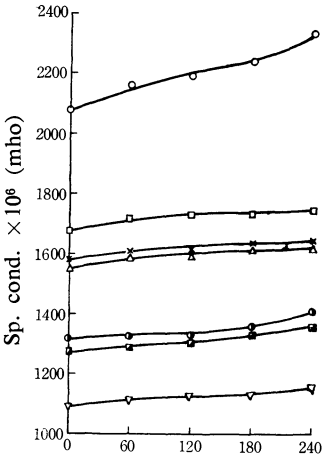



Fig. 12. Variation in sp. cond. in presence of non-electrolyte in sol A.

○—○ Without non-electrolyte
□—□ 2 ml. methanol
×—× 2 ml. acetone
△—△ 2 ml. ethanol
◑—◑ 5 ml. methanol
◪—◪ 5 ml. acetone
▽—▽ 5 ml. ethanol

pressure[12] of the medium are low, resulting in a decrease in the rate of ultrasonic action.

## Summary

A negatively-charged cobalt ferrocyanide sol has been prepared ultrasonically subjecting the washed precipitate of cobalt ferrocyanide and distilled water to ultrasonic waves. The amount of dispersion increases with the time of exposure. The sol is rendered more stable in an ultrasonic field in the presence as well as in the absence of oxygen. The enhanced stability has been attributed to the increase in hydroxyl ions in the medium as a result of the hydrolysis of cobalt ferrocyanide sol. The stability, pH and specific conductivity values are very little affected in the presence of methanol, ethanol and acetone. The inhibition is due to the suppression of cavitation and to a lesser energy release on the collapse of cavitational bubbles.

The authors are grateful to the Council of Scientific and Industrial Research for the award of a research fellowship to one of the authors (O. P.).

*Department of Chemistry*
*University of Allahabad*
*Allahabad, India*

10) A. I. Virtanen and N. Ellfolk, *Acta Chem. Scand.*, **6**, 660 (1952).
11) T. F. Heuter and R. H. Bolt, "Sonics," John Wiley & Sons, New York (1955), p. 240.
12) S. C. Srivastava and N. Berkowitz, *Can. J. Chem.*, **41**, 1787 (1963).

# The Hydrogen Bond in the Diols. I

By Teijiro YONEZAWA, Hazime SAITÔ,* Shinichi MATSUOKA and Kenichi FUKUI

(Received August 18, 1964)

The diols form intramolecular as well as intermolecular hydrogen bonds with two hydroxyl groups in a molecule. Though the intramolecular hydrogen bonds of the diols were investigated by Kuhn[1] using infrared spectra, intermolecular hydrogen bonds have never, so far as we know, been elucidated.

In the NMR spectra, the term "hydrogen bond shift" is defined[2] as the extreme shift of the proton signal between the non-associated state and the completely-associated state. In the associated state of the diols, both the intra- and the intermolecular hydrogen bonds are involved.

In the present paper, the hydrogen bond of the diols will be investigated by a nuclear magnetic resonance technique, and a procedure for estimating the hydrogen bond shifts of the diols will be proposed. For this purpose, the non-associated (free) OH proton shift, which is necessary to evaluate the hydrogen bond shift, will be calculated theoretically, since it seems very difficult to measure free OH proton shifts. Not only is there the technical difficulties arising from the slight solubility of the diols in an inert solvent as well as from their higher boiling points, but also the intramolecular hydrogen bond may occur even in the gaseous state or in an infinitely dilute solution. Therefore, the free OH proton shift will be obtained by a theoretical treatment, wherein the local diamagnetic shielding constants of OH protons in the diols and the shielding constant due to the paramagnetic anisotropy of the oxygen attached to the proton will be calculated by a molecular orbital method.

The measurement of the OH proton shift will be made at a temperature just above the freezing point in a pure liquid state, since a completely hydrogen-bonded state is realized at this temperature. Hence, the hydrogen bond shift of the diols can be derived from the difference between the chemical shift in the completely associated state and the theoretical shift stated above.

The hydrogen bond shifts thus obtained will then be compared with that of ethanol and found to be smaller. From these results, we can point out that the proportion of intramolecular hydrogen bonds can not be ingnored in the hydrogen bonds of the diols.

## The Measurement of Proton Shifts

All materials used were of guaranteed grade. The vacuum distillation was made before use after drying over anhydrous sodium sulfate. The measurements of the NMR spectra were performed by a Varian DP-60 60 MC spectrometer equipped with a V-4340 variable temperature accessory at a temperature just above the freezing point. Samples were measured in a pure liquid state. The plots of the OH proton shift vs. the temperature are shown in Fig. 1. The bulk susceptibility correction was made in the observed chemical shifts, which are referred to methylene

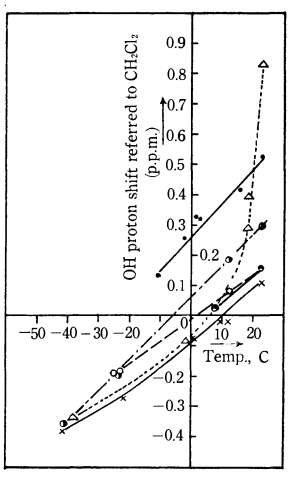



Fig. 1. Plots of OH proton shift vs. temperature. (uncorrected)
—×— 1,5-Pentanediol
—•— 2,3-Butanediol
···△··· Propylene glycol
--○-- Ethylene glycol
—◓— 1,4-Butanediol
··◑·· Trimethylene glycol

* Present address: Basic Research Laboratories, Toyo Rayon Co. Ltd., Tebiro, Kamakura.

1) L. P. Kuhn, *J. Am. Chem. Soc.*, **74**, 2492 (1952).

2) Cf. e. g., J. A. Pople, W. G. Schneider and H. J. Bernstein, "High-resolution Nuclear Magnetic Resonance," McGraw-Hill, New York (1959).

TABLE I. PROTON SHIFT OF THE DIOLS (referred to methylene chloride)

| | Temp. of measurement °C | $-\chi_v \times 10^{-6}$ | Bulk susceptibility correction | Proton shift observed (corrected) p. p. m. OH | CH | $CH_2$ | $CH_2$ | $CH_3$ |
|---|---|---|---|---|---|---|---|---|
| $HOCH_2CH_2OH$ | −25 | 0.695 | −0.08 | −0.28 | — | +1.74 | — | — |
| $HOCH_2CH(OH)CH_3$ | −39 | 0.689 | −0.09 | −0.43 | −1.58* | +1.92* | — | +4.28 |
| $HOCH_2CH_2CH_2OH$ | −42 | 0.701 | −0.07 | −0.43 | — | +1.83 | +3.77 | — |
| $CH_3CH(OH)CH(OH)CH_3$ | −11 | 0.705 | −0.06 | +0.07 | — | — | — | +4.20 |
| $HOCH_2CH_2CH_2CH_2OH$ | 8 | 0.705 | −0.06 | −0.03 | — | +1.80 | +3.87 | — |
| $HOCH_2CH_2CH_2CH_2CH_2OH$ | −42 | 0.705 | −0.06 | −0.44 | — | +1.88 | +3.96 | — |

* Values at a room temperature are quoted, because signals are not splited at −39°C.

chloride as an external standard. The volume susceptibility for correction is calculated from Pascal's rule. These shifs are listed, together with the temperature of measurement, in Table I.

### The Calculation of the Hydrogen Bond Shift

In order to obtain the hydrogen bond shift, free OH proton shifts were calculated theoretically by the following procedure. According to Pople,[3] the shielding constant of the free OH proton consits of the diamagnetic shielding constant, $\sigma_{dia}(OH)$, which depends on electrons around the proton in question, and the shielding constant, $\sigma_{para}(O)$, due to the paramagnetic anisotropy of the oxygen atom attached to the proton:[4]

$$\sigma(OH) = \sigma_{dia}(OH) + \sigma_{para}(O) \quad (1)$$

The free OH proton shift, $\delta(OH)$, referred to gaseous methane, is then given as:

$$\delta(OH) = \sigma_{dia}(OH) - \sigma_{dia}(CH_4) + \sigma_{para}(O) \quad (2)$$

since there is no contribution of the neighbor anisotropy in methane. The shielding constants, $\sigma_{dia}(OH)$, $\sigma_{dia}(CH_4)$ and $\sigma_{para}(O)$, are calculated by a simple LCAO MO method for $\sigma$-electron systems.

**The Diamagnetic Shielding Constant.**—It has been shown that the local diamagnetic shielding constant of a proton is given by:[3]

$$\sigma_{dia} = \lambda q_H \quad (3)$$

where $q_H$ is the total $\sigma$-electron density at the hydrogen atom and $\lambda$ is a constant. In the present paper, $\lambda$ is put as equal to 25 p. p. m.[5]

The total $\sigma$-electron density, $q_H$, is calculated by a simple LCAO MO method for sigma systems, where the $j$-th molecular orbital is expressed as a linear combination

TABLE II

| | |
|---|---|
| $\alpha_C = \alpha$ | $\beta_{CC'} = \beta$ |
| $\alpha_H = \alpha - 0.2\beta$ | $\beta_{CO} = 0.7\beta$ |
| $\alpha_O(sp^2) = \alpha + 0.4\beta$ | $\beta_{OH} = 1.2\beta$ |
| $\alpha_O(sp^3) = \alpha + 0.3\beta$ | $\beta_{CH} = 1.1\beta$ |
| | $\beta_{CC} = 0.4\beta$* |
| | $\beta_{OO}(sp^2) = 0.5\beta$ |
| | $\beta_{OO'}(sp^3) = 0.4\beta$* |

* Resonance integral between the different atomic orbitals of the same atom.

of the atomic orbitals constructing bonds in a molecule:

$$\varphi_j = \sum_r c_r^j \chi_r \quad (4)$$

The parameters adopted for the coulomb and resonanance integrals are nearly the same as in our previous paper;[6] they are listed in Table II. For the $H_2O$ molecule, we have adopted two different values for the coulomb integral of the oxygen atom with $sp^2$ and $sp^3$ hybrid orbitals and for the resonance integral between the two different hybrid orbitals of the oxygen atom. For the diols and alcohols, however, we have adopted the integrals for the oxygen of $sp^3$ hybridization.

The total $\sigma$-electron densities in the diols and some related compounds are given in Fig. 2. No remarkable variation in the electron density in the C-O-H bond is observed for the diols and alcohols.

**The Shielding Constant due to the Paramagnetic Anisotropy of the Oxygen Atom.**—The shielding constant arising from the magnetic anisotropy of the adjacent atom is written:

$$\sigma_{para}(O) = \frac{1}{3R^3H}\{\mu_x(1-3\cos^2\theta_x) + \mu_y(1-3\cos^2\theta_y) + \mu_z(1-3\cos^2\theta_z)\} \quad (5)$$

where $\mu_x$, $\mu_y$ and $\mu_z$ denote the components of the magnetic dipole moment induced at the oxygen atom by the paramagnetic current

3) J. A. Pople, *Proc. Roy. Soc.*, A239, 549, 557 (1954).

4) Evidently, the terms due to the neighbor anisotropy of other atoms do exist. These terms may be small since they are located rather far from the proton in question.

5) This value corresponds to the effective nuclear charge, $z=1.40$, in the Slater-type 1s orbital.

6) K. Fukui, H. Kato and T. Yonezawa, This Bulletin, 33, 1201 (1960); 34, 442 (1961); 35, 38 (1962).

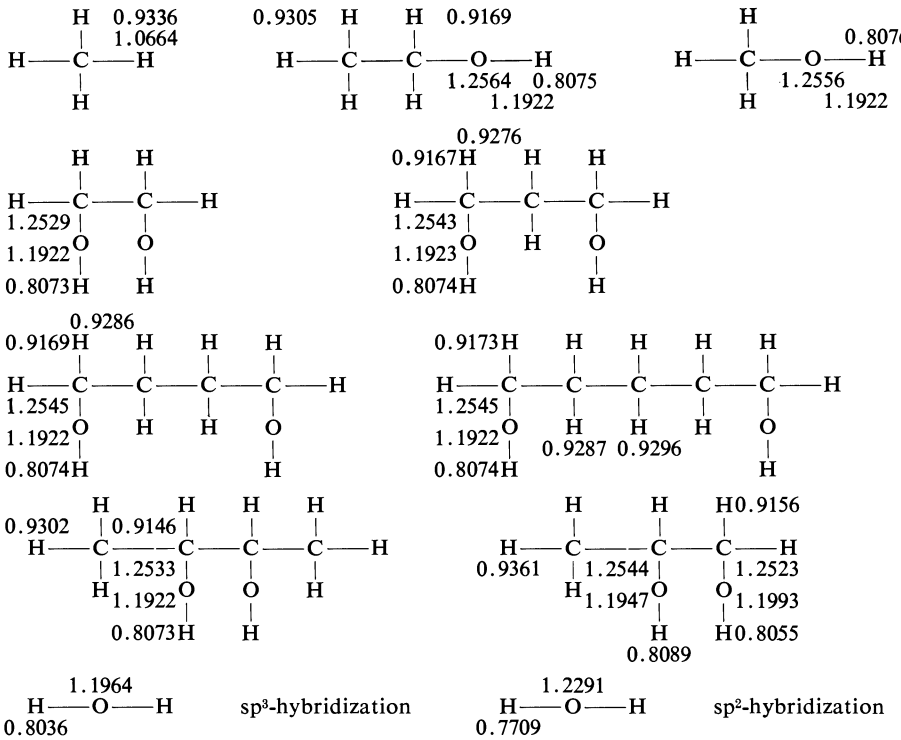
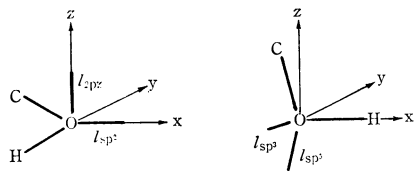



Fig. 2. Total $\sigma$-electon density in the diols and related compounds.

around the oxygen atom; $H$ is the external magnetic field; $\cos\theta_x$, $\cos\theta_y$ and $\cos\theta_z$ are the direction cosines of the vector, $\boldsymbol{R}$, connecting the oxygen atom to the hydrogen atom in question, and $R$ is the distance between them.




sp² hybridization sp³ hybridization

Fig. 3. Coordinate system used.

In the calculation of the magnetic dipole moment, as we do not have sufficient knowledge to determine whether the hybridization of the oxygen atom in the X-O-Y bond is of the $sp^3$ or the $sp^2$ type, the calculation has been performed for both cases. The coordinate system chosen in this treatment is shown in Fig. 3. The notations, $l_{2pz}$, $l_{sp^2}$ and $l_{sp^3}$ in Fig. 3 imply the lone pair electrons occupying 2pz, $sp^2$ and $sp^3$ hybrid orbitals respectively.

When we substitute the values of the direction cosines for two different cases, Eq. 5 becomes:

$$\left.\begin{aligned}\sigma_{para}(O)&=\frac{1}{12R^3H}(\mu_x+4\mu_z-5\mu_y)\\ &\qquad\text{for } sp^2 \text{ hybridization}\\ \sigma_{para}(O)&=\frac{1}{3R^3H}(\mu_y+\mu_z-2\mu_x)\\ &\qquad\text{for } sp^3 \text{ hybridization}\end{aligned}\right\}\quad(6)$$

The formulas for $\mu_x$, $\mu_y$ and $\mu_z$ of the oxygen atom in C-O-H and H-O-H bonds, which are derived in order to check the validity of the present treatment, are written as:

(1) COH

Case 1. oxygen of $sp^2$ hybridization

$$\left.\begin{aligned}\mu_x&=\frac{1}{2}\left(\frac{e\hbar}{mc}\right)^2H\left\{\frac{(a^*)^2}{\varepsilon^*_{OH}-\varepsilon_{l2pz}}+\frac{(c^*)^2}{\varepsilon^*_{CO}-\varepsilon_{l2pz}}\right\}\\ \mu_y&=\frac{1}{6}\left(\frac{e\hbar}{mc}\right)^2H\left\{\frac{(a^*)^2}{\varepsilon^*_{OH}-\varepsilon_{l2pz}}+\frac{(c^*)^2}{\varepsilon^*_{CO}-\varepsilon_{l2pz}}\right\}\\ \mu_z&=\frac{1}{3}\left(\frac{e\hbar}{mc}\right)^2H\left\{\frac{(a^*)^2}{\varepsilon^*_{OH}-\varepsilon_{lsp^2}}+\frac{(c^*)^2}{\varepsilon^*_{CO}-\varepsilon_{lsp^2}}+\frac{(ac^*)^2}{\varepsilon^*_{CO}-\varepsilon_{OH}}+\frac{(ca^*)^2}{\varepsilon^*_{OH}-\varepsilon_{CO}}\right\}\end{aligned}\right\}\quad(7)$$

Case 2. Oxygen of $sp^3$ hybridization

$$\left.\begin{aligned}
\mu_x &= \frac{2}{3}\left(\frac{e\hbar}{mc}\right)^2 H\left\{\frac{(c^*)^2}{\varepsilon^*_{CO}-\varepsilon_{lsp^3}}\right\}\\
\mu_y &= \frac{1}{4}\left(\frac{e\hbar}{mc}\right)^2 H\left\{\frac{3(a^*)^2}{\varepsilon^*_{OH}-\varepsilon_{lsp^2}}\right.\\
&\quad \left.+\frac{1}{3}\frac{(c^*)^2}{\varepsilon^*_{CO}-\varepsilon_{lsp^3}}\right\}\\
\mu_z &= \frac{1}{4}\left(\frac{e\hbar}{mc}\right)^2 H\left\{\frac{2(ac^*)^2}{\varepsilon^*_{CO}-\varepsilon_{OH}}\right.\\
&\quad +\frac{2(ac^*)^2}{\varepsilon^*_{OH}-\varepsilon_{CO}}+\frac{(a^*)^2}{\varepsilon^*_{OH}-\varepsilon_{lsp^3}}\\
&\quad \left.+\frac{(c^*)^2}{\varepsilon^*_{CO}-\varepsilon_{lsp^3}}\right\}
\end{aligned}\right\} \quad (8)$$

(2) HOH

Case 1. Oxygen of $sp^2$ hybridization

$$\left.\begin{aligned}
\mu_x &= \left(\frac{e\hbar}{mc}\right)^2 H\left\{\frac{(a^*)^2}{\varepsilon^*_{OH}-\varepsilon_{l2pz}}\right\}\\
\mu_y &= \frac{1}{3}\left(\frac{e\hbar}{mc}\right)^2 H\left\{\frac{(a^*)^2}{\varepsilon^*_{OH}-\varepsilon_{l2pz}}\right\}\\
\mu_z &= \frac{2}{3}\left(\frac{e\hbar}{mc}\right)^2 H\left\{\frac{(a^*)^2}{\varepsilon^*_{OH}-\varepsilon_{lsp^2}}\right.\\
&\quad \left.+\frac{(aa^*)^2}{\varepsilon^*_{OH}-\varepsilon_{OH}}\right\}
\end{aligned}\right\} \quad (9)$$

Case 2. Oxygen of $sp^3$ hybridization

$$\left.\begin{aligned}
\mu_x &= \frac{2}{3}\left(\frac{e\hbar}{mc}\right)^2 H\left\{\frac{(a^*)^2}{\varepsilon^*_{OH}-\varepsilon_{lsp^3}}\right\}\\
\mu_y &= \frac{5}{6}\left(\frac{e\hbar}{mc}\right)^2 H\left\{\frac{(a^*)^2}{\varepsilon^*_{OH}-\varepsilon_{lsp^3}}\right\}\\
\mu_z &= \frac{1}{2}\left(\frac{e\hbar}{mc}\right)^2 H\left\{\frac{2(aa^*)^2}{\varepsilon^*_{OH}-\varepsilon_{OH}}\right.\\
&\quad \left.+\frac{(a^*)^2}{\varepsilon^*_{OH}-\varepsilon_{lsp^3}}\right\}
\end{aligned}\right\} \quad (10)$$

These equations are derived according to the procedure of Pople.[3] In Eqs. 7, 8, 9 and 10, $\varepsilon_{XY}$ and $\varepsilon^*_{XY}$ denote the energies of the bonding and antibonding X-Y orbitals, and $\varepsilon_{l2pz}$, $\varepsilon_{lsp^2}$ and $\varepsilon_{lsp^3}$ are those of one electron of the lone pair in 2pz, $sp^2$ and $sp^3$ hybridized orbitals. The wave functions of the bonding and antibonding C-O and O-H obtitals are expressed, for the sake of simplicity, by the linear combination of two atomic orbitals with the coefficients which appear in Eqs. 7, 8, 9 and 10:

$$\left.\begin{aligned}
\varphi_{OH} &= a\chi_O + b\chi_H\\
\varphi^*_{OH} &= a^*\chi_O + b^*\chi_H\\
\varphi_{CO} &= c\chi_O + d\chi_C\\
\varphi^*_{CO} &= c^*\chi_O + d^*\chi_C
\end{aligned}\right\} \quad (11)$$

To carry out the numerical calculation, these energies and coefficients were determined by a similar procedure, one which appeared in one of our previous papers,[7] using empirical data such as the ionization potentials, bond moments and absorption spectra of related compounds, $R$ was taken as 0.958 Å, corresponding to a standard bond distance of the O-H bond. These values are summarized in Tables III and IV. All the energy levels in Table IV are given relative to the value of $\varepsilon_{OH}$ for the two cases stated above. Here we made a crude assumption that the variation in the molecular orbital coefficients and energies representing the characteristics of the O-H and C-O bonds for the diols and related compounds may be ignored.

TABLE III. MOLECULAR ORBITAL COEFFICIENTS

| MO Coefficients of MO's for | O-H | | C-O | |
|---|---|---|---|---|
| | $a^2$ | $(a^*)^2$ | $c^2$ | $(c^*)^2$ |
| $sp^2$ system | 0.600 | 0.400 | 0.500 | 0.500 |
| $sp^3$ system | 0.539 | 0.461 | 0.500 | 0.500 |

TABLE IV. MOLECULAR ORBITAL ENERGIES $\varepsilon_{X-Y}$'s

| Energy of $\varepsilon_{X-Y}$ in $sp^2$ system | Energy of $\varepsilon_{X-Y}$ in $sp^3$ system |
|---|---|
| $\varepsilon_{O-H}=0$ | $\varepsilon_{O-H}=0$ |
| $\varepsilon_{C-O}=-2.0$ eV. | $\varepsilon_{C-O}=-2.0$ eV. |
| $\varepsilon_{lsp^2}=+1.0$ eV. | $\varepsilon_{lsp^3}=+2.5$ eV. |
| $\varepsilon_{l2pz}=+2.0$ eV. | $\varepsilon^*_{O-H}=+10.0$ eV. |
| $\varepsilon^*_{C-O}=+12.0$ eV. | $\varepsilon^*_{C-O}=+12.0$ eV. |
| $\varepsilon^*_{O-H}=+10.0$ eV. | |

The shielding constants, $\sigma_{para}(O)$, thus calculated with the aid of Eq. 6 become:

| | $H_2O$ | COH |
|---|---|---|
| $sp^2$ system | +3.42 p.p.m. | +2.89 p.p.m. |
| $sp^3$ system | +2.02 p.p.m. | +2.18 p.p.m. |

On the shielding constant, $\sigma_{para}(O)$, for the proton in $H_2O$, Pople[3] obtained +2.75 p. p. m. by using the results of the LCAO MO SCF calculation performed by Ellison and Shull.[8] Using the same results, Matsuoka and Hattori[9] obtained an alternative value of +3.47 p. p. m. It may be concluded that the present result for $H_2O$ is reasonable.

With the shielding constants calculated by Eqs. 3 and 6, the free OH shift of the proton in $H_2O$ becomes −0.65 p. p. m. for the $sp^2$ hybrid system and −1.03 p. p. m. for the $sp^3$ system, whereas the chemical shift of gaseous $H_2O$ is −0.60 p. p. m.[10] Hence, the agreement between theoretical and experiment is

7) T. Yonezawa, K. Fukui, H. Kato, H. Kitano, S. Hattori and S. Matsuoka, This Bulletin, 34, 707 (1961).
8) E. O. Ellison and H. Shull, *J. Chem. Phys.*, 33, 2348 (1955).
9) S. Matsuoka and S. Hattori, unpublished.
10) J. A. Pople, W. G. Schneider and H. J. Bernstein, "High-resolution Nuclear Magnetic Resonance," McGraw-Hill, New York (1959), pp. 90, 410.

TABLE V. HYDROGEN BOND SHIFTS OF THE DIOLS (in units of p. p. m.)

| | Free OH proton[a] shift (calculated) | Maximum[a] OH proton shift | Hydrogen bond[a] shift (calculated) | Frequency shift of OH stretching due to intramolecular hydrogen bond in the infrared spectra ($cm^{-1}$) |
|---|---|---|---|---|
| $HOCH_2CH_2OH$ | −0.56 | −6.28 | 5.72 | 32[b] |
| $HOCH_2CH(OH)CH_3$ | −0.56 | −6.43 | 5.87 | 45[c] |
| $HOCH_2CH_2CH_2OH$ | −0.56 | −6.43 | 5.87 | 78[b] |
| $CH_3CH(OH)CH(OH)CH_3$ | −0.56 | −5.93 | 5.37 | 39[b] |
| $HOCH_2CH_2CH_2CH_2OH$ | −0.56 | −6.03 | 5.47 | 156[b] |
| $HOCH_2CH_2CH_2CH_2CH_2OH$ | −0.56 | −6.44 | 5.58 | 30[c] |

a) The observed proton shift referred to methylene chloride is converted to the shift referred to gaseous methane.
b) L. P. Kuhn, *J. Am. Chem. Soc.*, **74**, 2492 (1952).
c) Measured by present authors using Perkin-Elmer 125 spectrometer.

better when $sp^2$ hybridization is assumed for the oxygen atom. For ethanol, the OH shift calculated relative to gaseous methane becomes −0.97 p. p. m. if the hybridization of the oxygen atom is assumed to be $sp^3$ and if the experimental value is −0.48 p. p. m.[10] In the following calculation, the value of +2.60 p. p. m. is adopted for the shielding constant, $\sigma_{para}(O)$, in the diols, since better agreement is obtained if we adopt +2.60 p. p. m. for the shielding constant, $\sigma_{para}(O)$, which ranges from +2.89 p. p. m. to +2.18 p. p. m. with the change in the hybridization of the oxygen atom, as has been shown above.

## Results and Discussion

The hydrogen bond shift, $\Delta$, is defined as the difference between the free OH proton shift, $\delta_2$, and the maximum OH proton shift as measured in a pure liquid state referred to gaseous methane, $\delta_1$, as follows:

$$\Delta = \delta_2 - \delta_1 \qquad (12)$$

The free OH proton shift is obtained theoretically as has been described above, while the OH maximum shift is measured at a temperature just above the freezing point. The hydrogen bond shifts thus calculated are listed in Table V. The second column of the table shows free OH shifts; the third column, OH proton shifts referred to gaseous methane, and the final column, frequency shifts of the OH stretching vibrations due to intramolecular hydrogen bonds in the infrared spectra.

The hydrogen bond shifts listed in Table V show that the values for the diols are 5.37 −5.87 p. p. m. and are smaller than that of ethanol, 6.15 p. p. m.[11] This seems reasonable, since in the diols there exists a considerable number of intramolecular hydrogen bonds and probably some free OH groups, which cause a small hydrogen bond shift, while there is no free OH proton in the linear structure of the alcohols at a low temperature. The infrared spectra show the intramolecular hydrogen bond to be weaker than the intermolecular bond. This correlation in NMR spectra will be discussed in a following paper.

The authors are grateful for the help given by Dr. Yo-ichiro Mashiko, Dr. Kenkichi Nukada (present address: Toyo Rayon Co., Ltd.) and Dr. Osamu Yamamoto of the Government Chemical Industrial Research Institute, Tokyo, and by the Japan Electron Optics Laboratory Co., Ltd.

*Faculty of Engineering*
*Kyoto University*
*Sakyo-ku, Kyoto*
*(T. Y., H. S. & K. F.)*

*Faculty of Science*
*Kanazawa University*
*Kanazawa (S. M.)*

11) Ibid., p. 412.

# The Fractionation of Halogen Compounds through the Process of the Volatilization and the Sublimation from Volcanic Rocks on Heating*

By Minoru YOSHIDA, Ichiro MAKINO, Norinobu YONEHARA and Iwaji IWASAKI

(Received September 16, 1964)

The fractionation of elements through the deposition of the solid phases from magmatic gas is one of the most important processes in the differentiation of the magmatic emanation;[1] the solid phases thus formed appear in nature as volcanic sublimates. The "volcanic sublimates" observed at craters or fumaroles are not, however, always the true sublimates deposited from the magmatic emanation; they also include products of reactions among volcanic gases, surface waters and wall rocks. We can not yet clearly distinguish the true sublimates from others, such as the alteration products of the surrounding rocks.

Brun[2] reported in 1911 that ammonium chloride and some other chlorides sublimed from igneous rocks on heating. One of the present authors (M. Y.) reported in a previous paper[3] that small amounts of fluorine and chlorine were deposited on the surface of a silica-glass tube (or on the surface of a hard glass cap) on out-gassing the igneous rocks by heating them above 800°C, and that sodium and ammonium ions were found as the corresponding cations by qualitative tests. These results suggest that a detailed study of the sublimates formed in the laboratory experiments will give exact information about the sublimates directly derived from the magmatic emanation. The results of the previous study[3] and of the preliminary experiments indicate that the main parts of the sublimates are water-soluble and are composed mainly of chlorine, fluorine, sodium, potassium and ammonium.

To study the fractionation of these chemical species during sublimation, the sublimates deposited on the surface of the silica-glass tube were collected into several fractions, at 100°C intervals, by using a thermal-gradient furnace and silica-glass tubes designed for this purpose. The amounts of the chemical species mentioned above were determined separately in each fraction. Further, the amounts of bromine and iodine volatilized and sublimed from volcanic rocks were determined. Qualitative tests were also run in order to examine if there were some other compounds sublimed from the volcanic rock.

## Experimental

**Materials.**—The rock samples used in the study are listed in Table I, together with their chlorine, fluorine, sodium and potassium contents. The bromine and iodine in these rocks have not yet been determined. The bromine content of basalt from Ō-sima was reported by Sugiura et al.[4] as 0.00003%. The methods used in the determination of fluorine and chlorine in the rocks were the same as those used in the previous study.[3] The main chemical compositions of these rocks are also known.[5,6]

Reagent-grade chemicals and redistilled water were used in the preparation of all reagents and in the procedure described in the following section.

**Apparatus and Procedures.**—The apparatus used in this study is shown in Fig. 1. A platinum

TABLE I. HALOGEN AND ALKALI CONTENTS OF THE ROCK SPECIMENS USED IN THE PRESENT STUDY

| No. | Sample | F% | Cl% | Na% | K% |
|---|---|---|---|---|---|
| 1 | Basalt (lava of 1950 Mt. Mihara, Ō-sima Volcano, Tōkyō Metr.) | 0.011 | 0.031 | 1.5 | 0.37 |
| 2 | Basalt (lava of 1962 Miyake-zima Volcano, Tōkyō Metr.) | 0.020 | 0.060 | 2.1[6] | 0.52[6] |
| 3 | Andesite (lava of 1946 Sakura-zima Volcano, Kagosima Pref.) | 0.035 | 0.033 | 2.1[5] | 1.2[5] |
| 4 | Glassy andesite (lava of 1934 Shōwa-iwō-zima Volcano, Kagosima Pref.) | 0.055 | 0.060 | 2.5[5] | 1.4[5] |
| 5 | Liparite (Kōzu-sima Volcano, Tōkyō Metr.) | 0.025 | 0.091 | 3.3[5] | 1.3[5] |
| 6 | Obsidian (Imari, Saga Pref.) | 0.049 | 0.062 | 2.3[5] | 3.9[5] |

* A part of this report has been published in Japanese; *Bull. Volcanolog. Soc. Japan* (*Kazan*), 2nd Series, 9, 1 (1964).

1) I. Iwasaki, T. Ozawa, M. Yoshida, T. Katsura, B. Iwasaki, M. Kamada and M. Hirayama, *Bull. Tokyo Inst. Tech.*, No. 47, 1 (1962).

2) A. Brun, "Recherches sur l'Exhalation Volcanique," Libraire Kündig, Genéve (1911).

3) M. Yoshida, This Bulletin, 36, 773 (1963).

4) T. Sugiura, M. Takeuchi, M. Watabe and M. Nagao, Read at the Symposium on Geochemistry of the Geochemical Society of Japan and the Chemical Society of Japan, October, 1963.

5) Geological Survey of Japan, "Chemical Composition of Volcanic Rocks in Japan" (1962).

6) T. Matsuda and R. Morimoto, *Science* (*Kagaku*), 32, 578 (1962).

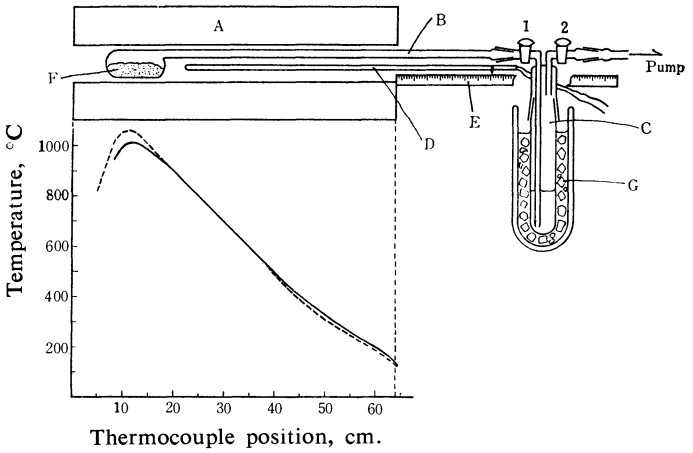



Fig. 1. Apparatus and thermogradient curve in the furnace.

A Thermal-gradient furnace
B Silica-glass tube
C Absorption vessel
D Thermocouple
E Stainless steel scale
F Sample
G Ice-water
1,2 Stopcock
—— Curve measured at the inside of the silica-glass tube
---- Curve measured at the outside of the silica-glass tube

TABLE II. METHODS OF ANALYSIS

| | Method | Concentration limit of determination | Precision |
|---|---|---|---|
| $F^-$ | *p*-Dimethylaminoazophenylarsonic acid - Zr method[7] | A 0.02—1 p. p. m.<br>B 0.2 —10 p. p. m. | ±0.02 p. p. m.<br>±0.1 p. p. m. |
| $Cl^-$ | Mercuric thiocyanate method (improved method[8]) | 0.05—20 p. p. m. | ±0.05 p. p. m. |
| $Br^-$ | Method by its catalytic action on the reaction between $I_2$ and $MnO_4^-$ [9] | 0.01—0.1 p. p. m. | ±0.004 p. p. m. |
| $I^-$ | Method by its catalytic action on the oxidation of $FeSCN^{2+}$ [10] | 1 —10 p. p. b. | ±0.2 p. p. b. |
| $NH_4^+$ | Nessler's method | 0.1 —20 p. p. m. | ±0.05 p. p. m. |
| $Na^+$ | Flame photometric method | 0.05—100 p. p. m. | ±5% in relative error |
| $K^+$ | Flame photometric method | 0.05—100 p. p. m. | ±5% in relative error |

resistance furnace (A) is so made as to obtain an almost linear thermal gradient of 20°C/cm. from 200°C to 1000°C. The temperature distribution is controlled by two transformers; one is connected to a main heater, and the other to an auxiliary heater. The temperature in the furnace is measured by a pyrometer with a movable platinum-platinum, 10% rhodium thermocouple (D); the thermocouple position is read by a stainless steel measure (E) attached to the furnace.

The temperature distribution curves in the furnace measured at the inside and at the outside of the silica-glass tube are also shown in Fig. 1. In the main experiments, the temperature was first measured at the outside and was then corrected to the inside value by means of these curves. The constancy of the distribution of the temperature during an experiment was enough for the present purpose.

The shape of the silica-glass tube used is also shown in Fig. 1 (B). The big end of the tube is 36 mm. in inside diameter and 10 cm. long, while the narrower part is 6 mm. in inside diameter and 65 cm. long. The narrower end of the tube is connected by a taper joint to the absorption vessel (C), which is made of borosilicate glass. To minimize the contamination, the tube was heated and washed twice before use.

Fifty grams of a finely-powdered sample were packed into the big end of the silica-glass tube by using a thistle tube like that used in Penfield's method for the determination of water in rocks. The tube was then connected to the absorption vessel and carefully evacuated to $10^{-1}$—$10^{-2}$ mmHg. The cock 1 was closed and about 10 ml. of redistilled water was introduced into the vessel. After

7) M. Kamada, T. Ōnishi and M. Ōta, This Bulletin, **28**, 148 (1955); M. Kamada and T. Ōnishi, *J. Chem. Soc. Japan, Pure Chem. Sec.* (*Nippon Kagaku Zasshi*), **80**, 275 (1959).
8) A. Tomonari, ibid., **83**, 693 (1962).
9) M. Shiota, S. Utsumi and I. Iwasaki, ibid., **80**, 753 (1959).
10) S. Utsumi, M. Shiota, N. Yonehara and I. Iwasaki, ibid., **85**, 32 (1964); I. Iwasaki, S. Utsumi and N. Yonehara, ibid., **85**, 36 (1964); N. Yonehara, This Bulletin, **37**, 1101 (1964).

the vessel had been sufficiently evacuated again, cock 1 was opened and cock 2 was closed. Then the silica-glass tube was inserted into the furnace, which had been heated beforehand to obtain the programed temperature distribution, at the sample site temperature of 1000°C. The absorption vessel was cooled by ice water.

About 15 min. were necessary for the stable temperature distribution to be attained. The temperature distribution in the furnace was charefully checked throughout the experiment and was controlled by the transformers if necessary. After 3 hours' heating, cock 1 was closed and the furnace was cooled. Small amounts of liquid water were condensed on the cold part of the tube.

After the furnace had been cooled, a part of the

TABLE III. THE AMOUNTS OF HALOGEN AND ALKALI RELEASED AT 1000°C AND SUBLIMED AT VARIOUS TEMPERATURES

Sample No. 1 Basalt, Ō-sima volcano

| | | μg. | | | | | | | Atomic ratio | | |
|---|---|---|---|---|---|---|---|---|---|---|---|
| | | F | Cl | Br | I | $NH_4$ | Na | K | F/Cl | Br/Cl | I/Cl |
| Abs. | | 240 | 3400 | 1.1 | 0.48 | 100 | 25 | 15 | 0.13 | $1.4\times10^{-4}$ | $3.9\times10^{-5}$ |
| Sub. | <200°C | 26 | 520 | 3.8 | 0.78 | 280 | 20 | 5 | $0.09_3$ | $3.2\times10^{-3}$ | $4.2\times10^{-4}$ |
| | 200—300 | 2 | 20 | 0.0 | 0.12 | 0 | 10 | 0 | 0.2 | $<2\times10^{-3}$ | $1.7\times10^{-3}$ |
| | 300—400 | 1 | 10 | 0.0 | 0.05 | 0 | 10 | 0 | (0.2) | $(<4\times10^{-3})$ | $(1\times10^{-3})$ |
| | 400—500 | 3 | 10 | 0.0 | 0.00 | 0 | 15 | 5 | (0.5) | $(<4\times10^{-3})$ | $(<3\times10^{-4})$ |
| | 500—600 | 2 | 30 | 0.0 | 0.00 | 10 | 10 | 10 | 0.1 | $<1\times10^{-3}$ | $<1\times10^{-4}$ |
| | 600—700 | 1 | 20 | 0.0 | 0.00 | 0 | 5 | 5 | (0.1) | $<2\times10^{-3}$ | $<2\times10^{-4}$ |
| | 700—800 | 1 | 0 | 0.0 | 0.00 | 0 | 0 | 0 | (>0.2) | — | — |
| | 800—900 | 1 | 0 | 0.0 | 0.00 | 0 | 0 | 0 | (>0.2) | — | — |
| Total sub. | | 37 | 610 | 3.8 | 0.95 | 290 | 70 | 25 | 0.11 | $2.8\times10^{-3}$ | $4.3\times10^{-4}$ |
| Total evolved | | 280 | 4000 | 4.9 | 1.43 | 390 | 95 | 40 | 0.13 | $5.4\times10^{-4}$ | $1.0\times10^{-4}$ |

Sample No. 2 Basalt, Miyake-zima volcano

| | | μg. | | | | | | | Atomic ratio | | |
|---|---|---|---|---|---|---|---|---|---|---|---|
| | | F | Cl | Br | I | $NH_4$ | Na | K | F/Cl | Br/Cl | I/Cl |
| Abs. | | 340 | 5100 | 4.0 | 0.98 | 75 | 0 | 5 | 0.12 | $3.5\times10^{-4}$ | $5.4\times10^{-5}$ |
| Sub. | <200°C | 40 | 350 | 8.0 | 0.15 | 195 | 5 | 5 | 0.21 | $1.0\times10^{-2}$ | $1.2\times10^{-4}$ |
| | 200—300 | 1 | 0 | 0.6 | 0.06 | 0 | 0 | 0 | (>0.2) | $>2\times10^{-2}$ | $>2\times10^{-3}$ |
| | 300—400 | 1 | 0 | 0.0 | 0.00 | 0 | 0 | 5 | (>0.2) | — | — |
| | 400—500 | 2 | 0 | 0.0 | 0.00 | 0 | 5 | 5 | >0.4 | — | — |
| | 500—600 | 2 | 30 | 0.5 | 0.00 | 0 | 20 | 15 | 0.12 | $7\times10^{-3}$ | $<1\times10^{-4}$ |
| | 600—700 | 1 | 100 | 0.6 | 0.00 | 0 | 45 | 20 | (0.02) | $3\times10^{-3}$ | $<3\times10^{-5}$ |
| | 700—800 | 2 | 0 | 0.0 | 0.00 | 0 | 0 | 0 | >0.4 | — | — |
| | 800—900 | 1 | 0 | 0.0 | 0.06 | 0 | 0 | 0 | (>0.2) | — | $>2\times10^{-3}$ |
| Total sub. | | 50 | 480 | 9.7 | 0.27 | 195 | 75 | 50 | 0.19 | $9.0\times10^{-3}$ | $1.6\times10^{-4}$ |
| Total evolved | | 390 | 5600 | 14 | $1.2_5$ | 270 | 75 | 55 | 0.13 | $1.1\times10^{-3}$ | $6.2\times10^{-5}$ |

Sample No. 3 Andesite, Sakura-zima volcano

| | | μg. | | | | | | | Atomic ratio | | |
|---|---|---|---|---|---|---|---|---|---|---|---|
| | | F | Cl | Br | I | $NH_4$ | Na | K | F/Cl | Br/Cl | I/Cl |
| Abs. | | 380 | 3200 | 1.7 | 0.90 | 75 | 10 | 5 | 0.22 | $2.4\times10^{-4}$ | $7.8\times10^{-5}$ |
| Sub. | <200°C | 150 | 550 | 5.8 | 0.78 | 350 | 5 | 5 | 0.51 | $4.7\times10^{-3}$ | $4.0\times10^{-4}$ |
| | 200—300 | 1 | 0 | 0.0 | 0.08 | 0 | 0 | 5 | (>0.2) | — | $>2\times10^{-3}$ |
| | 300—400 | 1 | 0 | 0.0 | 0.20 | 10 | 0 | 0 | (>0.2) | — | $>6\times10^{-3}$ |
| | 400—500 | 1 | 0 | 0.0 | 0.00 | 10 | 0 | 0 | (>0.2) | — | — |
| | 500—600 | 1 | 0 | 0.0 | 0.00 | 0 | 0 | 0 | (>0.2) | — | — |
| | 600—700 | 1 | 20 | 0.0 | 0.00 | 10 | 15 | 15 | (0.1) | $<2\times10^{-3}$ | $<2\times10^{-4}$ |
| | 700—800 | 1 | 0 | 0.0 | 0.00 | 10 | 0 | 0 | (>0.2) | — | — |
| | 800—900 | 0 | 0 | 0.0 | 0.00 | 0 | 0 | 0 | — | — | — |
| Total sub. | | 156 | 570 | 5.8 | $1.0_6$ | 390 | 20 | 25 | 0.51 | $4.5\times10^{-3}$ | $5.2\times10^{-4}$ |
| Total evolved | | 540 | 3800 | 7.5 | $1.9_6$ | 470 | 30 | 30 | 0.27 | $8.8\times10^{-4}$ | $1.5\times10^{-4}$ |

TABLE III (Continued)

Sample No. 4 Glassy andesite, Syōwa-iwō-zima volcano

| | | μg. | | | | | | | Atomic ratio | | |
|---|---|---|---|---|---|---|---|---|---|---|---|
| | | F | Cl | Br | I | $NH_4$ | Na | K | F/Cl | Br/Cl | I/Cl |
| Abs. | | 1600 | 11200 | 6.5 | 0.26 | 160 | 20 | 5 | 0.27 | $2.6\times10^{-4}$ | $6.5\times10^{-6}$ |
| Sub. | <200°C | 12 | 750 | 18.6 | 0.32 | 370 | 0 | 0 | 0.030 | $1.1\times10^{-2}$ | $1.2\times10^{-4}$ |
| | 200—300 | 7 | 25 | 0.3 | 0.03 | 0 | 0 | 0 | 0.5 | $5\times10^{-3}$ | $3\times10^{-4}$ |
| | 300—400 | 5 | 15 | 0.5 | 0.02 | 0 | 0 | 0 | 0.6 | $1.5\times10^{-2}$ | $4\times10^{-4}$ |
| | 400—500 | 3 | 35 | 0.1 | 0.03 | 0 | 15 | 15 | 0.2 | $1\times10^{-3}$ | $2\times10^{-4}$ |
| | 500—600 | 1 | 10 | 0.0 | 0.02 | 0 | 5 | 10 | (0.2) | ($<4\times10^{-3}$) | ($5\times10^{-4}$) |
| | 600—700 | 0 | 75 | 0.2 | 0.03 | 0 | 45 | 20 | <0.03 | $1\times10^{-3}$ | $1\times10^{-4}$ |
| | 700—800 | 0 | 0 | 0.0 | 0.03 | 0 | 0 | 0 | — | — | $>8\times10^{-4}$ |
| | 800—900 | 0 | 0 | 0.0 | 0.02 | 0 | 0 | 0 | — | — | $>5\times10^{-4}$ |
| Total sub. | | 28 | 910 | 19.7 | 0.50 | 370 | 65 | 45 | 0.057 | $9.6\times10^{-3}$ | $1.5\times10^{-4}$ |
| Total evolved | | 1630 | 12100 | 26.2 | 0.76 | 530 | 85 | 50 | 0.25 | $9.6\times10^{-4}$ | $1.8\times10^{-5}$ |

Sample No. 5 Liparite, Kōzu-sima

| | | μg. | | | | | | | Atomic ratio | | |
|---|---|---|---|---|---|---|---|---|---|---|---|
| | | F | Cl | Br | I | $NH_4$ | Na | K | F/Cl | Br/Cl | I/Cl |
| Abs. | | 780 | 29100 | 10 | 0·10 | 260 | 5 | 10 | 0.050 | $1.5\times10^{-4}$ | $9.6\times10^{-7}$ |
| Sub. | <200°C | 44 | 1310 | 57 | 1.1 | 660 | 5 | 5 | 0.063 | $1.9\times10^{-2}$ | $2.3\times10^{-4}$ |
| | 200—300 | 1 | 80 | 3.9 | 0.12 | 0 | 0 | 0 | (0.02) | $2.2\times10^{-2}$ | $4.2\times10^{-4}$ |
| | 300—400 | 1 | 15 | 0.8 | 0.03 | 0 | 0 | 0 | (0.1) | $2.4\times10^{-2}$ | $6\times10^{-4}$ |
| | 400—500 | 3 | 40 | 0.1 | 0.03 | 0 | 0 | 5 | 0.1 | $1\times10^{-3}$ | $2\times10^{-4}$ |
| | 500—600 | 4 | 155 | 0.2 | 0.03 | 10 | 30 | 35 | 0.05 | $6\times10^{-4}$ | $5\times10^{-5}$ |
| | 600—700 | 0 | 100 | 0.3 | 0.03 | 10 | 40 | 10 | <0.02 | $1\times10^{-3}$ | $8\times10^{-5}$ |
| | 700—800 | 0 | 0 | 0.0 | 0.02 | 0 | 0 | 0 | — | — | ($>5\times10^{-4}$) |
| | 800—900 | 0 | 0 | 0.0 | 0.03 | 0 | 0 | 0 | — | — | ($>8\times10^{-4}$) |
| Total sub. | | 53 | 1700 | 62 | 1.4 | 680 | 75 | 55 | 0.058 | $1.6\times10^{-2}$ | $2.3\times10^{-4}$ |
| Total evolved | | 830 | 30800 | 72 | 1.5 | 940 | 80 | 65 | 0.050 | $1.0\times10^{-3}$ | $1.4\times10^{-5}$ |

Sample No. 6 Obsidian, Imari

| | | μg. | | | | | | | Atomic ratio | | |
|---|---|---|---|---|---|---|---|---|---|---|---|
| | | F | Cl | Br | I | $NH_4$ | Na | K | F/Cl | Br/Cl | I/Cl |
| Abs. | | 1400 | 17000 | 13 | 0.50 | 55 | 5 | 5 | 0.15 | $3.4\times10^{-4}$ | $8.2\times10^{-6}$ |
| Sub. | <200°C | 85 | 560 | 12 | 0.30 | 270 | 0 | 5 | 0.28 | $9.5\times10^{-3}$ | $1.5\times10^{-4}$ |
| | 200—300 | 0 | 60 | 0.7 | 0.06 | 0 | 0 | 5 | <0.03 | $5\times10^{-3}$ | $3\times10^{-4}$ |
| | 300—400 | 2 | 15 | 0.0 | 0.00 | 0 | 0 | 0 | 0.2 | $<3\times10^{-3}$ | $<2\times10^{-4}$ |
| | 400—500 | 3 | 70 | 0.0 | 0.00 | 0 | 20 | 25 | 0.08 | $<6\times10^{-4}$ | $<5\times10^{-5}$ |
| | 500—600 | 8 | 80 | 0.0 | 0.00 | 0 | 20 | 25 | 0.19 | $<5\times10^{-4}$ | $<4\times10^{-5}$ |
| | 600—700 | 2 | 5 | 0.0 | 0.00 | 0 | 0 | 5 | (0.7) | ($<1\times10^{-2}$) | ($<6\times10^{-4}$) |
| | 700—800 | 0 | 0 | 0.0 | 0.00 | 0 | 0 | 0 | — | — | — |
| | 800—900 | 1 | 5 | 0.0 | 0.00 | 10 | 0 | 0 | (0.4) | ($<1\times10^{-2}$) | ($<6\times10^{-4}$) |
| Total sub. | | 101 | 800 | 13 | 0.36 | 280 | 40 | 65 | 0.28 | $7.7\times10^{-3}$ | $1.4\times10^{-4}$ |
| Total evolved | | 1500 | 17800 | 26 | 0.86 | 340 | 45 | 70 | 0.16 | $6.5\times10^{-4}$ | $1.4\times10^{-5}$ |

silica-glass tube where water was condensed was cut off and washed with water. The washing and the solution in the absorption vessel were combined and made up to 100 ml. in a volumetric flask. The other part of the tube was carefully observed by the naked eyes and by using a magnifying lens. The tube was cut into several pieces of lengths corresponding to the temperature intervals of 100°C. Each piece was washed with water, and the washings were analyzed for halogens and for sodium, potassium and ammonium ions.

The methods for the determination of these chemical species are listed in Table II, together with their precision and the concentration limits of the determination.

The solution in the absorption vessel was made

turbid by colloidal sulfur in some experiments. In these cases, an aliquot of the solution was heated by the addition of sodium peroxide to oxidize the sulfur compounds. The halogen content was determined from this solution. Another portion was treated with basic zinc carbonate to remove sulfides, and the ammonium ion content was determined from this. The sodium and potassium contents were determined from the original solution.

## Results

Two white spots were observed in the silica-glass tube in all the experiments; one was seen in the 100—200°C range and the other in the 500—700°C range. These two spots were soluble in water. A red or reddish-yellow spot was often found in the 500—700°C range; it was only partly soluble in water, but wholly soluble in 6 N hydrochloric acid. The washings of the pieces of the tube corresponding to the 500—700°C range showed reactions of ferric iron. It has not yet been confirmed what kinds of iron compounds were deposited and how iron was transported. A yellowish-white spot which was insoluble in water was observed in the 100—200°C range in some experiments; this was confirmed to be sulfur by qualitative tests.

The results of the determination of water-soluble halogens and alkalies are shown in Table III, together with the F/Cl, Br/Cl and I/Cl atomic ratios. In this table, "Abs." indicates the amounts of the chemical species found from the solution in the absorption vessel plus the liquid water condensed at the cold part of the silica-glass tube. "Sub." means the amounts of the chemical species found in the washings of each fraction of the tube cut out at 100°C intervals. In the columns of atomic ratios, ( ) means that the amounts of the halogens are fairly small and that the atomic ratio might, therefore, contain a comparatively larger error, while > means that the exact value of the atomic ratio can not be calculated, but only a lower limit of the value given, because the amount of chlorine evolved is smaller than the limit of exact determination.

The amounts of the chemical species contaminated in the experimental procedures were found to be smaller than the lower limit of the determination by means of blank tests.

## Discussion

First, comparison between the total amounts of the chemical species evolved from the rocks at 1000°C and those originally contained in the rocks are made. The $(X_{\text{total evolved}}/X_{\text{rock}}) \times 100$ values are calculated in Table IV for the elements the contents of which in the rocks are known.

TABLE IV

| Sample No. | $(X_{\text{total evolved}}/X_{\text{rock}}) \times 100$ | | | | |
|---|---|---|---|---|---|
| | F | Cl | Br | Na | K |
| 1 | 5.5 | 26 | 33 | 0.0013 | 0.0021 |
| 2 | 3.9 | 19 | — | 0.0007 | 0.0021 |
| 3 | 3.1 | 23 | — | 0.0003 | 0.0005 |
| 4 | 5.9 | 40 | — | 0.0007 | 0.0007 |
| 5 | 6.7 | 68 | — | 0.0005 | 0.0010 |
| 6 | 6.1 | 57 | — | 0.0004 | $0.0003_5$ |

The amounts of sodium and potassium volatilized from the rocks at 1000°C are very small compared with the amounts in the rocks. Fairly large amounts of chlorine and bromine are evolved from the rock at 1000°C, and the $(Br/Cl)_{\text{total evolved}}$ value is almost equal to the $(Br/Cl)_{\text{rock}}$ value, although there is only one datum on the bromine content in the rock. The $(Cl_{\text{total evolved}}/Cl_{\text{rock}}) \times 100$ value decreases with an increase in the amounts of the sample; this should be compared with the results of the previous report,[3] in which only 1 g. of the samples was used. The effect is more remarkable in the case of fluorine. The mean value of $(F_{\text{total evolved}}/F_{\text{rock}}) \times 100$ was about 50% in the previous study, but only about 5% in this study. The "$(F/Cl)_{\text{evolved}} < (F/Cl_{\text{rock}})$" relation is more clearly recognized in this study than in the previous study.

The second problem to be discussed is the distribution of the chemical species between "Abs." and "Sub." The $(X_{\text{total sub.}}/X_{\text{total evolved}}) \times 100$ values are calculated in Table V.

TABLE V

| Sample No. | $(X_{\text{total sub.}}/X_{\text{total evolved}}) \times 100$ | | | | | | |
|---|---|---|---|---|---|---|---|
| | F | Cl | Br | I | $NH_4$ | Na | K |
| 1 | 13 | 15 | 78 | 66 | 74 | 74 | 63 |
| 2 | 13 | 8.6 | 71 | 22 | 72 | 100 | 91 |
| 3 | 29 | 15 | 77 | 54 | 84 | 67 | 83 |
| 4 | 1.7 | 7.5 | 75 | 66 | 70 | 77 | 90 |
| 5 | 6.4 | 5.5 | 86 | 93 | 72 | 94 | 85 |
| 6 | 6.7 | 4.5 | 49 | 42 | 84 | 89 | 93 |

Large percentages of sodium, potassium, ammonium and bromine are deposited on the silica-glass tube. The amounts of chlorine and fluorine deposited are small as compared to those absorbed in water while the amounts of iodine deposited are comparable to those absorbed. The "$(F/Cl)_{\text{abs.}} \fallingdotseq (F/Cl)_{\text{total sub.}}$," "$(Br/Cl)_{\text{abs.}} < (Br/Cl)_{\text{total sub.}}$" and "$(I/Cl)_{\text{abs.}} < (I/Cl)_{\text{total sub.}}$" relations may, therefore, be recognized. On the other hand, Yoshida reported in a previous paper[3] that the $(F/Cl)_{\text{sub.}}$ ratio is always larger than the $(F/Cl)_{\text{abs.}}$ ratio. The discrepancy between the two reports may be ascribed to the difference between the materials

on which the halogens were deposited. In the present study, "sublimates" are deposited on the silica-glass surface only. On the other hand, in the previous study "sublimates" might be deposited not only on the silica-glass surface, but also on the hard-glass surface used as a cap for the connection to the absorption vessels. This difference indicates that the main portion of the fluorine determined as "Sub." in the previous study was not a true sublimate, but was deposited by the reaction with the silicate surface.

The third point to be discussed is the problem of how the chemical species are distributed among the sublimates deposited in various temperature regions. To see the general tendency of the distribution, $[X_{(t-t+100°C)\,sub.}/X_{total\,sub.}]\times 100$ values were calculated; their mean values are shown in Table VI.

TABLE VI

Mean values of the $[X_{(t-t+100°C)sub.}/X_{total\,sub.}]\times 100$ for 6 experiments

| Temp., °C | F | Cl | Br | I | $NH_4$ | Na | K |
|---|---|---|---|---|---|---|---|
| <200 | 76 | 80 | 94 | 73 | 97 | 11 | 11 |
| 200—300 | 6 | 3 | 2 | 12 | 0 | 2 | 4.5 |
| 300—400 | 4.5 | 1 | 0.5 | 5 | 0 | 2 | 1.5 |
| 400—500 | 5 | 3 | 0 | 1 | 0 | 17 | 18 |
| 500—600 | 5 | 5 | 1 | 1 | 1 | 23 | 32 |
| 600—700 | 1 | 7 | 1 | 1 | 0.5 | 44 | 32 |
| 700—800 | 1 | 0 | 0 | 1 | 0.5 | 0 | 0 |
| 800—900 | 1 | 0 | 1 | 5 | 0.5 | 0 | 0 |

The following facts may be seen in Table VI:

1) Chlorine and fluorine resemble each other in their distributions. About eighty per cent of each is deposited below 200°C and they show a second maximum in the region between 400°C and 700°C.

2) Almost all ammonium compounds are deposited below 200°C.

3) Large percentages of sodium and potassium are deposited between 400°C and 700°C.

4) Almost all bromine is deposited below 200°C, as in the case of the ammonium compound.

5) Iodine is also largely deposited below 200°C, but it is distributed in higher temperature regions, unlike bromine.

The equivalent relations between the total amounts of cations determined and those of anions are examined for every fraction in Table III. Cations are very deficient in the "Abs." fractions because of the existence of free halogen acids in the solutions. In most "Sub." fractions, the amounts of cations determined are equivalent to those of anions within the range of analytical error. The cations determined are fairly deficient in some fractions, that is, in the 200—300°C fraction and the 500—600°C fraction in the experiment on the obsidian from Imari; in the 200—300°C fraction and the 400—600°C fraction in the experiment on the liparite from Kōzu-sima, and in the 200—300°C fraction in the experiment on the glassy andesite from Syōwa-iwō-zima. Iron is found in the 400—700°C region qualitatively; it may be responsible for the definciency of cations in this temperature region. In the 200—300°C region, some other cations, such as calcium or magnesium must be present, but we have not been able to confirm their existence.

The distribution and equivalent relation of the chemical species determined show that water soluble sublimate deposited below 200°C is mainly composed of ammonium chloride and that that deposited in the 400—700°C region is mainly composed of sodium and potassium chloride.

The F/Cl value has no definite maximum point in any fraction from 100°C to 900°C. The Br/Cl value, in general, reaches its maximum in the 100—300°C region and the I/Cl value, in the 200—400°C region.

**A Comparison with Natural Volcanic Emanation.**—The Br/Cl (atomic ratio) value of the volcanic gases in Japan has been reported to be $(1—10)\times 10^{-4}$, and the I/Cl value, to be $(1—20)\times 10^{-5}$.[4,11,12] These value agree with the $(Br/Cl)_{abs.}$ and $(I/Cl)_{abs.}$ values obtained in the laboratory experiments. Bromine and iodine in the volcanic gases are, therefore, thought to be supplied from the magma; it is, in general, unnecessary to postulate any other sources.

The water-soluble component of volcanic ash was chosen as a representative of the natural volcanic sublimates in a previous paper,[3] and the "$(F/Cl)_{sublimate} > (F/Cl)_{gas}$" relation was obtained by comparison with natural volcanic gases. As has already been stated, fluorine is not enriched relative to chlorine in the "true sublimate" as compared with the gas phase, but it is enriched in the "so-called sublimate," probably by the reaction with silicates. The enrichment of fluorine in the natural "volcanic sublimates" may be caused by the reaction with silicates or other substances.

Iwasaki, Kamada and Miyaji[13] determined

11) T. Sugiura, Y. Mizutani and S. Oana, Read at the Symposium on Geochemistry of the Chemical Society of Japan, October, 1960.

12) K. Noguchi, T. Gotō, S. Ueno and M. Ichikuni, *Bull. Volcanolog. Soc. Japan* (*Kazan*), 2nd Series, 5, 163 (1961).

13) I. Iwasaki, M. Kamada and J. Miyaji, Read at the 11th Annual Meeting of the Chemical Society of Japan, April, 1958.

TABLE VII. ATOMIC RATIO AMONG HALOGENS IN NATURAL AMMONIUM CHLORIDE

| | Locality | F/Cl | Br/Cl | I/Cl |
|---|---|---|---|---|
| 1 | Syōwa-sinzan (Hokkaidō)*,[14] | 0.045 | 0.014 | $0.5\times10^{-5}$ |
| | (two analyses) | 0.092 | 0.016 | $0.6\times10^{-5}$ |
| 2 | Mt. Iwate (Iwate Pref.)[12] (three analyses) | — | $(0.9—1.4)\times10^{-3}$ | $1\times10^{-6}$ |
| 3 | Miyake-zima volcano (Tōkyō Metr.)[16] | | | |
| | Group A | — | $(0.4—1.7)\times10^{-2}$ | $(0.0—1)\times10^{-5}$ |
| | Group B | — | $(0.8—2.3)\times10^{-2}$ | $(0.1—5.6)\times10^{-4}$ |
| 4 | Miyake-zima volcano (Tōkyō Metr.)[15] | $0.5\times10^{-3}$ | $1.1\times10^{-3}$ | $1\times10^{-6}$ |
| 5 | Tokati-dake (Hokkaidō)[15] | $0.5\times10^{-3}$ | $1.3\times10^{-2}$ | $4.4\times10^{-6}$ |

* These samples are contaminated with about 15% sassolite.

TABLE VIII. ATOMIC RATIO AMONG HALOGENS AND ALKALIES IN NATURAL SODIUM AND POTASSIUM CHLORIDE[15]

| | Locality | F/Cl | Br/Cl | I/Cl | K/Na |
|---|---|---|---|---|---|
| 1 | Miyake-zima volcano (Tōkyō Metr.) | $1.2\times10^{-3}$ | $0.45\times10^{-3}$ | $1\times10^{-6}$ | 0.032 |
| 2 | Iwō-zima volcano (Kagosima Pref.) | $0.3\times10^{-3}$ | $2.7\times10^{-3}$ | $2\times10^{-6}$ | 0.16 |
| | (two analyses) | $0.7\times10^{-3}$ | $2.8\times10^{-3}$ | $1\times10^{-6}$ | 0.12 |

the iodine content in the water-soluble component of volcanic ash. Their study shows that the I/Cl value of the water-soluble component of volcanic ash was $(6—430)\times10^{-5}$, larger than that of volcanic gases. This relation coincides with that obtained in the laboratory experiment.

Ammonium chloride is widely distributed in active volcanoes. In Japan, it has been found in Syōwa-sinzan,[14] Tokati-dake,[15] Mt. Iwate,[12] Miyake-zima,[15,16] etc.[17] It has not, however, been clearly decided whether ammonia was derived from the magma as an essential component or was the result of contamination from other sources. The results of this study show that ammonia is a common constituent of volatiles from volcanic rocks when they are heated at 1000°C, and that it is deposited below 200°C as ammonium chloride. Mizutani[14] and Noguchi et al.[12,16] analyzed natural ammonium chloride. The atomic ratios among halogens calculated from their data and from our new data[15] are shown in Table VII.

Bromine is strongly enriched and fluorine is not enriched in natural ammonium chloride as compared with the gas phase, in good accordance with the results of the laboratory experiments. Iodine is not enriched in natural ammonium chloride. Mizutani[14] explained the enrichment of bromine in terms of the difference in volatility between ammonium chloride and ammonium bromide. According to this explanation, iodine must also be enriched; he stated that the unstable nature of iodide under fomarolic conditions might be the primary cause of the paucity.

From the results of the present study, the problem may be explained as follows: There is a tendency for iodine to be deposited in higher temperature regions than the region where ammonium chloride is deposited. The temperature gradient may be not so steep at orifice of the natural fumarole as in the furnace used in this study, and so iodine will be more effectively separated from chlorine and bromine.

Sodium chloride has been found as volcanic sublimates in Mt. Mihara, Ō-sima volcano,[18] Miyake-zima volcano[19] and Iwō-zima volcano[15],*; these volcanoes are the most active volcanoes in Japan. Potassium chloride is less common than ammonium and sodium chlorides. It was recently found with sodium chloride at the Kuromoe fumarole (where the orifice temperature is about 600°C) *at Iwō-zima volcano.

Chemical analysis shows that a small amount of potassium is also present in the sodium chloride found in Miyake-zima. The atomic ratios among halogens and alkalies are shown in Table VIII.

Bromine is not so highly enriched in sodium and potassium chloride as in ammonium chloride. Fluorine and iodine are also not enriched.

14) Y. Mizutani, *J. Earth Sci. Nagoya Univ.*, 10, 149 (1962).
15) Unpublished data by M. Yoshida et al.
16) K. Noguchi, S. Ueno and H. Kamiya, Read at the Meeting of the Volcanological Society of Japan, October, 1963.
17) I. Iwasaki "Chemistry of the Volcano" (in Japanese), Kawade Shobō, Tokyo (1948), p. 105.
18) J. Ossaka, private communication.
19) J. Ossaka and T. Ozawa, private communication.
* The specimen was collected by Minoru Yoshida as sodium chloride (March 1964). The existence of the sylvine phase was found by Jōyo Ossaka by X-ray analysis. The formula percentage of potassium chloride was found to be 12—16% by chemical analysis. A detailed description of alkali halides found as volcanic sublimates will be given in another paper.

## Conclusion

Ammonium chloride, sodium chloride, potassium chloride, iron compounds and sulfur, which have often been found in active volcanoes, have been proved to be capable of forming directly from the magmatic emanation.

By comparing the ratio among halogens in natural volcanic products and in products from the laboratory experiments, the following conclusions have been obtained. Bromine is more enriched in the ammonium chloride fraction as compared with the gas phase. Fluorine and iodine behave fairly differently from chlorine in volcanic phenomena. The mechanisms of the fractionation of fluorine and iodine from chlorine are essentially different from one another. The behavior of fluorine in volcanic phenomena is strongly affected by its reaction with silicates.

The authors are much obliged to Dr. Jōyo Ossaka and Mr. Takejirō Ozawa, Tokyo Institute of Technology, for kindly supplying the specimens of alkali halides they have found as volcanic sublimates and for their fruitful discussions.

*Laboratory of Analytical Chemistry*
*and Geochemistry*
*Tokyo Institute of Technology*
*Ookayama, Tokyo*

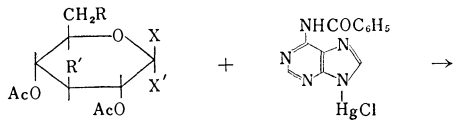
# Studies on Antibiotics and Related Substances. XX. The Synthesis of Adenine Nucleosides of 3-Amino-3-deoxyglucose and 6-Amino-6-deoxyglucose

By Shunzo FUKATSU and Sumio UMEZAWA

(Received October 30, 1964)

Several compounds obtained from streptomyces or fungi which contain purine or pyrimidine rings have shown an antibiotic or an antitumor property. The simplest examples are angustmycins,[1] nucleocidin,[2] cordycepin,[3] and nebularine.[4] Puromycin, an antibiotic purine derivative, belongs to the so-called aminonucleosides and exhibits carcinostatic and trypanocidal activities; its derivatives have been extensively synthesized by Baker and his coworkers.[5] Recently, 3'-amino-3'-deoxyadenosine[6] has been added to the group of aminonucleoside-antibiotics and shown to exhibit antitumor activity. We have also been interested in the aminonucleosides and have instituted a program aiming at the synthesis of nucleosides of rare aminosugars found in antibiotics. In this paper the syntheses of adenine nucleosides from chloromercuri-6-benzamidopurine and acetohalogeno derivatives of 3-amino-3-deoxy-D-glucose and 6-amino-6-deoxy-D-glucose, uncommon amino-sugars found as moieties of kanamycin, will be reported.

The required halogenoses, $\alpha$-1-bromo- and $\beta$-1-chloro-derivatives of 2, 4, 6-tri-*O*-acetyl-3-carbobenzoxyamino-1, 3-dideoxy-D-glucopyranose and 2, 3, 4-tri-*O*-acetyl-6-carbobenzoxyamino-1, 6-dideoxy-D-glucopyranose, were synthesized by the methods previously reported.[7]




Ia: R=NHCbz, R'=OAc, X=Cl, X'=H
Ib: R=NHCbz, R'=OAc, X=H, X'=Br
VIa: R=OAc, R'=NHCbz, X=Cl, X'=H
VIb: R=OAc, R'=NHCbz, X=H, X'=Br

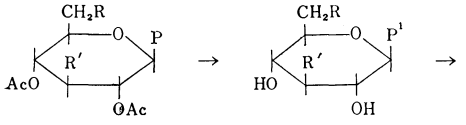
II

1) H. Yüntsen, *J. Antibiotics* (Japan), **11A**, 79 (1958); ibid., **11A**, 244 (1958); W. Schroeder and H. Hoeksema, *J. Am. Chem. Soc.*, **81**, 1767 (1959).
2) C. W. Waller, J. B. Patrick, W. Fulmor and W. E. Meyer, *J. Am. Chem. Soc.*, **79**, 1011 (1957).
3) H. R. Bentley, K. G. Cunningham and F. S. Spring, *J. Chem. Soc.*, **1951**, 2301.
4) N. Löfgren, B. Lüning and H. Hedström, *Acta Chem. Scand.*, **8**, 640 (1954); D. I. Magrath and G. B. Brown, *J. Am. Chem. Soc.*, **79**, 3252 (1957).
5) B. R. Baker, R. E. Schaub, J. P. Joseph and J. H. Williams, ibid., **77**, 12 (1955).
6) N. N. Gerber and H. A. Lechevalier, *J. Org. Chem.*, **27**, 1732 (1962).
7) Y. Ito, S. Koto and S. Umezawa, This Bulletin, **35**, 1618 (1962); S. Umezawa and S. Koto, ibid., **36**, 183 (1963).

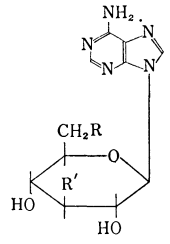
TABLE I. AMINONUCLEOSIDES AND THEIR BLOCKED DERIVATIVES

| Aminonucleoside and derivative | Starting anomer of acetohalogenose | Yield* % | UV Absorption $\lambda_{max}$, mμ | $[\alpha]_D$** |
|---|---|---|---|---|
| III | Ia | 84 (60) | 280 (ε 23100) m | −6.6 (*c* 1.21) c |
| III | Ib | 44 | 280 (ε 22500) m | −2.6 (*c* 1.35) c |
| IV | Ia | (55) | 260 (ε 21500) m | +8.0 (*c* 1.33) m |
| IV | Ib | (81) | 260 | −0.8 (*c* 1.23) m |
| V | Ia | 43 | 259 (ε 13300) w | +5.0 (*c* 1.40) w |
| V | Ib | 48 | 259 (ε 13700) w | +3.9 (*c* 1.27) w |
| VII | VIa | 53 | 280 (ε 20100) m | −7.9 (*c* 1.27) c |
| VII | VIb | 37 | 280 (ε 21700) m | −14.1 (*c* 1.32) c |
| VIII | VIa | (67) | 260 (ε 30600) mc | — |
| VIII | VIb | (38) | 260 mc | — |
| IX | VIa | 76 | 259 (ε 13600) w | +5.8 (*c* 1.56) w |
| IX | VIb | 77 | 259 (ε 13700) w | +3.5 (*c* 1.43) w |

* Figures in parentheses indicate yields of recrystallized products.
** Determined at room temperature. Exact value of specific rotation of VIII could not be c: Determined in chloroform., m: methanol, mc: methyl cellosolve, w: water



III: R=NHCbz, R′=OAc
VII: R=OAc, R′=NHCbz
IV: R=NHCbz, R′=OH
VIII: R=OH, R′=NHCbz
P=6-benzamidopurinyl-9
P¹=adenyl-9



V: R=$NH_2$, R′=OH
IX: R=OH, R′=$NH_2$

Chart A

The condensation of 2, 3, 4-tri-*O*-acetyl-6-carbobenzoxyamino-β-1-chloro-1, 6-dideoxyglucopyranose (Ia) with chloromercuri-6-benzamidopurine gave 6-benzamido-9-(2′, 3′, 4′-tri-*O*-acetyl-6′-carbobenzoxyamino-6′-deoxy-β-D-glucopyranosyl)-purine (III in Chart A). The hydrolysis of III with methanolic ammonia gave 9-(6′-carbobenzoxyamino-6′-deoxy-β-D-glucopyranosyl)-adenine (IV). Finally, the hydrogenolysis of the carbobenzoxy derivative with a palladium catalyst gave 9-(6′-amino-6′-deoxy-β-D-glucopyranosyl)-adenine (V). The structure of V was indicated by its elemental analyses, its ultraviolet spectrum, which was similary to that of a 9-substituted adenine, and its slightly negative rotation. The β-configuration of the aminonucleoside was deduced from Tipson's "trans rule"[8] as extended by Baker and his coworkers.[9] The values of the specific rotation of the aminonucleoside was consistent with the theoretical presumption and the reported values[10] for 9-β-D-glucopyranosyladenine. Hydrolysis with weak acid gave only adenine, 6-amino-6-deoxy-D-glucose and the unchanged nucleoside.

When 2, 4, 6-tri-*O*-acetyl-3-carbobenzoxyamino-β-1-chloro-1, 3-dideoxy-D-glucose (VIa) was used instead of the blocked acetohalogeno 6-aminoglucose (Ia), 6-benzamido-9-(2, 4, 6-tri-*O*-acetyl-3-carbobenzoxyamino-3-deoxy-β-D-glucopyranosyl)-purine (VII) was obtained. This was converted to the desired nucleoside (IX) by deacetylation and hydrogenolysis.

Applications of exactly identical series of reactions to α-bromo-anomers of 2, 3, 4-tri-*O*-acetyl-6-carbobenzoxyamino-1, 6-dideoxy-D-glucopyranose and 2, 4, 6-tri-*O*-acetyl-3-carbobenzoxyamino-1, 3-dideoxy-D-glucopyranose furnished 9-(6-amino-6-deoxy-β-D-glucopyranosyl)-adenine and 9-(3-amino-3-deoxy-D-glucopyranosyl)-adenine respectively; they were identical

8) R. S. Tipson, *J. Biol. Chem.*, **130**, 55, (1939); B. R. Baker, J. P. Joseph, R. E. Schaub and J. H. Williams, *J. Org. Chem.*, **19**, 1780 (1954); J. J. Fox and I. Wempen, *Advances in Carbohydrate Chem.*, **14**, 283 (1959); J. A. Montgomery and H. J. Thomas, ibid., **17**, 315 (1962).

9) B. R. Baker, *Ciba Foundation Symposium, Chem. and Biol. of Purines*, 120 (1957).

10) E. Fischer and B. Helferich, *Ber.*, **47**, 229 (1914); J. Davoll, B. Lythgoe and A. R. Todd, *J. Chem. Soc.*, 1946, 837. These workers reported $[\alpha]_D^{19}$ −10° (*c* 3.2, water) and $[\alpha]_D^{14}$ −9.7° (*c* 0.18, water) respectively.

FROM ANOMERS OF ACETOHALOGENOSES Ia AND Ib, VIa AND VIb

| Formula | Analysis, % | | | | | |
|---|---|---|---|---|---|---|
| | Found | | | Calcd. | | |
| | C | H | N | C | H | N |
| $C_{32}H_{32}N_6O_{11}$ | 58.46 | 4.92 | 12.29 | 58.15 | 4.89 | 12.70 |
| $C_{19}H_{22}N_6O_6$ | 53.09 | 5.11 | 19.44 | 53.00 | 5.15 | 19.54 |
| $C_{11}H_{16}N_6O_4$ | 43.98 | 5.47 | 28.45 | 44.56 | 5.44 | 28.38 |
| $C_{32}H_{32}N_6O_{11}\cdot H_2O$ | 56.48 | 4.80 | 12.07 | 56.50 | 4.97 | 12.07 |
| $C_{19}H_{22}N_6O_6$ | 53.00 | 5.15 | 19.47 | 53.24 | 5.29 | 19.54 |
| $C_{11}H_{16}N_6O_4$ | 43.84 | 5.30 | 27.80 | 44.56 | 5.44 | 28.38 |

determined because this derivative showed exceptionary low solubility in ordinary solvents tested.

with the above-mentioned $\beta$-anomers of aminonucleosides V and IX. Thus, it has been shown that the $\alpha$- and $\beta$-anomers of blocked acetohalogeno aminosugars (I, VI) both yield the same $\beta$-nucleosides (V, IX), a fact which can be interpreted adequately in terms of the extension of the "trans rule" made by Baker and his co-workers.[8]

The biological test of these compounds may be summarized as follows: compound IX possessed a weak anti-HeLa cell activity, but compound V was inactive in the antitumor tests. Both the compounds had a low toxicity.

## Experimental

The data of yields, of ultraviolet absorption, and of specific rotation and the analyses of title compounds are summarized in Table I.

**6-Benzamido-9-(2, 3, 4-tri-*O*-acetyl-6-carbobenzoxyamino-6-deoxy-$\beta$-D-glucopyranosyl)-purine (III).**—The method used here was virtually analogous to that described by Baker and his co-workers.[11] A mixture of Hyflo Super Cel (diatomaceous earth) (2.56 g.), the chloromercuric salt (II) (2.16 g.) of 6-benzamidopurine,[12] and toluene (265 ml.) was stirred and heated, while about 20 ml. of toluene was distilled off to remove azeotropically any moisture present. After the mixture had then been refluxed for 30 min. and cooled to approximately 60°C, 2,3,4-tri-*O*-acetyl-6-carbobenzoxyamino-$\beta$-1-chloro-1,6-dideoxy-D-glucopyranose (Ia) (2.26 g.) was added. The mixture was stirred and refluxed for 10 hr. and then filtered hot. The filter-cake was thoroughly washed with hot ethanol. The filtrate and washings were combined and evaporated to dryness in vacuo. The residue was dissolved in chloroform, and the solution was shaken with a 30% aqueous potassium iodide solution. The chloroform layer was separated, dried over anhydrous sodium sulfate, and evaporated to dryness in vacuo, leaving a dark gum (2.8 g.).

The crude product was purified by chromatography on alumina. To a solution of the crude product (2.8 g.) in methanol, alumina (5 g., aluminum oxide, Merck) was added, and then the mixture was evaporated to dryness. The residue was placed on a column (1.0×30 cm.) of alumina (34 g.) and developed with cyclohexane-ethyl acetate (1 : 1) ; eighty-seven fractions were cut, containing 7 ml. each. The ultraviolet absorption spectra of the residue obtained from tube Nos. 5—50 showed a characteristic absorption at 280 m$\mu$. The combined residues (2.49 g.) from the fractions were dissolved in a small quantity of methanol and filtered, and water was added to turbidity. After it had stood overnight, the solution deposited colorless crystals of the title compound (1.81 g.). The crystals had no definite melting point; a sample sintered from 96°C and became an opaque liquid. This compound was a 9-glucosyl derivative of adenine, as is shown by its ultraviolet absorption spectrum (Table I). In the infrared region, this compound in KBr showed absorptions at 3325 (NH), 1759 (C=O in OAc), 1718 ($\nu$C=C in Cbzo), 1608, 1589 (C=C), (C=N), 1219 ($\nu$C-O in OAc), 895 (shoulder, type 2b of pyranose ring), and 775, 739, 699 (phenyl) $cm^{-1}$.

The product was soluble in methanol, ethanol, benzene, dioxane or ethyl acetate, but practically insoluble in ether, ligroin, hexane, cyclohexane or water.

The same compound, III, was obtained by the condensation of the $\alpha$-bromo-anomer (Ib) of 2,3,4-tri-*O*-acetyl-6-carbobenzoxy-amino-1,6-dideoxy-D-glucopyranose with 6-benzamidopurine (II). The product showed an infrared spectrum identical with that of the specimen prepared from Ia and 6-benzamidopurine. The yield, the ultraviolet absorption, and the specific rotation are shown in Table I

11) B. R. Baker, J. P. Joseph and R. E. Schaub, *J. Org. Chem.*, **19**, 1780 (1954).
12) J. Davoll and B. A. Lowy, *J. Am. Chem. Soc.*, **73**, 1650 (1951).

comparison with those of a sample of III obtained from Ia.

**9-(6-Carbobenzoxyamino-6-deoxy-β-D-glucopyranosyl)-adenine (IV).** — A solution of III (3.1 g.) in absolute methanol (190 ml.) was saturated with ammonia at 0°C, and then the solution was allowed to stand in a refrigerator overnight. The solution was evaporated to dryness in vacuo, and the residue was washed with water in portions to give a slightly brown solid (1.5 g.). Recrystallization from *n*-propanol gave colorless crystals (0.79 g.) of the title compound. The product sintered at about 127—128°C and decomposed at 180°C with the evolution of gas. The ultraviolet spectrum of the product in methanol showed characteristic absorptions (Table I.).

The compound was soluble in methanol or ethanol but almost insoluble in benzene, petroleum ether or water.

**9-(6-Amino-6-deoxy-β-D-glucopyranosyl)-adenine (V).**—A solution of IV (1.5 g.) in 25% aqueous methanol (40 ml.) was shaken with 5% Pd-C (1.0 g.) and hydrogen at room temperature for 14 hr. After filtration, the filtrate was evaporated up to dryness under reduced pressure to give a colorless powder (0.825 g.). To a solution of the crude product (0.2 g.) in water, a solution of picric acid (1.45 g.) in methanol (14.5 ml.) was added; this mixture was then allowed to stand in a refrigerator to give a picrate (0.447 g.). Recrystallization from water gave yellow needles (0.226 g.). The picrate sintered at 168°C, gradually darkened, and decomposed at 215°C.

Found: C, 36.90; H, 3.27; N, 21.57. Calcd. for $C_{23}H_{22}N_{12}O_{18}$ (754.4): C, 36.59; H, 2.94; N, 22.29%.

The picrate (0.226 g.) was dissolved in water (8.2 ml.) and stirred with Dowex 1X2 ion exchange resin (OH form) (200—400 mesh, 10 ml.); the filtrate was passed through a column (1.5×30 cm.) of Dowex 1X2 (OH form). The column was then developed with water, and those fractions which showed characteristic ultraviolet absorptions at 259 mμ were collected. The product obtained by evaporation to dryness under reduced pressure was a colorless powder (84 mg.); the product sintered at about 205°C, darkened, and decomposed at 211°C, with the evolution of gas. The ultraviolet spectrum of the product in water showed absorptions characteristic of 9-substituted adenine.

The product showed a single ninhydrin-positive spot of $R_{fad}$ 0.36* upon the use of the descending method using an *n*-butanol - ethanol - water (10 : 5 : 7) solvent system and Toyo filter paper No. 52. The product was soluble in water, but nearly insoluble in methanol or ethanol.

A sample V was hydrolyzed with 1% acetic acid at room temperature for 5 days.

Chromatography on Toyo filter paper No. 50 by the ascending method using an *n*-butanol - acetic acid - water (4 : 2 : 1) solvent system showed two ninhydrin-positive spots ($R_f$ 0.12, 0.25) of 6-amino-6-deoxy-D-glucose and unchanged nucleoside, and another spot of adenine ($R_f$ 0.57), located by its slight opacity to the ultraviolet light of 2536 Å.

* $R_f$-Value relative to that of adenine taken as a unit.

**6-Benzamido-9-(2,4,6-tri-*O*-acetyl-3-carbobenzoxyamino-3-deoxy-β-D-glucopyranosyl)-purine (VII)** was prepared from 2,4,6-tri-*O*-acetyl-3-carbobenzoxyamino-1-β-chloro-1,3-dideoxy-D-glucopyranose (VIa) and 6-benzamidopurine (II) by a procedure analogous to that described in III; a sample purified by alumina chromatography and then by recrystallization from ethanol-water sintered at about 80°C.

The same compound, VII, was obtained in a similar condensation of the α-bromo anomer (VIb) of 2,4,6-tri-*O*-acetyl-3-carbobenzoxyamino-1,3-dideoxy-D-glucopyranose with 6-benzamidopurine (II). The product showed an infrared spectrum identical with that of the specimen prepared from VIa and 6-benzamidopurine. The yield, the ultraviolet absorption and the specific rotation are shown in Table I in comparison with those of a sample of VII obtained from VIa.

**9-(3-Carbobenzoxyamino-3-deoxy-β-D-glucopyrnosyl)-adenine (VIII)** was prepared from VII by a procedure analogous to that described in IV; a sample recrystallized from methanolic ammonia gradually darkened and decomposed at 233°C with the evolution of gas.

**9-(3-Amino-3-deoxy-β-D-glucosyl)-adenine (IX)** was prepared from VIII by a procedure analogous to that described in V. Picrate of IX: yield from a crude product, 84%; it gradually darkened and decomposed at 216—220°C.

Found: N, 21.55. Calcd. for $C_{23}H_{22}N_{12}O_{18}$ (754.4): N, 22.28%.

The yield of IX from its picrate was 92%. A sample purified with ion exchange resin Dowex 1X2 was recrystallized from water-ethanol; the product sintered a 170°C and decomposed at 191°C with the evolution of gas; the ultraviolet spectrum of the product in water showed the absorption characteristic of 9-substituted adenine. In the infrared region, this compound in KBr showed absorptions at 3320, 3180 (OH, NH), 1642, 1602 (C=N, C=C), 1058, 1043 (C-O), 890 $cm^{-1}$. (type 2b of the pyranose ring)

The product showed a single ninhydrin-positive spot of $R_{fad}$ 0.63 by a method similar to that used for V. The paper chromatographic analysis of the acid-hydrolyzate of a sample of IX by the same procedure as that used for V showed two ninhydrin-positive spots of 3-amino-3-deoxy-D-glucose ($R_f$ 0.16) and unchanged nucleoside ($R_f$ 0.41) and a spot of adenine ($R_f$ 0.57).

**Bioassays.**—It is interesting that IX shows antitumor activity. The minimum necessary concentration of IX for the anti-HeLa cell effect was 1 mg./ml. Preliminary tests indicated that IX possessed a weak antibacterial activity; IX completely inhibited the growth of Bacillus subtilis in the dilution of 1 : 1000. V showed almost no antitumor and antibacterial activity. V and IX had a low toxicity; V: $LD_0$ 500 mg./kg. (mice, i. v.), IX: $LD_0 > 500$ mg./mg./kg. (mice, i. v.).

## Summary

1) The subject amino-nucleoside have been synthesized from blocked acetohalogeno aminosugars and 6-benzamidopurine.

2) It has been shown that the $\alpha$- and $\beta$-anomers of blocked acetohalogeno aminosugars (Ia, Ib and VIa, VIb) both yield the same $\beta$-nucleosides (V, IX).

3) 9-(3-Amino-3-deoxy-$\beta$-D-glucopyranosyl)-adenine was found to possess a weak antitumor activity.

The authors are indebted to Professor Hamao Umezawa, of the National Institute of Health, Tokyo, for his antitumor assays. This work has been supported in part by a cancer research grant from the Ministry of Education, to which the authors' thanks are due. The authors are also grateful to Mr. Saburo Nakada for his microanalysis.

*Department of Applied Chemistry*
*Faculty of Engineering*
*Keio University*
*Koganei-shi, Tokyo*

# Studies on Antibiotics and Related Substances. XXII. Syntheses of Di(3-amino-3-deoxy-D-glucosyl)- and Di(6-amino-6-deoxy-D-glucosyl)-deoxystreptamine[1]

By Shinkiti KOTO, Yukio ITO and Sumio UMEZAWA

(Received January 28, 1965)

In a previous paper[2] we described the synthesis of di-*O*-(D-glucopyranosyl)-deoxystreptamine, in which two sugars are linked to C-4 and C-6 of deoxystreptamine in a manner analogous to that two amino sugars are linked in kanamycin. In an effort to determine the effect of amino groups on the antibiotic activity of glucosides of this kind, the amino glucosides of the title have been synthesized. The basis of the work of this series[3] arose with the recent discovery of a number of antibiotics which are the glucosides of deoxystreptamine but which differ primarily in the structures of their sugar moieties.

The condensation of *N*, *N'*-dicarbobenzoxydeoxystreptamine (II)[2] with an excess of 2, 4, 6-tri-*O*-acetyl-3-carbobenzoxyamino-3-deoxy-$\alpha$-D-glucopyranosyl bromide (I)[4] in nitromethane in the presence of mercuric cyanide gave 4, 6-di-*O*-(2, 4, 6-tri-*O*-acetyl-3-carbobenzoxyamino-3-deoxy-$\beta$-D-glucopyranosyl)-*N*, *N'*-dicarbobenzoxy-deoxystreptamine (III) in a 25% yield.

The deacetylation of III with methanolic ammonia gave 4, 6-di-*O*-(3-carbobenzoxyamino-3-deoxy-$\beta$-D-glucopyranosyl)-*N*, *N'*-dicarbobenzoxy-deoxystreptamine (IV) in a 68% yield.

The catalytic hydrogenolysis of IV with palladium black gave 4, 6-di-*O*-(3-amino-3-deoxy-$\beta$-D-glucopyranosyl)-deoxystreptamine (V) in an 80% yield.

The reaction sequence used in the synthesis of 4, 6-di-*O*-(6-amino-6-deoxy-$\beta$-D-glucopyranosyl)-deoxystreptamine (V') was analogous to that of V.

Since the structure of 4, 6-(tetra-*O*-acetyl-$\beta$-D-glucopyranosyl)-deoxystreptamine, which corresponds to the hydrogenolysis product of III had been previously[2] confirmed by means of periodate oxidation, the two amino sugar moieties in V and V' were assigned to the 4- and 6-positions in deoxystreptamine.

Futhermore, V' rapidly consumed about four moles of periodate, and the paper chromatography of the hydrolyzate of the oxidation mixture showed the presence of deoxystreptamine and the complete absence of 6-amino-6-deoxy-D-glucose. The survival of deoxystreptamine is indicative of glucosidation at the 4- and 6-positions of deoxystreptamine.

The designation of V and V' as $\beta$-anomers was based on their optical rotations and infrared spectra. The optical rotations of V and V' are $[\alpha]_D^{27}$ $-5.5°$ (*c* 1.2, water) and $[\alpha]_D^{15}$ $-0.1°$ (*c* 0.5, water) respectively. Compared with the optical rotation of the kanamycin free

1) Presented in part at the International Congress on Antibiotics, Prague, CSSR, June 15—19, 1964; S. Umezawa, Abstracts of Papers, 134 (1964).

2) S. Umezawa and Y. Ito, This Bulletin, **34**, 1540 (1961).

3) Previous papers of this series: S. Umezawa and T. Tsuchiya, *J. Antibiotics*, **A15**, 51 (1962); T. Suami, S. Ogawa and S. Umezawa, This Bulletin, **36**, 459 (1963); S. Umezawa and T. Tsuchiya, *J. Antibiotics*, **A16**, 173 (1963); T. Tsuchiya, H. Fujita and S. Umezawa, ibid., **A17**, 181 (1964); T. Tsuchiya and S. Umezawa, This Bulletin, **38**, 1181 (1965); Ref. 2.

4) Y. Ito, S. Koto and S. Umezawa, This Bulletin, **35**, 1619 (1962).

base $[\alpha]_D^{13}$ +140° (*c* 1.35, water)[5] with an α-configuration, that of V and V′ are levorotatory, and since the amino sugar moieties in V and V′ have a D-configuration, the assignment of β-configurations to V and V′ appears to be reasonable. The infrared spectra of V showed absorption band at 895 $cm^{-1}$, indicating a characteristic absorption band for β-glucoside, while the kanamycin free base showed absorption bands at 838 and 823 $cm^{-1}$ corresponding to two α-anomeric configurations.[6]

A similar condensation of *N*, *N*′-dicarbobenzoxy-deoxystreptamine with 3, 4, 6-tri-*O*-acetyl-2-carbobenzoxyamino-2-deoxy-α-D-glucopyranosyl bromide[7] was unsuccessful; only 4, 5-(3, 4, 6-tri-*O*-acetyl-D-glucopyrano)-2-oxazolone[8] was obtained.

## Experimental

**4, 6-Di-*O*-(2, 4, 6-tri-*O*-acetyl-3-carbobenzoxyamino-3-deoxy-β-D-glucopyranosyl)-*N*, *N*′-dicarbobenzoxy-deoxystreptamine (III).**—To a suspension of *N*, *N*′-dicarbobenzoxy-deoxystreptamine (0.38 g., 0.9 mmol.) and 2, 4, 6-tri-*O*-acetyl-3-carbobenzoxyamino-3-deoxy-α-D-glucopyranosyl bromide[4] (1.11 g., 2.2 mmol.) in nitromethane* (20 ml.), powdery mercuric cyanide (0.57 g., 2.3 mmol.) was addded, the suspension was then stirred at 27°C for 24 hr. The resulting mixture was filtered and the filtrate evaporated to dryness at about 40°C under reduced pressure. Extraction with chloroform was followed by repeated washings with water in order to remove mercuric salts. After drying over sodium sulfate, the chloroform solutions was evaporated to dryness under reduced pressure to give a residue (1.05 g.), which was washed with ether to give a crude product (250 mg.) (25%). Recrystallized from absolute ethanol; m. p. 277°C (decomp., sintered at about 277°C), $[\alpha]_D^{15}$ −13.0° (*c* 1.75, dioxane).

Found: C, 58.11; H, 5.75; N, 4.41; Mw, 1150. Calcd. for $C_{62}H_{72}O_{25}N_4$: C, 58.48; H, 5.70; N, 4.40%; Mw, 1273.

**4, 6-Di-*O*-(3-carbobenzoxyamino-3-deoxy-β-D-glucopyranosyl)-*N*, *N*′-dicarbobenzoxy-deoxystreptamine (IV).** — Three hundred and ten milligrams of III was suspended in 75 ml. of absolute methanol, and to this was added 50 g. of absolute methanol saturated with ammonia. Since, after this mixture had been left overnight, there was a considerable quantity of solid left in the mixture, absolute methanol saturated with ammonia was again added to the mixture. After again having been left overnight at room temperature, a clear solution was obtained; this was filtered, and the filtrate was concentrated under reduced pressure to yield colorless crystals, which were collected and washed with absolute methanol and chloroform in turn; 0.17 g., m. p. 264—265°C (decomp., sintered at about 200°C), $[\alpha]_D^{15}$ +5.0° (*c* 1.22, dimethyl formamide).

Found: C, 58.67; H, 5.60. Calcd. for $C_{50}H_{60}O_{19}N_4$: C, 58.81; H, 5.92%.

**4, 6-Di-*O*-(3-amino-3-deoxy-β-D-glucopyranosyl)-deoxystreptamine (V).** — One hundred and sixty milligrams of IV was suspended in 12 ml. of a dioxane-water mixture (7:5), and then this mixture was added to a prehydrogenated palladium black (50 mg.) in 1.5 ml. of a dioxane-water mixture (1:1). The mixture was hydrogenated under mechanical shaking at 23—25°C for 1.5 hr. and further at 30—31°C for 4 hr. A further suspension of 20 mg. of prehydrogenated palladium black in dioxane-water was added to the resulting mixture, and hydrogenolysis was continued at 38—42°C for about 7 hr. The resulting mixture was strongly alkaline. After the removal of the catalyst by filtration, the solution was evaporated under reduced pressure to give 60 mg. of an amorphous solid. The product was dissolved in hot methanol, and ethanol was added to yield a crystalline powder of the title compound, $[\alpha]_D^{27}$ −5.5° (*c* 1.2, water).

Found: C, 44.58; H, 7.30; N, 10.95. Calcd. for $C_{18}H_{36}O_{11}N_4$: C, 44.61; H, 7.49; N, 11.57%.

The infrared absorption spectrum of the product in Nujol contained absorptions at 3260 (NH, OH), 1665, 1595 (NH), 1040 (C-O) and 895 $cm^{-1}$ (type 2b of the pyranose ring).

**4, 6-Di-*O*-(6-amino-6-deoxy-β-D-glucopyranosyl)-deoxystreptamine (V′).** — To a suspension of *N*, *N*′-dicarbobenzoxy-deoxystreptamine (0.42 g., 1.0 mmol.) and 2, 3, 4-tri-*O*-acetyl-6-carbobenzoxyamino-6-deoxy-β-D-glucopyranosyl chloride[9] (1.00 g., 2.2 mmol.) in dry nitromethane (30 ml.), powdery mercuric cyanide (0.56 g., 2.2 mmol.) was added; then the suspension was shaken at about 27°C for 4 days in a dark room. The resulting mixture was filtered, and the filtrate was evaporated under reduced pressure. The residue was extracted with chloroform, and the chloroform extract was washed with water to remove mercuric salts. After it had been dried over sodium sulfate, the chloroform solution was evaporated under reduced pressure. The pale yellow syrup (1.1 g.) obtained was suspended in absolute methanol saturated with ammonia (62 g.). After having been left overnight at room temperature, the mixture was filtered, and the filtrate was evaporated under reduced pressure. The resulting syrup was treated several times with 2-ml. portions of water, and the residue was dried up under reduced pressure to give a colorless syrup (0.480 g.). The residue was dissolved in 10 ml. of 25% aqueous methanol, and to this solution was added a prehydrogenated palladium black (100 mg.). The mixture was hydrogenated under mechanical shaking at room temperatuer for 50 hr. During the hydrogenation, dilute hydrochloric acid was

5) Ph. D. thesis of K. Maeda, Keio University, 1958.
6) M. J. Cron, D. L. Evans, F. M. Palermiti, D. L. Whitehead, I. R. Hooper, Paul Chu and R. U. Lemieux, *J. Am. Chem. Soc.*, **80**, 4741 (1958).
7) L. Zervas and S. Konstas, *Chem. Ber.*, **93**, 435 (1960).
8) S. Konstas, A. I. Photake and L. Zervas, ibid., **92**, 1288 (1959); S. Umezawa, S. Koto and Y. Ito, This Bulletin, **36**, 186 (1963).
* Dry nitromethane obtained by distillation with phosphorus pentoxide.
9) S. Umezawa, S. Koto and Y. Ito, This Bulletin, **36**, 183 (1963).

added several times in order to acidify the reaction mixture.* After the catalyst had been removed, the solution was evaporated under reduced pressure to yield a syrup (324 mg.). Descending-paper chromatography of the product by ninhydrin coloration, using an *n*-butanol - pyridine - water - acetic acid (6 : 4 : 3 : 1) solvent system at room temperature for 19 hr., showed five spots of $R_{f6AG}$ 1.00, 0.65 (deoxystreptamine), 0.31, 0.10 and 0.04.** The spot of $R_{f6AG}$, 0.10, corresponded to the main product.

The product was mixed with cellulose powder (100—200 mesh) (1.0 g.) and water (3.0 ml.) and dried over phosphorus pentoxide in a desiccator under reduced pressure. It was then placed on a column (11×2.5 cm.) of cellulose powder (15 g.) and developed with the above-metioned solvent system at a rate of 10 ml./hr. The product of $R_{f6AG}$, 0.10, emerged from 340 to 800 ml. of the eluate. The fractions were then combined and evaporated under reduced pressure at 30—35°C. A solution of the residue (116 mg.) in water (1.0 ml.) free from carbon dioxide was placed on a column (0.5×5 cm.) of Dowex 1X2 (OH form) and developed with water free from carbon dioxide. The ninhydrin-positive fractions were then collected and evaporated under reduced pressure at about 20°C to give a colorless powder of the title compound (65 mg.) (13.5%). Purification for analysis was accomplished by dissolving the product in hot methanol, with the subsequent addition of ethanol; colorless amorphous powder, $[\alpha]_D^{15}$ −0.1° (*c* 0.5, water).

Found: C, 43.90; H, 7.25; N, 11.04. Mw, 480. Calcd. for $C_{18}H_{36}O_{11}N_4$: C, 44.61; H, 7.49; N, 11.57%. Mw, 484.

**The Periodate Oxidation of V′.**—An accurately-weighed sample (2.42 mg.) of V′ was dissolved in 5.0 ml. of a 0.03 M sodium periodate solution (acetate buffer, pH 4.4). The oxidation was carried out at 2—3°C. in the dark. To each one-ml. aliquot was added a measured excess of 0.05 M sodium arsenite at eight-hour intervals, beginning three hours after the dissolving of the sample, and then these solutions were titrated with a 0.01 M iodine solution. The product consumed 2.1 mol. of periodate at 3 hr. and 3.9 mol. at 24 hr. A parallel experiment using a sample (2.52 mg.) of kanamycin base gave a titration curve similar to that obtained from the product (V′); kanamycin consumed 2.6 mol. of periodate at 3 hr. and 4.0 mol. at 24 hr.

Another weighed sample (2.6 mg.) of V′ was oxidized similarly for 120 hr. After the addition of ethylene glycol (1.0 ml.), the mixture was again allowed to stand over night. To the mixture concentrated hydrochloric acid (5.0 ml.) was then added, and the mixture was heated at 90—95°C for 3 hr. The hydrolyzate was chromatographed on Toyo filter paper No. 51 by the descending method, using *n*-butanol - pyridine - water - acetic acid (6 : 4 : 3 : 1) for 16 hr. Detection by ninhydrin-coloration gave the spot corresponding to deoxystreptamine.

**The Paper Chromatography of the Acid Hydrolyzate of V′.**—Two 0.5 mg. samples of V′ were dissolved in 1.75 ml. of 2 N and 6 N hydrochloric acid respectively, and then allowed to stand at about 95°C for 6 hr. The hydrolyzates were chromatographed on Toyo filter paper No. 51 by the ascending method, using the above-mentioned solvent system, for 19 hr. Detection by ninhydrin-coloration gave only three spots, corresponding to 6-amino-6-deoxy-D-glucose, deoxystreptamine and unchanged V′.

**Bioassay.**—Compounds V and V′ did not show any antibacterial activity against *M. Pyogenes var. aureus* 209-p, *E. coli* and *Mycobacterium tuberculosis* 607 in a dilution of 1 : 1000.

The authors are indebted to Mr. Saburo Nakada for the microanalysis and to Mr. Yasushi Suzuki for his technical assistance. This research was supported in part by a grant from the Ministry of Education.

*Department of Applied Chemistry*
*Faculty of Engineering*
*Keio University*
*Koganei-shi, Tokyo*

* When the hydrogenation was effected without the addition of hydrochloric acid, the crude product (syrup) showed a remarkable inhibition against *B. subtilis* PCI 219. The antibacterial activity seems to be due to the presence of the complex diorthoester reported by R. U. Lemieux, C. I. C. Medal Lecture, "The Chemical Synthesis of Glucosides," Chemical Institute of Canada (1964).

** $R_{f6AG}$: $R_f$ values relative to the $R_f$ value of 6-amino-6-deoxy-D-glucopyranose taken as 1.0.

# Studies of the Chlorination of the Carboxylic Acids with *t*-Butyl Hypochlorite

By Yasuo SHIGEMITSU, Yoshinobu ODAIRA and Shigeru TSUTSUMI

(Received November 19, 1964)

Investigations of chlorination with *t*-butyl hypochlorite have been carried out for many years; recently Walling and his co-workers have indicated that the above hypochlorite is an efficient free-radical chlorinating agent for various hydrocarbons.[1-3]

We have been making studies of the extensive utilization of *t*-butyl hypochlorite, which can readily seprepared from *t*-butyl alcohol, in synthetic organic chemistry. As a part of these studies, our attention has been drawn to the telomerization using *t*-butyl hypochlorite.

In general, it is well-known that, with the exception of a few cases of using some such reagents as carbon tetrachloride or cyanogen chloride as a telogen, the telomerization affords a telomer with only one functional group, as is shown in the reactions of olefins with *N*-alkyl substituted formamides, acetic acid or alkyl acetates in the presence of di-*t*-butyl peroxide as the initiator.[4,5] However, when this hypochlorite is used in the telomerization, one would expect that the telomer with two functional groups at the both end sites, would be obtained, as is shown in the following scheme:

$$t\text{-BuOCl} \xrightarrow{h\nu} t\text{-BuO}\cdot + \text{Cl}\cdot \quad (1)$$

$$t\text{-BuO}\cdot + \text{RH} \rightarrow t\text{-BuOH} + \text{R}\cdot \quad (2)$$

$$\text{R}\cdot + n\text{R}'\text{-CH=CH}_2 \rightarrow \cdot(\text{CH}(\text{R}')\text{-CH}_2)_n\text{-R} \quad (3)$$

$$\cdot(\text{CH}(\text{R}')\text{-CH}_2)_n\text{-R} + t\text{-BuOCl} \rightarrow \text{Cl-}(\text{CH}(\text{R}')\text{-CH}_2)_n\text{-R} + t\text{-BuO}\cdot \quad (4)$$

We have already demonstrated that we have succeeded in the synthesis of 5-chloro-2-pentanone by means of this new telomerization using acetone and ethylene.[6] Since the carboxylic acids as well as acetone seem to be available for the telogen, we have first investigated the reactions of *t*-butyl hypochlorite with the carboxylic acids as an experiment preliminary to the telomerization using the carboxylic acids as the telogen. Now, in this paper, we wish to describe the reactions of *t*-butyl hypochlorite with a number of carboxylic acids in the presence of a solvent such as benzene or carbon tetrachloride and, especially, to demonstrate the effects of the acidity of the carboxylic acids and those of the solvents on the reactions, as well as to demonstrate the reactivities of the *t*-butoxy radical.

## Experimental

**Materials.** — *t*-Butyl hypochlorite was prepared according to the procedure of Teeter and Bell.[7] The hypochlorite was distilled before use; its b. p. was 79.5—80°C, and it was stored in the dark at 0°C. The purity was 95—99% as determined by iodometric analysis. The other materials were commercial-grade chemicals and were purified by the usual method and distilled or recrystallized before use.

**Reaction Procedures.** — All the reactions were carried out in a 200-ml. (or 300-ml.) four-necked flask equipped with a thermometer, a mechanical stirrer, a gas inlet and a condenser, to which a trap at −78°C and a gas holder were attached. *t*-Butyl hypochlorite and the carboxylic acid (and the solvent) were placed in the flask wrapped in aluminum foil designed to intercept the light. After completely replacing the system by nitrogen for 15 min. prior to irradiation, the aluminum foil was removed and the system was irradiated by a 60-watt incandescent light bulb at a distance of 5 cm. The conditions of the reaction are shown in Table I.

**Analytical Procedures.** — The gaseous products and the trapped fraction were analyzed by gas chromatography using a 2.5 m. silica gel and a 2.5 m. $\beta,\beta'$-oxydipropionitrile column. The low-boiling products and the solvent were distilled and determined quantitatively by gas chromatography using a 2.5 m. dinonyl phthalate column. Unreacted liquid carboxylic acids (acetic, propionic and *n*-butyric acids) were also distilled and titrated with 0.1 N sodium hydroxide, using phenolphthalein as

1) C. Walling and B. B. Jacknow, *J. Am. Chem. Soc.*, **82**, 6108 (1960).
2) C. Walling and B. B. Jacknow, ibid., **82**, 6113 (1960).
3) C. Walling and W. Thaler, ibid., **83**, 3877 (1961).
4) L. Friedman and H. Shechter, *Tetrahedron Letters*. 238 (1961).
5) J. Allen, *Chem. & Ind.*, **1962**, 1621.
6) Reported at the 17th Annual Meeting of the Chemical Society of Japan, Tokyo, March, 1964.
7) H. M. Teeter and E. W. Bell, "Organic Synthesis," **32**, 20 (1956).

TABLE I. REACTION CONDITIONS*1

| Exp. No. | Carboxylic acid | Solvent | *t*-BuOCl g. (mol.) | Carboxylic acid g. (mol.) | Solvent g. (mol.) |
|---|---|---|---|---|---|
| 1 | $CH_3COOH$ | None | 16.3 (0.15) | 90 (1.5) | — |
| 2 | $CH_3COOH$*2 | None | 27.1 (0.25) | 240 (4.0) | — |
| 3 | $CH_3COOH$ | $C_6H_6$ | 21.7 (0.2) | 12 (0.2) | 156 (2.0) |
| 4 | $CH_3COOH$ | $CCl_4$ | 10.9 (0.1) | 6 (0.1) | 154 (1.0) |
| 5 | $C_2H_5COOH$ | None | 16.3 (0.15) | 111 (1.5) | — |
| 6 | $C_2H_5COOH$ | $C_6H_6$ | 21.7 (0.2) | 14.8 (0.2) | 156 (2.0) |
| 7 | $n$-$C_3H_7COOH$ | None | 16.3 (0.15) | 132 (1.5) | — |
| 8 | $CH_2ClCOOH$ | $C_6H_6$ | 21.7 (0.2) | 18.9 (0.2) | 156 (2.0) |
| 9 | $CCl_3COOH$ | $C_6H_6$ | 10.9 (0.1) | 16.3 (0.1) | 78 (1.0) |
| 10 | $CCl_3COOH$ | $CCl_4$ | 16.3 (0.15) | 24.6 (0.15) | 115.5 (0.75) |
| 11 | None | $C_6H_6$ | 21.7 (0.2) | — | 156 (2.0) |

*1 All the reactions were carried out at 30°C.
*2 The high pressure mercury arc (Eikosha Type 400 W) was used.

an indicator. The high-boiling products were fractionally distilled under reduced pressure and determined quantitatively by gas chromatography, using a 2.5 m. dinonyl phthalate, a 2 m. polyethylene glycol-6000 or a 2.5 m. silicon DC-550 column; they were also determined qualitatively by means of their infrared spectra, by various spot tests, or by introduction to their derivatives. In the case of monochloroacetic acid, the high-boiling fractions, containing the unreacted acid, were treated with diazomethane and analyzed by gas chromatography, using a 3 m. tricresyl phosphate column. In the case of trichloroacetic acid in the presence of benzene, the low-boiling products and benzene were treated as has been described above. The residue was dissolved in water and extracted with benzene. The benzene extract was washed with 10% aqueous sodium carbonate and water successively. The residue obtained by the removal of benzene was a polymeric product; further investigation was not undertaken.

## Results

**Reactions with Acetic Acid.** — When *t*-butyl hypochlorite was illuminated by an incandescent light bulb in the presence of acetic acid, the acid was scarcely chlorinated, whereas the self-decomposition of *t*-butyl hypochlorite proceeded predominantly. As a consequence, acetone and methyl chloride were obtained as the main products, accompanied by small amounts of *t*-butyl alcohol, monochloroacetic acid, chloroacetone and chloro-*t*-butyl alcohol. The results on acetic acid are listed in Table II.

As Table II shows, the reactions in the presence of benzene or carbon tetrachloride gave the same results as the above, except that the formation of *t*-butyl alcohol increased somewhat. Interestingly, the formation of carbon dioxide suggests that the *t*-butoxy radical generated by the decomposition of *t*-butyl hypochlorite may abstract the hydrogen of the carboxyl group.

TABLE II. MAJOR PRODUCTS OF REACTIONS WITH ACETIC ACID

| Exp. No. | 1 | 2 | 3 | 4 |
|---|---|---|---|---|
| Product, mol. %* | | | | |
| *t*-Butyl alcohol | 16.2 | 16.7 | 35.1 | 32.5 |
| Acetone | 78.1 | 72.1 | 60.4 | 50.4 |
| Monochloroacetone | 2.9 | 4.8 | 1.6 | 1.1 |
| Chloro-*t*-butyl alcohol | 0.6 | 9.2 | 3.2 | 8.3 |
| Monochloroacetic acid | 6.4 | 1.3 | Trace | 4.2 |
| Chlorobenzene | — | — | 3.5 | — |
| Gaseous products | $CO_2$ $CH_3Cl$ | $CO_2$ $CH_3Cl$ | $CO_2$ $CH_3Cl$ | $CO_2$ $CH_3Cl$ |

* Basis on *t*-butyl hypochlorite used.

**Reactions with Propionic and *n*-Butyric Acids.** —Table III shows results of the reactions of *t*-butyl hypochlorite with propionic and *n*-butyric acids.

In the case of propionic acid, the major liquid products were *t*-butyl alcohol, acetone and $\alpha$- and $\beta$-chloropropionic acids. The

TABLE III. MAJOR PRODUCTS OF REACTIONS WITH PROPIONIC AND *n*-BUTYRIC ACIDS

| Exp. No. | 5 | 6 | 7 |
|---|---|---|---|
| Product, mol. %* | | | |
| *t*-Butyl alcohol | 59.4 | 45.3 | 52.3 |
| Acetone | 27.6 | 56.8 | 29.9 |
| Monochloroacetone | 5.8 | Trace | 2.2 |
| Chloro-*t*-butyl alcohol | 8.0 | 0.5 | 1.8 |
| Chlorinated carboxylic acid | 41.2 | 5.5 | 52.7 |
| Chlorobenzene | — | 4.9 | — |
| Gaseous products | $CO_2$ $CH_3Cl$ $C_2H_5Cl$ | $CO_2$ $CH_3Cl$ $C_2H_5Cl$ | $CO_2$ $CH_3Cl$ $n$-$C_3H_7Cl$ |

* Basis on *t*-butyl hypochlorite used.

yields of chlorinated carboxylic acids were considerably higher than those in the chlorination of acetic acid. On the other hand, in the presence of benzene as the solvent, the amounts of chlorinated carboxylic acids and *t*-butyl alcohol decreased, in contrast to an increase in those of acetone. From the formation of ethyl chloride along with carbon dioxide, we would conclude that the decarboxylation of the carboxylic acid might well occur. In Table III it can also be observed that *n*-butyric acid is more efficiently chlorinated than propionic acid by *t*-butyl hypochlorite. The isomer distributions of chlorinated carboxylic acids of propionic and *n*-butyric acids are summarized in Table IV.

TABLE IV. ISOMER DISTRIBUTIONS OF CHLORINATED CARBOXYLIC ACIDS

| Exp. No. | Carboxylic acid | $\alpha$-Isomer % | $\beta$-Isomer % | $\gamma$-Isomer % |
|---|---|---|---|---|
| 5 | $C_2H_5COOH$ | 61.2 | 38.8 | — |
| 6 | $C_2H_5COOH$ | 63.2 | 36.8 | — |
| 7 | $n$-$C_3H_7COOH$ | 20.6 | 46.4 | 33.0 |

The $\alpha$-isomer was rich in the case of propionic acid, but the ratio of $\alpha$- and $\beta$-isomers was constant, regardless of the presence or absence of the solvent. On the other hand, in the case of *n*-butyric acid, the $\beta$-isomer was predominantly formed and the $\gamma$-isomer was preferentially formed over the $\alpha$-isomer.

**Reactions with Other Acids.** — All the reactions with other acids were carried out in the presence of the solvent. The major products are listed in Table V.

TABLE V. MAJOR PRODUCTS OF REACTIONS WITH OTHER ACIDS

| Exp. No. | 8 | 9 | 10 | 11 |
|---|---|---|---|---|
| Product, mol. %* | | | | |
| *t*-Butyl alcohol | 32.4 | 41.9 | 12.6 | 41.8 |
| Acetone | 49.1 | Trace | 27.1 | 49.1 |
| Monochloro-acetone | 1.6 | Trace | 28.1 | 1.1 |
| Chloro-*t*-butyl alcohol | 4.6 | None | 12.3 | 1.4 |
| Chlorinated carboxylic acid | 0.4 | — | — | — |
| Chlorobenzene | 6.4 | 41.8 | — | 2.2 |
| Gaseous products | $CO_2$ $CH_3Cl$ | Iso-butene | $CH_3Cl$ | $CH_3Cl$ |

* Basis on *t*-butyl hypochlorite used.

The reaction of *t*-butyl hypochlorite with monochloroacetic acid gave the same results as in the case of acetic acid in the presence of benzene with the exception of the increase in the formation of chlorobenzene. The reactions of *t*-butyl hypochlorite with trichloroacetic acid provided very interesting results. When benzene was used as the solvent, the decomposition of *t*-butyl hypochlorite began immediately, without any illumination, as soon as the hypochlorite was dropped into the flask containing benzene and trichloroacetic acid. The products were *t*-butyl alcohol, chlorobenzene and isobutene, accompanied by trace amounts of acetone. Isobutene may be formed from *t*-butyl alcohol during distillation by the acid-catalytic action of trichloroacetic acid. On the other hand, using carbon tetrachloride as the solvent, the major products were acetone, methyl chloride, *t*-butyl alcohol, chloroacetone and chloro-*t*-butyl alcohol.

## Discussion

**The Effects of the Acidity of Carboxylic Acids.**—*t*-Butyl hypochlorite is often used as an electrophilic-chlorinating reagent in the presence of an acid-catalyst. For example, benzene has been efficiently chlorinated by *t*-butyl hypochlorite in the presence of sulfuric acid.[8] In our study, benzene was also chlorinated easily by *t*-butyl hypochlorite in the presence of trichloroacetic acid, which is a strong acid as well as a sulfuric acid, whereas scarcely any acetone was formed. From these results, it may be concluded that, in this reaction, the chlorination of benzene proceeds predominantly by the electrophilic attack of the chloro cation on the aromatic nucleus. The acidity of carboxylic acids in benzene and the yield of chlorobenzene are summarized in Table VI.

TABLE VI. THE YIELD OF CHLOROBENZENE IN THE PRESENCE OF THE CARBOXYLIC ACID

| Exp. No. | Carboxylic acid | p$K$ in $C_6H_6$*1 | Yield of chlorobenzene*2 % |
|---|---|---|---|
| 3 | $CH_3COOH$ | 5.18 | 3.5 |
| 6 | $C_2H_5COOH$ | | 4.9 |
| 8 | $CH_2ClCOOH$ | 1.75 | 6.2 |
| 10 | $CCl_3COOH$ | 0.70 | 41.8 |
| 11 | None | — | 2.2 |

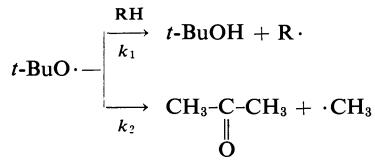
*1 V. K. LaMer and H. C. Dowens, *J. Am. Chem. Soc.*, **55**, 1860 (1933).
*2 Mol. % of *t*-butyl hypochlorite used.

In Table VI it can be observed that, although chlorobenzene was formed in a 2.2% yield by the homolytic decomposition of *t*-butyl hypochlorite in benzene, the yield of chlorobenzene was higher than 2.2% in the presence of the carboxylic acid, and that the yield of chlorobenzene increased with the increase in the

8) M. Anbar, Ph. D. Thesis, Hebrew University, Jerusalem (1953).

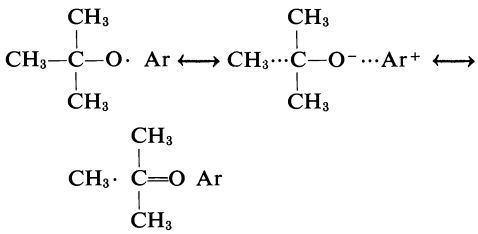
acidity of the carboxylic acids. Consequently, it may be presumed that the ionic process in the reaction becomes more important with the increase in the acidity of the carboxylic acids. However, in such weak acids as acetic and propionic acids, this ionic process may be almost ignored; we therefore studied in more detail the radical reactions of *t*-butyl hypochlorite with such weak acids.

**The Solvent Effects.**—As is well known, the *t*-butoxy radical formed by the photo-induced chain decomposition of *t*-butyl hypochlorite abstracts hydrogen or proceeds competitively via fragmentation, as is shown hereunder;



From the mole ratio of the *t*-butyl alcohol and acetone obtained from the above reactions, it is possible to calculate the $k_1/k_2$ ratio. Although, in our experiments, the $k_1/k_2$ rate ratio cannot be given precisely because of the further reactions of *t*-butyl alcohol or acetone with *t*-butyl hypochlorite, for convenience it is permissible to adopt the mole ratio of *t*-butyl alcohol and acetone as a measure of the reactivity of the *t*-butoxy radical.

Recently, Russel has investigated particularly the solvent effects in the decomposition of di-*t*-butyl peroxide in the presence of cyclohexane at 130°C,[9] he has shown that such aromatic solvents as benzene caused a decrease in the $k_1/k_2$ rate ratio due to the high dissociation of the aromatic hydrocarbon-*t*-butoxy radical $\pi$-complex. Moreover, Walling has also pointed out that the aromatic solvents stabilize the transition state for $\beta$-scission through the contribution of the charge-transfer type structure, as is shown below:[10]



Concerning the solvent effects, however, the dilution effect with a solvent must also be taken into consideration, because the hydrogen abstraction reaction by the *t*-butoxy radical is proportional to the concentration of the *t*-butoxy radical and RH. The $\beta$-scission becomes preferential in the presence of a solvent as a result of this dilution effect. This effect is summarized in Table VII.

Table VII. Dilution effect

| Exp. No. | $C_6H_6$/*t*-BuOCl Mole ratio | $R$*1,*2 Mole ratio |
|---|---|---|
| 11 | 10 | 0.83 |
| a*3 | 5 | 1.14 |
| b*3 | 14 | 0.7 |

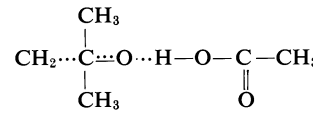
*1 $R = \dfrac{(t\text{-BuOH} + \text{chloro-}t\text{-BuOH})}{(\text{acetone} + \text{monochloroacetone})}$

*2 The value of $R$ may be influenced by reaction temperature, but we considered that there was no great difference of $R$ values within the range of 30°C to 40°C.

*3 C. Walling and B. B. Jacknow, *J. Am. Chem. Soc.*, **82**, 6111 (1960).

The mole ratio ($R$) of *t*-butyl alcohol and acetone decreases in proportion as the mole ratio of benzene and *t*-butyl hypochlorite increases. The $R$ ratio in this experiment is summarized in Table VIII.

In the case of propionic acid, the $R$ ratio is smaller than unity in the presence of benzene. In the reactions with monochloro- and trichloroacetic acids, $R$ is always smaller than unity. In the case of acetic acid, however, $R$ is, contrariwise, larger when the solvent is present than when there is no solvent. These results suggest that, as Walling has also described,[10] hydrogen bonding between the *t*-butoxy radical and acetic acid stabilizes the transition state of the $\beta$-scission.



In the case of propionic acid, however, this hydrogen bonding may be fairly unstable, the *t*-butoxy radical preferentially abstracts a hydrogen from the acid, and in the presence of the solvent, the $\beta$-scission of the radical proceeds predominantly as a results of the dilution effect.

**The Reactivities of the *t*-Butoxy Radical.**—Russell investigated the solvent effects in the photochlorination of hydrocarbons by molecular chlorine and found that, in the presence of some aromatic solvents, the chloro radical attacked hydrocarbons with a high selectivity.[11] Consequently, he considered that the selectivity may be ascribed to the formation of a $\pi$-complex between the chloro radical and the aromatic nucleus, and that this complex was less reactive and, therefore, more selective

9) G. A. Russell, *J. Org. Chem.*, **24**, 300 (1959).
10) C. Walling, *J. Am. Chem. Soc.*, **85**, 2333 (1963).
11) a) G. A. Russell, ibid., **80**, 4987 (1958); b) G. A. Russell, ibid., **80**, 4997 (1958); c) G. A. Russell, ibid., **80**, 5002 (1958).

TABLE VIII. MOLE RATIO ($R$) OF $t$-BUTYL ALCOHOL AND ACETONE AT 30°C

| Exp. No. | Carboxylic acid | Solvent | Solvent/$t$BuOCl Mole ratio | $R$* |
|---|---|---|---|---|
| 1 | $CH_3COOH$ | None | — | 0.21 |
| 2 | $CH_3COOH$ | None | — | 0.33 |
| 3 | $CH_3COOH$ | $C_6H_6$ | 10 | 0.62 |
| 4 | $CH_3COOH$ | $CCl_4$ | 10 | 0.89 |
| 5 | $C_2H_5COOH$ | None | — | 1.79 |
| 6 | $C_2H_5COOH$ | $C_6H_6$ | 10 | 0.8 |
| 7 | $n$-$C_3H_7COOH$ | None | — | 1.69 |
| 8 | $CH_2ClCOOH$ | $C_6H_6$ | 10 | 0.77 |
| 10 | $CCl_3COOH$ | $CCl_4$ | 5 | 0.44 |
| 11 | None | $C_6H_6$ | 10 | 0.83 |

* Considering further chlorinations of acetone and $t$-butyl alcohol, $R$ was corrected as follows.

$$R = M_a/M_d$$

$M_a$ = $t$-BuOH + Chloro-$t$-BuOH (mol.)
$M_d$ = Acetone + Monochloroacetone (mol.)

TABLE IX. ISOMER DISTRIBUTIONS — COMPARISON WITH OTHER DATA

| RCOOH | Method | $\alpha$-Isomer % | $\beta$-Isomer % | $\gamma$-Isomer % | Ref. |
|---|---|---|---|---|---|
| $C_2H_5$- | $t$-BuOCl + h$\nu$ | 61.2 | 38.8 | — | |
| $C_2H_5$- | $SO_2Cl_2$ + B. P. O. | 45 | 55 | — | a) |
| $n$-$C_3H_7$- | $t$-BuOCl + h$\nu$ | 20.6 | 46.4 | 33.0 | |
| $n$-$C_3H_7$- | $SO_2Cl_2$ + B. P. O. | 10 | 45 | 45 | a) |
| $n$-$C_3H_7$- | $Cl_2$ + h$\nu$ | 5 | 64 | 31 | b) |
| $n$-$C_3H_7$- | $Cl_2$ + $\gamma$-ray | 6 | 61 | 33 | c) |

a) M. S. Kharasch and H. C. Brown, *J. Am. Chem. Soc.*, **62**, 926 (1940).
b) A. Bruylants, M. Tits, C. Dieu and R. Gauthier, *Bull. soc. chim. Belges*, **61**, 266 (1952).
c) I. Rosen and J. P. Stallings, *Ind. Eng. Chem.*, **50**, 1512 (1958).

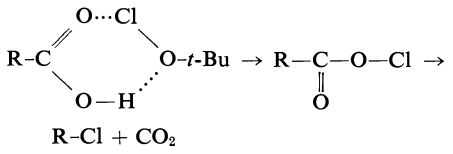
than the free chloro radical. On the other hand, Walling and his co-workers studied the similar chlorination by $t$-butyl hypochlorite.[1-3] They indicated that, even in the presence of an aromatic solvent, there was no change in the selectivitity of the $t$-butoxy radical as to the hydrogen abstraction. In our study of the chlorination of propionic acid as is shown in Table IV, the ratio of the $\alpha$- and, $\beta$-isomers was constant, regardless of the presence or absence of benzene. These facts suggest that the $t$-butoxy radical does not form a $\pi$-complex with the aromatic solvent because of the small electron affinity and the bulkiness of the $t$-butoxy radical.

Now we will discuss in more detail the selectivity of the $t$-butoxy radical in the hydrogen abstraction from the carboxylic acids. For this purpose, our data are compared with other data and the results summarized in Table IX.

Propionic acid was chlorinated somewhat predominantly in the $\alpha$-position in our study, but, on the contrary, in the $\beta$-position in Kharasch's experiment. On the other hand, chlorinations of $n$-butyric acid by all the methods listed in Table IX show a similar trend for the $\beta$-isomer to be formed most preferentially, followed by the $\gamma$-isomer. In our method, however, the formation of the $\alpha$-isomer increased to some extent as compared with the other methods. From these results, we would conclude that the direction of the hydrogen abstraction by a radical with a large electron affinity, such as the chloro radical, is greatly influenced by the electron density on the carbon atoms of the alkyl group (the values of 88 kcal./mol. was determined for the electron affinity of the chloro radical). Thus, the $\alpha$-position of propionic or $n$-butyric acid becomes inactive as a result of the electron-withdrawing effect of the carboxyl group. In $n$-butyric acid, the $\beta$-position is most reactive for the following two reasons. First, the inductive effect of the carboxyl group may be not so effective in the $\beta$-position as in the $\alpha$-position. Second, the hyperconjugation of the methyl group makes a contribution to the $\beta$-position. For these two reasons, the electron density on the carbon atoms of the alkyl group becomes greatest in the $\beta$-position; therefore, this position may be easily attacked by a highly-electrophilic chloro radical. On the other

hand, the electron affinity of the *t*-butoxy radical is not so high as the chloro radical (it is known that the electron affinity of the alkoxy radical is about 50 kcal./mol.) and, therefore, the electron density is not so effective in controlling the direction of the hydrogen abstraction from the alkyl group of the carboxylic acid by the *t*-butoxy radical. Consequently, *t*-butyl hypochlorite chlorinates *n*-butyric acid without selectivity, and the $\alpha$-isomers increase in number in the chlorination of propionic acid by *t*-butyl hypochlorite.

Although Walling has recently reported that the formation of carbon dioxide was not detected in the reaction of *t*-butyl hypochlorite in acetic acid,[12] the formation of carbon dioxide was observed in our study. The decarboxylation of the carboxylic acids may proceed through the formation of acyl hypochlorite, followed by decomposition to give carbon dioxide and the corresponding alkyl chloride, as is shown below:




*Department of Chemical Technology*
*Faculty of Engineering*
*Osaka University*
*Miyakojima-ku, Osaka*

12) C. Walling and P. J. Wagner, *J. Am. Chem. Soc.*, **86**, 3368 (1964).

# Magnetic Properties of Bi- and Uni-Nuclear Chromium(III) Complex Compounds at Low Temperatures

By Hanako KOBAYASHI,* Taiichiro HASEDA and Masayasu MORI

(Received November 30, 1964)

There are various theories on the mechanism of the superexchange interaction between magnetic ions in crystals. Kanamori,[1] for instance, studied the superexchange interaction, taking into consideration the symmetry of the electron orbitals of magnetic ions. It was shown that the sign** of the superexchange interaction is closely connected with the symmetry of the orbitals of the magnetic ions and non-magnetic ions which are in the path of the superexchange interaction. The cases in which each cation is subject to an octahedral cubic field and in which the lines connecting cations to the intervening anion make an angle of either 180° or 90° were discussed as simple and typical examples. His study suggested that the 180° superexchange interaction is antiferromagnetic and the 90° one, ferromagnetic in the case of $Cr^{3+}\cdots Cr^{3+}$ interaction. In the real crystals, there are usually both paths, 180° and 90°, of the superexchange interaction. The sign of the superexchange interaction in a magnetic substance depends on all the contributions from relevant paths. There is, in general, no simple and direct way to examine the above-cited theory by experimentation. Moreover, there have been few papers[2] which make clear any mechanism of the superexchange interaction actually occurring in the observed crystal.

It seems that the investigation of some sort of bi-nuclear complex salts, in which the superexchange interaction between two magnetic ions passes through only one path, either 180° or 90° would make possible a direct examination of the relation between the bond angle and the sign of the superexchange interaction.

The first part of the present paper will concern the study of the magnetic properties of bi-nuclear complex compounds. The experimental results of magnetic and optical measurements of the following four bi-nuclear complex salts will be discussed; $\mu$-hydroxo-bis-{pentamminechromium(III)} 3/2-chloride 7/2-perchlorate 1/2-hydrate,[3] $\mu$-hydroxo-{hydroxotetramminechromium(III)-pentamminechromium(III)}tetrachloride 1-hydrate, $\mu$-oxo-bis{pentamminechromium(III)}perchlorate, and

* Present address: Department of Chemistry, Faculty of Science, Kyoto University, Kyoto.

** Through this paper, a negative sign is used for the antiferromagnetic exchange interaction.

1) J. Kanamori, *J. Phys. Chem. Solids*, 10, 87 (1959).

2) J. Kondo, *Prog. Theor. Phys.*, 22, 41 (1959).

3) H. Kobayashi, T. Haseda, E. Kanda and M. Mori, *J. Phys. Soc. Japan*, 15, 1646 (1960).

μ-dihydroxo-bis{tetramminechromium(III)}dithionate 4-hydrate.

In the cases of μ-hydroxo-bis{pentamminechromium(III)}3/2-chloride 7/2-perchlorate 1/2-hydrate, μ-hydroxo{hydroxotetramminechromium(III)-pentamminechromium(III)}tetrachloride 1-hydrate and μ-oxo-bis{pentamminechromium(III)}perchlorate, the linkage of the superexchange interaction is considered to pass through a path of about 180°, connecting two chromic ions via one oxygen atom. In the case of μ-dihydroxo-bis{tetramminechromium-(III)}dithionate 4-hydrate, the linkage of the superexchange interaction is considered to turn at oxygen atoms, making angles of about 90°. We have already measured[3] the susceptibilities of some of these salts and have suggested some interpretations. We now add the salt which has a nearly 90° angle linkage. We shall discuss all of these experimental data from the above-mentioned point of view.

The second problem of the present paper is the comparison of the superexchange interaction among $Cr^{3+}$ ions which are octahedrally co-ordinated by various ligands. The interaction between two magnetic ions depends on the distance between the two ions and on the linkage from one magnetic ion to the other magnetic ion. If some ligands in a complex ion are replaced by other atoms or by atomic groups, leaving the distances almost the same as before substitution, the experimental results of the substituted compounds will contribute to an understanding of the interactions among magnetic ions through various linkages.

The following co-ordination compounds of $Cr^{3+}$ ions with various kinds of ligands were investigated: hexamminechromium(III) chloride, chloropentamminechromium(III) chloride, dibromo-diaquo-diamminechromium(III) bromide, and dihydroxo-diaquo-diamminechromium(III) bromide.

## Preparation

**μ-Hydroxo-bis{pentamminechromium(III)}3/2-chloride 7/2-perchlorate 1/2-Hydrate**[4] was prepared by Mori, Ueshiba and Yamatera's procedure (Ref. 5).

**μ-Hydroxo-{hydroxotetramminechromium(III)-pentamminechromium(III)}tetrachloride 1-Hydrate** was prepared by Jörgensen's procedure (Ref. 4).

**μ-Oxo-bis{pentamminechromium(III)}perchlorate.**—Two hundred milliliters of 30% perchloric acid (guaranteed grade) were carefully neutralized with sodium carbonate (guaranteed grade) until the mixture was only slightly acidic to methyl red. Twenty milliliters of concentrated aqueous ammonia was then added, and the mixture was filtered. To the filtrate was added 5 g. of μ-hydroxo-bis{pentamminechromium(III)}3/2-chloride 7/2-perchlorate 1/2-hydrate, and the mixture was cooled in an ice bath for 30 min. with occasional stirring. The deep blue precipitate was collected on a glass filter and washed with alcohol and ether. After it had been dried for several minutes under strong suction, the compound was kept in a desiccator with soda lime and dry ammonia gas under protection from light.

**μ-Dihydroxo-bis{tetramminechromium(III)}-dithionate 4-Hydrate.**—The procedure of preparation was that given by Dubsky in Ref. 6.

**Hexamminechromium(III) Chloride.**[7]—A green solution containing chromium(III) salt was prepared in a 1000 ml. beaker by mixing 30 g. of potassium dichromate, 40 ml. of ethanol and 80 ml. of concentrated hydrochloric acid. This solution was then transferred into a smaller beaker and covered with a 3-cm. layer of liquid paraffine. Sixty grams of pure zinc grains were added, and the mixture was heated to 80—90°C on a steam bath. When the solution had become perfectly blue, the container was cooled in running water, then the solution was removed, together with the mineral oil, into an Erlenmeyer flask containing a mixture of 200 ml. of concentrated aqueous ammonia, 50 g. of ammonia chloride and 50 g. of ammonium sulfate. The whole mixture was gently stirred and cooled in an ice bath for several minutes. To this was added 10 g. of powdered iron(II) ammonium sulfate. Finally the vessel was loosely stoppered and allowed to stand in an ice bath over night or longer. The yellow crystals thus formed were washed on a Buchner funnel with 50% ethanol, and dissolved in 400 ml. of water. After the addition of 2 ml. of concentrated aqueous ammonia and 2 ml. of 30% hydrogen peroxide, the solution was filtered, treated with 400 ml. of 12 N hydrochloric acid and 800 ml. of ethanol, and cooled in an ice bath. The yellow precipitate of hexamminechromium(III) chloride 1-hydrate thus obtained was dissolved in water, recrystallized by the addition of hydrochloric acid and ethanol, and dehydrated at 80°C until a constancy in weight was attained. The anhydrous salt was preserved in a desiccator under protection from light.

**Chloro-pentamminechromium(III) Chloride** was prepared by the procedure described in Ref. 8.

**Dibromo-diaquo-diamminechromium(III) Bromide:** Ref. 9.

**Dihydroxo-diaquo-diamminechromium(III) Bromide:** Ref. 9.

## Experimental Results

**The Magnetic Susceptibility of Bi-nuclear Complex Salts.**—The magnetic susceptibilities

4) S. M. Jörgensen, *J. prakt. Chem.*, 25, 321 (1882).
5) M. Mori, S. Ueshiba and H. Yamatera, This Bulletin, 32, 89 (1959).
6) J. B. Dubsky, *J. prakt. Chem.*, 90, 60 (1914).
7) S. M. Jörgensen, ibid., 30, 6 (1884); M. Mori, *J. Chem. Soc. Japan, Pure Chem. Sec.* (*Nippon Kagaku Zassi*), 74, 253 (1953).
8) H. Biltz and W. Biltz, "Laboratory Methods of Inorganic Chemistry" (Translated by W. T. Hall and A. A. Blanchard), 2nd Ed., John Wiley & Sons, New York, N. Y. (1928) p. 185.
9) A. Werner and J. L. Klein, *Ber.*, 35, 285 (1902).

were measured by an a.c. bridge method in the temperature range between 1.5°K and room temperature. The a.c. bridge was constructed so as to enable to measure magnetic susceptibilities of the order of $10\times10^{-6}$ c.g.s.e.m.u. with an accuracy of $\pm1\%$, when the amount of the sample was about 1 g. The cryostat and the procedure for measurment have been described in the literature.[10] The susceptibility is given in molar units for each compound. The calibration for diamagnetism was made by using the values listed in Table I.

TABLE I. CALIBRATION FOR DIAMAGNETISM

| Atomic or atomic group | $\chi$, c.g.s.e.m.u. |
|---|---|
| $Br^-$ | −0.000031 |
| $Cl^-$ | −0.000025 |
| $ClO_4^-$ | −0.000033 |
| $Cr^{3+}$ | −0.000015 |
| $H_2O$ | −0.000013 |
| $NH_3$ | −0.000001 |
| -O- | −0.000005 |
| -OH- | −0.000009 |

The molar magnetic susceptibility of $\mu$-dihydroxo-bis{tetramminechromium(III)}dithionate 4-hydrate is shown as a function of the temperature for a couple of $Cr^{3+}$ ions in Figs. 1 and 2, together with the results for the other bi-nuclear complexes which were studied before.[3] The susceptibility of this salt decreased with a decrease in the temperature in the liquid hydrogen and helium regions.

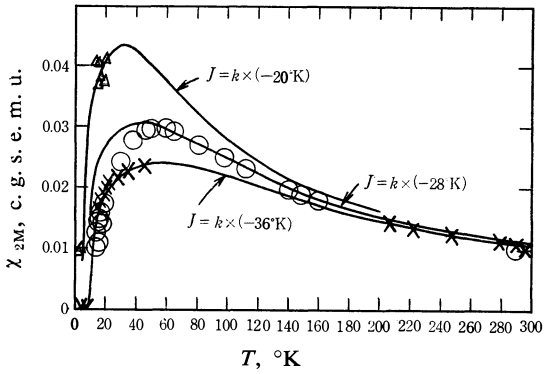



Fig. 1. Molar magnetic susceptibilities as a function of temperature.
○ : $\mu$-Hydroxo-bis{pentamminechromium(III)}3/2-chloride 7/2perchlorate 1-hydrate
× : $\mu$-Hydroxo-{hydroxotetramminechromium(III)-pentamminechromium(III)}tetrachloride 1-hydrate
△ : $\mu$-Dihydroxo-bis{tetramminechromium(III)}dithionate 4-hydrate

10) H. Kobayashi, thesis, Tohoku University, Sendai, 1962.

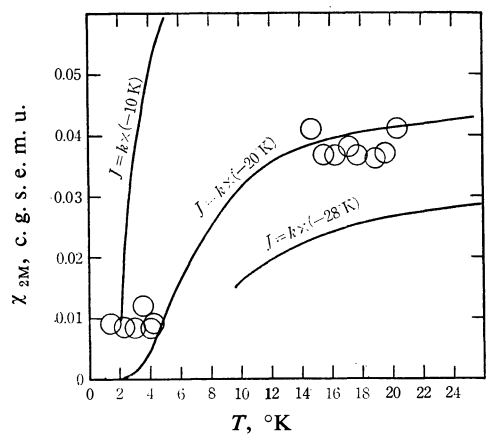



Fig. 2. Molar magnetic susceptibility of $\mu$-dihydroxo-bis{tetramminechromium(III)} dithionate 4-hydrate as a function of temperature.

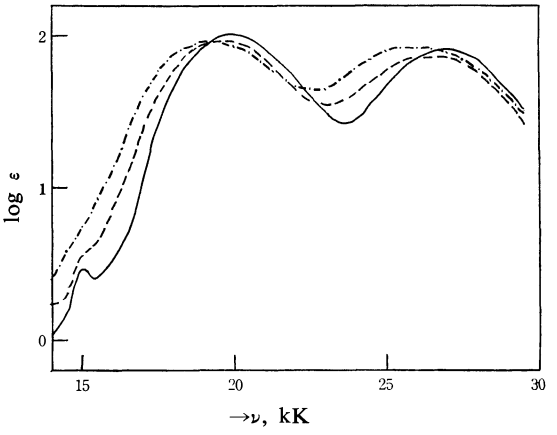



Fig. 3. Absorption Spectra of Binulear Chromammines.
——— $[Cr(NH_3)_5OHCr(NH_3)_5]Br_5\ H_2O$
— — — $[Cr(NH_3)_5OHCr(NH_3)_4OH_2]Br_5\ H_2O$
·—·—· $[Cr(NH_3)_5OHCr(NH_3)_4OH]Br_4\ H_2O$

Figure 3 gives the absorption spectra of aqueous $\mu$-hydroxo-bis{pentamminechromium(III)}bromide 1-hydrate, $\mu$-hydroxo-{hydroxotetramminechromium(III)-pentamminechromium(III)}bromide 1-hydrate and $\mu$-hydroxo-{aquotetramminechromium(III)-pentamminechromium(III)}bromide 1-hydrate. These spectra resemble each other. The former two salts have the cations in common with the salts studied magnetically, though their anions are not the same.

**The Magnetic Susceptibility of Uni-nuclear Co-ordination Compounds of $Cr^{3+}$ Ions.**—The reciprocals of the molar magnetic susceptibilities of hexamminechromium(III) chloride are shown as a function of the temperature in Fig. 4 and Table II. These salts have magnetic

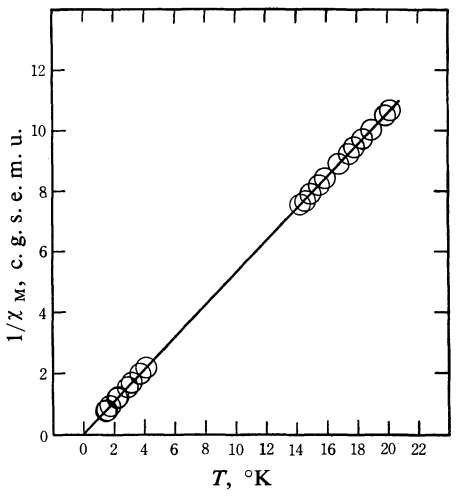



Fig 4. Reciprocal of molar magnetic susceptibility of hexamminechromium(III) chloride as a function of temperature.

TABLE II. MOLAR MAGNETIC SUSCEPTIBILITY OF HEXAMMINECHROMIUM(III) CHLORIDE

| $T$, °K | $\chi_M$ c.g.s.e.m.u. | $P$ | $T$, °K | $\chi_M$ c.g.s.e.m.u. | $P$ |
|---|---|---|---|---|---|
| 20.27 | 0.0939 | 3.9 | 3.43 | 0.551 | 3.9 |
| 19.46 | 0.0981 | 3.9 | 3.29 | 0.565 | 3.9 |
| 18.97 | 0.0993 | 3.9 | 3.02 | 0.615 | 3.9 |
| 18.46 | 0.1026 | 3.9 | 3.00 | 0.629 | 3.9 |
| 17.92 | 0.1065 | 3.9 | 2.78 | 0.672 | 3.9 |
| 17.50 | 0.1093 | 3.9 | 2.54 | 0.741 | 3.9 |
| 16.89 | 0.1126 | 3.9 | 2.49 | 0.745 | 3.9 |
| 15.93 | 0.1189 | 3.9 | 2.29 | 0.806 | 3.8 |
| 15.57 | 0.1203 | 3.9 | 2.03 | 0.920 | 3.9 |
| 15.02 | 0.1250 | 3.9 | 1.84 | 1.044 | 3.9 |
| 14.61 | 0.1295 | 3.9 | 1.76 | 1.057 | 3.9 |
| 14.33 | 0.1316 | 3.9 | 1.74 | 1.107 | 3.9 |
| 4.22 | 0.445 | 3.9 | 1.57 | 1.232 | 3.9 |
| 3.80 | 0.491 | 3.9 | 1.45 | 1.264 | 3.8 |

susceptibilities which follow the Curie-Weiss law.

The molar magnetic susceptibility of dibromo-diaquo-diamminechromium(III) bromide is shown in Fig. 6 as a function of the temperature, while that of dihydroxo-diaquo-diamminechromium(III) bromide is shown in Fig. 7. The susceptibilities of both salts follow the Curie-Weiss law down to the temperature region of liquid hydrogen and have maxima at about 3°K and about 3.5°K respectively. The shape of the maximum is broad in the former and steep in the latter.

## Discussion

**Bi-nuclear Complex Salts.**—The magnetic susceptibilities of $\mu$-hydroxo-bis{pentamminechromium(III)}3/2-chloride 7/2-perchlorate 1/2-hydrate and $\mu$-hydroxo{hydroxo-tetramminechromium(III) - pentamminechromium(III)}-tetrachloride 1-hydrate are similar, as is shown in Fig. 1. They have broad maxima near 50°K and become very small in the temperature region of liquid helium. The magnetic behavior of these salts indicates that their electronic structures and the mechanisms of their magnetic interaction are similar. The resemblance of the absorption spectra of these complex cations, as may be seen in Fig. 3, also seems to support this.[11] In this case, the difference in anions is probably of little importance since it is complex cations that are mainly responsible for both the absorption spectra and the magnetic susceptibilities of these compounds.

The energy levels of $Cr^{3+}$ spins ($S=3/2$) in the bi-nuclear salts can easily be calculated under the following simplified conditions. If the orbital angular momentum of the $Cr^{3+}$ ion in the bi-nuclear complex salts is assumed to be completely quenched, the spins of $Cr^{3+}$ ions in the same cation are expressed as $S_1$ and $S_2$, with the expectation value of $S=3/2$. In this case, the Hamiltonian of the two spins under a magnetic field, $H$, can then be written as:

$$\mathscr{H} = JS_1S_2 + g\mu_B (S_1+S_2)H$$

where $J$ is a coefficient of the exchange interaction between the two $Cr^{3+}$ ions and is negative in the case of these two salts. The magnetic susceptibility can be calculated by a standard method. The calculated curves of $\chi_{2M}$ with a parameter of $J$ are shown in Fig. 1 as a function of the temperature, where $g$ is assumed to be 2.00. The experimental values of $\mu$-hydroxo-bis{pentamminechromium(III)}-3/2-chloride 7/2-perchlorate 1/2-hydrate fit well the calculated curve with $J=k\times(-28°K)$, and the values of $\mu$-hydroxo-{hydroxotetramminechromium(III)-pentamminechromium(III)}tetrachloride 1-hydrate agree with the calculated curve with $J=k\times(-36°K)$. Judging from the chemical or photo-chemical inspections,[12] angle made by the lines connecting the two $Cr^{3+}$ ions to the intervening oxygen atom of the hydroxide group seems to be nearly 180°. The agreement of the experimental results with the above-mentioned calculations indicates that the superexchange interaction between two $Cr^{3+}$ ions through the oxygen of the hydroxide in these bi-nuclear complex cations has a constant of the superexchange interaction of about $k\times(-28°K)-k\times(-36°K)$.

11) Y. Inamura and Y. Kondo, *J. Chem. Soc. Japan, Pure Chem. Sec.* (*Nippon Kagaku Zassi*), **74**, 627 (1953).
12) W. K. Wilmarth, H. Graff and S. T. Gustin, *J. Am. Chem. Soc.*, **78**, 2683 (1956).

The magnetic property of $\mu$-oxo-bis{pentamminechromium(III)}perchlorate was expected to show the typical character of the 180° superexchange interaction of $3d^3$ electrons through a linear linkage. The minute details of the temperature dependence of the susceptibility could not be determined because of its change is too small. If the same calculation is applied as with the former two salts, $J$ is negative and is quite large ($>|k\times 200°K|$), as was expected. This means the antiferromagnetic interaction between $Cr^{3+}$ ions by the hydroxide group in the former two complex salts is much weaker than that of the perfect 180° bridge because of their deviation from linear linkage. $\mu$-Dihydroxo-bis{tetramminechromium(III)}dithionate 4-hydrate is a sample which is considered to have two nearly-90° bridges between two $Cr^{3+}$ ions. In the case of the 90° path between two $Cr^{3+}$ ions, the sign of the superexchange interaction may be expected to be plus.[1] The results of the measurements of magnetic susceptibility are shown in Figs. 1 and 2. In the region of the liquid hydrogen temperature, the experimental curve roughly agrees with the calculated curve, with negative $J\simeq k\times(-20°K)$.

From these results, we may conclude that $\mu$-oxo-bis{pentamminechromium(III)}perchlorate has 180° superexchange interaction and that the paths of the superexchange interaction of $\mu$-hydroxo-bis{pentamminechromium(III)}-3/2-chloride 7/2-perchlorate 1/2-hydrate and $\mu$-hydroxo-{hydroxotetramminechromium(III)-pentamminechromium(III)}tetrachloride 1-hydrate deviate from linear linkage. The path of $\mu$-dihydroxo-bis{tetramminechromium(III)}-dithionate 4-hydrate shows the smallest value of J, but it does not yet show a positive sign.

**Uni-nuclear Complex Salts.**—The crystalline structure of hexamminechromium(III) chloride is of the bismuth fluoride type. Each $Cr^{3+}$ ion is octahedrally co-ordinated by six ammonia molecules in the salt. The exchange interaction among the magnetic ions in this salt is through the following path:

$$Cr^{3+}\cdots\cdots NH_3\cdots\cdots Cl^-\cdots\cdots H_3N\cdots\cdots Cr^{3+}$$

ligand anion ligand

The experimental magnetic susceptibility curve as a function of the temperature follows the Curie-Weiss law quite well, with the absolute value of the Curie-Weiss constant, $\Theta$, smaller than 0.01°K, as is shown in Fig. 4. The sign of the $\Theta$ could not be determined from the experiment with the above-mentioned accuracy. The spectroscopic splitting factor, $g$, can be calculated from the next equation when the absolute value of $\Theta$ is smaller than 0.01°K:

$$\chi_M=\frac{N\mu_B^2\ g^2S(S+1)}{3k\ (T-\Theta)}$$

The mean $g$-value at the temperatures of liquid helium and liquid hydrogen is 2.00± 0.02. The very small absolute value of the Curie-Weiss constant implies quite a weak interaction among $Cr^{3+}$ ions in this salt.

The co-ordination of the ligands of chloropentamminechromium(III) chloride is not of the pentamminerhodium(I) chloride type, but of the chloropentamminerhodium(III) chloride type: that is, a ligand ammonia of the hexamminechromium(III) ion is replaced by a chlorine ion. The crystalline structure of this salt is of the calcium fluoride type,[13] so the paths of the interactions among $Cr^{3+}$ ions may be considered to pass through any of the following:

$$Cr^{3+}\cdots\cdots Cl^-\cdots\cdots Cl^-\cdots\cdots H_3N\cdots\cdots Cr^{3+}$$

ligand anion ligand

$$Cr^{3+}\cdots\cdots Cl^-\cdots\cdots Cl^-\cdots\cdots Cl^-\cdots\cdots Cr^{3-}$$

ligand anion ligand

$$Cr^{3+}\cdots\cdots NH_3\cdots\cdots Cl^-\cdots\cdots H_3N\cdots\cdots Cr^{3+}$$

ligand anion ligand

$$Cr^{3+}\cdots\cdots Cl^-\cdots\cdots H_3N\cdots\cdots Cr^{3+}$$

ligand ligand

$$Cr^{3+}\cdots\cdots Cl^-\cdots\cdots Cl^-\cdots\cdots Cr^{3+}$$

ligand ligand

$$Cr^{3+}\cdots\cdots NH_3\cdots\cdots H_3N\cdots\cdots Cr^{3+}$$

ligand ligand

From the magnetic susceptibility curve as a function of the temperature, a Curie-Weiss constant, $\Theta$, of about −0.8°K was obtained, as is shown in Fig. 5. This shows that the superexchange interaction between $Cr^{3+}$ ions

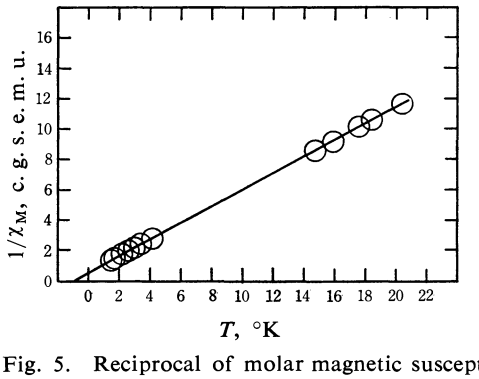



Fig. 5. Reciprocal of molar magnetic susceptibility of chloropentamminechromium(III) chloride as a function of temperature

13) Y. Nakao, S. Oi, Y. Komiyama and H. Kuroya, The 13th Symposium on Co-ordination Chemistry, Nagoya, 1963.

is considerably large than that of hexamminechromium(III) chloride, which may reasonably be attributed to the presence of the paths of the latter three types. The latter three paths, which do not pass through anions, are shorter than the former, and the presence of a large ion in the path strengthens the superexchange interaction. The mean value of $g$ is $1.95\pm0.09$ in the temperature region of liquid helium and liquid hydrogen, when 3/2 is given as the spin quantum number, $S$.

The crystal structure of dibromo-diaquo-diamminechromium(III) bromide has not yet been analyzed. However, some paths of the superexchange interaction can be considered to be the shortest, as in the case of chloropentamminechromium(III) chloride. The Curie-Weiss constant, $\Theta$, is estimated to have a larger absolute value than that of chloropentamminechromium(III) chloride, because the number of large $Br^-$ ligands is two in this salt, one more than in the case of chloropentamminechromium(III) salt. The $\Theta$ obtained was about $-3$°K. The curve of the molar magnetic susceptibility as a function of the temperature has a broad maximum at 2.5°K, showing a transition to an antiferromagnetic state (Fig. 6).

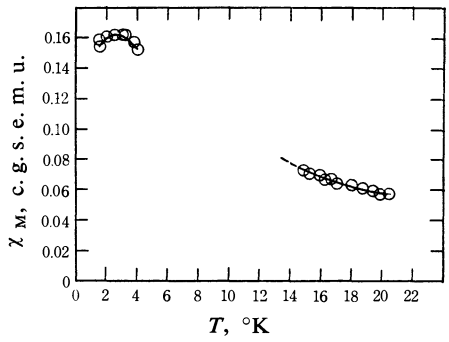



Fig. 6. Molar magnetic susceptibility of dibromo-diaquo-diamminechromium(III) bromide as a function of temperature

Dihydroxo - diaquo - diamminechromium(III) bromide has two hydroxyl groups in place of two bromine ligands of dibromo-diaquo-diamminechromium(III) bromide. The crystalline structure is not yet known. The experiment of the magnetic susceptibility gave a Curie-Weiss constant of about $-9$°K and a mean $g$-value of about $2.00\pm0.01$, when $S$ was taken as 3/2. This Curie-Weiss consant is larger than that of dibromo-diaquo-diamminechromium(III) bromide. The magnetic susceptibility-versus-temperature curve shows a steep peak at about $3.5\text{°K}\pm0.2\text{°K}$, as is shown in Fig. 7. Perhaps this is a transition to an antiferromagnetic state, though its shape is different from the typical antiferromagnetic transition.

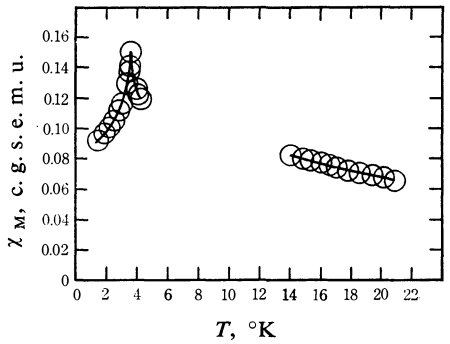



Fig. 7. Molar magnetic susceptibility of dihydroxo-diaquo-diamminechromium(III) bromide as a function of temperature

It may be noted that dihydroxo-diaquo-diamminechromium(III) salts are almost insoluble in water, although all chromammines with similar chemical formulae are known to be freely soluble. This peculiar insolubility and the comparatively large superexchange interaction of dihydroxo-diaquo-diamminechromium(III) bromide may be an indication that this compound is a co-ordination polymer, with each hydroxyl group ligated to different chromium ions. If this is the case, the above nomenclature must be revised somewhat, although names correctly expressing their true status will be hard to devise.

## Summary

The experimental study of the magnetic properties of bi- and uni-nuclear chromium(III) complex compounds in the low temperature

TABLE III.

| Multi-nuclear Cr(III) complex ion | Estimated angle of Cr-O-Cr linkages | Coefficient of the superexchange interactions |
|---|---|---|
| $(NH_3)_5Cr\text{-}O\text{-}Cr(NH_3)_5$ | 180° | $k\times(-200\text{°K})$ |
| $(NH_3)_5Cr\text{-}OH\text{-}Cr(NH_3)_5$ | ~180° | $k\times(-28\text{°K})$ |
| $(NH_3)_5Cr\text{-}OH\text{-}Cr(OH)\text{-}(NH_3)_4$ | ~180° | $k\times(-36\text{°K})$ |
| $(NH_3)_4Cr\langle^{OH}_{OH}\rangle Cr(NH_3)_5$ | 90° | $k\times(-20\text{°K})$ |

TABLE IV.

| Uni-nuclear Cr(III) complex salt | Transition point | Curie-Weiss constants | $g$-Values |
|---|---|---|---|
| $[Cr(NH_3)_6]Cl_3$ | | $\lvert\Theta\rvert<0.01$°K | $2.00\pm0.02$ |
| $[CrCl(NH_3)_5]Cl_2$ | | $-0.8$°K | $1.95\pm0.09$ |
| $[CrBr_2(OH_2)_2(NH_3)_2]\text{-}Br$ | ca. 2.5°K | $-3$°K | $1.69\pm0.04$ |
| $[Cr(OH)_2(OH_2)_2\text{-}(NH_3)_2]Br$ | ca. 3.5°K | $-9$°K | $2.00\pm0.01$ |

region has given the results summarized in Tables III and IV. As has been mentioned above, the results listed in Table III show the tendency expected from the superexchange interaction theories.

The authors would like to thank Professor Eizo Kanda for his continuous interest in this problem.

*Research Institute for Iron, Steel and Other Metals*
*Tohoku University*
*Katahira-cho, Sendai (H.K. & T.H.)*

*Faculty of Science*
*Osaka City University*
*Sumiyoshi-ku, Osaka (M.M.)*

# A Study of Unnatural Amino Acids and Their Peptides. I. The Synthesis of DL-β-(2-Furyl)-α-alanine*1

By Hiroshi WATANABE, Shigeru KUWATA, Shigeru NAKAJIMA*2
Kazuo KOSHIDA*3 and Motoshige HAYASHI*4

(Received December 7, 1964)

With the development of the chemistry of antibiotics and other microbial products, or of the constituents of microbes themselves, e. g., the cell wall of bacteria, it has been clarified that there are many sorts of amino acids which have not hitherto been encountered in common proteins. One of them is the D-amino acid, e. g., D-phenylalanine in gramicidin S[1] or tyrocidine,[2] D-serine in cycloserine,[3] and D-glutamic acid in the capsular substance of *Bact. anthracis*.[4] Another group is the amino acid with a hetero-ring, e. g., β-(2-thiazole)-β-alanine in bottromycin[5] or 3-oxy-2-picolic acid and 4-oxopipecolic acid in staphylomycin[6] and ostreogrycin.[7]

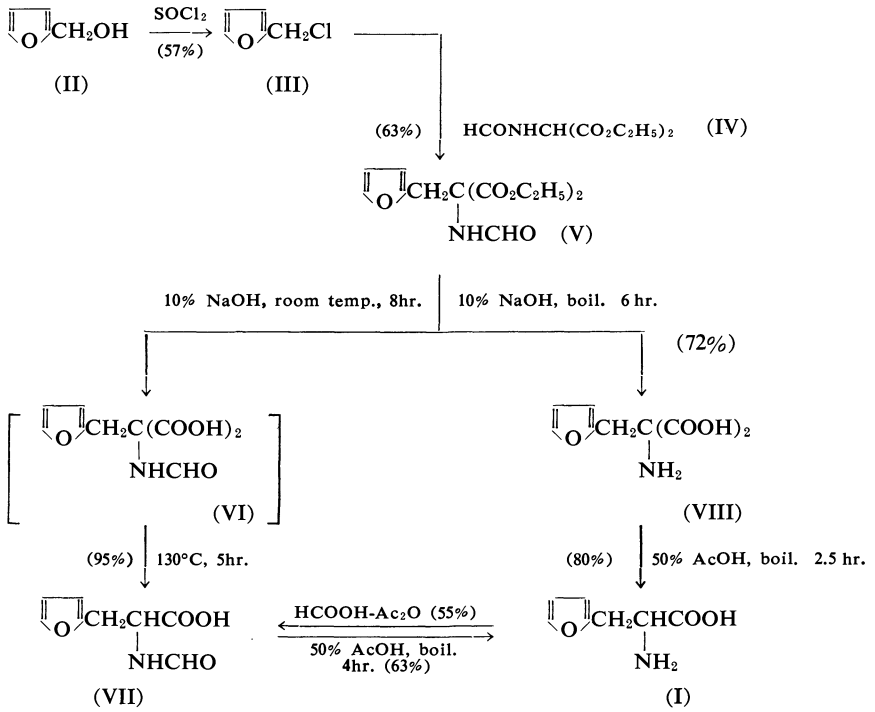
We are interested in these "unnatural amino acids" and in their peptides, especially those of the latter group, in connection with their biological properties. Therefore, we intend to begin to study in this field. In this paper the synthesis of DL-β-(2-furyl)-α-alanine (I), an amino acid with a furyl residue in place of the phenyl residue in phenylalanine, will be reported.

This amino acid has not yet been found in nature, but it has been synthesized in many ways, such as through the condensation of furfural with hydantoin,[8] rhodanine,[9] diketopiperazine,[10] or hippuric acid.[11] The condensation of furfurylchloride with acetamidomalonate[12] or acetamidocyanoacetate[12] has also been utilized for this purpose. Of these, the rhodanine method was tested first, but this was found not suitable for large-scale preparations. The acetamidomalonate method was then tried. The condensation of furfurylchloride (III) with ethyl acetamidomalonate proceeded smoothly, but no promising results were obtained in the hydrolysis of the condensation product. Although this difficulty can be avoided, according to Herz,[12] by using acetamidocyanoacetate instead of acetamidomalonate, the total yield is still too low. Thus ethyl formamidomalonate (IV) was chosen because the removal of formyl group is, in general, far easier than that of the acetyl group, and because, moreover, the formylfurylalanine itself may be useful as an intermediate for the further peptide synthesis.

*1 This work was presented at the 17th Annual Meeting of the Chemical Society of Japan, April, 1964.

*2 Present address; Kobe Electric Machinery Co., 14, Naka 5-Chome, Oyodo-cho, Oyodo-ku, Osaka.
*3 Present address; Japan Catalytic Chemical Industry Co., 5—8, Nishiotabi-cho, Suita, Osaka.
*4 Present address; Sekisui Sponge Ind. Co., Kanto Factory, 1433—2, Shimohenmi, Sowa-mura, Sashima-gun, Ibaragi-ken.

1) R. L. M. Synge, *Biochem. J.*, **39**, 363 (1945); F. Sanger, ibid., **40**, 261 (1946).
2) H. N. Christensen and O. M. Hegsted, *J. Biol. Chem.*, **158**, 593 (1945).
3) F. A. Huehl, Jr., F. J. Wolf, N. R. Trenner, R. L. Peck, E. Howe, B. D. Hunnewell, G. Downing, E. Newstead and K. Folkers, *J. Am. Chem. Soc.*, **77**, 2344 (1955).
4) G. Ivanovics and V. Bruckner, *Z. Immunitätsforsch.*, **90**, 304 (1937).
5) J. M. Waisvisz, M. G. VAN DER Hoeven and B. TE Nijenhuis, *J. Am. Chem. Soc.*, **79**, 4524 (1958).
6) H. Vanderhaeghe and G. Parmentier, ibid., **82**, 4414 (1960).
7) F. W. Eastwood, B. K. Snell and Sir A. Todd, *J. Chem. Soc.*, **1960**, 2286.
8) V. Deulofeu, *Z. physiol. Chem.*, **204**, 214 (1932).
9) C. Gränacher, *Helv. Chim. Acta.*, **5**, 610 (1922).
10) T. Sasaki, *Ber.*, **54**, 2056 (1921).
11) L. Flatow, *Z. physiol. Chem.*, **64**, 367 (1910).
12) W. Herz, K. Dittmer and S. J. Cristol, *J. Biol. Chem.*, **171**, 383 (1947).




Diethyl formamido-(2-furfuryl)-malonate (V) was obtained as a well-crystallizable compound in a 63% yield by the reaction of III and IV in ethanol using sodium as a condensing agent.

Acylamidomalonates can be hydrolyzed smoothly with mineral acid in one step, but in our case such an acid hydrolysis is inapplicable because of the sensitivity of the furan ring. In fact, when furylalanine was boiled with 6 N hydrochloric acid, it was decomposed very rapidly and the ninhydrin reaction became completely negative.

The alkaline hydrolysis of acylamidomalonate needs a step-by-step treatment, as has been shown in the synthesis of tryptophan[13]; hence, the hydrolysis conditions were investigated. First, V was refluxed with a 10% sodium hydroxide solution for one hour. The extraction of the acidified hydrolysate with ethyl acetate gave a crystalline product, a part of which decomposed at about 120°C under effervescence, though it all melted clearly at 145°C. Comparing these figures with the melting point of formylfurylalanine (VII), 144—146°C, we suspected that the product obtained here might be formylfurylalanine contaminated with a compound decomposing at about 120°C, probably VI, a precursor of formylfurylalanine. In order to verify this assumption, the product was heated at 130°C for 5 hr. Then it was observed that it melted at 146°C without preliminary effervescence and showed a good agreement with an authentic sample of formylfurylalanine prepared by the formylation of furylalanine (as ascertained by a mixed melting point determination and by a comparison of the infrared spectra).

When the refluxing period was elongated to 6 hr., the hydrolysate gave plenty of white precipitates at pH ca. 5.6 (72% yield), which showed a positive ninhydrin reaction and which could be formylated with formic acid and acetic anhydride, the product of which, in turn, afforded formylfurylalanine when heated at 120°C for about 3 hr. From these results we assumed this compound to be amino-(2-furfuryl)-malonic acid (VIII), though, unfortunately, we did not succeed in ascertaining this by analysis. Schlossberger and Kuch[14] have also obtained an intermediate analogous to ours during the synthesis of tryptophan derivatives.

The decarboxylation of the substituted malonic acid (VIII) was attempted by heating it in water. The reaction was found to be very slow, even under prolonged refluxing, but it proceeded smoothly at 190°C in an autoclave. The paper chromatogram of the reaction product showed its almost complete conversion into furylalanine, though a faint spot was still

13) N. F. Albertson, S. Archer and C. M. Suter, *J. Am. Chem. Soc.*, **66**, 500 (1944); H. R. Snyder and C. W. Smith, ibid., **60**, 350 (1944).

14) H. G. Schlossberger and H. Kuch, *Ann.*, **662**, 132 (1963).

observed near the position corresponding to the starting material even after 6 hrs' heating. By the elongation of the reaction time, this spot became more distinct, and refluxing it with hydrochloric acid could not extinguish it. Those facts indicate that this spot does not respond to the original malonic acid derivative (VIII), but to some further degradated product. The comparison of its $R_f$-value with that of DL-aspartic acid proved the identity of the two compounds. It is probable, as will be seen later, that part of the furylalanine produced by the decarboxylation is oxidized further at the furan ring during the reaction into aspartic acid.

In the investigation of the tryptophan synthesis, Schlossberger[14] has used 50% acetic acid and obtained good results in the decarboxylation of aminomalonic acid derivatives with an acid labile indole nucleus. Thus, the decarboxylation was carried out according to his method, that is, by heating it in 50% acetic acid, because furylalanine itself was found, in a preliminary test, to be stable under such conditions. The reaction proceeded very rapidly without any formation of aspartic acid; thus we could obtain furylalanine in an excellent yield (80%).

In order to obtain formylfurylalanine, an intermediate for the peptide synthesis, it will be enough to hydrolyze the ester V into VI, reserving the formyl group, and to decarboxylate the reaction product. Thus V was stirred with a 10% sodium hydroxide solution for 8 hr. at room temperature, and then the product was heated at 130°C for 5 hr.; we thus succeeded in obtaining formylfurylalanine almost quantitatively.

The method of deformylating formylfurylalanine was also investigated. In general, the formyl-protecting group is removed by either oxidative cleavage or acid solvolysis. The former method was found, however, not to be applicable to furylalanine, for furylalanine, when treated with hydrogen peroxide even under mild conditions, is oxidized into DL-aspartic acid very rapidly; this was confirmed by a mixed melting point determination, by a comparison of the infrared spectra, and by paper electrophoresis with an authentic sample. The acid hydrolysis with hydrochloric acid in dioxane at room temperature was attempted, but it was also found to be impractical because of its low yield. With hydrochloric acid in methanol, deformylation and esterification occurred simultaneously and the methyl ester of furylalanine, also an important intermediate in the peptide synthesis, was obtained in one step, but the yield was not as satisfactory. On the other hand, the hydrolysis with alkali or 50% acetic acid gave good results; the yields were 59% and 63% respectively.

An attempt to obtain furylalanine in one step from V by treating it with 50% acetic acid proved unpromising. The reaction was too slow and not complete even after 20 hr.

These results described above are summarized in the scheme.

## Experimental

**DL-β-(2-Furyl)-α-alanine (I) by the Rhodanine Method.**—According to Gränacher,[9] rhodanine[15] was condensed with furfural to 5-furfulidene-rhodanine (m. p. 2282—28.5°C) in a 89% yield, and was then hydrolyzed with 3 N sodium hydroxide to β-(2-furyl)-α-thioketopropionic acid (m. p. 113—116°C) in a 99% yield. The thioketoacid was then converted by the action of hydroxylamine into β-(2-furyl)-α-oximino-propionic acid (m. p. 138—140°C) in a 56% yield. The reduction of the oximino acid with lactic acid and the sodium-amalgam afforded I in a 64% yield; m. p. 251—252°C (from 80% ethanol); lit.[9] m. p. 252°C (decomp.). $R_f$=0.60—0.64 (circular paper chromatography, *n*-butanol - acetic acid - water (4 : 2 : 1) system). Furylalanine showed a characteristic color reaction by ninhydrin on paper (greenish or reddish gray at first, but gradually changing to gray).

**DL-β-(2-Furyl)-α-alanine (I) by the Formamidomalonate Method.**—*α-Furfurylchloride (III).*—The chloride was prepared from furfuryl alcohol and thionyl chloride in a 57% yield; b. p. 49—50°C/27 mmHg; lit.[16] b. p. 49.6—50°C/27 mmHg. The chloride was so unstable that it was used at once after distillation.

*Diethyl Formamidomalonate (IV).*—According to Shaw and Nolan,[17] diethyl malonate was converted by the action of sodium nitrite and acetic acid to diethyl oximinomalonate in a 89% yield, then isolated as an addition compound with sodium acetate, and finally reduced with zinc and formic acid to diethyl formamidomalonate in a 79% yield; m. p. 51—53°C; lit.[17] m. p. 53—54°C.

*Diethyl Formamido-(2-furfuryl)-malonate (V).*—IV (20.5 g.) was dissolved in a sodium ethoxide solution (absolute ethanol 100 ml., sodium 2.3 g.), into which III (12 g.) was then added at once. After the mixture had been refluxed for 2 hr., sodium chloride was filtered out and washed with hot ethanol. The combined ethanolic solution was concentrated in vacuo. Water (100 ml.) was added to the residue, and the mixture was left to stand overnight in a refrigerator. Brown needle crystals (22.8 g.) were filtered off and recrystallized from hot ethanol; yield 18 g. (63%). Slightly brown needles; m. p. 98—99.5°C (from aqueous ethanol).

Found: C, 55.20; H, 5.97; N, 4.98. Calcd. for $C_{13}H_{17}O_6N$; C, 55.12; H, 6.05; N, 4.95%.

***N*-Formyl-DL-β-(2-furyl)-α-alanine (VII).**—*a) From Furylalanine (I).*—Acetic anhydride (16.6 ml.)

15) C. E. Redmann, R. N. Icke and G. A. Alles, "Org. Synth.," Coll. Vol. II, 763 (1955).
16) W. R. Kirner, *J. Am. Chem. Soc.*, **50**, 1955 (1928).
17) K. N. F. Shaw and C. Nolan, *J. Org. Chem.*, **22**, 1668 (1957).

was added drop-by-drop into a solution of I (3.1 g.) in 88% formic acid (5 ml.) at 50—60°C. After it had been stirred at room temperature for 2 hr., the mixture was diluted with ice water (16 ml.) and concentrated in vacuo. The crystalline residue was then dissolved again in water, decolorized and, after a small amount of hydrochloric acid had been added, extracted with ethyl acetate. White crystals were obtained on evaporating the solvent; yield 2 g. (55%); m. p. 143—145°C. Recrystallized from ethyl acetate - petroleum ether; m. p. 144—145°C.

Found; C, 52.29; H, 4.88; N, 7.63. Calcd. for $C_8H_9O_4N$: C, 52.46; H, 4.95; N, 7.65%.

*(b) From Diethyl Formamido-(2-furfuryl)-malonate (V).*—V (52 g.) was suspended in 10% sodium hydroxide (270 ml.) and stirred at room temperature. After 5 hr. all the crystals were dissolved. Stirring was continued for another period of 3 hr., and then the solution was left to stand overnight. After the unreacted material had been extracted with ethyl acetate, the solution was made strongly acidic with concentrated hydrochloric acid and extracted with ethyl acetate. After the solvent had been evaporated, the residue was heated at 120—130°C for 5 hr. and the resultant product was dissolved in ethanol and decolorized. White crystals were obtained on evaporating off the solvent; yield 32 g. (95%); m. p. 143.5—145.5°C. Recrystallized from ethyl acetate, m. p. 144.5—146°C. The identity of this compound with that obtained by a) was confirmed by a mixed melting point determination and by a comparison of the infrared spectra.

When hydrolysis was carried out by refluxing with 10% sodium hydroxide, the yield was decreased with the elongation of the reaction time as follows; 0.5 hr., 65%; 1 hr., 50%; 2 hr., 39%; 3 hr., 16%.

*Amino-(2-furfuryl)-malonic Acid (VIII).*—V (358 g.) was refluxed with a 10% sodium hydroxide solution (1900 ml.) for 6 hr. After the unreacted V had been removed by extraction with ethyl acetate, the solution was acidified with hydrochloric acid. A white precipitate was obtained at pH ca. 5.6; yield 180 g. (72%); m. p. 285—288°C (from aqueous ethanol). $R_f$=0.48.

When this compound (10 g.) was formylated by the usual method with 85% formic acid and acetic anhydride, crystals (4 g.) melting at ca. 120—135°C with effervescence were obtained. After they had been heated at 120°C for several hours, the crystals melted at 143—145°C; they showed no depression of melting point when mixed with authentic formylfurylalanine.

**DL-β-(2-Furyl)-α-alanine (I).**—*a) From Amino-(2-furfuryl)-malonic Acid (VIII).*—i) VIII (3 g.) was dissolved in water and heated at 190°C for 6 hr. in an autoclave. After being decolorized and concentrated to dryness, the product was recrystallized from aqueous ethanol; yield 1.5 g. (64%); m. p. 244—247°C.

ii) VIII (20 g.) was refluxed with 50% acetic acid for 2.5 hr. and then concentrated to dryness after decolorization. The residue was dissolved in water, and a small amount of ethanol was added. On cooling, colorless crystals were separated; yield 12.5 g. (80%).

*b) From N-Formyl-DL-β-(2-furyl)-α-alanine (VII).*—i) VII (1 g.) was boiled with 25% sodium hydroxide (2 ml.) for 10 hr. After being decolorized and neutralized with hydrochloric acid, the mixture was filtered and the filtrate was made to have a pH value of 5 with hydrochloric acid. When the solution was cooled and a small amount of ethanol added, white crystals were obtained; yield 0.5 g. (59%).

ii) VII (1 g.) was boiled with 50% acetic acid (3 ml.) for 4 hr. and treated as above; yield 0.53 g. (63%); m. p. 248—250°C.

The identity of both the compounds with authentic furylalanine was confirmed by the mixed melting point determination of the purified samples and by a comparison of the $R_f$ values in paper chromatography.

*Laboratory of Chemistry*
*Faculty of Science*
*Konan University*
*Okamoto, Higashinada, Kobe*

# Vibrational Spectra of Triethylfluorosilane

By Toshio TANAKA and Shigezo MURAKAMI

(Received December 11, 1964)

One of the present authors has previously reported on the normal vibrations of methyltrimethoxysilane, $CH_3Si(OCH_3)_3$,[1] in which the methyl groups were treated as one particle. The vibrational spectra of this molecule can be explained by assuming the point group $C_{3v}$ for the molecular symmetry. Triethylhalogenosilanes, $(C_2H_5)_3SiX$ (X=halogen atoms), can be treated as $YM(XZ)_3$-type molecules with regard to their skeletal vibrations in the same way as methyltrimethoxysilne.

Among triethylhalogenosilanes, the Raman spectrum has been obtained previously only for triethylchlorosilane. Tentative assignments have been made for this compound.[2] The present paper will report on the infrared and the Raman spectra of triethylfluorosilane and a normal coordinate treatment for the skeletal modes by Wilson's ***FG*** matrix method[3] using a simple Urey-Bradley potential function.

## Experimental

**Material.**—Triethylfluorosilane was prepared by the reaction of triethylchlorosilane with hydrofluoric acid (a 46% aqueous solution) in a copper flask.[4] A sample for measuring the infrared and Raman spectra was purified by two fractional distillations through a Stedman column (about 25 plates); b. p. 110°C/760 mmHg, $n_D^{25}$ 1.3895; (lit. b. p. 109°C/730 mmHg, $n_D^{25}$ 1.3900[4]).

**Spectra.**—The infrared spectrum of the neat liquid sample was recorded using a Reitz infrared spectrophotometer equipped with an NaCl or KBr prism. The Raman spectrum was measured by the photographic method using a Japan Yūki-gōsei Raman Spectrograph. The observed and calculated frequencies are shown together in Table III.

## Normal Coordinate Treatment

It has been assumed that the molecule belongs to the point group $C_{3v}$ and has the structure shown in Fig. 1, in which an F–Si–C–C plane and a C–Si–C plane, including the same Si–C bond, has an interplanar angle of 120°. This molecule has twelve skeletal vibrations; five of $A_1$ species, one of $A_2$ species, and six of E species. One of the six skeletal vibrations of the E species is the torsional oscillation of the $Si–CH_2–CH_3$ group. All vibrations except the $A_2$ torsional mode are active in both the infrared and the Raman spectra. The $Si–CH_2–CH_3$ torsional vibration of the E species could not, however, be observed in the present experiment. This may be due to the weak intensity of this band, which may appear in the region lower than 100 $cm^{-1}$, where any weak band is difficult to measure with the spectrograph used here. For this reason, the $Si–CH_2–CH_3$ torsional oscillation of the E species has not been considered in the normal coordinate treatment.

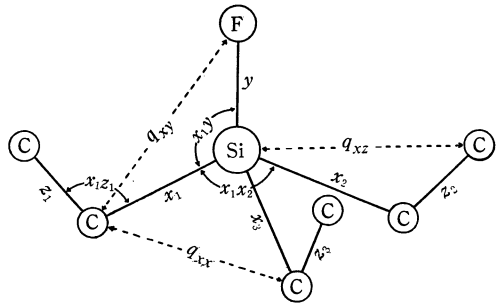



Fig. 1. Internal coordinates of the skeletal modes of triethylfluorosilane.

The orthonormal symmetry coordinates are shown in Table I. The numbering of these symmetry coordinates corresponds to that of the fundamentals in Table III.

The types of ***F*** matrix elements in the simple Urey-Bradley force field are the same as those reported earlier for methyltrimethoxysilane,[1] in which ∠Si–O–C was represented by a general angle of $\theta$. In the present molecule, the corresponding angle of Si–C–C is tetrahedral. The ***G*** matrix elements used previously for methyltrimethoxysilane[1] were also used, changing the masses of the atoms or groups concerned and replacing $\theta$ with a tetrahedral angle.

At first we adopted the force constants transferred or estimated from those obtained

* Present address: Research Division, Sumitomo Electric Industries Co. Ltd., Konohana-ku, Osaka.

1) T. Tanaka, This Bulletin, 33, 446 (1960).
2) H. Murata, *J. Chem. Soc. Japan, Pure Chem. Sec. (Nippon Kagaku Zassi)*, 73, 465 (1952).
3) E. B. Wilson, Jr., *J. Chem. Phys.*, 7, 1047 (1939); 9, 76 (1941).
4) N. S. Marans, L. H. Sommer and F. C. Whitmore, *J. Am. Chem. Soc.*, 73, 5127 (1951).

TABLE I. INTERNAL SYMMETRY COORDINATES OF TRIETHYLFLUOROSILANE

| | | |
|---|---|---|
| | $S_1=\Delta(z_1+z_2+z_3)/\sqrt{3}$ | C-C sym. str. |
| | $S_2=\Delta y$ | Si-F str. |
| $A_1$ | $S_3=\Delta(x_1+x_2+x^3)/\sqrt{3}$ | Si-C sym. str. |
| | $S_4=\Delta(x_1z_1+x_2z_2+x_3z_3)/\sqrt{3}$ | Si-C-C sym. def. |
| | $S_5=\Delta(x_1x_2+x_1x_3+x_2x_3-x_1y-x_2y-x_3y)/\sqrt{6}$ | $FSiC_3$ sym. def. |
| $A_2$ | $S_6$ | Si-C-C torsion |
| | $S_7=\Delta(2z_1-z_2-z_3)/\sqrt{6}$ | C-C deg. str. |
| | $S_8=\Delta(2x_1-x_2-x_3)/\sqrt{6}$ | Si-C deg. str. |
| E | $S_9=\Delta(2x_1z_1-x_2z_2-x_3z_3)/\sqrt{6}$ | Si-C-C deg. def. |
| | $S_{10}=\Delta(2x_1x_2-x_1x_3-x_2x_3)/\sqrt{6}$ | $SiC_3$ deg. def. |
| | $S_{11}=\Delta(2x_1y-x_2y-x_3y)/\sqrt{6}$ | Si-F def. |
| | $S_{12}$ | Si-C-C deg. torsion |

TABLE II. MOLECULAR AND POTENTIAL CONSTANTS OF TRIETHYLFLUOROSILANE

Bond distances and bond angles

$x=r(\text{Si-C})=1.89$ Å[5]
$y=r(\text{Si-F})=1.57$ Å[5]
$z=r(\text{C-C})=1.54$ Å

$\angle$C-Si-C, $\angle$C-Si-F, $\angle$Si-C-C $=109°28'$

| Potential constants | |
|---|---|
| Type | md./Å |
| $K_x(\text{Si-CH}_2)$ | 2.70 |
| $K_y(\text{Si-F})$ | 4.10 |
| $K_z(\text{CH}_2\text{-CH}_3)$ | 4.00 |
| $H_{xx}(\text{CH}_2\text{-Si-CH}_2)$ | 0.13 |
| $H_{xy}(\text{CH}_2\text{-Si-F})$ | 0.15 |
| $H_{xz}(\text{Si-CH}_2\text{-CH}_3)$ | 0.15 |
| $F_{xx}(\text{CH}_2\cdots\text{CH}_2)$ | 0.04 |
| $F_{xy}(\text{CH}_2\cdots\text{F})$ | 0.22 |
| $F_{xz}(\text{Si}\cdots\text{CH}_3)$ | 0.25 |
| $\kappa(C_3SiF)$ | $0.10\times$ Å$^2$ |

TABLE III. RAMAN AND INFRARED DATA, CALCULATED WAVE NUMBERS AND THE ASSIGNMENT FOR TRIETHYLFLUOROSILANE

| $\nu$. Obs. Raman | $\nu$. Obs. Infrared | $\nu$. Calcd. | Assignment | Modes of vibration* |
|---|---|---|---|---|
| 131(0) | | 150 | $\nu_5(A_1)$ | $FSiC_3$ sym. def. + Si-C-C sym. def. |
| 241(3b) | | 195 | $\nu_{11}(E)$ | Si-F def. + Si-C-C deg. def. |
| 279(1b) | | 258 | $\nu_{10}(E)$ | $SiC_3$ deg. def. |
| 297(2b) | | 286 | $\nu_4(A_1)$ | Si-C-C sym. def. + $FSiC_3$ sym. def. |
| 377(0) | | 371 | $\nu_9(E)$ | Si-C-C deg. def. + Si-F def. |
| 571(10) | 577(vw) | 638 | $\nu_3(A_1)$ | Si-C sym. str. ? |
| 587(9) | 587(vw) | | | |
| 679(1b) | 679(w) | | | (Si-)$CH_2$ rocking |
| 737(3) | 742(vs) | 752 | $\nu_8(E)$ | Si-C deg. str. |
| 835(1) | 834(vs) | 849 | $\nu_2(A_1)$ | Si-F str. |
| 980(3) | 984(w) | 998 | $\nu_1(A_1)$ | C-C sym. str. |
| 991(1) | | | | |
| | 1005(sh) | | | |
| 1011(2) | 1016(s) | 999 | $\nu_7(E)$ | C-C deg. str. |
| 1242(3) | 1244(m) | | | (C-)$CH_3$ rocking |
| 1304(3) | | | | (Si-)$CH_2$ wagging |
| 1380(2) | 1383(sh) | | | (C-)$CH_3$ sym. def. |
| 1418(4) | 1419(m) | | | (Si-)$CH_2$ scissors |
| 1468(6b) | 1467(m) | | | (C-)$CH_3$ deg. def. |
| 2885(10b) | | | | |
| 2912(7) | 2913(s) | | | (Si-)$CH_2$ str. |
| 2940(6) | | | | (C-)$CH_3$ str. |
| 2966(7) | 2981(sh) | | | |

* (Si-)$CH_2$ and (C-)$CH_3$ represent the methylene group attached to silicon and methyl group attached to carbon, respectively.

5) R. L. Gunton, J. F. Ollon and H. N. Rexroad, *J. Chem. Phys.*, **22**, 1942 (1954).

in many related compounds which had previously been studied on the basis of a simple Urey-Bradley force field;[6] the values of $F'$ in the $\boldsymbol{F}$ matrix elements were assumed to be equal to $-F/10$. These trial force constants were then modified so as to give a good agreement between the observed and the calculated frequencies. The molecular parameters and final potential constants used in the calculation are shown in Table II.

The value of $K_x$(Si–F) used in the present calculations is considerably smaller than that of tetrafluorosilane.[6] This may reflect the tendency for the bond distance of Si–F bond to increase as the number of fluorine atoms attached to silicon decreases; 1.54, 1.565, 1.577 and 1.595 Å for $SiF_4$, $HSiF_3$, $H_2SiF_2$ and $H_3SiF$ respectively.[7] The tendency of a bond-stretching force constant is quite similar to that for Si–O bond, whose stretching force constant in methylmethoxysilanes, $(CH_3)_nSi(OCH_3)_{4-n}$, ($n=0-3$), decreases with the number of oxygen atoms attached to silicon, as has been described previously by one of the present authors.[8] The other potential constants in Table II seem reasonable considering those in related compounds.

## Results and Assignment

The calculated frequencies are shown in Table III, together with the observed wave numbers of the infrared and Raman spectra. The calculated wave numbers of $\nu_{10}$ and $\nu_{11}$ are considerably lower than the observed values. This seems to be due to the neglect of the Si–$CH_2$–$CH_3$ torsional oscillation of E species in the normal coordinate treatment. The $\boldsymbol{L}$ matrices and the distribution of potential energy in symmetry coordinates have been calculated for the skeletal normal modes; the results are shown in Tables IV and V respectively. The skeletal vibrations have been assigned on the basis of the potential energy distribution in the symmetry coordinates; also, the hydrogen vibrations have been tentatively assigned.

The most characteristic line in the Raman spectrum of triethylfluorosilane is the strong doublet observed at 571 and 587 $cm^{-1}$. The corresponding bands in the infrared spectrum are very weak. This doublet can be assigned to the symmetric-stretching vibration of Si–C bonds on the basis of the intensities of the infrared and Raman spectra, although the observed wave numbers are somewhat lower than the calculated values. There are no corresponding doublets in the vibrational spectra of triethylchlorosilane,[2] methyltrimethoxysilane,[1] and triethyltinchloride,[9] which are considered to have a symmetry similar to that of the present molecule. It is not clear from the present work why the doublet appears for the symmetric-stretching vibration of the Si–C bond in this molecule.

As is shown in Table V, the Si–C–C symmetric deformation and $FSiC_3$ symmetric deformation modes of the $A_1$ species, and the Si–C–C degenerate deformation and Si–F deformation modes of the E species, are coupled with each other considerably. This coupling behavior is similar to that found for methyltrimethoxysilane.[1] However, the symmetric-stretching mode of the Si–C bonds is not so coupled with the Si–F stretching mode as with the vibrational coupling between Si–C and

Table IV. The $\boldsymbol{L}$ matrices of the skeletal normal vibrations of triethylfluorosilane

$A_1$ Vibrations

| | $Q_1$ | $Q_2$ | $Q_3$ | $Q_4$ | $Q_5$ |
|---|---|---|---|---|---|
| $S_1$ | +1.17 | +0.02 | +0.08 | −0.06 | −0.02 |
| $S_2$ | 0.00 | −0.89 | +0.31 | +0.04 | 0.00 |
| $S_3$ | −0.27 | +0.47 | +0.72 | −0.15 | +0.01 |
| $S_4$ | −0.27 | −0.60 | −0.67 | −0.50 | +0.29 |
| $S_5$ | −0.43 | −0.59 | −0.23 | −0.50 | −0.32 |

E Vibrations

| | $Q_7$ | $Q_8$ | $Q_9$ | $Q_{10}$ | $Q_{11}$ |
|---|---|---|---|---|---|
| $S_7$ | +1.15 | −0.23 | +0.04 | −0.01 | −0.01 |
| $S_8$ | −0.41 | −1.01 | −0.01 | −0.03 | +0.01 |
| $S_9$ | −0.25 | +0.45 | +0.73 | −0.14 | +0.37 |
| $S_{10}$ | −0.04 | +0.21 | −0.21 | −0.82 | −0.08 |
| $S_{11}$ | +0.39 | +0.26 | −0.70 | +0.07 | +0.40 |

Table V. Potential energy distribution $F_{ii}L_{ia}^2/\lambda_a$ for the skeletal normal vibrations of triethylfluorosilane

$A_1$ Vibrations

| | $\nu_1$ | $\nu_2$ | $\nu_3$ | $\nu_4$ | $\nu_5$ |
|---|---|---|---|---|---|
| $S_1$ | 0.96 | 0.00 | 0.01 | 0.03 | 0.01 |
| $S_2$ | 0.00 | 0.82 | 0.18 | 0.02 | 0.00 |
| $S_3$ | 0.03 | 0.16 | 0.67 | 0.16 | 0.00 |
| $S_4$ | 0.00 | 0.06 | 0.13 | 0.38 | 0.44 |
| $S_5$ | 0.02 | 0.05 | 0.01 | 0.37 | 0.55 |

E Vibrations

| | $\nu_7$ | $\nu_8$ | $\nu_9$ | $\nu_{10}$ | $\nu_{11}$ |
|---|---|---|---|---|---|
| $S_7$ | 0.93 | 0.06 | 0.01 | 0.00 | 0.00 |
| $S_8$ | 0.08 | 0.93 | 0.00 | 0.00 | 0.00 |
| $S_9$ | 0.00 | 0.04 | 0.48 | 0.04 | 0.45 |
| $S_{10}$ | 0.00 | 0.00 | 0.03 | 0.95 | 0.02 |
| $S_{11}$ | 0.00 | 0.00 | 0.45 | 0.01 | 0.52 |

6) T. Shimanouchi, ibid., 17, 245, 743, 848 (1949); *J. Chem. Soc., Japan, Pure Chem. Sec.* (*Nippon Kagaku Zassi*), 74, 266 (1953).
7) E. A. V. Ebsworth, "Volatile Silicon Compounds," Pergamon Press, Oxford (1963), p. 56.
8) T. Tanaka, This Bulletin, 34, 1752 (1961).
9) T. Tanaka, to be published.

Si–O stretching modes in methyltrimethoxysilane.[1] This is because the vibrational frequency of the stretching vibration of the Si–F bond is not so close to that of Si–C bonds in triethylfluorosilane.

## Summary

The infrared and the Raman spectra of triethylfluorosilane have been measured, and the normal vibrations for the skeletal modes have been calculated by Wilson's ***FG*** matrix method, using a simple Urey-Bradley force field and assuming point group $C_{3v}$ for the molecular symmetry. The skeletal vibrations have been assigned quantitatively on the basis of the normal coordinate treatment, and the hydrogen vibrations have been tentatively assigned. The vibrational spectra of this molecule have also been discussed in comparison with those of triethylchlorosilane and methyltrimethoxysilane.

*Department of Applied Chemistry*
*Osaka University*
*Miyakojima-ku Osaka*

# The Reaction of the Copper(II) Chelate of Ethyl Acetoacetate with Bromine* and the Reactions of the Copper(II) Chelates of Acetylacetone and Ethyl Acetoacetate with Dry Hydrogen Bromide**

By Tetsuya OGURA, Yoshitane KOJIMA, Yukio NAKAMURA and Shinichi KAWAGUCHI

(Received December 17, 1964; in revised form January 12, 1965)

In a previous paper[1] we have reported on the reaction of bis(acetylacetonato)copper(II) with bromine in dichloromethane. When 2 mol. of bromine was added to 1 mol. of the chelate at room temperature, copper(II) bromide and 3-bromoacetylacetone were formed, but if 1.5 mol. or less of bromine was employed against 1 mol. of the chelate, copper(I) bromide resulted instead of copper(II) bromide. The pathway of the reaction is not yet clear. Therefore, similar reactions of the copper(II) chelate of ethyl acetoacetate with bromine and dry hydrogen bromide have been studied, as has been the reaction of bis(acetylacetonato)-copper(II) with the latter reagent, in hopes of determining some reaction intermediates.

## Experimental

**Materials.**—The copper(II) chelate of ethyl acetoacetate was prepared according to the method of Wislicenus[2] by adding an ether solution of ethyl acetoacetate to an ammoniacal solution of copper sulfate. The complex thus obtained was then recrystallized from a hot chloroform solution. M. p. 193°C (lit., 192—193°C). (Found: Cu, 19.65; C, 44.79; H, 5.96%). Bis(acetylacetonato)copper(II) was also synthesized by a standard method reported previously.[1]

Commercial bromine was washed with pure water repeatedly (more than five times) and then distilled from an aqueous solution containing potassium bromide. The distillation of bromine was further repeated over calcium oxide in order to exclude all water.

Dry hydrogen bromide was prepared by dropping purified bromine into tetralin which had previously been dried and fractionally distilled. The evolved gas was passed through a column of calcium bromide and condensed in a trap immersed in a dry ice-methanol bath. Hydrogen bromide was then evaporated and absorbed in dry dichloromethane.

Dichloromethane from a commercial source was washed with a 5% solution of sodium hydrogen carbonate and then with pure water. After having been dried with calcium chloride, it was fractionally distilled through a Widmer column.[3]

**Reaction Procedure.**—In the reaction of the copper(II) chelate of ethyl acetoacetate with bromine, dry or wet dichloromethane was adopted as the reaction medium. The "dry" solvent was found by the Karl Fischer method to contain water in the concentration of $4.9\times10^{-3}$ mol./l. (8.8 mg. water in 100 ml. dichloromethane). In the experiment to clarify the role of water, dichloromethane saturated with water was employed; the water content was estimated to be 0.14 mol./l. (0.189 g. water in 100 g. dichloromethane) at 25°C.[4] The

* Presented at the 12th Symposium on the Chemistry of Metal Co-ordination Compounds of the Chemical Society of Japan, Tokyo, November, 1962.

** Presented at the 16th Annual Meeting of the Chemical Society of Japan, Tokyo, April, 1963.

1) Y. Nakamura and S. Kawaguchi, This Bulletin, **38**, 954 (1965).

2) W. Wislicenus, *Ber.*, **31**, 3151 (1898).

3) A. I. Vogel, *J. Chem. Soc.*, **1948**, 1833.

4) Weissberger, et al. (ed.), "Organic Solvents," Interscience Publishers, Inc. (1955), p. 192.

reaction was caused to proceed by dropping the bromine solution of a particular concentration (around 0.1 mol./l.) into a chelate solution of a similar concentration under vigorous agitation. Mole ratios of the metal chelate to bromine of 1 : 1, 1 : 1.5 and 1 : 2 were examined. In the latter two cases, the precipitate formed in the reaction mixture was filtered, washed with the solvent, dried, weighed and then analyzed for copper and bromine. The filtrate was also applied to the analysis of organic bromine. In the first case (1 : 1), when the desired amount of the bromine solution was added, a gray colloidal precipitate was formed; this was difficult to filter and so was separated from the solution by centrifugation after it had stored one day in a dessicator.

In the reaction of the copper(II) chelate of acetylacetone or ethyl acetoacetate with hydrogen bromide, dry dichloromethane was employed exclusively as a solvent. A desired amount of a hydrogen bromide solution was added from a burette to a chelate solution drop by drop or at full speed under vigorous agitation. Alternatively, a chelate solution was added gradually to a hydrogen bromide solution in experiments to investigate the effect of an excess of hydrogen bromide.

**Analysis.** — The concentration of hydrogen bromide in the dichloromethane solution was determined by titration, after the addition of dilute acetic acid, with a silver nitrate solution employing Eosin as the indicator.

The precipitate formed in the dry reaction medium was generally a mixture of copper(I) and copper(II) bromide. It was dissolved in aqueous ammonia and was kept standing in air overnight. A small amount of sodium hydroxide was then added to the solution, and it was heated in order to expel any ammonia. A black precipitate of copper(II) oxide was filtered off to be submitted to the electrolytic analysis of copper, and the bromide ion in the filtrate was determined gravimetrically to be silver bromide.

The precipitate formed in the reaction of the copper(II) chelate of ethyl acetoacetate with bromine in a wet solvent was a mixture of copper(I) bromide, copper(II) bromide and copper(II) hydroxide. When the precipitate was treated with acetic acid, copper(II) compounds were dissolved, but copper(I) bromide remained insoluble. The solution was then submitted to iodometry in order to determine the copper(II) content. On the other hand, the whole copper and bromine contents in the precipitate were determined as above.

The brominated $\beta$-dicarbonyl compound contained in the organic filtrate of each experiment was concentrated under reduced pressure and added to an acetic acid solution of potassium iodide. Iodine liberated in the solution was titrated with a solution of sodium thiosulfate.

## Results

**The Reaction of the Copper(II) Chelate of Ethyl Acetoacetate with Bromine in Dry Dichloromethane.**—The results of the analysis of reaction products under the dry conditions are listed in Table I. When the copper(II) chelate reacted with bromine in the mole ratio of 1 : 2, the precipitate formed was found to be practically copper(II) bromide. The filtrate contained ethyl $\alpha$-bromoacetoacetate; this was determined by iodometry as has been described in the Experimental section. Copper could not be detected in the filtrate. Thus, the net reaction may be represented by the following equation:

$$Cu(HA)_2 + 2\,Br_2 = CuBr_2 + 2HABr \qquad (1)$$

where $H_2A$ stands for the ethyl acetoacetate molecule, HA, for the enolate anion, and HABr, for ethyl $\alpha$-bromoacetoacetate. The yield of the bromoester listed in the last column of Table I was calculated on the basis of Eq. 1.

In the reaction of the 1 : 1.5 mole ratio, the precipitate formed was essentially copper(I)

Table I. Products of reaction between copper(II) chelate of ethyl acetoacetate and bromine in dry dichloromethane at room temperature

| Mole ratio chelate to bromine | Chelate used, g. (mmol.) | Ppt. recovered g. | Composition of precipitate: Cu, g. (mg.-atom) | Br, g. (mg.-atom) | Atom ratio Br/Cu | $\alpha$-Bromoester formed, mmol. (% yield) |
|---|---|---|---|---|---|---|
| 1 : 2 | 3.073 (9.548) | 2.069 | 0.5872 (9.243) | 1.471 (18.89) | 1.991 | 18.71 (97.85) |
| | 1.024 (3.182) | 0.7078 | 0.2012 (3.168) | 0.4608 (5.766) | 1.820 | 5.912 (92.88) |
| 1 : 1.5 | 1.022 (3.176) | 0.4779 | 0.1997 (3.143) | 0.2755 (3.448) | 1.097 | 5.659 (89.10) |
| | 3.455 (10.74) | 1.501 | 0.6578 (10.35) | 0.8414 (10.53) | 1.017 | 21.16 (98.52) |
| 1 : 1* | 5.174 (16.03) | 1.560 | 0.6712 (10.56) | 0.7742 (9.694) | 0.9190 | 21.29 (99.62) |

* The solution contained excess of chelate, which was determined by the electrolytic analysis of copper to be 5.031 mmol. (94.14% of the theoretical value calculated on the basis of Eq. 3).

TABLE II. PRODUCTS OF THE REACTION BETWEEN THE EQUIMOLAR COPPER(II) CHELATE OF ACETOACETATE AND BROMINE IN DICHLOROMETHANE SATURATED WITH WATER AT ROOM TEMPERATURE

| Chelate used, g. (mmol.) | Ppt. recovered g. | Composition of ppt. | | | α-Bromoester formed, mmol. (% yield) |
|---|---|---|---|---|---|
| | | Total Cu, g. (mg.-atom) | Cu(II) mg.-atom | Br, g. (mg.-atom) | |
| 5.537 | 2.601 | 0.9099 | | 1.026 | 18.1 |
| (17.21)* | | (14.34)* | 12.52 | (12.84) | (105) |
| 2.891 | 1.396 | 0.4072 | | 0.4862 | 9.08 |
| (8.983) | | (6.61) | 6.554 | (6.092) | (101) |

* The difference between these figures is due to incomplete transfer of the muddy precipitate from the reaction vessel into the glass filter.

bromide, and no copper remained in the solution. The stoichiometry of the reaction may satisfactorily be represented by the equation:

$$Cu(HA)_2 + 3/2\ Br_2 = CuBr + 2HABr \quad (2)$$

When an equimolar amount of bromine was added to the chelate solution, copper(I) bromide precipitated. In this case the solution still contained unchanged copper(II) chelate, which was determined to amount to about one-third of the original quantity. The material balance may be represented by the equation:

$$Cu(HA)_2 + Br_2 = 1/3\ Cu(HA)_2 + 2/3\ CuBr + 4/3\ HABr \quad (3)$$

The net change in this case should also be shown by Eq. 2.

Besides dichloromethane, chloroform and benzene (in the dark) were also used as solvents. The pattern of the reactions was the same as in dichloromethane.

**The Reaction of the Copper(II) Chelate of Ethyl Acetoacetate with Bromine in Wet Dichloromethane.**—When dichloromethane saturated with water was employed as the solvent, the precipitate formed in the reaction of the 1:1 mole ratio consisted essentially of copper(II) compounds, as is shown in Table II. This is in marked contrast to the case in a dry solvent, where copper(I) bromide was exclusively obtained in the 1:1 reaction (Table I). These results may be well reconciled with the following equation:

$$Cu(HA)_2 + Br_2 + H_2O = 1/2\ CuBr_2 + 1/2\ Cu(OH)_2 + HABr + H_2A \quad (4)$$

No trace of copper could be detected in the filtrate. The difference between the total copper content and that of copper(II) corresponds to that of copper(I), and ethyl α-bromoacetoacetate is obtained beyond the theoretical yield calculated on the basis of Eq. 4. These are considered to be formed in the following slow reaction:

$$2CuBr_2 + H_2A = 2CuBr + HABr + HBr \quad (5)$$

Copper(II) halide is known to react easily with acetone[5] and other compounds containing active hydrogen.[6] Reaction 5 really proceeds gradually at room temperature.

**The Reaction of the Copper(II) Chelate of Ethyl Acetoacetate with Bromine under Other Conditions.**—When dichloromethane containing ethyl alcohol or diethyl ether instead of water is employed as the reaction medium, the color of the reaction mixture changes from deep green to light blue on the addition of bromine, and the appearance of a precipitate is remarkably retarded. However, the precipitate is formed immediately on the addition of water.

When a 1:1 reaction is conducted in dry dichloromethane at −78°C, a grayish black muddy precipitate is formed; this changes to white copper(I) bromide when it is warmed to room temperature, reproducing thereby some quantity of the original copper(II) chelate. The dark precipitate is soluble in alcohol or ether, giving a light blue solution which is stable even at room temperature.

**The Reactions of Copper(II) Chelates of Acetylacetone and Ethyl Acetoacetate with Dry Hydrogen Bromide.**—In the reaction of these chelates with bromine in a mole ratio of 1:2, copper(II) bromide is formed exclusively, as has been reported above. However, it is not certain whether copper(II) bromide is directly produced through some intermediate or is formed secondarily by the reaction between copper(I) bromide and an excess of bromine. This problem is expected to be solved by an investigation of the reaction of the copper(II) chelates with hydrogen bromide, since even an excess of hydrogen bromide has no ability to oxidize copper(I) bromide once produced.

The analytical results of reaction products when the hydrogen bromide solution was added gradually to the chelate solution in various mole ratios, are summarized in Tables III and IV. In either case the sum of copper and

5) J. K. Kochi, *J. Am. Chem. Soc.*, 77, 5274 (1955).
6) E. M. Kosower, W. J. Cole, G.-S. Wu, D. E. Cardy and G. Meisters, *J. Org. Chem.*, 28, 630 (1963); E. M. Kosower and G.-S. Wu, ibid., 28, 633 (1963).

TABLE III. REACTION PRODUCTS FORMED WHEN A HYDROGEN BROMIDE SOLUTION WAS ADED GRADUALLY TO A SOLUTION OF BIS(ACETYLACETONATO)COPPER(II)

| Mole ratio chelate to HBr | Chelate used, g. (mmol.) | Ppt. obtained g. | Composition of the precipitate | | | | 3-Bromoketone | |
|---|---|---|---|---|---|---|---|---|
| | | | Cu, g. (mg.-atom) | Br, g. (mg.-atom) | CuBr mmol. (%) | $CuBr_2$ mmol. (%) | Found mmol. | Calcd. mmol. |
| 1 : 2 | 0.7171 (2.739) | 0.3186 | 0.1345 (2.117) | 0.1825 (2.284) | 1.950 (92.1) | 0.167 (7.9) | 1.200 | 1.261 |
| | 0.7171 (2.739) | 0.3103 | 0.1306 (2.055) | 0.1794 (2.245) | 1.865 (90.8) | 0.190 (9.2) | 1.009 | 1.243 |
| | 0.3545 (1.354) | 0.1734 | 0.0751 (1.18) | 0.0979 (1.23) | 1.13 (95.8) | 0.05 (4.2) | 0.645 | 0.652 |
| 1 : 1.5 | 0.6417 (2.451) | 0.2872 | 0.1257 (1.978) | 0.1600 (2.002) | 1.954 (98.8) | 0.024 (1.2) | 1.136 | 1.210 |
| | 0.5299 (2.024) | 0.2535 | 0.1115 (1.755) | 0.1426 (1.784) | 1.726 (98.4) | 0.029 (1.6) | 0.921 | 0.995 |
| 1 : 1* | 0.6417 (2.451) | 0.2497 | 0.1085 (1.708) | 0.1386 (1.735) | 1.681 (98.4) | 0.027 (1.6) | | |
| | 0.3545 (1.354) | 0.1249 | 0.0547 (0.861) | 0.0700 (0.876) | 0.846 (98.3) | 0.015 (1.7) | | |

* The product solution of a 1 : 1 reaction contains some quantity of remaining excess of chelate which disturbs the determination of 3-bromoacetylacetone.

TABLE IV. REACTION PRODUCTS FORMED WHEN A HYDROGEN BROMIDE SOLUTION WAS ADDED GRADUALLY TO A SOLUTION OF COPPER(II) CHELATE OF ETHYL ACETOACETATE

| Mole ratio chelate to HBr | Chelate used, g. (mmol.) | Ppt. obtained g. | Composition of the precipitate | | | | α-Bromoester | |
|---|---|---|---|---|---|---|---|---|
| | | | Cu, g. (mg.-atom) | Br, g. (mg.-atom) | CuBr mmol. (%) | $CuBr_2$ mmol. (%) | Found mmol. | Calcd. mmol. |
| 1 : 2 | 0.5139 (1.597) | 0.2114 | 0.0920 (1.45) | 0.1194 (1.494) | 1.41 (96.9) | 0.044 (3.1) | 0.720 | 0.773 |
| | 0.5139 (1.597) | 0.2144 | 0.0932 (1.47) | 0.1207 (1.510) | 1.43 (97.3) | 0.040 (2.7) | 0.722 | 0.775 |
| 1 : 1.5 | 0.8090 (2.514) | 0.3235 | 0.1424 (2.241) | 0.1805 (2.259) | 2.223 (99.2) | 0.018 (0.8) | 1.167 | 1.245 |
| 1 : 1* | 1.0278 (3.194) | 0.3325 | 0.1436 (2.260) | 0.1812 (2.267) | 2.253 (99.7) | 0.007 (0.3) | | |
| | 0.8598 (2.672) | 0.2787 | 0.1186 (1.867) | 0.1495 (1.871) | 1.863 (99.8) | 0.004 (0.2) | | |

* The bromination product in the solution could not be determined accurately because of the disturbance by the remaining chelate.

bromine found in the precipitate coincides quite well with the weight of the precipitate, indicating that the latter contains nothing but copper and bromine. The atomic ratio of bromine to copper in the precipitate is slightly larger than 1, showing that the reaction product is a mixture of copper(I) bromide and a small amount of copper(II) bromide. The number of millimoles of copper(I) bromide and that of copper(II) bromide were calculated from these equations:

$$CuBr = 2\ \text{Total Cu} - \text{Total Br}$$

$$CuBr_2 = \text{Total Br} - \text{Total Cu}$$

They are listed in Tables III and IV.

The results obtained in reactions at mole ratios of 1 : 1 and 1 : 1.5 are essentially simillar to those obtained in analogous reactions with bromine; they can be represented by the following equation:

$$Cu(HA)_2 + 3/2\ HBr = CuBr + 3/2\ H_2A + 1/2HABr \qquad (6)$$

where $H_2A$ stands for acetylacetone or ethyl acetoacetate, and HABr, for 3-bromoacetylacetone or ethyl α-bromoacetoacetate. The presence of free acetylacetone or ethyl acetoacetate in the solution was confirmed, after solvent evaporation in vacuo, by the nuclear magnetic resonance absorptions. The theoretical yield of brominated β-dicarbonyl compounds listed in the last column of Tables III and IV was calculated on the ground that 2 mol. of the original chelate produced 1 mol. of the

TABLE V. REACTION PRODUCTS FORMED WHEN A HYDROGEN BROMIDE SOLUTION WAS ADDED RAPIDLY FROM A BURETTE TO A SOLUTION OF COPPER(II) CHELATE OF ACETYLACETONE OR ETHYL ACETOACETATE (MOLE RATIO OF THE CHELATE TO BROMINE, 1 : 2)

| Cu chelate of | Chelate used, g. (mmol.) | Ppt. obtained g. | Composition of the precipitate | | | | Brominated product | |
|---|---|---|---|---|---|---|---|---|
| | | | Cu, g. (mg.-atom) | Br, g. (mg.-atom) | CuBr mmol. (%) | $CuBr_2$ mmol. (%) | Found mmol. | Calcd. mmol. |
| Acetylacetone | 0.3545 (1.354) | 0.1744 | 0.0710 (1.12) | 0.1032 (1.292) | 0.948 (84.8) | 0.172 (15.2) | 0.547 | 0.571 |
| | 0.7027 (2.684) | 0.3759 | 0.1437 (2.262) | 0.2263 (2.832) | 1.692 (74.8) | 0.570 (25.2) | 0.911 | 1.004 |
| Ethyl acetoacetate | 0.5139 (1.597) | 0.1875 | 0.0760 (1.20) | 0.1115 (1.395) | 1.005 (83.3) | 0.195 (16.7) | 0.667 | 0.667 |
| | 0.5139 (1.597) | 0.2159 | 0.0894 (1.41) | 0.1263 (1.580) | 1.240 (87.9) | 0.170 (12.1) | 0.679 | 0.700 |

TABLE IV. ANALYSIS OF THE PRECIPITATE FORMED WHEN A SOLUTION OF COPPER(II) CHELATE OF ACETYLACETONE OR ETHYL ACETOACETATE WAS ADDED GRADUALLY TO A SOLUTION OF HYDROGEN BROMIDE (MOLE RATIO OF THE CHELATE TO HYDROGEN BROMIDE, 1 : 2)

| Cu chelate of | Chelate used, g. (mmol.) | Ppt. obtained g. | Composition of the precipitate | | | |
|---|---|---|---|---|---|---|
| | | | Cu, g. (mg.-atom) | Br, g. (mg.-atom) | CuBr mmol. (%) | $CuBr_2$ mmol. (%) |
| Acetylacetone | 0.4147 (1.584) | 0.2941 | 0.0861 (1.36) | 0.2099 (2.602) | 0.118 (8.7) | 1.242 (91.3) |
| Ethyl acetoacetate | 0.8090 (2.514) | 0.5070 | 0.1475 (2.321) | 0.3602 (4.508) | 0.134 (5.8) | 2.187 (94.2) |

brominated compound, according to Eq. 6. A necessary correction for the occurrence of reaction 7 was made on the basis of the yield of copper(II) bromide.

As Tables III and IV show, a very small amount of copper(II) bromide is formed in the reaction at a mole ratio of 1 : 1.5 or 1 : 1; this is considered to result from the following reaction, which is analogous to Eq. 1:

$$Cu(HA)_2 + 2HBr = CuBr_2 + 2H_2A \qquad (7)$$

The relative amount of copper(II) bromide produced in comparison with copper(I) bromide indicates the relative probability of the occurrence of reaction 7 compared with reaction 6. Even in the reaction at a mole ratio of 1 : 2, the quantity of copper(II) bromide formed is far less than that of copper(I) bromide, suggesting that the reaction according to Eq. 6 proceeds far more rapidly than the reaction represented by Eq. 7 under such reaction conditions. The yield of copper(II) bromide might depend upon the speed of feeding hydrogen bromide to the intermediate.

Table V shows the results obtained when the hydrogen bromide solution was caused to flow at full speed from a burette into the chelate solution. The amount of copper(II) bromide produced in each experiment is much larger than that shown in Tables III and IV. In other experiments, the chelate solution was dropped gradually from a burette into a solution containing twice as many moles of hydrogen bromide. In these cases copper(II) bromide was produced predominantly, as was expected (Table VI). It must be noticed, however, that a small amount of copper(I) bromide was also produced, even when such a circumstance as an excess of hydrogen bromide should favor the reaction path of Eq. 7.

## Discussion

The stoichiometry of the reaction between the copper(II) chelate of ethyl acetoacetate and bromine in dry dichloromethane has been established for the two cases of the reactants mole ratio represented by Eqs. 1 and 2. In either case, the copper(II) chelate is decomposed by the attack of bromine, and the product is copper(II) or copper(I) bromide, depending upon whether 2 or 1.5 mol. of bromine is added to 1 mol. of the chelate. There are two possible reaction pathways to be considered: (i) copper(I) bromide is produced first, and then it is oxidized to copper(II) bromide by an excess of bromine. (ii) Copper(II) bromide is formed at first, and then it is reduced to copper(I) bromide by an excess of the chelate or the free ester produced. Copper(I) bromide is oxidized by bromine very rapidly, but copper(II) bromide is reduced by these compounds rather slowly; thus, the second pathway could not be responsible for the rapid formation of

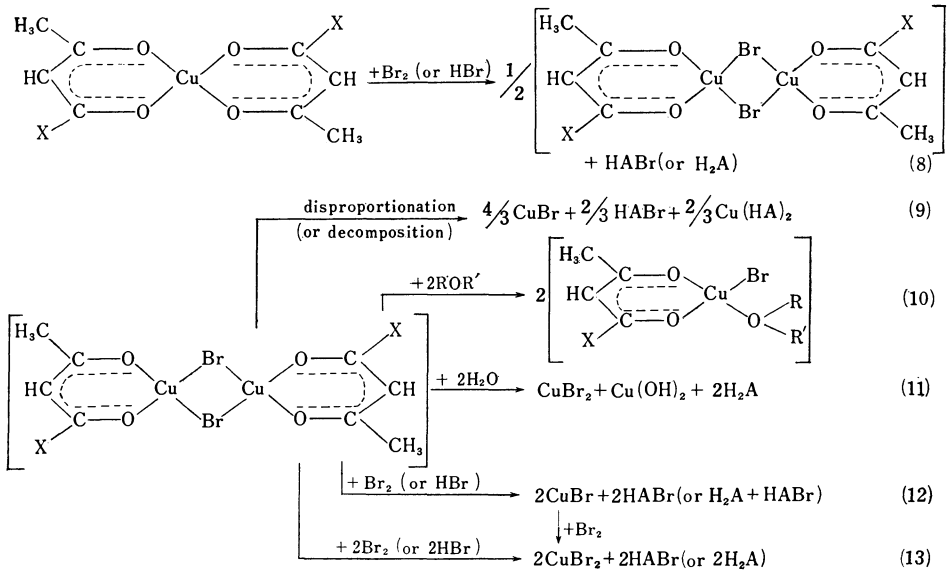



Fig. 1. Suggested pattern of the reaction between the copper(II) chelate of acetylacetone (X=$CH_3$) or ethyl acetoacetate (X=$C_2H_5O$) and bromine or hydrogen bromide. Bracketed species are still unidentified; their structures are only postulated here. ROR' represents alcohol or ether.

copper(I) bromide in the present case. Furthermore, the results obtained in the reaction of copper(II) chelates with hydrogen bromide strongly support the former reaction course under such reaction conditions.

The dark precipitate which is produced in the 1 : 1 reaction mixture of copper(II) chelate of ethyl acetoacetate and bromine at −78°C looks like a precursor of copper(I) bromide in the reaction pathway; it changes, in fact, to copper(I) bromide whenever warmed to room temperature. The precipitate is, however, soluble in alcohol or ether and does not produce copper(I) bromide in these solutions, even when warmed. Furthermore, in dichloromethane containing alcohol or ether, the formation of copper(I) bromide is greatly suppressed in the 1 : 1 reaction at room temperature. The water contained in dichloromethane also prohibits the formation of copper(I) bromide, so copper(II) bromide and hydroxide are produced instead. Thus, we may presume an intermediate with some stability, which decomposes (or disproportionates), spontaneously to copper(I) bromide and the original chelate, reacts with alcohol or ether to form some more stable species, or reacts with water to produce copper(II) bromide and hydroxide. It must be emphasized that, though one-third of the chelate employed is recovered in a 1 : 1 reaction (Eq. 3), it is not really unchanged, but is reproduced through an intermediate. We may now assume the following structure for this intermediate, and can picture the entire reaction pattern by virtue of it, as Fig. 1 shows. The experimental results obtained in the reactions of the copper(II) chelates with hydrogen bromide can also be explained by means of the same pattern.

An intermediate containing a double bridge of bromine is assumed to be formed in process 8. In the reactions at a mole ratio of 1 : 1, the intermediate disproportionates (or decomposes) according to Eq. 9, reproducing one-third of the original chelate. In the reaction at a mole ratio of 1 ; 1.5, copper(I) bromide is formed by process 12. In reactions with hydrogen bromide, copper(II) bromide can be produced only when two molecules of hydrogen bromide attack an intermediate molecule cooperatively, as is shown by Eq. 13.

The reactions represented by Eqs. 9, 12 and 13 are all very fast, and the competition between them is influenced by the chance of an encounter between the intermediate and the bromine or hydrogen bromide molecule. These reactions may not be elementary processes, and even their relative rates are not yet certain. Further extensive investigations are needed to elucidate the mechanisms of these reactions.

The preparation of the copper chelate of ethyl α-bromoacetoacetate was attempted but was unsuccessful, in contrast with that of 3-bromoacetylacetone.[1] This was due to the

lower stability of the copper(II) chelate of the $\alpha$-bromoester, and is related to Pedersen's finding[7] that copper(II) ions can not catalyze the second step of the bromination of ethyl acetoacetate by bromine in an aqueous solution, although it can accelerate the first step remarkably.

## Summary

When the copper(II) chelate of ethyl acetoacetate reacts with bromine in dry dichloromethane, the chelate is broken, forming the $\alpha$-bromoester and copper(I) or copper(II) bromide depending on the reactants' mole ratio. However, in the reaction between bromine and the chelate at a mole ratio of 1 : 1 in dichloromethane saturated with water, copper(I) bromide is not produced primarily; instead copper(II) hydroxide is formed, as is copper(II) bromide.

In the reactions of the copper(II) chelate of acetylacetone or ethyl acetoacetate with dry hydrogen bromide at the mole ratio of 1 : 1 or 1 : 1.5, more than 98% of the total copper precipitated as copper(I) bromide. Even when 2 mol. of hydrogen bromide was employed against 1 mol. of the chelate, more than 90% of the original copper changed to copper(I) bromide, in contrast with the results obtained in a similar reaction with bromine.

The entire reaction pattern has been suggested employing a presumed intermediate binuclear complex containing a bromine double brigde.

The authors wish to thank Dr. Kazuo Tōri of the Shionogi Research Laboratory, Shionogi & Co., Ltd., for the NMR spectral data. The cost of this research has been partly defrayed by a Scientific Research Grant from the Ministry of Education, to which the authors thanks are also due.

*Faculty of Science*
*Osaka City University*
*Sumiyoshi-ku, Osaka*

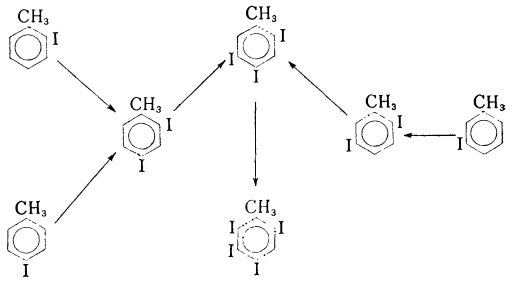
7) L. J. Pedersen, *Acta Chem. Scand.*, 2, 252 (1948).

# The Anomalous Behavior of Some 2, 6-Disubstituted Iodobenzenes in the Jacobsen Reaction[1]

By Hitomi SUZUKI, Kazuhiro MARUYAMA and Ryozo GOTO

(Received December 19, 1964)

Aromatic iodo compounds containing electron-releasing groups in the nucleus readily undergo disproportionation in the presence of sulfuric acid to give polyiodo compounds.[2] This is the Jacobsen reaction. The reaction proceeds like a progressive iodination of the starting material, an entering iodine atom always taking the position of higher electron density and smaller steric hindrance, in accordance with the orientation rule of the usual electrophilic substitution. An example is the conversion of iodotoluenes to polyiodotoluenes:



As has been reported in previous papers of this series,[2] however, some 2, 6-disubstituted iodobenzenes, such as 2-iodo-*m*-xylene, 2, 3-diiodotoluene, and 1, 2, 3-triiodobenzene, exhibit anomalous behavior in the reaction, affording none of the expected vicinal (or asymmetrical) compounds, but only symmetrically-substituted products; that is, the

1) The Reaction of Polysubstituted Aromatics. VI; this series of studies hereafter will be called by this title. Part V: This Bulletin, **37**, 1858 (1964).

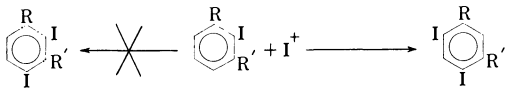
2) R. Goto and H. Suzuki, *J. Chem. Soc. Japan, Pure Chem. Sec.* (*Nippon Kagaku Zasshi*), **84**, 167 (1963); H. Suzuki and R. Goto, ibid., **84**, 284 (1963); H. Suzuki and R. Goto, This Bulletin, **36**, 389 (1963).

Table I. Action of sulfuric acid on 2-iodo-*m*-xylene

| Expt. No. | 2-Iodo-*m*-xylene g. | Sulfuric acid g. | | Reaction temp. °C | Reaction time hr. | Product g. | Main component |
|---|---|---|---|---|---|---|---|
| 1 | 2.3 | 6.0 | | 20—23 | 3 | 0.7 | 4,6-Diiodo-*m*-xylene<br>Tetraiodo-*m*-xylene |
| 2 | 2.3 | 1.0 | | 20—23 | 1 | 1.6 | 2- and 4-Iodo-*m*-xylene |
| 3 | 2.3 | 0.2 | | 20—23 | 4 | 1.9 | 2- and 4-Iodo-*m*-xylene |
| 4 | 2.3 | 1.0 | | 20—23 | 3.5 | 1.1 | 2- and 4-Iodo-*m*-xylene<br>2,4- and 4,6-diiodo-*m*-xylene |
| 5 | 2.3 | 6.0 | | 20—22 | 0.6 | 0.9 | 4,6- and 2,4-diiodo-*m*-xylene<br>4-Iodo-*m*-xylene |
| 6 | 2.3 | 6.0 | Water 1.2 | 20—22 | 1 | 2.1 | Only 2-iodo-*m*-xylene |
| 7 | 2.3 | 1.0 | Mesitylene 2.4 | 20—22 | 0.3 | 3.4 | 2-Iodo-*m*-xylene<br>Mesitylene<br>Iodomesitylene |
| 8 | 2.3 | | PPA 7.0 | ca. 140—150 | 2.5 | 1.9 | 2- and 4-Iodo-*m*-xylene |

PPA = Polyphosphoric acid

iodine atom located in the position 2 in the original compound migrates to the position 4 in the final product, as is shown in the following scheme:



In the present paper, the authors wish to report the results of their mechanistic study of this novel reaction. We used only 2-iodo-*m*-xylene as the reagent because of its ease of synthesis. To get more precise knowledge about the reaction, we also prepared four isomeric diiodo-*m*-xylenes and subjected them to the several conditions of the Jacobsen reaction; the results of these experiments will, however, be described in a succeeding paper. The reaction products were identified by an inspection of their infrared spectra and gas chromatogram.

## Experimental

**Procedure.** — Weighed 2-iodo-*m*-xylene and sulfuric acid (or PPA) were placed in a small, stoppered flask and then stirred magnetically at a given temperature for a definite time. Then the mixture was diluted with water, and the precipitated solid or oily matter was separated by extraction and purified through an alumina column, using petroleum ether as the eluant. The solid or oily matter which remained after the evaporation of the solvent was then subjected to infrared spectroscopic or gas chromatographic inspection. The reaction conditions and the products are summarized in Table I.

**Materials.** — 2-Iodo- and 4-iodo-*m*-xylene were prepared from the corresponding *m*-xylidines (Tokyo Kasei products, G. R. grade) by the ordinary procedure: 2-iodo-*m*-xylene[3] (b. p. 100—101°C/12 mmHg), 4-iodo-*m*-xylene[4] (b. p. 108—109°C/12 mmHg). The synthesis of four isomeric diiodo-*m*-xylenes will be reported in the succeeding paper.

## Results and Discussion

In the presence of an excess of sulfuric acid, the disproportionation of 2-iodo-*m*-xylene was completed so fast that in order to find out any possible intermediates it was necessary to carry out the reactions in the system containing an insufficient amount of sulfuric acid. As one molecule of *m*-xylene-4-sulfonic acid was inevitably formed for every intermolecular migration of an iodine atom, the disproportionation was considerably suppressed and the isomerization became prominent.[5] As may be seen from Fig. 2a and Fig. 3a, at an early stage of the reaction only a slight formation of diiodo-*m*-xylenes was found on the gas chromatogram, while on the infrared spectrogram the absorption bands characteristic of 2-iodo-*m*-xylene (698 and 767 $cm^{-1}$) were already much weakened and the absorption bands due to 4-iodo-*m*-xylene (805 and 872 $cm^{-1}$) were considerably strengthened. Even in the presence of a slight amount of sulfuric acid, 2-iodo-*m*-xylene gradually isomerized to the 4-iodo isomer during a prolonged reaction time. These facts clearly establish the prior isomerization of 2-iodo-*m*-xylene to the 4-iodo isomer.

Figure 3b indicates that two diiodo-*m*-xylenes were formed at an early stage of the reaction,

3) S. F. Birch, R. A. Dean, T. A. Tidler and R. A. Lowry, *J. Am. Chem. Soc.*, **71**, 1362 (1949).

4) A. Klages and C. Liecke, *J. prakt. Chem.*, **61**, 307 (1900).

5) 4-Iodo-*m*-xylene sulfonic acid is in part hydrolyzed to give 4-iodo-*m*-xylene and sulfuric acid, whereas *m*-xylene-4-sulfonic acid is very stable under ordinary conditions.

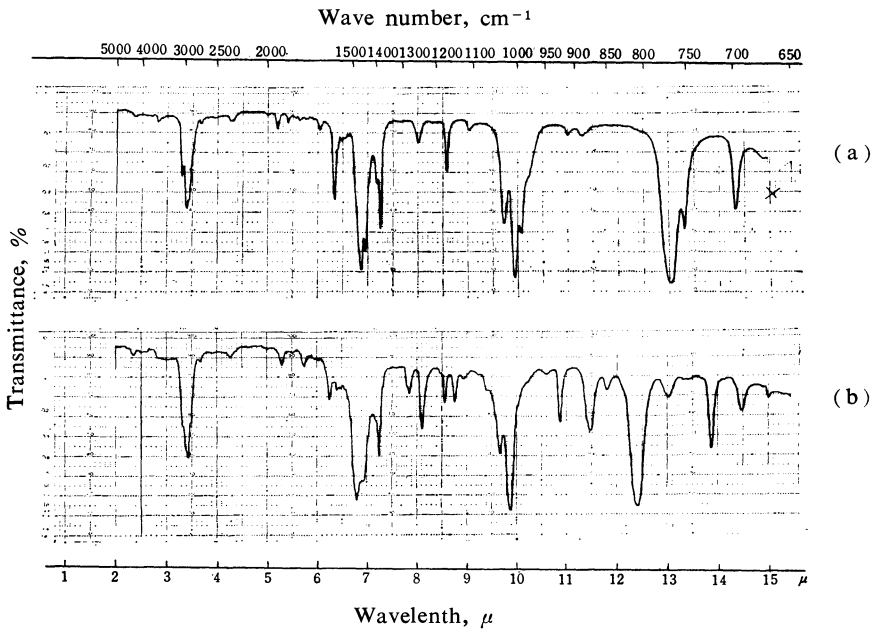



Fig. 1. Infrared spectra of iodo-*m*-xylenes.

(a) 2-Iodo-*m*-xylene
(b) 4-Iodo-*m*-xylene

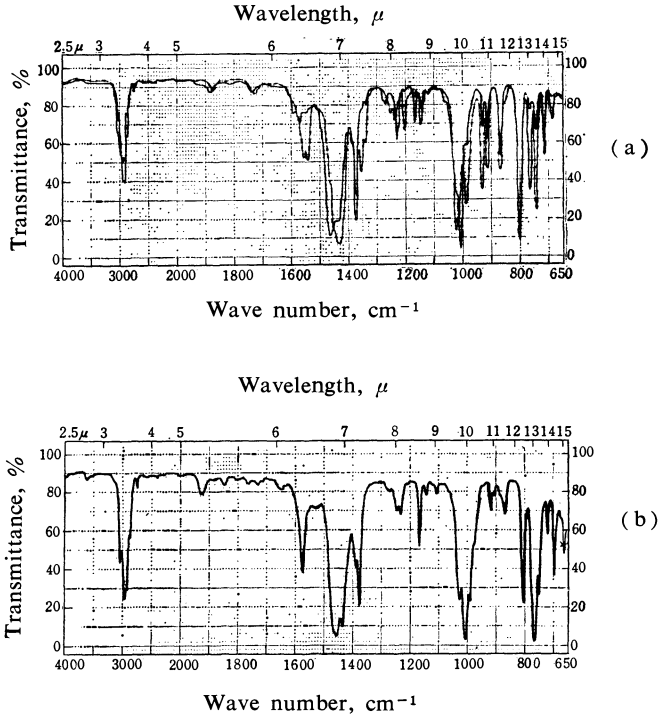



Fig. 2. Infrared spectra of reaction products.

(a) Full line Exp. No. 4
Dotted line Exp. No. 5
(b) Exp. No. 8

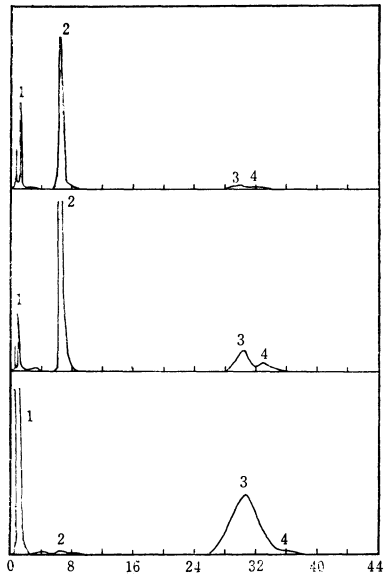



Fig. 3. Gas chromatogram of reaction products.
(a) Exp. No. 3 (b) Exp. No. 5 (c) Exp. No. 1
Peak 1 Solvent (benzene or petroleum ether)
2 2- or 4-Iodo-*m*-xylene
3 4,6-Diiodo-*m*-xylene
4 2,4-Diiodo-*m*-xylene
Stationary phase: Apiezon grease L, 3 m.
Carrier gas: Hydrogen
Column temperature: 245—246°C

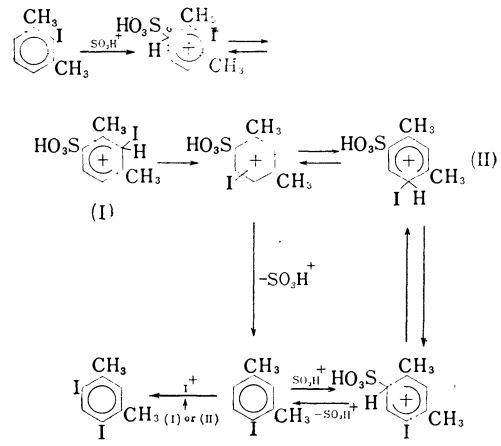
but one of them was gradually diminished during the usual Jacobsen reaction, which was carried out with a large excess of sulfuric acid. This minor precursor was identified as 2,4-diiodo-*m*-xylene. As will be described in the succeeding paper, however, 2,4-diiodo-*m*-xylene is comparatively stable towards the action of sulfuric acid and does not isomerize so readily to 4,6-diiodo-*m*-xylene under these conditions. Therefore, this compound cannot be considered to be a major intermediate.

In the crossed Jacobsen reaction of *m*-xylene-4-sulfonic acid with *p*-iodocumene (this compound readily liberates the iodinium cation in sulfuric acid), a considerable amount of elementary iodine was liberated, and the iodinated *m*-xylenesulfonic acid could not be isolated from the reaction mixture. Thus, it is reasonable not to postulate the complete detachment of the migrating iodine atom during the isomerization, because the iodinium cation formed under those conditions cannot be so active as to iodinate the *m*-xylene-4-sulfonic acid successfully. Little liberation of elementary iodine or sulfur dioxide during the reaction also supports this view.

An effort to isolate 2-iodo-*m*-xylene sulfonic acid from the reaction mixture was fruitless; *m*-xylene-4-sulfonic acid was always obtained, together with small amounts of 4-iodo-*m*-xylene-6-sulfonic acid. This may be interpreted as indicating that the migration of the iodine atom from the hindered (=2) to the less hindered position (=4) occurs prior to the completion of the sulfonation. If the reaction was carried out with an excess of mesitylene, the iodine atom was readily transferred to give iodomesitylene. This fact indicates that the iodine atom migrates to the position of higher electron density, because mesitylene is supposed to be much more basic than either 2- or 4-iodo-*m*-xylene. Characteristic color changes which always accompany the halogen migration were also observed during the reaction, and the color disappeared upon the addition of water.

In this connection, another interesting phenomenon was observed in the similar isomerization of 2-iodo-*m*-xylene caused by polyphosphoric acid (PPA) of a high temperature (Fig. 2b). Here, however, only an intramolecular migration of the iodine atom was observed, and the reaction needed more severe conditions and a much longer time in order to be completed.

From the results described above, we may conclude that the reaction proceeds mainly through the prior isomerization of 2-iodo-*m*-xylene to the 4-isomer, followed by the usual disproportionation; this process may be formulated as follows:




2-Iodo-*m*-xylene reacts reversibly with sulfuric acid to form a $\sigma$-complex, a benzenonium intermediate (I), in which the iodine atom, blocked on both sides by two ortho methyl groups, is jammed so hard by the entry of a bulky sulfo group that it is crowded out and migrates through $\pi$ and $\sigma$-complex transition states to the position of the next

highest electron density. If it settles down at the position 4 of the same molecule or replaces the sulfo group at the position 6, the isomerization occurs; if another molecule attacks the intermediate I or II nucleophilically and if the iodine is transferred, a disproportionation results. The easy transfer of the iodine atom generally found in the crossed Jacobsen reaction of some aromatic iodo compounds with highly alkylated benzenes[6] may also be explained consistently by this mechanistic scheme, assuming that the benzenonium intermediate formed by the entry of the sulfo group is attacked by the highly basic polyalkylbenzenes. The differences in the ease of migration between the reaction caused by sulfuric acid and that brought about with PPA is best interpreted as follows: in PPA 2-iodo-*m*-xylene is first protonated to form a benzenonium intermediate in which the iodine atom is less hindered than in a corresponding sulfonic acid intermediate (I) and thus migrates at a slower rate intramolecularly to the position 4.

This anomalous Jacobsen reaction draws our attention for the very interesting reason that the migrating group is not that one which is replaced directly by the attacking group (this type of replacement is the most general one encountered in the anomalous electrophilc substitution of aromatic compounds), but is one which is present at a position (meta) distant from the place where the actual reaction occurs. Further evidence to support the above mechanism will be reported in the succeeding paper.

6) H. Suzuki, T. Sugiyama and R. Goto, This Bulletin, 37, 1858 (1964).

**Summary**

Some 2, 6-disubstituted iodobenzenes undergo an anomalous Jacobsen reaction and so afford none of the expected vicinal, but only symmetrical diiodo products. This anomaly has been investigated using 2-iodo-*m*-xylene as the reagent. The reaction has been found to proceed mainly through the rapid isomerization of 2-iodo-*m*-xylene to the 4-iodo isomer, followed by the normal disproportionation to 4, 6-diiodo-*m*-xylene. A possible mechanism has also been proposed on the basis of the results obtained.

*Department of Chemistry*
*Faculty of Science*
*Kyoto University*
*Sakyo-ku, Kyoto*

# Solvent Extraction Studies of Tellurium(IV) with Dithizone

By Hisao MABUCHI and Isao OKADA

(Received January 6, 1965)

Dithizone (diphenylthiocarbazone, designated in this paper as $H_2Dz$) has previously been widely used for the extraction or the colorimetric determination of various metals. In a previous paper, one of the present authors reported that tellurium(IV), when shaken with a dithizone solution, was extracted into an organic layer, thus forming a complex compound with dithizone.[1] Generally, however, relatively little is known about the species and about the nature of the tellurium complex which is extracted by organic solvents. Therefore, we investigated the behavior of tellurium(IV) in the solvent extraction process by using dithizone.

1) H. Mabuchi, This Bulletin, **29**, 842 (1956).

## Experimental

**Dithizone Solution.** — The Merck product dithizone was purified by the ammonia water extraction method given by Sandell.[2] The purity of dithizone in carbon tetrachloride was checked spectrophotometrically by the use of the ratio of $E_{620}/E_{450}$, where $E_{620}$ and $E_{450}$ stand for the extinction of dithizone at 620 and 450 m$\mu$ respectively.[3] When this ratio is higher than 1.67, the solution may be considered sufficiently pure. The concentration of dithizone was determined spectrophotometrically each time it was used.

**Carbon Tetrachloride.**—Reagent-grade chemicals

2) E. B. Sandell, "Colorimetric Determination of Traces of Metals," Interscience Publishers, New York, London (1959), p. 170.

3) S. S. Cooper and M. L. Sullivan, *Anal. Chem.*, **23**, 613 (1951).

were distilled once, and the middle fraction of the distillate was used.

**Ammonium Hydroxide.**—A Concentrated C. P. reagent was distilled and absorbed in redistilled water. The ammonia solution used for the purification of dithizone was prepared by diluting this purified solution.

**Hydrochloric Acid.**—A concentrated C. P. reagent was distilled, and the middlle fraction of the distillate was used.

**Water.**—Water was distilled twice in an all-glass distilling apparatus.

All other chemicals were of the reagent grade and were used without further purification.

**The Preparation of a Tellurium Carrier Solution.**—Tellurium dioxide was prepared from a tellurium crystal by the method described in "Inorganic Syntheses"[4]; then it was dissolved in acid solutions. The concentrations were determined gravimetrically.

**The Preparation of Radioactive Tellurium.**—Radioactive tellurium was produced by Sb (p, $x$n) reactions ($x$=1—4) by bombarding an antimony metal target with the 56 MeV. proton at the Institute for Nuclear Study, the University of Tokyo. After several weeks of cooling, carrier-free tellurium(IV) was separated from the antimony target by the dithizone-extraction method.[5] Since short-lived tellurium nuclides must already have decayed, the radioactive tellurium solution may be supposed to have been mainly composed of a mixture of Te-121m ($T_{1/2}$=154 d.) and Te-123 m ($T_{1/2}$=104 d.).

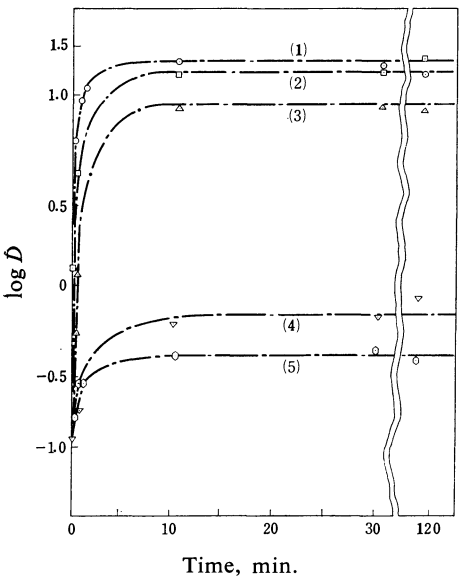



Fig. 1. Effect of shaking time on the extraction.

$H_2Dz$ in $CCl_4$: —⊙— (1) $9.60\times10^{-4}$ M, —⊡— (2) $2.00\times10^{-3}$ M, —△— (3) $1.00\times10^{-3}$ M, —▽— (4) $2.82\times10^{-4}$ M, —⬡— (5) $1.20\times10^{-4}$ M

$HClO_4$: (1) and (5) 2.43 M, (2), (3) and (4) 0.179 M

Shaking temp.: 20°C

Te(IV): $\sim10^{-11}$ M

**The Measurement of the Distribution Ratio.**—Two milliliters of a carbon tetrachloride solution of dithizone was equilibrated by shaking it with 2 ml. of an aqueous solution containing tracer amounts of tellurium(IV) ($\sim10^{-11}$ M) for 30 min. in a 15-ml. flask with a glass-stopper at 25°C. One milliliter of each layer was then put into a test tube and its radioactivity measured with a well-type NaI scintillation counter. The distribution ratio, $D$, for tellurium(IV) is given by the radioactivity of the organic layer divided by that of the aqueous layer.

Similarly, with macro amounts of tellurium the distribution ratio was measured radiometrically by using radioactive tellurium as a tracer.

**Spectrophotometric Measurements.**—All absorptiometric works were carried out with a Cary recording spectrophotometer, model 14.

**The Attainment of Equilibrium.**—This was investigated by shaking a number of tubes, each containing 2 ml. of an organic layer and 2 ml. of an aqueous layer, for various lengths of time (Fig. 1). The equilibrium between the two layers was attained within about 10 min.

## Results and Discussion

**The Chemical Composition of the Tellurium Dithizonate in the Organic Layer.**—The dependence of the distribution ratio, $D$, on the dithizone concentration in carbon tetrachloride, $(H_2Dz)_{org}$, was studied in the perchloric acid - sodium perchlorate media, using tracer amounts of radioactive tellurium. The results are shown in Fig. 2. It may be seen from Fig. 2 that the plot of $\log D$ vs. $\log (H_2Dz)_{org}$ at the constant $(H^+)_{aq}$ has a straight line whose slope is 2. This suggests, as is established below, that each tellurium(IV) cation in the organic layer is combined with two dithizonate anions.

In general, if one expresses the chemical species of tellurium in the acidic aqueous layer after the attainment of equilibrium as $(Te(OH)_n(HDz)_m)^{(4-m-n)+}$, and those in the organic layer as $Te(OH)_{4-p}(HDz)_p$, the slope of $\log D$ vs. $\log (H_2Dz)_{org}$, $\partial \log D/\partial \log (H_2Dz)_{org}=\bar{p}-\bar{m}$, where $\bar{m}$ and $\bar{p}$ are the average number of $HDz^-$ per tellurium(IV) cation in the aqueous and organic layers respectively. Here polymerized species of tellurium are neglected. This assumption may be valid as far as tracer experiments of tellurium are concerned.

As $HDz^-$ is a bidentate ligand, the coordination number, $N=4-p+2p$. From these considerations, one finds the two equations, (1) and (2):

$$\bar{p}-\bar{m}=2 \quad (1)$$

$$p+4=N \quad (2)$$

4) "Inorganic Syntheses," Vol. III, 143 (1950).

5) Y. Yokoyama, H. Mabuchi, H. Shoji and N. Saito, This Bulletin, 36, 352 (1963).

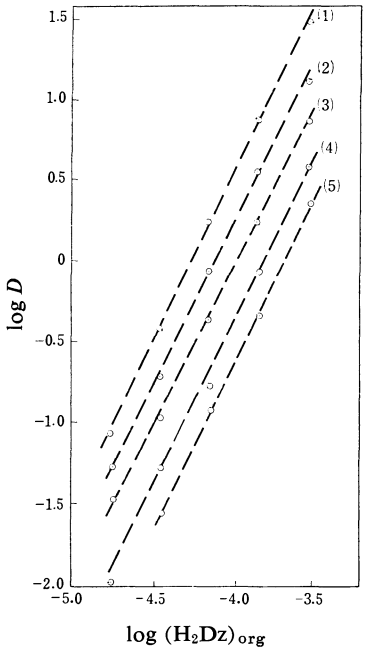



Fig. 2. Dependence of distribution ratio on the dithizone concentration.

$HClO_4$: (1) 0.10 M, (2) 0.23 M, (3) 0.55 M, (4) 1.31 M, (5) 3.12 M
Ionic strength: 3.12
Shaking temp.: 25°C
Shaking time: 30 min.
Slope of broken lines is 2.

The coordination number of the quadrivalent tellurium that appears in the solid compounds is 4 or 6. Although no data have been reported concerning its coordination number in solution, one may consider it not to exceed 6. If $N=4$, the extraction of tellurium with dithizone would not be possible, for in that case $p=0$. The only solution that satisfies Eqs. 1 and 2 is $N=6$, $\bar{p}=p=2$ and $\bar{m}=0$.

Therefore, the chemical species of tellurium extracted is supposed to be $Te(OH)_2(HDz)_2$* and the process of the extraction may be written as follows:

$$Te(OH)_n^{(4-n)+}\ (aq.) + 2H_2Dz\ (org.) = Te(OH)_2(HDz)_2\ (org.) + (4-n)H^+\ (aq.) + (n-2)H_2O\ (aq.) \quad (3)$$

The distribution ratios of macro amounts of tellurium whose initial concentration in the aqueous layer is $4.25\times10^{-5}$ M are shown in Fig. 3. Since, in the case of macro amounts, the concentration of dithizone at the extraction equilibrium differs from the initial concentration, the concentrations of dithizone were corrected on the assumption that the complex of dithizone contained two dithizonate anions to one tellurium cation. Plotting the logarithm of the distribution ratios against that of the concentrations of dithizone at equilibria, one could also obtain a straight line whose slope was 2 (Fig. 3).

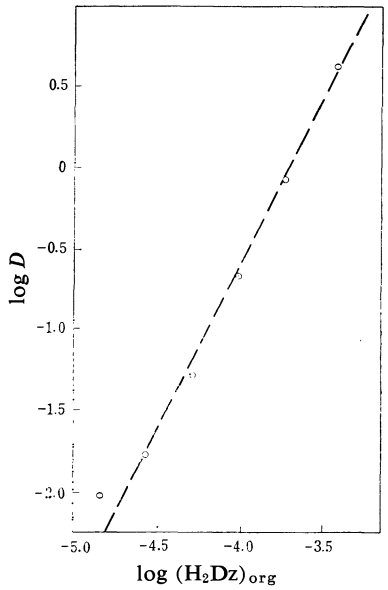



Fig. 3. Dependence of distribution ratio on the dithizone concentration.
Te(IV) before shaking: $4.25\times10^{-5}$ M
$HClO_4$: 1.17 M
Shaking temp.: 20°C
Shaking time: 30 min.
Slope of broken line is 2.

**The Tellurium Species in the Aqueous Layer.** —In order to determine the species of tellurium in an acidic aqueous solution, the distribution ratio was measured as a function of the hydrogen ion concentration. The results are shown in Fig. 4, where $\log D$ is plotted against $\log (H^+)$.

The equilibrium quotients for Eq. 3 are represented as:

$$K_n = \frac{(Te(OH)_2(HDz)_2)_{org}(H^+)_{aq}^{(4-n)}(H_2O)_{aq}^{(n-2)}}{((Te(OH)_n)^{(4-n)+})_{aq}(H_2Dz)_{org}^2} \quad (4)$$

The distribution ratio is given by:

$$D = \frac{(Te(OH)_2(HDz)_2)_{org}}{\sum_n (Te(OH)_n^{(4-n)+})_{aq}} \quad (5)$$

* $TeO(HDz)_2$ or $TeDz_2$ is also expected as the species of tellurium(IV) dithizonate. However, since $TeDz_2$ should be in the so-called "enol form,"[6] $TeDz_2$ may be excluded; because the "enol form" does not appear in other metal dithizonates extracted from a strongly acidic aqueous solution. At any rate, from this experiment, it is impossible to distinguish between $Te(OH)_2(HDz)_2$ and $TeO(HDz)_2$.

6) E. B. Sandell, "Colorimetric Determination of Traces of Metals," Interscience Publishers, New York, London (1959), p. 140.

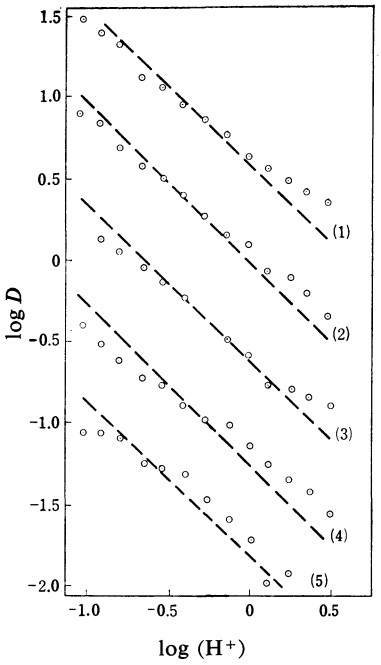



Fig. 4. Dependence of distribution ratio on the acid concentration.

$H_2Dz$ in $CCl_4$: (1) $2.76\times10^{-4}$ M, (2) $1.38\times10^{-4}$ M, (3) $6.90\times10^{-5}$ M, (4) $3.45\times10^{-5}$ M, (5) $1.73\times10^{-5}$ M
Ionic strength: 3.12
Shaking temp.: 25°C
Shaking time: 30 min.
Slope of broken lines is −1.

In this formulation the tellurium species containing dithizonate anions in the aqueous layer are neglected. This assumption may be valid under the present experimental conditions. Taking the partial derivative of log $D$ with respect to log $(H^+)$,

$$\partial \log D/\partial \log (H^+) = -4+f_1+2f_2+3f_3+4f_4+5f_5+6f_6 \qquad (6)$$

where;

$$f_n=\frac{(Te(OH)_n^{(4-n)+})}{(Te^{4+})+(Te(OH)^{3+})+\cdots+(Te(OH)_6^{2-})}$$

and

$$0 \leqq f_n \leqq 1$$

By using Eq. 6 and the value of $\partial \log D/\partial \log (H^+)$ experimentally obtained, one can calculate the average number of hydroxyl groups attached to one tellurium atom. As can be seen from Fig. 4, $\partial \log D/\partial \log (H^+)$ is nearly −1, so $f_3$ is the predominant factor, corresponding to $Te(OH)_3^+$.

That tellurium(IV) exists as $Te(OH)_3^+$ in acid solutions (0.10—3.0 M) agrees with the results obtained from solubility[7,8] and ion-exchange studies[9]. Thus, the overall reaction of tellurium(IV) with dithizone in the extraction process may be written as follows:

$$Te(OH)_3^+(aq.)+2H_2Dz(org.) = Te(OH)_2(HDz)_2(org.)+H^+(aq.)+H_2O(aq.) \qquad (7)$$

**The Effect of the Temperature on the Distribution Ratio.**—In order to determine the effect of the temperature on the extraction, measurements of the distribution ratio of tellurium were made at 3, 10, 20, 30 and 40°C. The results are shown in Fig. 5.

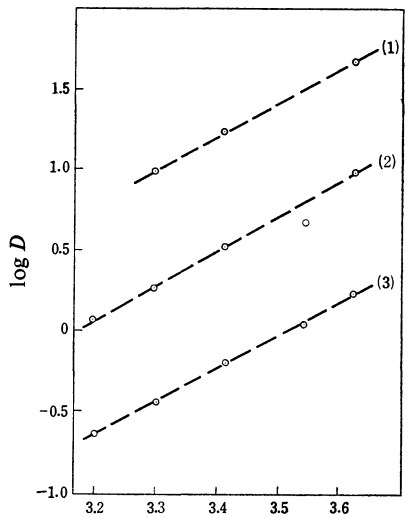



Fig. 5. Effect of temperature on the distribution ratio.

$H_2Dz$ in $CCl_4$: (1) $5.80\times10^{-4}$ M, (2) $2.54\times10^{-4}$ M, (3) $1.27\times10^{-4}$ M
Aqueous medium: $HClO_4$ 2.00 M
Shaking time: 30 min.

In general, for the equilibrium constant, $K$, of a reaction and the absolute temperature, $T$, the following thermodynamical relation holds:

$$(\partial \ln K/\partial(1/T))_p = -\Delta H^\circ/\boldsymbol{R} \qquad (8)$$

where $-\Delta H^\circ$ is the standard enthalpy change, $\boldsymbol{R}$ is the gas constant, and the subscript, $p$, implies that the pressure is constant.

The equilibrium constant, $K$, for Eq. 7 is written as follows:

$$K=\frac{[Te(OH)_2(HDz)_2][H^+]}{[Te(OH)_3^+][H_2Dz]^2} \qquad (9)$$

7) S. R. Schuhmann, *J. Am. Chem. Soc.*, **47**, 361 (1925).
8) I. M. Issa and S. A. Awad, *J. Phys. Chem.*, **58**, 948 (1954).
9) Y. Sasaki, *Japan Analyst (Bunseki-Kagaku)*, **4**, 637 (1955).

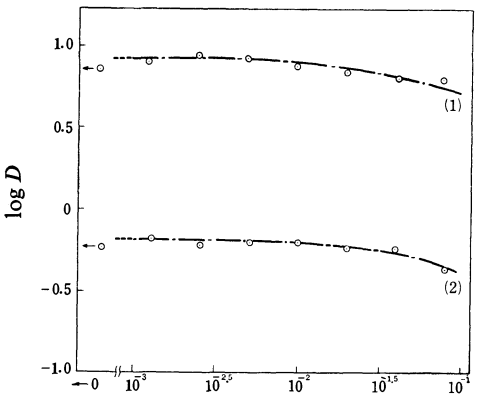



Fig. 6. Effect of fluoride on the distribution ratio.
$H_2Dz$ in $CCl_4$: (1) $2.60\times10^{-4}$ M, (2) $9.00\times10^{-5}$ M
$HClO_4$: 2.00 M+NaF
Shaking temp.: 20°C
Shaking time: 50 min.

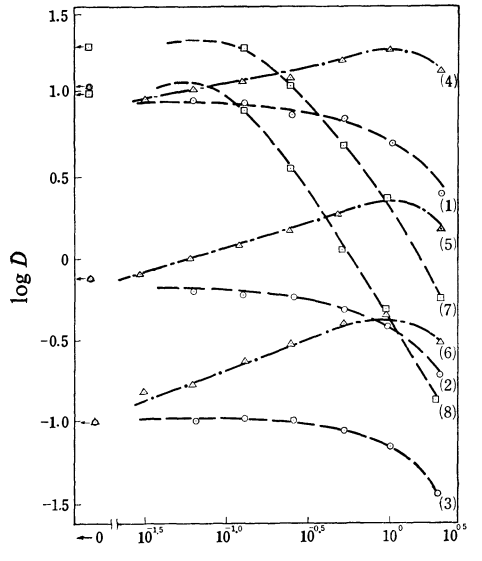



Fig. 7. Effect of chloride, bromide and iodide on the distribution ratio.
$H_2Dz$ in $CCl_4$: (1) and (4) $3.39\times10^{-4}$ M, (2) and (5) $9.00\times10^{-5}$ M, (3) and (6) $4.50\times10^{-5}$ M, (7) $5.70\times10^{-4}$ M, (8) $2.89\times10^{-4}$ M
(1), (2) and (3): chloride
(4), (5) and (6): bromide
(7) and (8): iodide
$[H^+]$: 2.00 M
Shaking temp.: 20°C
Shaking time: 50 min.
Ionic strength: 2.00

where the square brackets indicate the thermodynamical activity of the corresponding species. Equation 9 is rewritten as:

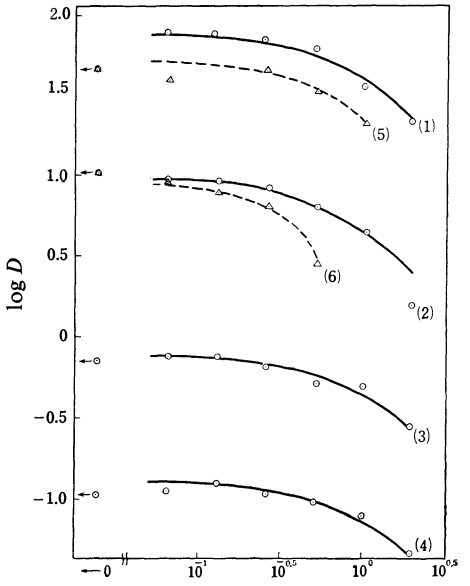



Fig. 8. Effect of bisulfate and nitrate on the distribution ratio.
$H_2Dz$ in $CCl_4$: (1) and (5)* $7.78\times10^{-4}$ M, (2) and (6)* $3.39\times10^{-4}$ M, (3) $9.00\times10^{-5}$ M, (4) $4.50\times10^{-5}$ M
(1), (2), (3) and (4): bisulfate
(5) and (6): nitrate
$[H^+]$: 2.00 M
Shaking temp.: 20°C
Shaking time: 50 min.
Ionic strength: 2.00
* After shaking dithizone was partially oxidized by nitric acid.

$$K=D\times\gamma_2\times\gamma_H\times(H^+)/\gamma_1\times\gamma_D{}^2\times(H_2Dz)^2 \quad (10)$$

where $\gamma_1$, $\gamma_2$, $\gamma_H$ and $\gamma_D$ are the activity coefficients of the tellurium(IV) ion, tellurium dithizonate, the hydrogen ion and dithizone respectively. Since the concentration of the solutes in the organic layer is very low, both $\gamma_2$ and $\gamma_D$ could be regarded as unity. When one assumes that the temperature dependence of the ratio, $\gamma_H/\gamma_1$, is very small, one can take the following formulation:

$$(\partial \ln K/\partial(1/T))_p \cong (\partial \ln D/\partial(1/T))_p \quad (11)$$

Thus, by plotting $\log D$ vs. $1/T$, one can obtain straight lines. From the slope of the lines in Fig. 5, the enthalpy change, $\Delta H°$, may be roughly estimated to be $-10.4$ kcal./mol.

**The Effect of Various Anions on the Distribution Ratio.** — Figures 6, 7 and 8 show the effects of fluoride, chloride, bromide, iodide, bisulfate and nitrate on the distribution ratios of tellurium(IV). In each case, the ionic strength was kept constant with perchloric acid. In the experiments involving fluoride, the extraction was carried out in glass tubes

Table I. Effect of various acids on the extraction

| Substance | Concn. M | $(D_x/D_0)\times100$*1 (1) | (2) |
|---|---|---|---|
| Formic acid | 1.0 | 100 | 100 |
| Acetic acid | 1.0 | 100 | 100 |
| Oxalic acid | 0.01 | 86 | 94 |
| Malonic acid | 0.01 | 85 | 94 |
| Succinic acid | 0.01 | 92 | 87 |
| Fumaric acid | 0.05 | 100 | 100 |
| Maleic acid | 0.05 | 84 | 86 |
| Citric acid | 0.01 | 87 | 84 |
| Tartaric acid | 0.01 | 93 | 97 |
| Orthophosphoric acid | 0.5 | 95 | 92 |
| Orthoboric acid | 0.1 | 97 | 99 |
| Metasilicic acid | 0.01 | 91 | 95 |
| NTA*2 | 0.01 | 100 | 100 |
| EDTA | 0.01 | 93 | 94 |
| CyDTA*3 | 0.01 | 100 | 92 |
| DTPA*4 | 0.01 | 99 | 100 |
| GEDTA*5 | 0.01 | 91 | 100 |

*1 Extracted with (1) $3.39\times10^{-5}$ M, (2) $9.00\times10^{-5}$ M $H_2Dz$ in $CCl_4$
$D_0$: Distribution ratio of Te(IV) when extracted from 2.00 M $HClO_4$.
$D_x$: Distribution ratio of Te(IV) when extracted from 2.00 M $HClO_4$ + a corresponding acid.
*2 NTA: Nitrilotriacetic acid
*3 CyDTA: 1,2-cyclohexanediaminetetraacetic acid
*4 DTPA: Diethylenetriaminepentaacetic acid
*5 GEDTA: Glycoletherdiaminetetraacetic acid
Shaking temp.: 20°C
Shaking time: 50 min.

the insides of which were coated with "Silicone."*

Another series of experiments extracting tellurium by dithizone were carried out in the presence of various acids, including phosphoric acid, boric acid, silicic acid and several organic acids. The results are shown in Table I.

**The Absorption Spectrum and the Molar Extinction Coefficient of Tellurium Dithizonate in Carbon Tetrachloride.**—Four milliliters of perchloric, sulfuric, hydrochloric or nitric acid solutions of tellurium(IV) were shaken with 4 ml. of a freshly-purified dithizone carbon tetrachloride solution. An aliquot of the organic layer was then diluted with carbon tetrachloride and subjected to the spectrophotometric measurement.

In all these cases, one could not obtain a pure tellurium dithizonate solution, only a mixture of dithizone and tellurium dithizonate. For example, the absorption spectrum for the extract from sulfuric acid is shown in Fig. 9. Assuming that the absorption peak at 620 mμ is wholly due to dithizone, one can analyze the curve into two components and assign the maximum absorption of tellurium dithizonate at 427 mμ, as Fig. 9 shows.

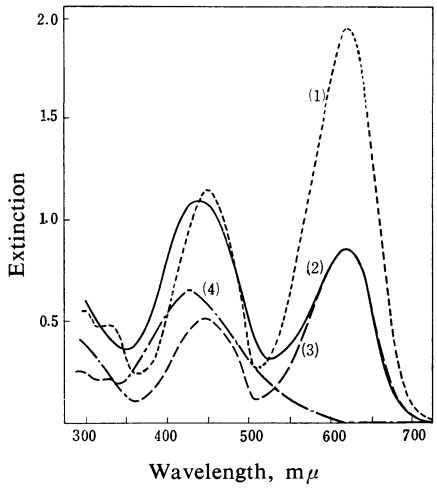



Fig. 9. Absorption spectra of dithizone and tellurium dithizonate in carbon tetrachloride.
----- (1): Absorption spectrum of dithizone ($5.66\times10^{-5}$ M)
——— (2): Absorption spectrum of a mixture of tellurium dithizonate ($1.58\times10^{-5}$ M) and dithizone ($2.50\times10^{-5}$ M)
——— (3): Assumed absorption spectrum of dithizone in (2)
— — — (4): Resulting absorption spectrum of tellurium dithizonate in (2), that is: (2) − (3).

Table II. Molar extinction coefficient of tellurium dithizonate in carbon tetrachloride

| Aqueous medium | Concn. M | Initial concn. of Te(IV) M | $\varepsilon_{427\,m\mu}$ $M^{-1}cm^{-1}$ |
|---|---|---|---|
| $HClO_4$ | 1.90 | $9.77\times10^{-5}$ | $4.13\times10^4$ |
| $H_2SO_4$ | 0.692 | $4.88\times10^{-3}$ | $4.12\times10^4$ |
| | 0.433 | $1.63\times10^{-3}$ | $4.17\times10^4$ |
| HCl | 1.07 | $8.02\times10^{-3}$ | $4.03\times10^4$ |
| | 0.230 | $3.76\times10^{-4}$ | $4.07\times10^4$ |
| $HNO_3$ | 0.814 | $8.34\times10^{-4}$ | $3.90\times10^4$ |

The molar extinction coefficients at 427 mμ were calculated for several extracts; they are tabulated in Table II. Since the wavelengths of the maximum absorption and the molar extinction coefficients are equal for all these extracts within the range of experimental error, they are supposed to be identical entities.

* Polone T, made by Shin-etsu Kagaku Co., Ltd., Japan.

**Summary**

Tellurium(IV) can be extracted into organic layers with dithizone. The analysis of the experimental results suggests, as the main process of extraction:

$$Te(OH)_3^+ \text{ (or } TeOOH^+) \text{ (aq.)} + 2H_2Dz \text{ (org.)} = Te(OH)_2(HDz)_2 \text{ (or } TeO(HDz)_2) \text{ (org.)} + H^+ \text{(aq.)} + xH_2O \text{ (aq.)}$$

The spectrophotometric measurements show that tellurium dithizonate in carbon tetrachloride has an absorption maximum at 427 mμ, where the molar extinction coefficient is $4.10 \times 10^4$ M$^{-1}$ cm$^{-1}$.

The authors wish to thank Professor Nobufusa Saito, Dr. Yukiyoshi Sasaki, Dr. Akira Yamasaki and Mr. Hitoshi Shoji for their helpful advice and discussions.

*Department of Chemistry*
*Faculty of Science*
*The University of Tokyo*
*Hongo, Tokyo*

# The Reaction of Tropoids with Quinone Derivatives. VIII. The Reaction of Several Tropolones with *p*-Benzoquinonemonobenzenesulfonimide

By Yukio NISHIYAMA

(Received January 11, 1965)

The reactions of tropolones with quinone derivatives have been investigated in our laboratory several times. For example, in one earlier paper of this series[1], it was reported that the reactions of *p*-benzoquinonedibenzenesulfonimide with tropolone and its bromo derivatives in the presence of a catalytic amount of triethylamine gave *N*-(tropolon-5-yl)-*N*,*N*'-dibenzenesulfonyl-*p*-phenylenediamine and its bromo derivatives in comparatively good yields.[2,3]

The present paper will describe the determination of the structure of the products of the reaction of *p*-benzoquinonemonobenzenesulfonimide (I)[4] with tropolone and its bromo derivatives without a catalyst.

The addition of tropolone to *p*-benzoquinonemonobenzenesulfonimide (I) dissolved in a mixture of methanol and benzene resulted in an orange solution. When this mixture had been allowed to stand overnight at room temperature, colorless crystals (II) were precipitated out. The analytical values of II corresponded to the molecular formula $C_{19}H_{15}O_{55}$·NS, and its ultraviolet and infrared absorption spectra revealed that the tropolone ring was retained. Furthermore, from an analogy to the reaction of quinonediimide derivatives,[5-8] it was assumed that the *N*-benzenesulfonyl-*p*-aminophenol moiety entered into the 5-position of the tropolone ring. The experimental results described below support this assumption.

In order to ascertain the position where the tropolone ring links, a similar reaction was carried out with 3-bromotropolone and 3,7-dibromotropolone in place of tropolone itself; pale yellow crystals III and yellow crystals IV were obtained respectively. The analytical values of III and IV agreed with the formulae for the monobromo and dibromo derivatives of II respectively.

The hydrogenolysis of III and IV in the presence of palladium-carbon afforded II. Since the electrophilic substitution of tropolone is

1) S. Seto, H, Yamazaki and Y. Nishiyama, This Bulletin, 33, 1081 (1960).

2) See also Y. Nishiyama, Y. Ikegami and S. Seto, ibid., 38, 72 (1965).

3) It was reported in an earlier paper of this series[1] that the structures of the reaction products of *p*-benzoquinonedibenzenesulfonimide with tropolone and its bromo derivatives were 5-(2',5'-dibenzenesulfonamidophenyl)tropolone and its bromo derivatives. However, further examination of these reaction products has revealed that they were *N*-(tropolon-5-yl)-*N*,*N*'-dibenzenesulfonyl-*p*-phenylenediamine and its bromo derivatives.[2]

4) R. Adams and J. H. Looker, *J. Am. Chem. Soc.*, 73, 1145 (1951).

5) S. Seto and H. Sato, This Bulletin, 35, 349 (1961).

6) S. Seto and Y. Nishiyama, *J. Pharm. Soc. Japan* (*Yakugaku Zasshi*), 82, 590 (1962).

7) S. Seto and Y. Nishiyama, This Bulletin, 35, 1010 (1962).

8) Y. Nishiyama, *Bull. Chem. Research Inst. of Non-aqueous Solutions, Tohoku Univ.*, 12, 55 (1963).

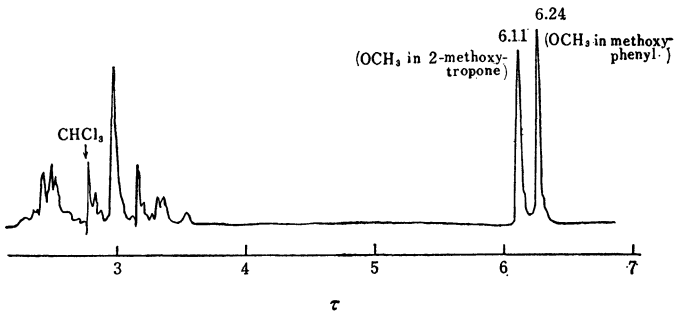
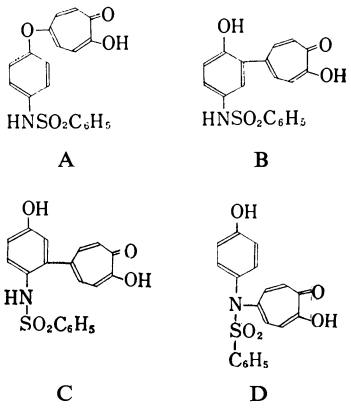



Fig. 1. The NMR spectrum of X.

known to occur at the 3, 5, and 7-position, these facts clearly indicate that the *N*-benzenesulfonyl-*p*-aminophenol moiety in II, III and IV is situated in the 5-position of the tropolone ring. Accordingly, formulae A, B, C and D have been taken into consideration in determining the structure of II.




The heating of II in a sealed tube with concentrated hydrochloric acid afforded the *p*-aminophenol derivative V.

The acetylation of II and V afforded diacetyl derivative VI and triacetyl derivative VII respectively, these acetyl derivative did not exhibit any absorption band due to the NH and OH groups in their infrared spectra.

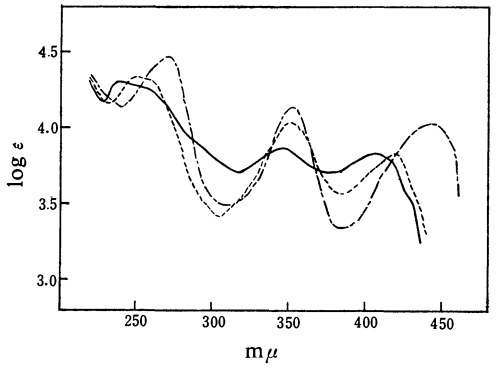



Fig. 2. Ultraviolet absorption spectra of II (——), III(----) and IV(-·--) in methanol.

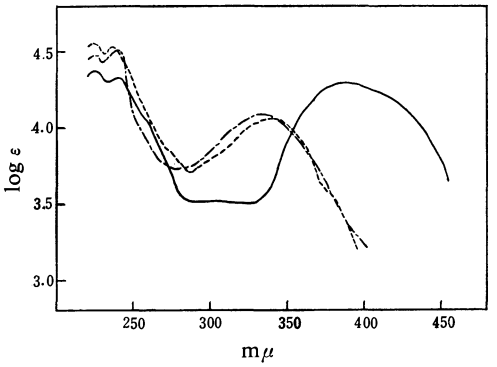



Fig. 3. Ultraviolet absorption spectra of V (——), VI(----) and VII(-·--) in methanol.

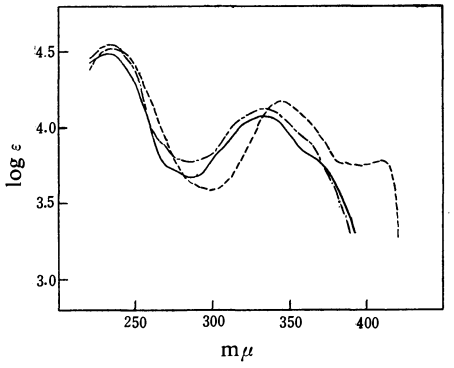
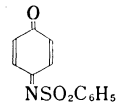


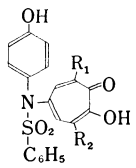

Fig. 4. Ultraviolet absorption spectra of VIII (——), IX(----) and X(-·--) in methanol.

The reaction of II with diazomethane afforded a methyl ether, the analytical values of which corresponded to those of the monomethyl compound VIII. Its ultraviolet absorption spectrum and the absence of coloration with ferric chloride revealed that VIII was a 2-methoxytropone derivative. The methylation of II with dimethyl sulfate in the presence of potassium hydroxide gave another monomethyl ether derivative, IX, which showed coloration with ferric chloride. The further methylation

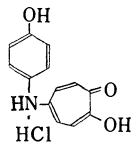
of IX with diazomethane afforded a dimethyl compound, X, that showed no coloration with ferric chloride. The infrared spectrum of X does not show any absorption band due to the NH and OH groups, and in the NMR spectrum[9] the signals for the protons of the $OCH_3$ groups in methoxyphenyl and 2-methoxytropone appear at 6.24 and 6.11 $\tau$[2] respectively, with almost equal intensities. If X had the $NCH_3$ group, the signal for the $NCH_3$ group would appear near 6.8—6.9 $\tau$.[2] Therefore, X, was identified as *N*-benzenesulfonyl-*N*-(2-methoxytropon-5-yl)-*p*-anisidine.



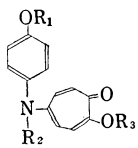
I



II: $R_1=R_2=H$
III: $R_1=Br$, $R_2=H$
IV: $R_1=R_2=Br$



V



VI: $R_1=R_3=COCH_3$, $R_2=SO_2C_6H_5$
VII: $R_1=R_2=R_3=COCH_3$
VIII: $R_1=H$, $R_2=SO_2C_6H_5$, $R_3=CH_3$
IX: $R_1=CH_3$, $R_2=SO_2C_6H_5$, $R_3=H$
X: $R_1=R_3=CH_3$, $R_2=SO_2C_6H_5$

From these facts, formulae A, B and C must be excluded for structure of II; thus it may be concluded that the reaction product of *p*-benzoquinone-monosulfonimide (I) with tropolone is *N*-benzenesulfonyl-*N*-(tropolon-5-yl)-*p*-aminophenol (II), and that III and IV are monobromo and dibromo derivatives of II respectively.

## Experimental[10]

***N*-Benzenesulfonyl-*N*-(tropolon-5-yl)-*p*-aminophenol (II).**—A solution of *p*-benzoquinonemonobenzenesulfonimide (I) (200 mg.) and tropolone (180 mg.) in 9 ml. of a mixture (3 : 1 by volume) of benzene and methanol was allowed to stand at room temperature. After 24 hr., the colorless crystals (120 mg.) which precipitated were collected by filtration. Recrystallization from ethanol afforded 110 mg. of II; m. p. 228°C.

Found: C, 61.90; H, 4.27; N, 3.74. Calcd. for $C_{19}H_{15}O_5NS$: C, 61.81; H, 4.06; N, 3.79%.

UV $\lambda_{max}^{MeOH}$ m$\mu$ (log $\varepsilon$): 235 (4.28), 345 (3.84), 403 (3.82).

***N*-Benzenesulfonyl-*N*-(3-bromotropolon-5-yl)-*p*-aminophenol (III).**—To a solution of I (300 mg.) in 7 ml. of benzene-methanol (3 : 1 by volume) was added a solution of 3-bromotropolone (490 mg.) in 2 ml. of the same solvent; the mixture was then allowed to stand at room temperature. After 2 days, the solvent was evaporated under reduced pressure. To this residue, a small amount of ethanol was added, whereupon pale yellow crystals (270 mg.), m. p. 240°C (decomp.) were obtained.

Found: C, 51.22; H, 3.96. Calcd. for $C_{19}H_{14}O_5NSBr$: C, 50.89; H, 3.13%.

UV $\lambda_{max}^{MeOH}$ m$\mu$ (log $\varepsilon$): 250 (4.32), 350 (4.04), 420 (3.83).

The filtrate left after the separation of III was evaporated under reduced pressure. When the residue was sublimed at 2 mmHg in a bath of 130°C, 130 mg. of 3-bromotropolone was recovered.

***N*-Benzenesulfonyl-*N*-(3,7-dibromotropolon-5-yl)-*p*-aminophenol (IV).**—When treated in the same way as above, I (400 mg.) and 3,7-dibromotropolone (480 mg.) afforded 670 mg. of yellow crystals, m. p. 197°C (decomp.).

Found: C, 43.47; H, 2.79; N, 2.39. Calcd. for $C_{19}H_{13}O_5NSBr_2$: C, 43.26; H, 2.47; N, 2.66%.

UV $\lambda_{max}^{MeOH}$ m$\mu$ (log $\varepsilon$): 270 (4.47), 353 (4.13), 445 (4.02).

**The Hydrogenolysis of III.**—A solution of the monobromo derivative III (50 mg.) in water (6 ml.) and ethanol (2 ml.) containing potassium hydroxide (100 mg.) was shaken in a hydrogen atmosphere over palladium-carbon (50 mg.) at room temperature. When the absorption of hydrogen had ceased, the catalyst was filtered off, the filtrate was acidified with diluted sufuric acid, and the precipitate thereby formed was collected by filtration. Recrystallization from ethanol afforded 30 mg. of colorless crystals, m. p. 227—228°C, undepressed on admixture with II. The ultraviolet and infrared absorption spectra of these two substances were also in complete agreement.

**The Hydrogenolysis of IV.**—A solution of the dibromo derivative IV (150 mg.) in water (6 ml.) and ethanol (4 ml.) containing potassium hydroxide (200 mg.) was added to palladium-carbon (50 mg.). The mixture was then treated as in the foregoing example. The recrystallization of the precipitate gave 70 mg. of crystals with a m. p. of 227—228°C, undepressed on admixture with II. The

9) The NMR spectrum was measured in deuteriochloroform, using a Varian 4301 high-resolution NMR spectrometer (60 Mc.); the measurements were performed by Assistant Professor Tsuneo Ikenoue of this Institute, to whom the author is indebted.

10) All melting points are uncorrected. The microanalyses were carried out by Misses Yoko Endo and Yukiko Endo in this Institute. The measurements of the ultraviolet and infrared spectra were made, respectively, with a Hitachi EPI-2A-type spectrophotometer in methanol and with a Hitachi EPI-S2-type infrared spectrophotometer using a potassium bromide disk.

ultraviolet and infrared absorption spectra of this product were also in agreement with those of II.

**The Reaction of II with Concentrated Hydrochloric Acid.** — A mixture of II (100 mg.) and concentrated hydrochloric acid (2 ml.) was heated in a sealed tube at 130°C for 5 hr. When it had cooled, the tube was opened and the orange red crystals that separated out were collected by filtration. Recrystallization from dilute hydrochloric acid gave 20 mg. of the hydrochloride of *N*-(tropolon-5-yl)-*p*-aminophenol (V) as orange red crystals, m. p. 265—266°C (decomp.).

Found: C, 58.04; H, 4.34; N, 5.44. Calcd. for $C_{13}H_{10}O_3NCl$: C, 59.20; H, 4.55; N, 5.31%.

UV $\lambda_{max}^{MeOH}$ mμ (log ε): 225 (4.37), 240 (4.32), 390 (4.26).

***N*-Benzenesulfonyl-*N*-(2-acetoxytropon-5-yl)-*p*-acetoxyaniline (VI).**—A mixture of II (200 mg.) and acetic anhydride (4 ml.) was heated at 130°C for 1 hr. The mixture was then evaporated under reduced pressure, and the residue was crystallized from ethanol to give 60 mg. of colorless crystals, melting at 139—140°C.

Found: C, 60.57; H, 4.33; N, 3.15. Calcd. for $C_{23}H_{19}O_7NS$: C, 60.95; H, 4.19; N, 3.09%.

UV $\lambda_{max}^{MeOH}$ mμ (log ε): 225 (4.54), 235 (4.48), 340 (4.05).

***N*-Acetyl-*N*-(2-acetoxytropon-5-yl)-*p*-acetoxyaniline (VII).**—A mixture of the hydrochloride V (150 mg.), anhydrous sodium acetate (50 mg.) and acetic anhydride (2 ml.) was heated at 130°C for 2 hr. The mixture was then evaporated under reduced pressure, and the residue was washed with water. The crystalline residue was recrystallized from ethyl acetate to give 80 mg. of colorless crystals, m. p. 173—174°C.

Found: C, 65.08; H, 5.04; N, 4.38. Calcd. for $C_{19}H_{17}O_6N$: C, 64.26; H, 4.79; N, 3.94%.

UV $\lambda_{max}^{MeOH}$ mμ (log ε): 225 (4.48), 240 (4.50), 335 (4.09).

***N*-Benzenesulfonyl-*N*-(2-methoxytropon-5-yl)-*p*-aminophenol (VIII).**—An ether solution of diazomethane was added to a suspension of II (150 mg.) in methanol (10 ml.). The mixture was then allowed to stand overnight, and the crystals that separated out were collected by filtration. Recrystallization from a methanol and chloroform mixture afforded 400 mg. of colorless needles, m. p. 160—162°C.

Found: C, 62.97; H, 5.04; N, 3.32. Calcd. for $C_{20}H_{17}O_5NS$: C, 62.68; H, 4.44; N, 3.65%.

UV $\lambda_{max}^{MeOH}$ mμ (log ε): 232.5 (4.48), 332 (4.07).

This product does not show any coloration with ferric chloride.

**The Methylation of II with Dimethyl Sulfate.**—A solution of II (300 mg.) in 2 N sodium hydroxide (16 ml.) was stirred at room temperature. To this solution, dimethyl sulfate (1 ml.) was added. A colorless solid began to separate after a few minutes. After 30 min., the solid was collected by filtration and suspended in a small amount of water. The mixture was then acidified with dilute sulfuric acid, and the solid that remained was collected and recrystallized from ethanol to give 130 mg. of *N*-benzenesulfonyl-*N*-(tropolon-5-yl)-*p*-methoxyaniline (IX) as colorless needles, m. p. 169—170°C.

Found: C, 63.62; H, 4.63; N, 3.89. Calcd. for $C_{20}H_{17}O_5NS$: C, 62.68; H, 4.44; N, 3.65%.

UV $\lambda_{max}^{MeOH}$ mμ (log ε): 235 (4.51), 345 (4.17), 407 (3.76).

This compound showed a positive color reaction with ferric chloride.

The filtrate left after the separation of IX was acidified with dilute sulfuric acid, and the solid that precipitated was collected. Recrystallization from ethanol gave 120 mg. of colorless crystals m. p. 228°C, undepressed on admixture with II.

**The Reaction of IX with Diazomethane.**—An ether solution of diazomethane was added to a suspension of IX (100 mg.) in methanol (4 ml.). After the mixture had been allowed to stand overnight, the crystals that separated were collected. Recrystallization from ethanol afforded 40 mg. of *N*-benzenesulfonyl-*N*-(2-methoxytropon-5-yl)-*p*-methoxyaniline as colorless crystals, m. p. 175—176°C.

Found: C, 63.91; H, 4.89; N, 3.64. Calcd. for $C_{21}H_{19}O_5NS$: C, 63.49; H, 4.78; N, 3.52%.

UV $\lambda_{max}^{MeOH}$ mμ (log ε): 235 (4.54), 332 (4.15).

Compound X did not show any coloration with ferric chloride.

The author wishes to express his gratitude to Professor Shuichi Seto for his kind guidance and encouragement throughout this work. A part of the expenses was defrayed by the Sankyo Co., Ltd., to which the author is deeply indebted.

*The Chemical Research Institute of Non-Aqueous Solutions*
*Tohoku University*
*Katahira-cho, Sendai*

# The Crystal Growth of Synthetic Fluor-phlogopite by the Moving Crucible Technique

By Tokiti NODA, Nobutoshi DAIMON, Michio INAGAKI, Mitsuru TANAKA
Takashi AMANO and Minoru HIRAO

(Received January 18, 1965)

Fluor-phlogopite crystallizes from a melt with a composition corresponding approximately to the composition of mica, [$KMg_3AlSi_3O_{10}F_2$]. In the earlier stage of our experiments, the crystal growth of mica in the melt of a large mass was carried out and thus large mica crystals were obtained.[1] A carbon granular resistance furnace was used for the melting and crystallization of mica. A batch of 30 kg. of a raw material mixture was heated in an aluminous clay or graphite crucible until a clear melt was obtained. The melt was then cooled at a cooling rate of 2 to 5°C per hour and left to cool to room temperature. The solidified mass was composed of interlocking mica crystals of various sizes. The maximum size of single crystals was about 5 cm. by 5 cm., but the yield of crystals of this size was small.

In order to increase the yield of large crystals in a given batch, it is necessary to prevent the formation of excess crystal nuclei at the beginning of crystallization and to give a preferred orientation to the growing crystals. Van Valkenburg and Pike[2] used an elliptical crucible with a wedge-shaped bottom for the melting and crystallization of fluor-phlogopite. With a steep temperature gradient within the melt (larger than 50°C between the top and the bottom of the melt) and a slow rate of cooling (less than 1°C/hr.), a good development of the vertical and lateral orientation of mica crystals was obtained.

The Electrotechnical Experimental Station, Bureau of Mines,[3] has developed an internal-electrical-resistance melting process for the manufacture of fluor-mica. This process can be used for the melting of a large quantity of a mica batch, but it usually results in the formation of a large number of interlocking crystals. Noda and Sumiyoshi[4] used two sets of graphite electrodes placed vertically one over the other and thus obtained a development of the vertical orientation of growing crystals by changing the ratio of the electrical current passing through the upper and the lower parts of the mica melt with the internal-electrical-resistance melting process.

Daimon et al.[5] applied the Kyropoulos (or Czockralski) technique of single-crystal growing to the crystal-growing of fluor-phlogopite, but they could not continue to grow crystals because of the change in the chemical composition of the surface layer of the melt caused by the evaporation of fluorine compounds.

Noda and Tsujimura[6] used a stationary crucible technique of single crystal growing for fluor-mica single-crystal growing. The furnace used for the experiments had three platinum ribbon heaters placed at the bottom, the top, and the side of the furnace chamber, the electrical current of each heater being regulated separately. A platinum crucible containing the fluor-phlogopite batch mixture was placed in the chamber and heated to a temperature above the melting point of the mica. The average temperature gradients obtained by changing the electrical current of heaters ranged vertically from 10 to 80°C/cm., with the extreme temperature at the top. The fluctuation of temperature around the crucible could be kept within ±0.1°C by using fine alumina powder as a thermal insulator between the heaters and the crucible. A charge of 20 to 40 g. was melted and crystallized at a cooling rate ranging from 0.5 to 90°C/min. Mica crystals grew with their basal planes vertically parallel to the temperature gradient when the temperature gradient was larger than 40°C/cm. However, no lateral orientation was developed, and the breadth of the crystals was limited by the intersection of the neighbor crystals. Good crystals of a length equal to the depth of the melt were grown with an estimated rate of growth (the rate of the descent of the crystal-melt boundary) of less than 1 mm./hr. Sometimes a few crystals were observed to have grown to project above the surface of the melt.

1) a) T. Noda, *J. Am. Ceram. Soc.*, **38**, 147 (1955); b) T. Noda and Y. Sumiyoshi, This Bulletin, **32**, 54 (1959).
2) Alvin Van Valkenburg and R. G. Pike, *J. Res. Nat. Bur. Standards*, **48**, 360 (1952).
3) R. A. Hatch, R. A. Humphrey and E. C. Worden, Synthetic Mica Investigations III. Report of Investigation 5283, Bureau of Mines, December, 1956.
4) M. Sumiyoshi and T. Noda, *J. Chem. Soc. Japan, Ind. Chem. Sec.* (*Kogyo Kagaku Zasshi*), **63**, 2069 (1960).
5) a) N. Daimon, *J. Ceram. Assoc. Japan* (*Yogyo Kyokaishi*), **60**, 179 (1952); b) N. Daimon, S. Shimizu, N. Ando and K. Kasuya, *J. Chem. Soc. Japan, Ind. Chem. Sec.* (*Kogyo Kagaku Zassi*), **59**, 1335 (1956).
6) T. Noda and S. Tsujimura, ibid., **61**, 477 (1958).

With a given temperature gradient, the maximum depth of the melt is limited by the highest temperature, which is in turn limited by the furnace used. Also, too high a temperature should be avoided because of the increase in the evaporation of the fluorine compound from the melt. Therefore, the size of the grown crystals can not be made large when a large temperature gradient is required for the growing of single crystals with the stationary crucible technique.

### Crystal Growth Without Seed Crystals
(Noda, Inagaki, Tanaka)

It is well known that the thermal history of melt affects the nucleation in the melt. In order to reduce the number of nuclei available for new crystal formation, the melt should be heated at a high enough temperature or for a long enough time for it to become a clear melt without any residual particles of raw material which may induce the nucleus formation.[7] On the other hand, when the melt is heated for an excessively long time or at too high a temperature, the melt cools, with a large undercooling which causes the sudden formation of a very large number of nuclei, once the nucleation begins.[8] Therefore, the control of the amount of nucleus formation needs a very delicate operation of the heating procedure.

**Apparatus and Experimental Procedure.**—The apparatus used for the moving crucible technique was a furnace the chamber of which was divided into two sections by a baffle plate.[9] The sections were heated by separate platinum-rhodium ribbon heaters in order to control the temperature of each room separately and in order to get a desired temperature gradient in the chamber. A charge of the fluor-phlogopite batch mixture was contained in a thin-walled platinum crucible 9 to 20 mm. in diameter, 20 to 30 mm. high, and with a conical bottom. The angle of the cone was 60°, and the apex of the cone was held on a platinum rod 5 mm. in diameter and 150 mm. long, the opposite end of which was in contact with the upper end of a stainless steel rod of the descending device. The crucible and the platinum rod were covered with refractory cases. The space between the crucible and the refractory case was filled with alumina powder so that no possible leakage of the batch melt might damage the wall of the furnace chamber.

The contact of the crucible apex with the platinum rod was designed to cool the apex preferentially by thermal conduction through the rod and to get so sharp a temperature gradient in the melt of the conical part of the crucible that the nucleation would take place only in the apex.

The rate of descent could be changed within the range of 0.1 to 1.0 mm./hr., because it was found from preliminary experiments that a rate of descent of 0.1 to 1.0 mm./hr. was good enough to grow single crystals of a good quality.

As raw materials, powdered fluor-phlogopite crystals or pre-melted blocks of fluor-phlogopite crystals were used. A crucible containing a charge of 20 to 300 g. of raw material was sealed by welding in order to prevent any change in the chemical composition of the charge by decomposition.

First, the crucible was placed in the upper section of the furnace; then the temperature of the furnace was raised. After the highest temperature of the furnace had reached about 1400°C, the temperature distribution in the furnace was measured and the crucible was moved to the position indicated as A in Fig. 1. In the figure the temperature distribution in the furnace is schematically described. The crucible was left there for a fixed time in order to complete the melting of the charge, and then it was manually moved to the position B, where the temperature of the crucible apex reached a definite temperature almost equal to or a little below the crystallization point of fluor-phlogopite (1375°C[8]). The crucible was

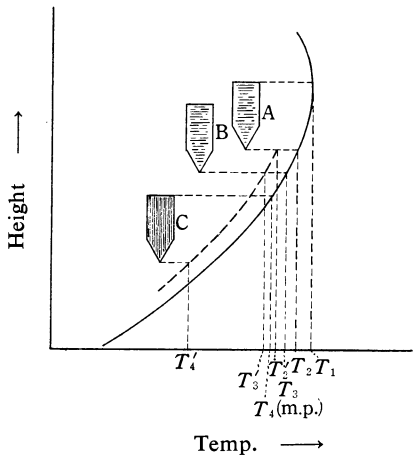



Fig. 1. Position of crucible in relation to the temperature gradient in the furnace in the growth of fluor-phlogopite crystal with the moving crucible technique.
—— Temperature of furnace
---- Temperature of apex of crucible

7) T. Noda and S. Sugiyama, ibid., 46, 1082 (1943).
8) S. Naka and T. Noda, ibid., 63, 232, 777, 946, 950, 954, 1325 (1960).
9) D. C. Stockbarger, "Crystal Growth," *Discussions Faraday Soc.*, 5, 299 (1949).

TABLE I. EXPERIMENTAL DATA OF FLUOR-PHLOGOPITE CRYSTAL GROWTH BY MOVING CRUCIBLE TECHNIQUE WITHOUT SEED CRYSTALS

| Exp. No. | Position A: Temp. of crucible apex | Position A: Holding time at $T'_2$ | Position A: Furnace temp. at the level of crucible apex | $T_2 - T'_2$ | Position B: Temp. of crucible apex at the beginning of descent | Position B: Holding time at $T'_3$ | Position B: Furnace temp. at the level of crucible apex | Rate of descent | Rate of* cooling of crucible apex |
|---|---|---|---|---|---|---|---|---|---|
| Series I | $T'_2$, °C | $t_2$, min. | $T_2$, °C | °C | $T'_3$, °C | $t_3$, min. | $T_3$, °C | mm./hr. | °C/hr. |
| 50 | 1373 | 30 | 1423 | 70 | 1329 | 30 | 1389 | 0.75 | 2.0 |
| 54(A) | 1355<br>1375 | 30<br>90 | 1409 | 34 | 1338 | 30 | 1368 | 0.75 | 2.0 |
| 55(A) | 1350<br>1368 | 30<br>30 | 1413 | 45 | 1325 | 30 | 1378 | 0.75 | 1.7 |
| 57 | 1348<br>1362 | 30<br>15 | 1427 | 65 | 1338 | 30 | 1387 | 0.76 | 2.3 |
| Series II | | | | | | | | | |
| 44 | 1390—1380 | 90 | 1450 | 70 | 1340 | 120 | 1415 | 0.75 | 2.0 |
| 47 | 1360 | 10 | 1430 | 70 | 1308 | 110 | 1390 | 0.75 | 3.0 |
| 58 | 1345<br>1360 | 10<br>25 | 1430 | 70 | 1320 | 30 | 1380 | 0.80 | — |

* The rate of cooling was calculated from the rate of descent and the temperature gradient in the furnace by the following relation:

Rate of cooling $(\Delta\theta/\Delta t)$ = Temperature gradient $(\Delta\theta/\Delta l) \times$ Rate of Descent $(\Delta l/\Delta t)$

where $t$ is time, $\theta$ temperature and $l$ distance.

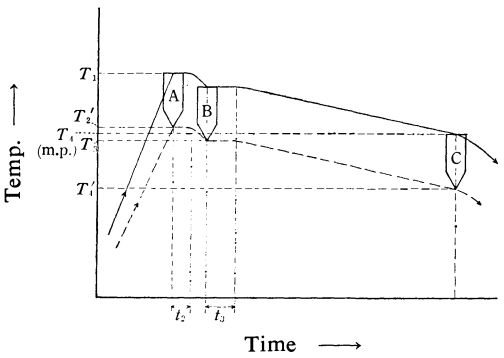



Fig. 2. Schematical heating program in the growth of fluor-phlogopite crystal with the moving crucible technique.

left there for a fixed time in order to form nuclei in the apex; then it was moved downward automatically at the rate of 0.75 mm./hr. The whole heating program is shown schematically in Fig. 2. When the top of the charge had passed the level of the crystallization temperature (the position C) and all of the melt was supposed to have crystallized, the furnace was cooled to room temperature. The temperature of the apex was measured by a thermocouple inserted between the crucible apex and the top of the platinum rod.

**Results.** — Some of experimental data are shown in Table I. When the apex of the crucible was placed directly on the platinum rod, the cooling effect of the rod was so large that the temperature of the apex was about 50—70°C lower than the furnace temperature of the same level. The temperature difference was reduced to about half (25—45°C) when a sintered alumina disk 1 mm. thick was inserted between the apex and the rod. The experiments with this inserted alumina disk are marked (A) in Table I.

In series I of the experiments, powdered crystals of fluor-phlogopite were used as raw material, while in series II of the experiments premelted blocks of fluor-phlogopite crystals were used. The premelted blocks were opaque white and were composed of minute, entangled crystals of mica.

In Exp. No. 50, in which the apex was held for 30 min. at the crystallization point of the mica, a very small number of unmelted crystals remained in the apex and a few single crystals of a good quality grew vertically from the apex to the top of the charge, orienting their basal planes parallel to the direction of growth, but without any lateral orientation (Plate I-1). Similar results were obtained with Exp. No. 55 (A) and 57, in which the apex temperature was held a little below the melting point of the mica (Plate I-2, -3). In Exp. No. 54, in which the apex was held for 90 min. at the crystallization point of mica, the resultant mass was composed of many randomly-oriented crystals (Plate I-4).

In Exp. No. 44, in which the apex was kept at 1390—1380°C for 90 min., the resultant mass was white, porcelain-like, and opaque, and was composed of a large number of minute



Plate I-1



Plate I-2

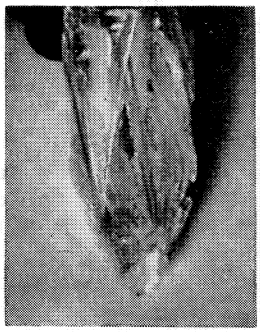


Plate I-3



Plate I-4

Plate I. Crystals grown by the moving crucible technique without seed crystals showing the effect of thermal history of melt.

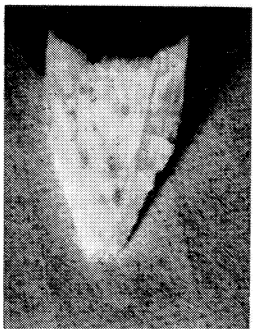


Plate II-1



Plate II-2

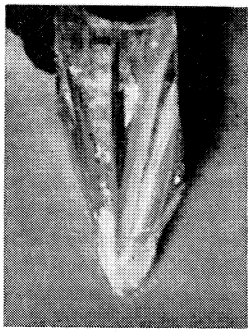


Plate II-3

Plate II. Crystals grown by the moving crucible technique without seed crystals showing the effect of thermal history of melt.

mica crystals and a small amount of needle crystals, probably chondrodite, all oriented vertically along the direction of growth (Plate II-1). In Exp. No. 47, in which the apex was kept a little below the crystallization point for a short time, small crystals remained at the apex; the size of the crystals deposited was small, but it became larger in the upper part of crucible, even though the apex was kept for 90 min. at 1300°C before the descent (Plate II-2). In Exp. No. 58, the thermal history of which was very similar to that of No. 57, single crystals of a good quality grew from the apex to the top of the charge (Plate II-3). This result was very similar to that obtained in Exp. No. 57. It can be seen from the similar results obtained in Exps. Nos. 57 and 58 that either powdered crystals or premelted crystalline aggregates can be used as raw material for the successful growing of fluor-phlogopite crystals.

As can be seen from the above experiments, the excessive heat treatment of the melt resulted in a large undercooling, which in turn resulted in the sudden formation of a large number of nuclei once the crystallization began. On the other hand, a number of seed crystals remained unmelted when the melting was insufficient. Experiments No. 54 and No. 44 are cases of excessive heat treatment, and Exp. No. 47 seems to be a case of insufficient melting, even though the apex was kept for a long time at a temperature a little below the crystallization point. Just to melt crystals down to the apex part may be the optimum

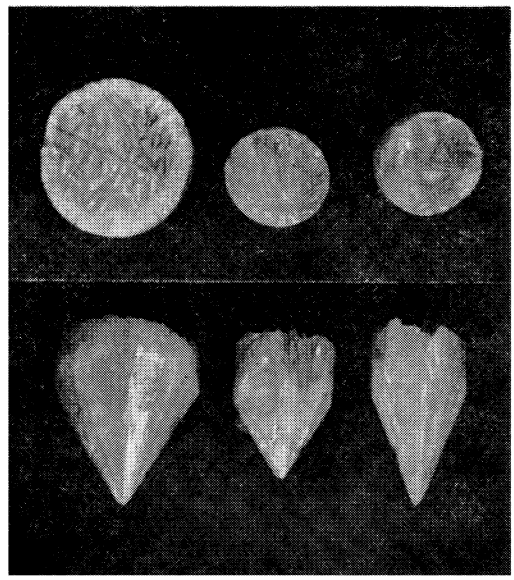


Plate III. Crystals grown by the moving crucible technique without seed crystals showing vertical and lateral orientation.

heat treatment for the growing of a few single crystals from the apex to the top of charge. This heat treatment can, however, be carried out only by a very careful control of the apex temperature. Experiments Nos. 50, 55 and 58 have heat treatments very close to the optimum.

With the moving crucible technique, the height of the charge is not necessarily as limited as it is with the stationary crucible technique, but the situation, in which the lateral orientation of grown crystals is random, is the same as with the latter technique. Some of the crystals grown by the moving crucible technique are shown in Plate III; they show a very good vertical orientation but a poor lateral orientation of crystal growth.

### Crystal Growth Using Seed Crystals
(Daimon, Hirao, Amano)

One of the authors (Daimon) invented a technique of using parallel-packed sheets of fluor-phlogopite as seeds with the moving crucible technique for growing single crystals of fluor-phlogopite.[10]

As seed crystals, transparent, apparently flawless sheets were cut from fluor-phlogopite crystals which had been hand-splitted from crystal aggregates produced by the internal-electrical-resistance melting method. Platinum crucibles with square sections were made by welding platinum sheets 0.03 mm. thick by an oxygen-city gas torch. Several sheets of seed crystals were put together parallel to each other in order to make a book-like packet; they were then placed on the bottom in the crucible with their basal planes parallel to the vertical axis of the crucible, as is shown in Fig. 3. The raw material of fluor-phlogopite

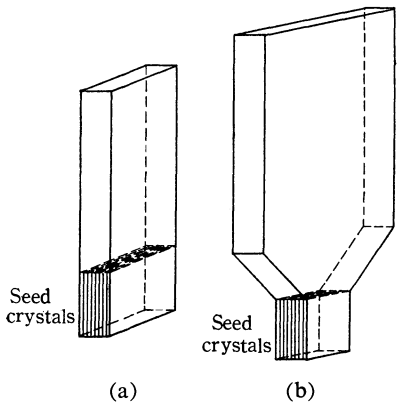



Fig. 3. Shaped crucible for the moving crucible technique with seed crystals.

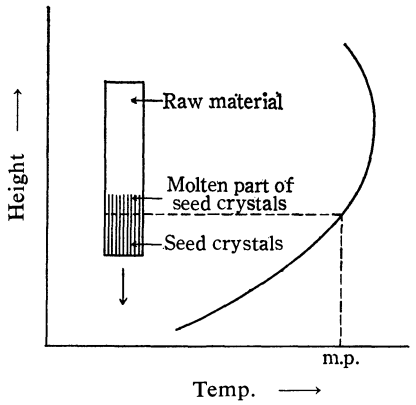



Fig. 4. Temperature gradient across the crucible in the moving crucible technique with seed crystals.

composition was put in the space over the seed crystals in the crucible, and the crucible was sealed by welding it in order to prevent the decomposition of the content. The crucible encased in a refractory sagger was placed in such a position in the furnace that when the highest-temperature part in the furnace was raised to 1400°C, the total charge of the raw material and the uppermost part of the seed crystals were to be melted. The temperature gradient across the crucible at the beginning of the descent is shown schematically in Fig. 4.

The sagger was connected with a descending device, the rate of descent being varied from 0.4 to 35 mm./hr. The temperature of the highest-temperature part in the furnace was kept at 1400°C during the descent. The temperature gradient around the crystal-melt boundary was estimated from the temperature difference between 1400°C and 1375°C, the crystallization point of fluor-phlogopite, divided by the distance between the seed crystal-grown crystal boundary and the highest temperature (1400°C) level in the furnace. The temperature gradient varied from 60 to 10°C/cm.

Powdered crystals of fluor-phlogopite, pre-melted blocks of fluor-phlogopite crystals, and a batch mixture of chemicals the composition of which corresponded to that of fluor-phlogopite or its pre-melted blocks were used as raw materials. When a batch mixture of an off composition was used, the concentration of fluor-phlogopite in the melt gradually decreased and, consequently, the crystallization temperature of fluor-phlogopite gradually decreased,[11] as the crystallization proceeded. This situation is in general not favorable for the growth of single crystals in the melt.

10) a) N. Daimon, Y. Ito and M. Hirao, *Memoir. Fac. Eng. Nagoya Univ.*, **12**, 136 (1960); b) N. Daimon, Japanese Pat. 254583 (1959); Brit. Pat. 832168 (1960); German Pat. 1088940 (1960); U. S. Pat. 3009788 (1961).

11) T. Noda, *J. Am. Ceram. Soc.*, **38**, 147 (1955).

As the result of a number of growing experiments,[12,13] the optimum temperature gradient in the growing zone was found to be about 40°C/cm. and a good, clear "booklet" of mica crystals was obtained with the rate of descent of 1.0 to 0.4 mm./hr. (Plate IV). It seems that better crystals may be grown with a smaller rate of descent. A booklet as large as 10 cm.×5 cm.×1 cm. was grown in the authors' laboratory.[14] (Plate V)

Synthetic fluor-phlogopite has been reported to have a monoclinic monolayer (1 M) structure. The optical angles (2V) of the mica reported range from 0 to 14°.[15-18] The results of the measurement of a large number of both seeds and grown crystals of fluor-phlogopite showed that the optical angles were distributed in the range from 0 to 16°, with a maximum distribution at angles less than 9 and around 15°. The optical angles of the grown crystals were mostly the same as those of their seed crystals; only a few had smaller or larger angles than those of their seeds.[13]

Weissenberg X-ray photographs of the single

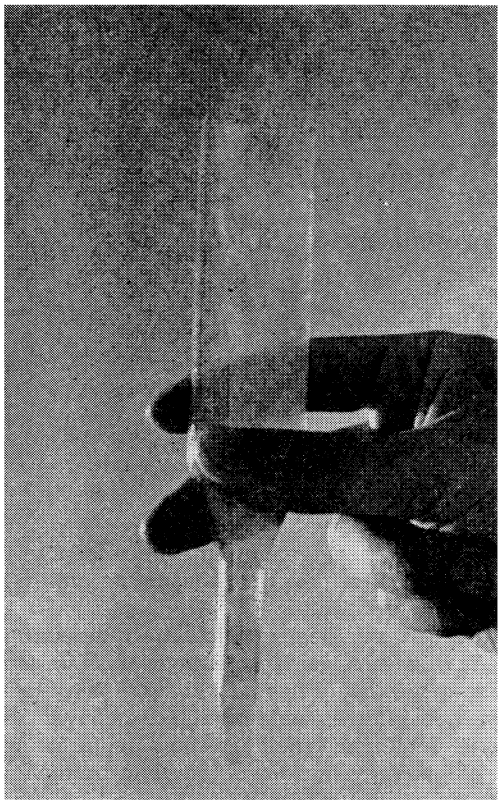


Plate IV. A booklet of fluor-phlogopite crystals grown by the moving crucible technique with seed crystals.

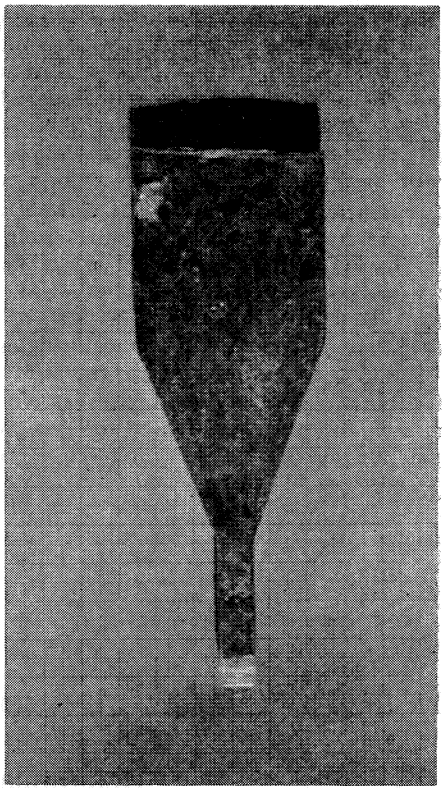
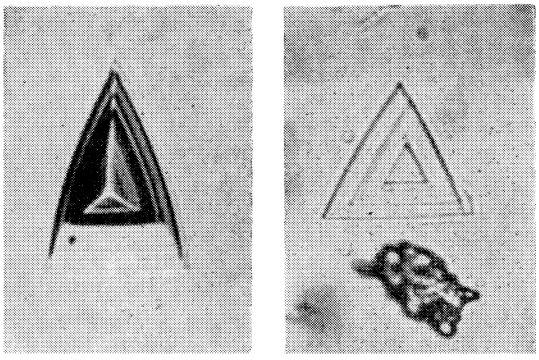


Plate V. A booklet of fluor-phlogopite grown by the moving crucible technique with seed crystals; length 14 cm., width 5 cm., thickness 1 cm.



(a) (b)

Plate VI. Etch figures of fluor-phlogopite crystals.
(a) 1 M type (b) Polysynthetic type

12) N. Daimon, Y. Ito and M. Hirao, *J. Chem. Soc. Japan, Ind. Chem. Sec.* (*Kogyo Kagaku Zasshi*), **64**, 1530 (1961).
13) N. Daimon and T. Amano, ibid., **65**, 507 (1962).
14) N. Daimon, *Electronics* (*Erekutoronikusu*), **6**, 126 (1961).
15) H. S. Yoder and H. P. Eugster, *Geoch. Cosmoch. Acta*, **6**, 157 (1954).
16) J. A. Kohn and R. A. Hatch, *Am. Mineral.*, **40**, 10 (1955).
17) J. V. Smith and H. S. Yoder, *Mineral. Mag.*, **31**, 209 (1956).
18) S. Naka and T. Noda, *J. Chem. Soc. Japan, Ind. Chem. Sec.* (*Kogyo Kagaku Zasshi*), **63**, 232 (1960).

crystal of fluor-phlogopite with an optical angle around 14° showed the 1 M symmetry, while that of the crystal with an optical angle of less than 9° gave reflection spots which could be interpreted by the polysynthetic-twin model.[19]

By etching fluor-phlogopite crystals with gaseous hydrogen fluoride or its concentrated aqueous solution, isosceles trianglar etch pits were observed on the surface of crystals with optical angles around 15° (Plate VI-a) and apparent equilateral trigons (Plate V-b) on the surface of crystals with optical angles of less than 9°, corresponding to the 1 M and polysynthetic twin-type structure respectively.[20]

The etch pit concentration of crystals grown at a smaller rate was smaller than those grown at a larger rate; for example, the etch pit concentration of crystals grown at the rate of 1.5 mm./hr. was $0.3—0.5\times10^4/cm^2$, about half that of crystals grown at the rate of 13 mm./hr. The etch pit concentration of seed crystals, which were produced by the internal-electrical-resistance melting method, was about the same as those grown at the rate of 13 mm./hr.[21]

*Department of Applied Chemistry*
*Faculty of Engineering*
*Nagoya University*
*Chikusa-ku, Nagoya*
*(T. N., M. I. & M. T.)*

*Department of Industrial Chemistry*
*Faculty of Engineering*
*Shinshu University*
*Nagano-shi, Nagano*
*(N. D., T. A. & M. H.)*

19) T. Amano and N. Daimon, ibid., **66**, 1416 (1963).
20) N. Daimon and T. Amano, ibid., **67**, 1860 (1964).
21) N. Daimon and T. Amano, ibid., **67**, 1865 (1964).

# The Spectrophotometric Determination of Anions by Solvent Extraction with Metal Chelate Cations. XIII. A New Method for the Determination of Picric Acid

By Shigehiko HAYASHI, Keiya KOTSUJI, Toshiyuki SAKURAI, Kenji KIMURA and Yuroku YAMAMOTO

(Received January 18, 1965)

Several procedures for the determination of picric acid have been published in the literature. In the well-known alkalimetric assay procedure, however, it is evident that a fictiously high value of the picric acid content is given because of the presence of lower-nitrated phenols as contaminates. Similarly, Bolliger's titration method,[1] based upon the principle that methylene blue picrate is extracted into chloroform, while methylene blue is not extractable, has been found by Baker[2] not to be universally applicable. Moreover, a titration method described by Johnson et al.,[3] in which the Koppeschaar method is applied to the procedure, is not desirable because of its experimental complexities.

Gravimetric methods using nitron[2,4,5] or 4-*n*-octyloxyphenylguanidine chloride[6] as a precipitant are too time-consuming and lack sensitivity.

Mites et al.[7] have studied the reduction of picric acid at a mercury cathode under a constant potential. Tur'yan et al.[8] have also investigated the polarographic behavior of picric acid, but their method requires the preliminary separation of some nitrophenols.

In an earlier work, Ruchhoft et al.[9] have described a spectrophotometric method of measuring the absorbance of ammonium picrate. Stöhr et al.[10] have reported that color is produced by heating picric acid with glucose in a weakly-alkaline medium.

Although it has been generally known that

1) A. Bolliger, *Analyst*, **64**, 416 (1939).
2) P. R. W. Baker, ibid., **79**, 289 (1954).
3) L. D. Johnson, W. M. McNabb and E. C. Wagner, *Anal. Chem.*, **27**, 1494 (1955).
4) M. Bush and G. Blume, *Z. angew. Chem.*, **21**, 354 (1908).
5) W. C. Cope and J. Barab, *J. Am. Chem. Soc.*, **39**, 504 (1917).
6) C. Pasini and A. Vercellone, *Z. anal. Chem.*, **143**, 172 (1954).
7) L. Meites and T. Meites, *Anal. Chem.*, **28**, 103 (1956).
8) Ya. I. Tur'yan and P. M. Zaitsev, *Zhur. Anal. Khim.*, **17**, 231 (1962); *Chem. Abstr.*, **57**, 56 (1962).
9) C. C. Ruchhoft and F. I. Norris, *Ind. Eng. Chem., Anal. Ed.*, **18**, 480 (1946).
10) R. Stöhr and F. Scheibl, *Mikrochemie ver Mikrochim. Acta*, **36/37**, 362 (1951).

picric acid can be quite well extracted into organic solvents with cationic dyes, such as methylene blue[1] and crystal violet[11], little attention has been paid to employing such solvent extraction techniques for the spectrophotometric determination of picric acid.

On the other hand, it has been found by the present authors that the 2, 2'-dipyridyl iron(II) chelate is extracted into nitrobenzene from an aqueous solution in the presence of picric acid as well as of pentachlorophenol[12] and that the color intensity of the nitrobenzene extract is proportional to the amount of picric acid.

On the basis of these facts, this work was undertaken in order to establish a method for the determination of picric acid by solvent extraction, followed by the measurement of the absorbance of the extracted picrate of the 2, 2'-dipyridyl iron(II) chelate. The proposed method has the advantage of being simpler, and the extraction is adequate to remove the interference of moderate amounts of mono- and dinitrophenols.

## Experimental

**Apparatus and Reagents.**—Unless otherwise stated, the apparatus and reagents were the same as those described in a preceding paper.[13]

**Standard Picric Acid Solution.**—A standard solution containing 1 mg. of picric acid per milliliter was prepared by dissolving purified picric acid (m. p. 120—121°C) in distilled water, as has been described by Meites et al.[7] This standard solution was then diluted to the concentration required for the experiments.

**Other Nitrophenols.**—All were purified until they had the proper constant melting points, *o*-nitrophenol by steam distillation and the others by recrystallization.

All other reagents of the analytical grade were used without further purification.

*Procedure.*—Mix a 2, 2'-dipyridyl solution ($6\times10^{-3}$ M), a ferrous ammonium sulfate solution ($1.5\times10^{-3}$ M), a sodium acetate solution (3 M) and a standard picric acid solution in the proper concentration. Adjust the pH of the solution to the required value and dilute it to 25 ml. with distilled water. To this, add 10.0 ml. of nitrobenzene and shake the solution for 5 min. After the solution has stood for 30 min., transfer the organic layer into a flask containing 1 g. of anhydrous sodium sulfate and shake it vigorously in order to make the solution transparent. Then transfer it through a folded filter paper into a 10 mm. cell. Measure the absorbance of the solution at 528 m$\mu$, using a reagent blank solution or nitrobenzene as a reference. Measure the pH of the aqueous layer after the separation.

## Results and Discussion

**The Absorption Spectrum.**—The spectral absorbance curves using nitrobenzene as a reference are shown in Fig. 1. Curve 1 is a spectrum of the extract when picric acid is absent, while curve 2 is that of the extract with picric acid. Curve 2 corresponds essentially to a spectrum of the 2, 2'-dipyridyl iron(II) chelate in an aqueous solution. The maximum absorbance is shifted from 522 m$\mu$ in an aqueous solution, and to 528 m$\mu$ in nitrobenzene. As Joshi and Bhargava[14] have shown that picric acid forms a 2:1 complex with $Cu(NH_3)_4^{2+}$, the extracted species is assumed to be a complex of 1 part 2, 2'-dipyridyl iron(II) chelate and 2 parts picric acid.

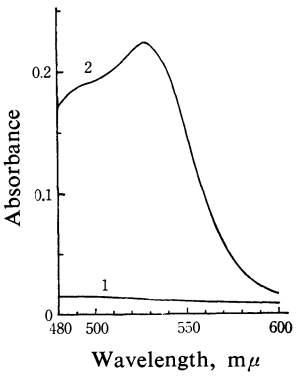



Fig 1. Absorption spectra.
Reference: Nitrobenzene, pH: 2.5
Curve 1: Spectrum of organic phase extracted from the aqueous solution (25 ml.) contained Dip. $2.4\times10^{-4}$ M, Fe(II) $6\times10^{-5}$ M, NaAc 0.24 M but picric acid is absent.
Cueve 2: Spectrum of organic phase extracted from the aqueous solution (25 ml.) containing 4 p. p. m. of picric acid in addition to the same component as that of curve 1.

**The Effect of Reagents.**—*The Effect of the 2, 2'-Dipyridyl Iron(II) Chelate Concentration.*—The formation of extractable species may be governed mainly by the concentration of the 2, 2'-dipyridyl iron(II) chelate cation.

Various amounts of ferrous ammonium sulfate and 2, 2'-dipyridyl were added to a solution containing a definite amount of picric acid, the mole ratio of dipyridyl to ferrous iron being kept at 4 to 1. In this case, because of the high stability of the chelate,[15]

11) M. Rebek and M. K. Semlitsch, *Monatsh. Chem.*, **92**, 254 (1961).
12) Y. Yamamoto, K. Kotsuji and T. Sakurai, *J. Chem. Soc. Japan, Pure Chem. Sec. (Nippon Kagaku Zasshi)*, **86**, 519 (1965).
13) Y. Yamamoto and K. Kotsuji, This Bulletin, **37**, 785 (1964).
14) D. P. Joshi and P. P. Bhargava, *J. Indian Chem. Soc.*, **40**, 19 (1963).
15) K. B. Yatsimirskii and V. P. Vasilev, "Instability Constants of Complex Compounds," Pergamon Press, Oxford (1960), p. 139.

the molar concentration of the 2, 2'-dipyridyl iron(II) chelate was assumed to be equivalent to that of the ferrous iron added. The pH of the solutions was kept at 2.5, and the extraction was then carried out. As is shown in Fig. 2, an excess of the 2, 2'-dipyridyl iron(II)

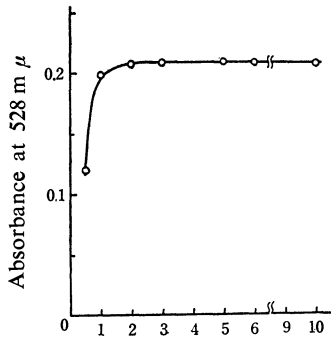



Fig. 2. Effect of 2, 2'-dipyridyl iron(II) chelate concentration.
Concentration of picric acid, 4 p. p. m.
pH of aqueous layer, 2.5
Mole ratio of Dip. to iron(II), 4
Shaking time, 5 min.
Reference, Reagent blank

chelate is necessary to obtain a quantitative recovery; therefore, the concentration of ferrous ammonium sulfate was usually kept at 6 $\times 10^{-5}$ M in this work.

*The Effect of the 2, 2'-Dipyridyl Concentration.*—While the concentrations of ferrous iron, sodium acetate and picric acid in the final solutions were kept at $6\times 10^{-5}$ M, 0.24 M and 4 p. p. m. respectively, various amounts of 2, 2'-dipyridyl were added in which the mole ratio of dipyridyl to ferrous iron was varied from 3 to 5. The experiments were then carried out in a manner similar to that described above. The variation in the mole ratio did not effect any measurable change in the absorbance of the extracts. This mole ratio was always kept at 4 to 1 in this work.

*The Effect of the Sodium Acetate Concentration.*—When the concentration of sodium acetate was low in the solution, it took much time to separate the two layers because of the formation of an emulsion. When, however, the acetate concentration was kept between 0.2 to 0.3 M, the formation of an emulsion could be prevented. Thus, the concentration of the acetate was kept at 0.24 M in this work.

**The Effect of the Shaking Time.**—Although a good recovery could be obtaind with a one-minute shaking, the shaking time was fixed at 5 min. in this work.

**The Effect of pH.**—The effect of changes in the pH on the extraction is shown in Fig. 3 (curve 1). The absorbances of the extracts are at a maximum and are uniform over the pH range of the aqueous solution from 2.2 to 11.5. In addition, it was found that the extraction behavior of dinitrophenols was similar to that of picric acid in this system, while dinitrophenols were scarcely extracted into nitrobenzene from an aqueous solution at low

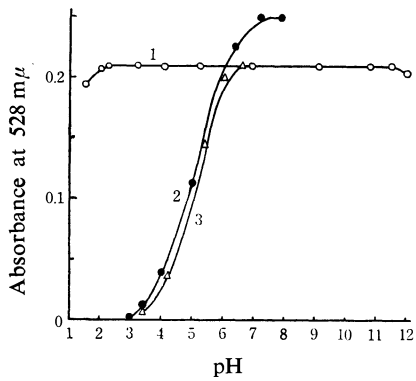



Fig. 3. Effect of pH.
The concentrations of dipyridyl, iron(II) and acetate in the final solutions were $2.4\times 10^{-4}$ M, $6\times 10^{-5}$ M and 0.24 M respectively.
Curve 1: Picric acid, 4 p. p. m.
Curve 2: 2, 4-Dinitrophenol, 5 p. p. m.
Curve 3: 2, 6-Dinitrophenol, 5 p. p. m.
Reference, Reagent Blank

pH values (pH 2—3). Thus, the pH of the solution to be extracted was adjusted to 2.5, because it appeared feasible that the interference of moderate amounts of dinitrophenols were avoided by the extraction procedure described above.

**The Stability of the Color.**—The color intensity of the extract in the transmission cell with a stopper was stable, even after 24 hr.

**The Choice of an Organic Solvent.**—The extracting solvents, such as nitrobenzene, benzene, cyclohexanone, 1, 2-dichloroethane, chloroform, carbon tetrachloride, isoamylalcohol and methylisobutylketone, were tested; of these, nitrobenzene proved to give the highest net absorbance.

The effect of the times of extraction was examined in the following manner. An aqueous solution containing a definite amount of picric acid and an optimum amount of the reagents was prepared; the extraction was then carried out with successive portions of nitrobenzene. The absorbance at 528 mμ was measured for the nitrobenzene solution obtained by each extraction. As Fig. 4 shows, the second extract has an appreciable absorbance, but the absorbance of the third extract is

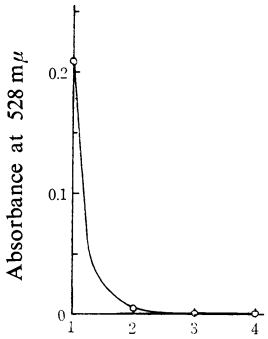



Fig. 4. Effect of times of extraction.
The concentrations of ferrous iron, dipyridyl, sodium acetate and picric acid in the aqueous solution before the first extraction were $6\times10^{-5}$ M, $2.4\times10^{-4}$ M, 0.24 M and 4 p. p. m. respectively, and the absorbance was measured for the nitrobenzene solution obtained by each extraction.
Reference, Reagent blank

almost negligible. Thus, a single extraction was used in this work.

**Calibration Curve.**—One milliliter of the 2, 2'-dipyridyl solution, 1 ml. of the ferrous ammonium sulfate solution, 2 ml. of the sodium acetate solution, and varying amounts (1—10 ml.) of the standard picric acid solution (20 p. p. m.) were mixed; the pH of this solution was then adjusted to 2.5 with a dilute sulfuric acid. The resulting solution was diluted to 25 ml. with distilled water. Then 10.0 ml. of nitrobenzene was added, and the mixture was treated by the preceding procedure. As can be seen from Fig. 5, up to 8 p. p. m. of picric acid obeys Beer's law.

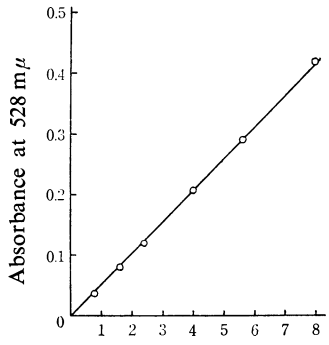



Fig. 5. Calibration curve.
Dip.: $2.4\times10^{-4}$ M
Fe(II): $6\times10^{-5}$ M
NaAc: 0.24 M
pH: 2.5
Reference, Reagent blank

Table I. Effect of nitrophenols on extraction and determination of picric acid
(4 p. p. m. of picric acid taken in each case)

| Compound | Compound concn. p. p. m. | Absorbance at 528 mμ |
|---|---|---|
| None | — | 0.209* |
| 2, 4-Dinitrophenol | 20 | 0.211 |
| 2, 4-Dinitrophenol | 40 | 0.216 |
| 2, 5-Dinitrophenol | 20 | 0.209 |
| 2, 5-Dinitrophenol | 40 | 0.210 |
| 2, 6-Dinitrophenol | 20 | 0.210 |
| 2, 6-Dinitrophenol | 40 | 0.211 |
| *o*-Nitrophenol | 40 | 0.209 |
| *o*-Nitrophenol | 100 | 0.212 |
| *m*-Nitrophenol | 40 | 0.210 |
| *m*-Nitrophenol | 100 | 0.214 |
| *p*-Nitrophenol | 40 | 0.210 |
| *p*-Nitrophenol | 100 | 0.213 |
| Phenol | 40 | 0.209 |
| Phenol | 100 | 0.212 |

pH of aqueous layer: 2.5, other variables were the same as that of the calibration curve.
* The absorbance of 4 p. p. m. of picric acid without nitrophenols.

Table II. Effect of diverse ions on extraction and determination of picric acid
(4 p. p. m. of picric acid taken in each case)

| Ion | Ion concn. p. p. m. | Absorbance at 528 mμ |
|---|---|---|
| None | — | 0.209* |
| $SO_4^{2-}$ | 3800 | 0.209 |
| $PO_4^{3-}$ | 1900 | 0.209 |
| $NO_3^-$ | 5 | 0.210 |
| $NO_3^-$ | 12 | 0.216 |
| $Cl^-$ | 700 | 0.210 |
| $Cl^-$ | 1400 | 0.214 |
| $Br^-$ | 64 | 0.209 |
| $Br^-$ | 160 | 0.215 |

* The absorbance of 4 p. p. m. of picric acid without diverse ions.

**Interferences.**—A study was made of the effects of the appropriate substances which commonly occur in picric acid. Absorbance measurements were made for the nitrobenzene extracts from solutions containing various amounts of each substance with 4 p. p. m. of picric acid. The results are given in Table I. No interference was found in concentrations as high as 40 p. p. m. for nitrophenols, except with 2, 4-dinitrophenol. Although satisfactory results were obtained in the presence of large amounts of sulfate and phosphate, a small amount of nitrate produced a positive error.

**Summary**

The solvent extraction method has been applied to the spectrophotometric determination of minute amounts of picric acid with the 2, 2'-dipyridyl iron(II) chelate. The selectivity of the procedure is largely dependent on the pH of the solution. At pH 2.5 the extraction is selective for picric acid in the presence of nitrophenols.

The authors are grateful to Miss Fumiko Shibata for her assistance in this work.

*Department of Chemistry*
*Faculty of Science*
*Hiroshima University*
*Higashisenda, Hiroshima* (*Y. Y.*)

*Faculty of Liberal Arts*
*Fukui University*
*Makinoshima, Fukui*
(*S. H., K. K., T. S. & K. K.*)

# The Peracid Oxidation of Ketones. III. The Reaction of $\alpha, \beta$-Unsaturated Ketones with Peroxybenzoic Acid*[1]

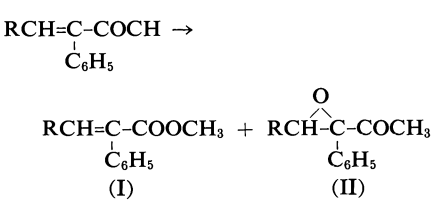
By Tai YOKOYAMA and Fujio NOHARA

(Received January 22, 1965)

In preceding papers[1] it was reported that the rate sequence of the peracid oxidation of ketones was the reverse to that of their oximation, and that the ketone peroxide was rearranged in the presence of both acid and peracid. It was concluded that the rate-determining step was the rearrangement of the addition intermediate which is formed by the nucleophilic attack of the peracid on the ketone. From the migratory aptitude in cycloalkylphenylketones,[2] it was considered that the most bulky group which is conformationally trans to the leaving carboxyl group migrates preferentially. Recently, Howthorne and his co-workers[3] reported that the rate-determining step was the acid-catalyzed decomposition of the peracid-ketone adduct and suggested that, in migration, although both electronic and steric effects were important, the electronic interpretation appeared to be the most promising.

In the present paper, the peracid oxidation of $\alpha, \beta$-unsaturated ketones will be undertaken in an attempt to provide additional information. Böeseken and his co-workers[4] studied the peroxyacetic acid oxidation of 4-phenyl-3-buten-2-one and 3-methyl-4-phenyl-3-buten-2-one; they were found to give mainly the enol acetates of phenylacetaldehyde and of phenylacetone respectively. The authors also carried out the peroxybenzoic acid oxidation of the same ketones and obtained the same products exclusively. These results show that mainly the unsaturated group rearranges. It is interesting to compare the migratory aptitude of the unsaturated group with that of the phenyl group, which has a superior migratory ability. When the peroxybenzoic acid oxidation of 1, 3-diphenyl-2-propen-1-one and 2-methyl-1, 3-diphenyl-2-propen-1-one was carried out, the analysis of the product showed phenyl migrations of 20 and 14% respectively. It is considered that the reaction proceeds through the process described in Scheme 1, that the migratory aptitude of the 1-methyl-2-phenylethenyl group is somewhat larger than that of the 2-phenylethenyl group, and that the migratory ability of the 2-phenylethenyl group is about three times that of the phenyl group.

Meanwhile, it has been reported by Wenkert and Rubin[5] that $\alpha$-phenyl-$\alpha, \beta$-unsaturated



(I) (II)

*[1] Presented at the 15th Annual Meeting of the Chemical Society of Japan, Kyoto, April, 1962.

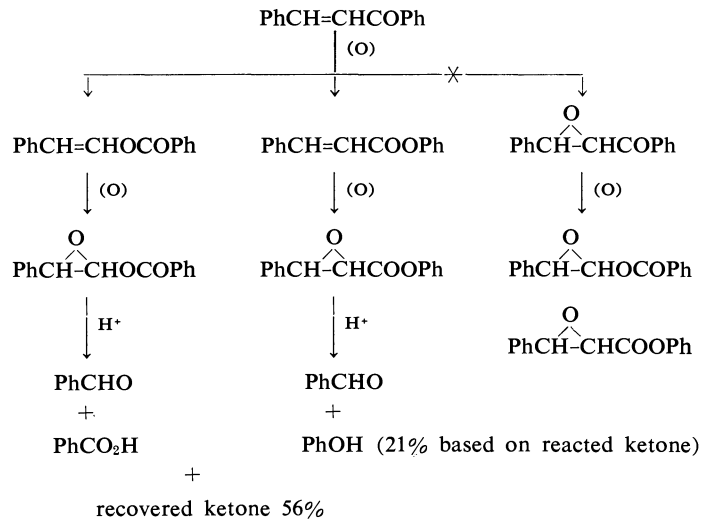
1) Y. Yukawa and T. Yokoyama, *J. Chem. Soc. Japan, Pure Chem. Sec.* (*Nippon Kagaku Zassi*), **73**, 370 (1952); *Memoirs of Inst. of Sci. and Ind. Research*, **IX**, 180 (1952); ibid., **XII**, 159 (1655).

2) Y. Yukawa and T. Yokoyama, *J. Chem. Soc. Japan, Pure Chem. Sec.* (*Nippon Kagaku Zassi*), **77**, 190 (1956); *J. Inst. Polytech., Osaka City Univ.*, Vol. 5, No. 1., *Seri. C.*, 158 (1956).

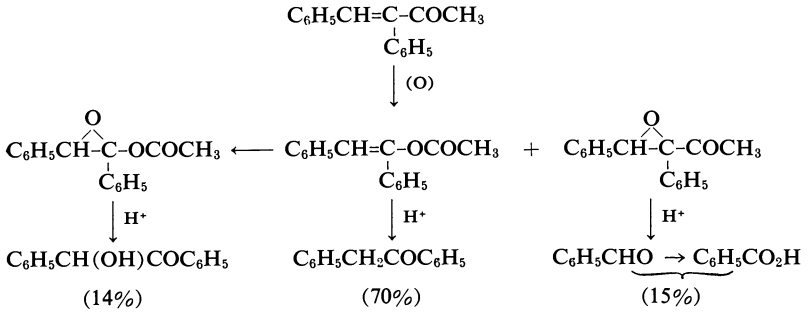
3) M. F. Howthorne, W. D. Emmons and K. S. McCallum, *J. Am. Chem. Soc.*, **80**, 6393 (1958).

4) L. Böeseken and A. L. Soeman, *Rec. trav. chim.*, **52**, 874 (1933); J. Böeseken and J. Jacobs, ibid., **55**, 786 (1936).

5) E. Wenkert and M. Rubin, *Nature*, **170**, 708 (1952); C. H. Hassall, "Organic Reaction," Vol. 9, 81 (1957).




Scheme 1




Scheme 2

ketone reacted with peroxyacetic acid to give a mixture consisting mainly of compounds I and II.

This indicates that the methyl group migrates exclusively. To confirm this point, the proxybenzoic acid oxidation of 3,4-diphenyl-3-buten-2-one was carried out. The hydrolysis of the peracid oxidation products gave desoxybenzoin as a main product, plus small amounts of bezoin, benzaldehyde and benzoic acid. On the other hand, the peroxybenzoic acid oxidation of methyl $\alpha$-phenyl cinnamate gave neither benzoin nor desoxybenzoin. These results show that the reaction proceeds through the process described in Scheme 2 and that the unsaturated group migrates exclusively.

These results indicate that the unsaturated group migrates exclusively as compared to the methyl group, that the migratory aptitude of the 2-phenylethenyl group is about three times that of the phenyl group, and that the more bulky groups migrate favorably. These results and the kinetic results*2 (the rate of the peroxybenzoic acid oxidation of 4-phenyl-3-buten-2-one was $2\times10^2$ faster than that of acetophenone) suggest that the favored transition state involves the participation of the carbon-carbon double bond.

*2 The kinetic studies are now in progress.

## Experimental*3

**Materials.**—*1, 3-Diphenyl-2-propen-1-one* was prepared from benzaldehyde and acetophenone according to the procedure of Kohler and Chadwell[6]; m. p. 56—57°C.

*2-Methyl-1, 3-diphenyl-2-propen-1-one* was prepared from benzaldehyde and propiophenone according to a procedure similar to the above one. B. p. 173—174°C/3 mmHg.

*3, 4-Diphenyl-3-buten-2-one* was prepared from benzaldehyde, phenylacetone, benzene and piperidine with a Dean and Stark distillation apparatus according to the procedure of Zimmerman, Singer and Thyagarajan.[7] B. p. 162—163°C/3 mmHg, m. p. 55—56°C.

**The Peroxybenzoic Acid Oxidation of 1, 3-Diphenyl-2-propen-1-one.**—10.69 g. (0.0514 mol.) of the ketone was added to a chloroform solution

*3 All melting points are uncorrected.

6) E. P. Kohler and H. W. Chadwell, "Organic Syntheses," Coll. Vol. I, 78 (1948).

7) H. E. Zimmerman, L. Singer and B. S. Thyagarajan, *J. Am. Chem. Soc.*, **81**, 108 (1959).

containing 0.0624 mol. of peroxybenzoic acid. The reaction mixture was swirled at intervals and then kept for 45 hr. in a thermostat maintained at 25°C. The reaction mixture was then extracted with an aqueous sodium bicarbonate solution in order to remove acids; then it was extracted with water. The aqueous phase was combined and extracted with ether. The ethereal layer was combined with the chloroform solution and dried over anhydrous sodium sulfate. After the solvent had been removed under reduced pressure, the residue was hydrolyzed by refluxing it for 10 hr. with 15% sulfuric acid and the hydrolysate was extracted with ether in a continuous extraction apparatus for 10 hr. The ethereal solution was shaken with a 15% sodium hydroxide solution and distilled under reduced pressure. The following fractions were obtained:

Fraction I: 1.64 g., b. p. 41—48°C/3 mmHg
Fraction II: 5.99 g., b. p. 159—187°C/3 mmHg
Residue: 1.62 g.

Fraction I was benzaldehyde (0.0155 mol.), identified as its 2,4-dinitrophenylhydrazone, m. p. 236 237°C; when it was mixed with an authentic sample, its melting point was not depressed.

Fraction II was the recovered ketone (0.0288 mol.); melting point and mixed melting point with an authentic sample, 54—55°C after recrystallization from ethyl acetate and petroleum ether.

To the alkaline solution dilute hydrochloric acid was added until a small amount of precipitate appeared, and then sodium bicarbonate was added. The mixture was then shaken violently and extracted with ether 10 hr. in a continuous extraction apparatus. The removal of the solvent gave 0.43 g. (0.0047 mol.) of phenol, which was then converted to tribromophenol (m. p. 87—89°C, melting point and mixed melting point with an authentic sample, 94—95°C after recrystallization from ethanol). To the aqueous solution, concentrated hydrochloric acid was added and then extracted with ether. The ethereal extracts were dried over anhydrous sodium sulfate. After the removal of the solvent, 1.89 g. (0.0155 mol.) of benzoic acid was obtained. The ratio of phenol to the reacted ketone, which corresponds to the extent of phenyl migration, was 20.8%. The repetition of the experiment showed a 21.3% phenyl migration.

The ester content in the products was analyzed by a saponification test. Thus, 0.576 g. of the peracid oxidation product mixture was stirred with 50 ml. of a 0.096 N sodium hydroxide solution for 20 hr. at room temperature, and then the excess alkali was back-titrated with 0.102 N hydrochloric acid. 11.9 ml. of the alkaline solution was consumed. It was ascertained that the starting ketone and 2,3-epoxy-1,3-diphenyl-2-propen-1-one consumed only 0.3 ml. and 0.5 ml. of the alkaline solution, respectively, under the same conditions. These results indicate that the product mixture was exclusively made up of the epoxy ester (0.0012 mol.) and the starting ketone (0.0013 mol.).

**The Peroxybenzoic Acid Oxidation of 1,3-Diphenyl-2-methyl-2-propen-1-one.**—15.81 g. (0.071 mol.) of the ketone was treated with peroxybenzoic acid (0.0763 mol.) at 25°C for 118 hr. When the reaction product was then treated as above, 1.98 g. (0.0187 mol.) of benzaldehyde and 8.66 g. (0.0389 mol.) of the recovered ketone were obtained from the neutral fraction. From the acidic fraction, 3.08 g. (0.0253 mol.) of benzoic acid and 0.49 g. (0.00477 mol.) of phenol were obtained. The yield of phenol based on the reacted ketone was 14.3%; the extent of phenyl migration was estimated to be 14.3%. The repetition of the experiment showed 13.6%.

**The Peroxybenzoic Acid Oxidation of 3,4-Diphenyl-3-buten-2-one.** — 13.380 g. (0.060 mol.) of the ketone was treated with peroxybenzoic acid (0.0712 mol.) at 27°C. From the acidic fraction of the hydrolysate, 0.854 g. (0.007 mol.) of benzoic acid was obtained. From the neutral fraction, the following fractions were obtained.

Fraction I: 1.353 g., b. p. ~110°C
Fraction II: 0.216 g., b. p. 52—57°C/6 mmHg
Fraction III: 10.110 g., b.p. 162—182°C/6 mmHg
Residue: 0.844 g.

Fraction II was benzaldehyde (0.002 mol.) identified as its 2,4-dinitrophenylhydrazone; a mixed melting point determination with an authentic sample showed no depression. From fraction III, crystals of benzoin (1.74 g.) were separated; melting point and mixed melting point with an authentic sample, 131—132°C after recrystallization from ethanol. The 2,4-Dinitrophenylhydrazone of the liquid part was fractionally crystallized from ethyl acetate and an orange yellow crystal (m. p. 198—199°C) was obtained. This was identified with the 2,4-dinitrophenylhydrazone of desoxybenzoin on the basis of a mixed melting point determination. From the mother liquor, small amounts of red crystals (m. p. 200—201°C) were obtained. A mixed melting point determination with the 2,4-dinitrophenylhydrazone of the starting ketone gave no depression. It was shown that the neutral fraction was made up of 1.74 g. (0.0082 mol.) of benzoin, 8.37 g. (0.043 mol.) of desoxybenzoin, 0.22 g. (0.002 mol.) of benzaldehyde, 0.85 g. (0.007 mol.) of benzoic acid, and a small amount of the recovered ketone.

The authors wish to express their thanks to Professor Yasuhide Yukawa of Osaka University for his helpful advice and kind encouragement. We are also grateful to Miss Shizuko Kuriyama for her helpful assistance.

*Department of Chemistry*
*Faculty of Literature and Science*
*Toyama University*
*Gofuku, Toyama*

# The Peracid Oxidation of Ketones. IV. The Peroxybonzoic Acid Oxidation of Cyclopentenone Derivatives*

By Tai YOKOYAMA and Noriaki IZUI

(Received January 22, 1965)

In the preceding paper,[1] the peracid oxidations of 4-phenyl-3-buten-2-one and its 3-substituted derivatives, and of 1, 3-diphenyl-2-propen-1-one and its 2-methyl derivative, were carried out. It was found that the unsaturated group migrated exclusively as compared to the methyl group, that the migratory aptitude of the 2-phenylethenyl group was about three times that of the phenyl group, and that the more bulky group migrated favorably.

In the present paper, the peroxybonzoic acid oxidation of the cyclic $\alpha$, $\beta$-unsaturated ketone was studied. The peracid oxidation of cyclic $\alpha$, $\beta$-unsaturated ketone has not been studied except for one example[2] of the trifluoroperoxyacetic acid oxidation of 2-cyclopentenone, which gave 2-hydroxyadipic acid. In this paper, the peroxybenzoic acid oxidation of 3-phenyl- and 2, 3-diphenyl-2-cyclopentenone was carried out. The acid obtained from the alkaline extract of the oxidation product was polymeric, and its crystalline derivatives could not be obtained. After the oxidation product had been esterified, the ester was hydrolyzed with dilute alkali at room temperature; the crystalline acid could thus be obtained in a 50% yield. This acid showed a m. p. of 115—116°C after recrystallization from petroleum ether and ethyl acetate. This acid and its *S*-benzylisothiouronium salt (m. p. 130—130.5°C) have the compositions of $C_{10}H_{10}O_3$ and $C_{18}H_{20}O_3N_2S$ respectively; the acid was found in a mixed meltlng point determination to be identical with $\beta$-benzoylpropionic acid.

From the alkaline extract of the peracid oxidation product of 2, 3-diphenyl-2-cyclopentenone, the acid A (m. p. 121.5—122°C) was obtained in a nearly quantitative yield, as based on the reacted ketone. The oxidation of A with potassium permanganate gave $\beta$-benzoylpropionic acid. The reduction of A with hydroiodic acid gave an acid with a m. p. of 134—135°C. Its methyl ester was identical in melting point and in mixed melting point with methyl $\gamma$-benzoyl-$\gamma$-phenylbutyrate prepared from desoxybenzoin, methyl acrylate and sodium ethoxide according to the procedure of Bertocchio and Dreux.[5]

It is considered that the peracid oxidation of 3-phenyl- and 2, 3-diphenyl-2-cyclopentenone proceeds through the process described in Fig. 1.

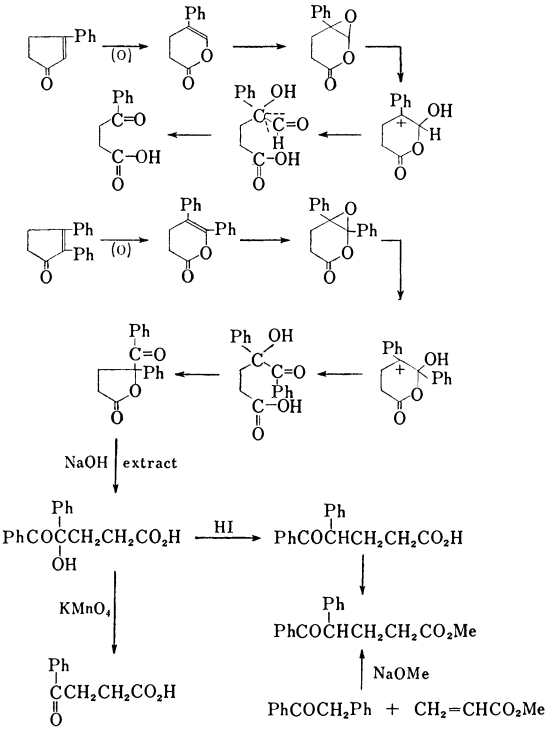



Fig. 1

These results can be explained as follows. In the favored transition state of the peracid rearrangement of cyclic $\alpha$, $\beta$-unsaturated ketone, the ring has a stable half-chair conformation, and the carbon-carbon double bond participate in the oxygen-oxygen fission (Fig. 2).

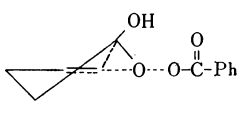



Fig. 2

* Presented at the 17th Annual Meeting of the Chemical Society of Japan, Tokyo, April, 1964.

1) T. Yokoyama and F. Nohara, This Bulletin, **38**, 1498 (1965).

2) E. E. Smissman and F. B. Block, *J. Am. Pharm. Assoc. Sci. Ed.*, Vol. XLVIII, No. 9, 526 (1959).

## Experimental**

**Materials.**—*3-Phenyl-2-cyclopentenone* was prepared from 2% sodium hydroxide and ethyl α-phenacyl acetoacetate, which in turn had been prepared from phenacyl bromide and ethyl acetoacetate according to the procedure of Borsche and Fels;[3] m. p. 82.5—83°C (recrystallized from ethyl acetate and petroleum ether).

*2,3-Diphenyl-2-cyclopentenone* was obtained from 2% sodium hydroxide and ethyl α-phenyl-α-phenacylacetoacetate, which had been prepared from ethyl α-phenacylacetoacetate, phenacyl bromide and sodium in ether according to the procedure of Borsche and Klein.[4] M. p. 94—95°C.

**The Peroxybenzoic Acid Oxidation of 3-Phenyl-2-cyclopentenone.**—a) Ten grams of the ketone was added to a chloroform solution of peroxybenzoic acid and kept for 45 hr. at 25°C. The reaction mixture was then extracted with sodium bicarbonate solution in order to remove acids, and then it was extracted with water. The aqueous layer was combined and extracted with ether. The ethereal layer was combined with the chloroform solution and extracted with a 5% sodium hydroxide solution. When the neutral solution remaining after the sodium hydroxide extraction was evaporated, 4.8 g. of a crystalline solid was obtained. This was recovered ketone (0.03 mol.); melting point and mixed melting point with an authentic sample, 82—83°C after recrystallization from ethyl acetate and petroleum ether. The basic extracts were acidified with concentrated hydrochloric acid and extracted with ether. After the removal of the ether, 3.8 g. of an acid was obtained. This was again dissolved in ether and extracted with a sodium bicarbonate solution. From the basic extracts, 2.1 g. of an acid was obtained. This acid was a brown, viscous oil; no crystalline derivatives could be obtained.

b) 25.01 g. (0.158 mol.) of the ketone was treated with peroxybenzoic acid (0.233 mol.) at 28°C. The reaction mixture was extracted with a sodium bicarbonate solution, and then with water. The aqueous phase was combined and extracted with ether. The ethereal layer was combined with the chloroform solution and dried over anhydrous sodium sulfate. After the solvent had been removed the residual oil was refluxed 8 hr. with 240 ml. of ethanol and 12 ml. of concentrated sulfuric acid. The reaction mixture was then extracted with ether. The ethereal solution was extracted with a sodium bicarbonate solution, and the ethereal layer was dried over anhydrous sodium sulfate. The solvent was then removed, and the residue was distilled under reduced pressure. The following fractions were obtained:

Fraction I: 36.689 g., b. p. 90—100°C/20 mmHg
Fraction II: 17.411 g., b. p. 132—197°C/4 mmHg
Residue: 6.90 g.

Fraction I was ethyl benzoate. Fraction II was stirred for 2.5 hr. with 100 ml. of a 10% sodium hydroxide solution at room temperature and then the hydrolysate was extracted with ether. From the ethereal layer, the recovered ketone was obtained, (2.592 g. 0.0164 mol.). The aqueous layer was acidified with concentrated hydrochloric acid and extracted with ether. After the removal of the ether, 11.003 g. of an acid was obtained, m. p. 115—116°C. The infrared spectrum of this acid showed no band in the 3000—4000 $cm^{-1}$ region originating in the hydroxyl group.

Found for this acid: C, 66.88; H, 5.53. Calcd. for $C_{10}H_{10}O_3$: C, 67.40; H, 5.66%.

*S*-Benzylisothiouronium salt of this acid, m. p. 130—130.5°C.

Found: C, 63.28; H, 5.64. Calcd. for $C_{18}H_{20}O_3N_2S$: C, 62.80; H, 5.81%.

From these results, this acid was confirmed to be β-benzoylpropionic acid; identification was established by a mixed melting point determination with an authentic sample. The yield of β-benzoylpropionic acid was 50% on the basis of the reacted ketone.

**The Peroxybenzoic Acid Oxidation of 2,3-Diphenyl-2-cyclopentenone.**—24.59 g. (0.105 mol.) of the ketone was added to 0.14 mol. of peroxybenzoic acid at 28°C for 24 hr. After the acids had been removed with sodium bicarbonate, 30.76 g. of a crude reaction product was obtained. This was dissolved in ether and extracted with a 10% sodium hydroxide solution. From the ethereal solution after the sodium hydroxide extraction, 13.016 g. (0.0556 mol.) of the recovered ketone was obtained. To the basic extracts, concentrated hydrochloric acid was added and then extracted with ether. The ethereal solution was extracted with the sodium bicarbonate solution. From the ethereal solution after the sodium bicarbonate extraction, 1.73 g. of an oil was obtained. The morpholide of this oil showed a m. p. of 188—188.5°C and showed no depression on a mixed melting point determination with the morpholide of the crude oxidation product. It was confirmed that this oil was the lactone of the acid A and that the peracid oxidation product contained this lactone.

To the sodium bicarbonate extracts, concentrated hydrochloric acid was added and then extracted with ether. After the removal of the ether, 12.088 g. of an acid A was obtained (m. p. 121.5—122°C, recrystallized from ethyl acetate and petroleum ether). This acid showed an infrared absorption band at 3450 $cm^{-1}$ (OH) and gave a benzoyl derivative, m. p. 40—41.5°C. The oxidation of A with potassium permanganate in an acidic media gave an acid, m. p. 115—116°C, a mixed melting point determination with β-benzoylpropionic acid showed no depression. To the acid A, was added an excess of 57% hydroiodic acid; this mixture was then refluxed for one hour under a constant stream of dry nitrogen. The mixture was then dissolved in ether and dried. The removal of the solvent gave an acid, m. p. 134—134.5°C; its methyl ester had a m. p. of 60—61.5°C. This methyl ester was methyl γ-benzoyl-γ-phenylbutyrate; identification was made by means of a mixed melting point determination with an authentic sample which had been prepared from methyl acrylate, desoxybenzoin and sodium ethoxide according to the procedure of

** All melting points are uncorrected.
3) W. Borsche and A. Fels, *Ber.*, **39**, 1809, 1922 (1906).
4) W. Borsche and A. Klein, ibid., **72B**, 2082 (1939).

Bertocchio and Dreux.[5] The acid A also showed no depression on admixture with an authentic specimen. The yield of A was 86% and that of the lactone of A was 12% on the basis of the reacted ketone.

The authors wish to express their deep thanks to Professor Yasuhide Yukawa of Osaka University for his helpful suggestions and kind encouragement throughout this work. The authors also wish to thank Dr. Toshikazu Ibata and Miss Kayo Kabazawa of the Institute of Science and Industrial Research of Osaka University for their measurements of infrared spectra, and Dr. Noboru Takabayashi of Toyama University for his elementary analysis. We are also grateful to Mr. Norihiko Sakamoto and Miss Chiiko Fukumura for their helpful assistance.

*Department of Chemistry*
*Faculty of Literature and Science*
*Toyama University*
*Gofuku, Toyama*

5) R. Bertocchio and J. Dreux, *Bull. soc. chim. France*, **1962**, 823.

# Oxidation of Alcohols with *t*-Butyl Chromate. III. The Oxidation of Alicyclic Alcohols*1

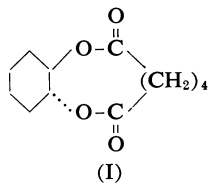
By Takayuki SUGA and Tamon MATSUURA

(Received January 26, 1965)

The previous papers[2,3] of this series have shown that the *t*-butyl chromate oxidation of the primary alcohol with an olefinic double bond or a phenyl group adjacent to a carbinol carbon gave the corresponding aldehyde, but did not produce the ester, and that the oxidation of the alcohol without these functional groups produced a mixture of the corresponding ester, aldehyde and acid. We have now attempted the *t*-butyl chromate oxidation of primary alicyclic alcohols, a secondary alicyclic alcohol and cyclic $\alpha$-glycols as an extension of our study of the oxidation of alcohols.[2,3]

**The Oxidation of Primary Alicyclic Alcohol.**—The oxidation of cyclohexylcarbinol (Exp. 1) at 1—2°C for 6 hr. with a benzene solution of *t*-butyl chromate prepared in the 1 : 1 mole ratio of the alcohol to this chromate gave the corresponding aldehyde (40% yield based on the alcohol), acid (28%) and ester, i. e., cyclohexylcarbinyl cyclohexanecarboxylate (19%). This oxidation is in contrast to that of benzyl alcohol,[3] which gave no ester but did give the corresponding aldehyde. The reason for the difference between these oxidations will be discussed in Part IV. The oxidation of myrtenol (Exp. 2) under the same conditions as in Exp. 1 produced no ester but did give the corresponding aldehyde (66%) and acid (5%). This finding agrees with those obtained in the oxidation of geraniol,[2] benzyl alcohol,[3] and *trans*-cinnamyl alcohol.[3]

**The Oxidation of Secondary Alicyclic Alcohol and Cyclic $\alpha$-Glycol.**—The oxidation of cyclohexanol at 35°C for 6 hr. with the oxidant solution prepared in the 1 : 3 mole ratio of the alcohol to the oxidant gave only the corresponding ketone (85%) (Exp. 3), but the oxidation for 48 hr. produced the cleavage product, adipic acid (7%), together with the ketone (68%) (Exp. 4). The oxidation of cyclohexane-*trans*-1, 2-diol*2 at 35°C for 3.5 hr. (Exp. 5) afforded no corresponding diketone, but it did afford adipic acid (57%) and a cyclic ester, *trans*-1, 2-adipoxycyclohexane (I) (7%).



(I)

*1 The oxidation of cyclohexanol and cyclohexane-*trans*-1, 2-diol, which composes a part of the present work, has been reported in Ref. 1 by one of the present authors. The other part was presented at the 4th Symposium on Perfume, Terpene and Essential Oil Chemistry of the Chemical Society of Japan, Sapporo, July, 1960.

1) T. Suga, *J. Chem. Soc. Japan, Pure Chem. Sec.* (*Nippon Kagaku Zasshi*), **80**, 918 (1959).

2) T. Suga, K. Kihara and T. Matsuura, This Bulletin, **38**, 893 (1959).

3) T. Suga, K. Kihara and T. Matsuura, ibid., **38**, 1141 (1965).

*2 L. P. Kuhn (Ref. 4) showed the two hydroxyl groups to be in the equatorial orientation.

4) L. P. Kuhn, *J. Am. Chem. Soc.*, **74**, 2492 (1952).

That the corresponding diketone was not obtained may be explained as being because this diketone, produced transiently, was immediately subjected to an oxidative fission to yield adipic acid. The formation of the ester (I) has not yet been reported in the oxidation of this diol; the mechanism will be discussed in Part IV. The oxidation of *p*-menthane-*trans*-3, 4-diol*[3] at 30°C for three different reaction times and with the oxidant prepared in the 1 : 1 mole ratio, as in Exps. 1 and 2, gave only the corresponding hydroxyketone (47, 60 and 63% in Exps. 6, 7 and 8 respectively). As regards the cyclic $\alpha$-glycol with a secondary and a tertiary hydroxyl group, a secondary hydroxyl group was oxidized to a ketone group, and only the corresponding hydroxyketone was formed, in contrast to the oxidation of cyclohexane-*trans*-1, 2-diol.

## Experimental

**Samples.** — Cyclohexylcarbinol was synthesized from cyclohexyl bromide and formaldehyde according to the known method[6]: b. p. 91.8°C/23.5 mmHg. Myrtenol was prepared by the oxidation of $\alpha$-pinene with selenium dioxide in a solvent of *t*-butyl alcohol according to the work[7] performed by one of the present authors: b. p. 96°C/9 mmHg. Cyclohexanol was obtained from a commercial source: b. p. 160—161°C. Cyclohexane-*trans*-1, 2-diol[8] (m. p. 103—104°C) and (+)-*p*-menthane-*trans*-3, 4-diol[5,9] (m. p. 76.5—77°C; $[\alpha]_D^{25}$ +27.5°, *c*, 1 in methanol) were prepared by the hydroxylation of cyclohexene and (+)-*p*-menth-3-ene respectively with performic acid. All the samples were purified by distillation or recrystallization just before use.

**The Oxidation, and the Treatment of a Reaction Mixture.**—A benzene solution of *t*-butyl chromate was prepared in the same manner as used in a preceding paper.[2] In Table I, the quantity of each component and the concentration of *t*-butyl chromate in this benzene solution are shown, together with the quantity of the sample alcohol and its solvent. After the oxidation was carried out under the conditions described above in a manner similar to that described in Ref. 2, the reaction mixture was treated with oxalic acid and water, as has also been shown in Ref. 2. The separated benzene solution containing a reaction product was subjected to the described examinations in each experiment. Each of the constituents of the reaction product was identified by a comparison of its infrared spectrum with that of an authentic sample and by a mixed melting point determination of a constituent or its crystalline derivatives; the yield of the constituents is shown above. Liquid-column chromatographic separation was made on a silica gel with a mixture of ethyl acetate and *n*-hexane.

**The Oxidation of Cyclohexylcarbinol (Exp. 1).** —The removal of the solvent from the separated benzene solution gave a reaction product (30.1 g.). The distillation of the reaction product gave cyclohexylaldehyde (b. p. 60—62°C/26.5 mmHg; $\nu_{aldehyde}^{liq.}$

Table I. The weights of the alcohol used and each component in the oxidant, and conditions of the oxidation

| Exp. | Sample: Alcohol[a] | Sample: $C_6H_6$ | Oxidant[b]: $CrO_3$ | Oxidant[b]: *t*-BuOH | Oxidant[b]: $C_6H_6$ | Temp. | Time |
|---|---|---|---|---|---|---|---|
| | | g. | g. | g. | g. | °C | hr. |
| 1 | Cyclohexyl-carbinol | 30.0 | 58 | 26.3 | 52.6 | 99 | 1—2 | 6 |
| 2 | Myrtenol | 7.4 | 11 | 4.9 | 9.7 | 18 | 1—2 | 6 |
| 3 | Cyclohexanol | 20.0 | 20 | 60.0 | 111.0 | 600 | 35 | 6 |
| 4 | Cyclohexanol | 25.0 | 25 | 75.0 | 139.0 | 750 | 35 | 48 |
| 5 | Cyclohexane-*trans*-1, 2-diol | 30.0 | 26 | 77.4 | 143.4 | 774 | 35 | 3.5 |
| 6 | *p*-Menthane-*trans*-3, 4-diol | 3.0 | 13 | 1.75 | 3.5 | 18 | 30 | 2.5 |
| 7 | *p*-Menthane-*trans*-3, 4-diol | 20.0 | 88 | 11.7 | 23.3 | 132 | 30 | 4.5 |
| 8 | *p*-Menthane-*trans*-3, 4-diol | 3.0 | 13 | 1.75 | 3.5 | 18 | 30 | 8.5 |

a) The concentration of the alcohol in 1000 g. of benzene is 4.5 mol. in Exps. 1 and 2, 10 mol. in Exps. 3—5, and 1.3 mol. in Exps. 6—8.

b) The concentration of *t*-butyl chromate in the benzene solution is 35% in Exps. 1 and 2, 16% in Exp. 7, and 18% in the others.

*[3] T. Suga et al. (Ref. 5) showed the two hydroxyl groups to be retained in the axial orientation.

5) T. Suga, T. Shishibori and T. Matsuura, This Bulletin, 37, 310 (1964).
6) H. Gilman and W. E. Catlin, "Organic Syntheses," Coll. Vol. I, 182 (1948).
7) T. Matsuura, Y. Tokutomi and W. Shinoda, unpublished data obtained in our laboratory.
8) A. Roebuck and H. Adkins, "Organic Syntheses," Vol. 28, 35 (1948).
9) Y.-R. Naves, *Helv. Chim. Acta*, 42, 1174 (1959).

2857, 2810, 2707, 1725, 955 $cm^{-1}$; 2,4-dinitrophenylhydrazone, m. p. 173—174°C), cyclohexanecarboxylic acid (b. p. 103—108°C/7 mmHg, m. p. 30.5—31.5°C, acid number, 436) and cyclohexylcarbinyl cyclohexanecarboxylate (b. p. 136—137°C/7 mmHg, $n_D^{25}$ 1.4727, $d_4^{25}$ 0.9763; $\nu_{ester}^{liq.}$ 1736, 1173 $cm^{-1}$); no original alcohol remained. The hydrolysis of the ester afforded cyclohexylcarbinol (its phenylurethane, m. p. 81.8—82.2°C) and cyclohexanecarboxylic acid (m. p. 30—31°C).

**The Oxidation of Myrtenol (Exp. 2).** — The separated benzene solution was extracted with a sufficient volume of a 3% sodium bicarbonate solution, which then gave myrtenic acid ($\nu^{liq.}$ a broad band of 2700—3500, 1686, 1424, 1270, 949 (COOH), 1623, 841 (trisubstd. C=C) $cm^{-1}$) on acidification. The removal of the solvent from the neutral benzene solution gave a neutral product (6.3 g.). The liquid-column chromatography of the neutral product gave myrtenal (b. p. 84—87°C/9 mmHg; $\nu_{aldehyde}^{liq.}$ 2816, 2733, 1682 $cm^{-1}$; 2,4-dinitrophenylhydrazone, m. p. 217—218°C), unchanged alcohol ($\nu_{OH}^{liq.}$ 3374, 1014 $cm^{-1}$; 3% yield), and a resinous substance (9%), probably a polymer.

**The Oxidation of Cyclohexanol (Exps. 3 and 4).** —The separated benzene solution was treated as in Exp. 2. The product (b. p. 153—155°C) obtained from the neutral benzene solution was then examined by infrared spectroscopy and chromatostrip chromatography,[10] while cyclohexanone was estimated by the 2,4-dinitrophenylhydrazine method.[11] The sodium bicarbonate extracts were combined with the aqueous solution used for hydrolyzing the residual oxidant. Adipic acid (m. p. 151—152°C) was obtained by extracting the combined solution with ether after acidification. No original alcohol remained in either experiment.

**The Oxidation of Cyclohexane-*trans*-1,2-diol (Exp. 5).**—The removal of the solvent from the separated benzene solution gave a viscous, neutral product (6.1 g.) and adipic acid (m. p. 151—152°C), which was also obtained from the aqueous solution used for hydrolyzing the residual oxidant (cf. Exps. 3 and 4). The neutral product deposited a crystalline mass (2.2 g.; m. p. 125—125.5°C; $\nu_{ester}^{KBr}$ 1733, 1271, 1155 $cm^{-1}$).

Found: C, 63.44; H, 8.29; ester number, 247.8. Calcd. for $C_{12}H_{18}O_4$: C, 63.70; H, 8.02%; ester number, 248.0.

The hydrolysis of the crystalline ester gave, quantitatively, cyclohexane-*trans*-1,2-diol (m. p. 103—104°C) and adipic acid (m. p. 151—152°C). Therefore, the ester was confirmed to be *trans*-1,2-adipoxycyclohexane (I).

No cyclohexane-1,2-dione was detected, and the other, resinous part of the neutral product looked like a polymer.

**The Oxidation of (+)-*p*-Menthane-*trans*-3,4-diol (Exps. 6—8).**—The separated benzene solution was treated in the same manner as in Exp. 2. The sodium bicarbonate extracts did not give any reaction product. The liquid-column chromatography of the reaction product obtained from the neutral benzene solution gave (−)-4-hydroxymenthone (b. p. 104—105°C/13 mmHg; $[\alpha]_D^{25}$ −96.7° (neat); $\nu^{liq.}$ 3493, 1154 (OH), 1709 (C=O), 1430 ($-CH_2-CO-$) $cm^{-1}$; 2,4-dinitrophenylhydrazone, m. p. 102.5—103°C; Found: N, 15.73. $C_{16}H_{22}O_5N_4$ requires N, 15.99%). (−)-4-Hydroxymenthone 2,4-dinitrophenylhydrazone was produced on treating the keto alcohol with a 2 N hydrochloric acid solution of 2,4-dinitrophenylhydrazine. On the other hand, the treatment of the keto alcohol with an ethanol-sulfuric acid solution of 2,4-dinitrophenylhydrazine gave (±)-*p*-menth-3-en-5-one 2,4-dinitrophenylhydrazone (m. p. 147.5—148.5°C).

## Summary

1) The *t*-butyl chromate oxidation of myrtenol gave no ester, but it did give the corresponding aldehyde as the main product, while the oxidation of cyclohexylcarbinol gave a mixture of the corresponding aldehyde, acid and ester in comparable yields.

2) A similar oxidation of cyclohexanol afforded the corresponding ketone in a high yield, while the oxidation of cyclohexane-*trans*-1,2-diol produced no corresponding diketone, but it did produce the glycol fission product and a cyclic ester such as *trans*-1,2-adipoxycyclohexane (a new compound). On the other hand, *p*-menthane-*trans*-3,4-diol yielded only the corresponding hydroxyketone in a good yield.

The authors are indebted to Messrs. Keiichi Kihara and Tsuyoshi Shishibori for their help in this research. This work was also aided by a grant from the Ministry of Education.

*Department of Chemistry*
*Faculty of Science*
*Hiroshima University*
*Hiroshima*

10) J. G. Kirchner, J. M. Miller and G. J. Keller, *Anal. Chem.*, **23**, 420 (1951); J. M. Miller and J. G. Kirchner, ibid., **25**, 1107 (1953).
11) H. A. Iddles, A. W. Low, B. D. Rosen and R. T. Hart, *Ind. Eng. Chem., Anal. Ed.*, **11**, 102 (1939).

# Cobalt(II) Complexes of Schiff Bases Derived from Salicylaldehyde and Aromatic Amines[1]

By Hiroaki NISHIKAWA and Shoichiro YAMADA

(Received January 26, 1965)

The preparation and the configuration of cobalt complexes of Schiff bases derived from salicylaldehyde and alkyl amines have been described in previous papers.[2] On the other hand, there have also been a comparatively large number of papers available about cobalt complexes of *N*-aryl-salicylideneimines.[3] As a conclusion of the previous studies, it has generally been postulated that quadri-co-ordinate cobalt(II) complexes do not exist with Schiff bases which have substituents on the ortho-carbon atom in Fig. 1. In fact, bis-(*N*-*o*-methoxyphenyl-salicylideneiminato)-cobalt(II) was synthesized, but its formation

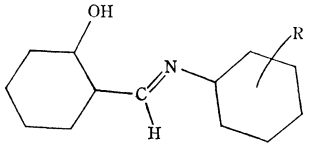



Fig. 1. *N*-Aryl-salicylideneimine.

was regarded as due to stabilization through the sexa-co-ordination attained by the additional linkage of the oxygen atoms of the methoxy groups with the cobalt(II) ion.[3] The present authors have recently succeeded in preparing several cobalt(II) complexes with Schiff bases which have substituents on the *o*-carbon atom. In the present paper the syntheses of bis(*N*-aryl-salicylideneiminato)cobalt-(II) complexes will be described, and the configurations of these complexes will be examined on the basis of the results of the preceding papers.

## Experimental

**Meterials.** — Salicylideneiminato-cobalt(II) complexes with *N*-*o*-substituted aryl groups were generally prepared in the following way. A yellow powder of $Co(sal)_2 \cdot 2H_2O$ was mixed with an excess (1.5 to 4.5 times the theoretical amount) of one of the amines to yield orange-colored paste; the notation "*sal*" denotes an anion which is formed when a molecule of salicylaldehyde loses a proton. A suitable organic solvent was boiled in another flask until the flask was filled with its vapor above the liquid phase. The paste of the mixture was then placed into the flask, and immediately the flask was closed tightly. The reaction was continued at a temperature just below the boiling point of the solvent. The period required for the reaction varied depending upon the amine used. After the reaction was over, the solution was cooled very slowly. The solution underwent oxidation when the temperature was appreciably higher than room temperature.

For the preparation of bis(*N*-*o*-tolylsalicylideneiminato)cobalt(II), $Co(sal)_2 \cdot 2H_2O$ (1.0 g.) and *o*-toluidine (3.0 g.) were used as the starting materials and ethanol (30 ml.) as a solvent. The general method described above was followed. After the flask had been closed tightly, the reaction was continued for about fifteen minutes at 70°C to 75°C; then the solution was allowed to stand until its temperature went down to room temperature. After it had been kept for a day or two at −15°C, the compound was obtained in deep-red, hexagonal plates.

Found: C, 69.9; H, 5.08; N, 5.92. Calcd. for $C_{28}H_{24}N_2O_2Co$: C, 70.2; H, 5.05; N, 5.84%.

For the preparation of bis(*N*-*o*, *m*-xylidyl-salicylideneiminato)cobalt(II), $Co(sal)_2 \cdot 2H_2O$ (1.0 g.) and *o*, *m*-xylidine (1.2 ml.) were used as the starting materials and methanol (22 ml.) as a solvent. After the flask had been closed tightly, the reaction was continued for about four hours at 60°C. Then the solution was allowed to cool slowly to −15°C. After the solution had been kept at −15°C for three days, the deep-red needles which separated out were collected.

Found: C, 70.7; H, 5.53; N, 5.86. Calcd. for $C_{30}H_{28}N_2O_2Co$: C, 71.0; H, 5.56; N, 5.52%.

For the preparation of bis(*N*-*o*, *o'*-xylidyl-salicylideneiminato)cobalt(II), $Co(sal)_2 \cdot 2H_2O$ (1.0 g.) and *o*, *o'*-xylidine (1.4 g.) were used as the starting materials and methanol (40 ml.) as a solvent. The reaction was continued for several hours at 60°C. Then the orange powder of $Co(sal)_2 \cdot 2H_2O$ was completely dissolved, giving a bright red solution. The reaction was then continued for several more hours until the red crystals started to separate out. Then the solution was cooled to 15°C, and the red crystals of the product were collected. The compound was also synthesized by the reaction of

1) A brief account has previously been published as a Short Communication. H. Nishikawa and S. Yamada, This Bulletin, **35**, 1430 (1962).

2) a) H. Nishikawa and S. Yamada, This Bulletin, **37**, 8 (1964); H. Nishikawa, S. Yamada and R. Tsuchida, *Z. Naturforsch.*, **17b**, 78 (1962); *Z. anorg. u. allgem. Chem.*, **316**, 278 (1962); S. Yamada and H. Nishikawa, This Bulletin, **36**, 755 (1963), etc. b) L. Sacconi, P. L. Orioli, P. Paoletti and M. Ciampolini, *J. Am. Chem. Soc.*, **85**, 411 (1963); L. Sacconi, M. Ciampolini, F. Maggio and F. P. Cavasino, ibid., **84**, 3246 (1962), etc.

3) B. O. West, *Nature*, **173**, 1187 (1954); *J. Chem. Soc.*, **1952**, 3115; ibid., **1960**, 4944; ibid., **1962**, 1374, etc.

theoretical amounts of cobalt(II) acetate tetrahydrate, *o*, *o'*-xylidine, salicylaldehyde and sodium hydrogencarbonate in ethanol, stirring the solution for about four hours at room temperature. Recrystallization from methanol yielded pure crystals of the product.

Found: C, 71.1; H, 5.52; N, 5.22. Calcd. for $C_{30}H_{28}N_2O_2Co$: C, 71.0; H, 5.56; N, 5.52%.

For the preparation of bis(*N*-*α*-naphthyl-salicylideneiminato)cobalt(II), $Co(sal)_2 \cdot 2H_2O$ (1.0 g.) and *α*-naphthyl amine were used as the starting materials and methanol as a solvent. After the flask had been closed tightly, the reaction was continued. As the orange powder of $Co(sal)_2 \cdot 2H_2O$ was dissolved, red crystals started to separate out. The flask was cooled very slowly to room temperature.

Found: C, 73.6; H, 4.36; N, 4.96. Calcd. for $C_{34}H_{24}N_2O_2Co$; C, 74.0; H, 4.39; N, 5.08%.

For the preparation of bis(*N*-*o*-chlorophenyl-salicylideneiminato)cobalt(II), $Co(sal)_2 \cdot 2H_2O$ (1.0 g.) and *o*-chloroaniline (3.3 g.) were used as the starting materials and ethanol (45 ml.) as a solvent. After the flask had been closed, the reaction was continued for four hours at 70°C to 75°C. The flask was cooled to room temperature, and the solution was kept at −15°C for one day, A brownish black mass was obtained. By extracting the mass with pyridine, orange-yellow crystals of $Co(O \cdot C_6H_4 \cdot CH : N \cdot o\text{-}Cl \cdot C_6H_4)_2 \cdot 2py$ were obtained.

Found: C, 63.5; H, 4.31; N, 8.51; Cl, 10.21. Calcd. for $C_{36}H_{28}N_4O_2Cl_2Co$: C, 63.7; H, 4.16; N, 8.26; Cl, 10.5%.

After the pyridine adduct had been left at 70°C in vacuo for several hours, an orange-yellow powder of bis(*N*-*o*-chlorophenyl-salicylideneiminato)cobalt-(II) was obtained.

Found: C, 60.3; H, 3.61; N, 5.22. Calcd. for $C_{26}H_{18}N_2O_2Cl_2Co$: C, 60.0; H, 3.49; N, 5.38%.

For the preparation of bis(*o*, *p*, *o'*-trichlorophenyl-salicylideneiminato)cobalt(II), a theoretical amount of potassium metal (0.8 g.) dissolved in ethanol (10 ml.) was stirred into a solution of cobalt acetate tetrahydrate (2.5 g.) and *N*-*o*, *p*, *o'*-trichlorophenyl-salicylideneimine (6.2 g.) in lukewarm ethanol (25 ml.). The vessel was then tightly closed and left to stand for a day at −15°C. The orange powder which sparated out was collected by filtration and washed with ether. The compound was soluble in chloroform and benzene.

Found: C, 47.5; H, 2.45; N, 4.15. Calcd. for $C_{26}H_{14}N_2O_2Cl_6Co$: C, 47.5; H, 2.14; N, 4.26%.

For the preparation of bis(*o*, *p*, *o'*-tribromophenyl-salicylideneiminato)cobalt(II), salicylaldehyde (4.9 g.) and tribromoaniline (13.2 g.) were refluxed for two hours in 150 ml. of amyl alcohol. Then piperidine (4.0 g.) and cobalt acetate tetrahydrate (4.9 g.) were added to the solution, and it was refluxed for about two hours. About 100 ml. of toluene was then added to the solution, and it was refluxed for about ten minutes. After the solution had been gradually evaporated at about 100°C to a volume of about 70 to 80 ml., it was cooled and allowed to stand at −15°C for a few days. The compound was obtained as an orange-red crystalline powder, which was then washed with benzene and chloroform.

Found: C, 33.8; H, 1.66; N, 3.13. Calcd. for $C_{26}H_{14}N_2O_2Br_6Co$: C, 33.6; H, 1.52; N, 3.01%.

Bis(*N*-phenyl-salicylideneiminato)cobalt(II), bis-(*N*-*m*-substituted aryl-salicylideneiminato)cobalt(II) and bis(*N*-*p*-substituted aryl-salicylideneiminato)-cobalt(II) were prepared by the method of West.[3]

All these compounds in the solid state are stable to the atmosphere.

**Measurements.**—The electronic absorption spectra of the compounds in soltuion were determined with a Beckman DU spectrophotometer in the near-infrared, visible and ultraviolet regions. Beer's law was generally obeyed in the concentration range between $10^{-3}$ and $10^{-5}$ mol./l., except for the trichlorophenyl derivative of cobalt(II). Pyridine for a solvent is purified by distillation after having been dried with potassium carbonate.

## Results and Discussion

**Bis(*N*-aryl-salicylideneiminato)cobalt(II).**—It seems to be significant that bis(*N*-*o*-substituted aryl-salicylideneiminato)cobalt(II) complexes were prepared as crystals in this work. It has generally been believed that, because of the serious strain to the tetrahedral co-ordination around the cobalt(II) ion, quadri-co-ordinate cobalt(II) complexes can not be formed with the Schiff bases which are shown as having a substituent on the ortho-carbon atom in Fig. 1. One success in preparing these compounds, however, shows that this is definitely not the case. The preparation of bis(*N*-*o*-tolyl-salicyli-

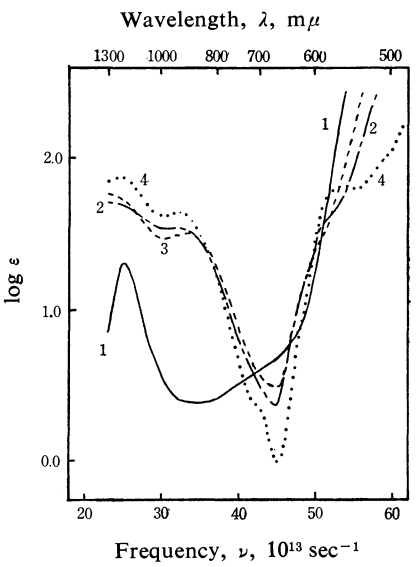



Fig. 2. Electronic absorption spectra of: 1, $Co(O \cdot C_6H_4 \cdot CH : N \cdot CH_2CH_2N : CH \cdot C_6H_4 \cdot O)$ in chloroform (——); 2, $Co(O \cdot C_6H_4 \cdot CH : N \cdot o\text{-}CH_3 \cdot C_6H_4)_2$ in benzene (—·—); 3, $Co(O \cdot C_6H_4 \cdot CH : N \cdot p\text{-}CH_3 \cdot C_6H_4)_2$ in benzene (----); 4, $Co(O \cdot C_6H_4 \cdot CH : N \cdot t\text{-}C_4H_9)_2$ in benzene (·····).

deneiminato)cobalt(II) has also been announced quite recently by West.

As has been shown previously,[2] the electronic absorption spectrum of the cobalt(II) complex depends upon the configuration of the complex, and it may be used diagnostically in the discussion of the configuration of the cobalt(II) complexes. For substituents such as methyl and chloro groups, bis(*N*-*o*-substituted aryl-salicylideneiminato)cobalt(II) complexes in non-co-ordinating solvents (Figs. 2 and 3) all show similar absorption spectra which are different from the spectra characteristic of the planar cobalt(II) complexes,[4] but which bear a close resemblance to the spectra regarded as being characteristic of quadri-co-ordinate, tetrahedral cobalt(II) complexes.[2] It may, therefore, be concluded that all these cobalt(II) complexes take a tetrahedral co-ordination around the cobalt(II) ion. The same configuration may be concluded for the trichlorophenyl- and the tribromophenyl- complexes in non-co-ordinating solvents (Fig. 3), although these complexes were not stable enough for us to determine the exact absorption spectra in solution. When a group attached to N is $\alpha$-naphthyl, the situation is similar to that with the corresponding complex with *o*-substituted phenyl for R; the comparison of the spectra, which are shown in Fig. 2, indicates that bis(*N*-$\alpha$-naphthyl-salicylideneiminato)-cobalt(II) also has a tetrahedral co-ordination.

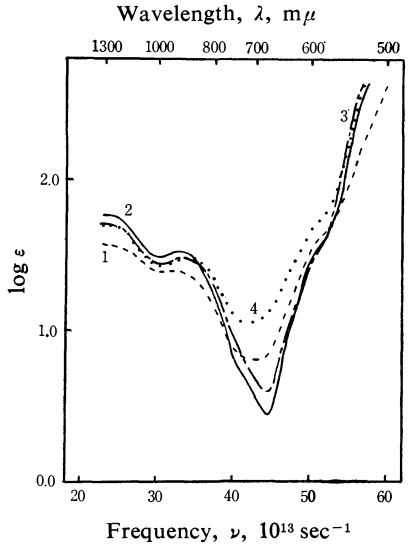



Fig. 3. Electronic absorption spectra of Co(O·$C_6H_4$·CH : N·R)$_2$ in benzene: 1, R=*o*-Cl·$C_6H_4$ (----); 2, R=*m*-$CH_3$·$C_6H_4$ (——); 3, R=*p*-Cl·$C_6H_4$ (—·—); 4, R=*m*-Cl·$C_6H_4$ (……).

4) H. Nishikawa and S. Yamada, This Bulletin, 37, 8 (1964).

Bis(*N*-*m*- and bis(*N*-*p*-substituted aryl-salicylideneiminato)cobalt(II) complexes were concluded previously from magnetic measurements to have a tetrahedral configuration.[3] The electronic absorption spectra examined in this work (Fig. 3) also support this conclusion. The absorption bands at about $24\times10^{13}$ sec$^{-1}$ may be tentatively assigned as a $^4A_2\rightarrow{}^4T_1(F)$ transition in the notation of the $T_d$ field symmetry.

It may be concluded that the co-ordination around the cobalt(II) ion in these compounds is tetrahedral, whether the substituent is on the *o*-, *m*- or *p*-position. It should be noted that the cobalt(II) complexes of the *o*,*o*'-disubstituted and of the mono-substituted ligands have a tetrahedral configuration, while the corresponding compounds of copper(II) and nickel(II) are known to take a planar co-ordination. Thus, it is again found that, in general, a tetrahedral configuration is more favorable for the cobalt(II) complex than for the copper(II) and the nickel(II) complexes, in agreement with the conclusion reached by the simple crystal field theory.

Bis(*N*-*o*-methoxyphenyl-salicylideneiminato)-cobalt(II) shows the ligand field bands at about 33 and $20\times10^{13}$ sec$^{-1}$, as may be seen in Fig. 4. These bands bear a resemblance to those of the other cobalt(II) compounds of the Schiff bases prepared in the present work. A slight difference between the *o*- and the *p*-derivatives, however, is seen in the ligand field bands of the complexes, the bands of the *o*-methoxy-derivative, for instance, being broader

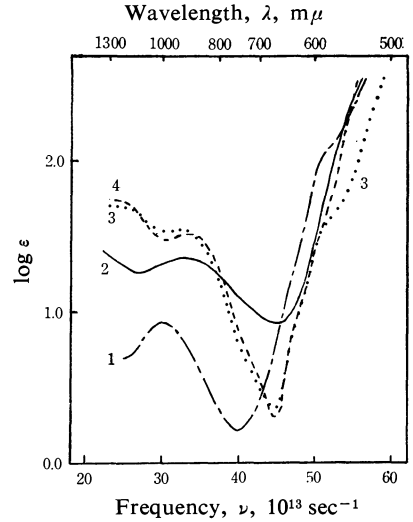



Fig. 4. Electronic absorption spectra of Co(O·$C_6H_4$·CH : N·R)$_2$: 1, R=*o*-$OCH_3$·$C_6H_4$, in pyridine (—·—); 2, R=*o*-$OCH_3$·$C_6H_4$, in chloroform (——); 3, R=*o*-$CH_3$·$C_6H_4$, in benzene (……); 4, R=*p*-$OCH_3$·$C_6H_4$, in benzene (----).

than those of bis(*N*-*p*-methoxyphenyl- as well as those of bis(*N*-*o*-tolyl-salicylideneiminato)-cobalt(II). This fact suggests that the configuration of the cobalt(II) complex with the *o*-methoxyphenyl group is somewhat anomalous compared with those of the other compounds of a similar type, in agreement with the view of West,[3] who postulated a weak interaction between the oxygen atom of the methoxy group and the central cobalt(II) ion. Since the absorption spectrum of the compound, however, is quite different from that of a typical sexa-co-ordinate cobalt(II) compound, the interaction between the oxygen atom and the cobalt(II) ion may not be very strong.

**The Configuration of Bis(*N*-aryl-salicylideneiminato)cobalt(II) Complexes in Pyridine.** — When R represents *m*- and *p*-methyl radicals, the steric condition does not greatly differ from that of the corresponding phenyl compound. The absorption spectra of these complexes (Fig. 5) clearly show that their configurations, which are all tetrahedral in non-donor solvents, are sexa-co-ordinate, octahedral in pyridine.[5] The absorption bands at about 30 and $51.5\times10^{13}$ sec$^{-1}$ may be tentatively identified as $^4T_1\rightarrow{}^4T_2$ and $^4T_1\rightarrow{}^4T_1(P)$ transitions respectively. Judging from the steric condition, it is quite difficult for the two molecules of pyridine to be co-ordinated to the central cobalt(II) ion in the bis(*N*-*o*, *o*'-xylidyl-salicylideneiminato) complex to complete a sexa-co-ordination around the cobalt(II) ion. The absorption spectra of these cobalt(II) complexes in pyridine (Fig. 6) differ definitely, though not greatly, from the spectra of the tetrahedral cobalt(II) complexes. The presence of the sexa-co-ordinate pyridine adduct of this complex may be excluded since (1) the steric factor is quite unfavorable for the octahedral configuration around the cobalt(II) ion, and (2) the absorption curve shows no clear peak in the frequency region, where the octahedral pyridine adduct is expected to absorb. It is, therefore, most likely that the quinque-co-ordinate complex with one molecule of pyridine is present in the pyridine solution. Thus, the inspection of the absorption curve seems to indicate that in the pyridine solution there is an equilibrium consisting of the quadri-co-ordinate, the tetrahedral and the quinque-co-ordinate complexes.[6] Evidence for the existence of the quinque-co-ordinate complex may be afforded by the isolation of the possibly

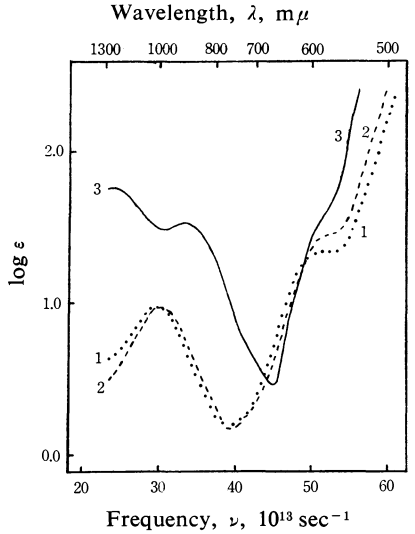



Fig. 5. Electronic absorption spectra of Co(O·$C_6H_4$·CH : N·R)$_2$: 1, R=*o*-$CH_3$·$C_6H_4$, in pyridine (·····); 2, R=*m*-$CH_3$·$C_6H_4$, in pyridine (----); 3, R=*m*-$CH_3$·$C_6H_4$, in benzene (——).

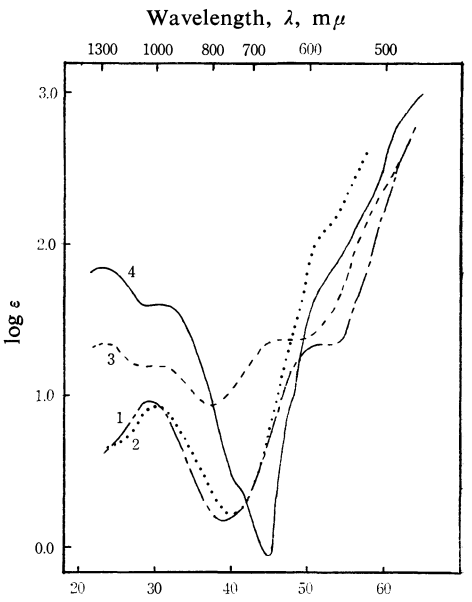



Fig. 6. Electronic absorption spectra of Co(O·$C_6H_4$·CH : N·R)$_2$: 1, R=*o*-$CH_3$·$C_6H_4$, in pyridine (——); 2, R=*o*-$OCH_3$·$C_6H_4$, in pyridine (·····); 3, R=*o*, *o*'-$(CH_3)_2$·$C_6H_3$, in pyridine (----); 4, R=*o*, *o*'-$(CH_3)_2$·$C_6H_3$, in benzene (——).

5) About the *N*-phenyl-complex of cobalt(II), the same result was reported previously; L. Sacconi, M. Ciampolini, F. Maggio and F. P. Cavasino, *J. Am. Chem. Soc.*, **84**, 3246 (1962).

6) Quite recently, Sacconi and Ciampolini (private communication) studied the equilibrium between bis-(salicylaldehyde)-*N*, *N*-disubstituted polymethylenediiminato cobalt(II) complexes and their pyridine adducts in solution, and found that, in some cases, the first step of the equilibrium was that between the original tetrahedral complex and the quinque-co-ordinate cobalt(II) adduct with one pyridine molecule.

quinque-co-ordinate adduct of the *o,o'*-dimethyl complexes with one pyridine molecule, which is quite a different color from that of the parent compound.[7] The reflection spectrum of the compound is obviously different from any of the known spectra of the tetrahedral, square-planar and octahedral complexes of cobalt(II).[7]

The adducts with two pyridine molecules were generally isolated for the corresponding cobalt(II) complexes of most *N*-aryl-substituted Schiff bases and show absorption bands which are considered to be characteristic of the octahedral complexes.

When a group attached to N is an *o*-methoxyphenyl radical, the absorption spectrum of the cobalt(II) complex in pyridine (Fig. 4) is quite different from that in chloroform; it shows the band at $30\times10^{13}\,\mathrm{sec}^{-1}$ ($\log\varepsilon$ about 0.9) which is considered to be the ligand field band of the sexa-co-ordinated cobalt(II) complex formed by the co-ordination of two molecules of pyridine.[8] It is most likely, therefore, that the weak bond originally present between the oxygen atom of the methoxy group and the cobalt(II) ion is broken in pyridine, so that the molecules of pyridine are combined with the cobalt(II) ion to yield another sexa-co-ordinate cobalt(II) complex.

7) S. Yamada and H. Nishikawa, This Bulletin, **38**, 683 (1965).

8) The electronic spectrum of the *o*-methoxyphenyl complex in chloroform in Fig. 4 is essentially the same as the spectrum of the same complex in benzene.

## Summary

Bis(*N*-aryl-salicylideneiminato)cobalt(II) complexes, including several new compounds, have been prepared and their configurations examined. These cobalt(II) compounds have been concluded, from their electronic spectra, to have a tetrahedral configuration around the cobalt(II) ion. All these compounds in pyridine have been concluded to take an octahedral configuration with the exception of the *N-o,o'*-disubstituted cobalt(II) compounds.

The authors wish to thank the Ministry of Education for financial support.

*Department of Chemistry*
*College of General Education*
*Osaka University*
*Toyonaka, Osaka*

# The Determination of Micro Amounts of Polythionates. I.* A Photometric Method for the Determination of Pentathionate by Means of Its Cyanolysis

By Tomozo KOH

(Received January 26, 1965)

Although it is important and desirable, from the viewpoints of geochemistry and medical science, to determine the amounts of polythionates in hot springs, there have been no suitable procedures for determining the polythionates in such micro amounts as are present in hot springs. Many investigations[1-15] have been made regarding the analysis of the polythionates. None of these methods, however, is suitable for micro quantities of polythionates.

Nietzel and DeSesa[16] have proposed a method for the estimation of a small amount of tetrathionate which is based on the reaction:

* Presented at the Scientific Meeting on Chemistry, Tokyo, November, 1964.

1) F. Raschig, *Z. angew. Chem.*, **33**, 260 (1920).
2) A. Kurtenacker and A. Fritsch, *Z. anorg. Chem.*, **117**, 262 (1921).
3) A. Kurtenacker, ibid., **134**, 265 (1924).
4) A. Kurtenacker and E. Goldbach, *Z. anorg. u. allgem. Chem.*, **166**, 177 (1927).
5) M. Goehring, *Z. anal. Chem.*, **128**, 6 (1948).
6) M. Goehring, U. Feldmann and W. Helbing, ibid., **129**, 346 (1949).
7) A. Kurtenacker and K. Bittner, *Z. anorg. u. allgem. Chem.*, **142**, 119 (1925).
8) R. Lang and H. Kurtenacker, *Z. anal. Chem.*, **123**, 169 (1942).
9) B. Singh and I. Ilahi, *J. Indian Chem. Soc.*, **14**, 376 (1937).
10) W. Feld, *Z. angew. Chem.*, **24**, 290 (1911).
11) R. R. Jay, *Anal. Chem.*, **25**, 288 (1953).
12) H. Ishikawa and T. Murooka, *Rikagaku Kenkyuzyo Iho* (*Sci. Rep. Res. Inst. Phys. Chem.*), **6**, 407 (1927).
13) T. Murayama, *J. Chem. Soc. Japan, Pure Chem. Sec.* (*Nippon Kagaku Zassi*), **74**, 349 (1953).
14) W. Furness and W. C. Davies, *Analyst*, **77**, 697 (1952).
15) A. Iguchi, This Bulletin, **31**, 597 (1958).
16) O. A. Nietzel and M. A. DeSesa, *Anal. Chem.*, **27**, 1839 (1955).

$$S_4O_6^{2-} + 3CN^- + H_2O = S_2O_3^{2-} + SO_4^{2-} + 2HCN + SCN^-$$

followed by the photometric determination of the thiocyanate with ferric iron. They have pointed out that their method might also be suitable for pentathionate and hexathionate, because the higher polythionates react more easily with cyanide to form thiocyanate. Recently, Urban[17] has improved the Nietzel and DeSesa's method and applied it to the evaluation of *n*, the mean number of sulfur atoms in the formula, $S_nO_6^{2-}$, for polythionate above trithionate, in order to indicate the polythionate composition of the solution.

In the present investigation, it is confirmed that pentathionate is not quantitatively converted into thiocyanate under the conditions of the Nietzel-DeSesa's and the Urban's methods,[16,17] because of the partial alkaline decomposition arising from the higher pH value caused by the addition of a sodium cyanide solution. Consequently, their methods are not suitable for the higher polythionate, pentathionate. The present author has, therefore, investigated, in greater detail, a photometric method for the determination of a small amount of pentathionate which is dependent on the reaction:

$$S_5O_6^{2-} + 4CN^- + H_2O = S_2O_3^{2-} + SO_4^{2-} + 2HCN + 2SCN^-$$

and he has established an excellent method, finding the most suitable conditions for the reaction of pentathionate with cyanide to go well to completion and to be stoichiometric.

This paper will be concerned with the results of this investigation and with the determination of pentathionate by means of its cyanolysis.

## Experimental

**Apparatus.**—The photometric measurements were made with a Hirama photometer with a 460 mμ filter (maximum transmission at 460 mμ) and with 10.0 mm. cells.

All pH measurements were made with a Toa Denpa Model HM-5A pH meter.

The desired temperatures were controlled by a Taiyo Model K-II thermostat.

The standard pentathionate solution was kept in a Hitachi Model R-104K refrigerator, the temperature of which was maintained at 5±2°C.

Potassium pentathionate was kept in a Sanyo Model HF-33 freezer in which the temperature was maintained at −8±2°C.

Volumetric flasks of 25 ml. were coated with black paint, except for small vertical areas on opposite sides near the top graduation.

17) P. J. Urban, *Z. anal. Chem.*, **180**, 110 (1961).

**Materials.**—Potassium pentathionate was prepared according to the procedure of Goehring and Feldmann.[18] The pentathionate obtained was recrystallized twice with 0.5 N hydrochloric acid and dried at room temperature for 4 days. The total water content in the pentathionate, including the water of crystallization, was estimated to be 8.2% by the Karl Fischer method. This result indicates that some moisture is adsorbed on the pentathionate besides the water of crystallization of one and a half molecules which corresponds to 7.5%.

*The Purity of the Potassium Pentathionate.*—The purity of this salt was estimated by determining the total sulfur and potassium as follows. The pentathionate was oxidized[19,20] by bromine in an alkaline medium on heating; the sulfate ion formed was determined by the usual gravimetric method.

The potassium pentathionate is decomposed into potassium sulfate by heating;

$$K_2S_5O_6 \rightarrow K_2SO_4$$

The potassium was determined by weighing[19] the potassium sulfate thus formed.

Table I. Determination of S for the potassium pentathionate* used in the present study

| Sample taken | As $K_2S_5O_6$ | Found as $BaSO_4$ | K found for $K_2S_5O_6$ | K calcd. for $K_2S_5O_6$ |
|---|---|---|---|---|
| mg. | mg. | mg. | % | % |
| 133.1 | 122.1 | 423.7 | 47.65 | 47.92 |
| 101.5 | 93.1 | 322.3 | 47.54 | |

* Total water content including the water of crystallization was 8.2%.

Table II. Determination of K for the potassium pentathionate* used in the present study

| Sample taken | As $K_2S_5O_6$ | Found as $K_2SO_4$ | S found for $K_2S_5O_6$ | S calcd. for $K_2S_5O_6$ |
|---|---|---|---|---|
| mg. | mg. | mg. | % | % |
| 310.2 | 284.8 | 148.8 | 23.44 | 23.38 |
| 215.4 | 197.7 | 103.2 | 23.43 | |

* Total water content including the water of crystallization was 8.2%.

The results listed in Tables I and II show that this potassium pentathionate is pure enough for the purpose of this study.

*The Standard Pentathionate Solution.*—182.2 mg. of the potassium pentathionate was dissolved in redistilled water and diluted to 500 ml. to give a $1.0\times10^{-3}$ M solution. This standard solution proved to be stable; even after four months, no measurable change was found by the present method when it was kept in a refrigerator at the temperature of

18) M. Goehring and U. Feldmann, *Z. anorg. Chem.*, **257**, 223 (1948).

19) F. Martin and L. Metz, *Z. anorg. u. allgem. Chem.*, **127**, 83 (1923).

20) C. Mishima, *Bull. Tokyo Inst. Tech.*, No. 1, 27 (1951).

5±2°C. This was diluted to the concentration required for the experiments.

*The Standard Thiocyanate Solution.* — The stock solution of thiocyanate was prepared by dissolving guaranteed potassium thiocyanate in redistilled water; it was then standardized acording to Volhard's method. The working thiocyanate solutions were prepared by diluting the stock solution properly; they were used as standards to ascertain whether or not the reaction of pentathionate with cyanide went to completion and was stoichiometric.

*Buffer Solutions.*—A 0.2 M sodium dihydrogenphosphate solution was mixed with a 0.2 N sodium hydroxide solution, at various ratios, in order to obtain the buffer solutions from pH 6.0 to 8.0.

*The Sodium Cyanide Solution.*—The working cyanide solutions were prepared by diluting a 1 M solution properly.

*The Ferric Nitrate - Perchloric Acid Solution.* — 303.0 g. of guaranteed ferric nitrate, $Fe(NO_3)_3 \cdot 9H_2O$, was dissolved in a small volume of redistilled water containing 217.4 ml. of concentrated perchloric acid; then the mixture was diluted to 500 ml. to give a 1.5 M ferric nitrate - 4 N perchloric acid solution.

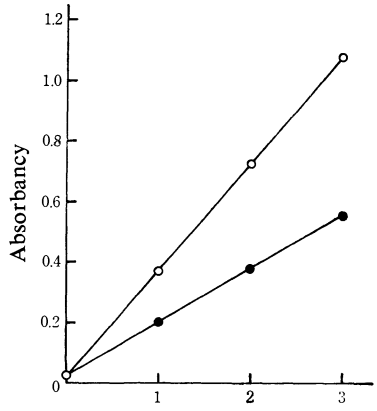
**Procedure.** — 10.0 ml. of the standard pentathionate solution is placed in a 25 ml. volumetric flask. To this solution are added first 4.0 ml. of the buffer solution of pH 7.4, and then 2.6 ml. of 0.05 M sodium cyanide; the pH of the solution is thereby brought to 8.6.

The volumetric flask is kept in the thermostat at 40°C for 30 min.; pentathionate is thereby converted into thiocyanate quantitatively. Then, 3.0 ml. of 1.5 M ferric nitrate - perchloric acid solution is added. After the flask has been filled with redistilled water to the mark, the contents are mixed well. The absorbancy of the solution of the ferric-thiocyanate complex thus formed is measured at the wavelength of 460 mμ, using distilled water as a reference.

## Results and Discussion

**Calibration Curves.** — The calibration curves shown in Figs. 1 and 2 were obtained by a procedure using standard pentathionate and thiocyanate solutions of known concentrations.

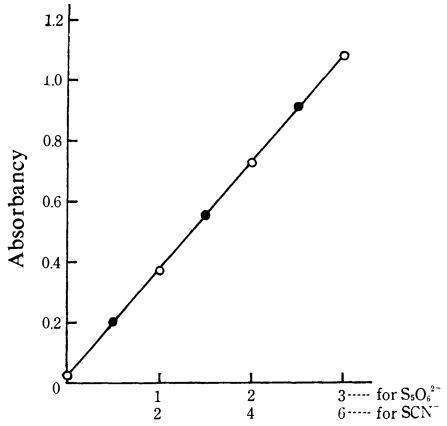
As can be seen in Figs. 1 and 2, the absorbancy and the concentration were in a good linear relationship. When one ion of pentathionate undergoes cyanolysis, two ions of thiocyanate are formed. Consequently, if the pentathionate is pure enough and if it is, moreover, converted into thiocyanate quantitatively, the sensitivity of the pentathionate should be just twice as much as that of thiocyanate. In fact, Fig. 1 shows that the calibration curve for pentathionate is twice as sensitive as that for thiocyanate. As can also be seen in Fig. 2, the calibration curve of pentathionate exactly coincides with that of thiocyanate when the scale of thiocyanate concentration is made to a half of the pentathionate




Concn. of $S_5O_6^{2-}$ and $SCN^-$, $\times 10^{-4}$ M

Fig. 1. Cablibration curves.

○ Pentathionate, ● Thiocyanate




Concn. of $S_5O_6^{2-}$ and $SCN^-$, $\times 10^{-4}$ M

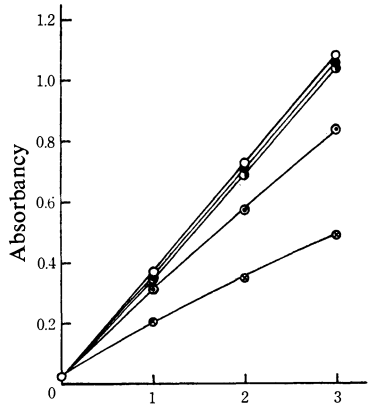
Fig. 2. Calibration curves.

○ Pentathionate, ● Thiocyanate

concentration, demonstrating that a stoichiometric reaction has occurred.

**The Effect of the Amount of Sodium Cyanide.** — In measuring the effect of the amount of sodium cyanide on the cyanolysis, from 0.5 to 6.0 ml. of a 0.05 M sodium cyanide solution was added to a standard pentathionate solution containing 4.0 ml. of the buffer solution of pH 7.4. Then, the mixiture was kept in the thermostat at 40°C for 30 min. and then treated as in the procedure described above. The experimental results are shown in Fig. 3.

When up to 2.6 ml. of a sodium cyanide solution, the more of it was added, the more the calibration curves approach the theoretical curve (see I, II and III). On the contrary, when more than 3.0 ml. was added, the more the absorbancies deviated from the theoretical value (see IV and V), except for the absorbancy of

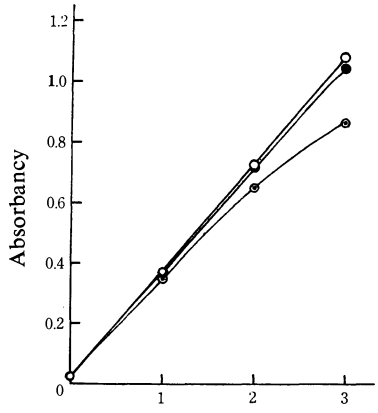



Concn. of pentathionate, $\times 10^{-4}$ M

Fig. 3. Effect of sodium cyanide amount.

Use is made of 4.0 ml. of the buffer solution of pH 7.4 in all cases.
Concn. of sodium cyanide solution: 0.05 M
Cyanolysis time: 30 min. at 40°C
⊗ 0.5 ml. (I) ⊙ 1.0 ml. (II)
○ 2.6 ml. (III) ● 4.0 ml. (IV)
◑ 6.0 ml. (V)

the reagent blank, which remains constant (see I—V). These facts led the author to the conclusion that the pH has a great effect on the cyanolysis and that pentathionate undergoes a partial alkaline decomposition as a result of the higher pH caused by the addition of the cyanide. As will be disclosed below, it was confirmed that the optimum pH for the reaction of pentathionate with cyanide is within a range from 8.0 to 8.8 under the conditions of the above procedure. A solution of from 0.5 to 4.0 ml. of 0.05 M sodium cyanide was employed; in all cases the solution is buffered over the optimum pH. The effect of the amount of sodium cyanide on the cyanolysis is shown in Fig. 4. The calibration curves with 0.5 and 1.0 ml. do not form straight lines (see I and II), indicating that the conversion of pentathionate is not quantitative because of the insufficient amounts of cyanide. Figure 4 shows that 2.0 ml. of a 0.05 M sodium cyanide solution is sufficient for the quantitative cyanolysis and that the amount of sodium cyanide does not have any effect on the method as long as it is sufficient and the pH is adjusted to an optimum value.




Concn. of pentathionate, $\times 10^{-4}$ M

Fig. 4. Effect of sodium cyanide amount.

The pH was adjusted over a range from 8.0 to 8.8 in all cases.
Cyanolysis time: 30 min. at 40°C
⊙ 0.5 ml. (I) ● 1.0 ml. (II)
○ 2.0, 2.6 and 4.0 ml. (III)

**The Effect of the pH.**—At higher pH levels, pentathionate also undergoes the alkaline decomposition, so the procedure should be carried out below a pH value of 8.8. Figure 5 shows the dependence of the rate of cyanolysis on the pH of the solutions at 20°C.

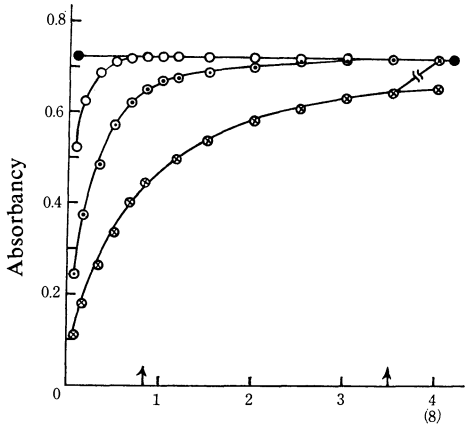



Fig. 5. Effect of pH on the rate of cyanolysis at 20°C.

● $4.0\times10^{-4}$ M $SCN^-$
○ pH 8.7 (I)
⊙ pH 8.0 (II)
⊗ pH 7.5 (III)
} $2.0\times10^{-4}$ M $S_5O_6^{2-}$

The maximum absorbancy, which means the quantitative cyanolysis, is reached in 50 min. at pH 8.7; then it remains constant (see I). The reaction at pH 7.5 does not go to completion in 4 hr.; however, it goes stoichiometrically to completion after 8 hr. (see III).

In order to accelerate the rate of cyanolysis, the reaction temperature was raised from 20°C to 40°C and 70°C. At 40°C, the reaction goes well to completion and is stoichiometric in 15 min. at pH 8.7 (see I in Fig. 6); the reactions at pH 8.0 and 7.5 go well to completion in 30 min. and 1 hr. 20 min. respectively (see II and III in Fig. 6). At 70°C, thermodecomposition occurs in addition to cyanolysis, so

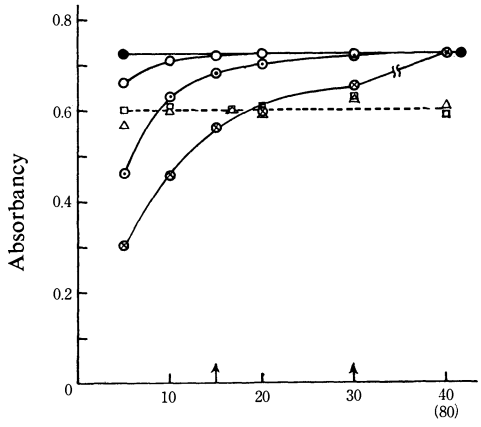



Fig. 6. Effect of pH on the rate of cyanolysis.

—●— $4.0\times10^{-4}$ M $SCN^-$
—○— pH 8.7 (I) } at 40°C
—⊙— pH 8.0 (II) } at 40°C
—⊗— pH 7.5 (III) } at 40°C
--△-- pH 8.7 (IV) } at 70°C
--□-- pH 8.0 (IV) } at 70°C
} $2.0\times10^{-4}$ M $S_5O_6^{2-}$

the reaction is not stoichiometric (see IV in Fig. 6).

In order to study the effect of the pH on the cyanolysis, the reaction of pentathionate with cyanide was carried out both at 20°C for 70 min. and at 40°C for 30 min. The results are shown in Fig. 7, where the reaction at 20°C for 70 min. gives maximum absorbancies over the pH range from 8.8 to 8.4 (see I) and that at 40°C for 30 min., over the pH range from 8.8 to 8.0 (see II). The decrease in absorbancy above the pH value of 9.0 may be attributed to the alkaline decomposition of pentathionate. The optimum pH range for the reaction with cyanide can be extended from both 8.0 and 8.4 to a lower pH value by making the cyanolysis time longer, because the rate of cyanolysis decreases with the lowering of the pH.

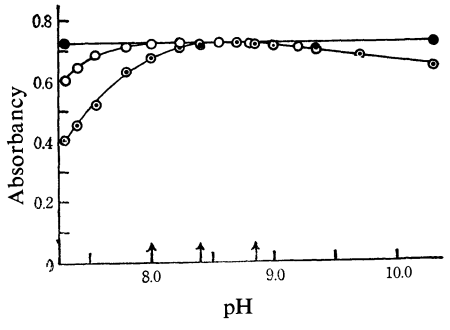



Fig. 7. Effect of pH.

● $4.0\times10^{-4}$ M $SCN^-$
○ 30 min. at 40°C (II) } $2.0\times10^{-4}$ M $S_5O_6^{2-}$
⊙ 70 min. at 70°C (I) } $2.0\times10^{-4}$ M $S_5O_6^{2-}$

**The Amount of Ferric Ntirate.** — It is well known that the phosphate interferes with the color development of ferric-thiocyanate because of the formation of a ferric-phosphate complex.

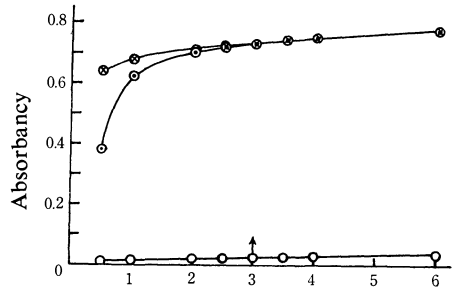



Fig. 8. Effect of ferric nitrate amount.
Use is made of 1.5 M ferric nitrate - 4 N perchloric acid solution

⊗ $4.0\times10^{-4}$ M thiocyanate without buffer solution.
⊙ $4.0\times10^{-4}$ M thiocyanate with 4.0 ml. of 0.2 M phosphate buffer solution of pH 7.4.
○ Reagent blank with 4.0 ml. of 0.2 M phosphate buffer solution of pH 7.4

Figure 8 shows how the phosphate buffer solution interferes; it also shows that 3.0 ml. of a 1.5 M ferric nitrate - perchloric acid solution is sufficient in the recommended procedure.

A similar method for the determination of micro amounts of hexathionate will be reported on in another paper. Moreover, the effect of diverse ions on the method and a detailed study regarding the stability of polythionate solutions will also be reported on.

## Summary

The photometric method for the determination of a small amount of pentathionate has been developed; it is based on the formation of thiocyanate equivalent to the pentathionate, and on the determination of thiocyanate with an excess of ferric iron.

The buffer solution is first added to the standard pentathionate solution so that the pH values of the mixture solution after the addition of the cyanide solution may be over an optimum range; othewise the pentathionate undergoes alkaline decomposition because of the higher pH value which results from the addition of the cyanide.

The conditions under which the reaction of pentathionate with cyanide is rapid and goes well to completion have been established by varying the cyanide amount, the pH, the reaction time, and the temperature.

The author wishes to express his gratitude to Professor Iwaji Iwasaki of the Tokyo Institute of Technology for his kind guidance throughout this study. He is also much indebted to Dr. Satori Utsumi and Mr. Takejiro Ozawa for their valuable advice. In addition, he wishes to express his hearty appreciation to the members of the Laboratory of Analytical Chemistry and Geochemistry, Tokyo Institute of Technology, for their helpful discussion, and to Dr. Kaname Muroi, the Central Research Laboratory of Mitsubishi Chemical Industries, Ltd., for the determination of the water content in the pentathionate by the Karl Fischer method.

*Laboratory of Analytical Chemistry*
*and Geochemistry*
*Tokyo Institute of Technology*
*Ookayama, Tokyo*

# The Oxidation-Reduction Potential of the System of Mn(II)EDTA-Mn(III)EDTA Complexes and the Stability Constant of Mn(III)EDTA Complex

By Nobuyuki TANAKA, Takashi SHIRAKASHI and Hiroshi OGINO

(Received January 26, 1965)

Recently Yoshino and his co-workers[1] have succeeded in preparation of a manganese(III) complex with ethylenediaminetetraacetate (EDTA), and its decomposition has been studied by several authors.[1-3] The thermodynamic properties of this complex, however, have not been reported yet. Meanwhile, the stability constant of the corresponding chromium(III) complex has been determined by Pecsok et al.[4] This urged us to undertake the determination of the stability constant of the manganese(III)-EDTA complex.

A preliminary investigation of the complex revealed that the change with time in the concentration of the Mn(III)EDTA complex can be followed by measuring the limiting current at the dropping mercury electrode, and the change with time in the equilibrium potential of the Mn(III)EDTA-Mn(II)EDTA system can be followed by measuring the zero-current potential at the rotated platinum electrode. In this paper, the standard oxidation-reduction potential of the Mn(III)EDTA-Mn(II)EDTA system and the stability constant of Mn(III)EDTA complex are presented.

## Theoretical

The following reactions are considered:

$$Mn^{3+} + e \rightleftharpoons Mn^{2+}, \quad E^{\circ}_{Mn} \qquad (1)$$

$$MnY^{-} + e \rightleftharpoons MnY^{2-}, \quad E^{\circ}_{MnY} \qquad (2)$$

$$Mn^{2+} + Y^{4-} \rightleftharpoons MnY^{2-}, \quad K_{Mn(II)Y} \qquad (3)$$

$$Mn^{3+} + Y^{4-} \rightleftharpoons MnY^{-}, \quad K_{Mn(III)Y} \qquad (4)$$

where $Y^{4-}$ is a quadrivalent anion of EDTA, $E^{\circ}_{Mn}$ and $E^{\circ}_{MnY}$ are the standard oxidation-reduction potentials for Eqs. 1 and 2 and $K_{Mn(II)Y}$ and $K_{Mn(III)Y}$ are the stability constants of $MnY^{2-}$ and $MnY^{-}$, respectively.

From Eqs. 1 and 2, one obtains,

$$Mn^{3+} + MnY^{2-} \rightleftharpoons Mn^{2+} + MnY^{-} \qquad (5)$$

and

$$E^{\circ}_{Mn} - E^{\circ}_{MnY} = 0.0591 \log K^{Mn(III)}_{Mn(II)}, \text{ at } 25°C \qquad (6)$$

where $K^{Mn(III)}_{Mn(II)}$ is the equilibrium constant of Eq. 5 given as,

$$K^{Mn(III)}_{Mn(II)} = \frac{[Mn^{2+}][MnY^{-}]}{[Mn^{3+}][MnY^{2-}]} = \frac{K_{Mn(III)Y}}{K_{Mn(II)Y}} \qquad (7)$$

All the activity coefficients are assumed to be unity.

From Eqs. 6 and 7,

$$\log K_{Mn(III)Y} = \frac{E^{\circ}_{Mn} - E^{\circ}_{MnY}}{0.0591} + \log K_{Mn(II)Y}, \quad \text{at } 25°C \qquad (8)$$

is obtained. In Eq. 8, the values of $E^{\circ}_{Mn}$ and $\log K_{Mn(II)Y}$ are referred from the literature. The value of $E^{\circ}_{MnY}$ is obtained in the present experiment.

The equilibrium potential $E_{t=0}$ is expressed as,

1) Y. Yoshino, A. Ouchi, Y. Tsunoda and M. Kojima, *Can. J. Chem.*, 40, 775 (1962).
2) Y. Yoshino, A. Ouchi and Y. Tsunoda, *Sci. Papers. Coll. Gen. Educ. Univ. Tokyo*, 13, 27 (1963).
3) K. A. Schroeder and R. E. Hamm. *Inorg. Chem.*, 3, 391 (1964).
4) R. L. Pecsok, L. D. Shields and W. P. Schaefer, ibid., 3, 114 (1964).

$$E_{t=0}=E^{\circ}_{MnY}-0.0591\log\frac{[Mn(II)Y]_0}{[Mn(III)Y]_0},\ \text{at } 25^{\circ}C \quad (9)$$

where $t$ means the time after the dissolution of the Mn(III)EDTA complex, and the subscript 0 represents $t=0$. The value of $E^{\circ}_{MnY}$ in Eq. 9 can be determined from the plot of $E_{t=0}$ vs. $\log([Mn(II)Y]_0/[Mn(III)Y]_0)$.

## Experimental

Mn(III)EDTA complex, $KMn(C_{10}H_{12}O_8N_2)2\cdot 5H_2O$, was prepared according to the method of Yoshino.[1] In an aqueous solution, it decreases in concentration gradually due to the thermal decomposition. Therefore, it was weighed at each measurement and dissolved into the solution. The time when the complex was dissolved was considered to be the initial time of decomposition; the dissolution was readily completed by bubbling nitrogen gas through the solution. To avoid the effect of light, the measurements were made with a brown-colored cell under the safety lamp in a dark room. A DME and a rotated platinum electrode were inserted into an electrolysis cell; the former was connected to a Yanagimoto Galvarecorder Model GR-103 and the latter to a potentiometer to follow the change in the limiting current and the equilibrium potential as a function of time, respectively. The limiting current was measured at −0.5 V. vs. SCE. The pH of the solution was adjusted to be 4.63±0.03 with sodium acetate-acetic acid buffer and the ionic strength, to be 0.2 with potassium chloride.

## Results and Discussion

The measurements were made with the solutions given in Table I at 25.0±0.1°C. In Fig. 1, the equilibrium potentials at time $t$, $E_{t=t}$, measured with the rotated platinum electrode were plotted against time $t$. Since the equilibrium potentials at $t=0$, $E_{t=0}$, are not accurately determined from Fig. 1, they were obtained by the following procedure.

Table I. Concentrations of Mn(II)EDTA and Mn(III)EDTA complexes in the solutions*

| Expt. No. | Concn. of Mn(II)Y mM | Concn. of Mn(III)Y** mM | pH |
|---|---|---|---|
| 1 | $0.101_0$ | $1.02_8$ | $4.6_4$ |
| 2 | $0.252_5$ | $1.00_2$ | $4.6_3$ |
| 3 | $0.505_0$ | $1.00_6$ | $4.6_5$ |
| 4 | $1.01_0$ | $1.00_3$ | $4.6_1$ |
| 5 | $1.76_8$ | $0.992_5$ | $4.6_6$ |
| 6 | $5.05_0$ | $0.988_8$ | $4.6_0$ |
| 7 | $10.1_0$ | $0.984_1$ | $4.6_0$ |

* Containing 0.05 M sodium acetate-acetic acid buffer and about 1 mM uncomplexed ethylenediaminetetraacetate, $\mu=0.2$ (KCl).
** Approximately 21 mg. of the complex were dissolved in 50 ml. of solution.

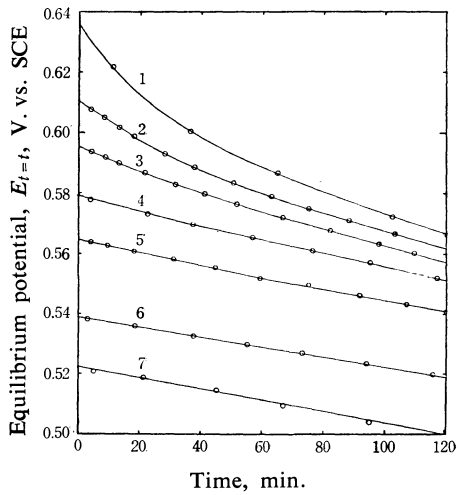



Fig. 1. $E_{t=t}$ as a function of time. Figures on the curves indicate experimental numbers given in Table I.

It was assumed that the decomposition product would have the same oxidation potential as the Mn(II)EDTA complex, and consequently, Eq. 9′ was derived from Eq. 9.

$$E_{t=t}=E^{\circ}_{MnY}-0.0591\times\log\frac{[Mn(II)Y]_0+[Mn(III)Y]_0-[Mn(III)Y]_t}{[Mn(III)Y]_t} \quad (9')$$

where the subscript $t$ means $t=t$. In Eq. 9′ the value of $[Mn(III)Y]_t$ was determined from the limiting current obtained with the DME at −0.5 V. vs. SCE; the limiting current of the Mn(III)EDTA complex was proved to be diffusion-controlled.* The values of $E_{t=t}$ were plotted against $\log\{([Mn(II)Y]_0+[Mn(III)Y]_0-[Mn(III)Y]_t)/[Mn(III)Y]_t\}$. Linear plots were obtained, and the more accurate values were determined for the equilibrium potential $E_{t=0}$ by the extrapolation of those plots to the points where the logarithmic terms equal to the values of $\log([Mn(II)Y]_0/[Mn(III)Y]_0)$.

According to Eq. 9, the values of $E_{t=0}$ determined by the above procedure were plotted against $\log([Mn(II)Y]_0/[Mn(III)Y]_0)$ which was calculated from Table I. Since this plot was very linear and its slope was found to be 57.2 mV., which was close to 59 mV. of the theoretical value, the above assumption and the determination of $E_{t=0}$ by the above procedure were considered to be valid and correct. From Fig. 2, the value of $E^{\circ}_{MnY}$ was determined to be $0.57_9$ V. vs. SCE at the point of

* The datails will be published elsewhere.

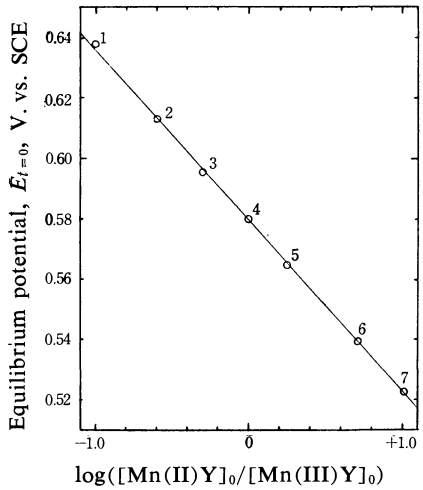



Fig. 2. Relation between equilibrium potential $E_{t=0}$ and log([Mn(II)Y]$_0$/[Mn(III)Y]$_0$) in Eq. 9. Figures on the plot indicate experimental numbers given in Table I.

log([Mn(II)Y]$_0$/[Mn(III)Y]$_0$)=0. Introducing into Eq. 8 the values of $E^\circ_{Mn}=1.49$ V. vs. NHE,[5] log $K_{Mn(II)Y}=13.64$[6] and $E^\circ_{MnY}=0.57_9$ V. vs. SCE (i. e. $0.82_3$ V. vs. NHE), the value of log $K_{Mn(III)Y}$ was calculated to be 24.9. As $E^\circ_{Mn}$ and $E^\circ_{MnY}$ are not determined under the identical condition, however, the value of the log $K_{Mn(III)Y}$ may involve a somewhat minor error. The logarithmic stability constants of EDTA complexes of some transition metals are given in Table II. The value of log $K_{Mn(III)Y}$ seems to be appropriate in comparison with those of other metals.

Table II. Logarithmic stability constants of EDTA complexes of some transition metals

| Metal | Cr | Mn | Fe | Co |
|---|---|---|---|---|
| log $K_{M(II)Y}$ | 13.6[4] | 13.64[6] | 14.33[7] | 15.71[6] |
| log $K_{M(III)Y}$ | 23.40[4] | 24.9 | 25.1[7] | 40.6[8] |

## Summary

The standard oxidation-reduction potential of the system of Mn(II)EDTA-Mn(III)EDTA complexes has been determined to be $E^\circ_{MnY}=0.57_9$ V. vs. SCE from the potentiometric measurement with the rotated platinum electrode. From this value the logarithmic stability constant of the Mn(III)EDTA complex (log $K_{Mn(III)Y}$) has been calculated to be 24.9 at 25.0°C and $\mu=0.2$.

The authors wish to thank the Ministry of Education for the financial support granted for this research.

*Department of Chemistry*
*Faculty of Science*
*Tohoku University*
*Katahira-cho, Sendai*

5) K. J. Vetter and G. Manecke, *Z. phys. Chem.*, **195**, 270 (1950).
6) H. Ogino, This Bulletin, **38**, 771 (1965).
7) G. Schwarzenbach and J. Heller, *Helv. Chim. Acta*, **34**, 576 (1951).
8) N. Tanaka and H. Ogino, This Bulletin, **38**, 1054 (1965).

# Vinyl Polymerization. CXVI.[1] The Effects of Several Sulfides and Oxides on Radical Polymerization

By Kazuichi TSUDA, Shigeru KOBAYASHI and Takayuki OTSU

(Received January 29, 1965)

It is known that some aliphatic disulfides can act as the initiator in radical polymerization.[2,3] Many studies have been made of the reaction and of the mechanism of the radical decomposition of these sulfides. Tobolsky[3] and Otsu et al.,[4] for example, investigated the polymerization of styrene or methyl methacrylate initiated by tetraalkylthiuramdisulfides. On the other hand, little progress has been made in the field of aromatic disulfide, although Pierson[5] and Otsu[6] used some aromatic disulfides, including diphenyl disulfide, as

1) Part CXV: T. Nakata, Y. Kinoshita, T. Otsu and M. Imoto, *J. Chem. Soc. Japan, Ind. Chem. Sec.* (*Kogyo Kagaku Zasshi*), **68**, 864 (1965).
2) R. J. Kern, *J. Am. Chem. Soc.*, **77**, 1382 (1955).
3) T. E. Ferington and A. V. Tobolsky, ibid., **77**, 4510 (1955).
4) T. Otsu, K. Nayatani, I. Muto and M. Imai, *Makromol. Chem.*, **27**, 142 (1958).
5) R. M. Pierson, A. J. Constanza and A. H. Weinstein, *J. Polymer Sci.*, **17**, 221 (1955).
6) T. Otsu, ibid., **21**, 559 (1956).

initiators and chain transfer agents of radical polymerization.

The present paper will deal with the polymerization of styrene and methyl methacrylate in the presence of aromatic sulfide or oxide. Some sulfides and oxides of a similar structure were employed in order to see (1) how these compounds act as initiators or chain transfer agents in radical polymerization, and (2) how the differences in structure affect on the radical polymerization.

The compounds used here are:

1) Sulfides: diphenyl sulfide (DPS), diphenyl disulfide (DPDS), dibenzyl sulfide (DBS), and dibenzyl disulfide (DBDS).

2) Oxides: diphenyl ether (DPE), and dibenzyl ether (DBE).

## Experimental

**Preparation and Purification of Materials.**—*Diphenyl Sulfide (DPS).*—Hartman's method[7] was adopted in preparing DPS, and the product obtained was purified by distillation. B. p. 160—161°C/23 mmHg (Found: C, 77.37; H, 5.47; S, 17.39. Calcd. for $C_{12}H_{10}S$: C, 77.37; H, 5.41; S, 17.22%).

*Diphenyl Disulfide (DPDS).*—This sulfide was obtained by the oxidation of thiophenol with iodine in ethanol. The crude product was recrystallized from dichloroethane. M. p. 58.8—59.0°C (Found: C, 66.33; H, 4.59; S, 29.21. Calcd. for $C_{12}H_{10}S_2$: C, 66.01; H, 4.62; S, 29.37%).

*Dibenzyl Sulfide (DBS).*—This was prepared by Seriner's process,[8] and the resulting DBS was purified by recrystallization. M. p. 47.5—48.0°C (lit.[8] 49.0°C) (Found: C, 78.43; H, 6.60; S, 14.85. Calcd. for $C_{14}H_{14}S$: C, 78.45; H, 6.59; S, 14.96%).

*Dibenzyl Disulfide (DBDS).*—Frank's process[9] was adopted for the preparation of this sulfide, and the product was recrystallized from dichloroethane. M. p. 69.0—69.5°C (lit.[9] 69—70°C) (Found: C, 67.96; H, 5.72; S, 25.99. Calcd. for $C_{14}H_{14}S_2$: C, 68.25; H, 5.73; S, 26.03%).

*Oxides.*—Commercial diphenyl ether was purified by distillation and recrystallization, while dibenzyl ether was purified by distillation alone.

*The Purification of the Other Reagents.*—Monomers were purified by the standard methods. Azobisisobutyronitrile (AIBN) was recrystallized from alcohol. M. p. 102.0—102.5°C.

**Polymerization.** — Bulk polymerization by the glass-tube method was employed. Given amounts of the monomer and of sulfide or oxide were charged into a tube and evacuated by the usual method. Thermal polymerizations were carried out at 60°C under shaking. During the polymerization, the outside light was completely excluded. Photo-polymerizations were made at room temperature by applying the ultraviolet rays from a mercury lamp. The conversion of both cases was controlled below 10%. The rate of polymerization was decided by the weight of the polymer obtained after it had been put into a quantity of methanol, let pass through glass filters, and dry.

**The Determination of Degree of Polymerization and the Chain Transfer Constants.**—The polymer obtained was precipitated again from a benzene solution by pouring it into methanol. The intrinsic viscosity $[\eta]$ was determined in benzene at 30°C by using Ubbelohde's viscometer. The number-average degree of polymerization ($\bar{P}_n$) was calculated by formulas 1 and 2:

For polystyrene[10] $\log \bar{P}_n = 3.205 + 1.37 \log[\eta]$ (1)

For polyMMA[11] $\log \bar{P}_n = 3.420 + 1.13 \log[\eta]$ (2)

The chain transfer constants ($C$) to sulfides or oxides were determined by Mayo's formula 3:

$$\frac{1}{\bar{P}_n} = \frac{1}{\bar{P}_0} + C\frac{[S]}{[M]} \qquad (3)$$

where [S] and [M] are the initial concentrations of the chain transfer agent and the monomer respectively.

## Results

**The Results of Thermal Polymerization.**—The results of thermal polymerization conducted at 60°C in the presence of sulfides or oxides are shown in Table I.

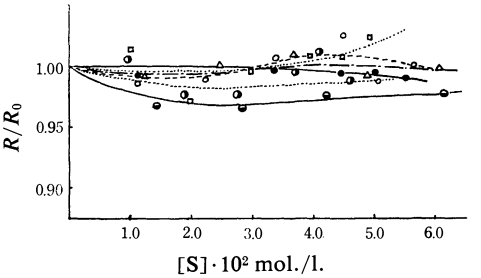



Fig. 1. The effect of sulfides or oxides on styrene polymerization.
--○-- DBS —△— DBE —◒— DPE
…□… DBDS —●— DPS …◑… DPDS

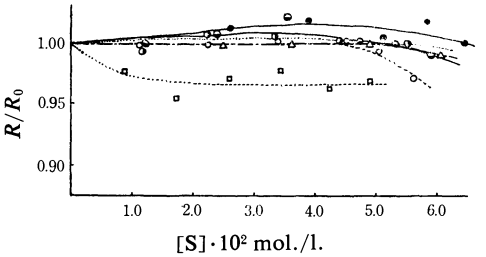



Fig. 2. The effect of sulfides or oxides on MMA polymerization.
Marks are the same as in Fig. 1.

7) W. W. Hartman, L. A. Smith and J. B. Dickey, "Organic Syntheses," Coll. Vol. 2, 242 (1948).
8) R. L. Seriner, H. C. Struck and W. J. Jopison, *J. Am. Chem. Soc.*, **52**, 2066 (1930).
9) R. L. Frank and J. R. Blegen, "Organic Syntheses," Coll. Vol. 3, 116 (1955).
10) F. R. Mayo, R. A. Gregg and M. S. Mathieson, *J. Am. Chem. Soc.*, **73**, 1691 (1951).
11) B. Baysal and A. V. Tobolsky, *J. Polymer Sci.*, **9**, 171 (1952).

TABLE I. THE RESULTS OF THERMAL POLYMERIZATION IN THE PRESENCE OF SULFIDES AND OXIDES AT 60°C

| Initiator | Styrene | | | MMA | | |
|---|---|---|---|---|---|---|
| | $[I]\cdot10^2$ mol./l. | Time min. | Yield % | $[I]\cdot10^2$ mol./l. | Time min. | Yield % |
| DPS | 1.16 | 730 | 1.64 | 1.10 | 480 | 1.83 |
| | 4.64 | 730 | 1.46 | 4.40 | 480 | 1.75 |
| | 6.96 | 730 | 1.25 | 6.59 | 480 | 1.53 |
| | 0 | 730 | 1.14 | 0 | 480 | 1.07 |
| DPE | 1.18 | 480 | 0.26 | 1.17 | 330 | 1.04 |
| | 5.90 | 480 | 0.26 | 7.02 | 330 | 0.95 |
| | 0 | 480 | 0.32 | 0 | 330 | 1.36 |
| DBS | 2.24 | 360 | 0.62 | 2.24 | 360 | 0.65 |
| | 5.60 | 360 | 0.84 | 5.60 | 360 | 0.49 |
| | 0 | 360 | 0.57 | 0 | 360 | 0.65 |
| DBDS | 2.45 | 360 | 0.65 | | | |
| | 4.91 | 360 | 0.66 | | | |
| | 0 | 360 | 0.53 | | | |
| DBE | 1.21 | 390 | 0.67 | 1.21 | 240 | 0.42 |
| | 6.05 | 390 | 0.89 | 6.05 | 240 | 0.89 |
| | 0 | 390 | 0.59 | 0 | 240 | 0.50 |

As may be easily seen from Table I, the concentration of the sulfides or oxides used does not have much effect on the rate of polymerization. As compared with the result in the absence of these compounds, they may safely be said to show little ability either to initiate or to retard.

Figures 1 and 2 show the effect of sulfides or oxides on the polymerizations of styrene and MMA, when AIBN was empolyed as the initiator in the presence and absence of sulfides or oxides.

It may be noted from Figs. 1 and 2 that sulfides or oxides have little effect on the reterdation or acceleration of the polymerization. Thus, the results shown here are much the same as those obtained when sulfides or oxides were employed in thermal polymerization. In order to determine the chain transfer constants to the sulfides or oxides, $1/\overline{P_n}$ was plotted against [S]/[M] according to Mayo's formula 3 as Figs. 3 and 4 show. The linear relationships were observed, but their intercepts did not converge at one point in all cases. The reason for this is not clear at the present time.

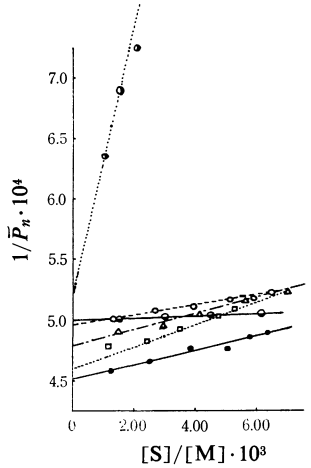



Fig. 3. Mayo's plott on styrene polymerization.
Marks are the same as in Fig. 1.

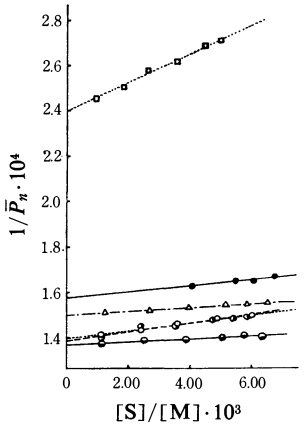



Fig. 4. Mayo's plott on MMA polymerization.
Marks are the same as in Fig. 1.

The apparent chain transfer constants to the sulfides or oxides calculated in terms of the slopes of the lines in Figs. 3 and 4 are given in Table II.

**The Results of Photo-polymerization.**—The results of the photo-polymerization where sulfides and oxides were used as photo-sensitizers are given in Figs. 5 and 6. Figures 7 and 8 show the results of photo-polymerizations in the presence of AIBN and sulfides or oxides.

TABLE II. APPARENT CHAIN TRANSFER CONSTANTS ($C \cdot 10^3$) IN THE POLYMERIZATION OF STYRENE AND MMA AT 60°C
[AIBN] $= 2.0 \times 10^{-3}$

| Sulfides or oxides | DPS | DPE | DBS | DBDS | DBE | DPDS |
|---|---|---|---|---|---|---|
| Styrene | 5.48 | 0.786 | 3.35 | 8.78 | 6.24 | 10.3 |
| MMA | 1.32 | 0.913 | 1.54 | 6.27 | 0.80 | 1.76 |

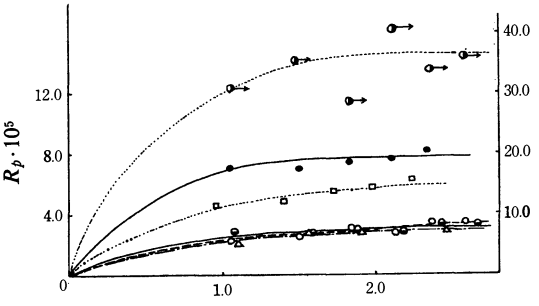



Fig. 5. Photo-polymerization of styrene using sulfides and oxides as photo-sensitizers.
Marks are the same as in Fig. 1.

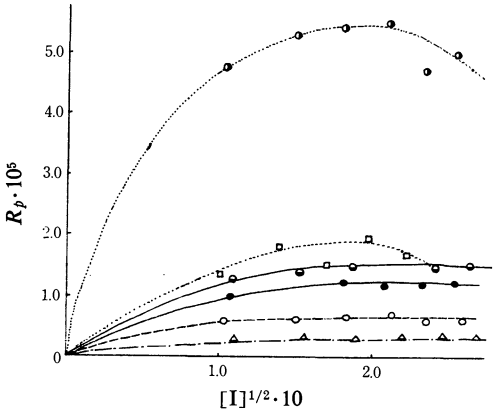



Fig. 6. Photo-polymerization of MMA using sulfides and oxides as photo-sensitizers.
Marks are the same as in Fig. 1.

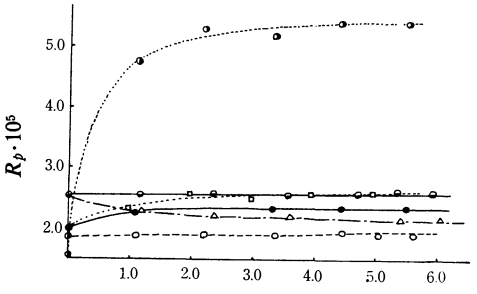



Fig. 7. The effect of sulfides or oxides on photo-polymerization of styrene.
[AIBN] $= 2.0 \times 10^{-3}$ mol./l.
Marks are the same as in Fig. 1.

In all these cases, it may be noted that none of the sulfides or oxides except DPDS affect

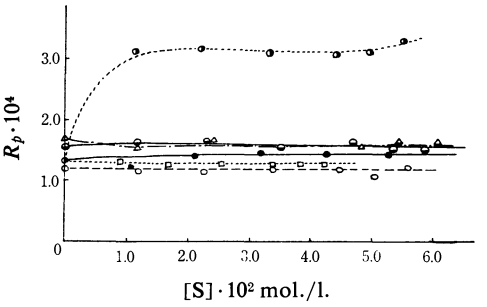



Fig. 8. The effect of sulfides or oxides on photo-polymerization of MMA.
[AIBN] $= 2.0 \times 10^{-3}$ mol./l.
Marks are the same as in Fig. 1.

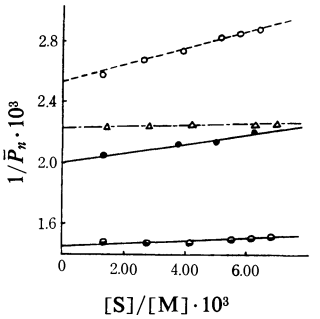



Fig. 9. Mayo's plott on styrene polymerization. (Initiator AIBN)
Marks are the same as in Fig. 1.

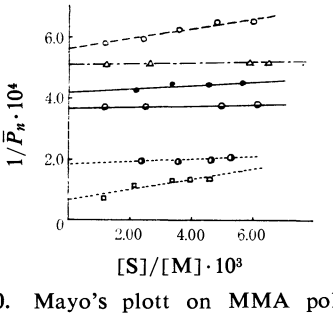



Fig. 10. Mayo's plott on MMA polymerization. (Initiator AIBN)
Marks are the same as in Fig. 1.

the rate of polymerization. Figures 9 and 10 show the plots of $1/\bar{P}_n$ with [S]/[M] according to Mayo's formula 3. From the slopes of the line in these figures, the apparent chain transfer constants have been determined to be as shown in Table III.

Table III. Apparent chain transfer constants ($C \cdot 10^3$) in the photo-polymerization of styrene and MMA
[AIBN] $= 2.0 \times 10^{-3}$

| Sulfides or oxides | DPS | DPDS | DPE | DBS | DBDS | DBE |
|---|---|---|---|---|---|---|
| Styrene | 32.5 | — | 0.794 | 54.8 | — | 7.16 |
| MMA | 5.54 | 17.4 | 0.642 | 18.3 | 134 | 1.04 |

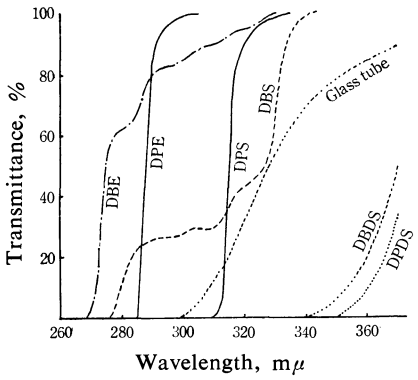



Fig. 11. Absorption spectra of sulfides and oxides.

## Discussion

As may be readily seen from Table I, it was found that the sulfides or oxides show little activity as initiators or retarders in the thermal polymerizations of styrene and MMA at 60°C. Accordingly, it may be concluded that the S-S or C-S bonds do not decompose spontaneously at 60°C.

The behavior of the sulfides and oxides as photo-sensitizers, as is shown in Figs. 5 and 6, may be taken to mean that the sulfides are subjected to radical decomposition in contact with light, though they showed no activity in thermal polymerizations. Similar phenomena may be observed from Figs. 7 and 8, which show the results of the experiment in which AIBN was employed as a photo-sensitizer in the presence of sulfides or oxides. Figures 5 and 6 show that DPDS is an excellent photo-sensitizer. It may be of some interest to note, however, that an increase in the concentration of the sulfides used here does not serve to increase the rate of polymerization very much. It is to be inferred that the sulfide radical produced by the application of the light of a mercury lamp starts the initiation, and that at the same time termination occurs; hence, the apparent rate of polymerization begins to decrease. This is why the rate of polymerization here is not in proportion to the square root of the amount of the sulfides or oxides used as the initiators, as Figs. 5 and 6 show.

As may be seen in Table II, when the chain transfer constants to sulfides and oxides as indicated in Table II are compared with the chain transfer constants to benzene ($0.28 \cdot 10^{-5}$, as determined by Misra et al.[12] in the polymerization of styrene and with the constant to benzene of $0.40 \cdot 10^{-5}$ in the polymerization[13] of MMA, the chain transfer constants to the sulfides or oxides are quite large. It may be said, therefore, that the transfer constants of these compounds result from the attack of the polymer radical on the S-S bond or C-S bond. The chain transfer constants to the oxides are much smaller than those to the sulfides of a similar structure.

As is shown in Figs. 5—8, DPDS alone could serve as an effective photo-sensitizer in the sulfides and oxides used. This result may be explained in terms of the transmittance of light under the conditions of polymerization referred to in this work. Figure 11 shows the absorption spectra of the sulfides or oxides at the concentration used and the transparency of the glass tube used. A comparison of the transparency of the glass tube with the light absorption of sulfides has shown that DPDS and DBDS could absorb effective sufficient light under the present conditions, while other sulfides or oxides did not. It may, therefore, be said that the activities of the compounds employed as photo-sensitizers depend more on the transmittance of the glass tubes than on the structure and the absorbancy of the compounds. The characteristic absorptions of these sulfides exist at nearly 243, 249, 255, and 261 mμ. It is to be expected that interesting results may be obtained by applying the lights of these wavelengths.

## Summary

A study has been made to see how some sulfides, such as diphenyl disulfide, diphenyl sulfide, dibenzyl disulfide, and dibenzyl sulfide, and such oxides as diphenyl ether and dibenzyl ether affect the radical polymerization of styrene or methyl methacrylate. None of these compounds acted effectively either as an initiator or as a retarder in the thermal

12) G. S. Misra and R. N. Chadha, *Makromol. Chem.*, **23**, 134 (1957).
13) R. N. Chadha, J. S. Shukla and G. S. Misra, *Trans. Faraday Soc.*, **53**, 230 (1957).

polymerization at 60°C. When employed as photo-sensitizers, the disulfides have been proven to have a remarkable activity of initiation, the monosulfides acting less effectively as initiators. Moreover, the oxides showed no such activity at all. When sulfides were used as photo-sensitizers, the rate of polymerization did not obey the equation of the square root of the concentrations of the sulfides. This may be attributable to the participation of the sulfide radicals in the initiation and termination. The chain transfer constants of these compounds at 60°C were in the order of disulfides>monosulfides>oxides.

The authors wish to thank Professor Minoru Imoto for his kind suggestions.

*Faculty of Engineering*
*Osaka City University*
*Sumiyoshi-ku Osaka*

# *t*-Amyloxycarbonyl as a New Protecting Group in Peptide Synthesis. I. The Synthesis and Properties of *N*-*t*-Amyloxycarbonylamino Acids and Related Compounds

By Shumpei SAKAKIBARA, Masaru SHIN, Masahiko FUJINO,* Yasutsugu SHIMONISHI, Sumiko INOUE and Noriyoshi INUKAI**

(Received February 1, 1965)

The *t*-butoxycarbonyl group (BOC group) is well known as a useful *N*-protecting group in the preparation of complicated peptides. Although *t*-butyl azidoformate,[1] *t*-butyl *p*-nitrophenyl carbonate[2] and *t*-butyl cyanoformate[3] have been recommended as *t*-butoxycarbonylating reagents, these can not be synthesized as easily as carbobenzoxy chloride. Thus, there is as yet no good practical method for synthesizing BOC-amino acids on a large scale. If *t*-butyl chloroformate, which corresponds to carbobenzoxy chloride, were stable against water or amines under normal conditions, it would be a most useful reagent for the purpose.[2,4]

In the present investigation, the *t*-amyloxycarbonyl group (AOC group) was found to be a much more convenient *N*-protecting group than BOC in many cases. The AOC group could be introduced quite readily into amino acid esters by using *t*-amyl chloroformate (I) as a reagent. Reagent I was originally prepared by Merck's group in 1912 as a material for hypnotics.[5] According to the description of the patent, it was synthesized by adding quinoline to a cold mixture of *t*-amyl alcohol and phosgene. When this procedure was tested, however, it was found that the product was colored and decomposed spontaneously within few days, even in a deep freezer at −20°C. Therefore, the procedure was improved in the present study. It was found that pyridine was a better condensing reagent than quinoline, and that excess phosgene was necessary to obtain a good yield of reagent I. The reagent thus obtained was a colorless liquid, which did not decompose when stored for over ten days in a deep freezer. The *N*-acylation reaction with amino acid esters was carried out readily in chloroform in the presence of triethylamine, with an almost quantitative yield. The AOC-esters were then converted to their respective free acids or hydrazides by the normal procedure. Generally, the hydrogenation of benzyl esters gave better yields of free acids than the saponification of ethyl or methyl esters. The yields, physical constants and analytical data of the AOC-amino acids are listed in Table I.

Since reagent I was unstable in the presence of water, it was not possible to get AOC-amino

* Present address: Research Laboratories, Takeda Chemical Industries Ltd., Higashiyodogawa-ku, Osaka.

** Present address: Yamanouchi Pharmaceutical Co. Ltd., Azusawa-cho, Itabashi-ku, Tokyo.

1) L. A. Carpino, *J. Am. Chem. Soc.*, **79**, 98, 4427 (1957); **81**, 955 (1959); **82**, 2725 (1960); R. Schwyzer, P. Sieber and H. Kappeler, *Helv. Chim. Acta*, **42**, 2622 (1959).

2) G. W. Anderson and A. C. McGregor, *J. Am. Chem. Soc.*, **79**, 6180 (1957).

3) L. A. Carpino, ibid., **82**, 2725 (1960).

4) A. R. Choppin and J. W. Rogers, ibid., **70**, 2967 (1948).

5) Merck, German. Pat. 254471 (1912); *Chem. Zentr.*, **1913 I**, 346.

TABLE I. YIELDS AND PROPERTIES OF *N*-*t*-AMYLOXYCARBONYLAMINO ACIDS

| AOC-deriv. of | Parent ester | Recryst. solvent | Yield, % | M. p., °C | $[\alpha]_D^{21}$ (*c* in EtOH) |
|---|---|---|---|---|---|
| L-Alanine | Benzyl | | 91 | Oil | |
| β-Methyl-L-aspartate | *p*-Nitrobenzyl | | 72 | Oil | |
| γ-Methyl-L-glutamate | *p*-Nitrobenzyl[a] | | 80 | Oil | |
| Glycine[b] | Ethyl | AcOEt - Pet. ether | 82 | 82.5—84 | |
| L-Isoleucine | Methyl | | 73 | Oil | |
| L-Isoleucine | Benzyl | | 100 | Oil | |
| L-Leucine[c] | Ethyl | EtOH-Water | 79 | 61—63 | −18.6°(1.9) |
| L-Lysine (di-AOC-deriv.) | Benzyl | | 96 | Oil | |
| α-Carbobenzoxy L-lysine[d] | Methyl | | 98 | Oil | |
| L-Methionine | Methyl | | 76 | Oil | |
| δ-Carbobenzoxy L-ornithine | Methyl | | 87 | Oil | |
| L-Phenylalanine | Ethyl | | 97 | Oil | |
| D-Phenylalanine | Methyl | | 93 | Oil | |
| L-Proline[e] | Benzyl | AcOEt - Pet. ether | 90 | 94—95.5 | −47.2°(1.7) |
| L-Serine | Methyl | | 98 | Oil | |
| L-Tryptophan[f] | Methyl | AcOEt - Pet. ether | 86 | 121—123 | +7.1°(1.2) |
| L-Tyrosine | Methyl | | 67 | Oil | |
| L-Valine | Ethyl | | 69 | Oil | |
| L-Valine | Benzyl | | 94 | Oil | |

a) *N*-AOC-γ-methyl-α-*p*-nitrobenzyl-L-glutamate was crystallized; m. p. 66—67°C, $[\alpha]_D^{22}$ −21.9° (*c* 2, EtOH). Found: C, 55.60; H, 6.39; N, 6.83. Calcd. for $C_{19}H_{26}O_8N_2$; C, 55.68; H, 6.24; N, 6.80%. b) Found: C, 50.91; H, 8.10; N, 7.42. Calcd. for $C_8H_{15}O_4N$: C, 50.78; H, 7.99; N, 7.40%. c) Crystallized as monohydrate. Found: C, 55.08; H, 9.48; N, 5.42. Calcd. for $C_{12}H_{23}O_4N \cdot H_2O$: C, 54.72; H, 9.57; N, 5.31%. d) cf. B. Bezas and L. Zervas, *J. Am. Chem. Soc.*, **83**, 719 (1961). e) Found: C, 57.57; H, 8.21; N, 5.97. Calcd. for $C_{11}H_{19}O_4N$: C, 57.62; H, 8.35; N, 6.11%. f) Found: C, 64.68; H, 7.14; N, 8.59. Calcd. for $C_{17}H_{22}O_4N_2$: C, 64.13; H, 6.97; N, 8.80%.

acids directly by the Schotten-Baumann procedure; this was a disadvantage of the method. Some AOC-amino acids were prepared as oils, but usually good crystalline derivatives could be derived from them, as with BOC-derivatives. These crystalline derivatives are listed in Table II. When the cleavage of the AOC group from various derivatives was tested, it was found that trifluoroacetic acid or anhydrous hydrogen chloride in an organic solvent decomposed AOC readily at room temperature. This property was quite similar to that of the corresponding BOC-derivatives in all cases. Since it is possible to prepare several moles of reagent I within 24 hr., this procedure should be of great use in the practical synthesis of complicated peptides.

Incidentally, 3-methyl-3-pentyl chloroformate (II) was synthesized, and several kinds of 3-methyl-3-pentoxycarbonylamino acids (MPC-acids) were prepared by following the same procedure as was used in the case of AOC-amino acids. These data are listed in Table III. Although the MPC group could be removed, as in the case of the AOC group, the difficulty of obtaining 3-methyl-3-pentanol would limit the application of the procedure.

## Experimental

***t*-Amyl Chloroformate (I).**—Dried phosgene (105 g., 1.06 mol.) was introduced into a solution of *t*-amyl alcohol (46 g., 0.52 mol.) in dry ether (500 ml.), and then the mixture was cooled to −60°C in an acetone - dry ice bath. A solution of pyridine (41 g., 0.52 mol.) in dry ether (500 ml.) was added dropwise into the cooled mixture with vigorous stirring. Then the reaction mixture was stored overnight in a deep freezer at −20°C. The pyridine hydrochloride which formed was removed by filtration, and the mother liquor was concentrated to a small volume (about 120 ml.) in an ice water bath under reduced pressure. The product thus obtained was used without further purification in the following reactions. Its purity was determined by acylating a known amount of phenylalanine methyl ester as described below; it was found that about 4 ml. of the product corresponded to 0.01 mol. The yield was about 60%.

**3-Methyl-3-pentyl Chloroformate (II).**—When 3-methyl-3-pentanol (b. p. 119—122°C; 31 g., 0.3 mol.) was allowed to react with phosgene (99 g., 1 mol.) as in the case of I using pyridine (24 g., 0.3 mol.), crude II was obtained as a colorless liquid (about 135 ml.). About 15 ml. of the product corresponded to 0.01 mol. The yield was about 30%.

TABLE II. CRYSTALLINE DERIVATIVES OF *N*-*t*-AMYLOXYCARBONYLAMINO ACIDS

| Compound | Recryst. solvent | M. p., °C | Yield % | $[\alpha]_D^{21}$ (*c* in Ethanol) | Empirical formula | Anal. Calcd. Found. C % | H % | N % |
|---|---|---|---|---|---|---|---|---|
| **A)** Dicyclohexylamine salt of AOC-deriv. of | | | | | | | | |
| L-Alanine | Ether-Pet. ether | 124—126 | 78 | +4.7°(2.4)[a] | $C_{21}H_{40}O_4N_2$ | 65.59<br>65.88 | 10.48<br>10.45 | 7.29<br>7.40 |
| β-Methyl-L-aspartate | AcOEt-Pet. ether | 123—124 | 91 | +19.4°(1.93)[b] | $C_{23}H_{42}O_6N_2$ | 62.34<br>62.41 | 9.55<br>9.57 | 6.38<br>6.33 |
| γ-Methyl-L-glutamate | AcOEt-Pet. ether | 133—134 | 70 | +13.5°(1.97)[b] | $C_{24}H_{44}O_6N_2$ | 63.32<br>63.13 | 9.61<br>9.71 | 6.09<br>6.14 |
| L-Isoleucine | Ether-Pet. ether | 101.5—102 | 71 | +3.9°(1.6)[a] | $C_{24}H_{46}O_4N_2$ | 67.56<br>67.65 | 10.87<br>10.89 | 6.57<br>6.76 |
| α-Carbobenzoxy-L-lysine | AcOEt | | 80 | +5.54°(3.1)[a] | $C_{32}H_{53}O_6N_3$ | 66.75<br>66.82 | 9.28<br>8.90 | 7.30<br>7.18 |
| L-Methionine | AcOEt-Pet. ether | 105—107 | 75 | +17.4°(1.3) | $C_{23}H_{44}O_4N_2S$ | 62.12<br>61.96 | 9.97<br>9.82 | 6.03[d]<br>6.17 |
| L-Phenylalanine | AcOEt | 198—199 | 85 | +27.4°(0.79) | $C_{27}H_{44}O_4N_2$ | 70.40<br>70.15 | 9.63<br>9.48 | 6.08<br>5.97 |
| L-Tyrosine | AcOEt-MeOH | 203—204 | 78 | +44.3°(1.0)[a] | $C_{27}H_{44}O_5N_2$ | 68.03<br>67.89 | 9.31<br>9.23 | 5.88<br>5.89 |
| L-Valine | Ether-Pet. ether | 119—121.5 | 79 | +2.0°(1.7) | $C_{23}H_{44}O_4N_2$ | 66.95<br>66.61 | 10.75<br>10.75 | 6.79<br>6.72 |
| **B)** *p*-Nitrophenyl ester of AOC-deriv. of | | | | | | | | |
| L-Leucine | Ether-Pet. ether | 59—61 | 79 | −49.3°(1.3) | $C_{18}H_{26}O_6N_2$ | 59.00<br>58.96 | 7.15<br>7.08 | 7.65<br>7.62 |
| L-Lysine (di-AOC deriv.) | Ether-Pet. ether | 65—68 | 46 | −25.2°(1.8) | $C_{24}H_{37}O_8N_3$ | 58.16<br>58.43 | 7.53<br>7.41 | 8.49<br>8.40 |
| δ-Carbobenzoxy-L-ornithine | AcOEt-Pet. ether | 110—112 | 50 | −27.5°(2.3)[c] | $C_{25}H_{31}O_8N_3$ | 59.87<br>59.83 | 6.23<br>6.32 | 8.38<br>8.56 |
| L-Phenylalanine | AcOEt-Pet. ether | 128—129 | 83 | −14.6°(1.3) | $C_{21}H_{24}O_6N_2$ | 62.99<br>63.02 | 6.04<br>6.07 | 7.00<br>6.92 |
| D-Phenylalanine | AcOEt-Pet. ether | 128—128.5 | 81 | +15.4°(1.0) | $C_{21}H_{24}O_6N_2$ | 62.99<br>63.00 | 6.04<br>6.08 | 7.00<br>7.05 |
| **C)** AOC-L-serine hydrazide | AcOEt | 98—100 | 82 | −5.0°(1.0) | $C_9H_{19}O_4N_3$ | 46.34<br>46.32 | 8.21<br>8.33 | 18.02<br>17.98 |

a) 22°C. b) 20°C. c) 24°C. d) Calcd.: S, 7.21. Found: S, 7.04%.

**AOC- and MPC-amino Acids.**—Into a solution of an amino acid-ester hydrochloride or tosylate (0.1 mol.) in chloroform (200 ml.), portions of I or II and triethylamine (0.1 mol.) were added alternately at −5 to −10°C. The addition of I or II was continued untill the ninhydrin-positive material had disappeared from the reaction mixture; this was checked by thin-layer chromatography. Then, the reaction mixture was washed successively with water, 0.5 N hydrochloric acid and a 5% sodium bicarbonate solution. The solution was dried over anhydrous magnesium sulfate and then concentrated to an oil. The yied of the oil (AOC-ester) was generally quantitative. Then the esters were subjected to saponification in acetone or, if benzyl esters, to hydrogenation in a suitable organic solvent (such as methanol); the AOC- or MPC-amino acids were obtained after following the usual purification procedures (Tables I and III).

**AOC-L-serine Hydrazide.**—AOC-L-serine methyl ester, which was obtained from L-serine methyl ester hydrochloride (3.9 g., 0.025 mol.), was dissolved in ethanol (18 ml.), and then hydrazine hydrate (4 ml.) was added to the solution. After the solution had stood for about 20 hr. at room temperature, it was concentrated to dryness, and the residue was recrystallized from ethyl acetate (Table II).

**Dicyclohexylamine Salts of AOC- and MPC-amino Acids.**—Each AOC- or MPC-amino acid was mixed with an equimolar amount of dicyclohexylamine in dry ether. The crystals which appeared were filtered off and recrystallized from a suitable solvent system. When the product was soluble in ether, it was precipitated by the addition of petroleum ether to the solution. The data are listed in Tables II and III.

**AOC-amino Acid *p*-Nitrophenyl Ester.**—A solution of each AOC-amino acid and an equimolar amount of *p*-nitrophenol in ethyl acetate was treated with an equimolar amount of dicyclohexylcarbodiimide at −10°C for one hour, and then the mixture was allowed to react for an additional 2 hr. at room temperature. The dicyclohexylurea which formed was removed by filtration, and the mother liquor was concentrated to dryness. The residual product was recrystallized from a suitable solvent system. The data are listed in Table II.

TABLE III. 3-METHYL-3-PENTOXYCARBONYLAMINO ACIDS AND THEIR DICYCLOHEXYLAMINE SALTS

| Compound | Recryst. solvent | M. p., °C | Yield % | $[\alpha]_D^{24}$ (*c* in Ethanol) | Empirical formula | Anal. Calcd. / Found | | |
|---|---|---|---|---|---|---|---|---|
| | | | | | | C % | H % | N % |
| A) MPC-deriv. of | | | | | | | | |
| Glycine | AcOEt-Pet. ether | 71.5—73 | 84 | | $C_9H_7O_4N$ | 53.19<br>53.02 | 8.43<br>8.42 | 6.89<br>7.00 |
| L-Leucine | | Oil | 84 | | | | | |
| L-Proline | | Oil | 90 | | | | | |
| B) Dicyclohexylamine salt of MPC-deriv. of | | | | | | | | |
| L-Leucine | Pet. ether | 114—116.5 | 63 | −4°(2) | $C_{25}H_{48}O_4N_2$ | 68.14<br>68.17 | 10.98<br>10.91 | 6.36<br>6.55 |
| L-Proline | AcOEt-Pet. ether | 127.5—128.5 | 77 | −29.5°C(2) | $C_{24}H_{44}O_4N_2$ | 67.88<br>67.56 | 10.45<br>10.22 | 6.60<br>6.51 |

**The Cleavage of the AOC Group from AOC-glycine.**—a) AOC-glycine (1.14 g., 0.006 mol.) was dissolved in trifluoroacetic acid (3 ml.). After the solution had been kept at room temperature for 40 min., it was concentrated to dryness. The residue was dissolved in ethanol (10 ml.), and the solution was neutralized with triethylamine. The crystals which appeared were collected by filtration and washed well with ethanol. The recrystallization of the product from water-ethanol afforded glycine (0.42 g., 93% yield), which was identified with an authentic sample by infrared spectral analysis.

b) AOC-glycine (1.90 g., 0.01 mol.) was dissolved in 10% anhydrous hydrogen chloride in acetic acid (4 ml.). After about 30 min. ether (20 ml.) was added to the reaction mixture in order to precipitate the product completely, and the latter was collected by filtration. Then the crystals were dissolved in ethanol (25 ml.), and the solution was neutralized with pyridine (about 1.2 ml.) to precipitate free glycine. The product (glycine) was collected by filtration, washed well with ethanol, and then recrystallized from water-ethanol; the yield of glycine was 97% (0.730 g.).

**Summary**

It has been shown that the *t*-amyloxycarbonyl group (AOC group) can be introduced quite readily into amino acid esters by using *t*-amyl chloroformate as a reagent, and that the AOC group can be cleaved as smoothly as the *t*-butoxycarbonyl group (BOC group) under acidic conditions. Since this reagent is much easier to prepare than any other reagents used for the introduction of the BOC group, the new procedure is considered to be of great use in the practical synthesis of complicated peptides. 3-Methyl-3-pentoxycarbonylamino acids were also prepared by following the same procedure as was used in the case of AOC-amino acids.

*Peptide Center*
*Institute for Protein Research*
*Osaka University*
*Kita-ku, Osaka*

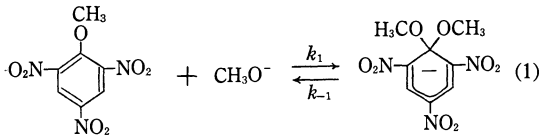
# Kinetic Studies of the Formation and Decomposition of the Meisenheimer Complex of 2, 4, 6-Trinitroanisole with Sodium Methoxide in Methanol

By Takehiro ABE, Toshihiko KUMAI and Hiroko ARAI

(Received February 5, 1965)

It has been widely accepted that aromatic polynitro-compounds react with alkalis to form colored intermediates of Meisenheimer's type. However, no investigation of the kinetics of both the coloration and the decoloration reactions has hitherto been reported on the color reaction of a polynitrobenzene in an alkaline solvent, although there have been several papers reporting the activation energy for either the coloration or the decoloration. In the present work, therefore, an attempt has been made to obtain the activation energies for the formation and decomposition of the Meisenheimer complex of 2, 4, 6-trinitroanisole with sodium methoxide in methanol.

It has been reported that 2, 4, 6-trinitroanisole reacts with the methoxide ion as follows:[1-9]




The Meisenheimer complex

The Meisenheimer complex in methanol has two absorption maxima, at about 485 and 415 mμ.[8,9]

## Experimental

**Materials.** — Commercial-grade 2,4,6-trinitroanisole was purified by several recrystallizations from methanol to a constant melting point. The Meisenheimer complex used was prepared by the same method as in the previous paper.[8] A solution of sodium methoxide in methanol was prepared by mixing freshly-cut pieces of sodium in methanol. The concentration was determined by the titration of samples diluted with water against a standard aqueous solution of hydrochloric acid. Methanol of a commercial grade was used without further purification.

**Measurements.**—Each run of the decomposition of the Meisenheimer complex prepared was started by the dissolution of very small pieces of the complex in methanol at the temperature of the thermostat. The rate of decomposition was followed by measuring the absorbancy at 480 mμ.

Each run of the formation of the Meisenheimer complex was started by pipetting 1 ml. of the methanolic sodium methoxide solution ($2.025\times10^{-3}$ M) into 2 ml. of the methanolic solution of 2,4,6-trinitroanisole ($3.980\times10^{-5}$ M) in a cell at the temperature of the thermostat. The resulting solution was then stirred by bubbles of nitrogen gas. The change in the absorbancy at 410 mμ was followed.

In the wavelength region above 400 mμ, 2,4,6-trinitroanisole scarcely absorbs at the low concentration of $2.65\times10^{-5}$ M, but it does at higher concentrations. The Meisenheimer complex absorbs more intensely at 410 mμ than at 480 mu. Moreover, it is likely that, at high concentrations of the methoxide ion, 2,4,6-trinitroanisole further reacts with the methoxide ion to form a second complex,[9] possibly absorbing in the visible region. (Details of this will be published later.) Accordingly, the absorbances at 410 mμ were measured for the runs of the formation of the Meisenheimer complex. The methoxide ion does not absorb in this wavelength range. On the other hand, the Meisenheimer complex slowly dissolves and rapidly decomposes in methanol. For convenience, therefore, the colored solutions for the runs of the decomposition were prepared by dissolving the Meisenheimer complex in methanol at arbitrary concentrations. The solutions contained considerable amounts of 2,4,6-trinitroanisole which results from the decomposition of the Meisenheimer complex. Consequently, the runs for the decomposition were followed by measuring the absorbancy at the longer wavelength of 480 mμ, at which scarcely any 2,4,6-trinitroanisole absorbs at high concentrations.

The absorbancies were measured with a Hitachi EPU-2A quartz spectrophotometer, a pair of 1 cm. cells with ground glass-stoppers being used in a thermostatted cell housing at constant temperatures. The temperature control in all cases was better than ±0.1°C. Methanol was used as a blank.

## Results

**The Decomposition of the Meisenheimer Complex.**—The decomposition of the Meisenheimer complex in methanol obeyed the first-order equation:

$$-\log A=(t-t_0)k_{-1}/2.303-\log A_0 \qquad (2)$$

1) J. Meisenheimer, *Ann. Phys. Lpz.*, **323**, 205 (1902).
2) J. B. Ainscough and E. F. Caldin, *J. Chem. Soc.*, **1956**, 2528.
3) R. Foster, *Nature*, **183**, 1042 (1959).
4) R. C. Farmer, *J. Chem. Soc.*, **1959**, 3425.
5) L. K. Dyall, ibid., **1960**, 5160.
6) S. Nagakura, *Tetrahedron*, **19**, 361 (1963).
7) J. Miller, *J. Am. Chem. Soc.*, **85**, 1628 (1963).
8) T. Abe, This Bulletin, **37**, 508 (1964).
9) V. Gold and C. H. Rochester, *J. Chem. Soc.*, **1964**, 1687.

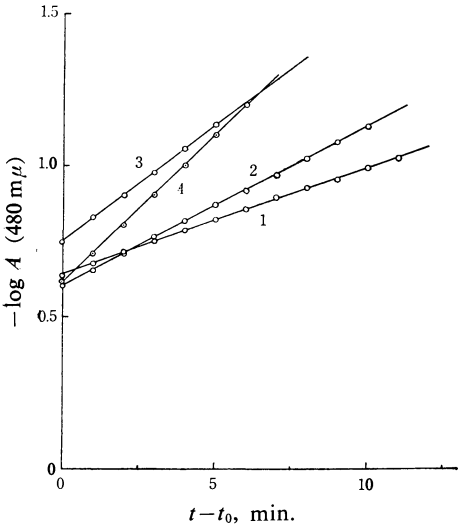



Fig. 1. Rates of decoloration reaction of the Meisenheimer complex in methanol.
1: 20.0°C 2: 25.0°C
3: 30.0°C 4: 34.0°C

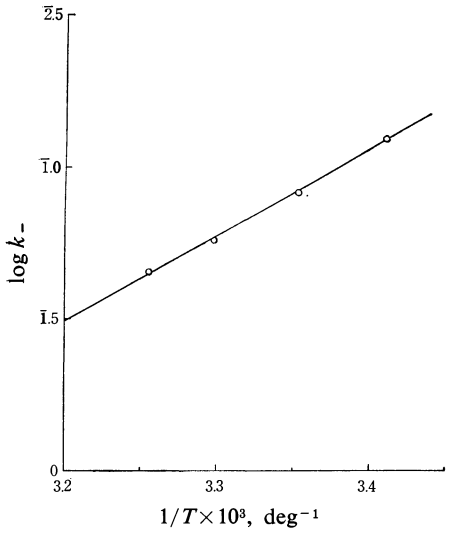



Fig. 2. Plots of $\log k_{-1}$ against reciprocal absolute temperature $1/T$°K.

Here $A$ is the absorbancy of the solution measured at time $t$, and the subscript zero indicates the starting time. By the least-squares calculations for the observed values in Fig. 1, we obtained the rate constants, $k_{-1}$'s, from whose temperature dependency in Fig. 2 the activation energy, $E_{-1}$, was found to be 12.9 kcal./mol.

**The Formation of the Meisenheimer Complex.**—The result of the runs for the reaction between 2, 4, 6-trinitroanisole and sodium methoxide are shown in Fig. 3. It is obvious from the figure that the reaction is exothermic,

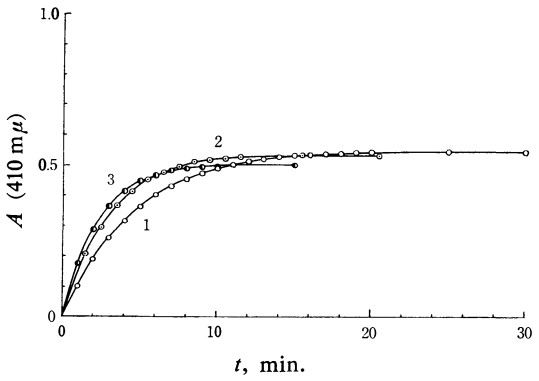



Fig. 3. Rates of reaction of 2,4,6-trinitroanisole ($2.653\times10^{-5}$ M) with sodium methoxide ($6.75\times10^{-4}$ M) in methanol.
1: 20.0°C 2: 25.0°C 3: 30.0°C

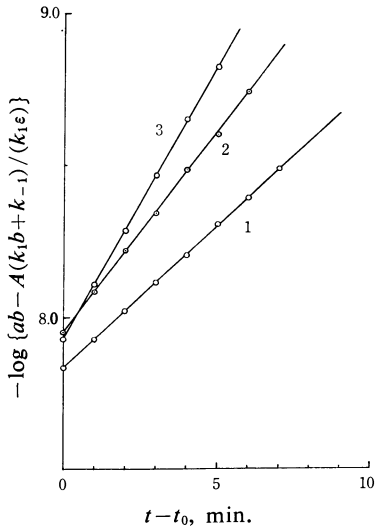



Fig. 4. Plots of $-\log\{ab-A(k_1b+k_{-1})/(k_1\varepsilon)\}$ against $(t-t_0)$.
1: 20.0°C, $(k_1b+k_{-1})/(k_1\varepsilon)=3.23\times10^{-8}$ mol./l.
2: 25.0°C, $(k_1b+k_{-1})/(k_1\varepsilon)=3.24\times10^{-8}$ mol./l.
3: 30.0°C, $(k_1b+k_{-1})/(k_1\varepsilon)=3.50\times10^{-8}$ mol./l.

because the absorbancy at the equilibrium point becomes lower as the temperature increases. If the initial concentration of 2, 4, 6-trinitroanisole ($a$) is considerably smaller than that of sodium methoxide ion ($b$), reaction mechanism 1 gives the kinetic equation of the second order as:

$$t-t_0=2.303\,[\log\{ab-A_0(k_1b+k_{-1})/(k_1\varepsilon)\}-\log\{ab-A(k_1b+k_{-1})/(k_1\varepsilon)\}]/(k_1b+k_{-1}) \quad (3)$$

where $k_1$ is the rate constant of the forward reaction, and $\varepsilon$ is the molar extinction coefficient of the Meisenheimer complex. By the trial-and-error method we found the values of

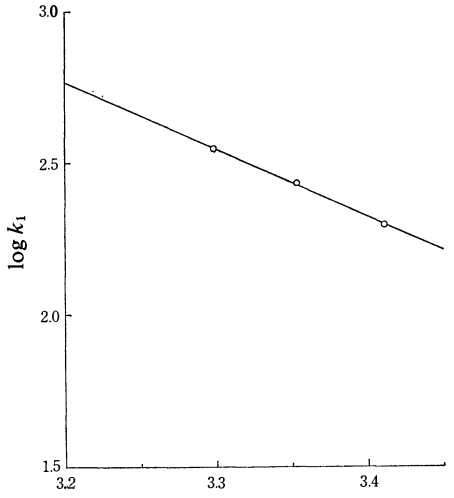



Fig. 5. Plots of $k_1$ against reciprocal absolute temperature $1/T$°K.

$(k_1b+k_{-1})/(k_1\varepsilon)$ that gave the best straight lines for the plots of $-\log\{ab-A(k_1b+k_{-1})/(k_1\varepsilon)\}$ against $(t-t_0)$ to be those shown in Fig. 4. From the slopes of the plots the values of $k_1$ were determined to be those listed in Table I, where the values of $k_{-1}$ determined above were used. The activation energy, $E_1$, obtained from Fig. 5 is 10.1 kcal./mol. The equilibrium constants $k_1$'s, for equilibrium 1 were estimated from the values of $k_1/k_{-1}$. The values of $\varepsilon$ in Table I were estimated from $(k_1b+k_{-1})/(k_1\varepsilon)$.

TABLE I. RATE CONSTANTS AND EQUILIBRIUM CONSTANTS FOR THE REACTION OF 2,4,6-TRINITROANISOLE WITH METHOXIDE ION IN METHANOL

| Temp. °C | $k_1$ l./mol. min. | $10k_{-1}$ min$^{-1}$ | $K_1$ l./mol. | $10^{-4}\varepsilon$ 410 m$\mu$ |
|---|---|---|---|---|
| 20.0 | 200 | 0.814 | 2450 | 3.35 |
| 25.0 | 273 | 1.21 | 2260 | 3.45 |
| 30.0 | 354 | 1.74 | 2030 | 3.34 |
| 34.0 | — | 2.23 | — | — |

## Discussion

It is evident from Fig. 6 that the Meisenheimer complex of 2,4,6-trinitroanisole is quite stable. This leads to the interpretation of why the complex is easily prepared.

Assuming that 2,4,6-trinitroanisole at $3.43\times10^{-5}$ M was completely converted into the Meisenheimer complex at the methoxide concentration of $1.28\times10^{-1}$ M, Gold and Rochester[9] obtained the value of $7.7\times10^3$ l./mol. for $k_1$ at 25°C and the value of $2.42\times10^4$ for $\varepsilon$ at 410 m$\mu$. This $K_1$ value is much higher than the present one of $2.26\times10^3$ l./mol. They estimated the rough values of 240 l./mol. min. and $3\times10^{-2}$/min. for $k_1$ and $k_{-1}$ respectively at 25°C.

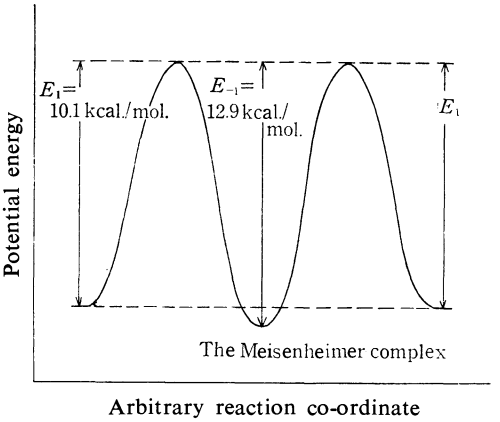



Fig. 6. The energy profile for the reaction of 2,4,6-trinitroanisole with sodium methoxide in methanol.

Our activation energy of 10.1 kcal./mol. for the forward reaction corresponds to Ainscough and Caldin's value of 13.1 kcal./mol. for the "slow" reaction of 2,4,6-trinitroanisole with ethanolic sodium ethoxide at temperatures from −20° to 10°C.[2]

Miller[7] calculated the activation energies for the same reaction, utilizing bond energies, electron affinities and solvation energies. According to his calculation, the values of $E_1$ and $E_{-1}$ are 14 and 16 kcal./mol., respectively; these values accord fairly well with our experimental values. By means of the simple LCAO MO method, Abe[8] also made the same calculation, although he did not consider the important solvation energy. His value of 15.7 kcal./mol., for $E_{-1}$ is, however, fairly good. This seems to be due to the cancellation of the solvation energies for a $\sigma$- and a $\pi$-part in his calculation.

*The College of General Education*
*Tohoku University*
*Kawauchi, Sendai*

# The Chemistry of Polyazanes. I. The Decomposition of 1, 3, 5-Tri-*p*-tolyl-1, 4-pentazdiene

By Hiroshi MINATO and Masayoshi OKU*

(Received February 19, 1965)

Although the organic compounds containing a chain of more than three nitrogen atoms appear to be very interesting, they have not been fully investigated. Our laboratories have, therefore, been investigating the chemistry of various polyazanes; in this paper the chemistry of 1, 3, 5-tri-*p*-tolyl-1, 4-pentazdiene (TTP) will be described.

Pechmann and Frobenius[1] studied the syntheses of TTP and other pentazdienes and found that these compounds underwent the following decomposition:

$$C_6H_5\text{-}N{=}N\text{-}\underset{\underset{Me}{|}}{N}\text{-}N{=}N\text{-}C_6H_5 \xrightarrow[\text{organic solvents}]{HCl} C_6H_5N_2Cl + MeNHN{=}NC_6H_5$$

$$\xrightarrow[H_2O]{HCl} C_6H_5OH + C_6H_5NH_2 + MeOH + N_2$$

Wicklatz[2] prepared TTP and other pentazdienes, and used these compounds as the initiators of the emulsion polymerization of butadiene and styrene at 0—50°C. Hall and Seed[3] used 1, 5-diaryl-3-alkyl-1, 4-pentazdienes as the initiators of the polymerization of ethylene at 120—150°C and of methyl methacrylate at 40°C. Rondestvedt and Davis[4] reported on the syntheses of 1, 5-diaryl-3-methyl-1, 4-pentazdienes as the by-products of the syntheses of triazenes. However, the spontaneous decomposition of 1, 3, 5-trisubstituted 1, 4-pentazdienes has never been investigated.

## Results and Discussion

1, 3, 5-Tri-*p*-tolyl-1, 4-pentazdiene (TTP) was obtained as a yellow solid when two moles of *p*-toluenediazonium chloride and one mole of *p*-toluidine were coupled in the presence of sodium methoxide, according to the method of Pechmann and Frobenius.[1] TTP is sparingly soluble in diethyl ether, alcohols or ligroin. It dissolves in acetone, benzene or chloroform, with a rapid evolution of nitrogen, at room temperature. The recrystallization of TTP is possible when it is handled quickly in ether, benzene or acetone-water at 0°C.

The spontaneous decomposition of TTP was investigated by dissolving one gram of TTP in one hundred milliliters of cumene at lower temperatures and by keeping the solution at 0°C, 15.0°C or 25.8°C. The decomposition followed good first-order kinetics, as may be seen in Fig. 1. The first-order rate constants at those three temperatures are shown in Table I, together with the half-lives. When $\ln(k/T)$ was plotted against $1/T$, a straight line was obtained, as may be seen in Fig. 2. The values of activation parameters obtained from the slope of Fig. 2 were $\Delta H^{\ddagger} = 22.6$ kcal./mol. and $\Delta S^{\ddagger} = 3.8$ e. u. Table II lists the products obtained from the decomposition of TTP at 25.8°C.

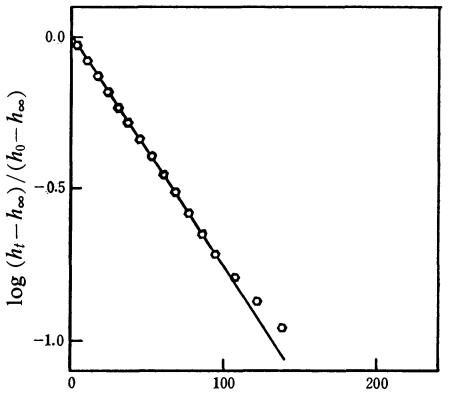



Fig. 1. Rate of decomposion of TTP in cumene at 15.0°.
$h_0$, $h_t$ and $h_\infty$ are the difference of the mercury heights at $t=0$, $t=t$ and $t=\infty$, respectively.

TABLE I. RATES OF DECOMPOSITION OF TTP IN CUMENE

| Temp. °C | $k_1$ sec$^{-1}$ | Half life min. |
|---|---|---|
| 25.8 | $12.9\times10^{-4}$ | 8.95 |
| 15.0 | $2.93\times10^{-4}$ | 39.2 |
| 0.0 | $0.325\times10^{-4}$ | 354 |

* American Chemical Society-Petroleum Research Fund Scholar.

1) H. V. Pechmann and L. Frobenius, *Ber.*, **27**, 705 (1894).
2) J. E. Wicklatz, U. S. Pat. 2530497 (1950); 2564632 (1951).
3) W. Hall and L. Seed, Japanese Pat. 11791 (1960).
4) C. S. Rondestvedt, Jr., and S. J. Davis, *J. Org. Chem.*, **22**, 200 (1957).

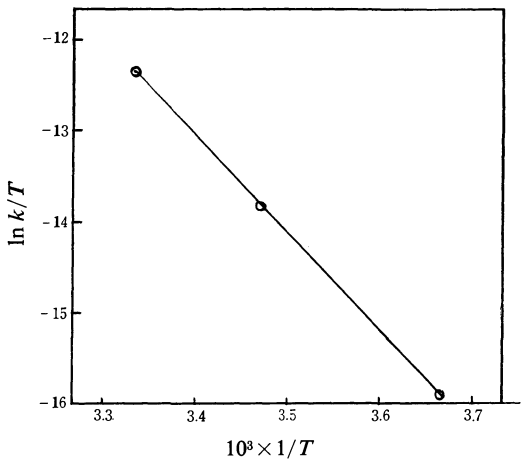



Fig. 2. $\ln k/T$ versus $1/T$ for the decomposition of TTP.

TABLE II. PRODUCTS OF DECOMPOSITION OF TTP IN CUMENE AT 25.8°*

| Product | mmoles | moles/mole TTP |
|---|---|---|
| $N_2$ | 2.52 | 0.871 |
| $MeC_6H_4N{=}NNHC_6H_4Me$ | 2.90 | 0.994 |
| $MeC_6H_5$ | 2.58 | 0.884 |
| $(C_6H_5CMe_2)_2$ | 1.18 | 0.405 |

* 1.000 g. of TTP (2.91 mmol.) was dissolved in 100.0 ml. of cumene, and decomposed at 25.8°C for 20 hr. in the absence of air.

The three most plausible mechanisms of the decomposition of TTP in inert solvents are the following:

$$MeC_6H_4\text{-}N{=}N\text{-}\underset{\displaystyle C_6H_4Me}{\underset{|}{N}}\text{-}N{=}N\text{-}C_6H_4Me \rightarrow MeC_6H_4\text{-}N{=}N\text{-}\underset{\displaystyle C_6H_4Me}{\underset{|}{N^{\ominus}}} + N_2 + {}^{\oplus}C_6H_4Me \quad (1)$$

$$MeC_6H_4\text{-}N{=}N\text{-}\underset{\displaystyle C_6H_4Me}{\underset{|}{N}}\text{-}N{=}N\text{-}C_6H_4Me \rightarrow MeC_6H_4\cdot + N_2 + \cdot\ddot{N}\text{-}C_6H_4Me + N_2 + \cdot C_6H_4Me \quad (2)$$

$$MeC_6H_4\text{-}N{=}N\text{-}\underset{\displaystyle C_6H_4Me}{\underset{|}{N}}\text{-}N{=}N\text{-}C_6H_4Me \rightarrow MeC_6H_4\text{-}N{=}N\text{-}\underset{\displaystyle C_6H_4Me}{\underset{|}{N}}\cdot + N_2 + \cdot C_6H_4Me \quad (3)$$

Mechanism 1 cannot, however, account for the production of toluene and 2, 3-dimethyl-2, 3-diphenylbutane. Mechanism 2 can account for the production of these two hydrocarbons, but it cannot account for the production of 1, 3-di-*p*-tolyl-triazene. Only mechanism 3 is consistent with the experimental results. Thus the mode of the decomposition of TTP resembles that of azohydrocarbons, which decompose to yield a nitrogen molecule and two free radicals.

In Table III the rate of the decomposition of TTP is compared with the rates of the decomposition of several azohydrocarbons. The fact that TTP decomposes about 300 times as fast as 1′, 1′, 1′-triphenylbenzeneazomethane is rather surprising. The order of the increasing ease of decomposition in the series of azomethane, azobisisobutyronitrile, 1′, 1′-diphenylbenzeneazomethane and 1′, 1′, 1′-triphenylbenzeneazomethane may be ascribed to the production of free radicals with an increasing stability. However, it is difficult to suppose that the resonance energy of $MeC_6H_4\dot{N}\text{-}N{=}N\text{-}C_6H_4Me$ is greater than that of the triphenylmethyl radical. Therefore, some factors in addition to the resonance energy must be responsible for the rapid decomposition of TTP.

It has been found that peroxyoxalates decompose relatively fast among various peroxyesters.[10-15] The similarity of the rate of decomposition of ethyl *t*-butylperoxyoxalate to

$$EtO\text{-}\overset{\displaystyle O}{\overset{\|}{C}}\text{-}\overset{\displaystyle O}{\overset{\|}{C}}\text{-}O\text{-}O\text{-}CMe_3 \quad \text{Half life at 60°C, 35.6 min.}$$

$$Ph_2CH\text{-}\overset{\displaystyle O}{\overset{\|}{C}}\text{-}O\text{-}O\text{-}CMe_3 \quad \text{Half life at 60°C, 26 min.}$$

that of *t*-butyl diphenylperoxyacetate suggests that the ethoxycarbonyl radical is about as stable as the diphenylmethyl radical. However, since the ethoxycarbonyl radical has no special structural characteristic which might account for this apparent stabilization, it is likely that the rate difference is due to the ease of the cleavage of the carbon-carbon bond of oxalates rather than to any special stabilization of the carbon radical formed. This reasoning may also be applicable to the rapid decomposition of TTP. Just as the decomposition of peroxyoxalates is aided by the repulsion

5) C. G. Overberger, M. T. O'Shaughnessy and H. Shalit, *J. Am. Chem. Soc.*, **71**, 2661 (1949).
6) O. K. Rice and D. V. Sickman, *J. Chem. Phys.*, **4**, 239, 242, 608 (1936).
7) S. G. Cohen and C. H. Wang, *J. Am. Chem. Soc.*, **77**, 3628 (1955).
8) S. G. Cohen and C. H. Wang, ibid., **75**, 5504 (1953).
9) M. G. Alder and J. E. Leffler, ibid., **76**, 1425 (1954).
10) P. D. Bartlett and R. R. Hiatt, ibid., **80**, 1398 (1958).
11) P. D. Bartlett, E. P. Benzing and R. E. Pincock, ibid., **82**, 1756 (1960).
12) P. D. Bartlett and R. E. Pincock, ibid., **82**, 1769 (1960).
13) P. D. Bartlett and H. Sakurai, ibid., **84**, 3269 (1962).
14) P. D. Bartlett, B. A. Contarev and H. Sakurai, ibid., **84**, 3101 (1962).
15) P. D. Bartlett and L. B. Gortler, ibid., **85**, 1864 (1963).

TABLE III. RATES OF DECOMPOSITION OF VARIOUS AZO COMPOUNDS

| Azo compound | Solvent | Temp. °C | $10^4 k_1$ $sec^{-1}$ | Ref. |
|---|---|---|---|---|
| Me-N=N-Me | (Gas) | 300 | 5.6 | 6) |
| $Me_2(NC)C-N=N-C(CN)Me_2$ | Xylene | 80 | 1.53 | 5) |
| $Ph-N=N-CHPh_2$ | Decalin | 54 | 1.01 | 7) |
| $Ph-N=N-CPh_3$ | Toluene | 53 | 2.25 | 8) |
| | Benzene | 25 | 0.042 | 9) |
| $C_7H_7-N=N-N(C_7H_7)-N=N-C_7H_7$ | Cumene | 25.8 | 12.9 | |

of the two central positively-polarized carbon atoms, the decomposition of TTP is aided by the repulsion of the electronegative nitrogen atoms, which weakens the bond between $N_b$ and $N_c$ in the structure $MeC_6H_4-N_a=N_b-N_c-(C_6H_4Me)-N_b=N_a-C_6H_4Me$.

In a number of cases, polar substituent effects have been discerned in the reactions of homolytic cleavage. For instance, Bartlett and Rüchardt[16] found that the thermal decomposition of substituted phenylperoxyacetates fits the Hammett equation when $\sigma^+$ is used rather than $\sigma$, and the observed $\rho$ value was $-1.04$ at 100°C. The transition state has been pictured as a resonance hybrid of ionic and radical structures:

$$XC_6H_4CH_2\bullet\cdots C(=O)\cdots\bullet OCMe_3 \longleftrightarrow XC_6H_4CH_2^{\oplus}\cdots C(=O)\cdots{}^{\ominus}OCMe_3$$

In a similar fashion, the transition state of the decomposition of TTP can be presented as a resonance hybrid of ionic and radical structures:

$$MeC_6H_4\bullet\cdots N\equiv N\cdots\bullet N(C_6H_4Me)-N=N-C_6H_4Me \longleftrightarrow MeC_6H_4^{\oplus}\cdots N\equiv N\cdots{}^{\ominus}N(C_6H_4Me)-N=N-C_6H_4Me$$

The ionic form had a negative charge on the electronegative nitrogen atom, and this is a favorable form. The contribution of the ionic form to the transition state will reduce the activation energy required for the decomposition of TTP. Hence, this may be one of the factors responsible for the rapid decomposition of TTP.

One of the remarkable features of TTP is that it is very stable as a solid, whereas it is unstable in a solution. As has been described above, the half life of TTP is 9.0 min. at 25.8°C, but no apparent decomposition was observed for the solid TTP when it was allowed to stand at room temperature for several weeks. Such unusual behavior was never observed in other free radical initiators, such as peroxides and azohydrocarbons. The reason for the abnormal behavior of TTP is not clear, but the following speculation is attractive.

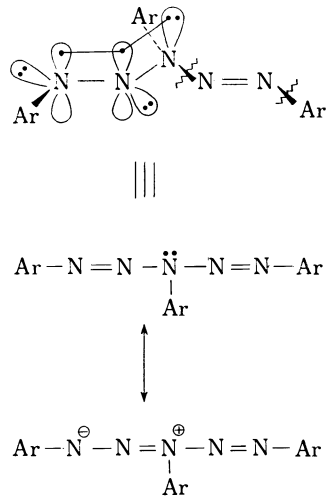


Fig. 3(a)

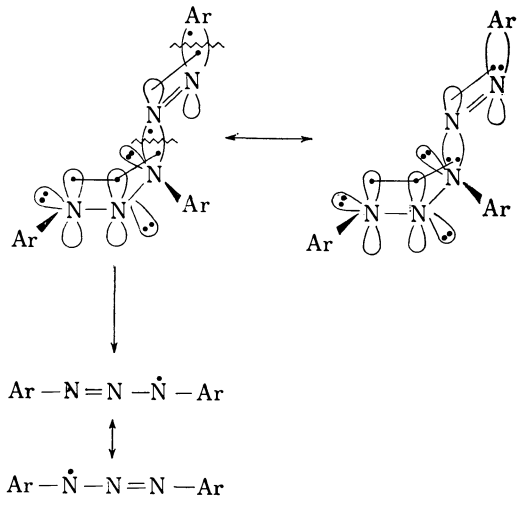


Fig. 3(b)

The lone pair electrons of the central nitrogen atom of TTP are in resonance with the *p*-orbitals of azo linkages, and hence these orbitals are parallel with one another, as is shown in Fig. 3(a). The structure of solid TTP is

16) P. D. Bartlett and C. Rüchardt, ibid., 82, 1756 (1960).

fixed as such. However, when the molecule of TTP with the structure shown in Fig. 3(a) is to decompose, the radical $MeC_6H_4N=\dot{N}NC_6H_4Me$ to be formed at the transition state does not have the resonance energy which is available for the molecules with the structure 3(b). The rotation of the groups in 3(a) to obtain 3(b) is possible in solution, but it is not possible in solids. This might be the reason why TTP is very unstable in solutions, though it is very stable as a solid.

Wicklatz[2] reported that a mixture of 72 parts of butadiene and 28 parts of styrene slowly polymerized and that the conversion of 90.6% was attained in 11 hr. when the monomers were mixed with 180 parts of water, 5 parts of soap flakes and 3.43 parts of TTP at 50°C. The slow rate of the decomposition of TTP in this system is surprising compared with the half life of 9.0 min. in cumene at 25.8°C. Although TTP dissolves in styrene, it does not dissolve in ligroin, diethyl ether or alcohols, and hence it would probably not dissolve in butadiene. The solubility of TTP in the mixture of butadiene and styrene may be very small, especially when they are scattered as oil droplets covered with soap molecules in the aqueous phase. Therefore, the slow prolonged polymerization may be ascribed to the fact that TTP is sparingly soluble in this emulsified system. As soon as molecules of TTP dissolve at 50°C, they will quickly decompose to yield free radicals, which in turn initiate the polymerization of butadiene and styrene.

## Experimental

**Materials.**—Tokyo Kasei Co. G. R. cumene was shaken wih portions of concentrated sulfuric acid until the acid layer no longer became colored upon long shaking. After it had been washed with water, a sodium bicarbonate solution, and water again, the cumene was dried with calcium chloride and distilled from sodium through a 90-cm. column packed with glass helices. The center fraction boiling at 152—152.3°C was stored under a nitrogen atmosphere and used.

All the other chemicals were of the best grade commercially available and were used without further purification.

**The Synthesis of 1, 3, 5-Tri-*p*-tolyl-1, 4-pentazdiene (TTP).** — The method of Pechmann and Frobenius[1] was modified a little and used for the synthesis of TTP. 10.7 g. of *p*-toluidine (0.1 mol.) in 15 ml. of water was diazotized by the addition of 6.9 g. of sodium nitrite (0.1 mol.) in 20 ml. of water and 25.1 g. of 35% hydrochloric acid (0.1 mol.) at 0°C. 5.1 g. of sodium (0.22 mol.) was dissolved in 150 ml. of methanol, and to this sodium methoxide solution 5.35 g. of *p*-toluidine (0.05 mol.) in 110 ml. of methanol was added. Then this methanolic solution was stirred, drop by drop, within half an hour to the aqueous soluion of *p*-toluenediazonium chloride. The yellow TTP precipitated was filtered and washed with cold ether. When the crude TTP was quickly recrystallized from cold ether, 5.5 g. of yellow crystals was obtained (16%). M. p. 84.5 — 85.0°C (decomp.) (literature:[1] 85.0°C).

When the ethereal solution of TTP was kept at −3°C for 36 hr., all the TTP were found to have decomposed. When TTP was added to acetone, benzene, ether or chloroform at room temperature, it quickly dissolved, with a rapid evolution of nitrogen. When TTP was added to chloroform, the decomposition was accompanied with a strong smell which resembled that of phenyl isocyanide. When the chloroform solution was viewed against pure chloroform in the infrared region, an absorption at 2220 $cm^{-1}$ was observed; this may be ascribed to *p*-tolyl isocyanide.

**Kinetic Procedure.**—One gram of TTP was placed in a container attached to one end of a U-shaped tube, while 100 ml. of cumene was placed in a container attached to the other end of the U-shaped tube, as is shown in Fig. 4. These two were degassed and then mixed at −78°. This U-tube was attached to an evacuated system of a known volume

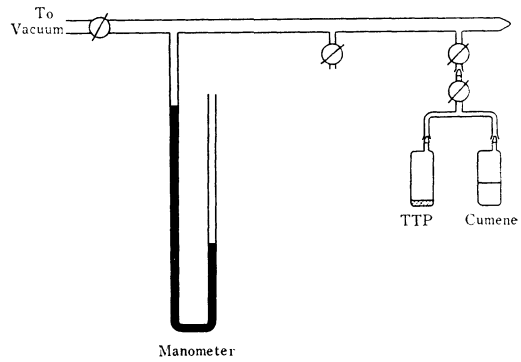



Fig. 4. Vacuum system used for kinetic and product studies.

with a mercury manometer. Then a water bath of a constant temperature (0.00, 15.00 or 25.80± 0.05°C) was raised so that the U-tube was immersed in the bath. By turning a cock, the U-tube was opened to the evacuated system, and the increase in the pressure of the system was measured versus the time. After the U-tube had been warmed to the temperature of the bath, the plots of the increase in the pressure showed good first order behavior. The infinity point was taken after about ten half lives.

**Procedure for Product Studies.**—The TTP solution used for kinetic studies was analyzed for the products of decomposition. The amount of nitrogen was determined from the data on the pressure, the volume and the temperature of the system. The cumene solution was distilled to yield brownish solids and a distillate. When the distillate was investigated by a Shimadzu Gas Chromatograph GC-2B, the only peaks observed were those of toluene and cumene. The amount of toluene was determined by using benzene as the internal standard.

When the brown residue was recrystallized from cold petroleum ether, brownish yellow crystals of 1,3-di-*p*-tolyltriazene were obtained, while upon the evaporation of the filtrate crystals of 2,3-dimethyl-2,3-diphenylbutane (bicumyl) were obtained. The melting points and the infrared spectra of these two products were the same as those of authentic samples.

Grateful acknowledgment is made to the donors of The Petroleum Research Fund, administered by the American Chemical Society, for support of this research.

*Department of Chemistry*
*International Christian University*
*Mitaka, Tokyo*

# The Preparation of Heteropoly Salts of Selenium and Molybdenum

By Sarju PRASAD and Virendra Nath GARG

(Received November 30, 1964)

Gibbs[1] and Péchard[2] seem to have been the first to observe the formation of heteropoly acids and their salts of selenium and molybdenum with different ratios of selenium dioxide and molybdenum trioxide. Rosenheim and Krause[3] prepared ammonium salt, $3(NH_4)_2O \cdot 2SeO_2 \cdot 8MoO_3 \cdot 6H_2O$, by treating one mole of selenium dioxide with one mole of molybdenum trioxide; they also prepared another type of ammonium salt, $2(NH_4)_2O \cdot 5SeO_2 \cdot 5\,MoO_3 \cdot 8H_2O$. Prandtl and Blochin[4] isolated ammonium salt ($2(NH_4)_2O \cdot 2SeO_2 \cdot 5MoO_3 \cdot 3H_2O$), rubidium salt ($2Rb_2O \cdot 2SeO_2 \cdot 5MoO_3 \cdot 5H_2O$), and also barium salt ($2BaO \cdot 2SeO_2 \cdot 5MoO_3 \cdot 7H_2O$). By acidifying a boiling ammoniacal solution of selenium dioxide and molybdenum trioxide in a molar ratio of 1 : 6 with nitric acid, Prandtl, Blochin and Obpacher[5] obtained a compound with the composition of $(NH_4)_2O \cdot SeO_2 \cdot 6MoO_3 \cdot 4H_2O$.

The present communication will deal with the preparation of and the properties of two new ammonium molybdoselenites and their heavy metal salts, which have been confirmed by conductometric titrations.

## Experimental and Results

All the chemicals used were of Merck's or B.D.H. quality of purity.

**Ammonium Salt of Molybdoselenite, Type, I.**—*Preparation.*—Seleneous acid and molybdic acid in the molar ratio of 1 : 4 were dissolved in aqueous ammonia and refluxed for 6 hr. at about 110°C. The clear solution thus obtained was evaporated to a small volume and then acidified with acetic acid to pH 3. On cooling, a white crystalline powder appeared; this was then recrystallized from water. It was analyzed after dried by successive washings with alcohol and finally by keeping it in a vacuum desiccator.

*Analytical Results and Properties.* — Found: $(NH_4)_2O$, 9.39; $SeO_2$, 13.82; $MoO_3$, 42.90; $H_2O$, 33.89. Calcd. for $3(NH_4)_2O \cdot 2SeO_2 \cdot 5MoO_3 \cdot 30H_2O$: $(NH_4)_2O$, 9.62; $SeO_2$, 13.52; $MoO_3$, 44.10; $H_2O$, 32.76%.

It is a white crystalline powder stable at room temperature, but it decomposes when heated, giving a residue containing molybdenum trioxide and a small amount of selenium dioxide. It is soluble in water, and insoluble in alcohol, ether, benzene and nitrobenzene. Dilute nitric acid or dilute hydrochloric acid produces a slight change in color when boiled with this compound.

**Silver Salt of Molybdoselenite, Type I.** — A yellowish white compound was produced when silver nitrate was added to the ammonium salt solution.

Found: $Ag_2O$, 37.15; $SeO_2$, 11.09; $MoO_3$, 36.46; $H_2O$, 15.42. Calcd. for $3Ag_2O \cdot 2SeO_2 \cdot 5MoO_3 \cdot 17H_2O$: $Ag_2O$, 36.6; $SeO_2$, 11.4; $MoO_3$, 37.14; $H_2O$, 15.83%.

**Lead Salt of Molybdoselenite, Type I.**—This salt was prepared by adding an aqueous solution of lead nitrate to the ammonium salt solution. It is dirty white in color.

Found: PbO, 42.1; $SeO_2$, 13.3; $MoO_3$, 40.2; $H_2O$, 3.4. Calcd. for $3PbO \cdot 2SeO_2 \cdot 5MoO_3 \cdot 3H_2O$: PbO, 41.01; $SeO_2$, 13.09; $MoO_3$, 42.1; $H_2O$, 3.2%.

**Ferric Salt of Molybdoselenite, Type I.**—This is a powdery, yellow precipitate, insoluble in water and alcohol, formed when a dilute solution of ferric chloride is added in excess to the solution of the ammonium salt.

Found: $Fe_2O_3$, 10.09; $SeO_2$, 14.26; $MoO_3$, 45.6; $H_2O$, 27.5. Calcd. for $Fe_2O_3 \cdot 2SeO_2 \cdot 5MoO_3 \cdot 24H_2O$: $Fe_2O_3$, 10.4; $SeO_2$, 14.48; $MoO_3$, 46.9; $H_2O$, 28.4%.

**Cerous Salt of Molybdoselenite, Type I.**—A light yellow salt is obtained by adding a cerous nitrate solution to a dilute solution of the ammonium salt.

1) W. Gibbs, *Ber.*, **18**, 1089 (1885).
2) M. E. Péchard, *Ann. chim. phys.*, (6) **30**, 395 (1893).
3) A. Rosenheim and L. Krause, *Z. anorg. u. allgem. Chem.*, **118**, 177 (1921).
4) W. Prandtl and W. von Blochin, ibid., **93**, 45 (1915).
5) W. Prandtl, W. von Blochin and H. Obpacher, ibid., **93**, 70 (1915).

TABLE I. COMPOSITIONS OF LEAD, FERRIC AND CEROUS MOLYBDOSELENITE, TYPE I, ESTIMATED BY CONDUCTIVITY TITRATIONS

Volume of titration mixture: 65 ml.
Temperature: 30±0.5°C

| Molarity of ammonium salt | Molarity of titrant | Volume of titrant in ml. | Molar ratio ammonium salt : titrant |
|---|---|---|---|
| | Titration with lead nitrate | | |
| $6.738\times10^{-5}$ | $10.09\times10^{-3}$ | 0.64 | 1 : 2.94 |
| $10.107\times10^{-5}$ | $10.09\times10^{-3}$ | 0.97 | 1 : 2.96 |
| $13.476\times10^{-5}$ | $10.09\times10^{-3}$ | 1.30 | 1 : 2.94 |
| $16.845\times10^{-5}$ | $10.09\times10^{-3}$ | 1.59 | 1 : 2.94 |
| $20.214\times10^{-5}$ | $10.09\times10^{-3}$ | 1.94 | 1 : 2.95 |
| | Titration with ferric chloride | | |
| $10.107\times10^{-5}$ | $10.15\times10^{-3}$ | 0.65 | 1 : 2.95 |
| $13.476\times10^{-5}$ | $10.15\times10^{-3}$ | 0.86 | 1 : 2.93 |
| $16.845\times10^{-5}$ | $10.15\times10^{-3}$ | 1.08 | 1 : 2.94 |
| $20.214\times10^{-5}$ | $10.15\times10^{-3}$ | 1.31 | 1 : 2.96 |
| | Titration with cerous nitrate | | |
| $10.107\times10^{-5}$ | $10.28\times10^{-3}$ | 0.63 | 1 : 2.91 |
| $13.476\times10^{-5}$ | $10.28\times10^{-3}$ | 0.84 | 1 : 2.94 |
| $16.845\times10^{-5}$ | $10.28\times10^{-3}$ | 1.05 | 1 : 2.93 |

Found: $Ce_2O_3$, 23.31; $SeO_2$, 15.1; $MoO_3$, 48.94; $H_2O$, 10.7. Calcd. for $Ce_2O_3\cdot2SeO_2\cdot5MoO_3\cdot9H_2O$: $Ce_2O_3$, 22.9; $SeO_2$, 15.5; $MoO_3$, 50.27; $H_2O$, 11.3%.

**Ammonium Salt of Molybdoselenite, Type II.**—This compound was prepared by dissolving seleneous acid and molybdic acid in a molar ratio of 1:4 in aqueous ammonia and by then acidifying the boiling solution with nitric acid. A yellow compound was precipitated. The compound is insoluble in water, alcohol, and ether, but soluble in dilute hydrochloric acid.

Found: $(NH_4)_2O$, 10.56; $SeO_2$, 10.18; $MoO_3$, 67.4; $H_2O$, 11.86. Calcd. for $4(NH_4)_2O\cdot2SeO_2\cdot9MoO_3\cdot12H_2O$: $(NH_4)_2O$, 10.71; $SeO_2$, 11.43; $MoO_3$, 66.8; $H_2O$, 11.1%.

**Conductometric Titrations.**—0.01 M solutions of ammonium molybdoselenite, type I, and the titrants (i.e., silver nitrate, lead nitrate, ferric chloride and cerous nitrate), were prepared in conductivity water. The titrants were added from a micro buret in small amounts to different volumes of the ammonium salt solution (0.001 M) diluted to 65 ml., the mixture was stirred well, and the readings were recorded after allowing the precipitate to settle down. The end point was obtained graphically by plotting the volume of the titrant added against the conductance. The results are given in Table I.

## Discussion

The compounds present great difficulty in determining their structure because of the large size of the molecule. However, the compositions of the salts have been determined on the basis of our analytical results, which have been proved further by conductometric titrations.

Conductometric titrations of the ammonium salt, type I, with the titrants with univalent, bivalent or trivalent cations have been carried out. In all the cases except silver nitrate, sharp breaks at the molar ratios of the ammonium salt to the titrant of 1:3 (divalent) and 1:2 (trivalent) cations lend support to the formation of the salts reported.

In the case of silver nitrate, apparently there is no formation of the salt at that particular dilution; this results in a regular increase in the conductance giving a straight line.

The authors are thankful to the authorities of the Banaras Hindu University for providing facilities. One of the authors (V. N. G.) is also grateful to the C. S. I. R., New Delhi, for its financial assistance.

*Chemical Laboratories*
*Banaras Hindu University*
*Varanasi-5, India*

# The Polymerization of Butene Isomers*

By Akihiko SHIMIZU, Takayuki OTSU and Minoru IMOTO

(Received January 11, 1965)

In a previous paper,[1] the effect of the substituents on the radical polymerization of three propenyl chloride isomers, isopropenyl, *trans*-propenyl and *cis*-propenyl chlorides, has been reported. The results obtained may be summarized as follows: 1) All of these isomers homopolymerize with a radical or an ionic initiator only with difficulty, 2) the reactivity of these isomers toward an attack by a polymer radical decreases in the order of isopropenyl$\gg$*trans*-propenyl$\geq$*cis*-propenyl chloride, and 3) isopropenyl chloride copolymerizes with maleic anhydride easier than other isomers to yield a high-molecular-weight alternate copolymer. These results can be interpreted in terms both of the steric effect and the allylic termination of the substituents in these isomers.

In order to further clarify the effect of the substituents on vinyl polymerization, a study of the polymerization of four butene isomers, *n*-butene-1 (NB), isobutene (IB), *trans*-butene-2 (TB) and *cis*-butene-2 (CB), was taken up and will be reported on the present work. Several studies of the polymerization of butenes have been reported,[2-7] but no detailed study as to the polymerization of the respective butene monomers under similar conditions has been found. The present paper will deal with the effect of the methyl substituents on the polymerization and copolymerization of pure butene monomers in the presence of a radical or an ionic initiator.

## Experimental

**Materials.** — Butene monomers (Matheson Co.) were dried over calcium hydride and then purified by distillation. The physical properties of the butene monomers used in this work are shown in Table I, in which their purities as determined by gas chromatography are also indicated. The gas chromatography of the respective butene isomers was carried out by using an acetonyl-aceton column in a stream of hydrogen (30 ml./min.) at 0°C.

The vinyl acetate (VAC), acrylonitrile (AN), methyl methacrylate (MMA) and maleic anhydride (MAH) used as comonomers were purified by conventional methods.[8] Azobisisobutyronitrile (AIBN) was recrystallized from ethanol. Boron trifluoride-diethyl etherate was used after distillation. Butyllithium (Hans Heinrich Hütte), triethylaluminum (Ethyl Corp.), and titanium trichloride (Staufer Chem. Co.) were used without further purification.

**Polymerization Procedure.**—In a hard glass tube with a 20-ml. content, the required amount of initiator, solvent and comonomers were placed; this tube was then connected to a vacuum system. After degassing its contents by a repeated freezing and thawing technique, the required amount of butene monomer (which had been weighed beforehand in the vacuum system) was charged into the tube by distillation, and then the tube was sealed off.

In the case of ionic polymerization, a hard glass tube provided with a rubber stopper and from which catalytst had been charged through a syringe, besides a connecting part to vacuum system was used. The polymerization and copolymerization were carried out under shaking in a thermostat maintained at a constant temperature for a given time. After polymerization, the contents of the tube were poured into a large amount of methanol (ether was used in the case of MAH) to precipitate the polymer. The resulting polymer was washed thoroughly, filtered, dried under a vacuum at 40°C, and then weighed. In the case of the polymerization with the Ziegler catalyst, the contents of the tube were poured into a large amount of a hydrochloric acid - isopropyl alcohol mixture to precipitate the polymer, and then the polymer was purified by reprecipitation with isopropyl alcohol from a hot *n*-heptane solution. The rate of conversion was calculated from the weight of the dry polymer obtained.

The composition of the unreacted monomers after cationic or coordinated anionic polymerization was determined by gas chromatography in order to confirm the isomerization of butenes during the polymerization.

**The Analysis of the Polymer.**—The composition of the resulting polymer was determined by elemental analyses on carbon and hydrogen. The

* Vinyl Polymerization. CXIII.

1) T. Otsu, A. Shimizu and M. Imoto, *J. Polymer Sci.*, A3, 615 (1965).

2) V. N. Ipatiev and B. B. Carson, *Ind. Eng. Chem.*, **27**, 1069 (1935).

3) R. L. Meier, *J. Chem. Soc.*, **1950**, 3656.

4) A. I. Medalia, A. Orzechowski, J. A. Trinchera and J. P. Morley, *J. Polymer Sci.*, **41**, 241 (1959).

5) J. Gresser and M. Szwarc, *J. Am. Chem. Soc.*, **83**, 3005 (1961).

6) M. H. Jones and M. P. Thorne, *Can. J. Chem.*, **40**, 1510 (1962).

7) H. R. Allcock and A. M. Easthana, ibid., **41**, 932 (1963).

8) E. R. Blout, W. P. Hohenstein and H. Mark, "Monomer," Interscience, New York (1949); T. Otsu and K. Takemoto "Experimental Method of Vinyl Polymerization," Kyoritsu, Tokyo (1960).

TABLE I. PURITIES AND PROPERTIES OF THE BUTENE ISOMERS

| Monomer | Purity[a] % | B. p. °C | $d$ | Relative retention volume[b] | Composition of butenes[c] | | | |
|---|---|---|---|---|---|---|---|---|
| | | | | | IB | NB | TB | CB |
| IB | 99.27 | −6.7 | 0.674(−49°C) | 435 | 99.7 | 0.3 | 0.0 | 0.0 |
| NB | 97.90 | −6.3 | 0.669(−46°C) | 405 | 0.0 | 100.0 | trace | trace |
| TB | 99.35 | 0.9 | 0.635(−42°C) | 531 | trace | 0.0 | 99.7 | 0.3 |
| CB | 99.16 | 3.6 | | 633 | trace | 0.0 | 0.4 | 99.6 |

a) Determined by gas chromatography.
b) Relative retention volume of the butenes was calculated taking the retention time of air as unity.
c) Corrected wt. % in the butenes determined by gas chromatography.

structure of the resulting polymers was also checked by means of the infrared spectra of their films, which were made from an ethyl ether or a hot *n*-heptane solution.

The monomer reactivity ratios ($r_1$ and $r_2$) were calculated by the Fineman-Ross method.[9]

**The Determination of the Chain Transfer Constants of Butene Monomers.** — The apparent chain transfer constants ($C_m$) of butene monomers toward an attack by the polymethyl methacrylate radical were determined at 40, 50 and 60°C. The intrinsic viscosity of the resulting polymer was determined by the viscosity measurement of its dilute chloroform solution at 30°C. The number-average degree of polymerization ($\bar{P}_n$) was then calculated from the intrinsic viscosity, [$\eta$], according to the following equation:[10]

$$\log \bar{P}_n = 3.261 + 1.256 \log [\eta]$$

## Results

**The Homopolymerization of Butene Monomers.** —The results of the homopolymerization of butene monomers with various initiators are summarized in Table II. These monomers were found not to be polymerized in the presence of AIBN or of *n*-butyllithium.

In the cationic polymerization of the $BF_3 \cdot O(C_2H_5)_2$ catalyst, the reactivities of these monomers were quite low and decreased in the order of IB≫NB>TB—CB. In all cases the resulting polymers were colorless, oily and viscous. The isomerization of the respective butene monomers to the other isomers during the cationic polymerization was not observed, as Table II indicates.

Figure 1 shows the infrared spectra of the resulting polymers, in which the absorption bands characteristic of the sequences of the respective monomer units are observed in their polymers: the absorption bands due to the sequence of the butene-2 unit (1125 $cm^{-1}$),[11] the ethyl group (766 $cm^{-1}$),[12] and

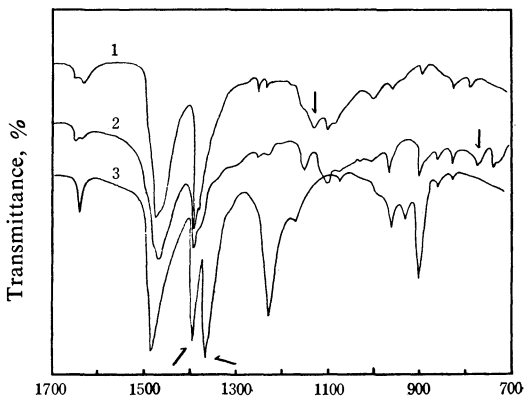



Fig. 1. Infrared spectra of polybutenes obtained with $BF_3 \cdot O(C_2H_5)_2$ (liquid film): (1) poly-*cis*-butene-2, (2) poly-*n*-butene-1, (3) polyisobutene.

*gem.*-dimethyl groups (1370, 1389 $cm^{-1}$)[13] were observed in the resulting polymers obtained from butene-2 (TB and CB), NB and IB, respectively.

In the coordinated anionic polymerization of these butene monomers by the $(C_2H_5)_3$-Al-$TiCl_3$ catalyst, as is also shown in Table II, their reactivities were in the order of NB≫CB—TB≫IB. From the results of the composition analyses (Table II) of unreacted butene monomers after the polymerization of IB and NB, the isomerization was not observed in the presence of any catalysts. However, the isomerizations from butene-2 (TB and CB) to NB and from CB to TB (or TB to CB) during the polymerization in the presence of the $(C_2H_5)_3Al$-$TiCl_3$ catalyst were observed.

Figure 2 shows the infrared spectra of these resulting polymers. It was clear that the polymers obtained from IB and NB showed absorption bands due to IB and NB units, respectively, in their infrared spectra. On the other hand, the infrared spectra of the

9) M. Fineman and S. D. Ross, *J. Polymer Sci.*, 5, 269 (1950).
10) B. Baysal and A. V. Tobolsky, ibid., 8, 529 (1952).
11) J. V. Schooten, E. W. Duck and R. Berkenbosch, *Polymer*, 2, 357 (1961).
12) M. C. Harvey and A. D. Ketley, *J. Appl. Polymer Sci.*, 5, 247 (1961).
13) L. J. Bellamy, "The Infrared Spectra of Complex Molecules," Wiley, New York (1958), p. 24.

TABLE II. RESULTS OF POLYMERIZATION OF BUTENES

| Initiation | Monomer | [M] mol./l. | Temp. °C | Time hr. | Yield % | Composition of butenes recovered after polymn.[c] IB | NB | TB | CB |
|---|---|---|---|---|---|---|---|---|---|
| [AIBN] = $1.68\times10^{-2}$ | IB | 2.10 | 60 | 20 | 0 | — | — | — | — |
| mol./l. in ethyl acetate | NB | 2.09 | 60 | 20 | 0 | — | — | — | — |
| | TB | 1.99 | 60 | 20 | 0 | — | — | — | — |
| | CB | 1.99 | 60 | 20 | 0 | — | — | — | — |
| [$BF_3\cdot O(C_2H_5)_2$] | IB[a] | 10.00 | 0 | 36 | 5.7 | — | — | — | — |
| $=3.0\times10^{-2}$ mol./l. | NB[a] | 9.99 | 0 | 36 | 0.2 | — | — | — | — |
| in bulk | NB | 11.93 | 27—30 | 240 | 3 | 0.0 | 97.9 | 0.9 | 1.2 |
| | TB | 11.34 | 27—30 | 240 | 0.5 | 0.0 | 0.0 | 99.8 | 0.2 |
| | CB | 11.34 | 27—30 | 240 | 1 | 0.0 | 0.1 | 1.5 | 98.4 |
| [$n$-$C_4H_9Li$] $10^{-1}$ | IB | 6.02 | −78 | 41 | 0 | — | — | — | — |
| mol./l. in toluene | NB | 5.97 | −78 | 41 | 0 | — | — | — | — |
| | TB | 5.67 | −78 | 41 | 0 | — | — | — | — |
| | CB | 5.67 | −78 | 41 | 0 | — | — | — | — |
| [$(C_2H_5)_3$Al-$TiCl_3$][b] | IB | 5.97 | 60 | 12 | 0.5 | 100.0 | trace | 0.0 | 0.0 |
| in $n$-heptane | NB | 6.03 | 60 | 0.83 | 73.1 | 0.0 | 100.0 | 0.0 | 0.0 |
| | TB | 6.08 | 60 | 12 | 1.0 | trace | 2.1 | 97.9 | trace |
| | TB | 6.08 | 80 | 28 | 17.5 | trace | 3.1 | 65.7 | 31.2 |
| | CB | 5.93 | 60 | 12 | 4.5 | trace | 2.6 | 27.1 | 70.3 |
| | CB | 5.93 | 80 | 28 | 18.0 | trace | 3.5 | 55.6 | 40.9 |

a) [$BF_3\cdot O(C_2H_5)_2$] = $5.0\times10^{-2}$ mol./l. in toluene
b) [$TiCl_3$] = $5.0\times10^{-2}$ mol./l., Al/Ti=2.0, Aging of catalyst: 27°C, 1 hr.
c) Corrected wt. % in the recovered butenes determined by gas chromatography

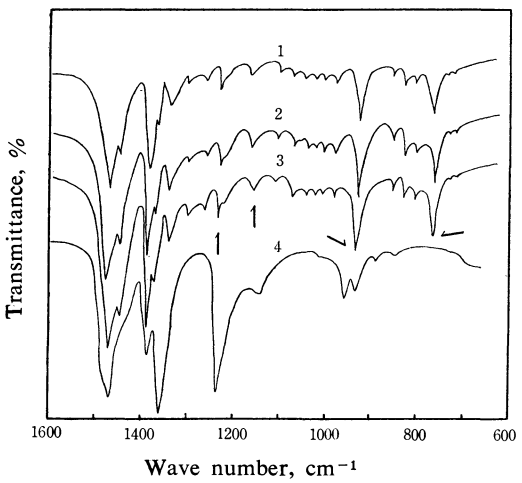



Fig. 2. Infrared spectra of the polymer resulted from $n$-butene-1 (1), *trans*-butene-2 (2), *cis*-butene-2 (3) and isobutene (4) with $(C_2H_5)_3$Al-$TiCl_3$ (film).

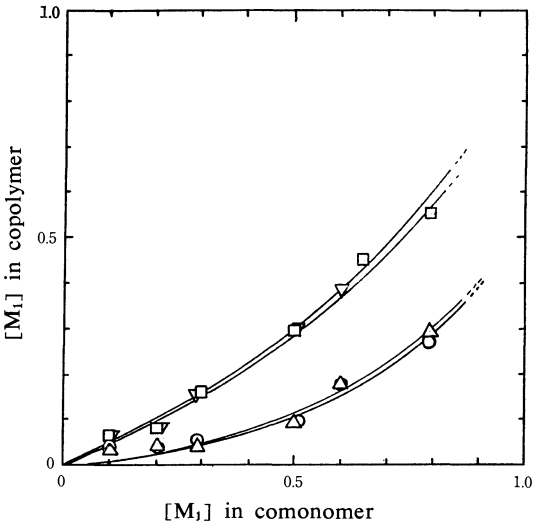



Fig. 3. Monomer-copolymer composition curves for copolymerization of butenes ($M_1$) with VAC ($M_2$) initiated by AIBN at 60°C: (□) IB-VAC system; (▽) NB-VAC system; (△) TB-VAC system; (○) CB-VAC system.

polymers from TB and CB showed no absorption bands due to the respective butene-2 units, although the absorption bands at 766 (ethyl group), 925 and 1221 $cm^{-1}$ (crystal. bands)[12] which are characteristic of the polymer of NB were observed.

**Copolymerization with VAC.** — The results of the radical copolymerization of butene monomers with VAC initiated by AIBN at 60°C are shown in Table III, in which the rate of copolymerization markedly decreases as the concentration of the butene monomer

TABLE III. RESULTS OF COPOLYMERIZATION OF THE BUTENES WITH VAC, AND AN AT 60°C; [AIBN] = $1.68 \times 10^2$ mol./l. IN BENZENE

| Polymerization system | [$M_1$] in comonomer mol. % | Time hr. | Yield % | Rate of copolymerization %/hr. | Copolymer C % | Copolymer H % | Copolymer [$M_1$] mol. % |
|---|---|---|---|---|---|---|---|
| IB($M_1$)-VAC($M_2$) | 9.98 | 2 | 11.6 | 5.8 | 57.11 | 7.24 | 6.54 |
| | 19.70 | 3 | 13.3 | 4.5 | 57.41 | 7.47 | 8.01 |
| | 29.80 | 4.5 | 7.1 | 1.6 | 59.25 | 7.95 | 16.68 |
| | 50.21 | 8 | 3.4 | 0.4 | 62.13 | 8.60 | 29.21 |
| | 66.17 | 42 | 12.9 | 0.3 | 66.33 | 9.29 | 45.55 |
| | 80.17 | 49 | 3.0 | 0.1 | 69.17 | 10.15 | 55.51 |
| NB($M_1$)-VAC($M_2$) | 9.91 | 2 | 5.6 | 2.8 | 57.12 | 7.13 | 6.58 |
| | 19.93 | 3 | 2.3 | 1.9 | 57.61 | 7.36 | 8.97 |
| | 28.30 | 4.5 | 5.5 | 1.2 | 59.14 | 7.79 | 16.20 |
| | 50.00 | 8 | 1.2 | 0.2 | 62.52 | 8.59 | 30.82 |
| | 59.97 | 42 | 4.6 | 0.1 | 64.45 | 8.95 | 38.49 |
| | 79.70 | 49 | 0.9 | 0.02 | — | — | — |
| TB($M_1$)-VAC($M_2$) | 10.19 | 2 | 8.9 | 4.4 | 56.48 | 7.12 | 3.41 |
| | 19.86 | 3 | 8.0 | 2.7 | 56.59 | 7.20 | 3.97 |
| | 28.15 | 4.5 | 7.1 | 1.6 | 56.61 | 7.25 | 4.06 |
| | 49.89 | 8 | 3.8 | 0.5 | 57.50 | 7.38 | 8.45 |
| | 59.86 | 42 | 9.2 | 0.2 | 59.62 | 7.85 | 18.36 |
| | 79.09 | 49 | 2.4 | 0.1 | 62.15 | 8.40 | 29.29 |
| CB($M_1$)-VAC($M_2$) | 10.19 | 2 | 7.7 | 3.8 | 56.51 | 7.16 | 3.56 |
| | 19.86 | 3 | 7.4 | 2.5 | 56.44 | 7.17 | 3.20 |
| | 28.15 | 4.5 | 2.5 | 0.6 | 56.60 | 7.20 | 4.01 |
| | 49.89 | 8 | 2.3 | 0.3 | 57.58 | 7.48 | 8.84 |
| | 59.86 | 42 | 8.2 | 0.2 | 59.44 | 7.80 | 17.53 |
| | 79.09 | 49 | 2.4 | 0.1 | 61.42 | 8.49 | 26.22 |
| IB($M_1$)-AN($M_2$) | 9.90 | 0.5 | 1.6 | 3.1 | 69.04 | 6.47 | 6.10 |
| | 19.83 | 1 | 1.8 | 1.8 | 71.59 | 7.53 | 19.91 |
| | 29.77 | 1.3 | 1.6 | 1.2 | 73.14 | 7.91 | 28.40 |
| | 39.74 | 2 | 1.7 | 0.9 | 73.81 | 8.12 | 32.10 |
| | 59.74 | 4 | 1.8 | 0.4 | 75.06 | 9.55 | 39.05 |
| | 79.83 | 21 | 5.6 | 0.3 | 75.62 | 9.47 | 42.17 |
| NB($M_1$)-AN($M_2$) | 10.08 | 0.5 | 4.7 | 9.3 | 67.95 | 5.86 | 0.26 |
| | 20.20 | 1 | 7.4 | 7.4 | 68.32 | 6.26 | 2.25 |
| | 29.60 | 1.3 | 3.9 | 3.0 | 68.33 | 6.22 | 2.30 |
| | 39.54 | 2 | 2.2 | 1.1 | 68.80 | 6.41 | 4.82 |
| | 59.54 | 4 | 2.4 | 0.6 | 71.25 | 7.57 | 18.05 |
| | 79.69 | 21 | 4.6 | 0.2 | 73.94 | 8.27 | 32.83 |
| TB($M_1$)-AN($M_2$) | 9.89 | 0.5 | 3.7 | 7.4 | 66.94 | 5.84 | 0 |
| | 19.92 | 1 | 3.3 | 3.3 | 67.46 | 6.06 | 0 |
| | 30.09 | 1.3 | 2.5 | 2.0 | 68.06 | 6.20 | 0.85 |
| | 40.41 | 2 | 2.2 | 1.1 | 68.26 | 6.28 | 1.92 |
| | 59.87 | 4 | 1.4 | 0.3 | 68.85 | 6.87 | 5.08 |
| | 78.86 | 8 | 0.4 | 0.1 | 71.37 | 8.27 | 18.71 |
| CB($M_1$)-AN($M_2$) | 9.89 | 0.5 | 4.1 | 8.3 | 67.05 | 5.96 | 0 |
| | 19.92 | 1 | 4.4 | 4.4 | 66.92 | 5.98 | 0 |
| | 30.09 | 1.3 | 1.7 | 1.3 | 67.59 | 6.19 | 0 |
| | 40.41 | 2 | 1.9 | 0.9 | 67.81 | 5.93 | 0 |
| | 59.87 | 4 | 1.1 | 0.3 | 69.21 | 7.26 | 7.01 |
| | 78.86 | 21 | 1.2 | 0.1 | 71.11 | 7.81 | 17.29 |

TABLE IV. RESULTS OF COPOLYMERIZATION OF BUTENES ($M_1$) WITH MAH ($M_2$) AT 60°C; [AIBN] = $1.68 \times 10^{-2}$ mol./l. IN BENZENE

| $M_1$ | [$M_1$] in comonomer mol. % | Time hr. | Yield % | Rate of copolymerization %/hr. | Copolymer C % | Copolymer H % | Copolymer [$M_1$] mol.% | $\eta_{sp}/C$[a] |
|---|---|---|---|---|---|---|---|---|
| IB | 19.87 | 0.17 | 6.8 | 41.0 | 61.02 | 6.37 | 46.05 | — |
| | 39.87 | 0.17 | 12.2 | 73.4 | 61.32 | 6.47 | 46.96 | 1.20 |
| | 59.80 | 0.08 | 13.9 | 167 | 61.35 | 6.66 | 47.06 | — |
| | 79.69 | 0.33 | 4.2 | 12.7 | 61.48 | 6.45 | 47.44 | — |
| NB | 20.07 | 20 | 20.4 | 1.0 | 61.04 | 6.37 | 46.10 | — |
| | 39.67 | 20 | 27.7 | 1.4 | 61.33 | 6.18 | 47.72 | 0.08 |
| | 60.05 | 20 | 45.5 | 2.3 | 61.70 | 6.24 | 48.11 | — |
| | 80.09 | 4.3 | 13.7 | 3.2 | 61.81 | 6.70 | 48.44 | — |
| TB | 19.79 | 20 | 7.0 | 0.4 | 60.15 | 6.12 | 43.33 | — |
| | 39.79 | 20 | 13.0 | 0.6 | 60.85 | 6.13 | 45.52 | 0.06 |
| | 59.74 | 20 | 14.7 | 0.7 | 61.23 | 6.57 | 46.68 | — |
| | 79.81 | 4.3 | 3.2 | 0.8 | 61.26 | 6.24 | 46.78 | — |
| CB | 19.79 | 20 | 9.2 | 0.5 | 60.34 | 6.27 | 43.92 | — |
| | 39.79 | 20 | 16.9 | 0.8 | 60.76 | 6.12 | 45.24 | 0.05 |
| | 59.74 | 20 | 22.1 | 1.1 | 61.16 | 6.00 | 46.47 | — |
| | 79.81 | 4.3 | 5.0 | 1.2 | 61.22 | 6.62 | 46.65 | — |

a) Determined by viscosity measurement of 0.4% tetrahydrofuran solution in an Ubbelohde viscometer.

increases. On the basis of the results of Table III, the monomer-copolymer composition curves are shown in Fig. 3.

**Copolymerization with AN.** — The results of the copolymerization of butene monomers with AN initiated by AIBN are shown in Table III, from which the monomer-copolymer composition curves are shown in Fig. 4.

**Copolymerization with MAH.** — The results of the copolymerization of the butene monomers with MAH initiated by AIBN at 60°C are shown in Table IV, from which the monomer-copolymer composition curves are shown in Fig. 5. As is clearly indicated in Table IV, the composition of the resulting copolymers was found to be independent of

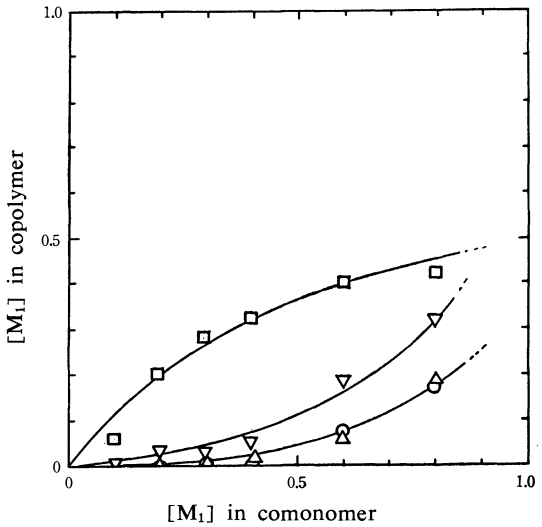



Fig. 4. Monomer-copolymer composition curves for copolymerization of butenes ($M_1$) with AN ($M_2$) initiated by AIBN at 60°C: (□) IB-AN system; (▽) NB-AN system; (△) TB-AN system; (○) CB-AN system.

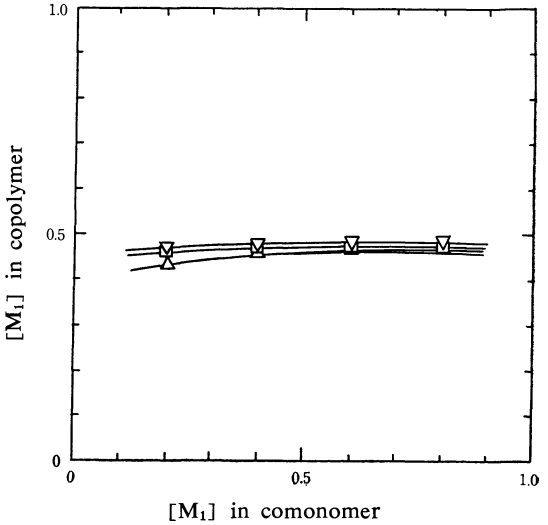



Fig. 5. Monomer-copolymer composition curves for copolymerization of butenes ($M_1$) with MAH ($M_2$) initiated by AIBN at 60°C: (□) IB-MAH system; (▽) NB-MAH system; (△) TB-MAH system; (○) CB-MAH system.

TABLE V. MONOMER REACTIVITY RATIOS ($r_1$, $r_2$) AND $Q_1$, $e_1$ VALUES FOR BUTENES

| $M_1$ | $M_2$ | $r_1$ | $r_2$ | $1/r_2$ | Relative reactivity | $Q_1$ | $e_1$ |
|---|---|---|---|---|---|---|---|
| IB | VAC | 0.31 | 2.15 | 0.47 | 3.8 | 0.014 | −0.86 |
| IB | AN | 0.00 | 0.80 | 1.25 | 17.6 | — | — |
| NB | VAC | 0.34 | 2.0 | 0.50 | 4.0 | 0.012 | −0.69 |
| NB | AN | 0.10 | 8.0 | 0.13 | 2.0 | — | — |
| TB | VAC | 0.07 | 7.0 | 0.14 | 1.1 | 0.004 | −1.06 |
| TB | AN | 0.00 | 14.0 | 0.07 | 1.0 | — | — |
| CB | VAC | 0.07 | 8.0 | 0.13 | 1.0 | 0.004 | −0.98 |
| CB | AN | 0.00 | 14.0 | 0.07 | 1.0 | — | — |

the monomer feed ratio and to be a 1 : 1 molar composition of MAH and the butene monomer.

IB copolymerized quite readily with MAH to give a colorless polymer which had a relatively high specific viscosity. However, the other butene monomers copolymerized at a rather slow rate, and light yellow-colored copolymers of a lower specific viscosity were obtained. Accordingly, it was clear that the tendency of these butene monomers to alternate copolymerization with MAH decreased in the order of IB≫NB≥CB≥TB.

The rate of the copolymerization of butene monomers with MAH increased with an increase in the initial concentration of the butene monomer and showed the maximum shown in Fig. 6.

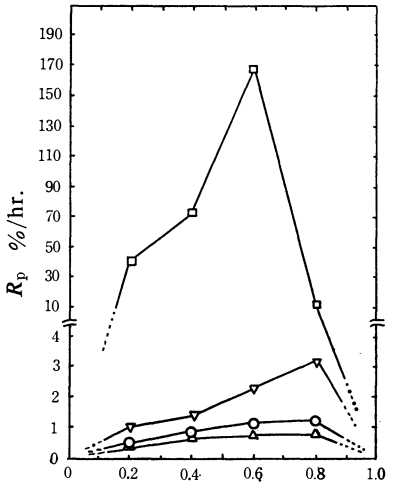



Fig. 6. Relationship between $R_p$ and monomer feed ratio for copolymerization of butenes ($M_1$) with MAH ($M_2$) initiated by AIBN at 60°C.

□ Isobutene
▽ *n*-Butene
△ *trans*-Butene
○ *cis*-Butene

**The Monomer Reactivity Ratio and the *Q* and *e* Values for Butene Monomers.**—The monomer reactivity ratios ($r_1$ and $r_2$) were calculated for these copolymerizations according to the Fineman-Ross method.[9] The results are summarized in Table V. From the values of $r_1$ and $r_2$ for the copolymerization with VAC, the $Q$ and $e$ values for butene monomers were calculated by assuming that $Q=0.026$ and $e=-0.22$ for VAC.[14]

As may be understood from this table, the values of $Q_1$ for butene monomers and the values of $1/r_2$ which might indicate the reactivity of butene monomers to polymer radicals were found to have the same tendency in their reactivities to cationic polymerization.

**The Chain Transfer Constants of Butene Monomers.**—Since it was confirmed from the elemental analyses and the infrared spectra of the resulting polymers that these butene monomers scarcely copolymerized with MMA at all, the apparent chain transfer constant of

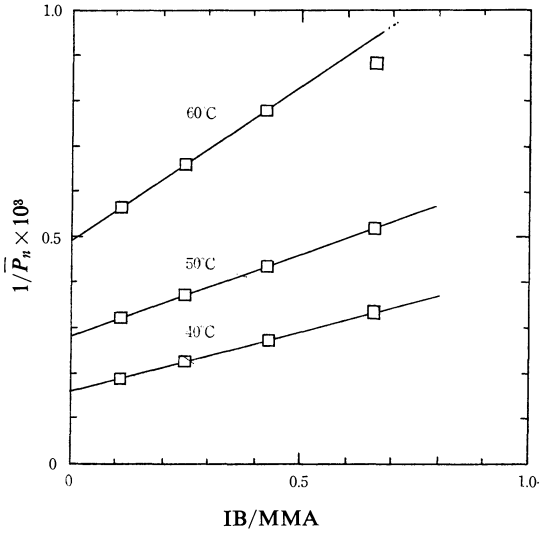



Fig. 7. Relationship between $1/\bar{P}_n$ and IB/MMA for copolymerization of isobutene with MMA.

14) L. J. Young, *J. Polymer Sci.*, **54**, 411 (1961).

TABLE VI. RATE CONSTANTS OF BUTENES TOWARD ATTACK OF RADICALS

| Butene | $k_2/k_1$ (65°C) | $k_3/k_2$ (65°C) | $C_m \times 10^3$ (40°C) | (50°C) | (60°C) |
|---|---|---|---|---|---|
| IB | 35.6 | 0.06 | 0.25 | 0.44 | 0.69 |
| NB | 26.9 | 0.25 | 0.31 | 0.51 | 0.73 |
| TB | 6.9 | 0.72 | 0.30 | 0.52 | 1.08 |
| CB | 3.3 | 0.95 | 0.32 | 0.49 | 1.12 |

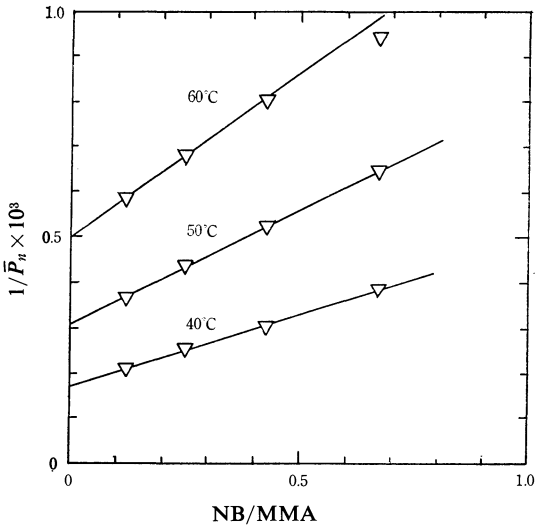



Fig. 8. Relationship between $1/\bar{P}_n$ and NB/MMA for copolymerization of *n*-butene with MMA.

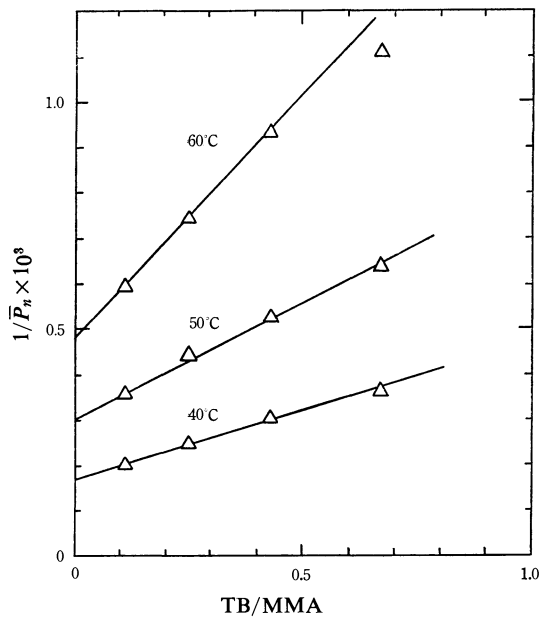



Fig. 9. Relationship between $1/\bar{P}_n$ and TB/MMA for copolymerization of *trans*-butene with MMA.

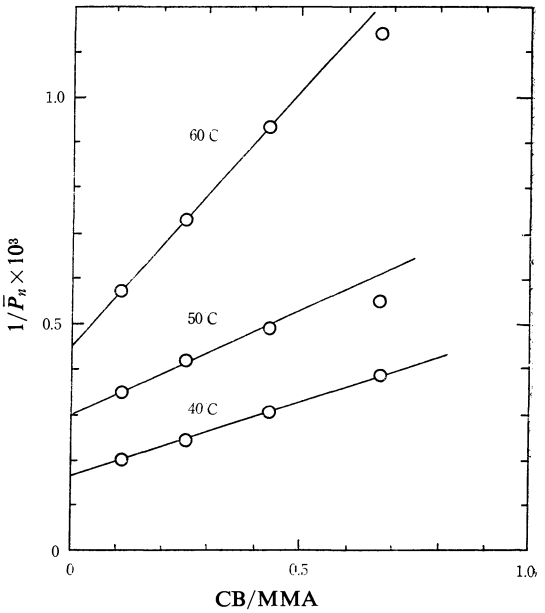



Fig. 10. Relationship between $1/\bar{P}_n$ and CB/MMA for copolymerization of *cis*-butene with MMA.

these butene monomers toward an attack by a polymethyl methacrylate radical were determined. The results are shown in Figs. 7—10 and Table VI.

Table VI also shows the relative reactivities of a methyl radical to butene isomers determined by Szwarc and his co-workers.[15] In this table, $k_1$, $k_2$ and $k_3$ are the rate constants, respectively, for hydrogen abstraction from isooctane, for addition to butenes, and for hydrogen abstraction from butenes toward the attack of a methyl radical.

## Discussion

In Tables II and III it was observed that these butene monomers did not homopolymerize in the presence of a radical initiator and that their copolymerization reactivities with VAC were in the order of IB≫NB>TB—CB. The

15) R. P. Buckley, F. Leavitt and M. Szwarc, *J. Am. Chem. Soc.*, **78**, 5557 (1956); R. P. Buckley and M. Szwarc, *Proc. Royal Soc.*, **A240**, 396 (1957).

results for butene isomers were almost the same as those for propenyl chloride isomers.[1)]

The low reactivitities of butene-2 monomers which are 1,2-disubstituted ethylene may be understood as the result of an increased steric effect of the substituents. It is also supported by the smaller $Q$ values of TB and CB than those of IB and NB, as Table V shows.

In the copolymerizations of propenyl chloride isomers, it was found that the trans-isomers were about two or three times more reactive than the cis-isomer toward attacks by polymer radicals. However, TB and CB were found to have almost the same reactivity. This result may be interpreted as indicating that CB takes a coplanar structure just like that of TB in the transition state.

From Table IV it is obvious that the tendency of the butene monomers to alternate copolymerization with MAH decreases in the order of IB$\gg$NB$>$CB$\geq$TB, which is similar to the findings concerning propenyl chloride isomers.[1)] This order in the reactivity of butene isomers was also similar to that of their hydrogen abstractions by the methyl radical and the polymethyl methacrylate radical, as is shown in Table VI. Accordingly, it may be concluded that the degradative chain transfer reactivity of butene isomers, which might be determined by their steric effects, is an important factor in their polymerizations and copolymerizations in the presence of a radical initiator.

The rate of the copolymerization of butene or propenyl chloride isomers with MAH markedly decreases with an increase in the concentration of butene or propenyl chloride in the monomer mixture. However, it is interesting that the rates of the copolymerizations of butenes with MAH gave a maximum as a function of the monomer concentration, as is shown in Fig. 6. This result might indicate that the specific stabilization of the transition state in alternating propagation which would lead to an energy-lowering is significant, as has been pointed out by Price[16)] and Walling[17)].

As can be seen from Table II, no butene monomers could be homopolymerize in the presence of *n*-butyl lithium, and only IB could be homopolymerized by $BF_3 \cdot O(C_2H_5)_2$. Their reactivities for cationic polymerization decreased in the order of IB$\gg$NB$>$TB—CB, and no isomerization was observed during the polymerization.

As is clearly shown in Table II, however, NB, TB and CB could be easily homopolymerized in the presence of the $(C_2H_5)_3Al$-$TiCl_3$ catalyst to give high-molecular-weight polymers. It was noted that TB and CB, which were known[18)] not to homopolymerize because of the steric effect, could homopolymerize at rather high temperatures. It was confirmed by infrared spectra and X-ray diffraction analyses that all of the polymers resulting from TB and CB consisted of the NB sequence.

The isomerization from TB to CB or NB and that from CB to TB or NB during the polymerization were observed in the presence of this coordinated catalyst. Accordingly, it was deemed that TB and CB isomerized into NB in the presence of $(C_2H_5)_3Al$-$TiCl_3$ catalyst and then polymerized to give a high-molecular-weight polymer of NB. The mechanism of the polymerization of butene-2 by the Ziegler-Natta catalyst will be described in detail in the next paper.

## Summary

The effect of the methyl substituents of four butene isomers (IB, NB, TB and CB) on their polymerizations and copolymerizations has been investigated. None of these monomers homopolymerized in the presence of an ordinary radical or in that of anionic catalysts, but they were homopolymerized by cationic catalysts. The reactivity of these monomers toward their cationic polymerizations and radical copolymerizations has been found to decrease in the order of IB$\gg$NB$>$TB—CB. These results have been interpreted on the basis of the steric effect and the chain transfer reactivity of the methyl substituents in these monomers.

These monomers, except for IB, can easily be homopolymerized by the Natta catalyst in the reactivity order of NB$\gg$TB—CB. The resulting polymers from TB and CB have been confirmed to be the same as the polymer from NB, which consisted of the recurring unit of *n*-butene-1.

The authors wish to thank Dr. Riichiro Imoto of the Toyo Soda Co. for his helpful suggestions and encouragement.

*Department of Applied Chemistry*
*Faculty of Engineering*
*Osaka City University*
*Sumiyoshi-ku, Osaka*

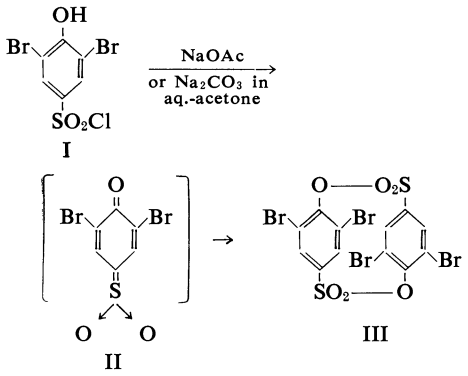
16) C. C. Price, *J. Polymer Sci.*, **1**, 83, (1946); **2**, 101 (1947); **3**, 772 (1948).
17) C. Walling, E. R. Briggs, K. B. Wolfstirn and F. R. Mayo, *J. Am. Chem. Soc.*, **70**, 1537 (1948); C. Walling, D. Seymour and K. B. Wolfstirm, ibid., **70**, 1544 (1948).
18) G. Natta, G. Dall'Asta, G. Mazzanti, I. Pasquon, A. Valvassori and A. Zambelli, ibid., **83**, 3343 (1961).

# The Reaction of 3, 5-Dibromo-4-hydroxybenzenesulfonyl Chloride with Weak Bases (The Question of the "Quinoid Sulfene" Intermediate*)

By Shigeru OAE and Reiko KIRITANI

(Received February 22, 1965)

Many decades ago, Zincke[1] and his coworkers suggested the formation of the "sulfene" intermediate (II) in the reaction of 3, 5-dibromo-4-hydroxybenzenesulfonyl chloride (I) with either sodium acetate or carbonate in an aqueous acetone solution; they made this suggestion on the basis of their observations that a bright yellow color is formed and then gradually disappears during the reaction, finally giving a colorless precipitate which was presumed to have structure (III).

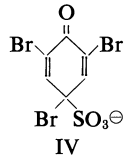



I II III

The possibility of this "quinoid sulfene" intermediate is rather fascinating in view of the recent interest in aliphatic "sulfene."[2] However, there has been no legitimate evidence to substantiate the formation of the intermediate during the reaction, nor has the product ever been proved to have structure III.

We have investigated this reaction, first by following the change in the ultraviolet absorption and then by determining the structure of the product. When an acetone solution of 3, 5-dibromo-4-hydroxybenzenesulfonyl chloride was mixed with a 20% aqueous solution containing an equimolar amount of potassium acetate, a bright yellow color developed immediately. Meanwhile, colorless precipitates started to form gradually and the yellow color faded away. Then the ultraviolet absorption was swept at several time intervals. The results are shown in Fig. 1. At an early stage of the reaction, when the yellow color was still strong, one saw a clear maximum at 310 m$\mu$, but this maximum gradually faded away as time passed. The strong absorption around 310 m$\mu$ might be due to the quinoid structure of the intermediate "sulfene."

However, Cannell[3] has recently shown that the quinoid intermediate (IV) formed during the bromination of sodium 3, 5-dibromo-4-hydroxybenzenesulfonate has a strong absorption around 280 m$\mu$ ($\varepsilon = 11400$).




IV

The process was also followed by the sweeping of the infrared spectrum around 1500—2000 $cm^{-1}$, in order to detect the presence of a conjugated carbonyl group. However, as Fig. 2 shows, there was no detectable absorption of any carbonyl function in the spectrum.

Since quinoid compounds are known to undergo electron transfer with phenolic compounds, thus forming fairly stable radicals, usually detectable by means of ESR spectroscopy,[4] the color which appeared in this reaction was suspected of being associated with the formation of an radical. The ESR spectrum was taken during the process of color formation. However, no detectable signal was observed.

Therefore, we have at present no concrete evidence to support the formation of the "quinoid sulfene" intermediate, nor can we offer any alternative suggestion as to the nature of the yellow color or of the incipient ultraviolet absorption perk at 310 m$\mu$.

When triethylamine was used in place of sodium acetate, it was found to effect the same reaction. In fact, with the tertiary amine one

* Presented at the 14th Annual Meeting of the Chemical Society of Japan, April, 1961. Paper V of "Reactions of Phenols and Phenolic Esters."

1) a) T. Zincke and W. Glahn, *Ber.*, **40**, 3039 (1907); b) T. Zincke and R. Brune, ibid., **41**, 902 (1908).

2) a) W. E. Truce, J. J. Breiter, D. J. Abraham and J. R. Norell, *J. Am. Chem. Soc.*, **84**, 3030 (1962); b) G. Optiz and H. Adalph, *Angew. Chem.*, **74**, 77 (1962); c) G. Optiz and K. Fischer, *Z. Naturforsch*, **186**, 775 (1963).

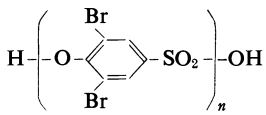
3) L. G. Cannell, *J. Am. Chem. Soc.*, **79**, 2927 (1957).

4) Private communication from Dr. R. Konaka.

can use anhydrous conditions and usually get better results. However, in this case the product appeared to be slightly more soluble in benzene, nitrobenzene or dioxane, possibly because of the lower molecular weight. Several attempts were made to freeze the intermediate for physical measurement by running the reaction in a dry-ice acetone bath. However, as soon as the solvent was evaporated, only a colorless precipitate remained.

The colorless precipitate, which was presumed to have structure III, is insoluble in most common solvents but only sparingly soluble in benzene and a little more soluble in nitrobenzene. It has no melting or decomposition points below 350°C. Since the amorphous precipitate is sparingly soluble in benzene and nitrobenzene, the molecular weight determination in these solvents was not successful, despite repeated careful attempts.

When this material was refluxed in a 6 N sodium hydroxide solution for an hour, the precipitate dissolved completely to give a clear solution. From the clear solution 3, 5-dibromo-4-hydroxybenzenesulfonic acid was recovered almost quantitatively as its *S*-benzylthiuronium salt. The mode of the facile hydrolysis was very similar to that with phenyl benzenesulfonate.[5] The acid hydrolysis was very sluggish and was found to take place only above 160°C in a sealed tube using 10 N hydrochloric acid, similar to the case of phenyl benzenesulfonate.[6] When it was hydrolyzed at 180°C for 24 hr., 3, 5-dibromo-4-hydroxybenzenesulfonic acid was recovered in an almost quantitative yield as its *S*-benzylthiuronium salt. These observations on the hydrolyses, together with the analytical data, seem to suggest that the precipitate has a structure similar to phenyl benzenesulfonate, possibly a linear oligomer such as V.



V

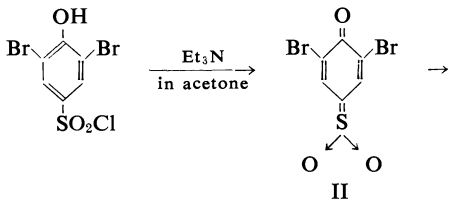
Both the infrared and the ultraviolet spectra of the material is almost identical with those of 3, 5-dibromo-4-hydroxybenzenesulfonic acid. Zincke's cyclic structure will not give similar ultraviolet and infrared spectra, because the molecule of the structure would be terribly strained and might be expected to change the nature of the electronic behavior considerably.

A rough determination of the terminal hydroxy group was carried out by reacting with phenyl isocyanate the precipitate obtained in the reaction with triethylamine. The product, presumably the urethan of the oligomer V, obtained in this reaction did not melt below 350°C, but its analytical composition is that of the phenyl urethan of either tetramer or pentamer of V, or a mixture of both.

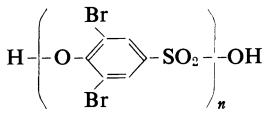
It is interesting to note that the oligomer can be crystallized from benzene, but that the crystals become amorphous powder when benzene is completely evaporated. A preliminary X-ray analysis[7] revealed the same phenomena.

Since the crystals were rather short-lived outside of the benzene solution, no further attempt was made to determine the structure. However, they are most likely a kind of clathrate complex, the oligomer and benzene being the host and the guest molecules respectively.

In conclusion, the reaction of 3, 5-dibromo-4-hydroxybenzenesulfonyl chloride (I) with a base such as triethylamine produces an quasi-stable intermediate, possibly the "quinoid sulfene" intermediate (II), which is sufficiently long-lived to find a few similar partner with which to oligomerize to the oligomer V, as is shown below:



II



V

## Experimental

**3, 5-Dibromo-4-hydroxybenzenesulfonyl Chloride.** — Sodium 3, 5-dibromo-4-hydroxybenzenesulfonate was obtained by the methods reported by Huston and Neeley,[8] and by Oshima[9] (yield 88%). The product was recrystallized from water and identified as 3, 5-dibromo-4-hydroxybenzenesulfonic acid *S*-benzylthiuronium salt; m. p. 192—193°C.

Found: C, 33.23; H, 2.81. Calcd. for $[C_6H_3Br_2O_4S]^-[C_6H_5CH_2SC(NH_2)_2]^+$: C, 33.05; H, 2.60%.

When the product was then allowed to react with a mixture of phosphorus oxychloride and

5) D. R. Christman and S. Oae, *Chem. & Ind.*, **1959**, 1251.
6) S. Oae, T. Fukumoto and R. Kiritani, ibid., **36**, 346 (1963).
7) We are indebted to Professor M. Kakudo for his generous collaboration.
8) R. C. Huston and A. H. Neeley, *J. Am. Chem. Soc.*, **57**, 2177 (1935).
9) See "Benzenesulfonic Acid" in "Yukikagaku Goseiho," Vol. I, Gihodo, Inc., Tokyo (1953), p. 31.

phosphorous pentachloride,[1a] 3,5-dibromo-4-hydroxybenzenesulfonyl chloride was obtained (66% yield from sodium salt). The sulfonyl chloride thus obtained was recrystallized from benzene; m. p. 128—129°C (Found: C, 20.2; H, 0.82%).

**The Reaction of 3,5-Dibromo-4-hydroxybenzenesulfonyl Chloride with Sodium Acetate.**[1b]—A solution of 3,5-dibromo-4-hydroxybenzenesulfonyl chloride (2 g., 0.0058 mol.) and 5 ml. of acetone was cooled in an ice-water bath. As soon as an equimolar amount of a 20% aqueous sodium acetate solution (3.5 ml.) was slowly added to the solution, the mixture turned a bright yellow; this color gradually disappeared during the reaction, and white precipitates were formed. The mixture was heated to reflux gently for a few minutes and then allowed to stand. The colorless solid product was obtained in a 30—35% yield based on the starting sulfonyl chloride. It could be recrystallized from nitrobenzene (no m. p. below 350°C). Together with the water-insoluble solid, the hydrolysis product, 3,5-dibromo-4-hydroxybenzenesulfonic acid, was also obtained from the filtrate; it was identified as a *S*-benzylthiuronium salt. The unchanged reactant was also recovered.

**The Reaction of 3,5-Dibromo-4-hydroxybenzenesulfonyl Chloride with Triethylamine.**—An acetone solution of 3,5-dibromo-4-hydroxybenzenesulfonyl chloride (2 g. in 5 ml. of acetone) was cooled and added to an equimolar amount of triethylamine. The reaction was nearly identical with that in an aqueous acetone solution with sodium acetate. The water-insoluble colorless product (yield 30—35%) was slightly soluble in hot benzene (no m. p. below 350°C). Recrystallization from benzene gave colorless shiny prismatic crystals in the bottom of the benzene layer; however, when the crystals were collected on filter paper, they gradually pulverized to an amorphous white powder. The analytical values of the colorless precipitate are as follows:

| | C% | H% | Br% | S% |
|---|---|---|---|---|
| Calcd. for III | 22.92 | 0.64 | 50.93 | 10.21 |
| Calcd. for $V_{n=5}$ | 22.69 | 0.76 | 50.33 | 10.10 |
| Found (by Zincke et al.) | 23.36 | 0.40 | 50.75 | 10.07 |
| Present investigation | 22.59 | 0.77 | 50.83 | 9.99 |

**The Alkaline Hydrolysis of the Colorless Precipitate.**—The colorless precipitate (1 g.) was added to a 20% aqueous sodium hydroxide solution (25 ml.); the mixture was refluxed for 1.5 hr., neutralized with hydrochloric acid, and finally evaporated down to 2 ml. When a few drops of hydrochloric acid and *S*-benzylthiuronium chloride (0.7 g.) were added to this solution, the *S*-benzylthiuronium salt of 3,5-dibromo-4-hydroxybenzenesulfonic acid (1.5 g.) was obtained (in a nearly quantitative yield).

**The Acid Hydrolysis of the Colorless Precipitate.**—The colorless precipitate (1 g.) and 10 N hydrochloric acid (20 ml.) were sealed in a tube and heated at 180°C for 24 hr. The resultant mixture was filtered, and the filtrate was treated with *S*-benzylthiuronium chloride as described above; the *S*-benzylthiuronium salt of 3,5-dibromo-4-hydroxybenzenesulfonic acid (1.3 g.) was obtained. The precipitate was found to be the unchanged polymer (0.1 g., 10%).

**The Reaction of the Colorless Precipitate with Phenyl Isocyanate.**[10]—Phenyl isocyanate (0.3 g., 0.0025 mol.) was added to a solution of the colorless precipitate (1.6 g., 0.0025 mol. as the linear dimer) in 20 ml. of dioxane, and then a few drops of anhydrous pyridine were added to the mixture. After the mixture has been refluxed for one hour, the solvent was removed. The residual precipitate was washed thoroughly with a large quantity of ice-water. Thus, a light brown precipitate partially soluble in benzene was obtained (1.6 g.) (no m. p. below 350°C). The analytical values of the product recrystallized from benzene, shown below, indicate that the urethan derivative of the oligomer was a mixture of the tetramer and the pentamer.

Found: C, 26.43; H, 1.15; Br, 46.46; S. 9.31; N, 0.88. Calcd. for $C_{37}H_{17}O_{17}Br_{10}S_5N$ (pentamer): C, 26.03; H, 1.00; Br, 46.82; S, 9.39; N, 0.82, for $C_{31}H_{15}O_{14}Br_8S_4N$ (tetramer): C, 26.73; H, 1.09; Br, 45.90; S, 9.21; N, 1.01%.

**Ultraviolet Spectra.**—The ultraviolt spectra of the "quinoid sulfene" intermediate, the colorless precipitate and 3,5-dibromo-4-hydroxybenzenesulfonyl chloride are shown in Fig. 1.

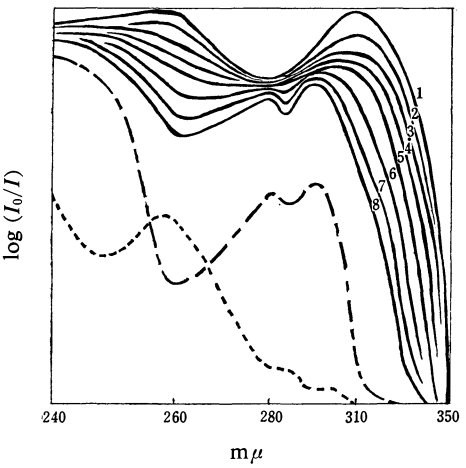



Fig. 1

—— UV spectra of quinoid sulfene intermediate: 1, 2, 3, ···, 8, after mixing the 3,5-dibromo-4-hydroxybenzenesulfonyl chloride in dioxane with an aqueous equimolar amount solution of potassium acetate, 30 sec., 5, 10, 20, 30, 40, 50, and 60 min.

—·— The oligomer V

---- 3, 5-Dibromo-4-hydroxybenzenesulfonyl chloride ($4\times10^{-7}$ mol./ml.) in *n*-hexane

A known amount of 3,5-dibromo-hydroxybenzenesulfonyl chloride was dissolved in pure dioxane ($1\times10^{-5}$ mol./10 ml.), and also an aqueous solution in which has been dissolved an equimolar amount of potassium acetate solution ($1\times10^{-5}$

10) See "Urethans" in "The Systematic Identification of Organic Compounds," by R. L. Shriner and R. C. Fuson, John Wiley & Sons, New York, N. Y. (1956), p. 211.

mol./10 ml.) was prepared. The two solutions were separately cooled in an ice-salt bath before mixing. As soon as the cooled dioxane solution was mixed with the aqueous solution, the ultaviolet spectra of the mixed solution were followed from time to time by a ultraviolet photospectrometer, with special attention paid to the absorption band at 310 mμ.

**Infrared.**—The infrared spectrum of the "quinoid sulfene" intermediate, sweeping at around 1500—2000 $cm^{-1}$, is shown in Fig. 2.

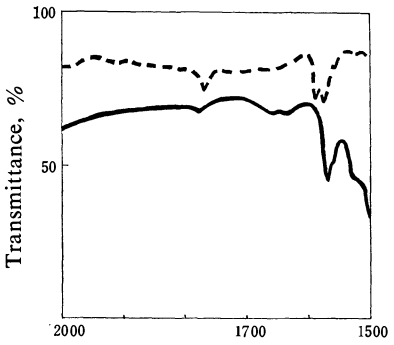



Fig. 2

—— Infrared spectra of quinoid sulfene intermediate: after mixing the 3,5-dibromo-4-hydroxybenzenesulfonyl chloride in dioxane with triethylamine, 1 min.

---- 3,5-Dibromo-4-hydroxybenzenesulfonyl chloride in dioxane

A triethylamine-dioxane solution (1 mol. soln.) was put into a liquid cell (0.5 mm. thick) containing the same amount of a solution of 3,5-dibromo-4-hydroxybenzenesulfonyl chloride in dioxane (1 mol. soln.). After the mixture has been sufficiently shaken, the absorption of the carbonyl group was followed as soon as possible. The infrared spectrum of the solid precipitate, the oligomer V, is shown in Fig. 3.

At 3450 $cm^{-1}$, the absorption of the hydroxy group is clearly observed, while at 1210—1150, 1060—1030 and near 650 $cm^{-1}$ the absorption of the $-SO_3H$ and $-SO_3-$ groups are observed in contrast with that of the reactant. The figure is simple and resembles the combined infrared absorption spectra of 3,5-dibromo-4-hydroxybenzenesulfonic acid phenyl benzenesulfonate.

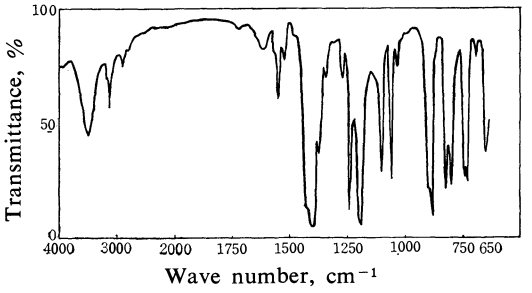



Fig. 3. Infrared spectrum of polymer in KBr disk.

**Electron Spin Resonance.**—All the ESR measurements were performed at X band frequencies, using a spectrometer equipped with a 100 Kc. modulation unit. A solution of 3,5-dibromo-4-hydroxybenzenesulfonyl chloride in dioxane (1.43 mol. soln.) was put into a quartz cell, and then a few drops of a triethylamine or potassium acetate-dioxane solution were added. Before the yellow color had disappeared, the samples were measured at room temperature and −180°C (the *g*-factor was 2.05—1.95). As no electron spin resonance signals were detected, the radical concentration was presumed to be below $10^{-6}$ mol.

## Summary

The formation of the "quinoid sulfene" intermediate, II, during the reaction between 3,5-dibromo-4-hydroxybenzenesulfonyl chloride and a weak base has been investigated by following the ultraviolet spectra of the reaction mixture. It has been suggested that the colorless precipitate formed as the final product of the reaction is an oligomer and has structure V.

*Department of Applied Chemistry*
*Faculty of Engineering*
*Osaka City University*
*Sumiyoshi-ku, Osaka (S. O.)*

*Department of Chemistry*
*Radiation Center of Osaka Prefecture*
*Sakai, Osaka (R. K.)*

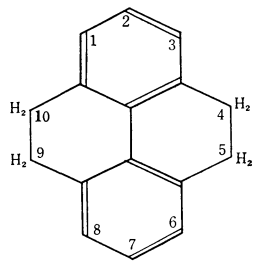
# Line-Width Alternation in the Electron Spin Resonance Spectra of the Anion Radicals of Hydropyrenes[1)]

By Masamoto IWAIZUMI and Taro ISOBE

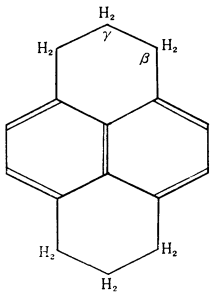
(Received February 23, 1965)

Recently, a number of ESR spectra have been reported in which the line width alternate in magnitude from one hyperfine component to another. This althernating line-width has been observed in the spectra of the durosemiquinone cation,[2)] the naphthazarine semiquinone cation,[3)] the dinitrodurene anion,[4)] the *m*-dinitrobenzene anion,[5)] the pyracene anion,[6)] and several other radicals.[7)] In the former two cases, the phenomenon has been attributed to the hindered rotation or rotational isomerization of the hydroxy groups, and in the dinitrodurene radical, to the hindered rotation of the nitro groups. On the other hand, in the case of the *m*-dinitrobenzene anion, the phenomenon has been ascribed to the effect of the collisions with solvent molecules or to the effect of formation of short-lived solvent complexes, and in the case of the pyracene anion, to the effect of the movement of the associated counter ions.

In this paper, we will report on the ESR of the anion radicals of 4, 5, 9, 10-tetrahydropyrene (I) and 1, 2, 3, 6, 7, 8-hexahydropyrene




(I)




(II)

(II). The ESR spectra of these radicals vary with the temperature remarkably and exhibit a marked line-width alternation effect, which may be attributed to the conformational interconversion: the inversion in the tetrahydropyrene anion radical, and the isomerization between the chair-like conformation and the boat-like one in the hexahydropyrene anion radical. Recently, de Boer et al.[8)] found the same phenomenon in the hexahydropyrene anion radical. We will indicate, furthermore, that the ESR spectrum of the hexahydropyrene anion radical, when the radical is prepared with sodium or with potassium in THF, shows one more additional line-width alternation effect, which may be attributed to the effect of the associated counter ions, as in the case of the alkali-pyracene radical ion.

## Experimental

Commercial tetrahydropyrene and hexahydropyrene were purified by chromatography. The radicals were prepared by an alkali metal reduction method. The alkali metals used were lithium, sodium, and potassium, and the solvents used were 1,2-dimethoxyethane (DME) and tetrahydrofuran (THF). The ESR spectra were measured with a Hitachi X-band ESR spectrometer, model MPU-3B, using field modulation at 100 kc./s. The temperature was controlled by letting dry and cooled nitrogen gas flow through a Dewar jacket passing through the sample cavity, and the temperature was varied by changing the flow rate of the gas. The temperature was measured with a copper-constantan thermocouple.

1) Presented at the symposium on Electron Spin Resonance, Tokyo, November, 1964.

2) J. R. Bolton and A. Carrington, *Mol. Phys.*, **5**, 161 (1962); A. Carrington, ibid., **5**, 425 (1962).

3) J. R. Bolton, A. Carrington and P. F. Todd, ibid., **6**, 169 (1963).

4) J. H. Freed and G. K. Fraenkel, *J. Chem. Phys.*, **37**, 1156 (1962).

5) J. H. Freed, P. H. Rieger and G. K. Fraenkel, ibid., **37**, 1881 (1962).

6) E. de Boer and E. L. Mackor, *Proc. Chem. Soc.*, **1963**, 23; E. de Boer and E. L. Mackor, *J. Am. Chem. Soc.*, **86**, 1513 (1964).

7) J. H. Freed, I. Bernal and G. K. Fraenkel, *Bull. Am. Phys. Soc.*, **7**, 44 (1962); R. W. Fessenden and R. H. Schuler, *J. Chem. Phys.*, **39**, 2147 (1963); I. Bernal and G. K. Fraenkel, *J. Am. Chem. Soc.*, **86**, 1671 (1964); J. H. Freed and G. K. Fraenkel, *J. Chem. Phys.*, **41**, 699 (1964); S. H. Glarum and J. H. Marshall, ibid., **41**, 2182 (1964).

8) E. de Boer and A. P. Praat, *Mol. Phys.*, **8**, 291 (1964).

## Results and Discussion

**The ESR Spectra of the Tetrahydropyrene Anion Radical.**—All the anion radicals of the tetrahydropyrene prepared under the respective conditions mentioned above exhibit similar spectra, though the spectra are not strictly identical in respect to the broadening, probably because of the coupling with metal ions. Representative spectra are shown in Fig. 1. At elevated temperatures, +63°C, the spectrum is well resolved and can be interpreted as arising from a triplet splitting due to the two equivalent protons, a fairly small nonet splitting from eight equivalent protons, and a still smaller quintet splitting from four equivalent

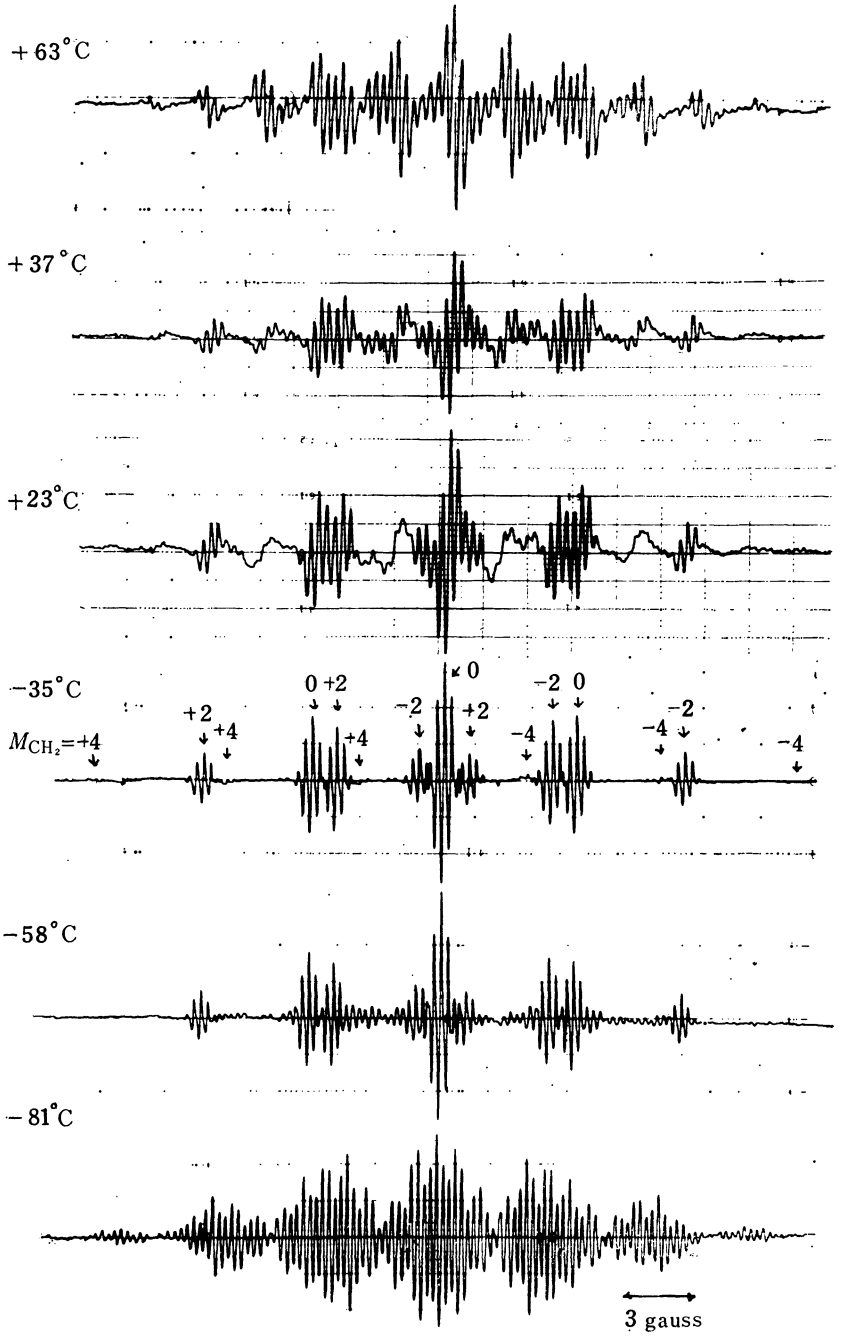
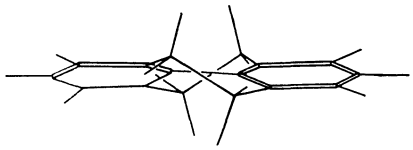



Fig. 1. ESR spectra of 4,5,9,10-tetrahydropyrene anion radical in DME at various temperatures with $K^+$ as counter ion.

protons. Based on the symmetry of the molecule, one can unambiguously attribute the triplet splitting to the coupling at position 2, the nonet splitting, to the coupling with aliphatic protons, and the quintet splitting, to the coupling at position 1. On the other hand, at room temperature or below, the spectrum exhibits a marked line-width alternation effect: let $M_{CH_2}$ be the total $z$ component of the nuclear spin angular momenta of the methylene protons; the hyperfine components with $M_{CH_2} = \pm 1$ and $\pm 3$ are then broadened considerably, and at $-35°C$, they are not observed in a spectrum recorded at a low amplitude of the field modulation. At still lower temperatures, this alternation effect again disappears, and the splittings due to the methylene protons are divided into two quintet splittings, the hyperfine splitting constants being 3.78 and 0.79 gauss. The variation in the spectra with the temperature was completely reversible except that, about 50°C, a diminution in the signal intensity due to the decomposition of the radicals was observed. The observed hyperfine splitting constants are listed in Table I.

Here, one would like to consider the structure of the tetrahydropyrene anion radical. In view of the results obtained by Braude et al.,[9] it is likely that the tetrahydropyrene anion radical is in a non-planar conformation (III)



(III)

and that the two methylene protons are not in the same situation: one of them is placed in the axial conformation, while the other is in the equatorial. When the inversion of the molecular conformation occurs, the situations of the two methylene protons will be reversed. If the life time of the individual configuration, $\tau$, is sufficiently short compared with $|\gamma(a_{equ.} - a_{ax.})|^{-1}$, where $\gamma$ is the gyromagnetic ratio of the electron and where $a_{equ.}$ and $a_{ax.}$ are the respective hyperfine splitting constants for the equatorial and the axial protons, the hyperfine splitting due to the methylene protons will be an average of the axial and the equatorial proton splittings. If the life time of the individual configuration is sufficiently long, the respective splittings due to the equatorial and the axial protons will be observed. However, when the life time of the individual configuration is comparable with $|\gamma(a_{equ.} - a_{ax.})|^{-1}$, the line-width alternation effect will be observed. Experiments at various temperatures yield spectra corresponding to each of these situations. The spectrum observed at 63°C corresponds to $|\gamma(a_{equ.} - a_{ax.})|^{-1} \ll \tau$, that observed at $-81°C$, to $|\gamma(a_{equ.} - a_{ax.})|^{-1} \gg \tau$, and that observed at intermediate temperatures, to $|\gamma(a_{equ.} - a_{ax.})|^{-1} \approx \tau$. Therefore, it seems reasonable to conclude that the variation in the spectra with the temperature and the line-width alternation effect may be attributed to the dynamical motion of the inversion of the molecular conformation. The two hyperfine coupling constants for the methylene protons, observed at $-81°C$, are assigned to the couplings with the axial and the equatorial protons, the larger to the axial protons and the smaller to the equatorial, on the basis of theoretical considerations.[10] Recently, Ōki et al.[11] examined the rate of the inversion of $o,o'$-bridged biphenyls by the NMR technique. In their technique, the rate of the inversion of the tetrahydropyrene was found to be too fast for the two kinds of methylene protons to be observed separately.

Using the hyperfine coupling constants for the equatorial and the axial protons, the life time of the individual configuration can be calculated to be in the range of $10^{-7}$—$10^{-9}$ sec. From the temperatures of their upper and lower limits, the inversion barrier may be estimated to be 4—5 kcal./mol.

Table I. Hyperfine splitting constants for the tetrahydropyrene anion radical
(in gauss)

| | +23°C | −81°C |
|---|---|---|
| $a_1$ | 0.32 | 0.28 |
| $a_2$ | 5.68 | 5.68 |
| $a_{ax.}$ | — | 3.81 |
| $a_{equ.}$ | — | 0.79 |
| $a_{ax.}+a_{equ.}$ | 4.65 | 4.60 |

Table II. Hyperfine splitting constants for the hexahydropyrene anion radical
(in gauss)

| | +23°C | −81°C |
|---|---|---|
| $a_4$ | 1.68 | 1.68 |
| $a_\gamma$ | 0.41 | 0.51 |
| $a_{\beta.ax.}$ | — | 8.00 |
| $a_{\beta.equ.}$ | — | 2.02 |
| $a_{\beta.ax.}+a_{\beta.equ.}$ | 9.87 | 10.02 |

**The ESR Spectra of the Hexahydropyrene Anion Radical.**—In the spectrum of the hexahydropyrene anion radical too, drastic changes in the hyperfine structure with the temperature were observed, as is shown in Fig. 2.

9) E. A. Braude and W. F. Forbes, *J. Chem. Soc.*, **1955**, 3776.

10) C. H. Heller and H. M. McConnell, *J. Chem. Phys.*, **32**, 1535 (1960).

11) M. Ōki, H. Iwamura and N. Hayakawa, This Bulletin, **36**, 1542 (1963); **37**, 1865 (1964).

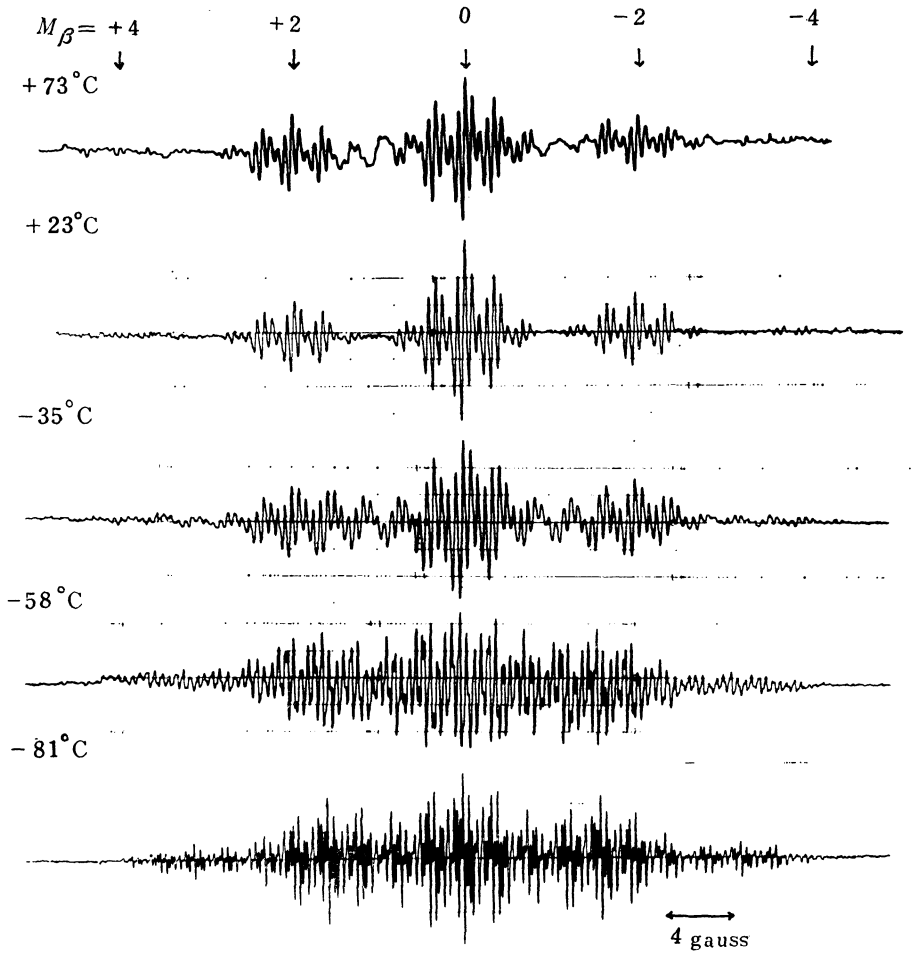
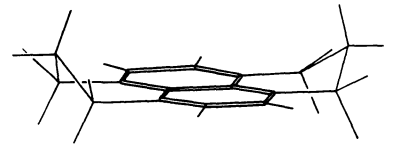
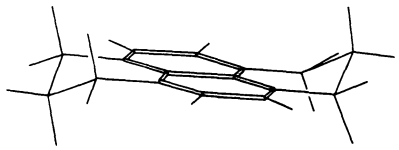



Fig. 2. ESR spectra of 1,2,3,6,7,8-hexahydropyrene anion radical in DME at various temperatures with $K^+$ as counter ion.

These changes in the spectrum with the temperature can be explained, as has recently been reported by de Boer et al.,[8] in terms of the dynamical equilibrium between the boat-like (IV) and the chair-like (V) conformations of the radical ions. This causes modulations in the isotropic hyperfine splittings, giving rise to a pronounced line-width alternation effect. The spectrum at a lower temperature is well explained by the hyperfine splittings coming from the fixed conformations of the radical. The hyperfin splitting constants are listed in Table II. However, when the temperature of the solution is raised, a marked alternation in the widths of the hyperfine components of the $\beta$ proton multiplet is observed. At room temperature, only the five components with $M_\beta$= 0, $\pm 2$ and $\pm 4$ and with statistical weights of 18 : 8 : 1 are observed, where $M_\beta$ is the total $z$ component of the nuclear spin angular momenta of the methylene protons at the $\beta$ position. The other components are broadened and unobservable at a low field amplitude of the field modulation, and the mean life time of the individual configuration may be comparable with the hyperfine separation between two $\beta$ protons, $\sim 10^{-8}$ sec.



(IV)



(V)

As compared with the spectra in Fig. 2,

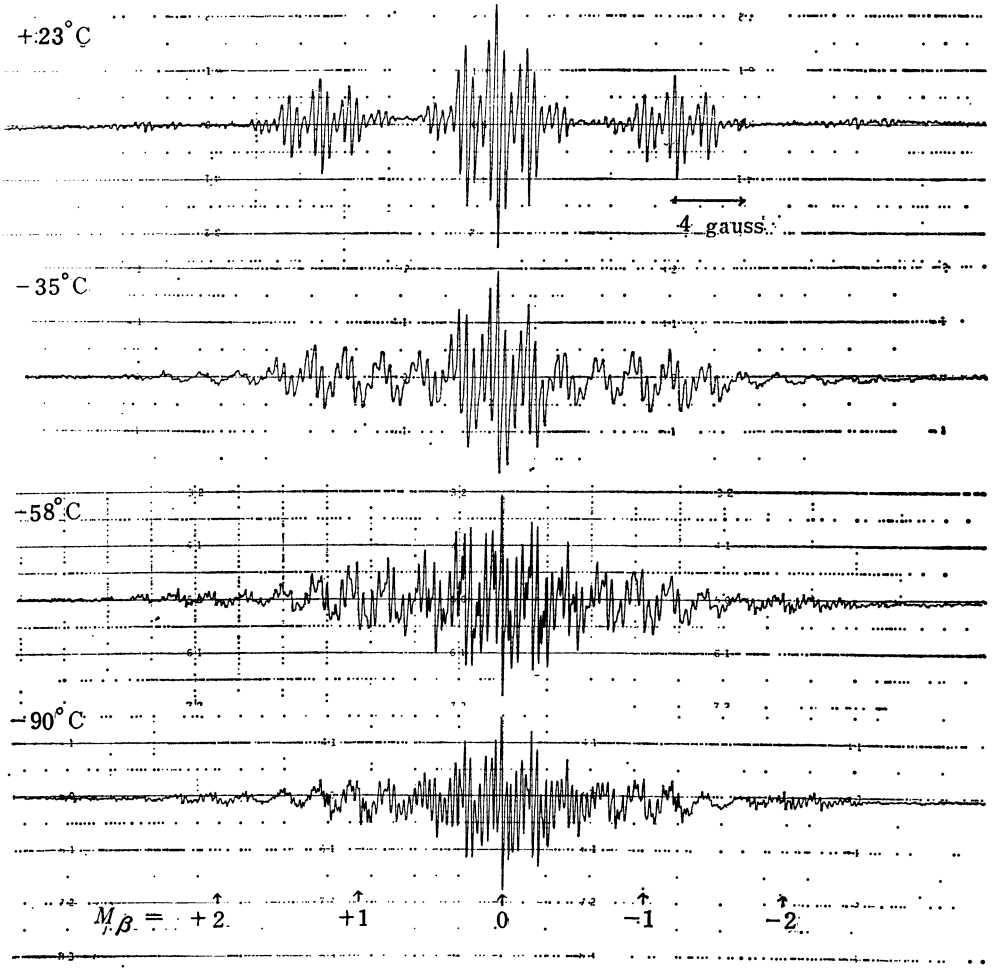
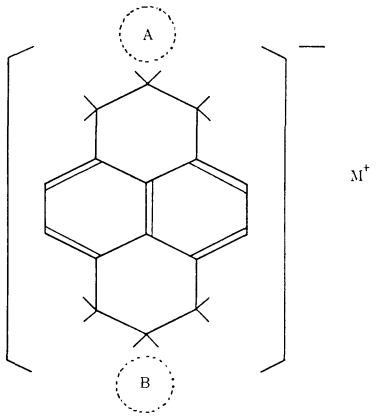



Fig. 3. ESR spectra of 1,2,3,6,7,8-hexahydropyrene anion radical in THF at various temperatures with $K^+$ as counter ion.

however, the spectra coming from the radicals prepared by the reduction with potassium or sodium in THF show somewhat different features, at lower temperatures, from those in Fig. 2, as is shown in Fig. 3. In these spectra, a marked alternation in the widths of the hyperfine components of the axial protons at the $\beta$ position is observed; the hyperfine components with $M_{\beta.ax.}=\pm1$ are broader than those with $M_{\beta.ax.}=0$ and $\pm2$, where $M_{\beta.ax.}$ is the total $z$ component of the nuclear spin angular momenta of the axial protons at the $\beta$ position.

Recently, de Boer et al.[6] observed a line width alternation effect in the ESR spectrum of the alkali-pyracene radical ion. In this case the phenomenon was ascribed to the effect of the motion of the associated alkali metal ion between two equivalent positions in the anion radical. In the present case the situation seems similar to that of the pyracene anion radical. Therefore, the following may be considered. In DME the alkali metal-hexahydropyrene radical is completely dissociated into ions, whereas in THF an ion pair (VI)




(VI)

occurs, and a dynamic equilibrium exists between the two possible conformations of the ion pair. Considering it analogously to the alkali-pyracene radical ion, the alkali metal may be placed on two symmetrical positions, A and B.

**The Hyperfine Splitting Constants of the Aliphatic Protons.** — The isotropic hyperfine splitting constants of aliphatic protons in a variety of hydrocarbon-free radicals have been determined by ESR studies. Heller and McConnell[10] have suggested that the hyperfine splitting constants for protons at the $\beta$ position* can be described by the relation:

$$a_{\beta}^{H} = (A + B\cos^2\theta)\,\rho_C^{\pi}$$

where $\rho_C^{\pi}$ is the spin density in the p orbital of the contiguous carbon atom, $\theta$ is the angle between the axis of the p orbital and the C-H bond, both projected on a plane perpendicular to the C-Ar bond, and $A$ and $B$ are constants. This equation has been justified by the studies of a variety of irradiated single crystals of alkyl carboxylic acids and others.[12] In these crystals the protons are frequently considered to be in fixed orientations.

In our experiments, at a sufficiently low temperature, the radicals reveal the hyperfine splitting constants in a fixed orientation, although the radicals are in solutions. If it is assumed that $A=0$, $B=46$ gauss and $\theta_{ax.}=\theta_{equ.}-120°$, where $\theta_{ax.}$ and $\theta_{equ.}$ are the $\theta$ values for the axial and the equatorial protons, from the above relation one may calculate that $\theta_{ax.}=3°$ and $\rho_C^{\pi}=0.08$ for the tetrahydropyrene anion radical, and $\theta_{ax.}=0°$ and $\rho_C^{\pi}=0.17$ for the hexahydropyrene anion radical. These angles are approximately that found in models of these molecules. The values of $\rho_C^{\pi}$ are comparable to the spin densities, 0.11 and 0.20, at the corresponding positions in the naphthalene and the biphenyl anion radicals,[13] which have conjugation systems similar to those of the tetrahydropyrene and the hexahydropyrene anion radicals respectively. For the $\gamma$ protons of the hexahydropyrene anion radical, one would expect two different splitting constants. However, only a single $\gamma$ splitting constant was observed. Theoretical calculations of the spin distribution in these radicals are in progress.

The authors wish to express their thanks to Miss Akie Sakai for her help in the purification of the samples.

*Chemical Research Institute of*
*Non-Aqueous Solutions*
*Tohoku University*
*Katahira-cho, Sendai*

* The proton positions are defined by the notation: Ar-$\overset{\beta}{C}H_2$-$\overset{\gamma}{C}H_2$-.

12) D. Pooley and D. H. Whiffen, *Mol. Phys.*, **4**, 81 (1961); A. Horsfield, J. R. Molton and D. H. Whiffen, ibid., **4**, 425 (1961), **5**, 115 (1962), N, M. Atherton and D. H. Whiffen, ibid., **3**, 103 (1960); D. Pooley and D. H. Whiffen, *Trans. Faraday Soc.*, **57**, 1445 (1961); I. Miyagawa and K. Itoh, *J. Chem. Phys.*, **36**, 2157 (1962).

13) A. D. McLachlan, *Mol. Phys.*, **3**, 233 (1960).

# The Optical Resolution of DL-Aspartic Acid, DL-Glutamic Acid, DL-Asparagine and DL-Glutamine by Preferential Crystallization*

By Kaoru HARADA

(Received December 28, 1964)

Several studies of optical resolutions of organic compounds by mechanical sorting[1,2] and by preferential crystallization[3-11] have been reported.

DL-Asparagine was first resolved by Piutti[2] using Pasteur's mechanical sorting method.[1] Ostromisslensky[3] also resolved DL-asparagine by seeding its supersaturated aqueous solution

* Contribution No. 46 of the Institute of Molecular Evolution, University of Miami.

1) L. Pasteur, *Ann. Chem. Phys.*, [3] **24**, 442 (1848).
2) A. Piutti, *Compt. rend.*, **103**, 134 (1886).
3) I. Ostromisslensky, *Ber.*, **41**, 3035 (1908).
4) K. Freudenberg, "Stereochemie," Franz Deuticke, Leipzig, (1932), p. 565.
5) J. Read, I. G. M. Campbell and T. V. Baker, *J. Chem. Soc.*, **1929**, 2305.
6) R. Puschinsky, *J. Soc. Chem. Ind.*, **53**, 10 (1934).
7) F. Kögl, Hoppe-Seyler's, *Z. Physiol. Chem.*, **258**, 57 (1939).
8) L. Velluz and G. Amiard, *Bull. soc. chim. France*, [5] **20**, 342, 903 (1953).
9) Japanese Pat. 2972 (1956); *Chem. Abstr.*, **51**, 2135 (1957); T. Akashi, *J. Chem. Soc. Japan, Pure Chem. Sec.* (*Nippon Kagaku Zasshi*), **83**, 417, 421, 532 (1962).
10) British Pat. 773660; *Chem. Abstr.*, **51**, 17984; U. S. Pat. 2790001; *Chem. Abstr.*, **51**, 13910.
11) K. Harada and S. W. Fox, *Nature*, **124**, 768 (1962).

with crystals of glycine, which has no asymmetric carbon. Although the optical activity of the resolved asparagine was not recorded, one seeding experiment resulted in the crystallization of the L-form, while the other induced crystallization of the D-from. The investigator could not predict which from of asparagine would crystallize in any given experiment. L-Histidine hydrochloride and some D-histidine hydrochloride were isolated by the successive crystallizations of the mixture of DL-histidine hydrochloride and L-histidine hydrochloride. DL-Threonine was resolved by seeding with L-threonine.[8] DL-Aspartic acid was partially resolved by preferential crystallization with optically active glutamic acid.[10] DL-Aspartic acid was totally resolved from its supersaturated copper complex solution by seeding it with an L- or D-aspartic acid copper complex.[11] DL-Glutamic acid was resolved completely from its supersaturated aqueous solution by seeding.[9] This type of simple optical resolution by the preferential crystallization procedure is the most advantageous method providing we can obtain an optically pure isomer. However, in the resolution of the DL-amino acids, most of the methods used are impractical or result in a partial resolution, with the exception of DL-glutamic acid[9] and the copper complex of DL-aspartic acid.[11]

In this report, the total optical resolution of DL-$\alpha$-amino acid from its supersaturated solution by an inoculation procedure will be described. The method will be applied to the optical resolution of DL-aspartic acid, DL-glutamic acid, DL-asparagine, and DL-glutamine.

One important condition in the optical resolution by the crystallization procedure is that the attraction between L- and D-isomers be weak; preferably, the compound should be a racemic mixture (conglomerate). However, most $\alpha$-amino acids form racemic compound crystals upon crystallization from an aqueous solution.[12,13] For this reason the seeding procedure did not give any optically active aspartic acid when a pure aqueous DL-aspartic acid solution was seeded by an optically active isomer.[11] The ammonium formate which was added to the aqueous aspartic acid solution may act as an agent (I) to stabilize the supersaturated solution, (II) to slow down the crystallization rate, and (III) to weaken the attraction between the D- and L-molecules, thus forming a racemic compound.

Formate ($HCOO^-$) and ammonium ($NH_4^+$) ions might not be essential for this type of resolution of amino acid. An aqueous solution of glycine was also used for this purpose. However, the results of the resolution using glycine were not as good as those obtained using ammonium formate.

12) T. Ogawa, *J. Chem. Soc. Japan, Ind. Chem. Sec.* (*Kōgyō Kagaku Zasst*), **52**, 69, 71, 102, 103, 104 (1949).
13) M. Tsuboi and T. Takenishi, This Bulletin, **32**, 726 (1959).

## Experimental

**The Resolution of DL-Aspartic Acid.**—DL-Aspartic acid (14.0 g.) was dissolved in a mixture of ammonium formate (25.0 g.) and 30 ml. of water at 80°C in a water bath. The hot solution was then filtered and cooled slowly to 43°C. Into this supersaturated solution 0.50 g. of finely-pulverized L-aspartic acid ($[\alpha]_D^{25}$ +24.6°, 6 N HCl) was seeded and mixed. The mixing is important, and the procedure should be standardized in order to obtain the best results. This is also true in the resolution of other amino acids. The seeded solution was allowed to stand undisturbed at room temperature (23°C) for 15 min. The crystals which were precipitated were filtered and washed with cold water. 1.57 g. of L-aspartic acid (including seed) was obtained (1st L-asp). When this was recrystallized from 39 ml. of water, 1.28 g. of purified L-aspartic acid crystals were obtained; $[\alpha]_D^{25}$ +24.6°, (*c* 2.13, 6 N HCl).

Found: C, 36.09; H, 5.34; N, 10.57. Calcd. for $C_4H_7O_4N$: C, 36.09; H, 5.30; N, 10.52%.

Into the filtrate, 0.50 g. of pulverized D-aspartic acid ($[\alpha]_D^{25}$ −24.3°, 6 N HCl) was added. The mixture was then kept undisturbed at room temperature (23°C) for 45 min. 1.69 g. of crystals (including seed) was thus obtained (1st D-asp). When this was recrystallized from water, 1.39 g. of purified D-aspartic acid was obtained; $[\alpha]_D^{25}$ −23.6° (*c* 2.03, 6 N HCl). (Found: C, 36.11; H, 5.30; N, 10.24%.) In the mother liquor, 2.50 g. of DL-aspartic acid was dissolved at 80°C. The solution was then filtered and cooled to 43°C at room temperature. Into the supersaturated solution, 0.50 g. of L-aspartic acid was seeded. After 15 min., 1.79 g. of 2nd L-asp was obtained. By seeding the filtrate with D-aspartic acid, 1.70 g. of 2nd D-asp was obtained after the solution had stood for 45 min. The same procedures were used to obtain 3rd L-asp, 1.79 g. and 3rd D-asp, 1.78 g. after dissolving 2.50 g. of DL-aspartic acid in the mother liquor. The nitro-

TABLE I. THE RESOLUTION OF DL-ASPARTIC ACID

| | Yield, g.*1 | $[\alpha]_D^{25}$*2 | Optical purity, %*3 |
|---|---|---|---|
| 1st L | 1.57 | +24.6 | 99 |
| 1st D | 1.69 | −23.6 | 95 |
| 2nd L | 1.79 | +24.4 | 98 |
| 2nd D | 1.70 | −23.7 | 96 |
| 3rd L | 1.79 | +24.8 | 100 |
| 3rd D | 1.78 | −23.0 | 93 |

*1 DL-Aspartic acid, 14.0 g., was resolved by seeding of 0.50 g. of L- and D-aspartic acids.
*2 Specific rotations were measured in 6 N hydrochloric acid.
*3 Specific rotation of pure L-aspartic acid: $[\alpha]_D^{25}$ +24.8°, 6 N hydrochloric acid.

gen analyses of 2nd L-, 2nd D-, 3rd L-, and 3rd D-aspartic acids agreed with the theoretical values. The specific rotations are listed in Table I.

**The Resolution of DL-Glutamic Acid.**—DL-Glutamic acid monohydrate (5.0 g.) was dissolved in a mixture of 20 ml. of water and 5.0 g. of ammonium formate at 80°C. The solution was then filtered, and the filtrate was cooled slowly. 0.25 g. of L-glutamic acid ($[\alpha]_D^{25}$ +31.5°, 6 N HCl) was seeded in the supersaturated solution at 43°C. The L-glutamic acid which was crystallyized was filtered after it had stood 20 min. at room temperature (23°C). L-Glutamic acid (0.97 g.) (1st L-glu) was obtained. This was recrystallized from 12 ml. of water. $[\alpha]_D^{25}$ +28.5° (*c* 2.05, 6 N HCl).

Found: C, 40.96; H, 6.18; N, 9.62. Calcd. for $C_5H_9O_4N$: C, 40.81; H, 6.17; N, 9.52%.

To the filtrate, 0.25 g. of D-glutamic acid ($[\alpha]_D^{25}$ −30.1°, 6 N HCl) was seeded. After it had stood 20 min. at room temperature (23°C), 1.04 g. of crystals were obtained (1st D-glu). The D-glutamic acid was recrystallized from water. $[\alpha]_D^{25}$ −27.5° (*c* 2.10, 6 N HCl). (Found: C, 40.83; H, 6.21; N, 9.65%.) 1.50 g. of DL-glutamic acid monohydrate was dissolved in the mother liquor, and the resolution procedures were repeated to isolate 2nd L- (0.87 g.), 2nd D- (0.90 g.), 3rd L- (1.13 g.), and 3rd D- (1.03 g.) glutamic acids. The specific rotations of these isolated glutamic acids are listed in Table II. The results of the nitrogen analyses

Table II. The resolution of DL-glutamic acid

| | Yield, g.*1 | $[\alpha]_D^{25}$*2 | Optical purity, %*3 |
|---|---|---|---|
| 1st L | 0.97 | +28.5 | 91 |
| 1st D | 1.04 | −27.5 | 88 |
| 2nd L | 0.87 | +30.8 | 99 |
| 2nd D | 0.90 | −26.3 | 84 |
| 3rd L | 1.13 | +27.2 | 87 |
| 3rd D | 1.03 | −27.5 | 88 |

*1 DL-Glutamic acid, 5.0 g., was resolved by seeding of 0.25 g. of L- and D-glutamic acids.
*2 Specific rotations were measured in 6 N hydrochloric acid.
*3 Specific rotation of pure L-glutamic acid: $[\alpha]_D^{25}$ +31.2°, 6 N hydrochloric acid.

of 2nd L-, 2nd D-, 3rd L- and 3rd D-glutamic acids agreed with the theoretical values.

**The Resolution of DL-Asparagine.**—DL-Asparagine monohydrate (10.0 g.) was dissolved at 60°C in 40 ml. of water containing 10.0 g. of ammonium formate. After the solution had been filtered and cooled slowly to about 40°C, it was seeded with 0.50 g. of L-asparagine monohydrate ($[\alpha]_D^{25}$ +30.6°, 3.4 N HCl). The solution was then kept undisturbed at room temperature for 30 min. The crystals which were precipitated were filtered and washed with cold water and ethanol. A total of 2.43 g. of L-asparagine monohydrate (1st L-asp $NH_2$) was obtained. When this was recrystallized from 12 ml. of water and 24 ml. of ethanol, 1.98 g. of purified L-asparagine was obtained; $[\alpha]_D^{25}$ +28.6° (*c* 3.10, 3.6 N HCl).

Found: C, 31.92; H, 6.44; N, 18.52. Calcd. for $C_4H_{10}O_4N_2$: C, 32.00; H, 6.11; N, 18.66%.

0.50 g. of D-asparagine ($[\alpha]_D^{25}$ −30.3°, 3.4 N HCl) was seeded in the filtrate. After 30 min. of undisturbed standing at room temperature, the crystals which were precipitated were isolated (1st D-asp $NH_2$). Yield, 3.05 g. This was recrystallized from water and alcohol; 2.54 g., $[\alpha]_D^{25}$ −29.7° (*c* 2.93, 3.6 N HCl). (Found: C, 32.32; H, 6.79; N, 18.76%.) In the mother liquor 4.50 g. of DL-asparagine monohydrate was then dissolved. The resolution procedures were repeated in a manner similar to that described above. Second L- (2.68 g.) and 2nd D- (2.48 g.) asparagines were thus obtained. The specific rotations are listed in Table III. The elemental analyses of 2nd L- and D-asparagines agreed with the theoretical values.

Table III. The resolution of DL-asparagine

| | Yield, g.*1 | $[\alpha]_D^{25}$*2 | Optical purity, %*3 |
|---|---|---|---|
| 1st L | 2.43 | +28.6 | 93 |
| 1st D | 3.05 | −29.7 | 97 |
| 2nd L | 2.68 | +30.0 | 98 |
| 2nd D | 2.48 | −28.9 | 94 |

*1 DL-Asparagine monohydrate, 10.0 g., was resolved by seeding of 0.50 g. of L- and D-asparagine monohydrate.
*2 Specific rotations were measured in 3.6 N hydrochloric acid.
*3 Specific rotation of pure L-asparagine: $[\alpha]_D^{25}$ +30.6°, 3.6 N hydrochloric acid.

**The Resolution of DL-Glutamine.**—DL-Glutamine was resolved under the same conditions as were used with DL-asparagine (DL-glutamine 10.0 g.; ammonium formate, 10.0 g., and 40 ml. of water). 0.5 g. of L-glutamine ($[\alpha]_D^{25}$ +32.8°, 1 N HCl) was seeded in a supersaturated glutamine solution. After 20 min., 2.05 g. of L-glutamine (1st L-glu $NH_2$) was obtained. This was recrystallized from 16 ml. of water and 30 ml. of ethanol; 1.65 g., $[\alpha]_D^{25}$ +32.8° (*c* 2.22, 1 N HCl).

Found: C, 41.06; H, 7.00; N, 18.67. Calcd. for $C_5H_{10}O_3N_2$: C, 41.09; H, 6.90; N, 19.19%.

From the filtrate, 2.32 g. of D-glutamine (1st D-glu $NH_2$) was obtained by the seeding of D-glutamine

Table IV. The resolution of DL-glutamine

| | Yield, g.*1 | $[\alpha]_D^{25}$*2 | Optical purity, %*3 |
|---|---|---|---|
| 1st L | 2.05 | +32.8 | 100 |
| 1st D | 2.32 | −31.4 | 96 |
| 2nd L | 2.45 | +32.5 | 99 |
| 2nd D | 2.38 | −31.1 | 95 |
| 3rd L | 2.04 | +32.9 | 100 |
| 3rd D | 2.15 | −30.5 | 93 |

*1 DL-Glutamine, 10.0 g., was resolved by seeding of 0.5 g. of each L-glutamine and D-glutamine.
*2 Specific rotations were measured in 1 N hydrochloric acid.
*3 Specific rotation of pure L-glutamine: $[\alpha]_D^{25}$ +32.8°, 1 N hydrochloric acid.

after 30 min.'s standing. This was recrystallized from water and alcohol; 1.86 g., $[\alpha]_D^{25}$ −31.4° (*c* 2.31, 1 N HCl). (Found: C, 41.48; H, 6.99; N, 19.21%.)

To the mother liquor 4.40 g. of DL-glutamine was then added and the resolution procedures repeated. Second L- (2.45 g.), 2nd D- (2.38 g.), 3 rd L- (2.04 g.) and 3rd D-glutamines (2.15 g.) were obtained. The results are shown in Table IV. The results of the nitrogen analysis of 2nd L-, 2nd D-, 3rd L- and 3rd D-glutamines agreed with the theoretical values.

This work was supported by Grant NsG-173-62 and NsG-689 from the National Aeronautics and Space Administration. Thanks are extended to Dr. Sidney W. Fox for his encouragement and to Mr. Arthur I. Holden for his measurement of optical rotation.

*Institute of Molecular Evolution*
*and Department of Chemistry*
*University of Miami*
*Coral Gables, Florida, U. S. A.*

# NOTES

## Thermodynamic Functions of the Ionisation of Aminobenzoic Acids

By H. C. SARASWAT and Uma Dutta TRIPATHI

(Received August 1, 1964)

Studies of the ionisation of substituted benzoic acids have received the attention of numerous workers in recent years.[1-5] Besides the value of the knowledge of p$K$ and related functions in chelate chemistry,[6] these data have been found to be extremely significant in elucidating a number of structural features, such as hydrogen bonding and the dipolar ion.[7] It is for the latter purposes that not only the change in the free energy of ionisation but also such other thermodynamic quantities as the changes in entropy or in heat content, have been found to be of importance. It was, therefore, considered worthwhile to undertake a systematic study of the thermodynamic functions of the ionisation of a few substituted benzoic acids; the results of the investigation of *o*-, *m*- and *p*-aminobenzoic acids will be reported in the present communication.

1) S. P. Datta and A. K. Grzybowski, *Trans. Faraday Soc.*, **54**, 1179 (1958).
2) K. Laidler, ibid., **55**, 1725 (1959).
3) E. King, *J. Am. Chem. Soc.*, **88**, 3577 (1960).
4) N. A. Ramaiah and R. K. Chaturvedi, *Proc. Ind., Acad. Sci.*, **51**, 177 (1960).
5) R. K. Chaturvedi and S. S. Katiyar, This Bulletin, **35**, 1416 (1962).
6) A. E. Martell and M. Calvin, "Chemistry of Metal Chelate Compounds," Prentice-Hall, Inc., Englewood Cliffs, N. J., p. 386.
7) H. C. Brown, D. H. McDaniel and O. Haflinger, "Determination of Organic Structures by Physical Methods," Ed. by E. A. Braude and F. C. Nachod, Acad. Press, New York (1937), pp. 59, 2365.

### Experimental

Oxalic acid and *m*-aminobenzoic acid were analar samples of B. D. H. *o*-Aminobenzoic acid was crystallised from alcohol while *p*-aminobenzoic acid was recrystallised from water.[8] Sodium hydroxide was a Mercks guaranteed reagent.

**Procedure.**—pH metric titrations were carried out with a Beckman pH meter model H2. The temperature was maintained with an accuracy of $\pm 0.1$°C. Nitrogen was bubbled in the solution before and during the titrations.

### Results and Discussion

p$K$ values were calculated by plotting the values of pH against $(HA)/(A^-)$, where the terms in parantheses refer to the activity of undissociated acid and the anions. The concentration of anions present at any stage of titration was calculated by the method of Britton,[9] while the activity coefficients were calculated in the usual manner, using the values of the Debye and Hückel constant given by Bales and his coworkers;[10] the activity coefficient of undissociated acid was taken as unity.

8) "Dictionary of Organic Compounds," Vol. I, Eyre and Spottiswoode, London (1946), p. 60.
9) H. T. S. Britton, "Hydrogen Ions," Chapman and Hall, London (1955), p. 170.
10) G. G. Manov, R. G. Bates, W. H. Hamer and S. E. Acree, *J. Am. Chem. Soc.*, **65**, 1765 (1943).

Figure 1 gives a typical set of titration curves of *o*-aminobenzoic acid at different temperatures. It may be seen that these curves show a marked inflexion, as is the case with most of the benzoic acids. Similar titration curves were obtained for other acids also. The values of p$K$ at different temperatures were obtained by the graphical procedure given in Fig. 2. These data are given in Table I.

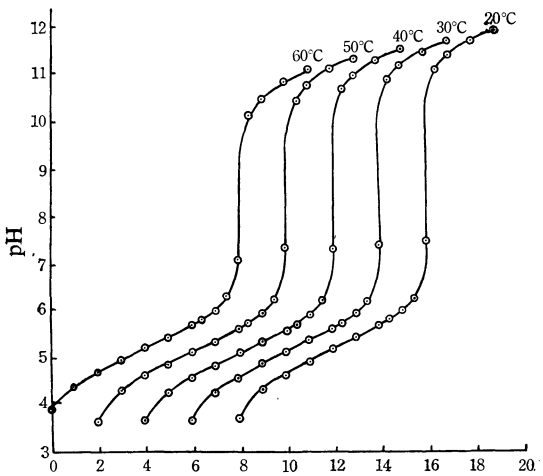



Fig. 1. pH metric titration of *o*-aminobenzoic acid.

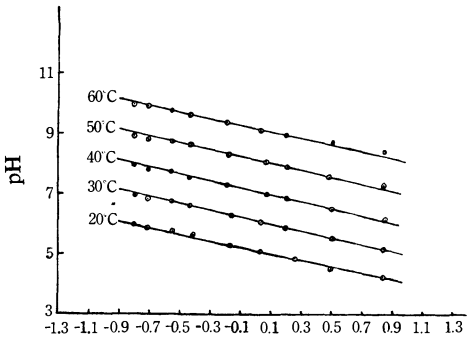



Fig. 2

TABLE I. THERMODYNAMIC DISSOCIATION CONSTANTS OF AMINOBENZOIC ACIDS

| Temp. °K | *o*-Amino-benzoic acid p$K_a$ | *m*-Amino-benzoic acid p$K_a$ | *p*-Amino-benzoic acid p$K_a$ |
|---|---|---|---|
| 293 | 5.125 | 4.90 | 4.95 |
| 303 | 5.025 | 4.75 | 4.90 |
| 313 | 5.030 | 4.675 | 4.95 |
| 323 | 5.100 | 4.600 | 5.10 |
| 333 | 5.200 | 4.70 | 5.25 |

The variation in p$K$ with the temperature has been studied theoretically by Harned and Robinson.[11] When the data in Table I are examined on the basis of the equation of Harned and Robinson, the following equations were derived:

*o*-Aminobenzoic acid

$$T\text{p}K = 13.589\times10^3 - 83.07T + 1.427\times10^{-1}T^2$$

*m*-Aminobenzoic acid

$$T\text{p}K = 12.929\times10^3 - 76.12T + 1.261\times10^{-1}T^2$$

*p*-Aminobenzoic acid

$$T\text{p}K = 13.73\times10^3 - 85.9T + 1.5\times10^{-1}T^2$$

The validity of these equations was established by the close agreement between observed and calculated values of p$K$. From the parameters of these equations, the values of the thermodynamic functions of ionisation were calculated in the usual way.[11] These are given in Table II.

TABLE IIA. THERMODYNAMIC FUNCTIONS OF IONISATION OF *o*-AMINOBENZOIC ACID

| Temp. °K | $\Delta F$ kcal./ mol. | $\Delta H$ kcal./ mol. | $\Delta S$ cal./ degree, mol. | $\Delta C_p$ cal./ mol., degree |
|---|---|---|---|---|
| 293 | 6.916 | 6.091 | −2.636 | −386.3 |
| 303 | 6.963 | 2.242 | −15.63 | −396.4 |
| 313 | 7.191 | −1.793 | −28.74 | −409.6 |
| 323 | 7.558 | −6.243 | −41.85 | −422.6 |
| 333 | 7.971 | −10.23 | −54.87 | −435.6 |

TABLE IIB. THERMODYNAMIC FUNCTIONS OF IONISATION OF *m*-AMINOBENZOIC ACID

| Temp. °K | $\Delta F$ kcal./ mol. | $\Delta H$ kcal./ mol. | $\Delta S$ cal./ degree, mol. | $\Delta C_p$ cal./ mol., degree |
|---|---|---|---|---|
| 293 | 6.643 | 9.665 | 10.17 | −335.7 |
| 303 | 6.597 | 6.229 | −1.283 | −350.1 |
| 313 | 6.689 | 2.655 | −12.92 | −360.8 |
| 323 | 6.825 | −1.013 | −24.39 | −373.3 |
| 333 | 7.191 | −4.817 | −39.02 | −385.0 |

TABLE IIC. THERMODYNAMIC FUNCTIONS OF IONISATION OF *p*-AMINOBENZOIC ACID

| Temp. °K | $\Delta F$ kcal./ mol. | $\Delta H$ kcal./ mol. | $\Delta S$ cal./ degree, mol. | $\Delta C_p$ cal./ mol., degree |
|---|---|---|---|---|
| 293 | 6.643 | 3.938 | −9.166 | −402.9 |
| 303 | 6.825 | −0.142 | −22.82 | −416.6 |
| 313 | 7.101 | −3.93 | −36.67 | −430.4 |
| 323 | 7.558 | −8.758 | −50.42 | −444.1 |
| 333 | 8.061 | −13.25 | −64.16 | −458.0 |

11) H. S. Harned and R. A. Robinson, *Trans. Faraday Soc.*, **36**, 973 (1940).

As was expected on the basis of the resonance effect and in accordance with deductions from physico-chemical measurements[12] the data obtained in the present work also suggest that there is a greater tendency for meta acid than for ortho and para acids to exist in the form of the dipolar ion.

12) E. J. Cohn and J. T. Edsall, "Proteins, Amino Acids and Peptides," Reinhold Publishing Corporation, New York (1943), p. 147.

The authors wish to take this opportunity to thank Sri N. Abraham, Principal, Christ Church College, Kanpur, for his interest in the work and Dr. R. K. Chaturvedi, H. B. T. I., Kanpur, for his stimulating discussions. Thanks are also due to the U. P. Scientific Research Committee for its contingency grant.

*Department of Chemistry*
*Christ Church College*
*Kanpur, U. P., India*

# Extraction of the Bismuth-Thiourea Complex with Tributyl Phosphate from a Perchloric Acid Medium

By Fumio Aoki and Hideo Tomioka

(Received February 23, 1965)

Though the colorimetric method for bismuth based on the formation of a bismuth-thiourea complex has been widely known, the literature does not seem to contain any report on the solvent extraction of the complex compound.

The present writers have found, however, that the complex can be quantitatively extracted with tributyl phosphate from a perchloric acid solution with an acidity ranging from 0.1 to 0.6 M.

The absorption curve of the extract, exactly like that of the aqueous solution, has two absorption peaks due to the complex. They are located at 322 nm and 470 nm, their molar absorptivities being $2.45\times10^4$ and $6.97\times10^3$ respectively. The 470 nm peak is thought to be better for analytical purposes, in spite of its lower sensitivity, since the 322 nm peak suffers more from the interference of diverse ions and has a poorer reproducibility. Beer's low is obeyed up to 45 $\mu$g./ml. of bismuth when the absorbance is measured at 470 nm. The colored system is stable for at least 3 hr.

Chloroform, carbon tetrachloride, benzene, methyl isobutyl ketone, ethyl ether, *n*-butyl alcohol and butyl acetate do not extract the complex.

On the basis of these observations we propose the following procedure:

A sample solution containing up to 400 $\mu$g. of bismuth is taken in a separatory funnel; 2.5 ml. of 60% perchloric acid and 25 ml. of 12% thiourea solution are added, and the solution is diluted to 50 ml. with water. Then exactly 10 ml. of tributyl phosphate is added, and the funnel is vigorously shaken for 2 min. Twenty minutes after the extraction the absorbance of the organic phase is measured at 470 nm. in a 1 cm. cell.

Osmium, ruthenium, and palladium interfere seriously with the determination of bismuth. Molybdenum and antimony also interfere to some extent.

A full paper will be published soon in Japanese.

*The Government Chemical Industrial Research Institute, Tokyo*
*Shibuya-ku, Tokyo*

# Evidence for the Activity Difference between Pure and Supported Nickel Catalysts

By Yoshie HIRONAKA and Kozo HIROTA

(Received February 3, 1965)

In a previous paper,[1] we reported on the difference in catalytic activity between nickel alone and nickel supported on $\gamma$-alumina (Ni : $Al_2O_3$ = 1 : 1 in weight) in the isotopic hydrogen exchange of propene with deuterium oxide. From the infrared and NMR spectroscopic data then obtained, we suggested that vinyl hydrogens are more exchangeable than methyl hydrogens on nickel and that the ratio of the exchangeability of the vinyl group to that of the methyl group was about 3.4, while supported nickel shows the opposite exchangeability (i. e., methyl hydrogens are more exchangeable). By the microwave spectroscopic method,[2-4] this suggestion was not only confirmed quantitatively, but also detailed knowledge could be obtained, as has been reported already.[2,3]

Table I shows the experimental conditions, while Table II shows the subspecies distribution of $d_1$ determined by the microwave spectroscopic method, as well as the $d_y$-distribution determined by a mass spectrometer.

TABLE I. EXPERIMENTAL CONDITIONS

| No. | Catalyst | | Reaction | | Sample | |
|---|---|---|---|---|---|---|
| | | | Temp. | Time | $C_3H_6$ | $D_2O$ |
| | | g. | °C | hr. | mol. $\times 10^3$ | |
| 3513 | Ni | 1.65 | 17 | 25 | 2.18 | 10 |
| A9 | $Ni\text{-}Al_2O_3$ | 5.0 | 18.6 | 354 | 6.00 | 18.1 |

The $\phi$ values of the two samples are nearly equal, both being ca. eight, so that their $d_y$-distribution shows the initial stage of the reaction in these cases. By comparing the amount of catalyst (only the weight of nickel) and the reaction time, it may be seen that the exchange rate is markedly decreased, by 7—8 times, if nickel is supported on $\gamma$-alumina. Besides, important information was obtained from the difference between the infrared spectra of No. 3513 (Ni) and No. A9 ($Ni\text{-}Al_2O_3$). However, the spectrum of No. 3513 (Ni) is not shown because it is almost identical with that of No. A4, which has already been shown in a previous report.[1] A completely different feature can be seen in the region of the C-D stretching band, suggesting that the catalytic activities of the two catalysts are different.

According to a comparison of the subspecies distribution of the $d_1$ of No. 3513 with that of No. A9, methine hydrogen is the most exchangeable on nickel (No. 3513), while methyl hydrogens are the most exchangeable on supported nickel (No. A9). The subspecies distribution of $d_1$ in the product of the catalytic exchange reaction shows some similarity between supported nickel (No. A9) and palladium in that methyl hydrogens became exchangeable to some extent, though methine hydrogen was still more exchanged on supported nickel than on palladium.[2] Such a tendency has been recognized in the exchange reaction of para-xylene with deuterium oxide,[5] though in this system only methyl hydrogens were exchanged on nickel, while both methyl and aromatic hydrogens became exchangeable on palladium and on supported nickel. Such a tendency in the exchangeability with respect to the double bond showed a tendency opposite to that of the present system.

From Table II, it may be seen that the exchangeability of methine hydrogen was larger than that of methylene hydrogen on both catalysts. The result of No. A9 may be interpreted in terms of the existence of two different active sites on supported nickel for this reaction. One of the sites (A), ascribable to nickel, has an activity similar to that of unsupported nickel, and the subspecies distribution of $d_1$ may, consequently, be similar to that of No. 3513, as is shown in Table II. The other site (B) has an activity similar to that of palladium, and the subspecies distribution of $d_1$ may become similar to that of palladium.[2] It may, therefore, be concluded that the activity of the A site has no interaction with the $\gamma$-alumina and that the activity of the B site may result from the interaction with $\gamma$-alumina. The subspecies distribution of $d_1$ of No. A9 may, therefore, be regarded as a mean value of two different distributions.

1) K. Hirota and Y. Hironaka, This Bulletin, **37**, 535 (1964).
2) K. Hirota, Y. Hironaka and E. Hirota, *Tetrahedoron Letters*, **1964**, 1645.
3) K. Hirota and Y. Hironaka, *J. Catalysis*, to be published.
4) Y. Morino and E. Hirota, *J. Chem. Soc. Japan, Pure Chem. Sec.* (*Nippon Kagaku Zasshi*), **85**, 535 (1964).
5) K. Hirota and T. Ueda, This Bulletin, **33**, 423 (1960).

TABLE II. DEUTERIUM DISTRIBUTION (%) AND SUBSPECIES DISTRIBUTION OF $d_1$ (%)

| Subspecies | No. A9(Ni-$Al_2O_3$) | No. 3513(Ni)** | No. 3315(Pd)** |
|---|---|---|---|
| $CH_2DCH=CH_2$ | 45.3±2.5(15.1)* | 22.5±2.7(7.5)* | 59.2±2.2(19.7) |
| *t*-$CH_3$ CH=CHD | 12.5±1.5 | 9.5±2.1 | 16.4±1.5 |
| *c*-$CH_3$ CH=CHD | 11.3±1.7 | 9.9±2.2 | 13.4±2.1 |
| $CH_3$ CD=$CH_2$ | 30.9±2.8 | 58.1±5.1 | 16.1±2.4 |
| $d_0$ | 63.6 | 58.4 | 51.3 |
| $d_1$ | 29.8 | 33.3 | 36.8 |
| $d_2$ | 5.9 | 7.3 | 10.7 |
| $d_3$ | — | 1.0 | 1.6 |
| $\phi=\frac{1}{6}\sum_{y=1}^{6} yd_y$ | 7.4 | 8.5 | 10.4 |

* Numerals in parenthesis are the ones alloted per one hydrogen atom.
** These data, already published,[2] were shown for the sake of comparison.

Morikawa and Nozaki[6] reported that both free metallic nickel and nickel atoms forming chemical bonds with $\gamma$-alumina existed in supported nickel. These states seem to correspond to the two states mentioned above.

The catalytic activity of supported nickel decreased as compared with that of nickel, as has been mentioned already. This decrease in activity may be attributed to the formation of nickel oxide with the oxygen absorbed on $\gamma$-alumina, because neither nickel oxide nor $\gamma$-alumina could catalyze this reaction. However, since the answers to these problems are not evident, further investigation is necessary on this point.

The authors wish to express their thanks to Professor Yonezo Morino and Dr. Eizi Hirota, the University of Tokyo, who kindly measured the samples with the microwave-spectroscopic method and discussed the results.

*Department of Chemistry*
*Faculty of Science*
*Osaka University*
*Toyonaka, Osaka*

6) K. Morikawa and F. Nozaki, *J. Chem. Soc. Japan, Ind. Chem. Sec.* (*Kogyo Kagaku Zasshi*), **64**, 1562 (1961).

# The Effect of Pressure on the Fluorescence Spectra of Anthracene, Chrysene and Pyrene

By Jiro TANAKA,* Takao KODA, Shigeo SHIONOYA and Shigeru MINOMURA

(Received February 17, 1965)

Recently the fluorescence spectra of aromatic molecular crystals have been found to be intimately connected with the crystal structure; the anomalous, long wavelength emission has been explained in terms of the formation of the excited dimer state.[1-3] In this note we will present a study of the effect of static high pressure on the fluorescence spectra of anthracene, chrysene and pyrene.

A Drickamer-type optical cell[4] available for measurement under high pressure up to 52 kb. was used. A small amount of pure crystal was put in the optical cell and excited by a 365 m$\mu$ mercury light. The measurement of the fluorescence spectra was made with a Bausch and Lomb 250 mm. monochromator and by a sensitive-photomultiplier detecting system.

The emission peaks of these crystals were found to shift remarkably to lower frequencies almost linearly with an increase in the pressure, the shift being 80 $cm^{-1}$/kb. for anthracene and 40 $cm^{-1}$/kb. for chrysene and pyrene (cf. Fig. 1). The vibrational structures in the fluorescence spectra were blurred under high pressure. The red shifts could be reversed for pyrene and chrysene by applying and releasing the pressure, but the shift was irreversible for anthracene. The fluorescence

* Present address: Department of Chemistry, Nagoya University, Chikusa, Nagoya.

1) J. Ferguson, *J. Chem. Phys.*, **28**, 765 (1958).
2) B. Stevens, *Spectrochim. Acta*, **18**, 439 (1962).
3) J. Tanaka, This Bulletin, **36**, 1237 (1963).
4) R. A. Fitch, T. E. Slykhouse and H. G. Drickamer, *J. Opt. Soc. Am.*, **47**, 1015 (1957).

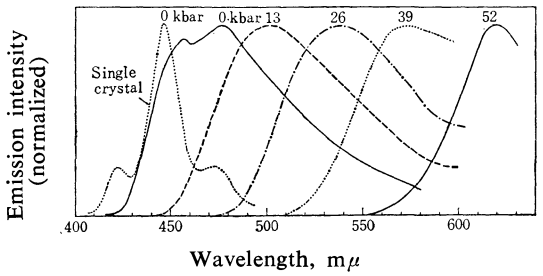



Fig. 1. Shifts of fluorescence bands.
The values for anthracene were determined from the reduced zero pressure value (475 mμ).

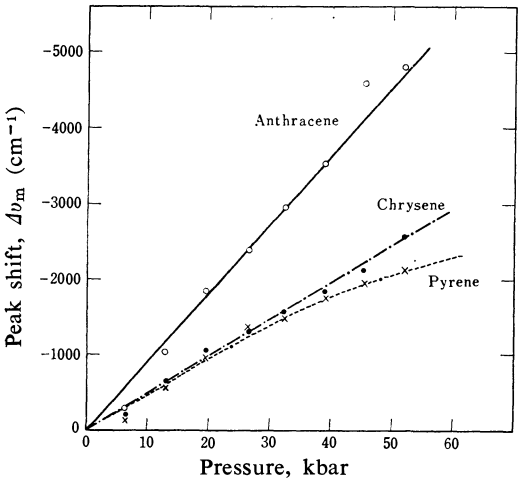



Fig. 2. Change in the fluorescence spectrum of anthracene with an increase in the pressure at room temperature.

of anthracene did not recover completely to the original spectrum once it had been pressed under high pressure, and it showed a strong broad emission in the 475 mμ region (cf. Fig. 2). The red shift of the crystal might be explained by assuming a potential energy diagram in which the curve for the ground state is steeper than that of the excited state and in which the minimum of the excited state is located at a smaller configurational coordinate than the ground state.[5]

The larger red shift of the anthracene crystal needs some comment. According to Wiederhorn and Drickamer,[6] the absorption spectrum of the anthracene crystal shifts to frequencies lower by 45 cm$^{-1}$/kb. with an increase in the pressure. The red shift of 80 cm$^{-1}$/kb. of the fluorescence will be partly due to the shift of the $^1L_a$ excited level. The second point to be considered is that the 475 mμ emission occurs even after the pressure is released. This might be explained by assuming the formation of an emission center of the dimer type produced under the high pressure. As a result of the hysteresis effect of the pressure, the emission center will remain in the crystal and the 475 mμ band will occur from this emission site, even if the pressure is released. This idea is supported by the observation that the 475 mμ band disappears when the pressed crystal is warmed up in vacuo.

*The Institute for Solid State Physics*
*The University of Tokyo*
*Azabu, Tokyo*

5) P. D. Johnson and F. E. Williams, *Phys. Rev.*, **95**, 69 (1954).
6) S. Wiederhorn and H. G. Drickamer, *J. Phys. Chem. Solids*, **9**, 330 (1959).

# The Copolymerization of β-Substituted Styrenes with Maleic Anhydride*

By Shunsuke MURAHASHI, Shun'ichi NOZAKURA, Kazuo EMURA and Katsutoshi YASUFUKU

(Received February 19, 1965)

It has been reported that 1, 2-disubstituted ethylenes, such as *p*-dioxene,[1] dihydropyrane,[2] butene-2,[3] and stilbene,[4] do not homopolymerize by a radical mechanism, but do copolymerize with maleic anhydride (MAn) to yield copolymers with a 1 : 1 alternating composition. The present paper will describe copolymerizations of some β-substituted styrenes with MAn by a radical mechanism and will compare their reactivities.

The copolymerizations were carried out in

* Paper III in a series on "The Polymerization of Internal Olefins;" for the preceding paper, see This Bulletin, **38**, 156 (1965). Presented at the Annual Meeting of Polymer Science, Kyoto, June, 1964.

1) S. Iwatsuki, Y. Tanaka and Y. Yamashita, *J. Chem. Soc. Japan, Ind. Chem. Sec.* (*Kogyo Kagaku Zasshi*), **67**, 1467 (1964).

2) R. D. Kimbough, Jr., Wm. P. Dickson and J. M. Wilkerson, *J. Polymer Sci.*, **B2**, 85 (1964).

3) T. Otsu, A. Shimizu and M. Imoto, ibid., **B2**, 973 (1964).

4) T. Wagner-Jauregg, *Chem. Ber.*, **63B**, 3213 (1930).

Table I. Copolymerization of β-substituted styrenes ($M_2$) with MAn ($M_1$) in benzene
$[M_1]=[M_2]=1.0$ mol./l. $[AIBN]=1.0\times10^{-2}$ mol./l.

| β-Substituent of $M_2$ | | Time hr. | Yield % | %/hr. | Copolymer C% | H% | $m_1/m_2$ | Soft. P., °C | $\eta_{sp}/c$* |
|---|---|---|---|---|---|---|---|---|---|
| -Ph | t | 1.0 | 15.7 | 15.7 | 76.48 | 5.06 | 1.06 | >300 | insol. |
| $-OCH_3$ | t | 5.0 | 25.0 | 5.0 | 66.17 | 5.16 | 1.08 | 230—250 | 0.209 |
| $-CH_3$ | t | 1.12 | 2.13 | 1.9 | 71.15 | 5.78 | 0.96 | 260—270 | 0.127** |
| $-CO_2CH_3$ | t | 23.2 | 34.8 | 1.5 | 64.45 | 4.74 | 0.95 | 180—200 | 0.148 |
| -Cl 67% | t | 18.7 | 5.05 | 0.27 | Cl% | 14.31 | 1.12 | 240—250 | 0.039 |
| $-COCH_3$ | t | 19.6 | 4.9 | 0.25 | 63.28 | 3.78 | 2.34 | 240—250 | — |
| -Ph | cis | 17.3 | 3.3 | 0.19 | 71.70 | 5.20 | 1.21 | 230—250 | — |
| -H | | 0.24 | 32.6 | (136) | 70.07 | 5.34 | 0.88 | — | — |

t: trans 100%
*: $\eta_{sp}/c$ was measured in acetone (1%) 30°C.
**: Mol. wt. determined by a vapor pressure osmometer was 2000—2100.

Table II. Copolymerization of *p*-substituted β-methylstyrenes ($M_2$) with MAn ($M_1$)
$[M_1]=[M_2]=1.0$ mol./l. $[AIBN]=1.0\times10^{-2}$ mol./l.

| *p*-Substituent of $M_2$ | | Time hr. | Yield % | %/hr. | Copolymer C% | H% | $m_1/m_2$ | Soft. p., °C | $\eta_{sp}/c$ |
|---|---|---|---|---|---|---|---|---|---|
| $CH_3O$- | t | 0.61 | 6.1 | 10.0 | 66.83 | 5.87 | 0.99 | 260—270 | insol. |
| $CH_3$- | t | 3.45 | 8.6 | 2.49 | 71.56 | 6.26 | 0.97 | 270—290 | 0.390 |
| H- | t | 1.12 | 2.13 | 1.90 | 71.15 | 5.78 | 0.96 | 260—270 | 0.127 |
| Cl- | t | 13.65 | 10.8 | 0.79 | Cl% | 13.20 | 1.20 | 220—240 | — |

t: trans 100%.

Table III. Effect of the monomer feed ratios on the copolymerization of *p*-substituted β-methylstyrenes ($M_2$) with (MAn ($M_1$)
$[M_1+M_2]=2.0$ mol./l. $[AIBN]=1.0\times10^{-2}$ mol./l.

| $M_1/M_2$ | *p*-Substituent $CH_3O$- $m_1/m_2$ | %/hr. | $CH_3$- $m_1/m_2$ | %/hr. | H- $m_1/m_2$ | %/hr. | Cl- $m_1/m_2$ | %/hr. |
|---|---|---|---|---|---|---|---|---|
| 0.43 | — | — | — | — | 0.92 | 0.8 | — | — |
| 0.67 | — | — | — | — | 0.93 | 1.2 | — | — |
| 1.00 | 0.99 | 10.0 | 0.97 | 2.5 | 0.96 | 2.1 | 1.20 | 0.97 |
| 1.50 | 1.07 | 12.6 | 0.97 | 2.9 | 1.04 | 2.9 | 1.33 | 1.11 |
| 2.33 | 1.02 | 14.7 | 0.97 | 5.3 | 0.98 | 3.5 | 1.09 | 1.29 |
| 4.00 | 1.05 | 29.7 | 1.02 | 5.8 | 1.08 | 4.2 | 1.05 | 1.83 |
| 9.00 | 1.06 | 22.3 | 1.02 | 5.9 | 1.00 | 4.6 | 1.06 | 1.33 |

a sealed glass tube at 60°C, using 2, 2'-azobisisobutyronitrile as the initiator and benzene as the solvent. β-Substituted styrenes of a known isomeric purity were used. The results are shown in Tables I, II and III.

All the β-substituted styrenes were found to be markedly less reactive than styrene. The general low reactivity may be attributed to the steric factor of the β-substituent,[5] and the magnitude of the steric factor may be considered to differ from one substituent to another. In Table I, however, a tendency is observed for the rate of the copolymerization of the β-substituted styrenes with MAn to decrease approximately with the increase in the electron-attracting character of β-substituents, except for the case of stilbenes. Thus, the effect of β-substituents is rather complicated; they exert a predominant steric effect and a

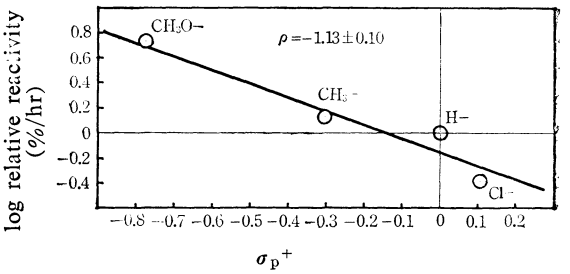



Fig. 1. Correlation of log relative reactivity and $\sigma_p^+$ for the copolymerization of *p*-substituted-β-methyl-Sts with MAn.

5) T. Alfrey, Jr., J. Bohrer and H. Mark, "Copolymerization," Interscience Pub. Inc., N. Y. (1952), p. 51.

polar effect as well as, presumably, a resonance effect.

On the other hand, the effect of *p*-substituents of β-methylstyrenes is a little more clean-cut, as is shown in Table II. Since these systems gave 1 : 1 copolymers as Table III shows, the logarithms of the relative reactivities (%/hr. in Table II) of *p*-substituted β-methylstyrenes to that of β-methylstyrene are plotted against Brown-Okamoto $\sigma_p^+$ values for the substituents (in Fig. 1). When the Hammett $\sigma_p$ was used instead of $\sigma_p^+$, the correlation was worse, the standard deviation of $\rho$ being $\pm 0.9$. A better linearity was observed for $\sigma_p^+$ with the $\rho$ value of $-1.13 \pm 0.10$, showing that the polar effect operates in this case. This result seems reasonable, since the steric factor around the double bond may not be altered by the *p*-substituent.

Table III demonstrates that these β-methylstyrenes formed 1 : 1 alternating copolymers with MAn independent of the monomer feed ratios, and that the rate of copolymerization increased with the increase in the fraction of MAn, sometimes showing maxima.

It should be noted that β-substituted styrenes of a comparatively high reactivity show thermal copolymerization with MAn, and that these copolymerization mixtures exhibit a deep yellow color. The phenomena of discoloring may be due to the formation of charge transfer complexes between the donor molecules (β-substituted-St-derivatives) and the accepter molecule (MAn), as reported by Walling[6] and Barb.[7] We are now studying whether the complex makes any contribution to the copolymerization reaction.

*Department of Polymer Science*
*Faculty of Science*
*Osaka University*
*Nakanoshima, Osaka*
*(S.M., S.N. & K.E.)*

*Institute of Physical & Chemical Research*
*Bunkyo-ku, Tokyo (K.Y.)*

6) C. Walling, D. Seymour and K. B. Wolfstirn, *J. Am. Chem. Soc.*, 70, 1544 (1947).
7) W. G. Barb, *Trans. Faraday Soc.*, 49, 143 (1953).

## SHORT COMMUNICATIONS

# Stain Film Formed Photochemically on Silicon

By Yasuo NAKAI

(Received May 21, 1965)

It is known that stain film can contribute to the stabilization of transistors.[1] The stain film has been obtained hitherto by reaction with hydrogen fluoride-nitric acid[2] or by anodic oxidation in hydrogen fluoride solution.[3]

In this experiment, it was found that the formation of stain film can be effected by the photochemical reaction of HF-$O_3$ with silicon crystal. For example, oxygen gas (1200 cc./min.) containing 5% ozone (in weight) and HF-$N_2$ gas (500 cc./min.) was brought into contact with the (111) surface of 2- to 80-chm-cm. n-type silicon crystals for 0.5 to 2 hr. at room temperature and under irradiation from a high-pressure mercury lamp (1 kW.) through filters transmitting at 5800, 5460, 4358, 4047 and 3650 Å. Ozone was obtained by a silent discharge. The mixture of HF-$N_2$ gas was obtained by bubbling nitrogen gas through a 24 N hydrogen fluoride solution at 25°C.

It was found to be necessary, for the formation of stain film, to irradiate the silicon surface with photons of energy higher than approximately 2.7 eV.

Infrared, optical absorption, electron spin resonance and solid mass spectra were investigated in studying the physicochemical properties of stain film.

1) K. Oho and K. Koso, *ECL. Tech. Jour.*, **10**, 1741 (1961); S. Y. Ellis, *J. Appl. Phys.*, **28**, 1262 (1957).
2) D. R. Turner, "The Electrochemistry of Semiconductors," Ed. by P. T. Holms, Academic Press, New York (1962).
3) R. J. Archer, *J. Phys. Chem. Solids*, **14**, 104 (1960); A. Uhlier, *Bell. Syst. Tech. J.*, **35**, 333 (1956).

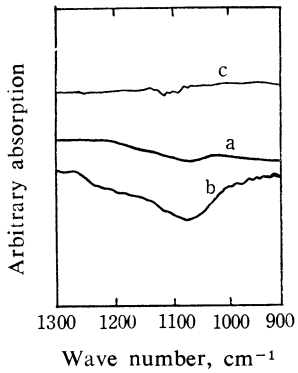



Fig. 1. The infrared spectra of stain film (a) before and (b) after thermal treatment at 250°C for 10 hr., and (c) of silicon crystal.

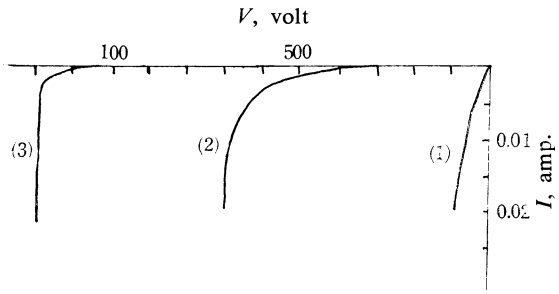



Fig. 2. Reverse characteristic (*I-V* curve) of a $p^+-n$ diode on which stain film was photochemically formed.
(1) Before heat treatment (2) after being kept at 250°C for 2 hr. in air, and (3) after being kept at 250°C for 10 hr. in air.

Figure 1 shows the infrared spectrum of stain film. The band at 1080 $cm^{-1}$, whose intensity is weak before heat treatment (as is shown by curve 1a), appears strongly after being kept at 250°C for approximately 10 hr. in air (curve 1b). The band at 1080 $cm^{-1}$ is assigned to the Si-O stretching mode; its shape is similar to that of amorphous silica.

The electron-spin resonance-absorption curve of stain film at an operation microwave frequency in the vicinity of 9.2 kMc./sec. exhibits three peaks ($g_1=2.0068$, $g_2=2.0048$ and $g_3=2.0000$) at 77°K. Two optical absorption bands were observed, at 7500Å and 5000Å. Silicon, oxygen and fluorine atoms were detected in stain film by solid mass spectroscopy, but its molecular formula is not clear at present.

Stain film was photochemically formed upon the junction of mesa $p^+-n$ diodes. A typical variation of the reverse *I-V* curve with aging is shown in Fig. 2. Diodes had a very inferior reverse characteristic just after forming stain film, but the breakdown voltage became stable and the drift decreased after they had been kept at 250°C for 10 hr. in air.[4]

*Central Research Laboratory*
*Tokyo Shibaura Electric Co., Ltd.*
*Kawasaki-shi, Kanagawa*

4) Y. Nakai, T. Owada, S. Fukasaku, M. Urakabe and T. Oi, *J. Electrochem. Soc.*, to be published.

# The Synthesis of a Heptadecapeptide Amide Corresponding to a Modified Sequence in the Corticotropin Structure

By Hideo OTSUKA, Ken INOUYE, Makoto KANAYAMA and Fusako SHINOZAKI

(Received June 9, 1965)

In order to examine whether or not the level of hormonal potency depends simply on the degree of basicity at positions 15—18 of the corticotropin (ACTH) molecule, we have synthesized a heptadecapeptide amide, H-Gly-Tyr-Ser-Met-Glu-His-Phe-Arg-Try-Gly-Lys-Pro-Val-Gly-Lys-Arg - Arg - $NH_2$ ($\alpha^{1-14,16-18}$ - Gly$^1$-ACTH-18-$NH_2$) (I);*1 The peptide I has bene found to possess 1.26 and 2.72 USP units per mg. of steroidogenic activity, as estimated in vitro[1] and in vivo[2] respectively.*2 On the other hand, the peptide I has been found to elicit a high lipolytic activity at minimal effective doses of 0.0037 $\mu$g. in rat adipose tissue and of 0.00042 $\mu$g. in rabbit.[3],*2

Cbz-Arg($NO_2$)-OH (II) was converted, via

* All amino acid residues are of the L-configuration with the exception of glycine. In this communication, the following abbreviations will be used: Cbz, carbobenzoxy; BOC, *t*-butyloxycarbonyl; Ac, acetyl; But, *t*-butyl; CMC, carboxymethyl cellulose.

1) M. Saffran and A. V. Schally, *Endocrinol.*, **56**, 523 (1955).

2) By a slight modification of Lipscomb and Nelson (H. S. Lipscomb and D. H. Nelson, ibid., **71**, 13 (1962)).

*2 The authors are much indebted to Dr. Akira Tanaka for these biological assays.

3) A. Tanaka, B. T. Pickering and C. H. Li, *Arch. Biochem. Biophys.*, **99**, 294 (1962).

a mixed anhydride, into Cbz-Arg($NO_2$)-$NH_2$ (m. p. 220—221°C, $[\alpha]_D^{24}$ +4.9° (*c* 1.95, dimethylformamide); lit.[4] m. p. 219—220°C); this was then treated with HBr/AcOH to obtain H-Arg($NO_2$)-$NH_2$·HBr (III) (m. p. 237—239°C, $[\alpha]_D^{26}$ +13.7° (*c* 2.6, water)). The coupling of II with III by the mixed anhydride procedure gave Cbz-Arg($NO_2$)-Arg($NO_2$)-$NH_2$ (IV), (m. p. 115—115.5°C, $[\alpha]_D^{25}$ −6.2° (*c* 2.1, 50% AcOH)). Cbz-Lys(BOC)-Pro-Val-Gly-Lys(BOC)-$N_3$, which was derived from the hydrazide,[5] was allowed to react with H-Arg($NO_2$)-Arg($NO_2$)-$NH_2$·HBr (m. p. 153—156°C decomp., $[\alpha]_D^{23.5}$ +14.1° (*c* 2.0, water)), which had been obtained from IV by the HBr/AcOH treatment, to give Cbz-Lys(BOC)-Pro-Val-Gly-Lys(BOC)-Arg($NO_2$)-Arg($NO_2$)-$NH_2$ (V) ($[\alpha]_D^{25.5}$ −40.4° (*c* 1.8, methanol)). Compound V was then hydrogenolyzed to obtain H-Lys(BOC)-Pro-Val-Gly-Lys(BOC)-Arg-Arg-$NH_2$ (VI) ($[\alpha]_D^{24}$ −44.8° (*c* 1.5, 50% AcOH).

The activated decapeptide ester, BOC-Gly-Tyr-Ser-Met-Glu($\gamma$-Bu$^t$)-His-Phe-Arg-Try-Gly-ON(CO-$CH_2$)$_2$[6], was allowed to react with VI to afford BOC-Gly-Tyr-Ser-Met-Glu($\gamma$-Bu$^t$)-His-Phe-Arg-Try-Gly-Lys(BOC)-Pro-Val-Gly-Lys(BOC)-Arg-Arg-$NH_2$ (VII). A crude sample of VII was, after having been treated with thioglycollic acid, purified by CMC column chromatography ($[\alpha]_D^{23.5}$ −35.8° (*c* 0.44, 50% AcOH). The purified VII was treated with 90% trifluoroacetic acid in order to liberate the heptadecapeptide I. $\lambda_{max}^{0.1N\ NaOH}$ = 281.5 mμ (ε 7070), 288.5 mμ (ε 6850). $[\alpha]_D^{23.5}$ −57.4° (*c* 0.5, 0.1 N AcOH). Amino acid ratios in acid ratios in acid hydrolysate:[7] Gly 2.81, Tyr 0.99, Ser 0.86, Met 1.00, Glu 1.00, His 1.01, Phe 0.91, Arg 2.74, Lys 2.12, Pro 1.04, Val 1.02, Try 0.57*3, $NH_3$ 1.30. Tyr/Try ratio in the intact I:[8] 1.00 : 1.14.

*Biochemistry Division*
*Shionogi Research Laboratory*
*Shionogi & Co., Ltd.*
*Fukushima-ku, Osaka*

4) H. van Orden and E. L. Smith, *J. Biol. Chem.*, **208**, 751 (1954).
5) H. Otsuka, K. Inouye and Y. Jono, This Bulletin, **37**, 1471 (1964).
6) H. Otsuka, K. Inouye, M. Kanayama and F. Shinozaki, ibid., **38**, 679 (1965).
7) D. H. Spackman, W. H. Stein and S. Moore, *Anal. Chem.*, **30**, 1191 (1958).
*3 Decomposed partially with acid.
8) T. W. Goodwin and R. A. Morton, *Biochem. J.*, **40**, 628 (1946); G. H. Beavan and E. R. Holliday, *Advances in Protein Chemistry*, **7**, 319 (1952).

# The Mechanism of the Copolymerization of Some Olefins with Maleic Anhydride*

By Chuji Aso and Toyoki KUNITAKE

(Received June 11, 1965)

Alternating free-radical copolymerization have been explained as resulting from the polar interaction of a growing radical and a monomer,[1] from the stabilization of the transition state of propagation due to electron transfer,[2] and from the charge-transfer complex between monomers.[3]

Although $\omega$-phenylalkenes copolymerize with maleic anhydride easily,[4] it has been found in this laboratory that 4-cyclohexyl-1-butene (CHBu) does not give a copolymer with maleic anhydride under the conditions under which 4-phenyl-1-butene copolymerizes. For example, the phenylbutene (1.0 mol./l.) and maleic anhydride (1.0 mol./l.) in methyl ethyl ketone, with azobisisobutyronitrile ($0.25\times10^{-2}$ mol./l.) as an initiator, gave 21% of a copolymer (M. W.> 2000) with an approximately 60 : 40 composition at 70°C in 5 hr. On the other hand, 4-cyclohexyl-1-butene and 1-octene gave trace amounts of solid products under the same conditions. This difference in reactivity cannot be considered to be due wholly to the different inductive effects of the benzene and cyclohexane rings, since these rings are separated from the double bond by two methylene groups.

Assuming similar initiation and termination

* Contribution No. 71 from Department of Organic Synthesis, Faculty of Engineering, Kyushu University.

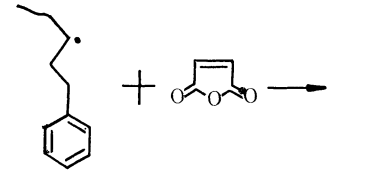
1) C. C. Price, *J. Polymer Sci.*, **1**, 83 (1946).

2) C. Walling, E. R. Briggs, K. B. Wolfstirn and F. R. Mayo, *J. Am. Chem. Soc.*, **70**, 1537 (1948).

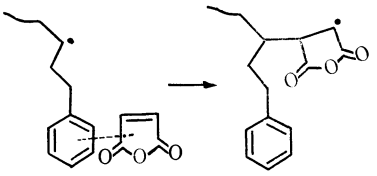
3) S. Iwatsuki, Y. Tanaka and Y. Yamashita, *J. Chem. Soc. Japan, Ind. Chem. Sec.* (*Kogyo Kagaku Zasshi*), **67**, 1464 1467, 1470 (1964).

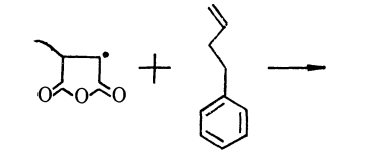
4) M. M. Martin and N. P. Jensen, *J. Org. Chem.*, **27**, 1201 (1962).

reactions, the higher copolymerizability of 4-phenyl-1-butene may be attributable to the following propagation mechanisms, which are specific to this monomer:

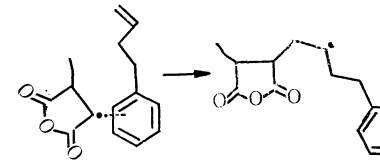


(1)





(2)



In Eq. 1, the benzene ring of the propagating radical and maleic anhydride form a charge-transfer complex, while in Eq. 2 the propagating maleic anhydride radical forms a similar complex with the phenylbutene monomer.[5]

A third possibility to be considered is the intramolecular complex-formation of the phenylbutene radical, as may be assumed in the polymerization of vinyl benzoate.[6] The radical would then become a kind of ocnjugated free radical, and would show a very different reactivity from that of the cyclohexylbutene radical.

Which of these three schemes contributes most to the higher copolymerizability of the phenylbutene remains to be clarified. However, the process depicted by Eq. 2 seems important in the copolymerization of styrene and maleic anhydride; evidence which supports this mechanism has been presented elsewhere.[7]

*Department of Organic Synthesis*
*Faculty of Engineering*
*Kyushu University*
*Hakozaki, Fukuoka*

5) M. M. Martin and G. J. Gleicher, *J. Am. Chem. Soc.*, **86**, 233 (1964).
6) G. F. Santee, R. H. Marchessault, H. G. Clark and J. J. Kearny, *Makromol. Chem.*, **73**, 177 (1964).
7) C. Aso, T. Kunitake and K. Watanabe, Papers presented at the 13th Discussion Meeting of the Society of High Polymers, Japan, November, 1964, p. 38.

# A Mössbauer Study of the Hot-atom Effect of EC Decay in Cobalt(II) Oxalate

By Hirotoshi SANO and Fukiko HASHIMOTO

(Received June 22, 1965)

Mössbauer spectroscopy provides unambiguous information about the chemical consequences of nuclear transformations. It is especially useful as a method for studying such effects on a rapid time scale which is inaccessible to classical chemical experimentation. The first excited state in the $^{57}$Fe nuclide is populated by the EC decay of $^{57}$Co, followed by the emission of a 123 keV. gamma ray from the second excited state. It has been found that the electron shake-off Auger cascade resulting from these precursor events gives rise to iron atoms in both $3d^5$ and $3d^6$ configurations, in cobalt(II) oxide,[1] cobalt(III) acetylacetonate[2] and biscyclopentadienyl cobalt(III) salts[3].

The Mössbauer study of the radiolysis of iron(III) oxalate has shown that iron(II) oxalate is formed as an irradiation product.[4] It has been also reported that the $G(Co^{2+})$ value in the $\gamma$-ray irradiated oxalatocobalt(III) complexes increases with an increase in the

1) G. K. Wertheim, *Phys. Rev.*, **124**, 764 (1961).
2) G. K. Wertheim, W. R. Kingston and R. H. Herber, *J. Chem. Phys.*, **37**, 687 (1962).
3) G. K. Wertheim and R. H. Herber, ibid., **38**, 2106 (1963).
4) N. Saito, H. Sano, T. Tominaga and F. Ambe, This Bulletin, **38**, 681 (1965).

oxalate ion content of the complexes,[5] and that ninety percent or more of the radiocobalt atoms are found as cobalt(II) species after the dissolution of the neutron-irradiated oxalatocobalt(III) complexes.[6] In the present study, the Mössbauer spectrum of $^{57}Fe$ produced from $^{57}Co$ in the $CoC_2O_4 2H_2O$ host crystal will be determined.

Pale pink-colored crystal of cobalt(II) oxalate was made by adding oxalic acid to cobalt(II) nitrate solution (containing 2 millicurie of $^{57}Co$). The cobalt content was determined radiochemically. The Mössbauer spectrum was measured with a stainless steel absorber moving at various constant velocities at room temperature. The spectra were also measured with iron(II) oxalate and iron(III) oxalate absorbers, using a $^{57}Co$ diffused copper foil source.

Typical spectra are shown in Fig. 1. With respect to a stainless steel source, iron(II) oxalate and iron(III) oxalate give isomer shifts of 1.28 and 0.49 mm./sec., and quadrupole splitting of 1.73 and 0.43 mm./sec., respectively. In the case of $^{57}Co$-labeled cobalt(II) oxalate, it may be expected that the EC precursor event leaves the daughter $^{57}Fe$ atom not only in the same oxidation state as that of parent cobalt atom, but also in a different oxidation state from those observed in cobalt(II) oxide, cobalt(III) acetylacetonate and biscyclopentadienyl cobalt(III) salts. However, no evidence for ionic charge states other than 2+ is observed. As may be seen in Fig. 1, the electron configuration around the $^{57}Fe$ atom produced in the cobalt(II) oxalate crystal is essentially identical to that in ferrous oxalate. This may be explained by assuming that higher charge species—even if formed as a consequence of the prior nuclear event—have been reduced by the oxalate ions in times brief compared to $10^{-7}$ sec. at room temperature; this is in accordance with the remarkable reducing power of oxalate ions observed in the radiolyses of iron(III) oxalate,[4] potassium trisoxalatoferrate(III)[7] and oxalatocobalt(III) complexes,[5] and with hot-atom effect of the latter.[6]

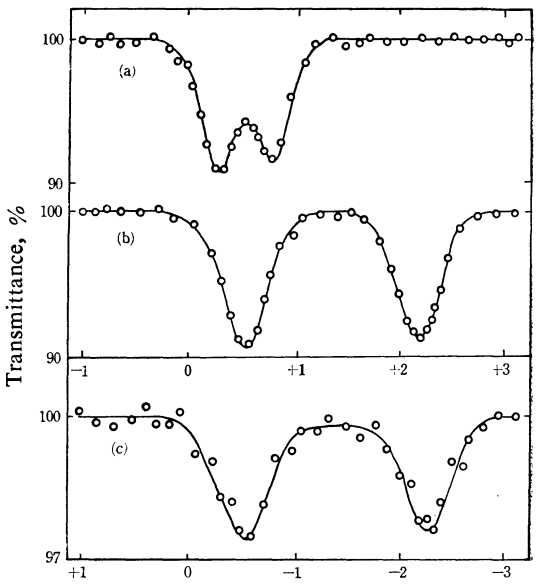



Fig. 1. Mössbauer spectra (at 22°C).

(a) Absorber, $Fe_2(C_2O_4)_3 5H_2O$; source, $^{57}Co$ in Cu

(b) Absorber, $FeC_2O_4 2H_2O$; source, $^{57}Co$ in Cu (Abscissa is normalized to stainless steel source)

(c) Source, $^{57}CoC_2O_4 2H_2O$; absorber, stainless steel

*Department of Chemistry*
*Faculty of Science*
*Ochanomizu University*
*Otsuka, Tokyo*

5) H. Sano, N. Matsubara and N. Saito, ibid., **38**, 333 (1965).

6) N. Saito, H. Sano and T. Tominaga, *Chem. & Ind.*, **1964**, 1622.

7) H. Sano and T. Fukuroi, Presented at the 17th Annual Meeting of Chemical Society of Japan, Tokyo April, 1964.

# The Infrared Spectra of Alkylaluminum-Ether Complexes*1

By Saburo TAKEDA and Ryokichi TARAO

(Received July 30, 1964)

Because of experimental difficulties, the infrared spectra of alkylaluminum-ether complexes have never been reported except for Hoffmann's report dealing with the triethylaluminum - diethyl ether complex along with nine alkylaluminum compounds.[1] As the importance of compounds of this type is increasing from both theoretical and practical points of view, however, fifteen kinds of such complexes have now been prepared and a systematic study of their infrared spectra has been carried out.

Their spectra have been assigned in the 2000 —350 $cm^{-1}$ region, although some of them are tentative. Hoffmann's assignment of the infrared spectrum of the triethylaluminum - diethyl ether complex has been partly corrected. Special attention has been paid to two absorption bands corresponding to the C-O antisymmetric and the C-O symmetric stretching vibration of ether. These C-O bands shift to lower frequencies when ether forms an alkylaluminum complex; the magnitudes of the shifts caused by trimethylaluminum and triethylaluminum complex formation have been compared with each other. The magnitudes of the shifts caused by $AlR_3$-, $AlR_2X$- or $AlRX_2$- (R=methyl, or ethyl, X=halogen) diethyl ether complex formation have also been compared. The infrared spectra of five kinds of ethylaluminum ethoxide have also been measured.

## Experimental

**Preparation of Alkylaluminum-Ether Complexes.** —Trialkylaluminums, dialkylaluminum halides and alkylaluminum dihalides, which were distilled just before use, were mixed with dimethyl ether, tetrahydrofuran, ethyl methyl ether and diethyl ether which had been dried and distilled just before use, in a molar ratio of 1 : 1, and distilled in vacuo. All manipulations were carried out under an atmosphere of purified nitrogen. Trimethylaluminum, dimethylaluminum chloride, and methylaluminum dichloride

TABLE I. ALKYLALUMINUM-ETHER COMPLEXES

| Complex | B. p., °C (mmHg) | Al, % | | Mol. wt. | |
|---|---|---|---|---|---|
| | | Calcd. | Found*1 | Calcd.*2 | Found*3 |
| $AlMe_3 \cdot Me_2O$*4 | 41.5 (10) | 22.8 | 22.7 | 118.2 | 121.6 |
| $AlMe_3 \cdot THF$ | 54.0—55.5 (2) | 18.7 | 18.5 | 144.2 | 146.4 |
| $AlMe_3 \cdot MeOEt$ | 55.5—56.5 (10) | 20.4 | 20.0 | 132.2 | 134.4 |
| $AlMe_3 \cdot Et_2O$ | 45.5—47.0 (4) | 18.5 | 18.3 | 146.2 | 149.5 |
| $AlMe_2Cl \cdot Me_2O$ | 85.5—87.0 (10.5) | 19.5 | 19.8 | 138.6 | 151.7 |
| $AlMe_2Cl \cdot Et_2O$ | 73.0—74.5 (2.5) | 16.2 | 16.4 | 166.6 | 199.7 |
| $AlMeCl_2 \cdot Et_2O$ | 123.0—125.0 (7) | 14.4 | 14.5 | 187.0 | 226.3 |
| $AlEt_3 \cdot Me_2O$ | 76.5—78.0 (3) | 16.8 | 17.5 | 160.2 | 176.3 |
| $AlEt_3 \cdot THF$ | 123.0—125.0 (9) | 14.5 | 14.8 | 186.3 | 198.6 |
| $AlEt_3 \cdot MeOEt$ | 82.0—83.5 (3.5) | 15.5 | 16.1 | 174.3 | 185.2 |
| $AlEt_3 \cdot Et_2O$ | 88.5—91.5 (3.5) | 14.3 | 14.8 | 188.3 | 205.8 |
| $AlEt_2Br \cdot Et_2O$ | 97.5—99.5 (2.5) | 11.3 | 11.6 | 239.1 | 261.1 |
| $AlEt_2Cl \cdot Et_2O$ | 92.0—93.0 (3.5) | 13.9 | 14.2 | 194.7 | 202.9 |
| $AlEtBr_2 \cdot Et_2O$ | 161.0—165.0 (15) | 9.3 | 9.9 | 290.0 | 324.5 |
| $AlEtCl_2 \cdot Et_2O$ | 122.0—130.0 (5.5) | 13.4 | 13.9 | 201.1 | 213.2 |

*1 Analysis was carried out by volumetric method (oxine complex salt method).
*2 Molecular weights were calculated for monomeric forms.
*3 Determined by measuring freezing point depression of benzene solution; values listed are mean values of several measurements.
*4 Me=$CH_3$, Et=$C_2H_5$, THF=tetrahydrofuran; these abbreviations are used throughout Tables I—VII.

*1 Presented partly at the 17th Annual Meeting of the Chemical Society of Japan, Tokyo, April, 1964.

1) E. G. Hoffmann, *Z. Elektrochem.*, 64, 616 (1960).

TABLE II. OBSERVED FREQUENCIES OF METHYLALUMINUM-ETHER COMPLEXES IN $cm^{-1}$ AND VIBRATION ASSIGNMENT

| $AlMe_3 \cdot Me_2O$ | $AlMe_3 \cdot THF$ | $AlMe_3 \cdot MeOEt$ | $AlMe_3 \cdot Et_2O$ | $AlMe_2Cl \cdot Me_2O$ | $AlMe_2Cl \cdot Et_2O$ | $AlMeCl_2 \cdot Et_2O$ | Assignment |
|---|---|---|---|---|---|---|---|
| | 1476 vw | 1474 m | 1479 vw | 1466 sh | | 1478 vw | $CH_3$ degenerate deformation |
| 1462 s | 1459 m | | 1469 s | 1456 s | 1469 s | 1467 s | $CH_2$ scissoring |
| | 1451 sh | 1451 m | 1448 m | | 1449 m | 1448 m | |
| | | 1393 m | 1393 s | | 1395 s | 1395 s | $CH_3$-C symmetric deformation |
| | 1372 w | | | | | | |
| | 1350 m | | | | | | |
| | 1319 vw | 1312 w | 1327 m | | 1328 m | 1328 m | $CH_2$ wagging |
| | 1294 vw | | 1282 m | | 1282 m | 1280 m | $CH_2$ twisting |
| 1250 w | 1244 w | 1255 vw | 1254 vw | 1252 m | 1255 w | 1256 vw | |
| 1185 vs | 1182 vs | 1185 vs | 1187 s | 1194 s | 1194 s | 1201 s | $CH_3$ rocking |
| 1153 m | | 1150 m | 1151 s | 1151 m | 1150 s | 1149 s | |
| | | 1091 m | 1091 s | | 1092 s | 1092 s | |
| | 1040 vw | | | | | | |
| 1046 vs | 1017 vs | 1042 vs | 1036 vs | 1031 vs | 1023 vs | 1009 vs | C-O antisymmetric stretching |
| | 958 w | 966 s | 996 m | | 993 vw | 990 sh | C-C stretching |
| | 919 m | | | | | | |
| 891 s | 869 vs | 833 s | 898 s | 882 s | 893 s | 884 s | C-O symmetric stretching |
| | | 800 m | 834 m | | 834 w | 833 m | $CH_2$ rocking |
| | | | 781 m | | 774 w | 771 s | |
| | | | | 854 vw | | | |
| | | | | 822 vw | | | |
| | | | | 769 vw | | | |
| 710 s | 707 s | 708 s | 706 s | | | | Al-C degenerate stretching |
| 622 m | 616 m | 625 m | 624 m | | | | |
| | | | 576 vw | | | | |
| 525 m | 519 m | 525 m | 526 m | | | | Al-C symmetric stretching |
| | | 507 vw | 506 vw | | | | |
| 473 m | 455 vw | 456 vw | 462 w | | | | Al-O stretching |
| | | | | 690 vs | 685 vs | | Al-C antisymmetric stretching |
| | | | | 582 s | 580 s | | Al-C symmetric stretching |
| | | | | 489 m | 517 m | | Al-O stretching |
| | | | | | (488 w) | | Al-Cl stretching |
| | | | | 407 m | 409 m | | |
| | | | | | | 673 s | Al-C stretching |
| | | | | | | 534 m | Al-O stretching |
| | | | | | | 489 m | Al-Cl antisymmetric stretching |
| | | | | | | 408 m | Al-Cl symmetric stretching |

were purchased from Texas Alkyls, Inc., and triethylaluminum, diethylaluminum chloride and ethylaluminum dichloride, from the Ethyl Co. Diethylaluminum bromide and ethylaluminum dibromide were prepared by the method of Grosse and Mavity.[2] Table I shows the boiling points, aluminum contents, and molecular weights of alkylaluminum-ether complexes prepared as above.*2

**Preparation of Ethylaluminum Ethoxides.** — Diethylaluminum ethoxide, and ethylaluminum diethoxide were prepared by the method of Grosse and Mavity.[2] Ethylethoxyaluminum chloride and ethylethoxyaluminum bromide were prepared by the reaction of ethylaluminum sesquihalide and aluminum triethoxide.[3] Ethylethoxyaluminum iodide was prepared by the reaction of diethyl aluminum iodide and anhydrous ethanol.[4] Table VI shows the boiling points, aluminum contents, and molecular weights of the ethylaluminum ethoxides thus obtained.

**Measurements of the Infrared Spectra.**—A Japan Spectroscopic Co. model DS-402G infrared spectrophotometer was used for the infrared absorption measurements. Thin liquid films of the samples were used in all cases. Freshly-distilled samples were injected in KRS-5 airtight cells in a glove box filled with purified nitrogen; this operation had to be performed as rapidly as possible, because even

2) A. V. Grosse and J. M. Mavity, *J. Org. Chem.*, 5, 106 (1940).

*2 The authors are indebted to Mr. Takao Tsunoda and Mr. Makoto Iizuka of our laboratory for their help in the synthetical work, and to Mr. Hitoshi Shinkoda of our laboratory for his aluminum analysis.

3) Brit. Pat. 858498 (1959).

4) N. Davidson and H. C. Brown, *J. Am. Chem. Soc.*, 64, 316 (1942).

in an atmosphere of carefully-purified nitrogen long exposure of samples brings about contamination with oxidation as a result of the trace amount of oxygen present. Absorption bands due to oxidized contaminants were discriminated by comparing the spectrum obtained with the spectrum obtained with the intentionally airoxidized samples. To make sure that samples did not react with window materials, the observed spectrum was compared with that taken by the polyethylene-sandwich method. No absorption band disappeared even if the polyethylene-sandwich method was applied, showing that no absorption bands due to reaction products with window materials could be detected at all.

## Results and Discussion

**Methylaluminum-Ether Complexes.**—The observed frequencies of the infrared spectra of seven kinds of methylaluminum-ether complexes in the 2000—350 $cm^{-1}$ region are shown in Table II. Figure 1 shows three typical spectra charts. As the spectrum of trimethylaluminum has no absorption band in the 1150—800 $cm^{-1}$ region,[1] and that of dimethyl ether has two bands, 1094 and 920 $cm^{-1}$ (C-O antisymmetric and symmetric stretching vibrations),[5] the absorption bands of the trimethylaluminum-dimethyl ether complex at 1046 and 891 $cm^{-1}$ are assigned to the C-O antisymmetric and symmetric stretching vibrations

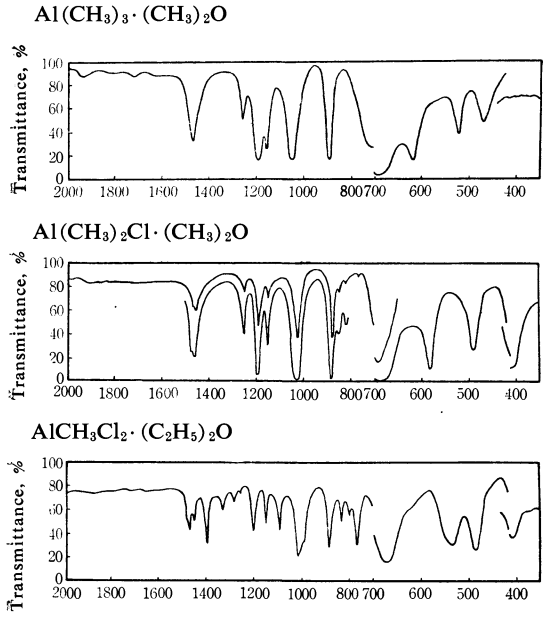



Fig. 1. Spectra of methylaluminum-ether complexes.

5) Y. Mashiko, *J. Chem. Soc. Japan, Pure Chem. Sec.* (*Nippon Kagaku Zassi*), **79**, 470 (1958); Y. Mashiko, ibid., **80**, 593 (1959).

respectively. These two C-O stretching bands are also easily found for the six other complexes. Table III shows the shifts of the C-O bands of dimethyl ether, tetrahydrofuran, ethyl methyl ether and diethyl ether upon trimethylaluminum-complex formation. The assignments of the other bands have been made by comparing the spectra of these seven complexes with one another.

Table III. Shifts of the C-O vibration bands of ethers on $AlMe_3$ complex formation

| | $\nu_{as}$(CO) ($cm^{-1}$) | | $\nu_s$(CO) ($cm^{-1}$) | |
|---|---|---|---|---|
| | Ether* | Complex | Ether* | Complex |
| $AlMe_3 \cdot Me_2O$ | 1094 | 1046 | 920 | 891 |
| $AlMe_3 \cdot THF$ | 1073 | 1017 | 913 | 869 |
| $AlMe_3 \cdot MeOEt$ | 1120 | 1042 | 925 | 833 |
| $AlMe_3 \cdot Et_2O$ | 1120 | 1036 | 926 | 898 |

* The values listed are taken from Mashiko's data in $CCl_4$ solution for $Me_2O$, MeOEt, and $Et_2O$.[5] For THF, the frequencies obtained by us in the pure liquid state are used.

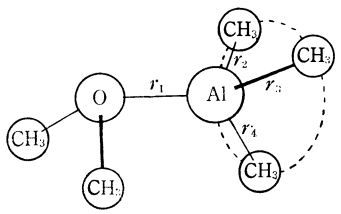



Fig. 2. Molecular model and internal coordinates of $Al(CH_3)_3 \cdot (CH_3)_2O$.

The assignment in the KBr prism region is guided by a consideration of the molecular model $Al(CH_3)_3 \cdot (CH_3)_2O$, as is illustrated in Fig. 2.*3 On the assumption that the trimethylaluminum-dimethyl ether complex has the $C_s$ symmetry only, the symmetry coordinates for each type of vibration in the model are as given in Table IV. Table IV also summarizes the symmetry coordinates for the dimethylaluminum chloride-dimethyl ether complex (in which $r_4$ represents the Al-Cl distance) and the methylaluminum dichloride-diethyl ether complex (in which $r_3$ and $r_4$ represent the two Al-Cl distances).

The assignments for the trimethylaluminum-dimethyl ether, -tetrahydrofuran, -ethyl

*3 Bauer and his co-workers measured the bond lengths and the angles of the boron trifluoride-dimethyl ether complex. They found that all angles of $BF_3 \cdot (CH_3)_2O$ are 109.5° and that the carbon atoms are staggered relative to the fluorine atoms. [S. H. Bauer, G. R. Finlay and A. W. Laubengayer, *J. Am. Chem. Soc.*, **67**, 339 (1945).]

Although the bond lengths and angles of $Al(CH_3)_3 \cdot (CH_3)_2O$ have not been measured, it seems most probable in this case that we may assume a staggered conformation as in the case of $BF_3 \cdot (CH_3)_2O$.

TABLE IV. SYMMETRY COORDINATES

| Complex | Coordinate | Description |
|---|---|---|
| $AlMe_3 \cdot Me_2O$ | $\Delta r_1$ | Al-O stretching |
| | $(\Delta r_2+\Delta r_3+\Delta r_4)/\sqrt{3}$ | Al-C symmetric stretching |
| | $(2\Delta r_2-\Delta r_3-\Delta r_4)/\sqrt{6}$ | Al-C degenerate stretching* |
| | $(\Delta r_3-\Delta r_4)/\sqrt{2}$ | |
| $AlMe_2Cl \cdot Me_2O$ | $\Delta r_1$ | Al-O stretching |
| | $(\Delta r_2+\Delta r_3)/\sqrt{2}$ | Al-C symmetric stretching |
| | $(\Delta r_2-\Delta r_3)/\sqrt{2}$ | Al-C antisymmetric stretching |
| | $\Delta r_4$ | Al-Cl stretching |
| $AlMeCl_2 \cdot Et_2O$ | $\Delta r_1$ | Al-O stretching |
| | $\Delta r_2$ | Al-C stretching |
| | $(\Delta r_3+\Delta r_4)/\sqrt{2}$ | Al-Cl symmetric stretching |
| | $(\Delta r_3-\Delta r_4)/\sqrt{2}$ | Al-Cl antisymmetric stretching |

* If only $AlMe_3 \cdot O$ part of the skeleton is taken into consideration, the symmetry is $C_{3v}$ and these two coordinates must be doubly degenerate. When the two methyl groups are attached to the oxygen atom, the over all symmetry of the complex becomes $C_s$ and these degenerate frequencies split into two. See also Ref. 6.

TABLE V. OBSERVED FREQUENCIES OF ETHYLALUMINUM-ETHER COMPLEXES IN $cm^{-1}$ AND VIBRATION ASSIGNMENTS

| $AlEt_3 \cdot Me_2O$ | $AlEt_3 \cdot THF$ | $AlEt_3 \cdot MeOEt$ | $AlEt_3 \cdot Et_2O$ | Assignment |
|---|---|---|---|---|
| 1468 s | | 1468 s | 1466 s | $CH_3$ degenerate deformation |
| | 1459 s | | | $CH_2$ scissoring (ether) |
| 1456 w | 1452 sh | 1454 s | 1452 sh | |
| 1436 sh | | | | |
| 1411 s | 1411 s | 1412 s | 1409 s | $CH_2$ scissoring ($-CH_2-Al$) |
| | | 1393 s | 1392 s | $CH_3$-C symmetric deformation |
| 1375 w | 1372 w | 1374 w | | |
| 1339 vw | 1350 w | | | |
| | 1317 vw | 1313 m | 1326 m | $CH_2$ wagging (ether) |
| | 1296 vw | | 1283 m | $CH_2$ twisting (ether) |
| 1253 m | 1244 vw | 1254 vw | | |
| 1225 m | 1224 w | 1215 m | 1223 m | $CH_2$ wagging ($-CH_2-Al$) |
| 1188 s | 1186 s | 1187 s | 1189 s | $CH_2$ twisting ($-CH_2-Al$) |
| 1155 s | | 1151 s | 1146 s | $CH_3$ rocking |
| | 1120 vw | | | |
| | | 1091 s | 1089 s | |
| | 1040 vw | | | |
| 1049 vs | 1018 vs | 1042 vs | 1035 vs | C-O antisymmetric stretching |
| 986 s | 986 s | 985 s | 988 vs | C-C stretching |
| 947 m | 947 m | 966 s | 946 s | |
| | | 948 m | | |
| 918 sh | 918 m | 918 w | 913 sh | |
| 886 vs | 865 vs | 829 vs | 894 s | C-O symmetric stretching |
| | | 800 m | 835 m | $CH_2$ rocking (ether) |
| | | | 774 s | |
| 649 vs | 647 vs | 647 vs | 648 vs | Al-C degenerate stretching |
| 629 s | 630 s | 631 s | 630 s | $CH_2$ rocking ($-CH_2-Al$) |
| 597 w | 599 sh | 600 sh | 600 w | Al-C degenerate stretching |
| 496 w | 494 w | 511 m | 510 w | Al-C symmetric stretching |
| 472 w | 455 vw | 458 vw | 457 w | Al-O stretching |

TABLE V. (Continued)

| $AlEt_2Br \cdot Et_2O$ | $AlEt_2Cl \cdot Et_2O$ | $AlEtBr_2 \cdot Et_2O$ | $AlEtCl_2 \cdot Et_2O$ | Assignment |
|---|---|---|---|---|
| 1468 s | 1468 s | 1468 s | 1469 s | $CH_3$ degenerate deformation |
| 1449 w | 1449 sh | 1448 w | 1450 m | $CH_2$ scissoring (ether) |
| 1409 w | 1410 w | | | $CH_2$ scissoring ($-CH_2-Al$) |
| 1394 s | 1394 s | 1395 s | 1396 s | $CH_3$-C symmetric deformation |
| 1379 sh | 1379 sh | | | |
| 1362 vw | | 1362 vw | | |
| 1327 m | 1328 m | 1326 m | 1329 w | $CH_2$ wagging (ether) |
| 1282 m | 1282 m | 1280 w | 1283 w | $CH_2$ twisting (ether) |
| 1256 w | 1255 w | 1255 vw | 1257 vw | |
| 1223 w | 1224 w | 1222 vw | 1224 vw | $CH_2$ wagging ($-CH_2-Al$) |
| 1191 m | 1190 m | 1191 m | 1193 m | $CH_2$ twisting ($-CH_2-Al$) |
| 1149 m | 1149 m | 1149 m | 1151 m | $CH_3$ rocking |
| 1091 s | 1091 s | 1092 s | 1092 s | |
| 1021 vs | 1027 vs | 1006 vs | 1010 vs | C-O antisymmetric stretching |
| 992 s | 991 s | | 990 vw | C-C stretching |
| 952 m | 951 m | 958 vw | 957 vw | |
| 921 w | 919 w | 923 w | 922 vw | |
| 889 s | 890 s | 881 s | 884 s | C-O symmetric stretching |
| 832 m | 831 s | 832 m | 833 m | |
| | | (795 w) | (796 w) | $CH_2$ rocking (ether) |
| 772 s | 771 s | 766 s | 769 s | |
| 650 vs | | | | Al-C antisymmetric stretching |
| 623 s | | | | $CH_2$ rocking ($-CH_2-Al$) |
| 593 sh | | | | |
| 553 s | | | | Al-C symmetric stretching |
| 516 w | | | | |
| 464 w | | | | Al-O stretching |
| 356 w | | | | Al-Br stretching |
| | 650 vs | | | Al-C antisymmetric stretching |
| | 625 s | | | $CH_2$ rocking ($-CH_2-Al$) |
| | 595 vw | | | |
| | 556 m | | | Al-C symmetric stretching |
| | 515 w | | | Al-O stretching |
| | 406 m | | | Al-Cl stretching |
| | | | 629 s | $CH_2$ rocking ($-CH_2-Al$) |
| | | | 609 sh | Al-C stretching |
| | | | 532 m | Al-O stretching |
| | | | 502 s | Al-Cl antisymmetric stretching |
| | | | 405 w | Al-Cl symmetric stretching |

methyl ether and - diethyl ether complexes are given straightforwardly in Table II, the band appearing at 473—455 $cm^{-1}$ being assigned to the Al-O stretching mode.

The assignments for the methylaluminum dichloride -, the ethylaluminum dichloride - and the diethylaluminum bromide - diethyl ether complexes can also be given straightforwardly, as in Tables II and V (see also Fig. 3). The two Al-Cl vibrations appear at 489 and 408 $cm^{-1}$ for the methylaluminum dichloride complex and at 502 and 405 $cm^{-1}$ for the ethylaluminum dichloride complex. The Al-Br vibration appears at 356 $cm^{-1}$ for the diethylaluminum bromide complex.*4 The Al-O stretching vibrations are assigned for these molecules in Tables II and V. These assignments for the Al-O stretching vibrations are reasonable when we compare them with the B-O stretching vibration assigned by Begun, Fletcher and Palko.[6],*5

The spectra in the KBr region of the dimethylaluminum chloride - dimethyl ether, the dimethylaluminum chloride - diethyl ether and

*4 We also measured the spectrum of the ethylaluminum dibromide - diethyl ether complex. It has 425 and 362 $cm^{-1}$ bands, which are assigned to two Al-Br stretching bands.

6) G. M. Begun, W. H. Fletcher and A. A. Palko, *Spectrochim. Acta*, **18**, 655 (1962).

*5 The difference between 670 $cm^{-1}$ (the B-O stretching vibration) and 530—460 $cm^{-1}$ (the Al-O stretching vibration) can be explained in terms of the difference between the masses of boron and aluminum atoms.

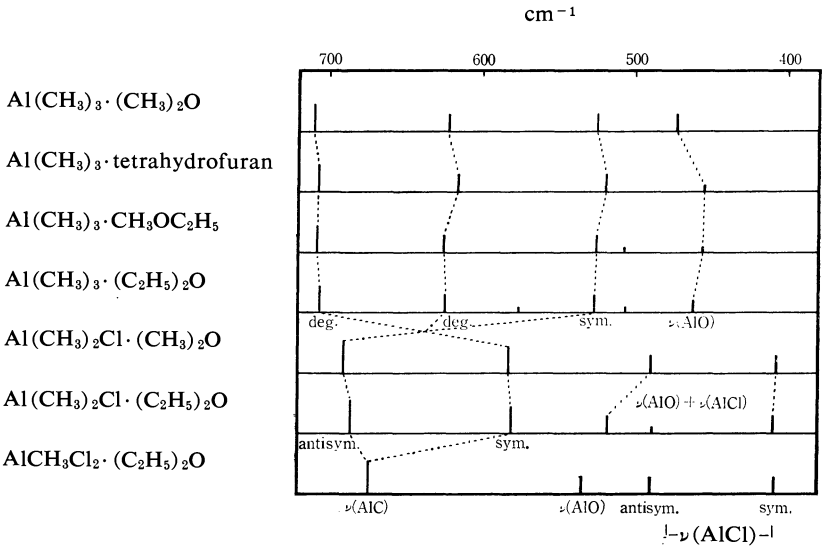



Fig. 3. The KBr region spectra of methylaluminum-ether complexes.

TABLE VI. ETHYLALUMINUM ETHOXIDES

| Ethoxide | B. p., °C (mmHg) | Al, % | | Mol. wt. | |
|---|---|---|---|---|---|
| | | Calcd. | Found*1 | Calcd.*2 | Found*3 |
| $AlEt_2OEt$ | 59.0 (1.5) | 20.7 | 20.4 | 260.3 (2) | 278.7 |
| $AlEt(OEt)_2$ | 155.0—165.0 (3) | 18.5 | 19.0 | 438.5 (3) | 450.4 |
| AlEt(OEt)Cl | 96.0—97.0 (4.5) | 19.8 | 19.7 | 409.7 (3) | 395.9 |
| AlEt(OEt)Br | 130.0 (7) | 14.9 | 15.0 | 362.0 (2) | 374.5 |
| AlEt(OEt)I | 120.0—122.0 (4) | 11.8 | 11.8 | 456.0 (2) | 471.8 |

*1 Method of analysis is the same as in Table I.
*2 Molecular weights were calculated by assuming degree of polymerization as shown in parentheses.
*3 Experimental method is the same as in Table I. AlEt(OEt)Cl isomerized from dimeric to trimeric form in a few days and AlEt(OEt)Br in a few months (see footnote in Appendix). The data listed for these two compounds come from measurements at the time one week after they had been synthesized.

the diethylaluminum chloride - diethyl ether complexes, given in Tables II and V, are somewhat complex. They have two bands in this region, 489 and 407 $cm^{-1}$ for the dimethylaluminum chloride - dimethyl ether, 517 and 409 $cm^{-1}$ for the dimethylaluminum chloride - diethyl ether, and 515 and 406 $cm^{-1}$ for the diethylaluminum chloride - diethyl ether complex. These bands can only be understood in terms of the strong coupling between the Al-O stretching and the Al-Cl stretching vibrations. As has been mentioned above, the Al-O stretching vibration of the trimethylaluminum complex appears near 460 $cm^{-1}$, while that of the methylaluminum dichloride complex appears near 534 $cm^{-1}$. These two facts suggest that the A-O stretching bands of the dimethylaluminum chloride complex appear in the region between 470 and 500 $cm^{-1}$. In this region the Al-Cl stretching vibration is also expected to appear. Therefore, it is very probable that these two bands are coupled with each other and appear as two bands, as has been postulated above.

**Ethylaluminum-Ether Complexes.**—The observed frequencies of the infrared spectra of eight kinds of ethylaluminum-ether complexes in the 2000—350 $cm^{-1}$ region are shown in Table V. Figure 4 shows three typical spectra charts. The assignments are almost self-evident if one uses the results of the assignments of methylaluminum-ether complexes.

Hoffmann assigned the absorption band near 770 $cm^{-1}$ of the triethylaluminum - diethyl ether complex to the C-O symmetric stretching vibration.[1] The above assignment for the C-O symmetric stretching band of the trimethylaluminum - dimethyl ether complex, however, suggests that the band at 894 $cm^{-1}$ originates from the C-O symmetric stretching. Since only the diethyl ether complexes of

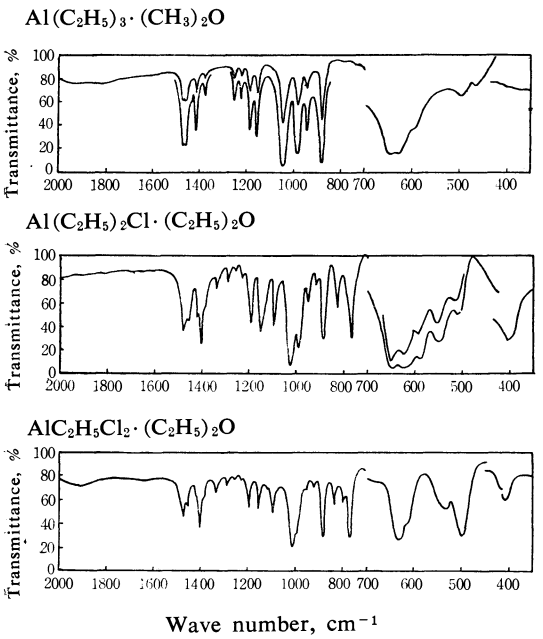



Fig. 4. Spectra of ethylaluminum-ether complexes.

alkylaluminums show an absorption band near 770 $cm^{-1}$, while the dimethyl ether, tetrahydrofuran and ethyl methyl ether complexes do not, this band is assigned to the $CH_2$ rocking vibration of diethyl ether, as is shown in Tables II and V.

In the KBr prism region, the $CH_2$ rocking band of the $CH_2$ group adjacent to the aluminum atom appears near 630 $cm^{-1}$ and the spectra of ethylaluminum-ether complexes become more complicated than those of methylaluminum-ether complexes.[1] The spectrum of the ethylaluminum dibromide-diethyl ether complex in the 710—350 $cm^{-1}$ region is not simple and no adequate assignment has been made.

**Shifts of the C-O Antisymmetric and Symmetric Stretching Bands of Ether on Forming Complex.**—Both the C-O antisymmetric stretching (near 1100 $cm^{-1}$) and the symmetric stretching vibration bands (near 920 $cm^{-1}$) of ether shift to lower frequencies when a complex is formed either with trimethylaluminum (Tables II and III) or with triethylaluminum (Table V). For trimethylaluminum and triethylaluminum, the magnitudes of the shifts are almost the same. These facts suggest that, in the alkylaluminum-ether complex, the C-O bonds of ether are somewhat weaker than those in the free ether molecule because an unshared pair of electrons of the oxygen atom coordinates to the aluminum atom.

If we compare the magnitudes of the shifts of the C-O antisymmetric and symmetric stretching bands of diethyl ether caused by the complex formation with trimethylaluminum, dimethylaluminum chloride and methylaluminum dichloride, the shifts become larger in this order. As regards the magnitudes of the shifts of these two bands of diethyl ether caused by the complex formation with triethylaluminum, diethylaluminum halide and ethylaluminum dihalide, the shifts become larger in this order. Figure 5 shows the shifts of the C-O stretching bands in eight kinds of diethyl ether complexes. From this figure, the following two conclusions can be drawn.

i) The electron-accepting tendency of alkylaluminum becomes larger in the order of $AlR_3 < AlR_2X < AlRX_2$ (R=methyl or ethyl, X=halogen).

ii) The electron-accepting tendencies of $Al(CH_3)_nX_{3-n}$ and $Al(C_2H_5)_nX_{3-n}$ ($n$=1, 2, 3) are almost the same.

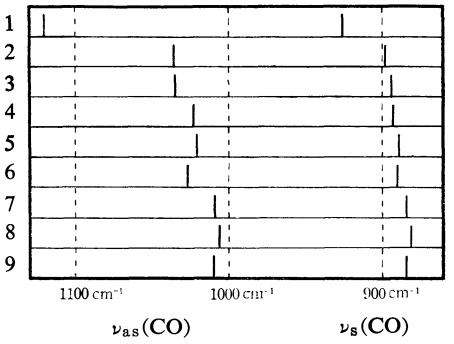



Fig. 5. Shifts of the absorption bands of CO antisymmetric and symmetric stretching vibration of ether on complex formation.

1 $(C_2H_5)_2O$
2 $Al(CH_3)_3 \cdot (C_2H_5)_2O$
3 $Al(C_2H_5)_3 \cdot (C_2H_5)_2O$
4 $Al(CH_3)_2Cl \cdot (C_2H_5)_2O$
5 $Al(C_2H_5)_2Br \cdot (C_2H_5)_2O$
6 $Al(C_2H_5)_2Cl \cdot (C_2H_5)_2O$
7 $AlCH_3Cl_2 \cdot (C_2H_5)_2O$
8 $AlC_2H_5Br_2 \cdot (C_2H_5)_2O$
9 $AlC_2H_5Cl_2 \cdot (C_2H_5)_2O$

As has been mentioned previously, the Al-O stretching vibration bands of trialkylaluminum-diethyl ether and alkylaluminum dihalide-diethyl ether complexes appear near 460 and 534 $cm^{-1}$ respectively. This fact suggests that the Al-O co-ordination bond in alkylaluminum dihalide-diethyl ether complexes is stronger than that in trialkylaluminum-diethyl ether complexes. This interpretation corresponds closely with the above two conclusions, i) and ii).

Lehmkuhl has reported, in comparing the thermal stabilities of complex salts, that the tendency of ethylaluminum compounds to form

a $K^+[Al(C_2H_5)_3Cl]^-$-type complex salt with alkali halides increases in the order of triethylaluminum < diethylaluminum chloride < ethylaluminum dichloride.[7] It is of interest that the electron-accepting tendencies of alkylaluminum compounds obtained by the thermal and the infrared spectroscopic methods give the same order: trialkylaluminum < dialkylaluminum halide < alkylaluminum dihalide.

## Summary

Fifteen samples of alkylaluminum-ether complexes (alkyl=methyl or ethyl) have been prepared, and their infrared spectra have been measured in the 2000—350 $cm^{-1}$ region. Most of the absorption bands in this region have been assigned. In the KBr prism region, the assignments of the absorption bands of the trimethylaluminum - dimethyl ether complex have been made on the assumption that this complex has the $C_s$ symmetry only. The absorption bands of these complexes have been found to shift to lower frequencies in the C-O antisymmetric and symmetric streching vibrations in the order of trialkylaluminum-ether < dialkylaluminum halide - ether < alkylaluminum dihalide - ether complexes. The infrared spectra of five samples of ethylaluminum ethoxides have also been measured in the 2000—350 $cm^{-1}$ region.

The authors are indebted to Professor Takehiko Shimanouchi of the University of Tokyo for his valuable discussions throughout this work.

*Research Center*
*Chisso Co., Ltd.*
*Kanazawa-ku, Yokohama*

## Appendix

**Ethylaluminum Ethoxides.** — These compounds were studied as model substances of partly-oxidized ethylaluminum derivatives. The infrared spectra of five kinds of ethylaluminum ethoxides in the 2000—350 $cm^{-1}$ region are shown in Table VII. Figure 6 shows three typical spectra charts. The infrared spectrum of ethylaluminum diethoxide is reported to have been studied by Schomburg, but his result is not easily accesible.[8] The spectrum of ethylethoxyaluminum chloride has been reported by

TABLE VII. OBSERVED FREQUENCIES OF ETHYLALUMINUM ETHOXIDES IN $cm^{-1}$

| $AlEt_2OEt$ | $AlEt(OEt)_2$ | AlEt(OEt)Cl | AlEt(OEt)Br | AlEt(OEt)I |
|---|---|---|---|---|
| 1482 w | 1484 w | 1480 s | 1480 s | 1481 w |
| 1462 sh | 1463 sh | 1465 vw | 1466 vw | 1464 sh |
| 1451 s | 1449 s | 1447 s | 1450 s | 1451 m |
| 1409 m | 1409 w | 1407 vw | 1407 sh | 1406 vw |
| 1394 s | 1391 s | 1393 s | 1395 s | 1397 s |
| 1374 vw | 1373 vw | 1372 vw | 1374 vw | 1380 vw |
| 1288 m | 1285 w | 1299 m | 1298 m | 1291 w |
| 1254 w | 1253 vw | 1265 w | 1256 w | 1256 sh |
| 1222 w | 1223 w | 1222 w | 1224 w | 1219 vw |
| 1193 s | 1193 s | 1201 m | 1200 m | 1196 m |
| 1163 m | 1163 s | 1167 s | 1166 s | 1165 m |
| 1100 s | 1101 s | 1094 s | 1097 s | 1100 s |
| 1058 vs | 1060 vs | 1041 m | 1042 vs | 1035 vs |
| 985 s | 986 s | 997 s | 995 s | 991 m |
| 948 m | 951 m | 960 vw | 959 w | 955 w |
| 914 w | 918 sh | 926 w | 923 w | 921 m |
| 894 s | 895 s | 896 w | 895 s | 895 s |
| | | 851 s | 848 s | 846 w |
| 806 s | 806 m | 809 vw | 811 vw | |
| | | 675 s | 671 s | 674 s |
| 652 vs | 633 vs | 641 s | 627 s | 620 s |
| | | | 598 w | 591 w |
| | | 555 vw | | |
| 481 w | 523 sh | 527 m | 519 m | 514 m |
| | 431 w | 447 m | 442 w | 430 w |
| | | | | 387 w |
| | | | 355 w | |

7) H. Lehmkuhl, *Angew. Chem.*, 75, 1090 (1963).

8) G. Schomburg, Dissertation, Technische Hochschule Aachen (1956).

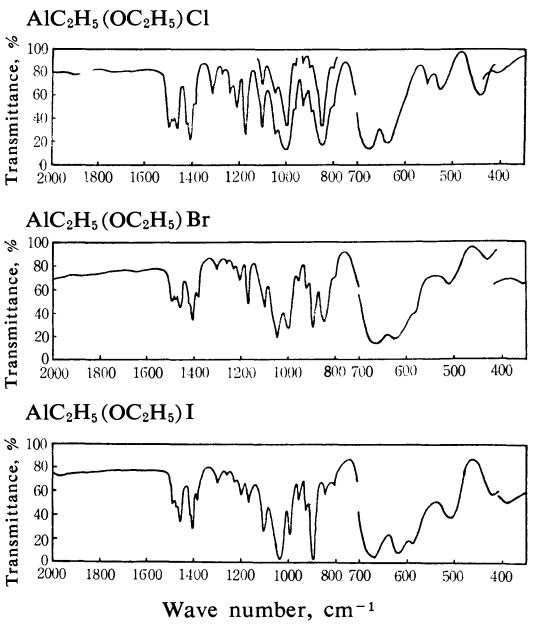



Fig. 6. Spectra of ethylaluminum ethoxides.

Scherer and Seydel ;[9] a comparison of our spectrum with theirs shows a good qualitative agreement.* The spectra of diethylaluminum ethoxide, ethylethoxyaluminum bromide and ethylethoxyaluminum iodide have not been published as yet. All five spectra show very strong bands near 1050 $cm^{-1}$; these bands may be due to the C-O stretching vibration band. The assignments of other bands are also still uncertain.

9) H. Scherer and G. Seydel, *Angew. Chem.*, **75**, 846 (1963).

* Scherer and Seydel found that ethylethoxyaluminum chloride was dimeric just after it was synthesized, but that it isomerized to the trimeric form in a few days; they also reported a corresponding change in the infrared spectrum (intensity changes of four bands at 9.6, 10.0, 11.14 and 11.7 $\mu$). The present authors recognized the same phenomenon. Our spectrum in this paper corresponds to that obtained by the measurement of an aged sample. In our laboratory it was found that ethylethoxyaluminum bromide and ethylethoxyaluminum iodide behaved analogously (isomerization from the dimeric to the trimeric form with a corresponding change in the infrared spectrum - intensity changes of four bands at 9.6, 10.05, 11.2 and 11.8 $\mu$ for ethylethoxyaluminum bromide - though the isomerization was much slower and the change of spectrum was less striking than in the case of ethylethoxyaluminum chloride).

# Transition Metal Complex Catalysts for the Oligomerization of Butadiene. II. The Reaction of Catalyst Components

By Katsumi TAMAI, Taro SAITO, Yasuzo UCHIDA and Akira MISONO

(Received August 11, 1964)

There have been several reports on the remarkable activities of catalysts composed of transition metal complexes and organometallic compounds on the oligomerization of butadiene.[1] The present authors have reported in previous papers[2),3)] that butadiene dimerizes into 3-methyl-hepta-1, 4, 6-triene with the catalyst system consisting of cabalt(III) acetylacetonate and triethylaluminum, and that it trimerizes into *n*-dodeca-1, 3, 6, 10-tetraene with iron(III) acetylacetonate and triethylaluminum. In these reactions, it has been found that the order of the mixing of the catalyst components and butadiene has a great effect on the rate of the formation of oligomers; this has been explained[4)] as being true because in the presence of butadiene, triethylaluminum reduces cobalt(III) or iron (III) acetylacetonate and makes butadiene coordinate to the low valent metal, while without butadiene, cobalt(III) or iron(III) acetylacetonate and triethylaluminum react to form a complex to which butadiene coordinates only with difficulty. The present investigation was undertaken in order to acquire knowledge about the behavior of catalyst components in these reactions. The structure of the catalysts, the oxidation states of the transition metals, the role of triethylaluminum, and the mechanism of the reactions will be discussed on the basis of the results of the magnetic

1) Studiengesellschaft Kohle, *Austrian.* 219580 (1962); G. Wilke, *Angew. Chem.*, **75**, 10 (1963); S. Ohtsuka, T. Taketomi and T. Kikuchi, *J. Chem. Soc. Japan, Ind. Chem. Sec.* (*Kogyo Kagaku Zasshi*), **66**, 1094 (1963); *J. Am. Chem. Soc.*, **85**, 3709 (1963); H. Takahashi, *J. Org. Chem.*, **28**, 1409 (1963); S. Tanaka, K. Mabuchi and N. Shimazaki, ibid., **29**, 1636 (1964).

2) T. Saito, T. Ohno, Y. Uchida and A. Misono, *J. Chem. Soc. Japan, Ind. Chem. Sec.* (*Kogyo Kagaku Zasshi*), **66**, 1094 (1963).

3) M. Hidai, Y. Uchida and A. Misono, This Bulletin, to be published.

4) T. Saito, Y. Uchida and A. Misono, ibid., **37**, 105 (1964).

susceptibility, infrared spectra, gasometry, and electron spin resonance spectra of the reaction solutions.

## Experimental

**Reagents.**—The reagents used in these experiments were prepared and purified in the way which has been described in previous reports.

**Magnetic Susceptibility Measurements.**—Most of the reactions were carried out in a specially-made Erlenmeyer flask (100 ml.) with a small cell on its side. Known amounts of cobalt(III) acetylacetonate or iron(III) acetylacetonate (benzene solution) and triethylaluminum (benzene solution), one introduced in the main body of the flask and the other in the side cell separately under an atmosphere of nitrogen, were mixed by inclining the flask. The reaction solution was then transfused into a Gouy tube with a hypodermic syringe.

The magnetic susceptibility was measured using a Gouy balance. The Gouy tube was 250 mm. long and 10 mm. in diameter and was calibrated with distilled water. The sample transfused into the Gouy tube was placed in the field of 10000 gauss, and the measurements ware carried out at room temperature. The calculations of the magnetic susceptibility and the magnetic moment were performed with the following equations:

$$\chi_M = (\chi_g - \sum_i w_i \chi_{gi}) M/w$$

$$\mu_{eff} = 2.84\sqrt{\chi_M T}$$

where $\chi_M$: the moalr susceptibility based on the cobalt or the iron atom
$\chi_g$: the gram susceptibility of the sample solution
$\sum_i w_i \chi_{gi}$: the diamagnetic correction
$M$: the molecular weight of $Co(acac)_3$ or $Fe(acac)_3$
$w$: the weight fraction of $Co(acac)_3$ or $Fe(acac)_3$
$\mu_{eff}$: the effective magnetic moment (B.M.)
$T$: the absolute temperature

**Gasometry.**—The reaction was carried out in a 300 ml. four-necked flask equipped with a gas burette and a dropping funnel. With a magnetical stirring of the benzene solution of cobalt(III) acetylacetonate or iron(III) acetylacetonate, a certain quantity of a benzene solution of triethylaluminum in the funnel was dropped intermittently, with an allowed interval long enough to complete the gas evolution after each addition. During the measurement, the temperature was kept at 25°C. A change in the order of mixing the components was achieved by interchanging the contents of the flask and the funnel. The gas volume was converted into that at 0°C.

**Infrared Spectra.**—The infrared spectra of the samples were measured by a Hitachi EPI-S2 spectrometer for the sodium chloride region and by a Nihon-bunko Model 201 for the potassium bromide region. A certain amount of cobalt(III) acetylacetonate or iron(III) acetylacetonate was weighed in the same reaction apparatus as was used in the gasometry, and then dissolved in benzene. After the air in the flask has been displaced with nitrogen triethylaluminum in benzene was introduced into the solution, which was kept at room temperature and stirred magnetically. Then a part of the miexed solution was transfused into a KRS-5 cell (0.1 mm. path length) with a glass syringe.

**Electron Spin Resonance Spectra.**—The spectra were recorded in the X-band (9400 Mc.), with 100 kc. modulation, by a Nihon-denshi Model JES-3B ESR spectrometer. The method of sample preparation was similar to that described as having been used for the magnetic susceptibility measurements.

## Results and Discussion

**Infrared Spectra Analysis.**—When triethylaluminum was added to cobalt(III) acetylacetonate, the green color of $Co^{3+}$ faded and the reaction solution changed to purple and then black, with heat and gas generation. Changes in the infrared spectra of the reaction solution were observed with the variation in the amount of triethylaluminum added. A significant change in the absorption band was recognized between 1260 and 1300 $cm^{-1}$. In this region the following bands were assigned[5]: 1261 $cm^{-1}$ for the C-C stretching + C-$CH_3$ stretching of cobalt(II) acetylacetonate, 1284 $cm^{-1}$ for that of cobalt(III) acetylacetonate, and 1288 $cm^{-1}$ for that of aluminum(III) acetylacetonate. The changes in these bands of the solution due to the increase in triethylaluminum added are shown in Fig. 1. As triethylaluminum was added to cobalt(III) acetylacetonate, the band at 1284 $cm^{-1}$ gradually decreased, and a new band at 1261 $cm^{-1}$ began to grow; then a new band at 1288 $cm^{-1}$ was also observed. These results indicate the reduction of cobalt(III) acetylacetonate with triethylaluminum and the resultant formation of cobalt(II) acetylacetonate and aluminum(III) acetylacetonate. At a molar ratio of triethylaluminum to cobalt(III) acetylacetonate of

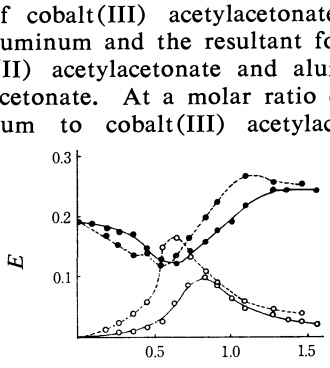



Fig. 1. Variation of the absorbance of IR spectra in 1260—1290 $cm^{-1}$ region upon addition of $AlEt_3$ to $Co(acac)_3$ in benzene ($8.12 \times 10^{-2}$ M) in the presence (—) or in the absence (···) of butadiene.
○ for 1261 $cm^{-1}$, ● for 1284—1288 $cm^{-1}$

5) K. Nakamoto, P. J. McCarthy, A. Ruby and A. E. Martell, *J. Am. Chem. Soc.*, **83**, 1066, 1272 (1961).

about 0.5, the amount of cobalt(II) acetylactonate formed suddenly increased; then the amount of cobalt(II) acetylacetonate reached a maximum and gradually decreased with the increase in the amounts of triethylaluminum added. The band at 1288 $cm^{-1}$ of aluminum-(III) acetylacetonate increased until the amounts of triethylaluminum added reached a level about 1.5 times that of cobalt(III) acetylacetonate. In the presence of butadiene, the addition of triethylaluminum changes the benzene solution of cobalt(III) acetylacetonate from green to purple, and then to wine red. In this case, the formation of cobalt(II) acetylacetonate was less than in the former case, as is shown in Fig. 1, which suggests that the presence of butadiene made the further reduction of cobalt(II) faster by means of complex formation.

When iron(III) acetylacetonate was employed instead of cobalt(III) acetylacetonate, almost the same tendency was observed, as is shown in Fig. 2. In this case the band at 1276 $cm^{-1}$ decreased; new bands were observed at 1288 $cm^{-1}$ and 1265 $cm^{-1}$ with the adddition of triethylaluminum. The band at 1265 $cm^{-1}$ reached a maximum at an Al/Fe ratio of about 0.5 and then gradually decreased in just the same way as the band at 1261 $cm^{-1}$ of cobalt-(II) acetylacetonate. The behavior of the band at 1288 $cm^{-1}$ was also similar to the case of the cobalt(III) acetylacetonate and triethylaluminum system. The bands at 1276 $cm^{-1}$ and 1288 $cm^{-1}$ were assigned to the C-C stretching + $C-CH_3$ stretching of iron(III) acetylacetonate and aluminum(III) acetylacetonate respectively[5]. The band of 1265 $cm^{-1}$ was assigned to the C-C stretching + $C-CH_3$ stretching of iron(II) acetylacetonate from the infrared observation of iron(II) acetylacetonate prepared by the method described by Buckingham.[6] Thus, in either the presence or absence of butadiene, iron(III) acetylacetonate, as well as cobalt(III) acetylacetonate, may be supposed to be reduced via the bivalent state to the zero valent state by the addition of triethylaluminum, with the resultant formation of aluminum(III) acetylacetonate.

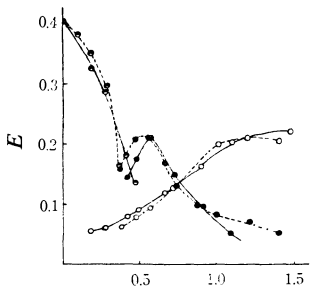



Fig. 2. Variation of the absorbance of IR spectra in 1260—1290 $cm^{-1}$ region upon addition of $AlEt_3$ to $Fe(acac)_3$ in benzene (6.76 $\times 10^{-2}$ M) in the presence (—) or in the absence (···) of butadiene.
● for 1265 $cm^{-1}$, ◓ for 1276 $cm^{-1}$
○ for 1288 $cm^{-1}$

In order to acquire knowledge about the variation in metal-oxygen band through the reaction, the infrared spectra of several reaction, mixture were recorded in the potassium bromide region from 18 $\mu$ to 27 $\mu$. When more than 0.5 mol. of triethylaluminum to 1.0 mol. of cobalt(III) acetylacetonate was added, the band at 21.4 $\mu$, assigned to the $Co^{3+}$-O stretching of cobalt(III) acetylacetonate almost disappered, new bands appeared at 20.5 $\mu$ and about 23.6—23.7 $\mu$. The former band was assigned to the Al-O stretching of aluminum(III) acetylacetonate, while the band at 23.6—23.7 $\mu$ was assigned to the overlap of the $Co^{2+}$-O stretching of cobalt(II) acetylacetonate and the out-of-plane bending of aluminum(III) acetylacetonate. Although the exchange of the ligand from cobalt to aluminum was confirmed, a quantitative treatment was unsuccessful because of the overlapping bands.

**Gasometry.**—When triethylaluminum was added drop-by-drop into the cobalt(III) acetylacetonate - benzene solution, gas evolved. This gas evolution was gradual until the amount of triethylaluminum added reached about a half of the cobalt(III) acetylacetonate in the solution, whereupon a sudden violent gas evolution was observed. The amount of gas evolved by the violent reaction was nearly 1.5—2 times the total amount of that which had been evolved before. The further addition of triethylaluminum made more gas evolve; the gradients of the plots of the evolved gas and the triethylaluminum added before and after the violent gas evolution are nearly equal as shown in Fig. 3. When nearly the same amount of triethylaluminum as cobalt(III) acetylacetonate in the solution was added, the gas evolution ceased. These observations suggest that, in the first step of the reaction, triethylaluminum reacts with cobalt(III) acetylacetonate in the following way to from cobalt(II) acetyl acetonate:

$$AlEt_3 + Co(acac)_3 =$$
$$AlEt_2(acac) + Co(acac)_2 + \cdot Et$$

It is considered that the diethylaluminum monoacetylacetonate and cobalt(II) acetylacetonate thus formed exist in a meta-stable state with residual cobalt(III) acetylacetonate

6) D. A. Buckingham, J. L. E. Cheong, J. E. Fergusson and C. J. Wilkins, *J. Chem. Soc.*, **1963**, 3461.

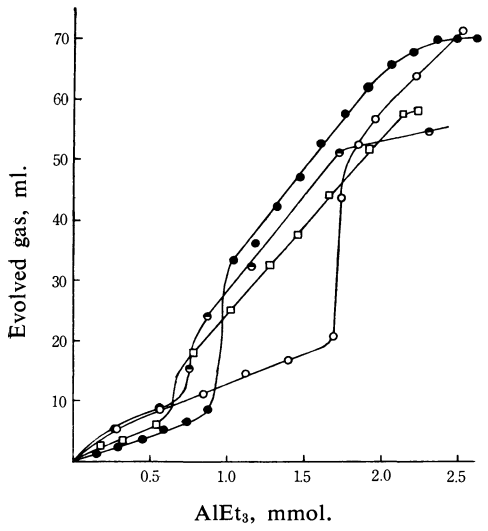



Fig. 3. Plots of amounts of evolved gas upon addition of $AlEt_3$ to $Co(acac)_3$ or $Fe(acac)_3$ in benzene.
- ○ 0.278 M of $AlEt_3$ in benzene was added to 3.66 mmol. of $Co(acac)_3$ in 20 ml. of benzene.
- ◓ 0.571 M of $AlEt_3$ in benzene was added to 1.41 mmol. of $Co(acac)_3$ in 20 ml. of benzene.
- ● 0.292 M of $AlEt_3$ in benzene was added to 2.31 mmol. of $Co(acac)_3$ in 20 ml. of benzene.
- □ 0.336 M of $AlEt_3$ in benzene was added to 1.46 mmol. of $Fe(acac)_3$ in 20 ml. of benzene.

by solvation or complex formation. The violent reaction, induced by the further addition of only one drop of triethylaluminum to the solution when about a half of the triethylaluminum was added to the cobalt(III) acetylacetonate, can be understood by considering that the meta-stable state is destroyed by the decrease in the amount of cobalt(III) acetylacetonate to less than that of cobalt(II) acetylacetonate. It is considered that the following reactions occurred in this case:

$$AlEt_2(acac) + 2Co(acac)_3 = Al(acac)_3 + 2Co(acac)_2 + 2\cdot Et$$

$$AlEt_2(acac) + Co(acac)_2 = Al(acac)_3 + Co^0 + 2\cdot Et$$

This mechanism was supported by the infrared observations. Thus, cobalt(III) is supposed to be reduced to cobalt(II), and then to the zero valent state:

$$Co(acac)_3 \rightarrow Co(acac)_2 \rightarrow Co^0$$

Cobalt(I) acetylacetonate is probably too unstable to exist as an intermediate state. The same results were found in the case of the iron(III) acetylacetonate and triethylaluminum system (Fig. 3).

When cobalt(III) acetylacetonate was added to an excess of triethylaluminum, cobalt(III) seemed to be reduced immediately to the zero valent state (Fig. 4).

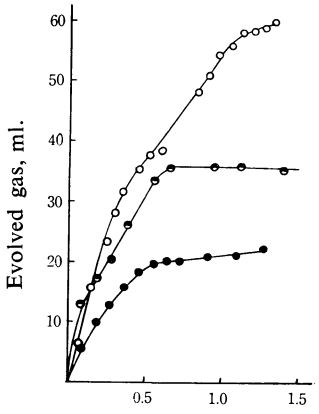



Fig. 4. Plots of amounts of evolved gas upon addition of $Co(acac)_3$ in benzene to $AlEt_3$.
- ○ 0.0734 M of $Co(acac)_3$ in benzene was added to 2.22 mmol. of $AlEt_3$ in 20 ml. of benzene.
- ◓ 0.0914 M of $Co(acac)_3$ in benzene was added to 1.11 mmol. of $AlEt_3$ in 10 ml. of benzene.
- ● 0.0894 M of $Co(acac)_3$ in benzene was added to 1.11 mmol. of $AlEt_3$ in 20 ml. of benzene.

The amount of gas observed in the gasometry was 50—60% of the theoretical value. When the composition of the evolved gas was determined by gas chromatography, it was found that the gas was about 85% ethane and 15% ethylene. The deficiency in gas evolution compared with the theoretical value could be explained by the dissolution of gas in benzene and by the chemisorption of ethylene to the complex formed with the reduced cobalt or iron.

**Magnetic Susceptibility Measurements.**—The composition and the gram magnetic susceptibility for the sample solution are shown in Table I.

a) When cobalt(III) acetylacetonate in benzene was added to an excess of triethylaluminum, the magnetic moment of the solution was 0.6 B. M. (at Al/Co=7.3). This shows that the cobalt complex in the solution is probably diamagnetic. With the addition of cobalt(III) acetylacetonate, the magnetic moment of the solution increased and reached a maximum at an Al/Co ratio equal to 1. At the same time, the solution turned from brown

Table I. Composition and magnetic susceptibility of the benzene solution of $Co(acac)_3$ (or $Fe(acac)_3$) and $AlEt_3$

(a) $Co(acac)_3$ was added to $AlEt_3$.
(b) $Co(acac)_3$ and $AlEt_3$ were mixed simultaneously.
(c) $AlEt_3$ was added to $Co(acac)_3$.
(d) $Fe(acac)_3$ was added to $AlEt_3$.

| Al/Co | Weight fraction | | | $\chi_g \times 10^6$ |
|---|---|---|---|---|
| | $C_6H_6$ | $Co(acac)_3$ or $Fe(acac)_3$ | $AlEt_3$ | |
| (a) 1.1 | 0.978 | 0.0150 | 0.0053 | +2.06 |
| 2.0 | 0.975 | 0.0155 | 0.0100 | +1.26 |
| 3.2 | 0.969 | 0.0150 | 0.0156 | +0.081 |
| 4.1 | 0.964 | 0.0155 | 0.0202 | −0.597 |
| 5.9 | 0.954 | 0.0153 | 0.0306 | −0.675 |
| 7.3 | 0.951 | 0.0146 | 0.0340 | −0.695 |
| (b) 0.5 | 0.964 | 0.0312 | 0.0050 | +2.32 |
| 0.9 | 0.956 | 0.0340 | 0.0096 | +4.71 |
| 1.0 | 0.959 | 0.0309 | 0.0098 | +4.12 |
| 2.2 | 0.972 | 0.0167 | 0.0115 | +1.50 |
| 3.0 | 0.952 | 0.0248 | 0.0237 | +0.938 |
| 4.0 | 0.981 | 0.0084 | 0.0109 | −0.530 |
| 4.4 | 0.927 | 0.0306 | 0.0427 | −0.205 |
| 5.3 | 0.915 | 0.0311 | 0.0535 | −0.405 |
| 6.7 | 0.968 | 0.0102 | 0.0218 | −0.486 |
| 6.8 | 0.947 | 0.0166 | 0.0361 | −0.624 |
| (c) 1.0 | 0.944 | 0.0435 | 0.0107 | +6.75 |
| 8.1 | 0.949 | 0.0142 | 0.0366 | +0.334 |
| (d) 0.8 | 0.982 | 0.0144 | 0.0036 | +1.30 |
| 1.3 | 0.980 | 0.0147 | 0.0061 | +4.55 |
| 2.4 | 0.972 | 0.0155 | 0.0122 | +5.07 |
| 4.8 | 0.962 | 0.0149 | 0.0228 | +1.93 |
| 5.8 | 0.945 | 0.0190 | 0.0356 | +1.13 |
| 8.9 | 0.949 | 0.0147 | 0.0420 | +0.285 |

to black, and a precipitate formed. Here an extraordinarily large $\mu_{eff}$ value of 12.1 was observed, which could not be attributed to the paramagnetism arising from first transition metals. If the magnetic moment is considered to be attributed only to the electron spin of the first transition metal, the value can not be expected to be higher than 6. The contribution of orbital motion will probably not be large enough to explain the extraordinarily large magnetic moment. These phenomena can only be explained in terms of the ferromagnetism due to the coagulation of the reduced zero valent cobalt to the unstable metallic state. The above observation suggest that the excess triethylaluminum has the ability to stabilize the cobalt of the zero valent by the formation of a complex like that suggested by Sartori and Costa in such a way as that shown below[9]:

$$Co(acac)_3 + 3AlEt_3 \rightarrow Co^0 \cdots [AlEt_2(acac)]_3 + \frac{3}{2}(C_2H_4 + C_2H_6)$$

As $Co^0$ has a $d^7s^2$ ground state, the diamagnetism can be explained by the assumption of a dimer structure or of cobalt hydride, for example. As cobalt(III) acetylacetonate was then added to the reaction mixture which included the above complex, the remaining ethyl groups of $AlEt_2(acac)$ were also used for the reduction of the cobalt atom. The resultant $AlEt(acac)_2$ or $Al(acac)_3$ perhaps has no ability to stabilize $Co^0$ or to prevent its coagulation.

b) When cobalt(III) acetylacetonate and triethylaluminum were mixed at the same time, it was observed that the magnetic moment was somewhat larger than in the case of a) in the region of an Al/Co ratio greater than four. These results are understood to indicate that small coagulations of cobalt occurred during the mixing.

c) In the case of the addition of triethylaluminum to cobalt(III) acetylacetonate, the magnetic moment also reached a maximum ($\mu_{eff}=12$) at an Al/Co ratio around unity, but the further addition of triethylaluminum to this solution made the $\mu_{eff}$ decrease to some degree. This phenomenon can be explained in terms of the fact that the added triethylaluminum dissolved the coagulated cobalt by the complex formation, as has been mentioned above. It may be supposed that the bonds formed by the coagulation of cobalt are either so weak or so active that they have a tendency to enter into the reaction. This was elucidated by the decrease in $\mu_{eff}$ caused by the addition of some organic compounds. The addition of butadiene in the solution prepared by adding triethylaluminum to cobalt(III) acetylacetonate in a Al/Co ratio of unity decreased the $\mu_{eff}$ value to 7.8. This shows some coordination of butadiene to reduced cobalt, but the amount is not so large that the dependency of the rate of the formation of methylheptatriene on the mixing order ($Co(acac)_3 + AlEt_3$ + butadiene) is small.[2,4] When methanol was added to the solution of cobalt(III) acetylacetonate and triethylaluminum (Al/Co=1) and the mixture was brought into contact with air, the coagulated cobalt dissolved and the solution changed red. From the infrared spectra it was considered that cobalt was oxidized to cobalt(II) acetylacetonate. The magnetic moment ($\mu_{eff}=5.1$) also supported this supposition.

d) When iron(III) acetylacetonate instead of cobalt(III) acetylacetonate was added to triethylaluminum, the curve of the relation between the Al/Fe ratio and the magnetic

7) H. Sinn and F. Patat, *Angew. Chem.*, **75**, 805 (1963).
8) T. Saito, Y. Uchida and A. Misono, This Bulletin, to be published.
9) G. Sartori and G. Costa, *Z. Elektrochem.*, **63**, 105 (1959).

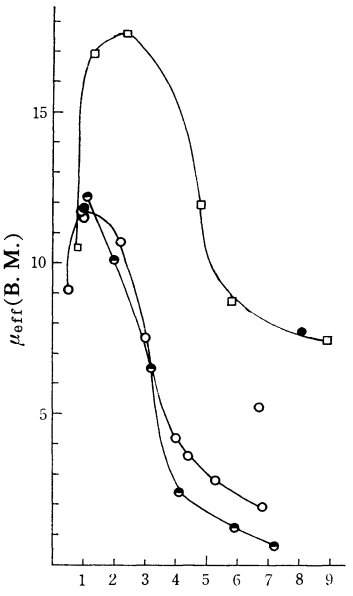



Fig. 5. Variation of the effective magnetic moment with the molar ratio of $AlEt_3$ to $Co(acac)_3$ or $Fe(acac)_3$.
○ $Co(acac)_3$ and $AlEt_3$ were mixed at once.
◓ $Co(acac)_3$ was added to $AlEt_3$.
● $AlEt_3$ was added to $Co(acac)_3$.
□ $Fe(acac)_3$ was added to $AlEt_3$.

moment showed almost the same tendency as in the system of cobalt(III) acetylacetonate and triethylaluminum. In this case, however, the $\mu_{eff}$ value of the solution was much larger than in the case of cobalt throughout the Al/Fe ratio range. The extraordinarily large $\mu_{eff}$ value of the iron system, even when there is excessive triethylaluminum, may be due to the unstability of the complex between reduced iron and aluminum derivatives of this sort.

**ESR Spectra.**—With the view of deciding whether the extraordinarily large magnetic moments are aroused by paramagnetism or by ferromagnetism, the electron spin resonance spectra of a benzene solution of cobalt(III) acetylacetonate and triethylaluminum were recorded. A single line signal was observed at a *g*-value of 2.128. The signal was hardly observed at all in the Al/Co ratio region about 0.5—1, where an extraordinarily large magnetic moment was shown. However, the intensity of the signal increased as the Al/Co ratio became as large as 3—5, which is a tendency opposite to that of the magnetic moment. At an Al/Co ratio of 3—5, the presence of an unpaired electron was supposed, but the spin concentration was quite small. Thus, it is obvious that the large susceptibility is not due to paramagnetism, but to ferromagnetism.

## Summary

In order to obtain some knowledge on the behavior of catalysts in the oligomerization of butadiene, the reaction between cobalt(III) acetylacetonate or iron(III) acetylacetonate and trietylaluminum has been investigated by means of magnetic susceptibility measurements, infrared spectra, gasometry, and electron spin resonance spectra.

When triethylaluminum was added to an excess of cobalt(III) acetylacetonate, the infrared spectra and gasometry suggested that the latter was reduced via stable cobalt(II) acetylacetonate to zero valent cobalt and that, at the same time, the former was transformed into aluminum(III) acetylacetonate. The extraordinarily large magnetic moment ($\mu_{eff}$= 12) and the absence of the signal of the electron spin resonance specra suggested the formation of metallic cobalt. The metallic cobalt was active enough to be readily oxidized by the addition of methanol. The addition of butadiene to this solution decreased the magnetic moment to 7.8. This shows some coordination of butadiene to reduced cobalt.

When cobalt(III) acetylacetonate was reduced in the presence of an excess of triethylaluminum (Al/Co>4), the zero valent cobalt was stablilized as a result of the formation of a certain diamagnetic complex with triethylaluminum. However, the addition of cobalt (III) acetylacetonate to this reaction mixture decomposed the above complex, and the very large magnetic moment indicated the formation of metallic cobalt.

Iron(III) acetylacetonate was, like cobalt(III) acetylacetonate, reduced to zero valent iron via stable iron(II) acetylacetonate. In the presence of an excess of triethylaluminum, however, zero valent iron did not form a stable complex with triethylaluminum, and from the ferromagnetism metallic iron was observed toresult.

*Department of Industrial Chemistry*
*Faculty of Engineering*
*The University of Tokyo*
*Hongo, Tokyo*

# Basic Bile Acids. V. On the Syntheses and Properties of Basic Bile Acids and Their Derivatives

By Yasuo SATOH

(Received December 7, 1964)

In the previous papers of the series,[1] the syntheses and properties of the several basic bile acids and their derivatives have been reported. The present paper will summarize the syntheses and properties of the basic bile acids, including new derivatives.

## 3-Amino Derivatives

In the catalytic reduction of the oxime of 3-keto bile acid, it was found that the configurations of the amino groups formed are identical with those of the hydroxyl groups formed in the case of 3-keto steroids.[2] That is, in the catalytic reduction of the oxime in an acidic medium, a 3$\beta$-amino derivative is formed, with a speedy absorption of hydrogen, as in the case of 3-keto bile acids. The configuration of this product has been determined by a comparison of its properties with those of the 3$\beta$-amino derivative prepared by Walden's inversion of 3$\alpha$-tosylate with liquid ammonia. Moreover, in the catalytic reduction of the oxime in a neutral medium, a 3$\alpha$-amino derivative is formed, with a slow absorption of hydrogen, contrary to that formed in the case of an acidic medium.

On the other hand, in the metallic reduction of the oxime, a 3$\alpha$-amino derivative is obtained which has the same configuration as the hydroxyl group formed in the case of the reduction of 3-keto steroids.[2]

These results agree well with the facts obtained previously from the reduction of the oxime of 5$\beta$-cholestan-3-one by Shoppee et al.[3,4]

The reaction of the 3-amino derivatives with nitrous acid was also examined. It has generally been confirmed that the course of the deamination of cyclohexylamines and decalylamines is conformationally specific[5,6]: if the amino group is equatorial in the most stable conformation of the molecule, deamination gives an alcohol of the same configuration; if it is axial, elimination and inversion occur.

In basic steroids, the same result has been reported by several workers.[4,7] When the reaction is examined with respect to the synthesized 3-aminocholanic acids, the following results are obtained:

3$\alpha$-Amino derivative ($C_3$–$NH_2$: e) $\rightarrow$
3$\alpha$-Hydroxy derivative ($C_3$–OH: e)

3$\beta$-Amino derivative ($C_3$–$NH_2$: a) $\rightarrow$
3$\beta$-Hydroxy derivative ($C_3$–OH: a)
+ 3-Cholenic acid

These results coincide with the experiential rule described above for the deamination of alicyclic and steroidal amines.

The additive charactor of the molecular rotation has generally been proposed to exist in the steroid field.[8] When the molecular rotations of methyl 3-acetamidocholanates are calculated from that of the 3-acetamido-5$\beta$-cholestane prepared by Shoppee et al.,[3] the results are as follows:

$M_D$ of 3$\alpha$-acetamido-5$\beta$-cholestane $= +206$ (a)

$M_D$ of 3$\beta$-acetamido-5$\beta$-cholestane $= +112$ (b)

$M_D$ of 5$\beta$-cholestane $= +97$ (c)

(a) $-$ (c) $= (+206) - (+97) = +109$

$\Delta M_D$ of 3$\alpha$-$NHCOCH_3$ in the 5$\beta$ series

(b) $-$ (c) $= (+112) - (+97) = +15$

$\Delta M_D$ of 3$\beta$-$NHCOCH_3$ in the 5$\beta$ series

$M_D$ of methyl cholanate $= +80$ (d)

(d) + ($\Delta M_D$ of 3$\alpha$-$NHCOCH_3$ in 5$\beta$ series)
$= (+80) + (+109) = +189$

1) Y. Satoh and A. Hagitani, *J. Chem. Soc. Japan, Pure Chem. Sec.* (*Nippon Kagaku Zasshi*), **80**, 1310 (1959): Y. Satoh, ibid., **84**, 829 (1963); **85**, 54 (1964).

2) L. F. Fieser and M. Fieser, "Natural Products Related to Phenanthrene," Reinhold Publ. Corp., New York (1949), p. 99; W. Klyne, "The Chemistry of the Steroids," Methuen & Co. Ltd., London (1957), p. 80; D. H. R. Barton and C. H Robinson, *J. Chem. Soc.*, **1954**, 3045.

3) J. H. Pierce, C. W. Shoppee and G. H. R. Summers, ibid., **1955**, 690; J. H, Pierce, C. W. Shoppee, H. C. Richards, R. J. Stephenson and G. H. R. Summers, ibid., **1955**, 694; H. C. Richards, C. W. Shoppee, J. C. P. Sly and G. H. R. Summers, ibid., **1956**, 1054; C. W. Shoppee, D. E. Evans, H. C. Richards and G. H. R. Summers, ibid., **1956**, 1649.

4) C. W. Shoppee, D. E. Evans and G. H. R. Summers, ibid., **1957**, 97; C. W. Shoppee, R. J. W. Cremlyn, D. E. Evans and G. H. R. Summers, ibid., **1957**, 4364.

5) A. K. Bose, *Experimentia*, **9**, 256 (1953).

6) J. A. Mills, *J. Chem. Soc.*, **1953**, 260.

7) W. G. Dauben, R. C. Tweit and C. Mannerskantz, *J. Am. Chem. Soc.*, **76**, 4420 (1954).

8) D. H. R. Barton, *J. Chem. Soc.*, **1945**, 813; **1946**, 512; **1946**, 1116.

calculated value of $M_D$ for methyl 3$\alpha$-acetamidocholanate

(d) + ($\Delta M_D$ of 3$\beta$-NHCOCH$_3$ in 5$\beta$ series)
= (+80) + (+15) = +95

Calculated value of $M_D$ for methyl 3$\beta$-acetamidocholanate

Observed values:

Methyl 3$\alpha$-acetamidocholanate = +177

Methyl 3$\beta$-acetamidocholanate = +95

From the good agreement between the calculated values and the observed values, the configurations previously deduced from each methyl ester acetate seem indeed to be correct; almost no effect of the side chain in $C_{17}$ is present, and, in these substances, the additive character of the molecular rotation holds.

### 7-Amino Derivatives

The 7-position of cholanic acid suffers a larger steric hindrance than that in the 3-position, considered not only from the molecular model but from the following facts. In the catalytic reduction of 7-keto bile acid, it is well known that the 7$\alpha$-hydroxyl group ($C_7$–OH: a) is mainly formed either in an acidic or in a neutral medium, in contrast to the behavior of the 3-keto bile acids. That is, in the catalytic reduction of 3$\alpha$-hydroxy-7-ketocholanic acid, the main product is chenodeoxycholic acid ($C_7$–OH: a) rather than ursodeoxycholic acid ($C_7$–OH: e), which has a stable equatorial hydroxyl group in the 7-position.[9,10] Moreover, in the reduction of that acid with sodium ethoxide, the results are similar to those in the case of catalytic reduction.[9] On the basis of these data and the results of catalytic reduction in an acidic medium for decalones, their oximes[11,12] and the oxime of 3-keto 5$\beta$-steroid,[3] it seems reasonable to assume that the product obtained from the oxime of 7-ketocholanic acid by catalytic reduction in an acidic medium is 7$\alpha$-aminocholanic acid.

In order to determine more precisely the configuration of this product, a reaction with nitrous acid was attempted with the methyl ester of 7-amino acid similar to that described above for the 3-amino derivatives. As has been described in the previous paper,[1] an unsaturated compound is obtained from the methyl 7-aminocholanate in this reaction. The 7-amino group formed by the catalytic reduction of the oxime, therefore, may be assigned the $\alpha$-configuration (axial).

Furthermore, the unsaturated compound formed by the reaction of methyl 7$\alpha$-aminocholanate with nitrous acid is assumed to be 7-cholenate. This assumption is based on the consideration that, although two axial hydrogens at the $C_6$- and $C_8$-positions, are present in this compound, elimination between $C_8$–H and $C_7$–NH$_2$ may be expected according to the Saytzeff rule. A similar situation has also been reported in the case of deamination for 6$\beta$-amino-5$\alpha$-cholestane.[4]

In order to confirm the structure of the unsaturated product in this reaction, it was desirable to examine the propriety of the structure presumed above by the application of the additive character in molecular rotation:

$\Delta M_D$ of $C_7$-double bond = +119[2] (a)

$M_D$ of methyl cholanate = +80[13] (b)

(a) + (b) = (+119) + (+80) = +199 Calculated value of $M_D$ for methyl 7-cholenate

Observed value: +195

This good agreement between calculated and observed values gives further confirmation that the product from the reaction with nitrous acid and the 7-amino derivative is methyl 7-cholenate, and that the reduction product of the oxime in an acidic medium is 7$\alpha$-aminocholanic acid.

A number of years ago attempts by several workers to prepare the 7$\beta$-hydroxy derivative from 7-keto bile acid were unsuccessful.[9,10,14] It was reported by Hoshino et al.[15] in 1954, however, that ursodeoxycholic acid could be obtained in a good yield by reduction with sodium and *n*-propanol. In order to prepare the 7$\beta$-amino derivative from the oxime of 7-ketocholanic acid, therefore, this procedure was used. The results showed that the methyl ester acetate of the product is different from the 7$\alpha$-amino epimer (obtained from the oxime by catalytic reduction) in melting point, infrared spectrogram, thin-layer chromatogram and specific rotation, while their elementary analyses are the same. It might, therefore, be concluded that the product is 7$\beta$-aminocholanic acid.

### 12-Amino Derivative

The 12-position of cholanic acid suffers a larger steric hindrance than the 3- or 7-position. This can easily be understood from the fact that the acetylation and oxidation of the 7$\alpha$-hydroxyl group are more easily accomplished

9) S. Miyaji, *Z. physiol. Chem.*, **250**, 31 (1932).
10) T. Iwasaki, ibid., **244**, 191 (1936).
11) H. D. Orhloff, *Chem. Revs.*, **54**, 347 (1954).
12) D. H. R. Barton, *J. Chem. Soc.*, **1954**, 1027.
13) M. Z. Nazer and C. H. Issidorides, *J. Org. Chem.*, **26**, 839 (1961).
14) M. Tsukamoto, *Biochem.*, **32**, 461 (1940).
15) T. Kanazawa, A. Shimazaki, T. Satoh and T. Hoshino, *Proc. Japan Acad.*, **30**, 391 (1954).

than in the case of the 12$\alpha$-hydroxyl group ($C_{12}$–OH : a).[16] Moreover, in the reductions of 12-ketocholanic acid[17] and 12-hydroxyiminocholan,[18] 12$\alpha$-epimers with a thermodynamically-unstable bond are predominantly formed as a result of the steric hindrances, while under the same conditions, unhindered ketone gives an equatorial hydroxyl group. Also, in the reduction of the respective oxime it has been found in the present work that the reaction rates have the same relationship.

When the hydroxyimino group at such a highly-hindered position was reduced with sodium and *n*-propanol, as has been described in the case of the 7-position, the product obtained was the same as that of the catalytic reduction in an acidic medium. Since this position has such a large steric hindrance compared with the 7-position, it seems reasonable to assume, from the results, that the factor in determining the direction of the reaction is concerned rather with the steric approach control than with the product development control.

The configuration of the amino group in the basic bile acid prepared from the 12-hydroxyimino derivative by catalytic reduction is presumed to the axial by deduction from the cases of the 3- and 7-derivatives. When this substance is allowed to react with nitrous acid, a product which gives a positive tetranitromethane test and which has an absorption band at 1635 $cm^{-1}$ in its infrared spectrum is obtained. From these results, it may be inferred that elimination has occurred in this reaction. On the basis of these data, it was concluded that the basic derivative obtained from the oxime is 12$\alpha$-aminocholanic acid ($C_{12}$–$NH_2$ : a).

### Methyl 3$\alpha$-Acetoxy-12$\alpha$-acetamidocholanate

The molecular rotation of this substance is as follows:

$M_D$ of methyl 12$\alpha$-acetamidocholanate $= +397$ (a)

(a) $-$ ($M_D$ of methyl cholanate)
$= (+397) - (+80) = +317$

$\Delta M_D$ of 12$\alpha$-$NHCOCH_3$ in 5$\beta$ series (b)

$\Delta M_D$ of 3$\alpha$-$OCOCH_3$ in 5$\beta$ series $= +114$ (c)

Calculated value of $M_D$ for methyl 3$\alpha$-acetoxy-12$\alpha$-acetamidocholanate
$= (M_D$ of methyl cholanate$) + (b) + (c)$
$= (+80) + (+317) + (+114) = +511$

Observed value : $+547$

The observed value is in fairly good agreement with the calculated value. The small difference may come from the molecule's being subject to a little strain due to the $\alpha$-orientated two groups.

### On the Leuckart-Wallach Reaction of Methyl Ketocholanate

This reaction had already been attempted by Hadáček et al. for methyl 7-keto-3$\alpha$, 12$\alpha$-dihydroxycholanate and methyl 3, 7, 12-triketocholanate,[19] but, as their results seemed to be inadequate for a determination of the structure, it was reinvestigated. They reported that the configuration of the formamido groups in the products is equatorial. In view of the following points, however, the determination of this configuration seems to contain an error.

1) The configuration of the formamido group formed was determined by Hadáček et al. by means of the formation of a free amino group by hydrolysis. That is, the configuration was determined only on the basis that the melting point of this amino derivative was virtually identical with that of the 7-amino-3$\alpha$, 12$\alpha$-dihydroxycholanic acid prepared from the 7-hydroxyimino derivative with sodium and isoamyl alcohol by Webb et al.[20] According to Barton, the reduction of a ketoxime with sodium and alcohol gives an equatorial amino group predominantly.[12] Then, on the basis of the Barton report, Hadáček et al. determined that the configuration of the amino group in the product formed by Webb et al. has a 7$\beta$-orientation ($C_7$–$NH_2$ : e), and, since the melting points of both this 7$\beta$-amino derivative and their product derived from formamido derivative by hydrolysis were almost the same, they concluded that the product of the Leuckart-Wallach reaction of methyl 7-keto-3$\alpha$, 12$\alpha$-dihydroxycholanate might be methyl 7$\beta$-amino-3$\alpha$, 12$\alpha$-dihydroxycholanate. However, Barton's theory seems inadequate to determine the configuration of the 7-position in bile acids, because the reaction of this position gives a result different from that of the 3-position, as has been mentioned above for the catalytic reduction of the 7-ketone.

16) C. W. Shoppee, "Chemistry of the Steroids," Butterworths Sci. Publ., London (1958), p. 83.
17) J. W. Huffman, D. M. Alabran and T. W. Bethea, *J. Org. Chem.*, **27**, 3382 (1962); J. W. Huffman, D. M. Alabran, T. W. Bethea and A. C. Ruggles, ibid., **29**, 2963 (1964).
18) M. Alauddin and M. Martin-Smith, ibid., **28**, 886 (1963).
19) J. Hadáček, and B. Čajánek, *Publs. Fac. Sci. Univ. Masaryk*, **395**, 259 (1958).
20) S. P. James, F. Smith and M. Webb, *J. Chem. Soc.*, **1946**, 665; A. S. Jones, M. Webb and F. Smith, ibid., **1946**, 2164.

2) They carried out an elementary analysis and measured the melting point of this substance, but they did not report its optical rotatory power.

Hadáček et al. determined, as has been described above, that the product of the Leuckart-Wallach reaction of methyl 7-keto-3$\alpha$, 12$\alpha$-dihydroxycholanate is the 7$\beta$-amino derivative, with an equatorial amino group, they did this on the agreement of the basis of the melting point with the literature.[20] They then deduced that the reaction gave an equatorial amino group in all other positions, also. They concluded, therefore, that the product of this reaction of 3, 7, 12-triketocholanic acid is 3$\alpha$, 7$\beta$, 12$\beta$-triaminocholanic acid ($C_3$–, $C_7$– and $C_{12}$–$NH_2$: e). For the reasons pointed out above, however, the present author cannot accept this conclusion. From the experimental results[1] and the consideration of them in the present work, it may be firmly concluded that the configuration of the amino group formed from the ketone of bile acid in this reaction is axial, and, at the same time, that the presumed configuration proposed by Hadáček et al.[19] should be corrected.

## Thin-layer Chromatography of Methyl Acetamidocholanates

This chromatography was carried out using the technique of Hara[21] for the methyl esters of bile acids; results are listed in Table I.

On the relationship between the configuration of substituted groups and adsorbability, it has been reported that axial epimers are generally adsorbed more weakly than equatorial epimers.[22]

It would be interesting to compare this general rule with the reults obtained in the present work for acetamido derivatives. In the 3-substituted compounds, the adsorbability of axial-bonded derivatives ($\beta$) is larger than that of the equatorial-bonded derivative ($\alpha$), while in the 7-substituted compounds that relation is reversed (e>a). Although this relation seems to be inconsistent with the general rule, this inconsistency may be accounted for by considering the overall shape of the molecule. The 3$\alpha$(e)- and 7$\alpha$(a)-bonds are oriented almost parallel to the axis of the steroidal nucleus; in other words, these bonds correspond to the axial bonds in the cyclohexane ring. Therefore, the adsorbability of 3$\alpha$- and 7$\alpha$-derivatives is smaller than that of 3$\beta$- and 7$\beta$-derivatives, and, consequently, the former moves more quickly than the later in thin-layer chromatography. In the case of the thin-layer chromatography of both epimer of methyl 3-acetoxycholanate, the same relations are also observed (Solvent, benzene/pet.-ether: 3$\alpha$-OAc (e), $R_f$ 0.74; 3$\beta$-OAc (a), $R_f$ 0.65).

TABLE I. $R_f$ VALUES OF METHYL ACETAMIDOCHOLANATES IN THIN-LAYER CHROMATOGRAPHY

| Compound | Configuration of acetamido group | $R_f$ Value |
|---|---|---|
| 3$\alpha$-Derivative(m) | e | 0.36 |
| 3$\beta$-Derivative(c) | a | 0.26 |
| 3$\beta$-Derivative(w) | a | 0.26 |
| 3$\beta$-Derivative(f) | a | 0.26 |
| 7$\alpha$-Derivative(c) | a | 0.62 |
| 7$\alpha$-Derivative(f) | a | 0.62 |
| 7$\beta$-Derivative(m) | e | 0.47 |
| 12$\alpha$-Derivative(c) | a | 0.81 |
| 12$\alpha$-Derivative(f) | a | 0.81 |
| 12$\alpha$-Derivative(m) | a | 0.81 |

m, metallic reduction; c, catalytic reduction; w, Walden's inversion of the tosylate; f, Leuckart-Wallach's reaction

Adsorbent, Wako-gel B-5; thickness of layer, 0.5 mm.; activation temperature, 130°C/1 hr.; solvent system, benzene/ether (8/2, v/v); indicator, concentrated sulfuric acid

21) S. Hara, *Kagaku-no-Ryoiki*, 17, 196 (1963).

## On the Infrared Spectrography of Mathyl Acetamidocholanates

Some of the characteristic bands of individual methyl acetamidocholanates are listed, with their wave numbers, in Table II.

In an associated acyl amide derivative, the stretching vibration of C=O has been observed to shift to a lower wave number, the bending vibration of N–H has been observed to shift to a higher wave number, and the stretching vibration of N–H and unknown vibration appear above 3000 $cm^{-1}$.[23]

Each absorption band in a chloroform solution of these methyl acetamidocholanates, as is shown in Table II-I, is almost identical with the standard value for the non-associated second-amide type, while the values in the cases of the KBr disk method are observed to shift to longer wavelengths than those values for $\nu_{N-H}$ and $\nu_{C=O}$ and to shorter wavelength than those values for $\delta_{N-H}$. In view of the above facts, the conclusion may be drawn that these compounds may exist in the non-associated state in such a solution and in the associated state in the KBr disk.

Moreover, with reference to Table II-Ia, in the 7$\alpha$-acetamido derivative only one absorption band above 3000 $cm^{-1}$ was observed, while

22) L. F. Fieser and M. Fieser, "Steroids," Reinhold Publ. Corp., New York (1959), p. 14.

23) K. Nakanishi, "IR Absorption Spectroscopy: Practical," Nanko-do, Tokyo (1960), p. 51.

Table II. Some of the characteristic absorption bands of methyl acetamidocholanates in IR spectra (wave number)

| Compound | $\nu_{N-H}$ | Unknown vibration | $\nu_{C=O}$ | $\nu_{C=O}$ | $\delta_{N-H}$ |
|---|---|---|---|---|---|
| Ia KBr disk method*1 | | | | | |
| 3α-Derivative | 3238 | 3075 | 1725 | 1638 | 1558 |
| 3β-Derivative | 3382<br>3262 | 3078 | 1726 | 1620 | 1570 |
| 7α-Derivative | 3373 | — | 1735 | 1639 | 1539 |
| 7β-Derivative | 3260 | 3076 | 1745 | 1638 | 1557 |
| 12α-Derivative | 3265 | 3075 | 1735 | 1635 | 1553 |
| Ib KBr disk method*2 | | | | | |
| 3α-Derivative | 3279<br>3280*3 | 3075<br>3076*3 | 1735<br>1736*3 | 1634<br>1636*3 | 1554<br>1556*3 |
| 3β-Derivative | 3382 | — | 1743 | 1641 | 1536 |
| 7α-Derivative | 3378 | — | 1738 | 1640 | 1539 |
| 7β-Derivative | 3260 | 3080 | 1745 | 1634 | 1558 |
| 12α-Derivative | 3273<br>3275*3 | 3080<br>3079*3 | 1737<br>1740*3 | 1637<br>1638*3 | 1557<br>1554*3 |
| II Chloroform solution | | | | | |
| 3α-Derivative | 3410 | — | 1717 | 1653 | 1512 |
| 3β-Derivative | 3410 | — | 1717 | 1652 | 1514 |
| 7α-Derivative | 3440 | — | 1719 | 1652 | 1517 |
| 7β-Derivative | 3435 | — | 1720 | 1653 | 1518 |
| 12α-Derivative | 3440 | — | 1725 | 1657 | 1506 |

*1 The sample was prepared by drying at 25°C/760 mmHg/24 hr.
*2 The sample was prepared by drying at 105—110°C/1 mmHg/6 hr.
*3 The sample was prepared by drying at 160—165°C/1 mmHg/8 hr.

the other derivatives show two bands. However, one of the two bands of the 3β-acetamido derivative above 3000 $cm^{-1}$ disappeared for the sample in Table II-Ib. In a chloroform solution the absorption bands above 3000 $cm^{-1}$ of all derivatives are shifted to about 3400 $cm^{-1}$, where the values are identical with those of the stretching vibration of N-H for the non-associated secondary amide type, as has been described above. A band at 3070 $cm^{-1}$, for which the assignment has not yet been distinctly made, was not observed for the 3β-derivative when it was dried at 105—110°C under 1 mmHg; on the other hand, in the 3α- and 12α-acetamido derivatives, the band does not disappear even at 160—165°C under 1 mmHg. Moreover, these compounds with an absorption band at about 3070 $cm^{-1}$ (e. g., methyl esters of 3α-, 7β- and 12α-acetamidocholanic acids) also possess an absorption band near 720 $cm^{-1}$ with a broad shape. (This band is called an amide V band and has been reported to possess only a secondary associated-amide type.[24]) Though the absorption bands of these derivatives are considered to shift as a result of their crystalline structure, the shift may be smaller than that arising from association. On the basis of the facts that, in Table II-Ib, considerable shifts of the absorption bands of $\nu_{N-H}$, $\nu_{C=O}$ and $\delta_{N-H}$ are observed and that the absorption band near 720 $cm^{-1}$ is presented, it seems reasonable to assume that the 3α-, 7β- and 12α-acetamido derivatives exist in the associated states in the KBr disk.

The author wishes to express his gratitude to Professor Akira Hagitani for his discussions and encouragement throughout the course of this work. He is also indebted to Professor Yuzo Kakiuchi for his valuable discussions of the infrared spectra.

*Department of Chemistry*
*Faculty of Science*
*St. Paul's University*
*(Rikkyo Daigaku)*
*Toshima-ku, Tokyo*

24) C. J. Bellamy, "The Infrared Spectra of Complex Molecules," Methuen & Co., Ltd., London (1958), p. 205.

# The Isocyanurates. I. A Novel Method of Synthesizing Trialkyl Isocyanurates

By Kenichi FUKUI, Fumio TANIMOTO and Hisao KITANO

(Received December 18, 1964)

Some esters of isocyanuric acid are interesting as heat resistant resins[1,2] because of their symmetrical triazine ring structure. Only a few of the isocyanurates have, however, been used as practical chemical intermediates. This is because of the methods of synthesizing them are not sufficiently economical for general use.

Hofmann first indicated that trimethyl isocyanurate had been prepared by the thermal isomerization of trimethyl cyanurate both without[3] or with[4] methyl iodide. The trimethyl cyanurate was synthesized from cyanuric chloride and methyl alcohol in the presence of alkali hydroxide. However, his method was applied only to the preparation of lower alkyl esters. Other classical preparative methods of isocyanurates were by the reaction of alkyl iodides with silver cyanurate[5] and by that of potassium alkyl sulfate with potassium cyanate or potassium cyanurate.[6] The trimerization of alkyl isocyanates to isocyanurates catalyzed by phosphines or tertiary amines[7-9] has been used in laboratory techniques. Since, however, this method involves the treatment of poisonous and expensive isocyanates, it is not preferable to synthesizing many isocyanurates.

Although Kaiser and his co-workers reported[10] that the reaction of alkali cyanates with alkyl halides in acetonitrile as a solvent under pressure afforded alkyl isocyanurates, the yield was generally very low and it was difficult to purify the products to an extent similar to that of the other known methods. Kaiser also reported that the syntheses of unsaturated carbamates from potassium cyanate and alkenyl halides in alcohols were accompanied by the formation of alkenyl isocyanurates as a by-product.[11] De Pree reported that, in the syntheses of isocyanates from the reaction of alkyl halides with alkali cyanates catalyzed by tertiary amines, considerable amounts of isocyanurates were formed, along with isocyanates.[12]

In the previous works of our laboratory,[13-22] several aprotic solvents, such as dimethylformamide, dimethyl sulfoxide, dimethylacetamide, tetramethylene sulfoxide, tetramethyl urea, *N*-formyl morpholine, and *N*-formyl piperidine, were found to be powerful solvents for the nucleophilic displacement reaction of organic halides with metal cyanates and for the subsequent trimerization of isocyanates to isocyanurates.

Recently Frazier[23] reported an improvement of the isocyanurates synthesis by means of the reaction of alkenyl halides with cyanuric acid in aqueous alkali in the presence of cuprous chloride. Tazuma and his co-worker patented[24] a method of synthesizing isocyanurates from potassium cyanate and alkyl halides with tertiary amines in inert solvents. As an improvement of Frazier's method, Francis showed that the reaction of alkyl halides with alkali cyanurates proceeded smoothly in dimethylformamide as a reaction medium.[25]

In the present paper, the reactions between alkyl halides and potassium cyanate in aprotic solvents, such as dimethylformamide and dimethyl sulfoxide, have been studied. The

1) H. M. Day and J. G. Affleck, *SPE Journal*, **9**, No. 2, 22 (1953); H. M. Day and D. G. Patterson, *Modern Plastics*, **29**, No. 11, 116 (1952).
2) K. Thinius and G. v. Hintzenstern, *Plaste und Kautschuk*, **6**, 275, 375, 439 (1959).
3) A. W. Hofmann, *Ber.*, **3**, 264 (1870); A. W. Hofmann and O. Olshausen, ibid., **3**, 269 (1870); A. W. Hofmann, ibid., **19**, 2063 (1886); P. Klason, *J. prakt. Chem.* (2), **33**, 129 (1886).
4) E. Bilmann and J. Bjerrum, *Ber.*, **50**, 503 (1917).
5) Leukart, *J. prakt. Chem.* (11), **21**, 1 (1880); J. Ponomarew, *Ber.*, **18**, 3261 (1885).
6) A. W. Hofmann, ibid., **14**, 2728 (1881).
7) J. C. Saunders and R. J. Slocombe, *Chem. Revs.*, **43**, 212 (1948).
8) R. C. Arnold, J. A. Nelson and J. J. Verbanc, ibid., **57**, 47 (1957).
9) F. E. G. Tate and J. H. Wild, Brit. Pat. 856372 (1961); E. C. Juenge and W. C. Francis, *J. Org. Chem.*, **26**, 3334 (1961).
10) D. W. Kaiser, O. Greenwich and D. Holm, U. S. Pat. 2536849 (1951).
11) D. W. Kaiser, U. S. Pat. 2697720 (1954).
12) D. O. De Pree, U. S. Pat. 2866803 (1958).
13) K. Fukui and H. Kitano, Japanese Pat. 270734 (1960).
14) K. Fukui and H. Kitano, Japanese Pat. 276856 (1961).
15) K. Fukui and H. Kitano, Japanese Pat. 277389 (1961).
16) K. Fukui and H. Kitano, Japanese Pat. 281924 (1961).
17) K. Fukui and H. Kitano, Japanese Pat. 282405 (1961).
18) K. Fukui and H. Kitano, Italian Pat. 60082 (1960).
19) K. Fukui and H. Kitano, Brit. Pat. 858810 (1961).
20) K. Fukui and H. Kitano, German Pat. 1124957 (1962).
21) K. Fukui and H. Kitano, U. S. Pat. 3037979 (1962).
22) K. Fukui and H. Kitano, Canadian Pat. 635454 (1964).
23) T. C. Frazier, U. S. Pat. 3065231 (1962).
24) J. J. Tazuma and R. Miller, U. S. Pat. 3075979 (1963).
25) W. C. Francis, Brit. Pat. 912964 (1962).

TABLE I. YIELD AND PROPERTIES OF ISOCYANURATES

| Substituent of isocyanurate | Yield % | B. p. °C/4 mmHg | $n_D^{25}$ | Composion | Analysis, N % | |
|---|---|---|---|---|---|---|
| | | | | C H O N | Found | Calcd. |
| Trimethyl[a] | 90 | 274[b] | — | $C_6H_9O_3N_3$ | 24.52 | 24.55 |
| Triethyl[c] | 88 | 106[d] | — | $C_9H_{15}O_3N_3$ | 19.70 | 19.71 |
| Tri-*n*-propyl[e] | 85 | 136[f] | 1.4746 | $C_{12}H_{21}O_3N_3$ | 16.40 | 16.46 |
| Tri-*n*-butyl | 85 | 162[g] | 1.4720 | $C_{15}H_{27}O_3N_3$ | 14.20 | 14.13 |
| Tri-*n*-amyl | 80 | 186[h] | 1.4725 | $C_{18}H_{33}O_3N_3$ | 12.45 | 12.39 |
| Tri-*n*-hexyl | 88 | 212[i] | 1.4730 | $C_{21}H_{39}O_3N_3$ | 11.08 | 11.01 |
| Tri-*n*-heptyl | 75 | 232[j] | 1.4733 | $C_{24}H_{45}O_3N_3$ | 9.94 | 9.92 |
| Tri-*n*-octyl | 73 | 257[k] | 1.4730 | $C_{27}H_{51}O_3N_3$ | 9.07 | 9.02 |
| Tri-*n*-nonyl | 70 | 281 | 1.4720 | $C_{30}H_{57}O_3N_3$ | 8.41 | 8.28 |
| Tri-*n*-decyl | 68 | 300 | 1.4730[l] | $C_{33}H_{63}O_3N_3$ | 7.77 | 7.64 |
| Tri-isobutyl[m] | 70 | 145—147 | — | $C_{15}H_{27}O_3N_3$ | 14.15 | 14.13 |
| Tri-*s*-butyl | 75 | 138—139 | 1.4600[n] | $C_{15}H_{27}O_3N_3$ | 14.25 | 14.13 |
| Tri-isoamyl | 70 | 176/3 | 1.4710[l] | $C_{18}H_{33}O_3N_3$ | 12.44 | 12.39 |
| Tri-*s*-heptyl[o] | 57 | 208 | 1.4750[l] | $C_{24}H_{45}O_3N_3$ | 10.04 | 9.92 |
| Tri-isooctyl[p] | 80 | 221/3 | 1.4762[l] | $C_{27}H_{51}O_3N_3$ | 9.14 | 9.02 |
| Tri-isononyl[q] | 75 | 244 | 1.4712[l] | $C_{30}H_{57}O_3N_3$ | 8.40 | 8.28 |
| Tribenzyl[r] | 83 | 382[s] | — | $C_{24}H_{21}O_3N_3$ | 10.49 | 10.52 |
| Tris-(2-methoxyethyl) | 55 | 194—195/6 | 1.4865[l] | $C_{12}H_{21}O_6N_3$ | 13.77 | 13.86 |
| Tris-(2-ethoxyethyl) | 51 | 193—194/3 | 1.4766[l] | $C_{15}H_{27}O_6N_3$ | 12.21 | 12.17 |
| Tris-(2-butoxyethyl) | 70 | 234 | — | $C_{21}H_{39}O_6N_3$ | 9.83 | 9.78 |
| Tris-(2-vinyloxyethyl)[t] | — | 175—178[u] | — | $C_{15}H_{39}O_6N_3$ | 12.35 | 12.38 |

a) Melted at 177°C. b) Boiling point at ordinary pressure. c) M. p. 95°C. d) B. p. 276°C/760 mmHg. e) M. p. 24°C. f) B. p. 286°C/760 mmHg. g) B. p. 318°C/760 mmHg. h) B. p. 336°C/760 mmHg. i) 356°C/760 mmHg. j) B. p. 373°C/760 mmHg. k) B. p. 388°C/760 mmHg. l) $n_D^{20}$. m) M. p. 50—51°C. n) $n_D^{15}$. o) 1-Ethylpentyl-. p) 2-Ethylhexyl-. q) 3,5,5-Trimethylhexyl-. r) M. p. 157°C. s) Boiling point at ordinary pressure, slightly decomposed. t) M. p. 59°C. u) Partial polymerization was observed.

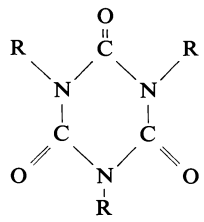
TABLE II. THE INFLUENCE OF WATER CONTENT IN THE REACTION MIXTURES

| $H_2O$ g. | $\frac{H_2O}{C_4H_9Br}$ mol./mol. | $\frac{H_2O}{DMF+KCNO}$ wt.% | Yield of raw urea g. | Yield of raw urea % | Yield of isocyanurate g. | Yield of isocyanurate % | Conversion of water % | Total yield % |
|---|---|---|---|---|---|---|---|---|
| 0.0 | 0.0 | — | trace | — | 25 | 84.2 | — | 84.2 |
| 0.5 | 0.09 | 0.33 | 4.0 | 15.5 | 21 | 70.7 | 84 | 86.2 |
| 1.0 | 0.19 | 0.67 | 6.0 | 23.2 | 17 | 67.3 | 63 | 80.5 |
| 1.5 | 0.28 | 1.00 | 9.5 | 36.8 | 13 | 43.8 | 67 | 80.6 |
| 2.0 | 0.39 | 1.33 | 13 | 50.4 | 8.5 | 28.9 | 68 | 79.3 |
| 2.5 | 0.47 | 1.66 | 17 | 65.9 | 6 | 20.2 | 71 | 86.1 |
| 2.7 | 0.50 | 1.79 | 18 | 69.7 | 4 | 13.4 | 70 | 83.1 |
| 3.0 | 0.56 | 1.99 | 19.5 | 75.2 | 2 | 6.7 | 68 | 81.9 |

yield of the isocyanurates was generally good enough to be applied to the synthetic purpose, and the techniques of synthesis and the purification of the products were also easy. The reactions may be written as follows:

$$RX + KCNO \xrightarrow[\text{or DMSO}]{\text{in DMF}} RNCO + KX \quad (1)$$

$$3\ RNCO \xrightarrow[\text{or DMSO}]{\text{in DMF}} \quad (2)$$



As a side reaction, the formation of 1,3-dialkyl ureas from moisture and alkyl isocyanates were observed as follows:

$$2\ RNCO + H_2O \xrightarrow[\text{or DMSO}]{\text{in DMF}} (RNH)_2CO + CO_2 \quad (3)$$

Although the rate of the reaction 3 of isocyanates with miosture was faster than that of the reaction 2, the formation of ureas was effectively avoided by drying the solvents and reactants before use. The condition of reactions 1 and 2 were moderate. The preferable conditions were a reaction temperature of 110—150°C and a molar ratio of the solvent to the halide of at least 2.5. The yields and the

properties of isocyanurates are listed in Table I.

The trialkyl isocyanurates and tris-(2-alkoxyethyl) isocyanurates shown in Table I were relatively thermostable compounds, could be distilled under atmospheric pressure without decomposition, and were resistant to chemicals at ordinary temperatures. Tris-(2-vinyloxyethyl) isocyanurate was easily polymerized with a cationic catalyst such as boron trifluoride etherate in a hydrocarbon solvent, leading to a heat-stable polymer.

The urea formation was affected by the amount of water involved in the reaction mixture. The influence of water was observed in the reaction of *n*-butyl bromide with potassium cyanate. The results are listed in Table II.

To increase the yield of isocyanurate, it is extremely necessary to remove the water in the reaction mixture carefully. The total yield of tri-*n*-butyl isocyanurate and 1, 3-di-*n*-butyl urea was 80—87%.

## Experimental[26]

**1) Materials.**—Alkyl halides were prepared from the corresponding alcohols by the usual method and were purified by fractional distillation. 2-Alkoxyethyl bromides were prepared by the reaction of alkyl cellosolves with phosphorus tribromide, and crude products were fractionally distilled to give pure samples. 2-Vinyloxyethyl chloride was obtained by the elimination distillation of bis-(2-chloroethyl)ether with sodium hydroxide. The raw product was dried over potassium carbonate and then fractionally distilled. A distillate which boiled at 109—110°C was collected.[27]

Potassium cyanate was prepared by a method of fusing analytical-grade anhydrous potassium carbonate and pure urea,[28] while the hard blocks of potassium cyanate were pulverized by a closed-type ball-mill in order to get them through a 40 mesh sieve. The fine potassium cyanate was then dried over phosphorus pentoxide in vacuo. The purity was determined by the use of a silver nitrate solution. There was a min. of 98% of potassium cyanate. If the blocks of potassium cyanate formed by the fusion method had dull surfaces, the potassium cyanate content was 70% (max.), indicating the presence of unreacted potassium carbonate.

Commercial dimethylformamide (DMF) or dimethyl sulfoxide (DMSO) was mixed with about 10% benzene and distilled to remove water as by the benzene-water azeotrope process. After most of the water had been removed, the aprotic solvent was dried over porous barium oxide overnight and then fractionally distilled under reduced pressure.[29-31] The pure DMF had a boiling point of 72—73°C/41 mmHg, while the pure DMSO boiled at 73—74°C/10 mmHg.

**2) Trimethyl Isocyanurate.**—In a 1 l. four-necked flask fitted with a reflux condenser, a thermometer, a stirrer and a dropping funnel, 105 g. (1.3 mol.) of potassium cyanate and 300 g. (4.0 mol.) of DMF were placed. The mixture was then heated to 130—134°C in an oil bath, and 142 g. (1 mol.) of methyl iodide was added from the dropping funnel over a period of about 1 hr. with stirring. The temperature was kept at 100—110°C for about 2 hr. From the reaction mixture, a precipitate of potassium iodide was then filtered off and washed with 50 ml. of acetone. After the solvents had been removed from the combined filtrate, the residue was recrystallized from aqueous ethanol to give trimethyl isocyanurate, m. p. 176—177°C.[32] (Yield, 51 g. (90%)).

**3) Triethyl Isocyanurate.**—A mixture of 47 g. (0.3 mol.) of ethyl iodide, 110 g. (1.3 mol.) of DMSO and 30 g. (0.37 mol.) of potassium cyanate was kept, with stirring, at 70—80°C for about 3 hr. (until no refluxing of ethyl iodide was observed in the condenser). The temperature was then raised to 135°C and maintained at that point for about 1 hr. After the reaction mixture had then been cooled, 50 ml. of ethanol was added for filtration. The filtrate yielded, on the evaporation of the solvents under reduced pressure and recrystallization from aqueous ethanol, triethyl isocyanurate, m. p. 94—95°C (Ref. 32 : 95°C).

**4) Tri-*n*-propyl Isocyanurate.**—*n*-Propyl bromide (124 g.) (1 mol.) was dropped into a mixture of 105 g. (1.3 mol.) of potassium cyanate and 250 ml. (3.6 mol.) of DMSO at 110°C with stirring. After all of the bromide had been added over a 1.5-hr. period, the reaction mixture was gradually heated to 130°C and the stirring was continued for an additional 2 hr. The reaction mixture was then poured into cold water, and the product was extracted with ether. The extract was washed, dried over anhydrous magnesium sulfate, and distilled.

**5) Tributyl Isocyanurates.**—To a mixture of 105 g. of potassium cyanate (1.3 mol.) and 200 g. (2.7 mol.) of DMF, 137 g. (1 mol.) of butyl bromide was added drop-by-drop at 135—140°C. The reaction time depended on the reactivity of the bromide, generally it took 1—3 hr. after addition of the bromide. The reaction mixture was then cooled, and a white precipitate of potassium bromide was filtered off and washed with small portions of ethyl methyl ketone. From the combined filtrated, tributyl isocyanurate was yielded by the evaporation of the solvents and by the fractional distillation of the residue.

**6) Tri-*s*-heptyl Isocyanurate.**—A mixture of 108 g. (1.35 mol.) of potassium cyanate, 179 g. (1 mol.) of 3-bromo-heptane and 250 g. (3.4 mol.) of DMF was heated to 140—145°C while being stirred in

26) The boiling points and melting points are uncorrected.
27) L. H. Cretcher et al., *J. Am. Chem. Soc.*, **47**, 1175 (1925).
28) A. Scattergood, "Inorganic Syntheses," Vol. 2, 86 (1946).
29) D. P. Ames, and P. G. Sears, *J. Phys. Chem.*, **59**, 16 (1955).
30) P. G. Sears, E. D. Wilhorit and L. R. Dawson, ibid., **59**, 373 (1955).
31) A. B. Thomas and E. G. Rochow, *J. Am. Chem. Soc.*, **79**, 1843 (1957).
32) E. M. Smolin and L. Rapoport, "The Chemistry of Heterocyclic Compounds, *s*-Triazines and Derivatives," Interscience Publ., N. Y. (1959), p. 404.

an oil bath. As the reaction proceeded, the reaction temperature was seen to become lower as a result of the formation of heptenes as by-products. When most of the bromide had been added, the reaction temperature was lowered to about 100°C, the reaction was then continued for 3 hr. more. The reaction mixture was then cooled, poured into ice-cold water, and filtered after which the filtrate was extracted with ether. The ethereal solution was separated and dried over calcium chloride. After the ether had been removed, heptenes (13.5 g.) (20%), 3-bromo-heptane (3.5 g.) (2%) and crude tri-*s*-heptyl isocyanurate (73 g.) (57%) were obtained. Tri-*s*-heptyl isocyanurate was redistilled to give a pure sample. The above-mentioned precipitate, which had been separated from the water extract, was recrystallized from boiling water to give mono-potassium isocyanurate (about 1 g.).

**7) Tribenzyl Isocyanurate.**—To a suspension of 105 g. (1.3 mol.) of potassium cyanate in 250 ml. (3.2 mol.) of DMF, 126.6 g. (1 mol.) of benzyl cholride was added through a dropping funnel, the reaction mixture was then stirred at 140—145°C for 3 hr. The reaction mixture was then cooled and poured into cold water. The flocculated product was collected by filtration, crushed into small particles, and recrystallized from ethanol to give colorless needles. (The m.p. in Ref. 33 is 157°C, while that in Ref. 32 is 165°C.)

**8) Tri-higher Alkyl Isocyanurate.**—Two moles of potassium cyanate and 1 mol. of higher alkyl bromide were reacted in 300 g. (4 mol.) of DMF in a manner which has been described in Experiments 5). The temperature of the reaction mixture should be kept at 140—150°C for at least 3 hr. The mixture was then poured into cold water and extracted with benzene. After the extract had been dried with anhydrous magnesium sulfate and the solvents had been removed, the residue was distilled to yield pure tri-higher alkyl isocyanurate.

**9) Tris-(2-alkoxyethyl) Isocyanurates.**—A mixture of 200 g. (2.7 mol.) of DMF, 88 g. (1.1 mol.) of potassium cyanate and 153 g. (1 mol.) of 2-ethoxyethyl bromide was heated to 135—140°C while being stirred for 2 hr. After it had then been cooled, the reaction mixture was poured into cold water and extracted with benzene. The extract was washed with water, dried with anhydrous potassium carbonate, and distilled. Other tris-(2-alkoxyethyl) isocyanurates were prepared by a similar method from corresponding bromides.

**10) Tris-(2-vinyloxyethyl) Isocyanurate.**—Into a suspension of 249 g. (3 mol.) of potassium cyanate in 500 ml. (6.5 mol.) of DMF, 213 g. (2 mol.) of 2-vinyloxyethyl chloride (freshly distilled) was gradually stirred through a dropping funnel for about 2 hr. After half of the solvent had been removed under reduced nitrogen pressure, the reaction mixture was poured into brine and extracted with benzene. Under a nitrogen current, the solvent was carefully removed; the residue was then distilled to collect a 130—180°C/4 mmHg fraction. The distillate was recrystallized from ethanol to give pure tris-(2-vinyloxyethyl) isocyanurate as colorless needles. (Precaution should be taken against polymerization during the distillation.)

One gram of the tris-(2-vinyloxyethyl) isocyanurate was dissolved in 250 ml. of pure *n*-heptane by slightly warming it, yielding a clear solution. To this solution 0.1 g. of boron trifluoride etherate was added, and the mixture was stirred for about an hour. The resulting white precipitate was then filtered, washed with ether, and dried under reduced pressure to give poly-tris-(2-vinyloxyethyl) isocyanurate. The polymer did not show a weight loss on 1 hr.'s exposure to 200°C in a nitrogen stream and did not dissolve in ethanol, acetone or DMF.

**11) The Influence of Water in the Reaction System.**—In a 300-ml. flask, 41 g. (0.3 mol.) of *n*-butyl bromide, 40.5 g. (0.5 mol.) of potassium cyanate and 110 g. (1.5 mol.) of DMF were mixed; then a calculated quantity of water was added. After the temperature of the mixture had been raised to 130°C, the reaction mixture was stirred at 128—130°C for 3 hr. The solvent was then removed after the filtration of the potassium bromide. The residue was mixed with a 1/2 vol. of petroleum ether and cooled to −3°C. 1,3-Di-*n*-butyl urea was then separated as white crystals. Tri-*n*-butyl isocyanurate was obtained after the evaporation of the petroleum ether and weighed. The results are shown in Table II. The crude 1,3-*n*-butyl urea was recrystallized from a ligroin-methyl ethyl ketone mixture to form a pure sample melting at 74°C; this was identified by means of comparison with an authentic specimen.

## Summary

Reactions of alkyl halides with potassium cyanate have been carried out in several aprotic solvents. Dimethylformamide and dimethyl sulfoxide have been proved to play a superior role as aprotic solvents in the displacement reaction and also in the subsequent trimerization of the isocyanates. Several trialkyl isocyanurates have been obtained in yields better than those of the other known methods.

From 2-alkoxyethyl halides and 2-vinyloxyethyl chloride respectively, tris-(2-alkoxyethyl) isocyanurates and tris-(2-vinyloxyethyl) isocyanurate have been synthesized.

The presence of water in the reaction mixture results in the formation of 1,3-dialkyl ureas, consequently decreasing the yield of isocyanurates.

*Department of Fuel Chemistry*
*Faculty of Engineering*
*Kyoto University*
*Sakyo-ku, Kyoto*

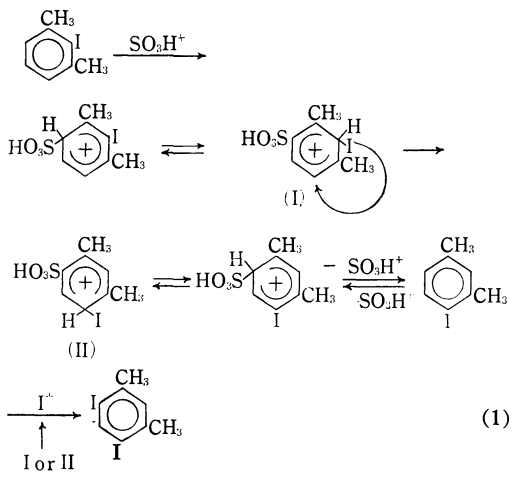
33) N. A. Lange, "Handbook of Chemistry," Handbook Publishers, Inc. Sandusky, Ohio, Ninth Edition, (1956), p. 426.

# The Synthesis of Four Isomeric Diiodo-*m*-xylenes. Their Isomerization in Sulfuric and Polyphosphoric Acids[1)]

By Hitomi SUZUKI, Kazuhiro MARUYAMA and Ryozo GOTO

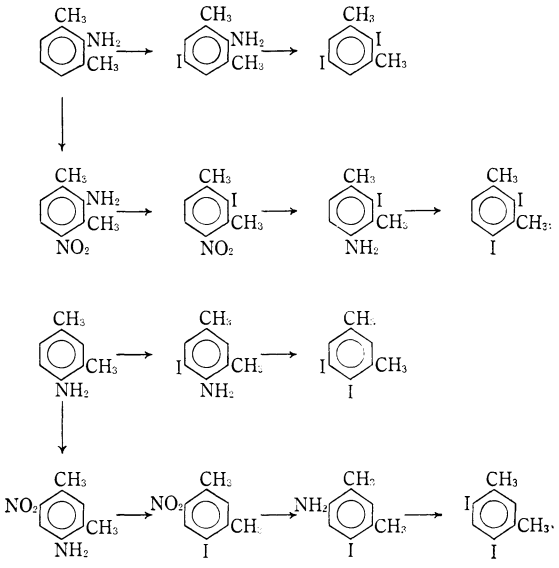
(Received December 21, 1964)

Since the general pattern of the Jacobsen reaction of aromatic iodo compounds is the progressive iodination of the starting materials, vicinally-substituted 2, 4-diiodo-*m*-xylene may be expected to be a main product in the reaction of 2-iodo-*m*-xylene. As has been shown in a previous paper,[1)] however, the latter compound readily undergoes disproportionation to give 4, 6-diiodo-*m*-xylene and *m*-xylene-4-sulfonic acid. The mechanism proposed for this unexpected result involves the migration of the iodine atom of 2-iodo-*m*-xylene from the hindered position (=2) to a less hindered one (=4), facilitated by the increased steric stress caused by the entry of a bulky sulfo group in the position meta to the iodine atom. The 4-iodo-*m*-xylene thus formed, undergoing the normal Jacobsen reaction, affords 4, 6-diiodo-*m*-xylene as a final product. This is shown by the following scheme:



(1)

The present work aims to provide definite evidence for the interpretation that the sulfo group in the position meta to the iodine atom plays an important role in such an easy intramolecular migration of an iodine atom. In the pursuit of this problem, it was necessary to ascertain whether any other isomers might be formed during the reaction, and if so, how they would behave under those conditions. Because of the difficulties encountered in the separation of each isomer, we inspected the product spectroscopically and gas chromatographically. Therefore, four isomeric diiodo-*m*-xylenes were prepared as authentic specimens. As little was known about diiodo-*m*-xylenes, we synthesized them from *m*-xylidines by the procedure shown below:



The direct iodination of 2-*m*-xylidine in a weakly alkaline medium proceeded smoothly and afforded a fairly high yield of the product, whereas that of 4-*m*-xylidine afforded a poorer yield under the same conditions, with much tarry matter formed. The diazotizations of the iodo-xylidines were carried out in concentrated sulfuric acid, while in an aqueous acid solution the diazotization was incomplete and the yields were often very poor. The replacement of the diazo group by an iodine atom was always accompanied by a remarkable formation of black resinous substances, which lowered the yields of the products considerably. The infrared spectra of four isomers are shown in Fig. 1. Absorption bands due to the aromatic C–I bond (990—1050 $cm^{-1}$) show remarkable changes according to the differences in relative positions of the iodine atoms in

1) The Reaction of Polysubstituted Aromatics, Part VII. Part VI: This Bulletin, 38, 1474 (1965).

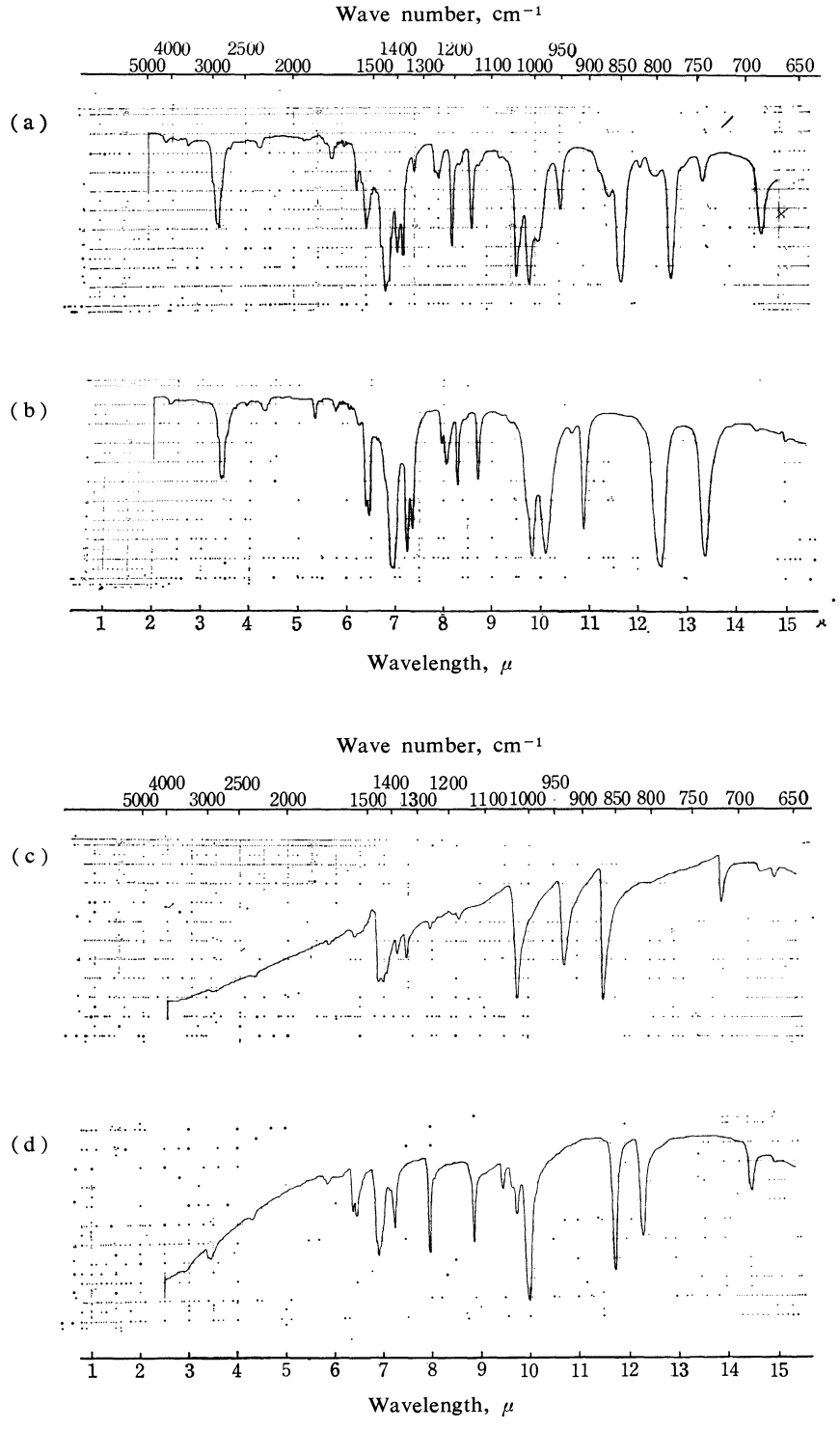



Fig. 1. Infrared spectra of diiodo-*m*-xylenes.

(a) 4,5-Diiodo-*m*-xylene (liquid film)
(b) 2,4-Diiodo-*m*-xylene (liquid film)
(c) 4,6-Diiodo-*m*-xylene (KBr disk)
(d) 2,5-Diiodo-*m*-xylene (KBr disk)

the nucleus. The appearance of the doubling of the band in the 990—1040 $cm^{-1}$ region may be correlated with the presence of the iodine atoms at hindered positions. Both 4, 5- and 2, 4-diiodo-*m*-xylenes show a strong doubling in this region, whereas the 2, 5-diiodo isomer shows an incomplete doubling and the 4, 6-diiodo isomer no doubling. Similar doublings are also observed in the infrared spectrogram of some other aromatic polyiodo compounds carrying hindered iodine atoms. However, these findings are not conclusive.

**The Isomerization of Diiodo-*m*-xylenes in Concentrated Acids.**—Two of the four diiodo-*m*-xylenes, 2, 4- and 4, 5-diiodo-*m*-xylenes underwent the isomerization easily in concentrated sulfuric acid and fairly readily in polyphosphoric acid (PPA) at a high temperature, but not at all in concentrated hydrochloric acid or perchloric acid. All four isomers underwent disproportionation with hot sulfuric acid to give mixtures of tri- and tetraiodo-*m*-xylenes.

*In Sulfuric Acid.*—The instability of diiodo-*m*-xylenes in sulfuric acid was found to be in the increasing order of 4, 5->2, 4->2, 5->4, 6-. The iodine atom located in the position of highest crowding migrated to the position which was less hindered and of the next highest electron density. Figure 2a shows the isomerization of 2, 4-diiodo-*m*-xylene to 4, 6-diiodo-*m*-xylene; after 5 hr. there still remained strong absorption bands due to the vicinal compound (803 $cm^{-1}$), while those due to the symmetrical compound (865 $cm^{-1}$) were comparatively weak. This indicates that 2, 4-diiodo-*m*-xylene cannot be a possible major intermediate of reaction 1, because 2-iodo-*m*-xylene is rapidly converted to 4, 6-diiodo-*m*-xylene under the same conditions. The increase in temperature (up to 50—60°C), however, brought about an immediate disproportionation to give mixtures of tri- and tetraiodo-*m*-xylenes, with little liberation of elementary iodine. 2, 5-Diiodo-*m*-xylene was more stable towards sulfuric acid than was 2-iodo-*m*-xylene and underwent disproportionation only at an elevated temperature. 1, 3-Dimethyl-5-*t*-butyl-2-iodobenzene was also comparatively stable in reaction to cold sulfuric acid, whereas iodomesitylene readily underwent disproportionation. These facts clearly indicate the importance of the buttressing effect of the sulfo groups taking the meta position to the iodine atom; that, is, the bulky substituent group (the iodine atom or the *t*-butyl group) at position 5 inhibits the entry of a sulfo group

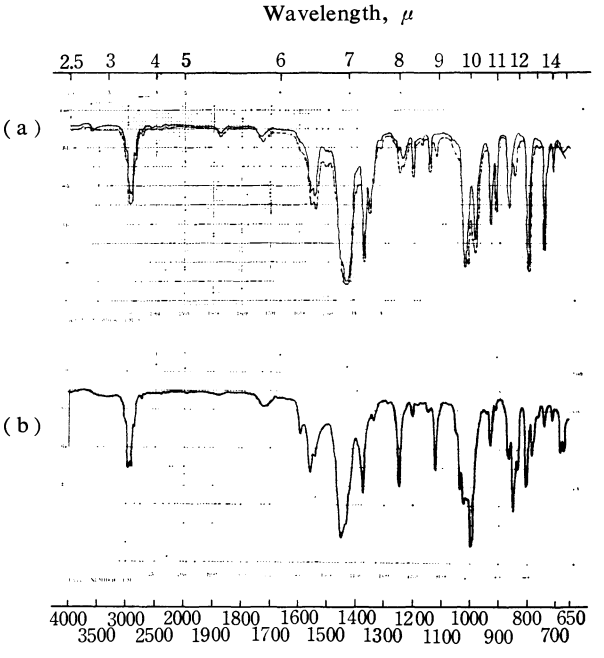



Fig. 2. Infrared spectra of reaction products (liquid film).
(a) Full line Exp. No. 1
Dotted line Exp. No. 2
(b) Exp. No. 4*
* This spectrum was taken with the uncrystallized oily part of the product.

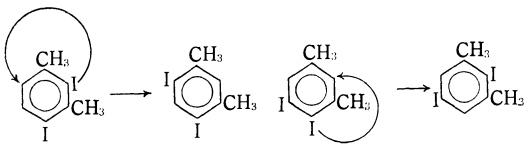
TABLE I. ACTION OF SULFURIC AND POLYPHOSPHORIC ACIDS UPON DIIODO-*m*-XYLENES

| Expt. No. | Diiodo-*m*-xylene g. | | Sulfuric acid g. | PPA* g. | Temp. °C | Time hr. | Product g. | Main component |
|---|---|---|---|---|---|---|---|---|
| 1 | 2,4- | 1.0 | 5.0 | | 15—20 | 3 | 0.8 | 2,4- and 4,6-diiodo-*m*-xylene |
| 2 | 2,4- | 1.5 | | 10.0 | 180—190 | 1 | 0.9 | 2,4- and 4,6-diiodo-*m*-xylene |
| 3 | 4,5- | 0.9 | 5.0 | | 15—20 | 3 | 0.6 | 2,5- and 4,5-diiodo-*m*-xylene |
| 4 | 4,5- | 1.0 | | 7.0 | 180—190 | 1 | 0.5 | 2,5- and 4,5-diiodo-*m*-xylene |
| 5 | 2,5- | 1.2 | | 5.0 | 180—190 | 1 | 0.9 | 2,5-diiodo-*m*-xylene |
| 6 | 2,5- | 0.8 | 5.0 | | 50—60 | 3 | 0.5 | tri- and tetraiodo-*m*-xylene |
| 7 | 4,6- | 1.0 | 5.0 | | 15—20 | 3 | 0.7 | 4,6-diiodo-*m*-xylene<br>tri- and tetraiodo-*m*-xylene |
| 8 | 4,6- | 1.0 | | 7.0 | 180—190 | 1 | 0.6 | 4,6-diiodo-*m*-xylene |

* PPA=polyphosphoric acid

into the unoccupied position so greatly that the iodine atom at the 2-position, in spite of the similar structural conditions, resists both intra- and intermolecular migration. We could not detect any diiodo-*m*-xylenes other than 4,6-isomer in the final reaction products from 2- and 4-iodo-*m*-xylenes.

*In Polyphosphoric Acid (PPA).* — The isomerization of aromatic iodo compounds in PPA seems never to have been described. Diiodo-*m*-xylenes were stable in cold PPA, but they gradually decomposed in resinous substances and in elementary iodine in acid at high temperature; in PPA only 2,4- and 4,5-diiodo-*m*-xylenes, which have an iodine atom at the highly-hindered position, underwent a slow isomerization to 4,6- and 2,5-diiodo-*m*-xylenes respectively (Figs. 2a and 2b).



Under the same conditions, 4,5-diiodo-*m*-xylene isomerized much more readily than the 2,4-isomer. The migration caused by PPA differs from those caused by sulfuric acid in the following two points: first, the migration of the iodine atom needs much more severe conditions and a longer reaction time, and second, the reaction is limited to the isomerization — no disproportionation is observed. The possibility of a thermal isomerization was excluded, because no change was observed in the absence of the acid at those temperatures. These facts may be taken to indicate that the migration of an iodine atom proceeds through a benzenonium intermediate, as is shown in Eq. 1, where the iodine atom expelled by a proton migrates, seeking the position of the next highest electron density, intramolecularly (isomerization). The substantial steric stress developed in the benzenonium intermediate is relieved during the migration of the iodine atom from the 2- to the 4-position, thus contributing to the ease of migration.

From these and related previous studies,[2] it may be concluded that this new type of rearrangement observed in the Jacobsen reaction of some 2,6-disubstituted iodobenzenes, especially 2-iodo-*m*-xylene, is essentially caused by the entry of a bulky and powerfully electron-attracting sulfo group in the position meta to the iodine atom blocked on both sides by substituent groups. This conclusion follows from these observations: (1) 2,4-diiodo-*m*-xylene did not isomerize so readily as 2-iodo-*m*-xylene under the same conditions; (2) 2,5-diiodo-*m*-xylene and 5-*t*-butyl-1,3-dimethyl-2-iodobenzene were rather more stable in relation to sulfuric acid than was 2-iodo-*m*-xylene; (3) isomerization occurred more readily in sulfuric acid than in PPA, and diluted sulfuric acid could not bring about any isomerization; (4) some color changes were observed during the reaction, and the color disappeared upon the addition of water; (5) the iodinium cation, when completely detached from the nucleus, could not attack *m*-xylene-4-sulfonic acid to any great extent, and (6) in the presence of an excess of mesitylene, the iodine atom of 2-iodo-*m*-xylene was readily transferred to the hydrocarbon, resulting in the formation of iodomesitylene and *m*-xylene-4-sulfonic acid. The reaction mechanism described at the beginning of this paper is consistent with these experimental observations.

## Experimental

**General Procedure for Isomerization.**—The reactions were carried out with magnetic stirring in small stoppered vessels which were heated externally. The mixtures were diluted with water;

2) H. Suzuki and R. Goto, *J. Chem. Soc. Japan, Pure Chem. Sec.* (*Nippon Kagaku Zasshi*), **84**, 284 (1963); H. Suzuki, This Bulletin, **36**, 1642 (1963).

the precipitated substances were separated and then chromatographed on an alumina column to remove higher iodinated products. The solid or oily substances which remained after the evaporation of the solvent were inspected by means of infrared spectroscopy and gas chromatography as has been described in the preceding paper.[1]

**Synthesis of Four Isomeric Diiodo-*m*-xylenes.**—All the procedures employed in these preparations were well-known to exclude the possibility of the migration of the iodine atom under ordinary conditions, so the definite location of the substituent groups attached to the ring could readily be ascertained by the annexed scheme. The structure proof of each isomer was also achieved by means of infrared spectroscopy (Fig. 1).

**2-Amino-4-nitro-*m*-xylene (I).**—A solution of 22 g. of 2-*m*-xyledine in 220 g. of concentrated sulfuric acid was cooled to 5°C; then 18 g. of concentrated nitric acid ($d$=1.38) was slowly but vigorously stirred in. During this operation, the temperature of the reaction mixture was held below 15°C. After 30 minutes' agitation, the mixture was poured onto crushed ice; the resulting aqueous solution was neutralized with a sodium hydroxide solution with cooling. The precipitated amine was collected by filtration and recrystallized from a petroleum ether - tetrahydrofuran mixture. The yield was 26 g. (86%); the product, golden yellow needles, melted at 81—82°C (reported,[3] 81—82°C).

**2-Iodo-4-nitro-*m*-xylene (II).**—To a solution of 21 g. of I in 300 ml. of sulfuric acid was added, with stirring and cooling to hold the temperature below 5°C, 10 g. of finely powdered sodium nitrite. The mixture was stirred for an additional 30 min. and then poured onto crushed ice. The resulting solution of the diazonium salt was filtered, and the filtrate was added slowly to a solution of 33 g. of potassium iodide in a little water. After the mixture had stood overnight, the precipitated tan solid was collected by filtration and chromatographed through a short alumina column with benzene. The evaporation of the benzene afforded 28 g. of pale yellow crystals of a pure iodo compound; m. p. 51—52°C. Yield, 80%.

Found: C, 34.60; H, 2.66; N, 4.93. Calcd. for $C_8H_9INO_2$: C, 34.68; H, 2.90; N, 5.06%.

**2-Iodo-4-amino-*m*-xylene (III).**—One hundred grams of stannous chloride dihydrate was dissolved in 200 ml. of hydrochloric acid diluted with 200 ml. of ethanol. To this solution was slowly but vigorously stirred in 25 g. of finely powdered II. The reaction preceeded with a moderate evolution of heat, the white crystalline solid which was gradually precipitated was collected by filtration. This material was then suspended in water, and an excess of a sodium hydroxide solution was added until the precipitated stannic hydroxide redissolved. The resulting solution was steam-distilled until the distillate became clear. The product was then separated from the distillate by ether extraction. The evaporation of the ether gave 17.0 g. of a pale yellow oil, which solidified to white needles in an ice box and which melted at 17—18°C. Yield, 76%.

Acetanilide; white needles from aqueous ethanol, m. p. 171—172°C.

Found: C, 41.82; H, 4.38; N, 4.58. Calcd. for $C_{10}H_{12}NIO$: C, 41.55; H, 4.19; N, 4.84%.

**2,4-Diiodo-*m*-xylene (IV).**—A solution of 17 g. of 2-iodo-4-amino-*m*-xylene in 150 ml. of concentrated sulfuric acid was cooled to 5°C and diazotized by the addition of 8.5 g. of sodium nitrite at 5—10°C. After 30 minutes' agitation, the mixture was poured onto crushed ice and the resulting solution was filtered. The filtrate was added slowly to a solution of potassium iodide dissolved in a small amount of water. The mixture was then allowed to stand overnight, and the black oil which precipitated was separated by decantation and chromatographed through an alumina column with petroleum ether. The evaporation of the solvent, followed by distillation, gave 11.5 g. of a colorless oil, boiling at 176—177°C/18 mmHg, which solidified in an ice box and which melted at 6—7°C. The yield was 47%.

Found: C, 26.93; H, 2.23. Calcd. for $C_8H_8I_2$: C, 26.84; H, 2.25%.

The infrared spectrum showed a band at 803 $cm^{-1}$ for two adjacent hydrogen atoms. The pattern in the 1650—2000 $cm^{-1}$ region also confirms the vicinal structure. Aromatic carbon-iodine bands were observed at 990 and 1017 $cm^{-1}$.

**2-Amino-5-iodo-*m*-xylene (V).**—To a suspension of 17 g. of sodium hydrogen carbonate in 150 ml. of water, 10 g. of 2-*m*-xylidine and 80 ml. of ether were added; the mixture was then stirred rapidly while 20 g. of iodine was added at such a rate that the color of the free iodine disappeared within a few minutes. Stirring was then continued for an additional hour, after which the reaction mixture was steam-distilled until 4 l. of the distillate had been collected. The amine separated as white needles in the distillate, which was filtered and recrystallized from boiling petroleum ether. The resulting large needles weighed 11.0 g. and melted at 52—53°C. Yield, 49%.

Found: C, 39.20; H, 4.14; N, 5.70. Calcd. for $C_8H_9IN$: C, 38.88; H, 4.08; N, 5.67%.

**2, 5-Diiodo-*m*-xylene (VI).**—Ten grams of V was diazotized in 80 ml. of sulfuric acid with 5.0 g. of sodium nitrite in the same manner as has been described above. The mixture was then poured onto crushed ice, and the resulting solution was, after filtration, added to a concentrated solution of 16.0 g. of potassium iodide in water. The mixture was allowed to stand overnight, and the brown solid which precipitated was removed by filtration and chromatographed through a short alumina column, using light-boiling ligroin as an eluant. The evaporation of the solvent gave 3.6 g. of the product, white needles with a m. p. of 64—65°C. The yield was low (25%) because of the formation of a large amount of resinous matter.

Found: C, 27.05; H, 2.30. Calcd. for $C_8H_8I_2$: C, 26.84; H, 2.25%.

The infrared spectrum showed a band at 850 $cm^{-1}$ which may be attributed to one isolated ring-hydrogen. The absence of ring CH absorption in the

3) E. Noelting, A. Braun and G. Thesmar, *Ber.*, **34**, 2242 (1901).

910—950 $cm^{-1}$ region was associated with the presence of a center of symmetry ($A_2$ vibration). The pattern in the 1650—2000 $cm^{-1}$ region also supports the 1,2,3,5-tetra substitution. Aromatic carbon-iodine band was observed at 1000 and 1023 $cm^{-1}$.

**4-Amino-5-iodo-*m*-xylene (VII).** — 4-*m*-Xylidine was directly iodinated with free iodine by the same method as has been used above. In this case, however, the reaction proceeded with some difficulty and resinous matter was formed in an appreciable amount. The product separated out as white needles from the steam-distillate. Recrystallization from boiling petroleum ether gave white needles, m. p. 65°C. Reported,[4] 65°C. The yield was 16% on the basis of the *m*-xylidine used.

**4,5-Diiodo-*m*-xylene (VIII).** — The diazonium salt solution prepared from VII was slowly added to a solution of potassium iodide in water. The mixture was then allowed to stand overnight, and the black oil which precipitated was chromatographed as usual. The evaporation of the solvent, followed by the distillation of the residual oil, afforded a pale pink-colored oil, boiling at 176—177°C/18 mmHg, which did not solidify upon standing in an ice box. The yield was very poor.

Found: C, 27.00; H, 2.31. Calcd. for $C_8H_8I_2$: C, 26.84; H, 2.25%.

The infrared spectrum showed a peak at 849 $cm^{-1}$ which may be attributed to one isolated ring-hydrogen. A band at 950 $cm^{-1}$ was attributed to the B vibration of the ring CH bond which distinguished 4,5-diiodo-*m*-xylene from the 2,5-diiodo isomer. Aromatic carbon-iodine bands were observed at 1012 and 1040 $cm^{-1}$.

**4-Amino-6-nitro-*m*-xylene (IX).** — 4-*m*-Xylidine was dissolved in concentrated sulfuric acid and nitrated as in the preparation of I. The crude amine obtained was then triturated and extracted several times with small amounts of cold tetrahydrofuran in order to remove the accompanying isomer, 2-nitro-4-amino-*m*-xylene. Then the product was recrystallized from an aqueous ethanol solution. The yield was 50%, and the product, orange yellow needles, melted at 122—124°C. Reported,[5] 124°C.

**4-Iodo-6-nitro-*m*-xylene (X).**—The amine IX was converted into this compound by the same method as that used in the preparation of II. The product was purified through an alumina column using light-boiling ligroin as an eluant. Recrystallization from boiling petroleum ether afforded large pale yellow crystals which melted at 87—88°C. The yield was 60%.

Found: C, 34.96; H, 2.27; N, 4.87. Calcd. for $C_8H_9INO_2$: C, 34.68; H, 2.90; N, 5.05%.

**4-Iodo-6-amino-*m*-xylene (XI).**—Fifty grams of stannous chloride dihydrate was dissolved in a mixture of 200 ml. of concentrated hydrochloric acid and 200 ml. of ethanol; to the resultant solution 12.5 g. of X was added and it was gradually heated to a gentle refluxing. After the complete dissolution of the crystal, refluxing was continued for an additional 2 hr., and then the mixture was cooled. An excess of sodium hydroxide was added to redissolve the precipitated tin hydroxide, after which the mixture was steam-distilled. The amine was readily steam-distilled and solidified in a condenser as white crystals, which were collected and recrystallized from boiling petroleum ether. The product was obtained as a cluster of white leaflets which weighed 9.4 g. (84%); m. p. 68—69°C.

Found: C, 39.03; H, 4.27; N, 5.45. Calcd. for $C_8H_9NI$: C, 38.88; H, 4.08; N, 5.67%.

**4,6-Diiodo-*m*-xylene (XII).**—The amine XI was diazotized and converted into this compound by the same procedure as that used in the preparation of IV. The crude product was purified through an alumina column using petroleum ether, from which 4,6-diiodo-*m*-xylene separated as large plates, m. p. 72—74°C. Reported,[6] 72°C. The yield was 72%.

Found: C, 27.17; H, 2.53. Calcd. for $C_8H_8I_2$: C, 26.84; H, 2.25%.

Peaks (865 and 931 $cm^{-1}$) and a pattern (1650—2000 $cm^{-1}$) indicating the appropriate aromatic substitution were present in the infrared spectrum. Aromatic carbon-iodine band was observed at 1023 $cm^{-1}$.

## Summary

Four isomeric diiodo-*m*-xylenes have been synthesized and their isomerization in concentrated acids investigated in order to elucidate the mechanism of the new rearrangement observed in the Jacobsen reaction of 2-iodo-*m*-xylene. 2,4- and 4,5-Diiodo-*m*-xylene, in the presence of cold sulfuric or hot polyphosphoric acid, isomerize to 4,6- and 2,5-diiodo-*m*-xylene respectively. All four isomers readily undergo disproportionation with hot sulfuric acid to give mixures of tri- and tetraiodo-*m*-xylenes. No disproportionation has been observed in the reaction with polyphosphoric acid. The important role played by a sulfo group in this reaction has been discussed.

*Department of Chemistry*
*Faculty of Science*
*Kyoto University*
*Sakyo-ku, Kyoto*

4) M. Kerschbaum, ibid., **28**, 2798 (1895).
5) E. C. Kleiderer and R. Adams, *J. Am. Chem. Soc.*, **53**, 1576 (1931); E. Noelting and A. Collin, *Ber.*, **17**, 265 (1884).
6) A. Töhl and E. Bauch, ibid., **26**, 1105 (1893).

# The Chemical Behavior of Low Valence Sulfur Compounds. I. Oxidation of Elemental Sulfur with Compressed Oxygen in Aqueous Ammonia Solution

By Mu-Chang SHIEH, Hiroshi OTSUBO and Taijiro OKABE

(Received December 28, 1964)

Recently, the chemistry of sulfane (hydrogen sulfide), sulfane monosulfonic acid (the family of the derivatives of thiosulfuric acid formulated as $H_2S_{x+1}O_3$ or $H_2S_x \cdot SO_3$) and sulfane disulfonic acid (polythionic acids formulated as $H_2S_{x+2}O_6$ or $H_2S_x \cdot 2SO_3$) has been splendidly systematized, as a series of sulfane derivatives, by the excellent work of Feh'er[1] and Schmidt[2]. Nevertheless, the details of the mechanisms by which these compounds react are still obscure, because of the lack of reliable methods of chemical analysis and because of the complexity of the reactions. Knowledge of these mechanisms has, in fact, so far been based mainly on speculation.

In the well-known work of Forward[3] on the hydrometallurgy of nonferrous metals, which involves the leaching of complex sulfide ores containing nickel, cobalt and copper with ammonia solution and compressed air, it has yet been reported that the metal sulfides can be easily converted into sulfate through thiosulfate trithionate and sulfamate as intermediates, but no concrete evidence for their mechanism has been provided. The formation of sulfate by the oxidation of thiosulfate has been observed by Glund[4] in the high pressure oxidation of sodium thiosulfate, but the reaction mechanism has not yet been reported.

The intention of this paper is to clarify the reaction mechanism of the oxidation of sulfide to sulfate, when elemental sulfur suspended in aqueous ammonia is used as the starting material. This study will show that, under optimum conditions, 50% or more of the sulfur can be converted into ammonium sulfamate, a compound which is expected to become an important raw material for various products, as weed killers, fire-proofing agents, and sweetening agents. This oxidation can, therefore, profitably be applied to the manufacture of sulfamate-form sulfur-bearing materials.

1) F. Feh'er, W. Laue and G. Winkhaus, *Z. anorg. u. allgem. Chem.*, **288**, 113 (1956); ibid., **290**, 52 (1957).
2) M. Schmidt, "Sulfur Polymer," in "Inorganic Polymer," Vol. 2, Ed. by F. G. A. Stone and W. A. G. Graham, Academic Press Inc., New York (1962), p. 98.
3) F. A. Forward, *Trans. Canad. Inst. Min. Metall.*, **66**, 191 (1957).
4) W. Gluud, *Ber.*, **54**, 2425 (1921).

## Experimental

**Apparatus.**—A Sakashita Seisakusho Model SR-50 autoclave with a 500-ml. capacity and made of SUS 32 stainless steel, which is the same as alloy AISI 316 or V4A, was used for the reaction. The apparatus is depicted schematically in Fig. 1.

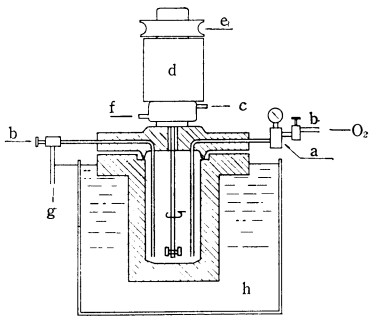



Fig. 1. Experimental apparatus.

| | | | |
|---|---|---|---|
| (a) | Oil trap | (e) | Pulley |
| (b) | Needle valve | (f) | Cooling water |
| (c) | Ammonia gage | (g) | Sampling pipe |
| (d) | Magnetic stirrer | (h) | Glycerine bath |

**Procedure.**—After the addition of the sulfur and aqueous ammonia, the autoclave was kept in a heated glycerine bath regulated within 1°C. After one hour the disproportionation reaction had been completed; oxygen was then introduced through a control valve and carefully kept at a constant pressure. Every few hours, 10 ml. aliquots of the solution were withdrawn for analysis.

**Analysis.**—The sample solution did not contain any sulfite or dithionate. Although the presence of polythionates, such as 3-, 4-, and 5-thionate, was proved by the the paper chromatography proposed by Pollard,[5] their concentrations were too low to permit their determination by chemical analysis. Therefore, after it had been diluted to a suitable concentration, the sample solution was analyzed for sulfides, thiosulfate, sulfate, and sulfamate as follows:

$S_x^{2-}$: a 1N cadmium acetate solution was added to the diluted solution; the cadmium sulfide precipitated, after being separated by filtration, was oxidized to sulfate with nitric acid and potassium chlorate and weighed as barium sulfate.

5) F. H. Pollard, *Brti. Med. Bull.*, **10**, 187 (1954).

$S_2O_3^{2-}$ : One portion of the sample solution was directly titrated with a 0.02 N iodine solution.

$SO_3NH_2^-$ : After the addition of a 1 N silver nitrate solution, the sample solution was heated on a water bath in order to convert $S_2O_3^{2-}$ into $SO_4^{2-}$ by the following reaction:

$$S_2O_3^{2-} + 2Ag^+ + 2OH^- = Ag_2S + SO_4^{2-} + H_2O$$

The silver sulfide was then removed by filtration, and the sulfate ions and excess silver nitrate in the filtrate were precipitated, as barium sulfate and silver chloride respectively, by the addition of a barium chloride solution. Then the filtered solution was acidified with dilute hydrochloric acid and heated to boiling, after a sufficient amount of sodium nitrite had been added to decompose the $SO_3NH_2^-$ as follows:

$$SO_3NH_2^- + NO_2^- = SO_4^{2-} + N_2 + H_2O$$

The sulfate ion formed was determined by the ordinary method as barium sulfate, and the amount of sulfamate was estimated.

## Results

**General View of the Entire Reaction.**—When elemental sulfur is heated in aqueous ammonia at about 100°C, the solution gradually becomes reddish brown and is found to contain polysulfide and thiosulfate, as is shown in Table I and II. Although these results are not completely accurate, as the result of a poor sampling, the molar ratio, $S_x^{2-}/S_2O_3^{2-}$, seems to indicate that the value of $x$ has a tendency to decrease from about 8 to 5 during the course of the reaction. This fact can be explained by assuming the successive formation of $S_8^{2-}$ and $S_5^{2-}$. When oxygen is introduced into a solution in which the sulfur has been entirely disproportionated, the red color of the solution rapidly fades away and the temperature of the solution rises; at the same time a large amount of thiosulfate is formed. The oxidation of polysulfide which proceeds faster than that of thiosulfate, appears to be the rate-determining step for the over-all reaction; thus thiosulfate temporarily reaches a maximum concentration and then gradually changes into sulfate and sulfamate, the final products. If oxygen is introduced at the beginning of the reaction, both the disproportionation and the oxidation will occur in the early stages. These aspects are shown schematically in Fig. 2. The kinetics of these reactions could not be determined, because free ammonia is continuously consumed in the course of the reaction and, consequently, the partial pressure of oxygen increases under a constant pressure. These relations become even more complicated when the changes in temperature are taken into account.

**The Effect of the Ammonia Concentration.**—The ammonia concentration varied from 4 N to 16 N. An increase in the concentration of ammonia caused a remarkable increase in the reaction rate and improved the yield of sulfamate.

**The Effect of the Oxygen Pressure.**—The effect of the oxygen pressure was examined in the 20—100 kg./cm² range. This pressure includes the vapor pressure of the solution. As is shown in Fig. 3, the increase in the reaction rate is proportional to the oxygen pressure, but only at pressures below 50 kg./cm². On the other hand, while high oxygen pressures cause a small improvement in the yield of sulfamate, this enhancement of the yield of sulfamate is not as great as that due to a decrease in the temperature or that due to an increase in the ammonia concentration.

Table I. Composition of the disproportionate solution of sulfur

| Reaction temp., °C | 90 | 110 | 110 | 110 | 110 | 130 | 130 | 150 |
|---|---|---|---|---|---|---|---|---|
| Ammonium concn., N | 8.30 | 4.16 | 7.88 | 12.14 | 15.97 | 8.16 | 8.16 | 8.30 |
| Reaction time, hr. | 1 | 1 | 1 | 1 | 1 | 1 | 1 | 1 |
| $S_x^{2-}$ (S-g. atom/l.) | 0.42 | 0.69 | 1.34 | 1.89 | 1.92 | 1.78 | 1.79 | 1.75 |
| $S_2O_3^{2-}$ (S-g. atom/l.) | 0.12 | 0.12 | 0.25 | 0.55 | 0.35 | 0.32 | 0.29 | 0.32 |
| Total S (S-g. atom/l.) | 0.54 | 0.81 | 1.57 | 2.40 | 2.27 | 2.10 | 2.08 | 2.07 |
| $S_x^{2-}/S_2O_3^{2-}$ | 3.5 | 5.8 | 5.4 | 3.4 | 5.5 | 5.6 | 6.2 | 5.5 |

$S_x^{2-}/S_2O_3^{2-}$ : Sulfur atom ratio of polysulfide ion to thiosulfate ion.

Table II. Composition of the disproportionate solution of sulfur

| Reaction time, hr. | 0 | 3 | 6 | 12 | 18 | 24 |
|---|---|---|---|---|---|---|
| $S_x^{2-}$ (S-g. atom/l.) | 3.95 | 3.74 | 3.92 | 3.89 | 3.90 | 3.93 |
| $S_2O_3^{2-}$ (S-g. atom/l.) | 0.51 | 0.63 | 0.67 | 0.61 | 0.72 | 0.73 |
| Total S (S-g. atom/l.) | 4.46 | 4.37 | 4.59 | 4.50 | 4.62 | 4.66 |
| $S_x^{2-}/S_2O_3^{2-}$ | 7.7 | 5.9 | 5.8 | 6.4 | 5.4 | 5.4 |

Reaction temp., 130°C Stirring speed, 500 r. p. m. Ammonium concn., 16.9 N
Partial pressure of $NH_3$, 16.0 kg./cm²

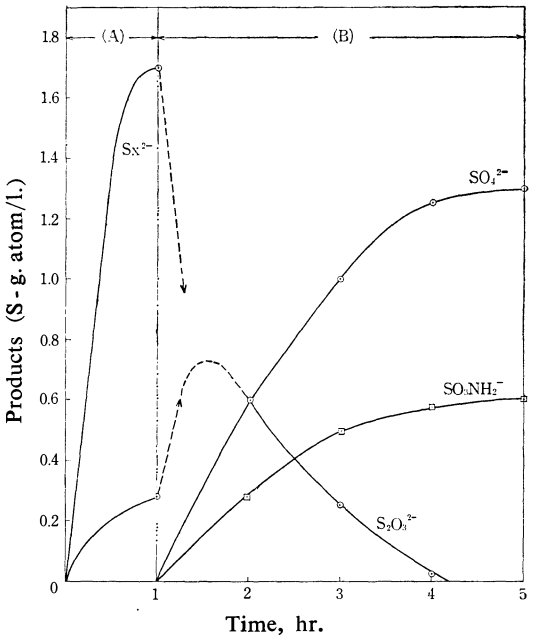



Fig. 2. General view of the whole reaction
Disproportionation and oxidation of sulfur.
(A) Disproportionation reaction
(B) Oxidation reaction under oxygen pressure

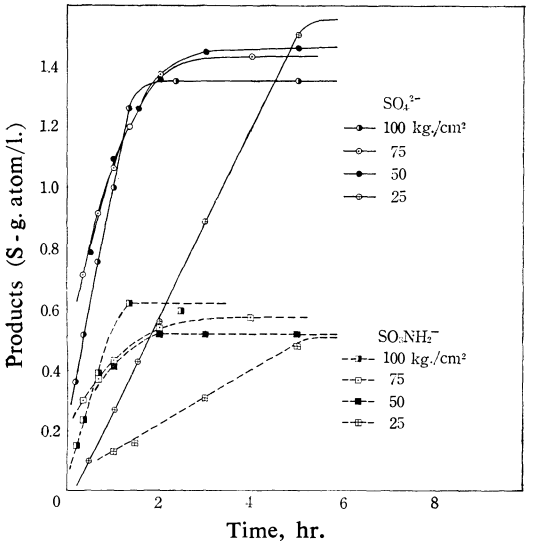



Fig. 3. Effect of oxygen pressure on the reaction of sulfur oxidation.
Temperature 130°C
Ammonia concentration 8 N

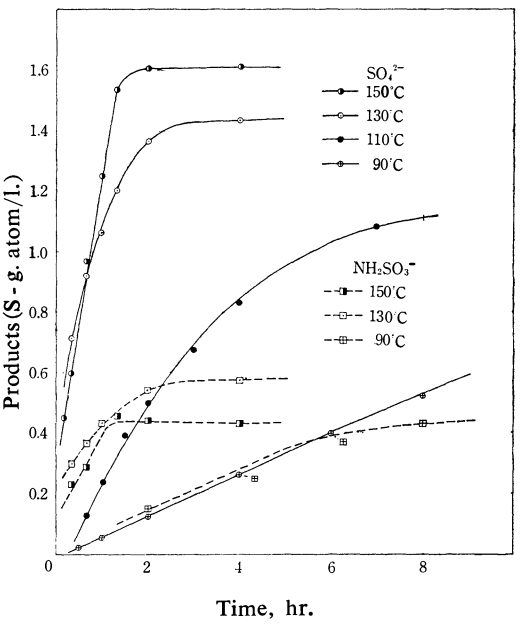



Fig. 4. Effect of temperature on the reaction of sulfur oxidation.
Oxygen pressure 75 (kg./cm²)
Ammonia concentration 8 N

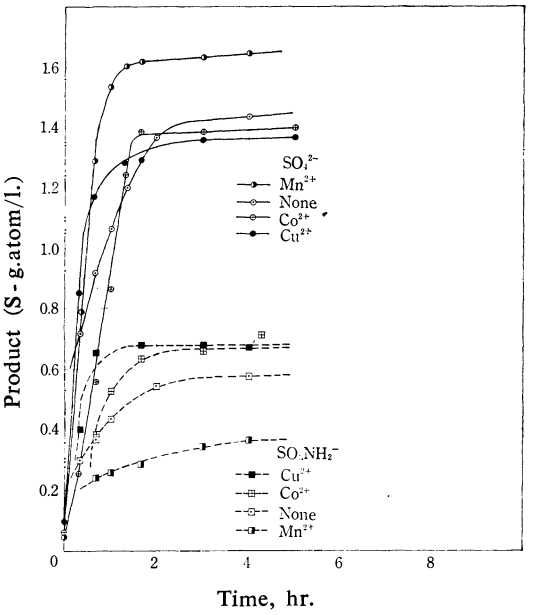



Fig. 5. Effect of metal ion on the reaction of sulfur oxidation.
Temperature 130°C
Oxygen pressure 75 (kg./cm²)
Ammonia concentration 8 N

**The Effect of the Reaction Temperature.**—The reaction rate is increased by raising the reaction temperature, but the yield of sulfamate is thus decreased, probably because of the decomposition of trithionate into sulfate by the hydrolysis. The results are shown in Fig. 4.

**The Catalytic Effect of Metal Ions.**—The transition metals, such as cobalt, nickel, and

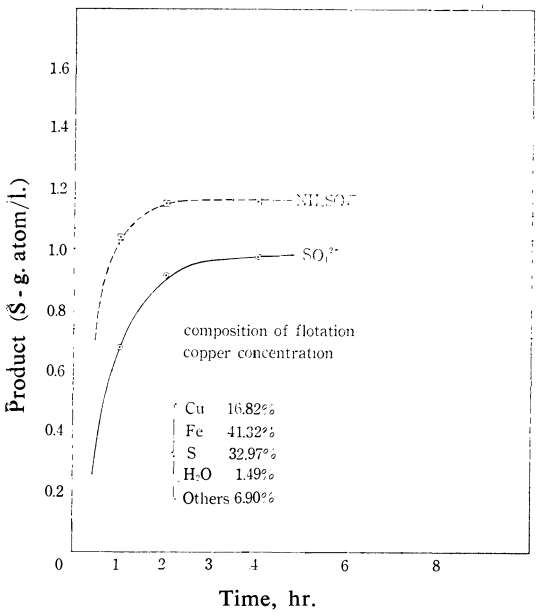



Fig. 6. Effect of flotation copper concentrate on the reaction of sulfur oxidation.

| | |
|---|---|
| Temperature | 110°C |
| Oxygen pressure | 75 (kg./cm²) |
| Ammonia concentration | 11.74 N |

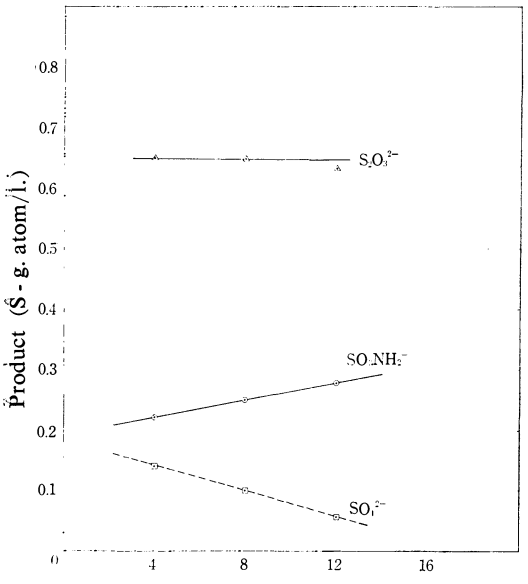



Fig. 7. Effect of ammonia concentration on the decomposition of trithionate.
Reaction temperature 110°C

copper, are known to accelerate remarkably the oxidation of sulfite with oxygen. The expected catalytic effects of these metals on the above oxidation of sulfur are shown in Figs. 5 and 6. The reaction rate is significantly affected by the presence of these metals, but the effect is not as large as that in the sulfite oxidation. However, the yield of sulfamate can be remarkably increased by the addition of copper sulfide ores. Since most of the dissolved copper is precipitated as sulfide in the course of the reaction, there are very few copper ions to serve as catalysts.

**The Decomposition of Trithionate.**—Related experiments were made on trithionate; the results, shown in Fig. 7, indicate that the yield of sulfamate ions increases with the concentration of ammonium hydroxide, while that of sulfate ions shows a reverse tendency.

## Discussion

Although the reaction mechanism has not yet been fully established, the main course of the reaction is roughly disclosed by this study. The oxidation of sulfur does not occur as a series of simultaneous reactions; Rather, it proceeds through the following series of consecutive steps:

**The Disproportionation of Sulfur.**—According to Pryor's review,[6] the most widely-accepted mechanisms of the disproportionation of sulfur in an alkaline solution are as follows;

$$\frac{1}{2}S_8 + 4NaOH = Na_2S_2O_3 + 2NaHS + H_2O \qquad (100-200°C)$$

$$\frac{1}{2}S_8 + 5NH_4OH = (NH_4)_2SO_4 + 3NH_4SH + H_2O \qquad (250-350°C)$$

However, the present study, at 100°C, revealed that unstable ammonium octasulfide forms at the beginning and that this polysulfide gradually degrades to pentasulfide. This behavior can be understood easily by assuming that the eight-membered ring of the sulfur molecule is broken open to form an octasulfide by the attack of the ammonia, and that the octasulfide is then converted into the stable pentasulfide by the step-by-step elimination of three sulfur atoms. Consequently, the disproportionation can be represented as follows:

$$\frac{3}{2}S_8 + 6NH_4OH = 2(NH_4)_2S_5 + 2(NH_4)_2S_2O_3$$

**The Oxidation of Sulfide.**—Bloxam[7] reported

6) W. A. Payor, "Mechanisms of Sulfur Reaction," McGraw-Hill Inc., New York (1962), p. 12.
7) W. P. Bloxam, *J. Chem. Soc.*, **67**, 277 (1895), see also E. Schulek and E. Koros, *Acta Chim. Acad. Sci. Hung.*, **3**, 125 (1953); *Chem. Abstr.*, **47**, 10390 (1953).

the formation of thiosulfate in the oxidation of ammonium sulfide under atmospheric pressure at room temperature, but the reaction velocity must be very small under such conditions. It has been found that, if compressed oxygen is employed, the oxidation of sulfide to thiosulfate is almost instantaneous. The rise in the temperature of the reaction mixture must be due to a strongly exothermic reaction, such as the following:

$$2(NH_4)_2S_5 + 6NH_4OH + 6O_2 = 5(NH_4)_2S_2O_3 + 3H_2O + 640\ \text{kcal.}$$ [8]

**The Oxidation of Thiosulfate.**—Most thiosulfates can hardly be oxidized at all with oxygen under ordinary pressures. The oxidation of thiosulfate by air was first studied by Gluud,[4] who employed a pressure of 10 atm. at 100°C for the sodium salt. The thiosulfate was found to afford only sulfate in alkaline solutions, but in neutral solutions it was converted into free sulfur and sulfate. Moreover, Forward[3] reported that ammonium thiosulfate is first oxidized to trithionate with compressed air at 175—300°C. From the fact that thiosulfate is usually oxidized to tetrathionate with iodine and other mild oxidants, it is most reasonable to regard tetrathionate as the product first formed from thiosulfate. The decomposition of the tetrathionate produces trithionate, pentathionate and thiosulfate; the pentathionate then further decomposes, thus forming both trithionate and thiosulfate. Therefore, it now remains to clarify the behavior of trithionate in an aqueous ammonia solution. Its yield is improved by an increase in the ammonia concentration, as Fig. 7 shows. The decomposition of trithionate must, therefore, proceed mainly as:

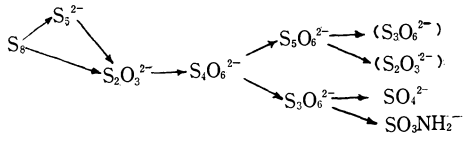
$$S_3O_6^{2-} + NH_3 + OH^- = SO_3NH_2^- + S_2O_3^{2-} + H_2O$$

but partly as:

$$S_3O_6^{2-} + 2OH^- = SO_4^{2-} + S_2O_3^{2-} + H_2O$$

When these reactions are considered, the reason for the increase in the yield of the sulfamate with the increase in the ammonia concentration becomes obvious.

Consequently, although further studies are required, the oxidation of sulfur in an aqueous ammonia solution may be considered to proceed via the following course:




## Summary

1) The oxidation of sulfur with compressed oxygen proceeds through the following sequence of steps: (a) The disproportionation of sulfur to both pentasulfide and thiosulfate. (b) The oxidation of pentasulfide to thiosulfate. (c) The oxidation of thiosulfate to sulfate and sulfamate through a series of complicated intermediates.

2) Sulfamate forms only in the decomposition of trithionate.

3) The over-all reaction of the oxidation is prompted by a rise in the temperature, an increase in the ammonia concentration, and the addition of transition metal ions, especially copper ions.

*Department of Applied Chemistry*
*Faculty of Engineering*
*Tohoku University*
*Katahira-cho, Sendai*

8) F. D. Rossini "Selected Values of Chemical Thermodynamic Properties. Part 1. Tables," Department of Commerce, U. S. A. (1961).

# An Attempt to Determine Fluorescein's S*–T Transition Probability and a Preliminary Investigation of the Behavior of Its Semiquinone in an Alkaline Solution

By Yoshihiro MOMOSE, Kengo UCHIDA and Masao KOIZUMI

(Received January 6, 1965)

Having previously reported on the determination of $\varphi_{S-T}$* for eosine,[1] we will report here on a similar attempt with fluorescein. Although a value of $2.01\times10^{-2}$ for $\phi_{S-T}$ at pH 7.0 has been reported by Oster et al.,[2] it seems desirable to repeat this experiment and to examine more critically the conditions necessary for this method to be applicable. For example, a more detailed investigation of the rate formula and of the steps in the reaction following the formation of semiquinone seems to be required. Moreover, the pH value at which their experiment was made may have been the cause of some ambiguity, because in this pH region divalent and monovalent anions exist simultaneously.[3,4] We have, therefore, chosen a pH >10.9 and used disodium ethylenediaminetetraacetate (EDTA) and allylthiourea (ATU) as the reducing agents. In addition, it must be recalled that leuco-fluorescein can be oxidized photochemically by using fluorescein as a sensitizer in the evacuated state.[5,6] If the product of the photoreduction with EDTA or ATU is really a leuco compound, a similar phenomenon may be expected; therefore, this fact must be taken into consideration in order to obtain an exact kinetic treatment. Hence, the behavior of the reaction product was investigated; the effect of the addition of the reducing agents on the sensitized oxidation of leucofluorescein was also examined to some extent.

It was established that semiquinone is formed as a rather stable intermediate product and that the behavior of the final product differs from that of the product obtained by the photoreduction in an alcoholic solution. It was further found that most of the semiquinone is gradually converted to the oxidized form in the dark and, quite astonishingly, in the ratio of 1 : 1.

A simple rate formula could not always be given, and even a rather tentative value of $\varphi_{S-T}$ was determined only under special conditions.

## Experiment

**Materials.**—*Allylthiourea.*—Tokyo Kasei G. R. 1-allyl-2-thiourea was recrystallized three times from the aqueous solution.

*Disodium Ethylenediaminetetraacetate, Dihydrate (DOTITE 2 Na).*—The special grade reagent of the Dojindo Pharm. Ltd., was used.

*Fluorescein.*—Commercial material was repeatedly recrystallized from ethanol.

*Leuco-fluorescein.*—Fluorescein was reduced with sodium amalgam and, after repeated recrystallizations from ethanol solution, desiccated in a high vacuum.[5]

*Sodium Hydroxide.*—A saturated solution was prepared from the G.R. reagent of the Wako Junyaku Co. The supernatant liquid was diluted to the desired concentration.

*Disodium Hydrogen Phosphate.*—A G. R. reagent of Wako Junyaku Co. was recrystallized three times from the aqueous solution.

**Apparatus.**—The apparatus is shown in Fig. 1.

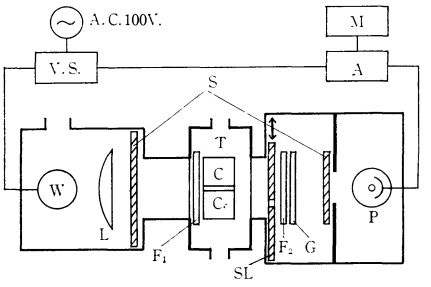



Fig. 1.

V. S. Voltage stabilizer
W Tungsten lamp L Collimating lens
S Shutter T Thermostat
C Sample cell $C_0$ Reference cell
$F_1$ Cut-off filter (>430 m$\mu$)
$F_2$ Interference filter (peak 490 m$\mu$)
SL Slit for changing light path
G Frosted glass P Photoelectric tube
A Amplifier M Microammeter

* $\varphi_{S-T}$ is the S*→T transition probablity. As to the general purpose for which the present investigations have been made, seen Ref. 1.

1) T. Ohno, Y. Usui and M. Koizumi, This Bulletin, 38, 1022 (1965).
2) A. H. Adelman and G. Oster, *J. Am. Chem. Soc.*, 78, 3977 (1956).
3) V. Zanker and W. Peter, *Chem. Ber.*, 91, 572 (1958).
4) L. Lindqvist, *Arkiv Kemi*, 16, 79 (1960).
5) K. Uchida, S. Kato and M. Koizumi, This Bulletin, 35, 16 (1962).
6) K. Uchida and M. Koizumi, ibid., 35, 1871 (1962).

**Procedure.**—The light source, L, was a tungsten lamp (Kondo Projection Lamp 100 V.-500 W.); this was always operated at 50.0 V. All the experiments were carried out at 25°C in a thermostat. The fluorescein solution was ordinarily made up in a $1\times10^{-5}$ M aqueous solution. The concentration of reducing agents (ATU or EDTA) was $3\times10^{-2}$—$3\times10^{-3}$ M. The sample solutions were made up in a sodium hydroxide-disodium hydrogen phosphate buffer at pH 10.95 or in a $1.0\times10^{-1}$ N, $5.0\times10^{-2}$ N, or $1.0\times10^{-3}$ N sodium hydroxide solution. The solution was usually degassed five times by using a mercury diffusion pump, melting and freezing being repeated each time. After degassing, the solution was poured into a reaction cell 1 cm. thick. The fading and coloring of the solution was followed with a photoelectric tube (Toshiba 7211). The absorption spectra of the solutions were measured with a Hitachi EPU-2A spectrophotometer or a Hitachi EPS-2 recording spectrophotometer. The absolute intensity of the light falling on the reaction cell was determined with a calibrated thermopile (Kipp & Zonen, type E 5) with a sensitivity of $1.02\times10^{-5}$ V./W. of radiant energy.

## Results and Discussion

**Preliminary Observation.**—A check was made to ensure that the addition of EDTA or ATU did not essentially affect the absorption spectra of the dye, and that no dark reaction occurred. When the sample was illuminated with visible light, the absorption spectra in the visible region always declined monotonously, without any even slight shift. When EDTA was used as a reducing agent, the absorption due to semiquinone was readily apparent near 394 m$\mu$, and at the same time, the decrease in the absorbance near 300 m$\mu$ was somewhat less. The last phenomenon[7] is considered to be due to the formation of leuco-uranine. Figure 2 shows a typical example. In the case of ATU, the absorption spectrum of the product could not be obtained in detail, because ATU absorbs up to $\lambda=310$ m$\mu$. The increase in the absorbance near 394 m$\mu$, however, could be clearly detected, although the intensity of the absorbance near 394 m$\mu$ was much less than in the case of EDTA.

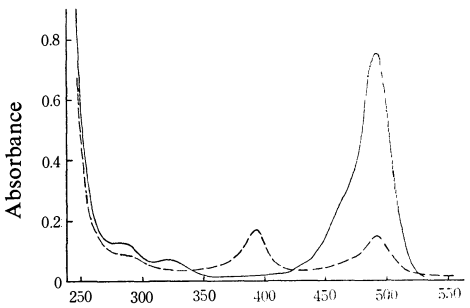



Fig. 2. Change of the absorption spectra of fluorescein by irradiation.
$[U]_0=1\times10^{-5}$ M, $[EDTA]_0=4.0\times10^{-3}$ M, $[NaOH]=0.1$ N
—— before irradiation
---- immediately after 28.3 min. irradiation

**Studies of the Reaction Products.**—*The Formation of Semiquinone and Its Kinetic Behavior.*—Since semiquinone was found to be formed as a rather stable product both when EDTA and when ATU were used, its behavior was investigated in some detail. Figure 3 shows a typical example of the change in the absorption spectra when the irradiated solution involving EDTA was kept in the dark. It shows that the gradual dercrease in the height of the peak at 394 m$\mu$ is accompanied by an increase in the main absorption of the dye. An isosbestic point is seen at 430 m$\mu$. The behavior agrees quite well with that, in ethanol-water or in isopropanol-water, observed by Imamura.[7] The molar absorbance of semiquinone at $\lambda=394$ m$\mu$ was determined in the following way.

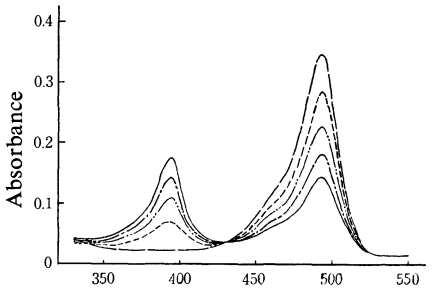



Fig. 3. Change of the absorption spectra when the solution having the spectra --- in Fig. 2, is kept in the dark.
—— after 2 min. 35 sec.
—— after 20 min. 25 sec.
—— after 45 min. 15 sec.
---- after 129 min.
—— after 1000 min.

After the absorbances at 394 and 490 m$\mu$ of the partially-bleached solution had been measured, air was introduced into the solution and changes in the absorbances were examined immediately. Since it was confirmed that only semiquinone is converted to the original dye by this procedure, $\varepsilon_{394}$ can easily be obtained by using the $\varepsilon_{490}$ value of uranine ($7.80\times10^4$ at pH 9). Table I gives some of the results.

The value, $5.0\times10^4$, obtained from the mixture of uranine and leuco-uranine is a little

7) M. Imamura, This Bulletin, 31, 962 (1958).

TABLE I. THE DETERMINATION OF $\varepsilon_{394}$ OF SEMIQUINONE

A)

| $[L]_0$* M | $[U]_0$* M | [NaOH] N | Change in absorbance at 490 mμ | Change in absorbance at 394 mμ | $\varepsilon_{394}$ |
|---|---|---|---|---|---|
| $30.3\times10^{-6}$ | $7.7\times10^{-6}$ | 1.0 | 1.003 | 0.650 | $5.05\times10^{4}$ |
| $31.5\times10^{-6}$ | $6.5\times10^{-6}$ | $5.0\times10^{-2}$ | 0.702 | 0.438 | $4.88\times10^{4}$ |
| | | | | | Av. $5.0\times10^{4}$ |

B) $[U]_0=1\times10^{-5}$ M, [NaOH]=0.1 N

| Concn. of EDTA M | Change in absorbance at 490 mμ | Change in absorbance at 490 mμ | $\varepsilon_{394}$ |
|---|---|---|---|
| $3.0\times10^{-2}$ | 0.238 | 0.147 | $4.82\times10^{4}$ |
| $1.0\times10^{-2}$ | 0.247 | 0.142 | $4.98\times10^{4}$ |
| $1.0\times10^{-2}$ | 0.261 | 0.148 | $4.42\times10^{4}$ |
| $6.0\times10^{-3}$ | 0.256 | 0.146 | $4.45\times10^{4}$ |
| $6.0\times10^{-3}$ | 0.217 | 0.128 | $4.60\times10^{4}$ |
| $6.0\times10^{-3}$ | 0.242 | 0.150 | $4.84\times10^{4}$ |
| $4.0\times10^{-3}$ | 0.261 | 0.180 | $5.38\times10^{4}$ |
| $4.0\times10^{-3}$ | 0.256 | 0.144 | $4.38\times10^{4}$ |
| $3.0\times10^{-3}$ | 0.265 | 0.151 | $4.44\times10^{4}$ |
| $3.0\times10^{-3}$ | 0.254 | 0.145 | $4.45\times10^{4}$ |
| $6.0\times10^{-3}$** | 0.272 | 0.154 | $4.42\times10^{4}$ |
| | | | Av. $4.6_5\times10^{4}$ |

* $[L]_0$ and $[U]_0$ are the initial concentrations of leuco-uranine and uranine.
** [NaOH]=$5.0\times10^{-2}$ N.

larger than that ($4.7\times10^{4}$) found for the solution containing EDTA. Since, however, the former agrees quite well with the published date ($\varepsilon_{394}=5\times10^{4}$ (Lindqvist[4]; 0.01 N NaOH), $\varepsilon_{395}=4.9\times10^{4}$* (Imamura; water-ethanol or water-isopropanol alkaline solution)), it may be accepted as reliable.

Using $\varepsilon_{394}=5.0\times10^{4}$, the quantities of semiquinone produced under various conditions were evaluated. It was found that when the alkaline solution, 0.1 N sodium hydroxide, containing $1\times10^{-5}$ M fluorescein and various amounts of EDTA was illuminated for twenty minutes, about one-half of the bleached dye was present as a semiquinone. Some of the results are shown in Table II.

TABLE II. THE CHANGE IN THE ABSORBANCE AT 490 mμ ($-D_{ox}$) AND AT 394 mμ ($+D_{sem}$) DURING THE PHOTOREDUCTION BY EDTA

| Concn. of EDTA, M | $-D_{ox}$ | $+D_{sem}$ | $R(-\frac{D_{sem}}{D_{ox}})$ | $f_{sem}$ |
|---|---|---|---|---|
| $1\times10^{-2}$ | 0.506 | 0.142 | 0.28 | |
| $1\times10^{-2}$ | 0.462 | 0.148 | 0.32 | |
| $6\times10^{-3}$ | 0.562 | 0.146 | 0.26 | |
| $6\times10^{-3}$ | 0.563 | 0.128 | (0.22) | |
| $4\times10^{-3}$ | 0.544 | 0.180 | 0.33 | |
| $4\times10^{-3}$ | 0.546 | 0.144 | 0.32 | |
| $3\times10^{-3}$ | 0.544 | 0.151 | 0.27 | |
| $3\times10^{-3}$ | 0.433 | 0.145 | 0.33 | |
| | | Av. | 0.29±0.03 | 0.45±0.05 |

* Imamura's value was recalculated since the method of evaluation was found to involve some misunderstanding.

The ratio of the quantity of the produced semiquinone to that of the consumed dye, $f_{sem}$, is 0.45±0.05.

In the case of ATU, the quantity of produced semiquinone is much smaller and appears to change according to the experimental conditions. Table III gives the values of $f_{sem}$ obtained, when 0.1 N aqueous sodium hydroxide solutions of fluorescein, $1\times10^{-5}$ M, containing various amounts of ATU were irradiated for twenty minutes.

TABLE III. $f_{sem}$ FOR ATU

| Concn. of ATU, M | $-D_{ox}$ | $f_{sem}$ |
|---|---|---|
| $3.0\times10^{-2}$ | 0.534 | 0.04 |
| $1.6\times10^{-2}$ | 0.532 | 0.03 |
| $1.0\times10^{-2}$ | 0.532 | 0.07 |
| $6.0\times10^{-3}$ | 0.530 | 0.06 |
| $(4.0\times10^{-3}$ | 0.631 | 0.02) |

Thus, $f_{sem}$ value for ATU is only few hundredths for EDTA. Furthermore, in the mixed solvent of ethanol and water containing $3\times10^{-2}$—$4\times10^{-3}$ M ATU and $5\times10^{-2}$ N sodium hydroxide, $f_{sem}$ reaches 0.34 (the average of four determinations). From these results, one may characterize the reaction as follows. The reducing agent, $RH_2$, attacks the triplet dye, $D^t$, and forms a transient intermediate consisting of semiquinone and a half-oxidized reducing agent. If the intermediate simply dissociates into its two components, then the semiquinone would remain as a stable product,

while if the cleavage involves a hydrogen transfer, then leuco-uranine or a leuco-type compound would be produced. Schematically, this may be written as follows:

$$D^t + RH_2 \rightarrow DH\cdots RH$$

$$DH\cdots RH \rightarrow DH + RH \quad (a)$$

$$DH\cdots RH \rightarrow DH_2 + R \quad (b)$$

Thus, the behavior of the D-R redox-intermediate is quite different in EDTA and ATU; the reaction in the former case proceeds along both paths, a and b, with equal probabilities, while in the latter case the principal path is b.

When a solution which had been illuminated and which contained some semiquinone was kept in the dark, semiquinone gradually returned to the oxidized form. For example, when the solution containing about $3\times10^{-6}$ M of semiquinone, obtained by illuminating the 0.1 N sodium hydroxide solution containing $1\times10^{-5}$ M uranine and $3.0\times10^{-2}$ M EDTA, was kept in the dark, $2.58\times10^{-6}$ M of semiquinone disappeared and $3.07\times10^{-6}$M of dye was recovered in about 220 min. The ratio is close to one, indicating that 1 M semiquinone is converted into the 1 M oxidized form. This is quite unexpected, because the disproportionation of the semiquinone is generally considered to be the normal process.

Analogous results were obtained for the irradiated solution containing $5.0\times10^{-2}$ N sodium hydroxide, $9.0\times10^{-6}$ M leuco-uranine and a small quantity of uranine. The illumination of this solution for about 20 min. produced $5.04\times10^{-6}$ M of semiquinone. When the solution thus obtained was kept in the dark for five hours, the decrease in semiquinone and the increase in the oxidized form were, respectively, $3.46\times10^{-6}$M and $3.15\times10^{-6}$M; after an additional twelve hours, the two quantities increased, respectively, to $5.04\times10^{-6}$ M and $4.87\times10^{-6}$M. The ratios of the two quanties in the two cases are, respectively, 1.10 and 1.03, again indicating that the main reaction is $2DH \rightarrow 2D + H_2$. Even in the presence of ATU or EDTA, illumination converts leuco-uranine into semiquinone (see below) and the ratio of the decrease in semiquinone to the increase in uranine is also about one. All these results suggest that semiquinone, once produced, is not affected very much by EDTA, ATU, leuco or oxidized dye.

This view was further supported by the fact that semiquinone in all cases disappears according to the second order rate formula, although the rate constant itself is affected moderately by the presence of the reducing agent. Some of the rate constants in various conditions are given in Table IV. Figure 4 gives some examples of the second order plots.

Although the data are still preliminary, it can be said that the rate constant is very sensitive to the pH value. Further, it appears that the addition of EDTA or ATU increases the rate costant to some extent.

*The Behavior of the Leuco Dye.*—As has already been reported (in 1962),[5] leuco-uranine is oxidized to uranine by a photosensitized reaction using uranine as a photosensitizer.

TABLE IV. SECOND ORDER RATE CONSTANTS FOR THE DISAPPEARANCE OF SEMIQUINONE

| $[U]_0$ M | [NaOH] N | $[L]_0$ M | [EDTA] or [ATU], M | Wavelength used for analysis, mμ | $k$, $sec^{-1}M^{-1}$ |
|---|---|---|---|---|---|
| $1.0\times10^{-6}$ | 1.0 | $37.0\times10^{-6}$ | 0 | 394 | 8.1 |
| $6.4\times10^{-6}$ | 1.0 | $31.6\times10^{-6}$ | 0 | 394 | 1.1 |
| $1.0\times10^{-6}$ | $5.0\times10^{-2}$ | $9.0\times10^{-6}$ | 0 | 394 | 19.9 |
| $7.1\times10^{-6}$ | $5.0\times10^{-2}$ | $1.9\times10^{-6}$ | 0 | 394 | 24.6 |
| $1.0\times10^{-6}$ | $5.0\times10^{-2}$ | $37.0\times10^{-6}$ | 0 | 394 | 9.73 |
| $3.8\times10^{-6}$ | $5.0\times10^{-2}$ | $34.2\times10^{-6}$ | 0 | 394 | 6.22 |
| $3.5\times10^{-6}$ | $1.0\times10^{-3}$ | $34.5\times10^{-6}$ | 0 | 394 | 4280 |
| $4.1\times10^{-6}$ | $1.0\times10^{-3}$ | $33.9\times10^{-6}$ | 0 | 394 | 4000 |
| $4.2\times10^{-6}$ | $1.0\times10^{-3}$ | $33.8\times10^{-6}$ | 0 | 394 | 4760 |
| $4.3\times10^{-6}$ | $1.0\times10^{-3}$ | $33.7\times10^{-6}$ | 0 | 394 | 4270 |
| $1.0\times10^{-5}$ | $1.0\times10^{-1}$ | 0 | E $3.0\times10^{-2}$ | 394 | 181 |
| $1.0\times10^{-5}$ | $5.0\times10^{-2}$ | 0 | E $1.0\times10^{-2}$ | 490 | 49.5 |
| $1.0\times10^{-5}$ | $5.0\times10^{-2}$ | 0 | E $6.0\times10^{-3}$ | 490 | 90.1 |
| $1.0\times10^{-5}$ | $1.0\times10^{-1}$ | 0 | E $4.0\times10^{-3}$ | 394 | 83.4 |
| $1.0\times10^{-6}$ | $5.0\times10^{-2}$ | $9.0\times10^{-6}$ | A $4.0\times10^{-3}$ | 394 | 86.1 |
| $1.0\times10^{-6}$ | $5.0\times10^{-2}$ | $9.0\times10^{-6}$ | A $4.0\times10^{-3}$ | 394 | 296 |
| $1.0\times10^{-6}$ | $5.0\times10^{-2}$ | $9.0\times10^{-6}$ | E $4.0\times10^{-3}$ | 394 | 911 |
| $4.5\times10^{-6}$ | $5.0\times10^{-2}$ | $5.5\times10^{-6}$ | E $4\times10^{-3}$ | 394 | 866 |

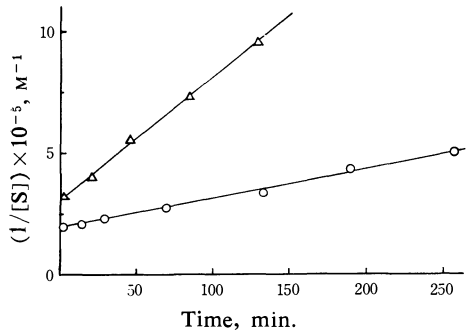



Fig. 4. Decay of the semiquinone as the second order process.
○ for the solution $[L]_0=9.0\times10^{-6}$ M, $[U]_0=1.0\times10^{-6}$ M, [NaOH]=0.05 N, irradiated for 19.5 min. $k=19.9\ M^{-1}\ sec^{-1}$
△ for the solution $[U]_0=1\times10^{-5}$ M $[EDTA]_0=4.0\times10^{-3}$ M, [NaOH]=0.1 N, irradiated for 28.3 min. $k=83.4\ M^{-1}\ sec^{-1}$

In order to compare the behavior of the photoproduct (other than semiquinone) obtained in the present experiments with that of leuco dye, the above photooxidation of leuco-uranine was reinvestigated. The results obtained in the present investigation were somewhat different from those that had been obtained before.

For instance, in the previous experiments, leuco-uranine was photooxidized to the dye, with the peak at 490 m$\mu$ rising monotonously, whereas in the present experiments the absorbance at 490 m$\mu$ showed a distinct maximum in the course of irradiation. For example, when a $5.0\times10^{-2}$ N aqueous sodium hydroxide solution of $9.0\times10^{-6}$ M leuco-uranine containing $1.0\times10^{-6}$ M uranine was irradiated, the peak at 490 m$\mu$ rose at first, but soon, within a few minutes, it reached a maximum, equivalent to $3.38\times10^{-6}$ M, and then fell to a constant value. After about twenty minutes' illumination, the concentrations of the oxidized dye and of the semiquinone reached, respectively, $2.11\times10^{-6}$ M and $5.04\times10^{-6}$ M. In another example using a similar solution, illumination caused the peak at 490 m$\mu$ to increase until, after 1.75 min., it reached a maximum value, equivalent to $2.64\times10^{-6}$ M; after 50 minutes' illumination, the concentration of the oxidized form decreased to $0.90\times10^{-6}$ M, while the concentration of semiquinone rose to $5.82\times10^{-6}$ M.

These results imply that the oxidized form is produced in the initial stage, perhaps by the reaction c, $D^t+DH_2\rightarrow 2D+H_2$, that at the same time, semiquinone is also produced, perhaps according to the reaction d, $D^t+DH_2\rightarrow 2DH$, and, furthermore, that the latter reaction gradually supersedes the former, causing a decrease in the oxidized form. It is evident from the above results that the entire quantity of D produced by the reaction $D^t+DH_2\rightarrow 2D+H_2$ is actually much larger than the increment of D at the maximum point, as long as one can consider that the formation of semiquinone is due to the reaction $D^t+DH_2\rightarrow 2DH$. When the solution was kept in the dark, semiquinone was gradually converted to the oxidized form, as has been mentioned already. When this solution was illuminated again, a steady decrease in the peak at 490 m$\mu$ was observed. A typical series of experiments is shown in Fig. 5.

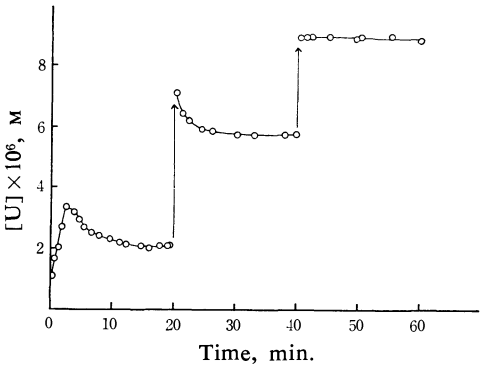



Fig. 5. Change of the dye concentration when the solution, $[L]_0=9.0\times10^{-6}$ M, $[U]_0=1.0\times10^{-6}$ M, [NaOH]=0.05 N, is irradiated.
↑ Change when the solution is kept in the dark for several days.

It appears that when the concentration of the oxidized dye exceeds a certain value, the peak at 490 m$\mu$ falls from the starting point instead of undergoing an initial increase; apparently a large excess of the oxidized form favors the reaction d. Although the present results are very curious and apparently differ from the previous results, the overall reaction is the same in both cases, i.e., $D^t+DH_2\rightarrow 2D+H_2$.

The oxidation of leuco-uranine is observed even in the presence of a moderate quantity of ATU or EDTA. The quantum yields for the production of the oxidized form at the initial stage are $3.3\times10^{-2}$, $1.6\times10^{-2}$, and $8.4\times10^{-3}$ when the concentrations of added ATU are zero, $4.0\times10^{-3}$ and $1.0\times10^{-2}$ M respectively. In the case of $4.0\times10^{-3}$ M EDTA, the quantum yield is $2.0\times10^{-2}$ under otherwise similar conditions. The behavior during the course of illumination is at least qualitatively similar to that in the absence of any reducing agent. Thus the quantity of the oxidized form usually reaches a maximum after a few minutes and then decreases. The quantity of semiquinone produced during irradiation varies,

however, according to the experimental conditions. When the solution is kept in the dark for a long time, about the same quantity of the oxidized form as that of semiquinone is produced.

The cause of the discrepancy between these results and those obtained previously is at present unknown.

*The Final Products when the Reducing Agent is EDTA.*—It was established that when EDTA is used as a reducing agent in an alkaline solution, the reaction product consists mainly of semiquinone and leuco-uranine. The evidence will be given below.

Firstly, the absorbances for uranine, leuco-uranine and semiquinone were determined at two wavelengths in order to make the analysis spectroscopically. The extinction coefficients given in Table V were obtained by the following procedures.

TABLE V. THE EXTINCTION COEFFICIENTS OF URANINE, LEUCO-URANINE AND SEMIQUINONE AT 285 AND 300 mμ

| | 285 mμ | 300 mμ |
|---|---|---|
| Uranine: $\varepsilon_U$ | $1.3\times10^4$ | $7.2\times10^3$ |
| Leuco-uranine: $\varepsilon_L$ | $6.1\times10^3$ | $6.1\times10^3$ |
| Semiquinone: $\varepsilon_S$ | $5.8\times10^3$ | $4.9\times10^3$ |

$\varepsilon_U$: from the alkaline solution of uranine at a known concentration.
$\varepsilon_L$: from the solution of leuco-uranine at a known concentration.
$\varepsilon_S$: from the irradiated solution of (leuco+uranine) at a known concentration ($[L]+[U])_0$.

The concentration of semiquinone produced by the reaction $D^t+DH_2\rightarrow 2DH$ was evaluated from $\varepsilon_S$ at 394 mμ, where $\varepsilon_U$ and $\varepsilon_L$ are practically nil. The concentration of uranine was obtained from the absorbance at 490 mμ. The concentration of leuco-uranine was calculated from $[L]+[S]+[U]=([L]+[U])_0$. Two examples of analysis by the use of the above data are given in Table VI.

Thus, the sum of [L] and [S] agrees with the total concentration of bleached dye within the range of experimental error. The above data confirm the afore-mentioned result that semiquinone forms about one-half of the total dye that has disappeared.

A remarkable fact that was found is that the leuco dye produced in this case goes back to the oxidized form, although very slowly. When the solution is kept in the dark, the reaction proceeds as a second order reaction in regard to [L]. This may be due to the reaction between leuco dye and the oxidized product of EDTA. A few examples of the second order plot are given in Fig. 6.

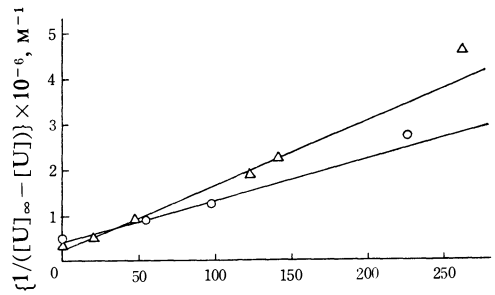



Fig. 6. Second order plot for the recovery of dye from the final product obtained by illuminating the solution containing uranine and EDTA.
○ for the solution, $[U]_0=1\times10^{-5}$ M, $[EDTA]_0=3.0\times10^{-2}$M, $[NaOH]=0.1$N, $k=2.7$ sec$^{-1}$ M$^{-1}$
△ for the solution, $[U]_0=1\times10^{-5}$ M, $[EDTA]_0=1.0\times10^{-2}$M, $[NaOH]=0.05$N, $k=4.0$ sec$^{-1}$ M$^{-1}$

Some of the rate constants obtained are:

i) $[NaOH]=1.0\times10^{-1}$ N; $[U]_0=1\times10^{-5}$ M; $[EDTA]_0=3.0\times10^{-2}$ M; $k=2.7$ sec$^{-1}$ M$^{-1}$ (181 sec$^{-1}$ M$^{-1}$)

ii) $[NaOH]=5.0\times10^{-2}$ N; $[U]_0=1\times10^{-5}$ M; $[EDTA]_0=1.0\times10^{-2}$ M; $k=4.0$ sec$^{-1}$ M$^{-1}$ (49.5 sec$^{-1}$ M$^{-1}$)

The values in parentheses refer to the second order rate constant for the decay of semiquinone. The order of magnitude for the two rate constants being different, one can treat the two processes separately. The total dye recovered from the solution usually reached about 90% of the original quantity.

*The Product when ATU was Used.* — The absorption spectra of the reaction product could not be investigated, because ATU absorbs

TABLE VI. ANALYSIS OF THE PRODUCTS

| Irradiated solution | | | [L], M | [S], M | Total of the bleached dye, M |
|---|---|---|---|---|---|
| $1.0\times10^{-1}$ N [NaOH], | $1\times10^{-5}$ M $[U]_0$, | $4.0\times10^{-3}$ M $[EDTA]_0$, | $6.1\times10^{-6}$* $6.0\times10^{-6}$** | $3.5\times10^{-6}$ | $7.8\times10^{-6}$ |
| $1.0\times10^{-1}$ N [NaOH], | $1\times10^{-5}$ M $[U]_0$, | $6.0\times10^{-3}$ M $[EDTA]_0$, | $5.4\times10^{-6}$* $4.9\times10^{-6}$** | $3.4\times10^{-6}$ | $8.7\times10^{-6}$ |

* From $\varepsilon_{285}$ ** From $\varepsilon_{300}$

up to 310 mμ. Hence, the reaction product, other than semiquinone, was examined by means of a paper chromatograph. As a developer, a mixture of water (75 vol.%), ethanol (15 vol.%) and a 28% ammonia solution (10 vol.%) was used. The spots after development were detected by the emitted fluorescence.[5] Table VII gives the results obtained in one experiment.

Table VII. The results for a paper chromatograph

| | Sample | $R_f$ Uranine | $R_f$ Leuco |
|---|---|---|---|
| 1) | Aq. soln. of uranine | 0.79 (yellow) | |
| 2) | Aq. soln. of (ATU+ Leuco) | 0.79 (faint yellow) | 0.85 (dark yellow) |
| | | 0.78 (faint yellow) | 0.85 (dark yellow) |
| 3) | Leuco -uranine | 0,78 (faint yellow) | 0.84 (dark yellow) |
| 4) | The irradiation product of uranine (buffer soln.) | 0.77 (weak) | 0.95 (?) |

The product does not seem to be leuco-uranine. ATU and leuco dye might form some kind of intermolecular complex. The solution, after being kept in the dark for a day, showed no change in the absorption spectra.

In connection with the nature of the photoproduct in the case of ATU, it is important to note that if the main product were leuco-uranine (the quantity of semiquinone forms only a small percentage, as has already been stated), the photoreduction should cease at a certain point, since the rate of the reverse reaction is quite large. However, this is not the case, as is evident from Fig. 7. This is additional evidence that the photoproduct is not leuco-uranine in the case of ATU.

*Concluding Remarks.*—When EDTA is used as a reducing agent, the photoproduct consists of semiquinone and leuco dye in the ratio of about 1. Semiquinone is rather indifferent to EDTA and very slowly returns to the oxidized form, mainly by the $2DH \rightarrow 2D + H_2$ reaction but this does not affect the rate of the photoreduction under ordinary conditions. Leuco-uranine, on the other hand, reacts according to $D^t + DH_2 \rightarrow 2D + H_2$ or $D^t + DH_2 \rightarrow 2DH$; either process would affect the overall reduction rate in the opposite direction. It may, therefore, be inferred that the effect of the product on the rate would not be very large.

When ATU is used as a reducing agent, the quantity of semiquinone forms only a small percentage of the total product and the main product is some substance other than leuco-uranine. The effect of this substance on the rate is quite unknown at present.

**Kinetic Studies and the Determination of $\varphi_{S-T}$.***—Most of the experiments concerning the effect of various factors upon the rate were made using ATU as a reducing agent in a sodium hydroxide - disodium hydrogen phosphate buffer solution (pH=10.94). However, the simple rate formula did not generally hold for this solution, while it did hold when a strong alkaline solution of sodium hydroxide was used. Hence, the later experiments for determining $\varphi_{S-T}$ were performed in such a solution.

*Rate Formula.*—The following two rate formulas were tested:

a) First order rate formula with respect to the quantity of absorbed light:

$$-\frac{dc}{dt} = \Phi\frac{I_0}{d}(1-e^{-\alpha c d}) \times 1000$$

By integration:

$$\ln(e^{\alpha c d}-1) = \ln(e^{\alpha c_0 d}-1) - 1000\Phi\alpha I_0 t$$

where $\Phi$, $\alpha$, $d$, $c$ and $I_0$ are, respectively, the quantum yield, the mean absorption coeffecient, the length of the light path, the concentration of dye, and the number of input photons (in mole) per $cm^2$. The above relation corresponds to the situation where bleaching is simply proportional to the absorption of light.

b) Second order rate formula;

$$\frac{1}{C} - \frac{1}{C_0} = kt$$

Although neither a) nor b) can reproduce the general bleaching curve when ATU is present in the buffer solution, it seems that when the concentration of ATU is large enough, the relation a holds approximately; it seems further that the relation holds better at lower dye concentrations. On the other hand, at lower concentrations of ATU and higher concentrations of dye the relation b seems to hold better. Some examples are shown in Fig. 7.

These results suggest that the D-R mechanism[1] predominates in the higher concentration region of ATU, whereas the D-D mechanism[1] begins to play a part in its lower concentration region. This suggestion is consistent with

* Details of the method were described in a previous paper. See Ref. 1.

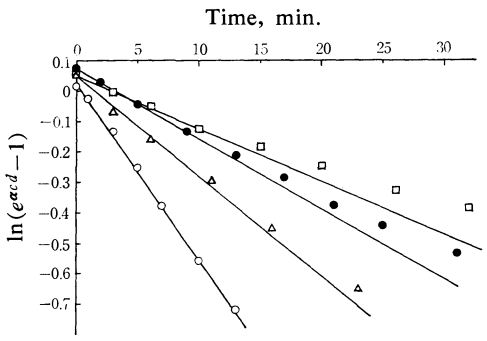



Fig. 7. Plot of $\ln(e^{acd}-1)$ vs. time for the buffer solution (pH 10.94), $[U]_0=1\times10^{-5}$ M. The concentration of ATU is;
○ $3.0\times10^{-2}$ M; △ $1.5\times10^{-2}$ M;
● $7.0\times10^{-3}$ M; □ $3.5\times10^{-3}$ M

the following rate constants reported by Lindqvist[4]:

$$D^t+D \rightarrow 2D \qquad 5\times10^7\ M^{-1}\,sec^{-1}$$

$$D^t+D \rightarrow D^-+D^+ \qquad 5\times10^7\ M^{-1}\,sec^{-1}$$

$$D^t+ATU \begin{cases} \nearrow D^-+(ATU)^+ \\ \searrow D+ATU \quad 2\times10^5\ M^{-1}\,sec^{-1} \end{cases}$$

(all in the alkaline region)

*Intensity Effect.*—Using a buffer* solution of $1\times10^{-5}$ M uranine containing $6.0\times10^{-3}$ M ATU, the effect of the intensity of the exciting light was examined. When the metallic net with a transmission coefficient of 39.3% was inserted into the light path, the rate decreased to 36% of the original value. The rate is thus proportional to the intensity of light.

*The Effect of the Dye Concentration on the Rate.*—Using a solution containing $4.0\times10^{-3}$ M ATU, and $5.0\times10^{-2}$ N sodium hydroxide the concentration of the dye was varied from 4.6 to $23\times10^{-6}$ M. The $1/\Phi$** vs. $[U]_0$ plot given in Fig. 8 clearly demonstrates that, in contrast to the case of eosine, the concentration of fluorescein has little effect on the quantum yield.

This different behavior may be accounted for by the value of the rate constant for:

$$D^t+D \begin{cases} \nearrow 2D \\ \searrow D^-+D^+ \end{cases}$$

and for:

$$D^t+ATU \begin{cases} \nearrow D^-+(ATU)^+ \\ \searrow D+ATU \end{cases}$$

* A sample solution with a pH value of 10.9 was usually prepared from a 1/5 M $Na_2HPO_4$ - 1/10 N NaOH solution.

** is evaluated from the initial slope of the ln $(e^{acd}-1)$ vs. $t$ plot.

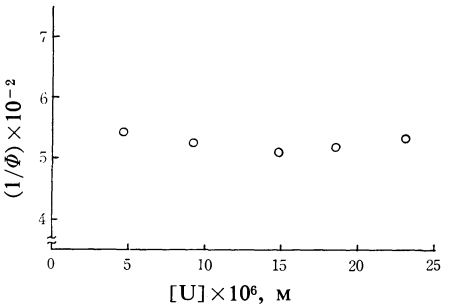



Fig. 8. $1/\Phi$ vs. $[U]_0$ plot for the solution containing $[ATU]_0=4.0\times10^{-3}$ M, [NaOH]= 0.05 N.

(The values for fluorescein are given above; the values for eosine are, respectively, $8.8\times10^8\ M^{-1}\,sec^{-1}$ and $3.4\times10^5\ M^{-1}\,sec^{-1}$)

*The Effect of the Reaction Product.*—Using a buffer solution containing $5.0\times10^{-3}$ M ATU and $1\times10^{-5}$ M uranine, the effect of the reaction product on the rate was examined. The solution was irradiated and the initial rate was measured. After about 70% of dye had been bleached, the concentration of uranine was again increased to $1.2\times10^{-5}$ M and the experiment was repeated. The rate in the second run was found to be about one-half of that in the first run.

*The Determination of $\varphi_{S-T}$ under Various Conditions.*—The rate formula a holds practically in $5.0\times10^{-2}$ N and $1.0\times10^{-1}$ N sodium hydroxide alkaline solution when the concentration of ATU is in the $4\times10^{-3}$—$3\times10^{-2}$ M range. The plot of $1/\Phi$ against $1/[ATU]_0$ as shown in Fig. 9, gives a satisfactorily straight line.

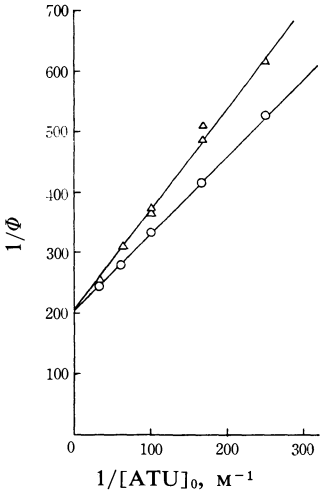



Fig. 9. $1/\Phi$ vs. $1/[ATU]_0$ plot ($1\times10^{-6}$ M $[U]_0$).
△ 0.1 N [NaOH]; ○ 0.05 N [NaOH]

TABLE VIII. QUANTUM YIELDS UNDER VARIOUS CONDITIONS

a) ATU

| $[ATU]_0$ M | $1.0\times10^{-3}$ N [NaOH] | $5.0\times10^{-2}$ N [NaOH] | $1.0\times10^{-1}$ N [NaOH] |
|---|---|---|---|
| $3.0\times10^{-2}$ | $2.8\times10^{-3}$ | $4.1\times10^{-3}$ | $3.9\times10^{-3}$ |
| $1.6\times10^{-2}$ | | $3.6\times10^{-3}$ | $3.2\times10^{-3}$ |
| $1.0\times10^{-2}$ | $1.5\times10^{-3}$ | $3.0\times10^{-3}$ | $2.7\times10^{-3}$ |
| $6.0\times10^{-3}$ | $0.99\times10^{-3}$ | $2.4\times10^{-3}$ | $2.1\times10^{-3}$ |
| $4.0\times10^{-3}$ | | $1.9\times10^{-3}$ | $1.6\times10^{-3}$ |

b) EDTA

| $[EDTA]_0$ M | $5.0\times10^{-2}$ N [NaOH] | $1.0\times10^{-1}$ N [NaOH] |
|---|---|---|
| $3.0\times10^{-2}$ | $7.2\times10^{-3}$ | $11\times10^{-3}$ |
| $1.0\times10^{-2}$ | $4.6\times10^{-3}$ | $7.2\times10^{-3}$ |
| $6.0\times10^{-2}$ | $3.8\times10^{-3}$ | $5.7\times10^{-3}$ |
| $4.0\times10^{-3}$ | $3.4\times10^{-3}$ | $4.2\times10^{-3}$ |
| $3.0\times10^{-3}$ | $2.5\times10^{-3}$ | $3.2\times10^{-3}$ |

TABLE IX. A SUMMARY OF THE $\varphi_{S-T}$ VALUES

| Reducing agent | $[U]_0$, M | [NaOH], N | $\varphi_{S-T}$ | $k_7/k_6$ |
|---|---|---|---|---|
| ATU | $1.0\times10^{-5}$ | $5.0\times10^{-2}$ | $4.9\times10^{-3}$ | $6.2\times10^{-3}$ |
| ATU | $1.0\times10^{-5}$ | $1.0\times10^{-1}$ | $4.9\times10^{-3}$ | $8.2\times10^{-3}$ |
| EDTA | $1.0\times10^{-5}$ | $5.0\times10^{-2}$ | $8.7\times10^{-3}$ | $7.2\times10^{-3}$ |
| EDTA | $1.0\times10^{-5}$ | $1.0\times10^{-1}$ | $1.5\times10^{-2}$ | $10.8\times10^{-3}$ |

As for EDTA, the rate formula a also holds for $5.0\times10^{-2}$ N and $1.0\times10^{-1}$ N sodium hydroxide solutions. However, we could not get a satisfactory plot of $1/\Phi$—$1/[EDTA]_0$, as Fig. 10 shows. The $\varphi_{S-T}$ value obtained from these plots is, therefore, not very accurate.

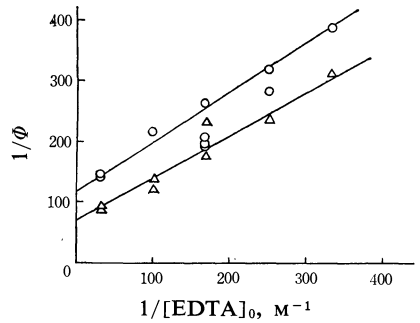



Fig. 10. $1/\Phi$ v. s. $1/[EDTA]_0$ plot ($1\times10^{-5}$ M $[U]_0$).
△ 0.1 N [NaOH]; ○ 0.05 N [NaOH]

Table VIII gives a summary of the quantum yields under various conditions.

Table IX gives the value of $\varphi_{S-T}$ obtained in this paper. The value of $k_7/k_6$ was evaluated from the inclination and the intercept.

Since the validity of the present method for obtaining $\varphi_{S-T}$ values has by no means been established beyond doubt, only a brief additional comment will be made on them. As is evident from the present studies, the main reaction product in the case of ATU is believed to be some leuco-like compound which is produced directly by the interaction of $D^t$ and ATU and which is believed to have little effect on the reduction rate at the initial stage. In view of the fact that the rate is simply proportional to the absorption of light until about 50% of dye is bleached, the value of $\varphi_{S-T}$ for ATU is considered to be more reliable.

On the other hand, the product in the case of EDTA consists mainly of semiquinone and leuco-dye. The former will not affect the reduction rate very much, but the latter will do so to some extent, probably by increasing it. In any case, these facts must be taken into consideration if we try to obtain a reliable $\varphi_{S-T}$ value. Moreover, it is not unlikely that the two reducing agents cause simple deactivation of $D^t$. The value of $\varphi_{S-T}$ obtained for ATU is, therefore, still tentative.

## Summary

An attempt to obtain a reliable value of $\varphi_{S-T}$ for fluorescein in an alkaline solution has been unsuccessful since the values for EDTA and ATU were quite different. It has been found that a large quantity of semiquinone is produced when EDTA is used as a reducing agent. In the case of ATU, the quantity of semiquinone produced is very small. Semiquinone in an alkaline solution reverts to the oxidized dye by the second-order thermal reaction and, quite astonishingly, mostly by the reaction $2DH \rightarrow 2D+H_2$. The photochemical behavior of leuco-fluorescein has been invesigated to some extent in the presence of and in the absence of a reducing agent.

*Department of Chemistry*
*Faculty of Science*
*Tohoku University*
*Katahira-cho, Sendai*

# A Study of Concentrated Solutions of Mixed Electrolytes. Ultrasonic Velocities and Viscosities of Mixtures of Aqueous Solutions of Potassium and Sodium Chlorides at High Concentrations

By J. KUPPUSAMI, A. S. LAKSHMANAN, R. LAKSHMINARAYANAN, N. RAJARAM and C. V. SURYANARAYANA

(Received January 11, 1965)

Stearn,[1] Ruby and Kawai,[2] and Smith and Gortner[3] determined the conductivity of concentrated aqueous mixtures of alkali halides. The conductivity of mixed salt solutions is not strictly additive. In these mixtures, the ion of a higher mobility is slowed down while that of a lower mobility is speeded up. Onsager and Fuoss[4] and Van Rysselberghe and Nutting[5] gave quantitative theories for the mobility changes occuring in mixed electrolyte solutions. However, the rather anomalous behaviour of mixtures of electrolyte solutions has not been properly explained; often such behaviour may be attributed to the ion pairing on complex formation and ionic hydration. O'Connor[6] examined mixtures of calcium and strontium dithionates in different proportions and found the same equivalent conductivity throughout the concentration range examined. It has been felt by previous workers that the effect of the hydration of the ions on the electrical conductivity is a factor of major importance. Against this background, we have undertaken a very systematic study of mixtures of potassium and sodium chlorides from the points of view of ionic hydration and viscosity.

## Experimental Procedure

**The Preparation of Solutions.**—All solutions were made by weighing the constituents. At a chosen constant molality of one salt, mixtures were made in such a way that the molality of the other salt was increased in steps. This was repeated systematically by choosing different increasing molalities of the first salt. For instance, 0.1, 0.5, 1.0, 1.5, 2.0, 2.5, 3.0, 3.5, 4.0 and 4.5 m of sodium chloride could be obtained at each of the potassium chloride molalities of 0.1, 0.5, 1.0, 1.5, 2.0 and 2.5, subject to both the constituents being soluble. The potassium and sodium chlorides used were of the B. D. H. Analar variety. Solutions were prepared in distilled water.

**Ultrasonic Velocities.**—The measurements of ultrasonic velocities were made by the Debye and Sears[7] diffraction method. The frequency of the piezo-electric quartz oscillator used in our experiments was 5 Mc./s. The third-order diffraction fringes were taken in all the cases for measurement. Hilger's X-ray microphotometer L 486 was used with a Multiflex galvanometer with a sensitivity of $8\times10^{-9}$ amp./mm. to measure the distance between the fringes.

The hydration numbers were calculated by Passynsky's method:[8]

$$\text{Hydration number}=\frac{n_1}{n_2}\left\{1-\frac{\beta}{\beta_0}\right\} \qquad (1)$$

where $n_1$ and $n_2$ are the numbers of the moles of the solvent and of the solute respectively, and $\beta$ and $\beta_0$ are the adiabatic compressibilities of the solution and solvent respectively. The adiabatic compressibility is given by:

$$\beta_s=\frac{1}{u^2\rho} \qquad (2)$$

where $u$ is the ultrasonic velocity and $\rho$, the density of the medium.

For measuring the ultrasonic velocity of the solutions at 34.9±0.05°C, a special water-jacketted stainless-steel cubical cell with a chromium-plated inside was fabricated with two optical-plane glass windows cemented on opposite faces to give a perfect transmission of the sodium light. The cell was thermostated at 34.9±0.05°C.

**The Measurement of Viscosities.**—A Cannon-Fenske type viscometer was used, immersed in a glass-walled thermostat at 34.9±0.05°C. The viscosity values reported herein are subject to an error of ±0.5%. The flow time of the solutions ranged from 62.0 sec. to 93.0 sec. measured to an accuracy of ±0.2 sec.

**Density.**—A 10 ml. picnometer was used. Care was taken that the picnometer and its contents attained the thermostat temperature before they were weighed. A Sartorius semi-micro single-pan balance accurate to the fifth place was used for weighing.

1) A. E. Stearn, *J. Am. Chem. Soc.*, **44**, 670 (1922).
2) C. E. Ruby and J. Kawai, ibid., **48**, 1119 (1926).
3) A. K. Smith and R. A. Gortner, *J. Phys. Chem.*, **37**, 79 (1933).
4) L. Onsager and R. M. Fuoss, ibid., **36**, 2689 (1932).
5) P. Van Rysselberghe and L. Nutting, *J. Am. Chem. Soc.*, **56**, 1435 (1934).
6) E. A. O'Connor, *Nature*, **139**, 151 (1937).
7) P. Debye and F. W. Sears, *Proc. Nat. Acad. Sci.*, **18**, 409 (1932).
8) A. Passinski, *Acta Physicochimica*, **8**, 385 (1938).

## Results and Discussion

Figures 1A and 1B show that the viscosity varies exponentially with the ionic strength of the electrolyte mixture:

$$\eta = A\exp[B\mu] \quad (3)$$

where A and B are constants, and $\mu$ and $\eta$ are the ionic strength and viscosity of the solution respectively. In Fig. 1A, a few points at a higher ionic strength in a solution of lower potassium chloride concentrations are off the straight line. In Fig. 1B, the exponential relationship is valid in most cases, except at low ionic strengths containing lower sodium chloride concentrations. Up to a 1.0 m sodium chloride concentration, the viscosity falls or remains almost constant initially, and

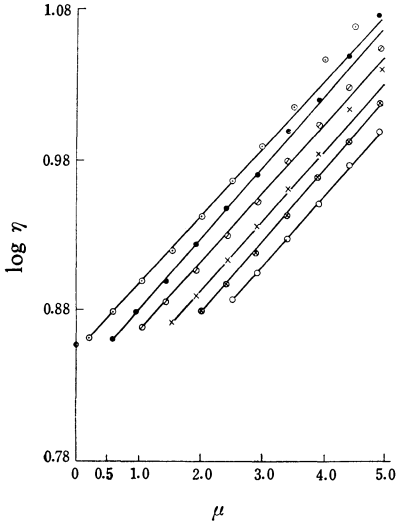



Fig. 1A

⊙——⊙ 0.1 m kcl Base
●——● 0.5 m kcl Base
⊖——⊖ 1.0 m kcl Base
×——× 1.5 m kcl Base
⊗——⊗ 2.0 m kcl Base
○——○ 2.5 m kcl Base

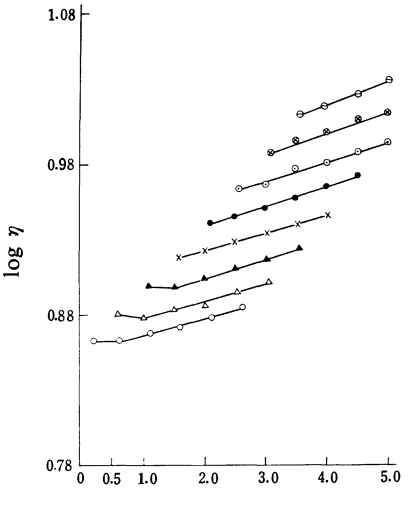



Fig. 1B

○——○ 0.1 m NaCl
△——△ 0.5 m NaCl
▲——▲ 1.0 m NaCl
×——× 1.5 m NaCl
●——● 2.0 m NaCl
⊙——⊙ 2.5 m NaCl
⊗——⊗ 3.0 m NaCl
⊖——⊖ 3.5 m NaCl

then there is a linear rise. The initial effect may be ascribed to the well-known negative viscosity effects due to potassium chloride.

Table IIA gives the intercepts and slopes of the linear plots of Figs. 1A and 1B. In all the cases, the intercepts, ideally speaking should have corresponded to $\log_{10}\eta_{H_2O}$, which is 0.858. In Fig. 1A all intercept values are less than 0.858, whereas the reverse is the case with the intercepts in Fig. 1B, excepting that which corresponds to 0.1 m sodium chloride. One interesting observation is that, for purposes of viscosity, the solution of a constant molality chosen as the base of reference, in which varying concentrations of the other salts are investigated, acts as the

TABLE I. DENSITY OF THE MIXED ELECTROLYTE SOLUTIONS ($\rho$ in g./ml.)

| Molal concn. of NaCl | Molal concn. of KCl | | | | | |
|---|---|---|---|---|---|---|
| | 0.1 | 0.5 | 1.0 | 1.5 | 2.0 | 2.5 |
| 0.1 | 1.00253 | 1.02144 | 1.04194 | 1.06310 | 1.08098 | 1.10225 |
| 0.5 | 1.01807 | 1.03636 | 1.05631 | 1.07760 | 1.09489 | 1.11368 |
| 1.0 | 1.03683 | 1.05437 | 1.07343 | 1.09806 | 1.11016 | 1.12972 |
| 1.5 | 1.05421 | 1.07248 | 1.09004 | 1.10960 | 1.12588 | 1.14371 |
| 2.0 | 1.07230 | 1.09071 | 1.10607 | 1.12523 | 1.14085 | 1.15895 |
| 2.5 | 1.08870 | 1.10449 | 1.12246 | 1.13824 | 1.15435 | 1.16478 |
| 3.0 | 1.10482 | 1.12344 | 1.13649 | 1.15440 | 1.16845 | — |
| 3.5 | 1.12058 | 1.13575 | 1.15105 | 1.16946 | — | — |
| 4.0 | 1.14251 | 1.15162 | 1.16521 | — | — | — |
| 4.5 | 1.15056 | 1.16811 | 1.17921 | — | — | — |

TABLE IIA. VALUES OF INTERCEPTS AND SLOPES OF PLOTS IN GRAPHS IA AND IB

Graph IA

| Molality of KCl kept constant | Intercept | Slope | 0.858−Col. (2) |
|---|---|---|---|
| 0.1 | 0.8493 | 0.0445 | +0.0087 |
| 0.5 | 0.8250 | 0.0483 | +0.033 |
| 1.0 | 0.8099 | 0.0476 | 0.0481 |
| 1.5 | 0.7909 | 0.0454 | 0.0671 |
| 2.0 | 0.7758 | 0.0472 | 0.0822 |
| 2.5 | 0.7686 | 0.0456 | 0.0894 |

Graph IB

| Molality of NaCl kept constant | Intercept | Slope | 0.858−Col. (2) |
|---|---|---|---|
| 0.1 | 0.8546 | 0.0119 | +0.0034 |
| 0.5 | 0.8646 | 0.0126 | −0.0066 |
| 1.0 | 0.8815 | 0.0132 | −0.0235 |
| 1.5 | 0.8994 | 0.0118 | −0.0414 |
| 2.0 | 0.9115 | 0.0134 | −0.0535 |
| 2.5 | 0.9299 | 0.0129 | −0.0719 |
| 3.0 | 0.9543 | 0.0125 | −0.0963 |

solvent. For example, mixtures of varying concentrations of sodium chloride in a solution of 2.5 m potassium chloride of a constant molality, give, on extrapolation, an intercept of 0.881 at an ionic strength of 2.5; the $\log_{10}$ of the viscosity of a 2.5 m potassium chloride solution alone is 0.879. In the case of almost all the plots of Figs. 1A and 1B the above observation is fully verified when compared with the respective viscosities of individual solutions of sodium and potassium chloride reported earlier.[9]

The intercept corresponding to zero ionic strength is always lower than for pure water in the case of the plots in Fig. 1A. In general, this may be ascribed to the lowering of the viscosity by potassium chloride. From Table IIA the ratio of the corresponding slopes of the plots in Figs. IA and IB may be seen to be a constant around 3.68.

Table III gives the ultrasonic velocities measured by us in different mixtures. Table IV gives the compressibility values calculated using Eq. 2.

Table V gives hydration numbers calculated from Eq. 1.

Figures 2A and 2B give plots of the hydration numbers vs. the total concentrations the mixtures. The plots in Fig. 2A are from the point of view of potassium chloride solutions to which varying amounts of sodium chloride have been added, whereas Fig. 2B gives the plots from the point of view of sodium chloride as the base of reference. For one thing, these

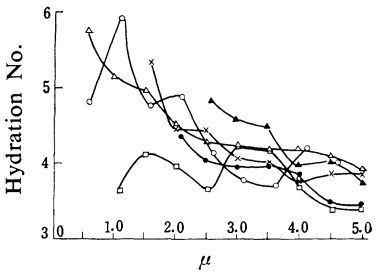



Fig. 2A

○—○ 0.1 m KCl △—△ 0.5 m KCl
□—□ 1.0 m KCl ×—× 1.5 m KCl
●—● 2.0 m KCl ▲—▲ 2.5 m KCl

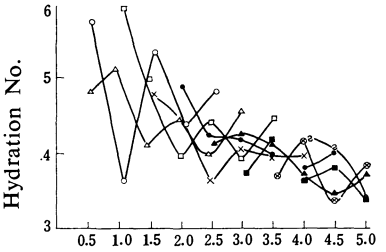



Fig. 2B

○—○ 0.1 m NaCl △—△ 0.5 m NaCl
□—□ 1.0 m NaCl ×—× 1.5 m NaCl
●—● 2.0 m NaCl ▲—▲ 2.5 m NaCl
■—■ 3.0 m NaCl ⊗—⊗ 3.5 m NaCl
ȣ—ȣ 4.0 m NaCl

hydration number plots do not satisfactorily explain the conductance data obtained by previous workers. No single plot in any graph gives a uniform variation. Peaks and troughs occur too often, and both the sets of graphs are rather difficult to explain. A very broad trend seems, however, to be that, with an increasing total molality, the hydration declines.

With an increasing salt mixture concentration, either the water molecules required for the hydration of ions are not enough to go around all the ions, or ion pairing occurs preferentially. The viscosity behaviour and the hydration data of these mixed electrolyte solutions do not throw any light on the conductivity behaviour they exhibit and they at last leave us in the same position we were in previously.

A quantity called "Relative Association" was defined by some previous workers[10,11] as:

$$\text{R. A.} = \frac{\rho_c}{\rho_0} \cdot \left(\frac{u_0}{u_c}\right)^{1/3} \qquad (4)$$

where $\rho_0$ and $\rho_c$ are the densities of water at 0°C and of a solution at room temperature,

9) C. V. Suryanarayana and V. K. Venkatesan, This Bulletin, 31, 442 (1958).

10) G. W. Marks, *J. Acoust. Soc. Am.*, 31, 936 (1959).

11) S. V. Subrahmanyam and I. Bhimasenachar, ibid., 32, 835 (1960).

TABLE II. VISCOSITIES OF THE MIXED ELECTROLYTE SOLUTIONS IN MILLIPOISES

| Molal concn. of NaCl | Molal concn. of KCl | | | | | |
|---|---|---|---|---|---|---|
| | 0.1 | 0.5 | 1.0 | 1.5 | 2.0 | 2.5 |
| 0.1 | 7.292 | 7.291 | 7.390 | 7.444 | 7.558 | 7.694 |
| 0.5 | 7.589 | 7.562 | 7.683 | 7.729 | 7.865 | 7.999 |
| 1.0 | 7.940 | 7.931 | 8.075 | 8.198 | 8.250 | 8.421 |
| 1.5 | 8.311 | 8.394 | 8.495 | 8.597 | 8.736 | 8.861 |
| 2.0 | 8.744 | 8.845 | 8.945 | 9.074 | 9.239 | 9.398 |
| 2.5 | 9.222 | 9.269 | 9.496 | 9.578 | 9.739 | 9.867 |
| 3.0 | 9.708 | 9.910 | 10.012 | 10.222 | 10.307 | — |
| 3.5 | 10.302 | 10.416 | 10.582 | 10.857 | — | — |
| 4.0 | 11.020 | 11.095 | 11.213 | — | — | — |
| 4.5 | 11.540 | 11.795 | 11.933 | — | — | — |

TABLE III. ULTRASONIC VELOCITIES IN (KCl+NaCl) MIXTURES IN METRES PER SECOND

| Molal concn. of NaCl | Molal concn. of KCl | | | | | |
|---|---|---|---|---|---|---|
| | 0.1 | 0.5 | 1.0 | 1.5 | 2.0 | 2.5 |
| 0.1 | 1514 | 1546 | 1540 | 1595 | 1593 | 1637 |
| 0.5 | 1541 | 1560 | 1562 | 1592 | 1599 | 1653 |
| 1.0 | 1582 | 1584 | 1578 | 1612 | 1619 | 1679 |
| 1.5 | 1587 | 1596 | 1585 | 1625 | 1646 | 1674 |
| 2.0 | 1618 | 1611 | 1635 | 1649 | 1664 | 1710 |
| 2.5 | 1615 | 1639 | 1660 | 1661 | 1662 | 1717 |
| 3.0 | 1620 | 1662 | 1656 | 1696 | 1682 | — |
| 3.5 | 1641 | 1696 | 1656 | 1731 | — | — |
| 4.0 | 1703 | 1722 | 1685 | — | — | — |
| 4.5 | 1732 | 1735 | — | — | — | — |

TABLE IV. COMPRESSIBILITIES OF (KCl+NaCl) MIXTURES ($\beta \times 10^6$ atm$^{-1}$)

| Molal concn. of NaCl | Molal concn. of KCl | | | | | |
|---|---|---|---|---|---|---|
| | 0.1 | 0.5 | 1.0 | 1.5 | 2.0 | 2.5 |
| 0.1 | 43.51 | 40.91 | 40.47 | 36.95 | 36.45 | 33.82 |
| 0.5 | 41.36 | 39.61 | 38.80 | 36.61 | 35.71 | 32.84 |
| 1.0 | 38.52 | 37.77 | 37.38 | 35.01 | 34.35 | 31.38 |
| 1.5 | 37.66 | 36.56 | 36.48 | 34.10 | 32.77 | 31.2 |
| 2.0 | 35.62 | 35.31 | 33.78 | 32.68 | 31.63 | 29.48 |
| 2.5 | 35.19 | 33.67 | 32.30 | 31.83 | 31.36 | 29.09 |
| 3.0 | 34.46 | 32.22 | 32.05 | 30.11 | 30.23 | — |
| 3.5 | 33.14 | 30.60 | 31.65 | 28.52 | — | — |
| 4.0 | 30.18 | 29.25 | 30.22 | — | — | — |
| 4.5 | 28.94 | 28.41 | — | — | — | — |

TABLE V. HYDRATION NUMBERS IN (KCl+NaCl) MIXTURES

| Molal concn. of NaCl | Molal concn. of KCl | | | | | |
|---|---|---|---|---|---|---|
| | 0.1 | 0.5 | 1.0 | 1.5 | 2.0 | 2.5 |
| 0.1 | 0.83 | 5.74 | 3.64 | 5.31 | 4.36 | 4.81 |
| 0.5 | 4.81 | 5.11 | 4.11 | 4.47 | 4.02 | 4.57 |
| 1.0 | 5.91 | 4.96 | 3.97 | 4.40 | 3.94 | 4.46 |
| 1.5 | 4.76 | 4.50 | 3.64 | 4.04 | 3.95 | 3.96 |
| 2.0 | 4.87 | 4.24 | 4.19 | 3.98 | 3.82 | 4.00 |
| 2.5 | 4.12 | 4.22 | 4.13 | 3.75 | 3.47 | 3.71 |
| 3.0 | 3.76 | 4.14 | 3.68 | 3.83 | 3.41 | — |
| 3.5 | 3.70 | 4.15 | 3.39 | 3.84 | — | — |
| 4.0 | 4.17 | 4.07 | 3.41 | — | — | — |
| 4.5 | 4.07 | 3.88 | — | — | — | — |

TABLE VI. RELATIVE ASSOCIATION

| Molal concn. of NaCl | Molal concn. of KCl | | | | | |
|---|---|---|---|---|---|---|
| | 0.1 | 0.5 | 1.0 | 1.5 | 2.0 | 2.5 |
| 0.1 | 0.9825 | 0.9929 | 1.0149 | 1.0236 | 1.0416 | 1.0523 |
| 0.5 | 0.9911 | 1.0044 | 1.0245 | 1.0387 | 1.0533 | 1.0593 |
| 1.0 | 1.0017 | 1.0171 | 1.0359 | 1.0533 | 1.0633 | 1.0704 |
| 1.5 | 1.0171 | 1.033 | 1.0514 | 1.0623 | 1.0724 | 1.0838 |
| 2.0 | 1.0273 | 1.0474 | 1.0563 | 1.0714 | 1.0827 | 1.0901 |
| 2.5 | 1.0445 | 1.0543 | 1.0663 | 1.0817 | 1.0964 | 1.0943 |
| 3.0 | 1.0583 | 1.0673 | 1.0806 | 1.088 | 1.104 | — |
| 3.5 | 1.0693 | 1.0714 | 1.0943 | 1.0964 | — | — |
| 4.0 | 1.0765 | 1.0806 | 1.1007 | — | — | — |
| 4.5 | 1.0786 | 1.0932 | — | — | — | — |

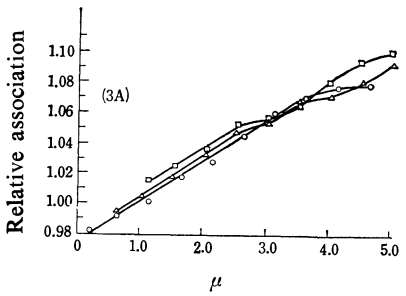



Fig. 3A

○——○ 0.1 m KCl base
△——△ 0.5 m KCl base
□——□ 1.0 m KCl base

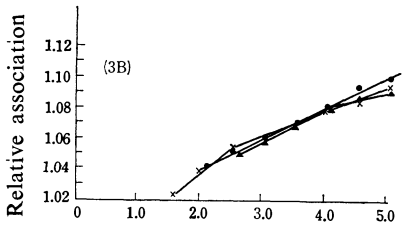



Fig. 3B

×——× 1.5 m KCl base
●——● 2.0 m KCl base
▲——▲ 2.5 m KCl base

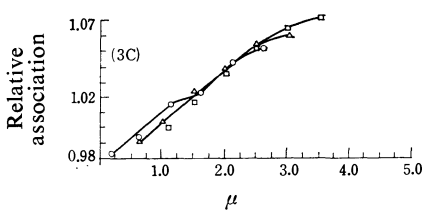



Fig. 3C

○——○ 0.1 m NaCl
△——△ 0.5 m NaCl
□——□ 1.0 m NaCl

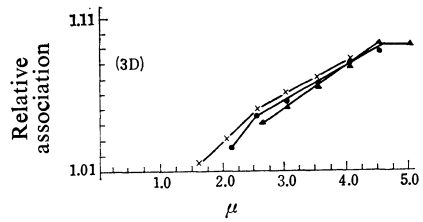



Fig. 3D

×——× 1.5 m NaCl
●——● 2.0 m NaCl
▲——▲ 2.5 m NaCl

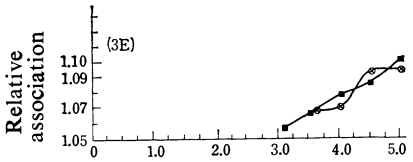



Fig. 3E

■——■ 3.0 m NaCl
⊗——⊗ 3.5 m NaCl

and $u_0$ and $u_c$ are the velocities of ultrasonic waves in water at 0°C and in a solution at room temperature. Figures 3A, 3B, 3C, 3D and 3E show the plots of the "Relative Association" vs. the total molality. The general trend is for relative association to increase steadily, almost linearly, in most of the cases examined. All the plots have approximately the same slope. One must, therefore, doubt whether "Relative Association" is a measure of the hydration at all.

## Summary

The electrical conductance of mixtures of aqueous solutions of potassium and sodium chlorides has been studied by previous workers. However, no valid explanation has been given for the conductance behaviour of the mixtures.

We have reported herein the results of our ultrasonic and viscometric studies of the same mixtures. Even now the hydration numbers and the viscosity variation are inadequate to explain the conductance behaviour of the mixtures. We have observed that all the mixtures follow the exponential relation, $\eta = A_e^{B\mu}$, where $A$ and $B$ are constants; $\eta$ the viscosity of the mixture, and $\mu$, the ionic strength.

Our thanks are due to Professor K. S. G. Doss, Director of the Central Electrochemical Research Institute, for his kind encouragement.

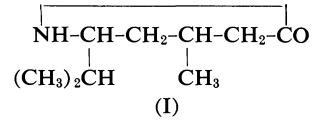
*Central Electrochemical Research Institute*
*Karaikudi*-3, *India*

# Optically Active Polymers. III.* Polymers of 1, 3-Dimethylbutyl Methacrylate

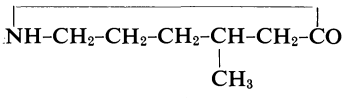
By Minoru IMOTO and Yoshiyuki KUMATA

(Received January 16, 1965)

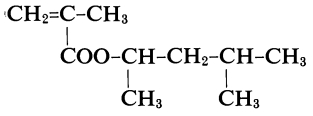
In an earlier study, Imoto and Sakurai[1] synthesized a polymer of (−)-*l*-4-methyl-7-isopropyl-2-oxohexamethyleneimine (I) and found that its optical rotation increased with the molecular weight. Recently Overberger and Jabloner[2] obtained a polymer of D-(−)-β-methyl-ε-caprolactam (II), measured its rotatory dispersion, and concluded that the polymer showed no definite proof for the assignment of a helical structure. However, if we can assume that the longer the molecule, the greater is the portion of molecular-structural (helical) asymmetry, an increase in molecular rotation with molecular weight is understandable.



(I)

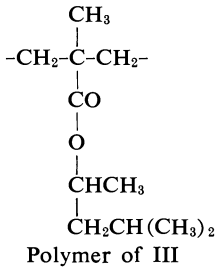


(II)

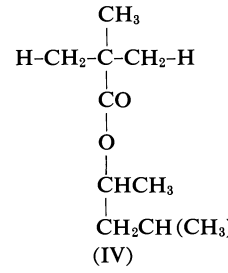


(III)

Arcus and West[3] synthesized (+)-1, 3-dimethylbutyl methacrylate (III) and carried out its polymerization in the presence of benzoyl peroxide or azobisisobutyronitrile. The molecular rotation [M] of the polymer and (+)-1, 3-dimethylbutyl pivalate (IV) was determined for five wavelengths at 25°C in tetrachloroethane. Compound IV could be recognized as the unit of the polymer of compound III.



Polymer of III



(IV)

Moreover, the difference between the values of [M] of IV and the polymer of III was considered to be that part of the [M] which was due to structural features other than the individual ester units. For example, at 4358 Å, the values of [M] were determined as follows: IV, +82°; Polymer of III, +60°, and the difference, −22°. It was concluded that the contribution of the difference was due to disymmetric coiling of the main chain.

This paper will deal with the preparation of three kinds of polymers of (+)-1, 3-dimethylbutyl methacrylate (III), polymers which were assumed to be isotactic, syndiotactic and atactic, as well as with the determination of the optical rotatory dispersion of the polymers. Moreover, the polymerization of optically impure (−)-1, 3-dimethylbutyl methacrylate and the optical rotatory dispersion of the polymers will be investigated.

* Part II: M. Imoto and S. Kimura, *Makromol. Chem.*, 53, 210 (1962).

1) M. Imoto, H. Sakurai and T. Kono, *J. Polymer Sci.*, 50, 467 (1961).

2) C. G. Overberger and J. Jabloner, *J. Am. Chem. Soc.*, 85, 3431 (1963).

3) C. L. Arcus and D. West, *J. Chem. Soc.*, 1959, 2699.

It is known that methyl methacrylate can be polymerized with *n*-BuLi at −78°C to give an isotactic polymer, while with azobisisobutyronitril (AIBN) at a higher temperature it gives an atactic polymer, and at about −40°C, a syndiotactic polymer. Granting that these specific polymerizations of methyl methacrylate could also be applied to 1,3-dimethylbutyl methacrylate, isotactic, syndiotactic and atactic polymers of optically active 1,3-dimethylbutyl methacrylate may be obtained.[4] It seemed an interesting problem to investigate the relationship between the change in the optical rotatory power of a polymer, with its molecular weight, and the stereospecific configuration of the polymer molecule. However, no definite result could be obtained.

## Experimental

**Syntheses of Optically Active Monomers.** — 1) The resolution of *dl*-1,3-dimethylbutanol was carried out through the salt of 1,3-dimethylbutyl hydrogen phthalate with brucine, according to the method of Kenyon et al.[5] In recrystallization from acetone, the salt of *d*-ester crystallized out first. accordingly, optically pure *d*-1,3-dimethylbutanol could be obtained. However, the *l*-isomer was recovered in a less optically pure state. The specific rotations observed were as follows:

*d*-1,3-dimethyl butanol $[\alpha]_D^{14}$ +20.41°

*l*-1,3-dimethyl butanol $[\alpha]_D^{17}$ −7.53°

2) 1,3-Dimethylbutyl methacrylate was prepared by the reaction of the alcohol with methacrylic chloride, according to the method of Arcus et al.[3] *d*-, *l*- and *dl*-1,3-Dimethylbutyl methacrylate (DBMA) were purified by repeated distillation in the stream of nitrogen and in the presence of picric acid (an inhibitor for polymerization). Their boiling points were 75—78°C/20 mmHg and 65°C/15 mmHg.

| | | |
|---|---|---|
| *d*-DBMA | $[\alpha]_D^{20}$ +58.1° | $n_D^{24}$ 1.4232[a] |
| *l*-DBMA | $[\alpha]_D^{20}$ −21.8° | $n_D^{24}$ 1.4229 |
| *dl*-DBMA | $d_4^{25}$ 0.8698[b] | $n_D^{24}$ 1.4237 |

a) $n_D^{24}$ 1.4224 (Arcus, West[3]).
b) $d_4^{20}$ 0.8714 (Crawford[6]).

**Hydrogenation of the *d*-Monomer to *d*-1,3-Dimethylbutyl Pivalate.** — Three milliliters of the *d*-monomer in *n*-hexane was hydrogenated in the presence of 0.3 g. of the palladium charcoal catalyst with shaking. After the absorption of hydrogen had stopped, the content was filtered and fractionated. The yield was 1.8 g. B. p. 75°C/21.5 mmHg; $n_D^{23}$ 1.4053; $[\alpha]_D^{23}$ ±1 (lit.[3]: b. p. 78°C/22 mmHg, $n_D^{23}$ 1.4070). The structure was identified from its infrared spectrum.

**Polymerization.**—*Isotactic Polymerization.*—To a solution of 5 ml. of DBMA in 10 ml. of purified toluene, 0.2 ml. of a 4 N *n*-butyl lithium solution in heptane was added at −78°C. After it had stood for 2 hr., the mixtue was poured into mixture of a large amount of methanonl and a small quantity of hydrogen chloride. What was assumed to be isotactic polymer was precipitated out.

*Atactic Polymerization.*—To 0.005 g. of azobisisobutyronitrile in a hard glass tube, 5 ml. of DBMA was added. The tube was then deaerated, sealed and heated at 60°C for 5.5 hr. while being shaken. The contents were dissolved in benzene and then poured into methanol to isolate the atactic poly-DBMA.

*Syndiotactic Polymerization.*—A solution of 0.02 g. of azobisisobutyronitrile in 5 ml. of DBMA was placed in a tube. The tube was deaerated, sealed, cooled at −35°C—−50°C, and irradiated for 30—36 hr. The light was obtained from a high-voltage mercury lamp of the Mazda SHL-100 type and filtered through $UVD_1$-filter. The contents were dissolved in a mixture of benzene and a small quantity of hydroquinone, and then poured into methanol. What was assumed to be syndiotactic poly-DBMA was isolated. These poly-DBMA's were then purified by the reprecipitation method using benzene and methanol.

**Fraction of the Polymer of DBMA.**—One gram of the polymer was dissolved in 50 ml. of benzene. When, to this solution, methanol was added portion-by-portion, 4—7 fractions were obtained.

**Measurement of the Softening Temperature (Ts).** — The Ts was measured by the deck-glass method, using an electroheating melting point apparatus and raising the temperature by one degree per minute.

**Optical Rotation and Dispersion.**—The apparatuses used were a Lippich-type polarimeter, a dispersion polarimeter (the Rudolf 260/655/850/810 type) and a spectrophotometer equipped with a polarimetric attachment (the Shimadzu QR-50 type). The two types of dispersion polarimeters gave the same results.

## Results and Discussion

**Polymerization of DBMA.**—The results obtained are shown in Table I. All the polymers were colorless and soluble in petroleum ether, acetone, benzene, toluene, dioxane, chloroform and dichloroethane, while they were insoluble in methanol and swelled in ethanol. The tacticities of the polymers could be observed from their softening temperatures (Ts) and from their infrared spectra. Ts's of the isotactic, atactic and syndiotactic polymers fell in the ranges of the Ts's of the isotactic, atactic and syndiotactic polymethyl methacrylates which have previously been described by Fox, Stroupe et al.[7]

4) T. Tsuruta and H. Kanai (XII Annual Meeting of the Polymer Society of Japan, Preliminary Issue, [A17], p. 26 (1963)) stated that ethyl-, isopropyl- and *t*-butylesters of methacrylic acid could be polymerized to polymers having the same tacticity as methyl methacrylate, by the methods applied to methyl methacrylate.
5) J. Kenyon and H. E. Strauss, *J. Chem. Soc.*, **1949**, 2153.
6) J. W. C. Crawford, *J. Soc. Chem. Ind.*, **68**, 201 (1949).
7) T. G. Fox, B. S. Garrett, W. E. Goode, S. Gratch, J. F. Kincaid, A. Spell and J. D. Stroupe, *J. Am. Chem. Soc.*, **80**, 1769 (1958); J. D. Stroupe and R. E. Hughes, ibid., 2341.

Table I. Results of polymerization of DBMA and some properties of the polymer

| No.*1 | Monmer ml. | Initiator mol./l. | Temp. °C | Time hr. | Yield % | $[\eta]$*2 dl./g. | Ts °C | $[\alpha]_D$, in dioxane |
|---|---|---|---|---|---|---|---|---|
| RI | *dl*-, 5 | *n*-Bu-Li, 0.08 | −78 | 2.5 | 86.2 | (0.79) | — | — |
| DI | *d*-, 5 | 0.08 | −78 | 2 | 81.7 | 0.31 | 83—87 | +9° |
| LI | *l*-, 4 | 0.09 | −78 | 2.5 | 73.9 | 0.43 | 86—95 | −15° |
| RA | *dl*-, 5 | AIBN, 0.0055 | 60 | 4.5 | 66.0 | (2.32) | — | — |
| DA | *d*-, 5 | 0.0080 | 60 | 4 | 87.5 | 2.81 | 98—104 | +17° |
| LA | *l*-, 4 | 0.0061 | 60 | 5.5 | 95.5 | 2.06*3 | 90—119*3 | −18°*3 |
| RS | *dl*-, 5 | AIBN, 0.0291 | −35——40 | 30 | 73.7 | (1.03) | — | — |
| DS | *d*-, 5 | 0.0294 | −40——50 | 33 | 56.6 | 1.93 | 118—126 | +14.5° |
| LS | *l*-, 4 | 0.0282 | −35——40 | 36 | 71.5 | 2.08 | 128—135 | −17° |

*1 R, D and L mean racemic, dextro and laevo, respectively. I, A and S mean isotactic, atactic and syndiotactic polymer.
*2 At 30°C in $CHCl_3$. $[\eta]$ in parentheses were measured at 30°C in toluene.
*3 Soluble part in dioxane.

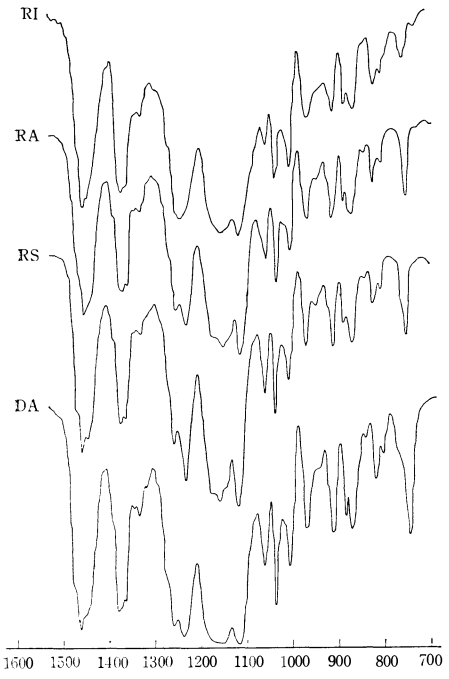



Fig. 1. IR-spectra of poly-DBMA.
RI: racemic-isotactic RA: racemic-atactic
RS: racemic-syndiotactic DA: dextro-atactic

The infrared spectra of the polymers are shown in Fig. 1. From the figure, the relative intensities of the absorption bands for the three kinds of poly-DBMA's (RS, RA and RI) were tabulated as in Table II.

The orders of the intensities in this table coincide with those for polymethylmethacrylates which were described Baumann et al.[8] From

8) U. Baumann, H. Schreiber and K. Tessmar, *Makromol. Chem.*, **36**, 81 (1959).

Table II. The relative intensities of the infrared absorption bands of poly-DBMA

| $cm^{-1}$ | 752 | 806 | 825 | 915 | 1060 | 1238 |
|---|---|---|---|---|---|---|
| $\mu$ | 13.38 | 12.40 | 12.12 | 11.00 | 9.45 | 8.08 |
| RS | 4+ | + | 2+ | 4+ | 4+ | 3+ |
| RA | 4+ | + | 2+ | 4+ | 3+ | 2+ |
| RI | 2+ | + | + | 2+ | 1+ | 0 |

the order of the Ts's and from the comparison of the intensities of the absorptions with the data obtained by Baumann et al., it was concluded that the polymers obtained in the present work consisted principally of isotactic, atactic and syndiotactic poly-DBMA's) respectively. Furthermore, Fig. 1 shows that the spectra of DA (atactic (+)-polymer) and RA (atactic (±) polymer) were almost exactly the same. This means that the presence of asymmetric carbon in the side chain had no effect on the stereospecific polymerization.

**Optical Rotation of Poly-DBMA.**—The values of specific rotation ($[\alpha]_D$ (20°C, in chloroform)) given in Table III were measured at the concentrations of 1.0—1.5 g./dl. In other measurement, it was confirmed that $[\alpha]_D$ was constant over such a range of concentrations.

From the data in Table III, the relationships between specific rotations and molecular weights may be illustrated as in Fig. 2. It seems that, in the cases of DI(isotactic (+)-polymer) and DA, the specific rotation increases with the molecular weight, while in the cases of DS (syndiotactic (+)-polymer), LS (syndiotactic (−)-polymer) and LA (atactic (−)-polymer), the specific rotation remains constant during the change in molecular weight. It may be assumed that the difference between isotactic (DI) and syndiotactic polymers (DS) suggests a difference in the molecular conformation.

TABLE III. RESULTS OF FRACTIONATIONS OF POLYMERS AND SPECIFIC ROTATIONS OF EACH FRACTIONATES

| No. of fraction | DI | | | DA | | | DS | | |
|---|---|---|---|---|---|---|---|---|---|
| | Yield % | $[\eta]$ | $[\alpha]_D$ | Yield % | $[\eta]$ | $[\alpha]_D$ | Yield % | $[\eta]$ | $[\alpha]_D$ |
| 1 | 13 | 0.59 | +23.5 | 12 | 4.50 | +27.3 | 5 | 3.76 | +19.6 |
| 2 | 33 | 0.37 | +14.3 | 16 | 3.11 | +15.1 | 25 | 2.87 | +16.8 |
| 3 | 13 | 0.33 | +14.0 | 26 | 2.26 | +15.8 | 28 | 0.78 | +17.2 |
| 4 | 35 | 0.15 | +13.4 | 20 | 1.63 | +12.6 | 23 | 0.75 | +16.3 |
| 5 | 3 | — | — | 9 | 1.53 | +10.9 | | | |
| 6 | | | | 7 | 1.51 | +19.2 | | | |
| 7 | | | | 5 | — | — | | | |
| Total | 97 | | | 95 | | | 81 | | |

| No. of fraction | LI | | | LA | | | LS | | |
|---|---|---|---|---|---|---|---|---|---|
| | Yield % | $[\eta]$ | $[\alpha]_D$ | Yield % | $[\eta]$ | $[\alpha]_D$ | Yield % | $[\eta]$ | $[\alpha]_D$ |
| 1 | — | 0.62 | −17.8<br>−16.9 | 2 | — | — | 25 | 3.30 | −8.0 |
| 2 | — | 0.55 | −8.8 | 37 | 5.35 | −6.0<br>−4.4 | 25 | 2.21 | −9.0 |
| 3 | — | 0.51 | −8.3 | 20 | 3.46 | −5.9 | | | |
| 4 | — | 0.17 | −8.5 | 9 | 2.32 | −5.9 | 20 | 0.98 | −8.0 |
| 5 | | | | 25 | 2.03 | −7.8<br>−8.6 | 26 | 0.27 | −4.7 |
| 6 | | | | | | | | | |
| 7 | | | | 5 | 1.53 | −8.4 | | | |
| Total | — | | | 88 | | | 96 | | |

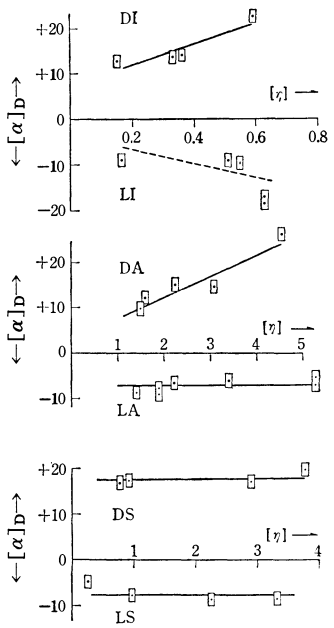



Fig. 2. Relation between specific rotation of poly-DBMA and their molecular weights.

DI: dextro-isotactic LI: laevo-isotactic
LA: laevo-isotactic DS: dextro-syndiotactic

**Optical Rotatory Dispersion of the Polymer.** —The optical rotatory dispersions of the polymers are illustrated in Fig. 3. The dispersion curves of the polymers from the *d*-monomer could not be compared with those of the polymers from the *l*-monomer because of the optical impurity of the *l*-monomer. If $[\alpha]$ comes only from asymmetric carbon, the relation between $[\alpha]$ and the wavelength, $\lambda$, may be given by the simple Drude equation (1):

$$[\alpha]=\frac{k\lambda_c^2}{\lambda^2-\lambda_c^2} \qquad (1)$$

where $\lambda_c$ is the dispersion constant and $k$ is the rotatory constant. The results are illustrated in Figs. 4 and 5. As the figures shows, the results of poly-DBMA did not fit the equation, while the *d*-monomer and its hydrogenated compound obeyed the equation.

Recently, Klabunovskii et al.[9] obtained poly-(+)-2-methylbutyl methacrylate and investigated its structure spectro-polarimetrically. Their polymerization was carried out with radical and ionic catalysts (benzoyl peroxide and phenyl magnesium bromide). The optical dispersion curves in the 302—589 m$\mu$ range

9) E. I. Klabunovskii, M. I. Shwarzman and Y. I. Petrov, *Vysokomolec. Soed.*, 6, 1579 (1964).

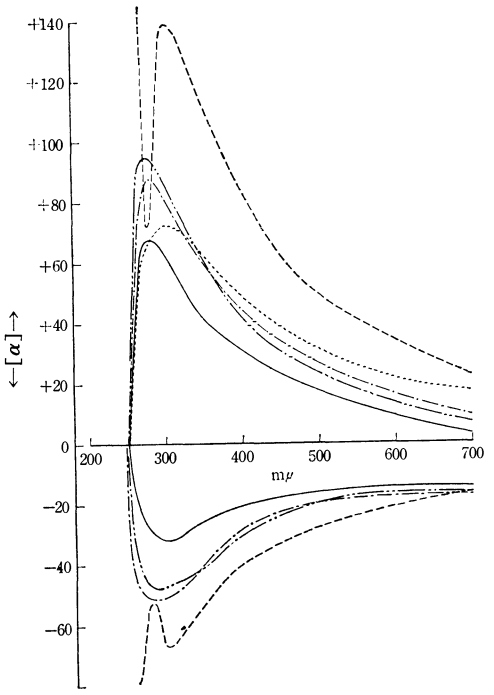



Fig. 3. Optical rotatory dispersion of DBMA, 1,3-dimethylbutyl pivalate and poly-DBMA.

------ Monomer (DBMA)
..... Pivalate
—·—· Isotactic polymer
—··— Atactic polymer
——— Syndiotactic polymer

were determined and could be described by Drude's single term equation. The value of $\lambda_c$ for the monomer was close to that of both polymers (173 m$\mu\pm$14).

As is known from the studies of polypeptides, if the optical activity comes from assymmetric carbon and the molecular helical structure, $[\alpha]$ may obey Moffitt's equation (2):

$$\frac{3}{n^2+2}\cdot\frac{M}{100}[\alpha]=\frac{a\lambda_0^2}{\lambda^2-\lambda_0^2}+\frac{b\lambda^4}{(\lambda^2-\lambda_0^2)^2} \quad (2)$$

where $n$ is the refractive index of the solvent; $M$ is the molecular weight of the structural unit of the polymer; $a$ is a term for the helix and the residue, and $b$ is a constant for the helical structure. As Fig. 6 shows, if a value of 212 was adopted for $\lambda_0$, a straight line was obtained in the case of the atactic *d*-polymer (DA). (In the case of polypeptides, a value of 212 is also suitable.) From the inclination of the straight line, it was deduced that $b$ was −64.3. This value of $b$ would correspond to about 10% of the right-hand helical structure if we were dealing with polypeptide. However, the polymer which we have dealt with is not a polypeptide. Therefore, no definite

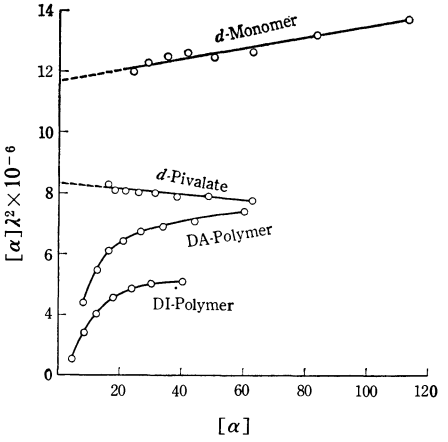



Fig. 4. Adaptability of the Drude equation for *d*-monomer and *d*-polymers.

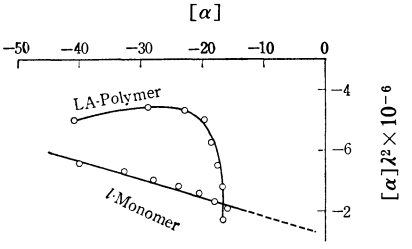



Fig. 5. Adaptability of the Drude equation for *l*-monomer and *l*-polymer.

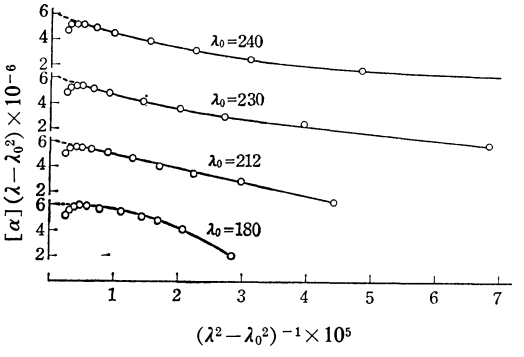



Fig. 6. Adaptability of the Moffit equation for DA.

conclusion as to its molecular asymmetry can be made. In the cases of isotactic and syndiotactic *d*-polymers (Dl and Sl), a straight line could not be obtained by using a value of 212 for $\lambda_0$. However, it could be concluded qualitatively that the $b$ constant for Dl was negative, and for those for LA, LI and LS, positive.

## Summary

The polymerization of (+)-1, 3-dimethylbutyl methacrylate and its optically impure

(−)-isomer have been carried out through different three initiations:

(1) *n*-BuLi in toluene at −78°C gave isotactic polymers (DI and LI). (2) Azobisisobutyronitrile at 60°C gave atactic polymers (DA and LA). (3) Photopolymerization in the presence of azobisisobutyronitrile at −35—−50°C gave syndiotactic polymers (DS and LS). The tacticities of the resulting polymers have been deduced from their softening temperatures and their infrared spectra. Optically active polymers have been fractionated from a benzene solution by adding methanol. In the cases of DI and DA, the specific rotation $[\alpha]_D$ increased with the molecular weight, while in the cases of DS, LS and LA, $[\alpha]_D$ remained constant during the change in molecular weight. The optical rotatory dispersion of the polymers has been measured. Drude's equation does not hold. In the case of DA, however, a straight line was obtained by Moffitt's equation, giving −64.3 as the *b*-values.

The authors wish to thank Professor Naokazu Sakota of Ehime University, Professor Takayuki Otsu of Osaka City University and Assistant Professor Hideki Sakurai of Kyoto Univesity for their helpful discussions. Besides, they wish to express their deep thanks to Professor Sakota for his permission to use dispersion polarimeter. The authors are also much indebted to the Shionogi Research Laboratory, Shionogi and Co., Ltd., for measuring the rotatory dispersion.

*Department of Applied Chemistry*
*Faculty of Engineering*
*Osaka City University*
*Sumiyoshi-ku, Osaka*

# Studies of Thermosetting Resin. I. The Infrared Analysis of Cured Epoxy Resins

By Tadao SUGITA and Mitsuko ITO

(Received January 18, 1965)

Recently many investigations of epoxy resins has been made. However, as analyses of thermosetting resins are generally difficult, a method of identifying the curing agents used has not yet been established for cured epoxy resins.

We have learned that the infrared analysis of pyrolyzates, which Harms[1] has successfully applied with various resins and elastomers and McGarvey[2] and Tanaka[3,4] with elastomers only, is very useful for thermosetting resins. Therefore, we have applied this method, along with a more standard procedure, in the analyses of cured epoxy resins. Some studies[5-10] of amine-cured resins performed by means of the infrared spectroscopic technique have been published, but only a single study[11] has been reported on acid anhydride cured resins.

In the present paper, only cured epoxy resins which contain no other materials (e.g., fillers and plasticizers) will be studied. Infrared spectra are recorded for the powders of cured epoxy resins and their pyrolyzates as a means to establish a method of identifying the curing agents.

Although Harms identified the types of resins, he did not identify the types of curing agents in the case of epoxy resins. From the infrared spectra of the powders of cured epoxy resins, we can determine only whether the cured resin is an acid anhydride or an amine-cured type. However, from the spectra of the pyrolyzates of cured epoxy resins, we can readily identify the types of acid anhydrides which were used in the curing process.

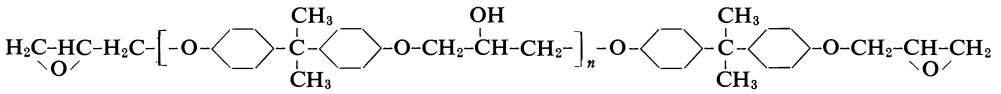
1) D. L. Harms, *Anal. Chem.*, **25**, 1140 (1953).
2) J. W. McGarvey, *Technical Report* Nr. **58—2159.**, Rock Island Arsenal Laboratory, Illinois (1958).
3) T. Tanaka, *J. Soc. Rubber Ind. Japan* (*Nippon Gomu Kyokaishi*), **29**, 998 (1956).
4) T. Tanaka, H. Kano and H. Higashi, ibid., **30**, 762 (1957).
5) H. Lee and K. Neville, "Epoxy Resins," McGraw-Hill, New York (1957).
6) H. Dannenberg and W. R. Harp, *Anal. Chem.*, **28**, 86 (1956).
7) L. A. O'Neill and C. P. Cole, *J. Appl. Chem.*, **6**, 356 (1956).
8) D. E. Peerman, W. Tolberg and D. E. Floyd, *Ind. Eng. Chem.*, **49**, 1091 (1957).
9) C. E. Feazel and E. A. Verchot, *J. Polymer Sci.*, **25**, 351 (1957).
10) H. C. Anderson, PB **151150** (1957).
11) A. Shimazaki and M. Kojima, *J. Chem. Soc. Japan, Ind. Chem. Sec.* (*Kogyo Kagaku Zasshi*), **66**, 1610 (1963).

Here the infrared spectra of the pyrolyzates of seven acid anhydride-cured epoxy resins will be studied in detail.

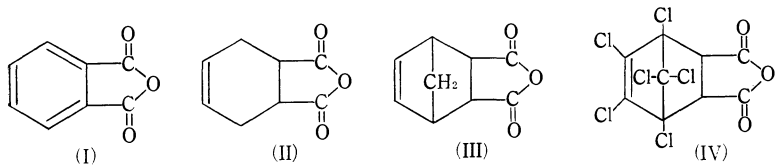
## Experimental

**Measurements.**—Spectra were scanned using a Perkin-Elmer Model 21 infrared spectrophotometer, with a sodium chloride prism in the 600 $cm^{-1}$- to -4000 $cm^{-1}$ region.

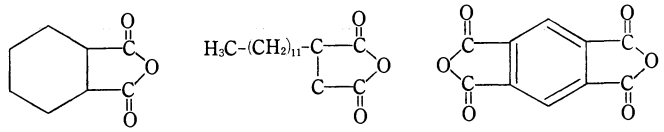
**The Preparation of Cured Epoxy Resins.**—As the epoxy resin, Epon 828 (Shell Chemical Corp.) was used. Figure 1 shows the structures of Epon 828 and the curing agents. Table I shows the mixing composition and the curing conditions accepted as standard. The solid curing agent was stirred



Epon 828



(I) (II) (III) (IV)



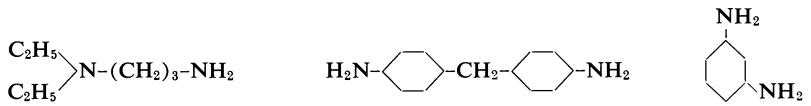
(V) (VI) (VII)

$H_2N-C_2H_4-NH-C_2H_4-NH_2$

(VIII)

$H_2N-C_2H_4-NH-C_2H_4-NH-C_2H_4-NH_2$

(IX)



(X) (XI) (XII)

Fig. 1. Structure of Epon 828 and curing agents.
(I) Phthalic anhydride (PA). (II) Tetrahydrophthalic anhydride (THPA). (III) Endomethylenetetrahydrophthalic anhydride (EMTHPA). (IV) Chlorendic anhydride (HET). (V) Hexahydrophthalic anhydride (HHPA). (VI) Dodecenyl succinic anhydride (DDSA) (VII) Pyromellitic dianhydride (PMDA). (VIII) Diethylene triamine (DETA). (IX) Triethylene tetramine (TETA). (X) Diethylamino propyl amine (DEAPA). (XI) *p, p'*-Diamino diphenyl methane (DDM) (XII) *m*-Phenylene diamine (MPDA).

TABLE I. MIXING COMPOSITION AND CURING CONDITION

| Type | Curing agent | Parts per 100 parts of Epon | Curing condition |
|---|---|---|---|
| Acid anhydride | PA | 60 | 130°C 2 hr. + 150°C 10 hr. |
| | THPA | 80 | 80°C 2 hr. + 150°C 4 hr. |
| | EMTHPA | 80 | 80°C 2 hr. + 150°C 4 hr. |
| | HET | 100 | 100°C 1 hr. + 200°C 1 hr. |
| | HHPA | 80 | 80°C 2 hr. + 150°C 4 hr. |
| | DDSA | 130 | 100°C 6 hr. |
| | PMDA | 31 | 120°C 3 hr. + 220°C 20 hr. |
| Amine | DETA | 8 | 20°C 2 hr. + 115°C 30 min. |
| | TTA | 14 | Room temp. 4 days |
| | DEAPA | 8 | 115°C 1 hr. |
| | MPDA | 14 | 100°C 1 hr. + 200°C 1 hr. |
| | DDM | 27 | 150°C 2 hr. + 125°C 4 hr. |

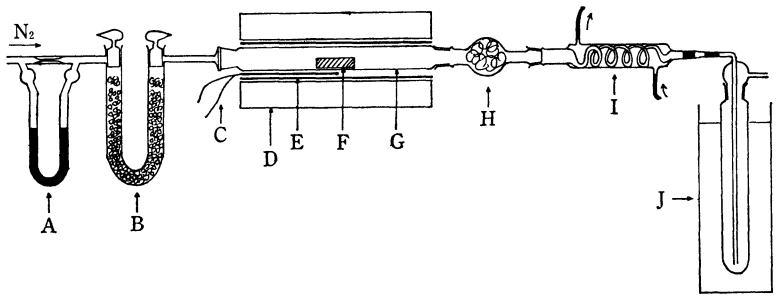



Fig. 2. Equipment of pyrolysis.

| | | | |
|---|---|---|---|
| A | Flowmeter | F | Sample |
| B | U tube with silica gel | G | Borosilicate glass tube |
| C | Thermocouple | H | Air-cooled trap (with glass wool) |
| D | Electric Furnace | I | Water cooled trap |
| E | Porcelain tube | J | Freezing mixture trap |

TABLE II. PROPERTIES OF PYROLYZATES

| Type of acid anhydride | | Spectrum number and pyrolysis temperature I room temp. —300°C | II 300—350°C | III 350—400°C | IV 400—450°C | V 450—500°C |
|---|---|---|---|---|---|---|
| PA | Properties of pyrolyzates | Needles | Needles + Yellow liq. | Fine crystal + Yellow liq. | Yellow liq. | Yellow liq. |
| | Method of measurement | K ◎ | K ◎ | K | K | K |
| THPA | ibid. | White crystal | Pale purple liq. | Pale purple liq. + Brown liq. | Brown liq. | Brown liq. |
| | ibid. | K ◎ | S | S | S | S |
| EMTHPA | ibid. | White crystal | Yellow liq. | Yellow liq. | Yellow liq. | Yellow liq. |
| | ibid. | K ◎ | S | S | S | S |
| HET | ibid. | White crystal | Reddish purple liq. | Reddish purple liq. + Brown liq. | Yellow brown liq. | Yellow brown liq. |
| | ibid. | K ◎ | S | S | S | S |
| HHPA | ibid. | Colorless liq. | Yellow liq. | Yellow liq. | Yellowish brown liq. | brown liq. |
| | ibid. | S | S ◎ | S | S | S |
| DDSA | ibid. | Yellow liq. | Yellow liq. | Yellow liq. | Yellowish brown liq. | Yellowish brown liq. |
| | ibid. | S ◎ | S ◎ | S | S | S |
| PMDA | ibid. | Yellowish brown solid | Brown purple soild | Yellow brown liq. (a)+White solid (b) | Yellow brown liq. (a)+White solid (b) | Yellow brown liq. |
| | ibid. | K | K | S (a), K (b) | S (a), K (b) | S |
| None (Epon 828 only) | ibid. | Pale-yellow liq. | Pale-yellow liq. | Yellow liq. | Yellow liq. | Yellow liq. |
| | ibid. | S | S | S | S | S |

* K KBr pellet technique, S Sandwich technique, ◎ Indicates the fractions utilized for identification of the curing agents used.

into warmed Epon 828, stirring was continued and the mixture was heated until the curing agent had been dissolved uniformly into the resin. The liquid curing agent was thoroughly mixed with the resin at room temperature. Then the sample was cured in an oven.

**The KBr Pellet Technique of Cured Resins.**—A file was used to reduce a block of cured resin to small particles. This method was found to be very simple and convenient for preparing a powdered sample for infrared analysis. The powdered sample thus obtained was passed through a 200 mesh screen. About 1 mg. of the sieved sample was thoroughly mixed with about 200 mg. of KBr powder, and a KBr pellet about 1 mm. thick was then prepared.

**The Method of Pyrolysis.**—Figure 2 shows the equipment of pyrolysis. About 2 g. of a sieved sample was placed into a horizontal borosilicate glass tube in an electric furnace. In the case of Epon 828, the sample was inserted into the furnace in a platinum boat. Then the temperature was raised at the rate of 2°C/min.; pyrolysis was continued until the temperature reached 500°C under a stream of high-purity nitrogen at a flow rate of 32 cc./min. Pyrolysis products were trapped in five temperature sections: (I) room temperature to 300°C; (II) 300—350°C; (III) 350—400°C; (IV) 400—450°C, and (V) 450—500°C (Table II). As can be seen from Fig. 2, three traps, the air-, water- and dry ice-cooled traps, were connected in series. Liquid and crystalline pyrolyzates caught in the traps were washed out with acetone. After the acetone had evaporated, the infrared spectra were recorded using the KBr-pellet technique or the sandwich technique.

## Results and Discussion

The infrared spectra of Epon 828 (the top of Fig. 5) and acid anhydrides (the top of Figs. 6 through 12) used as curing agents were recorded for reference. All anhydrides show two characteristic carbonyl absorption bands near 1780 and 1850 $cm^{-1}$.

**The Infrared Spectra of Cured Epoxy Resins.**—In the case of the amine-cured resins, a hydroxyl group is formed by the reaction of the amine with the epoxy group. Accordingly, the absorption band of the epoxy group at 907 $cm^{-1}$ disappears and the absorption intensity of the hydroxyl group in the 3400 $cm^{-1}$ region increases. Examples of two spectra (DETA- and MPDA- cured resins) are shown in Fig. 3. The spectra of three other types (DEAPA-, TTA- and DDM-cured resins) give patterns very similar to the first two (DETA and MPDA). Therefore, while the spectra of these cured resins can not be used to identify the specific type of amine utilized as the curing agent, the characteristic pattern can be used to determine that an amine and not an anhydride was used in the curing process.

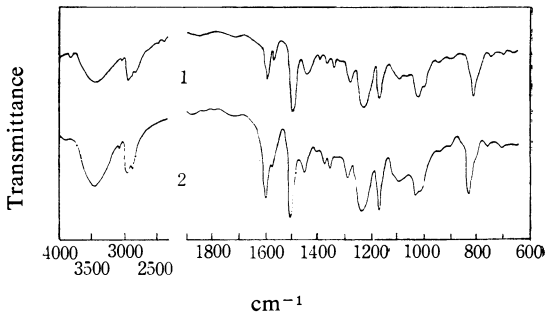



Fig. 3. Spectra of amine cured epoxy resins.
1 DETA-cured resin
2 MPDA-cured resin

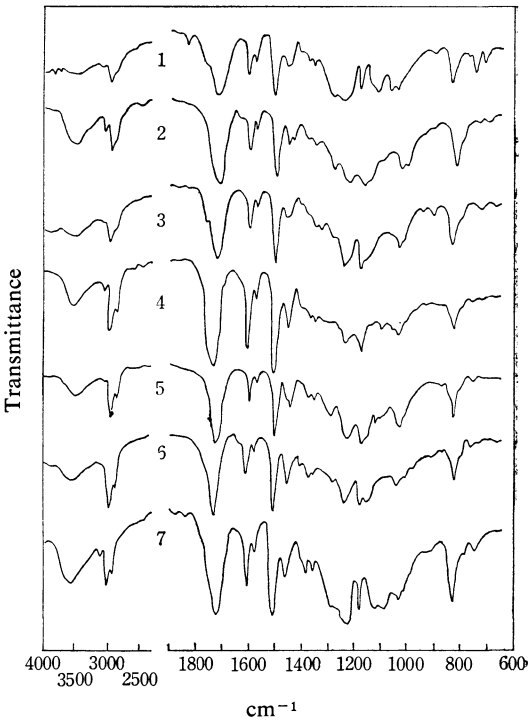



Fig. 4. Spectra of acid anhydride cured epoxy resins.
1 PA-cured resin
2 THPA-cured resin
3 EMTHPA-cured resin
4 HET-cured resin
5 HHPA-cured resin
6 DDSA-cured resin
7 PMDA-cured resin

In the case of acid anhydride-cured resins (Fig. 4), an ester-linkage is formed by the reaction of the anhydride with the hydroxyl group and an acid with the epoxy group, while a further ether linkage is formed by the reaction of the epoxy group with the hydroxyl group. Therefore, the absorption band of the epoxy group at 907 $cm^{-1}$ disappears and a strong ester carbonyl band appears at 1730 $cm^{-1}$.

Furthermore, small differences in the spectra are observed for each acid anhydride in the 1300—1000 $cm^{-1}$ region. The spectra of these anhydride-cured resins can not be utilized to identify the types of anhydrides used as curing agents, but they are useful in determining whether or not the resin is an anhydride-cured epoxy resin by the form of the curve, especially through the presence of a strong carbonyl band.

**The Infrared Spectra of Pyrolyzates of Cured Epoxy Resins.**—As the amounts of pyrolyzates caught in the water- and dry ice - cooled traps were very small, their infrared spectra were not studied. Most of the pyrolyzates caught in the air-cooled trap were studied by means of their infrared spectra. As can be seen from the properties of the pyrolyzates (Table II) and their infrared spectra (Figs. 6 through 12), pyrolyzates of PA-, THPA-, EMTHPA-, and HET-cured epoxy resin obtained at room temperature through 300°C were crystalline, and their infrared spectra gave nearly the same patterns as those of the individual acid anhydride-curing agents. Meanwhile, the pyrolyzates of HHPA- and DDSA-cured epoxy resins obtained at room temperature through 350°C were liquid, and each of the acid anhydride-curing agents used could be identified by the finger-print region of their infrared spectra.

In the spectra of the pyrolyzates of HHPA-cured resin, the formation of aliphatic compounds was observed. In the case of PMDA-cured resin, the infrared spectra of pyrolyzates did not give the pattern of PMDA utilized for curing at a low pyrolysis temperature, but did give the specific pattern at a high pyrolysis temperature; this pattern was different from those shown in the cases of other acid anhydride-cured resins. The ordinary acid anhydride used as a curing agent can be identified by the characteristic curve shown by the infrared spectra of pyrolyzates, while the presence of PMDA as a curing agent may be presumed from the fact that the spectra of the pyrolyzates do not have the absorption bands of PMDA, in contrast with the other acid anhydride-cured resins.

The experimental results with Epon 828 and each acid anhydride cured-epoxy resin will be discussed in detail below.

**Epon 828 (Fig. 5).**—Epoxy resin itself was also investigated as a related study. The infrared spectrum of the pyrolyzate obtained at room temperature through 350°C is almost the same as that of the original sample. At temperatures above 350°C, the intensities of the absorptions at about 3400 $cm^{-1}$ ($\nu$OH) and 1700 $cm^{-1}$ ($\nu$C=O) increase. At temperatures above 400°C the intensities of the absorptions at about 1025 $cm^{-1}$ (ether linkage $\nu$ C–O–C) and 907 $cm^{-1}$ (stretching vibration of epoxy ring) decrease; the characteristic spectrum is obtained from the sample at temperatures between 400—450°C.

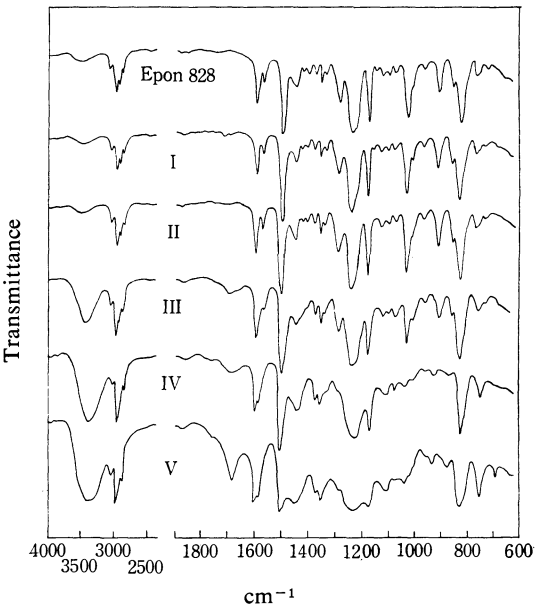



Fig. 5. Spectra of Epon 828 and its pyrolyzates.

This typical spectrum appears in every spectrum of the pyrolyzates above 350°C of cured epoxy resins subsequently mentioned, and so it is referred to as the *characteristic spectrum* hereafter. From these spectra, the opening of epoxy rings, the scission of ether linkages and the formation of hydroxyl groups may be assumed.

The main absorption bands of this *characteristic spectrum* are assigned as follows: 755 $cm^{-1}$: CH out-of-plane vibration of the mono-substituted benzene ring; 830 $cm^{-1}$: CH out-of-plane vibration of the para-substituted benzene ring; 1240, 1514 and 1610 $cm^{-1}$: vibrations related to the benzene ring; 1695 $cm^{-1}$: C=O stretching vibration.

Further, when an ethyl alcohol solution of 2, 4-dinitrophenylhydrazine acidified with hydrochloric acid was added to an ethyl alcohol solution of fractions IV and V, brown oily products separated out. From this fact and from the absorption near 1695 $cm^{-1}$ in spectra IV and V, the formation of carbonyl compound may be assumed.

**PA-Cured Resin (Fig. 6).**—Spectrum I is the same as that of PA. Pyrolyzate II is a mixture of a crystalline and a yellow liquid material, but except for the absorption of PA, only the absorption of the hydroxyl group (near 3400

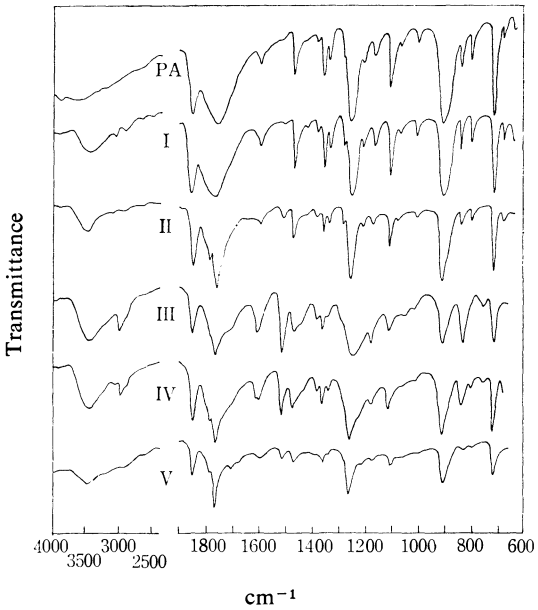



Fig. 6. Spectra of PA and pyrolyzates of PA-cured resin.

$cm^{-1}$) appears. Pyrolyzate III and IV show the absorptions of PA (at 1845, 1763, 1107, 905, and 715 $cm^{-1}$) overlapped with the *characteristic spectrum*. From the absorption as a shoulder at 1700 $cm^{-1}$ the formation of a carboxyl group may be assumed. Even in spectrum V the absorptions of PA (at 1845, 1763, 1260, 905, and 715 $cm^{-1}$) are clearly observed.

**THPA-Cured Resin (Fig. 7).**—Spectrum I is nearly the same as that of THPA. In spectrum II the absorptions of THPA are also observed at 1831, 1770, 1179, 1090, 995, 964, 933, 772, and 730 $cm^{-1}$. In spectrum III the *characteristic spectrum* strongly appears, while the absorptions of THPA are not clearly observed. The absorption curve becomes broad in spectrum IV.

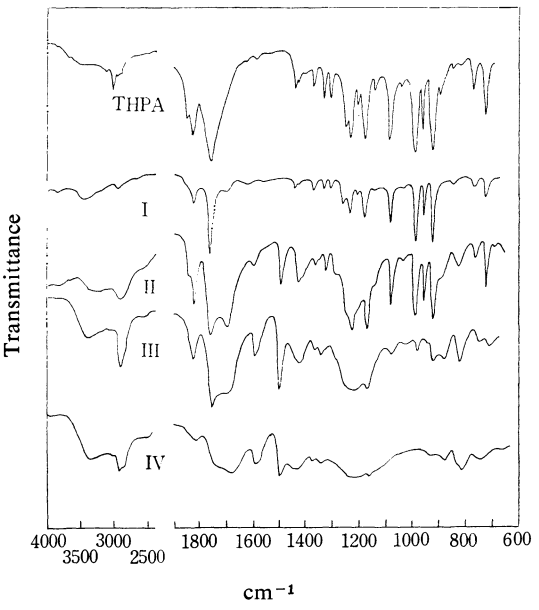



Fig. 7. Spectra of THPA and pyrolyzates of THPA-cured resin.

**EMTHPA-Cured Resin (Fig. 8).**—In spectrum I the absorption bands at 1860, 1770, 1335, 1293, 1117, 1078, 910, 791, and 732 $cm^{-1}$ are identical with those of EMTHPA. In spectra II, III, and IV the *characteristic spectrum* appears strongly, but the absorptions of EMTHPA could not be clearly observed. However, unlike the case of PA and THPA, the higher the pyrolysis temperature, the lower the carbonyl band shifts in the wave numbers of the spectrum (for example, 1725, 1717, 1695 and 1680 $cm^{-1}$ in II, III, IV and V respectively).

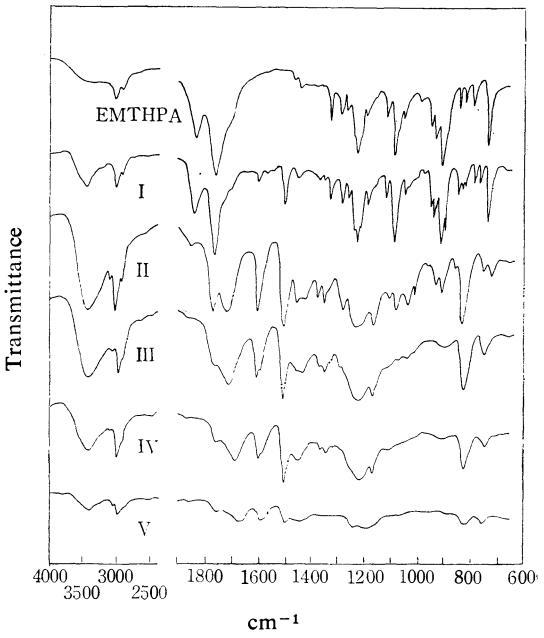



Fig. 8. Spectra of EMTHPA and pyrolyzates of EMTHPA-cured resin.

When an ethylalcohol solution of 2, 4-dinitrophenylhydrazine acidified with hydrochloric acid was added to the fractions from I to V, yellow oily products separated out, except for fraction I.

The amount of the products is highest in fractions III and IV. From this fact and from the above-mentioned carbonyl band shifts, the formation of a carbonyl compound may be assumed.

**HET-Cured Resin (Fig. 9).**—Pyrolyzate I is crystalline, and HET is identified by the absorptions at 1883, 1782, 1598, 1243, 1216, 1067,

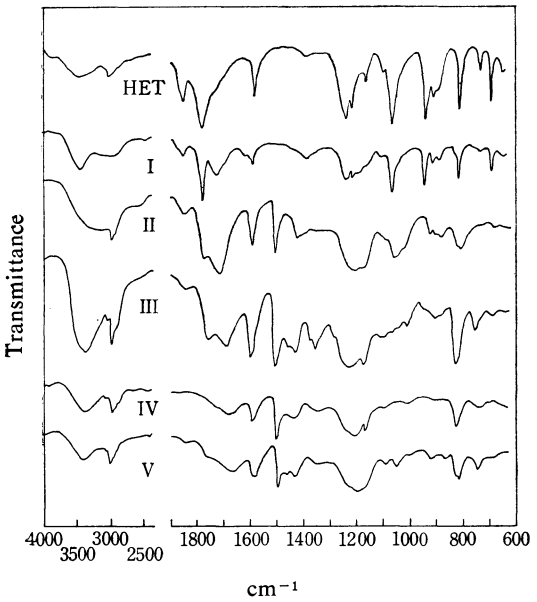



Fig. 9. Spectra of HET and pyrolyzates of HET-cured resin.

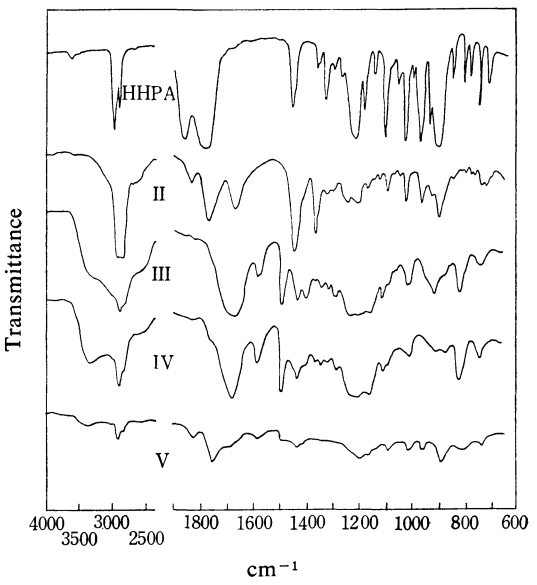



Fig. 10. Spectra of HHPA and pyrolyzates of HHPA-cured resin.

942, 817, and 695 $cm^{-1}$. The *characteristic spectrum* becomes strong in the spectra of the sample obtained above 300°C; the absorption bands of HET could not be identified. Similarly, in the case of EMTHPA, at the higher pyrolysis temperatures, the carbonyl band shifts to a lower wave number (for example, 1725, 1722, 1692, 1680, and 1675 $cm^{-1}$ in I, II, III, IV and V respectively).

In this case 2, 4-dinitrophenylhydrazine test was omitted, but the formation of a carbonyl compound may be assumed.

**HHPA-Cured Resin (Fig. 10).**—The amount of pyrolyzate I was too small to get a satisfactory spectrum. From spectrum II HHPA is identified by the absorptions at 1841, 1780, 1100, 1027, 971, and 900 $cm^{-1}$. Furthermore, strong absorption bands appear near 2800, 1450, and 1380 $cm^{-1}$. From this fact, the formation of aliphatic chain compounds by the opening of the cyclohexane ring of HHPA may be assumed. The *characteristic spectrum* becomes strong in the spectra of the samples obtained above 350°C. Furthermore, in contrast with other acid anhydrides, the carbonyl bands of this acid anhydride could not be observed, while the carbonyl band appears strongly near 1675 $cm^{-1}$. After several experiments, it was recognized that the two carbonyl bands of HHPA appeared when the spectra were measured immediately after the pyrolysis. Therefore, a high reactivity of HHPA was assumed.

**DDSA-Cured Resin (Fig. 11).**—As DDSA is a liquid with an aliphatic chain, its pyrolyzate is also a liquid, as would be expected. DDSA

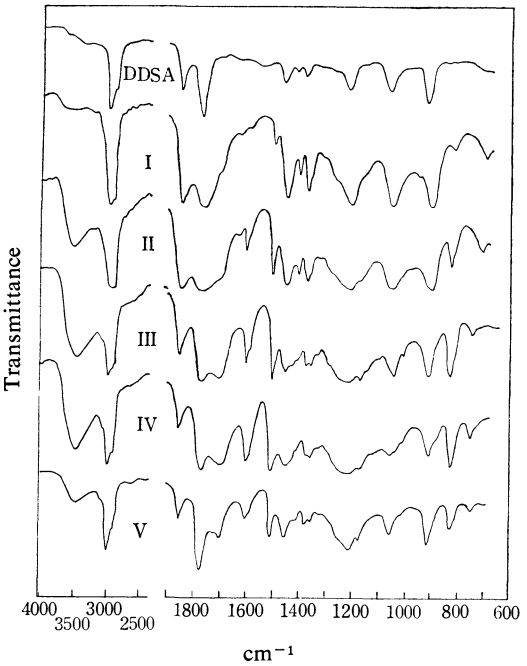



Fig. 11. Spectra of DDSA and pyrolyzates of DDSA-cured resin.

is identified from spectra I and II. With a rise in the temperature of the pyrolysis, spectra III, IV, and V give a pattern similar to the *characteristic spectrum.*

**PMDA-Cured Resin (Fig. 12).**—The spectra of pyrolyzates I and II are almost identical with the *characteristic spectrum.* Pyrolyzate III is a mixture of liquid and a small amount of

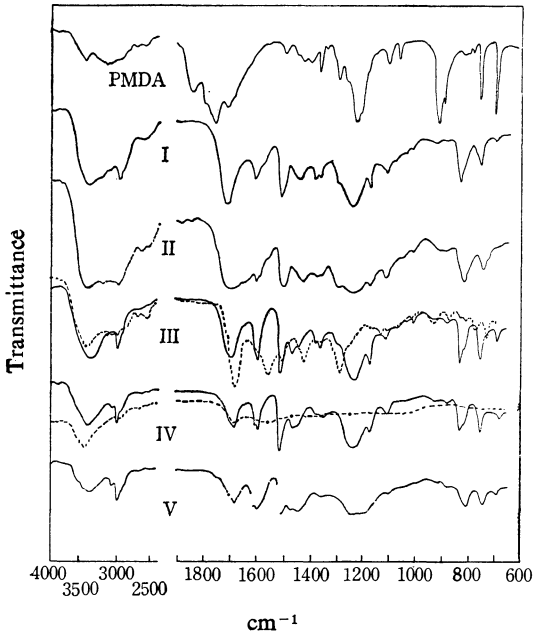



Fig. 12. Spectra of PMDA and pyrolyzates of PMDA-cured resin.
III, IV: — liquid, --- solid

solid. The liquid portion gives almost the same spectra as the pyrolyzates I and II. Meanwhile, the spectrum of the solid portion is very specific, but it has not been identifide as yet. Only in the case of PMDA-cured resin is the original acid anhydride used as a curing agent (PMDA) not formed by pyrolysis. However, PMDA can be assumed by a comparison of the pyrolyzate spectra of PMDA-cured resin with those of another acid anhydride resins.

**Summary**

To pulverize the cured hard resins for the infrared KBr technique, the method using a file is very simple and convenient.

From the infrared spectra of the powder of cured epoxy resins using the KBr-pellet technique, the curing agent used can be readily identified by type whether it is an amine or an acid-anhydride type by the absence or presence of the carbonyl absorption band.

Furthermore, in the case of the acid anhydride-cured epoxy resins, the acid anhydride used as the curing agent can be identified by type from the spectra of the resin pyrolyzate. Namely, PA, THPA, EMTHPA, HET, and DDSA may be identified immediately from the spectra of pyrolyzates between room temperature and 300°C, and HHPA, from the spectrum of the pyrolyzate between 300 and 350°C. The results of these experiments are summarized in Table II.

PMDA used as a curing agent can not be so straightforwardly identified as in the other cases, but even this may be identified by a comparison of the spectra of the pyrolyzates of PMDA-cured resin with those of the pyrolyzates of each resin.

The authors are indebted to Dr. Shigeyuki Tanaka, Associate Professor of the University of Tokyo, for his helpful advice and comments.

*Central Research Laboratory*
*Fuji Electric Co., Ltd.*
*Nagasaka, Yokosuka*

# Intramolecular Hydrogen Bonds. III.[1] Cyanoalkanols

By Nobuo MORI, Satoshi ŌMURA,* Hiroyuki YAMAKAWA and Yojiro TSUZUKI

(Received January 25, 1965)

The intramolecular hydrogen bonding in some cyanoalkanols in dilute carbon tetrachloride solutions was previously investigated by means of infrared measurements in the OH-stretching region near 3 $\mu$.[2,3] Acetaldehyde- and cyclohexanone-cyanohydrins show only one absorption band, at 3604 and 3594 $cm^{-1}$ respectively, the latters are lower by ca. 20 $cm^{-1}$ than those of the corresponding unsubstituted secondary and tertiary alcohols. Flett[2] suggested that the lowering in frequency is to be attributed to the electron-attracting effect of the cyano group and that the OH bands are, then, due to the free OH group. On the other hand, Allerhand and Schleyer[3] attributed the lowering in frequency to the formation of an internal

1) Part II: N. Mori, S. Ōmura and Y. Tsuzuki, This Bulletin, 38, 1037 (1965).

* Present address: The Kitasato Institute, Minatoku, Tokyo.

2) M. St. C. Flett, *Spectrochimica Acta*, 10, 21 (1957).

3) A. Allerhand and P. von R. Schleyer, *J. Am. Chem. Soc.*, 85, 866 (1963).

hydrogen bond of the OH group with the $\pi$-electrons of the cyano group; they based their suggestion on a comparison with the OH frequency (3620 $cm^{-1}$) of propargyl alcohol, which had been assigned to the OH group internally banded to the $\pi$-electrons of the triple bond.[4] However, the re-investigation of propargyl alcohol, which has recently been reported,[5] shows the frequency to be that of the free OH group. Thus, the basis for the assignment given for the cyanoalkanols by Allerhand and Schleyer has been lost. Accordingly, we must re-investigate to determine whether or not such $\alpha$-cyanoalkanols form intramolecular hydrogen bonding. This problem has now been solved through the infrared measurements of a series of $\alpha$-cyanoalkanols. Further, this paper will report on the limitation of intramolecular hydrogen bonding* through the length of an alkylene chain in the series of $\omega$-cyanoalkanols, $NC(CH_2)_nOH$.

## Experimental

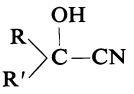
$\alpha$-Cyanoalkanols were prepared from the corresponding aldehydes and ketones in the usual manner, while 4- and 10-cyanoalkanols were synthesized from the corresponding haloalkanols by reaction with potassium cyanide[6]; b. p. 130°C/14 mmHg ($n_D^{25}$ = 1.4371) and 178—179°C/8 mmHg. $\beta$-Cyanoethanol was commercially obtained and was fractionally distilled; b. p. 110°C/15 mmHg.

Infrared measurements in the OH-stretching region were carried out at 25°C with solutions of 0.004 mol./l. in carbon tetrachloride on a Perkin Elmer 21 spectrophotometer equipped with a lithium fluoride prism. The cell used was 3 cm. long, and the slit width was always 0.029 mm. The observed frequencies were calibrated on the standard of atmospheric vapor and within a range of error of $\pm 1$ $cm^{-1}$. At that concentration, there was observed, in addition to a strong absorption band near 3600 $cm^{-1}$, a very weak and broad bond at 3470—3490 $cm^{-1}$ which varied with the concentration; the latter is indicative of some intermolecular hydrogen bonding. The infrared data are summarized in Table I.

## Results and Discussion

The spectrum of cyclohexanone cyanohydrin (V) includes only one symmetric sharp band, at 3591 $cm^{-1}$, while the other $\alpha$-cyanoalkanols (I—IV) each show a band rather broadened on the higher frequency side. 4- and 10-cyanoalkanols (VIII and IX) each show a band somewhat broadened on the lower frequency side. The lack of symmetry of the bands may be produced by the overlap of symmetric bands of the Lorentz type, which should be assigned to the OH groups in the conformational isomers possible by rotation around the $C_\alpha$-O bond, as will be presented below. The symmetric bands can graphically be separated from the original unsymmetric band, e.g., as is shown in Fig. 1. $\beta$-Cyanoethanol (VI) apparently

Table I. Summary of infrared data



| Compound | R | R′ | $\nu_{OH}$ ($cm^{-1}$)* | log $I_0/I$ | $\Delta\nu_{1/2}$ |
|---|---|---|---|---|---|
| I | H | H | (3623) | 0.16 | 16 |
| | | | 3610 | 0.86 | 28 |
| II | H | Me | (3615) | 0.10 | 12 |
| | | | 3604[a] | 1.00 | 27 |
| III | Me | Me | (3608) | 0.10 | 8 |
| | | | 3599 | 1.02 | 22 |
| IV | Me | Et | (3606) | 0.15 | 8 |
| | | | 3599 | 0.97 | 24 |
| V | $-(CH_2)_5-$ | | 3591[b] | 1.08 | 23 |

$NC-(CH_2)_n-OH$

| | $n$ | | | |
|---|---|---|---|---|
| VI | 2 | (3631)[c] | 0.57 | 28 |
| | | (3610)[c] | 0.46 | 28 |
| VII | 3 | 3640[3] | | |
| VIII | 4 | 3638[d] | 0.68 | 20 |
| | | (3622) | 0.19 | 18 |
| IX | 10 | 3637 | 0.70 | 24 |
| | | (3621) | 0.20 | 10 |

a) reported 3604[2] or 3607[3]; b) reported 3594[2]; c) reported 3625 and 3610[2] or 3632 and 3617[3], respectively; d) reported 3639.[3]

* Parentheses show separated-band frequencies, the errors for which are in a range of $\pm 2$ $cm^{-1}$.

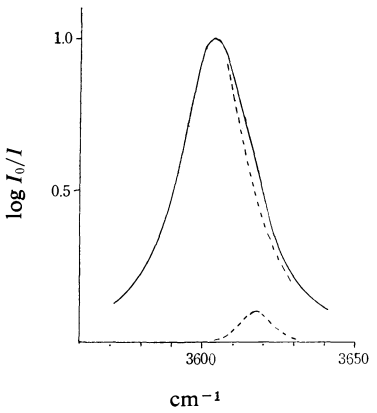



Fig. 1. IR Spectrum of $\alpha$-cyanoethanol (II).

4) P. von R. Schleyer, D. S. Trifan and R. Bacskai, ibid., 80, 6691 (1958).

5) B. Jordanov, A. Jovtscheff, S. Spassov, B. Blagoev and M. Agova, *Tetrahedron*, 20, 903 (1964).

* The term "Hydrogen bonding" will herein be replaced by the term "Interaction," which has been proposed for hydrogen bonding between an OH group and $\pi$-electrons by M. Ōki and H. Iwamura, This Bulletin, 32, 567 (1959).

6) P. Chuit and J. Hausser, *Helv. Chim. Acta*, 12, 463 (1929).

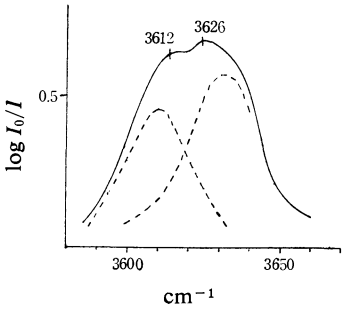



Fig. 2. IR Spectrum of β-cyanoethanol (VI).

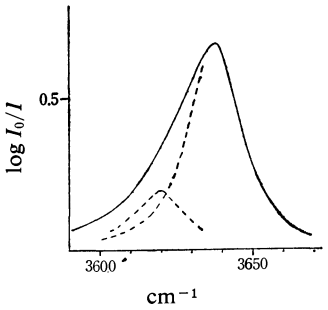
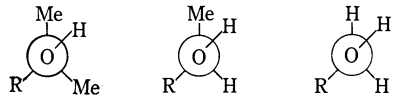



Fig. 3. IR Spectrum of 4-cyanobutanol (VIII).

shows partially-resolved doublet, with maxima at 3626 and 3612 cm$^{-1}$, whose frequencies agree with those previously reported by Flett,[2] but this doublet can not be separated into two symmetric bands which have maxima at the above frequencies and which by overlapping with each other can reproduce the doublet. However, it can be synthesized from the two symmetric bands whose maxima are at 3631 and 3610 cm$^{-1}$, as Fig. 2 shows. This separation seems to be rather reasonable as will be discussed below. The frequencies of the separated bands are summarized in Table I, but they are somewhat rough because of the graphical separation and the relatively poor resolving power of the spectrophotometer employed.

According to the infrared study by Ōki and Iwamura[7] of the rotational isomerism around the C-O bond in alcohols, a methyl group skew to the OH group has a steric effect serving to make the OH frequency lower by ca. 13 cm$^{-1}$, as is shown in Table II.

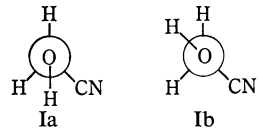
TABLE II. THE ROTATIONAL ISOMERS OF ALCOHOLS AND THEIR OH FREQUENCIES




| | (A) | (B) | (C) |
|---|---|---|---|
| $\nu_{OH}$ cm$^{-1}$ | 3617 | 3627 | 3640 |

R : H or alkyl.

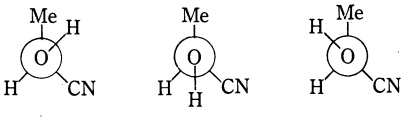
In consideration of the above assignments, the lower and the higher frequency band of cyanomethanol (I) should be assigned to the OH groups of Ia and Ib respectively.



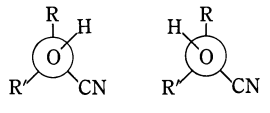

3610 cm$^{-1}$ 3623 cm$^{-1}$ $\Delta\nu$ : 13 cm$^{-1}$

The shift of the higher frequency band by 17 cm$^{-1}$ from that of the corresponding rotational isomer (C) of ethanol, may be attributed to the electron-attracting effect of the cyano group; this is also true with the other α-cyanoalkanols, but the shifts is drastically decreased by the intervention of a methylene group, as may be seen in β-cyanoethanol (VI), whose free OH frequency is 3631 cm$^{-1}$. Although the separation between the two bands, $\Delta\nu$, is only 13 cm$^{-1}$, equal to that in the case of ethanol, the OH grop in Ia interacts with the π-electrons of the cyano group, because its absorption intensity is very high with respect to that of the OH in Ib.

Similarly, the follwing assignment may be given for the other α-cyanoalkanols (II—V):




For II 3604 cm$^{-1}$ ca. 3615 cm$^{-1}$ $\Delta\nu$ : 11 cm$^{-1}$




For III and IV 3599 cm$^{-1}$ ca. 3607 cm$^{-1}$ $\Delta\nu$ : 8 cm$^{-1}$

For V 3591 —

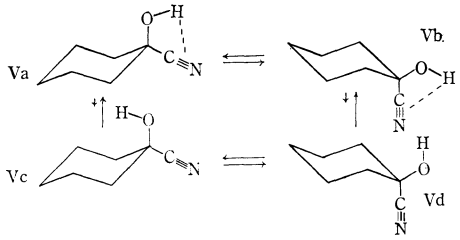
The difference in frequency between Ib and IIc, 8 cm$^{-1}$, may result from the steric effect of the methyl group.

In the case of compound II, the 3604 cm$^{-1}$ of the symmetric, interacted OH band lies just between the OH frequencies of forms Ia and IIIa. This compound can take two interacted forms, IIa and IIb, which correspond to forms IIIa and Ia respectively. Accordingly, one may say that the OH frequencies of forms IIa and IIb are close to 3604 cm$^{-1}$, that the major component of the band is due to the OH group

7) M. Ōki and H. Iwamura, This Bulletin, 32, 950 (1959). The same assignments were also reported by F. Dalton, G. D. Meakins, J. H. Robinson and W. Zaharia, *J. Chem. Soc.*, **1962**, 1566.

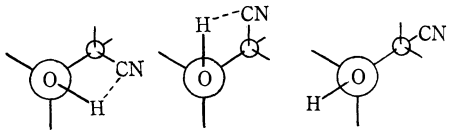
in form IIb, and that its minor component is due to the OH in form IIa, since form IIb should be thermodynamically more stable than form IIa.

The OH band of cyclohexanone cyanohydrin (V) is symmetric, as has been mentioned above; this indicates that all the molecules substantially exist in at least one of the interacted forms, Va or Vb:




Form Vc may be negligible because the axial hydrogens on $C_3$ and $C_5$ sterically repel the hydroxyl-hydrogen atom, thus directing it towards the cyano group, and form Vd is less stable than Vb because, similarly, the latter is possibly more stabilized through the interaction between the OH group and the $\pi$-electrons of the cyano group. Let us now consider which of the forms, Va or Vb, is more stable. The difference in free energy between the equatorial and the axial OH group is 0.4—0.9 kcal./mol.,[8] which is higher than the value of 0.15—0.25 kcal./mol. for the cyano group.[9] The difference between the respective, averaged values, 0.45 kcal./mol., corresponds to a $K$ value of 2.1 in the van't Hoff isotherm: $\Delta G^\circ = -RT \ln K$. This means that the number of molecules taking form Vb is larger by a factor of roughly 2.1 than that taking form Va. Further, the symmetric shape of the band can be confirmed from this population of molecules and by the fact that the difference in frequency between axial and equatorial tertiary OH groups is generally 6 $cm^{-1}$ at most.[10] That the frequency of this compound is lower by 8 $cm^{-1}$ than those of compound III and IV may be explained in terms of the *gem*-dialkyl effect,[11] by which the O-$C_\alpha$-CN bond angle is decreased, thus bringing the OH and the cyano group closer together.

For $\beta$-cyanoethanol (VI), one may consider nine rotational isomers to be possible by rotation around the single bonds: three (the number of rotational isomers around the $C_\alpha$-O bond) times three (the number of rotational isomers around the $C_\alpha$-$C_\beta$ bond). Eight of these form four pairs of mirror images, and only one pair of VIa and VIb are those favorable for intramolecular interaction. Since forms VIa and VIb contain, in addition to the methyl effect, interaction between the OH and the $\beta$-cyano group, the interacted OH frequency will be lower than the 3627 $cm^{-1}$ of the above-mentioned ethanol B. On the other hand, form VIc may be the least strained conformation of those free from interaction. Thus the OH frequency will be near the 3640 $cm^{-1}$ of ethanol C. The observed frequencies of 3610 and 3631 $cm^{-1}$ are in accordance with those expected and are rather more reasonable values than those of the apparent peaks (3612 and 6326 $cm^{-1}$). The interacted OH frequency of 3617 $cm^{-1}$ reported by Allerhand and Schleyer might be incorrect because the frequency was that of the shoulder of band.




Compounds VIII and IX are free from intramolecular interaction. The bands at 3622 and 3637 $cm^{-1}$ may be due to the free OH groups in the rotational isomers formed by rotation around the $C_\alpha$-O bond, such as forms B and C of ethanol respectively. The absence of interaction may be due to the formation of a larger ring through interaction being thermodynamically more difficult.

From the above findings, it may be concluded that the OH group in the $\alpha$-cyanoalkanols interacts with the $\pi$-electrons of the cyano group, and that the interaction in the series of $NC(CH_2)_n$-OH occur when $n$ is 1 or 2, as has previously been reported[3].

The authors wish to express their gratitude to Professor Dr. Michinori Ōki of the University of Tokyo for his kind advice and suggestions concerning the OH-$\pi$ interaction, and to Mr. Teruo Kajiura and Mr. Tadao Tamura of the Government Chemical Industrial Research Institute of Tokyo for their infrared measurements.

*Department of Chemistry*
*Tokyo College of Science*
*Kagurazaka Shinjuku-ku*
*Tokyo (N. M., H. Y. and Y. T.)*

*Research Institute of Fermentation*
*The University of Yamanashi*
*Kofu (S. O.)*

8) E. L. Eliel, "Stereochemistry of Carbon Compounds," McGraw-Hill Book Company, New York, N. Y. (1962), p. 236.
9) N. L. Allinger and W. Szkryblo, *J. Org. Chem.*, **27**, 4601 (1962); B. Rickborn and F. R. Jensen, ibid., **27**, 4606 (1962).
10) A. R. H. Cole, G. T. A. Müller, D. W. Thornton and R. L. S. Willix, *J. Chem. Soc.*, **1959**, 1218.
11) P. von R. Schleyer, *J. Am. Chem. Soc.*, **83**, 1368 (1961), and the references cited therein.

# Intramolecular Hydrogen Bonds. IV.[1] Phenylalkane-diols

By Nobuo Mori, Satoshi Ōmura* and Yojiro Tsuzuki

(Received January 25, 1965)

The present investigation is concerned with intramolecular hydrogen bonding in the systems of poly-functional compounds in which one or more proton-donating groups can form a hydrogen bond with a few proton-accepting groups. Such systems are complicated because various types of intramolecular hydrogen bonding may simultaneously appear, depending on the thermodynamical stability of the geometries to be formed through the intramolecular hydrogen bonding between the groups. Of such compounds, some phenylalkane-diols, such as diaryl pinacols[2] and phenylcycloalkane-diols,[3] have recently been investigated by means of infrared spectroscopy in the OH-stretching region.

This paper will deal with intramolecular hydrogen bonding in phenyl-$\alpha,\omega$-alkane-diols and with its limitation through the length of an alkylene chain intervening between the hydroxyl groups.

Intramolecular hydrogen bonding occurs in $\alpha,\omega$-alkane-diols HO-$(CH_2)_n$-OH and in $\omega$-phenylalkanols Ph-$(CH_2)_n$-OH when $n$ is an integer of from 2 to 4* in the former[5,6] and from 1 to 2 in the latter.[7,8] As $n$ increases, the separation between the free and the bonded OH band ($\Delta\nu$) increases from 32 through 78 to 156 $cm^{-1}$ in the former[5] and from 17 to 30 $cm^{-1}$ in the latter.[8] Moreover, the intensity ratio of the free OH band to the bonded OH generally grows with the increasing $n$.

In consideration of these facts, it is to be expected, in the present series of Ph-CHOH-$(CH_2)_n$-OH, that the primary alcoholic hydroxyl group will predominantly form a hydrogen bond with both the secondary hydroxyl group and the $\pi$-electrons of the phenyl group when $n$ is equal to 1, and with only the former when $n$ is 2 or 3. However, it forms a hydrogen bond with neither of them when $n$ is 4. At the same time, the secondary hydroxyl group may be expected to form a hydrogen bond with both the proton-accepting groups when $n$ is an interger of from 1 to 3, but with the $\pi$-electrons only when $n$ is 4.

In this paper, the free OH group is that OH which contains an unbonded H atom, i.e., which includes an OH group not participating in any hydrogen bond and an OH group whose oxygen atom hydrogen-bonds to the hydrogen of another OH. The bonding of the oxygen atom of a free OH group to the hydrogen of another OH group has, in general, little effect upon the frequency of the free OH group.[5,10] Accordingly, the following discussion and assignments will be made mainly on the basis of the frequencies and the intensities of the bonded OH bands, with some

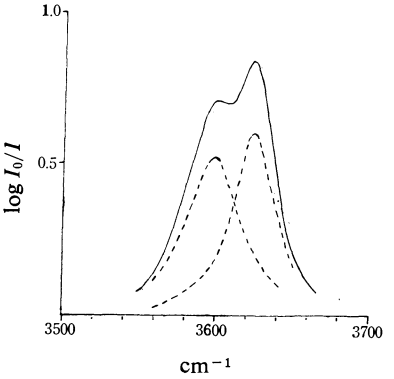



Fig. 1. IR spectrum of phenylethane-1,2-diol (I).

1) Part III: N. Mori, S. Ōmura, H. Yamakawa and Y. Tsuzuki, This Bulletin, **38**, 1627 (1965).

* Present address: The Kitasato Institute, Minatoku, Tokyo.

2) E. J. Moriconi, F. T. Wallenberger, L. P. Kuhn and W. F. O'Connor, *J. Org. Chem.*, **22**, 1651 (1957); E. J. Moriconi, W. F. O'Connor, L. P. Kuhn, E. A. Keneally and F. T. Wallenberger, *J. Am. Chem. Soc.*, **81**, 6472 (1962); P. Tomboulian, *J. Org. Chem.*, **26**, 2652 (1951); W. A. Mosher and N. D. Heindel, ibid., **28**, 2154 (1963).

3) a) D. C. Kleinfelter and P. von R. Schleyer, *J. Am. Chem. Soc.*, **83**, 2329 (1961); M. T. Davies, D. F. Dobson, D. F. Hayman, G. B. Jackman, M. G. Lester, V. Petrow, O. Stephenson and A. A. Webb, *Tetrahedron*, **18**, 751 (1956); E. Galantay, ibid., **19**, 319 (1963). b) E. M. Philbin, T. S. Wheeler, F. V. Brutcher and W. Bauer, *J. Org. Chem.*, **27**, 4114 (1962); D. C. Staiff and A. C. Huitric, ibid., **28**, 3531 (1963); H. M. Fales and W. C. Wildman, *J. Am. Chem. Soc.*, **85**, 784 (1963).

* Kuhn and Wires[4] have recently reported that a slight intramolecular hydrogen bonding appears also when $n$ is 5, although other investigators[6,9] previously reported its absence in this case.

4) L. P. Kuhn and R. A. Wires, *J. Am. Chem. Soc.*, **86**, 2161 (1964).

5) L. P. Kuhn, ibid., **74**, 2492 (1952).

6) A. B. Foster, A. H. Haines and M. Stacey, *Tetrahedron*, **16**, 177 (1961).

7) P. von R. Schleyer, D. S. Trifan and R. Bacskai, *J. Am. Chem. Soc.*, **80**, 6691 (1958).

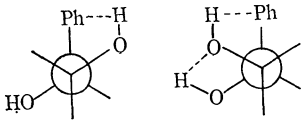
8) M. Ōki and H. Iwamura, This Bulletin, **32**, 1135 (1959).

9) D. W. Davidson, *Can. J. Chem.*, **39**, 2139 (1961).

10) L. P. Kuhn, *J. Am. Chem. Soc.*, **80**, 5950 (1958).

consideration also of those of the free OH bands.

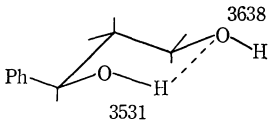
The spectrum of phenylethane-1,2-diol (I) contains a partially resolved doublet with maxma at 3624 and 3600 $cm^{-1}$; this doublet can graphically be separated into two symmetric components, as is shown in Fig. 1, which can reproduce almost the same doublet as the original one by overlapping with each other. The former frequency accords with the free $\nu_{OH}$ of 3627 $cm^{-1}$ of $\alpha$-phenylethanol,[8] and the latter, with the bonded $\nu_{OH}$ of ca. 3605 $cm^{-1}$ of $\beta$-phenylethanol.[7,8,11] Consequently, diol I may predominantly take form Ia rather than form Ib:



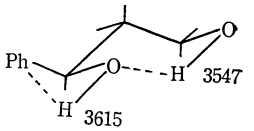

Ia Ib

The secondary OH group in Ia is completely free, but in Ib it is hydrogen-bonded with the primary one. Form Ib may be absent because this diol shows no OH band near 3550 $cm^{-1}$, at which point *cis*-1-phenylcyclohexane-1,2-diol containing a hydrogen-bonded conformation similar to form Ib shows a strong band due to the tertiary OH group bonded to the secondary OH.[3a] Also, the diol may be free from hydrogen bonding between the secondary OH group and the $\pi$-electrons because there is no absorption band near 3616 $cm^{-1}$, at which point $\alpha$-phenylethanol shows a bonded OH band.[8]

1-Phenylpropane-1,3-diol (II) shows two unsymmetric bands at 3615 and 3547 $cm^{-1}$, the former having a shoulder on the higher frequency side and the latter, a shoulder on the lower frequency side. Therefore, the bands can be resolved into four substantially symmetric components by graphical separation, as is shown in Fig. 2. The bands at 3638 and 3531 $cm^{-1}$ may be assigned to the free and the bonded OH group, as in IIa, and similarly, the other pair of 3615 and 3547 $cm^{-1}$, to the bonded OH groups, as in IIb.




IIa




IIb

The separation between the primary OH bands is 91 $cm^{-1}$, but for the secondary OH bands it is 84 $cm^{-1}$. In the latter case, however, it is increased to a reasonable value of 93 $cm^{-1}$ by replacing the bonded secondary OH frequency in IIb by the free one of 3624 $cm^{-1}$ of compound I.

1-Phenylbutane-1,4-diol (III) similarly shows two unsymmetric bands, with peaks at 3614 and 3452 $cm^{-1}$, which have shoulders at about 3636 and 3473 $cm^{-1}$ respectively, as Fig. 3 shows. The former band could graphically be separated into two components, whose maxima are at 3636 and 3614 $cm^{-1}$, but the latter band was difficult to divide into components and the apparent shoulder was taken to be the peak of the additional unresolved components. As is shown in forms IIIa and IIIb, these bands may, respectively, be assigned to the free

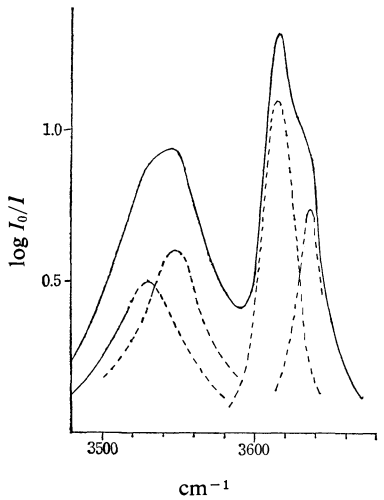



Fig. 2. IR spectrum of 1-phenylpropane-1,3-diol (II).

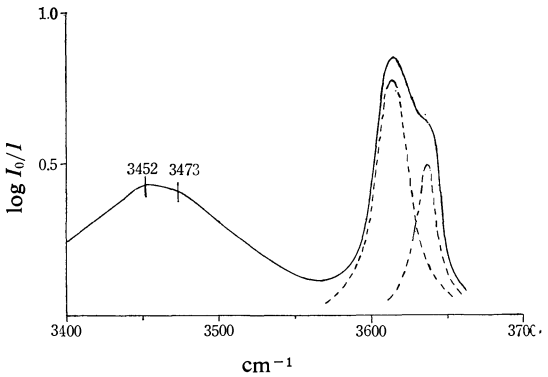
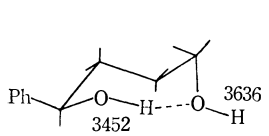


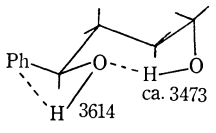

Fig. 3. IR spectrum of 1-phenylbutane-1,4-diol (III).

11) F. Dalton, *J. Chem. Soc.*, **1962**, 1566.

primary OH group, the secondary OH bonded to the $\pi$-electrons, the primary OH bonded to the secondary OH, and the secondary OH bonded to the primary OH.




IIIa




IIIb

1-Phenylpentane-1, 5-diol (IV) shows a strong band at 3615 $cm^{-1}$ and a very weak, broad band at about 3491 $cm^{-1}$. The former has a shoulder on the higher frequency side and can be separated into two symmetric bands, at 3636 and 3615 $cm^{-1}$, which may be due to the free primary OH group and the secondary OH bonded to the $\pi$-electrons respectively. Since the absorbance of the free primary OH band is lower than that of the secondary OH band, the weak band is probably due to the primary OH group whose H atom hydrogen-bonds with the oxygen of the bonded secondary OH group, in spite of the fact that the phenyl group makes the secondary OH group more acidic than the primary OH.[3a] 5-Methoxypentanol shows a weak, broad band due to the internally bonded OH group at 3501 $cm^{-1}$.[6]

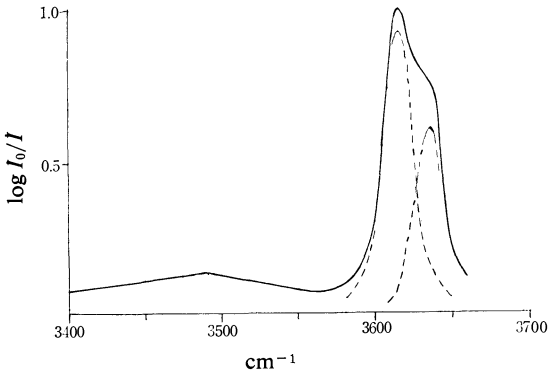
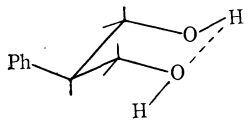



Fig. 4. IR spectrum of 1-phenylpentane-1, 5-diol (IV).

2-Phenylpropane-1, 3-diol (V) shows two almost symmetric bands at 3634 and 3553 $cm^{-1}$, which accord with those of 2-alkylpropane-1, 3-diols.[12] The following internally-bonded form Va may be the most favorable for this compound:




Va

12) P. von R. Schleyer, *J. Am. Chem. Soc.*, **83**, 1368 (1961).

The phenylalkane-diols will also contain a certain proportion of molecules in which both the OH groups are free and/or one of them is free and the other forms a hydrogen bond with the phenyl group; this proportion may not be significantly high in the case of diols other than I and IV.

TABLE I. SUMMARY OF INFRARED DATA FOR Ph-CHOH-$(CH_2)_n$-OH

| Compound | $n$ | $\nu_{OH}$, $cm^{-1}$ | log $I_0/I$ | $\Delta\nu_{1/2}$ |
|---|---|---|---|---|
| I | 1 | 3624 | 0.60 | 35 |
| | | 3600 | 0.52 | 46 |
| II | 2 | 3638 | 0.74 | 25 |
| | | 3615 | 1.10 | 30 |
| | | 3547 | 0.60 | 52 |
| | | 3531 | 0.50 | 60 |
| III | 3 | 3636 | 0.49 | 16 |
| | | 3614 | 0.76 | 25 |
| | | 3473, 3452 | 0.43 | 136 |
| IV | 4 | 3636 | 0.61 | 22 |
| | | 3615 | 0.94 | 23 |
| | | 3491 | 0.13 | |
| V | | 3634 | 0.19 | 27 |
| | | 3553 | 0.12 | 24 |

## Experimental

Compound I was prepared from styrene by the method described in the literature.[13] Compounds II and V were synthesized in the usual way by the hydrogenolysis of ethyl $\beta$-phenyl-$\beta$-hydroxypropionate[14] and diethyl phenylmalonate[15] with lithium aluminum hydride, while compounds III and IV were similarly prepared from the ethyl esters of $\omega$-benzoyl-propionic and -butyric acid[16] and recrystallized from ether. Their properties and data of analysis are shown in Table II.

TABLE II

| Compound | M. p., °C (B. p., °C/mmHg) | Calcd. C | Calcd. H | Found C | Found H |
|---|---|---|---|---|---|
| I | 65—66[13] | | | | |
| II | (152/5[17]) $n_D^{25}=1.4528$ | | | | |
| III | 75 (155/2) | For $C_{10}H_{14}O_2$ 72.26 | 8.49 | 72.53 | 8.78 |
| IV | 53.5 (165—166/4) | For $C_{11}H_{16}O_2$ 73.30 | 8.95 | 73.25 | 9.35 |
| V | 48.5—49.5[18] (167/9) | | | | |

13) N. A. Milas and S. Sussmann, ibid., **59**, 2345 (1937).
14) E. C. Horning (Editor-in-chief), "Organic Syntheses", Coll. Vol. III, 408 (1955).
15) A. H. Blatt (Editor-in-chief), ibid., Coll, Vol. II, 288 (1948).
16) A. H. Blatt, ibid., Coll. Vol. II, 81 (1948).
17) A. St. Pfau and P. Plattner, *Helv. Chim. Acta*, **15**, 1250 (1632).
18) H. Adkins and H. R. Billica, *J. Am. Chem. Soc.*, **70**, 3121 (1948).

The infrared measurements were carried out by a method previously reported,[1] at a concentration of 0.004 mol./l. in carbon tetrachloride, except that saturated solutions of compounds I and V were used because of their low solubility. The infrared data are summarized in Table I.

The authors wish to express their thanks to Mr. Teruo Kajiura and Mr. Tadao Tamura of the Government Chemical Industrial Research Institute of Tokyo for the infrared measurements.

*Department of Chemistry*
*Tokyo College of Science*
*Kagurazaka, Shinjuku-ku, Tokyo*
*(N. O. & Y. T.)*

*The University of Yamanashi*
*Research Institute of Fermentation*
*Kofu, Yamanashi (S. Õ.)*

# A Study of the Growth of Particles in Silica Sol and Hydrogel as a Factor Determining the Final Structure of Silica Gel

By Hiroshi OTOUMA and Hiroshi UKIHASHI

(Received February 2, 1965)

Many investigations have been made of the polymerization of silicic acid. However, few studies have been undertaken of the systems with relatively high concentrations and of the changes in the turbidity of the silicic acid sol in relation to the growth of the ultimate particles comprising the sol after its gelation.

The purpose of the present work is to gain new information, by the light scattering method, about the growth of particles at a relatively high concentration of silicic acid before and after the gelation of its sol, which is prepared by adding sodium silicate solutions to sulfuric acid; we also eventually hope to find some relationship with the final structure of dried silica gel.

In the sol state the changes in particle size with time was indirectly determined by the weight-average molecular weights obtained by the dilution method. After gelation, the dissymmetry, which is especially related to the size of the large particles, and the turbidity were measured at frequent intervals in pursuit of the growth of primary particles and the state of their aggregation. The surface area of dried gel was measured in seeking its relationship with the size of the primary particles as determined by light scattering. The light scattering behavior of the sol and hydrogel will be consistently discussed in connection with the growth of the primary and secondary produced particles by aggregation.

## Experimental

**The Preparation of the Silica Sol and the Gel.**—Samples with various pH values were prepared by controlling the addition of sodium silicate solutions ($SiO_2 : Na_2O = 3.22$) to sulfuric acid. The concentrations and other experimental conditions are listed in Table I. The sodium silicate solutions, sulfuric acid and sols prepared were purified by the use of glass filters (No. 4 and No. 5) and a solvent filtration apparatus. The sols which were used for determination of the particle size were filtered with great care. The turbidity of the distilled water used in the dilution was below $5 \times 10^{-5}$ $cm^{-1}$. Silica hydrosol changed into hydrogel after a definite time. Both the sols and the hydrogels were always kept at 30°C in a thermostat except when measurements were being made.

**Light Scattering Measurement and Equipment.**—Light scattering measurements were made on a Shimadzu Photoelectric Light-Scattering Photometer Model-21 type, with a green light (546 m$\mu$). The turbidity was evaluated against the incident beam from the scattering intensity at a direction of 90 degrees. The calibration of the turbidity was made by using a glass block. In the sol state small portions of samples, immediately after being taken up at definite intervals after their formation, were diluted to a concentration of $10^{-3}$ g./ml. in distilled water maintained at 30°C, then they were measured.

By using Eq. 1,[1] the weight-averge molecular weight, $\overline{M}_w$, was determined from the reciprocal of the intercept on the $Hc/\tau$ axis. Particle sizes were obtained by assuming the spheres to have the uniform density 2.2 g./cm$^3$.[2]

$$\frac{Hc}{\tau} = \frac{1}{\overline{M}_w} + Ac \qquad (1)$$

where :

1) P. Debye, *J. Phys. Chem.*, **51**, 18 (1947).
2) R. K. Iler, "Colloid Chemistry of Silica and Silicates," Cornell University Press, Ithaca, N. Y. (1955).

$$H=\frac{32\pi^3}{3\lambda^4 N}\cdot n_0^2\cdot\left(\frac{dn}{dc}\right)^2$$

$c$: the concentration of solute in g./ml.
$\tau$: the turbidity
$\overline{M}_w$: the weight-average molecular weight
$A$: a constant
$N$: Avogadro's number
$\lambda$: the wavelength of the light in vacuum
$n_0$: the refractive index of the solvent
$\frac{dn}{dc}$: the refractive index increment

$\frac{dn}{dc}=0.151$ (determined by the differential refractometery)

After gelation, the change in the dissymmetry Z, the ratio of the intensity of the scattered light at 45° to that at 135°, was sought together with the intensity of the scattered light at 90°. For the measurement of the surface area, parts of the hydrogel were taken out at appropriate intervals after gelation and then repeatedly washed and dried at 200°C for 2 hr. Surface area was determined after calcination at 540°C for 4 hr. by the BET method.

## Results and Discussion

Figure 1 shows the variation, with time, of the particle diameters in the sol state as calculated from the weight-average molecular weights.

The variation in the intensity of scattered light, and that in the dissymmetry, with the time elapsed after gelation are shown in Fig. 2 and Fig. 3 respectively. The curves of the scattering intensity are of the sigmoid type, with a maximum slope immediately after gelation. An almost constant value (not shown in Fig. 2) was reached in every case after a long period. In the curves in Fig. 3, on the other hand, the dissymmetry increases rapidly near the gelation point and finally reaches a constant value after only about two hours. The relations between the increase in the scattering intensity and the decrease in the surface area are shown in Fig. 4.

The experimental data on the changes in particle diameters in the sol state indicate

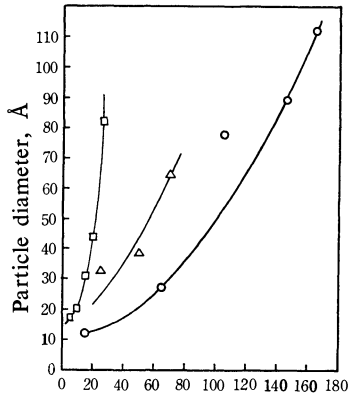



Fig. 1. Variation of particle size as a function of time.
□ Sample I △ Sample II ○ Sample III

Table I. The Preparation of the Silica Hydrosol

| Sample | Concn. | pH for preparation | Time of gelation* (at 30°C) |
|---|---|---|---|
| I | 6N $H_2SO_4$+8.5% (as $SiO_2$) $Na_2O\cdot 3.22SiO_2$ | 4.05 | 32 min. |
| II | 6N $H_2SO_4$+8.5% (as $SiO_2$) $Na_2O\cdot 3.22SiO_2$ | 3.53 | 100 min. |
| III | 6N $H_2SO_4$+8.5% (as $SiO_2$) $Na_2O\cdot 3.22SiO_2$ | 3.25 | 175 min. |
| IV | 2.1N $H_2SO_4$+3.0% (as $SiO_2$) $Na_2O\cdot 3.22SiO_2$ | 10.40 | 10 day** |

* The time of gelation was taken as the earliest time at which the samples in the beaker became stiff enough not to move when the beaker was tilted.
** The surface area (274 $m^2$/g.) was obtained of silica xerogel which had been prepared from hydrogel taken out immediately after gelation.

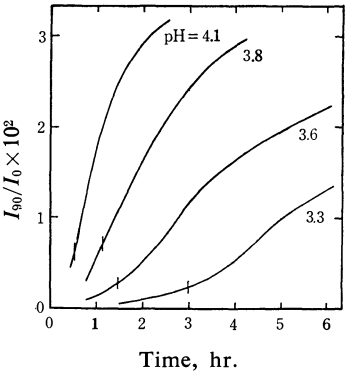



Fig. 2. Variation of scattering intensity with time. The vertical lines show the period of gelation.
$I_0$: incident beam, $I_{90}$: scattering light at 90° to the incident beam.

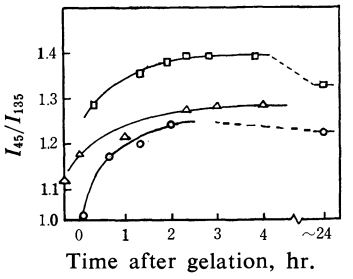



Fig. 3. Variation of dissymmetry for hydrogels.
pH: □ 3.8, △ 3.3, ○ 3.6

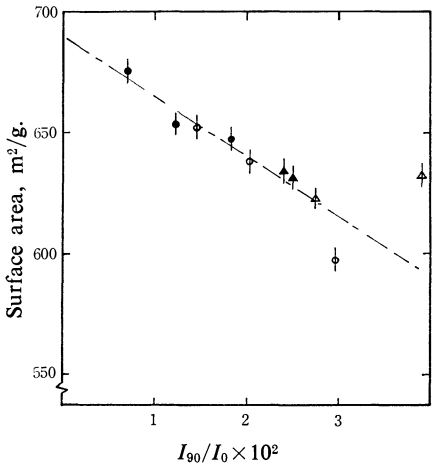
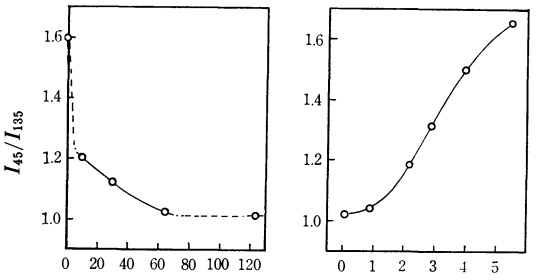



Fig. 4. Decrease of the surface area of silica gel with increasing scattering intensity of hydrogel from which the gels were prepared.
pH: ▲ 3.5, ○ 3.6, ● 4.0, △ 4.1




Figs. 5(a), 5(b). Variation of dissymmetry for sample IV.

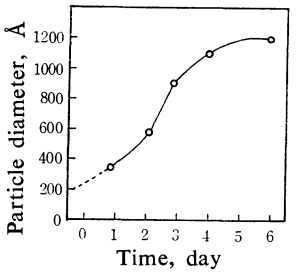



Fig. 6. Change of particle size with time determined from dissymmetry.

that it is likely that the following changes are likely when sodium silicate solutions are added to sulfuric acid.

First of all, particles with diameters of about 10—20Å rapidly appear in the mixture, as is estimated from Fig. 1, where three curves extrapolated to time zero intercept the coordinate at about 10—20Å, though their exact values in the initial stage could not be obtained because of the undue light scattering caused by impurities. The rapid growth of particles at the start, as seen in the results of sample IV (Fig. 5a), has also been predicted by Greenberg's[3] and Debye's[4] experiments. As Fig. 5a shows the large dissymmetry at $t=0$ is possibly due to impurities included rapidly decreased during the initial one hundred minutes, and then slowly increased with the growth of the particles, until gelation is completed ten days after. The interpretation of the rapid decrease in the dissymmetry in the initial stage would be: the light scattering arising from rapidly-growing particles after mixing surpassed that of impurities. Therefore, the decreased dissymmetry observed after one hundred minutes or so was due largely to the particles thus grown; these, however, were not so large as to make the dissymmetry deviate greatly from unity, so a value of around unity was obtained. Thus, the rapid decrease in the dissymmetry gives evidence of the rapid growth of particles at the start.

Greenberg obtained the particle diameter, at $t=0$, of approximately 200Å from his dissymmetry measurements. A similar observation has been reported elsewhere.[4]

In view of these facts, it may be concluded that the rapid growth occurred soon after mixing.

In the initial stage, as has been mentioned in the literature,[4] the association of particles seems to occur to a minor extent. According to Greenberg's experiment, the diameter of the particles at zero time is approximately 200Å. We, however, obtained the corresponding value of 10—20Å. This marked discrepancy can only be ascribed to the association-dissociation process, in which particles of 10—20Å are very weakly bounded together to form associated particles in a "highly solvated state"[3] and in which, upon progressive dilution, the aggregates dissociate into smaller particles 10—20Å in diameter.

This is also suggested by the negative value of $A$ (a constant in Eq. 1) being obtained only in the initial stage.

In the final stage, in turn, bonds between primary particles became stronger to such an extent that aggregates no longer dissociated into components upon dilution. This would be the reason why the particle size obtained in the final stage (Fig. 1) was substantially larger than that (only 40—45Å) which could be presumed from the BET surface area of dried gel[2] (Fig. 4). In this connection the data on sample IV are very interesting, in this

3) S. A. Greenberg and D. Sinclair, *J. Phys. Chem.*, **59**, 435 (1955).
4) P. Debye and R. V. Nauman, ibid., **65**, 10 (1961).

case the change in particles size was followed by the measurements of the dissymmetry. A particle size of approximately 1200Å before gelation is shown in Fig. 6. Dried gel after gelation, however, shows a surface area of 274 $m^2/g.$, which may indicate a primary particle only 110Å in diameter.[2)]

These observations suggest that, in the final stage of the sol, not only the continued growth of ultimate particles but also association and partial gelation occur.

So far discussions have been made on primary and secondary particles and their growth in the sol state. Our further remarks will be centered upon the continued polymerization, resulting in the growth of primary particles, and upon the continued aggregation in the gel state.

Although the value of the dissymmetry and the scattering intensity are measures of the growth of particles, their behaviors with time in the same sample are markedly different from each other (Figs. 2 and 3). A possible explanation may be based on the fact that the increase in dissymmetry shows an increase in the size of secondary particles and that gel is built up as a result of three-dimensional linkages of such secondary particles. Though hydrogel is seemingly of a solid state at the gelation point, the networks are not completed. It takes still more time for the gel to form a complete network. Therefore, the time would be shown by the point of constant dissymmetry, when the net works are finished, since the aggregation accompanies gelation. The final diameter of the secondary particles in this experiment may be of the order of 800Å as calculated from the final dissymmetry uncorrected for concentrations.

A slight fall in the dissymmetry observed after a long time would be the result of a decrease in the size of secondary particles by dehydration condensation.

The change in scattering intensity is, on the other hand, due not only to the growth of primary particles but also to that of secondary particles. The increase in the earlier parts of the curves is probably due to the light scattering from secondary particles. While the dissymmetry reached a constant about two hours after gelation, the intensity of the scattered light continuously increased. Accordingly, the growth in the size of secondary particles would stop at the time given above. The fact that the intensity of scattered light exhibits a continuous increase furnishes evidence of the continued growth of primary particles as a result of the reaction of primary particles with the silicate ions remaining unreacted in gel. This reaction or polymerization certainly accompanies the change in the weight of secondary particle, but it does not accompany the change in size.

A series of surface area measurements of samples after gelation elucidated the light scattering behavior in connection with the internal change in the gel. The increase in the scattering intensity was clearly shown to be accompanied by an increase in the size of primary particles as determined from the surface area measurement. Accordingly, a decrease in the surface area will be related to an increase in the intensity of light scattering.

Although it seemed difficult to obtain a priori the relationship from the light scattering data because of the effects of secondary particles in gel and of the relatively high concentrations, resulting in interference between particles, nevertheless the following equation was derived from the straight line shown in Fig. 4 within a limited pH range:

$$S=690-21.5\cdot(I_{90}/I_0\times10^{-2})$$

where $S$ is the surface area in $m^2/g.$

## Summary

The growth of particles in the polymerization of silicic acid has been investigated by means of light scattering. The following results were obtained:

1) Polymerization does occur for a long period, even after gelation.

2) While the aggregation is predominant near the gelation point, it seems to occur to a lesser extent even in the initial stage. The aggregate finally grows to as much as 800Å in diameter. It is of a porous and sponge-like structure, including the solvent in it.

3) Hydrogel must be understood as an entity built up of secondary particles which also consist of primary ones. Consequently, hydrogel has prime structure and a substructure, by the former three-dimensional linkages among secondary particles are meant, while by the latter are meant those among primary particles.

4) There is a linear relationship between the scattering intensity of the hydrogel and the surface area of dried gel.

*Research Laboratory*
*Asahi Glass Co., Ltd.*
*Kanagawa-ku, Yokohama*

# Semi-empirical Self-consistent Field Molecular Orbital Calculation of the Electronic Structure of the Base Components of Nucleic Acids

By Chikayoshi NAGATA, Akira IMAMURA, Yusaku TAGASHIRA and Masahiko KODAMA

(Received February 2, 1965)

Investigations of the $\pi$-electronic structure of such base components as adenine, guanine, cytosine, thymine and uracil are of importance in connection with the biological activities of deoxyribonucleic acid (DNA) and ribonucleic acid (RNA). Pullman[1] and Ladik[2] have calculated the $\pi$-electronic structures of base components by means of the Hückel MO method, and have compared them with experimental results; various kinds of physicochemical properties of bases and nucleic acids, such as the relative stability of the base paring or the base tautomers, the positions of attack in the hydration of pyrimidine bases, etc., have been well explained. However, in the Hückel MO method an ambiguity in choosing the parameters cannot be avoided, and, furthermore, the method has failed to explain such optical properties of the bases as the absorption wavelength and the oscillator strength. That is, as was pointed out by Ladik,[2] the calculated wavelengths are larger than the experimental results by 150 m$\mu$ or more (cf. Table II).

In view of this disagreement between the theories and experiments with absorption spectra, calculation by means of the SCF MO method may be valuable since the iterative procedure in this method is known to eliminate the parameter dependence. Veillard and Pullman[3] have carried out semi-empirical SCF MO calculations on the bases and the base analogs, but they have not attempted to explain such optical properties of bases as their absorption wavelengths and their oscillator strengths. Recently Nesbet[4] has calculated the wavelengths and oscillator strengths for adenine, guanine, cytosine and thymine and also for the base-pair, but no attempt to explain the direction of polarization has been made. Furthermore, in Veillard's treatment, no SCF MO calculations on the thymine molecule were carried out, and Nesbet has calculated the electronic structure of thymine by neglecting the methyl group. They did this bacause of the difficulty of estimating the energy of the valence state and the repulsion integral for the methyl group. The present authors have attempted in this paper to compare the calculated wavelengths, oscillator strengths and directions of polarization with the experimental results for adenine, guanine, cytosine, thymine, uracil, 9-methyladenine and 1-methylthymine. In the estimation of two-center repulsion integral, two alternative methods have been used, the Pariser-Parr[5] and Mataga-Nishimoto approximations.[6] Veillard and Pullman[3] used the former method, and Nesbet,[4] the latter. In our calculation, both these methods of approximation have been used and have been compared.

## Calculation Procedure

In the calculation, only $\pi$-electrons have been taken into account explicitly. The Hamiltonian of the system is written in this form:

$$H=\sum_{\mu}\left\{-\frac{\hbar^2}{2m}\Delta_{\mu}+V(\mu)\right\}+\sum_{\mu>\nu}\frac{e^2}{r_{\mu\nu}} \tag{1}$$

and the molecular orbitals have been formed by a linear combination of atomic orbitals:

$$\varphi_j=\sum_{r} C_{jr}\chi_r \tag{2}$$

Then, the energies and coefficients have been determined by solving the secular equation;

$$\begin{vmatrix} F_{11}-E & F_{12}\cdots\cdots & F_{1m} \\ F_{21} & F_{22}-E\cdots\cdots & F_{2m} \\ \cdots\cdots & \cdots\cdots & \\ \cdots\cdots & \cdots\cdots & \\ F_{m1} & F_{m2}\cdots\cdots & F_{mm}-E \end{vmatrix}=0 \tag{3}$$

where

$$F_{rr}=\alpha_r+\sum_{t}^{m}P_{tt}(rr\,|\,tt)-\frac{1}{2}P_{rr}(rr\,|\,rr) \tag{4}$$

1) A. Pullman and B. Pullman, *Bull. soc. chim. France*, 1958, 766; 1959, 594.
2) J. Ladik and T. A. Hoffmann, *Biopolymers, Symposia*, No. 1, 117 (1964).
3) A. Veillard and B. Pullman, *J. Theoret. Biol.*, 4, 37 (1963).
4) R. K. Nesbet, *Biopolymers, Symposia*, No. 1, 129 (1964).
5) R. Pariser and R. G. Parr, *J. Chem. Phys.*, 21, 466 (1953).
6) N. Mataga and K. Nishimoto, *Z. physik. Chem., Neue Folge*, 13, 140 (1957).

$$F_{rs}=\beta_{rs}-\frac{1}{2}P_{rs}(rr\,|\,ss) \tag{5}$$

with

$$\alpha_r=\int\chi_r(1)\Big(-\frac{\hbar^2}{2m}\Delta_1+V(1)\Big)\chi_r(1)\mathrm{d}\tau_1$$
$$=\int\chi_r(1)\Big(-\frac{\hbar^2}{2m}\Delta_1+U_r(1)\Big)\chi_r(1)\mathrm{d}\tau_1$$
$$+\sum_{s\neq r}\int\left[\chi_r(1)\left\{U_s^0(1)-\int\frac{\chi_s^2(2)e^2}{r_{12}}\mathrm{d}\tau_2\right\}\right]\times$$
$$\chi_r(1)\mathrm{d}\tau_1\fallingdotseq W_{2p}-\sum_{s\neq r}\{(s:rr)+(rr\,|\,ss)\} \tag{6}$$

$$\beta_{rs}=\int\chi_r(1)\Big(-\frac{\hbar^2}{2m}\Delta_1+V(1)\Big)\chi_s(1)\mathrm{d}\tau_1 \tag{7}$$

and

$$(rr\,|\,ss)=\iint\chi_r(1)\chi_r(1)\frac{e^2}{r_{12}}\chi_s(2)\chi_s(2)\mathrm{d}\tau_1\mathrm{d}\tau_2 \tag{8}$$

In Eq. 6, the Coulomb penetration integral $(s:rr)$ is neglected, as usual. $W_{2p}$ is taken as equal to $-I$; $I$ is the ionization potential of the atomic valence state. One-center repulsion integral $(rr\,|\,rr)$ is usually estimated as $I$-$A$, where $A$ is the electron affinity. In our calculation the values of $I$ and $A$ have been taken from the paper of Hinze and Jaffé.[7] As was stated above, two alternative ways of estimating the two center repulsion integral have been used; the Pariser-Parr and Mataga-Nishimoto approximations. In the former method, the following equations are used: at the $R\leqq 2.8$ Å distances;

$$(rr\,|\,ss)=1/2\{(rr\,|\,rr)+(ss\,|\,ss)\}+aR+bR^2 \tag{9}$$

and at $R>2.8$ Å:

$$(rr\,|\,ss)=7.1975(1/\sqrt{R^2+1/4(R_r+R_s)^2}$$
$$+1/\sqrt{R^2+1/4(R_r-R_s)^2}) \tag{10}$$
$$R_r=(4.597/Z^*)\times10^{-8}\,\mathrm{cm}.$$

where $R$ is the internuclear distance, and $a$ and $b$ are parameters determined from Eq. 10 when $R$ is equal to 2.8 Å and 3.7 Å respectively. $Z^*$ is the effective nuclear charge.

In the case of the Mataga-Nishimoto approximation, the following relation is used:

$$(rr\,|\,ss)=e^2/(R_{rs}+a_{rs}) \tag{11}$$

The constant, $a_{rs}$ is determined by using the relation:

$$(rr\,|\,rr)=14.39/a=I_r-A_r \tag{12}$$

For the case of two-heteronuclear centers, i.e. carbon and nitrogen, the value of $a$ is taken as the harmonic mean of $a_C$ and $a_N$.

The above two methods of approximation have been used in our calculations, and their results have been compared with each other and also with the experimental results.

Several ways of evaluating the values of $\beta_{rs}$ have been proposed[4,5,8]; Pariser-Parr's method, which determins $\beta_{rs}$ from the spectroscopic data for only the nearest neighbor atomic orbitals, has especially been used. However, we used the following relation:

$$\beta_{rs}=lS_{rs} \tag{13}$$

where $S_{rs}$ is the overlap integral between the $r$th $\pi$-atomic orbital and $s$th one, and $l$ is a parameter, which was determined as $-12.65$ from the mean of the following values:

$\beta_{CO}=-2.70$ eV. $S_{CO}=0.2063$

$\beta_{CN}=-2.39$ eV. $S_{CN}=0.1957$

Moreover, in our calculation, $\beta_{rs}$ was taken into account not only for the nearest neighbors but also for all pairs of $r$ and $s$.

The oscillator strengths of the transitions from the ground state to the excited states have been calculated by using the following equation;

$$f=1.085\times10^{-5}\,\sigma_{ob}\,\boldsymbol{m}_{ob}^2 \tag{14}$$

where $\sigma_{ob}$ is the wave number of the transition from the ground state to the excited state $b$. $\boldsymbol{m}_{ob}$ in Eq. 14 is given by:

$$\boldsymbol{m}_{ob}=\int\Psi_{ob}\sum_i\boldsymbol{r}_i\,\Psi_b\,\mathrm{d}\tau \tag{15}$$

in which $\Psi_o$ and $\Psi_b$ are the wave functions of the ground and excited states respectively, and $\boldsymbol{r}_i$ is the position coordinate of the $i$th electron.

## Choice of Parameters

Values of $W_{2p}$ and $(rr\,|\,rr)$ semi-empirically evaluated are tabulated in Table I.

Table I. Semi-empirically evaluated values of $W_{2p}$ and $(rr|rr)$

| $r$ | $W_{2p}$ | $(rr\|rr)$ |
|---|---|---|
| C | −11.16 | 11.13 |
| O | −17.28 | 15.27 |
| N(azo) | −14.12 | 12.34 |
| N(amino) | −28.53 | 16.57 |
| OH | −34.75 | 21.18 |
| $H_3$* | −10.256 | 9.326 |

* Hyperconjugation in the methyl group is taken into account, and the group orbital of $H_3$ is assumed to overlap with $\pi$-orbitals.

The values of $W_{2p}$ and $(rr\,|\,rr)$ for the carbon, oxygen and azo-nitrogen are taken from the paper of Hinze and Jaffé.[7] It is difficult to

7) J. Hinze and H. H. Jaffé, *J. Am. Chem. Soc.*, **84**, 540 (1962).
8) G. Leroy, *J. chim. phys.*, **60**, 1270 (1963).

choose the values of $W_{2p}$ for such atoms as amino-nitrogen, which contribute two electrons to the $\pi$-system; many different values for this atom have been adopted by different authors.[3,9-11] In the present paper, we have adopted the value of $-28.526$ eV. for the $W_{2p}$ of amino-nitrogen (that is, $N^+(t_r t_r t_r, \pi) \rightarrow N^{++}(t_r t_r t_r)$) from the following relations:

$$N^+(s^2p^2) \rightarrow N^+(t_r t_r t_r, \pi) \quad 9.814 \text{ eV.}$$

$$N^+(s^2p^2) \rightarrow N^{++}(s^2p) \quad 29.41 \text{ eV.}$$

$$N^{++}(s^2p) \rightarrow N^{++}(t_r t_r t_r) \quad 8.930 \text{ eV.}$$

Similarly, the values of $W_{2p}$ and $(rr|rr)$ for the quasi-$\pi$ orbital of $H_3$ in the methyl group are difficult to evaluate semi-empirically, therefore, no calculation has ever been carried out for thymine and its analogs. The values adopted in our calculation are presented in Table I; the values have been determined by Morita for the SCF MO calculation of the benzenium ion by taking hyperconjugation into account.[12] By using these values, he has successfully explained the experimental results of the absorption spectra of the benzenium ion.

The values of the interatomic distances for adenine, guanine, cytosine and thymine are taken from the paper of Spencer,[13] while the values for uracil are taken from Wyckoff's table.[14] For such methylderivatives as 1-methylthymine and 9-methyladenine, the data for their parent molecules, i. e., thymine and adenine are used except for the distance of the N-$CH_3$ bond. The value for this N-C distance is tentatively taken as 1.46 Å, which is the distance between the carbon and the nitrogen in $CH_3NH_2$ molecules.

All the calculations in this paper have been carried out on the NEAC 2101 electronic computer in this Institute.

## Results and Discussion

**Wavelength and Oscillator Strength.** — The results of the calculation of the transition energies and oscillator strengths for adenine, guanine, thymine, cytosine and uracil are presented in Table II in comparison with the experimental values. The experimental data of the absorption spectra have been given by Beaven et al.[15] For the sake of comparison, the values obtained in the Hückel MO method, taken from the paper of Ladik,[2] are also indicated. It may clearly be seen that the SCF MO treatment improves the results strikingly and that the agreement between the theoretical results and experiments is satisfactory, especially for adenine and cytosine. That is, if the 6→7 transition of adenine and 5→6 transition of cytosine are assigned to the first bands of these molecules respectively, the calculated wavelengths coincide with experimental values within the limits of 15—20 Å. Agreements between the theory and experiment for these transitions are very good also for the values of the oscillator strengths.

The calculated wavelength for thymine is shorter than the experimental value by about 60 m$\mu$ in the case of the Pariser-Parr approximation. This is the largest discrepancy between theory and experiment among the bases calculated in this paper. First of all, an inappropriate choice of the semi-empirical parameter for the methyl group was deemed the cause of this large discrepancy. Therefore, calculation has been carried out for demethylated thymine, and the wavelength of 198 m$\mu$ has been obtained. This result shows that the cause of the disagreement for thymine is not in the unsuitable choice of the parameter of methyl group. In general, it is known that the agreement between the calculated and experimental wavelengths for the compounds which contain two oxygens is not very good for other compounds. Thus, the calculated wavelength for parabenzoquinone gave a value 50 m$\mu$ shorter than the experimental value.[16] Many attempts have been made to improve the theoretical results by changing the values of the semi-empirical parameters, but no remarkable improvement has been achieved.[16,17] It may be expected that the theoretical wavelength for thymine can be improved in connection with these compounds.

The wavelengths and oscillator strengths for the transitions other than the maximum wavelength have been calculated; they are indicated in Table II, together with the observed values. From a comparison of these values, the following assignments may be made: the bands at 210 m$\mu$ in cytosine, 246 m$\mu$ in guanine and 207 m$\mu$ in thymine might be assigned to the transitions of 4→6 or 5→7 in cytosine, 7→9 in guanine and 5→8 in thymine respectively. The transitions of 6→8 and 5→7 in thymine may be neglected, because the calculated

9) S. Yomosa, *Biopolymers, Symposia*, No. 1, 1 (1964).
10) B. Grabe, ibid., 1, 283 (1964).
11) S. Mataga and N. Mataga, *Z. physik. Chem., Neue Folge*, 19, 231 (1959).
12) T. Morita, This Bulletin, 33, 1486 (1960).
13) M. Spencer, *Acta Cryst.*, 12, 59 (1959).
14) R. W. G. Wyckoff, "Crystal Structure," Supplement IV, Interscience Publishers (1959), p. 128.
15) G. H. Beavens, E. R. Holiday and E. A. Johnson, "The Nucleic Acids," Vol. I, Ed. by E. Chargaff and J. N. Davidson, Academic Press, New York (1955), p. 493.
16) J. W. Sidman, *J. Chem. Phys.*, 27, 429 (1957).
17) A. Kuboyama and K. Wada, Preprint of the 17th Annual Meeting of the Chemical Society of Japan (1964), p. 496; Preprint of the Discussion for the Electronic State of Molecules (1964) p. 63.

TABLE II. COMPARISON OF THE CALCULATED WAVELENGTH AND OSCILLATOR STRENGTH WITH EXPERIMENTS

| Compound | Absorption max., mμ | | | | Oscillator strength | | | |
|---|---|---|---|---|---|---|---|---|
| | Exp. | Pariser-Parr | Mataga-Nishimoto | Hückel MO* | Exp.** | Pariser-Parr | Mataga-Nishimoto | Hückel MO* |
| Adenine | 260.5 | 262(6→7) | 253(6→7) | 396 | 0.30 (13.35) | 0.387 | 0.472 | 0.51 |
| | | 232(6→8) | 238(6→8) | | | 0.471 | 0.379 | |
| | | 178(5→7) | 199(5→7) | | | 0.181 | 0.161 | |
| Cytosine | 276 | 278(5→6) | 289(5→6) | 366 | 0.17 (10.0) | 0.182 | 0.299 | 0.43 |
| | 210 | 197(4→6) | 192(4→6) | | (9.7) | 0.616 | 0.689 | |
| | | 181(5→7) | 194(5→7) | | | 0.618 | 0.601 | |
| Guanine | 275.5 | 299(7→8) | 325(7→8) | 353 | (8.15) | 0.395 | 0.361 | 0.44 |
| | 246 | 239(7→9) | 268(7→9) | | (10.7) | 0.575 | 0.416 | |
| | | 173(6→8) | 194(6→8) | | | 0.149 | 0.146 | |
| Uracil | 259 | 290(5→6) | 300(5→6) | 335 | 0.25 (8.2) | 0.177 | 0.313 | 0.50 |
| | | 185(5→7) | 198(5→7) | | | 0.622 | 0.616 | |
| | | 188(4→6) | 183(4→6) | | | 0.611 | 0.516 | |
| Thymine | 264.5 | 200(6→7) | 221(6→7) | 342 | 0.21 (7.89) | 0.730 | 0.993 | 0.50 |
| | 207 | 172(5→8) | 175(5→8) | | (9.5) | 0.394 | 0.440 | |
| | | 162(6→8) | 211(6→8) | | | 0.005 | 0.072 | |
| | | 190(5→7) | 199(5→7) | | | 0.039 | 0.041 | |

* Theoretical values in the Hückel MO method were taken from the paper of Ladik and Hoffmann (Ref. 2).

** Numerals in parenthesis are $\varepsilon \times 10^{-3}$, where $\varepsilon$ is the absorption coefficient.

oscillator strengths of these transitions are very small, i. e., 0.005 and 0.038 respectively.

It is difficult to determine the relative merits of the Pariser-Parr and Mataga-Nishimoto approximations.

**The Direction of Polarization.**—It may be of interest to compare the polarized absorption spectra of bases with the theoretically-determined directions of polarization. As far as we are aware, the experimental data for the polarized absorption spectra of bases or their analogs have been obtained only for 9-methyladenine and 1-methylthymine. That is, Stewart and Davidson[18] have obtained the polarized absorption spectra of the single crystal of 9-methyladenine, 1-methylthymine and the A-T dimer.[18] As a result, for 1-methylthymine the first absorption band has been shown to polarize close to the $N_1$–$C_4$ axis, and the second band, approximately perpendicular to the first, and for 9-methyladenine the direction of polarization has been determined along the shorter axis, $D_4$–$C_5$. From the results for 9-methyladenine, Stewart and Davidson also assumed that the main band of adenine ($\lambda_{max}=261$ mμ) should be assigned to a short-axis polarized band and the weak shoulder ($\lambda_{max}=267$ mμ), to a long-axis band

The theoretical treatment of Tinoco and DeVoe[19] has led to the same assignment; that is, by using the Hückel MO method they have assigned the 6→8 transition to the main band of adenine and the 6→7 transition to the shoulder band. On the other hand, Mason has attributed the intense absorption (261 mμ) in adenine to a long-axis polarized band.[20] Thus, the assignments of the transitions in adenine and 9-methyladenine contradict to one another; in view of this contradiction, it may be worth while to determine the directions of polarization for adenine and 9-methyladenine by means of the SCF MO calculation and to compare them with the experimental values.

As may be seen in Fig. 1, the theoretically-predicted direction of polarization of the 7→9 transition for 9-methyladenine is close to the $C_4$–$C_5$ axis (short-axis polarized), whereas the 7→8 transition is nearly perpendicular to the direction of the 7→9 transition. This is true in both methods of approximations, the Pariser-Parr and Mataga-Nishimoto methods. When these results are compared with those of the experiment of Stewart and Davidson,[18] it may

18) R. F. Stewart and N. Davidson, *J. Chem. Phys.*, **39**, 255 (1963).

19) H. DeVoe and I. Tinoco, Jr., *J. Mol. Biol.*, **4**, 518 (1962).

20) S. F. Mason, *J. Chem. Soc.*, **1954**, 2071.

TABLE III. COMPARISON OF THE CALCULATED WAVELENGTH AND OSCILLATOR STRENGTH WITH EXPERIMENTS FOR 9-METHYLADENINE AND 1-METHYLTHYMINE

| Compound | Absorption max., mμ | | | Oscillator strength | | |
|---|---|---|---|---|---|---|
| | Exp.* | Pariser-Parr | Mataga-Nishimoto | Exp.* | Pariser-Parr | Mataga-Nishimoto |
| 9-Methyladenine | 261 | 263(7→8) | 254(7→8) | 0.28 | 0.377 | 0.479 |
| | 206 | 231(7→9) | 238(7→9) | 0.62 | 0.482 | 0.389 |
| | | 199(7→10) | 204(7→10) | | 0.188 | 0.191 |
| | | 180(6→8) | 200(6→8) | | 0.199 | 0.165 |
| | | 178(6→9) | 184(6→9) | | 0.435 | 0.447 |
| | | 164(6→10) | 172(6→10) | | 0.358 | 0.408 |
| 1-Methylthymine | 273 | 200(7→8) | 222(7→8) | 0.19 | 1.007 | 0.985 |
| | 207 | 162(7→9) | 213(7→9) | 0.28 | 0.005 | 0.074 |
| | | 154(7→10) | 165(7→10) | | 0.098 | 0.125 |
| | | 190(6→8) | 199(6→8) | | 0.042 | 0.049 |
| | | 172(6→9) | 175(6→9) | | 0.396 | 0.428 |
| | | 129(6→10) | 138(6→10) | | 0.203 | 0.087 |

* These are spectra in solution. Spectra in crystal state are 275 and 230 mμ for 1-methylthymine and 275, 255 and 230 mμ for 9-methyladenine (Ref. 18).

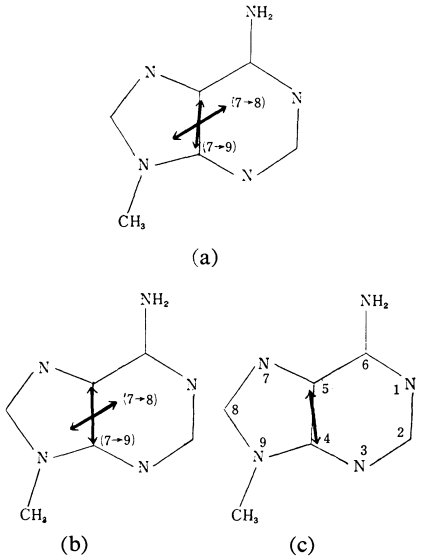



Fig. 1. Comparison of the predicted direction of polarization of 9-methyladenine with the experiment: (a) Calculation according to Mataga-Nishimoto and (b) Pariser-Parr approximations. (c) Experiment of Stewart and Davidson (Ref. 18).

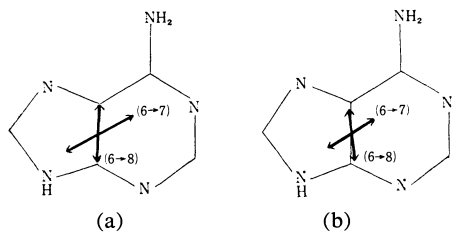



Fig. 2. Predicted directions of polarization of adenine: (a) Mataga-Nishimoto approximation and (b) Pariser-Parr approximation.

be seen that the intense band which is polarized to the $C_4$-$C_5$ axis may be assigned to the second transition, 7→9. Similarly, the first (6→7) transition of adenine is predicted to polarize to the long-axis, and the second (6→8) transition, to be short-axis polarized (Fig. 2). If Stewart's assignment for adenine were true, 6→7 and 6→8 transitions in adenine should be assigned to the weak shoulder (267 mμ) and to the main band (261 mμ) respectively. However, as has been stated above, Mason[20] attributed the long-axis polarized band to the main band of adenine. From this point of view, the 6→7 transition may reasonably be assigned to the main band. In these controversial circumstances, it is difficult to determine which assignment is true for adenine and 9-methyladenine. From a comparison of the calculated transition energy and the experimental results, the main band of adenine was assigned to the 6→7 transition; in this point Mason's assignment is supported. Thus, the first and the second bands of 9-methyladenine (261 mμ and 206 mμ respectively) may be assigned to the 7→8 and 7→9 or 7→10 transitions (Table III). As may be seen in Table III, the 7→9, 7→10, 6→8, 6→9 and 6→10 transitions in 9-methyladenine have nearly the same energies of absorption; therefore, the absorption of 206 mμ may consist of these transitions. The magnitude of the oscillator strength of this absorption may well be understood if it is assigned as above.

The calculated optical indexes for 1-methylthymine are also shown in Table III, in comparison with the experimental results. The

calculated oscillator strength of the first band, i.e., the 7→8 transition, is the largest, and that of the 6→9 transition is next largest. The strengths of the other transitions are relatively weak compared with these two transitions, and, as may be seen in Fig. 3, the directions of these transitions agree well with the experimentally-determined values. With regard to the transition energy, agreement between theory and experiment is very poor,

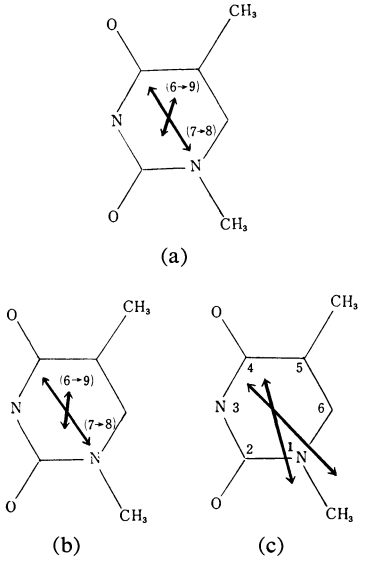



Fig. 3. Comparison of the predicted direction of polarization of 1-methylthymine with the experiment: (a) Calculation according to the Mataga-Nishimoto and (b) Pariser-Parr approximations. (c) Experiment of Stewart and Davidson (Ref. 18).

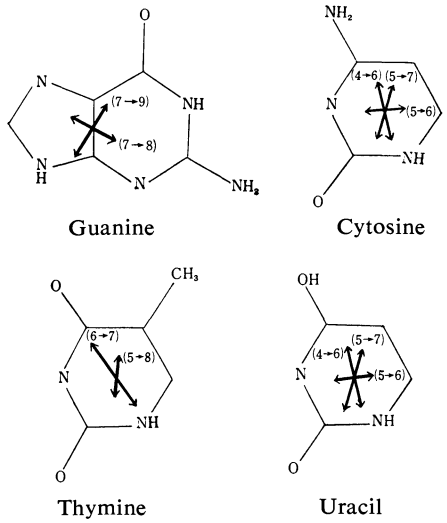



Fig. 4. Predicted directions of polarization of guanine, cytosine, thymine and uracil (Pariser-Parr approximation).

as in the case of thymine itself; in this case, the results of the Mataga-Nishimoto approximation are better than those of the Pariser-Parr method.

Similarly, the theoretically-determined direction of the polarization for guanine, thymine, cytosine and uracil are indicated in Fig. 4. Although the experiments have not yet been carried out for these compounds, the theoretical results may give an insight into the direction of the polarization and the assignment of the optical transition. In determining the direction of polarization, calculations were carried out by means of the Pariser-Parr approximation. The results using the Mataga-Nishimoto approximation are nearly the same in all these molecules. DeVoe and Tinoco,[19] from their Hückel MO calculation, have predicted the directions of polarization of these molecules and of adenine. It is worth noticing that their results are very similar to those of our SCF MO treatment. Therefore, it may be said that the direction of the transition moments is not sensitive to the degree of approximation.

**The Orbital Energy and the π-Electron Distribution.** — The energies of the highest-occupied and lowest-vacant orbitals are indicated in Table IV. The meanings of the orbital energy in the Hückel and SCF MO methods are not necessarily the same, but it may be of interest to compare the relative magnitudes of the orbital energies obtained by the two methods. The order of the energies

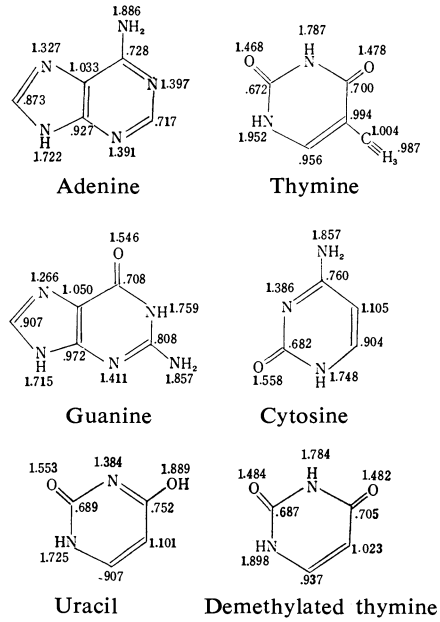
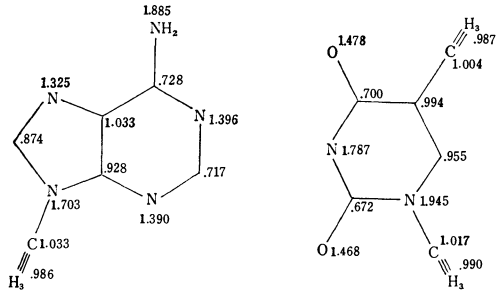



Fig. 5. π-Electron distributions of bases by means of SCF MO method (Pariser-Parr approximation).

TABLE IV. THE ENERGIES OF THE HIGHEST OCCUPIED AND LOWEST VACANT ORBITALS OF BASES (in eV.)

| Compound | Energies of the highest occupied levels | | Energies of the lowest vacant levels | |
|---|---|---|---|---|
| | Pariser-Parr | Mataga-Nishimoto | Pariser-Parr | Mataga-Nishimoto |
| Thymine | −12.045 | −10.131 | −1.450 | −1.861 |
| Uracil | −10.472 | −9.419 | −1.332 | −2.109 |
| Cytosine | −10.460 | −9.401 | −1.145 | −1.914 |
| Adenine | −9.513 | −9.029 | +0.132 | −0.980 |
| Guanine | −9.236 | −8.289 | −0.314 | −1.305 |




9-Methyladenine 1-Methylthymine

Fig. 6. $\pi$-Electron distributions of 9-methyladenine and 1-methylthymine (Pariser-Parr approximation).

of the highest-occupied level of bases is written, in the order of decreasing energy, as follows; guanine>adenine>cytosine>uracil. This order is in accordance with that obtained by Veillard and Pullman,[3] and also with the results of the Hückel MO method.[1,2] For thymine, however, the results by the SCF MO and Hückel MO methods are not in accord; in the former method, the energy of the highest-occupied level of this molecule is the lowest among the bases, but the latter method gives a value between those of cytosine and adenine.

The $\pi$-electron distributions of adenine, thymine, guanine, cytosine, uracil, 9-methyladenine and 1-methylthymine are shown in Figs. 5 and 6. The relative magnitude of the $\pi$-electron density for guanine and cytosine is the same as that of the SCF MO calculation of Veillard and Pullman[3] and also that of the Hückel MO calculation by Pullman,[1] but for adenine the relative magnitude is in disagreement; that is, the order is $N_1>N_3>N_7$ in our calculation, whereas it is $N_7>N_1>N_3$ in Veillard and Pullman.[3] The protonation has been known to occur at the $N_1$ position of adenine,[21,22] and this fact is in accord with the results of the present authors.

21) J. M. Broomhead, *Acta Cryst.*, **1**, 324 (1948); **4**, 92 (1951).
22) W. Cochram, ibid., **4**, 81 (1951).

As may be seen in Figs. 5 and 6, the electron densities for 9-methyladenine and 1-methylthymine are nearly the same as those of its parent molecules, adenine and thymine. Thus, the changes in the $\pi$-electron distributions due to the methyl substitution are known to be small. The changes in the transition wavelengths due to the methyl substitution are zero and 10 m$\mu$ for 9-methyladenine and 1-methylthymine respectively (cf. Tables II and III). The fact that there is no shift due to the methyl substitution in adenine seems very curious; the spectra of adenine and 9-methyladenine should be measured under the same conditions.

## Summary

SCF MO calculations have been carried out for adenine, guanine, thymine, cytosine, uracil, 9-methyladenine and 1-methylthymine. In evaluating the two-center repulsion integral, the Pariser-Parr and Mataga-Nishimoto approximations have both been used, and the results compared with each other and with the experimental data on the optical properties. In the calculation of thymine, 9-methyladenine, and 1-methylthymine, the hyperconjugation of the methyl group has been taken into account. The calculated wavelength and the oscillator strength of the singlet-singlet transition for the above-mentioned molecules explain the experimental values well except for thymine and 1-methylthymine. The theoretically-determined directions of the polarization of the transition moments have been compared with the experimental results for adenine, 9-methyladenine and 1-methylthymine. With regard to the direction of the polarization of the transition moments of the first and the second absorptions of adenine and 9-methyladenine, the results are questionable. From the theoretical point of view, it is difficult to determine which assignment is correct, however, in view of the wavelength and the oscillator strength, the first absorption may

reasonably be assigned to the long-axis polarized band. The calculated and the experimentally-determined direction of polarization for 1-methylthymine agree well with each other. The energies of the highest and lowest vacant orbitals and the $\pi$-electron densities for the molecules treated in the present paper have been calculated and compared with the results obtaied by the Hückel MO method.

*Division of Biophysics,*
*National Cancer Center Research Institute*
*Tsukiji, Chuo-ku, Tokyo*

# The Benzene-Photosensitized cis-trans Isomerization of Butene-2

By Masahiro TANAKA, Terumi TERAO and Shin SATO

(Received February 4, 1965)

Recently there have been a number of reports on the photochemical cis-trans isomerization of olefins by organic sensitizers.[1-3] Hammond et al.[1,2] have examined the photosensitized isomerization in the liquid phase, using mainly carbonyl compounds as sensitizers. Cundall and his co-workers[3] studied the gas-phase-photosensitized isomerization of butene-2, using several organic sensitizers. They showed that the photostationary trans-to-cis ratio was 1.37 when benzene and pyridine were used as sensitizers.

The photosensitization by organic substances seems to be of great importance not only in elucidating intermolecular energy transfer phenomena in general, but also in solving the problem of assimilation in plants.

This paper will describe the benzene-photosensitized cis-trans isomerization of butene-2 in the gas phase.[4]

## Experimental

The benzene used was a special-grade reagent which had been fractionally distilled; the middle third was used. The *cis*- and *trans*-butene-2 were commercially available substances whose vapor-phase chromatography showed to be 99.9% pure. They were thus used without further purification.

Special care was taken to keep the vacuum line free of mercury. The light source used was a low-pressure mercury arc lamp. Between the lamp and the quartz reaction vessel, a UV25 filter (supplied by the Toshiba Denki Co.) which eliminated the light shorter than 2300 Å was placed.

The analysis was carried out gas chromatographically, using dimethylsulfolane on celite as a separation column.

In the course of the experiment, it was shown that the light absorbed by benzene did not obey Lambert-Beer's law. When necessary, the ratio of absorbed light and incident light, $I_a/I_0$, was obtained as follows: the light transmitted was measured by the mercury-photosensitized decomposition of ethylene[5,6] in a cell just behind the reaction cell, which contained various pressures of benzene. This procedure gave the relation $\log_{10}(I_0/I_t) = 0.0205p - 0.0000883p^2$, where $I_0$ and $I_t$ are the intensities of transmitted light when the reaction cell contains no benzene and $p$ mmHg benzene respectively. From this relation, $I_a/I_0$ ratio could be calculated at any benzene pressure.

All experiments were carried out at room temperature.

## Results

The reaction was very clean, no products other than the isomerized butene-2 being detected.

Figure 1 shows the time dependence of the cis-to-trans ratio, both *cis*- and *trans*-butene-2 being used as starting materials. The photostationary cis-to-trans ratio may be seen from the figure to be about unity.

The effect of the benzene pressure on the cis-to-trans isomerization rate is summarized in Table I. It can be seen from the Table that the isomerization rate increases with the pressure of benzene. The rate tends to decrease, however, after the benzene pressure reaches a certain value. The ratio of the absorbed light to the isomerization rate is also seen to increase with the pressure of benzene.

The dependence of the isomerization rate on

1) G. S. Hammond and J. Saltiel, *J. Am. Chem. Soc.*, **84**, 4938 (1962).
2) G. S. Hammond, J. Saltiel, A. A. Lamola, N. J. Turro, J. S. Bradshaw, D. O. Cowan, R. C. Counsell, V. Vogt and C. Dalton, ibid., **86**, 3197 (1964).
3) R. B. Cundall, F. J. Fletcher and D. G. Milne, *Trans. Faraday Soc.*, **60**, 1149 (1964).
4) S. Sato, K. Kikuchi and M. Tanaka, *J. Chem. Phys.*, **39**, 239 (1963).
5) A. B. Callear and R. J. Cvetanović, ibid., **24**, 873 (1956).
6) Kang Yang, *J. Am. Chem. Soc.*, **86**, 3941 (1964).

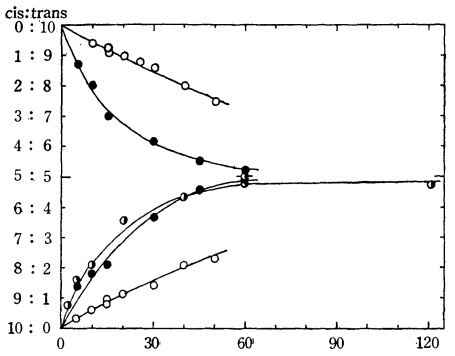



Fig. 1. The time dependence of the cis-trans isomerization.

○ Butene-2, 20 mmHg ; benzene, 47.2 mmHg
● Butene-2, 5 mmHg ; benzene, 47.2 mmHg
◑ Butene-2, 11 mmHg ; benzene, 69 mmHg ; The incident light intensity is not the same as the above two series.
-◑- Started from *trans*-butene-2. The other conditions are the same as just the above series.

TABLE I. BENZENE PRESSURE DEPENDENCE OF THE PHOTOSENSITIZED ISOMERIZATION

Initial *cis*-butene-2 pressure, 20.7±0.4 mmHg
Irradiation period, 15 min.

| Benzene mmHg | $I_a/I_0$ | Conversion % | Isomerization rate mmHg/min. |
|---|---|---|---|
| 0 | 0 | 0.65 | 0 |
| 3.18 | 0.139 | 2.52 | 0.0258 |
| 4.48 | 0.187 | 2.76 | 0.0291 |
| 5.68 | 0.230 | 3.48 | 0.0391 |
| 6.6 | 0.261 | 3.78 | 0.0433 |
| 14.5 | 0.474 | 5.69 | 0.0696 |
| 14.5 | 0.474 | 5.70 | 0.0698 |
| 15.6 | 0.497 | 5.81 | 0.0712 |
| 18.7 | 0.556 | 7.01 | 0.0878 |
| 28.6 | 0.694 | 8.65 | 0.104 |
| 47.2 | 0.831 | 9.60 | 0.124 |
| 49.0 | 0.839 | 9.74 | 0.125 |
| 64.4 | 0.890 | 10.5 | 0.136 |
| 75.2 | 0.909 | 10.1 | 0.130 |
| 92.6 | 0.927 | 9.83 | 0.127 |
| 93.5 | 0.929 | 9.29 | 0.119 |

the butene-2 pressure was also examined. The results are summarized in Table II, which shows that the rate increases monotonously as the pressure increases, while at high pressures it tends to saturate.

## Discussion

Table I clearly shows that scarcely any cis-trans isomerization of butene-2 occurs in the absence of benzene, but that the rate increases

TABLE II. BUTENE-2 PRESSURE DEPENDENCE OF PHOTOSENSITIZED ISOMERIZATION

Benzene pressure, 69 mmHg
Irradiation period, 2 min.

| *cis*-Butene-2 mmHg | Isomerization rate mmHg/min. |
|---|---|
| 3.16 | 0.0264 |
| 3.85 | 0.0283 |
| 6.05 | 0.0325 |
| 6.49 | 0.0464 |
| 9.08 | 0.0459 |
| 9.52 | 0.0461 |
| 14.9 | 0.0565 |
| 28.5 | 0.0596 |

markedly as the pressure of benzene increased. It is evident from this fact that the energy transfer from excited benzene to butene-2 induces the ovserved isomerization. Among the excited states of benzene, the lowest-excited singlet ($^1B_{2u}$, 4.7 eV.)[7,8] and the lowest triplet ($^3B_{1u}$, 3.6 eV.)[8] are conceivably involved in the reaction when, as is the case in the present study, the 2537 Å mercury resonance line is employed. A possible reaction mechanism involving these excited states is

$$B + h\nu \longrightarrow {}^1B_n \quad (1)$$

$${}^1B_n + M \longrightarrow {}^1B_0 + M \quad (2)$$

$${}^1B_0 \longrightarrow B + h\nu' \quad (3)$$

$$\longrightarrow {}^3B_n \quad (4)$$

$${}^1B_0 + B \longrightarrow B + B \quad (5)$$

$${}^3B_n + M \longrightarrow {}^3B_0 + M \quad (6)$$

$${}^3B_0 \longrightarrow B(+ h\nu'') \quad (7)$$

$${}^3B_0 + B \longrightarrow B + B \quad (8)$$

$${}^1B_0 + C \longrightarrow B + {}^1C \quad (9)$$

$${}^3B_0 + C \longrightarrow B + {}^3C \quad (10)$$

$$\left.\begin{array}{l} {}^1C \xrightarrow{1-\alpha} C \\ \quad\xrightarrow{\alpha} T \end{array}\right\} \quad (11)$$

$$\left.\begin{array}{l} {}^3C \xrightarrow{1-\beta} C \\ \quad\xrightarrow{\beta} T \end{array}\right\} \quad (12)$$

where B, C and T refer to benzene, *cis*- and *trans*-butene-2 respectively, where the superscripts and subscripts denote the electronic multiplicities and the vibrational quantum numbers respectively and where M indicates any third body carrying away the vibrational energy of excited benzene. The steady-state treatment gives the following equation:

7) M. Goeppert-Meiyer and A. L. Sklar, *J. Chem. Phys.*, 6, 645 (1938).
8) R. Pariser, ibid., 24, 250 (1956).

$$R_T \equiv \frac{[dT]}{dt} = \frac{\alpha k_9[C] I_a}{k_3+k_4+k_5[B]+k_9[C]} + \frac{\beta k_{10}[C]}{k_7+k_8[B]+k_{10}[C]} \cdot \frac{k_4 I_a}{k_3+k_4+k_5[B]+k_9[C]} \quad (1)$$

The photochemical cis-trans isomerization of olefins by organic sensitizers has been extensively studied in the liquid phase by Hammond et al.,[1,2] the results being best understood in terms of a triplet energy transfer from sensitizer to olefin. Since butene-2 has little absorption in the neighborhood of 2500 Å, and since the life-time of a singlet excited state is much shorter than that of a triplet, the excitation of butene-2 by an energy transfer from a singlet-excited benzene to butene-2 is unlikely; the intersystem crossing from an excited-singlet benzene to its lowest triplet would be much faster than the energy transfer to butene-2. Therefore, it may be safe to say that the isomerization we observed resulted from a triplet state of butene-2 formed by the energy transfer from the triplet benzene to butene-2. By applying $k_4 \gg k_9[C]$ to Eq. 1, we obtain:

$$\frac{\beta I_a}{R_T} = \frac{k_3+k_4+k_5[B]}{k_4}\left(1+\frac{k_7+k_8[B]}{k_{10}[C]}\right) \quad (2)$$

Equation 2 requires that, under a constant pressure of benzene, a linear relationship should hold between the reciprocal of the isomerization rate and that of the butene-2 pressure. As may be seen from Fig. 2, this is indeed the case. The ratio of the slope to the intercept gives $(k_7+k_8[B])/k_{10}$. We may assume $k_7$ to be negligibly small compared with $k_8[B]$, since the triplet benzene seems to have a rather long life-time, of the order of magnitude $10^{-4}$ to $10^{-5}$ sec., as has been found for other aromatic molecules,[9] and we obtain 11.2 as the value of $k_{10}/k_8$. That is, butene-2 quenches triplet benzene more efficiently than does benzene.

The relation between the reciplocal of the isomerization rate and the pressure of benzene is shown in Fig. 3. Although the plots show a considerable scatter a straight line may be drawn. This linear relationship[10] may be expected from Eq. 2 in two cases: (1) $k_3+k_4 \gg k_5[B]$, or (2) $1 \gg (k_7+k_8[B])/k_{10}[C]$. In case 1, the ratio of the slope to the intercept gives $k_8/(k_7+k_{10}[C])$. Neglecting $k_7$ compared with $k_{10}[C]$, one obtains the value of $k_{10}/k_8$ as 12.8, which is comparable to the value (11.2) ob-

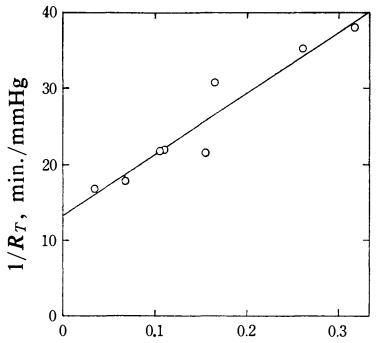



Fig. 2. The relation between the reciprocal of isomerization rate and that of butene-2 pressure.
Benzene, 69 mmHg; irradiation time, 2 min.

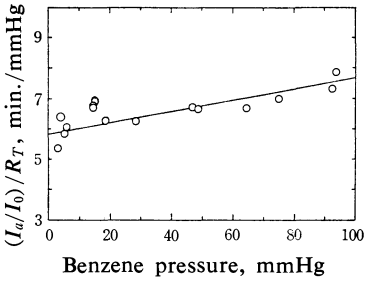



Fig. 3. The relation between the reciprocal of isomerization rate and the pressure of benzene.
*cis*-Butene-2, 20.7 mmHg; irradiation time, 15 min.

tained from the relation between $1/R_T$ and the butene-2 pressure. Because our experiment was carried out below 100 mmHg of benzene, the condition $k_3+k_4 \gg k_5[B]$ will be satisfied if we take 10 as the value of the ratio $(k_3+k_4)/k_5[B]$ at 100 mmHg of benzene, which gives $(k_3+k_4)/k_5 = 1\times10^3$ mmHg. In case 2, the slope to intercept ratio gives $k_5/(k_3+k_4)$. The value of $(k_3+k_4)/k_5$ thus obtained is $3.05\times10^2$ mmHg. If we take the ratio $(k_7+k_8[B])/k_{10}[C]$ to be 1/10 at 100 mmHg of benzene, the highest pressure employed in our experiment, the condition $(k_7+k_8[B])/k_{10}[C] \ll 1$ will be satisfied. Neglecting $k_7$, we obtain from this relation 48.3 as the value of $k_{10}/k_8$.

Ishikawa and Noyes[11] have obtained the value of $k_5$ of $4.6\times10^{-3}$ ml./molec./sec. $= 1.5\times10^4$/mmHg/sec., taking $k_3+k_4 = 1.7\times10^6$ sec$^{-1}$. The value of $(k_3+k_4)/k_5$ calculated from these values is $1.2\times10^2$ mmHg, which is smaller than the values estimated above in both cases. The true value of $(k_3+k_4)/k_5$ might somewhat larger than the value given by Ishikawa and Noyes,

9) G. Porter and F. G. Wright, *Trans. Faraday Soc.*, 51, 1205 (1955).
10) The linear relationship between the ratio of the benzene pressure to the rate of isomerization ($[B]/R_T$) and the benzene pressure has been discarded in the previous note,[4] in which the correction to light absorption was not made.
11) H. Ishikawa and W. A. Noyes, Jr., *J. Chem. Phys.*, 37, 583 (1962).

although the considerable scatter of our data makes questionable the accuracy of our value. It cannot be decided at this stage whether case 1 or case 2 is actually operative under our experimental conditions; more precise experiments must be carried out before further discussions can be made.

A crude estimation of the quantum yield can be made. Behind the reaction cell another quartz cell was placed; in this cell the mercury-photosensitized decomposition of ethylene was carried out. Using 0.502 as the quantum yield of hydrogen production in the mercury-photosensitized decomposition of ethylene,[6] the light quanta transmitted through a cell containing various pressures of benzene were obtained. On the basis of these measurements the quantum yield of the formation of *trans*-butene-2 in the benzene-photosensitized isomerization was calculated to be 1.5. Since the incident light beam was not a parallel one and since the light was reflected on the surfaces of the reaction vessels, the light absorbed by benzene must have been estimated too low by a factor of about 3. The true quantum yield seems to be nearly 0.5, the value which is to be expected from a full utilization of the light absorbed by benzene in the isomerization and from $\beta=0.5$. The isomerization observed in the present experiment, therefore, can be said to have proceeded very efficiently.

The observed photostationary cis-to-trans ratio was about 1.0 in our experiment. The value obtained by Cundall and his co-workers[3] was 0.73 in the benzene and pyridine sensitizations. The reason for this discrepancy is not clear, but the difference in the light sources employed by them (possibly a medium-pressure mercury arc lamp) and by us (a low-pressure mercury arc lamp) might be responsible for it.

The energy curve of the ground singlet state as a function of the relative angle of the rotation of two methyl groups around the axis passing through the two central carbon atoms of butene-2 would have its maximum at 90°. On the other hand, the energy of the lowest-triplet butene-2 would go down from 4.2 eV.[12] at 0° to a minimum at 90°. Thereby the two energy curves are very likely to intersect each other. That the triplet benzene sensitizes the isomerization implies that the energy of the crossing point is smaller than 3.6 eV., the energy of triplet benzene. The cis-to-trans ratio at the photostationary state may depend, according to Landau and Zener,[16] on the angle of the crossing of singlet and triplet energy curves and on the speed at the crossing point. Accordingly, the cis-to-trans ratio may depend on the energy of the sensitizers and on the pressure of the system. A detailed study along these lines is now in progress in this laboratory.

## Summary

The benzene-photosensitized cis-trans isomerization of butene-2 has been investigated in the gas phase. The results have been discussed on the basis of a mechanism involving triplet-energy transfer from benzene to butene-2.

The quantum yield measurements indicate that the reaction occurs at a very high efficiency. The triplet-benzene quenching efficiency of butene-2 has been shown to be considerably greater than that of the ground-state benzene.

The photostationary cis-to-trans ratio has been about unity, unlike the value obtained by Cundall et al. A mechanism which may explain the dependence of the ratio on the pressure and on the energy of the sensitizer has been suggested.

*Department of Applied Physics*
*Tokyo Institute of Technology*
*Ookayama, Tokyo*

12) Although the energy of the triplet butene-2 has not been measured, this value was estimated as follows: The energy of triplet ethylene has been measured by Kupperman and Raff[13] by electron diffraction method and by Evans[14] spectroscopically. Kupperman and Raff gave the value of 4.8 eV., possibly a vertical one. Comparing the excitation energies of ethylene and butene-2 calculated by Sato and Cvetanović,[15] together with the above measured value of the triplet energy of ethylene, we obtain 4.2e V. as the value of the triplet energy of butene-2.

13) A. Kupperman and L. M. Raff, *J. Chem. Phys.* **37**, 2497 (1962).

14) D. F. Evans, *J. Chem. Soc.*, **1960**, 1735.

15) S. Sato and R. J. Cvetanović, *J. Am. Chem. Soc.*, **81**, 3223 (1959).

16) L. Landau, *Physik. Z. Sowjetunion*, **2**, 46 (1932); C. Zener, *Proc. Royal Soc.*, **A137**, 696 (1932).

# Studies of the Organic Reaction of Metal Carbonyl. VII.* The Acceleration Effect of the Addition of Inorganic Compounds on the Reaction of Olefin Oxide with Cobalt Hydrocarbonyl

By Yoshinobu TAKEGAMI, Chikao YOKOKAWA, Yoshihisa WATANABE and Hiromitsu MASADA

(Received February 5, 1965)

Previous work[1] in this laboratory has shown that the reaction of olefin oxide with cobalt hydrocarbonyl is accelerated by the addition of even a relatively small amount of such organic compounds as alcohol, ketone, ether and esters.

In the present paper, the effects of the addition of various inorganic compounds will be examined for this type of reaction. The results obtained in this investigation indicate that some inorganic compounds, such as cuprous oxide and halide, silver oxide and aluminum chloride, also have an acceleration effect on this reaction.

## Experimental

**Reaction Procedures.** — The reactions of olefin oxide with cobalt hydrocarbonyl were carried out in the way which has been described in a previous paper.[2] Into a 100 ml. four-necked flask, fitted with a 50 ml. dropping funnel, a stirrer and a rubber stopple and connected with a 500 ml. gas buret, various amounts of inorganic compounds were introduced, and the air in the system was replaced with carbon monoxide. By the use of a syringe, 50 ml. of a 0.09 M cobalt hydrocarbonyl solution in toluene or in *n*-hexane and various amounts of organic compounds were put into the flask. To this system, 0.5 ml. of propylene oxide (1.6 mol./mol. cobalt hydrocarbonyl) was then introduced, after which the reaction mixture was agitated at 0°C for several hours.

**Analytical Procedures.** — The reaction products (ethyl $\beta$-hydroxybutyrate and ethyl $\gamma$-chloro-$\beta$-hydroxybutyrate) were analyzed by gas chromatography and by means of infrared spectra which were taken on a Shimadzu model IR-27 infracord spectrophotometer. The details were given in the previous paper.[2]

**Materials.** — All of the materials used in this study were commercial products.

## Results and Discussion

**The Reaction of Propylene Oxide with Cobalt Hydrocarbonyl in the Presence of Various Inorganic Compounds.** — All reactions were carried out at 0°C and under one atmosphere of carbon monoxide, and with the mole ratio*

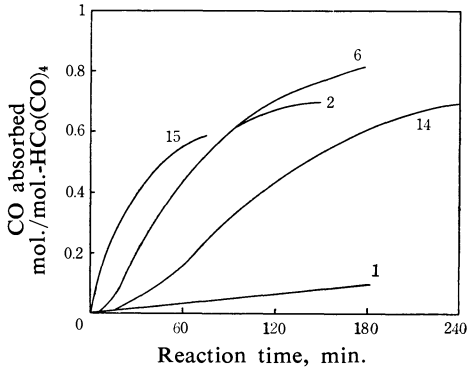



Fig. 1. CO absorption vs. time plots for the reaction of propylene oxide in the presence of inorganic additives.
Number: Exp. No.

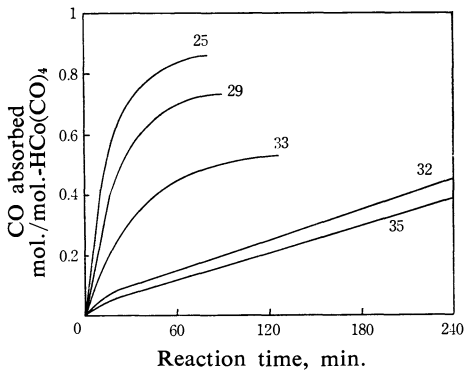



Fig. 2. CO absorption vs. time plots for the reaction of propylene oxide in the presence of inorganic additives.
Number: Exp. No.

* Part VI: Y. Takegami, C. Yokokawa, Y. Watanabe, H. Masada and Y. Okuda, This Bulletin, 38, 787 (1965).

1) Y. Takegami, C. Yokokawa and Y. Watanabe, This Bulletin, 37, 934 (1964).

2) Y. Takegami, C. Yokokawa, Y. Watanabe and H. Masada, ibid., 37, 672 (1964).

* Mole of propylene oxide per mole of cobalt hydrocarbonyl used.

of propylene oxide fixed at 1.6. Under these conditions, the reaction without additives proceeds very slowly (Exp. 1 in Table I).[2] The results of the reactions which were carried out in the presence of inorganic additives are summarized in Figs. 1 and 2 and in Tables I—III. The values of the gas absorption rate at the early stage of the reactions relative to the absorption rate of Exp. 1 are shown as a measure of the acceleration effect.

As the gas absorption curves in Fig. 1 show, the gas absorption rate was highly promoted by the addition of a relatively small amount of cupric and cuprous chloride; the gas absorption rate at the early stage of the reaction was about twenty times as large as that of Exp. 1, which was carried out without additives. The amount of cupric chloride necessary for this acceleration effect seemed to be about 0.05 mol. or less, since the gas absorption rates of Exps. 3—5 (0.1, 0.2 and 0.8 mol. of cupric chloride were added respectively) were comparable to that of Exp. 2. Cuprous chloride also had an effect similar to that of cupric chloride, as Exps. 6—9 and curve 6 show. In all of these reactions, an induction period of

TABLE I. THE REACTION OF PROPYLENE OXIDE WITH COBALT HYDROCARBONYL IN THE PRESENCE OF CUPRIC AND CUPROUS HALIDE AT 0°C

| Exp. No. | Additives | mol./mol. $HCo(CO)_4$ | Reaction*1 time, min. | CO absorbed mol./mol.-$HCo(CO)_4$ | CO absorbed Relative rate*2 | Product ester*3 mol./mol.-$HCo(CO)_4$ |
|---|---|---|---|---|---|---|
| 1 | None | | 180 | 0.10 | 1 | 0.1 |
| 2 | $CuCl_2$ | 0.05 | 140 | 0.70 | 20 | 0.50 |
| 3 | $CuCl_2$ | 0.10 | 110 | 0.70 | 20 | 0.50 |
| 4 | $CuCl_2$ | 0.20 | 160 | 0.77 | 20 | 0.60 |
| 5 | $CuCl_2$ | 0.80 | 180 | 0.70 | 20 | 0.4 |
| 6 | CuCl | 0.05 | 210 | 0.81 | 20 | 0.5 |
| 7 | CuCl | 0.20 | 180 | 0.86 | 20 | 0.5 |
| 8 | CuCl | 0.20 | 150 | 0.75 | 20 | 0.4 |
| 9 | CuCl | 0.40 | 180 | 0.89 | 20 | 0.5 |
| 10 | CuI | 0.20 | 170 | 0.75 | 20 | 0.4 |
| 11 | CuCN | 0.20 | 260 | 0.75 | 15 | 0.5 |
| 12 | $CuCl_2 \cdot 2H_2O$ | 0.20 | 180 | 0.73 | 15 | 0.4 |
| 13*4 | CuCl | 1.2 | 400 | 0.92 | — | — |

*1 Other reaction conditions: 1.6 mol. of propylene oxide per mole of cobalt hydrocarbonyl used, under one atmosphere of carbon monoxide. The speed of stirring was 900 r. p. m.
*2 The relative value of the gas absorption rate at the early stage of the reaction to the rate of Exp. 1.
*3 Ethyl β-hydroxy-*n*-butyrate.
*4 Without propylene oxide.

TABLE II. THE REACTION OF PROPYLENE OXIDE IN THE PRESENCE OF VARIOUS METAL COMPOUNDS

| Exp. No. | Additives | mol./mol.-$HCo(CO)_4$ | Reaction*1 time, min. | CO absorbed mol./mol.-$HCo(CO)_4$ | CO absorbed Relative rate*2 | Ester*3 mol./mol.-$HCo(CO)_4$ |
|---|---|---|---|---|---|---|
| 14 | AgCl | 0.20 | 300 | 0.72 | 9 | 0.4 |
| 15 | $AlCl_3$ | 0.2 | 80 | 0.60 | 30 | 0.3 |
| 16 | $SnCl_4$ | 0.2 | 320 | 0.47 | 5 | 0.2 |
| 17 | KCl | 0.2 | 90 | 0.05 | 1 | — |
| 18 | $MgCl_2 \cdot 2H_2O$ | 0.1 | 60 | 0.03 | 1 | — |
| 19 | $ZnCl_2$ | 0.2 | 240 | 0.1 | 1 | — |
| 20 | $FeCl_3$ | 0.2 | 60 | 0.03 | 1 | — |
| 21 | $NiCl_2$ | 0.2 | 60 | 0.04 | 1 | — |
| 22 | $PdCl_2$ | 0.2 | 300 | 0 | — | 0 |
| 23 | $TiCl_4$ | 0.2 | 150 | 0 | — | — |

*1 Other reaction conditions: 1.6 mol. of propylene oxide, under one atmosphere of carbon monoxide.
*2 The relative value of the gas absorption rate to the rate of Exp. 1.
*3 β-Hydroxy-*n*-butyrate.

Table IIIa. The reaction of propylene oxide in the presence of cuprous and cupric oxide at 0°C

| Exp. No. | Additives | mol./mol. $HCo(CO)_4$ | Reaction*1 time, min. | CO absorbed mol./mol.-$HCo(CO)_4$ | CO absorbed Relative rate*2 | Ester*3 mol./mol.-$HCo(CO)_4$ |
|---|---|---|---|---|---|---|
| 24 | $Cu_2O$ | 0.001 | 120 | 0.73 | 40 | 0.4 |
| 25 | $Cu_2O$ | 0.005 | 80 | 0.85 | 75 | 0.5 |
| 26 | $Cu_2O$ | 0.05 | 60 | 0.70 | 72 | 0.5 |
| 27 | $Cu_2O$ | 0.10 | 60 | 0.50 | 72 | 0.3 |
| 28 | CuO | 0.005 | 120 | 0.67 | 27 | 0.4 |
| 29 | CuO | 0.02 | 100 | 0.73 | 55 | 0.4 |
| 30 | CuO | 0.10 | 60 | 0.67 | 55 | 0.4 |
| 31 | CuO | 0.20 | 50 | 0.60 | 60 | 0.4 |
| 32 | Cu powder | 0.1 | 420 | 0.66 | 4 | 0.4 |
| 33 | $Ag_2O$ | 0.10 | 130 | 0.53 | 27 | 0.3 |
| 34 | $Al_2O_3$ | 0.10 | 120 | 0.07 | 1 | — |
| 35*4 | $Cu_2O$ | 0 | 420 | 0.50 | 3 | 0.3 |
| 36*4 | CuCl | 0 | 300 | 0.35 | 2 | — |

Table IIIb. The reaction in *n*-hexane

| | | | | | | |
|---|---|---|---|---|---|---|
| 37 | $Cu_2O$ | 0.05 | 150 | 0.45 | 14 | 0.3 |
| 38 | CuCl | 0.10 | 200 | 0.57 | 5 | — |
| 39*5 | None | | 250 | 0.78 | — | 0.6 |

*1 Other condition: 1.6 mol. of propylene oxide and under one atmosphere of carbon monoxide.
*2 The relative value of the gas absorption rate to Exp. 1.
*3 β-Hydroxy-*n*-butyrate.
*4 25 ml. of toluene refluxed with cuprous oxide and chloride was added respectively.
*5 6.2 mol. of propylene oxide. The rate of the gas absorption in *n*-hexane is about one-fourth that in toluene.[1]

about 5 min. was observed. As the main product in these reactions, ethyl β-hydroxy-*n*-butyrate* was obtained.

Accordingly, it may be concluded that the carbonylation of propylene oxide, i.e. the formation of β-hydroxy-*n*-butyrylcobalt carbonyl, is promoted by the addition of cupric or cuprous chloride.

Gas absorption was observed in the reaction system of cobalt hydrocarbonyl and cuprous chloride (Exp. 13). The gas chromatography, however, gave no indication of the presence of an organic product, and the amount of the gas evolved by treatment with iodine was comparable to the sum of the amount of the gas absorbed and that to be expected from the cobalt hydrocarbonyl used, indicating that the gas absorption is due to the formation of cuprous carbonyl chloride. This interpretation is supported by the facts that a 0.1 N hydrogen chloride - cuprous chloride aqueous solution readily absorbs carbon monoxide and that the gas absorbed was evolved by the treatment with iodine. However, the formation of cuprous carbonyl chloride seemed to be independent of its acceleration effect, since no gas absorption was observed in the reaction system of cobalt hydrocarbonyl and cupric chloride.

Cuprous iodide and cyanide and cupric chloride dihydrate had an acceleration effect almost equal to that of cuprous and cupric chloride (Exps. 10—12).

Silver chloride also had an effect which was smaller than that of cuprous chloride, and it had a longer induction period (about 15 min.) (Exp. 14 and curve 14). Aluminum trichloride had a larger acceleration effect than cuprous chloride and had no induction period (Exp. 15 and curve 15).

The reaction system of cobalt hydrocarbonyl and aluminum trichloride gradually caused gas to evolve, with a color change from yellow to pale green, suggesting that the aluminum chloride decomposed the cobalt hydrocarbonyl.

Tin tetrachloride seemed to have a relatively small acceleration effect (Exp. 16). However, zinc chloride, nickel chloride, ferric chloride, potassium chloride and magnesium chloride-dihydrate had no effect at all on this reaction (Exps. 17—21). The addition of palladium chloride and titanium chloride caused the color of the reaction system to change rapidly from yellow to brown black and green brown

* Obtained from the corresponding acylcobalt carbonyl by cleavage with iodine and ethyl alcohol.

respectively, without gas absorption or evolution, and it gave no ethyl β-hydroxy-*n*-butyrate as a product, suggesting that some reaction other than the carbonylation reaction of propylene oxide occurred (Exps. 22 and 23).

Cuprous and cupric oxide had an acceleration effect similar to that of their chlorides, but the effects of these oxides are several times larger than that of the chlorides (Table III). When more than 0.005 mol. of cuprous oxide or more than 0.02 mol. of cupric oxide was added, the rates of the gas absorption were, respectively, about seventy and sixty times as large as that of the standard run (curves 25 and 29 in Fig. 2). However, the acceleration effect decreased with the decrease in the amount of cuprous and cupric oxide, as Exps. 24 and 28 show. This indicates the following relation: 0.001 mol.<enough cuprous oxide for this reaction<0.005 mol. and 0.005 mol.<enough cupric oxide<0.02 mol.

Copper powder also had a promoting effect, one which seems to be about one-fifth that of cuprous chloride (Exp. 32 and curve 32). Silver oxide had a promoting effect about three times as large as that of silver chloride (Exp. 33). On the other hand, aluminum oxide had no effect on this reaction (Exp. 34).

These inorganic additives are insoluble in toluene. Even 0.005 mol. of cuprous oxide (3.5 mg. in 50 ml. of toluene) seemed not to dissolve in the reaction solution. From the standpoint of solubility, the inorganic additives differ from the organic additives, which are very soluble in toluene. It may reasonably be considered that the inorganic additives are effective for the reaction as the solid state. This consideration is supported by the following fact: when 25 ml. of toluene,* refluxed with cuprous oxide or chloride for one hour, was used in the reaction after the separation of the solid phase, only a relatively small acceleration effect was observed (Exps. 35 and 36).

As has been mentioned above, various compounds of copper and silver, but not aluminum chloride, significantly promote the carbonylation reaction of propylene oxide, suggesting that compounds of metals which belong to Periodic Group Ib have an acceleration effect on this type of reaction. This acceleration effect may be attributed to the formation of some active complex from propylene oxide and the inorganic additives. This theory is supported by the fact that the inorganic additives have no effect on the reaction of styrene or ethyl acrylate with cobalt hydrocarbonyl.

* 25 ml. of a 0.18 M cobalt hydrocarbonyl solution in toluene was diluted with 25 ml. of this refluxed toluene in the experiment.

Cuprous oxide and chloride have also an effect in *n*-hexane (Exps, 37 and 38), but the effect in this solvent seems to be one-fourth that of the reaction in toluene (cf. Exps. 6 and 26). Without additives, however, the reaction in *n*-hexane seems to proceed about one-fourth as fast as in toluene (Exp. 39), suggesting that this reaction is highly influenced by the solvent. However, the additives seem to be effective in the reaction independently of the solvent.

**The Reactions of Propylene Oxide and Epichlorohydrin in the Presence of Inorganic and Organic Additives.** — As has previously been reported,[1] the reaction of olefin oxide with cobalt hydrocarbonyl is remarkably promoted by the addition of various organic compounds, such as ethyl alcohol and tetrahydrofuran. The effect of the combination of the inorganic additives described above with organic additives has, therefore, been examined, the results are summarized in Tables IV and V and in Fig. 3.

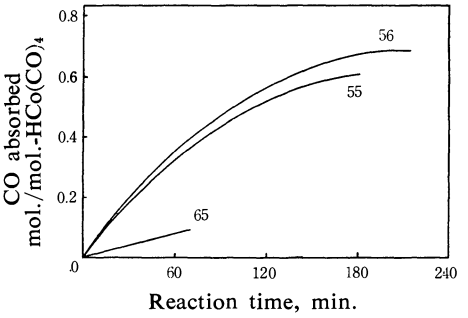



Fig. 3. CO absorption vs. time plots for the reaction of epichlorohydrin in the presence of cuprous oxide or ethyl alcohol.
Number: Exp. No.

As Exps. 41 and 42 clearly show, the reaction of propylene oxide is further promoted by the combination of cuprous chloride with ethyl alcohol, suggesting that such a combination has a synergistic effect.

The combination of cuprous chloride with various organic additives, such as tetrahydrofuran (30*[1]), acetone (25*[1]), ethyl acetate (12*[1]) and ethyl ether (6*[1]), also has a synergistic effect (Exps. 45 and 48). Cupric chloride and cuprous oxide in combination with ethyl alcohol have also a synergistic effect (Exps. 50 and 52). However, the combination of cuprous chloride with cupric chloride has no synergistic effect (Exp. 51). Ethylene chlorohydrin (10) has no synergistic effect, even when combined with cuprous oxide (75) (Exp. 53).

The relative rates of the reactions with 2.0 mol. of ethyl alcohol (Exp. 44) and with 2.0

*1 The relative values of the gas absorption rate when only these compounds were added to the reaction system.

TABLE IV. THE REACTION OF PROPYLENE OXIDE IN THE PRESENCE OF INORGANIC AND ORGANIC ADDITIVES AT 0°C

| Exp. No. | Additives mol./mol. $HCo(CO)_4$ | | | | Reaction*1 time, min. | CO absorbed mol./mol.-$HCo(CO)_4$ | CO absorbed Relative rate*2 | Ester*3 mol./mol.-$HCo(CO)_4$ |
|---|---|---|---|---|---|---|---|---|
| 40 | CuCl | 0.10, | EtOH | 0.5 | 100 | 0.82 | 30 | 0.50 |
| 41 | CuCl | 0.10, | EtOH | 1.0 | 50 | 0.85 | 80 | 0.5 |
| 42 | | | EtOH | 1.0 | 90 | 0.77 | 40 | 0.50 |
| 43 | CuCl | 0.10, | EtOH | 2.0 | 50 | 0.83 | 120 | 0.5 |
| 44 | | | EtOH | 2.0 | 90 | 0.93 | 120 | 0.5 |
| 45 | CuCl | 0.10, | Tetrahydro-furan | 3.0 | 50 | 0.70 | 60 | — |
| 46 | CuCl | 0.10, | Acetone | 3.0 | 80 | 0.78 | 50 | 0.6 |
| 47 | CuCl | 0.10, | Ethyl acetate | 3.0 | 70 | 0.78 | 38 | 0.5 |
| 48 | CuCl | 0.10, | Ether | 2.0 | 70 | 0.70 | 30 | 0.4 |
| 49 | CuCl | 0.10, | Ethylene chlorohydrin | 3.0 | 60 | 0.45 | 23 | 0.2 |
| 50 | $CuCl_2$ | 0.1, | EtOH | 1.0 | 80 | 0.89 | 55 | 0.7 |
| 51 | CuCl | 0.1, | $CuCl_2$ | 0.1 | 110 | 0.70 | 20 | 0.4 |
| 52 | $Cu_2O$ | 0.01, | EtOH | 1.0 | 60 | 0.80 | 90 | 0.6 |
| 53 | $Cu_2O$ | 0.01, | Ethylene chlorohydrin | 3.0 | 120 | 0.65 | 55 | 0.5 |

*1 Other conditions: 1.6 mol. of propylene oxide and under one atmosphere of carbon monoxide.
*2 The relative value of the gas absorption rate to Exp. 1.
*3 β-Hydroxy-*n*-butyrate.

TABLE V. THE REACTION OF EPICHLOROHYDRIN WITH COBALT HYDROCARBONYL IN THE PRESENCE OF CUPROUS OXIDE AND ETHYL ALCOHOL AT 0°C

| Exp. No. | Additives mol./mol. $HCo(CO)_4$ | | | | Epichloro-hydrin | Reaction*1 time, min. | CO absorbed mol./mol.-$HCo(CO)_4$ | CO absorbed Relative rate*2 | Ester*3 mol./mol.-$HCo(CO)_4$ |
|---|---|---|---|---|---|---|---|---|---|
| 55 | | | EtOH | 1.0 | 14.5 | 180 | 0.61 | 1 | 0.4 |
| 56 | $Cu_2O$ | 0.1 | | | 14.5 | 220 | 0.67 | 1 | 0.3 |
| 57 | $Cu_2O$ | 0.2 | | | 14.5 | 200 | 0.70 | 1 | 0.3 |
| 58 | $Cu_2O$ | 0.1, | EtOH | 2.0 | 14.5 | 120 | 0.60 | 1.4 (2.0*4) | 0.2 |
| 59 | $Cu_2O$ | 0.1, | EtOH | 3.0 | 14.5 | 160 | 0.76 | 2.1 (3.0) | 0.6 |
| 60 | $Cu_2O$ | 0.1, | EtOH | 4.0 | 14.5 | 140 | 0.66 | 2.9 (4.0) | 0.3 |
| 61 | $Cu_2O$ | 0.1, | EtOH | 8.0 | 14.5 | 90 | 0.57 | 6.3(10) | 0.5 |
| 62 | $Cu_2O$ | 0.1, | EtOH | 8.0 | 5.8 | 120 | 0.54 | 2.6 (4.0) | — |
| 63 | $Cu_2O$ | 0.1, | EtOH | 8.0 | 8.7 | 70 | 0.53 | 4.0 (6.0) | — |
| 64 | $Cu_2O$ | 0.1, | EtOH | 8.0 | 11.6 | 60 | 0.55 | 5.1 (8.0) | 0.3 |
| 65 | None | | | | 14.5 | 70 | 0.1 | — | — |

*1 Other condition: Under one atmosphere of carbon monoxide.
*2 The value of the gas absorption rate relative to the rate of Exp. 55.
*3 γ-Chloro-β-hydroxy-*n*-butyrate.
*4 The relative values of the gas absorption rate when cuprous oxide is absent.

mol. of ethyl alcohol and 0.10 mol. of cuprous chloride (Exp. 43) are comparable. This may be interpreted as follows: under the reaction conditions (the apparatus, the speed of stirring, etc.) used, the maximum rate of gas absorption seems to be about 120 of the relative value.

The results with epichlorohydrin are summarized in Table V and Fig. 3, in which the values of the gas absorption rates relative to that of Exp. 55, carried out in the presence of 1.0 mol. of ethyl alcohol at a 14.5 mol. ratio*2 of epichlorohydrin, are shown as a measure of the acceleration effect.

As the results in Fig. 3 show, cuprous oxide also had an acceleration effect on this reaction (Exp. 56). The effect of cuprous oxide is almost comparable to that of 1.0 mol. of ethyl alcohol. The main product of these reactions

*2 Mole of epichlorohydrin per mole of cobalt hydrocarbonyl used.

has been proved to be $\gamma$-chloro-$\beta$-hydroxy-*n*-butyrate.[2] Thus, the carbonylation reaction is similarly promoted by the addition of cuprous oxide as ethyl alcohol.

However, the combination of cuprous oxide with ethyl alcohol has a retardation effect on this reaction. As Exps. 58—64 show, the relative values of the gas absorption rate in the presence of both cuprous oxide and ethyl alcohol decreased to about two thirds of those in the presence of ethyl alcohol alone. Thus, the equation*3 of the gas absorption rate at the early stage of the reaction, obtained in the presence of ethyl alcohol alone, may be corrected by the combination of ethyl alcohol with cuprous oxide as follows:

$$\text{Rate} = 0.6 - 0.7\,k \times [\text{epichlorohydrin}]\,[\text{ethyl alcohol}]$$

In the light of the above equation, cuprous oxide seems to lose its own acceleration effect and to retard some of the active complex formation of ethyl alcohol with epichlorohydrin.

## Summary

The reaction of olefin oxide with cobalt hydrocarbonyl in the presence of inorganic (and organic) additives has been investigated.

1) The addition of relatively small amounts of various compounds of copper and silver promote the carbonylation of propylene oxide. The order of the promoting effect of these compounds is $Cu_2O$, 70>CuO, 60>($AlCl_3$, 30)>$Ag_2O$, 27>$CuCl_2$, CuCl and CuI, 20>CuCN, 15>AgCl, 9>Cu powder, 4>None, 1 (the numbers indicating the relative rates of the gas absorption at the early stage of the reaction). Among these, cuprous oxide has the largest effect. The amount of cuprous oxide necessary for this effect is only about 0.005 mol./mol. $HCo(CO)_4$. $\beta$-Hydroxy-*n*-butyrate has been the main reaction product obtained. On the other hand, chlorides of zinc, nickel, ferric, potassium, magnesium, palladium and titanium have no promoting effect on the reaction.

2) The combination of cuprous halide (and oxide) with various organic additives, which also have a promoting effect,[1] has a synergistic effect on the reaction of propylene oxide.

3) The reaction of epichlorohydrin is also promoted by the addition of cuprous oxide. However, in this case cuprous oxide combined with ethyl alcohol has a retardation effect.

*Departmeat of Fuel Chemistry*
*Faculty of Engineering*
*Kyoto University*
*Sakyo-ku, Kyoto*

*3 When only ethyl alcohol is present, the gas absorption rate at the early stage of the reaction is represented as follows:[1] Rate=$k$[epichlorohydrin] [ethylalcohol].

# Quinoxaline Derivatives. VI.[1] An Unusual Chlorine Substitution during the Reaction of 3-Hydroxy-2-phenylquinoxaline 1-Oxide with Acetyl Chloride

By Yusuf AHMAD, M. S. HABIB,*[1] ZIAUDDIN and Naz BASHIR

(Received February 8, 1965)

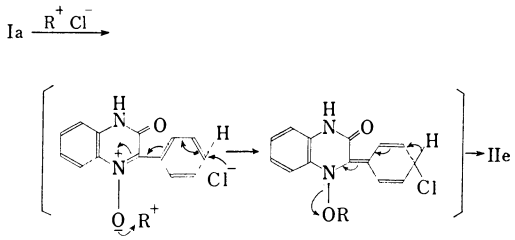
During an attempted acetylation of 3-hydroxy-2-phenylquinoxaline 1-oxide[2] (Ia) with acetyl chloride, it was observed that, instead of the normal acetyl derivative, a compound X was obtained; it was analysed as $C_{14}H_9ClN_2O$. The parent compound ($C_{14}H_{10}N_2O_2$) had gained a chlorine atom at the expense of one hydrogen and one oxygen atom, and the chlorine in the molecule was in the non-ionic form. The same compound X was obtained if the *N*-oxide (Ia) was heated with a mixture of concentrated hydrochloric acid and acetic acid (1 : 1 by volume). The reactions seemed to be general ones, as 7-chloro-, 7-ethoxy-, 7-methoxy- derivatives (Ib—d) of 3-hydroxy-2-phenylquinoxaline 1-oxide behaved similarly and gave the corresponding chlorine-substituted compounds. Although the *N*-oxide function was lost during the transformation, electrophilic chlorination by the chlorine generated at the expense of the *N*-oxide function was ruled out, as in each case a uniform single-chlorinated compound was obtained in almost a quantitative yield.

1) Part V: Y. Ahmad, M. S. Habib, M. Iqbal and Ziauddin, This Bulletin, **38**, 562 (1965).

*1 Burroughs Wellcome & Co. (Pakistan), Ltd., D/43 S. I. T. E., Karachi, Pakistan.

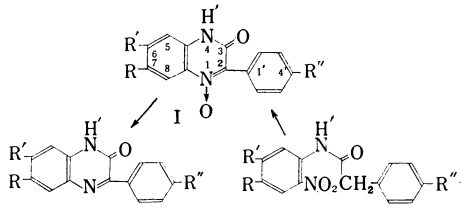
2) Y. Ahmad, M. S. Habib, Ziauddin and N. Bashir, *Tetrahedron*, **21**, 861 (1965).

The evidence presented in earlier papers[1,3,4] strongly indicated that the presence of an oxide function at $N_{(1)}$, coupled with an electron-withdrawing group on $C_{(2)}$ in the quinoxaline molecule, made $C_{(2)}$ strongly electrophilic. The acetylation (or protonation) of the *N*-oxide would further enhance this effect, making the nucleophilic chlorination of the molecule quite feasible. However, in the case of 3-hydroxy-2-phenylquinoxaline 1-oxide, this effect was not expected to remain localised at $C_{(2)}$; it could have been relayed further, through the mesomeric effect, making the 4'-position of the phenyl ring at $C_{(2)}$ liable to the attack by a nucleophile (in the present case a chloride anion). The reaction was expected to take the course indicated below:



(R=Ac or H)

To test the feasibility of this hypothesis, an authentic sample of 2-(*p*-chlorophenyl)-3-hydroxyquinoxaline (IIe) was synthesised in order to compare it with compound X, by the condensation of *o*-nitroaniline with *p*-chlorophenylacetyl chloride, and the resulting α-(*p*-chlorophenyl)-*o*-nitroacetanilide (IIIe) was cyclised with hot aqueous alkali to 2-(*p*-chlorophenyl)-3-hydroxyquinoxaline 1-oxide (Ie), which, on deoxygenation with sodium dithionite in aqueous ethanol, gave IIe. However, the infrared spectrum, melting point and other properties of compound X indicated it to be different from 2-(*p*-chlorophenyl)-3-hydroxyquinoxaline (IIe).

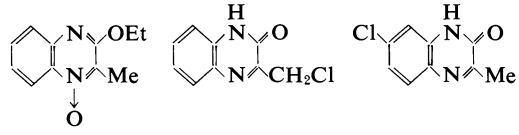


II III

| | R | R′ | R″ | | R | R′ | R″ |
|---|---|---|---|---|---|---|---|
| (a) | H | H | H | (g) | H | Cl | H |
| (b) | Cl | H | H | (h) | Cl | Cl | H |
| (c) | EtO | H | H | (i) | EtO | Cl | H |
| (d) | MeO | H | H | (j) | MeO | Cl | H |
| (e) | H | H | Cl | (k) | H | Cl | Cl |
| (f) | Cl | H | Cl | (l) | Cl | Cl | Cl |

7-Chloro-2-(*p*-chlorophenyl)-3-hydroxyquinoxaline 1-oxide (If) was obtained by a similar sequence of reactions: [*p*-chlorophenylacetyl chloride + 4-chloro-2-nitroaniline → 4-chloro-α-(*p*-chlorophenyl)-2-nitroacetanilide (IIIf) → If]. Ie and If, derivatives of 3-hydroxyquinoxaline 1-oxide, had, at position 2, a phenyl ring, in which the *p*-position was already blocked. Even these compounds, on being heated with acetyl chloride, lost the *N*-oxide and gained an extra chlorine atom in the molecule. These observations indicated that probably the point of the attack of the chloride anion was not in the phenyl ring at position 2 of these quinoxaline derivatives, but at position 5, 6 or 8 of the molecule. Position 7 was excluded, as 2-phenyl-7-chloro-3-hydroxyquinoxaline (IIb), the synthesis of which has already been reported in Part IV,[2] was different (infrared spectra and melting point) from the compound X.

A survey of the literature brought to our notice a similar case. Nowbold and Spring,[5] on heating 3-ethoxy-2-methylquinoxaline 1-oxide (IV) with ethanolic hydrochloric acid, obtained a chlorine substituted quinoxaline, to which they assigned the 2-chloromethyl-3-hydroxyquinoxaline (V) structure, obviously on considerations similar to those above and on some spectroscopic evidence. Later,[6] when they synthesised 2-chloromethyl-3-hydroxyquinoxaline by an unambiguous route, it turned out

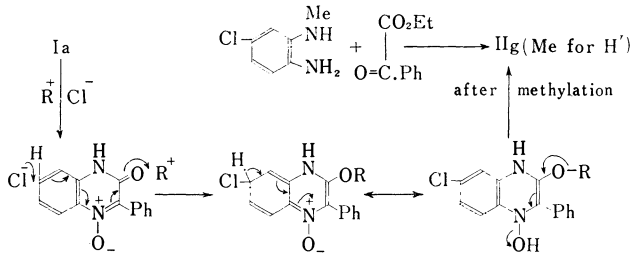


IV V VI

to be different from their earlier chloro-derivative, which they then proved to be 6-chloro-3-hydroxy-2-methyl quinoxaline (VI) through another synthesis. Spring et al.[5,6] had proposed no mechanism for this unusual chlorination, which they had earlier considered to have taken place on the methyl at position 2 and had later found to replace $C_{(6)}$ of the quinoxaline molecule.

In view of the above observation, 6-chloro-3,4-dihydro-4-methyl-3-oxo-2-phenylquinoxaline (IIg, Me for H′) was synthesised by two different routes: (a) 5-chloro-2-nitro-*N*-methylaniline with phenylacetyl chloride gave 5-chloro-*N*-methyl-2-nitro-α-phenylacetanilide

3) Y. Ahmad, M. S. Habib and Ziauddin, ibid., **20**, 1107 (1964).
4) M. S. Habib and C. W. Rees, *J. Chem. Soc.*, **1960**, 3371, 3384, 3386.
5) G. T. Newbold and F. S. Spring, ibid., **1948**, 519.
6) W. Dawson, G. T. Newbold and F. S. Spring, ibid., **1949**, 2579.




(R=Ac or H)

(IIIg, Me for H′), which, with hot aqueous alkali, cyclised to 6-chloro-3,4-dihydro-4-methyl-3-oxo-2-phenylquinoxaline 1-oxide (Ig, Me for H′), and its deoxygenation with sodium dithionite in boiling aqueous ethanol gave IIg (Me for H′). (b) 2-Amino-5-chloro-*N*-methylaniline, on condensation with ethyl phenylglyoxalate, gave IIg (Me for H′). The chloro-base (IIg, Me for H′) as prepared by either of the methods was identical (infrared spectra and mixed melting point) with the product of the methylation of the compound X.

The dichloro-compound obtained by heating 7-chloro-3-hydroxy-2-phenylquinoxaline 1-oxide (Ib) with acetyl chloride in a sealed tube was identical (infrared spectra and mixed melting point) with 6, 7-dichloro-3-hydroxy-2-phenylquinoxaline (IIh), which was synthesised by the condensation of 4, 5-dichloro-*o*-phenylenediamine with ethyl phenylglyoxalate. The trichloro-compound, which resulted when 7-chloro-2-(*p*-chlorophenyl)-3-hydroxyquinoxaline 1-oxide (If) and acetyl chloride were heated together in a sealed tube, was identical (infrared spectra and mixed melting point) with 6, 7-dichloro-2-(*p*-chlorophenyl)-3-hydroxyquinoxaline (III), an authentic sample of which, for the sake of comparison, was prepared by following sequence of reactions: [4, 5-dichloro-2-nitroaniline + *p*-chlorophenylacetyl chloride → 4, 5-dichloro-$\alpha$-(*p*-chlorophenyl)-2-nitroacetanilide (IIII), which cyclised with alkali → 6, 7-dichloro-2-(*p*-chlorophenyl-3-hydroxyquinoxaline 1-oxide (II), which on deoxygenation gave → III].

The above reactions clearly establish that 3-hydroxy-2-phenylquinoxaline 1-oxide and its derivatives, when heated with acetyl chloride or a mixture (1 : 1) of concentrated hydrochloric acid and acetic acid, undergoes chlorination at position 6 with simultaneous deoxygenation. By analogy, the chloro compounds similarly obtained from 2-(*p*-chlorophenyl)-3-hydroxyquinoxaline 1-oxide (Ie) and 7-ethoxy- and 7-methoxy- derivatives (Ic and Id) of Ia should be formulated as IIk, IIi and IIj respectively. In this reaction, powerful electron-withdrawing properties of the *N*-oxide function at $N_{(1)}$, augmented by the interaction of an $Ac^+$ (or $H^+$)*2 with the oxygen function at $C_{(3)}$ of quinoxaline molecule, made position 6 prone to nucleophilic attack by the chloride anion (as shown below), particularly so if position 2 was already occupied. The presence of an oxygen function at position 3 of the quinoxaline 1-oxides seemed to be essential for directing this nucleophilic chlorination to position 6. Otherwise[8] either the chlorination did not take place at all under the conditions of this reaction, or, if it did take place, it was directed to the substituent at position 2.

This mechanism† satisfactorily accounted for the cases of chlorination with the simultaneous deoxygenation of quinoxaline *N*-oxide derivatives reported above, and also for all such cases reported earlier by other workers.[5,6,9]

On the other hand, when 3-hydroxy-2-phenylquinoxaline 1-oxide (Ia) was heated with fuming hydrobromic acid, the product isolated, instead of being 6-bromo-3-hydroxy-2-phenylquinoxaline (IIg, Br for Cl), was the halogen-free deoxygenated base, i. e., 3-hydroxy-2-phenylquinoxaline (IIa). This was not entirely unexpected, as Loudon et al.[10,11] had obtained chlorinated quinoline derivatives when they

*2 Acetyl chloride, when used as a reaction medium, has been shown[7] to ionise as $CH_3COCl \rightleftarrows CH_3CO^+ + Cl^-$. Therefore, hydrochloric acid and acetyl chloride can be considered to follow the same course of reaction, to effect the nucleophilic chlorination reaction in the present investigation.

7) K. K. Desai and B. C. Halder, *J. Indian Chem. Soc.*, **41**, 116 (1964).

8) Y. Ahmad et al., unpublished work.

† We do not wish to imply that the initial attack of the reagent on the *N*-oxide is to be excluded here. This probably takes place and helps in further enhancing the electron-withdrawing properties of the *N*-oxide. However, this alone does not seem to direct the attack of the nucleophile ($Cl^-$) to position 6 of the quinoxaline molecule. It is the attack (or simultaneous attack) of the reagent at the oxygen function at $C_{(3)}$ which seems to control it. For the sake of brevity, the attack of the reagent on the *N*-oxide is, therefore, not shown in the mechanism.

9) J. W. Clark-Lewis and G. F. Katekar, *J. Chem. Soc.*, **1959**, 2825.

10) J. D. Loudon and I. Wellings, ibid., **1960**, 3470.

11) J. D. Loudon and G. Tennant, ibid., **1962**, 3092.

reacted *o*-nitrobenzaldehyde with compounds containing an active methylene group in the presence of hydrogen chloride. However, when they replaced hydrogen chloride by hydrogen bromide, the compounds isolated, although similar in structure, were free from halogen.

Further work is in progress.

## Experimental*3

**α-(*p*-Chlorophenyl)-2-nitroacetanilide (IIIe).** — *o*-Nitroaniline (0.1 mol.) and *p*-chlorophenylacetyl chloride[12] (0.12 mol.) dissolved in minimum quantity of dry benzene were heated together under reflux for 25—30 min. More benzene was then added and, the solution was washed with 5% aqueous hydroxide and with water and then dried (sodium sulphate). The residue obtained after the removal of the solvent under reduced pressure was crystallised from light petroleum as yellow plates of the anilide (IIIe) in 80% yield, m. p. 91—92°C.

Found: N, 9.4. Calcd. for $C_{14}H_{11}ClN_2O_3$: N, 9.6%. The same procedure was followed for the preparation of the anilides described below.

**4-Chloro-α-(*p*-chlorophenyl)-2-nitroacetanilide (IIIf).**—4-Chloro-2-nitroaniline,[13] when treated by the above method, gave, in a 86% yield, yellow plates (from benzene-light petroleum) of the dichloroanilide (IIIf), m. p. 127—128°C.

Found: C, 51.9; H, 3.3; Cl, 21.2; N, 7.9. Calcd. for $C_{14}H_{10}Cl_2N_2O_3$: C, 51.7; H, 3.1; Cl, 21.8; N, 7.7%.

**4,5-Dichloro-α-(*p*-chlorophenyl)-2-nitroacetanilide (IIII).**—4,5-Dichloro-2-nitroaniline[14] gave, in 78% yield, yellow needles (from benzene) of the trichloroanilide (IIII), m. p. 150—151°C.

Found: Cl, 30.2; N, 7.6. Calcd. for $C_{14}H_9Cl_3N_2O_3$: Cl, 29.6; N, 7.8%.

**5-Chloro-*N*-methyl-2-nitro-α-phenylacetanilide (IIIg; H′=Me).** — 5-Chloro-2-nitro-*N*-methylaniline,[15] on being allowed to react with phenylacetyl chloride[16] as described above, gave, in 83% yield, yellow microneedles (from benzene-light petroleum) of the 5-chloro-*N*-methylanilide (IIIg; H′=Me), m. p. 140—141°C.

Found: N, 8.9. Calcd for $C_{15}H_{14}ClN_2O_3$: N, 9.2%.

**2-(*p*-Chlorophenyl)-3-hydroxyquinoxaline 1-Oxide (Ie).**—A solution of the anilide (IIIe) (4.0 g.) in pyridine (20 ml.) was heated with 20% aqueous potassium hydroxide (20 ml.) on a water bath for 1 hr. The reaction mixture, after dilution with water and acidification with dilute hydrochloric acid, gave a solid which crystallised from ethanol as yellow needles of the *N*-oxide (Ie) in 65% yield, m. p. 316—318°C (decomp.).

Found: N, 10.1. Calcd. for $C_{14}H_9ClN_2O_2$: N, 10.3%.

These needles, on being heating with an excess of sodium dithionite in 50% aqueous ethanol, was deoxygenated, and, on removal of the excess solvent, gave a solid which crystallised from benzene as yellow needles of *2-(p-chlorophenyl)-3-hydroxyquinoxaline (IIe)* in 82% yield, m. p. 291—292°C.

Found: N, 10.5. Calcd. for $C_{14}H_9ClN_2O$: N, 10.9%.

The *N*-oxides described below were obtained and deoxygenated by the procedures outlined above.

**7-Chloro-2-(*p*-chlorophenyl)-3-hydroxyquinoxaline 1-Oxide (If).**—The compound IIIf when treated by the above method, gave yellow microneedles (from dimethylformamide-ethanol) of the dichloro-*N*-oxide (If) in 62% yield, m. p. 333°C (decomp.).

Found: C, 54.4; H, 2.9; N, 8.9. Calcd. for $C_{14}H_8Cl_2N_2O_2$: C, 54.7; H, 2.6; N, 9.1%; these microneedles, on reduction with sodium dithionite in 50% aqueous acetic acid, gave pale yellow microneedles (from benzene) of *7-chloro-2-(p-chlorophenyl)-3-hydroxyquinoxaline (IIf)* in quantitative yield, m. p. 220—222°C.

Found: C, 57.0; H, 2.8; N, 9.8. Calcd. for $C_{14}H_8Cl_2N_2O$: C, 57.7; H, 2.7; N, 9.6%.

**6,7-Dichloro-2-(*p*-chlorophenyl)-3-hydroxyquinoxaline 1-Oxide (II).** — The anilide (IIII) gave, in 64% yield, yellow needles (from ethanol) of the trichloro *N*-oxide (II), m. p. 310°C (decomp.).

Found: Cl, 30.5; N, 8.2. Calcd. for $C_{14}H_7Cl_3N_2O_2$: Cl, 31.2; N, 8.2%.

**6,7-Dichloro-2-(*p*-chlorophenyl)-3-hydroxyquinoxaline (III).**—a) The *N*-oxide (II), on reduction with sodium dithionite in 50% aqueous ethanol, gave, in good yield, pale yellow microneedles (from ethanol) of the trichloroquinoxaline (III), m. p. 320—323°C.

Found: C, 51.3; H, 2.2; N, 8.5. Calcd. for $C_{14}H_7Cl_3N_2O$: C, 51.6; H, 2.15; N, 8.6%.

b) The *N*-oxide (If) (0.5 g.) and acetyl chloride (30 ml.) were heated together in a sealed tube at 100°C for 72 hr. The excess solvent was then removed, and the residue was washed with water and the crystallised from ethanol as pale yellow microneedles of the trichloroquinoxaline (III) in 75% yield, m. p. 322—323°C. This was identical (infrared spectra and mixed melting point) with the sample described under a).

**6-Chloro-3,4-dihydro-4-methyl-3-oxo-2-phenylquinoxaline 1-Oxide (Ig; H′=Me).** — The anilide (IIIg; H′=Me) cyclised in 58% yield as pale yellow plates (from methanol) of the 6-chloro-dihydro *N*-oxide (Ig; H′=Me), m. p. 191—192°C.

Found: Cl, 12.0; N, 9.9. Calcd. for $C_{15}H_{11}ClN_2O_2$: Cl, 12.3; N, 9.75%.

**6-Chloro-3,4-dihydro-4-methyl-3-oxo-2-phenylquinoxaline (IIg; H′=Me).** — a) The above *N*-oxide, on reduction with sodium dithionite in 50% aqueous ethanol, gave, in a good yield, pale yellow microneedles (from ethanol) of the 6-chloro-dihydroquinoxaline (IIg; H′=Me), m. p. 123°C.

Found: Cl, 13.3; N, 10.2. Calcd. for $C_{15}H_{11}ClN_2O$: Cl, 13.1; N, 10.35%.

*3 All melting points are uncorrected. Infrared spectra were measured in Nujol mull. Light petroleum used was of 60—80°C boiling range.

12) E. Friedmann and C. Masse, *Biochem. Z.*, **27**, 97 (1910).

13) M. K. Bose, *J. Indian Chem. Soc.*, **22**, 169 (1945).

14) F. Beilstein and A. Kurbatow, *Liebig's Ann.*, **196**, 214 (1879).

15) F. Kehrmann and H. Muller, *Ber. Dtsch. Chem. Ges.*, **34**, 1095 (1901).

16) F. M. Hamer, *J. Chem. Soc.*, **1956**, 1480.

b) 5-Chloro-2-nitro-*N*-methylaniline[15] (1.0 g.) in benzene (40 ml.) was reduced with hydrogen over Pd-C. The catalyst was then filtered off, and the solvent from the dried (sodium sulphate) solution was completely removed under reduced pressure. The residue in a minimum of ethanol was heated with ethyl phenylglyoxalate[17] (1.2 g.) under reflux for 3 hr. The solid obtained on cooling was crystallised from ethanol as colourless microneedles of IIg (H′=Me), m. p. 122—123°C. It was identical (infrared spectrum and mixed melting point) with the product obtained under a).

**6-Chloro-3-hydroxy-2-phenylquinoxaline (IIg).**—3-Hydroxy-2-phenylquinoxaline 1-oxide[2] (Ia) (1.0 g.) and acetyl chloride (40 ml.) or a mixture of hydrochloric acid and acetic acide (1 : 1) were heated under reflux for 6—8 hr. The excess solvent was then removed under reduced pressure, and the residue was washed with water and then crystallised from ethanol as pale yellow microneedles of the 6-chloroquinoxaline (IIg) in 88% yield, m. p. 274—275°C.

Found: C, 65.55; H, 3.9; Cl, 13.5; N, 10.7. Calcd. for $C_{14}H_9ClN_2O$: C, 65.5; H, 3.5; Cl, 13.8; N, 10.9%.

This, on being methylated with methyl sulphate in the presence of anhydrous sodium carbonate in acetone, gave, in a good yield, colourless microneedles (from ethanol) of the 6-chloro-3,4-dihydro-4-methyl-3-oxo-2-phenylquinoxaline (IIg; H′=Me), m. p. 123—124°C; these microneedles were identical (infrared spectra and mixed melting point) with the sample prepared under a) and b) above.

**6, 7-Dichloro-3-hydroxy-2-phenylquinoxaline (IIh).** — a) A mixture of 7-chloro-3-hydroxy-2-phenylquinoxaline 1-oxide[2] (Ib) (1.0 g.) and acetyl chloride (40 ml.) was heated in a sealed tube at 100°C for 72 hr. After the acetyl chloride had then been removed, the residue was washed with water. The solid thus obtained (in a quantitative yield) was crystallised from ethanol as yellow needles of the dichloroquinoxaline (IIh), m. p. 305—306°C.

Found: Cl, 24.3; N, 9.75. Calcd. for $C_{14}H_8Cl_2N_2O$: Cl, 24.4; N, 9.6%.

It was identical (infrared spectra and mixed melting point) with an authentic sample synthesised as described below.

b) A solution of 4,5-dichloro-*o*-phenylenediamine (obtained in situ by reduction with hydrogen of 4,5-dichloro-2-nitroaniline[14] (1.0 g.) in ethanol over Pd-C) and ethyl phenylglyoxalate[17] (1.2 g.) in ethanol (about 10 ml.) was heated under reflux for 3 hr. The solid obtained on cooling was crystallised from ethanol (in a quantitative yield) as yellow needles of 6,7-dichloro-3-hydroxy-3-phenylquinoxaline (IIh), m. p. 305—306°C.

**6-Chloro-7-ethoxy-3-hydroxy-2-phenylquinoxaline (IIi).** — 7-Ethoxy-3-hydroxy-2-phenylquinoxaline 1-oxide[2] (Ic) (1.0 g.) and a mixture of concentrated hydrochloric acid and acetic acid (1 : 1) (40 ml.) were heated under reflux for 6 hr. The mixture, after the excess acetic acid had been removed, was diluted with water and chilled overnight; a solid was thereby obtained (yield 70%) which crystallised from ethanol as yellow needles of the chloroethoxyquinoxaline (IIi), m. p. 283—284°C.

Found: Cl, 11.5; N, 9.4. Calcd. for $C_{16}H_{13}ClN_2O_2$: Cl, 11.8; N, 9.3%.

**6-Chloro-7-methoxy-3-hydroxy-2-phenylquinoxaline (IIj).** — 7-Methoxy-3-hydroxy-2-phenylquinoxaline 1-oxide[2] (Id), on being heated with acetyl chloride under reflux for 15 hr. (and being worked up as usual) gave, in a quantitative yield, yellow needles (from ethanol) of the chloromethoxyquinoxaline (IIj), m. p. 260—261°C.

Found: Cl, 12.3; N, 10.2. Calcd. for $C_{15}H_{11}ClN_2O_2$: Cl, 12.4; N, 9.8%.

**6-Chloro-2-(*p*-chlorophenyl)-3-hydroxyquinoxaline (IIk).**—2-(*p*-Chlorophenyl)-3-hydroxyquinoxaline 1-oxide (Ie) (1.0 g.), on being heated under reflux for 12 hr. with a mixture of concentrated hydrochloric acid and acetic acid (1 : 1) (40 ml.) (an additional 5 ml. of concentrated hydrochloric acid was added every hour) and on being worked up as usual, gave a solid which crystallised from ethanol as pale yellow microneedles (yield 95%) of the dichlorophenylquinoxaline (IIk), m. p.>325°C.

Found: Cl, 22.9; N, 9.1. Calcd. for $C_{14}H_8Cl_2N_2O \cdot H_2O$: Cl, 23.0; N, 9.1%.

**The Action of Hydrobromic Acid on 3-Hydroxy-2-phenylquinoxaline 1-Oxide (Ia).** — The *N*-oxide[2] (Ia) (1.0 g.), on being heated with a mixture of fuming hydrobromic acid and acetic acid (1 : 1) (40ml.) at 100°C for 12 hr., gave after the excess acids had been removed and it had been washed with water, a product which crystallised from ethanol as pale yellow microneedles (yield 60%) of the 3-hydroxy-2-phenylquinoxaline (IIa), m. p. 243—245°C. It was identical (infrared spectrum) with an authentic sample prepared[2] by the condensation of *o*-phenylenediamine with ethyl phenylglyoxalate.

## Summary

3-Hydroxy-2-phenylquinoxaline 1-oxide (Ia), on being heated with acetyl chloride, instead of giving the acetyl derivative, gives a chloro compound (IIg), with a simultaneous loss of its *N*-oxide function. Ia, on being refluxed with a mixture of concentrated hydrochloric acid and acetic acid, undergoes the same transformation. Other derivatives (Ib—f) of Ia behave similarly and give the corresponding chlorine-substituted bases (IIh—l), the structure of which has been established by authentic syntheses.

A nucleophilic mechanism of this chlorination has been proposed, in which the presence of an oxygen function a position 3 of the 2-substituted quinoxaline 1-oxides seems to direct the chlorine substitution to position 6.

The authors wish to thank Dr. S. Siddiqui F. R. S. Chairman, Pakistan Council of Scientific and Industrial Research, for his interest and encouragement. Analyses were carried out by M/S. Pascher & Pascher, Bonn (W. Germany);

17) J. Vene, *Bull. soc. chim. France*, **12**, 506 (1945).

M/S. Alfred Bernhardt, Mulheim (W. Germany) and the Microanalytical Section of Central Laboratories of Pakistan Council of Scientific and Industrial Research, Karachi.

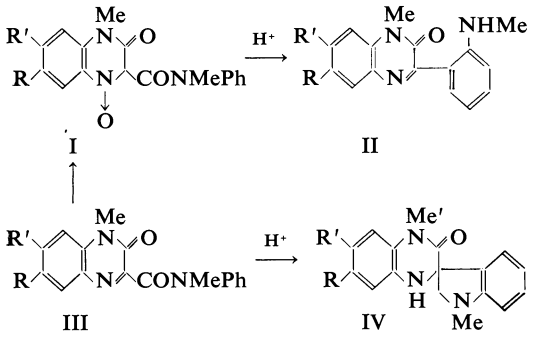
*Chemical Research Division*
*Central Laboratories*
*Pakistan Council of Scientific and Industrial Research*
*Karachi, Pakistan*

# Quinoxaline Derivatives. VII.[1] The Mechanism of the Formation of 6-Chloro-1, 2, 3, 4, 2′, 3′-hexahydro-4, 1′-dimethyl-3, 2′-dioxoquinoxaline-2-spiro-3′-indole from a Quinoxaline *N*-Oxide Derivative by Nucleophilic Chlorination

By Yusuf Ahmad, M. S. Habib,* M. Iqbal, M. I. Qureshi and Ziauddin

(Received February 8, 1965)

Usherwood and Whiteley[2] found that 3, 4-dihydro-4-methyl-2-(*N*-methyl-*N*-phenylcarbamoyl)-3-oxoquinoxaline 1-oxide (Ia), on reaction with ethanolic hydrogen chloride, was converted to the compound $C_{17}H_{16}ClN_3O_2$, whereas with acetyl chloride it gave the compound $C_{19}H_{18}ClN_3O_3$. The latter compound apparently was the acetyl derivative of the former, and in both the compounds chlorine was inactive. However, no structures were proposed for these products. Clark-Lewis and Katekar[3] in 1959 re-examined the problem and revised the molecular formula of these compounds to $C_{17}H_{14}ClN_3O_2$ and $C_{19}H_{16}ClN_3O_3$ respectively; on the basis of spectroscopic data, the study of the degradation products and the synthesis of 6-chloro-3, 4-dihydro-4-methyl-2-(*o*-methylaminophenyl)-3-oxoquinoxaline (IIb, the major product of the degradation of $C_{19}H_{16}ClN_3O_3$), they deduced the structure of the compound $C_{17}H_{14}ClN_3O_2$ to be 6-chloro-1, 2, 3, 4, 2′, 3′-hexahydro-4, 1′-dimethyl-3, 2′-dioxoquinoxaline-2-spiro-3′-indole (IVb), the acetylation of which with acetyl chloride gave a product which was identical with the other compound, $C_{19}H_{16}ClN_3O_3$. However, no synthesis of the compound, which would have confirmed the proposed structure of the spiro-indole (IVb) had previously been reported. It has now been accomplished and is reported below.




Clark-Lewis and Katekar[3] discounted the electrophilic chlorination of the molcule in this interaction of the *N*-oxide (Ia) with acetyl chloride (or ethanolic hydrogen chloride) on the grounds that the "formation of such chlorinating species would consume the *N*-oxide function, and subsequent cyclisation would then be difficult to understand." According to them, for this chlorination, the protonation of the *N*-oxide (Ia) to the conjugate acid (V) is the first step; the powerful inductive effect of the hydroxylammonium ion then promotes the intramolecular electrophilic substitution at the ortho-position of the methylanilide moiety by the quinoxaline 2-C-atom, giving the *N*-hydoxy-compound (VI). The known nucleophilic substitution by chloride ions (i.e., *N*-phenylhydroxylamine with hydrochloric acid → *p*-chloro-aniline[4]) with the intermediate (VI) then leads to the formation of the 6-chloro-spiro-indole (IVb). If this order

1) Part VI: Y. Ahmad, M. S. Habib, Ziauddin and N. Bashir. This Bulletin, **38**, (1965).

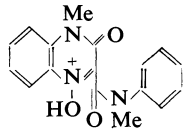
* Burroughs Wellcome & Co. (Pakistan), Ltd., D/43 S. I. T. E., Karachi, Pakistan.

2) E. H. Usherwood and M. A. Whiteley, *J. Chem Soc* **1923**, 1069.

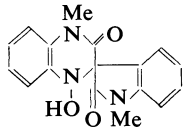
3) J. W. Clark-Lewis and G. F. Katekar, ibid., **1959**, 2825.

4) C. K. Ingold, "Structure and Mechanism in Organic Chemistry," Bell, London (1953), p. 621; H. E. Heller, E. D. Hughes and C. K. Ingold, *Nature*, **168**, 909 (1951).

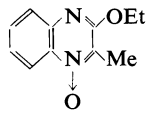
of the two steps for this nucleophilic chlorination is accepted, then the analogy drawn by



V

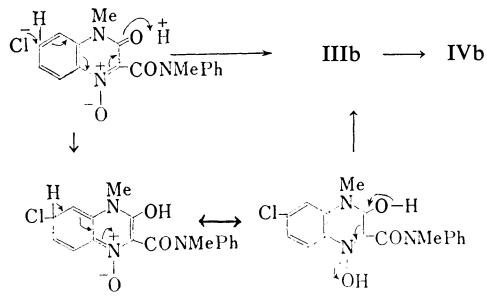


VI



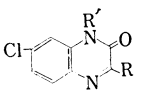
VII

the same authors between this substitution by chlorine in the 6-position of this quinoxaline spiro-indole (IVb) and the reported[5] conversion of 3-ethoxy-2-methyl-quinoxaline 1-oxide (VII) into 6-chloro-3-hydroxy-2-methylquinoxaline (VIIIa; R=Me) cannot be explained, as the cyclisation step to convert VII into an *N*-hydroxy intermediate analogous to VI is not possible in the latter case. The mechanism proposed in Part VI[1] for this type of nucleophilic chlorination of quinoxaline *N*-oxides satisfactorily accounts for both the cases, as, according to it, this nucleophilic chlorination takes place as a result of the combined action of the protonation of oxygen functions at $C_{(3)}$ and $N_{(1)}$ of the quinoxaline molecule, whereby $C_{(6)}$ becomes prone to the attack of the nucleophile (chloride anion), irrespective of the substituent at position 2.

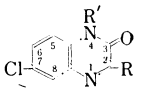



Accordingly, the *N*-oxide (Ia) first gives the chloroquinoxalineanilide (IIIb), which then immediately undergoes the known[6,12] acid-catalysed rearrangement to the isomeric 6-chloro-spiro-indole (IVb).

It is now well established, on the basis of the studies made in earlier papers,[6,12] that 3, 4-dihydro-4-methyl-2-(*N*-methyl-*N*-phenylcarbamoyl)-3-oxoquinoxaline (IIIa), when treated with concentrated sulphuric acid or ethanolic hydrogen chloride, isomerises to 1, 2, 3, 4, 2′, 3′-hexahydro-4, 1′-dimethyl-3, 2′-dioxoquinoxaline-2-spiro-3′-indole (IVa). Substituted derivatives of IIIa behave similarly and give the corresponding spiro-indoles.[12] On the other hand, the *N*-oxides of IIIa and its substituted derivatives, with concentrated sulphuric acid, undergo rearrangement,[13] accompanied by dehydration and decarboxylation, to give the corresponding amines (IIa and its substituted derivatives).



VIII



IX

| | R | R′ | | R | R′ |
|---|---|---|---|---|---|
| (a) | H | H | (f) | $CONH_2$ | H |
| (b) | $CO_2Et$ | H | (g) | $CONH_2$ | Me |
| (c) | $CO_2Et$ | Me | (h) | CONHPh | H |
| (d) | $CO_2H$ | H | (i) | CONMePh | H |
| (e) | $CO_2H$ | Me | (j) | CN | H 1-oxide |

For the synthesis of spiro-indole IVb, 6-chloro-3, 4-dihydro-4-methyl-3-oxoquinoxaline-2-carboxylic acid (VIIIe, see below) was converted to its methylanilide (IIIb) by the usual methods.[12,13] IIIb, when heated with ethanolic hydrogen chloride, rearranged intramolecularly to the isomeric spiro-indole (IVb), which was identical (infrared spectrum and mixed melting point) with the product obtained by the action of ethanolic hydrogen chloride on the chlorine free *N*-oxide (Ia), as described by Clark-Lewis and Katekar.[3] The position of the entering chlorine atom in the molecule in the latter reaction is thereby fully established.

7-Chloro-3-hydroxyquinoxaline-2-carboxylic acid (IXd) was converted to its methylanilide (IXi), and then this was further methylated to IIIc. IXi and IIIc, on being heated with ethanolic hydrogen chloride, rearranged, as expected,[6,12] to their corresponding 7-chloro-spiro-indoles IVc (H for Me′) and IVc. IIIb and IIIc both were smoothly converted to their *N*-oxides (Ib and Ic) with hydrogen peroxide and acetic acid. Both of these *N*-oxides (Ib and Ic) underwent intramolecular rearrangement, accompanied by dehydration and decarboxylation, in concentrated sulphuric acid, yielding 6-chloro-3, 4-dihydro-4-methyl-2-(*o*-methylaminophenyl)-3-oxoquinoxaline (IIb) and the 7-chloro-isomer (IIc) respectively, which were identical (infrared spectrum and mixed melting point) with the synthetic samples provided by Professor J. W. Clark-Lewis.

As expected,[14] the methylanilide IXi, on reaction with hydrogen peroxide in hot acetic acid, yielded 6-chloro-2, 3-dihydroxyquinoxaline (IXa; R=OH) instead of giving its *N*-oxide.

During the preparation of the intermediates needed for this investigation, it was observed

5) W. Dawson, G. T. Newbold and F. S. Spring, *J. Chem. Soc.*, **1949**, 2579.
6) M. S. Habib and C. W. Rees, ibid., **1962**, 123.

that if a large excess of ethyl mesoxalate was not used in its condensation with 4-chloro-*o*-phenylenediamine or 4-chloro-2-methylaminoaniline, instead of the expected quinoxaline-2-carboxylic esters, products of a very high melting point were formed; these probably resulted from the further condensation of the ethoxycarbonyl moiety of the esters formed with another molecule of the *o*-phenylenediamines, as these products[7] were sparingly soluble in, and stable to, acids and alkalies. 4-Chloro-2-methylaminoaniline, on being heated with an excess of ethyl mesoxalate in ethanol (or dry benzene), gave, in a good yield, the ester VIIIc, which, on being shaken with aqueous potassium hydroxide, hydrolysed to the acid VIIIe. The ester which was separated in a good yield by the reaction of 4-chloro-*o*-phenylenediamine with ethyl mesoxalate under similar conditions was the 7-chloro isomer (IXb); its hydrolysis with aqueous alkali gave the corresponding acid (IXd), which, on decarboxylation, gave 6-chloro-2-hydroxyquinoxaline (IXa), identical with a sample[8] which had previously been obtained by an unambiguous route. The 6-chloro isomeric ester (VIIIb), which was the second expected product of the reaction, was formed to a much lesser extent and remained in the mother liquor; on hydrolysis in situ with aqueous alkali it gave 6-chloro-3-hydroxyquinoxaline-2-carboxylic acid (VIIId), which, on decarboxylation, in turn gave the known 6-chloro-3-hydroxyquinoxaline (VIIIa). The structure of this acid (VIIId) was further confirmed by methylation, with methyl sulphate in acetone in the presence of anhydrous potassium carbonate, to lead to a product identical (infrared spectrum and mixed melting point) with the 6-chloro-3,4-dihydro-4-methyl-3-oxoquinoxaline-2-carboxylic acid (VIIIe) described above.

## Experimental

The infrared spectra were measured in Nujol mulls with a Perkin-Elmer spectrophotometer model 137. The light petroleum used had a boiling range of 60—80°C.

**The Condensation of 4-Chloro-*o*-phenylenediamine with Ethyl Mesoxalate.**—4-Chloro-*o*-phenylenediamine (8.4 g.), obtained by the reduction of 4-chloro-2-nitroaniline[9] (10 g.) with stannous chloride and hydrogen chloride (by adopting the procedure of Dawson et al.[5]), was taken up in dry benzene (150 ml.), and then the solution was added portion-by-portion to ethyl mesoxalate (35 ml.). After the mixture had been heated under reflux for 1 hr., about half of the solvent of the mixture was removed under reduced pressure. On cooling, a yellow solid separated (10.5 g.); this was collected and crystallised from ethanol as yellow needles of ethyl 7-chloro-3-hydroxyquinoxaline-2-carboxylate (IXb), m. p. 206—207°C.

Found: Cl, 13.9; N, 11.3. Calcd. for $C_{10}H_9ClN_2O_3$: Cl, 14.05; N, 11.1%.

This compound, which separated as the major product of the condensation, gave, on hydrolysis, an acid the decarboxylation of which afforded the known 6-chloro-2-hydroxyquinoxaline (IXa, see below); this established its structure as a 7-chloro-ester (IXb).

The 6-chloro-ester (VIIIb), the other expected product of the condensation, remained in the mother liquor and was hydrolysed in situ by heating it with 3 N aqueous potassium hydroxide (50 ml.) on a steam bath for 2 hr. The dark red mixture was filtered, and the filtrate, on acidification with concentrated hydrochloric acid, gave a precipitate (purified by dissolution in aqueous potassium hydrogen carbonate and reprecipitation with acid) of 6-chloro-3-hydroxyquinoxaline-2-carboxylic acid (VIIId), m. p. 194—196°C (decomp.).

Found: Cl, 15.2; N, 11.6. Calcd. for $C_9H_5ClN_2O_3 \cdot H_2O$: Cl, 14.7; N, 11.55%.

This acid (VIIId), on being heated to its melting point, gave 6-chloro-3-hydroxyquinoxaline (VIIIa), m. p. 251—252°C, for which Crowther et al.[10] have recorded a m. p. of 270°C (decomp.). VIIId, on methylation, gave the methylated acid (VIIIe), which was identical with the product of the hydrolysis of the authentic ester (VIIIc, see below).

**Ethyl 6-Chloro-3,4-dihydro-4-methyl-3-oxoquinoxaline-2-carboxylate (VIIIc).** — 4-Chloro-2-methylaminoaniline (6.2 g.), obtained from 5-chloro-*N*-methyl-2-nitroaniline (7.5 g.) according to the method of Dawson et al.[5]; was taken up in dry benzene (125 ml.) and then the solution was added to ethyl mesoxalate (28 ml.). After the mixture had been heated under reflux on a water bath for 1.5 hr., the excess solvent was removed under reduced pressure. The solid which separated (in a 60% yield) on cooling was crystallised from ethanol as light yellow needles of the 6-chloro-*N*-methyl ester (VIIIc), m. p. 134—135°C.

Found: Cl, 12.8; N, 9.9. Calcd. for $C_{12}H_{11}ClN_2O_3$: Cl, 13.3; N, 10.5%.

The mother liquor contained more of the ester, as the residue obtained on its evaporation to dryness, on hydrolysis with aqueous alkali, gave an additional amount of the 6-chloro-4-methyl acid (VIIIe, see below).

In the preparation of the esters VIIIc and IXb above, if a large excess of ethyl methoxalate was not used, products with very high melting points were formed; these probably resulted from the further condensation of the ethoxycarbonyl moiety of these esters with another molecule of the *o*-phenylenediamines. These products[7] were stable and sparingly soluble in, acids and alkalies.

7) Cf. H. Ohle and W. Gross, *Ber.*, **68**, 2262 (1935).
8) Y. Ahmad, M. S. Habib and Ziauddin, *Tetrahedron*, **20**, 1107 (1964).
9) M. K. Bose, *J. Indian Chem. Soc.*, **22**, 169 (1945).
10) A. F. Crowther, F. H. S. Curd, D. G. Davy and G. J. Stacey, *J. Chem. Soc.*, **1949**, 1260.
11) F. Kehrmann and H. Muller, *Ber.*, **34**, 1095 (1901).
12) Y. Ahmad, M. S. Habib, M. Iqbal and M. I. Qureshi, *J. Chem. Soc.*, **1964**, 4053.
13) M. S. Habib and C. W. Rees, ibid., **1960**, 3371.
14) M. S. Habib and C. W. Rees, ibid., **1960**, 3386.

**6-Chloro-3, 4-dihydro-4-methyl-3-oxoquinoxaline-2-carboxylic Acid (VIIIe).**—a) 6-Chloro-*N*-methyl ester (VIIIc; 5 g.) was shaken with 20% aqueous potassium hydroxide (100 ml.) at room temperature for 2 hr., during which period it dissolved. On acidification with 25% sulphuric acid with cooling, a light brown precipitate was obtained; this crystallised from ethanol as cream-coloured needles of the 6-chloro-4-methyl acid (VIIIe), m. p. 186—187°C (decomp.). Yield 3.9 g.

Found: Cl, 14.3; N, 11.4. Calcd. for $C_{10}H_7ClN_2O_3$: Cl, 14.8; N, 11.7%.

b) The acid VIIId (1 g.), methyl sulphate (0.5 ml.) and anhydrous potassium carbonate (2 g.) were heated together under reflux in an acetone suspension (100 ml.) for 3 hr. The mixture was then evaported to dryness and acidified with dilute hydrochloric acid. The solid which separated was collected and crystallised from ethanol as cream-coloured needles, m. p. 188—189°C (decomp.), identical (infrared spectrum and mixed melting point) with the 6-chloro-4-methyl acid (VIIIe) described under a).

**7-Chloro-3-hydroxyquinoxaline-2-carboxylic Acid (IXd).**—The ester (IXb) and 3 N aqueous potassium hydroxide were heated on a steam bath for 1 hr. The reaction mixture was then filtered, and the filtrate, on acidification with concentrated hydrochloric acid, gave the 7-chloro acid (IXd) in quantitative yield, m. p. 308—310°C (decomp.).

Found: Cl, 15.5; N, 12.8. Calcd. for $C_9H_5ClN_2O_3$: Cl, 15.8; H, 12.5%.

This could, when heated at 310°C, be decarboxylated to 6-chloro-2-hydroxyquinoxaline (IXa), m. p. 320—321°C, identical with that of a sample[8] (m. p. 320—321°C) obtained by the reduction of 7-chloro-2-cyano-3-hydroxyquinoxaline 1-oxide (IXj) with sodium dithionite in boiling 50% aqueous ethanol.

**7-Chloro-3, 4-dihydro-4-methyl-3-oxoquinoxaline-2-carboxylic Acid (IXe).**—The ester (IXb) in acetone was methylated with methyl sulphate in the presence of anhydrous potassium carbonate to give the 7-chloro-4-methyl ester (IXc) (crystallised from ethanol as yellow needles) in a good yield, m. p. 125—126°C.

Found: Cl, 10.4; N, 12.8. Calcd. for $C_{12}H_{11}ClN_2O_3$: Cl, 10.5; N, 13.3%.

This ester, on hydrolysis with 3 N aqueous potassium hydroxide, gave yellow cubes (from ethanol) of the 7-chloro-4-methyl acid (IXe) (yield 80%), m. p. 198—199°C (decomp.).

Found: Cl, 13.9; N, 11.9. Calcd. for $C_{10}H_7ClN_2O_3$: Cl, 14.8; N, 11.7%.

**7-Chloro-3-hydroxyquinoxaline-2-carboxyamide (IXf).**—The ester (IXb), on being heated with concentrated ammonia on a steam bath for 2 hr., afforded a solid which crystallised from ethanol as yellow micro-crystals of the amide (IXf) in a quantitative yield, m. p. 310—311°C.

Found: Cl, 15.2; N, 18.4. Calcd. for $C_9H_6ClN_3O_2$: Cl, 15.8; N, 18.8%.

**7-Chloro-3,4-dihydro-4-methyl-3-oxoquinoxaline-2-carboxyamide (IXg).**—Similarly, the ester (IXc) with concentrated ammonia gave yellow needles (from ethanol) of the 4-methyl amide (IXg) in a good yield, m. p. 325—326°C (decomp.).

Found: Cl, 13.7; N, 16.6. Calcd. for $C_{10}H_8ClN_3O_2 \cdot H_2O$: Cl, 13.9; N, 16.4%.

**6-Chloro-3, 4-dihydro-4-methyl-2-(*N*-methyl-*N*-phenylcarbamoyl)-3-oxoquinoxaline (IIIb).**—The acid (VIIIe) (1 g.) and thionyl chloride (20 ml.) were heated under reflux for 1 hr. The solid obtained after the removal of thionyl chloride was taken up in a small amount of dry benzene and added portion-by-portion to a solution of *N*-methylaniline (8 ml.) in dry benzene (10 ml.). The reaction mixture was then heated on a steam bath for 10 min. and washed with 2 N hydrochloric acid. The solid which separated was crystallised from ethanol as light yellow cubes of the 4-methyl-*N*-methylanilide (IIIb); yield 80%; m. p. 192—193°C.

Found: C, 62.7; H, 4.6; Cl, 10.6. Calcd. for $C_{17}H_{14}ClN_3O_2$: C, 62.3; H, 4.3; Cl, 10.8%.

This general procedure was also used for the preparation of the other anilides described below.

**7-Chloro-3-hydroxy-2-(*N*-phenylcarbamoyl)-quinoxaline (IXh).**—The acid chloride from the acid (IXd), on reaction as above, gave with aniline yellow needles (from glacial acetic acid) of the anilide (IXh); yield 90%, m. p. >340°C.

Found: Cl, 11.45. Calcd. for $C_{15}H_{10}ClN_3O_2$: Cl, 11.85%.

**7-Chloro-3, 4-dihydro-4-methyl-2-(*N*-methyl-*N*-phenylcarbamoyl)-3-oxoquinoxaline (IIIc).**—Similarly, the acid chloride from the acid (IXd) with methylaniline gave yellow needles (from ethanol) of 7-chloro-3-hydroxy-2-(*N*-methyl-*N*-phenylcarbamoyl)-quinoxaline (IXi); yield 70%; m. p. 285°C.

Found: Cl, 10.9; N, 13.7. Calcd. for $C_{16}H_{12}ClN_3O_2$: Cl, 11.3; N, 13.4%.

The methylation of this anilide with methyl sulphate and anhydrous potassium carbonate in acetone gave cream-coloured cubes (from benzene-light petroleum) of 4-methyl-*N*-methylanilide (IIIc) in a good yield, m. p. 164—166°C.

Found: Cl, 10.7. Calcd. for $C_{17}H_{14}ClN_3O_2$: Cl, 10.8%.

**6-Chloro-1, 2, 3, 4, 2', 3'-hexahydro-4, 1'-dimethyl-3, 2'-dioxoquinoxaline-2-spiro-3'-indole (IVb).**—The anilide (IIIb) (0.5 g.) was boiled under reflux for 2 hr. with saturated ethanolic hydrogen chloride (25 ml.), and then the mixture was evaporated under reduced pressure to dryness. The residue crystallised from ethanol as colourless needles of the spiro-indole (IVb), m. p. 239—240°C, in a good yield. The spiro-indole was identical (infrared spectrum and mixed melting point) with a sample[2] obtained by the action of ethanolic hydrogen chloride on 3, 4-dihydro-4-methyl-2-(*N*-methyl-*N*-phenylcarbamoyl)-3-oxoquinoxaline 1-oxide (Ia). The above procedure was used for the preparation of the following spiro-indoles.

**7-Chloro-1, 2, 3, 4, 2', 3'-hexahydro-1'-methyl-3, 2'-dioxoquinoxaline-2-spiro-3'-indole (IVc; H for Me').**—The anilide (IXi), on being treated with ethanolic hydrogen chloride as above, gave white needles (from acetic acid) of the spiro-indole (IVc; H for Me'); yield 70%; m. p. 320°C (decomp.).

Found: C, 61.6; H, 4.5; Cl, 11.7. Calcd. for $C_{16}H_{12}ClN_3O_2$: C, 61.2; H, 3.8; Cl, 11.3%.

**7-Chloro-1, 2, 3, 4, 2', 3'-hexahydro-4, 1'-dimethyl-3,2'-dioxoquinoxaline-2-spiro-3'-indole (IVc).**—Similarly, the anilide (IIIc) gave light yellow needles (from ethanol) of the 4-methyl spiro-indole (IVc); yield 80%; m. p. 260—262°C (decomp.).

Found: Cl, 61.8; H, 4.1. Calcd. for $C_{17}H_{14}ClN_3O_2$: C, 62.3; H, 4.3%.

**6-Chloro-3, 4-dihydro-4-methyl-2-(*N*-methyl-*N*-phenylcarbamoyl)-3-oxoquinoxaline 1-Oxide (Ib).**—The anilide (IIIb) (1.0 g.), acetic acid (10 ml.), and 30% hydrogen peroxide (1 ml.) were heated at 55—60°C for 72 hr.; the acetic acid was removed under reduced pressure, and the residue was crystallised from benzene-light petroleum as yellow crystals of the 1-oxide (Ib); yield 25%; m. p. 160—162°C.

Found: C, 57.9; H, 3.8; N, 12.0. Calcd. for $C_{17}H_{14}ClN_3O_3 \cdot 1/2H_2O$: C, 57.9; H, 4.0; N, 11.9%.

**7-Chloro-3, 4-dihydro-4-methyl-2-(*N*-methyl-*N*-phenylcarbamoyl)-3-oxoquinoxaline 1-Oxide (Ic).**—Similarly, the anilide (IIIc) gave yellow crystals (from benzene-light petroleum) of the 1-oxide (Ic); yield 40%; m. p. 180—182°C.

Found: N, 12.5. Calcd. for $C_{17}H_{14}ClN_3O_3$: N, 12.2%.

**6-Chloro-2, 3-dihydroxyquinoxaline (IXa; R=OH).**—The anilide (IXi), on being treated with a mixture of hydrogen peroxide and glacial acetic acid at 60°C, gave colourless flakes (from glacial acetic acid) of the dihydroxyquinoxaline (IXa; R=OH); yield 50%; m. p. >350°C, identical (infrared spectrum) with an authentic sample.[10]

**6-Chloro-3, 4-dihydro-4-methyl-2-(*o*-methylaminophenyl)-3-oxoquinoxaline (IIb).**—The *N*-oxide (Ib) (0.5 g.) was stirred gradually into concentrated sulphuric acid (2 ml.) at room temperature. After the evolution of carbon dioxide had ceased, the solution was poured on ice and filtered. The basification of the filtrate gave a precipitate which crystallised from ethanol as orange needles of the 6-chloro-amine (IIb) (yield 40%); m. p. 186—188°C; identical (infrared spectrum and mixed melting point) with the synthetic sample[3] supplied by Professor J. W. Clarke-Lewis.

**7-Chloro-3, 4-dihydro-4-methyl-2-(*o*-methylaminophenyl)-3-oxoquinoxaline (IIc).**—The *N*-oxide (Ic) (0.5 g.) obtained by the above method yielded the 7-chloroamine (IIc); yield 50%; m. p. 163—164°C; indentical (infrared spectra and mixed melting point) with a synthetic sample[3] supplied by Professor J. W. Clark-Lewis.

## Summary

The compound IVb named in the title has been obtained by an unambiguous route. It has been shown to be identical with the product of the reaction of the *N*-oxide (Ia) with ethanolic hydrogen chloride. Clark-Lewis and Katekar's mechanism[3] for the nucleophilic chlorination in the latter case has been discussed, and a modified mechanism proposed.

Isomeric 7-chloro-spiro-indole (IVc) has also been obtained by the rearrangement of the anilide IIIc. Similarly, the anilide IXi gives spiro-indole (IVc; H for Me').

The anilides IIIb and IIIc give normal *N*-oxides Ib and Ic, which, with concentrated sulphuric acid, decompose and afford the amines IIb and IIc. IXi, instead of giving its *N*-oxide, yields 6-chloro-2, 3-dihydroxyquinoxaline.

The authors wish to thank Dr. S. Siddiqui, F. R. S., Chairman, Pakistan Council of Scientific and Industrial Research, for his interest and encourgement. Analyses were carried out by M/S. Pascher and Pascher, Germany; Wellcome Research Laboratories (through the courtesy of Dr. H. T. Openshaw), England; and Microanalytical Section, Central Laboratories, Pakistan Council of Scientific and Industrial Research, Karachi. We are also indebted to Professor J. W. Clark-Lewis for the samples of 6-chloro- and 7-chloro-3, 4-dihydro-4-methyl-2-(*o*-methylaminophenyl)-3-oxoquinoxalines (IIb and IIc).

*Chemical Research Division*
*Central Laboratories*
*Pakistan Council of Scientific and Industrial Research*
*Karachi, Pakistan*

# Equilibria in the System $FeO$–$Fe_2O_3$–$MgO$ at 1160°C

By Takashi KATSURA and Shigeyuki KIMURA

(Received February 15, 1965)

The system $FeO$–$Fe_2O_3$–$MgO$ is one of the most important systems not only for ceramics, but also for metallurgy and geochemistry. The subsolidus study of this system may establish the fundamental thermodynamic properties of both magnesioferrite and magnesiowüstite solid solutions. This knowledge will in turn furnish chemical data for the investigation of the system $FeO$–$Fe_2O_3$–$MgO$–$SiO_2$, which is very important since it includes the stability relationship between the pyroxene solid solution, $FeSiO_3$–$MgSiO_3$, and the olivine solid solution, $Fe_2SiO_4$–$Mg_2SiO_4$, which usually coexist in igneous rocks. However, no investigation of a complete isothermal phase diagram of the system Fe–Mg–O at a subsolidus temperature under various oxygen partial pressures has yet been published.

Darken and Gurry[1] studied the system Fe–O and precisely re-determined the thermodynamic properties of metallic iron, wüstite, and magnetite in their equilibrated states. Richards and White[2] and Woodhouse and White[3] studied the system Fe–Mg–O at high temperatures, up to 1650°C, in air and constructed a modified phase diagram showing the extensive solid solubility of iron(II) oxide and iron(III) oxide in periclase. Phillips, Sōmiya, and Muan[4] also studied the system and determined the phase relations in air at temperatures up to 1800°C by means of the quenching technique. Moreover, Brynestad and Flood[5] studied this system at 1400°C and at various oxygen partial pressures in order to clarify the equilibrium between ferrous and ferric iron in wüstite containing various amounts of magnesium oxide; these data were then used for a discussion of the applicability of the mass-action law on the redox equilibrium. Roberts and Merwin[6] investigated the system $FeO$–$Fe_2O_3$–$MgO$ at temperatures above 1000°C in an isobar 1/5 atmosphere of $O_2$. As for the binary system $MgO$–$Fe_2O_3$, they found no compound other than $MgO \cdot Fe_2O_3$ which dissociates slightly on heating, and established that the solid solution extends from this compound for a short distance toward MgO. On the basis of studies by Schenck and Dingmann[7] and of those by Roberts and Merwin[6] and Bowen and Schairer[8] on the system $FeO$–$MgO$, White[9] constructed approximate phase relations for the system Fe–Mg–O.

The purpose of the present study is to determine the detailed phase equilibria in the system $FeO$–$Fe_2O_3$–$MgO$ at 1160°C by varying partial oxygen pressures from 0.21 atm. to $10^{-13.5}$ atm. The temperature of 1160°C was adopted for convenience in studying the subsolidus equilibria in the system $FeO$–$Fe_2O_3$–$MgO$–$SiO_2$.

## Experimental Methods

**General Procedures.**—The different experimental methods were used in the present investigation—quenching and thermogravimetric methods as previously described by Katsura and Muan.[10]

In the thermogravimetric method, pellete of oxide mixtures of iron(III) oxide and magnesium oxide were suspended by a thin platinum wire from one beam of an analytical balance, and the weight changes were recorded as a function of the oxygen pressure at 1160°C. The data thus obtained were used to locate oxygen isobars. According to Richards and White,[2] no change was observed in the weight of mixtures of iron(III) oxide and magnesium oxide in any ratio when the mixtures (starting materials) were heated at 700°C and in air. In the present study, we checked the fact mentioned above. The weight in air at 700°C was taken as the reference state for calculation of the amount of $Fe^{2+}$ produced in drawing the isobaric line, and subsequently in determining the phase boundary.

In the quenching method, oxide samples were heated at 1160°C and at a chosen oxygen pressure until equilibrium was attained among gas and condensed phases. The samples were then quenched rapidly to the temperature of ice by burning away the thin platinum wire with an electric current. The sample thus obtained were used for determining

1) L. S. Darken and R. W. Gurry, *J. Am. Chem. Soc.*, **67**, 1398 (1945); ibid., **68**, 798 (1946).
2) R. G. Richards and J. White, *Trans. Brit. Ceram. Soc.*, **53**, 422 (1954).
3) D. Woodhouse and J. White, ibid., **54**, 333 (1955).
4) B. Phillips, S. Sōmiya and A. Muan, *J. Am. Ceram. Soc.*, **44**, 167 (1961).
5) J. Brynestad and H. Flood, *Z. Elektrochem.*, **62**, 953 (1958).
6) H. S. Roberts and H. E. Merwin, *Am. J. Sci.*, **21**, 145 (1931).
7) R. Schenck and H. Dingmann, *Z. anorg. u. allgem. Chem.*, **166**, 133 (1927).
8) N. L. Bowen and J. F. Schairer, *Am. J. Sci.*, [5th Series], **29**, 151 (1935).
9) J. White, *J. Iron and Steel Inst.*, **148**, 579 (1943).
10) T. Katsura and A. Muan, *Trans. AIME*, **230**, 77 (1964).

the phases present by X-ray and the microscopic examinations and for the determination of the compositions by chemical analysis. The amounts of ferrous iron determined by thermogravimetric and by chemical analysis were in good agreement.

**Materials.**—Guaranteed reagents of iron(III) oxide and magnesium oxide were used as the starting materials. Each oxide was heated separately in air at 1000°C for several hours. Mixtures of the desired ratios of the two oxides were then prepared. Each mixture was finely ground by an agate mortar, mixed, and heated at 1250 to 1300°C in air for 3 to 12 hr., depending on the composition. The sintered mixture was again finely ground and repeatedly heated in air at 1300°C. A suitable starting material for thermogravimetry was obtained by this treatment. Some of the mixed samples thus prepared were heated for several hours at 1160°C and at the low oxygen pressures necessary to produce the magnesiowüstite. Reduced samples with the same iron/magnesium ratios were obtained by this treatment, and equilibrium could be approached in opposite directions by using these reduced samples in subsequent equilibration runs, as will be described later.

**The Control of the Atmosphere.**—Atmospheres of the desired oxygen pressures were obtained by using pure oxygen, air, carbon dioxide, and $CO_2$-$H_2$ mixtures. The $CO_2$-$H_2$ mixtures were prepared by proportioning the two gas components in the desired ratios in a gas mixer principally similar to that described by Darken and Gurry.[1] Oxygen pressures in the $CO_2$-$H_2$ mixtures were calculated from the thermodynamic data summarized by Elliot and Gleiser.[11] The fluctuation of the $CO_2/H_2$ ratio was within ± 1% throughout the present study, the fluctuation of the value of $\log P_{O_2}$ due to the maximum variation in the $CO_2/H_2$ ratio is thus about 0.01. The oxygen partial pressures at 1160°C were checked by means of the relationship between the chemical composition of wüstite and the oxygen pressure at which the composition is equilibrated as has previously been established by Darken and Gurry,[1] Katsura and Muan,[10] and Taylor.[12] The purities of the carbon dioxide and hydrogen used in the present study were sufficient for the present purposes.

**Furnaces and Temperature Control.**—A vertical tube quench furnace with an 80%Pt20%Rh winding was used for the equilibration runs. A brass-made attachment for quenching was connected with the lower end of a mullite furnace tube with a 30 mm. diameter. The gases used for controlling the oxygen partial pressure were passed through the furnace from bottom to top.

The furnace temperatures were kept constant to approximately ±2° by means of electric controllers activated by a Pt-87%Pt13%Rh thermocouple inserted close to the hot spot of the furnace. The actual temperatures within the furnace were measured with another Pt-90%Pt10%Rh thermocouple which was calibrated against the melting points of diopside ($CaMgSi_2O_6$), 1391.5°C, and Gold (Au), 1063°C. (This thermocouple was provided by the courtesy of Dr. E. F. Osborn and Dr. A. Muan, of the Pennsylvania State University).

**The Identification of Phases and the Determination of the Lattice Parameter.**—The phases present in the quenched samples were identified by an X-ray diffractometer. Silicon powder was used as the standard in determining the lattice parameters of the phase present.

An indirect and useful check on the phases present is afforded by the location and shape of the oxygen isobars, as determined in the thermogravimetric study. These relations have been explained in detail in recent papers by Taylor[12] and Katsura and Muan.[10]

The presence of metallic iron in the phase assemblages was evidenced by the liberation of hydrogen gas when samples were dipped in hydrochloric acid. This test is sensitive enough to detect iron in amounts as small as 0.2%.

**Chemical Analysis.**—The ferrous iron content of the quenched samples was determined volumetrically by the method described in detail by Iwasaki et al.,[13] while the total iron content was determined by the zinc-amalgam method described by Katsura.[14] In cases of small amounts of iron, the colorimetric method was adopted to determine the total iron by using $\alpha, \alpha'$-dipyridyl.

**Checking Equilibration and Quenching Procedures.**—First, the most suitable linear rate of flow of a homogeneous mixture of gases through the mixing apparatus to the furnace was checked for the equilibration within the gas phase at 1160°C. When the linear rates of flow was kept at 5 mm/sec., and 4 mm./sec. respectively, the equilibrium state in the condensed phases was never attained. That is to say, the chemical composition was not constant in each run of the same starting material under identical conditions; even in a quenched pellet with about a 1 cm. cube, an appreciable difference was observed in appearance. When we adopt 2.5 mm./sec., the equilibrium was approached within a reasonable period of time and the relationships between the oxygen partial pressures and the chemical compositions of both magnetite and wüstite were just the same as those obtained by Darken and Gurry[1] although they used a mixture of $CO_2$-CO instead of $CO_2$-$H_2$ to obtain constant oxygen partial pressure. In the present study, the linear rate of flow, therefore, was kept close to 2.5 mm./sec.

The rate of approach to equilibrium was studied thermogravimetrically. Mixtures with identical iron/magnesium ratios but of different initial degrees of oxidation were used in these experiments to ensure that the equilibrium measured was independent of the time and could be established from both sides. The procedures were as follows: A pellet with a fixed ratio of iron/magnesium which has been heated preliminarily at 700°C was heated at 1160°C in air for 3 hr. After ensuring no

11) J. F. Elliot and M. Gleiser, "Thermochemistry for Steelmaking," Addison-Wesley Publishing Co., Inc., Reading, Mass. (1960).
12) R. W. Taylor, *Am. Mineralogist*, **49**, 1016 (1964).
13) I. Iwasaki, T. Katsura, M. Yoshida and T. Tarutani, *Japan Analyst*, **6**, 211 (1957).
14) T. Katsura, "Zikken Kagaku Koza," Vol. 15, Maruzen Shuppan, Tokyo (1959), pp. 272—275.

change in the weight by the thermobalance, the degree of weight-loss was followed by the thermobalance at a desired oxygen partial pressure. When there was no recognizable change in weight over, at least, one hour, the weight thus obtained was regarded as the nearest point to the equilibrated state during the course from the oxidized state to the reduced state. Then the oxygen pressure was very greatly decreased to form magnesiowüstite with a large amount of ferrous iron. After fixing the desired oxygen partial pressure as the same as that in the course from the oxidized state to the reduced state, the degree of weight-gain was measured. The results obtained from both sides were identical within the limits of experimental error.

The thermogravimetric determination of ferrous iron was also ascertained by chemical analysis after rapid quenching. In addition, the composition of both the inside and the outside of a pellet equilibrated after a reasonable period of time was determined to check whether or not there was an uniform compositional distribution, as has been pointed out by Katsura[15] in the case of magnetite solid solution. These careful checks showed that the equilibrium point with regard to composition was experimentally determined by the thermogravimetric method.

Whereas the total compositions of condensed phases remained constant during the quenching, the phase assemblages present after the quenching were not always the same as they were at the end of the equilibration. For instance, the magnesiowüstite of the composition in the vicinity of the magnesiowüstite-spinel boundary curve could not be quenched. In such cases, the phase evidence given by the thermogravimetric data (the shape and location of oxygen isobars) is more reliable than that obtained by the quenching technique.

## Results and Discussion

The equilibrium data obtained at 1160°C are summarized in Table I, while they are illustrated graphically in Fig. 1.

Three oxide phases are stable under the present experimental conditions : hematite, $Fe_2O_3$, with a rhombohedral structure ; an oxide solid solution with a spinel structure (it is simply called spinel in this paper), and an oxide solid solution with sodium chloride structure (simply called magnesiowüstite). The detailed phase relations were studied mainly in those areas with both spinel and magnesiowüstite phases.

Figure 2 shows the relationship between the oxygen partial pressure (as $-\log P_{O_2}$) and the mole fraction of iron(II) oxide produced in a starting material of iron(III) oxide. We can see the discontinuous points in Fig. 2 as marked by letters from a to e. These may reasonably be responsible for the points where the starting material is in characteristic states at specified,

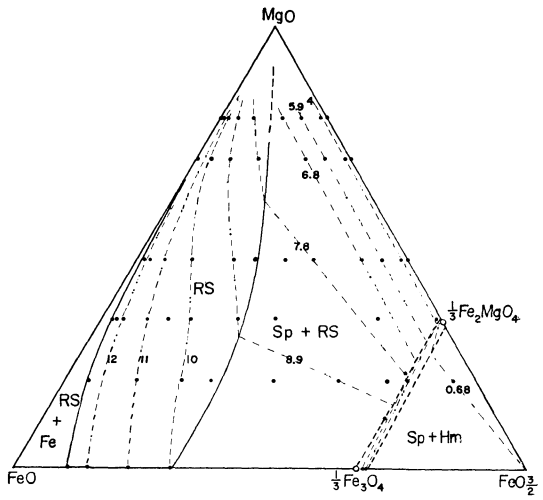



Fig. 1. Diagram illustrating phase relationship in the system $FeO$-$Fe_2O_3$-$MgO$. For convenience, the three components are taken as FeO, $FeO_{3/2}$, and MgO. Heavy lines are boundary curves. Heavy dashed lines are for the approximate spinel phase, and light dashed lines are isobaric lines with numbers meaning $-\log P_{O_2}$. Solid circles represent compositions, as shown in Table I. Abbreviations used have the following meaning : Hm= hematite, Sp=oxide with spinel structure, RS=oxide with NaCl structure, and Fe= metallic iron.

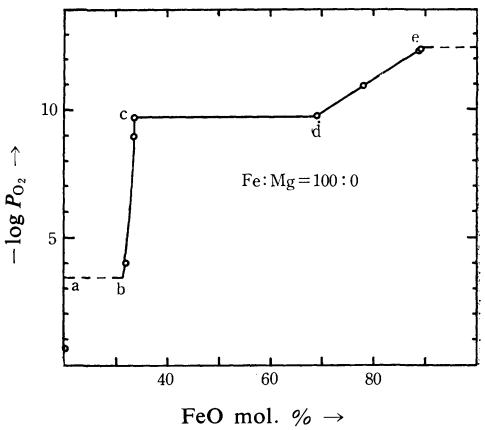



Fig. 2. The relationship between the oxygen partial pressure and the mole fraction of FeO produced in a starting material of $Fe_2O_3$.

respective oxygen pressures, and they represent the points where the equilibrium relationship among condensed phases greatly changes. In view of the experimental results, the line a—b shows the stable coexistence of hematite and magnetite, b—c is for one phase region of magnetite, c—d is for the stable coexistence of magnetite and wüstite, d—e is for one phase region of wüstite, and the right side of e shows the

15) T. Katsura, *Bull. Phys. Soc. Japan*, **19**, 21 (1964).

TABLE I.

| Starting material $Fe_2O_3$ : MgO mol. % | $P_{O_2}$ | FeO mol. %* in product | Phases present** | Startion material $Fe_2O_3$ : MgO mol. % | $P_{O_2}$ | FeO mol. %* in product | Phases present** |
|---|---|---|---|---|---|---|---|
| 100 : 0 | $10^{-0.68}$ | 0.1 | Hm | 25.8 : 47.2 | $10^{-7.80}$ | 18.4 | |
| | $10^{-4.04}$ | 31.9 | Sp | | $10^{-8.10}$ | 23.9 | Sp+RS |
| | $10^{-9.00}$ | 33.4 | Sp | | $10^{-8.34}$ | 29.8 | Sp+RS |
| | $10^{-9.73}$ | 33.4 | Sp | | $10^{-8.89}$ | 33.7 | |
| | $10^{-9.78}$ | 69.0 | RS | | $10^{-10.0}$ | 42.0 | |
| | $10^{-10.98}$ | 77.9 | | | $10^{-11.0}$ | 47.6 | RS |
| | $10^{-12.38}$ | 89.2 | RS | | $10^{-12.0}$ | 50.6 | RS |
| | $10^{-12.40}$ | | Fe | | $10^{-12.8}$ | 51.1 | RS |
| 80.2 : 19.8 | $10^{-0.68}$ | 4.6 | Hm+Sp | | $10^{-12.9}$ | | RS+Fe |
| | $10^{-4.04}$ | 13.4 | Sp | 30.0 : 70.0 | $10^{-0.68}$ | 0.2 | Sp+RS |
| | $10^{-7.81}$ | 14.5 | Sp | | $10^{-4.04}$ | 1.6 | Sp+RS |
| | $10^{-8.34}$ | 17.4 | Sp+RS | | $10^{-5.89}$ | 4.7 | |
| | $10^{-8.88}$ | 27.0 | | | $10^{-6.82}$ | 8.8 | Sp+RS |
| | $10^{-9.10}$ | 39.7 | | | $10^{-7.80}$ | 17.8 | Sp+RS*** |
| | $10^{-9.42}$ | 51.8 | Sp+RS*** | | $10^{-8.89}$ | 23.5 | |
| | $10^{-10.0}$ | 57.7 | Sp+RS*** | | $10^{-10.0}$ | 27.5 | RS |
| | $10^{-11.0}$ | 66.8 | RS | | $10^{-12.0}$ | 29.7 | |
| | $10^{-12.5}$ | 75.1 | RS | | $10^{-12.5}$ | 29.3 | |
| | $10^{-12.6}$ | | RS+Fe | | $10^{-12.7}$ | 29.3 | |
| 66.3 : 33.7 | $10^{-0.68}$ | 0.4 | Sp | | $10^{-12.9}$ | 29.7 | |
| | $10^{-4.04}$ | 1.5 | | | $10^{-13.0}$ | 29.7 | RS |
| | $10^{-7.65}$ | 12.6 | Sp+RS | | $10^{-13.1}$ | | RS+Fe |
| | $10^{-8.75}$ | 32.7 | Sp+RS | 20.7 : 79.3 | $10^{-0.68}$ | 0.2 | Sp+RS |
| | $10^{-8.90}$ | 39.9 | Sp+RS | | $10^{-4.04}$ | 1.3 | Sp+RS |
| | $10^{-9.00}$ | 41.4 | | | $10^{-5.89}$ | 5.2 | |
| | $10^{-9.95}$ | 49.2 | | | $10^{-6.82}$ | 8.7 | Sp+RS |
| | $10^{-10.45}$ | 53.5 | | | $10^{-7.81}$ | 14.1 | |
| | $10^{-10.97}$ | 57.5 | RS | | $10^{-8.87}$ | 17.3 | |
| | $10^{-11.98}$ | 62.4 | RS | | $10^{-10.0}$ | 19.4 | |
| | $10^{-12.47}$ | 63.8 | RS | | $10^{-11.0}$ | 20.1 | RS |
| | $10^{-12.62}$ | | RS+Fe | | $10^{-12.0}$ | 20.4 | |
| 52.8 : 47.2 | $10^{-0.68}$ | 0.3 | Sp+RS | | $10^{-13.0}$ | 20.6 | |
| | $10^{-4.04}$ | 1.6 | | | $10^{-13.2}$ | 20.6 | |
| | $10^{-5.89}$ | 5.4 | Sp+RS | | $10^{-13.5}$ | | RS+Fe |
| | $10^{-6.82}$ | 9.2 | | | | | |

* FeO mol. % was calculated on the basis of $FeO+FeO_{3/2}+MgO=100$.

** Abbreviations used have the following meaning: Hm=hematite, Sp=oxide with spinel structure, RS=oxide with NaCl structure, and Fe=metallic iron.

*** The phases at 1160°C could not be quenched.

stable coexistence of wüstite and metallic iron. These assignments are generally consistent with the Gibbs' Phase Rule. Figure 3 (a—e) was constructed on the basis of the treatment described above, but with different ratios of iron/magnesium in the starting materials. Figure 1 shows the phase boundaries over the whole system of $FeO-Fe_2O_3-MgO$ based on the results obtained from Fig. 2 and Fig. 3. The isobaric lines are also given by the broken lines Fig. 1. Each isobaric line is uniquely bent on the phase boundary curve.

The compositions of the spinel solid solution are generally represented by the formula $(Fe, Mg)_3O_4$. However, the solid solubility of the iron(III) oxide component into spinel extends pretty widely, as is approximately shown by the heavy broken line in Fig. 1. In addition, this solid solution seems to be stable, with a small deviation in the oxygen-to-cation ratio below the stoichiometric 4 : 3 value and with, at least, a 1 mole per cent of excess FeO. Table II shows the chemical composition of spinel with excess FeO at various oxygen partial pressures and at 1160°C. The lattice parameters of these metal-rich spinels were almost identical; $a_0=8.398\pm0.003$ Å. The lattice parameter of the stoichiometric spinel solid solution was also measured, but the difference was very small, ranging from 8.396 Å

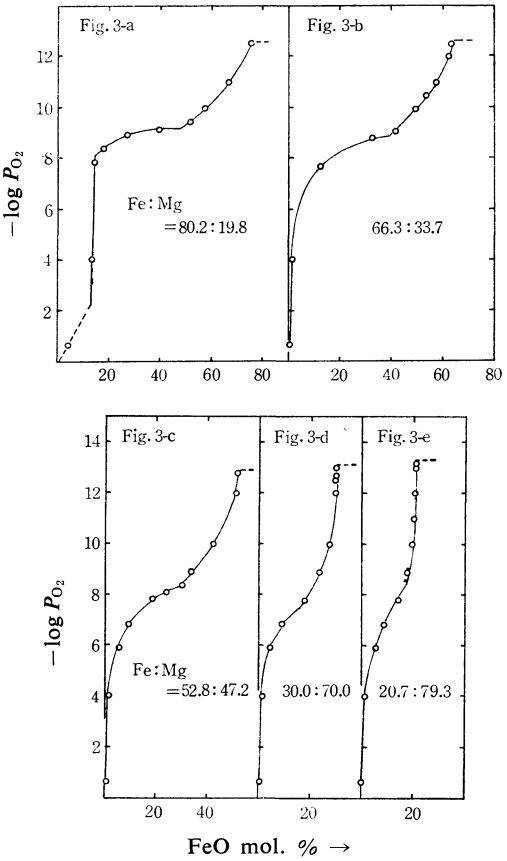



Fig. 3. The relationship between the oxygen partial pressure and the mole fraction of FeO produced in starting materials with different ratios of Fe/Mg.

TABLE II. CHEMICAL COMPOSITION OF METAL-RICH OXIDES WITH SPINEL STRUCTURE

| $\frac{Mg}{Mg+Fe}$ | FeO, mol. %* | $\frac{Metal}{Oxygen}$ | $P_{O_2}$(atom) |
|---|---|---|---|
| 0.307 | 3.7 | 3.012 : 4 | $10^{-4.04}$ |
| 0.202 | 13.7 | 3.006 : 4 | $10^{-7.58}$ |
| 0.120 | 22.6 | 3.014 : 4 | $10^{-8.90}$ |

* FeO has the same meaning as in Table I.

of $Fe_3O_4$ to 8.399 Å of $MgFe_2O_4$.

The wüstite phase is characterized by wide variations in the iron/oxygen ratios; a continuous areal solid solution (magnesiowüstite) with sodium chloride structure is seen in Fig. 1. The present results sustain the observations of Brynestad and Flood[5] that the magnesiowüstite field in the $FeO$-$Fe_2O_3$-$MgO$ ternary system has an extensive range of stable existence at 1400°C and at various oxygen pressures ranging from $10^{-3.1}$ atm. to $10^{-7.46}$ atm. Figure 4 shows the relationship between the mole fraction of MgO and the ratio of $Fe^{3+}/(Fe^{2+}+Fe^{3+})$ within the field of magne siowüstite. It may be seen

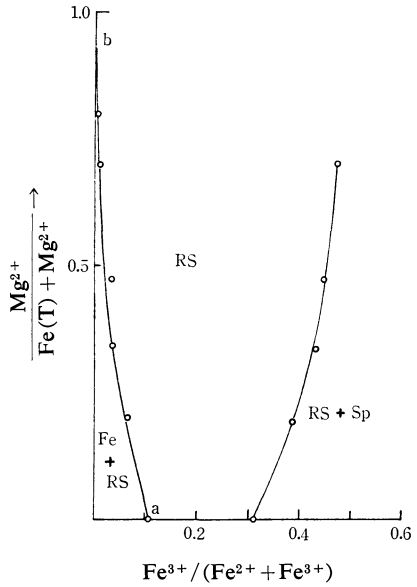



Fig. 4. The relationship between mole fraction of $Mg^{2+}$ and the ratio of $Fe^{3+}/(Fe^{2+}+Fe^{3+})$ within the field of magnesiowüstite. The curve a—b is the equilibrium boundary between magnesiowüstite and metallic iron + magnesiowüstite.

from Fig. 4 that the amount of $Fe^{2+}$ increases with an increse in the amount of magnesium on the equilibrium boundary between magnesiowüstite and metallic iron + magnesiowüstite (a—b in Fig. 4); the ratio of $Fe^{3+}/(Fe^{2+}+Fe^{3+})$ becomes nearly zero when the $Mg^{2+}/(Fe_{total}+Mg^{2+})$ ratio exceeds 0.7, while, as has been established by Darken and Gurry,[1] wüstite is unstable when the $Fe^{3+}/(Fe^{2+}+Fe^{3+})$ ratio becomes smaller than 0.10 (0.106 in the present study) at 1160°C.

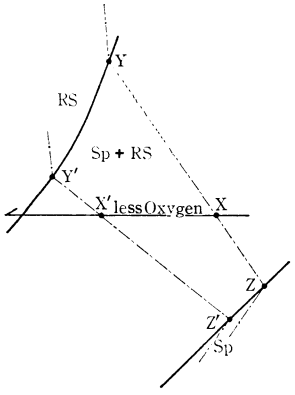



Fig. 5. A distorted diagram illustrating the equilibrated compositions within the field of spinel + magnesiowüstite.
Heavy lines are the boundary curves.
Light dash-hot lines are isobaric lines.

The area between the field of the magnesiowüstite solid solution and that of the magnetite-magnesioferrite solid solution is for the two phases. A mixed oxide witha composition within this area, say X, consists of an extremely reduced spinel, lettered Z and an extremely oxidized magnesiowüstite, letteredY as in Fig. 5.

The left side of the area of magnesiowüstite is for the two phases comprising metallic iron and magnesiowüstite. The metallic iron in equilibrium with magnesiowüstite within the range of oxygen pressures used in the present investigation is assumed to be pure because of the great stability of MgO. Therefore, consider the reaction:

$$Fe_{metal}+1/2\,O_2=(FeO)_{ss}$$

where $(FeO)_{ss}$ means the molality in the solid solution considered. The equilibrium constant $K$ is, therefore, expressed by:

$$K=a_{FeO}/a_{Fe}\cdot(P_{O_2})^{1/2}=a_{FeO}/(P_{O_2})^{1/2}$$

where $a$ means activity. When we assume that Raoult's law is applicable in the vicinity of $N_{FeO}\cong 1$, we have

$$K=N_{FeO}/P_{O_2}{}^{1/2}$$

where $N$ indicates the mole fraction.

According to the present study the maximum value of $N_{FeO}$ in pure wüstite was 0.894 at 1160°C (see Fig. 2) and log $P_{O_2}$ was $-12.40$, while the interpolated values based on the results of Darken and Gurry[1] were 0.903 and $-12.48$ respectively. From the present values, we get:

$$\log K=6.15$$

and

$$\log N_{FeO}=1/2\log P_{O_2}+6.15$$

The calculated values of $N_{FeO}$ in magnesiowüstite in equilibrium with matallic iron are plotted against $-\log P_{O_2}$ in Fig. 6 on the basis of the present study. The dotted line shows the experimental values in order to facilitate comparison with the calculated values. It is clear from Fig. 6 that a solid solution with more than 30 mole per cent of magnesium oxide deviates significantly from ideality. On the other hand, the calculated values agree rather well with the experimental values in the oxide solid solution with less than 30 mole per cent of magnesium oxide. This means that the assumption of Raoult's law may be correct near the composition $N_{FeO}\cong 1$. On the basis of this assumption, we can calculate the standard free energy of the formation of the stoichiometric ferrous iron oxide, $FeO_{1.000}$, which has never been synthesized in the standard state:

$$\Delta F^\circ{}_{1160^\circ C}=-RT\ln K=-40.3\ \text{kcal./mol.}$$

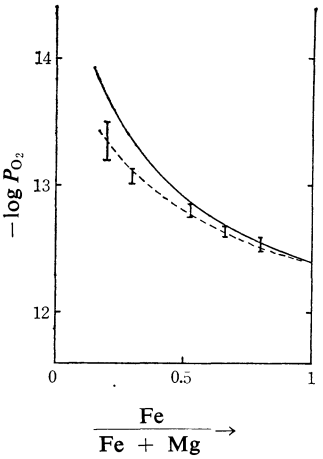



Fig. 6. The deviation from the Raoult's law in magnesiowüstite solid solution in equilibrium with metallic iron. Solid line is for calculated values, and dashed line is for observed with the width of experimental error.

When we compare this with the standard free energy of the formation of the most reduced and the actual wüstite, $FeO_{1.053}$ ($N_{FeO}=0.894$), we recognize that the stoichiometric compound, $FeO_{1.000}$, is unstable by $+0.4$ kcal. based on the following calculations: we calculate the free energy change on the reaction,

$$1.053\,FeO_{1.000}=0.053Fe+FeO_{1.053}$$

to be

$$\Delta F^\circ=1.053\times(-40.7)-1.053\times(-40.3),\ \text{(cal.)}$$

Here, the standard free energy of the formation of $FeO_{1.053}$ is equal to $1.053\,RT\ln P_{O_2}$ where $P_{O_2}$ is $10^{-12.40}$ atm.

Hahn and Muan[16] studied the activity of wüstite "FeO" in "FeO"-MgO solid solution in the temperature interval from 1100 to 1300°C by equilibrating oxide samples with pure metallic iron in atmospheres of known oxygen partial pressures. In their study, the component iron(III) oxide in the solid solution was neglected; they pointed out that the system shows a considerable positive deviation from Raoult's low. However, when we discuss the deviation from ideality, we must not neglect the actual component iron(III)oxide in magnesiowüstite; that is to say, we have to plot the values of $a_{FeO}$ against the actual values of $N_{FeO}$ instead of $(1-N_{MgO})$, which is equal to the marked "FeO." The results derived from the Gibbs-Duhem equation will, therefore, inform us only about the approximate thermodynamic properties of systems involving an iron(II) oxide component.

16) W. C. Hahn, Jr., and A. Muan, *Trans. AIME*, **224**, 416 (1962).

The authors wish to express their thanks to Dr. Elburt F. Osborn and Dr. Arnulf Muan, of Pennsylvania State University. They are also indebted to Dr. Syun-iti Akimoto, the Institute for Solid State Physics, The University of Tokyo. Dr. Iwaji Iwasaki, Professor of the Tokyo Institute of Technology, also encouraged us throughout the present study.

*Department of Chemistry*
*Tokyo Institute of Technology*
*Ookayama, Tokyo*

# Kinetic Studies of Ammonia Oxidation in Shock Waves. I. The Reaction Mechanism for the Induction Period

By Tetsu TAKEYAMA and Hajime MIYAMA

(Received February 16, 1965)

The catalytic oxidation of ammonia has been studied extensively. On the contrary, however, because of the relatively lower reactivity of ammonia, only a few works can be found on non-catalytic oxidation. Stephens and Pease obtained only qualitative results from their flow[1] and static[2] experiments. Volders and Van Tiggelen[3] proposed a mechanism involving $NH_2$, OH and NOH for the slow thermal reaction. Recently, Husain and Norrish[4] investigated the photolytic oxidation of ammonia by the flash photolysis method and by kinetic spectroscopy. They postulated a mechanism in which a relatively stable intermediate, HNO, plays the role as a degenerate branching reagent, although they themselves could not actually detect it.

However, no information can be found with respect to the mechanism responsible for the high-temperature oxidation of ammonia. In order to clarify this, we have made experiments at temperatures between 1550 and 2300°K by using the shock-tube technique combined with the spectroscopic method. In this paper, we will report on the results obtained from the measurements of the induction periods for the appearance of OH and of the time relations among the concentration changes of NH, $NH_2$, NO and OH.

## Experimental

The experimental arrangements were much the same as have been reported previously:[5] by means of a Shimadzu QR-50 monochromator and an R106 photomultiplier, the ultraviolet absorptions of OH and NH and the intensity distributions of light emitted at various wavelengths were measured.

The reaction mixtures were prepared in an all-glass apparatus with a 10 l. reservoir and were stirred magnetically for an hour before being used. Commercial ammonia (99.98%), oxygen (99.5%) and argon (99.999%) were used without further purification.

## Results

**Induction Period.**—The induction period for the appearance of OH absorption was measured in reflected shock waves for two mixtures at initial pressures from 50 to 110 mmHg. The experimental conditions covered are presented in Table I.

The induction period was found to be dependent neither on the ammonia concentration nor on the product of the ammonia and oxygen concentration, but on the oxygen concentration alone over the 1.5—0.67 range of the ammonia to oxygen ratio, as is shown in Fig.

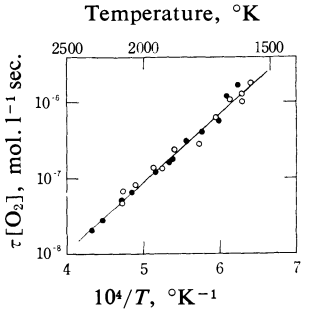



Fig. 1. Induction period for appearance of OH-absorption vs. reciprocal temperature. Open and solid circles are obtained from mixtures I and II (see Table I), respectively.

1) E. R. Stephens and R. N. Pease, *J. Am. Chem. Soc.*, **72**, 1188 (1950).
2) E. R. Stephens and R. N. Pease, ibid., **74**, 3480 (1952).
3) A. Volders and A. Van Tiggelen, *Bull. soc. chim. Belg.*, **63**, 542 (1954).
4) D. Husain and R. G. W. Norrish, *Proc. Roy. Soc.*, **A 273**, 245 (1963).
5) T. Takeyama and H. Miyama, This Bulletin, **38**, 936, (1965).

Table I. Experimental conditions

| Mixture | $\%O_2$ | $\%NH_3$ | %Ar | Temp. range °K | Press. range atm. | $[O_2]$ range $10^{-3}$ mol./l. |
|---|---|---|---|---|---|---|
| I | 6 | 4 | 90 | 1550—2110 | 3.5—5.5 | 1.23—2.47 |
| II | 4 | 6 | 90 | 1600—2300 | 3.5—4.5 | 0.741—1.37 |

1. The least-squares line in the figure is expressed by:

$$\log \tau [O_2]\,(\text{mol.}\,l^{-1}\text{sec.}) = -11.71 + (9300 \pm 270)/T$$

where the temperature dependence corresponds to an activation energy of 42.5±1.2 kcal./mol.

The pressure of the reaction system was measured simultaneously at the same location in the tube by a quartz transducer. However, the pressure increase due to the reaction was far less than that found by us in the oxidation of hydrogen,[6] acetylene[5] and methane[7]; it was not appreciable in most runs.

**The Spectroscopic Identification of Reaction Intermediates.**—The reaction intermediates, the NH radical, nitric oxide and the $NH_2$ radical, were identified by measuring the intensity distribution of light emitted in the ultraviolet and visible region:

*The NH Radical.*—Since NH has a strong band emission at 3360 Å due to its $^3\Pi \rightarrow {}^3\Sigma$ transition,[8] the intensities of light emitted at 1960±10°K were measured over the 3270—3430 Å wavelength range. The width of the exit slit of the monochromator was set at 0.20 mm., allowing a band pass of about 12Å. The results are shown in Fig. 2, where the intensities given in the ordinate are corrected with the spectral response of the R106 photomultiplier and divided by the intensities, which were measured simultaneously by means of an interference filter (Baird-Atomic, Inc., $\lambda_{max}$: 3070Å, transmission at $\lambda_{max}$: 13%, half width: 120Å) and an RCA 1P28 photomultiplier. There is a sharp peak at 3360 Å; hence, the existence of the NH radical is definite.

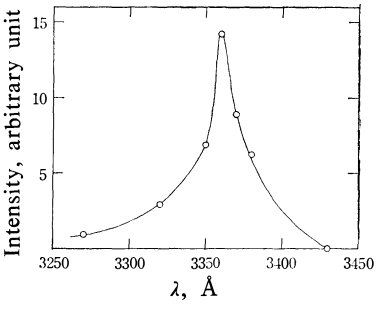



Fig. 2. Intensity distribution of light emitted between 3250 and 3450Å.
Mixture II, initial pressure 55.0 mmHg, shock temperature 1960±10°K

*Nitric Oxide.*—The β-band of nitric oxide has weak emissions at 4303 and 4310Å because of its $B^2\Pi \rightarrow X^2\Pi$ transition.[9] Therefore, the intensity distribution was measured over the 4215—4360Å wavelength range, with the slit width of the monochromator being set at 0.25 mm. and the band pass at 30Å. The results obtained at 2120±30°K are shown in Fig. 3, where the intensities are treated as has been described above. Although the peak near 4300Å is less definite than that found at 3360 Å, it may be attributed to nitric oxide, for there is no other possible emitter at this wavelength.

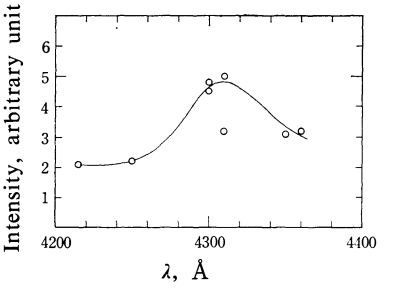



Fig. 3. Intensity distribution of light emitted between 4200 and 4400Å.
Mixture I, initial pressure 50.0 mmHg, shock temperature 2120±30°K

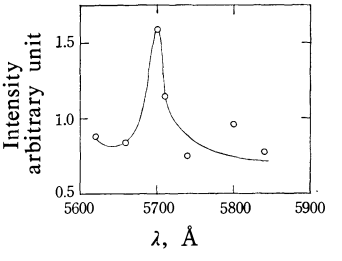



Fig. 4. Intensity distribution of light emitted between 5600 and 5900Å.
Mixture II, initial pressure 55.0 mmHg, shock temperature 1970±20°K

*The $NH_2$ Radical.*—The visible emission of $NH_2$, which is found in oxy-ammonia flames

6) H. Miyama and T. Takeyama, *J. Chem. Phys.*, **41**, 2287 (1964).
7) H. Miyama and T. Takeyama, ibid., **40**, 2049 (1964); This Bulletin, **38**, 37 (1965).
8) A. G. Gaydon, "The Spectroscopy of Flames," Chapman & Hall Ltd., London (1957), p. 242.
9) R. W. B. Pearse and A. G. Gaydon, "The Identification of Molecular Spectra," Chapman & Hall Ltd., London (1950), p. 180.

and is called the ammonia $\alpha$-band, is composed of a very large number of fine lines as a result of its rotational structure.[10] We have tried to find the bright band at about 5705 Å,[10] measuring the intensities of light emitted at 1970±20°K over the 5620—5840Å wavelength range; the slit width of the monochromator was set at 0.1 mm., which allows a band pass of 30Å. As is shown in Fig. 4, a peak is observed at 5700Å, thus confirming the existence of $NH_2$ radicals.

**Concentration Changes of Intermediate Species with Time.**—In order to observe the concentration changes of the above-described intermediates in the course of the reaction, the changes in the absorption and/or the emission of these species were followed by means of a monochromator with a photomultiplier. Since, however, the experimental arrangement does not allow the simultaneous measurements of absorptions or emissions of all these species, the ultraviolet emission, which was measured simultaneously at the auxiliary observation station by a Baird-Atomic interference filter and an RCA 1P28 photomultiplier, has been used as a reference standard for the time scale. A typical example of the changes observed in this way can be seen in Fig. 5, which was obtained by shock-heating the reaction mixture II at an initial pressure of 65.0 mmHg to 1840 ±10°K.

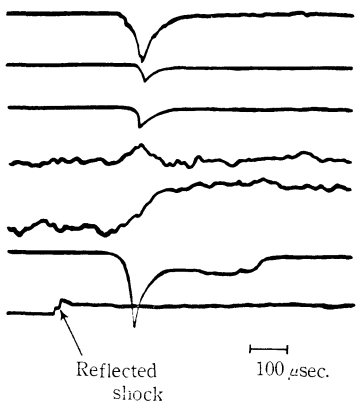



Fig. 5. Changes in absorption and/or emission of various intermediates with time.
Traces represent, from top to bottom, $NH_2$-, NO- and NH-emission, NH- and OH-absorption, the ultraviolet emission measured by an interference filter, and pressure.
Mixture II, initial pressure 65.0 mmHg, shock temperature 1840±10°K

The general features observed under various conditions are as follows: (a) the absorptions of OH and NH appear at the same time, after the arrival of the reflected shock; (b) the emissions of NH and nitric oxide appear and reach their maxima at almost the same time, while the emission of $NH_2$ seems to reach its maximum a little earlier than do those of NH and nitric oxide; and (c) the absorption of NH reaches its maximum earlier than that of OH and decays within a few tens of micro seconds.

## Discussion

The experimental observations a and b, concerning the time relations of various intermediates, lead us to postulate the following reaction scheme as the main steps governing the induction period of the high-temperature, homogeneous oxidation of ammonia:

$$NH_2+O_2 \rightarrow NH+HO_2 \quad (I)$$

$$NH+O_2 \rightarrow NO+OH \quad (II)$$

$$OH+NH_3 \rightarrow NH_2+H_2O \quad (III)$$

The $HO_2$ radical produced in Reaction I is unstable at these high temperatures[6] and so may soon decompose into OH and O by Reaction IV rather than reacting with ammonia.

$$HO_2 \rightarrow OH+O \quad (IV)$$

The oxygen atom will then abstract hydrogen from ammonia by Reaction V; the reactions between such intermediates as $NH_2$, NH, OH and O should be excluded from the reaction scheme for the induction period.[6,7]

$$O+NH_3 \rightarrow OH+NH_2^{\cdot} \quad (V)$$

An application of the treatment given by Schott and Kinsey for the hydrogen-oxygen reaction[11] to Reactions I—V will explain the dependence of the induction period on the oxygen concentration and the activation energy obtained from the temperature coefficient. By assuming that the principal chain carrier is the $NH_2$ radical, and that the OH, O, NH and $HO_2$ radicals are steady-state intermediates, [OH] and the rate of formation of the $NH_2$ radical are expressed by Eqs. 1 and 2 respectively:

$$[OH]=3k_1[O_2][NH_2]/k_3[NH_3] \quad (1)$$

$$d[NH_2]/dt=3k_1[O_2][NH_2] \quad (2)$$

Here, $k_1$ and $k_3$ are the rate constants of Reactions I and III respectively.

The integrated form of Eq. 2, assuming that the concentrations of ammonia and oxygen are not decreased during the induction period, is:

$$[NH_2]=[NH_2]_0 \exp\{3k_1[O_2](t-t_0)\} \quad (3)$$

10) Ref. 9, p. 178.

11) G. L. Schott and J. L. Kinsey, *J. Chem. Phys.*, **29**, 1177 (1958).

where $t_0$ is any reference time following which Eqs. 2 and 3 are valid, and the concentration with the subscript zero represents the concentration at $t=t_0$. It is assumed that at $t_0=0$ the rate of the chain branching becomes equal to the rate of initiation, although the initiation step can not be identified in the present study. [OH] can then be expressed by Eq. 4 and builds up exponentially, as has been found experimentally:

$$[OH] = [OH]_0 \exp(3k_1 [O_2] t) \quad (4)$$

$[OH]_0$ is given by Eq. 1.

Therefore,

$$\log\{[OH]_\tau / [OH]_0\} = 1.303\, k_1 [O_2] \tau \quad (5)$$

$[OH]_\tau$ being the concentration at the end of the induction period.

If it can be assumed, as in the hydrogen-oxygen reaction,[11] that the $[OH]_\tau / [OH]_0$ ratio remains approximately constant over the temperature range studied, the following relation is obtained from Eq. 5:

$$\tau [O_2] \propto 1/k_1 \quad (6)$$

Therefore, a plot of $\log(\tau [O_2])$ against $1/T$ would give a straight line, the slope of which corresponds to the activation energy of Reaction I. This has been found to be true, as has been described in the preceding section; the straight line shown in Fig. 1 gives an experimental activaion energy of 42.5±1.2 kcal./mol. for Reaction I, which is endothermic by 41 kcal./mol., if the bond energies of NH–H and H–$O_2$ are taken to be, respectively, 88[12,16] and 47[16] kcal./mol. The relatively small difference between the activation energy and the endothermicity may be due to the low activation barrier which is usually found in free radical reactions.[17] The results from the induction period measurements, therefore, suggest strongly that Reaction I is rate-controlling.

In the photolytic oxidation of ammonia, Husain and Norrish[4] have found NH, OH and nitric oxide to be absent in the initial stages of the reaction and have, therefore, postulated the following scheme:

$$NH_2 + O_2 \rightarrow HNO + OH \quad (VI)$$

$$OH + NH_3 \rightarrow NH_2 + H_2O \quad (VII)$$

$$HNO \rightarrow H + NO \quad (VIII)$$

$$2HNO \rightarrow H_2O + N_2O \quad (IX)$$

where they regarded the HNO intermediate as a degenerate branching reagent, although they could not detect it. At high temperatures such as those studied by us, the HNO molecule cannot be stable enough to play such a role. Furthermore, it is impossible for their scheme VI—IX to account for the experimental activation energy of 42.5 kcal./mol. and for Findings a and b.

Volders and Van Tiggelen[3] studied, by the static method, the slow oxidation of ammonia around 800°K and proposed the following mechanism:

$$NH_3 \overset{\text{wall}}{\rightarrow} NH \quad (X)$$

$$NH + O_2 \rightarrow NO + OH \quad (XI)$$

$$OH + NH_3 \rightarrow NH_2 + H_2O \quad (XII)$$

$$NH_2 + O_2 \rightarrow NOH + OH \quad (XIII)$$

$$OH + NO \rightarrow HNO_2 \quad (XIV)$$

Since NOH was not detected, Reaction XIII is rather speculative and open to question. In addition, the heterogeneous Reaction X yielding NH should be ruled out for the reaction in shock waves.

Therefore, our mechanism accounts most reasonably for the experimental findings concerning the induction period, i.e., for those except Finding c. In order to explain this, it is necessary to obtain the reaction profile after the induction period by using the values of rate constants, the concentrations of intermediates, and their thermochemical properties. Unfortunately, the available data at present are inadequate for carrying out such a numerical calculation.

## Summary

The oxidation of ammonia has been studied at temperatures between 1550 and 2300°K by using the shock-tube technique combined with ultraviolet absorption spectroscopy.

The measurements of the induction periods for the appearance of OH have shown that they are strongly dependent on the concentration of oxygen and that the activation energy required is 42.5±1.2 kcal./mol.

The intermediates of the reaction, NH, NO and $NH_2$, have been detected spectroscopically, and the time relations between their appearance and their accumulation have been determined.

As a result, the following mechanism has been postulated as the main steps governing the induction period of the high-temperature oxidation of ammonia:

12) E. D. Coon, *Proc. N. Dakota Acad. Sci.*, 7, 46 (1953); This value is also calculated from the values of the bond energies of $NH_2$–H and N–H and of the average N–H bond energy in ammonia, if they are taken to be 106,[13] 85[14] and 93[15] kcal./mol., respectively.

13) S. N. Foner and R. L. Hudson, *J. Chem. Phys.*, 29, 442 (1958).

14) A. G. Gaydon "Dissociation Energies and Spectra of Diatomic Molecules," Chapman and Hall Ltd., London (1953), p. 228.

15) Ref. 14, p. 170.

16) A. P. Altshuler, *J. Chem. Phys.*, 22, 1947 (1954).

17) N. N. Semenov, "Some Problems in Chemical Kinetics and Reactivity," Vol. I, Princeton University Press (1958), p. 4.

$$NH_2+O_2 \rightarrow NH+HO_2 \quad (I)$$

$$NH+O_2 \rightarrow NO+OH \quad (II)$$

$$OH+NH_3 \rightarrow NH_2+H_2O \quad (III)$$

$$HO_2 \rightarrow OH+O \quad (IV)$$

$$O+NH_3 \rightarrow OH+NH_2 \quad (V)$$

where Reaction I is considered to be rate-controlling.

We are grateful to Mr. Kazutoshi Sugiyama for his help in performing the experiments.

*Basic Research Laboratories*
*Toyo Rayon Company, Ltd.*
*Tebiro, Kamakura*

# A Study of the Charge-Transfer Complexes. I. The Interaction of Pyromellitic Dianhydride with Polymethylbenzenes*

By Yusuke NAKAYAMA, Yukihiko ICHIKAWA and Taku MATSUO

(Received February 20, 1965)

The formation of molecular complexes between pyromellitic dianhydride and aromatic compounds, such as anisole, tetralin etc., was first reported by Seka and Sedlatschek as early as 1926.[1] In spite of the remarkable advances made thereafter in the investigation of charge-transfer complexes, however, no further paper had been published on the phenomena until Heaton and others recognized pyromellitic dianhydride as a strong electron acceptor.[2] Heaton and his co-workers studied the complexes by the spectroscopic method and concluded that pyromellitic dianhydride was one of the strongest electron acceptors which had yet been found. Recently, Briegleb reported on the electron affinity of pyromellitic dianhydride, among other compounds, as estimated from the charge-transfer band.[3] Nothing else is known about the charge-transfer complexes of pyromellitic dianhydride, which is in contrast with the abundance of information about the behavior of such other acceptors as halogens, quinones, and nitro compounds. A little further investigation is reported, in this paper, into the complex formation of pyromellitic dianhydride (abbreviated as PMDA hereafter) with polymethylbenzenes, both in a solution and in the solid phase. Polymethylbenzenes were chosen as the donor to be studied for the following reasons.

1) The basicity or the ionization potential of each molecule is well known.[4]

2) The frame work of the $\pi$-electron system can be taken as a simple hexagon throughout the system.

3) The introduction of the methyl group into the benzene nucleus results in only a small perturbation in the $\pi$-electron system to be treated theoretically.

4) The charge-transfer complexes between polymethylbenzenes and iodine or chloranil have been studied fairly well in the past.[4b),5,6)]

Consequently, the discussion of the experimental results becomes much easier than in the case of other aromatic donors, which have many complicated unknown factors. This experiment was designed with some emphasis on the investigation of the nature of the solid molecular complexes.

## Experimental

*o*- and *p*-Xylenes were purified by repeated distillations and recrystallizations from commercial products until the purity in the gas chromatograph exceeded 98%. Tetralin was purchased from the Wako Pure Chemical Company, Ltd.; it was purified and proved to be free from naphthalene. Indan was synthesized by the reduction of indanone which had been prepared from cinnamic acid through 3-phenylpropionic acid.[7] Mesitylene was synthesized from acetone[8] and was determined to be pure by

* Contribution No. 80 from the Department of Organic Synthesis, Faculty of Engineering, Kyushu University, Fukuoka.

1) R. Seka and H. Sedlatschek, *Monatsh. Chem.*, **47**, 516 (1962).

2) L. L. Ferstandig, W. G. Toland and C. D. Heaton, *J. Am. Chem. Soc.*, **83**, 1151 (1961).

3) G. Briegleb, *Angew. Chem.*, **76**, 326 (1964).

4) a) Cf. R. L. Flurry, Jr., and P. G. Lykos, *J. Am. Chem. Soc.*, **85**, 1033 (1963), and the references therein for the basicity; b) Cf. R. E. Merrifield and W. D. Phillips, ibid., **80**, 2778 (1958) for the ionization potential.

5) L. J. Andrews and R. M. Keefer, ibid., **74**, 4500 (1952).

6) N. Smith, Ph. D. Thesis, University of Chicago, Illinois, cf. J. N. Murrell, *J. Am. Chem. Soc.*, **81**, 5037 (1959).

7) S. Gabriel and J. Zimmerman, *Ber.*, **13**, 1680 (1880).

8) R. Adams and R. W. Hufferd, "Organic Syntheses," Coll. Vol. I, 341 (1958).

CH analysis, infrared spectra and gas chromatography. Durene, penta- and hexamethylbenzenes were prepared by succesive Friedel-Crafts reactions and were purified by several fractional distillations and recrystallizations from either methanol or a methanol-benzene mixture. Infrared spectra and CH analysis were used to identify the prepared methylbenzenes, whose melting points are as follows: durene (80.8—81.0°C), pentamethylbenzene (52.7—53.2°C), and hexamethylbenzene (168.0—168.3°C).

Pyromellitic dianhydride was prepared by the dehydration of pyromellitic acid, a reagent-grade product of Tokyo Kasei Kogyo Co., Ltd., through refluxing in acetic anhydride for several hours. The product was then recrystallized from purified ethylacetate and proved to be free from any trace of the original acid. (Found: C, 55.05: H, 0.93%: m. p. 299.8—300.0°C). The melting points are the values as observed on a Kofler micro hot-stage and are uncorrected.

Solid molecular complexes were prepared by adding pyromellitic dianhydride either to a donor or to an ethyl acetate solution of the donor at an elevated temperature and then cooling the solution to room temperature. The formation of charge-transfer molecular complex could easily be noticed by the precipitation of crystals with a characteristic shape and color. Extra care was taken here to avoid the coprecipitation of the uncomplexed pyromellitic dianhydride. The degree of heating and the relative ratio of the donor to the pyromellitic dianhydride in the best conditions varied from case to case.

The ultraviolet and visible spectra were measured by a conventional method using an EPS-2U model Hitachi recording spectrophotometer.

The solid complexes were ground on an agate mortar and were dispersed evenly in approximately ten times as much talcum powder (as determined by weight). The sample was packed in a cylindrical cell and was mounted on the wall of the integrating sphere of the reflectance attachment of an EPU-2A model Hitachi photoelectric spectrophotometer. The reflectance of the sample was determined against a standard sample of talcum powder under the same geometrical conditions.

The X-ray diffraction data of the powdered solid samples were obtained by the use of a Norelco X-ray spectrophotometer.

## Results and Discussion

**Complexes in Solution.**—After many attempts, ethyl acetate was found to be the best solvent for the complexes of PMDA with a wide variety of aromatic compounds. The newly-appeared absorption bands due to the complex formation of mesitylene, durene, penta- and hexamethylbenzenes with PMDA in ethylacetate are shown in Fig. 1. There is no appreciable absorption due to the donor in the longer-wavelength region beyond 330 mμ (Fig. 2). The absorption of PMDA is practically negligible in the visible range under

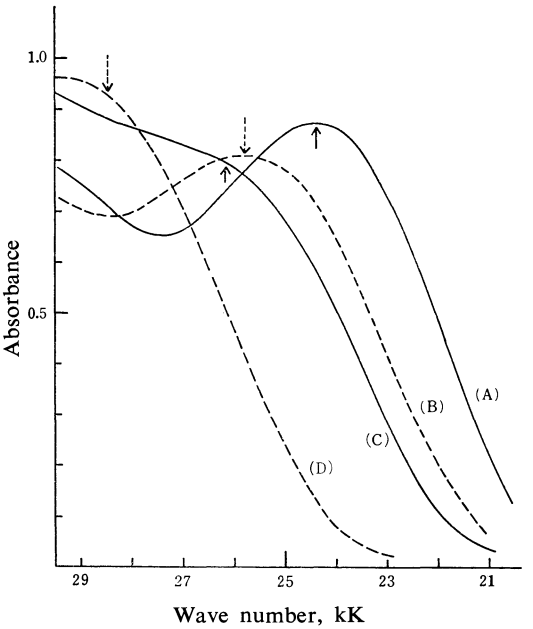



Fig. 1. The charge-transfer absorption bands of PMDA-polymethylbenzene complexes in ethyl acetate (18±1°C).
(A) Hexamethylbenzene ($4.0\times10^{-2}$ mol./l.)-PMDA
(B) Pentamethylbezene ($7.3\times10^{-2}$ mol./l.)-PMDA
(C) Durene ($1.5\times10^{-1}$ mol./l.)-PMDA
(D) Mesitylene ($2.4\times10^{-1}$ mol./l.)-PMDA
The concentration of PMDA is $1.0\times10^{-2}$ mol./l.

these experimental conditions (Fig. 2). An unmistakable charge-transfer absorption band is observed for each complex of hexa- and pentamethylbenzenes with PMDA. The peak still appears as a shoulder in the case of durene, but it is not at all obvious in the case of the mesitylene complex.

Since the charge-transfer absorptions in general are expected to be sensitive to the solvent polarity, the charge transfer bands of the well-known chloranil complexes with polxmethylbenzenes or pyrene were studied in several solvents; the results are summarized in Table I. It may be seen from this table that the charge-transfer band shows a hypsochromic shift as the solvent polarity increases. In addition, the apparent peak height decreases considerably if the donor-acceptor pair is present in a polar medium. The frequency of the charge-transfer band $\nu$ is correlated with the electron affinity ($E_A$) of the acceptor and the ionization potential ($I_D$) of the donor by Eq. 1:

$$h\nu = I_D - E_A + \Delta \quad (1)$$

where $\Delta$ is a correction term mainly due to

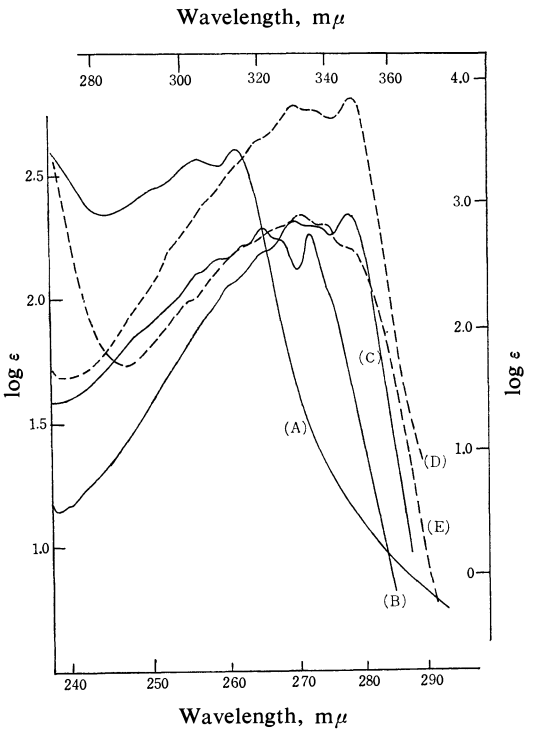



Fig. 2. Absorption spectra of PMDA and polymethylbenzenes used in the experiments. The upper and the right scales are to be used for PMDA only.
(A) PMDA (B) Mesitylene (C) Durene (D) Pentamethylbenzene (E) Hexamethylbenzene

TABLE I. THE CHARGE-TRANSFER ABSORPTION BANDS OF CHLORANIL COMPLEXES IN VARIOUS SOLVENTS*1

| Donor | Solvent | | |
|---|---|---|---|
| | $CCl_4$ | Butyl ether*2 | Ethyl acetate |
| Mesitylene | 23.5±0.1 | 24.4 | 24.2±0.1 |
| Durene | 20.5±0.1 | 21.3 | 21.9±0.1 |
| Pentamethylbenzene | 20.3±0.1 | 20.8 | 21.4±0.1 |
| Hexamethylbenzene | 19.2±0.1 | 19.8 | 20.1±0.1 |
| Pyrene | 16.5±0.1 | — | 17.5±0.1 |

*1 The values are expressed in kilo-kaysers (kK).
*2 Quoted from the Ref. 6.

the Coulombic interaction of $D^+$ and $A^-$.[9] Thus, the hypsochromic shifts observed above may be interpreted mainly as due to the decrease in the electron affinity of the acceptor level as a consequence of the solvation by the polar molecules. If the last term in Eq. 1 is approximately constant among the complexes with donors of a similar type, the band separation among the polymethylbenzene-chloranil complexes in ethyl acetate can be used to estimate the difference in the ionization potentials of the donors in the same solvent. Using these values and taking hexamethylbenzene as the standard, the location of the charge-transfer band of each polymethylbenzene-PMDA complex is calculated. The values are indicated by the arrows in Fig. 1. Then the newly-appeared absorptions of the polymethylbenzene-PMDA complex are resolved into two bands of a different nature. The first band is found at the frequency indicated by the arrow in Fig. 1; it is, of cause, believed to originate from the transfer of an electron from the highest-occupied donor orbital to the lowest unoccupied acceptor orbital. The band moves to the longer-wavelength region as the number of methyl groups increases. The second band, with a rather diffuse shape, is noticed clearly on the higher frequency side in the case of the hexamethylbenzene complex in Fig. 1. The first band becomes less distinct in comparison with the second band as the number of methyl groups decreases. In the case of the mesitylene complex, finally, the first band appears to be merged in the second band. The origin of this second band is not certain. Obviously, however, it is not the so-called "second charge-transfer band," which is defined as due to the electron transfer from the second highest occupied orbital of the donor to the lowest unoccupied orbital of the acceptor. It is more likely that the second band comes from the combination of many complexes with different geometries and electronic states, including the contact charge transfer.[10]

No matter where they come from, these newly-appeared absorption bands can be used to estimate the equilibrium constants of the charge-transfer complexes in the solution. It must be remembered, however, that the equilibrium constants thus obtained are contributed by charge-transfer complexes of various types.[11] The original Benesi-Hildebrand equation[12] for a one-to-one complex was modified into the follwing form:

$$\frac{1}{(\mathrm{ArH})} = \frac{[\mathrm{PMDA}] \times l}{\mathrm{ABS}} \times K\varepsilon - K \qquad (2)$$

where (ArH) is the concentration of methylbenzenes in mole fractions; [PMDA] is the concentration of PMDA in mol./l.; $l$ stands

9) J. N. Murrell, *Quart. Revs.*, **16**, 191 (1962).

10) R. S. Mulliken, *Rec. trav. chim. Pays-Bas*, **75**, 845 (1956).
11) L. E. Orgel and R. S. Mulliken, *J. Am. Chem. Soc.*, **79**, 4839 (1957).
12) H. A. Benesi and J. H. Hildebrand, ibid., **71**, 2703 (1949).

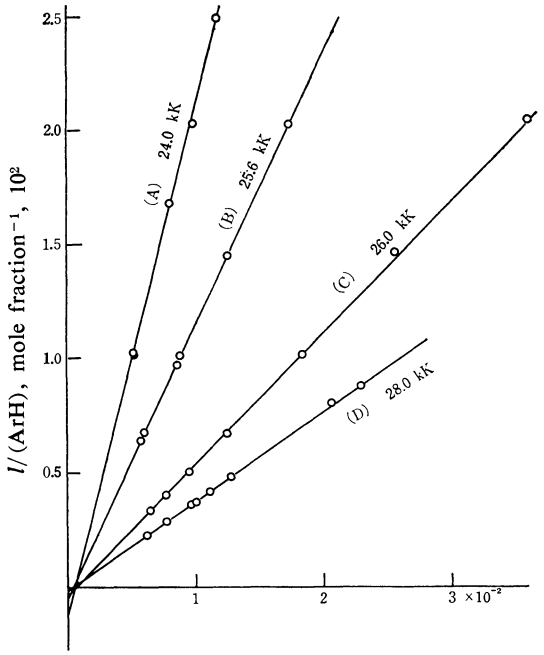



Fig. 3. Determintion of $K$ and $K\varepsilon$. The concentration of each component is as follows.
(A) Hexamethylbenzene: $0.4\times10^{-1}$—$1.0\times10^{-1}$ mol./l.
(B) Pentamethylbenzene: $0.4\times10^{-1}$—$1.6\times10^{-1}$ mol./l.
(C) Durene: $0.5\times10^{-1}$—$3.0\times10^{-1}$ mol./l.
(D) Mesitylene: $1.2\times10^{-1}$—$4.6\times10^{-1}$ mol./l.
and PMDA: $0.1\times10^{-1}$ mol./l. or less
The plots are made after converting the donor concentrations into mole fractions.

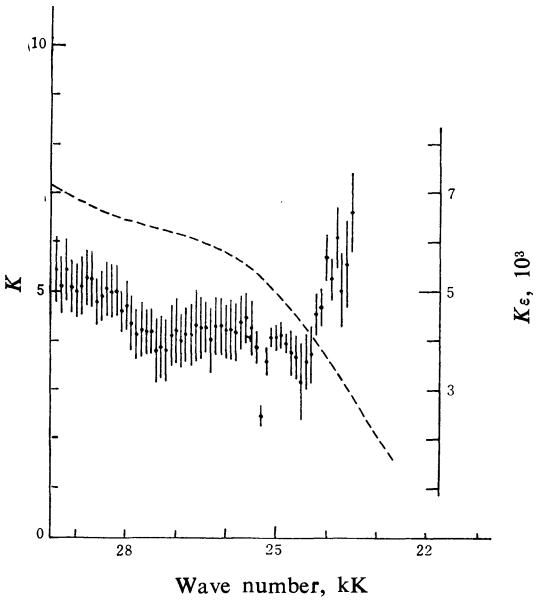



Fig. 4. The stability constant $K$ as calculated by the modified Benesi-Hildebrand equation at various positions of the charge-transfer band of durene-PMDA complex in ethylacetate (18°C).
Molar fractions were used in the calculation as the units of donor concentration. The dotted line represents $K\varepsilon$ which is obtained from the slope of the modified Benesi-Hildebrand equation.

for the length of the absorption cell in cm.; $K$ is the equilibrium constant (dimensionless quantity), and ABS and $\varepsilon$ are the absorbance and the extinction coefficient (l./mol.) for the complex at a particular wavelength respectively.

Plotting 1/(ArH) vs. [PMDA]$\times l$/ABS at a fixed wavelength yields the equilibrium constant and $K\varepsilon$ as the intercept and the slope of the straight line respectively. Examples are shown in Fig. 3, where the plots are made by using the data of four polymethylbenzene complexes at their absorption maxima. Rather low donor concentrations were used in these experiments because of the limited solubilities. The equilibrium constants of the complexes, however, hardly ever exceed ten, as may be found below. Therefore, a simple calculation shows that the concentrations of the complexed species are negligibly small in comparison with that of the added donor in the experiments. Thus the basic condition for the applicability of the Benesi-Hildebrand equation is fulfilled. The plotting of the experimental data as in Fig. 3 gives a straight line and verifies the correctness of the treatment. The equilibrium constants and $K\varepsilon$'s were evaluated by applying the method of least squares to the data at various frequencies of the absorption bands; an example is shown in Fig. 4. The arithmetic means of the values obtained over the absorption band of each complex are summarized in Table II. The equilibrium constants of the methylbenzene-chloranil complexes are also quoted from Smith's data[6] in the third column of Table II. The trends in both

Table II. The equilibrium constants of polymethylbenzene complexes with PMDA and chloranil*1

| Donor | PMDA*2 | Chloranil*3 |
|---|---|---|
| Mesitylene | 1.3±0.3 | 1.17 |
| Durene | 4.2±0.3 | 3.02 |
| Pentamethylbenzene | 5.7±0.3 | 5.32 |
| Hexamethylbenzene | 11.4±0.6 | 9.08 |

*1 The values are dimensionless since the donor concentrations were expressed in mole fractions (see the text).
*2 In ethylacetate solution, 18±1°C.
*3 In butylether.[6]

series are in good agreement and indicate that the methyl groups have similar stabilizing effects on the charge-transfer complexes of both types, as was expected. No direct comparison was made of the present results with those reported by Heaton et al.,[2] since the donors and the solvents used in the two experiments are quite different. It appears, however, that the equilibrium constants obtained in ethyl acetate are less than those measured in carbon tetrachloride. An attempt is now being made to investigate the solvent effect by employing donors whose equilibrium constants in complex formation can be determined in either solvent with a satisfactory accuracy.

**Solid Complexes.**—The relative diffuse reflectance, $R$, of a solid material is correlated with the absorption coefficient, $k$, by the following Kubelka-Munk remission function, $f(R)$ :

$$f(R)=\frac{k}{S}=(R-1)^2/2R \qquad (3)$$

where $S$ denotes a scattering coefficient.[13]

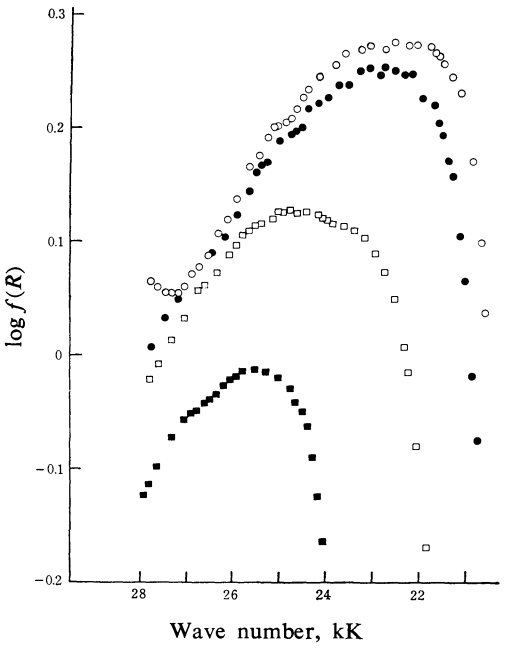



Fig. 5. The diffuse reflectance spectra of PMDA-polymethylbenzene complexes.
Filled square: Mesitylene complex (120 mg./400 mg. talc)
Filled circle: Durene complex (38 mg./400 mg. talc)
Open square: Pentamethylbenzene complex (33 mg./415 mg. talc)
Open circle: Hexamethylbenzene complex (44 mg./405 mg. talc)

Kortum and Braun successfully applied Eq. 3 in their studies of the pyrene- and anthracene-trinitrobenzene complexes.[14]

The diffuse reflectances of PMDA-polymethylbenzene complexes obtained above were then used to calculate the $f(R)$ function; the results are shown in Fig. 5. When Fig. 5 is compared with Fig. 1, it may be noticed that the spectra of PMDA-polymethylbenzene complexes in the solid state show a regular red-shift from those in solution. The red-shift of the absorption of the durene-PMDA complex, however, is extraordinarily large, showing that the band is situated between those of penta- and hexamethylbenzene complexes. Apparently, the durene molecule takes a more favorable position with regard to the PMDA molecule in the charge-transfer complex than do other polymethylbenzenes. This odd behavior of durene in the solid state will be discussed, together with that of *o*-xylene, in the following section.

Heaton et al. noticed that the equilibrium constant of the *o*-xylene-PMDA complex exceeded those of meta and para isomers, and explained this as being due to the dipole moment of *o*-xylene.[2] In solid states, the

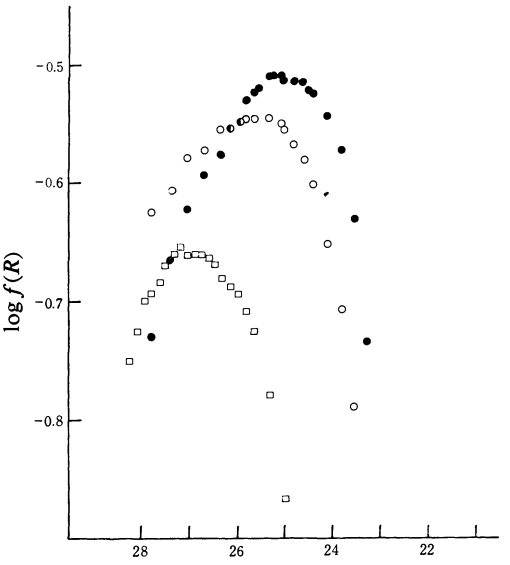



Fig. 6. The diffuse reflectance spectra of PMDA-xylene complexes.
Open circle: *o*-Xylene complex (53 mg./380 mg. talc)
Open square: *m*-Xylene complex (43 mg./380 mg. talc)
Filled circle: *p*-Xylene complex (45 mg./370 mg. talc)

13) G. Schreyer, *Z. Phys. Chem., N. F.*, **18**, 123 (1958).

14) G. Kortum and W. Braun, ibid., **18**, 242 (1958).

TABLE III. THE MOLAR RATIOS OF PMDA COMPLEXES WITH POLYMETHYLBENZENES

| Donor | Sample mg. | Loss mg. | Molar ratio Donor/PMDA | Condition |
|---|---|---|---|---|
| *o*-Xylene | 81.5 | 40.0 | 1.98 | 80°C/20 mmHg |
| Tetralin | 73.1 | 40.3 | 2.01 | 80°C/20 mmHg |
| Indan | 83.3 | 43.2 | 1.99 | 80°C/20 mmHg |
| Toluene | 62.3 | 18.5 | 1.00 | 70°C/50 mmHg |
| *p*-Xylene | 68.0 | 22.2 | 1.00 | 80°C/20 mmHg |
| Mesitylene | 104.8 | 37.0 | 0.99 | 70°C/50 mmHg |
| Durene | 20.85 | 7.95 | 1.00 | 120°C/1 atm |
| Pentamethylbenzene | 16.95 | 7.30 | 1.01 | 140°C/1 atm |
| Hexamethylbenzene | 10.70 | 4.70 | 1.05 | 160°C/1 atm |

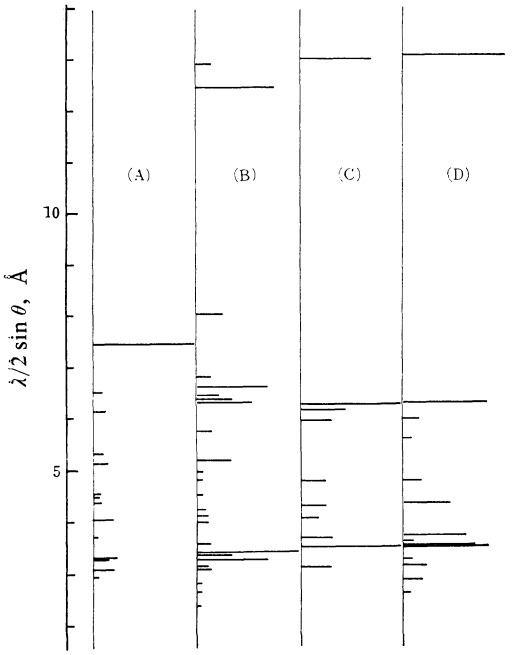



Fig. 7. X-Ray diffraction from the powered samples of the PMDA complexes with xylene isomers and the analogues. The relative intensity of diffraction at a Bragg angle $\theta$ is represented by the length of horizontal line.
(A) *p*-Xylene - PMDA (C) Indan-PMDA
(B) *o*-Xylene - PMDA (D) Tetralin-PMDA

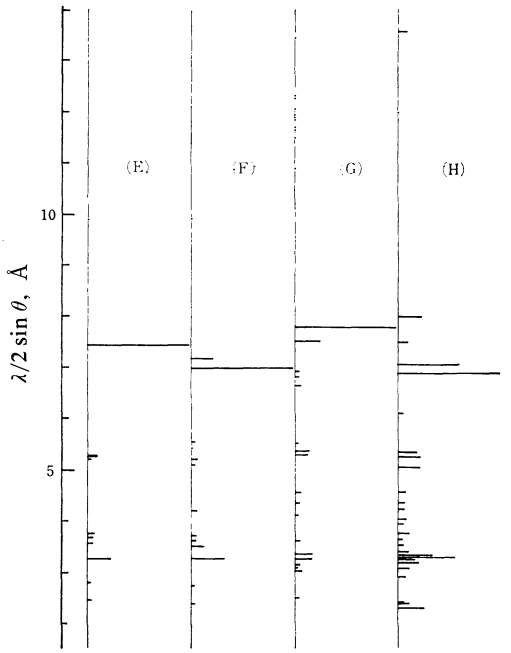



Fig. 8. X-Ray diffraction from the powered samples of the PMDA complexes with highly methylated benzenes.
(E) Hexamethylbenzene-PMDA
(F) Pentamethylbenzene-PMDA
(G) Durene-PMDA (H) Mesitylene-PMDA

absorptions of PMDA-xylene complexes are fairly sharp, as is indicated by $f(R)$ functions in Fig. 6, and simple, well defined structures may be expected for the molecular complexes. A comparison of the peak positions does not give any fruitful results in this case, since the solution spectra of the corresponding complexes are too broad to make a fine argument. The anomalous behavior of *o*-xylene becomes clear when the molar ratios of the donor to the acceptor in xylene-PMDA complexes are compared. The molar ratio was determined by heating the solid samples up to 80°C under reduced pressure and by then measuring the weight decrease due to the loss of the donor molecule. The results are summarized in Table III.

Included in the same table are complexes of tetralin and indan, which are taken as the analogues of *o*-xylene. These *o*-xylene analogues are seen to make definite two-to-one complexes with PMDA. All of the other polymethylbenzenes, dimethoxybenzene isomers, and polycyclic aromatic hydrocarbons, without exception, make one-to-one complexes. Therefore, the formation of two-to-one complexes with PMDA is a special characteristic of the *o*-xylene analogues which have two alkyl groups at adjacent positions on a benzene nucleus.

X-Ray diffraction from the powdered sample affords another method to differentiate between two-to-one and one-to-one complexes. As may be seen from Figs. 7 and 8, the two-to-one complexes show characteristic diffraction in the neighborhood of 13Å. Analogously strong peaks are observed around 7Å in the case of the one-to-one complexes. Not only the X-ray diffraction patterns but also the crystalline form of the complex changes vividly from monoclinic needles to leaflets as the molar ratio increases. Obviously, the arrangement of the molecules differs considerably for these two types of solid complexes. As is generally agreed, the smallest unit of a charge-transfer complex with $\pi, \pi$-interaction is a donor and acceptor pair, their molecular planes facing each other. Thus the structure of the one-to-one complex is considered to consist of the layers of the PMDA-donor pair in succession.

The presence and position of the second donor molecule in the two-to-one complex is more difficult to explain. In order to understand this problem more fully, the $\pi$-electron systems of PMDA and donor molecules were studied by the simple LCAO MO method. The coefficients of the atomic orbitals contributing to the lowest unoccupied molecular orbital of PMDA are shown in Fig. 9. On the basis of these figures, it is reasonable to consider PMDA as a bifunctional electron acceptor consisting of two molecules of maleic anhydride. The same LCAO MO calculation was made on polymethylbenzenes, assuming an inductive model for the methyl group. The energies and the coefficients of AO's for the

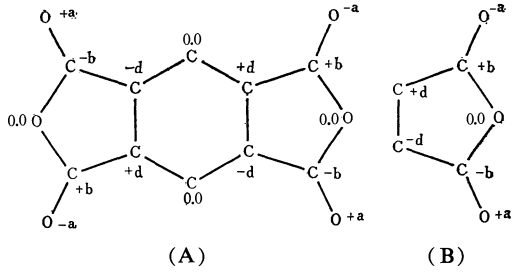



Fig. 9. The coefficients of AO's in the lowest unoccupied molecular orbital of anhydride.
(A) PMDA: $a=0.317$, $b=0.283$, $d=0.263$
$E=\alpha+0.11\beta$
(B) Maleic anhydride: $a=0.449$, $b=0.401$, $d=0.372$
$E=\alpha+0.11\beta$

The parameters used in the calculation are as the following, $h_{\dot{O}}=1.0$, $h_{\ddot{O}}=2.0$, $k_{C=O}=1.0$, $k_{C-O}=0.8$ and an auxiliary inductive parameter as suggested by Streitwieser (A. Streitwieser, Jr., "Molecular Orbital Theory," John Wiley & Sons, Inc., New York (1961), p. 135).

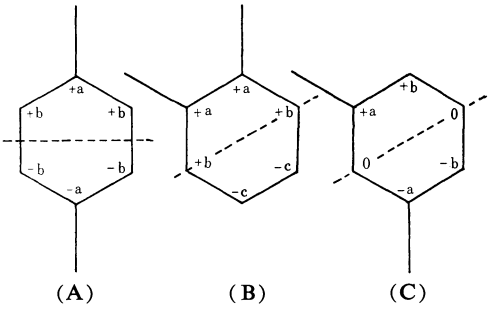



Fig. 10. The symmetry properties of the highest occupied MO's of xylene isomers as calculated by the simple LCAO MO method.

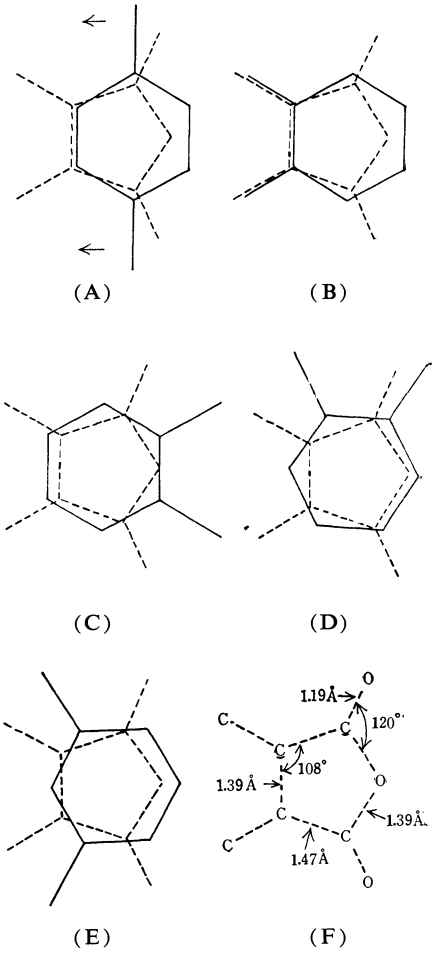



Fig. 11. Possible orientations of xylene isomers with respect to PMDA.
(A) *p*-Xylene (B), (C), (D) *o*-Xylene
(E) *m*-Xylene

The dotted lines indicate the right hand half of PMDA molecule. The dimensions as shown in (F) are assumed for PMDA on the basis of the reported X-ray data about maleic anhydride (R. E. Marsh, E. Ubell and H. E. Wilcox, *Acta Cryst.*, **15**, 35 (1962)).

occupied orbitals are listed in Table IV. The highest occupied MO's of xylene isomers are also shown in Fig. 10.

One of the most important conditions for a stable charge-transfer complex is a good overlapping between the acceptor orbital (the MO, as illustrated in Fig. 9(A) in this case) and the donor orbital (the highest occupied orbital of the donor in general). From this point of view, the symmetry properties of the above MO's may be seen to indicate that the anhydride group of PMDA would work as a better electron-accepting site to the donors under consideration than the central benzene ring in the same molecule. In addition to this electronic factor, the van der Waals repulsion should affect, to some extent, the relative orientation of the donor-acceptor pair. The highest occupied molecular orbital of *p*-xylene, for example, is ideal for "lock and

TABLE IV. THE OCCUPIED MOLECULAR ORBITALS OF METHYLBENZENES AS CALCULATED BY SIMPLE LCAO MO METHOD*,**

| Toluene | | | | | | |
|---|---|---|---|---|---|---|
| Energy | (1) | 2 | 3 | 4 | 5 | 6 |
| 1.93 | 0.32 | 0.39 | 0.44 | 0.45 | 0.44 | 0.39 |
| 1.00 | 0.00 | 0.50 | 0.50 | 0.50 | −0.50 | −0.50 |
| 0.84 | 0.55 | 0.37 | −0.24 | −0.57 | −0.24 | 0.37 |
| *p*-Xylene | | | | | | |
| Energy | (1) | 2 | 3 | (4) | 5 | 6 |
| 1.85 | 0.37 | 0.43 | 0.43 | 0.37 | 0.43 | 0.43 |
| 1.00 | 0.00 | 0.50 | 0.50 | 0.00 | −0.50 | −0.50 |
| 0.69 | 0.54 | 0.32 | −0.32 | −0.54 | −0.32 | 0.32 |
| *o*-Xylene | | | | | | |
| Energy | (1) | 2 | 3 | 4 | 5 | (6) |
| 1.87 | 0.31 | 0.42 | 0.48 | 0.48 | 0.42 | 0.31 |
| 0.93 | 0.24 | 0.59 | 0.31 | −0.31 | −0.59 | −0.24 |
| 0.73 | 0.54 | 0.12 | −0.45 | −0.45 | 0.12 | 0.54 |
| *m*-Xylene | | | | | | |
| Energy | 1 | (2) | 3 | 4 | 5 | (6) |
| 1.86 | 0.37 | 0.35 | 0.44 | 0.48 | 0.44 | 0.35 |
| 0.91 | 0.66 | 0.30 | −0.24 | −0.52 | −0.24 | 0.30 |
| 0.78 | 0.00 | 0.44 | 0.56 | 0.00 | −0.56 | −0.44 |
| Mesitylene | | | | | | |
| Energy | (1) | 2 | (3) | 4 | (5) | 6 |
| 1.77 | 0.38 | 0.43 | 0.38 | 0.43 | 0.38 | 0.43 |
| 0.78 | −0.50 | −0.32 | 0.25 | 0.64 | 0.25 | −0.32 |
| 0.78 | 0.00 | 0.56 | 0.44 | 0.00 | −0.44 | −0.56 |
| Durene | | | | | | |
| Energy | 1 | (2) | (3) | 4 | (5) | (6) |
| 1.69 | 0.45 | 0.38 | 0.38 | 0.45 | 0.38 | 0.38 |
| 0.85 | 0.61 | 0.26 | −0.26 | −0.61 | −0.26 | 0.26 |
| 0.50 | 0.00 | 0.50 | 0.50 | 0.00 | −0.50 | −0.50 |
| Pentamethylbenzene | | | | | | |
| Energy | 1 | (2) | (3) | (4) | (5) | (6) |
| 1.61 | 0.52 | 0.42 | 0.36 | 0.34 | 0.36 | 0.42 |
| 0.67 | −0.57 | −0.19 | 0.35 | 0.60 | 0.35 | −0.19 |
| 0.50 | 0.00 | 0.50 | 0.50 | 0.00 | −0.50 | −0.50 |
| Hexamethylbenzene | | | | | | |
| Energy | (1) | (2) | (3) | (3) | (5) | (6) |
| 1.50 | 0.41 | 0.41 | 0.41 | 0.41 | 0.41 | 0.41 |
| 0.50 | 0.58 | 0.29 | −0.29 | −0.58 | −0.29 | 0.29 |
| 0.50 | 0.00 | 0.50 | 0.50 | 0.00 | −0.50 | −0.50 |

* An inductive model was used for the methyl group ($h_C = -0.5$).

** The energy (in $\beta$ units) is shown with respect to $\alpha$. The integers stand for the numbering of carbon atoms. Parentheses are added if the atom is attached by a methyl group.

key" fitting[2] to the accepting orbital of the anhydride group, as is shown, in Fig. 11(A). The distance between the molecular planes is assumed to be 3.3Å, which is the value commonly found in the cases of chloranil- and trinitrobenzene complexes with aromatic hydrocarbons. Some van der Waals repulsion results from the methyl and carbonyl groups being in an exact superposition. This repulsion is relieved by shifting the donor molecule horizontally in the direction indicated by the arrows. The *o*-xylene analogues represent a case where the van der Waals repulsion between the substituents and PMDA strongly depends on their mutual orientation if the inter-planar distance is held at 3.3Å. In the orientation as is illustrated in Fig. 11(B), a considerable change in the van der Waals repulsion may be expected if the comparison is made between the complexes of *o*-xylene and tetralin or indan. Since all of these *o*-xylene analogues show similar complexing behavior, it is unlikely that a coordination of this type really exists. Furthermore, both models, B and C, may be eliminated by considering the symmetry properties of the MO's concerned. The model D is the only one left as a possible structure. Certainly it is not the best one as judged on the maximum overlap principle. The van der Waals repulsion mentioned above, however, is at a minimum in this configuration. Similar arguments predict model E as the most probable structure for the *m*-xylene - PMDA complex. This situation is rather satisfactory in view of both the electronic interaction and the intermolecular repulsion.

Coming back to the case of the two-to-one complex, the above theoretical considerations do not give any explanation of why it is found only in the *o*-xylene analogue. In any case, however, a donor molecule is taken to be located directly above one of the anhydride groups of PMDA. Therefore, there is not enough room left for another donor on the same side of PMDA. The second donor may come in freely from the back of PMDA, as is shown in Fig. 12. The formation of such a donor-acceptor-donor sandwich, if one exists, should be favored by a strong electron donor such as hexamethylbenzene or anthracene. Since this is not the actual case, however, such a system has very poor prospects to be the unit of the *o*-xylene analogue-PMDA complex in the solid state. As has been pointed out by Heaton et al.,[2] the existence of large dipolement is an important characteristic of the *o*-xylene and its analogue, differentiating them the isomers. The donor-acceptor pair in the charge-transfer complex

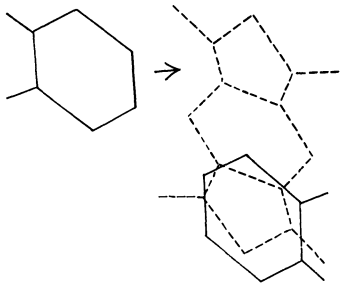


Fig. 12. One of the possible routes for the second donor to approach PMDA.

is also polar by its own nature. Therefore, the truth may be that the second *o*-xylene (or its analogue) is paired off to the first donor-PMDA couple in such a way as to stabilize the whole system in the solid state. The role may be close to that played by the water of crystallization in ionic crystals. Of course, some charge-transfer-type interaction is to be expected between the second donor and the unoccupied anhydride group. Therefore, it may be predicted that the second donor will be found somewhere close to the vacant electron-accepting site of PMDA. The final answer must, however, await the results of the X-ray diffraction and spectroscopic studies of a single crystal of the complex.

In the above discussion of the xylene complexes, the second-highest-occupied MO (abbreviated as SHO MO) of the donor is not taken into consideration. This treatment may be justified on the basis of the following facts:

(1) The SHO level of xylene is located between the highest occupied levels of toluene and benzene, as may be seen in Table IV.

(2) No solid complex is formed between benzene and PMDA, while the complex yielded from toluene is rather unstable.

The treatment, however, can not be applied to the highly methylated benzenes any more. In some of these donors, the energy of the SHO MO is too close to that of the highest occupied orbital to be neglected in the discussion. The difference between the highest-occupied and the SHO MO's is seen in their symmetry properties. The highest occupied MO's of mesitylene, durene, penta- and hexamethylbenzenes are shown schematically in Fig. 13(A). It should be noticed here that the coefficients are antisymmetric and symmetric with respect to the x and the y axes respectively. Exactly reverse situations are found for the coefficients in the corresponding SHO MO's (or the counterparts of the degenerate pairs in the cases of mesitylene and hexamethylbenzene), as Fig. 13(B) shows.

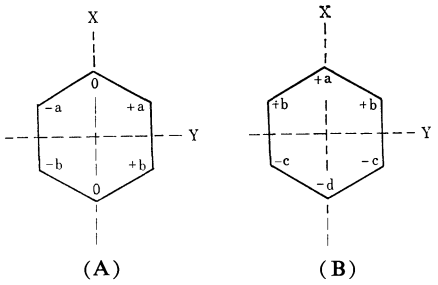



Fig. 13. The symmetry properties of the highest and the second highest occupied molecular orbitals of the highly methylated benzenes.

The lowest unoccupied MO of PMDA, on the other hand, is antisymmetric with respect to the longitudinal axis of symmetry, as is shown in Fig. 9.

As far as the symmetry properties are concerned, therefore, the predicted orientation of the donor molecule with relation to PMDA is approximately ninety degrees apart, depending on the particular orbital used in the interaction. In other words, the electronic interaction between PMDA and the highest occupied MO is counteracted by that due to the SHO MO. The higher the energy level of the SHO MO, the stronger the interaction. If a strong counteraction is exerted, the actual orientation of the donor molecule becomes less favorable to the overlapping between the highest occupied MO and the acceptor orbital. Furthermore, the best orientation of the SHO MO's results in the worst situation for the van der Waals repulsion due to the methyl groups. As may clearly be seen in Table IV, the SHO MO of durene is located considerably lower than those of mesitylene, penta- and hexamethylbenzenes. Therefore, the anomalous peak position observed in the solid spectra of durene-PMDA complex may be explained as being due to the more effective overlapping between the highest occupied MO of the donor and the acceptor orbital than in the cases of other polymethylbenzenes.

The above theoretical prediction seems to explain the behavior of polymethylbenzene-PMDA complexes very well. The findings regarding simple LCAO MO method, however, should be applied to actual cases with great care. It is well known that the quantitative results obtained by the method differ considerably from the true values. Even a qualitative prediction is sometimes in error, as in the case of the iodine-benzene complex.[15] The situation is expected to be a little better for the $\pi-\pi^*$ charge-transfer complexes, where no other arrangement of the donor acceptor pair is conceivable except a sandwich type with their molecular planes facing each other. Many atomic orbitals in both the donor and the acceptor molecules are involved in the overlapping of the MO's. Consequently, a minor change in the relative orientation of the molecules causes an appreciable difference in the overlap integral between the donor and the acceptor orbitals. Therefore, the symmetry consideration of the problem would be more fruitful than it is in the cases of the other type of complexes. Nevertheless, it is advisable to evaluate the results of the simple LCAO MO method with some reservations. Further studies are required to solve the problem.

In summary, the study of PMDA-polymethylbenzene solid complexes reveals many characteristics which are not found in the complexes in solution. These phenomena may be explained as representing the finer differences in the donor properties, such as the polarity of the molecule, the symmetry of the orbitals concerned, and the van der Waals repulsion due to the substituents. The compact and well-defined arrangement of the donor-acceptor pair in the solid state is considered to be responsible for the appearance of these phenomena.

The authors are grateful to Miss Katsumi Mera for measuring the ultraviolet and visible spectra reported in this paper. They are also indebted to Miss Tsuneko Ito and Miss Mizue Moritomo for their help in preparing the manuscript.

*Department of Organic Synthesis*
*Faculty of Engineering*
*Kyushu University*
*Hakozaki, Fukuoka*

15) R. S. Mulliken, *J. Am. Chem. Soc.*, 74, 811 (1952).

# The Mössbauer Spectra of Several Inorganic Iron Salts

By Yoshimasa TAKASHIMA* and Shigeru OHASHI*

(Received February 25, 1965)

Since the discovery of the Mössbauer effect, a number of papers have appeared concerning this phenomenon, which consists of the recoilless emission and resonant recoilless absorption of nuclear gamma radiation. However, the great majority of previous investigations of the Mössbauer effect have been concerned almost exclusively with nuclear physics, solid state physics and theoretical physics.

Takashima et al.[1] and Fluck et al.[2] have, in earlier reviews pointed out the applicability and significance of the Mössbauer effect in chemical research. In recent years, chemical Mössbauer studies of iron cyanide complexes,[3] iron carbonyl complexes,[4,5] ferrocene derivatives[6] and iron phenanthroline complexes[7] have, therefore, been carried out by several groups of workers. However, a large number of other compounds are still unexplored. Meanwhile, increasing interest is being shown in chemical applications of the Mössbauer effect.

The purpose of the present work is to measure the isomer shift and the quadrupole splitting for the 14.4 keV. $\gamma$-transition of $^{57}Fe$ in various iron compounds, in the hope that the wealth of the resultant data will make clear any correlation between these values and the chemical binding of iron atoms.

## Theoretical Considerations

The very low gamma ray level used in Mössbauer study tells us that the vibrational and rotational states in the molecule will have little effect on the Mössbauer spectrum. The shape of the spectrum is mainly affected by the electronic charge distribution around the iron atom. As has been shown in previous papers,[4-7] the Mössbauer measurements can give extremely valuable information about the electronic charge distribution in the molecule as a function of the structure.

Two quantities, the isomer shift and the quadrupole splitting, are readily derived from Mössbauer spectra. The magnitude of these values is considered to be closely related to the molecular structure with which $^{57}Fe$ is concerned.

The isomer shift, $\delta$, is given in first approximation by the formula:

$$\delta = C(R_e^2 - R_g^2)[|\psi_a(0)|^2 - |\psi_s(0)|^2]$$

where $C$ is a constants; $R_e$ and $R_g$ are the effective charge radii in the excited and ground states respectively, and $|\psi_a(0)|^2$ and $|\psi_s(0)|^2$ are, respectively, the $s$-electron densities at the iron nucleus in the absorber and in the source. This density is greatest for the inner $s$-electrons, but it is nonzero for even the outermost $s$-electrons.

If we consider two atoms of the same element that differ only in respect to the molecule in which they are bound, the difference in the electron density at the nucleus will reflect the difference in the chemical nature. Thus the extent of the isomer shift will give semiquantitative information as to the chemical binding.

The quadrupole slitting, $\varepsilon$, is characterized by the $1/4\, e^2qQ$, quantity where $e$ is the electronic charge, $q$ is the electronic field gradient at the nucleus, and $Q$ is the quadrupole moment of the nucleus. Splitting occurs if the electronic charge distribution at the atom is not spherically symmetrical.

Therefore, the quadrupole splitting provides a measure of the crystal field parameters in various compounds. However, there is, at present, no general method for predicting the relative isomer shift (or the quadrupole splitting) of various compounds with different types of bindings.

## Experimental

**Materials.**—The following chemicals were used, all were commercial reagent grade products, and all were used without further purification.

Iron(III) chromate $\{Fe_2(CrO_4)_3\}$, Basic iron(III) chromate $(Fe_2O_3 \cdot 4CrO_3 \cdot H_2O)$, Iron(III) arsenate $(FeAsO_4)$, Iron(III) phosphate $(FePO_4 \cdot 4H_2O)$, Iron(III) pyrophosphate $Fe_4(P_2O_7) \cdot 9H_2O$, Iron(II)

* Present address: Department of Chemistry, Faculty of Science, Kyushu University, Hakozaki, Fukuoka.

1) Y. Takashima and S. Ohashi, "*Bussei*", **4**, 243 (1963).
2) E. Fluck, W. Kerler and W. Neuwirth, *Angew. Chem.*, **75**, 461 (1963).
3) J. F. Duncan and P. W. R. Wigley, *J. Chem. Soc.*, **1963**, 1120.
4) R. H. Herber, W. R. Kingston and G. K. Wertheim, *Inorg. Chem.*, **2**, 153 (1963).
5) W. Kerler, W. Neuwirth, E. Fluck, P. Kuhn and B. Zimmermann, *Z. Physik*, **173**, 321 (1963).
6) G. K. Wertheim, *J. Chem. Phys.*, **38**, 2106 (1963).
7) L. M. Epstein, ibid., **40**, 435 (1964).

phosphate $Fe_3(PO_4)_2 \cdot 8H_2O$, Graham's salt $\{(NaPO_3)_n\}$, Iron oxides ($Fe_2O_3$ and $Fe_3O_4$), Potassium ferricyanide $K_3[Fe(CN)_6]$.

Most of the samples studied were especially prepared for the measurements.

*Metal Ferricyanide Complexes $M_3[Fe(CN)_6]_2$ (M= Zn, Cd, Ni and Co).*—Solutions (approximately 0.1 M) of metal sulfate and potassium ferricyanide were prepared. Equivalent quantities of the former were then added to the latter, so that four different precipitates were obtained. After that, the precipitate was centrifuged off, washed with water, and dried on filter paper.

*Alkali-Iron(III) Double Sulfates $M'Fe(SO_4)_2 \cdot 12H_2O$, (M'=K, Rb and Cs).*—A saturated solution of metal sulfate was mixed with an equivalent amount of an iron(III) sulfate solution. The mixture was then placed in a desiccator for several days until crystals formed. The precipitate was filtered off and dried on filter paper.

*Glassy Substances Consisting of $(NaPO_3)_n$-$Fe_2O_3$ and $(NaPO_3)_n$-$Fe_3O_4$.*—Graham's salts (10 g.), prepared by the thermal dehydration of dihydrogen phosphate, was mixed with varying amounts of $Fe_2O_3$ (or $Fe_3O_4$) in a platinum crucible so that the P/Fe ratios became 5, 7, 10 and 50. The mixtures were then fused by heating them at 900°C for one hour and then rapidly cooling them. The products were all brownish, glassy substances.

*Cement.*—A vinyl cemedine*-chloroform solution was used to cement the sample on a sample holder disk.

**Apparatus.** — Our experimental arrangements, shown in Fig. 1, were essentially the same as those described by De Pasquali et al.[8] (1960) and by Shirley et al.[9] (1961).

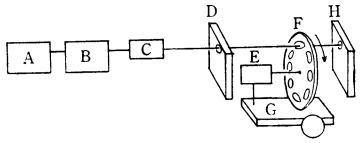



Fig. 1. Experimental arrangement.

A Scaler
B Single channel pulse height analyser
C NaI detecter
D Slit
E Synchronous motor
F Absorber disk
G Angle changer
H Source

About 5 mc. of $^{57}Co$ electroplated on metallic copper was used as a source. The main advantage of such a large amount of source material is the feasibility of time-saving measurements.

The constant velocity drive consists of a constant speed synchronous motor (4 r.p.m.) with a round absorber disk (7.4 cm. in diameter). The absorber disk has eight open windows in which a sample is mounted. The gamma ray passing through the disk sees, in its direction of motion, a velocity component, $r\omega \sin\theta$, where $r$ is the distance from the axis of rotation to the point where the gamma ray passes through the absorber, and where $\theta$ is the angle between the gamma ray and the axis of motion.

The gamma ray (14.4 keV.) was measured by means of a single-channel pulse-height analyzer equipped with a thin NaI scintillation detector (1 cm.×2 cm., 1 mm. thick). The detector face was located 40 cm. from the source. The absorber was placed between the source and detector face, at a distance 9 cm. from the source. The instrumental conditions were unchanged for many months.

A multichannel pulse-height analyzer,[10] coupled with an instantaneous velocity measurement of the gamma ray source, was also used for the measurement of several samples, but only when enough sample for the previous technique was not available.

**Procedure.** — A known amount of a powdered sample was mounted on an absorber disk by using a vinyl cemedine-chloroform solution. The total amount of sample taken varied within the range from 0.8 to 2.4 g. (10—20 mg. Fe/cm²), depending on its iron content. The sample sheet was made as uniform as possible.

The gamma ray transmissions were measured at room temperature for each Doppler velocity, these velocity were arbitrarily selected by changing the angle of the absorber disk. The relationship between the intensity of the transmitted radiation and the relative velocity of the absorber was plotted in graphical form, and then both the isomer shift and the quadrupole splitting were read out from the curve. All the values of the isomer shift were represented by the shifts (mm./sec.) relative to the stainless steel. The activity was measured by counting the $\sim 10^5$ total for each point. Statistical error ($\pm\sqrt{n}\cdots n$=counts) was taken into account in drawing the spectral lines. The reading errors of $\delta$ and $\varepsilon$ depend on the sharpness of the absorption peak. The estimated error for metal ferricyanides was about $\pm 0.01$ mm./sec. On the other hand, the error increased to $\pm 0.02$ mm./sec. in the case of the $(NaPO_3)_n$-$Fe_2O_3$ system.

## Results and Discussion

The results obtained for the isomer shift and the quadrupole splitting are summarized in Table I, together with some of the data obtained by other workers.[2] The data cited from other papers were normalized to our data, which were obtained by using a $^{57}Co$-Cu source and a stainless steel reference. In all our measurement the source absorber were held at room temperature (20—25°C).

In a closely-related series of compounds, such as metal ferricyanides $\{M_x[Fe(CN)_y]\}$, small differences in the Mössbauer spectra are to be expected because of the similar $s$-electron

* Commercial name.

8) DePasquali, H. Frauenfelder, S. Margulies and R. N. Peacock, *Phys. Rev. Letters*, 4, 71 (1960).

9) E. A. Shirley, M. Kaplan and P. Axel, *Phys. Rev.*, 123, 816 (1961).

10) K. Ôno and A. Ito, *J. Phys. Soc. Japan*, 17, 1012 (1962).

TABLE I. ISOMER SHIFT, $\delta$, AND QUADRUPOLE SPLITTING, $\varepsilon$, OF VARIOUS INORGANIC IRON COMPOUNDS

| Compound | $\delta$ mm./sec. | $\varepsilon=\frac{1}{4}e^2qQ$ mm./sec. |
|---|---|---|
| $K_3[Fe(CN)_6]$ | 0.00 | 0.14 |
| $Zn_3[Fe(CN)_6]_2$ | −0.02 | 0.00 |
| $Cd_3[Fe(CN)_6]_2$ | −0.05 | 0.00 |
| $Ni_3[Fe(CN)_6]_2$ | −0.06 | 0.24 |
| $Co_3[Fe(CN)_6]_2$ | −0.06 | 0.17 |
| $Ag_3[Fe(CN)_6]$*1 | −0.08 | 0.39 |
| $Cu_3[Fe(CN)_6]_2$*1 | −0.09 | 0.24 |
| $KFe(SO_4)_2\cdot 12H_2O$ | +0.49 | 0 |
| $RbFe(SO_4)_2\cdot 12H_2O$ | +0.51 | 0 |
| $CsFe(SO_4)_2\cdot 12H_2O$ | +0.55 | 0 |
| $(NaPO_3)_n$-$Fe_2O_3$ (P/Fe=5) | +0.49 | 0 |
| $(NaPO_3)_n$-$Fe_2O_3$ (P/Fe=10) | +0.52 | 0.17 |
| $(NaPO_3)_n$-$Fe_2O_3$ (P/Fe=50) | +0.52 | 0.21 |
| $(NaPO_3)_n$-$Fe_3O_4$*2 (P/Fe=5) | +0.48 | 0.21 |
| $(NaPO_3)_n$-$Fe_3O_4$*2 (P/Fe=7) | +0.48 | 0.22 |
| $(NaPO_3)_n$-$Fe_3O_4$*2 (P/Fe=10) | +0.51 | 0.23 |
| $(NaPO_3)_n$-$Fe_3O_4$*2 (P/Fe=50) | +0.53 | 0.24 |
| $Fe_4(P_2O_7)_3\cdot 9H_2O$ | +0.49 | 0 |
| $FePO_4\cdot 4H_2O$ | +0.43 | 0.15 |
| $Fe_3(PO_4)_2\cdot 8H_2O$ | +0.13 | 1.36 |
| $Fe_2O_3$*3 | +0.47 | 0.21 |
| $Fe_3O_4$*3 | +0.87 | 0 |
| | +0.46 | 0 |
| $Fe_2(CrO_4)_3$ | +0.34 | 0.38 |
| | +0.38 | 0 |
| $Fe_2O_3\cdot 4CrO_3\cdot H_2O$ | +0.37 | 0.33 |
| $FeAsO_4$ | +0.59 | 0.19 |

*1 See Ref. 2.
*2 Most Fe(II) in $Fe_3O_4$ must be oxidized into Fe(III) in the course of the sample preparation. Therefore these four formulas do not represent their true constituents.
*3 See Ref. 10.

density around the Mössbauer nucleus. This rule appeared to be only roughly valid for the group of compounds. Our results on metal ferricyanides and metal-iron double sulfates seem to indicate that small differences in the isomer shifts and the quadrupole splittings exist.

In a series of metal ferricyanide complexes, the absorption peak appeared close to zero velocity in every case, showing the strong covalent character of the bond between Fe and CN. The "outside" metal, separated from the iron atom by more than about 4 Å, was considered to have very little effect on the peak position. However, our results seemed to show a systematic change in the isomer shifts depending on the electronegativity of the "outside" metal. The positive shifts of the isomer shift were observed with a decrease in the electronegativities of the metals. This rule was also observed in the case of a series of metal-iron double sulfates. Lithium and sodium containing double sulfate were not measured because of the difficulty in preparing such compounds.

All the Mössbauer spectra of the metal-iron double sulfates studies displayed a single peak. On the contrary, all the metal ferricyanide salts, except zinc and cadmium salts, gave small quadrupole splittings. As examples, three spectra are illustrated in Fig. 2.

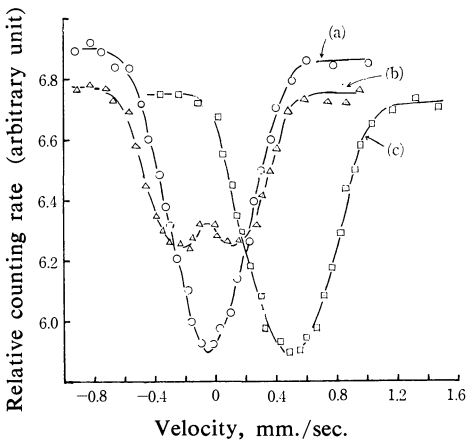



Fig. 2. Mössbauer spectra of $Cd_3[Fe(CN)_6]_2$ (a), $Co_3[Fe(CN)_6]_2$ (b) and $KFe(SO_4)_2\cdot 12H_2O$ (c).

Since these ferricyanide complexes have no water molecule in them, a direct comparison of the data is possible; i. e., one can neglect the influence of water molecules on the spectral shape. The sharp single absorption peak in the spectra for zinc and cadmium ferricyanide complexes indicates that the iron atoms in these complexes have spherically symmetric electron distribution.

As has been discussed earlier, the quadrupole splitting is caused by a nonzero electric field gradient at the iron nucleus. Moreover, the electric field gradient depends on various collective factors, i. e., the bonding character and the crystallographic character of the compound, the electronegativity of the neighboring atoms, etc. In this case, however, it appears that the sizable quadrupole splitting of these metal ferricyanides is to be attributed to their crystallographic distortion from a cubic structure caused by the "outside" metals. A noticeable broadening of the spectral lines in some ferricyanide complexes (nickel and cobalt) has been observed. This might be due to a small unresolved quadrupole splitting.

The purpose of the present investigation of the glassy substances of iron-phosphate was to elucidate the bonding character between the iron and the phosphate group in the materials. Originally, it was thought that one of the fundamental requirements for the Mössbauer effect to arise was that Mössbauer atoms should be bound in a crystal lattice. It was, however, shown in an earlier paper[11] that there is a high possibility of observing the effect even in amorphous substances (or in solid solutions).

In view of the above fact, we chose a series of fused products or iron-phosphate as samples. The spectral shapes of two series of the substances, the $(NaPO_3)_n$-$Fe_2O_3$ system and the $(NaPO_3)_n$-$Fe_3O_4$ system, were essentially identlcal, and both exhibited characteristic peaks at about 0.50 mm./sec. This fact means that iron(II) in $Fe_3O_4$ was oxidized into iron-(III) in the course of the sample preparation.

It is very difficult to conclude from the present data whether the isomer shifts obtained are due to the original iron(III) oxide or to new bonding between iron and the phosphate group. At any rate, the iron atoms are supposed to be surrounded predominantly by oxygen atoms. Therefore, relatively close values of isomer shift were observed for $Fe_2O_3$, $Fe_4(P_2O_7)_3 \cdot 9H_2O$ and $FePO_4 \cdot 4H_2O$, as is shown in Table I. However, there is one thing to be noted: the spectral characteristics of $(NaPO_3)_n$-$Fe_2O_3$ (P/Fe=5) differ from those of iron(III) oxide itself. The former displayed no quadrupole splitting, and the isomer shift value agreed well with that of $Fe_4(P_2O_7)_3 \cdot 9H_2O$. In view of this fact, all one can conclude at present is that the iron(III) pyrophosphate type of bonding grew, at least in $(NaPO_3)_n$-$Fe_2O_3$ (P/Fe=5).

The samples chosen for the remaining studies were iron(III) arsenate and iron(III) chromates. The results obtained suggest that the bonding between Fe and $AsO_4$ is typically ionic, while the bonding between Fe and $CrO_4$ (or $CrO_3$) is more or less covalent.

The Mössbauer spectrum of iron(III) chromate is shown in Fig. 3a. It can be resolved into two components (dotted curves), showing that iron(III) chromate has two different isomer shifts. This fact obviously indicates that there are two sites for iron atoms in the iron-(III) chromate crystal. Consequently, it is recommended that the chemical formula of iron(III) chromate be written as $Fe[Fe(CrO_4)_3]$ instead of $Fe_2(CrO_4)_3$. We interpreted the single peak as being due to ionic Fe ($\delta$=0.38 mm./sec.), while we attributed the doublet to

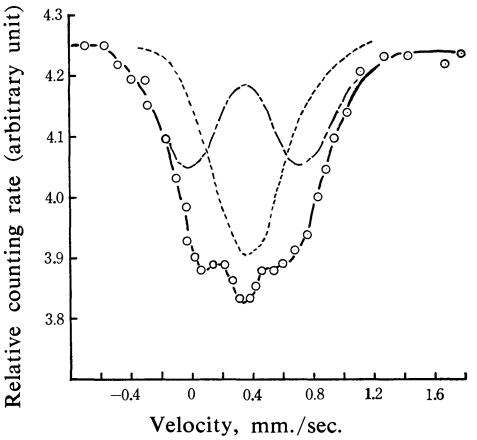



Fig. 3a. Mössbauer spectrum of iron(III) chromate.

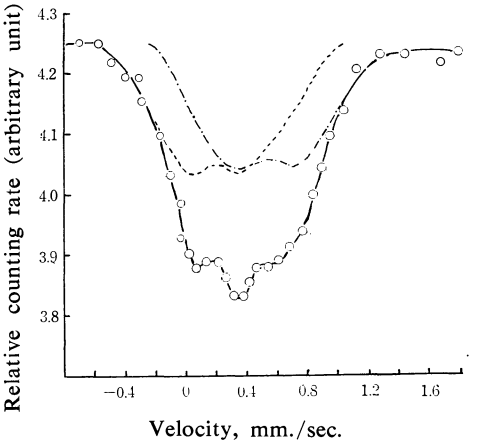



Fig. 3b. Mössbauer spectrum of iron(III) chromate.

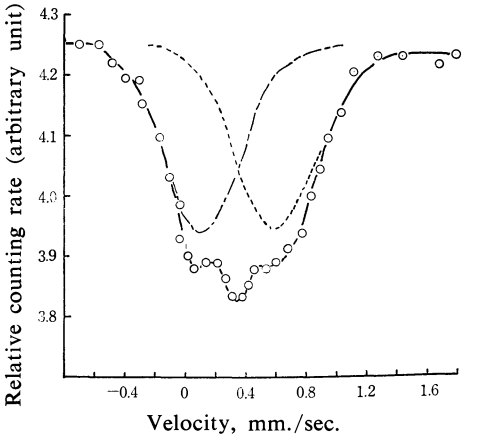



Fig. 3c. Mössbauer spectrum of iron(III) chromate.

covalent iron atoms ($\delta$=0.34 mm./sec., $\delta$=0.38 mm./sec.). It should be noted that the spectrum may also be resolved in the two ways

11) V. A. Bryukhanov, V. I. Col'danskii, N. N. Delyagin, L. A. Korytko, E. F. Makarov, I. P. Suzdalev and V. S. Shpinel, *Soviet Phys., JETP*, **16**, 321 (1963).

shown in Fig. 3b ($\delta_1 = +0.58$, $\delta_2 = +0.10$ mm./sec.) and in Fig. 3c. ($\delta_1 = +0.21$, $\delta_2 = +0.52$ mm./sec.).

As has been described elsewhere, however, the magnitude of one of the isomer shifts (+0.10 mm./sec.) in Fig. 3b is not in the region of iron(III) salts. Though the isomer shifts obtained from Fig. 3c are reasonable, any possible analysis of the spectrum can be made only in a rough manner. The assumption of the presence of two different types of iron atoms should be confirmed chemically in future study.

We have as yet comparatively little knowledge as to what chemical information can be obtained from the Mössbauer spectrum. More extensive studies and discussion by many workers are desired.

## Summary

The Mössbauer spectra of a variety of as-yet-unexplored iron compounds have been investigated by using 14.4 keV. gamma rays from $^{57}Fe$. The isomer shifts and the quadrupole splitting extracted from the spectra have been discussed in terms of the electronegativity of the atoms connected to the iron atom. The correlation of these values with the bond character and the chemical structure has also been discussed qualitatively. The results obtained for a series of glassy substances of iron-phosphate suggest that the Mössbauer spectra may permit us to study the chemical structure of iron compounds in an amorphous substance.

The authors are indebted to Drs. Kazuo Ôno, Atsuko Ito, Masatake Honda, Hideo Yamatera, Masako Shima, Hirotoshi Sano and Kunihiko Mizumachi for their helpful discussions. Grateful aknowledgement is also made to Messrs. Terumasa Nakamura and Fumitoshi Inenaga for their technical assistance in the preparation of several samples.

*The Institute for Solid State Physics*
*The University of Tokyo*
*Azabu, Tokyo*

# Mössbauer Spectra of Various Organic Iron Chelates

By Yoshimasa TAKASHIMA and Yasuyuki TATEISHI

(Received February 25, 1965)

In a previous paper,[1] the Mössbauer spectra of various inorganic iron compounds were studied and some significant aspects of the spectra were discussed. The results showed that such an investigation can give valuable information concerning the change in the charge distribution in the molecule as a function of the chemical structure or bindings.

In the studies reported on in this paper, the work on the Mössbauer spectra was extended to a variety of organic iron chelates. The choice of organic iron chelates as an absorber was made because a series of structurally-related compounds are readily available and because various kinds of bindings are included in the organic iron chelates.

The two parameters of major interest, the isomer shift and the quadrupole splitting, will be discussed, as will the correlation between the above values and the molecular structure.

Special attention will be paid to the effect on the isomer shift of varying ligands bonded to the iron atom.

## Experimental

**Apparatus and Procedure.** — The apparatus and procedure employed were essentially the same as those described in the previous paper.[1] All measurements were made at room temperature and with respect to a $^{57}Co$ source diffused into metallic copper. The isomer shifts were referred to the stainless steel absorber.

Minor variations in technique were matters of convenience in the cases of hygroscopic and light-sensitive substances. Such samples were stored under a vacuum in the dark until they were mounted to the absorber disk. The mounted samples were then covered with a piece of black paper and adhesive tape to avoid light and moisture respectively.

**Materials.** — Most of the chemicals used were commercial reagent-grade products which were used without any further purification. (The Mössbauer effect is not very sensitive to a small impurity.) Several samples were prepared in the laboratory because of the lack of commercial ones. Two

1) Y. Takashima and S. Ohashi, This Bulletin, **38**, 1684 (1965).

samples, bis(salicylaldehyde)ethylenediimine iron(III) chloride and oxide, were provided by Professor Tamotsu Yoshino of Kyushu University.

The commercially-obtained samples were the following:

Monosodium-ethylenediaminetetraacetato-iron(III), (Na·Fe-EDTA), iron(III)-nitrilotriacetate, (Fe(III)-NTA), iron(III)-acetylacetonate, {Fe(III)-$(AA)_3$}, iron(III)-trifluoroacetylacetonate, {Fe(III)-$(TAA)_3$}, iron(III)-thenoyltrifluoroacetonate, {Fe(III)-$(TTA)_3$}.

The above chemicals were obtained from Dojin Pharmaceutical Laboratories, Kumamoto. All the other chemicals, shown below, were purchased from Wako Pure Chemical Industries, Ltd., Osaka:

Iron(III) formate $\{Fe(HCO_2)_3 \cdot H_2O\}$, iron(III) succinate $\{Fe_2(C_3H_4O_4)_3\}$, iron(III) tartrate $\{Fe_2(C_4H_4O_6)_3 \cdot H_2O\}$, iron(III) malate $\{Fe_2(C_4H_4O_5)_3\}$, iron(III) citrate $\{FeC_6H_5O_7 \cdot 5H_2O\}$ ammonium iron(III) citrate $\{(NH_4)_3[Fe(C_6H_5O_7)_2]\}$, basic iron(III) benzoate $\{[Fe_3(C_6H_5COO)_6 \cdot (OH)_2](OH)\}$, iron(II) oxalate $(FeC_2O_4 \cdot 2H_2O)$, iron(II) lactate $\{Fe(C_3H_5O_3)_2 \cdot 3H_2O\}$, iron(II) gluconate $\{Fe(C_3H_6O_4)\}$, iron(II) tartrate $(FeC_4H_4O_6 \cdot H_2O)$.

The following samples were prepared in the laboratory. The preparation techniques were based on "Gmelins Handbuch der anorganishen Chemie" in most cases. Trisalicylaldehyde-diimine iron(III), phenylnitrosohydroxylamine-iron(III) oxide and phenylnitrosohydroxylamine iron(III) were made by Tsumaki's method.[2]

*Iron(III) Acetate A.* — Wet iron(III) hydroxide containing 10% iron was dissolved in 95% acetic acid. The solution was then allowed to stand over concentrated sulfuric acid in a vacuum desiccator for several days until the precipitate appeared.

*Iron (III) Acetate B.* — Wet iron(III) hydroxide containing 20% iron was dissolved in pure acetic acid. The following procedures were the same as those described above.

*Iron(III)+Cr(III) Acetate (Cr : Fe=1 : 2 and 2 : 1).* —These compounds were prepared in a way similar to that described in the case of iron(III) acetate A. However, the initial hydroxides used were mixed hydroxides of iron(III) and chromium(III) having ratios (atom) of 1 : 2 and 2 : 1.

*Iron(III) Salicylate.* — To 50 ml. of an aqueous solution of 4.8 g. of sodium salicylate, 40 ml. of ether and 50 ml. of an aqueous solution of 2.7 g. iron(III) chloride were added. After the mixture had stood for several hours, the red precipitate formed was filtered. The precipitate was dried over calcium chloride.

*1,10-Phenanthroline Iron(II) Chloride,* $\{(Phen)_3Fe\}Cl_2 \cdot 7H_2O$.—Ethanolic solutions of both 1,10-phenanthroline and iron(II) chloride were mixed. The precipitate was obtained by the addition of acetone. The resultant red precipitate was recrystallized from a small amount of water.

*1,10-Phenanthroline Iron(III) Chloride,* $[(Phen)_2Fe(OH)_2Fe(Phen)_2]Cl_4$. — The method of preparation was essentially the same as that described above. The only exception was the use of iron(III) chloride instead of iron(II) chloride.

*Hexaureo-iron(III) Chloride,* $\{[Fe(CON_2H_4)_6]Cl_3 \cdot 3H_2O\}$.[3]—Concentrated iron(III) chloride and urea solutions were mixed. The mixture was then evaporated in a vacuum desiccator containing sulfuric acid until the precipitate was produced.

*Potassium Iron(III) Diglycolate,* $\{K[Fe(CH_2O \cdot COO)_2] \cdot H_2O\}$.[4]—To 2 ml. of a 1 M iron(III) chloride solution was added 40 ml. of a 2 M potassium glycolate solution. The addition of alcohol to the mixture yielded a pale green precipitate.

*Iron(III) Oxalate,* $Fe_2(C_2O_4)_3$. — Iron(III) nitrate and oxalic acid were dissolved in 65% nitric acid to saturation. The yellow solution thus obtained was then let stand over sulfuric acid in a vacuum desiccator until the precipitate was formed.

*Bis(quinaldinato) Iron(II),* $\{Fe(C_{10}H_6O_2N)_2\}$. — Iron(II) chloride (5 g.) was added to 50 ml. of an aqueous solution made up with 10 g. of quinaldic acid. A red precipitate was formed almost immediately. After the mixture had stood for several hours, the color of the precipitate changed from red to purple. This purple precipitate (cis form) was used for the Mössbauer measurement.

## Results and Discussion

The isomer shifts and the quadrupole splittings obtained for a variety of organic iron compounds are summarized in Table I.

The magnitudes of the isomer shift can, in principle, be related to the details of the bonding between iron and the ligands; i.e., the isomer shifts decrease regularly with the increasing covalency. In this connection, we indicated in the previous paper[1] that even atoms well separated from the iron affect the isomer shift.

The general tendency to be noticed from Table I is that the compound of more complicated chemical structures show the larger values of the isomer shift and of the quadrupole splitting within the series of chemically-related compounds.

Comparing the results for the isomer shifts and the quadrupole splittings for a series of iron-carboxylic acid compounds, it can be interpreted that the simpler compounds have a more covalent tendency in their bonds between the iron atom and carboxylic acid groups.

It was noted that[5] there was negligible quadrupole splitting in the case of the ionic ferric compound because of its $3d^5$ electron configuration. However, in almost all the organic iron chelates investigated, splitting did occur. This probably was caused by the field gradient from the neighboring atoms rather than by the iron atom itself. Presumably, the magnitude of the quadrupole splitting can be a measure of the crystallographic asymmetry.

2) T. Tsumaki, *J. Chem. Soc. Japan (Nippon Kwagaku Kwaishi)*, **55**, 1245 (1934).

3) G. A. Barbieri, *Chem. Zent.*, **84**, 1035 (1913).

4) Ad. Paira, *Ber.*, **47**, 1773 (1914).

5) S. DeBenedetti, G. Lang and R. Ingalls, *Phys. Rev. Letters*, **6**, 60 (1961).

TABLE I. ISOMER SHIFT, $\delta$ AND QUADRUPOLE SPLITTING, $\varepsilon$, OF VARIOUS ORGANIC IRON COMPOUNDS

| Compound | | $\delta$, mm./sec. | $\varepsilon=\frac{1}{4}e^2qQ$ mm./sec. |
|---|---|---|---|
| $Fe(HCO_2)_3\cdot H_2O$ | Iron(III) formate | +0.32 | 0.17 |
| $[Fe_3(CH_3COO)_6(OH)_2]CH_3COO$ | Iron(III) acetate A (Basic) | +0.46<br>+0.44 | 0<br>0.33 |
| $[Fe_3(CH_3COO)_6](CH_3COO)_3$ | Iron(III) acetate B | +0.46<br>+0.44 | 0<br>0.36 |
| $[Fe_2Cr(CH_3COO)_6(OH)_2]CH_3COO$ | | +0.47<br>+0.43 | 0<br>0.33 |
| $[FeCr_2(CH_3COO)_6(OH)_2]CH_3COO$ | | +0.44 | 0.27 |
| $K[Fe(CH_2OCO_2)_2]\cdot H_2O$ | Potassium-iron(III) diglycolate | +0.52 | 0.15 |
| $Fe_2(C_2O_4)_3\cdot 5H_2O$ | Iron(III) oxalate | +0.36 | 0 |
| $(NH_4)_3[Fe(C_2O_4)_3]\cdot 3H_2O$ | Ammonium tris(oxalato) ferrate(III) | Absorption not observed | |
| $K_3[Fe(C_2O_4)_3]$ | Potassium tris(oxalato) ferrate(III) | Absorption not observed | |
| $Fe_2(C_3H_4O_4)_3$ | Iron(III) succinate | +0.39 | 0.20 |
| $Fe_2(C_4H_4O_6)_3$ | Iron(III) tartrate | +0.44 | 0.25 |
| $Fe_2(C_4H_4O_5)_3$ | Iron(III) malate | +0.45 | 0.25 |
| $FeC_6H_5O_7\cdot 5H_2O$ | Iron(III) citrate | +0.56 | 0.16 |
| $(NH_4)_3Fe(C_6H_5O_7)_2$ | Iron(III) ammonium citrate | +0.49 | 0.55 |
| $[Fe_3(C_6H_5COO)_6(OH)_2]OH$ | Iron(III) benzoate | +0.36<br>+0.53 | 0<br>0.33 |
| $[Fe_3(C_6H_5OHCOO)_6(OH)_2\cdot C_6H_5OHCOO\cdot 3H_2O$ | Iron(III) salicylate | +0.49<br>+0.51 | 0.16<br>0.55 |
| $Fe(C_2O_4)\cdot 2H_2O$ | Iron(II) oxalate | +1.32 | 1.03 |
| $Fe(C_3H_5O_3)_2\cdot 3H_2O$ | Iron(II) lactate | +1.20 | 1.39 |
| $Fe(C_3H_6O_4)$ | Iron(II) gluconate | +1.08 | 1.30 |
| $Fe(C_4H_4O_6)\cdot H_2O$ | Iron(II) tartrate | +1.47 | 1.31 |
| $Fe(C_{10}H_6O_2N)_2$ | Bis(quinaldinato) iron(II) | +1.09 | 1.24 |
| Na·Fe(III)-EDTA | Monosodium iron(III) ethylenediamine tetraacetate | −0.16<br>+0.60 | 0<br>0 |
| Fe(III)-NTA | Iron(III) nitrilotriacetate | +0.41 | 0 |
| $[C_{16}H_{14}O_2N_2Fe]_2O$ | Bis(salicylaldehyde) ethylenediimine iron(III) oxide | +0.46 | 0.40 |
| $[C_{16}H_{14}O_2N_2Fe]Cl$ | Bis(salicylaldehyde) ethylenediimine iron(III) chloride | +0.54 | 0.71 |
| $(C_{21}H_{15}O_3N_2Fe)(C_6H_5O_2)$ | Tris(salicylaldehydediimine iron(III) + nitrobenzene | +0.61 | 0.18 |
| $[(Phen)_3Fe^{II}]Cl\cdot 7H_2O$ | 1,10-Phenanthroline iron(II) chloride | +0.29 | 0 |
| $[(Phen)_2Fe(OH)_2Fe(Phen)_2]Cl_4$ | 1,10-Phenanthroline iron(III) chloride | +0.64 | 0.41 |
| Fe(III)-$(AA)_3$ | Iron(III) acetylacetonate | Absorption not observed | |
| Fe(III)-$(TAA)_3$ | Iron(III) trifluoroacetylacetonate | Absorption not observed | |
| Fe(III)-$(TTA)_3$ | Iron(III) thenoyltrifluoroacetonate | Absorption not observed | |
| $[Fe(CON_2H_4)_6]Cl_3\cdot 3H_2O$ | Hexaureo-iron(III) chloride | Absorption not observed | |
| $(C_{12}H_{10}O_4Fe)_2O$ | Phenylnitrosohydroxylamine-iron(III) oxide | Absorption not observed | |
| $(C_6H_5O_2N_2)_3Fe$ | Phenylnitrosohydroxylamine-iron(III) | Absorption not observed | |

Considering all of the above concepts, we are now in a position to discuss some characteristics in each particular spectrum.

**Iron(III) Oxalate.**—The iron atoms in $Fe_2(C_2O_4)_3\cdot 5H_2O$, $K_3[Fe(C_2O_4)_3]$ and $(NH_4)_3[Fe(C_2O_4)_3]$ have been considered to be located in similar chemical environments. Nevertheless, the latter two compounds showed no absorption, while the former displayed a single absorption peak at room temperature. Unfortunately, it is hardly possible at present to make a detailed discussion. However, one

possible interpretation is that there may be different types of iron atoms in these compounds; i.e., the one shows absorption, but the other does not for some unidentified reason. Suppose we write the molecular formula as $Fe^*[Fe(C_2O_4)_3]\cdot 5H_2O$ instead of $Fe_2(C_2O_4)_3\cdot 5H_2O$, the asterisked iron atom differing in its binding mode from the other iron atom. This situation may be favorably compared with that of iron(III) chromate discussed in the previous paper.[1] Experiments to elucidate this assumption need to be conducted at a lower temperature. The chemical ascertainment of the structure of iron oxalate is also needed.

**Iron(III) Acetates and Iron(III) Benzoate.**—The spectra of these compounds have triple absorption peaks. They may be resolved either into two single lines or into one doublet and one single line. We tried out both analyses and felt that the latter is more reasonable. Thus, the spectrum was interpreted as the superposition of a quadrupole split and a single line. This may naturally be explained by the presence of different types of iron atoms in these compounds as a result of their polynuclear structure. For example, the spectrum and a generally-adopted structural formula of iron(III) acetate A are given in Figs. 1a and 1b:

The components of the composite spectra are shown by the broken line. The first analysis, shown in Fig. 1a, does not support the structure described above, because the split peak should be assigned to the central iron atom in view of its intensity. This fact is inconsistent with the general rule that a central atom is in a more symmetrical environment than are outside atoms. This difficulty was overcome by using the other analysis, shown in Fig. 1b, where two outer lines correspond to

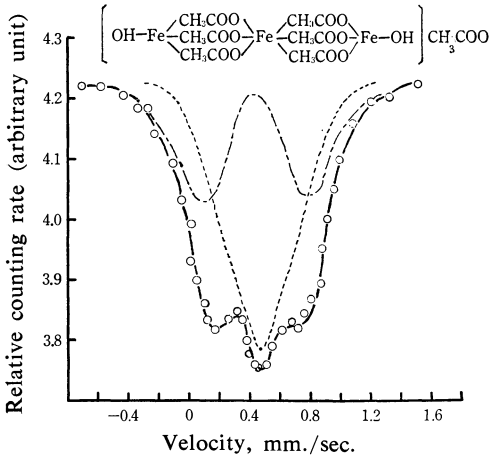



Fig. 1a. Mössbauer spectrum of iron(III) acetate A.

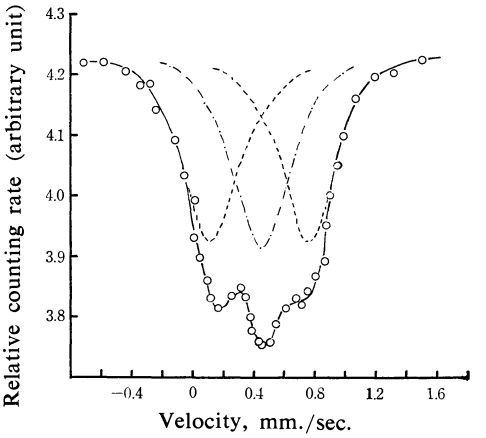



Fig. 1b. Mössbauer spectrum of iron(III) acetate A.

the quadrupole splitting due to two "outside" iron atoms and the central single line assigned to a central iron atom.

The spectra for iron(III) acetate A and B were almost identical. The minor difference observed must have arisen from the slightly different molecular structures of these acetates.

A particularly instructive case was the comparison of the spectra obtained for iron(III)+chromium(III) acetates with that obtained previously for iron(III) acetate A. The middle single peak was slightly decreased in intensity in the case of the mixed acetate (Fe : Cr = 2 : 1), and it disappeared almost completely in the case of the other mixed acetate (Fe : Cr = 1 : 2), while the outer double peaks remained essentially unchanged in shape. This fact could be interpreted qualitatively as meaning that chromium atoms can occupy any iron sites in the molecule, while the resultant distribution of chromium is not uniform but one-sided.

**Iron(III) Salicylates.**—The Mössbauer spectrum of this compound showed four resonance

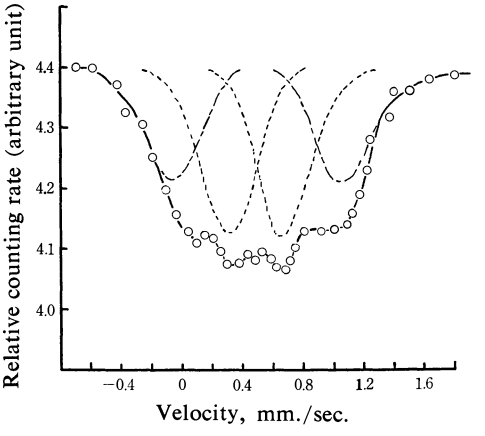



Fig. 2. Mössbauer spectrum of iron(III) salicylate.

absorption maxima (Fig. 2). The spectrum was analyzed by assuming that the quadrupole pair were of equal intensity. Thus, it was concluded that this spectrum is resolved into two doublets (dotted curves), the middle one showing an isomer shift of 0.49 mm./sec., while that for the outer one is 0.51 mm./sec. The measured values of the quadrupole splitting of the middle and outer doublets are 0.17 and 0.55 mm./sec. respectively. By assuming a trinuclear structure for the compounds, both the outside and central iron atoms can be considered to be situated at a point where the electric field gradient is nonzero.

**Na·Fe(III)-EDTA, Fe(III)-NTA.**—The spectra of these compounds showed main single peaks at +0.60 and +0.41 mm./sec. respectively. This fact indicates that the bondings are primarily ionic and that the iron atoms are in an octahedral symmetry. This conclusion is not in agreement with that of a previous infrared spectroscopic study,[6] in which the bonding between iron and EDTA has been reported to be covalent. It seems possible that this disagreement may be ascribed to an ambiguous definition of terms, ionic and covalent.

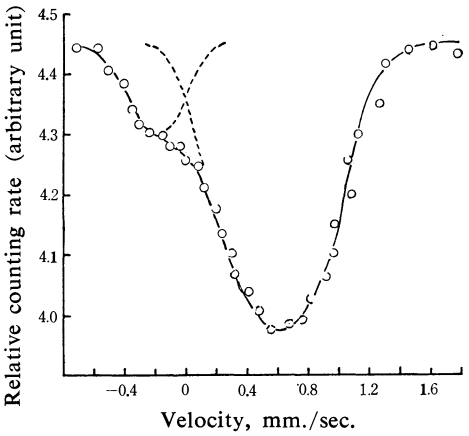



Fig. 3. Mössbauer spectrum of Na·Fe(III)-EDTA.

One peculiar anomaly of the spectrum was observed in the case of the Fe(III)-EDTA sample. As is shown in Fig. 3, the spectrum exhibited considerably more line broadening than other typical spectra. In addition, a shoulder appeared at −0.16 mm./sec. This shoulder can not be readily explained, but it could possibly be attributed to some impurity which has a strong covalent character. The investigation of this possibility must be the subject of future research.

6) D. T. Sawyer and J. M. McKinnie, *J. Am. Chem. Soc.*, **82**, 4191 (1960).

**Bis(salicylaldehyde)ethylenediimine Iron(III) Chloride and Oxide.** — As may be seen from Fig. 4, these two compounds are closely related

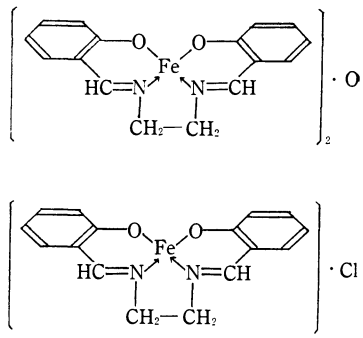



Fig. 4. Structural formulas of bis(salicylaldehyde)ethylenediimine iron(III) chloride and the oxide.

in chemical structure. Accordingly, no large differences in the isomer shift and quadrupole splitting were expected between them. Nevertheless, the experimental observations showed relatively large differences in their magnitude. This fact must be attributed to the molecular architecture of these compounds. In this connection we should note that, in a book by Martell and Calvin[7] on the chemistry of the metal chelate compound, they mentioned that the cobalt chelate of salicylaldehyde ethylenediimine crystallizes in layers, with holes running through the layers. The results of our Mössbauer study of the iron chelates also support the view of such a planar structure of the compounds. The oxygen or chlorine atoms may be interposed between two closely adjacent pairs of the unit cell, so that they behave as an atom covalently bonded to two adjacent iron atoms. The electronic charge distribution around the iron atoms which determine the isomer shift and quadrupole splitting can be considerably affected by the oxygen or chlorine in the molecule because of their high electronegativity.

**1, 10-Phenanthroline Iron(II) Chloride.**—This compound, which is regarded as a very stable covalent compound, showed a small isomer shift, suggesting greater covalency, whereas the relatively unstable iron(III) compound of 1, 10-phenanthroline shows a large isomer shift, suggesting a small covalent contribution. Since the bonding arrangement of the former compound resembles that of the ferrocyanide complex, the spectrum showed a single peak.

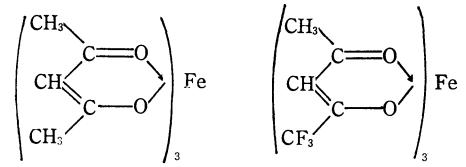
7) A. E. Martell and M. Calvin, "Chemistry of the Metal Chelate Compounds," Prentice-Hall, Inc. Englewood Cliffs, N. J. (1956), pp. 270, 342.

On the contrary, the latter displayed a double-peaked spectrum which may have arisen from the binuclear structure of the molecule.

**Divalent Iron Organic Compounds.**—Table I includes the values of the isomer shift and quadrupole splitting for several divalent iron compounds. The magnitude of these values were, of course, far larger than those of trivalent iron compounds. However, the present data may not be very accurate because of instrumental limitations; i.e., our instrument is not designed for a wide-range Doppler velocity, but is, rather, most useful in the neighborhood of zero velocity covering the $\pm 1.0$ mm./sec. range. For this reason, these data will not be further discussed here.

**Compounds Whose Resonance Absorption was not Observed at Room Temperature.** — In our observation, there are several iron-bearing organic compounds that did not show any resonance absorption. The chemical structures of the compounds studied are shown in Fig. 5.

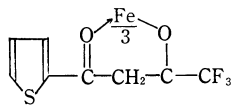
All these compounds are characteristic in their binding nature; i.e., in all cases an iron atom is coordinated with oxygen atoms. There is no a priori reason why the resonance absorption does not occur in these compounds.



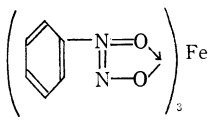
(I)



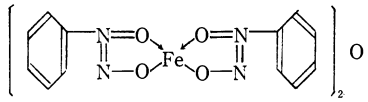
(II)



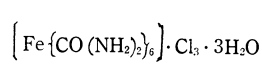
(III)



(IV)



(V)



(VI)

Fig. 5. Structural formulas of some organic iron(III) chelates.

(I) Iron(III) acetylacetonate
(II) Iron(III) trifluoroacetylacetonate
(III) Iron(III) thenoyltrifluoroacetonate
(IV) Phenylnitrosohydroxylamine-iron(III)
(V) Phenylnitrosohydroxylamine-iron(III) oxide
(VI) Hexaureo-iron(III) chloride

In any event, however, the absence of the Mössbauer effect should be attributed to either the low Debye temperature or the high recoil probability of the compound. Nevertheless, although such data for these organic compounds are not available at present, our speculation would prefer the interpretation that the disappearence of the absorption is caused by the latter.

It should be noted that the Mössbauer effect was not observed in the case of a dry cation exchanger (Dowex 50) saturated with iron(III) ions (thickness $=\sim 10$ mg. Fe/cm$^2$). The further measurement of these compounds at a low temperature would be an interesting subject for future research.

## Summary

Continuing our previous studies of the Mössbauer spectra of inorganic iron compounds,[1] we have found some characteristic features of the spectra of some organic iron compounds. There is a general tendency, in a series of related compounds, for the isomer shift and the quadrupole splitting to increase regularly with increase in the structural complexity of the compounds.

The data for iron(III) acetate, benzoate and salicylate suggest the polynuclear structure of these compounds. The observed isomer shifts for other organic iron compounds may also be interpreted in terms of the chemical binding in the molecule.

No resonance absorption was observed for a few groups of organic iron chelates (1, 3 diketone derivatives, etc.). Though our interpretation is still conjectual, the reason for this is believed to rest in the high recoil probability of these compounds.

This work was done at The Institute for Solid State Physics, The University of Tokyo. The authors wish to express their gratitude to Professor Tamotsu Yoshino for his gifts of two samples used in this work. The authors are also indebted to Drs. Kazuo Ono, Atsuko Ito, Masatake Honda, Shigeru Ohashi, Hideo Yamatera, Masako Shima, Hirotoshi Sano and Kunihiko Mizumachi for their helpful discussions.

*Department of Chemistry*
*Faculty of Science*
*Kyushu University*
*Hakozaki, Fukuoka (Yo. T.)*

*The Institute for Solid State Physics*
*The University of Tokyo*
*Azabu, Tokyo (Ya. T.)*

# The Far-infrared Spectra of Some Phenols

By Kunio FUKUSHIMA

(Received March 5, 1965)

Many greatly-successful infrared investigations of substances with the X-H···Y hydrogen bond have been made using the X-H stretching absorption band. However, it seems that these have not given any information on the minute differences in the conformation of the X-H···Y group.

The infrared absorption band due to a vibration of the X-H···Y group, which is expected to give more information about the conformation of the X-H···Y group, appears in the far-infrared spectral region. Green et al. have found a band in the far-infrared spectra of phenol in the crystalline state; they have tentatively assigned it to the stretching vibration of the O-H···O group.[1] Stanevich has measured the far-infrared spectra of crystalline phenol, *m*- and *p*-nitrophenols, hydroquinone, resorcinol, *o*-nitrophenol, and 2,6-dinitrophenol. He has found that only in the case of phenol does a frequency shift when it is dissolved into a non-polar solvent.[2]

In the present investigation, the far-infrared spectra of *o*- and *p*-hydroxybenzaldehydes and *o*- and *p*-methoxyphenols will be measured and compared with those of carbon tetrachloride solutions.

## Experimental

**Material Employed.**—*o*- and *p*-Hydroxybenzaldehydes and *o*- and *p*-methoxyphenols were of the reagent grade. Phenol was recrystallized from its carbon tetrachloride solution.

**Infrared Spectra.**—The infrared spectra were recorded with a Perkin-Elmer model 201C far-infrared spectrometer in the region from 80 to 350 $cm^{-1}$, and with a Perkin-Elmer model 221 spectrophotometer equipped with a LiF prism in the region from 2800 to 3800 $cm^{-1}$.

The spectra of crystals were measured in Nujol mull sandwiched between two polyethylene plate 1 mm. thick while those of solutions were measured using liquid cells with polyethylene windows 3 mm. thick. The concentrations of the solutions and the cell thicknesses are listed in Table I. The sample solution of phenol in carbon tetrachloride was prepared by the dilution of its saturated solution with carbon tetrachloride in a volume ratio of 1 to 12.5. The spectra obtained are shown in Figs. 1—8.

TABLE I. CONCENTRATION OF SOLUTIONS AND CELL THICKNESS

| Substance | Concn. | Cell thickness | |
|---|---|---|---|
| $C_6H_5(OH)$ | | 2 | |
| *o*-$(CHO)C_6H_4(OH)$ | 0.38 | 2 | (Fig. 5) |
| | 0.15 | 5 | (Fig. 6) |
| *o*-$(CH_3O)C_6H_4(OH)$ | 0.46 | 2 | (Fig. 8(A)) |
| | 0.18 | 5 | (Fig. 8(B)) |

* Concentration in mol./l.; Cell thickness in mm.

## Results and Discussion

As Figs. 1—3 show, it is clear from the frequency values of O-H stretching bands in the 3$\mu$ region (phenol, 3279 $cm^{-1}$; *p*-hydroxybenzaldehyde, 3175 $cm^{-1}$) that strong hydrogen bonds are formed in phenol and *p*-hydroxybenzaldehyde in the crystalline state. Both these compounds have a band in the region from 170 to 180 $cm^{-1}$ (phenol, 172 $cm^{-1}$; *p*-hydroxybenzaldehyde, 180 $cm^{-1}$). The band at 170 $cm^{-1}$ of phenol has been assigned to the stretching vibration of the O-H···O group by Stanevich, on the basis of its frequency change observed through the change in the state from crystal to solution.[1] This frequency

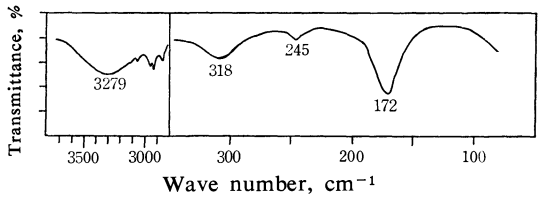



Fig. 1. Far-infrared spectra of phenol in crystalline state.

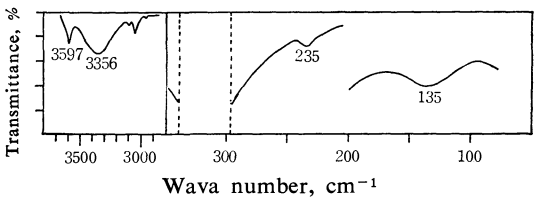



Fig. 2. Far-infrared spectra of phenol in carbon tetrachloride solution.

1) J. H. S. Green, W. Kynaston and H. A. Gebbie, *Nature*, **195**, 595 (1962).
2) A. E. Stanevich, *Optics and Spectroscopy*, **16**, 539 (1964).

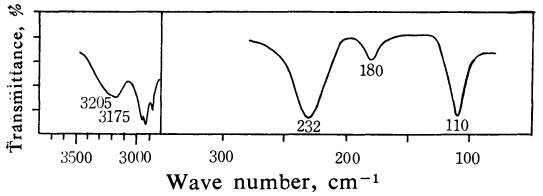



Fig. 3. Far-infrared spectra of *p*-hydroxybenzaldehyde in crystalline state.

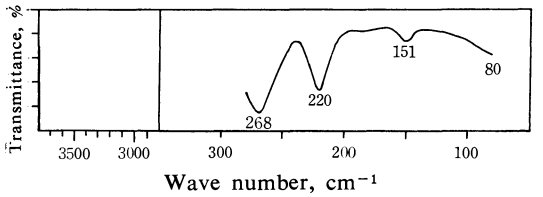



Fig. 4. Far-infrared spectra of *o*-hydroxybenzaldehyde in liquid state.

change was confirmed by the present investigation, as Figs. 1 and 2 show. Among the three bands in the spectra of *p*-hydroxybenzaldehyde (Fig. 3, 80—300 $cm^{-1}$ region), two bands, at 110 $cm^{-1}$ and 232 $cm^{-1}$, can be assigned to the vibrations of the CHO-C group by a comparison of the spectra with those of benzaldehyde,* no other bands are expected to appear in the region from 100 to 300 $cm^{-1}$ except for the stretching vibration of the O-H···O group. Therefore, the band at 180 $cm^{-1}$ of *p*-hydroxybenzaldehyde is considered to correspond to the stretching vibration of the intermolecular hydrogen bond.

The band at 179 $cm^{-1}$ in the far-infrared spectra of *p*-methoxyphenol in the crystalline state may correspond to the stretching vibration of the intermolecular hydrogen bond.

It may be suggested, from the fact that the frequency values of the stretching vibration of the intermolecular hydrogen bond are nearly the same in phenol, in *p*-hydroxybenzaldehyde and in *p*-methoxyphenol, that the types of the intermolecular hydrogen bond of *p*-hydroxybenzaldehyde and *p*-methoxyphenol are similar to that of the phenol crystal.[3]

In the case of *o*-hydroxybenzaldehyde in the liquid state, which is considered to have an intramolecular hydrogen bond on the basis of the frequency value of the O-H stretching band in its 3$\mu$ region and the geometry of its molecule, no band was observed in the region from 100 to 200 $cm^{-1}$, except for a band at 151 $cm^{-1}$. This band can be assigned to a vibration of the CHO-C group by a comparison of the spectra with those of benzaldehyde. When *o*-hydroxybenzaldehyde is diluted with carbon tetrachloride, no change takes place in the spectra, as Figs. 5 and 6 show. Therefore, the bands at 268, 220, 151 and about 80 $cm^{-1}$ in Fig. 4 may reasonably be interpreted as being due to the vibrations of non-associated molecules. As the three bands, 268, 220 and 151 $cm^{-1}$, can be assigned to the vibrations of the CHO-C group, we might assign the band at about 80 $cm^{-1}$ to the stretching vibration of an intramolecular hydrogen bond. In the spectra of a solution of *o*-methoxyphenol in carbon tetrachloride, the O-H stretching bands were observed at 3565 and 3470 $cm^{-1}$. The former is due to the O-H stretching vibration of free molecules, while the latter is due to

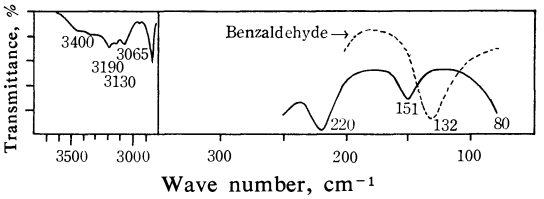



Fig. 5. Far-infrared spectra of *o*-hydroxybenzaldehyde in carbon tetrachloride solution.

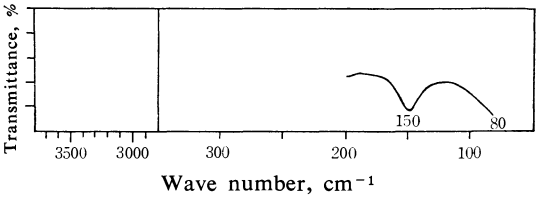



Fig. 6. Far-infrared spectra of *o*-hydroxybenzaldehyde in carbon tetrachloride solution.

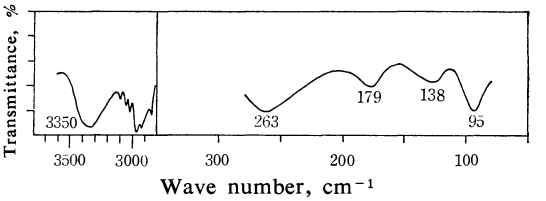



Fig. 7. Far-infrared spectra of *p*-methoxyphenol in crystalline state.

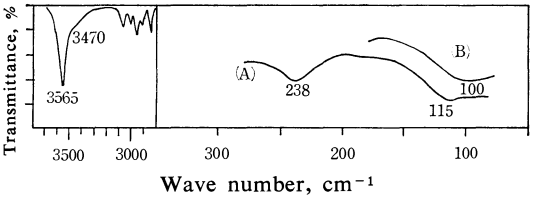



Fig. 8. Far-infrared spectra of *o*-methoxyphenol in carbon tetrachloride solution.

* Benzaldehyde has three bands, 130, 224 and 235 $cm^{-1}$, in the region from 80 to 250 $cm^{-1}$, these are assigned to the vibrations of the CHO-C group[1].

3) C. Scheringer, O. J. Wehrhahn und M. v. Stackelberg, *Z. Elektrochem.*, **64**, 381 (1960).

that of the hydrogen-bonded O-H group. As the intensity of the latter band is very weak, it is expected that the amount of molecules forming a hydrogen bond is not great. Corresponding to this fact, no band that is considered to be due to the stretching vibration of the O-H···O group was observed in the far infrared region, as is shown in Fig. 8.

On the basis of the experimental results in the present investigation, it may be suggested that the frequency value of the stretching vibration of the O-H···O group in the far-infrared region is very sensitive to the structural difference of the O-H···O group and can be useful in the study of molecular structure.

*Institute for Protein Research*
*Osaka University*
*Kita-ku, Osaka*

# The Rapid Solvent Extraction and Simultaneous Spectrophotometric Determination of Palladium with TTA - Methyl Propyl Ketone

By Asha V. RANGNEKAR and S. M. KHOPKAR

(Received March 8, 1965)

The chelating agent 2-thenoyltrifluoroacetone (TTA) has been extensively utilised for the extraction, separation and spectrophotometric determination of numerous metals.[1] From a slightly acidic solution palladium(II) gives an orange yellow chelate with TTA which is extractable into methyl propyl ketone (MPK), giving a brilliant orange yellow solution. It appears that MPK exerts a synergestic effect on the extraction of palladium with TTA.

Dimethylglyoxime[2] is commonly used for the solvent extraction separation of palladium in chloroform. 2-Nitroso-1-naphthol in toluene[3] was used for the extraction and colorimetric determination at 370 m$\mu$. In a highly alkaline medium it was extracted with diethyldithiocarbamate.[4] Its complex with dibenzyldithiooxamide[5] was extracted and measured at 450 m$\mu$ in order to determine palladium in the presence of platinum. The iodide complex[6] was extracted with tri-*n*-butyl phosphate, whereas the pyridine thiocyanate complex[7] aminoquinoline complexes[8] or chloroiodopyridine complexes[9] were extracted in chloroform and were determined colorimetrically.

In this paper, systematic investigations of the liquid-liquid extraction behaviour of the palladium(II) TTA chelate at different pH's and spectrophotometric studies of it will be described. It will also offer a simple and rapid procedure for the rapid solvent extraction and simultaneous spectrophotometric determination of palladium(II) at the microgram level. (A preliminary note on this work has been published.[10])

## Experimental

**Apparatus.**—Absorbance measurements were carried out with a quartz CØ4 spectrophotometer, using matched 10-mm. quartz cells, while pH measurements were made with a Cambridge pH meter (Marshal model). Reagents grade chemicals were used. TTA (B. D. H.) solutions in MPK (about 0.15 M) were used. A stock solution of palladium chloride was prepared by dissolving about 0.6334 g. of palladous chloride in one litre of distilled water containing 1 per cent hydrochloric acid. The diluted solution was then prepared by ten-fold dilution and was standardized gravimetrically with dimethyl glyoxime (II). The diluted solution contained 6.334 $\gamma$ of palladium per millilitre.

**General procedure.**—An aliquot of the palladous chloride solution (3 ml.), containing 6.334 $\gamma$ of palladium(II) per millilitre, was adjusted to the desired pH with 0.01 N hydrochloric acid and 0.01 N sodium hydroxide, using a pH meter. For the study of diverse ions, a solution containing the ion under investigation was added prior to the pH

1) S. M. Khopkar and A. K. De, *J. Sci and Ind. Res.*, 21A, 131 (1962).
2) R. S. Young, *Analyst*, 76, 46 (1951).
3) K. L. Cheng, *Anal. Chem.*, 26, 1894 (1954).
4) H. Bode, *Z. Anal. Chem.*, 144, 165 (1955).
5) J. T. Pyle and W. D. Jacobs, *Talanta*, 9, 761 (1962).
6) C. H. Faye and W. R. Inman, *Anal. Chem.*, 35, 985 (1963).
7) J. H. W. Forsythe, R. J. Magee and C. L. Wilson, *Talanta*, 3, 324—329 (1960).
8) V. K. Gustin and T. R. Sweet, *Anal. Chem.*, 35, 44 (1963).
9) R. A. Egli, *Z. Anal. Chem.*, 194, 401 (1963).
10) A. V. Rangnekar and S. M. Khopkar, *Sci. and Culture*, to be published.

control. The aqueous solution, unless otherwise mentioned, was adjusted to pH ~4.0. Final volume was maintained with water at 25 ml. in each case. It was introduced into a separatory funnel (250 ml.) and shaken for 10 min. with 10 ml. of 0.15 M TTA-MPK. The lower aqueous layer was transferred to a beaker, and the upper MPK layer, to a 10 ml. volumetric flask. The MPK extract was made up exactly to 10 ml. with MPK, and the absorbance was read at 430 mμ against a reagent blank. The amount of palladium extracted was directly obtained from the calibration curve. The aqueous layers at the end of extraction were saved for the pH measurement.

## Results and Discussion

**Absorption Curve.**—The absorption spectrum of a solution of the palladium(II) - TTA complex ($Pd=1.78\times10^{-5}$ M), extracted at pH 4.0, is illustrated in Fig. 1, the reagent blank being used as the reference solution. The spectrum of the reagent blank against MPK was also taken. The orange-yellow palladium(II) chelate solution shows a maximum absorbtion at 415 mμ. Then the curve steadily falls untill the absorbance becomes negligible beyond 500 mμ. The reagent blank itself has a strong absorption up to 400 mμ; this becomes insignificant, compared to the chelate solution, from 420 mμ onward. All the absorbance measurements were performed at 430 mμ. The absorptivity at 430 mμ is $4.2\times10^5\pm51.4$ (calculated on the basis of the palladium content).

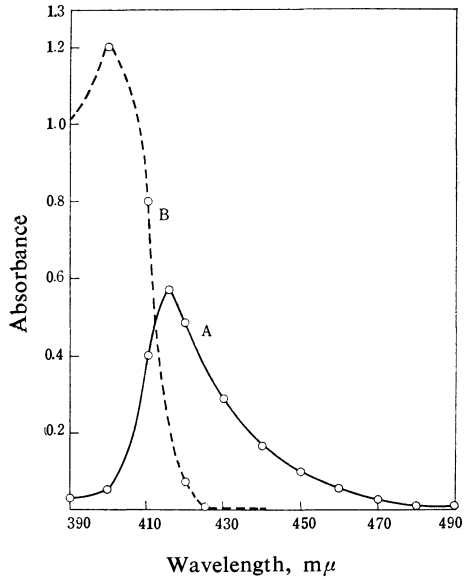



Fig. 1. Absorption spectrum.
A Palladium(II)-TTA chelate in MPK against reagent blank.
Pd(II) $1.78\times10^{-5}$ M at pH 4.0
B Reagent blank against MPK.
TTA $15\times10^{-2}$ M at pH 4.0

**The Effect of the pH Value.**—The pH range from 0.8 to 6.2 was studied in order to investigate the liquid-liquid extraction behaviour of the palladium(II)-TTA system. At higher pH values the precipitation of palladium hydroxide causes trouble. The distribution ratios, $D$, were calculated from the extraction curve in a manner described earlier[12] (Fig. 2 and Table I). The extraction starts after pH 1.6 and becomes 100% at pH 4.0. In the pH range from 3.4 to 4.9 extraction occurs to the extent of 80% or more. The extraction curve drops sharply beyond pH 5.0 and terminates at pH 6.0, corresponding to

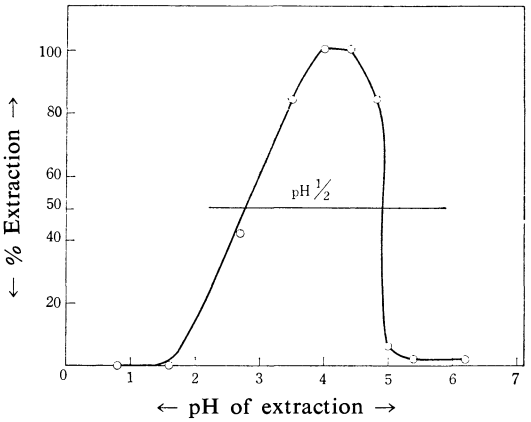



Fig. 2. Extraction of Pd-TTA chelate with MPK as the function pH.

Table I. Distribution ratios of palladium(II)-thenoyl trifluoroacetone between MPK and aqueous solution as a function of pH

| pH | % Palladium extraction in MPK | $D$ |
|---|---|---|
| 0.8 | 0.0 | 0.0 |
| 1.6 | 0.0 | 0.0 |
| 2.1 | 18.4 | 0.56 |
| 2.7 | 42.1 | 1.8 |
| 3.0 | 65.7 | 4.7 |
| 3.5 | 84.2 | 13.3 |
| 3.6 | 84.2 | 13.3 |
| 4.0 | 100.0 | 2500 |
| 4.4 | 100.0 | 2500 |
| 4.6 | 18.4 | 0.56 |
| 4.8 | 84.2 | 13.3 |
| 5.0 | 7.8 | 0.21 |
| 5.4 | 2.6 | 0.06 |
| 5.8 | 5.2 | 0.13 |
| 6.2 | 2.6 | 0.06 |

11) A. I. Vogel, "The Text Book of Quantitative Inorganic Analysis," ELBS Series (1960), p. 511.

12) S. M. Khopkar and A. K. De, *Anal. Chem.*, 32, 478 (1960).

zero extraction. The pH for the 50% extraction is 2.8 and 4.9.

Beyond pH 6.2, hydroxide precipitation commences and inhibits the extraction procedure.

**Calibration Curve.**—Different amounts of palladium(II) were taken and extracted as above at pH 4.0, and the corresponding absorbances were measured against the reagent blank at various wavelengths (420, 430 and 440 mμ) in order to observe the adherence of the coloured system to Beer's law. In each case the solution of palladium(II) was exhaustively extracted for 10 min.; the aqueous phase was always clear and colourless. Table II indicates that the palladium(II)-TTA system closely obeys Beer's law at 430 mμ over the concentration range from 0.60 to 6 γ of palladium per millilitre.

TABLE II. ADHERENCE TO BEER'S LAW

| Palladium(II) taken, γ | Absorbance | | |
|---|---|---|---|
| | 420 mμ | 430 mμ | 440 mμ |
| 3.16 | 0.065 | 0.040 | 0.025 |
| 6.33 | 0.140 | 0.095 | 0.055 |
| 9.49 | 0.210 | 0.140 | 0.080 |
| 12.66 | 0.265 | 0.195 | 0.105 |
| 15.82 | 0.340 | 0.240 | 0.140 |
| 18.99 | 0.410 | 0.300 | 0.170 |
| 22.15 | 0.470 | 0.350 | 0.190 |
| 25.32 | 0.540 | 0.400 | 0.220 |
| 28.48 | 0.610 | 0.460 | 0.255 |

**The Stability of the Colour.**—The absorbance of the MPK solution of the palladium(II)-TTA complex, prepared according to the general procedure at pH 4.0, was measured at elapsed times of 30 min., 1, 24, 48, 72, 96, 144 and 190 hr. The corresponding absorbances were 0.300, 0.300, 0.300, 0.300, 0.300, 0.310, 0.320 and 0.320 respectively. It is evident that the colour is stable up to 72 hr., at the end of 94 hr. the absorbance increases by about 3%, and after 144 hr. by about 8%. Hence, it is suggested that the colour be measured within 72 hr.

TABLE III. EFFECT OF REAGENT CONCENTRATION

19 γ of palladium(II) after extraction by TTA-MPK at pH 4.0 gives an absorbance of 0.300 ±0.005 in 10 ml. of MPK.

| TTA Concn., M | TTA added, ml. | Absorbance at 430 mμ |
|---|---|---|
| 0.50 | 10 | 0.310 |
| 0.25 | 10 | 0.300 |
| 0.15 | 10 | 0.300 |
| 0.10 | 10 | 0.210 |
| 0.075 | 10 | 0.210 |
| 0.050 | 10 | 0.200 |
| 0.025 | 10 | 0.195 |
| 0.015 | 10 | 0.120 |
| 0.15 | 1 | 0.150 |
| 0.15 | 2 | 0.170 |
| 0.15 | 4 | 0.210 |
| 0.15 | 6 | 0.220 |
| 0.15 | 8 | 0.280 |

**Reagent Concentration.**—With other factors constant, the concentration of TTA was varied from 0.015 M to 0.5 M. The results in Table III prove that the optimum reagent concentration is 0.15 M. The absorbance is constant, even at such a higher reagent concentration as 0.50 M. With a dilute solution of the reagent, e.g., 0.025 or 0.015 M, the extraction is incomplete.

TABLE IV. DIVERSE IONS

Palladium(II) = 19 γ pH = 4.0

| Foreign ion | Added as | Ion concen. mg./ml. | Absorbance at 430 mμ 0.300±0.010 |
|---|---|---|---|
| None | — | — | |
| $Pb^{2+}$ | $Pb(NO_3)_2$ | 5.0 | 0.310 |
| $Hg^{2+}$ | $Hg(NO_3)_2 \cdot H_2O$ | 1.5 | 0.320 |
| $Tl^{+}$ | $Tl_2SO_4$ | 2.0 | 0.295 |
| $Cu^{2+}$ | $CuSO_4 \cdot 5H_2O$ | 2.0 | 1.650 |
| $Cd^{2+}$ | $Cd(NO_3)_2$ | 5.0 | 0.295 |
| $Sb^{3+}$ | $Sb_2(SO_4)_3$ | 5.0 | 0.310 |
| $Bi^{3+}$ | $Bi_2(CO_3)_3$ | 1.0 | 0.290 |
| $Sn^{4+}$ | $SnCl_2$ | 2.0 | 0.040 |
| $Pt^{4+}$ | $H_2PtCl_6 \cdot 6H_2O$ | 2.5 | 0.310 |
| $Fe^{3+}$ | $Fe(NO_3)_3 \cdot 6H_2O$ | 2.0 | 1.350 |
| $Al^{3+}$ | $Al(NO_3)_3 \cdot 9H_2O$ | 10.0 | 0.295 |
| $Zn^{2+}$ | $ZnSO_4 \cdot 7H_2O$ | 5.0 | 0.305 |
| $Mn^{2+}$ | $MnSO_4 \cdot 7H_2O$ | 2.0 | 0.400 |
| $Co^{2+}$ | $Co(NO_3)_2 \cdot 6H_2O$ | 2.0 | 0.400 |
| $Ni^{2+}$ | $NiSO_4 \cdot 7H_2O$ | 2.0 | 0.290 |
| $U^{6+}$ | $UO_2(NO_3)_2 \cdot 6H_2O$ | 2.5 | 1.000 |
| $Th^{4+}$ | $Th(NO_3)_4 \cdot 4H_2O$ | 1.0 | 0.285 |
| $Zr^{4+}$ | $Zr(NO_3)_4$ | 2.0 | 0.295 |
| $Ce^{4+}$ | $Ce_2(SO_4)_3$ | 2.5 | 0.800 |
| $Ca^{2+}$ | $Ca(NO_3)_2 \cdot 4H_2O$ | 2.5 | 0.340 |
| $Sr^{2+}$ | $SrCl_2 \cdot 6H_2O$ | 2.5 | 0.275 |
| $Ba^{2+}$ | $Ba(NO_3)_2$ | 2.5 | 0.275 |
| $Mg^{2+}$ | $MgCl_2 \cdot 6H_2O$ | 3.0 | 0.295 |
| $Li^{+}$ | LiCl | 1.0 | 0.320 |
| Ascorbate$^{2-}$ | Ascorbic acid | 2.0 | 0.04 |
| Oxalate$^{2-}$ | Oxalic acid | 2.0 | 0.04 |
| $Cit^{3-}$ | Citric acid | 2.0 | 0.015 |
| $Tart^{3-}$ | Tartaric acid | 2.0 | 0.110 |
| $PO_4^{3-}$ | $H_3PO_4$ | 2.0 | 0.295 |
| $CH_3COO^{-}$ | $CH_3COOH$ | 2.0 | 0.305 |
| $WO_4^{2-}$ | $Na_2WO_4$ | 1.0 | 0.285 |
| $CN^{-}$ | KCN | 2.0 | 0.04 |
| $SO_4^{2-}$ | $Na_2SO_4$ | 2.0 | 0.310 |
| $CrO_4^{2-}$ | $K_2CrO_4$ | 2.5 | 0.290 |
| $VO_4^{3-}$ | $Na_3VO_4$ | 0.50 | 0.285 |
| $AsO_3^{3-}$ | $Na_3AsO_3$ | 2.0 | 0.275 |

**Diverse Ions.**—The following ions (~2.0—10 mg.) were carried through the procedure, the pH being maintained at about 4.0:
$Pb^{2+}$, $Hg^{2+}$, $Tl^{+}$, $Cu^{2+}$, $Cd^{2+}$, $Sb^{3+}$, $Bi^{3+}$, $Sn^{4+}$, $Pt^{4+}$, $Fe^{3+}$, $Al^{3+}$, $Zn^{2+}$, $Mn^{2+}$, $Co^{2+}$, $Ni^{2+}$, $U^{6+}$, $Th^{4+}$, $Zr^{4+}$, $Ce^{4+}$, $Ca^{2+}$, $Sr^{2+}$, $Ba^{2+}$, $Mg^{2+}$ $Li^{+}$, $SO_4^{2-}$, $PO_4^{3-}$, $WO_4^{2-}$, $CN^{-}$, $CH_3COO^{-}$, $C_2O_4^{2-}$, $CrO_4^{2-}$, $VO_4^{3-}$, $AsO_3^{3-}$, citrate$^{3-}$, tartrate$^{3-}$, ascorbate$^{2-}$.

The results in Table IV show that about 5—10 mg. of lead(II), thallium(I), cadmium(II), antimony(III), bismuth(III), platinum(IV), aluminum(III), zinc(II), nickel(II), zirconium-(IV), chromate, phosphate, acetate and sulphate do not interfere, whereas copper(II), iron(III), uranium(VI), and cerium(IV) give colour reactions. Palladium can tolerate less than 5 mg. each of mercury(II), thorium(IV), calcium(II), strontium(II), barium(II), magnesium(II), lithium, vanadate, tungstate and arsenite. The ions showing strong interferences are tin(IV), manganese(II), cobalt(II), ascorbate, oxalate, citrate, tartarate and cyanide.

Because palladium(II) is extracted from weakly acidic solutions, metals that yield chelates with TTA under these conditions may be expected to interfere if present in large amounts.

The interferences due to ascorbate, oxalate, citrate, tartarate and cyanide can be easily eliminated by passing them on an anion exchange resin like Dowex 21 K (chloride form). These anions are retained in the resin bed, while palladium(II) passes through. Palladium-(II) may then be extracted as usual with 0.15 M TTA in MPK at pH 4.0.

## Recommended Procedure

Take an aqueous solution containing 19 $\gamma$ of palladium(II) and adjust the pH ~4.0 with a pH meter by using 0.01 N hydrochloric acid and 0.01 N sodium hydroxide. Introduce the solution into a 250 ml. separatory funnel. Shake for 10 min. with 10 ml. of a 0.15 M TTA-MPK solution. Allow the layers to settle; transfer the aqueous layer into a beaker and the MPK layer into a 10 ml. volumetric flask, and measure the absorbance as 430 m$\mu$ against the reagent blank. In nine runs with 19 $\gamma$ of palladium(II), the absorbance found was 0.296 ±0.005. The standard deviation was ±1.2%. Different amounts of palladium(II) were taken and determined by the recommended procedure. The results (Table V) are accurate to within ±1.5%.

TABLE V. ACCURACY OF METHOD

| Palladium(II) taken, $\gamma$ | Absorbance at 430 m$\mu$ | Palladium(II) found, $\gamma$ | % Error |
|---|---|---|---|
| 9.5 | 0.145 | 9.25 | +2.7 |
| 12.66 | 0.195 | 12.66 | 0.0 |
| 19.00 | 0.300 | 19.00 | 0.0 |
| 25.33 | 0.380 | 24.0 | +5.2 |
| 28.50 | 0.450 | 28.5 | 0.0 |
| | | | Av. ±1.5% |

Thus the proposed method is fairly precise, being accurate to within ±1.5%. The total operation for each run requires only 20—25 minutes. As little as 1 $\gamma$ of palladium(II) can be detected.

## Summary

A spectrophotometric method has been developed for the determination of palladium-(II) at microgram levels; the method is based on the colour reaction with 2-thenoyltrifluoro-acetone (TTA) in methyl propyl ketone (MPK). The bright orange-yellow-coloured palladium(II) - TTA chelate solution follows Beer's law at 430 m$\mu$ over the 0.6—6.0 $\gamma$ range of palladium(II) per millilitre. At pH values from 3.4 to 4.9, about 80% or more of palladium(II) is removed from an aqueous solution of TTA-MPK in a single extraction. The coloured system is stable for 72 hr. It can tolerate lead(II), thallium(I), cadmium(II), antimony(III), bismuth(III), platinum(IV), aluminium(III), zinc(II), nickel(II), zirconium-(IV), phosphate, chromate, acetate and sulphate, whereas tin(IV), manganese(II), cobalt(II), ascorbate, oxalate, citrate, tartarate and cyanide seriously interfere. Mercury(II), thorium(IV), calcium(II), strontium(II), barium(II), magnesium(II), vanadate and tungstate are moderately tolerated. The method is accurate and reproducible to within ±1.5%, and it offers a simple procedure for the simultaneous extraction and spectrophotometric determination of palladium(II).

*Department of Chemistry*
*Indian Institute of Technology*
*Bombay, India*

# Studies of the Aqueous Solution of a Surface Active Substance by Means of an Ultrasonic Interferometer. I. Determinations of the Critical Concentration and Compressibility of Micelles of Several Alkyl Sulfates

By Koji SHIGEHARA*

(Received March 9, 1965)

The dissolved state and the properties, especially the micelle formation and the solubilization, of surface active substances in an aqueous solution have been studied by various methods of measurements, such as light scattering, X-ray diffraction, diffusion, electrolytic conductance, osmometry and dialysis.[1] The hydration of the surface active substance in a solution has been studied by many authors, it also is important for the study of the properties of an aqueous solution of a surface active substance. Among such studies, Stigter, Williams and Mysels[2] have estimated the hydration of micelles to be monomolecular, a theory which is in accordance with the light scattering and micelle diffusion data. However, little is known about the hydration of the solute in the state of a single molecule, which is rather important in relation to the amphipathic nature of the substance in question and also in relation to the builder action of the inorganic salt usually added to enhance the surface activity. In this connection, ultrasonic interferometry offers another useful method, since the compressibility of a solution of a surface active substance, as calculated from the sound velocity, is closely related to the hydration of the solute in a solution, which is often difficult to measure by other methods. Thus, a number of studies have been reported on the hydration of inorganic and organic substances using an ultrasonic interferometer.[3,4] However, similar studies have not yet been reported of solutions of surface active substances. This is mainly due to the fact that the accuracy of the sound velocity of $\pm 0.5$ m./sec. attainable by an ordinary ultrasonic interferometer is still insufficient for a study which requires the measurement of such a small difference in sound velocity as that between pure water and dilute solution of the most surface active substance near CMC. The present investigation, therefore, used a differential ultrasonic interferometer with an accuracy of $\pm 3$ cm./sec. which had already been devised by Sasaki and Yasunaga.[5]

The present paper will describe the results of measurements of the sound velocity and compressibility of aqueous solutions of homologues of alkyl sulfates and sodium hydrogen sulfate. Further, the CMC's will be determined and the compressibility of micelles calculated from sound velocity data.

## Experimental

**Materials.**—The alkyl sulfates used were sodium *n*-tetradecyl (STS), *n*-dodecyl (SDS), *n*-octyl (SOS) and methyl (SMS) sulfates. They were prepared from their corresponding alcohols and then purified, except for SMS, which was prepared from a commercial product by drying it over silica gel. Sodium hydrogen sulfate (SHS) was also used for the sake of comparison. Its aqueous solution was prepared by dissolving an equimolar amount of pure sulfuric acid and recrystallized sodium sulfate in water.

**Apparatus and Procedure.**—The apparatus used for the measurement of the sound velocity was the usual ultrasonic interferometer, somewhat modified so as to determine the change in the sound wavelength in the solution resulting from the change in the concentration of the solute by measuring the change in the length of a series of several hundred stationary sound waves. The main part of the cell (Fig. 1) consisted of a glass tube 34 cm. long and 1.8 cm. in diameter, to one end of which a quartz ultrasonic generator plate 2.5 cm. in diameter and with a frequency of $f=1.432$ Mc./sec. was attached, while to the opposite end there was connected a vertical glass tube so that a vertical glass reflector

* Present address: Ocean Research Institute, University of Tokyo, Nakano-ku, Tokyo.

1) M. E. McBain and E. Hutchinson, "Solubilization and Related Phenomena," Academic Press, New York (1955); A. M. Schwartz and J. W. Perry, "Surface Active Agents," Vol. I, Interscience Publishers, New York (1949), pp. 289—315; T. Yamamoto, S. Okazaki and T. Sasaki, *Kolloid-Z.*, **178**, 97 (1961).

2) D. Stigter, R. J. Williams and K. J. Mysels, *J. Phys. Chem.*, **59**, 330 (1955).

3) A. Passynski, *Acta Physicochimica USSR*, **8**, 385 (1938); T. Yasunaga and T. Sasaki, *J. Chem. Soc. Japan, Pure Chem. Sec. (Nippon Kagaku Zassi)*, **72**, 87, 89 and 336 (1951); K. Tamura and T. Sasaki, This Bulletin, **36**, 975 (1963).

4) Y. Miyahara, This Bulletin, **26**, 390 (1953); H. Shiio, T. Ogawa and H. Yoshihashi, *J. Am. Chem. Soc.*, **77**, 4890 (1955); etc.

5) T. Sasaki and T. Yasunaga, *Chem. & Chem. Ind. (Kagaku to Kogyo)*, **7**, 138 (1954).

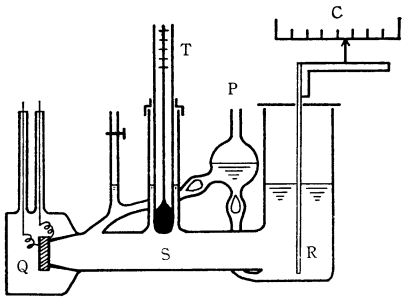



Fig. 1. Differential ultrasonic interferometer.
S Cell with solution
Q Quartz ultrasonic generator
R Reflector plate
C Comparator
P Circulation pump
T Thermometer

plate could move in the solution contained in the cell by means of a comparator with a $\pm 0.002$ mm. accuracy. The sample liquid in the cell was circulated during the measurement by means of an all-glass circulation pump. The cell was immersed in a thermostat of $30.00 \pm 0.003$°C.

The principle of measurement is based on the fact that if we fix the reflector plate of the interferometer to the $n$'th node (counting from the quartz ultrasonic generator plate) of the stationary wave produced in the sample solution, as in the case of ordinary ultrasonic interferometry, and trace the change in the position ($\Delta L$) of the same node due to the increase in the wavelength ($\Delta\lambda$) produced by the change in the concentration ($C$) of the solution, we can calculate $\Delta\lambda$ and the change in the sound velocity ($\Delta U$) by:

$$\Delta\lambda = \Delta L/n \qquad (1)$$

and

$$\Delta U = f \times \Delta\lambda \qquad (2)$$

The actual position we follow shifts from the node by a constant amount equal to the phase difference of the sound wave at the reflector plate, but this dose not alter the above relation, since it is considered to be constant and does not affect $\Delta L$.

To carry out the experiment, it is necessary to increase the concentration gradually, starting from pure water, and following carefully the shift of the specified node of the stationary sound wave produced in it. For this purpose, 250 cc. of distilled and degassed water was first introduced in the cell, and then the reflector plate was fixed to an appropriate node corresponding to the minimum of the interference current. Then a certain volume (10—50 cc.) of water in the cell was replaced by an equal volume of the sample solution of a known concentration, and the concentration of the solution in the cell was slightly changed. The reflector plate was then shifted in order to follow the resulting change in the position of the node to which the plate was initially fixed. The distance ($\Delta L$) traveled by the plate was recorded. $\Delta\lambda$ was then calculated by means of Eq. 1. Here the $n$ value was calculated from the distance between the quartz oscillator and the reflector divided by the exactly-measured wavelength of the stationary sound wave.* The value of $n$ was a definite integer near 300. From the value of $\Delta\lambda$, we calculated change in the sound velocity by means of Eq. 2. From the measurements of a series of such successive increments $\Delta U$ corresponding to the successive values of concentration $C$, we obtain the relation:

$$\Delta U = F(C) \quad \text{or} \quad U_c = U_w + \Delta U = U_w + F(C)$$

where $U_w$ and $U_c$ denote the sound velocity in pure water and in the solution with the concentration $C$ respectively, and $F(C)$, the measured concentration function of the sound velocity. The value of $U_w = 1509.44$ m./sec. was used in the present experiment.[6] The error introduced in the measurement of $\Delta U$ was $\pm 3$ cm./sec. for $n = 300$.

The density of the solution at 30°C was calculated from the measurement of its change from the value of pure water, which was taken as a standard,[7] by using an ordinary float balance[8] in a thermostat controlled to $\pm 0.001$°C (measurement being possible down to $\pm 10^{-6}$ g./cc.), except for the measurement of concentrated solutions of SOS and SHS where a pycnometer was used at 30 $\pm 0.01$°C.

The compressibility ($\beta$) of the solution was further calculated from the sound velocity and the density ($\rho$) by the Laplace equation:

$$\beta = 1/U^2\rho$$

and was also expressed as a function of the solute concentration.

## Results and Discussion

Figures 2 and 3 show the sound velocity vs. concentration diagrams, and Figs. 4 and 5, the compressibility vs. concentration diagrams for aqueous solutions of SHS, SMS, SOS, SDS and STS. It can be seen in these figures that the diagrams for SMS and SHS solutions consist of a single straight line, while in the cases of

Table I. Values of CMC

| Substance | CMC value ($10^{-3}$ mol./l. unit) Ultrasonic method | Conductivity method[a] | Surface tension[b] |
|---|---|---|---|
| SOS | 130 | 130 | 130* |
| SDS | 8.0 | 8.1 | 6.9—8.0 |
| STS | 2.2 | — | 2.0—2.2 |

* Measured by the present author using the drop weight method.

a F. D. Haffner, F. A. Piccione and C. Rosenblum, *J. Phys. Chem.*, **46**, 662 (1942).

b J. Powney and C. C. Addison, *Trans. Faraday Soc.*, **33**, 1243 (1937); A. Lottermoser and F. Stoll, *Kolloid-Z.*, **63**, 49 (1933).

* Calculated by the measurement of the total length of 10 successive waves produced in the solution.

6) M. Greenspan and C. E. Tschiegg, *J. Research Natl. Bur. Standards*, **59**, 249 (1957).

7) "International Critical Tables," Vol. III, McGraw-Hill Book Co., New York (1928), p. 25.

8) T. W. Richards and J. W. Shipley, *J. Am. Chem. Soc.*, **34**, 599 (1912); T. W. Richards and G. W. Harris, ibid., **38**, 1000 (1916).

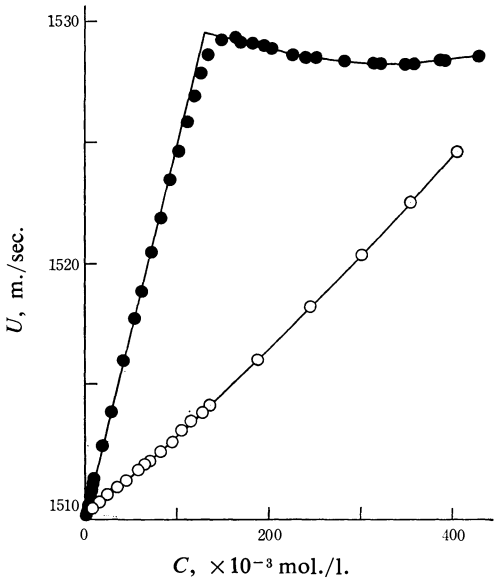



Fig. 2. Sound velocity vs. concentration.
○ SHS ● SOS

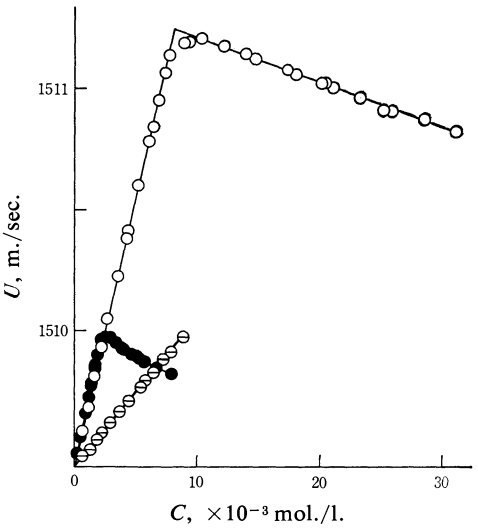



Fig. 3. Sound velocity vs. concentration
⊖ SMS ○ SDS ● STS

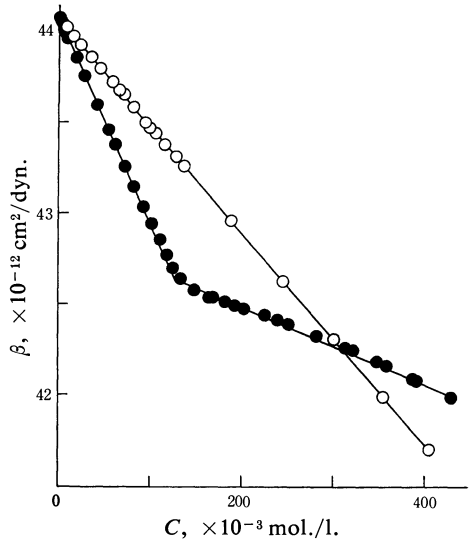



Fig. 4. Compressibility vs. concentration.
○ SHS ● SOS

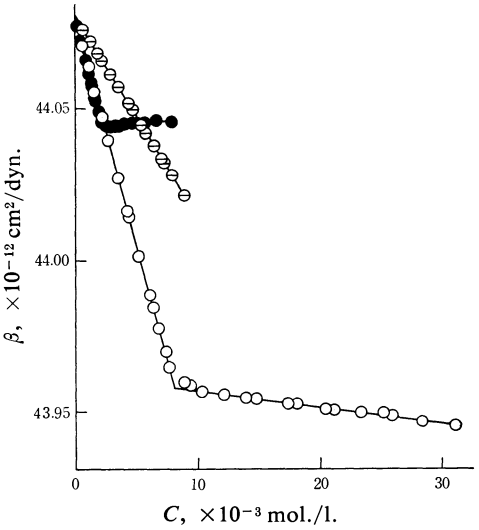



Fig. 5. Compressibility vs. concentration.
⊖ SMS ○ SDS ● STS

STS, SDS and SOS solutions each of the diagrams, especially that for compressibility, consists of two linear portions with a break point between them. This break point coincided with the CMC of the respective solute, as is shown in Table I. This proves the differential ultrasonic interferometry to be a useful method for the measurement of the CMC.

Figure 6 further shows that the inclination of the $\beta$ vs. concentration diagram ($d\beta/dC$) above and below CMC is in a linear relation with the number of carbon atoms ($N$) in the solute molecule, and that when extrapolated the two straight lines to $N=0$ coincide with each other and with the $d\beta/dC$ value for sodium hydrogen sulfate of a moderate concentration of about 0.1 mol./l., where it is considered to behave as a uni-univalent electrolyte composed of $HSO_4^-$ and $Na^+$.[9] These relations are expressed by the following equations:

$$d\beta/dC = -5.94\times10^{-12} + 0.445\times10^{-12}\times N \quad (3)$$

for solutions above CMC, and:

$$d\beta/dC = -5.94\times10^{-12} - 0.776\times10^{-12}\times N \quad (4)$$

9) I. M. Klotz and C. F. Eckert, *J. Am. Chem. Soc.*, **64**, 1878 (1942); P. L. Khare, *Trans. Faraday Soc.*, **58**, 359 (1962).

for solutions below CMC, where $d\beta/dC$ is expressed as $(cm^2/dyn.)/(mol./1.)$. This suggests that the dissolved state of the $SO_4Na$ radical of alkyl sulfates in an aqueous solution is the same as that of $HSO_4Na$, whether they are in the state single ions or micelles, and that the contribution to $d\beta/dC$ of each $CH_2$-chain in the solute molecule is constant, which is different in signs according to their dissolved states. Since the value of $-5.94\times10^{-12}$ in Eq. 4 expresses the compressibility decrease due to the introduction of one mole of $Na^+$ and $HSO_4^-$ in water, the portion of the ordinate of the lower line below the dotted horizontal line in Fig. 6 expresses the additional decrease

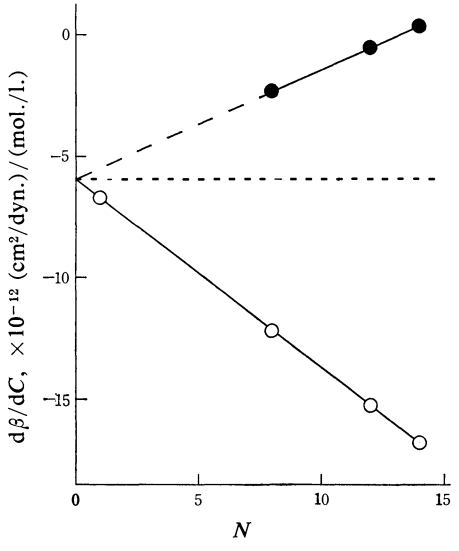



Fig. 6. $d\beta/dC$ vs. $N$.
○ $d\beta/dC$ below CMC
● $d\beta/dC$ above CMC
Dotted line: $d\beta/dC$ for SHS

in compressibility due to the dissolution of one mole of alkyl chains of the respective carbon numbers in a molecule in the state of molecular dispersion in water, and the portion of the ordinate between the dotted horizontal line and the upper straight line expresses a similar increase in compressibility due to the introduction of one mole of alkyl chains in a micellar state in water. Both of these values may, therefore, be considered to be proportional to the carbon number in the solute molecule, and Eqs. 3 and 4 may be expected to intersect at the zero point of the carbon number in the solute molecule.

Similar results are obtained for the partial molar volume ($\bar{V}$) of alkyl sulfate by the measurement of the density for the solution. Figure 7 shows the results. Here the diagram of $\bar{V}$ vs. the carbon number ($N$) in the solute molecule consists of two straight lines, above

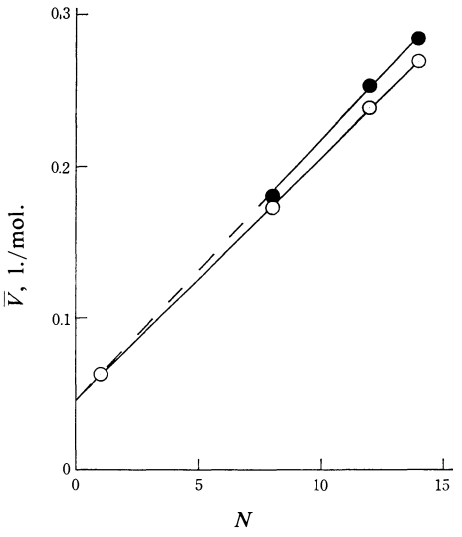



Fig. 7. $\bar{V}$ vs. $N$.
○ $\bar{V}$ below CMC
● $\bar{V}$ above CMC

and below CMC, which coincide with each other at $N=0$. These ralations are expressed by the following equations:

$$\bar{V}=0.0171\,N+0.046 \tag{5}$$

for solutions above CMC, and:

$$\bar{V}=0.0159\,N+0.046 \tag{6}$$

for solutions below CMC, where $\bar{V}$ is expressed in l./mol.

To derive theoretically the equations corresponding to those of Eqs. 3 and 4, the solution of the volume ($V$) and compressibility ($\beta$) as a whole is assumed to consist of several volume elements ($V_1$, $V_2$, $\cdots$) of different compressibilities ($\beta_1$, $\beta_2$, $\cdots$). Therefore, we have:

$$V=V_1+V_2+\cdots \tag{7}$$

$$V\beta=V_1\beta_1+V_2\beta_2\cdots \tag{8}$$

From these equations and with an additional assumption, usually accepted,[3] that such an ionic radical as $HSO_4^-$ or $-SO_4^-$ of alkyl sulfate, together with its water of hydration, is incompressible and is independent of the micellization of the solute, as may reasonably be understood from Fig. 6, the following equations are derived for solutions above CMC:

$$d\beta/dC=V_mN\ (\beta_m-\beta_1)-V_s\beta_1 \tag{9}$$

$$\bar{V}=V_mN+V_s-n_xV_1 \tag{10}$$

where $\bar{V}$ denotes the partial molar volume of alkyl sulfate; $V_1$ and $V_m$, the molar volume of free water and of $CH_2$ in micelle respectively; $\beta_1$ and $\beta_m$, the compressibility of free water and the hydrocarbon part of the micelle

TABLE II

| Substance: Hydrocarbon or alkyl sulfate | State of aggregation | Compressibility ($10^{-12}$ cm²/dyne) of hydrocarbon: Solid or liquid | Compressibility ($10^{-12}$ cm²/dyne) of hydrocarbon: Micelle | Molar vol. (cc./mol.) of $CH_2$ in: Solid or liquid[17] | Molar vol. (cc./mol.) of $CH_2$ in: Micelle | Amount of hydration of $SO_4Na$ (mol./mol.) | Molar vol. (cc./mol.) of hydrated $SO_4Na$ |
|---|---|---|---|---|---|---|---|
| *n*-$C_8$ | Liquid | 109.0[a] | | 20.57 | | | |
| *n*-$C_{10}$ | Liquid | 93.50[b] | | 19.66 | | | |
| *n*-$C_{12}$ | Liquid | 84.68[b] | 70.1 | 19.11 | 17.1 | 4.9 | 135 |
| *n*-$C_{14}$ | Liquid | — | | 18.70 | | | |
| *n*-$C_{16}$ | Liquid | 74.5[c] | | 18.45 | | | |
| Paraffin | Solid | — | | 15.5 | | 5.7 | |
| | | 26* | | | | for aq. | |
| Polyethylene | Solid | 25.2** | | 15.2 | | $NaHSO_4$ | |

* Calculated by the present author.
** Value at 20°C, Ref. 18.
a B. B. Freyer, J. C. Hubbard and D. H. Andrews, *J. Am. Chem. Soc.*, **51**, 759 (1929).
b A. Weissler and V. A. Del Grosso, *J. Am. Chem. Soc.*, **72**, 4209 (1950).
c F. Danusso and E. Fadigati, *Rendiconti Accad. Naz. Lincei, Cl. Sci. Fis. Mat. e Natur.*, **14**, 81 (1953).
d "International Critical Tables," Vol. II, p. 314 (1927) and Vol. III, pp. 27 (1928), McGraw-Hill Book Co., New York, etc.
e P. Heydemann, *Acustica*, **9**, 446 (1959).

respectively; $n_x$, the mole number of hydration water per mole of $SO_4Na$, and $V_s$, the molar volume of the $SO_4Na$ radical, together with the volume of $n_x$ moles of hydration water.

By comparing Eq. 9 with Eq. 3, and Eq. 10 with Eq. 5, the $V_s$, $V_m$, $n_x$ and $\beta_m$ values are calculated to be as shown in Table II.

It may be seen in this table that the compressibility of the micelle and the mole volume of the $CH_2$ radical in the micellar state are constant, independent of the number of the carbon atoms of the alkyl sulfate molecule, and that they are nearer to the value for liquid rather than solid hydrocarbon. These facts are additional evidence for the view that the hydrocarbon interior of the ionic micelle is liquid-like rather than solid-like.[10] The amount of hydration, $n_x=4.9$, for the $SO_4Na$ radical is comparable with the corresponding value of 5.7 for $NaHSO_4$ near a 0.1 molar solution, where the solution as a whole is considered to contain $HSO_4^-$ and $Na^+$ ions,[9] although we can cite other data which is somewhat different.[11]

## Summary

The sound velocity and the density of aqueous solutions of sodium hydrogen (SHS), methyl (SMS), octyl (SOS), dodecyl (SDS) and tetradecyl (STS) sulfates have been measured by using, respectively, a differential ultrasonic interferometer and a float balance, and the compressibility ($\beta$) has then been calculated from these results. Each of these three quantities, when plotted against the concentration ($C$), has shown a nearly straight line for SHS and SMS, while it consists of two nearly straight lines, with a break point between them at CMC, in the cases of SOS, SDS and STS. The values of $d\beta/dC$ below and above CMC, when plotted against the number of carbon atoms in the alkyl chain of the solute molecule, again showed two straight lines which intersected with each other at the zero number of carbon atoms. This value of $d\beta/dC$ is equal to that of SHS at a moderate concentration. These results have been explained by taking account of the dissolved state of these solutes. The compressibility of the micelle ($\beta_m$), the molar volume of the $CH_2$ radical in the micellar state ($V_m$), and the ionic hydration number of solute have been calculated; the values of $\beta_m$ and $V_m$ show evidence for the view that the hydrocarbon interior of the ionic micelle is liquid-like rather than solid-like.

The author wishes to express his deep gratitude to Professor Tsunetaka Sasaki of our University for his kind direction and valuable criticism. The cost of this research has been defrayed by a grant of the Ministry of Education given to Professor Sasaki.

10) G. S. Hartley, "Aqueous Solutions of Paraffin Chain Salts," Hermann et Cie, Paris (1936); K. Shinoda and T. Soda, *J. Phys. Chem.*, **67**, 2072 (1963); etc.
11) T. F. Young and L. A. Blatz, *Chem. Revs.*, **44**, 93 (1949).

*Department of Chemistry*
*Faculty of Science*
*Tokyo Metropolitan University*
*Setagaya-ku, Tokyo*

# The Calculation of the Adsorptive Separation Factors of Hydrogen Isomers

By Shozo FURUYAMA and Nozomu EBARA

(Received March 11, 1965)

Static and gas chromatographic studies of hydrogen mass isomers and spin isomers have been carried out by many authors.[1-8] Recently the gas chromatographic separation of radioactive isomers has been carried out at the temperature of liquid nitrogen in separate experiments by Carter and Smith,[9] King,[10] and West and Marston[11]; an apparent separation factor between each pair among the nine isomers has thus been determined. On the other hand, a quantum mechanical explanation of the separation between para- and ortho-hydrogen has been given by several other investigators, and a qualitative agreement with experiments has been obtained.[12-16]

There are still, however, several problems left to be resolved. (i) Why is the elution of tritium hydride, which is composed of two atoms of different weights (a hetero-isomer) faster than that of deuterium, which is composed of two like atoms (a homo-isomer), although they have the same mass? (ii) Ortho-hydrogen and hydrogen deuteride can hardly be separated at all by gas chromatography, except for a single experiment of one of the present authors using an interconverting double-column method. Why does the mass effect play an insignificant role in this case? (iii) Para- and ortho-tritium have not yet been separated. Is it not possible to separate them experimentally?

This paper will deal with a quantum mechanical treatment of the separation factors of hydrogen isomers at the temperature of liquid nitrogen using Evett's model,[12a] with particular emphasis on the explanation of the trend for hetero-isomers to be adsorbed strongly on an adsorbent surface than homo-isomers.

## Theory

It is assumed that each atom of a molecule to be adsorbed on an adsorbent surface is subjected to a potential of the Lennard-Jones type along an axis perpendicular to the adsorbent surface. The potential is expanded in powers of the distance in the vicinity of the equilibrium position, and the higher terms are disregarded.

$$V=-U+\frac{1}{2}K(Z_a-Z_0)^2-U+\frac{1}{2}K(Z_b-Z_0)^2 \qquad (1)$$

Here $Z_a$ and $Z_b$ are, respectively, the distances from the adsorbent surface to the atoms a and b; $Z_0$ is the equilibrium distance and $K$ and $U$ are constants. $Z_a$ and $Z_b$ can be replaced by $Z+m_b d\cos\theta/(m_a+m_b)$ and $Z-m_a d\cos\theta/(m_a+m_b)$ respectively, where $Z$ is the distance from the center of the gravity of the molecule to the adsorbent surface; $m_a$ and $m_b$ are the atomic weights and $\theta$ is the angle between the molecular axis and the axis normal to the adsorbent surface. We then have:

$$\begin{aligned}V=&-2U+K(Z-Z_0)^2\\&+|m_a-m_b|\,Kd(Z-Z_0)\cos\theta/(m_a+m_b)\\&+(m_a^2+m_b^2)Kd^2\cos^2\theta/2(m_a+m_b)^2\end{aligned} \qquad (2)$$

where $d$ is the distance between the centers of the atoms in the molecule. The second term leads to vibrational wave functions for a harmonic oscilator:

$$G_n(\xi)=(2MK/\pi^2\hbar^2)^{1/8}(2^n n!)^{-1/2}H_n(\xi)e^{-\xi^2/2}$$
$$\xi=(2MK/\hbar^2)^{1/4}(Z-Z_0)$$

1) Y. L. Sandler, *J. Phys. Chem.*, **58**, 58 (1954); *J. Chem. Phys.*, **29**, 97 (1958).
2) C. M. Cunningham and H. L. Johnston, *J. Am. Chem. Soc.*, **80**, 2377 (1958); Cunningham, Chapin and Johnston, ibid., **80**, 2382 (1958).
3) S. Ohkoshi, Y. Fujita and T. Kwan, This Bulletin, **31**, 770 (1958); S. Ohkoshi, S. Tenma, Y. Fujita and T. Kwan, ibid., **31**, 772, 773 (1958); T. Kwan, *J. Res. Ins. Catalysis, Japan*, **8**, 18 (1960); I. Fujita and T. Kwan, *Japan Analyst*, **12**, 15 (1963).
4) W. R. Moore and H. R. Ward, *J. Am. Chem. Soc.*, **80**, 2909 (1958); *J. Phys. Chem.*, **64**, 832 (1960).
5) C. O. Thomas and H. A. Smith, ibid., **63**, 427 (1959).
6) W. A. Van Hook and P. H. Emett, ibid., **64**, 673 (1960).
7) H. A. Smith and P. P. Hunt. ibid., **64**, 384 (1960); P. P. Hunt and H. A. Smith, ibid., **65**, 87 (1961).
8) S. Furuyama and T. Kwan, ibid., **65**. 190 (1961).
9) E. H. Carter, Jr., and H. A. Smith, ibid., **67**, 1512 (1963).
10) J. King, ibid., **67**, 1397 (1963).
11) D. L. West and A. L. Marston, *J. Am. Chem. Soc.*, **86**, 4731 (1964).
12) a) A. A. Evett, *J. Chem. Phys.*, **31**, 565 (1959); b) A. A. Evett, ibid., **33**. 789 (1960).
13) D. White and E. N. Lassettre, ibid., **32**, 72 (1960).
14) E. M. Mortensen and H. Eyring, *J. Phys. Chem.*, **64**, 433 (1960).
15) T. Takaishi, presented at the 13th Annual Meeting of the Chemical Society of Japan, Tokyo, April, 1960.
16) S. Ono and I. Yasumori, presented at the 17th Annual Meeting of the Chemical Society of Japan, Tokyo, April, 1964.

where $M$ is the total mass. The third term has matrix elements only between vibrational states of different quantum numbers and is regarded as a perturbation. The last term leads to hindered rotational wave functions. Following Wilson, the rotational wave functions are expanded in powers of $\cos\theta(=x)$ and the recursive method is used to calculate the coefficients $a_{l,m,2k}$ and $a_{l,m,2k+1}$ in wave functions[17]:

$$F^{e}{}_{l,m}(x) = (2\pi)^{-1/2}(1-x^2)^{m/2}e^{im\varphi}\sum_{k=0} a_{l,m,2k}x^{2k}$$

$$F^{o}{}_{l,m}(x) = (2\pi)^{-1/2}(1-x^2)^{m/2}e^{im\varphi}\sum_{k=0} a_{l,m,2k+1}x^{2k+1}$$

In carrying out the calculation, the term

$$(2I_{ab}/\hbar^2)(Kd^2/2)(m_a^2+m_b^2)/(m_a+m_b)^2=\lambda^2$$

is regarded as a parameter.

If $m_a$ and $m_b$ are equal, the third term of 2 vanishes identically and 2 reduces to Evett's equation.[12a] The unperturbed hindered rotational energies $\mu$ of hetero-isomers, as well as those of homo-isomers, are obtained in units of $\hbar^2/2I_{ab}$, where $I_{ab}$ is the moment of inertia of the molecule. For a partition function of a hydrogen molecule at a low temperature (the temperature of liquid nitrogen), only a few low-lying energy levels are important. For para-hydrogen, ortho-deuterium and para-tritium, the exclusion principle requires that their rotational states should be associated only with even $l$ values. For ortho-hydrogen, para-deuterium and ortho-tritium, on the other hand, states are associated with odd $l$ values. The symmetry consideration violates the exclusion principle for hetero-molecules. Hence, for the calculation of the partition function, the energy levels to be taken into account are $F^{e}{}_{0,0}(x)$ for para-hydrogen, ortho-deuterium and para-tritium; $F^{e}{}_{1,1}(x)$ for ortho-hydrogen, para-deuterium and ortho-tritium, and both states for hetero-isomers. These two energy levels are both even states with respect to $\cos\theta$.

The term $K|m_a-m_b|d\cos\theta(Z-Z_0)/(m_a+m_b)$ is treated as a perturbation. As this term is an odd function with respect to both $(Z-Z_0)$ and $\cos\theta$, the first-order perturbation energy and the second-order contribution from even states vanish identically, and it is enough to consider only the first excited state of the vibration combined with odd states of rotation. The second-order perturbation energy is:

$$E''=\hbar^2/2K(m_a+m_b)\times 4K^2d^2(m_a-m_b)^2/(m_a+m_b)^2\times\langle 0|\xi|1\rangle^2\sum_{l'}\langle l,m|x|l',m\rangle^2/(\Delta E_{vib}+\Delta E_{rot}) \quad (3)$$

17) A. H. Wilson, *Proc. Roy. Soc.*, **118A**, 623 (1928).

TABLE I. SECOND ORDER PERTURBATION ENERGIES OF HYDROGEN DEUTERIDE, TRITIUM HYDRIDE AND TRITIUM DEUTERIDE AT SEVERAL POTENTIAL BARRIERS B

| Species | States $m$ | Perturbation energy $E''$, cal./mol. $B/\Lambda$ 4 | 8 | 12 |
|---|---|---|---|---|
| HD | 0 | 16.87 | 24.45 | 29.23 |
| | 1 | 10.98 | 19.14 | 25.16 |
| HT | 0 | 32.59 | 44.91 | 54.97 |
| | 1 | 22.10 | 37.68 | 50.00 |
| DT | 0 | 5.00 | 6.74 | |
| | 1 | 3.74 | 6.11 | |

It is evaluated for hydrogen deuteride, tritium hydride and tritium deuteride at several potential barriers, $B$, in Table I, where

$$B=\lambda^2\Lambda I_{H_2}(m_a+m_b)^2/2I_{ab}(m_a^2+m_b^2)=Kd^2/4$$

and

$$\Lambda=\hbar^2/2I_{H_2}$$

The energies:

$$E=\mu\Lambda I_{H_2}/I_{ab}+E''$$

are plotted against the potential barrier, $B$, in Figs. 1 and 2.

So far as the separation factor between isomers of the same molecular weight is concerned, only rotational energies need be considered. However, for hydrogen isomers of different molecular weights, A and B, translational and vibrational factors should also be taken into account. The separation factor is defined as:

$$S=([A]/[B])_{gas}/([A]/[B])_{ads} \quad (4)$$

Here the following arrangement is to be understood:

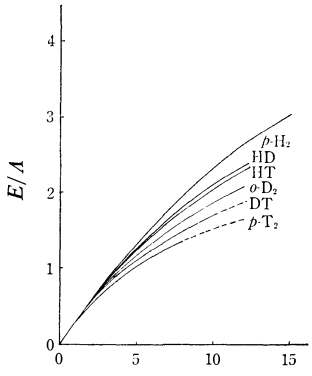



Fig. 1. The rotational energies combined with the second-order perturbation energies against the potential barrier $B$. State: $l=0$, $m=0$

TABLE II. SEPARATION FACTORS

| Species A | Species B | Experimental: Carter and Smith[9] I*1 | Experimental: Carter and Smith[9] II*2 | Experimental: King[10] *2 | Calculated B/A = 4 | Calculated B/A = 8 | Calculated B/A = 12 |
|---|---|---|---|---|---|---|---|
| $p$-$H_2$ | $o$-$H_2$ | 1.37 | | | 1.05 | 1.27 | 1.48 |
| $o$-$D_2$ | $p$-$D_2$ | 1.09*1,4) 1.10*3,3) | | | 1.02 | 1.03 | 1.08 |
| $p$-$T_2$ | $o$-$T_2$ | | | | 0.85 | 0.92 | 0.94 |
| HT | $D_2$ | 1.12 | 1.05 | 1.13 | 1.10 | 1.13 | 1.27 |
| $o$-$H_2$ | HD | (1.00) | | | 1.26 | 1.44 | 1.59 |
| $p$-$H_2$ | HD | (1.37) | | | 1.33 | 1.83 | 2.36 |
| $p$-$H_2$ | HT | 2.01 | | | 1.46 | 2.42 | 3.36 |
| $p$-$H_2$ | $D_2$ | 2.25 | | | 1.64 | 2.69 | 4.10 |
| $p$-$H_2$ | DT | 3.30 | | | 1.73 | 3.37 | 5.90 |
| $p$-$H_2$ | $T_2$ | 3.86 | | | 2.00 | 4.20 | 8.58 |
| $H_2$ | HD | | 1.22 | | 1.31 | 1.71 | 2.12 |
| $H_2$ | HT | | 1.42 | 1.23 | 1.44 | 2.27 | 3.02 |
| $H_2$ | $D_2$ | | 1.49 | 1.38 | 1.61 | 2.52 | 3.68 |
| $H_2$ | DT | | 1.85 | | 1.70 | 3.16 | 5.29 |
| $H_2$ | $T_2$ | | 2.08 | 1.68 | 1.97 | 3.98 | 7.69 |

*1 Active alumina
*2 Ferric oxide on alumina
*3 Molecular sieves 5A

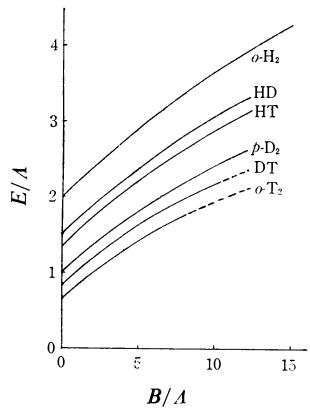



Fig. 2. The rotational energies combined with the second-order perturbation energies against the potential barrier $B$. State; $l=1$, $m=1$

(i) Between spin isomers, A should be the molecule in a state associated with an even $l$.

(ii) Between molecules of different weights, A should be the lighter molecule.

(iii) Between isobaric molecules, i.e., between tritium hydride and deuterium, A should be the tritium hydride.

Assuming that Langmuir's adsorption equation is obeyed and that the relation $[A]_{ads} \propto b_A[A]_{gas}$ holds approximately (because the extent of adsorption is small), 4 can be written in terms of Langmuir's adsorption coefficient, $b$, as $S=b_B/b_A$. When A and/or B is a mixture of spin isomers, $b_A$ is expressed approximately as $b_{A_1} \times b_{A_2}/(x_{A_1}b_{A_2}+x_{A_2}b_{A_1})$, where the suffix on A refers to the kind of spin isomer and where $x$ is the mole fraction in the adsorbed phase. As the translational and vibrational parts of $b_{A_1}$ and $b_{A_2}$ are equal, 4 is rewritten as:

$$S=(b_B/b_A)_{trans,vib} \times \left(\frac{x_{A_1}/b_{A_1}+x_{A_2}/b_{A_2}}{x_{B_1}/b_{B_1}+x_{B_2}/b_{B_2}}\right)_{rot} \quad (5)$$

In order to simplify the calculation of the separation factor, we assume that, in the adsorbed phase, a translational degree of freedom along the Z axis is replaced by a vibrational degree of freedom along the same axis and that the other modes of translation and vibration are almost the same as in the gas phase. The separation factor, $S$, is then expressed as:

$$S=\sqrt{\frac{M_A}{M_B}} \exp\left(\frac{(1/2)\hbar(\nu_A-\nu_B)}{kT}\right) \times \frac{x_{A1}(Q/q)_{A_1}+x_{A_2}(Q/q)_{A_2}}{x_{B_1}(Q/q)_{B_1}+x_{B_2}(Q/q)_{B_2}} \quad (6)$$

where $M$ is the molecular weight; $\nu$ the frequencies of vibration along the Z axis ($\sqrt{2K/4\pi^2M}$) and $Q$ and $q$ the partition functions of rotation in the gas phase and in the adsorbed phase respectively.

The calculated values of the separation factor at the temperature of liquid nitrogen are summarized in Table II for potential barriers of $4A$, $8A$ and $12A$.

## Discussion

The adsorptive separation factor of a pair of isomers can be separated into three parts:

$S_{trans}$, $S_{vib}$ and $S_{rot}$. $S_{trans}$ depends solely on the total mass ratio of molecules and decreases with an increase in the mass ratio, running from 1 to 0.577. It is, however, always less than unity. $S_{vib}$ depends on both $B$ and the mass ratio, and it increases either with an increase in the mass or in the mass ratio. It runs from 1 to 3.78 when $B=8\Lambda$, and from 1 to 5.11 when $B=12\Lambda$. $S_{rot}$ is a complicated function. In general, it increases as $B$ and the total mass ratio increase, but the reverse may be the case at particular values of $B$ and the mass ratio.

White and Lassettre have assumed that the molecule is not completely free to move along directions parallel to the adsorbent surface and that it is confined within a definite range of the surface.[13] In this case, $S_{trans}$ may exceed unity, depending on the area of the cage. However, this situation may conveniently be disregarded, as the contribution of $S_{trans}$ is not very large. The most important contribution comes from $S_{vib}$, which increases exponentially as $B$ increases. Therefore, the value of $B$ should be carefully estimated when a separation factor between isomers of different molecular weights is going to be considered.

Comparing the calculated values with the experimental results (Table II), it can be seen that the values at $B=8\Lambda$ conform well to the experiment I of Carter and Smith using a highly active alumina column, and the values at $B=4\Lambda$, to the experiment II of Carter and Smith and to that of King, using ferric oxide on alumina column. At $B=12\Lambda$, the calculated values deviate greatly from the experimental results. Therefore, for an alumina column or its modifications, the value of $B$ is most likely to fall within the range from $4\Lambda$ to $8\Lambda$. The agreement is plausible, except for several cases which we shall discuss later.

In spite of having the same mass, the elution of tritium hydride become faster than deuterium. The calculated values, 1.10 ($B=4\Lambda$) and 1.13 ($B=8\Lambda$), can be compared with the experimental values, 1.12 (alumina), and 1.05 and 1.13 (ferric oxide on alumina). This surprising agreement may in part be accidental, for the introduction of another potential, $V_\phi$, which is to be discussed later, somewhat reduces the values. To anticipate the later discussion, the decrement is small, however. Moreover, we can see from Table II that the elution of lighter molecules tends to be faster than that of heavier molecules.

There are still several disagreements. For the separation factor between para- and ortho-hydrogen, $B$ should take a value as large as $10\Lambda$ in order to obtain the best fit with the experimental value (1.37). Evett, in his first paper,[12a] estimated $B$ to be $14\Lambda$ in order to account for both the experiment of Sandler at 90°K (1.67)[1] and that of Cunningham and Johnston at 20°K (16).[2] In his later work, however, Evett found that the value of $B$ could be reduced to about $6\Lambda$, which was thought to account for the heat of adsorption (2000 cal./mol.), if another potential in the direction of $\phi$ was introduced:[12b]

$$V_\phi = D\cos 2\phi$$

This assumption is acceptable, for we may consider the substrate surface to be an array of attractive centers. In the present case, also, the potential favors the separation of para- and ortho-hydrogen and may bring about the agreement of the calculated value with the experimental value at an appropriate $B$ value.

It may also be the case for the separation of ortho-hydrogen and hydrogen deuteride, where the agreement is somewhat poor. We have good reason to assume that the potential $V_\phi$ may reduce the separation factor considerably, as the level associated with $m=1$ is affected greater than with $m=0$.

The potential $V_\phi$ may not be very important for separation factors between heavy molecules or between molecules in states of the same $m$ values. Hence, the correction should be small for values which are already in good agreement.

The separation factors between para-tritium and ortho-tritium are very close to unity. Here, the partition among various energy levels is taken into account, as they are closer together for heavier molecules. The result is practically the same as that which is obtained disregarding higher levels. The separation factor is a very insensitive function in this case, running from 1 ($B=0$) to 0.98 ($B=\infty$). Therefore, it is very probable that the experimental separation of para- and ortho-tritium is very difficult, if not impossible.

*Department of Chemistry*
*College of General Education*
*The University of Tokyo*
*Komaba, Tokyo*

# π-Electronic Energy Levels of *o*-Benzoquinone

By Akira KUBOYAMA and Kōichi WADA*

(Received March 12, 1965)

Previously, π-electronic energy levels of quinones have been studied by one[1] of the present authors using the simple MO calculation. In that study, an attempt to explain the electronic spectra of quinones on the basis of calculated results was made. However, in order to clarify the whole aspect of the electronic spectra of quinones, it is desirable that the electronic energy levels of quinones be studied by the MO calculation using a Hamiltonian which includes electronic interaction terms. Among quinones, *p*-benzoquinone alone has been studied by many authors[2] with such a calculation. However, *o*-benzoquinone and anthraquinone are also important compounds among the quinones. We have, therefore, carried out such a calculation concerning *o*-benzoquinone and anthraquinone. In this paper the results obtained for *o*-benzoquinone will be shown.

## The Method of Calculation

In the MO calculation of a π-electronic system which contains hetero atoms such as quinones, it is desirable to use the self-consistent field (SCF) technique. In Sidman's work[2d] on carbonyl compounds and *p*-benzoquinone, Pople's SCF MO method[3] was used, but the values of the electron repulsion integrals were obtained according to Pariser-Parr's uniformly-charged sphere approximation[4] instead of Pople's point-charge approximation. The configuration interaction among low-energy excited states were also calculated. This Sidman calculation gives, on the whole, reasonable results. Therefore, our calculation was carried out according to Sidman's method.

The integrals used are shown in Table I. O and C denote oxygen and carbon atoms respectively and, for example, (OO|OO) and (OO|CC) denote the one-center electron repulsion integral of the oxygen atom and the two-center Coulomb repulsion integral over the oxygen and carbon atoms respectively. The values in Table I are those in Sidman's Table except for the formula for (OO|OO) and the values of the core-exchange integrals for the C-C bonds ($\beta_{CC'}$) ($R$=1.46, 1.49Å). The formula for (OO|OO) was obtained from the value of (OO|OO) and the formula for (OO|O'O') (for $R>2.8$Å) in Sidman's Table.[2d] Sidman regarded the $U$-term in Pople's SCF MO method as the valence-state orbital energy corrected for the fact that the atom is no longer isolated, but is now a part of a molecule. The value of $U_{CC}$ is the same as that used in Hush and Pople's paper.[5] The value of $U_{OO}$ was determined from a comparison of the valence-state ionization potentials of the oxygn and carbon atoms. As will be shown later, the energy levels are not sensitive to the value of $U_{OO}$. The values of $\beta_{CC'}$ were obtained according to the Pariser-Parr method. The value of $\beta_{CO}$ is that presented by Parks and Parr.[6]

Table I. Integral values (eV., $R$ (interatomic distance) in Å)

| | | | | |
|---|---|---|---|---|
| (OO\|OO) | 14.671 | $U_{OO}$ | | −13.00 |
| (CC\|CC) | 10.842 | $U_{CC}$ | | − 9.50 |
| (OO\|CC) | $12.757-3.966R_{CO}$ | $\beta_{CO}$ | | − 3.00 |
| | $+0.4169R^2_{CO}$ | | | |
| | | $\beta_{CC'}$ | | |
| (CC\|CC) | $10.842-2.821R_{CC'}$ | $R_{CC'}$=1.35 | | − 2.92 |
| | $+0.2454R^2_{CC'}$ | 1.46 | | − 1.76 |
| (OO\|OO) | $14.671-4.748R_{OO'}$ | 1.47 | | − 1.68 |
| | $+0.5012R^2_{OO'}$ | 1.49 | | − 1.52 |

In this work an electronic computer (NEAC 2101) was used.[7] SCF calculations were repeated until the coefficients of the symmetry orbitals[8] in the SCF MO's become consistent to three decimal places.

It is assumed that *o*-benzoquinone is planar

* Present address: The Yokohama Customs House, Naka-ku, Yokohama.

1) A. Kuboyama, a) This Bulletin, **31**, 752 (1958); b) ibid., **32**, 1226 (1959); c) ibid., **33**, 917 (1960).

2) H. Kon, ibid., **28**, 275 (1955); b) M. Okuda, *J. Chem. Phys.*, **25**, 1083 (1956); c) T. Anno, I. Matubara and A. Sadô, This Bulletin, **30**, 168 (1957); T. Anno, A. Sadô and I. Matubara, *J. Chem. Phys.*, **26**, 967 (1957); d) J. W. Sidman, ibid., **27**, 429 (1957).

3) J. A. Pople, *Trans. Faraday Soc.*, **49**, 1375 (1953).

4) R. Pariser and R. G. Parr, a) *J. Chem. Phys.*, **21**, 466 (1953); b) ibid., **21**, 767 (1953).

5) J. M. Parks and R. G. Parr, ibid., **32**, 1657 (1960).

6) N. S. Hush and J. A. Pople, *Trans. Faraday Soc.*, **51**, 600 (1955).

7) The program for eigenvalue problem was made by Dr. O. Yamamoto of this institute.

8) To simplify the calculation, symmetry orbitals were used instead of atomic orbitals.

and that its symmetry group is $C_{2v}$. Since the molecular dimension of *o*-benzoquinone has never been reported, it was determined as follows. At first, the SCF calculation was carried out with the molecular dimension which has been obtained according to the bond order - bond distance relation[9] from the bond orders previously obtained by the simple MO calculation.[10] From the bond orders obtained by this SCF MO calculation, the molecular dimension which is shown in Fig. 1 was obtained and used in the final SCF MO calculation. The numerals in parentheses in Fig. 1 denote the numbering for the atoms.

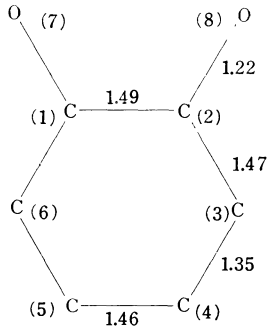



Fig. 1. The assumed molecular dimension (Å).

## Results

The molecular orbital ($\phi_i$)[11] and their orbital energies ($\varepsilon_i$) are shown in Table II. Among the excitation energies of the excited singlet and triplet configurations,[12] the lower ones are shown in Table III, along with the corresponding Coulomb and exchange integrals and transition dipole strengths ($\mu^2$) from the ground state (for singlet configurations). Configuration interactions among five low energy-excited singlet and triplet configurations in Table III were calculated. The obtained excited state wave functions ($^{1,3}\Phi_i$), their excitation energies ($^{1,3}E_i - E_0$), the transition dipole strengths from the ground state and the interconfigurational matrix elements ($\Phi_{i\to j}|H|\Phi_{k\to l}$) are shown in Table IV.

The calculated and observed energy levels[13]

Table II. SCF MO's and their energies

| Symmetry | SCF MO's | Orbital energies, eV. |
|---|---|---|
| $b_1$ | $\phi_1=0.4431(\chi_1+\chi_2)+0.2981(\chi_6+\chi_3)+0.2774(\chi_5+\chi_4)+0.3712(\chi_7+\chi_8)$ | −13.588 |
| $a_2$ | $\phi_2=0.3944(\chi_1-\chi_2)+0.3000(\chi_6-\chi_3)+0.1806(\chi_5-\chi_4)+0.4710(\chi_7-\chi_8)$ | −11.977 |
| $b_1$ | $\phi_3=0.2567(\chi_1+\chi_2)-0.3195(\chi_6+\chi_3)-0.4844(\chi_5+\chi_4)+0.3120(\chi_7+\chi_8)$ | −11.667 |
| $a_2$ | $\phi_4=0.1362(\chi_1-\chi_2)-0.4680(\chi_6-\chi_3)-0.3890(\chi_5-\chi_4)+0.3333(\chi_7-\chi_8)$ | − 9.777 |
| $b_1$ | $\phi_5=0.2744(\chi_1+\chi_2)+0.3938(\chi_6+\chi_3)-0.3571(\chi_5+\chi_4)-0.3770(\chi_7+\chi_8)$ | 0.351 |
| $a_2$ | $\phi_6=0.3492(\chi_1-\chi_2)+0.2788(\chi_6-\chi_3)-0.4636(\chi_5-\chi_4)-0.2923(\chi_7-\chi_8)$ | 2.449 |
| $b_1$ | $\phi_7=0.4030(\chi_1+\chi_2)-0.3924(\chi_6+\chi_3)+0.2468(\chi_5+\chi_4)-0.3503(\chi_7+\chi_8)$ | 2.572 |
| $a_2$ | $\phi_8=0.4516(\chi_1-\chi_2)-0.3364(\chi_6-\chi_3)+0.3181(\chi_5-\chi_4)-0.2858(\chi_7-\chi_8)$ | 4.446 |

Table III. Excitation energies and transition dipole strengths of the configurations and electronic repulsion integrals

| $i\to j$ | Symmetry | $^1E_{i\to j}-E_0$, eV. | $\mu^2$, Å$^2$ | $^3E_{i\to j}-E_0$, eV. | $J_{ij}$, eV. | $K_{ij}$, eV. |
|---|---|---|---|---|---|---|
| 4→5 | $A_1\to B_2$ | 5.207 | 0.733 | 3.803 | 6.325 | 0.702 |
| 2→5 | $A_1\to B_2$ | 6.930 | 0.017 | 5.882 | 6.446 | 0.524 |
| 4→7 | $A_1\to B_2$ | 6.943 | 0.036 | 6.055 | 6.294 | 0.444 |
| 3→5 | $A_1\to A_1$ | 7.190 | 1.179 | 5.716 | 6.302 | 0.737 |
| 4→6 | $A_1\to A_1$ | 7.263 | 1.126 | 5.859 | 6.367 | 0.702 |
| 3→6 | $A_1\to B_2$ | 8.517 | | 7.643 | 6.321 | 0.440 |
| 4→8 | $A_1\to A_1$ | 8.782 | | 7.902 | 6.473 | 0.437 |
| 2→7 | $A_1\to B_2$ | 8.885 | | 7.789 | 6.232 | 0.464 |
| 3→7 | $A_1\to A_1$ | 8.935 | | 8.007 | 6.210 | 0.481 |
| 2→6 | $A_1\to A_1$ | 9.178 | | 8.216 | 6.760 | 0.548 |

9) C. A. Coulson, "Valence," Oxford Univ. Press, Oxford (1952), p. 253.

10) S. Nagakura and A. Kuboyama, *J. Chem. Soc. Japan, Pure Chem. Sec.* (*Nippon Kagaku Zasshi*), **74**, 499 (1953); *J. Am. Chem. Soc.*, **76**, 1003 (1954).

11) $\chi_i$ denotes the $2p\pi$ atomic orbital of *i*-atom.

12) $\Phi_0$ and $E_0$ denote the wave function and the energy of the ground state respectively. $^1\Phi_{i\to j}$, $^1E_{i\to j}$ and $^3\Phi_{i\to j}$, $^3E_{i\to j}$ denote the wave functions and the energies of the singlet and triplet configurations, respectively, in which one electron is excited from an occupied orbital $\chi_i$ to an unoccupied orbital $\chi_j$. The excitation energy of each excited configuration is given by the following formula.

$$\left.\begin{matrix}{}^1E_{i\to j}\\ {}^3E_{i\to j}\end{matrix}\right\} - E_0 = (\varepsilon_j - \varepsilon_i) - (J_{ij} - K_{ij}) \begin{cases} +K_{ij} \\ -K_{ij} \end{cases}$$

$J_{ij}$ and $K_{ij}$ denote Coulomb and exchange integrals over $\Phi_i$ and $\Phi_j$ respectively.

13) S. Goldschmidt and F. Graef, *Ber.*, **61**, 1858 (1928). The $n\to{}^1\pi^*$ band of *o*-benzoquinone is at ca. 600 m$\mu$.

TABLE IV. WAVE FUNCTIONS, EXCITATION ENERGIES AND TRANSITION DIPOLE STRENGTHS OF EXCITED STATES AND INTERCONFIGURATIONAL MATRIX ELEMENTS

(1) Singlet states

| Symmetry | $^{1,3}\Phi_i$ | $^{1,3}E_i - E_0$, eV. | $\mu^2$, Å$^2$ |
|---|---|---|---|
| $^1B_2$ | $^1\Phi_1 = 0.9880\,^1\Phi_{4\to5} - 0.1337\,^1\Phi_{2\to5} - 0.0780\,^1\Phi_{4\to7}$ | 5.171 | 0.711 |
| $^1B_2$ | $^1\Phi_2 = 0.1494\,^1\Phi_{4\to5} + 0.6928\,^1\Phi_{2\to5} + 0.7055\,^1\Phi_{4\to7}$ | 6.615 | 0.007 |
| $^1A_1$ | $^1\Phi_3 = 0.7522\,^1\Phi_{3\to5} - 0.6589\,^1\Phi_{4\to6}$ | 6.949 | 0.014 |
| $^1B_2$ | $^1\Phi_4 = 0.0403\,^1\Phi_{4\to5} + 0.7086\,^1\Phi_{2\to5} - 0.7044\,^1\Phi_{4\to7}$ | 7.294 | 0.068 |
| $^1A_1$ | $^1\Phi_5 = 0.6589\,^1\Phi_{3\to5} + 0.7522\,^1\Phi_{4\to6}$ | 7.504 | 2.290 |

(2) Triplet states

| | | |
|---|---|---|
| $^3B_2$ | $^3\Phi_1 = 0.9798\,^3\Phi_{4\to5} - 0.0800\,^3\Phi_{2\to5} - 0.1831\,^3\Phi_{4\to7}$ | 3.745 |
| $^3A_1$ | $^3\Phi_2 = 0.7286\,^3\Phi_{3\to5} + 0.6849\,^3\Phi_{4\to6}$ | 4.630 |
| $^3B_2$ | $^3\Phi_3 = 0.1822\,^3\Phi_{4\to5} + 0.7336\,^3\Phi_{2\to5} + 0.6547\,^3\Phi_{4\to7}$ | 4.778 |
| $^3A_1$ | $^3\Phi_4 = 0.6849\,^3\Phi_{3\to5} - 0.7286\,^3\Phi_{4\to6}$ | 6.945 |
| $^3B_2$ | $^3\Phi_5 = 0.0820\,^3\Phi_{4\to5} - 0.6748\,^3\Phi_{2\to5} + 0.7334\,^3\Phi_{4\to7}$ | 7.217 |

(3) Interconfigurational matrix elements

| | Singlet state eV. | Triplet state eV. |
|---|---|---|
| $(\Phi_{4\to5}\|H\|\Phi_{2\to5})$ | 0.210 | −0.054 |
| $(\Phi_{4\to5}\|H\|\Phi_{4\to7})$ | 0.092 | 0.332 |
| $(\Phi_{2\to5}\|H\|\Phi_{4\to7})$ | −0.354 | −1.222 |
| $(\Phi_{3\to5}\|H\|\Phi_{4\to6})$ | 0.275 | −1.155 |

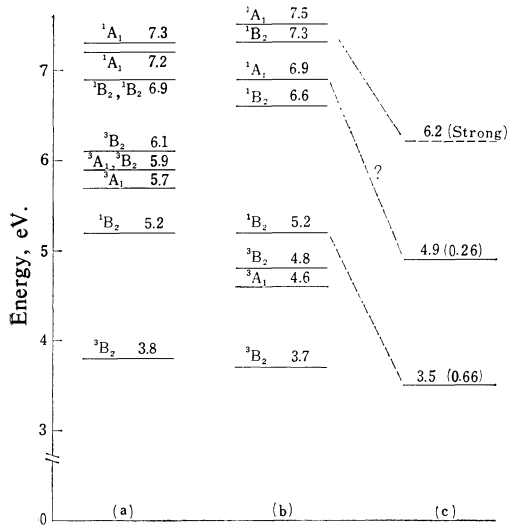



Fig. 2. Energy levels.

(a) Without configuration interaction
(b) With configuration interaction (high triplet levels not described)
(c) Observed

are shown in Fig. 2. In Fig. 2, numerical values on or below the energy levels are the excitation energies rounded to the first decimal in eV., while those in parentheses on the observed levels are the dipole strengths calculated from the observed oscillator strengths. The dipole strength of the 4.9 eV. band is not so accurate because of the overlapping of neighboring bands. As for the observed highest level at 6.2 eV., the corresponding absorption peak has never been observed, but it is certain that an absorption band whose intensity is far greater than the other two observed bands exists near 200 m$\mu$ (which corresponds to ca. 6.2 eV.).

## Discussion

In *o*-benzoquinone, all singlet $\pi$-electronic transitions are allowed and the transitions $^1A_1 \to {}^1A_1$ and $^1A_1 \to {}^1B_2$ are polarized parallel to and perpendicular to the symmetry axis respectively. In Fig. 2, considering the values of dipole strengths, the two observed levels at 3.5 and 6.2 eV. may reasonably be assigned to the $^1B_2$ level at 5.2 eV. and to the $^1A_1$ level at 7.5 eV. respectively. The calculated and observed dipole strengths for the 3.5 eV. band are in good agreement. It is noticeable that the excited-state wave function of this band ($^1\Phi_1$) consists for the most part of $^1\Phi_{4\to5}$, as may be seen in Table IV. The assignment of the observed level at 4.9 eV. is uncertain. The dipole strengths for the two $^1A_1$ configurations whose energy levels are at 7.2 and 7.3 eV. are large and nearly equal to each other. Therefore, if the mixing of these two configurations differs slightly from that given in Table IV, the dipole strength for the $^1A_1$ level at 6.9 eV. will increase to some extent. Therefore, the observed level at 4.9 eV. may be assigned to the $^1A_1$ level at 6.9 eV.

In the results described above, it is noticeable that the calcluated singlet excited levels are much higher than the observed ones. In the case of *o*-benzoquinone studied by Sidman,

TABLE V. EXCITATION ENERGIES OF THE CONFIGURATION ($^1\Phi_{4\to5}$) IN VARIOUS CASES

| | a | b | c | d | e | f | g | h | obs. |
|---|---|---|---|---|---|---|---|---|---|
| $^1E_{4\to5}-E_0$, eV. | 5.21 | 4.98 | 5.12 | 5.13 | 4.94 | 4.57 | 4.14 | 4.60 | 3.5 |

a) The value in Table III.
b) The two center Coulomb repulsion integrals obtained by the Mataga-Nishimoto's method[14] were used.
c) The value (−14.00 eV.) for $U_{OO}$ was used.
d) The value (−10.00 eV.)for $U_{CC}$ of the carbonyl carbon atoms was used.
e) $\beta$'s obtained by Kon's method[2a] were used.
f) For $\beta$'s of the conventional double and single bonds, the values (−2.7 and −1.9 eV. respectively) were used.
g) For $\beta$'s of the conventional double and single bonds, the values (−2.5 and −2.0 eV. respectively) were used.
h) For $\beta$'s the values smaller than those in the case a by the factor (0.8) were used.

TABLE VI. SIMPLE MO'S AND THEIR ENERGIES

| Symmetry | Simple MO's | Orbital energies |
|---|---|---|
| $b_1$ | $\phi_1=0.4655(\chi_1+\chi_2)+0.2820(\chi_6+\chi_3)+0.2419(\chi_5+\chi_4)+0.3811(\chi_7+\chi_8)$ | $(\alpha+)$ 1.7657$\beta$ |
| $a_2$ | $\phi_2=0.4114(\chi_1-\chi_2)+0.2801(\chi_6-\chi_3)+0.1454(\chi_5-\chi_4)+0.4808(\chi_7-\chi_8)$ | 1.3268$\beta$ |
| $b_1$ | $\phi_3=0.2231(\chi_1+\chi_2)-0.3197(\chi_6+\chi_3)-0.5136(\chi_5+\chi_4)+0.2902(\chi_7+\chi_8)$ | 1.2226$\beta$ |
| $a_2$ | $\phi_4=0.0990(\chi_1-\chi_2)-0.4908(\chi_6-\chi_3)-0.3852(\chi_5-\chi_4)+0.3177(\chi_7-\chi_8)$ | 0.6740$\beta$ |
| $b_1$ | $\phi_5=0.2682(\chi_1+\chi_2)+0.3889(\chi_6+\chi_3)-0.3484(\chi_5+\chi_4)-0.3943(\chi_7+\chi_8)$ | −0.5164$\beta$ |
| $a_2$ | $\phi_6=0.3640(\chi_1-\chi_2)+0.2374(\chi_6-\chi_3)-0.4641(\chi_5-\chi_4)-0.3095(\chi_7-\chi_8)$ | −1.1115$\beta$ |
| $b_1$ | $\phi_7=0.4020(\chi_1+\chi_2)-0.4086(\chi_6+\chi_3)+0.2373(\chi_5+\chi_4)-0.3393(\chi_7+\chi_3)$ | −1.1218$\beta$ |
| $a_2$ | $\phi_8=0.4341(\chi_1-\chi_2)-0.3526(\chi_6-\chi_3)+0.3393(\chi_5-\chi_4)-0.2686(\chi_7-\chi_8)$ | −1.1693$\beta$ |

a similar trend was observed. We examined the lowering of the calculated singlet excited levels by using modified values of various kinds of integrals. Since the $^1B_2$ level at 5.2 eV. is much lower than the other singlet excited levels, and since its state almost entirely consists of the configuration ($^1\Phi_{4\to5}$), as is mentioned above, the energy level of this configuration is thought to be reasonably usable as a measure of the lowering of the calculated singlet excited levels. The calculated energy levels of that configuration in various cases where the values of one of the three kinds of integrals (two-center Coulomb repulsion integrals, $U$ and $\beta$) are modified are shown in Table V. As may be seen in Table V, the lowering of that level is small except for the cases (f, g, h) where modified values of $\beta$ are used. From the results in Table V, it may be concluded that a satisfactory lowering of the calculated singlet excited levels cannot be expected unless values of $\beta$ are used which are much modified from those generally used. This disagreement between the calculated singlet energy levels and the observed ones may be attributed to a peculiar electronic structure of quinones, one different from those of usual aromatic compounds.

The Coulomb and exchange integrals in the simple MO method appropriate to simulate the simple MO's to the SCF MO's obtained here for *o*-benzoquinone were searched for with the trial-and-error method. The integral values obtained are shown in Fig. 3. The Coulomb integral of the oxygen atoms and the exchange integrals of the conventional single bonds are far smaller (in $\beta$ units) than those generally used. Similar results have been reported by other authors.[14,15] The MO's of *o*-benzoquinone obtained using these integral values are shown in Table VI. The molecular diagrams of the SCF and simple MO's are shown in Fig. 4. The charge densities of the oxygen atoms and the carbonyl carbon atoms in Fig. 4a are similar to those (−0.149e and +0.131e) of *p*-benzoquinone calculated with Sidman's SCF MO's.[2d] The dipole moment

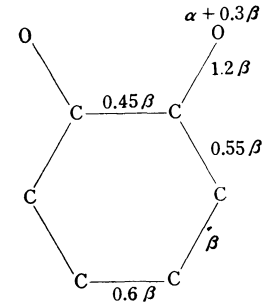
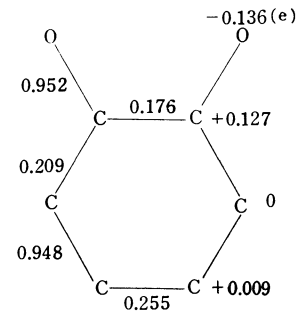
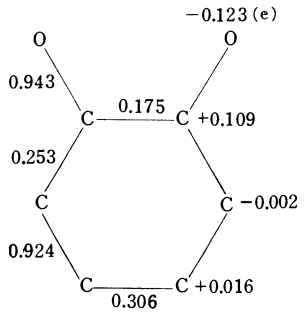



Fig. 3. Integral values in the simple Mo method.

14) N. Mataga and K. Nishimoto, *Z. physik. Chem. N. F.*, **12**, 335 (1957).
15) a) R. Mcweeny and T. E. Peacock, *Proc. Phys. Soc.*, **A69**, 41 (1957); b) R. D. Brown and M. L. Heffernan, *Trans. Faraday Soc.*, **54**, 757 (1958).




(a) SCF MO




(b) Simple MO

Fig. 4. Molecular diagrams (charge densities and bond orders).

calculated from the charge densities in Fig. 4a is 1.56 D. The observed dipole moment of *o*-benzoquinone in benzene is 5.1 D.[10] In *o*-benzoquinone, the lone-pair moment of two oxygen atoms and the $\sigma$-moment cannot be estimated with certainty, but the former[16] may be quite large. Even considering this, the $\pi$-moment obtained here seems too small.

## Summary

The $\pi$-electronic energy levels of *o*-benzoquinone have been obtained by using Pople's SCF MO method, while the electron repulsion integrals have been obtained by the Pariser-Parr method. The absorption band near 360 m$\mu$ and the strong band which is thought to exist near 200 m$\mu$ have unambiguously been assigned to the first $^1A_1 \rightarrow {}^1B_2$ and the second $^1A_1 \rightarrow {}^1A_1$ transitions respectively. The calculated singlet excited energy levels are much higher than the observed levels. The reason for this has been examined by SCF MO calculations using modified values of various kinds of electron repulsion integrals and core integrals. It has been concluded that a satisfactory lowering of the calculated singlet excited energy levels cannot be expected unless values of the core resonance integrals ($\beta$) are used which are much modified from those generally used. Simple MO parameters for *o*-benzoquinone adequate to simulate the simple MO's to the SCF MO's have been obtained.

*Government Chemical Industrial Research Institute, Tokyo*
*Shibuya-ku, Tokyo*

16) The lone-pair moments of sp- and $sp^2$-hybridized oxygen atoms are 1.6 D and 1.5 D respectively.

# Studies on the Liquid-Liquid Partition Systems. II. The Determination of Water Activity by the Solvent Extraction Technique

By Yuko HASEGAWA and Tatsuya SEKINE

(Received March 12, 1965)

In the course of our study on the liquid-liquid partition systems, we desired to find a way to ascertain the water activity of various electrolyte solutions easily.

As Robinson and Stokes[1] have stated, the vapour pressure method is very accurate; the limit of the error is usually less than 0.01%. However, the method is not always easy to carry out because special apparatus must be prepared and a careful control of the experimental conditions is indispensable.

It seems that the water activity in an aqueous solution can be determined by the solvent extraction technique without any special difficulty, because the water content in an organic solvent in equilibrium with the solution can be measured by Karl Fischer titration, and it will be proportional to the water activity in the solution.

1) R. A. Robinson and R. H. Stokes, "Electrolyte Solutions," Butterworths, London (1959).

Högfeldt and his co-workers[2] have studied the extraction of water and acids from various acid solutions into organic solvents by Karl Fischer titration. In these systems, the water in the organic phase consists of two fractions, the free water and the hydrated water. They calculated the hydrated water content from the difference between the total water content as determined by Karl Fischer titration and the free water content as calculated from the water activity cited in the literature.

The present work was carried out to ascertain the accuracy of the value of the water activity determined by the solvent extraction method. For this purpose, benzene was equilibrated with various electrolyte solutions, and the concentration of water in the benzene phase was determined by Karl Fischer titration. Then the water activity of the solution was calculated.

The results were compared with the data in the literature, which had been determined by the vapor-pressure method.

## Statistical Treatment

*Symbols.*

| | |
|---|---|
| $\{H_2O\}$ | water activity |
| $[H_2O]$ | water concentration |
| $\gamma$ | activity coefficient |

The following subscripts denote the activity, concentration or activity coefficient of water in:

"*aq*" an aqueous phase
"*org*" an organic phase
"0" pure water, or an organic phase in equilibrium with pure water
"*n*" an electrolyte solution, or an organic phase in equilibrium with the aqueous phase

When an aqueous solution is in equilibrium with an immiscible organic solvent, the distribution constant of water is defined as:

$$H_2O_{(aq)} \rightleftharpoons H_2O_{(org)} \quad (1)$$

$$K=\{H_2O\}_{org}/\{H_2O\}_{aq} \quad (2)$$

Moreover, an equation can be introduced for the ratio of the water activity in the organic phase in equilibrium with an electrolyte solution and pure water as:

$$\{H_2O\}_{aq,n}/\{H_2O\}_{aq,0}=\{H_2O\}_{org,n}/\{H_2O\}_{org,0} \quad (3)$$

When the water activity in pure water is defined as unity, Eq. 3 can be described, using the activity coefficient as:

$$\{H_2O\}_{aq,n}=\gamma_{org,n}[H_2O]_{org,n}/\gamma_{org,0}[H_2O]_{org,0} \quad (4)$$

Here the following will be assumed.

(i) The activity coefficient of water in the organic phase is constant when the water concentration in it is low.

(ii) The distribution of a small amount of the organic solvent in the aqueous phase does not change the character of the solution.

(iii) No extraction of species which carries water as hydrated water occurs.

On the basis of the first assumption $\gamma_{org,n}$ is equal to $\gamma_{org,0}$ and the water activity in the aqueous solution can be calculated as:

$$\{H_2O\}_{aq,n}=[H_2O]_{org,n}/[H_2O]_{org,0} \quad (5)$$

Thus the water activity of a certain solution can be determined from the ratio of the water concentration in two organic phases if these three assumptions can be made.

## Experimental

**Materials.**—The following chemicals (of a specially-purified grade) were employed without further purification: benzene, potassium bichromate, potassium nitrate, potassium chloride, sodium chloride, strontium chloride, magnesium nitrate, and magnesium chloride. Solutions for Karl Fischer titration were obtained from the Mitsubishi Kasei Co. The sodium chloride was dried in an air-bath at 120°C for several hours and then stored in a desiccator. Sodium chloride solutions of various concentrations were prepared by weighing the dried sodium chloride. Saturated-salt stock solutions were prepared from the metal salts.

**Procedures.**—All of the procedures were carried out in a thermostated room at 25±0.3°C. Twelve milliliters of benzene and 5 ml. of the sample solution were placed in glass-stoppered tubes (volume, 20 ml.). For the experiments with saturated solutions, 0.3—0.5 g. of the salt crystals was added to the sample solution in order to ensure saturation. A mechanical rotator (20 r. p. m.) was used for the agitation of the two phases in the tube; this rotation was continued overnight. It was confirmed by preliminary experiments that the distribution equilibrium was reached within one hour by this rotation. Then the two phases were centrifuged about 5 min. at 2000 r. p. m. This seems to be enough for the separation, because a centrifugation for over 15 min. at 3500 r. p. m. gave the same results.

Ten milliliters of the benzene were then pipetted out and the water content was titrated with a Karl Fischer apparatus (Kyoto Denshi Kogyo Co.).

Blank titration was carried out, and a small correction was made for the water coming from the air.

## Results

The results are given in the following tables.

2) E. Högfeldt and B. Bolander, "Arkiv for Kemie," Band 21, nr 16, Almqvist & Wiksell, Stockholm (1963).

Table I. The water concentration in the benzene phase in an equilibrium with pure water

| Reference | Water concn., mol./l. |
|---|---|
| This work | 0.034* |
| Högfeldt, Bolander[2] | 0.032 |
| Clifford[3] | 0.026 |
| Groschuff[4] | 0.033 |
| Hill[5] | 0.035 |
| Joris, Taylor[6] | 0.025 |
| Rosenbaum, Walton[7] | 0.024 |
| Stavely et al.[8] | 0.033 |

* The average of the results. The original data are as follows:
0.0342 0.0340 0.0340 0.0342 0.0342 0.0339
0.0339 0.0342 0.0342 0.0342 0.0340 0.0340
0.0341 0.0342

Table II. Water activity in various saturated salt solutions

| Salt | $\{H_2O\}_{aq}$ Determined | | | Average | $\{H_2O\}_{aq}$ From Ref. 1 |
|---|---|---|---|---|---|
| $K_2Cr_2O_7$ | 0.976 | 0.980 | 0.976 | $0.97_7$ | 0.980 |
| $KNO_3$ | 0.941 | 0.937 | 0.942 | $0.94_0$ | 0.925 |
| KCl | 0.854 | 0.857 | 0.850 | $0.85_4$ | 0.843 |
| NaCl | 0.756 | 0.757 | 0.762 | $0.75_8$ | 0.753 |
| $SrCl_2$ | 0.693 | 0.707 | 0.697 | $0.69_9$ | 0.708 |
| $Mg(NO_3)_2$ | 0.529 | 0.536 | 0.530 | $0.53_2$ | 0.529 |
| $MgCl_2$ | 0.326 | 0.326 | 0.320 | $0.32_4$ | 0.330 |

Table III. Water activity in sodium chloride solution

| Concn. of NaCl (molality) | $\{H_2O\}_{aq}$ Determined | | | Average | $\{H_2O\}_{aq}$ From Ref. 1 |
|---|---|---|---|---|---|
| 0.50 | 0.984 | 0.983 | 0.985 | $0.98_4$ | 0.984 |
| 1.0 | 0.970 | 0.967 | 0.970 | $0.96_9$ | 0.967 |
| 2.0 | 0.931 | 0.938 | 0.931 | $0.93_3$ | 0.932 |
| 3.0 | 0.889 | 0.892 | 0.908 | $0.89_6$ | 0.893 |
| 4.0 | 0.855 | 0.856 | 0.854 | $0.85_5$ | 0.852 |
| 5.0 | 0.812 | 0.815 | 0.814 | $0.81_3$ | 0.807 |

## Discussion

In these systems, the water concentration in benzene is very low (maximum: 0.034 M water per liter of benzene), and the benzene concentration in the aqueous phase is also very low (maximum: 0.01 M benzene per liter of water). Thus, the first and second assumptions seem to be established in the present systems.

From the results in the tables, we may also conclude that the present method is accurate to less than 1% when the procedures are carried out properly. The error of Karl Fischer titration may be 0.1—0.5% at most.

By the use of this method, the water activity of several electrolyte solutions can be determined.

## Recommended Procedures

On the basis of the present results, the following procedures can be recommended:

**Organic Solvents.**—Benzene seems to be a suitable solvent for this purpose. If the solvent is not very pure, it should be washed several times with distilled water in order to back-extract hydrophilic impurities.

**Procedures.**—Twelve to fifteen milliliters of benzene and a few milliliters of the sample solutions are placed in glass-stoppered tubes. They are agitated until the distribution equilibrium is reached, and then centrifuged. Ten milliliters of benzene is pipetted out, and the water content is titrated with a Karl Fishcer solution 1 ml. of which is equivalent to about 1 mg. of water.

The following would be useful suggestions for the experiments:

i) The phase separation should be made completely. The present experiment showed that a centrifugation at 2000 r. p. m. for 5 min. is enough for the phase separation if the viscosity of the solution is not high.

ii) The solubility of water in an organic phase is sometimes very sensitive to impurities; the blank test to determine the $[H_2O]_{org,0}$ in Eq. 5 should be made.

iii) The extraction of chemical species which co-extract water as the hydrated water should be checked. The extraction of such species increases the apparent water activity determined by this method. The extraction of chemical species which may react with the Karl Fischer reagent should also be checked.

iv) Chemical species which will change the mutual solubility should be avoided. The change in the mutual solubility may influence the distribution of water (cf. assumptions i and ii).

v) The mutual solubility between an organic solvent and an aqueous solution should not be very high, for the high solubulity changes the properties of each solution.

## Summary

An attempt has been made to apply the solvent extraction technique to the determination of the water activity in various electrolyte solutions.

3) C. W. Clifford. *Ind. Eng. Chem.*, **13**, 631 (1921).
4) E. Z. Groschuff, *Elektrochemie*, **17**, 348 (1911).
5) A. E. Hill, *J. Am. Chem. Soc.*, **45**, 1143 (1923).
6) G. G. Joris and H. S. Taylor, *J. Chem. Phys.*, **16**, 45 (1948).
7) C. K. Rosenbaum and J. H. Walton, *J. Am. Chem. Soc.*, **52**, 3568 (1930).
8) L. A. K. Staverly and J. A. E. Moy, *Trans. Faraday Soc.*, **39**, 5 (1943).

Benzene was agitated with a sample solution until the distribution equilibrium was attained, the water content in the benzene was then measured by Karl Fischer titration. The water activity was calculated on the basis of the water content.

The results agree with the data obtained by the vapor pressure method. On the basis of these, a solvent extraction procedure has been recommended as an easy and rapid method to determine the water activity in various electrolyte solutions.

*Department of Chemistry*
*Tokyo College of Science*
*Kagurazaka, Shinjuku-ku, Tokyo*

# A Kinetic Study of the Catalytic Isotopic Hydrogen Exchange of Propene with Deuterium Oxide on Palladium Black

By Yoshie HIRONAKA and Kozo HIROTA

(Received May 16, 1965)

It has already been reported[1,2] that methyl hydrogen is, of all the hydrogen atoms in propene, the most exchangeable on palladium black, while methine hydrogen is the most exchangeable on nickel judging from the subspecies-distribution of propene-$d_1$ in the product.

On the other hand, when the kinetic study of this reaction was carried out on nickel, it was concluded that the exchange of vinyl hydrogen attained equilibrium faster than that of methyl hydrogen.[3]

Since the mechanism of the reaction has been discussed in the case of palladium black only in terms of the subspecies-distribution of $d_1$,[1,2] information concerning the mechanism has been insufficiently detailed for us to reach a final conclusion. The present work was therefore undertaken in order to confirm kinetically the mechanism of the isotopic hydrogen exchange of propene with deuterium black.

## Experimental

**Materials.**—Propene obtained from the Takachiho Industrial Co. (purity: 99.7%) was used without any further purification. Deuterium oxide obtained from the Showa Denko K. K. (the deuterium content, 99.7%) was used also without any further purification. The palladium black used as a catalyst, obtained from the Mitsuwa Kagaku Yakuhin K. K., was reduced at 180°C with hydrogen which had been purified by diffusion through a palladium tube, until no water was produced, followed by degassing for at least four hours at the same temperature.

**Procedure.**—Propene and deuterium oxide were throughly outgassed and were charged in vacuo at the temperature of liquid nitrogen in an ampoule (200 cc.) in which the catalyst had already been prepared. The ampoule was kept at reaction temperature. In order to carry out a kinetic run, about one milliliter (corresponding to 0.5% in a reactor) of gas was sampled from the ampoule at each reaction time. The gas was subjected to mass spectrometric analysis in order to determine the $d_y$-distribution (Hitachi RMU-5B). The infrared method was also applied to the qualitative analysis of the product in order to study the activation energy of exchange for each hydrogen atom in propene.

## Results

**The Kinetics of the Reaction.**—Table I shows the $d_y$-distribution obtained at various times at 50°C, $d_y$ representing the percentage of the isotopic species containing $y$ deuterium atoms at time $t$, while $\phi$ is defined by Eq. 1:

$$\phi = \sum_{y=1}^{6} y d_y \qquad (1)$$

The exchange rate constants measured at 50°C were calculated by assuming the reaction to be first order with respect to the concentration of propene ($d_0$). They are shown in Table I. The triangles in Fig. 1 show the plots of the log $(d_{0t} - d_{0\infty})$ vs. the time (curve a), while the circles show the plots of the log $(\phi_\infty - \phi)$ vs. the time (curve b), with the equilibrium value of $\phi$ denoted by $\phi_\infty$. Both plots show approximately straight lines. Such a tendency was not found in nickel.[3]

1) K. Hirota, Y. Hironaka and E. Hirota, *Tetrahedron Letters*, **1964**, 1945.
2) K. Hirota and Y. Hironaka, *J. Catalysis*, **4**, No. 5 (1965).
3) K. Hirota and Y. Hironaka, This Bulletin, **37**, 535 (1964).

TABLE I. $d_y$-DISTRIBUTION IN KINETIC STUDY

| No. | Time, hr. | $d_0$ | $d_1$ | $d_2$ | $d_3$ | $d_4$ | $d_5$ | $d_6$ | $\phi$% |
|---|---|---|---|---|---|---|---|---|---|
| 1 | 0.25 | 84.3 | 14.4 | 1.3 | — | — | — | — | 16.0 |
| 2 | 0.75 | 66.9 | 27.6 | 5.0 | 0.5 | — | — | — | 38.6 |
| 3 | 2.0 | 41.7 | 39.2 | 15.7 | 3.1 | 0.3 | — | — | 81.1 |
| 4 | 3.5 | 27.0 | 40.2 | 24.0 | 7.6 | 1.2 | — | — | 115.8 |
| 6 | 7.5 | 11.0 | 29.5 | 33.0 | 19.3 | 6.3 | 0.9 | — | 183.1 |
| 8 | 13.0 | 4.0 | 18.3 | 32.5 | 28.7 | 13.5 | 3.0 | — | 238.4 |
| 9 | 17.0 | 2.6 | 13.4 | 29.4 | 30.3 | 18.3 | 5.2 | 0.7 | 267.2 |
| 10 | 23.0 | 1.8 | 9.7 | 24.6 | 31.9 | 22.9 | 8.2 | 1.2 | 294.4 |

Pd: 3.26 g. $C_3H_6$: 7.26 mmol. $D_2O$: 29.5 mmol. Temp.: 50°C.

TABLE II. THE TEMPERATURE DEPENDENCY OF THE REACTION RATE

| No. | Temp., °C | Time, hr. | $d_0$ | $d_1$ | $d_2$ | $d_3$ | $d_4$ | $\phi$ | $k$, $hr^{-1}$ |
|---|---|---|---|---|---|---|---|---|---|
| 4227 | 50 | 5.5 | 29.7 | 39.8 | 22.7 | 6.6 | 1.2 | 109.8 | 20.0 |
| 4308 | 55 | 4.0 | 32.1 | 40.8 | 20.9 | 5.4 | 0.8 | 102.0 | 28.6 |
| 4311 | 60 | 3.0 | 34.0 | 40.4 | 19.7 | 5.0 | 0.9 | 98.3 | 42.9 |

Catalyst: 3.26 g. $C_3H_6$: 7.26 mmol. $D_2O$: 30 mmol.

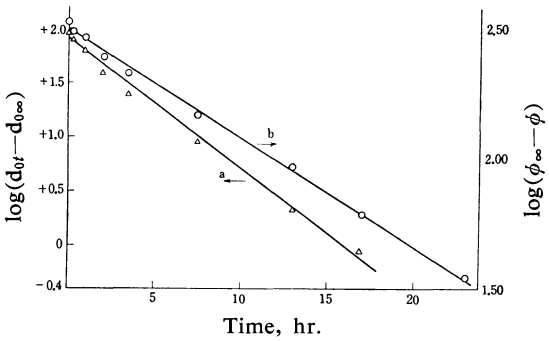



Fig. 1. The plots of $\log(d_{0t}-d_{0\infty})$ vs. time (△) and $\log(\phi_\infty-\phi)$ vs. time (○).

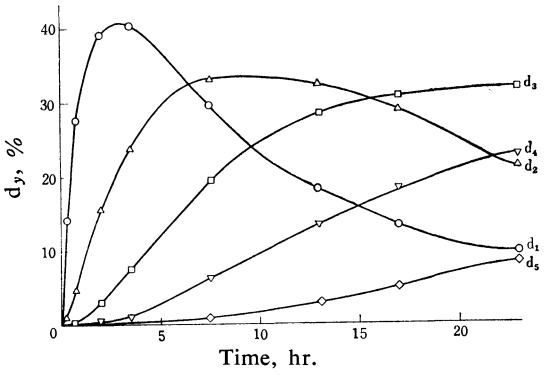



Fig. 2. Time dependency of $d_y$-species.

The time-dependency of the $d_1$—$d_5$ species produced (%) is shown in Fig. 2, with $\sum d_y = 100\%$. Both $d_1$ and $d_2$ rose to a maximum and then decreased, while the others increased for 23 hr.

**Activation Energy.**—The exchange was carried out at 55 and 60°C, as well as at 50°C, on the same palladium black, which was reduced with purified hydrogen gas prior to each run. When the activity was checked in the final run under the same conditions as in the initial run, the two examinations agreed well.

The $d_y$ and $\phi$ values, as well as the $k$ values, are summarized in Table II.

The apparent activation energy obtained from the first order rate constant, $k$, was 9 kcal./mol. The infrared spectra of three runs are practically identical over the range of the C-D stretching region (2100—2300 $cm^{-1}$).

## Discussion

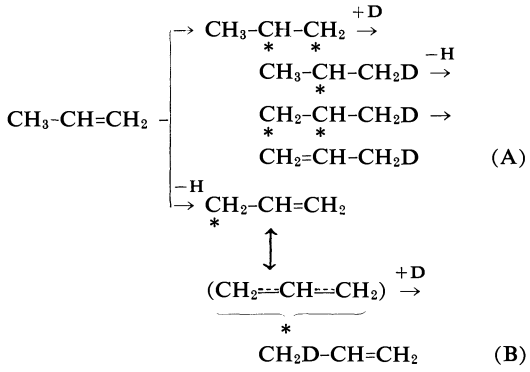
From the data obtained by microwave analysis,[1] methyl hydrogen of propene was the most exchangeable of the three kinds of hydrogens atoms at the initial stage of the reaction (3-$d_1$=59.1%, 2-$d_1$=14.1%, t-1-$d_1$=13.1%, c-1-$d_1$=13.7%[1]*)

Nevertheless, there still remains a question whether or not the exchange occurred according to the mechanism concluded from the analysis of the subspecies-distribution of $d_1$ in the reaction process. This question can be solved by measuring the rate of this reaction. Crawford and Kemball[4] suggested that the $\log(\phi_\infty-\phi)$ curve was composed of two or more straight lines if the molecule has two or more kinds of hydrogen atoms different in their exchangeabilities. In the present case, since the $\log(\phi_\infty-\phi)$ vs. time plot shows a straight line in Fig. 1, the exchange rate of

* This data is shown in Ref. 1.

4) E. Crawford and C. Kemball, *Trans. Faraday Soc.*, **58**, 2452 (1962).

all the hydrogen atoms in propene may be equal, regardless of the groups to which they belong. However, for the purposes of explaining the finding that 3-$d_1$ is most abundant in the subspecies-distribution of $d_1$, it seems convenient to say that there are two different paths of methyl hydrogen exchange;



(A)

(B)

i. e., double-bond migration (A) and the dissociative adsorption of methyl hydrogen (B), the former isomeric mechanism having already been proposed.[3]

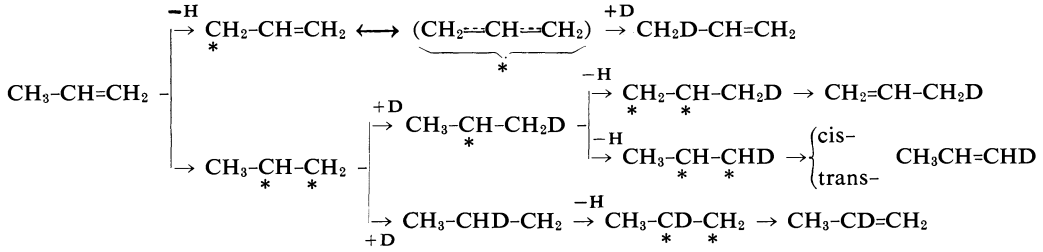
If the rate-determining step of the exchange is the adsorption of propene, the activation energies would be different between the A and B mechanisms, while the activation energy for methyl and methylene hydrogen exchange would be equal as they passed through the A reaction process. Secondly, if some other step is the rate-determining step, the activation energies of A and B would not be very different in general. The activation energy as determined by means of the rate constant, about 9 kcal./mol., would be the same with respect to the six hydrogen atoms in propene, because the infrared spectra of all three runs are practically identical, as has been mentioned above, as are their $d_y$-distributions (Table II).

The activation energy observed on palladium black is smaller than the value (13.7 kcal./mol.) obtained by Twigg,[5] who studied the exchange between deuterium gas and propene on nickel catalyst. The above value, however, is reasonable, because palladium is generally known to be more active than nickel in the catalytic hydrogenation of ethylene. On the other hand, the activation energies were 21.4 kcal./mol. and 23.7 kcal./mol. in the isotopic hydrogen exchanges of ethane[6] and propane[7] respectively with deuterium gas on evaporated palladium film.

Considering these facts, a higher activation energy seems to be required for the exchange of the hydrogen atom of saturated hydrocarbon. Nevertheless, for the exchange of methyl hydrogen in propene the activation energy is given as only 9 kcal./mol. If we assume the mechanism of methyl hydrogen exchange in propene is likely to be similar to that of ethane or propane, the activation energy would be higher. Considering that the existence of the dissociated propene on palladium black as an allyl-type intermediate ($CH_2{=}CH{=}CH_2$) is highly probable, as has been mentioned already,[2] the activation energy for the methyl exchange of propene would become smaller than that of propane or ethane, because the allyl-type intermediate is more stable than a propyl or ethyl intermediate. Though the rate-determining step could not be determined in this study, it may be considered that methyl exchange occurs according to both mechanisms, A and B, the exchange rates of which are given as nearly equal on the basis of the subspecies-distribution of $d_1$ and of kinetic studies.

Accordingly, the reaction scheme would be shown in Scheme 1.

On the other hand, it is possible that the exchange occurs according to either a multiple or a step-by-step mechanism[8] when the $d_2$-species are produced. Morino and Hirota[9] calculated the subspecies-distribution of $d_2$ using a statistical method. Their calculated values



Scheme 1

5) G. H. Twigg, ibid., 35, 934 (1939).
6) J. R. Anderson and C. Kemball, *Proc. Roy. Soc.*, A233, 361 (1954).
7) F. G. Gault and C. Kemball, *Trans. Faraday Soc.*, 57, 1771 (1961).
8) Cf. G. C. Bond, "Catalysis by Metals," Academic Press, London and New York (1962), p. 191.
9) Y. Morino and E. Hirota, *J. Chem. Soc. Japan, Pure Chem. Sec.* (*Nippon Kagaku Zasshi*), 85, 535 (1964).

agreed well with the observed values. However, it was still impossible to determine which of the two mechanisms is the more probable.

If the exchange occurred according to the multiple process, highly-deuterated species would appear, even at the initial stage of reaction. If, on the other hand, the exchange occurred step-by-step, highly deuterated species would not exist at the initial stage of reaction. Therefore, the step-by-step mechanism may be more suitable in this reaction, because highly-deuterated species do not appear at the initial stage of reaction, as is shown in Table I; moreover, the amounts of $d_1$ and $d_2$ species rose to maxima and then decreased as Fig. 2 shows.

It was found to be obviously unreasonable to rely only on the $d_y$-distribution in determining the mechanism of reaction, because even if the $d_y$-distribution is the same between two different samples, subspecies-distributions of $d_y$ are not always the same as has been pointed out in a previous paper.[1] For instance, $d_y$-distributions of propene at the initial stage of exchange reaction were nearly the same on palladium and on nickel, even though the subspecies-distributions of $d_1$ were clearly different.

**Summary**

A reaction mechanism for the catalytic isotopic hydrogen exchange of propene with deuterium oxide on palladium has been offered on the basis of the observed reaction rate and activation energy.

It has been concluded from the observed similarity in the $d_y$-distribution and infrared spectra of the products at different temperatures that the exchange rates of the six hydrogen atoms in propene are nearly equal, while their activation energies are all 9 kcal./mol.

The exchange of methyl hydrogen atoms has been estimated to occur according to the double-bond migration mechanism as well as the dissociation mechanism.

A difference in catalytic activity has been found between palladium and nickel, even when their $d_y$-distributions are nearly the same.

*Chemistry Department*
*Faculty of Science*
*Osaka University*
*Nakanoshima, Osaka**

* New address since July, 1965: Kitatoneyama, Toyonaka, Osaka.

# The Formation of Crystal Violet by the Reaction of *N, N*-Dimethylaniline with Aluminum Chloride

By Hiroyasu SATO*

(Received March 18, 1965)

As has been reported in a previous paper,[1] aniline and *N*-methylaniline adsorbed on aluminum chloride show electronic absorption spectra which are different from those of gaseous molecules; in these spectra the bands are brought nearer to those of toluene and ethylbenzene. This finding was interpreted from the LCMO point of view, and it was concluded that there was a rise in the ionization potential of the amino- or *N*-methylamino-group on adsorption.[2] It was also assumed that the lone-pair electrons of the nitrogen atom in these molecules interact with an electron-accepting center on aluminum chloride to form a Lewis acid-base type, i. e., a sigma-type complex.[1,2] In this paper, the reaction of *N, N*-dimethylaniline with aluminum chloride will be studied. No molecular complex such as is found in the cases of aniline and *N*-methylaniline is formed. The formation of crystal violet is observed in its stead.

## Experimental

Aluminum chloride was prepared from silver chloride and aluminum foils in vacuo according to Wallace and Willard's procedure.[3] *N, N*-Dimethylaniline of the Tokyo Kasei, G. P. grade, was dried with sodium hydroxide and distilled in vacuo before use. The middle fraction was used for the

* Present address: Faculty of Engineering Science, Osaka University, Toyonaka, Osaka,

1) H. Sato, K. Hirota and S. Nagakura, This Bulletin, **38**, 962 (1965).

2) H. Sato, S. Nagakura and K. Hirota, This Bulletin, **38**, 1730 (1965).

3) C. H. Wallace and J. E. Willard, *J. Am. Chem. Soc.*, **72**, 5275 (1950).

experiment. Since the system studied here is very sensitive to moisture, the adsorption and spectrometry procedures were carried out in vacuo. The vacuum system apparatus used in this experiment was the same as that already reported,[1] except for one point — a glass tube for the ESR measurement was attached directly to the quartz cell. Aluminum chloride was sublimed by heating it over a free flame via a break-off seal into the cell-system composed of the quartz cell and the ESR tube. Then the vapor of *N*, *N*-dimethylaniline was introduced by opening the stopcock. The electronic spectrum recorded after the evacuation of this cell system did not show the presence of any adsorbed species, contrary to the cases of aniline and *N*-methylaniline.[1] Therefore, a larger amount of *N*, *N*-dimethylaniline was distilled in vacuo into the cell system. The distilled liquid, initially colorless, gradually became blue. This blue color deepened with time, until finally a deep blue solution was obtained. The electronic and ESR spectra of this solution were then recorded. The electronic spectra were recorded by a Hitachi recording spectrophotometer, model EPS-2.

The electronic spectra of commercial crystal violet $C_{25}H_{30}N_3Cl \cdot 9H_2O$ in *N*, *N*-dimethylaniline and in methanol were also measured for the purpose of comparison.

## Results and Discussion

The electronic spectrum of the blue solution is shown in Fig. 1a. It was stable, even for several months, when kept in vacuo. When the cell system was opened to air, however, a muddy greenish color developed (with another absorption band around 400—430 m$\mu$) and a gel-like precipitate (presumably a hydrolyzed product of aluminum chloride) appeared, and finally the liquid phase turned violet. This violet liquid was also obtained when methanol was added to the greenish mixture. The electronic spectrum of this methanol solution is shown in Fig. 1b. No ESR signal was detected for these solutions. In Fig. 2 the electronic spectra of crystal violet in *N*, *N*-dimethylaniline and in methanol are presented. The spectrum of an aqueous solution (Merrill and Spencer[4]) is reproduced in the figure for the sake of convenience. The spectra shown in Fig. 1a and Fig. 1b seem to be identical to those of crystal violet.

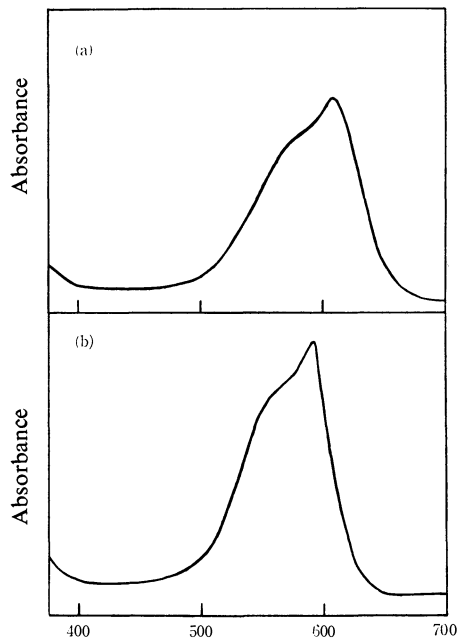



Fig. 1. The electronic spectra of the blue solution obtained by the reaction of *N*, *N*-dimethylaniline and aluminum chloride (a), and of the violet solution obtained when methanol was added to the reaction mixture (b).

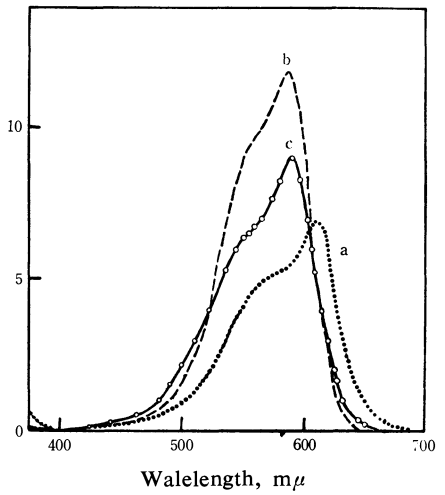



Fig. 2. The electronic spectra of crystal violet.
(a) in *N*, *N*-dimethylaniline ($1.1\times10^{-4}$ mol./l.)
(b) in methanol ($1.1\times10^{-5}$ mol./l.)
(c) in water[4] ($1.0\times10^{-5}$ mol./l.)
The ordinate shows $10^{-3}\varepsilon$ ($\varepsilon$=molar extinction coefficient) for a and $10^{-4}\varepsilon$ for b and c.

Adams and Rosenstein[5] have already shown that a green or a yellow solution is obtained when crystal violet is dissolved in hydrochloric acid (the color depending on the concentration of the acid), and that the color fades in sunlight. According to these authors, such a

4) R. C. Merrill and R. W. Spencer, ibid., **70**, 3683 (1948).

5) E. Q. Adams and L. Rosenstein, ibid., **36**, 1452 (1914). Analyzing the spectra of crystal violet in hydrochloric acid, these authors proved the presence of three colored species in equilibrium (violet with $\lambda_{max}$=590 m$\mu$, green with $\lambda_{max}$=630 m$\mu$ and yellow with $\lambda_{max}$ not located). In the present study these findings were reinvestigated and confirmed. The $\lambda_{max}$ for the yellow species was found to be 430 m$\mu$.

characteristic is common in the chromogens derived from triphenylmethane, and is especially pronounced in the cases of methyl violet and crystal violet. These facts seem to explain what happened when the cell system was opened to air. The moisture reacted with aluminum chloride to give hydrochloric acid and aluminum hydroxide on the surface of the reaction mixture, the acid reacting with crystal violet to give green species. With time this green color was faded by sunlight and/or by the reaction of hydrochloric acid with the remaining *N,N*-dimethylaniline. Finally, by the complete reaction with moisture, there developed the violet color which is like the color of crystal violet dissolved in water. These experimental findings seem to prove the presence of crystal violet in the reaction system. though chemical analysis was impossible.

The formation of crystal violet results from the oxidation of *N,N*-dimethylaniline by aluminum chloride, though the detailed mechanism of the reaction is not clear. The low ionization potential of *N,N*-dimethylaniline will facilitate this reaction. The central carbon atom in the crystal violet may come from the methyl group in the *N,N*-dimethylaniline molecule. The formation of crystal violet ions, $C_{25}H_{30}N_3^+$, will require one electron per ion to be caught in the gegen-anion or elsewhere. In the present case this electron may rest in the vacant orbital of aluminum chloride. Therefore, the finding that the blue solution gave no ESR signal could be interpreted, among other ways, in terms of the possibility that the electron may be paired in the vacant orbital.

Eastman et al.[6] have observed that *N,N*-dimethylaniline and chloranil react to give crystal violet as the final product via the formation of a charge-transfer (CT) complex. Their CT complex has an absorption maximum at 650 m$\mu$. This CT complex has also been found by Briegleb et al.[7] and Mukherjee et al.[8] In the present case also, such a CT complex might be formed during the course of the reaction, though it was not found in the present study.

## Summary

The reaction of *N,N*-dimethylaniline with aluminum chloride in vacuo has given a deep blue solution. This blue solution turns violet because of moisture or the added methanol. The electronic spectra of these solutions seem to be identical with that of crystal violet. The finding that transient green species appear when the vacuum cell system is opened to air can be interpreted in terms of the color of crystal violet dissolved in hydrochloric acid. From these findings the formation of crystal violet has been concluded.

The present author wishes to express his deep gratitude to Professor Kozo Hirota, Faculty of Science, Osaka University, for his continued interest and generous encouragement throughout the work. The author is also indebted to Mr. Toshinobu Imanaka of the same department for his useful suggestions concerning experimental techniques for preparing the evaporated film of aluminum chloride. Thanks are also due to Mr. Koichi Nishikida of the same department for the ESR measurement.

*Department of Chemistry*
*Faculty of Science*
*Osaka University*
*Toyonaka, Osaka*

6) J. W. Eastman, G. Engelsma and M. Calvin, *J. Am. Chem. Soc.*, **84**, 1339 (1962).

7) G. Briegleb and J. Czekalla, *Z. Electrochem.*, **58**, 249 (1954).

8) D. C. Mukherjee and A. K. Chandra, *J. Phys. Chem.*, **68**, 477 (1964).

# The Radiolysis of Ethylene Glycol Diacetate

By Toshiro ISOYA, Kozo HIROTA and Motoyoshi HATADA

(Received March 19, 1965)

There have been a number of reports on the radiolysis, in the liquid phase, of various monoacetates[1-7] which have an ester group in the molecule, but the radiolysis of diacetate or polyacetate, each of which has two or more groups in the molecule, has not yet been reported. The present paper, which will describe the radiolysis of ethylene glycol diacetate (EGDA), the lowest member of diacetate, which was attempted in order to investigate the effect on radiolysis of the number of ester groups in the molecule; the paper will, it is hoped, make possible a better understanding of the radiolysis of such polymers as polyacetates, because diacetate may, in a way, be ragarded as the lowest member of these polymers.

## Experimental

**Material.** — Commercially-available EGDA was refluxed with acetic acid and then purified by distillation in vacuo. By gas chromatographic analysis, two small peaks were found in the sample, before and after the peak of EGDA; the impurities, which could not be identified, were ca. 0.8%.

**Irradiations.**—In each run, a liquid sample of 2 ml. of EGDA was by the conventional vacuum technique, degassed in a glass ampoule fitted with a break seal; the ampoule was sealed off and was then subjected to irradiation at room temperature with cobalt-60 gamma rays. The dose rate, which was determined by the use of a Fricke ferrous sulfate dosimeter, was $1.2\times10^{16}$ eV. $sec^{-1}$ $ml^{-1}$, the correction in the electron density difference between the sample and the dosimeter solution being taken into account.

**The Analysis of the Liquid Products.**—The liquid products were identified by gas chromatographic and mass spectrometric analyses. The gas chromatograph used was a Shimadzu GCIB apparatus, its operating conditions for identification being as follows: adsorbent=polyethyleneglycol (PEG) 6000; column temperature=65°C and 130°C, and adsorbent=dioctyl phthalate, column temperature=110°C, column length=3.75 m., and flow rate of the carrier gas (nitrogen)=30 cc./min. The fractions separated by the gas chromatograph were collected by fraction collectors and subjected to mass spectrometry in order to identify them. To obtain the data for kinetics, the following operating conditions were adopted: column length=3.75 m., adsorbent=PEG 6000, the flow rate of the carrier gas (nitrogen) =30 cc./min., column temperatures=65°C (and 135°C for only methyl cellosolve acetate).

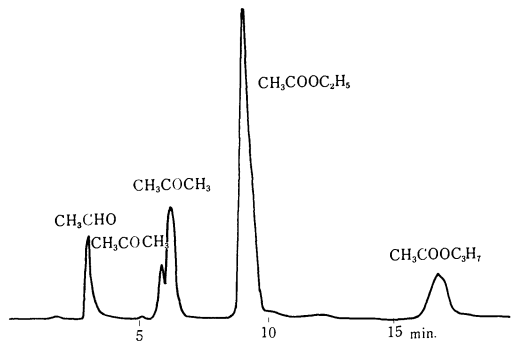



Fig. 1. Gas chromatogram of irradiated ethylene glycol diacetate.
PEG 6000 3.75 m.
$N_2$ gas 30 cc./min.
Column temp. 65°C

Figure 1 shows a typical gas chromatogram of the irradiated EGDA.

**The Analysis of the Gaseous Products.** — The gaseous products were separated into two fractions with a Toepler pump at −78°C and −196°C and were subjected to mass spectrometry.

**The Measurement of the Mass Spectra.**—The mass spectra were obtained by the use of a Hitachi RMU-5-type mass spectrometer, which was a 90°-sector-type instrument of magnetic scanning; the following conditions were adopted: accelerating potential=1500 V., bombarding electron voltage=90 V., and total electron current=100 $\mu$amp.

**The Measurement of the ESR Spectrum.**—The ESR spectrum was measured at −196°C on EGDA, which was degassed in a "Spectrosil" silica tube and irradiated with 1.5 MeV. electron beams (dose rate=$9.3\times10^{18}$ eV. $g^{-1}$ $sec^{-1}$, and total dose=$3.1\times10^{21}$ eV. $g^{-1}$) from a Van de Graaff accelerator at −196°C. The apparatus was of the X-band type, equipped with a Varian V-4500 ESR spectrometer.

## Results and Discussion

1) Figures 2 and 3 show the yields of products as a function of the energy absorbed.

1) E. M. Kindermann, Report WADC-TR-57-465, Stanford Research Institute, September, 1957.
2) A. S. Newton and P. O. Strom, *J. Phys. Chem.*, **62**, 24 (1958).
3) G. E. Adams, J. H. Baxendale and R. D. Sedgwick, ibid., **63**, 854 (1959).
4) P. Ausloos and C. N. Trumbore, *J. Am. Chem. Soc.*, **81**, 3866 (1959).
5) R. W. Wagner and L. H. Towle, Report WADC-TR-58-683, Stanford Research Institute, March, 1959.
6) R. W. Hummel, *Trans. Faraday Soc.*, **56**, 234 (1960).
7) P. Ausloos, *J. Am. Chem. Soc.*, **83**, 1056 (1961).

The yields increased linearly with the dose in most cases; acetaldehyde and ethyl acetate were the exceptions. The $G$ values of the eleven products are listed in Table I. These values were obtained from the best-fitting lines through the experimental points in Fig. 2 and Fig. 3.

The effect of DPPH addition is shown in Table II. The yields of hydrogen, carbon dioxide, acetaldehyde and ethyl acetate decreased at the concentration of $5.5\times10^{-3}$ mol./l., but the yields of the other products were scarcely affected at all by DPPH addition at this concentration. The yields of all the products, however, decreased as the concentration became higher. Some products were affected even at the lowest concentration ($5.5\times10^{-3}$ mol./l.), while other products were not, but all the products were affected at the highest concentration ($9.2\times10^{-2}$ mol./l.). DPPH may play not only the role of a scavenger of the radicals escaping from "cage," but also that of energy-acceptor.[4]

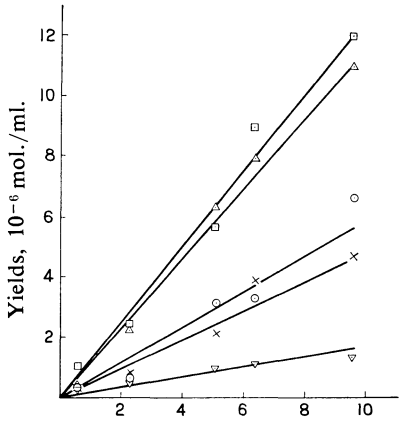



Fig. 2. Yields of gaseous products as a function of energy absorbed.
⊡ CO ⊙ $H_2$ ▽ $C_2H_6$
△ $CH_4$ × $CO_2$

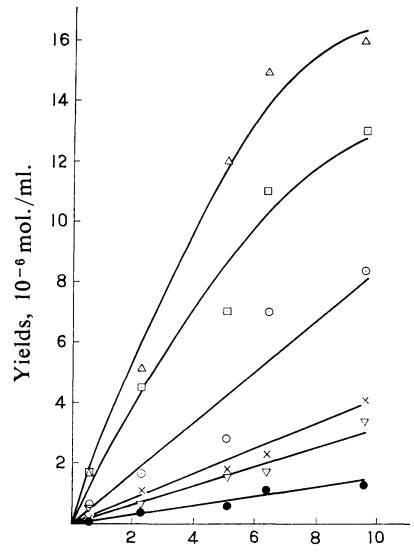



Fig. 3. Yields of liquid products as a function of energy absorbed.
△ $CH_3CHO$ × $CH_3COOC_3H_7$
⊡ $CH_3COOC_2H_5$ ▽ $CH_3COCH_3$
⊙ $CH_3COOCH_3$ ● $CH_3OCH_2CH_2OOCCH_3$

Table I. $G$ Values of products
(dose rate $1.2\times10^{16}$ eV. $ml^{-1}$ $sec^{-1}$)
(dose $6.3\times10^{20}$ eV. $ml^{-1}$)

| Product | $G$ Value |
|---|---|
| $CH_4$ | 0.70 |
| $C_2H_6$ | 0.10 |
| $H_2$ | 0.34 |
| CO | 0.76 |
| $CO_2$ | 0.28 |
| Acetaldehyde | 1.4 |
| Acetone | 0.18 |
| Methyl acetate | 0.50 |
| Ethyl acetate | 1.0 |
| *n*-Propyl acetate | 0.25 |
| Methyl cellosolve acetate | 0.10 |

Figure 4 shows the mass spectrum of EGDA. The ions of $m/e=29$ and 61 are assigned to $HCO^+$ and $CH_3COOH_2^+$, which are formed by some rearrangement processes. These rearrangement peaks have often been reported in the mass spectra of various acetates.[9-13] The ion of $m/e=86$ is assigned to $CH_3COOC_2H_3^+$, which may come from the C–O bond scission of the parent molecule after a rearrangement process including an H atom transfer, and the ion of $m/e=116$ may be formed by $CH_2O$ elimination from the parent molecule.

Figure 5 shows the ESR spectrum of the irradiated EGDA.

This spectrum may be ascribed to $CH_3COOCH_2$ and/or $\dot{C}H_2COOCH_2CH_2OOCCH_3$.

The ratio of the number of carbon, hydrogen and oxygen atoms found in the products is calculated to be C : H : O = 5.0 : 10 : 2.7, clearly indicating that an excess of H is incorporated

8) R. O. Bolt and J. G. Carroll, "Radiation Effects on Organic Materials," Academic Press, New York and London (1963).
9) A. G. Sharkey, Jr., J. L. Schultz and A. Friedel, *Anal. Chem.*, **31**, 87 (1959).
10) J. H. Beyonen, R. A. Saunders and A. E. Williams, ibid., **33**, 221 (1961).
11) E. W. Goldbole and P. Kebarle, *Trans. Faraday Soc.*, **58**, 1897 (1962).
12) C. E. Brion and W. J. Dunning, ibid., **59**, 647 (1963).
13) D. R. Black, W. H. McFadden and J. W. Corse, *J. Phys. Chem.*, **68**, 1237 (1964).

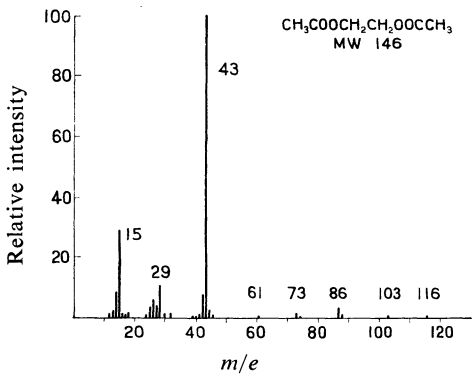



Fig. 4. Mass spectrum of ethylene glycol diacetate.

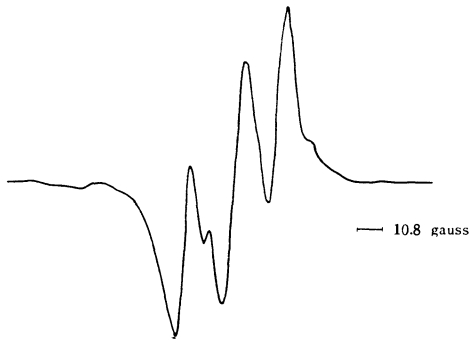



Fig. 5. ESR spectrum of irradiated ethylene glycol diacetate at −196°C.

in the products in comparison with the empirical formula for EGDA, C : H : O = 6.0 : 10 : 4.0. In addition, a brown substance remained after the unreacted EGDA had been distilled away from the irradiated sample. The elemental analysis of this residue gave C : H : O = 6.2 : 10 : 4.1, the C and O contents being slightly larger than those of EGDA. These findings suggest the formation of such undetectable products as dimers, which may come from the radicals, $\dot{C}H_2COOCH_2CH_2OOCCH_3$ and $CH_3COO\dot{C}HCH_2OOCCH_3$, formed by the primary processes 1 and 2, as well as from unsaturated compounds of a higher molecular weight.

The dimers may be formed by the recombination reaction of radicals, $\dot{C}H_2COOCH_2CH_2OOCCH_3$ and/or $CH_3COO\dot{C}HCH_2OOCCH_3$. They may be produced by abstracting a hydrogen atom from EGDA with the radicals produced primarily, such as H, $\dot{C}H_3$, $CH_3\dot{C}O$, $CH_3COO\dot{C}H_2$ and $CH_3COOCH_2\dot{C}H_2$. On the above assumption, the yields of dimers may be given by the following equation:

$$G_{\text{dimers}} = G_{H_2} + 1/2(G_{CH_4} + G_{CH_3CHO} + G_{CH_3COOCH_3} + G_{CH_3COOC_2H_5})$$

The $G_{\text{dimers}}$ value calculated by this equation is 2.1, which gives a calculated C : H : O ratio of the system of 6.0 : 10 : 3.7, a ratio close to that of EGDA, 6.0 : 10 : 4.0.

2) The following reaction scheme is possible judging from the radiolytic products and the mass spectrum of EGDA. A part of the products can be explained by recombination reactions of these radicals.

$$CH_3\overset{\overset{O}{\|}}{C}OCH_2CH_2O\overset{\overset{O}{\|}}{C}CH_3$$

$$\xrightarrow{(1)} H + \dot{C}H_2\overset{\overset{O}{\|}}{C}OCH_2CH_2O\overset{\overset{O}{\|}}{C}CH_3$$

$$\xrightarrow{(2)} H + CH_3\overset{\overset{O}{\|}}{C}O\dot{C}HCH_2O\overset{\overset{O}{\|}}{C}CH_3$$

$$\xrightarrow{(3)} CH_3\overset{\overset{O}{\|}}{C}O + \dot{C}H_2CH_2O\overset{\overset{O}{\|}}{C}CH_3$$

$$\searrow^{(4)}$$

$$\dot{C}H_3 + CO_2 + \dot{C}H_2CH_2O\overset{\overset{O}{\|}}{C}CH_3$$

$$\nearrow_{(6)}$$

$$\xrightarrow{(5)} \dot{C}H_3 + \dot{C}OCH_2CH_2O\overset{\overset{O}{\|}}{C}CH_3$$

$$\searrow^{(7)}$$

$$\dot{C}H_3 + CO + \dot{O}CH_2CH_2O\overset{\overset{O}{\|}}{C}CH_3$$

$$\nearrow_{(9)}$$

$$\xrightarrow{(8)} CH_3\overset{\overset{O}{\|}}{\dot{C}} + \dot{O}CH_2CH_2O\overset{\overset{O}{\|}}{C}CH_3$$

$$\xrightarrow{(10)} CH_3\overset{\overset{O}{\|}}{C}O\dot{C}H_2 + \dot{C}H_2O\overset{\overset{O}{\|}}{C}CH_3$$

Some other products can be explained by the following rearrangement and recombination reactions:

$$CH_3COOCH_2CH_2OOCCH_3$$

$$\xrightarrow{(11)} CH_3COOCH_2CH_2OCH_3 + CO$$

$$\xrightarrow{(12)} CH_3COOCH_2CH_2CH_3 + CO_2$$

$$CH_3COOCH_2CH_2\dot{O} + \dot{C}H_3$$

$$\xrightarrow{(13)} CH_3COOCH_2CH_2OCH_3$$

$$CH_3COOCH_2\dot{C}H_2 + \dot{C}H_3$$

$$\xrightarrow{(14)} CH_3COOCH_2CH_2CH_3$$

Table II. Yields in the presence of DPPH
(dose rate $1.2\times10^{16}$ eV. ml$^{-1}$ sec$^{-1}$)
(dose $6.3\times10^{20}$ eV. ml$^{-1}$)

| ($10^{-6}$ mol./ml.) | Concentration of DPPH ($10^{-2}$ mol./l.) | | | | | Decrease* in the presence of DPPH |
|---|---|---|---|---|---|---|
| | 9.2 | 6.5 | 1.3 | 0.55 | 0 | % |
| $H_2$ | 1.7 | 1.5 | 1.8 | 1.9 | 3.3 | 48 |
| $CH_4$ | 4.2 | 4.0 | 6.2 | 7.6 | 7.9 | 47 |
| $C_2H_6$ | 0.9 | 0.9 | 1.0 | 1.2 | 1.1 | 18 |
| CO | 7.9 | 7.5 | 9.0 | 9.0 | 8.9 | 11 |
| $CO_2$ | 2.4 | 2.4 | 2.4 | 2.8 | 3.9 | 38 |
| Acetaldehyde | 6.4 | 8.5 | 8.9 | 11.7 | 15.0 | 57 |
| Acetone | 1.2 | 1.3 | 2.0 | 2.6 | 2.7 | 56 |
| Methyl acetate | 1.4 | 1.4 | 1.4 | 2.1 | 2.0 | 80 |
| Ethyl acetate | 5.5 | 5.5 | 6.9 | 5.7 | 11.0 | 50 |
| *n*-Propyl acetate | 1.2 | 1.7 | 2.1 | 2.5 | 2.3 | 48 |
| Methyl cellosolve acetate | 0.90 | 0.75 | 1.0 | 1.1 | 1.1 | 18 |

* $(G_{DPPH(0)}-G_{DPPH(9.2)})/G_{DPPH(0)}\times100$

Carbon monoxide is produced by the molecular rearrangement or the reaction in the cage 11, as well as by the radical decomposition processes 7 and 9. Similarly, carbon dioxide is produced by the reactions 12, 4 and 6. The effect of DPPH shows that a larger part of CO and $CO_2$ is produced through reactions 11 and 12, implying that a part of the methyl cellosolve acetate is formed by reaction 11, and the remaining part, by 13. Reactions 11 and 12 are supported by the ions of $m/e=28$ and $m/e=44$, ascribable to $CO^+$ and $CO_2^+$ respectively, in the mass spectrum of EGDA. *n*-Propyl acetate is formed by reactions 12 and 14. Reaction 12 proceeds almost as that reaction 14, judging from the effect of DPPH addition.

Ethyl acetate is formed by the reaction of such radicals as $CH_3COO\dot{C}H_2$ and $\dot{C}H_3$, $CH_3COOCH_2\dot{C}H_2$ and H, while hydrogen, methane, acetaldehyde, and methyl acetate are formed by the reaction of the hydrogen radical with the corresponding radical and by hydrogen abstraction by the three radicals from the parent molecule. Since the $CH_3COO$ radical is unstable,[14,15] the reaction of $CH_3COO$ and $\dot{C}H_3$ is disregarded; in fact, acetic acid was not actually found. 80% of the methyl acetate and 50% of the ethyl acetate were formed by some processes unaffected by DPPH.

Acetone and ethane are formed by the radical reactions 15 and 16 respectively, and to some extent by molecular processes in the cage:

$$CH_3\dot{C}O+\dot{C}H_3 \xrightarrow{(15)} CH_3COCH_3$$

$$\dot{C}H_3+\dot{C}H_3 \xrightarrow{(16)} C_2H_6$$

3) Most data on the monoacetates' radiolysis so far published have been obtained by electron-beam irradiation. In order to compare our results with those for monoacetates, the total gaseous yields of deaerated EGDA was determined by the use of electron irradiation from a Van de Graaff accelerator (dose rate: $1.0\times10^{19}$ eV. ml$^{-1}$ sec$^{-1}$, and dose: $6.7\times10^{20}$ eV. ml$^{-1}$ rads) at room temperature. The results are shown in Table III, as well as those for monoacetates.

Table III. Total gaseous yields of various acetates

| | $G_{gas}$ |
|---|---|
| Methyl acetate[1,8] | 3.40 |
| *n*-Propyl acetate[1,5,8] | 2.4 |
| Isopropyl acetate[1,5,8] | 3.62 |
| Benzyl acetate[1,5,8] | 2.66 |
| EGDA | 1.45 |

The stability of EGDA against the radiation is about twice as much as that of the monoacetates. Similarly, as in the case of monoacetates, the most labile bond of EGDA is the acyl-oxygen bond, a finding from the product yields and from the mass spectrum of EGDA. The above conclusion implies that the yields of the products (acetaldehyde, acetone, carbon monoxide and methyl cellosolve acetate) formed by this bond scission are more than those of others formed by other bond scissions, the sum of the height of the peaks, $m/e=43$ ($CH_3CO^+$) and $m/e=103$ ($CH_3COOCH_2CH_2O^+$), which result from this bond scission occupies

14) L. Jaffe, E. J. Prosen and M. Szwarc, *J. Chem. Phys.*, 27, 416 (1957).
15) P. Ausloos, *Can. J. Chem.*, 36, 383 (1958).

the largest part of the total ion intensity in the mass spectrum of EGDA.

In comparison with the yield of gaseous products from methyl acetate (MA) and EGDA (Table IV), the $G_{MA}/G_{EGDA}$ ratio ranges between ca. 2 and 3. The molecular weights of MA and EGDA are 74.08 and 146.14, and the absorption energy per molecule of EGDA is about two times as much as that of MA. The ratio of the decomposition of MA to that of EGDA is 1.6, smaller than the others.

Table IV. *G* Values of gaseous products of methyl acetate and EGDA

| | Methyl acetate | EGDA | $G_{MA}/G_{EGDA}$ |
|---|---|---|---|
| $G_{-M}$ | 4.1[6] | 2.5 | 1.6* |
| $G_{H_2}$ | 0.87(0.76)[4] | 0.34 | 2.6(2.2) |
| $G_{CO}$ | 1.57(1.64) | 0.76 | 2.1(2.2) |
| $G_{CO_2}$ | 0.78(0.95) | 0.28 | 2.8(3.4) |
| $G_{CH_4}$ | 2.07(2.03) | 0.70 | 3.0(2.9) |
| $G_{C_2H_6}$ | 0.27(0.34) | 0.10 | 2.7(3.4) |

* Only this numeral denotes the ratio of decomposition of MA to that of EGDA.

The yield of each gas per molecule of MA is 1—1.5 times as much as that of EGDA. This means that the formation mechanisms of these gaseous products from EGDA are very similar to those from MA.

**Summary**

The radiolysis of air-free ethylene glycol diacetate by $^{60}Co$ $\gamma$-rays has been studied at room temperature. The following results have been obtained: a) irradiation gives five gaseous products and six liquid products; b) the *G* value of the total of all the gaseous products is 2.18; c) the *G* value of the EGDA decomposition is 2.5. The effect of DPPH addition on the radiolytic products, the relation between radiolytic products and the mass spectrum of unirradiated EGDA, and the ESR spectrum of irradiated EGDA have also been studied. No remarkable difference in the products has been found between EGDA and various monoacetates except in the gaseous products, the yields from EGDA being 1/2—1/3 of those from methyl acetate.

*Osaka Laboratories*
*Japanese Association for Radiation Research on Polymers*
*Neyagawa, Osaka (T. I., K. H. & M. H.)*

*Department of Chemistry*
*Faculty of Science*
*Osaka University*
*Toyonaka, Osaka (K. H.)*

*Technical Research Laboratory*
*Asahi Chemical Industry Co., Ltd.*
*Itabashi-ku, Tokyo (T. I.)*

# Adsorption Measurements during the Synthesis of Methanol at Lower Pressures*

By Susumu TSUCHIYA and Tadao SHIBA

(Received March 20, 1965)

Various mechanisms of the methanol synthesis reaction have been proposed by many workers.[1-6] In deducing these mechanisms, however, the adsorption during the reaction has indirectly been estimated on the basis of either a Langmuir-Hinshelwood or a Temkin-Pyzhev-type mechanism. The importance of the adsorption measurements during surface catalysis has recently been emphasized by Tamaru.[7] In his method, the adsorption on the catalyst surface, as well as its reaction rate, can be directly measured; such reactions as the decomposition of formic acid on metal catalysts[8] and the synthesis and decomposition of ammonia[9,10] have already been studied by means of this new approach.

In order to obtain further information on the mechanism of the methanol synthesis reaction, the present authors used the new

* Presented at Annual Meeting of Catalysis Club of Japan, April, 1962.

1) G. Natta, P. Pino, G. Mazzanti and I. Pasquon, *Chimica e Industria*, **35**, 705 (1953).

2) G. Natta and G. Pastonesi, ibid., **19**, 313 (1937), **20**, 587 (1938).

3) A. Ozaki and T. Saita, *Shokubai* (*Tokyo*), **3**, 158 (1961).

4) V. M. Cheredinichenko and M. I. Temkin, *Zhur. Fiz. Khim.*, **31**, 1072 (1957).

5) H. Uchida and Y. Ogino, This Bulletin, **31**, 45 (1958).

6) I. Pasquon, *Chemica e Industria*, **42**, 352 (1960).

7) K. Tamaru, This Bulletin, **31**, 666 (1958).

8) K. Tamaru, *Trans. Faraday Soc.*, **55**, 824, 1191 (1959).

9) K. Tamaru, ibid., **57**, 1410 (1961).

10) K. Tamaru, "Actes du deuxième Congr. Catalyse," Edition Technip Paris (1961), p. 325.

method to measure the adsorption during the reaction.

## Experimental

The apparatus employed in these experiments was a closed circulating system, as Fig. 1 shows. A is a cylindrical reaction vessel 85 mm. long and 25 mm. in internal diameter. Passing through the central tube of the vessel, the circulating gas was pre-heated before reaching the catalyst bed, which was 45 mm. thick. B is an electric heater, regulated within ±2°C, and D is a thermocouple. K is a circulating pump; a piece of iron sealed in a glass piston, M, was driven reciprocally by means of an electromagnet, L. During the course of the reaction, the stop-cocks, I, J, P, Q, R, S, Y, were closed. The synthesis reaction usually proceeded in such a way that the methanol produced was

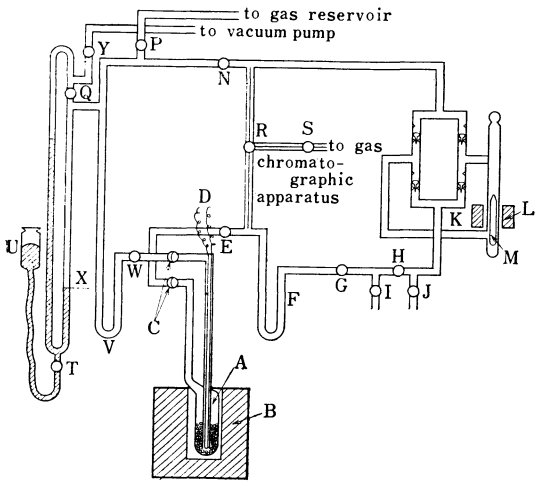



Fig. 1. Apparatus.
A Reaction vessel
B Electric heater
D Thermocouple
F Trap cooled with liquid nitrogen
K Circulation pump

collected in a trap, F, maintained at the temperature of liquid nitrogen. The volume of the circulating system corresponded to about 433 ml. at a reaction temperature of 250°C.

Known amounts of the reactants, pure hydrogen and carbon monoxide, in a synthesis reaction, and methanol in a decomposition reaction, were introduced into the system; the reaction followed, the pressure and composition of the circulating gas being measured at suitable time intervals. The amounts of products condensed in the trap, F, were determined at the end of each run. Gas chromatography as described by Murakami[11] was used for the analyses of gases and condensed products. In this method, the amounts of hydrogen, carbon monoxide, methane, and carbon dioxide were simultaneously determined, using two columns, one (80 cm. long) packed with silica gel as an adsorbent, and the other (2 m. long) packed with 13x Molecular Sieves, successively at room temperature, where herium was employed as a carrier gas. In the analyses of methanol and water, on the other hand, the amounts of carbon monoxide co-existing in the trap, F, were first estimated, and then the ratios of the amounts of the methanol and water to that of carbon monoxide were determined, using successively two columns (1 m. long), packed with polyethylene glycol on celite 545 and with 5A Molecular Sieves, at 60°C, where the carrier gas was hydrogen.

The amounts of the gases adsorbed on the catalyst were obtained as either hydrogen or carbon monoxide from the amounts of reactants introduced into the system, the pressure and the composition of the circulating gas, and the amounts of products trapped. Due allowance was made for the analytical samples removed from the apparatus.

Carbon monoxide was prepared by decomposing sodium formate with sulfuric acid, and it was purified by repeated fractional distillation at the temperature of liquid nitrogen after having passed through a soda-lime column. Hydrogen was obtained from a commercial cylinder, and purified over palladium asbestos at 350°C. Methanol was purified by repeated distillation after having been dried over calcium oxide.

The catalyst employed had the composition Zn : Cr : Cu = 1.0 : 0.49 : 0.16, and it was reduced at 280°C under atmospheric pressure, initially in a hydrogen stream for 60 hr. and then in a hydrogen stream saturated with methanol vapor at room temperature for 50 hr. Before each run, the catalyst was evacuated for 3 hr. at 400°C. Thus the experimental results were satisfactorily reproducible.

## Results and Discussion

The measurements of the adsorption and of the reaction rate were carried out at 250°C. A typical result during the methanol synthesis reaction is shown in Fig. 2. The amounts of the adsorption of hydrogen and carbon monoxide during the reaction were greater than those separately adsorbed, which are represented by solid symbols, when the corresponding amounts of gases were introduced. This fact can be explained as indicating a marked mutual influence on the adsorption of hydrogen and carbon monoxide in the presence of the other gas. It was thus suggested that the adsorption behavior during the reaction can not be estimated from the results observed in the absence of the other gas. A similar effect was reported during the ammonia synthesis reaction.[10] The amounts of methanol formed were far less than those calculated from the equilibrium constant and from the circulating rate. The circulating rate was occasionally measured by means of a soap film meter, connected with the system through the stop-cocks I and J, precautions being taken to prevent the

11) Y. Murakami, This Bulletin, 32, 316 (1959).

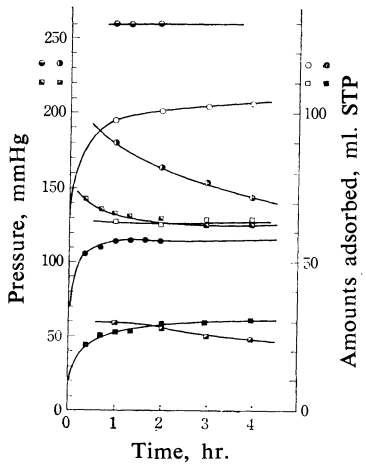



Fig. 2. Adsorption measurements during methanol synthesis at 250°C.
Amounts introduced: $H_2$, 183.3 ml.; CO, 92.0 ml., (STP)
○ $H_2$ adsorbed
□ CO adsorbed
◑ Ambient $H_2$ pressure
◪ Ambient CO pressure
● $H_2$ adsorption in the absence of CO
■ CO adsorption in the absence of $H_2$
◒ $H_2$ pressure in the absence of CO
◩ CO pressure in the absence of $H_2$

water vapor from contaminating the catalyst. The observed products of the reaction were usually identified as methanol and carbon dioxide and, depending on the reaction conditions, small amounts of water and a trace of methane.

The surface area of the catalyst was estimated to be $1.0\times10^7$ cm$^2$ by using the B. E. T. method for nitrogen adsorption at −196°C after the catalyst had been reduced.

The ratios of adsorbed hydrogen to carbon monoxide during the synthesis and the decomposition reaction of methanol are plotted against the ratios of their ambient pressures in Fig. 3. The compositions of the adsorbed phase did not depend on those of the gas phase, in spite of the wide change (about eight thousand-fold) of the partial pressure ratio. The composition of the adsorbed phase would reasonably depend on their partial pressure ratios if the two gases were separately adsorbed. The marked constancy of the composition of the adsorbed species suggests, accordingly, that most of the adsorbed hydrogen and carbon monoxide (more than 80% of the hydrogen and 75% of the carbon monoxide) form a complex, and the average value, 1.5, suggests that the stoichiometric formula of the complex is $CH_3O$.

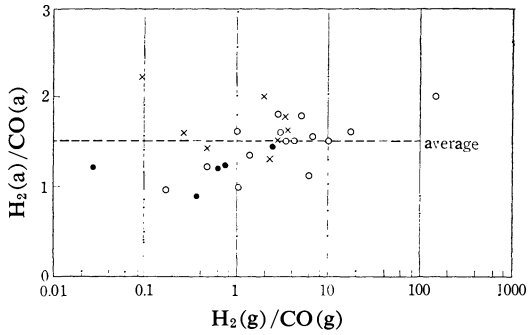



Fig. 3. Relationship between $H_2(g)/CO(g)$ and $H_2(a)/CO(a)$.
○ Synthesis with liquid nitrogen trap
● Synthesis without liquid nitrogen trap
× Decomposition

Figures 4 and 5 give two examples of the plots of the average synthesis rate against the ambient pressure, as well as the amounts of adsorption of hydrogen and carbon monoxide. The rates of methanol synthesis reaction were represented by the cumulative amounts of methanol synthesized over a four-hour period, the rates being too slow to determine with time. The ambient pressure and the amounts of the adsorption of hydrogen and carbon monoxide were represented by their average value over the four-hour period. As is shown

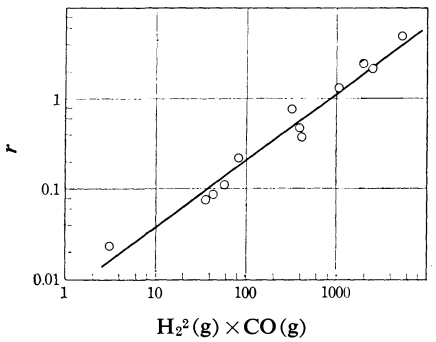



Fig. 4. Synthesis rate vs. $H_2^2(g)\times CO(g)$.

in Fig. 4, the synthesis rate of methanol can be expressed by Eq. 1:

$$r=k(P_{H_2}{}^2P_{CO})^n \qquad (1)$$

where $P_{H_2}$ and $P_{CO}$ are the ambient pressures of hydrogen and carbon monoxide respectively; $k$, the rate constant, and $n$, a constant, which is 0.75. Uchida and Ogino[5] previously reported Eq. 2:

$$r=k(P_{H_2}{}^2P_{CO})^{1-\alpha} \qquad (2)$$

where $\alpha$ is a constant equal to 0.3. These equations are in good agreement in spite of the different conditions of the experiments (at 300—360°C, under 90—150 kg./cm$^2$ by Uchida and Ogino, but at 250°C, under 100—760

TABLE I. ADSORPTION OF HYDROGEN AND CARBON MONOXIDE DURING THE METHANOL SYNTHESIS AT VARIOUS CONDITIONS (250°C)

| Amounts introduced | | Ratio | Gas phase volume | | Amounts adsorbed | | |
|---|---|---|---|---|---|---|---|
| $H_2$, ml. (STP) | CO, ml. (STP) | $H_2$/CO | $H_2$, ml. (STP) | CO, ml. (STP) | $H_2$, ml. (STP) | CO, ml. (STP) | Total, ml. (STP) |
| 229.8 | 107.1 | 2.15 | 99.5 | 34.6 | 125.8 | 69.2 | 195.0 |
| 185.8 | 137.8 | 1.35 | 82.4 | 57.7 | 100.6 | 75.2 | 175.8 |
| 148.3 | 69.4 | 2.14 | 73.7 | 12.0 | 72.8 | 57.0 | 129.9 |
| 80.9 | 180.6 | 0.45 | 18.3 | 105.4 | 62.1 | 65.9 | 138.0 |
| 339.4 | 47.6 | 7.15 | 239.8 | 1.5 | 93.4 | 45.9 | 139.3 |
| 348.5 | 206.5 | 1.69 | 235.5 | 90.7 | 91.9 | 94.3 | 186.2 |
| 318.5 | 137.7 | 2.32 | 193.7 | 62.5 | 106.0 | 66.3 | 172.3 |
| 139.2 | 68.0 | 2.05 | 63.5 | 16.9 | 73.9 | 48.8 | 122.7 |
| 200.6 | 92.0 | 2.09 | 106.4 | 29.7 | 91.1 | 56.2 | 147.3 |
| 76.8 | 178.9 | 0.43 | 5.3 | 112.4 | 71.5 | 58.2 | 128.7 |
| 275.1 | 92.8 | 3.37 | 173.5 | 34.3 | 94.8 | 53.8 | 148.6 |
| 316.4 | 151.5 | 2.09 | 172.5 | 59.8 | 129.2 | 67.9 | 197.1 |

mmHg by the present authors). These equations can be interpreted as implying that the catalyst surface is partially covered with adsorbate, assuming that a Langmuir-type adsorption is valid. It is, however, found that considerable amounts of adsorption on the surface are involved, as is shown in Table I.

It thus seems inappropriate to apply the Langmuir-type adsorption. Moreover, the results reported by Uchida and Ogino[12] indicate that the rate of the reaction of methanol synthesis can not be expressed by any equation based on the Langmuir-type adsorption.

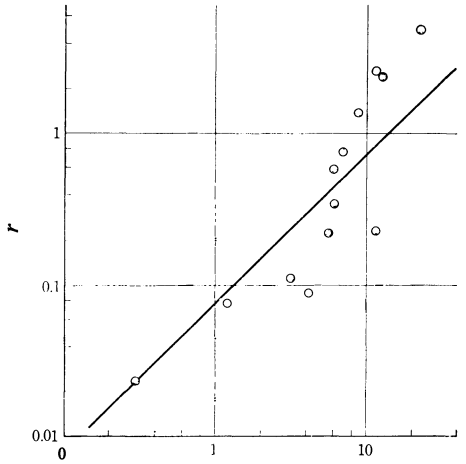



Fig. 5. Synthesis rate vs. $H_2(g)\times CO(a)$.

As Fig. 5 shows, the synthesis rate may also be expressed by Eq. 3:

$$r=kP_{H_2}A_{CO} \qquad (3)$$

where $A_{CO}$ is the amount of carbon monoxide adsorbed in any form combined or not combined with hydrogen on the surface. The adsorbed carbon monoxide mostly forms a complex, so:

$$A_{CO}\fallingdotseq A_X$$

where $A_X$ is the amount of the surface complex. Taking the surface complex to have the $CH_3O$ composition, the Eley-Rideal-type hydrogenation of the adsorbed complex would be the rate-determining step of the over-all reaction:

$$CH_3O(a)+H_2(g) \xrightarrow{-A-} CH_3OH(a)+H(a)$$

The synthesis rate is thus expressed by Eq. 4:

$$r=kP_{H_2}A_{CH_3O} \qquad (4)$$

It may, accordingly, be concluded that the Eley-Rideal-type hydrogenation of the surface complex is the rate-determining step of the methanol synthesis reaction.

## Summary

Adsorption has been studied on a three-component methanol synthesis catalyst during the synthesis of methanol in a closed circulating system. It has been shown that the adsorption of hydrogen and carbon monoxide are both enhanced by the presence of the other. The composition of the adsorbed phase has scarcely been affected at all by the ratio of the partial pressure of hydrogen to carbon monoxide, and the formation of surface complex has been suggested. The rate-determining step of the synthesis of methanol has been suggested to be the process of the Eley-Rideal type hydrogenation of the surface complex.

The authors are grateful to Professor Yoshisada Ogino of Tohoku University for providing the catalyst sample.

*Tokyo Institute of Technology*
*Ookayama, Tokyo*

12) H. Uchida and Y. Ogino, Annual Meeting of Catalysis Club of Japan, April, 1957.

# The Electronic Spectra of Aniline and *N*-Methylaniline Adsorbed on Aluminum Chloride. II. The Theoretical Treatment

By Hiroyasu SATO,* Saburo NAGAKURA and Kozo HIROTA

(Received March 23, 1965)

In the preceding paper,[1] the electronic spectra of aniline and *N*-methylaniline adsorbed on aluminum chloride were measured and compared with those of gaseous aniline, *N*-methylaniline, toluene and ethylbenzene. In the case of adsorbed *N*-methylaniline, the spectrum was almost the same as that of gaseous ethylbenzene, while in the case of adsorbed aniline, a spectrum with a strong band at 192 m$\mu$ and a weak hidden band at about 218 m$\mu$ was obtained. The spectra of the adsorbed species were there discussed qualitatively by considering the location of the intramolecular charge-transfer (CT) configurations relative to those of the locally-excited (LE) configurations. In the adsorbed molecules, the former has a higher energy than in gaseous molecules, as a result of the rise of the ionization potential of the electron-donating group. This rise in the ionization potential was attributed to the interaction of the lone-pair electrons in the adsorbed molecule with some electron-accepting center on aluminum chloride, presumably with the vacant $sp^3$-orbital of the aluminum atom.

In the present paper, the electronic spectra of adsorbed molecules will be studied, by the LCMO treatment, in comparison with those of gaseous molecules. The results can explain satisfactorily the experimental findings mentioned in the preceding paper.[1]

## Calculation Procedure

The calculation was carried out according to the intramolecular charge-transfer model, which is based on the idea that the molecules to be treated consist of an electron-accepting group (the benzene ring in this case) and an electron-donating group (X=$NH_2$, $NHCH_3$, $CH_3$ and $C_2H_5$ groups). Only $\pi$-electrons were taken into account. In the case of aniline or *N*-methylaniline, the lone pair electrons on the nitrogen atom were assumed to belong to the pure 2p$\pi$ atomic orbital. For toluene and ethylbenzene, the hyperconjugation was taken into account, and two $\pi$-electrons were counted for the methyl- or ethyl-group respectively. For adsorbed aniline and adsorbed *N*-methylaniline, an intermediate situation between gaseous aniline and toluene, and between gaseous *N*-methylaniline and ethylbenzene, respectively, is to be expected, as was discussed in the preceding paper. Hence, in these cases also, two $\pi$-electrons may be taken into account for the adsorbed amino-group or the adsorbed *N*-methylamino-group respectively.

After the procedure of Longuet-Higgins and Murrell,[2] configuration interaction was considered among seven electron configurations constructed from the $\pi$-electron orbitals of the benzene ring ($\phi_1, \phi_2, \cdots, \phi_6$) and the 2p$\pi$ (or the pseudo-2p$\pi$) orbital on the electron-donating group, X. They include two CT configurations and four LE configurations, besides the ground configuration. Assuming the molecule $C_6H_5X$ to belong to the point group $C_{2v}$, these configurations can be divided into two symmetry species, $A_1$ and $B_2$. The wave functions which are obtained by the linear combination of the orbital wave functions associated with those configurations are:

$$
\begin{aligned}
A_1:\ & \psi_G = 1/\sqrt{8!}\,|\phi_1\bar{\phi}_1\phi_2\bar{\phi}_2\phi_3\bar{\phi}_3\chi\bar{\chi}| \\
& \psi_P = 1/\sqrt{2}\,\{1/\sqrt{2}\,(\phi_3^{-1}\phi_4+\bar{\phi}_3^{-1}\bar{\phi}_4) \\
& \qquad -1/\sqrt{2}\,(\phi_2^{-1}\phi_5+\bar{\phi}_2^{-1}\bar{\phi}_5)\} \\
& \psi_{\beta'} = 1/\sqrt{2}\,\{1/\sqrt{2}\,(\phi_3^{-1}\phi_4+\bar{\phi}_3^{-1}\bar{\phi}_4) \\
& \qquad +1/\sqrt{2}\,(\phi_2^{-1}\phi_5+\bar{\phi}_2^{-1}\bar{\phi}_5)\} \\
& \psi_{CT} = 1/\sqrt{2}\,(\chi^{-1}\phi_5+\bar{\chi}^{-1}\bar{\phi}_5) \\
B_2:\ & \psi_\alpha = 1/\sqrt{2}\,\{1/\sqrt{2}\,(\phi_2^{-1}\phi_4+\bar{\phi}_2^{-1}\bar{\phi}_4) \\
& \qquad -1/\sqrt{2}\,(\phi_3^{-1}\phi_5+\bar{\phi}_3^{-1}\bar{\phi}_5)\} \\
& \psi_\beta = 1/\sqrt{2}\,\{1/\sqrt{2}\,(\phi_2^{-1}\phi_4+\bar{\phi}_2^{-1}\bar{\phi}_4) \\
& \qquad +1/\sqrt{2}\,(\phi_3^{-1}\phi_5+\bar{\phi}_3^{-1}\bar{\phi}_5)\} \\
& \psi_{CT'} = 1/\sqrt{2}\,(\chi^{-1}\phi_4+\bar{\chi}^{-1}\bar{\phi}_4)
\end{aligned}
\qquad (1)
$$

Here the suffix G denotes the ground configuration; $\alpha$, P, $\beta$ and $\beta'$, the locally-excited configurations, CT and CT', the two charge-transfer configurations respectively. Considering the configuration interaction among these configurations, the energy levels of the molecule

* Present address: Faculty of Engineering Science, Osaka University, Toyonaka, Osaka.

1) H. Sato, K. Hirota and S. Nagakura, This Bulletin, **38**, 962 (1965).

2) H. C. Longuet-Higgins and J. N. Murrell, *Proc. Roy. Soc.*, **A68**, 601 (1955); J. N. Murrell, ibid., **A68**, 969 (1955).

can be obtained by taking the energy of the ground configuration to be zero. The energies of the LE configurations were taken to be equal to the observed excitation energies of benzene (Kimura and Nagakura[3]), while those of the CT configurations can be evaluated by the following equations:

$$\left.\begin{aligned} H_{CT} &= I_X - A_\phi - C \\ H_{CT'} &= I_X - A_\phi - C' \end{aligned}\right\} \qquad (2)$$

where $I_X$ and $A_\phi$ are the ionization potential of the electron donating group, X, and the electron affinity of the benzene molecule respectively.

The Coulombic attraction energies, $-C$ or $-C'$, can be calculated by the uniformly-charged sphere model of Pariser and Parr.[4] In order to carry out the calculation, one must know the bond length, C-X. For toluene this length has already been determined to be 1.52 Å.[5] For aniline, however, there is no data available so far. The available data on $r_{CN}$ are as follows: 1.35 Å (aniline hydrochloride), 1.39 Å (*o*-methylaniline hydrochloride), 1.45 Å (*p*-tolidine hydrochloride), 1.37 Å (*p*-nitroaniline)[6] and 1.407 Å (2, 5-dichloroaniline)[7]. In the present calculations, the $r_{CN}$ value of aniline was taken to be 1.37 Å. The C-N distance for the adsorbed aniline molecule was assumed, however, to be equal to the C-N single bond length, 1.47 Å, because the conjugation between the amino-group and the benzene ring is weakened in this case and, hence, a considerable loss of the double-bond character can be expected. The experimental analysis of molecular structure of *N*-methylaniline and ethylbenzene still has not been made. For these two substances and adsorbed *N*-methylaniline, the C-X distances were assumed to be the same as those of aniline, toluene and adsorbed aniline respectively.

The off-diagonal matrix elements can be determined as follows:

$$\left.\begin{aligned} H_{G\cdot CT} &= \sqrt{2}\int \phi_5 H\chi d\tau \\ H_{\beta'\cdot CT} &= -H_{p\cdot CT} = 1/\sqrt{2}\int \phi_2 H\chi d\tau \\ H_{G\cdot\beta'} &= H_{G\cdot p} = H_{\beta'\cdot p} = 0 \\ H_{\alpha\cdot CT} &= H_{\beta\cdot CT} = 1/\sqrt{2}\int \phi_2 H\chi d\tau \\ H_{\alpha\cdot\beta} &= 0 \end{aligned}\right\} \qquad (3)$$

In evaluating $\int \phi_5 H\chi d\tau$ and $\int \phi_2 H\chi d\tau$, Kimura's procedure[8] was adopted; i. e., besides the core resonance integral between X and the adjacent carbon atom ($\beta$), the corresponding integral between X and the ortho-carbon atom ($\beta'$) was taken into account. In estimating the values of $\beta$ and $\beta'$ for aniline and *N*-methylaniline, their proportionality to the overlap integral was assumed. The obtained values for $\beta$ (and $\beta'$) are $-1.9$ eV. (and $-0.3$ eV.) for aniline and *N*-methylaniline, and $-1.6$ eV. (and $-0.2$ eV.) for adsorbed aniline and adsorbed *N*-methylaniline[9] respectively. For toluene and ethylbenzene, $\beta$ was equated to 0.7 $\beta_0$[10] ($\beta_0$ being $\beta_{CC}$ in benzene), while $\beta'$ was estimated from this $\beta$ by assuming its proportionality to the overlap integral. The values of $-1.6$ eV. and $-0.3$ eV. were thus obtained for $\beta$ and $\beta'$.

The *I-A* values were determined by the following procedure, regarding them as parameters. Calculations were carried out for a certain range of *I-A* values, and the "best" *I-A* value was determined by observing the best fit with the observed transition energy of each substance.

Numerical calculations were carried out with a NEAC 2101 computer set up in the Protein Research Institute of Osaka University.

## Results and Discussion

The calculated results are shown in Fig. 1 and Table I. The experimental results are plotted in the figure at the position which shows the best fit with the calculated values.

As is shown in Fig. 1, a satisfactory agreement can be obtained between calculated and experimental energy values if we assign 11.0, 11.3, 11.5, 11.8, 11.8 and about 12.5 eV. to the *I-A* values of *N*-methylamino-, amino-, adsorbed amino-, adsorbed *N*-methylamino-, ethyl and methyl groups respectively. In the case of both aniline and *N*-methylaniline, the rise in the ionization potential of the electron-donating group (0.2 eV. and 0.8 eV.) is found to be a result of adsorption on aluminum

3) K. Kimura and S. Nagakura, *Molecular Physics*, **9**, 117 (1965).
4) R. Pariser and R. G. Parr, *J. Chem. Phys.*, **21**, 466, 767 (1953).
5) F. A. Keidel, quoted by S. H. Bauer et al., *Ann. Rev. Phys. Chem.*, **4**, 236 (1953).
6) These values are obtained from L. E. Sutton, ed., "Interatomic Distances," Special Publication No. 11, The Chemical Society, London (1958).
7) T. Sakurai, M. Sundaralingam and G. A. Jefferey, *Acta Cryst.*, **16**, 354 (1963).
8) K. Kimura, H. Tsubomura and S. Nagakura, This Bulletin, **37**, 1336 (1964).
9) The change in hybridization which is possibly effected by adsorption is neglected in the evaluation of these numerals. Such a smaller (in absolute terms) value of the resonance integrals for the adsorbed molecules may be caused by a joint effect of bond elongation and hybridization change.
10) The factor of 0.7 has already been used by several authors in the Hückel MO calculation of toluene: cf. C. A. Coulson and U. A. Crawford, *J. Chem. Soc.*, **1953**, 2052; A. Pullman and J. Metzger, *Bull. soc. chim. France*, **15**, 1021 (1948); B. Pullman, M. Magot and G. Berthier, *J. Chem. Phys.*, **18**, 257 (1950).

TABLE I. CALCULATED ENERGY LEVELS, WAVE FUNCTIONS AND OSCILLATOR STRENGTHS ($f$) TAKING ($I$-$A$) AS A PARAMETER, T, AA AND GA DENOTING TOLUENE-TYPE, ADSORBED ANILINE-TYPE AND GASEOUS ANILINE-TYPE CALCULATION, RESPECTIVELY

| Energy, eV. | Wave function | $f$ |
|---|---|---|
| T, $I$-$A$=12.5 eV. | | |
| 0.00 | $\psi_1=0.9900\psi_G-0.0169\psi_p+0.0150\psi_{\beta'}+0.1390\psi_{CT}$ | — |
| 5.92 | $\psi_2=0.0799\psi_G+0.8521\psi_p-0.2787\psi_{\beta'}-0.4357\psi_{CT}$ | 0.16 |
| 6.85 | $\psi_3=-0.0478\psi_G+0.4360\psi_p+0.8461\psi_{\beta'}+0.3027\psi_{CT}$ | 0.99 |
| 8.55 | $\psi_4=-0.1055\psi_G+0.2890\psi_p-0.4540\psi_{\beta'}+0.8362\psi_{CT}$ | 0.06 |
| 4.85 | $\psi_5=0.9668\psi_\alpha+0.0817\psi_\beta+0.2423\psi_{CT'}$ | 0.0054 |
| 6.79 | $\psi_6=-0.1762\psi_\alpha+0.8994\psi_\beta+0.4000\psi_{CT'}$ | 0.91 |
| 8.71 | $\psi_7=-0.1852\psi_\alpha-0.4294\psi_\beta+0.8839\psi_{CT'}$ | 0.27 |
| T, $I$-$A$=12.0 eV. | | |
| 0.00 | $\psi_1=0.9886\psi_G-0.0180\psi_p+0.0160\psi_{\beta'}+0.1484\psi_{CT}$ | — |
| 5.82 | $\psi_2=0.0977\psi_G+0.7907\psi_p-0.3048\psi_{\beta'}-0.5218\psi_{CT}$ | 0.21 |
| 6.81 | $\psi_3=-0.0527\psi_G+0.5261\psi_p+0.7817\psi_{\beta'}+0.3307\psi_{CT}$ | 0.88 |
| 8.23 | $\psi_4=-0.1014\psi_G+0.3125\psi_p-0.5438\psi_{\beta'}+0.7722\psi_{CT}$ | 0.12 |
| 4.82 | $\psi_5=0.9550\psi_\alpha+0.0936\psi_\beta+0.2816\psi_{CT'}$ | 0.0070 |
| 6.70 | $\psi_6=-0.2254\psi_\alpha+0.8460\psi_\beta+0.4832\psi_{CT'}$ | 0.79 |
| 8.36 | $\psi_7=-0.1930\psi_\alpha-0.5249\psi_\beta+0.8290\psi_{CT'}$ | 0.38 |
| AA, $I$-$A$=12.0 eV. | | |
| 0.00 | $\psi_1=0.9860\psi_G-0.0190\psi_p+0.0168\psi_{\beta'}+0.1648\psi_{CT}$ | — |
| 5.82 | $\psi_2=0.1134\psi_G+0.7620\psi_p-0.3039\psi_{\beta'}-0.5605\psi_{CT}$ | 0.23 |
| 6.82 | $\psi_3=-0.0612\psi_G+0.5664\psi_p+0.7406\psi_{\beta'}+0.3561\psi_{CT}$ | 0.83 |
| 8.06 | $\psi_4=-0.1057\psi_G+0.3133\psi_p-0.5990\psi_{\beta'}+0.7293\psi_{CT}$ | 0.16 |
| 4.87 | $\psi_5=0.9565\psi_\alpha+0.0882\psi_\beta+0.2781\psi_{CT'}$ | 0.0062 |
| 6.73 | $\psi_6=-0.2237\psi_\alpha+0.8336\psi_\beta+0.5050\psi_{CT'}$ | 0.77 |
| 8.26 | $\psi_7=-0.1873\psi_\alpha-0.5452\psi_\beta+0.8171\psi_{CT'}$ | 0.40 |
| AA, $I$-$A$=11.5 eV. | | |
| 0.00 | $\psi_1=0.9838\psi_G-0.0203\psi_p+0.0180\psi_{\beta'}+0.1770\psi_{CT}$ | — |
| 5.65 | $\psi_2=-0.1385\psi_G-0.6665\psi_p+0.3147\psi_{\beta'}+0.6614\psi_{CT}$ | 0.29 |
| 6.77 | $\psi_3=-0.0632\psi_G+0.6756\psi_p+0.6380\psi_{\beta'}+0.3641\psi_{CT}$ | 0.66 |
| 7.84 | $\psi_4=0.0943\psi_G-0.3144\psi_p+0.7026\psi_{\beta'}-0.6314\psi_{CT}$ | 0.28 |
| 4.84 | $\psi_5=0.9376\psi_\alpha+0.1032\psi_\beta+0.3320\psi_{CT'}$ | 0.0084 |
| 6.59 | $\psi_6=-0.2955\psi_\alpha+0.7398\psi_\beta+0.6045\psi_{CT'}$ | 0.59 |
| 7.98 | $\psi_7=-0.1832\psi_\alpha-0.6649\psi_\beta+0.7241\psi_{CT'}$ | 0.58 |
| GA, $I$-$A$=11.5 eV. | | |
| 0.00 | $\psi_1=0.9775\psi_G+0.0287\psi_p+0.0255\psi_{\beta'}+0.2075\psi_{CT}$ | — |
| 5.45 | $\psi_2=0.1733\psi_G-0.6158\psi_p-0.3397\psi_{\beta'}-0.6895\psi_{CT}$ | 0.34 |
| 6.83 | $\psi_3=-0.0604\psi_G-0.7079\psi_p+0.6344\psi_{\beta'}+0.3045\psi_{CT}$ | 0.64 |
| 8.05 | $\psi_4=0.1042\psi_G+0.3447\psi_p+0.6939\psi_{\beta'}-0.6235\psi_{CT}$ | 0.24 |
| 4.84 | $\psi_5=0.9033\psi_\alpha+0.1445\psi_\beta+0.4040\psi_{CT'}$ | 0.016 |
| 6.51 | $\psi_6=-0.3751\psi_\alpha+0.7231\psi_\beta+0.5800\psi_{CT'}$ | 0.62 |
| 8.16 | $\psi_7=-0.2083\psi_\alpha-0.6755\psi_\beta+0.7073\psi_{CT'}$ | 0.60 |
| GA, $I$-$A$=11.0 eV. | | |
| 0.00 | $\psi_1=0.9737\psi_G-0.0308\psi_p+0.0274\psi_{\beta'}+0.2241\psi_{CT}$ | — |
| 5.21 | $\psi_2=-0.1998\psi_G-0.5338\psi_p+0.3248\psi_{\beta'}+0.7548\psi_{CT}$ | 0.37 |
| 6.80 | $\psi_3=-0.0588\psi_G+0.7759\psi_p+0.5549\psi_{\beta'}+0.2944\psi_{CT}$ | 0.52 |
| 7.91 | $\psi_4=0.0926\psi_G-0.3348\psi_p+0.7654\psi_{\beta'}-0.5417\psi_{CT}$ | 0.34 |
| 4.69 | $\psi_5=0.8618\psi_\alpha+0.1651\psi_\beta+0.4797\psi_{CT'}$ | 0.020 |
| 6.38 | $\psi_6=-0.4684\psi_\alpha+0.6220\psi_\beta+0.6275\psi_{CT'}$ | 0.40 |
| 7.99 | $\psi_7=-0.1947\psi_\alpha-0.7654\psi_\beta+0.6134\psi_{CT'}$ | 0.75 |

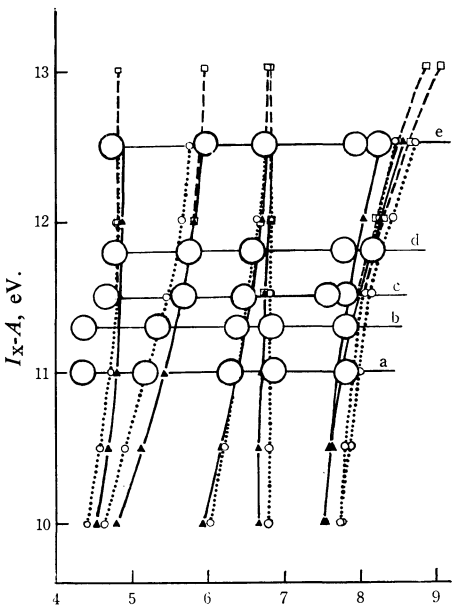



Fig. 1. Calculated and observed energies of excited states.
····· Calcd. for gaseous aniline and *N*-methylaniline
—— Calcd. for adsorbed aniline and *N*-methylaniline
---- Calcd. for toluene and ethylbenzene
○ Observed
a) *N*-Methylaniline b) Aniline
c) Adsorbed aniline
d) Ethylbenzene and adsorbed *N*-methylaniline e) Toluene

chloride, if the change in the electron affinity of benzene ring can be disregarded.

In the calculated results one can find a general tendency for bands to shift and intensities to change with an increase in the *I-A* values. The band corresponding to the $2A_1$ state (hereafter abbreviated to "$2A_1$") shifts to a shorter wavelength with a decrease in the intensity. The "$2B_2$" and "$3A_1$" bands approach each other with an increase in the intensity. For adsorbed *N*-methylaniline, ethylbenzene and toluene, these bands nearly overlap, forming a band corresponding to the degenerate $\beta$ and $\beta'$ bands of benzene. The "$4A_1$" and "$3B_2$" bands show a tendency to separate from each other with a decrease in the intensity. These general trends are just the same as those observed in the spectra of *N*-methylaniline, aniline, adsorbed aniline, adsorbed *N*-methylaniline, ethylbenzene and toluene, according to this order. Such being the case, adsorbed aniline and *N*-methylaniline clearly show intermediate spectra between aniline and toluene, and between *N*-methylaniline and ethylbenzene, respectively.

In the spectra of toluene and ethylbenzene reported by Hammond et al.,[11] more than two bands are found near 150—160 m$\mu$. They assigned them as Rydberg bands. In the light of the present calculations, however, it may be, rather, possible to assign two of these bands as CT bands. In the spectrum of adsorbed aniline,[1] two peaks are found near 160 m$\mu$, though they are weak and less-resolved than other peaks. These bands may also have much of a CT character.

Why the spectra of adsorbed aniline and adsorbed *N*-methylaniline become nearer to those of toluene and ethylbenzene is a difficult question to answer. It may result from the interaction of the lone pair electrons on the nitrogen atom of the adsorbate molecule and a vacant $sp^3$ orbital of the aluminum atom.

## Summary

The electronic spectra of aniline and *N*-methylaniline adsorbed on aluminum chloride have been examined by the LCMO method and have been compared with those of gaseous aniline, *N*-methylaniline, toluene and ethylbenzene. All of these molecules can be treated by the intramolecular charge-transfer model. In order for us to be able to interpret the spectra from the LCMO point of view, the ionization potential of the electron donating group in aniline and *N*-methylaniline molecules should rise upon adsorption on aluminum chloride.

The authors would like to express their gratitude to Dr. Katsumi Kimura, Faculty of Engineering Science, Osaka University, for his helpful discussions. The authors are also indebted to Professor Tatsuo Miyazawa, The Protein Research Institute of Osaka University, for numerical calculations with a NEAC 2101 computer.

*Department of Chemistry*
*Faculty of Science*
*Osaka University*
*Toyonaka, Osaka (H. S. & K. H.)*

*The Institute of Solid State Physics*
*The University of Tokyo*
*Azabu, Tokyo (S. N.)*

### Note Added in Proof

The details of Terenin's work referred in the part I of this paper (*2 in p. 962) was published in *Acta Phys. Chem. URSS*, **18**, 210 (1943) (in English).

11) V. J. Hammond, W. C. Price, J. P. Teegan and A. D. Walsh, *Discussions Faraday Soc.*, **9**, 53 (1950).

# The Vibrational Assignment, Rotational Isomerism and Force Constants of 1, 2-Ethanedithiol

By Michiro HAYASHI, Yuji SHIRO, Toshiyuki OSHIMA and Hiromu MURATA

(Received April 1, 1965)

Many experimental data have been accumulated concerning the rotational isomerism of 1, 2-disubstituted ethanes.[1] Still, a number of molecules have not yet been studied in detail. The present work is the first of a series of papers which will deal with a group of molecules containing sulfur atoms. In this paper, we will first consider the rotational isomerism of 1, 2-ethanedithiol, and then we will determine a set of force constants in a modified Urey-Bradley force field. These force constants will then, in the subsequent paper,[2] be transferred to the other members of the series with similar structures. Finally, they will be transferred to the calculations attempted for polyethylene disulfide, which will be reported in the near future.

## Experimental

The sample used for the measurements was prepared in the following way.[3]

1, 2-Dichloroethane was refluxed over thiourea in ethanol, and the product was treated by a concentrated potassium hydroxide solution and subsequently neutralized by concentrated sulfuric acid. b. p. 70°C/48 mmHg, $n_D^{20}$ 1.5591.

A deuterated species, $DSCH_2CH_2SD$, was prepared from 1, 2-ethanedithiol by a direct exchange of hydrogen with $D_2O$ in the presence of a small amount of potassium carbonate. However, only 30% of the hydrogen was replaced by deuterium.

The infrared spectra in the crystalline state were recorded for the sample cooled with liquid nitrogen at about −120°C. In the gaseous state the infrared spectra were recorded at ten different temperatures in the range from 60 to 220°C.

## The Assignment of the Spectra

If this substance had a unique molecular form, it would show twenty-four fundamental frequencies. However, as we observed too many spectra for one molecular form and since, especially, we found that some of the spectra vanish in the crystalline state we may conclude that rotational isomers exist. Since the mass of a SH group is nearly equal to the mass of a chlorine atom, the spectra of this substance might be close to those of 1, 2-dichloroethane, which were examined in detail.[4]

Actually, this substance gives spectra very similar to those of 1, 2-dichloroethane in the region between 1000 and 1450 $cm^{-1}$. For 1, 2-dichloroethane we have the trans and gauche isomers, and only the trans isomer persists in the crystalline state. For 1, 2-ethanedithiol, the similarity of the spectra and the similar behavior of the spectra upon solidification suggest that the trans and gauche isomers around the C-C bond also exist.

From the well-known assignments for 1, 2-dichloroethane, the assignments of the observed frequencies are easy in this region, where we may have two $CH_2$ bending vibrations, two $CH_2$ wagging vibrations, two $CH_2$ twisting vibrations and one C-C stretching vibration for one molecular form. These frequencies are easily identified at nearly the same frequencies as those for 1, 2-dichloroethane. The spectra relating to the gauche isomer vanish in the crystalline state.

The spectral pattern in the region from 1000 to 650 $cm^{-1}$ looks very different from that of 1, 2-dichloroethane. In this region, we may have two $CH_2$ rocking, two CSH deformation and two C-S stretching vibrations for one molecular form. A deuterated species, $DSCH_2CH_2SD$, was measured for the purpose of the use of its spectra as an aid in the assignment of the observed spectra in this region. For this deuterated species we would expect the CSH deformation vibrations alone to be shifted strongly to the lower frequency region, where no other spectra are expected. Actually, we observed that two new bands are present at 600 and 619 $cm^{-1}$. If the deuteration were perfect, we could expect that the frequencies of two CSH deformation vibrations would vanish or become weaker. Since, however, the deuteration was, unfortunately, not perfect, we could not identify the CSH deformation frequencies directly.

However, a simple application of the product

1) S. Mizushima, "Structure of Molecules and Internal Rotation," Academic Press, New York (1954).
2) M. Hayashi, Y. Shiro and Murata, to be published.
3) J. Spaziale, "Organic Syntheses," Vol. XXX, 35 (1950).
4) For example, I. Nakagawa and S. Mizushima, *J. Chem. Phys.*, **21**, 2195 (1953).

rules reveals that 800 and 890 $cm^{-1}$ should be the CSH deformation vibrations corresponding to the CSD deformation vibrations at 600 and 619 $cm^{-1}$; as 800 $cm^{-1}$ disappears in the crystalline state, it is assigned to the gauche isomer.

We assigned the bands at 718 and 699 $cm^{-1}$ for the trans and those at 664 and 639 $cm^{-1}$ for the gauche to the C-S stretching vibrations on the basis of the assignments given to such similar molecules as methyl mercaptan, dimethyl sulfide and ethyl methyl sulfide.[5]

There remain three unassigned observed frequencies (972, 942 and 769 $cm^{-1}$) in this region; all three disappear in the crystalline state, and 974 $cm^{-1}$ is observed only in the Raman spectra. Some of these frequencies are regarded as the $CH_2$ rocking vibrations on the basis of the assignments given to ethyl methyl sulfide,[6] diethyl sulfide,[7] and $\beta$-chloroethyl methyl sulfide.[8]

Since the bands at 972, 942 and 796 $cm^{-1}$ vanish in the crystalline state, they are not for the trans isomer. There are no unassigned spectra persisting in the crystalline state, and we regarded the band at 718 $cm^{-1}$ as two overlapping frequencies, one for a C-S stretching vibration and the other for a $CH_2$ rocking vibration for the trans isomer. This is a reasonable choice from the selection rule of the trans isomer, as we will discuss in the following section. The other $CH_2$ rocking vibration is assigned to 1030 $cm^{-1}$. For the gauche isomer we have three possibilities: (A) 972 and 769 $cm^{-1}$; (B) 972 and 942 $cm^{-1}$ and (C) 942 and 769 $cm^{-1}$. The band at 942 $cm^{-1}$ is much weaker than that at 972 $cm^{-1}$ and appears as a shoulder of 972 $cm^{-1}$; if we take the pair C as the $CH_2$ rocking vibrations, the strong band at 972 $cm^{-1}$ remains unassigned. We compared the spectra with those of $\beta$-thiamethyl ethyl mercaptan[2]

Table I. Infrared and Raman spectra of 1,2-ethanedithiol ($cm^{-1}$)

| $HSCH_2CH_2SH$ Infrared | | | $DSCH_2CH_2SD$ | | Molecular[a] form | Assignment |
|---|---|---|---|---|---|---|
| Gas | Liquid | Solid | Raman Liquid | Infrared Liquid | | |
| | | | 255 w | | T | C-S torsion |
| | | | 267 s | | G | CCS def. A |
| | | | 299 w | | T | CCS def. $A_g$ |
| | 400 w | | 403 w | | G | CCS def. B |
| | 641 m | | 639 m | 641 m | G | C-S str. A |
| | 662 sh | | 664 m | 699 m | G | C-S str. B |
| 696 s | 699 s | 686 vs | | 699 m | T | C-S str. $B_u$ |
| 710 sh | 718 sh | 715 s<br>720 s | 720 s | 721 s | T | $CH_2$ rock. $A_u$, C-S str. $A_g$ |
| 768 w | 769 w | | 774 m | 771 m | G | $CH_2$ rock. B |
| 794 w | 800 w | | 800 w | 600 m | T, G | CSH def. $A_g$, A (CSD def.) |
| 890 m | 890 w | 887 s | 896 m | 619 m | T, G | CSH def. $B_u$, B (CSD def.) |
| 942 sh | 942 sh | | | | | |
| 970 m | 972 s | | 974 w | 965 m | G | $CH_2$ rock. A |
| 1029 w | 1030 m | | 1027 m | 1008 m | T, G | $CH_2$ rock. $B_g$, C-C str. A |
| | | | 1035 m | | T | C-C str. $A_g$ |
| 1145 m | 1145 s | | 1150 w | 1143 s | G | $CH_2$ twist. B |
| | 1155 sh | 1155 s | | 1148 sh | T | $CH_2$ twist. $A_u$ |
| | 1203 sh | | 1200 w | 1200 sh | G | $CH_2$ twist. A |
| 1217 s | 1220 vs | 1221 s | | 1214 s | T | $CH_2$ wag. $B_u$ |
| 1272 s | 1273 vs | | 1275 m | 1272 s | G | $CH_2$ wag. A |
| 1289 sh | 1292 vs | | 1289 s | 1293 s | T, G | $CH_2$ wag. $A_g$, B, twist. $B_g$ |
| 1419 s | 1420 vs | | 1418 s | 1420 s | T, G | $CH_2$ bend. $A_g$, B |
| | | 1423 s | | | | |
| 1426 s | 1428 vs | | 1425 s | 1438 s | T, G | $CH_2$ bend. $B_u$, A |
| 2570 s | 2570 vs | 2570 s | | 1854 s | T, G | S-H str. (S-D str.) |
| | 2920 vs | | 2920 vs | | T, G | C-H str. |
| 2950 vs | | 2950 vs | | 2950 s | | |
| | 2970 vs | | 2968 vs | | T, G | C-H str. |

a) Molecular forms around the C-C bond.

5) M. Hayashi, *J. Chem. Soc. Japan, Pure Chem. Sec.* (*Nippon Kagaku Zassi*), **78**, 627 (1957).
6) M. Hayashi, T. Shimanouchi and S. Mizushima, *J. Chem. Phys.*, **26**, 608 (1957).
7) M. Hayashi, *J. Chem. Soc. Japan, Pure Chem. Sec.* (*Nippon Kagaku Zassi*), **77**, 1804 (1956).
8) M. Hayashi, ibid., **80**, 1084 (1959).

and found that a band corresponding to 940 $cm^{-1}$ does not exist, while bands corresponding to 972 and 769 $cm^{-1}$ are found at 959 and 776 $cm^{-1}$. Therefore, we took the pair A as the $CH_2$ rocking vibrations.

For 1, 2-dichloroethane and also for many molecules with a $-CH_2CH_2-$ structure, it is well-known that the frequency difference of two $CH_2$ rocking vibrations strongly depends on the azimuthal angle around the C-C bond.

For 1, 2-dichloroethane the frequency differences are 221 $cm^{-1}$ for the trans and 62 $cm^{-1}$ for the gauche; their ratio is 0.28. For 1, 2-ethanedithiol, according to the above assignments, the frequency differences are 312 $cm^{-1}$ for the trans and 203 $cm^{-1}$ for the gauche, while their ratio is 0.65. This ratio seems too large compared with that for 1, 2-dichloroethane. However, 0.64 is also obtained for both $\beta$-thiamethyl ethyl mercaptan and $\beta$-chloroethyl mercaptan.

Furthermore, a refined calculation of nomal vibrations, which will be described afterwards, gave a reasonable set of force costants from this assignment, while the solved force constants obtained from the other possibilities are not acceptable.

From the observed frequencies we have:

$$\sum\nu_i^2(T) = 6.334 \times 10^7$$
$$\sum\nu_i^2(G) = 6.321 \times 10^7 \quad (0.21\% \text{ difference})$$

Therefore, the assignments of the observed frequencies are quite satisfactory. Recently, Fujiyama et al.[9] published a discussion of the vibrational spectra of succinonitrile. According to their assignment, the $CH_2$ rocking frequencies of this substance also have a large ratio of frequency differences (0.62). For the $CH_2$ rocking vibrations, then, the difference of the ratio from that of 1, 2-dichloroethane might arise from the influence of some special character of sulfur atoms attached to the $-CH_2CH_2-$ group. The assignments are given in Table I.

## The Molecular Form of Isomers

In the preceding section, we have assumed that the isomers are the trans and gauche forms around the C-C bond.

The assignment of the spectra discussed above leads to the conclusion that the spectra in the crystalline state show the mutual exclusion rule between the infrared and the Raman spectra. Therefore, the isomer in this state should have the center of symmetry. This requires that the isomer have the trans form around the C-C bond.

9) T. Fujiyama, K. Tokumaru and T. Shimanouchi, *Spectrochim. Acta*, 20, 415 (1964).

We made the calculation of normal vibrations for skeletal frequencies in order to find the molecular form of the isomer disappearing in the crystalline state.

In this treatment, SH and $CH_2$ group were regarded as dynamic units, and, accordingly, only the internal rotation around the C-C bond was taken into consideration. About the force constants used in the Urey-Bradley potential function adopted for this treatment, one of the present authors reported that reasonable values were obtained from the observed vibrational frequencies of molecules with similar structures, such as dimethyl sulfide, methyl mercaptan and ethyl mercaptan.[5] These are $K(CH_2\text{-}SH) = 2.60$, $K(CH_2\text{-}CH_2) = 3.7$, $H(CH_2\text{-}CH_2\text{-}SH) = 0.15$ and $F(CH_2\cdots SH) = 0.50$ md./Å. The calculation was carried out for seven different molecular forms around the C-C bond. Skeletal deformation frequencies produce large frequency changes, as Fig. 1 shows,

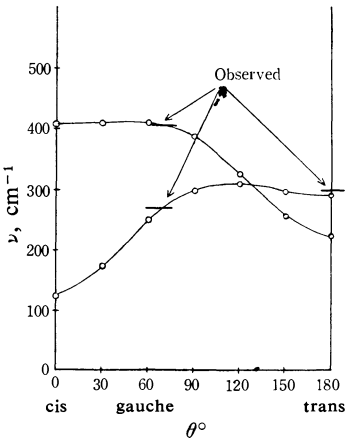



Fig. 1. Observed and calculated frequencies of skeletal deformation modes.

where arrows indicate the observed Raman lines below 450 $cm^{-1}$. The Raman line observed at 299 $cm^{-1}$ is understood to be one of the skeletal deformation vibrations for the trans form, and the other frequency is considered to be Raman-inactive from the symmetry of the trans isomer, while the lines at 267 and 407 $cm^{-1}$ are regarded as the frequencies for the gauche form around the C-C bond. Therefore, we concluded that the isomer disappearing in the crystalline state is the gauche form around the C-C bond.

When we take the rotational isomerism around two C-S bonds into consideration, we would have ten different isomers altogether. Four of them have the trans form, and six have the gauche form, around the C-C bond. The form with the center of symmetry arises twice among the four trans isomers.

We will use symbols T, G and G′ for each rotational axis to designate their molecular forms. For example, GTG′ means an isomer with the gauche, the trans and the gauche form for the first C–S, C–C and the second C–S bond respectively, where the gauche form for the second C–S bond is obtained by a 120° rotation of the hydrogen in the second SH group from its trans position to the opposite direction against the hydrogen in the first SH group. In these notations, two trans forms with a center of symmetry can be expressed as TTT and GTG′ respectively.

Since a Raman line at 255 $cm^{-1}$ is found from the refined normal vibration calculation described in the following section, as a C–S torsion, we have no unassigned spectra persisting in the crystalline state.

Since it is hard to consider that two sets of the spectra arising from TTT and GTG′ would overlap perfectly, and since the results of the normal vibration treatment also indicate that perfect overlapping never happens between two sets of the spectra of TTT and GTG′, we have concluded that only one molecular form exists in the crystalline state. About the molecular form disappearing in the crystalline state, we have not enough information to determine how many molecular forms there are and what the molecular forms are. We have only an unassigned band at 942 $cm^{-1}$ which disappears in the crystalline state; this fact suggests that two or more molecular forms probably exist. From the above discussion about skeletal deformation vibrations, it may be said that the main molecular form is the gauche form around the C–C bond. However, the complete determination of the molecular forms around the C–S bonds is a difficult problem on the basis only of the experimental data available at present.

However, it is worthwhile to note that, as we will discuss in detail, the force constants as determined by the least-squares treatment on the assumption of such molecular forms as TTT and TGT, are considered to be reasonable and can be successfully transferred to other substances with similar structures, while the force constats obtained on the assumption of such molecular forms as GTG′ and GGG are not only unreasonable but also less transferable. We believe that this is a good reason to conclude that the isomer in the crystalline state is TTT with $C_{2h}$ symmetry and that the main isomer vanishing in the crystalline state is TGT with $C_2$ symmetry.

## Energy Difference between Isomers

In the gaseous state at ten different temperatures, we made measurements of the relative absorption intensity of the bands at 1289 and 1272 $cm^{-1}$, which were assigned to the $CH_2$ wagging frequencies for the trans and gauche isomers respectively.

From the observed optical densities, we found that the energy difference of the isomer is $0.6_3$ kcal./mol. where the trans is more stable than the gauche. In order to check the accuracy of this, the measurement was made for 1,2-dichloroethane, which was reported to have an energy difference of $1.1_4$ kcal./mol.,[1] we obtained a very satisfactory agreement.

An attempt was made to measure the intensities in the liquid state at room temperature, at the temperature of ice water, and at the temperature of an ice-alcohol mixture. However, no change could be seen in the absorption intensities. This shows that the isomer have almost the same energy in the liquid state.

## Normal Vibration Calculation

We have attempted to make the normal vibration calculation, including all the vibrational freedoms, in order to get a reliable set of force constants which can then be transferred to molecules with similar structures.

For 1,2-dichloroethane we have established that the usual simple Urey-Bradley force field is not enough to reproduce the observed frequencies. Modifications of the force field have, therefore, been proposed:[10]

1) Torsional freedom is added, with the torsional force constant $Y$.

2) C–H bond interaction constants, $p$, are introduced.

3) Angle-interaction constants, $l$, are considered.

4) Trans and gauche interaction constants, $t$ and $g$, are added between the angles of different $CH_2$ groups.

For 1,2-ethanedithiol we did not know to what extent the force field should be modified. Therefore, we made a trial calculation in a simple Urey-Bradley force field with torsional freedoms for TTT and TGT isomers.

Since we have no observed C–C torsional bands and since the 255 $cm^{-1}$ Raman line is still uncertain as a C–S torsional vibration at this stage, the torsional force constant $Y$(C–S) for the C–S torsional frequencies was computed from the barrier height reported for methyl mercaptan,[11] while the $Y$(C–C) for the C–C torsional frequencies was assumed to be the same value as that for 1,2-dichloroethane.

10) T. Shimanouchi, "Proc. Intern. Sym. Mol. Str. and Spectroscopy," Tokyo, C 216 (1962).
11) T. Kojima and T. Nishikawa, *J. Phys. Soc. Japan*, **12**, 680 (1957).

Since the results have indicated that the 255 $cm^{-1}$ Raman line can be regarded as one of the C–S tortional bands for TTT isomers (species $B_g$), we made a slight change in $Y$(C–S) in order to predict the frequency better. 0.05 md. Å was obtained as a $Y$(C–S) force constant, which made the barrier height 1.7 kcal./mol. This is a little higher than that for methyl mercaptan (1.27 kcal./mol.). The assumed $Y$(C–C) is 0.15 md. Å, which corresponds to the barrier height of 4.8 kcal./mol. We have fixed these two values throughout the following treatments. The first column of Table II presents the set of force constants which best predicts the observed frequencies in the simple Urey-Bradley force field. This set has been obtained by adjusting the force constants little by little in order best to predict the observed frequencies for TTT and TGT isomers. From a comparison of the observed and the calculated frequencies for 1,2-ethanedithiol, it has been found that the force field should also be modified. Especially, as is shown in the second column of Table III, the $CH_2$ wagging, twisting and rocking frequencies strongly suggest the necessity of some modifications of the force field. For example, the observed frequency differences of two $CH_2$ wagging, two $CH_2$ twisting and two rocking vibrations are 68, 140, and 317 $cm^{-1}$ for TTT, and 19, 58, and 203 $cm^{-1}$ for TGT, respectively. The calculated values, 12, 9, and 106 $cm^{-1}$ for TTT and 69, 20, and 160 $cm^{-1}$ for TGT, are much smaller than the observed.

As the first trial of the modification, we have added $p$ and $l$, that is, the C–H bond interaction and the angle interaction terms. The set of force constants obtained is listed in the second column of Table II. As the third column of Table III shows, the above-mentioned frequency differences are improved very much. However, a large difference still remains in the $CH_2$ twisting frequencies for TTT.

As the second trial of the modification, we have added the trans and gauche interaction

TABLE II. FORCE CONSTANTS
$F' = -(1/10)F$

| Force const. | | No. 1 | No. 2 | No. 3 | No. 4 |
|---|---|---|---|---|---|
| $K$(S-H) | (md./Å) | 3.65 | 3.49 | 3.46 | 3.41 |
| $K$(C-S) | (md./Å) | 1.80 | 1.96 | 1.92 | 1.90 |
| $K$(C-C) | (md./Å) | 2.36 | 2.25 | 2.20 | 2.20 |
| $K$(C-H) | (md./Å) | 4.35 | 4.32 | 4.33 | 4.31 |
| $H$(HSC) | (md./Å) | 0.18 | 0.13 | 0.09 | 0.06 |
| $H$(SCC) | (md./Å) | 0.11 | 0.09 | 0.05 | 0.05 |
| $H$(HCC) | (md./Å) | 0.16 | 0.14 | 0.16 | 0.15 |
| $H$(HCS) | (md./Å) | 0.14 | 0.30 | 0.29 | 0.28 |
| $H$(HCH) | (md./Å) | 0.46 | 0.34 | 0.33 | 0.33 |
| $F$(H·S·C) | (md./Å) | 0.35 | 0.36 | 0.62 | 0.70 |
| $F$(S·C·C) | (md./Å) | 0.61 | 0.53 | 0.56 | 0.56 |
| $F$(H·C·C) | (md./Å) | 0.43 | 0.47 | 0.46 | 0.47 |
| $F$(H·C·S) | (md./Å) | 0.43 | 0.21 | 0.19 | 0.23 |
| $F$(H·C·H) | (md./Å) | 0.01 | 0.20[b] | 0.20[b] | 0.20[b] |
| $\kappa$ | (md.·Å) | −0.01 | 0.07 | 0.06 | 0.06 |
| $Y$(C-S) | (md.·Å) | 0.05 | 0.05 | 0.05 | 0.05 |
| $Y$(C-C) | (md.·Å) | 0.15[b] | 0.15[b] | 0.15[b] | 0.15[b] |
| $p$[c] | (md./Å) | | −0.11 | −0.11 | −0.11 |
| $l$[c] | (md.·Å) | | 0.05 | 0.06 | 0.06 |
| $t$[c] | (md.·Å) | | | 0.14 | 0.14 |
| $g$[c] | (md.·Å) | | | −0.05 | −0.05 |
| $t'$[c] | (md.·Å) | | | | −0.04 |
| $g'$[c] | (md.·Å) | | | | −0.04 |
| Averaged error in % | | 2.3 | 1.7 | 0.4 | 0.4 |

a) Averaged error between the observed and the calculated frequencies.
b) Assumed.
c) $p$; C-H bands interaction.
$l$; angles interaction in a $CH_2$ group.
$t$, $g$; trans and gauche interaction between different $CH_2$ group.
$t'$, $g'$; trans and gauche interaction between a $CH_2$ group and a CSH group.

TABLE III. OBSERVED AND CALCULATED FREQUENCIES OF $CH_2$ HYDROGEN DEFORMATION VIBRATIONS ($cm^{-1}$)

| Molecular form | | | Obs. | | Calcd. No. 1 | | Calcd. No. 2 | | Calcd. No. 3 | | Calcd. No. 4 | |
|---|---|---|---|---|---|---|---|---|---|---|---|---|
| TTT | $CH_2$ wag. | $A_g$ | 1292 | (68) | 1202 | (12) | 1289 | (88) | 1305 | (90) | 1305 | (88) |
| | | $B_u$ | 1220 | | 1214 | | 1201 | | 1215 | | 1217 | |
| | $CH_2$ twist. | $A_u$ | 1153 | (140) | 1152 | (9) | 1154 | (19) | 1161 | (130) | 1160 | (131) |
| | | $B_g$ | 1292 | | 1143 | | 1173 | | 1291 | | 1291 | |
| | $CH_2$ rock. | $A_u$ | 718 | (312) | 701 | (106) | 730 | (235) | 714 | (308) | 715 | (308) |
| | | $B_g$ | 1030 | | 807 | | 965 | | 1022 | | 1023 | |
| TGT | $CH_2$ wag. | A | 1273 | (19) | 1182 | (69) | 1281 | (13) | 1257 | (42) | 1257 | (42) |
| | | B | 1292 | | 1251 | | 1294 | | 1299 | | 1299 | |
| | $CH_2$ twist. | A | 1203 | (58) | 1147 | (29) | 1164 | (18) | 1195 | (45) | 1197 | (47) |
| | | B | 1145 | | 1137 | | 1146 | | 1150 | | 1150 | |
| | $CH_2$ rock. | A | 972 | (203) | 829 | (160) | 923 | (158) | 974 | (198) | 974 | (199) |
| | | B | 769 | | 769 | | 765 | | 776 | | 775 | |

TABLE IV. OBSERVED AND CALCULATED FREQUENCIES OF 1,2-ETHANEDITHIOL ($cm^{-1}$)

| | Trans (TTT) | | | | Gauche (TGT) | | | |
|---|---|---|---|---|---|---|---|---|
| | Obs. | Calcd. | | | Obs. | Calcd. | | Assignment |
| | | No. 1[a] | No. 3[b] | | | No. 1[a] | No. 3[b] | |
| | 2920 | 2910 | 2908 | | 2920 | 2913 | 2901 | C-H str. |
| | 2570 | 2583 | 2570 | | 2570 | 2583 | 2570 | S-H str. |
| | 1420 | 1411 | 1426 | | 1428 | 1429 | 1426 | $CH_2$ bend. |
| $A_g$ | 1292 | 1202 | 1305 | | 1273 | 1182 | 1257 | $CH_2$ wag. |
| | 1035 | 1027 | 1037 | | 1030 | 1023 | 1020 | C-C str. |
| | 800 | 815 | 806 | | 800 | 815 | 802 | CSH def. |
| | 718 | 723 | 721 | A | 639 | 615 | 642 | C-S str. |
| | 299 | 297 | 301 | | 267 | 284 | 267 | CCS def. |
| | 2968 | 2975 | 2972 | | 2968 | 2965 | 2963 | C-H str. |
| | 1155 | 1152 | 1161 | | 1203 | 1147 | 1195 | $CH_2$ twist. |
| $A_u$ | 718 | 701 | 714 | | 972 | 829 | 974 | $CH_2$ rock. |
| | — | 232 | 236 | | — | 209 | 210 | C-S torsion |
| | — | 115 | 118 | | — | 102 | 100 | C-C torsion |
| | 2968 | 2963 | 2961 | | 2968 | 2972 | 2969 | C-H str. |
| $B_g$ | 1292 | 1143 | 1291 | | 1145 | 1137 | 1150 | $CH_2$ twist. |
| | 1030 | 807 | 1022 | | 769 | 769 | 776 | $CH_2$ rock. |
| | 255 | 249 | 255 | | — | 229 | 236 | C-S torsion |
| | 2920 | 2934 | 2929 | | 2920 | 2930 | 2925 | C-H str. |
| | 2570 | 2583 | 2570 | B | 2570 | 2583 | 2570 | S-H str. |
| | 1428 | 1429 | 1420 | | 1420 | 1424 | 1422 | $CH_2$ bend. |
| $B_u$ | 1220 | 1214 | 1215 | | 1292 | 1251 | 1299 | $CH_2$ wag. |
| | 890 | 878 | 889 | | 890 | 883 | 886 | CSH def. |
| | 699 | 695 | 690 | | 664 | 641 | 665 | C-S str. |
| | — | 227 | 173 | | 403 | 408 | 401 | CCS def. |

a) Using a simple Urey-Bradley force field corresponding to a set of force constants No. 1 in Table II.
b) Using a modified Urey-Bradley force field corresponding to a set of force constants No. 3 in Table II.

terms between the angles of different $CH_2$ groups. As the fourth column of Table III shows, a very satisfactory agreement has thus been obtained. The set of force constants in this modified Urey-Bradley force field was obtained by the application of the least-squares method. We have twenty-two force constants, of which two for torsinal freedoms are fixed at the values mentioned before.

Forty-two observed frequencies could be predicted with an average error of 0.4%; the maximum error was 1.5%.

By the use of the set of force constants so obtained, the frequencies for $DSCH_2CH_2SD$ species were calculated; the observed frequencies have been reproduced with an average error of 0.8%. The calculated and the observed frequencies are tabulated in Table IV.

As we mentioned before, we tried to check the molecular forms. At first, as may be seen in Table V, we calculated the frequencies for GTG′ and GGG isomers as well as for TTT and TGT isomers. We concluded that the C–C stretching, $CH_2$ rocking, CSH deformation and C–S stretching frequencies for GTG′ and GGG isomers can be observed separately from those for TTT and TGT isomers if they exist. As we have no unassigned spectra in the expected region, however, GTG′ and GGG isomer may not exist.

Secondly, we tried, by the least-squares method, to get a set of force constants on the assumption that the molecular forms were GTG′ and GGG isomers. In this attempt, we found that the force constants did not converge well in a reasonable range of values. Therefore, we might say that GTG′ and GGG isomers are not actual molecular forms. We have concluded that TTT and TGT are the actual molecular forms, as we mentioned in the preceding section.

Another modification of the force field has also been attempted. As the last modification, we introduced the trans and gauche interaction terms between the angles of different $CH_2$ groups. Similar interaction terms, $t'$ and $g'$,

Table V. Observed and calculated frequencies in different molecular forms of 1,2-ethanedithiol[a] ($cm^{-1}$)

| | Obs. | Calcd. | | Obs. | Calcd. | |
|---|---|---|---|---|---|---|
| | | TTT | GTG′ | | TGT | GGG |
| CC str. | 1035 | 1037 | 1016 | 1030 | 1020 | 992 |
| CS str. | 718 | 720 | 691 | 664 | 665 | 650 |
| | 699 | 696 | 694 | 639 | 642 | 630 |
| $CH_2$ rock. | 1030 | 1022 | 1011 | 972 | 974 | 970 |
| | 718 | 719 | 718 | 769 | 776 | 779 |
| CSH def. | 890 | 892 | 898 | 890 | 886 | 896 |
| | 800 | 804 | 877 | 800 | 802 | 845 |

a) Frequencies unaffected by the molecular forms are omitted from the table.

are possible between the angles of a $CH_2$ group and a CSH angle. The last column of Table V shows a set of force constants adjusted in this modified force field by the least-squares method. However, as we see in the last column of Table III, this modification has no appreciable influence on the $CH_2$ wagging, twisting and rocking vibrations or on the CSH deformation vibrations, and no appreciable improvement of the average errors could be obtained. Therefore, we have concluded at present that this kind of modification is not necessary for 1, 2-ethanedithiol.

The transferability of the force constants has been checked by the use of the set of the force constants of the second modification of the Urey-Bradley force field. For *n*-propyl mercaptan, β-thiamethyl ethyl mercaptan, β-halogenoethyl mercaptan and 1, 2-dithiamethyl ethane, the set can predict the observed frequencies with a very satisfactory agreement,[2] as will be reported on in the subsequent papers of this series.

*Department of Chemistry*
*Faculty of Science*
*Hiroshima University*
*Higashisenda-machi, Hiroshima*

# The Vibrational Assignment and Rotational Isomerism of β-Halogenoethyl Mercaptan

By Michiro HAYASHI, Yuji SHIRO, Masahiro MURAKAMI and Hiromu MURATA

(Received April 1, 1965)

In a previous paper,[1] we dealt with the vibrational spectra of 1, 2-ethanedithiol in relation to the rotational isomerism. The present work, the second of a series of papers, will deal with the vibrational spectra of β-chloroethyl mercaptan and β-bromoethyl mercaptan. We have two objects in studying the spectra of these substances. First, these molecules are suitable for checking the transferability of the force constants obtained from the observed spectra of 1, 2-ethanedithiol. Second, they can be obtained by the exchange of an oxygen in ethylene chlorohydrin with a sulfur atom. For ethylene chlorohydrin, extensive studies were reported by Mizushima and his coworkers[2] about the rotational isomerism. They reported that two rotational isomers exist in the gaseous and the liquid states, where the gauche isomer is more stable than the trans. In the crystalline state, the gauche isomer alone was found to persist. For other 1, 2-disubstituted ethanes, the trans isomer was usually found to be more stable than the gauche, and in

1) M. Hayashi, Y. Shiro. T. Oshima and H. Murata, This Bulletin, 38, 1734 (1965).

2) S. Mizushima, T. Shimanouchi, T. Miyazawa, K. Abe and M. Yasumi, *J. Chem. Phys.*, 19, 1477 (1951); S. Mizushima, T. Shimanouchi, K. Kuratani and T. Miyazawa, *J. Am. Chem. Soc.*, 74, 1378 (1952).

the crystalline state, the trans isomer alone was found to persist. It was understood that this irregularity in the case of ethylene chlorohydrin appears because of the presence of an intramolecular hydrogen bond between a chlorine and a OH group in the gauche form.

Since a SH group is expected to have a very weak power to make a hydrogen bond with a halogen atom, in contrast to the fact that a OH group has a strong power, the findings concerning β-halogenoethyl mercaptan are expected to be interesting.

## Experimental

β-Chloroethyl and β-bromoethyl mercaptans were prepared by adding dry hydrochloric acid and hydrobromic acid respectively to ethylene sulfide.

β-Chloroethyl mercaptan: b. p. 113°C/760 mmHg

β-Bromoethyl mercaptan: b. p. 52°C/ 28 mmHg

The purity of the samples was checked by gas chlomatography.

The Raman spectra were measured with a Cary 81 spectrometer, while the infrared spectra were recorded with EPI-S2 (Hitachi Co. Ltd.) with NaCl optics in the region from 4000 to 650 $cm^{-1}$.

The infrared spectra in the crystalline state were recorded for the samples cooled with liquid nitrogen at about −120°C.

## Rotational Isomerism

A comparison of the observed spectra in the gaseous and the liquid states with those in the crystalline state immediately reveals the existence of rotational isomers for these substances, since many infrared bands vanish in the crystalline state.

As we reported in the previous paper, in the case of 1, 2-ethanedithiol, large shifts of frequencies may be expected, depending on the molecular forms around the C-C bond, while the molecular forms around the C-S bond will cause rather smaller shifts in frequency. As we have very similar spectra to those of 1, 2-ethanedithiol, the above conclusion might also be true for β-halogenoethyl mercaptan. Therefore, we will disregard for a moment the molecular forms around the C-S bond. If the isomers are the trans and the gauche forms around the C-C bond, the trans form might be a less polar form than the gauche form. We may expect then that the spectra for the trans form will get their relative absorption intensities when a mixture is made with a non-polar substance as a solvent, while the spectra for the gauche form will get their relative intensities in a mixture with a polar solvent. Measurements were made with cyclohexane, carbon disulfide, acetone and nitromethane as a solvents for β-chloroethyl mercaptan. Around 750 $cm^{-1}$, five infrared bands (778, 753, 724, 699 and 675 $cm^{-1}$) are seen, of which two (675 and 778 $cm^{-1}$) vanish in the crystalline state. It has been found that the bands at 675 and 778 $cm^{-1}$ become stronger as the solvent becomes polar. Therefore, for β-chloroethyl mercaptan the molecular form in the crystalline state is probably the less polar form or the trans form around the C-C bond, and the other which exists only in the gaseous and liquid states, is probably the more polar form or the gauche form. Similar results have been obtained for β-bromoethyl mercaptan.

The skeletal normal vibration calculation has also given the same conclusion for both substances. We have calculated the skeletal frequencies as a four-body problem in an Urey-Bradley force field with the force constants reported in the literature.[3] They are $K(CH_2\text{-}CH_2)=3.7$, $K(CH_2\text{-}SH)=2.43$, $K(CH_2\text{-}Cl)=2.9$, $K(CH_2\text{-}Br)=2.4$, $H(CH_2\text{-}CH_2\text{-}SH)=0.15$, $H(CH_2\text{-}CH_2\text{-}Cl)=0.17$, $H(CH_2\text{-}CH_2\text{-}Br)=0.15$, $F(CH_2\cdots SH)=0.466$, $F(CH_2\cdots Cl)=0.49$ and $F(CH_2\cdots Br)=0.40$ md./Å. Seven different isomers around the C-C bond were considered as molecular forms.

For these substances there are two skeletal deformation frequencies for an unique molecular form, which would be expected below 500 $cm^{-1}$. For β-chloroethyl mercaptan, four Raman lines are seen, at 406, 300, 255 and 220 $cm^{-1}$. It has been concluded from the calculation that 406 and 255 $cm^{-1}$ correspond to the calculated frequencies (406 and 248 $cm^{-1}$) for the gauche form and that 300 $cm^{-1}$ corresponds to that (282 $cm^{-1}$) for the trans form. The line at 220 $cm^{-1}$ might not be another skeletal deformation frequency for the trans form even though the calculated frequency is 221 $cm^{-1}$, since this has been calculated as 186 $cm^{-1}$ from the refined treatment of normal vibrations to be described afterwards, and since the calculation has shown that 220 $cm^{-1}$ might be the C-S torsional frequencies for the gauche form.

For β-bromoethyl mercaptan we have three observed Raman lines, at 210, 245 and 375 $cm^{-1}$; the calculated frequencies are 375 and 225 $cm^{-1}$ for the gauche form and 235 and 169 $cm^{-1}$ for the trans form. Therefore, 245 $cm^{-1}$ corresponds to that for the trans form, while 210 and 375 $cm^{-1}$ correspond to those for the gauche form. In the gaseous and the liquid states, both the trans and the gauche isomers exist. Measurements of the relative absorption

3) S. Mizushima, T. Shimanouchi, I. Nakagawa and A. Miyake, *J. Chem. Phys.*, **21**, 215 (1953); M. Hayashi, *J. Chem. Soc. Japan, Pure Chem. Sec.* (*Nippon Kagaku Zassi*), **77**, 1692 (1956); **78**, 627 (1957).

TABLE I. INFRARED AND RAMAN SPECTRA OF β-CHLOROETHYL MERCAPTAN ($cm^{-1}$)

| Infrared Gas | Infrared Liquid | Infrared Solid | Raman Liquid | Assignment[a] |
|---|---|---|---|---|
| | | | 220 vw | torsion |
| | | | 255 w | skel. def. (G) |
| | | | 300 s | skel. def. (T) |
| | | | 406 w | skel. def. (G) |
| | | | 640 s | C-S str. (G) |
| 675 w | 675 sh | | 680 sh | C-Cl str. (G) |
| 705 sh | 702 vs | 699 vs | 695 s | C-S str. (T) |
| 720 vs | 724 m | 724 m | 720 s | $CH_2$ rock. (T) |
| 754 vw | 754 w | 753 s | 753 vs | C-Cl str. (T) |
| 766 w | 778 m | — | | $CH_2$ rock. (G) |
| 855 w | 860 m | 860 m | 860 m | CSH def. (TT, GT) |
| — | 888 w | — | | CSH def. (GG) |
| 920 vw | 928 m | — | 920 w | CSH def. (TG, GG') |
| 972 s | 969 vs | — | 970 w | $CH_2$ rock. (TG) |
| 1034 m | 1021 w | 1021 w | 1025 m | $CH_2$ rock. (TT), C-C str. (G) |
| 1052 w | 1048 m | 1048 s | 1045 m | C-C str. (T) |
| 1136<br>1146 m | 1143 s | 1143 s | 1142 w | $CH_2$ twist. (T, G) |
| 1226 vs | 1227 vs | 1224 vs | 1210 w | $CH_2$ wag. (T) |
| 1280 vs | 1283 vs | 1268 w | 1275 sh | $CH_2$ twist. (T), $CH_2$ wag. (G) |
| 1296 vs | 1298 vs | 1294 s | 1295 vs | $CH_2$ wag. (T) |
| 1305 sh | 1306 vs | — | 1310 sh | $CH_2$ wag. (G) |
| 1431 vs | 1423 s<br>1445 vs | 1421 s<br>1443 vs | 1430 s<br>1435 s | $CH_2$ bend. (T, G)<br>$CH_2$ bend. (T, G) |
| 2570 m | 2570 s | 2570 s | 2570 vs | S-H str. (T, G) |
| 2950 s | 2950 vs | 2950 vs | 2950 vs | C-H str. (T, G) |
| 2995 s | 2995 s | 2995 s | 2990 s | C-H str. (T, G) |

a) Molecular forms around the C-C bond are shown in parentheses. For CSH deformations, molecular forms around both the C-C bond and the C-S bond are shown.

intensities of $CH_2$ wagging frequencies around 1250 $cm^{-1}$ were attempted in order to ascertain the energy differences in the isomers in both the gaseous and the liquid states.

In the gaseous state measurements were made at ten different temperatures in the range from 50 to 160°C. In the liquid state they were made at five different temperatures in the range from −30 to 70°C. The measurements indicated that for these substances the trans isomer is more stable than the gauche isomer in both the gaseous and the liquid state. In the gaseous state the energy differences are computed from the observed optical densities as $0.5_2$ and $0.9_5$ kcal./mol. for β-chloroethyl and β-bromoethyl mercaptan respectively. In the liquid state they are computed as $0.1_6$ and $0.6_2$ kcal./mol. respectively.

However, the spectra used for the trans and the gauche isomers are situated so close together that the errors might be expected to be relatively large (±300 cal./mol.).

## Normal Coordinate Treatment

The normal vibration calculation has been attempted for two purposes:

1) In order to use the results as an aid in the assignment of the spectra and for the consideration of the detailed molecular forms of the isomers, and

2) In order to test the set of force constants which we obtained from the observed spectra of 1, 2-ethanedithiol and to ascertain whether or not the set is applicable to these substances.

There are five possible molecular forms for these substances. In the notation described in the previous paper, these are TT, TG, GT, GG and GG' (where the first letter refers to the molecular form around the C-C bond, and the second, to those around the C-S bond). In this treatment all the vibrational freedoms were taken into account, including two torsional freedoms, and a modified Urey-Bradley force field was used which included the following modifications:[4]

(1) Torsional force constants, $Y$; (2) C-H bond interaction constants, $p$; (3) angle interaction constants, $l$, for $CH_2$ groups, and (4) trans and gauche interaction constants, $t$ and $g$, between angles of different $CH_2$ groups.

4) T. Shimanouchi, *Pure and Appl. Chem.*, 7, 131 (1963); T. Shimanouchi, "Proc. Intern. Sym. Mol. Str. and Spectroscopy," Tokyo, C 216 (1962).

TABLE II. INFRARED AND RAMAN SPECTRA OF β-BROMOETHYL MERCAPTAN ($cm^{-1}$)

| Infrared Gas | Infrared Liquid | Infrared Solid | Raman Liquid | Assignment[a] |
|---|---|---|---|---|
| | | | 210 w | skel. def. (G) |
| | | | 245 m | skel. def. (T), torsion (T) |
| | | | 375 w | skel. def. (G) |
| | | | 555 s | C-Br str. (G) |
| | | | 612 vs | C-Br str. (T) |
| 665 m | 665 w | — | 662 m | C-S str. (G) |
| 710 m | 710 m | 713 s | 710 s | $CH_2$ rock. (T) |
| 743 m | 743 m | 742 s | 735 s | C-S str. (T) |
| 765 m | 765 m | — | | $CH_2$ rock. (G) |
| 848 w | 852 s | 852 s | 837 s | CSH def. (TT), (GT) |
| | 858 sh | — | | CSH def. (GG) |
| 900 s | 903 m | 910 m | 895 w | CSH def. (TG), (GG′) |
| 950 m | 964 vs | — | 960 w | $CH_2$ rock. (TG) |
| 1033 w | 1022 w | 1022 w | 1028 w | $CH_2$ rock. (TT), C-C str. (G) |
| | 1043 w | 1043 m | 1045 s | C-C str. (T) |
| 1122 m | 1122 vs | | 1123 w | $CH_2$ twist. (G) |
| | | 1135 vs | 1140 s | $CH_2$ twist. (T) |
| 1199 vs | 1199 vs | 1199 vs | 1195 m | $CH_2$ wag. (T), $CH_2$ twist. (G) |
| 1259 s | 1260 vs | — | | $CH_2$ wag. (G) |
| 1273 s | 1271 sh | 1271 vs | 1275 vs | $CH_2$ wag. (T), twist. (T) |
| 1295 sh | 1291 s | — | | $CH_2$ wag. (G) |
| 1415 s | 1416 s | 1419 s | 1425 s | $CH_2$ bend. (T, G) |
| 1431 s | 1431 vs | 1430 vs | 1430 s | $CH_2$ bend. (T, G) |
| 2570 m | 2570 s | 2570 s | 2562 vs | S-H str. (T, G) |
| 2950 s | 2950 vs | 2950 vs | 2962 sh | C-H str. (T, G) |
| 3000 s | 3000 s | 3000 s | 3010 m | C-H str. (T, G) |

a) Molecular forms around the C-C bond are shown in parentheses. For CSH deformations, molecular forms around both the C-C bond and the C-S bond are shown.

There was no modification made between the CSH angle and those of $CH_2$ groups. Therefore, the force field remained unchanged even when the molecular form around the C–S bond changed. All of five molecular forms were considered for β-chloroethyl mercaptan, while for β-bromoethyl mercaptan only two isomers (TT and GT) were considered. Twenty-six force constants were used in the calculation; among them twenty force constants were transferred from those obtained for 1, 2-ethanedithiol. Six other force constants, which were related to halogen atoms, were determined in order to predict the observed spectra in the best possible way. They are listed in Table III; the calculated frequencies are listed in Tables IV and V with the observed frequencies, which we will discuss afterwards. The agreement between the observed and the calculated frequencies has been found to be very satisfactory; we have concluded that the set of force constants obtained in the previous paper is also applicable to these substances.

## Vibrational Assignment and Molecular Form

The assignments of these spectra can easily be found by comparing them with the spectra of 1, 2-ethanedithiol. They are given in Tables I and II. We found differences from the results of 1, 2-ethanedithiol in the region from 950 to 800 $cm^{-1}$, where we would expect CSH deformation frequencies. In this region, we have four infrared bands for both β-chloroethyl and β-bromoethyl mercaptan. As we have only one CSH deformation frequency for a unique molecular form, these are too many for two isomers.

In the previous paper on 1, 2-ethanedithiol, we noted, from the refined treatment of normal vibration calculations, that C–C stretching, C–S stretching, one of two $CH_2$ rockings and one of two CSH deformation frequencies are shifted slightly if the molecular form around the C–S bond is different. Since we had no unassigned spectra for 1, 2-ethanedithiol and since the results of normal vibration calculation gave reasonable force constants for the trans form around the C–S bonds, while the gauche form did not, we determined tentatively that the molecular form is the trans around the C–S bond.

The situation is different for β-halogenoethyl mercaptan. For β-chloroethyl mercaptan, the molecular form in the crystalline state is regarded as TT, since, from the absorption

TABLE III. FORCE CONSTANTS

Force constants transferred from the set obtained from 1, 2-ethanedithiol.

| | | | | | |
|---|---|---|---|---|---|
| $K$(C-H) | md./Å | 4.33 | $F$(HCS) | md./Å | 0.192 |
| $K$(S-H) | md./Å | 3.46 | $F$(HCC) | md./Å | 0.459 |
| $K$(C-C) | md./Å | 2.2 | $F$(SCC) | md./Å | 0.560 |
| $K$(C-S) | md./Å | 1.9 | $F$(CSH) | md./Å | 0.620 |
| $H$(HCH) | md./Å | 0.331 | $Y$($CH_2SH$) | md.·Å | 0.052 |
| $H$(HCS) | md./Å | 0.294 | $Y$($CH_2CH_2$) | md.·Å | 0.15 |
| $H$(HCC) | md./Å | 0.156 | $\kappa$($CH_2S$) | md.·Å | 0.058 |
| $H$(SCC) | md./Å | 0.052 | $l$($CH_2$) | md.·Å | 0.057 |
| $H$(CSH) | md./Å | 0.086 | $t$($CH_2CH_2$) | md.·Å | 0.136 |
| $F$(HCH) | md./Å | 0.2 | $g$($CH_2CH_2$) | md.·Å | −0.051 |

Force constants determined to predict the observed spectra best.

| | | | | | |
|---|---|---|---|---|---|
| $K$(C-Cl) | md./Å | 2.0 | $F$(CCCl) | md./Å | 0.60 |
| $K$(C-Br) | md./Å | 1.75 | $F$(HCCl) | md./Å | 0.20 |
| $H$(CCCl) | md./Å | 0.10 | $F$(CCBr) | md./Å | 0.58 |
| $H$(HCCl) | md./Å | 0.29 | $F$(HCBr) | md./Å | 0.19 |
| $H$(CCBr) | md./Å | 0.09 | $\kappa$($CH_2Cl$) | md.·Å | 0.05 |
| $H$(HCBr) | md./Å | 0.28 | $\kappa$($CH_2Br$) | md.·Å | 0.05 |

$F' = -(1/10)F$ $l$; interaction term within $CH_2$ group $t$, $g$; trans and gauche interaction terms for $CH_2CH_2$ group $Y$; torsional vibration force constant.

TABLE IV. OBSERVED AND CALCULATED FREQUENCIES OF β-CHLOROETHYL MERCAPTAN ($cm^{-1}$)

| Trans (C-C) | | | Gauche (C-C) | | | | |
|---|---|---|---|---|---|---|---|
| Obs. | Calcd. | | Obs. | Calcd. | | | Assignment |
| | TT | GT | | TG | GG | GG′ | |
| 1445 | 1429 | 1429 | 1445 | 1429 | 1429 | 1429 | $CH_2$ bend. |
| 1423 | 1415 | 1415 | 1423 | 1417 | 1418 | 1418 | $CH_2$ bend. |
| 1298 | 1295 | 1289 | 1306 | 1292 | 1285 | 1286 | $CH_2$ wag. |
| 1227 | 1202 | 1197 | 1283 | 1249 | 1248 | 1248 | $CH_2$ wag. |
| 1283 | 1289 | 1287 | | 1177 | 1168 | 1168 | $CH_2$ twist. |
| 1143 | 1157 | 1159 | 1143 | 1145 | 1146 | 1145 | $CH_2$ twist. |
| 1121* | 1015 | 985 | 969 | 971 | 968 | 966 | $CH_2$ rock. |
| 724 | 709 | 705 | 778 | 774 | 775 | 760 | $CH_2$ rock. |
| 1048 | 1024 | 1028 | 1021 | 1010 | 1000 | 986 | C-C str. |
| 754 | 724 | 713 | 675 | 657 | 652 | 657 | C-Cl str. |
| 702 | 688 | 689 | 640 | 625 | 628 | 626 | C-S str. |
| 860* | 857 | 907 | 860* | 850 | 889 | 919 | CSH def. |
| 300 | 303 | 304 | 406 | 418 | 424 | 417 | skel. def. |
| | 186 | 186 | 255 | 258 | 260 | 277 | skel. def. |
| (220) | 246 | 253 | (220) | 221 | 221 | 208 | torsion |
| | 119 | 118 | | 102 | 100 | 101 | torsion |

* The values are the observed frequencies for trans form around C-S bond. Observed frequencies for other forms should be referred to Table I.

intensity measurements in mixtures, the bands persisting in the crystalline state are found to be the less polar form and since one of two $CH_2$ rocking modes in the higher frequency was calculated to be 1015 $cm^{-1}$ for TT, and 985 $cm^{-1}$ for TG, while we have only 1021 $cm^{-1}$ in the crystalline state and no corresponding band can be seen around 985 $cm^{-1}$. In the region from 950 to 800 $cm^{-1}$, there is only one infrared band, at 860 $cm^{-1}$, in the crystalline state. Therefore, this is assigned to the CSH deformation mode for the TT isomer. We have two other bands in this region where no other vibrational modes is to be expected, except for CSH deformation modes. Therefore, we may conclude that more polar form is not a unique molecular form but a group of isomers.

From the normal vibration calculation described in the preceding section, we have

Table V. Observed and calculated frequencies of β-bromoethyl mercaptan ($cm^{-1}$)

| Trans (TT) | | Gauche (TG) | | Assignment |
|---|---|---|---|---|
| Obs. | Calcd. | Obs. | Calcd. | |
| 1431 | 1428 | 1431 | 1428 | $CH_2$ bend. |
| 1416 | 1418 | 1416 | 1417 | $CH_2$ bend. |
| 1271 | 1294 | 1291 | 1291 | $CH_2$ wag. |
| 1199 | 1201 | 1260 | 1245 | $CH_2$ wag. |
| 1271 | 1275 | 1199 | 1172 | $CH_2$ twist. |
| 1135 | 1150 | 1122 | 1141 | $CH_2$ twist. |
| 1022 | 1013 | 964 | 968 | $CH_2$ rock. |
| 710 | 708 | 765 | 774 | $CH_2$ rock. |
| 1043 | 1022 | 1022 | 1007 | C-C str. |
| 743 | 715 | 665 | 667 | C-S str. |
| 612 | 623 | 555 | 557 | C-Br str. |
| 852 | 856 | 852 | 849 | CSH def. |
| 245 | 251 | 375 | 392 | skel. def. |
| | 173 | 210 | 215 | skel. def. |
| (245) | 246 | (245) | 255 | torsion |
| | 112 | | 86 | torsion |

also relatively large shifts in frequency for the CSH deformation, and one of two rocking modes for β-chloroethyl mercaptan, for different isomers around the C-S bond. For $CH_2$ rocking modes we have so many spectra in the expected region that the overlapping of the spectra might hide the differences. However, for CSH deformation modes we have found infrared bands corresponding to the calculated frequencies for different isomers. That is, 928 $cm^{-1}$ corresponds to the calculated frequency, 907 $cm^{-1}$, for TG and to that, 919 $cm^{-1}$, for GG', 888 $cm^{-1}$, to the calculated frequency, 989 $cm^{-1}$, for GG, and 860 $cm^{-1}$, to the calculated frequency, 857 $cm^{-1}$, for TT and to that, 850 $cm^{-1}$, for GT. We could not determine whether all five isomers exist or not. However, at least three rotational isomers definitely exist, TT, GG and either TG or GG'. For β-bromoethyl mercaptan, we have also found results similar to those in the case of β-chloroethyl mercaptan, since we have similar spectra for CSH deformation modes. This substance, though the band at 903 $cm^{-1}$ is assigned to either TG or GG', might have a component arising from impurity; it persists in the crystalline state, the absorption intensity rapidly increases as the temperature increases in the gaseous state, and the band never loses its intensity again, even when it was cooled to room temperature.

For GG', there is a possibility of finding an intramolecular hydrogen bond between a SH group and a halogen atom. However, we could not find any evidence, though careful measurements were made with different solvents for SH stretching modes around 2570 $cm^{-1}$.

It should be noted that, even when the trans isomer consists of two molecular forms (TT and TG) and the gauche isomer consists of three molecular forms (GG, GT and GG'), the influences can not be seen for frequencies other than for CSH deformation frequencies; that is, the spectra for all the components coincide with each other except for CSH deformation modes. Therefore, we can find only two sets of the spectra for the trans and the gauche forms around the C-C bond. The assignments are shown in Tables I and II.

### Comparison with Ethylene Chlorohydrine

The following are the differences between the results for β-halogenoethyl mercaptan and those for ethylene chlorohydrin:

| | β-Halogenoethyl mercaptan | Ethylene chlorohydrin |
|---|---|---|
| 1) Molecular form around the C-C bond in the crystalline state | trans | gauche |
| 2) More stable molecular form around the C-C bond in the gaseous state | trans | gauche |
| 3) More stable molecular form around the C-C bond in the liquid state | trans | gauche |
| 4) Intramolecular hydrogen bond between XH and a halogen (X=O and S) | not be found | exists |
| 5) Molecular form around the C-S bond | several isomers | not proved |

It is very clear from the above comparison that the irregularity of the molecular form in the crystalline state and the stabilities in the gaseous and the liquid states for ethylene chlorohydrin come from the influences of the intramolecular hydrogen bonding between OH and Cl, as Mizushima and his co-workers pointed out. The results for β-halogenoethyl mercaptan strongly confirm this conclusion. For β-halogenoethyl mercaptan, the lack of the intramolecular hydrogen bonding probably makes it easy to find the different isomers around the C-S bond, since this makes the CSH deformation bands of these substances sharper than the COH deformation bands of ethylene chlorohydrin.

The author wish to express their gratitude to Mrs. Michiko Fukuyama of the Tokyo Industrial Research Institute for her measurements of the Raman spectra.

*Department of Chemistry*
*Faculty of Science*
*Hiroshima University*
*Higashisenda-machi, Hiroshima*

# Metal Complexs of Amino Acids. I. The Circular Dichroism of Copper(II) Complexes with Optically Active Amino Acids

By Takaji YASUI

(Received April 5, 1965)

It is well known that copper(II) complexes show a broad absorption band, which is due to the d→d transition, in the visible region. There have been many reports[1,2] concerning the assignments of the absorption components of this band, but most of these studies have been made on the basis of the absorption spectrum.

Pfeiffer and Christeleit[3] have studied the optical rotatory dispersion (ORD) of copper(II) complexes with optically active amino acids; their ORD data suggest that the Cotton effect in the visible absorption region is only one. It may be expected from the recent circular dichroism (CD) studies by other workers[4] that the split components of the d→d transition of the copper(II) complexes with optically active amino acids may also be separated by the CD method.

In the present paper, the CD curves of [Cu(am)$_2$]-type complexes (am=L- and D-alanine, L-serine, L-valine, L-threonine, L-allothreonine, L-proline and L-hydroxyproline) have been reported in the region from 1000 to 400 m$\mu$ in aqueous solutions. A preliminary letter on this subject was published recently.[5]

## Experimental

**Measurements.**—The CD curves were obtained by a Shimadzu QR-50 spectrophotometer with a CD attachment. All measurements were made at 10—12°C in the region from 1000 to 400 m$\mu$. Saturated, 1/40 or 1/20 mol./l. solutions in water, pyridine or ethylene glycol were used. The cell length employed was 1 cm. The aqueous solutions of bis(DL-threoninato)copper(II) or bis(sarcosinato)copper(II) monohydrate were used as the reference solutions instead of water.

The absorption measurements were made by a Beckman DU spectrophotometer at room temperature.

**Materials.**—All of the copper(II) amino acid complexes were prepared from copper(II) hydroxide by a modification of the method of Abderhalden and Schnitzler.[6]

1) *Bis(L-alaninato)copper(II), [Cu(L-ala)$_2$].*—To a solution containing 4.5 g. of L-alanine in 30 ml. of warm water, 2.2 g. of copper(II) hydroxide was added; the mixture was then heated for a few minutes on a water bath. After the solution had been filtered, a small amount of alcohol was added drop-by-drop to the filtrate and the solution was cooled in an ice bath. The crystals which separated were collected and washed with alcohol and then ether. Recrystallization was carried out from an aqueous alcohol solution.

Found: C, 30.31; H, 4.91; N, 11.64. Calcd. for Cu($C_3H_6NO_2$)$_2$: C, 30.06; H, 5.05; N, 11.69%.

2) *Bis(D-alaninato)copper(II), [Cu(D-ala)$_2$].*—This compound was prepared by the same procedure as was used in 1).

3) *Bis(L-serinato)copper(II), [Cu(L-ser)$_2$].*—One gram of copper(II) hydroxide was added to a solution containing 2.1 g. of L-serine in 30 ml. of warm water. The mixture was then filtered and left to stand at room temperature. When a proper amount of alcohol was added to the filtrate, blue crystals were deposited. They were washed with alcohol and then with ether. The complex was recrystallized from an aqueous alcohol solution.

Found: C, 26.75; H, 4.42; N, 10.19. Calcd. for Cu($C_3H_6NO_3$)$_2$: C, 26.52; H, 4.46; N, 10.31%.

4) *Bis(L-valinato)copper(II) Monohydrate, [Cu(L-val)$_2$]·$H_2O$.*—The compound was obtained by a method similar to that used in 1). It forms bluish-violet crystals.

Found: C, 40.63; H, 6.95; N, 9.45; $H_2O$, 6.08. Calcd. for Cu($C_5H_{10}NO_2$)$_2$·$H_2O$: C, 40.60; H, 6.81; N, 9.47; $H_2O$, 5.74%.

5) *Bis(L-threoninato)copper(II) Monohydrate, [Cu(L-thr)$_2$]·$H_2O$.*—Bluish-violet crystals were separated by the method that was used in 3).

Found: C, 32.04; H, 5.39; N, 9.39; $H_2O$, 5.91. Calcd. for Cu($C_4H_8NO_3$)$_2$·$H_2O$: C, 32.05; H, 5.38; N, 9.35; $H_2O$, 5.67%.

6) *Bis(L-allothreoninato)copper(II) Monohydrate, [Cu(L-allothr)$_2$]·$H_2O$.*—The needle crystals of a bluish-violet color were separated by a method similar to that used in 3).

Found: C, 32.01; H, 5.48; N, 9.14; $H_2O$, 5.85. Calcd. for Cu($C_4H_8NO_3$)$_2$·$H_2O$: C, 32.05; H, 5.38; N, 9.35; $H_2O$, 5.67%.

7) *Bis(L-prolinato)copper(II) Dihydrate, [Cu(L-prol)$_2$]·$2H_2O$.*—To a solution containing 3 g. of L-proline in 20 ml. of water, 1.2 g. of copper(II) hydroxide was added; then a sufficient amount of

1) J. Bjerrum, C. J. Ballhausen and C. K. Jørgensen, *Acta Chem. Scand.*, **8**, 1275 (1954).
2) C. K. Jørgensen, ibid., **10**, 887 (1956).
3) P. Pfeiffer and W. Christeleit, *Z. physiol. Chem.*, **245**, 197 (1937).
4) B. E. Douglas, R. A. Haines and J. G. Brushmiller, *Inorg. Chem.*, **2**, 1194 (1963).
5) T. Yasui, J. Hidaka and Y. Shimura, *J. Am. Chem. Soc.*, **87**, 2762 (1965).
6) E. Abderhalden and E. Schnitzler, *Z. physiol. Chem.*, **163**, 94 (1927).

acetone was added to the solution until crystals deposited. These crystals were collected and washed with acetone. The needle crystals were obtained in blue by recrystallizing them from an aqueous acetone solution. The complex prepared by the method of Pfeiffer and Christeleit[3] was hygroscopic, but the crystals separated by the present method were not so.

Found: C, 41.57; H, 5.53; N, 9.53; $H_2O$, 11.06. Calcd. for $Cu(C_5H_8NO_2)_2 \cdot 2H_2O$: C, 41.16; H, 5.53; N, 9.60; $H_2O$, 10.99%.

The anhydrous compound was prepared by the dehydration of bis(L-prolinato)copper(II) dihydrate in a vacuum oven at 75°C.

*8) Bis(L-hydroxyprolinato)copper(II) Trihydrate, $[Cu(L\text{-}hydprol)_2] \cdot 3H_2O$.*—The compound, obtained by the same method as was used in 7) was trihydrate and blue plates.

Found: C, 37.02; H, 5.04; N, 8.58; $H_2O$, 14.95. Calcd. for $Cu(C_5H_8NO_3)_2 \cdot 3H_2O$: C, 37.08; H, 4.99; N, 8.65; $H_2O$, 14.31%.

## Results and Discussion

The CD and absorption data in an aqueous solution are shown in Figs. 1—3 and in Table I. As is shown in Fig. 1, the absorption curve of $[Cu(L\text{-}ala)_2]$ shows a simple broad band, while the CD curve shows three bands in the region (namely, a positive band at about 730 mμ and two negative band, at 630 and 565 mμ). The CD curve of the copper complex with D-alanine is also plotted for the comparison. The CD curve of $[Cu(L\text{-}ser)_2]$ is similar to that of $[Cu(L\text{-}ala)_2]$ on the whole; namely, it has a small positive peak at about 730 mμ, a negative band at 595 mμ, and a negative shoulder at about 640 mμ. However, another small positive shoulder (about 820 mμ) is observed on the longer wavelength side of the positive peak at about 730 mμ. Similar trends are also observed in the curves of $[Cu(L\text{-}thr)_2]$, $[Cu(L\text{-}val)_2]$, and $[Cu(L\text{-}allothr)_2]$ (Figs. 1 and 2). These facts suggest that the broad positive bands in the 900—700 mμ region are composed of two weak positive CD components. As may be seen in Fig. 1, it also seems likely that the observed broad negative bands of $[Cu(L\text{-}thr)_2]$ and $[Cu(L\text{-}val)_2]$ are

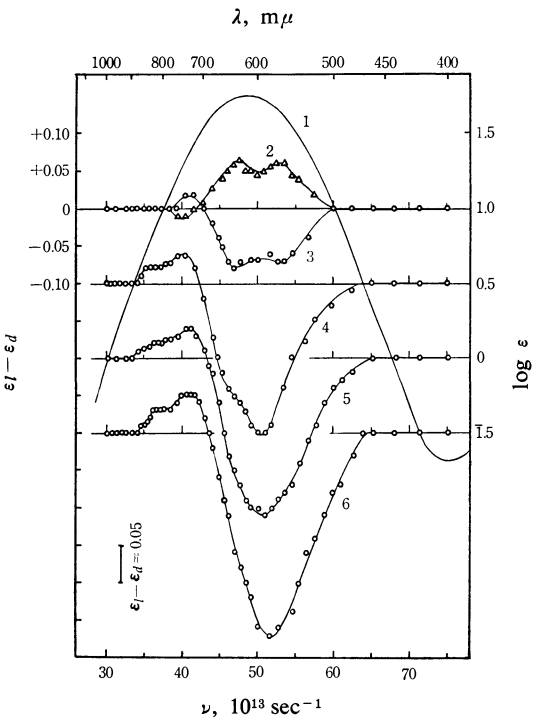



Fig. 1. Absorption curve of (1) $[Cu(L\text{-}ala)_2]$ and CD curves of (2) $[Cu(D\text{-}ala)_2]$, (3) $[Cu(L\text{-}ala)_2]$, (4) $[Cu(L\text{-}ser)_2]$, (5) $[Cu(L\text{-}thr)_2] \cdot H_2O$ and (6) $[Cu(L\text{-}val)_2] \cdot H_2O$ in aqueous solutions.

caused by the superposition of two negative CD bands.

From these results, it is concluded that the $[Cu(L\text{-}am)_2]$ complex shows *four* CD components of the d→d transitions, which are related to the magnetic dipole-allowed transitions under the symmetry of $C_2$. The signs of these CD components of the L-amino acid complexes are (+), (+), (−) and (−), listing from longer to shorter wavelengths. The single ORD inversion observed by Pfeiffer and Christeleit[3] may be thought to be a superposition of four Cotton effects.

The CD and absorption curves of the $[Cu(L\text{-}thr)_2]$ and $[Cu(L\text{-}allothr)_2]$ complexes are shown in Fig. 2. The L-threonine or L-allothreonine

Table I. Circular dichroism and absorption data of $[Cu(am)_2]$ in aqueous solutions

| Complex | CD Band ν, $10^{13}$ sec$^{-1}$ ($\{\varepsilon_l - \varepsilon_d\}_{max}$) | | | | Absorption band ν, $10^{13}$ sec$^{-1}$(log ε) |
|---|---|---|---|---|---|
| $[Cu(L\text{-}ala)_2]$ | | 41.1(+0.02) | 47.6(−0.07) | 53.1(−0.07) | 48.78(1.75) |
| $[Cu(D\text{-}ala)_2]$ | | 40.5(−0.01) | 47.6(+0.06$_5$) | 53.1(+0.06) | 48.78(1.75) |
| $[Cu(L\text{-}ser)_2]$ | sh ca. 36.1(+0.02) | 40.0(+0.03$_5$) | sh ca. 46.9(−0.15) | 50.4(−0.20) | 48.50(1.71) |
| $[Cu(L\text{-}val)_2] \cdot H_2O$ | sh ca. 36.6(+0.03) | 41.1(+0.05) | | 51.7(−0.27) | 49.16(1.77) |
| $[Cu(L\text{-}thr)_2] \cdot H_2O$ | sh ca. 36.1(+0.02) | 41.1(+0.04) | | 50.9(−0.21) | 49.50(1.72) |
| $[Cu(L\text{-}allothr)_2] \cdot H_2O$ | 36.6(+0.02$_5$) | 39.5(+0.02) | sh ca. 46.9(−0.30) | 49.6(−0.35) | 48.39(1.66) |

sh: Shoulder

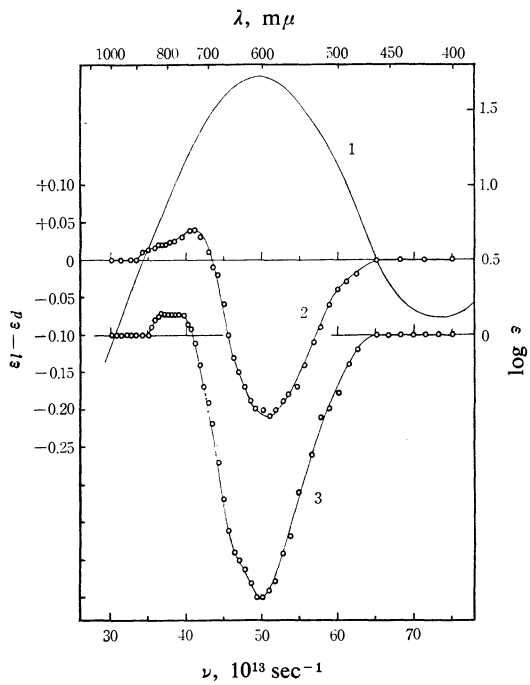



Fig. 2. Absorption curve of (1) $[Cu(L\text{-thr})_2]\cdot H_2O$ and CD curves of (2) $[Cu(L\text{-thr})_2]\cdot H_2O$ and (3) $[Cu(L\text{-allothr})_2]\cdot H_2O$ in aqueous solutions.

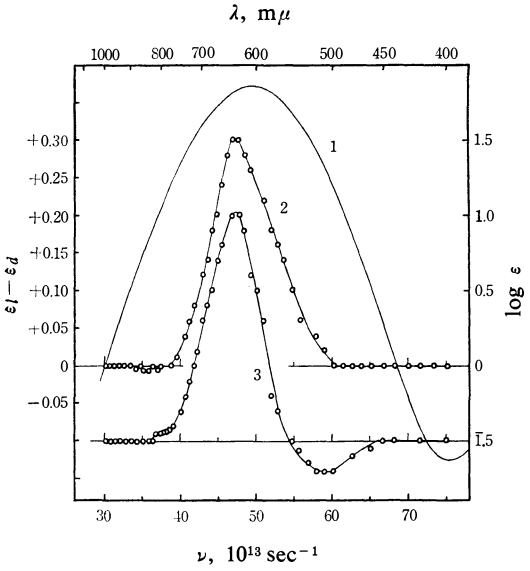



Fig. 3. Absorption curve of (1) $[Cu(L\text{-prol})_2]\cdot 2H_2O$ and CD curves of (2) $[Cu(L\text{-hydprol})_2]\cdot 3H_2O$ and (3) $[Cu(L\text{-prol})_2]\cdot 2H_2O$ in aqueous solutions.

molecule has two asymmetric carbon atoms, located in $\alpha$- and $\beta$-positions. The CD behavior of $[Cu(L\text{-thr})_2]$ is, on the whole, almost the same as that of $[Cu(L\text{-allothr})_2]$ except for a small difference in their intensities. These facts suggest that the vicinal effect caused by the $\alpha$-asymmetric carbon atom, which is located in the five-membered chelate ring containing a central copper atom, is more effective than that of the $\beta$-asymmetric atom, which is located in the side chain of the chelate ring. Similar work concerning the $\alpha$- and $\beta$-asymmetry of optically active amino acids has been reported on the basis of ORD study in another wavelength region,[7] but it resulted in no definite conclusion.

As may be seen in Fig. 3, the CD curve of $[Cu(L\text{-prol})_2]$ is considerably different from those of the other amino acid complexes. This may be attributed to the stereospecific activation of the nitrogen atom in the coordinated ligand, because the construction of the molecular models of the complexes shows that the nitrogen atom of the coordinated L-proline takes a forced asymmetric configuration, and that of the coordinated D-proline, the enantiomorphous configuration. This was also supported by the X-ray analysis of the $[Cu(L\text{-prol})(D\text{-prol})]\cdot 2H_2O$ crystal.[8] The $[Cu(L\text{-hydprol})_2]$ may be said to have the same conditions as $[Cu(L\text{-prol})_2]$ in view of the similarity of their CD behavior. These CD behavior will suggest that the vicinal effect from the activated nitrogen atom will be more effective than that from the $\alpha$-asymmetric carbon atom, since the nitrogen atom is directly

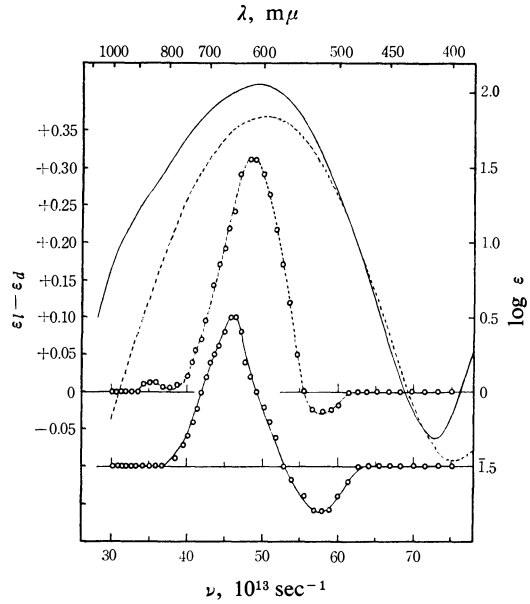



Fig. 4. Absorption and CD curves of $[Cu(L\text{-prol})_2]$ in ethylene glycol (----) and in pyridine (——).

7) N. Izumiya, M. Winitz, S. M. Birnbaum and J. P. Greenstein, *J. Am. Chem. Soc.*, **78**, 1602 (1956).
8) A. M. Mathieson and H. K. Welsh, *Acta Cryst.*, **5**, 599 (1952).

attached to the copper atom, while the carbon atom is attached indirectly.

The CD and absorption data of [Cu(L-prol)$_2$] in pyridine or ethylene glycol are shown in Fig. 4. This complex can be kept in these solvents without decreasing its optical activity. The absorption maxima of this complex in these solvents are almost the same as that in an aqueous solution, though the absorption intensity is slightly higher in pyridine than in the other two solvents. On the other hand, the intensity of the CD band in pyridine is less than that in ethylene glycol or in water. It may be considered, however, that these differences in behavior in these different solvents do not suggest any essential differences in the CD components.

## Summary

On the basis of the CD measurements of the complexes of the [Cu(L-am)$_2$] type, four CD components have been observed in the region of the d→d absorption band, namely, (+), (+), (−) and (−), listing from longer to shorter wavelengths. The L-configuration of the amino acids determines the signs of these CD components.

Judging from the CD curves of the copper-(II) complexes with L-threonine and with L-allothreonine, it has been suggested that the vicinal effect caused by the $\alpha$-asymmetric carbon atom is stronger than that caused by the $\beta$-asymmetric one.

It has also been suggested that, when L-proline or L-hydroxyproline is coordinated to copper, the nitrogen atoms of these ligands are activated by the configurational stereospecificity.

The author is grateful to Assistant Professor Yoichi Shimura and Dr. Jinsai Hidaka for their advice and discussions relating to this work.

*Depatment of Chemistry*
*Faculty of Science*
*Osaka University*
*Toyonaka, Osaka*

# A Molecular Orbitals Study of the Nucleophilic Substitution in Methyl Chloride

By Hiroshi KATO, Keiji MOROKUMA, Teijiro YONEZAWA and Kenichi FUKUI

(Received April 9, 1965)

The mechanism of the $S_N2$-type nucleophilic substitution of aliphatic compounds has been discussed in many experimental studies.[1] Some quantitative and semi-quantitative interpretations of this type of reaction have been carried out by using semi-empirical theory[2,3] or by means of a simple LCAO-MO method.[4] No attempt, however, has yet been made to throw light on the mechanism of the electronic process of this type of reaction. Recently Hoffmann has proposed an extended Hückel method in which an MO (molecular orbital) is represented by linear combination of valence AO's (atomic orbitals) in the molecule.[5] As will be shown in the next section, this procedure, along with the Born-Oppenheimer adiabatic approximation, is particularly convenient and effective for treating the electronic structure of unstable intermediates or such molecules as contain atoms with an unusual valency, as well as ordinary stable molecules.

Accordingly, in the present paper we intend to apply this method to a discussion of the electronic structure of the molecular system which would appear near the transition state of the typical $S_N2$-type reaction, $CH_3Cl+Cl^- \rightarrow Cl^-+CH_3Cl$. This species may be written schematically as $(Cl\cdots CH_3\cdots Cl)^-$.

The calculated results will help us to ascertain the characteristic role which might be

1) E. g., C. K. Ingold, "Structure and Mechanism in Organic Chemistry," Cornell Univ. Press, Ithaca, N. Y. (1953).

2) P. B. D. de la Mare, L. Fowden, E. D. Hughes, C. K. Ingold and J. D. H. Mackie, *J. Chem. Soc.*, **1955**, 3200; I. Dostrovsky, E. D. Hughes and C. K. Ingold, ibid., **1946**, 173.

3) S. Glasstone, K. J. Laidler and H. Eyring, "The Theory of Rate Process," McGraw-Hill, New York (1941).

4) R. Daudel, R. Lefebre and C. Moser, "Quantum Chemistry Method and Application," Interscience Pub., New York (1963); A. Streitwieser, Jr., "Molecular Orbital Theory for Organic Chemists," John Wiley, New York (1961).

5) R. Hoffmann, *J. Chem. Phys.*, **39**, 1397 (1963); **40**, 2474, 2480, 2745 (1964).

played by each atomic orbital during the electronic interaction of this process.

### The Parameters Used and the Coordinates

The MO's to describe these systems are represented by a linear combination of valence AO's; that is, the 1s orbital of the hydrogen atom, the 2s, 2px, 2py and 2pz orbitals of the carbon atom, and the 3s, 3px, 3py and 3pz orbitals of the chlorine atom.

The Coulomb integrals of these AO's, $H_{ii}$, are given as follows:

$$H_{ii}(1s, H) = -13.60 \text{ eV.}$$
$$H_{ii}(2s, C) = -21.43 \text{ eV.}$$
$$H_{ii}(2p, C) = -11.42 \text{ eV.}$$
$$H_{ii}(3s, Cl) = -25.26 \text{ eV.}$$
$$H_{ii}(3p, Cl) = -15.09 \text{ eV.}$$

These values are cited from Pritchard and Skinner's paper[6] while that of the 3s orbital of the chlorine atom is estimated by means of the observed atomic spectra.[7] For the negative chlorine ion, the values of $H_{ii}$ is tentatively assumed to be same as that of the neutral atom.

The resonance intergral between $i$th and $j$th AO's, $H_{ij}$, is calculated by the equation:

$$H_{ij} = 0.5K(H_{ii} + H_{jj})S_{ij}$$

where $S_{ij}$ is the overlap integral and where the value of $K$ is taken to be 1.75 as in Hoffmann's paper.[5]

The effective nuclear charges for these atoms are $Z_H = 1.00$, $Z_C = 3.25$ and $Z_{Cl} = 6.10$ (for both the ionic and neutral chlorine atoms).

The coordinates of this system are presented in Fig. 1, where the carbon atom is situated at the origin of the coordinate system and where the line of $Cl_2$-C-$Cl_1$ is taken as the Y axis. (The symbol $Cl_2$ refers to the attacking chlorine atom, while $Cl_1$ refers to the one in the isolated methyl chloride at the initial stage of reaction.) The $Cl_1$-C-$H_1$ plane lies in the Y-Z plane, and the angle of $Cl_1$-C-H is named $\theta$. The C-$H_2$ bond inclines in the +X direction, and the C-$H_3$ bond, in the −X direction. The px, py, and pz orbitals of the carbon and chlorine atoms direct their positive parts in the X, Y and Z directions respectively.

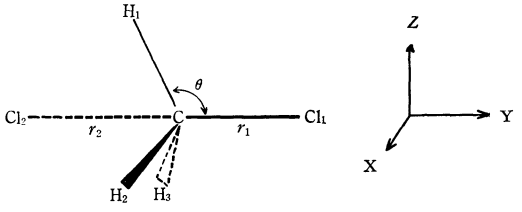



Fig. 1. The coordinate.

### The Electronic Structure of the $CH_3Cl$ Molecule

The calculated MO energies (in units of eV.), together with their irreducible representation and the values of the coefficients of the AO's of $CH_3Cl$, are summarized in Table I, where the geometry of this molecule is given as follows:[8] The C-H distance is 1.1 Å, the C-Cl distance is 1.784 Å and the angle of Cl-C-H, $\theta$, is 110°, and the molecule belongs to the $C_{3v}$ point group.

Frost and McDowell,[9] in their electron impact experiment, studied the electronic structure of methyl chloride; they give the electronic configuration of this molecule as $(a_1)^2(a_1)^2(e)^4(a_1)^2(e)^4$, where the MO energies, except for the lowest $a_1$ MO, are −18.71, −13.02, −12.07 and −11.42 eV. respectively, and where the bracket (A) refers to a molecular orbital belonging to the irreducible representation, A. This order of MO energy agrees with our results, as may be seen in Table I. However, our calculated values are uniformly ca. 3 eV. lower than the above-cited experimental values.

As is shown in Table I, the highest occupied orbital of this molecule is a $\pi$-type orbital consisting of the chlorine atom and the methyl group, which is the C-H bonding in the methyl group and which is C-Cl antibonding, and the electrons in this orbital are largely localized on the chlorine atom. Thus, this orbital may be characterized as a lone-pair orbital, as in Ref. 9. The lowest vacant orbital is now a $\sigma$-type orbital and is strongly antibonding on the C-Cl bond. This result agrees with our previous result.[10] This orbital energy, that is, +1.08 eV., seems to be too high, however, and the energy difference between the highest occupied and the lowest vacant orbitals becomes about 15 eV., while the experimental value, obtained by means of the spectroscopic data, is about 8 eV.[11]

6) H. A. Skinner and H. O. Pritchard, *Chem. Revs.*, **55**, 745 (1955).
7) C. E. Moore, "Atomic Energy Levels," National Bureau of Standards, Washington (1949).
8) "Table of Interatomic Distances and Configuration in Molecules and Ions," Ed. by A. D. Mitchell, L. C. Cross, L. E. Sutton and D. G. Jenkin, The Chemical Society, London (1958).
9) D. C. Frost and C. A. McDowell, *Proc. Roy. Soc.*, **A241**, 194 (1957).
10) T. Yonezawa, H. Kato, H. Saito and K. Fukui, This Bulletin, **35**, 1814 (1962).
11) M. J. Kamlet, "Organic Spectra Data," Vol. I, Interscience, N. Y. (1960).

TABLE I. MOLECULAR ORBITALS OF $CH_3Cl$

| Irreducible representation | $a_1$ | $a_1$ | e | e | $a_1$ | e*1 | e*1 | $a_1$*2 |
|---|---|---|---|---|---|---|---|---|
| Orbital energy, eV. | −27.78 | −21.75 | −16.00 | −16.00 | −15.76 | −13.80 | −13.80 | +1.09 |
| $S_C$*3 | 0.427 | −0.415 | 0.0 | 0.0 | 0.005 | 0.0 | 0.0 | 0.218 |
| $X_C$ | 0.0 | 0.0 | −0.246 | 0.316 | −0.0 | −0.293 | −0.351 | 0.0 |
| $Y_C$ | 0.064 | 0.185 | 0.0 | 0.0 | 0.383 | 0.0 | 0.0 | 1.094 |
| $Z_C$ | 0.0 | 0.0 | 0.316 | 0.246 | 0.0 | −0.351 | 0.293 | 0.0 |
| $H_1$ | 0.076 | −0.177 | 0.239 | 0.186 | −0.125 | −0.294 | 0.245 | 0.171 |
| $H_2$ | 0.076 | −0.177 | −0.281 | 0.114 | −0.125 | −0.066 | −0.378 | 0.171 |
| $H_3$ | 0.076 | −0.177 | 0.041 | −0.300 | −0.125 | 0.359 | 0.132 | 0.171 |
| $S_{Cl}$ | 0.676 | 0.644 | 0.0 | 0.0 | −0.117 | 0.0 | 0.0 | −0.585 |
| $X_{Cl}$ | 0.0 | 0.0 | −0.421 | 0.542 | 0.0 | 0.472 | 0.565 | 0.0 |
| $Y_{Cl}$ | −0.030 | 0.213 | 0.0 | 0.0 | −0.784 | 0.0 | 0.0 | 0.764 |
| $Z_{Cl}$ | 0.0 | 0.0 | 0.542 | 0.421 | 0.0 | 0.565 | −0.472 | 0.0 |

*1 The highest occupied orbitals (degenerated).
*2 The lowest vacant orbital.
*3 The symbols $S_C$, $X_C$, $Y_C$ and $Z_C$ denote the 2s, 2px, 2py and 2pz orbitals of the carbon atom and $H_i$ denotes the 1s orbital of the $i$th hydrogen atom. The $S_{Cl}$, $X_{Cl}$, $Y_{Cl}$ and $Z_{Cl}$ refer to the 3s, 3px, 3py and 3pz orbital of the chlorine atom.

The calculated results for the charge distributions[12] are as follows: The atomic orbital populations, $N$(r), are:

$$N(S_H)=0.875$$

$$N(S_C)=1.140 \quad N(X_C)=N(Z_C)=1.111 \quad N(Y_C)=0.683$$

$$N(S_{Cl})=1.819 \quad N(X_{Cl})=N(Z_{Cl})=1.998 \quad N(Y_{Cl})=1.513$$

where the notations, $S_H$, $S_C$ and $X_C$ etc., denote the hydrogen 1s orbital, the carbon 2s and 2px orbitals, and so on. The atomic populations, $M$(A), are calculated as 4.045 on the carbon atom and as 7.329 on the chlorine atom.

The atomic bond populations, $M$(A-B), are $M$(C-H) = 0.802, $M$(C-Cl) = 0.564, $M$(H···H) = −0.074 and $M$(H···Cl) = −0.067. The calculated values of the atomic orbital bond population, $N$(r-s), between the r and s atomic orbitals are listed in Table II. For the C-Cl bond, the value of $N(Y_C-Y_{Cl})$ is 0.338 and is the largest, and the magnitude of $N(Y_C-S_{Cl})$ and $N(S_C-Y_{Cl})$ is of the same order, while $N(X_C-X_{Cl})$ and $N(Z_C-Z_{Cl})$ are both negative and very small.

TABLE II. THE $N$(r-s) VALUES BETWEEN AO'S OF THE C-Cl AND C-H BONDS IN $CH_3Cl$

| | $S_C$ | $X_C$ | $Y_C$ | $Z_C$ |
|---|---|---|---|---|
| $S_{Cl}$ | 0.022 | 0 | 0.142 | 0 |
| $X_{Cl}$ | 0 | −0.034 | 0 | 0 |
| $Y_{Cl}$ | 0.128 | 0 | 0.338 | 0 |
| $Z_{Cl}$ | 0 | 0 | 0 | −0.034 |
| $H_1$ | 0.238 | 0 | 0.048 | 0.517 |
| $H_2$ | 0.238 | 0.388 | 0.048 | 0.129 |
| $H_3$ | 0.238 | 0.388 | 0.048 | 0.129 |

Accordingly, the C-Cl bond is a $\sigma$-type bond and is mainly dependent upon the interaction between the carbon 2py orbital and the chlorine 3py orbital, whereas the 3px and 3pz orbitals of the chlorine atom do not participate in the bond formation and stand for lone-pair orbitals. On the other hand, the $N$(r-s) values of the pairs between AO's of C-H bond indicate that the carbon 2px and 2pz orbitals do participate in the C-H bonding and not in the C-Cl bonding.

## The Electronic Structure of the "Transient Species" $(Cl\cdots CH_3\cdots Cl)^-$

In this section, we will treat, on the assumption of adiabaticity, the electronic structure of the systems in which the attacking chlorine ion ($Cl_2$) interacts with the isolated methyl chloride with various assumed configurations. It is well established, in normal $S_N2$-type halogen substitutions of alkyl halides, that the replacement proceeds most often in such a way that the attacking reagent, the central carbon atom and the substitution atom lie co-linear and the hybridization of the central carbon atom shifts from $sp^3$ to $sp^2$, which is finally reached in the transition state. However, the reaction path of this reaction has not yet been strictly established. Accordingly, we have tentatively selected two hypothetical processes, a and b, and have investigated the electronic structure of the species $(Cl\cdots CH_3\cdots Cl)^-$. This is neither a stable molecule nor an unstable intermediate,

12) K. Morokuma, H. Kato, T. Yonezawa and K. Fukui, This Bulletin, 33, 1263 (1965).

but rather corresponds to a certain configuration near the transition state. The electronic structure is calculated with respect to several different configurations in each process. These calculated configurations are shown in Table III, together with the calculated total electronic energy values (in eV.), where the C–$Cl_1$ bond distance is denoted as $r_1$ and the C–$Cl_2$ distance as $r_2$, and where the $Cl_1$–C–H angle is $\theta$. The C–H distances are kept constant, as equal to 1.10Å throughout both the a and b processes. In both processes a chlorine ion approaches the isolated methyl chloride along the Y axis from the −Y direction, as may be seen in Fig. 1, and these two processes start at $r_2=3.0$Å, $r_1=1.784$Å and $\theta=110°$; the process a ends with $r_2=r_1=2.20$Å and $\theta=90°$, and the process b with $r_2=r_1=2.05$Å and $\theta=90°$ (Ingold et al.[2] adopted the value $r_2=r_1=2.05$Å, and Spinner,[13] 2.17Å, as the C–Cl bond distances at the transition state of the chlorine substitution reaction of methyl chloride.).

Table III. The various configurations and the calculated total electronic energy values (eV.) in the $(Cl\cdots CH_3\cdots Cl)^-$ systems

| $r_1$ Å | $r_2$ Å | $\theta$ ° | Total energy eV. |
|---|---|---|---|
| 1.784 | 3.0 | 90 | −389.07 |
| | | 100 | −390.15 |
| | | 110 | −390.36 |
| 1.9 | 2.8 | 95 | −390.15 |
| | | 100 | −390.43 |
| | | 110 | −390.34 |
| 2.0 | 2.6 | 95 | −390.08 |
| | | 100 | −390.20 |
| | | 110 | −389.80 |
| 2.1 | 2.4 | 90 | −389.46 |
| | | 95 | −389.60 |
| | | 100 | −389.52 |
| 2.15 | 2.3 | 90 | −389.18 |
| | | 95 | −389.20 |
| | | 100 | −388.99 |
| 2.2 | 2.2 | 90 | −388.85 |
| | | 95 | −388.73 |
| | | 100 | −386.96 |
| 1.85 | 2.8 | 100 | −390.17 |
| | | 110 | −390.36 |
| 1.9 | 2.6 | 95 | −389.52 |
| | | 100 | −389.73 |
| | | 110 | −389.48 |
| 1.95 | 2.4 | 95 | −388.71 |
| | | 100 | −388.77 |
| | | 110 | −388.14 |
| 2.0 | 2.2 | 90 | −387.16 |
| | | 95 | −387.25 |
| | | 100 | −387.05 |
| 2.05 | 2.05 | 90 | −386.01 |
| | | 95 | −385.85 |

When we refer to the calculated values of the total electronic energies in Table III, we can see that those values have a minimum, with a variation of $\theta$ at fixed $r_1$ and $r_2$ distances. This may tentatively be referred to as a "local" minimum. The value of $\theta$ at local minima gradually decrease from 110° at the initial state to 90° at the symmetrical configuration ($r_1=r_2$, $\theta=90°$).

For the sake of simplicity, several sets of $r_1$ and $r_2$ values were selected for each process, a and b. The electronic structure was calculated with respect to the configurations in which the value of $\theta$ corresponds to a local minimum at this fixed $r_1$ and $r_2$. These configurations are summarized in Table IV, where they are named a-I, a-II,···, a-VI and b-I, b-II, ···, b-VI respectively (a-I and b-I have the same configuration.).

Now let us investigate the process of the nucleophilic reaction of aliphatic compounds. The configurations which we adopted allow

Table IV. The selected configuration and the calculated values of the total electronic energy (eV.) $E$, and the atomic population, $M$(A), of each atom in the a and b processes

| Process | $r_1$ | $r_2$ | $\theta$ | $E$ | $M$(C) | $M$(H) | $M$($Cl_1$) | $M$($Cl_2$) |
|---|---|---|---|---|---|---|---|---|
| a-I | 1.784 | 3.0 | 110 | −390.36 | 4.056 | 0.872 | 7.333 | 7.995 |
| II | 1.9 | 2.8 | 100 | −390.43 | 3.986 | 0.869 | 7.413 | 7.994 |
| III | 2.0 | 2.6 | 100 | −390.20 | 3.924 | 0.869 | 7.491 | 7.979 |
| IV | 2.1 | 2.4 | 95 | −389.60 | 3.852 | 0.868 | 7.618 | 7.925 |
| V | 2.15 | 2.3 | 95 | −389.20 | 3.829 | 0.869 | 7.691 | 7.873 |
| VI | 2.2 | 2.2 | 90 | −388.85 | 3.820 | 0.870 | 7.784 | 7.784 |
| b-I | 1.784 | 3.0 | 110 | −390.36 | 4.056 | 0.872 | 7.333 | 7.995 |
| II | 1.85 | 2.8 | 100 | −390.17 | 4.013 | 0.869 | 7.386 | 7.995 |
| III | 1.9 | 2.6 | 100 | −389.73 | 3.979 | 0.869 | 7.428 | 7.986 |
| IV | 1.95 | 2.4 | 100 | −388.77 | 3.938 | 0.869 | 7.492 | 7.961 |
| V | 2.0 | 2.2 | 95 | −387.25 | 3.882 | 0.874 | 7.611 | 7.883 |
| VI | 2.05 | 2.05 | 90 | −386.01 | 3.862 | 0.880 | 7.749 | 7.749 |

13) E. Spinner, *Aust. J. Chem.*, 13, 218 (1960).

TABLE V. THE CALCULATED ATOMIC ORBITAL POPULATION, $N(r)$, VALUES ON THE CARBON AND CHLORINE ATOMS IN THE a AND b PROCESSES

| Process | $N(S_C)$ | $N(Y_C)$ | $N(X_C)$ $N(Z_C)$ | $N(S_{Cl_1})$ | $N(Y_{Cl_1})$ | $N(X_{Cl_1})$ $N(Z_{Cl_1})$ | $N(S_{Cl_2})$ | $N(Y_{Cl_2})$ | $N(X_{Cl_2})$ $N(Z_{Cl_2})$ |
|---|---|---|---|---|---|---|---|---|---|
| a-I | 1.149 | 0.680 | 1.113 | 1.820 | 1.516 | 1.998 | 1.998 | 1.999 | 1.999 |
| II | 1.184 | 0.627 | 1.087 | 1.869 | 1.543 | 2.000 | 1.999 | 1.996 | 1.999 |
| III | 1.206 | 0.538 | 1.090 | 1.904 | 1.587 | 2.000 | 1.998 | 1.984 | 1.998 |
| IV | 1.227 | 0.453 | 1.086 | 1.938 | 1.680 | 2.000 | 1.990 | 1.937 | 1.998 |
| V | 1.234 | 0.421 | 1.087 | 1.952 | 1.740 | 2.000 | 1.983 | 1.894 | 1.998 |
| VI | 1.236 | 0.414 | 1.085 | 1.968 | 1.818 | 2.000 | 1.968 | 1.818 | 2.000 |
| b-I | 1.149 | 0.680 | 1.113 | 1.820 | 1.516 | 1.998 | 1.998 | 1.999 | 1.999 |
| II | 1.175 | 0.665 | 1.086 | 1.851 | 1.535 | 2.000 | 2.000 | 1.997 | 1.999 |
| III | 1.189 | 0.612 | 1.089 | 1.871 | 1.556 | 2.000 | 1.999 | 1.991 | 1.998 |
| IV | 1.205 | 0.546 | 1.093 | 1.894 | 1.598 | 2.000 | 1.996 | 1.971 | 1.997 |
| V | 1.219 | 0.485 | 1.089 | 1.923 | 1.689 | 2.000 | 1.982 | 1.906 | 1.997 |
| VI | 1.219 | 0.466 | 1.089 | 1.953 | 1.799 | 2.000 | 1.953 | 1.799 | 2.000 |

us to derive a certain semi-quantitative conclusion concerning the electronic distribution in the process of the reaction.*

**The Electronic Energy and the Atomic Population.**—The calculated values of the total electronic energy (in eV.) and the atomic population, $M(A)$, of each atom in these configurations in both processes are given in Table IV. The calculated results show that, in both processes, the total energies become higher and higher as the C–$Cl_2$ distance decreases.

On the other hand, the calculated values of $M(A)$ lead to the following results: The $M(Cl_2)$ values decrease from 7.995 at the initial state to 7.784 at the a-VI state, while the $M(C)$ values decrease from 4.056 to 3.820 and the $M(Cl_1)$ values increase from 7.333 to 7.784 through the process a. This tendency is similar to that in the process b. That is, the negative charge located on the chlorine ion at the initial configuration gradually migrates to the $Cl_1$ atom, and at the symmetrical configuration the $M(A)$ values of $Cl_2$ and $Cl_1$ atoms become equal.

In order to discuss this further, the calculated values of the atomic orbital populations, $N(r)$, of various AO's are collected in Table V, while the relation between the magnitude of $N(r)$ and the configuration at various stages is plotted in Fig. 2. In the process a, $N(S_C)$ increases gradually from 1.149 to 1.236 and $N(Y_C)$ remarkably decreases from 0.680 to 0.414, while the values of the $X_C$ and $Z_C$ orbitals are almost invariable. As for the $Cl_1$ atom, the change of $N(Y_{Cl_1})$ is the largest, i. e. from 1.516 to 1.818; that of $N(S_{Cl_1})$ is the next, and the $N(r)$ values of $X_{Cl_1}$ and $Z_{Cl_1}$ orbitals are almost constant, i. e., ca. 2.000 through the process a. The $N(r)$ values of the $Cl_1$ atom show a tendency to be the inverse of that of the $Cl_2$ atom. Thus, it is noticed that the changes in the $M(A)$ values are mainly governed by that of the 2py orbital at the carbon atom and the 3py orbitals at the chlorine atoms, whereas the $N(r)$ values of the 3px and 3pz orbitals of the chlorine atoms remain constant and these orbitals have a lone-pair orbital, as in nature. These results will be accepted more easily in the light of the discussion in the following section.

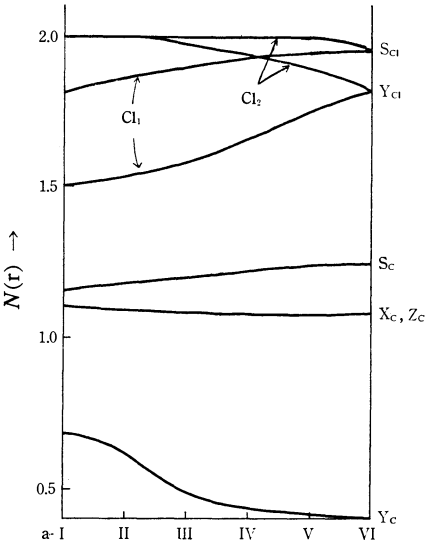



Fig. 2. The change of the $N(r)$ values of the carbon and chlorine atoms through the process a.

**The Bond Population in the C–Cl Bond.**—Tables VI and VII list, respectively, the calculated values of the atomic bond populations, $M(A–B)$, between various atoms, and also those of the atomic orbital bond populations,

* If we adopt the $M(A)$ or $M(A–B)$ values with a little different $\theta$ values from those in Tables IV and VI, our conclusions will be not seriously affected, since the variations in these magnitudes are limited within 0.02.

$N$(r-s), between various AO's. The values of $M$(C-$Cl_1$) and $M$(C-$Cl_2$) vary inversely proportionally to their bond distance; both are positive and equal at the symmetrical configuration. The value of $M$(H-C) shows only a slight change during the course of both processes, a and b, in its overall magnitude, but it varies remarkably in its terms. This point will be discussed again in a later section.

The $M$(C-$Cl_1$) values decrease rapidly in both processes, that is, from 0.558 to 0.102 in the process a and from 0.558 to 0.098 in the process b. The magnitudes of the contributions of several factors to the rapid decrease in $M$(C-$Cl_1$) may be roughly estimated as follows: a) The contribution from the change in the $\theta$ value. This magnitude may be estimated by the difference between the values of $M$(C-$Cl_1$) at $r_1=r_2=r_0$, $\theta=90°$, and the value at $r_1=r_2=r_0$, $\theta=110°$. The value of $r_0$ is taken as 2.20Å in the process a and as 2.05Å in the process b. That is, it is calculated as $-0.038$ at the process a and at $-0.018$ at the process b. b) The contribution from the interaction with the $Cl_2$ atom. This magnitude may be estimated by means of the difference between $M$(C-$Cl_1$) at $r_1=r_2=r_0$, $\theta=90°$, and the value at $r_1=r_0$, $r_2=\infty$ and $\theta=90°$, it is $-0.158$ in the process a and $-0.242$ in the process b. c) The contribution from the streching of the C-$Cl_1$ bond. This is estimated by means of the difference between $M$(C-$Cl_1$) at $r_1=r_0$, $r_2=\infty$, $\theta=110°$, and that at $r_1=1.784$Å, $r_2=\infty$, $\theta=110°$. This is $-0.246$ in the process a and $-0.160$ in the process b. On the basis of these estimations, it may be concluded that the decrease in the $M$(C-$Cl_1$) value is mainly brought about by the interaction with the $Cl_2$ atom and the streching of the C-$Cl_1$ bond, while the effect of the change in $\theta$ is very small.

On investigating the values of $N$(r-s) in the C-Cl bond given in Table VI and Fig. 3, it may be seen that a remarkable change during the processes is observed in the values of $N(Y_C-Y_{Cl_1})$ and $N(Y_C-Y_{Cl_2})$; i. e., the former decreases and the latter increases in both processes, while there is a less remarkable

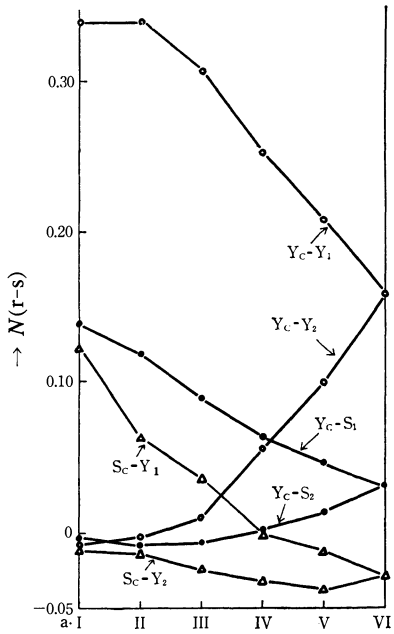



Fig. 3. The change of the $N$(r-s) values between some AO's of the carbon and chlorine atoms in the process a, where $S_1$ and $S_2$, etc. refer to the 3s orbitals of the chlorine 1 and 2 atom and so on.

change in the $N(Y_C-S_{Cl_1})$ and $N(S_C-Y_{Cl_1})$ values. In the symmetrical configuration, the magnitude $N$(r-s) decreases in the order of $N(Y_C-Y_{Cl})>N(Y_C-S_{Cl})>N(S_C-Y_{Cl})$, where the $N(S_C-Y_{Cl})$ value is negative. Accordingly, the C-Cl bond is considered to be formed mainly through the interaction between the 3py orbitals of the two chlorine atoms and the 2py orbital of the carbon atom. The interaction between the chlorine 3py and the carbon 2s orbitals is not concerned with this bond formation, especially near the symmetrical configuration. The values of $N(X_C-X_{Cl})$ and $N(Z_C-Z_{Cl})$ are almost unchangeable and are negligibly small throughout the process.

**The Change of $N$(r-s) in the C-H Bond.**— The $N$(r-s) values between AO's of the hydrogen and carbon atoms in both processes are

TABLE VI. THE CALCULATED VALUES OF THE ATOM BOND POPULATIONS, $M$(A-B) IN THE a AND b PROCESSES

| Process | C-H | C-$Cl_1$ | C-$Cl_2$ | H-$Cl_1$ | H-$Cl_2$* | Process | C-H | C-$Cl_1$ | C-$Cl_2$ | H-$Cl_1$ | H-$Cl_2$* |
|---|---|---|---|---|---|---|---|---|---|---|---|
| a-I | 0.804 | 0.558 | −0.026 | −0.068 | −0.006 | b-I | 0.804 | 0.558 | −0.026 | −0.068 | −0.006 |
| II | 0.816 | 0.456 | −0.030 | −0.064 | −0.012 | II | 0.814 | 0.486 | −0.032 | −0.072 | −0.012 |
| III | 0.822 | 0.376 | −0.040 | −0.056 | −0.024 | III | 0.820 | 0.444 | −0.052 | −0.066 | −0.024 |
| IV | 0.830 | 0.256 | −0.010 | −0.056 | −0.040 | IV | 0.832 | 0.380 | −0.072 | −0.068 | −0.048 |
| V | 0.834 | 0.192 | 0.022 | −0.056 | −0.052 | V | 0.844 | 0.254 | −0.028 | −0.082 | −0.080 |
| VI | 0.836 | 0.102 | 0.102 | −0.060 | −0.060 | VI | 0.854 | 0.098 | 0.098 | −0.100 | −0.100 |

* The notation, A-B denotes the $M$(A-B) value between the A and B atoms.

TABLE VII. THE CALCULATED $N$(r-s), VALUES BETWEEN THE C-$Cl_1$ AND C-$Cl_2$ BONDS IN THE a AND b PROCESSES

| Process | S-$S_1$ | S-$Y_1$ | X-$X_1$ Z-$Z_1$ | Y-$S_1$ | Y-$Y_1$ | S-$S_2$ | S-$Y_2$ | X-$X_2$ Z-$Z_2$ | Y-$S_2$ | Y-$Y_2$* |
|---|---|---|---|---|---|---|---|---|---|---|
| a-I | 0.020 | 0.124 | −0.034 | 0.140 | 0.340 | −0.006 | −0.008 | −0.001 | −0.004 | −0.006 |
| II | −0.012 | 0.064 | −0.030 | 0.122 | 0.340 | −0.008 | −0.012 | −0.002 | −0.006 | −0.001 |
| III | −0.018 | 0.038 | −0.020 | 0.092 | 0.308 | −0.016 | −0.022 | −0.004 | −0.004 | 0.012 |
| IV | −0.030 | 0.0 | −0.018 | 0.066 | 0.254 | −0.026 | −0.030 | −0.008 | 0.004 | 0.058 |
| V | −0.030 | −0.010 | −0.014 | 0.050 | 0.210 | −0.034 | −0.036 | −0.012 | 0.016 | 0.100 |
| VI | −0.036 | −0.028 | −0.014 | 0.034 | 0.160 | −0.036 | −0.028 | −0.014 | 0.034 | 0.160 |
| b-I | 0.020 | 0.124 | −0.034 | 0.140 | 0.340 | −0.006 | −0.008 | −0.001 | −0.004 | −0.006 |
| II | −0.008 | 0.076 | −0.036 | 0.138 | 0.352 | −0.008 | −0.011 | −0.002 | −0.006 | −0.004 |
| III | −0.015 | 0.058 | −0.030 | 0.122 | 0.338 | −0.016 | −0.020 | −0.004 | −0.009 | 0.001 |
| IV | −0.023 | 0.035 | −0.025 | 0.104 | 0.314 | −0.030 | −0.036 | −0.009 | −0.009 | 0.021 |
| V | −0.041 | −0.004 | −0.025 | 0.083 | 0.267 | −0.047 | −0.045 | −0.017 | 0.009 | 0.088 |
| VI | −0.054 | −0.035 | −0.025 | 0.049 | 0.187 | −0.054 | −0.035 | −0.025 | 0.049 | 0.187 |

* The notations, S, $S_1$ and $S_2$··· refer to the 2s orbital of the carbon atom and the 3s orbitals of the chlorine 1 and chlorine 2 atoms and so on.

TABLE VIII. THE CALCULATED $N$(r-s) VALUES BETWEEN THE $H_1$-C BOND IN THE a AND b PROCESSES

| Process | $H_1$-$S_C$ | $H_1$-$Y_C$ | $H_1$-$Z_C$* | Process | $H_1$-$S_C$ | $H_1$-$Y_C$ | $H_1$-$Z_C$* |
|---|---|---|---|---|---|---|---|
| a-I | 0.253 | 0.026 | 0.530 | b-I | 0.253 | 0.026 | 0.530 |
| II | 0.267 | 0.021 | 0.527 | II | 0.263 | 0.023 | 0.528 |
| III | 0.280 | 0.016 | 0.525 | III | 0.273 | 0.021 | 0.527 |
| IV | 0.297 | 0.005 | 0.527 | IV | 0.288 | 0.017 | 0.526 |
| V | 0.304 | 0.003 | 0.527 | V | 0.310 | 0.005 | 0.529 |
| VI | 0.309 | 0.0 | 0.528 | VI | 0.322 | 0.0 | 0.532 |

* The notation $H_1$-$S_C$ denotes the $N$(r-s) value between the 1s orbital of the hydrogen 1 and the 2s orbital of the carbon atom.

listed in Table VIII, where the $H_1$ 1s orbital does not overlap with the carbon 2px orbital, as is shown in Fig. 1, hence, the $N(H_1\text{-}X_C)$ values are omitted in Table VIII. By referring to the calculated results, it may clearly be seen that $N(H_1\text{-}S_C)$ values increase and $N(H_1\text{-}Z_C)$'s are almost invariable in both processes. Thus, the carbon 2s orbital is concluded to play an important role in the C–H bond-formation near the symmetrical configuration. In other words, in this state the s-nature of the C–H bond increases. This result may correspond to the change in the hybridization of the central carbon atom from $sp^3$ in the direction of $sp^2$ at the transition state of the $S_N2$-type reaction.

The discussions above concerned with the roles of various AO's in the interactions of these systems may be summarized as follows: At the carbon atom, the 2s orbital takes part in the C–H and C–Cl bondings at the initial state, whereas at the symmetrical state it participates only in the C–H bonding. The 2px and 2pz orbitals take part in the C–H bonding only, and the 2py orbital alone contributes always to the C–Cl bonding throughout the process. At the chlorine atoms, the 3s orbitals take part partially in the C–Cl bonding, while the 3py orbitals play a dominant part in the C–Cl bonding. The 3px and 3pz orbitals remain as lone-pair orbitals.

**The Energy Levels in the Symmetrical Configuration.**—The calculated values of MO energy, their irreducible representation, and those of the coefficients of AO's in the symmetrical configuration (a-VI and b-VI) are listed in Tables IX(i) and (ii), where these systems belong to the $D_{3h}$ point group. The characteristic features of these MO's may be pointed out briefly as follows: The $a_1'$ and $a_2''$ orbitals are $p\sigma$-type orbitals, the e′ orbitals are $p\pi$-type orbitals, and the e″ orbitals are lone-pair orbitals of the chlorine atoms.

Judging from the population analysis in Tables VII and VIII, the $a_2''$ occupied orbitals may be said to make an important contribution to the C–Cl bonding, while the other MO's make a minor contribution. On the other hand, the highest-occupied orbital belonging to $a_1'$ has a C–Cl antibonding and a C–H bonding character and its energy is very sensitive to the C–Cl distance, which is, in our approximation, interpreted in terms of the magnitude of the overlap between the carbon

TABLE IX. THE MOLECULAR ORBITALS OF THE SYMMETRICAL CONFIGURATION

(i) a-VI State ($r_1=r_2=2.2$Å, $\theta=90°$)

| Irreducible representation | $a_1'$ | $a_2''$ | $a_1'$ | e' | e' | $a_2''$ | e'' | e'' | e' | e' | $a_1'$*1 | $a_2''$*2 |
|---|---|---|---|---|---|---|---|---|---|---|---|---|
| Orbital energy | −27.26 | −25.43 | −21.76 | −16.02 | −16.02 | −15.86 | −15.09 | −15.09 | −14.13 | −14.13 | −13.63 | −6.33 |
| $S_C$ | 0.410 | 0.0 | 0.471 | 0.0 | 0.0 | 0.0 | 0.0 | 0.0 | 0.0 | 0.0 | −0.168 | 0.0 |
| $X_C$ | 0.0 | 0.0 | 0.0 | −0.206 | 0.338 | 0.0 | 0.0 | 0.0 | −0.378 | 0.229 | 0.0 | 0.0 |
| $Y_C$ | 0.0 | 0.114 | 0.0 | 0.0 | 0.0 | 0.311 | 0.0 | 0.0 | 0.0 | 0.0 | 0.0 | 1.034 |
| $Z_C$ | 0.0 | 0.0 | 0.0 | 0.338 | 0.206 | 0.0 | 0.0 | 0.0 | −0.229 | −0.378 | 0.0 | 0.0 |
| $H_1$ | 0.097 | 0.0 | 0.154 | 0.301 | 0.183 | 0.0 | 0.0 | 0.0 | −0.170 | −0.281 | −0.144 | 0.0 |
| $H_2$ | 0.097 | 0.0 | 0.154 | −0.309 | 0.169 | 0.0 | 0.0 | 0.0 | −0.159 | 0.288 | −0.144 | 0.0 |
| $H_3$ | 0.097 | 0.0 | 0.154 | 0.008 | −0.352 | 0.0 | 0.0 | 0.0 | 0.329 | −0.007 | −0.144 | 0.0 |
| $S_{Cl}$*3 | 0.488 | 0.684 | −0.519 | 0.0 | 0.0 | −0.092 | 0.0 | 0.0 | 0.0 | 0.0 | 0.132 | −0.247 |
| $X_{Cl}$*3 | 0.0 | 0.0 | 0.0 | −0.237 | 0.389 | 0.0 | 0.0 | −0.707 | 0.466 | −0.282 | 0.0 | 0.0 |
| $Y_{Cl}$*3 | −0.022 | 0.007 | −0.147 | 0.0 | 0.0 | −0.611 | 0.0 | 0.0 | 0.0 | 0.0 | −0.711 | 0.426 |
| $Z_{Cl}$*3 | 0.0 | 0.0 | 0.0 | 0.389 | 0.237 | 0.0 | −0.707 | 0.0 | 0.282 | 0.466 | 0.0 | 0.0 |

(ii) b-VI State ($r_1=r_2=2.05$Å, $\theta=90°$)

| Irreducible representation | $a_1'$ | $a_2''$ | $a_1'$ | e' | e' | $a_2''$ | e'' | e'' | e' | e' | $a_1'$*1 | $a_2''$*2 |
|---|---|---|---|---|---|---|---|---|---|---|---|---|
| Orbital energy | −27.76 | −25.51 | −20.95 | −16.26 | −16.26 | −15.99 | −15.08 | −15.08 | −13.76 | −13.76 | −12.61 | −3.52 |
| $S_C$ | 0.416 | 0.0 | −0.443 | 0.0 | 0.0 | 0.0 | 0.0 | 0.0 | 0.0 | 0.0 | −0.208 | 0.0 |
| $X_C$ | 0.0 | 0.0 | 0.0 | −0.211 | 0.321 | 0.0 | 0.0 | 0.0 | −0.335 | 0.313 | 0.0 | 0.0 |
| $Y_C$ | 0.0 | 0.137 | 0.0 | 0.0 | 0.0 | 0.310 | 0.0 | 0.0 | 0.0 | 0.0 | 0.0 | 1.083 |
| $Z_C$ | 0.0 | 0.0 | 0.0 | 0.321 | 0.211 | 0.0 | 0.0 | 0.0 | −0.313 | −0.335 | 0.0 | 0.0 |
| $H_1$ | 0.089 | 0.0 | −0.145 | 0.289 | 0.190 | 0.0 | 0.0 | 0.0 | −0.229 | −0.245 | −0.197 | 0.0 |
| $H_2$ | 0.089 | 0.0 | −0.145 | −0.309 | 0.155 | 0.0 | 0.0 | 0.0 | −0.098 | 0.321 | −0.197 | 0.0 |
| $H_3$ | 0.089 | 0.0 | −0.145 | 0.020 | −0.345 | 0.0 | 0.0 | 0.0 | 0.327 | −0.076 | −0.197 | 0.0 |
| $S_{Cl}$*3 | 0.473 | 0.673 | 0.524 | 0.0 | 0.0 | −0.112 | 0.0 | 0.0 | 0.0 | 0.0 | 0.206 | −0.311 |
| $X_{Cl}$*3 | 0.0 | 0.0 | 0.0 | −0.249 | 0.379 | 0.0 | 0.0 | −0.707 | 0.402 | −0.375 | 0.0 | 0.0 |
| $Y_{Cl}$*3 | −0.023 | 0.010 | 0.215 | 0.0 | 0.0 | −0.601 | 0.0 | 0.0 | 0.0 | 0.0 | −0.701 | 0.474 |
| $Z_{Cl}$*3 | 0.0 | 0.0 | 0.0 | 0.379 | 0.249 | 0.0 | −0.707 | 0.0 | 0.375 | 0.402 | 0.0 | 0.0 |

*1 The highest occupied orbital.

*2 The lowest vacant orbital.

*3 The notation, $S_{Cl}$ and $Y_{Cl}$ denote $(S_{Cl_1}+S_{Cl_2})$ and $(Y_{Cl_1}+Y_{Cl_2})$ in the $a_1'$ orbitals and $(S_{Cl_1}-S_{Cl_2})$ and $(Y_{Cl_1}-Y_{Cl_2})$ in the $a_2''$ orbitals, for $X_{Cl}$ and $Z_{Cl}$, they represent $(X_{Cl_1}+X_{Cl_2})$ and $(Z_{Cl_1}+Z_{Cl_2})$ in the e' orbitals and $(X_{Cl_1}-X_{Cl_2})$ and $(Z_{Cl_1}-Z_{Cl_2})$ in the e'' orbitals respectively.

and chlorine atoms. Thus, this orbital originates from the splitting of the $a_1$ lowest vacant orbital of the isolated methyl chloride. The mode may be represented by the scheme:

$$a_1(C_{3v}) \rightarrow a_1' \text{ and } a_2'' \ (D_{3h})$$

Accordingly, it may be said that the unstable character and the C–Cl lengthened bond result mainly from this kind of orbital, $a_1'$.

From the above-mentioned results, it may be concluded that the $a_2''$ orbitals play an important role in the stabilization of these systems,[4] but that the $a_1'$ orbitals should be taken into account in the more rigorous treatment.

## Summary

The electronic structures of $CH_3Cl$ and a "transient" species $(Cl\cdots CH_3\cdots Cl)^-$ have been calculated by an extended Hückel method. The calculated results of $CH_3Cl$ correlate well with the experimental facts. The main features of the electronic structure of $(Cl\cdots CH_3\cdots Cl)^-$ may be summarized as follows:

1) The 3py orbitals of the chlorine atoms and the 2py orbital of the central carbon atom ($p\sigma$-orbitals) play an important role in the interaction between the C–Cl bonds.

2) The 2s orbital of the central carbon atom at the symmetrical configuration makes no contribution to the C–Cl bonding; rather, this orbital, together with the 2px and 2pz orbitals, participates in the C–H bonding.

3) The 3px and 3pz orbitals of the chlorine atoms form the lone-pair orbitals.

The natures of the MO's of the symmetrical configuration have also been briefly discussed.

It should be noticed, however, that the present treatment is not yet sufficiently qualified as a method to allow an interpretation of the stable configuration of a molecular system, since it does not explicitly take into account the nuclear repulsion and the electronic interaction. Accordingly, there remains room for criticism with respect to the theoretical significance which the configuration of such a local minimum will have in the true electronic process on the reaction path. This point will be examined further in the future.

The calculations have been carried out on an IBM 7090 computer at the Japan IBM Co., with the permission of the UNICON committee, which the authors wish to thank.

*Department of Fuel Chemistry*
*Faculty of Engineering*
*Kyoto University*
*Sakyo-ku, Kyoto*

# Small-angle Scattering from Methane, Ammonia and Water by Fast Electrons†,*

By Takao IIJIMA, Russell A. BONHAM, Claude TAVARD, Monique ROUX and Marguerite CORNILLE

(Received April 17, 1965)

With the advent of improved methods for the calculation of the wave functions for a many-electron system, it has become of interest to obtain experimental measurements of quantities with direct relationships to the computed wave functions. Scattering experiments with fast electrons are of interest in this connection, since they provide direct information concerning the shape of electron-charge distributions in atoms and molecules.[1-8]

Some one-center wave functions, which are now available for the molecular systems methane, ammonia and water[9,10] have been

† Contribution No. 1295 from the Chemical Laboratories of Indiana University.

* The authors wish to thank the U. S. Atomic Energy Commission and the U. S. Air Force Office of Aerospace Research for their support of this work; one of us (R.A.B.) also wishes to thank the John Simon Guggenheim foundation and the U. S. Educational Commission in Japan for their help.

1) L. S. Bartell and L. O. Brockway, *Phys. Rev.*, **90**, 833 (1953).

2) M. Roux and M. Cornille, *Cah. Phys.*, **16**, 45 (1962).

3) R. A. Bonham and T. Iijima, *J. Phys. Chem.*, **67**, 1472, 2266, 2769 (1963).

4) C. Tavard, *Cah. Phys.*, **17**, 165 (1963).

5) T. Iijima and R. A. Bonham, *Acta Cryst.*, **16**, 106 (1963).

6) C. Tavard, M. Rouault, M. Roux and M. Cornille, *J. Chem. Phys.*, **39**, 2390 (1963).

7) C. Tavard, M. Rouault, M. Roux and M. Cornille, *J. chim. phys.*, **61**, 1324, 1330 (1964).

8) R. A. Bonham and T. Iijima, *J. Chem. Phys.*, **42**, 2612 (1965).

9) M. Allavena and S. Bratož, *J. chim. phys.*, **59**, 1199 (1963).

10) R. Moccia, *J. Chem. Phys.*, **40**, 2164, 2176, 2186 (1964).

used to calculate the total scattering intensity for fast electrons in the first Born approximation.[4,6] When these results are compared with those of the independent-atom model, a contribution from the binding electrons is seen to appear on the first ring of scattered intensities. This last calculation may be performed using the best available wave functions for each atom in these molecules. It is therefore, the purpose of this work to compare recently-obtained experimental results with these theoretical predictions.

Sector electron-diffraction photographs of methane, ammonia, water and helium were obtained over the $s$ ($s=(4\pi/\lambda)\sin\theta/2$) range $1<s<8$ using a newly-constructed electron-fraction unit, in the Electron Diffraction Laboratory of Indiana University; this unit, to be described elsewhere,[11] has a nozzle-to-photographic plate distance of 65 cm. and an accelerating voltage of 40 kV. The diffraction patterns were recorded on Kodak process plates with an exposure time ranging from 1 to 3 min. and with a beam current of about 0.1 $\mu$ amp. The sample pressure was nearly 80 mmHg (except in the case of water, for which the pressure was $\sim$20 mmHg); the gas was expanded into the vacuum chamber through an orifice 0.15 mm. in diameter. The chamber pressure was maintained at better than $2\times10^{-4}$ mmHg during the entire exposure time by the use of a fast pumping system. The optical density of the plates as a function of the scattering angle was measured using a newly-constructed automatic recording densitometer.[12]

The optical density measurements were made with a precision of better than $\pm0.5\%$; the $s$ scale was also determined with a precision better than $\pm0.5\%$ at a maximum $s$ value ($s=8.0$). The maximum optical density on any given plate was on the order of 0.35, and the intensity of electrons striking the plate was assumed to be proportional to the optical density. The intensity of electrons on Kodak process plates characteristically exhibits a quadratic dependence on the optical density that is usually less than 10% of the linear term. The recognition of this fact, coupled with the use of a sector correction based on helium to correct the experimental intensities, further compensates for the lack of an emulsion correction. Calculations showed that, for a nonlinear term of 10% in the optical density, an error of less than 2% was introduced into the experimentally-corrected intensities due to the neglect of the emulsion calibration.

The observed intensity curves were corrected for extraneous scattering by the use of a blank photograph taken under conditions identical with those encountered in the experiments. The helium experimental results were then matched, at $s=6$, with the best available theoretical results, using a single multiplicative scale factor. A wave function of the form:

$$\psi(\vec{r}_1,\vec{r}_2)=\{\exp[-Z_1r_1-Z_2r_2]+\exp[-Z_1r_2-Z_2r_1]\}\times(1+b\exp[-\alpha r_{12}])$$

was used to calculate the first Born-approximation elastic and inelastic scattering factors[13] employed in the calculation of the theoretical helium intensity. The parameters used in the above wave function were $Z_1=1.4079$, $Z_2=2.2085$, $b=-0.5780$ and $\alpha=0.2925$ (in atomic units). The total energy given by this wave function is 2.90188 Hartrees. The necessary expressions for the scattered intensity can all be obtained in terms of closed-form analytical functions. The ratio of the calculated to the observed helium intensities was then employed to correct the methane, ammonia and water intensities for uncertainties in the shape of the rotating sector, for magnetic disturbances from the sector-bearing, and for the lack of an emulsion calibration.

For the final analysis, the three best helium plates were selected in constructing the sector correction. The helium results are shown in Fig. 1. The best two plates each for methane, ammonia and water were selected; these results,

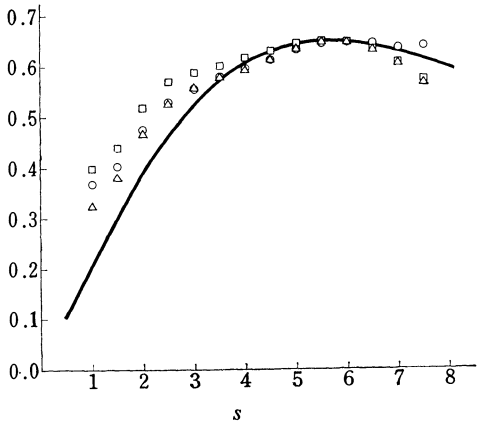



Fig. 1. Comparison of theoretical (——) and experimental (△, □, ○) intensities for atomic helium using an $s^3$ sector. The intensity scale is in arbitrary units. The theoretical and experimental curves are matched at $s=6$.

11) F. Momany, T. Iijima, D. A. Kohl, M. Williams and R. A. Bonham, to be published.

12) D. A. Kohl and M. Williams, to be published.

13) One of us (R.A.B.) wishes to thank the students in his advanced quantum mechanics class for calculating the analytical functions for the elastic and inelastic scattering factors used for the analysis of the helium intensity.

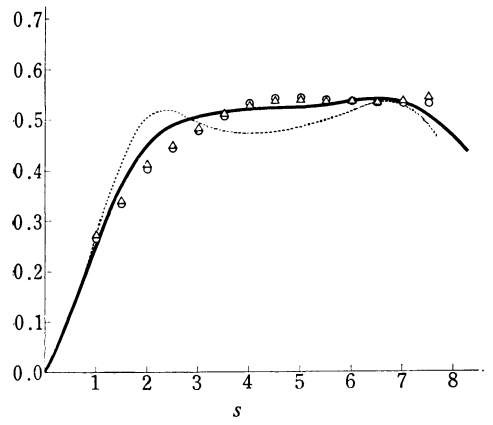



Fig. 2. Experimental and theoretical intensities for methane on an arbitrary intensity scale with results matched at $s=6$.
1. Experimental points: △, ○
2. Theory including binding effects ——
3. Independent-atom model ----

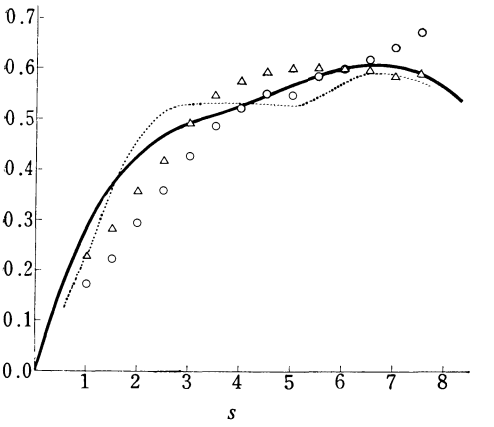



Fig. 3. Experimental and theoretical intensities for ammonia on an arbitrary intensity scale with results matched at $s=6$.
1. Experimental points: △, ○
2. Theory including binding effects ——
3. Independent-atom model ----

after having been sector-corrected, are compared with the theoretical results in Figs. 2, 3 and 4. The agreement with theory in the case of methane is quite gratifying. Unfortunately, the reproducibility of the ammonia and water results indicates only a general qualitative agreement with the theory.

The uncertainty in the present results possibly occurs because of extraneous scattering or intermolecular multiple scattering. Further improvement of the experimental conditions in order to reduce such effects is currently in progress. A further possible source of confusion is the neglect of polarization effects in the theoretical scattering calculations. There

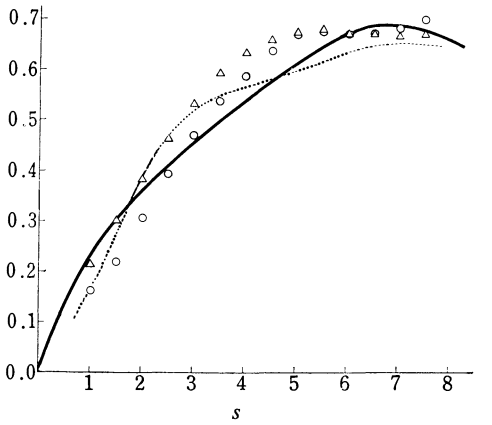



Fig. 4. Experimental and theoretical intensities for water on an arbitrary intensity scale with results matched at $s=6$.
1. Experimental points: △, ○
2. Theory including binding effects ——
3. Independent-atom model ----

are also uncertainties involved in the comparison of theoretical and experimental results because of the approximate nature of the molecular wave functions used. This error should be at a maximum for water, while it should have its smallest value for methane.

In principle there are two effects associated with chemical-bond formation on the scattered intensity from polyatomic molecules. The first is the size effect, which is the main effect in the case of molecular hydrogen; this has been discussed previously.[3,8] The size effect is essentially a change in the effective volume occupied by a fixed percentage of the electrons in the molecule when the independent-atom model goes over to the case where chemical bonds are formed. A comparison between the theoretical results for the independent-atom model and the experimental results or the theoretical calculation including chemical-binding effects shows that the formation of a stable molecular system is accompanied by a decrease in the volume occupied by a fixed percentage of the electrons.

The results of experiments on molecular hydrogen, reported elsewhere,[3,8] are essentially a measure of the effective volume occupied by a fixed percentage of the electrons in the molecule. This decrease indicates an increase in the kinetic energy over that of the independent-atom system; hence, by the use of the virial theorem, it also indicates a lowering of the total energy. Because the independent-atom model represents the size and, thus, the total energy of the system without bond formation, the difference between this curve and the experimental curve is directly related to the binding energy of the system. Unfortunately,

however, the total intensity is also related to the total number of electrons in the system, so the magnitude of the change between the independent-atom model and the experimental results will be proportional to the ratio of the number of electrons involved in the binding to the total number of electrons in the system. Thus the binding effects in systems containing large numbers of electrons, only a few of which are involved in chemical binding, will be quite small. This effect can also be observed in the differences, shown in Figs. 2, 3 and 4, between the independent-atom results (dotted curve) and the results including binding effects (solid curve). According to the simple ideas of valence theory; the magnitude of the binding effects for covalent bonds should be 8/10 for methane, 6/10 for ammonia and 4/10 for water, as compared with the effect in molecular hydrogen.[3,8] (A more detailed examination, appealing to electronegativity concepts, gives ratios slightly different from these.)

The second effect due to bonding arises because of the dipolar character of hetero-atom pairs. In the case of hetero-atoms, the scattering is sensitive to the shifts of charge from one atom to another which occur due to differences in the electronegativity of the atoms involved. This is especially significant in molecules possessing permanent dipole moments; it has been discussed previously by Altshuler.[14] The scattered intensity is proportional to $\mu^2/3s^2$, where $\mu$ is the permanent dipole moment, in the limit as $s$ goes to zero. Unfortunately, this effect may tend to be obscured by polarization effects.

Since size effects and dipole effects occur together, it is of some interest to attempt to isolate one effect from the other. One possibility which suggests itself is to analyze the molecular wave function into "ionic" and "atomic" parts according to the scheme suggested by Shull.[15] In this fashion, the scattered intensity using the "atomic"-like wave function with and without ionic contributions could be calculated. The difference between these cases could then possibly be interpreted in terms of charge drifts due to electronegativity differences in the hetero-polar chemical bonds. Unfortunately, it is felt that both the experimental and theoretical results presented in the present analysis are too crude to allow any conclusions to be drawn regarding the dipole character of the scattering. At any rate, however, the foregoing remarks point out the desireability of obtaining quantitative theoretical relationships between size and dipole effects, on the one hand, and experimental measurements of a limited part of the differential scattering cross section, on the other.

Work is presently under way to obtain more precise measurements, both experimental and theoretical, of the type of scattering presented here so that more detailed comparisons may be made. While this type of experiment is somewhat limited in the kind of information that can be obtained about charge distributions, there are many other possibilities of the use of scattering techniques to obtain such information. Indeed, many of these possibilities have already been previously discussed in the literature.[16-19]

## Summary

The total differential scattering cross sections for the 40 kV. electron from the methane, ammonia and water molecules obtained experimentally over the $1 \leqslant s \leqslant 8$ $s$ range have been compared with the theoretical results. Good agreement with the theoretical results have been obtained in the case of methane. In the cases of ammonia and water the results are in qualitative agreement with the theoretical predictions, but uncertainties in both the theory and experiment prevent a detailed comparison from being made in these cases.

The authors wish to thank Mr. Lao-Sao Su, Mr. Hollace Cox, Mr. Denis A. Kohl and Mr. Howard Brown for their help in obtaining the experimental data. Thanks are also due to Drs. Savo Bratož, M. Allavena and Roberto Moccia for the use of their wave functions prior to publication.

*Department of Chemistry*
*Faculty of Science*
*Hokkaido University*
*Sapporo (T. I.)*

*Department of Chemistry*
*Faculty of Science*
*The University of Tokyo*
*Hongo, Tokyo*
*and*
*Department of Chemistry*
*Indiana University*
*Bloomington, Indiana, U. S. A. (R. A. B.)*

*Laboratoire de Diffraction Electronique*
*Institut d'Electronique*
*Faculte des Sciences-Orsay*
*Seine et Oise, France (C. T.)*

*Centre de Mechanique Ondulatoire Appliquee*
*23, Rue de Maroc, Paris XIXe, France*
*(M. R. & M. C.)*

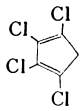
14) S. Altshuler, *Phys. Rev.*, 107, 114 (1957).
15) H. Shull, *J. Phys. Chem.*, 44, 2320 (1962).
16) L. S. Bartell and R. M. Gavin, Jr., *J. Am. Chem. Soc.*, 86, 3493 (1964).
17) R. A. Bonham, *J. Chem. Phys.*, 36, 3260 (1962).
18) J. Karle, ibid., 35, 963 (1961).
19) D. A. Swick, *Rev. Sci. Instr.*, 31, 525 (1960).

# The Crystal Structure of 1, 2, 3-Tribromo-6-(*o*-methoxyphenyl)fulvene

By Yukio KATO,* Yoshio SASADA and Masao KAKUDO

(Received May 4, 1965)

Sesquifulvalene (cycloheptatrienylidenecyclopentadiene), recently synthesized by Prinzbach and Rosswog,[1] is an interesting substance of non-alternant hydrocarbons. Kitahara, Murata, Funamizu and Asano[2] have attempted to obtain the tetrachloro derivative of this compound by the reaction of 1, 2, 3, 4-tetrachlorocyclopentadiene (I) and tropone (II) in a large volume of methanol.

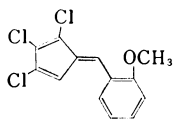


(I)

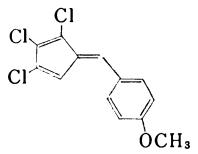


(II)

Contrary to their expectation, however, they got two kinds of products: red prisms (m. p. 117—118°C) and reddish-orange needles (m. p. 77—78°C). Elementary analysis indicated that both of these products had the molecular formula $C_{13}H_9OCl_3$. By some chemical consideration, and with the help of infrared, ultraviolet and NMR spectra, in was concluded that these isomers were trichloro-6-(*o*-methoxyphenyl)fulvene (III) and trichloro-6-(*p*-methoxyphenyl)fulvene (IV).



(III)



(IV)

Thus they have shown that the reaction of I and II in methanol results in an entirely new type of rearrangement reaction, in which the methoxy group enters the seven-membered ring (a six-membered ring after the rearrangement) and in which a chlorine atom in the five-membered ring is librated. The conformations of these molecules were also discussed on the basis of the NMR spectra.

The reaction between tropone and 1, 2, 3, 4-tetrabromocyclopentadiene followed an entirely analogous course; red plates (m. p. 128—129°C) and red prisms (m. p. 90—91°C) were obtained.[2] These compounds were supplied to us so that we could undertake an independent verification of the structures by means of X-ray.

The present paper will describe the structure determination of 1, 2, 3-tribromo-6-(*o*-methoxyphenyl)fulvene.

## Experimental

Crystals of 1,2,3-tribromo-6-(*o*-methoxyphenyl)-fulvene (hereafter termed the "bromo derivative") and 1,2,3-trichloro-6-(*o*-methoxyphenyl)fulvene (hereafter the "chloro derivative") were supplied by Professor Kitahara of Tohoku University. Both of them are stable red laths elongated along the c axis.

From oscillation, Weissenberg and precession photographs of these crystals, the unit cell dimensions and space groups were determined. The crystal and physical data are summarized in Table I.

TABLE I. CRYSTAL AND PHYSICAL DATA

| | Bromo derivative | Chloro derivative |
|---|---|---|
| M. p. | 128—129°C | 117—118°C |
| $a$ | 11.46 Å | 11.65 |
| $b$ | 14.53 | 14.61 |
| $c$ | 7.85 | 7.64 |
| $\beta$ | 96°35′ | 98°58′ |
| Space group | $P2_1/c$ | $P2_1/c$ |
| $Z$ | 4 | 4 |
| $\rho_{obs.}$ | 2.17 g.cm$^{-3}$ | 1.50 |
| $\rho_{calcd.}$ | 2.15 | 1.49 |

Intensity data were collected only for the bromo derivative. Equi-inclination Weissenberg photographs around the c axis were taken with Cu$K\alpha$ radiation for $l$ values from 0 to 6. The crystal used had a cross section of 0.1×0.2 mm. In order to determine the scale factors among the $l$ layers, photographs for zero and first layers around the b axis were taken, also. Reflections from 2060 planes were observed out of 2900 possible ($hkl$)'s. In order to correlate the strong and the weak reflections, a multiple-film technique was applied, the relative intensities being ranged between 1 to 7000. The intensities were measured by a visual comparison with a standard intensity scale prepared with the same crystal. Lorentz and polarization corrections were made in the usual way. Since the main interest of this work was in determining the molecular conformation, the correction for absorption was omitted in spite of its large effect as a

* On leave from Research Laboratory, Teijin Co., Ltd., Iwakuni.

1) H. Prinzbach and W. Rosswog, *Angew. Chem.*, 73, 543 (1961).

2) Y. Kitahara, I. Murata, M. Funamizu and T. Asano, This Bulletin, 37, 1399 (1964).

result of the high bromine content. Tentative scale and temperature factors were estimated by Wilson statistics, the latter being $B=3.1$ Å$^2$.

## Structure Determination

The three-dimensional Patterson function was synthesized on an electronic computer (IBM 7040) with a programme written by the authors. Figure 1 shows the Patterson section

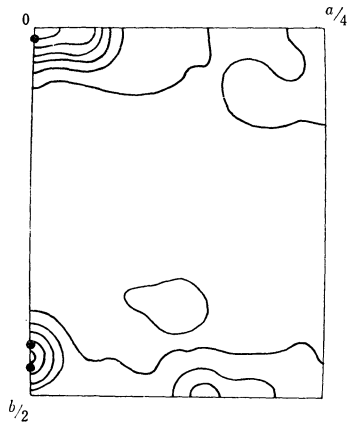



Fig. 1. Harker section $P(u,v,1/2)$. Contours are at equal intervals on an arbitrary scale. Black circles show Br-Br vectors from the final result.

$P(u,v,1/2)$. There should appear on the $u=0$ line peaks due to vectors between atoms related to each other by the c glide operation. Only two significant peaks were observed on this line, however, at $v=0$ and at $v=0.45$. Since there should be three heavy atoms in an asymmetric unit, the peak at $v=0.45$ may be supposed to be a superimposed one due to two independent bromine atoms. Therefore, the $y$ coordinate of one bromine atom was

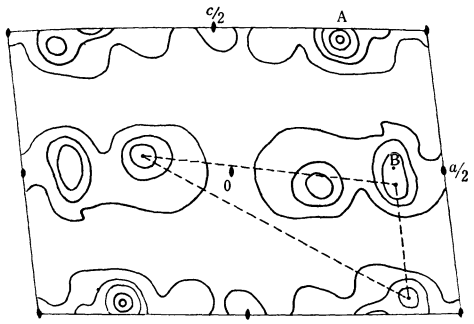



Fig. 2. Harker section $P(u,1/2,w)$. Contours are at equal intervals on an arbitrary scale. Three peaks linked by dashed lines correspond to vectors between the bromine atoms related by two-fold screw axis.

$\pm 0.250$, while those of the remaining two were $\pm 0.025$.

The interpretation of the Harker section at $v=1/2$ was very ambiguous, because there appeared not only peaks between atoms related by a two-fold screw axis, but also peaks between independent atoms, the difference between whose $y$ coordinates are, by accident, a half of the b axis. Figure 2 shows the Harker section $P(u,1/2,w)$.

The first clue to the structure was obtained by examining the intramolecular heavy atom vectors in the three-dimensional Patterson function. Chemical information tells us that three bromine atoms attached to the fulvene ring form a two-lateral triangle whose sides are 3.6, 3.6 and 5.8 Å long. Figure 3 gives a

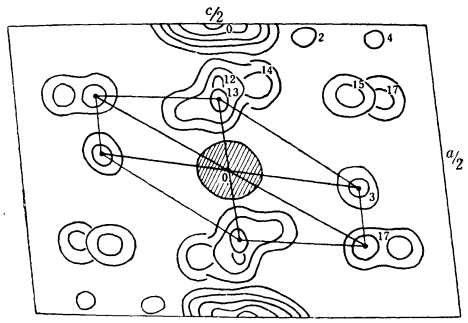



Fig. 3. Three-dimensional Patterson function. Composite diagram of sections parallel to (0 1 0). Height of section is added to each peak in unit of 1/60. Contours are at equal intervals on an arbitrary scale. Black circles show intramolecular Br-Br vector peaks.

composite three-dimensional Patterson function, showing peaks which lie within, say, 7 Å from the point of origin. Although some intermolecular vectors between the bromine atoms were observed at distances of about 4 Å from the point of origin, a constellation of Patterson peaks corresponding to the vector set of such a bromine triangle was clearly recognized, as is illustrated by the solid lines in Fig. 3. With the help of the orientation of the bromine triangle so found, the Harker section at $v=1/2$ was again examined and true Harker peaks were assigned, as is shown by the dash-line triangle in Fig. 2. The atomic coordinates of the three bromine atoms obtained were (0.605, $-0.027$, 0.225) for $Br_1$, (0.310, 0.027, 0.272) for $Br_2$ and (0.301, 0.250, 0.470) for $Br_3$. The non-Harker peak A in Fig. 2 was explained as a vector between the $Br_1$ of one molecule and the $Br_2$ of the molecule related by the c glide, and the B peak, as that between $Br_3$ atoms related to each other by the center of symmetry in different molecules.

Structure factors were computed with these

three bromine atoms with $B=3.1$ Å$^2$, the discrepancy factor, $R=\Sigma||F_o|-|F_c||/\Sigma|F_o|$, being 0.45. The first Fourier synthesis of the three-dimensional electron density distribution was carried out with signs based on the three bromine atoms. Significant peaks appearing in the Fourier map gave a reasonable molecular shape. Although some ghost peaks were observed in the map, it seemed quite certain that the molecular structure has been established by this stage. To be more precise, however, only three bromine atoms and five carbon atoms in the fulvene ring were introduced into the second calculation of the structure factors, and the *R* factor dropped to 0.36. The second Fourier synthesis looked very refined, and the coordinates of all the atoms could be read off from it. These coordinates of atoms gave reasonable bond lengths and angles. The third calculation of the structure factors resulted in an *R* factor of 0.30. At this stage, the scaling factors among the layers were corrected by the use of these calculated structure factors. All of these computations were executed on an IBM 7040 with programmes devised by the authors.

The atomic coordinates and temperature factors (anisotropic for the bromine atoms only) were refined by the successive block-diagonal matrix (9×9) least-squares method, the programmes for which were written by Tamaichi Ashida of this laboratory. Each cycle of the refinement on the IBM 7040 using all reflections took about 15 min. After four cycles, the *R* factor decreased to 0.126 (if non-observed reflections were omitted, the *R* factor was 0.113).

The final atomic coordinates and temperature factors of each atom are listed in Tables II and III respectively. The observed and calculated structure factors are shown in Table IV. Figure 4 gives the superimposed (0 0 1) sections of the final electron density distribution as taken through the atomic centers in the molecule.

TABLE II. THE FINAL ATOMIC COORDINATES

| Atom | *x/a* | *y/b* | *z/c* |
|---|---|---|---|
| $Br_1$ | 0.6048 | −0.0195 | 0.2265 |
| $Br_2$ | 0.3089 | 0.0372 | 0.2778 |
| $Br_3$ | 0.3051 | 0.2582 | 0.4716 |
| $C_1$ | 0.5512 | 0.0874 | 0.3176 |
| $C_2$ | 0.4434 | 0.1080 | 0.3340 |
| $C_3$ | 0.4418 | 0.1975 | 0.4248 |
| $C_4$ | 0.5492 | 0.2303 | 0.4586 |
| $C_5$ | 0.6282 | 0.1630 | 0.3942 |
| $C_6$ | 0.7470 | 0.1593 | 0.4034 |
| $C_7$ | 0.8270 | 0.2338 | 0.4754 |
| $C_8$ | 0.7992 | 0.3288 | 0.4509 |
| $C_9$ | 0.8748 | 0.3942 | 0.5216 |
| $C_{10}$ | 0.9858 | 0.3683 | 0.6090 |
| $C_{11}$ | 1.0194 | 0.2752 | 0.6364 |
| $C_{12}$ | 0.9346 | 0.2099 | 0.5596 |
| $C_{13}$ | 1.0759 | 0.0862 | 0.6479 |
| O | 0.9584 | 0.1167 | 0.5790 |

## Discussion

The very reasonable three-dimensional electron density distribution (shown in Fig. 4)

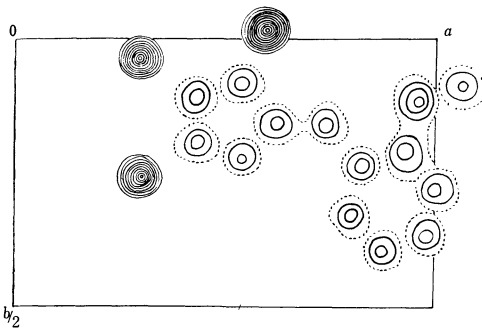



Fig. 4. The final electron density distribution. Composite diagram of sections parallel to (0 0 1). Contours are at intervals of 3 e.Å$^{-3}$ with dashed contour of 2 e.Å$^{-3}$. For bromine, contours are at intervals of 6 e.Å$^{-3}$, beginning with 6 e.Å$^{-3}$.

TABLE III. THE FINAL TEMPERATURE FACTORS

For heavy atoms, temperature factors are in the form of
$\exp\{-(B_{11}h^2+B_{22}k^2+B_{33}l^2+B_{12}hk+B_{23}kl+B_{31}lh)\}$.

| Atom | $B_{11}$ | $B_{22}$ | $B_{33}$ | $B_{12}$ | $B_{23}$ | $B_{31}$ |
|---|---|---|---|---|---|---|
| $Br_1$ | 0.00788 | 0.00346 | 0.01357 | 0.00180 | −0.00473 | −0.00209 |
| $Br_2$ | 0.00627 | 0.00377 | 0.01458 | −0.00255 | −0.00137 | −0.00375 |
| $Br_3$ | 0.00515 | 0.00468 | 0.01179 | 0.00091 | −0.00264 | 0.00172 |

| Atom | $B$(Å$^2$) | Atom | $B$(Å$^2$) | Atom | $B$(Å$^2$) | Atom | $B$(Å$^2$) |
|---|---|---|---|---|---|---|---|
| $C_1$ | 2.40 | $C_5$ | 2.09 | $C_9$ | 4.10 | $C_{13}$ | 4.19 |
| $C_2$ | 2.74 | $C_6$ | 2.61 | $C_{10}$ | 3.75 | O | 3.08 |
| $C_3$ | 2.17 | $C_7$ | 2.40 | $C_{11}$ | 3.69 | | |
| $C_4$ | 2.47 | $C_8$ | 3.27 | $C_{12}$ | 2.62 | | |

TABLE IV. OBSERVED AND CALCULATED STRUCTURE FACTORS

| $h$ | $k$ | $l$ | $F_{obs.}$ | $F_{calcd.}$ | $h$ | $k$ | $l$ | $F_{obs.}$ | $F_{calcd.}$ | $h$ | $k$ | $l$ | $F_{obs.}$ | $F_{calcd.}$ | $h$ | $k$ | $l$ | $F_{obs.}$ | $F_{calcd.}$ |
|---|---|---|---|---|---|---|---|---|---|---|---|---|---|---|---|---|---|---|---|
| 2 | 0 | 0 | 11.11 | −13.84 | 8 | 4 | 0 | 17.18 | −17.01 | 4 | 9 | 0 | 19.59 | −17.94 | 2 | 1 | 1 | 10.84 | −11.73 |
| 3 | 0 | 0 | 46.60 | 60.38 | 9 | 4 | 0 | 8.45 | − 7.70 | 5 | 9 | 0 | 8.97 | 8.36 | 2 | 1 | −1 | 5.35 | 6.20 |
| 4 | 0 | 0 | 7.69 | − 7.48 | 10 | 4 | 0 | 22.22 | 21.45 | 6 | 9 | 0 | 10.62 | 10.02 | 3 | 1 | 1 | 31.06 | 32.55 |
| 5 | 0 | 0 | 14.68 | −14.55 | 11 | 4 | 0 | 11.47 | −11.44 | 7 | 9 | 0 | 2.14 | − 5.13 | 3 | 1 | −1 | 36.25 | −41.93 |
| 6 | 0 | 0 | 5.77 | 5.33 | 12 | 4 | 0 | 2.69 | 2.84 | 8 | 9 | 0 | 9.16 | − 9.38 | 4 | 1 | 1 | 37.97 | −38.81 |
| 7 | 0 | 0 | 24.41 | 24.87 | 13 | 4 | 0 | 11.51 | 11.91 | 9 | 9 | 0 | 19.20 | 16.56 | 4 | 1 | −1 | 26.61 | 28.08 |
| 8 | 0 | 0 | 27.56 | −27.26 | 14 | 4 | 0 | 3.81 | − 4.77 | 10 | 9 | 0 | 4.76 | − 4.35 | 5 | 1 | 1 | 10.01 | 8.49 |
| 9 | 0 | 0 | 7.69 | − 5.46 | 1 | 5 | 0 | 55.18 | −59.65 | 11 | 9 | 0 | 9.34 | −10.44 | 5 | 1 | −1 | 4.23 | 3.59 |
| 10 | 0 | 0 | 22.10 | 21.52 | 2 | 5 | 0 | 42.02 | 41.27 | 12 | 9 | 0 | 9.58 | 12.09 | 6 | 1 | 1 | 32.02 | 27.78 |
| 11 | 0 | 0 | 14.50 | −12.03 | 3 | 5 | 0 | 11.63 | 10.81 | 0 | 10 | 0 | 13.52 | −12.82 | 6 | 1 | −1 | 25.63 | −24.35 |
| 12 | 0 | 0 | 9.40 | 8.72 | 4 | 5 | 0 | 41.93 | −40.44 | 1 | 10 | 0 | 4.61 | 3.80 | 7 | 1 | 1 | 30.24 | −29.27 |
| 13 | 0 | 0 | 13.40 | 15.26 | 5 | 5 | 0 | 6.44 | 6.48 | 2 | 10 | 0 | 26.43 | 23.97 | 7 | 1 | −1 | 33.45 | 30.76 |
| 14 | 0 | 0 | 5.25 | − 6.17 | 6 | 5 | 0 | 12.67 | 12.90 | 3 | 10 | 0 | 16.91 | −16.42 | 8 | 1 | 1 | 14.82 | 12.74 |
| 1 | 1 | 0 | 18.01 | −19.64 | 7 | 5 | 0 | 12.63 | −11.22 | 4 | 10 | 0 | 9.06 | − 8.79 | 8 | 1 | −1 | 1.56 | − 1.22 |
| 2 | 1 | 0 | 28.99 | 38.08 | 8 | 5 | 0 | 14.71 | −14.63 | 5 | 10 | 0 | 20.26 | 18.79 | 9 | 1 | 1 | 9.88 | 7.88 |
| 3 | 1 | 0 | 13.24 | 15.81 | 9 | 5 | 0 | 20.72 | 19.92 | 6 | 10 | 0 | 13.86 | −11.92 | 9 | 1 | −1 | 9.36 | − 7.78 |
| 4 | 1 | 0 | 28.32 | −30.78 | 10 | 5 | 0 | 8.06 | − 7.04 | 7 | 10 | 0 | 9.64 | − 9.19 | 10 | 1 | 1 | 6.09 | − 5.18 |
| 5 | 1 | 0 | 6.74 | 5.87 | 11 | 5 | 0 | 16.48 | −15.52 | 8 | 10 | 0 | 10.41 | 9.97 | 10 | 1 | −1 | 15.34 | 12.48 |
| 6 | 1 | 0 | 26.18 | 25.66 | 12 | 5 | 0 | 11.96 | 13.20 | 10 | 10 | 0 | 8.55 | − 9.52 | 13 | 1 | 1 | 2.09 | 2.14 |
| 7 | 1 | 0 | 12.51 | −12.52 | 13 | 5 | 0 | 2.14 | − 1.35 | 11 | 10 | 0 | 4.36 | 4.20 | 13 | 1 | −1 | 3.13 | − 3.32 |
| 8 | 1 | 0 | 8.09 | 7.37 | 0 | 6 | 0 | 8.48 | − 7.11 | 12 | 10 | 0 | 2.23 | 2.08 | 14 | 1 | 1 | 2.94 | − 3.69 |
| 9 | 1 | 0 | 19.96 | 18.84 | 1 | 6 | 0 | 14.31 | −11.46 | 1 | 11 | 0 | 7.51 | − 8.21 | 14 | 1 | −1 | 2.96 | 3.61 |
| 10 | 1 | 0 | 8.03 | − 7.33 | 2 | 6 | 0 | 4.79 | 5.53 | 2 | 11 | 0 | 19.71 | 16.89 | 0 | 2 | 1 | 20.03 | −17.32 |
| 11 | 1 | 0 | 10.01 | − 9.19 | 4 | 6 | 0 | 16.97 | −16.05 | 3 | 11 | 0 | 12.42 | −12.01 | 1 | 2 | 1 | 14.10 | 10.99 |
| 12 | 1 | 0 | 9.77 | 8.52 | 5 | 6 | 0 | 27.65 | 29.27 | 4 | 11 | 0 | 13.67 | 14.49 | 1 | 2 | −1 | 15.37 | −14.10 |
| 14 | 1 | 0 | 5.83 | − 6.70 | 6 | 6 | 0 | 11.90 | −11.56 | 5 | 11 | 0 | 3.02 | 2.63 | 2 | 2 | 1 | 15.42 | 13.49 |
| 0 | 2 | 0 | 4.61 | 3.92 | 7 | 6 | 0 | 12.79 | −12.02 | 6 | 11 | 0 | 8.64 | − 7.81 | 2 | 2 | −1 | 1.62 | − 0.28 |
| 1 | 2 | 0 | 26.40 | −26.26 | 8 | 6 | 0 | 17.94 | 17.88 | 7 | 11 | 0 | 8.51 | 8.28 | 3 | 2 | 1 | 5.21 | − 5.97 |
| 2 | 2 | 0 | 8.88 | 7.73 | 9 | 6 | 0 | 5.28 | − 5.69 | 1 | 13 | 0 | 10.99 | −11.25 | 3 | 2 | −1 | 8.04 | 6.66 |
| 3 | 2 | 0 | 11.05 | 10.50 | 12 | 6 | 0 | 3.54 | 3.65 | 2 | 13 | 0 | 12.94 | 13.53 | 4 | 2 | 1 | 16.76 | −15.42 |
| 4 | 2 | 0 | 20.51 | −27.33 | 13 | 6 | 0 | 1.98 | − 3.06 | 3 | 13 | 0 | 8.06 | − 6.95 | 4 | 2 | −1 | 1.54 | 1.39 |
| 5 | 2 | 0 | 15.78 | 16.74 | 1 | 7 | 0 | 9.52 | 10.33 | 4 | 13 | 0 | 6.78 | − 5.53 | 5 | 2 | 1 | 5.19 | 6.71 |
| 6 | 2 | 0 | 13.61 | −12.62 | 2 | 7 | 0 | 15.59 | 13.61 | 8 | 13 | 0 | 5.52 | − 5.41 | 5 | 2 | −1 | 12.95 | −13.48 |
| 7 | 2 | 0 | 4.97 | − 3.10 | 3 | 7 | 0 | 20.63 | −19.04 | 9 | 13 | 0 | 5.22 | 6.23 | 7 | 2 | 1 | 11.19 | − 8.85 |
| 8 | 2 | 0 | 11.57 | 10.27 | 4 | 7 | 0 | 6.32 | 6.05 | 0 | 14 | 0 | 14.53 | −16.02 | 7 | 2 | −1 | 9.36 | 7.96 |
| 9 | 2 | 0 | 8.79 | − 6.55 | 5 | 7 | 0 | 3.60 | 2.45 | 1 | 14 | 0 | 6.74 | 6.87 | 8 | 2 | 1 | 1.65 | 2.91 |
| 10 | 2 | 0 | 6.07 | 6.19 | 6 | 7 | 0 | 5.43 | − 3.95 | 2 | 14 | 0 | 9.03 | 10.23 | 8 | 2 | −1 | 8.40 | − 7.90 |
| 11 | 2 | 0 | 7.97 | − 6.34 | 7 | 7 | 0 | 2.90 | 2.64 | 3 | 14 | 0 | 8.91 | − 9.53 | 9 | 2 | 1 | 10.95 | − 8.71 |
| 14 | 2 | 0 | 3.57 | − 3.91 | 8 | 7 | 0 | 7.35 | − 6.68 | 5 | 14 | 0 | 8.88 | 9.28 | 9 | 2 | −1 | 5.21 | 3.78 |
| 1 | 3 | 0 | 2.26 | 0.91 | 9 | 7 | 0 | 3.05 | 1.52 | 6 | 14 | 0 | 4.61 | − 4.64 | 10 | 2 | 1 | 1.56 | 2.20 |
| 2 | 3 | 0 | 3.23 | 2.83 | 10 | 7 | 0 | 4.21 | − 2.71 | 7 | 14 | 0 | 5.46 | − 6.82 | 10 | 2 | −1 | 2.72 | 1.66 |
| 3 | 3 | 0 | 14.47 | −13.43 | 11 | 7 | 0 | 2.75 | − 1.45 | 8 | 14 | 0 | 7.42 | 8.59 | 11 | 2 | 1 | 0. | − 0.39 |
| 4 | 3 | 0 | 17.43 | 16.66 | 12 | 7 | 0 | 3.33 | 3.42 | 3 | 15 | 0 | 9.25 | − 9.68 | 11 | 2 | −1 | 2.72 | 2.15 |
| 6 | 3 | 0 | 10.53 | − 9.54 | 13 | 7 | 0 | 3.08 | − 3.80 | 4 | 15 | 0 | 5.37 | 6.73 | 12 | 2 | 1 | 2.44 | 3.06 |
| 7 | 3 | 0 | 9.49 | 9.42 | 0 | 8 | 0 | 27.89 | 25.76 | 6 | 15 | 0 | 9.95 | −11.04 | 12 | 2 | −1 | 0. | − 0.43 |
| 10 | 3 | 0 | 7.48 | 5.80 | 1 | 8 | 0 | 5.58 | − 6.39 | 7 | 15 | 0 | 5.86 | 7.29 | 13 | 2 | 1 | 2.03 | − 3.02 |
| 11 | 3 | 0 | 5.98 | 4.96 | 3 | 8 | 0 | 17.52 | 15.09 | 0 | 16 | 0 | 5.92 | − 6.80 | 13 | 2 | −1 | 0. | 1.71 |
| 14 | 3 | 0 | 2.41 | 2.79 | 4 | 8 | 0 | 6.74 | − 4.79 | 1 | 16 | 0 | 3.72 | 3.67 | 0 | 3 | 1 | 8.42 | 7.01 |
| 0 | 4 | 0 | 51.48 | 54.44 | 6 | 8 | 0 | 4.03 | 3.41 | 1 | 17 | 0 | 3.20 | − 3.84 | 1 | 3 | 1 | 17.31 | −14.94 |
| 1 | 4 | 0 | 39.25 | −39.59 | 7 | 8 | 0 | 7.26 | 6.45 | 2 | 17 | 0 | 3.11 | 4.15 | 1 | 3 | −1 | 2.85 | − 1.92 |
| 2 | 4 | 0 | 31.04 | −30.11 | 9 | 8 | 0 | 3.02 | − 3.89 | 3 | 17 | 0 | 3.63 | − 5.10 | 2 | 3 | 1 | 4.42 | 3.93 |
| 3 | 4 | 0 | 36.41 | 37.69 | 10 | 8 | 0 | 7.63 | 6.66 | 4 | 17 | 0 | 2.72 | 3.43 | 2 | 3 | −1 | 20.52 | 18.21 |
| 4 | 4 | 0 | 14.07 | −13.86 | 11 | 8 | 0 | 4.49 | − 4.38 | 0 | 18 | 0 | 3.97 | − 5.08 | 3 | 3 | 1 | 31.66 | 30.30 |
| 5 | 4 | 0 | 14.80 | −14.39 | 13 | 8 | 0 | 2.53 | 3.82 | 1 | 18 | 0 | 3.02 | 4.48 | 3 | 3 | −1 | 36.79 | −36.40 |
| 6 | 4 | 0 | 10.93 | 8.62 | 1 | 9 | 0 | 34.97 | −33.23 | 1 | 1 | 1 | 2.28 | − 2.44 | 4 | 3 | 1 | 30.76 | −33.24 |
| 7 | 4 | 0 | 15.87 | 15.43 | 2 | 9 | 0 | 34.82 | 32.30 | 1 | 1 | −1 | 9.52 | 9.08 | 4 | 3 | −1 | 25.05 | 24.93 |

TABLE IV. (Continued)

| *h* | *k* | *l* | $F_{obs.}$ | $F_{calcd.}$ | *h* | *k* | *l* | $F_{obs.}$ | $F_{calcd.}$ | *h* | *k* | *l* | $F_{obs.}$ | $F_{calcd.}$ | *h* | *k* | *l* | $F_{obs.}$ | $F_{calcd.}$ |
|---|---|---|---|---|---|---|---|---|---|---|---|---|---|---|---|---|---|---|---|
| 5 | 3 | 1 | 13.58 | 11.88 | 4 | 5 | 1 | 13.77 | −12.49 | 10 | 7 | −1 | 0. | 0.07 | 4 | 10 | 1 | 14.21 | −13.25 |
| 5 | 3 | −1 | 0. | 1.76 | 4 | 5 | −1 | 19.65 | 17.62 | 11 | 7 | 1 | 8.23 | 7.62 | 4 | 10 | −1 | 9.25 | 8.04 |
| 6 | 3 | 1 | 12.68 | 12.19 | 5 | 5 | 1 | 0. | − 0.59 | 11 | 7 | −1 | 2.47 | − 1.04 | 5 | 10 | 1 | 14.10 | 14.56 |
| 6 | 3 | −1 | 34.05 | −32.31 | 5 | 5 | −1 | 4.53 | 2.98 | 0 | 8 | 1 | 2.03 | − 2.50 | 5 | 10 | −1 | 17.12 | −17.48 |
| 7 | 3 | 1 | 25.82 | −23.88 | 6 | 5 | 1 | 15.78 | 14.18 | 1 | 8 | 1 | 2.06 | − 1.85 | 6 | 10 | 1 | 13.03 | −12.53 |
| 7 | 3 | −1 | 19.43 | 17.40 | 6 | 5 | −1 | 13.09 | −12.32 | 1 | 8 | −1 | 21.21 | 17.31 | 6 | 10 | −1 | 12.70 | 12.69 |
| 8 | 3 | 1 | 13.36 | 11.22 | 7 | 5 | 1 | 17.40 | −16.16 | 2 | 8 | 1 | 21.84 | 18.88 | 7 | 10 | 1 | 6.67 | − 6.56 |
| 8 | 3 | −1 | 6.53 | − 4.78 | 7 | 5 | −1 | 17.31 | 15.49 | 2 | 8 | −1 | 24.12 | −21.70 | 7 | 10 | −1 | 4.72 | − 3.91 |
| 9 | 3 | 1 | 0. | 0.25 | 8 | 5 | 1 | 7.87 | 6.43 | 3 | 8 | 1 | 20.39 | −18.67 | 8 | 10 | 1 | 7.02 | 6.70 |
| 9 | 3 | −1 | 9.49 | − 7.65 | 8 | 5 | −1 | 13.12 | −11.31 | 3 | 8 | −1 | 10.21 | 9.23 | 8 | 10 | −1 | 10.07 | −10.43 |
| 10 | 3 | 1 | 13.66 | −11.58 | 9 | 5 | 1 | 0. | 0.19 | 4 | 8 | 1 | 1.65 | − 2.23 | 9 | 10 | 1 | 4.31 | − 4.19 |
| 10 | 3 | −1 | 0. | − 0.95 | 9 | 5 | −1 | 2.69 | − 3.36 | 4 | 8 | −1 | 21.07 | 18.73 | 9 | 10 | −1 | 12.02 | 12.44 |
| 11 | 3 | 1 | 2.63 | 3.71 | 10 | 5 | 1 | 0. | − 1.07 | 5 | 8 | 1 | 28.81 | 27.30 | 0 | 11 | 1 | 2.55 | − 2.28 |
| 11 | 3 | −1 | 0. | 1.21 | 10 | 5 | −1 | 9.82 | 8.16 | 5 | 8 | −1 | 27.36 | −26.13 | 1 | 11 | 1 | 12.02 | 11.70 |
| 12 | 3 | 1 | 1.65 | 0.84 | 11 | 5 | 1 | 2.55 | 1.25 | 6 | 8 | 1 | 19.81 | −18.69 | 1 | 11 | −1 | 11.44 | − 9.94 |
| 12 | 3 | −1 | 1.78 | − 0.04 | 11 | 5 | −1 | 6.94 | − 6.20 | 6 | 8 | −1 | 11.06 | 9.85 | 2 | 11 | 1 | 7.79 | − 7.48 |
| 13 | 3 | 1 | 2.80 | 0.65 | 13 | 5 | 1 | 2.52 | 1.91 | 7 | 8 | 1 | 11.69 | 11.03 | 2 | 11 | −1 | 9.30 | 8.57 |
| 13 | 3 | −1 | 0. | − 1.88 | 13 | 5 | −1 | 0. | − 0.60 | 7 | 8 | −1 | 13.25 | 12.59 | 3 | 11 | 1 | 7.46 | − 7.11 |
| 14 | 3 | 1 | 2.61 | − 3.99 | 0 | 6 | 1 | 6.06 | − 4.89 | 8 | 8 | 1 | 13.66 | 12.42 | 3 | 11 | −1 | 6.94 | − 6.22 |
| 14 | 3 | −1 | 2.77 | 3.20 | 1 | 6 | 1 | 14.82 | −12.41 | 8 | 8 | −1 | 11.55 | − 9.79 | 4 | 11 | 1 | 7.11 | 6.53 |
| 0 | 4 | 1 | 6.72 | − 5.40 | 1 | 6 | −1 | 2.39 | 0.92 | 9 | 8 | 1 | 10.40 | −10.36 | 4 | 11 | −1 | 11.66 | −11.15 |
| 1 | 4 | 1 | 16.57 | 14.21 | 2 | 6 | 1 | 18.82 | 16.81 | 9 | 8 | −1 | 0. | − 1.49 | 5 | 11 | 1 | 1.92 | 2.19 |
| 1 | 4 | −1 | 13.01 | 10.63 | 2 | 6 | −1 | 21.37 | −18.14 | 10 | 8 | 1 | 0. | 0.29 | 5 | 11 | −1 | 6.06 | 5.77 |
| 2 | 4 | 1 | 23.82 | 18.59 | 3 | 6 | 1 | 17.81 | −15.77 | 10 | 8 | −1 | 2.61 | 3.52 | 6 | 11 | 1 | 5.46 | − 5.17 |
| 2 | 4 | −1 | 24.06 | −21.12 | 3 | 6 | −1 | 10.67 | 9.44 | 11 | 8 | 1 | 5.49 | 5.53 | 6 | 11 | −1 | 0. | 1.48 |
| 3 | 4 | 1 | 11.22 | −10.24 | 4 | 6 | 1 | 16.19 | −13.67 | 11 | 8 | −1 | 0. | − 0.93 | 7 | 11 | 1 | 0. | 0.61 |
| 3 | 4 | −1 | 9.27 | 7.72 | 4 | 6 | −1 | 13.06 | 11.58 | 0 | 9 | 1 | 6.28 | 5.76 | 7 | 11 | −1 | 5.41 | − 5.30 |
| 4 | 4 | 1 | 4.39 | 3.26 | 5 | 6 | 1 | 28.29 | 27.21 | 1 | 9 | 1 | 9.25 | 7.50 | 8 | 11 | 1 | 3.59 | 3.71 |
| 4 | 4 | −1 | 26.31 | 24.71 | 5 | 6 | −1 | 25.22 | −23.02 | 1 | 9 | −1 | 19.56 | −16.46 | 8 | 11 | −1 | 0. | − 0.42 |
| 5 | 4 | 1 | 24.39 | 23.56 | 6 | 6 | 1 | 13.86 | −13.79 | 2 | 9 | 1 | 20.88 | −19.89 | 9 | 11 | 1 | 5.19 | − 5.76 |
| 5 | 4 | −1 | 28.86 | −27.19 | 6 | 6 | −1 | 20.33 | 18.51 | 2 | 9 | −1 | 2.28 | 2.85 | 9 | 11 | −1 | 1.12 | 1.81 |
| 6 | 4 | 1 | 20.63 | −18.79 | 7 | 6 | 1 | 6.72 | − 5.82 | 3 | 9 | 1 | 10.87 | 9.55 | 11 | 11 | 1 | 4.12 | 4.76 |
| 6 | 4 | −1 | 10.37 | 9.55 | 7 | 6 | −1 | 4.97 | 3.40 | 3 | 9 | −1 | 13.03 | 11.76 | 11 | 11 | −1 | 0. | − 2.11 |
| 7 | 4 | 1 | 5.35 | − 4.20 | 8 | 6 | 1 | 13.88 | 12.83 | 4 | 9 | 1 | 2.47 | 2.58 | 0 | 12 | 1 | 8.01 | 7.55 |
| 7 | 4 | −1 | 9.85 | 8.81 | 8 | 6 | −1 | 15.37 | −14.09 | 4 | 9 | −1 | 7.68 | − 6.29 | 1 | 12 | 1 | 4.64 | 4.14 |
| 8 | 4 | 1 | 18.36 | 16.21 | 9 | 6 | 1 | 6.12 | − 4.39 | 5 | 9 | 1 | 11.19 | −10.84 | 1 | 12 | −1 | 13.09 | 12.61 |
| 8 | 4 | −1 | 14.87 | −13.86 | 9 | 6 | −1 | 9.03 | 8.05 | 5 | 9 | −1 | 0. | − 1.18 | 2 | 12 | 1 | 3.81 | 3.12 |
| 9 | 4 | 1 | 8.94 | − 7.94 | 11 | 6 | 1 | 3.51 | 1.98 | 6 | 9 | 1 | 0. | − 0.99 | 2 | 12 | −1 | 9.30 | − 8.26 |
| 9 | 4 | −1 | 5.32 | 4.40 | 11 | 6 | −1 | 4.44 | − 3.81 | 6 | 9 | −1 | 6.97 | 6.29 | 3 | 12 | 1 | 0. | − 0.83 |
| 10 | 4 | 1 | 4.72 | − 4.00 | 1 | 7 | 1 | 10.32 | 9.08 | 7 | 9 | 1 | 3.84 | 4.12 | 3 | 12 | −1 | 2.72 | − 3.82 |
| 10 | 4 | −1 | 2.74 | 2.24 | 1 | 7 | −1 | 11.08 | − 8.76 | 7 | 9 | −1 | 3.84 | 4.16 | 4 | 12 | 1 | 3.87 | − 4.15 |
| 11 | 4 | 1 | 4.53 | 3.71 | 2 | 7 | 1 | 2.77 | − 2.98 | 8 | 9 | 1 | 7.68 | 6.83 | 4 | 12 | −1 | 10.21 | 9.44 |
| 11 | 4 | −1 | 3.76 | − 2.48 | 2 | 7 | −1 | 24.28 | 22.49 | 8 | 9 | −1 | 0. | − 1.10 | 5 | 12 | 1 | 11.22 | 12.35 |
| 12 | 4 | 1 | 0. | − 0.06 | 3 | 7 | 1 | 2.06 | − 0.44 | 9 | 9 | 1 | 5.84 | − 6.71 | 5 | 12 | −1 | 13.36 | −13.49 |
| 12 | 4 | −1 | 6.86 | − 5.66 | 3 | 7 | −1 | 19.95 | −18.03 | 9 | 9 | −1 | 7.52 | 6.57 | 6 | 12 | 1 | 13.33 | −14.24 |
| 13 | 4 | 1 | 1.89 | − 3.00 | 4 | 7 | 1 | 6.53 | − 5.98 | 10 | 9 | 1 | 4.14 | 4.20 | 6 | 12 | −1 | 0. | 0.98 |
| 13 | 4 | −1 | 3.57 | 3.55 | 4 | 7 | −1 | 2.14 | 0.79 | 10 | 9 | −1 | 6.09 | 5.56 | 7 | 12 | 1 | 4.42 | 5.12 |
| 14 | 4 | 1 | 1.95 | 1.61 | 5 | 7 | 1 | 5.21 | 5.41 | 11 | 9 | 1 | 3.57 | 2.84 | 7 | 12 | −1 | 5.21 | 6.02 |
| 14 | 4 | −1 | 2.09 | 1.99 | 5 | 7 | −1 | 8.51 | 7.97 | 11 | 9 | −1 | 7.57 | − 8.04 | 8 | 12 | 1 | 5.82 | 6.76 |
| 0 | 5 | 1 | 5.41 | 3.58 | 6 | 7 | 1 | 2.47 | 3.42 | 0 | 10 | 1 | 5.35 | 4.54 | 8 | 12 | −1 | 7.33 | − 7.86 |
| 1 | 5 | 1 | 2.17 | 2.75 | 6 | 7 | −1 | 13.97 | −12.68 | 1 | 10 | 1 | 18.05 | −17.15 | 9 | 12 | 1 | 9.38 | −10.19 |
| 1 | 5 | −1 | 6.06 | − 4.86 | 7 | 7 | 1 | 11.72 | −10.71 | 1 | 10 | −1 | 2.41 | 2.46 | 9 | 12 | −1 | 3.10 | 4.42 |
| 2 | 5 | 1 | 19.51 | −17.01 | 7 | 7 | −1 | 8.15 | 7.71 | 2 | 10 | 1 | 10.43 | 8.97 | 10 | 12 | 1 | 5.13 | 4.79 |
| 2 | 5 | −1 | 18.49 | 14.72 | 8 | 7 | 1 | 8.12 | 7.12 | 2 | 10 | −1 | 8.45 | − 7.71 | 10 | 12 | −1 | 0. | − 1.91 |
| 3 | 5 | 1 | 25.49 | 24.00 | 8 | 7 | −1 | 8.92 | − 8.21 | 3 | 10 | 1 | 4.36 | − 4.28 | 0 | 13 | 1 | 6.09 | 5.69 |
| 3 | 5 | −1 | 9.66 | − 7.06 | 10 | 7 | 1 | 5.84 | − 4.82 | 3 | 10 | −1 | 0. | 1.25 | 1 | 13 | 1 | 10.56 | 10.05 |

TABLE IV. (Continued)

| h | k | l | $F_{obs.}$ | $F_{calcd.}$ | h | k | l | $F_{obs.}$ | $F_{calcd.}$ | h | k | l | $F_{obs.}$ | $F_{calcd.}$ | k | h | l | $F_{obs.}$ | $F_{calcd.}$ |
|---|---|---|---|---|---|---|---|---|---|---|---|---|---|---|---|---|---|---|---|
| 1 | 13 | −1 | 12.81 | −13.62 | 1 | 16 | −1 | 7.00 | 8.21 | 3 | 1 | −2 | 17.80 | 19.77 | 3 | 3 | 2 | 11.65 | −11.09 |
| 2 | 13 | 1 | 10.56 | −10.31 | 2 | 16 | 1 | 2.28 | − 2.59 | 4 | 1 | 2 | 19.17 | −19.77 | 3 | 3 | −2 | 6.06 | − 6.15 |
| 2 | 13 | −1 | 5.46 | 5.59 | 2 | 16 | −1 | 1.78 | − 1.07 | 4 | 1 | −2 | 15.90 | −17.31 | 4 | 3 | 2 | 32.58 | 31.66 |
| 3 | 13 | 1 | 4.72 | 4.85 | 3 | 16 | 1 | 2.17 | 3.14 | 5 | 1 | 2 | 2.85 | 2.98 | 4 | 3 | −2 | 31.68 | 35.12 |
| 3 | 13 | −1 | 10.56 | 10.57 | 3 | 16 | −1 | 4.97 | − 5.72 | 5 | 1 | −2 | 11.62 | 10.67 | 5 | 3 | 2 | 0. | − 2.02 |
| 4 | 13 | 1 | 10.10 | 10.42 | 4 | 16 | 1 | 1.43 | − 1.77 | 6 | 1 | 2 | 15.75 | 15.71 | 5 | 3 | −2 | 12.69 | −11.81 |
| 4 | 13 | −1 | 7.16 | − 7.00 | 4 | 16 | −1 | 5.57 | 6.84 | 6 | 1 | −2 | 18.49 | 16.95 | 6 | 3 | 2 | 19.77 | −20.18 |
| 5 | 13 | 1 | 4.58 | − 5.33 | 6 | 16 | 1 | 2.80 | − 4.70 | 7 | 1 | 2 | 0. | − 1.36 | 6 | 3 | −2 | 16.08 | −16.59 |
| 5 | 13 | −1 | 3.76 | − 3.85 | 6 | 16 | −1 | 0. | 0.26 | 7 | 1 | −2 | 15.60 | −13.93 | 7 | 3 | 2 | 11.86 | 10.20 |
| 6 | 13 | 1 | 4.39 | − 4.32 | 7 | 16 | 1 | 3.43 | 5.00 | 8 | 1 | 2 | 9.84 | − 8.17 | 7 | 3 | −2 | 11.18 | 10.49 |
| 6 | 13 | −1 | 8.53 | 9.05 | 7 | 16 | −1 | 1.40 | 2.11 | 8 | 1 | −2 | 5.80 | 4.24 | 8 | 3 | 2 | 13.32 | 12.85 |
| 7 | 13 | 1 | 8.86 | 9.30 | 0 | 17 | 1 | 2.83 | 3.83 | 9 | 1 | 2 | 10.37 | 9.87 | 8 | 3 | −2 | 8.80 | 8.14 |
| 7 | 13 | −1 | 4.12 | − 3.81 | 3 | 17 | 1 | 1.26 | − 1.06 | 9 | 1 | −2 | 9.24 | 7.38 | 9 | 3 | 2 | 15.60 | −16.47 |
| 8 | 13 | 1 | 4.25 | − 4.68 | 3 | 17 | −1 | 6.67 | 7.68 | 10 | 1 | 2 | 0. | − 1.58 | 9 | 3 | −2 | 19.97 | −18.94 |
| 8 | 13 | −1 | 3.84 | − 4.94 | 4 | 17 | 1 | 4.91 | 5.81 | 10 | 1 | −2 | 8.71 | − 5.84 | 10 | 3 | 2 | 6.48 | 6.12 |
| 9 | 13 | 1 | 3.59 | − 3.71 | 4 | 17 | −1 | 6.15 | − 4.92 | 11 | 1 | 2 | 3.92 | − 4.03 | 10 | 3 | −2 | 9.21 | 8.98 |
| 9 | 13 | −1 | 3.84 | 4.66 | 5 | 17 | 1 | 4.55 | − 6.14 | 11 | 1 | −2 | 5.77 | − 5.99 | 11 | 3 | 2 | 11.59 | 12.28 |
| 10 | 13 | 1 | 3.37 | 4.34 | 5 | 17 | −1 | 0.82 | − 0.73 | 12 | 1 | 2 | 0. | 1.20 | 11 | 3 | −2 | 11.44 | 10.93 |
| 10 | 13 | −1 | 1.10 | 2.22 | 0 | 18 | 1 | 5.93 | 8.45 | 12 | 1 | −2 | 6.63 | 7.47 | 12 | 3 | 2 | 8.32 | −10.14 |
| 0 | 14 | 1 | 8.53 | 8.88 | 2 | 18 | 1 | 0. | − 0.13 | 13 | 1 | 2 | 2.82 | 4.17 | 12 | 3 | −2 | 12.10 | −11.77 |
| 1 | 14 | 1 | 12.35 | −13.48 | 2 | 18 | −1 | 3.51 | 5.21 | 13 | 1 | −2 | 0. | − 1.25 | 14 | 3 | −2 | 4.07 | 5.56 |
| 1 | 14 | −1 | 0. | − 0.75 | 3 | 18 | 1 | 4.39 | 5.02 | 14 | 1 | 2 | 2.08 | − 4.62 | 0 | 4 | 2 | 12.22 | −10.07 |
| 2 | 14 | 1 | 5.98 | 6.52 | 3 | 18 | −1 | 3.13 | − 4.66 | 14 | 1 | −2 | 1.19 | − 3.77 | 1 | 4 | 2 | 28.15 | 24.12 |
| 2 | 14 | −1 | 6.01 | 6.70 | 1 | 0 | 2 | 38.04 | 46.58 | 0 | 2 | 2 | 86.40 | −90.78 | 1 | 4 | −2 | 15.75 | −13.00 |
| 3 | 14 | 1 | 4.58 | 4.36 | 1 | 0 | −2 | 20.72 | 16.40 | 1 | 2 | 2 | 45.83 | 47.48 | 2 | 4 | 2 | 28.74 | −26.67 |
| 3 | 14 | −1 | 3.76 | − 4.06 | 2 | 0 | 2 | 25.35 | −25.30 | 1 | 2 | −2 | 31.33 | 33.26 | 2 | 4 | −2 | 9.12 | 7.53 |
| 4 | 14 | 1 | 5.76 | − 5.86 | 2 | 0 | −2 | 7.19 | 8.67 | 2 | 2 | 2 | 18.78 | 18.43 | 3 | 4 | 2 | 13.02 | −11.01 |
| 4 | 14 | −1 | 4.50 | 5.40 | 3 | 0 | 2 | 10.43 | −10.35 | 2 | 2 | −2 | 32.37 | 34.47 | 3 | 4 | −2 | 0. | − 1.21 |
| 5 | 14 | 1 | 4.28 | 4.22 | 3 | 0 | −2 | 16.08 | −19.21 | 3 | 2 | 2 | 34.00 | −36.60 | 4 | 4 | 2 | 25.89 | 25.17 |
| 5 | 14 | −1 | 3.54 | − 4.03 | 4 | 0 | 2 | 34.57 | 35.06 | 3 | 2 | −2 | 36.83 | −43.94 | 4 | 4 | −2 | 10.82 | 9.72 |
| 6 | 14 | 1 | 0. | − 0.34 | 4 | 0 | −2 | 4.79 | 3.98 | 4 | 2 | 2 | 5.80 | 6.16 | 5 | 4 | 2 | 26.78 | −26.63 |
| 6 | 14 | −1 | 7.90 | 8.04 | 5 | 0 | 2 | 16.70 | −16.62 | 4 | 2 | −2 | 16.41 | 17.38 | 5 | 4 | −2 | 15.16 | −15.97 |
| 7 | 14 | 1 | 0. | 0.06 | 5 | 0 | −2 | 15.96 | −17.57 | 5 | 2 | 2 | 9.48 | 11.38 | 6 | 4 | 2 | 4.22 | 3.93 |
| 7 | 14 | −1 | 3.79 | − 4.60 | 6 | 0 | 2 | 0. | 1.76 | 5 | 2 | −2 | 18.70 | 18.52 | 6 | 4 | −2 | 15.57 | 14.98 |
| 8 | 14 | 1 | 0. | − 0.58 | 6 | 0 | −2 | 19.41 | 19.55 | 6 | 2 | 2 | 0. | 0.95 | 7 | 4 | 2 | 3.75 | 2.79 |
| 8 | 14 | −1 | 3.84 | − 2.67 | 7 | 0 | 2 | 9.01 | 7.93 | 6 | 2 | −2 | 13.23 | −13.32 | 7 | 4 | −2 | 9.72 | 9.18 |
| 9 | 14 | 1 | 2.39 | − 3.31 | 7 | 0 | −2 | 7.40 | − 7.60 | 7 | 2 | 2 | 22.86 | −20.77 | 8 | 4 | 2 | 12.28 | −11.55 |
| 9 | 14 | −1 | 5.38 | 6.09 | 8 | 0 | 2 | 0. | 1.09 | 7 | 2 | −2 | 13.70 | −13.76 | 8 | 4 | −2 | 16.47 | −15.36 |
| 1 | 15 | 1 | 2.55 | 2.81 | 8 | 0 | −2 | 18.22 | −17.23 | 8 | 2 | 2 | 25.17 | 24.16 | 9 | 4 | 2 | 2.91 | − 2.67 |
| 1 | 15 | −1 | 2.52 | − 3.51 | 9 | 0 | 2 | 4.96 | − 4.48 | 8 | 2 | −2 | 21.07 | 18.86 | 9 | 4 | −2 | 15.13 | 14.12 |
| 2 | 15 | 1 | 0. | 0.40 | 9 | 0 | −2 | 16.67 | 14.84 | 9 | 2 | 2 | 9.99 | 8.40 | 10 | 4 | 2 | 4.99 | − 4.79 |
| 2 | 15 | −1 | 2.55 | 3.15 | 10 | 0 | 2 | 1.55 | − 2.32 | 9 | 2 | −2 | 4.84 | 3.64 | 10 | 4 | −2 | 0. | − 0.31 |
| 3 | 15 | 1 | 6.04 | − 6.46 | 10 | 0 | −2 | 11.59 | −10.97 | 10 | 2 | 2 | 19.71 | −20.15 | 11 | 4 | 2 | 6.57 | 7.35 |
| 3 | 15 | −1 | 2.50 | 2.60 | 11 | 0 | 2 | 10.05 | 10.14 | 10 | 2 | −2 | 21.94 | −20.24 | 11 | 4 | −2 | 0. | 1.04 |
| 4 | 15 | 1 | 5.79 | 6.33 | 11 | 0 | −2 | 0. | − 1.30 | 11 | 2 | 2 | 12.36 | 13.64 | 12 | 4 | 2 | 6.60 | − 7.44 |
| 4 | 15 | −1 | 5.38 | − 7.06 | 12 | 0 | 2 | 7.04 | − 8.46 | 11 | 2 | −2 | 9.96 | 8.82 | 12 | 4 | −2 | 4.49 | 3.71 |
| 5 | 15 | 1 | 0. | 0.77 | 12 | 0 | −2 | 2.68 | 2.97 | 12 | 2 | 2 | 4.25 | 4.65 | 0 | 5 | 2 | 15.04 | 13.56 |
| 5 | 15 | −1 | 4.55 | 5.53 | 13 | 0 | 2 | 2.85 | − 3.14 | 12 | 2 | −2 | 4.64 | 5.11 | 1 | 5 | 2 | 0. | 0.22 |
| 6 | 15 | 1 | 4.06 | − 3.90 | 13 | 0 | −2 | 0. | − 0.77 | 13 | 2 | 2 | 6.81 | −10.25 | 1 | 5 | −2 | 15.04 | 11.63 |
| 6 | 15 | −1 | 4.20 | 2.70 | 14 | 0 | 2 | 2.38 | 5.85 | 13 | 2 | −2 | 14.98 | −15.23 | 2 | 5 | 2 | 17.63 | −16.20 |
| 7 | 15 | 1 | 3.95 | 4.39 | 14 | 0 | −2 | 0. | 1.00 | 14 | 2 | −2 | 4.28 | 5.53 | 2 | 5 | −2 | 6.96 | − 6.36 |
| 7 | 15 | −1 | 4.94 | − 6.26 | 1 | 1 | 2 | 34.54 | −34.45 | 0 | 3 | 2 | 5.74 | − 4.84 | 3 | 5 | 2 | 25.59 | 24.32 |
| 8 | 15 | 1 | 0. | 1.57 | 1 | 1 | −2 | 26.10 | 26.07 | 1 | 3 | 2 | 34.57 | 33.60 | 3 | 5 | −2 | 4.93 | 2.89 |
| 8 | 15 | −1 | 4.55 | 3.49 | 2 | 1 | 2 | 1.81 | − 0.88 | 1 | 3 | −2 | 48.09 | 50.27 | 4 | 5 | 2 | 7.10 | − 5.95 |
| 0 | 16 | 1 | 7.41 | 9.27 | 2 | 1 | −2 | 32.93 | 39.53 | 2 | 3 | 2 | 30.02 | −28.95 | 4 | 5 | −2 | 11.06 | − 9.53 |
| 1 | 16 | 1 | 2.33 | − 2.78 | 3 | 1 | 2 | 14.03 | 13.51 | 2 | 3 | −2 | 32.55 | −33.80 | 5 | 5 | 2 | 13.17 | −11.96 |

TABLE IV. (Continued)

| *h* | *k* | *l* | $F_{obs.}$ | $F_{calcd.}$ | *h* | *k* | *l* | $F_{obs.}$ | $F_{calcd.}$ | *h* | *k* | *l* | $F_{obs.}$ | $F_{calcd.}$ | *h* | *k* | *l* | $F_{obs.}$ | $F_{calcd.}$ |
|---|---|---|---|---|---|---|---|---|---|---|---|---|---|---|---|---|---|---|---|
| 5 | 5 | −2 | 6.21 | 6.13 | 8 | 7 | −2 | 7.61 | 6.62 | 12 | 9 | −2 | 0. | − 1.55 | 8 | 12 | −2 | 8.50 | − 9.95 |
| 6 | 5 | 2 | 11.03 | 10.17 | 9 | 7 | 2 | 20.09 | −20.89 | 0 | 10 | 2 | 6.93 | − 5.95 | 9 | 12 | 2 | 0. | 0.36 |
| 6 | 5 | −2 | 0. | − 0.44 | 9 | 7 | −2 | 16.97 | −17.12 | 1 | 10 | 2 | 4.58 | 4.87 | 9 | 12 | −2 | 2.29 | 0.98 |
| 7 | 5 | 2 | 3.83 | 3.67 | 10 | 7 | 2 | 4.67 | 5.67 | 1 | 10 | −2 | 8.71 | 7.13 | 10 | 12 | 2 | 5.68 | 7.96 |
| 7 | 5 | −2 | 14.65 | −14.12 | 10 | 7 | −2 | 2.82 | 2.91 | 3 | 10 | 2 | 3.89 | 4.92 | 10 | 12 | −2 | 9.96 | 7.91 |
| 8 | 5 | 2 | 5.71 | − 4.62 | 11 | 7 | 2 | 7.91 | 9.66 | 3 | 10 | −2 | 9.75 | − 9.26 | 11 | 12 | −2 | 3.69 | − 5.59 |
| 8 | 5 | −2 | 11.00 | 12.01 | 11 | 7 | −2 | 12.25 | 12.85 | 4 | 10 | 2 | 5.65 | − 5.27 | 0 | 13 | 2 | 8.74 | 9.08 |
| 10 | 5 | 2 | 5.68 | 5.53 | 12 | 7 | 2 | 9.99 | −12.15 | 4 | 10 | −2 | 10.02 | 9.47 | 1 | 13 | 2 | 0. | − 0.83 |
| 10 | 5 | −2 | 8.20 | − 7.30 | 12 | 7 | −2 | 11.29 | −12.40 | 5 | 10 | 2 | 0. | − 1.46 | 1 | 13 | −2 | 5.05 | 4.74 |
| 11 | 5 | 2 | 3.69 | − 4.09 | 0 | 8 | 2 | 13.29 | 11.92 | 5 | 10 | −2 | 5.71 | − 4.95 | 2 | 13 | 2 | 5.02 | − 5.59 |
| 11 | 5 | −2 | 2.79 | 3.20 | 1 | 8 | 2 | 12.48 | 10.90 | 6 | 10 | 2 | 5.05 | 6.42 | 2 | 13 | −2 | 5.05 | − 5.47 |
| 12 | 5 | 2 | 3.86 | − 4.78 | 1 | 8 | −2 | 5.97 | − 4.19 | 6 | 10 | −2 | 5.80 | − 5.92 | 3 | 13 | 2 | 12.57 | 14.37 |
| 12 | 5 | −2 | 0. | 0.30 | 2 | 8 | 2 | 21.40 | −19.50 | 7 | 10 | 2 | 4.07 | − 4.67 | 3 | 13 | −2 | 5.80 | 6.16 |
| 13 | 5 | 2 | 4.34 | 6.62 | 2 | 8 | −2 | 11.95 | −10.32 | 7 | 10 | −2 | 5.83 | 3.72 | 4 | 13 | 2 | 8.03 | −10.33 |
| 13 | 5 | −2 | 0. | 0.18 | 3 | 8 | 2 | 14.68 | 13.59 | 9 | 10 | 2 | 5.08 | 6.12 | 4 | 13 | −2 | 8.62 | − 8.86 |
| 0 | 6 | 2 | 36.53 | −34.83 | 3 | 8 | −2 | 10.08 | 8.09 | 9 | 10 | −2 | 1.78 | − 2.23 | 5 | 13 | 2 | 0. | − 0.88 |
| 1 | 6 | 2 | 13.82 | 10.99 | 4 | 8 | 2 | 14.98 | 13.69 | 10 | 10 | 2 | 4.43 | − 2.92 | 5 | 13 | −2 | 4.87 | − 4.83 |
| 1 | 6 | −2 | 24.02 | 21.24 | 4 | 8 | −2 | 7.85 | 6.41 | 10 | 10 | −2 | 0. | − 0.91 | 6 | 13 | 2 | 7.82 | 8.95 |
| 2 | 6 | 2 | 12.57 | 11.63 | 5 | 8 | 2 | 21.07 | −21.61 | 11 | 10 | 2 | 3.00 | − 3.29 | 6 | 13 | −2 | 7.67 | 8.85 |
| 2 | 6 | −2 | 14.15 | 11.91 | 5 | 8 | −2 | 23.51 | −22.15 | 11 | 10 | −2 | 0. | 1.67 | 7 | 13 | 2 | 5.38 | − 6.75 |
| 3 | 6 | 2 | 11.98 | −10.18 | 6 | 8 | 2 | 13.23 | 12.91 | 1 | 11 | 2 | 14.86 | 13.87 | 7 | 13 | −2 | 7.64 | − 8.78 |
| 3 | 6 | −2 | 34.36 | −33.53 | 6 | 8 | −2 | 9.10 | 8.59 | 1 | 11 | −2 | 29.72 | 25.96 | 0 | 14 | 2 | 2.85 | 3.44 |
| 4 | 6 | 2 | 5.08 | 4.59 | 7 | 8 | 2 | 10.85 | 9.93 | 2 | 11 | 2 | 16.91 | −16.83 | 1 | 14 | 2 | 6.36 | − 6.72 |
| 4 | 6 | −2 | 19.38 | 17.19 | 7 | 8 | −2 | 10.67 | 9.69 | 2 | 11 | −2 | 22.02 | −21.02 | 1 | 14 | −2 | 1.55 | 0.13 |
| 5 | 6 | 2 | 8.47 | 7.79 | 8 | 8 | 2 | 8.20 | − 9.51 | 3 | 11 | 2 | 4.96 | 4.72 | 2 | 14 | 2 | 3.98 | 2.30 |
| 5 | 6 | −2 | 6.60 | 5.64 | 8 | 8 | −2 | 16.20 | −15.13 | 3 | 11 | −2 | 9.81 | 7.97 | 2 | 14 | −2 | 0. | − 2.14 |
| 6 | 6 | 2 | 0. | − 0.90 | 10 | 8 | 2 | 5.17 | 5.26 | 4 | 11 | 2 | 6.48 | 6.37 | 3 | 14 | 2 | 3.89 | 4.59 |
| 6 | 6 | −2 | 9.72 | − 7.79 | 10 | 8 | −2 | 3.89 | 4.47 | 4 | 11 | −2 | 14.39 | 14.11 | 3 | 14 | −2 | 0. | 1.29 |
| 7 | 6 | 2 | 10.05 | −10.38 | 11 | 8 | 2 | 0. | − 0.06 | 5 | 11 | 2 | 0. | − 1.69 | 4 | 14 | 2 | 3.77 | − 4.33 |
| 7 | 6 | −2 | 8.89 | − 7.55 | 11 | 8 | −2 | 5.53 | − 6.03 | 5 | 11 | −2 | 7.13 | − 5.42 | 4 | 14 | −2 | 0. | 2.42 |
| 8 | 6 | 2 | 5.02 | 6.33 | 12 | 8 | 2 | 3.36 | − 4.70 | 6 | 11 | 2 | 4.07 | − 4.15 | 6 | 14 | 2 | 3.33 | 4.00 |
| 8 | 6 | −2 | 8.00 | 7.03 | 12 | 8 | −2 | 0. | − 1.66 | 6 | 11 | −2 | 0. | − 1.70 | 6 | 14 | −2 | 3.51 | − 4.40 |
| 9 | 6 | 2 | 5.02 | 6.00 | 0 | 9 | 2 | 11.95 | 10.94 | 8 | 11 | 2 | 4.52 | 6.04 | 7 | 14 | 2 | 1.49 | − 2.04 |
| 9 | 6 | −2 | 5.05 | 5.19 | 1 | 9 | 2 | 5.35 | 5.43 | 8 | 11 | −2 | 6.72 | 8.19 | 7 | 14 | −2 | 3.21 | 3.93 |
| 10 | 6 | 2 | 10.05 | −11.65 | 1 | 9 | −2 | 14.45 | 13.03 | 9 | 11 | 2 | 5.74 | − 7.33 | 8 | 14 | 2 | 2.44 | − 3.67 |
| 10 | 6 | −2 | 11.89 | −11.71 | 2 | 9 | 2 | 25.00 | −24.31 | 9 | 11 | −2 | 8.77 | −10.45 | 8 | 14 | −2 | 0. | − 1.37 |
| 11 | 6 | 2 | 5.02 | 6.41 | 2 | 9 | −2 | 7.85 | − 6.44 | 10 | 11 | 2 | 2.76 | 3.96 | 1 | 15 | 2 | 0. | 3.18 |
| 11 | 6 | −2 | 9.01 | 9.18 | 3 | 9 | 2 | 22.29 | 21.70 | 10 | 11 | −2 | 1.19 | 1.94 | 1 | 15 | −2 | 6.57 | 7.26 |
| 13 | 6 | 2 | 2.82 | − 4.94 | 3 | 9 | −2 | 6.24 | 5.56 | 11 | 11 | 2 | 3.12 | 5.19 | 2 | 15 | 2 | 5.23 | − 5.82 |
| 13 | 6 | −2 | 6.84 | − 8.37 | 4 | 9 | 2 | 12.10 | −12.12 | 11 | 11 | −2 | 5.62 | 6.73 | 2 | 15 | −2 | 8.38 | − 8.81 |
| 0 | 7 | 2 | 12.99 | 11.57 | 4 | 9 | −2 | 5.91 | − 5.59 | 0 | 12 | 2 | 14.39 | 14.63 | 3 | 15 | 2 | 3.60 | 4.77 |
| 1 | 7 | 2 | 40.81 | 41.85 | 5 | 9 | 2 | 10.14 | − 8.24 | 1 | 12 | 2 | 10.40 | − 9.81 | 3 | 15 | −2 | 3.66 | 4.91 |
| 1 | 7 | −2 | 36.47 | 34.55 | 5 | 9 | −2 | 4.76 | 5.25 | 1 | 12 | −2 | 1.55 | − 1.95 | 6 | 15 | 2 | 0. | 2.04 |
| 2 | 7 | 2 | 37.21 | −35.54 | 6 | 9 | 2 | 6.45 | 6.30 | 2 | 12 | 2 | 15.34 | −15.77 | 6 | 15 | −2 | 3.77 | 4.29 |
| 2 | 7 | −2 | 39.38 | −37.87 | 6 | 9 | −2 | 6.33 | 6.10 | 2 | 12 | −2 | 15.31 | −14.62 | 7 | 15 | 2 | 3.33 | − 4.57 |
| 3 | 7 | 2 | 0. | − 0.71 | 7 | 9 | 2 | 4.13 | − 3.62 | 3 | 12 | 2 | 9.21 | 9.83 | 7 | 15 | −2 | 1.34 | − 2.86 |
| 3 | 7 | −2 | 17.89 | −14.99 | 7 | 9 | −2 | 7.10 | − 5.54 | 3 | 12 | −2 | 13.94 | 13.30 | 0 | 16 | 2 | 8.32 | 9.98 |
| 4 | 7 | 2 | 21.10 | 21.15 | 8 | 9 | 2 | 0. | 0.69 | 4 | 12 | 2 | 0. | 1.58 | 1 | 16 | 2 | 3.36 | − 4.18 |
| 4 | 7 | −2 | 25.77 | 24.62 | 8 | 9 | −2 | 7.70 | 7.01 | 4 | 12 | −2 | 4.13 | 4.37 | 1 | 16 | −2 | 4.16 | − 5.87 |
| 5 | 7 | 2 | 5.14 | − 3.60 | 9 | 9 | 2 | 3.80 | − 4.77 | 5 | 12 | 2 | 14.92 | −15.77 | 2 | 16 | 2 | 2.32 | − 3.80 |
| 5 | 7 | −2 | 13.08 | −12.26 | 9 | 9 | −2 | 3.98 | 2.97 | 5 | 12 | −2 | 8.20 | − 8.81 | 2 | 16 | −2 | 3.33 | − 3.32 |
| 6 | 7 | 2 | 12.19 | −11.87 | 10 | 9 | 2 | 4.84 | 5.97 | 6 | 12 | 2 | 6.24 | 7.24 | 3 | 16 | 2 | 6.63 | 8.03 |
| 6 | 7 | −2 | 10.49 | −10.28 | 10 | 9 | −2 | 4.55 | − 4.22 | 6 | 12 | −2 | 6.39 | 7.12 | 3 | 16 | −2 | 4.58 | 5.54 |
| 7 | 7 | 2 | 4.93 | 5.31 | 11 | 9 | 2 | 0. | − 2.41 | 7 | 12 | 2 | 3.72 | 5.18 | 4 | 16 | 2 | 0. | − 1.70 |
| 7 | 7 | −2 | 10.37 | 9.33 | 11 | 9 | −2 | 3.98 | 3.60 | 7 | 12 | −2 | 9.10 | 9.81 | 4 | 16 | −2 | 1.49 | 0.11 |
| 8 | 7 | 2 | 10.49 | 12.09 | 12 | 9 | 2 | 1.87 | − 2.73 | 8 | 12 | 2 | 7.19 | − 8.34 | 6 | 16 | 2 | 2.08 | 2.97 |

TABLE IV. (Continued)

| h | k | l | $F_{obs.}$ | $F_{calcd.}$ | h | k | l | $F_{obs.}$ | $F_{calcd.}$ | h | k | l | $F_{obs.}$ | $F_{calcd.}$ | h | k | l | $F_{obs.}$ | $F_{calcd.}$ |
|---|---|---|---|---|---|---|---|---|---|---|---|---|---|---|---|---|---|---|---|
| 6 | 16 | −2 | 1.19 | 0.83 | 8 | 2 | −3 | 10.05 | 10.87 | 3 | 5 | 3 | 9.81 | − 9.50 | 7 | 7 | −3 | 5.49 | − 4.49 |
| 1 | 17 | 2 | 3.45 | − 4.44 | 9 | 2 | 3 | 4.00 | 4.73 | 3 | 5 | −3 | 23.48 | 24.64 | 8 | 7 | 3 | 4.86 | − 4.70 |
| 1 | 17 | −2 | 2.02 | − 3.41 | 9 | 2 | −3 | 3.91 | 4.23 | 4 | 5 | 3 | 21.05 | 21.12 | 8 | 7 | −3 | 5.63 | 6.00 |
| 2 | 17 | 2 | 0. | 0.93 | 11 | 2 | 3 | 2.55 | − 3.41 | 4 | 5 | −3 | 7.92 | − 7.48 | 9 | 7 | 3 | 6.05 | 6.54 |
| 2 | 17 | −2 | 3.39 | − 2.06 | 11 | 2 | −3 | 4.77 | 4.10 | 5 | 5 | 3 | 11.53 | −11.40 | 9 | 7 | −3 | 2.82 | − 3.18 |
| 3 | 17 | 2 | 3.92 | 5.65 | 12 | 2 | 3 | 0. | − 0.35 | 5 | 5 | −3 | 8.30 | − 8.56 | 10 | 7 | 3 | 1.78 | − 2.72 |
| 3 | 17 | −2 | 3.72 | 5.67 | 12 | 2 | −3 | 4.39 | 3.58 | 6 | 5 | 3 | 1.33 | − 1.97 | 10 | 7 | −3 | 4.68 | − 5.37 |
| 4 | 17 | 2 | 4.84 | − 7.30 | 0 | 3 | 3 | 4.86 | − 4.67 | 6 | 5 | −3 | 19.24 | 19.92 | 11 | 7 | 3 | 2.08 | − 3.05 |
| 4 | 17 | −2 | 3.39 | − 4.24 | 1 | 3 | 3 | 9.84 | 7.07 | 7 | 5 | 3 | 12.54 | 13.46 | 11 | 7 | −3 | 7.38 | 7.19 |
| 5 | 17 | 2 | 1.87 | 0.17 | 1 | 3 | −3 | 12.84 | 9.99 | 7 | 5 | −3 | 14.14 | −13.98 | 12 | 7 | 3 | 3.94 | 4.87 |
| 5 | 17 | −2 | 0. | − 2.31 | 2 | 3 | 3 | 11.06 | 10.49 | 8 | 5 | 3 | 8.48 | − 8.16 | 12 | 7 | −3 | 1.04 | − 2.45 |
| 0 | 18 | 2 | 2.88 | 4.04 | 2 | 3 | −3 | 15.98 | −15.90 | 8 | 5 | −3 | 0. | 0.65 | 0 | 8 | 3 | 5.04 | − 5.87 |
| 1 | 18 | 2 | 2.73 | − 4.02 | 3 | 3 | 3 | 11.27 | −12.61 | 9 | 5 | 3 | 0. | 1.44 | 1 | 8 | 3 | 7.74 | 7.54 |
| 1 | 18 | −2 | 0. | − 0.06 | 3 | 3 | −3 | 18.15 | 19.83 | 9 | 5 | −3 | 2.82 | 2.10 | 1 | 8 | −3 | 0. | − 1.61 |
| 1 | 1 | 3 | 9.28 | 7.99 | 4 | 3 | 3 | 26.00 | 26.37 | 10 | 5 | 3 | 5.93 | 6.18 | 2 | 8 | 3 | 11.27 | −11.36 |
| 1 | 1 | −3 | 6.70 | − 7.04 | 4 | 3 | −3 | 7.35 | − 7.94 | 10 | 5 | −3 | 0. | − 0.57 | 2 | 8 | −3 | 8.09 | 6.82 |
| 2 | 1 | 3 | 4.89 | − 4.62 | 5 | 3 | 3 | 7.03 | − 8.61 | 11 | 5 | 3 | 4.06 | − 4.17 | 3 | 8 | 3 | 5.60 | 5.11 |
| 2 | 1 | −3 | 11.47 | −14.05 | 5 | 3 | −3 | 12.81 | −13.51 | 11 | 5 | −3 | 0. | − 1.85 | 3 | 8 | −3 | 7.98 | 6.72 |
| 3 | 1 | 3 | 22.92 | −25.45 | 6 | 3 | 3 | 5.46 | − 6.53 | 0 | 6 | 3 | 6.05 | 4.81 | 4 | 8 | 3 | 2.61 | 3.43 |
| 3 | 1 | −3 | 20.76 | 29.83 | 6 | 3 | −3 | 20.10 | 20.94 | 1 | 6 | 3 | 6.79 | − 6.43 | 4 | 8 | −3 | 15.42 | −13.52 |
| 4 | 1 | 3 | 27.84 | 31.79 | 7 | 3 | 3 | 23.16 | 23.14 | 1 | 6 | −3 | 18.92 | −16.44 | 5 | 8 | 3 | 13.05 | −13.76 |
| 4 | 1 | −3 | 15.36 | −19.65 | 7 | 3 | −3 | 17.08 | −18.46 | 2 | 6 | 3 | 21.70 | −17.72 | 5 | 8 | −3 | 14.29 | 15.05 |
| 5 | 1 | 3 | 22.80 | −22.86 | 8 | 3 | 3 | 12.13 | −12.96 | 2 | 6 | −3 | 23.81 | 22.32 | 6 | 8 | 3 | 17.73 | 17.60 |
| 5 | 1 | −3 | 10.08 | −12.34 | 8 | 3 | −3 | 0. | 1.25 | 3 | 6 | 3 | 23.93 | 21.84 | 6 | 8 | −3 | 7.68 | − 7.43 |
| 6 | 1 | 3 | 15.09 | −15.16 | 9 | 3 | 3 | 2.82 | − 2.06 | 3 | 6 | −3 | 3.56 | − 3.30 | 7 | 8 | 3 | 0. | − 0.42 |
| 6 | 1 | −3 | 24.58 | 27.27 | 9 | 3 | −3 | 9.22 | 8.69 | 4 | 6 | 3 | 4.06 | − 3.83 | 7 | 8 | −3 | 6.85 | − 6.73 |
| 7 | 1 | 3 | 21.85 | 22.46 | 10 | 3 | 3 | 4.74 | 5.06 | 4 | 6 | −3 | 22.48 | −21.23 | 8 | 8 | 3 | 7.32 | − 8.37 |
| 7 | 1 | −3 | 13.73 | −13.35 | 10 | 3 | −3 | 7.47 | − 6.91 | 5 | 6 | 3 | 19.93 | −20.02 | 8 | 8 | −3 | 9.78 | 9.85 |
| 8 | 1 | 3 | 18.41 | −16.95 | 11 | 3 | 3 | 2.49 | − 2.64 | 5 | 6 | −3 | 26.57 | 28.52 | 9 | 8 | 3 | 6.88 | 7.43 |
| 8 | 1 | −3 | 3.65 | − 3.06 | 11 | 3 | −3 | 3.88 | 2.33 | 6 | 6 | 3 | 22.30 | 23.92 | 9 | 8 | −3 | 9.61 | − 9.80 |
| 9 | 1 | 3 | 0. | 0.94 | 13 | 3 | 3 | 0.89 | − 2.13 | 6 | 6 | −3 | 1.78 | − 2.67 | 10 | 8 | 3 | 3.26 | − 3.25 |
| 9 | 1 | −3 | 10.97 | 10.44 | 13 | 3 | −3 | 2.97 | 3.15 | 7 | 6 | 3 | 5.57 | − 4.87 | 10 | 8 | −3 | 3.68 | − 2.55 |
| 10 | 1 | 3 | 4.80 | 5.26 | 0 | 4 | 3 | 10.38 | 9.56 | 7 | 6 | −3 | 11.30 | −11.46 | 0 | 9 | 3 | 5.54 | − 5.55 |
| 10 | 1 | −3 | 6.32 | − 5.27 | 1 | 4 | 3 | 5.93 | − 5.63 | 8 | 6 | 3 | 9.37 | − 9.92 | 1 | 9 | 3 | 7.09 | − 6.38 |
| 11 | 1 | 3 | 2.55 | − 1.14 | 1 | 4 | −3 | 2.13 | − 1.67 | 8 | 6 | −3 | 11.80 | 10.46 | 1 | 9 | −3 | 8.21 | 7.40 |
| 11 | 1 | −3 | 0. | 0.39 | 2 | 4 | 3 | 9.64 | − 8.06 | 9 | 6 | 3 | 9.58 | 10.73 | 2 | 9 | 3 | 6.29 | 5.91 |
| 12 | 1 | 3 | 2.19 | − 2.73 | 2 | 4 | −3 | 9.13 | 7.62 | 9 | 6 | −3 | 0. | 0.91 | 2 | 9 | −3 | 8.69 | − 8.27 |
| 12 | 1 | −3 | 0. | − 1.25 | 3 | 4 | 3 | 16.16 | 14.31 | 10 | 6 | 3 | 2.58 | 2.80 | 3 | 9 | 3 | 5.28 | − 5.85 |
| 13 | 1 | 3 | 0. | 0.60 | 3 | 4 | −3 | 2.43 | − 2.31 | 10 | 6 | −3 | 5.54 | − 5.61 | 3 | 9 | −3 | 2.55 | 3.23 |
| 13 | 1 | −3 | 2.19 | 2.63 | 4 | 4 | 3 | 0. | 1.51 | 11 | 6 | 3 | 4.48 | − 4.78 | 4 | 9 | 3 | 3.85 | − 3.56 |
| 14 | 1 | −3 | 1.60 | − 3.01 | 4 | 4 | −3 | 15.92 | −16.22 | 11 | 6 | −3 | 0. | 1.35 | 4 | 9 | −3 | 5.90 | 6.09 |
| 1 | 2 | 3 | 6.14 | 4.12 | 5 | 4 | 3 | 13.85 | −14.30 | 12 | 6 | 3 | 1.72 | 2.54 | 5 | 9 | 3 | 7.89 | − 7.68 |
| 1 | 2 | −3 | 10.02 | −10.10 | 5 | 4 | −3 | 13.43 | 13.53 | 12 | 6 | −3 | 4.48 | 4.00 | 5 | 9 | −3 | 5.46 | − 5.45 |
| 2 | 2 | 3 | 4.80 | − 4.37 | 6 | 4 | 3 | 9.04 | 9.86 | 13 | 6 | −3 | 2.43 | − 3.04 | 6 | 9 | 3 | 2.82 | − 2.48 |
| 2 | 2 | −3 | 10.05 | 8.89 | 6 | 4 | −3 | 6.91 | − 7.06 | 0 | 7 | 3 | 9.43 | − 8.37 | 6 | 9 | −3 | 6.26 | 5.56 |
| 3 | 2 | 3 | 8.92 | 8.37 | 7 | 4 | 3 | 1.48 | 2.17 | 1 | 7 | 3 | 1.19 | − 1.99 | 7 | 9 | 3 | 2.79 | 3.99 |
| 3 | 2 | −3 | 3.23 | − 4.03 | 7 | 4 | −3 | 9.04 | − 7.99 | 1 | 7 | −3 | 17.23 | 15.15 | 7 | 9 | −3 | 0. | − 1.62 |
| 4 | 2 | 3 | 3.85 | − 3.55 | 8 | 4 | 3 | 6.26 | − 6.46 | 2 | 7 | 3 | 11.83 | 11.07 | 8 | 9 | 3 | 5.99 | − 6.31 |
| 4 | 2 | −3 | 12.84 | −14.70 | 8 | 4 | −3 | 7.59 | 6.91 | 2 | 7 | −3 | 10.76 | − 8.53 | 8 | 9 | −3 | 0. | 1.49 |
| 5 | 2 | 3 | 15.86 | −14.57 | 9 | 4 | 3 | 7.47 | 7.23 | 3 | 7 | 3 | 9.96 | − 9.86 | 9 | 9 | 3 | 3.50 | 3.43 |
| 5 | 2 | −3 | 9.78 | 10.71 | 9 | 4 | −3 | 3.97 | − 3.52 | 3 | 7 | −3 | 3.85 | − 2.72 | 9 | 9 | −3 | 4.66 | 5.00 |
| 6 | 2 | 3 | 10.14 | 10.37 | 0 | 5 | 3 | 12.13 | −10.65 | 4 | 7 | 3 | 4.95 | 4.29 | 10 | 9 | 3 | 0. | 0.29 |
| 6 | 2 | −3 | 1.19 | − 2.22 | 1 | 5 | 3 | 4.36 | 2.98 | 4 | 7 | −3 | 3.32 | 3.32 | 10 | 9 | −3 | 2.46 | − 2.81 |
| 7 | 2 | 3 | 5.81 | − 5.84 | 1 | 5 | −3 | 6.40 | 4.31 | 5 | 7 | 3 | 3.71 | 4.42 | 11 | 9 | 3 | 1.63 | − 3.16 |
| 7 | 2 | −3 | 5.34 | − 4.88 | 2 | 5 | 3 | 11.21 | − 9.03 | 5 | 7 | −3 | 2.49 | − 2.44 | 11 | 9 | −3 | 0. | 0.07 |
| 8 | 2 | 3 | 12.04 | −11.43 | 2 | 5 | −3 | 19.48 | −19.17 | 7 | 7 | 3 | 0. | 0.41 | 1 | 10 | 3 | 2.67 | − 3.26 |

TABLE IV. (Continued)

| *h* | *k* | *l* | $F_{obs.}$ | $F_{calcd.}$ | *h* | *k* | *l* | $F_{obs.}$ | $F_{calcd.}$ | *h* | *k* | *l* | $F_{obs.}$ | $F_{calcd.}$ | *h* | *k* | *l* | $F_{obs.}$ | $F_{calcd.}$ |
|---|---|---|---|---|---|---|---|---|---|---|---|---|---|---|---|---|---|---|---|
| 1 | 10 | −3 | 13.70 | −12.80 | 8 | 12 | −3 | 4.15 | 4.40 | 3 | 17 | −3 | 0. | − 2.49 | 2 | 2 | −4 | 16.20 | −17.87 |
| 2 | 10 | 3 | 8.09 | − 7.47 | 9 | 12 | 3 | 2.43 | 2.68 | 4 | 17 | −3 | 0. | 3.25 | 3 | 2 | 4 | 10.91 | 9.09 |
| 2 | 10 | −3 | 14.80 | 13.82 | 9 | 12 | −3 | 5.99 | − 6.58 | 1 | 0 | 4 | 38.34 | −33.78 | 3 | 2 | −4 | 8.56 | 8.08 |
| 3 | 10 | 3 | 13.19 | 14.45 | 10 | 12 | −3 | 2.43 | 3.86 | 1 | 0 | −4 | 17.22 | −17.96 | 4 | 2 | 4 | 28.32 | −30.29 |
| 3 | 10 | −3 | 0. | − 1.29 | 0 | 13 | 3 | 2.82 | − 3.07 | 2 | 0 | 4 | 11.19 | − 9.94 | 4 | 2 | −4 | 8.19 | 8.56 |
| 4 | 10 | 3 | 0. | 1.34 | 3 | 13 | 3 | 3.88 | 4.33 | 2 | 0 | −4 | 23.84 | −39.22 | 5 | 2 | 4 | 17.90 | 17.17 |
| 4 | 10 | −3 | 14.29 | −13.12 | 3 | 13 | −3 | 3.94 | − 3.69 | 3 | 0 | 4 | 19.94 | 19.65 | 5 | 2 | −4 | 9.31 | 11.15 |
| 5 | 10 | 3 | 16.01 | −17.12 | 4 | 13 | 3 | 3.77 | − 4.36 | 3 | 0 | −4 | 15.61 | 21.68 | 6 | 2 | 4 | 3.62 | 2.22 |
| 5 | 10 | −3 | 18.59 | 18.44 | 4 | 13 | −3 | 5.49 | 5.99 | 4 | 0 | 4 | 0. | − 1.42 | 6 | 2 | −4 | 14.75 | −15.93 |
| 6 | 10 | 3 | 14.88 | 17.00 | 5 | 13 | 3 | 2.55 | 2.68 | 4 | 0 | −4 | 21.02 | −27.12 | 7 | 2 | 4 | 5.47 | − 5.23 |
| 6 | 10 | −3 | 2.08 | − 0.53 | 5 | 13 | −3 | 4.63 | − 5.28 | 5 | 0 | 4 | 6.89 | − 5.85 | 7 | 2 | −4 | 3.52 | 3.88 |
| 7 | 10 | 3 | 8.18 | − 9.29 | 6 | 13 | 3 | 3.35 | 1.96 | 5 | 0 | −4 | 20.47 | −21.58 | 8 | 2 | 4 | 0. | − 1.65 |
| 7 | 10 | −3 | 10.53 | −10.46 | 6 | 13 | −3 | 1.78 | − 3.20 | 6 | 0 | 4 | 0. | 0.43 | 8 | 2 | −4 | 18.98 | 17.90 |
| 8 | 10 | 3 | 5.69 | − 6.46 | 7 | 13 | 3 | 2.99 | − 3.98 | 6 | 0 | −4 | 14.04 | 13.11 | 9 | 2 | 4 | 10.08 | 9.28 |
| 8 | 10 | −3 | 10.20 | 10.01 | 7 | 13 | −3 | 0. | 0.80 | 7 | 0 | 4 | 19.76 | 19.08 | 9 | 2 | −4 | 10.11 | −16.53 |
| 9 | 10 | 3 | 7.21 | 8.11 | 0 | 14 | 3 | 6.61 | − 7.13 | 7 | 0 | −4 | 0. | 3.42 | 10 | 2 | 4 | 2.63 | 0.67 |
| 9 | 10 | −3 | 0. | 0.07 | 1 | 14 | 3 | 1.78 | 3.34 | 8 | 0 | 4 | 15.95 | −15.34 | 10 | 2 | −4 | 6.31 | 5.52 |
| 10 | 10 | 3 | 3.26 | − 3.36 | 1 | 14 | −3 | 4.68 | − 4.68 | 8 | 0 | −4 | 14.07 | −13.10 | 11 | 2 | 4 | 9.99 | −10.96 |
| 10 | 10 | −3 | 0. | − 0.35 | 2 | 14 | 3 | 3.74 | − 3.86 | 9 | 0 | 4 | 4.85 | − 3.37 | 11 | 2 | −4 | 6.03 | 5.24 |
| 0 | 11 | 3 | 3.91 | − 4.45 | 2 | 14 | −3 | 0. | − 0.22 | 9 | 0 | −4 | 5.60 | − 4.93 | 12 | 2 | 4 | 8.35 | 9.70 |
| 1 | 11 | 3 | 6.79 | − 6.82 | 3 | 14 | 3 | 1.33 | 1.83 | 10 | 0 | 4 | 17.75 | 18.12 | 12 | 2 | −4 | 8.01 | − 7.34 |
| 1 | 11 | −3 | 18.29 | 18.05 | 3 | 14 | −3 | 4.57 | 6.15 | 10 | 0 | −4 | 17.19 | 14.45 | 0 | 3 | 4 | 39.05 | −32.76 |
| 2 | 11 | 3 | 16.07 | 17.79 | 4 | 14 | 3 | 0. | 0.92 | 11 | 0 | 4 | 12.12 | −12.94 | 1 | 3 | 4 | 17.10 | 13.03 |
| 2 | 11 | −3 | 0. | − 0.97 | 4 | 14 | −3 | 7.26 | − 8.69 | 11 | 0 | −4 | 9.80 | − 9.60 | 1 | 3 | −4 | 13.11 | −12.90 |
| 3 | 11 | 3 | 4.89 | − 5.35 | 5 | 14 | 3 | 3.97 | − 4.92 | 12 | 0 | 4 | 0. | − 1.22 | 2 | 3 | 4 | 13.23 | 11.47 |
| 3 | 11 | −3 | 13.11 | −13.57 | 5 | 14 | −3 | 6.94 | 7.86 | 12 | 0 | −4 | 4.92 | − 3.96 | 2 | 3 | −4 | 5.22 | − 4.64 |
| 4 | 11 | 3 | 4.00 | − 5.04 | 6 | 14 | 3 | 6.58 | 8.43 | 13 | 0 | −4 | 11.69 | 11.19 | 3 | 3 | 4 | 20.74 | −20.18 |
| 4 | 11 | −3 | 8.92 | 7.82 | 6 | 14 | −3 | 0. | − 0.69 | 0 | 1 | 4 | 12.68 | 12.20 | 3 | 3 | −4 | 5.32 | 5.72 |
| 5 | 11 | 3 | 7.41 | 7.89 | 7 | 14 | 3 | 2.49 | − 4.19 | 1 | 1 | 4 | 29.18 | −25.19 | 4 | 3 | 4 | 6.59 | 4.59 |
| 5 | 11 | −3 | 2.67 | 4.16 | 7 | 14 | −3 | 3.97 | − 5.30 | 1 | 1 | −4 | 4.95 | − 9.25 | 4 | 3 | −4 | 11.69 | 12.48 |
| 6 | 11 | 3 | 3.85 | 4.95 | 8 | 14 | 3 | 0.65 | − 2.37 | 2 | 1 | 4 | 4.82 | 4.31 | 5 | 3 | 4 | 10.51 | 9.07 |
| 6 | 11 | −3 | 6.29 | − 9.07 | 8 | 14 | −3 | 5.01 | 6.00 | 2 | 1 | −4 | 23.84 | 31.98 | 5 | 3 | −4 | 11.59 | −11.74 |
| 7 | 11 | 3 | 7.32 | − 8.84 | 9 | 14 | −3 | 1.75 | − 3.32 | 3 | 1 | 4 | 13.14 | 12.62 | 6 | 3 | 4 | 14.07 | −13.77 |
| 7 | 11 | −3 | 3.85 | 4.22 | 0 | 15 | 3 | 6.08 | − 7.40 | 3 | 1 | −4 | 5.16 | 6.31 | 6 | 3 | −4 | 3.31 | − 2.94 |
| 8 | 11 | 3 | 0. | 0.47 | 1 | 15 | 3 | 3.47 | − 4.15 | 4 | 1 | 4 | 17.03 | −15.06 | 7 | 3 | 4 | 12.03 | −10.45 |
| 8 | 11 | −3 | 3.68 | 3.83 | 1 | 15 | −3 | 7.86 | 9.67 | 4 | 1 | −4 | 19.60 | −22.21 | 7 | 3 | −4 | 16.11 | 15.95 |
| 9 | 11 | 3 | 6.43 | 7.66 | 2 | 15 | 3 | 5.87 | 7.70 | 5 | 1 | 4 | 4.02 | − 2.64 | 8 | 3 | 4 | 9.37 | 8.56 |
| 9 | 11 | −3 | 3.35 | − 3.58 | 2 | 15 | −3 | 0. | − 0.02 | 5 | 1 | −4 | 9.06 | 9.79 | 8 | 3 | −4 | 15.61 | −15.25 |
| 10 | 11 | 3 | 4.66 | − 6.71 | 3 | 15 | 3 | 1.19 | − 2.15 | 6 | 1 | 4 | 12.43 | 11.90 | 9 | 3 | 4 | 4.79 | − 3.74 |
| 10 | 11 | −3 | 3.53 | − 3.79 | 3 | 15 | −3 | 7.21 | − 8.83 | 6 | 1 | −4 | 3.15 | 3.28 | 9 | 3 | −4 | 2.01 | − 1.89 |
| 0 | 12 | 3 | 6.91 | − 6.92 | 4 | 15 | 3 | 5.28 | − 6.68 | 7 | 1 | 4 | 0. | 0.12 | 10 | 3 | 4 | 5.78 | − 5.68 |
| 1 | 12 | 3 | 12.96 | 13.89 | 4 | 15 | −3 | 6.49 | 7.02 | 7 | 1 | −4 | 10.45 | −10.50 | 10 | 3 | −4 | 8.87 | 6.57 |
| 1 | 12 | −3 | 2.82 | − 2.88 | 5 | 15 | 3 | 4.80 | 6.00 | 8 | 1 | 4 | 9.77 | − 9.30 | 11 | 3 | 4 | 2.16 | 3.36 |
| 2 | 12 | 3 | 2.82 | − 4.57 | 5 | 15 | −3 | 1.78 | 3.22 | 8 | 1 | −4 | 0. | 1.11 | 11 | 3 | −4 | 2.66 | − 2.11 |
| 2 | 12 | −3 | 2.82 | − 2.70 | 6 | 15 | 3 | 2.91 | 3.83 | 9 | 1 | 4 | 8.41 | 8.37 | 12 | 3 | 4 | 3.40 | 3.92 |
| 3 | 12 | 3 | 0. | − 0.00 | 6 | 15 | −3 | 4.57 | − 7.21 | 9 | 1 | −4 | 8.84 | 6.65 | 12 | 3 | −4 | 7.11 | − 7.07 |
| 3 | 12 | −3 | 4.00 | 4.92 | 0 | 16 | 3 | 6.88 | − 8.71 | 10 | 1 | 4 | 2.63 | 1.68 | 0 | 4 | 4 | 47.52 | 40.58 |
| 4 | 12 | 3 | 4.83 | 5.51 | 1 | 16 | 3 | 7.71 | 10.12 | 10 | 1 | −4 | 7.98 | − 7.19 | 1 | 4 | 4 | 24.18 | −19.78 |
| 4 | 12 | −3 | 8.92 | − 8.63 | 1 | 16 | −3 | 0. | 0.45 | 11 | 1 | 4 | 4.02 | − 5.30 | 1 | 4 | −4 | 14.65 | −16.59 |
| 5 | 12 | 3 | 5.43 | − 6.39 | 2 | 16 | 3 | 2.91 | − 3.66 | 11 | 1 | −4 | 6.06 | − 6.14 | 2 | 4 | 4 | 8.32 | − 6.72 |
| 5 | 12 | −3 | 2.22 | 3.17 | 2 | 16 | −3 | 5.34 | − 8.26 | 12 | 1 | 4 | 3.65 | 4.09 | 2 | 4 | −4 | 15.40 | −14.13 |
| 6 | 12 | 3 | 5.19 | 5.64 | 3 | 16 | 3 | 3.35 | − 4.55 | 12 | 1 | −4 | 8.81 | 8.17 | 3 | 4 | 4 | 9.80 | 9.08 |
| 6 | 12 | −3 | 5.25 | − 6.26 | 3 | 16 | −3 | 4.60 | 6.54 | 0 | 2 | 4 | 18.12 | 13.52 | 3 | 4 | −4 | 35.21 | 36.50 |
| 7 | 12 | 3 | 3.38 | − 3.46 | 2 | 17 | 3 | 2.22 | − 3.02 | 1 | 2 | 4 | 42.94 | −36.96 | 4 | 4 | 4 | 0. | 0.44 |
| 7 | 12 | −3 | 0. | 1.39 | 2 | 17 | −3 | 0. | 1.45 | 1 | 2 | −4 | 14.28 | 14.62 | 4 | 4 | −4 | 13.29 | −12.62 |
| 8 | 12 | 3 | 1.48 | 0.48 | 3 | 17 | 3 | 2.37 | 4.02 | 2 | 2 | 4 | 33.88 | 31.21 | 5 | 4 | 4 | 3.52 | − 3.56 |

TABLE IV. (Continued)

| h | k | l | $F_{obs.}$ | $F_{calcd.}$ | h | k | l | $F_{obs.}$ | $F_{calcd.}$ | h | k | l | $F_{obs.}$ | $F_{calcd.}$ | h | k | l | $F_{obs.}$ | $F_{calcd.}$ |
|---|---|---|---|---|---|---|---|---|---|---|---|---|---|---|---|---|---|---|---|
| 5 | 4 | −4 | 6.28 | − 5.90 | 9 | 6 | −4 | 7.95 | − 7.85 | 4 | 9 | −4 | 15.46 | −15.32 | 2 | 12 | 4 | 2.78 | − 2.80 |
| 6 | 4 | 4 | 5.97 | − 5.05 | 11 | 6 | 4 | 5.01 | − 5.71 | 5 | 9 | 4 | 0. | − 1.49 | 2 | 12 | −4 | 4.88 | 5.67 |
| 6 | 4 | −4 | 11.38 | 10.92 | 11 | 6 | −4 | 5.47 | 5.74 | 5 | 9 | −4 | 8.81 | 7.52 | 3 | 12 | 4 | 6.15 | − 7.22 |
| 7 | 4 | 4 | 11.16 | 11.63 | 12 | 6 | −4 | 2.91 | − 2.70 | 6 | 9 | 4 | 4.85 | 5.23 | 3 | 12 | −4 | 5.60 | 5.15 |
| 7 | 4 | −4 | 3.68 | 3.69 | 0 | 7 | 4 | 17.84 | −16.19 | 6 | 9 | −4 | 2.32 | 2.66 | 4 | 12 | 4 | 7.57 | 8.49 |
| 8 | 4 | 4 | 11.66 | −11.46 | 1 | 7 | 4 | 0. | − 0.51 | 7 | 9 | 4 | 1.98 | − 2.05 | 4 | 12 | −4 | 4.79 | − 5.11 |
| 8 | 4 | −4 | 8.25 | − 7.13 | 1 | 7 | −4 | 20.34 | −18.52 | 7 | 9 | −4 | 2.81 | − 2.88 | 6 | 12 | 4 | 6.74 | − 8.28 |
| 9 | 4 | 4 | 6.15 | − 6.27 | 2 | 7 | 4 | 25.78 | 23.15 | 8 | 9 | 4 | 5.60 | − 6.83 | 6 | 12 | −4 | 8.66 | 10.82 |
| 9 | 4 | −4 | 0. | − 1.38 | 2 | 7 | −4 | 3.25 | − 3.82 | 8 | 9 | −4 | 3.86 | − 4.56 | 7 | 12 | 4 | 4.27 | 5.67 |
| 10 | 4 | 4 | 8.75 | 10.37 | 3 | 7 | 4 | 26.74 | −25.98 | 9 | 9 | 4 | 7.95 | 9.80 | 7 | 12 | −4 | 4.24 | − 4.04 |
| 10 | 4 | −4 | 10.42 | 9.56 | 3 | 7 | −4 | 6.28 | 5.24 | 9 | 9 | −4 | 7.76 | 8.42 | 8 | 12 | 4 | 1.76 | 1.21 |
| 11 | 4 | 4 | 6.09 | − 6.60 | 4 | 7 | 4 | 6.46 | 6.96 | 10 | 9 | 4 | 4.98 | − 5.46 | 8 | 12 | −4 | 0. | − 0.95 |
| 11 | 4 | −4 | 5.84 | − 5.40 | 4 | 7 | −4 | 2.47 | 2.87 | 10 | 9 | −4 | 0. | − 0.95 | 9 | 12 | −4 | 4.27 | 4.84 |
| 0 | 5 | 4 | 5.29 | − 2.79 | 5 | 7 | 4 | 14.78 | 14.23 | 11 | 9 | −4 | 7.23 | − 7.83 | 1 | 13 | 4 | 2.72 | − 2.49 |
| 1 | 5 | 4 | 20.74 | −18.52 | 5 | 7 | −4 | 9.00 | − 8.98 | 0 | 10 | 4 | 11.32 | −10.62 | 1 | 13 | −4 | 10.94 | −13.36 |
| 1 | 5 | −4 | 32.77 | −29.02 | 6 | 7 | 4 | 8.44 | − 8.90 | 1 | 10 | 4 | 1.85 | 3.02 | 2 | 13 | 4 | 6.00 | 6.52 |
| 2 | 5 | 4 | 28.88 | 25.40 | 6 | 7 | −4 | 0. | 0.76 | 1 | 10 | −4 | 3.71 | 3.58 | 2 | 13 | −4 | 11.87 | 14.45 |
| 2 | 5 | −4 | 21.36 | 21.45 | 7 | 7 | 4 | 0. | − 1.44 | 2 | 10 | 4 | 12.15 | 12.90 | 3 | 13 | 4 | 1.85 | − 2.93 |
| 3 | 5 | 4 | 3.86 | 3.59 | 7 | 7 | −4 | 12.52 | 13.18 | 2 | 10 | −4 | 4.76 | 3.26 | 3 | 13 | −4 | 3.80 | − 4.24 |
| 3 | 5 | −4 | 5.72 | 5.03 | 8 | 7 | 4 | 4.73 | 4.53 | 3 | 10 | 4 | 6.89 | − 7.93 | 4 | 13 | 4 | 3.52 | 3.18 |
| 4 | 5 | 4 | 11.53 | −11.59 | 8 | 7 | −4 | 10.20 | − 9.99 | 3 | 10 | −4 | 8.78 | − 7.94 | 4 | 13 | −4 | 5.87 | − 5.88 |
| 4 | 5 | −4 | 18.92 | −20.12 | 9 | 7 | 4 | 4.36 | 4.43 | 4 | 10 | 4 | 2.84 | − 3.77 | 5 | 13 | 4 | 1.24 | − 2.70 |
| 5 | 5 | 4 | 1.85 | 2.08 | 9 | 7 | −4 | 2.78 | − 3.51 | 4 | 10 | −4 | 4.85 | − 4.17 | 5 | 13 | −4 | 6.21 | 7.05 |
| 5 | 5 | −4 | 10.73 | 10.96 | 10 | 7 | 4 | 8.50 | − 9.62 | 5 | 10 | 4 | 12.86 | 14.63 | 9 | 13 | −4 | 2.54 | 3.55 |
| 6 | 5 | 4 | 15.40 | 15.34 | 10 | 7 | −4 | 10.11 | 10.99 | 5 | 10 | −4 | 7.48 | 8.10 | 0 | 14 | 4 | 9.58 | −10.52 |
| 6 | 5 | −4 | 9.09 | 9.21 | 11 | 7 | 4 | 3.37 | 4.44 | 6 | 10 | 4 | 6.09 | − 6.73 | 1 | 14 | 4 | 3.59 | 4.85 |
| 7 | 5 | 4 | 4.88 | − 4.61 | 11 | 7 | −4 | 4.64 | − 5.21 | 6 | 10 | −4 | 3.71 | − 4.05 | 1 | 14 | −4 | 0. | 1.44 |
| 7 | 5 | −4 | 9.65 | − 9.69 | 0 | 8 | 4 | 12.74 | 11.40 | 7 | 10 | 4 | 3.62 | − 3.64 | 2 | 14 | 4 | 3.49 | 4.81 |
| 8 | 5 | 4 | 8.44 | − 8.23 | 1 | 8 | 4 | 2.50 | − 2.76 | 7 | 10 | −4 | 7.30 | − 8.76 | 2 | 14 | −4 | 4.39 | 5.75 |
| 8 | 5 | −4 | 2.78 | − 2.85 | 1 | 8 | −4 | 14.87 | −13.34 | 8 | 10 | 4 | 8.38 | 8.89 | 3 | 14 | 4 | 6.71 | − 7.58 |
| 9 | 5 | 4 | 15.24 | 15.99 | 2 | 8 | 4 | 2.57 | − 2.75 | 8 | 10 | −4 | 11.16 | 13.18 | 3 | 14 | −4 | 4.98 | − 6.52 |
| 9 | 5 | −4 | 14.13 | 14.57 | 2 | 8 | −4 | 8.56 | − 7.37 | 10 | 10 | 4 | 3.09 | − 4.47 | 5 | 14 | 4 | 4.05 | 5.39 |
| 10 | 5 | 4 | 4.88 | − 5.95 | 3 | 8 | 4 | 7.48 | − 7.04 | 10 | 10 | −4 | 3.65 | − 4.66 | 5 | 14 | −4 | 3.22 | 4.21 |
| 10 | 5 | −4 | 3.90 | − 4.37 | 3 | 8 | −4 | 16.60 | 16.32 | 11 | 10 | −4 | 4.33 | 5.55 | 6 | 14 | 4 | 3.46 | − 4.29 |
| 11 | 5 | 4 | 5.78 | − 6.56 | 4 | 8 | 4 | 7.23 | 6.97 | 0 | 11 | 4 | 17.59 | −17.61 | 6 | 14 | −4 | 0. | − 1.54 |
| 11 | 5 | −4 | 8.44 | − 8.19 | 4 | 8 | −4 | 17.34 | −19.41 | 1 | 11 | 4 | 3.99 | 2.87 | 7 | 14 | 4 | 0. | − 1.61 |
| 12 | 5 | 4 | 5.78 | 8.50 | 6 | 8 | 4 | 5.66 | − 6.46 | 1 | 11 | −4 | 6.31 | − 5.32 | 7 | 14 | −4 | 5.19 | − 6.36 |
| 12 | 5 | −4 | 9.31 | 10.33 | 6 | 8 | −4 | 6.83 | 5.68 | 2 | 11 | 4 | 8.93 | 9.18 | 8 | 14 | −4 | 3.52 | 5.24 |
| 0 | 6 | 4 | 2.07 | − 3.14 | 7 | 8 | 4 | 7.36 | 8.09 | 2 | 11 | −4 | 0. | 0.61 | 0 | 15 | 4 | 3.25 | − 4.00 |
| 1 | 6 | 4 | 23.56 | −20.09 | 7 | 8 | −4 | 4.88 | − 4.71 | 3 | 11 | 4 | 15.46 | −17.27 | 1 | 15 | 4 | 3.18 | 4.74 |
| 1 | 6 | −4 | 19.88 | 16.78 | 8 | 8 | 4 | 0. | 0.34 | 3 | 11 | −4 | 0. | 0.72 | 1 | 15 | −4 | 2.16 | − 2.89 |
| 2 | 6 | 4 | 26.28 | 24.83 | 8 | 8 | −4 | 3.96 | − 4.30 | 4 | 11 | 4 | 6.25 | 7.35 | 3 | 15 | 4 | 6.12 | − 7.13 |
| 2 | 6 | −4 | 0. | − 0.21 | 9 | 8 | 4 | 4.76 | − 5.76 | 4 | 11 | −4 | 2.01 | 2.75 | 3 | 15 | −4 | 3.80 | − 4.40 |
| 3 | 6 | 4 | 4.11 | − 3.77 | 9 | 8 | −4 | 0. | 1.15 | 5 | 11 | 4 | 3.83 | 3.73 | 4 | 15 | 4 | 7.17 | 9.72 |
| 3 | 6 | −4 | 3.12 | − 2.72 | 10 | 8 | 4 | 4.02 | 5.14 | 5 | 11 | −4 | 0. | − 0.45 | 4 | 15 | −4 | 3.62 | 3.65 |
| 4 | 6 | 4 | 17.10 | −15.76 | 10 | 8 | −4 | 0. | 1.55 | 6 | 11 | 4 | 7.33 | − 7.28 | 5 | 15 | 4 | 0. | − 1.20 |
| 4 | 6 | −4 | 2.32 | 1.63 | 11 | 8 | 4 | 2.75 | 1.96 | 6 | 11 | −4 | 7.27 | − 7.18 | 5 | 15 | −4 | 2.72 | 2.91 |
| 5 | 6 | 4 | 16.63 | 15.73 | 11 | 8 | −4 | 6.09 | − 5.91 | 7 | 11 | 4 | 1.24 | 1.86 | 6 | 15 | −4 | 4.76 | − 6.47 |
| 5 | 6 | −4 | 12.58 | 12.12 | 0 | 9 | 4 | 5.22 | − 4.77 | 7 | 11 | −4 | 5.90 | 6.00 | 7 | 15 | −4 | 3.06 | 5.88 |
| 6 | 6 | 4 | 6.21 | − 6.14 | 1 | 9 | 4 | 17.13 | −17.30 | 8 | 11 | 4 | 0. | 1.13 | 1 | 16 | 4 | 5.22 | 6.11 |
| 6 | 6 | −4 | 8.69 | − 8.44 | 1 | 9 | −4 | 25.69 | −24.37 | 8 | 11 | −4 | 5.50 | − 5.81 | 1 | 16 | −4 | 1.05 | − 2.03 |
| 7 | 6 | 4 | 5.66 | − 5.32 | 2 | 9 | 4 | 17.87 | 16.94 | 9 | 11 | 4 | 2.84 | 3.72 | 2 | 16 | 4 | 3.49 | − 4.18 |
| 7 | 6 | −4 | 5.50 | − 5.11 | 2 | 9 | −4 | 21.86 | 20.33 | 9 | 11 | −4 | 0.93 | − 2.24 | 2 | 16 | −4 | 0. | 1.73 |
| 8 | 6 | 4 | 0. | 1.33 | 3 | 9 | 4 | 6.74 | − 6.56 | 10 | 11 | −4 | 3.65 | 4.36 | 3 | 16 | 4 | 2.20 | − 2.86 |
| 8 | 6 | −4 | 10.54 | 10.16 | 3 | 9 | −4 | 0. | 0.60 | 1 | 12 | 4 | 6.31 | 6.44 | 3 | 16 | −4 | 0. | 1.34 |
| 9 | 6 | 4 | 3.71 | 3.76 | 4 | 9 | 4 | 6.28 | − 6.04 | 1 | 12 | −4 | 2.01 | − 2.40 | 0 | 1 | 5 | 2.36 | 1.29 |

TABLE IV. (Continued)

| *h* | *k* | *l* | $F_{obs.}$ | $F_{calcd.}$ | *h* | *k* | *l* | $F_{obs.}$ | $F_{calcd.}$ | *h* | *k* | *l* | $F_{obs.}$ | $F_{calcd.}$ | *h* | *k* | *l* | $F_{obs.}$ | $F_{calcd.}$ |
|---|---|---|---|---|---|---|---|---|---|---|---|---|---|---|---|---|---|---|---|
| 1 | 1 | 5 | 6.51 | − 4.61 | 2 | 4 | −5 | 11.57 | −11.19 | 1 | 7 | 5 | 5.48 | − 5.22 | 0 | 10 | 5 | 7.92 | 7.39 |
| 1 | 1 | −5 | 0. | − 0.03 | 3 | 4 | 5 | 15.76 | −15.02 | 1 | 7 | −5 | 5.35 | − 5.35 | 1 | 10 | 5 | 5.02 | − 4.03 |
| 2 | 1 | 5 | 3.82 | 2.70 | 3 | 4 | −5 | 4.23 | 2.03 | 2 | 7 | 5 | 0. | − 1.30 | 1 | 10 | −5 | 0. | 1.22 |
| 2 | 1 | −5 | 11.37 | 15.09 | 4 | 4 | 5 | 4.48 | 4.49 | 2 | 7 | −5 | 4.40 | 3.25 | 2 | 10 | 5 | 6.18 | 7.04 |
| 3 | 1 | 5 | 7.30 | 7.43 | 4 | 4 | −5 | 12.94 | 12.98 | 3 | 7 | 5 | 6.76 | 7.01 | 2 | 10 | −5 | 0. | − 0.27 |
| 3 | 1 | −5 | 12.57 | −15.23 | 5 | 4 | 5 | 9.54 | 10.70 | 3 | 7 | −5 | 6.39 | − 6.16 | 3 | 10 | 5 | 0. | 0.90 |
| 4 | 1 | 5 | 24.85 | −24.23 | 5 | 4 | −5 | 14.10 | −14.20 | 4 | 7 | 5 | 7.80 | − 7.33 | 3 | 10 | −5 | 10.08 | − 9.85 |
| 4 | 1 | −5 | 3.28 | 3.81 | 6 | 4 | 5 | 16.14 | −16.49 | 4 | 7 | −5 | 0. | − 1.31 | 4 | 10 | 5 | 0. | 2.06 |
| 5 | 1 | 5 | 16.93 | 15.29 | 6 | 4 | −5 | 0. | − 1.58 | 5 | 7 | 5 | 7.14 | 7.73 | 4 | 10 | −5 | 8.71 | 9.02 |
| 5 | 1 | −5 | 15.43 | 16.32 | 7 | 4 | 5 | 8.71 | 8.85 | 5 | 7 | −5 | 4.85 | 4.92 | 5 | 10 | 5 | 4.77 | 5.59 |
| 6 | 1 | 5 | 3.44 | − 2.08 | 7 | 4 | −5 | 9.08 | 7.97 | 6 | 7 | 5 | 0. | − 0.96 | 5 | 10 | −5 | 2.90 | − 2.52 |
| 6 | 1 | −5 | 17.01 | −17.30 | 8 | 4 | 5 | 6.02 | 6.59 | 6 | 7 | −5 | 7.88 | − 7.88 | 6 | 10 | 5 | 8.42 | −10.14 |
| 7 | 1 | 5 | 18.09 | −17.67 | 8 | 4 | −5 | 7.09 | − 5.74 | 7 | 7 | 5 | 4.85 | − 5.86 | 6 | 10 | −5 | 0. | − 0.18 |
| 7 | 1 | −5 | 9.29 | 7.27 | 9 | 4 | 5 | 6.43 | − 6.93 | 7 | 7 | −5 | 6.18 | 5.79 | 7 | 10 | 5 | 6.47 | 7.50 |
| 8 | 1 | 5 | 14.60 | 15.16 | 9 | 4 | −5 | 3.57 | − 3.95 | 8 | 7 | 5 | 4.52 | 4.83 | 7 | 10 | −5 | 3.32 | 4.58 |
| 8 | 1 | −5 | 6.02 | 5.23 | 10 | 4 | 5 | 0. | − 0.25 | 8 | 7 | −5 | 3.53 | 3.14 | 8 | 10 | 5 | 0. | − 0.18 |
| 9 | 1 | 5 | 3.36 | − 3.43 | 10 | 4 | −5 | 7.63 | 6.99 | 9 | 7 | 5 | 3.94 | − 4.62 | 8 | 10 | −5 | 4.40 | − 4.41 |
| 9 | 1 | −5 | 10.08 | − 9.07 | 0 | 5 | 5 | 8.63 | 7.14 | 9 | 7 | −5 | 4.77 | − 4.29 | 0 | 11 | 5 | 7.09 | 7.23 |
| 0 | 2 | 5 | 5.10 | 3.80 | 1 | 5 | 5 | 7.18 | − 5.96 | 0 | 8 | 5 | 3.32 | − 2.00 | 3 | 11 | 5 | 2.49 | 2.60 |
| 1 | 2 | 5 | 7.18 | 5.13 | 1 | 5 | −5 | 14.35 | −14.56 | 1 | 8 | 5 | 6.72 | 5.10 | 3 | 11 | −5 | 3.53 | 4.95 |
| 1 | 2 | −5 | 6.60 | 7.45 | 2 | 5 | 5 | 0. | − 1.58 | 1 | 8 | −5 | 11.41 | 11.06 | 4 | 11 | 5 | 0. | 1.37 |
| 2 | 2 | 5 | 7.72 | 5.00 | 2 | 5 | −5 | 12.90 | 11.43 | 2 | 8 | 5 | 3.44 | 3.36 | 4 | 11 | −5 | 3.53 | − 4.31 |
| 2 | 2 | −5 | 6.18 | − 4.75 | 3 | 5 | 5 | 5.35 | 6.19 | 2 | 8 | −5 | 12.40 | −11.15 | 7 | 11 | 5 | 0. | 1.03 |
| 3 | 2 | 5 | 4.60 | − 3.72 | 3 | 5 | −5 | 4.81 | − 5.15 | 3 | 8 | 5 | 16.43 | −17.55 | 7 | 11 | −5 | 3.11 | 3.20 |
| 3 | 2 | −5 | 3.65 | − 3.47 | 4 | 5 | 5 | 6.55 | − 6.61 | 3 | 8 | −5 | 0. | − 0.38 | 0 | 12 | 5 | 3.44 | 2.36 |
| 4 | 2 | 5 | 8.38 | 7.16 | 4 | 5 | −5 | 4.19 | − 4.65 | 4 | 8 | 5 | 0. | 1.10 | 1 | 12 | 5 | 2.90 | − 3.46 |
| 4 | 2 | −5 | 7.30 | 7.18 | 5 | 5 | 5 | 9.75 | 8.97 | 4 | 8 | −5 | 15.43 | 15.92 | 1 | 12 | −5 | 4.89 | 4.91 |
| 5 | 2 | 5 | 7.92 | 6.69 | 5 | 5 | −5 | 9.46 | 8.59 | 5 | 8 | 5 | 10.66 | 12.46 | 2 | 12 | 5 | 6.72 | 7.67 |
| 5 | 2 | −5 | 9.17 | − 8.15 | 6 | 5 | 5 | 3.53 | − 2.53 | 5 | 8 | −5 | 15.35 | −15.26 | 2 | 12 | −5 | 0. | − 1.15 |
| 6 | 2 | 5 | 3.44 | − 4.04 | 6 | 5 | −5 | 12.03 | −10.76 | 6 | 8 | 5 | 14.39 | −16.90 | 3 | 12 | 5 | 7.30 | − 8.00 |
| 6 | 2 | −5 | 0. | 1.05 | 7 | 5 | 5 | 3.57 | − 3.66 | 6 | 8 | −5 | 0. | − 0.38 | 3 | 12 | −5 | 2.49 | − 1.29 |
| 0 | 3 | 5 | 5.72 | − 4.09 | 7 | 5 | −5 | 3.48 | 3.76 | 7 | 8 | 5 | 4.69 | 5.50 | 4 | 12 | 5 | 0. | 1.38 |
| 1 | 3 | 5 | 4.98 | − 3.58 | 8 | 5 | 5 | 6.80 | 8.31 | 7 | 8 | −5 | 11.20 | 10.87 | 4 | 12 | −5 | 7.47 | 9.27 |
| 1 | 3 | −5 | 1.04 | − 1.93 | 8 | 5 | −5 | 1.87 | − 2.42 | 8 | 8 | 5 | 5.23 | 5.66 | 5 | 12 | 5 | 5.02 | 6.67 |
| 2 | 3 | 5 | 9.96 | 8.35 | 1 | 6 | 5 | 1.66 | 1.65 | 8 | 8 | −5 | 10.33 | − 9.83 | 5 | 12 | −5 | 8.42 | − 9.92 |
| 2 | 3 | −5 | 11.74 | 12.61 | 1 | 6 | −5 | 2.86 | 2.37 | 9 | 8 | 5 | 6.76 | − 7.55 | 6 | 12 | 5 | 8.17 | − 9.55 |
| 3 | 3 | 5 | 8.34 | 7.45 | 2 | 6 | 5 | 3.11 | 2.95 | 9 | 8 | −5 | 0. | 0.92 | 6 | 12 | −5 | 0. | 0.88 |
| 3 | 3 | −5 | 15.97 | −18.01 | 2 | 6 | −5 | 2.90 | − 3.27 | 0 | 8 | 5 | 6.93 | 7.40 | 7 | 12 | 5 | 4.19 | 5.94 |
| 4 | 3 | 5 | 19.29 | −18.55 | 3 | 6 | 5 | 9.75 | − 8.95 | 1 | 9 | 5 | 6.97 | 7.20 | 7 | 12 | −5 | 6.26 | 7.35 |
| 4 | 3 | −5 | 5.19 | 4.54 | 3 | 6 | −5 | 10.37 | − 9.73 | 1 | 9 | −5 | 13.36 | −13.12 | 8 | 12 | −5 | 3.44 | − 4.91 |
| 5 | 3 | 5 | 16.80 | 17.39 | 4 | 6 | 5 | 4.81 | 4.32 | 2 | 9 | 5 | 8.63 | − 9.23 | 0 | 13 | 5 | 4.60 | 6.33 |
| 5 | 3 | −5 | 11.82 | 12.15 | 4 | 6 | −5 | 16.88 | 16.05 | 2 | 9 | −5 | 6.02 | 5.43 | 1 | 13 | 5 | 3.19 | 2.23 |
| 6 | 3 | 5 | 6.02 | 5.75 | 5 | 6 | 5 | 4.98 | 5.96 | 3 | 9 | 5 | 3.57 | 4.40 | 1 | 13 | −5 | 8.63 | −10.06 |
| 6 | 3 | −5 | 17.75 | −18.24 | 5 | 6 | −5 | 8.71 | − 8.75 | 3 | 9 | −5 | 7.01 | 7.73 | 2 | 13 | 5 | 6.97 | − 9.07 |
| 7 | 3 | 5 | 11.28 | −12.16 | 6 | 6 | 5 | 11.82 | −12.24 | 4 | 9 | 5 | 0. | − 0.63 | 2 | 13 | −5 | 4.56 | − 2.89 |
| 7 | 3 | −5 | 10.08 | 8.83 | 6 | 6 | −5 | 0. | 0.00 | 4 | 9 | −5 | 4.98 | − 4.98 | 3 | 13 | 5 | 1.66 | 3.02 |
| 8 | 3 | 5 | 11.62 | 10.71 | 7 | 6 | 5 | 3.53 | 4.26 | 5 | 9 | 5 | 3.53 | − 4.69 | 3 | 13 | −5 | 9.54 | 10.81 |
| 8 | 3 | −5 | 4.98 | 3.45 | 7 | 6 | −5 | 9.38 | 7.77 | 5 | 9 | −5 | 0. | − 0.36 | 4 | 13 | 5 | 4.81 | 6.08 |
| 9 | 3 | 5 | 1.87 | − 2.03 | 8 | 6 | 5 | 4.69 | 4.81 | 6 | 9 | 5 | 4.77 | − 4.69 | 4 | 13 | −5 | 7.05 | − 7.33 |
| 9 | 3 | −5 | 6.18 | − 5.16 | 8 | 6 | −5 | 6.18 | − 6.52 | 6 | 9 | −5 | 3.57 | 4.66 | 5 | 13 | 5 | 4.36 | − 5.16 |
| 10 | 3 | 5 | 2.07 | − 2.51 | 9 | 6 | 5 | 6.64 | − 8.29 | 7 | 9 | 5 | 5.43 | 5.73 | 5 | 13 | −5 | 1.66 | − 3.09 |
| 10 | 3 | −5 | 5.97 | 5.28 | 9 | 6 | −5 | 0. | 2.04 | 7 | 9 | −5 | 0. | − 1.93 | 7 | 13 | −5 | 4.77 | − 5.36 |
| 0 | 4 | 5 | 6.14 | − 5.57 | 10 | 6 | 5 | 1.24 | 4.17 | 8 | 9 | 5 | 0. | − 0.54 | 0 | 14 | 5 | 5.06 | 7.20 |
| 1 | 4 | 5 | 2.49 | − 1.19 | 10 | 6 | −5 | 0. | − 2.05 | 8 | 9 | −5 | 3.32 | − 4.07 | 1 | 14 | 5 | 6.35 | − 8.96 |
| 1 | 4 | −5 | 11.41 | 12.57 | 11 | 6 | −5 | 1.24 | 2.92 | 9 | 9 | 5 | 5.48 | − 6.20 | 1 | 14 | −5 | 2.95 | 2.01 |
| 2 | 4 | 5 | 9.67 | 8.64 | 0 | 7 | 5 | 7.59 | 7.33 | 9 | 9 | −5 | 0. | 1.74 | 2 | 14 | 5 | 1.66 | 1.54 |

TABLE IV. (Continued)

| h | k | l | $F_{obs.}$ | $F_{calcd.}$ | h | k | l | $F_{obs.}$ | $F_{calcd.}$ | h | k | l | $F_{obs.}$ | $F_{calcd.}$ | h | k | l | $F_{obs.}$ | $F_{calcd.}$ |
|---|---|---|---|---|---|---|---|---|---|---|---|---|---|---|---|---|---|---|---|
| 2 | 14 | −5 | 4.98 | 5.70 | 5 | 2 | −6 | 5.31 | 5.40 | 11 | 4 | −6 | 7.80 | − 7.63 | 6 | 7 | 6 | 3.82 | − 4.28 |
| 3 | 14 | 5 | 0. | 1.64 | 6 | 2 | 6 | 0. | 1.49 | 12 | 4 | −6 | 5.52 | 5.80 | 6 | 7 | −6 | 0. | − 0.68 |
| 3 | 14 | −5 | 5.68 | − 7.58 | 6 | 2 | −6 | 10.88 | −10.58 | 0 | 5 | 6 | 28.72 | 24.78 | 7 | 7 | 6 | 3.52 | 3.18 |
| 0 | 0 | 6 | 6.21 | − 9.50 | 7 | 2 | 6 | 9.08 | − 9.09 | 1 | 5 | 6 | 7.42 | − 5.77 | 7 | 7 | −6 | 5.26 | 5.03 |
| 1 | 0 | 6 | 24.17 | 31.36 | 7 | 2 | −6 | 0. | 0.75 | 1 | 5 | −6 | 18.86 | 15.71 | 8 | 7 | 6 | 3.44 | 4.30 |
| 1 | 0 | −6 | 18.14 | −22.34 | 8 | 2 | 6 | 5.62 | 6.05 | 2 | 5 | 6 | 18.73 | −16.57 | 8 | 7 | −6 | 2.69 | 2.45 |
| 2 | 0 | 6 | 23.33 | −24.54 | 8 | 2 | −6 | 2.82 | 2.57 | 2 | 5 | −6 | 7.67 | 6.56 | 9 | 7 | 6 | 5.34 | − 6.83 |
| 2 | 0 | −6 | 8.49 | 19.63 | 9 | 2 | 6 | 0. | 1.43 | 3 | 5 | 6 | 21.02 | 19.64 | 9 | 7 | −6 | 6.11 | − 5.61 |
| 3 | 0 | 6 | 7.98 | − 6.61 | 9 | 2 | −6 | 2.80 | 2.49 | 3 | 5 | −6 | 13.29 | −10.60 | 10 | 7 | −6 | 0. | 1.47 |
| 3 | 0 | −6 | 3.85 | − 6.51 | 10 | 2 | 6 | 7.67 | − 8.46 | 4 | 5 | 6 | 4.39 | − 4.21 | 11 | 7 | −6 | 4.82 | 5.43 |
| 4 | 0 | 6 | 22.38 | 24.43 | 10 | 2 | −6 | 7.72 | − 6.67 | 4 | 5 | −6 | 2.05 | − 3.09 | 0 | 8 | 6 | 7.60 | 5.20 |
| 4 | 0 | −6 | 12.29 | −16.91 | 11 | 2 | −6 | 5.52 | 5.27 | 5 | 5 | 6 | 10.98 | −10.78 | 1 | 8 | 6 | 6.26 | 4.46 |
| 5 | 0 | 6 | 12.52 | −11.97 | 0 | 3 | 6 | 5.67 | − 3.75 | 5 | 5 | −6 | 12.22 | 11.27 | 1 | 8 | −6 | 11.91 | −10.20 |
| 5 | 0 | −6 | 2.31 | − 3.90 | 1 | 3 | 6 | 10.91 | 9.67 | 6 | 5 | 6 | 7.70 | 7.79 | 2 | 8 | 6 | 13.99 | −12.71 |
| 6 | 0 | 6 | 0. | − 3.17 | 1 | 3 | −6 | 11.45 | 10.19 | 6 | 5 | −6 | 0. | − 0.03 | 2 | 8 | −6 | 1.98 | 1.82 |
| 6 | 0 | −6 | 12.09 | 12.25 | 2 | 3 | 6 | 6.93 | − 5.18 | 7 | 5 | 6 | 5.72 | 6.01 | 3 | 8 | 6 | 3.46 | 2.98 |
| 7 | 0 | 6 | 4.44 | 4.32 | 2 | 3 | −6 | 17.89 | −14.79 | 7 | 5 | −6 | 12.83 | −11.65 | 3 | 8 | −6 | 2.80 | 1.37 |
| 7 | 0 | −6 | 0. | 0.01 | 3 | 3 | 6 | 3.49 | − 2.96 | 8 | 5 | 6 | 5.75 | − 6.33 | 4 | 8 | 6 | 3.44 | 3.93 |
| 8 | 0 | 6 | 5.67 | 5.73 | 3 | 3 | −6 | 2.05 | − 1.35 | 8 | 5 | −6 | 12.11 | 10.71 | 4 | 8 | −6 | 2.82 | − 1.74 |
| 8 | 0 | −6 | 12.34 | −12.74 | 4 | 3 | 6 | 4.21 | 4.22 | 9 | 5 | 6 | 0. | − 1.67 | 5 | 8 | 6 | 8.42 | − 8.25 |
| 9 | 0 | 6 | 6.78 | − 7.84 | 4 | 3 | −6 | 11.78 | 10.33 | 9 | 5 | −6 | 3.80 | 3.33 | 5 | 8 | −6 | 3.46 | − 3.78 |
| 9 | 0 | −6 | 16.55 | 15.26 | 5 | 3 | 6 | 0. | 0.71 | 10 | 5 | 6 | 2.49 | 7.39 | 6 | 8 | 6 | 0. | 2.52 |
| 10 | 0 | 6 | 0. | 0.55 | 5 | 3 | −6 | 10.75 | − 9.18 | 10 | 5 | −6 | 9.83 | − 7.98 | 6 | 8 | −6 | 2.82 | 3.09 |
| 10 | 0 | −6 | 3.28 | − 2.83 | 6 | 3 | 6 | 10.03 | − 8.88 | 11 | 5 | −6 | 4.16 | 3.73 | 7 | 8 | 6 | 0. | 2.27 |
| 11 | 0 | −6 | 7.57 | − 6.03 | 6 | 3 | −6 | 0. | − 0.94 | 12 | 5 | −6 | 2.16 | 3.25 | 7 | 8 | −6 | 3.88 | 4.17 |
| 12 | 0 | −6 | 8.98 | 8.75 | 7 | 3 | 6 | 0. | − 1.05 | 0 | 6 | 6 | 18.09 | −15.07 | 8 | 8 | 6 | 2.39 | − 2.13 |
| 0 | 1 | 6 | 13.01 | 18.22 | 7 | 3 | −6 | 7.62 | 6.48 | 1 | 6 | 6 | 6.80 | 5.01 | 8 | 8 | −6 | 7.75 | − 7.84 |
| 1 | 1 | 6 | 11.01 | −10.54 | 8 | 3 | 6 | 3.70 | 4.55 | 1 | 6 | −6 | 10.68 | 8.32 | 9 | 8 | −6 | 5.21 | 5.41 |
| 1 | 1 | −6 | 0. | 0.17 | 8 | 3 | −6 | 0. | − 1.59 | 2 | 6 | 6 | 3.77 | − 2.60 | 0 | 9 | 6 | 20.63 | 17.32 |
| 2 | 1 | 6 | 8.01 | − 7.03 | 9 | 3 | 6 | 6.47 | − 6.41 | 2 | 6 | −6 | 9.55 | 7.74 | 1 | 9 | 6 | 6.03 | − 4.77 |
| 2 | 1 | −6 | 8.44 | 9.82 | 9 | 3 | −6 | 4.82 | − 4.62 | 3 | 6 | 6 | 5.85 | 5.31 | 1 | 9 | −6 | 10.96 | 8.76 |
| 3 | 1 | 6 | 12.29 | 11.69 | 10 | 3 | 6 | 0. | 1.47 | 3 | 6 | −6 | 19.35 | −15.02 | 2 | 9 | 6 | 10.78 | −10.13 |
| 3 | 1 | −6 | 5.85 | − 6.53 | 10 | 3 | −6 | 4.52 | 3.82 | 4 | 6 | 6 | 7.72 | − 7.36 | 2 | 9 | −6 | 4.90 | 4.03 |
| 4 | 1 | 6 | 4.44 | − 4.25 | 11 | 3 | −6 | 3.98 | 3.57 | 4 | 6 | −6 | 15.19 | 13.52 | 3 | 9 | 6 | 16.60 | 16.24 |
| 4 | 1 | −6 | 11.55 | −13.60 | 12 | 3 | −6 | 6.29 | − 6.57 | 5 | 6 | 6 | 0. | − 0.44 | 3 | 9 | −6 | 8.75 | − 7.09 |
| 5 | 1 | 6 | 10.44 | − 9.07 | 0 | 4 | 6 | 3.90 | − 1.96 | 5 | 6 | −6 | 1.95 | 1.27 | 4 | 9 | 6 | 3.36 | − 3.83 |
| 5 | 1 | −6 | 5.70 | 6.22 | 1 | 4 | 6 | 28.20 | 25.29 | 6 | 6 | 6 | 7.70 | 7.65 | 4 | 9 | −6 | 0. | 0.20 |
| 6 | 1 | 6 | 7.21 | 6.51 | 1 | 4 | −6 | 13.60 | −11.07 | 6 | 6 | −6 | 8.21 | − 7.24 | 5 | 9 | 6 | 7.62 | − 7.51 |
| 6 | 1 | −6 | 6.54 | − 6.73 | 2 | 4 | 6 | 23.74 | −22.14 | 7 | 6 | 6 | 7.83 | − 9.10 | 5 | 9 | −6 | 3.44 | 2.66 |
| 7 | 1 | 6 | 5.95 | 5.46 | 2 | 4 | −6 | 15.65 | 13.03 | 7 | 6 | −6 | 4.49 | 4.19 | 6 | 9 | 6 | 7.24 | 7.55 |
| 7 | 1 | −6 | 12.24 | −11.93 | 3 | 4 | 6 | 1.82 | 1.61 | 8 | 6 | 6 | 0. | 2.43 | 6 | 9 | −6 | 1.80 | 1.66 |
| 8 | 1 | 6 | 9.80 | − 9.74 | 3 | 4 | −6 | 4.72 | 4.18 | 8 | 6 | −6 | 2.77 | 2.66 | 7 | 9 | 6 | 0. | 1.84 |
| 8 | 1 | −6 | 9.60 | 9.14 | 4 | 4 | 6 | 19.04 | 18.37 | 9 | 6 | 6 | 3.00 | 4.10 | 7 | 9 | −6 | 9.78 | − 9.86 |
| 10 | 1 | 6 | 5.59 | 5.83 | 4 | 4 | −6 | 7.57 | − 5.19 | 9 | 6 | −6 | 4.13 | − 4.73 | 8 | 9 | 6 | 2.57 | − 3.72 |
| 10 | 1 | −6 | 9.06 | − 7.76 | 5 | 4 | 6 | 8.21 | − 7.44 | 11 | 6 | −6 | 3.57 | 3.17 | 8 | 9 | −6 | 7.26 | 6.85 |
| 12 | 1 | −6 | 4.70 | 4.68 | 5 | 4 | −6 | 2.57 | − 2.35 | 0 | 7 | 6 | 5.34 | 2.99 | 10 | 9 | −6 | 7.37 | − 8.36 |
| 0 | 2 | 6 | 15.63 | −15.88 | 6 | 4 | 6 | 0. | 0.57 | 1 | 7 | 6 | 9.78 | 7.21 | 1 | 10 | 6 | 8.65 | − 6.70 |
| 1 | 2 | 6 | 15.37 | 12.71 | 6 | 4 | −6 | 8.60 | 10.47 | 1 | 7 | −6 | 16.66 | 13.91 | 1 | 10 | −6 | 4.90 | 5.24 |
| 1 | 2 | −6 | 3.21 | 3.69 | 7 | 4 | 6 | 3.88 | 4.16 | 2 | 7 | 6 | 13.70 | −11.61 | 2 | 10 | 6 | 5.18 | 4.03 |
| 2 | 2 | 6 | 1.49 | 0.57 | 7 | 4 | −6 | 3.98 | − 3.73 | 2 | 7 | −6 | 14.22 | −11.81 | 2 | 10 | −6 | 4.47 | − 4.14 |
| 2 | 2 | −6 | 14.50 | 14.06 | 8 | 4 | 6 | 5.70 | 5.05 | 3 | 7 | 6 | 5.65 | 4.61 | 3 | 10 | 6 | 7.67 | 7.43 |
| 3 | 2 | 6 | 3.36 | − 3.71 | 8 | 4 | −6 | 8.73 | − 8.47 | 3 | 7 | −6 | 3.82 | 2.61 | 3 | 10 | −6 | 9.32 | − 9.36 |
| 3 | 2 | −6 | 17.17 | −20.99 | 9 | 4 | 6 | 9.47 | − 9.25 | 4 | 7 | 6 | 0. | 1.54 | 4 | 10 | 6 | 8.83 | − 8.81 |
| 4 | 2 | 6 | 3.18 | − 3.08 | 9 | 4 | −6 | 10.65 | 9.56 | 4 | 7 | −6 | 12.52 | 11.01 | 4 | 10 | −6 | 9.21 | 8.71 |
| 4 | 2 | −6 | 12.16 | 13.56 | 10 | 4 | 6 | 0. | 2.22 | 5 | 7 | 6 | 3.44 | 2.88 | 6 | 10 | 6 | 6.57 | 7.38 |
| 5 | 2 | 6 | 0. | − 0.47 | 10 | 4 | −6 | 3.11 | − 2.67 | 5 | 7 | −6 | 4.88 | − 3.65 | 6 | 10 | −6 | 9.75 | − 9.05 |

TABLE IV. (Continued)

| *h* | *k* | *l* | $F_{obs.}$ | $F_{calcd.}$ | *h* | *k* | *l* | $F_{obs.}$ | $F_{calcd.}$ | *h* | *k* | *l* | $F_{obs.}$ | $F_{calcd.}$ | *h* | *k* | *l* | $F_{obs.}$ | $F_{calcd.}$ |
|---|---|---|---|---|---|---|---|---|---|---|---|---|---|---|---|---|---|---|---|
| 7 | 10 | 6 | 4.03 | − 5.40 | 4 | 11 | 6 | 3.41 | − 3.60 | 4 | 12 | 6 | 1.05 | − 0.44 | 3 | 13 | −6 | 0. | 1.04 |
| 7 | 10 | −6 | 6.21 | 5.45 | 4 | 11 | −6 | 6.21 | 5.64 | 4 | 12 | −6 | 0. | 0.20 | 4 | 13 | 6 | 4.77 | − 6.12 |
| 8 | 10 | −6 | 3.11 | 2.94 | 5 | 11 | 6 | 2.69 | 2.79 | 5 | 12 | 6 | 2.90 | − 4.50 | 4 | 13 | −6 | 0. | − 0.15 |
| 9 | 10 | −6 | 3.39 | − 3.16 | 5 | 11 | −6 | 8.47 | − 8.43 | 5 | 12 | −6 | 2.31 | − 2.55 | 6 | 13 | −6 | 3.98 | 4.67 |
| 0 | 11 | 6 | 3.34 | 3.17 | 0 | 12 | 6 | 7.70 | 7.95 | 7 | 12 | −6 | 4.11 | 5.73 | 1 | 14 | 6 | 5.67 | − 6.18 |
| 1 | 11 | 6 | 3.82 | 2.43 | 1 | 12 | 6 | 1.28 | − 1.90 | 0 | 13 | 6 | 7.47 | 8.22 | 1 | 14 | −6 | 3.08 | 3.57 |
| 1 | 11 | −6 | 12.57 | 12.66 | 1 | 12 | −6 | 1.82 | − 2.10 | 1 | 13 | 6 | 4.49 | − 5.03 | 2 | 14 | 6 | 2.90 | 4.06 |
| 2 | 11 | 6 | 6.75 | − 6.12 | 2 | 12 | 6 | 2.98 | − 2.99 | 1 | 13 | −6 | 3.67 | 3.93 | 2 | 14 | −6 | 1.92 | − 3.21 |
| 2 | 11 | −6 | 11.45 | −10.46 | 2 | 12 | −6 | 1.82 | 1.12 | 2 | 13 | 6 | 1.80 | − 2.72 | 3 | 14 | 6 | 3.44 | 4.43 |
| 3 | 11 | 6 | 3.62 | 3.76 | 3 | 12 | 6 | 6.11 | 5.91 | 2 | 13 | −6 | 0. | 0.89 | 3 | 14 | −6 | 0. | − 1.86 |
| 3 | 11 | −6 | 0. | − 1.09 | 3 | 12 | −6 | 3.98 | 3.46 | 3 | 13 | 6 | 5.57 | 8.25 | 4 | 14 | −6 | 2.05 | 3.63 |

and the low value of the discrepancy factor obtained by the block-diagonal matrix least-squares refinement guarantee that the three-dimensional molecular structure determined here is quite reliable. Thus the molecular structure of this compound, derived by chemical reasoning, has been verified by independent X-ray analysis.

As was mentioned in the previous paragraph, we used only one chemical fact to interpret the Patterson function, the fact that three bromine atoms combine with the fulvene ring. The first Fourier synthesis, computed with signs based on the three bromine atoms, gave the whole molecular shape definitely. Two low and broad peaks were observed near the position of $C_8$ in the first Fourier synthesis. They were quite a bit lower than those of O and $C_{13}$. Although another molecular model, in which the methoxybenzene rotates by 180° about the $C_6$–$C_7$ bond, seemed to be least probable, we made a least-squares refinement for it. After three least-squares, cycles the ***R*** factor dropped to 0.16 without non-observed reflections ($R=0.18$ including them). A Fourier map corresponding to the last cycle of the least-squares procedure gave peaks whose heights were only 10% of those of the other carbon atoms near these assumed atomic positions (the temperature factors for these atoms became 8.1 and 7.5 Å$^2$ in the least-squares procedure) and rather high peaks at the positions of O and $C_{13}$ where, in this calculation, we did not put any atom. Therefore, the reliability of the present analysis is further confirmed.

This molecular structure explains the NMR spectra well. For example, the $H_6$ signal of this compound (7.63 p. p. m.) shifts into a field lower by 0.41 p. p. m. than that of the *p*-methoxy compound (7.22 p. p. m.). The shift may be due to the magnetic anisotropy of the oxygen atom which is disposed near the hyrogen, $H_6$, in this configuration.

The bond lengths and angles are illustrated in Fig. 5. The average estimated standard deviations of the coordinates are 0.003, 0.022 and 0.015 Å for bromine, carbon and oxygen atoms respectively. Therefore, the estimated standard deviations of the bonds are 0.022 Å for C–Br, 0.027 Å for C–O, and 0.031 Å for C–C. In the fulvene ring, $C_1$–$C_2$ and $C_3$–$C_4$ may be double bonds, the mean bond length being 1.31 Å. The bonds $C_2$–$C_3$, $C_4$–$C_5$ and $C_5$–$C_1$ are thought to be single bonds, their mean length being 1.48 Å. The bond $C_5$–$C_6$ seems to be double, and the C–C distances in the benzene ring are within the range from 1.36 to 1.44 Å. The lengths of $C_{12}$–O (1.39 Å) and O–$C_{13}$ (1.46 Å) are reasonable if the standard deviations in the bond lengths are allowed for. The mean C–Br distance is 1.86 Å, in good agreement with the normal value of this pair (1.85 Å).[3]

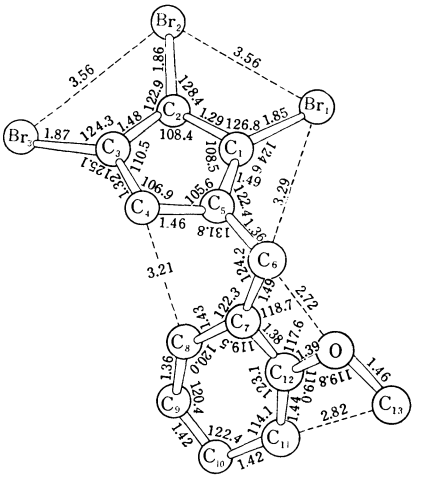



Fig. 5. Bond lengths (Å) and bond angles (°) in the molecule of 1,2,3-tribromo-6-(*o*-methoxyphenyl)fulvene.

3) "Tables of Interatomic Distances and Configuration in Molecules and Ions," The Chemical Society, London (1958).

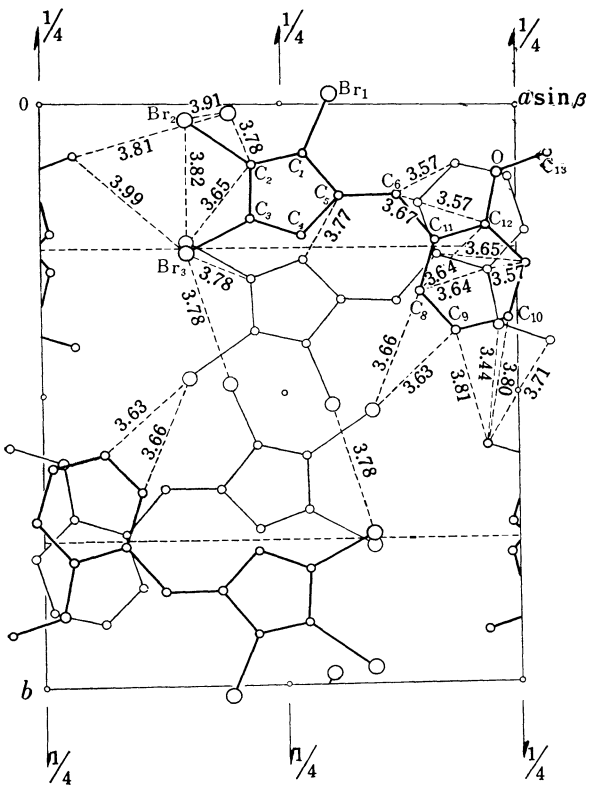



Fig. 6. Arrangement of molecules in the unit cell viewed along the c axis, with short intermolecular distances (Å).

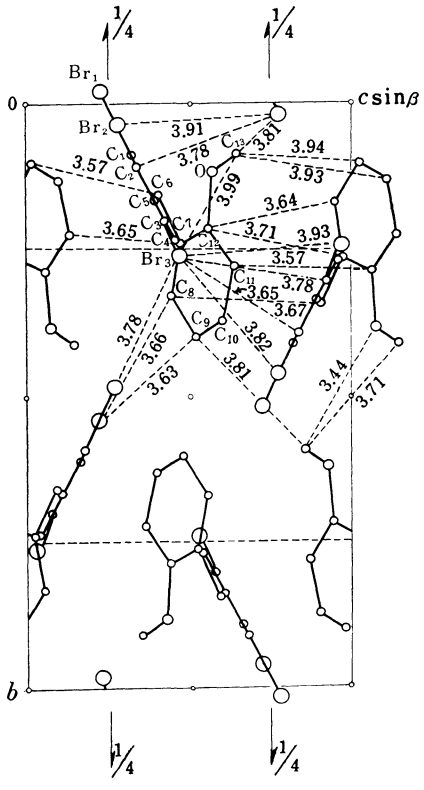



Fig. 7. Arrangement of molecules viewed along the a axis.

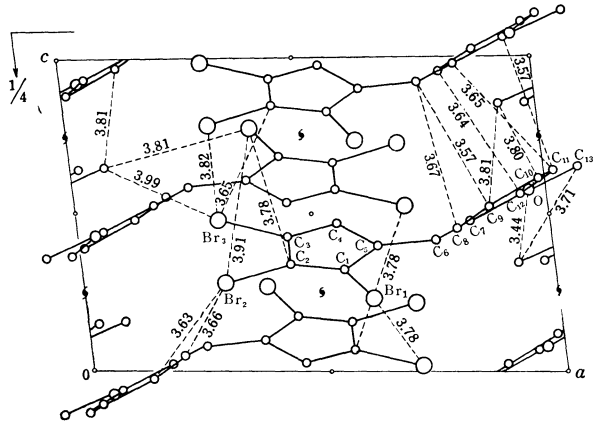



Fig. 8. Arrangement of molecules viewed along the b axis.

The benzene ring is approximately planar, the best plane being represented by the equation;

$$Y=-12.76X+27.80Z+51.01$$

where $X=x\sin\beta$, $Y=y$, and $Z=z+x\cos\beta$. The coefficients were determined by the least-squares method. The fulvene ring is also nearly planar, the best plane being described by the equation:

$$Y=0.1836X+1.859Z-3.159$$

The perpendicular displacements of the atoms from these mean planes are listed in Table V. The plane of the benzene ring makes an angle of 38°54′ with the plane of the fulvene ring. This angle between two planes mainly occurs as a result of the twisting about the bond $C_6$–$C_7$. The distance between the non-bonded atoms $C_4$ and $C_8$ is 3.21 Å; contact between

TABLE V. DEVIATIONS FROM THE LEAST-SQUARES PLANES (Å)

| Atom | From the benzene plane | Atom | From the fulvene plane |
|---|---|---|---|
| $C_7$ | 0.03 | $C_1$ | 0.00 |
| $C_8$ | −0.02 | $C_2$ | −0.01 |
| $C_9$ | −0.00 | $C_3$ | 0.01 |
| $C_{10}$ | −0.03 | $C_4$ | −0.00 |
| $C_{11}$ | 0.02 | $C_5$ | 0.00 |
| $C_{12}$ | 0.00 | $Br_1$ | 0.10 |
| $C_1$ | 0.61 | $Br_2$ | 0.12 |
| $C_2$ | 1.36 | $Br_3$ | −0.07 |
| $C_3$ | 1.98 | $C_6$ | 0.07 |
| $C_4$ | 1.56 | $C_7$ | 0.04 |
| $C_5$ | 0.67 | $C_8$ | −0.77 |
| $Br_1$ | −0.30 | $C_9$ | −0.75 |
| $Br_2$ | 1.79 | $C_{10}$ | 0.01 |
| $Br_3$ | 3.09 | $C_{11}$ | 0.83 |
| $C_6$ | 0.03 | $C_{12}$ | 0.77 |
| O | 0.04 | O | 1.53 |
| $C_{13}$ | −0.15 | $C_{13}$ | 2.20 |

them might cause this twisting. If the positions of the hydrogen atoms bonding to $C_4$ and $C_8$ are estimated with conventional C–H length and angles, the distance between them is approximately 1.9 Å; this value might be reasonable for the contact of such hydrogens.

The methyl group in the methoxy group deviates from the plane of the benzene ring, the $C_{11}$–$C_{13}$ distance being 2.82 Å. Three bromine atoms and $C_6$ are out of the plane of the fulvene ring, probably because of the mutual repulsion among these substituted atoms and this group. The $Br_1$–$Br_2$, $Br_2$–$Br_3$ and $Br_1$–$C_6$ distances are 3.56, 3.56 and 3.29 Å respectively.

Figures 6, 7 and 8 show the crystal structures projected along the c, a and b axes respectively. If the van der Waals radii of the bromine, oxygen and methyl groups are taken to be 1.95, 1.40 and 2.0 Å respectively, and if the half thickness of the aromatic ring is 1.70 Å, as is usually accepted, all the intermolecular approaches observed are equal to or longer than the sums of the radii of the corresponding atoms within the range of errors. It might be concluded from Figs. 6, 7 and 8 that the molecules are well packed by the van der Waals interactions. The benzene rings which are related to each other by the c glide plane are nearly parallel, because the plane of any benzene ring makes a very small angle with the b axis. Therefore, these nearly parallel benzene rings are piled up at a distance of about 3.5 Å in the direction of the c axis, as may be seen from Fig. 8.

Although the dipole moment of the present compound has not been measured, it is, expected to show a considerable value, judging from the value of the related chloro derivative (4.72D). If the crystal structure of the present compound is discussed in view of the arrangement of such dipolar molecules, it may be compared to that of 3-bromo-2-methoxytropone,[4] although there is a slight difference in the direction of the glide planes, the c glide in the former and the a glide in the latter.

From the similarity of the unit cell dimensions between the present crystal and that of the chloro derivative, it may be deduced that the molecular packing of the latter is essentially the same as that of the former, which has been described here.

We wish to express our deep thanks to Professor Yoshio Kitahara and Dr. Ichiro Murata of Tohoku University for supplying the materials and for their helpful discussions. We are also grateful to Dr. Tamaichi Ashida and all our collaborators for their kind suggestions on the structure analysis and computing programmes, while we are indebted to the staff of the computing center of Teijin Co., Ltd., for the numerical calculations.

*Institute for Protein Research*
*Osaka University*
*Kita-ku, Osaka*

4) K. Furukawa, Y. Sasada, A. Shimada and T. Watanabe, This Bulletin, 37, 1871 (1964).

# The Heat Capacity and the Entropy of Transition of Würster's Blue Perchlorate

By Hideaki CHIHARA, Minoru NAKAMURA and Syûzô SEKI

(Received May 4, 1965)

Würster's Blue perchlorate

$$[(CH_3)_2N\text{-}C_6H_4\text{-}N\text{-}(CH_3)_2]^+ ClO_4^-$$

is one of the free radical crystals that are stable at room temperatures. Other similar crystals include those of diphenylpicryl hydrazyl (DPPH) and 1, 3-bisdiphenylene-2-phenyl allyl (BDPA), which are believed to become antiferromagnetic below 1.73 and 0.2°K respectively.[1] The heat capacity measurements of BDPA indicated the occurrence of linear antiferromagnetic chains below its Néel point; the heat capacity shows a sharp spike at 1.73°K and a broad maximum at higher temperatures, centering at about 3°K.[2] The magnetic properties of BDPA and DPPH are also consistent with the idea of spin ordering into an antiferromagnetic array at low temperatures.

Würster's Blue perchlorate, on the other hand, has a transition at a relatively high temperature (190°K), as is revealed by the magnetic susceptibility measurements.[3] This transition has sometimes been referred to as antiferromagnetic transition. McConnell's electron spin resonance studies[4] showed the existence of a triplet exciton state below the transition temperature and give support to Hausser's idea that the cation radicals are dimerized to give a singlet ground state and a triplet excited state.[5] Chesnut[6] presented a simple theory, based on these experimental facts, to account for the transition in terms of cooperative interaction between triplet excitons.

The present paper will describe some results of the measurements of the heat capacities of powdered Würster's Blue perchlorate, measurements conducted in an attempt to discriminate among various possible mechanisms of the transition.

## Experimental

The calorimeter, the cryostat, and their operations were the same as have been described previously.[7]

Fine flakes of Würster's Blue perchlorate (WB) were a donation from Dr. K. Suzuki of Kwansei Gakuin University, who will describe their preparation elsewhere. The molar magnetic susceptibility of the specimen as received was $1.28\times10^{-3}$ e.m.u./mol. at room temperature (12°C), which corresponded to that of about 100% free radical; it did not show any change after having been stored in dark, dry air for a year. As the amount of the specimen available was small, only 0.7079 g. or 0.002684 mol., of powdered WB was used in the measurement of the heat capacity; as a result, the error in the heat capacity values amounted to about 2% under the most unfavorable conditions, when the empty calorimeter contributed about 3/4 to the total heat capacity. The results of the measurements to be reported in the following section are for the fresh WB of a 100 ±3% free radical. After these measurements in the copper calorimeter with a few mmHg of helium exchange gas in it, the specimen was stored in situ for about half a year, during which time the apparata were moved to the North Campus of the University. The second series of runs which were then taken did not give consistent results in the phase transition region; however, the normal portion of the heat capacity agreed with that obtained in the first series of runs within the range of experimental error. The molar magnetic susceptibility after the second run was about 73% of the intial value for the fresh WB.

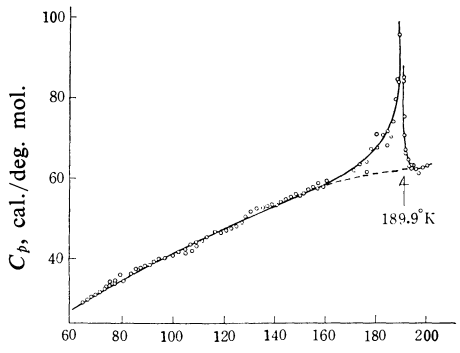



Fig. 1

1) A. S. Edelstein, *J. Chem. Phys.*, **40**, 488 (1964). This paper lists the earlier bibliography.
2) J. P. Goldsborough, M. Mandel and G. E. Pake, Proc. VIIth Intern. Conf. Low Temp. Phys., Toronto, 702 (1961); A. S. Edelstein and M. Mandel, *J. Chem. Phys.*, **35**, 1130 (1961); W. O. Hamilton and G. E. Pake, ibid., **39**, 2694 (1963).
3) K. Okumura, *J. Phys. Soc., Japan*, **18**, 69 (1963); see also W. Duffy, Jr., *J. Chem. Phys.*, **36**, 490 (1962).
4) a) H. M. McConnell and R. Lynden-Bell, ibid., **37**, 794 (1962); b) D. D. Thomas, H. Keller and H. M. McConnell, ibid., **39**, 2321 (1963).
5) K. H. Hausser and J. N. Murrell, ibid., **27**, 500 (1957).
6) D. B. Chesnut, ibid., **40**, 405 (1964).
7) T. Shinoda, H. Chihara and S. Seki, *J. Phys. Soc. Japan*, **19**, 1637 (1964).

## Results and Discussion

The primary experimental results are plotted in Fig. 1. There is a sharp rise in the heat capacity at 189.9°K, with a tail extending down to about 160°K. Although the temperature did not exactly stop at the transition point, it is highly probable that the transition is of the first order. Two independent runs were performed for the determination of the enthalpy change of the transition; it was 408.6±4.5 cal./mol. The entropy of the transition was 2.19±0.02 cal./deg.mol. It should be noted that this entropy change is very close to $R \ln 3$, which is 2.18 cal./deg.mol.

The temperature of the transition has been reported differently by different investigators: Duffy's susceptibility curve[3] shows a sudden decrease at 186°K, Okumura's one[3] at 189°K, Edelstein[1] gave 175±5°K, and Suzuki's differential thermal analysis[8] showed a peak at about 190°K. The present study agrees with Suzuki's probably because specimens from the same batch were used in both experiments. As has been mentioned in experimental section, the lowering of the transition temperature may be due to the partial dying of the free radicals.

We shall now compare our experimental results with several models hitherto presented to account for this transition.

**a) The Paramagnetic-antiferromagnetic Scheme.**—The shape of the curve showing the temperature dependence of the susceptibility near 190°K is similar to that in an antiferromagnetic, as has been pointed out by Elliot and Wolfsberg[9] and by Duffy[3]. Edelstein[1] developed a theory for a linear Ising chain of half spins and applied it successfully to the cases of BDPA and PAC. Here inter-chain coupling was approximated by the molecular field treatment. However, although he estimated the intra-chain exchange intergral for WB as $J/k = -27 \pm 10$, he did not explicitly mention that WB was an antiferromagnetic. Also, Duffy and Okumura pointed out that the Curie temperature, $|\theta| =$ 23°K, derived from the high temperature susceptibilities is too small, compared to the transition temperature, for an antiferromagnetic transition. The entropy of the transition to be predicted for such a scheme is $R \ln 2$; the experimental results can rule out such possibility if the transition arises solely from an order-disorder problem of the spin system. If an attempt is made to divide the total entropy of the transition into contributions from the latent heat portion and those from the low temperature tail of Fig. 1, the latter amounts to 1.36 cal./deg.mol. and is close to what one would expect for an antiferromagnetic transition. The rest of the entropy would then come from some structural changes. In fact, X-ray diffraction studies, cited by McConnell,[4b] show that the transition is accompanied with a small structural change from the room-temperature orthorhombic phase to the low temperature monoclinic phase. The X-ray density does not appear to change substantially, and the angular tilt is only 2.7°. A single crystal does not shatter in going through the transition. It is difficult to assess the entropy of a structural change, but it should come from a variation in the lattice frequency spectrum, which must also be seen in the normal part of the heat capacity below and above the transition point. As the smooth dash-line curve in Fig. 1 suggests, such a variation would appear to be small.

**b) The Dimerization Scheme.**—Hausser's study[5,10] of the electronic absorption spectra of WB in solution and in solid is believed to indicate the presence of dimerized species in solid WB at low temperatures. Suzuki's spectroscopic study also supports this view.[11] The idea of dimerization has, moreover, been indirectly substantiated by McConnell's electron spin resonance studies, in which the triplet exciton resonance, free from a nuclear hyperfine structure, was observed at low temperatures. The X-ray diffraction findings that the unit cell lengths become doubled in the directions of the a and b axes can also be regarded as showing that dimerization occurs at the transition temperature. From the temperature dependence of the ESR signal intensity, McConnell was able to derive the energy of exitation from the ground singlet state to the triplet exciton state of a dimer as 246 $cm^{-1}$. The heat capacity should see the consequence of this energy gap that a Schottky-type anomaly occurs, with the maximum of 1.02 cal./deg.mol. at 123°K. Unfortunately, no anomaly of this magnitude is discernible in Fig. 1 because of the lack of precision in the measurements. A simple calculation shows, however, that the total gain in entropy due to the Schottky anomaly is $(1/2)\ R \ln 4$ and that about 69% of this would have been acquired when the crystal reaches the transition point. Therefore, the transition would be concerned only with the dissociation of the dimerized species and the rest of the spin disordering. The dissociation does not itself contribute to the entropy, except, of course,

8) K. Suzuki, 16th Annual Meeting of the Chemical Society of Japan, Tokyo, April, 1963, Abstract of Paper 2U12.

9) N. Elliot and M. Wolfsberg, *Phys. Rev.*, **91**, 435A (1953).

10) K. H. Hausser, *Z. Naturforsch.*, **11a**, 20 (1956).

11) Private communication.

for the structural change which accompanies it.

The entropy of spin disordering at the transition is, thus, no larger than 31% of $(1/2)\boldsymbol{R}\ln 4$, or 0.42 cal./deg.mol., even if it is assumed that the rest of the Schottky anomaly is replaced by the cooperative disordering of spins.

c) **Exciton Interaction.**—Since the formation of cation dimers in WB at low temperatures and the excitation transfer of the triplet level of the dimers have been well established, another possible approach to the mechanism of the transition would be to incorporate the cooperative interaction between the excitons. Chesnut[6] showed that a type of order-disorder transition does occur if one includes in the interaction a term which is quadratic in the excitation density, $\rho$, and writes the Helmholtz energy for the $N$ cations as:

$$F=\frac{1}{2}N[\varepsilon_0\rho+\frac{1}{2}\varepsilon_1\rho^2-\boldsymbol{k}T\{\rho\ln g-\rho\ln\rho-(1-\rho)\ln(1-\rho)\}]$$

where $g$ is the multiplicity ($g=3$), $\varepsilon_0$ is the singlet-triplet excitation energy, and $\varepsilon_1$ is the inter-exciton energy. The justification for the quadratic energy term has already been discussed.[12,13] A diffuse first-order transition stems from the Helmholtz energy expression, and the entropy change will be:

$$\Delta S=\frac{1}{2}\boldsymbol{R}\Delta\rho\ln g$$

where $\Delta\rho$ is the change in the excitation density at the transition. The total entropy of the transition will now be:

$$\Delta S=\frac{1}{2}\times\frac{3}{4}\boldsymbol{R}\ln 3=0.82\ \text{cal./deg.mol.}$$

at the maximum since, in the limit of high temperature, the population in the triplet state would be $(3/4)N$.

We have now evaluated three possible interpretations of the transition and have found that no single mechanism can satisfactorily account for the observed change in entropy by the transition, 2.19 cal./deg.mol. Actually, if one considers only the spin system as the source of entropy creation at the transition, it is almost hopeless to get a larger value than $\boldsymbol{R}\ln 2$ out of it. One of the recourses in such a situation is to assume some disordering in the orientation of perchlorate ions; this, however, has not been substantiated in WB experimentally. If this tetrahedral ion can assume one of two equally probable orientations in the high temperature phase and can then become frozen in either one of them at low temperatures, an entropy of $\boldsymbol{R}\ln 2$ would appear at the transition point. In fact, the combination of this type of disorder with the mechanism c, or the exciton cooperation, gives the total entropy of 2.20 cal./deg.mol., a value which is very close to what has been found by experiment. A refined X-ray diffraction study will give us some direct clue to the answer of this problem.

12) H. M. McConnell and Z. Soos, *J. Chem. Phys.*, **40**, 586 (1964).
13) D. B. Chesnut, ibid., **41**, 472 (1964).

## Summary

The heat capacity of Würster's Blue perchlorate (*N, N, N', N'*-tetramethyl-*p*-phenylenediamine perchlorate) has been measured between 66 and 200°K. A phase transition occurs at 189.9°K with its tail extending down to about 160°K. The transition is probably of the first order. The heat and the entropy of the transition are 408.6±4.5 cal./mol. and 2.19±0.02 cal./deg.mol. respectively. The magnetic susceptibility of the specimen at room temperature indicates that the paramagnetic spin density is 100±3%. The experimental results have been compared with current theories, and it has been inferred that some unknown structural changes are involved in the phase transition.

The authors would like to thank Professor Keisuke Suzuki of Kwansei Gakuin University, who gave us a sample of Würster's Blue perchlorate; the discussions with him have been helpful. The measurements of the magnetic susceptibility made, at our request, by Dr. Shuichi Tazawa of Osaka University helped to solve inconsistencies in the primary heat capacity results; to him the authors' deep gratitude is extended. Thanks are also due to Dr. Takako Shinoda, who helped us in part of the measurements.

*Department of Chemistry*
*Faculty of Science*
*Osaka University*
*Toyonaka, Osaka*

# Phase Transitions in Crystalline Divalent Metal Dicalcium Propionates. I. Calorimetric and Dielectric Investigations of Strontium- and Lead Dicalcium Propionates

By Nobuo NAKAMURA, Hiroshi SUGA, Hideaki CHIHARA and Syûzô SEKI

(Received May 6, 1965)

There are three substances known as the double propionates of divalent metals: barium-, strontium- and lead-dicalcium propionates. The room temperature modification of the barium salt is known to be cubic.[1] The X-ray crystal structure analysis of this phase was made in 1935 by Nitta and Watanabé,[2] and also, independently, by Harris and Biefeld,[3] and its space group was found to be $O^4$–$F4_13$. In 1951, it was found in our laboratory by the use of the calorimetric method, that this material undergoes a phase transition at −8.5°C.[4] Taking account of the crystal symmetry and molecular shape, this phase transition was supposed to be a kind of order-disorder type with regard to the motion of the propionate anions in the crystal lattice.

In the case of strontium salt, the spontaneous polarization was measured by Matthias and Remeika in 1957; it was thus revealed that this salt becomes ferroelectric below 8.5°C.[5] The crystal symmetry of this compound at room temperature is tetragonal,[1] and the ferroelectric axis is the c-axis. Orioli and Pieroni applied the X-ray method to this salt in 1959 and proposed a probable space group, $D_4^4$–$P4_12_12$ or $D_4^8$–$P4_32_12$; they also determined the positions of the heavy atoms.[6] The crystal symmetry and the space group of the lower temperature phase was determined by Kobayashi and Yamada in 1962, the modification being found to be tetragonal, while the space group is either $C_4^4$–$P4_3$ or $C_4^3$–$P4_2$.[7]

The lead salt at room temperature is of tetragonal symmetry and is isomorphous to the strontium salt.[1] Using the differential thermal analysis method, the authors have found a new phase transition at about −80°C. The crystal structure analysis of its room temperature phase was made by Ferroni and Orioli in 1959; they obtained a structure similar to that for the room temperature phase of the strontium.[8] Yamada analyzed the lower temperature phase of the compound and found that it to be of tetragonal symmetry, the space group being either $C_4^4$ or $C_4^3$.[9]

It seems highly desirable to obtain further information about the mechanism of the phase transitions of these three compounds. For this purpose, the present authors have studied the thermal properties of the strontium- and the lead salts and the dielectric properties of the lead salt. In the present paper, such experimental data will be presented, and the mechanisms of the phase transitions in these two salts will be discussed.

## Experimental Procedures

**Materials.** — *a)* $SrCa_2(CH_3CH_2CO_2)_6$.—An aqueous solution of sodium carbonate (extra pure grade, manufd. by Wako Chem. Ind., Ltd.) was added to an aqueous solution of strontium chloride (Merck). The strontium carbonate precipitates were then washed with water and dried at 40°C. Powdered strontium carbonate and calcium carbonate were mixed together in the molar ratio of 1 : 2, and the mixture was dissolved in an aqueous solution of propionic acid, which, by evaporation at 40°C, yielded colorless crystals. The crystals obtained were, then, recrystallized from an aqueous solution, fed into the calorimeter vessel, and then dried in a vacuum of $10^{-4}$ mmHg at room temperature for about 30 hr.

*b)* $PbCa_2(CH_3CH_2CO_2)_6$. — The sample for the calorimetric study was prepared by a method similar to that used for strontium salt. Lead carbonate was prepared from lead dichloride (extra pure grade, manufd. by Wako Chem. Ind., Ltd.) and sodium carbonate (see in a)). For the measurement of the dielectric constant, the sample for calorimetry was dissolved again in water and kept at 25°C in a thermostated bath for about 20 days, in order to grow a single crystal about 15 mm. across. Disk specimens were then cut out with the

1) A. Fitz and F. Sansoni, *Z. Krist.*, **6**, 68 (1882); P. Groth, "Chemische Krystallographie," Vol. III, Verlag von Wilhelm Engelmann, Leipzig (1910), p. 203.
2) I. Nitta and T. Watanabé, *Sci. Papers Inst. Phys. Chem. Research (Tokyo)*, **26**, 164 (1935).
3) L. P. Harris and P. M. Biefeld, *J. Am. Chem. Soc.*, **57**, 396 (1935).
4) S. Seki, M. Momotani, K. Nakatsu and T. Ôshima, *J. Chem. Phys.*, **19**, 1061 (1951); This Bulletin, **28**, 411 (1955).
5) B. T. Matthias and J. P. Remeika, *Phys. Rev.*, **107**, 1727 (1957).
6) P. Orioli and M. Pieroni, *La Ricerca Sci.*, **29**, 295 (1959).
7) J. Kobayashi and N. Yamada, *Bull. Science and Engineering Research Lab., Waseda Univ.*, **18**, 63 (1962).
8) E. Ferroni and P. Orioli, *Z. Krist.*, **111**, 362 (1959).
9) Y. Yamada, Private communication.

parallel planes corresponding to the crystallographic (110) and (001) planes. The directions of the axes were identified by taking Laue photographs. For the dielectric measurements, the specimen was sandwiched between the electrodes and dried in situ under $10^{-5}$ mmHg pressure for 5 hr. at room temperature.

**Calorimetry.** — The calorimetric measurements were made on single loadings of 25.97 g. (0.04287 mol.) and 29.53 g. (0.04071 mol.) for the strontium and the lead salts respectively. The measurements were carried out with an adiabatic calorimeter in the temperature region from 15 to 300°K. The details of the apparatus and the methods of operation have already been described.[10]

**Dielectric Measurements.** — The dielectric constants of the lead salt were measured for the planes (100) and (001) with a Cole-type mutual-inductance bridge (Ando Elec. Co., Ltd.) in the frequency range between 100 c.p.s. and 1 Mc.p.s., covering the temperature region from the liquid nitrogen temperature to 90°C. Temperatures were measured with two copper-constantan thermocouples attached to the electrodes; the errors are estimated to be within 0.5°. The details of the apparatus and the method. of operation have been described elsewhere.[11]

**Dilatometry.**—By using a simple glass-tube dilatometer, with mercury as the confining liquid, a preliminary dilatometric study was carried out with a powdered specimen of the lead salt in the temperature region from room temperature to 70°C.

## Experimental Results

**The Thermodynamic Properties of $SrCa_2(CH_3CH_2CO_2)_6$ and $PbCa_2(CH_3CH_2CO_2)_6$.**— The heat capacity curves for the strontium and the lead salts obtained are shown in Figs. 1 and 2 respectively. The smoothed values of the heat capacities, enthalpies, entropies and Gibbs energy functions are tabulated in Tables I and II for the strontium and lead salts respectively. These values are expressed in terms of the defined thermochemical calorie, equal to 4.1840 absolute joules. The ice point is taken to be 273.15°K. The experimental errors in the heat capacity were estimated to be within 1% and 0.3% in the liquid hydrogen and the liquid nitrogen temperature regions respectively. The thermodynamic functions at the standard state are shown in Table III.

As a result of this experiment on the strontium salt, we found a new phase transition at 104°K. At an ordinary cooling rate, the temperature of the calorimeter went down to the liquid hydrogen temperature with no indication of any transition. When the calorimeter was then heated, an exothermic effect appeared at around 83°K, and the crystal was

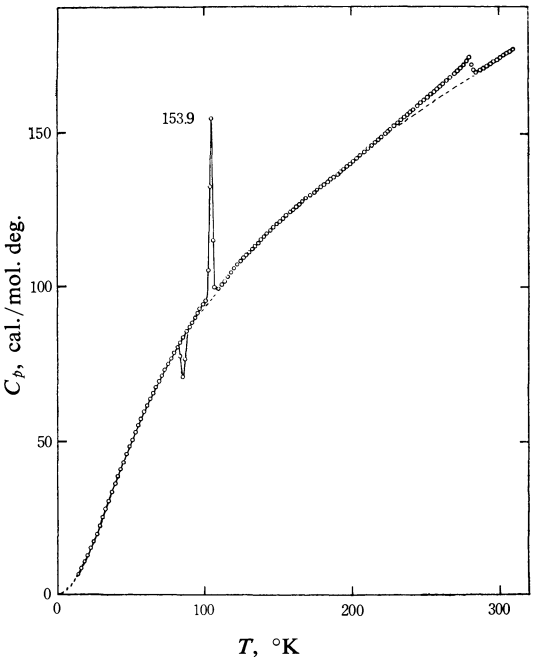



Fig. 1. Heat capacity of $SrCa_2(CH_3CH_2CO_2)_6$. Dashed curve shows the estimated normal heat capacity. Three points around 83°K below the normal curve correspond to the exothermic effect described in the text.

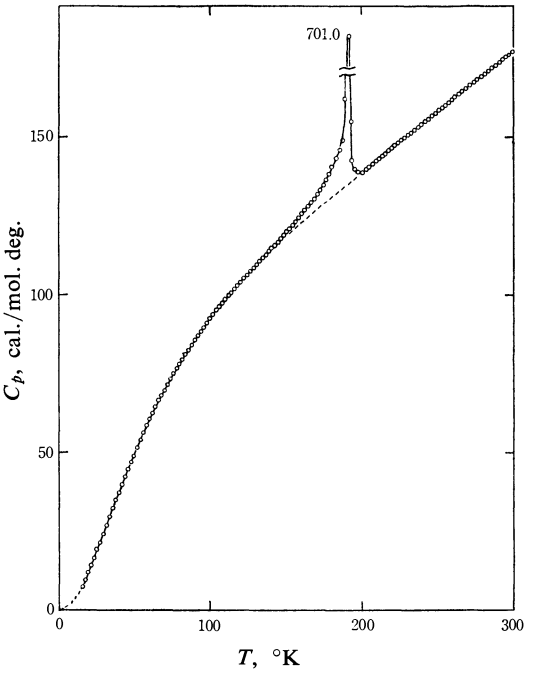



Fig. 2. Heat capacity of $PbCa_2(CH_3CH_2CO_2)_6$. Dashed curve shows the estimated normal heat capacity.

10) H. Suga and S. Seki, This Bulletin, **38**, 1000 (1965).
11) H. Chihara, S. Okawa and S. Seki, This Bulletin, **37**, 1373 (1964).

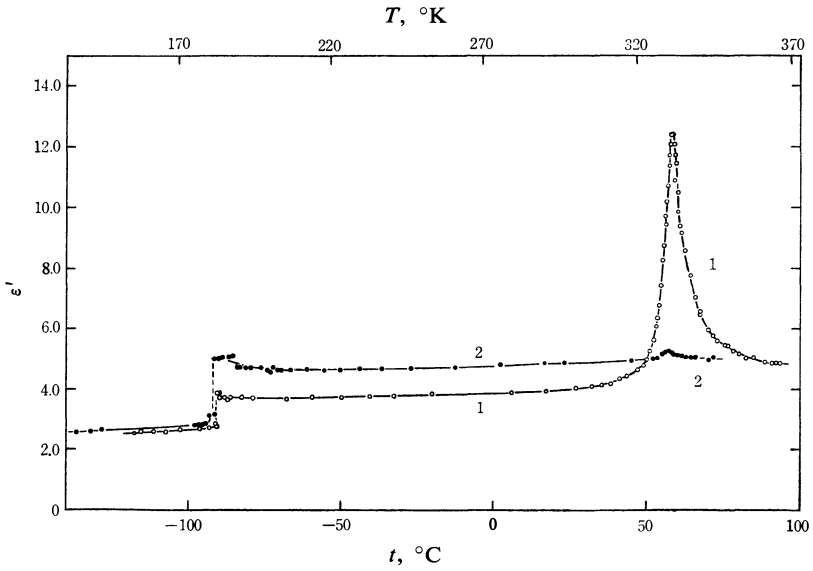



Fig. 3. Dielectric constants of $PbCa_2(CH_3CH_2CO_2)_6$ at 10 kc.p.s.
Curve 1: Parallel to c-axis, (001). Curve 2: Perpendicular to c-axis, (110)

TABLE I. THERMODYNAMIC PROPERTIES OF $SrCa_2(CH_3CH_2CO_2)_6$

| $T$ °K | $C_p°$ cal./mol./deg. | $S°$ cal./mol./deg. | $(H°-H_0°)/T$ cal./mol./deg. | $-(G°-H_0°)/T$ cal./mol./deg. |
|---|---|---|---|---|
| 5 | (0.28) | (0.10) | (0.07) | (0.02) |
| 10 | (1.96) | (0.69) | (0.50) | (0.19) |
| 20 | 11.97 | 4.88 | 3.61 | 1.31 |
| 30 | 23.61 | 11.88 | 8.27 | 3.61 |
| 40 | 35.78 | 20.39 | 13.67 | 6.72 |
| 50 | 46.44 | 29.57 | 19.22 | 10.37 |
| 60 | 58.10 | 39.10 | 24.76 | 14.36 |
| 70 | 68.81 | 48.88 | 30.31 | 18.59 |
| 80 | 78.23 | 58.70 | 35.71 | 22.99 |
| 90 | 85.90 | 68.40 | 40.89 | 27.49 |
| 100 | 94.36 | 77.82 | 45.75 | 32.05 |
| 100.5 | 95.25 | 78.28 | 45.99 | 32.29 |
| 104.2±0.5 | | Lower transition | | |
| 106.0 | 97.04 | 88.19 | 53.39 | 34.80 |
| 110 | 99.38 | 92.11 | 56.48 | 35.64 |
| 130 | 110.71 | 109.68 | 64.01 | 45.70 |
| 150 | 120.05 | 126.20 | 70.87 | 55.33 |
| 170 | 128.61 | 141.76 | 77.18 | 64.60 |
| 190 | 136.38 | 156.50 | 82.98 | 73.50 |
| 210 | 144.43 | 170.53 | 88.46 | 82.08 |
| 230 | 152.56 | 184.04 | 93.69 | 90.37 |
| 250 | 161.02 | 197.11 | 98.74 | 98.38 |
| 270 | 169.76 | 209.83 | 104.28 | 105.55 |
| 280 | 174.88 | 216.09 | 106.72 | 109.37 |
| 282.6±0.1 | | Upper transition | | |
| 285 | 170.27 | 219.17 | 107.89 | 111.28 |
| 290 | 171.73 | 222.14 | 108.99 | 113.17 |
| 310 | 177.77 | 233.78 | 113.22 | 120.58 |

TABLE II. THERMODYNAMIC PROPERTIES OF $PbCa_2(CH_3CH_2CO_2)_6$

| $T$ °K | $C_p°$ cal./mol./deg. | $S°$ cal./mol./deg. | $(H°-H_0°)/T$ cal./mol./deg. | $-(G°-H_0°)/T$ cal./mol./deg. |
|---|---|---|---|---|
| 5 | (0.24) | (0.10) | (0.07) | (0.02) |
| 10 | (2.29) | (0.72) | (0.55) | (0.17) |
| 20 | 13.96 | 5.64 | 4.16 | 1.48 |
| 30 | 26.82 | 13.74 | 9.58 | 3.20 |
| 40 | 39.46 | 23.18 | 15.46 | 7.72 |
| 50 | 50.77 | 33.22 | 21.42 | 11.81 |
| 60 | 61.09 | 43.40 | 27.18 | 16.23 |
| 70 | 70.51 | 53.56 | 29.30 | 24.26 |
| 80 | 78.83 | 63.53 | 37.95 | 25.55 |
| 90 | 86.43 | 73.26 | 43.88 | 29.37 |
| 100 | 92.69 | 82.70 | 48.47 | 34.23 |
| 120 | 104.26 | 100.62 | 56.81 | 43.81 |
| 140 | 114.89 | 117.50 | 64.34 | 53.16 |
| 160 | 126.08 | 133.56 | 71.34 | 62.19 |
| 170 | 132.70 | 141.40 | 74.76 | 66.64 |
| 180 | 140.56 | 149.19 | 78.18 | 71.01 |
| 185 | 146.35 | 153.11 | 79.95 | 73.16 |
| 186.5 | 148.95 | 154.30 | 80.47 | 73.81 |
| 187.5 | 151.70 | 155.09 | 80.86 | 74.24 |
| 191.5±0.5 | | Lower transition | | |
| 194.5 | 140.54 | 168.60 | 92.16 | 76.44 |
| 196.0 | 137.17 | 169.65 | 92.35 | 77.30 |
| 197.5 | 138.39 | 170.72 | 91.71 | 79.02 |
| 200 | 138.77 | 172.45 | 92.31 | 80.16 |
| 220 | 146.66 | 186.05 | 96.87 | 89.17 |
| 240 | 154.33 | 199.12 | 101.34 | 97.80 |
| 260 | 162.07 | 211.79 | 105.71 | 106.07 |
| 280 | 169.89 | 224.07 | 110.02 | 114.08 |
| 300 | 177.66 | 236.07 | 114.27 | 121.80 |

TABLE III. THERMODYNAMIC FUNCTIONS AT STANDARD STATE

| Substance | $C_p°_{298.15}$ cal./mol./deg. | $(H°_{298.15}-H_0°)/T$ cal./mol./deg. | $S°_{298.15}$ cal./mol./deg. | $(G°_{298.15}-H_0°)/T$ cal./mol./deg. |
|---|---|---|---|---|
| $SrCa_2(C_2H_5CO_2)_6$ | 174.1±0.7 | 110.7±0.4 | 226.9±0.9 | −116.2±0.5 |
| $PbCa_2(C_2H_5CO_2)_6$ | 177.0±0.7 | 113.9±0.5 | 235.0±0.9 | −121.1±0.5 |

TABLE IV. TRANSITION TEMPERATURES, ENTHALPIES AND ENTROPIES OF TRANSITIONS

| Substance | $T_t$, °K | $\Delta H_t$, cal./mol. | $\Delta S_t$, e.u. |
|---|---|---|---|
| $SrCa_2(C_2H_5CO_2)_6$ | 104.2±0.5 | 255±5 | 3.2±0.1 |
| | 282.6±0.1 | 159.6±0.5 | 0.61±0.02 |
| $PbCa_2(C_2H_5CO_2)_6$ | 191.5±0.5 | 1160.0±5.0 | 5.82±0.03 |
| $BaCa_2(C_2H_5CO_2)_6$ | 266.9 | 1741 | 6.50 |

transformed into the stable lower temperature phase, as is shown in Fig. 1. The heat capacities of the stable and the metastable phases below the transition point are nearly equal within the range of experimental error and, therefore, the exothermic effect does not modify the interpretation of the results given in the following section.

For the lead salt, we also found two phase transition phenomena, as will be mentioned later. The upper transition, however, was not studied by the calorimetric method because of the limited capability of the apparatus. Table IV lists the transition temperatures and the heats and the entropies of transition obtained for the strontium and lead salt, together with those previously obtained for the barium salt for the sake of comparison.

**The Dielectric Properties of $PbCa_2(CH_3CH_2CO_2)_6$.**—As is shown in Fig. 3, the dielectric constants in each crystallographic plane, measured only in the cooling direction, jump abruptly at about 183°K; this temperature corresponds to the transition temperature observed by the

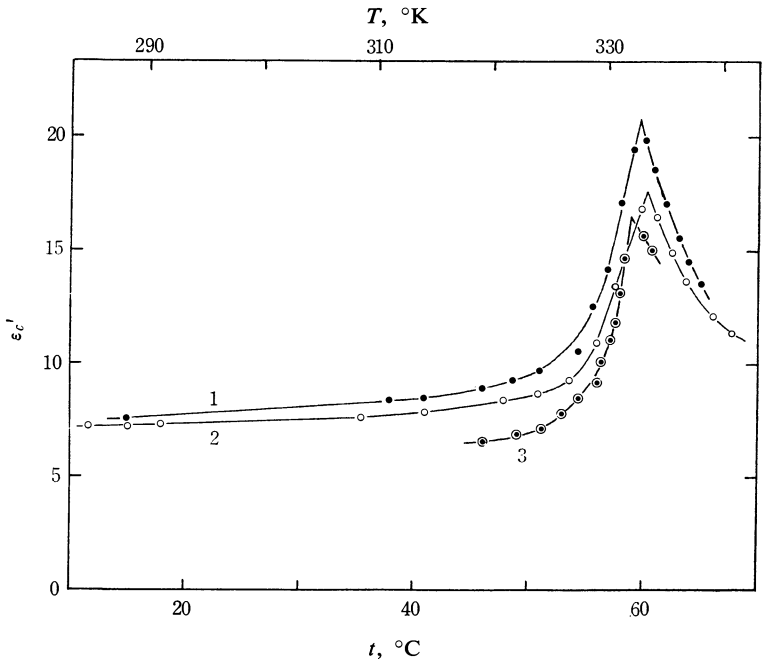



Fig. 4. Frequency dependence of dielectric constant of $PbCa_2(CH_3CH_2CO_2)_6$ (parallel to c-axis).
Curve 1: 300 c.p.s. Curve 2: 1 kc.p.s. Curve 3: 10 kc.p.s.

calorimetry, as has been mentioned above. The discrepancy in the transition temperatures found by these two methods may be due to thermal hysteresis, accompanied by a phase transition. The crystals were shattered below this temperature, and measurements in the heating direction were not possible.

No anomalous dispersion was observed in the temperature region from that of liquid nitrogen to room temperature. On further heating, we found another anomaly, around 60°C, in both directions; it is more prominent when the electric field is perpendicular to the (001) plane. The maximum temperature of the $\varepsilon'$ seems to be independent of the frequency, as is shown in Fig. 4.

With regard to this dielectric anomaly, further study was made by use of a dielectric hysteresis bridge,[12] but no hysteresis phenomenon characteristic of ferroelectricity and/or antiferroelectricity was detected either above or below this transition point. For the lower transition (183°K), no such experiment was attempted, because it has already been shown by Remeika that the crystal is not ferroelectic below room temperature.[13]

**The Thermal Expansion of $PbCa_2(CH_3CH_2CO_2)_6$.**—The results of the dilatometry of the lead salt are shown in Fig. 5. A conspicuous change in the expansion coefficient was detected at about 58°C, a change which corresponds to the anomaly found by the dielectric method. The shape of the change is indicative of what is called a higher-order transition.

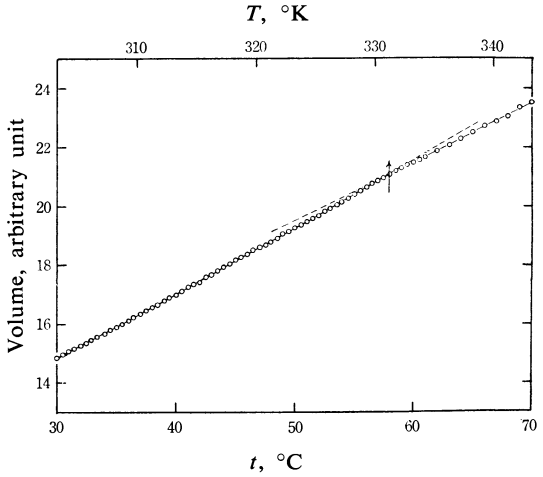



Fig. 5. Volume expansion of $PbCa_2(CH_3CH_2CO_2)_6$.

## Discussion

**$SrCa_2(CH_3CH_2CO_2)_6$.**—As the crystal structure is not precisely known, it seems difficult to propose a detailed molecular mechanism of

12) H. Diamant, K. Drenck and R. Pepinsky, *Rev. Sci. Instr.*, **28**, 30 (1957).
13) F. Jona and G. Shirane, "Ferroelectric Crystals," Pergamon Press, Oxford (1962), p. 357.

TABLE V. TRANSITION TEMPERATURES AND CRYSTALLINE DATA

| Substance | $T_t$, °K | Phase | Symmetry | Space group |
|---|---|---|---|---|
| $SrCa_2(C_2H_5CO_2)_6$ | 282.6 | III | tetragonal | $D_4^4$–$P4_12_12_1$ or $D_4^8$–$P4_32_12$ |
| | 104.2 | II | tetragonal | $C_4^4$–$P4_3$ or $C_4^3$–$P4_2$ |
| | | I | — | — |
| $PbCa_2(C_2H_5CO_2)_6$ | 333 | III | — | — |
| | 191.5 | II | tetragonal | $D_4^4$–$P4_12_12$ or $D_4^8$–$P4_32_12$ |
| | | I | tetragonal | $C_4^4$–$P4_3$ or $C_4^3$–$P4_2$ |
| $BaCa_2(C_2H_5CO_2)_6$ | 266.9 | II | cubic | $O^4$–$F4_13$ |
| | | I | — | — |

the ferroelectric phase transition. However, by a comparison of the crystalline data given in Table V with those for the barium salt, of which a much more precise X-ray analysis has been carried out, and also from the behavior of the heat capacity curve, it would be reasonable to assume for the strontium salt a kind of orientational order-disorder transition with respect to the methyl groups in the propionate anions.

In the room temperature phase, each methyl group must be found at two equivalent positions with an equal probability in order to satisfy the required two-fold symmetry about the axis connecting the carboxyl- and the $\alpha$ carbon atoms. Figure 6 illustrates one of the possible models assumed for this modification, the orientational disorder of the methyl groups being indicated by broken lines.

For the lower temperature phase, only the space group has been determined by Kobayashi and Yamada.[7] However, it would be plausible to consider that such disorder would gradually disappear as the absolute zero of temperature is approached. Thus, in the ordered state, each methyl group will be located in only one of the crystallographically equivalent sites of the two possible orientations (broken lines) depicted in Fig. 6(b).

If these two different structures are assumed for the higher and the lower temperature phases, the phase transition between them may be treated, as a first approximation, by the Bragg-Williams theory. According to this theory, with $T_t=282.6$°K determined by calorimetry, the potential difference between the two possible sites of a methyl group becomes 560 cal. mol$^{-1}$. As both the upper and the lower temperature phases have a tetragonal symmetry, it may be anticipated that, among the six propionate anions in the unit cell, only four, those in which the $C_{carboxyl}$–$C_\alpha$ axes are in the c-plane of the crystal, contribute to the phase transition. The height of the jump in heat capacity and the entropy change associated with the transition can be obtained theoretically, the values being calculated to be 11.9 cal. mol$^{-1}$ deg$^{-1}$ and 5.5 e.u. respectively. The experimental values are, on the other hand, 5.7 cal. mol$^{-1}$ deg$^{-1}$ and 0.6 e.u. for the heat capacity jump and the entropy of transition. The agreement beween the theoretical and the experimental values is thus not very good; this suggests that the short range or other correlations, including the heavy atoms, should be taken into consideration in a more detailed discussion.

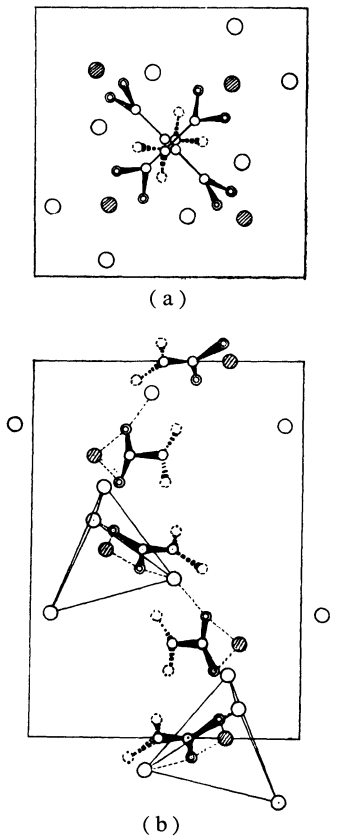



Fig. 6. Crystal structure of $SrCa_2(C_2H_5CO_2)_6$.
(a) (001) projection, (b) (100) projection
Sr Ca C O

In the next place, we should like to proceed to the problem of the temperature dependence

of the spontaneous polarization, $P_s$. The greater part of the $P_s$ value may arise from the displacement of the metallic cations relative to the negative propionate anions, and by the electronic polarization of the large oxygen atoms. However, it seems reasonable to assume as the 1st approximation, that, each propionate anion having a small dipole moment, the change in the direction of this dipole moment, accompanied by some kind of motion in the methyl group, reflects the change in the macroscopic $P_s$ value. The motions responsible for the effective change in this quantity may be assumed to consist of the torsional oscillation of the methyl group about the $C_{carboxyl}$–$C_\alpha$ axis, and also of the population difference between the two possible sites of the methyl groups mentioned above. Here we may assume that the magnitude of a dipole moment of one propionate anion, $\mu_0$, at absolute zero will decrease to $\mu_0 \cos\theta$ when the methyl group of the anion rotates about the $C_{carboxyl}$–$C_\alpha$ axis through an angle, $\theta$, around its equilibrium position at elevated temperatures. In the simple harmonic approximation, the potential function, $U$, is represented by $U=1/2\,\kappa\theta^2$; where $\kappa$ is the effective force constant for the torsional oscillation of the methyl group. According to classical statistical mechanics, the mean value of the dipole moment at a given temperature, $T$, $\overline{\mu_{vib}(T)}$, is given by:

$$\overline{\mu_{vib}(T)} = \frac{\int \mu_0 \cos\theta \exp(-U/\boldsymbol{k}T)\,d\theta}{\int \exp(-U/\boldsymbol{k}T)\,d\theta} = \frac{\int \mu_0 \cos\theta \exp(-\kappa\theta^2/\boldsymbol{k}T)\,d\theta}{\int \exp(-\kappa\theta^2/\boldsymbol{k}T)\,d\theta} = \mu_0 \exp(-\boldsymbol{k}T/2\kappa) \quad (1)$$

where $\boldsymbol{k}$ is the Boltzmann constant; the kinetic part of the partition function was not considered because it is not relevant to the present discussion.

Another contribution which decreases the mean value of the dipole moment comes from the inversion of the moment due to the order-disorder transition. In the Bragg-Williams approximation, an order parameter $x$ is introduced which varies from unity at completely ordered, to zero at completely disordered, states. Therefore, the probability of the moment being in one of the positions is given by $(1/2)(1+x)$, and that of its being in the other, inverse, position, by $(1/2)(1-x)$.

If the contributions from the torsional oscillation, as well as from the order-disorder transition, are taken into account, the effective dipole moment at $T$°K is represented by:

$$\overline{\mu(T)} = \mu_0 \exp(-\boldsymbol{k}T/2\kappa)\{1/2(1+x) - 1/2(1-x)\} = \mu_0 x \exp(-\boldsymbol{k}T/2\kappa) \quad (2)$$

where the force constant for the torsional osillation is assumed to be the same for the two sites of the methyl group. The macroscopic spontaneous polarization, $P_s(T)$, at $T$°K becomes:

$$P_s(T) = N\mu_0 x \exp(-\boldsymbol{k}T/2\kappa) = P_s(0)x \exp(-\boldsymbol{k}T/2\kappa) \quad (3)$$

by the use of Eq. 2, where $N$ is the number of those propionate anions per unit volume that have their $C_{carboxyl}$–$C_\alpha$ axes in the c-plane, and where $P_s(0)$ is the spontaneous polarization at absolute zero.

The value of $\kappa$ was evaluated semi-quantitatively from Eq. 3, using the $P_s(0)=0.6$ coulomb $cm^{-2}$ value obtained by the extrapolation of the experimental $P_s$ vs. $T$ curve[5,7] to absolute zero, and fitting the theoretical $P_s(T)$ to the experimental data at 188°K or at 262°K. The values obtained are 1.1 and $1.6\cdot10^{-3}$ md. $Å^{-1}$ respectively. Figure 7 shows the experimental[5,7] and the theoretical $P_s$ curves calculated for these two $\kappa$ values (curves 1, 2 and 3). The agreement of the experimental and the theoretical curves is fairly good if the difficulties in the accurate measurement of the spontaneous polarization are taken into account.

Now that the force constant, $\kappa$, and $\overline{\mu_{vib}(T)}$ have been obtained, we may discuss the mean maximum amplitude of the torsional oscillation of the methyl groups at each temperature on the basis of classical statistical mechanics. If the mean maximum amplitude of oscillation is represented by $\theta_1$, the mean value of the dipole moment, $\overline{\mu_{vib}(\theta_1)}$, can be given as follows:

$$\overline{\mu_{vib}(\theta_1)} = \int_{-\theta_1}^{+\theta_1} \mu_0 \cos\theta \cdot p(\theta)\,d\theta \Big/ \int_{-\theta_1}^{+\theta_1} p(\theta)\,d\theta = \mu_0 \cdot J_0(\theta_1) \quad (4)$$

where $p(\theta)$ is the probability of the dipole being rotated by an angle, $\theta$, and $J_0(\theta_1)$ the Bessel function of zeroth order. It may easily be shown that $p(\theta)$ is proportional to $(\theta_1^2-\theta^2)^{-1/2}$. By setting $\overline{\mu_{vib}(\theta_1)}$ to be equal to $\overline{\mu_{vib}(T)}$ in Eq. 1, $\theta_1$ can be calculated for each temperature. The results of the calculation for the two $\kappa$ values are shown in Fig. 7 (curves 4 and 5). The force onstant, $\kappa$, and the mean amplitude, $\theta_1$ will be discussed in a following paper.

The features of the newly-found phase transition of this crystal at 104°K were described

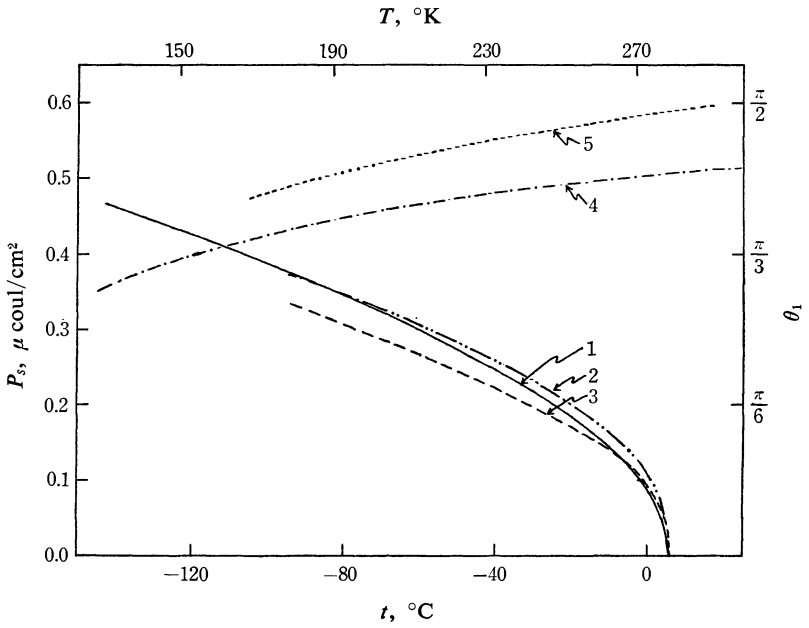



Fig. 7. Spontaneous polarization and maximum amplitude of torsional oscillation of the methyl groups in $SrCa_2(CH_3CH_2CO_2)_6$.

Curve 1: $P_s$, experimental (See refs. 5 and 7)
Curve 2: $P_s$, theoretical, fitted at 188°K
Curve 3: $P_s$, theoretical, fitted at 262°K
Curve 4: $\theta_1$, calculated from curve 2
Curve 5: $\theta_1$, calculated from curve 3

in the previous section. Recently, Kobayashi informed us that there is a slight, discontinuous change in $P_s$ values at about −177°C.[14] However, more detailed analyses for this transition phenomenon will require other experimental data, especially on the crystal structure of the lowest temperature phase.

**$PbCa_2(CH_3CH_2CO_2)_6$.** — In this salt, the enthalpy and entropy changes for the phase transition at 191.5°K are larger than those of the strontium salt, and it is noticeable that the value of $\Delta S_t = 5.8$ e.u. is rather close to that for the barium salt[4] (see Table IV).

If the mechanism assumed for the strontium and barium salts also applies to this salt, the calculated value of the entropy of transition, 5.5 e.u., agrees fortuitously well with the experimental value of 5.8 e.u.

The phase transition at about 60°C found by dielectric and dilatometric measurements may be due to some displacement of the metallic ions,* but no detailed discussion can be made at present.

No possibility of the appearence of ferroelectricity in the lead- and barium salts has been confirmed by Remeika below room temperature,[13] or by the present work for the phase above 60°C. The considerable difference between the dielectric properties of the strontium salt and those of the lead salt as well as of the barium salt is difficult to interpret from only the standpoint of the motions of the propionate anions assumed in the present paper.

A detailed discussion of the difference in the behavior of the propionate anions in these salts will be made in the following paper.

14) J. Kobayashi, Private communication.

* A preliminary X-ray analysis was undertaken for a powdered specimen of the lead salt, above 60°C; it was thus found that the symmetry of the phase is lower than cubic.

## Summary

Heat capacities have been measured for strontium and lead dicalcium propionates from 15 to 300°K with an adiabatic-type calorimeter in connection with the ferroelectric phase transition of strontium salt. The heat capacities, enthalpies, entropies and Gibbs energy functions in the standard state have been determined. For the strontium salt, the transition temperature, the heat of transition, and the entropy of transition for the ferroelectric phase transition are 282.6°K, 159.6 cal. $mol^{-1}$, and 0.6 e.u. respectively. Another phase transition was discovered at 104°K; the heat and entropy of this transition amount to 255 cal. $mol^{-1}$ and 3.2 e.u. respectively.

For the lead salt, a phase transition was found at 191.5°K, and the heat and the entropy of the transition are 1160.0 cal. $mol^{-1}$ and 5.8 e.u.

respectively. Low frequency dielectric constants have been measured for the lead salt from the liquid nitrogen temperature to 90°C. A discontinuous change in the dielectric constants at 183°K and another dielectric anomaly at 60°C have been observed. The absence of evidence of ferroelectricity above room temperature has also been confirmed.

The ferroelectric phase transition of the strontium salt has been treated by the Bragg-Williams theory. The temperature dependence of the spontaneous polarization has tentatively been interpreted with torsional oscillations of the methyl groups of the propionate anions.

The authors wish to express their thanks to Professor Jinzo Kobayashi of Waseda University for his helpful discussions, and to Dr. Yasusada Yamada of Osaka University for taking an X-ray photograph of the low temperature modification of the lead salt. They are also grateful to Miss Masako Ohtsuru for her help in the dielectric measurements.

*Department of Chemistry*
*Faculty of Science*
*Osaka University*
*Toyonaka, Osaka*

# NOTES

## The Differentiation of Diastereoisomers of 1-Phenyl-2-acetamidopropane-1-ol Derivatives by Means of the NMR Spectrum

By Haruhisa SHIRAHAMA and Takeshi MATSUMOTO

(Received November 24, 1964)

During the course of studies[1] of the synthesis of 1-phenyl-2-aminopropane-1-ol derivatives, it became disirable to find a simple method for determining whether the 1-phenyl-2-acetamidopropane-1-ol derivatives belonged to the *threo* or the *erythro* series. The differentiation of these isomers by means of the infrared spectrum has been studied by Suzuki and Shindo.[2] In the present paper, we should like to show that these compounds may also be distinguished by their NMR spectra.

The hydroxyl groups of *threo* and *erythro* $\alpha$-glycols have been shown to exhibit in the NMR spectra distinctly different chemical shifts when measured in pyridine - trifluoroacetic acid.[3] Namely, the resonance line arising from the exchanging-hydroxyl group of the threo isomers appears at a higher field than that of the erythro isomer.

A similar comparison of the NMR peaks of *threo* and *erythro* 1-phenyl-2-acetamidopropane-1-ol and 1-phenyl-2-acetamido-3-ethoxypropane-1-ol[1] (Table I) also shows that the peak due to the exchanging-hydroxyl and amide protons in the threo isomer appears at the higher field. Although only two pairs have been measured, this tendency of the threo isomer to

TABLE I

| Sample | Concn. mol. % | Shift[a] c. p. s. |
|---|---|---|
| Solvent (3.80 mol. solution of trifluoroacetic acid in pyridine) | | 375.8 |
| *N*-Acetylnorephedrine (*erythro*) | 1.973 | 230.5 |
| *N*-Acetylnor-$\phi$-ephedrine (*threo*) | 1.973 | 158.7 |
| *erythro*-1-Phenyl-2-acetamido-3-ethoxypropane-1-ol | 0.7305 | 283.1 |
| *threo*-1-Phenyl-2-acetamido-3-ethoxypropane-1-ol | 0.7305 | 204.5 |

a) The NMR spectra were measured on a Varian V 4300 high resolution spectrometer at a fixed frequency of 40 Mc./sec. Shift is relative to the signal of the $\gamma$ proton of pyridine.

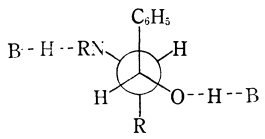
1) T. Matsumoto, T. Nishida and H. Shirahama, *J. Org. Chem.*, **27**, 79 (1962); H. Shirahama and T. Matsumoto, This Bulletin, **38**, 1289, 1293 (1965).,

2) M. Suzuki and H. Shindo, *J. Pharm. Soc. Japan*, **76**, 927 (1956).

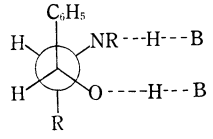
3) S. Fujise, G. Hazato, T. Ikenoue, S. Sasaki and Y. Senda, unpublished results; Y. Senda, M. Sc. Thesis, Tohoku University (1958). Our thanks are due to Dr. Tsuneo Ikenoue, Tohoku University, for informing us of these results prior to publication and for his valuable discussions. For the concentration shift of *threo* and *erythro* $\alpha$-glycols in pyridine and in acetic acid, see S. Fujise, G. Hazato, T. Ikenoue, S. Sasaki and Y. Senda, This Bulletin, **25**, 1742 (1962).

exhibit its resonance peak at higher fields is presumably quite general, since similar results have been obtained, without exception, with the eight $\alpha$-glycols so far examined.[3]

An explanation for the above findings may be added here, although it is only tentative. The chemical shift of an exchanging proton depends on the time-averaged environment of the active hydrogen. Assuming that all proton exchanges take place by way of hydrogen-bonded structures,[4] the interaction between the most stable form of each acetamido alcohol and surrounding species can be illustrated as follows:[5]




erythro



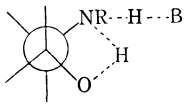

threo

The interaction is clearly more effective in the *erythro* isomer, and, therefore, the exchangeable proton in the erythro form is more deshielded.

*Department of Chemistry*
*Faculty of Science*
*Hokkaido University*
*Sapporo*

4) J. A. Pople, W. G. Schneider and H. J. Bernstein, "High Resolution Nuclear Magnetic Resonance," McGraw-Hill Book Company, New York (1959), See. 15-6 and p. 441.

5) B represents one of pyridine, trifluoroacetate ion and trifluoroacetic acid. The species with an intramolecular hydrogen bond, as illustrated below, may be neglected in a pyridine-trifluoroacetic acid solution.



# The Synthesis and Polymerization of β-Propiolactam and α-Phenyl-β-propiolactam

By Toshiyuki KODAIRA, Hideo MIYAKE*, Koichiro HAYASHI and Seizo OKAMURA

(Received November 25, 1964)

There have been several reports concerning the polymerization of α, β-substituted[1] or *N*-substituted[2] β-propiolactam. In this note, the syntheses and polymerizations of unsubstituted β-propiolactam and α-phenyl-β-propiolactam will be reported. It was found by the present study that, in the presence of such anionic catalysts as butyl lithium, sodium methoxide or potassium hydroxide, β-propiolactam and α-phenyl-β-propiolactam polymerized easily in dimethyl sulfoxide (DMSO) under mild conditions, as is shown in Tables I and II. However, a cationic catalyst, boron trifluoride, was not effective for the polymerization. Further, it was observed that the polymerization of unsubstituted lactam took place rapidly in DMSO, but very slowly when it was polymerized in the solid state. The polymer yield was slightly influenced by the reaction temperature when polymerization was carried out in DMSO (Fig. 1 and Fig. 2).

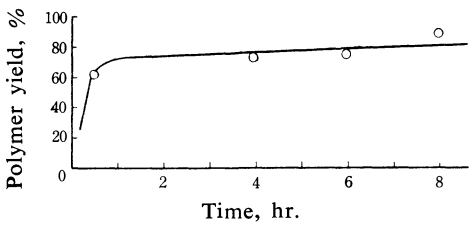



Fig. 1. Polymerization of 3-phenyl-β-propiolactam.
(M) : 3.16 mol./l.
(BuLi) : $4.3\times10^{-3}$ mol./monomer mol.
Solvent : DMSO, Temp. : 25°C

The polymerizability of β-propiolactam was larger than that of α-phenyl-β-propiolactam because of the electron-donating character of the phenyl substituent.

The infrared spectra of both polymers had characteristic absorption bands attributable to NH linkage (3300 $cm^{-1}$) and to the poly-amide structure (1655 $cm^{-1}$). The infrared spectrum of poly-β-propiolactam agreed well with those

* Present address: Chalmers Tekniska Högskala Institutinen för Organisk Kemi, Gibraltargatan 5A, Göteborg S., Sweden.

1) R. Graf, G. Lohaus, K. Börner, E. Schmidt and H. Bestian, *Angew. Chem.*, 74, 523 (1962).

2) T. Kagiya, H. Kishimoto, S. Narusawa, T. Sano and K. Fukui, The Symposium of Rubber and High Polymers, Nagoya, November, 1963.

Table I. Polymerization of β-propiolactam

| No. | Cat. | Solvent | (M) mol./l. | (C) mol./mol. | Temp. °C | Polymerization time, min. | Conv. % |
|---|---|---|---|---|---|---|---|
| 1 | BuLi | DMSO | 0.17 | $5.4\times10^{-3}$ | 30 | 20 | 35.7 |
| 2 | BuLi | DMSO | 0.18 | $5.3\times10^{-3}$ | 60 | 5 | 25.7 |
| 3 | BuLi | Ether | 0.071 | $4.3\times10^{-3}$ | 30 | 40 | 0.7 |
| 4* | BuLi | Ether | 0.25 | $5.3\times10^{-3}$ | 30 | 40 | 0.6 |
| 5* | BuLi | Toluene | 0.23 | $4.0\times10^{-3}$ | 30 | 40 | 0.5 |
| 6** | $CH_3ONa$ | DMSO | 0.23 | $9.5\times10^{-2}$ | 30 | 40 | 40.8 |
| 7** | KOH | DMSO | 0.23 | $7.8\times10^{-2}$ | 30 | 40 | 36.8 |
| 8 | $BF_3OEt_2$ | $CH_2Cl_2$ | 2.25 | $5.0\times10^{-2}$ | 30 | 300 | ~0 |

* Solid state polymerization ** Heterogeneous catalyst

Table II. Polymerization of 3-phenyl-β-propiolactam

| No. | Cat. | Solvent | (M) mol./l. | (C) mol./mol. | Temp. °C | Polymerization time, min. | Conv. % |
|---|---|---|---|---|---|---|---|
| 9 | BuLi | DMSO | 0.23 | $1.22\times10^{-2}$ | 30 | 80 | 20.6 |
| 10 | BuLi | DMSO | 3.16 | $4.3\times10^{-3}$ | 30 | 20 | 70.2 |
| 11 | BuLi | DMSO | 0.23 | $1.22\times10^{-2}$ | 60 | 5 | 6.5 |
| 12* | BuLi | Ether | 0.23 | $1.22\times10^{-2}$ | 30 | 40 | 1.0 |
| 13* | BuLi | *n*-Hexane | 0.23 | $1.22\times10^{-2}$ | 30 | 20 | 0.5 |
| 14* | BuLi | Toluene | 0.23 | $1.22\times10^{-2}$ | 30 | 40 | 0.3 |
| 15** | $CH_3ONa$ | DMSO | 0.23 | $9.1\times10^{-2}$ | 30 | 40 | 71.4 |
| 16** | KOH | DMSO | 0.23 | $12.9\times10^{-2}$ | 30 | 40 | 42.5 |
| 17 | $BF_3OEt_2$ | $CH_2Cl_2$ | 1.87 | $5.0\times10^{-2}$ | 30 | 300 | ~0 |

* Solid state polymerization ** Heterogeneous catalyst

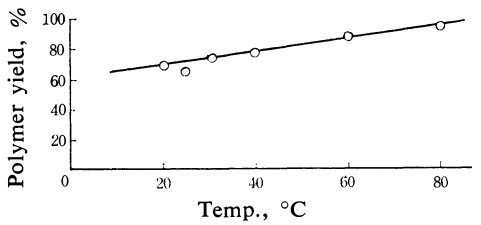



Fig. 2. Polymerization of 3-phenyl-β-propiolactam, influence of polymerization temperature.
(M) : 3.16 mol./l.
(BuLi) : $4.3\times10^{-3}$ mol./monomer mol.
Solvent: DMSO, Polym. time: 20 min.

of the polymer obtained from the polycondensation reaction of dithiocarbonylethoxy-dicarbonyl-β-alanine.[3] Further, the polymers had higher melting points (>300°C) and larger viscosities (the $[\eta]$ values were 0.7—1.0 in a 0.5% dichloroacetic acid solution at 35°C) than those of the polymers obtained by poly-condensation[3] or by the hydrogen-transfer polymerization of acryl-amide.[4]

The results of the X-ray diffraction diagram show that the poly-β-propiolactam has a higher crystalline structure ($2\theta$: 18°46′, 26°26′, 28°40′ and 32°6′), while poly-α-phenyl-β-propiolactam has a lower one, because of the bulky substituent of the phenyl group.

## Experimental

**The Synthesis of β-Propiolactam.** — β-Alanine-ethyl ester hydrochloride (I) was prepared from β-alanine by a method similar to that used for the synthesis of α-alanine-ethyl ester hydrochloride.[5] It was recrystallized from a chloroform-ether mixture.[6] Yield 93%, m. p. 64—65°C. The β-Alanine-ethyl ester was prepared from I by a procedure similar to that used for the glycine derivative.[7] Yield 32%, b. p. 58°C/14 mmHg. β-Propiolactam (m. p. 74—75°C) was synthesized by the method of Holley.[8] The synthesis of 3-phenyl-β-propiolactam (m. p. 119—120°C) followed the method of Testa.[9] The polymerizations were carried out under a dry nitrogen stream, and the polymers obtained were precipitated in methanol.

*Department of Polymer Chemistry*
*Faculty of Engineering*
*Kyoto University*
*Sakyo-ku, Kyoto*

3) H. Kato, K. Suzuoki, T. Higashimura and S. Okamura, unpublished results.
4) N. Ogata, This Bulletin, **33**, 906 (1960), *Makromol. Chem.*, **40**, 55 (1960).
5) S. D. Brewer and R. M. Herbst, *J. Org. Chem.*, **6**, 870 (1941).
6) W. J. Hale and E. M. Honan, *J. Am. Chem. Soc.*, **41**, 774 (1919).
7) E. Fischer, *Ber.*, **34**, 436 (1901).
8) W. Holley and Am. D. Holley, *J. Am. Chem. Soc.*, **71**, 2129 (1949).
9) E. Testa, F. Fava and L. F. Liebig, *Ann. Chem.*, **614**, 167 (1958).

# Basic Bile Acids. IV. On the Syntheses of 7β-Amino-, 12α-Amino-, and 3α-Hydroxy-12α-aminocholanic Acid and Their Derivatives*1

By Yasuo SATOH

(Received November 5, 1964)

In the previous papers of this series,[1] the syntheses and properties of 3α-, 3β-, 7α-, and 12α-aminocholanic acid and their derivatives have been reported. The present paper will describe the syntheses of 7β-amino-, 12α-amino-,*2 and 3α-hydroxy-12α-aminocholanic acid and their derivatives.

Derivatives of 7β- and 12α-aminocholanic acid were synthesized from the oximes of each ketone by reduction with sodium and *n*-propanol. Moreover, as a basic bile acid containing a hydroxyl group, 3α-hydroxy-12α-aminocholanic acid was synthesized. For the synthesis of this basic bile acid, deoxycholic acid was chosen as the starting material, and the reduction of the oxime was carried out according to the methods described for the cases of the 3-, 7-, and 12-positions.[1]

## Experimental*3,*4

**7β-Aminocholanic Acid Hydrochloride (II).***5— Into a boiling solution of 3.5 g. of 7-hydroxyiminocholanic acid (I) in 105 ml. of dried *n*-propanol, 10.5 g. of sodium cut into small pieces was gradually stirred. When all the sodium had been added, 15 ml. of ethanol was slowly added to the reaction mixture through the reflux condenser until the few remaining pieces of sodium had completely reacted. After the reaction mixture had then stood for 14 hr. at room temperature, 90 ml. of water was added, the separated lower layer was taken off, and 220 ml. of water was added to the upper layer. The solution, now consisting of two layers, was acidified with hydrochloric acid (1 : 1) and concentrated to half-volume under reduced pressure, and then this solution was cooled. The resultant crystals were collected, washed with water, and dried. The yield of a slightly brownish amorphous substance was 3.17 g. Attempts to crystallize the hydrochloride were unsuccessful, and so it was used for the next step without purification. IR (KBr disk): 3440, 1721, 1602 and 1508 $cm^{-1}$.

**Methyl 7β-Aminocholanate Hydrochloride (III).** —This substance was prepared according to the procedure described earlier for the synthesis of the 7α-isomer.[1] The crystallization of the resultant solid from methanol - petroleum ether gave 1.92 g. of the methyl ester from 2.7 g. of II; colorless plates, m. p. 248.5—249.5°C (which changed to needles at about 204°C), and $[\alpha]_D^{25}$ +28.5° (*c* 2.01, methanol). IR (KBr disk): 3250, 1742, 1604, 1508, and 1170 $cm^{-1}$.

**Methyl 7β-Acetamidocholanate (IV).** — The synthesis of this substance was carried out using the technique described for the synthesis of the 7α-isomer.[1] Attempts to crystallize the acetamido derivative from the ether extracts were unsuccessful. IR (KBr disk): 3264, 1732, 1636, 1559, and 1164 $cm^{-1}$.

When the syrupy material was submitted to thin-layer chromatography on Wako-gel B-5 (thickness, 0.5 mm.) with benzene-ether (1 : 2), a spot at 0.3 in $R_f$ value and another weak spot at the original point were observed. Therefore, the above-described syrupy substance was subjected to separation using a large-area layer (20×20 $cm^2$; thickness, 0.5 mm.). A separated band, which was detected with concentrated sulfuric acid, was scraped off and extracted with warm methanol. The methanolic solution was filtered, and the filtrate was evaporated under reduced pressure. Crystallization of the residue from benzene - petroleum ether afforded a crude acetamido derivative, m. p. 115—117°C; yield 165 mg. Two crystallizations of this substance from the same solvent raised the melting point to 120—121°C; $[\alpha]_D^{20}$ +22.0° (*c* 1.01, chloroform). IR (KBr disk): 3260, 1745, 1638, 1557, and 1165 $cm^{-1}$.

Found: C, 75.05; H, 10.48; N, 3.20. Calcd. for $C_{27}H_{45}O_3N$: C, 75.12; H, 10.51; N, 3.26%.

**12α-Aminocholanic Acid Hydrochloride (VIm).**— This substance was prepared according the procedure described above for the synthesis of the 7β-isomer (II). The crystallization of the resultant solid from methanol gave 2.86 g. of the amino acid hydrochloride from 3.3 g. of the oxime (V) of 12-ketocholanic acid; m. p. 285.5—287°C, $[\alpha]_D^{25}$ +42.9° (*c* 1.89, ethanol). IR (KBr disk): 3432, 1702, 1611, and 1521 $cm^{-1}$.

The melting point of this derivative was not depressed by admixture with a sample VIc prepared by the catalytic reduction of the oxime,[1] and this derivative was identical in infrared spectrum with a sample of VIc.

When the oxime was reduced with sodium and ethanol, the amino derivative formed was identical with a specimen of VIm.

---

*1 Presented at the Local Meeting of the Chemical Society of Japan, Morioka, September, 1964.

*2 The method of the synthesis of this derivative used here differs from that of the previous work.

1) Y. Satoh and A. Hagitani, *J. Chem. Soc. Japan, Pure Chem. Sec.* (*Nippon Kagaku Zasshi*), **80**, 1310 (1959); Y. Satoh, ibid., **84**, 829 (1963); **85**, 54 (1964).

*3 All melting points are uncorrected.

*4 The infrared absorption spectra were measured with a Shimadzu model IR-27B infrared spectrophotometer.

*5 This compound is an epimer of the 7-amino derivative described in our previous paper.[1]

**Methyl 12α-Aminocholanate Hydrochloride (VII).**—This substance was prepared according to the procedure described earlier for the synthesis of the 7α-isomer.[1] The crystallization of the resultant solid from methanol gave 810 mg. of the methyl ester from 1 g. of VIm; m. p. 205.5—207°C, $[\alpha]_D^{25}$ +40.1° (*c* 1.00, ethanol). IR (KBr disk): 3220, 1730, 1605, and 1521 $cm^{-1}$. No depression in melting point was observed upon its admixture with a sample prepared by the catalytic reduction of the oxime.[1]

**Methyl 12α-Acetamidocholanate (VIII).**—The synthesis of this substance was carried out using the technique described for the synthesis of the 7α-isomer.[1] Two-hundred and forty-four milligrams of this substance (octagonal crystals; m. p. 231—232°C, $[\alpha]_D^{28}$ +29.1° (*c* 2.00, chloroform) was obtained from 500 mg. of VII. The melting point of this substance was not depressed by admixture with methyl 12α-acetamidocholanate derived from the oxime by catalytic reduction.[1] IR (KBr disk): 3272, 1735, 1636 and 1554 $cm^{-1}$.

Found: C, 75.09; H, 10.29; N, 3.20. Calcd. for $C_{27}H_{45}O_3N$: C, 75.12; H, 10.51; N, 3.26%.

**3α-Hydroxy-12-hydroxyiminocholanic Acid (X).**—This preparation followed the general method used for the synthesis of the steroidal ketoxime from 3α-hydroxy-12-ketocholanic acid (IX): m. p. 131—132°C, $[\alpha]_D^{20}$ +149.7° (*c* 0.35, chloroform). IR (KBr disk): 3310, 1704, 1644, and 938 $cm^{-1}$.

**The Synthesis of 3α-Hydroxy-12α-aminocholanic Acid Hydrochloride (XI) from the Oxime.**—*i) Catalytic Reduction.*—The method used here was identical with that described for the 7α-isomer.[1] The crystallization of the residue from methanol yielded 751 mg. of the amino acid from 1 g. of the oxime; m. p. 279—281°C, $[\alpha]_D^{25}$ +51.5° (*c* 0.91, ethanol). IR (KBr disk): 3344, 1708, 1608, and 1518 $cm^{-1}$.

Found: C, 68.01; H, 9.91; N, 3.20; Cl, 8.20. Calcd. for $C_{24}H_{43}O_3NCl$: C, 67.37; H, 9.82; N, 3.27; Cl, 8.30%.

*ii) Reduction with Sodium and n-Propanol.*—This reaction was carried out according to the procedure described above for the synthesis of the 7β-isomer (II). The crystallization of the resultant solid from methanol gave 0.96 g. of the amino acid hydrochloride from 1.6 g. of the oxime; m. p. 280.5—282.5°C, $[\alpha]_D^{25}$ +52.7° (*c* 0.68, ethanol). IR (KBr disk): 3340, 1708, 1609, and 1518 $cm^{-1}$.

Found: C, 67.54; H, 9.82; N, 3.32; Cl, 8.23. Calcd. for $C_{24}H_{42}O_3NCl$: C, 67.37; H, 9.82; N, 3.27; Cl, 8.30%.

The melting point of this derivative was not depressed by its admixture with a sample prepared by method i.

Moreover, when the oxime was reduced with sodium and ethanol, it was found that the product was identical with the samples XIc and XIm*6.

**Methyl 3α-Hydroxy-12α-aminocholanate Hydrochloride (XII).**—This substance, m. p. 255—256°C, $[\alpha]_D^{22}$ +42.7° (*c* 0.35, chloroform), was prepared from XIc and XIm with absolute methanol and dry hydrogen chloride gas. IR (KBr disk): 3344, 1723, 1613, and 1529 $cm^{-1}$. The mixed melting point of the two esters was 254—256°C.

Found: C, 68.20; H, 9.83; N, 3.26; Cl, 7.95 (XIIc) and C, 68.06; H, 9.87; N, 3.19; Cl, 7.91 (XIIm). Calcd. for $C_{25}H_{44}O_3NCl$: C, 67.95; H, 9.97; N; 3.17; Cl, 8.04%.

**Methyl 3α-Acetoxy-12α-acetamidocholanate (XIII).**—This derivative, m. p. 248—249°C, $[\alpha]_D^{25}$ +111.9° (*c* 2.10, chloroform), was prepared from XIIc and XIIm with acetic anhydride and absolute pyridine by heating it for 4 hr. at 100°C. The mixed melting point of XIIIc and XIIIm was 247.5—249°C. IR (KBr disk): 3260, 1723, 1632, 1550, and 1250 $cm^{-1}$ (XIIIc); 3263, 1722, 1632, 1551, and 1251 $cm^{-1}$ (XIIIm).

Found: C, 71.39; H, 9.51; N, 2.86 (XIIIc) and C, 71.37; H, 9.56; N, 2.88 (XIIIm). Calcd. for $C_{29}H_{47}O_5N$: C, 71.17; H, 9.61; N, 2.86%.

The author is grateful to Professor Akira Hagitani of St. Paul's University for many helpful discussions and suggestions during this work; thanks are to be given to Miss Itsuko Sano and Mr. Akira Satomura for their assistance in the experimental work.

*Department of Chemistry*
*Faculty of Science*
*St. Paul's University (Rikkyo Daigaku)*
*Toshima-ku, Tokyo*

*6 XIc and XIm are samples prepared by the methods i and ii respectively.

# The Extraction of Thallium(III) from Hydrochloric Acid Solutions with Ethyl Acetate

By T. N. Srivastava and D. C. Rupainwar

(Received December 14, 1964)

The extraction of thallium(III) from hydrochloric acid solutions into ether and other organic solvents has been reported by several investigators.[1-4] It has been developed into an analytical method for the separation of thallium from most elements, excepting iron(III), gallium(III), gold(III), and a few others. Irving and Rossotti,[5] while studying the extraction of indium(III) from hydrochloric acid solutions, have given a comparative account of the extraction of the $HMX_4$ species (M= $Ga^{3+}$, $In^{3+}$, $Fe^{3+}$, $Au^{3+}$; X=Cl, Br, I) with various organic solvents, including ethyl acetate. However, no information is available on the extraction of the corresponding halothallic acids ($HTIX_4$). The present communication will give the details of the extraction of thallium(III) from its solutions in hydrochloric acid, using ethyl acetate as an extracting solvent.

## Experimental

Stock solutions of thallic chloride were prepared by dissolving freshly-precipitated thallium(III) oxide in hydrochloric acid solutions of the desired strength.

Ethyl acetate (British Drug House) was distilled once and used in that form. All the other reagents and solutions were prepared from "Analar" compounds, and their concentrations were ascertained by conventional methods.

Known volumes of an aqueous thallic chloride solution of the desired strength in hydrochloric acid of an appropriate concentration were shaken for a constant time (1 min.) with an equal volume of ethyl acetate (pre-equilibriated with acid of a corresponding strength), in a glass-stoppered measuring cylinder. The layers were allowed to separate, and the final volumes were recorded. Known aliquots from the organic and the aqueous layers were withdrawn and analysed volumetrically for their thallium and chloride contents.

1) H. M. Irving, *Quart. Revs.*, **5**, 200 (1951).
2) H. M. Irving and F. J. C. Rossotti, *Analyst*, **77**, 2440 (1957).
3) D. L. Horrocks and A. F. Voigt, *J. Am. Chem. Soc.*, **79**, 2440 (1957).
4) K. S. Venkateswarlu and P. C. Das, *J. Inorg. & Nuclear Chem.*, **25**, 730 (1963).
5) H. M. Irving and F. J. C. Rossotti, *J. Chem. Soc.*, 1955, 1906, 1918.

## Results and Discussion

**Optimum Conditions for Extraction.**—The extraction yield of thallium(III) at 1.0 N hydrochloric acid was found to be as high as 72%; the percentage extraction and the distribution coefficient increase gradually with an increase in the acid concentration, attain a maxima at 6.0 N hydrochloric acid, and then fall to a lower value (Fig. 1). As the changes in the phase miscibility, due to the hydrolysis of ethyl acetate, are relatively small up to 6.0 N hydrochloric acid, the experimental conditions at this stage correspond approximately to the ideal state, but at a higher concentration of the acid, the hydrolysis of the ester becomes significant and the volume of the organic layer decreases. This consequently brings about a decrease in the activity of the extractable species, and results in the lower values for the percentage extraction and the distribution coefficient.

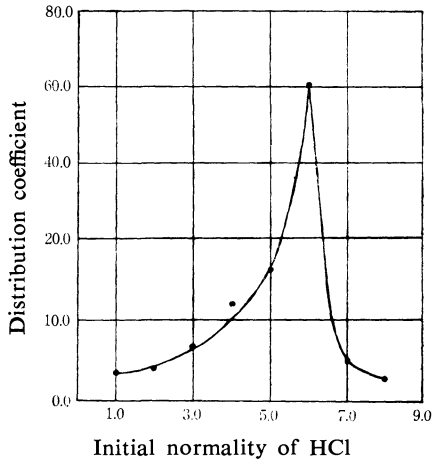



Fig. 1. Distribution of thallium(III) between ethyl acetate and hydrochloric acid.

**The Nature of the Extracted Species.**—The empirical formula of the extracted species corresponds to $HTICl_4$, because almost equimolar quantities of thallic chloride and hydrogen chloride are extracted from aqueous solutions containing less than 6.0 N hydrochloric acid.

Beyond this concentration, an increasingly greater quantity of hydrochloric acid is co-extracted. This fact cannot be attributed to the formation of a thallium complex with a larger amount of hydrochloric acid, e. g., $H_2TlCl_5$, as this species has already been shown by Horrocks and Voigt[3] to be inextractable. A plausible explanation may be a salting-out effect of thallium(III).

**The Effect of the Metal Concentration.**—The studies of the extraction of thallium(III) at various concentrations in 6 N hydrochloric acid solutions have shown that the percentage extraction and the distribution coefficient increase with the increase in the concentration of the metal. This may be due to a self-salting-out effect caused by thallium(III) itself, similar to that reported for the extraction of gallium(III) and iron(III) from hydrochloric acid solutions.[6] The mechanism of this phenomenon may be explained by assuming the formation of $[Tl(H_2O)_6]^{3+}$ ions in more concentrated solutions of thallium, which replace the protons in the species $[H^+(TlCl_4)]$, thereby giving enhanced values of the distribution coefficient and of the percentage extraction.

**Salting-out Effects.**—The extraction of thallium(III) from its solution in 2 N hydrochloric acid and in the presence of 1.0 M $MCl_x$ (where M=Li, Na, K, $NH_4$, Ca, Mg, and Al, and $x$, the valency of the cation) was studied. The presence of metal chloride results in a considerable increase in the percentage extraction and distribution coefficient. When univalent chlorides were used, the distribution coefficient followed the order Li>K—Na>$NH_4$. For other metal chlorides, an order of the Li>Al >Mg>Ca>$NH_4$ type is obtained. This may be attributed to the relative differences in the water activity in the presence of these cations. Lithium, being the most strongly hydrated, has the greatest effect.

**The Effect of the Dilution of the Solvent.**—Ethyl acetate diluted with such solvents as petroleum ether (B. range 85—100°C), benzene, chloroform and carbon tetrachloride was employed for the extraction of thallium(III). The results indicate that the distribution coefficient decreases with the increasing molar polarisation of the diluent. This happens to be in conformity with a generalisation given previously.[7]

A plot of the log of the distribution coefficient against the log of the concentration of ethyl acetate did not give a definite value of $n$, the solvation number. It appears that the solvation of the metal varies significantly with the extent of dilution; hence, a definite stiochiometric ratio can not be obtained.

**The Separation of Thallium(III) from $Al^{3+}$, $Ga^{3+}$, and $In^{3+}$.**—Experimentation on other metals of the III-B group has, however, shown that the extraction percentages of aluminum, gallium and indium are 0, 96.7, and 3.72 respectively at an initial hydrochloric acid concentration of 6.0 N. Aluminum does not from a tetrahedral-extractable species of the chloride complex in an aqueous solution, while indium under similar conditions shows a marked tendency to remain predominantly octahedral[7]; hence, very low values for the percentage extraction are obtained.

The fact that thallium(III) is extracted by 72.26% at a 1.0 N hydrochloric acid concentration, at which concentration gallium and indium are only negligibly extracted, has been utilised in separating it from these two metals. A batch-by-batch extraction with ethyl acetate at 1.0 N hydrochloric acid effects a quantitative separation of thallium from other members of the III-B group. The presence of other metals, particularly aluminum, on the other hand, results in a salting-out effect of thallium and enhances the percentage extraction.

## Summary

Ethyl acetate has been employed as a solvent for extracting thallium(III) from its hydrochloric acid solutions. The empirical formula of the extracted metal entity has been found to be $HTlCl_4$. Optimum conditions for the extraction of the metal have been determined, and the effect of various factors, e. g., metal concentration, salting-out agents, and the dilution of the solvent, have been investigated. It has been possible to separate thallium(III) from aluminum(III), gallium(III) and indium-(III) by performing a batch-by-batch extraction at a 1.0 N hydrochloric acid concentration.

1) The extracted species is an acid with an approximate formula of $HTlCl_4$, the distribution of the species between the two phases depends upon the concentration of the hydrochloric acid present in the system.

2) The extracted species is ionic and may associate in the organic phase to from ion pairs, ion triplets and higher clusters. This is evident from the fact that an increase in the metal concentration causes an increase in the distribution coefficient.

3) There is no primary solvation of thallium, which is tetrahedrally surrounded by chloride ions and which is apparently saturated. This is supported by the observation that the metal

6) N. H. Nachtrieb and R. E. Fryxell, *J. Am. Chem. Soc.*, **71**, 4035 (1949); **70**, 3522 (1948).
7) Y. Marcus, *Chem. Revs.*, **63**, 139 (1963).

could not be extracted from its solution in perchloric acid.

4) The proton of the chlorothallic acid may be solvated (and possibly hydrated, too) in the organic phase, the solvation number being indefinite.

5) Ion pairing results in the formation of an extractable complex and a general mechanism of the type:

$$H(S)^+ + [Tl(S)_2Cl_4]^- \rightleftharpoons [(HS^+)(Tl(S_2)Cl_4)^-]$$

may be expected, where S is either $H_2O$ or ethyl acetate.

The above equation may well represent qualitatively various reactions at different relative water and ethyl acetate activities.

In general, the system is a simple ion-association extraction system and is quite similar to the extraction of iron(III) and gallium(III) chloride with oxygenated solvents.

The authors are thankful to the Chairman of their Chemistry Department for providing laboratory facilities. The authors' thanks are also due to the CSIR, New Delhi, for awarding a junior research fellowship to one of them (D. C. R.).

*Chemistry Department*
*Lucknow University*
*Lucknow, India*

# Temperature Dependence of A. C. Polarographic Waves

By G. H. Aylward and J. W. Hayes*

(Received February 23, 1965)

There are few published data on the temperature dependence of a. c. polarographic waves. The most extensive study is that of Bauer and Goodwin[1] who reported the temperature coefficients of the peak heights for the reduction of a number of metal ions and compared these values with the values for the corresponding d. c. polarographic step heights. These temperature coefficients were expressed as a percentage. Randles and Somerton[2] have reported the activation energies of electron transfer reactions involving several inorganic depolarizers. These results were obtained from faradaic impedance measurements.

Vlček[3] has proposed that the temperature dependence of d. c. polarographic step heights be expressed in terms of an activation energy obtained from an Arrhenius type plot. The values obtained should be independent of the temperature range used and activation energies have a deeper physical meaning than temperature coefficients expressed as a percentage. For a diffusion controlled limiting current, this value expresses the activation energy of diffusion. At low frequencies and high values of the electron transfer rate constant, the a. c. polarographic current is determined by mass transfer terms, and hence if this mass transfer is a diffusion process, it should be possible to obtain a value for the activation energy of diffusion from the a. c. polarographic wave height. If the mass transfer is not a diffusion process (e. g. involves a coupled chemical reaction) then this fact should be detectable from the form of Arrhenius plot obtained. Electrode processes, where the rate of electron transfer is slow enough to affect the a. c. polarographic current at low frequencies, should also show a different form of Arrhenius plot. Thus it should be possible, from the temperature dependence of the peak height, to obtain some useful information about the nature of the electrode process.

At low frequencies and high values of the electron transfer rate constant and for mass transfer by diffusion, the faradaic admittance at the peak of an a. c. polarographic wave, $Y$, is given by:[4]

$$Y=\frac{n^2F^2AC^0(\omega D)^{1/2}}{4RT} \qquad (1)$$

where $C^0$ is the concentration of depolarizer in the bulk of the solution, $\omega$ the angular

* Present address: School of Chemistry, University of Sydney, N.S.W., Australia.

1) H. H. Bauer and P. B. Goodwin, *Aust. J. Chem.*, **14**, 460 (1961).

2) J. E. B. Randles and K. W. Somerton, *Trans. Faraday Soc.*, **48**, 937, 951 (1952).

3) A. A. Vlček, *Coll. Czech. Chem. Comm.*, **24**, 3538 (1959).

4) H. H. Baure, *J. Electroanal. Chem.*, **3**, 150 (1962).

frequency, $D$ the diffussion coefficient of the depolarizer, and $n, F, A, R$, and $T$ have their usual meanings. Assuming that all quantities in Eq. 1 except $D$ and $T$ are independent of temperature, and that the temperature dependence of $D$ may be written :[3]

$$D = D_0 \exp\left(\frac{-Q_D}{RT}\right) \qquad (2)$$

where $D_0$ is a constant and $Q_D$ is the activation energy of diffusion, the temperature dependence of the faradaic admittance may be written :

$$YT = \alpha \exp\left(\frac{-1/2\, Q_D}{RT}\right) \qquad (3)^*$$

where $\alpha$ is a constant made up of the temperature independent terms. A plot of log $YT$ against $1/T$ should yield a straight line of slope $-Q_D/4.61\,R$ for cases where the above conditions are valid. The activation energy determined in this way should be comparable with that determined from the d. c. polarographic limiting current. According to Vlček[3] the values of $Q_D$ usually fall in the range 4—6 kcal. mol$^{-1}$.

Table I shows some results obtained for systems of several types. For systems numbers 1 and 2 the electrode process is known to be reversible,[5] and the values of $Q_D$ obtained from a. c. and d. c. polarography are comparable and of the expected order of magnitude. In system number 3 an irreversible chemical reaction follows the reversible electron transfer reaction[5] viz.

$$EuY^{2-} + Ca^{2+} \rightarrow Eu^{2+} + CaY^{2-}$$

where Y represents ethylenediaminetetraacetic acid (EDTA). Although the d. c. limiting current is diffusion controlled, the height of the a. c. wave is affected by the rate of the chemical reaction.[5] Consequently, the value of $Q_D$ obtained from d. c. polarography is comparable with that obtained for system number 2, whilst a linear plot is not obtained for the a. c. case. Figure 1 shows the difference in the Arrhenius plots from the a. c. polarograms in presence and absence calcium chloride.

TABLE I. TEMPERATURE DEPENDENCE OF POLAROGRAPHIC WAVES

Frequency : 60 c. p. s.
Amplitude : 15 mV. r. m. s.
Temperature range : 25—65°C

| | System studied | $Q_D$, kcal. mol$^{-1}$ D. C. polarography | $Q_D$, kcal. mol$^{-1}$ A. C. polarography |
|---|---|---|---|
| (1) | $1.0\times10^{-3}$M $Cd^{2+}$ in 0.5M KCl + 0.5M HCl | 4.4 | 4.4 |
| (2) | $2.0\times10^{-3}$M Eu(III)-EDTA in 0.2M ammonia buffer + $1.0\times10^{-3}$M Ca(II)-EDTA + $2\times10^{-4}$% Triton X-100 | 4.0 | 5.1 |
| (3) | as (2) + $5\times10^{-2}$M $CaCl_2$ | 3.7 | curve |
| (4) | $1.0\times10^{-3}$M $Zn^{2+}$ in 1M KCl | 3.8 | curve |

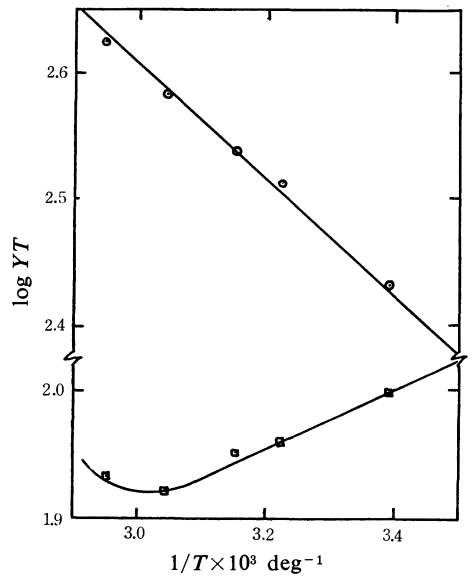



Fig. 1. Temperature dependence of a. c. polarographic wave heights for reduction of Eu(III)-EDTA in absence ⊙ and presence ⊡ of calcium chloride (for conditions see Table I).

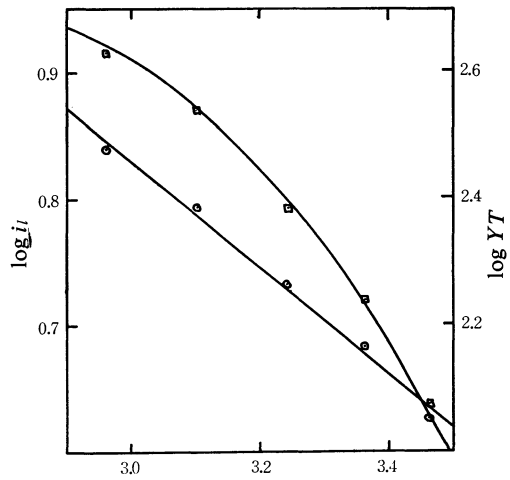



Fig. 2. Temperature dependence of limiting current ⊙, and a. c. polarographic wave height ⊡ for reduction of zinc ions (for conditions see Table I).

5) G. H. Aylward and J. W. Hayes, *Anal. Chem.*, 37, 195 (1965).

* Added in Proof : Since submission of this paper, T. Kambara and K. Kunimatsu in *Review of Polarography*, 13, 20 (1965) have published a development of Eq. 3 and its application to quasi-reversible systems.

By means of a plot of the logarithm of the rate constant against $1/T$, the activation energy of the chemical reaction has been determined.[5]

System number 4 is a well known quasi-reversible system, and the height of the a. c. wave is influenced by the rate of the electron transfer reaction. Although a linear Arrhenius plot is obtained from the d. c. polarograms, and the value $Q_D$ obtained from the limiting current is in the expected range of magnitude, marked non-linearity is found from a. c. polarograms, see Fig. 2.

Further work in this field should prove useful in the assignment of mechanisms to electrode processes.

*School of Chemistry*
*University of New South Wales*
*Kensington, N. S. W. Australia*

# Interatomic and Intermolecular Scattering in Gas Electron Diffraction†

By Yonezo MORINO, Kozo KUCHITSU and R. A. BONHAM*

(Received March 29, 1965)

The effect of interatomic and intermolecular scattering on the total intensity of electrons scattered from a narrow beam of atoms or molecules in the gaseous state can be written as:

$$I_T(s) = I(s)\left\{1+4\pi\left(\frac{N}{V}\right)\times\int_0^\infty dr r^2[e^{-V(r)/kT}-1]\frac{\sin sr}{sr} +4\pi\left(\frac{N}{V}\right)\int_0^\infty dr r^2\frac{\sin sr}{sr}\right\} \quad (1)$$

in the first Born approximation, where $I(s)$ is the usual Debye intensity expression for scattering from atoms or molecules.[1] In Eq. 1, $N$ refers to the number of atoms or molecules in the volume, $V$, undergoing scattering. It should be noted that Eq. 1 is the equation previously derived by Debye and Menke[2] for the X-ray scattering from liquids. The second term on the right of the equal sign in Eq. 1 represents electron scattering from a pair of atoms separated by distances close to the position of the minimum of the interatomic or intermolecular potential, $V(r)$. The third term represents the scattering of electrons from atom pairs separated by large distances and makes no contribution to the intensity.[1] Since the second term on the right of the equal sign in Eq. 1 makes a periodic contribution to the differential scattering cross section, it is of interest to investigate this term in order to ascertain if corrections for its effect on the electron diffraction analysis are needed.

It is convenient to define a reduced molecular intensity function for interatomic or intermolecular scattering as:

$$N(s) = 9.221\times10^{-2}(P_0/T)\times\int_0^\infty dr r^2[e^{-V(r)/kT}-1]\frac{\sin sr}{sr} \quad (2)$$

where $P_0$ is the average pressure in the gas beam in fractions of an atmosphere, and $T$ is the temperature in degrees of atoms or molecules in the gas beam. In Fig. 1 $N(s)$ is calculated for an argon gas beam with $P_0=10^{-2}$ atm. and $T=300°K$. The $V(r)$ potential is approximated by a Lennard-Jones 6-12 expression using parameters obtained from Ref. 3. It is obvious from Fig. 1 that interatomic or intermolecular effects at sample pressures of the order of 10 mmHg will usually not create any difficulty in the analysis of electron diffraction data. On the other hand, an interesting question arises as to whether or not the potential function, $V(r)$, can be obtained experimentally by carrying out electron diffraction experiments with high beam pressures. This appears to be a feasible experiment provided gas pressures greater than

† Contribution Number 1286 from the Chemical Laboratories of Indiana University.

* This author wishes to thank the U. S. Educational Commission in Japan, the John Simon Guggenheim Foundation, and the Alfred P. Sloan Foundation for their support.

1) P. Debye, *J. Chem. Phys.*, **9**, 55 (1941).
2) P. Debye and H. Menke, *Physik. Z.*, **31**, 797 (1930).
3) R. H. Fowler and E. A. Guggenheim, "Statistical Themodynamics," Cambridge at the University Press, London, Cambridge, England (1939), Chapter VII, Table 3, p. 285.

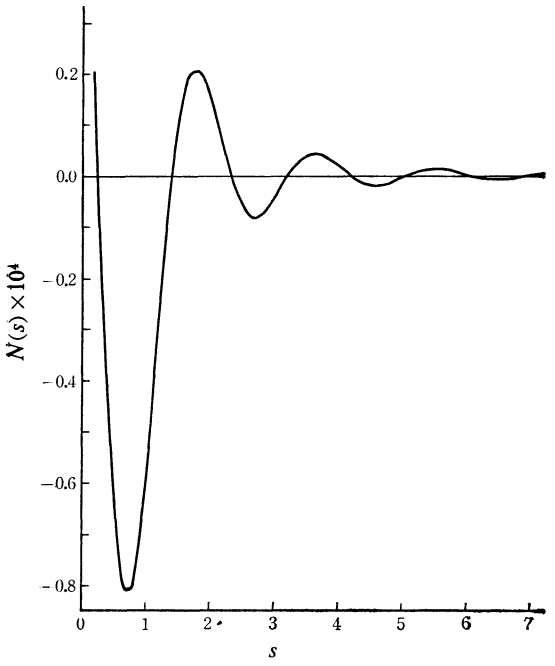



Fig. 1

1 atm. can be obtained while conditions for an optimum diffraction experiment are maintained. That is, the volume of gas undergoing scattering must be small (i. e., $10^{-3}$ cubic mm.), and the vacuum in the diffraction chamber should be at least $10^{-4}$ mm. of Hg away from the beam. At high pressures of the gas beam it is possible, in the case of many atoms and molecules, to obtain diffraction pictures in a few hundredths of a second with 40 kV. electrons. By taking a diffraction photograph during the instant following the formation of a gas beam by expansion through a small orifice (~0.1 mm.), it should be possible to maintain a reasonably good chamber pressure during the course of the exposure.

It is also important to consider the effect of multiple scattering on Eq. 1. The Karles[4] have discussed such effects previously; it appears, on the basis of their analysis, that such effects mainly contribute to the background term, $I(s)$, in a smooth fashion. It is, of course, possible for coherent contributions of these effects to the frequency such as those in Eq. 2 to arise from multiple scattering from closely-grouped clusters of three or more atoms. However, Bunyan[5] has shown that the intensity from triple scattering, for extremely heavy atoms, amounts to probably no more than 10% of the coherent scattering intensity from a cluster of three atoms in close proximity. Since in gases, even at fairly high pressures, there must be many more clusters with two atoms than with three atoms, the appearance of coherent features from multiple scattering seems rather improbable.

It is also important to note that the amplitude of $N(s)$ depends, in a sensitive manner, on the depth of the energy minimum of $V(r)$. This means that an increase in the density of the potential minimum of $V(r)$ will greatly enhance the amplitude of $N(s)$. Thus, the possibility of observing the function $N(s)$ experimentally for krypton or xenon should be even better than for argon.

*Department of Chemisty*
*Faculty of Science*
*The University of Tokyo*
*Hongo, Tokyo*
*(Y. M., K. K. & R. A. B.)*

*Department of Chemistry*
*Indiana University*
*Bloomington, Indiana (R. A. B.)*

4) I. L. Karle and J. Karle, *J. Chem. Phys.*, **18**, 963 (1950).
5) P. J. Bunyan, *Proc. Phys. Soc.*, **82**, 1051 (1963).

# The Correction of the Relation of the Optical Density Ratio to the Stretch Ratio on the Dichroic Spectra*

By Yoshié TANIZAKI

(Received April 26, 1965)

Previously,[1] in order to analyze the dichroic spectra and determine the transition directions of the electronic bands of molecules in the stretched PVA sheet, an expression was proposed for the density ratio ($R_d=D_{\parallel}/D_{\perp}$) as a function of the stretch ratio ($R_s$). In the course of the derivation, however, the author made a mistake in the description of the surface element, $\rho(\theta_0)$; therefore, the distribution function was not correct. For that reason, the proposed expression was also incorrect, though it could explain some experimental results obtained under certain conditions.[1,2]

In the present communication the author shall give the correct description of $\rho(\theta_0)$ and derive anew the distribution function $f(\theta)$ and the $R_d$ expression. Further, it will be shown how the orientation angle of the transition moment can be obtained practically.

Figure 1 illustrates schematically the previous statement[1] of the deformation of a sphere with a unit radius into a spheroid with the same volume. The long axis of the spheroid is taken as the Z axis (the stretching direction). On the assumption that the deformation is made under a constant volume, the angle $\theta_0$ of any unit vector in the sphere will be transformed into $\theta$ in the spheroid as follows:

$$\tan\theta_0=R_s\tan\theta \tag{1}$$

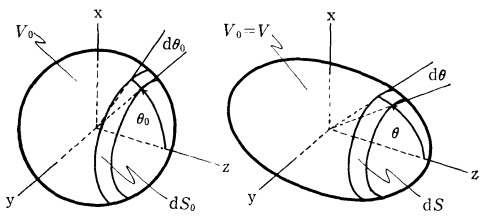
where both $\theta_0$ and $\theta$ are defined in the region $0-\pi/2$. The distribution function, $f(\theta)$, after stretching, is expressed as:

$$f(\theta)=\int_0^{\pi/2}G(\theta,\theta_0)F(\theta_0)\,d\theta_0$$
$$=\int_0^{\pi/2}\delta(\theta-\theta_0)\rho(\theta_0)F(\theta_0)\,d\theta_0 \tag{2}$$

where $F(\theta_0)$ $(=\sin\theta_0)$ is the distribution before stretching; $G(\theta,\theta_0)$, the transformation function, and $\delta$, the delta function. From the relation $dV_0=dV$ (Fig. 1), we have:

$$h/h_0=dS_0/dS=\rho(\theta_0)$$

hence:




$dS_0=2\pi\sin\theta_0\,d\theta_0$ $\quad dS=\dfrac{2\pi R_s^{2/3}\sin\theta\,d\theta}{\sqrt{1+(R_s^2-1)\sin^2\theta}}$

$dV_0=h_0\,dS_0$ $\quad dV=h\,dS$

Fig. 1. The schematic illustration for the deformation from a sphere to a spheroid under a constant volume.

$$\rho(\theta_0)=R_s^{-2/3}\sqrt{1+(R_s^2-1)\sin^2\theta}\,\frac{\sin\theta_0}{\sin\theta}\,\frac{d\theta_0}{d\theta}$$
$$=R_s^{1/3}\sqrt{1+(R_s^2-1)\sin^2\theta}\,\frac{\sin\theta_0}{\sin\theta}\,\frac{\cos^2\theta_0}{\cos^2\theta}$$

because, by Eq. 1, we can write $d\theta_0/d\theta=R_s\cos^2\theta_0/\cos^2\theta$. Therefore, Eq. 2 becomes:

$$f(\theta)=\int_0^{\pi/2}\delta(\theta-\theta_0)R_s^{1/3}\sqrt{1+(R_s^2-1)\sin^2\theta}\times\frac{\sin^2\theta_0\cos^2\theta_0}{\sin\theta\cos^2\theta}\,d\theta_0$$
$$=\int_0^{\pi/2}\delta(\theta-\theta_0)R_s^{1/3}\frac{\sqrt{1+(R_s^2-1)\sin^2\theta}}{\sin\theta\cos^2\theta}\times\frac{\tan^2\theta_0}{(1+\tan^2\theta_0)^2}\,d\theta_0$$

By eliminating $\tan\theta_0$ by Eq. 1, that is to say, by carrying out the integration with respect to $\theta_0$, we obtain:

$$f(\theta)=R_s^{1/3}\frac{\sqrt{1+(R_s^2-1)\sin^2\theta}}{\sin\theta\cos^2\theta}\times\frac{R_s^2\tan^2\theta}{(1+R_s^2\tan^2\theta)^2}$$

or

$$=R_s^{7/3}\sin\theta\{1+(R_s^2-1)\sin^2\theta\}^{-3/2}$$

The further integration of $f(\theta)$ with respect to $\theta$ in the region of $0-\pi/2$ gives $R_s^{1/3}$. Therefore, $R_s^{-1/3}f(\theta)$ is normalized. Rewriting this normalized function by $f(\theta)$ again, the distribution function becomes:

$$f(\theta)=R_s^2\sin\theta\{1+(R_s^2-1)\sin^2\theta\}^{-3/2} \tag{3}$$

---

* Dichroism of Dyes in the Stretched PVA Sheet. V. IV: Y. Tanizaki and H. Ono, This Bulletin, 33, 1207 (1960).

1) Y. Tanizaki, This Bulletin, 32, 75 (1959).

2) Y. Tanizaki, ibid., 33, 979 (1960).

Equation 3 is the corrected distribution function required.

The correct $R_d$ equation against $R_s$ for a parameter $r$, therefore, can be obtained as follows, using the same procedure as that described in the previous paper:[1]

$$\left.\begin{aligned} R_d &= \frac{2+2(2r^2-1)T}{(2r^2+1)-(2r^2-1)T} \\ T &= \frac{R_s^2}{R_s^2-1}\left[1-\left\{\frac{\pi}{2}-\tan^{-1}(R_s^2-1)^{-1/2}\right\}\times(R_s^2-1)^{-1/2}\right] \\ R_s &> 1 \end{aligned}\right\} \quad (4)$$

The parameter $r$ has the following meaning: $\cot^{-1} r$ provides the angle of the transition moment against the orientation axis which is considered to be peculiar to the molecular species.

If the orientation axis is peculiar to the molecular species, namely, if the $r$-value is independent of $R_s$, the orientation angle of the transition moment must be decided from Eq. 4 by substituting the observed $R_d$ and $R_s$ values. According to our experiences with the dichroic measurement, however, in some cases, the $r$-value is not invariant with $R_s$, as in the examples shown in Fig. 2. In that case, the $r$-value extrapolated to $R_s=1$ should be employed.

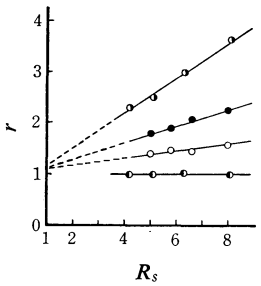



Fig. 2. Examples of the relations of $r$ vs. $R_s$.
Sodium 4'-hydroxyazobenzene-4-sulfonate:
◑ at 365 mμ, ◐ at 244 mμ
Chrysoidine:
● at 460 mμ, ○ at 240 mμ

The warrant for the appropriate deformation of the sample sheet by stretching will be given by the fact that the ratio of $(D_{\parallel}+2D_{\perp})$ for any $R_s$ to $D$ for $R_s=1$ (i.e., nonstretching) at the same wavelength is invariant for the observed region.

The author wishes to thank Dr. Yasuji Kobayashi, Assistant Professor of the Tokyo Metropolitan University, for pointing out the mistake in the distribution function in the previous paper.

*Department of Chemistry*
*Tokyo Institute of Technology*
*Ookayama, Tokyo*

## SHORT COMMUNICATIONS

# The Proton Magnetic Resonance of Thianaphthenes. III.* The Long-range Coupling Observed in Side-chain Methyl Hydrogens in Some Methylthianaphthenes

By Kensuke TAKAHASHI, Tatsuo KANDA and Yasuo MATSUKI

(Received June 2, 1965)

In this report we will discuss the coupling observed in methyl hydrogens in some methylthianaphthenes. The signal of the methyl hydrogens in 2- or 3-methylthianaphthene splits into a doublet with a splitting of about 1 c. p. s. as a result of its coupling with an adjacent ring hydrogen. However, the signal of methyl hydrogens in 4-, 5-, 6- or 7-methylthianaphthene shows a more complex structure than the doublet observed in 2- or 3-methylthianaphthene. This means that there exists some coupling between methyl hydrogens and their non-adjacent ring hydrogens in addition to the

* See Refs. 1 and 2 for Parts I and II.

1) K. Takahashi, T. Kanda and Y. Matsuki, This Bulletin, 37, 768 (1964).
2) K. Takahashi, T. Kanda, F. Shoji and Y. Matsuki, ibid., 38, 508 (1965).

TABLE I. PMR DATA OF SOME THIANAPHTHENE DERIVATIVES IN CARBON TETRACHLORIDE, REFERRED TO CYCLOHEXANE AT 60 Mc./sec.
Parenthesis shows the chemical shift of the substituent.

| Substituent | Chemical shift p. p. m. | | | | | | Coupling c. p. s. |
|---|---|---|---|---|---|---|---|
| | 2-H | 3-H | 4-H | 5-H | 6-H | 7-H | $J_{23}$ |
| 5-Br[2] | 5.93 | 5.74 | 6.45 | — | 5.94 | 6.21 | 5.6 |
| 6-$COOCH_3$[2] | 6.13 | 5.88 | 6.35 | 6.54 | (2.47) | 7.13 | 5.4 |
| 2-$CH_3$[1] | (1.09) | 5.40 | ~6.1 | ~5.7 | ~5.7 | ~6.1 | 1.1 |
| 3-$CH_3$[1] | 5.51 | (0.96) | ~6.2 | ~5.8 | ~5.8 | ~6.2 | $1.0_5$ |
| 2,3-$(CH_3)_2$ | (1.00) | (0.80) | ~6.1 | ~5.8 | ~5.8 | ~6.1 | $0.7_5$ |
| 2,3-$(CH_3)_2$, 6-$COCH_3$ | (1.05) | (0.83) | 6.00 | 6.35 | (1.10) | 6.77 | 0.7 |



Fig. 1. The PMR spectrum of 2,3-dimethylthianaphthene in the 5.2 mol. % solution in carbon tetrachloride at 60 Mc./sec. Applied magnetic field increasing from left to right.

coupling between the methyl hydrogens and their adjacent ring hydrogens. Similar results have already been presented for some other aromatics.[3] In the spectrum of 2, 3-dimethylthianaphthene, two methyl signals, at 0.80 and 1.00 p. p. m. with reference to cyclohexane, corresponding to 3-methyl and 2-methyl hydrogens respectively, have quartet structures, as is shown on the right side of Fig. 1. The magnitude of these splittings is about 0.7 c. p. s. This may be attributed to the coupling between two methyl hydrogens in 2, 3-dimethylthianaphthene. The present results give us some information about the mechanism of the side-chain coupling in methylthianaphthenes and indicate that it is similar to that in methylthiophenes.[4]

Hoffman described the methyl substitution technique used to check the mechanism of coupling.[5] Some compounds were taken up in order to compare the coupling of $J_{23}$ in thianaphthenes. Table I lists the observed PMR data of the first-order analyses. $J_{2\text{-H},\ 3\text{-H}}$ is about 5 c. p. s. in thianaphthenes. When we substitute a methyl group for a 2- or 3-positioned ring hydrogen, a $J_{2\text{-}CH_3,\ 3\text{-H}}$ or $J_{2\text{-H},\ 3\text{-}CH_3}$ value of about 1 c. p. s. is observed, showing a great decrease as compared with $J_{2\text{-H},\ 3\text{-H}}$. After the further substitution of a methyl group for the remaining 2- or 3-positioned ring hydrogen, we get a $J_{2\text{-}CH_3,\ 3\text{-}CH_3}$ value of about 0.7 c. p. s., which has the same order of magnitude as $J_{2\text{-H},\ 3\text{-}CH_3}$ or $J_{2\text{-}CH_3,\ 3\text{-H}}$. This leads to the conclusion that the side-chain coupling in methylthianaphthenes is mainly due to the $\pi$-electron contact contribution.

*The Chemical Research Institute of Non-Aqueous Solutions*
*Tohoku University*
*Katahira-cho, Sendai*

3) R. A. Hoffman and S. Gronowitz, *Arkiv. Kemi*, **16**, 563 (1960); K. Takahashi, Y. Matsuki, Y. Miyake and G. Hazato, This Bulletin, **34**, 1599 (1961); G. P. Newsoroff and S. Sternhell, *Tetrahedron Letters*, **1964**, 3499.

4) S. Gronowitz, Bo Gestblom and R. A. Hoffman, *Acta Chem. Scand.*, **15**, 1201 (1961).

5) R. A. Hoffman and S. Gronowitz, *Arkiv. Kemi*, **16**, 471 (1960).

# Radiation-Induced Catalytic Activity of Nickel Oxide

By Toshiro YAMASHINA and Masakatsu SANO

(Received June 11, 1965)

The fact that the irradiation of nickel oxide with $\gamma$-rays results in changes in surface phenomena and in the reduction process by hydrogen has been suggested previously.[1] The present communication will present evidence that the induced catalytic activity with $\gamma$-irradiation leading to the decomposition of hydrogen peroxide solution is closely connected with the chemisorbed oxygen induced by radiation.

The pure nickel oxide sample was prepared in a manner identical with that described previously.[1] The samples were irradiated to total doses of $\sim 8 \times 10^8$ r. in air at room temperature, with Co-60 gamma-rays. The catalytic activity of the nickel oxide was then determined by using the decomposition of a 7.5% hydrogen peroxide solution as a model reaction, in which the rate of the reaction was followed by reading the volume of oxygen evolved per minute. A 0.2 g. catalyst sample was used for each run. The reaction temperature was 40°C. The chemisorbed oxygen was estimated by its ability to oxidize potassium iodide in a hydrochloric acid solution, in fact, the quantity of $Ni^{3+}$ ions was determined. Therefore, the results are represented as excess oxygen, two $Ni^{3+}$ ions corresponding to one $O^{2-}$ ion.

The catalytic activity and chemisorbed oxygen due to $\gamma$-irradiation are presented as a function of the radiation dose in Fig. 1. Both values were found to increase with the radiation dose, being remarkable over a total dose of about

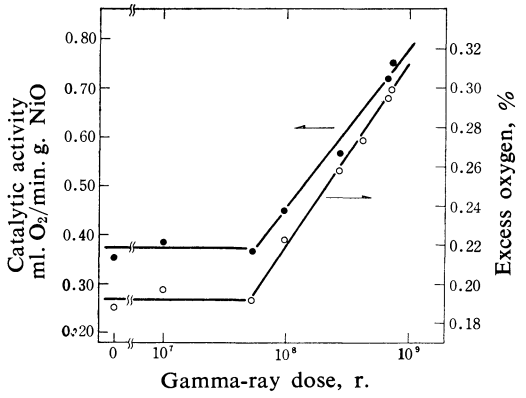



Fig. 1. Catalytic activity and excess oxygen as a function of $\gamma$-ray dose.

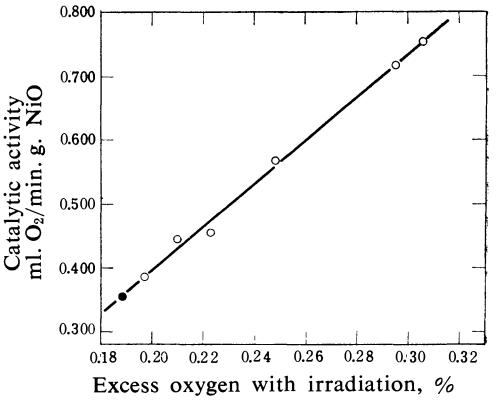



Fig. 2. Catalytic activity vs. excess oxygen with $\gamma$-irradiation.

$1 \times 10^8$ and reaching a level over twice as great as not-irradiated nickel oxide. No differences in the B. E. T. surface area with the irradiation were observed. Figure 2 shows the induced catalytic activity as a function of the oxygen chemisorbed with irradiation; a linear relationship was obtained. Similar relations have been observed in the case of oxidized chromina-alumina catalysts.[2,3] From the present results, it can be concluded that the catalytic sites on nickel oxide are closely associated with the oxygen chemisorbed on the surface with $\gamma$-irradiation.

Although some investigators[4,5] have shown the radiation induced catalytic activity on nickel oxide to be concerned with the characterization of defects with radiation damage, the mechanism of its catalysis is still not clear.

We, however, would like to suggest that catalytic action takes place preferentially at the oxygen chemisorbed with irradiation. Further study is now in progress to reveal which state of adsorbed oxygen, $O_2^-$, $O^-$ or $O^{2-}$, contributes to the catalysis.

*Faculty of Engineering*
*Hokkaido University*
*Sapporo*

1) T. Yamashina and T. Nagamatsuya, This Bulletin, **38**, 507 (1965).

2) I. Maxim and T. Braun, *J. Phys. Chem. Solids*, **24**, 537 (1963).

3) S. E. Volts and S. W. Weller, *J. Am. Chem. Soc.*, **76**, 1568 (1654).

4) Y. Matsunaga, This Bulletin, **30**, 984 (1957).

5) H. B. Charman, R. M. Dell and S. S. Teale, *Trans. Faraday Soc.*, **59**, 453 (1963).

6) H. B. Charman and R. M. Dell, ibid., **59**, 470 (1963).

# The Selective Debenzylation of *N*-Acyl-*O*-benzylhydroxylamines

By Mitsuo MASAKI, Junzo OHTAKE, Masatoshi SUGIYAMA and Masaki OHTA

(Received June 25, 1965)

It has been shown in our laboratory[1] that the catalytic hydrogenation of *N*-leucyl-*O*-benzylhydroxylamine (I) yields *N*-leucylhydroxylamine (II). This hydrogenolytic method was applied to *N*-acyl-*O*-benzylhydroxylamines and found to yield either hydroxamic acid or amide selectively in either the presence or absence of a trace of pyridine.

$$\underset{\text{(I)}}{\textit{iso}\text{-}C_4H_9\overset{\displaystyle NHR}{\overset{|}{C}}HCONHOCH_2C_6H_5} \rightarrow \underset{\text{(II)}}{\textit{iso}\text{-}C_4H_9\overset{\displaystyle NHR}{\overset{|}{C}}HCONHOH}$$

R=H, $C_3H_7COCH_2$

*N*-(2-Bromo-4-methylvaleryl)-*O*-benzylhydroxylamine (III-a) prepared from 2-bromo-4-methylvaleryl chloride and *O*-benzylhydroxylamine according to the usual method[1] was dissolved in 1 N sodium hydroxide, and the solution was neutralized with 1 N hydrochloric acid to afford *N*-(2-hydroxy-4-methylvaleryl)-*O*-benzylhydroxylamine (III-b), m. p. 76—77°C (Found: C, 66.04; H, 8.27; N, 6.04. Calcd. for $C_{13}H_{19}NO_3$: C, 65.80; H, 8.07; N, 5.90%). When III-b was hydrogenated with hydrogen-5% palladium on charcoal at an initial pressure of 40 kg./cm$^2$ in ethanol, only the corresponding amide (IV-b) was obtained in a 81% yield, m. p. 79—81°C (lit.[2] m. p. 51—52°C) (Found: C, 54.90; H, 9.82; N, 11.90. Calcd. for $C_6H_{13}NO_2$: C, 54.94; H, 9.99; N, 10.68%), instead of the expected hydroxamic acid (V-b).

When I is compared with III-b, the difference is found to consist only in substituents of the $\alpha$-position, amino- and hydroxyl-groups; thus some effect of the basic amino-group of I might cause the difference in the course of hydrogenation.

$$\underset{\text{(III)}}{\textit{iso}\text{-}C_4H_9\overset{\displaystyle X}{\overset{|}{C}}HCONHOCH_2C_6H_5}$$

$$\textit{iso}\text{-}C_4H_9\overset{\displaystyle X}{\overset{|}{C}}HCONH_2 \quad \text{(IV)}$$

$$\textit{iso}\text{-}C_4H_9\overset{\displaystyle X}{\overset{|}{C}}HCONHOH \quad \text{(V)}$$

a, X=Br b, X=OH c, X=H

The catalytic reduction of III-b by a similar technique was then carried out in the presence of a few drops of pyridine; this yielded exclusively the corresponding hydroxamic acid (V-b), which was isolated by conversion into the copper salt, followed by treatment of the latter with hydrogen sulfide; 73% yield, m. p. 104—105.5°C (Found: N, 9.67. Calcd. for $C_6H_{13}NO_3$: N, 9.52%). The hydroxamic acid gives a wine red color with ferric chloride.

In a similar manner, *N*-(4-methyl-2-pentenoyl)-*O*-benzylhydroxylamine (VI), prepared from 4-methylpentenoyl chloride and *O*-benzylhydroxylamine, was catalytically hydrogenated in the presence of a few drops of pyridine to yield *N*-(4-methylvaleryl)hydroxylamine (V-c) in a 56% yield, m. p. 57—58.5°C (Found: N, 10.94. Calcd. for $C_6H_{13}NO_2$: N, 10.68%), which gave a wine-red ferric reaction, while the catalytic hydrogenation of VI in the absence of pyridine gave only the corresponding amide (IV-c) in a 96% yield.

*Laboratory of Organic Chemistry*
*Tokyo Institute of Technology*
*Ookayama, Tokyo*

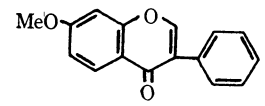
1) M. Masaki and M. Ohta, *J. Org. Chem.*, **29**, 3165 (1964).
2) P. Nicolle, *Bull. soc. chim. France*, **39**, 55 (1926).

# A New Method for the Synthesis of Isoflavones

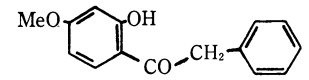
By Kenji FUKUI and Mitsuru NAKAYAMA

(Received July 1, 1965)

Of the several known methods[1] for synthesizing isoflavones, the formylation reaction, consisting of the condensation of benzyl 2-hydroxyphenyl ketones (*o*-hydroxydeoxybenzoins), is considered to be the most convenient. The Duff reaction,[2] in which formylation is effected by hexamine, has been used for the preparation of *o*-hydroxyaromatic aldehydes from phenols. The action of hexamine on the ketones has now been studied, since formylation at the reactive methylene group should lead to an isoflavone directly. Under the conditions used for the formylation of phenols, an isoflavone could be isolated in a highly pure state. This new method may be illustrated by the preparation of 7-methoxyisoflavone (I).[3] Benzyl 2-hydroxy-4-methoxyphenyl ketone (II)[4] was refluxed for several hours with an excess of hexamine in acetic acid. The resulting solution, when treated with hydrochloric acid and then poured into water, gave the isoflavone (I).




I




II

The general applicability of the method has been studied by the preparation of a number of other isoflavones, including dehydro-*O*-dimethylsophorol.[5] The results are summarized in Table I. This simple method proceeds satisfactorily when all the hydroxyl groups in the

TABLE I

| | Isoflavone | Ketone from which prepared | Yield % | Form (solvent) | M. p. and mixed m. p., °C |
|---|---|---|---|---|---|
| 1 | 7-Methoxy (I) | Benzyl 2-hydroxy-4-[4] methoxyphenyl (II) | 10 | Plates (EtOH) | 155—156 [3,4] |
| 2 | 7-Benzyloxy | Benzyl 4-benzyloxy-2-[a] hydroxyphenyl (II) | 15 | Plates (EtOH) | 170—171 [a] |
| 3 | 7-Methoxy-3′, 4′-methylenedioxy | 2-Hydroxy-4-methoxyphenyl[b] 3, 4-methylenedioxybenzyl | 10 | Needles (EtOH) | 179—180 [c] |
| 4 | 7-Benzyloxy-3′, 4′-methylenedioxy | 4-Benzyloxy-2-hydroxyphenyl[d] 3, 4-methylenedioxybenzyl | 20 | Needles (EtOH) | 167—168 [c] |
| 5 | 7, 2′, 4′, 5′-Tetramethoxy | 2-Hydroxy-4-methoxyphenyl[e] 2, 4, 5-trimethoxybenzyl | 5 | Plates (EtOH) | 190—191 [e] |
| 6 | 7-Benzyloxy-2′, 4′, 5′-trimethoxy | 4-Benzyloxy-2-hydroxyphenyl[e] 2,4,5-trimethoxybenzyl | 15 | Plates (EtOH) | 143—144 [f] |
| 7 | 7, 2′-Dimethoxy-4′, 5′-methylenedioxy (Dehydro-*O*-dimethyl[5]-sophorol) | 2-Hydroxy-4-methoxyphenyl[g] 2-methoxy-4, 5-methylenedioxybenzyl | 20 | Needles (MeOH) | 209—210 [h] |

a) H. S. Mahal, H. S. Rai and K. Venkataraman, *J. Chem. Soc.*, **1934**, 1120.
b) E. Späth and O. Schmidt, *Monatsh. Chem.*, **53-54**, 454 (1929).
c) K. Fukui, M. Nakayama and M. Hatanaka, *J. Chem. Soc. Japan, Pure Chem. Sec. (Nippon Kagaku Zasshi)*, **84**, 189 (1963).
d) H. S. Mahal, H. S. Rai and K. Venkataraman, *J. Chem. Soc.*, **1934**, 1769.
e) K. Fukui, M. Nakayama, M. Hatanaka, T. Okamoto and Y. Kawase, This Bulletin, **36**, 397 (1963).
f) New compound (Found: C, 71.99; H, 5.27. Calcd. for $C_{25}H_{22}O_6$: C, 71.76; H, 5.30%).
g) H. Suginome, *Tetrahedron Letters*, No. **19**, 16 (1960).
h) K. Fukui, M. Nakayama and K. Okazaki, *J. Chem. Soc. Japan, Pure Chem. Sec. (Nippon Kagaku Zasshi)*, **86**, 960 (1965).

1) W. K. Warburton, *Quart. Rev.*, **8**, 67 (1954); T. A. Geissman, "The Chemistry of Flavonoid Compounds," Pergamon Press, London (1962), p. 353.
2) J. C. Duff, *J. Chem. Soc.*, **1941**, 547; **1945**, 276.
3) Y. Kawase, M. Nakayama and S. Matsutani, This Bulletin, **35**, 1369 (1962).
4) W. Baker, J. Chadderton, J. B. Harbone and W. D. Ollis, *J. Chem. Soc.*, **1934**, 1120.
5) H. Suginome, *J. Org. Chem.*, **24**, 1655 (1959).

ketone except the one involved in cyclization are protected, but it fails with polyhydroxyketones.

*Department of Chemistry*
*Faculty of Science*
*Hiroshima University*
*Higashi-Sendamachi, Hiroshima*

# A New Red Platinum(II)-Platinum(IV) Compound

By Sigeo KIDA

(Received July 3, 1965)

A number of compounds, e. g., $[PtBr_2(NH_3)_2]$-$[PtBr_4(NH_3)_2]$ and $[PtCl_2en][PtCl_4en]$,[1] have been known as platinum(II)-platinum(IV) compounds, which can be regarded as consisting of platinum(II) and platinum(IV) complexes. The characteristic feature of these compounds is their intense color, which can not be expected from the component complexes. This anomalous color has been believed, on the basis of X-ray[2] and ultraviolet[3] investigations to be due to the platinum(II)-halogene-platinum(IV) interaction. Among these compounds the red Wolffram salt,[1,4] $[Ptea_4][PtCl_2ea_4]$-$Cl_4 \cdot 4H_2O$ (where "ea" denotes ethylamine), has attracted much interest; its prominent properties are its clear red color, the distinct dichroism, and the colorlessness of its aqueous solution. This compound has been believed to be unique in containing ethylamine, since, according to Reihlen and Flohr,[5] the substitution of ethylamine with other amines (or ammonia) does not lead to the formation of homologue compounds.

In this paper, in spite of Reihlen's statment, a new red platinum(II)-platinum(IV) compound, which should be one of the homologues of Wolffram's salt and which yet has no ethylamine, will be reported.

This compound was obtained in the course of synthetic work on $[Pten_3](ClO_4)_4$ (where "en" denotes ethylenediamine). Hexachloroplatinic acid was heated with an excess of ethylenediamine in 96% ethanol for 1.5 hr. The resulting light yellow precipitate was filtered and then extracted with a small amount of water. When to this solution, 60% aqueous perchloric acid was added, red crystals appeared.

This compound was found by elementary analyses to have the formula $Pten_2Cl(ClO_4)_2$ (Found: Pt, 35.80; C, 8.83; H, 3.13; N, 10.42; Calcd.: Pt, 35.49; C, 8.74; H, 2.93; N, 10.42%). The properties of this compound are similar to those of Wolffram's salt. The crystal shows a remarkable dichroism, is red (when parallel to the needle) and a very light yellow (when perpendicular to the needle). It is stable in the air, decomposes above 220°C, and is soluble in water, forming a colorless solution from which the red crystals can be recrystallized by adding concentrated perchloric acid.

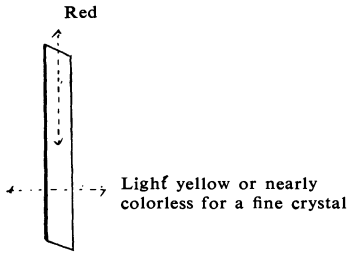



Fig. 1. Microscopic observation and dichroism of the red crystal.

The compound was directly sythesized from the colorless solution of $[Pten_2]Cl_2$ and $[PtCl_2$-$en_2]Cl_2$ at an equimolar ratio by adding 60% perchloric acid. Elementary analyses, infrared spectra, and microscopic observations indicated that the two products, obtained by different methods, are the same compound.

From the above facts, a rational formula would be $[Pten_2][PtCl_2en_2](ClO_4)_4$; this compound is undoubtedly one of the homologues of Wolffram's red salt.

A number of combinations of platinum(II) and platinum(IV) complexes are now being investigated in an attempt to obtain new compounds of this type.

*Department of Chemistry*
*Wakayama University*
*Masago-cho, Wakayama*

1) "Gmelins Handbuch," Platin, Teil D (1957), pp. 616–624.
2) C. Brosset, *Arkiv. Kemi Mineral. Geol.*, **A25**, 14 (1948).
3) S. Yamada and R. Tsuchida, This Bulletin, **29**, 894 (1956).
4) H. Wolffram, Dissertation, Konigsberg, 1900.
5) H. Reihlen and F. Flohr, *Ber.*, **67**, 2010 (1934).

# The Preparation of 2-Substituted Benzimidazoles and 2-Phenylnaphtho-[1, 2-d]imidazole from *N*-Arylamidines

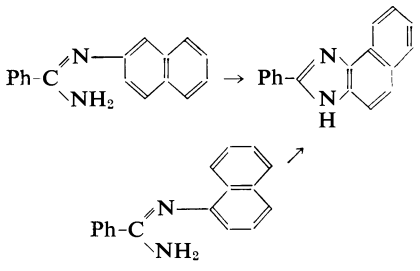
By Eiichi HARUKI, Toshihiro INAIKE and Eiji IMOTO

(Received August 2, 1965)

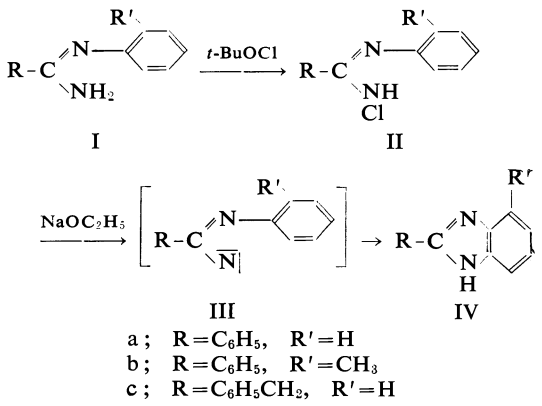
Grenda et al.[1] have recently reported the preparation of benzimidazoles from *N*-aryl-*N'*-haloamidines in an aqueous solvent. Independently of them, we also discovered an analogous method for the preparation of substituted benzimidazoles and 2-phenylnaphtho-[1, 2-d]imidazole during the course of a research program into the preparation and the reactivity of *N*-haloamidines. In our case, the benzimidazole derivatives and 2-phenylnaphtho[1, 2-d]-imidazole were obtained by the treatment of *N*-aryl-*N'*-chloroamidines with an equivalent amount of sodium ethoxide in benzene-ethanol.

To 3.9 g. (0.02 mol.) of *N*-phenylbenzamidine in 15 ml. of dry benzene and 15 ml. of absolute ethanol, there was added 2.3 g. of *t*-butyl hypochlorite at 0—−5°C. After the mixture had been stirred at the same temperature for two hours, 0.9 g. of sodium in 10 ml. of absolute ethanol was added; the mixture was then refluxed for three hours. When the mixture was cooled and poured into ice water, brown precipitates were obtained. Recrystallization from aqueous ethanol gave 3.1 g. (80% yield) of a pure product, m. p. 289—290°C. This compound was identified as 2-phenylbenzimidazole by means of infrared and ultraviolet spectroscopic measurements, and by a mixed melting point test with an authentic sample which had been prepared according to the method described in the literature.[2]

By the same procedure, *N*-(*o*-tolyl)benzamidine was converted to 4-methyl-2-phenylbenzimidazole in a 76% yield, and *N*-phenylphenylacetamidine, to 2-benzylbenzimidazole in a 35% yield. However, the attempt to convert *N*-phenylacetamidine to 2-methylbenzimidazole was unsuccessful. Both *N*-(α-naphthyl)benzamidine and *N*-(β-naphthyl)benzamidine afforded the same product, 2-phenylnaphtho-[1, 2-d]imidazole, in 24% and 64% yields respectively.



Our proposed mechanism for this reaction is as follows:



a; R=$C_6H_5$, R'=H
b; R=$C_6H_5$, R'=$CH_3$
c; R=$C_6H_5CH_2$, R'=H

Amidines react with *t*-butyl hypochlorite to give *N*-chloroamidines (II), which are isolated as discrete intermediates. The reaction of sodium ethoxide with *N*-haloamidines would produce the nitrene intermediate (III), which attacks the benzene nucleus to give the benzimidazole ring.

The usual syntheses of the benzimidazole ring system utilize *o*-phenylenediamine or *o*-nitroaniline as starting materials.[3] In either case, the cyclization involves a coupling at the *o*-phenylene nitrogens. It is interesting to note that the benzimidazole ring can be prepared without using *o*-phenylenediamine derivatives.

*Department of Applied Chemistry*
*Faculty of Engineering*
*University of Osaka Prefecture*
*Sakai, Osaka*

1) V. J. Grenda, R. E. Jones, G. Gale and M. Sletzinger, *J. Org. Chem.*, **30**, 259 (1965).
2) B. A. Porai-Koshits, O. F. Ginzburg and L. S. Eflos, *J. Gen. Chem. (U. S. S. R.)*, **17**, 1768 (1947).
3) K. Hoffman, "Heterocyclic Compounds. Imidazoles and Derivatives," Part I, Interscience Publishers, New York (1953), pp. 258—273.

# A Novel Method for the Preparation of Carbodiimides from *N*-Haloamidine

By Eiichi HARUKI, Toshihiro INAIKE and Eiji IMOTO

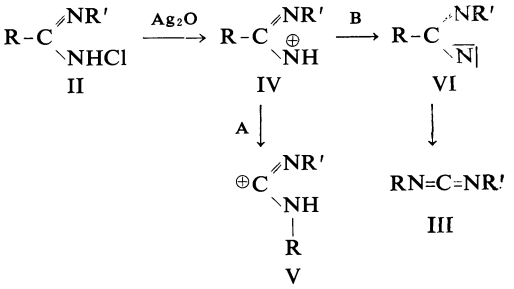
(Received August 2, 1965)

In a previous communication,[1] we have shown that *N*-aryl-*N'*-haloamidines react with sodium ethoxide to form benzimidazole derivatives or 2-phenylnaphtho[1, 2-d]imidazole depending on the structure of the haloamidines. In this communication we wish to report on the reaction of *N*-aryl-*N'*-haloamidines with silver oxide. The *N*-haloamidines were mixed with silver oxide in ligroin or benzene, and these mixtures were refluxed. This treatment caused a rearrangement, thus forming the carbodiimides.

To 2.3 g. of *N*-chloro-*N'*-phenylbenzamidine in 10 ml. of dry ligroin, 5.0 g. of silver oxide was added. The mixture was stirred under reflux for two hours, and then silver oxide and silver chloride were removed by filtration. After the solvent had been evaporated from the filtrate in vacuo, diphenylcarbodiimide b.p. 140—144°C/14 mmHg, was obtained in a 80% yield. Its infrared spectrum showed the characteristic carbodiimide absorption at 2150 $cm^{-1}$ and agreed completely with that of an authentic sample prepared by the method described in the literature.[2] Chemical evidence for structure III was given by the reaction with hydrochloric acid. When refluxed in dilute hydrochloric acid, diphenylcarbodiimide was converted quantitatively into *N*, *N'*-diphenylurea.

In a similar manner, *N*-phenylphenylacetamidine (Ib) and *N*-phenylacetoamidine (Ic) yielded *N*-benzyl-*N'*-phenylcarbodiimide (IIIb, 52% yield) and *N*-methyl-*N'*-phenylcarbodiimide (IIIc, 36% yield) respectively.

The mechanism of the described conversion of *N*-chloroamidines to carbodiimides may be supposed to be as follows:




a; $R=C_6H_5$, $R'=C_6H_5$
b; $R=C_6H_5CH_2$, $R'=C_6H_5$
c; $R=CH_3$, $R=C_6H_5$

Whether the rearrangement proceeds through route A or route B is not certain. However, it is sure that this reaction involves the migration of the R group to an electron-deficient nitrogen.

*Department of Applied Chemistry*
*Faculty of Engineering*
*University of Osaka Prefecture*
*Sakai, Osaka*

1) E. Haruki, T. Inaike and E. Imoto, This Bulletin, **38**, 1805 (1965).
2) P. Schlack and G. Keil, *Ann.*, **661**, 164 (1963).

# The Proton Magnetic Resonance Spectrum of Hydrogen Sulfide and HDS

By Kensuke TAKAHASHI and Genjiro HAZATO

(Received August 3, 1965)

The proton magnetic resonance spectrum of HDS has not yet been observed. Our interest is drawn to the proton-deuteron coupling constant of HDS and its isotope shift with reference to hydrogen sulfide. The equilibrium of the following exchange reaction, another point of interest, has been studied by many authors:[1]

$$H_2O+HDS \rightleftarrows H_2S+HDO$$

This equilibrium suggests one possibility of observing the multiplet spectrum of HDS if the exchange rate is not too rapid. We have estimated that the gas phase is suitable for observing the spectrum of HDS because we can easily expect a slower exchange rate in gas than in liquid.

About equal volumes of $D_2O$ and liquid hydrogen sulfide were therefore introduced into a 5 mm. glass tube in a vacuum, using a small amount of tetramethylsilane as an internal reference. Measurements for a gaseous mixture of hydrogen sulfide and HDS were carried out at about 24°C in contact with a liquid mixture of hydrogen sulfide and $D_2O$ in a sealed glass tube; we could thus estimate the total pressure of hydrogen sulfide and HDS to be about 20 atmospheres. This mixture of hydrogen sulfide and $D_2O$ gave the signal of hydrogen sulfide 0.25 p. p. m. downfield from that of tetramethylsilane in the gas phase. The triplet of HDS was centered $0.028\pm0.003$ p. p. m. upfield from the hydrogen sulfide resonance, as is shown in Fig. 1, in which one of the triplet lines of HDS seems to overlap with the signal of hydrogen sulfide. The observed proton-deuteron spin-spin coupling constant is $2.1\pm0.2$ c. p. s. The proton-proton spin-spin coupling constant for hydrogen sulfide can be readily obtained by multiplying the experimentally-determined $J_{HD}$ by the ratio of the gyromagnetic ratios, $\gamma_H/\gamma_D=6.51$; we thus get $J_{HH}=13.7\pm1.3$ c. p. s. It can be estimated that the rate of the exchange reaction between hydrogen sulfide and HDS in the gas phase, with the saturated vapor pressure at 24°C, is slower than 0.5 $sec^{-1}$, a value which is derived from the observed proton-deuteron coupling constant. Without $D_2O$, the signal of hydrogen sulfide is observed 0.89 and 0.25 p. p. m. downfield from tetramethylsilane in the liquid and gas phases respectively. The difference of 0.64 p. p. m. between the chemical shifts of the liquid and the gas of hydrogen sulfide may be due to the weak hydrogen-bonded association of hydrogen sulfide in a liquid, as has previously been discussed by Schneider et al.[2]

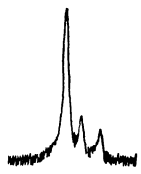


Fig. 1. The proton magnetic resonance spectrum of a gaseous mixture of $H_2S$ and HDS at 24°C in contact with a liquid mixture of $H_2S$ and $D_2O$ in a sealed glass tube. The applied magnetic field increases from left to right.

*The Chemical Research Institute of Non-Aqueous Solutions Tohoku University Katahira-cho, Sendai*

1) For example, J. Garaud and R. Amanrich, *J. Chim. Phys.*, **56**, 532 (1959); R. Haul, H. Behnke and H. Dietrich, *Angew. Chem.*, **71**, 64 (1959).

2) W. G. Schneider, H. J. Bernstein and J. A. Pople, *J. Chem. Phys.*, **28**, 601 (1958).

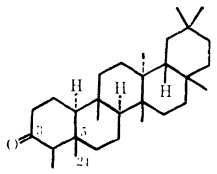
# The Synthesis of 3β-Hydroxyfriedelan-24-oic Lactone

By Toshio FUKUDA, Takahiko TSUYUKI, Yoshiaki TANAHASHI and Takeyoshi TAKAHASHI

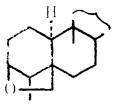
(Received August 16, 1965)

The structure of friedelin (I) has been established,[1] and the presence of a methyl group at $C_5$ has been demonstrated by degradation and by acid-catalyzed rearrangement, as well as by means of biogenetic considerations.[1] However, no direct chemical proof has yet been furnished for this methyl group.

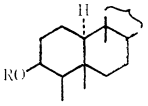
A recent communication[2] on the structure of friedelan-*y*-al, in which the synthesis of 3β,24-oxidofriedelane (II) is registered, has prompted us to report our results in a preliminary form.



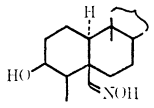
(I)



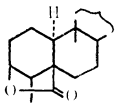
(II)



(III) R=H
(IV) R=NO



(V)



(VI)

3β-Hydroxyfriedelane (III) was, by treatment with nitrosyl chloride in pyridine, converted almost quantitatively into 3β-friedelanyl nitrite (IV); m.p. 261—263°C, $\nu_{max}^{Nujol}$ 1645 and 1610 $cm^{-1}$ (nitrite), $C_{30}H_{51}O_2N$. (Found: N, 3.02. Calcd.: N, 3.06%.) The photolysis of the nitrite (IV) in dry benzene by the Barton procedure[3] using a 100 W. mercury lamp gave 24-oximinofriedelan-3β-ol (V); m.p. 249.5—251°C, $\nu_{max}^{Nujol}$ 3570 and 3300 $cm^{-1}$, $C_{30}H_{51}O_2N$. (Found: N, 3.11. Calcd.: N, 3.06%.) This oxime (V), when treated with chromic trioxide - sulfuric acid, afforded 3β-hydroxyfriedelan-24-oic lactone (VI), m.p. 287—287.5°C, $\nu_{max}^{Nujol}$ 1765 $cm^{-1}$, $C_{30}H_{48}O_2$ (Found: C, 82.20; H, 11.19. Calcd.: C, 81.76; H, 10.98%), whose mass spectrum[4] shows a peak at *m/e* 440 ($M^+$), together with other peaks due to skeletal fragmentations.

The same γ-lactone (VI) was also obtained by an alternative route. A solution of 3β-hydroxyfriedelane (III) in cyclohexane was refluxed for 1.5 hr. with lead tetraacetate in the presence of iodine under irradiation with a 250 W. lamp. The residue obtained, when treated with chromic trioxide - sulfuric acid, gave, after separation by thin-layer chromatography, a lactone, m.p. 286—287°C, $\nu_{max}^{Nujol}$ 1765 $cm^{-1}$, identical (IR, m.p. and mixed m.p.) with 3β-hydroxyfriedelan-24-oic lactone (VI).

The synthesis of 3β-hydroxyfriedelan-24-oic lactone thus achieved furnishes chemical evidence for the presence in friedelin of an axial β-methyl group at $C_5$.

*Department of Chemistry*
*Faculty of Science*
*The University of Tokyo*
*Hongo, Tokyo*

1) E. J. Corey and J. J. Ursprung, *J. Am. Chem. Soc.*, **77**, 3667, 3668 (1955); **78**, 5041 (1956); G. Brownlie, F. S. Spring, R. Stevenson and W. S. Strachan, *J. Chem. Soc.*, **1956**, 2419; T. Takahashi and G. Ourisson, *Bull. soc. chim. France*, **1956**, 353; H. Dutler, O. Jeger and L. Ruzicka, *Helv. Chim. Acta*, **38**, 1268 (1955), and the references cited therein.

2) J. L. Courtney and W. Stern, *Tetrahedron Letters*, No. 21, 1607 (1965).

3) D. H. R. Barton, J. M. Beaton, L. E. Geller and M. M. Pechet, *J. Am. Chem. Soc.*, **82**, 2640 (1960); **83**, 4076 (1961), and related papers.

4) Measured using the Hitachi Mass Spectrometer RMU-6 Type, at the Naka Works, Hitachi, Ltd., to which company the authors' thanks are due.

# Effect of the *N*-Substituent on the Course of the Reaction of α-Aminonitriles with Organometallic Reagents[1]

By Juji Yoshimura, Yoshiaki Ohgo and Tetsuo Sato

(Received August 12, 1964)

It is generally known that Grignard reagents or lithium alkyls react with nitriles to afford ketimines or ketones. On the other hand, one of the present authors has previously reported that the cyano group of *N*-phenyl-3, 4; 5, 6-di-*O*-isopropylidene-D-glucosaminonitrile was predominantly substituted with alkyls of various Grignard reagents or lithium alkyls to afford levo- and dextro-rotating diasteromers respectively.[2] Such substituted products have often been obtained along with the normal addition products[3] by Grignard reactions using a nitrile with an amino or a hydroxyl group on its α-carbon.

In the present work, the reactions of Grignard or lithium alkyl reagents with various *N*-substituted α-aminonitriles will be examined in order to clarify the factors governing the reaction courses, namely, the substitution and addition reactions.

## Materials

*N*-Phenyl-3,4-*O*-isopropylidene-D-threosamino- and -erythrosaminonitrile (Ib and Ic), the corresponding *N*-benzyl derivatives (Id and Ie),[4] diastereomeric mixtures of the *N*-ethyl and *N*-dimethyl derivatives (Ia and Ig), and racemic α-phenyl α-dimethylaminoacetonitrile (III)[5] were prepared by the reaction of the corresponding amines, hydrogen cyanide, and either acetone-D-glyceraldehyde or benzaldehyde.

3, 4-*O*-Isopropylidine-*N*-acetyl-*N*-benzyl-D-threosaminonitrile (If) and α-acetamido butyronitrile (II) were prepared by the acetylation of the corresponding α-aminonitriles produced by the above-mentioned procedure.

Table I. Cyanide ion (%) liberated in the reaction of α-aminonitriles with organometallic reagents, and products

| Run | α-Amino-nitrile | Reagent | $CN^-$ liberated % | 2,4-Dinitro-phenylhydrazine test | Product |
|---|---|---|---|---|---|
| 1 | Ia | PhMgBr | 43 | | VIa |
| 2 | Ib | PhMgBr | 60 | | VIb+VIc |
| 3 | Ic | PhMgBr | 55 | | VIb+VIc |
| 4 | Id | PhMgBr | 56 | | VId+VIe |
| 5 | Ie | PhMgBr | 73 | | VId+VIe |
| 6 | If | PhMgBr | 0 | + | IVf+Vf |
| 7 | Ig | PhMgBr | 51 | | VIg |
| 8 | II | PhMgBr | 0 | + | VIII |
| 9 | Ia | PhLi | 87 | | VIa |
| 10 | Ib | PhLi | 91 | | VIb+VIc |
| 11 | Ic | PhLi | 99 | | VIb+VIc |
| 12 | Id | PhLi | 91 | | VId+VIe |
| 13 | Ie | PhLi | 99 | | VId+VIe |
| 14 | If | PhLi | 0 | + | — |
| 15 | Ig | PhLi | 0 | + | — |
| 16 | II | PhLi | 7 | + | VII+VIII |
| 17 | III | EtLi | 0 | + | IX |

1) A part of this work was presented at the 15th Annual Meeting of the Chemical Society of Japan, April, 1962.
2) J. Yoshimura, This Bulletin, 35, 536 (1962).
3) M. S. Kharasch and O. Reinmuth, "Grignard Reactions of Nonmetallic Substances," Prentice-Hall, New York (1954).
4) J. Yoshimura, Y. Ohgo and T. Sato, This Bulletin, 34, 1197 (1961).
5) T. S. Stevens, J. M. Cowan and J. Mackinnon, *J. Chem. Soc.*, 1931, 2568.

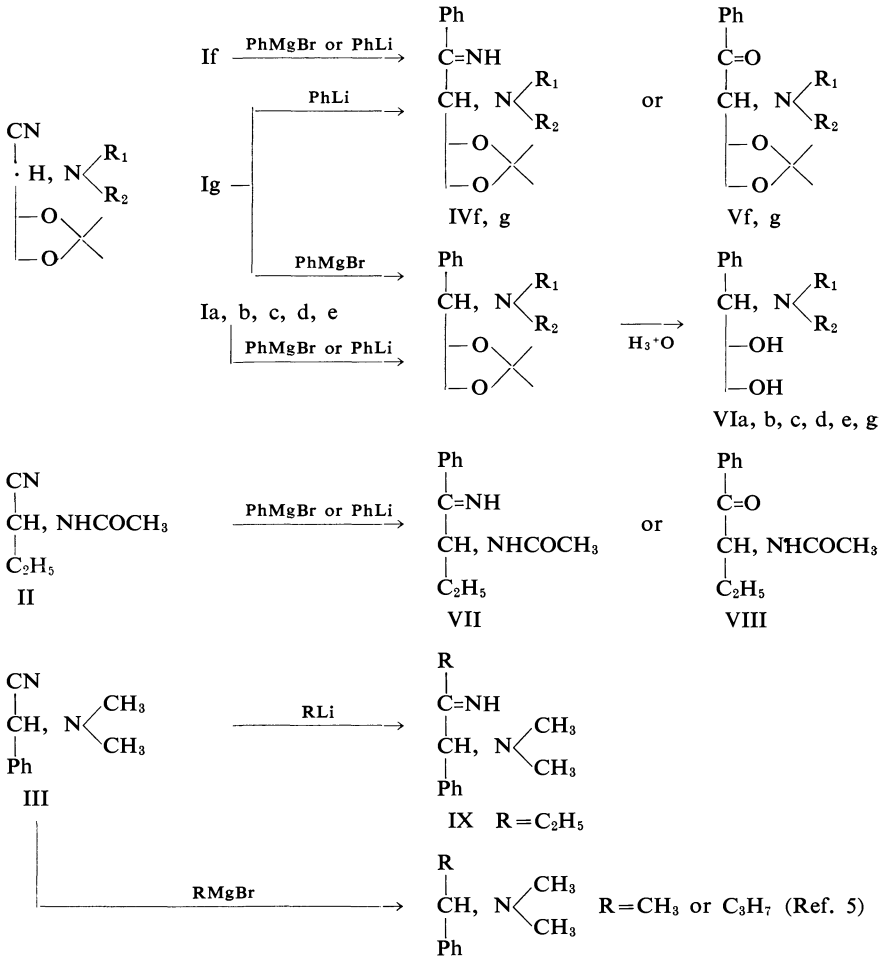
## Results and Discussion

*N*-Substituted 3, 4-*O*-isopropylidene-D-tetrosaminonitriles (Ia—Ig), $\alpha$-acetamido butyronitrile (II) and $\alpha$-phenyl $\alpha$-dimethylaminoacetonitrile (III) were treated with phenylmagnesium bromide, phenyllithium or ethyllithium in ether, and each reaction mixture was decomposed with ice-water.

The amount of cyanide ions liberated in the water layer was determined by titration with a 0.5 N silver nitrate solution; the results are summarized in Table I.

The 2, 4-dinitrophenylhydrazine test was applied to the syrup obtained from the reaction mixtures in which no detectable amount or only a very small amount of cyanide ions was produced. As shown in Table I, the test was positive in all the cases tried. Moreover, elemental analyses of each fraction isolated by high-vacuum distillation from runs 6, 8, 16 and 17 agreed with the structures of the addition products, IV (V),* VIII, VII (VIII)* and IX respectively, as shown in Scheme 1. (Yield: 20—30%; see Experimental section.)

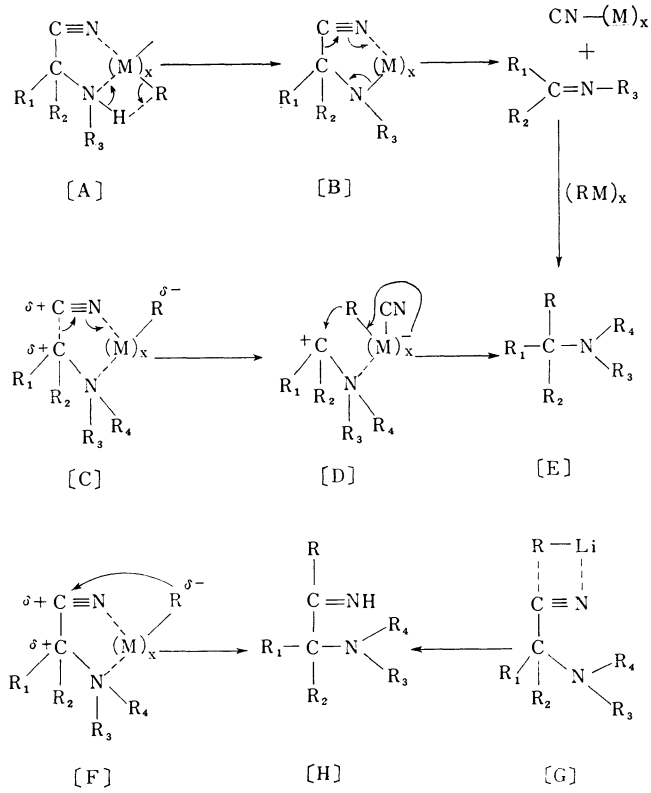
When a considerable amount of cyanide ions was detected in the reaction mixture, the substituted products were derived to VI by treatment with hot 6 N hydrochloric acid and isolated in yields of 20—50%, as shown in Scheme 1.




| | $R_1$ | $R_2$ | Configuration | | $R_1$ | $R_2$ | Configuration |
|---|---|---|---|---|---|---|---|
| a | H | Ethyl | A diastereomeric mixture | b | H | Phenyl | Threo |
| c | H | Phenyl | Erythro | d | H | Benzyl | Threo |
| e | H | Benzyl | Erythro | f | Benzyl | Acetyl | Threo |
| g | Methyl | Methyl | A diastereomeric mixture | | | | |

Scheme 1

* The substance in parenthesis is a minor product.



$(M)_x$ means that x molecules of organometallic reagents are involved in the transition state.

Scheme 2

The structure of VId was confirmed[6] by leading it to the known *N*-acetyl-D(−)-phenylglycine, while those of VIa, VIb, VIc, VIe and VIg were presumed from the analogy of these infrared absorption spectra with that of VId and from their analytical data. VIb and VIc or VId and VIe are diastereomeric to each other.

The analytical data, physical properties, and configurational assignments of the substituted products have been shown in a previous paper.[6]

The results are summarized in Scheme 1.

As runs 1—5 and 9—13 show, both the Grignard reagent and lithium alkyl attack not nitrile carbon but α-carbon to give a substituted product when the α-aminonitrile has an active hydrogen on its aminonitrogen.

Active hydrogen is known to be highly sensitive to organometallic reagents.[3] Consequently, in the case of the α-aminonitrile with an active hydrogen on the aminonitrogen, this reagent may expel the hydrogen in the first step via coordination, thus making an *N*-metal covalent bond. The metal in this state will be coordinated with the neighboring cyano group to form a five-membered ring.

This cyclic chelation may be favored for electron migration, as shown in diagram [B], and the cyano group could smoothly migrate to the metal. The imines thus formed are attacked by another molecule of organometallic reagents to give substituted products [E].

On the other hand, a marked difference appeared in the products between Grignard and lithium alkyl reactions with α-dialkylaminonitriles; Grignard reagents attack α-carbon to give substituted products, but lithium alkyls attack nitrile carbon (runs 5, 15 and 17).

Since there is no place to make a *N*-metal covalent bond in dialkylaminonitriles, this marked differnce between Grignard and lithium alkyl reactions may be attributed to the difference in the coordination ability of the reagents. The elimination of the cyano group of α-dialkylaminonitriles in the Grignard reaction may be interpreted by assuming the initial formation of a coordinative complex [C]. The formation of the complex decreases electron density not only at the nitrile carbon but also at the α-carbon, and it may facilitate the dissociation of the $C_\alpha$–CN bond to form

6) J. Yoshimura, Y. Ohgo and T. Sato, *J. Am. Chem. Soc.*, 86, 3858 (1964).

the cyanide ion and a carbocation [D].* Lithium alkyls would not have as strong a power of attracting electron from these ligands as magnesium, and they would be considered to form the four-center transition state [G],[7] which in turn leads to ketimines. This seems to be related to the fact that the addition reaction of conjugeted carbonyl compounds with lithium alkyls gives the 1, 2 addition product predominantly, while that with Grignard reagents the 1, 4 addition product[8].

Runs 6, 8, 14 and 16 shows that the aminonitriles bearing acetyl group on its aminonitrogen are not attacked at $\alpha$-carbon but at nitrile carbon with both the reagents, thus giving the addition products.

It may be considered that the dissociation of the $C_\alpha$–CN bond of these aminonitriles does not occur, for aminonitrogen whose basicity is weakened by the acetyl group can not coordinate to the metal.

From the above mechanism concerning the Grignard reaction, it may be expected that the existence of factors to prevent the coordination of the aminonitrogen suppress the substitution reaction. In fact, certain $\alpha$-aminonitriles with oxygen in the dialkylamino portion are attacked at nitrile carbon to afford ketones predominantly.[9]

Recent investigations[10] on the composition of Grignard compounds in a solution have shown that a Grignard solution is an equilibrium mixture of several species, such as $R_2Mg$, $MgX_2$, RMgX, $(RMgX)_2$ and $R_2Mg \cdot MgX_2$, and that the natures of the alkyl group, the halogen atom and the solvent all have an effect on the equilibrium.

It would be of interest to investigate which species do play a principal role in the substitution or the addition reaction.

## Experimental

**The General Procedure for the Reaction of $\alpha$-Aminonitriles with an Organometallic Reagent.**—Into an ethereal solution of phenyllithium or phenylmagnesium bromide, prepared from 0.06 mol. of bromobenzene and 0.12 mol. of metal lithium or 0.06 mol. of magnesium, was added 0.02 mol. of aminonitrile with stirring at 0—5°C. The mixture was refluxed for about ten hours, and then it was cautiously poured into ice water covered with 100 ml. of ether. The water layer was separated from the ether layer and extracted twice 50 ml. of ether. The water layer was then titrated by a 0.5 N silver nitrate solution, using potassium iodide as an indicator, in order to determine the amount of cyanide ions liberated in the reaction mixture. In the case of the Grignard reaction, 25 ml. of a 4 N potassium hydroxide solution had previously been added to the water layer in order to prevent the cyanide ions from escaping as hydrogen cyanide; also, an amorphous precipitate was removed by filtration. The filtrate was used for the quantitative determination of the cyanide ions. The ether layer was washed with water, dried, and concentrated in vacuo to a syrup. When a considerable amount of cyanide ion were detected in the water layer, the above syrup was subjected to hydrolysis with a 6 N hydrochloric acid solution (20 ml.) at 100°C for two hours. After tar-like substances insoluble in hydrochloric acid had been removed by filtration through activated carbon, followed by steam distillation, the filtrate was decolorized with activated carbon. After the filtrate had been adjusted to pH 10 with a sodium hydroxide solution it was extracted four times with 50 ml. of ethyl acetate.

The combined ethyl acetate solution was washed twice with 50 ml. of water and dried with anhydrous sodium sulfate. After the ethyl acetate fraction had been concentrated under reduced pressure to dryness, a crude diastereomeric mixture of 1-*C*-phenyl-1-alkylamino-1-deoxy-D-glyceritol became crystals, except for the product from run 9, whose yields were from 20 to 50%.

When no remarkable amount of cyanide ion was detected in the water layer, a small portion of the syrup from the ether layer was tested for the precipitation reaction by 2,4-dinitrophenylhydrazine after the removal of isopropylidene group; in some cases the isolation of addition products from the residual syrup was attempted by high-vacuum distillation.

***N*-Ethyl-3, 4-*O*-isopropylidene-D-tetrosaminonitrile (A Diastereomeric Mixture) (Ia).**—A benzene solution (1.2 l.) of acetone-D-glyceraldehyde[11] prepared from 40 g. of diacetone-D-mannitol by oxidative scission using lead tetraacetate (70 g.) was neutralized with a 50 per cent aqueous potassium carbonate solution (50 ml.). The benzene layer was separated, dried with anhydrous sodium sulfate, and then shaken with 70 per cent ethylamine (50 ml.) for thirty minutes. The resulting reaction mixture was concentrated under reduced pressure to about 200 ml., and to it was added ethanol (100 ml.) and hydrogen cyanide (40 ml.) with cooling. The mixture was then left to stand overnight in a refrigerator and then concentrated in vacuo to a syrup; the syrup was then purified by distillation under reduced pressure.

Yield, 18.9 g. B. p. 88°C (0.35 mmHg).

Found: C, 58.18; H, 9.09; N, 14.59. Calcd. for $C_9H_{16}O_2N_2$: C, 58.67; H, 8.75; N, 15.21%.

***N*-Dimethyl-3, 4-*O*-isopropyridene-D-tetrosaminonitrile (A Diastereomeric Mixture) (Ig).**—A benzene

* In the Grignard reaction a minor path from [F] to [H] may be included.

7) E. A. Braude, "Progress in Organic Chemistry," 3, Butterworths Scientific Publications, London (1955), p. 185.

8) A. Lüttringhaus, *Chem. Ber.*, 67, 1602 (1934); H. Gilman and R. H. Kirby, *J. Am. Chem. Soc.*, 63, 2046 (1941); S. H. Tucker and M. Whalley, *J. Chem. Soc.*, **1949**, 50; E. A. Braude and J. A. Coles, ibid., **1950**, 2012; **1952**, 1425.

9) L. H. Goodson and H. Christopher, *J. Am. Chem. Soc.*, 72, 358 (1950).

10) R. M. Salinger and H. S. Mosher, ibid., 86, 1782 (1964); E. C. Ashby and M. B. Smith, ibid, 86, 4363 (1964); 85, 118 (1963).

11) E. Baer and H. O. L. Fisher, *J. Biol. Chem.*, 128, 463 (1939).

solution of 50 g. of acetone-D-glyceraldehyde was shaken with 60 ml. of a 30 per cent dimethylamine solution. The mixture was concentrated to about 200 ml. under reduced pressure, mixed with 100 ml. of ethanol and 30 ml. of hydrogen cyanide with chilling, and then left to stand in a refrigerator overnight. The reaction mixture was then concentrated to a syrup, which was distilled to give 21.2 g. of the product. B. p. 81°C (0.2 mmHg).

Found: C, 58.16; H, 8.40; N, 14.21. Calcd. for $C_9H_{16}O_2N_2$: C, 58.67; H, 8.75; N, 15.21%.

**N-Benzyl-N-acetyl-3, 4-O-isopropylidene-D-threosaminonitrile (If).**—To a solution of 4 g. of *N*-benzyl-3,4-*O*-isopropylidene-D-threosaminonitrile (m. p. 86—87°C) in 40 ml. of pyridine 15 ml. of acetic anhydride was added with cooling. After the reaction mixture had been left standing at room temperature for two days, it was poured into ice water. The suspension was extracted with chloroform, and the chloroform layer was repeatedly washed with water, dried, and concentrated to a syrup. The syrup was dissolved in a suitable amount of ethanol and then left to stand overnight in a refrigerator. The crystals which appeared were recrystallized from ethanol-petroleum ether to give colorless plates (2.8 g.). M. p. 81—82°C, $[\alpha]_D$ −34° (*c* 1.03, ethanol).

Found: C, 66.03; H, 7.23; N, 9.73. Calcd. for $C_{16}H_{20}N_2O_3$: C, 66.64; H, 6.99; N, 9.72%.

**N-Acetylbutyronitrile (II).** — To a 100 ml. of ethanol containing 7.4 g. of ammonia was added 25 g. of propionaldehyde and then 40 ml. of hydrogen cyanide with chilling. After the reaction mixture had been left standing in a refrigerator for two hours, it was concentrated carefully under reduced pressure. The syrup obtained was dissolved in 50 ml. of pyridine and then 50 ml. of acetic anhydride was added to the solution with chilling. After it had stood two days at room temperature, the reaction mixture was poured into ice water and extracted with 200 ml. of ethyl acetate. The ethyl acetate layer was separated, washed with water, and dried over anhydrous sodium sulfate. After the ethyl acetate had been removed under reduced pressure, a syrup was obtained by distillation; 101°C (0.03 mmHg).

Found: C, 56.77; H, 7.93; N, 22.48. Calcd. for $C_6H_{10}N_2O$: C, 57.11; H, 7.99; N, 22.21%.

**Addition Products.**—When no cyanide ion could be detected in the reaction mixture, the isolation of the addition product from the ether fraction was attempted by high vacuum distillation in some cases. The addition products were obtained as follows.

*Addition Products from Run 6.* — Three fractions were obtained by the distillation of the syrup from run 6.

I. B. p. 125—126°C (0.01 mmHg); 0.25 g.

Found: N, 4.82%.

The analytical value in nitrogen was agreed with that of the carbonyl structure (V).

II. B. p. 143—144°C (0.002—0.003 mmHg)/bath temp. 197°C; 0.25 g.

Found: N, 7.13%.

III. B. p. 200—205°C (0.005 mmHg); m. p. 159—161°C; 1.4 g.

Found: C, 72.58; H, 6.35; N, 7.78. Calcd. for $C_{22}H_{26}O_3N_2$: C, 72.10; H, 7.15; N, 7.65%.

The analytical values of this fraction agreed with those of the imino compound (IV).

*The Addition Product from Run 8 (VIII).* — The evolution of ammonia gas was perceived from the reaction mixture of run 8 after it has stood for a week. An oily substance was obtained, besides a small amount of biphenyl, on the distillation of the syrup. Yield, 1.1 g.; b. p. 125°C (0.08 mmHg); $R_f$ 0.89 (BuOH saturated with water).

Found: C, 70.79; H, 7.17; N, 6.78. Calcd. for $C_{12}H_{17}O_2N$: C, 70.22; H, 7.37; N, 6.82%.

*The Addition Products from the Reaction Mixture of Run 16.*—The evolution of ammonia gas was perceived from the reaction mixture of run 16. The distillation of the syrup gave the following fractions.

I. B. p. 135—140°C (0.1—0.2 mmHg); 0.5 g.

The infrared spectrum of this syrup was consistent with VIII.

II. B. p. Over 150°C (0.1 mmHg); 0.3 g. The fraction became crystals. Its analytical value in nitrogen was agreed with that of VII.

Found: N, 13.12. Calcd. for $C_{12}H_{16}N_2O$: N, 13.72%.

III. A small amount of a crystalline product condensed at the top of the thermometer. This substance was identical in analytical value with the substance of fraction II.

Found: N, 13.82. Calcd. for $C_{12}H_{16}N_2O$: N, 13.72%.

*The Addition Product from Run 17 (IX).* — B. p. 111—112°C (20 mmHg).

Found: N, 14.48. Calcd. for $C_{12}H_{18}N_2$: N, 14.75%.

## Summary

The reactions between various *N*-substituted-α-aminonitriles and organometallic reagents have been investigated in order to clarify the effect of the *N*-substituent on the reaction course.

The results indicate that:

(1) Both Grignard reagent and lithium alkyl attack not nitrile carbon but α-carbon to give substituted product when the α-aminonitrile has an active hydrogen on its aminonitrogen.

(2) In the case of α-dialkylaminonitriles, Grignard reagents attack the α-carbon to give substituted products, but lithium alkyls attack the nitrile carbon.

(3) The aminonitriles bearing acetyl group on its aminonitrogen are not attacked at α-carbon but at nitrile carbon by both the reagents, thus giving addition products.

The authors wish to express their hearty thanks to the members of the Laboratory of Organic Analysis, Tokyo Institute of Technology, for their microanalysis.

*Laboratory of Organic Chemistry*
*Tokyo Institute of Technology*
*Ookayama, Tokyo*

# The Adsorption of Copper(II), Dichromate(II) and Oxalate(II) by Different Samples of Precipitated Hydrous Beryllium Oxide

By Rup DUTTA

(Received August 13, 1964)

In an earlier communication[1] we have described the precipitation of hydrous beryllium oxide by different alkalis, like sodium, potassium and ammonium hydroxides, from a beryllium sulfate solution. It has been shown that hydrous beryllium oxide is always associated with sulfate and sodium or potassium, according to whether the medium of precipitation is acidic or alkaline. This behavior has been attributed to the fact that at lower pH values, the precipitated hydrous oxide is basic in character and adsorbs anions, while at higher pH values it is predominantly acidic in character and preferentially adsorbs cations from the solution (Table IV). This shows, therefore, the amphoteric nature of the hydrous oxide in media of different pH values. It is worthwhile to mention here that, at different stages of precipitation, the ions adsorbed by the hydrous beryllium oxide could not be removed by washing it with hot water or even by heating the precipitated mass.

Extensive studies[2-7] of the adsorption of dyestuffs by precipitated hydrous oxides have been carried out in these laboratories. Tewari, Dey and Ghosh,[8] from a consideration of the adsorption of dyestuffs by hydrous oxides, attempted to elucidate the mechanism of the ageing of metal hydroxide.

It has been thought desirable to study the adsorption of some inorganic ions by different samples of hydrous beryllium oxide, prepared with different amounts of alkali, this paper will record the observation of the association of copper(II), dichromate(II) and oxalate(II) with the samples of hydrous beryllium oxide.

## Experimental and Results

**Materials.**—Beryllium sulfate, copper sulfate, potassium dichromate and sodium thiosulfate solutions of the desired strengths were prepared from B. D. H., AnalaR grade chemicals and standardized by the usual methods (Arthur I. Vogel).

**The Preparation of the Samples of Hydrous Oxide.**—The samples, A, B and C, of the hydrous oxide were obtained by adding calculated amounts of a standard solution of sodium hydroxide to 500 ml. of a 0.5 M beryllium sulfate solution at 25°C.

A: precipitated with an equivalent sodium hydroxide
B: precipitated with a 10% deficient sodium hydroxide
C: precipitated with a 10% excess sodium hydroxide

These samples were thoroughly washed by decantation with distilled water the washings were free from a majority of the sulfate and hydroxyl ions. (The hydroxyl ions were removed completely, but the last traces of sulfate ions could not be removed completely due to the increasing tendency of the hydrous oxide to form a colloidal solution on further washing.)

These samples were then allowed to age for a month in Jena glass bottles. The volumes of these suspensions were raised by dilution with water to 0.2 M of beryllium oxide per liter after ageing; the pH values of A, B and C were then found to be 6.1, 5.6 and 6.9 respectively.

**Adsorption Experiments.**—To 5 ml. of suspension (0.001 M), varying amounts of the electrolyte solution were added, and the volumes were raised to 15 ml. The systems were then allowed to equilibrate for 24 hr. at 30°C. In the supernatant liquids, the concentrations of the ions were estimated, copper and dichromate iodometrically and oxalate against a standard permanganate solution. The amounts of ions adsorbed, $x/m$, where $x$ is the amount of adsorbent adsorbed on $m$ g. of adsorbate, are given below.

TABLE I. ADSORPTION OF CUPRIC IONS BY VARIOUS SAMPLES OF HYDROUS BERYLLIUM OXIDE

| Initial concn. M×10⁶ | Values of cupric ion adsorbed $x/m$ | | |
|---|---|---|---|
| | Sample A | Sample B | Sample C |
| 159.6 | 88.7 | 94.2 | 43.5 |
| 128.7 | 67.2 | 71.7 | 34.2 |
| 106.0 | 52.0 | 55.0 | 25.9 |
| 85.2 | 37.5 | 39.7 | 19.9 |
| 53.3 | 17.0 | 18.2 | 10.0 |
| Total: | 262.4 | 278.8 | 133.5 |

Adsorptive capacities of samples A, B and C are in the sequence B>A>C.

1) R. Dutta and S. Ghosh, *Kolloid-Z*, to be published.
2) A. K. Dey and S. Ghosh, *Proc. Natl. Acad. Sci. India*, **15A**, 143 (1946).
3) S. N. Tewari, *Kolloid-Z*, **19**, 128 (1962).
4) R. B. Hajela and S. Ghosh, *Proc. Natl., Acad. Sci. India*, **28A**, 59, 118, 130 (1959).
5) S. N. Tewari and S. Ghosh, ibid., **21A**, 29, 41 (1952).
6) R. Prasad and A. K. Dey, *J. Phys. Chem.*, **65**, 1272 (1961).
7) R. Prasad and A. K. Dey, *J. Inorg. Nucl. Chem.*, **24**, 1018 (1962).
8) S. N. Tewari, A. K. Dey and S. Ghosh, *Z. anong. Chem.*, **271**, 150 (1953).

TABLE II. ADSORPTION OF DICHROMATE IONS BY VARIOUS SAMPLES OF HYDROUS BERYLLIUM OXIDE

| Initial concn. $M\times10^6$ | Values of $x/m$ | | |
|---|---|---|---|
| | Sample A | Sample B | Sample C |
| 26.70 | 11.00 | 5.75 | 11.50 |
| 21.45 | 7.90 | 4.70 | 9.80 |
| 17.75 | 7.85 | 4.05 | 8.50 |
| 14.20 | 6.30 | 3.40 | 7.45 |
| Total : | 38.55 | 20.35 | 42.15 |

Adsorptive capacities of samples A, B and C in the sequence are C>A>B.

TABLE III. ADSORPTION OF OXALATE IONS BY VARIOUS SAMPLES OF HYDROUS BERYLLIUM OXIDE

| Initial concn. $M\times10^6$ | Values of $x/m$ | | |
|---|---|---|---|
| | Sample A | Sample B | Sample C |
| 79.95 | 26.40 | 11.85 | 31.50 |
| 53.30 | 22.65 | 9.40 | 25.65 |
| 42.60 | 19.75 | 7.85 | 23.40 |
| 26.65 | 13.60 | 5.70 | 17.35 |
| Total : | 82.40 | 34.80 | 97.90 |

Adsorptive capacities of samples A, B and C in the sequence are C>A>B.

## Discussion

The above tables conclusively show that in the case of the adsorption of cupric ions, the amount of adsorption reaches a maximum for sample B, prepared from deficient amount of alkali, and a minimum for sample C, prepared from an excess of alkali, and is in the order of B>A>C. In the case of oxalate and dichromate, the order of adsorption, as noted, is C>A>B, showing thereby that sample C, prepared from an excess of alkali, has the maximum adsorptive capacity for the ions.

It is well known that amphoteric bodies depend on environmental conditions to display their acidic and basic characters. A sample prepared from an excess of alkali should have an acidic character and should adsorb cations. Similarly, an acidic character and should adsorb cations. Similarly, a sample prepared from a deficient quantity of alkali should have a basic property and should preferentially adsorb anions.

In the case of beryllium hydroxide, however, the results show that the adsorption is in the reverse order; i.e., sample C displays a basic character and shows a maximum adsorption for dichromate or oxalate anions. Similarly, sample B shows an acidic character and results in a maximum adsorption for copper cation. It has been explained in an earlier communication,[1] that during the precipitation of hydrous beryllium oxide by different alkalis, the precipitated mass always contains sodium or potassium or sulfate according as the medium of precipitation is, respectively, alkaline or acidic (cf. Table IV). Moreover, as has been said earlier, these adsorbed ions could not be removed by either washing with hot water or heating the precipitated mass.

Table IV shows the amounts of beryllium oxide (in mg.) obtained in the residue and $SO_3$ obtained in the filtrate, when the precipitation of beryllium from beryllium sulfate was carried out with sodium hydroxide. The pH change during the precipitation has also been recorded. It is clear from Table IV that, when the pH of the precipitating medium is made less than 9 by the addition of deficient alkali, the adsorption of $SO_3$ is prominent on the beryllium oxide precipitate (which is represented by sample B), but that as soon as the pH

TABLE IV. PRECIPITATION OF BERYLLIUM HYDROXIDE BY SODIUM HYDROXIDE AND ESTIMATION OF BeO IN THE RESIDUE AND $SO_3$ IN THE FILTRATE AT DIFFERENT pH VALUES

Beryllium sulphate of 0.1 M taken—20 ml.
Total volume—100 ml.

| Ratio Be : $OH^-$ | pH | BeO obtained, mg. | | $SO_3$ obtained, mg. | |
|---|---|---|---|---|---|
| | | Theoretical calculation | Experimental | Theoretical calculation | Experimental |
| 1 : 1.0 | 5.3 | 25 | 0.0 | 160.0 | 160.0 |
| 1 : 1.2 | 5.65 | 30 | 12.4 | 160.0 | 158.0 |
| 1 : 1.4 | 5.75 | 35 | 26.4 | 160.0 | 156.0 |
| 1 : 1.6 | 5.90 | 40 | 43.4 | 160.0 | 151.0 |
| 1 : 1.8 | 6.20 | 45 | 58.6 | 160.0 | 149.0 |
| 1 : 2.0 | 9.80 | 50 | 63.6 | 160.0 | 157.0 |
| 1 : 2.2 | 11.05 | 50 | 62.6 | 160.0 | 160.5 |
| 1 : 2.4 | 11.35 | 50 | 62.0 | 160.0 | 160.3 |
| 1 : 2.6 | 11.60 | 50 | 61.6 | 160.0 | 160.2 |
| 1 : 3.0 | 11.70 | 50 | 61.6 | 160.0 | 160.1 |
| 1 : 4.0 | 11.85 | 50 | 61.5 | 160.0 | 160.1 |

goes above 9 upon the addition of an excess of alkali, sodium ions are preferentially adsorbed by the beryllium oxide (which is represented by sample C).

These results, therefore, conclusively show that sample B, prepared from a deficient quantity of a alkali, which is already associated with anion sulfate, prevents the further association of other oxalate or dichromate anions, and showing thereby the least adsorption value for these anions. Similarly, sample C, prepared from an excess of alkali, is already associated with the cation sodium, prevents the further association of any other cation like copper from the solution.

## Summary

Three samples, A, B and C, of hydrous beryllium oxide were prepared by adding different amounts of alkali to a fixed volume of a beryllium sulfate solution.

Sample A prepared with an equivalent amount of alkali, sample B prepared with a 10% deficient amount of alkali, sample C prepared with a 10% excess amount of alkali.

These samples were washed thoroughly and allowed to age for a month. The adsorption capacities of these samples for the ions copper(II), oxalate(II) and dichromate(II) were then studied. The adsorption of copper(II) by different samples was found to be in the order B>A>C, whereas in the case of oxalate and dichromate the order of adsorption, is C>A>B.

The author wishes to thank Dr. A. K. Day for his valuable suggestions. The author is also thankful to the Council of Scientific and Industrial Research for awarding a fellowship to him.

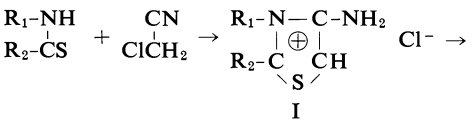
*Chemical Laboratory*
*University of Allahabaa*
*Allahabad, India*

# The Reaction of "4-Thiazone Imine" Derivatives with Acetic and Benzoic Anhydride[1]

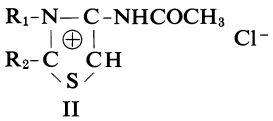
By Chung-gi SHIN and Masaki OHTA

(Received December 8, 1964)

In a previous paper of this series, the synthesis of some new meso-ionic compounds, 4-thiazone imine hydrochlorides (Ia), by the condensation of thioamides with $\alpha$-halonitriles was reported.[2] The acetylation of Ia by acetic anhydride at 100°C afforded hydrochlorides of an acetyl derivative IIa, which in turn gave a free acetyl derivative III when treated with an aqueous solution of sodium hydrogen carbonate.[2]

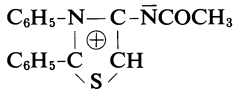


I

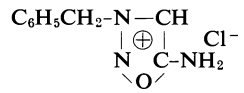


II

Ia : $R_1=C_6H_5$, $R_2=C_6H_5$
b : $R_1=C_6H_5$, $R_2=CH_3$
c : $R_1=CH_3$, $R_2=C_6H_5$
d : $R_1=p\text{-}ClC_6H_4$, $R_2=C_6H_5$
IIa : $R_1=C_6H_5$, $R_2=C_6H_5$
b : $R_1=C_6H_5$, $R_2=CH_3$
c : $R_1=CH_3$, $R_2=C_6H_5$
d : $R_1=p\text{-}ClC_6H_4$, $R_2=C_6H_5$



III

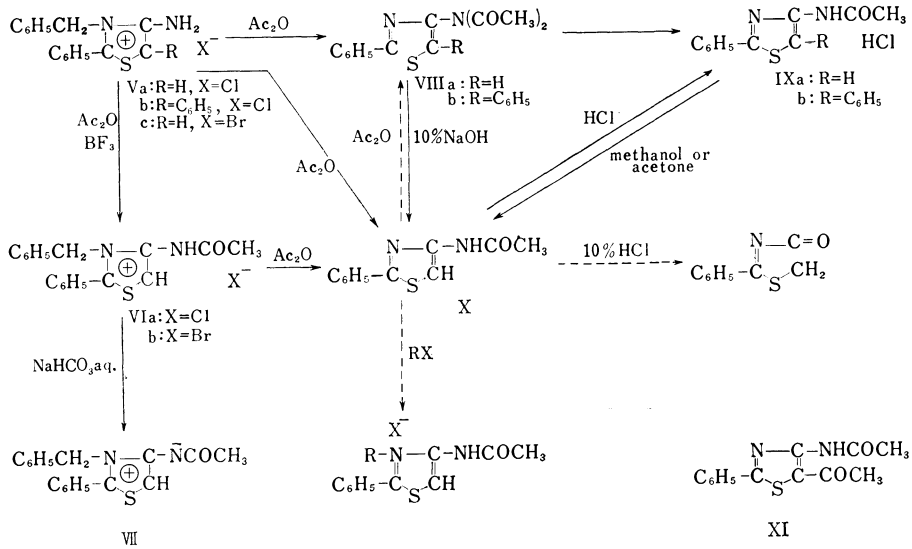


IV

Recently, the thermal instability of sydnone imine hydrochlorides possessing an aralkyl group, such as the benzyl group in the 3-position (IV), has been reported by Daeniker and Druey,[3] but the structures of the decomposition products have not yet been described.

In the course of our studies of the acylation of 4-thiazone imine salts, the present authors

1) This paper is the part XXIII of "Studies on Meso-ionic Compounds."
2) H. Chosho, K. Ichimura and M. Ohta, This Bulletin, 35, 1670 (1964).
3) H. U. Daeniker and J. Druey, *Helv. Chim. Acta*, 45, 2426 (1962).



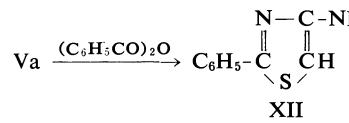

have found that 3-benzyl derivatives behave peculiarly towards acylation under special conditions. When 3-benzyl-2-phenylthiazone imine hydrochloride (Va) was treated with acetic anhydride in the presence of boron trifluoride in acetic acid at room temperature for about two weeks, until all of the solids dissolved, the monoacetyl derivative VIa was obtained in a good yield as colorless prisms. Compound VIa gave the free acetyl derivative VII upon treatment with an aqueous solution of sodium hydrogen carbonate. On the other hand, we found that when Va was refluxed with acetic anhydride, 4-diacetylamino-2-phenylthiazole (VIIIa) or a mixture of VIIIa and 4-acetylamino-2-phenylthiazole (X) was obtained, depending upon the reaction temparature and the duration of the heating. Thus, the benzyl group was eliminated and one or two acetyl groups were introduced in this reaction. The elimination of the benzyl group as benzyl chloride was confirmed by the gas chromatographic analysis of the mother liquor. The action of acetic anhydride on VIa under reflux for 45 min. gave X, also.

When an acetone solution of VIIIa was treated with 30% ethanolic hydrogen chloride at room temperature, the hydrochloride of the monoacetyl derivative IXa was obtained in an almost quantitative yield, while under a brief reflux in acetone or methanol, IXa gave the monoacetyl derivative X. This free base could also be obtained by boiling VIIIa with a 10% sodium hydroxide solution for a few minutes. Considering that 4-thiazone, with no substituent at the 5-position, is acetylated at the 5-position (XI) by heating it with acetic anhydride,[4] it is probable that one of the acetyl groups in VIIIa may be located at the 5-position, but when 3-benzyl-2, 5-diphenylthiazone imine hydrochloride (Vb) was refluxed with acetic anhydride, a diacetyl derivative VIIIb was also obtained, and it in turn gave monoacetyl derivative IXb upon hydrolysis. Only a very few 4-aminothiazole derivatives can be found in the literature. In order to establish the structure of the new acetyl derivatives, VIII and X, we tried the synthesis of X using thiobenzamide and chloroacetonitrile under various conditions; however, these attempts resulted only in the formation of resinous matter. The acetylation of Ia was reported in our previous paper,[2] in which 4-thiazone imine hydrochloride was heated with acetic anhydride at 100°C for many hours. When Ia–d were refluxed with acetic anhydride for one hour, monoacetylated thiazone imine hydrochlorides IIa–d were obtained in a good yield without the elimination of the substituent at the 3-position. The facile elimination of the benzyl group at the 3-position is, of course, due to the stability of the benzyl cation.

An attempted preparation of the 5-bromo derivative of Va with bromine in chloroform at room temperature afforded, in a high yield, yellow tablets of 3-benzyl-2-phenylthiazone imine hydrobromide (Vc), the structure of which was indicated by elemental analysis and by its infrared absorption spectrum, which was essentially identical with that of Va. It shows the same reactivity as compounds Va and Vb. Thus, by the action of acetic anhydride as in the case of Ia, Vc gave the monoacetyl derivative VIb at room temperature, while under

4) Part XVIII: M. Ohta, H. Chosho, C. Shin and K. Ichimura, *J. Chem. Soc. Japan, Pure Chem. Sec.* (*Nippon Kagaku Zasshi*), **85**, 440 (1964).

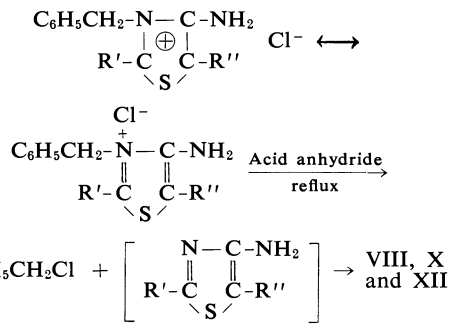
reflux, it gave X, also. An attempted preparation of VIIIa from X with acetic anhydride was not successful. Also not successful were the alkylation of X with benzyl chloride or methyl iodide and the hydrolysis of X with 10% hydrochloric acid. Moreover, we found that when Va was fused with benzoic anhydride in an oil bath for 10 min., 4-benzoylaminothiazole (XII) was obtained in a good yield.



XII

The structures of these 4-aminothiazole derivatives, VIII, IX, X and XII, were assigned on the basis of elemental analyses and their infrared absorption spectra. The elemental analysis of VIIIa is consistent with either one of two structures, VIIIa or XI; the infrared absorption spectrum showed the sharp stretching bands of two carbonyl groups, at 1700 and 1650 $cm^{-1}$, as in the case of VIIIb, which showed bands at 1720 and 1700 $cm^{-1}$. The disappearance of the $-NH_2$ stretching band at 3250 $cm^{-1}$ and the characteristic sharp absorptions of the 4-thiazone imine ring at about 1630, 1570 and 1500 $cm^{-1}$ in the cases of VIIIa and VIIIb, however, suggest the formation of *N*-diacetylated 4-aminothiazole derivatives. Compounds X and XII showed typical secondary amide absorptions, the former at 3200, 1650 and 1290 $cm^{-1}$, and the latter at 3250, 1660 and 1265 $cm^{-1}$.

Daeniker et al.[3,5] have reported the facile removal of the benzyl group of *N*-acetyl-3-benzylsydnone imine by reduction and the formation of *N*-substituted diazoacetamide. They explained its formation in terms of an intermediate formation of the 1, 2, 3-oxadiazole derivative. The formation of VIII, X and XII by reaction with acid anhydride can very possibly be explained by a similar sequence of reactions, which can be shown as follows:



5) H. U. Daeniker and J. Druey, *Helv. Chim. Acta*, **46**, 805 (1963).

We expected the reaction of acid anhydride with *N*-acyl-3-benzylsydnone imine hydrochloride to be similar and we have found that the same type of reaction does indeed take place. The details of this will be the subject of a future report.

## Experimental

**3-Benzyl-2-phenyl-*N*-acetylthiazone Imine Hydrochloride (VIa).**—A suspension of 1 g. of Va in 10 ml. of acetic anhydride and 3 drops of boron trifluoride in acetic acid was heated on a steam bath for 4—5 hr. and then kept standing for about two weeks until all the solid had dissolved. The color of the solution turned brown. The removal of acetic anhydride by evaporation under reduced pressure afforded a brown oil. Upon the addition of anhydrous acetone, colorless prisms crystallized out. Recrystallization from chloroform-ether also afforded colorless prisms. Yield, 0.7 g.; m. p. 150—151°C.

Found: C, 62.90; H, 5.01; N, 8.42. Calcd. for $C_{18}H_{17}ClN_2OS$: C, 62.70; H, 4.93; N, 8.13%.

**2, 3-Diphenyl-*N*-acetylthiazone Imine Hydrochloride (IIa).**—A suspension of 2 g. of Ia in 20 ml. of acetic anhydride was heated under reflux for one hour, until all of the solids had dissolved; the removal of half of the acetic anhydride by evaporation under reduced pressure then afforded colorless precipitates. The precipitates were collected by means of suction and washed with acetone (yield, about 1 g.). An additional 1 g. was obtained from the brown filtrate. Recrystallization from ethanol-ether gave colorless prismatic needles. The total yield of IIa was 1.6 g.; m. p. 291—292°C (decomp.). The melting point and the infrared spectrum of IIa were shown to the identical with those of an authentic sample. In exactly the same manner as in the case of IIa, *N*-monoacetylated 4-thiazone imine hydrochlorides, IIb, IIc and IId, were prepared from the corresponding thiazone imine hydrochlorides.

IIb: m. p. 228—229°C (decomp.), yellow needles.
Found: C, 53.42; H, 4.92; N, 10.74 Calcd. for $C_{12}H_{13}ClN_2OS$: C, 53.63; H, 4.84; N, 10.43%.

IIc: m. p. 215—216°C (decomp.), yellow needles.
Found: N, 10.54. Calcd. for $C_{12}H_{13}ClN_2OS$: N, 10.43%.

IId: m. p. 279—280°C (decomp.), colorless prisms.
Found: N, 7.76. Calcd. for $C_{17}H_{14}Cl_2N_2OS$: N, 7.67%.

**3-Benzyl-2-phenyl-4-thiazone Imine Hydrobromide (Vc).**—Into a solution of 10 g. of Ia in 100 ml. of chloroform, 5.3 g. of bromine in 30 ml. of chloroform were gradually added and stirred for 2 hr. at room temperature. When the chloroform was removed by evaporation under reduced pressure without heating, a brown residual oil was obtained. Yellow precipitates were crystallized out from the oil by the addition of acetone. Yield, 9.3 g.; m. p. 194—195°C (decomp.).

Found: C, 55.06; H, 4.64; N, 8.09. Calcd. for $C_{16}H_{15}BrN_2S$: C, 55.34; H, 4.32; N, 8.07%.

In the same manner as in the case of Ic, 2, 3-diphenyl-4-thiazone imine hydrobromide was obtained from the corresponding hydrochloride (Ia) (2 g.) and recrystallized from ethanol-ether as yellow needles. Yield, 1.8 g.; m. p. 209—210°C (decomp.).

Found: C, 54.26; H, 3.29; N, 8.52. Calcd. for $C_{15}H_{13}BrN_2S$: C, 54.05; H, 3.90; N, 8.41%.

**3-Benzyl-2-phenyl-*N*-acetylthiazone Imine Hydrobromide (VIb).**—A suspension of 2 g. of Vc in 20 ml. of acetic anhydride and 1 ml. of boron trifluoride in acetic acid was swirled on a steam bath for 2 hr., by which time all of the solids had dissolved. The removal of the acetic anhydride of the solution by evaporation under reduced pressure afforded a brown oil. White precipitates were crystallized out from the oil by the addition of acetone. Recrystallization from ethyl acetate-ethanol gave colorless prismatic needles. Yield, 1.5 g.; m. p. 160—161°C.

Found: C, 55.85; H, 4.70; N, 7.40. Calcd. for $C_{18}H_{17}BrN_2OS$: C, 55.52; H, 4.37; N, 7.20%.

**3-Benzyl-2-phenyl-*N*-acetylthiazone Imine (VII).**—To 20 ml. of an aqueous solution of VIa (4.5 g.), 10 ml. of a saturated aqueous solution of sodium hydrogen carbonate was added, and the mixture was shaken with benzene. The benzene layer was then washed with water and dried with sodium sulfate. The removal of the benzene afforded 3.5 g. of yellow crystals, which were then recrystallized from acetone-petroleum ether. Yield, 2.8 g.; m. p. 155—156°C.

Found: C, 69.87; H, 5.02; N, 9.43. Calcd. for $C_{18}H_{16}N_2OS$: C, 70.13; H, 5.19; N, 9.25%.

**2-Phenyl-4-diacetaminothiazone (VIIIa).**—A suspension of 7 g. of Va in 50 ml. of acetic anhydride was heated gently under reflux for 30 min.; the subsequent removal of the acetic anhydride of the solution by evaporation under reduced pressure afforded colorless needles. Recrystallization from a small amount of methanol afforded colorless prismatic needles. Yield, 3.8 g.; m. p. 98—99°C. The crystals showed $\lambda_{max}^{EtOH}$ 290 mμ (ε=11700) and 296 mμ (ε=21100).

Found: C, 60.00; H, 4.62; N, 10.77. Calcd. for $C_{13}H_{12}N_2O_2S$: C, 60.01; H, 4.55; N, 11.06%.

In the same manner as in the case of VIIIa, VIIIb was obtained from Vb (1 g.) and recrystallized from methanol as colorless needles. Yield, 0.5 g.; m. p. 108—109°C. The crystals showed $\lambda_{max}^{EtOH}$ 230 mμ (ε=18700), 240 mμ (ε=18500), 285 mμ (ε=12600) and 304 mμ (ε=13500).

Found: C, 67.44; H, 4.77; N, 8.40. Calcd. for $C_{19}H_{16}N_2O_2S$: C, 67.85; H, 4.80; N, 8.33%.

**2-Phenyl-4-acetaminothiazole Hydrochloride (IXa).**—To a solution of 0.5 g. of VIIIa in 6 ml. of anhydrous acetone, 3 ml. of a 30% ethanolic hydrogen chloride solution was added portion-by-portion at room temperature; small colorless needles were thereby crystallized out. The crystals were filtered and washed with acetone. Yield, 0.45 g.; m. p. 165—166°C (decomp.).

Found: C, 52.22; H, 4.59; N, 11.61. Calcd. for $C_{11}H_{10}ClN_2OS$: C, 51.87; H, 4.32; N, 11.01%.

In the same manner as in the case of IXa, IXb was obtained from VIII (1 g.) and recrystallized from acetone as yellow prisms. Yield, 0.6 g.; m. p. 182—183°C (decomp.).

Found: C, 61.94; H, 4.29; N, 8.75. Calcd. for $C_{17}H_{15}ClN_2OS$: C, 61.73; H, 4.54; N, 8.47%.

**2-Phenyl-4-acetaminothiazole (X).**—*a) From Va.*—A solution of 2 g. of Va in 50 ml. of acetic anhydride was heated under reflux for 1 hr.; the subsequent removal of the acetic anhydride from the solution by evaporation under reduced pressure afforded colorless precipitates, to which 8 ml. of acetone was then added and the solution filtered. To the filtrate was added, portion-by-portion, 10 ml. of a 30% ethanolic hydrogen chloride solution at room temperature. In a few minutes, small colorless needles began to separate out. After 20 min., the products were filtered and washed with acetone. Recrystallization from methanol afforded colorless tablets. Yield, 0.6 g.; m. p. 169—171°C. The crystals showed $\lambda_{max}^{EtOH}$ 238 mμ (ε=24600) and 315 mμ (ε=10900).

Found: C, 60.36; H, 4.69; N, 12.99. Calcd. for $C_{11}H_{10}N_2OS$: C, 60.54; H, 4.62; N, 12.84%.

*b) From Vc.*—A suspension of 2 g. of Vc in 20 ml. of acetic anhydride was heated under reflux for 45 min., during which time Vc was gradually dissolved in it. The removal of the acetic anhydride by evaporation under reduced pressure afforded colorless tablets. Yield, 0.6 g.; m. p. 170—171°C. This material was shown, by mixed melting point determination and by a comparison of their infrared absorption spectra, to be identical with the X obtained from Va.

*c) From VIa.*—A solution of 1 g. of VIa in 10 ml. of acetic anhydride was heated under reflux for 45 min.; then the acetic anhydride was removed by evaporation under reduced pressure. Crude colorless precipitates were obtained. Recrystallization from benzene gave colorless tablets. Yield, 0.3 g. In the same manner as in the case of c), X was obtained from VIb.

*d) From VIIIa.*—A suspension of 2 g. of VIIIa in a 10% aqueous sodium hydroxide solution was heated under reflux for a few minutes, during which time the crystal form of Va was gradually changed. After cooling, the products were collected by filtration. Recrystallization from methanol afforded colorless tablets. Yield, 1.2 g.; m. p. 170—171°C.

*e) From IXa.*—A suspension of IXa (0.45 g.) in acetone was heated under reflux for 20 min.; crude crystals were crystallized out after the removal of the acetone. Recrystallization from methanol afforded colorless tablets. Yield, 0.25 g.; m. p. 170—171°C.

**2-Phenyl-4-benzoylaminothiazole (XII).**—Two grams of Va and 1.5 g. of benzoic anhydride were fused at 200—210°C in an oil bath for 10 min. The reaction mixture turned brown, and then in a few minutes, colorless prisms were separated out. After these had cooled, anhydrous ether was added, and the products were filtered and washed with anhydrous ether. Recrystallization from ethanol gave colorless needles. Yield, 0.8 g.; m. p. 128—129°C. The material showed $\lambda_{max}^{EtOH}$ 315 mμ (ε=24100).

Found: C, 68.66; H, 4.43; N, 10.04. Calcd. for $C_{16}H_{12}N_2OS$: C, 68.58; H, 4.29; N, 10.00%.

The authors are indebted to Miss Toshiko Aoyagi for her elementary analysis.

*Laboratory of Organic Chemistry*
*Tokyo Institute of Technology*
*Ookayama, Tokyo*

# The Reaction of Nitriles and Dicyandiamide

By Yoshio IWAKURA, Keikichi UNO and Shinsaku SHIRAISHI

(Received December 9, 1964)

Guanamine formations from dicyandiamide and nitriles[1-5] and their application to the preparation of various compounds[6,7] have been investigated by many workers, but the systematic investigation of the reaction of dinitriles with dicyandiamide has not yet been reported. This paper will, therefore, describe the formation of mono and diguanamines from dinitriles and dicyandiamide, the reaction of cyano groups in polymer molecules with dicyandiamide, and the chemical behavior of the cyano group of β-cyanopropioguanamine.

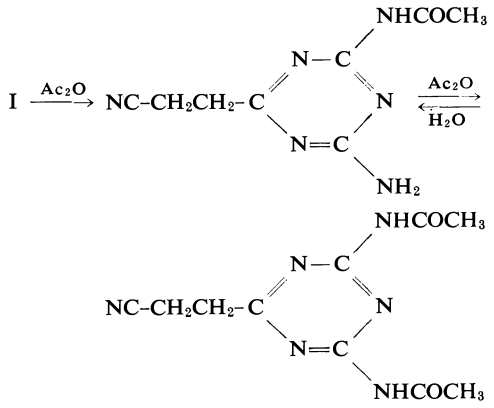
The reaction of one mole of succinonitrile and two moles of dicyandiamide with sodium methoxide as a catalyst in methanol gave an addition compound consisting of one molecule of each starting material instead of the expected succinoguanamine. The structure of the addition compound (I) was determined to be β-cyanopropioguanamine by identifying it with an authentic sample prepared from ethyl β-cyanopropionate and biguanide.

Succinoguanamine (II) was obtained by the reaction of I with dicyandiamide at 130—140°C in either dimethylformamide or methyl cellosolve in the presence of either sodium methoxide or potasium hydroxide. It was also identified with the authentic sample prepared from dimethyl succinate and biguanide. The reaction of one mole of succinonitrile and two moles of dicyandiamide at 130—140°C in methyl cellosolve in the presence of potassium hydroxide also gave succinoguanamine.

When the reaction of succinonitrile with dicyandiamide was carried out in methanol, I was precipitated from the reaction mixture in an almost pure state as a result of its insolubility to methanol, even if an excess dicyandiamide was employed. On the other hand, in methyl cellosolve, diguanamine was obtained with two moles of dicyandiamide and one mole of succinonitrile, or with one mole each of I and dicyandiamide. The reaction of each mole of succinonitrile and dicyandiamide in methyl cellosolve gave I, together with a trace amount of II.

The results suggest that mono and diguanamine selectively can be obtained from the dicyano compound and dicyandiamide, depending on the reaction temperature and solvent employed. Similar reactions of dicyandiamide with various nitriles were carried out under various reaction conditions; the results are summarized in Tables I and II. The yields of mono and diguanamines from dinitriles with odd numbers of methylene groups were comparatively low.

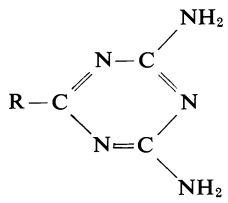
The acetylation of I with acetic anhydride gave mono and diacetyl derivatives. The diacetyl derivative was easily hydrolyzed to form the monoacetyl derivative by heating it in glacial acetic acid or water. This behavior is similar to that of acetoguanamine.[8]




The hydrolysis of I with 6 N hydrochloric acid or with a 1 N sodium hydroxide solution, followed by the neutralization of the reaction

1) A. Ostrogovich and Gh. Gheorghiu, *Gazz. chim. ital.*, **60**, 648 (1930).
2) U. S. Pat. 2302162 (1942); *Chem. Abstr.*, **37**, 2016 (1943).
3) Brit. Pat. 642409 (1950); ibid., **46**, 146 (1952).
4) U. S. Pat. 2532519 (1950); ibid., **45**, 3429 (1951).
5) Brit. Pat. 758601 (1956); ibid., **51**, 10594 (1957).
6) H. J. Sims, H. B. Parseghian and P. L. de Benneville, *J. Org. Chem.*, **23**, 724 (1958).
7) L. S. Luskin, P. L. de Benneville and S. Meland, ibid., **23**, 1082 (1958).
8) A. A. Ryabinin, *Zhur. Obschchei Khim.*, **22**, 541 (1952).

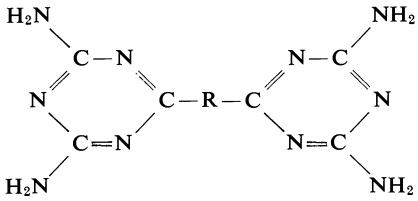
TABLE I. SYNTHESIS OF MONOGUANAMINES



| R- | Reaction time, hr. | Yield % | M. p. °C | Recryst. solvent | N, anal. Found | N, anal. Calcd. |
|---|---|---|---|---|---|---|
| $CH_3$- | a) | — | | | | |
| $C_2H_5$- | a) | — | | | | |
| $C_{13}H_{27}$- | 4[a] | —[1] | | | | |
| $C_{17}H_{35}$- | 5[a] | Trace | Wax | | | |
| NC-$CH_2$- | a) | —[2] | | | | |
| NC-$(CH_2)_2$- | 1/4—1/2[a] | 60—70 | 241.5—242.0 | Water | 51.47 | 51.19 |
| NC-$(CH_2)_3$- | 5[a] | 10 | 163—167 | Water | 47.0 | 47.17 |
| NC-$(CH_2)_4$- | 6[a] | 50 | 253—255 (d.) | 50% MCS* | 43.5 | 43.72 |
| NC-$(CH_2)_7$- | 2.5[b] | 30[3] | 195—199 | 85% methanol | 36.8 | 35.87 |
| $C_6H_5$- | 7[a] | 25 | 221—222 | | | |
| *o*-NC-$C_6H_4$- | 1/4—1/2[a] | 60—85 | 230.5—231.5 | Water | 39.85 | 39.61 |
| | 2[b] | 85 | | | | |
| *m*-NC-$C_6H_4$- | 1[a] | 65 | 265—273 | 50% MCS | 39.6 | 39.61 |
| | 1[b] | 80 | | | | |
| *p*-NC-$C_6H_4$- | 1[a] | 50 | 329.5—330.5 | 80% MCS | 39.1 | 39.61 |
| | 1[b] | 90 | | | | |

a) Methanol and sodium methoxide were used as the reaction solvent and catalyst respectively.
b) Methyl cellosolve and potassium hydroxide were used as the reaction solvent and catalyst respectively.
1) Not characterized adduct was obtained; m. p. >330°C. When it was heated in water, mirystonitrile was separated on the surface.
2) Tar-like substance was obtained.
3) When methanol was used as the reaction solvent, guanamine was not obtained.
* MCS indicates methyl cellosolve (ethyleneglycol monomethyl ether).

TABLE II. SYNTHESIS OF DIGUANAMINES



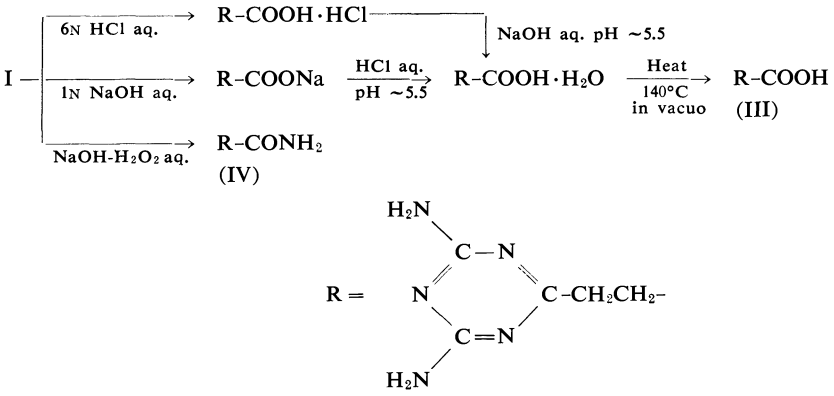
| -R- | Reaction time hr. | Yield % | M. p. °C | N, anal. Found | N, anal. Calcd. |
|---|---|---|---|---|---|
| -$(CH_2)_2$- | 1 | 70 | >360 | *1 | |
| -$(CH_2)_3$- | 2 | 25*[2] | 265—270 | *1 | |
| -$(CH_2)_4$- | 3 | 90 | 285 (d.) | 50.57 | 50.70 |
| -$(CH_2)_7$- | 4 | 50*[2] | | *1 | |
| -$C_6H_4$-(*o*-) | 7 | 60 | 343—345 | 44.9 | 44.57*[3] |
| (*m*-) | 1 | 90 | >360 | 47.4 | 47.26 |
| (*p*-) | 6 | 90 | >360 | *1 | |

*1 Elemental analyses of these compounds were done several times but the analytical values varied each time. Identification of these compounds was done by their infrared spectra.
*2 One mole of nitriles were treated with four moles of dicyandiamide.
*3 Calcd. as monohydrate of isophthaloguanamine. The result of carbon and hydrogen analyses also coincided with the value of the monohydrate.

TABLE III. THE REACTION OF AS RESINS AND DICYANDIAMIDE

| Exp. No. | AS resin g. | | Dicy. g. | KOH g. | MCS ml. | DMF ml. | React. time hr. | N*1 anal. % | Conv.*2 % |
|---|---|---|---|---|---|---|---|---|---|
| 1 | AS1 | 2 | 3 | 0.2 | 20 | 20 | 7.5 | 10.30 | 9 |
| 2 | | 2 | 3 | 0.2 | 20 | 20 | 5 | 9.90 | 8 |
| 3 | | 2 | 2.2 | 0.2 | 20 | 20 | 5 | 10.84 | 10 |
| 4 | AS2 | 2 | 2 | 0.2 | 20 | 25 | 5 | 7.87 | 3 |
| 5 | AS3 | 1.5 | 2.6 | 0.2 | 35 | 25 | 5.5 | — | 1*3 |
| 6 | | 1 | 0.8 | 0.1 | 50 | 10 | 2 | — | 1*3 |

*1 The nitrogen content of starting AS resins were 8.30% (AS1), 7.30% (AS2) and 5.39% (AS3).
*2 Conversion means the ratio of the number of cyano groups converted to diamino-*sym*-triazine to those of the starting polymers.
*3 Determined from infrared spectra.




mixture up to pH 5.5, gave β-carboxypropioguanamine (III). The hydrolysis of I with an alkaline aqueous solution of hydrogen peroxide gave β-(4, 6-diamino-*sym*-triazin-2-yl) propionamide (IV). Each compound, III and IV, combines with one molecule of water, and the dehydration of the hydrates can be conducted by heating them at a temperature above 140°C under reduced pressure.

The reaction of dicyandiamide with cyano groups in polymer molecules was studied in order to modify the properties of the polymers. Polyacrylonitrile and acrylonitrile-styrene copolymers (AS resins) were used as the polymers. Copolymers containing 4, 6-diamino-*sym*-triazine were obtained from the AS resins, but not from polyacrylonitrile. The reaction mixture with polyacrylonitrile gelled and colored in the presence of potassium hydroxide. The mixture of dimethylformamide and methyl cellosolve was suitable for the reaction solvent. The infrared spectra of the modified AS resins obtained here showed new peaks at 3025—3060 (two peaks), 1630, 1545 and 824 $cm^{-1}$, the locations of the characteristic bands of guanamines.[9] The ratio of the number of cyano groups converted to diamino-*sym*-triazine to that of the starting polymer was determined by nitrogen analysis. The acrylonitrile contents of the starting copolymers were 47.3 mol.% (AS1), 42.8 mol.% (AS2) and 33.3 mol.% (AS3). The results obtained are summarized in Table III. It can be concluded that no degradation of the polymer main chain occurred in the course of the reaction; only a small change in reduced specific viscosity was observed (0.84 before to 0.78 after the reaction for the sample of Exp. No. 2).

The modified AS resins gave insoluble and infusible substances when treated with an aqueous solution of formaldehyde. However, the reaction, as well as the properties of the products, has not yet been investigated in detail.

9) W. M. Padgett, II, and W. F. Hamner, *J. Am. Chem. Soc.*, **80**, 803 (1958).

## Experimental

**β-Cyanopropioguanamine (I).**—To a mixture of 30 g. of succinonitrile and 31 g. of dicyandiamide in 230 ml. of absolute methanol, 50 ml. of methanol containing 3 g. of sodium was added. The reaction mixture was then heated and stirred under reflux for 30 min. After the mixture had then cooled, the resulting precipitate was filtered, washed twice with 30 ml. of methanol, and dried. It was recrystallized from water; m. p. 241.5—242°C (colorless needles); yield, 40 g. (66%); IR, 3505, 3440,

3370 (N-H), 2270 (C≡N), 1672, 1645, 1543, 1425 and 818; UV, 258 mμ ($\varepsilon_{max}$=3800).

Found: C, 44.35; H, 5.05; N, 51.47. Calcd. for $C_6H_8N_6$: C, 43.89; H, 4.90; N, 51.19%.

**Succinoguanamine (II).** — Into a solution of 1.8 g. of I and 0.9 g. of dicyandiamide in 20 ml. of dimethylformamide there was added 5 ml. of a methanolic solution of sodium methoxide which had been freshly prepared from 0.1 g. of sodium; the mixture was then heated at 130—140°C for 3 hr. After the mixture had then been cooled, a white precipitate formed was filtered and washed with hot water. It did not melt at 360°C. The infrared spectrum showed the absorption bands characteristic to guanamines, but not around the 2250 $cm^{-1}$ of C≡N. When methyl cellosolve was used as the reaction solvent, potassium hydroxide was used as the catalyst.

**Guanamines.** — *o-Cyanobenzoguanamine.* — a) (In methanol) To a solution of 6.2 g. of phthalonitrile and 4.2 g. of dicyandiamide in 40 ml. of methanol, there was added a sodium methoxide solution which had been made by dissolving 0.5 g. of sodium in 10 ml. of methanol. The mixture was refluxed for 30 min. The white precipitate thus formed was filtered and recrystallized from water; yield, 8.8 g. (85%); m. p. 230.5—231.5°C.

Found: C, 56.19; H, 4.19; N, 39.85. Calcd. for $C_{10}H_8N_6$: C, 56.59; H, 3.80; N, 39.61%.

b) (In methyl cellosolve) A mixture of 1.1 g. of phthalonitrile, 0.8 g. of dicyandiamide and 0.1 g. of potassium hydroxide in 15 ml. of methyl cellosolve was heated at 130—140°C for 2 hr. The reaction mixture was then poured into cold water. A white precipitate was collected by filtration and recrystallized from water; yield, 1.6 g. (80%); m. p. 230—231°C.

*Phthaloguanamine.*—a) (From *o*-cyanobenzoguanamine) A mixture of 1.1 g. of *o*-cyanobenzoguanamine, 0.5 g. of dicyandiamide, 0.1 g. of potassium hydroxide and 20 ml. of methyl cellosolve was heated at 130—140°C for 8 hr. The white powder which was thus precipitated was filtered and washed with methanol. M. p. 340—343°C.

b) (From phthalonitrile) A mixture of 1.3 g. of phthalonitrile, 1.7 g. of dicyandiamide, 0.2 g. of potassium hydroxide and 30 ml. of methyl cellosolve was heated at 130—140°C for 7 hr. The white powder which was thus precipitated was filtered and washed with methanol. M. p. 340-343°C.

Other mono and diguanamines were synthesized by similar procedures. The results are summarized in Tables I and II.

**2-Acetamino-4-amino-6-β-cyanoethyl-1, 3, 5-triazine.**—A solution of 6 g. of I in 30 ml. of acetic anhydride was heated under reflux for several minutes, thus precipitating a white solid. This was collected by filtration and recrystallized from water; m. p. 230—231°C.

Found: N, 41.02. Calcd. for $C_8H_{10}N_6O$: N, 40.76%.

**2, 4-Diacetamino-6-β-cyanoethyl-1, 3, 5-triazine.**—When the above reaction was continued without the isolation of the monoacetate, the precipitate disappeared once, thus forming a clear solution. After another hour of reflux, however, a grayish precipitate was deposited. This was collected by filtration and recrystallized from acetic anhydride; m. p. 213—215°C.

Found: N, 33.7. Calcd. for $C_{10}H_{12}N_6O_2$: N, 33.86%.

**The Monohydrochloride of I.**—A solution of 1 g. of I in 10 ml. of cold 6 N hydrochloric acid was allowed to stand overnight in ice box. The white precipitate which was thus formed was filtered and washed with methanol; m. p. 208—209°C (decomp.); IR, 2280 (C≡N).

Found: N, 41.61; HCl, 18.5 (from the neutralization value with 0.1 N NaOH aq.). Calcd. for $C_6H_8N_6 \cdot HCl$: N, 41.90; HCl, 18.2%.

**The Acidic Hydrolysis of I.**—*β-(4,6-Diamino-sym-triazin-2-yl)propionic Acid (III).*—A mixture of 3 g. of I in 60 ml. of 6 N hydrochloric acid was heated to reflux for 5 hr. The white precipitate which was thus formed was filtered and recrystallized from water, giving colorless needles of a monohydrochloride of III. They did not melt, but they did decomposed at a temperature above 250°C, forming a black mass.

Found: N, 31.72 (Kjeldahl method). Calcd. for $C_6H_9N_5O_2 \cdot HCl$: 31.89%.

A solution of 2 g. of the monohydrochloride in 100 ml. of water was neutralized with a 1 N sodium hydroxide aqueous solution to a pH value of 5.5. The white precipitate which was thus formed was collected and recrystallized from water, giving a monohydrate of III; m. p. 262°C (decomp.). The infrared spectrum of this compound showed absorption bands at 3350 (broad), 2800—2500 $cm^{-1}$ (COOH) and other regions characteristic of guanamines.

Found: N, 35.03 (Kjeldahl method). Calcd. for $C_6H_9N_5O_2 \cdot H_2O$: N, 34.81%.

The monohydrate was dehydrated by heating it at 140°C in vacuo for 5 hr., thus forming III; m. p. 262°C (decomp.); IR, 3450, 3300 (N-H), 2800—2500 $cm^{-1}$ (COOH).

Found: N, 38.00 (Kjeldahl method). Calcd. for $C_6H_9N_5O_2$: N, 38.24%.

**The Alkaline Hydrolysis of I.**—A mixture of 2 g. of I and 1 g. of sodium hydroxide in 25 ml. of water was refluxed for 30 min. The evolution of ammonia was observed. After it had then been cooled, the mixture was neutralized with 5 N hydrochloric acid to a pH value of 5.5. The product precipitated was the same as the monohydrate of III obtained in the preceding section.

**β-(4, 6-Diamino-*sym*-triazin-2-yl)propionamide (IV).**—A solution of 2 g. of I and 0.1 g. of sodium hydroxide in 40 ml. of a 9% hydrogen peroxide aqueous solution was heated at 60—65°C for 40 min. The precipitate which was thus formed was collected by filtration and recrystallized from water, giving a monohydrate of IV; m. p. 250—251°C (decomp.).

Found: C, 36.33; H, 6.14; N, 42.26. Calcd. for $C_6H_{10}N_6O \cdot H_2O$: C, 36.00; H, 6.04; N, 41.98%.

The monohydrate was dehydrated by the same procedure as that used for III to give IV; m. p. 251—252°C (decomp.).

Found: N, 46.52. Calcd. for $C_6H_{10}N_6O$: N, 46.13%.

**The Reaction of AS Resins with Dicyandiamide.** —(Exp. No. 2). To a solution of 2 g. of AS1 in 20 ml. of dimethylformamide, 20 ml. of methyl cellosolve and 3 g. of dicyandiamide were added. The mixture was then heated at 130°C until a clear solution was obtained. To this solution there was added 0.2 g. of potassium hydroxide. The mixture was then kept at 130°C for 5 hr., after which it was poured into methanol. The polymer thus precipitated was filtered, washed with methanol, and purified by reprecipitation with a dimethylformamide-methanol system. The reduced specific viscosity of AS1 and of the modified polymer obtained here were, respectively, 0.84 and 0.78, at 30°C at the concentration of 0.2 g. of polymer in 100 ml. of dimethylformamide.

The other reactions of AS resins with dicyandiamide were carried out similarly; the results are summarized in Table III.

*Department of Synthetic Chemistry*
*Faculty of Engineering*
*The University of Tokyo*
*Hongo, Tokyo*

# The Catalytic Effect of the Support on Terpene Compounds in Gas-Liquid Chromatography

By Shûichi HAYASHI, Katsumi YANO, Naruo YOKOYAMA and Tamon MATSUURA

(Received January 22, 1965)

At the present time, diatomaceous earth or its manufactures are in general use as the solid support of a packed column in gas-liquid chromatography because these materials are porous and, consequently, have a large surface area. In the gas chromatography of terpene compounds using these solid supports, unfortunately, erroneous results due to the catalytic action of the support have occasionally been observed. Naves,[1] for instance, has observed dehydration, condensation and other reactions in the gas chromatography of essential oils by the use of diatomaceous earth or firebrick. Cartoni[2] has observed the decomposition of oxygen-containing terpene compounds in gas chromatography using Sterchamol. Using diatomaceous earth, Celite 545, Chromosorb or C-22 firebrick, Vilkas,[3] Zubyk,[4] Lukes[5] and the present authors[6] have reported the isomerisation of $\alpha$-pinene into such compounds as camphene, dipentene and *p*-cymene, and also of $\beta$-pinene into such compounds as $\alpha$-pinene, camphene, dipentene and *p*-cymene. Besides, the liquid phase on diatomaceous earth or fireblick is also rapidly decomposed,[7] as has been shown in Polyethylene glycol-1500 impregnated on Shimalite.[8] Also, the authors[6] have done preliminary research on the catalytic action of several solid materials (commercial supports, rock crystal, glass, etc.), using nearly fifty kinds of monoterpene compounds (hydrocarbons 16, alcohols 11, esters 13, carbonyl compounds 8, etc.); they have found a remarkable catalytic decomposition of terpene compounds by commercial solid supports.

Thus, in order to get a correct gas chromatogram it will be necessary to find a support possessing no catalytic action or a weak one.

In the present investigation, the catalytic action of several materials, such as glass, rock crystal, quartzite, sea sand and unglazed porcelain, and that of several commercial solid supports, such as Shimalite,*1 Diasolid-M,*2 Microsorb-W, -S, -SS and -F,*3 towards six monoterpene compounds and five sesquiterpene alcohols, which were chosen as representative compounds, will be examined in detail.

## Experimental

**Apparatus and Procedure.** — A Shimadzu Gas Chromatograph GC-2 furnished with a katharometer-type detector was used. A coiled copper tube (3 m. long, 4 mm. inner diameter) packed with the

1) Y.-R. Naves, *J. Soc. Cosmetic Chemists*, **9**, 101 (1958).
2) G. P. Cartoni and A. Liberti, *J. Chromatog.*, **3**, 121 (1960).
3) M. Vilkas and N. A. Abraham, *Bull. soc. chim. France*, **1959**, 1651.
4) W. J. Zubyk and A. Z. Connor, *Anal. Chem.*, **32**, 912 (1960).
5) V. Lukes, R. Komers and V. Herout, *J. Chromatog.*, **3**, 303 (1960).
6) T. Matsuura, T. Aratani, H. Komae and S. Hayashi, *J. Chem. Soc. Japan, Ind. Chem. Sec.* (*Kogyo Kagaku Zasshi*), **64**, 795 (1960).
7) A. Kele, R. Bate, B. Costa and P. Forman, *J. Chromatog.*, **8**, 157 (1962).
8) S. Akiyoshi, T. Matsuda and K. Akune, *Japan Analyst* (*Bunseki Kagaku*), **10**, 960 (1961).

*1 Commercial solid support put on sale by Shimadzu Seisakusho Ltd., Kyoto, Japan.
*2 Commercial solid support by the Nippon Kuromato Kôgyô Co., Ltd., Tokyo, Japan.
*3 Commercial solid support by the Tôsin Gôsei Kôgyô Co., Ltd., Tokyo, Japan.

bare material (28—48 mesh) to be examined was connected between a sample injector and a separation column (Fig. 1). The operating temperature and the flow rate of the helium carrier were set as follows: 140°C and 60 ml./min. for the monoterpene compound, 200°C and 30 ml./min. for the sesquiterpene alcohol.

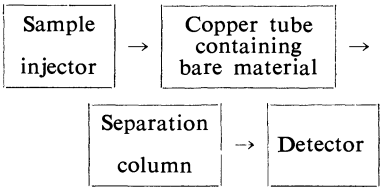



Fig. 1. Scheme of apparatus.

If an injected terpene compound suffers isomerization and/or decomposition by the bare material, its isomerization and/or decomposition products are separated by the next separation column and recorded on a chromatogram. Accordingly, by a comparison of this chromatogram with the chromatogram obtained from a blank test performed without the connection of a column packed with the bare material, one can get information about the catalytic activity and the adsorptivity of this bare material.

Crushed rock crystals (150—200 mesh) coated with 5% Thermol-1*[4] were employed in the separation column throughout this research. The sample size to be injected at one run was in the range from 0.5 to 1.5 $\mu$l.; the value was varied according to the extent of the isomerization and/or the decomposition of the sample. The electric current of the detector cell and the sensitivity of the recorder were set at 200 mamp. and 2 mV. respectively.

**The Preparation of the Solid Materials to be Examined.** — For the preparation of the solid materials (supports) to be examined, the following substances were used: soda-lime glass tubing, scraps of rock crystal from which the quartz oscillator has been cut out, quartzite ($SiO_2$ 99.88%, snow-white color) dug out in Yamanashi Prefecture, Japan, and unglazed porcelain tubing. When these substances were crushed separately in a stainless-steel mortar, 28—48 mesh particles were collected. To these particles ten portions (in volume) of aqua regia were added, and the mixture was boiled for two hours in order to dissolve any metallic impurities that entered during the crushing process. The cleaned particles were washed with water, dried, and heated at 300°C for two hours.

Sea sand ($SiO_2$ 99.02%, $Al_2O_3$ 0.52%, $Fe_2O_3$ 0.32%, trace of CaO, light brown beads), collected in Kam-ranh Bay, Viet Nam, was treated in the same way as above.

All the commercial solid supports examined are manufactured from diatomaceous earth. Of these Shimalite belongs to a usual type, Diasolid is a support which has been treated at a high temperature in order to diminish the adsorptivity for oxygen-containing compounds, and Microsorb is a firebrick precoated with Polyflon,*[5] presumably in order to diminish its adsorptivity and its catalytic activity.

**The Preparation of Terpene Compounds.** — Six monoterpene compounds, that is, $\alpha$-pinene, limonene, linalool, $\alpha$-terpineol, linalyl acetate, and geranyl acetate, were chosen from the standpoint of their sensitivity to the catalytic action. Five sesquiterpene alcohols, that is, $\alpha$- and $\beta$-santalol, $\alpha$-cadinol, patchouli alcohol and elemol, were adopted because they were easily available in our laboratory.

$\alpha$-Pinene (b. p. 156°C, $d_4^{25}$ 0.8544, $n_D^{25}$ 1.4638, $[\alpha]_D$ −39.51°) was isolated from a commercial turpentine oil, while limonene (b. p. 175.5°C, $d_4^{25}$ 0.8397, $n_D^{25}$ 1.4711, $[\alpha]_D$ +117.6°) was isolated from an essential oil of Citrus Natsudaidai Hayata. These two compounds were then each purified by repeated fractional distillation. The other monoterpene samples were commercial materials supplied by the Abrack Co., Ltd. and were used without further purification.

$\alpha$-Santalol and $\beta$-santalol were isolated from an essential oil of the sandal-wood tree through their phthalic ester; each was purified by repeated fractional distillation. The infrared absorption spectrum of $\alpha$-santalol (b. p. 160°C (10 mmHg), $d_4^{25}$ 0.9722, $n_D^{25}$ 1.4998) obtained here coincided with that reported by Herout[10] and Chakravarti[11]. $\beta$-Santalol (b. p. 164°C (10 mmHg), $d_4^{25}$ 0.9703, $n_D^{25}$ 1.5063) was recognized to be contaminated with a small amount of $\alpha$-santalol by a comparison of its infrared spectrum here with that obtained by Chakravarti.[11]

$\alpha$-Cadinol (b. p. 147°C (8 mmHg), $d_4^{25}$ 0.9375, $n_D^{25}$ 1.4960, $[\alpha]_D$ −23.63) was isolated from an essential oil of the hinoki tree,[12] by preparing its sodium alcoholate, and then fractionated. The infrared spectrum of this sample coincided with that reported by Motl et al.[13]

Patchouli alcohol was separated in the crystalline form by cooling commercial Patchouli oil in a refrigerator; it was then recrystallized three times from *n*-hexane. This preparation melted at 59—60°C, a slightly higher point than that shown in Büchi's reported (55—56°C).[14]

Elemol was isolated from Citronella oil by fractional distillation; it was then purified by elution chromatography using silica gel and *n*-hexane. This sample melted at 48—49°C, a value which coincided with that reported by Halsall,[15] and its phenyl urethane melted at 111—112°C, a value which

*[1] Commercial stationary liquid put on sale by Shimadzu Seisakusho, Ltd. Thermol-1 has been confirmed by the present authors to be excellent for the separation of terpene alcohols.[9]

9) T. Matsuura, T. Aratani, H. Komae and S. Hayashi, *J. Chem. Soc. Japan, Ind. Chem. Sec.* (*Kogyo Kagaku Zasshi*), **64**, 799 (1961).

*[5] Tetrafluoroethylene polymer (Teflon) produced at the Osaka Kinzoku Co., Ltd., Osaka, Japan.

10) V. Herout, V. Jarolim and J. Pliva, *Collection Czech. Chem. Commun.*, **22**, 773 (1957).

11) K. K. Chakravarti, *Perfumery Essent. Oil Record*, **46**, 330 (1955).

12) S. Hayashi, K. Yano and T. Matsuura, This Bulletin, **37**, 474 (1964).

13) O. Motl, V. Sýkora, V. Herout and F. Šorm, *Collection Czech. Chem. Commun.*, **23**, 1297 (1958).

14) G. Büchi, R. E. Erickson and N. Wakabayashi, *J. Am. Chem. Soc.*, **83**, 927 (1961); **84**, 3205 (1962).

15) T. G. Halsall, D. W. Theobald and K. B. Walshaw, *J. Chem. Soc.*, **1964**, 1029.

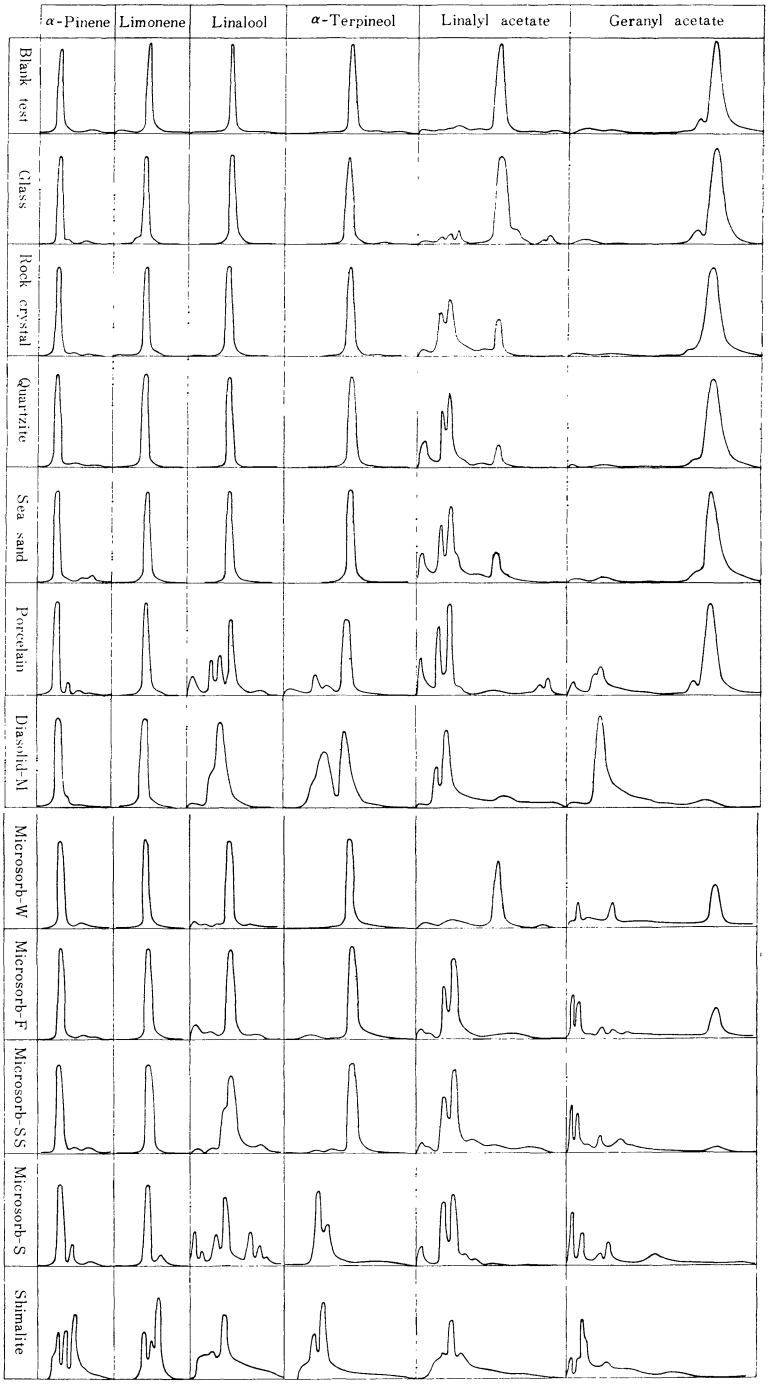



Fig. 2. Catalytic effect of bare supporting material toward monoterpene compound.
Column packed with bare material: 4 mm. × 3 m.
Separation column (Thermol-1 on crushed rock crystal): 4 mm. × 3 m.
Operating temperature: 140°C
Flow rate of helium: 60 ml./min.

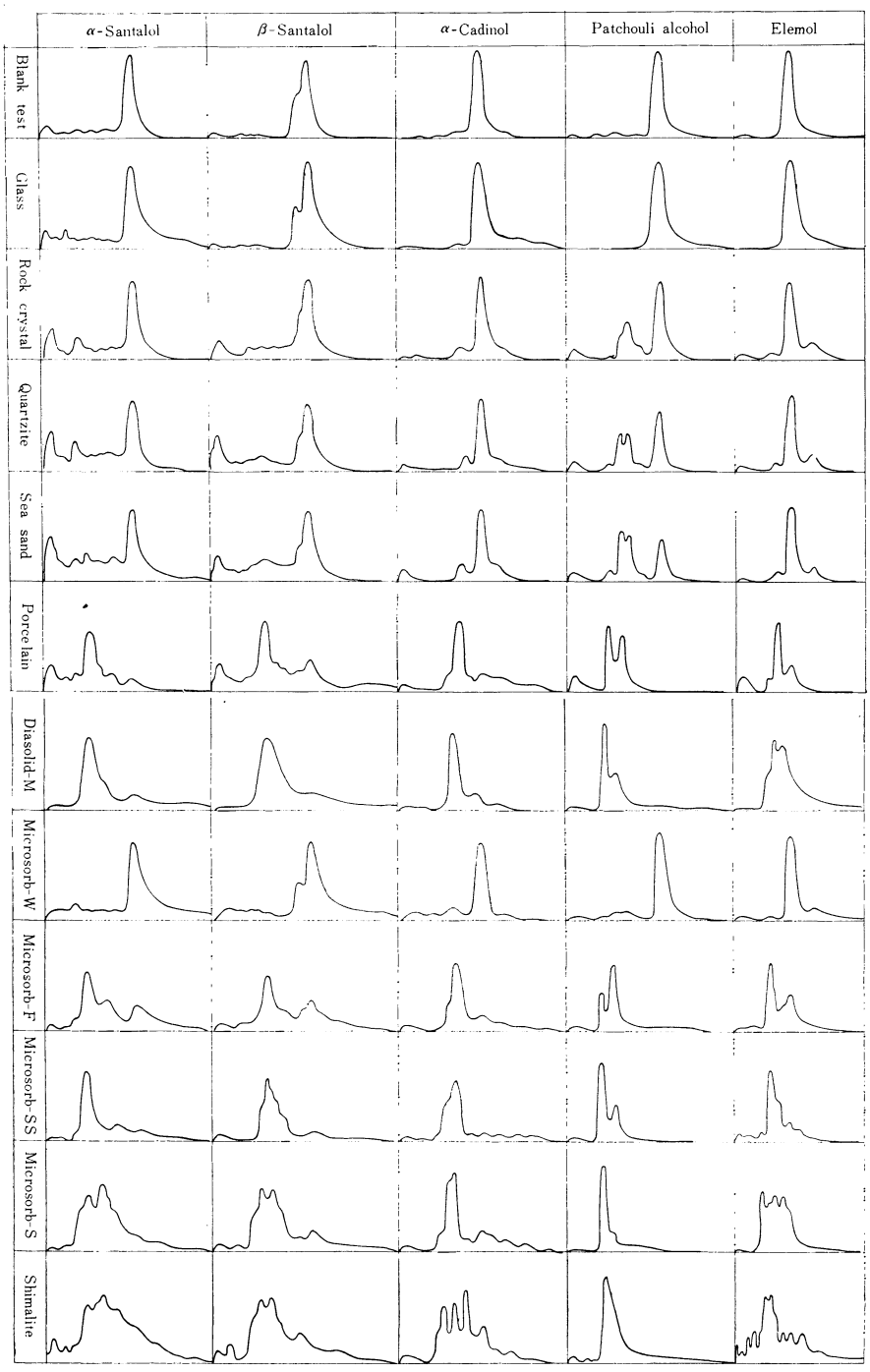



Fig. 3. Catalytic effect of bare supporting material toward sesquiterpene alcohol.
Column packed with bare material: 4 mm.×3 m.
Separation column: 4 mm.×3 m.
Operating temperature: 200°C
Flow rate of helium: 30 ml./min.

agreed with the melting point reported in the literature.[16]

## Results and Discussion

Gas chromatograms of monoterpene compounds and sesquiterpene alcohols, which were obtained by an apparatus furnished with a column containing the bare material to be examined, are shown in Figs. 2 and 3. Each run was carried under the same operating conditions. However, the same component did not show an identical retention time in each chromatogram on account of the difference in adsorptivity, depending on the kind of bare material. Every chromatogram shown in Figs. 2 and 3 was corrected, for the sake of convenience, by multiplying a certain factor, one which was special for each material, since the peak of the same component could be seen at an identical position in each gas chromatogram.

In these figures, the top lines represent the results of the blank test, that is, gas chromatograms of terpene compounds obtained without a column packed with the examined bare material. Therefore, if gas chromatograms regarding a certain examined material are compared with those of the corresponding blank test, information about the catalytic activity and the adsorptivity of this material can be obtained.

**Glass.** — As will be seen in Figs. 2 and 3, chromatograms obtained using a connection of a column packed with glass are simpler than chromatograms of the cases employing other bare materials. Besides, the chromatograms where glass was used closely resemble those of the blank test except for the cases of linalyl acetate and of $\alpha$-santalol. In the chromatograms of linalyl acetate and $\alpha$-santalol, several small peaks appear in addition to the main peak; these small peaks are probably due to the catalytic action of glass.

From these observations, the catalytic activity of glass seems to be the feeblest among the examined materials.

**Rock Crystal.**—When a rock crystal-packed column was used, each chromatogram of a monoterpene compound is almost identical with that obtained in the case of glass or the blank test except for the case of linalyl acetate; chromatograms of linalyl acetate and of sesquiterpene alcohols are compared with those in the case of glass. In the chromatogram of linalyl acetate, the peaks, which are small in shape in the case of glass, appear large. In the case of patchouli alcohol, new moderate-size peaks appear besides the main peak. These newly-formed or newly-enlarged peaks are perhaps due to the catalytic action of the bare material.

Therefore, the catalytic activity of rock crystal is slightly stronger than that of glass.

**The Adsorpitivity of Glass Support.** — There have been several papers[17] which have recommended glass beads as a solid support for impregnation with a liquid phase in a low concentration. The present authors[9] and Takayama[18] have, however, pointed out that glass is not suitable as a solid support, because the oxygen-containing compound has shown a broad peak and a remarkable tailing phenomenon when glass has been employed as a solid support, Takeuchi,[19] who has introduced the "tailing coefficient" as a measure to indicate quantitatively the degree of peak tailing, recently compared several solid supports by the tailing coefficient as calculated from the peak of butyl alcohol. According to his results, the tailing coefficient of glass is not small.

The uncorrected retention time of the main peak of each chromatogram involving glass and rock crystal (cf. Figs. 2 and 3) is listed in Table I. In the case of the glass-packed column, the retention time of each compound is ca. 1.5 times as large as that in the case of the rock crystal-packed column, in which the retention time is practically the same as in the blank test.

The peak width measured at half-height is shown in Table II. The peak width of each of the hydrocarbons and the esters is nearly the same in both glass and rock crystal, whereas

TABLE I. COMPARISON OF RETENTION TIME (min.) OF TERPENE COMPOUNDS

| Compound | Bare supporting material connected to the separation column | | |
|---|---|---|---|
| | Blank test | Glass | Rock crystal |
| $\alpha$-Pinene | 2.4 | 3.5 | 2.4 |
| Limonene | 3.7 | 5.3 | 3.6 |
| Linalool | 4.1 | 6.7 | 4.3 |
| $\alpha$-Terpineol | 6.7 | 11.1 | 6.8 |
| Linalyl acetate | 8.2 | 14.0 | 8.5 |
| Geranyl acetate | 14.9 | 25.1 | 14.0 |
| $\alpha$-Santalol | 9.4 | 15.2 | 9.8 |
| $\beta$-Santalol | 10.6 | 17.1 | 11.0 |
| $\alpha$-Cadinol | 8.8 | 13.8 | 8.6 |
| Patchouli alcohol | 10.2 | 15.7 | 10.2 |
| Elemol | 6.6 | 10.1 | 6.4 |

16) V. Sýkora, V. Herout, J. Pliva and F. Šorm, *Collection Czech. Chem. Commun.*, **19**, 124 (1954).

17) C. Hishta, J. P. Messerly and R. F. Reschke, *Anal. Chem.*, **32**, 1730 (1960); P. R. Datta and H. Susi, ibid., **34**, 1028 (1962); D. H. Frederick, B. T. Miranda and W. D. Cooke, ibid., **34**, 1521 (1962); J. W. Ashley and C. N. Reilley ibid., **34**, 1537 (1962).

18) Y. Takayama, *J. Japan Chem.* (*Kagaku no Ryoiki*), **15**, 369 (1961).

19) T. Takeuchi and T. Setsuda, *J. Chem. Soc. Japan, Ind. Chem. Sec.* (*Kogyo Kagaku Zasshi*), **66**, 1648 (1963).

Table II. Comparison of peak width (min.) measured at one half of peak height

| Compound | Bare supporting material connected to the separation column | | |
|---|---|---|---|
| | Blank test | Glass | Rock crystal |
| α-Pinene | 3.4 | 4.2 | 3.5 |
| Limonene | 3.6 | 4.8 | 3.8 |
| Linalool | 4.7 | 5.6 | 4.6 |
| α-Terpineol | 5.4 | 7.8 | 5.7 |
| Linalyl acetate | 6.6 | 8.7 | 6.8 |
| Geranyl acetate | 10.4 | 14.6 | 10.4 |
| α-Santalol | 13.0 | 21.0 | 13.0 |
| β-Santalol | 20.0 | 25.0 | 20.1 |
| α-Cadinol | 13.0 | 19.7 | 12.8 |
| Patchouli alcohol | 9.0 | 11.6 | 9.0 |
| Elemol | 7.5 | 8.8 | 7.3 |

the peak width of each alcohol is very much larger in glass than in rock crystal. Generally, the peak width in rock crystal is the same as in the blank test.

Such prolongation of the retention time and broadening of the peak width observed in the case of glass are probably due to the adsorption of the oxygen-containing compound on the surface of the glass used as the bare material. In fact, when the bare glass-packed column was set between the injector and the separation column, a considerable tailing phenomenon was observed in the chromatography of oxygen-containing terpene compounds, as compared with the results in the blank test.

Glass showed practically no catalytic action on terpene compounds, but it did show the adsorption or the tailing phenomenon to some extent on oxygen-containing terpene compounds. A further examination of the glass support is being attempted in our laboratory.

**Quartzite and Sea Sand.**—The chromatograms obtained by using quartzite and those in the case of sea sand are almost identical. Besides, the chromatograms in both these cases closely resemble the chromatograms obtained using rock crystal. Therefore, of rock crystal, quartzite and sea sand, it may be said that there is little difference in catalytic activity.

**Unglazed Porcelain.**—All the chromatograms in the case of unglazed porcelain are remarkably complicated compared with those of glass, rock crystal, quartzite and sea sand. Especially, linalyl acetate, α-santalol, α-cadinol and patchouli alcohol do not show the peak corresponding to the original sample in their chromatograms. On the basis of such results, it is obvious that all monoterpene and sesquiterpene compounds suffered an intense action by unglazed porcelain. That is, the catalytic activity of this material is certainly very strong, in spite of the recommendation of Lukes[5] that it has a weak activity.

**Commercial Solid Supports.**—Three groups of commercial solid supports, Shimalite, Diasolid and Microsorb, show chromatograms with characteristic features.

The chromatograms obtained with the Shimalite-packed column are the most complicated; they consist of many peaks projected on a large mountain. In these chromatograms, however, the peak corresponding to the original sample is not observed except in the chromatograms of α-pinene and limonene.

On the basis of such complex chromatograms, it may be assumed that all the terpene compounds examined suffered greatly from various catalytic actions, such as dehydration, dehydrogenation, decarboxylation, isomerization, and the cleavage of a carbon-carbon bond.

On the other hand, the chromatograms obtained by using the Diasolid-packed column show simple features, with only a few peaks, although the catalytic action of Diasolid is obviously vigorous, because the peak corresponding to the original sample is not observed in the chromatograms obtained using this material, except in the case of α-pinene and limonene. Although Diasolid has been subjected to the high temperature-treatment to diminish the catalytic activity of diatomaceous earth, it is not yet satisfactory for the gas chromatography of terpene compounds.

Regarding Microsorb, four manufactures of different grades of activity, W, F, SS and S, were examined. These materials commonly show less-tailling chromatograms than the case with Shimalite or Diasolid. Of these, Microsorb-W gives the simplest chromatograms in shape, that is, the number of peaks is the least; largely the peak corresponding to the original sample is left in these chromatograms. Therefore, the catalytic action of Microsorb-W is assumed to be the weakest among the commercial solid supports examined, and to be nearly the same as that of glass on the basis of a comparison of the two kinds of chromatograms.

**The Gas Chromatography of Terpene Compounds Using Microsorb-W.** — Microsorb-W, which showed the feeblest catalytic action among the commercial solid supports examined, was used for the gas chromatography of terpene compounds.

This support, impregnated with 7% Thermol-1, was packed into a column (4 mm. in internal diameter, 3 m. long), and the conditioning of the column was carried out at 140°C for five hours. Two chromatograms of the mixture which was prepared from ten oxygen-containing compounds are shown in Figs. 4A and 4B.

4A is a chromatogram which has been obtained immediately after the conditioning, while 4B is a chromatogram which has been obtained after 40 hr. In A, there is a large, gently sloping hill; it has been confirmed to be attributable to a trace of water contained in the terpene mixture. On the other hand, no such hill is to be seen in B. Besides, in B the peak resolution is very good, and the retention times of the peaks are also remarkably shortened in comparison with the corresponding peaks in A.

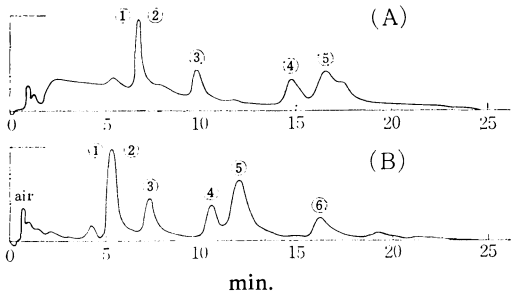



Fig. 4. Gas chromatography of terpene compounds using Microsorb-W.
A: After conditioning at 140°C for 5 hr.
B: After the use of 40 hr.
Stational liquid: Thermol-1 (7%)
Column temp.: 160°C
Flow rate of helium: 40 ml./min.
(1) Ethyl valerianate (2) Benzyl alcohol
(3) Linalool (4) Camphor
(5) Menthol (6) α-Terpineol
(7) Pulegone (8) Hydroxycitronellal
(9) α-Terpinyl acetate (10) α-Pinene

The difference observed between the two chromatograms, of A and of B, is assumed to result from an increase in the surface area of the stationary phase and from a decrease in its thickness, as a result of the evaporation and/or the decomposition of the precoating material. In such a support as Microsorb-W, the activity centers will gradually be exposed from the precoating material. Thus, this support appears unsatisfactory for the gas chromatography of terpene compounds.

**The Catalytic Action of the Stationary Phase Prepared from Diasolid-M.**—The controlling of the catalytic activity on Microsorb by precoating with a high polymer has been shown in the above section. Geranyl acetate, even when Shimalite is used, has been gas-chromatographed without decomposition by the impregnation of

TABLE III. CATALYTIC ACTION OF STATIONARY PHASE PREPARED FROM DIASOLID-M

| Compound | Stationary liquid: Termol-1 (20%) | Polycarbonate (5%) + PEG-6000 (5%) | PEG-6000 (5%) | Result in Figs. 2 and 3 |
|---|---|---|---|---|
| | | Monoterpene | | |
| Column temp. | 140°C | 140°C | 140°C | 140°C |
| Citronellal | ○ | + | + | −− |
| Hydroxycitronellal | ○ | ○ | + | −− |
| Nerol | + | ++ | ++ | −− |
| Geraniol | + | ++ | + | −− |
| Linalool | + | + | +++ | +++ |
| Citronellol | + | + | ++ | −− |
| Phenyl ethyl alcohol | ○ | + | + | −− |
| α-Terpineol | ○ | ○ | ○ | ++ |
| Geranyl acetate | + | + | + | ++++ |
| Linalyl acetate | ++ | ++ | ++ | ++++ |
| | | Sesquiterpene | | |
| Column temp. | 180°C | 160°C | 160°C | 200°C |
| α-Santalol | ++ | +++ | +++ | ++++ |
| β-Santalol | + | + | ++ | ++++ |
| α-Cadinol | ○(?) | +++ | +++ | ++++ |
| Elemol | ○ | ○ | ○ | ++ |
| Patchouli alcohol | +(?) | +(?) | + | ++++ |

○: No decomposition nor isomerization
+: Slight decomposition
++: D is roughly equal to U, where D is total area depending upon decomposition components, and U is peak area of unchanged original sample.
+++: D is larger than U.
++++: Complete decomposition with no peak of original sample.

a large quantity of Polyethylene glycol-1500.[20]

In order to clarify the extent of the controlling, several monoterpene compounds were separatly gas-chromatographed using three kinds of stationary phases prepared from Diasolid-M, that is, by the impregnation of 5% Polyethylene glycol-6000 or 20% Thermol-1 into Diasolid-M, and by the impregnation of 5% Polyethylene glycol-6000 into Diasolid-M precoated with 5% polycarbonate.*6 The results are listed in Table III.*7 In the right-hand column of this table, the results regarding Diasolid-M, which has been illustrated in Figs. 2 and 3, are represented using the same symbols for convenience in comparison.

Judging from the results in Table III, it seems difficult to prepare the stationary phase, which is adequately suitable for the gas chromatography of every terpene compound, even by the impregnation of a large quantity of a stationary liquid on Diasolid-M.

20) G. Indo and H. Yukawa, *J. Japan Chem.* (*Kagaku no Ryoiki*), Addendum for Gas Chromatography, No. 3, Nankodo, Tokyo (1962), p. 105.

*6 Presented by the Teijin Kasei Co., Ltd., Matsuyama, Japan.

*7 This experiment was carried out using a flame ionization-type gas chromatograph, because Diasolid is manufactured to use when impregnated with a low concentration of a stationary liquid.

**Summary**

The catalytic action of several solid supports, that is, glass, rock crystal, quartzite, sea sand, unglazed porcelain and commercial supports, have been examined. Glass shows practically no catalytic action in the examined terpene compounds, except for linalyl acetate and $\alpha$-santalol, which were decomposed and/or isomerized slightly, but this support does show an adsorption of oxygen-containing compounds. The catalytic action of rock crystal is slightly greater than that of glass, but the adsorptivity of rock crystal is extremely small. Commercial diatomaceous earth supports show a remarkable catalytic action.

The authors wish to express their thanks to Tôyô Tsûshin, Tôyô Kôgyô, Shiono Kôryô and the Soda Kôryô Co., Ltd., for the donation of materials.

*Department of Chemistry*
*Faculty of Science*
*Hiroshima University*
*Higashi-sendamachi, Hiroshima*

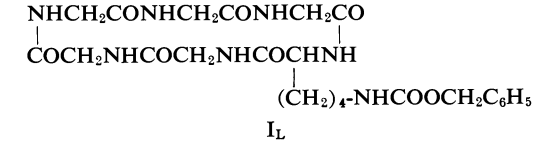
# The Synthesis of Cyclo-pentaglycyl-L-lysyl and Its Hydrolysis by Trypsin

By Motonori OHNO and Nobuo IZUMIYA

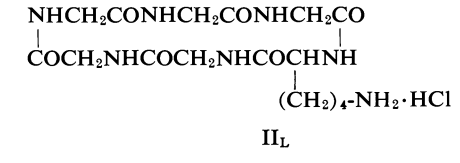
(Received January 22, 1965)

In a previous paper from this laboratory, it was shown that L-phenylalanyl- and L-valyl-L-lysine anhydrides are not hydrolyzed by trypsin at the lysine carbonyl linkage.[1] Although the reason why the dipeptide anhydrides are not susceptible to the enzyme is not yet clear, it is possible that a certain minimum ring size is necessary in order that a cyclic peptide can be hydrolyzed by the enzyme. From the literature, it appears that cyclic tri-, tetra- and pentapeptides are difficult to synthesize,[2] but cyclic hexapeptides have been prepared without difficulty.[2,3] Therefore, we attempted to synthesize a cyclic hexapeptide containing a lysine residue.

In the present investigations, the synthesis of cyclo-pentaglycyl-ε-benzyloxycarbonyl-L-lysyl ($I_L$) was studied in detail in an attempt to obtain fundamental information about the syntheses of cyclic peptides; then, cyclo-pentaglycyl-L-lysyl hydrochloride ($II_L$), which had been obtained by the hydrogenolysis of $I_L$, was tested by the trypsin.



$I_L$



$II_L$

1) N. Izumiya, T. Kato, Y. Fujita, M. Ohno and M. Kondo, This Bulletin, **37**, 1809 (1964).
2) R. Schwyzer, *CIBA Foundation Symposium of Amino Acids and Peptides with Antimetabolic Activity*, 171 (1958).
3) T. Kato, M. Kondo, M. Ohno and N. Izumiya, This Bulletin, **38**, 1202 (1965).

Various methods for the synthesis of cyclo-pentaglycyl-ε-benzyloxycarbonyllysyl were undertaken. Since the cyclization of a linear active ester gave a better yield than the other cyclization methods,[2] we first attempted to prepare the cyclic peptide by the active ester method. In the present series of syntheses of the cyclic peptide, a benzyloxycarbonyl group was used for the selective blocking of the ε-amino group of the lysine residue.

$$\text{TRI-Gly}_2\text{-OH} + \varepsilon\text{-Z-L-Lys-OEt}\cdot\text{TsOH} \xrightarrow[\text{M.A. 77\%}]{\text{NEt}_3}$$

$$\text{TRI-Gly}_2\text{-}\varepsilon\text{-Z-L-Lys-OEt} \xrightarrow{\text{HCl-MeOH}}$$

III

$$\text{H-Gly}_2\text{-}\varepsilon\text{-Z-L-Lys-OEt}\cdot\text{HCl} \xrightarrow[\text{TRI-Gly}_3\text{-OH, M.A. 68\%}]{\text{NEt}_3}$$

IV

$$\text{TRI-Gly}_5\text{-}\varepsilon\text{-Z-L-Lys-OEt} \xrightarrow[91\%]{\text{OH}^- \text{ and } \text{H}^+}$$

V

$$\text{TRI-Gly}_5\text{-}\varepsilon\text{-Z-L-Lys-OH} \xrightarrow{\text{NPS, pyridine}}$$

VI

$$\text{TRI-Gly}_5\text{-}\varepsilon\text{-Z-Lys-ONP} \xrightarrow{\text{CF}_3\text{COOH, H}_2\text{O}}$$

$\text{VII}_{\text{PR}}$

$$\text{H-Gly}_5\text{-}\varepsilon\text{-Z-Lys-ONP}\cdot\text{CF}_3\text{COOH} \xrightarrow[33\% \text{ from VI}]{\text{pyridine}}$$

$\text{VIII}_{\text{PR}}$

$$\varepsilon\text{-Z-}\underbrace{\text{Lys Gly}_5}_{\text{I}_{\text{PR}}} \xrightarrow[\text{HCl-MeOH}]{\text{H}_2/\text{Pd}} \underbrace{\text{Lys Gly}_5}_{\text{II}_{\text{PR}}}\cdot\text{HCl}$$

Fig. 1. Synthesis of cyclic hexapeptide via $\text{VII}_{\text{PR}}$: TRI, trityl; Z, benzyloxycarbonyl; TsOH, *p*-toluenesulfonic acid; $\text{NEt}_3$, triethylamine; M.A., mixed anhydride method; NPS, di-*p*-nitrophenyl sulfite; ONP, *p*-nitrophenoxy.

Figure 1 indicates the sequence of reactions via the linear hexapeptide *p*-nitrophenyl ester, in which ε-benzyloxycarbonyllysine was the *C*-terminal amino acid. The product obtained in a fairly good yield by the cyclization reaction of $\text{VIII}_{\text{PR}}$ was found to be a monomer with a molecular weight in agreement with that of cyclic hexapeptide ($\text{I}_{\text{PR}}$). However, it was found that the lysine residue in the compound $\text{I}_{\text{PR}}$ is partially racemized, since the specific rotation of $\text{I}_{\text{PR}}$ was +0.5, whereas that of optically-pure cyclo-pentaglycyl-ε-benzyloxycarbonyl-L-lysyl ($\text{I}_{\text{L}}$) was +0.9. When calculations are based on the specific rotation, $\text{I}_{\text{PR}}$ is found to contain about 78 per cent of the L-compound ($\text{I}_{\text{L}}$) and 22 per cent of the D-compound. Furthermore, $\text{II}_{\text{PR}}$ derived from $\text{I}_{\text{PR}}$ was not completely hydrolyzed by trypsin. The cyclo-pentaglycyllysyl which remained unchanged appeared to have a D-configuration (see Fig. 8). We assume that a partial racemization had taken place at the step of the *p*-nitrophenyl esterification of VI by di-*p*-nitrophenyl sulfite and pyridine, since Iselin and Schwyzer had reported that a partially-racemized benzyloxycarbonyl dipeptide *p*-nitrophenyl ester was obtained when benzyloxycarbonyl dipeptide was treated with di-*p*-nitrophenyl sulfite and pyridine.[4] Furthermore, since it has been reported that no racemization occurs when the benzyloxycarbonyl dipeptide *p*-nitrophenyl ester which was obtained from benzyloxycarbonyl amino acid and amino acid *p*-nitrophenyl ester is coupled with the amino acid ethyl ester,[5] no racemization may be expected at the step of the formation of $\text{I}_{\text{PR}}$ from $\text{VIII}_{\text{PR}}$ by intramolecular peptide bond formation. Therefore, a glycine or proline residue should be selected as the *C*-terminal amino acid of the *N*-blocked peptide in the case of its *p*-nitrophenyl esterification with di-*p*-nitrophenyl sulfite and a base.

$$\text{VI} \xrightarrow[71\%]{\text{AcOH, H}_2\text{O}} \text{H-Gly}_5\text{-}\varepsilon\text{-Z-L-Lys-OH}$$

IX

$$\xrightarrow[\text{less than 4.7\%}]{\text{DCC}} \text{I}_{\text{PR}} \text{ or } \text{I}_{\text{L}}$$

Fig. 2. Synthesis of cyclic hexapeptide with IX and DCC: DCC, dicyclohexylcarbodiimide.

Figure 2 indicates an attempt to cyclize pentaglycyl-ε-benzyloxycarbonyl-L-lysine with two equivalents of dicyclohexylcarbodiimide. The yields were, however, found to be very poor. Contrary to this study, syntheses of cyclic hexa-,[6] hepta-[7] and octapeptide[8] from the pertinent linear peptides with carbodiimide have been reported.

Figures 3 and 4 indicate attempts to cyclize the linear hexapeptide azides. Although it has been reported that cyclo-hexaglycyl is obtained in a good yield by dimerization reaction from triglycine azide,[9] both triglycyl-ε-benzyloxycarbonyl-L-lysylglycylglycine azide and pentaglycyl-ε-benzyloxycarbonyl-L-lysine azide gave only a very small amount of $\text{I}_{\text{L}}$. Sheehan and McGregor reported that the cyclization of tripeptide azide did not give the desired

4) B. Iselin and R. Schwyzer, *Helv. Chim. Acta*, **43**, 1760 (1960).
5) M. Goodman and K. C. Stueben, *J. Am. Chem. Soc.*, **81**, 3980 (1959).
6) K. D. Kopple and K. E. Nitecki, ibid., **83**, 4103 (1961); **84**, 4457 (1962); T. Wieland and K. W. Ohle, *Ann.*, **605**, 179 (1957).
7) R. O. Studer, W. Lergier and K. Vogler, *Helv. Chim. Acta*, **46**, 612 (1963); K. Vogler, R. O. Studer, P. Lanz, W. Lergier, E. Böhni and B. Fust, ibid., **46**, 2823 (1963).
8) K. Vogler, R. O. Studer, W. Lergier and P. Lanz, ibid., **43**, 1751 (1960); R. O. Studer, K. Vogler and W. Lergier, ibid., **44**, 131 (1961).
9) J. C. Sheehan and W. L. Richardson, *J. Am. Chem. Soc.*, **76**, 6329 (1954); **77**, 6391 (1955).

BOC-Gly-OH + IV $\xrightarrow[88\%]{DCC}$

BOC-$Gly_3$-ε-Z-L-Lys-OEt $\xrightarrow[93\%]{OH^-\text{ and }H^+}$
X

BOC-$Gly_3$-ε-Z-L-Lys-OH $\xrightarrow[77\%]{H\text{-}Gly_2\text{-}OBz,\ DCC}$
XI

BOC-$Gly_3$-ε-Z-L-Lys-$Gly_2$-OBz $\xrightarrow[93\%]{NH_2NH_2}$
XII

BOC-$Gly_3$-ε-Z-L-Lys-$Gly_2$-$NHNH_2$ $\xrightarrow{HCl\text{-}MeOH}$
XIII

H-$Gly_3$-ε-Z-L-Lys-$Gly_2$-$NHNH_2\cdot 2HCl$ $\xrightarrow{HNO_2}$

H-$Gly_3$-ε-Z-L-Lys-$Gly_2$-$N_3\cdot HCl$ $\xrightarrow{NaHCO_3}$ Trace of $I_L$

Fig. 3. Attempt to synthesize cyclic hexapeptide via XIII: BOC, *t*-butyloxycarbonyl.

V $\xrightarrow[71\%]{NH_2NH_2}$ TRI-$Gly_5$-ε-Z-L-Lys-$NHNH_2$ $\xrightarrow[77\%]{HCl\text{-}MeOH}$
XIV

H-$Gly_5$-ε-Z-L-Lys-$NHNH_2\cdot 2HCl$ $\xrightarrow{HNO_2}$
XV

H-$Gly_5$-ε-Z-L-Lys-$N_3\cdot HCl$ $\xrightarrow{NaHCO_3}$ Trace of $I_L$

Fig. 4. Attempt to synthesize cyclic hexapeptide via XIV.

cyclic hexapeptide.[10]

Figure 5 illustrates the sequence of reactions via the peptide active ester in which glycine is the *C*-terminal amino acid. The optical purity of the L-lysine residue should be maintained in this reaction sequence, since the coupling of *N*-blocked peptide hydrazide (XVIII) and the dipeptide ester is performed

pMZ-Gly-OH + IV $\xrightarrow[87\%]{NEt_3,\ M.A.}$
XVI

pMZ-$Gly_3$-ε-Z-L-Lys-OEt $\xrightarrow[79\%]{NH_2NH_2}$
XVII

pMZ-$Gly_3$-ε-Z-L-Lys-$NHNH_2$ $\xrightarrow{HNO_2}$
XVIII

pMZ-$Gly_3$-ε-Z-L-Lys-$N_3$ $\xrightarrow[71\%\text{ from XVIII}]{H\text{-}Gly_2\text{-}OBz}$

pMZ-$Gly_3$-ε-Z-L-Lys-$Gly_2$-OBz $\xrightarrow[75\%]{OH^-\text{ and }H^+}$
XIX

pMZ-$Gly_3$-ε-Z-L-Lys-$Gly_2$-OH $\xrightarrow{NPS}$
XX

pMZ-$Gly_3$-ε-Z-L-Lys-$Gly_2$-ONP $\xrightarrow{CF_3COOH,\ anisole}$
XXI

H-$Gly_3$-ε-Z-L-Lys-$Gly_2$-ONP$\cdot CF_3COOH$ $\xrightarrow[42\%\text{ from XX}]{pyridine}$

ε-Z-L-Lys $\overbrace{\text{Gly}_5}$ $\xrightarrow[66\%]{H_2/Pd,\ HCl}$ L-Lys $\overbrace{\text{Gly}_5}\cdot HCl$

$I_L$ $II_L$

Fig. 5. Synthesis of cyclic hexapeptide via XXI: pMZ, *p*-methoxybenzyloxycarbonyl.

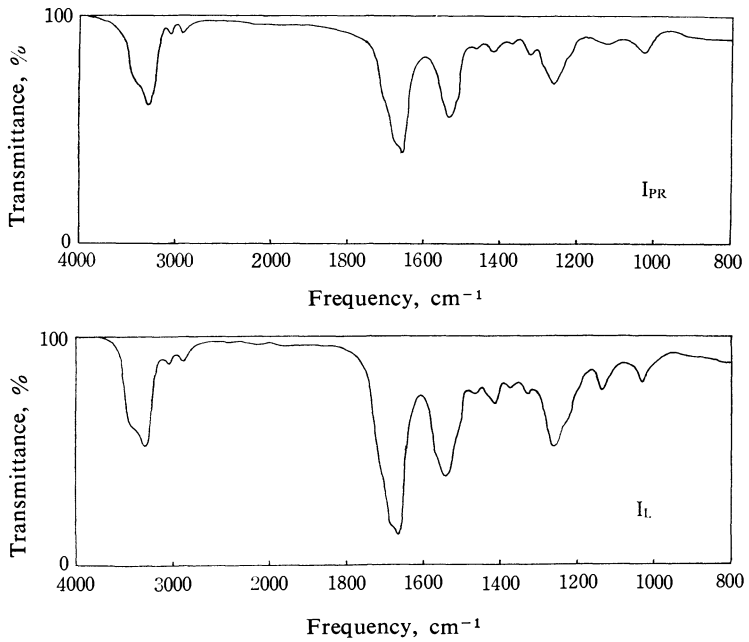



Fig. 6. Infrared spectra of cyclo-pentaglycyl-ε-benzyloxycarbonyllysyl ($I_{PR}$) and cyclo-pentaglycyl-ε-benzyloxycarbonyl-L-lysyl ($I_L$).

10) J. C. Sheehan and D. N. McGregor, ibid., **84**, 3000 (1962).

by the azide method, in which the *C*-terminal amino acid residue is known to be remarkably resistant to racemization.[11] Furthermore, the *p*-nitrophenyl esterification of XX does not cause any racemization since *C*-terminal amino acid is glycine. During this study, we found that the *p*-methoxybenzyloxycarbonyl group was superior to trityl or *t*-butyloxycarbonyl as a group protecting the *N*-terminal amino group of a linear peptide *p*-nitrophenyl ester. The *p*-methoxybenzyloxycarbonyl group is easily, in a few minutes, released at 0°C with trifluoroacetic acid in the absence of water, while the trityl group requires successive treatments with trifluoroacetic acid and water. The experiment, as shown in Fig. 1, indicates that the sensitive *p*-nitrophenyl ester group is degraded partially in the presence of water. Furthermore, we found that the *t*-butyloxycarbonyl peptide could not afford the desired *t*-butyloxycarbonyl peptide *p*-nitrophenyl ester with di-*p*-nitrophenyl sulfite and a base.[12] The yield of $I_L$ from XXI was fairly good, as is shown in Fig. 5. The infrared absorption spectra of $I_L$ was identical with that of $I_{PR}$ (Fig. 6), as were the $R_f$ values of $II_{PR}$ and $II_L$ in the paper chromatography. The hydrogenolysis of $I_L$ yielded the desired cyclic peptide, $II_L$. The homogeneity of $II_L$ wa asscertained by chromatography and by elemental analyses.

It was observed that cyclo-pentaglycyl-L-lysyl is completely hydrolyzed by trypsin to pentaglycyl-L-lysine. This agrees well with the fact that a linear peptide containing L-lysine is susceptible to the hydrolytic action of trypsin at the linkage of lysine carbonyl.[13] An authentic pentaglycyl-L-lysine hydrochloride (XXII) was synthesized, as Fig. 7 shows. This finding is of great interest, because this is the first example of how trypsin can hydrolyze a cyclic peptide. However, glycyl-L-lysine anhydride, a cyclic dipeptide, was found not to be hydrolyzed by trypsin, but it did not inhibit the hydrolysis of $\alpha$-benzoyl-L-arginine amide by trypsin.[14] These enzymatic experiments show that even a cyclic dipeptide containing a L-lysine residue has no affinity to trypsin, while a cyclic hexapeptide, cyclo-pentaglycyl-L-lysyl, can form an enzyme-substrate complex which is finally decomposed to the enzyme and the product. Further experiments on the preparation of cyclic peptides, cyclo-(glycyl$_n$-L-lysyl)$_2$ ($n$=2 and 4), and on their susceptibility to trypsin are in progress in this laboratory.

$$\text{IX} \xrightarrow[80\%]{\text{H}_2/\text{Pd, HCl-MeOH}} \underset{\text{XXII}}{\text{H-Gly}_5\text{-L-Lys-OH}\cdot\text{HCl}}$$

Fig. 7. Synthesis of pentaglycyl-L-lysine hydrochloride.

## Experimental

The melting points were not corrected. The optical rotations were measured on a Yanagimoto Photometric Polarimeter, OR-20 type. The paper chromatography was carried out on Toyo Roshi No. 52 chromatography paper. The thin-layer chromatography was carried out on Merck silica gel G. The developing solvents were *n*-butanol - acetic acid - pyridine - water (4 : 1 : 1 : 2) and *t*-butanol - formic acid - water (75 : 15 : 10). Spots of materials possessing a free amino group on a thin layer plate were detected by spraying ninhydrin, and those of the amino group-blocked materials, by spraying 47 per cent hydrobromic acid and then ninhydrin.

**Trityldiglycyl - ε - benzyloxycarbonyl - L - lysine Ethyl Ester (III).**—The mixed anhydride prepared at −5°C from 18.7 g. (50 mmol.) of tritylglycylglycine,[15] 6.7 ml. (50 mmol.) of isobutyl chloroformate and 7.0 ml. (50 mmol.) of triethylamine in 150 ml. of tetrahydrofuran was coupled with 24.0 g. (50 mmol.) of ε-benzyloxycarbonyl-L-lysine ethyl ester *p*-toluenesulfonate[16] dissolved in a chilled mixture of 7.0 ml. (50 mmol.) of triethylamine and 150 ml. of chloroform. The reaction mixture was allowed to stand overnight and then evaporated to dryness in vacuo. The oily residue was dissolved in 250 ml. of ethyl acetate, and the solution was washed successively with 100-ml. portions of 0.5 N acetic acid, a 3% sodium bicarbonate solution and water, dried over sodium sulfate, and then evaporated to dryness in vacuo. The oily residue was then solidified by adding petroleum ether. Yield: 25.7 g. (77%). For analysis, the product was recrystallized from ethyl acetate - ether - petroleum ether; m. p. 107—108°C, $[\alpha]_D^{20}$ −7.1° (*c* 2, methanol).

Found: C, 70.42; H, 6.57; N, 8.45. Calcd. for $C_{39}H_{44}O_6N_4$: C, 70.46; H, 6.67; N, 8.43%.

**Diglycyl-ε-benzyloxycarbonyl-L-lysine Ethyl Ester Hydrochloride (IV).**—To a solution of 6.64 g. (10 mmol.) of III in 50 ml. of methanol, 15 ml. of N hydrogen chloride in methanol was added; then the solution was boiled for 2 min. The solution was concentrated in vacuo and ether was added to the residue. The resulting white crystals were collected by filtration and washed with ether (3.72 g.). The product was recrystallized from methanol - ether. Yield: 3.44 g. (75%); m. p. 144—146°C, $[\alpha]_D^{20}$ −13.2° (*c* 2, methanol).

Found: C, 52.17; H, 6.71; N, 11.84. Calcd. for $C_{20}H_{30}O_6N_4\cdot HCl$: C, 52.34; H, 6.59; N, 12.21%.

11) N. F. Albertson, "Organic Reactions." Vol. 12 (1962), p. 168.
12) M. Ohno and N. Izumiya, unpublished.
13) H. Neurath and G. W. Schwert, *Chem. Revs.*, **46**, 69 (1950); N. Izumiya, T. Yamashita, H. Uchio and K. Kitagawa, *Arch. Biochem. Biophys.*, **90**, 170 (1960).
14) T. Yamamoto and N. Izumiya, unpublished.
15) R. Schwyzer, B. Iselin, W. Rittel and P. Sieber, *Helv. Chim. Acta*, **39**, 872 (1956).
16) T. Kato, S. Makisumi, M. Ohno and N. Izumiya, *J. Chem. Soc. Japan, Pure Chem. Sec.* (*Nippon Kagaku Zasshi*), **83**, 1151 (1962).

**Tritylpentaglycyl-ε-benzyloxycarbonyl-L-lysine Ethyl Ester (V).**—The mixed anhydride prepared at −5°C from 4.32 g. (10 mmol.) of trityldiglycylglycine,[15] 1.3 ml. (10 mmol.) of isobutyl chloroformate and 1.4 ml. (10 mmol.) of triethylamine in a mixture of 30 ml. of tetrahydrofuran and 20 ml. of chloroform was coupled with 4.59 g. (10 mmol.) of IV dissolved in a chilled mixture of triethylamine and 30 ml. of chloroform. The reaction mixture was allowed to stand overnight and then evaporated to dryness in vacuo. The oily residue was dissolved in 200 ml. of chloroform, and the solution was washed successively with 0.5 M citric acid, a 3% sodium bicarbonate solution and water, dried over sodium sulfate, and then evaporated to dryness in vacuo. The oily residue was easily solidified by adding ether and petroleum ether (6.19 g.). The product was recrystallized from acetone-ether. Yield: 5.68 g. (68%); m. p. 94—96°C, $[\alpha]_D^{20}$ −4.7° (*c* 2, dimethylformamide).

Found: C, 64.35; H, 6.56; N, 11.33. Calcd. for $C_{45}H_{53}O_9N_7$: C, 64.65; H, 6.39; N, 11.73%.

**Tritylpentaglycyl-ε-benzyloxycarbonyl-L-lysine (VI).**—To a solution of 1.80 g. (2.15 mmol.) of V in a mixture of 10 ml. of dioxane and 5 ml. of methanol, 2.5 ml. of N sodium hydroxide was added. After 2 hr., the solution was concentrated in vacuo to remove methanol, and the residual solution was diluted with water and acidified with 3.0 ml. of M citric acid under cooling. The precipitate was collected by filtration under cooling and washed with cold water. The product was recrystallized from ethanol-ether. Yield: 1.58 g. (91%). For analysis, this was further recrystallized from ethanol-ether; m. p. 109—112°C, $[\alpha]_D^{20}$ −6.5° (*c* 2, dimethylformamide).

Found: C, 63.25; H, 6.20; N, 12.22. Calcd. for $C_{43}H_{49}O_9N_7$: C, 63.92; H, 6.11; N, 12.14%.

**Tritylpentaglycyl-ε-benzyloxycarbonyllysine *p*-Nitrophenyl Ester ($VII_{PR}$).**—A solution of 1.62 g. (2 mmol.) of VI and 1.30 g. (4 mmol.) of di-*p*-nitrophenyl sulfite[4] dissolved in 10 ml. of pyridine was allowed to stand at room temperature for 15 hr. The solvent was then removed in vacuo, and the oily residue was solidified by adding a mixture of ether and petroleum ether (1 : 1) and scratching. The product was collected by filtration and washed with a mixture of ether and petroleum ether (1 : 1) until the yellow color could not be discerned upon the addition of N sodium hydroxide to the filtrate. A faintly yellow product was obtained. Yield: 1.80 g.; $[\alpha]_D^{20}$ −1.6° (*c* 2, dimethylformamide).

Found: N, 11.43. Calcd. for $C_{49}H_{52}O_{11}N_8$: N, 11.93%.

The solution of 3.04 mg. of this product in 50 ml. of methanol was diluted with N sodium hydroxide to 100 ml. ($c=3.27\times10^{-5}$ M). The absorption of this solution was measured at 404 mμ and compared with a standard curve which had been determined with the benzyloxycarbonyl-L-leucine *p*-nitrophenyl ester in the same solvent.[17] The value of the absorbance of this sample corresponded to $c=3.46\times10^{-5}$ M. Therefore, the *p*-nitrophenyl ester content of this product was estimated to be 106%.

**Pentaglycyl-ε-benzyloxycarbonyllysine *p*-Nitrophenyl Ester Trifluoroacetate ($VIII_{PR}$).**—A solution of 1.0 g. of $VII_{PR}$ dissolved in 18 ml. (25 g.) of trifluoroacetic acid was cooled to −5°C, and then 15 ml. of cold water was added slowly to this solution. After 15 min., the precipitate of triphenylcarbinol was filtered off. The filtrate was lyophilized, and the oily residue was solidified by adding ether and scratching. The powdery solid was collected by filtration and washed thoroughly with a mixture of ether and petroleum ether (1 : 1) until the yellow color could not be discerned upon the addition of N sodium hydroxide to the filtrate. A faintly yellow powder was obtained; 0.660 g. (apparent yield, 86%).

The *p*-nitrophenyl ester content of this product was estimated by the same method as has been described previously except that a mixture of dimethylformamide and N sodium hydroxide (1 : 1) was used as a solvent and the measurement was performed at 411 mμ. The *p*-nitrophenyl ester content was estimated to be 81%. Therefore, the true yield of the compound $VIII_{PR}$ was 70%.

**Cyclo-pentaglycyl-ε-benzyloxycarbonyllysyl ($I_{PR}$).**—A solution of 0.610 g. (0.762 mmol.) of $VIII_{PR}$ in a mixture of 15 ml. of dimethylformamide and 0.15 ml. of acetic acid was stirred drop by drop into 140 ml. of pyridine kept at 55—60°C over a 9-hr. period. The solution was stirred at this temperature for another 2 hr. and then evaporated to dryness in vacuo. The dried residue was dissolved in 160 ml. of a hot mixture of water and methanol (1 : 1), and insoluble materials were filtered off. The filtrate was passed successively through columns (1×14 cm.) of Dowex-50 ($H^+$ form) and Dowex-1 ($OH^-$ form) which had been washed with a mixture of water and methanol (1 : 1). The columns were then washed with a mixture of water and methanol (1 : 1). The filtrate and washings (total 400 ml.) were combined and evaporated to dryness in vacuo. The weight of the dried residue was 0.229 g. (39% from $VII_{PR}$). The crude cyclic product was recrystallized from methanol-water. Yield: 0.193 g. (33% from $VII_{PR}$); m. p. 261—262°C, $[\alpha]_D^{20}$ +0.5° (*c* 1.33, dimethylformamide).

Found: C, 51.90; H, 6.33; N, 17.19. Calcd. for $C_{24}H_{34}O_8N_7\cdot1/2H_2O$: C, 51.62; H, 6.33; N, 17.59%.

The air-dried compound lost 1.62% of its weight after being dried for 2 hr. at 130°C, 0.1 mmHg. Calcd. for $1/2H_2O$: 1.62%. The molecular weight was determined by the micro Rast method with a solvent of hexahydro-*p*-aminobenzoic acid lactam.[18] Calcd.: 549. Found: 557, 510.

**Cyclo-pentaglycyllysyl Hydrochloride ($II_{PR}$).**—A solution of 5.56 mg. (0.01 mmol.) of $I_{PR}$ dissolved in a mixture of 0.4 ml. of 0.025 N hydrochloric acid and 0.2 ml. of water was hydrogenolyzed in the presence of palladium black. After the filtrate had been evaporated to dryness, the residue was filtered with the aid of acetone; yield, 3.0 mg. The homogeneity of $II_{PR}$ was established by

17) R. Schwyzer and P. Sieber, *Helv. Chim. Acta*, **40**, 624 (1957).

18) G. Wendt, *Chem. Ber.*, **75**, 425 (1942).

chromatography ($R_f$[19] 0.27, $R_f$[20] 0.42 and $R_f$[21] 0.13). These values of $R_f$ are identical as those of analytically-pure cyclo-pentaglycyl-L-lysyl hydrochloride ($II_L$).

**Pentaglycyl-ε-benzyloxycarbonyl-L-lysine (IX).**—When 1.0 g. (1.24 mmol.) of VI suspended in 20 ml. of 50 per cent aqueous acetic acid was boiled for 2 min., it dissolved and triphenylcarbinol was deposited.[22] Ten milliliters of water was then added, and the solution was kept in a refrigerator for several hours, after which the carbinol was removed by filtration (0.298 g.). The filtrate was evaporated to dryness in vacuo. The product was filtered with the aid of ethanol (0.630 g.). This was recrystallized from water-ethanol. Yield: 0.500 g. (71%); m. p. 213—214°C (decomp.), $[\alpha]_D^{20}$ −2.4° (*c* 2, 0.2 N hydrochloric acid).

Found: C, 49.44; H, 6.28; N, 17.13. Calcd. for $C_{24}H_{35}O_9N_7 \cdot 1/2H_2O$: C, 49.39; H, 6.39; N, 16.80%.

**An Attempt to Cyclize IX by Dicyclohexylcarbodiimide.**—To a suspension of 0.234 g. (0.414 mmol.) of IX in 10 ml. of dimethylformamide, 0.170 g. (0.828 mmol.) of dicyclohexylcarbodiimide was added. The reaction mixture was kept at 0°C with stirring for 24 hr. and then evaporated to dryness in vacuo. The residue was extracted with 50 ml. of a hot mixture of water and methanol (1 : 1). After the extract had been cooled, the dicyclohexylurea deposited was removed by filtration and the filtrate was passed successively through columns of Dowex-50 ($H^+$ form) and Dowex-1 ($OH^-$ form). The filtrate and washings were then combined and evaporated to dryness in vacuo (0.011 g.). This product contained cyclo-pentaglycyl-ε-benzyloxycarbonyllysyl since the hydrogenolyzed material gave a single spot of $R_f$ 0.27[19] which was identical with $II_{PR}$.

***t*-Butyloxycarbonyltriglycyl-ε-benzyloxycarbonyl-L-lysine Ethyl Ester (X).**—To a stirred solution of 3.50 g. (20 mmol.) of *t*-butyloxycarbonylglycine[23] and 9.18 g. (20 mmol.) of IV in 200 ml. of chloroform, 2.8 ml. (20 mmol.) of triethylamine was added. The solution was then cooled to 0°C, and 4.12 g. (20 mmol.) of dicyclohexylcarbodiimide was stirred into it. The reaction mixture was stirred at 0°C for one hour and then kept in a refrigerator overnight. Dicyclohexylurea was removed by filtration. The filtrate was washed successively with 0.5 M citric acid, a 3% sodium bicarbonate solution and water, dried over sodium sulfate, and then evaporated to dryness in vacuo (9.88 g.). The product was twice recrystallized from ethyl acetate-petroleum ether. Yield: 8.88 g. (79%); m. p. 115—117°C, $[\alpha]_D^{20}$ −8.4° (*c* 2, methanol).

Found: C, 56.11; H, 7.35; N, 11.71. Calcd. for $C_{27}H_{41}O_9N_5$: C, 55.94; H, 7.13; N, 12.08%.

***t*-Butyloxycarbonyltriglycyl-ε-benzyloxycarbonyl-L-lysine (XI).**—To a solution of 8.42 g. (15 mmol.) of X in 45 ml. of methanol, 18 ml. of N sodium hydroxide was added. Saponification was carried out at room temperature for 2 hr. After the removal of the methanol in vacuo, the aqueous solution was acidified with 23 ml. of M citric acid under cooling and the oil deposited was extracted two times with 50-ml. portions of ethyl acetate. The combined ethyl acetate solution was then washed with water, dried over sodium sulfate, and evaporated to dryness in vacuo. The residue was solidified by adding petroleum ether. Yield: 7.44 g. (93%). For analysis, the product was twice recrystallized from ethyl acetate-ether; m. p. 66—67°C, $[\alpha]_D^{20}$ +2.6° (*c* 2, methanol).

Found: C, 54.11; H, 6.60; N, 12.22. Calcd. for $C_{25}H_{37}O_9N_5$: C, 54.43; H, 6.76; N, 12.70%.

***t*-Butyloxycarbonyltriglycyl-ε-benzyloxycarbonyl-L-lysylglycylglycine Benzyl Ester (XII).**—To a stirred, faintly cloudy solution of 5.52 g. (10 mmol.) of XI and 3.94 g. (10 mmol.) of glycylglycine benzyl ester *p*-toluenesulfonate in 200 ml. of chloroform, 1.4 ml. (10 mmol.) of triethylamine was added. The solution was then cooled to 0°C and 2.06 g. (10 mmol.) of dicyclohexylcarbodiimide was added to it. After the mixture had been stirred at 0°C for 4 hr., it was kept in a refrigerator for 2 days and then evaporated in vacuo. The residue was filtered with the aid of water and petroleum ether, and washed with 0.5 M citric acid, a 3% sodium bicarbonate solution and water. The dried mixture was dissolved in methanol and kept in a refrigerator for several hours, and the dicyclohexylurea was removed by filtration. These operations were repeated several times, thus removing almost all the dicyclohexylurea. Finally the filtrate was evaporated to dryness in vacuo. The oily residue was solidified by adding ether and petroleum ether. Yield: 5.80 g. (77%). For analysis, the product was twice recrystallized from methanol-ethyl acetate-ether; m. p. 132—156°C, $[\alpha]_D^{20}$ −0.5° (*c* 2, dimethylformamide).

Found: C, 56.83; H, 6.51; N, 12.38. Calcd. for $C_{36}H_{49}O_{11}N_7 \cdot 1/2H_2O$: C, 56.54; H, 6.35; N, 12.82%.

***t*-Butyloxycarbonyltriglycyl-ε-benzyloxycarbonyl-L-lysylglycylglycine Hydrazide (XIII).**—A solution of 1.51 g. (2 mmol.) of XII and 0.20 g. (4 mmol.) of hydrazine hydrate in 14 ml. of methanol was allowed to stand at room temperature for 24 hr. The solution was then evaporated to dryness in vacuo, after which the oily residue was immediately solidified by adding a mixture of ether and petroleum ether (1 : 1). This product was recrystallized from methanol-ether. Yield: 1.27 g. (93%); m. p. 159—172°C.

Found: C, 50.17; H, 6.66; N, 18.41. Calcd. for $C_{29}H_{45}O_{10}N_9 \cdot H_2O$: C, 49.92; H, 6.79; N, 18.07%.

**An Attempt to Synthesize Cyclic Hexapeptide via XIII by the Azide Method.**—A solution of 1.01 g. (1.49 mmol.) of XIII in a mixture of 8.5 ml.

19) The $R_f$ of the paper chromatography refers to the *n*-butanol-acetic acid-pyridine-water (4 : 1 : 1 : 2) system.
20) The $R_f$ of the paper chromatography refers to the *t*-butanol-formic acid-water (75 : 15 : 10) system.
21) The $R_f$ of the thin layer chromatography with Merck silica gel G refers to the *n*-butanol-acetic acid-pyridine-water (4 : 1 : 1 : 2) system.
22) L. Zervas and D. M. Theodoropoulos, *J. Am. Chem. Soc.*, **78**, 1359 (1956); G. C. Stelakatos, D. M. Theodoropoulos and L. Zervas, ibid., **81**, 2884 (1959).
23) This was prepared from glycine and *t*-butyloxycarbonyl azide by the general method developed by Schwyzer et al. (R. Schwyzer, H. Kappeler, B. Iselin, W. Rittel and H. Zuber, *Helv. Chim. Acta*, **42**, 2622 (1959)).

of methanol and 20 ml. of 2.84 N hydrogen chloride in methanol was allowed to stand at room temperature for 2 hr.[24] The solution was then evaporated to dryness in vacuo, and the residue was kept under high vacuum for 2 hr. The main portion of the residue was regarded as triglycyl-ε-benzyloxycarbonyl-L-lysylglycylglycine hydrazide dihydrochloride. The residue was dissolved in 8 ml. of 0.2 N hydrochloric acid. To the solution was then added a solution of 0.111 g. (1.6 mmol.) of sodium nitrate in 1 ml. of water under cooling. After it had stood for 15 min. at 0°C, the solution was poured into 1.5 l. of cold water containing 5.6 g. of sodium bicarbonate. The solution was kept at 4°C for 24 hr., and then the pH was brought to 5 with 2 N hydrochloric acid. The solution was passed successively through columns of Dowex-50 ($H^+$ form) and Dowex-1 ($OH^-$ form). The filtrate and washings were combined and evaporated to dryness in vacuo. Only a few milligrams of $I_L$ were obtained.

**Tritylpentaglycyl-ε-benzyloxycarbonyl-L-lysine Hydrazide (XIV).**—A solution of 0.836 g. (1 mmol.) of V and 0.150 g. (3 mmol.) of hydrazine hydrate in 5 ml. of methanol was allowed to stand at room temperature for 24 hr. The solution was then concentrated in vacuo to a small volume, ether was added, and the resulting crystals were collected by filtration (0.70 g.). The product was recrystallized from methanol-ether. Yield: 0.580 g. (71%); m. p. 162—167°C, $[\alpha]_D^{20}$ −3.0° (*c* 2, dimethylformamide).

Found: C, 62.70; H, 6.36; N, 14.75. Calcd. for $C_{43}H_{51}O_8N_9$: C, 62.83; H, 6.25; N, 15.34%.

**Pentaglycyl-ε-benzyloxycarbonyl-L-lysine Hydrazide Dihydrochloride (XV).**—A solution of 0.476 g. (0.58 mmol.) of XIV in a mixture of 8 ml. of methanol and 2.4 ml. of 0.5 N hydrogen chloride in methanol was boiled for 2 min. Then the solution was evaporated in vacuo, and the resulting crystals were filtered with the aid of a mixture of ethanol and ether. The product was recrystallized from methanol-ethanol-ether. Yield: 0.292 g. (77%); m. p. 196—198°C.

Found: N, 18.33. Calcd. for $C_{24}H_{39}O_8N_9Cl_2 \cdot 2H_2O$: N, 18.29%.

**An Attempt at the Cyclization of XV by the Azide Method.**—To a cold solution of 0.255 g. (0.39 mmol.) of XV dissolved in 4 ml. of 0.1 N hydrochloric acid, a cold solution of 0.028 g. (0.40 mmol.) of sodium nitrate in 0.3 ml. of water was added. After it had stood for 15 min. at 0°C, the golden yellow solution was poured into 300 ml. of cold water containing 1.8 g. of sodium bicarbonate. The solution was kept at 4°C for 45 hr., and the pH was adjusted to 5 with 2 N hydrochloric acid. The solution was passed successively through columns of Dowex-50 and Dowex-1. The filtrate and washings were combined and evaporated to dryness in vacuo. Only a trace of $I_L$ was thus obtained.

***p*-Methoxybenzyloxycarbonylglycine (XVI).**—The synthetic procedure[25] was revised as follows. A mixture of 2.25 g. (30 mmol.) of glycine, 45 ml. of water, 45 ml. of dioxane, 6.72 g. (80 mmol.) of sodium bicarbonate and 8.07 g. (39 mmol.) of *p*-methoxybenzyloxycarbonyl azide was stirred at room temperature for 24 hr. The solution was then evaporated in vacuo in order to remove the dioxane. After it had been extracted with ethyl acetate, the solution was acidified with 80 ml. of M citric acid and then extracted with ethyl acetate. The ethyl acetate solution was dried and evaporated to dryness in vacuo. The crystals were washed with petroleum ether. Yield: 6.93 g. (97%); m. p. 95—96°C. Reported value, m. p. 94—96°C.[25]

***p*-Methoxybenzyloxycarbonyltriglycyl-ε-benzyloxycarbonyl-L-lysine Ethyl Ester (XVII).**—The mixed anhydride prepared from 3.59 g. (15 mmol.) of XVI, 1.95 ml. (15 mmol.) of isobutyl chloroformate and 2.10 ml. (15 mmol.) of triethylamine in 30 ml. of chloroform was coupled with 6.89 g. (15 mmol.) of IV dissolved in a chilled mixture of 2.10 ml. (15 mmol.) of triethylamine and 60 ml. of chloroform. After the organic solvents had been removed in vacuo, water was added to the residue and it was kept in a refrigerator. The product was collected by filtration and washed successively with M citric acid, a 3% sodium bicarbonate solution and water (9.0 g.). The product was recrystallized from methanol-ether-petroleum ether. Yield: 8.2 g. (87%); m. p. 108—112°C, $[\alpha]_D^{20}$ −6.1° (*c* 2, dimethylformamide).

Found: C, 57.19; H, 6.38; N, 10.93. Calcd. for $C_{31}H_{41}O_{10}N_5$: C, 57.84; H, 6.42; N, 10.88%.

***p*-Methoxybenzyloxycarbonyltriglycyl-ε-benzyloxycarbonyl-L-lysine Hydrazide (XVIII).**—A solution of 7.53 g. (12 mmol.) of XVII and 12 ml. (240 mmol.) of hydrazine hydrate in 24 ml. of dimethylfomamide was allowed to stand at room temperature for 2 days. The excess hydrazine was then evaporated in vacuo, and the residual solution was diluted with 400 ml. of water. The product was collected by filtration (6.30 g.). This was recrystallized from methanol-ether. Yield: 5.82 g. (79%); m. p. 182—184°C, $[\alpha]_D^{20}$ −3.9° (*c* 2, dimethylformamide).

Found: C, 55.17; H, 6.25; N, 15.79. Calcd. for $C_{29}H_{39}O_8N_7$: C, 55.31; H, 6.24; N, 15.57%.

***p*-Methoxybenzyloxycarbonyltriglycyl-ε-benzyloxycarbonyl-L-lysylglycylglycine Benzyl Ester (XIX).**—To a cooled solution of 4.30 g. (7 mmol.) of XVIII in 20 ml. of dimethylformamide and 7.7 ml. of N hydrochloric acid, a cold solution of 0.531 g. (7.7 mmol.) of sodium nitrate in 3 ml. of water was added. After it had stood for 5 min. at −5°C, the solution was diluted to a volume of 350 ml. with cold water and extracted two times with 80-ml. portions of ethyl acetate. The ethyl acetate solution was twice washed with a sodium bicarbonate solution and with water, dried over sodium sulfate, and then added to a cold solution of 2.56 g. (7 mmol.) of glycylglycine benzyl ester *p*-toluenesulfonate in 0.98 ml. (7 mmol.) of triethylamine and 4 ml. of dimethylformamide. The reaction mixture was kept at 3°C with stirring for 2 days. A gelatinous material deposited in the course of the reaction. The mixture was then evaporated in vacuo in order to remove the ethyl acetate, and the resulting solution was diluted with cold water. The product deposited was collected

24) E. Klieger and H. Gibian, *Ann.*, **649**, 183 (1961).
25) F. Weygand and K. Hunger, *Chem. Ber.*, **95**, 1 (1962).

by filtration and washed with a citric acid solution, a sodium bicarbonate solution and water (4.08 g.). The product was recrystallized from dimethylformamide - ether - petroleum ether. Yield: 4.0 g. (71%); m. p. 183—186°C, $[\alpha]_D^{20}$ −2.2° (*c* 2, dimethylformamide).

Found: C, 57.96; H, 6.27; N, 11.82. Calcd. for $C_{40}H_{49}O_{12}N_7$: C, 58.60; H, 6.02; N, 11.96%.

***p*-Methoxybenzyloxycarbonyltriglycyl-ε-benzyloxycarbonyl-L-lysylglycylglycine (XX).**—Into a suspension of 2.41 g. (3 mmol.) of XIX in 35 ml. of dioxane, 33 ml. of 0.1 N sodium hydroxide was stirred at 0°C. By thin-layer chromatography,[21] the hydrolysis was found to be complete after 1.5 hr.; it gave only one detectable product. The solution was then evaporated in vacuo in order to remove the dioxane and then further treated with a mixture of ether and petroleum ether (1 : 1) in order to extract the residual dioxane. The acidification of the aqueous solution with 4 ml. of M citric acid yielded a gelatinous product. After the solution had stood in a refrigerator overnight, the product was collected by filtration and washed with cold water (1.83 g.). The product was recrystallized from dimethylformamide - water. Yield: 1.64 g. (75%); m. p. 190—195°C, $[\alpha]_D^{20}$ −3.8° (*c* 2, dimethylformamide).

Found: C, 54.49; H, 6.06; N, 12.87. Calcd. for $C_{33}H_{43}O_{12}N_7$: C, 54.31; H, 5.94; N, 13.44%.

***p*-Methoxybenzyloxycarbonyltriglycyl-ε-benzyloxycarbonyl-L-lysylglycylglycine *p*-Nitrophenyl Ester (XXI).**—To a solution of 1.05 g. (1.43 mmol.) of XX in a mixture of 0.24 ml. (1.72 mmol.) of triethylamine and 6 ml. of dimethylformamide, 1.02 g. (3.14 mmol.) of di-*p*-nitrophenyl sulfite was added. The solution was then allowed to stand at room temperature overnight. The solvent was removed in vacuo, and the oily residue was solidified by adding a mixture of ether and petroleum ether (1 : 1) and scratching. The product was then filtered with the aid of petroleum ether (1.53 g.). The *p*-nitrophenyl ester content in this product was estimated to be 106% by means of the method described in the preparation of $VII_{PR}$. This product was used for the next reaction without further purification.

**Cyclo-pentaglycyl-ε-benzyloxycarbonyl-L-lysyl- ($I_L$).**—To a mixture of 1.53 g. of XXI and 1.3 ml. of anisole, 13 ml. of trifluoroacetic acid was added at −5°C.[25] After 10 min., the reaction mixture formed a reddish-brown solution. The removal of the trifluoroacetic acid in vacuo and the addition of ether yielded a faintly brown powder. The product was collected by filtration, washed with ether, and then dissolved in a mixture of 0.5 ml. of acetic acid and 25 ml. of dimethylformamide. A solution containing triglycyl-ε-benzyloxycarbonyl-L-lysylglycylglycine *p*-nitrophenyl ester trifluoroacetate was stirred drop by drop into 300 ml. of pyridine kept at 70—80°C over a 5.5-hr. period. The solution was then stirred at 70°C for another hour. After the solvents had been removed in vacuo, the residue was dissolved in 140 ml. of methanol and a small amount of insoluble material was filtered off. The methanolic solution was diluted with 140 ml. of water and passed successively through columns (2.5×10 cm.) of Dowex-50 and Dowex-1. The filtrate and washings were then combined and evaporated to dryness in vacuo. The residue was dissolved in 50 ml. of methanol, and insoluble materials were filtered off. The filtrate was concentrated to a small volume (0.4 ml.), and 4 ml. of ether and then 4 ml. of petroleum ether were added, to afford crystals; yield, 0.435 g. This gave only one spot in a paper chromatogram, $R_f$ 0.70.[21] Careful recrystallization from methanol - ether - petroleum ether afforded 0.335 g. (42% from XX); m. p. 262°C, $[\alpha]_D^{20}$ +0.9° (*c* 1.33, dimethylformamide).

Found: C, 52.35; H, 5.99; N, 17.77. Calcd. for $C_{24}H_{34}N_8O_7$: C, 52.54; H, 6.25; N, 17.87%.

**Cyclo-pentaglycyl-L-lysyl Hydrochloride ($II_L$).**—A solution of 0.083 g. (0.15 mmol.) of $I_L$ in a mixture of 6 ml. of methanol and 0.165 ml. of N hydrochloric acid was hydrogenolyzed in the presence of palladium black. The filtrate was then evaporated in vacuo and the concentrated solution was diluted to a volume of 0.5—0.6 ml. with water, whereupon a very small amount of an insoluble material was filtered off. After the filtrate had been concentrated to a small volume (0.3 ml.), addition of 0.3 ml. of ethanol and then 2 ml. of acetone yielded crystals. Yield: 0.045 g. (66%); m. p. 247°C (decomp.), $[\alpha]_D^{20}$ +15.6° (*c* 1.3, water); $R_f$ 0.27,[19] 0.42[20] and 0.13[21].

Found: C, 39.87; H, 6.82; N, 20.46. Calcd. for $C_{16}H_{30}O_6N_7Cl \cdot 2H_2O$: C, 39.46; H, 6.83; N, 20.13%.

**Pentaglycyl-L-lysine Hydrochloride (XXII).**—A solution of 0.300 g. (0.53 mmol.) of IX dissolved in a mixture of 7 ml. of water and 3 ml. of 0.2 N hydrochloric acid was hydrogenolyzed in the presence of palladium black. The filtrate was evaporated to a small volume, and ethanol was added to afford crystals (0.230 g.). The product was recrystallized from water - ethanol. Yield: 0.202 g. (80%); m. p. 210—212°C (decomp.), $[\alpha]_D^{20}$ 0° (*c* 1.33, water).

Found: C, 40.03; H, 6.62; N, 20.03. Calcd. for $C_{16}H_{30}O_7N_7Cl \cdot 1/2H_2O$: C, 40.29; H, 6.76; N, 20.55%.

**The Action of Trypsin on Glycyl-L-lysine Anhydride Hydrochloride, $II_{PR}$ and $II_L$.**—Hydrolysis experiments of substrates by trypsin[26] were carried out at pH 7.8, 30°C. The initial concentration of the substrates was 0.01 M, and the enzyme concentration was 0.05 mg. protein nitrogen per milliliter. The progress of the reactions was checked by thin-layer and paper chromatographies in the course of time. Table I shows the compositions of the reaction mixtures. Number 2 in Table I indicates the control experiment without the enzyme. No. 1 was performed in order to determine whether or not the trypsin autolysis took place. The control experiments (1 and 2) showed that neither the hydrolysis of cyclo-pentaglycyllysyl in the absence of the enzyme nor the autolysis of trypsin occurred. Experiment No. 3 indicated that glycyl-L-lysine anhydride hydrochloride[27] was not hydrolyzed at

26) This was a salt-free, crystalline sample from the Nutritional Biochemicals Corporation, U. S. A.

27) The synthesis of the compound (by M. Kondo and N. Izumiya) is unpublished; $R_f$ 0.34.[19]

TABLE I. COMPOSITION OF THE MIXTURES OF THE ENZYME REACTION

| Experimental No. | Substrate | Weighed amount of substrate | 0.2 M Tris buffer (pH 7.8) | Trypsin solution (0.2 mg. protein nitrogen per ml.) | Water | Total volume |
|---|---|---|---|---|---|---|
| 1 | | | 0.50 ml. | 0.25 ml. | 0.25 ml. | 1.0 ml. |
| 2 | Lys Gly$_5$·HCl ($II_{PR}$) | 0.01 mmol. | 0.50 | | 0.50 | 1.0 |
| 3 | L-Lys Gly·HCl | 0.01 | 0.50 | 0.25 | 0.25 | 1.0 |
| 4 | Lys Gly$_5$·HCl ($II_{PR}$) | 0.01 | 0.50 | 0.25 | 0.25 | 1.0 |
| 5 | L-Lys Gly$_5$·HCl ($II_L$) | 0.01 | 0.50 | 0.25 | 0.25 | 1.0 |

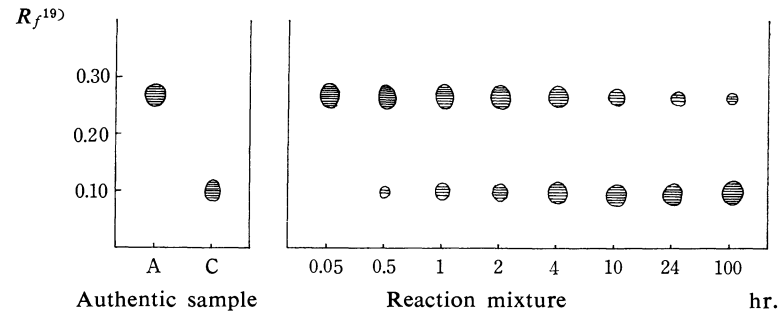



Fig. 8. Paper chromatograms of reaction mixtures of the experiment No. 4 in Table I.
Authentic sample : A, cyclo-pentaglycyllysyl hydrochloride ($II_{PR}$) ; C, pentaglycyl-L-lysine hydrochloride (XXII).

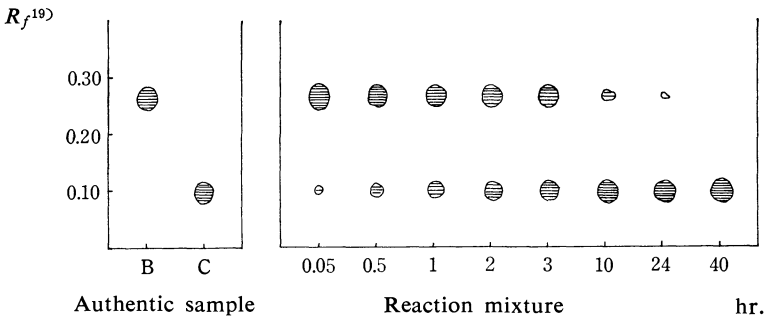



Fig. 9. Paper chromatograms of reaction mixtures of the experiment No. 5 in Table I.
Authentic sample: B, cyclo-pentaglycyl-L-lysyl ($II_L$) ; C, pentaglycyl-L-lysine hydrochloride (XXII).

all by trypsin, even after 48 hrs.' incubation. Cyclo-pentaglycyllysyl hydrochloride ($II_{PR}$) was partially hydrolyzed by the enzyme (Fig. 8). After 100 hrs.' incubation, a great part of the $II_{PR}$ was hydrolyzed to the linear pentaglycyl-L-lysine, as may be seen in Fig. 8, while the rest of the material remained unchanged as the cyclic hexapeptide, presumably of the D-configuration. On the other hand, cyclo-pentaglycyl-L-lysyl hydrochloride ($II_L$) was completely hydrolyzed by trypsin after 40 hr. (Fig. 9). That the product of the two latter reactions was the corresponding linear hexapeptide, pentaglycyl-L-lysine, was proved by the chromatographic comparison of it with an authentic sample of pentaglycyl-L-lysine hydrochloride (XXII) synthesized as has been described above.

## Summary

A cyclic hexapeptide, cyclo-pentaglycyl-L-lysyl hydrochloride ($II_L$), has been synthesized in an attempt to obtain fundamental information about the syntheses of cyclic peptides; it has also been subjected to the action of trypsin.

*p*-Methoxybenzyloxycarbonyltriglycyl-ε-benzyloxycarbonyl-L-lysylglycylglycine (XX) has

been prepared by the saponification of the di-*N*-blocked hexapeptide ester which had been obtained by the condensation of *p*-methoxybenzyloxycarbonyltriglycyl-ε-benzyloxycarbonyl-L-lysine azide with the glycylglycine benzyl ester. XX has been converted to the relevant *p*-nitrophenyl ester by the action of di-*p*-nitrophenyl sulfite, and, after the removal of the *p*-methoxybenzyloxycarbonyl group with trifluoroacetic acid, the hexapeptide *p*-nitrophenyl ester has been transformed, by means of a large amount of pyridine, to the cyclic benzyloxycarbonyl-substituted hexapeptide. It has then been hydrogenolyzed in the presence of palladium black to furnish the desired product, $II_L$.

Several different synthetic methods for obtaining $II_L$ have been adopted. However, they are not satisfactory with regard to the optical purity of the L-lysine residue or the yield.

It has been observed that $II_L$ is completely hydrolyzed to pentaglycyl-L-lysine by trypsin. This appears to be the first example of how trypsin can hydrolyze a cyclic peptide. A smaller cyclic peptide, glycyl-L-lysine anhydride, could not be hydrolyzed.

*Laboratory of Biochemistry*
*Faculty of Science*
*Kyushu University*
*Fukuoka*

# Some Reactions of Mercuridiacetaldehyde*

By Shunsuke MURAHASHI, Shun'ichi NOZAKURA and Saburo FUJI

(Received January 28, 1965)

Mercuridiacetaldehyde $Hg(CH_2CHO)_2$ was first prepared by Nesmeyanov and his group in 1955; it has since been used for the synthesis of various kinds of vinyl ethers.[1-7] Mercuridiacetaldehyde and chloromercuriacetaldehyde show O-vinylation by means of the reaction of the Hg–O with C-halogen bonds in substrates. In some cases, however, the reaction proceeds in an alternative way, one in which the C-alkylation reaction takes place by means of the Hg–C bonds.[2,8] Thus mercuridiacetaldehyde can also be regarded as divinyloxymercury, a mercuric salt of vinyl alcohol. A number of vinyloxymetal compounds have been reported in the literature, such as aluminum,[9] titanium,[10] lithium,[5] sodium,[5] iron,[5] and silicon.[6] However, the chemical behavior of the unsaturated bonds in these compounds is scarcely known at all.

In the course of their synthetic study of vinyloxymetal compounds with mercuridiacetaldehyde, the present authors noticed that the latter compound was easily converted, in various organic solvents, into an insoluble and infusible substance. This phenomenon led the authors to suspect that the insoluble substance might be a polymeric material which was formed by the addition reaction of C=C double bonds in the form of divinyloxymercury. The object of the present work is to elucidate the chemical structure of the insoluble substance, and also to obtain further information on the chemical structure of the starting material, mercuridiacetaldehyde.

As a compound closely-related to mercuridiacetaldehyde, Nef's so-called mercuric salt of vinyl alcohol was also reinvestigated in the light of recent knowledge.

## Results and Discussion

**On Mercuridiacetaldehyde.**—Two tautomeric structures, I and II, can be assumed for mercuridiacetaldehyde in view of its dual reactivities:[12]

$Hg(CH_2CHO)_2$ (I) $\quad$ $Hg(OCH{=}CH_2)_2$ (II)

* Presented at the Symposium on Organometallic Compounds, Nagoya, October 1963.

1) A. N. Nesmeyanov, K. M. Khomtov and I. F. Lutsenko, *Izvest. Akad. Nauk SSSR, Otdet. Khim. Nauk*, **1957**, 942.

2) A. N. Nesmeyanov, I. F. Lutsenko and Z. M. Tumanova, ibid., **1949**, 601.

3) I. F. Lutsenko and R. M. Khomtov, *Dokl. Akad. Nauk SSSR*, **102**, 97 (1955).

4) I. F. Lutsenko, *Izvest, Akad. Nauk SSSR, Otdel. Khim. Nauk*, **1956**, 27.

5) A. N. Nesmeyanov and I. F. Lutsenko, *Dokl. Akad. Nauk SSSR*, **120**, 1049 (1958).

6) A. N. Nesmeyanov and I. F. Lutsenko, ibid., **128**, 551 (1959).

7) A. N. Nesmeyanov, *Zhur. Obshchei Khim.*, **29**, 2817 (1959).

8) D. N. Kursanov, M. E. Volpin and I. S. Okhrem, *Dokl. Akad. Nauk SSSR*, **120**, 531 (1958).

9) L. I. Zakharkin, *Izvest. Akad. Nauk SSSR, Otdel. Khim. Nauk*, **1961**, 378.

10) J. H. Haslam, U. S. Pat. 2708205 (1955).

11) J. U. Nef, *Ann.*, **298**, 316 (1897).

12) A. N. Nesmeyanov and I. F. Lutsenko, *Dokl. Akad. Nauk SSSR*, **59**, 707 (1948).

Type I should show infrared absorptions of the carbonyl group, while type II shows those of the C=C double bond. The infrared spectrum of mercuridiacetaldehyde shows a strong band at around 1645 $cm^{-1}$ (Table I). Nesmeyanov and Lutsenko[13] assigned the band to the stretching vibration of the carbonyl group, taking into account the fact that the ultraviolet spectrum of the compound showed the absorption maximum at 296 $m\mu$ ($\log \varepsilon = 2.90$) which is characteristic of the carbonyl absorption. In order to exlain both the large bathochromic shift of the carbonyl band and the dual reactivities of the compound, they proposed a $\sigma$-$\pi$ conjugated structure.[13,14]

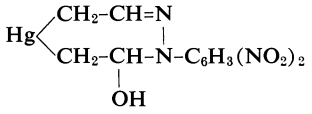
As the infared spectrum of mercuridiacetaldehyde showed an absorption band at 2720 $cm^{-1}$ which seemed to be a normal position for the C–H stretching vibration of an aldehyde group, the reactions of the compound with typical aldehyde reagents were studied. The reactions of the compound with sodium bisulfite, 2, 4-dinitrophenylhydrazine, semicarbazide hydrochloride, and hydroxylamine hydrochloride were found to take place as follows:

$$Hg(CH_2CHO)_2 + NaHSO_3 \rightarrow$$



(III)

$$Hg(CH_2CHO)_2 + NH_2NHC_6H_3(NO_2)_2 \rightarrow$$



(IV)

$$Hg(CH_2CHO)_2 + NH_2NHCONH_2 \cdot HCl \rightarrow$$

$$ClHgCH_2CH{=}NNHCONH_2$$

(V)

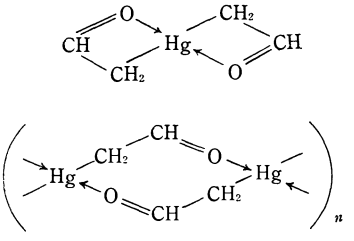
$$Hg(CH_2CHO)_2 + NH_2OH \cdot HCl \rightarrow$$

$$ClHgCH_2CH{=}NOH$$

(VI)

The structural assignment of these products was based on analysis and on a study of their infrared spectra. Structure IV is tentatively assigned as in the case of levulinaldehyde.[15] The reaction with hydrazine hydrate led to the liberation of metallic mercury. Thus, it was shown that mercuridiacetaldehyde behaved like usual aldehydes.

The infrared spectrum of mercuridiacetaldehyde (Table I) shows a band at 553 $cm^{-1}$ which may be assigned to Hg–C. The wave number is almost the same as that reported for dimethylmercury (550 $cm^{-1}$),[16] suggesting a covalent nature of the Hg–C bond. As the carbonyl absorption at about 1645 $cm^{-1}$ corresponds to an intermediate of a metal chelate (1600—1530 $cm^{-1}$) and normal carbonyl, the carbony oxygen group in the compound might be weakly chelated to the mercury atom in the same molecule or form a polymer through coordination to the mercury atom in the next molecule. Thus, the structure may be best represented by VII, as has been suggested by Nesmeyanov.



(VII)

The structure of the decomposition product, which will be discussed below, also seems to support these chelated structures.

**The Decomposition of Mercuridiacetaldehyde in Alcohol.**—Mercuridiacetaldehyde synthesized according to the method described in the literature[3] showed a melting point of 84—86°C, which was rather low compared with the reported value (91°C).

Purification by recrystallization from various solvents was unsuccessful, because of the instability of the crude compound in solution. Table II shows the solubility of the compound in ordinary organic solvents and its stability after it has stood overnight. Water was the best solvent, and in its dilute solution the compound was considerably stable, but in a concentrated solution the compound decomposed rapidly with the separation of metallic mercury. The compound, after the solvent treatment, generally showed much higher melting points, became insoluble, and showed a higher mercury-content than the original sample. Since a survey of the infrared spectra of the high-melting sapmles thus obtained usually showed new common absorption bands, the change brought about by this treatment is considered to be due to the formation of the same decomposition product. In order to elucidate the decomposition reaction, therefore, the reaction in ethanol was then studied in more detail.

13) A. N. Nesmeyanov and I. F. Lutsenko, ibid., **127**, 115 (1959).
14) A. N. Nesmeyanov, *Zhur. Obshchei Khim.*, **25**, 41 (1955).
15) C. Harries and M. Boegemann, *Chem. Ber.*, **42**, 442 (1901).
16) K. Bradersen, ibid., **90**, 2703 (1957).

TABLE I. INFRARED SPECTRA OF MERCURIDIACETALDEHYDE AND THE RELATED COMPOUNDS

| $Hg(CH_2CHO)_2$ | $ClHgCH_2CHO$ | $Hg_2(CH_2CHO)_2$ (Decomp. product) | Nef's Compd. |
|---|---|---|---|
| 2720 (w) | 2720 (w) | 2720 (w) | 2720 (w) |
| 1645 (vs) | 1645 (vs) | 1650 (m) | 1650 (m) |
| | | 1580 (s) | 1580 (s) |
| 1410 (m) | 1425 (w) | 1420 (w) | |
| 1390 (m) | 1390 (m) | 1400 (w) | 1400 (w) |
| | 1300 (w) | 1300 (w) | |
| 1148 (s) | 1152 (s) | 1160 (s) | 1160 (m) |
| | | 1120 (w) | 1140 (m) |
| 1058 (m) | 1080 (m) | 1050 (m) | 1030 (w) |
| 1025 (s) | 1020 (m) | 1020 (w) | |
| 930 (w) | 955 (w) | 940 (w) | 940 (w) |
| 553 (m) | 553 (m) | 545 (m) | 545 (m) |
| | | 541 (m) | |
| 456 (s) | 488 (m) | 448 (s) | 448 (m) |

TABLE II. SOLUBILITY AND STABILITY OF MERCURIDIACETALDEHYDE IN VARIOUS SOLVENTS

| Treatment[a] | Solubility[b] | Hg% after treatment | Change of m. p. after the treatment, °C |
|---|---|---|---|
| Untreated | | 69.9 | 84 |
| Ethanol | + | | 200—250 (d) |
| Ethanol, refluxed for 5—6 hr. | | 77.3 | 200—250 (d) |
| Benzene | − | 64.7 | |
| Benzene, refluxed for 5—6 hr. | | 72.6 | 250 (d) |
| Acetone | ++ | 63.3 | |
| Acetone, 3 days | | 78.4 | 250 (d) |
| Ethyl methyl ketone | + | 78.4 | 250 (d) |
| Tetrahydrofuran | + | 74.0 | 250 (d) |
| Methanol | ++ | | 200—250 (d) |
| Water | ++ | | 78—79 |

a) A mixture of about 1 g. of sample and 1 ml. of a solvent was allowed to stand overnight and then the solvent was evaporated in vacuo.
b) −, insoluble; +, soluble; ++, readily soluble.

When an ethanol solution of mercuridiacetaldehyde was kept under reflux, a white precipitate separated after one or two hours. After the refluxing had continued for 4 hr., the mercury content of the precipitate increased to 77.3% from the original 69.9%; it remained constant thereafter. Alternatively, when a catalytic amount of an ethanol solution of sodium ethoxide was added to the solution at room temperature, the white precipitate appeared immediately. In this case, the mercury content of the product increased to 80.7%.

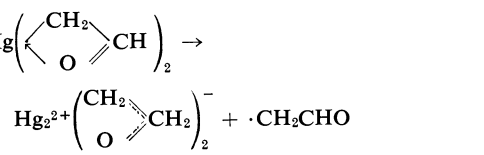
Associated with the decomposition phenomenon, the infrared spectra showed a marked change in some respects. The $\nu C{=}O$ band at 1645 $cm^{-1}$ and the bands at 1150 and 1050 $cm^{-1}$ diminished and new bands appeared at 1580, 1300 and 1120 $cm^{-1}$. The $\nu Hg{-}C$ band at 553 $cm^{-1}$ shifted to the doublet at 545 and 541 $cm^{-1}$. The $\nu C{-}H$ of aldehyde at 2720 $cm^{-1}$ showed no appreciable change.

When decomposition product was treated with bromine, bromacetaldehyde was obtained as a sole organic product. This fact suggests the existence of the $Hg{-}CH_2CHO$ group in the decomposition product.

$$-Hg{-}CH_2CHO + Br_2 \rightarrow -HgBr + BrCH_2CHO$$

The new band at 1580 $cm^{-1}$ is considered to be due to a carbonyl bond which is weaker than that of the original mercuridiacetaldehyde (a bathochromic shift of 60 $cm^{-1}$). A bathochromic shift of the $\nu Hg{-}C$ bond also suggests a weaker Hg–C bond in the decomposition compound than in the original compound.

From the above-mentioned facts, the authors concluded that most of the mercuridiacetaldehyde was converted into a mercurous compound, $Hg_2(CH_2CHO)_2$ by the decomposition of the Hg–C bonds.



This conclusion is supported by the fact that the $\nu C{=}O$ bands in mercuric and mercurous acetates are 1570 and 1540 $cm^{-1}$ respectively, showing a bathochromic shift of 30 $cm^{-1}$ in the change from mecuric to mercurous. The bathochloric shift of the $\nu Hg{-}C$ bond seems to be compatible with the fact that mercurous compound are generally more ionic than the corresponding mercuric compounds.

The decomposition reaction could, practically speaking, not be brought to completion, as may be seen from the analytical results and the infrared spectra, probably because of the insolubility of the product.

The decomposition of mercuridiacetaldehyde in ethanol may be interpreted in terms of a homolytic fission of the Hg–C bonds or by a nucleophilic substitution on mercury, followed by a homolytic cleavage of the $Hg{-}OC_2H_5$ bonds.

$$Hg(CH_2CHO)_2 \rightarrow HgCH_2CHO + \cdot CH_2CHO$$

or

$$Hg(CH_2CHO)_2 + C_2H_5OH \rightarrow C_2H_5OHgCH_2CHO + CH_3CHO$$

The formation of acetaldehyde was confirmed by a gas chromatographic analysis of the volatile component of the reaction mixture: about 40% of the theoretical amount of acetaldehyde was thereby detected as 2, 4-dinitrophenylhydrazone.

In the case of the base-catalyzed decomposition, it seems that the first step is a nucleophilic attack by the ethoxide anion on mercury, followed by the cleavage of the $Hg{-}OC_2H_5$ bonds. The acetaldehyde liberated during the alkaline decomposition was not detected, but it seemed to be converted into a brown polymeric material by the alkali.

As a compound closely related to mercuridiacetaldehyde, Nef's compound was reexamined. Nef[11] reported the synthesis of a mercuric salt of vinyl alcohol by the reaction of fresh mercuric oxide and aqueous acetaldehyde in the presence of sodium hydroxide. The infrared examination of Nef's compound indicated that the compound was identical with the decomposition product of the mercuridiacetaldehyde which had been obtained in the presence of sodium ethoxide.

## Experimental

**The Analysis of Mercury.** — According to the method of Hirai and Hayatsu,[17] a sample containing mercury was digested with concentrated sulfuric acid and 30% aqueous hydrogen peroxide until a colorless solution was obtained. The mercuric ion content was determined by the usual Volhard method.

**The Synthesis of Mercuridiacetaldehyde.**—The method of Nesmeyanov[3] was taken, using yellow mercuric oxide, vinyl isobutyl ether, water and a catalytic amount of mercuric acetate. The crude yield was 86—89% (m. p. 82—83°C (91°C in the literature)). It was used without further purification. The presence of mercuric acetate as a catalyst was not essential for the reaction, particularly in the small-scale preparation. The yield in this case was 76—80% (m. p. 82—84°C). However, when the synthesis was carried out on a larger scale and without the addition of merric acetate, a rapid exothermic reaction after some induction period frequently resulted in the decomposition of a part of the product.

**Reactions with the Aldehyde Reagents.** — The sodium bisulfite adduct, 2,4-dinitrophenylhydrazone and semicarbazone were prepared in the usual manner. The sodium bisulfite adduct, which was recrystallized from water, decomposed at 133—138°C; yield, 62%. The infrared spectrum showed a $\nu O{-}H$ band at 3450(s), bands of the sulfonate group at 1140(vs) and 650(s), a sulfite band at 980(s), and a $\nu Hg{-}C$ band at 530 $cm^{-1}$.

Found: Na, 10.3; Hg, 44.0. Calcd. for $C_2H_4O_7S_2Na_2Hg$: Na, 10.20; Hg, 44.50%.

The 2,4-dinitrophenylhydrazone which was recrystallized from ethanol decomposed at 138—139°C; yield, 54%. The infrared spectrum showed a $\nu O{-}H$ band at 3300(m), a $\nu C{=}N$ band at 1620(s), and a $\nu Hg{-}C$ band at 588(m) $cm^{-1}$.

Found: N, 11.4; Hg, 44.8. Calcd. for $C_{10}H_{10}O_5N_4Hg$: N, 11.99; Hg, 42.97%.

The semicarbazone recrystallized from ethanol decomposed at 159—160°C; yield, 31%. The infrared spectrum showed the $\nu N{-}H$ bands of the amide group at 3420(m) and 3320(m), a $\delta N{-}H$ band at 1540(s), and a $\nu C{=}O$ band at 1660(s) $cm^{-1}$.

Found: N, 14.56. Calcd. for $C_3H_6ON_3HgCl$: N, 14.21%.

The reaction with hydroxylamine was carried out by mixing a freshly-prepared solution of mercuridiacetaldehyde (5 g.) in water (15 ml.) and a mixed aqueous solution of 2 g. of hydroxylamine hydrochloride and 2.8 g. of potassium acetate. A white precipitate was filtered out and recrystallized from ethanol. The yield was 11.4%. M. p. 115—116°C, with decomposition. The infrared spectrm showed a chelated $\nu O{-}H$ band at 3170(m), $\nu{=}CH$ bands at 3025(m) and 3045(m), a $\nu C{=}N$ band at 1658(s), and a $\delta{=}CH$ band at 840(s) $cm^{-1}$.

Found: N, 4.60. Calcd. for $C_2H_4ONHgCl$: N, 4.76%.

**The Decomposition of Mercuridiacetaldehyde in Ethanol.**—A solution of 9.87 g. of mercuridiacetaldehyde in 80 ml. of ethanol, after filtration, was refluxed for 5 to 6 hr., yielding 8.81 g. of an insoluble white precipitate (1.06 g. of weight loss).

17) M. Hirai and R. Hayatsu, *Yakugaku Zasshi*, **70**, 76 (1956).

The volatile portion of the filtrate was found by gas chromatography to contain acetaldehyde; this acetaldehyde was converted into 2,4-dinitrophenylhydrazone in the usual manner (m. p. 163°C). The mixed melting point test with an authentic sample did not show any depression. The yield was 2.43 g., which corresponded to 0.44 g. of acetaldehyde and to a 41.5% loss of the weight of the starting material. The insoluble product was found to contain 77.3% Hg, and it decomposed at 200—250°C.

The insoluble product (3.0 g.) was decomposed by an excess of a chloroform solution of bromine at room temperature. The chloroform solution, after filtration, was found by gas chromatography to contain bromacetaldehyde; it was then converted into 2,4-dinitrophenylhydrazone, the yield being 1.48 g. (m.p. 150—152°C (from ethanol)). The mixed melting point test did not show any depression.

Found: C, 31.05; H, 2.20; N, 18.38; Br, 17.01. Calcd. for $C_8H_7O_4N_4Br$: C, 31.68; H, 2.28; N, 18.48; Br, 16.40%.

Into a solution of mercuridiacetaldehyde (3.0 g.) in 30 ml. of ethanol, a few drops of a solution of sodium ethoxide in ethanol (1 N) were added; the immediate formation of a white precipitate was observed. This precipitate (2.12 g.) contained 80.7% Hg.

**Nef's Compound.** — Nef's procedure was used, yielding 6.6 g. of the product from 8.0 g. of mercuric chloride, 4.0 g. of acetaldehyde, and 20.0 g. of sodium hydroxide. The product decomposed at about 190—210°C, changing in color from white to orange. It was soluble in oranganic solvents and in water. The infrarred spectrum is presented in Table I. It was found to contain 77.02% Hg.

## Summary

Mercuridiacetaldehyde is soluble in polar solvents and rather instable in the state of solution, yielding an insoluble and infusible substance. The decomposition reaction has been proved to include the formation of mercuri(I)-acetaldehyde $Hg_2(CH_2CHO)_2$ by the cleavage of one of the Hg–C bonds. On the other hand, mercuridiacetaldehyde reacted with aldehyde reagents as usual aldehydes. The change in the infrared spectra on these reactions has been interpreted in terms of $\sigma$-$\pi$ conjugation, as has been suggested previously by Nesmeyanov.

Nef's compound, which is considered to be a mercuric salt of vinyl alcohol, has been found to be almost identical with the mercuri-(I)-acetaldehyde.

*Department of Polymer Science*
*Faculty of Science*
*Osaka University*
*Toyonaka, Osaka*

# Kinetic Studies of Solvolysis. X.* Transition from a van't Hoff to an Arrhenius Intermediate Caused by Steric Hindrance at the Product-Formation Step of $S_N1$ Reactions

By Kunio OKAMOTO, Yoshihisa MATSUI and Haruo SHINGU

(Received February 1, 1965)

The kinetics of the two-step mechanism for the $S_N1$ reaction, in which an ion-pair is assumed as an intermediate, can well be treated by the steady-state approximation; the overall rate is then shown by Eq. 1:

$$RX \underset{k_{-1}}{\overset{k_1}{\rightleftarrows}} \text{(ion-pair intermediate)} \xrightarrow{k_2[Y]} RY$$

$$d[RX]/dt = k_1k_2[RX][Y]/(k_{-1}+k_2[Y]) \quad (1)$$

In typical $S_N1$ reactions, the first ionization step is rate-determining, and $k_2$, the rate constant for the reaction of a nucleophile with the intermediate, is much larger than $k_{-1}$, the rate constant for the reversal of the ionization step. This intermediate formed at the rate-determining step can be classified as a van't Hoff intermediate.[1] If, on the other hand, $k_{-1}$ is larger than $k_2$, a pre-equilibrium will be approximately established, followed by a rate-determining step. Here the intermediate is defined as an Arrhenius intermediate[1] and the reaction obeys second-order kinetics despite its initiation by the $S_N1$ ionization mechanism:

$$d[RX]/dt = k_1k_2[RX][Y]/k_{-1} \quad (2)$$

Although the literature contains several

* Presented at the 17th Annual Meeting of the Chemical Society of Japan, Tokyo, April, 1964. Pnrt IX: K. Okamoto, K. Takeuchi and H. Shingu, This Bulletin, 37, 276 (1964).

1) a) A. Skrabal, "Homogenkinetik," T. Steinkopf, Dresden (1941), pp. 38—43; b) A. Skrabal, *Monatsh. Chem.*, 51, 93 (1929).

TABLE I. SUMMARY OF THE FIRST-ORDER RATE CONSTANTS OF THE $S_N1$ REACTIONS OF BENZHYDRYL CHLORIDE IN THE PRESENCE OF POTASSIUM PHENOXIDE IN ACETONITRILE

| Temp. °C | Initial concn. RCl, M | Initial concn. $C_6H_5OK$, M | $k_1$[a] $min^{-1}$ | $k_2$[a] $min^{-1}\ M^{-1}$ |
|---|---|---|---|---|
| 140.0 | | | (0.6—1.4)[b] | |
| 120.0 | 0.0584 | 0.0986 | $2.82\times10^{-1}$ | (4.27) |
| | 0.0488 | 0.0488 | $2.56\times10^{-1}$ | (5.28) |
| 90.0 | 0.0318 | 0.0786 | $7.12\times10^{-2}$ | (0.906) |
| | 0.0344 | 0.0508 | $7.03\times10^{-2}$ | (1.33) |
| 70.0 | 0.0445 | 0.0590 | $1.58\times10^{-2}$ | (0.317) |
| | 0.0234 | 0.0550 | $1.59\times10^{-2}$ | (0.295) |
| | 0.0241 | 0.0474 | $1.52\times10^{-2}$ | (0.305) |
| | 0.0200 | 0.0378 | $1.55\times10^{-2}$ | (0.413) |
| | 0.0197 | 0.0316 | $1.53\times10^{-2}$ | (0.503) |
| | 0.0198 | 0.0308 | $1.54\times10^{-2}$ | (0.502) |
| | 0.0214 | 0.0214 | $1.43\times10^{-2}$ | (0.710) |

a) Initial rate constants calculated by the graphical method.
b) Extrapolated from data at 70.0, 90.0 and 120.0°C.

TABLE II. SUMMARY OF THE SECOND-ORDER RATE CONSTANTS OF THE $S_N1$ REACTIONS OF BENZHYDRYL CHLORIDE WITH SOME HINDERED NUCLEOPHILES IN ACETONITRILE

| Nucleophiles | Temp. °C | Initial concn. RCl, M | Initial concn. nucleophile M | $k_2$ $min^{-1}\ M^{-1}$ |
|---|---|---|---|---|
| Potassium 2,6-di-*t*-butyl-4-methylphenoxide (I) | 110.0 | 0.0385 | 0.0594 | $6.82\times10^{-1}$ |
| | 120.0 | 0.0368 | 0.0564 | 1.62 |
| | | 0.0500 | 0.0500 | 1.62 |
| | | 0.0196 | 0.0334 | 1.65 |
| | 140.0 | | | (6.3)[a] |
| Tri-*n*-butylammonium phenoxide (II) | 140.0 | 0.0840 | 0.1240 | $3.52\times10^{-1}$ |
| | | 0.0527 | 0.0750 | $3.63\times10^{-1}$ |
| | | 0.0500 | 0.0500 | $3.71\times10^{-1}$ |
| Tri-*n*-butylamine | 140.0 | 0.0905 | 0.1370 | $3.66\times10^{-2}$ |
| Tri-*n*-butylammonium 2,6-di-*t*-butyl-4-methyl phenoxide (III) | 140.0 | 0.0930 | 0.1340 | $2.84\times10^{-2}$ |

a) Extrapolated from data at 110 and 120°C.

references[2] to the $S_N1$ reaction involving Arrhenius intermediates, there have been reported to date no examples which clearly demonstrate such a transition of an carbonium-ion pair intermediate from a van't Hoff to an Arrhenius type.

We will report on an example of such a transition caused by a series of nucleophiles which have various steric requirements at the product-formation stage of the $S_N1$ reaction. The results of our kinetic runs and product studies[3] show that the $S_N1$ reactions of benzhydryl chloride with potassium 2,6-di-*t*-butyl-4-methylphenoxide (I), tri-*n*-butylamine, tri-*n*-butylammonium phenoxide (II), and tri-*n*-butylammonium 2,6-di-*t*-butyl-4-methylphenoxide (III) proceed through an Arrhenius intermediate and obey good second-order kinetics in acetonitrile, whereas the reaction with potassium phenoxide is a typical $S_N1$ reaction with a vant't Hoff intermediate. We will also report on the details of product studies which reveal the occurrence of a one-electron transfer reaction between the carbonium-ion intermediate and these hindered nucleophiles.

**Rate Measurements and Kinetic Interpretation.**—The titrimetric rate constants for the reaction of benzhydryl chloride with potassium phenoxide are given in Table I. The integrated first-order rate constants tended to show a slight decrease as the reaction progressed; therefore, the rate constant was calculated from the initial slope of a plot of the $\log(a-x)$ vs. the time, where $a$ is the initial concentration of the chloride and $x$ is the concentration

2) For triphenylmethyl chloride see R. F. Hudson and B. Saville, *J. Chem. Soc.*, **1955**, 4130; C. G. Swain and E. E. Pegues, *J. Am. Chem. Soc.*, **80**, 812 (1958); C. G. Swain and A. MacLachlan, ibid., **82**, 6095 (1960); L. J. Andrews and R. M. Keefer, ibid., **83**, 3708 (1961).

3) Some of the results of the product studies and kinetic runs have been published: K. Okamoto, Y. Matsui and H. Shingu, This Bulletin, **38**, 153 (1965).

of the chloride consumed. The $S_N1$ characteristic of the reaction was confirmed from the invariability of the first-order constants in the various initial concentrations (0.02—0.05 M). This is illustrated in Fig. 1. For purposes of comparison, the rate constants calculated for the second-order kinetics are included in Table I. In contrast to the first-order rate constants, the second-order rate constants display a clear trend toward larger rate constants in higher initial concentrations of the nucleophile.

Table II gives the second-order rate constants for the reactions of benzhydryl chloride with I, II, III and tri-*n*-butylamine in acetonitrile. The reactions were followed to about 70—80% completion; in all cases good second-order behaviors were observed. The plot of the log $a(b-x)/b(a-x)$ vs. the time, $t$, of a representative run is illustrated in Fig. 2, where $a$ is the initial concentration of benzhydryl chloride and $b$ is the initial concentration of the nucleophile. The definitely-curved plot for the first-order kinetics is also illustrated in Fig. 2.

An examination of the data in Tables I and II reveals that the $S_N1$ reaction of potassium phenoxide proceeds at a rate higher than any of the second-order reactions of these hindered nuclophiles. This fact evidently shows the existence of an ionized $S_N1$ intermediate, not only in the reaction medium where the first-order reaction of potassium phenoxide proceeded, but also in the environments in which the second-order reactions of the hindered nucleophiles were observed.

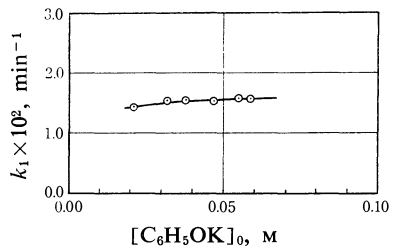



Fig. 1. First-order rate constants of the $S_N1$ reaction of benzhydryl chloride in acetonitrile in the presence of potassium phenoxide at 70.0°C. The initial concentrations of benzhydryl chloride, 0.02—0.04 M.

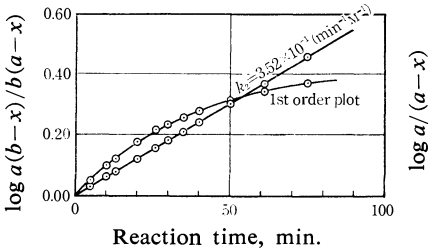



Fig. 2. Reaction rate of benzhydryl chloride in acetonitrile in the presence of tri-*n*-butylammonium phenoxide (II) at 140.0°C.
The initial concentration: the chloride, 0.0840 M; II, 0.1240 M

Thus two mechanisms for the second-order reactions of the hindered nucleophiles are possible. First, because of the large steric hindrance, the rate of a reaction between a nucleophile and the ionized intermediate became lower than the return rate of the intermediate, i.e., $k_2[Y] \ll k_{-1}$ in Eq. 1. Consequently, the reaction order changed from the first to the second, as is shown in Eq. 2, and the intermediate became an Arrhenius type. Secondly, if $k_2[Y]$ was extremely small compared with $k_{-1}$, the $S_N1$ reaction would be completely suppressed; then the $S_N2$ reactions between benzhydryl chloride and these hindered nucleophiles might appear, despite its sluggishness arising from the steric hindrance.

The first mechanism is more probable in view of the fact that a carbonium-ion type intermediate exists in acetonitrile in all the reactions of these nucleophiles. As has been briefly reported,[3] the results of product studies and of relevant control experiments have disclosed the formation of the compounds, which is unexplicable on the basis of the $S_N2$ mechanism but is conceivable as being due to a one-electron transfer reaction between the $S_N1$ intermediate and the nucleophile. Thus the $S_N1$ mechanism with an Arrhenius intermediate remains as the most probable one for the reaction with hindered nucleophiles.

**Products Studies and Mechanistic Considerations.**—The results of product studies, along with the reaction orders, are summarized in Table III. The products resulting from the $S_N1$ reaction of benzhydryl chloride and potassium phenoxide in acetonitrile at 82°C were isolated after ten half-periods; column chromatography showed that benzhydryl phenyl ether (93% yield) and *p*-benzhydrylphenol (3% yield) were formed. These are the expected products from the nucleophilic substitution of such an ambident anion.[4]

The reaction with potassium 2,6-di-*t*-butyl-4-methylphenoxide (I) was carried out in acetonitrile at 83—85°C, while the reactions with tri-*n*-butylamine and with tri-*n*-butylammouium phenoxide (III) were performed in the same solvent in a bomb at 140—160°C. The products of reactions with these hindered

4) For a general discussion of the nucleophilic substitution by an ambident anion, see N. Kornblum, R. A. Smiley, R. K. Blackwood and D. C. Iffland, *J. Am. Chem. Soc.*, 77, 6269 (1955).

TABLE III. SUMMARY OF THE YIELDS OF REACTION PRODUCTS OF $S_N1$ REACTIONS OF BENZHYDRYL HALIDES IN ACETONITRILE

| Nucleophile | Temp. °C | Conversion, %[a] (Reaction time, hr.) | Reaction products, %[b] Benzhydryl phenyl ether | *p*-Benzhydrylphenol | IV[g] | *sym*-Tetraphenylethane | Diphenylmethane | Reaction order[c] |
|---|---|---|---|---|---|---|---|---|
| | | | Substrate: Benzhydryl chloride | | | | | |
| $C_6H_5OK$ | 82 | 97 (2.5) | 93.2 | 3.1[h] | — | 0.0 | 0.0 | First |
| I[g] | 82—85[d] | 82 (18.3) | — | — | 28.7 | 40.2 | 0.0 | Second |
| II[g] | 143—150[e] | 95 (4.0) | 83.0 | 11.5[h] | — | 0.0 | 0.0 | Second |
| $(n\text{-Bu})_3N$ | 146—156[e] | 68 (6.5) | — | — | — | 64.5 | 3.0 | Second |
| III[g] | 141—158[e] | 82 (6.5) | — | — | 0.0 | 22.5 | 0.0 | Second |
| | | | Substrate: Benzhydryl bromide | | | | | |
| I | 82[d] | 97 (6.9) | — | — | 24.1 | 3.0 | 0.0 | — |
| $(n\text{-Bu})_3N$ | 90—93[f] | 91 (18.3) | — | — | — | 22.8 | 34.4 | — |

a) Conversion on the halide, calculated from determination of the halogen ion formed during the reaction.
b) Based on the halide.
c) See Tables I and II.
d) Reflux temperature.
e) Reaction in a stainless-steel bomb.
f) Reaction in a sealed tube.
g) I, Potassium 2,6-di-*t*-butyl-4-methylphenoxide; II, Tri-*n*-butylammonium phenoxide; III, Tri-*n*-butylammonium 2,6-di-*t*-butyl-4-methylphenoxide: IV, 1-(3',5'-di-*t*-butyl-4'-hydroxyphenyl)-2,2-diphenylethane.
h) Contaminated with the ortho-isomer.

nucleophiles were also isolated after ten half-periods and separated by column chromatography.

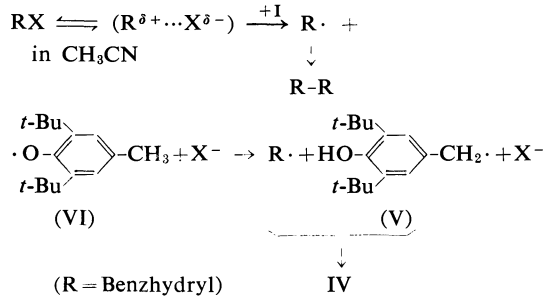
Much as with the reaction with potassium phenoxide, tri-*n*-butylammonium phenoxide and benzhydryl chloride resulted in benzhydryl phenyl ether (83% yield) and *p*-benzhydrylphenol (11.5% yield). In contrast to the reactions with these phenoxides, however, I and benzhydryl chloride yielded not the expected ether but rather *sym*-tetraphenylethane (40% yield), together with 1-(3',5'-di-*t*-butyl-4'-hydroxyphenyl)-2,2-diphenylethane (IV) (29% yield).[5] The reactions with tri-*n*-butylamine and with III gave also *sym*-tetraphenylethane as a major product in, respectively, 65% and 23% yields; in addition, a small amount of diphenylmethane (3% yield) was obtained in the former reaction.

Although kinetic runs were not carried out for benzhydryl bromide, the reaction of this bromide with I, much as in the reaction of the chloride, gave rise to no benzhydryl 2,6-di-*t*-butyl-4-methylphenyl ether in acetonitrile. Instead, IV (24% yield) and *sym*-tetraphenylethane (3% yield) were obtained at 83°C after a 23 hr. reaction. Tri-*n*-butylamine and benzhydryl bromide in the solvent also gave *sym*-tetraphenylethane (23% yield) and diphenylmethane (34% yield) in a sealed tube after 18 hr. at 90—93°C.

Evidently, the formation of both *sym*-tetraphenylethane and diphenylmethane indicates the transient existence of a benzhydryl radical in the reaction path from the benzhydryl halide. The formation of IV is also realized as being due to coupling between a benzhydryl radical and a 3,5-di-*t*-butyl-4-hydroxybenzyl radical (V). It has been known that a benzyl radical such as V can easily be formed from a 2,6-di-*t*-butyl-4-methylphenoxy radical (VI).[6] Consequently, the formation of IV indicates that, in the reaction of the benzhydryl halide and I, a one-electron transfer reaction occurs from a 2,6-di-*t*-butyl-4-methylphenoxide anion to a benzhydryl cation or to a $S_N1$ intermediate containing a benzhydryl cation. This may be formulated as follows:

5) For the structural assignment, see Ref. 3.

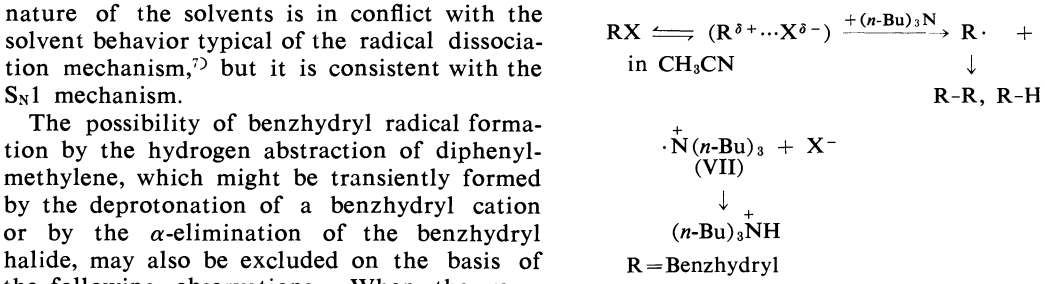
6) C. D. Cook, N. G. Nash and H. R. Flanagan, *J. Am. Chem. Soc.*, 77, 1783 (1955).



The possibility of benzhydryl radical formation by the radical dissociation of the benzhydryl halide in acetonitrile may be eliminated by a comparison of the rates in acetonitrile and in a non-polar solvent such as decalin. From the rate determination of the reaction of benzhydryl chloride and tri-*n*-butylamine in decalin at 150°C, it is estimated that only 4% or less of the starting chloride decomposes in 6.5 hr. Under identical reaction conditions, the reaction in acetonitrile proceeds to a more than 68% decomposition (Table III). Such rate sensitiveness to the nature of the solvents is in conflict with the solvent behavior typical of the radical dissociation mechanism,[7] but it is consistent with the $S_N1$ mechanism.

The possibility of benzhydryl radical formation by the hydrogen abstraction of diphenylmethylene, which might be transiently formed by the deprotonation of a benzhydryl cation or by the $\alpha$-elimination of the benzhydryl halide, may also be excluded on the basis of the following observations. When the reaction of benzhydryl bromide and tri-*n*-butylamine was carried out in the presence of 1, 1-diphenylethylene, a powerful scavenger of diphenylmethylene,[8] no addition product of the diphenylmethylene, i.e., 1, 1, 2, 2-tetraphenylcyclopropane, was obtained. Instead, in addition to *sym*-tetraphenylethane (13% yield) and diphenylmethane (20% yield), 1, 1, 3, 3-tetraphenyl-1-propene (VIII) was obtained in a 13% yield after a 65-hr. reaction in acetonitrile at 91°C. In the absence of tri-*n*-butylamine, benzhydryl bromide and 1, 1-diphenylethylene also yielded VIII in a 82% yield under identical reaction conditions. In the latter reaction, VIII is evidently produced by the electrophilic addition of the $S_N1$ intermediate to 1, 1-diphenylethylene and by the succeeding dehydrobromination. Therefore, the formation of VIII in the former reaction is conceivably, realized by the same addition-elimination mechanism, and the possibility of the formation of VIII as an insertion product of diphenylmethylene to 1, 1-diphenylethylene is ruled out.

In comparison with the mechanism for the reaction of hindered phenoxides, the mechanism of benzhydryl radical formation in the presence of tri-*n*-butylamine can be explained as the reduction of an $S_N1$ intermediate (i.e., a benzhydryl cation or a benzhydryl ion-pair) by the tertiary amine. It has been known that a tertiary amine such as triethylamine readily yields a charge-transfer complex with tetracyanoethylene[9a] and 7, 7, 8, 8-tetracyanoquinodimethane.[9b] Furthermore, the existence of a charge transfer complex of the amine has been suggested in certain reactions of polyhalomethane and trialkylamine, in which a homolytic cleavage of carbon-halogen bond was observed.[10] Thus, for the reaction of the benzhydryl halide and tri-*n*-butylamine in acetonitrile, the reaction scheme may be shown as follows:



A part of the amminium ion radical (VII) seems to be stabilized by forming tri-*n*-butylammonium ion, which has been identified as the halide, in a yield of 50—60% in these reactions. The source of hydrogen atoms in tri-*n*-butylammonium ions and in diphenylmethane, R–H, has not yet been established.

As for the detailed mechanism of the reduction of the $S_N1$ intermediate by tertiary amine, there seem to be two possible pathways. One is a direct reduction of the cation by the tertiary amine. The other is the reduction through a charge-transfer complex, or a complex of Weitz's quinhydrone type,[11] between the $S_N1$ intermediate and the amine. In the course of these reactions, we could not observe any deep coloration due to such complex formation. However, the possibility of the formation of such a complex between the

7) For hexaphenylethane, see K. Ziegler, L. Ewald and P. Orth, *Ann.*, **479**, 277 (1930); K. Ziegler, P. Orth and K. Weber, ibid., **504**, 131 (1933); K, Ziegler, A. Seib, K. Knoevenagel, P. Herte and F. Andreas, ibid., **551**, 150 (1942).

8) For example, see R. M. Etter, H. S. Skovronek and P. S. Skell, *J. Am. Chem. Soc.*, **81**, 1008 (1959).

9) a) O. W. Webster, W. Mahler and R. E. Benson, *J. Am. Chem. Soc.*, **84**, 3678 (1962); b) L. R. Melby, R. J. Harder, W. R. Hertler, W. Mahler, R. E. Benson and W. E. Mochel, ibid., **84**, 3374 (1962).

10) D. P. Stevenson and G. M. Coppinger, *J. Am. Chem. Soc.*, **84**, 149 (1962); M. G. Reinecke, *J. Org. Chem.*, **29**, 299 (1964).

11) E. Weitz, *Angew. Chem.*, **66**, 658 (1954).

$S_N1$ intermediate of the carbonium-ion type and the amine can not be excluded. This will be the subject of a future paper.

## Experimental[12]

**Materials.**—Benzhydryl chloride was prepared by the reaction of thionyl chloride with benzhydryol;[13] b. p. 131.0—133.5°C/7 mmHg. Benzhdryl bromide was prepared by the reaction of bromine with diphenylmethane;[14] b. p. 139—143°C/3 mmHg. Potassium phenoxide was prepared by refluxing a mixture of potassium with a slight excess of purified phenol in dried benzene. After the potassium had completely disappeared, the phenoxide was filtered in a nitrogen stream and dried at 50°C to a constant weight in vacuo. Potassium 2,6-di-*t*-butyl-4-methylphenoxide (I) was prepared from potassium and 2,6-di-*t*-butyl-4-methylphenol (m. p. 68.0—71.0°C), by a procedure identical with that for potassium phenoxide. 1,1-Diphenylethylene (b.p. 102.5—104.5°C/2 mmHg) was prepared by the dehydration of methyldiphenylcarbinol, which had been prepared by the reaction of phenylmagnesium bromide and ethyl acetate.[15] Tri-*n*-butylamine was fractionally distilled in vacuo; b. p. 75.0—76.0°C/5 mmHg. Acetonitrile was refluxed over phosphorus pentoxide and distilled; b. p. 81.4—82.0°C. Decalin was refluxed over sodium and distilled; b. p. 190—191.5°C. Phenol was dried over calcium chloride and distilled; b. p. 178.5°C.

**Kinetic Measurements.**—A sealed-ampoule technique similar to that previously described[16] was employed. The diminution of the concentrations of the nucleophiles was followed by titration with standard perchloric acid in acetic acid, using crystal violet as an indicator. Each run was followed to 70—80% completion, and the thermostat was controlled to ±0.05—0.1°C.

**The Reaction of Benzhydryl Chloride and Potassium Phenoxide in Acetonitrile.**—A solution of potassium phenoxide was prepared in a 500-cc. round-bottomed flask equipped with a reflux condenser and a calcium chloride tube by boiling a mixture of 3.00 g. (0.0227 mol.) of potassium phenoxide and 300 cc. of acetonitrile. Benzhydryl chloride (2.94 g., 0.0145 mol.) was then added in one portion to the warm solution, and the mixture was boiled under reflux for 2.5 hr. The reaction mixture was filtered, the filtrate was concentrated by distillation, and then ether was added to the residue. The ethereal solution was washed with water, dried over magnesium sulfate, and evaporated in vacuo to give 3.79 g. of viscous oil. The potassium chloride which precipitated during the reaction was filtered after the reaction and dissolved in water, and the chloride ion concentration was determined by the Volhard method. The yield of potassium chloride based on the starting chloride was estimated as 97%. A part (0.550 g.) of the viscous oil so obtained was chromatographed over 25 g. of basic alumina. Elution with *n*-hexane afforded 0.51 g. of benzhydryl phenyl ether; m. p. 48.3—51.1°C (lit. m. p. 54°C[17] and 55°C[18]), $\lambda^{KBr}$ (infrared) 8.10 $\mu$ (C-O-C). With ethanol as the eluent, 0.04 g. of benzhydrylphenol ($\lambda^{KBr}$ (infrared) 2.73 $\mu$ (monomeric OH) and 2.80 $\mu$ (polymeric OH)) was obtained. The other part (3.24 g.) of the oil precipitated some crystals after being left overnight; the recrystallization of the crystals afforded 1.76 g. of benzhydryl phenyl ether, m. p. 51.2—53.5°C, $\lambda^{KBr}$ (infrared) identical with the sample mentioned above. When the mother liquors were chromatographed, 1.23 g. of additional benzhydryl phenyl ether (total 3.50 g., 93.2% of the starting chloride), m. p. 47.8—50.4°C (identical in the infrared spectrum), and 0.07 g. of benzhydrylphenol (total 0.11 g., 3.1%), m. p. 109.5—114.3°C (lit. m. p. 112°C) (*p*-benzhydrylphenol)[18] and 125°C (*o*-benzhydrylphenol)[17,18] almost identical in infrared spectrum with that of the authentic para isomer, were obtained.

**The Reaction of Benzhydryl Chloride and Potassium 2,6-Di-*t*-butyl-4-methylphenoxide (I) in Acetonitrile.**—A solution of 6.30 g. (0.0244 mol.) of potassium 2,6-di-*t*-butyl-4-methylphenoxide in 500 cc. of acetonitrile was prepared in a 1-l. three-necked flask with a reflux condenser, equipped with a sodalime tube, and a thermometer under a nitrogen atmosphere by refluxing the mixture. To the warm solution 4.01 g. (0.0198 mol.) of benzhydryl chloride was added; the mixture was then refluxed in a stream of nitrogen at 82—85°C for 18.3 hr. The reaction mixture was then filtered and potassium chloride was dissolved in distilled water in order to determine the chloride ion concentration by the Volhard method. The amount of the chloride ions liberated during the reaction was estimated to be 82% of the starting chloride. The filtrate was concentrated and the residue dissolved in benzene. The benzene solution was washed with water, dried with magnesium sulfate, and then concentrated in vacuo to give 7.90 g. of an oily material, which was then chromatographed over 200 g. of basic alumina. *n*-Hexane, benzene, ether and finally ethanol were used as the eluents. The first-half of the *n*-hexane fractions afforded 0.51 g. of 2,6-di-*t*-butyl-4-methylphenol, m. p. 67—70°C, identical in infrared spectrum with the authentic sample. From the second-half fractions, 2.20 g. (28.7% of the chloride) of 1-(3′,5′-di-*t*-butyl-4′-hydroxyphenyl)-2,2-diphenylethane (IV), m. p. 113—115°C (ethanol), was obtained. The structural assignment for IV has already been reported.[3] Elution with benzene afforded 1.33 g. (40.2%) of *syn*-tetraphenylethane, m. p. 207.5—208.5°C (lit. m. p. 207—208°C[19]) (identity established by m.m.p.

12) The melting points are uncorrected. The microanalyses were performed by the Microanalytical Center, Kyoto University, Kyoto. The infrared spectra were obtained from a Shimadzu model IR-27 spectrometer.
13) H. Gilman and J. E. Kirby, *J. Am. Chem. Soc.*, **48**, 1735 (1926).
14) J. F. Norris, R. Thomas and B. M. Brown, *Ber.*, **43**, 2959 (1910).
15) C. F. H. Allen and S. Converse, "Organic Syntheses," Coll. Vol. I, 2nd Ed., 226 (1958).
16) K. Okamoto and H. Shingu, This Bulletin, **34**, 1131 (1961).
17) P. Schorigin, *Ber.*, **59**, 2508 (1926).
18) M. Busch and R. Knoll, ibid., **60**, 2247 (1927).
19) G. Wittig and H. Witt, ibid., **74**, 1474 (1941).

207—209°C, and the infrared spectrum). Elution with ethanol gave 1.71 g. of a brown oil, which contained a dienone, $\lambda^{neat}$ (infrared) 6.00 and 6.06 $\mu$ (doublet). This oil was not identified further. No diphenylmethane was identified from the *n*-hexane fractions.

**The Reaction of Benzhydryl Chloride and Tri-*n*-butylammonium Phenoxide (II) in Acetonitrile.**—Phenol (1.229 g., 0.0130 mol.) 2.40 g. (0.0130 mol.) of tri-*n*-butylamine, 30 cc. of acetonitrile and finally 2.00 g. (0.00985 mol.) of benzhydryl chloride were placed in a stainless-steel bomb (50 cc.). After 4 hours of heating at 143—150°C, the mixture was distilled to remove the acetonitrile; ether was added to the residue. After the ethereal solution had been washed with cold water, the titration of a part of the combined water-washings by the Volhard method indicated that 95% of the starting chloride had reacted to give chloride ions. The evaporation of the ethereal solution under reduced pressure afforded 2.71 g. of an oil, a part (0.65 g.) of which was chromatographed over 25 g. of basic alumina. Elution with benzene afforded 0.51 g. (corresponding to 83% of the starting chloride) of benzhydryl phenyl ether, m. p. 50.1—52.3°C (identity established by m.m.p. 50.1—52.5°C and the infrared spectrum). The ether fractions gave 0.07 g. (corresponding to 11.5% of the starting chloride) of benzhydrylphenol, containing mainly of the para isomer (identity established by the infrared spectrum).

**The Reaction of Benzhydryl Chloride and Tri-*n*-butylamine in Acetonitrile.**—A mixture of 1.62 g. (0.0080 mol.) of benzhydryl chloride, 1.63 g. (0.00881 mol.) of tri-*n*-butylamine and 40 cc. of acetonitrile was heated in a stainless-steel bomb at 146—156°C for 6.5 hr. The reaction mixutre was then filtered to give 0.6 g. (45% yield) of *sym*-tetraphenylethane, m. p. 208—209°C (identity established by m.m.p. 207.0—208.5°C and the infrared spectrum). The filtrate was concentrated to give an additional 0.21 g. (15.8% yield) of *sym*-tetraphenylethane, m. p. 207.0—209°C) (identity established by m.m.p. 207.0—208.5°C and the infrared spectrum). The mother liquors were washed with water and concentrated to give 1.01 g. of an oily material, which was then chromatographed on basic alumina (25 g.). Elution with *n*-hexane gave 0.04 g. (3.0% yield) of diphenylmethane (identity established by the infrared spectrum) from early fractions. Succeeding fractions gave 0.05 g. (3.7% yield) of *sym*-tetraphenylethane (total yield, 64.5%), m. p. 204.5—207.0°C (identity established by the infrared spectrum). The combined water washings were then concentrated to give 1.47 g. of hygroscopic white crystals, which was found by the Volhard method to contain 64.6% of the chloride ions of the starting chloride. These crystals were dissolved in 1 N sodium hydroxide, and an oily material was extracted with ether. The etheral solution was concentrated to give 1.05 g. of the residue, which, after distillation in vacuo, gave 0.85 g. (52.2% of the starting amine) of tri-*n*-butylamine, b. p. 84.0°C/14 mmHg (identity established by the infrared spectrum).

**The Reaction of Benzhydryl Chloride and Tri-*n*-butylammonium 2,6-Di-*t*-butyl-4-methylphenoxide (III) in Acetonitrile.**—A mixture of 1.62 g. (0.00800 mol.) of benzhydryl chloride, 1.63 g. (0.00881 mol.) of tri-*n*-butylamine and 2.12 g. (0.00881 mol.) of 2,6-di-*t*-butyl-4-methylphenol was heated in a stainless-steel bomb (50 cc.) at 141—158°C for 6.5 hr. After the mixture had been concentrated, 0.29 g. (21.8% yield) of *sym*-tetraphenylethane, m. p. 207.5—208.5°C (identity established by m.m.p. 207.5—209.0°C and the infrared spectrum) was obtained. The filtrate and the mother liquors from the recrystallization were then combined, concentrated, taken up with *n*-hexane, washed with water, and worked up to give 3.5 g. of an oily material, which was then chromatographed over 100 g. of basic alumina. Elution with benzene afforded 0.01 g. (0.7% yield) of additional *sym*-tetraphenylethane, m. p. 198—204°C (identity established by the infrared spectrum), 0.03 g. (2.1% yield) of benzophenone (identity established by the infrared spectrum), and finally 0.05 g. of 2,6-di-*t*-butyl-4-methylphenol (identity established by the infrared spectrum). A part of the water washings was titrated by the Volhard method in order to determine the chloride ion concentration; the total amount of chloride ions was estimated to be 82% of the starting chloride. The water washings were then concentrated to give 1.33 g. of hygroscopic crystals, from which 0.76 g. (46.4% of the starting amine) of tri-*n*-butylamine, (b. p. 67—73°C/17 mmHg) (identity established by the infrared spectrum) was obtained after the usual working-up.

**The Reaction of Benzhydryl Bromide and Potassium 2,6-di-*t*-butyl-4-methylphenoxide (I) in Acetonitrile.**—A solution of 2.31 g. (0.00896 mol.) of I in 250 cc. of acetonitrile was prepared in a 500-cc. round-bottomed flask equipped with a reflux condenser and a sodalime tube. After the addition of 2.01 g. (0.00850 mol.) of benzhydryl bromide, the mixture was refluxed for 6.9 hr. After the filtration of the potassium bromide, a part of the filtrate (1.000 cc.) was titrated by the Volhard method in order to determine the unchanged benzhydryl bromide. The conversion of benzhydryl bromide was estimated as 97% of the starting bromide. The filtrate was then concentrated, taken up with benzene, washed with water, dried with magnesium sulfate, and finally evaporated to give 3.26 g. of an oily material, a part (0.863 g.) of which was then chromatographed over 25 g. of basic alumina. Elution with *n*-hexane afforded 0.567 g. of an oil containing a solid, which gave 0.0104 g. of *sym*-tetraphenylethane, m. p. 197—204°C (identity established by the infrared spectrum) and 0.139 g. of IV, m. p. 116—117.5°C (identity established by m.m.p. 112—116°C, and the infrared spectrum) after fractional crystallization with ethanol. Benzene-*n*-hexane (1 : 1 by volume) fractions yielded an additional 0.057 g. of IV, m. p. 112—115°C (identity established by the infrared spectrum). From these results, the yields of *sym*-tetraphenylethane and of IV were estimated to be 3.0 and 24.1% respectively.

**The Reaction of Benzhydryl Bromide with Tri-*n*-butylamine in Acetonitrile.**—In a 100-cc. ampoule were placed 2.98 g. (0.0121 mol.) of benzhydryl

bromide, 2.45 g. (0.0132 mol.) of tri-*n*-butylamine, and 60 cc. of acetonitrile. The free space of the ampoule was then filled with nitrogen. After being sealed, the ampoule was kept at 90—93°C for 18.3 hr. Ether (100 cc.) was added to the cooled mixture, and the ethereal solution was washed with ice water. The bromide ion concentration of the water washings was determined by the Volhard method; the conversion of the starting bromide was estimated to be 91%. The dried ethereal solution was evaporated to give 2.72 g. of an oil containing some crystals. After recrystallization from ethanol, 0.10 g. (5.0% yield) of *sym*-tetraphenylethane, m. p. 196—200°C (identity established by m.m.p. and the infrared spectrum) was obtained. The mother liquors were concentrated to give 2.59 g. of an oil, a part (0.288 g.) of which was chromatographed over 25 g. of basic alumina. Some diphenylmethane (0.0775 g.) (identity established by the infrared spectrum) was left after the evaporation of the *n*-hexane fractions. Elution with *n*-hexane - benzene (7 : 3 by volume) afforded 0.0709 g. of crystals, which were then fractionally recrystallized from ethanol to give 0.0400 g. of *sym*-tetraphenylethane, m. p. 199—203°C (identity established by the infrared spectrum) and 0.028 g. of dibenzhydryl ether, m. p. 107—110°C (lit. m. p. 110°C[20]). Benzene fractions gave 0.0055 g. of benzophenone (identity established by the infrared spectrum), while ether fractions afforded 0.0185 g. of benzhydrol (identity established by the infrared spectrum). From these results, the yields of diphenylmethane and *sym*-tetraphenylethane were estimated as 22.8 and 34.4% respectively.

**The Reaction of Benzhydryl Chloride and Tri-*n*-butylamine in Decalin.**—The rate of chloride ion formation was determined at 150°C, using the sealed ampoule technique. The initial concentrations of benzhydryl chloride and tri-*n*-butylamine were 0.187 and 0.207 M respectively. The conversion of the starting chloride was estimated as 4.0% after a 6.5-hr. reaction. The conversion of the chloride under same reaction conditions was 3.0% in the absence of tri-*n*-butylamine. Product analyses for these runs were not carried out.

**The Reaction of Benzhydryl Bromide and Tri-*n*-butylamine in Acetonitrile in the Presence of 1, 1-Diphenylethylene.**—In a 100-cc. ampoule a mixture of 2.88 g. (0.0117 mol.) of benzhydryl bromide, 2.45 g. (0.0132 mol.) of tri-*n*-butylamine, 2.16 g. (0.0120 mol.) of 1, 1-diphenylethylene, and 60 cc. of acetonitrile was placed; after being sealed, the ampoule was kept at 90—91°C for 6.5 hr. To the cooled mixture was then added 100 cc. of ether, and the ethereal solution was washed with ice water. From the determination of the bromide ion concentration by the Volhard method, the conversion of starting bromide was estimated to be 95%. After the concentration of the ethereal solution, 3.69 g. of a brown oil was obtained; this was chromatographed over 145 g. of basic alumina. From *n*-hexane fractions a mixture (1.95 g., b. p. 103—107°C/3 mmHg) of diphenylmethane and 1,1-diphenylethylene was obtained. The composition of the mixture was estimated to be 0.388 g. (19.8% of the starting bromide) of diphenylmethane and 1.28 g. of 1, 1-diphenylethylene on the basis of the infrared spectrum of the mixture, taken in carbon disulfide. The characteristic bands used for the estimation were 13.5 $\mu$ for diphenylmethane and 11.1 $\mu$ for 1, 1-diphenylethylene. The first half of the benzene-*n*-hexane (1 : 9 by volume) fractions afforded 0.395 g. of a solid, which was then recrystallized from ethanol-benzene (5 : 1 by volume) to give 0.187 g. (4.5% of the starting bromide) of 1,1,3,3-tetraphenylpropene, m. p. 122—127°C (lit. m. p. 127—127.5°C[21]) (identity established by the infrared spectrum). From the second-half fractions 0.741 g. of an oil was obtained with a solid, which was then recrystallized from ethanol-benzene (5 : 1 by volume) to afford 0.212 g. (12.7% yield) of *sym*-tetraphenylethane, m. p. 203—205.5°C (identity established by the infrared spectrum). After the concentration of the mother liquors and recrystallization from ethanol-benzene (5 : 1 by volume), 0.341 g. (8.2% yield) of additional 1,1,3,3-tetraphenylpropene, m. p. 127—128°C (identity established by m.m.p. 125—126°C and the infrared spectrum) was obtained. Elution with *n*-hexane - benzene (3 : 1 by volume) gave 0.12 g. of crystals of a hydrocarbon containing a benzene nucleus (confirmed by the infrared spectrum), m. p. 165—167°C (Found: C, 93.27; H, 6.69%). The crystals showed a mixed melting point of 139—169°C on admixture with 1,1,2,2-tetraphenylcyclopropane (m. p. 164.5—166°C). Further identification for these crystals has not been carried out. From fractions eluted with ether 0.066 g. (3.1% yield) of benzophenone (identity established by the infrared spectrum) was obtained. The water washings were extracted with ether after the addition of sodium hydroxide, and the extracts were worked up to give 2.00 g. of tri-*n*-butylamine, b. p. 75—76°C/5 mmHg (identity established by the infrared spectrum).

**The Reaction of Benzhydryl Bromide and 1, 1-Diphenylethylene in Acetonitrile.**—In a 100-cc. ampoule were placed 2.98 g. (0.0121 mol.) of benzhydryl bromide, 2.16 g. (0.0120 mol.) of 1, 1-diphenylethylene and 60 cc. of acetonitrile; after it had been sealed, the ampoule was kept at 90—91°C for 63.9 hr. The white crystals (ca. 0.3 g.) which deposited on the glass wall in the upper part of the free space of the ampoule were examined in order to determine their bromide ion content by the Volhard method; Calcd. for $CH_3CN(HBr)_2$: Br, 78.8. Found: Br, 75.8%. The crystals, which precipitated in the acetonitrile solution, were filtered and washed with ether to give 2.66 g. (63.5% yield) of 1,1,3,3-tetraphenylpropene, m. p. 127—128°C (identity established by the infrared spectrum). A part of the filtrate (1.000 cc.) was added to 10 cc. of ether and washed with ice water, and the ethereal solution was titrated in order to estimate the unchanged benzhydryl bromide by the Volhard method. The conversion of the starting bromide was estimated as 97%. The mother liquors were concentrated and the residue was taken up with benzene, washed with water, dried

20) J. U. Nef, *Ann.*, **298**, 232 (1897).

21) J. E. Hodgkins and M. P. Hughes, *J. Org. Chem.*, **27**, 4189 (1962).

with magnesium sulfate and concentrated to give 1.56 g. of a solid, which in turn afforded 0.80 g. (19.2% yield) of 1,1,3,3-tetraphenylpropene, m. p. 124—126°C, (identity established by the infrared spectum) after recrystallization with benzene. The filtrate was concentrated to give 0.50 g. of an oil, which was chromatographed over 25 g. of basic alumina. Elution with *n*-hexane gave a mixture of 1,1-diphenylethylene (0.097 g.) and diphenylmethane (0.130 g., 6.4% yield). The composition was estimated by the infrared analysis mentioned above. The last fractions eluted with benzene gave 0.114 g. (5.2% yield) of benzophenone (identity established by the infrared spectrum), while those eluted with ethanol afforded 0.013 g. of benzhydrol (identity established by the infrared spectrum).

## Summary

1. The $S_N1$ reactions of benzhydryl halides and hindered nucleophiles, i. e., potassium 2, 6-di-*t*-butyl-4-methylphenoxide (I), tri-*n*-butylammonium 2, 6-di-*t*-butyl-4-methylphenoxide (III), tri-*n*-butylamine and tri-*n*-butylammonium phenoxide (II), proceed through an Arrhenius intermediate[1] and obey good second-order kinetics in acetonitrile at 110—140°C, whereas in the same solvent the reaction with potassium phenoxide is a typical $S_N1$ reaction with a van't Hoff intermediate[1] at 70—120°C. This transition of the characteristics of the intermediates from a van't Hoff to an Arrhenius type has been explained as being due to steric hindrance at the product-formation step of the $S_N1$ reactions.

2. The reactions of benzhydryl halides and some hindered nucleophiles, i. e., tri-*n*-butylamine, I and III, afford not products anticipated for the nucleophilic substitution in acetonitrile, but rather products derived from benzhydyl radicals, i. e., *sym*-tetraphenylethane, diphenylmethane and 1-(3′, 5′-di-*t*-butyl-4′-hydroxyphenyl)-2, 2-diphenylethane, whereas potassium phenoxide and II give rise to substitution products typical of the nucleophilic reactions, i. e., benzhydryl phenyl ether and *p*-benzhydrylphenol. A one-electron transfer mechanism between these hindered nucleophiles, such as tri-*n*-butylamine, I and III, and the $S_N1$ intermediate has been suggested for the formation of benzhydryl radicals.

The authors are indebted to Mrs. Yukiko Takemura, who carried out some of the kinetic measurements.

*Department of Fuel Chemistry*
*Faculty of Engineering*
*Kyoto University*
*Sakyo-ku, Kyoto*

# The Solution State of Cationic Polysoap Derived from Polyallyl Chloride

By Yutaka ISHIGAMI and Hideo NARASAKI

(Received February 5, 1965)

Polysoap differs from colloidal electrolytes in exhibiting no critical micelle concentration (CMC), and in it solubilization occurs over the entire polysoap concentration range. This means that a unit polymer specy in a true molecular solution acts as a micelle.[1]

In a preceding paper,[2] one of the present authors has already reported on the synthesis and some properties of cationic polysoaps, which consist of short polymer chains with chemically-attached soap-like groups. These polysoaps were prepared by quaternizing *N*-dodecylpiperidine or dimethyl dodecylamine with polyallyl chloride, and by quaternizing *N*-dodecylpiperidine with a copolymer of allyl chloride and vinyl acetate (1 : 1 molar ratio). Their CMCs in water were determined by the three independent methods, such as conductivity, dye absorption, and surface tension. The CMC values obtained by the three methods were in good agreement. From these results, it was concluded that the micelle formation of such a polysoap in water was indeed true.

The present work was undertaken in order to examine, by means of light-scattering and surface-tension measurements, the CMC, the micellar weight, the micellar charge in water and surface excess at the air-solution interface of a cationic polysoap which consists of a

1) M. E. L. McBain and E. Hutchinson, "Solubilization and Related Phenomena," Academic Press, New York (1955), p. 236.

2) H. Narasaki, *J. Chem. Soc. Japan, Ind. Chem. Sec.* (*Kogyo Kagaku Zasshi*), **65**, 793 (1962).

relatively short polymer chain. Moreover, the results involved the effect of added sodium chloride on them.

## Experimental

**Material.** -- Polyallyl chloride was prepared by polymerizing allyl chloride at 65°C for 75 hr., using benzoyl peroxide (5% by weight of the monomer) as a polymerization initiator in an atmosphere of nitrogen, then the unreacted monomer was removed by steam distillation. The number-average molecular weight ($\overline{M}_n$) of the polyallyl chloride, as determined by freezing point depression in benzene, was 647, while the degree of polymerization ($\overline{P}_n$) calculated from $\overline{M}_n$ was 8.46. The chlorine content was 43.2% (calculated 46.4%) by a modification of the Volhard method.[3] The polysoap was prepared by quaternizing *N*-dodecylpiperidine with polyallyl chloride, using nitrobenzene as a solvent, at 150°C for 70 hr. in nitrogen. The reaction product was then isolated by precipitation into *n*-hexane. The precipitate was repeatedly washed with a large amount of benzene and dried at 55°C in a vacuum. Then it was obtained as a powder-like white material. This polysoap will be referred to as SP-100. The total chlorine content was 11.99%, as determined by a modification of the Volhard method, and the quaternized chlorine, as determined by the Volhard method, was 11.89%. Therefore, the degree of the quaternization of polyallyl chloride was calculated to be 99.2%, and the molecular weight of SP-100 was 2770.

**Light Scattering.**—Light-scattering measurements were carried out at a room temperature of about 25°C and with a wavelength of 436 m$\mu$, by using a light-scattering photometer (Shimadzu Instr. Co.). The apparatus was calibrated against redistilled benzene as a reference standard. Scattered light was measured at 45°, 90° and 135° relative to the incident beam. The dissymmetry ($Z_{45}$) was determined for all solutions, only the solutions in which $Z_{45}$ did not differ significantly from unity were used as light-scattering data. The $Z_{45}$ of the pure solvent (water) clarified in the manner described below was less than 1.03. Therefore, it is thought that the optical clarification of the solvent is accomplished.

The optical clarification of the solution to be examined was achieved as follows. Stock solutions were prepared on a weight/volume basis. The solution was centrifuged for 1 hr. at 21000 g. and the upper 2/3 parts of the solution were used for the light-scattering measurements. Then aliquots of the solution thus obtained were diluted volumetrically. Redistilled water or an aqueous sodium chloride solution clarified by the above procedure was used as the solvent. After the prepared solutions had been allowed to stand overnight in order to assure equilibrium, they were then clarified by filtration, by using suction through an ultrafine sintered glass filter directly into a light-scattering cell.

3) W. Kimura, ibid., 37, 1310 (1934).

The refractive index increments were determined with a differential refractometer (Shimadzu Instr. Co.) at a room temperature of about 25°C and with a wavelength of 436 m$\mu$. The refractometer was standardized with an aqueous potassium chloride solution. The refractive index increments, $dn/dc$, of SP-100 were found to be effectively independent of the added sodium chloride concentration in the range from 0 to 0.3 mol./l., and the value was 0.175 ml./g.

For an accurate analysis, one should treat the light scattering data as a three-component system, for the present system which was composed of SP-100, water and sodium chloride. However, Strauss and Williams,[4] and Orofino and Flory[5] have suggested that hardly any relative errors in the molecular weight of polysoaps and polyelectrolytes between two component and three component treatments, can be found. Therefore, we treated it as a two-component system composed of SP-100 and water.

In order to evaluate the micellar weight and the slope of the Debye plot of SP-100 from the light scattering data, the Debye equation below was used;

$$K(C-C_0)/(R_{90}-R_{90,\mathrm{CMC}}) = 1/M + 2A_2(C-C_0)$$

$K = 2\pi^2 n_0^2 (dn/dc)^2 / N\lambda_0^4$, where $R_{90}$ is the reduced intensity of the solution at 90°; $R_{90,\mathrm{CMC}}$ is $R_{90}$ at the CMC; $n_0$ is the refractive index of the solvent; $n$ is the refractive index of the solution; $C$ is the surfactant concentration in g./ml.; $\lambda_0$ is the wavelength of the incident light in a vacuum; $N$ is the Avogadro number; $M$ is the micellar weight; $A_2$ is the apparent second virial coefficient and $C_0$ is the CMC.

**Surface Tension.**— Surface tension measurements were carried out by the drop-weight method in a thermostat maintained at 30.0+0.2°C by using the correction of Harkins and Brown.[6] In the measurement, about one minute was allowed for the formation of each drop of the solution, since it was clear from a preliminary experiment that the solutions reached a constant value one minute after the drop formation.

## Results and Discussion

The reduced intensity of the aqueous solutions of SP-100 is plotted against the surfactant concentration in Fig. 1. The CMC was obtained from the inflection point on a curve. The scattering curve for SP-100 in water apparently shows two break points, as 0.10% and 0.22%. The CMC value in water, as determined by the minimum concentration of the surface tension, is in better agreement with 0.22% than with 0.10%, in terms of light scattering. However, this value (0.22%) gives discrepancies when compared with the system composed of added salt in the Debye plot. The Debye plot in water crosses many other

4) U. P. Strauss and B. L. Williams, *J. Phys. Chem.*, 65, 1390 (1961).
5) T. A. Orofino and P. J. Flory, ibid., 63, 283 (1959).
6) W. D. Harkins and F. E. Brown, *J. Am. Chem. Soc.*, 41, 499 (1919).

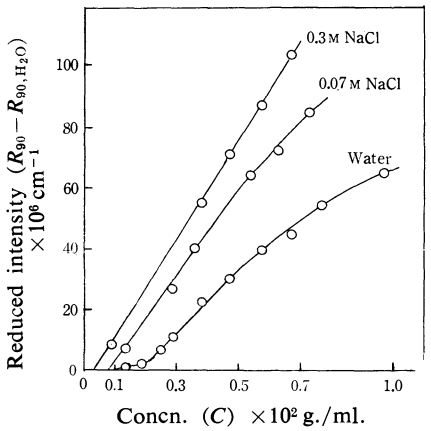



Fig. 1. Reduced intensity vs. concentration curves of SP-100 (wavelength 436 mμ, 25°C).

plots, and the extrapolation of the plot to the ordinate gives the micellar weight of about thirty thousand (Fig. 3). This means that, in the micellar weight vs. the molarity of sodium chloride relation (Fig. 4), a minimum exists at 0.03 M sodium chloride. On the other hand, the CMC value of 0.10% can easily explain the relation between the systems composed of water and of added salt in Fig. 3 and Fig. 4. Therefore, the CMC has been given as 0.10%.

The CMC of SP-100 ($3.64\times10^{-4}$ mol./l. in water) was much lower than the $10^{-2}$ mol./l. value of ordinary ionic monosoaps with the nearly same lipophilic properties, and it was of the same order of magnitude as those of nonionic monosoaps. It seems probable that a surfactant which has some soap-like groups in a molecule, such as SP-100, can more easily form a micelle than those which have only one soap group in a molecule.

As is shown in Fig. 2, when the logarithmic relation between the CMC and the total gegen ion concentration is plotted, the curve can be divided into two regions. One shows that added salt has little effect on the CMC at concentrations below about 0.07 mol./l. The other shows that the effect of added salt predominates beyond this concentration and that the CMC is linearly lowered with an increase in the total gegen ion concentration ($cl^-$). It is well known that the logarithmic relation between the CMC of a univalent ionic monosoap and the univalent gegen ion concentration can be expressed by the equation;

$$\log \mathrm{CMC} = A - B\log(\text{total gegen ion concn.})$$

where $A$ and $B$ are constants. The above phenomenon of SP-100 has never been observed for any ionic monosoaps. The dependence of the CMC of SP-100 on the total gegen ion concentration in the linear portion of the curve is given by;

$$\log \mathrm{CMC} = -4.122 - 0.547\log(cl^-)$$
$$(0.07 \leqq (cl^-) \leqq 0.6 \text{ mol./l.})$$

$K(C-C_0)/(R_{90}-R_{90,\mathrm{CMC}})$ vs. $(C-C_0)$ curves are illustrated in Fig. 3. The plots form straight lines within this range of experimental accuracy. The uncertainties in the Debye plots can be seen in water, especially at lower micellar concentration of SP-100. The slopes of the Debye plots were smaller than those of ionic monosoaps.

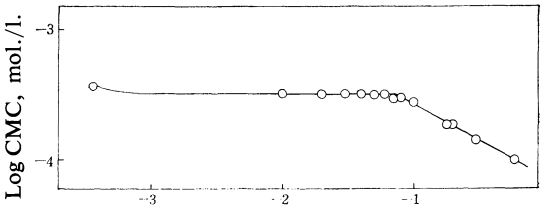



Fig. 2. Log CMC vs. log total gegen ion concentration curve of SP-100.

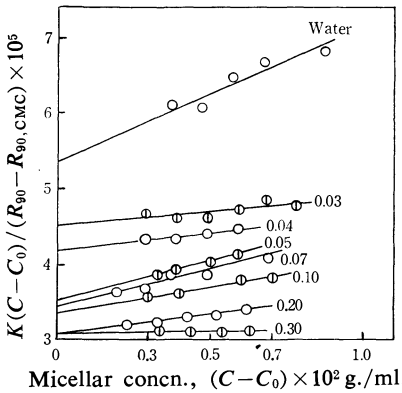



Fig. 3. Light-scattering of SP-100 in water and in aqueous sodium chloride solution (wavelength 436 mμ, 25°C). Numericals in this figure show the concn. of sodium chloride (mol./l.).

Strauss et al.[4] studied the transition from a typical polyelectrolyte to a polysoap of poly-4-vinylpyridine derivatives; they showed that a much more extended polyelectrolyte may be seen to have a much larger second virial coefficient. Inoue[7] pointed out that, in poly-2-vinylpyridine derivatives, the Huggins constant increased and the second virial coefficient decreased with an increase in their alkyl content. This reflects the interaction between their polar groups.

The micellar charge of SP-100 may, therefore, be expected to be quite small, though it may be improvable from the slope of the Debye plot. The charge on the micelle, $p$, can be

7) H. Inoue, *Kolloid-Z. U. Z. Polymere*, **195**, 102 (1964).

TABLE I. THE MICELLAR PROPERTIES OF SP-100 IN AQUEOUS SOLUTIONS

| NaCl mol./l. | CMC mol./l. $\times 10^4$ | $M$ $\times 10^{-3}$ | $1/AM_1$ | $B$ $\times 10^4$ | $m(2)$ | $n$ 8.46 $m$ | $p$ | $p/n$ |
|---|---|---|---|---|---|---|---|---|
| 0 | 3.64 | 18.8 | 6.79 | 17.70 | 6.98 | 59.0 | 0.76 | 0.01 |
| 0.01 | 3.16 | — | — | — | — | — | — | — |
| 0.02 | 3.15 | — | — | — | — | — | — | — |
| 0.03 | 3.16 | 22.2 | 8.00 | 3.75 | 8.11 | 68.6 | 3.38 | 0.05 |
| 0.04 | 3.18 | 24.0 | 8.65 | 4.63 | 8.78 | 74.3 | 4.68 | 0.06 |
| 0.05 | 3.18 | 28.4 | 10.23 | 10.28 | 10.52 | 89.0 | 9.30 | 0.10 |
| 0.06 | 3.17 | — | — | — | — | — | — | — |
| 0.07 | 2.88 | 29.1 | 10.49 | 9.85 | 10.78 | 91.2 | 11.99 | 0.13 |
| 0.08 | 2.88 | — | — | — | — | — | — | — |
| 0.10 | 2.74 | 29.9 | 10.77 | 6.92 | 11.03 | 93.3 | 11.27 | 0.12 |
| 0.18 | 1.86 | — | — | — | — | — | — | — |
| 0.20 | 1.84 | 32.5 | 11.71 | 5.06 | 12.04 | 101.8 | 14.87 | 0.15 |
| 0.30 | 1.43 | 32.3 | 11.64 | 0.42 | 11.76 | 99.5 | 5.16 | 0.05 |
| 0.60 | 0.99 | — | — | — | — | — | — | — |

$M$: Micellar weight
$1/AM_1$: Apparent aggregation number; $A$=intercept of the Debye plot, and $M_1$=formula weight of SP-100
$B$: Slope of the Debye plot
$m(2)$: Aggregation number as computed from Eq. 2
$n$: Number of soap-like groups per micelle of SP-100
$p$: Micellar charge

obtained from the derived equation of Princen and Mysels[8] as follows;

$$p=[BM_1(n_1+fn_3) + \sqrt{2B(n_1+n_3)}]/A(1-AM_1E/2) \quad (1)$$
$$E=(n_1+fn_3)/(n_1+n_3)$$

where $B$ is the slope of the Debye plot; $M_1$ is the formula weight of the surfactant; $n_1$ and $n_3$ are the CMC and the added simple salt concentration both in mol./ml. respectively; $A$ is the intercept of the Debye plot, and $f$ is the ratio of the molar refractive index increment of the added salt to that of the surfactant. Once the charge has been computed, the aggregation number, $m$, is given by;

$$m=\frac{1}{2}(pE+1/AM_1) + \frac{1}{2}\sqrt{(pE+1/AM_1)^2-(p^2+p)E^2} \quad (2)$$

The results thus obtained are represented in Table I. At a lower concentration range of added salt, the $p/n$ value is much smaller than those values found for ionic monosoaps. This result may certainly be interpreted as follows. The SP-100 molecules interpenetrate each other in the interior of the micelle, and so the mutual repulsive force between the polar groups in the micelle is weakened by the shielding effect of the lipophilic groups. Many of the charged polar heads are buried so deeply in the interior of the micelle that they are effectively shielded. As a result of this shielding effect, the net charge on the micelle may be small even if the charge on single molecules is larger. On the other hand, the micellar charge increases with an increase in the added salt concentration, as is indicated in Table I. It seems probable that the micellar charge increases with the number of polar groups on the micellar surface, because the aggregated configuration of molecules in a micelle can be altered from the "*interpenetrated*" form mentioned above to a more regular one.

As Fig. 4 shows, it is noteworthy that the micellar weight of SP-100 increases much

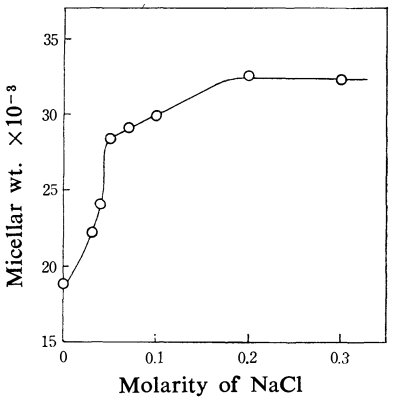



Fig. 4. Dependence of the micellar weight of SP-100 on the concentration of sodium chloride.

8) L. I. Osipow, "Surface Chemistry," Reinhold Publishing Co., New York (1962), p. 176; L. H. Princen and K. J. Mysels, *J. Colloid Sci.*, **12**, 594 (1957).

faster with an increase in the concentration of salt below about 0.06 M. On the contrary, the CMC remained essentially constant in the range from 0.01 to 0.07 M of salt. It is well known that, in ionic monosoap solutions, the addition of salt decreases the CMC and increases the micellar weight. The discrepancy between the CMC and micellar growth of SP-100 in the diluted salt solutions may be interpreted as follows. The effect of the addition of salt on the CMC and on the micellar weight of SP-100 may be distinguished as two concentration ranges. One holds in the case of the diluted SP-100 solutions below the CMC, while the other holds with solutions more concentrated than the CMC. Nakagawa and Inoue[9] considered theoretically that an intramolecular association between alkyl groups would occur in a polysoap, which did not aggregate between the molecules, even in a quite diluted solution when the cohesive power between alkyl groups was extremely strong. The degree of association between alkyl groups is large under some conditions, even in the case of a polysoap with fewer soap-like groups. In view of this, it is probable that an intramolecular association between dodecyl groups of a SP-100 molecule occurs. A small amount of added salt can not give a cohesive power level, whom SP-100 molecules require to form a micelle, to the SP-100 molecules at the lower concentrations of SP-100 just below the CMC, because the intramolecular association is expected to predominate at the lower concentrations of SP-100. Cohesive power sufficient to form a micelle may not be given to the molecules in the solution before the salt concentrtion reaches 0.07 M. On the other hand, upon the addition of a small amount of salt, the micellar weight of SP-100 increases much faster with an increase in the concentration of salt in the case of higher surfactant concentrations, because of the accessibility between the SP-100 molecules in the solution.

Surface tension vs. the logarithm of the SP-100 concentration curves are given in Fig. 5. The uppermost curve shows the system composed of water, while the lowest two curves illustrate the effect of the presence of sodium chloride on the surface activity of the surfactant. Surface tension can be regarded as entirely a linear function of $\log C$ in the concentration range of the surfactant below but near the CMC, and the $-d\gamma/d\log C$ values in these three curves are in fair agreement.

The slope of the surface tension vs. the logarithm of the concentration of an ionic surfactant has different physical meanings under

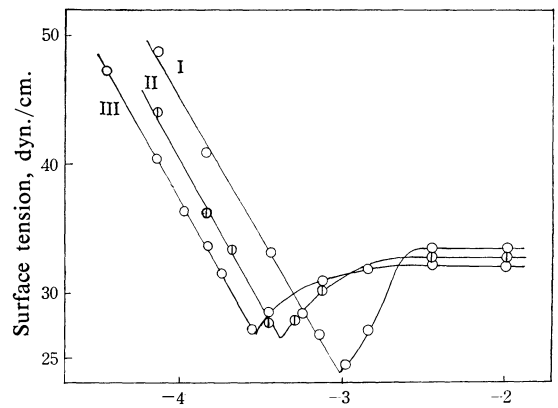



Fig. 5. Surface tension vs. log concentration curves of SP-100 at 30°C.
I Distilled water II 0.05 M NaCl
III 0.10 M NaCl

various conditions. The surface excess of SP-100 at the air-solution interface can be determined from the slope of the surface tension vs. the logarithm of the SP-100 concentration containing a definite amount of sodium chloride. In this case, Gibbs adsorption isotherm is expressed by Shinoda and Nakayama[10] as

$$-d\gamma/\boldsymbol{RT}\, d\ln X_2 = \Gamma_2 + (X_2/X_3)\Gamma_3 \qquad (3)$$

where $\gamma$ is the surface tension; $\boldsymbol{R}$ is the gas constant; $T$ is the absolute temperature; $\Gamma_2$ and $\Gamma_3$ are the surface excesses of the surfactant ion and the gegen ion at the air-solution interface respectively; and $X_2$ and $X_3$ are the mole fractions of components. Because $X_3$ is much larger than $X_2$ in the concentration region of SP-100 examined, and since $\Gamma_3$ is supposed to be at most commensurate with $\Gamma_2$, Eq. 3 reduces to

$$-d\gamma/\boldsymbol{RT}\, d\ln X_2 = \Gamma_2 \qquad (4)$$

Strictly speaking, the sample must be purified until it shows no minimum in $\gamma$ - $\log C$ curves. However, in the present system, it is difficult for us to do so; moreover, the sample itself includes fatal uncertainties in molecular weight distribution, quaternized degree distribution, and end group, etc. Therefore, we have greater interest in the comparison of the surface excesses of monosoaps and ordinary polysoaps than in the determination of the absolute value.

The $\Gamma_2$ value of SP-100, as calculated from Eq. 4 is $3.78\times10^{-10}$ mol./cm$^2$; the corresponding surface area ($A$) is obtained as 44 Å$^2$/mol. by the equation of $A=10^{16}/\boldsymbol{N}\Gamma_2$, where $\boldsymbol{N}$ is the Avogadro number. The $\Gamma_2$ value is of the same order of magnitude as those found for

9) T. Nakagawa and H. Inoue, *Kolloid-Z. u. Z. Polymere*, **195**, 93 (1964).

10) K. Shinoda and H. Nakayama, *J. Colloid Sci.*, **18**, 705 (1963).

ordinary ionic monosoaps. However, since the molecular weight of SP-100 is of the order of $10^3$, as determined on a weight basis, the surface excess of SP-100 is much larger than those of ionic monosoaps.

## Summary

Cationic polysoap (SP-100, mol. wt. 2770), consisting of a short polymer chain with chemically-attached soap-like groups, has been prepared by quaternizing *N*-dodecylpiperidine with polyallyl chloride (mol. wt. 647). Some properties of the aqueous solution of SP-100 has been investigated by the light-scattering and surface-tension methods in the absence of and in the presence of sodium chloride.

We have found that the solution of such a polysoap exhibited the CMC value and that the concentration was $3.64\times10^{-4}$ mol./l. (light scattering).

When the logarithmic relation between the CMC and the total gegen ion concentration was plotted, the curve thus obtained could be divided into two regions. Namely, the curve was almost flat at lower total gegen ion concentrations, followed by a depressed portion.

The micellar weight of SP-100 was 18800 in water and 32300 in a 0.3 M sodium chloride solution. The charges of SP-100 in aqueous solutions were calculated from the slope of the Debye plots by the derived equation of Princen and Mysels; on the basis of these results, the micellar charge of SP-100 in water is quite small.

The surface excess ($\Gamma_2$), together with the corresponding surface area ($A$), of SP-100 at the air-solution interface has been calculated from the slopes of the surface tension vs. the logarithm of polysoap concentration curve slightly below the CMC by applying the Gibbs equation. The $\Gamma_2$ value thus obtained was $3.78\times10^{-10}$ mol./cm$^2$, while $A$ was 44 Å$^2$/mol. The $\Gamma_2$ value of SP-100 in mol./cm$^2$ was of nearly the same order of magnitude as those of ionic monosoaps.

The authors wish to express their hearty thanks to Dr. Toshio Kamata for his valuable advice.

*Government Chemical Industrial Research Institute, Tokyo*
*Shibuya-ku, Tokyo*

# The Electron Paramagnetic Resonance Absorption of Chromium Ions Dispersed on Silica-alumina. II. The Variation in the Spectrum under Several Chemical Treatments

By Akira MATSUMOTO, Hazime TANAKA and Nobuhisa GOTO

(Received February 5, 1965)

The structural change in chromium ions with the variation in the chemical composition of the supporting material was examined by the authors in a preceding report (Part I of this series)[1] through the analysis of the line shape in the $\gamma$-absorption on the electron paramagnetic resonance (EPR), which has been attributed to $Cr^{5+}$ ions. This paper will be concerned mainly with the spectral change in the EPR of the same materials under several chemical treatments.

A few investigators have examined the behavior of the EPR spectra of chromium ions dispersed on silica-alumina under the influence of chemical reagents. Pecherskaya and Kazanskii[2-5] have reported on a series of experiments on this problem, attaching importance to the catalytic activity in the polymerization of ethylene. They have considered that $Cr^{5+}$ ions are the catalytic-active sites. They have also examined the influence of the chemical composition of the supporting materials on the EPR spectra and the catalytic activity.

On the other hand, Cossee and Van Reijen[6] have investigated a similar substance by means

1) A. Matsumoto, H. Tanaka and N. Goto, This Bulletin, 38, 45 (1965).

2) Yu. I. Pecherskaya, V. B. Kazanskii and V. V. Voevodskii, 2nd International Congress on Catalysis (Paris), 1960, paper no. 108.

3) F. M. Bukanaeva, Yu. I. Pecherskaya, V. B. Kazanskii and V. A. Dzis'ko, *Kin. i Kat.*, 3, 358 (1962).

4) V. B. Kazanskii and Yu. I. Pecherskaya, ibid., 4, 244 (1963).

5) G. K. Boreskov, F. M. Bukanaeva, V. A. Dzis'ko, V. B. Kazanskii and Yo. I. Pecherskaya, ibid., 5, 434 (1964).

6) P. Cossee and L. L. Van Reijen, 2nd International Congress on Catalysis (Paris), 1960, paper no. 82.

of EPR and magnetic susceptibility under the influence of hydrogen, sulfur dioxide, benzene, etc. They think that reduction at a relatively low temperature produces mainly $Cr^{4+}$ ions, and they discussed the influence of the supporting materials as well as the methods of reduction. However, they did not very much consider the nature of active sites in the polymerization of ethylene. Recently they also reported on interesting work on the same sort of material in relation to the catalytic-active sites in the dehydrogenation reactions.[7]

The authors intend in this paper to demonstrate the influence of the chemical composition of the supporting materials on the variation in EPR spectra under the action of air, water vapor, cyclohexane. The effect of evacuation will also be investigated. Then, with these results added to those of Part I, the relation between the stability of the $3d^1$ state or chromium ions and the catalytic activity in the polymerization of ethylene and in the decomposition of hydrogen peroxide will be discussed.

## Experimental

**Materials and Treatment.**—The supporting materials and the method of preparing dispersed samples were the same as those described in Part I. The calcination of samples was carried out in a stream of dry air at 500°C for 4 or 17 hr. Immediately after the calcination, the measurement of the EPR and the chemical treatments were started. The samples used in the experiment are listed in Table I.

**The Measurement of the EPR Spectra.**—The EPR spectra were observed with the K-band superheterodyne spectrometer described in the preceding paper. When the measurement was performed at elevated temperatures, a cavity equipped with a heater was employed. A small quantity of coal powder was fixed in the cavity as a standard of the relative intensity of the EPR absorption.

A silica tube which contained the sample was inserted into the cavity and connected with a vacuum system. The cavity had previously been heated at a fixed temperature. After evacuation for several minutes, each reagent was introduced and the measurement of EPR was started. Dry air was conducted from a flask containing phosphorus(V) oxide. Water vapor was then introduced from a glass tube in which a small quantity of deaerated water had been sealed off. Ethylene was taken from the same material as those used in the polymerization experiment in this laboratory. The reaction of cyclohexane was followed in the open air.

In some cases samples were treated outside the cavity and were measured in an ordinary cavity at room temperature. Especially the evacuation of the samples not calcined was carried out in another tube at room temperature for 24 hr. with an oil diffusion pump, and then the samples were transferred into a tube for measurement and sealed off. When the samples not calcined were evacuated, a color change occurred, even at room temperature.

**The Oxidation Number.**—The oxidation number was determined by the iodometry described in Part I.[1] When the determination was carried out after reduction with cyclohexane, the samples were dried, with evacuation, at room temperature. After treatment with ethylene, however, it was impossible to determine the oxidation number because the polymer covered the samples.

**The Polymerization of Ethylene.**—The activity in the polymerization of ethylene was determined at 135°C by means of the decrease in the pressure of ethylene starting from 1 atm. and from 40 kg./cm$^2$ without a solvent. About 200 mg. of the sample calcined was placed in a glass tube dipped in an oil bath at 135°C; then, after the air had been removed with a rotary vacuum pump for five minutes, ethylene was introduced up to 1 atm. The volume of the system was about 600 cc. (N.T.P.). Then the decrease in the pressure was observed. Some of the samples were taken out during this treatment and their EPR spectra measured.

When the experiment was performed starting from 40 kg./cm$^2$, about 500 mg. of the sample was placed in a stainless steel autoclave (100 cc.). After the repeated replacement of the atmosphere with nitrogen, the autoclave was heated to 135°C and ethylene was introduced up to 40 kg./cm$^2$. The decrease in the pressure was observed, and after a definite time the weight of the polymer produced was measured. The volume of the system was about 125 cc. (N.T.P.).

**Decomposition of Hydrogen Peroxide.**—The decomposition of hydrogen peroxide was investigated at 30°C, using an apparatus which was similar to that of Deren et al.[8] About 100 mg. of the sample was placed in an ampoule and 30 cc. of 30% hydrogen peroxide was added. By running water out from the burettes connected to the system, a manometer was balanced and the volume of the generated oxygen was determined nearly continuously. The decomposition proceeded linearly with time. The measurement was continued for about an hour.

## Results

**The Variation in EPR Absorption in the Atmospheres of Different Gases.**—*The Appearance of the γ-Absorption by Evacuation and Its Disappearance with Air and Water Vapor.*—Impregnated samples which had merely been dried at 120°C in open air gave a broad so-called β-absorption of EPR without a sharp line of γ-absorption or with only a very weak one. When these materials were evacuated, the γ-absorption appeared and increased, even at room temperature. This absorption, however, was more affected by air and water vapor than that of the calcined samples. Figures 1

7) L. L. Van Reijen, W. M. H. Sachtler, P. Cossee and D. M. Brouwer, 3rd International Congress on Catalysis (Amsterdam), 1964.

8) J. Deren, J. Haber, A. Podgorecka and J. Burzyk, *J. Cat.*, 2, 161 (1963).

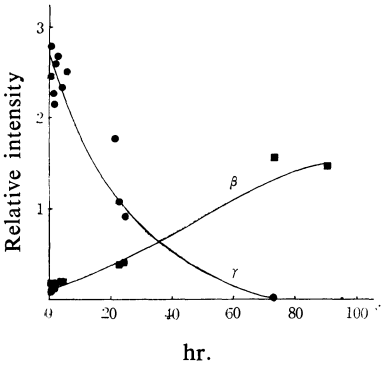



Fig. 1. The variation of the intensity of EPR absorptions in dry air. Sample No. 5, not heat treated and evacuated, at room temperature. (The unit of the intensity is not the same in two absorptions.)

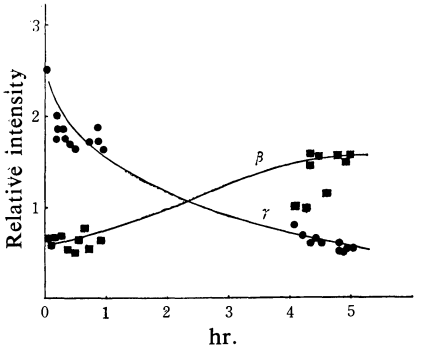



Fig. 2. The variation of the intensity of EPR absorptions in water vapor. Sample No. 5, not heat treated and evacuated, at room temperature. (The unit of the intensity is not the same in two absorptions.)

and 2 shows the decrease in this absorption in atmospheres of dry air and water vapor at room temperature. It may be seen that water vapor is 10 times as effective in causing this decrease as dry air.

*Dry Air and Water Vapor.*—Figure 3 shows the variation in the intensity of EPR absorption in a vacuum, in dry air and in water vapor at three different temperatures. The sample is No. 5, i.e., the sample with a commercial silica-alumina base, in Table I, and

TABLE I. THE SAMPLES USED IN THE EXPERIMENTS

| Sample No. | Base material* | Cr cont. % |
|---|---|---|
| 1 | Silica gel (635) | 4.88 |
| 2 | Silica : alumina 4 : 1 (279) | 4.27 |
| 3 | Silica : alumina 1 : 1 (306) | 5.40 |
| 4 | Gamma alumina (233) | 5.45 |
| 5 | Silica : alumina 10 : 1** | 2.36 |

* Figures indicate BET surface area in $m^2/g$.
** Commercial silica-alumina.

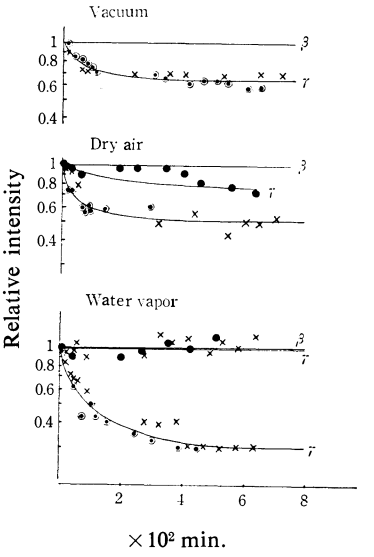



Fig. 3. The variation of the intensity of EPR absorptions.
Sample No. 5; ● 50°C, ◉ 80°C, × 120°C

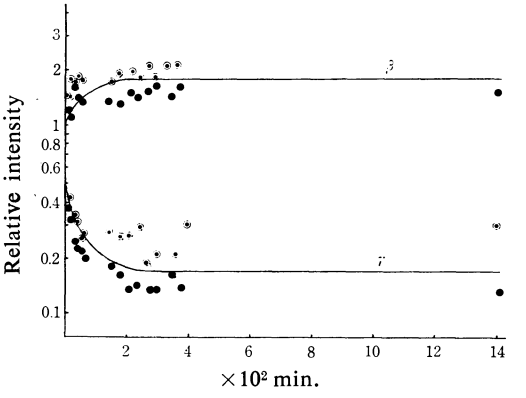



Fig. 4(a). The variation of the intensity of EPR absorptions in cyclohexane at 70°C.
Sample No. 5; ● 50°C, ◉ 80°C

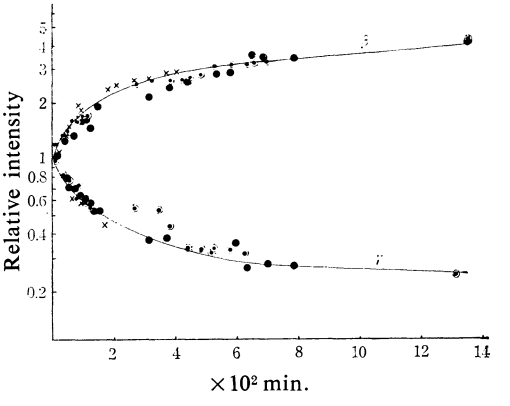



Fig. 4(b). The variation of the intensity of EPR absorptions in ethylene.
Sample No. 5; ● 50°C, ◉ 80°C, × 120°C

it is calcined at 500°C for 17 hr. Concerning the $\beta$-absorption, no marked increase is seen. The decrease in the intensity of the $\gamma$-absorption is accelerated by water vapor and temperature, but the acceleration does not linearly correlate with the temperature.

*Cyclohexane and Ethylene.*—The same material was treated with cyclohexane and ethylene ;

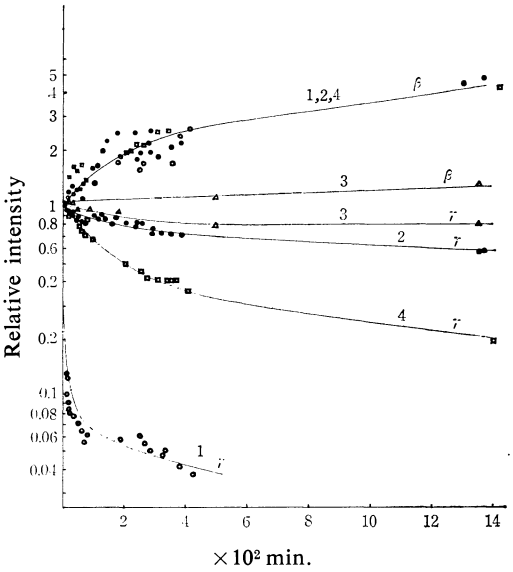



Fig. 5. The variation of the intensity of EPR absorptions by the contact of ethylene in the samples with different supporting materials at 70°C. Figures indicate sample numbers.

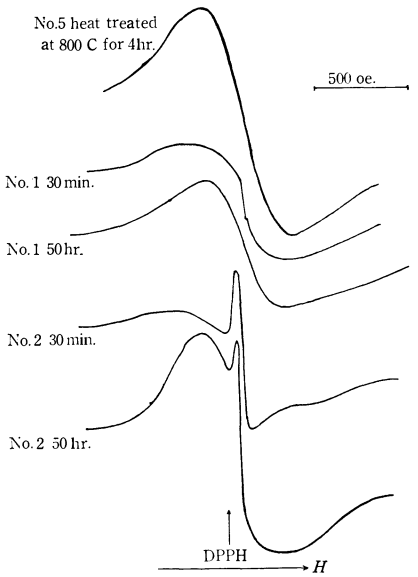



Fig. 6(a). EPR spectra after the treatment with ethylene at 1 atm. The first indicates the spectrum of the sample No. 5 heat treated in air at 800°C for 4 hr.

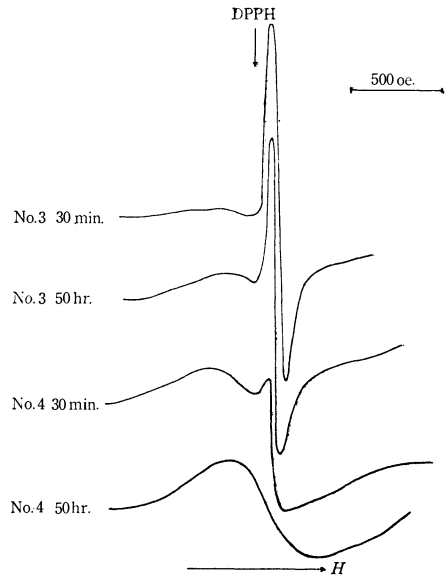



Fig. 6(b). EPR spectra after the treatment with ethylene at 1 atm.

the results are shown in Fig. 4. Another series of experiments was carried out in order to compare the samples with different supporting materials. Figure 5 shows the intensity variation in each sample at 70°C in an atmosphere of ethylene. Figure 6 shows the line shapes of the EPR of samples which were picked out in the course of the polymerization experiment to be described below.

It may be seen that in these atmospheres the $\beta$-absorption grows rapidly and that the decrease in $\gamma$-absorption is also remarkable. The variation does not depend on temperatue very much, from 50°C to 120°C, in the atmosphere of ethylene. The supporting material markedly affects the behavior of the $\gamma$-absorption. As may be seen in Figs. 5 and 6, the

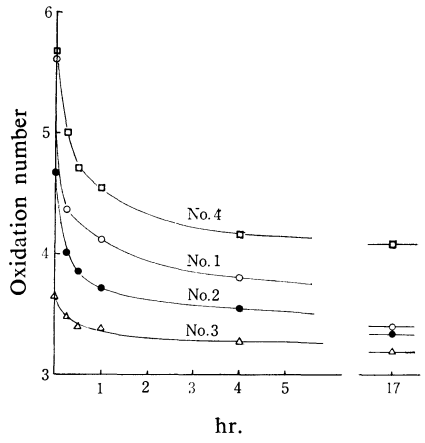



Fig. 7. The variation of the oxidation number by the treatment with cyclohexane at 60°C.

sample with a silica gel base loses the $\gamma$-absorption quite rapidly, with the sample with a gamma-alumina base next. In the sample with a silica-alumina I (silica : alumina=4 : 1) base, the $\gamma$-absorption is rather stable, and in the sample of silica-aluminaII (silica : alumina= 1 : 1) the $\gamma$-absorption hardly changes at all during the measurement.

Figure 7 indicates the variation in the oxidation number of the four kinds of samples by the treatment with cyclohexane at 60°C. The oxidation number of the silica-gel-base sample also decreases quickly. The sample with a silica-alumina II base keeps a low oxidation number from the beginning. It may be noticed that the sample with a gamma-alumina base keeps a relatively high oxidation number, even after long treatment.

**The Polmerization of Ethylene.** — When the samples calcined at 500°C for 4 hr. were brought into contact with ethylene of 1 atm. at 135°C, a decrease in the pressure was observed in the cases of the samples with a silica gel base and with a silica-alumina I base, as is shown in Fig. 8. The polymers which

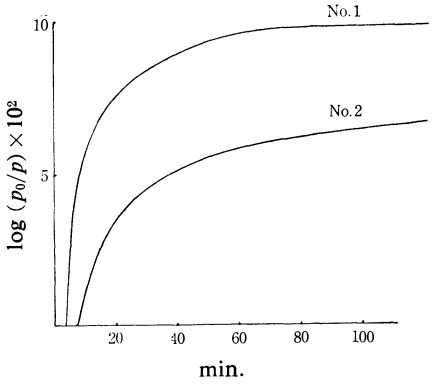



Fig. 8. The pressure decrease of the ethylene with the contact of the samples (at 135°C, from 1 atm.).

melted during the reaction, including the particles of the samples, formed a plate. The reproducibility of the experiment was not very good, but the relative inclination was always similar. Figure 8 indicates the average curves of several runs. In all cases a short period of induction was observed. This period was shorter in the silica-gel-base sample than in the silica-gel-alumina I base sample, and the initial rate of the reaction was faster in the former. After about an hour of the rapid decrease in the pressure, a gradual drop continued for a long time.

For the samples with a silica-alumina II base and with a gamma-alumina base, no decrease in the pressure could be observed. The

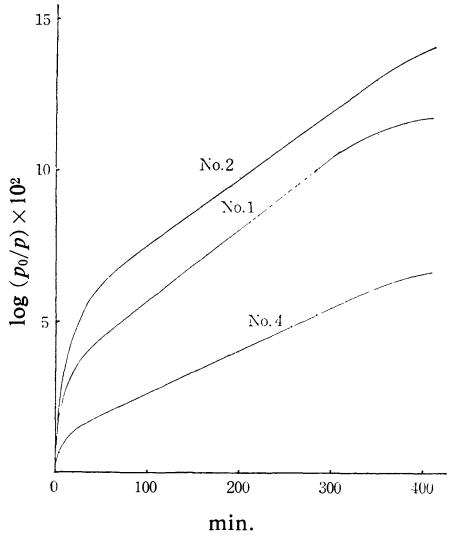



Fig. 9. The pressure drop of the ethylene with the contact of the samples (at 135°C, from 40 kg./cm$^2$).

color of the samples turned green from the initial orange or orange yellow for the samples with a silica gel base and with a silica-alumina I base, but for the sample with a silica-alumina II base the color changed little remaining brown.

Figure 9 shows the results of the experiments with an autoclave. In this case decrease in the pressure was observed even with the sample with a gamma-alumina base, but the rate was slower than with the samples with a silica gel base and with a silica-alumina I base. The difference between the latter two samples was not as clear as in the experiment started from 1 atm. The polymer produced after 20 hr. was 4—5 g. per 1 g. of the sample in the cases of silica gel and silica-alumina I, and about 1.5 g. per 1 g. of the sample in the case of a gamma-alumina base. However, as the polymerization proceeds, the samples are covered with the molten polymer and the diffusion of ethylene into the polymer becomes important in the reaction. Also, the heat of the reaction necessarily elevates the temperature at the surface of the sample, so it is difficult to decide the activity directly on the basis of these values. The sample with a silica-alumina II base did not bring about the pressure drop at 40 kg./cm$^2$ either.

**The Decomposition of Hydrogen Peroxide.**— In Table II the amount of oxygen liberated in one minute per gram of chromium in the sample and that oxidation number are shown for the four kinds of samples, each of which was measured before and after treatment with cyclohexane. This treatment was the same as

that for the determination of the variation in the oxidation number, and the duration was fixed at thirty minutes.

The activities per chromium differ, but if the activity is expressed by the value per oxidation number, they are not very different. Even after the reduction, these values remain constant, except for the sample with a silica gel base, where the activity per oxidation number becomes more than two times as large.

TABLE II. THE CATALYTIC ACTIVITY IN THE DECOMPOSITION OF $H_2O_2$

| Sample | Before reduction | After reduction* |
|---|---|---|
| Liberated $O_2$ cc./min./g. of Cr | | |
| 1 | $9.79\times10^{12}$ | $7.98\times10^{12}$ |
| 2 | 9.00 | 5.02 |
| 3 | 3.14 | 1.57 |
| 4 | 1.47 | 1.04 |
| Liberated $O_2$ cc./min./g. of $Cr^{6+}$ ** | | |
| 1 | $11.9\times10^{12}$ | $25.8\times10^{12}$ |
| 2 | 16.8 | 17.1 |
| 3 | 13.3 | 10.7 |
| 4 | 16.8 | 18.7 |

* Treated in cyclohexane for 30 min. at 60°C.
** Determined by the method of the analysis of oxidation number.

## Discussion

**The Stability of $\gamma$-Absorption Sites Against Chemical Reagents.** — The authors showed in Part I of this series that thermal stability of $\gamma$-absorption sites in the dispersed chromia was affected by the chemical composition of the supporting material. The sample with a silica gel base held a high mean oxidation state and showed the $\gamma$-absorption up to a higher temperature of the heat treatment. The addition of alumina to the base material lowered the thermal stability of the high oxidation state and $\gamma$-absorption sites. Pure gamma-alumina had a somewhat different inclination as a supporting material.

On the contrary, the reduction with chemical reagents proceeds most easily in the sample with a silica gel base, and the disappearance of the $\gamma$-absorption upon contact with ethylene occurs most rapidly in this sample. The sample with a silica-alumina II base, which has a relatively low oxidation number from the beginning and which shows a strong $\gamma$-abserption, is quite inert; the $\gamma$-absorption is hardly changed at all by the treatment with ethylene, as is shown in Figs. 5 and 6. The absorption of the sample with a gamma-alumina base behaved in an intermediate manner under this treatment.

As was mentioned in Part I, the $\gamma$-absorption site of the pure silica-gel-base sample must be present in the cluster of chromia, possibly at the surface. Its concentration is low, and the coordination field around the $Cr^{5+}$ ions is a symmetric. It may be considered that under such conditions chromium ions react easily with chemical reagents.

When alumina is added to the supporting material, isolated chromium ions appear. The concentration of $Cr^{5+}$ ions increases, and the coordination field around them becomes more symmetric. The chemical stability of these sites increases, though they are not very stable against heat treatment. It is natural to think that this effect is caused by aluminum ions or by the defects made by aluminum ions. It is, however, not clear at present whether the $\gamma$-absorption sites are present at the isolated chromium or in the clusters of chromia, but at least there are several $\gamma$-absorption sites which are different in the chemical stability, and the addition of alumina to the supporting material makes for an increase in the number of chemically-stable sites or for an increase in the general stability of the sites against chemical reagents.

Gamma-alumina acts as an intermediate supporting material. The line shape of the $\gamma$-absorption is most symmetric in the sample with this base and the coordination is most regular. Unlike silica-alumina, gamma-alumina is rather a regular substance, so the dispersion of chromia on this material is more regular, though the interaction between chromia and alumina is strong. The fact that the oxidation number does not go below four upon treatment with cyclohexane indicates the different state of the chromium ions on this material.

Kazanskii et al.[5] reported similar findings concerning variation in the line shape of the EPR in different supporting materials, though they thought mainly in terms of a substitution of the chromium atom for the silicon atom. The interaction of chromium with silica-alumina has also been discussed by a few investigators.[9-11] Topchiev et al.[9,10] considered the formation of aluminum chromate, with reference to the work of Pode et al.,[12] and concluded that the stability of the high oxidation state of chromium is determined by the form of the chromates.

As has been seen earlier, the evacuation of a sample not calcined produces $\gamma$-absorption

9) A. V. Topchiev, B. A. Krentsel, A. I. Perel'man and K. G. Miesserov, *J. Polymer Sci.*, **34**, 129 (1959).
10) A. V. Topchiev, ibid., **53**, 195 (1961).
11) K. G. Miesserov, *Neftekhimiya*, **2**, 681 (1962); *Chem. Abstr.*, **58**, 8042e.
12) T. V. Rode, V. B. Kazanskii and Yu. I. Pecherskaya, *J. Phys. Chem. SSSR*, **35**, 2370 (1961).

sites which easily disappear upon contact with air, even, at room temperature. Perhaps the nature of these sites is similar to that on silica gel. The EPR spectra of the samples calcined do not change very much in a vacuum or in dry air. Particularly the $\beta$-absorption does not increase. This means that the ionic state of chromium in the dispersed clusters of chromia does not essentially change. On the contrary, in the samples not calcined, a rise in the $\beta$-absorption is seen in response to a fall in the $\gamma$-absorption. The effect of water vapor is more rapid and clear, and the $\beta$-absorption appears gradually, even in the calcined sample. These phenomena correlate with the process of stabilization, indicating the formation of certain coordination states.

**The Activity in the Polymerization of Ethylene.**—The initial reaction rate of ethylene at 1 atm. is the fastest with a silica gel base, but the chromium ions on the same base are most easily reduced. This may correlate with the fact that when used as the supporting material the pure silica gel makes the catalyst most easily deactivated.[13] The addition of alumina produces the more stable active sites. However, addition in excess increases the number of inactive chromium ions.

The nature of the active sites in these substances in the polymerization of ethylene is not yet clear. It is, however, possible to consider that such sites exist in the dispersed clusters of chromia, where chromium ions are placed in a field of distorted octahedron. In the course of the present experiment, it was established that the samples become yellow or orange yellow when subjected to heat treatment in dry air. If the activation was carried out in wet air, the samples turned green. After the polymerization, the color generally turned green. The green samples played no part in the polymerization, as is well known. The teatment of the activated samples by cyclohexane caused a color change to brown and not to green.

Van Reijen et al.[7] also paid attention to the color change of chromia-alumina and chromia-silica. They measured the EPR and the magnetic susceptibility and concluded that, in a light blue sample, chromium ions become $Cr^{2+}$ and active in the dehydrogenation of cyclohexane, while in a green sample chromium ions are $Cr^{3+}$ and inactive.

These colors reflect the electronic state of the active chromium ions. From the facts that the oxidation state of chromium easily changed by the treatment with cyclohexane and that, in general, the catalyst is dispersed in some hydrocarbon before coming in contact with the solution of ethylene, the valence state of chromium has to be below $5^+$ at the moment of reaction. Accordingly, the existence of chromium ions which are easily reduced to a low valence state, but yet keep some coordination condition, may be essential for the polymerization.

The life of the active site is decided by the ease of the transfer from an active to an inactive coordination state. The effect of the addition of alumina can be understood from the increase in the symmetry of the coordination field and from the subsequent increase in the stability of the state, which is reflected by the increase in the symmetry and width of the $\gamma$-absorption.

About the poisoning of the activity by water, Kazanskii and Pecherskaya[4] proposed a mechanism of the strong attaching of water to $Cr^{5+}$ sites, which they considered to be the active sites in the polymerization reaction. This is a possibility, but at the same time it is possible to consider that water accelerates the transfer of chromium ions into an inactive state. This is because, if the air of the heat treatment is wet, the color of the sample becomes green, the presence of water produces a green sample both in a reductive atmosphere and in an oxidative.

There are a few articles about the mechanism of the polymerization of ethylene with this sort of catalyst.[10,14-19] Clark et al.[20] reported that the treatment of the catalyst by carbon monoxide above 250°C or by ethylene above 15°C produces a complex of the carboxylate type on the surface, and that only the catalyst accompanying this complex is active in the polymerization of ethylene at low temperature. The role of this complex has not yet been made clear.

Before the catalyst is introduced into the reactor, it is dispersed and held in the solvent. This procedure may, like the penetration of the solvent, be useful in making the complex. As may be seen in Fig. 8, the polymerization at 1 atm. shows an induction period, which may correspond to the complex formation. Topchiev et al.[21] have shown that the pretreatment of the catalyst by ethylene or isooctane reduces this induction period.

13) Phillips Petro. Co., Belg. Pat. 530617, July 23 (1954); 535082, Jan. 22 (1955); 551826, Oct. 16 (1956).

14) F. Eirich and H. Mark, *J. Colloid Sci.*, **11**, 748 (1956).
15) E. C. Curphey, *Brit. Plastic*, **31**, 63 (1958).
16) T. Tsuruta, *Kagaku*, **13**, 614 (1958).
17) A. Takahashi, *Yuki Gosei Kagaku*, **18**, 624 (1960).
18) Stanislaw Benbenek, *Przemysl Chem.*, **41**, 719 (1962); *Chem. Abstr.*, **58**, 12677h; *Przemysl Chem.*, **43**, 28 (1964); *Chem. Abstr.*, **60**, 13320d.
19) A. Clark and G. C. Bailey, *J. Cat.*, **2**, 230 (1963).
20) A. Clark, J. N. Finck and B. H. Ashe, 3rd International Congress on Catalysis (Amsterdam), 1964.
21) K. V. Topchieva, O. K. Sharaev, A. I. Perel'man and A. V. Topchiev, *Neftekhimiya*, **1**, 780 (1961); *Chem. Abstr.*, **57**, 6111c, *Neftekhimiya*, **2**, 187 (1962); *Chem. Abstr.*, **58**, 4649f.

The dispersion of chromia in the form of thin-layer clusters is convenient for the multi-point adsorption; also, if this assembly of chromia has the character of an *n*-type semiconductor in the reducing atmosphere, the $d^1$ or $d^2$ state of chromium is conductive to the adsorption from the point of view of the ligand field stabilization energy. The adsorption is also possible in a Zeise-type $\pi$-complex, such as Cossee suggested in the case of the Zieglar-type catalyst.[23] In any case, ethylene monomers are adsorbed on the surface of the cluster of chromia collectively. If the carboxylate ions cited above serve to initiate the process, the polymerization proceeds in a manner like that proposed by Duck[23] in a Ziegler-type catalyst or by Friedlander[24,25] in a standard-type catalyst. It is interesting that Eishens observed the same type of carboxylate ions on the Ni–NiO treated with CO.[26]

**The Decomposition of Hydrogen Peroxide.**— There have been several reports concerning the activity of chromia dispersed on the supporting materials in the decomposition of hydrogen peroxide. Voltz and Weller[27] and Matsunaga[28] have shown that the activity of the chromia-alumina system depends on the excess oxygen over a wide range of the chromium concentration; the activity per excess of oxygen is constant. Tarama et al.[29] have reported that the $Cr^{6+}$ site and the $Cr^{5+}$ site both have catalytic activity. On the other hand, Deren et al.[8,30] showed that the aggregative state of $Cr^{6+}$ affects the activation energy in the decomposition reaction. From the low concentration range of chromium where an atomic dispersion occurred, to the higher concentration which resulted in the clusters, the activation energy gradually lowered and the activity increased as a whole.

In the present experiment, the decomposition activity is related to the excess oxygen of the samples in many cases. The difference in the supporting material does not produce a great difference in the specific activity. The reduction by cyclohexane lowers the total activity, but the activity per excess unit of oxygen remains constant. Only in the case of the sample with a silica gel base is the activity per excess unit of oxygen about two times larger after the reduction; the lowering of the activity is not so great as that of the oxidation number.

This phenomenon may be correlated with the coordination state of the chromium ion. If the decomposition of hydrogen peroxide by these materials proceeds via the cycle of oxidation-reduction mentioned in the case of $MnO_2$,[31] the quantity of the excess oxygen is only a measure of the sites in the oxidation state. In general, the rate-determining step of the reaction involves only the acceptor site. There are two possibilities in the case of the sample with a silica gel base. First, the reduction does not destroy the active site, though its oxidation state is changed. Second, both the acceptor site and the donor site contribute to the rate determination step in some coordination state. The former enlarges the finding of Tarama et al. that $Cr^{4+}$ is also a reactive site. The results of Deren et al. are also useful in understanding special features of the chromia cluster. It would be expected that the assembly would produce an lowering of the activation energy. This must be a characteristic of this dispersion.

## Summary

The dispersed state of chromium and the effect of heat treatment have been compared in Part I in chromium dispersed on different supporting materials. The behavior of the EPR absorption of the same materials in the reaction of several chemical reagents have been observed in the present work. The catalytic activities of these samples in the polymerization of ethylene and in the decomposition of hydrogen peroxide have also been measured.

The $\gamma$-absorption sites of the samples had different stabilities. In the sample with a silica gel base, this absorption disappeared quite easily in a reductive atmosphere, but that of the sample with a silica : alumina 1 : 1 base was stable in the same atmosphere. The former showed the greatest initial reaction rate in the polymerization of ethylene at 1 atm., while the latter had no catalytic activity in the polymerization, even at 40 kg./cm$^2$. The sample with a gamma-alumina base showed an intermediate character in many respects. The activity in the decomposition of hydrogen peroxide generally corresponded to the oxidation number of the samples, even after reduction with cyclohexane, but in the case of the silica gel base different behavior was observed.

22) P. Cossee, *J. Cat.*, **3**, 80 (1964).
23) E. W. Duck, *J. Polymer Sci.*, **24**, 86 (1958).
24) H. N. Friedlander, ibid., **38**, 91 (1959).
25) H. N. Friedlander and K. Oita, *Ind. Eng. Chem.*, **49**, 1885 (1957).
26) R. P. Eischens and W. A. Pliskin, *Advan. Catalysis*, **10**, 25 (1958).
27) S. E. Voltz and S. W. Weller, *J. Am. Chem. Soc.*, **76**, 1586 (1954).
28) Y. Matsunaga, This Bulletin, **30**, 984 (1957).
29) K. Tarama, S. Teranishi and H. Yoshida, *Shokubai*, **4**, 341 (1962).
30) J. Deren, J. Haber and J. Siechowski, 3rd International Congress on Catalysis (Amsterdam), 1964.
31) J. Mooi and P. W. Selwood, *J. Am. Chem. Soc.*, **72**, 4333 (1950).

Taking the present and the preceding results into account, the character of this type of catalyst has been discussed. Its nature must essentially be due to the cluster-form dispersion of chromia; the addition of alumina to the supporting material gives an effect of stabilization to the active site, which extends the life of the catalyst, though an excess in the addition results in an inactive material. The $3d^3$ state of the chromium ions is inactive in the polymerization of ethylene, probably because of the lack of a beneficial adsorptive property to the monomer. The ease in the transfer among $d^0$, $d^1$ and $d^2$ states of chromium ions may decide the activity, while the transfer into the $d^3$ state may decide tha life of the catalyst. Water accelerates the latter and deactivates the catalyst.

The authors wish to express their thanks to Messrs. Kunihiko Nakamura and Hiroshi Fukunaga for their help in the course of the experiment.

*The Central Research Laboratory*
*Showa Denko K. K.*
*Ota-ku, Tokyo*

# The Preparation of Hydride-free Triethylaluminum and Its Reaction with Titanium Tetrachloride

By Yukichi TAKASHI and Itsuho AISHIMA

(Received February 6, 1964)

In order to clarify the mechanism of the Ziegler catalysis for the polymerization of $\alpha$-olefins, many investigations concerning the reaction between the catalyst components, namely, triethylaluminum and titanium tetrachloride, have been reported. All authors have observed the rapid reduction of titanium tetrachloride to the lower valency states.

Roha et al.[1] proposed that the reduction of titanium tetrachloride during the reaction with triethylaluminum was due to the effect of the diethylaluminum hydride present in the triethylaluminum. They stated that the diethylaluminum hydride present as an impurity in triethylaluminum has a strong reducing power and that the triethylaluminum, which had been treated with ethylene at a high pressure in an attempt to decrease the hydride content, did not show any appreciable reduction of titanium tetrachloride, although a clear orange solution was obtained.

In order to study the true behavior of triethylaluminum, hydride-free triethylaluminum was prepared and the reactivity of trialkylaluminum with titanium tetrachloride was investigated.

## Experimental

**Material.**—*Crude Triethylaluminum.*—A commercial reagent (Texas Alkyls Corp.) was used.

*Diethylzinc.*—A commercial reagent (Sankyo Yuki Co.) was distilled at 50°C/64 mmHg.

*Titanium Tetrachloride.*—A commercial reagent (Kishida Chem. Co.) was distilled at 136—137°C.

*n-Hexane.*—Commercial-grade *n*-hexane (Phillips Petroleum Co.) was refluxed on sodium wire, distilled, and stored over a molecular sieve.

*Ethylene.*—Commercial high-purity ethylene (Nihon Sekiyu Co.) was used after having been dried with a molecular sieve.

*Analysis.*—Elemental analysis was done according to the standard methods as follows: aluminum, gravimetric oxine method; zinc, titration method using ethylenediamine tetraacetic acid; carbon and hydrogen, microcombustion method. The determination of the alkyl group or hydrogen bound to aluminum or zinc was accomplished by the hydrolysis and the volumetric measurement of the alkane and hydrogen evolved. The above gaseous hydrolysis products were analyzed by gas chromatography at room temperature using a column 5 m. long×4.5 mm. diameter packed with alumina containing 25% acetonylacetone (for hydrogen) and with "C-22" (Shimadzu Seisakusyo) containing 25% liquid paraffin (for hydrocarbons). Furthermore, the trace of diethylaluminum hydride in triethylaluminum was analyzed qualitatively by means of the infrared spectrum and the isoquinoline test. Diethylaluminum hydride shows a deep infrared absorption at about 5.7 $\mu$[2] and forms a deep red complex with isoquinoline.[3] For the measurement of the infrared spectrum, a Perkin-Elmer model 137 was used.

1) M. Roha, U. C. Kreider, M. R. Frederic and W. L. Beears, *J. Poly. Sci.*, **38**, 51 (1959).

2) G. Schomberg and E. C. Hoffman, *Z. Elektrochem.*, 61, 1110 (1957).

3) F. Bonitz, *Chem. Ber.*, **88**, 742 (1955).

**The Preparation of Hydride-free Triethylaluminum.**—Crude triethylaluminum (45 cc.) and 100 cc. of *n*-hexane were introduced, under a nitrogen atmosphere, into a 200 cc. flask equipped with a dropping funnel, a stirring bar, and a gas outlet connected to a nitrogen surge tube. The flask was set in a bath kept at −30°C using dry ice - *n*-hexane. Diethylzinc (5 cc.) dissolved in 100 cc. of *n*-hexane was dropped into the stirred solution of crude triethylaluminum. A white precipitate was thus formed. After the dropping was completed, the temperature of the flask was gradually raised to room temperature. The white precipitate then turned dark gradually. At about 20°C the precipitate instantaneously turned black. The supernatant colorless liquid was distilled under reduced pressure. A main fraction (a colorless liquid), distilled at 64—66°C/6 mmHg, was analyzed as follows: Found: Al, 23.56; C, 63.27; H, 13.21; Zn, 0.00; Calcd. for $Al(C_2H_5)_3$: Al, 23.63; C, 63.12; H, 13.24%. The results of the determination of the hydride by means of the infrared spectrum, the isoquinoline test and hydrolysis are shown in Table I.

Table I. The analysis of triethylaluminum

| $AlEt_3$ | | | Crude | Purified |
|---|---|---|---|---|
| Infrared spectrum (5.7 $\mu$) | | | + | − |
| Isoquinoline test | | | + | − |
| Hydrolysis | Gas evolved | mol./mol. $AlEt_3$ | 2.98 | 2.98 |
| | Ethane | vol. % | 93.16 | 98.44 |
| | Ethylene | vol. % | 0.33 | 0.00 |
| | *n*-Butane | vol. % | 3.14 | 1.56 |
| | Hydrogen | vol. % | 3.37 | 0.00 |

**The Reaction of Crude Triethylaluminum with Diethylzinc.**—Crude triethylaluminum (9.2 g., 0.081 mol.) was introduced under a nitrogen atmosphere into a 50 cc. test tube equipped with a magnetic stirrer, a gas outlet connected to a gas burette, and a dropping funnel. The test tube was then set in an oil bath kept at 60°C. To the stirred crude triethylaluminum, 10.0 g. (0.088 mol.) of diethylzinc was added from the dropping funnel over a 10 min. period, after which stirring was continued for a further 20 min. The reaction thus proceeded, separating a black metallic powder, and 6.2 mmol. of gas was evolved during the reaction. The composition of the gaseous products, as determined by gas chromatographic analysis, is shown in Table II.

Table II. The composition of the gaseous products evolved during the reaction between crude $AlEt_3$ and $ZnEt_2$

| Component | Vol. % |
|---|---|
| Hydrogen | 70.0 |
| Ethane | 29.1 |
| *n*-Butane | trace |

When the black precipitate was filtered, washed with dried *n*-hexane, and dried, 0.46 g. of a matallic solid was obtained. It was 97.37% zinc and 0.24% aluminum, and so it seems to be almost pure zinc metal. (Zn, 6.85 m atom).

To the filtrate a few drops of diethylzinc were then added. No further change was observed. On the other hand, when a few drops of crude triethylaluminum were added to the filtrate, a black precipitate separated again.

**The Treatment of Crude Triethylaluminum with Ethylene.**—A solution of 10 g. (0.088 mol.) of triethylaluminum in 50 cc. of dry *n*-hexane was treated with ethylene at 40—60 kg./cm² at 90°C for 18.5 hr. in an autoclave. Ethylene (0.56 mol.) was absorbed smoothly. *n*-Hexane was then stripped from the resultant to obtain 25.7 g. of a colorless liquid. The average chain length (carbon number) was calculated as 6.3 on the assumption that all the ethylene absorbed was consumed in the "Aufbau Reaktion." The reaction product was hydrolyzed as usual. The composition of the evolved gas was analyzed by gas chromatography. Table III shows the composition of the evolved gas.

Table III. The composition of the gas evolved upon hydrolysis

| Component | Composition vol. % |
|---|---|
| Ethane | 11.3 |
| *n*-Butane | 86.7 |
| Hydrogen | 2.0 |
| (Total gas | 1.73 mmol./g.-Product) |

Table IV. The distribution of the groups bound to aluminum

| Group | Composition mol. % |
|---|---|
| Ethyl | 1.9 |
| *n*-Butyl | 14.6 |
| Hydride | 0.3 |
| Longer alkyls | 83.2* |

* Calculated as 100 minus the sum of the percentages of the above groups.

Table V. The reaction of trialkylaluminum with titanium tetrachloride

| Run No. | $AlR_3$ | Ethylene* treatment | Reaction |
|---|---|---|---|
| 1 | Crude $AlEt_3$ | − | A dark brown precipitate was formed instantaneously |
| 2 | Crude $AlEt_3$ | + | A dark brown precipitata was formed instantaneously |
| 3 | Pure $AlEt_3$ | − | A dark brown precipitata was formed instantaneously |
| 4 | Pure $AlEt_3$ | + | A dark brown precipitate was formed instantaneously |
| 5 | $AlEt_3$ treated with ethylene at a high pressure | − | Clear yellow solution (slightly orange-colored) |
| 6 | $AlEt_3$ treated with ethylene at a high pressure | + | Clear yellow solution |

* Ethylene was passed into the $AlR_3$ benzene solution at atmospheric pressure and at room temperature for 30 min.

The distribution of the groups bound to aluminum is shown in Table IV.

**The Reaction of Various Trialkylaluminum Species with Titanium Tetrachloride.**—To trialkylaluminum (0.274 g.) dissolved in 200 cc. of dry benzene in a 300 cc. conical flask, titanium tetrachloride (3 cc.) in benzene (1 mmol./cc.) was added drop by drop at room temperature.

The same procedure was then repeated using a benzene solution of trialkylaluminums which had been treated with ethylene bubbled in at atmospheric pressure and at room temperature for 30 min.

The results of the reactions are shown in Table V.

## Discussion

**The Preparation of Hydride-free Triethylaluminum.**—Triethylaluminum free from hydride can be prepared by treating triethylaluminum containing the hydride with diethylzinc. It is postulated that the reaction proceeds according to the following equations:

$$Et_2AlH + Et_2Zn \longrightarrow Et_3Al + EtZnH \quad (1)$$

$$Et_2AlH + EtZnH \longrightarrow Et_3Al + ZnH_2 \quad (2)$$

$$2EtZnH \longrightarrow Et_2Zn + ZnH_2 \quad (3)$$

$$EtZnH \longrightarrow Zn + EtH \quad (4)$$

$$ZnH_2 \longrightarrow Zn + H_2 \quad (5)$$

Equations 4 and 5 are supported by the fact that the reaction gives metallic zinc and a nearly equimolar quantity of a gas consisting mainly of hydrogen and ethane.

The gas evolved during the reaction contained 70 mol. % of hydrogen. However, it is uncertain that the second-step alkylation shown in Eq. 2 can proceed. The disproportionation of ethylzinc hydride as shown in Eq. 3 should also be considered.

Assuming that the reactions of 1—5 proceeded quantitatively, the hydride-group content in the groups bound to the aluminum of crude triethylaluminum was calculated to be 4.3%. This value nearly coincided with the analytical value of 3.4% (Table I).

**The Reaction of Ziegler-catalyst Components.**—In order to clarify the mechanism of Ziegler catalysis, many investigations concerning the reaction of the catalyst components, e. g., triethylaluminum and titanium tetrachloride, have been reported. All the authors agree that titanium tetrachloride is alkylated by triethylaluminum and that then the alkyl-titanium bond is decomposed to yield titanium species of lower valency states. Although some catalysts which are comprised only quadrivalent titanium species have been proposed,[2] the reduction of titanium in the case of a Ziegler catalyst consisting of triethylaluminum and titanium tetrachloride is noticeable as a reaction important to an analysis of the catalytic mechanism. However, the mechanism of the reduction of titanium tetrachloride has not yet been clarified in detail.

Roha et al.[1] found that the triethylaluminum treated with ethylene at a high pressure and temperature does not reduce titanium tetrachloride; they therefore proposed that the reduction of titanium tetrachloride is due to the effect of the diethylaluminum hydride present as an impurity in triethylaluminum, which hydride has a stronger reducing ability.

Sinn et al.[4] proposed that the presence of a small quantity of water is necessary for Ziegler catalysis.

In fact, it is important to notice the effects of the components present in small quantities in the catalyst system.

In order to study the role of the impurities present in trialkylaluminum, we studied the reactions between titanium tetrachloride and various trialkylaluminums, namely, commercial crude triethylaluminum which contained a small quantity of the hydride (diethylaluminum hydride), purified triethylaluminum free from hydride, and trialkylaluminum which had been obtained by the treatment of commercial triethylaluminum with ethylene at a high pressure and temperature.

The experimental results showed that even when the purified triethylaluminum was used, the instantaneous reduction of titanium tetrachloride occured, just as in the case of crude triethylaluminum containing diethylaluminum hydride.

On the other hand, trialkylaluminum with longer alkyl chains, which had been obtained by treating crude triethylaluminum with ethylene at a high pressure and temperature, could not reduce titanium tetrachloride to the lower valency states; rather, a clear yellowish-orange solution was obtained.

The fact that the triethylaluminum treated with ethylene at a high pressure and temperature, even though with a detectable amount of an aluminum-hydrogen bond, did not reduce titanium tetrachloride might be explained in terms of the steric hindrance of its long alkyl groups.

We might also conclude that the reduction of titanium tetrachloride with triethylaluminum is not caused only by the hydride present in it as an impurity.

## Summary

Hydride-free triethylaluminum has been prepared by destroying diethylaluminum hydride by reaction with diethylzinc.

4) Hj. Sinn, H. Winter and W. v. Tirpitz, *Makromol. Chem.*, **48**, 59 (1961).

The reaction of hydride-free triethylaluminum and titanium tetrachloride in benzene shows the instantaneous reduction of titanium tetrachloride. It has been concluded that the reduction of titanium tetrachloride is not caused only by the presence of diethylaluminum hydride as an impurity in triethylaluminum, as has been proposed by Roha. Triethylaluminum treated with ethylene at a high pressure does not reduce titanium tetrachloride under ordinary conditions, even though it contains appreciable amounts of the hydride.

On the basis of the above facts, the reaction of Ziegler-catalyst component has been discussed.

*Polymerization Research Laboratory*
*Asahi Chemical Ind. Co., Ltd.*
*Nobeoka, Miyazaki*

# The Interaction of Cumulene Systems with Organometallic $\pi$-Complexes. III.[1] Iron Carbonyl Complexes of Hexapentaene and of Tetra- and Dimethylbutatriene*

By Akira NAKAMURA**

(Received February 16, 1965)

The stabilization of unstable organic compounds by the formation of organometallic $\pi$-complexes has provided a base for the occurrence of such unstable reaction intermediate species as cyclobutadiene.[2] We have reported the formation of a very stable tetraphenylcyclobutadiene complex of cobalt by the reaction of diphenylacetylene with some organocobalt compounds. In continuation of our study of the stabilization of unstable organic compounds by $\pi$-complex formation, we have found that the unsubstituted butatriene, a very unstable compound, can be stabilized by the formation of a stable iron carbonyl complex, $C_4H_4Fe_2(CO)_5$.[3] A brief communication describing the preparation of a tetraphenylbutatriene complex of iron carbonyl has also been published.[4] Unsubstituted hexapentaene, one of the unknown higher homologues of the butatriene, seems to be much more unstable than the unsubstituted butatriene. The successful isolation of the butatriene iron carbonyl complex led us to investigate the corresponding iron carbonyl complexes of the hexapentaene. We also investigated the preparation of alkyl derivatives of the butatriene complexes in order to get a better understanding of their structures and bonding by a study of their electronic, vibrational and NMR spectra.

**Hexapentaene Complexes.**—By an extension of the method of the preparation of the unsubstituted butatriene complex, which involves the dehalogenation of dihalobutyne, an analogous dehalogenation of dihalohexadiyne with zinc powder in the presence of tri-iron dodecacarbonyl was attempted:

$$\underset{\displaystyle X \quad X}{H_2C\text{-}C{\equiv}C\text{-}CH_2} + Fe_3(CO)_{12} + Zn \rightarrow (H_2C{=}C{=}C{=}CH_2)Fe_2(CO)_5$$

$$\underset{\displaystyle X \qquad X}{H_2C\text{-}C{\equiv}C\text{-}C{\equiv}C\text{-}CH_2} + Fe_3(CO)_{12} + Zn \rightarrow (H_2C{=}C{=}C{=}C{=}C{=}CH_2)Fe_3(CO)_{7-8}$$

Thus, 1,6-dichlorohexadiyne was treated with an excess of zinc powder and tri-iron dodecacarbonyl in refluxing benzene. A vigorous gas evolution was observed during the reaction. From the reaction mixture, the product was purified by chromatography, followed by crystallization, to give deep purple-red crystals. The main difficulty in obtaining the product was its exceedingly small yield (1.2%) and the separation from the remaining tri-iron dodecacarbonyl. The product I was found to have the composition: $C_6H_4Fe_3(CO)_{7-8}$.

* Presented at the Symposium on Organometallic Compounds, Osaka, November, 1964.

** Present address: Faculty of Engineering Science, Osaka University, Toyonaka, Osaka.

1) For previous paper of this series, A. Nakamura, P.-J. Kim and N. Hagihara, *J. Organometal. Chem.*, 3, (1965) in press.

2) For review article, see, E. O. Fischer and H. Werner, *Angew. Chem.*, 75, 64 (1963). For the cyclobutadiene-cobalt complex, see, A. Nakamura and N. Hagihara, *J. Chem. Soc. Japan, Pure Chem. Sec.* (*Nippon Kagaku Zasshi*), 84, 339 (1963); This Bulletin, 34, 452 (1961).

3) A. Nakamura, P.-J. Kim and N. Hagihara, *J. Organometal. Chem.*, 3, 7 (1965).

4) A. Nakamura, P.-J. Kim and N. Hagihara, This Bulletin, 37, 292 (1964).

The number of carbonyl groups in the complex is rather ambiguous considering the accuracy of the elemental analysis. Moreover, the molecular weight of I is not very accurate as a result of its slight solubility in many organic solvents. The infrared spectrum of I was found to have very strong carbonyl bands at 2088, 2065, 2045 and 2005 $cm^{-1}$, thus indicating some similarity with that of the corresponding butatriene complex. The electronic spectrum of I had its maximum at 567 m$\mu$. The position of this maximum is, significantly, at a longer wavelength than that of the butatriene complex. The NMR spectrum was very similar to that of the butatriene complex in that it showed two signals at 5.20 and 5.71 $\tau$, although the very low solubility of I prevented the obtaining of a well-resolved spectrum. Therefore, no splitting of the signals were observed.

The most interesting property of I is its thermal and air stability. For example, it is stable up to 250°C in nitrogen, stable in air as crystals, and also stable as a solution in carbon tetrachloride. Since unsubstituted butatriene has been reported[5] to be stable only at very low temperatures in nitrogen, unsubstituted hexapentaene, if prepared, will probably be much more unstable than the butatriene. Hence, the preparation of unsubstituted hexapentaene has not been reported to date and a comparison of the stability of the free and the complexed hexapentaene is impossible. However, the stabilization of the hexapentaene by means of the $\pi$-complex formation is apparent; it is another example of such stabilization.

In order to furnish further evidence for the presence of a hexapentaene system in the complex, tetraphenylhexapentaene was reacted with iron pentacarbonyl and with tri-iron dodecacarbonyl. A very deep brown solid II was obtained; it was stable in air. However, it was very difficult to obtain the product in a crystalline state, and attempts to purify it by chromatography on activated or deactivated alumina resulted in decomposition in the column. The infrared spectrum of II showed a similarity with that of I in the absorption pattern of the terminal metal carbonyl-stretching region (maxima at 2071, 2036, 2009 and 2001 $cm^{-1}$). The absence of an uncomplexed tetraphenylhexapentaene system in the product was shown by the absence of any maxima in the visible region. The structures of these hexapentaene complexes are difficult to infer, but they are probably similar to those of the butatriene complexes described below. Attempts to prepare analogous hexapentaene complexes of cobalt and chromium have all failed. Now, however, it may be said with considerable certainty that the interaction of cumulene systems with iron carbonyls is great enough to give stable $\pi$-complexes generally.

**1, 1, 4, 4-Tetramethyl- and 1, 4-Dimethylbutatriene Iron Carbonyl Complexes.**—Unsubstituted butatriene and tetraphenylbutatriene complexes of iron carbonyl have already been prepared and described in detail in a previous paper of this series.[3] We have here attempted to prepare methyl-substituted analogues by the application of the dehalogenation method to methyl-substituted dihalobutynes. The preparation of the methyl analogues will allow us to compare the electronic and vibrational spectra of the complexes and will give us very interesting NMR spectra, which might in turn lead to the determination of the correct structure of the complexes. 2, 5-Dichlorohexyne-3 (1, 4-dimethyl-1, 4-dichlorobutyne-2) was reacted with an excess of zinc powder in the presence of tri-iron dodecacarbonyl in just the same way as in the preparation of butatriene di-iron pentacarbonyl (III). A reddish-orange, air-stable crystalline compound IV was obtained in a 4.1% yield (based on the iron carbonyl used). It was very similar to the butatriene complex III in appearance, solubility, volatility and stability. The close similarity to III in its infrared metal carbonyl-stretching absorption pattern and also in its electronic spectrum, together with the elemental analysis and molecular weight data, showed it to be a dimethyl derivative of III.

$$\begin{matrix} R_1 \\ R_2 \end{matrix}\!\!>\!C(X)\!-\!C\equiv C\!-\!C(X)\!<\!\!\begin{matrix} R_1 \\ R_2 \end{matrix} + Zn + Fe_3(CO)_{12} \rightarrow$$

$$\left(\begin{matrix} R_1 \\ R_2 \end{matrix}\!\!>\!C=C=C=C<\!\!\begin{matrix} R_1 \\ R_2 \end{matrix}\right)Fe_2(CO)_5$$

III: $R_1=R_2=H$, X=Br
IV: $R_1=H$, $R_2=CH_3$, X=Cl
V: $R_1=R_2=CH_3$, X=Cl

2, 5-Dichloro-2, 5-dimethylhexyne-3 (1, 1, 4, 4-tetramethyl-1, 4-dichlorobutyne-2) was used to prepare an analogous tetramethyl derivative in the same way. The reddish-orange, air-stable compound V obtained in this way, in a 4.4% yield, was also very similar to III and IV in many ways. Apart from the similarity in the infrared and electronic spectra of these compounds, their NMR spectra provided the confirmation of IV and V as, respectively, di- and tetramethyl derivatives of III.

## Discussion

The method of preparation, the yield and various physical constants of the cumulene

5) W. M. Schubert, T. H. Liddicoet and W. A. Lanka, *J. Am. Chem. Soc.*, **76**, 1929 (1954).

TABLE I

| | $\left(\begin{matrix}H\\H\end{matrix}\right)C=C=C=C\left(\begin{matrix}H\\H\end{matrix}\right)Fe_2(CO)_5$ (III) | $\left(\begin{matrix}CH_3\\H\end{matrix}\right)C=C=C=C\left(\begin{matrix}CH_3\\H\end{matrix}\right)Fe_2(CO)_5$ (IV) |
|---|---|---|
| Method of preparation | Dehalogenation | Dehalogenation |
| Color | Red-orange | Red-orange |
| Yield, % | 16.7 | 4.1 |
| M. p. °C | 69—70 (air) | 104 (air) |
| Decomposition (°C) | 230 (air) | 240—250 ($N_2$) |
| Sublimation temp., °C/mmHg | 40—50/3 | 80/3 |
| Infrared, $\nu C\equiv O$, $cm^{-1}$ | 2090<br>2052<br>2022/1995<br>1963 | 2088<br>2051<br>2020<br>1958 |
| Visible and ultraviolet, $m\mu$, (log $\varepsilon$)*1 | 448 (3.356)<br>346 (3.734)<br>286 sh | 452 (3.303)<br>342 (3.728)<br>298 (3.83) |
| NMR, $\tau$ | 5.22 (d)*2 1*3<br>5.85 (d) 1 | 8.17 (d) 3<br>4.42 (q) 1 |
| Coupling constant | $J$=1.5 c. p. s. | $J$=6.0 c. p. s. |

| | $\left(\begin{matrix}CH_3\\CH_3\end{matrix}\right)C=C=C=C\left(\begin{matrix}CH_3\\CH_3\end{matrix}\right)Fe_2(CO)_5$ (V) | $\left(\begin{matrix}Ph\\Ph\end{matrix}\right)C=C=C=C\left(\begin{matrix}Ph\\Ph\end{matrix}\right)Fe_2(CO)_5$ (VI) |
|---|---|---|
| Method of preparation | Dehalogenation | Direct reaction |
| Color | Red-orange | Red |
| Yield, % | 4.4 | 26 |
| M. p. °C | 118 ($N_2$) | Decomp. |
| Decomposition (°C) | 240—250 ($N_2$) | 200 (air) |
| Sublimation temp., °C/mmHg | 90—100/3 | 180/3 (decomp.) |
| Infrared, $\nu C\equiv O$, $cm^{-1}$ | 2087<br>2039<br>2010<br>1953 | 2072<br>2035<br>1998<br>1988 |
| Visible and ultraviolet, $m\mu$, (log $\varepsilon$)*1 | 470 (3.299)<br>340 sh<br>299 (3.86) | No maximum |
| NMR, $\tau$ | 7.81 (s) 1<br>7.98 (s) 1 | — |
| Coupling constant | — | — |

*1 Measured in ethanol *2 s : singlet, d : doublet, q : quartet. *3 ratio of area

complexes prepared by us are listed in Table I. The successful preparation of the di- and tetramethyl derivatives of III showed that the preparation of such derivatives is possible by the same dehalogenation route and that the alkyl derivatives have a stability similar to that of the unsubstituted compound III. The preparation of the tetraphenyl derivative VI, as has been reported previously, also shows that the tetra-aryl derivatives will be similarly stable and can be prepared by the direct route in good yields.

A comparison of the infrared spectra of butatriene complexes, III—VI, also seems of interest. A small but significant lowering of the metal carbonyl-stretching frequency in the III to VI series is apparent. This lowering is obviously caused by the introduction of the substituents into the butatriene system. A lowering of the metal carbonyl-stretching frequency has been attributed to the increase in electron density around the metal atom,[6] because such an increase results in the enhanced contribution of the resonance species of M=C=O, as is shown below:

$$\left[L\text{-}\overset{(-)}{M}\text{-}C\equiv\overset{(+)}{O} \longleftrightarrow L\text{-}M=C=O\right]$$

It is conceivable that, in the case of the substituted butatriene complexes, electron-donating methyl groups on the butatriene part push the electron to the iron atom through the butatriene part and cause the lowering of the metal carbonyl-stretching frequency. Phenyl groups are known to have an electron-attracting inductive effect, but they are also known to have an electron-releasing resonance polar effect. The tetraphenylbutatriene complex VI has the lowest metal carbonyl-stretching

6) R. D. Fischer, *Chem. Ber.*, **93**, 165 (1960); E. O. Fischer and H. Werner, *Angew. Chem.*, **75**, 60 (1963).

frequency among the butatriene complexes prepared heretofore. Therefore, the electron-releasing resonance polar effect may be operating here. The complexes, III—VI, resemble each other in metal carbonyl-stretching pattern so closely that only difference in the frequency distinguish them.

The electronic spectra of the butatriene compounds are also very similar. Here again, only small differences in the position of the absorption maxima are observed. The longest wavelength maxima of these complexes shift towards even longer wavelengths upon the successive introduction of methyl groups. The introduction of two methyl groups shifts the maximum by 4 m$\mu$, and that of four methyl groups, by 22 m$\mu$. This shifts reminds us of the mell-known Woodward rule,[7] which states that the introduction of one methyl group into the conjugated diene system results in a shift of 5 m$\mu$ in the K-band.

The NMR spectrum of III has already been discussed in the previous paper. No definite conlusion concerning the structure of III was there obtained, however. The spectrum indicated that two kinds of protons are present and that the coupling constant of the two protons is small (ca. 1.5 c. p. s.). As expected, two kinds of methyl signals were observed in the NMR spectrum of the tetramethyl derivative V. The difference in the chemical shift (0.17 p. p. m.) between the methyl signals is significantly smaller than that between the two proton signals of III (0.63 p. p. m.). In the NMR spectrum of the corresponding dimethyl derivative IV, only one methyl signal is observed; it is split into a doublet by an adjacent olefinic proton. The olefinic proton signal is split into a symmetrical quartet (ratio of areas: 1 : 3 : 3 : 1) by the adjacent methyl group. The coupling constant between these methyl and olefinic protons was, as expected, found to be 6.0 c. p. s. These results show that the two methyl groups are equivalent, and so are the two olefinic protons.

From an examination of the NMR spectra of these three compounds, III—V, the following conclusions can be drawn:

i) The Ha and Hb protons (also Hc and Hd) are not equivalent.

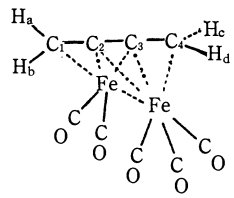
$$\left(\begin{matrix}Ha\\Hb\end{matrix}\right)C=C=C=C\left(\begin{matrix}Hc\\Hd\end{matrix}\right)Fe_2(CO)_5$$

(III)

ii) The splitting observed in the spectrum of III probably arises from the geminal coupling between Ha and Hb.

iii) No appreciable long-range coupling is observed between the terminal protons of III.

A planar structure of the butatriene part and a symmetrical attachment of the iron carbonyl groups do not easily explain the difference between Ha and Hb. A twisted structure, as shown below, explains the observed NMR spectrum more easily than the other possible




structures. In the twisted structure, the two terminal protons are not equivalent because of the unsymmetrical attachment of the two iron carbonyl groups, $Fe(CO)_3$ and $Fe(CO)_2$. However, a repeated intramolecular transfer of one of the CO groups from the iron tricarbonyl group to the iron dicarbonyl group would make the two terminal protons equivalent. The Ha and Hb protons are made non-equivalent by the attachment of the iron carbonyl group on one side of the plane defined by Hc–$C_4$–Hd. Therefore, Hb and Hd may be expected to be nearer to the iron carbonyl groups than Ha and Hc. The difference in the environment will make the protons, Ha and Hb, non-equivalent. For the tetramethyl compound V, the situation is quite similar, and two methyl signals are observed. In the dimethyl compound IV, the two methyl groups probably occupy the positions of Ha and Hc because of the bulkiness of the methyl group, and they remain equivalent.

The NMR results obtained so far can be explained, as above, on the assumption of a straight C4 chain, but there is no clear indication of the straightness of the C4 chain. Actually, it might well be a bent structure. The NMR results are not very sensitive to such a deformation, and, unfortunately, they do not definitely establish the correct structure for the butatriene complexes. Therefore, an X-ray structure analysis of these complexes is necessary in order to establish the correct structure.*

## Experimental

All melting points are uncorrected; they were measured by a micro-melting point apparatus, Yanagimoto Model MP-S2. The melting points and decomposition points in nitrogen were measured in a sealed capillary filled with nitrogen. The infrared spectra were obtained by Hitachi Model EPI-2

7) R. B. Woodward, *J. Am. Chem. Soc.*, **64**, 72 (1942).

* A private communication from Professor O. S. Mills told us that he and his co-workers were carrying out an X-ray analysis of the tetraphenyl butatriene iron carbonyl complex.

and Jasco Model DS-402G grating spectrophotometers. The visible and ultraviolet spectra were taken by a Beckman DK-2 spectrophotometer. The NMR spectra were recorded by a Varian Model A-60 instrument using tetramethylsilane as an internal standard in carbon tetrachloride. The alumina used for the chromatography had an activity grade of I and was of a 200—300 mesh size. The elemental analysis was performed by Mr. T. Shibano of this Institute. The elemental analysis for oxygen was performed by Mr. I. Shimidzu of the Japan Synthetic Rubber Company. The molecular weights were measured in a benzene solution using a Mechrolab Vapor Pressure Osmometer Model 301A.

**Materials.**—Dichloro- and dibromohexadiyne-2, 4,[8] 2, 5-dichlorohexyne-3,[9] 2, 5-dimethyl-2, 5-dichlorohexyne-3,[10] tetraphenylhexapentaene,[11] butatriene di-iron pentacarbonyl[3] and tetraphenylbutatriene di-iron pentacarbonyl[3] were prepared in manners described in the literature.

**The Preparation of the Hexapentaene Iron Carbonyl Complex (I).**—A mixture of 3.0 g. of freshly prepared and distilled dichlorohexadiyne-2, 4, 4.2 g. of tri-iron dodecacarbonyl, 5.0 g. of zinc powder in 25 ml. of isooctane and 20 ml. of benzene was heated, with vigorous magnetic stirring, under nitrogen for 4 hr. at 80—90°C. During the reaction period, a total of about 1250 ml. of a gas evolved. The deep green solution was then filtered by gravity in air, and the brown precipitates were washed well with benzene. The evaporation of the filtrate and the wash gave almost black crystalline solids, which were then dissolved again in benzene and purified by chromatography on alumina. Elution with benzene gave a deep purple-red eluate. (A considerable decomposition of the product was observed when the elution was carried out with *n*-hexane.) The evaporation of the eluate gave almost black crystals (0.1 g.), which were purified further by crystallization from benzene (5 ml.) to give deep purple-red crystals (45 mg.) (I). The insoluble part in benzene consists mainly of tri-iron dodecacarbonyl

Found: C, 35.73; H, 1.19; O, 30.05±3%; mol. wt., 500—700. Calcd. for $C_{14}H_4Fe_3O_8$: C, 35.94; H, 0.87; O, 27.36%; mol. wt. 467.6.

**The Preparation of the Tetraphenylhexapentaene Iron Carbonyl Complex (II).**—Tetraphenylhexapentaene was reacted with an excess of iron pentacarbonyl in *p*-xylene for 3.5 hr. under nitrogen. The color turned deep brown upon heating at 140°C. The reaction mixture was then evaporated under reduced pressure to give a deep-reddish-brown semisolid (II), m. p. (decomp.) ca. 220°C in air. This semisolid did not crystallize from the solution in benzene or in a *n*-hexane-benzene mixture. A similar reaction using tri-iron dodecacarbonyl in benzene at 90°C for 3 hr. gave similar results.

**Tetramethylbutatriene Di-iron Pentacarbonyl (V).**—A mixture of 1.2 g. of freshly distilled 2, 5-dimethyl-2, 5-dichlorohexyne-3, 2.2 g. of tri-iron dodecacarbonyl and 3.0 g. of zinc powder in 20 ml. of dry isooctane was stirred magnetically under nitrogen and heated at 90—100°C on a water bath. During the 3 hr. of the reaction, the evolution of a gas continued. After 150 ml. of the gas had evolved, however, the evolution almost stopped. The brownish suspension was filtered by gravity in air, and the precipitates were washed with a small amount of benzene. The deep brown filtrate was then evaporated under reduced pressure at room temperature to give a deep brown semisolid.

The semisolid was then dissolved in a small amount of *n*-hexane and chromatographed on alumina. Elution with *n*-hexane gave a deep red eluate, which in turn gave a red viscous oil upon evaporation under reduced pressure. Most of the oil crystallized when the mixture was chilled to −20°C in a refrigerator overnight. The red crystals (52 mg.) (V) were collected on a clay plate and washed well with a small amount of *n*-hexane. The crystals were purified further by sublimation at 80°C/3 mmHg to afford an analytical sample. A further crop (12 mg.) of the crystals could be obtained from the oily part of the eluate through fractional sublimation and through drying on a clay plate.

Found: C, 43.56; H, 3.35; mol. wt., 357. Calcd. for $C_{13}H_{12}Fe_2O_5$: C, 43.38; H, 3.36%; mol. wt., 360.

**Dimethylbutatriene Di-iron Pentacarbonyl (IV).**—The title compound IV was obtained by essentially the same method as that described for the tetramethyl compound V, using 0.9 g. of 2, 5-dichlorohexyne-3, 2.0 g. of tri-iron dodecacarbonyl and 3.0 g. of zinc powder in 20 ml. of isooctane. The analytical sample (31 ml.) was obtained from 38 mg. of the crude product by sublimation. A further crop (16 mg.) was obtainable by working up the oily part in the manner described above for V.

Found: C, 40.22; H, 2.33; O, 23.04; mol. wt., 360. Calcd. for $C_{11}H_8Fe_2O_5$: C, 39.85; H, 2.43; O, 24.10%; mol. wt., 332.

## Summary

The reaction of 1, 6-dihalohexadiyne-2, 4 with tri-iron dodecacarbonyl in the presence of an excess of zinc powder have given a hexapentaene iron carbonyl complex, $C_6H_4Fe_3(CO)_{7-8}$, as deep purple-red, air-stable crystals in a 1.2% yield. Essentially the same reaction using methyl-substituted 1, 4-dichlorobutyne-2 have given substituted butatriene iron carbonyl complexes, $(R_1R_2C{=}C{=}C{=}CR_1R_2)Fe_2(CO)_5$, where $R_1{=}R_2{=}CH_3$ (V), $R_1{=}H$, and $R_2{=}CH_3$ (IV), in low yields. The vibrational, electronic and NMR spectra of these new complexes have been discussed in connection with their structures.

8) J. B. Armitage and M. C. Whiting, *J. Chem. Soc.*, **1952**, 2005.
9) C. L. Cook, E. R. H. Jones and M. C. Whiting, ibid., **1952**, 2883; R. Ya. Levina and Yu. S. Shabarov, *Doklady Acad. Nauk. SSSR.*, **84**, 709 (1952); *Chem. Abstr.*, **47**, 3219 (1953).
10) W. Reppe, *Ann.*, **596**, 25 (1955); A. I. Zhakharova and G. D. Ilina, *Zhur. Obshchei. Khim.*, **24**, 2144 (1954).
11) H. D. Hartzler, *J. Am. Chem. Soc.*, **83**, 4996 (1961).

The author wishes to express his appreciation to Professor Nobue Hagihara for his continued interest in and many helpful suggestions for this work. He also wishes to thank Mr. Haruo Masai for his experimental assistance and the Japan Synthetic Rubber Company for its oxygen analysis.

*The Institute of Scientific and Industrial Research*
*Osaka University*
*Sakai, Osaka*

# Studies on the Chemical Decomposition of Simple Sugars. XVI. Pyruvic Acid Formation from D-Glucose-1-$^{14}$C*

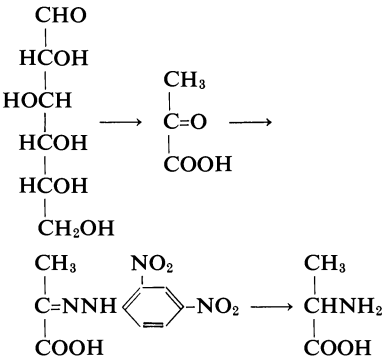
By Sinichi OTANI**

(Received February 20, 1965)

The fragmentation reaction of reducing sugars is well known in both acid and alkaline media,[1,2] but the mechanism of this reaction has not been satisfactorily elucidated. Especially, the formation of pyruvic acid has remained to be studied on account of its instability, its low yield, and the difficulty of isolating it. Nodzu et al.,[2,3] however, obtained pyruvic acid from a weakly alkaline and a weakly acid solution of glucose, and proposed a mechanism which included acetylformoin as a direct precursor of pyruvic acid. Recently, Hayami et al. effectively used the $^{14}$C-labeled sugars[4,5] and the methylated sugars[6] for the investigation of the mechanism of the acetol formation, and presented another mechanism in which they inferred the formation of pyruvic acid, though they had no experimental evidence.

The present purpose was to obtain pyruvic acid by the decomposition of D-glucose-1-$^{14}$C in a weakly acid phosphate solution, and to determine the relative distribution of a label in pyruvic acid in order to elucidate the mechanism of the pyruvic acid formation.

The present author obtained a mixture of pyruvic acid 2, 4-dinitrophenylhydrazone and other kinds of acid hydrazone or osazone; he then reduced them to amino acids, while the pyruvic acid 2, 4-dinitrophenylhydrazone was reduced to alanine.[7] The alanine was separated[8] and subjected to the degradation, by which means the relative distribution of a label in pyruvic acid was determined.



Scheme 1.

The alanine was decomposed with ninhydrin in nitrogen gas after some modification of the method of Virtanen et al.[9] The methyl part and the center carbon of the alanine were converted into acetaldehyde, and the carboxylic acid part was converted into carbon dioxide,

* The present work was presented at the Symposium on the Mechanism of Organic Chemical Reaction of the Chemical Society of Japan, Nagoya, October, 1964.

** Present address: Department of Liberal Arts and Science, Kyoto University, Kyoto.

1) H. J. Dakin and H. W. Duddley, *J. Biol. Chem.*, **15**, 127 (1913); J. U. Nef, *Ann.*, **357**, 214 (1907); **376**, 1 (1910); **403**, 204 (1914); W. L. Evans, *J. Org. Chem.*, **1**, 1 (1937); R. Nodzu, This Bulletin, **10**, 122 (1935); R. Nodzu and K. Matsui, ibid., **10**, 467 (1935); R. Nodzu and R. Goto, ibid., **11**, 381 (1936); R. Goto, ibid., **15**, 103 (1940); R. Nodzu and R. Goto, ibid., **15**, 209 (1940); R. Goto, *J. Chem. Soc. Japan (Nippon Kwagaku Kwaisi)*, **64**, 999, 1054, 1183 (1943); L. Sattler and F. W. Zerban, *J. Am. Chem. Soc.*, **70**, 1975 (1948); M. Gibbs, ibid., **72**, 3964 (1950); E. Waldmann and V. Prey, *Monatsh.*, **82**, 856 (1951); **83**, 65 (1952); V. Prey, E. Waldmann, H. Berbalk and F. Sommer, ibid., **85**, 1186 (1954); V. Prey, E. Waldmann, H. Berbalk and F. Ludwig, ibid., **84**, 551 (1953); R. Weidenhagen, *Zucker*, **12**, 244 (1959).

2) R. Nodzu, K. Matsui, R. Goto and S. Kunichika, *Mem. Coll. Sci. Kyoto Imp. Univ.*, **20**, 197 (1937).

3) R. Nodzu, *J. Biochem. Soc. Japan (Nippon Seikagaku Kaishi)*, **18**, 237 (1944).

4) R. Goto, J. Hayami, K. Kudo and S. Otani, This Bulletin, **34**, 753 (1961).

5) J. Hayami, ibid., **34**, 924 (1961).

6) J. Hayami, ibid., **34**, 927 (1961).

7) G. H. N. Towers, J. F. Thompson and F. C. Steward, *J. Am. Chem. Soc.*, **76**, 2392 (1954).

8) C. H. W. Hirs, S. Moore and W. H. Stein, *J. Biol. Chem.*, **192**, 669 (1951).

9) A. I. Virtanen, T. Laine and T. Toivonen, *Z. physiol. Chem.*, **266**, 193 (1940).

which was then caught in a sodium hydroxide solution and counted in the form of barium carbonate. Acetaldehyde was caught as an adduct of sodium bisulfite and converted into iodoform and formic acid. From the combustion of the iodoform, the radioactivity of the methyl carbon of the alanine was determined.

By the method mentioned above, the radioactivity of both terminal carbons of the alanine was determined, but it was impossible to determine of the center carbon directly. Therefore, the radioactivity of the center carbon was indirectly deduced from the results of the two terminal carbons and from that of the three carbon atoms of the alanine.

## Experimental

**Radioactive Sugars and Assay Method.** — D-Glucose-1-$^{14}$C was prepared from D-arabinose by a cyanohydrin synthesis.[10]

For an assay, all samples were converted into barium carbonate by the Van Slyke-Folch wet combustion method. Barium carbonate was collected on a filter paper and counted, mostly in an infinite thickness, with a $2\pi$-gas flow counter. In the case of the combustion of iodoform, the barium carbonate obtained was counted in a medium thickness and corrected for an infinite thickness.

**The Decomposition of D-Glucose-1-$^{14}$C.**—A solution of 20 g. of the labeled D-glucose in 200 ml. of a concentrated potassium acid phosphate buffer solution (40%, pH 6.6) was heated and distilled. Water was added drop by drop in order to maintain a constant volume. About 100 ml. of the distillate was collected every 45 min., and the distillation was continued for 9 hr.

**The Isolation of Crude Pyruvic Acid 2, 4-Dinitrophenylhydrazone.** — The distillation residue was made up to one and a half in volume by the addition of 6 N hydrochloric acid; the precipitate formed was then removed by filtration after having been kept overnight. To the filtrate was added 2 l. of a saturated solution of 2, 4-dinitrophenylhydrazine in 2 N hydrochloric acid, and the precipitate formed was collected and dried in a vacuum. About ten grams of the precipitate were extracted with about 20 l. of isopropyl ether. The ether solution was then extracted with an equal volume of a 6% aqueous solution of sodium bicarbonate. After the extract had been slightly acidified with 6 N hydrochloric acid, it was again extracted with about an equal volume of isopropyl ether. The ether solution was evaporated under reduced pressure to give a brown residue (1.2 g.). It was shown by paper chromatography (solvent; *n*-butanol - 0.1 N aqueous ammonium hydroxide - methanol 4 : 1 : 1 v/v) that the residue contained pyruvic acid 2, 4-dinitrophenylhydrazone in a considerably high concentration.

**The Reduction of the Crude Pyruvic Acid 2, 4-Dinitrophenylhydrazone to Alanine.**—2, 4-Dinitrophenylhydrazone (600 mg.) was suspended in water (ca. 40 ml.) and hydrogenated with Adams' catalyst, platinum dioxide (147 mg.) under the atmospheric pressure of hydrogen gas.

**The Isolation of the Crude Alanine.**— After the removal of the catalyst by filtration, the filtrate and washings (25 ml.) were passed through a column (1.6×18 cm.) of Dowex 50W-X8 in the H form (200—400 mesh). Hydrochloric acid (1.5 N) was used as the eluting solvent. The effluent, which was positive for a ninhydrin test,[11] was then concentrated and passed through a column of Amberlite IR-400 (acetate form) in order to remove the chloride anions, using 0.5 N acetic acid as the eluting solvent. The effluent was then collected, concentrated under reduced pressure, and dried to a yellow powder.

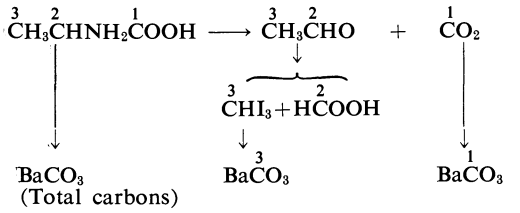
**The Purification of Alanine.**—This part was a modification of the method of Hirs, Moore and Stein.[8] An ammonium formate buffer solution (pH 3.7) was made by mixing 375 ml. of 2 N formic acid, 200 ml. of 1 N ammonium hydroxide, 400 ml. of ethanol and water to 1 l. Dowex 50W-X8 (200—400 mesh, 500 ml.) was placed in a column (3.5×55 cm.) with the aid of an ammonium formate buffer solution, which was used as an eluting solvent, and the crude alanine (ca. 50 mg.) was charged. The effluent was collected in about 10 ml. fractions with a flow-rate about 30 ml./hr. Aliquots (0.5 ml.) of the effluents were then analyzed by means of the ninhydrin test after the sublimation of ammonium formate. The fractions showing a positive reaction were collected and concentrated under reduced pressure. A yellow residue was obtained after the sublimation of ammonium formate. This residue was decolorized with active carbon and crystallized from a thick aqueous solution by adding anhydrous ethanol.

**The Degradation of Alanine.** — The procedure was carried out under a stream of nitrogen and under oxygen-free conditions. In a three-necked flask, 62.6 mg. of alanine, 168 g. of ammonium sulfate, and 11.5 g. of citric acid were dissolved in 150 ml. of water; the solution was then heated. After it had been boiled, 60 ml. of a 1% aqueous solution of ninhydrin was added drop by drop from a dropping funnel; the solution was then kept boiling for 90 min. The acetaldehyde formed was swept into 40 ml. of a 1% aqueous solution of sodium bisulfite passing through the Allihn condenser and caught in the form of an adduct. Carbon dioxide was introduced into 20 ml. of a 0.1 N sodium hydroxide solution, which was connected to the sodium bisulfite solution. The sodium bisulfite solution was treated with a 10% sodium hydroxide solution and a 10% iodine solution, and the iodoform formed was collected using a centrifugal separator, washed with water, and converted in a wet condition into barium carbonate by the Van Slyke-Folch wet combustion method. The carbon dioxide, caught in a sodium hydroxide solution, was treated with 360

10) H. S. Isbell, J. V. Karabinos, H. L. Frush, N. B. Holt, A. Schwebel and T. T. Galkowski, *J. Res. Natl. Bur. Std.*, **48**, 163 (1952).

11) E. W. Yemm and E. C. Cocking, *Analyst*, **80**, 209 (1955).

mg. of barium chloride; barium carbonate was thus obtained.




Scheme 2. Degradation process.

TABLE I. RADIOASSAY DATA

| Sample | Carbon atom(s) | Radioactivity c. p. m./mol. |
|---|---|---|
| D-Glucose-1-$^{14}$C | Total carbons | 562*2 |
| Pyruvic acid*1 | Total carbons | 162*2 |
| | $CH_3$ | 133*4 |
| | C=O | *5 |
| | COOH | 14*6 |

*1 Degraded in the form of alanine.
*2 Probable error was less than 1%.
*3 Probable error was less than 4%.
*4 Probable error was less than 2%.
*5 Not determined.
*6 Probable error was less than 15%.

## Results and Discussion

The results reported herein indicate that, in the case of D-glucose-1-$^{14}$C, the radioactivity is mostly found in the methyl carbon of the alanine. This means that the C-1 of the glucose was converted into the methyl carbon of the pyruvic acid.

In the case of the formation of acetol,[5-6] accompanied by pyruvic acid, the C-1 and C-6 of the original glucose were converted into the methyl carbon of the acetol, while the C-3 and C-4 of the original glucose were converted into the hydroxymethyl carbon of the acetol. In addition, the acetol-1-$^{14}$C, which was formed from D-glucose-3, 4$^{14}$-$C_2$, was found to preserve the molar radioactivity of the original glucose. This indicates that, in the formation of acetol, the C-1, 2, and 3 and the C-4, 5, and 6 of the original glucose behaved as units, and that no skeletal rearrangement in these $C_3$ units was involved. In the case of pentoses,[5] both terminal carbons were converted into the methyl carbon of the acetol. Hayami[6] has determined the mechanism of the formation of acetol on the basis of findings concerning labeled sugars and methylated sugars; he inferred that pyruvic acid should be formed by a similar mechanism. His inference consisted of two essential points, which he applied also to the case of the formation of acetol. One was $\beta$-hydroxy-carbonyl elimination, after the isomerization to 3-ketose or 4-ketose; the other was hydrolytic cleavage between the C-3 and C-4 of glucose. The present results support Hayami's inference.

From the common finding of these experiments with pyruvic acid and acetol, it may be deduced that the C-6 of glucose is converted into the methyl carbon of pyruvic acid, while the C-3 and C-4 are converted into the carbon of the carboxylic acid group of pyruvic acid.

From this point of view, comparing the molar radioactivity of the original D-glucose-1-$^{14}$C with that of the alanine found in the present study, the results show that the lower half of the glucose skeleton contributes more than the upper half to the formation of pyruvic acid.

Further experiments using other labeled sugars are, however, necessary to explain the mechanism of the formation of pyruvic acid.

The author wishes to express his thanks to Professor Ryozo Goto for his constant guidance and encouragement and to Dr. Jun'ichi Hayami for his kind suggestions throughout the course of this work. The author wishes also to thank Dr. Yo Miyagi for his assistance in synthesizing the labeled sugar.

*Institute of Chemistry*
*Faculty of Science*
*Kyoto University*
*Sakyo-ku, Kyoto*

# The Absorption Spectrum of the Cobalt(II) Ion Catalyst in the Reaction of Methanol with Carbon Monoxide and Hydrogen under a High Pressure

By Tsutomu MIZOROKI and Mikitake NAKAYAMA

(Received February 22, 1965)

The treatment of methanol with carbon monoxide or carbon monoxide - hydrogen mixtures under a high temperature and pressure results in the formation of acetic acid, acetaldehyde and ethanol, as in the following equations:

$$CH_3OH + CO = CH_3COOH + 33.0^{*1} \quad (1)$$

$$CH_3OH + CO + H_2 = CH_3CHO + H_2O + 24.6 \quad (2)$$

$$CH_3OH + CO + 2H_2 = C_2H_5OH + H_2O + 51.2 \quad (3)$$

In the acetic acid synthesis from methanol and carbon monoxide represented by Eq. 1, mixtures of the salts of transition metals (nickel, iron, cobalt etc.) and iodine or the iodides of these metals have been used as the catalyst,[1,2] and a mixture of cobalt(II) acetate and iodine had been reported as a catalyst of the homologation of methanol[3], as is represented by Eqs. 2 and 3. On the other hand, no works have been reported on reaction mechanisms with these catalysts, because the complex intermediates from these catalysts are too unstable to be isolated at room temperature and pressure.

The present authors investigated in detail these reaction, in the presence of a mixture of cobalt(II) acetate ($Co(AcO)_2 \cdot 4H_2O$*2) and with an iodide (lithium iodide, sodium iodide, potassium iodide, etc.) as the catalyst, by using an autoclave lined with Ti-Mn alloy. It was reported that the conversion of methanol into acetic acid or acetaldehyde increased with the amount of an iodide added and that ethanol was estimated to be formed from the hydrogenation of the acetaldehyde produced.[4,5] On the other hand, it is well known that the soluble salts of cobalt(II) ions form blue or green tetrahedral complex ions $[CoX_4]^{2-}$ ($X=Cl^-$, $Br^-$, $I^-$, $AcO^-$, $NCS^-$, etc.[6]) in organic solvents (glacial acetic acid, acetone, nitromethane, etc.). From these facts, it was assumed that, during the course of the reaction, most of cobalt(II) ions were surrounded with iodide ions, thus forming tetrahedral complex ions of the $[Co(AcO)_{4-n}I_n]^{2-}$ type ($n=1$—4), with which carbon monoxide was then activated.[7]

This work was undertaken in order to study the behavior of cobalt(II) ions and iodide ions in the course of the reaction of methanol with carbon monoxide and hydrogen by measuring the absorption spectra. For this purpose, a special autoclave, with which absorption spectra could be observed under a high temperature and pressure, was made of Ti-Mn alloy and a couple of thick pieces of quartz glass.

## Experimental

**The Apparatus for Taking an Electronic Absorption Spectrum under a High Temperature and Pressure.**—The special autoclave is illustrated in Fig. 1. A couple of thick quartz glass windows (15 mm. thick, 20 mm. in diameter) were set in teflon packings and pressed uniformly hard against the autoclave by high internal pressure introduced through a valve (1 in Fig. 1). These pieces of glass were proof against pressure lower than 250 kg./cm² at a temperature of 200°C. The inner volume of this autoclave was about 6 ml., and the thickness of a liquid sample was about 5.5 mm. The autoclave was heated by the electric furnace shown in Fig. 1. The temperature of the autoclave was kept constant (within ±0.5°C) by using an electronic thermo-controller (P. I. D. method), because the absorption spectrum of cobalt(II) ion was very dependent on the temperature. The autoclave was then placed with the electric furnace into the sample box of an automatic recording spectrophotometer (IV-50A type, Shimadzu Seisakusho Ltd.), and absorption spectra were recorded over the range from 340 to 1000 mμ.

**The Reaction Conditions.**—The reaction rate of the acetic acid synthesis by Eq. 1 was very slow at 200°C under pressure lower than 250 kg./cm². However, the reaction of the acetaldehyde synthesis

*1 $-\Delta H°$ (25°C) (kcal./mol.) obtained from the heats of combustion.

1) W. Reppe, *Ann. Chem.*, **582**, 72—83 (1953).

2) S. K. Bhattacharyya and S. Sourirajan, *J. Appl. Chem.*, **6**, 442 (1956); **9**, 126 (1959).

3) J. Berty and L. Marko, *Chem. Tech. (Berlin)*, **8**, 260 (1956).

*2 AcO=$CH_3COO$

4) T. Mizoroki, et al., *J. Chem. Soc. Japan, Ind. Chem. Sec. (Kogyo Kagaku Zasshi)*, **65**, 1049, 1054 (1962).

5) T. Mizoroki and M. Nakayama, This Bulletin, **37**, 236 (1964).

6) As for the literature, see Table I.

7) T. Mizoroki and M. Nakayama, *Catalyst (Shokubai)*, **5**, 203 (1963).

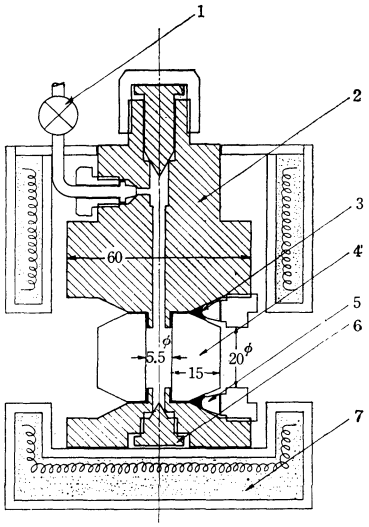



Fig. 1. A special autoclave with a couple of high pressure sight gasses.

1 A valve
2 Ti-Mn alloy
3 Teflon packing
4 Sight glass (Quartz)
5 Ti metal packing
6 Inlet of a liquid sample
7 Electric furnace

by Eq. 2 proceeded smoothly under the endurable condititons of the special autoclave, even if the amount of cobalt(II) acetate added was less than 0.10 mol. %. A preliminary experiment showed that the lowest partial pressures of carbon monoxide and hydrogen reacting with methanol to form acetaldehyde were, respectively, 70 and 30 kg./cm² at 200°C. From these experimental results, it was found that the following conditions were suitable for investigating the variation in the absorption spectrum of the cobalt(II) ion catalyst. The solution used was a mixture of methanol 9 and acetic acid*3 1 (mole ratio) containing 0.05 mol. % of cobal(II) acetate and a given amount of sodium iodide. After the solution of 3.0 ml. had been charged into the autoclave through inlet 6 in Fig. 1, carbon monoxide and hydrogen were introduced, up to 70 and 30 kg./cm² respectively (the total pressure, 100 kg./cm²). The autoclave was then heated up to 180—190°C within one hour. The methanol, acetic acid, cobalt(II) acetate and sodium iodide used were obtained from commercial sources, while the hydrogen and carbon monoxide were obtained from the electrolysis of water and the decomposion of formic acid respectively.

No attempt was made to evaluate the base line of a high temperature and pressure spectrum. Only the positions of the bands and the relative magnitude of the intensities of the recorded absorption spectra are important, since the transmittances, $I/I_0$ ($=T$), were determined at 840 mμ, at which point that of the liquid sample was nearly constant. The formation of acetaldehyde was confirmed by subjecting the liquid sample, after an experiment had been finished to gas chromatography.

*3 Acetic acid was added to prevent the catalyst from precipitating.

## Results and Discussion

**Visible Absorption Spectra.**—The variation in the absorption spectra due to the d-d transitions of cobalt(II) ions in the course of the reaction is recorded in Fig. 2. The amounts of the iodide ions of I, II, and III added in Fig. 2 are, respectively, 5, 10 and 20 times that of the cobalt(II) ion. IV shows a variation in the absorption spectrum of the cobalt(II) ion ($I^-/Co^{2+}=10$) in ethanol, with which carbon monoxide and hydrogen do not react under these conditions. V shows an absorption spectra of $[CoI_4]^{2-}$ and $[Co(AcO)_4]^{2-}$ in glacial

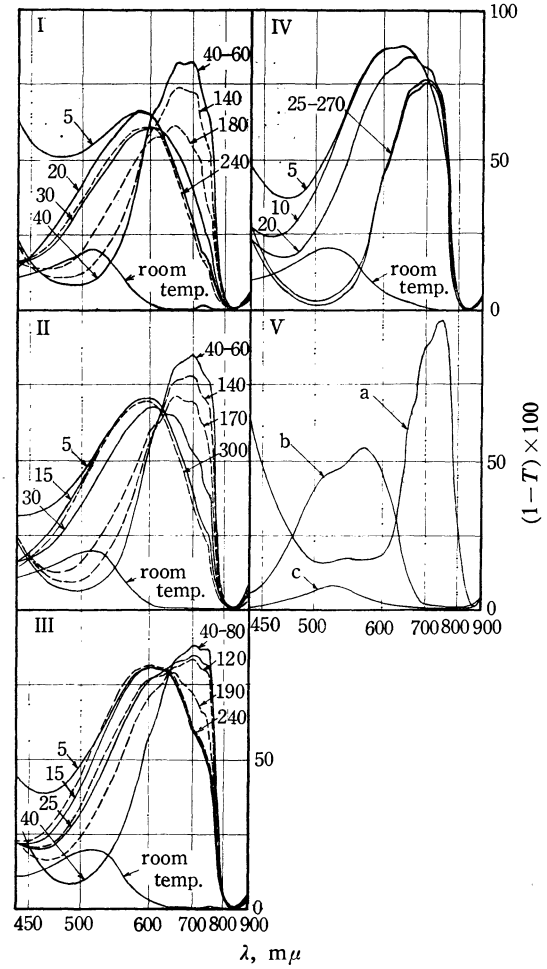



Fig. 2. The variation in the absorption spectra of cobalt(II) ions ($Co(AcO)_2 \cdot 4H_2O$ of 0.050 mol. %) in course of the reaction.

Numbers in the figure are the times (min.) after the temperature of the autoclave having reached 180°C. (I) $I^-/Co^{2+}=5$, (II) $I^-/Co^{2+}=10$, (III) $I^-/Co^{2+}=20$, (IV) $I^-/Co^{2+}=10$ in ethanol 9 : acetic acid 1 sol. and (V) the absorption spectra of $[CoI_4]^{2-}$ (a), $[Co(AcO)_4]^{2-}$ (b) and $[Co(H_2O)_6]^{2+}$ (c).

TABLE I. THE ABSORPTION SPECTRA OF TETRAHEDRAL COBALT(II) COMPLEX IONS

| Complex ion | Absorption range, mμ | λ, mμ (ε=max.) | ε ($mol^{-1}\,cm^{-1}$) | Solvent |
|---|---|---|---|---|
| $[Co(H_2O)_6]^{2+}$ | 450—550 | 530 | 17 | $H_2O$ |
| $[CoCl_4]^{2-}$ a) | 500—730 | 693 | 653 | $CH_3NO_2$ |
| $[CoBr_4]^{2-}$ a) | 520—750 | 698 | 790 | $CH_3NO_2$ |
| $[CoI_4]^{2-}$ a) | 600—800 | 733 | 1126 | $CH_3NO_2$ |
| $[CoCl_4]^{2-}$ b) | 560—720 | 697 | 612 | $CH_3COCH_3$ |
| $[CoBr_4]^{2-}$ b) | 620—750 | 723 | 1090 | $CH_3COCH_3$ |
| $[CoI_4]^{2-}$ b) | 650—830 | 777 | 1120 | $CH_3COCH_3$ |
| $[CoCl_4]^{2-}$ c) | 550—720 | 685 | 650 | AcOH |
| $[CoBr_4]^{2-}$ c) | 600—750 | 695 | 900 | AcOH |
| $[CoI_4]^{2-}$ e) | 620—810 | 755 | 1050 | AcOH |
| $[Co(AcO)_4]^{2-}$ d) | 450—650 | 565 | 1700 | AcOH |
| $[Co(CNS)_4]^{2-}$ c) | 550—670 | 620 | 2500 | AcOH |

a) N. S. Gill, R. S. Nyholm, *J. Chem. Soc.*, **1959**, 3977.
b) D. A. Fine, *J. Am. Chem. Soc.*, **84**, 1139 (1962).
c) P. J. Proll, L. H. Sutcliffe, *J. Phy. Chem.*, **65**, 1993 (1961).
d) P. J. Proll, L. H. Sutcliffe, J. Walkley, ibid, **65**, 455 (1961).
e) T. Mizoroki, Y. Andō, S. Furumi, The 16th Annual Meeting of the Chemical Society of Japan, Tokyo, April, 1963.

acetic acid: (a) is that of $[CoI_4]^{2-}$ formed at a room temperature from cobalt(II) acetate (2.0 mmol./l.) and sodium iodide (0.10 mol./l.); (b) is that of $[Co(AcO)_4$*4$]^{2-}$ formed at 150°C from cobalt(II) acetate (6.0 mmol./l.) and lithium acetate (0.10 mol./l.), and (c) is that of the hexaquo cobalt(II) ion $[Co(H_2O)_6]^{2+}$ (6.0 mmol./l.) in water.

Tetrahedral cobalt(II) complex ions of the $[CoX_4]^{2-}$ type, where X is $AcO^-$, $NCS^-$, $Cl^-$, $Br^-$ or $I^-$, have absorptions in a visible range, their extinction coefficients being about one hundred times stronger than that of the hexaquo cobalt(II) ion. According to the ligand field theory,[8] their absorptions are due to the electronic transitions of $d_\gamma \rightarrow d_\varepsilon$. The decrease in the strength of a ligand field decreases the difference between $d_\gamma$ and $d_\varepsilon$; the absorption, therefore, shifts toward longer wavelengths. The absorption spectra of $[CoX_4]^{2-}$ are represented in Table I. The decrease in the strength of a ligand field becomes larger in the order of $AcO^-$, $NCS^-$ $Cl^-$, $Br^-$ and $I^-$.

I, II and III of Fig. 1 show that the absorption corresponding to that of $[CoI_4]^{2-}$ obviously increases with the increase in the amount of iodide ions added. The extinction coefficient of $[Co(AcO)_4]^{2-}$ ($\varepsilon=1700$) is larger than that of $[CoI_4]^{2-}$. It seems, therefore, unreasonable that the absorption corresponding to $[CoI_4]^{2-}$ becomes stronger than that corresponding to $[Co(AcO_4)]^{2-}$. It is considered that those complex ions that have methanol, acetic acid or water as the ligand L are present in considerable quantities, together with $[Co(AcO)_4]^{2-}$, although it is nearly impossible to distinguish their absorption spectra from those of $[Co(AcO)_4]^{2-}$ and $[Co^{2+}(L)_6]$. Their extinction coefficients are probably smaller than that of $[Co(AcO)_4]^{2-}$. Therefore, the absorption corresponding to $[Co(AcO)_4]^{2-}$ recorded in Fig. 2 is not as strong as expected.

The variation in the absorption spectra may be divided into three parts. The first part lasts for about 20 min. after the temperature has reached 180°C, within which period no variation in the absorption of cobalt(II) ion is observed except that the absorption in the short-wavelength region gradually decreases. The second part lasts from about 20 to 100 min., within which period, as soon as the absorption from 500 to 650 mμ has started decreasing, that from 600 to 800 mμ goes on increasing until it reaches its maximum. The third part lasts from about 100 to 300 min., within which period the variation is the inverse of that of the second part. The absorption spectrum recorded after 200 to 300 min. becomes nearly the same as that of the first part. In the case of IV, the absorption from 500 to 650 mμ decreases very much within 25 min. after the temperature reaches 180°C; however, that from 600 to 800 mμ scarcely increases at all, and no variation is observed after 25 min. These are large differences from I, II and III.

The present authors would like to give the following estimates of these three parts of the variation. In the first part, most of the iodine molecules formed from iodide ions have been

*4 The octahedral species of the $[Co^{2+}(L)_6]$ type, where L represents $AcO^-$, AcOH or $H_2O$, are present in considerable quantities, together with $[Co(AcO)_4]^{2-}$.

8) L. E. Orgel, "An Introduction to Transition Metal Chemistry (Ligand Field Theory)," Methuen & Co. Ltd., London (1960).

reduced to iodide ions once again,*5 and the reaction does not start (an induction time). The second part is that in which the reaction starts and its rate reaches its maximum. The third part is that in which the partial pressure of carbon monoxide decreases in proportion as the reaction proceeds, until it nearly stops after 200 to 300 min. These estimates are supported by the following experimental results.

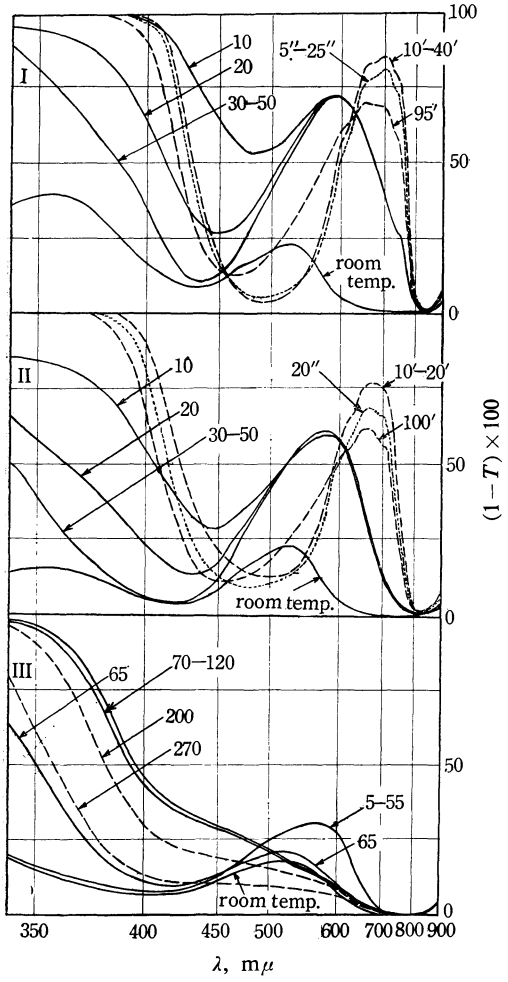



Fig. 3. The variation in the absorption spectra in course of the reaction under 200—220 kg./cm² ($CO/H_2=1$) at 185°C.
(I) $I^-/Co^{2+}=10$, (II) $I^-/Co^{2+}=2$ and (III) $I^-/Co^{2+}=0$. Numbers in the figure are the time (min.) since the temperature of the autoclave has reached 185°C and dashed numbers ($t'$ and $t''$) are those since the higher pressure gases have been introduced up to 220 kg./cm² at 185°C.

*5 The absorption in the short wavelengths is observed to decrease. See the near ultraviolet absorptions recorded in I and II of Fig. 3. It may be considered that most of the iodine molecules are formed according to the following reactions:

$$I^- + AcOH \rightleftarrows AcO^- + HI, \quad 2HI \rightleftarrows H_2 + I_2$$

The gases ($CO/H_2=1$) with a lower pressure (60 kg./cm²) than that in Fig. 2 were introduced at room temperature into the autoclave, in which the same solution as that of II in Fig. 2 had previously been placed. After the temperature had been kept constant at 185°C for about one hour (the variation in the absorption spectra within this period is shown by the full lines in I and II of Fig. 3), higher-pressure gases ($CO/H_2=1$) were introduced up to 220 kg./cm² at this temperature and the absorption spectra were taken (the broken lines). The results are summarized as I in Fig. 3. When the higher-pressure gases were introduced, most of the iodine molecules formed had already been reduced to iodide ions. The reaction, therefore, starts without exhibiting any induction time; the absorption from 600 to 800 mμ goes on increasing so fast that it reaches its maximum after about 10 min. After about 3 hr., the absorption spectrum returns to become nearly the same as it was before the reaction started. It may be expected that, if the higher pressure gases are once more introduced up to 220 kg./cm², nearly the same variation will again be observed. This is shown by the dotted lines in Fig. 3. II of Fig. 3 shows the results obtained when a small number of iodide ions are present in the solution ($I^-/Co^{2+}=2$).

These experimental results show that the reaction of methanol with carbon monoxide-hydrogen starts at the time that the iodine molecules formed have been mostly reduced to iodide ions, and that it is accompanied by an increase in the number of tetrahedral iodocobalt(II) complex ions.

**Near Ultraviolet Absorption Spectra.**—There may be expected to be five kinds of absorptions in a near ultraviolet region. 1) The absorption of an iodine. The strong absorption of an iodine molecule takes place from a visible part to a near ultraviolet one. This is due to the transition of non-bonding electrons in the iodine molecule ($n \rightarrow \sigma^*$).[9] This absorption is observed from 600 mμ toward the near ultraviolet region*6 of these absorption specra that are taken immediately after the temperature of the autoclave has reached 185°C (I and II of Fig. 3). 2) An electronic charge transfer from a coordinated iodine ion to the cobalt(II) ion. Whenever the reaction starts and the number of iodo-cobalt(II) complex ions increases, a new strong absorption takes place from 480 mμ to the shorter wavelengths, as is shown in I and II of Fig. 3. This absorption is probably due to an electronic charge

9) C. N. Rao, "Ultraviolet and Visible Spectroscopy," Butterworths, London (1961).

*6 This was confirmed by a preliminary experiment.

transfer of the $Co^{2+} + I^- \rightarrow Co^+ + I$ type, which may be correlated with the oxidation-reduction potential of cobalt(II) ions.[7] 3) An electronic charge transfer of the Mulliken type. If an iodine molecule or an iodide ion makes a weak bond with a solvent molecule, it may be expected that an electronic charge transfer of the Mulliken type[10] will take place in a near ultraviolet region. 4) The absorptions of cobalt carbonyls. III of Fig. 3 shows the variation in the absorption spectrum of the solution (methanol 9 : acetic acid 1) containing only cobalt(II) acetate (0.020 mol.%) under the same conditions as those of I, II and III of Fig. 2. After 50 to 60 min. since the temperature has been increased up to 180°C, the absorption corresponding to that of $[Co(AcO)_4]^{2-}$ decreases rapidly, while a new strong absorption takes place in the near ultraviolet region, although its intensity continues to decrease. This new absorption may be considered to be that of the cobalt carbonyl*7 formed from the following equations: $Co^{2+} + H_2 \rightarrow Co + 2H^+$, $2Co + 8CO \rightarrow Co_2(CO)_8$, $H_2 + Co_2(CO)_8 \rightarrow 2HCo(CO)_4 \rightarrow 2H^+ + 2[Co(CO)_4]^-$; it may also be considered that its decomposition into metallic cobalt[11] causes its absorption to decrease. 5) The absorption of acetaldehyde. Acetaldehyde formed has an absorption from 330 mμ to the shorter wavelengths ($n \rightarrow \pi^*$, $\varepsilon = 10—100$). However, the intensity of the near ultraviolet absorption due to the electronic charge transfer from iodine ions to cobalt(II) ions was so strong that it was difficult to confirm the formation of cobalt carbonyls during the course of the reaction.

From the variation in the visible absorption spectra of cobalt(II) ions in the course of the reaction of methanol with carbon monoxide and hydrogen, it may be considered that, when a comparatively large number of iodide ions are added to the solution, most of the cobalt(II) ions do not form cobalt carbonyls, but tetrahedral cobalt(II) complex ions, and that the equilibrium of the equation represented apparently by $[Co(AcO)_{4-n}I_n]^{2-} + I^- \rightleftarrows [Co(AcO)_{3-n}I_{n+1}]^{2-} + AcO^-$ inclines much toward the right side in the course of the reaction. This is greatly different from an oxo-reaction.

10) R. S. Mulliken, *J. Am. Chem. Soc.*, **74**, 811 (1952).

*7 This absorption is estimated to be the transition of the bonding electrons between a cobalt atom and carbon monoxides to an anti-bonding orbital (H. B. Gray et al., *J. Am. Chem. Soc.*, **84**, 3404 (1962); R. J. Angelici and F. Basolo, *Inorg. Chem.*, **2**, 728 (1963)).

11) P. H. Emett, "Catalysis," Vol. V. Reinhold Publ. Corp., New York (1957), p. 73.

## Summary

The absorption spectra during the course of the reaction of methanol with carbon monoxide-hydrogen mixtures in the presence of a mixture of cobalt(II) acetate and sodium iodide as the catalyst under high temperatures and pressures (180—185°C, 200—220 kg./cm²) have been taken, using an automatic recording spectrophotometer and special autoclave made of Ti-Mn alloy and a couple of thick pieces of quartz glass. Whenever the reaction starts, the absorption corresponding to that of $[Co(AcO)_4]^{2-}$ goes on decreasing, while that corresponding to $[CoI_4]^{2-}$ increases in place. It has been difficult to confirm the formation of cobalt carbonyls as $Co_2(CO)_8$ and $HCo(CO)_4$ during the course of the reaction, because their absortions overlap with those of the strong electronic charge transfer of tetrahedral iodocobalt(II) complex ions. From the experimental results and subsequent considerations, it has been shown that, when a comparatively large number of iodide ions are present in the solution, most of the cobalt(II) ions do not form cobalt carbonyls, but tetrahedral cobalt(II) complex ions of the $[Co(AcO)_{4-n}I_n]^{2-}$ type ($n = 1—4$) during the course of the reaction, and that the reaction is accompanied by an increase in the number of tetrahedral iodocobalt(II) complex ions.

The authors wish to express their thanks to Professor Yukio Yoneda, Faculty of Engineering, The University of Tokyo, for his discussions on the visible absorption spectra, and to Dr. Hiroshi Uchida for his invaluable advice.

*Government Chemical Industrial Research Institute, Tokyo*
*Meguro-ku, Tokyo*

# A New Method of Analyzing Thermogravimetric Data

By Takeo Ozawa

(Received February 23, 1965)

Various kinds of materials have been studied by thermogravimetric analysis, in which is recorded the weight-change of a sample heated at a constant rate of heating. Thermogravimetry has an advantage over measurement at a constant temperature, because in the latter a part of the sample may change while the sample is heated to the desired temperature. Especially at the degradation of high polymers, this initial structure change in the sample complicates the isothermal data and makes it difficult to analyze.

The many methods proposed for obtaining the kinetic parameters from the thermogravimetric data, though rather complicated, may be classified into two classes, in both of which the rates of decomposition must have the following form:

$$-\frac{dW}{dt}=A\exp\left(-\frac{\Delta E}{RT}\right)W^n \qquad (1)$$

where $W$ is the fractional residual weight of the sample; $T$, the absolute temperature; $R$, the gas constant; $t$, the time, and $A$, $\Delta E$ and $n$, the pre-exponential factor, the activation energy and the order of the reaction respectively.

In the first class of the analyzing method,[1-5] Eq. 1 is treated as a differential equation, and the fractional weight is derived by integration as a function of the temperature. In the other method,[6-10] from the plots of the logarithms of the terms of Eq. 1 the kinetic constants are obtained. These analyses are usually cumbersome. Complex quantities must be derived from the data or the trial-and-error fitting of the curve is required in the former cases, while the weight-temperature curve must be differentiated graphically in the latter cases. Furthermore, these methods are applicable only to the decomposition expressed by Eq. 1.

This paper will propose an approximate integral method similar to, but even simpler than, that of Doyle.[2] This method is more widely applicable than the others. For example, the random degradation of high polymers[11] can be analyzed by this treatment.

A few methods of estimating the thermal stability of polymeric materials have been reported.[12,13] In these papers, however, the effect of the heating rate has not been considered. In this paper these methods will be revised, considering the effect of heating rates, and it will be shown that a master curve may be derived from the data at different heating rates.

The applications of the method to the decomposition of calcium oxalate and to the degradation of nylon 6 will be shown. Finally, the applicability of the method to other types of thermal analyses and the possibility of extending it to thermal behavior under various conditions of temperature change will be discussed.

## Theoretical Consideration

Generally, the fractional weight, $W$, of a reacting material is expressed as a function of the fraction of a structural quantity, such as a group, a constituent, a broken bond, etc., which is represented by $x$:

$$W=f(x) \qquad (2)$$

where $x$ changes according to the ordinary kinetic equation:

$$-\frac{dx}{dt}=A\exp\left(-\frac{\Delta E}{RT}\right)g(x) \qquad (3)$$

By integration,

$$-\int_{x_0}^{x}\frac{dx}{g(x)}=A\int_{t_0}^{t}\exp\left(-\frac{\Delta E}{RT}\right)dt \qquad (4)$$

where $x_0$ is the value of $x$ at $t=t_0$. In most cases, the kinetics of the weight-change can be expressed as Eq. 1, where $x$ is equal to $W$.

1) D. W. van Krevelen, C. van Heerden and F. J. Huntjens, *Fuel*, **30**, 253 (1951).
2) C. D. Doyle, *J. Appl. Polymer Sci.*, **5**, 285 (1961).
3) C. D. Doyle, ibid., **6**, 639 (1962).
4) H. H. Horowitz and G. Metzger, *Anal. Chem.*, **35**, 1464 (1963).
5) A. W. Coats and J. P. Redfern, *Nature*, **201**, 68 (1964).
6) P. Kofstad, ibid., **179**, 1362 (1957).
7) E. S. Freeman and B. Carroll, *J. Phys. Chem.*, **62**, 394 (1958).
8) D. A. Anderson and E. S. Freeman, *J. Polymer Sci.*, **54**, 253 (1961).
9) H. C. Anderson, ibid., C, No. 6, 175 (1964).
10) H. L. Friedman, ibid., C, No. 6, 183 (1964).
11) R. Simha and L. A. Wall, *J. Phys. Chem.*, **56**, 707 (1952).
12) C. D. Doyle, *Anal. Chem.*, **33**, 77 (1961).
13) L. Reich and D. W. Levi, *Makromol. Chem.*, **66**, 102 (1963).

TABLE I. SEVERAL FORMS OF $f(x)$, $g(x)$ AND $\int dx/g(x)$

| Type of reaction | $f(x)$ | $g(x)$ | $\int dx/g(x)$ |
|---|---|---|---|
| 0th order reaction | $W$ | 1 | $W$ |
| 1st order reaction | $W$ | $W$ | $\ln W$ |
| 2nd order reaction | $W$ | $W^2$ | $-1/W$ |
| 3rd order reaction | $W$ | $W^3$ | $-2/W^2$ |
| Random degradation[11] | $(1-x)^{L-1}\left\{1+x\frac{(N-L)(L-1)}{N}\right\}$* | $-(1-x)$ | $-\ln(1-x)$ |

* $N$ is the initial degree of polymerization and $L$ is the least number of repeating units of polymer not volatilized. Following approximation can be made for $N \gg L$:
$f(x)=(1-x)^{L-1}\{1+(L-1)x\}$

In the random degradation of high polymers,[11] $x$ is a fractional number of the broken bond.

When the temperature of the sample is raised at a constant rate, $a$, the change in $x$ is given by Eq. 5:

$$-\int_{x_0}^{x}\frac{dx}{g(x)}=\frac{A}{a}\int_{T_0}^{T}\exp\left(-\frac{\Delta E}{RT}\right)dT \qquad (5)$$

where $T_0$ is the value of $T$ at $t=t_0$. Ordinarily, the rate of the reaction is very low at low temperatures. Therefore, the next approximation is valid:

$$\int_{T_0}^{T}\exp\left(-\frac{\Delta E}{RT}\right)dT=\int_{0}^{T}\exp\left(-\frac{\Delta E}{RT}\right)dT \qquad (6)$$

The value of the right side of Eq. 6 is expressed and tabulated by Doyle[2] as the following function, $p$:

$$\frac{\Delta E}{R}p\left(\frac{\Delta E}{RT}\right)=\int_{0}^{T}\exp\left(-\frac{\Delta E}{RT}\right)dT \qquad (7)$$

If $\Delta E/RT$ is larger than 20, $p(\Delta E/RT)$ can be approximated by the following formula:[3]

$$\log p\left(\frac{\Delta E}{RT}\right)\fallingdotseq -2.315-0.4567\frac{\Delta E}{RT} \qquad (8)$$

Now, for a given value of $W$, a single-valued function of $x$, the left side of Eq. 5 is a constant which does not depend on the heating rate. Therefore, if the weight decreases to a given fraction at the temperature, $T_1$, for the heating rate of $a_1$, at $T_2$ for $a_2$, and so on, the following equations can be obtained;

$$\frac{A\Delta E}{a_1 R}p\left(\frac{\Delta E}{RT_1}\right)=\frac{A\Delta E}{a_2 R}p\left(\frac{\Delta E}{RT_2}\right)=\cdots \qquad (9)$$

Using Eq. 8, the following linear relations can easily be derived:

$$-\log a_1-0.4567\frac{\Delta E}{RT_1}=-\log a_2-0.4567\frac{\Delta E}{RT_2}=\cdots \qquad (10)$$

Thus, the plots of $\log a$ versus the reciprocal absolute temperature for a given value of $W$ must give a straight line, the slope of which gives the activation energy. In other words, if the thermogravimetric curves are given as a plot of $W$ versus the reciprocal absolute temperature for various heating rates, the curves can be superposed upon each other by shifting them along the abscissa. The length of the lateral shift is proportional to the logarithm of the corresponding heating rate of the curve. By these superpositions there is obtained the master thermogravimetric curve, which is a standard and more accurate curve than individual ones; this procedure makes possible the mutual comparison of the thermogravimetric data at different heating rates.

The next step of the analysis is the determination of $A$, $f(x)$ and $g(x)$. For some typical kinetic processes, $f(x)$, $g(x)$ and $\int dx/g(x)$ are given in Table I, where $L$ is the

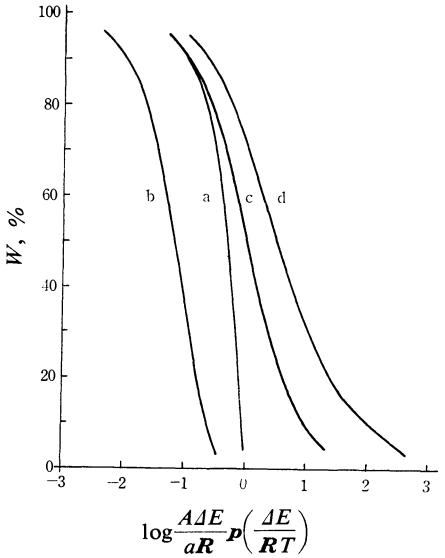



Fig. 1. The theoretical thermogravimetric curves for;
a, 0th order reaction; b, 1st order reaction;
c, 2nd order reaction; d, 3rd order reaction.

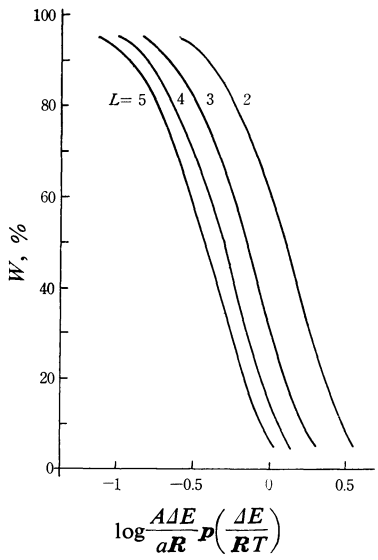



Fig. 2. The theoretical thermogravimetric curves of the random degradation of high polymers with the indicated values of $L$. Approximation is made for $N \gg L$.

least number of repeating units of the polymer not volatilized.[11] As $\int dx/g(x)$ is a function of $x$, which is equal to $(A\Delta E/aR)p(\Delta E/RT)$, and $W$ is a single-valued function of $x$, $W$ can be calculated as a function of $\log\{(A\Delta E/aR)p(\Delta E/RT)\}$, as is shown in Figs. 1 and 2. The plots of $W$ against $\log\{(A\Delta E/aR)p(\Delta E/RT)\}$ by using the experimental master thermogravimetric curve and the activation energy determined as shown above must be superposed upon one of the curves in Figs. 1 and 2 by a lateral shift. By this procedure the forms of $f(x)$ and $g(x)$ are determined, and the length of the lateral shift is found to be equal to $\log A$. An analogous, but more precise determination of $A$ can be made by the subtraction of $\log\{(\Delta E/aR)p(\Delta E/RT)\}$ from the $\int dx/g(x)$ of the determined form of $g(x)$, as is shown in Tables II and III.

Table II. The kinetic parameters of the decomposition of calcium oxalate

| $W$ | $\Delta E$ | $\log A$* |
|---|---|---|
| | kcal./mol. | |
| 0.95 | 87.4 | 28.60 |
| 0.90 | 80.3 | 28.57 |
| 0.85 | 76.7 | 28.56 |
| 0.80 | 82.7 | 28.56 |
| 0.75 | 74.8 | 28.58 |
| 0.70 | 77.9 | 28.58 |
| 0.65 | 76.9 | 28.59 |
| 0.60 | 77.0 | 28.62 |
| 0.55 | 79.2 | 28.63 |
| 0.50 | 80.1 | 28.64 |
| 0.45 | 80.1 | 28.64 |
| 0.40 | 82.1 | 28.67 |
| 0.35 | 78.0 | 28.67 |
| 0.30 | 78.7 | 28.68 |
| 0.25 | 76.3 | 28.69 |
| 0.20 | 75.6 | 28.70 |
| 0.15 | 77.0 | 28.72 |
| 0.10 | 73.7 | 28.69 |
| 0.05 | 67.0 | 28.69 |
| mean | 78.0±1.0 | 28.64±0.012 |

* The dimension of $A$ is $min^{-1}$.

Table III. The kinetic parameters of the degradation of nylon 6

| $W$ | $\Delta E$ | $\log A$* |
|---|---|---|
| | kcal./mol. | |
| 0.95 | 29.7 | 11.11 |
| 0.90 | 35.0 | 10.98 |
| 0.85 | 35.9 | 10.96 |
| 0.80 | 35.7 | 10.95 |
| 0.75 | 36.2 | 10.94 |
| 0.70 | 35.3 | 10.92 |
| 0.65 | 35.7 | 10.91 |
| 0.60 | 36.5 | 10.90 |
| 0.55 | 36.0 | 10.91 |
| 0.50 | 35.5 | 10.90 |
| 0.45 | 36.3 | 10.89 |
| 0.40 | 36.3 | 10.90 |
| 0.35 | 36.5 | 10.88 |
| 0.30 | 36.5 | 10.88 |
| 0.25 | 37.2 | 10.88 |
| 0.20 | 37.0 | 10.88 |
| 0.15 | 37.8 | 10.87 |
| 0.10 | 39.2 | 10.88 |
| 0.05 | 40.1 | 10.84 |
| mean | 36.2±0.5 | 10.91±0.014 |

* The dimension of $A$ is $min^{-1}$.

Thus, the kinetic parameters, e.g., $\Delta E$, $A$, $f(x)$ and $g(x)$, are determined; from these parameters, a theoretical curve can be drawn and compared with the experimental master thermogravimetric curve. If the successive adjustments of the parameters are made, more accurate values will be obtained.

## Experimental

The method was applied to two reactions: the decomposition of calcium oxalate into calcium carbonate and carbon monooxide, and the degradation of nylon 6. The calcium oxalate monohydrate was of a G.R. grade, purchased from the Showa Chemical Co., Ltd., and used without further purification. The nylon 6, kindly supplied by the Toyo Rayon Co., Ltd., was dissolved in formic acid, reprecipitated by water, and dried in vacuo. The viscosity-average molecular weight of 10300,

was obtained from the intrinsic viscosity as measured in formic acid at 25°C. The amino groups at the chain ends of the polymer were partly acetylated.

A 300 mg. sample of calcium oxalate monohydrate or a 100 mg. sample of nylon 6 was weighed in a glass sample pan 15 mm. in diameter and 10 mm. in depth. The sample of nylon 6 was dried in the sample pan at 180°C for one hour under a pressure of less than $1\times10^{-3}$ Torr. prior to the measurements.

A null-type continuously-recording thermobalance supplied by the Ohyo Rika Kogyo Co., Ltd., was employed for the thermogravimetric measurements. A chromel-alumel thermocouple was located directly above the sample. The linear increase in the furnace temperature was regulated by a PI-type program controller and a SCR regulator purchased from the Ohkura Electric Co., Ltd. The pyrolysis of calcium oxalate monohydrate was carried out in air at an ambient pressure, and that of nylon 6, under a pressure of less than $1\times10^{-3}$ Torr. The heating rates were varied from 12°C per hour to 140°C per hour. The samples were weighed before and after heating by an analytical balance.

## Results and Discussion

The results of the thermogravimetry at various heating rates are plotted against the reciprocal absolute temperature in Figs. 3 and 4. It is apparent that these curves can be superposed by lateral shifts. The logarithms of the heating rates are plotted against the reciprocal absolute temperature, until which point the weight of the sample decreases to a

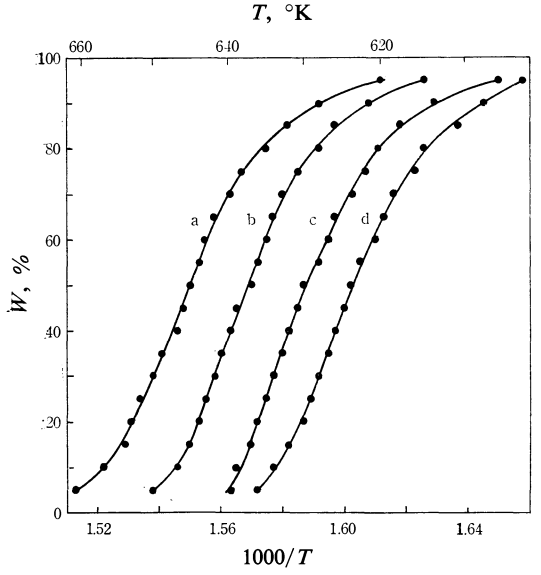



Fig. 3. The thermogravimetric curves of decomposition of calcium oxalate plotted against the reciprocal absolute temperature. Heating rate; a, 108°C/hr.; b, 54°C/hr.; c, 24.4°C/hr.; d, 12.5°C/hr.

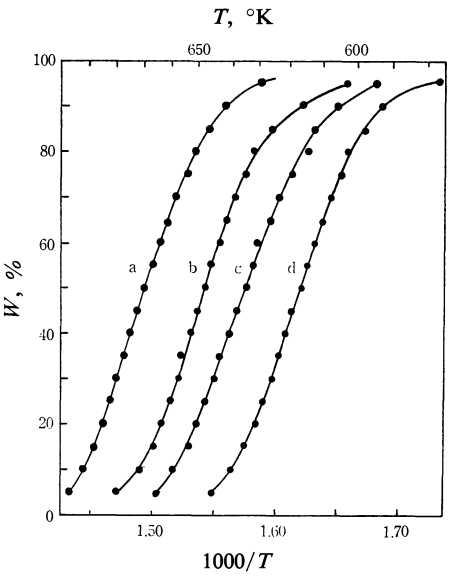



Fig. 4. The thermogravimetric curves of nylon 6 plotted against the reciprocal absoute temperature. Heating rate; a, 140°C/hr.; b, 48°C/hr.; c, 28°C/hr.; d, 14.3°C/hr.

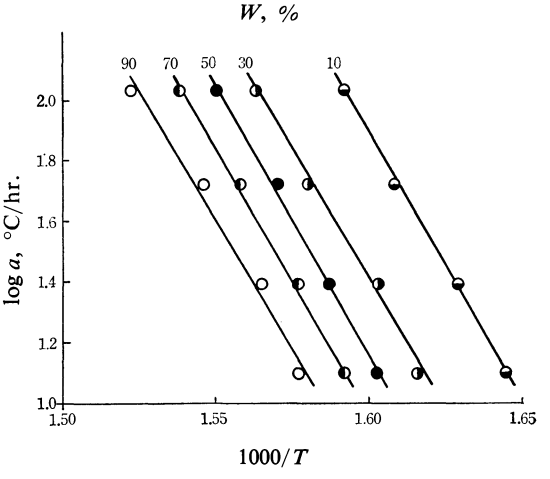



Fig. 5. The plots of logarithms of heating rate versus the reciprocal absolute temperature for indicated conversions of the decomposition of calcium oxalate.

given fraction, as Figs. 5 and 6 show. Straight lines are drawn by the method of the least squares; from these lines the activation energies are determined as listed in Tables II and III.

By using the activation energies thus determined, the weight changes are plotted against $\log\{(\Delta E/aR)p(\Delta E/RT)\}$ and compared with the curves in Figs. 1 and 2. From these comparisons, the mechanism of the decomposition of calcium oxalate may be elucidated to be of the 1st order; it is also found that the

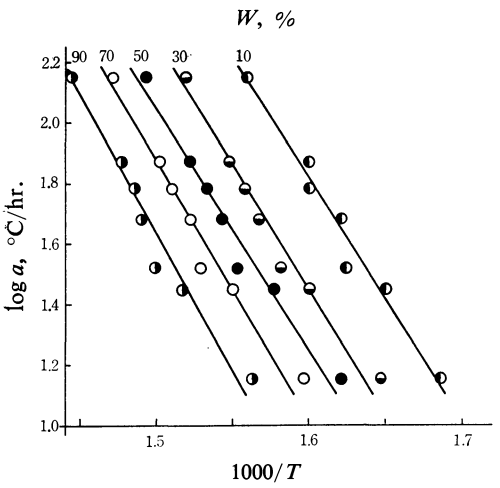



Fig. 6. The plots of logarithms of heating rate versus the reciprocal absolute temperature for indicated conversions of the degradation of nylon 6.

theoretical curve of random degradation with $L=2$ is best fitted to the experimental curve of nylon 6. A is determined by comparing $\log\{(\Delta E/aR)p(\Delta E/RT)\}$ with $\log\int dx/g(x)$ at every 5% of conversion; this tabulation is also in Tables II and III. In Freeman and Carrol's paper,[7] the activation energy and the order of the reaction of the decomposition of calcium oxalate were reported to be 74 kcal./mol. and 0.7 respectively, but the pre-exponential factor could not be evaluated by their method. The agreement between the results of this paper and theirs is good. For nylon 6, the activation energy and the order of the reaction were evaluated to be 37.0 kcal./mol. and 0 in Inoue and Sumoto's paper,[14] in which the mechanism of the unzipping of the monomer from carboxyl ends was postulated, whereas Straus and Wall[15] reported a mechanism of random degradation in which the activation energy is about 30 kcal./mol., the pre-exponential factor is of the order of $10^5$—$10^7$, and $L$ is 5. In both papers, the results were obtained by isothermal measurements, which contain some errors, as has been pointed out above. Considering these facts, the agreement seems fairly good. The experimental master curves at the heating rate of 60°C per hour are shown in Figs. 7 and 8, where they are also compared with the theoretical curves on the basis of the kinetic parameters obtained by the above analyses. The agreements between them are also good.

14) R. Inoue and M. Sumoto, *Chem. High Polymers*, **11**, 169 (1954).
15) S. Straus and L. A. Wall, *J. Res. Natl. Bur. Std.*, **60**, 39 (1958).

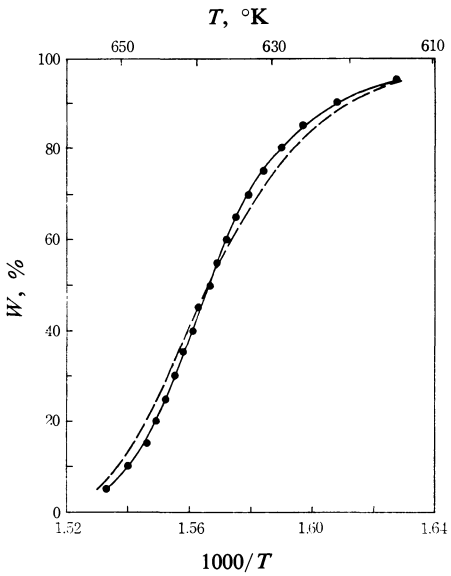



Fig. 7. The comparison of the experimental master curve (——) and the theoretical curve (----) of the decomposition of calcium oxalate.

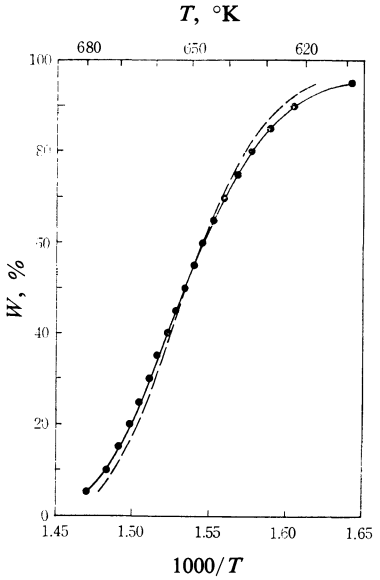



Fig. 8. The comparison of the experimental master curve (——) and the theoretical curve (----) of the degradation of nylon 6.

As may be seen in the above procedure, the method described in this paper is simple and applicable to the random degradation of polymers and other complicated reactions which can not be analyzed by other methods. However, if the weight changes in the manner of parallel reactions or consecutive reactions (in other words, if the weight-change is governed by two or more activation energies), the curves of the weight versus the reciprocal

absolute temperature at different heating rates can not be superposed, and the analysis mentioned above can not be applied. This is also the case for the other methods of analyzing thermogravimetric data.

Now we would like to discuss the applicability of the method to other types of thermal analyses, in which is recorded the change, or the rate of the change, of some property of the material heated at a constant rate.[16,17] If the property measured is a function of $x$ only, the change in the property can be treated similarly to the change in weight at the random degradation of polymers, and even if the exact form of $f(x)$ and/or $g(x)$ is unknown, the activation energy of the thermal behavior of the property can be estimated by a plot similar to Figs. 5 and 6. Furthermore, the change in the property under different conditions of temperature change can be predicted. Namely, the conversion of the property depends on the integral of the right side of Eq. 4, which has the dimension of time and which could be called "reduced time," $\theta$:

$$\theta = \int_{t_0}^{t} \exp\left(-\frac{\Delta E}{RT}\right) dt \tag{11}$$

When the change in the property is plotted against the logarithm of the reduced time by using the activation energy thus determined, the master curve of the change in the property under the various conditions of temperature change will be obtained. Below are shown the expressions of the reduced time, some of which have already been calculated in the literature.[18] (i) If the temperature is maintained at $T$ from time 0 to time $t$:

$$\theta = t \exp(-\Delta E/RT) \tag{12}$$

(ii) If the temperature is raised from $T_1$ to $T_2$ at the rate of $a$ and cooled from $T_2$ to $T_3$ at the rate of $b$:

$$\theta = (\Delta E/aR)\{p(\Delta E/RT_2) - p(\Delta E/RT_1)\} + (\Delta E/bR)\{p(\Delta E/RT_2) - p(\Delta E/RT_3)\} \tag{13}$$

(iii) If the temperature is changed from $T_1$ to $T_2$ according to Eq. 14:

$$T = a + b\exp(-\alpha t) \tag{14}$$

$$\theta = \left(\frac{1}{\alpha}\right)\left\{Ei\left(-\frac{\Delta E}{RT_2}\right) - Ei\left(-\frac{\Delta E}{RT_1}\right)\right\} - \left(\frac{1}{\alpha}\right)\exp\left(-\frac{\Delta E}{aR}\right)\left\{Ei\left(\frac{\Delta E}{aR} - \frac{\Delta E}{RT_2}\right) - Ei\left(\frac{\Delta E}{aR} - \frac{\Delta E}{RT_1}\right)\right\} \tag{15}$$

where:

$$Ei(x) = \frac{\exp(x)}{x}\left\{1 + \frac{1}{x} + \frac{2!}{x^2} + \frac{3!}{x^3} + \cdots\right\} \tag{16}$$

(iv) If the temperature is changed from $T_1$ to $T_2$ according to Eq. 17:

$$1/T = 1/T_0 - at \tag{17}$$

$$\theta = \left(\frac{R}{a\Delta E}\right)\left\{\exp\left(-\frac{\Delta E}{RT_2}\right) - \exp\left(-\frac{\Delta E}{RT_1}\right)\right\} \tag{18}$$

For the more complicated changes in the temperature, $\theta$ can be calculated according to its additivity, or according to its linearity in integration. It is also apparent from the above discussions that the thermal stability of the materials should be defined by using $\theta$ and $\Delta E$.

## Summary

A new method of obtaining the kinetic parameters from thermogravimetric curves has been proposed. The method is simple and applicable to reactions which can not be analyzed by other methods. The effect of the heating rate on thermogravimetric curves has been elucidated, and the master curve of the experimental curves at different heating rates has been derived.

The applications of the method to the pyrolyses of calcium oxalate and nylon 6 have been shown; the results are in good agreement with the reported values.

The applicability of the method to other types of thermal analyses has been discussed, and the method of the conversion of the data to other conditions of temperature change has been suggested. From these discussions, the definition of the thermal stability of materials has been criticized.

*Electrotechnical Laboratory*
*Tanashi-machi, Kitatama-gun, Tokyo*

16) C. B. Murphy, *Anal. Chem.*, **36**, 347R (1964).
17) Jen Chiu, Preprint presented at the National Meeting of Am. Chem. Soc. (Chicago, 1964).
18) H.-J. Frentz, *Elektrotechnische Z.*, A, **78**, 156 (1957).

# A New Colorimetric Method for the Determination of Minute Amounts of Bromide by Means of Its Catalytic Effect*

By Norinobu YONEHARA, Satori UTSUMI and Iwaji IWASAKI

(Received February 24, 1965)

A rapid and sensitive method for the determination of a minute amount of bromide is desirable. Two of the present authors (S. U. and I. I.) and Shiota[1] have previously reported a colorimetric method for the determination of bromide which is based on the catalytic effect of bromide on the oxidation of iodine to iodate by potassium permanganate in a sulfuric acid solution. Fishman and Skougstad[2] have studied this method further. However, it has been observed that some inevitable technical difficulties occur in keeping the reaction time and temperature constant, because this oxidation reaction proceeds fairly rapidly, even below room temperature.

By a further investigation of the oxidation of iodine to iodate employing various oxidizing agents, it was found that, when ceric ammonium sulfate is used as the oxidizing agent, this oxidation reaction is catalytically promoted by a minute amount of bromide in the presence of large amounts of potassium dichromate in a nitric acid solution. This reaction proceeds fairly slowly at room temperature, thus, favorable conditions for the procedure can be realized. In this paper a new method for the determination of a minute amount of bromide using this reaction will be described.

This oxidation reaction proceeds more rapidly in the presence of bromide than in its absence. Consequently, when this reaction was carried out at a given temperature for a given time, the higher the concentration of bromide was, the lower that of the unreacted iodine became. Thus, the determination of bromide can be made by determining the amount of this unreacted iodine. The oxidation reaction is stopped after a given time by the extraction of the unreacted iodine with carbon tetrachloride; the amount of iodine in the extract is then determined by adding an alcoholic solution of mercuric thiocyanate and a ferric ammonium sulfate solution and by measuring the absorbance of the resulting ferric thiocyanate.[3]

## Experimental

**Apparatus.**—A Hirama photoelectric-colorimeter with a 460 filter (with maximum transmission at 460 mμ) and 10 mm. cells was used to measure the absorbance.

The reactions were carried out at given temperatures (±0.1°C) using a water bath with a Taiyo Thermo Unit.

**Reagents.** — All the chemicals used were of guaranteed-reagent quality.

*The Ceric Ammonium Sulfate Solution (0.2 M in 2 N Sulfuric Acid).*—Dissolve 33.42 g. of ceric ammonium sulfate $[Ce(SO_4)_2 \cdot 2(NH_4)_2SO_4 \cdot 4H_2O]$ in a sulfuric acid solution (14 ml. of concentrated sulfuric acid +115 ml. of redistilled water) and dilute to 250 ml. with redistilled water.

*The Potassium Dichromate Solution (0.2 M).*—Dissolve 15.21 g. of potassium dichromate in redistilled water and dilute to 250 ml.

*The Potassium Iodide Solution (1 mg. of iodide per ml.).*—Recrystallized potassium iodide was used. Prepare about a 0.1 M potassium iodide solution, standardize by Volhard's method, and then dilute this solution to give 1000 p. p. m. of iodide.

*Concentrated Nitric Acid (sp. gr. 1.38).*

*The Mercuric Thiocyanate Solution.*—Solid mercuric thiocyanate[4] was prepared in our laboratory. Dissolve 0.3 g. of mercuric thiocyanate in 100 ml. of absolute ethyl alcohol.

*The Ferric Ammonium Sulfate Solution.*—Dissolve 6 g. of ferric ammonium sulfate in 100 ml. of a 6 N nitric acid solution and store in a brown glass bottle.

*The Standard Bromide Solution.*—Prepare about a 0.1 M potassium bromide solution using redistilled water and standardize by Volhard's method. Prepare the working solutions by diluting this solution adequately.

*The Standard Chloride Solution.*—Dissolve 1.649 g. of sodium chloride in redistilled water and dilute to exactly 1 l. This solution contains 1 mg. of chloride per milliliter. Prepare the working solutions by successive dilutions.

**Procedure and Calibration Curve.** — To 10.0 ml. of the sample in a 30 ml. glass tube with a glass

* Partly read at the symposium of the Japan Society for Analytical Chemistry, May, 1964.

1) M. Shiota, S. Utsumi and I. Iwasaki, *J. Chem. Soc. Japan, Pure Chem. Sec.* (*Nippon Kagaku Zasshi*), **80**, 753 (1959).

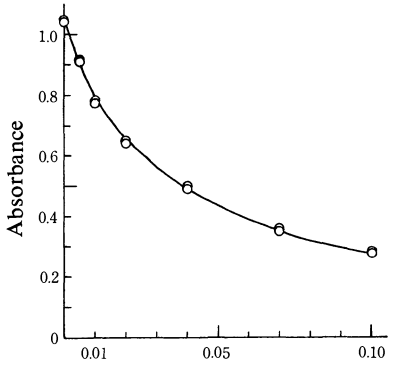
2) M. J. Fishman and M. W. Skougstad, *Anal. Chem.*, **35**, 146 (1963).

3) S. Utsumi, *J. Chem. Soc. Japan, Pure Chem. Sec.* (*Nippon Kagaku Zasshi*), **74**, 32 (1953); I. Iwasaki, S. Utsumi, A. Tomonari and I. Morita, ibid., **80**, 749 (1959).

4) S. Utsumi, *J. Chem. Soc. Japan, Pure Chem. Sec.* (*Nippon Kagaku Zasshi*), **73**, 835 (1952); I. Iwasaki, S. Utsumi, K. Hagino and T. Ozawa, This Bulletin, **29**, 860 (1956).

stopper add 1.5 ml. of the potassium iodide solution, 1.0 ml. of the potassium dichromate solution and 2.0 ml. of the nitric acid solution, and mix thoroughly. Place the glass tube in the water bath at 30°C for about 10 min. Start the reaction by adding 2.0 ml. of the ceric ammonium sulfate solution (at the same temperature), mixing thoroughly, and replacing the glass tube in the water bath.

Exactly 20 min. after the addition of the ceric ammonium sulfate solution, add 5 ml. of carbon tetrachloride and immediately shake the glass tube for 30 sec. After the layers have completely separated, remove the aqueous layer by using the pipet with a rubber bulb. As even a small amount of the remaining aqueous layer disturbs the subsequent procedure, it is necessary to remove it completely by the following procedure. Add about 5 ml. of redistilled water to the glass tube containing carbon tetrachloride along the inside wall of the tube, and then remove this water again in the manner described above. The aqueous layer that initially remains can be removed almost completely by repeating this procedure three times. To the carbon tetrachloride thus obtained in the glass tube, add 5.0 ml. of redistilled water, 1.0 ml. of the ferric ammonium sulfate solution and 0.5 ml. of the mercuric thiocyanate solution, and shake the glass tube for about one minute. Thus, the aqueous layer is colored with ferric thiocyanate. Measure the absorbance of this aqueous layer at 460 mμ using redistilled water as a reference.




Concn. of bromide, p. p. m.

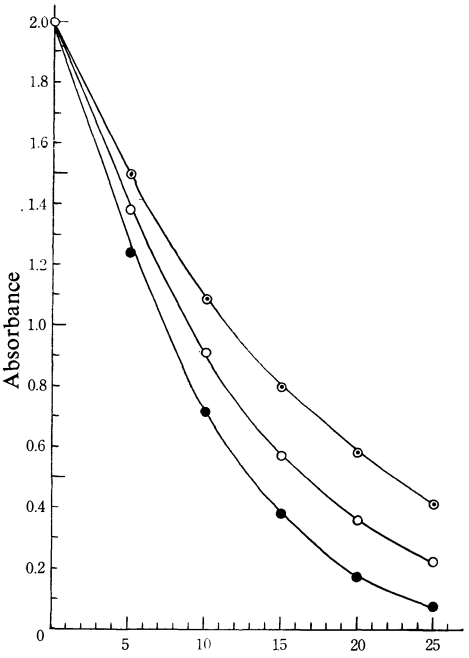
Fig. 1. Calibration curve.
30°C, 20 min.

The calibration curve shown in Fig. 1 was obtained by the procedure described above, using standard bromide solutions of known concentrations. The same calibration curve as that for bromide is obtained by using standard bromate solutions with the concentrations given as bromine.

This method is especially suitable for the determination of concentrations lower than 0.05 p. p. m.; concentrations of bromide as low as 0.005 p. p. m. can thus be determined.

## Results and Discussion

**The Reaction Rate Curves.** — The catalytic reactions were carried out in the same way using 10.0 ml. of a 0.10 p. p. m. bromide solution. After various intervals, the color was developed by using 10.0 ml. of redistilled water, 2.0 ml. of the ferric ammonium sulfate solution and 1.0 ml. of the mercuric thiocyanate solution. The reaction rate curve I shown in Fig. 2 was obtained by this experiment.




Time, min.

Fig. 2. Reaction rate curves.
30°C, Color reaction of $FeSCN^{2+}$ is done by using 10 ml. of $H_2O$, 2 ml. of ferric solution and 1 ml. of $Hg(SCN)_2$ solution.
—●— 0.10 p. p. m. $Br^-$ (I)
—○— 0.02 p. p. m. $Br^-$ (II)
—⊙— Redistilled water (III)

Curves II and III in Fig. 2 were obtained by using a 0.02 p. p. m. bromide solution and redistilled water. As can be seen from Fig. 2, the reaction rate increased with an increase in the concentration of bromide, and the differences in absorbances among the three curves increased with the reaction time. These results indicate that the sensitivity of the method increases with the reaction time. However, in the solution with 0.10 p. p. m. bromide, the reaction has been almost completed after 25 min. and the sensitivity became small. A reaction time of 20 min. was adequate at 30°C.

**The Amount of Iodide, the Reaction Time and the Temperature.**—Curves I and II in Fig. 3 show the combined effect of the reaction time and the temperature. Similar calibration curves were obtained when shorter periods of time were used for higher temperatures.

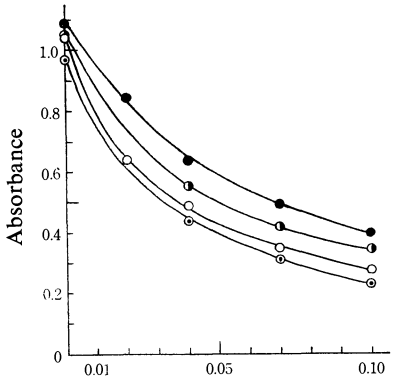



Fig. 3. Effects of reaction time, temperature and amounts of iodide.
—○— 30°C, 20 min., 1.5 ml. of iodide (I)
—●— 35°C, 10 min., 1.5 ml. of iodide (II)
—⊙— 30°C, 15 min., 1.0 ml. of iodide (III)
—◑— 30°C, 25 min., 2.0 ml. of iodide (IV)

The results with different amounts of iodide and different reaction times are shown by curves I, III and IV in Fig. 3. Similar curves were also obtained when longer periods of time were used for larger amounts of iodide. It was thought most favorable to use the reaction time of 20 min., the temperature of 30°C, and 1.5 ml. of the iodide solution.

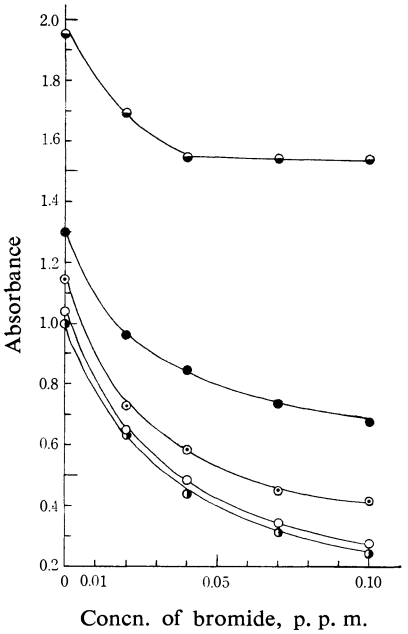



Fig. 4. Effect of amount of ceric solution.
30°C, 20 min., 0.2 M ceric solution is used.
—◒— 0.5 ml. —○— 2.0 ml.
—●— 1.0 ml. —◑— 2.5 ml.
—⊙— 1.5 ml.

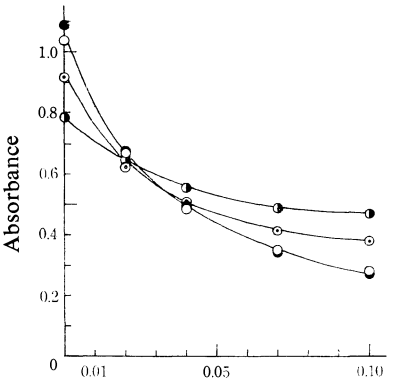



Fig. 5. Effect of amount of nitric acid.
30°C, 20 min., concentrated nitric acid is used.
—◑— 1.0 ml. —○— 2.0 ml.
—⊙— 1.5 ml. —●— 2.5 ml.

**The Concentration of Reagents.**—The effects of the ceric solution are shown in Fig. 4. The sensitivity increased with an increase in the amount of ceric solution added, but when more than 2.0 ml. of the ceric solution was used, no increase in sensitivity was obtained.

Figure 5 shows the effects of nitric acid. The larger the amount of nitric acid, the higher the absorbance of the blank solution and the lower that of the 0.10 p. p. m. bromide solution. However, by using 2.5 ml. of nitric acid, almost the same curve as that of 2.0 ml. was obtained. It appears that the nitric acid is necessary for this catalytic reaction. When sulfuric acid was used instead of nitric acid, no difference in absorbances between blank solution and 0.10 p. p. m. bromide solution was observed.

Dichromate is essential for this catalytic reaction. In its absence no difference in absorbance was obtained between blank and bromide solutions. In order to examine the

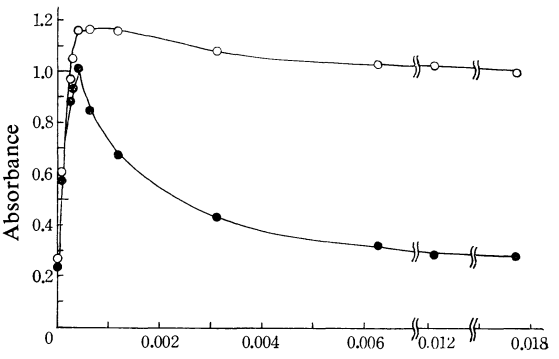



Fig. 6. Effect of concentration of dichromate.
30°C, 20 min.
—○— Redistilled water (I)
—●— 0.10 p. p. m. $Br^-$ (II)

effects of dichromate, the reactions were performed in the presence of various amounts of dichromate using the blank solution and the solution containing 0.1 p. p. m. of bromide. The results are shown in Fig. 6. The presence of small amounts of dichromate caused a sharp decrease in the reaction rate and only a slight difference in absorbance between the two curves I and II. However, at higher concentrations than 0.0004 M in the reaction solution, curve II deviated remarkably from curve I with the increase in the concentration of dichromate; they then ran parallel to each other.

In order to ascertain the most suitable conditions, the effects of the amount of the dichromate solution were further determined, as shown in Fig. 7.

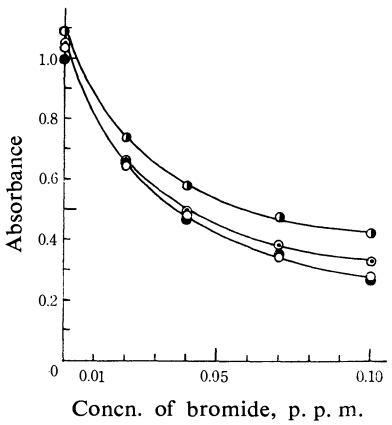



Fig. 7. Effect of amount of dichromate solution.
30°C, 20 min., 0.2 M dichromate solution is used.
—◑— 0.25 ml. —○— 1.0 ml.
—⊙— 0.5 ml. —●— 1.5 ml.

The sensitivity increased with an increase in the amount of dichromate solution added, but by using more than 1.0 ml. almost the same curves were obtained.

**The Effect of Diverse Ions.** — In order to make clear the effect of diverse ions on this method, some experiments were made in the presence of 0.04 p. p. m. of bromide ion and in its absence. The experimental results are given in Table I.

Nitrate and sulfate ions do not interfere at considerably high concentrations, but chloride ions interfere at 1 p. p. m. The effects of chloride ions will be described in detail in the following section. Iodide ions interfere slightly at 10 p. p. m. However, even if the sample contains more than 10 p. p. m. of iodide ions, the total amount of iodide in the reaction solution at the start of the oxidation can be

TABLE I. EFFECT OF DIVERSE IONS

| Ion | Added as | Concn. p.p.m. | Absorbance: Reagent blank | Absorbance: 0.04 p. p. m. $Br^-$ |
|---|---|---|---|---|
| None | | | 1.061 | 0.509 |
| | | | 1.046 | 0.495 |
| | | | 1.041 | 0.478 |
| $NO_3^-$ | $NaNO_3$ | 62000 (1 M) | 1.051 | 0.510 |
| $SO_4^{2-}$ | $K_2SO_4$ | 9600 (0.1 M) | 1.215 | 0.791 |
| | | 1000 | 1.061 | 0.507 |
| $CO_3^{2-}$ | $Na_2CO_3$ | 100 | 1.044 | 0.469 |
| $PO_4^{3-}$ | $Na_2HPO_4 \cdot H_2O$ | 10 | 1.044 | 0.507 |
| $F^-$ | NaF | 100 | 1.086 | 0.585 |
| | | 10 | 1.061 | 0.498 |
| $Cl^-$ | NaCl | 1 | 0.951 | 0.471 |
| $I^-$ | KI | 100 | 1.921 | 1.409 |
| | | 10 | 1.086 | 0.541 |
| $ClO_3^-$ | $KClO_3$ | 10 | 1.032 | 0.478 |
| $IO_3^-$ | $KIO_3$ | 10 | 1.061 | 0.495 |
| $NO_2^-$ | $NaNO_2$ | 10 | 1.043 | 0.482 |
| $CN^-$ | KCN | 10 | 0.770 | 0.376 |
| | | 1 | 1.043 | 0.470 |
| $SCN^-$ | KSCN | 10 | 0.772 | 0.367 |
| | | 1 | 1.051 | 0.467 |
| $S^{2-}$ | $Na_2S \cdot 9H_2O$ | 10 | 1.096 | 0.545 |
| | | 1 | 1.041 | 0.495 |
| $SO_3^{2-}$ | $Na_2SO_3 \cdot 7H_2O$ | 100 | 1.046 | 0.494 |
| $S_2O_3^{2-}$ | $Na_2S_2O_3 \cdot 5H_2O$ | 10 | 1.051 | 0.480 |
| $CrO_4^{2-}$ | $K_2CrO_4$ | 100 | 1.036 | 0.495 |
| $MnO_4^-$ | $KMnO_4$ | 1 | 0.801 | 0.388 |
| | | 0.1 | 1.046 | 0.457 |
| $H_2O_2$ | | 100 | 1.046 | 0.465 |
| Borate ion | $H_3BO_3$ | 10 | 1.032 | 0.479 |
| Silicate ion | (as $SiO_2$) | 100 | 1.000 | 0.434 |
| | | 50 | 1.036 | 0.509 |
| $Al^{3+}$ | $Al(NO_3)_3 \cdot 9H_2O$ | 100 | 1.046 | 0.476 |
| $Ca^{2+}$ | $Ca(NO_3)_2 \cdot 4H_2O$ | 100 | 1.046 | 0.488 |
| $Mg^{2+}$ | $Mg(NO_3)_2 \cdot 6H_2O$ | 100 | 1.046 | 0.478 |
| $Zn^{2+}$ | $ZnSO_4 \cdot 7H_2O$ | 100 | 1.035 | 0.478 |
| $Pb^{2+}$ | $Pb(NO_3)_2$ | 100 | 1.046 | 0.478 |
| $Cu^{2+}$ | $CuSO_4 \cdot 5H_2O$ | 100 | 1.035 | 0.478 |
| $Ni^{2+}$ | $NiSO_4 \cdot 7H_2O$ | 100 | 1.035 | 0.478 |
| $Co^{2+}$ | $CoSO_4 \cdot 7H_2O$ | 100 | 1.035 | 0.478 |
| $Cd^{2+}$ | $3CdSO_4 + 8H_2O$ | 100 | 1.035 | 0.478 |
| $Fe^{3+}$ | $Fe(NO_3)_3 \cdot 9H_2O$ | 100 | 1.046 | 0.509 |
| $Fe^{2+}$ | $FeSO_4 \cdot 7H_2O$ | 100 | 0.959 | 0.456 |
| $Ce^{4+}$ | $Ce(SO_4)_2$ | 100 | 1.046 | 0.471 |
| $Mn^{2+}$ | $Mn(NO_3)_2 \cdot 6H_2O$ | 1 | 0.480 | 0.206 |
| | | 0.1 | 0.932 | 0.431 |
| $Ag^+$ | $Ag_2SO_4$ | 0.1 | 0.883 | 0.367 |
| | | 0.01 | 1.036 | 0.480 |
| $Hg^{2+}$ | $HgSO_4$ | 0.1 | 0.747 | 0.325 |
| | | 0.01 | 1.046 | 0.495 |

kept at the constant concentration by decreasing the amount of the iodide reagent to be used. Permanganate and manganese(II) ions interfere at relatively low concentrations. Silver and mercuric ions interfere remarkably.

**The Determination of Bromide in the Presence of Chloride.**—This method is affected by 1 p.p.m. of chloride. As natural waters always contain small amounts of chloride, the effects of chloride were examined.

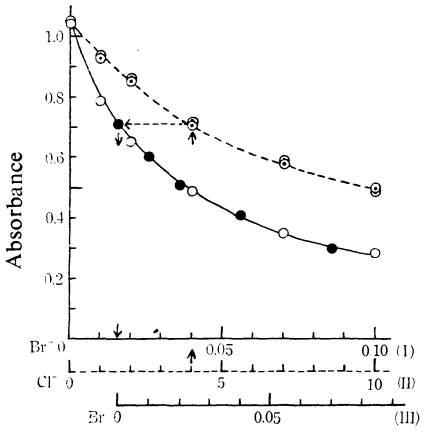



Fig. 8. Calibration curves.
30°C. 20 min.
—○— $Br^-$ (I)
--⊙-- $Cl^-$ (II)
—●— $Br^-$ in the presence of 4 p. p. m. $Cl^-$ (III)
←---- 4 p. p. m. $Cl^-$ (↑) is equivalent to 0.016 p. p. m. $Br^-$ (↓).

Curve II in Fig. 8 was obtained by this method by using standard chloride solutions of known concentrations. Curve I, the calibration curve of this method, is shown in Fig. 1. Chloride gives a curve similar to bromide when the concentrations of chloride are a hundred times larger than those of bromide. The experiments were also made by using standard bromide solutions containing 4 p. p. m. of chloride. The absorbances obtained are plotted against the concentrations of bromide on the abscissa III with solid circles. All these solid circles fall just on curve I. The concentration of bromide on the abscissa I minus that equivalent to 4 p. p. m. of chloride gives the value on the abscissa III. The same results were also obtained in the presence of different amounts of chloride. Thus, in samples containing small amounts of chloride, the concentration of bromide can be obtained by correcting the value for the chloride.

The concentration of chloride in the sample is first determined by the mercuric thiocyanate method.[4] By means of curves I and II in Fig. 8, a concentration of bromide ($A$ p. p. m.) equivalent to the concentration of chloride is obtained. Then the sample is treated by this method, and the value ($B$ p. p. m.) is obtained by curve I. Thus, the concentration of bromide in the sample is calculated as the difference between $B$ and $A$ [$(B-A)$ p. p. m.].

The bromide contents in several natural waters were also determined by this method. The results are given in Table II.

Table II. Determination of bromide contents in natural waters

| | Sample | Concn. of bromide p. p. m. | Concn. of chloride p. p. m. |
|---|---|---|---|
| No. 1 | Rain water*1 (I) | 0.005 | 0.17 |
| No. 2 | River water*2 (II) | 0.070 | 16.2 |
| No. 3 | River water*3 (III) | 0.060 | 15.2 |
| No. 4 | | 0.062 | |
| No. 5 | Sample added bromide*4 | 0.082 | |

*1 The sample was taken at Meguro-ku, Tokyo, July, 1963.
*2 The sample was taken in River Tamagawa, Noborito-bashi, Tokyo, June, 1963.
*3 The sample was taken in River Tamagawa, Futako-bashi, Tokyo, June, 1963.
*4 The sample contains 0.020 p. p. m. of added bromide and 0.061 p. p. m. of originally present bromide.

Sample I was analyzed by using 10 ml., while samples II and III were analyzed by using samples diluted 3 ml. to 10 ml. The results given in Table II are calculated to original concentrations. The value listed in No. 4 was obtained by using sample III diluted 5 ml. to 10 ml. The comparison of the two results of sample III shows a good agreement. The method was also checked by adding a known amount of bromide to sample III. The determination of the total bromide concentration of this sample was made by using a sample diluted 3 ml. to 10 ml. The original concentration was calculated from the value thus obtained; it is listed in No. 5. This result shows that the known amount of bromide added is satisfactorily determined.

By this method, minute amounts of bromide in natural waters can be determined rapidly and sensitively.

*Laboratory of Analytical Chemistry and Geochemistry*
*Tokyo Institute of Technology*
*Ookayama, Tokyo (N. Y. & I. I.)*

*Department of Science and Technology*
*Nihon University*
*Chiyoda-ku, Tokyo (S. U.)*

# Chemical Effects Associated with the $\beta$-Decay Process. II. A Kinetic Study of the Chemical Behavior of $^{144}Pr$ in the EDTA Complex System

By Takanobu SHIOKAWA and Takashi OMORI

(Received March 5, 1965)

Unusual chemical behavior of a radioactive daughter atom may result from an increase in the nuclear charge produced by $\beta^-$-decay.[1] The effects of the increase include such secondary processes as an electronic excitation due to a sudden change in the nuclear charge, and rotational and vibrational excitations due to recoil. It is very difficult to evaluate the effects associated with $\beta^-$-decay in the liquid system, in contrast to those taking place in the gas phase. In the Ce-Pr-144 system, however, the probability of a bond-rupture arising from the recoil by $\beta^-$-decay is expected to be much smaller, since the maximum recoil energy imparted to a free, isolated $^{144}Pr$ atom is only 1.6 eV. It was also suggested in the preceding paper[2] that the thermodynamical instability of a $^{144}Pr$ atom plays an important role in determining its chemical behavior. Accordingly, the experimental results could be explained qualitatively by a mechanism which includes the decomposition of an intermediate complex produced by intramolecular electron-transfer, in addition to the substitution reaction between the liberated $^{144}Pr$ ion and the cerium(III) ethylenediaminetetraacetate (Ce(III)-EDTA) complex.

More experimental evidence is needed to substantiate this model. The present authors have, therefore, attempted to elucidate quantitatively the chemical behavior of $^{144}Pr$ atoms in terms of the per cent yield of the $^{144}Pr$(III)-EDTA complex (the $^{144}PrY^-$-yield). Moreover, in order to study the kinetics of the $^{144}PrY^-$-yield, the substitution reactions of the cerium(III) ion and the Pr(III)-EDTA complex were investigated in an aqueous solution using $^{144}Ce$ as a tracer.

## Experimental

The chemicals employed were the same as those described previously.[2]

The kinetic runs were carried out as follows: an aqueous solution of the Pr(III)-EDTA complex was mixed with praseodymium(III) chloride containing $^{144}Ce$ at 25±0.1°C. The ionic strength was adjusted using 0.50 M sodium chloride, and then 0.04 M sodium acetate was added as a buffer. As will be mentioned later, the exchange rate is affected by the presence of acetate ions, so the total concentration of acetate ions was maintained at 0.04 M in order to minimize such effect. At suitable times, samples were withdrawn rapidly through a Dowex 50W-X8 column (0.5 g. of resin) which had been previously treated with an appropriate buffer. The column was then washed with a known amount of buffer, and the combined eluates (that is, the fraction containing the complex) were collected in a test tube. The separate experiments ensured that the free-ion fraction was separated quantitatively from the complex fraction.

The $^{144}PrY^-$-yield, which was defined as the ratio of the $\gamma$-activity of the eluate to the total activity, was obtained similarly, after a complete equilibration with respect to $^{144}Ce$ had been attained chemically.

The $\gamma$-activity of each liquid sample was determined with a well-type scintillation spectrometer. The $^{144}Ce$ and $^{144}Pr$ were assayed by essentially the same methods as had been employed previously.[2] The pH of the solution at the equilibrium was measured by a glass-electrode pH meter, with an accuracy of 0.01 pH.

## Results and Discussion

**The Substitution Mechanism.**—In the preliminary experiments on the isotopic exchange reaction of $^{144}Ce$(III) ion and Ce(III)-EDTA complex, it was found that the rate of the exchange reaction, $R$, may be expressed as:

$$R = k_{Ce,\,app}\,[CeY^-]\,[H^+] \qquad (1)$$

where $k_{Ce,\,app}$ is the apparent rate constant, depending on the concentration of acetate ions, and $Y^{4-}$ indicates a tetravalent EDTA anion. The main path leading to exchange is the acid-catalyzed dissociation of the Ce(III)-EDTA complex, which is in accordance with the mechanism suggested by Betts et al.[3]

The substitution reaction of the cerium(III)

1) S. Wexler, "Chemical Effects of Nuclear Transformations (Prague Conf.)," Vol. I, IAEA, Vienna (1961), p. 115.
2) T. Shiokawa, H. Kudo and T. Omori, This Bulletin, 38, 1340 (1965).
3) R. H. Betts, O. F. Dahlinger and D. M. Munro, "Radioisotopes in Scientific Research. Proceedings of the First UNESCO International Conference, Paris, 1957," Vol. II, Pergamon Press, New York (1958), p. 326.

ion and the Pr(III)-EDTA complex may be expressed stoichiometrically as follows:

$$^{144}Ce^{3+} + PrY^{-} \rightleftarrows {}^{144}CeY^{-} + Pr^{3+} \quad (2)$$

On the basis of the isotopic exchange reaction, the path of the substitution will be:

$$PrY^{-} + H^{+} \xrightarrow{k_{Pr,\,app}} Pr^{3+} + HY^{3-} \quad (3)$$

followed by a very fast reaction:

$$Ce^{3+} + HY^{3-} \xrightarrow{k'_{Ce}} CeY^{-} + H^{+} \quad (4)$$

The reverse reactions, whose rate constants are designated by $k'_{Pr}$ for Eq. 3 and $k_{Ce,\,app}$ for Eq. 4, would take place simultaneously. In these expressions, $Pr^{3+}$ and $Ce^{3+}$ represent the species in the cationic form, including acetate complexes. These, however, may be allowed, since the exchange rate is independent of the nature of the free metal ion. It is also permissible to set $k'_{Ce}=k'_{Pr}$. Hence, the overall rate equation is given by:

$$\frac{d[CeY^{-}]}{dt} = k_{Pr,\,app}[PrY^{-}][H^{+}]\frac{[Ce^{3+}]}{[Ce^{3+}]+[Pr^{3+}]} - k_{Ce,\,app}[CeY^{-}][H^{+}]\frac{[Pr^{3+}]}{[Ce^{3+}]+[Pr^{3+}]} \quad (5)$$

Since the kinetic measurements are carried out with solutions containing both the praseodymium(III) ion and the Pr(III)-EDTA complex in a large excess over carrier-free $^{144}Ce$, the substitution reaction can be treated as a pseudo-first order reaction; the reaction rate may thus be simplified as follows:

$$\frac{d[^{144}CeY^{-}]}{dt} = k_{Pr,\,app}[H^{+}]\frac{[PrY^{-}]_0}{[Pr^{3+}]_0}[^{144}Ce^{3+}] - k_{Ce,\,app}[H^{+}][^{144}CeY^{-}] \quad (6)$$

where the subscript $_0$ denotes the initial state. The concentrations of the praseodymium(III) ion and the Pr(III)-EDTA complex remain unchanged during the reaction; therefore, the following relation may be satisfied at equilibrium:

$$K_{app} = \frac{[PrY^{-}]_e[^{144}Ce^{3+}]_e}{[Pr^{3+}]_e[^{144}CeY^{-}]_e} = \frac{k_{Ce,\,app}}{k_{Pr,\,app}} \quad (7)$$

where $K_{app}$ corresponds to the reciprocal of the apparent equilibrium constant of Eq. 2 at a specified acetate concentration, and the subscript e denotes the equilibrium state. The apparent equilibrium constant, $K_{app}$, was found to be $2.10\pm0.08$ in the presence of 0.04 M acetate at 25°C.

The integration of Eq. 6, then, gives:

$$\ln\left\{\frac{[^{144}CeY^{-}]_e}{[^{144}CeY^{-}]_e-[^{144}CeY^{-}]}\right\} = \left\{k_{Pr,\,app}\frac{[PrY^{-}]_0}{[Pr^{3+}]_0}+k_{Ce,\,app}\right\}[H^{+}]t = k_{app}\cdot t \text{ (at a constant pH)} \quad (8)$$

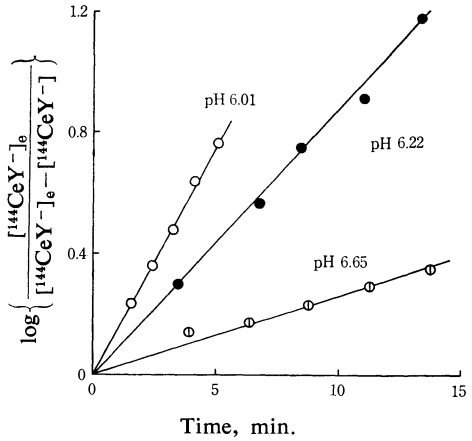



Fig. 1. $\log\left\{\frac{[^{144}CeY^{-}]_e}{[^{144}CeY^{-}]_e-[^{144}CeY^{-}]}\right\}$ vs. time.

| | $[PrY^{-}]_0$ | $[Pr^{3+}]_0$ |
|---|---|---|
| ○ and ● : | $1.82\times10^{-4}$ M ; | $7.62\times10^{-5}$ M |
| ① : | $9.52\times10^{-5}$ M ; | $7.62\times10^{-5}$ M |

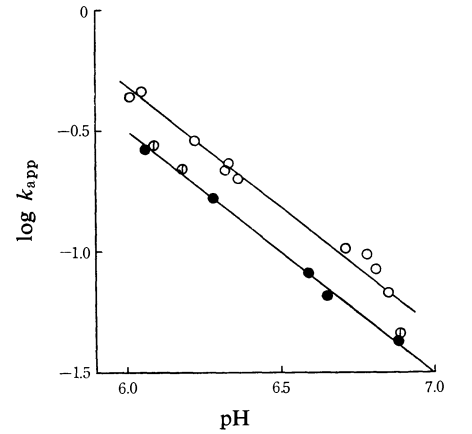



Fig. 2. Dependence of apparent rate constant, $k_{app}$, on pH at 25°C.

| | $[PrY^{-}]_0$ | $[Pr^{3+}]_0$ |
|---|---|---|
| ○ : | $1.82\times10^{-4}$ M ; | $8.00\times10^{-5}$ M |
| ● : | $9.52\times10^{-5}$ M ; | $7.62\times10^{-5}$ M |
| ① : | $1.82\times10^{-4}$ M ; | $1.64\times10^{-4}$ M |

Typical plots of the logarithmic term in Eq. 8 against $t$ are shown in Fig. 1. The zero-time exchange appears to be negligible. The apparent rate constant, $k_{app}$, is obtained from the slope of the straight line shown in Fig. 1. The dependence of $\log k_{app}$ on pH is given in Fig. 2, indicating the first order dependence of $k_{app}$ on the hydrogen ion concentration. Equation 7 also gives the relation:

$$k_{Ce,\,app} = K_{app}\cdot k_{Pr,\,app} = 2.10\,k_{Pr,\,app} \quad (7')$$

indicating that the exchange rate constants are in inverse order with regard to the stability constants of the EDTA complexes. Hence, as long as the substitution mechanism proposed

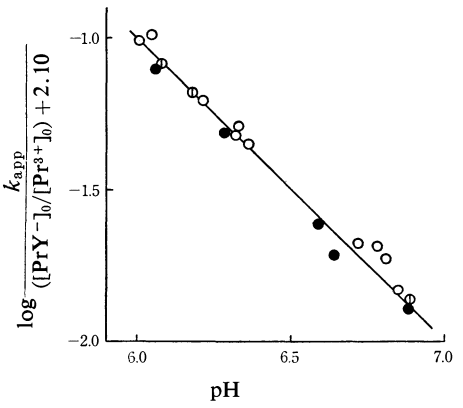



Fig. 3. $\log\frac{k_{app}}{([PrY^-]_0/[Pr^{3+}]_0)+2.10}$ vs. pH.

is valid, the plot of $\log k_{app}/\{([PrY^-]_0/[Pr^{3+}]_0)+2.10\}$ against the pH value must normalize the experimental values obtained under different conditions, giving a straight line with a unit slope. The value of $k_{Pr,\,app}$ can be determined from the intercept. The results are satisfactory, as Fig. 3 shows, and lend support to the kinetic mechanism proposed. The exchange rate constant, $k_{Pr,\,app}$, was determined to be:

$$k_{Pr,\,app}=1.0_1\times10^5\ \text{l. mol}^{-1}\text{min}^{-1}$$

and from the relation expressed by Eq. 7', $k_{Ce,\,app}$ was calculated as follows:

$$k_{Ce,\,app}=2.1_1\times10^5\ \text{l. mol}^{-1}\ \text{min}^{-1}$$

**The Chemical Behavior of $^{144}$Pr.**—In order to estimate the contribution of the thermal exchange reaction, the dependence of the $^{144}PrY^-$-yield on the pH value was investigated. As is shown in Fig. 4, the $^{144}PrY^-$-yield decreases gradually with the pH, indicating that the departure from the equilibrium value is large in higher pH regions.

If the $^{144}$Pr atoms which escape from the parent molecule distribute thermally between the praseodymium(III) ion and the Pr(III)-EDTA complex, the fraction of exchange that has taken place during the time, $t$, can be expressed as:

$$\ln\left\{\frac{[^{144}PrY^-]_e}{[^{144}PrY^-]_e-[^{144}PrY^-]}\right\}=k_{Pr,\,app}\left\{\frac{[Pr^{3+}]_0+[PrY^-]_0}{[Pr^{3+}]_0}\right\}[H^+]t \quad (9)$$

Of course, one must take into consideration the fact that, even in the case of the transformation of the $^{144}$Ce(III)-EDTA complex to the $^{144}$Pr(III)-EDTA complex without any net chemical change, a re-distribution of the praseodymium ions takes place because of the difference in the formation constants of their EDTA complexes.

First, let us assume that the extent of the bond-rupture by the $\beta^-$-decay process is insensitive to the pH, viz., that $t$ in Eq. 9 is a constant. When one plots the logarithmic fraction of the exchange vs. the pH, a straight line with a slope of -1 should be obtained. On the other hand, the value of $t$ in Eq. 9 can be determined by introducing the rate constants obtained in the preceding section. These results are given in Figs. 5 and 6. The non-unit slope, as shown in Fig. 5, means that the extent of formation of free $^{144}$Pr ions varies with the pH; that is, the reaction time

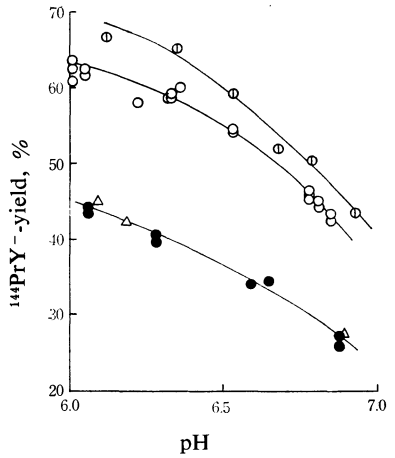



Fig. 4. Dependence of the $^{144}PrY^-$-yield on pH at 25°C.

| | $[PrY^-]_0$ | $[Pr^{3+}]_0$ |
|---|---|---|
| ①: | $2.40\times10^{-4}$ M; | $8.00\times10^{-5}$ M |
| ○: | $1.82\times10^{-4}$ M; | $7.62\times10^{-5}$ M |
| ●: | $9.52\times10^{-5}$ M; | $7.62\times10^{-5}$ M |
| △: | $1.82\times10^{-4}$ M; | $1.64\times10^{-4}$ M |

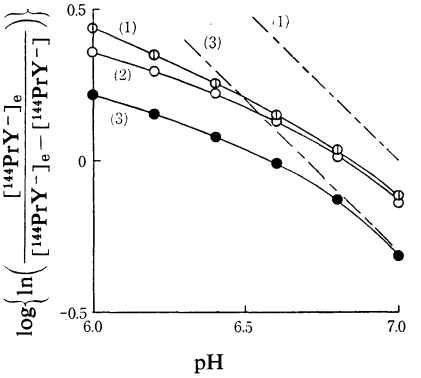



Fig. 5. $\log\left\{\ln\left(\frac{[^{144}PrY^-]_e}{[^{144}PrY^-]_e-[^{144}PrY^-]}\right)\right\}$ vs. pH.

| | $[PrY^-]_0$ | $[Pr^{3+}]_0$ |
|---|---|---|
| ①: | $2.40\times10^{-4}$ M; | $8.00\times10^{-5}$ M |
| ○: | $1.82\times10^{-4}$ M; | $7.62\times10^{-5}$ M |
| ●: | $9.52\times10^{-5}$ M; | $7.62\times10^{-5}$ M |

The dashed lines were calculated by Eq. 9.

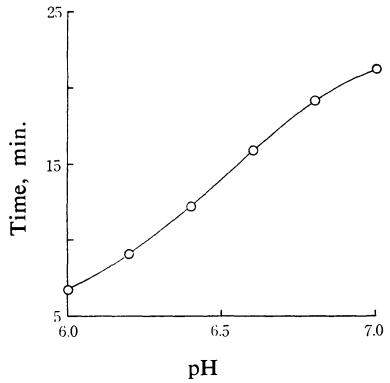



Fig. 6. Reaction time vs. pH.
$[PrY^-]_0=1.82\times10^{-4}$ M
$[Pr^{3+}]_0=7.62\times10^{-5}$ M

is not constant. However, even if the concept that the extent of bond rupture is sensitive to pH is valid, the values of the reaction time obtained are fairly small in the lower pH region, as compared with the average life of $^{144}Pr$, $\tau$, which is defined as:

$$\tau=t_{1/2}/0.693=25.3 \text{ min.}$$

These facts are strong evidence in support of the presence of an intermediate with a measurable lifetime produced by the $\beta^-$-decay of the $^{144}Ce$(III)-EDTA complex.

Before we consider the physical and chemical meanings of the intermediate complex, an attempt to treat the decomposition of this complex on the basis of kinetics will be discussed. The deviation of the $^{144}PrY^-$-yield from the equilibrium values leads to an assumption that the irreversible decomposition of the intermediate complex to produce the free $^{144}Pr$ ions is promoted by the action of either hydroxide ions or protonated EDTA anions ($HY^{3-}$), which are supplied steadily by the acid-catalyzed dissociation of the Pr(III)-EDTA complex. The latter mechanism is substantially analogous to the decomposition of the Mn-(III)-EDTA complex in the presence of an excess of EDTA.[4] The proposed mechanism excludes a direct bimolecular reaction between the intermediate and Pr(III)-EDTA complex to afford $^{144}Pr$-EDTA complex, because $^{144}Pr$ atoms were considerably enriched in the free-ion fraction. Hence, the decomposition process may be expressed as:

$$^{144}PrZ \xrightarrow[k_1]{OH^-,\ HY^{3-}} {}^{144}Pr^{3+} \underset{k_2}{\rightleftarrows} {}^{144}PrY^- \qquad (10)$$

where $^{144}PrZ$ represents the intermediate complex.

4) K. A. Schroeder and R. E. Hamm, *Inorg. Chem.*, **3**, 391 (1964).

The fraction of the $^{144}Pr$(III)-EDTA complex, $Z$, at the time, $t$, can be obtained by the following equation:

$$Z=\frac{[PrY^-]_0}{([Pr^{3+}]_0+[PrY^-]_0)2\sqrt{\alpha^2-\beta}} \times (r_2e^{r_1t}-r_1e^{r_2t}+2\sqrt{\alpha^2-\beta}) \qquad (11)$$

where:

$$k_1+k_2=2\alpha, \quad k_1k_2=\beta$$
$$r_1=-\alpha+\sqrt{\alpha^2-\beta} \quad r_2=-\alpha-\sqrt{\alpha^2-\beta}$$
$$k_1=k'[OH^-]+k''[H^+][PrY^-]_0/[Pr^{3+}]_0 \qquad (12)$$
$$k_2=k_{Pr,\ app}[H^+]([Pr^{3+}]_0+[PrY^-]_0)/[Pr^{3+}]_0$$

$k'$ and $k''$ are the rate constants for the hydroxide ion- and the protonated EDTA anion-dependent terms respectively. If one chooses suitable values for $k'$ and $k''$, the $^{144}PrY^-$-yield can be calculated from Eqs. 9 and 11, provided that the $^{144}Pr$ atoms produced by the $\beta^-$-decay of free $^{144}Ce$(III) ions are reduced instantaneously to stable $^{144}Pr$(III) ions through electron-transfer with surrounding substances.

By using the rate constants, $k'=10^{6.1}$ l. mol$^{-1}$. min$^{-1}$ and $k''=10^{4.4}$ l. mol$^{-1}$ min$^{-1}$, and the reaction time of $t=25.3$ min., the $^{144}PrY^-$-yields were calculated as in Fig. 7. The agreement

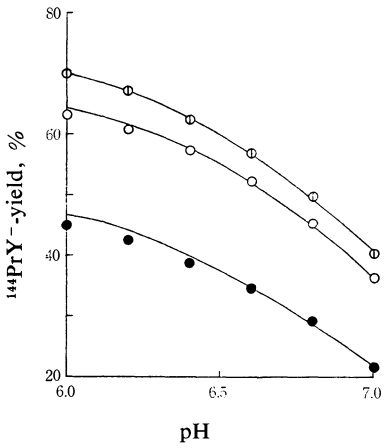



Fig. 7. The $^{144}PrY^-$-yield calculated by Eqs. 9 and 11.

| | $[PrY^-]_0$ | $[Pr^{3+}]_0$ |
|---|---|---|
| ① : | $2.40\times10^{-4}$ M ; | $8.00\times10^{-5}$ M |
| ○ : | $1.82\times10^{-4}$ M ; | $7.62\times10^{-5}$ M |
| ● : | $9.52\times10^{-5}$ M ; | $7.62\times10^{-5}$ M |

The circles indicate the experimental values obtained from the curves in Fig. 4.
The solid curves were calculated by Eqs. 9 and 11.

between the observed and calculated $^{144}PrY^-$-yields is satisfactory.

To confirm this mechanism, a similar experiment was carried out with the cerium(III) ion and Ce(III)-EDTA complex system. The

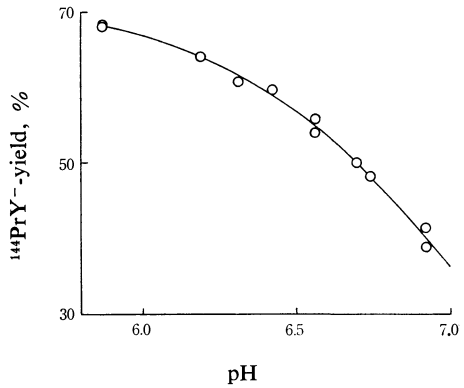



Fig. 8. Dependence of the $^{144}PrY^-$-yield on pH at 25°C in the $Ce^{3+}$-$CeY^-$ system.
$[CeY^-]_0=1.00\times10^{-4}$ M;
$[Ce^{3+}]_0=8.08\times10^{-5}$ M

relation between the $^{144}PrY^-$-yield and the pH is shown in Fig. 8. The substitution reaction for a $^{144}Pr$(III) ion and a Ce(III)-EDTA complex is expressed as follows:

$$\ln\left\{\frac{[^{144}PrY^-]_e}{[^{144}PrY^-]_e-[^{144}PrY^-]}\right\}=\left\{k_{Ce,\,app}\frac{[CeY^-]_0}{[Ce^{3+}]_0}+k_{Pr,\,app}\right\}[H^+]t \quad (13)$$

In this system, Eq. 11 will be rewritten as:

$$Z=\frac{2.10[CeY^-]_0}{([Ce^{3+}]_0+2.10[CeY^-]_0)2\sqrt{\alpha^2-\beta}}\times(r_2e^{r_1t}-r_1e^{r_2t}+2\sqrt{\alpha^2-\beta}) \quad (14)$$

and the rate constants for the processes in Eq. 10 are expressed, respectively, as follows:

$$k_1=k'[OH^-]+2.10k''[H^+][CeY^-]_0/[Ce^{3+}]_0$$

$$k_2=\{k_{Ce,\,app}[CeY^-]_0/[Ce^{3+}]_0+k_{Pr,\,app}\}[H^+] \quad (15)$$

As Fig. 9 shows, the excellent agreement between the $^{144}PrY^-$-yield calculated by Eqs. 13 and 14 and the experimental values further supports the proposed decomposition process of the intermediate complex.

These results indicate that at least the intermediate can not be regarded as the EDTA complex, the chemical behavior of which is treated reasonably by Eq. 9 or Eq. 13. EDTA is a reducing agent, one which reduces permanganate, chromate and cerium(IV) ions in an acidic solution,[5] but EDTA bound in a metal complex is not oxidized by permanganate ions.[6] Recently, it has been found that the photodecomposition of acid aquoethylenediaminetetraacetatoferrate(III) produces both iron(II) ions by electron-transfer and carbon

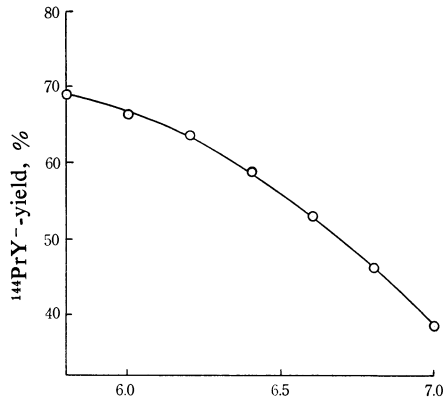



Fig. 9. The $^{144}PrY^-$-yield calculated by Eqs. 13 and 14.
$[CeY^-]_0=1.00\times10^{-4}$ M;
$[Ce^{3+}]_0=8.08\times10^{-5}$ M
○ indicates the experimental value obtained from the curve in Fig. 8.
The solid curve was calculated by Eqs. 13 and 14.

dioxide by the decarboxylation of a coordinated carboxylate group.[7] Schroeder and Hamm[4] also found that carbon dioxide and formaldehyde were produced in the case of the decomposition of the Mn(III)-EDTA complex. By taking into consideration the fact that the praseodymium(IV) ion is very unstable in solution, it is apparent that an intramolecular electron-transfer between the tetravalent praseodymium and the EDTA molecule will take place at the time of the $\beta^-$-decay of $^{144}Ce$ complexed with EDTA, as has been proposed in the previous paper.[2] The trivalent $^{144}Pr$ ion remains complexed with an oxidized EDTA radical, which is probably produced by the loss of one chelating carboxylate group; it does not escape from the molecule.

According to the formation constant of the cerium(III) acetate complex,[8] about 80 per cent of the cerium(III) ions complex with acetate ions under the experimental conditions. The tetravalent praseodymium produced by the $\beta^-$-decay of the $^{144}Ce$ acetate complex may be either reduced by the intramolecular electron-transfer or by the action of the surrounding substances. The reduced praseodymium(III) ion will escape easily from the molecule, because the acetate ion is a monodentate ligand and it forms labile complexes with praseodymium(III) ions. The process of the deactivation of the $^{144}Pr$ produced by the $\beta^-$-decay of $^{144}Ce$ is illustrated schematically in Fig. 10.

5) P. N. Palei and N. I. Udal'tsova, *Zhur. Anal. Khim.*, 15, 668 (1960); *Chem. Abstr.*, 55, 18424 (1961).
6) M. J. Beck, *Chemist-Analyst*, 50, 14 (1961).
7) J. K. Lambert, C. E. Godsey and L. M. Seitz, *Inorg. Chem.*, 2, 127 (1963).
8) S. K. Kolat and J. E. Powell, ibid., 1, 293 (1962).

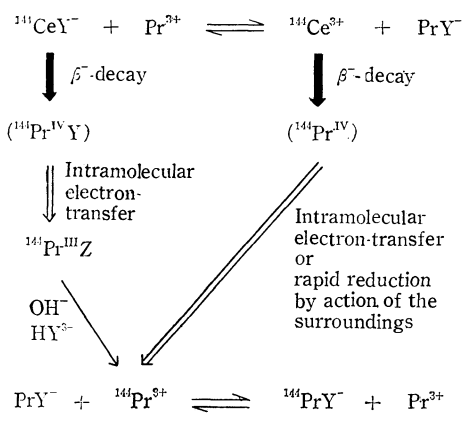



Fig. 10. De-activation proceses of $^{144}Pr$ atom produced by $\beta^-$-decay of $^{144}Ce$ in the EDTA complex system.

A satisfactory explanation for the experimental results can be offered on the assumption that all the decay events of the complexed $^{144}Ce$ lead to the formation of the intermediate. Nevertheless, the excited $^{144}Pr$ atoms may be stabilized by a different route; namely, the multiple charging due to internal conversion, at least in part, may cause an exhaustive decomposition, thus liberating the free $^{144}Pr$ ion. It must be noted, therefore, that the values obtained for the rate constants, $k'$ and $k''$, are not absolute, but include the various accompanying effects resulting from the $\beta^-$-decay process.

## Summary

The substitution reaction of $^{144}Ce$(III) ions with the $^{144}Pr$(III)-EDTA complex in an aqueous solution at 25°C has been investigated; the rate-determining step has been found to be the acid-catalyzed dissociation of the Pr(III)-EDTA complex.

On the basis of the above substitution mechanism, the chemical behavior of the $^{144}Pr$ atoms produced by the $\beta^-$-decay of $^{144}Ce$ has been satisfactorily explained in terms of a model which involves the formation of an intermediate complex. The kinetic treatment leads to the conclusion that the intermediate, produced as a results of an increase in the nuclear charge by the $\beta^-$-decay of the complexed $^{144}Ce$, is available for attack by hydroxide ions and protonated EDTA anions and, consequently, produces free $^{144}Pr$(III) ions.

The authors wish to thank Mr. Michio Hoshi* for his assistance in the experimental work.

*Department of Chemistry*
*Faculty of Science*
*Tohoku University*
*Katahira-cho, Sendai*

* Present address: Japan Atomic Energy Research Institute, Tokai, Ibaraki.

# Studies of Hydrogenolysis. XLIX.[1] The Selective Hydrogenolysis of $\alpha, \beta$-Epoxyketones*1

By Sekio MITSUI, Yasuhisa SENDA, Takashi SHIMODAIRA*2 and Hiroshi ICHIKAWA*3

(Received March 6, 1965)

It has been reported that the mechanism of catalytic hydrogenolysis depends on the adsorbed state of organic compounds,[2] especially on the orientation of molecules at the catalyst surface which is in turn determined by the chemical and steric structure of the molecules and by the nature of the catalysts.[3,4] We can now report that some $\alpha, \beta$-epoxyketones have been hydrogenated to give isomeric products at room temperature and at atmospheric pressure with different catalysts.

When benzalacetophenone oxide (I)[5] was

1) Part XLVIII: S. Mitsui and S. Imaizumi, *J. Chem. Soc. Japan, Ind. Chem. Sec.* (*Kogyo Kagaku Zasshi*), **68**, 816 (1965).

*1 Presented at the 17th Annual Meeting of Chemical Society of Japan, Tokyo, April, 1964.

*2 Presented address, Mitsubishi Petrochemical Co., Ltd., Tokyo, Japan.

*3 Presented address, Nippon Carbon Co., Ltd., Tokyo, Japan.

2) S. Mitsui and S. Imaizumi, This Bulletin, **34**, 744 1961); 36, 855 (1963).

3) S. Mitsui, Y. Senda and K. Konno, *Chem. & Ind.*, **1963**, 1354.

4) S. Mitsui and K. Iijima, *J. Chem. Soc. Japan, Pure Chem. Sec.* (*Nippon Kagaku Zasshi*), **84**, 833 (1963); **85**, 682 (1964).

5) E. Weitz and A. Scheffer, *Ber.*, **54**, 2329 (1921).

hydrogenated with either palladium charcoal-A[6],*4 (abbr. Pd-C-A) or palladium charcoal-B[7],*4 (abbr. Pd-C-B), 2-hydroxy-1, 3-diphenylpropan-1-one (II) (m. p. 66°C)[8] was produced with absorption of one mole of hydrogen, and 1, 3-diphenylpropane-1, 2-diol (III and III') (III: m. p. 84.5°C, III': m. p. 70°C),[9] with the absorption of two moles of hydrogen. The catalytic hydrogenation of III with Pd-C-A, to which small portions of concentrated hydrochloric acid had been added, yielded 1, 3-diphenylpropan-2-ol (IV) (*p*-nitrobenzoate (m. p. 79°C)).[10] The Raney nickel hydrogenation of I gave 1, 3-diphenylpropane-1, 3-diol (V and V') (V, racemic isomers; m. p. 130°C. V', meso isomer, m. p. 97°C).[11] V was converted into 1, 3-diphenylpropane (VI) (b. p. 126°C/0.6 mmHg)[12] by hydrogenation over Pd-C-A which contained a small amount of concentrated hydrochloric acid. I was also hydrogenated with platinum oxide; in this case both III' and V were reaction products.

The NMR spectrum of I shows that the signals of the epoxide protons are a doublet at 4.06 p.p.m. and 4.27 p.p.m.[13] The coupling constant for these protons in I is 1.7 c.p.s. This epoxide is confirmed as the trans isomer by the published data for simple epoxides.[14] The structures of II, III, III', IV, V, V' and VI were confirmed by analyses of them and of their benzoates and *p*-nitrobenzoates (except the VI) and by a comparison of their physical properties with those reported in the literature.[8-10,11a,12]

Differences similar to those observed in the hydrogenation of I with different catalysts, were also found in the hydrogenation of *cis*-dypnone oxide (VII).[15] The hydrogenation of VII over Pd-C-A or Pd-C-B gave 1, 3-diphenylbutane-1, 2-diol (VIII) (m. p. 90°C), while over Raney nickel 1, 3-diphenylbutane-1, 3-diol (IX) (m. p. 91°C) was obtained. The structures of VIII and IX were confirmed by analyses and by the reaction with periodic acid.

On the other hand, when benzalacetone oxide (X)[16] was hydrogenated with Pd-C-A, the hydrogen uptake ceased after one mole of hydrogen had been absorbed and 3-hydroxy-4-phenylbutan-2-one (XI) (b. p. 93.5°C/0.75 mmHg)[17] was obtained. XI was hydrogenated to give 1-phenylbutane-2, 3-diol (XII) (b. p. 118°C/0.18 mmHg)[16] with Raney nickel. Similarly, the hydrogenation of X over Raney nickel gave mainly XI when one mole of hydrogen was absorbed and XII when two moles of hydrogen were absorbed.

The X formed from benzaldehyde and chloroacetone under normal Darzen condensation was confirmed to be the trans isomer by Kwart and Kirk.[18] The structures of XI and XII were established by analyses of the semicarbazone of XI (m. p. 179°C)[17] and di-*p*-nitrobenzoate of XII (m. p. 130°C) and by a comparison of several of their physical properties with those of an authentic sample of 1-hydroxy-1-phenylbutan-3-one (XIII) (b. p. 106°C/0.11 mmHg, semicarbazone; m. p. 173°C), prepared by the reaction of benzaldehyde with acetone.[19]

XI and XII were recovered unchanged when they were shaken with hydrogen over Pd-C-A containing a small amount of concentrated hydrochloric acid. This fact also supports the theory that XI and XII are not benzyl-type alcohols.

It has been shown by Herz[9c] that the catalytic hydrogenation of benzalacetophenone oxide (I) yielded two dihydroxydiphenylpropanes, which he considered to be the diastereoisomeric $\alpha$-glycols.[20] From the present results, it is obvious that, on the hydrogenation of I and VII, the two isomeric products resulting from the cleavage of the carbon-oxygen bonds of the epoxide ring at different position were obtained according to the species of the catalysts. On the other hand, on the hydrogenation of X, which includes an acetyl group instead of the benzoyl group in I and VII, the cleavage of the $\beta$-carbon-oxygen bond

6) Method C; E. C. Horning, "Organic Syntheses," Coll. Vol. III, 686 (1955).

*4 These catalysts were named palladium charcoal-A or palladium charcoal-B respectively, by Mitsui and Saito as the catalysts contain trace acid or trace base: S. Mitsui and H. Saito, *J. Chem. Soc. Japan, Pure Chem. Sec.* (*Nippon Kagaku Zasshi*), **82**, 890 (1961).

7) Method B; E. C. Horning, "Organic Syntheses," Coll. Vol. III, 686 (1955).

8) P. L. Julian, E. W. Meyer, A. Magnani and W. Cole, *J. Am. Chem. Soc.*, **67**, 1203 (1945).

9) a) J. Levy and Dvoleitzka-Gombinska, *Bull. soc. chim. France*, **49**, 1765 (1931); b) P. Ruggli and A. H. Lutz, *Helv. Chim. Acta*, **30**, 1070 (1947); c) W. Herz, *J. Am. Chem. Soc.*, **74**, 2928 (1952).

10) P. Papa, E. Schwenk and B. Whitman, *J. Org. Chem.*, **7**, 587 (1942).

11) a) H. E. Zimmerman and J. English, Jr., *J. Am. Chem. Soc.*, **76**, 2285 (1954); b) A. S. Dreiding and J. A. Hartman, ibid., **75**, 3723 (1953); c) J. English, Jr., and A. D. Bliss, ibid., **78**, 4057 (1956).

12) D. J. Cram and H. Steinberg, ibid., **73**, 5691 (1951).

13) NMR spectrum was measured at 60 Mc./sec. on a modified Varian Model A-60 spectrometer. The sample was dissolved in $CDCl_3$ and contained tetramethylsilane as internal reference.

14) C. A. Relly and J. D. Swalen, *J. Chem. Phys.*, **32**, 1378 (1960).

15) H. H. Wasserman, N. E. Auberg and H. E. Zimmerman, *J. Am. Chem. Soc.*, **75**, 96 (1953).

16) T. I. Temnikova and V. F. Martynov, *J. Gem. Chem.* (*U. S. S. R.*), **15**, 499 (1945); *Chem. Abstr.*, **40**, 4695 (1945).

17) T. I. Temnikova and V. A. Kropachev, *Zhur. Obshchei. Khim.*, **19**, 2069 (1949); *Chem. Abstr.*, **44**, 3941 (1949).

18) H. Kwart and L. G. Kirk, *J. Org. Chem.*, **32**, 116 (1957).

19) D. S. Noyce and W. L. Reed, *J. Am. Chem. Soc.*, **80**, 5539 (1958).

20) H. E. Zimmerman and J. English, Jr. described in their work (Ref. 7a) that one of the diastereoisomeric $\alpha$-glycols, the 128° compound derived from benzalacetophenone oxide which was reported by W. Herz was assigned to 1, 3-diphenyl-1, 3-propanediol.

occurred irrespective of the kind of catalyst, giving an $\alpha$-hydroxyketone.

We have reported that the hydrogenolysis of optically active benzyl-type alcohols and alkyl ethers took different courses of reaction according to the species of the catalysts; it is considered that, on hydrogenolysis over Raney nickel, hydrogen may attack the asymmetric carbon atom from the same direction as the C*–O bond and that the reaction may proceed with the retention of the original configuration. On the other hand, over palladium catalyst the hydrogen may attack from behind the C*–O bond and the reaction may proceed with an inversion of the configuration; this would be caused by the differences, in the affinities of the catalysts for the oxygen atom.[3,4]

By taking account of the different properties of the nickel and palladium catalysts mentioned above, together with the consideration that the phenyl group may be adsorbed more strongly on the surface of the catalyst than the acetyl group, the adsorbed states of X on the catalyst may be assumed to be as shown in Figs. 1 and 2; it may also be assumed that the hydrogen adsorbed on the surface of the catalyst may attack the $\beta$-carbon atom.

On the other hand, as it is considered that the benzoyl group may be adsorbed more strongly than the phenyl group on the surface of the catalyst by means of its $\pi$ and lone-pair electrons of the carbonyl group, the adsorbed states of I and VII may be assumed to be as shown in Figs. 1 and 3. On this occasion, the surface-adsorbed hydrogen may attack the $\beta$-carbon atom, in the case of Fig. 1, and the $\alpha$-carbon atom, in the case of Fig. 3 so that in each case the corresponding products are obtained on the hydrogenation of I and VII. Besides, it may also be assumed that the hydrogenation of I, VII and X proceeds with a carbonium ion mechanism[2] (Fig. 4) to give $\alpha$-hydroxyketones; however, it is not possible to conclude whether or not this mechanism is responsible.

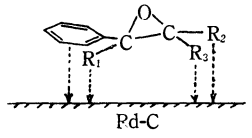



Fig. 1.

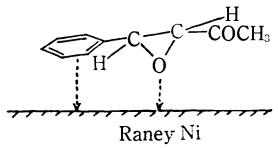



Fig. 2.

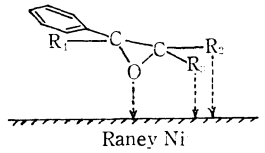



Fig. 3.

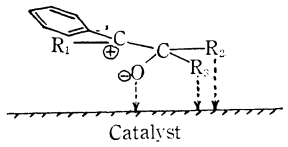



Fig. 4.

I: $R_1=H$, $R_2=H$, $R_3=COC_6H_5$
VII: $R_1=CH_3$, $R_2=COC_6H_5$, $R_3=H$
X: $R_1=H$, $R_2=H$, $R_3=COCH_3$

These considerations are also supported by the following experimental evidence: Optically-active $\alpha$-methyl or $\alpha$-ethylstyrene oxide was hydrogenolyzed, with the retention of the original configuration over Raney nickel and with an inversion over palladium charcoal, to give corresponding optically-active products.[21] On the hydrogenolysis of *trans*-dimethylstilbene oxide, the reaction products were *erythro*-2, 3-diphenylbutan-2-ol over palladium charcoal and the threo isomer over Raney nickel.[22]

The experimental results of the platinum oxide hydrogenation suggest that it possesses the characteristics of both nickel and palladium.

## Experimental

**Starting Material.**—$\alpha,\beta$-Epoxyketones (I,[5] VII[15] and X[16]) were prepared by the procedures reported in literatures.

**Catalytic Hydrogenation.**—The following general procedure was used. 1/100 mol. of the compounds, 0.2 g. of Pd-C or 1 g. of Raney nickel and 100 ml. of ethanol were stirred into hydrogen at an ordinary temperature and at atmospheric pressure. After the theoretical amount of hydrogen had been absorbed, the catalyst was filtered out and the ethanol was distilled off.

*Benzalacetophenone Oxide (I) over Pd-C (with 1 mol. of Hydrogen).*—The residue was recrystallized from ligroin to give 2-hydroxy-1,3-diphenylpropan-1-one (II) in an 86% yield. The melting point was 66°C.

Found: C, 79.41; H, 6.28. Calcd. for $C_{15}H_{14}O_2$: C, 79.62; H, 6.19%.

*Benzalacetophenone Oxide (I) over Pd-C (with 2 mol. of Hydrogen).*—The residual sirup was dissolved in hot ligroin and then cooled in an ice bath. Isomer-A-rich crystals of 1,3-diphenylpropane-1,2-diol were obtained (m. p. 65—77°C); they were

21) S. Mitsui and S. Imaizumi, *J. Chem. Soc. Japan, Pure Chem. Sec.* (*Nippon Kagaku Zasshi*), **86**, 219 (1965); *Chem and Ind.*, in press.
22) S. Mitsui and Y. Nagahisa, Presented at the 15th Symposium of Reaction Mechanism of Organic Compounds, Nagoya, October, 1964.

then recrystallized from ligroin to give the pure isomer-A (III) in a 59% yield (m. p. 85°C). When the mother liquor was concentrated and also cooled in an ice bath, isomer-B-rich crystals of 1,3-diphenylpropane-1,2-diol were obtained; they were recrystallized from ligroin to give the pure isomer-B (III') in a 7% yield (m. p. 70°C).

Found (for III): C, 78.83; H, 7.63. Calcd. for $C_{15}H_{16}O_2$: C, 78.92; H, 7.06%. Found (for III'): C, 78.81; H, 7.29. Calcd. for $C_{15}H_{16}O_2$: C, 78.92; H, 7.06%.

The dibenzoate of III melted at 157°C.

Found: C, 79.66; H, 5.33. Calcd. for $C_{29}H_{24}O_4$: C, 79.79; H, 5.54%.

*Benzalacetophenone Oxide (I) over Raney Nickel.*—The residual sirup was dissolved in a hot benzene-ligroin (1:1) mixture and then cooled in an ice bath. Crystals rich in the racemic isomer of 1,3-diphenylpropane-1,3-diol were obtained; they were recrystallized from ligroin to give the pure racemic isomer (V) in a 40% yield (m. p. 130°C). The mother liquor was concentrated and also cooled in an ice bath. Crystals rich in the meso isomer of 1,3-diphenylpropane-1,3-diol were obtained; they were recrystallized from ligroin to give the pure meso isomer (V') in 24% yield (m. p. 97°C).

Found (for V): C, 79.17; H, 7.22. Calcd. for $C_{15}H_{16}O_2$: C, 78.92; H, 7.06%. Found (for V'): C, 78.83; H, 7.35. Calcd. for $C_{15}H_{16}O_2$: C, 78.92; H, 7.06%.

The dibenzoate of V melted at 123—124°C.

Found: C, 79.61; H, 5.56. Calcd. for $C_{29}H_{24}O_4$: C, 79.79; H, 5.54%.

*Benzalacetophenone Oxide (I) over Platinum(IV) Oxide.*—The residual sirup was dissolved in hot petroleum benzine and then cooled to room temperature. The crystals obtained were recrystallized from petroleum benzine to give pure V in a 40% yield (m. p. 130°C). The mother liquor was concentrated to give III' in a 47% yield (m. p. 70°C).

*cis-Dypnone Oxide (VII) over Pd-C.*—The residue was recrystallized from a benzene-petroleum ether (1:1) mixture to give pure 1,3-diphenylbutane-1,2-diol (VIII) in a 70% yield. The melting point was 90°C.

Found: C, 79.21; H, 7.21. Calcd. for $C_{16}H_{18}O_2$: C, 79.31; H, 7.49%.

*cis-Dypnone Oxide (VII) over Raney Nickel.*—The residue was recrystallized from a benzene-petroleum ether (1:1) mixture to give pure 1,3-diphenylbutane-1,3-diol (IX) in a 50% yield. The melting point was 91°C.

Found: C, 79.72; H, 7.49. Calcd. for $C_{16}H_{18}O_2$: C, 79.31; H, 7.49%.

The mixed melting point of VIII and IX was 62—65°C.

*Benzalacetone Oxide (X) over Pd-C.*—The residual oil was distilled under reduced pressure to give 3-hydroxy-4-phenylbutane-2-one (XI) in an 88% yield (b. p. 93.5°C/0.75 mmHg). XI was identified as the semicarbazone (m. p. 174°C).

Found: C, 59.72; H, 7.35; N, 19.26. Calcd. for $C_{11}H_{15}O_2N_2$: C, 59,71; H, 6.83; N, 18.99%.

The mixed melting point of the semicarbazone of XI and of 1-hydroxy-1-phenylbutan-3-one (XIII) was 162—163.5°C.

*Benzalacetone Oxide (X) over Raney Nickel.*—The residual sirup was distilled under reduced pressure to give 1-phenylbutane-2,3-diol (XII) in a 72% yield (b. p. 118°C/0.18 mmHg), and di-*p*-nitrobenzoate, which melted at 130°C and which was recrystallized from ethanol.

Found: C, 62.00; H, 4.28; N, 5.93. Calcd. for $C_{24}H_{20}O_8N_2$: C, 62.06; H, 4.34; N, 6.03%.

*3-Hydroxy-4-phenylbutan-2-one (XI) over Raney Nickel.*—The residual sirup was distilled under reduced pressure to give 1-phenylbutane-2,3-diol (XII) in a 79% yield (b. p. 118°C/0.17 mmHg), and di-*p*-nitrobenzoate, which was recrystallized from ethanol and which melted at 129°C.

Found: C, 62.24; H, 4.38; N, 5.94. Calcd. for $C_{24}H_{20}O_8N_2$: C, 62.06; H, 4.34; N, 6.03%.

The mixed melting point of the di-*p*-nitrobenzoates of XII which was obtained by the hydrogenation of XI over Raney nickel and of X over Raney nickel remained undepressed.

*1,3-Diphenylpropane-1,2-diol (III) over Pd-C-A Containing Three Micro Drops of Concentrated Hydrochloric Acid.*—The residual oil was distilled under reduced pressure to give 1,3-diphenylpropan-2-ol (IV) in a 67% yield (b. p. 130—140°C/0.5 mmHg). The *p*-nitrobenzoate, which was recrystallized from ethyl acetate, melted at 79.5°C.

*1,3-Diphenylpropane-1,3-diol (V) over Pd-C-A Containing Three Micro Drops of Concentrated Hydrochloric Acid.*—The residual oil was distilled under reduced pressure to give 1,3-diphenylpropane (VI) in a 50% yield (b. p. 126—127°C/0.6 mmHg).

Found: C, 91.29; H, 8.19. Calcd. for $C_{15}H_{16}$: C, 91.78; H, 8.22%.

The infrared spectrum of VI showed that $\nu_{OH}$ vanished completely.

**1-Hydroxy-1-phenylbutan-3-one (XIII).**—XIII was prepared from acetone and benzaldehyde by the alkaline condensation reported by Noyce and Reed.[18] B. p. 106°C/0.11 mmHg; semicarbazone, m. p. 180—181.5°C.

Found: C, 59.91; H, 6.47; N, 18.84. Calcd. for $C_{11}H_{15}O_2N_2$: C, 59.71; H, 6.83; N, 18.99%.

**Periodic Acid Oxidation.**—This experiment was carried out by the method of Jackson.[23] Sample VIII consumed 1.09 equivalents of periodic acid, while sample IX did not consume any at all, after three hours of mixing diols with periodic acid.

The derivatives, such as benzoate, *p*-nitrobenzoate and semicarbazone, which are mentioned above were prepared by the usual procedure.

The authors are indebted to Misses Ayako Iwanaga and Mutsuko Suzuki and Mrs. Hide Arai of the Department of Chemistry of this University for their elementary microanalyses. They wish also to thank Dr. Shin-ichi Sasaki of the Department of Chemistry of this University for his kindness in measuring the infrared and NMR spectra.

*Department of Applied Science*
*Faculty of Engineering*
*Tohoku University*
*Katahira-cho, Sendai*

23) R. Adams, "Organic Reactions," Vol. II, 341 (1944).

# Some Acetylene Complexes of Vanadium*

By Ryuichiro TSUMURA** and Nobue HAGIHARA

(Received March 8, 1965)

It was previously reported[1] that $\pi$-dicyclopentadienyl-vanadium causes the catalytic polymerization of various acetylenes. Much attention was then drawn to a possible isolation of acetylene complexes of vanadium in an effort to elucidate the catalysis of the vanadium complex, which seems to be different from that of such nickel compounds as $(PPh_3)_2Ni(CO)_2$[2] and $NiCl_2 \cdot 2PPh_3$[3] in the catalytic polymerization of acetylenes. We will now report on the preparation, some properties and a proposed structure of some new acetylene complexes of vanadium, such as $\pi$-$C_5H_5(RC_2H)V(CO)_2$, prepared from the reactions of $\pi$-cyclopentadienyl-vanadium tetracarbonyl[4] with several acetylenes. The infrared and nuclear magnetic resonance spectra of the acetylene complexes are used as the basis of discussion of their structure and of the type of bonding by which the acetylenes may be bonded to metal. Regarding the bonding of the acetylenes to vanadium, the acetylene complexes described here are probably related to an intermediate in the catalytic polymerization mentioned above. Although a wide variety of acetylene complexes of such transition metals as manganese,[5,6] iron,[7] cobalt,[7-9] nickel,[7,9,10] tungsten,[11] and platinum[6,12,13] have been reported, some acetylene complexes described here are the first examples of vanadium.

## Preparation and Properties

$\pi$-Cyclopentadienyl-vanadium tetracarbonyl[4] (I) reacted with pressured acetylene in benzene near room temperature under the influence of the irradiation of light from a tungsten lamp. The reaction solution turned from orange to green to form an acetylene complex. Similar photochemical reactions of I with an excess of such 1-alkynes as 1-pentyne, 1-hexyne and *t*-butylacetylene proceeded with the evolution of approximately 2 mol. of carbon monoxide per atom of vanadium present and gave green acetylene complexes. On the other hand, in the interactions of an excess of I with 1-alkynes 2 mol. of carbon monoxide per mole of the alkynes present were evolved, and also the corresponding acetylene complexes were obtained. It is, therefore, reasonable to assume from these facts and from the results of the elemental and spectroscopic analyses to be described later, that the resulting compounds are acetylene complexes of vanadium (II) in which two carbonyl groups of the starting material, I, have been replaced by the corresponding acetylene molecule by the following reaction:

$$\underset{(I)}{\pi\text{-}C_5H_5V(CO)_4} + RC{\equiv}CH \xrightarrow{h\nu} \underset{(II)}{\pi\text{-}C_5H_5(RC_2H)V(CO)_2} + 2CO$$

(R=H, $n$-$C_3H_7$, $n$-$C_4H_9$ and $(CH_3)_3C$)

Acetylene complexes of vanadium II were purified through chromatography over alumina, followed by vacuum distillation. They are either viscous oils or low melting solids which crystallize spontaneously on cooling. All of them are quite sensitive to air, so they must be handled under oxygen-free nitrogen. These properties make it difficult to obtain satisfying values from the elemental analyses. The acetylene complexes II are easily soluble in most organic solvents. Their infrared and nuclear magnetic resonance spectra are shown in the Experimental section and in Table I respectively, together with some assignments.

* Presented at the 17th Annual Meeting of the Chemical Society of Japan, Tokyo, April, 1964.

** Present address: Central Research Laboratory, Tôyô-kôatsu Industries, Kuden-cho, Totsuka-ku, Yokohama.

1) R. Tsumura and N. Hagihara, This Bulletin, **37**, 1889 (1964).
2) L. S. Meriwether, M. F. Leto, E. F. Colthup and G. W. Kennerly, *J. Org. Chem.*, **27**, 3930 (1962).
3) W. E. Daniels, ibid., **29**, 2936 (1964).
4) E. O. Fischer and S. Vigoureux, *Chem. Ber.*, **91**, 2205 (1958).
5) W. Strohmeier and D. von Hobe, *Z. Naturforsch.*, **16b**, 402 (1961).
6) W. Strohmeier, H. Laporte and D. von Hobe, *Chem. Ber.*, **95**, 455 (1962); J. L. Boston, S. O. Grim and G. Wilkinson, *J. Chem. Soc.*, **1963**, 3468.
7) J. F. Tilney-Basset, ibid., **1963**, 4784.
8) H. Greenfield, H. W. Sternberg, R. A. Friedel, J. H. Wotiz, R. Markby and I. Wender, *J. Am. Chem. Soc.*, **78**, 120 (1956); W. G. Sly, ibid., **81**, 18 (1959).
9) J. L. Boston, D. W. A. Sharp and G. Wilkinson, *J. Chem. Soc.*, **1962**, 3488.
10) J. F. Tilney-Basset and O. S. Mills, *J. Am. Chem. Soc.*, **81**, 4757 (1959).
11) D. P. Tate, J. M. Augl, W. M. Ritchey, B. L. Ross and J. G. Grasselli, ibid., **86**, 3261 (1964).
12) J. Chatt, G. A. Rawe and A. A. Williams, *Proc. Chem. Soc.*, 208 (1957).
13) J. Chatt, R. G. Guy, L. A. Duncanson and D. T. Thompson, *J. Chem. Soc.*, **1963**, 5170.

TABLE I. NMR SPECTRA OF ACETYLENE COMPLEXES OF VANADIUM II[a]

| Compound[b] | Solvent | Band position ($\tau$)[c,d] | | | | |
|---|---|---|---|---|---|---|
| | | $\pi$-$C_5H_5$- | $HC_2$- | $-C_2CH_2$- | $-CH_2$- | $-CH_3$ |
| M($HC_2H$) | $CCl_4$ | 4.46(s)[e] | 4.92(s) | | | |
| | $C_6H_6$ | 4.88(s) | 5.63(s) | | | |
| M($HC_2C_3H_7$) | $CHCl_3$ | 4.50(s) | 4.93(s) | 6.61(t)[e] | 8.18(m)[e] | 9.01(t) |
| M($HC_2C_4H_9$) | $C_6H_6$ | 4.78(s) | 5.60(s) | 6.46(t) | 8.37(m) | 9.01(t) |
| M($HC_2CMe_3$) | $CCl_4$ | 4.48(s) | 4.90(s) | | | 8.76(s) |
| | $CHCl_3$ | 4.45(s) | 4.90(s) | | | 8.73(s) |

a) Measured at 60 Mc./sec. at room temperature.
b) M = $\pi$-$C_5H_5V(CO)_2$.
c) Relative to $SiMe_4$ ($\tau$ = 10) as the internal standard.
d) The relative intensities were essentially consistent with those to be expected from the assigned structure. The decomposition during the measurements sometimes also showed complex spectra containing absorptions of free acetylene molecules.
e) (s), (t) and (m) indicate multiplicity, singlet, triplet and complex multiplets respectively.

Attempts to make the complex I interact with phenylacetylene and tolane were made in order to obtain more stable and higher melting acetylene complexes than the complex II itself. The reactions occurred with the evolution of carbon monoxide and presumably formed the corresponding acetylene complexes of vanadium, but their isolation was unsuccessful because of the great difficulty of purifying them. Seeking to obtain a more stable and crystalline acetylene complex, we have investigated the preparation of a complex in which at least one of the two remaining carbonyl groups of the acetylene complexes II obtained above is replaced by triphenylphosphine.

The photochemical reaction of the carbonyl compound I with triphenylphosphine in a benzene solution at room temperature proceeded quantitatively, with the evolution of a mole of carbon monoxide equal to the mole of the vanadium compound present, and it gave orange crystals of a mono-substituted product (III) by the following reaction:

$$\pi\text{-}C_5H_5V(CO)_4 + PPh_3 \xrightarrow{h\nu} \pi\text{-}C_5H_5V(PPh_3)(CO)_3 + CO$$
(III)

The phosphine derivative III is completely air-stable in the solid state, and it is only slowly oxidized by air in solutions; these characteristics indicate that the stability of the new compound III is higher than that of I. It is fairly soluble in hot benzene and carbon tetrachloride, but poorly soluble in *n*-hexane, ethers and alcohols.

The reaction between III and tolane gave yellow crystals of the expected acetylene complex (IV):

$$\pi\text{-}C_5H_5V(PPh_3)(CO)_3 + PhC{\equiv}CPh \xrightarrow{h\nu} \pi\text{-}C_5H_5(PhC_2Ph)V(PPh_3)(CO) + 2CO$$
(IV)

The tolane complex IV could be recrystallized from *n*-hexane in a careful operation, though it is still sensitive to air. It is easily soluble in most organic solvents in the same manner as is II.

## Discussion

In general, acetylenes are known[14] to give many kinds of organometallic complexes upon reaction with transition metal carbonyl compounds. On the basis of the chemical and physical properties of the acetylene complexes of vanadium reported here, it is clear that they are monomeric compounds obtained through the replacement of two carbonyl groups in the complex I by the acetylene, and that the acetylene molecule is bonded to a single vanadium atom as a bidentate ligand. On the other hand, there are some examples of the $\pi$-bonding of acetylenes as monodentate ligands through a single electron pair of their triple bond to a metal, for instance, in such manganese complexes as $\pi$-$C_5H_5(PhC_2Ph)$-$Mn(CO)_2$,[5] which is prepared from the reaction of $\pi$-cyclopentadienyl-manganese tricarbonyl with tolane. It is very interesting that the bonding of acetylenes to the vanadium atom is assumed to be different from that in the manganese complexes even though the same types of acetylene complexes are derived from the similar reaction of $\pi$-cyclopentadienyl-metal carbonyl compounds with acetylenes.

The infrared spectra of all of the acetylene complexes II indicate that the wave numbers of the two carbonyl bands are a little smaller than those in the original compound, I, as a result of the replacement of two carbonyl groups in I by the acetylene. The infrared

14) M. A. Bennet, *Chem. Revs.*, **62**, 611 (1962); R. G. Guy and B. L. Shaw, "Advances in Inorganic Chemistry and Radiochemistry," Vol. 4, Academic Press Inc., New York (1962), p. 78.

spectra of the alkyne complexes II (R=alkyl) showed no absorptions in the region of 3300 $cm^{-1}$ due to the presence of the acetylenic hydrogen atoms and of the band at 2100 $cm^{-1}$ arising from the stretching vibrations of the terminal triple bonds. The lack of the characteristic absorptions of 1-alkynes suggests that their triple bond nature is weakened in the acetylene complexes. The stretching absorptions of the coordinated acetylenic bond are reported to be situated at 1919 $cm^{-1}$ in the manganese complex, $\pi$-$C_5H_5(CF_3C_2CF_3)Mn(CO)_2$,[6] in which the acetylene is merely acting as a donor. In contrast, they have been found in the 1700 $cm^{-1}$ region in such complexes of platinum, rhenium and tungsten as $(RC_2R)Pt(PPh_3)_2$,[12] $(PhC_2H)_2ReCl$,[15] and $(RC_2R)_3W(CO)$[11] respectively, in which the acetylenes are considered to be $\sigma$-bonded or doubly $\pi$-bonded to the metal, apparently as a bidentate ligand. In the vanadium compounds II, however, it was impossible to assign any band to the stretching vibration of the coordinated multiple bond with certainty. The two broad, strong absorptions of the carbonyls could also be presumed to cover the absorption band in question.

The nuclear magnetic resonance spectra of the acetylene complexes II given in Table I indicate what the property of the coordinated acetylenic bond might be. All of the compounds II possess essentially the same chemical shifts for the acetylenic hydrogens, at $\tau$ 4.9 in carbon tetrachloride and chloroform or at $\tau$ 5.6 in benzene. In carbon tetrachloride and chloroform, the spectra of the acetylenic protons of the coordinated acetylenes are shifted about $\tau$ 2.7 toward the lower-magnetic field than those of the corresponding free acetylenes; they are thus located in the region of olefinic protons. As a result of the coordination of the acetylenes to vanadium metal, the chemical shift of the acetylenic hydrogens is expected to be mainly influenced by a diamagnetic effect due to d-electrons of the metal on the one hand, and, on the other hand, by a paramagnetic effect which is brought about through the loss of the diamagnetic anisotropy of the triple bond. In this case, the great paramagnetic shift observed might be presumed to result from the more remarkable effect of the latter than the former.

These facts, consistent with the results of the infrared spectra described above, suggest that the triple bond of the acetylenes in II may be reduced effectively to a double bond by their bonding to vanadium metal. The higher shielding of the acetylenic protons in benzene than that in the other chlorinated hydrocarbons may be considered to result from a solvent effect due to the remarkable diamagnetic anisotropy and plane form of the benzene molecule. Such a shielding due to the solvent effect of benzene is seen also in the chemical shifts of the cyclopentadienyl ring protons, though it is not so great as in those of the acetylenic hydrogens. A comparison of the spectra in the different solvents tested indicates that of all kinds of hydrogens present in the acetylene complexes II, the acetylenic protons are affected by solvents most sensitively.

On the basis of these experimental results, various possible structures of the acetylene complexes of vanadium II might be considered: The structure formulated in Fig. 1(A), in which the acetylene is $\pi$-bonded to the metal by only a single $\pi$-electron pair, as in the above-mentioned complexes[5,6] of manganese; the structure presented in Fig. 1(B), in which the acetylenic carbon atoms are substantially rehybridized toward the $sp^2$ configuration and the acetylene is bonded to the metal through two $\sigma$-bondings, as in the above-described complexes of platinum[12] and rhenium[15], and a possible intermediate structure, one between structures A and B.

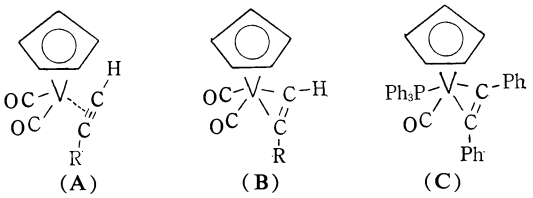



Fig. 1. Acetylene complexes of vanadium.

It may be concluded from the experimental evidence that the most probable structure of the vanadium complexes II is consistent with, or at least near, structure B, even if it may be intermediate between structures A and B. The tolane complex IV prepared from the phosphine derivative III is presumed in the same way to have the structure given in Fig. 1(C).

In the catalysis of dicyclopentadienyl-vanadium for the polymerization of acetylenes, it appears reasonable to assume that the polymerization proceeds through the initial formation of an acetylene complex in which the acetylene molecule is bonded to a vanadium atom by a bonding similar to that in the structure B of the isolated complexes II.

Further investigation has led to the successful preparation of a few acetylene complexes in which an acetylene molecule is probably $\sigma$-bonded to a vanadium metal, one simultaneously having two coordinated cyclopentadienyl

15) R. Colton, R. Levitus and G. Wilkinson, *Nature*, **186**, 233 (1960).

rings. The findings on such acetylene complexes will be soon presented elsewhere.

## Experimental

All preparations, chromatographic separations, distillations and analytical measurements were carried out under an atmosphere of dry, oxygen-free nitrogen or in a vacuum. Solvents were distilled and saturated with nitrogen before use. All melting points are uncorrected.

**Preparation.** —*π-Cyclopentadienyl - acetylene - vanadium Dicarbonyl.*—In a 70ml. glass autoclave acetylene was pressured into a solution of 0.58 g. (2.5 mmol.) of π-cyclopentadienyl-vanadium tetracarbonyl[4] (I) in 30 ml. of benzene up to about 5 kg./cm². The resultant orange solution was irradiated with a 500 W. tungsten lamp for ca. 4 hr. while being cooled with running water; it thus turned dark green and had an evolution of small bubbles from the bottom of the vessel. After the solvent had been removed at room temperature, the oily residue was chromatographed over alumina which had been treated with nitrogen before use. The elution of the column with benzene gave, at first, a light orange solution of the unchanged material I and then a clear green solution. When the green fraction was concentrated in vacuo at room temperature, a green oil was left; this was then distilled in 0.1 mmHg at ca. 70°C. The resulting green viscous distillate crystallized spontaneously upon being cooled, yielding 0.10 g. of green crystals, m. p. 27—30°C.

Found: C, 55.7; H, 3.7; mol. wt. (cryoscopic in benzene), 183. Calcd. for $C_9H_7O_2V$: C, 54.6; H, 3.6%; mol. wt., 198.

The yield of the isolation procedure virtually depended upon the decomposition of the product during the manipulations. The discrepancy in the elemental analysis for the acetylene complex may be due to the instability of the complex, which could not be purified by recrystallization.

*π-Cyclopentadienyl-(1-pentyne)-vanadium Dicarbonyl.*—Into a 100 ml. fiask connected to a gas-measuring vessel a solution of 0.815 g. (3.57 mmol.) of I in 30 ml. of benzene and 2.0 ml. of 1-pentyne was placed. The reaction system was then magnetically stirred and irradiated with a tungsten lamp while being cooled with running water. The color of the solution gradually turned from orange to green, and was a gas evolved. Irradiation was continued for 8 hr., until the evolution of the gas had ceased. The carbon monoxide evolved amounted to approximately 165 ml. (7.05 mmol.). The reaction mixture was then chromatographed and distilled as has been described above, yielding 0.35 g. of a green oil.

Found: C, 61.0; H, 5.6. Calcd. for $C_{12}H_{13}O_2V$: C, 60.0; H, 5.5%.

*π-Cyclopentadienyl-(1-hexyne)-vanadium Dicarbonyl and π-Cyclopentadienyl-(t-butylacetylene)-vanadium Dicarbonyl.*—A mixture of I and the 1-alkyne in benzene was treated in the manner described for the pentyne complex.

Hexyne gave a green oil of the acetylene complex.

Found: C, 62.1; H, 6.3. Calcd. for $C_{13}H_{15}O_2V$: C, 61.4; H, 6.0%.

Tertiary butylacetylene gave green crystals of the acetylene complex, m. p. 31—32°C.

Found: C, 62.0; H, 5.9; CO, 21.7. Calcd. for $C_{13}H_{15}O_2V$: C, 61.4; H, 6.0; CO, 22.0%.

*π-Cyclopentadienyl-triphenylphosphine-vanadium Tricarbonyl.*—A mixture of 5.85 g. (25.5 mmol.) of I and 7.02 g. (26.8 mmol.) of triphenylphosphine, dissolved in 80 ml. of benzene, was photochemically treated in a manner similar to that described above. A gas evolved smoothly, and fine orange crystals separated. Irradiation was then continued for about 15 hr., until the evolution of the gas almost ceased. The carbon monoxide evolved amounted to 570 ml. (24.4 mmol.). The reaction mixture was then filtered, and the precipitate washed well with cold benzene and dried under reduced pressure to yield 9.40 g. (87.8%) of orange crystals of a mono-substituted product III, m. p. 160—161°C.

Found: C, 67.38; H, 4.53; V, 11.23. Calcd. for $C_{26}H_{29}O_3PV$: C, 67.55; H, 4.36; V, 11.02%.

Furthermore, 0.50 g. of III was recovered by recrystallization from the orange filtrate.

*π-Cyclopentadienyl - tolane - triphenylphosphine - vanadium Carbonyl.*—A mixture of 0.658 g. (1.42 mmol.) of III and 0.267 g. (1.49 mmol.) of tolane in 50 ml. of benzene was worked up in the same way. The carbon monoxide evolved amounted to 50 ml. (2.14 mmol.), though there was a slower evolution of the gas. The reaction mixture was then evacuated and chromatographed over alumina with benzene, and the resulting yellow-green eluate was evaporated to dryness under reduced pressure. The residue was recrystallized from *n*-hexane at the temperature of dry ice to yield 0.25 g. of a yellow crystalline powder, m. p. 35—37°C.

Found: C, 78.02; H, 5.35; mol. wt. (cryoscopic in benzene), 559. Calcd. for $C_{38}H_{30}OPV$: C, 78.08; H, 5.17%; mol. wt., 584.

**Infrared Spectra.** — Measurements were made with a Hitachi EPI-2 spectrophotometer. The spectra and some assignments are shown below:

π-$C_5H_5(HC_2H)V(CO)_2$[a]: 3100 w[c] 2940 w 2860 w 1996 vs[d] 1925 vs[d] 1528 w 1434 m[e] 1363 vw 1009 m[e] 950 m 810 s[e] 787 sh 695 m.

π-$C_5H_5(HC_2C_3H_7)V(CO)_2$[b]: 3120 vw[c] 2960 m[f] 2932 sh[f] 2875 w[f] 1985 vs[d] 1905 vs[d] 1635 vw 1520 vw 1460 w 1431 w[e] 1378 vw 1098 w 1063 w 1010 m[e] 980 vw 953 w 895 vw 866 vw 806 s[e] 700 sh.

π-$C_5H_5(HC_2C_4H_9)V(CO)_2$[b]: 1990 vs[d] 1910 vs[d]

π-$C_5H_5(HC_2CMe_3)V(CO)_2$[a]: 3130 vw[c] 3060 vw 2970 s[f] 2910 sh[f] 2880 m[f] 1994 vs[d] 1920 vs[d] 1632 w 1474 sh 1458 m 1435 w[e] 1389 w 1361 s 1227 m 1205 sh 1116 vw 1060 vw 1030 vw 1010 m[e] 955 w 931 w 885 vw 857 vw 805 s[e] 772 vw 750 vw 718 vw

π-$C_5H_5V(PPh_3)(CO)_3$[a]: 3060 vw[c] 1950 vs[d] 1855 vs[d] 1840 vs[d] 1587 vw 1473 m 1435 s[e] 1307 w 1183 m 1160 w 1119 vw 1090 s 1071 w 1025 w 1013 m[e] 996 m 969 vw 920 vw 909 vw 833 m 819 s[e] 750 sh 744 s[g] 718 vw 700 sh 688 s[g].

π-$C_5H_5(PhC_2Ph)V(PPh_3)(CO)$[a]: 1825 vs[d]

a) measured in Nujol and hexachlorobutadiene; b) measured as thin films of the pure oil; c) a C-H stretch of π-$C_5H_5$; d) a C≡O stretch; e) π-$C_5H_5$ frequencies; f) a C-H stretch of alkyl groups; g) phenyl absorptions.

**Nuclear Magnetic Resonance Spectra.**—Measurements were made on a Varian A 60 spectrometer. The spectra and conditions of measurements are given in Table I.

## Summary

Some acetylene complexes of vanadium of the $\pi$-$C_5H_5(RC_2H)V(CO)_2$ (R=H, *n*-$C_3H_7$, *n*-$C_4H_9$ and $(CH_3)_3C$) and $\pi$-$C_5H_5(PhC_2Ph)V(PPh_3)(CO)$ types have been prepared by the photochemical reaction of the corresponding acetylene with $\pi$-cyclopentadienyl-vanadium tetracarbonyl and its phosphine derivative respectively. It has been proposed, on the basis of their infrared and nuclear magnetic resonance spectra, that the acetylene complexes of vanadium have a structure in which the acetylene molecule is bonded via two $\sigma$-bondings to a vanadium atom.

We wish to thank Mr. Shibano of our laboratory for his elemental analyses, and Mr. Ishikawa and Mr. Naoki, Faculty of Science, Osaka University, for their spectroscopic measurements.

*The Institute of Scientific and Industrial Research*
*Osaka University*
*Sakai, Osaka*

# The Preparation and Polymerization of Divinyl Carbonate*

By Shunsuke MURAHASHI, Shun'ichi NOZAKURA, Saburo FUJI and Kiyoshi KIKUKAWA

(Received March 15, 1965)

Since Butler[1] found the principle of the intra-inter polymerization of divinyl compounds, many divinyl compounds have been reported to undergo cyclopolymerization, yielding soluble polymers.

Divinyl carbonate seems, considering its structural analogy to divinyl thiocarbonate,[2] to be a monomer with the possibility of cyclopolymerization. The hydrolysis of the cyclized polymer might yield polyvinyl alcohol, which in turn might show some features of the cyclopolymer with stereoregularity.[3] The present study started from such point of view.

Divinyl carbonate has not previously been successfully prepared. In the present paper we wish to report the synthesis of divinyl carbonate and its polymerization, emphasis being laid on the cyclopolymerization of the monomer under various conditions. The identification of cyclic units in the polymer and the estimation of the degree of cyclization have been made by means of infrared analysis based on the study of model compounds.

## Experimental

**The Preparation of Divinyl Carbonate.**—Divinyl carbonate was synthesized by the reaction of mercuridiacetaldehyde with phosgene in tetrahydrofuran. A mixture of 220 g. of mercuridiacetaldehyde,[4] 150 ml. of tetrahydrofuran, and 0.5 g. of hydroquinone was placed in a 500 ml. three-necked flask equipped with a reflux condenser with a calcium chloride tube, a stirrer and a glass gas inlet tube, the flask was then cooled with an ice bath. Phosgene (29 ml.), which had been condensed in a graduated trap cooled in a dry ice-acetone bath, was gradually evaporated through a phosphorus pentoxide tube into the flask while its contents were being stirred. The flask was then kept at 0°C for 1 hr. while being stirred, kept at room temperature for another hour, and then warmed slowly up to 60°C. The reaction, which was not complete at 0°C, yielded vinyl chlorocarbonate as a main product. The volatile components of the reaction mixture were collected by vacuum distillation at room temperature, and then the distillate was subjected to fractional distillation at reduced pressure using a fractional column of about 30 theoretical plates. The yield was 17 g., 40% based on mercuridiacetaldehyde. Colorless liquid, b. p. 103.5—104.5°C, 49.0—49.2°C/98 mmHg, m. p. −38.0—−38.5°C, $n_D^{25}$ 1.4135, $d_4^{25}$ 1.0095.

Found: C, 51.92; H, 5.22. Calcd. for $C_5H_6O_3$: C, 52.63; H, 5.25%.

**The Synthesis of Carbonates.** — Trimethylene carbonate was prepared by a known method[5] from 45 g. of diethyl carbonate, 25 g. of 1,3-propanediol and 0.2 g. of sodium. B. p. 115—116°C/2 mmHg; m. p. 47.0—47.5°C (recrystallized from ether). Yield 27%.

* Part of this paper was presented at the 17th Annual Meeting of the Chemical Society of Japan, April, 1964.

1) G. B. Butler and R. J. Angelo, *J. Am. Chem. Soc.*, **79**, 3128 (1957).

2) H. R. Ringsdorf and C. G. Overberger, *Makromol. Chem.*, **44/46**, 418 (1961).

3) S. Murahashi, H. Yuki, T. Sano, U. Yonemura, H. Tadokoro and Y. Chatani, *J. Polymer Sci.*, **62**, 577 (1964).

4) A. N. Nesmeyanov, R. M. Khomtov and I. F. Lutsenko, *Izvest. Akad. Nauk SSSR., Otdel. Khim. Nauk*, **1957**, 942.

5) L. Hough and J. E. Priddle, *J. Chem. Soc.*, **1961**, 581.

2,3-Butanediol cyclic carbonate was prepared from 25 g. of 2,3-butanediol, 45 g. of diethyl carbonate and 0.1 g. of sodium. The mixture was then heated for 5 hr. at 120°C, the ethanol thus formed being distilled through a Vigreux column. After the distillation of ethanol had ceased, the reaction mixture was distilled under reduced pressure twice, thus yielding 19 g. of the product (60%), b. p. 78—79°C/4 mmHg.

Found: C, 51.78; H, 6.88. Calcd. for $C_5H_8O_3$: C, 51.72; H, 6.89%.

2,4-Pentanediol cyclic carbonate was prepared in a manner similar to that used for 2,3-butanediol cyclic carbonate, using 10 g. of 2,4-pentanediol, 15 g. of diethyl carbonate and 0.1 g. of sodium. The yield was 7 g. (54%). B. p. 129—130°C/7 mmHg, m. p. 12.5—13.0°C.

Found: C, 55.37; H, 7.78. Calcd. for $C_6H_{10}O_3$: C, 55.39; H, 7.75%.

For the preparation of ethyl vinyl carbonate, a mixture of 60 g. mercuridiacetaldehyde, 15 g. of ethyl chlorocarbonate and 30 ml. of tetrahydrofuran was stirred in a three-necked flask equipped with a reflux condenser and a stirrer, first at room temperature for several hours, and then at gradually increased temperatures up to 65°C. The volatile component of the reaction mixture was collected in a trap cooled by a dry ice - acetone bath in a vacuum, and then fractionally distilled, yielding 11 g. of the product (69%), b. p. 71—72°C/176 mmHg.

Found: C, 50.98; H, 6.75. Calcd. for $C_5H_8O_3$: C, 51.72; H, 6.89%.

Propylene carbonate, a commercial product, was used after distillation and the gas chromatographic comfirmation of its purity.

The solvents for the polymerization experiments were purified by standard procedures.

**Polymerization.**—An ampoule containing a monomer, a solvent and benzoylperoxide (0.5 mol.% of the monomer) or 2,2'-azobisisobutyronitrile was degassed three times in a high-vacuum manipulation and then sealed. Polymerization was carried out in a thermostat at 60±0.05°C.

In the photo-sensitized polymerization, a solution of the monomer and 2,2'-azobisisobutyronitrile in benzene was irradiated with a ultraviolet lamp (Toshiba SHL 100-UV) in a vacuum, using a vessel with a fused silica window.

After polymerization, a small amount of an inhibitor, *p-t*-butylcatechol, was introduced into the polymerization mixture, and then the residual monomer and the solvent are stripped in a vacuum at room temperature. The residual crude polymer was treated with acetone. The acetone-soluble fraction was precipitated with petroleum ether. In some experiments the polymerization mixture was poured into a large amount of hexane, yielding a precipitate of the polymer. The polymer was dried at room temperature in vacuo.

A typical example of the analysis of the polymer is shown below for the sample of Exp. No. 1 in Table V.

Found: C, 52.61; H, 5.29. Calcd. for $C_5H_6O_3$: C, 52.62; H, 5.31%.

**Infrared Spectra.**—The absorption coefficients of the model compounds were determined in chloroform, as it was confirmed that the Lambert-Beer law was applicable at concentrations from 0.02 to 0.5 mol./l. The infrared spectra of the polymer were taken by the KBr-tablet method.

## Results

**The Infrared Analysis of the Polymer Structure.**—An infrared spectrum of the polymer, shown in Fig. 1, has two carbonyl absorptions, at 1810 and 1760 $cm^{-1}$, and a double bond absorption at 1660 $cm^{-1}$. To identify these absorptions, the infrared spectra of model compounds were studied, they are listed in Table I. It can there be seen that the band at 1810 $cm^{-1}$ in the polymer corresponds to 2,3-butanediol cyclic carbonate (1810) and closely corresponds to propylene carbonate (1800), thus indicating that the 1810 band may be due to the presence of a 5-membered carbonate. The band at 1760 $cm^{-1}$ of the polymer corresponds to 2,4-pentanediol cyclic carbonate (1750), trimethylene carbonate (1755), and also to ethyl vinyl carbonate (1760), indicating that this band may originate from the unsaturated carbonate of 1,2-addition type, presumably being overlapped with a 6-membered cyclic carbonate. Thus, the structure of the polymer may be represented by Formula I:

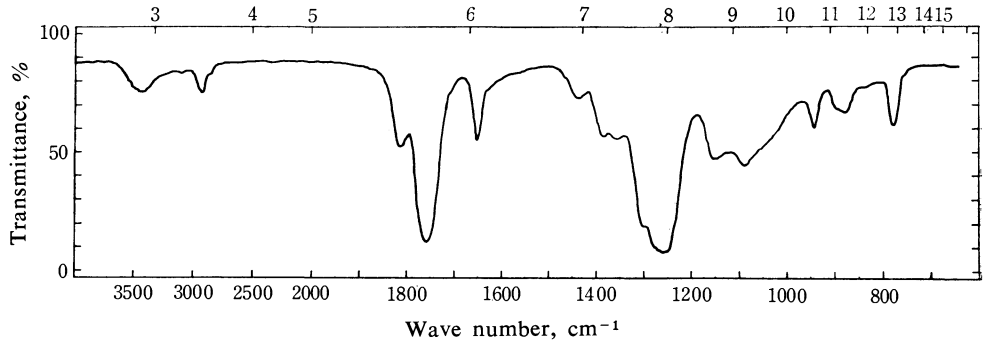
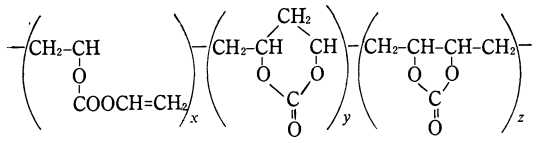



Fig. 1. Infrared spectrum of polydivinylcarbonate.



I

Using the following notations:

| Polymer structure | Molar concn. | Absorption coefficient | | Observed absorbance |
|---|---|---|---|---|
| Unsaturated carbonate | $C_1$ | C=C | $\varepsilon_1$ | $D_1$ (1660 $cm^{-1}$) |
| | | C=O | $\varepsilon_2$ | |
| 6-Membered carbonate | $C_2$ | | $\varepsilon_3$ | $D_2$ (1760 $cm^{-1}$) |
| 5-Membered carbonate | $C_3$ | | $\varepsilon_4$ | $D_3$ (1810 $cm^{-1}$) |

the molar concentrations of the three structural units can be expressed as;

$$C_1 = D_1/\varepsilon_1 l$$
$$C_2 = (D_2 - \varepsilon_2 D_1/\varepsilon_1)/\varepsilon_3 l$$
$$C_3 = D_3/\varepsilon_4 l$$

where $l$, denotes the thickness of a specimen. Assuming that the absorption coefficients of the three structural units can be represented by those of the corresponding model compounds in solution, the following expressions result:

$$C_1 = D_1/494l$$
$$C_2 = (D_2 - 2.97D_1)/1819l$$
$$C_3 = D_3/1960l$$

The relative amounts of $C_1$, $C_2$ and $C_3$ can be calculated independently of the thickness, $l$. The absorption bands at 1810 and 1760 $cm^{-1}$ in the polymer, which overlapped each other, were separated as shown in Fig. 2. The 6-membered cyclic carbonate content was not determined directly, but it was calculated on the basis of the difference in the observed absorbance of unsaturated carbonate as calculated from the $\nu_{C=C}$ band at 1660 $cm^{-1}$. Therefore, its value is likely to have some error and to be less reliable. Cross-linking due to the pendant unsaturation may not be large,

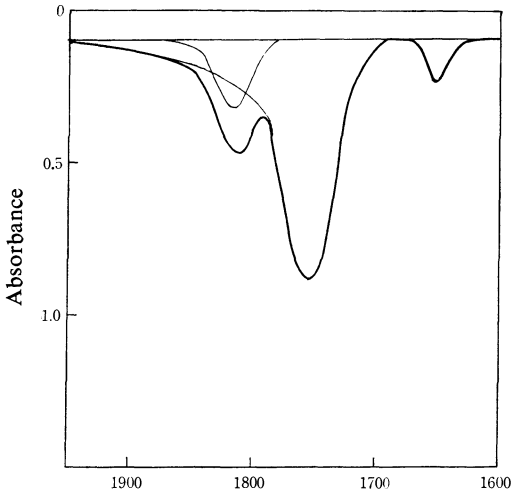



Fig. 2. Analysis of an infrared spectrum of polydivinyl carbonate.

but its increase will result in the overestimation of the 6-membered carbonate in the above calculations. This is another source of error in the estimation of the 6-membered carbonate.

**The Effect of Polymerization Variables on Polymer Properties.**—Gel point conversion may represent a qualitative measure of the degree of cyclization.[2] The effect of the monomer concentration on the gel point conversion is shown in Table II. When a visible gellation had taken place, almost the entire polymer was found to become insoluble; the monomer concentration in this case did not have any appreciable effect on the gel point conversion.

As it has been shown that, at a gel point conversion, almost the entire polymer becomes insoluble, the solubility of the polymers was examined at various points of conversion. The polymer was fractionated into a soluble part and an insoluble part by digesting the precipitated polymer with acetone at room temperature. The results are shown in Table III. The first appearance of gellation was observed after about 75 min. polymerization, but the insoluble

Table I. Infrared absorption coefficients of the related model compounds

| Carbonate | $\nu_{C=O}$, $cm^{-1}$ | $\varepsilon$ | $\nu_{C=C}$, $cm^{-1}$ | $\varepsilon$ |
|---|---|---|---|---|
| Divinyl carbonate | 1775 | 1460 | 1660 | 752 |
| Vinyl ethyl carbonate | 1765 | 1470 | 1665 | 494 |
| Diethyl carbonate | 1745 | 1110 | | |
| 2,3-Butanediol cyclic carbonate | 1810 | 1960 | | |
| Propylene carbonate | 1800 | 1490 | | |
| Trimethylene carbonate | 1755 | 1970 | | |
| 2,4-Pentanediol cyclic carbonate | 1750 | 1810 | | |
| Poly(vinylene carbonate)[a] | 1825 | | | |

a) H. C. Haas and N. W. Schuler, *J. Polymer Sci.*, **31**, 237 (1958).

TABLE II. POLYMERIZATION AND POLYMER STRUCTURE OF DIVINYL CARBONATE AT VARIOUS MONOMER CONCENTRATION IN BENZENE

60±0.05°C; [BPO]=0.5 mol. % of monomer

| Exp. No. | 1 | 2 | 3 | 4 |
|---|---|---|---|---|
| Monomer concn., % by Vol. | 70 | 50 | 30 | 10 |
| Time, min. | 52 | 77 | 112 | 1080 |
| Conversion, %[a] | 12.2 | 13.9 | 11.1 | 14.7 |
| Sol. and insol. part, % | 0.9 10.0 | 0.5 10.9 | 0.4 8.4 | 0.0 14.0 |
| 1,2-Addition, % | — 72 | 56 69 | 59 52 | — — |
| 6-Membered ring, % | — 12 | 31 18 | 25 27 | — — |
| 5-Membered ring, % | — 16 | 13 13 | 16 21 | — — |

a) Polymerization was stopped at the first appearance of gellation except for No. 5 where no visible gellation was observed.

TABLE III. PROPERTIES OF POLYMERS OBTAINED AT VARIOUS CONVERSIONS

[M]=30 vol. % in benzene; [AIBN]=0.5 mol. % of monomer; 60±0.05°C

| Exp. No. | 5 | 6 | 7 | 8 | 9 |
|---|---|---|---|---|---|
| Time, min. | 30 | 60 | 90 | 120 | 180 |
| Conversion, % | 5.8 | 8.5 | 11.6 | 14.0 | 20.5 |
| Sol. and insol. part, % | 5.3 0.0 | 3.7 4.7 | 1.3 9.5 | 1.1 12.1 | 0.5 20.0 |
| 1,2-Addition, % | — — | 59 52 | — — | 48 51 | 59 48 |
| 6-Membered ring, % | — — | 25 27 | — — | 36 31 | 21 33 |
| 5-Membered ring, % | — — | 16 21 | — — | 16 19 | 20 19 |

Intrinsic viscosity of the soluble part of Nos. 5 and 6 are 0.109 and 0.118 dl./g. in acetone.

TABLE IV. EFFECT OF SOLVENTS ON POLYMERIZATION OF DIVINYL CARBONATE

[M]=30 vol. %, [AIBM]=0.5 mol. % of monomer; 60±0.05°C

| Exp. No. | 10 | | 11 | | 12 | | 13 | | 14 | | 15 | |
|---|---|---|---|---|---|---|---|---|---|---|---|---|
| Solvent | Benzene | | Toluene | | Cumene | | $CCl_4$ | | Aceto-nitrile | | Nitro-benzene | |
| Time, min.[a] | 75 | | 140 | | No gel. | | 135 | | 140 | | No gel. | |
| Conversion, % | 20.1 | | 20.1 | | 7 | | (70.1)[b] | | 25.6 | | 0 | |
| Sol. and insol. part, % | 0.5 | 20.0 | 1.5 | 15.3 | 7 | 0 | (21.0) | (48.6) | 5.5 | 19.6 | 0 | |
| 1,2-Addition, % | 59 | 52 | 61 | 60 | 61 | — | 91 | 52 | 40 | 48 | — | — |
| 6-Membered ring, % | 25 | 27 | 21 | 21 | 26 | — | 0 | 29 | 21 | 19 | — | — |
| 5-Membered ring, % | 16 | 21 | 18 | 19 | 14 | — | 9 | 19 | 39 | 33 | — | — |

Intrinsic viscosity of the soluble part of Nos. 12 and 14 are 0.062 and 0.080 dl./g. in acetone.

a) Time at the first appearance of gellation.

b) Cl%=19.76. Figures in parentheses are values corrected for chlorine, assuming that $CCl_4$ was incorporated by a chain transfer reaction.

TABLE V. BULK POLYMERIZATION OF DIVINYL CARBONATE AT VARIOUS TEMPERATURES

Monomer, 2 ml.; AIBN 0.1 mmol.

| Exp. No. | 1 | 2[a] | 3 | 4[a] | 5[a] | 6[a] |
|---|---|---|---|---|---|---|
| Temperature, °C[c] | 60 | 45 | 30 | 15 | 0 | −30 |
| Time, min. | 14 | 3 | 1215 | 70 | 25 | 105 |
| Conversion, %[b] | 9.9 | 4.1 | 5.7 | 7.5 | 8.2 | 0.5 |
| 1,2-Addition, % | 71 | 90 | 76 | 88 | 86 | 85 |
| 6-Membered ring, % | 21 | 5.5 | 22 | 11 | 14 | 15 |
| 5-Membered ring, % | 7.9 | 4.0 | 2.3 | 1.2 | 0.5 | 0 |

a) Photo-sensitized polymerization.

b) Polymerization was stopped shortly after gellation except for No. 6.

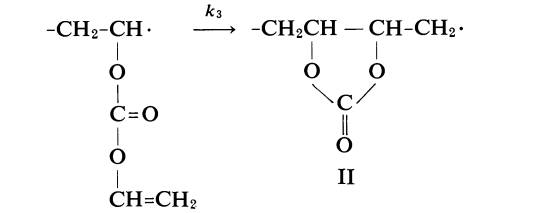
c) Temperature was kept constant within ±0.5°C.

polymer had been formed prior to the apparent gellation. At a conversion as low as 6%, the polymer was soluble in acetone, and thereafter the fraction of the insoluble polymer increased rapidly with conversion. The soluble part softened at 250—270°C with a slight discoloring. The polymer structure did not show appreciable change during the course of polymerization.

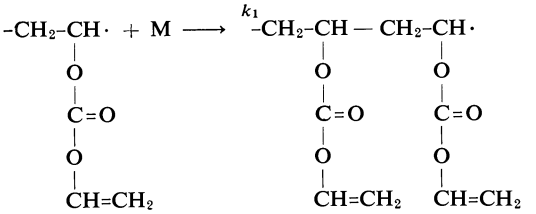
The solvent was expected to influence the solubility and the structure of the resulting polymer because of the differences in the chain transfer reaction and in the polarity, the latter of which might have some special influence on the conformation of the monomer molecule and of the polymer end in solution. The results are listed in Table IV. Even carbon tetrachloride, which is known to have a large chain transfer constant in the vinyl acetate polymerization, could not prevent the gel formation. However, polymerization in acetonitrile gave a polymer of a relatively high solubility. The extraordinary high yield of the polymer in carbon tetrachloride was unexpected: the reason can not be determined at present. Hydrocarbon solvents with high chain transfer constants, such as toluene and cumene, did not have any effect on the polymer structure, but a polar solvent, acetonitrile, showed such an effect, increasing the relative content of the 5-membered cyclic carbonate structure.

**The Effect of the Polymerization Temperature on the Polymer Structure.**—The formation of the 5-membered cyclic structure means the head-to-head addition of two vinyl groups in the same molecule. Head-to-head addition in usual vinyl monomers is known to have a higher activation energy than that of head-to-tail addition, and so it is to be expected that the polymerization temperature will have an effect on the content of cyclic units. The results are shown in Tables V and VI. The ratios of $C_3/C_1$, that is, the mole ratio of the 5-membered cyclic unit to the unsaturated carbonate units, is taken in an Arrhenius plot, giving the difference in the activation energies (Fig. 3):

$$E_3-E_1=6.21\pm0.29 \text{ kcal./mol. in a 50\% benzene solution}$$
$$=8.44\pm0.48 \text{ kcal./mol. in bulk polymerization}$$



II



III

Since

$$\frac{k_3}{k_1}=\frac{1}{(M)}\times\frac{A_3}{A_1}\exp\left(-\frac{E_3-E_1}{RT}\right)$$

Where (M) represents the monomer concentration in terms of the vinyl group, it follows

Table VI. Photosensitized polymerization of divinyl carbonate at various temperature in benzene (1 : 1 vol.)

Monomer, 2 ml.; Benzene 2 ml.; AIBM 0.1 mmol.

| Exp. No. | 7 | 8 | 9 | 10 |
|---|---|---|---|---|
| Temperature, °C[a] | 40 | 30 | 20 | 10 |
| Time, min. | 40 | 48 | 60 | 85 |
| Conversion, %[b] | 13.6 | 12.0 | 13.0 | 14.5 |
| 1,2-Addition, % | 68 | 71 | 71 | 81 |
| 6-Membered ring, % | 25 | 24 | 25 | 16 |
| 5-Membered ring, % | 7.7 | 5.1 | 4.1 | 3.0 |

a) Temperature was kept constant within ±0.1°C.
b) Polymerization was stopped shortly after gellation.

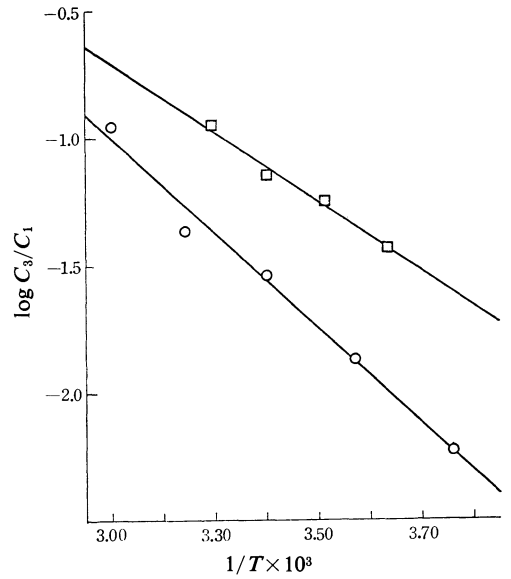



Fig. 3. Dependency of relative abundance of 5-membered ring on temperature of polymerization.
□ Solution polymerization in benzene (50 vol. %)
○ Bulk polymerization

that;

$A_3/A_1 = 2.04 \times 10^4$ in a 50% benzene solution

$= 5.85 \times 10^5$ in bulk polymerization

## Discussion

The experimental facts concerning the polymerization of divinyl carbonate at low conversions may be summarized thus:

i) The polymer structure has been found to be composed of a 5-membered cyclic carbonate unit, a 6-membered cyclic carbonate unit, and an unsaturated carbonate unit.

ii) Cyclopolymerization is not a predominant mode of propagation, leaving not less than half a mole of unsaturation per unit structure. Hence, the polymers are likely to be cross-linked.

iii) The polymerization variables, i.e., the concentrations of the monomer, the conversion, and the solvent, had no appreciable effect on the polymer structure except for the polymerization in acetonitrile (Table IV).

iv) The polymerization temperature had a strong influence on the polymer structure, raising temperature resulting in an increased content of the 5-membered cyclic carbonate unit.

Divinyl compounds which undergo cyclopolymerization may be classified into two types. The one is compounds with unsaturated groups relatively inactive towards a radical, such as diallyl compounds and divinyl acetals. The other one is monomers with the reactive double bonds, like acrylic anhydride and its derivatives. Recently, it has been suggested, from a study of the electronic spectra, that two double bonds in a molecule of the latter type have a mutual interaction in solution and that the molecule takes a special conformation favorable to cyclization.[6] The vinyl groups in divinyl carbonate belong to the latter type, its reactivity is not very different from that of vinyl acetate.[7] The fact that divinyl carbonate is unlikely to undergo genuine cyclopolymerization might be due to the lack of a conformation favorable to cyclopolymerization in this case.

Gellation at the stage of low conversion is explained as being due simply to the prior existence of a large amount of the pendant vinyl groups in the polymer and to the high reactivity of the vinyl group.

The temperature dependency of the polymer structure is significant. The intramolecular formation of the 5-membered cyclic unit has a larger activation energy, from 6 to 8 kcal./mol., than the intermolecular propagation. The difference in the activation energies between the head-to-head addition and the head-to-tail addition of the usual monomers is reported to be 1 to 3 kcal./mol.[8] The formation of the 5-membered cyclic unit of divinyl carbonate implies an intramolecular cyclization as well as a head-to-head addition. Therefore, the cyclization reaction may need an additional activation energy to be able to take a conformation favorable to the ring closure.

The frequency factor of the 5-membered cyclization reaction ($A_3$) is larger than that of the intermolecular propagation ($A_1$) by a magnitude of $10^4$ to $10^5$. The ratios observed in other vinyl monomers range from 0.1 to 0.7.[8] This large difference may not be unreasonable when it is considered that the reacting vinyl group in the cyclization reaction always exists in the vicinity of the reacting polymer radical. In other words, the intramolecular cyclization needs less decrease of entropy at the activated state than does the intermolecular propagation.

## Summary

The preparation of divinyl carbonate has been described. The cyclopolymerization of the monomer has been studied under various reaction conditions, and it has been found that cyclopolymerization is not a predominant mode of propagation, for it leaves not less than half a mole of unsafuration per unit structure. The polymer structure has been analyzed by the infrared method and found to contain the 5-membered cyclic carbonate unit, the 6-membered cyclic carbonate unit and the pendant unsaturated carbonate unit.

The polymerization temperature has been shown to have a significant effect on the 5-membered cyclic unit content, increasing the temperature resulting in an increase in the 5-membered unit. The activation energy difference between the intramolecular 5-membered cyclization and the intermolecular propagation has been estimated to be $6.21 \pm 0.29$ kcal./mol. in the polymerization in a 50% benzene solution and $8.44 \pm 0.48$ kcal./mol. in bulk polymerization.

*Department of Polymer Science*
*Faculty of Science*
*Osaka University*
*Nakanoshima, Osaka*

6) G. B. Butler and J. W. Brooks, *J. Org. Chem.*, **28**, 2699 (1963).

7) S. Murahashi, S. Nozakura and K. Kikukawa, to be published.

8) I. Rosen, G. H. McCain, A. L. Endrey and C. L. Sturm, *J. Polymer Sci.*, **A1**, 951 (1963).

# The Electrodeposition of Ruthenium from a Ruthenium(III) and Ruthenium(IV) Solution and a Fission Products Solution

By Yoshii KOBAYASHI,* Hideo YAMATERA and Hisateru OKUNO

(Received March 20, 1965)

Ruthenium in an aqueous solution may be present as a variety of chemical species, and its chemical behavior is affected by various factors. Thus the complete separation of ruthenium is one of the most difficult problems in the separation of fission products. In order to solve this problem, various separation methods, including solvent extraction,[1,2] ion exchange[3] and ruthenium-tetroxide distillation[4], have been proposed. Since ruthenium is one of the noble metals, the electrochemical method should be useful for the separation of ruthenium from fission products. Although some electrochemical studies of ruthenium have been reported (they will be described below), no electrochemical method has yet been applied successfully to the separation of ruthenium from fission products.

The electrochemical studies of ruthenium were carried out by Griess and Lietzke,[5,6] by Haissinsky and El Guebely[7,8] and by other investigators. Griess and Lietzke reported that the complete electrodeposition of ruthenium was possible from a ruthenium nitrosyl chloride solution at concentrations higher than $5\times10^{-5}$ M, while an 80% deposition was obtained at concentrations of $5\times10^{-6}$ M or less. Haissinsky and Guebely investigated the electrodeposition of ruthenium on the cathode and the anodic oxidation of ruthenium sulfate using a sulfuric acid solution.

In this study, we will attempt to find an electrochemical method of separating ruthenium from fission products. For this purpose, the electrodeposition will be investigated with sample solutions containing $^{106}$Ru-labeled ruthenium in the form of ruthenium chloride and ruthenium nitrosyl chloride. Moreover, the electrodeposition method will be successfully applied to the separation of ruthenium from fission products. The ruthenium deposited on a platinum electrode is easily recovered into a solution by anodic oxidation, using sodium hydroxide as the electrolyte.

## Experimental

**Cells for Electrolyses.**—Cells of two types were used for the electrolyses: one of them was a Joliot cell[9] made of Plexiglass, while the other, shown in Fig. 1, was a cylindrical glass cell clamped on the cathode plate by a brass stand. The latter was used for the electrolyses at elevated temperatures and for the separation of ruthenium from fission products. Silver-coated copper ($20\times0.5$ mm.) and platinum ($20\times0.05$ mm.) plates were used as the cathode, and a platinum wire ($0.50\times100$ mm.), as the anode. As the reference electrode, a saturated calomel electrode was used for the Joliot cell and a silver-silver chloride electrode for the cylindrical glass cell. The cathode potential was kept at a given potential against the reference electrode by a potential regulator.

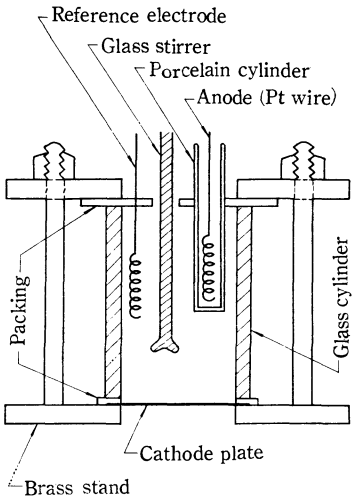



Fig. 1. Cylindrical glass cell.

**The Preparation of a Ruthenium Sample Solution and the General Procedure.**—Radioruthenium-106 (as ruthenium chloride) in a hydrochloric acid

* Present address: Chemistry Division, Tokai Laboratory, Japan Atomic Energy Research Institute, Tokai, Ibaraki-ken.

1) T. Kiba, S. Ohashi and T. Maeda, This Bulletin, **33**, 810 (1960).

2) W. Merrit, *Can. J. Chem.*, **36**, 426 (1958).

3) E. Minami, M. Honda and Y. Sasaki, This Bulletin, **31**, 372 (1958).

4) R. Overstreet, L. Jacobson and J. G. Hamilton, MDDC-1275 (1946).

5) J. C. Griess, *J. Electrochem. Soc.*, **100**, 429 (1953).

6) M. H. Lietzke and J. C. Griess, ibid., **100**, 434 (1953).

7) M. A. El Guebely and M. Haissinsky, *J. Chim. Phys.*, **54**, 290 (1954).

8) M. Haissinsky and M. A. El Guebely, ibid., **56**, 744 (1956).

9) F. Joliot, ibid., **27**, 119 (1930); N. Matsuura and H. Yumoto, *Radioisotopes* (Tokyo), **8**, 28 (1959). The Joliot cell was available through the courtesy of Dr. N. Matsuura.

solution was imported from the Radiochemical Center, Amersham, England. A $1\times10^{-7}$ M ruthenium chloride sample solution was prepared by evaporating the radioruthenium chloride and by dissolving the residue in 0.1 M hydrochloric acid. A $2\times10^{-4}$ M ruthenium chloride solution was prepared by the following method. Radioruthenium was added to a ruthenium chloride solution of an appropriate concentration ($\sim10^{-3}$ M), and then ruthenium tetroxide was distilled. The distilled ruthenium tetroxide, containing radioruthenium, was absorbed in dilute hydrochloric acid containing a small amount of hydrogen peroxide. The solution was then evaporated to dryness, and the residue was dissolved in 0.1 M hydrochloric acid. The ruthenium concentration was determined by the colorimetric method with a ruthenium thiourea complex. Ruthenium nitrosyl chloride was prepared according to the method of Griess; the resulting ruthenium nitrosyl chloride was dissolved in 0.1 M hydrochloric acid.

Five milliliters of the sample solution was placed in a cell equipped with a silver-coated copper plate as the cathode, a platinum wire as the anode, and a motor-driven glass stirrer. The solution was then electrolyzed while being continuosly stirred for a given period of time. In some cases, a Geiger counter was placed close to the outside of the cathode plate, which constituted a part of the wall of the cell, in order to measure the radiation from the inside. The rate of increase in the counting rate was directly related to the rate of electrodeposition. The activity of the electrolyte solution was measured with a well-type NaI(Tl) scintillation counter, and the activity of the electrodeposited ruthenium on the cathode plate, with a Geiger counter.

**The Electrolysis of the Fission Products.**—The gross fission products in a nitric acid solution were imported from the Oak Ridge National Laboratory, U. S. A., and aged for about 3.5 years, until they consisted mainly of $^{144}$Ce-$^{144}$Pr, $^{90}$Sr-$^{90}$Y, $^{137}$Cs, and $^{106}$Ru-$^{106}$Rh. An aliquot of this sample was evaporated to dryness and dissolved in 0.1 M hydrochloric acid. Ten milliliters of the solution was electrolyzed in the cylindrical glass cell by the general procedure except that a platinum plate was used as the cathode and the cathode and anode electrolytes were separated.

**The Determination of the Total Ruthenium Activity in the Fission Products.**—Aliquots of the fission products solution before and after electrolysis were converted from a hydrochloric into a sulfuric acid solution and mixed with a ruthenium carrier (0.5 mg.) in a sulfuric acid solution. Then the solution was made alkaline with some sodium hydroxide solution, and antiformine (a commercial sodium hypochlorite solution) was added in order to oxidize the ruthenium to ruthenate or perruthenate. To this solution, carbon tetrachloride was then added, after which the solution was slightly acidified with sulfuric acid. After the solution had been shaken for about two minutes, the ruthenium was completely extracted with carbon tetrachloride as ruthenium tetroxide, while the other fission products remained in the aqueous phase. In this method, the activity of the ruthenium extracted in carbon tetrachloride was measured on the fission products solution before and after the electrolysis, and the percentage of ruthenium electrodeposited from fission products was calculated.

**The Dissolution of the Ruthenium Deposited on a Platinum Plate.**—In order to remove the ruthenium deposited on a platinum plate, anodic oxidation was performed by the following procedure. An electrolytic cell was equipped with the platinum plate carrying the ruthenium deposit as the anode (and a copper wire as the cathode). With 0.1 M hydrochloric acid as the electrolyte, electrolysis was carried out for ten minutes at room temperature. The anode potential was maintained at a given potential (each of the potentials presented in Fig. 8) against a silver-silver chloride electrode.

The anodic oxidation was also carried out with a 0.1 M sodium hydroxide solution without controlling the anode potential. In this case, the current was supplied by a six-volt storage battery and controlled to give a rapid evolution of oxygen gas at the anode. By this method, the deposited ruthenium was completely removed from the platinum in ten minutes; the cleaned platinum plate was thereafter used repeatedly.

## Results

**Ruthenium Chloride and Ruthenium Nitrosyl Chloride.**—Figure 2 shows the results of the electrolysis of $1\times10^{-7}$ M ruthenium chloride in 0.1 M hydrochloric acid for 90 min. There was no deposition of ruthenium at the cathode potential of $-0.2$ V. vs. SCE. The ruthenium deposition increased with the decrease in the cathode potential until it reached a maximum at $-0.55$ V. vs. SCE; it decreased with the further decrease in the cathode potential. The deposition curve for $2\times10^{-4}$ M ruthenium

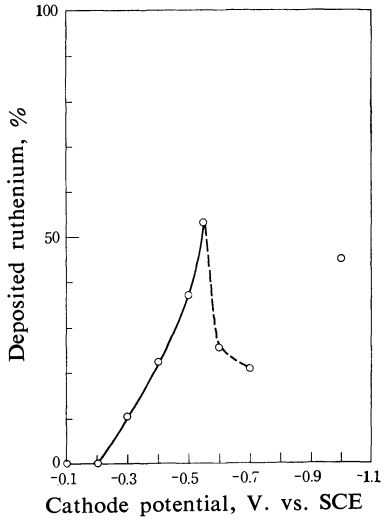



Fig. 2. Deposition curve of $1\times10^{-7}$ M ruthenium chloride (0.1 M HCl, room temperature, 90 min.).

chloride is presented in Fig. 3. This curve is unlike the cuve for $1\times10^{-7}$ M ruthenium chloride and has no maximum. In Figs. 4 and 5, the activity of the ruthenium deposited on the cathode plate is plotted against the loss of ruthenium activity from the electrolyte. The findings on $2\times10^{-4}$ M ruthenium chloride at cathode potentials between $-0.4$ and $-0.8$ V. fell on a straight line, as would naturally be expected, but the findings on $1\times10^{-7}$ M deviated from the linear relationship at cathode potentials lower than $-0.6$ V.

Figure 6 shows the results on electrolyses of $1\times10^{-7}$ M ruthenium nitrosyl chloride in 0.1 M hydrochloric acid for 60 min. The deposition curve has a maximum at $-0.6$ V. vs. SCE. A comparison of Fig. 6 with Fig. 2 will indicate that ruthenium nitrosyl chloride more easily produces a metal deposit than does ruthenium

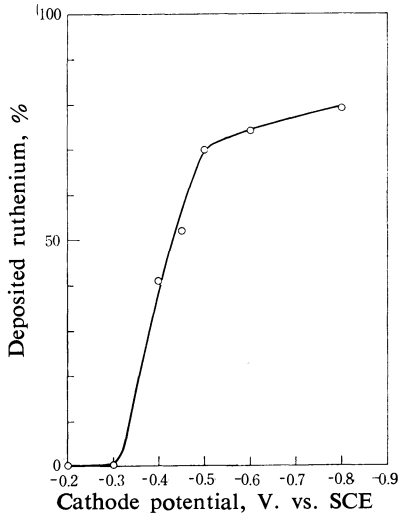



Fig. 3. Deposition curve of $2\times10^{-4}$ M ruthenium chloride (0.1 M HCl, room temperature, 30 min.).

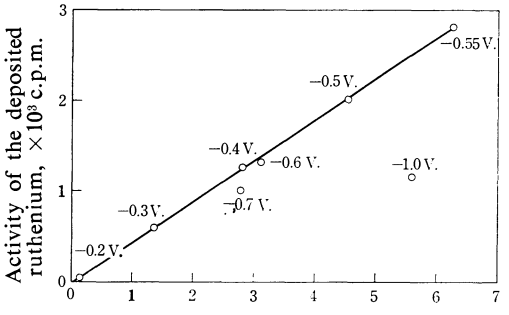



Fig. 5. Relationship between the deposited and the lost ruthenium from a $2\times10^{-4}$ M ruthenium chloride electrolyte.

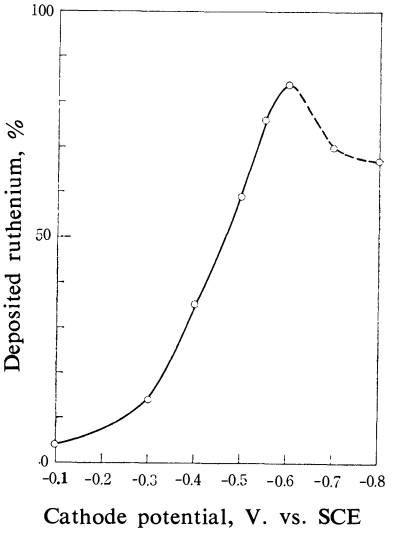



Fig. 6. Deposition curve of $1\times10^{-7}$ M ruthenium nitrosyl chloride (0.1 M HCl, room temperature, 60 min.).




Fig. 4. Relation ship between the deposited and the lost ruthenium from a $1\times10^{-7}$ M ruthenium chloride electrolyte.

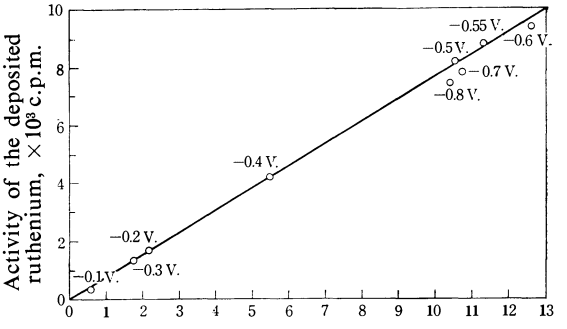



Fig. 7. Relationship between the deposited and the lost ruthenium from a $1\times10^{-7}$ M ruthenium nitrosyl chloride electrolyte.

TABLE I. ELECTRODEPOSITION OF Ru FROM Ru NITROSYL NITRATE IN 0.1 M $HNO_3$ (one hour)

| Cathode pot. vs. SCE | % Ru deposited |
|---|---|
| −0.3 | 15.8 (14.4) |
| −0.4 | 18.6 (36.4) |
| −0.5 | 36.3 (69.2) |
| −0.6 | 34.6 (84.0) |
| −0.7 | 21.1 (70.8) |

Values in parentheses are data of Ru nitrosyl chloride in 0.1 M hydrochloric acid.

chloride. The relationship between the activity of the ruthenium deposit on the cathode plate and the loss of ruthenium activity from the electrolyte is presented in Fig. 7, which also shows deviation from a linear relationship at lower cathode potentials.

Experiments with a 0.1 M nitric acid solution were also carried out, since nitrosyl ruthenium normally occurs in a nitric acid solution. The results are given in Table I. The ruthenium depositions were not as good as those from a 0.1 M hydrochloric acid solution.

Since about six hours were required to obtain a 90% deposition of ruthenium from a $1\times10^{-7}$ M ruthenium chloride solution at a cathode potential of −0.5 V. vs. SCE at room temperature, some experiments were attempted in an attempt to speed up the rate of ruthenium deposition. The results showed that a platinum plate was more useful as the cathode than a silver-coated copper plate; it gave an 85% deposition in two hours at 45°C. When 100 $\gamma$ of hexachloroplatinic(IV) acid was added to the electrolyte as the carrier, 97% of the ruthenium was deposited in one hour at room temperature using a platinum plate as the cathode.

**The Dissolution of the Deposited Ruthenium.**—The results of the anodic oxidation are presented in Fig. 8. The ruthenium deposited on a platinum plate was completely removed from the plate in a 0.1 M hydrochloric acid solution in ten miutes at anode potentials higher than 1.2 V. vs. a silver - silver chloride electrode. At these potentials, oxygen gas evolved at the anode plate. The dissolution of the ruthenium deposited on a platinum plate was also complete within ten minutes when electrolysis without the anode potential control was carried out in 0.1 M sodium hydroxide with a current strong enough to produce a violent evolution of oxygen gas at the anode.

**Fission Products.**—On the basis of the experimental results described above, the separation of ruthenium from fission products was carried out under the following conditions: the cathode potential was −0.5 V. vs. a silver - silver chloride electrode, and the cathode electrolyte solution (fission products solution) and the anode electrolyte solution (0.1 M hydrochloric acid) were separated by a diaphragm in order to prevent the oxidation of ruthenium-(III) or ruthenium(IV) to higher oxidation states. The results are presented in Table II. The nuclide separated by this method was identified as ruthenium-106 by gamma-spectrometry.

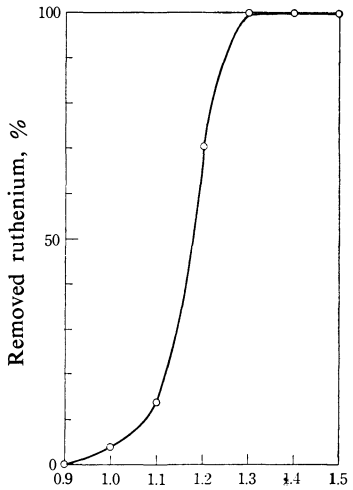



Fig. 8. Anodic oxidation of deposited ruthenium on platinum electrode (0.1 M HCl, room temperature, 10 min.).

TABLE II. ELECTRODEPOSITION OF Ru FROM FISSION PRODUCTS

| Temperature | % Ru deposited |
|---|---|
| Room temp. | 72.8 |
| Room temp. | 73.0 |
| 75°C | 97.5 |
| 75°C | 95.5 |
| Room temp. | 100 (Ru carrier; 0.5 mg.) |

## Discussion

Haissinsky and Guebely carried out experiments on the electrodeposition of ruthenium from solutions at the concentration of $5\times10^{-9}$ g.equiv./l. in sulfuric acid without separating the cathode and the anode electrolyte; they found that the ruthenium deposited on the cathode decreased at lower cathode potentials. They thought that this decrease in the electrodeposition might be attributed to the rapid evolution of hydrogen gas at the cathode at lower potentials partially preventing the ruthenium deposition, although they also found, in their experiments on anodic oxidation, that the ruthenium oxide or hydroxide was deposited on the wall of the cell. On the other

hand, Griess, who carried out electrolyses using a salt bridge to separate the cathode and the anode electrolyte, did not report any decrease in the ruthenium deposition on the cathode at lower potentials.

In the present study, the same tendency as had been reported by Haissinsky and Guebely was observed in experiments with a $1\times10^{-7}$ M ruthenium solution, while a different tendency was observed at the concentration of $2\times10^{-4}$ M.

If the decrease in ruthenium deposition had been effected mainly by the evolution of hydrogen gas at the cathode, the abnormal decrease should have been observed not only in the experiments at $1\times10^{-7}$ M and in those by Haissinsky and Guebely, but also in the experiments at $2\times10^{-4}$ M and in those by Griess, and a linear relationship would naturally exist between the activity of the deposited ruthenium and the activity of the ruthenium lost from the electrolyte, even at lower cathode potentials (−0.6 V.) Actually, however, no mention was made of any such abnormality by Griess, and a deviation from the linear relationship was observed in some of the present experiments (Fig. 4, 5 and 7).

From these facts, the abnormal phenomenon can be explained as follows. At lower cathode potentials, especially at −1.0 V., where gases rapidly evolved from the cathode and anode, an appreciable portion of the ruthenium in a $1\times10^{-7}$ M solution disappeared from the electrolyte, probably due to oxidation to higher oxidation states, followed by deposition on the wall of the cell and the anode and/or by volatilization as ruthenium tetroxide. With a $2\times10^{-4}$ M ruthenium solution, the portion of ruthenium oxidized was negligible as compared with the total, and a normal deposition curve resulted. Although no decisive conclusion could be derived from the present study, it seems very probable that the anodic oxidation of ruthenium, as well as the evolution of hydrogen gas at the cathode, is responsible for the abnormality in the deposition of ruthenium from the $1\times10^{-7}$ M solution.

Griess and Lietzke reported the dissolution of the ruthenium deposited on a gold or platinum electrode. When they carried out electrolysis in a strong sodium cyanide solution using a gold or platinum electrode as the anode, the ruthenium deposited on the gold or platinum plate was completely removed from the plate by the electrochemical dissolution of the base gold or platinum metal. In the present study, however, our tentative conclusion is that the removal of the ruthenium that had been deposited on a platinum plate was effected by the anodic oxidation of the ruthenium, for an electrolytic solution (acidic or alkaline) took on an orange-yellow color when ruthenium in a macro amount was electrolytically removed from a platinum plate, whereas the solution was colorless with ruthenium in a micro amount.

It has been shown that this electrochemical method for the separation of ruthenium may be successfully applied to fission products. Unlike other methods, such as tetroxide distillation method and some solvent extraction methods, this method does not require the addition of an oxidizing, a reducing or a complexing agent and is free from trouble in the subsequent steps needed for the separation of other nuclides.

## Summary

The electrodeposition of ruthenium from ruthenium chloride and ruthenium nitrosyl chloride solution has been studied and has been applied to the separation of the radioactive ruthenium contained in fission products. When the amount of the ruthenium deposited in a given time was plotted against the cathode potential, the curves for $1\times10^{-7}$ M solutions of chloride and nitrosyl chloride showed a maximum. The decrease in the electrodeposition at lower cathode potentials may be due to the anodic oxidation of ruthenium as well as to the evolution of hydrogen gas at the cathode. The rate of electrodeposition was found to depend on the material used as the cathode, and to be increased by an increase in the temperature and by the addition of the carrier platinum or ruthenium. A complete separation of radio-ruthenium from fission products resulted when electrolysis was carried out with a 0.1 M hydrochloric acid solution of fission products containing carrier ruthenium under the appopriate conditions mentioned in the text. The ruthenium electrodeposited on the platinum electrode was completely recovered into the solution by anodic oxidation.

The authors wish to express their deep thanks to Professor Niro Matsuura (The University of Tokyo) for his invaluable suggestions and for providing the Joliot electrolysis cell. They are also indebted to Professor Tatsujiro Ishimori and Professor Kunihiko Mizumachi (St. Paul's University) for their useful discussions. The expenses of the work were partly defrayed by a grant from the Ministry of Education, to which the authors' thanks are due.

*Department of Chemistry*
*St. Paul's University (Rikkyo Daigaku)*
*Ikebukuro, Tokyo*

10) E. B. Sandell, "Colorimetric Determination of Traces of Metal," Interscience Publishers Inc., New York (1959).

# The Photolysis of Ethyl Chloroformate in Hydrocarbons

By Chyongjin PAC and Shigeru TSUTSUMI

(Received March 22, 1965)

It has been reported that alkoxycarbonyl radicals are produced by the reactions of alkyl formates with alkyl[1,2] or methoxy[3] radicals, and by those of methyl chloroformate with methyl radicals.[4] In the peroxide-induced reaction of methyl formate with an olefin such as oct-1-ene, the formation of methyl pelargonate can arise from the addition of methoxycarbonyl radicals to the olefin.[5] Although the alkoxycarbonyl radicals would also be produced in some of the primary steps in the photolysis of alkyl formates[6] or esters of aliphatic carboxylic acids,[7] this photolytic decomposition mainly takes place in the formyl- or acyl-alkoxy bond fission. An illustration is provided by the fact that the photolysis of methyl formate in cyclohexane gives cyclohexylcarbinol as the major product.[8] The photolysis of esters of formic and other aliphatic carboxylic acids, therefore, is not suitable for the generation of alkoxycarbonyl radicals. Photolyses of ethyl cyanoformate and diethyl oxalate have been reported from this laboratory to give ethoxycarbonyl radicals, though the photolyses are related to the cyanation[9] and the $\alpha$-ketocarboxylation[10] of the substrates respectively.

Although the thermodynamic properties of alkoxycarbonyl radicals have been discussed by Gray and Thynne,[2] little information concerning the stability and the reactivity of the radicals has been given for lack of convenient methods for the generation of such radicals. In a previous communication,[11] we have reported that the photolysis of ethyl chloroformate affords ethoxycarbonyl radicals and supplies a method for the direct carboxylation of hydrocarbons. The present paper will show the full results of the photolysis of ethyl chloroformate (ECF) in hydrocarbons; these results indicate the occurrence of selective carbon-chlorine bond breaking to give ethoxycarbonyl radicals. The reactivity of the radical in such hydrocarbons as cyclohexane, cyclohexene, oct-1-ene, and benzene will also be discussed in some detail.

## Results and Discussion

The photolysis of ECF was carried out with an unfiltered high pressure mercury arc without a solvent, or in cyclohexane, cyclohexene, oct-1-ene, and benzene. During the course of the

TABLE I. GASEOUS PRODUCTS FORMED BY THE PHOTOLYSIS OF ECF IN CYCLOHEXANE AND CYCLOHEXENE

| ECF | Hydrocarbon | Irradiation time | Product | | | | | | |
|---|---|---|---|---|---|---|---|---|---|
| | | | Volume* | Ratio** | | | | | |
| g. | g. | hr. | cc. | CO | : | $CO_2$ | : | $C_2H_6$ | : $C_2H_4$ |
| 100 | — | 25 | 700 | 0.1> | : | 1 | : | 0.56 | : 0.056 |
| 80 | Cyclohexane, 20 | 4 | 240 | *** | : | 1 | : | 0.73 | : 0.05 |
| 18 | Cyclohexane, 40 | 4 | 200 | *** | : | 1 | : | 1 | : *** |
| 80 | Cyclohexene, 20 | 4 | 7 | *** | : | 1 | : | 0.14 | : 0.11 |
| 18 | Cyclohexene, 40 | 4 | 7 | *** | : | 1 | : | 0.13 | : 0.13 |

* Volumes of neutral gaseous products ($CO+C_2H_6+C_2H_4$)

** The products-ratios were determined by gas chromatography using 1 m. of silica-gel column at 25°C.

*** The amounts were too small to be measured.

1) J. C. J. Thynne, *Proc. Chem. Soc.*, **1961**, 18; *Trans. Faraday Soc.*, **58**, 1533 (1962).
2) P. Gray and J. C. J. Thynne, *Nature*, **191**, 1357 (1961).
3) J. C. J. Thynne, *Proc. Chem. Soc.*, **1962**, 295.
4) J. C. J. Thynne and P. Gray, ibid., **1962**, 141.
5) C. Walling and E. S. Huyser, "Organic Reactions," Vol. 13, John Wiley & Sons, Inc., New York (1963), p. 111.
6) R. Borkowski and P. Ausloos, *J. Am. Chem. Soc.*, **83**, 1053 (1961).
7) P. Ausloos, ibid., **80**, 1310 (1958); M. H. J. Wijnen, ibid., **82**, 1847 (1960).
8) K. Shima and S. Tsutsumi, *J. Chem. Soc. Japan, Ind. Chem. Sec. (Kogyo Kagaku Zasshi)*, **64**, 1945 (1961).
9) T. Tominaga, Y. Odaira and S. Tsutsumi, This Bulletin, **37**, 596 (1964).
10) Y. Odaira, T. Tominaga, T. Sugihara and S. Tsutsumi, *Tetrahedron Letters*, **1964**, 2527.
11) C. Pac and S. Tsutsumi, This Bulletin, **36**, 234 (1963).

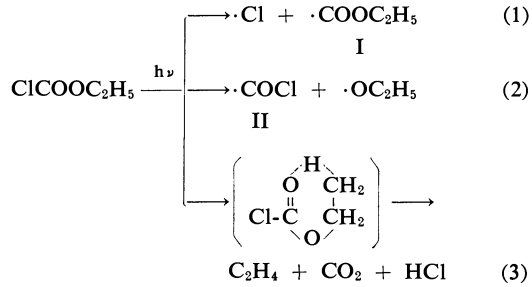
Table II. Gaseous* and liquid products formed by the photolysis of ECF in hydrocarbons

| ECF g. | Hydrocarbon g. | Irradiation time hr. | Product** mmol. | |
|---|---|---|---|---|
| 83 | Cyclohexane, 168 | 6 | Carbon dioxide | 60 |
| | | | Ethane | 60 |
| | | | Ethyl cyclohexanecarboxylate | 6 |
| | | | Bicyclohexyl | 9 |
| 83 | Cyclohexene, 164 | 14 | Carbon dioxide | 7 |
| | | | Ethane | 1 |
| | | | Ethylene | 1 |
| | | | Ethyl cyclohexanecarboxylate | 18 |
| | | | Ethyl cyclohexene-3-carboxylate | *** |
| | | | 3, 3'-Bicyclohexenyl | 21 |
| 60 | Oct-1-ene, 178 | 12 | Carbon dioxide | 8 |
| | | | Ethane | 2 |
| | | | Ethylene | 2.6 |
| | | | Ethyl pelargonate | 6—7 |
| | | | Ethyl 3-chloropelargonate | *** |
| 80 | Benzene, 22 | 50 | Carbon dioxide | 5 |
| | | | Ethane | 5 |
| | | | Ethylene | *** |
| | | | Ethyl benzoate | 50—100 mg. |
| | | | Biphenyl | *** |

* In all cases, traces of carbon monoxide, ethyl chloride, and acetaldehyde were detected.
** In the case of cyclohexane, traces of ethylene, chlorocyclohexane, ethylcyclohexane, and diethyl carbonate were found. In the case of oct-1-ene, other unidentified products were observed.
*** The amounts were negligible.

irradiation, hydrogen chloride and the other gases were evolved; small amounts of the condensable products were trapped at −60°C at the end of the irradiation. The condensable products, which were analyzed by gas chromatography, mainly consisted of ethyl chloride, along with traces of acetaldehyde, while *n*-butane could not be detected. The gases formed, which were also analyzed by gas chromatography, included carbon monoxide, carbon dioxide, ethane, and ethylene. Both in cyclohexane and in the absence of a solvent, carbon dioxide and ethane were the major products, while carbon monoxide and ethylene were found to be the minor products. In the case of cyclohexene, the yields of gaseous products were very small, and the product-ratios were different from those found in the case of cyclohexane. The results concerning gaseous products obtained from the photolysis of ECF in cyclohexane and cyclohexene are summarized in Table I. The liquid products found in the photolysis of ECF in cyclohexane, cyclohexene, oct-1-ene, and benzene are listed in Table II.

**Primary Processes of the Photolysis of ECF.** —On the basis of the suggestions regarding the photolysis of esters of formic or aliphatic carboxylic acids,[7] the possible primary processes of the photolysis of ECF might be shown as follows:




(1)
(2)
(3)

The ethoxycarbonyl radical I, produced by the breaking of the carbon-chlorine bond (Eq. 1), is decomposed into carbon dioxide and an ethyl radical (Eq. 4-a) with an activation energy somewhat greater than 1—2 kcal./mol.[2] The chloroformyl radical II produced by the homolysis of the chloroformyl-ethoxy bond (Eq. 2) breaks down into carbon monoxide and a chlorine atom (Eq. 4-b) with the activation energy of 6.3 kcal./mol.[12]

$$\underset{\text{I}}{\cdot COOC_2H_5} \rightarrow CO_2 + \cdot C_2H_5 \qquad (4\text{-a})$$

$$\underset{\text{II}}{\cdot COCl} \rightarrow CO + \cdot Cl \qquad (4\text{-b})$$

According to schemes 1, 3, and 4-a, if ethyl radicals are quantitatively converted to ethane

12) W. G. Burn and F. S. Dainton, *Trans. Faraday Soc.*, **48**, 39 (1952).

and/or ethylene by their hydrogen-abstraction from a substrate or by disproportionation, the stoichiometric relationship between $C_2$-hydrocarbons and carbon dioxide must be given by Eq. 5:

$$([C_2H_4] + [C_2H_6])/[CO_2] = 1 \quad (5)$$

where $[C_2H_4]$, $[C_2H_6]$, and $[CO_2]$ indicate the moles of the corresponding compounds. It has been suggested that the disproportionation of ethyl radicals is suppressed by the use of organic solvents and that, in some cases, it does not take place at all.[13] The proportion of ethylene in gaseous products, therefore, might be expected to determine how process 3 participates in the photolysis of ECF. As is shown in Table I, with the increase in the amount of cyclohexane added. the values of the $C_2$-hydrocarbons/$CO_2$ ratio were changed from 0.62 to unity. When ECF was sufficiently diluted with cyclohexane, equal amounts of ethane and carbon dioxide were obtained, and the formation of ethylene became negligible. The dilution with cyclohexane apparently completes the conversion of ethyl radicals to ethane:

$$\cdot C_2H_5 + \bigcirc \rightarrow C_2H_6 + \cdot\bigcirc \quad (6)$$

and Eq. 5 is satisfied. These results, therefore, strongly suggest that process 3 does not play an important role in the primary processes of the photolysis of ECF in cyclohexane.

On the other hand, the amounts of carbon monoxide might indicate the extent of the primary process 2. The findings in Table I show that the amounts of carbon monoxide are very small in all cases; hence process 2 would be negligible. From a comparison of the activation energy for the decomposition of the radical II with that for the decomposition of the radical I, however, it might be expected that a significant amount of the former radical might be likely to react with the other species before the decomposition. Contrary to the above expectation, however, the liquid products obtained from the photolysis of ECF in excess cyclohexane were not contaminated with cyclohexanecarbonyl chloride. Moreover, the amounts of acetaldehyde and diethyl carbonate which are derived from ethoxy radicals produced through process 2 are very small:

$$C_2H_5O\cdot + R\cdot \rightarrow CH_3CHO + RH \quad (7)$$

$$2C_2H_5O\cdot \rightarrow CH_3CHO + C_2H_5OH \quad (7')$$

$$C_2H_5O\cdot \xrightarrow{\text{hydrogen donor}} C_2H_5OH \quad (8)$$

$$C_2H_5OH + ClCOOC_2H_5 \rightarrow (C_2H_5O)_2CO + HCl \quad (9)$$

13) J. Smid, A. Rembaum and M. Szwarc, *J. Am. Chem. Soc.*, 75, 3315 (1956); M. Matsuoka, P. S. Dixon, A. P. Stefani and M. Szwarc, *Proc. Chem. Soc.*, **1962**, 304; J. N. Bradley, *J. Chem. Phys.*, 35, 748 (1961).

$$C_2H_5O\cdot + \cdot COOC_2H_5 \rightarrow (C_2H_5O)_2CO \quad (10)$$

These results are consistent with the conclusion that the primary process 2 plays a negligible role in the photolysis of ECF.

Thus we may decide that, in the photolysis of ECF, the breaking of the carbon-chlorine bond occurs in a selective manner, and that the photolysis of ECF can serve for the generation of ethoxycarbonyl radicals.

**The Reactions of Ethoxycarbonyl Radicals.** —As Table II shows, the liquid products from the photolysis of ECF in cyclohexane consisted of ethyl cyclohexanecarboxylate, bicyclohexyl, and traces of a mixture of chlorocyclohexane, ethylcyclohexane, and diethyl carbonate, while cyclohexanecarbonyl chloride could not be detected in any liquid fraction.

With respect to the formation of ethyl cyclohexanecarboxylate, two alternative interpretations are possible, as is shown in schemes 11 and 12, the radical-association scheme and the chain-reaction scheme. In the latter scheme, if a cyclohexyl radical is generated, the ester

$$\bigcirc\cdot + \cdot COOC_2H_5 \rightarrow \bigcirc\text{-}COOC_2H_5 \quad (11)$$

$$\bigcirc\cdot + \begin{matrix} Cl \\ | \\ C{=}O \\ | \\ OC_2H_5 \end{matrix} \rightarrow \bigcirc\text{-}COOC_2H_5 + \cdot Cl \quad (12)$$

must be produced. When the dibenzoyl peroxide-catalyzed reaction of ECF in cyclohexane was carried out, the ester was not observed, but bicyclohexyl was produced. Therefore, the latter interpretation (chain reaction) is ruled out; the association scheme 11 can be adopted in this case.

Assuming that the radical I diffuses in the solvent and associates with a cyclohexyl radical, the dimerization product, diethyl oxalate, may be expected to be formed, since carbamoyl radicals, $\cdot CONH_2$, can dimerize to give oxamide.[14] The difference in these reactions must be ascribed to the difference in stability between the radical I and the carbamoyl radical, not to a difference in electronic properties. The radical I might not have life time enough to dimerize. Therefore, it is very unlikely that the radical I diffuses in the solvent; it should be considered that ethyl cyclohexanecarboxylate might be produced in a solvent cage, involving the cage wall.

$$\left[\bigcirc + \cdot Cl + \cdot COOC_2H_5\right] \rightarrow \left[\bigcirc\cdot + \cdot COOC_2H_5 + HCl\right] \rightarrow \bigcirc\text{-}COOC_2H_5 + HCl \quad (13)$$

14) D. Elad and J. Rochach, *J. Org. Chem.*, 29, 1855 (1964).

Gray and Thynne have shown that the activation energies for the decomposition of alkoxycarbonyl radicals are somewhat greater than those for the decomposition of acyloxy radicals.[2] An acetyloxy radical, even in the liquid phase, does not attack alkanes; the entity of the radical reaction in such a system has been suggested to be a methyl radical,[15] though acetyloxy radicals are scavenged by iodine molecules.[16] In our experiments, the ratio of the association of the radical I with a cyclohexyl radical to the decomposition exhibits values of 0.1 or less, showing, in the liquid phase, fairly good accordance with the above authors' suggestion. The radical I might have life time enough to associate with a cyclohexyl radical in the solvent cage.

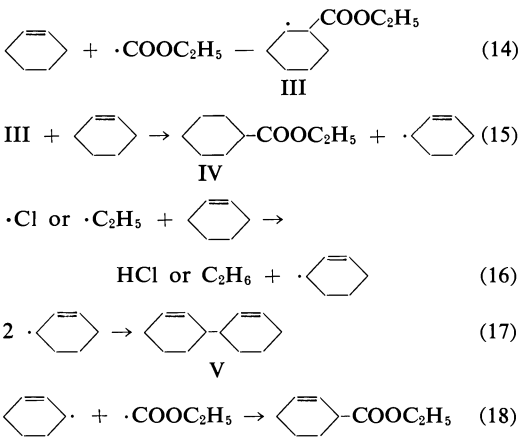
In order to observe the reactivity of the radical I to double bonds, cyclohexene and oct-1-ene were employed as solvents. The dilution with cyclohexene suppressed the formation of gases to a great extent, but the amounts of gases formed did not vary, though the concentration of ECF in cyclohexene was greatly changed. These results might indicate that a facile addition of the radical I to cyclohexene takes place, and that the decomposition is greatly suppressed. This interpretation is well supported by the results in Table II and by the well-known fact that olefins are good scavengers of various radicals.

The ratio of ethyl cyclohexanecarboxylate to carbon dioxide might give a measure of the reactivity of the radical I to cyclohexene. The value of the ratio, 2.5, indicates that the addition of the radical I to cyclohexene predominates over the decomposition at least 2.5 times. It is, however, difficult to explain why the amount of $C_2$-hydrocarbons were much less than that of carbon dioxide, and why ethylcyclohexane was not detected. It is most likely that ethyl radicals add to cyclohexene, and that the resulting species react further with cyclohexene to give unreclaimed, heavier compounds.

In the photolysis of esters of formic and aliphatic carboxylic acids[6] it has been suggested that the migration of a hydrogen atom (process 3) takes place in the excited singlet state. Therefore, the formation of ethylene via process 3 might not be quenched by cyclohexene. On the other hand, the formation of carbon dioxide might be much suppressed by the facile addition of the radical I to cyclohexene, and some of the ethyl radicals from the decomposition of the radical I might be trapped by cyclohexene. Thus, the proportion of ethylene in gaseous products is increased, and that of ethane is decreased compared with the results in the case of cyclohexane or in the absence of a solvent.

It was expected that the radical I would associate with a cyclohexen-3-yl radical in a manner similar to that in the case of cyclohexyl radicals to give an amount of ethyl cyclohexene-3-carboxylate comparable with that of ethyl cyclohexanecarboxylate obtained from the photolysis of ECF in cyclohexane. However, the amount of ethyl cyclohexene-3-carboxylate was negligible. These unexpected results can be explained by assuming that the addition of the radical I to cyclohexene is very rapid. Since the radical I is almost scavenged by cyclohexene, the concentration of the radical I might be so lowered that the association with the cyclohexen-3-yl radical, even in a solvent cage, can not take place to any appreciable extent.

The reaction scheme is shown as follows:



According to the above scheme, a stoichiometry is given by Eq. 19:

$$([HCl] + [C_2H_6] + [IV])/2[V] = 1 \quad (19)$$

where [HCl], [$C_2H_6$], [IV], and [V] indicate the moles of the corresponding products. Since the number of chlorine atoms is equivalent to the amount of the radical I, [HCl] can be approximately replaced by [$CO_2$]+[IV]:

$$([CO_2] + [C_2H_6] + 2[IV])/2[V] \sim 1 \quad (20)$$

The observed values of the ratio in Eq. 20 are 1.05, showing good accordance with those expected from the scheme.

Another possible product, ethyl 2-chlorocyclohexanecarboxylate, could not be detected in any appreciable amounts. Although a methyl radical has been reported to abstract the chlorine atom in methyl chloroformate in the vapor phase,[4] the species III might not abstract the chlorine atom in ECF. The above finding can be interpreted in three ways: 1) The chlorine

15) L. Herk and M. Szwarc, *J. Am. Chem. Soc.*, **82**, 3558 (1960).
16) H. J. Shine and D. H. Hoffman, ibid., **83**, 2782 (1961).

atom-abstraction may be sterically hindered by the configuration of the cyclohexane ring. 2) Since cyclohexene has highly labile allylic hydrogen atoms, the species III may predominantly abstract the hydrogen atoms. 3) The chlorine atom in ECF may be insensitive to abstraction with radical species other than a methyl radical in the liquid phase.

A chain terminal olefin, such as oct-1-ene, eliminates such steric hindrance and does not have so reactive hydrogen atoms. When the photolysis of ECF in oct-1-ene was carried out, a variety of products was formed, including a moderate amount of ethyl pelargonate and traces of ethyl 3-chloropelargonate. Moreover, the amount of ethyl chloride found was very small in all cases. Therefore, it is likely that the third possibility is correct, that is, that the chlorine atom in ECF is insensitive to abstraction with the species III and VI and with ethyl radicals in the liquid phase.

$$C_6H_{13}\text{-}\dot{C}HCH_2COOC_2H_5$$

VI

The formation of a variety of products is ascribed to the competing reactions of various radicals formed primarily and secondarily. All of the liquid fractions obtained, however, showed essentially identical infrared absorption spectra, exhibiting strong bands corresponding to esters of aliphatic carboxylic acid without any other carbonyl bands. Moreover, the amounts of gases formed and the product ratios were comparable to those in the case of cyclohexene. These results show that the radical I adds not only to cyclohexene, but also to oct-1-ene, and with less decomposition.

In the case of benzene, the effective light for the photolysis of ECF appears to be quenched by benzene, since the absorption maximum of ECF lies below 2500 Å. Therefore, a precise investigation could not be undertaken, though small amounts of ethyl benzoate and traces of biphenyl were detected.

## Experimental

**Materials.**—ECF, cyclohexane, and benzene were obtained commercially and purified in usual ways. Cyclohexene was prepared by the dehydration of cyclohexanol,[17] and oct-1-ene, by the pyrolysis of *n*-octyl acetate.[18] All of the materials were distilled before use.

**The Analysis of Gaseous and Condensable Products.**—In the study of gaseous products for Table I, the photolysis of ECF was carried out in a quartz cell (50 cm. long, 2 cm. in diameter) immersed in a water bath maintained at room temperature, and with a high-pressure mercury arc (600 W.) mounted 1 cm. from the cell. The gases formed were passed through an aqueous alkaline solution after a trap at −60°C and were collected in a gas buret, with which the volumes of the neutral gaseous products were measured. The product ratios were determined by gas chromatographic measurements (silica-gel column: 1 m. at 25°C). At the end of the irradiation, a slow stream of nitrogen was bubbled into the irradiated mixture, and the condensable products collected in the trap were subjected to gas chromatography (tricresyl phosphate column: 3 m. at 25°C). Acetaldehyde was identifed by the paper chromatography of its 2,4-dinitrophenylhydrazone.

**The Photolysis of ECF in Cyclohexane.**—A mixture of ECF (83 g.) and an excess of cyclohexane (168 g.) was irradiated with an internally-mounted high-pressure mercury arc (600 W.) at room temperature for 6 hr. in an atmosphere of nitrogen. During the course of the irradiation, 1400 cc. of neutral gaseous products was evolved. After the unchanged materials had been removed from the irradiated mixture, the remaining oil was distilled under reduced pressure to yield traces of a mixture of chlorocyclohexane, ethylcyclohexane, and diethyl carbonate (b. p. 30—60°C/35 mmHg), 1 g. of ethyl cyclohexanecarboxylate (b. p. 93—96°C/35 mmHg, $n_D^{26}$ 1.4510) and 1.5 g. of bicyclohexyl (b. p. 65—70°C/3 mmHg, $n_D^{26}$ 1.4743). The mixture of chlorocyclohexane, ethylcyclohexane, and diethyl carbonate was analyzed by gas chromatography (silicone-oil column: 3 m. at 80°C). The fraction of ethyl cyclohexanecarboxylate showed only one peak in its gas chromatogram (silicone-oil column: 3 m. at 170°C) and an infrared absorption spectrum identical with that of an authentic sample. An anilide derived from this fraction showed no melting point depression upon admixture with an authentic anilide; melting point and mixed melting point 143—143.5°.

(Found: C, 76.69; H, 8.06. Calcd. for $C_{18}H_{17}ON$: C, 76.81; H, 8.43%)

The fraction of bicyclohexyl was analyzed by gas chromatography (silicone-oil column: 3 m. at 170°C); it was contaminated with only a small amount of ethyl cyclohexanecarboxylate (3.8 wt.%).

**The Photolysis of ECF in Cyclohexene.**—The photolysis of ECF (83 g.) in cyclohexene (164 g.) for 14 hr. gave 50 cc. of neutral gaseous products and two fractions, one of them with a b. p. of 88—99°C/28 mmHg ($n_D^{26}$ 1.4570, 3.1 g.) and the other with a b. p. of 110—132°C/28 mmHg ($n_D^{26}$ 1.4953, 2.9 g.); both of these showed two peaks in their gas chromatograms (silicone-oil column: 3 m. at 170°C). One of the peaks had the same retention time as that of ethyl cyclohexanecarboxylate, while the other was considered to be the peak of 3,3'-bicyclohexenyl on the basis of findings to be described later. The area-ratios of the former peak to the latter in two fractions showed the values of 5.7 and 0.15 respectively; thus the yields of ethyl cyclohexanecarboxylate and 3,3'-bicyclohexenyl were each calculated to be 3 g. The lower boiling fraction was further analyzed by gas chromatography under

17) G. H. Coleman and H. F. Johnstone, "Organic Syntheses," Coll. Vol. 1, 183 (1956).
18) W. J. Bailey and W. H. Hale, *J. Am. Chem. Soc.*, **81**, 647 (1959).

different conditions (dioctyl sebatate column: 4 m. at 120°C); this analysis showed the presence of a trace of ethyl cyclohexene-3-carboxylate.[19] This fraction showed an infrared absorption spectrum essentially identical with that of ethyl cyclohexanecarboxylate, and an anilide derived from the fraction showed no melting point depression upon admixture with anilide of cyclohexanecarboxylic acid (m. p. 143.5°C and mixed m. p. 143—143.5°C). The higher boiling fraction showed the absorption bands characteristic of double bonds at 3040 and 1640 $cm^{-1}$ and, on treatment with bromine, afforded two white crystals, the one (m. p. 153—156°C) more soluble and the other (m. p. 187—189°C) less soluble in chloroform; these were considered to be tetrabromides of 3, 3'-bicyclohexenyl (lit.[20] the more soluble isomer, m. p. 159—162°C, and the less soluble one, m. p. 188—190°C).

**The Photolysis of ECF in Oct-1-ene.**—The photolysis of ECF (60 g.) in oct-1-ene (178 g.) for 12 hr. gave 100 cc. of neutral gaseous products and the following fractions; b. p. 109—115°C/27 mmHg, 1.7 g. and b. p. 125—149°C/1 mmHg, 1.9 g. These two fractions exhibited infrared absorption spectra essentially identical with the strong bands of the aliphatic carboxylic acids at 1740 (C=O) and 1160 (C-O) $cm^{-1}$ respectively. The lower boiling fraction showed five peaks in its gas chromatogram (silicone oil column: 1.5 m. at 165°C), in which the largest peak had the same retention time as that of ethyl pelargonate, while the retention time of the smallest one was identical with that of ethyl 3-chloropelargonate. An anilide derived from the lower boiling fraction showed no melting point depression upon admixture with anilide of pelargonic acid; m. p. 56.5—57.5°C and mixed m. p. 56.5—58°C.

(Found: C, 77.33; H, 9.91. Calcd. for $C_{15}H_{23}ON$: C, 77.25; H, 9.87%)

The higher boiling fraction was analyzed by gas chromatography (silicone oil column: 1.5 m. at 165°C) and found to consist of seven or more components; these were not, however, identified.

**The Photolysis of ECF in Benzene.**—When a mixture of ECF (80 g.) and benzene (22 g.) was photolyzed for 50 hr., 100 cc. of neutral gaseous products and 100 mg. of a fraction (b. p. 65—75°C/10 mmHg) were obtained. The liquid fraction, when analyzed by gas chromatography (silicon oil column: 3 m. at 160°C), was found to consist of ethyl benzoate, along with traces of biphenyl and only a small amount of another, unidentified component. Further investigations were not carried out.

**The Dibenzoyl Peroxide-Catalyzed Reaction of ECF in Cyclohexane.**—A mixture of ECF (18 g.) and cyclohexane (40 g.) containing 2 g. of dibenzoyl peroxide was refluxed at 83—85°C for 24 hr. under a nitrogen atmosphere. During the course of the reaction, carbon dioxide was evolved, but no other gaseous products were observed. After the unchanged materials had been removed, the remaining oil was distilled under reduced pressure to yield 0.2 g. of a fraction (b. p. 100—130°C/25 mmHg). During the distillation, benzoic acid was sublimed. In the gas chromatogram of the fraction, a peak showed the same retention time as that of bicyclohexyl, but there was no peak with a retention time the same as or near the same as that observed in ethyl cyclohexanecarboxylate (silicone oil column: 3 m. at 170°C).

## Summary

The photolysis of ECF in cyclohexane, cyclohexene, oct-1-ene, and benzene has been carried out. It has been concluded that carbon-chlorine bond breaking has occurred to give ethoxycarbonyl radicals in a selective manner. The reactions of the radical in hydrocarbons have been qualitatively discussed, and it has been suggested that the radical had a life long enough to associate with a cyclohexyl radical in a solvent cage, but not a life long enough to dimerize and be added to carbon-carbon double bonds with less decomposition. Thus, cyclohexane, cyclohexene, oct-1-ene, and benzene were carboxylated. No chain reactions were observed in light- and dibenzoyl peroxide-induced reactions of ECF in hydrocarbons; i. e., ECF was unreactive to alkyl radicals and radicals bearing an ethoxycarbonyl group on their $\alpha$-carbon. The photolysis of ECF supplies a convenient method for the generation of ethoxycarbonyl radicals.

The authors wish to express their hearty thanks to Dr. Yoshinobu Odaira for his kind advice and encouragement throughout this work. Thanks are also due to Mr. Kikuhiko Koyama for his kind advice.

*Department of Chemical Technology*
*Faculty of Engineering*
*Osaka University*
*Miyakojima-ku, Osaka*

19) An authentic sample was prepared according to directions of Boorman and Linstead; *J. Chem. Soc.*, **1935**, 258.

20) E. H. Farmer and C. G. Moor, ibid., **1951**, 131.

# The Copolymerization of the Vinyl Monomer with a Cyclic Compound. I. The Cationic Copolymerization of Some Vinyl Monomers with 3, 3-Bis(chloromethyl)oxetane*

By Shuzo AOKI, Yoshiyuki HARITA, Takayuki OTSU and Minoru IMOTO

(Received March 25, 1965)

Several attempts to copolymerize the vinyl monomer with cyclic ether have been made. Recently, Tsuruta and Fujio[1] prepared the copolymer of methyl vinyl ketone with propylene oxide or epichlorohydrin, using aluminum isopropoxide as an anionic catalyst. The acrylonitrile - ethylene oxide[2] and - propylene oxide[3] copolymers have been prepared in the radiation-induced copolymerization at a low temperature. The cationic copolymerizations of cyclic ethers with vinyl monomers have also been patented.[4,5] Höhr et al.[6] have reported a detailed mechanism of the cationic copolymerization of trioxane with styrene.

The present investigation was undertaken to evaluate the reactivities of vinyl monomers and cyclic ether in their copolymerizations by Lewis acids. Styrene (St), $\alpha$-methylstyrene ($\alpha$-MeSt) and isobutyl vinyl ether (IBVE), having different reactivities for cationic polymerization, were used as the vinyl monomers. 3, 3-Bis(chloromethyl)oxetane (BCMO) was adopted as the cyclic ether, and boron trifluoride-diethyl etherate ($BF_3 \cdot Et_2O$), stannic chloride ($SnCl_4$) and triethylaluminum-water ($AlEt_3$-$H_2O$) were used as the cationic catalysts. The copolymerizations were carried out in methylene chloride at 0°C.

## Experimental

**Materials.**—Commercial St, $\alpha$-MeSt and IBVE were distilled over calcium hydride under reduced pressure. BCMO was prepared by the method described by Farthing[7] and distilled over calcium hydride under reduced pressure; b. p. 80.5—81.5°C/10 mmHg, $n_D^{20}$ 1.4858 (lit.[7] b. p. 80.2—81.5°C/10 mmHg, $n_D^{20}$ 1.4858).

Commercial $BF_3 \cdot Et_2O$ and $SnCl_4$ were purified by distillation before use. $AlEt_3$ (Ethyl Corp.) was used without further purification. The $AlEt_3$-$H_2O$ catalyst was prepared in methylene chloride ($AlEt_3$/$H_2O$=1 in mole).

Methylene chloride was shaken with a sodium carbonate solution, washed with pure water, and then distilled over phosphorous pentoxide. The other materials were purified by ordinary methods.

**Copolymerization Procedure.**—The copolymerizations were carried out in a glass-stoppered tube, except in the case of the $AlEt_3$-$H_2O$ catalyst, for which a serum type-stoppered tube was used as the reaction vessel. The initial concentrations of the total monomer mixture and of the catalyst were kept constant at 3.0 and 0.07 mol./l. respectively. After the monomers and the solvent had been charged, dry nitrogen gas was flashed into the tube, which had previously been chilled in an ice-water bath. A known quantity of the catalyst solution in methylene chloride was then added to this tube, and it was sealed off. After it had been polymerized for a given time, the reaction mixture was poured into a large amount of methanol in order to stop the reaction and isolate the polymer produced. In the cases of $SnCl_4$ and $AlEt_3$-$H_2O$ catalysts, methanol containing a small amount of hydrochloric acid was used as the precipitant in order to avoid the precipitation of metal hydroxide. The resulting polymer was washed by methanol and dried under reduced pressure at room temperature.

**The Analysis and Fractionation of the Polymer.**—The compositions of the polymers were determined from their chlorine contents. In order to check whether or not the copolymer was obtained, the polymer was separated with chloroform into insoluble and soluble fractions. The chloroform-soluble fraction was then fractionated into several fractions by the successive addition of methanol.

The molecular weight of the polymer was determined by the cryoscopic method in benzene. The infrared spectra of the polymers were determined in a KBr disk.

## Results

**The St-BCMO-$BF_3 \cdot Et_2O$ System.**— The results of the copolymerization of St and BCMO as catalyzed by $BF_3 \cdot Et_2O$ are tabulated in Table I. The rate of the polymerization ($R_p$) of St was remarkably lowered by the presence of BCMO. As is indicated in Table I, the reactivity of St for the copolymerization with BCMO

* Vinyl Polymerization. CIV.

1) T. Tsuruta and R. Fujio, *Makromol. Chem.*, **64**, 219 (1963).

2) S. Okamura, K. Hayashi and H. Watanabe, *Isotopes and Radiation (Doitai to Hoshasen)*, **3**, 512 (1960).

3) S. Okamura, K. Hayashi and H. Watanabe, *J. Chem. Soc. Japan, Ind. Chem. Sec. (Kogyo Kagaku Zasshi)*, **65**, 740 (1962).

4) R. Merten, Ger. Pat. 1083055; *Chem. Abstr.*, **55**, 14998 (1961).

5) British Industrial Plastics, Ltd., Berg. Pat. 610580; *Chem. Abstr.*, **57**, 11401 (1962).

6) L. Höhr, H. Cherdron and W. Kern, *Makromol. Chem.*, **52**, 59 (1962).

7) A. C. Farthing, *J. Chem. Soc.*, **1955**, 3648.

TABLE I. COPOLYMERIZATION OF St AND BCMO BY $BF_3 \cdot Et_2O$ IN METHYLENE CHLORIDE AT 0°C
([Monomer] = 3, $[BF_3 \cdot Et_2O]$ = 0.07 mol./l.)

| Exp. No. | Monomer compn.* | | Time min. | Conversion, % | $R_p$ %/min. | Cl content in polymer, % | Polymer compn.* | |
|---|---|---|---|---|---|---|---|---|
| | St | BCMO | | | | | St | BCMO |
| 11 | 0.00 | 1.00 | 35 | 3.9 | 0.11 | (45.73)** | 0.00 | 1.00 |
| 12 | 0.20 | 0.80 | 15 | 11.2 | 0.75 | 45.67 | 0.00 | 1.00 |
| 13 | 0.30 | 0.70 | 15 | 8.7 | 0.58 | 45.50 | 0.01 | 0.99 |
| 14 | 0.40 | 0.60 | 10 | 4.8 | 0.48 | 45.62 | 0.00 | 1.00 |
| 15 | 0.50 | 0.50 | 20 | 6.4 | 0.32 | 45.11 | 0.02 | 0.98 |
| 16 | 0.60 | 0.40 | 20 | 3.1 | 0.16 | 44.36 | 0.04 | 0.96 |
| 17 | 0.70 | 0.30 | 25 | 3.5 | 0.14 | 43.97 | 0.06 | 0.94 |
| 18 | 0.80 | 0.20 | 20 | 2.4 | 0.12 | 43.42 | 0.07 | 0.93 |
| 19 | 1.00 | 0.00 | 0.5 | 90.2 | 180 | — | 1.00 | 0.00 |

* In mole fraction
** Calculated value for BCMO

TABLE II. COPOLYMERIZATION OF α-MeSt AND BCMO BY $BF_3 \cdot Et_2O$ IN METHYLENE CHLORIDE AT 0°C
([Monomer] = 3, $[BF_3 \cdot Et_2O]$ = 0.07 mol./l.)

| Exp. No. | Monomer compn.* | | Time min. | Conversion, % | $R_p$ %/min. | Cl content in polymer, % | Polymer compn.* | |
|---|---|---|---|---|---|---|---|---|
| | α-MeSt | BCMO | | | | | α-MeSt | BCMO |
| 11 | 0.00 | 1.00 | 35 | 3.9 | 0.11 | — | 0.00 | 1.00 |
| 32 | 0.21 | 0.79 | 20 | 5.9 | 0.30 | 45.16 | 0.02 | 0.98 |
| 33 | 0.31 | 0.69 | 158 | 5.6 | 0.04 | 43.05 | 0.05 | 0.95 |
| 34 | 0.31 | 0.69 | — | 13.8 | — | 45.25 | 0.01 | 0.99 |
| 35 | 0.41 | 0.59 | 14 | 3.4 | 0.24 | 43.69 | 0.06 | 0.94 |
| 36 | 0.41 | 0.59 | 135 | 3.0 | 0.02 | 40.15 | 0.17 | 0.83 |
| 37 | 0.51 | 0.49 | 865 | 35.9 | — | 34.56 | 0.26 | 0.74 |
| 38 | 0.51 | 0.49 | 105 | 1.7 | 0.02 | 31.61 | 0.33 | 0.67 |
| 39 | 0.61 | 0.39 | 195 | 13.9 | — | 29.58 | 0.42 | 0.58 |
| 40 | 0.61 | 0.39 | 92 | 3.8 | 0.03 | 18.49 | 0.66 | 0.34 |
| 41 | 0.61 | 0.39 | 25 | 2.1 | 0.08 | 31.18 | 0.38 | 0.62 |
| 42 | 0.71 | 0.29 | 124 | 7.8 | 0.06 | 20.66 | 0.61 | 0.39 |
| 43 | 0.71 | 0.29 | 77 | 4.1 | 0.05 | 6.76 | 0.88 | 0.12 |
| 44 | 0.81 | 0.19 | 80 | 9.7 | 0.12 | 1.65 | 0.97 | 0.03 |
| 45 | 0.81 | 0.19 | 41 | 1.6 | 0.04 | 16.20 | 0.70 | 0.30 |
| 46 | 0.81 | 0.19 | 60 | 8.2 | 0.14 | 3.46 | 0.94 | 0.06 |
| 47 | 1.00 | 0.00 | 0.5 | 30.2 | 60 | — | 1.00 | 0.00 |

* In mole fraction

TABLE III. FRACTIONATION OF THE POLYMER OBTAINED IN THE SYSTEM α-MeSt - BCMO - $BF_3 \cdot Et_2O$

| Fraction | Wt. g. | Wt. % | Cl % | BCMO unit* | Wt. g. | Wt. % | Cl % | BCMO unit* | Wt. g. | Wt. % | Cl % | BCMO unit* |
|---|---|---|---|---|---|---|---|---|---|---|---|---|
| Sample | Exp. No. 37** | | | | Exp. No. 39 | | | | Exp. No. 40 | | | |
| | 0.9752 | — | 34.56 | 0.70 | 0.4980 | — | 29.58 | 0.58 | 0.0964 | — | 18.49 | 0.34 |
| 1 ($CHCl_3$-insol.) | 0.7303 | 74.89 | 44.02 | 0.95 | 0.3170 | 63.65 | 45.97 | 1.00 | 0.0290 | 30.08 | 42.96 | 0.92 |
| 2 | 0.0054 | 0.55 | 39.05 | 0.82 | 0.0504 | 10.12 | 20.09 | 0.37 | 0.0657 | 68.15 | 12.89 | 0.23 |
| 3 | 0.1054 | 10.81 | 11.04 | 0.20 | 0.0698 | 14.02 | 2.11 | 0.04 | — | — | — | — |
| 4 | 0.0186 | 1.91 | 7.60 | 0.13 | 0.0205 | 4.12 | — | — | — | — | — | — |
| 5 ($CHCl_3$-sol.) | 0.0248 | 2.54 | 1.29 | 0.02 | — | — | — | — | — | — | — | — |
| 6 | 0.0029 | 0.29 | — | — | — | — | — | — | — | — | — | — |
| Total | 0.8874 | 90.99 | | | 0.4577 | 91.91 | | | 0.0947 | 98.23 | | |

* In mole fraction
** Molecular weight of $CHCl_3$-soluble part was 724 (Cl: 5.07%), while that of homopolyα-MeSt (Exp. No. 47) was 1270.

was extremely low, and the homopolymer of BCMO was obtained.

**The α-MeSt - BCMO - $BF_3 \cdot Et_2O$ System.**— The results of the copolymerization of α-MeSt and BCMO by $BF_3 \cdot Et_2O$ are summarized in Table II. The rate of copolymerization decreased as compared with the respective homopolymerization rates. Colorless, powdered polymers, composed of both monomer units, were obtained. The monomer-polymer composition curve in this system is shown in Fig. 1.

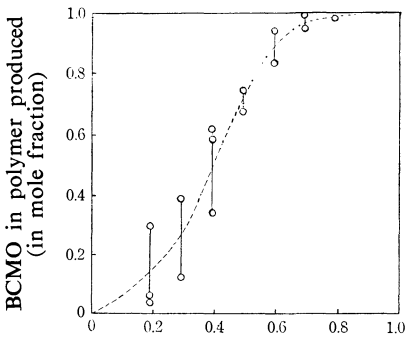



Fig. 1. Monomer-polymer composition curve for the copolymerization of α-MeSt and BCMO by $BF_3 \cdot Et_2O$ in methylene chloride at 0°C.

Since the molecular weights of the polymers obtained under the present conditions were low (see Table III), it may be assumed that the low molecular weight polymer mainly consisted of α-MeSt units is partly soluble in methanol as a precipitant. Accordingly, the curve in Fig. 1 should be shifted in a small extent, however, any further discussion will be not disturbed.

In order to check whether or not the copolymer was produced, some of the polymers obtained were fractionated into several fractions. The analytical results of these fractions are shown in Table III, while their infrared spectra are indicated in Fig. 2.

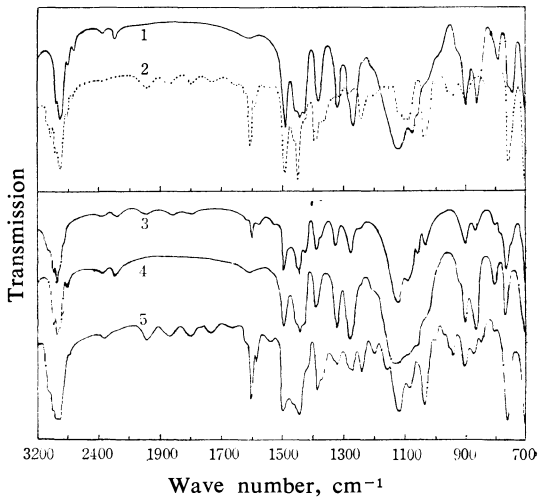



Fig. 2. Infrared spectra of the polymer (Exp. No. 37) obtained in the system of α-MeSt - BCMO - $BF_3 \cdot Et_2O$ in methylene chloride at 0°C. 1. PolyBCMO, 2. Polyα-MeSt, 3. Unfractionated polymer, 4. Chloroform-insoluble fraction, 5. Chloroform-soluble fraction

Because the infrared spectra and chlorine contents of the chloroform-insoluble fractions were nearly identical with those of polyBCMO, it was obvious that this fractions were homopolymers of BCMO. On the other hand, the infrared spectrum of the chloroform-soluble fraction showed the absorption bands due to the α-MeSt unit and the C-O-C band at 1120 $cm^{-1}$ from the BCMO unit, as is shown in Fig. 2. This fraction was, therefore, further fractionated into several fractions which contained considerable amounts of chlorine. The molecular weight of the chloroform-soluble fraction (Exp. No. 37) was found to be 724 (Cl: 5.07%). This value corresponds approximately to the calculated value (746) of the

TABLE IV. COPOLYMERIZATION OF α-MeSt AND BCMO BY $SnCl_4$ IN METHYLENE CHLORIDE AT 0°C ([Monomer] = 3, $[SnCl_4]$ = 0.07 mol./l.)

| Exp. No. | Monomer compn.* α-MeSt | Monomer compn.* BCMO | Time min. | Conversion, % | $R_p$ %/min. | Cl content in polymer, % | Polymer compn.* α-MeSt | Polymer compn.* BCMO |
|---|---|---|---|---|---|---|---|---|
| 51 | 0.00 | 1.00 | 2460 | 0.02 | 0.000 | — | 0.00 | 1.00 |
| 52 | 0.21 | 0.79 | 685 | 0.10 | 0.000 | — | — | — |
| 53 | 0.31 | 0.69 | 450 | 0.8 | 0.002 | 2.67 | 0.95 | 0.05 |
| 54 | 0.41 | 0.59 | 410 | 3.9 | 0.01 | 1.73 | 0.97 | 0.03 |
| 55 | 0.51 | 0.49 | 405 | 9.9 | 0.02 | 2.03 | 0.97 | 0.03 |
| 56 | 0.61 | 0.39 | 350 | 24.9 | 0.07 | — | — | — |
| 57 | 0.71 | 0.29 | 300 | 41.8 | 0.14 | — | — | — |
| 58 | 0.81 | 0.19 | 15 | 11.8 | 0.79 | 0.83 | 0.98 | 0.02 |
| 59 | 1.00 | 0.00 | 1 | 84.2 | 84 | — | 1.00 | 0.00 |

* In mole fraction

TABLE V. COPOLYMERIZATION OF α-MeSt AND BCMO BY $Al(C_2H_5)_3$-$H_2O$ IN METHYLENE CHLORIDE AT 0°C
([Monomer]=3, $[Al(C_2H_5)_3]$=0.07 mol./l.)

| Exp. No. | Monomer compn.* | | Time min. | Conversion, % | $R_p$ %/min. | Cl content in polymer, % | Polymer compn.* | |
|---|---|---|---|---|---|---|---|---|
| | α-MeSt | BCMO | | | | | α-MeSt | BCMO |
| 62 | 0.21 | 0.79 | 300 | 1.2 | 0.004 | 43.65 | 0.06 | 0.94 |
| 63 | 0.31 | 0.69 | 300 | 0.6 | 0.002 | 43.41 | 0.07 | 0.93 |
| 64 | 0.51 | 0.49 | 470 | 0.9 | 0.002 | 46.42 | 0.00 | 1.00 |
| 65 | 0.61 | 0.39 | 360 | 1.3 | 0.004 | 40.88 | 0.13 | 0.87 |
| 66 | 0.71 | 0.29 | 460 | 0.2 | 0.001 | 43.37 | 0.07 | 0.93 |
| 67 | 0.81 | 0.19 | 240 | 0.2 | 0.001 | — | — | — |
| 68 | 1.00 | 0.00 | 18 | 4.4 | 0.24 | — | 1.00 | 0.00 |

* In mole fraction

TABLE VI. COPOLYMERIZATION OF IBVE AND BCMO BY $BF_3 \cdot Et_2O$ IN METHYLENE CHLORIDE AT 0°C
([Monomer]=3, $[BF_3 \cdot Et_2O]$=0.07 mol./l.)

| Exp. No. | Monomer compn.* | | Time sec. | Conversion, % | Cl content in polymer, % | Polymer compn.* | |
|---|---|---|---|---|---|---|---|
| | IBVE | BCMO | | | | IBVE | BCMO |
| 11 | 0.00 | 1.00 | 210 | 3.9 | — | 0.00 | 1.00 |
| 72 | 0.20 | 0.80 | 120 | 5.0** | 7.97 | 0.89 | 0.11 |
| 73 | 0.30 | 0.70 | 30 | — | 2.84 | 0.96 | 0.04 |
| 74 | 0.40 | 0.60 | 30 | 19.6 | 0.27 | 1.00 | 0.00 |
| 75 | 0.50 | 0.50 | 30 | 31.4 | 0.21 | 1.00 | 0.00 |
| 76 | 0.60 | 0.40 | 45 | 32.9 | 0.22 | 1.00 | 0.00 |
| 77 | 0.70 | 0.30 | 15 | 40.5 | 0.07 | 1.00 | 0.00 |
| 78 | 0.80 | 0.20 | 10 | 46.7 | 0 | 1.00 | 0.00 |
| 79 | 1.00 | 0.00 | 10 | 69.3 | — | 1.00 | 0.00 |

* In mole fraction
** $CHCl_3$-insoluble part: 18.42 wt.% (Cl: 41.74%); $CHCl_3$-soluble part: 81.58 wt.% (Cl: 0.68%)

polymer, which consisted of five α-MeSt units and one BCMO unit (Cl: 9.5%). Therefore, this soluble fraction may be taken as a mixture of the homopolymers of α-MeSt and of polyα-MeSt containing one terminal BCMO unit.

**The α-MeSt - BCMO - $SnCl_4$ System.**—The results of the copolymerization of α-MeSt and BCMO with $SnCl_4$ as the catalyst are tabulated in Table IV. BCMO was hardly polymerized at all by $SnCl_4$, and only a polyα-MeSt was obtained in this system.

**The α-MeSt - BCMO - $AlEt_3$-$H_2O$ System.**—The results of the copolymerization of α-MeSt and BCMO by the $AlEt_3$-$H_2O$ catalyst are tabulated in Table V. The polymer, mainly consisting of BCMO units, was obtained in the copolymerization of various monomer compositions, though the homopolymerizations of both α-MeSt and BCMO proceeded without difficulty when this catalyst system was used.

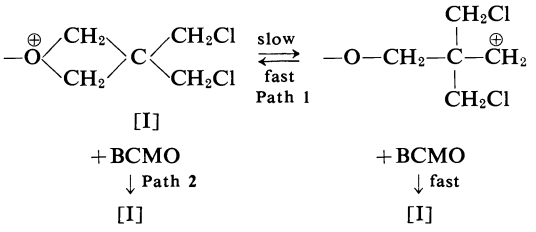
**The IBVE-BCMO-$BF_3 \cdot Et_2O$ System.** — The results of the copolymerization of IBVE and BCMO by $BF_3 \cdot Et_2O$ are tabulated in Table VI. Tacky and pale yellow polymers were obtained from this system. The homopolyIBVE was obtained in the copolymerization at a higher concentration of IBVE, while a polymer containing both IBVE and BCMO units was obtained through the system which used a higher concentration of BCMO. This polymer, containing both IBVE and BCMO units, was fractionated with chloroform, and a polymer mainly consisting of BCMO units and homopolyIBVE were separated.

## Discussion

In the cationic copolymerizations of the St-BCMO-$BF_3 \cdot Et_2O$, α-MeSt - BCMO - $SnCl_4$ and α-MeSt - BCMO - $AlEt_3$-$H_2O$ systems, only the homopolymer of a vinyl or a cyclic compound was obtained (Tables I, IV and V). On the other hand, in the copolymerization of α-MeSt or IBVE by $BF_3 \cdot Et_2O$, the composition analyses showed that the resulting polymer contained both monomer units (Tables II and VI, and Fig. 1). The S-shaped monomer-polymer composition curve in the copolymerization of α-MeSt and BCMO (Fig. 1) indicated that both monomer reactivity ratios ($r_1$ and $r_2$) were larger than unity, and that the homopropagating reactivities of both growing chain ends were very important. Furthermore, from the fractionation experiments of the resulting polymers

(see Table III), it was clarified that no copolymer was obtained, although a mixture of the homopolymers of BCMO and $\alpha$-MeSt, and of poly$\alpha$-MeSt containing one BCMO unit which might be attached as an end group, was obtained. Similar results were obtained in the case of IBVE-BCMO copolymerization (see Table VI). The phenomenon in which a mixture of homopolymers was produced through the copolymerization (this is expressed in terms of independent copolymerization) may be observed when the reactivities of the two monomers are close to each other.

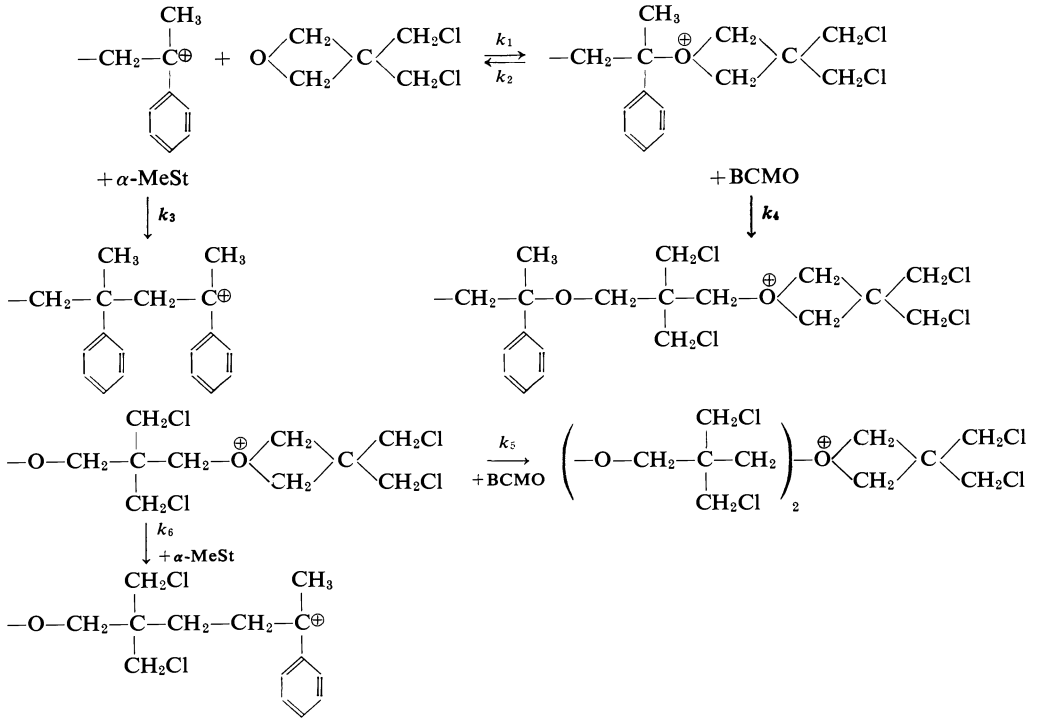
The following two paths may be considered in the propagation of BCMO:




The rate of propagation should be proportional to the concentration of the propagating cation in path 1 and to the concentrations of both the propagating cation and the monomer in path 2. Penczek and Penczek[8] proved kinetically that the propagation in BCMO polymerization was a bimolecular reaction of the propagating cation and the monomer. Therefore, path 1 may be eliminated. The propagation takes place through the reaction of the terminal oxonium ion with the monomer molecule.

The reaction scheme of the cationic copolymerization of $\alpha$-MeSt and BCMO is expressed below.

The reactions of $k_3$ and $k_5$ are the homopolymerizations of $\alpha$-MeSt and BCMO respectively; their rates must be larger than that of cross propagation, if only a mixture of both homopolymers is produced. The stability of the $\alpha$-MeSt cation participates in this copolymerization fairly importantly. If the growing carbonium ion from the vinyl monomer is unstable, it is very easy in the reaction with ether to form a stable oxonium ion, and the polymerization of the vinyl monomer is inhibited by the presence of ether. It is understandable, in view of this, that the greater reactivity of $\alpha$-MeSt for cationic polymerization by $BF_3 \cdot Et_2O$ was much depressed, being it close to that of BCMO in its copolymerization with BCMO. In the St-BCMO system, the polymerization reactivity of St by $BF_3 \cdot Et_2O$ was also greatly depressed, and scarcely any polymers containing St units were obtained. The inhibiting effect of ethers in the cationic




8) I. Penczek and S. Penczek, *Makromol. Chem.*, **67**, 203 (1963).

polymerization of St has been reported previously.[9]

The phenomenon that the copolymer was not obtained in the cationic copolymerization of α-MeSt and BCMO may result from the difference in reactivity based on the structures of the propagating cations; namely, the poly-α-MeSt cation is the carbonium ion, while the polyBCMO cation is the oxonium ion. A similar consideration was postulated by Yamashita et al.[10] for the cationic copolymerization of BCMO and β, β-dimethyl-β-propiolactone.

In the $SnCl_4$-catalyzed copolymerization, only a homopolymer of α-MeSt was obtained, because the polymerization reactivity of BCMO by this catalyst is quite small. In the $AlEt_3$-$H_2O$- catalyzed copolymerization, homopolyBCMO was obtained, though the homopolymerization of α-MeSt proceeded without difficulty when this catalyst system was used. Recently it was proposed by Furukawa et al.[11] that this catalyst system could act as does Lewis acid for the polymerization of BCMO.

These differences in the results according to the kind of catalyst may result from the fact that the effect of the gegen ion in the cationic polymerization is very important.

The relationship between the monomer and the resulting polymer compositions in the copolymerization is expressed by Eq. 1[12];

$$\frac{[m_1]}{[m_2]}=\frac{[M_1]}{[M_2]}\frac{r_1[M_1]+[M_2]}{[M_1]+r_2[M_2]} \qquad (1)$$

where $m_1$ and $m_2$ are the monomer units in the copolymer, and $M_1$ and $M_2$ are those in the monomer mixture. If $r_1$ and $r_2$ are infinity, Eq. 1 is converted into Eq. 2:

$$\frac{[m_1]}{[m_2]}=\frac{[M_1]^2}{[M_2]^2} \qquad (2)$$

However, if absolutely no cross propagation occurs (independent copolymerization), $[m_1]/[m_2]$ must be proportional to the ratio of the rates of homoplymerizations of $M_1$ and $M_2$. On the basis of the postulations of the rate equations and the rate constants, including the term of the catalyst concentration in the homopolymerizations of $M_1$ and $M_2$, the relation between monomer and polymer compositions in the independent copolymerization is shown in Fig. 3a—c.

As can be seen from Fig. 3, the relation of Eq. 2 is only an example of independent copolymerization; the S-shaped composition

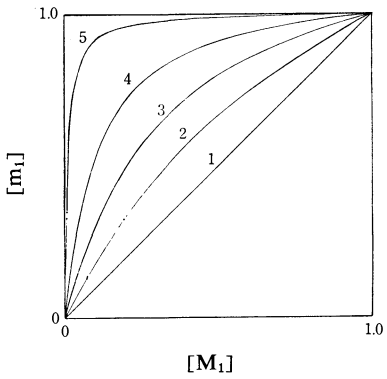



Fig. 3a. Relation between monomer and polymer compositions in independent copolymerization.
The case $R_{p1}=k_1[M_1]$ ; $R_{p2}=k_2[M_2]$
1. $k_1=k_2$, 2. $k_1=2k_2$, 3. $k_1=4k_2$,
4. $k_1=10k_2$, 5. $k_1=100k_2$

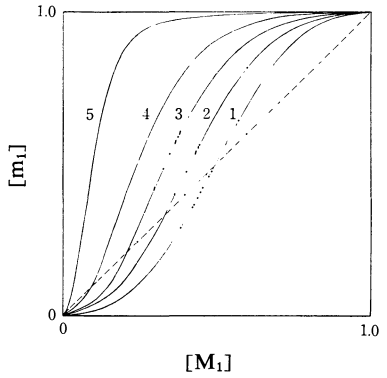



Fig. 3b. Relation between monomer and polymer compositions in independent copolymerization.
The case $R_{p1}=k_1[M_1]^2$ ; $R_{p2}=k_2[M_2]^2$
1. $k_1=k_2$, 2. $k_1=2k_2$, 3. $k_1=4k_2$,
4. $k_1=10k_2$, 5. $k_1=100k_2$

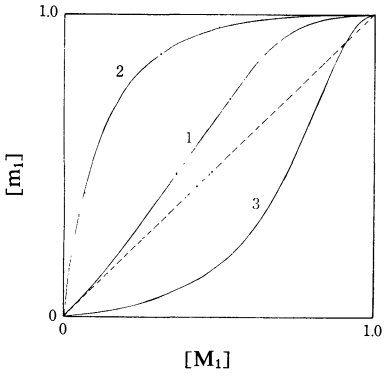



Fig. 3c. Relation between monomer and polymer compositions in independent copolymerization.
The case $R_{p1}=k_1[M_1]$ ; $R_{p2}=k_2[M_2]^2$
1. $k_1=k_2$, 2. $k_1=10k_2$, 3. $k_1=1/10k_2$

9) M. Imoto and S. Aoki, ibid., 63, 141 (1963).
10) Y. Yamashita, T. Tsuda, Y. Ishikawa and T. Shimizu, *J. Chem. Soc. Japan, Ind. Chem. Sec.* (*Kogyo Kagaku Zasshi*), 66, 1493 (1963).
11) J. Furukawa, *Polymer*, 3, 487 (1962); T. Saegusa, H. Imai and J. Furukawa, *Makromol. Chem.*, 65, 60 (1963).
12) T. Alfrey, J. J. Bohrer and H. Mark, "Copolymerization," Interscience, New York (1952), p. 8.

curve is not essential. However, in actuality, no clear relation such as is shown in Fig. 3 is observed because of the complicated effects in the ionic polymerization.

It is known that the block copolymer is obtained occasionally in the ionic copolymerization. Tada, Saegusa and Furukawa[13] proved that this phenomenon occurs with the cationic copolymer of BCMO and β-propiolactone.

Equation 1 can be simply adopted for a copolymerization in which the monomer units are distributed statistically in the resulting copolymer chain. Therefore, if a block copolymer or a mixture of copolymer and homopolymer was obtained through the copolymerization, the resulting monomer reactivity ratios ($r_1$ and $r_2$), which indicate the ratio of the rate constants of homo- and cross-propagation, may become less significant.

13) K. Tada, T. Saegusa and J. Furukawa, *Makromol. Chem.*, **71**, 71 (1964).

**Summary**

The copolymerization of several vinyl monomers, such as styrene, α-methylstyrene and isobutyl vinyl ether, with 3,3-bis(chloromethyl)oxetane catalyzed by Lewis acids (boron trifluoride-diethyl etherate, stannic chloride and triethylaluminum-water) in methylene chloride at 0°C has been investigated. In these copolymerizations, the copolymers were not obtained, though a mixture of the corresponding homopolymers was obtained in some cases. The results have been explained on the basis of the differences in reactivity resulting from the structures of the two propagating chain ends.

*Faculty of Engineering*
*Osaka City University*
*Sumiyoshi-ku, Osaka*

# The Copolymerization of the Vinyl Monomer with a Cyclic Compound. II. The Cationic Copolymerization of Some Vinyl Monomers with β-Propiolactone*

By Shuzo AOKI, Yoshiyuki HARITA, Takayuki OTSU and Minoru IMOTO

(Received March 25, 1965)

In a preceding paper,[1] the cationic copolymerization of some vinyl monomers with 3, 3-bis(chloromethyl)oxetane catalyzed by Lewis acids was investigated. It was found that the copolymers were not obtained in all systems, but that mixtures of the corresponding homopolymers were produced in some cases. The present paper is concerned with the cationic copolymerization of vinyl monomers with β-propiolactone (β-PL) catalyzed by Lewis acids.

It is interesting to prepare the copolymer of the vinyl monomer with β-PL, which gives the ester linkage in the main chain of the resulting copolymer. With such a purpose in mind, Okamura et al.,[2] for instance, attempted the radiation-induced copolymerization of styrene (St), acrylonitrile and methyl methacrylate with β-PL. Shimosaka, Tsuruta and Furukawa[3] prepared the copolymer of acrylonitrile with β-PL through the copolymerization catalyzed by organometallic compounds. Yamashita et al.[4] reported the copolymerization of St with β, β-dimethyl-β-propiolactone by stannic chloride.

In the present paper, St, α-methylstyrene (α-MeSt) and isobutyl vinyl ether (IBVE) will be used as vinyl monomers. Boron trifluoride-diethyl etherate ($BF_3 \cdot Et_2O$), stannic chloride ($SnCl_4$) and triethylaluminum-water ($AlEt_3$-$H_2O$) will be used as cationic catalysts. From the copolymerization results, the reactivity of β-PL with vinyl monomers will be evaluated and discussed.

## Experimental

**Materials.**—Commercial β-PL, St, α-MeSt and IBVE were distilled over calcium hydride under reduced pressures.

* Vinyl Polymerization. CV.

1) S. Aoki, Y. Harita, T. Otsu and M. Imoto, This Bulletin, **38**, 1922 (1965).

2) S. Okamura, K. Hayashi, Y. Kitanishi and M. Nishii, *Isotopes and Radiation* (*Doitai to Hoshasen*), 3, 510 (1960).

3) Y. Shimosaka, T. Tsuruta and J. Furukawa, *J. Chem. Soc. Japan, Ind. Chem. Sec.* (*Kogyo Kagaku Zasshi*), **66**, 1498 (1963).

4) Y. Yamashita, T. Tsuda, Y. Ishikawa and T. Shimizu, ibid., **66**, 1493 (1963).

$BF_3 \cdot Et_2O$, $SnCl_4$ and methylene chloride were purified and the $AlEt_3$-$H_2O$ catalyst was prepared in the methods described in the preceding paper.[1] The other materials were purified by the ordinary methods.

**Copolymerization Procedure.**—The copolymerization procedure was the same as that described in the preceding paper.[1]

**The Fractionation of the Polymer.**—The polymer obtained in the copolymerization of β-PL and St was fractionated to determine whether this polymer was the copolymer or a mixture of the homopolymers. Since polySt was isoluble in acetic acid, while polyβ-PL was soluble, the chloroform solution of the resulting polymer was poured into a large amount of acetic acid in order to separate it into acetic acid-soluble and acetic acid-insoluble fractions. Both fractions were then further fractionated by the chloroform-methanol system.

**The Analysis of the Polymer.**—The compositions of the polymers obtained in various monomer compositions were determined by means of their infrared spectra and by means of elementary analyses on carbon.

The molecular weight of the polymer was determined with a Mechrolab vapor pressure osmometer, model 301-A.

The inherent viscosity of the polymer was measured in a one per cent solution of it in choroform at 30°C.

## Results

**The β-PL - St - $BF_3 \cdot Et_2O$ or - $SnCl_4$ System.**—The results of the copolymerization of β-PL with St catalyzed by $BF_3 \cdot Et_2O$ or $SnCl_4$ are summarized in Tables I and II. The copolymerization proceeded without difficulty with both catalysts, and a colorless, powdered polymer was obtained. The infrared spectra of the resulting polymer showed the characteristic absorption bands at 1725 and 1603 $cm^{-1}$ based on the ester linkage (β-PL unit) and

Table I. Copolymerization of St and β-PL by $BF_3 \cdot Et_2O$ in methylene chloride at 0°C ([Monomer]=3, $[BF_3 \cdot Et_2O]$=0.07 mol./l.)

| Exp. No. | Monomer compn.* | | Time min. | Conversion % | $R_p$ %/min. | Polymer resulted | | | | | |
|---|---|---|---|---|---|---|---|---|---|---|---|
| | | | | | | I.R.S.** | | Analysis*** | | Compn.* | |
| | St | β-PL | | | | St | β-PL | C% | H% | St | β-PL |
| 11 | 1.00 | 0.00 | 0.5 | 89 | 187 | (+) | (−) | (92.26) | (7.74) | 1.00 | 0.00 |
| 12 | 0.60 | 0.40 | 8 | 2.9 | 0.36 | | | 91.34 | 7.99 | 0.97 | 0.03 |
| 13 | 0.50 | 0.50 | 5 | 2.2 | 0.45 | + | + | 90.88 | 7.68 | 0.95 | 0.05 |
| 14 | 0.40 | 0.60 | 65 | 2.7 | 0.04 | + | + | 90.20 | 7.74 | 0.93 | 0.07 |
| 15 | 0.30 | 0.70 | 30 | 1.6 | 0.05 | + | + | 89.68 | 7.66 | 0.91 | 0.09 |
| 16 | 0.20 | 0.80 | 60 | 0.7 | 0.01 | + | + | 83.49 | 7.30 | 0.73 | 0.27 |
| 17 | 0.00 | 1.00 | 900 | 8.8 | 0.01 | (−) | (+) | (49.99) | (5.61) | 0.00 | 1.00 |

* In mole fraction
** Infrared spectrum
*** Figures in parentheses are the calculated value.

Table II. Copolymerization of St and β-PL by $SnCl_4$ in methylene chloride at 0°C ([Monomer]=3, $[SnCl_4]$=0.07 mol./l.)

| Exp. No. | Monomer compn.* | | Time min. | Conversion % | $R_p$ %/min. | Polymer resulted | | | | | |
|---|---|---|---|---|---|---|---|---|---|---|---|
| | | | | | | I.R.S. | | Analysis | | Compn.* | |
| | St | β-PL | | | | St | β-PL | C% | H% | St | β-PL |
| 21 | 1.00 | 0.00 | 2 | 35 | 18 | (+) | (−) | — | — | 1.00 | 0.00 |
| 22 | 0.60 | 0.40 | 2.5 | 15.8 | 6.3 | + | + | 90.53 | 7.96 | 0.94 | 0.06 |
| 23 | 0.60 | 0.40 | 2 | 21.8 | 10.9 | + | + | 90.45 | 7.79 | 0.94 | 0.06 |
| 24 | 0.50 | 0.50 | 4 | 16.8 | 4.2 | + | + | 90.30 | 7.80 | 0.93 | 0.07 |
| 25 | 0.50 | 0.50 | 3 | 19.2 | 6.4 | + | + | 90.62 | 7.77 | 0.94 | 0.06 |
| 26 | 0.40 | 0.60 | 6.5 | 13.7 | 2.1 | + | + | 89.85 | 7.68 | 0.92 | 0.08 |
| 27 | 0.40 | 0.60 | 4 | 13.8 | 3.4 | + | + | 90.09 | 7.89 | 0.93 | 0.07 |
| 28 | 0.30 | 0.70 | 8 | 8.6 | 1.1 | + | + | 89.55 | 7.69 | 0.91 | 0.09 |
| 29 | 0.30 | 0.70 | 7 | 8.0 | 1.1 | + | + | 89.06 | 7.67 | 0.89 | 0.11 |
| 30 | 0.20 | 0.80 | 12 | 6.2 | 0.5 | + | + | 82.21 | 7.23 | 0.69 | 0.31 |
| 31 | 0.20 | 0.80 | 9.5 | 4.2 | 0.4 | + | + | 85.95 | 7.50 | 0.80 | 0.20 |
| 32 | 0.00 | 1.00 | 80 | 29.3 | 0.4 | (−) | (+) | — | — | 0.00 | 1.00 |

* In mole fraction

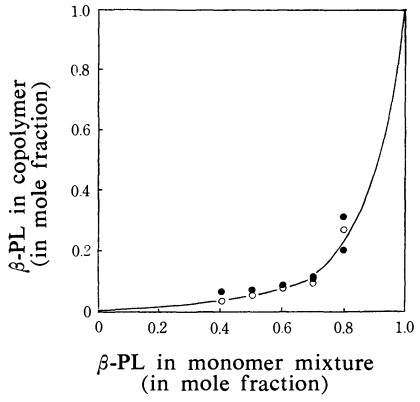



Fig. 1. Monomer-polymer composition curve for the copolymerization of St and β-PL.
(○) $BF_3 \cdot Et_2O$ catalyst, (●) $SnCl_4$ catalyst

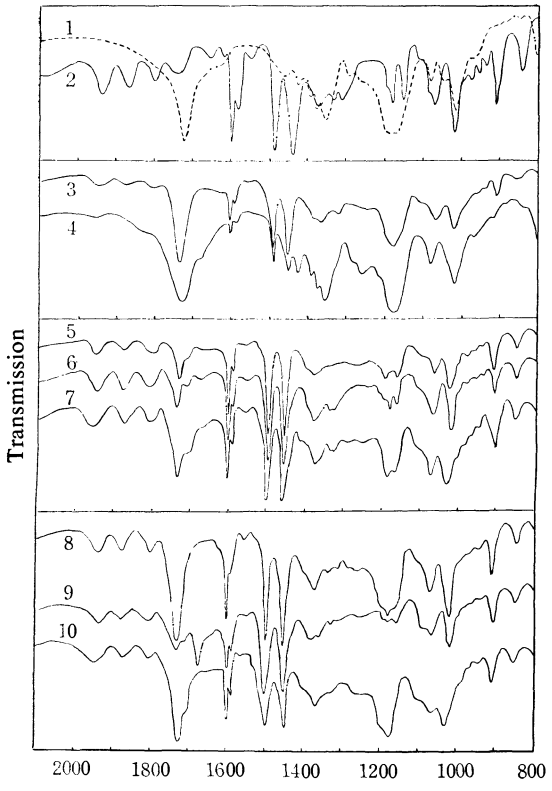



Fig. 2. Infrared spectra of the β-PL - St copolymer (in KBr disk).
1. Poly-β-PL, 2. PolySt, 3. No. 16 unfractionated, 4. No. 16 AcOH-soluble, 5. No. 24 unfractionated, 6. No. 24 AcOH-isoluble, 7. No. 24 AcOH-soluble, 8. No. 28 unfractionated, 9. No. 28 AcOH-insoluble, 10. No. 28 AcOH-soluble

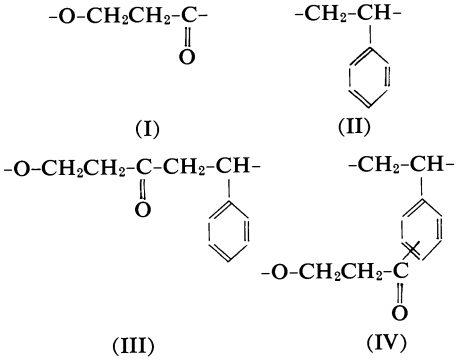
the benzene nucleus (St unit) respectively (see Fig. 2). The monomer-polymer composition curve for this copolymerization is shown in Fig. 1.

No difference between $BF_3 \cdot Et_2O$ and $SnCl_4$ catalysts was observed in the monomer-polymer composition relation. The apparent monomer reactivity ratios were estimated, by the curve-fitting method, to be $r_{(\beta\text{-PL})}=0.2$ and $r_{(St)}=20$ respectively.

In order to determine whether the polymer obtained here was the copolymer or a mixture of the corresponding homopolymers, the resulting polymer was fractionated into several fractions. The results are given in Table III, while the infrared spectra of soluble and insoluble fractions in acetic acid are shown in Fig. 2.

It was proved, by infrared spectra and elementary analysis, that the insoluble fraction of the resulting copolymer in acetic acid, which is known to be a solvent for only polyβ-PL, contained the β-PL unit; while its soluble fraction contained the St unit. The molecular weight of the fractionated copolymer was not very low (see Table III). These results indicated that the copolymer of β-PL with St was produced in their copolymerizations with such Lewis acids as $BF_3 \cdot Et_2O$ and $SnCl_4$.

Some of the infrared spectra of the unfractionated and fractionated copolymers showed absorption bands at 1680 and 1710 $cm^{-1}$ in addition to the characteristic bands mentioned above (see Fig. 2). It is assumed that the structure of the β-PL - St copolymer contains the following four types of repeating units:




The structures I and II are the repeating units of polyβ-PL and polySt, and show the characteristic absorption bands in the infrared spectra at 1725 and 1603 $cm^{-1}$ respectively. The structure III must be formed through the copolymerization in which the opening of the β-PL ring, followed by an attack on the vinyl double bond of St, takes place to form carbonyl cations as the propagating species. Since the infrared absorption band at 1710 $cm^{-1}$ agreed with that of a carbonyl group of aliphatic ketone, it was obvious that this copolymer contained the structure III. If the

carbonyl cation formed from β-PL attacks the benzene nucleus of monomeric or polymeric St through the chain-transfer reaction, the structure IV may be formed. The absorption band at 1680 $cm^{-1}$ may be assigned to a carbonyl group of aromatic ketone. It was therefore concluded that this copolymer contained the structure IV.

In order to obtain further evidence for the existence of the structure IV in the copolymer, the polymerization of β-PL in the presence of ethylbenzene in place of St was performed. The existence of the ketonic carbonyl group in the resulting polymer was also confirmed by the reaction with 2, 4-dinitrophenylhydrazine.

**The β-PL - St - $AlEt_3$-$H_2O$ System.**—The results of the copolymerization of β-PL with St catalyzed by $AlEt_3$-$H_2O$ are summarized in Table IV. In contrast with the case of the $BF_3 \cdot Et_2O$ or the $SnCl_4$ catalyst, no copolymer was obtained in this catalyst system.

**The β-PL - α-MeSt - $BF_3 \cdot Et_2O$ or - $SnCl_4$ System.**—The results of the copolymerization of β-PL with α-MeSt by the $BF_3 \cdot Et_2O$ or the $SnCl_4$ catalyst are summarized in Tables V and VI. The absence of the β-PL unit in the resulting polymers was confirmed by their infrared spectra.

**The β-PL - α-MeSt - $AlEt_3$-$H_2O$ System.**—The results of the copolymerization of β-PL and α-MeSt by the $AlEt_3$-$H_2O$ catalyst are shown in Table VII. The resulting polymers were found to be homopolymers of β-PL, much as in the case of β-PL - St - $AlEt_3$-$H_2O$.

**The β-PL - IBVE - $SnCl_4$ System.**—The results of the copolymerization of β-PL and IBVE by $SnCl_4$ are tabulated in Table VIII. The polymerization was very rapid, and the resulting

Table III. Fractionation of the β-PL - St copolymer

| Fraction | Wt., g. | Wt., % | Analysis | | Composition | |
|---|---|---|---|---|---|---|
| | | | C% | H% | St | β-PL |
| | | | Exp. No. 24 | | | |
| Sample | $0.294_9$ | — | 90.30 | 7.79 | 0.93 | 0.07 |
| 1 | $0.194_1$* | 65.8 | 90.59 | 8.05 | 0.94 | 0.06 |
| 2 (Insoluble in acetic acid) | $0.008_6$ | 2.9 | 86.64 | 8.14 | 0.82 | 0.18 |
| 3 (Soluble in acetic acid) | $0.067_2$** | 22.8 | 85.91 | 7.76 | 0.80 | 0.20 |
| | | | Exp. No. 28 | | | |
| Sample | $0.170_6$ | — | 89.55 | 7.69 | 0.91 | 0.09 |
| 1 (Insoluble in acetic acid) | $0.035_5$ | 20.8 | 90.29 | 7.78 | 0.93 | 0.07 |
| 2 | $0.063_2$ | 37.1 | 85.32 | 7.57 | 0.78 | 0.22 |
| 3 | $0.017_5$ | 5.9 | — | — | — | — |
| 4 (Soluble in acetic acid) | $0.033_3$ | 19.5 | 82.67 | 7.41 | 0.70 | 0.30 |

* Molecular weight 3250
** Molecular weight 2120

Table IV. Copolymerization of St and β-PL by $AlEt_3$-$H_2O$ in methylene chloride at 0°C
([Monomer] = 3, [$AlEt_3$-$H_2O$] = 0.07 mol./l.)

| Exp. No. | Monomer compn.* | | Time min. | Conversion, % | $R_p \times 10^3$ %/min. | I.R.S. of polymer | |
|---|---|---|---|---|---|---|---|
| | St | β-PL | | | | St | β-PL |
| 41 | 1.00 | 0.00 | 180 | 0.2 | 0.9 | (+) | (−) |
| 42 | 0.80 | 0.20 | 420 | 3.3 | 7.8 | − | + |
| 43 | 0.60 | 0.40 | 420 | 1.2 | 2.9 | − | + |
| 44 | 0.50 | 0.50 | 420 | 1.2 | 2.9 | − | + |
| 45 | 0.40 | 0.60 | 420 | 2.0 | 4.8 | − | + |
| 46 | 0.30 | 0.70 | 1365 | 3.2 | 2.4 | − | + |
| 47 | 0.20 | 0.80 | 630 | 0.7 | 1.1 | − | + |
| 48 | 0.00 | 1.00 | 100 | 0.2 | 2.0 | (−) | (+) |

* In mole fraction

TABLE V. COPOLYMERIZATION OF α-MeSt AND β-PL BY $BF_3 \cdot Et_2O$ IN METHYLENE CHLORIDE AT 0°C
([Monomer] = 3, $[BF_3 \cdot Et_2O]$ = 0.07 mol./l.)

| Exp. No. | Monomer compn.* | | Time min. | Conversion, % | $R_p$ %/min. | I.R.S. of polymer | |
|---|---|---|---|---|---|---|---|
| | α-MeSt | β-PL | | | | α-MeSt | β-PL |
| 51 | 1.00 | 0.00 | 0.75 | 53.4 | 71 | (+) | (−) |
| 52 | 0.80 | 0.20 | 2 | 22.5 | 11.3 | + | − |
| 53 | 0.70 | 0.30 | 0.5 | 6.9 | 13.9 | + | − |
| 54 | 0.60 | 0.40 | 0.5 | 7.2 | 15.0 | + | − |
| 55 | 0.50 | 0.50 | 11 | 19.9 | 1.8 | + | − |
| 56 | 0.40 | 0.60 | 1 | 5.0 | 5.0 | + | − |
| 57 | 0.30 | 0.70 | 2 | 2.1 | 1.1 | + | − |
| 58 | 0.20 | 0.80 | 2 | 0.2 | 0.1 | + | − |
| 17 | 0.00 | 1.00 | 900 | 8.8 | 0.01 | (−) | (+) |

* In mole fraction

TABLE VI. COPOLYMERIZATION OF α-MeSt AND β-PL BY $SnCl_4$ IN METHYLENE CHLORIDE AT 0°C
([Monomer] = 3, $[SnCl_4]$ = 0.07 mol./l.)

| Exp. No. | Monomer compn.* | | Time sec. | Conversion, % | $R_p$ %/min. | I.R.S. of polymer | |
|---|---|---|---|---|---|---|---|
| | α-MeSt | β-PL | | | | α-MeSt | β-PL |
| 61 | 1.00 | 0.00 | 30 | 73 | 147 | (+) | (−) |
| 62 | 0.80 | 0.20 | 135 | 54 | 24 | + | − |
| 63 | 0.70 | 0.30 | 75 | 29.8 | 23.8 | + | − |
| 64 | 0.60 | 0.40 | 60 | 30.0 | 30.0 | + | − |
| 65 | 0.50 | 0.50 | 90 | 19.8 | 12.7 | + | − |
| 66 | 0.40 | 0.60 | 60 | 8.7 | 8.7 | + | − |
| 67 | 0.30 | 0.70 | 120 | 5.9 | 2.9 | + | − |
| 68 | 0.20 | 0.80 | 215 | 1.6 | 0.4 | + | − |
| 32 | 0.00 | 1.00 | 4800 | 29.3 | 0.4 | (−) | (+) |

* In mole fraction

TABLE VII. COPOLYMERIZATION OF α-MeSt AND β-PL BY $AlEt_3$-$H_2O$ IN METHYLENE CHLORIDE AT 0°C
([Monomer] = 3, $[AlEt_3$-$H_2O]$ = 0.07 mol./l.)

| Exp. No. | Monomer compn.* | | Time min. | Conversion, % | $R_p \times 10^3$ %/min. | I.R.S. of polymer | |
|---|---|---|---|---|---|---|---|
| | α-MeSt | β-PL | | | | α-MeSt | β-PL |
| 71 | 1.00 | 0.00 | 2550 | 0.03 | 0.01 | (+) | (−) |
| 72 | 0.70 | 0.30 | 2550 | 1.1 | 0.4 | − | + |
| 73 | 0.50 | 0.50 | 1400 | 0.9 | 0.7 | − | + |
| 74 | 0.40 | 0.60 | 1450 | 0.9 | 0.7 | − | + |
| 75 | 0.20 | 0.80 | 1450 | 1.3 | 0.9 | − | + |
| 48 | 0.00 | 1.00 | 100 | 0.2 | 2.0 | (−) | (+) |

* In mole fraction

TABLE VIII. COPOLYMERIZATION OF IBVE AND β-PL BY $SnCl_4$ IN METHYLENE CHLORIDE AT 0°C
([Monomer] = 3, $[SnCl_4]$ = 0.07 mol./l.)

| Exp. No. | Monomer compn.* | | Time sec. | Conversion, % | $R_p$ %/min. | I.R.S. of polymer | |
|---|---|---|---|---|---|---|---|
| | IBVE | β-PL | | | | IBVE | β-PL |
| 81 | 1.00 | 0.00 | 5 | 69 | 830 | (+) | (−) |
| 82 | 0.60 | 0.40 | 5 | 29.9 | 357 | + | − |
| 83 | 0.50 | 0.50 | 5 | 27.2 | 326 | + | − |
| 84 | 0.40 | 0.60 | 5 | 19.8 | 237 | + | − |
| 85 | 0.20 | 0.80 | 10 | 5.0 | 30 | + | − |
| 32 | 0.00 | 1.00 | 4800 | 29.3 | 0.4 | (−) | (+) |

* In mole fraction

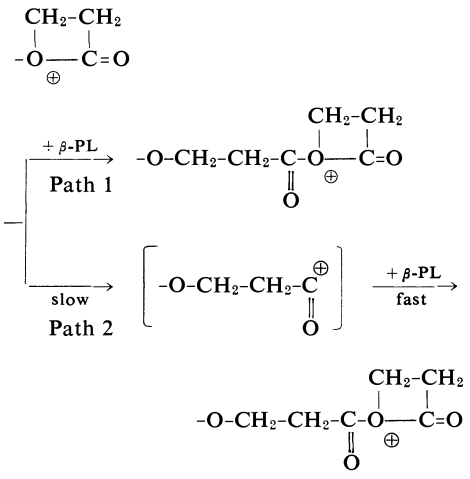
polymer was confirmed by infrared spectra to be polyIBVE.

## Discussion

The results of the copolymerization of vinyl monomers with β-PL are summarized in Table IX. As this table shows, the β-PL - St - $BF_3 \cdot Et_2O$ or - $SnCl_4$ system gave copolymer. This copolymer contained infrared absorption bands at 1680 and 1710 $cm^{-1}$ which could be assigned to the carbonyl groups of aromatic and aliphatic ketones respectively. These results indicate that the ring-opening of β-PL takes place at the acyl-oxygen bond, as has been reported by Cherdron et al.[5] The presence of aromatic and aliphatic ketones also indicates that the copolymers obtained here include a graft copolymer of polySt containg a pendant polyester chain derived from β-PL.

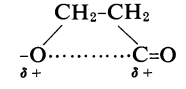
In our previous paper,[1] it was suggested that the copolymer was not obtained in the copolymerization of monomers which propagate via different propagating species, carbonium and oxonium ions. Accordingly, the fact that the copolymer is formed in the present case may lead to the conclusion that the propagating species of β-PL in this cationic polymerization is that of carbonium ions, although an oxonium-ion mechanism was proposed by Yamashita et al.[6]

In order to clarify this ambiguity, the homopolymerization of β-PL was undertaken. The results are tabulated in Table X. The rate of polymerization increased with an increase in the concentration of the monomer, but the molecular weight of the resulting polymer, as deduced from its inherent viscosity, was little affected. The propagation scheme in β-PL polymerization may, then, be expressed by the following two paths:




In path 1, an oxonium ion of the propagating β-PL directly attacks the β-PL monomer. On the other hand, in path 2, the propagation includes a carbonium-ion intermediate. From the difference in the stabilities of the oxonium and carbonium ions, it may reasonably be assumed that, in path 2, the rate-determining step is the formation of the carbonium-ion intermediate. If the termination of the β-PL polymerization is an unimolecular reaction of the growing cation, the molecular weight of the resulting polymer is proportional to the monomer concentration in path 1, while it is independent of it in path 2.

The results in Table X support the mechanism of path 2. In practice, however, the carbonyl cation derived from β-PL may be considered to exist as an intramolecular-solvated state, an intermediate between oxonium and carbonium ions. Therefore, the β-PL-growing cation contains an intermediate structure of both oxonium and carbonium ions (V):




(V)

In a polar solvent the character of the carbonium ion may be emphasized, but the reverse holds in a nonpolar solvent. Thus, it may be concluded that β-PL copolymerizes with St via β-PL carbonium ions and with 3, 3-bis(chloromethyl)oxetane[7] via oxonium ions.

The reaction scheme of the copolymerization of β-PL and St can be given as follows:

TABLE IX. COPOLYMERIZATION BEHAVIOR OF β-PL

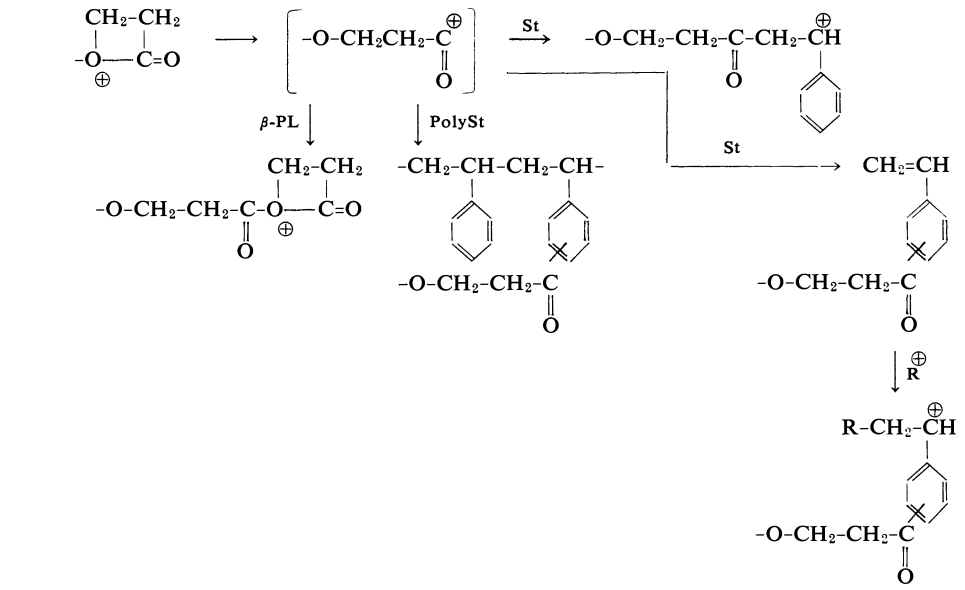
| Catalyst | Comonomer | | |
|---|---|---|---|
| | St | α-MeSt | IBVE |
| $BF_3 \cdot Et_2O$ | Copolymer | Polyα-MeSt | — |
| $SnCl_4$ | Copolymer | Polyα-MeSt | PolyIBVE |
| $AlEt_3$-$H_2O$ | Polyβ-PL | Polyβ-PL | — |

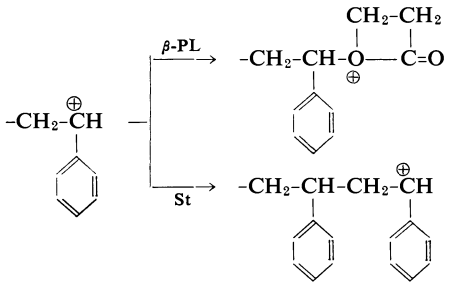
TABLE X. HOMOPOLYMERIZATION OF β-PL BY $SnCl_4$ IN METHYLENE CHLORIDE AT 0°C
([$SnCl_4$] = 0.07 mol./l.)

| [β-PL] mol./l. | Time min. | Conversion, % | $R_p \times 10^3$ mol./l. min. | $\eta_{sp}/C$* dl./g. |
|---|---|---|---|---|
| 0.5 | 270 | 36.5 | 0.7 | 0.07 |
| 1.0 | 150 | 28.3 | 1.9 | 0.07 |
| 2.0 | 250 | 35.2 | 2.8 | 0.09 |
| 2.0 | 345 | 46.6 | 2.7 | 0.09 |
| 3.0 | 80 | 29.3 | 11.0 | 0.09 |

* In 1% chloroform solution at 30°C.

5) H. Cherdron, H. Ohse and F. Korte, *Makromol. Chem.*, **56**, 179 (1962).
6) Y. Yamashita, Y. Ishikawa, T. Tsuda and S. Miura, *J. Chem. Soc. Japan, Ind. Chem. Sec.* (*Kogyo Kagaku Zasshi*), **66**, 104 (1963).
7) K. Tada, T. Saegusa and J. Furukawa, *Makromol. Chem.*, **71**, 71 (1964).





It should be noted that the copolymerization results on $\alpha$-MeSt and IBVE by $BF_3 \cdot Et_2O$ or $SnCl_4$, as shown in Table IX, may be understood to be caused by the higher reactivity of these vinyl monomers than that of St. The difference between the results obtained using $BF_3 \cdot Et_2O$ and $SnCl_4$, and $AlEt_3$-$H_2O$ as catalysts may result from the difference in the effect of gegen ions.


## Summary

The copolymerization of several vinyl monomers, such as styrene (St), $\alpha$-methylstyrene and isobutyl vinyl ether, with $\beta$-propiolactone ($\beta$-PL) as catalyzed by Lewis acids has been investigated in methylene chloride at 0°C. In the copolymerization of $\beta$-PL and St using boron trifluoride-diethyl etherate or stannic chloride as a catalyst, the copolymer was obtained. The apparent monomer reactivity ratios were estimated to be as follows:

$$r_{(\beta\text{-PL})}=0.2\,;\ r_{(St)}=20$$

In the other copolymerization systems, the copolymer was not obtained. The mechanism of these copolymerizations has been discussed.



*Faculty of Engineering*
*Osaka City University*
*Sumiyoshi-ku, Osaka*

# The Effect of Hydrogen-Bonding on the g-Value of Diphenyl Nitric Oxide

By Takashi KAWAMURA, Shoichi MATSUNAMI, Teijiro YONEZAWA and Kenichi FUKUI

(Received March 29, 1965)

The solvent effects on the hyperfine structure of the ESR spectra of semiquinones,[1,2] nitro-compounds[3-5] and aromatic nitric oxides[6,7] have been reported on. However, only a few studies of the solvent effect upon the g-value have been reported.[8] Stone has derived the gauge-invariant g-tensor[9] and an equation as for calculating the g-value of a π-radical.[10] His work suggests that the g-value of a π-radical which contains an oxygen atom in conjugated systems would deviate considerably from the g-value of a free electron (2.00232) because of the large L-S coupling of oxygen as well as the small difference in energy between the odd-electron orbital and the oxygen lone-pair orbital. This has also been pointed out qualitatively by McConnell and Robertson.[11]

It may be expected that the formation of a hydrogen bond to an oxygen atom in a conjugated system would diminish the contribution of the oxygen atom to the g-value through lowering the lone-pair orbital energy and decreasing the odd-electron density on the oxygen atom, thus causing a variation in the g-value. In the present paper we will investigate the effect of the hydrogen bond on the g-value of diphenyl nitric oxide (DPNO); we will attempt a precise analysis.

## Experimental

**Materials.**—DPNO was synthesized by employing the method of Wieland and Roth,[12] recrystallized from methanol (m. p. 62—63°C), sealed in an ampoule under $10^{-4}$ mmHg vacuum, and stored in liquid nitrogen.[6] Carbon tetrachloride, chloroform, ethanol and toluene were purified by following the directions described in "Organic Solvents."[13] Phenylacetylene was purified by distillation from Drierite in a vacuum. Phenol was purified by the freezing method.

**The Measurement of the ESR Spectra.**—Several solvents were employed in preparing a dilute solution of DPNO. The solvents were dried over Drierite for at least one day and then distilled from Drierite under a $10^{-4}$—$10^{-5}$ mmHg vacuum into sample tubes which had previously been charged with DPNO. In the case of a phenol-toluene mixed solvent, a dilute solution of DPNO was prepared under ordinary atmospheric conditions, charged into a sample tube, and then degassed. The ESR spectrometer employed was a JES-3BX-type instrument with a 100 kc. modulation, made by the Japan Electron Optics Co. The static magnetic field was generated by a JES electro-magnet with 300 mmφ pole pieces, with a homogeneity of $1\times10^{-5}$. For the measurement of the g-value and hyperfine splittings, a glass capillary was attached to a sample. The capillary, as in the usual procedure, was filled, as a reference compound, with an aqueous solution of potassium peroxylamine disulfonate, the g-value and the hyperfine coupling constant of the $^{14}N$ of which had been reported to be $2.00550\pm0.00005$ and $13.0\pm0.1$ gauss.[14]

All the measurements of the ESR spectra and the visible spectra were performed at room temperature (10—20°C).

## Results

The numbering of the positions in the DPNO molecule is shown in Fig. 1c. The ESR spectrum of DPNO in carbon tetrachloride is shown in Fig. 1a, and a constructed spectrum with coupling constants of $a_{1\text{-H}}=a_{3\text{-H}}=1.845$, $a_{2\text{-H}}=0.810$ and $a_N=9.559$ gauss, in Fig. 1b. Figure 1b shows a good agreement with the observed spectrum in Fig. 1a. The g-value of DPNO in carbon tetrachloride proved to be $2.00572\pm0.00005$.

The g-value and hyperfine coupling constants of 1- and 3-protons are listed in Table I, together with the changes in them caused by

1) W. Stone and A. H. Maki, *J. Chem. Phys.*, **36**, 1944 (1962).
2) J. Gendell, J. H. Freed and G. L. Fraenkel, ibid., **37**, 2835 (1962).
3) L. H. Piette, P. Ludwig and R. N. Adams, *J. Am. Chem. Soc.*, **84**, 4212 (1962).
4) P. L. Kolker and W. A. Waters, *J. Chem. Soc.*, **1964**, 1136.
5) C. Corvaja and G. Giacometti, *J. Am. Chem. Soc.*, **86**, 2736 (1964).
6) Y. Deguchi, This Bulletin, **33**, 260 (1962).
7) K. Umemoto, Y. Deguchi and H. Takaki, ibid., **36**, 560 (1963).
8) In the course of our experiments, Zandstra has reported on the solvent effect of the g-value of *p*-benzosemiquinone, but his comparison is between in only two solvents, water and dimethylsulfoxide. R. J. Zandstra, *J. Chem. Phys.*, **41**, 3655 (1964).
9) A. J. Stone, *Proc. Roy. Soc.*, **A271**, 424 (1963).
10) A. J. Stone, *Mol. Phys.*, **6**, 509 (1963).
11) H. M. McConnell and R. E. Robertson, *J. Phys. Chem.*, **61**, 1018 (1957).
12) H. Wieland and K. Roth, *Ber.*, **53**, 216 (1920).
13) J. A. Riddick and E. E. Toops, Jr., "Organic Solvents," 2nd ed., Interscience Pub. Inc., N. Y. (1955).
14) J. Q. Adams and J. R. Thomas, *J. Chem. Phys.*, **39**, 1904 (1964).

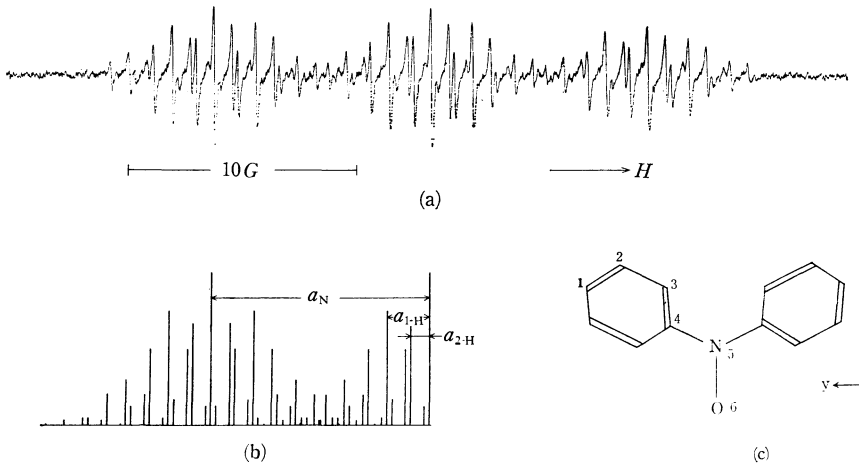



Fig. 1. (a) ESR spectrum of diphenyl nitric oxide in carbon tetrachloride.
(b) Reconstructed spectrum with $a_{1\text{-H}}=a_{3\text{-H}}=1.845$, $a_{2\text{-H}}=0.810$ and $a_N=9.559$ gauss.
(c) Numbering of positions in diphenyl nitric oxide molecule.

TABLE I. THE OBSERVED $g$-VALUE AND HYPERFINE COUPLING CONSTANTS OF 1- AND 3-PROTONS AND THEIR SHIFTS

| Solvent | $(g-g_{POA})\times10^5$ a) | $a_{1\text{-H}}=a_{3\text{-H}}$ b) Gauss | $\delta\Delta g\times10^5$ | $\delta a_{1\text{-H}}$ Gauss |
|---|---|---|---|---|
| Carbon tetrachloride | +22±1 | 1.845±0.008 | 0 | 0 |
| Phenylacetylene | +10±2 | 1.879±0.006 | −12 | +0.034 |
| Chloroform | +6±1 | 1.890±0.003 | −16 | +0.045 |
| Ethanol | +4±1 | 1.913±0.014 | −18 | +0.068 |
| Methanol | +0±1 | 1.917±0.002 | −22 | +0.072 |
| Phenol in toluene (4.4 mol./l. soln.) | −35±1 | 2.068±0.007 | −57 | +0.223 |
| Water | −42±1 | 2.105±0.003 | −64 | +0.260 |

a) The measurement of $g$-value is performed by employing peroxylamine disulfonate as a reference. The $g$-value of peroxylamine disulfonate is notated as $g_{POA}$.
b) Experimentally found values of $a_{1\text{-H}}$ and $a_{3\text{-H}}$ are equal in all solvents employed, although 1- and 3-protons are non-equivalent.

the variation in solvents employed. The differences of these values from those in carbon tetrachloride are denoted by $\delta\Delta g$ and $\delta a_{1\text{-H}}$ respectively, where $\Delta g$ means the difference in $g$-value from that of free spins, which is indicated in Eq. 1.

The visible spectra of DPNO in carbon tetrachloride, chloroform, ethanol and methanol are shown in Fig. 2.

In the visible spectrum of DPNO in carbon tetrachloride, the absorptions at 578 m$\mu$ (shoulder) ($\log\varepsilon=1.97$), 537 m$\mu$ (2.24) and 512 m$\mu$ (2.26) are taken to be the $n$-$\pi^*$ transition, and the absorptions at 473 m$\mu$ (2.66) and 395 m$\mu$ (3.17) are taken to be the $\pi$-$\pi^*$ transition, because the former three shift toward blue and the latter two, toward red when dissolved in hydrogen-bond-forming solvents.[15] Although the observed spectra show that the magnitude of the blue shift of the $n$-$\pi^*$ transition is parallel with the hydrogen-bonding ability of the solvents, and also with the shift of the $g$-value and the hyperfine coupling constants, the position of $n$-$\pi^*$ absorption in hydrogen-bonding solvents, unfortunately, can not be determined with accuracy.

15) H. McConnell, *J. Chem. Phys.*, 20, 700 (1952).

## Discussion

**Stone's Theory for the $g$-Value.**—Considering only one-center integrals and using the two-center $\sigma$-molecular orbital model, Stone has derived the following equation to give the $g$-value of a $\pi$-radical:[10]

$$g=2.00232+\Delta g \quad (1)$$

$$\Delta g=\sum_i \Delta g_i+\sum_j \Delta g_{nj} \quad (2)$$

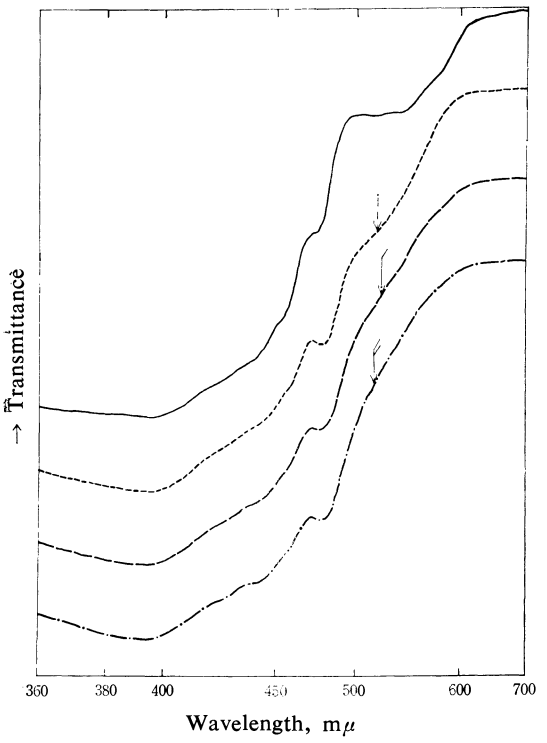



Fig. 2. Visible spectra of DPNO in carbon tetrachloride ——, in chloroform - - - -, in ethanol — — — and in methanol —·—·—. Arrows ↓, ↓ and ↓ show the position of $n$-$\pi^*$ transition of DPNO in chloroform, in ethanol and in methanol calculated from the $g$-value (see text).

$$\Delta g_i = \frac{2}{3}\sum_{m}^{a,b} \frac{\zeta_r(C^m_{rx})^2(C^p_r)^2+\zeta_s(C^m_{sx})^2(C^p_s)^2+(\zeta_r+\zeta_s)C^m_{rx}C^m_{sx}C^p_rC^p_s}{\varepsilon^p-\varepsilon^m_i} + \frac{2}{3}\sum_{m}^{a,b} \frac{\zeta_r(C^m_{ry})^2(C^p_r)^2+\zeta_s(C^m_{sy})^2(C^p_s)^2+(\zeta_r+\zeta_s)C^m_{ry}C^m_{sy}C^p_rC^p_s}{\varepsilon^p-\varepsilon^m_i} \quad (3)$$

$$\Delta g_{nj} = \frac{2}{3}\frac{\zeta_j\{(C^n_{jx})^2+(C^n_{jy})^2\}(C^p_j)^2}{\varepsilon^p-\varepsilon^n_j} \quad (4)$$

where $\Delta g_i$ and $\Delta g_{nj}$ are the contributions to $\Delta g$ from $i$th $\sigma$-bond and the $j$th lone-pair orbital respectively; the notation $\sum_i$ and $\sum_j$ in Eq. 2 indicate the sums over $\sigma$-bonds and over lone-pairs respectively. Throughout this paper, $g$ and all the $\Delta g$'s are the average with respect to three spatial axes. In Eq. 3, $a$ and $b$ indicate the bonding and the anti-bonding orbitals of the $i$th $\sigma$-bond between atoms $r$ and $s$. When the nodal plane of the $\pi$-orbital is the xy-plane, $C^p_r$ is the coefficient of the $P_z$ atomic orbital (AO) of the atom $r$ in the odd-electron orbital; $C^m_{rx}$ and $C^m_{ry}$ are coefficients of the $P_x$ and $P_y$ AO's of the atom $r$ in the $m$th $\sigma$-orbital, and so on. The notations $\zeta_r$ and $\zeta_s$ are L-S coupling constants about the $r$ and $s$ nuclei. The notations $C^n_{jx}$ and $C^n_{jy}$ in Eq. 4 are the coefficients of the $P_x$ and $P_y$ AO's in the $j$th lone-pair orbital, while $C^p_j$ and $\zeta_j$ are the coefficient in the odd-electron orbital and the L-S coupling constant of the atom which has the $j$th lone-pair. When many-center integrals are neglected, fully-occupied or vacant $\pi$-orbitals do not mix into the half-occupied $\pi$-orbital by means of the perturbation of the L-S coupling. Thus, the summation in Eq. 2 is only required over all of the $\sigma$-bonds and lone-pair orbitals.

**The Calculation of the $g$-Value of DPNO in Carbon Tetrachloride.**—The $\pi$-orbitals of DPNO were obtained by the Hückel molecular orbital method, with parameters of $\alpha_O=\alpha+\beta$, $\alpha_N=\alpha+2\beta$, $\beta_{NC}=0.7\beta$ and $\beta_{NO}=0.7\beta$.[16] The calculated odd-electron orbital energy, the odd-electron densities, $\rho_r=(C^p_r)^2$, and the odd-electron orbital bond-orders, $p^p_{rs}=C^p_r\times C^p_s$, are as follows:

$\varepsilon^p=\alpha+0.5090\beta=-8.33$ eV.[17],

$\rho_1=0.0551$, $\rho_2=0.0036$,

$\rho_3=0.0418$, $\rho_4=0.0268$,

$\rho_5=0.2160$, $\rho_6=0.4389$,

$p^p_{45}=-0.0761$, $p^p_{56}=-0.3079$

To obtain N–O and N–C $\sigma$-orbitals, an extended Hückel molecular orbital calculation[18] of $((CH_2)_2C)_2NO$ was performed, on the assumption that all bond angles were 120°, and that the C–H, C–C, C–N and N–O distances were 1.084 Å, 1.397 Å, 1.40 Å and 1.35 Å respectively in the co-planar structure. Then, by slightly modifying the $\sigma$-molecular orbitals, which are mainly localized in N–O and N–C bonds obtained by an extended Hückel method, we got:

the N–C anti-bonding orbital and its orbital energy:

$$\varphi^a_{NC}=0.9120\chi_{Ny}+0.1248\chi_{Cs}-0.3556\chi_{Cx}+0.6916\chi_{Cy}$$

$\varepsilon^a_{NC}=+4.25$ eV.

the N–C bonding orbital and its orbital energy:

16) A. Streitwieser, Jr., "Molecular Orbital Theory for Organic Chemists," John Wiley & Sons, Inc., N. Y. (1961), p. 135. A small $\beta_{NC}$ is used, because the phenyl ring plane would be somewhat twisted from the nodal plane of N–O $\pi$-orbital.

17) $\alpha=-7.06$ eV. and $\beta=-2.49$ eV. are used. Teijiro Yonezawa, Chikayoshi Nagata, Hiroshi Kato, Akira Imamura and Keiji Morokuma, "Ryōshikagaku Nyūmon (Introduction to Quantum Chemistry)," Kagaku Dōjin Co., Tokyo (1964), p. 130.

18) R. Hoffmann, *J. Chem. Phys.*, **39**, 1397 (1963); **40**, 2474, 2480, 2745 (1964).

$$\varphi^{b}_{NC}=0.7777\chi_{Ny}+0.0718\chi_{Cs}+0.3627\chi_{Cx}-0.2823\chi_{Cy}$$

$$\varepsilon^{b}_{NC}=-14.33\ \text{eV}.$$

the N–O anti-bonding orbital and its orbital energy:

$$\varphi^{a}_{NO}=0.5456\chi_{Os}+0.7031\chi_{Ox}-0.2846\chi_{Ns}+1.0517\chi_{Nx}$$

$$\varepsilon^{a}_{NO}=+0.10\ \text{eV}.$$

the N–O bonding orbital and its orbital energy:

$$\varphi^{b}_{NO}=-0.1804\chi_{Os}+0.8247\chi_{Ox}+0.0555\chi_{Ns}-0.3623\chi_{Nx}$$

$$\varepsilon^{b}_{NO}=-19.02\ \text{eV}.$$

Here $\chi_{Ns}$ and $\chi_{Ox}$ are the 2S AO of nitrogen and $2P_x$ AO of oxygen, and so on. These $\sigma$-orbitals would not be bad for N–C and N–O $\sigma$-orbitals in DPNO. In the present treatment, we assumed that a $2P_y$ AO is a lone-pair orbital of the oxygen atom. We estimated $\varepsilon^{p}-\varepsilon^{n}$ as 18620 $cm^{-1}$ from the observed $n$-$\pi^*$ absorption spectrum.

With the above-mentioned orbitals and by putting $\zeta_N=70\ cm^{-1}$ and $\zeta_O=152\ cm^{-1}$,[19] $\Delta g_i$'s and $\Delta g_{nj}$ were calculated as follows:

$$\Delta g_{NC}=+9.7\times10^{-5}$$

$$\Delta g_{NO}=+53.2\times10^{-5}$$

$$\Delta g_{n}=+238.8\times10^{-5}$$

For the sum of the $\Delta g_i$'s over the hydrocarbon part, which may be denoted by $\Delta g_{h.c.}$, Stone has proposed formula 5 semiempirically[10]:

$$\Delta g_{h.c.}=\sum_{i}^{carbons}\rho_i(24.7-19.3\lambda)\times10^{-5} \qquad (5)$$

where $\lambda$ is the coefficient of the odd-electron orbital energy, $\alpha+\lambda\beta$, and $\rho_i$ is the odd-electron density on the $i$th carbon. With Eq. 5, $\Delta g_{h.c.}$ of DPNO becomes:

$$\Delta g_{h.c.}=+5.1\times10^{-5}$$

The calculated $g$-value of DPNO is, therefore:

$$g_{calcd}=2.00232+2\Delta g_{NC}+\Delta g_{NO}+\Delta g_{n}+\Delta g_{h.c.}=2.00549$$

This value shows a good agreement with the $g$-value observed in carbon tetrachloride:

$$g_{obs}=2.00572\pm0.00005$$

**The Calculation of the Hydrogen-bond Effect on the $g$-Value.**—Bolton[20] has considered the protonation effect on the hyperfine structure of the ESR spectra of semiquinones as a perturbation which causes changes in the coulomb integral of the oxygen atom and the resonance integral of the C–O bond. In a similar way, in explaining the difference in the hyperfine coupling constants of semiquinones in dimethylsulfoxide and in an ethanol-water mixed solvent, Gendell and Fraenkel[2] regarded the solvent effect as a perturbation which causes a change in the coulomb integral of the oxygen atom.

Here we take the hydrogen-bond effect to be a perturbation which increases the coulomb integral of the oxygen atom. In the Hückel molecular orbital theory the perturbation, which increases the coulomb integral of the $t$th atom from $\alpha_t$ to $\alpha_t+\delta\alpha_t$, also increases the odd-electron density on the $r$th atom from $\rho_r$ to $\rho_r+\delta\rho_r$, the odd-electron orbital bond order between $r$th and $s$th atoms from $p^{p}_{rs}$ to $p^{p}_{rs}+\delta p^{p}_{rs}$, and the odd-electron orbital energy from $\varepsilon^{p}$ to $\varepsilon^{p}+\delta\varepsilon^{p}$, as is indicated in Eqs. 6—10.

$$\delta\rho_r=\pi^{p}_{r,t}\times\delta\alpha_t \qquad (6)$$

$$\delta p^{p}_{rs}=\pi^{p}_{rs,t}\times\delta\alpha_t \qquad (7)$$

$$\delta\varepsilon^{p}=\rho_t\times\delta\alpha_t \qquad (8)$$

$$\pi^{p}_{r,t}=2\sum_{k\neq p}\frac{C^{k}_{r}C^{k}_{t}C^{p}_{r}C^{p}_{t}}{\varepsilon^{p}-\varepsilon^{k}} \qquad (9)$$

$$\pi^{p}_{rs,t}=\sum_{k\neq p}\frac{C^{k}_{t}C^{k}_{r}C^{p}_{t}C^{p}_{s}+C^{k}_{t}C^{k}_{s}C^{p}_{t}C^{p}_{r}}{\varepsilon^{p}-\varepsilon^{k}} \qquad (10)$$

Here $C^{k}_{r}$ and $C^{p}_{r}$ are the coefficients of the AO of the $r$th atom in the $k$th and the odd-electron $\pi$-orbitals. The notations $\varepsilon^{k}$ and $\varepsilon^{p}$ are the orbital energies of the $k$th and the odd-electron $\pi$-orbitals. Calculated with the parameters mentioned in the preceding section, the values of $\pi^{p}_{r,t}$'s and $\pi^{p}_{rs,t}$'s are tabulated in Table II.

TABLE II. $\pi^{p}_{r,t}$ AND $\pi^{p}_{rs,t}$ (in unit of $1/\beta$)

| $\pi^{p}_{1,6}$ | $\pi^{p}_{2,6}$ | $\pi^{p}_{3,6}$ | $\pi^{p}_{4,6}$ |
|---|---|---|---|
| +0.1074 | +0.0139 | +0.0574 | +0.0932 |
| $\pi^{p}_{5,6}$ | $\pi^{p}_{6,6}$ | $\pi^{p}_{45,6}$ | $\pi^{p}_{56,6}$ |
| +0.0831 | −0.7696 | −0.1392 | +0.2297 |

From Eq. 6, in this connection we get:

$$\frac{\delta a_{1\text{-H}}}{a_1}=\frac{\delta\rho_1}{\rho_1}=\frac{\pi^{p}_{1,6}}{\rho_1}\times\delta\alpha_6$$

$$\frac{\delta a_{3\text{-H}}}{a_3}=\frac{\delta\rho_3}{\rho_3}=\frac{\pi^{p}_{3,6}}{\rho_3}\times\delta\alpha_6$$

where $a_1$ and $a_3$ are the coupling constants of 1- and 3-protons of DPNO dissolved in carbon tetrachloride respectively, and where $\delta a_{1\text{-H}}$ and $\delta a_{3\text{-H}}$ are their increases in hydrogen-bond solvents. It was observed that $a_1=a_3$ and $\delta a_{1\text{-H}}=\delta a_{3\text{-H}}$. Hence, for the purpose of obtaining the value of $\delta\alpha_6$, we may write approximately:

19) D. S. McClure, *J. Chem. Phys.*, **17**, 905 (1949).
20) J. R. Bolton, A. Carrington and J. dos Santos-Veiga, *Mol. Phys.*, **5**, 465 (1962).

$$\delta\alpha_6=(\delta a_{1\text{-H}}/a_1)/\{(1/2)(\pi^{p}{}_{1,6}/\rho_1+\pi^{p}{}_{3,6}/\rho_3)\} \quad (11)$$

In this way, we can calculate the increase in the coulomb integral of the oxygen atom, $\delta\alpha_6$, by means of formula 11. The results are listed in Table III.

Table III. Increase of the coulomb integral of the oxygen atom due to hydrogen bonding

| Solvent | $\delta\alpha_6$ ($\beta$) |
|---|---|
| Carbon tetrachloride | +0 |
| Phenylacetylene | +0.0111 |
| Chloroform | +0.0147 |
| Ethanol | +0.0222 |
| Methanol | +0.0235 |
| Phenol in toluene (4.4 mol./l. soln.) | +0.0728 |
| Water | +0.0848 |

The contribution to $\delta\Delta g$ from each $\sigma$-bond, the lone-pair and the hydrocarbon part are obtained from Eqs. 3—5 by considering their changes due to the increase in the coulomb integral of the oxygen atom, by considering, that is Eqs. 6—8. The results are as follows:

$$\delta\Delta g_{NC}=+14.5\times10^{-5}\times\delta\alpha_6/\beta \quad (12)$$

$$\delta\Delta g_{NO}=-55.3\times10^{-5}\times\delta\alpha_6/\beta \quad (13)$$

$$\delta\Delta g_{h.c.}=+7.0\times10^{-5}\times\delta\alpha_6/\beta \quad (14)$$

$$\delta\Delta g_{n}=-418.8\times10^{-5}\times\delta\alpha_6/\beta \quad (15)$$

Using these equations, $\delta\Delta g_i$'s are estimated to be as cited in Table IV.

Table IV. The variation of contribution to $\Delta g$ from $\sigma$-bonds and the lone-pair

| Solvent | $\delta\Delta g_{NO}$ $\times10^5$ | $\delta\Delta g_{NC}$ $\times10^5$ | $\delta\Delta g_{h.c.}$ $\times10^5$ | $\delta\Delta g_{n}$ $\times10^5$ |
|---|---|---|---|---|
| Carbon tetrachloride | 0 | 0 | 0 | 0 |
| Phenylacetylene | −0.6 | +0.2 | +0.1 | −4.6 |
| Chloroform | −0.8 | +0.2 | +0.1 | −6.2 |
| Ethanol | −1.2 | +0.3 | +0.2 | −9.3 |
| Methanol | −1.3 | +0.3 | +0.2 | −9.8 |
| Phenol in toluene (4.4 mol./l. soln.) | −4.0 | +1.1 | +0.5 | −30.5 |
| Water | −4.7 | +1.2 | +0.6 | −35.5 |

The values of the $\delta\Delta g_i$'s obtained from Eqs. 12—15 are the variations in $\Delta g_i$'s which are caused by the redistribution of the odd electron through the increase in the coulomb integral of the oxygen atom. Hence, the difference, $\delta'\Delta g_n$, as defined by the equation:

$$\delta'\Delta g_n=\delta\Delta g_{obs}-(2\delta\Delta g_{NC}+\delta\Delta g_{NO}+\delta\Delta g_{h.c.}+\delta\Delta g_n)$$

would be the change in $\Delta g_n$ caused by the increase in the difference between the odd-electron orbital and the lone-pair orbital energies, which brings out the blue shift of the $n$-$\pi^*$ transition. The blue shift of the $n$-$\pi^*$ transition can be represented by Eq. 16[21]:

$$\delta(\varepsilon^{p}-\varepsilon^{n})=-\frac{\delta'\Delta g_n}{\Delta g_n}\times18620\ \text{cm}^{-1} \quad (16)$$

The value of $\delta'\Delta g_n$ and the blue shift of the $n$-$\pi^*$ transition, $\delta(\varepsilon^{p}-\varepsilon^{n})$, are tabulated in Table V.

Table V. The blue shift of the $n$-$\pi^*$ transition calculated from the $g$-value

| Solvent | $\delta'\Delta g_n$ $\times10^5$ | $\delta(\varepsilon^{p}-\varepsilon^{n})$ cm$^{-1}$ |
|---|---|---|
| Carbon tetrachloride | 0 | 0 |
| Phenylacetylene | −7 | +550 |
| Chloroform | −9 | +700 |
| Ethanol | −8 | +600 |
| Methanol | −11 | +850 |
| Phenol in toluene (4.4 mol./l. soln.) | −24 | +1900 |
| Water | −26 | +2000 |

The positions of the $n$-$\pi^*$ transition as calculated from the $g$-value of DPNO in chloroform, ethanol and methanol are shown in Fig. 2. The agreement between the calculated $n$-$\pi^*$ transition energy and the observed spectra seems passable. The following factors might cause deviation. The value of $\delta'\Delta g_n$ is very sensitive to parameters in the Hückel calculation. Intermolecular forces other than hydrogen-bonding, orientation forces, inductive forces, dispersion forces and so on, might change the coulomb parameters of the conjugated system, and the solvation might cause a change in the $\beta_{NC}$ through the distortion of the phenyl ring. Thus, the value of $\delta'\Delta g_n$ obtained is only qualitatively reliable.

## Summary

The decrease in the $g$-value of diphenyl nitric oxide in hydrogen-bonding solvents has been examined. This decrease has been analyzed on the basis of Stone's theory for the $g$-value of a $\pi$-radical. The decrease in the $g$-value has been shown to be caused mainly by the decrease in the odd-electron density on the oxygen atom and the increase in the energy difference between the odd-electron and lone-pair orbitals. We have also attempted to

21) Thus determined $n$-$\pi^*$ transition energy is a weighted mean value of solvated and not solvated DPNO, because when the equilibrium is established with rapid exchange between two states, the observed ESR spectrum is a weighted mean spectrum of ones of the two states. H. M. McConnell, *J. Chem. Phys.*, **28**, 430 (1958).

estimate the blue shift of the $n$-$\pi^*$ transition from the $g$-value.

The authors are indebted to Professor Hideo Takaki and Professor Yasuo Deguchi for offering them a chance to use the ESR spectrometer. They also wish to express their thanks to Dr. Hiroshi Kato and Dr. Keiji Morokuma for their valuable discussions throughout this work.

*Faculty of Engineering*
*Kyoto University*
*Sakyo-ku, Kyoto*

# A Geochemical Study of Selenium in Volcanic Exhalation and Sulfur Deposits. II.* On the Behavior of Selenium and Sulfur in Volcanic Exhalation and Sulfur Deposits

By Tetsuro SUZUOKI

(Received April 1, 1965)

It has been reported by the present author that selenium is contained in the volcanic exhalations and sulfur deposits collected at the Nasudake and Kuju volcanoes. It has also been observed that the variations in the selenium content and in the sulfur/selenium ratio are closely related to the change in the temperature of fumarolic gases.[1] The main purpose of the previous study was to examine the content and the distribution of selenium in the matters emitted from volcanoes in Japan. From the results of the previous study, it is anticipated that the estimation of the conditions in natural vents from their inside to the outlets of the fumaroles may be possible by means of studying the change in the sulfur/selenium ratio with the temperature and with the concentration of selenium.

It has already been found, in the previous studies of the chemical equilibrium in volcanic gases, that some of the chemical constituents in volcanic gases are in equilibrium with respect to several chemical reactions associated with the volcanic activity.[2,3] It is also possible that a phase change such as vaporization plays an important role in the process of the occurrence of selenium and sulfur in volcanic gases because of the greater volatility of these substances. In the case of sulfur, as is well known, the hydrogen sulfide and sulfur dioxide which are in equilibrium with free sulfur are important in the transfer of sulfur in volcanic gases. As to the selenium, however, the chemical form of this element in volcanic gases is unknown. Therefore, it is necessary to estimate the chemical form of selenium by considering the chemical equilibria in the reactions with which selenium is possibly concerned. The effect of vapor pressure on the transfer of selenium into volcanic gases should also be studied.

Mizutani[4] found a linear relationship between the concentration of gaseous components and the temperature at the Showashinzan volcano; for this he gave the explanation that the low-temperature fumarolic gases are formed by the mixing of the original gases with water vapor. In this study, the author intends to examine whether or not similar processes are controlling the concentration of selenium in volcanic exhalations emitting from the Nasudake volcano.

From the above points of view, a thermodynamic consideration will be made in order to find the factors controlling the concentration of selenium and the sulfur/selenium ratio in volcanic matters. The cause and the mechanism producing the distribution of selenium and sulfur in the effusion process in the Nasudake volcano will also be discussed.

## Theoretical Considerations

**The Relation between the Temperature and the Equilibrium Constants.**—By combining the chemical components whose presence may be expected in volcanic gases, we find four possible reactions for selenium:

$$3/2Se_2 + 2H_2O = 2H_2Se + SeO_2 \quad (1)$$

*. Part I of this series: This Bulletin, 37, 1200 (1964).

1) T. Suzuoki, ibid., 37, 1200 (1964).

2) K. B. Krauskoph, *Econ. Geol.*, 52, 786 (1957).

3) S. Matsuo, *Bull. Volcanologique*, 24, 59 (1962).

4) Y. Mizutani, *J. Earth Sci., Nagoya Univ.*, 10, 135 (1962).

$$1/2Se_2+2SO_3=SeO_2+2SO_2 \quad (2)$$

$$Se_2+2H_2=2H_2Se \quad (3)$$

$$3H_2+SeO_2=H_2Se+2H_2O \quad (4)$$

The equilibrium constants of the above reactions were calculated; the thermodynamical data were refferred chiefly to Kubaschewski et al.,[5] Latimer,[6] Palmer et al.,[7] and Altschuller.[8] The equations expressing the relation between the equilibrium constants and the temperature in these reactions are as follows:

$$\log K_1=\frac{1.25\times10^4}{T}-88.16-0.3314\log T-0.2470\times10^{-3}T+0.5279\times10^{-7}T^2 \quad (5)$$

$$K_1=\frac{(SeO_2)\,(H_2Se)^2}{(Se_2)^{3/2}(H_2O)}$$

$$\log K_2=\frac{1.125\times10^4}{T}-81.45+7.432\log T-10.36\times10^{-3}T+2.396\times10^{-7}T^2-0.0038\times10^{-9}T^3 \quad (6)$$

$$K_2=\frac{(SeO_2)\,(SO_2)^2}{(Se_2)^{1/2}(SO_3)^3}$$

$$\log K_3=\frac{2.023\times10^3}{T}-22.94+1.220\log T-0.7526\times10^{-3}T+1.105\times10^{-7}T^2 \quad (7)$$

$$K_3=\frac{(H_2Se)^2}{(Se_2)\,(H_2)^2}$$

$$\log K_4=\frac{8.855\times10^3}{T}-64.11-1.264\log T+0.8798\times10^{-3}T-1.158\times10^{-7}T^2 \quad (8)$$

$$K_4=\frac{(H_2Se)\,(H_2O)^2}{(H_2)^3(SeO_2)}$$

The relations between the equilibrium constants and the temperature are illustrated in Fig. 1, in which the $K$-$T$ relations for sulfur are also shown for the sake of comparison. The reactions for sulfur are:

$$3/2S_2+2H_2O=2H_2S+SO_2 \quad (9)$$

and:

$$3H_2+SO_2=2H_2O+H_2S \quad (10)$$

where the $K$-$T$ relations are as follows:

$$\log K_9=-\frac{4.26\times10^4}{T^{2.}}+\frac{0.2031\times10^4}{T}+0.68-1.37\log T+4.77\times10^{-4}T \quad (11)$$

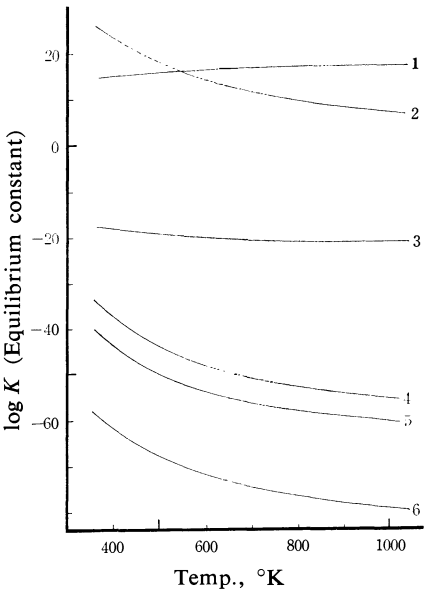



Fig. 1. Relation between temperature and equilibrium constant.

1, $\frac{[H_2Se]^2}{[Se_2][H_2]^2}$ 2, $\frac{[H_2S][H_2O]^2}{[H_2]^3[SO_2]}$

3, $\frac{[H_2S]^2[SO_2]}{[S_2]^{3/2}[H_2O]^2}$ 4, $\frac{[SeO_2][SO_2]}{[Se_2]^{1/2}[SO_3]^2}$

5, $\frac{[H_2Se][H_2O]^2}{[H_2]^3[SeO_2]}$ 6, $\frac{[H_2Se]^2[SeO_2]}{[Se]^{3/2}[H_2O]}$

$$K_9=\frac{(S_2)^{3/2}(H_2O)^2}{(H_2S)^2(SO_2)}$$

and

$$\log K_{10}=\frac{1.041\times10^4}{T}+5.45-2.82\log T-5.24\times10^{-4}T+3.28\times10^{-7}T^2-4.9\times10^{-11}T^3 \quad (12)$$

$$K_{10}=\frac{(H_2O)^2(H_2S)}{(H_2)^3(SO_2)}$$

**The Relation between the Vapor Pressure of Selenium and the Temperature.**—As to the data of the vapor pressure of selenium and sulfur, papers by Kubaschewski et al.,[5] West et al.,[9] and others[10] may be referred to. The empirical formulae for expressing the relation between the temperature and the vapor pressure of selenium and sulfur are given by the above authors as follows: For selenium:

$$\log P_{Se}=8.0886-4989.5/T \quad (13)$$

and for sulfur:

$(598°K>T>393°K)$

$$\log P_S=14.7-6.2238\times10^{-3}T-5405.1/T \quad (14)$$

5) O. Kubaschewski and E. Evans, "Metallurgical Thermochemistry," Pergamon Press, London (1956).
6) W. M. Latimer, "The Oxidation States of the Elements and their Potential in Aqueous Solution," Prentice Hall, New York (1952).
7) K. J. Palmer and N. Elliott, *J. Am. Chem. Soc.*, **60**, 1309 (1938).
8) A. P. Altschuller, *J. Phys. Chem.*, **61**, 509 (1957).
9) W. A. West and A. W. Menzies, ibid., **33**, 1880 (1929).
10) "International Critical Tables of Numerical Data," McGraw-Hill, London, **3**, 201 (1933).

($T>598$°K)

$$\log P_S = 7.4329 - 3268.2/T \quad (14')$$

where $P$ and $T$ are, respectively, the vapor pressure in mmHg and the absolute temperature, °K.

From the above equations, the ratios of the vapor pressure of sulfur to that of selenium are given by the following equations as functions of the temperature:

($598$°K$>T>393$°K)

$$\log P_S/P_{Se} = 6.6114 - 6.2238\times10^{-3}T - 415.6/T \quad (15)$$

($T>598$°K)

$$\log P_S/P_{Se} = -0.6557 + 1.7213/T \quad (15')$$

## Discussion

**The Chemical Form of Selenium and Sulfur in Volcanic Gases.**—As is shown in Fig. 1 the calculated equilibrium constants in reactions 1, 2, 3 and 4 at temperature between 400 and 1000°K range from $10^{-60}$ to $10^{-56}$, from $10^{-56}$ to $10^{-34}$, from $10^{14}$ to $10^{18}$, and from $10^{-60}$ to $10^{-40}$ respectively. The chemical equilibrium constants in reactions 1, 2 and 4 show that a gaseous form of selenium is most stable in the temperature range quoted above. On the contrary, the higher value of the equilibrium constants in reaction 3 shows that hydrogen selenide is more stable than gaseous selenium. However, it is known that hydrogen selenide tends to be unstable in the presence of much water. The volcanic gases usually contain an excess amount of water vapor (more than 99% of the total). Therefore, the hydrogen selenide would not remain stable in the volcanic gases. Thus, the most probable chemical form of selenium in volcanic gases near the outlet of a fumarole is gaseous, perhaps such elementary forms as $Se_2$ and $Se_6$. The value of the $Se_2/Se_6$ ratio depends on the equilibrium constants in the dissociation reaction, $Se_6=3Se_2$, which is given by the following equation as a function of the temperature: $\log K=-13000/T+18.40$, where $K=(Se_2)^3/(Se_6)$.[11] On the other hand, as is well known, most sulfur exists in the forms of sulfur dioxide and hydrogen sulfide in volcanic gases.

It should be noted that in volcanic gases the stable form of selenium is different from that of sulfur despite the similarity of these elements.

**The Vapor Pressure of Selenium and Sulfur in Their Respective Chemical Forms.**—It may be said that an abundance of selenium and sulfur in volcanic gases depends on the volatility of these chemical elements. Therefore, the effect of vapor pressure on the behavior of selenium and sulfur in volcanic gases must be examined.

The ratio of the vapor pressures of free sulfur and selenium is expressed by Eqs. 15 and 15′ as a function of the temperature. The relation between the temperature and the sulfur/selenium ratio is illustrated in Fig. 3 as a

TABLE I. THE S-Se ABUNDANCE RATIO FROM OBSERVATIONS AND DATA OF VAPOR PRESSURE

| Temp., °K | S/Se ratio | |
|---|---|---|
| | Observed | Estimated |
| 694 | $2.0\times10^4$ | 66.7 |
| 683 | 2.0 | 73.1 |
| 659 | 2.4 | 90.4 |
| 653.5 | 2.7 | 95.1 |
| 569 | 6.7 | 278 |
| 539 | 14 | 306 |
| 534 | 11 | 324 |
| 525 | 11 | 357 |
| 514 | 10 | 402 |
| 509 | 15 | 424 |
| 500 | 55 | 458 |
| 499 | 6.8 | 471 |
| 479 | 25 | 579 |
| 468 | 38 | 647 |
| 454 | 57 | 742 |
| 413 | 53 | 1100 |
| 393 | 310 | 1300 |
| 391 | 120 | 1310 |
| 391 | 200 | 1310 |

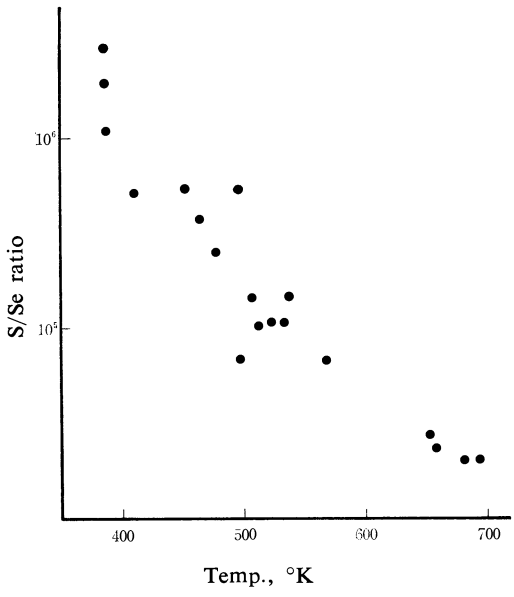



Fig. 2. Relation between S/Se ratio in fumarolic gases and gas temperature.

11) O. V. Al'tshuller, G. N. Zwinadadze and D. M. Chizhikow, *Zhur. Neorg. Khim.*, **2**, 1581 (1957).

straight line extending from about $10^2$ to $10^3$. As is shown in Table I and Fig. 2, however, the abundance ratio of sulfur to selenium in volcanic gases is much higher than the sulfur/selenium ratio shown in Fig. 3. This discrepancy is doubtless due to the presence of much sulfur dioxide and hydrogen sulfide. Therefore, the amount of $S_2$ vapor was calculated by using Eq. 11, putting into it the observed values of hydrogen sulfide and sulfur dioxide; the ratio of the elementary sulfur to selenium was thus obtained. It was found that the ratio of $S_2$ sulfur to selenium is nearly equal to or little less than the theoretical value of the sulfur/selenium ratio, as is shown in Fig. 3.

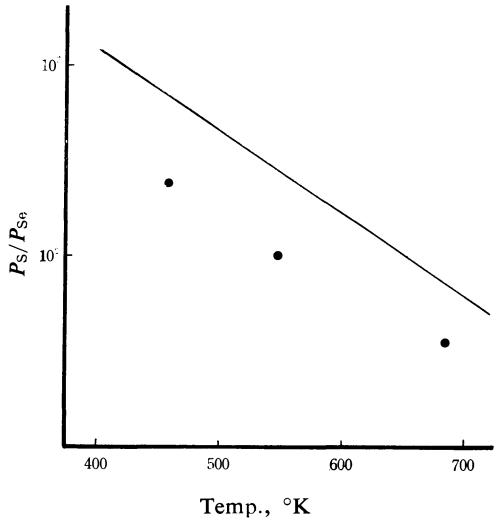



Fig. 3. Comparison of vapor pressure ratio $(P_S/P_{Se})_{saturation}$ with the ratio calculated from observations.
——: Vapor pres. of S/vapor pres. of Se
●: Calculated from observations

The above results suggest that the main part of the sulfur is present and is transferred in form other than that of free gaseous sulfur. Thus, it may be concluded that the behavior of selenium and sulfur in the transfer process is determined by the differences in their chemical forms and in the vapor pressure of each substance.

**The Absolute Concentration and the Distribution of Sulfur and Selenium.**—Regarding the vapor pressure of selenium and sulfur, the observed vapor pressure in volcanic gases have been compared with the saturated vapor pressure obtained by Eqs. 13, 14 and 14′ respectively. As Table II and Fig. 4 show, both selenium and sulfur in volcanic gases are present in quantities very much less than the saturation point. For instance, the degrees of saturation at 800°K for selenium and sulfur are as small as $10^{-6}$ and $10^{-4}$ respectively.

Table II. The degree of saturation for selenium and sulfur in volcanic gases (saturation=1)

| Temp., °K | Ratio to saturation: Sulfur | Selenium |
|---|---|---|
| 694 | 0.00045 | 0.0000015 |
| 683 | 0.00056 | 0.0000021 |
| 659 | 0.00084 | 0.0000033 |
| 653.5 | 0.00095 | 0.0000033 |
| 569 | 0.0084 | 0.000035 |
| 539 | 0.045 | 0.000093 |
| 534 | 0.014 | 0.000041 |
| 525 | 0.023 | 0.000075 |
| 514 | 0.040 | 0.00016 |
| 509 | 0.041 | 0.00012 |
| 500 | 0.16 | 0.00013 |
| 499 | 0.051 | 0.00035 |
| 479 | 0.32 | 0.00074 |
| 468 | 0.76 | 0.0013 |
| 454 | 1.6 | 0.0021 |
| 413 | 8.3 | 0.0017 |
| 393 | 29 | 0.012 |
| 391 | 13 | 0.014 |
| 391 | 21 | 0.014 |

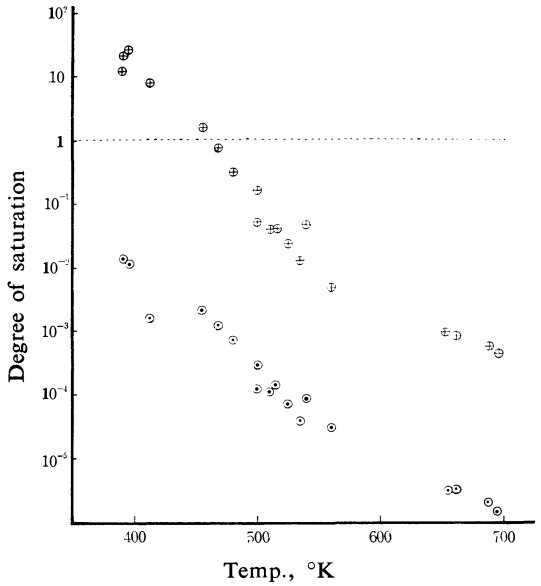



Fig. 4. The degree of saturation for selenium and sulfur in volcanic gases.
⊕: Sulfur
⊙: Selenium

Regarding the scantiness of both chemical elements in volcanic gases, two interpretations are possible. One is based on the static process, and the other, on the dynamic process. In the former, it is supposed that the vapors of selenium and sulfur in primary gases are

once in the equilibrium condition with their solid or liquid phases, that these are quenched in situ, and that the gases are then isolated from the source and transported. The unsaturation may result from the addition of water vapor to the primary gas mixtures. In the second interpretation, it is supposed that the gaseous selenium and sulfur have never been in equilibrium with other phases of the same elements because of the dynamic process of transfer. If the unsaturation results, as in the first interpretation, from only the dilution with water vapor with a temperature of 373°K, the mixing ratio of the latter to the primary gases will be about $10^5$. The addition of such a large amount of water vapor will decrease the temperature very much below the observed value. Therefore, the interpretation based on the static process is inadequate to explain the selenium and sulfur deficiency. It may, therefore, be said that the dynamic process is more probable than the static one in bringing about a deficiency of these elements at a high temperature.

**The Dilution of the Primary Gases with the Water Vapor near the Surface.**—As has been mentioned above, the gas emitted from each fumarole is considered to derive from a common source. In addition, if selenium and sulfur enter into the gases through, for instance, distillation taking place at certain zones in natural vents, and if there is no change in the composition of volcanic gases near the surface, the partial pressure of each component may not vary despite the temperature lowering, provided that the concentration is far below the saturation point. It was found from observation that the concentrations of selenium and sulfur show, respectively, a gradual decrease and a gradual increase with the decrease in the temperature, as is shown in Figs. 5 and 6. The decrease in selenium may be the result of dilution with recyclic water vapor near the surface. Here, the fumarolic gas with the highest temperature is assumed to represent the primary gas.

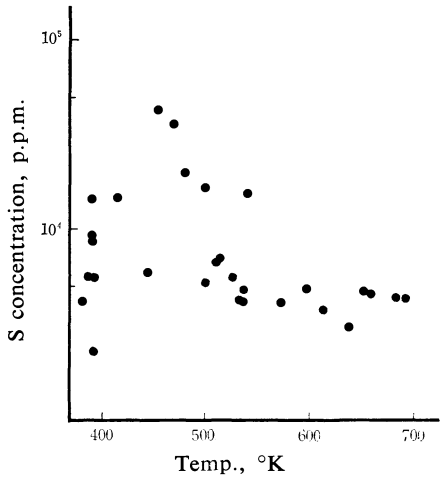



Fig. 6. Relation between temperature and sulfur content in fumarolic gases from Nasudake.

When the primary gases with a temperature of 873°K is diluted with a different amount of water vapor with a temperature of 373°K, the change in the fraction of the primary gases or in the concentration of selenium will be linear with respect to the temperature of the mixture as may be seen in Fig. 7. The calculation is made on the basis of the thermal balance in mixing the respective gases with different temperatures, as is represented in the following equation:

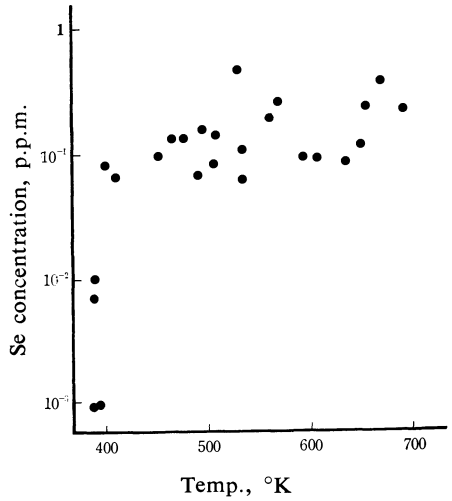



Fig. 5. Relation between temperature and selenium content in fumarolic gases from Nasudake.

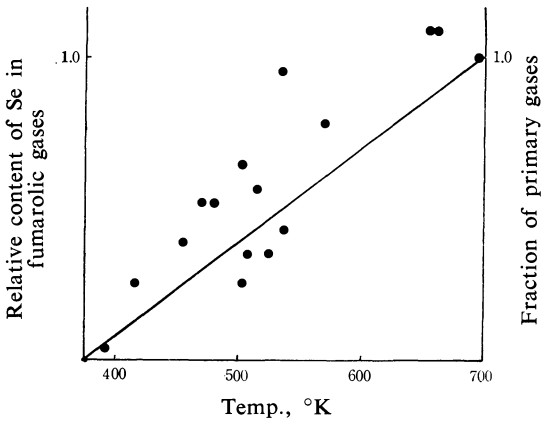



Fig. 7. Relation of selenium concentration and fraction of primary gases to gas temperature.

$$F(T)=\frac{\int_{T}^{873} Cp_{H_2O}dT}{\int_{373}^{T} Cp_{H_2O}dT+\int_{T}^{873} Cp_{H_2O}dT}$$

where $F(T)$ and $Cp_{H_2O}$ are a fraction of the primary gas in the observed mixture at the temperature $T$°K and the heat capacity of water respectively. The selenium contents are also plotted in Fig. 7 in a relative scale. As Fig. 7 shows, the agreement between the calculated and the observed changes in the fraction of selenium suggests that the decrease in the selenium concentration with the decrease in the temperature is mainly due to dilution by water vapor supplied near the earth surface (in the respective vents). As for sulfur, the increase with the decrease in the temperature may result from the addition of sulfur near the surface. This problem will be discussed in the following paper.

The addition or removal of the components in the primary gas may take place in the process of mixing it with water vapor. It may be possible to obtain useful information on the mixing problem by examining the variation in the concentrations of some constituents with the temperature. It may be said that selenium is one of the most promising constituents or indicators for this purpose.

Mizutani explained the origin of low-temperature fumarolic gases of the showashinzan volcano on the basis of the linear relation between the concentration of some gaseous components and the temperature.[4] The linear relation as found at the Showashinzan volcano was not observed at the Nasudake volcano for such components as chlorine, fluorine and boron. It is, therefore, necessary to determine the one component among others, in the primary and secondary gases which is applicable to the study of the mixing processes.

## Conclusion

Regarding the presence of selenium and sulfur in volcanic exhalations and sulfur deposits, it may be concluded that the different behavior of selenium and of sulfur is mainly due to the differences in the vapor pressures and in the chemical forms of these elements in volcanic gases. From thermodynamic considerations, it may also be concluded that the most probable chemical form of selenium in volcanic gases is free selenium.

It may be said that the amount of selenium and sulfur in fumarolic gases is controlled not only by the above factors but also by other factors, judging from the fact that these elements are seldom saturated in volcanic gases, especially at high temperature. It is thought that the undersaturation may occur in the course of the transfer of both elements through fractional distillation, which is controlled by the rates of flow and vaporization. Such dynamic processes may be important as controlling factors in the introduction of selenium and sulfur into volcanic gases in natural vents.

Unlike the Showashinzan volcano, the Nasudake volcano exhibits no linear relation between the temperature and the concentration of most of the gaseous components, except for selenium. The dilution process through mixing with water vapor of a ground-water origin seems to be the cause of the apparent variation in selenium content with the temperature at or near the surface.

Generally, the variation in the concentrations of the chemical components in volcanic gases gives valuable information for a study of the alteration of volcanic exhalation through the mixing of the other components and so on. However, in such a study, careful consideration is required in selecting components which are as practical indicators of the above processes.

It is found in the study of the Nasudake volcano that the selenium and sulfur in volcanic gases are useful indicators for the study of the mixing processes in the course of the alteration of volcanic gases. In this connection, the selenium content and the variation in its concentration in volcanic gases may be regarded as an interesting problem in the study of volcanoes in other areas.

## Summary

With regard to the temperature dependency of the sulfur/selenium ratio in volcanic gases, the factors which control the behavior of selenium and sulfur have been considered from the viewpoints of the chemical equilibrium, the vapor pressure and the thermal balance.

It has been found, from the examination of the equilibrium constants, that, unlike the case with sulfur, the most probable form of selenium in volcanic gases is free selenium. The effect of the vapor pressuse is significant in controlling the transfer of selenium and sulfur into volcanic gases. The results of the calculation of the thermal balance show that the observed wide variation in selenium concentration is due to the addition of water vapor.

On the other hand, it has been found that selenium and sulfur are extremely unsaturated at higher temperatures. This lack of saturation is caused by the dynamical processes of the introduction of these gases into volcanic gases.

The author wishes to thank Professor Yasuo Miyake and Dr. Sadao Matsuo, Department of

chemistry, Faculty of Science, Tokyo Kyoiku University, who gave him valuable advice on many points throughout this study.

Thanks are also due to Dr. Yoshihiko Mizutani, the Institute of Earth Sciences, Faculty of Science, Nagoya University, and Mr. Eitaro Wada and Mr. Osamu Matsubaya, Department of Chemistry, Faculty of Science, Tokyo Kyoiku University, for their help in the collection of samples.

*Department of Chemistry*
*Faculty of Science*
*Tokyo Kyoiku University*
*Otsuka, Tokyo*

# A Geochemical Study of Selenium in Volcanic Exhalation and Sulfur Deposits. III. On the Relation between Selenium and Certain Other Constituents, and on the Behavior of Volcanic Gases

By Tetsuro SUZUOKI

(Received April 1, 1965)

Regarding the relation beween selenium and other constituents in volcanic exhalations, it has been reported in previous papers[1,2] that the gas temperature at the outlets of fumaroles is one of the factors controlling the selenium content in volcanic gases and the amount of sulfur deposits. On the other hand, though the ratio of sulfur to selenium is correlated with the gas temperature at the outlets of fumaroles, the selenium content in the gases has little correlation with the contents of sulfur and chlorine. For instance, it was found that the sulfur content in gases of a certain area was several times higher than that in gases of other areas.

It has also been reported that difference in the behavior of sulfur and selenium in the transfer process of these chemical elements into volcanic gases is mainly caused by the difference in such of their characteristics as the chemical form and the vapor pressure. In addition, the variation of selenium and other constituents in volcanic gases is found to be due to the dilution process.

A continuous observation over a short period was undertaken in order to study the time variation in the contents of sulfur and selenium in volcanic gases from a fumarole at the Nasudake volcano. It was found that the time variation of the sulfur content in volcanic gases was small, while the selenium content showed a considerable variation.

It is necessary, therefore, to study the time variation of selenium in more detail, in connection with other components (sulfur, chlorine, fluorine and boron), by means of a continuous observation. It is also desirable to study the variation in the contents of these elements with the temperature in order to clarify the behavior of selenium and other elements in the effusion process of volcanic gases.

This study was carried out in order to examine the behavior of volcanic gases by observing the variation in the chemical nature of volcanic gases at the sub-surface of the Nasudake volcano.

## Sampling Site and Samples

Samples were collected during the years from 1961 to 1964 at the Nasudake volcano (36°07'N, 139°57'E). The condition of the field has been previously described, and a part of the data for the selenium and sulfur contents, previously reported.[1]

Two kinds of samples were collected; one was used to examine the variation in the constituents in fumarolic gases with the temperature and the other, to observed continuously the concentration of several components in the fumarolic gases.

The samples for the former purpose were collected from many fumaroles with different temperatures over a wide area of Nasudake. The samples for the latter purpose were collected at several fumaroles over a short period of time at intervals of 40 or 60 min. Simultaneous and continuous observation was made at two different fumaroles, representative ones in the NA and NB areas respectively.[1] The distribution of fumaroles at Nasudake is shown in Fig. 1.

1) T. Suzuoki, This Bulletin, 37, 1200 (1964).
2) T. Suzuoki, ibid., 38, 1940 (1965).

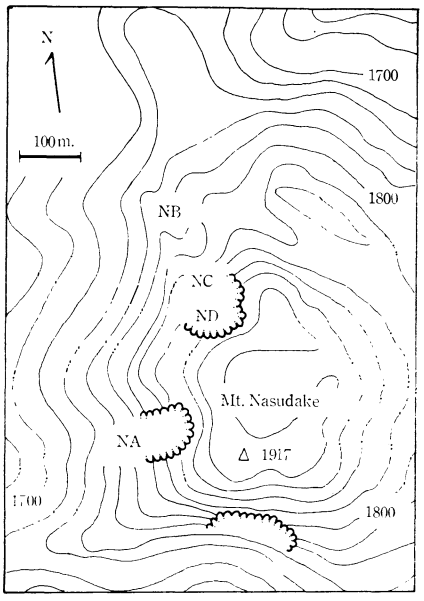



Fig. 1. Distribution of fumaroles at the Nasudake volcano.

## Analytical Methods

The selenium, sulfur, chlorine, fluorine and boron in volcanic gases, which were collected as condensed water (alkaline solution), were determined by the following methods.

**Selenium.** — A colorimetric method using 3,3′-diaminobenzidine. A solution of 10—20 ml. containing 5—25 $\mu$g. of selenium is oxidized with hydrogen peroxide, followed by the reduction of the selenium in 6 M hydrochloric acid solution and neutralization with ammonia.[1]

**Sulfur.**—The total amount of sulfur is determined by the gravimetric method as barium sulfate. A solution of 2—5 ml. is oxidized by hydrogen peroxide and acidified with a dilute hydrochloric acid solution. The $SO_2$-sulfur is determined in the same way as the total sulfur after the sulfide has been removed as cadmium sulfide. The filtrate is oxidized by hydrogen peroxide. Sulfide-sulfur is obtained by the subtraction of the $SO_2$-sulfur from the total sulfur.

**Chlorine.**—Mohr's titration method, or the colorimetric method using iron alum and mercury thiocyanate.[3] A solution of 1—2 ml. is oxidized with hydrogen peroxide.

**Fluorine.**—The colorimetric method using alizarin sodium monosulfonate and thorium nitrate. A solution of 1—2 ml. is oxidized, and then 100—300 mg. of silver oxide is added to avoid the disturbance from chlorine: fluorine is then distilled as hydrofluorosilicic acid.[4,5] The distillation apparatus is a little modified in order to apply it to volcanic samples.

**Boron.** — The titration method using a 0.002 N sodium hydroxide solution and mannitol. A solution of 10—20 ml. is oxidized and acidified by a dilute hydrochloric acid solution in order to expel the carbon dioxide, bicarbonate and carbonate; then the pH of the solution is adjusted to 7.0 with a sodium hydroxide solution before titration.[6]

## Results

A) The following results of analysis were obtained for condensed water from various fumarolic gases of the Nasudake volcano collected in 1964: The sulfur and selenium contents range from 2350 to 8730 p.p.m. and from 0.01 to 0.31 p.p.m. respectively. The chlorine,

Table I. The contents of selenium, sulfur, chlorine, fluorine and boron in volcanic gases from the Nasudake volcano

| Location No. | Temp. °C | Se | S | Cl | F | B |
|---|---|---|---|---|---|---|
| | | | | p.p.m. | | |
| NA-1b | 365 | 0.08 | 3050 | 295 | 10.9 | 81 |
| NA-2 | 325 | 0.09 | 4900 | 1010 | 12.5 | 54 |
| NA-3a | 339 | 0.09 | 3800 | 570 | 11.7 | 59 |
| NA-3b | 264 | 0.06 | 4900 | 880 | 14.5 | 41 |
| NB-2 | 170 | 0.07 | 5030 | 535 | 18.7 | 54 |
| NB-3 | 300 | 0.24 | 4180 | 595 | 21.1 | 51 |
| NB-4 | 130 | 0.08 | 6030 | 730 | 15.9 | 43 |
| NC-1 | 115 | 0.01 | 4220 | 913 | 4.3 | 57 |
| NC-2 | 119 | 0.01 | 2350 | 460 | 2.0 | 20 |
| ND-1 | 110 | 0.01 | 5600 | 782 | 4.0 | 39 |
| NE-1 | 120 | 0.01 | 8780 | 1350 | 7.2 | 34 |

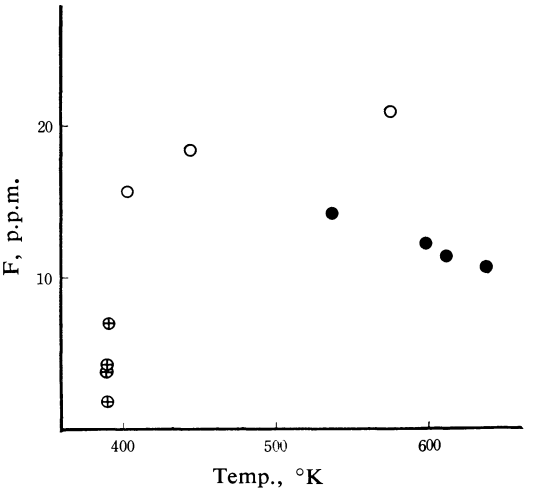



Fig. 2. Relation between fluorine content and gas temperature.

● Gases from the NA area
○ Gases from the NB area
⊕ Gases from the others

3) S. Utsumi, *J. Chem. Soc. Japan, Pure Chem. Sec.* (*Nippon Kagaku Zasshi*), **81**, 401 (1960).
4) J. M. Icken and B. M. Blank, *Anal. Chem.*, **25**, 1741 (1953).
5) J. Samachson, N. Slovik and A. E. Sobel, ibid., **29**, 1888 (1957).
6) ASTM, "Standard on Glass and Glass Products," 346 (1950).

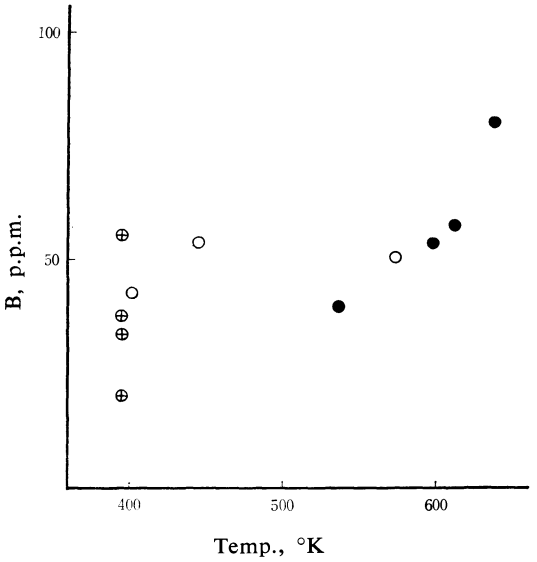



Fig. 3. Relation between boron content and gas temperature.

● Gases from the NA area
○ Gases from the NB area
⊕ Gases from the others

fluorine and boron contents range from 295 to 1350 p.p.m., 2.0 to 26.0 p.p.m. and 20 to 81 p.p.m. respectively. The results are listed in Table I.

The fluorine content in the NB area is higher than that in other areas. The boron content is a little higher in the NA area than that in other areas. Regarding the variation in chlorine, little correlation was found with the gas temperature or with the location of the fumarole. The correlation with the temperature found in the case of selenium content was not observed for some of the other elements over a wider area of Nasudake. The

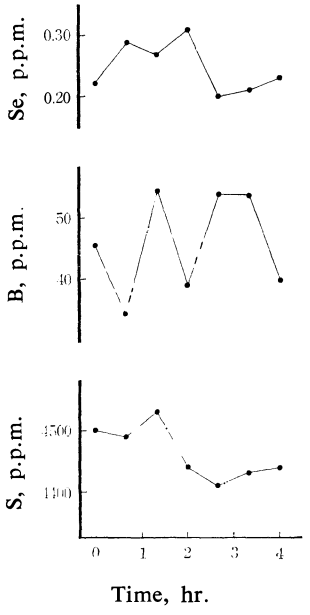



Fig. 4. Time variation of Se, B and S in volcanic gases (1962).

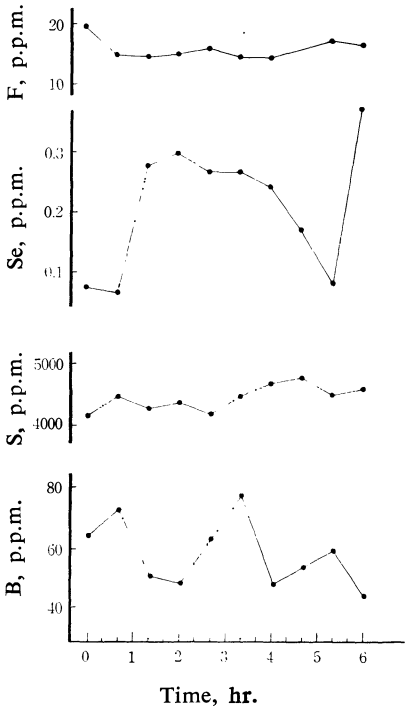



Fig. 5. Time variation of F, Se, S and B in volcanic gases (1963).

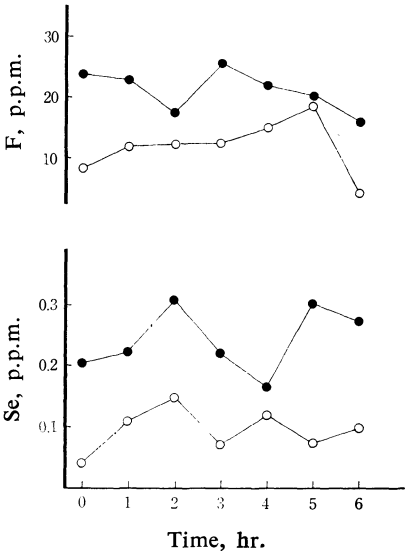



Fig. 6-a. Time variation of Se and F contents in volcanic gases (1964).

○ Collected at the NA area (612°K)
● Collected at the NB area (573°K)

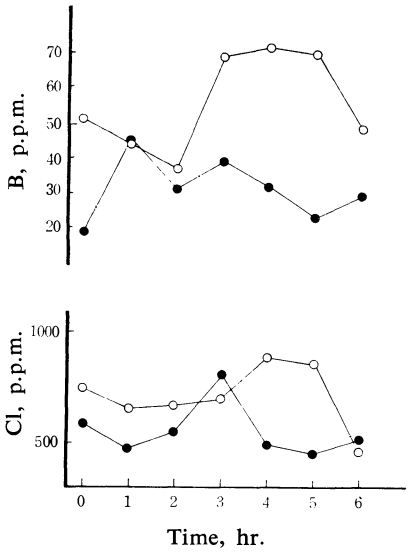



Fig. 6-b. Time variation of Cl and B contents in volcanic gases (1964).

○ Collected at the NA area (612°K)
● Collected at the NB area (573°K)

fluorine and boron contents, however, are likely to show the linear relation with the temperature in the NA area shown in Figs. 2 and 3.

B) The following results of analysis were obtained by the continuous observation of fumarolic gases at the Nasudake volcano in 1962, 1963 and 1964:

*Continuous Observation.* — The contents of sulfur, selenium, chlorine, fluorine and boron in condensed water samples, which were collected at several fumaroles at time intervals of 40 and 60 min., were determined in order to examine the time variations in the contents of those elements. As is shown in Figs. 4, 5 and 6, the contents of selenium, chlorine, fluorine and boron in volcanic gases show comparatively wide variations, while the sulfur content shows a smaller variation, as in the previous observation at the Nasudake volcano.

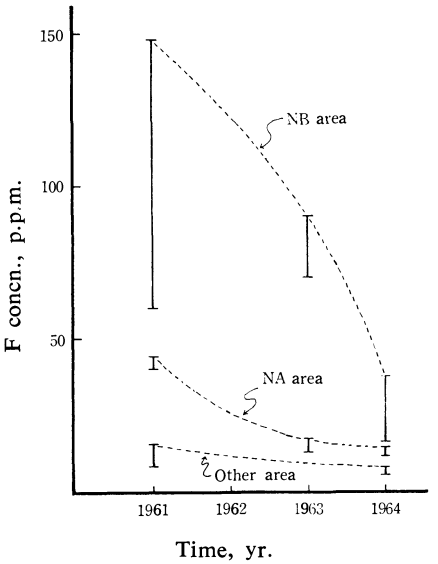



Fig. 8. Year to year variation of fluorine content in fumarolic gases from Nasudake.

*Simultaneous and Continuous Observations.*— A continuous observation for several hours was done simultaneously at two different fumarole areas (NA and NB) in order to examine the differences in several gaseous components with the location. As is shown in

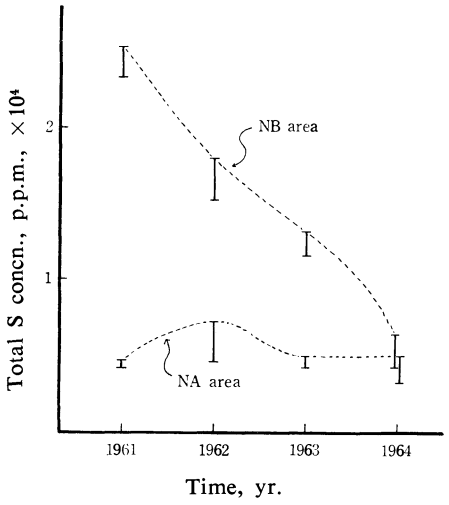



Fig. 7. Year to year variation of total sulfur content in fumarolic gases from Nasudake.

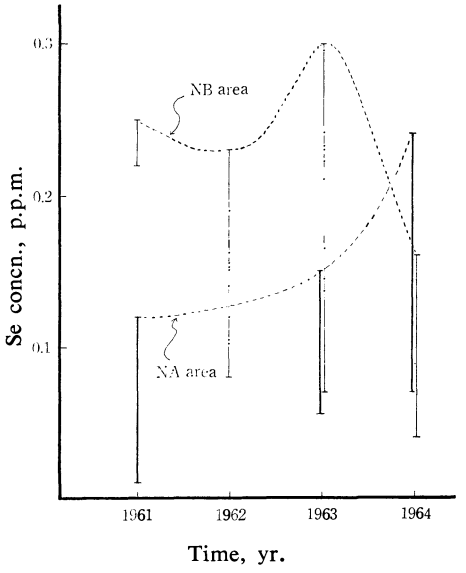



Fig. 9. Year to year variation of the selenium content in fumarolic gases from Nasudake.

Fig. 6, the mode of time variation in the contents of the constituents in gases were considerably different according to the fumarolic area of the volcano.

C) The following results were obtained concerning the year-to-year variations in the contents of sulfur, selenium and fluorine, and in the gas temperature.

As is shown in Figs. 7 and 8, it was found that the contents of sulfur and fluorine remarkably decrease with four years' lapse of time, except that the sulfur in the NA area and the fluorine in the NC and ND areas may be regarded as constant. On the other hand, the selenium content slightly decreased in the NA area and increased in the NB area, as is shown in Fig. 9. In 1964, it was found that the gas temperature in the NB area rose from 195°C to 300°C. It was also noted that the sulfur/selenium ratio in gases decreased slightly in the NA area and increased in the NB area, and that the local variation in the sulfur and fluorine contents in fumarolic gases through the wider areas became smaller during the four years' period.

## Discussion

It may be said that, in addition to the study of the behavior of selenium and sulfur, the study of the behavior of other chemical constituents is important in order to elucidate the effusion process of volcanic gases. Both selenium and boron form volatile compounds with halogens, especially with fluorine. However, there is no indication that these compounds play an effective role in controlling the respective concentrations of these elements in volcanic exhalations. It has already been found that the chemical composition of fumarolic gases gives an average value which is fairly reproducible with the repeated collection of samples when a sample of more than about 200 ml. of condensed water is collected. The results of continuous observation, however, show that the chemical composition varies considerably over a short period of time (i.e., several hours) when a small fraction of gases (less than about 50 ml.) is collected as condensed water. It was also found that the patterns of the time variations of several components are different; this finding indicates that there are some causes of the different patterns of the time variation with each components, besides the common effect over the wider area of the Nasudake volcano. Thus, it is likely that the observed time variation is due to a local effect superposed on the general and common change. The following local effects are to be considered as factors producing the time variation in each constituent in fumarolic gases: i) an accidental addition of particulated matters from wall rocks constituting the vents to volcanic gases, ii) the intermittent addition of water, in which some components are dissolved, and iii) a change in the fumarolic activity.

It is, however, difficult to give a right answer to the question of the variation in the content of substances in the volcanic gases, because of the insufficient data obtained so far.

It was reported in a previous paper[2] that the dilution effect of mixing the primary gases with water vapor is important in the content variation of selenium in fumarolic gases. In this paper, "primary gas" means the source gas of the Nasudake volcano, not a magmatic gas. If the same is true for the variations of sulfur, fluorine, chlorine and boron, a relation similar to that in the case of selenium of each component and the mixing ratio with the temperature should be obtained. The total sulfur content, however, increases with the decreasing temperature, as is shown in Fig. 10. Regarding boron, fluorine and chlorine, no intimate relation was found with respect to the temperature. As has been mentioned above, only the boron and fluorine contents have a linear relation with the temperature, and they only in the NA area, not in the NB area. It is also found that sulfur, boron and fluorine contents, except for chlorine, show a tendency to increase in the NB area. In the effusion process, it is not reasonable to expect that these components will be enriched in the lower-temperature gases if the presence of a single source for each

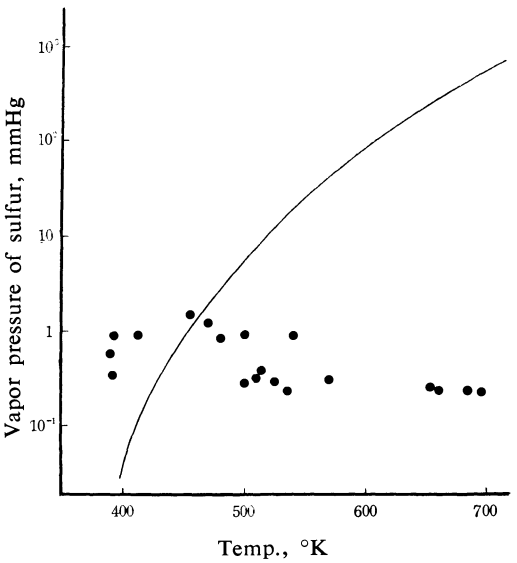



Fig. 10. Relation between vapor pressure ot sulfur and temperature.

● Obtained from observation

Table II. Year-to-year variations of total sulfur, selenium, fluorine and gas temperature in volcanic gases emitted at the Nasudake volcano during the four years' period (from 1961 to 1964)

| Year | Temp., °C | | Sulfur, p.p.m. | | Selenium, p.p.m. | | Fluorine, p.p.m. | |
|---|---|---|---|---|---|---|---|---|
| | NA | NB | NA | NB | NA | NB | NA | NB |
| 1961 | 410 | 200 | 4390 | 25400 | 0.25 | 0.12 | 44 | 148 |
| | | | 4430 | 23300 | 0.22 | 0.01 | 40 | 60 |
| 1962 | 421 | — | 7150 | 18100 | 0.23 | 0.12 | — | — |
| | | | 4500 | 15200 | 0.08 | — | — | — |
| 1963 | 396 | 266 | 4800 | 13100 | 0.30 | 0.15 | 17 | 90 |
| | | | 4200 | 11700 | 0.07 | 0.05 | 12 | 70 |
| 1964 | 360 | 300 | 4900 | 6030 | 0.15 | 0.22 | 14 | 36 |
| | | | 3050 | 3180 | 0.04 | 0.07 | 11 | 26 |

fumarolic gas is considered. Judging from the distribution and the year-to-year variation of these components, it may be expected that a part of the components is derived from the secondary source in the sub-surface, and also that the high-temperature gas from the NA area is closely related to the primary gas of Nasudake. In other words, it is likely that the source gas in the NB area is almost the same as that in the NA area, and that the sulfur, fluorine and boron in fumarolic gases of the NB area are concentrated in the sub-surface in this area when primary gas is encountered with the secondary source near the sub-surface. In the case of sulfur, the additional sulfur is derived from the distillation of the underlying sulfur deposits, which are the products of the past effusion process.

The results of the observation of year-to-year variation of sulfur (Fig. 7) show that the sulfur content in the NA area may be regarded as constant compared with that in the NB area, and that the lowest sulfur/selenium ratio in the NA area is close to the sulfur/selenium ratio in the primary gas. The fluorine content also shows a year-to-year variation like sulfur, whereas a gradual decrease in the fluorine content in the NA area is observed, as Fig. 8 shows. These results may be taken to indicate that the amount of the underlying source of sulfur and fluorine decreased during the four years' lapse of time. The result for selenium, on the other hand, indicates that the selenium in the NB area increases during the four years, as is shown in Fig. 9, while the temperature of the gases in this area is found to rise from 200 to 300°C as is listed in the second column of Table II. The increase in the selenium content might not be regarded as being due to the secondary source, unlike the sulfur and fluorine, but rather to the increase in the temperature of gases in the NB area. This fact also indicates that the selenium concentration has a strong temperature dependency, which reflect the peculiar nature of selenium and which is followed by a change in the fumarolic activity. As one of the causes of the higher concentration of fluorine in lower-temperature gases, it may be expected that fluorine has accumulated in the sub-surface in the form, like calcium fluoride, through the past effusion process of volcanic gases and that it is derived to the fumarolic gases by a leaching of calcium fluoride with water vapor or volcanic gases according to the change in fumarolic activity, for it is known that the reaction rate of calcium fluoride with water vapor increases with a lowering of the temperature and an increase of the silica content in the gases.[7,8]

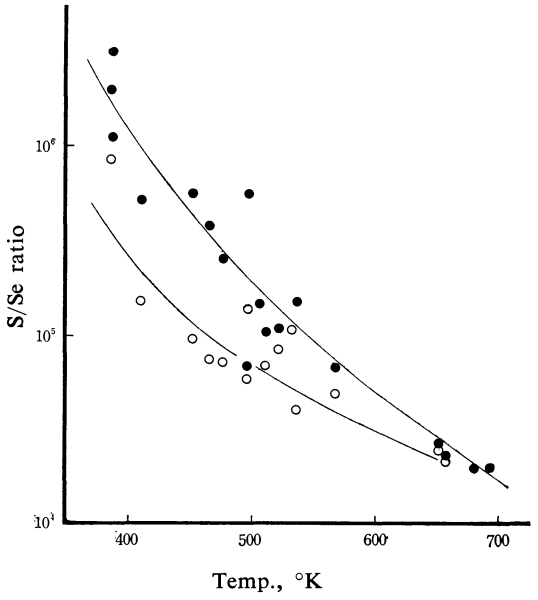



Fig. 11. Relation between S/Se ratio in fumarolic gases and gas temperature.
● Observed
○ Obtained by eliminating excess sulfur

7) H. S. Booth and R. M. Bidwell, *J. Am. Chem. Soc.*, **72**, 2570 (1950).
8) A. J. Ellis and W. A. Mahon, *Geochim. Cosmochim. Acta*, **28**, 1323 (1964).

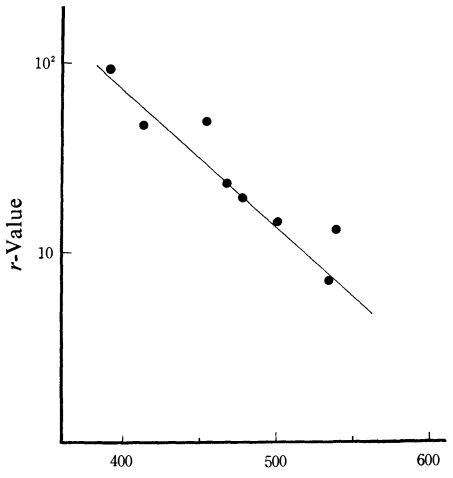



Fig. 12. Relation between gas temperature and S-Se fractionation factors ($r$).

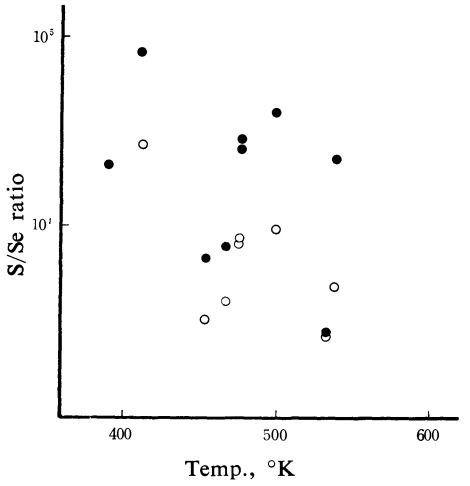



Fig. 13. Relation between S/Se ratio in sulfur deposits and gas temperature.

● Observed
○ Obtained by eliminating excess sulfur

On the basis of the above considerations, the observed sulfur/selenium ratio over the four-year period is corrected by eliminating the effect of the secondarily-added sulfur. The result gives the relation between the sulfur/selenium ratio and the gas temperature, as is shown in Fig. 11; this relation may represent the change in the ratio of sulfur/selenium with the temperature of primary gases. As Fig. 12 shows, it should be noted that a log-linear relation with the temperature is still maintained for the fractionation factors of selenium and sulfur between fumarolic gases and sulfur sublimates, regardless of the content variation of these elements in exhalations and in a dynamical process such as volcanic emission. The sulfur/selenium ratio in sulfur deposits from the primary gases is estimated to be as shown in Fig. 13 by using the above two relations. Accordingly, the proportion of the primary sulfur in the sulfur deposits can be estimated. The gas temperature and the sulfur/selenium ratio in gases co-existing at the time when the separation of sulfur deposits as free sulfur begins from the gaseous phase, can be estimated by means of sulfur/selenium ratio in the sulfur, solidified from the outflowing liquid, and by using the sulfur/selenium ratio in the curves, as is shown in Figs. 11, 12 and 13, which were obtained by the least-square method. Consequently, $1.0—1.7\times10^4$ were obtained for the sulfur/selenium ratio in the source gases from which the above-mentioned sulfur deposit was formed in the NA and NB areas. These data are consistent with the sulfur/selenium ratio ($1.8\times10^4$) which is estimated from the data for fumarolic gases.[1] This supports the supposition that the source gases in both areas are the same and suggests that the sulfur/selenium ratio in the original gases will be between $1—2\times10^4$. It might even be possible to guess the conditions of the formation of sulfur in the past effusion processes by means of the sulfur/selenium ratios in the deposits available at present.

The year-to-year variations in several components suggest that a certain mechanism through fractional distillation or occlusion process by the primary volcanic gases occurs in the sub-surface. It is thought that sulfur and selenium are derived by fractional distillation. In this case, it may be expected that the sulfur/selenium ratio will increase during the process, the stages of which may be divided into 4 steps as follows: I. The first step of distillation, in which only the sulfur content increases; II. The second step, in which the sulfur/selenium ratio remains nearly constant; III. The third step, in which the sulfur content decreases and the selenium content increases (decrease in the sulfur/selenium ratio); and IV. the last one, in which both sulfur and selenium contents decrease. It was mentioned above that there was the difference in sulfur and selenium content between the NA and NB area, and also that there has been a slight variation in the selenium content during the last four years. It may be said, on the basis of observation and the above considerations, that the process of fractional distillation certainly takes place in the sub-surface and the process in the NB area has proceeded from step II to III, and that in the NA area, from III to IV, during the last four years. In addition, it may also be said that the proportion of the secondary

to the primary origin is much higher in the cases of sulfur and fluorine than in that of selenium.

Regarding the differences in the chemical nature of gases among fumarole areas, two interpretations may be given. One is that, as there is originally no secondary source in a certain area (i. e., the NA area), the entry of several components through distillation or occlusion process has not occured in the course of the effusion process. The other is that, after the secondary process has been carried out over a broader area at the same time, an apparent difference in the evolution stages among fumarole areas is brought about at the present time on account of the difference in each fumarolic activity, which corresponds to the temperature conditions of each fumarolic gas. Our consideration and our field observation of several gaseous constituents show that the latter interpretation is more probable.

In connection with the behavior of the several constituents mentioned above, the movement of volcanic gases and the possible process occurring in the sub-surface are illustrated schematically in Fig. 14, which is based on the results obtained thus far.

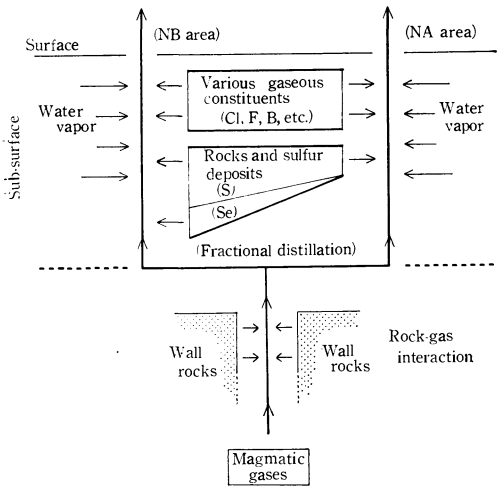



Fig. 14. Schematic diagram of behavior of volcanic gases at the sub-surface of volcano.

## Conclusion

Unlike the case of the Showashinzan volcano,[9] the gaseous components at the Nasudake volcano show no linear relation with the gas temperature with the exception of selenium.

It is to be expected that, at an old solfataric volcano like Nasudake, certain constituents will have been accumulated in the sub-surface during the past effusion processes. It may also be possible that the constituents thus accumulated are leached by the volcanic gases with the change in volcanic activity, and that the observed variations in sulfur, chlorine, fluorine and boron with temperature and time are brought about through such effects. On the other hand, the variation in the selenium content as a result of local effects is much smaller than those of other components; it can be regarded as characteristic in the primary gases. In the cases of a volcano with secondary effects of a considerable extent on the content variations, it may be concluded that the behavior of selenium and the fractionation of selenium and sulfur are applicable to the study of the behavior of volcanic gases according to the stages of the effusion processes and the changes in the chemical nature of volcanic gases in the sub-surface.

The variation in the content of some gaseous constituents with time is an interesting problem to study before we can study in detail the behavior of fumarolic gases near the surface in relation to the change in volcanic activity, the accidental addition of fine particles from wall rocks, and the intermittent addition of water vapor. The problem, however, is still unsolved because not enough data are available for us to make a detailed discussion. Thus, it is necessary to obtain more data with sampling method device suitable to this purpose, one which would make possible the successive collection of fumarolic gases.

As has been mentioned in a previous paper,[2] it may be concluded, from the results of geochemical work on selenium and sulfur, that the entry and transfer of selenium and sulfur into the primary volcanic gases are controlled by certain dynamic factors, such as the rate of vaporization, the rate of gas flow, the ratio of the amounts of gases and rocks, and the reaction time in the rock-gas interactions. It is likely that these processes contribute to the common and general change in the contents of several constituents in volcanic gases. On the other hand, it has also been concluded, from the present study, that the several constituents accumulated in the sub-surface are occluded by primary gases after volcanic gases have branched into smaller vents on the way to the surface. It is likely that the local change in the contents of several constituents is caused by these processes. It may be expected that the above two processes will superpose on each other in the volcanic processes and that, consequently, the distributions of several components at the outlet of fumaroles are as has now been observed.

9) Y. Mizutani, *J. Earth Sci., Nagoya Univ.*, **10**, 135 (1962).

**Summary**

Continuous observations of fumarolic gases have been made in order to study the chemical nature of volcanic gases. A very wide variation in the content of some gaseous constituents has been observed in continuous observation over several hours, and over four years.

Judging from the field observation and the mode of the content variation of several components with the time and the temperature, it is likely that process of the alteration of volcanic gases occurring in the sub-surface plays an important role in producing the difference in the chemical nature of fumarolic gases among the fumarole areas. In addition, the year-to-year variation of the contents of some constituents might provide an indication of the stage of some processes, such as distillation and occlusion, which have occurred in the sub-surface.

It has been found that components like selenium are useful in an examination of the behavior of volcanic gases at an old solfataric volcano like Nasudake, because it is expected that most of the constituents except for selenium have been accumulated in the sub-surface by the past effusion processes and that the accumulated constituents have been occluded in the primary volcanic gases with the change in volcanic activity.

The author wishes to thank Professor Yasuo Miyake and Dr. Sadao Matsuo, Department of Chemistry, Faculty of Science, Tokyo Kyoiku University, both of whom gave him valuable advice on many points throughout this study.

Thanks are also due to Dr. Yoshihiko Mizutani, Institute of Earth Sciences, Faculty of Science, Nagoya University, and author's colleagues, Messrs. Eitaro Wada, Osamu Matsubaya and Minoru Kusakabe, Department of Chemistry, Faculty of Science, Tokyo Kyoiku University, for their help in the collection of samples for present study.

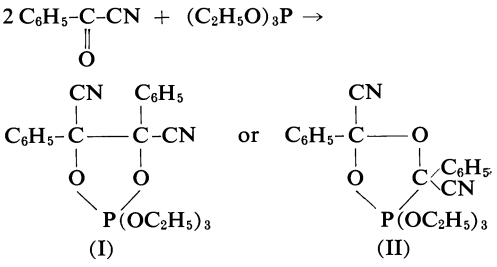
*Department of Chemistry*
*Faculty of Science*
*Tokyo Kyoiku University*
*Otsuka, Tokyo*

# The Reactions of Benzoyl Cyanide with Trivalent Phosphorus Compounds

By Teruaki MUKAIYAKA, Isao KUWAJIMA and Kiyotaka OHNO

(Received April 2, 1965)

The deoxygenation reactions of isocyanates,[1] diphenyl ketone,[1] and benzil[2] by means of trivalent phosphorus compounds have been described in previous papers. In the present study, the reactions of benzoyl cyanide with trivalent phosphorus compounds will be examined. When triethyl phosphite is added to two equivalents of benzoyl cyanide in anhydrous benzene at room temperature, the reaction takes place exothermically. After the mixture is warmed to 50°C for 30 min., a white solid is obtained in a high yield. An elemental analysis shows that this product is a 2 : 1 adduct.

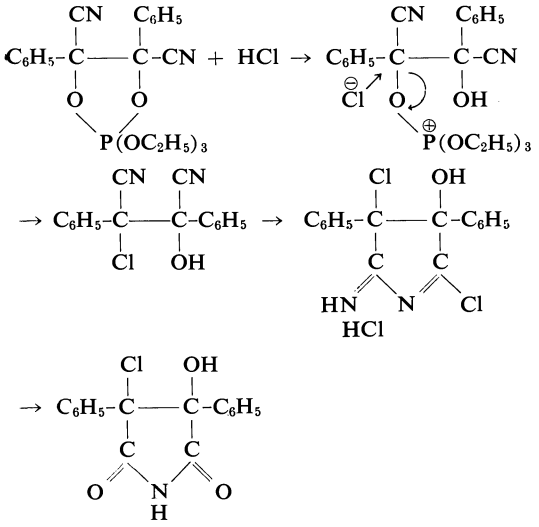


(I) or (II)

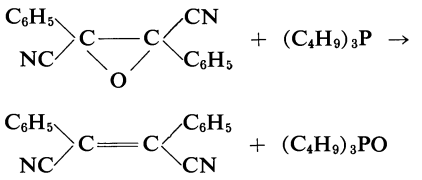
In order to confirm this structure, it was hydrolyzed in concentrated hydrochloric acid; 3,4-diphenyl-3-chloro-4-hydroxysuccinimide, whose infrared spectrum has characteristic bonds for carbonyl (1790 and 1720 $cm^{-1}$), for NH (3270 $cm^{-1}$) and for OH (3430 $cm^{-1}$), was thus obtained in a 62% yield. Mark[3] and Ramirez[4] reported that tris-dimethylamino phosphane or triethyl phosphite reacts with 2 mol. of aldehydes to form 2 : 1 adducts which

1) T. Mukaiyama, H. Nambu and M. Okamoto, *J. Org. Chem.*, **27**, 3651 (1962).
2) T. Mukaiyama, H. Nambu and T. Kumamoto., ibid., **29**, 2243 (1964).
3) V. Mark, *J. Am. Chem. Soc.*, **85**, 1884 (1963).
4) F. Ramirez, A. V. Patwardhan and S. R. Heller, ibid., **86**, 514 (1964).

posses phosphorus-carbon bond. However, in the present case the structure of the adduct may be designated as I, since the hydrolysis product obtained adove may be expected only from I through decomposition as is sketched below:



When the adduct was heated in xylene, it decomposed into $\alpha,\alpha'$-dicyanostilbene oxide (70%) and triethyl phosphate (100%). The former compound could be identified by its infrared spectrum which has characteristic absorption bonds attributable to the epoxide ring (1260, 870 and 790 $cm^{-1}$), and by the fact of its conversion to *cis*-$\alpha,\alpha'$-dicyanostilbene when treated with tri-*n*-butylphosphine at 160°C.

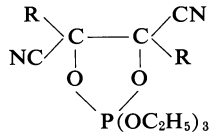


It has been reported by Wittig[5] that an inverted olefin is a predominant product when the epoxide is deoxygenated by tertiary phosphine. This suggests that the epoxide obtained above is in the trans-form. Similar adducts were obtained in the cases of *p*-nitro, *p*-chloro and *p*-methyl phenyl derivatives; they decomposed into the corresponding epoxides when they were refluxed in toluene or xylene (see Tables I and II).

In the case of *p*-anisoyl cyanide, however, a similar adduct was not obtained; rather $\alpha,\alpha'$-dicyano-*p*,*p'*-dimethoxystilbene was formed in a 64% yield.

Next, the reaction was attempted by using tri-*n*-butylphosphine in place of the triethyl phosphite used in the above experiment. When tri-*n*-butylphosphine was added drop-by-drop to an equimolar amount of benzoyl cyanide at room temperature, a red color was formed with a violent evolution of heat. After the solvent had been removed, a large amount of white crystals were obtained from the tarry reaction mixture. This product was shown to be *cis*-$\alpha,\alpha'$-dicyanostilbene by means of elemental analysis, its melting point[6] and its infrared spectrum (2400 $cm^{-1}$ for nitrile; 1600, 1580, 1500, 1470, 770 and 700 $cm^{-1}$ for the

Table I. The synthesis of 2:1 adduct from the reaction of aroyl cyanides with triethyl phosphite



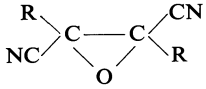
| R | Yield, % | M. p.,°C | | Analysis C, % | H, % | N, % | P, % |
|---|---|---|---|---|---|---|---|
| $C_6H_5$- | 97 | 117 | Found | 61.29 | 6.08 | 6.58 | 7.45 |
| | | | Calcd. | 61.68 | 5.84 | 6.54 | 7.24 |
| *p*-$CH_3$-$C_6H_4$- | 66 | 84 | Found | 62.98 | 6.40 | 6.32 | 7.01 |
| | | | Calcd. | 63.15 | 6.36 | 6.14 | 6.79 |
| *p*-Cl-$C_6H_4$- | 99 | 111—113 | Found | 53.13 | 4.41 | 5.76 | * |
| | | | Calcd. | 53.12 | 4.62 | 5.63 | |
| *p*-$NO_2$-$C_6H_4$- | 74 | 131 dec. | Found | | | 10.81 | 5.82 |
| | | | Calcd. | | | 10.81 | 5.63 |

* Due to its sublimation property, the analysis of phosphorus of this compound could not be carried out.

5) G. Wittig and W. Haag, *Ber.*, **88**, 1654 (1955); C. B. Scott, *J. Org. Chem.*, **22**, 1118 (1957); M. J. Boskin and D. B. Denney, *Chem. & Ind.*, **1959**, 330.

6) L. Chalanay and E. Knoevenagel, *Ber.*, **25**, 289 (1892).

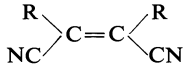
TABLE II. THE DECOMPOSITIONS OF 2 : 1 ADDUCTS INTO EPOXIDES AND TRIETHYL PHOSPHATE



| R | Yield, % | M. p., °C | | Analysis C, % | Analysis H, % | Analysis N, % | $(C_2H_5O)_3PO$, % |
|---|---|---|---|---|---|---|---|
| $C_6H_5$- | 70 | 162[a] | Found | 78.22 | 4.20 | 11.39 | 91 |
| | | | Calcd. | 78.03 | 4.09 | 11.38 | |
| *p*-$CH_3$-$C_6H_4$- | 22 | 150[b] | Found | 78.43 | 5.03 | 10.40 | 98 |
| | | | Calcd. | 78.81 | 5.14 | 10.21 | |
| *p*-Cl-$C_6H_4$- | 20 | 168[c] | Found | 61.12 | 2.39 | 9.10 | 77 |
| | | | Calcd. | 60.95 | 2.54 | 8.88 | |
| *p*-$NO_2$-$C_6H_4$- | 76 | 190[d] | Found | 57.22 | 2.34 | 16.82 | 71 |
| | | | Calcd. | 57.15 | 2.40 | 16.66 | |

The reactions were carried out by heating in xylene for 1.5 hr.
a) Recrystallized from ethanol. b) Recrystallized from ether.
c) Recrystallized from ethyl acetate. d) Recrystallized from benzene.

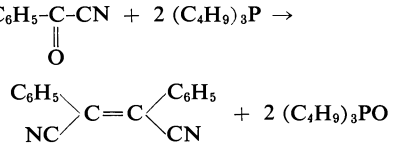
TABLE III. THE REACTIONS OF AROYL CYANIDES WITH TRI-*n*-BUTYLPHOSPHINE



| R | Yield, % | M. p., °C | | Analysis C, % | Analysis H, % | Analysis N, % |
|---|---|---|---|---|---|---|
| $C_6H_5$- | 39 | 159[a] | Found | 83.23 | 4.47 | 12.23 |
| | | | Calcd. | 83.45 | 4.38 | 12.17 |
| *p*-$CH_3$-$C_6H_4$- | 19 | 197[a] | Found | 83.67 | 5.68 | 11.04 |
| | | | Calcd. | 83.69 | 5.46 | 10.85 |
| *p*-$CH_3O$-$C_6H_4$- | 40 | 188[b] | Found | 74.65 | 5.15 | 9.69 |
| | | | Calcd. | 74.47 | 4.86 | 9.65 |
| *p*-Cl-$C_6H_4$- | 20 | 184[c] | Found | 64.34 | 2.61 | 9.49 |
| | | | Calcd. | 64.21 | 2.67 | 9.36 |

a) Recrystallized from ethanol. b) Recrystallized from benzene.
c) Recrystallized from ethyl acetate.

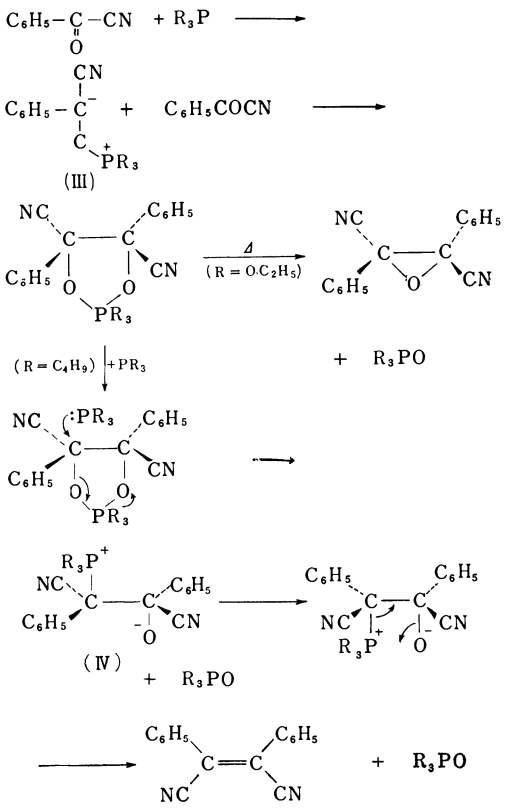
monosubstituted benzene ring). In order to ascertain whether the epoxide is an intermediate of this reaction, the deoxygenation of $\alpha,\alpha'$-dicyanostilbene oxide by tri-*n*-butylphosphine was next attempted under similar moderate conditions. However, the expected deoxygenation could not be observed, and the epoxide was recovered almost quantitatively. The results show that the epoxide is not a probable intermediate in this olefin formation. Similar results were observed in the cases of various *p*-substituted benzoyl cyanides, where the corresponding $\alpha,\alpha'$-dicyano olefines were obtained in 18—40% yields (see Table III).



The mechanisms of these reactions may be considered to be as follows; initially, benzoyl cyanide reacts with the trivalent phosphorus compound to form an adduct such as III, which may be stabilized by the strong electron-attracting effect of the cyano group. This is in turn transformed into 2 : 1 adduct by the electrophilic attack of another molecule of benzoyl cyanide. The electrophilic attack may occur at this stage so that two large groups, e. g., the phenyl group, conform in trans-position. Thus, the triethyl phosphite adduct, which is pyrolyzed, gives *trans*-epoxide, as is shown below.

In the case of tri-*n*-butylphosphine, the reaction may proceed through a similar adduct. The substitution reaction is expected to occur by the nucleophilic attack of the tertiary phosphine, accompanied by the elimination of the phosphine oxide. In the intermediate IV,

since the $\geqslant P^+$ part and $-O^-$ part are situated on opposite sides, it is necessary to rotate along the central carbon-carbon bond in order to accomplish the Wittig-type elimination of the tertiary phosphine oxide. Thus, *cis*-olefin may be formed predominantly.



## Experimental

**The Reaction of Benzoyl Cyanide with Triethyl Phosphite.** — A solution of triethyl phosphite (0.415 g., 0.0025 mol.) in 10 ml. of anhydrous benzene was added slowly to benzoyl cyanide (0.655 g., 0.005 mol.) in 20 ml. of anhydrous benzene at 50°C under nitrogen atmosphere. After this mixture had stood for 30 min. at 50°C, the benzene was distilled off in vacuo, and the solidified residue was recrystallized from ligroin. The 2 : 1 adduct (1.04 g., 97% ; m. p. 117°C) was obtained.

By a similar procedure, the corresponding adducts were obtained from *p*-methyl, *p*-chloro and *p*-nitro phenyl derivatives.

**The Reaction of Benzoyl Cyanide with Tri-*n*-butylphosphine.**—A solution of tri-*n*-butylphosphine (6.06 g., 0.03 mol.) in 10 ml. of anhydrous ether was added drop-by-drop to benzoyl cyanide (3.93 g., 0.03 mol.) in 20 ml. of anhydrous ether under cooling in an ice-salt bath. Then the bath was removed and the reaction mixture was kept for one day at room temperature. After the evaporation of the ether at reduced pressure, the deposited solid was filtered and recrystallized from ethanol. $\alpha,\alpha'$-Dicyanostilbene (1.35 g., 39% ; m. p. 160°C) was thus obtained. By the distillation of the residue, tri-*n*-butylphosphine oxide (4.00 g., 61% ; b. p. 125—130°C/0.5 mmHg) was then obtained.

**The Decomposition of the Adduct.**—The benzoyl cyanide-triethyl phosphite adduct (4.30 g.) was dissolved in anhydrous xylene and refluxed for 1.5 hr. Then the solvent was removed in vacuo and the reaction mixture was distilled, giving triethyl phosphate (1.80 g., 98% ; b. p. 105—107°C/22 mmHg). The residue was solidified by cooling it and then recrystallized from ethanol. $\alpha,\alpha'$-Dicyanostilbene oxide (1.75 g., 70% ; m. p. 162°C) was thus obtained.

**The Hydrolysis of the Adduct.**—When 10 ml. of concentrated hydrochloric acid was added to the adduct (1.00 g.), it turned into a yellow oil. After it had then been refluxed for an hour, the deposited white solid was filtered and recrystallized twice from benzene.

Found : C, 63.11 ; H, 4.37 ; N, 5.03. Calcd. for $C_{16}H_{12}NO_3Cl$ : C, 63.68 ; H, 3.98 ; N, 4.64%.

**The Conversion of $\alpha,\alpha'$-Dicyanostilbene Oxide into $\alpha,\alpha'$-Dicyanostilbene.**—A mixture of $\alpha,\alpha'$-dicyanostilbene oxide and tri-*n*-butylphosphine was heated at 160°C for 5 min. in nitrogen atmosphere. The reaction took place violently, and the reaction mixture turned black. After it had then been washed with ether, $\alpha,\alpha'$-dicyanostilbene (m. p. and m. m. p. 158—160°C) was obtained in a 48% yield.

No similar reaction could be observed at room temperature or at 100°C.

## Summary

The reactions of various *p*-substituted benzoyl cyanides with trivalent phosphorus compounds have been studied. They react with triethyl phosphite to form 2 : 1 adducts which, upon being heated in xylene, decomposed into the corresponding dicyanostilbene oxide and triethyl phosphate. The reaction with tri-*n*-butylphosphine, on the other hand, gives *cis*-dicyanostilbene derivatives. These reactions can be explained by a mechanism through similar intermediates.

*Laboratory of Organic Chemistry*
*Tokyo Institute of Technology*
*Ookayama, Tokyo*

# The Switch-over from the D–R to the D–D Mechanism in the Photoreduction of Methylene Blue

By Nobuo KOSUI, Kengo UCHIDA and Masao KOIZUMI

(Received April 3, 1965)

One of the present authors (M. K.) and his collaborators have found that some thiazine dyes undergo photoreduction in the absence of any reducing agents,[1,2] and that the primary process is an electron transfer between the triplet dye and the ground-state dye.[3,4] This finding has led to the expectation that the photoreduction of thiazine dyes may in general be classified into two types according to their primary processes. The first type begin with an electron transfer (or a hydrogen transfer) from the reductant to the dye (the D–R mechanism), whereas the second type is initiated by an electron transfer between the excited dye and the ground-state dye molecules (the D–D mechanism). However, evidence for a switch-over from one mechanism to the other has recently been presented for the first time in connection with the photoreduction of eosine by allythiourea (ATU).[5] The purpose of the present paper is to report a similar switch-over of mechanisms taking place in the photoreduction of methylene blue with such reductants as ATU and EDTA. The evidence was obtained in two ways, from an investigation of the rate formula for a run and from the effect of the dye concentration on the quantum yield of the photoreduction. In addition, an attempt was made to determine $\varphi_{S-T}$, the probabilities of a transition from the singlet-excited state to the triplet state.

## Experimental

**Material.** — *Methylene Blue.* — Grübler's special-grade sample was recrystallized three times from *n*-butanol. $\varepsilon_{max}=6.0\times10^4$.

ATU and EDTA and the other inorganic reagents were recrystallized three times from water.

**Apparatus and Procedure.**—The pH of the sample solution was controlled by a phosphate buffer solution (1/50 M), and most experiments were performed at pH 7.2. The sample was degassed thoroughly, freezing and thawing being repeated six times.

The apparatus and procedure were the same as have already reported on,[3] apart from the method of following the reaction.

The reactions were carried out in an apparatus equipped with a microammeter and photocell; the light beam entered through a cut-off filter, and passed through the reaction cell and then via an interference filter ($\lambda_{max}=669$ m$\mu$; half-width=18 m$\mu$) to the photocell.

When the shift in the absorption peak was observed, a new absorption spectrum in the 600 m$\mu$ to 700 m$\mu$ region was recorded on a Hitachi spectrophotometer (EPU-2A), and the kinetics were investigated by employing Blaisdell's method. The light intensity was measured by using a thermopile (Kipp & Zonen Co.). The reactions were all carried out at 30.0°C.

Both EDTA and ATU scarcely affect the absorption spectra of methylene blue at all. Usually photobleaching occurred without a shift of the absorption peak. When air was introduced at the end of the reaction, coloration was restored in a few minutes in the methylene blue - EDTA system, whereas a longer time was required in the case of the methylene blue - ATU system, about ten minutes being necessary for an 80% recovery of the original dye.

## Results and Discussion

**Rate Formula for a Run.**—In the case of EDTA, the relation between $\ln(e^{\alpha cd}-1)$ and time, $t$, ($\alpha$, $c$ and $d$ are, respectively, the average

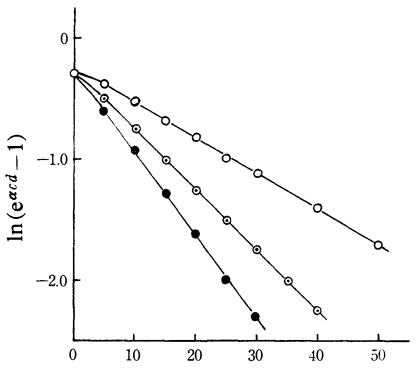



Fig. 1. Plots of $\ln(e^{\alpha cd}-1)$ against time.
pH=7.2, $[MB]_0=9.0\times10^{-6}$ M
○ : [EDTA] $=1.4\times10^{-3}$ M
⊙ : $3.0\times10^{-3}$ M ● : $2.0\times10^{-2}$ M

1) Y. Usui, H. Obata and M. Koizumi, This Bulletin, 34, 1649 (1961).
2) Y. Usui and M. Koizumi, ibid., 34, 1651 (1961).
3) M. Koizumi, H. Obata and S. Hayashi, ibid., 37, 108 (1964).
4) S. Kato, M. Morita and M. Koizumi, ibid., 37, 117 (1964).
5) K. Ohno, Y. Usui and M. Koizumi, ibid., 38, 1022 (1965).

molar absorption coefficient, the concentration of dye, and the thickness of the cell) is satisfactorily linear for all the experiments when the concentration of EDTA is larger than $1.0\times10^{-4}$ M and when the dye concentration is less than $10^{-5}$ M. As Fig. 1 shows, the linear relation holds in most cases until two-thirds or more of the dye had been bleached. This means that the rate is simply proportional to the absorption of light, for in this case the rate is given by:

$$\frac{-\mathrm{d}[\mathrm{D}]}{\mathrm{d}t}=\Phi I_{abs}=\frac{10^3 I_0\Phi}{d}(1-\mathrm{e}^{\alpha[\mathrm{D}]d}) \qquad (1)$$

where $\Phi$ is the quantum yield and $I_0$ is the intensity of the exciting light (expressed in moles per $cm^2$ per sec.), and one obtains, by integrating (1):

$$\ln(\mathrm{e}^{\alpha d[\mathrm{D}]}-1)-\ln(\mathrm{e}^{\alpha d[\mathrm{D}]_0}-1)=10^3\Phi I_0\alpha t \qquad (2)$$

where $[\mathrm{D}]_0$ is the initial concentration of dye. From the plots in Fig. 1 one can evaluate the quantum yield, $\Phi$, since $I_0\alpha$ is obtained easily by measuring the light absorption.

When the concentration of EDTA is reduced to $1\times10^{-4}$ M, the situation becomes a little different. Thus, when the original dye concentration is $5.6\times10^{-6}$—$1.6\times10^{-5}$ M relation 2 still holds until two-thirds of the original dye has been bleached, whereas when the dye concentration is higher, Eq. 2 ceases to be applicable and deviations become apparent when one-third of the dye has been bleached.

When ATU is the reducing agent, its concentration must be higher than $\sim4\times10^{-2}$ M for formula 2 to express a run down to a two-thirds bleaching of the original dye. When the concentration of ATU is decreased, although relation 2 still holds in the earlier stages down to $4.0\times10^{-3}$ M of ATU, it becomes less applicable as the reaction proceeds, until at a concentration of $\sim1\times10^{-3}$ M ATU it becomes entirely unsatisfactory. Parallel with this, the plot of 1/O.D. against $t$ becomes more linear, and when the concentration of ATU is $\sim10^{-3}$ M the linearity of the 1/O.D. versus $t$ plot becomes almost satisfactory. This implies that, with the decrease in ATU, the second-order reaction with regard to the dye becomes predominant. Thus, in this case:

$$\frac{1}{[\mathrm{D}]}-\frac{1}{[\mathrm{D}]_0}=kt \qquad (3)$$

or

$$\frac{1}{\mathrm{O.D}}-\frac{1}{(\mathrm{O.D})_0}=\frac{k}{\varepsilon d}t \qquad (3')$$

The above tendency is quite evident and always exists irrespective of the dye concentration, apart from the fact that the larger the dye concentration, the larger the concentration of ATU at which Eq. 2 deteriorates. Figures 2a and 2b show typical examples of the above tendency. The effect of the dye concentration on the rate formula will be discussed later.

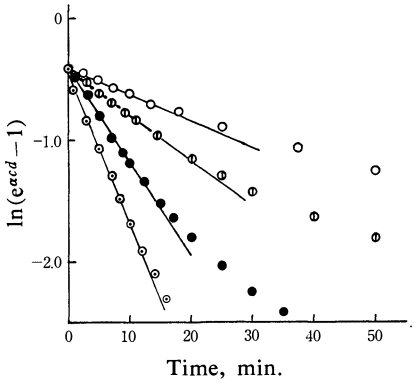



Fig. 2a. Plots of $\ln(e^{\alpha cd}-1)$ against time.
pH=7.2, $[\mathrm{MB}]_0=(8.2\pm0.2)\times10^{-6}$ M
○: [ATU]$=4.0\times10^{-3}$ M ◑: $8.0\times10^{-3}$ M
●: $1.4\times10^{-2}$ M ⊙: $4.0\times10^{-2}$ M

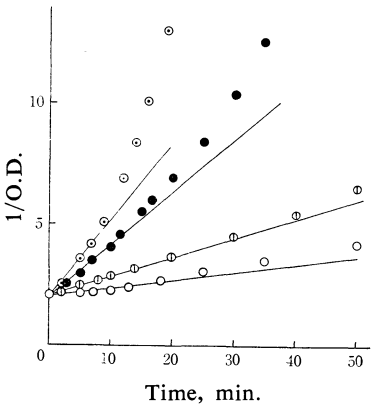
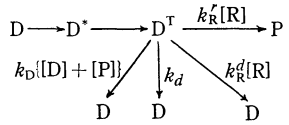



Fig. 2b. Plots of 1/O.D. against time.
pH=7.2, $[\mathrm{MB}]_0=(8.2\pm0.2)\times10^{-6}$ M
○: [ATU]$=4.0\times10^{-3}$ M ◑: $8.0\times10^{-3}$ M
●: $1.4\times10^{-2}$ M ⊙: $4.0\times10^{-2}$ M

An attempt to determine $\varphi_{S-T}$ from the effect of the reductant concentration on $\Phi$ was made as follows. When the concentration of reductant is large enough for Eq. 2 to hold, there is scarcely any doubt that the reaction proceeds as follows:




(P denotes the photoproduct, perhaps leuco dye)

On the basis of this scheme, the following rate formula is derived:

$$-\frac{d[D]}{dt}=\frac{\varphi_{S-T}k_R^r[R]I_{abs}}{k_d+k_R^S[R]+k_D[D]_0}$$

where $\varphi_{S-T}$ is the transition probability for the singlet excited state to the triplet state and $k_R^S$ is the sum of $k_R^r$ and $k_R^d$ (the rate constant for mere deactivation by R). Further, it is assumed that the ground-state dye and the leuco dye deactivate the triplet state at a diffusion-controlled rate.

From the above formula, it follows that:

$$\Phi=\frac{\varphi_{S-T}k_R^r[R]}{k_d+k_R^S[R]+k_D[D]_0} \quad (4)$$

Taking the inverse of Eq. 4, one gets:

$$\frac{1}{\Phi}=\frac{1}{\varphi_{S-T}}\frac{k_R^S}{k_R^r}+\frac{1}{\varphi_{S-T}}\left\{\frac{k_d}{k_R^r}+\frac{k_D[D]_0}{k_R^r}\right\}\frac{1}{[R]} \quad (5)$$

If one assumes that $k_R^S=k_R^r$, then the value of $\varphi_{S-T}$ can immediately be obtained by applying Eq. 5 to the experimental data. This was attempted first for the case of EDTA. Some of the necessary data are given in Table I, while the $1/\Phi$—$1/[R]$ plots are given in Fig. 3.

Table I

a) $[MB]=9.0\times10^{-6}$ M, pH=6.7

| $[EDTA]\times10^3$ M | $\Phi$ | $[EDTA]\times10^3$ M | $\Phi$ |
|---|---|---|---|
| 20 | 0.154 | 3.0 | 0.102, 0.099 |
| 10 | 0.144 | 2.0 | 0.080 |
| 6.0 | 0.127 | 1.6 | 0.067 |
| 5.0 | 0.133 | 1.4 | 0.061 |
| 4.0 | 0.116 | | |

b) $[MB]=9.0\times10^{-6}$ M, pH=7.2

| $[EDTA]\times10^3$ M | $\Phi$ | $[EDTA]\times10^3$ M | $\Phi$ |
|---|---|---|---|
| 20 | 0.170 | 3.0 | 0.103 |
| 10 | 0.165 | 2.0 | 0.080 |
| 5.0 | 0.133 | 1.4 | 0.066 |

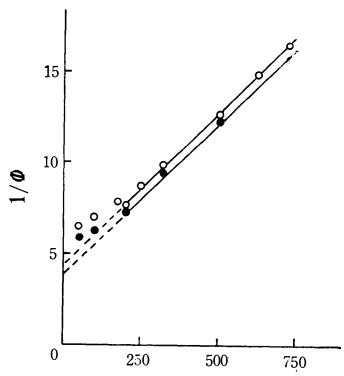



Fig. 3. Plots of $1/\Phi$ against EDTA concentration.
$[MB]_0=9.0\times10^{-6}$ M
○ : pH=6.7, ● : pH=7.2

As may be seen in Fig. 3 the linearity holds satisfactorily except in the region of very high concentrations of EDTA. The values of $\varphi_{S-T}$ obtained are 0.22 and 0.24, for pH=6.7 and 7.2 respectively. These values agree quite well with Oster's value of 0.21[6] at pH=7.0. Although there is some doubt concerning the assumption that $k_R^r=k_R^S$, we would like tentatively to take this value as a real value of $\varphi_{S-T}$. Besides, from the slope of the curves one gets:

$$\frac{k_d}{k_R^r}+\frac{k_D[D]_0}{k_R^r}=3.7\times10^{-3}\text{ M}$$

In the case of ATU, Eq. 2 holds when $[ATU]\gtrsim4\times10^{-3}$ M, at least in the earlier stages of bleaching; hence, as in the above case, an attempt was made to apply Eq. 2 to the results obtained under such experimental conditions. The necessary data are given in Table II, while the $1/\Phi$—$1/[R]$ plot is shown in Fig. 4.

Table II

$[MB]=(8.2\pm0.2)\times10^{-6}$ M, pH=7.2

| $[ATU]\times10^2$ M | $\Phi\times10^3$ | $[ATU]\times10^2$ M | $\Phi\times10^3$ |
|---|---|---|---|
| 0.40 | 0.96 | 2.0 | 2.92 |
| 0.48 | 1.15 | 4.0 | 5.0 |
| 0.80 | 1.60 | 6.0 | 6.9 |
| 1.0 | 2.10 | 8.0 | 7.4 |
| 1.4 | 2.81 | | |

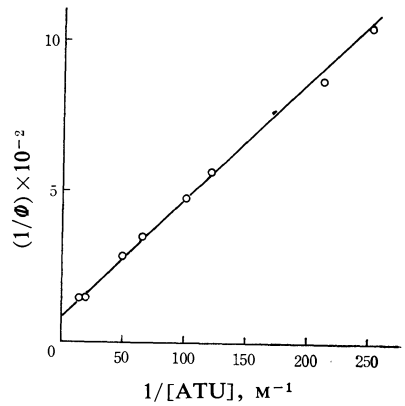



Fig. 4. Plot of $1/\Phi$ against $1/[ATU]$.
pH=7.2, $[MB]_0=(8.2\pm0.2)\times10^{-6}$ M

As can be seen from Fig. 4, the plot is linear, and from its slope and the intercept one gets $(k_d+k_D[D]_0)/\varphi_{S-T}k_R^r=3.9$ M and $k_R^S/k_R^r\varphi_{S-T}=80$. If one assumes that $k_R^S=k_R^r$, then one gets $\varphi_{S-T}=1.3\times10^{-2}$, which is very small compared with that for EDTA. The mere deactivation of the triplet dye by an ATU molecule seems quite plausible.

6) N. Wotherspoon and G. Oster, *J. Am. Chem. Soc.*, 79, 4836 (1957).

**The Effect of the Dye Concentration on $\Phi$.**— This can be dealt with in one of two different ways, depending on the situation. The first method is used in cases in which the D–R mechanism predominates. As may be judged from Eq. 2, the mere deactivation of the triplet dye by the ground state dye causes a decrease in the quantum yield with the increase in the dye concentration. However, when the D–D mechanism begins to take part, a deviation from Eq. 2 is to be expected. The other method is used in cases in which both D–R and D–D mechanisms participate and at the same order of magnitude. In these cases, since the kinetic features of the later steps of D–D mechanism are not clear, it is desirable to discuss the experimental data from a different angle.

Judging from the applicability of Eq. 2, the D–R mechanism is considered to hold for EDTA in general, while for ATU it is dominant only when $[ATU]>1.4\times10^{-2}$ M.

*EDTA.*—The effect of the dye concentration was examined at two fixed concentrations of EDTA. The results are given in Table III, while the $1/\Phi$—$[D]_0$ plot is given in Fig. 5.

TABLE III

| a) $[EDTA]=2.0\times10^{-3}$ M, pH=7.2 | | | |
|---|---|---|---|
| $[MB]\times10^6$ M | $\Phi\times10^2$ | $[MB]\times10^6$ M | $\Phi\times10^2$ |
| 11.4 | 6.55 | 4.8 | 8.71 |
| 9.8 | 7.50 | 4.5 | 8.20 |
| 9.1 | 7.96 | 3.4 | 9.50 |
| 7.8 | 7.75 | 2.6 | 9.70 |
| b) $[EDTA]=4.0\times10^{-4}$ M, pH=7.2 | | | |
| $[MB]\times10^6$ M | $\Phi\times10^2$ | $[MB]\times10^2$ M | $\Phi\times10^2$ |
| 3.2 | 2.23 | 8.6 | 1.75 |
| 5.6 | 2.01 | 9.5 | 1.70 |
| 6.6 | 1.90 | 9.9 | 1.58 |
| 7.2 | 1.85 | 12.7 | 1.41 |

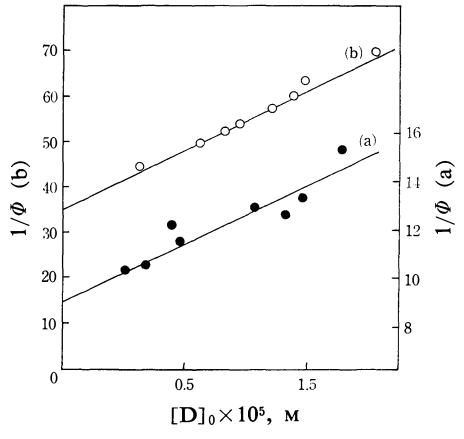



Fig. 5. Plots of $1/\Phi$ against initial dye concentration.
pH=7.2
○ : $[EDTA]=4.0\times10^{-4}$ M
● : $[EDTA]=2.0\times10^{-3}$ M

From Eq. 4, one gets (R is denoted as E) :

$$\frac{1}{\Phi}=\left\{\frac{1}{\varphi_{S-T}}+\frac{1}{\varphi_{S-T}}\frac{k_d}{k_R{}^r}\frac{1}{[E]}\right\}+\frac{1}{\varphi_{S-T}}\frac{k_D}{k_R{}^r[E]}[D]_0 \qquad (6)$$

and from the intercept and the slope of the line b in Fig. 5, one gets:

$$\frac{1}{\varphi_{S-T}}\left(1+\frac{k_d}{k_R{}^r[E]}\right)=9.0$$

$$\frac{1}{\varphi_{S-T}}\frac{k_D}{k_R{}^r[E]}=4.8\times10^5\ M^{-1}$$

With the value of $\varphi_{S-T}$ (0.24) obtained above and by putting $k_d=3.0\times10^4\ sec^{-1}$,[4] one can determine $k_R{}^r$ and $k_D$ separately.

From the results in a),

$$k_R{}^r=1.3\times10^7\ M^{-1}\ sec^{-1}$$

$$k_D=3.0\times10^9\ M^{-1}\ sec^{-1}$$

while from the results in b),

$$k_R{}^r=1.0\times10^7\ M^{-1}\ sec^{-1}$$

$$k_D=2.5\times10^9\ M^{-1}\ sec^{-1}$$

It is worth noting that, when $[D]_0=9.0\times10^{-6}$ M, $k_R{}^r[E]$, $k_D[D]_0$ and $k_d$ are, respectively, $2.6\times10^4$, $2.7\times10^4$ and $3.0\times10^4\ sec^{-1}$ and are of the same order of magnitude. The value of $\frac{1}{\varphi_{S-T}}\left(\frac{k_d}{k_R{}^r}+\frac{k_D}{k_R{}^r}[D]_0\right)$ (see Eq. 5), as calculated by using the above rate constants and by putting $[D]_0=9.0\times10^{-6}$ M, is $1.8\times10^{-2}$ M, which is in good agreement with the experimental value, $1.6\times10^{-2}$ M, obtained from the plot in Fig. 3. At $[EDTA]=1.0\times10^{-4}$ M, a wider range

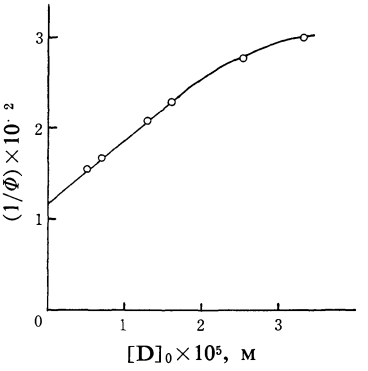



Fig. 6. Polt of $1/\Phi$ against initial dye concentration.
pH=7.2, $[EDTA]=1.0\times10^{-4}$ M

of dye concentrations was chosen, i.e., from $5.6\times10^{-6}$ to $3.3\times10^{-5}$ M. In the case of the higher concentrations of dye, a spacer (7 mm. thick) was used to measure the optical density accurately. Equation 2 holds until one-third of the original dye has been bleached, even when the dye concentration is $\sim2.5\times10^{-5}$ M. A $1/\Phi$—$[D]_0$ plot is shown in Fig. 6. It may be seen that the deviation from a linear plot begins at $2.5\times10^{-5}$ M of dye. By extrapolating the linear part, one gets from the intercept:

$$\frac{k_R^r[E]+k_d}{\varphi_{S-T}k_R^r[E]}=120$$

and from the slope:

$$\frac{k_D}{\varphi_{S-T}k_R^r[E]}=6.4\times10^6\ M^{-1}$$

With $\varphi_{S-T}=0.24$ and $k_d=3.0\times10^4\ sec^{-1}$, one gets:

$$k_R^r=1.1\times10^7\ M^{-1}\ sec^{-1}$$
$$k_D=1.7\times10^9\ M^{-1}\ sec^{-1}$$

From the above results, it may be concluded that as long as the concentration of EDTA is moderate, only the D–R mechanism prevails.

*ATU.*—Different behaviours are expected in the higher and the lower concentration regions of ATU, because the rate formula for a run is Eq. 2 in the former case and Eq. 3 in the latter case. Therefore, rather extensive studies were made by varying the concentration of ATU over a wide range.

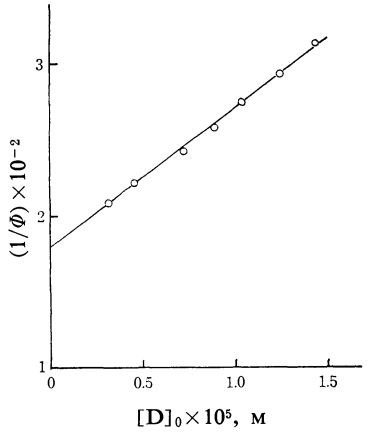



Fig. 7. Plot of $1/\Phi$ against initial dye concentration.
pH=7.2, $[ATU]=4.4\times10^{-2}$ M

Table IV

$[ATU]=4.4\times10^{-2}$ M, pH=7.2

| $[MB]\times10^6$ M | $\Phi\times10^3$ | $[MB]\times10^6$ M | $\Phi\times10^3$ |
|---|---|---|---|
| 14.4 | 3.21 | 7.1 | 4.15 |
| 12.5 | 3.4 | 4.6 | 4.51 |
| 10.3 | 3.65 | 3.2 | 4.8 |
| 8.8 | 3.9 | 2.6 | 5.80 |

When the concentration of ATU is $8.0\times10^{-2}$ or $4.4\times10^{-2}$ M, Eq. 2 fits as a rate formula. A plot of $1/\Phi$ against the original dye concentration is given in Fig. 7. Only the data for $[ATU]=4.4\times10^{-2}$ M are given in Table IV.

From the intercept and the slope of the plot shown in Fig. 8, one obtains:

$$\frac{1}{\varphi_{S-T}}\left\{\frac{k_R^S}{k_R^r}+\frac{k_d}{k_R^r[A]}\right\}=180$$

$$\frac{k_D}{\varphi_{S-T}k_R^r[A]}=9.0\times10^6\ M^{-1}$$

Using the value of $k_R^S/k_R^r\varphi_{S-T}=80$, one gets $k_D/k_R^r=9.5\times10^4$, and, further, by the use of the $k_d$-value;

$$k_R^r=1.1\times10^5\ M^{-1}\ sec^{-1}$$
$$k_D=1.0\times10^{10}\ M^{-1}\ sec^{-1}$$

$k_R^r$ can also be obtained by applying Eq. 5 to the plot in Fig. 4 and by using the value of $k_D/k_R^r$ obtained above. The value thus obtained is $1.8\times10^5\ M^{-1}\ sec^{-1}$, which is in good agreement with the above value. Although the values for $[ATU]=8\times10^{-2}$ M are not so accurate, the value of $k_R^r$ obtained is of the order of $10^5$.

To examine the dye concentration effect more extensively, the concentration of dye was varied over a wider range at a fixed ATU

Table V

$[ATU]=4.0\times10^{-2}$ M, pH=7.2

| $[MB]\times10^5$ M | $\Phi\times10^3$ | $[MB]\times10^5$ M | $\Phi\times10^3$ |
|---|---|---|---|
| 0.32 | 4.70 | 2.36 | 2.82 |
| 0.56 | 4.30 | 2.40 | 2.82 |
| 0.66 | 4.16 | 3.30 | 2.56 |
| 1.03 | 3.65 | 3.46 | 2.54 |
| 1.37 | 3.35 | | |

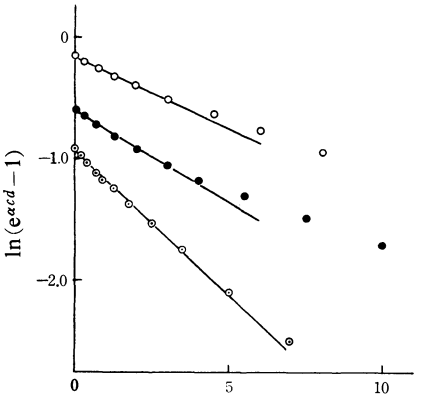



Fig. 8a. Plots of $\ln(e^{acd}-1)$ against time.
pH=7.2, $[ATU]=4.0\times10^{-2}$ M
○: $[MB]_0=3.46\times10^{-5}$ M
●: $2.36\times10^{-5}$ M ⊙: $5.6\times10^{-6}$ M

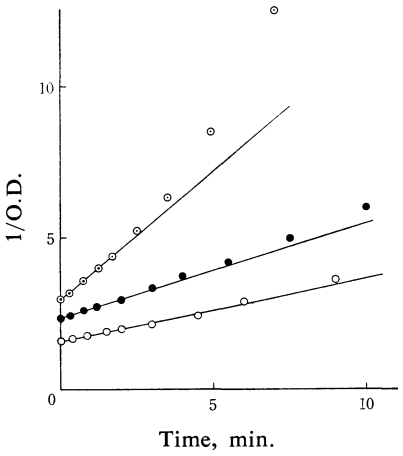



Fig. 8b. Plots of 1/O.D. against time.
pH=7.2, [ATU]=$4.0\times10^{-2}$ M
○ : $[MB]_0=3.46\times10^{-5}$ M
● : $2.36\times10^{-5}$ M ⊙ : $5.6\times10^{-6}$ M

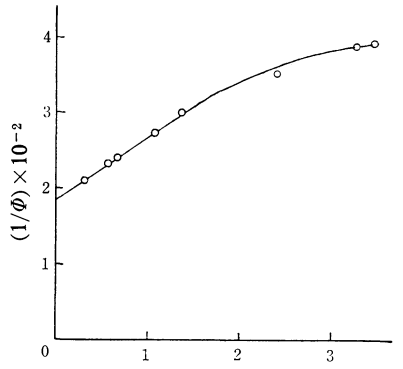



Fig. 9. Plot of $1/\Phi$ against initial dye concentration.
pH=7.2, [ATU]=$4.0\times10^{-2}$ M

concentration ($4.0\times10^{-2}$ M). The results are given in Table V. Figures 8a and 8b show that with the increase in the dye concentration, the applicability of Eq. 2 gets worse, while that of 3 gets better.

Figuare 9, which gives the $1/\Phi$—$[D]_0$ plot, shows that deviation becomes appreciable at $2\times10^{-5}$ M of dye. From the intercept and the slope of the straight part,

$$\frac{1}{\varphi_{S-T}}\left\{\frac{k_R^S}{k_R^r}+\frac{k_d}{k_R^r[A]}\right\}=185$$

$$\frac{k_D}{\varphi_{S-T}k_R^r[A]}=8.5\times10^6\ M^{-1}$$

With the use of $\varphi_{S-T}=0.24$ and $k_R^S/k_R^r=20$, one gets:

$$k_R^r=1.1\times10^5\ M^{-1}\ sec^{-1}$$

and $$k_D=9.0\times10^9\ M^{-1}\ sec^{-1}$$

When the concentration of ATU is low, Eq. 3′ instead of Eq. 2 becomes applicable, as Fig. 10 shows. At the same time, a slight shift in the main absorption peak of the dye becomes apparent. The kinetics were investigated, therefore, by employing Blaisdell's method.

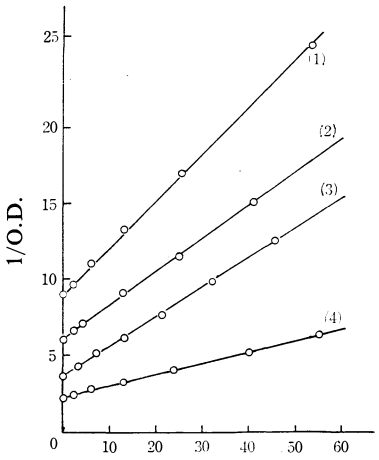



Fig. 10. Plot of 1/O.D. against time.
pH=7.2, [ATU]=$8.0\times10^{-4}$ M,
(1) : $[MB]_0=1.8\times10^{-6}$ M, (2) : $2.9\times10^{-6}$ M
(3) : $4.7\times10^{-6}$ M (4) : $7.9\times10^{-6}$ M

TABLE VI

a) [ATU]=$8.0\times10^{-4}$ M, pH=7.2

| [BM]$\times10^6$ M | $\Phi\times10^4$ | $\Phi_{D-R}\times10^4$ | $\Phi_{D-D}\times10^4$ |
|---|---|---|---|
| 9.6 | 6.03 | 1.50 | 4.53 |
| 7.9 | 6.70 | 1.73 | 4.97 |
| 6.1 | 7.51 | 2.07 | 5.44 |
| 5.2 | 7.63 | 2.33 | 5.30 |
| 4.7 | 8.20 | 2.43 | 5.77 |
| 3.9 | 7.51 | 2.71 | 4.80 |
| 3.5 | 7.13 | 2.87 | 4.26 |
| 2.9 | 6.42 | 3.20 | 3.22 |
| 2.2 | 5.88 | 3.55 | 2.33 |
| 1.9 | 6.10 | 3.77 | 2.33 |

b) [ATU]=$2.0\times10^{-3}$ M, pH=7.2

| [MB]$\times10^6$ M | $\Phi\times10^4$ | $\Phi_{D-R}\times10^4$ | $\Phi_{D-D}\times10^4$ |
|---|---|---|---|
| 21.5 | 3.03 | 1.93 | 1.10 |
| 17.6 | 3.70 | 2.22 | 1.48 |
| 15.3 | 4.47 | 2.57 | 1.90 |
| 13.4 | 4.90 | 2.85 | 2.05 |
| 10.8 | 5.77 | 3.44 | 2.33 |
| 10.5 | 5.96 | 3.48 | 2.48 |
| 9.3 | 6.89 | 3.79 | 3.10 |
| 8.6 | 7.60 | 4.02 | 3.58 |
| 7.1 | 7.67 | 4.32 | 3.35 |
| 6.2 | 7.87 | 5.04 | 2.83 |
| 5.6 | 7.74 | 5.32 | 2.42 |
| 5.2 | 7.90 | 5.65 | 2.25 |
| 2.8 | 9.25 | 7.84 | 1.41 |
| 1.27 | 11.2 | 10.6 | 0.6 |

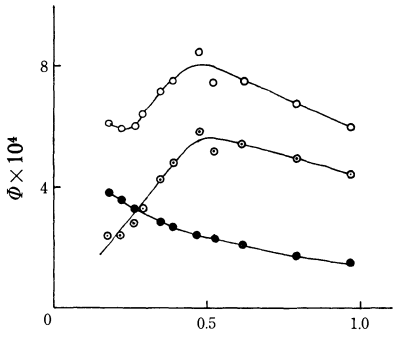



Fig. 11. Plots of $\Phi$, $\Phi_{D-R}$ and $\Phi_{D-D}$ against initial dye concentration.
pH=7.2, [ATU]=$8.0\times10^{-4}$ M
○ : $\Phi$ ● : $\Phi_{D-R}$ ⊙ : $\Phi_{D-D}$

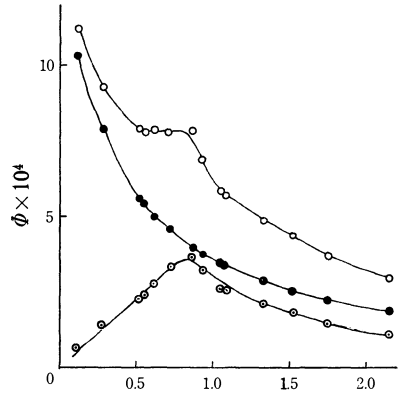
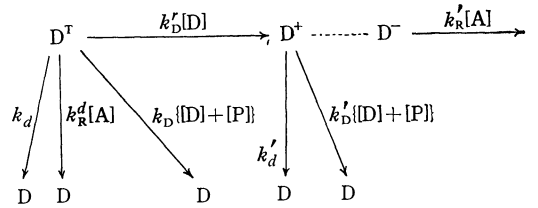



Fig. 12. Plots of $\Phi$, $\Phi_{D-R}$ and $\Phi_{D-D}$ against initial dye concentration.
pH=7.2, [ATU]=$2.0\times10^{-3}$ M
○ : $\Phi$ ● : $\Phi_{D-R}$ ⊙ : $\Phi_{D-D}$

Under such conditions, there is scarcely any doubt that, in addition to a D–R mechanism, a D–D mechanism plays a large part in the reaction. Hence, the total quantum yield should consist of two parts, $\Phi_{D-R}$ and $\Phi_{D-D}$, which are, respectively, the quantum yields due to the D–R and the D–D mechanisms. One can estimate $\Phi_{D-R}$ by inserting the values of the rate constants obtained above and the concentrations of ATU and dye into Eq. 4. $\Phi_{D-D}$, then, is obtained as the difference between $\Phi$ and $\Phi_{D-R}$. The results are shown in Table VI and in Fig. 11 and 12, which show that the curves for $\Phi_{D-D}$ are quite similar in the two series of experiments.

Thus, $\Phi_{D-D}$ increases with the dye concentration until it reaches its maximum at $[D]_0\approx(5—8)\times10^{-6}$ M, where $\Phi_{D-D}=(4—6)\times10^{-4}$, and then decreases again.

The results can be interpreted by assuming the analogous scheme proposed for the photoreduction in the absence of any reducing agent:[4]




From this scheme, one gets:

$$\Phi_{D-D}=\frac{\varphi_{S-T}k_D^r[D]k_R'[A]}{\{k_R^S[A]+k_d+k_D[D]_0\}\{k_R'[A]+k_D'[D]_0+k_d'\}} \quad (7)$$

At very low concentrations of D, $\Phi$ at the initial stage is approximated by:

$$\Phi_{D-D}\frac{\varphi_{S-T}k_D^r[D]_0k_R'[A]}{\{_R^S[A]+k_d\}\{k_R'[A]+k_d'\}}$$

which increases with $[D]_0$, while at high concentrations of D,

$$\Phi_{D-D}\frac{\varphi_{S-T}k_D^rk_R'[A]}{k_Dk_D'[D]_0}$$

which decreases with $[D]_0$.

If the second factor in the denominator in Eq. 7 is missing, then $\Phi_{D-D}$ should increase monotonously with $[D]_0$, without showing any maximum. Thus, in order to interpret the present results, it is necessary to take into account the deactivation of the redox intermediate, $D^+\cdots D^-$, by the ground state dye and (perhaps) by the leuco dye produced.

## Conclusions

It may be concluded from the present results that a switch-over in mechanism really does take place in the photoreduction of methylene blue by EDTA and ATU. This was verified consistently from the rate formula for a run and from the dye concentration effect on the quantum yield. The rate constants of the elementary reactions obtained in the present paper are summarized in the following table:

| | $\varphi_{S-T}$ | $k_R^r/k_R^S$ | $k_R^r M^{-1}sec^{-1}$ | $k_D M^{-1}sec^{-1}$ |
|---|---|---|---|---|
| EDTA | (0.23) | (1) | $1.2\times10^7$ | $2.4\times10^9$ |
| ATU | (0.23) | (0.052) | $1.1\times10^5$ | $9.5\times10^9$ |

These values were obtained by assuming that

$$k_d=3.0\times10^4\ sec^{-1}$$

It is seen from the above table that EDTA is a hundred times more efficient as a reducing agent than is ATU. The reason for the rather large difference in the values of $k_D$ for the two reducing agents is unknown.

As to the switch-over of the mechanism, it does not take place very easily in the case of EDTA; thus, even when the concentration of EDTA is $\sim 1\times10^{-4}$ M, the D–D mechanism only operates to a slight extent when the dye concentration is as high as $2.5\times10^{-5}$ M. On the other hand, in the case of ATU, the D–D mechanism becomes appreciable even with $4\times10^{-2}$ M of reductant and $2.5\times10^{-5}$ M of dye. When the concentration of ATU is $\sim 1\times10^{-3}$ M, the D–D mechanism operates to a large extent.

From these results it may be inferred that the proportion of leuco dye formed by the D–D mechanism is only one hundredth, or less, of that from the entire reaction between $D^T$ and D. This is consistent with a small value of $\Phi_{D-D}$.

Moreover, the rate of the reaction proceeding by the D–D mechanism is greatly reduced at higher concentrations of dye. Hence, it is rather difficult to study the D–D reaction separately. This is consistent with the scheme, proposed in the previous paper, in which the D–D intermediate or $D^+\cdots D^-$ is deactivated by the ground state dye as well as by the leuco dye.[3] Were this not the case, $\Phi_{D-D}$ would have reached a constant limiting value when the dye concentration was increased.

Another notable finding in the present paper is that, at a lower concentration of dye, $\Phi_{D-D}$ increases with the dye concentration. This is naturally to be expected from the scheme, but it was not observed in the photoreduction of toluidine blue and methylene blue in the absence of a reducing agent. This is perhaps due to the fact that the minimum dye concentration then used was $0.7\times10^{-5}$ M, while in the present investigation a concentration as low as $0.2\times10^{-5}$ M was employed.

Although the occurence of a switch-over in the mechanism of the photoreduction of methylene blue has now been proved, it is not so clear-cut as in the case of eosine.[5] This seems rather strange at first sight, because eosine, in contrast to thiazine dyes, does not bleach photochemically in the absence of a reducing agent. However, the reason is that, in the case of eosine, only the reverse reaction of $D^-\cdots D^+$ follows its formation on account of the absence of a simultaneous reaction, such as demethylation, to make the forword reduction feasible. On the other hand, there appear to be at least two reasons why eosine shows this change of mechanism more clearly than thiazine dyes. First, the triplet state of eosine has a longer life than thiazine dyes, so it has a greater chance to be attacked by the ground state dye. Second, its redox intermediate seems to be more easily attacked by ATU and less effectively attacked by the ground state dye than in the case of thiazine dyes.

Summarizing the results obtained so far on xanthene dyes and thiazine dyes, one may state, that as far as the primary processes of the D–D and the D–R mechanisms are concerned, there seems to be no essential difference between xanthene dyes and thiazine dyes.

*Department of Chemistry*
*Faculty of Science*
*Tohoku University*
*Katahiracho, Sendai*

# The Zeeman Effect of Nuclear Quadrupole Resonance Spectrum in $\alpha$-BHC Crystal

By Gen SODA, Masaharu TOYAMA and Yonezo MORINO

(Received April 17, 1965)

Pure quadrupole resonances of the $^{35}Cl$-nuclei for crystals of various isomers of benzene hexachlorides (BHC) have been studied by Duchesne, Monfils and Depireux,[1] and by Morino and others,[2-4] and the assignments of each spectral line to one of the six chlorine atoms have been carried out for $\alpha$- and $\gamma$-isomers, with reference to the crystal structure obtained by van Bommel[5] by the X-ray diffraction method. The apparatus and the method of analysis have been so greatly improved that the Zeeman study enables us to determine the

1) J. Duchesne, A. Monfils and J. Depireux, *Compt. rend.*, **243**, 144 (1956).
2) Y. Morino, I. Miyagawa, T. Chiba and T. Shimozawa, *J. Chem. Phys.*, **25**, 185 (1956).
3) Y. Morino, T. Chiba, T. Shimozawa and M. Toyama, *J. Phys. Soc. Japan*, **13**, 869 (1958).
4) Y. Morino, T. Chiba, T. Shimozawa, M. Toyama and K. Ito, *Rev. Univ. des Mines, 9e Ser. T.*, XV, 591 (1959).
5) A. J. Van Bommel, Private communication (1956).

exact locations of the principal axes of the field-gradient tensors at the chlorine nuclei. For instance, for $\delta$-BHC the direction of each axis was determined with an uncertainty of only 0.1° to 0.5°.[6] It has also been revealed that some of the C-Cl bonds are considerably distorted from the directions to be expected from the tetrahedral bond angles for each carbon atom. The purpose of the present study is to locate the field-gradient tensors in the racemic $\alpha$-BHC crystal by the use of the refined technique that was used for $\delta$-BHC.

The molecule of $\alpha$-BHC has two axial C-Cl bonds and four equatorial C-Cl bonds, one for each carbon atom in the cyclohexane ring. The configuration, which is shown in Fig. 1, is expressed as "*aaeeee*", where *a* and *e* denote the axial and equatorial C-Cl bonds respectively. The crystal is monoclinic, and the four molecules contained in a unit cell are all equivalent, although they are different in orientation. They may be classified into two groups; two molecules in each group are arranged antiparallel to each other, while the molecules in one group are located symmetrically with the molecules in the other group with respect to the crystal ac-plane.

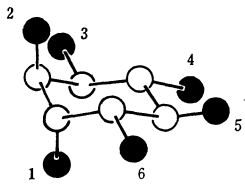



Fig. 1. Model structure of the $\alpha$-BHC molecule. Black and white circles denote the chlorine and carbon atoms respectively. The locations of hydrogen atoms are omitted.

## Experimental and Results

**Apparatus and Material.** — The spectrometer used was the same as that described in a previous paper on $\delta$-BHC.[6] The absorption spectra were detected by using a self-quenched super-regenerative spectrometer similar to that described by Dean, the modulation and the quench frequencies being 230 cycle/sec. and about 50 kc./sec. respectively. The magnetic field for the Zeeman study was supplied by an air-cooled Helmholtz coil. The field strength was continuously variable from zero to 162 gauss. All the Zeeman studies were carried out at room temperature.

The $\alpha$-BHC was recrystallized from a benzene solution. A single crystal with dimensions of $0.6\times2.0\times4.0$ cm$^3$ was prepared from the saturated solution by carefully evaporating the solvent. The crystal thus obtained was a good single crystal, as was supported by the fact that the spectra of this crystal did not show, even under a strong magnetic field, any unexpected disturbance, such as line-splitting and broadening, due to the coexistence of crystals with a different orientation.

**Principle of the Measurement.**—The principle used for the measurement was exactly the same as that used for $\delta$-BHC in the preceeding paper. The direction of the principal z-axis of the field-gradient tensor was determined by the method of "no-splitting locus" proposed by Das and Hahn.[7] The no-splitting locus is expressed by the formula of the first order with respect to $\eta$:

$$(\boldsymbol{H}\cdot\boldsymbol{Z})=\frac{1}{\sqrt{3}}\left\{1+\frac{\eta}{3}[1-3(\boldsymbol{X}\cdot\boldsymbol{H})^2]\right\} \qquad (1)$$

where $\boldsymbol{H}$ represents a unit vector in the direction of the generating line of the locus, and $\boldsymbol{Z}$ and $\boldsymbol{X}$, those in directions parallel to the principal z- and x-axes of the field-gradient $q$-tensor respectively. Equation 1 shows that, in the case of $\eta=0$, the no-splitting locus is a circular cone whose axis is parallel to $\boldsymbol{Z}$, and that the first-order term in $\eta$ represents a distortion from the circular cone. It would, therefore, be possible to determine not only the direction of $\boldsymbol{Z}$ from the axis of the observed cone, but also the asymmetry parameter, $\eta$, and the direction of $\boldsymbol{X}$ from its distortion. This method was, however, not applicable to the latter purpose in the present case, because our apparatus, because of its construction, does not give the whole locus; furthermore, the distortion of the locus from the circular cone is small for $\alpha$-BHC. Thus, $\eta$ and $\boldsymbol{X}$ were obtained by the measurement of the splitting and the intensity ratio of the outer and inner components of the Zeeman pattern when the magnetic field was applied nearly parallel to the direction of the intersection between the crystal ac-plane and the principal xy-plane of the field-gradient $q$-tensor.[6] At this setting of the magnetic field, the relative intensity, $P_r$, of the outer and the inner components of the Zeeman pattern is expressed by these formulae;

$$P_r=P(-)/\{P(+)+P(-)\}$$
$$=\frac{1}{2}\{1-(\eta/\Delta\nu)\cos 2\varphi_r\} \qquad (2)$$

and

$$\Delta\nu=(\eta^2+9\cos^2\theta_s)^{1/2} \qquad (3)$$

where $P(-)$ and $P(+)$ indicate the intensities

6) Y. Morino, M. Toyama and K. Itoh, *Acta Cryst.*, **16**, 129 (1963); M. Toyama, *J. Phys. Soc. Japan*, **14**, 1727 (1959).

7) T. P. Das and E. L. Hahn, Nuclear Quadrupole Resonance Spectroscopy," Academic Press, New York (1958).

of the outer and the inner components respectively, and $(\theta_r, \varphi_r)$ and $(\theta_s, \varphi_s)$ indicate, respectively, the directions of the r. f.-field and of the static magnetic field with reference to the principal coordinate system. $\Delta\nu$ designates a half of the difference between the frequency separations of the two pairs in units of $\nu_H = \gamma H/2\pi$, where $\gamma$ is the gyromagnetic ratio and $H$, the strength of the applied magnetic field.

**No-splitting Loci and the Principal z-Axes of Field-gradient Tensors.**—An approximate location of the no-splitting locus was first determined by observing the Zeeman pattern of each spectral line at various orientations of a relatively weak magnetic field (50—70 gauss). Next, a magnetic field of a suitable strength, from 100 to 160 gauss, was applied in directions near the locus thus roughly determined; the directions giving a no-splitting Zeeman component were determined within an uncertainty of about 0.2°. A no-splitting locus was drawn by tracing the directions thus obtained at intervals of 3—5°.

Table I. Pure quadrupole resonance frequencies of $^{35}Cl$ nuclei of α-BHC and their temperature dependence (Mc./sec.)

| | 291°K | 197°K | 77°K | 197—291°K | 77—197°K |
|---|---|---|---|---|---|
| A | 36.817 | 37.015 | 37.219 | 0.198 | 0.204 |
| B | 36.487 | 36.680 | 36.879 | 0.193 | 0.199 |
| C | 36.230 | 36.456 | 36.705 | 0.226 | 0.249 |
| D | 36.230 | 36.408 | 36.589 | 0.178 | 0.181 |
| E | 35.693 | 35.878 | 36.081 | 0.185 | 0.203 |
| F | 35.608 | 35.813 | 36.038 | 0.205 | 0.225 |

The six absorption lines are designated, for convenience, A, B, C, D, E and F, in the order of decreasing frequency, as is shown in Table I. The no-splitting loci of the spectral lines A, B, E and F were first determined with a single crystal mounted in such a way that the crystal b-axis was nearly parallel to the $Z_l$-axis of the laboratory coordinate system. The loci of the spectral lines C and D were not determined, because the frequency difference between the two lines was so small that the Zeeman pattern was complicated at this mounting. This run is called Experiment 1. Next, the crystal was remounted at such a position that the b-axis was located nearly parallel to the $X_l$-axis. At this mounting the no-splitting loci of the spectral lines from A through F were all determined. This run is called Experiment 2.

Figures 2a and 2b illustrate the no-splitting loci in a stereographic projection; they are projected on a horizontal plane, namely, on the $X_lY_l$-plane which passes through the center of the crystal as its origin. The symbols $\Theta$ and $\Phi$ denote the polar coordinates with reference to the laboratory coordinate system. The figures show that two no-splitting loci were found for each spectral line. This means that each line corresponds to two distinct field-gradient tensors which are equal in magnitude but different in direction; in other words, one

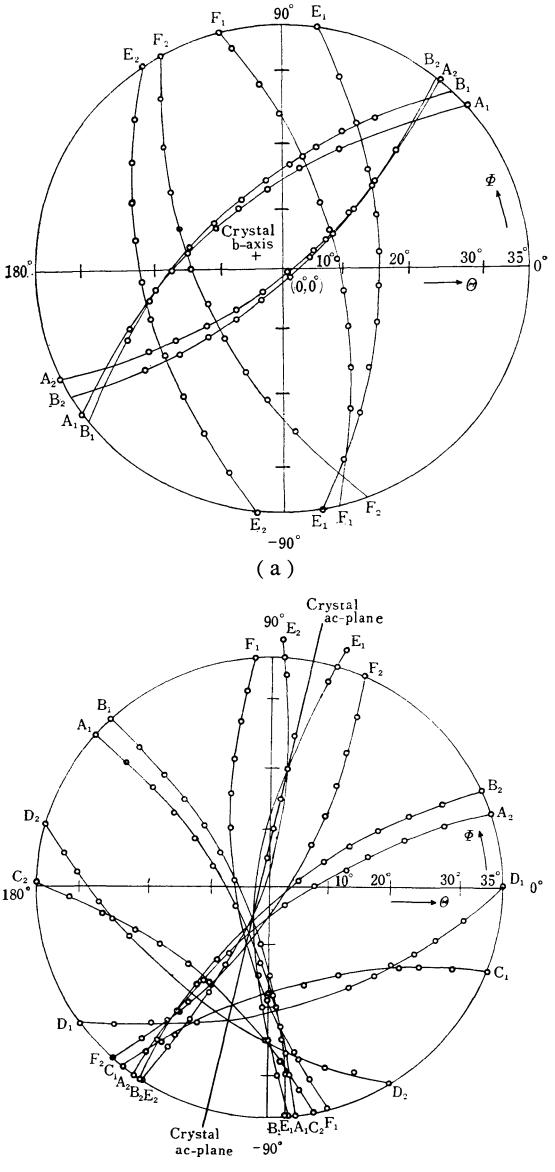



Fig. 2. Stereographic projection of the no-splitting loci.
(a) Experiment 1. Crystal b-axis oriented nearly parallel to the $Z_l$-axis of laboratory coordinate system.
(b) Experiment 2. Two pairs of no-splitting loci of each spectral line located symmetrically with respect to the crystal ac-plane.

TABLE II. DIRECTION COSINES OF THE PRINCIPAL Z-AXES OF THE FIELD-GRADIENT TENSORS FOR THE MOLECULES 1 AND 2, WITH REFERENCE TO THE CRYSTAL-FIXED COORDINATE SYSTEM

| | $X_c$ | $Y_c$ | $Z_c$ |
|---|---|---|---|
| $A_1$ | 0.3293±0.0023 | −0.6735±0.0020 | 0.6818±0.0015 |
| $A_2$ | 0.3283±0.0018 | −0.6730±0.0020 | −0.6628±0.0011 |
| $B_1$ | 0.3634±0.0030 | −0.6379±0.0021 | 0.6790±0.0025 |
| $B_2$ | 0.3607±0.0030 | −0.6369±0.0017 | −0.6815±0.0025 |
| $C_1$ | 0.0544±0.0137 | −0.8879±0.0062 | −0.4568±0.0119 |
| $C_2$ | 0.0516±0.0155 | −0.8940±0.0069 | 0.4452±0.0133 |
| $D_1$ | 0.9370±0.0014 | 0.2340±0.0040 | 0.2594±0.0024 |
| $D_2$ | 0.9381±0.0032 | 0.2304±0.0075 | −0.2588±0.0055 |
| $E_1$ | −0.5832±0.0014 | 0.0669±0.0022 | 0.8097±0.0009 |
| $E_2$ | −0.5819±0.0018 | 0.0660±0.0041 | −0.8106±0.0012 |
| $F_1$ | 0.6859±0.0020 | 0.0803±0.0050 | −0.7233±0.0017 |
| $F_2$ | 0.6850±0.0018 | 0.0761±0.0044 | 0.7250±0.0017 |

spectral line corresponds to two distinct C-Cl bonds which are different in direction. As will be seen later, the principal z-axes of the two field-gradients determined by two no-splitting loci were found to be symmetrical with respect to an axis which is common to all the six lines. This axis is the crystal b-axis. These results agree with those obtained by X-ray diffraction;[5] four equivalent C-Cl bonds in a unit cell are classified into two groups, as has been described in the introduction. All principal z-axes of the field-gradient tensors determined above were, therefore, uniquely classified into two groups according to the criterion that the mutual angles between the two directions of the principal z-axes which belong to the same group were nearly 180° or close to the tetrahedral angle. These two groups are distinguished by the suffixes 1 and 2; for example, $A_1$ and $A_2$ denote the field-gradient tensors belonging to group 1 and group 2 respectively.

There are two symmetry planes with respect to which two principal z-axes of the $q$-tensors of each spectral line are equivalent. One is the crystal ac-plane, and the other is a plane which is perpendicular to it. The latter symmetry planes intersect, on the crystal b-axis, with those for other field-gradient tensors. Accordingly, a bisecting line of the angle between the z-axes of $A_1$ and $A_2$ should be either on the ac-plane or parallel to the b-axis. This gives a method for determining the b-axis; that is, a direction common to either one of the bisecting lines for all of the six spectral lines, A to F, is parallel to the b-axis. As the observed directions of these bisecting lines deviated from A to F within a possible range of experimental error, an average of them was taken and designated as the $Z_c$-axis, the suffix c denoting a crystal-fixed coordinate system.

The $X_cY_c$-plane was easily given by a plane perpendicular to the $Z_c$-axis thus determined. The $X_c$- and $Y_c$-axes were defined, for the sake of convenience, by taking the direction of a bisecting line between the projections of the z-axes of the E and F tensors on the $X_cY_c$-plane. As the $X_cY_c$-plane does not exactly coincide with the ac-plane of the crystal because of experimental uncertainties, the projections of the two z-axes belonging either to the E or to the F tensors on the $X_cY_c$-plane are slightly different from each other. Thus, the $Y_c$-axis was determined by taking an average of them. The $X_c$-axis was determined as perpendicular to both the $Y_c$- and $Z_c$-axes.

Table II shows the final values of the directions of the principal axes referred to the crystal-fixed coordinate system. The details of the elimination of one of the two choices of $\varphi_r$ will be described later.

**Asymmetry Parameters and the Principal x- and y-Axes of Field-gradient Tensors.**—When a static magnetic field is applied in a direction which is in either of the two symmetry planes mentioned above, then the Zeeman pattern is reduced to a simple four-line pattern. For example, Fig. 3 shows a Zeeman pattern of a spectral line, F, for such a setting of the magnetic field. The spectra were recorded from the right to the left, with the magnetic field applied 12′ and 44′, respectively, from the intersection of the crystal ac-plane and the principal xy-plane of the $q$-tensor. The asymmetry parameter of $\alpha$-BHC is so small that the outer and the inner components of the Zeeman pattern overlap appreciably, as is shown in Fig. 3, and the apparent peak-to-peak separation recorded in the first derivative form is smaller than the correct value. Therefore, the values of $P(+)/P(-)$ and $\Delta\nu$ were determined from the observed Zeeman pattern in the following way.

If the shape of a single spectral line is

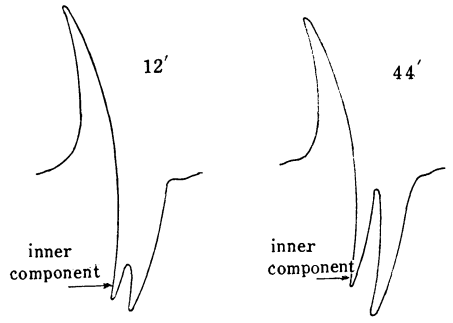



Fig. 3. Typical patterns of the Zeeman splittings of the spectral line F when the static magnetic field is applied near the principal xy-plane in the crystal ac-plane. Zeeman components on the higher frequency side were recorded in the first derivative form. The frequency increase from the left to the right.

assumed to be expressed by a Gaussian distribution function, then the first derivative curve of a doublet is given by the following equation:

$$g(x)=\frac{\{P(+)(x+\Delta\nu)e^{-a(x+\Delta\nu)^2}+P(-)xe^{-ax^2}\}}{(P(+)+P(-))} \quad (4)$$

where $\Delta\nu$ denotes the frequency separation. The two lines are assumed to have the same width, $(2/a)^{1/2}$. The three parameters, $a$, $\Delta\nu$ and $P(+)/P(-)$, involved in this formula were obtained by comparing the calculated curve with the observed one, with reference to the peak-to-peak separation and the widths at half-height positions of the two peaks. The asymmetry parameters of the six field-gradient tensors thus determined are given in Table III.

Table III. Asymmetry parameters of field-gradient tensors

| Absorption line | Asymmetry parameter $\eta$ |
|---|---|
| A | 0.0166±0.0014 |
| B | 0.0231±0.0031 |
| C | 0.0286±0.0031 |
| D | 0.036 ±0.010 |
| E | 0.0220±0.0025 |
| F | 0.0311±0.0031 |

The angle, $\theta_r$, of the r. f.-field with respect to the principal axes was determined, with an uncertainty of 10°, on the assumption that the r. f.-field was parallel to the axis of the r. f.-coil. The values of $\varphi_r$ are obtained from the intensity ratio, $P_r$, by the use of Eq. 2. However, the sign of $\varphi_r$ was not determined uniquely, because $\varphi_r$ is involved in Eq. 2 in the form of $\cos 2\varphi_r$. One of the alternatives was discarded by the following procedure. The approximate directions of the principal z-axes obtained above were refined for the first-order term given in Eq. 1, the magnitude of which depended on the choice of the direction of the principal x-axes. By using one of the values of the principal x-axes, the corrected directions of the principal z-axes for the two experiments, 1 and 2, coincided within the range of experimental error, whereas, for the other choice, they did not coincide beyond the range of experimental error. The former direction was, therefore, taken as the correct one. The measurements at different mountings were thus efficient in excluding the alternative choice of $\varphi_r$.

This method, however, could not be used for the spectral lines, C and D, not measured in Experiment 1. Nevertheless, in the case of D the direction of the principal x-axis was determined, because $|\varphi_r|$ was accidentally close to 90°. In the case of C, the directions of the principal axes were examined by the same method as was employed in a previous report:[6] first, two directions of the principal z-axes of the $q$-tensors were calculated, corresponding to the choices of the two principal x-axes, which are designated by $C_I$ and $C_{II}$, and then two directions of the intersection between the principal xy-plane and the crystal ac-plane were determined. The directions of the intersections for the other spectra were similarly calculated; the mutual angles between these

Table IV. Observed and calculated angles between the intersections of the principal xy-planes of field-gradient tensors with the crystal ac-plane

| | Observed | Calculated | Difference |
|---|---|---|---|
| ∠AB | 3°32′ | 3°32′ | 0′ |
| $\angle AC_I$ | 22°22′ | 22°32′ | 10′ |
| $\angle AC_{II}$ | 22°22′ | 22°51′ | 29′ |
| $\angle BC_I$ | 25°54′ | 26°05′ | 11′ |
| $\angle BC_{II}$ | 25°54′ | 26°25′ | 31′ |

Table V. Direction cosines of the principal x- and y-axes of the field-gradient tensors with reference to the crystal-fixed coordinate system (molecule 1)

| | | $X_c$ | $Y_c$ | $Z_c$ |
|---|---|---|---|---|
| A | x | 0.25 | −0.61 | −0.75 |
| | y | 0.91 | 0.41 | −0.03 |
| B | x | 0.90 | 0.44 | −0.07 |
| | y | 0.25 | −0.64 | −0.73 |
| C | x | 0.62 | −0.32 | 0.72 |
| | y | −0.78 | −0.32 | 0.54 |
| D | x | 0.17 | 0.34 | −0.92 |
| | y | 0.30 | −0.91 | −0.28 |
| E | x | 0.28 | −0.92 | 0.28 |
| | y | 0.76 | 0.39 | 0.52 |
| F | x | 0.68 | 0.26 | 0.68 |
| | y | 0.24 | −0.96 | 0.13 |

directions of the intersections are listed in Table IV, along with the values obtained in the course of the determination of $\eta$. If the choice is correct, the mutual angles among these calculated intersections should agree with those among the observed intersections. As Table IV shows, this requirement was actually satisfied for both assignments; of these, however, $C_I$ seems to be preferable because in it the deviation was found to be smaller. The final values of the directions of the principal z-axes and those of the principal x- and y-axes are tabulated in Tables II and V respectively.

## Discussion

**Assignment.**—Six absorption lines are assigned to six chlorine atoms by comparing the directions of the principal z-axes of the field-gradient tensors determined by the present study with those of the C-Cl bonds obtained by X-ray diffraction. Table VI shows the

TABLE VI. COMPARISON OF THE RESULTS OF THE ZEEMAN STUDY WITH THOSE OF X-RAY DIFFRACTION

| | Mutual angles between the two principal z-axes of the field-gradient tensors | Mutual angles between the C-Cl bonds by the X-ray diffraction by van Bommel | |
|---|---|---|---|
| A | 82°57′ | $C_3$-$Cl_3$ | 82°36′ |
| B | 85°43′ | $C_6$-$Cl_6$ | 86°22′ |
| C | 53°37′ | $C_4$-$Cl_4$ | 49°56′ |
| D | 30°02′ | $C_5$-$Cl_5$ | 30°36′ |
| E | 108°13′ | $C_2$-$Cl_2$ | 106°48′ |
| F | 92°48′ | $C_1$-$Cl_1$ | 92°48′ |

angles between the two principal z-axes of the field-gradient tensors belonging to each spectral line obtained by the Zeeman study and the angles between the C-Cl bonds which are symmetric with respect to the ac-plane. It may easily be seen that a mutual agreement is attained between the corresponding angles, if the absorption lines from A through F are assigned to the bonds shown on the same line in the table. The assignment of A and B has not yet been established because of the experimental error, ±4°, which accompanies the X-ray diffraction. The reliability factor proposed in the previous paper,

$$\langle \Delta\theta^2 \rangle^{1/2} = \left\{ \frac{1}{6} \sum_{i=1}^{6} (\Delta\theta_i)^2 \right\}^{1/2} \qquad (5)$$

decreases when the assignments A and B are interchanged, as is shown in Table VII. Here $\Delta\theta_i$ denotes the angle between the direction of the $i$-th C-Cl bond and that of the principal z-axis of the corresponding field-gradient tensor. For calculating $\Delta\theta_i$, it is necessary to describe the directions of the C-Cl bonds and those of the principal z-axes of

TABLE VII. PROBABLE ASSIGNMENT OF THE ABSORPTION LINES TO THE C-Cl BONDS OF α-BHC AND THE RELIABILITY FACTOR

| Spectral line | A | B | C | D | E | F | $\langle \Delta\theta^2 \rangle^{1/2}$ |
|---|---|---|---|---|---|---|---|
| Assignment 1 | 3 | 6 | 4 | 5 | 2 | 1 | 2°58′ |
| Assignment 2 | 6 | 3 | 4 | 5 | 2 | 1 | 2°44′ |

the $q$-tensors on the same coordinate system. The direction of the $Z_c$-axis as determined by X-ray diffraction coincides well with that obtained by the Zeeman study, because, as a result of the symmetry, the crystal b-axis was determined accurately in comparison with the other axes. On the other hand, the $Y_c$-axis which is obtained from the directions of the principal z-axes of the spectra E and F does not always coincide with the $Y_c$-axis as determined from the directions of the corresponding C-Cl bonds, 2 and 1, by X-ray diffraction. Because of the experimental errors, the directions of the two $Y_c$-axes thus determined might have a small deviation between them. The description of the results on a common coordinate system may be obtained by rotating either of the two coordinate systems about the $Z_c$-axis so as to minimize $\langle \Delta\theta^2 \rangle^{1/2}$. This minimum value of $\langle \Delta\theta^2 \rangle^{1/2}$ was calculated for each probable assignment as in Table VII. Here again the difference in $\langle \Delta\theta^2 \rangle^{1/2}$ between the two assignments is so small compared with the error, ±4°, that it would be premature to eliminate one of the two assignments.

The assignment obtained here agrees with the tentative one reported previously, and it is consistent with the temperature dependence of the resonance frequencies listed in Table I. According to Bayer's theory,[8] the absorption lines coming from the parallel C-Cl bonds should have the same temperature gradient. Two pairs of lines, A and B, and E and F, have nearly the same temperature gradients, but the curves of the C and D spectral lines cross each other slightly below room temperature. This indicates that the lines, A and B or E and F, may be assigned to the pair of C-Cl bonds which are parallel to each other, whereas C and D may be assigned to a pair of C-Cl bonds which are not parallel, in accord with the results obtained above.

**Molecular Structure.**—The α-BHC molecule in the gaseous state has a two-fold symmetry axis which passes through the middle point of the $C_1$-$C_2$ bond and that of the $C_4$-$C_5$ bond, as is shown in Fig. 1, and each of the pairs of chlorine atoms, ($Cl_1$-$Cl_2$), ($Cl_3$-$Cl_6$), or ($Cl_4$-$Cl_5$), is disposed symmetrically with respect to this axis. The molecules in the crystal are appreciably distorted from the configuration in

8) H. Bayer, *Z. Physik*, **130**, 227 (1951).

the gaseous state. Still, the molecules retain a pseudo-two-fold symmetry, as is easily shown by the fact that the principal z-axes of the $q$-tensors belonging to each of the above chlorine pairs are symmetrically oriented about the axis; the deviations were found to be within 45′ for the pairs, A and B, or E and F, and 3°, for the pair of C and D. The location of the x-axes is also another test for this symmetry; it shows a tendency to satisfy the symmetry, though fairly large errors were unavoidable in determining the x-axes.

Table VIII. Mutual angles between the principal z-axes of the field-gradient tensors in the α-BHC molecule

| | B (6) | C (4) | D (5) | E (2) | F (1) |
|---|---|---|---|---|---|
| A (3) | 2°59′ | 70°51′ | 71°12′ | 72°32′ | 72°08′ |
| B (6) | — | 73°43′ | 68°31′ | 72°40′ | 73°53′ |
| C (4) | — | — | 74°06′ | 62°51′ | 72°59′ |
| D (5) | — | — | — | 71°18′ | 61°51′ |
| E (2) | — | — | — | — | 11°18′ |

Table VIII shows the mutual angles of the directions of the principal z-axes of the $q$-tensors within a molecule, as calculated from the results listed in Table II. It exhibits considerable distortions of bond angles from 180° or from the tetrahedral angle. For instances, neither the opposite equatorial bonds, 3 and 6, nor the opposite axial bonds, 1 and 2, are parallel to each other; the deviations amount to 2°59′, or even to 11°18′. For the bond pairs, 2 and 4, and 1 and 5, which consist of an axial bond and an equatorial bond, the deviations from the tetrahedral angle (70°32′) amount to 7°41′ and 8°41′ respectively. A closer examination indicates that the distorting force tends to make the skeleton of the molecule planar, keeping the symmetry of the molecule at a maximum. Therefore, it is likely that the distortions are mainly due to intramolecular forces which act in accordance with the molecular symmetry, and only partly due to intermolecular forces which are not connected with the symmetry of the molecule.

The asymmetry parameters shown in Table III are of the same order of magnitude as those observed in the δ-BHC crystal.[6] This is another case in which the asymmetry parameters of the chlorine nuclei substituted to a saturated hydrocarbon have been measured. Two effects have been pointed out concerning the origin of the asymmetry of the field-gradient. One is the intramolecular effect, such as the deviation of the hybridization of carbon atoms from $sp^3$, which would be anticipated from the distortion of bond angles. The other is the effect of the crystal field; the electric charge on the neighboring atoms distorts the charge cloud around the chlorine nucleus, thus producing asymmetry in the field-gradient. For δ-BHC, the asymmetry parameters were of the same order of magnitude as that produced by the crystal field. For α-BHC it is likely that, in addition to the crystal field, the intramolecular effect also makes a considerable contribution to the asymmetry parameters, because the principal x-axes tend to satisfy the symmetry of the free molecule. In the δ-BHC crystal, the orientation of the x-axes were not examined except for line B, because the assignment was accompanied by a large uncertainty originating from the errors of the X-ray study, and because two choices between x-axes remained undetermined for the D, E and F spectra. The α-BHC reported here is a fortunate case where the directions of the x-axes have been determined by the pursuit of the measurement at two different mountings of the crystal.

## Summary

The Zeeman effect of the nuclear quadrupole resonance has been studied on the $^{35}Cl$-nuclei in the racemic α-BHC single crystal at room temperature. The directions of the principal x-, y- and z-axes of the field-gradient tensor at each nucleus have been determined through two runs of measurements of the no-splitting loci of each absorption line. The asymmetry parameters of the field-gradient tensor have also been determined. The C–Cl bonds have been found to be considerably distorted from the directions to be expected from the tetrahedral bond angles for each carbon atom. The distortion takes place in such a way that the skeleton of each molecule approachs a planar configuration. Since the principal axes show a tendency to satisfy the two-fold symmetry, the distorting force has been attributed mainly to the intramolecular forces, and only partly to the intermolecular forces. The previous assignment of the six absorption lines to the six chlorine atoms in the molecule has thus been confirmed.

The authors wish to express their deep thanks to Dr. Hideo Sueta, of the Research Laboratory of the Mitsubishi Chemical Industries, Ltd., for kindly supplying the pure sample of α-BHC. The expenses of the work were defrayed by the Ministry of Education of Japan, to which their thanks are also due.

*Department of Chemistry*
*Faculty of Science*
*The University of Tokyo*
*Hongo, Tokyo*

# Studies of the Liquid-Liquid Partition Systems. III. The Solvent Extraction of Americium(III) and Europium(III) Thiocyanate Complexes with Tributylphosphate

By Tatsuya SEKINE

(Received April 19, 1965)

Two different liquid-liquid partition methods have been applied to the determination of the stability constants of various metal complexes in aqueous solutions.

By the first method, the metal ion is extracted with an organophilic chelating acid in the organic phase. The complex formation is determined from the decrease in the chelate extraction caused by the complex formation in the aqueous phase.

By the second method, the metal ion is extracted, as an adduct of the neutral complex, with an organophilic neutral ligand in the organic phase. The complex formation is determined from the change in the metal extraction caused by the change in the relative concentration of the neutral complex in the aqueous phase.

The principles of these two methods are quite different, and the stability constants of metal complexes in an aqueous solution may be determined quite independently by the two methods.

The chelate extraction method has been applied to various complex formation systems; the stability constants thus determined have been found to agree with the constants determined by various other methods. On the other hand, the adduct extraction method has not often been applied except in some recent studies of the mononuclear hydrolysis of metal ions,[1] and no attempt seems to have been made to compare the results given by this method with the results given by the other methods.

The present work studied the thiocyanate complexes of trivalent americium and europium by the adduct extraction method.

As was reviewed in the previous paper,[2] a remarkable difference in ion-exchange behavior has been observed between the trivalent actinide and lanthanide ions in thiocyanate media; this has been explained in terms of the stronger complexing of actinides than of lanthanides with thiocyanate ions. The stability constants of these complexes in 5 M Na(SCN, $ClO_4$) were determined by the chelate extraction method at 25°C.[2] The results showed that americium(III) forms more stable thiocyanate complexes than does europium(III).

The extraction of the neutral metal thiocyanate complexes as an adduct of various extractants has been reported by many authors.[3] Yoshida[4] reported that europium(III) was extracted with tributylphosphate (TBP) from ammonium thiocyanate solutions and that the distribution ratio was quite different when the inert diluent of TBP was different; he concluded that the metal complex in the organic phase was a tetrasolvate of TBP.

In the present work, the distribution of americium(III) and europium(III) between hexane solutions of TBP and aqueous solutions of sodium thiocyanate will be studied. The stability constants of the complexes will be calculated from the distribution data and compared with the results given in Ref. 2. Some discussion will also be made of the salting-out of the metal ions by the electrolytes in the aqueous phase.

## Statistical Treatment

The formation of the metal thiocyanate complexes and the over-all stability constants can be described as follows:

$$M^{3+} + nSCN^- \rightleftarrows M(SCN)_n^{3-n} \quad (1)$$

$$\beta_n = [M(SCN)_n^{3-n}]/[M^{3+}][SCN^-]^n \quad (2)$$

In the present paper, the net distribution ratio of the metal ions between the organic and aqueous phases is always defined as:

$$D = [M(III)]_{org,total}/[M(III)]_{total} \quad (3)$$

The subscript " org " denotes a chemical species in the organic phase, while the absence of a

1) D. Dyrssen and T. Sekine, *J. Inorg. Nucl. Chem.*, **26** 981 (1964); D. Dyrssen and P. Lumme, *Acta Chem. Scand.*, **16**, 1785 (1962); T. Sekine, *Acta Chem. Scand.*, to be published.

2) T. Sekine, *J. Inorg. Nucl. Chem.*, **26**, 1463 (1964). The full paper will be published in *Acta Chem. Scand.*

3) The previous work is reviewed in G. H. Morrison and H. Freiser, " Solvent Extraction in Analytical Chemistry," John Wiley & Sons Inc., New York (1957); L. G. Sillén, and A. E. Martell, " Stability Constants," spec. pub. No. 17, The Chemical Society, London (1964). and revised edition to be published.

4) H. Yoshida, *J. Inorg. Nucl. Chem.*, **24**, 1257 (1962).

subscript denotes a chemical species in the aqueous phase.

**The Metal Chelate Extraction Method.**—The details of this method were given in Ref. 2; only the final equation will be given in the present paper:

$$D_0/D=K_0/K=1+\sum_1^n \beta_n[SCN^-]^n \quad (4)$$

In Eq. 4, the subscript "0" denotes the net distribution ratio of the metal or the metal chelate extraction constant when no complexes are formed in the aqueous phase. The metal chelate extraction and the extraction constant are described as:

$$M^{3+} + 3HA_{(org)} \rightleftarrows MA_{3(org)} + 3H^+$$

$$K_0=D_0[H^+]^3[HA]^{-3}{}_{org} \quad (5)$$

where HA denotes an organophilic chelating acid.

Equation 4 shows that the stability constants of the thiocyanate complexes, $MSCN^{2+}$, $M(SCN)_2{}^+$,$\cdots$ can be determined from the decrease in the metal chelate extraction and in the concentration of the ligand.

**The Adduct Extraction Method.**—In an aqueous solution where the metal complexes are formed with thiocyanate ions, the metal concentration can be written as:

$$[M(III)]_{total} = [M^{3+}] + [MSCN^{2+}] + [M(SCN)_2{}^+] + [M(SCN)_3] + [M(SCN)_4{}^-] + \cdots \quad (6)$$

When the neutral complex, $M(SCN)_3$, is extracted with an organophilic neutral ligand, N, the equilibrium constant is described as:

$$M(SCN)_3 + nN_{(org)} \rightleftarrows M(SCN)_3N_{n(org)} \quad (7)$$

$$K_n = [M(SCN)_3N_n]_{org}/[M(SCN)_3][N]^n{}_{org} \quad (8)$$

The total metal concentration in the organic phase is written as:

$$[M(III)]_{org,total}=[M(SCN)_3N]_{org} + [M(SCN)_3N_2]_{org} + \cdots \quad (9)$$

$$= \sum_1^n K_n[M(SCN)_3][N]^n{}_{org} \quad (10)$$

When the concentration of the extracting ligand, N, in the organic phase is constant, Eq. 10 can be written as:

$$[M(III)]_{org,total} = K_{DM}[M(SCN)_3] \quad (11)$$

From Eqs. 6 and 10, the net distribution ratio of M(III) in Eq. 3 can be written as:

$$D=K_{DM}[M(SCN)_3]/([M^{3+}] + [MSCN^{2+}] + [M(SCN)_2{}^+] + [M(SCN)_3] + [M(SCN)_4{}^-] + \cdots) \quad (12)$$

From Eqs. 2 and 12, the distribution of M(III) can be written as:

$$D = K_{DM}\beta_3[SCN^-]^3/(1 + \beta_1[SCN^-] + \beta_2[SCN^-]^2 + \beta_3[SCN^-]^3 + \beta_4[SCN^-]^4 + \cdots) \quad (13)$$

or it can also be written as:

$$D=K_{DM}/(\beta_3{}^{-1}[SCN^-]^{-3} + \beta_1\beta_3{}^{-1}[SCN^-]^{-2} + \beta_2\beta_3{}^{-1}[SCN^-]^{-1} + 1 + \beta_4\beta_3{}^{-1}[SCN^-] + \cdots) \quad (14)$$

Thus we can determine the stability constants, $\beta_n$, from the net distribution ratio, $D$, and the concentration of thiocyanate ions if the concentration of the extracting ligand in the organic phase is kept constant.

## Experimental

**Reagents.** — The europium 152+154 tracer was obtained from the Oak Ridge National Laboratory as a hydrochloric acid solution. The americium 241 tracer was obtained from the Radiochemical Center, Amersham, also as a hydrochloric acid solution. They were then diluted with 5 M sodium perchlorate or 5 M sodium thiocyanate and used as the stock solutions. All of the reagents used were of analytical grade. Sodium perchlorate was prepared from sodium carbonate and perchloric acid and recrystallized two times. Tributylphosphate (TBP) was washed with 0.1 M perchloric acid, water and 0.1 M sodium hydroxide, and then with water until the washed solution gave a neutral color on an indicator paper. Stock solutions of sodium perchlorate and sodium thiocyanate were also prepared. The concentration of the sodium perchlorate stock solution was determined from the difference in the weight of a portion of the stock solution before and after it had been dried in an air-bath at 120°C. The concentration of the thiocyanate stock solution was determined by argentimetry.

**Procedures.**—All of the procedures were carried out in a thermostatted room at 25±0.5°C. The tracer solution, various amounts of the sodium thiocyanate solution, the sodium perchlorate solution and the TBP hexane solution were placed in stoppered glass tubes. The aqueous phase was buffered at pH 4 to 5 with a small amount of acetate. The initial volume of both the organic and aqueous phases was 5.0 ml. The initial concentration of the tracer in the aqueous phase was less than $10^{-6}$ M.

The two phases in the tubes were agitated with a mechanical rotator at 20 r.p.m. for about two hours and centrifuged at 1500 r.p.m. for about three minutes. Two milliliters of the solution was then pipetted from both phases and transferred into small tubes. The $\gamma$-radioactivity of the solutions was determined with a well-type (NaI) scintillation counter, and the net distribution ratio of M(III) was determined to be:

$$D=\frac{\gamma\text{-count-rate per 2 ml. of the organic phase}}{\gamma\text{-count-rate per 2 ml. of the aqueous phase}} \quad (15)$$

## Results

In the present study, the hydrogen ion concentration of the aqueous solution was buffered at pH 4 to 5. This was enough to prevent the association of $SCN^-$ with $H^+$ and the hydrolysis of the metal ion. In the preliminary experiments, is was confirmed that the change in the pH value within this range did not change the metal distribution. The expression "5% TBP in hexane" will always mean a 5% TBP hexane solution as expressed by the volume percentage. The temperature was always 25±0.5°C. The description "5 M Na(SCN, $ClO_4$)" denotes that the concentration of sodium ions is always 5 M; the sum of the thiocyanate and perchlorate concentrations is also kept at 5 M.

**The Extraction of Americium(III) and Europium(III) from Sodium Thiocyanate Solutions.**—Figure 1 gives the plot of log $D$ vs. log [$SCN^-$] when the organic phase was 5% TBP in hexane and when the aqueous phase was sodium thiocyanate solutions (the total electrolyte concentration was not kept constant). We may see in the figure that the distribution of the metal ions increases drastically with the increase in the thiocyanate concentration. The slope d log $D$/d log [$SCN^-$] also increases with the increase in the thiocyanate concentration.

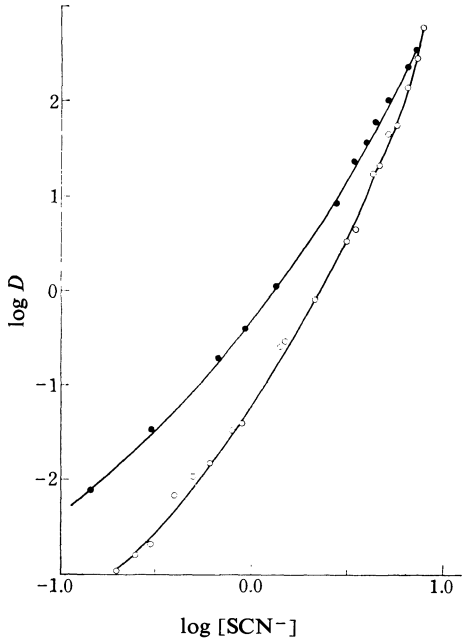



Fig. 1. Distribution of americium(III) (●) and europium(III) (○) between 5% TBP (by volume) in hexane and sodium thiocyanate solutions at pH 4 to 5 (total electrolyte concentration is not constant).

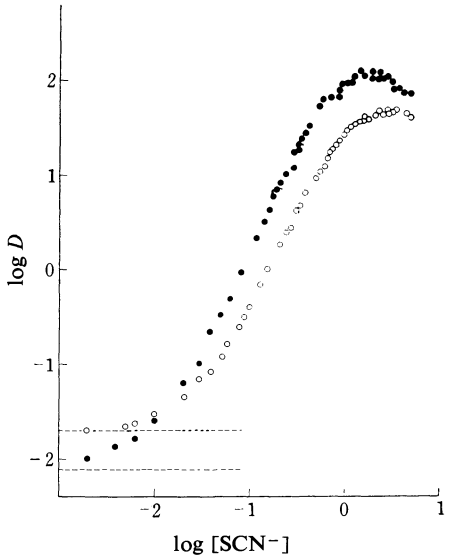



Fig. 2. Distribution of americium(III) (●) and europium(III) (○) between 5% TBP (by volume) in hexane and 5 M Na(SCN, $ClO_4$) at pH 4 to 5. The dotted lines give the distribution ratio of Am(III) (log $D=-2.10$) and Eu(III) (log $D=-1.70$) when the aqueous phase is 5 M $NaClO_4$ at pH 4 to 5.

The separation factor of americium(III) and europium(III), $D_{Am}/D_{Eu}$, is largest in the lowest thiocyanate concentration region; it decreases to unity in the highest region.

**The Extraction of Americium(III) and Europium(III) from 5 M Na(SCN, $ClO_4$).**—Figure 2 gives the plot of log $D$ vs. log [$SCN^-$] of americium(III) and europium(III) when the organic phase was 5% TBP in hexane and when the aqueous phase was 5 M Na(SCN, $ClO_4$). In the figure, we see that the distribution ratio of the metal ions is constant in the lowest thiocyanate concentration region. The distribution ratio increases with the increase in the thiocyanate concentration until it reaches a maximum, and then it decreases slightly in the highest concentration region.

From Eqs. 12 to 14 we may see that the slope d log $D$/d log [$SCN^-$] changes from +3 to $3-n$ with the change in the thiocyanate concentration corresponding to the dominant metal complex species, $M^{3+}$, $MSCN^{2+}$,…, $M(SCN)_n^{3-n}$ in the aqueous phase. It seems that the constancy of the distribution ratio in the lowest thiocyante concentration region can be explained by the extraction of the ion-pair of the metal ion with the perchlorate ion, $M^{3+}(ClO_4^-)_3\cdot(TBP)_n$. It may be also possible that mixed complexes are extracted from the aqueous solutions at a lower thiocyanate concentration and that the distribution ratio of the metal ions may generally be described as:

$$D=\sum_{0}^{3}[M(SCN)_a(ClO_4)_{3-a}]_{org}/\sum_{0}^{n}[M(SCN)_n^{3-n}] \quad (16)$$

The separation factor, $D_{Am}/D_{Eu}$, changes from 0.4 to 10 between a 0.1 M and a 1.0 M thiocyanate solution and decreases in the highest thiocyanate concentration region.

Table I. Two phase distribution of americium(III) and europium(III)

Organic phase; 5% (by volume) TBP in hexane
Aqueous phase; 5 M Na(SCN, $ClO_4$) at pH 4 to 5
Temperature 25±0.5°C

| log [SCN⁻] | log $D_{Am}$ | log [SCN⁻] | log $D_{Eu}$ |
|---|---|---|---|
| 0.681 | 1.86 | 0.681 | 1.64 |
| 0.644 | 1.87 | 0.644 | 1.65 |
| 0.623 | 1.86 | 0.501 | 1.68 |
| 0.602 | 1.87 | 0.477 | 1.68 |
| 0.556 | 1.91 | 0.477 | 1.71 |
| 0.532 | 1.91 | 0.415 | 1.66 |
| 0.505 | 1.94 | 0.398 | 1.65 |
| 0.501 | 1.90 | 0.362 | 1.64 |
| 0.477 | 2.01 | 0.342 | 1.65 |
| 0.477 | 2.01 | 0.322 | 1.63 |
| 0.477 | 2.01 | 0.301 | 1.64 |
| 0.415 | 2.00 | 0.279 | 1.62 |
| 0.398 | 2.08 | 0.255 | 1.65 |
| 0.362 | 2.07 | 0.230 | 1.58 |
| 0.342 | 2.03 | 0.230 | 1.60 |
| 0.301 | 2.02 | 0.176 | 1.56 |
| 0.279 | 2.07 | 0.146 | 1.56 |
| 0.230 | 2.03 | 0.146 | 1.58 |
| 0.176 | 2.08 | 0.114 | 1.53 |
| 0.176 | 2.06 | 0.114 | 1.56 |
| 0.114 | 2.03 | 0.079 | 1.51 |
| 0.079 | 1.99 | 0.079 | 1.51 |
| 0.000 | 1.96 | 0.041 | 1.53 |
| −0.036 | 1.90 | 0.000 | 1.43 |
| −0.046 | 1.87 | 0.000 | 1.48 |
| −0.076 | 1.83 | −0.046 | 1.37 |
| −0.131 | 1.84 | −0.097 | 1.33 |
| −0.155 | 1.81 | −0.119 | 1.30 |
| −0.208 | 1.80 | −0.143 | 1.26 |
| −0.268 | 1.73 | −0.167 | 1.23 |
| −0.366 | 1.54 | −0.194 | 1.20 |
| −0.409 | 1.47 | −0.222 | 1.14 |
| −0.444 | 1.38 | −0.222 | 1.13 |
| −0.468 | 1.33 | −0.252 | 1.07 |
| −0.495 | 1.26 | −0.301 | 0.99 |
| −0.523 | 1.25 | −0.398 | 0.82 |
| −0.585 | 1.09 | −0.468 | 0.70 |
| −0.620 | 1.08 | −0.509 | 0.64 |
| −0.658 | 0.90 | −0.553 | 0.49 |
| −0.699 | 0.86 | −0.602 | 0.42 |
| −0.745 | 0.79 | −0.658 | 0.30 |
| −0.796 | 0.66 | −0.796 | 0.01 |
| −0.854 | 0.52 | −0.886 | −0.14 |
| −0.921 | 0.36 | −1.000 | −0.38 |

**The Calculation of the Stability Constants.**— From the results in the Fig. 2, we can calculate the stability constants of the metal thiocyanate complexes in 5 M Na(SCN, $ClO_4$).

For the calculation of the stability constants, the data should be taken from the thiocyanate concentration region, where the extraction of the mixed complexes is practically negligible. In Fig. 2, we see that the slope d log $D$/d log [SCN⁻] is about +2 above log [SCN⁻]= −1.3, and so it may be possible to say that the $MSCN^+$ complex is dominant in this region and that only the $M(SCN)_3$ species is extracted into the organic phase. The results in Ref. 2 also seem to support this estimate.

From this, the data used for the calculation were taken from the thiocyanate concentration region above 0.1 M. The data are given in Table I.

In the present study, Eq. 14 was used for the calculation because it is not possible to calculate the $\beta_1$ without the distribution data in the region where both of the $M^{3+}$ and the $MSCN^{2+}$ species exist in the aqueous phase (and where the slope in Fig. 2 should be from

Table II. Equilibrium constants of americium(III) and europium(III) thiocyanate complexes in 5 M Na(SCN, $ClO_4$) at 25°C

$\beta_n=[M(SCN)_n^{3-n}]/[M^{3+}][SCN^-]^n$
$\beta_1\beta_3^{-1}=[MSCN^{2+}][SCN^-]/[M(SCN)_3]$
$\beta_2\beta_3^{-1}=[M(SCN)_2^+][SCN^-]/[M(SCN)_3]$
$\beta_4\beta_3^{-1}=[M(SCN)_4^-]/[M(SCN)_3][SCN^-]$
$K_{DM}=[M(SCN)_3]_{org}/[M(SCN)_3]$
(organic phase: 5% (by volume) TBP in hexane)

(A) Equilibrium constants obtained by the adduct extraction method (present work).

| | Am(III) | Eu(III) |
|---|---|---|
| $\beta_1\beta_3^{-1}$ | 1.68±0.84 | 2.48±0.24 |
| $\beta_2\beta_3^{-1}$ | no evidence | ∼0.9(<0.75) |
| $\beta_4\beta_3^{-1}$ | 0.74±0.51 | 0.34±0.07 |
| $K_{DM}$ | 321±146 | 113±10 |

(B) Equilibrium constants obtained by the chelate extaction method in Ref. 2.

| | Am(III) | Eu(III) |
|---|---|---|
| $\beta_1$ | 7.02±0.28 | 2.08±0.14 |
| $\beta_2$ | no evidence | ∼0.9(<1.5) |
| $\beta_3$ | 3.57±0.41 | 0.44±0.15 |
| $\beta_4$ | 1.00±0.12 | no evidence |
| $\beta_1\beta_3^{-1}$ | 2.0 | 4.7 |
| $\beta_2\beta_3^{-1}$ | no evidence | erroneous |
| $\beta_4\beta_3^{-1}$ | 0.28 | no evidence |

(the limit of error is $3\sigma$)

+3 to +2). The equilibrium constants thus calculated show the following:

$$\beta_1\beta_3^{-1}=[MSCN^{2+}][SCN^-]^2/[M(SCN)_3]$$

$$\beta_2\beta_3^{-1}=[M(SCN)_2^+][SCN^-]/[M(SCN)_3]$$

$$\beta_4\beta_3^{-1}=[M(SCN)_4^{-1}]/[M(SCN)_3][SCN^-]$$

The constants were first estimated graphically, and then the estimates were refined by a generallized least-squares method using the computer program "LETAGROP VRID."[5] The details of the calculation were the same as those given in previous work.[1,2] The equilibrium constants thus determined are given in Table II, together with the constants calculated from the results in Ref. 2. In the table, the limit of the error is $3\sigma$. The expression for the $\beta_2\beta_3^{-1}$ of europium(III), $\sim$0.3 ($<$0.75), means that the calculated value is 0.3 but it may range in the region $0 \leq \beta_2\beta_3^{-1} < 0.75$ if $3\sigma$ is employed as the limit of the error.

**The Change in the Distribution Ratio upon the Addition of Perchlorate.**—Figure 3 gives the plot of the distribution of europium(III), log $D$ vs. log [$SCN^-$], when the organic phase was 5% TBP in hexane and when the aqueous phase was (i) sodium thiocyanate, (ii) 3 M Na(SCN, $ClO_4$) and (iii) 5 M Na(SCN, $ClO_4$).

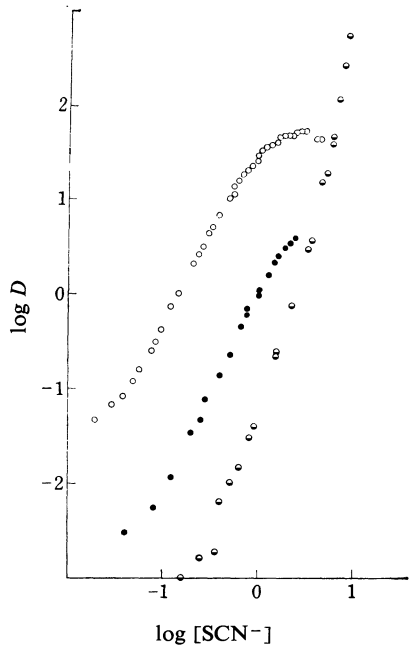



Fig. 3. Distribution of europium(III) between 5% TBP hexane (by volume) and (i) sodium thiocyanate (◒), (ii) 3 M Na(SCN, $ClO_4$) (●), (iii) 5 M Na(SCN, $ClO_4$) (○). pH of the aqueous phase is 4 to 5.

5) N. Ingri and L. G. Sillén, *Acta Chem. Scand.*, **16**, 173 (1962); *Arkiv Kemi*, **23**, 97 (1964).

In the figure we can see that the slope d log $D$/d log [$SCN^-$] increases drastically with the increase in the thiocyanate concentration when the aqueous phase contains only sodium thiocyanate, but that the slope changes only gradually when the total electrolyte concentration is kept constant at 3 M Na(SCN, $ClO_4$) or 5 M Na(SCN, $ClO_4$).' This indicates that the metal distribution is very much increased

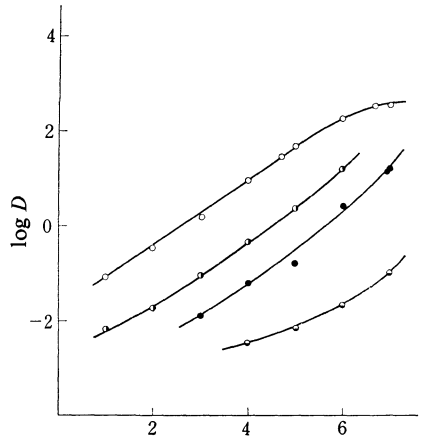



Fig. 4. Increase of the distribribution ratio of europium(III) by addition of sodium perchlorate. Organic phase: TBP 5% (by volume) in hexane. Aqueous phase: at pH 4 to 5
○ [$SCN^-$]=1.0 M, ◑ [$SCN^-$]=0.28 M,
● [$SCN^-$]=0.10 M, ◒ [$SCN^-$]=0 M.
The abscissa gives the total electrolyte concentration in the aqueous phase (the sum of the concentrations of sodium perchlorate and sodium thiocyanate).

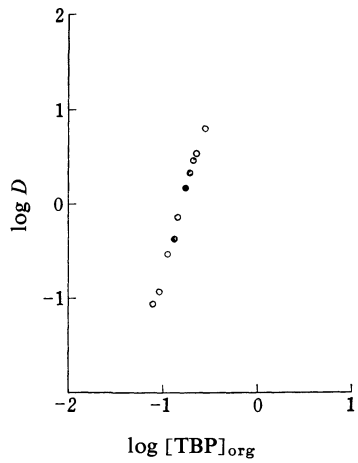



Fig. 5. Dependency of the distribution ratio of europium(III) on the concentration of tributylphosphate.
Organic phase: TBP in hexane.
Aqueous phase: 1 M NaSCN+2 M $NaClO_4$ at pH 4 to 5.

by the addition of sodium perchlorate, even when the concentration of thiocyanate ions is kept constant.

Figure 4 gives the change in the log $D$ when various amounts of sodium perchlorate are added to the solutions while the concentration of thiocyanate ion is kept constant.

In the figure we can see that the addition of perchlorate increases the distribution greatly.

Europium(III) is extracted with TBP, even from a sodium perchlorate solution, and the distribution ratio is also greatly increased by the increase in the perchlorate concentration.

**The TBP Dependency of the Metal Distribution.**—Figure 5 gives the plot of log $D$ vs. log$[TBP]_{org}$ when the aqueous phase contains 1 M sodium thiocyanate and 2 M sodium perchlorate. In this figure we can see that the TBP dependency of the metal distribution is between 3 and 4 in the TBP concentration range.

## Discussion

**The Stability Constants of the Metal Thiocyanate Complexes.**—The results in Fig. 2 and the equilibrium constants in Table II may be summarized as follows.

The constants determined by the chelate extraction method in Ref. 2 indicate that:

(i) The americium(III) thiocyanate complexes are always more stable than the europium(III) thiocyanate complexes.

(ii) No evidence of the complex $Am(SCN)_2^+$ can be observed. The stability constants for the $Eu(SCN)_2^+$ is erroneous, and it is not possible to recognize this species definitely.

(iii) The stability constants for the $Am(SCN)_4^-$ species can be determined, but no evidence of the $Eu(SCN)_4^-$ complex is observed when the thiocyanate concentration is below 5 M.

On the other hand, the results obtained by the present TBP adduct extraction method indicate that:

(i) In the lower thiocyanate concentration region, both americium(III) and europium(III) are extracted with perchlorate ions, and it is not possible to determine the constant for the equilibrium, $M^{3+} + SCN^- \rightleftarrows MSCN^{2+}$.

(ii) It is also not possible to determine the stability constants of the other complexes in Eq. 2. The equilibrium constants obtained are only for the formation of the $M(SCN)_3$ complex from the $MSCN^{2+}$, $M(SCN)_2^+$ and $M(SCN)_4^-$ complexes.

(iii) No evidence of the complex $Am(SCN)_2^+$ can be observed. The equilibrium constant, $\beta_2\beta_3^{-1} = [Eu(SCN)_2^+][SCN^-]/[Eu(SCN)_3]$, is very erroneous, and it is not possible to confirm this complex definitely.

(iv) The formation of the $Eu(SCN)_4^-$ complex, which was not observed in the chelate extraction method, is here observed in the heighest thiocyanate concentration region. The stability constant for the $Am(SCN)_4^-$ complex is higher than that obtained by the chlate extraction method.

(v) The distribution constant of the $Am(SCN)_3$ species between the aqueous and the organic phases, $K_{DM}$ in Eq. 11, is higher than that of the $Eu(SCN)_3$ species.

Thus, from Table II, we may conclude that the equilibrium constants as determined by these two methods nearly agree with each other except for the constant for the formation of the $Eu(SCN)_4^-$ complex.

In the highest thiocyanate concentration region, the anion in the aqueous phase is almost entirely changed from $ClO_4^-$ to $SCN^-$; this may cause some change in the activity of the chemical species in the aqueous phase, even when the total electrolyte concentration is kept constant.

However further information on these systems seems to be necessary in order for us to be able to explain the difference in the constants obtained by these two methods.

**The Effect of the Electrolyte Concentration on the Metal Distribution.**—The increase in the distribution of the metal ions by the addition of various amounts of perchlolate is very remarkable. The increase can be caused by: (i) the extraction of the mixed complexes with thiocyanate and perchlorate ions; (ii) the increase in the stability of the $M(SCN)_3$ species in the aqueous phase, or (iii) the increase in the distribution constant of the $M(SCN)_3$ complex, $K_{DM}$ in Eq. 11.

The extraction of the mixed complexs may not always be important, because the stability constants in Table II, obtained by calculations which neglect the mixed complexs, seem to be reasonable.

The increase in the stability of the $M(SCN)_3$ may also not be very important, because we see in Fig. 3 that the plot of log $D$ vs. log $[SCN^-]$ of the metal extraction from 3 M Na(SCN, $ClO_4$) is nearly parallel to that of the extraction from 5 M Na(SCN, $ClO_4$). If the difference in the distribution ratio is caused by the increase in the relative concentration of the $M(SCN)_3$, the shape of the extraction curve should be different (cf. Eqs. 12 to 14). However, it is not possible to discuss this problem in more detail before we know the equilibrium constants in 3 M Na(SCN, $ClO_4$).

The final explanation, that the addition of sodium perchlorate increases the $K_{DM}$ in Eq. 11, seems to be most reasonable. The increase in

the $K_{DM}$ can be caused both by the increase in the thermodynamical activity of the $M(SCN)_3$ species and by the decrease in the activity of water in the aqueous phase. The decrease in the activity of water may be favorable for the dissociation of the hydrated water of the $M(SCN)_3$ moleculces when they pass through the intersurface between the two phases. However, further information seems to be necessary before we can discuss this problem further.

In Fig. 1 we see that the distribution ratios always increase with the increase in the thiocyanate concentration. When the total electrolyte concentration is kept constant with sodium perchlorate, a slight decrease is observed in the highest thiocyanate concentration region for both americium and europium; this can be explained in terms of the formation of the negative charged species, $M(SCN)_4^-$. The continuous increase in the distribution ratios in Fig. 1, even above 5 M sodium thiocyanate, may be explained in terms of the salting-out effect of the sodium thiocyanate. The formation of the negative charged species by the increase in the thiocyanate concentration should decrease the relative concentration of the $M(SCN)_3$ species in the aqueous phase, and this in turn should decrease the metal distribution. However, as we see in Figs. 3 and 4, the salting-out in these systems is very large, and even though the relative concentration of the $M(SCN)_3$ is decreased by the increase in the thiocyanate concentration (which is not favorable for the metal distribution), the increase in the distribution constant of the $M(SCN)_3$, $K_{DM}$, by the salting-out exceeds the decrease by the former.

Thus, we may conclude that the addition of sodium thiocyanate in the experiment in Fig. 1 causes both the complex formation and the salting-out effect.

**The Solvation Number of TBP in the Adduct Complexes.**—The TBP dependency of the distribution ratio of europium(III) was estimated to be between 3 and 4. This means that if the activity coefficient of TBP in the organic phase can be assumed to be constant, the adduct complexes in the organic phase are a mixture of $Eu(SCN)_3(TBP)_3$ and $Eu(SCN)_3(TBP)_4$. This is a little different from the conclusion of Yoshida.[4] The difference in the composition of the aqueous phase can cause this difference.

## Summary

The two-phase distribution of americium(III) and europium(III) has been studied between the hexane solution of tributylphosphate (TBP) and the aqueous solution of sodium thiocyanate at 25°C. From the distribution data when the organic phase was 5% (by volume) TBP in hexane and the aqueous phase was 5 M Na(SCN, $ClO_4$), the following equilibrium constants have been obtained by a least-squares method:

| | Am(III) | Eu(III) |
|---|---|---|
| $\beta_1\beta_3^{-1}$ | 1.68±0.84 | 2.53±0.24 |
| $\beta_2\beta_3^{-1}$ | no evidence | ~0.3 (<0.75) |
| $\beta_4\beta_3^{-1}$ | 0.74±0.51 | 0.34±0.07 |
| $K_{DK}$ | 321±146 | 113±10 |

(The limit of error is $3\sigma$)

A remarkable salting-out effect has been observed when sodium perchlorate is added to the aqueous phase. This salting-out effect has been discussed, as has the solvation number of TBP in the adduct complexes in the organic phase.

Some part of this work was carried out at the Department of Inorganic Chemistry, the Royal Institute of Technology, Stockholm. The author is very grateful to Professors Lars-Gunnar Sillén and David Dyrssen. Another of this work was carried out at the Laboratory of Nuclear Chemistry, Institute of Physical and Chemical Research, Tokyo. The author is very grateful to Profesor Nobufusa Saito, the head of that laboratory. Some experimental work was carried out by Miss Yuko Hasegawa and Messrs. Mitsuo Sakairi and Takeshi Hamada in the present laboratory. The author is very grateful to them also.

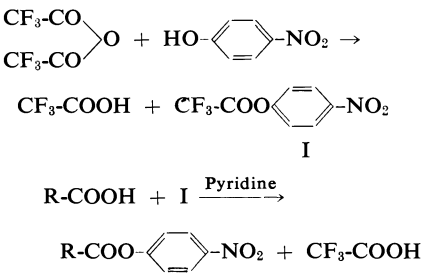
*Department of Chemistry*
*Tokyo College of Science*
*Kagurazaka, Shinjuku-ku, Tokyo*

# The Trifluoroacetate Method of Peptide Synthesis. I. The Synthesis and Use of Trifluoroacetate Reagents

By Shumpei SAKAKIBARA and Noriyoshi INUKAI*

(Received April 24, 1965)

In a preceding paper,[1] a new method for the preparation of the *p*-nitrophenylesters of ordinary carboxylic acids, using *p*-nitrophenyl trifluoroacetate (I) as a reagent, has been reported. Reagent I reacts smoothly with carboxylic acids in pyridine to give the *p*-nitrophenylesters by an ester-exchange reaction. In the present investigation, various active esters of trifluoroacetic acid were synthesized



as possible reagent, and the above-mentioned method was extended to the synthesis of the respective esters of acylated amino acids. In addition, a new procedure for the synthesis of peptides using these new reagents was developed.

First, various compounds, such as phenol, thiophenol and *N*-hydroxyimide derivatives, which are known to be hydroxylic partners of various active carboxylic acid esters, were converted to their respective trifluoroacetates by the procedure used for synthesizing reagent I. The physical constants of and analytical data on the trifluoroacetate reagents obtained are listed in Table I. Since these reagents were rather unstable against water, they had to be kept in sealed tubes or in tightly-closed bottles. Attempts to synthesize the trifluoroacetates of 2, 4-dinitrophenol, 2, 4, 6-trinitrophenol and 2, 4-dinitrothiophenol were unsuccessful under the present experimental conditions. Moreover, the trifluoroacetates of common alcohols, such as ethanol and benzyl alcohol, were found to be inactive as ester-exchange reagents in pyridine.

The reagents cited in Table I were each subjected to reaction with acylated amino acids in pyridine for the ester-exchange reactions;

TABLE I. PHYSICAL CONSTANTS AND ANALYTICAL VALUES OF THE TRIFLUOROACETATE REAGENTS

| Compound No. | Name | [m. p.] or (b. p.)[a] °C | Anal. % Found C | Found H | Found N | Calcd. C | Calcd. H | Calcd. N |
|---|---|---|---|---|---|---|---|---|
| I | *p*-Nitrophenyl trifluoroacetate[b] | [36—38] | 41.11 | 1.89 | 5.99 | 40.86 | 1.71 | 5.96 |
| II | Phenyl trifluoroacetate | (123) | 50.60 | 2.61 | | 50.54 | 2.65 | |
| III | *p*-Chlrophenyl trifluoroacetate | (50/5 mmHg) | 43.30 | 1.89 | | 42.78 | 1.80 | |
| IV | *p*-Bromophenyl trifluoroacetate | (135—142) | 35.71 | 1.56 | | 35.71 | 1.50 | |
| V | 2, 4, 5-Trichlorophenyl trifluoroacetate | Oil[c] | 34.41 | 0.97 | | 32.74 | 0.69 | |
| VI | Pentachlorophenyl trifluoroacetate | [64—66] | 26.49 | 0.00 | | 26.51 | 0.00 | |
| VII | *p*-Methoxyphenyl trifluoroacetate | (150—160) | 49.07 | 3.25 | | 49.10 | 3.21 | |
| VIII | Thiophenyl trifluoroacetate | (140—150) | 46.43 | 2.45 | | 46.60 | 2.44 | |
| IX | *p*-Nitrothiophenyl trifluoroacetate | Oil[c] | 38.76 | 1.85 | | 40.51 | 1.70 | |
| X | *N*-Hydroxysuccinimide trifluoroacetate | Oil[c] | 30.59 | 1.64 | | 34.14 | 1.91 | |
| XI | *N*-Hydroxyphthalimide trifluoroacetate | Oil[c] | 42.71 | 1.90 | | 46.34 | 1.56 | |

a) The boiling point indicates the boiling range, when the material was distilled in a simple distilling flask.
b) S. Sakakibara and N. Inukai, This Bulletin, **37**, 1231 (1964).
c) Purification was unsuccessful and correct analytical values were not obtained because of the instability of this material. Thus, this material should be prepared just before subsequent reactions.

* Present address: Yamanouchi Pharmaceutical Co., Ltd., Azusawa-cho, Itabashi-ku, Tokyo.

1) S. Sakakibara and N. Inukai, This Bulletin, **37**, 1231 (1964).

TABLE II. ACTIVE ESTER FORMATION OF ACYLAMINO ACIDS BY ESTER-EXCHANGE REACTION WITH THE TRIFLUOROACETATE REAGENTS IN PYRIDINE

| Product | Reagent used | Reaction conditions | Yield % | M. p., °C Found/Cited | $[\alpha]_D$ (°C) *c* 1, in DMF Found/Cited | Anal. % Found/Calcd. C | H | N |
|---|---|---|---|---|---|---|---|---|
| Z-L-CyS(MBz)-ONP | I | Room temp. 10—20 min. | 85 | 97—98.5<br>94—97[a] | −39.3(22)<br>−39.8(21) | 60.72<br>60.48 | 4.93<br>4.87 | 5.59<br>5.64 |
| BOC-L-Ala-ONP | I | Room temp. 10—20 min. | 80 | 81—82<br>83[b] | −51.6(26)<br>−52.5(22) | 54.08<br>54.19 | 5.75<br>5.85 | 9.08<br>9.03 |
| Ac-L-Ala-ONP | I | Room temp. 10—20 min. | 83 | 115—119[c] | 0 | 52.12<br>52.38 | 4.80<br>4.80 | 10.95<br>11.11 |
| Phth-L-Phe-ONP | I | Room temp. 10—20 min. | 84 | 169—171 | −204.7(23) | 66.62<br>66.34 | 3.82<br>3.81 | 6.83<br>6.73 |
| Tos-Gly-ONP | I | Room temp. 10—20 min. | 80 | 157—159 | | 51.55<br>51.42 | 4.19<br>4.03 | 7.95<br>8.00 |
| Z-L-Phe-OPh | II | Reflux 80 min. | 72.5 | 107—108<br>106—106.5[d] | −29.5(21)<br>−30.1(25) | 73.37<br>73.54 | 5.59<br>5.64 | 3.68<br>3.73 |
| Z-Gly-OCP | III | Reflux 35 min. | 71 | 105—107 | | 60.39<br>60.10 | 4.62<br>4.41 | 4.45<br>4.38 |
| Z-Gly-OBP | IV | Reflux 25 min. | 71 | 111—114.5 | | 52.83<br>52.76 | 3.71<br>3.87 | 3.82<br>3.85 |
| Z-Gly-OTCP | V | Room temp. 10—20 min. | 93 | 105—108<br>107—108[e] | | 49.39<br>49.45 | 3.05<br>3.11 | 3.47<br>3.60 |
| Z-L-Phe-OTCP | V | Room temp. 10—20 min. | 65 | 140—142<br>142[f] | −39.4(24)<br>−51 (22) | 58.02<br>57.70 | 3.85<br>3.79 | 2.92<br>2.93 |
| Z-Gly-OPCP | VI | Room temp. 10—20 min. | 78 | 133—134<br>185.5—187[g] | | 41.78<br>42.00 | 2.31<br>2.20 | 2.98<br>3.06 |
| Z-L-Phe-OPCP | VI | Room temp. 10—20 min. | 74 | 156—157<br>153—155.5[d] | −49.4(24)<br>−50.1(26) | 50.70<br>50.44 | 3.00<br>2.94 | 2.48<br>2.56 |
| Z-L-Val-OPCP | VI | Room temp. 10—20 min. | 80 | 140—141<br>140—142[d] | −22.8(24)<br>−22.5(26) | 45.77<br>45.67 | 3.30<br>3.23 | 2.76<br>2.80 |
| Z-L-Glu(OMe)-OPCP | VI | Room temp. 10—20 min. | 72.5 | 118—120<br>122—123[d] | −27.5(21)<br>−27.1(26) | 44.33<br>44.19 | 2.98<br>2.97 | 2.52<br>2.58 |
| Z-L-Met-OPCP | VI | Room temp. 10—20 min. | 69 | 129—131<br>130—131[d] | −30.7(21)<br>−26.9(26) | 43.15<br>42.92 | 2.95<br>3.03 | 2.58<br>2.63 |
| Z-Gly-OMP | VII | Reflux 20—30 min. | 71 | 86.5—88.5 | | 64.55<br>64.75 | 5.55<br>5.43 | 4.53<br>4.44 |
| Z-Gly-SPh | VIII | Reflux 2 hr. | 50 | 70—72<br>72[h] | | 63.77<br>63.77 | 4.98<br>5.02 | 4.63<br>4.65 |
| Z-L-Phe-SPh | VIII | Reflux 1 hr. | 81 | 128—130[c]<br>116—118[d] | 0<br>−78.2(26) | 70.38<br>70.56 | 5.53<br>5.41 | 3.52<br>3.58 |
| Z-Gly-SNP | IX | Room temp. 10—20 min. | 83.4 | 110—112<br>112.5[i] | | 55.13<br>55.48 | 4.02<br>4.07 | 7.98<br>8.09 |
| Z-L-Phe-SNP | IX | Room temp. 10—20 min. | 81 | 177—180.5<br>174—176[d] | −71.5(26)<br>−68.5(26) | 63.08<br>63.29 | 4.43<br>4.62 | 6.34<br>6.42 |
| Z-Gly-OHSI | X | Room temp. 10—20 min. | 55 | 113—114<br>113—114[j] | | 54.94<br>54.90 | 4.54<br>4.61 | 9.07<br>9.15 |
| Z-L-Phe-OHSI | X | Room temp. 10—20 min. | 90 | 134—136<br>140—140.5[k] | −53.8(24)<br>−17.3(25) | 63.67<br>63.63 | 5.14<br>5.09 | 7.02<br>7.07 |
| Z-Gly-OHPI | XI | Room temp. 10—20 min. | 23.8 | 122—125<br>124[l] | | 60.82<br>61.01 | 3.94<br>3.98 | 7.94<br>7.91 |
| *p*-Nitrophenyl laurate | I | Room temp. 10—20 min. | 86 | 44.5—47 | | 67.49<br>67.26 | 8.51<br>8.47 | 4.29<br>4.36 |
| *p*-Nitrophenyl palmitate | I | Room temp. 10—20 min. | 96.5 | 60—63 | | 70.18<br>69.99 | 9.35<br>9.35 | 3.64<br>3.71 |
| *p*-Nitrophenyl levulinate | I | Room temp. 10—20 min. | 76.5 | 60—62 | | 55.47<br>55.69 | 4.73<br>4.67 | 5.97<br>5.91 |

a) S. Sakakibara, Y. Nobuhara, Y. Shimonishi and R. Kiyoi, This Bulletin, **38**, 120 (1965).
b) E. Sandrin and R. A. Boissonnas, *Helv. Chim. Acta*, **46**, 1638 (1963).
c) This material racemized during the reaction.
d) These values were obtained from a compound prepared by the dicyclohexylcarbodiimide method.
e) J. Pless and R. A. Boissonnas, *Helv. Chim. Acta*, **46**, 1609 (1963).
f) The same lit. as in e). The same compound which was prepared in the laboratory according to the description of Pless and Boissonnas gave the following values; m. p. 139.5—141°C, $[\alpha]_D^{25}$ −39.8° (*c* 1, DMF).

g) *Chem Abstr.*, **57**, 7373 (1962). The cited value may have been a misprint.
h) T. Wieland, W. Schäfer and E. Bokelmann, *Ann.*, **573**, 99 (1951).
i) J. A. Farrington, G. W. Kenner and J. M. Turner, *Chem. & Ind.*, **1955**, 601.
j) G. W. Anderson, J. E. Zimmerman and F. M. Callahan, *J. Am. Chem. Soc.*, **86**, 1839 (1964).
k) The same lit. as in j). The optical rotation was determined in dioxan at C=2. This compound when prepared in this laboratory according to the description of Anderson et al. gave the following values; m. p. 134—136.5°C, $[\alpha]_D^{26}$ −52.8° (*c* 1, DMF). This material did not dissolved in dioxan at room temperature at *c*=2.
l) G. H. L. Nefkens, G. I. Tesser and R. J. F. Nivard, *Rec. trav. chim.*, **81**, 683 (1962).
Z=carbobenzoxy; BOC=*t*-butoxycarbonyl; Ac=acethyl; Phth=phthalyl; Tos=tosyl; NP=*p*-nitrophenyl; Ph=phenyl; CP=*p*-chlorophenyl; BP=*p*-bromophenyl; TCP=2, 4, 5-trichlorophenyl; PCP=pentachlorophenyl; MP=*p*-methoxyphenyl; HSI=*N*-hydroxysuccinimide residue; HPI=*N*-hydroxyphthalimide residue; DMF=dimethylformamide.

Table III. Stabilities of optical rotation of carbobenzoxy-L-phenylalanine active esters in pyridine at room temperature

| Compound[a] | Optical rotation change in pyridine (*c* 1) | | |
|---|---|---|---|
| | Starting value | Storage time at room temp. hr. | Observed value |
| Z-L-Phe-ONP | −24.3 | 19 | −24.2 |
| Z-L-Phe-OTCP | −40.6 | 22 | −39.6 |
| Z-L-Phe-OPCP | −49.5 | 1[b] | −45.4 |
| Z-L-Phe-SPh | −67.5 | 23 | −67.5 |
| Z-L-Phe-SNP | −57.1 | 2[b] | −57.4 |
| Z-L-Phe-OHSI | −31.8 | 1[b] | −30.7 |

No decomposition of these compounds was detectable by thin-layer chromatography during the period except in the cases with b) as a suffix.
a) See Table II for the abbreviations used.
b) Partial decomposition of this material was detected during the period by thin-layer chromatography.

the results are listed in Table II. In addition, the *p*-nitrophenylesters of some fatty acids and keto acid were also prepared. In general, the trifluoroacetates of 2, 4, 5-trichlorophenol (V), pentachlorophenol (VI), *p*-nitrothiophenol (IX) and *N*-hydroxysuccinimide (X) gave good results in the reaction. Reagents II, III, IV, VII and VIII, however, were found to be less reactive, and the reaction mixture had to be heated in order to accelerate the reaction. In the case of XI, a remarkable decomposition of the reagent was observed in pyridine, and the yield of the desired product was poor. Since amino acids with free functional groups on the side chains, such as serine, threonine, tyrosine and histidine, showed complicated side reactions with these trifluoroacetate reagents, these functional groups had to be protected before the compounds could be subjected to the reaction. Carbobenzoxy-L-asparagine also gave a poor yield. This may be due to intramolecular dehydration by the reagent.

No racemization was observed during the ester-exchange reaction of these reagents with phthalylamino acids or urethane-type acylamino acids. In the following cases, however, apparent racemization was observed: (1) When carbobenzoxy-L-phenylalanine was treated with VIII in boiling pyridine, and (2) when acetyl-L-alanine was treated with I at room temperature. The latter case seemed to be general for any of the reagents when usual acylamino acids, such as acetyl or benzoyl derivatives, were treated. Therefore, if racemization is to be avoided, the procedure should be limited to amino acids which are acylated through a phthalyl- or urethane-type group, since these are known to be resistant to racemization. Reagent VIII seemed to be exceptional in causing racemization with carbobenzoxy-L-phenylalanine. The thiophenylester of the compound, when once formed, may readily racemize in hot pyridine during the procedure. To check this possibility, authentic carbobenzoxy-L-phenylalanine thiophenylester was prepared by the dicyclohexylcarbodiimide method; the complete racemization of the compound was observed after treatment with boiling pyridine for one hour.

As can be seen in Table III and Fig. 1, the optical stabilities of other carbobenzoxy-L-phenylalanine active esters were measured in pyridine at room temperature; a distinct decrease in rotation was observed only with the pentachlorophenylester. This may be due not only to the partial racemization, but also to

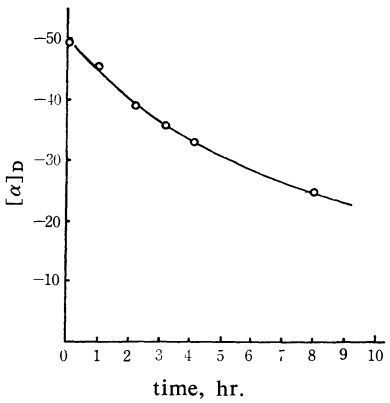



Fig. 1. Optical rotation change of carbobenzoxy-L-phenylalanine pentachlorophenylester in pyridine. $c=1$, 22°C.

the partial decomposition (probably the oxazolon formation) of the compound. Serious decomposition was also observed with the *p*-nitrothiophenylester wtihin two hours. Therefore, care should be taken with prolonged treatment of the materials with VI or IX. Finally, it was concluded that the *p*-nitrophenylesters, 2, 4, 5-trichlorophenylesters and *N*-hydroxysuccinimidesters of phthalyl or urethanetype acyl-L-amino acids can safely be prepared by the new procedure.

Next, the direct syntheses of peptides using the trifluoroacetate reagents I, V and X were studied. One advantage of the trifluoroacetate method in the preparation of active esters of acylamino acids is that the only co-product of the ester-exchange reaction is water-soluble trifluoroacetic acid, which can be removed from the product very easily. Therefore, in preparing peptides, a direct method becomes possible, a method in which the isolation of the active ester of the acylamino acid is not necessary before it is condensed with an amino component. This procedure is considered to be similar to that of the mixed anhydride method, in which the acylamino acid is activated by an acyl chloride reagent, and then the activated intermediate is condensed with an amino acid or peptide ester without being isolated from the reaction mixture.

As examples of the direct method, carbobenzoxy-L-phenylalanyl-L-phenylalanine benzylester, carbobenzoxy-L-phenylalanylglycine ethylester and carbobenzoxyglycyl-L-tyrosine ethylester were prepared, and the optimum conditions of each reaction were investigated. The relationship between the reactivity of each active ester and the amount of triethylamine added to a reaction mixture was interesting. In the cases of reaction with I or V, two equivalents of triethylamine were necessary to proceed the

TABLE IV. DIRECT SYNTHESIS OF PEPTIDES BY THE TRIFLUOROACETATE METHOD FROM CARBOBENZOXYAMINO ACID AND AMINO ACID ESTER HYDROCHLORIDES OR TOSYLATES

| Product | Reagent | Mole equiv. of triethylamine used | Reaction period for peptide formation | Yield % | M. p. °C | $[\alpha]_D$ ($c$, solvent) (°C) |
|---|---|---|---|---|---|---|
| Z-L-Phe- | I | 2 | 1 hr. | 85 | 147—151[a] | +8.2(2, $CHCl_3$) (25) |
| L-Phe-OBz | V | 2 | 1 hr. | 80 | 149—152 | +8.0(2, $CHCl_3$) (25) |
| | X | 0 | 5 days | 80 | 149—150 | +8.1(2, $CHCl_3$) (21) |
| | X | 1 | 2 days | 73 | 150—151 | +8.5(2, $CHCl_3$) (25) |
| | X | 2 | 1 hr. | 96 | 149—151 | +8.4(2, $CHCl_3$) (25) |
| | X[b] | 1 | 2 days | 94 | 152 | +8.2(2, $CHCl_3$) (25) |
| Z-L-Phe-Gly- | I | 2 | 6 hr. | 98 | 108—110[c] | −17.1(3, EtOH) (21) |
| OEt | V | 2 | 6 hr. | 94 | 109—111 | −17.4(3, EtOH) (21) |
| | V[b] | 1 | 1 day | 83 | 110—110.5 | −16.5(4, EtOH) (25) |
| | X | 1 | 2 days | 81 | 110—111 | −17.2(5, EtOH) (22) |
| | X[b] | 1 | 2 days | 93 | 110—111 | −16.9(5, EtOH) (22) |
| | X | 2 | 6 hr. | 95 | 109—111 | −17.1(3, EtOH) (21) |
| Z-Gly-L-Tyr- | I | 2 | 6 hr. | 89 | 123—125[d] | +19.1(3, EtOH) (21) |
| OEt | I[b] | 1 | 1 day | 97 | 125—126 | +19.3(3, EtOH) (21) |
| | V | 2 | 6 hr. | 95 | 125—127 | +19.1(3, EtOH) (21) |
| | X | 2 | 6 hr. | 92 | 125—126 | +19.0(3, EtOH) (21) |

a) Cited: m. p. 149—150°C, $[\alpha]_D^{25}$ +8.4 ($c$ 2, $CHCl_3$); T. Sugimura and W. K. Paik, unpublished data.
b) The intermediate, carbobenzoxyamino acid active ester, was isolated and then recrystallized before being subjected to reaction with amino acid ester hydrochloride or tosylate in pyridine.
c) Cited: m. p. 110—111°C, $[\alpha]_D^{25}$ −16.9 ($c$ 5, EtOH); R. W. Young, K. H. Wood, R. J. Joyce and G. W. Anderson, *J. Am. Chem. Soc.*, **78**, 2126 (1956).
d) Cited: m. p. 126—127°C, $[\alpha]_D^{24}$ +19.2 ($c$ 5, EtOH); G. W. Anderson, J. Blodinger and A. D. Welcher, ibid., **74**, 5309 (1952).

reaction; these may be consumed for liberating the free ester from the hydrochloride or tosylate and for neutralizing the trifluoroacetic acid formed. In the case of reaction with X, however, the addition of triethylamine was not necessary for the completion of the reaction, even if ester hydrochloride or tosylate was used, and the only contribution of the triethylamine to the reaction was to reduce the reaction period. The pyridine in the reaction mixture should act as the necessary base for the reaction (Table IV). The yields of the reaction products were excellent, and their purities were also quite satisfactory. The procedure should be useful for the step wise elongation method of peptide synthesis.

One advantage of the direct method for peptide synthesis is that the procedure can be applied whether or not the acylamino acid active ester can be crystallized. For the same reason, it should also be useful for the synthesis of long peptides by the fragment-condensation method or for the synthesis of cyclic peptides. Studies of these possibilities will be published in subsequent papers.

## Experimental

All melting points given were uncorrected, and all were determined by the capillary method in a sulfuric acid bath. The completion of the reaction was checked by simplified thin-layer chromatography[2] using Merck's silica gel G and with a mixture of chloroform, methanol and acetic acid (95 : 5 : 3 v/v) as the solvent. *N*-Carbobenzoxy or *t*-butoxycarbonyl compounds were developed on the plates by heating with hydrobromic acid, followed by treatment with ninhydrin.

**Materials.**—Trifluoroacetic anhydride was prepared according to the procedure of Bourne.[3] *p*-Nitrothiophenol was prepared according to the procedure of Price and Stacy,[4] as was 2, 4-Dinitrothiophenol. *N*-hydroxysuccinimide was prepared by the procedure of Anderson et al.[5] *N*-hydroxyphthalimide was prepared by the method of Nefkens and Tesser.[6] *p*-Chlorophenol, *p*-bromophenol, 2, 4, 5-trichlorophenol, pentachlorophenol, *p*-methoxyphenol and thiophenol were obtained from the Tokyo Kasei Co., Ltd., Tokyo. Acyl amino acids were prepared by standard procedures, and their physical constants were checked before the reactions. Pyridine was dried over potassium hydroxide pellets before use.

**The General Procedure for the Preparation of Trifluoroacetate Reagents.**—A mixture of trifluoroacetic anhydride (0.15 mol.) and a phenolic compound or an *N*-hydroxyimide derivative (0.1 mol.) in benzene (30 ml.) was refluxed for about 5 hr. until all the crystals had disappeared. The solution was then concentrated to dryness in order to obtain the product. The yield was generally quantitative, and the product was used without further purification in subsequent reactions. The trifluoroacetates of 2, 4, 5-trichlorophenol, *p*-nitrothiophenol, *N*-hydroxysuccinimide and *N*-hydroxyphthalimide did not give correct analytical data, because all the purification procedures tested, such as recrystallization and distillation, caused their partial decomposition. Other trifluoroacetates could, however, be purified for analysis by sublimation or distillation. Their physical constants and analytical data are listed in Table I.

**The General Procedure for the Preparation of Acylamino Acid-active Esters Using Trifluoroacetate Reagents.**—A solution of an acylamino acid (0.005 mol.) in pyridine (3 ml.) was treated with a trifluoroacetate reagent (0.006 mol.) until the starting material had disappeared; this was checked by thin-layer chromatography. After the reaction was complete, water (about 20 ml.) was added to the reaction mixture in order to precipitate the product as crystals; these were then separated by filtration and recrystallized from a suitable solvent system. The yields, properties and analytical data on these products are listed in Table II.

**The General Procedure for the Preparation of Carbobenzoxy Dipeptide Esters by the Direct Method.**—A solution of carbobenzoxy-amino acid (0.005 mol.) in pyridine (4 ml.) was treated with a trifluoroacetate reagent (0.006 mol.), I, V or X, as has been described above, and then water (0.018 ml.) was added to the reaction mixture in order to destroy the excess reagent. A solution of amino acid ester hydrochloride or tosylate (0.005 mol.) and triethylamine (2 mole equivalents) in chloroform (4 ml.) was added to the reaction mixture. After an adequate period, water was added to the solution, and the oil precipitated was extracted with ethyl acetate. The extract was washed successively with a 10% sodium bicarbonate solution or, if necessary, with N ammonia and N hydrochloric acid, and then dried over anhydrous magnesium sulfate. The dried solution was concentrated to dryness, and the residue was crystallized from a suitable solvent system. The data are listed in Table IV.

## Summary

The trifluoroacetates of various phenol, thiophenol and *N*-hydroxyimide derivatives, which are known as hydroxylic partners of various active carboxylic acid ester, have been synthesized, and it has been found that they are good reagents for the preparation of the respective active esters of acylamino acids by the ester-exchange reaction in pyridine. The new method is especially effective in the preparation of *p*-nitrophenyl, 2, 4, 5-trichlorophenyl and *N*-hydroxysuccinimide esters of acylamino acids, which are well known to be useful intermediates for peptide synthesis. The direct

2) K. Morita and F. Haruta, *J. Chromatog.*, **12**, 412 (1963).
3) E. J. Bourne, M. Stacey, J. C. Tatlow and J. M. Tedder, *J. Chem. Soc.*, **1949**, 2976.
4) C. C. Price and G. W. Stacy, *J. Am. Chem. Soc.*, **68**, 498 (1946).
5) G. W. Anderson, J. E. Zimmerman and F. M. Callahan, ibid., **85**, 3039 (1963); ibid., **86**, 1839 (1964).
6) G. H. L. Nefkens and G. I. Tesser, ibid., **83**, 1263 (1961).

syntheses of peptides using these reagents, without the isolation of the intermediates, have also been studied, and the new procedure has been found to be useful for the step wise elongation of peptides.

*Peptide Center*
*Institute for Protein Research*
*Osaka University*
*Kita-ku, Osaka*

# The Relative Reactivities of Different C–H Bonds in the Photochemical Sulfoxidation of *n*-Hexane[1]

By Yoshiro OGATA, Yasuji IZAWA and Takao TSUDA

(Received April 30, 1965)

The present authors have previously postulated,[2] in the photochemical sulfoxidation of *n*-hexane, a mechanism involving the simultaneous steps of a chain reaction via persulfonate radical and a molecular mechanism via excited sulfur trioxide; the primary process in the radical chain seems to involve two simultaneous processes, i. e., energy transfer and hydrogen abstraction with excited sulfur dioxide.

The relative reactivities of different C–H bonds in *n*-heptane towards ultraviolet light-excited sulfur dioxide have recently been estimated by Asinger, Fell and Pöttkamper.[3] In order to estimate the relative reactivities, the heptanesulfonic acids produced were converted to the corresponding methyl heptanesulfonates, which had been determined by gas chromatography.

The present paper will describe the results obtained in a study of the relative reactivities of different C–H bonds towards excited sulfur dioxide and sulfur trioxide in the photochemical sulfoxidation of *n*-hexane, together with the results of the comparison of these data with those of the photochemical chlorination.

## Experimental

**Materials.**—*n*-Hexane was purified by a previously reported procedure.[2] Acetic anhydride, dichloromethane, sulfur dioxide and oxygen were of commercial materials of an extra pure grade. Thionyl chloride (b. p. 78—79°C) and dimethyl formamide (b. p. 75—77°C/63 mmHg) were purified by the fractionation of commercial materials of an extra pure grade. Authentic 2-hexanesulfonyl chloride was prepared as follows: 2-hexanol (b. p. 79—80°C/81 mmHg; $n_D^{25}$ 1.4133 (lit.[4] $n_D^{25}$ 1.4136); its 3,5-dinitrobenzoate, m. p. 37.8—38.5°C (lit.[5] m. p. 38°C)) was prepared by Grignard synthesis from *n*-butyl bromide and acetaldehyde; it was converted by phosphorous tribromide to 2-hexyl bromide, which was then converted to 2-hexanesulfonyl chloride (b. p. 60—62°C/4.5 mmHg; $n_D^{25}$ 1.4630 (lit.[6] $n_D^{25}$ 1.4610)) via 2-hexyl thiocyanate.[7,8] Authentic 1-hexanesulfonyl chloride (b. p. 92—93°C/4 mmHg; $n_D^{25}$ 1.4612 (lit.[9] $n_D^{25}$ 1.4563)) and 3-hexanesulfonyl chloride (b. p. 64°C/5.5 mmHg; $n_D^{25}$ 1.4637) were similarly prepared from 1-hexanol (b. p. 156—157°C) and 3-hexanol (b. p. 134—135°C; $n_D^{25}$ 1.4134 (lit.[10] $n_D^{25}$ 1.4139); its 3,5-dinitrobenzoate, m. p. 75.2—75.5°C (lit.[5] m. p. 77°C)) respectively. The purities of all the alcohols, bromides, thiocyanates and sulfonylchlorides examined were confirmed by gas chromatography.

**The Sulfoxidation of *n*-Hexane.**—Sulfur dioxide (0.5—2 l./hr.) and oxygen (0.3—2 l./hr.) were introduced simultaneously into a mixture of *n*-hexane (0.3 mol., 40 ml.) and acetic anhydride (0.016 mol.) under ultraviolet light (Toshiba SHL-100 UV) at 1—28°C for 1 hr. After irradiation had ended, treatment in a way similar to that described in a previous paper[2] gave sodium hexanemonosulfonates.

**The Conversion of Sodium Hexanesulfonates to Their Sulfonyl Chlorides.**—The procedure employed was similar to that reported by Kirkland.[11] A mixture of the resulting sodium hexanesulfonates

1) Contribution No. 73. Presented in part at the 3rd Symposium on Oil Chemistry, Nagoya, November, 1964.
2) Y. Ogata, Y. Izawa and T. Tsuda, *Tetrahedron*, **21**, 1349 (1965).
3) F. Asinger, B. Fell and S. Pöttkamper, *Chem. Ber.*, **97**, 3092 (1964).
4) J. F. Norris and F. C. Cortese, *J. Am. Chem. Soc.*, **49**, 2645 (1927).
5) P. Sutter, *Helv. Chim. Acta*, **21**, 1266 (1938).
6) L. Spiegler and J. M. Tinker, *J. Am. Chem. Soc.*, **61**, 942 (1939).
7) J. B. Johnson and J. B. Douglass, ibid., **61**, 2548 (1939).
8) F. Asinger, B. Fell and H. Scherb, *Chem. Ber.*, **96**, 2831 (1963).
9) C. Ziegler and T. M. Tinker, *J. Org. Chem.*, **16**, 161 (1951).
10) F. Hovorka, H. P. Lamkelma and S. C. Stanford, *J. Am. Chem. Soc.*, **60**, 820 (1938).
11) K. Kirkland, *Anal. Chem.*, **32**, 1388 (1960).

(1.5 g.) and fresh thionyl chloride (50 ml.) in the presence of dimethyl formamide (1.5 ml.) was refluxed until the evolution of sulfur dioxide had subsided (1—2 hr.); then it was cooled. Dichloromethane (about 50 ml.) was added to the reaction product, and the precipitate of sodium chloride was filtered off. The unreacted thionyl chloride and the solvent were carefully removed by evaporation under moderately reduced pressure, and dichloromethane (3—5 ml.) was added to the remaining sulfonyl chloride. The isomeric hexanesulfonyl chloride content of the solution was determined by gas chromatography.

**The Determination of the Isomeric Hexanesulfonyl Chlorides by Gas Chromatography.**—The vapor-phase chromatographic determination of the isomers was carried out using a 5 m. column (diameter 4 mm.) containing polyethylene glycol 4000 (1% by weight)/C-22 (40—60 mesh), and with helium as a carrier gas (54 ml./min.) at 130°C (Fig. 1); the similarity of the retention times of the peaks of the authentic material to those of the peaks of the sample established their identity. The molar ratio of the isomers was calculated by means of the paper-peak-weight ratio. No appreciable decomposition of hexanesulfonyl chlorides to the corresponding hexyl chlorides was observed under these conditions.

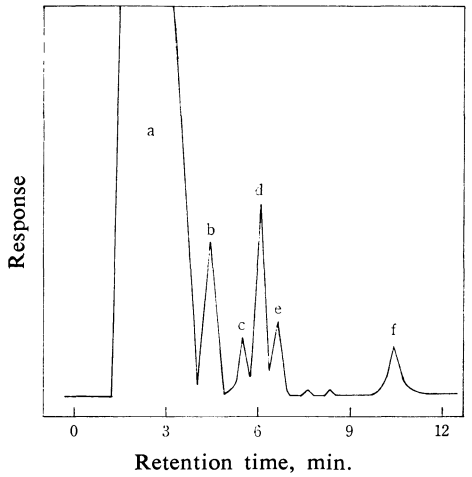



Fig. 1. Typical chromatogram of 1-, 2- and 3-hexanesulfonyl chlorides.
a: Dichloromethane, b: Dimethylformamide, c: Unknown, d: 3-Hexanesulfonyl chloride, e: 2-Hexanesulfonyl chloride and f: 1-Hexanesulfonyl chloride.

**The Photochlorination of *n*-Hexane.**—Chlorine (0.3—0.5 l./hr.) was introduced into *n*-hexane (0.3 mol., 40 ml.) under ultraviolet light at −10—+28°C for 1 hr. After the irradiation had ended, nitrogen was bubbled into the reaction mixture in order to remove the free chlorine and hydrogen chloride in the mixture. The resulting solution was washed with 1 N aqueous sodium hydrogen carbonate and then with water, and dried with sodium sulfate. The isomeric hexyl monochloride content was determined by gas chromatography, using a column similar to that used for hexanesulfonyl chloride at 37°C. The hexyl monochloride content as a whole in the resulting chlorinated hexane was about 83%.

## Results and Discussion

The sodium 1-, 2- and 3-hexanesulfonates obtained by the sulfoxidation of *n*-hexane were converted to the corresponding sulfonyl chlorides, and then the latter were estimated by gas chromatography. The relative reactivity ($R$) of different C–H bonds towards excited $SO_2$ and $SO_3$ is given by:

$$R=\left(\frac{\text{Mol.\% of the isomer in the product}}{\text{Total number of C–H bonds at the corresponding position}}\right)\Big/R_1$$

where

$$R_1=\frac{\text{Mol.\% of 1-isomer}}{\text{Total No. of C–H bonds at the 1-position}}$$

Table I summarizes the relative reactivities of different C–H bonds in the photochemical sulfoxidation and chlorination of the *n*-hexane in our hands, together with the results in the literature. As Table I shows, the relative reactivity, 2.1—3.6, for the secondary vs. the primary C–H bond of *n*-hexane approximates those in the photochemical sulfoxidation[12] and sulfochlorination[13] of *n*-dodecane and the photochlorination of *n*-heptane[14] and *n*-dodecane.[15,16] In contrast, it has recently been reported[3] that the relative reactivity for C(secondary) vs. $C_1$ in the photochemical sulfoxidation of *n*-heptane without acetic anhydride is about 30, although this value is very different from those obtained in photochemical reactions by other workers. At any rate, the increase in the relative reactivity of C(secondary) may be accounted for by the stability of the secondary carbon radical being greater than that of the primary radical.

On the other hand, since it may be expected that the $C_3$–H bond is more sterically hindered, it is surprising to observe that the reactivity of the $C_2$–H bond is lower than that of the $C_3$–H bond. This fact may be explained by assuming temporarily the tentative formation of a six-membered ring[17,18] of the 2-hexyl radical, which results in the inhibition of the approach of $SO_2$ or $SO_3$ to the 2-position, thus

12) F. Asinger, G. Geiseler and H. Eckoldt, *Chem. Ber.*, **89**, 1037 (1956).
13) F. Asinger, *Ber.*, **77**, 191 (1944).
14) B. Fell and Li-Hong Kong, *Angew. Chem.*, **75**, 165 (1963).
15) F. Asinger, *Ber.*, **75**, 668 (1942).
16) F. Asinger, G. Geiseler and K. Schmiedel, *Chem. Ber.*, **92**, 3085 (1959).
17) S. Tsutsumi, *Sekiyu & Sekiyukagaku* (*Petroleum and Petroleum Chemistry*), **6**, (6), 105 (1962).
18) B. Blouri, G. Lanchec and P. Rumpf, *Compt. rend.*, **253**, 3609 (1963).

TABLE I. RELATIVE REACTIVITIES OF C-H BONDS FOR TYPICAL PHOTOCHEMICAL REACTIONS OF *n*-ALKANES

| Reaction | Substrate | Temp. °C | Relative reactivity | | | |
|---|---|---|---|---|---|---|
| | | | $C_1$-H | $C_2$-H | $C_n$-H | $2_{ry}C$-H/$1_{ry}C$-H |
| Chlorination | *n*-Hexane | −7—28 | 1 | 2.9—3.5 | 3.0—3.8 ($n=3$) | 3.1—3.6 |
| | *n*-Heptane[14] | 98 | 1 | 3.4[a] | 3.3($n=3$)[a] 3.3($n=4$)[a] | 2.4[a] |
| | *n*-Dodecane[15] | 20 | 1 | 5.8[a] | 6.9[a] ($n=3$—6) | 6.7[a] |
| Sulfochlorination | *n*-Dodecane[13] | 25 | 1 | 1.6[a] | 3.8[a] ($n=3$—6) | 3.3 |
| Sulfoxidation | *n*-Hexane | 1—28 | 1 | 0.8—1.3 | 3.2—6.2 ($n=3$) | 2.1—3.6 |
| | *n*-Heptane[3] | 20 | 1 | 32[a] | 29($n=3$)[a] 27($n=4$)[a] | 30 |
| | *n*-Dodecane[12] | 30—80 | 1 | 3.1[a] | 5.7[a] ($n=3$—6) | 3.3 |

a) Calculated values based on the experimental data in the literature.[3,12-15]

TABLE II. EFFECT OF THE RATIO $[SO_2]/[O_2]$ ON THE RELATIVE REACTIVITIES OF C-H BONDS ($[n\text{-}C_6H_{14}]/[Ac_2O]$ : 19; Irradiation time: 1 hr.)

| $[SO_2]/[O_2]$ | Temp. °C | Relative reactivity | | | |
|---|---|---|---|---|---|
| | | $C_1$-H | $C_2$-H | $C_3$-H | $2_{ry}C$-H/$1_{ry}C$-H |
| 0.5 | 18—19 | 1 | 0.8 | 4.0 | 2.4 |
| 2 | 11—18 | 1 | 1 | 3.3 | 2.2 |
| 10 | 18—19 | 1 | 0.9 | 6.2 | 3.6 |

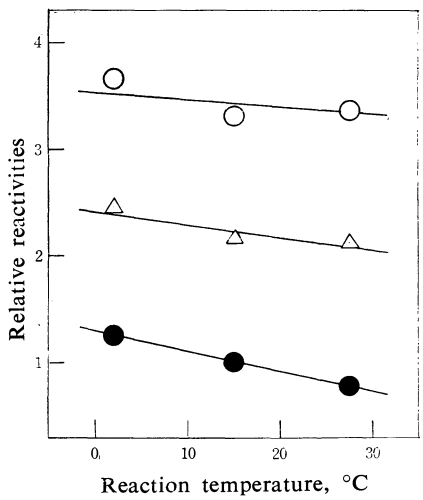



Fig. 2. Temperature dependence of the relative reactivities in photochemical sulfoxidation of *n*-hexane.
●: $C_2$-H, ○: $C_3$-H
△: (Secondary C-H)/(Primary C-H)

lowering the reactivity of $C_2$-H bonds compared with that of $C_3$-H bonds. This assumption may also explain the fact that the temperature dependence of the reactivity of $C_2$-H bonds is somewhat greater than that of $C_3$-H bonds (Fig. 2), for rings are formed more easily at a higher temperature. Since the C-H bond length is short, the five-membered ring from the 3-hexyl radical may approach the four-membered ring, which is less stabilized. Although the temperature effect on the reactivity is small in the 0—30°C range, an increase in the temperature results in a small decrease in the reactivity for photochemical sulfonates by sulfur trioxide, as is shown in Fig. 2. Furthermore, the ratio of $SO_2$ vs. $O_2$ also affects the relative reactivity, particularly for $C_3$-H bonds (Table II).

Table III shows the findings on the photochemical chlorination of *n*-hexane, where such steric hindrance of the six-membered ring seems to be small. In this case, the difference in the relative reactivities of $C_2$-H and $C_3$-H bonds is small. Such a difference in the behavior of chlorine and sulfur dioxide has been reported in the photochemical chlorination of

TABLE III. RELATIVE REACTIVITIES OF C-H BONDS IN THE PHOTOCHLORINATION OF *n*-HEXANE (Flow rate of $Cl_2$: 0.3—0.5 l./hr.; Irradiation Time: 1 hr.)

| Temp. °C | Relative reactivity | | |
|---|---|---|---|
| | $C_1$-H | $C_2$-H | $C_3$-H |
| −7—−5 | 1 | 3.5 | 3.0 |
| 21— 22 | 1 | 2.9 | 3.2 |
| 27— 28 | 1 | 3.4 | 3.8 |

isobutane, giving *t*-butyl chloride,[19] and the sulfochlorination of the same substrate, giving isobutanesulfonyl chloride alone.[20]

## Summary

The product mixture of isomeric hexanesulfonic acids in the ultraviolet light-induced sulfoxidation of *n*-hexane under various conditions has been analyzed by gas chromatography. On the basis of the data thus obtained, the relative reactivities of different C–H bonds in *n*-hexane towards light-excited sulfur dioxide and sulfur trioxide have been estimated. The ratio of the reactivities of $C_1$–H : $C_2$–H : $C_3$–H has been calculated to be 1 : 0.8—1.3 : 3.2—6.2. The higher reaction temperatures tend to lower the reactivity of $C_2$–H. The mole ratio of $SO_2$ vs. $O_2$ has an appreciable effect on the composition of the isomers. The lower reactivity of $C_2$–H than that of $C_3$–H may be explained by the intermediary formation of a six-membered ring.

The authors are grateful to the Seitetsu Chemical Co. for their gift of sulfur dioxide.

*Department of Applied Chemistry*
*Faculty of Engineering*
*Nagoya University*
*Chikusa-ku, Nagoya*

19) H. B. Hass, E. T. McBee and P. Weber, *Ind. Eng. Chem.*, **27**, 1192 (1935).
20) F. Asinger and F. Ebeneder, *Ber.*, **75**, 344 (1942).

# Traube's Rule for Soluble Monolayers of Homologous Strong Electrolytes

By Kunio TAMAKI

(Received May 8, 1965)

On the surface tension of dilute aqueous solutions of a homologous series of aliphatic alcohols or carboxylic acids, Traube[1] showed that the concentrations required for an equal lowering of the surface tension diminished by a constant factor for each additional methylene group in the hydrocarbon chain. This relation, commonly called Traube's rule, is conveniently expressed as;

$$C_n/C_{n+1}=K \tag{1}$$

where $C_n$ and $C_{n+1}$ are, respectively, the concentrations for successive members of the series with $n$ and $n+1$ methylene groups at the equal lowering of surface tension, and $K$, termed "Traube's factor" in this paper, is a constant. Many experimental data for the homologous series of nonelectrolytes, such as aliphatic alcohols, or of weak electrolytes, such as aliphatic carboxylic acids, indicate that $K$ is about 3.

On the other hand, Traube's factor for a homologous series of strong electrolytes seems to be about 2. The object of this paper is to interpret the significance of Traube's factor for soluble monolayers of homologous strong electrolytes, especially for perfluoro acids.

**Traube's Factor for Nonelectrolytes and Weak Electrolytes.**—Langmuir,[2] Tamamushi,[3] Ward[4] and Davies[5] interpreted Traube's rule in terms of the free energy of the adsorption of each additional methylene group.

The chemical potentials of a solute, $\mu$, in the surface film and in the water may be written, respectively, as;

$$\left.\begin{aligned}\mu_s&=\mu_s^\circ+\boldsymbol{R}\boldsymbol{T}\ln C_s\\ \mu_b&=\mu_b^\circ+\boldsymbol{R}\boldsymbol{T}\ln C_b\end{aligned}\right\} \tag{2}$$

where $\boldsymbol{R}$ is the gas constant; $T$, the absolute temperature, and $C$, the concentration; the superscript $\circ$ is used to identify the standard state, while the subscripts $s$ and $b$ refer to the surface and the bulk phases respectively. The activity coefficients are omitted in this paper. When surface and bulk are in equilibrium, $\mu_s=\mu_b$; therefore,

$$C_s=C_b\exp\frac{\mu_b^\circ-\mu_s^\circ}{\boldsymbol{R}\boldsymbol{T}}=C_b\exp\frac{-\Delta F^\circ}{\boldsymbol{R}\boldsymbol{T}} \tag{3}$$

where $\Delta F^\circ$ $(=\mu_s^\circ-\mu_b^\circ)$ is the standard free energy of the adsorption of the solute molecule from the bulk to be the surface, which is written as;

$$\Delta F^\circ=W_0+nW \tag{4}$$

1) I. Traube, *Ann. Chem. Liebigs*, **265**, 27 (1891).

2) I. Langmuir, *J. Am. Chem. Soc.*, **38**, 1948 (1917).

3) B. Tamamushi, This Bulletin, **9**, 363 (1934).

4) A. F. H. Ward, *Trans. Faraday Soc.*, **42**, 399 (1946).

5) J. T. Davies and E. K. Rideal, "Interfacial Phenomena," Academic Press, New York and London (1961), p. 154.

where $W$ is the free energy of the adsorption of an additional methylene group from the bulk to the surface and $W_0$ is the free energy contribution of a polar group. Then, from the great resemblance of the surface tension versus the logarithm of concentration curve for each homologous compound, it may be assumed that the surface concentration, $C_s$, is approximately equal at the equal lowering of surface tension for each compound. From the two equations corresponding to Eq. 3 for successive members of the series with $n$ and $n+1$ methylene groups, one obtains;

$$\frac{C_n}{C_{n+1}} = \exp\left(\frac{\Delta F_n^\circ - \Delta F_{n+1}^\circ}{RT}\right) \quad (5)$$

From Eqs. 1, 4 and 5, we obtain;

$$K = \exp(-W/RT) \quad (6)$$

At the air-water interface, the interchain cohesion increases with the adsorption and the standard free energy of the adsorption of long-chain molecules is dependent on the surface concentration, as has been discussed by Tamamushi[6] in his early work and by Davies[7] in recent years. If, however, we set $W=-650$ cal./mol. at 25°C, as an approximate value, in Eq. 6, Traube's factor becomes 3.0.

**Traube's Factor for Strong Electrolytes.**—For soluble ionized monolayers, one must take into consideration the electrical repulsive potential of the surface, which tends to make the adsorbed long-chain ions repel each other; the standard free energy of the adsorption per mole, $\Delta F^\circ$, is expressed as;

$$\Delta F^\circ = nW + NZe\phi \quad (7)$$

where $N$ is the Avogadro number; $Z$, the valency of the long-chain ion; $e$, the proton charge, and $\phi$, the electrical potential of the surface. According to Gouy's theory, $\phi$ may be given as;

$$\phi = \frac{2kT}{Ze}\sinh^{-1}\left(\sigma\sqrt{\frac{500\pi}{CDRT}}\right) \quad (8)$$

where $k$ is the Boltzmann constant; $\sigma$, the surface charge density; $C$, the molar concentration, and $D$, the dielectric constant of the solvent. Further, at a high potential, Eq. 8 may be simplified to;

$$\phi = \frac{kT}{Ze}\ln\frac{2000\sigma^2\pi}{CDRT} \quad (9)$$

The combination of Eqs. 7 and 9 gives;

$$\Delta F^\circ = nW + RT\ln\frac{2000\sigma^2\pi}{CDRT} \quad (10)$$

From the two equations corresponding to Eq. 10 for successive members of the series with $n$ and $n+1$ methylene groups, and by assuming that the surface charge density, $\sigma$, is approximately equal at equal lowerings of the surface tension for homologous compounds, as has been mentioned above, we obtain;

$$\Delta F_n^\circ - \Delta F_{n+1}^\circ = -W + RT\ln C_{n+1}/C_n \quad (11)$$

By the substitution of Eq. 11 into Eq. 5, we find that;

$$C_n/C_{n+1} = K = \exp(-W/2RT) \quad (12)$$

Table I summarizes the values of Traub's factor calculated from the published data of Kling and Lange[8] on the heptane-water interfacial tensions for sodium alkyl sulfates at 50°C. From this table Traube's factor is found to be about 2. With $W=-810$ cal./mol. as the free energy of the adsorption for each methylene group at the oil-water interface, Eq. 12 gives $K=1.9$. It may, therefore, be concluded that Eq. 12 can be used to obtain a very good approximation of Traube's factor for soluble monolayers of homologous strong electrolytes.

Table I. Calculation of the Traube's factor for sodium alkyl ($C_8$–$C_{16}$) sulfates at the heptane-water interface at 50°C using data of Kling and Lange[8]

| Substance | Concn. required to give interfacial tension of 30 dyne/cm., M | $K^2$ |
|---|---|---|
| $C_8$ | 0.021 | $(1.8)^2$ |
| $C_{10}$ | 0.0063 | $(2.0)^2$ |
| $C_{12}$ | 0.0016 | $(2.0)^2$ |
| $C_{14}$ | 0.00042 | $(2.0)^2$ |
| $C_{16}$ | 0.00011 | |

**Traube's Factor for Perfluoro Acids.**—Aranow and Witten[9] proposed a theory of Traube's rule on the assumption that on the surface each methylene group has 3 equal energy potential minima with respect to the torsion whose effect contributes $R\ln 3$ to the entropy, and that if the enthalpy increment per methylene group is zero, the increment in the free energy per methylene group is given by $RT\ln 3$. Further, they pointed out, as an example of the applicability of their theory, that Traube's factor for homologous series with perfluorochains is found to be about 3, and that this can be explained by similarily assuming that each $CF_2$ group has 3 positions of potential minima about carbon-carbon bonds, regardless of the different strengths of the interactions between water-$CF_2$ and water-$CH_2$.

According to our view, however, Traube's

6) B. Tamamushi, *Kolloid-Z.*, **71**, 150 (1935).
7) J. T. Davies, *J. Colloid Sci.*, **11**, 377 (1956).
8) W. Kling and H. Lange, "Proceedings of IInd International Congress on Surface Activity," Vol. 1, Butterworths, London (1957), p. 295.
9) R. H. Aranow and L. Witten, *J. Chem. Phys.*, **28**, 405 (1958), **35**, 1504 (1961).

rule for homologous perfluoro acids can be interpreted using Eq. 12, because perfluoro acids are of the strong electrolyte type. Phillips[10] obtained the free energy of the transfer of the $CF_2$ group from the water phase to the oil phase as about $-1300$ cal./mol. By the substitution of this value into Eq. 13, Traube's factor $K$ becomes 3.3 Therefore, it is a fortuitous fact that Traube's rule with the same constant holds for molecules with fluorocarbon chains as well as for hydrocarbon chains.

Recently, Kauzmann,[11] and Némethy and Scheraga[12] evaluated the thermodynamic parameters pertaining to the transfer of such nonpolar molecules as hydrocarbons from the water phase to the oil phase, termed the "hydrophobic bond" or "hydrophobic interaction"; they concluded that the entropy increment caused by the change of the "iceberg" around the nonpolar molecules to the original water is the most important part of the process. The entropy effect may be a main contribution to the free energy of the adsorption of nonpolar molecules from the water phase to the surface phase; however, this effect would not originate from the potential minima of the internal rotation about carbon-carbon bonds, but probably from the hydrophobic interaction. More recently, Spaull and Nearn[13] have discussed the thermodynamic parameters of the adsorption of fatty alcohols at the air-water interface along the same lines.

10) J. N. Phillips, *Trans. Faraday Soc.*, **51**, 561 (1955).
11) W. Kauzmann, *Advances in Protein Chem.*, **14**, 1 (1959).
12) G. Némethy and H. A. Scheraga, *J. Chem. Phys.*, **36**, 3382, 3401 (1962); *J. Phys. Chem.*, **66**, 1773 (1962).


## Summary

By using the free energy of the adsorption of the $CH_2$ or the $CF_2$ group from water to the surface, $W$, and the surface potential of Gouy's theory, Traube's factor, $K$, that is, the ratio of the respective concentrations, $C_n$ and $C_{n+1}$, required to effect the equal lowering of surface or interfacial tension for successive homologous strong electrolytes with $n$ and $n+1$ $CH_2$ or $CF_2$ groups, has been derived as;

$$K=C_n/C_{n+1}=\exp(-W/2\boldsymbol{R}T)$$

where $\boldsymbol{R}$ is the gas constant and $T$, the absolute temperature. This equation has been shown to be applicable also in obtaining a very good approximation for homologous sodium alkyl sulfates or perfluoro acids.


The author wishes to express his sincere gratitude to Professor Bun-ichi Tamamushi, of Tokyo Woman's Christian College, for his many helpful discussions throughout this work.

*Department of Chemistry*
*Yokohama City University*
*Kanazawa-ku, Yokohama*

13) A. J. B. Spaull and M. R. Nearn, ibid., **68**, 2043 (1964).

# The Preparation of Iminosulfonic Acid Derivatives by Means of Sulfinamides and *N*-Bromosuccinimide

By Hisashi TAKEI, Itaru WATANABE and Teruaki MUKAIYAMA

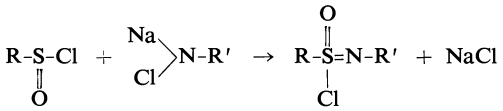
(Received May 15, 1965)

The preparation of *N*-alkyl and *N*-aryliminosulfonic acid derivatives by the reaction of sulfinamides with bromine or *N*-bromosuccinimide in the presence of amines or sodium *p*-nitrophenolate has been attempted on the assumption that the iminosulfonic acid derivatives might be useful as intermediates in the field of synthetic chemistry.

In this connection, Levchenko and his coworkers[1] have recently reported that *N*-sulfonyl, *N*-ethoxycarbonyl or *N*-acetyl iminosulfonyl chlorides may be prepared by the reaction of arylsulfinyl chlorides with sodium *N*-chlorosulfonamides, sodium ethyl *N*-chlorocarbamate or sodium *N*-chloroacetamide. The amides and esters of iminosulfonic acid are synthesized from the chlorides, and amines and sodium phenolate respectively:[2]

1) E. S. Levchenko, N. Ya. Derkach and A. V. Kirsanov, *Zhur. Obschei. Khim.*, **30**, 1971 (1960); *Chem. Abstr.*, **55**, 7335g (1961); *Zhur. Obschei. Khim.*, **31**, 1971 (1961); *Chem. Abstr.*, **55**, 27175g (1961); E. S. Levchenko, E. S. Kozlov and A. V. Kirsanov, *Zhur. Obschei. Khim.*, **31**, 2381 (1961); *Chem. Abstr.*, **56**, 4653h (1962); *Zhur. Obschei. Khim.*, **32**, 2585 (1962); *Chem. Abstr.*, **58**, 8947c (1963).

2) E. S. Levchenko, N. Ya. Derkach and A. V. Kirsanov, *Zhur. Obschei. Khim.*, **32**, 1208 (1962); *Chem. Abstr.*, **58**, 1388g (1963); E. S. Levchenko, E. S. Kozlov and A. V. Kirsanov, *Zhur. Obschei. Khim.*, **32**, 882 (1962); *Chem. Abstr.*, **58**, 2395f (1963); *Zhur. Obschei. Khim.*, **33**, 565 (1963); *Chem. Abstr.*, **59**, 2701f (1963).



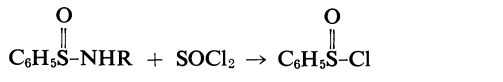
R=aryl
R'=arylsulfonyl, ethoxycarbonyl or acetyl

However, the method is not applicable to the synthesis of *N*-alkyl or *N*-aryliminosulfonic acid derivatives, because the sodium *N*-chloroalkyl or aryl amides are difficult to handle in the isolated state.

Iminochlorides are generally obtained by the reaction of carboxylic acid amides with phosgene, thionyl chloride or phosphorus pentachloride.[3] However, sulfonamides do not give the corresponding iminosulfonyl chlorides[4] when treated with the above-mentioned chlorinating reagents except in the case of diarylsulfonylimides[5] and *N*-dichlorophosphorylarylsulfonamides.[4a]

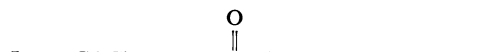
In the present experiment, the preparation of benzene-*N*-phenyliminosulfinyl chloride from benzenesulfinanilide (Ia) and thionyl chloride was attempted first. When a benzene solution of Ia and excess thionyl chloride was refluxed for half an hour, a 87% yield of be benzenesulfinyl chloride and a 88% yield of *N*-sulfinylaniline were obtained instead of the expected iminosulfinyl chloride. *N*-Cyclohexylbenzenesulfinamide (Ib) reacted with thionyl chloride to yield 11% of benzenesulfinyl chloride and 13% of *N*-sulfinylcyclohexylamine, along with a large amount of a dark-colored tarry product.

Similarly, the reaction of Ia with phosgene gave a 55% yield of benzenesulfinyl chloride and a 42% yield of phenyl isocyanate.

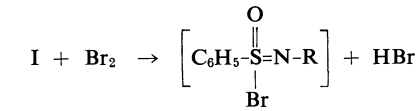


(Ia) R=$C_6H_5$

(Ib) R= 

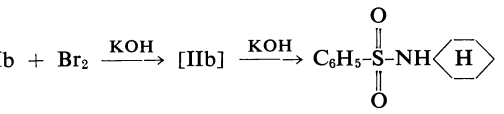


Since the preparation of iminosulfonyl halide or iminosulfinyl halide by a method similar to those used for iminochloride had proved unsuccessful, it was thought advisable to investigate the method of preparing the iminosulfonyl bromide by the oxidation of sulfinamides with bromine, a method shown in the following equation:

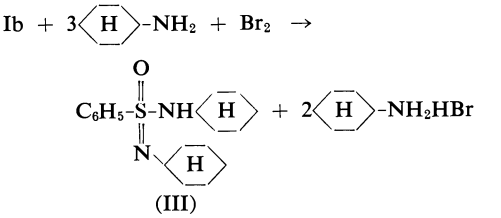


(II)

The expected product, benzene-*N*-cyclohexyliminosulfonyl bromide (IIb), could not be isolated by the addition of bromine to a suspension of Ib in carbon tetrachloride, but cyclohexylamine hydrobromide was obtained in a good yield. It is known that sulfinamides are unstable towards acid;[6] therefore, it seemed reasonable to assume that the hydrogen bromide initially produced rapidly react with Ib, thus giving cyclohexylamine hydrobromide. On the other hand, when bromine was added drop-by-drop to a solution of Ib and potassium hydroxide in 50% aqueous ethanol, *N*-cyclohexylbenzenesulfonamide, the oxidized product of Ib, was obtained in a 60% yield. This may be produced by the hydrolysis of the IIb initially formed.



It is to be expected that if the above reaction is carried out in the presence of primary or secondary amine instead of potassium hydroxide, IIb will rapidly react with the amine to yield iminosulfonamide. Indeed, when the reaction of Ib with bromine in carbon tetrachloride was attempted at 0°C in the presence of three times as many moles of cyclohexylamine, *N*-cyclohexylbenzene-*N*-cyclohexyliminosulfonamide (III) was obtained in a 32% yield, along with cyclohexylamine hydrobromide. The III was identified by elemental analyses and by means of its infrared spectrum, which has the characteristic bonds of the nitrogen hydrogen bond (3250 $cm^{-1}$) and of the iminosulfonyl group (1272 $cm^{-1}$, 1255 $cm^{-1}$ and 1135 $cm^{-1}$).[7]



(III)

3) These reactions have been reported by many workers, for example, O. Wallach, *Ann.*, **184**, 1 (1877); J. v. Braun and W. Pinkernelle, *Ber.*, **67**, 1218 (1934).

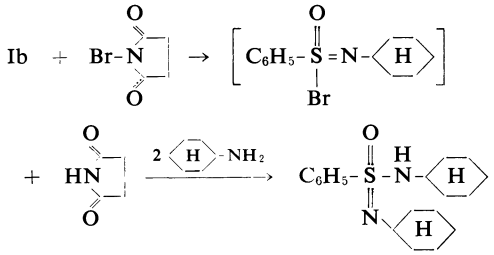
4) a) E. S. Levchenko and A. V. Kirsanov, *Zhur. Obscheĭ. Khim.*, 30, 1553 (1960); *Chem. Abstr.*, **55**, 3484g (1961). b) J. v. Braun and K. Waissbach, *Ber.*, **63B**, 2836 (1930).

5) E. S. Levchenko, N. Ya. Derkach and A. V. Kirsanov, *Zhur. Obschei. Khim.*, 32, 1212 (1962); *Chem. Abstr.*, **58**, 4456h (1963).

6) D. Klamann, Chr. Sass and M. Zelenka, *Chem. Ber.*, **92**, 1910 (1959).

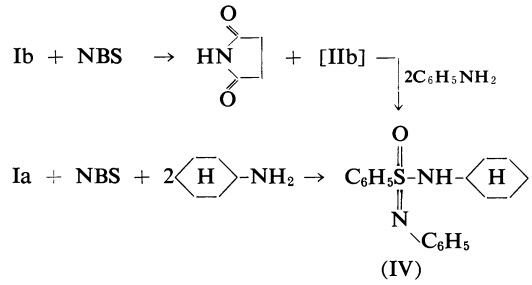
7) E. S. Levchenko, E. S. Kozlov, A. A. Kisilenko and A. V. Kirsanov, *Zhur. Obscheĭ. Khim.*, 33, 3065 (1963); *Chem. Abstr.*, **60**, 2451h (1964).

When *N*-bromosuccinimide (NBS) was used instead of bromine in the above experiment, III was obtained in a 69% yield, along with succinimide and cyclohexylamine hydrobromide. This reaction is considered to proceed through an initial formation of IIb and succinimide by a reaction of Ib with NBS similar to that of Ib with bromine. The IIb in turn reacts with cyclohexylamine to yield III.

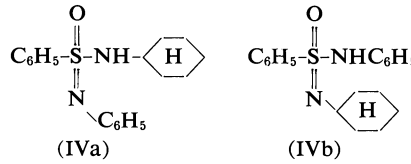


However, the treatment of Ib and NBS in the presence of aniline did not give *N*-cyclohexylbenzene-*N*-phenyliminosulfonamide (IV), presumably because of the facile reaction of NBS with aniline. Instead, IV was obtained in a 73% yield, along with succinimide and aniline hydrobromide, when NBS and Ib were stirred at 0°C for forty minutes in carbon tetrachloride and then two times as many moles of aniline were added to the reaction mixture. On the other hand, the yield of IV decreased to 39% when Ib and NBS were treated for three hours before the addition of aniline. Thus, it seemed reasonable to assume that the intermediate, *N*-cyclohexyliminobenzenesulfonyl bromide (IIb), may be unstable even at 0°C.

On the other hand, IV was also obtained in a 84% yield by the reaction of Ia with NBS in the presence of cyclohexylamine.



There may be two tautomeric forms of IVa and IVb for IV. The phenyl group has a greater tendency to attract electrons and IV should, therefore, tend to exist as formula IVa:



The results of the reactions of Ia or Ib and NBS in the presence of various amines are summarized in Table I.

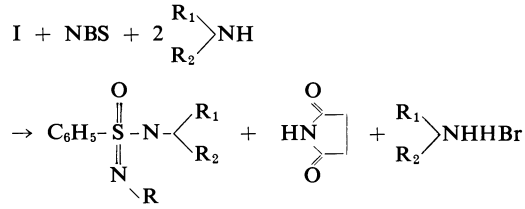
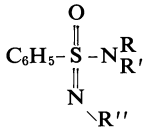


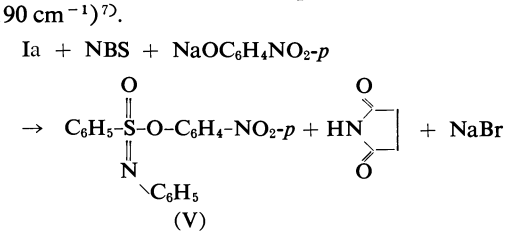
Table I. Preparation of benzeneiminosulfonamides



| $R\diagdown R'\diagup N-$ | R'' | Yield % | M. p. °C | Formula | C, % Found | C, % Calcd. | H, % Found | H, % Calcd. | N, % Found | N, % Calcd. |
|---|---|---|---|---|---|---|---|---|---|---|
| *n*-$C_6H_{13}NH-$ | H- | 53 | 52— 54[a,b] | $C_{18}H_{30}N_2OS$ | 66.66 | 67.05 | 9.61 | 9.38 | 8.93 | 8.68 |
| H-NH- | H- | 69 | 100—101[b] | $C_{18}H_{28}N_2OS$ | 67.39 | 67.47 | 8.81 | 8.81 | 8.50 | 8.74 |
| N- | H- | 55 | 75— 76[b] | $C_{17}H_{26}N_2OS$ | 66.71 | 66.64 | 8.75 | 8.55 | 9.21 | 9.44 |
| *n*-$C_4H_9NH-$ | $C_6H_5$- | 81 | 52— 53[b] | $C_{16}H_{20}N_2OS$ | 66.71 | 66.64 | 7.22 | 6.99 | 9.87 | 9.72 |
| *n*-$C_6H_{13}NH-$ | $C_6H_5$ | 94 | 49— 50[b] | $C_{18}H_{24}N_2OS$ | 68.32 | 68.33 | 7.83 | 7.65 | 9.14 | 8.85 |
| H-NH- | $C_6H_5$ | 84 | 149—150[c] | $C_{18}H_{22}N_2OS$ | 68.63 | 68.77 | 7.16 | 7.05 | 8.92 | 8.91 |
| N- | $C_6H_5$ | 95 | 115—116[d] | $C_{17}H_{20}N_2OS$ | 67.88 | 67.98 | 6.53 | 6.71 | 9.54 | 9.33 |
| O N- | $C_6H_5$ | 95 | 107—108[d] | $C_{16}H_{18}N_2O_2S$ | 63.78 | 63.56 | 6.22 | 6.00 | 9.34 | 9.27 |

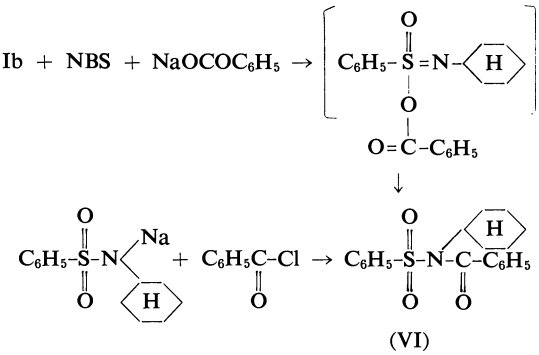
a) B. p. 168—172°C/0.13 mmHg. b) Recrystallized from petroleum ether. c) Recrystallized from alcohol. d) Recrystallized from ligroin.

Next, the preparation of the *p*-nitrophenyl ester of iminosulfonic acid by the reaction of Ia with NBS and sodium *p*-nitrophenolate was attempted. When the suspension of Ia, NBS and sodium *n*-nitrophenolate in carbon tetrachloride was stirred at 0°C for about 10 hr., *p*-nitrophenyl benzene-*N*-phenyliminosulfonate (V) was obtained in a 48% yield. The infrared spectrum of V contains characteristic bands assignable to a nitro group (1349 $cm^{-1}$) and a iminosulfonyl group (1250 $cm^{-1}$ and 1190 $cm^{-1}$)[7].



(V)

When the reaction of Ib, NBS and sodium benzoate was carried out, colorless needles were obtained in a high yield, along with succinimide and sodium bromide. These needles were identified as *N*-benzoyl-*N*-cyclohexylbenzenesulfonamide (VI) by elementary analyses and by a comparison of them with an authentic sample prepared by the reaction of sodium *N*-cyclohexylbenzenesulfonamide with benzoyl chloride. This finding suggests that an initially-formed IIb reacted with sodium benzoate to give the intermediate, iminosulfonic benzoic anhydride, which in turn rearranged to yield VI.[8]



(VI)

## Experimental

**Benzenesulfinanilide (Ia) and *N*-Cyclohexylbenzenesulfinamide (Ib).**—These compounds were prepared, according to the method of Klaman et al.,[6] from phenylmagnesium bromide and the corresponding *N*-sulfinylamine.

**The Reaction of Ia with Thionyl Chloride.**—To a suspension of Ia (2.17 g., 0.01 mol.) in anhydrous benzene, excess thionyl chloride (3.0 g., 0.025 mol.) was added, the mixture was then refluxed for half an hour. After the solvent and the excess thionyl chloride had been removed, benzenesulfinyl chloride (1.42 g., 88%; b. p. 90—93°C/4 mmHg) and *N*-sulfinylaniline (1.20 g., 87%; b. p. 96—98°C/18 mmHg) were obtained.

When Ib (2.23 g., 0.01 mol.) was used in place of Ia in the above experiment, benzenesulfinyl chloride (0.17 g., 11%) and *N*-sulfinylcyclohexylamine (0.19 g., 13%; b. p. 55°C/4 mmHg) were obtained, along with a large amount of a tarry product.

**The Reaction of Ia with Phosgene.**—To a suspension of Ia (2.17 g., 0.01 mol.) in anhydrous benzene, 30% phosgene in toluene (3.3 g., 0.01 mol.) was added drop-by-drop under cooling; the mixture was then refluxed for half an hour. A 55% yield of benzenesulfinyl chloride (0.88 g.) and a 42% yield of phenyl isocyanate (0.50 g.) were obtained by fractional distillation.

***N*-Cyclohexylbenzenesulfonamide.**—To a solution of Ib (2.23 g., 0.01 mol.) and potassium hydroxide (1.34 g., 0.034 mol.) in 50% aqueous ethanol, bromine (1.60 g., 0.01 mol.) was added drop-by-drop under cooling. The mixture was evaporated to dryness under reduced pressure, and the residue was extracted with hot ligroin to give colorless needles (1.43 g. (60%); m. p. 89—90°C (undepressed by admixture with an authentic sample)).

***N*-Cyclohexylbenzene-*N*-cyclohexyliminosulfonamide (III).**—a) To a mixture of Ib (2.23 g., 0.01 mol.) and cyclohexylamine (3.07 g., 0.031 mol.) in 30 ml. of carbon tetrachloride, bromine (1.60 g., 0.01 mol.) was added drop-by-drop under cooling; cyclohexylamine hydrobromide and succinimide were thus precipitated. The filtrate was evaporated, and the dark-colored residue was chromatographed on alumina. III was eluted with ether and recrystallized from petroleum ether (1.02 g. (32%); m. p. 100—101°C).

Found: C, 67.39; H, 8.81; N, 8.50; S, 10.18. Calcd. for $C_{18}H_{28}N_2OS$: C, 67.47; H, 8.81; N, 8.74; S, 9.99%.

b) A mixture of cyclohexylamine (3.07 g., 0.031 mol.), Ib (2.23 g., 0.01 mol.) and *N*-bromosuccinimide (NBS) (1.78 g., 0.01 mol.) in carbon tetrachloride was stirred for 3 hr. at 0°C and then for an additional 3 hrs. at room temperature. III was obtained from the filtrate in a 69% yield (2.20 g.; m. p. 100—101°C). Similarly, when *N*-bromophthalimide was used instead of NBS in the above experiment, III was obtained in a 50% yield.

***N*-Cyclohexylbenzene-*N*-phenyliminosulfonamide (IV).**—a) A mixture of Ia (2.17 g., 0.01 mol.) and NBS (1.78 g., 0.01 mol.) in carbon tetrachloride (30 ml.) was stirred for 40 min. at 0°C; then aniline (2.05 g., 0.022 mol.) was added, and the mixture was stirred for 3 more hr. The precipitate was collected and washed with water and weighed; 1.20 g., m. p. 140—143°C. The filtrate, after the solvent had been removed, gave an additional IV (1.10 g.); total yield, 2.30 g. (73%). The IV was recrystallized from ethanol (m. p. 149—150°C).

8) A similar rearrangement is observed in the case of the carboxylic imidic anhydride produced by the reaction of sodium carboxylate with imidoyl chloride; it yields diacylamides. O. Mumm, H. Hesse and H. Volquartz, *Ber.*, **48**, 388 (1915); F. Cramer and K. Baer, ibid., **93**, 1231 (1960).

Found: C, 68.63; H, 7.16; N, 8.92. Calcd. for $C_{18}H_{22}N_2OS$: C, 68.77; H, 7.05; N, 8.91%.

When a mixture of Ib and NBS in carbon tetrachloride was stirred for 3 hr. at 0°C before the addition of aniline as in the above experiment, the yield dropped to 1.22 g. (39%).

b) Similarly, when a mixture of Ib (2.17 g., 0.01 mol.), NBS (1.78 g., 0.01 mol.) and cyclohexylamine (3.07 g., 0.031 mol.) was stirred for 2 hr. at 0°C and then for an additional 3 hr. at room temperature, IV was obtained in a 84% yield (2.65 g.).

The other iminosulfonamides were prepared by the reaction of Ia or Ib, NBS and 2 mol. of the corresponding amines. The results are listed in Table I.

***p*-Nitrophenyl Benzene-*N*-phenyliminosulfonate (V).**—A mixture of Ia (2.23 g., 0.01 mol.), NBS (1.78 g., 0.01 mol.) and sodium *p*-nitrophenolate (1.78 g., 0.011 mol.) in 30 ml. of carbon tetrachloride was stirred for 10 hr. at 0°C. The filtrate, after the solvent had been removed, gave a dark-colored syrup. When a small portion of ethanol was added to the syrup, pale yellow V was crystallized out (1.70 g., 48%; m. p. 70—72°C). When it was recrystallized from ethanol, its m. p. was 72—73°C.

Found: C, 60.75; H, 3.91; N, 8.07. Calcd. for $C_{18}H_{14}N_2O_4S$: C, 61.01; H, 3.98; N, 7.91%.

***N*-Benzoyl-*N*-cyclohexylbenzenesulfonamide (VI).**—A mixture of Ib (2.23 g., 0.01 mol.), NBS (1.78 g., 0.01 mol.), and sodium benzoate (1.44 g., 0.01 mol.) in 30 ml. of carbon tetrachloride was stirred for 3 hrs. at 0°C and then for an additional 3 hr. at room temperature. The precipitate was collected and washed with water to give VI (2.44 g. (71%), m. p. 140—142°C). When it was then recrystallized from ethanol, its m. p. was 143—144°C. The infrared spectrum (KBr) showed strong absorptions at 1650 $cm^{-1}$ (C=O of amide linkage) and at 1330 $cm^{-1}$ and 1160 $cm^{-1}$ ($SO_2$ linkage).

Found: C, 66.18; H, 6.13; N, 3.82; S, 9.40. Calcd. for $C_{19}H_{21}NO_3S$: C, 66.46; H, 6.16; N, 4.08; S, 9.32%.

When the same reaction was carried out in tetrahydrofuran, methylene chloride or ether, the yield of VI decreased to 58%, 17% or 5% respectively.

This compound VI can also be prepared by the reaction of sodium *N*-cyclohexylbenzenesulfonamide with benzoyl chloride.

## Summary

It has been found that *N*-substituted benzenesulfinamides (I) react with thionyl chloride to give benzenesulfinyl chloride and the corresponding *N*-sulfinylamines, and that they are oxidized by treatment with bromine in an alkaline solution to give *N*-substituted sulfonamides.

When these benzenesulfinamides are treated with bromine or *N*-bromosuccinimide (NBS) in the presence of various primary or secondary amines, the corresponding benzeneiminosulfonamides are obtained in high yields. Similarly, the reaction of I, NBS and sodium *p*-nitrophenolate or sodium benzoate yields *p*-nitrophenyl benzeneiminosulfonate or *N*-benzoylbenzensulfonamide. These reactions are considered to proceed through the benzeneiminosulfonyl bromides formed by the oxidation of sulfinamides with bromine or NBS.

*Laboratory of Organic Chemistry*
*Tokyo Institute of Technology*
*Ookayama, Tokyo*

# A Study of Zinc Oxide - Chromium Oxide Catalysts. VI. The Changes Brought about by Heat Treatment in the Activity for Methanol Synthesis and in the Structure of the Raw Catalysts

By Hiroshi UCHIDA, Masaaki OBA and Michio ARAKI

(Received May 24, 1965)

A number of papers have appeared dealing with those methanol-synthesis catalysts which consist of the oxides of zinc and chromium.[1] However, most of these papers have described mainly the relation of the activity and of the catalyst structure to the chemical composition. The only exception is a series of papers by Kawamura and his associates,[3-6] who investigated the reduction process of the catalysts in detail and also the changes in the activity and in the structure of the reduced catalysts brought

1) See Ref. 2.
2) G. Natta, "Catalysis," III, Reinhold Publ., N. Y. (1955), p. 349.
3) M. Kawamura, T. Irie, T. Shiraishi and K. Tokunaga, *J. Chem. Soc. Japan, Ind. Chem. Sec.* (*Kogyo Kagaku Zassi*), **60**, 162 (1957).
4) M. Kawamura and T. Irie, ibid., **60**, 162 (1957).
5) M. Kawamura and T. Irie, ibid., **60**, 170 (1957).
6) T. Irie and T. Shiraishi, *J. Chem. Soc. Japan, Pure Chem. Sec.* (*Nippon Kagaku Zasshi*), **80**, 107 (1957).

about by heat treatment. In the course of our previous study[7] of the catalysts, it became evident that the activity declined considerably if a dry preparation from a slurry of zinc oxide powder in aqueous chromic acid was preheated in the air in the hope that the shrinkage of the catalyst bed during the synthesis might be avoided. This observation makes us suspect that a change in the catalyst structure might accompany this decline in activity. However, in order that a better understanding of the dependence of the catalyst performance upon the history of a catalyst may be obtained, a more detailed study on this subject is required.

## Experimental

**Catalyst Preparation and Activity Measurement.**—Catalysts with different chromium/zinc atomic ratios were prepared from commercial zinc oxide powder and chromic acid in the following way. A slurry of the zinc oxide powder in aqueous chromic acid was spread over a glass plate and evaporated to dryness in the air at room temperature. The resulting cake was then ground to a 100-mesh powder, and the powder was pelleted (4 mm. in diameter by 4 mm. high). The chromium/zinc atomic ratios in the catalysts thus prepared were 0.1, 0.5, and 1.0. Also, a catalyst not containing chromic acid was prepared by pelleting the zinc oxide powder to the same size.

Every kind of catalyst was treated as follows. A lot of the catalyst was divided into two parts. One part was reduced in a vessel different from the methanol synthesis reactor[7] and then immediately tested in the reactor for catalytic activity. The other part was first heated in the air at 400°C for 5 hr., and then reduced in the methanol synthesis reactor and tested for catalytic activity in situ. In this paper, the former class of catalysts will be denoted by the symbol "A," and the latter class, by the symbol "B." Also, if necessary, the numerals, 1, 2, 3, and 4, will be attached to the above symbols to indicate the chromium/zinc ratios of 0, 0.1, 0.5, and 1.0 respectively. Thus we will have A-1, A-2, etc.

In all cases, the reduction was carried out in a current of $2H_2$-1CO synthesis gas under atmospheric pressure; in the earlier stages of reduction, the temperature was gradually raised to 350°C over a 1.5 hr., period so that the glow phenomenon due to the rapid reduction of sexivalent chromium might be prevented in the catalyst bed. This final temperature was maintained for 4 hr.

The activity for methanol synthesis was measured by the use of the same apparatus as has been described previously.[8] Five milliliters of a catalyst sample (1—2 mm.) was placed to the reactor in order to fill the annular space between the walls of the reactor and the centrally-placed stainless-steel thermocouple protection tube (4 mm. in OD and 2 mm. in ID). The catalyst bed formed was 18 mm. in OD, 4 mm. in ID, and 22 mm. high. The longitudinal temperature difference throughout the whole catalyst bed remained within 2°C when the activity measurements were made with a $2H_2$-1CO synthesis gas containing 4% nitrogen under the following conditions; pressure=150 kg./cm$^2$, space velocity based on the feed rate (vol./hr. at S. T. P.) of synthesis gas=$1\times10^4\pm50$ hr$^{-1}$, and temperature range=300—390°C.

In the experiments with the catalyst samples A-3 and B-3, the samples, once they had been used in the methanol synthesis, were heated in a hydrogen stream at 500°C for 8 hr.; then activity measurements were again made on these hydrogen-treated samples (designated as A'-3 and B'-3).

**The Investigation of Catalyst Structures.**—The specific surface area, $S$, was determined by applying the BET equation to the argon adsorption isotherm at −196°C. The density, $\rho_t$, was measured by the helium displacement method. From the values of $S$ and $\rho_t$, the average particle diameter, $\bar{d}$, was calculated according to the formula $\bar{d}=6/\rho_t S$, on the basis of the assumption that the particles have the form of a sphere or cube. Moreover, the particle size and shape in catalyst granules were examined under an electron microscope of the JEM-6 type. The samples for the electron microscopic observation were prepared by grinding the catalyst with castor oil in a mortar.

The X-ray diffraction patterns for powdered samples of the catalysts were obtained with an

Table I. Samples used for the investigation of catalyst structures

| Sample | Cr/Zn atomic ratio | Remarks |
|---|---|---|
| $A_0$-1 | 0 | Catalysts as prepared from slurries. (These are the original samples for the preparation of the othe series of samples listed in this table.) |
| $A_0$-2 | 0.1 | |
| $A_0$-3 | 0.5 | |
| $A_0$-4 | 1.0 | |
| $A_1$-1 | 0 | Reduced in $2H_2$-1CO gas stream under atmospheric pressure at temperatures below 350°C after the preparation from slurries. |
| $A_1$-2 | 0.1 | |
| $A_1$-3 | 0.5 | |
| $A_1$-4 | 1.0 | |
| $A_2$-1 | 0 | Reduced under the afore-mentioned conditions after the preparation from slurries and subsequently used for methanol synthesis. |
| $A_2$-2 | 0.1 | |
| $A_2$-3 | 0.5 | |
| $A_2$-4 | 1.1 | |
| $B_0$-1 | 0 | Heated in air at 400°C for 5 hr. after the preparation from slurries. |
| $B_0$-2 | 0.1 | |
| $B_0$-3 | 0.5 | |
| $B_0$-4 | 1.0 | |
| $B_1$-1 | 0 | Treated in the same manner as samples $B_0$ after the preparation from slurries and then used for methanol synthesis. |
| $B_1$-2 | 0.1 | |
| $B_1$-3 | 0.5 | |
| $B_1$-4 | 1.0 | |
| A'$_2$-3 | 0.5 | Obtained by heating samples $A_2$-3 and $B_1$-3 in hydrogen stream at 500°C for 8 hr. |
| B'$_1$-3 | 0.5 | |

7) If reduced in the reactor, the catalyst bed shrinks with the progress of reduction and, consequently cannot be tested for catalytic activity in situ.

8) M. Oba, Y. Ogino and H. Uchida, *Rpt. Gov't, Chem. Ind. Research Inst., Tokyo*, **60**, 121 (1965).

X-ray diffractometer of the Geigerflex D-3F type. The nickel-filtered Cu$K\alpha$ radiation from a sealed-off X-ray tube equipped with beryllium windows and operated at 40 kV. and 18 mamp. was used.

The above measurements and observations were conducted on catalyst samples taken at various stages of catalyst treatment. These samples are listed in Table I. In the nomenclature used here, subscript numbers are attached to the catalyst class symbols A and B in order to indicate the different treatments to which the catalysts, A and B, were subjected. Thus the symbols $A_1$ and $B_{1,}$, for example, stand for those samples of a catalyst of Class A or B which were subjected to a specified treatment.

## Results

**Activity for Methanol Synthesis.**—The methanol concentration in the exit gas is plotted against the reaction temperature in Fig. 1 for the synthesis runs conducted with the catalysts of two series, A and B.[9] Also, for the purpose of a quantitative comparison of activities, the values of the rate constant of methanol synthesis at 330°C, $k_{330}$, taken as a measure of the activity are listed in Table II. The $k_{330}$ values for synthesis with the catalysts A'-3 and B'-3 are also included in this table. The $k_{330}$ values were calculated according to Eq. 1, which was in turn derived from Rate Eq. 2.[10]

$$k=\frac{SV}{273\boldsymbol{R}}\times \int_0^z \frac{\left[\nu_{CO}\nu_{H_2}{}^2 4P^3\{1+(1-n)z\}\left(\frac{n}{2}-z\right)\right]^{0.3}}{(1+2z)^2\left[\nu_{CO}\nu_{H_2}{}^2\frac{4P^3\{1+(1-n)z\}}{(1+n)^3}-\frac{\nu_{CH_3OH}Pz}{K}\right]} \quad (1)$$

$$r=k\{(f_{CO}f_{H_2}{}^2)^{0.7}-f_{CH_3OH}(f_{CO}f_{H_2}{}^2)^{-0.3}/K\} \quad (2)$$

In these equations, $SV$ ($hr^{-1}$) is the space velocity based on the feed rate of the synthesis gas; $\boldsymbol{R}$, the gas constant; $\nu_i$, the fugacity coefficient of the $i$th component; $P$ (atm.), the total pressure of the $H_2$-CO gas; $n$ the $H_2$/CO mol. ratio; $z$, the mole fraction of methanol in the exit gas; $r$ (mol./hr.), the rate of methanol formation; $f_i$ (atm.), the fugacity of the $i$th component, and $K$, the equilibrium constant of reaction. Both Fig. 1 and Table II show that the optimum chromium/zinc atomic ratio is 0.5 for each series of catalysts, and that all the catalysts of series A have higher activities than the corresponding catalysts of series B.

A comparison of the activity difference between catalysts A-3 and A'-3 with the difference between the catalysts B-3 and B'-3 (Fig. 2 and Table II) may give an approximate concept of the relative thermal stability of the two series, A and B. The stronger thermal stability of the catalysts of series A may be seen from the data.[11]

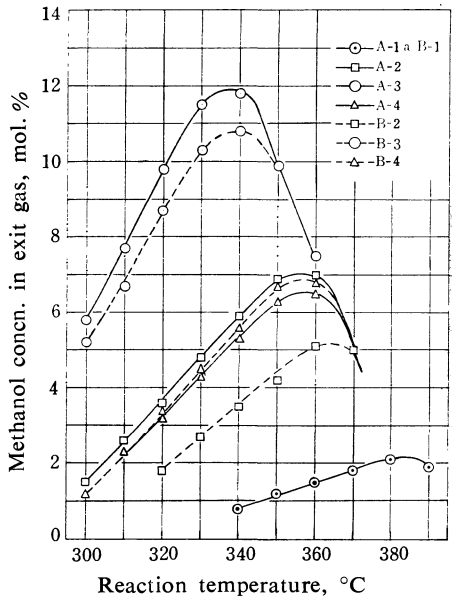



Fig. 1. Catalyst activity for methanol synthesis.

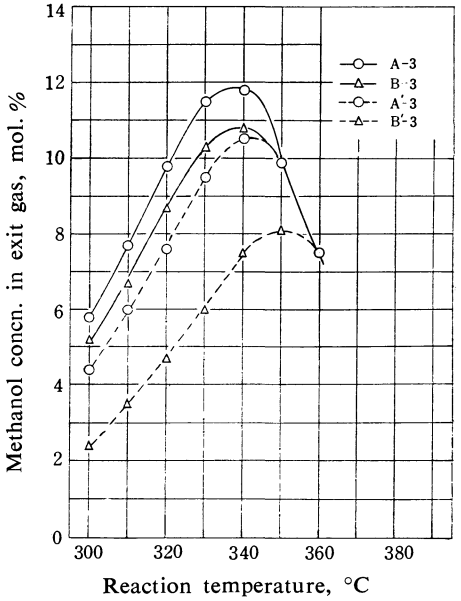



Fig. 2. Catalyst activity for methanol synthesis.

9) According to the nomenclature in Table I, these catalysts should be denoted by the symbols $A_1$ and $B_0$. However, for the sake of simplicitys, the symbols with the subscript numbers will not be used unless necessary.

10) H. Uchida and Y. Ogino, This Bulletin, 31, 45 (1958).

11) When catalysts A-3 and B-3 were heated in hydrogen for only 2 hr., their activities decreased to the same extent as when the catalysts were heated in the same medium for 8 hr.

TABLE II. RATE CONSTANT OF METHANOL SYNTHESIS AT 330°C ($k_{330}$), SPECIFIC RATE CONSTANT ($k'_{330}$), ACTIVATION ENERGY ($E$), AND FREQUENCY FACTOR PER UNIT SURFACE AREA ($A'$)

| Catalyst | $k_{330}$ $atm^{-2.1}hr^{-1}$ | $k'_{330}$ $atm^{-2.1}ml.hr^{-1}m^{-2}$ | $E$ kcal./mol. | $A'$ $atm^{-2.1}ml.hr^{-1}m^{-2}$ |
|---|---|---|---|---|
| A-1 | $0.50\times10^{-2}$ | $1.65\times10^{-4}$ | 33 | $1.44\times10^{8}$ |
| A-2 | $5.90\times10^{-2}$ | $11.5\times10^{-4}$ | 24 | $3.17\times10^{5}$ |
| A-3 | $17.9\times10^{-2}$ | $18.2\times10^{-4}$ | 21 | $4.79\times10^{4}$ |
| A-4 | $5.25\times10^{-2}$ | $4.29\times10^{-4}$ | 26 | $8.51\times10^{5}$ |
| B-1 | $0.50\times10^{-2}$ | $1.69\times10^{-4}$ | 33 | $1.47\times10^{8}$ |
| B-2 | $3.20\times10^{-2}$ | $1.43\times10^{-4}$ | 39 | $4.33\times10^{10}$ |
| B-3 | $15.2\times10^{-2}$ | $6.32\times10^{-4}$ | 21 | $3.56\times10^{4}$ |
| B-4 | $5.60\times10^{-2}$ | $2.64\times10^{-4}$ | 29 | $2.77\times10^{6}$ |
| A'-3 | $13.5\times10^{-2}$ | $16.0\times10^{-4}$ | 22 | $1.36\times10^{5}$ |
| B'-3 | $7.70\times10^{-2}$ | $18.7\times10^{-4}$ | 24 | $8.51\times10^{5}$ |

TABLE III. BED DENSITY ($\rho_b$), SURFACE AREA ($S$), HELIUM DENSITY ($\rho_t$), AVERAGE PARTICLE DIAMETER ($\bar{d}$), AND LATTICE CONSTANT ($a$)

| Catalyst | $\rho_b$ g./ml. | $S$ $m^2/g.$ | $\rho_t$ g./ml. | $\bar{d}$, Å | $a$, Å ZnO | $a$, Å $ZnCr_2O_4$ | Identification[b] |
|---|---|---|---|---|---|---|---|
| $A_0$-1 | 2.10 | 3.8 | 5.47 | 2900 | 3.252 | — | Z |
| $A_0$-2 | 1.44 | 3.0 | 3.78 | 5300 | 3.251 | — | Z+III$\beta$+I$\beta$(v.w.) |
| $A_0$-3 | 1.56 | 4.0 | 3.49 | 4300 | — | — | I$\beta$ |
| $A_0$-4 | 1.38 | 2.0 | 3.20 | 9400 | — | — | Zn bichromate presumably |
| $A_1$-1 | 2.08 | 5.2 | 5.23 | 3300 | | — | Z |
| $A_1$-2 | 1.38 | 120 | 4.37 | 110 | 3.251 | — | Z |
| $A_1$-3 | 1.17 | 128 | 3.69 | 130 | 3.250 | 8.482 | Z+S(w.) |
| $A_1$-4 | 1.26 | 93 | 3.90 | 170 | 3.246 | 8.482 | Z+S |
| $A_2$-1 | 2.08 | 13.5 | 5.47 | 810 | | — | Z |
| $A_2$-2 | 1.38 | 37 | 4.90 | 330 | 3.251 | 8.523 | Z+S(v.w.) |
| $A_2$-3 | 1.17 | 83.5 | 4.46 | 160 | 3.249 | 8.397 | Z+S |
| $A_2$-4 | 1.26 | 97 | 4.28 | 145 | — | | Z(v.w.)+S |
| $B_0$-2 | 1.33 | 14.3 | 5.04 | 830 | 3.251 | — | Z |
| $B_0$-3 | 1.46 | 15 | 4.51 | 880 | 3.250 | 8.434 | Z+S(v.w.)+? |
| $B_0$-4 | 1.24 | 6.2 | 3.62 | 2700 | — | 8.429 | Z(w.)+S+? |
| $B_1$-1 | 2.18 | 13.5 | 5.50 | 810 | 3.249 | — | Z |
| $B_1$-2 | 1.37 | 163 | 5.53 | 67 | 3.253 | — | Z+S(w.) |
| $B_1$-3 | 1.41 | 170 | 5.18 | 68 | 3.252 | 8.460 | Z+S |
| $B_1$-4 | 1.18 | 178 | 5.09 | 66 | — | 8.408 | Z(v.w.)+S |
| $A_2'$-3 | 1.56 | 54 | 4.52 | 240 | 3.256 | 8.470 | Z+S |
| $B_1'$-3 | 1.49 | 28 | 4.83 | 450 | 3.254 | 8.453 | Z+S |

b) The symbols Z and S stand for zinc oxide and zinc chromite while I$\beta$ and III$\beta$ for zinc hydroxychromates I$\beta$ and III$\beta$ respectively.

The liquid product of methanol synthesis, in general, contains small amounts of such by-products as dimethyl ether, methylformate, water, formaldehyde, and isobutanol. Therefore, the liquid products obtained in the synthesis runs conducted at 380°C with different catalysts were analyzed for such by-products.[12] The results show that the proportion of water in the liquid product obtained with a catalyst of a lower activity is greater than in the product obtained with a catalyst of a higher activity (e.g., 5% water in the case of the catalyst A-3 and 1.1% in the case of the catalyst A-1), whereas the proportions of the other by-products are nearly in dependent of catalyst species or of chromium content (0.7—1.5% dimethyl ether, 0.5—0.6% methylformate, and 0.1% formaldehyde).[13]

**Surface Area and Average Particle Diameter.** —The results of the surface-area determination are summarized in Table III. The surface areas of three original catalysts containing chromium, $A_0$-2, $A_0$-3, and $A_0$-4, are very small, even

12) The by-products were determined gas chromatographically except for formaldehyde, which was determined iodometrically.

13) The percentages are based on the weight of the liquid product. In no cases was isobutanol detectable.

smaller than the surface area of the original zinc oxide catalyst, $A_0$-1. If these chromium-containing catalysts are reduced in the synthesis gas, the reduced catalysts ($A_1$-2, $A_1$-3, and $A_1$-4) show quite large surface areas, 30—50 times as large as the surface areas before reduction. However, when these reduced catalysts are used for methanol synthesis, the surface area decreases more or less according to the chromium content; the smaller the chromium content, the smaller the surface area. (Compare the surface areas of the samples $A_1$ with those of the samples $A_2$.) On the other hand, if the original catalysts are heated in the air at 400°C, the surface area of the chromium-containing catalysts is slightly increased (see the data for the samples $B_0$), while when these heat-treated catalysts are used for methanol synthesis, the surface areas of such samples ($B_1$) are greater than those of the samples $A_2$. It is worth noting here that the surface area is nearly the same for all the samples $B_1$, being independent of the chromium content. On the other hand, when two catalyst samples once used for methanol synthesis, $A_2$-3 $B_1$-3, are heated in hydrogen at 500°C for 8 hr., the surface areas are markedly decreased, the extent of decrease being greater in the case of the sample $B_1$-3 (see the data for $A_2'$-3 and $B_1'$-3).[14]

The density, $\rho_t$, is the highest for the catalyst samples with no chromium; it tends to decrease with an increase in the chromium content.

The values of the average particle diameter are also listed in Table III. Particles in the chromium-containing original catalysts ($A_0$) are quite large, much larger than the particles in the original zinc oxide catalyst. However, when these catalysts are reduced in the synthesis gas, the particles are split into very fine particles.

**X-Ray Diffraction.**—The results obtained are summarized in Table III. In the case of the chromium-containing catalysts $A_0$, if the chromium/zinc ratio is smaller than the ratio for zinc hydroxychromate I$\beta$ ($ZnCrO \cdot Zn(OH)_2$, $Cr/Zn=0.5$), all the chromic acid added will react with zinc oxide to form zinc hydroxychromates. In fact, the X-ray diffraction pattern of the sample $A_0$-2 shows the presence of hydroxychromate III$\beta$ ($ZnCrO_4 \cdot 3\text{-}4Zn(OH)_2$), together with zinc oxide, whereas the diffraction pattern of the sample $A_0$-3 shows the presence of hydroxychromate I$\beta$ alone. If the proportion of chromic acid is further increased, there appears another diffraction pattern which has not yet been identified. Kawamura et al.,[3] however, attributed this diffraction pattern to a bichromate.

When the chromium-containing original catalysts ($A_0$) are reduced in the synthesis gas or are used for methanol synthesis, the resultant catalysts give diffraction diagrams quite different from those for the original catalysts. In such diagrams, no crystalline phase other than those of zinc oxide and zinc chromite is observed. This indicates that hydroxychromates has undergone decomposition in the synthesis gas. The decomposition of hydroxychromates is also caused by the heat treatment of the same original catalysts in the air at 400°C, as is evidenced by the diffraction data obtained with the $B_0$ catalysts. However, the results of the differential thermal analysis and the thermogravimetric analysis of the sample $A_0$-3 (Fig. 3)[15] show that the decomposition occurring

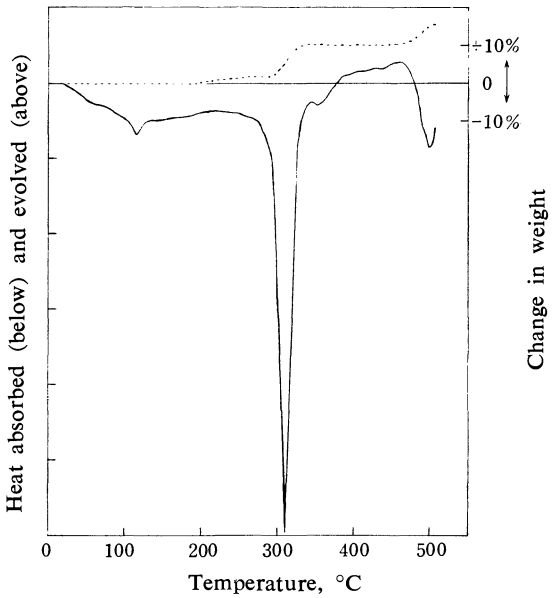



Fig. 3. Differential thermal analysis curve and thermogravimetric analysis curve.
—— D. T. A. ---- T. G. A.

in the air is different in type from the decomposition in the synthesis gas. The former type of decomposition is endothermic and takes place at ca. 310°C, whereas the latter type is exothermic and, according to Kawamura and Irie,[5] begins to take place at a much lower temperature, i. e., 200°C. The endothermic peak observed is due to the conversion of sexivalent chromium oxide by oxygen removal into the

14) When the catalysts A-3 and B-3 were heated in hydrogen for only 2 hr., the surface areas decreased to the same extent as when the catalysts were heated in the same medium for 8 hr.

15) Similar results, though not the same as those reported here, were presented by Kawamura et al.[3] for a variety of zinc oxide-chromium oxide catalysts, but their results for a catalyst similar to the present one are not identical with ours.

trivalent oxide, which combines with zinc oxide to form zinc chromite.

Besides the diffraction patterns due to zinc oxide and zinc chromite, the diffraction diagram of the sample $B_0$-4 shows complicated patterns, which, though not identified, give evidence for the formation of intermediates in the decomposition process.

On the basis of diffraction lines due to the (110) plane of zinc oxide and the (400) plane of zinc chromite, the lattice constants for the two components have been calculated; they are listed in Table III. The lattice constants calculated for the zinc oxide in the catalyst samples vary little among the samples and agree with the literature value (a=3.249 Å).[16] whereas the lattice constants found for the zinc chromite[17] in the catalyst samples are, in general, greater than the literature values[18] ($a$=8.32, 8.20 Å).[16] According to Irie and Shiraishi,[6] the zinc chromite produced by the reduction of the hydroxychromates at low temperatures occludes zinc oxide, and its lattice is enlarged to form a stressed structure. By taking their view into consideration, the present observation may be interpreted as follows: Where there is a non-stoichiometric structure of zinc chromite, $Zn^{2+}$ will enter the structure to occupy the empty interstices; as a result, the lattice will be enlarged, with stresses set up on it. The zinc chromite retains the enlarged lattice even when heated for a prolonged time in hydrogen at 500°C.

**Electron Microscopic Picture.**—Upon the addition of aqueous chromic acid to zinc oxide powder (Micrograph 1), the reaction between the two reagents takes place around the periphery of the powders. This fact can be seen, though not directly, from Micrograph 5 with reference to a low-chromium sample once used for the synthesis (the sample $A_2$-2). As the amount of chromic acid is increased, the reaction extends into the interior of the powders, producing large crystals of zinc hydroxychromate I$\beta$ (see Micrograph 2 for the sample $A_0$-3). According to Feitknecht and Hugi-Carmes,[19] the crystal of this hydroxychromate grows to a thin hexagonal plate of large dimensions. The present observation is in agreement with their statement in that the crystal grows in the form of a layer-structure; the only difference is that the crystal is a thin plate of an irregular shape. The crystals here observed may be the fragments into which the original hexagonal plate has been broken as a result of grinding the catalyst in the preparation of samples for electron microscopic observation. On the other hand, the electron microscopic picture of a reduced catalyst (the sample $A_1$-3) is entirely different from that of the original (the sample $A_0$-3). Micrograph 3 for the sample $A_1$-3 shows a number of caterpillar-like particles within the original fringe of the hydroxychromate crystal, particles which are as fine as about 50 Å wide. Seemingly, the particle is an aggregate of a few crystallites of a spheroid structure (ca. 50 Å in diameter). When the reduced catalyst is used for methanol synthesis, the particles become greater and more gaps are formed between them, with no substantial change in the pattern visible in the original fringe of the crystal. (Compare Micograph 4 for the sample $A_2$-3 with Micrograph 3.) This phenomenon may be simply due to the progress of sintering during the synthesis run. It should here be noted that these electron microscopic pictures are quite different from that of the catalyst prepared from a mixed solution of the nitrates and ammonia (see Refs. 8 and 20).

In spite of the fact that zinc hydroxychromate undergoes thermal decomposition in the heat treatment of catalysts in the air at 310°C,

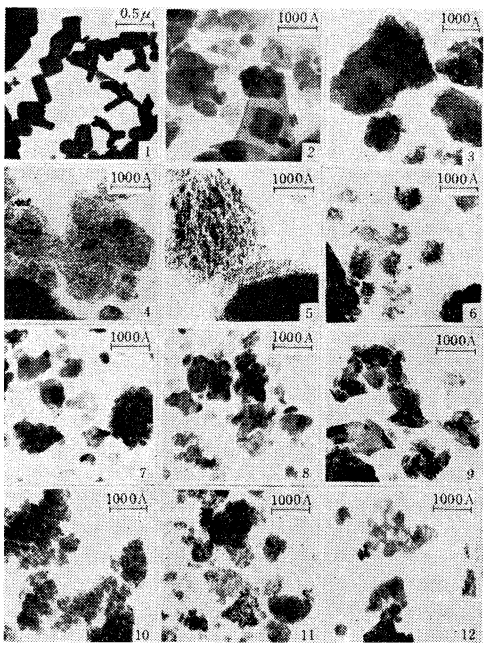



Fig. 4. Electron micrographs.

1, Sample $A_0$-1. 2, $A_0$-3. 3, $A_1$-3. 4, $A_2$-3. 5, $A_2$-2. 6, $A_2$-4. 7, $B_0$-3. 8, $B_1$-3. 9, $B_1$-4. 10, $A'_2$-3. 11, Residue from $A_2$-3. 12, Residue from $B_1$-3

16) A. S. T. M. Special Technical Publication 48-L, The X-ray Powder Data File, 1962.

17) Irie and Shiraishi[6] designated this structure as R and distinguished it from zinc chromite.

18) A sample with a chromium/zinc ratio of 1.98 was found to give the value of 8.331 Å after it was reduced and then heat-treated in the air at 800°C for 40 hr.

19) W. Feitknecht and L. Hugi-Carmes, *Helv. Chim. Acta*, 37, 2093 (1953).

the electron microscopic picture of a heat-treated catalyst (the sample $B_0$-3) is not essentially different from the original catalyst (the sample $A_0$-3). The only differences are that the crystal fragments are smaller and that massive fragments of an irregular shape are more abundant in the case of the sample $B_0$-3 than in the case of the sample $A_0$-3.

In contrast to the structural difference observed between the samples $A_0$-3 and $A_1$-3, no remarkable difference is found between the electron microscopic pictures of the samples $B_0$-3 and $B_1$-3 (i.e., the sample once used for methanol synthesis after heat treatment in the air). In the sample $B_1$-3, such a pattern as is observed in the micrograph for the sample $A_2$-3 appears only within a very small portion of the original fringe of the thin plate-like crystal; the major part remains so homogeneous that the individual particles, if present, are indistinguishable. This is also the case with the two samples of a high chromium content, $B_0$-4 and $B_1$-4 (see Micrograph 9).

When two samples once used for methanol synthesis, $A_2$-3 and $B_1$-3, are heated in hydrogen at 500°C, a marked crystal growth occurs, leading to the production of large crystals (compare Micrograph 10 with Micrograph 4), the growth being more pronounced in the sample $B_1$-3.[20]

**The Composition of Individual Particles.**—It yet remained unclarified whether the catalyst particles in a sample once used for methanol synthesis consist of the single component, zinc oxide or zinc chromite, or whether each particle is a composite substance made up of the two. For the study of this problem, two samples containing a large excess of zinc oxide, $A_2$-3 and $B_1$-3, in which the $ZnO/ZnCr_2O_4$ mol. ratio was 3, were treated with an aqueous ammonium acetate solution for half an hour at room temperature and the free zinc oxide removed;[22] the residues were then examined under an electron microscope.

The residue from the sample $A_2$-3 was found to have a chromium/zinc ratio of 1.79, which is approximately the ratio for zinc chromite. Its electron microscopic picture does not differ essentially from that of the initial sample (compare Micrograph 11 with Micrograph 4), although the caterpillar-like particles in the residue are thinner than in the initial sample and more white areas are observed. Therefore, it follows that most of the particles are aggregates of zinc oxide and zinc chromite crystallites, whereas the others consist of zinc oxide

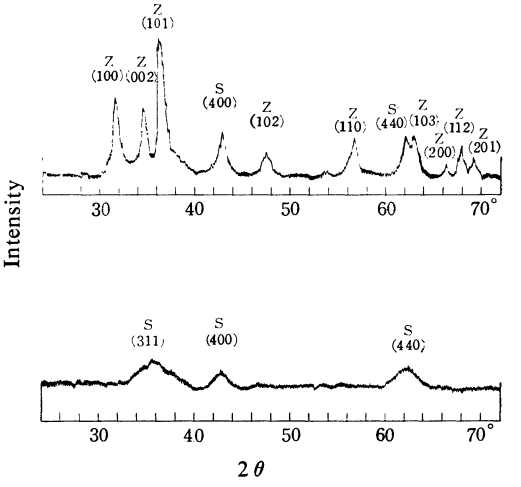



Fig. 5. X-Ray diffraction diagrams.
Above, sample $A_3$-3. Below, residue from sample $A_3$-3 after removal of zinc oxide.

alone or mainly of zinc oxide. This inference is also supported by a comparison of the X-ray diffraction diagram of the residue with that of the initial sample (Fig. 5). The X-ray diffraction diagram shows the presence of zinc chromite alone, and the diffraction lines due to zinc chromite are greatly broadened. The line-broadening effect is probably due to the stress imposed on the chromite lattice as a result of the removal of the zinc oxide initially present in the zinc chromite in excess of its stoichiometric proportion.

The electron microscopic picture of the residue from the sample $B_1$-3 (Micrograph 12) is somewhat different from that of the initial sample (Micrograph 8). Within the original fringe of the crystal there appear wide openings, in which presumably zinc oxide particles have predominated. Accordingly, either zinc oxide crystallites or zinc chromite crystallites are more or less concentrated locally within the fringe, and the mutual penetration of the two components seems to have been achieved not as thoroughly as in the case of the sample $A_2$-3.

## Discussion

**The Size and Shape of Particles.**—In general, the average particle diameter, $\bar{d}$, as calculated by use of the formula $\bar{d}=6/\rho_t S$, greatly differs from the size as estimated by electron microscopic observations. The shape one can imagine from the $\bar{d}$ for the particles in the sample $A_0$-3 is a sphere or cube about 4000 Å in diameter or in linear dimension. Similarly, the particle in the $A_2$-3 is considered to be a sphere or cube of the 160 Å size. However, electron

20) J. E. Germain and L. Ponsole, *Bull. soc. chim. France*, 1961, 1572.
21) Other electron micrographs will be presented elsewhere.
22) G. H. Osborn, *Analyst*, **76**, 114 (1951).

micrographs show a thin plate-like particle of several thousands Å size for the former sample, and a caterpillar-like particle about 50 Å in width for the latter. Such a discrepancy is also found in the case of the sample $A_2$-4. Particularly in the case of the sample $B_1$-3, the particle shape imaginable from the $\bar{d}$ differs markedly from the shape observed under the electron microscope. The $\bar{d}$ for the particles in this sample is calculated to be 70 Å. This size would be sufficiently large for the individual particles to be distinguished from one another in the electron micrograph if they could be assumed to be, for instance, spherical. However, most of the particles seen in the electron micrograph are relatively large and thin plates of a homogeneous structure.

These seemingly contradictory results may be interpreted as follows. In the sample $A_0$-3, thin plates of large dimensions are piled up, with no gaps between them, to form particles as thick as several thousand Å. These particles are more or less similar in shape to the one assumed in the calculation of $\bar{d}$; however, under the influence of the grinding action in the preparation of samples for electron microscopic observations, they collapse to yield thin plate-like particles. On the other hand, in the sample $A_2$-3, the particles are in the form of caterpillars and apparently different in shape from the one assumed in the calculation of $\bar{d}$; in the sample $A_2$-4, particles are of two different types, caterpillar-like particles and particles of irregular shape, whereas the particle shape assumed in the calculation is of a single type, a sphere or a cube. These considerations will account for the discrepancies noted above. However, it is not possible to give a satisfactory interpretation of the results for the sample $B_1$-3. At any rate, the $\bar{d}$ value is of minor significance for us in drawing the picture of individual particles.

The sum of the surface areas of all the particles in one gram of a catalyst, when calculated from their linear dimensions as estimated from the electron micrograph, can be considerably greater than the specific surface area of the same catalyst as measured by the BET method. In this respect, Nielsen[23] points out that the interfacial layers are apt to coalesce with the particles to a coherent surface, and that only where the distance between two particles, or the orientation, is too divergent does the interfacial layer split up in two surface areas. This coherent surface should be taken into consideration in attempting to understand the $k$ in terms of the specific activity and the specific surface area, because this is the surface where the reactants in the methanol synthesis reach.

**Specific Activity.**—The specific activity based on unit accessible surface area at a given reaction temperature, $k'$, is calculated by the following formula:

$$k' = k/\rho_b S \qquad (3)$$

where $\rho_b$ is the catalyst bed density (the values are listed in Table III). The $k'$ depends on the chromium/zinc ratio in nearly the same manner as the $k$ does.[24] From the Arrhenius plot of $k'$, the activation energy, $E$, and the frequency factor per unit surface area, $A'$, are calculated for each catalyst. The calculated values of $k'$ at 330°C ($k'_{330}$), $E$, and $A'$ are given in Table II.

In the case of the catalysts A, both the high $k'$ value and the moderately large $S$ value are responsible for the high $k$ value. On the other hand, in the case of the catalysts B, $k'$ is the sole factor affecting the $k$ value, because the surface area, $S$, in this particular case is almost the same for all the catalysts.

A comparison of the data for $k'$ values of the two series of catalysts show that the heat treatment of chromium-containing catalysts (the original catalysts, designated as $A_0$ in Tables I and III) in the air at 400°C results in a considerable decrease in $k'$. However, the heat-treated catalysts, after having been used for methanol synthesis, have a much greater surface area than the corresponding catalysts used for the synthesis without previous heat treatment in the air (see the data for $S$ of the samples $B_1$ and $A_2$ in Table III). Therefore, the decrease in $k'$ due to heat treatment is the main reason why the catalysts B have lower activities ($k$) than the catalysts A.

**Structural Factors Affecting the Specific Activity.**—The catalysts A have higher specific activtiies ($k'$) than the corresponding catalysts B. Moreover, the two series of catalysts are quite different in their electron microscopic pictures. The structural difference between the two series of catalysts may stem from the difference in the way of the decomposition of zinc hydroxychromate into zinc oxide and zinc chromite. The decomposition of, or the removal of excess oxygen from, the hydroxychromate proceeds more slowly but to a greater extent in the heat treatment of catalysts in the synthesis gas than in the treatment in the air.

23) A. Nielsen, "An Investigation on Promoted Iron Catalysts for the Synthesis of Ammonia," Jul. Gjellerups Forlag. Copenhagen (1956), p. 167.

24) The correlation between $k'$ and the chromium/zinc ratio in the range of high chromium/zinc ratios is different from that described in the previous paper.[25] This is mainly due to the different values of $S$ for the catalyst samples with a chromium/zinc ratio of 1.

25) Y. Ogino, M. Oba and H. Uchida, This Bulletin, 32, 284 (1954).

According to Irie and Shiraishi,[6] the decomposition of the hydroxychromate in the synthesis gas begins to take place at a temperature as low as 200°C, and the rate of decomposition gradually increases as the temperature is raised. The excess oxygen, in this case, is removed exothermically as carbon dioxide. Therefore, it is here considered that, in the earlier stages of the heat treatment of catalysts in the synthesis gas (i. e., treatment at low temperatures), a number of fine crystallites of zinc oxide and zinc chromite appear in the layer-structure of hydroxychromate and that, in the latter stages (i. e., treatment at higher temperatures), these crystallites will serve as nuclei for the formation of large particles by the aggregation of newly-born crystallites. In these particles, the mutual penetration of zinc oxide and zinc chromite is likely to be achieved as thoroughly as possible.

On the other hand, in the treatment of catalysts in the air, the decomposition of the hydroxychromate, as is exemplified in Fig. 3 for the catalyst A-3, occurs suddenly at a higher temperature, i. e., at 310°C. In this case, the whole layer-structure of hydroxychromate will be decomposed instantaneously into a great number of very fine crystallites of zinc oxide and zinc chromite, the crystallites being scattered within the initial fringe of the layer-structure; the removal of excess oxygen will remain rather incomplete. Accordingly, once this structure appears in the heat treatment of a catalyst in the air, the complete transformation of this structure into one capable of forming large particles in the heat treatment in the synthesis gas may be difficult, even though the catalyst is subsequently heated in the synthesis gas at temperatures not much higher.

The lattice constant of zinc chromite in catalysts is, in general, considerably greater than the normal value,[26] it varies a little among the catalysts studied. However, the specific activities of the chromium-containing catalysts of Series A greatly differ, from the specific activities of the corresponding catalysts of Series B. Hence, the specific activity can, by no means, be correlated with the lattice constant. The difference in specific activity is considered attributable to the difference in the degree of the mutual penetration of zinc oxide and zinc chromite rather than to the difference in the lattice constants.

This consideration is not contradictory to the observation that the specific activity of the catalyst B'-3 can be increased to the level of specific activity for the catalyst A-3 by heat treatment in hydrogen at 500°C, because the heat treatment favors the progress of the mutual penetration of zinc oxide and zinc chromite.

26) Irie and Shiraishi[6] state that the zinc chromite of the normal lattice constant shows scarcely any activity for methanol synthesis.

## Summary

The activity for methanol synthesis has been determined for two series of catalysts prepared from zinc oxide and chromic acid with and without subsequent heat treatment in the air. Also, the correlations between catalytic activity and other catalyst properties have been studied. Each catalyst series has consisted of four catalysts, three of them prepared from slurries of zinc oxide powder in aqueous chromic acid, and the other prepared directly from zinc oxide powder. The chromium/zinc ratios in the catalysts made from the slurries are 0.1, 0.5, and 1.0. The catalysts of one series have been heated in the air at 400°C after their preparation (the "heated series").

In both series, the activity and the specific activity have been found to be influenced by the chromium/zinc ratio. The catalysts not heated in the air after their preparation (the "unheated series") show higher activities than the corresponding catalysts of the heated series, though the former catalysts have much smaller surface areas.

The results of electron microscopic examination show that the two series of catalysts, after having been used for methanol synthesis, are structually different. The structural difference has been ascribed to the difference in the way of the decomposition of the layer-structure of zinc hydroxychromate. In the case of the unheated series, the layer-structure is decomposed into crystallites of zinc oxide and zinc chromite by reduction in the synthesis gas, whereas in the case of the heated series the layer-structure is decomposed by heat treatment in the air.

X-Ray diffraction data show that, in all cases, the lattice constant for the zinc oxide in catalysts is normal, whereas the lattice constant for the zinc chromite is larger than the normal value.

The average particle diameter as calculated from the surface area and density of catalysts does not agree with the size as estimated by electron microscopic observations.

The difference in specific activity between the two series may be due to the difference in the degree of the mutual penetration of zinc oxide and zinc chromite crystallites rather than to the variation in the zinc chromite lattice constant.

In addition, the effects upon the activity and

upon the catalyst structure of catalyst treatment in hydrogen at 500°C after methanol synthesis have been discussed.

*Government Chemical Industrial Research Institute, Tokyo*
*Shibuya-ku, Tokyo*

# The Effect of Temperature on Electrodialytic Demineralization

By Susan A. WEINER

(Received May 25, 1965)

Saline water conversion, a relatively new field, has shown considerable progress in the past ten years although the conversion of sea water by simply boiling it and collecting the vapors was practiced over two centuries ago. Among the various desalination techniques, distillation is still the most feasible one for highly saline waters. For the conversion of slightly brackish waters, however, electrodialysis is considered to be one of the most promising methods.

**Electrodialysis.**—In this process demineralization is achieved with the aid of electrical energy. Salt ions, confined into compartments bounded by ion-selective polymer membranes, move towards the oppositely charged electrodes from compartments 1, 3, 5, ···, etc. (see Fig. 1). Ions from compartments 2, 4, 6, ···, etc. cannot pass through the membranes because of the repulsion between the like charges on the ions and membranes. As a result, demineralization of the feed solution occurs in the odd numbered cells while the even numbered ones increase in concentration.

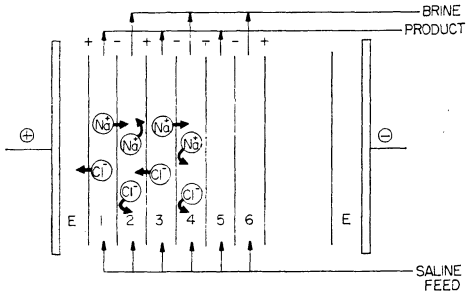



Fig. 1. Schematic of a multicompartment electrodialysis stack.

One of the major factors which limits the practical and economical application of electrodialysis is polarization. This phenomenon arises when a certain limiting current density is exceeded.[1] Under severe polarization conditions the current is used partly to transport salt ions, partly to transport $H^+$ and $OH^-$ ions. This not only results in decreased coulomb efficiency, but can give rise to harmful scale formation.

Polarization is a function of several variables: throughput velocity, stack geometry, feed concentration, temperature and others. This paper describes the changes observed when the feed solution temperature was varied from 5°C to 35.5°C and 40°C.

**Prior Work.** — Several variables influencing polarization characteristics were investigated at our Laboratory[2,3] using a modified Aquafresh stack (manufactured by the American Machine and Foundry Company). It was found that under 4 cm./sec. velocity a straight line correlation existed between the polarization parameter $J_{lim}/N_{do}$, (mamp./cm²)/(eq./l.) and the throughput velocity, but over 4 cm./sec. no such correlation could be established. In this region the limiting current density was found to be a function of the product normality and could be expressed as

$$J_{lim}=6400\ (N_{do})^{1.65}$$ for countercurrent NaCl solutions

$$J_{lim}=3000\ (N_{do})^{1.55}$$ for countercurrent San Francisco Bay water

where $J_{lim}$ = limiting current density (mamp./cm²) and $N_{do}$ = dialyzate stream concentration at the stack outlet (eq./l.) Feed solution temperatures in these experiments were all around 20°C.

## Experimental Procedure

The modified Aquafresh stack was used with 8 cell pairs in series. To obtain higher temperatures

1) N. W. Rosenberg and C. E. Tirrell, *Ind. Eng. Chem.*, 49, 780 (1957).

2) P. M. Rapier, S. A. Weiner and W. K. Baker, "Salt Water Demineralization with a Modified Aquafresh Electrodialytic Stack," Sea Water Convertion Laboratory Issue 28, University of California, Berkeley (1962), p. 24.

3) P. M. Rapier, S. A. Weiner and W. K. Baker, "Experimental Study of Some Basic Parameters in Electrodialysis," Sea Water Conversion Laboratory Report No. 63-4, University of California (1963), p. 43.

the brine and dialyzate feed tanks were equipped with immersion heaters; Fenwal thermoswitches served as regulators. Constant air agitation was used to insure uniform temperature throughout the five-gallon capacity containers. The dialyzate stream flow was approximately constant in all runs at around 6.5 cm./sec. Feed concentrations were varied from 0.0148 to 0.246 N.

A very simple but effective arrangement was used to obtain the desired low temperature. Water was placed in a three-gallon plastic pail which was embedded in a salted, crushed-ice bed. Circulation of the cooling water was achieved by a small Eastern pump. Four coils, constructed from 3/8" copper tubing, were immersed in each feed tank, connections were made from flexible plastic tubing. The recirculation created enough turbulence in the bucket to prevent ice formation next to the walls. Crushed ice was also added to the water directly. Temperatures as low as 3.5°C could easily be maintained with very little deviation. Our experiments were conducted around 5.3°C; the concentration of the feed solutions ranged from 0.0168 N to 0.245 N. For the complete set of experimental data see table below.

## Discussion and Results

The role of temperature in electrodialytic demineralization cannot be dismissed by simply stating that the total resistance of the system changes about 2% per °C. True, one of the advantages of operating at elevated temperatures is the reduced resistance, or in other words the decreased power consumption, but there is another very important factor to be considered. This is the variation of the limiting current density with temperature. Our experiments revealed that the limiting current density is increased at elevated temperatures. The straight line relationship between current density and product normality could be expressed as

$$J_{lim}=5500(N_{do})^{1.53} \text{ at } 40°C$$

$$J_{lim}=4600(N_{do})^{1.53} \text{ at } 35.5°C$$

and is plotted on Fig. 2. Should one operate at elevated temperatures, the current density could be increased (required membrane area decreased) or keeping the area constant a greater degree of demineralization could be achieved. The estimated 20—30% power reduction is another favorable feature. Experiments with a pilot-plant size stack, that was constructed at the University of California, yielded similar results.

In many parts of this country and abroad, well waters have considerably lower temperatures than 18—20°C. A good example is Webster, South Dakota, where the Office of Saline Water electrodialysis demonstration plant has to cope with a 9°C feed water. It was of interest, therefore, to examine the effect of low temperatures on the electrodialytic desalination process. Our experiments yielded the following observations: (a) while the limiting current density was found to be a function of product normality over 4 cm./sec. at feed temperatures of 15°C and over, no such correlation could be established for runs at approximately 5°C (Fig. 2); (b) with feeds more concentrated than 0.05 N (3000 p.p.m. sodium chloride) very strong back pressure in the electrode compartments was noticeable (in

Table I. Experimental data—AMF stack
(8 cell pairs in series*)

| Run No. | $N_o$ eq./l. | $N_{do}$ eq./l. | $I_{lim}$ amp. | $J_{lim}/N_{do}$ (mamp./cm²)/(eq./l.) | Dialyzate stream flow rate ml./min. | Velocity cm./sec. | $f$ % | Temp. dialyzate °C | Temp. brine °C | $R=E/I$ ohm. |
|---|---|---|---|---|---|---|---|---|---|---|
| 38 | 0.241 | 0.0438 | 1.60 | 942 | 38.0 | 6.26 | 81.8 | 35.5 | 35.4 | |
| 39 | 0.201 | 0.0380 | 1.31 | 886 | 38.8 | 6.40 | 81.1 | 35.6 | 35.0 | |
| 40 | 0.0528 | 0.0154 | 0.321 | 537 | 39.5 | 6.51 | 70.8 | 35.6 | 35.4 | |
| 41 | 0.0148 | 0.0058 | 0.078 | 345 | 39.7 | 6.55 | 60.8 | 36.4 | 36.4 | |
| 46 | 0.0315 | 0.0097 | 0.184 | 490 | 41.0 | 6.76 | 69.2 | 40.2 | 40.4 | 23.3 |
| 47 | 0.0522 | 0.0133 | 0.328 | 636 | 40.0 | 6.60 | 74.6 | 40.1 | 40.1 | 17.7 |
| 49 | 0.246 | 0.0431 | 1.59 | 952 | 38.8 | 6.40 | 82.6 | 40.0 | 40.2 | 6.62 |
| 50 | 0.140 | 0.0270 | 0.909 | 870 | 39.5 | 6.51 | 80.7 | 40.1 | 40.3 | 9.72 |
| 51 | 0.0173 | 0.0064 | 0.101 | 407 | 40.8 | 6.74 | 63.0 | 40.1 | 40.3 | 46.1 |
| 52 | 0.0168 | 0.0076 | 0.087 | 295 | 41.3 | 6.81 | 54.8 | 5.95 | 6.23 | 67.5 |
| 53 | 0.0334 | 0.0128 | 0.162 | 326 | 42.2 | 6.96 | 61.7 | 5.06 | 5.22 | 44.5 |
| 54 | 0.0528 | 0.0192 | 0.302 | 405 | 42.8 | 7.06 | 63.7 | 5.17 | 5.39 | 39.7 |
| 55 | 0.147 | 0.0589 | 0.813 | 357 | 42.3 | 6.98 | 60.1 | 4.78 | 5.01 | |
| 56 | 0.145 | 0.0489 | 0.888 | 496 | 42.8 | 7.06 | 66.3 | 5.45 | 5.50 | |
| 58 | 0.0900 | 0.0345 | 0.449 | 336 | 40.0 | 6.61 | 61.8 | 5.38 | 5.55 | |

* Countercurrent flow, NaCl feed in all runs, AMF membranes

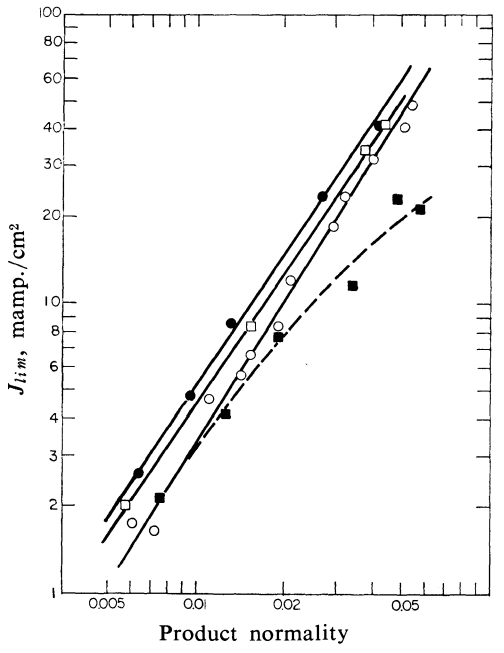



Fig. 2. Polarization characteristics-limiting current density varsus product normality.

■ ~5°C ○ Room temperature
□ ~35.5°C ● ~40°C

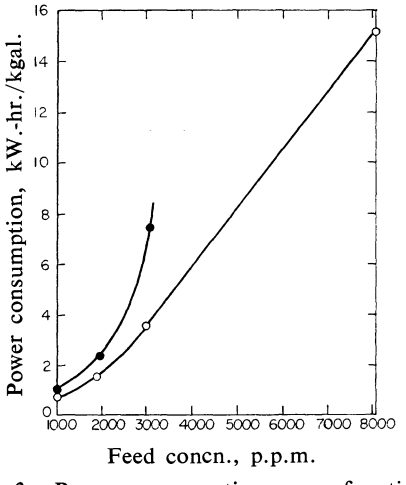



Fig. 3. Power consumption as a function of feed concentration at different temperatures. Values extrapolated to 350 p.p.m. product.

● ~5°C ○ ~40°C

the run with $N_0 = 0.245$ N this was so pronounced that the electrode rinse flow was completely stopped); (c) polarization occurred at decreased current densities; (d) by comparing power consumptions at 40°C and 5°C (Fig. 3) it can be seen that while there is no significant increase for feeds of 1000 p.p.m., the increase is considerable at $N_0 > 2000$ p.p.m.

## Conclusions

Our experiments quantitatively demonstrated that electrodialytic demineralization at elevated temperatures has two attractive features: higher limiting current density and lower power consumption. These savings cannot, however, be achieved without the installation (and maintenance) of expensive heat exchange equipment. The question arises: would the additional cost in equipment be counterbalanced by the gains resulting from elevated temperature operation. Only an extensive economic analysis could give a definite answer to this important question.

## Summary

The process of electrodialysis, as a means of demineralizing brackish water, is briefly described. Polarization, a limiting factor in the practical application of the process, is a function of several variables, one of which is temperature. In this study the temperature dependence of limiting current density and power consumption was examined. Experiments conducted at elevated temperatures (35.5°C and 40°C) showed that the limiting current densities are increased and the power consumption is decreased. At low temperatures (5°C) marked decrease in limiting current density was observed. Comparison of power consumption data at 40°C and 5°C show that significant differences occur with feeds more concentrated than 2000 p.p.m.

The author wishes to thank Professor E. D. Howe for his guidance and many helpful suggestions; the help of the Sea Water Conversion Laboratory staff is also gratefully acknowledged.

*Sea Water Conversion Laboratory*
*University of California*
*Berkeley, California, U. S. A.*

NOTES

# The Determination of Formaldehyde by Means of 3-Methyl-2-benzothiazolone Hydrazone. A New Procedure, Involving Extraction

By Eijiro KAMATA

(Received January 16, 1965)

A new solvent extraction procedure for the determination of formaldehyde with 3-methyl-2-benzothiazolone hydrazone (MBTH)[1] will be described. This procedure is particularly advantageous in the determination of a minute amount of the aldehyde in colored and/or turbid sample solutions.

## Experimental

**Reagents.**—*A Standard Solution of Formaldehyde.*—The stock solution of formaldehyde is standardized by the dimedon method.[2] The aliquot portion of the stock solution is then diluted in order to prepare the standard solution (1 $\mu$g./ml.).

*3-Methyl-2-benzothiazolone Hydrazone Hydrochloride (MBTH) Reagent.*—0.4% aqueous solution.

*1% Ferric Chloride Solution.*

*Saturated Sodium Chloride Solution.*

*Anhydrous Sodium Sulfate.*

*A Mixed Solvent, (1+1) Acetone-Chloroform.*

**Instruments.**—A Beckman model DU spectrophotometer. A Coleman model 14 spectrophotometer.

**Procedure.**—To 9 ml. of test solution, 1 ml. of a saturated sodium chloride solution is added, and then 2 ml. of a 0.4% MBTH aqueous solution is added. After the mixture has stood for 20 min., 0.5 ml. of a 1% ferric chloride solution is added. After an additional 10 min., 12.5 ml. of a (1+1) acetone-chloroform solvent is added to the mixture. Then the mixture is transferred into a separatory funnel and shaken twenty times.* The extract is poured into a 10 ml. measuring flask, and the flask is filled up to the mark with the solvent. Then the extract is quickly dehydrated in a stoppered test tube with 6 g. of anhydrous sodium sulfate.** The extract is filtered through a dry filter paper. The absorbance is read at the wavelength of 670 m$\mu$. The color is stable for at least two hours.

## Results and Discussion

In the reaction of MBTH with formaldehyde, a maximum coloration is obtained in the range of the concentration of sodium chloride from 0.5 mol. to 1.0 mol. The molar absorptivity is $6.9\times10^4$ in the sodium chloride solution, while it is $6.1\times10^4$ in a solution without sodium chloride. The absorbance is increased by 1.13 times in the sodium chloride solution. On the other hand, Sawicki et al.[1] give $6.5\times10^4$ as the molar absorptivity in a solution without

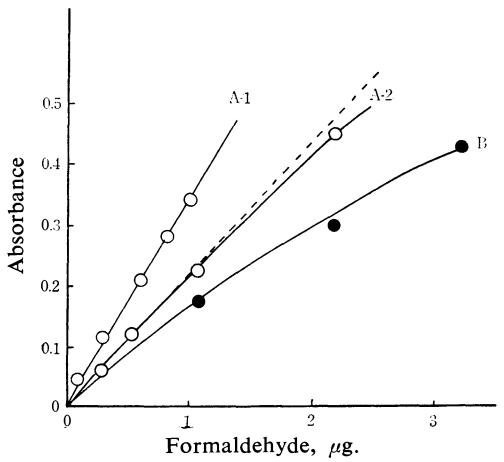



Fig. 1. Calibration curve fromaldehyde.

A. Extraction from 0.54 mol. sodium chloride solution. pH of the aqueous phase, 2.5.
1. 16 mm. light path at the wavelength of 670 m$\mu$. (Coleman spectrophotometer).
2. 10 mm. light path at the wavelength of 670 m$\mu$. (Beckman spectrophotometer).

B. Extraction from a solution without sodium chloride. pH of the aqueous phase, 2.45. 10 mm. light path at the wavelength of 670 m$\mu$. (Beckman spectrophotometer).

1) E. Sawicki, T. R. Hauser, T. W. Stanley and W. Elbert, *Anal. Chem.*, 33, 93 (1961).

2) J. H. Yoe and L. C. Reid, *Ind. Eng. Chem., Anal. Ed.*, 13, 238 (1941).

* After shaking the solvent decreases in volume to about 9.8 ml.

** The color is not stabilized for a longer period by using a smaller amount of sodium sulfate. Any decrease of the absorbance is not noticed by treating the extract with sodium sulfate and then a filter paper.

sodium chloride, while Hünig et al.[3] gives 7.6 $\times 10^4$ as the molar absorptivity of the pure product in acetone. A similar increase in the absorbance is also noticed in the reaction of acetaldehyde with MBTH. Sodium chloride seems to be effective in raising the yield of the color reaction of MBTH with aldehyde. Potassium chloride is less effective than sodium chloride for the enhancement of the sensitivity of the present method.

The addition of sodium chloride to the reaction mixture has another advantage. In the presence of sodium chloride, the extraction of the colored product is quantitative, while in a solution without sodium chloride more than 10% of the colored product remains in the aqueous phase (Fig. 1). Extraction is also advantageous for the determination of a minute amount of aldehyde in colored or turbid solutions, because the colored product of aldehyde is concentrated in a small volume of the organic phase. A prolonged contact of the organic phase with the aqueous phase reduces the absorbance. The extract must be rapidly dehydrated after extraction; delayed dehydration also causes a decrease in the absorbance.

The presence of 20 mg./l. of ferrous ions or 50 mg./l. of manganese ions does not interfere. The presence of 1 mg. of sugar gives only a minimum detectable absorbance. This is one of the advantages of the MBTH method here presented. By means of the method using chromotropic acid, a small amount of formaldehyde in the presence of a larger amount of sugar cannot be determined because sugar and formaldehyde are likely to react with the reagent.

The author wishes to thank Professor Motoharu Tanaka for his many helpful suggestions made during this work.

*Laboratory of Analytical Chemistry*
*Faculty of Science*
*Nagoya University*
*Chikusa-ku, Nagoya*

3) S. Hünig and K. H. Fritsch, *Ann.*, **609**, 172 (1957).

# Catalytic Tritium Exchange Reactions with Tritiated Active Methylene Compound

By Ken-ichi KUDO, Takayoshi ADACHI, Masaaki HAZUE and Michio ENDO

(Received February 18, 1965)

Although the isotopic hydrogen exchange reactions of a number of organic compounds catalyzed by a transition-metal have been investigated by many workers,[1] these exchange reactions have dealt almost exclusively with deuterium oxide,[1] deuterium,[1] and tritium oxide[2] as an isotope source.

The present paper will describe the catalytic tritium-hydrogen exchange using ethyl malonate-(active methylene-T) (I) as a tritium source. Table I shows that the alkyl hydrogens are, by the use of a catalyst, exchanged with I more easily than with tritium oxide. The catalytic activity of the transition-metal for benzene is in the following order: with I, Raney Ni>Pd-black>Pt-black; with tritium oxide, Pt-black>Pd-black>Raney Ni.

TABLE I. EXCHANGE BY TRITIUM OXIDE OR I*

| Catalyst | Substrate | % Approach to statistical equilibrium | |
|---|---|---|---|
| | | $T_2O$ | I |
| Pd-Black | *p*-Xylene | 4 | 99 |
| Pd-Black | Benzene | 77 | 10 |
| Pd-Black | Cyclohexane | 0 | 11 |
| Pt-Black | *p*-Xylene | 0 | 0 |
| Pt-Black | Benzene | 100 | 6 |
| Pt-Black | Cyclohexane | 0 | 3 |
| PtO | *p*-Xylene | 3 | 17 |
| PtO | Benzene | 98 | 45 |
| Raney Ni | *p*-Xylene | 2 | 90 |
| Raney Ni | Benzene | 62 | 76 |
| Raney Ni | Cyclohexane | 0 | 2 |

* At 130°C for 17 hr.

The results in Table II show that the exchanges of toluene and *m*-xylene catalyzed by Pd-black and Raney Ni occur mainly in the alkyl groups. Figure 1 indicates that the

1) J. L. Garnett, *Nucleonics*, 20, 86 (1962); A. Murray, III, and D. L. Williams, "Organic Syntheses with Isotopes," Vol. II, Interscience Publisher, New York (1948), p. 1594.

2) J. L. Garnett and W. A. Sollich, *J. Catalysis*, 2, 350 (1963).

TABLE II. TRITIUM DISTRIBUTION IN THE COMPOUNDS LABELED WITH I*

| Substrate | Catalyst | % of tritium | |
|---|---|---|---|
| | | Methyl | Ring |
| Toluene | Pd-Black | 100 | 0 |
| Toluene | Raney Ni | 89 | 11 |
| *m*-Xylene | Pd-Black | 98 | 2 |
| *m*-Xylene | Raney Ni | 97 | 3 |

* At 130°C for 17 hr.

TABLE III. EXCHANGES OF ORGANIC COMPOUNDS WITH I*

| Substrate | % Approach to statistical equilibrium | | |
|---|---|---|---|
| | Pd-Black | Pt-Black | Raney Ni |
| *m*-Xylene | 96 | 1 | 82 |
| *p*-Xylene | 99 | 0 | 91 |
| Toluene | 100 | 16 | 83 |
| Benzene | 10 | 6 | 76 |
| Diphenyl | 0 | 90 | 1 |
| *n*-Heptane | 5 | 0 | 2 |
| Cyclohexane | 11 | 3 | 2 |
| Tetralin | 67 | 77 | 85 |

* At 130°C for 17 hr.

extent of the isotopic exchanges with I is decreased considerably by the addition of water. Judging from the above results in this reaction, it may be expected that the mechanism of the exchange with I will be different from that with tritium oxide. The extent of the exchange of some organic compounds with I are shown in Table III.

These results indicate that the catalytic exchange of hydrogen with I is a good method for labeling an organic compound with hydrogen isotopes.

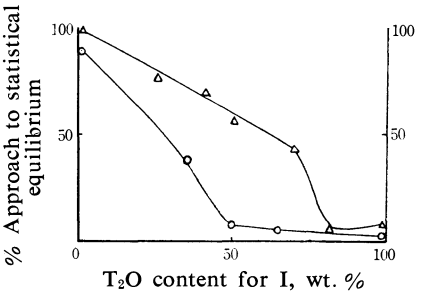



Fig. 1. Effects of water on exchange reaction of *p*-xylene by I at 130°C for 17 hr.
—△— With Pd-black
—○— With Raney Ni

## Experimental

**The Exchange of *p*-Xylene by Pd-Black.** — A mixture of 30 ml. of *p*-xylene, 1 ml. of I (41.1 μc./ml.), and 0.3 g. of Pd-black in an ampoule was shaken at about 130°C for 17 hr. After it had then been cooled, Pd-black was filtered off, the filtrate was hydrolyzed with 20 ml. of a 10% aqueous sodium hydroxide solution to give sodium malonate, and the reaction mixture was washed repeatedly with water, dried with sodium sulfate, and distilled to give 24 ml. (80%) of tritiated *p*-xylene (specific activity 1.36 μc./ml.) (99% approach to statistical equilibrium).

**The Determination of the Tritium Distribution in Toluene.**—A mixture of 2 ml. of tritiated toluene (0.179 mc./mM), 8 g. of potassium permanganate, and 96 ml. of water was heated under reflux for 3 hr. After it had cooled, the mixture was filtered and the filtrate was acidified with hydrochloric acid. The precipitate was then recrystallized from alcohol to give pure benzoic acid (specific activity $1.93\times10^{-2}$ μc./mM). Thus, the distribution of tritium in toluene was as follows: methyl, 89%; ring, 11%.

*Takarazuka Radiation Raboratory*
*Sumitomo Atomic Energy Ind., Ltd.*
*Takarazuka, Hyogo*

# The Anomalous Thermal Expansion of Hematite at a High Temperature

By Tatsuo SAITO

(Received February 20, 1965)

It has long been known that magnetic and specific heat anomalies are shown by hematite, $\alpha$-$Fe_2O_3$, in the 650—700°C region.

Néel[1] has suggested that this magnetic change comprises a transition from an antiferromagnetic state below 675°C to a paramagnetic one above this temperature.

However, when Willis and Rooksby[2] examined the crystal structure of hematite at elevated temperatures from 20°C to 950°C by means of a high temperature X-ray powder camera, they did not find any crystallogaphic phase transitions. However, at a temperature near 675°C the expansion coefficient of the $c_h$-axis in the hexagonal system showed a sudden increase. These results were interpreted in terms of the magnetic transition of pure hematite.

Finch and Sinha[3] observed the surface of a hematite single crystal by electron diffraction after heating it in air at 700°C; they concluded that $\gamma$-$Fe_2O_3$ was the stable form of $Fe_2O_3$ at high temperatures.

Blackman and Kaye[4] examined single crystals of hematite between 700°C and 1000°C by electron diffraction; they claimed that, in some cases, oriented layers of $Fe_3O_4$ occurred, but, in contrast to the results of Finch and Sinha, they found no evidence for the presence of $\gamma$-$Fe_2O_3$.

In view of these differences in the high temperature structural behavior of hematite, the present investigations were undertaken in order to determine the change in the unit cell of hematite precisely.

## Experimental

The materials used in this experiment were specular hematite, obtained from the Quebec-Cartier Company of Canada, and reagent grade hematite, $\alpha$-$Fe_2O_3$, obtained from the Fisher Scientific Company. The specular hematite, which was ground in a small tungsten carbide ball mill, contained about 2.5% $Fe_3O_4$ and a small percentage of $SiO_2$. This hematite ore powder was pre-heated at about 1000°C for 1 hr. because the original powder has lattice strains resulting from the grinding. Minus 325 mesh fractions of powder samples of both hematite ore and Fisher reagent were taken for X-ray measurements.

The equipment used was a Norelco X-ray difractometer, with, attached, a Materials Research Corporation Model X86-N furnace using a platinum ribbon heater.

The spacings of (10.4), (11.0) and (30.0) of hematite were measured at 50°C intervals, from room temperature to 1100°C, through the heating and cooling cycles. Both the heating and cooling rates of the furnace were 10°C per minute, and the specimens were kept at a constant temperature for 10 min. before performing the X-ray measurements.

The thermocouple measurements were calibrated by the data of the lattice parameter changes for magnesium oxide as a function of the temperature;[5] moreover, in this experiment the lattice strain of magnesium oxide due to the distorsion of the sample holder during heating was checked at each temperature by the above data of the lattice parameter for magnesium oxide.[5] The temperature control of the furnace was maintained within ±5°C.

The lattice parameters of the hexagonal cell, $a_h$ and $c_h$, at each temperature were computed from the measured average reflection angles, without taking corrections by the extraporation method. The rhombohedral unit cell dimensions, the cell edge, $a_R$, and the angle, $\alpha$, were computed from the hexagonal lattice parameters.

## Results and Discussion

The lattice parameter values at each temperature during heating and cooling are plotted in Figs. 1 and 2 as functions of the temperature. Figure 1 compares the thermal expansions of both $a_h$- and $c_h$-axes with one together. The values shown are $\Delta a_{ht}/a_{h20}$ and $\Delta c_{ht}/c_{h20}$ in percent for $a_h$- and $c_h$-axes expansions respectively. $a_{h20}$ or $c_{h20}$ means the lattice parameter value at 20°C, while $\Delta a_{ht}$ or $\Delta c_{ht}$ means the difference between each parameter value at 20°C and at $t$°C. In this case, the lattice parameter values at each temperature in the cooling stage were slightly larger than those in the heating stage. Figure 2 shows the expansion of the rhombohedral cell edge, $\Delta a_{Rt}/a_{R20}$, in percent. $a_{R20}$ is the value

1) L. Néel, *Ann. Phys., Paris*, **12**, 249 (1949).
2) B. T. M. Willis and H. P. Rooksby, *Proc. Phys. Soc.*, **65B**, 950 (1952).
3) G. I. Finch and K. P. Sinha, *Proc. Roy. Soc.*, **A241**, 1 (1957).
4) M. Blackman and G. Kaye, *Proc. Phys. Soc.*, **75**, 364 (1960).
5) W. J. Campbell, *U. S. Bureau of Mines, Reports of Investigation*, No. 6115 (1962).

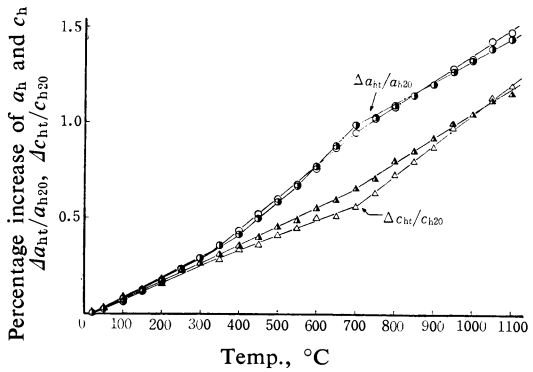



Fig. 1. Thermal expansion of hexagonal lattice parameters for hematite ore.

○—○ Heating stage
◑—◑ Cooling stage
△—△ Heating stage
◭—◭ Cooling stage

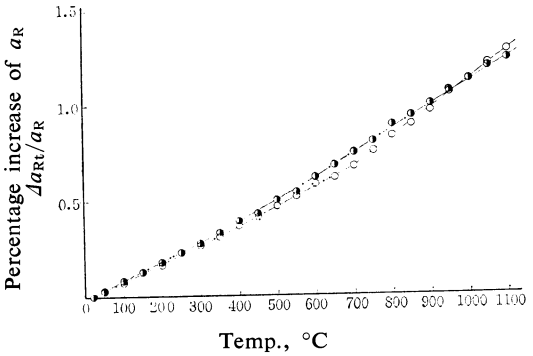



Fig. 2. Thermal expansion of rhombohedral lattice parameter for hematite ore.

○—○ Heating stage
◑—◑ Cooling stage

of the cell edge at 20°C. $\Delta a_{Rt}$ is the difference between the cell edge values at 20°C and at $t$°C. Figure 3 shows the rhombohedral angle-temperature curve for the expansion of the rhombohedral unit cell.

As may be seen in these figures, two anomalies, at about 300°C and 700°C, are observed for the thermal expansion curve of hematite.

The hexagonal lattice parameters increase uniformly from room temperature to about 300°C, and they also increase almost uniformly above about 700°C; however, in the temperature range from about 300°C to 700°C, the two axes show different expansion behavior.

Similar behavior is also observed in the experiment with Fisher hematite.

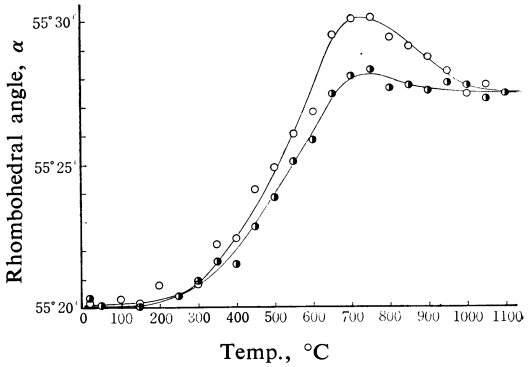



Fig. 3. Rhombohedral angle variation with temperature for hematite ore.

○—○ Heating stage
◑—◑ Cooling stage

It has, therefore, been found that the rhombohedral hematite has three stages of thermal expansion. Below about 300°C and above about 700°C the rhombohedral angle is almost constant, but in the temperature range from about 300°C to 700°C the rhombohedral angle increases. On the other hand, as may be seen in Fig. 3, the values of $\alpha$ in the 700—800°C range during heating are slightly larger than during cooling above 700°C. This irreversibility of the rhombohedral cell expansion at high temperatures during the heating and cooling cycles was also observed in the experiment with Fisher hematite. X-ray measurements were also performed in a nitrogen atmosphere, but no distinct differences were observed. On further heating above 1100°C, the rhombohedral unit cell of hematite underwent a complete deformation because of its dissociation to magnetite.

The work was done at the Institute of Mineral Research, Michigan Technological University, U. S. A., with financial support provided by that university. The author wishes to express his appreciation to Mr. M. E. Volin, Director of the Institute of Mineral Research, for his permission to publish this paper. The author also wishes to Thank Mr. W. A. Hockings, Research Engineer of the Institute of Mineral Research, for his helpful discussions.

*Government Chemical Industrial Research Institute, Tokyo*
*Shibuya-ku, Tokyo*

# The Spectrophotometric Determination of Chromium with 2-Hydroxy-1-(2-hydroxy-4-sulfo-1-naphthylazo)-naphthalein (Sodium Salt)

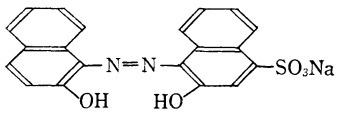
By Katsuya UESUGI and Yukiteru KATSUBE

(Received March 18, 1965)

2-Hydroxy-1-(2-hydroxy-4-sulfo-1-naphthylazo)-naphthalein (Sunchromine blue black R) has been examined spectrophotometrically in order to determine the molybdenum,[1] zirconium[2] and titanium[3] in a methanol-hydrochloric acid solution; it has also been examined as an indicator of the complexometric titration of calcium in the presence of magnesium.[4]

In this paper, a new method will be described for the spectrophotometric determination of trace amounts of chromium(III). The method is based on the stable blue complex formed by the reaction between chromium ions and 2-hydroxy-1-(2-hydroxy-4-sulfo-1-naphthylazo)-naphthalein.

The structure of the reagent is as follows:




## Experimental

**Reagents.**—The reagent solution was prepared by dissolving 0.1 g. of Sunchromine blue black R in 100 ml. of distilled water.

The standard solution, containing 100 $\mu$g. of chromium(III) per milliliter, was prepared by dissolving chromium alum (analytical grade) in 0.01 N sulfuric acid. The other reagents used were also of analytical grade.

**The Procedure for the Determination of Chromium.**—Transfer the solution containing 5 to 75 $\mu$g. of chromium to a 50 ml. volumetric flask, and add 5 ml. of the 0.1% reagent solution. Then add 10 ml. of a borax-sodium hydroxide buffer solution (pH 10), and make up to the mark with distilled water. After ten minutes, measure the absorbance at 630 m$\mu$, using a reagent blank solution as a reference.

## Results and Discussion

**Absorption Spectra.**—The absorption spectra of the complex are shown in Fig. 1. At pH 10, the maximum absorbance is at 630 m$\mu$.

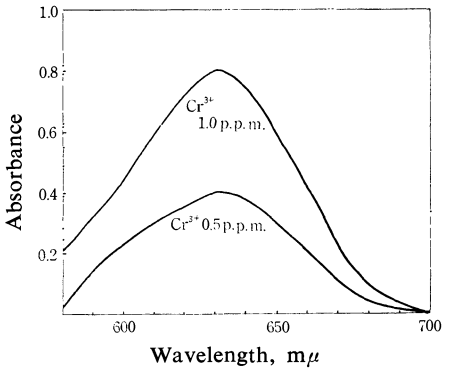



Fig. 1. Absorption spectra of the Cr-complex. pH 10, reagent 80 p. p. m., against reagent blank.

**The Effect of pH.**—A borax-sodium hydroxide buffer was satisfactory for the determination of chromium. The effect of pH on the color intensity of the complex is shown in Fig. 2. The complex has a maximum intensity in the pH range from 9.8 to 10.3.

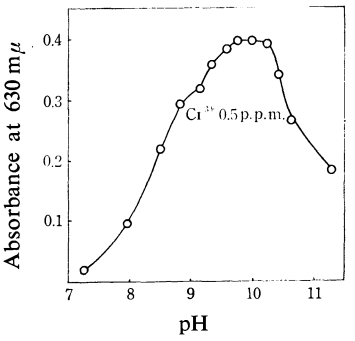



Fig. 2. Effect of pH on the Cr-complex.

**Rate of Color Formation.**—The color intensity reaches a maximum in ten minutes and remains constant for about an hour.

**Beer's Law.**—Beer's law is obeyed up to about 1.2 p. p. m. of chromium at 630 m$\mu$ (see Fig. 3).

**Sensitivity.**—The molar extinction coefficient is about 42000 at 630 m$\mu$, and the spectrophotometric sensitivity is 0.0013 $\mu$g. Cr/cm$^2$ for $\log I_0/I = 0.001$.

1) J. Korkisch, *Mikrochim. Acta*, **1961**, 564.
2) J. Korkisch, *Z. anal. Chem.*, **182**, 253 (1961).
3) J. Korkisch, *Mikrochim. Acta*, **1962**, 16.
4) G. P. Hildebrand and C. N. Reilley, *Anal. Chem.*, **29**, 259 (1957).

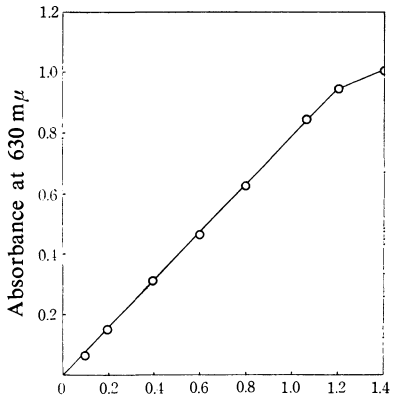



Fig. 3. Beer's law curve, pH 10.

**Interfering Ions.** — The effect of various cations was studied; it was found that aluminum, beryllium, iron(III), scandium, and large amounts of calcium, cobalt, zinc and titanium interfere. The presence of these interfering metal ions gives the smaller absorbance at 630 mμ. Hexavalent chromium, chloride and sulfate are without effect; 50 μg. of chromium(III) can thus be successfully determined in the presence of 100 mg. of any of these ions. The interfering metals must be removed or masked prior to the determination. Aluminum[5,6] and iron(III)[6] can be removed by the 8-hydroxyquinoline chloroform extraction method from chromium. The acetylacetone chloroform extraction method[7] effected a good separation of aluminum, iron(III) and beryllium from chromium.

## Summary

A spectrophotometric method for the determination of traces of chromium(III) with 2-hydroxy-1-(2-hydroxy-4-sulfo-1-naphthylazo)-naphthalein has been described. Beer's law is obeyed up to 1.2 p. p. m. of chromium. The spectrophotometric sensitivity is 0.0013 μg. Cr/cm$^2$ based on an absorbance of 0.001 unit at 630 mμ. The accuracy and precision are satisfactory. The interference of foreign ions can be avoided by 8-hydroxyquinoline chloroform extraction or by acetylacetone chloroform extraction.

*Himeji Institute of Technology*
*Idei-600, Himeji*

5) A. Classen, L. Bastings and J. Visser, *Anal. Chim. Acta*, 10, 373 (1954).
6) C. H. R. Gentry and L. G. Sherrington, *Analyst*, 75, 17 (1950).
7) E. B. Sandell, "Colorimetric Determination of Traces of Metals," 3rd Ed., Interscience Publishers, New York (1959), p. 58.

# The Preparation of Triorganosilyl Derivatives of Hydroquinone, Resorcinol, Bisphenol-A and Terephthalic Acid

By Minoru Abe, Masaru Niwano, Hideaki Kobuna and Toshio Akiguchi

(Received April 5, 1965)

In the course of the preparation of phenylene- and phthalate-siloxy copolymers with $-C_6H_4O-Si-$ and $-O_2CC_6H_4CO_2Si-$, di-triorganosilyl derivatives of hydroquinone and resorcinol, *1,4(1,3)-di-triorganosiloxy benzene* ($R_3HQ$ and $R_3RC$), those of bisphenol-A (BPA), *2,2-bis-(4-triorganosiloxyphenyl)-propane* ($R_3BPA$), and terephthalic acid, *bis-triorganosilyl terephthalate* ($R_3TPA$) were isolated in pure states. $R_3HQ$ and $R_3RC$ were prepared from the reaction of triorganochlorosilane with the diphenols; $R_3BPA$, from the reaction of chlorosilane with BPA in the presence of aniline as a hydrogen chloride acceptor, or with the sodium salt of BPA in an inert solvent, and $R_3TPA$, from the reaction of chlorosilane with dipotassium terephthalate. $R_3TPA$ was found to be extremely sensitive towards solvolysis, while the phenolic silyl-ethers, the former three, were rather stable in both hydrolysis and alcoholysis.

## Experimental

**Triorganochlorosilanes.** — A pure sample of trimethylchlorosilane (b. p. 58°C) was obtained from the Shinetsu Chemical Industrial Co. Dimethylbutylchlorosilane (b.p. 139—140°C), dimethylphenylchlorosilane (b. p. 76—78°C/2 mmHg) and diphenylmethylchlorosilane (b. p. 145—146°C/2.5 mmHg) were prepared by the Grignard route.[1] Triphenylchlorosilane (m. p. 98—99°C) was isolated from high

1) T. Takiguchi and M. Abe, *J. Chem. Soc. Japan, Ind. Chem. Sec.* (*Kogyo Kagaku Zasshi*), **66**, 625 (1963).

boiling residue[2] of the direct synthesis of phenylchlorosilanes. All the compounds were further purified by conventional methods just before use.

**The Preparation of $R_3HQ$ and $R_3RC$.** — The general procedure will be described using 1,4-bis-trimethylsiloxy-benzene ($Me_3HQ$) as an example. A mixed sample of hydroquinone (33 g., 0.3 mol.) and trimethylchlorosilane (54 g., 0.5 mol.) was refluxed until the hydroquinone dissolved completely to give a clear yellow solution. The resultant solution was evaporated to remove the excess chlorosilan and then distilled under a vacuum. The distillate at 107—110°C/4 mmHg was a viscous liquid which solidified on standing. Recrystallization from ether gave 59 g. (77%) of pure $Me_3HQ$ (m. p. 48°C) (lit. m. p. 46°C,[3] 52°C,[4] 48.9—49.3°C[5]); b. p. 239°C (lit. b. p. 252°C,[6] 246°C[3]). The following disilyl ethers of the diphenols were obtained by a very similar procedure: $Me_3RC$, b. p. 235—236°C, 92—93°C/2 mmHg (lit. b. p. 239°C,[6] 243°C[4], 237—240°C,[7] 116°C/7 mmHg[3]); $n_D^{20}$ 1.4755; $d_4^{20}$ 0.947. $Me_2BuHQ$, b. p. 158—195°C/1.5 mmHg; $n_D^{20}$ 1.4765; $d_4^{20}$ 0.925. $Me_2BuRC$, b. p. 161—162°C/3 mmHg; $n_D^{20}$ 1.4798; $d_4^{20}$ 0.923. $Me_2PhHQ$, b. p. 137—139°C/0.5 mmHg; $n_D^{20}$ 1.5720; $d_4^{20}$ 1.087. $MePh_2HQ$, b. p. 237—238°C/0.5 mmHg; $n_D^{20}$ 1.5882; $d_4^{20}$ 1.113. $Ph_3HQ$, m. p. 225—226°C (lit. m. p. 215.8—216.0°C[5]). ($Ph_3HQ$ was prepared from the reaction in aniline.)

*$Me_3HQ(RC)$.* — Found: Si, 21.0 (21.7); mol. wt., 238 (244) (in benzene); $MR_D$,[8] — (75.35). Calcd. for $C_{12}H_{22}O_2Si_2$: Si, 22.0%; mol. wt., 254; $MR_D$, 74.38.

*$Me_2BuHQ(RC)$.*—Found: Si, 16.4 (16.0); mol. wt., 318 (326); $MR_D$, 104.7 (104.3). Calcd. for $C_{18}H_{34}O_2Si_2$: Si, 16.6%; mol. wt., 339; $MR_D$, 104.7.

*$Me_2PhHQ$.* — Found: Si, 14.5; mol. wt., 377, 373; $MR_D$, 111.4. Calcd. for $C_{22}H_{26}O_2Si_2$: Si, 14.8%; mol. wt., 379; $MR_D$, 112.7.

*$MePh_2HQ$.* — Found: Si, 10.7; mol. wt., 491; $MR_D$, 152.2. Calcd. for $C_{32}H_{30}O_2Si_2$: Si, 11.2%; mol. wt., 503; $MR_D$, 150.9.

*$Ph_3HQ$.*—Found: Si, 8.2; mol. wt., 633 (1,4-dioxane). Calcd. for $C_{42}H_{34}O_2Si_2$: Si, 8.9%; mol. wt., 627.

$R_3HQ$ was fairly stable in hydrolysis; e.g., $Me_3HQ$ recovered unchanged even after 2 hr.' boiling with distilled water. $R_3RC$ was less stable than $R_3HQ$. However, both were hydrolyzed gradually by prolonged heating with 1/20 N sulfuric acid, yielding the diphenols and the corresponding disiloxanes. The produts were also characterized by their infrared absorption spectra.[9] X-Ray powder patterns for crystalline ethers are given below:

$Me_3HQ$

| | | | | | | | |
|---|---|---|---|---|---|---|---|
| $d, kX$: | 11.05 | 5.57 | 5.31 | 4.93 | 4.42 | 3.90 | 3.71 |
| | 3.47 | 3.04 | | | | | |
| $I/I_0$: | 1.00 | 0.39 | 0.29 | 0.14 | 0.24 | 0.29 | 0.26 |
| | 0.14 | 0.13 | | | | | |

$Ph_3HQ$

| | | | | | | | |
|---|---|---|---|---|---|---|---|
| $d, kX$: | 12.26 | 8.51 | 7.76 | 6.92 | 6.15 | 4.70 | 4.53 |
| | 4.37 | 4.17 | 4.02 | 3.59 | 3.48 | 3.39 | |
| $I/I_0$: | 0.19 | 0.45 | 0.36 | 0.28 | 0.93 | 1.00 | 0.48 |
| | 0.98 | 0.63 | 0.36 | 0.26 | 0.24 | 0.25 | |

**The Preparation of $R_3BPA$.**—A typical procedure will be detailed for 2,2-bis-(4-dimethylphenylsiloxyphenyl)-propane ($Me_2PhBPA$). A mixture of BPA (46 g., 0.2 mol.) and dimethylphenylchlorosilane (85 g., 0.5 mol.) was refluxed for 5 hr. After it had then been cooled to room temperature, a solution of aniline (37 g., 0.4 mol.) in 300 ml. of ether was vigorously stirred into the mixture, after which the mixture was refluxed for an additional 2 hr. The resultant solution was filtered to remove aniline hydrochloride and concentrated to a clear viscous liquid, from which crude $Me_2PhBPA$ boiling at 266—285°C (1.5 mmHg) was obtained by distillation. The redistillation of the fraction gave 74 g. (74%) of pure $M_2PhBPA$; b. p. 286—287°C/1.5 mmHg, $n_D^{20}$ 1.5746, $d_4^{20}$ 1.117.

It was found that the use of aniline as a hydrogen chloride acceptor was essential for the successful preparation; otherwise, the reaction was not completed, it was always accompanied by the formation of considerable amounts of mono-silyl ether, and the yield of bis-silyl ether was less than 40%.

In another preparation, an ethereal solution of dimethylphenylchlorosilane (85 g., 0.5 mol.) was added to a stirred slurry of sodium salt of BPA (54 g., 0.2 mol.) in ether. After it has been stirred for 2 hr. under refluxing, the mixture was filtered to remove sodium chloride; then the filtrate was evaporated to give an oily viscous liquid, which gave 66 g. (66%) of $Me_2PhBPA$ by fractionation under a vacuum. The following were obtained analogously in a consistent yield of 65—70%. $Me_3BPA$, b. p. 179—180°C/1.5 mmHg, $n_D^{20}$ 1.5178, $d_D^{20}$ 0.981; $Me_2BuBPA$, b. p. 211—214°C/1.5 mmHg, $n_D^{20}$ 1.5102, $d_4^{20}$ 0.976; and $MePh_2BPA$, b. p. 297—300°C/0.5 mmHg, $n_D^{20}$ 1.5777, $d_4^{20}$ 1.084.

Triphenylchlorosilane was found to be much less reactive to BPA than the other chlorosilanes. Therefore, a reaction in a high boilng solvent (toluene, xylene, etc.) using aluminum chloride as a catalyst was necessary; otherwise, the yield of bis-silyl-ether always remained below 20%. $Ph_3BPA$ was a fine crystalline substance melting at 151—152°C; it was obtained in a 47% (mean) yield by preparation in xylene. It was readily soluble in benzene, toluene and xylene, and insoluble in hexane, acetone, ethanol and methanol.

X-Ray powder diffraction data of $Ph_3BPA$:

| | | | | | | | |
|---|---|---|---|---|---|---|---|
| $d, kX$: | 8.93 | 7.48 | 6.86 | 6.42 | 5.83 | 5.28 | 5.19 |
| | 4.80 | 4.60 | 4.51 | 4.33 | 3.87 | 3.68 | |
| $I/I_0$: | 0.47 | 0.25 | 0.43 | 0.23 | 0.48 | 0.38 | 0.37 |
| | 0.31 | 0.55 | 0.73 | 1.00 | 0.22 | 0.38 | |

2) T. Takiguchi and M. Abe, ibid., **68**, 679 (1965).
3) M. G Voronkov and Z. I. Shabarova, *Zhur. Obshchei Khim.*, **30**, 1955 (1960).
4) F. A. Heinlein and J. Krämer, *Chem. Ber.*, **92**, 2585 (1959).
5) G. Illuminati and F. Tarli, *Ric. Sci., Rend. Sez.*, **A3**, 329 (1963).
6) M. Jacovic, *Z. anorg. u. allgem. Chem.*, **288**, 324 (1956).
7) S. H. Langer, S. Connell and I. Wender, *J. Org. Chem.*, **23**, 50 (1958).
8) E. L. Warrick, *J. Am. Chem. Soc.*, **68**, 2445 (1946); R. O. Sauer, ibid., **68**, 954 (1946).
9) T. Takiguchi, M. Abe and H. Kobuna, Presented at the 18th Annual Meeting of the Chemical Society of Japan, Osaka, April, 1965.

*$Me_2PhBPA$*.—Found: Si, 11.0; mol. wt., 506 (benzene); $MR_D$, 147.0. Calcd. for $C_{31}H_{36}O_2Si_2$: Si, 11.3%; mol. wt., 497; $MR_D$, 146.9.

*$Me_3BPA$*.—Found: Si, 14.7; mol. wt., 366; $MR_D$, 115.2. Calcd. for $C_{21}H_{32}O_2Si_2$: Si, 15.1%; mol. wt., 373; $MR_D$, 112.0.

*$Me_2BuBPA$*. — Found: Si, 11.9; mol. wt., 455; $MR_D$, 140.1. Calcd. for $C_{27}H_{44}O_2Si_2$: Si, 12.3%; mol. wt., 457; $MR_D$, 139.8.

*$MePh_2BPA$*. — Found: Si, 8.83; mol. wt., 617; $MR_D$, 191.3. Calcd. for $C_{41}H_{40}O_2Si_2$: Si, 9.1%; mol. wt., 621; $MR_D$, 188.5.

*$Ph_3BPA$*.—Found: Si, 7.1; mol. wt., 750. Calcd. for $C_{51}H_{44}O_2Si_2$: Si, 7.5%; mol. wt., 745.

The identifications of these bis-silyl ethers were further established by their hydrolytic cleavage. The hydrolysis of $Me_2BuBPA$ (22.8 g., 0.05 mol.) with 1/20 N sulfuric acid by refluxing it for 10 hr. afforded BPA (10.0 g., 0.044 mol.) and 1,3-dibutyltetramethyldisiloxane (b. p. 207—208°C; 11.3 g., 0.046 mol.). Infrared absorption data[9] were also recorded.

Throughout the infrared absorption spectra of all silyl ethers ($R_3BPA$, $R_3HQ$ and $R_3RC$), a very strong and characteristic absorption band in the 910—925 $cm^{-1}$ region was found to exist. Its assignment still remains uncertain; however, it is very probably due to the existence of phenylene- or phenyl-silyl ether bonding (-$C_6H_4$-O-Si- or $C_6H_5$-O-Si-) in these compounds. An entire absence of the band in BPA, diphenols and in phenol, and its appearance in the silyl derivatives of BPA, in diphenols and in all phenoxysilanes[10] seems to support this assignment strongly.

**Bis-triphenylsilyl Terephthalate.**—In a manner similar to that employed for $R_3TPA$ ($R_3$=$Me_3$, $Me_3Bu$, $Me_2Ph$ and $MePh_2$) in the preceding paper,[11] bis-triphenylsilyl terephthalate ($Ph_3TPA$) was obtained in 67% yield from the reaction of dipotassium terephthalate with triphenylchlorosilane in boiling toluene.

$Ph_3TPA$ was a fine acicular crystal melting at 242—243°C, hardly soluble in ordinary solvents at room temperature, and fairly soluble in boiling toluene, xylene, dioxane and chlorobenzene.

Found: Si, 7.7; mol. wt., 688, 692 (Rast method). Calcd. for $C_{44}H_{34}O_4Si_2$: Si, 8.2%; mol. wt., 683.

X-Ray powder diffraction data of $Ph_3TPA$:

| | | | | | | | |
|---|---|---|---|---|---|---|---|
| *d*, *kX*: | 8.93 | 7.83 | 7.31 | 7.28 | 5.79 | 5.13 | 5.10 |
| | 4.75 | 4.57 | 4.15 | 4.02 | | | |
| $I/I_0$: | 0.28 | 0.18 | 0.13 | 0.11 | 0.12 | 0.62 | 0.19 |
| | 0.39 | 1.00 | 0.34 | 0.21 | | | |

The authors' thanks are due to the Shinetsu Chemical Industrial Co. for the supply of pure organochlorosilanes.

*Department of Synthetic Chemistry*
*Kiryu College of Technology*
*Gumma University*
*Tenjin-cho, Kiryu*

10) T. Takiguchi, M. Abe and M. Niwano *J. Chem. Soc. Japan, Ind. Chem. Sec.* (*Kogyo Kagaku Zasshi*), in press.
11) M. Abe, ibid., in press.

# A New Cobalt(III) Complex: $K[Co(CN)_2dg_2] \cdot 3/2\ H_2O$

By Nobufumi MAKI

(Received April 9, 1965)

The dicyano-bis(dimethylglyoximato)cobaltate(III) complex, $K[Co^{III}(CN)_2dg_2] \cdot 3/2\ H_2O$,[1] has been prepared, and its absorption spectrum compared with those of the related dicyanocobalt(III) complexes.

A solution (200 ml.) containing 13.7 g. of potassium cyanide was mixed with a solution of 50 g. of bis(dimethylglyoximato)diamminecobalt(III) chloride, $[Co\ dg_2(NH_3)_2]Cl \cdot 5H_2O$,[2] under continuous stirring, and then heated on a water bath until the reaction mixture was evaporated to one-third of its former volume. From the smell of the ammonia evolved, it could be discerned that the following mild reaction was in progress:

$$[Co\ dg_2(NH_3)_2]Cl \cdot 5\ H_2O + 2\ KCN \rightarrow K[Co(CN)_2dg_2] \cdot 3/2\ H_2O + 2\ NH_3 + KCl$$

During the course of the reaction, an insoluble yellow matter was deposited. These crystalline deposits were eliminated from the solution quickly while it was in a hot state. These insoluble orange yellow crystals are probably tris(dimethylglyoximato)cobalt(III), $[Co(dgH)_3]$,[3] formed from the rupture of the hydrogen bonding due to the alkalinity of the cyanide solution.

After cooling, the lusterous silky yellow crystals which had been deposited were filtered and washed with cold 85% ethanol and ether.

1) N. Maki, *Nature*, **188**, 227 (1960).
2) L. Tschugaeff, *Z. anorg. u. allgem. Chem.*, **46**, 160 (1905).
3) J. Fujita, A. Nakahara and R. Tsuchida, *J. Chem. Phys.*, **23**, 1541 (1955).

When the mother liquor was concentrated on a water bath, more crystals were obtained and recrystallized from hot water. Large needle-shaped crystals were thus obtained.

Found: Co, 15.49; C, 31.60; N, 21.99; K, 10.22. Calcd. for $K[Co(C_8H_{14}O_4N_4)(CN)_2]$: Co, 15.50; C, 31.58; N, 22.10; K, 10.28%.

The anhydrous salt (dried at 110°C for 3 hr.) was hygroscopic.

*cis*-Dicyano-bis(ethylenediamine)cobalt(III) chloride[4] and dicyano-bis(propylenediamine)-cobalt(III) thiosulfate were prepared by the method of Rây and Sarma[5] or that of Gupta[6].

The visible and ultraviolet absorption spectra measurements were made manually by a Beckmann DU spectrophotometer in an aqueous solution.

## Results and Discussion

The absorption spectra of dicyano-cobalt(III) complexes are shown in Fig. 1. It can be seen that the first band in the visible region shifts towards the shorter wavelength in the following order of ligands:

tn en pn dg.

Table I shows the absorption maxima for dicyano-cobalt(III) complexes. These data were reported recently by Ohkawa, Fujita and Shimura[7] except for that of a dimethylglyoxime complex.

Figure 2 shows the absorption spectra for bis(dimethylglyoximato)cobalt(III) complexes of the $[Co^{III}dg_2X_2]$-type.[8] The order of the spectrochemical series of ligands is as follows:

$CN^-$ $NO_2^-$ $NH_3$ $dgH^-$ $Cl^-$

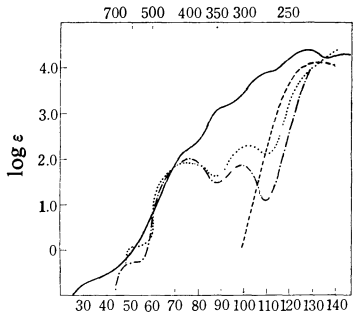



Fig. 1. The absorption spectra of dicyano-cobalt(III) complexes obtained in aqueous solution.
——— $K[Co(CN)_2dg_2]\cdot 3/2\,H_2O$
····· $[Co(CN)_2pn_2]_2S_2O_3\cdot H_2O$
—·—· $[Co(CN)_2en_2]Cl$
——— Dimethylglyoxime in ethanol

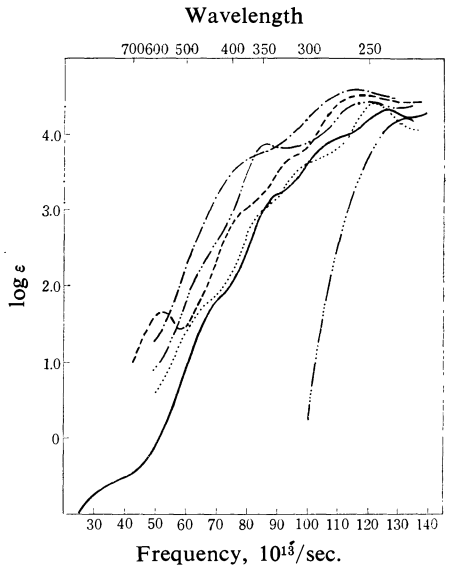



Fig. 2. The absorption spectra for dimethylglyoximato-cobalt(III) complexes.
—·—· $[Co(dgH)_3]$ in $H_2O$
—··—·· $NH_4[Co(NO_2)_2dg_2]\cdot H_2O$ in $H_2O$
—···— Dimethylglyoxime in ethanol
——— $H[CoCl_2dg_2]$ in 3 M HCl
····· $[Co(NH_3)_2dg_2]Cl\cdot 5\,H_2O$ in $H_2O$
——— $K[Co(CN)_2dg_2]\cdot 3/2\,H_2O$ in $H_2O$

TABLE I. ABSORPTION MAXIMA FOR DICYANO-COBALT(III) COMPLEXES

| Compound | Spin-forbidden band | | Spin-allowed band | | Allowed band | |
|---|---|---|---|---|---|---|
| | A | B | I | II | I | II |
| $K[Co(CN)_2dg_2]\cdot 3/2\,H_2O$ | — | — | ca. 78(2.3) | ca. 92(3.24)? | ca. 110(3.9)? | 125.2(4.45) |
| *cis*-$[Co(CN)_2en_2]Cl$* | 49.7(1.67) | — | 74.2(1.91) | 97.1(1.93) | 142.1(4.32) | |
| *cis*-$[Co(CN)_2pn_2]_2S_2O_3\cdot H_2O$* | 50.6(1.73) | — | 74.5(1.90) | 97.4(1.94) | 140.8(4.38) | |
| *cis*-$[Co(CN)_2tn_2]_2S_2O_3$* | 47.2(1.60) | — | 73.6(1.89) | 95.6(1.97) | 137.0(4.38) | |

* The absorption maxima data were adopted from Ref. 7.
tn=trimethylenediamine pn=propylenediamine

4) S. C. Chan and M. L. Tobe, *J. Chem. Soc.*, **1963**, 966.
5) P. R. Rây and B. Sarma, *J. Indian Chem. Soc.*, **28**, 59 (1951).
6) N. R. Sen Gupta, *Z. anorg. u. allgem. Chem.*, **326**, 108 (1963).
7) K. Ohkawa, J. Fujita and Y. Shimura, This Bulletin, **38**, 66 (1965).
8) A. Nakahara, ibid., **28**, 207 (1955).

As for the dicyano complex, two dimethylglyoximes co-ordinate with the central cobalt(III) ion in a planary manner as a pair of chelate rings with two hydrogen bonds, and two dicyano ligands co-ordinate with it at position above and below its coplanar structure. Each co-ordinate bond appears to have a strong $\pi$-bonding character in its co-ordination sphere. Therefore, this complex has a configuration similar to that of cobalamine (vitamin $B_{12}$) and shows a quite analogous behavior in solution.[1] This stable complex, in view of this, will be useful for the study of a catalytic reaction.

The author wishes to thank Professor Akitsugu Nakahara (Osaka University) and Dr. Junnosuke Fujita (Tohoku University) for their kindness to give him the data and suggestions throughout this work.

*Radiation Center of Osaka Prefecture*
*Shinke-cho, Sakai, Osaka*

# The Electrical Properties of the Poly(*N*-vinyl Carbazole) - Antimony(V) Chloride (or Iodine) Charge Transfer Complexes*

By Yoshihisa YAMAMOTO, Seiichi KANDA, Shigekazu KUSABAYASHI
Takeshi NOGAITO, Kazuo ITO and Hiroshi MIKAWA

(Received April 21, 1965)

Many investigations have been made of solid molecular complexes containing polycyclic aromatic hydrocarbons as donors and halogens[1,2] or antimony(V) chloride as acceptors.[3] Most of these complexes are good semiconductors and have a high conductivity, and they often show ESR absorption. Charge transfer complexes derived from polyvinylanthracene,[4] polyvinylpyridine,[5] polyvinylnaphthalene,[6] polyvinylmesitylene[6] and polyvinylcarbazole[7] have already been reported.

It may be expected that vinyl polymer with a $\pi$-electron system of aromatic amines may form a charge transfer complex with antimony(V) chloride or iodine. Although vinyl polymers are real insulating materials, some electrical conductivity may be expected in the resulting complex. It may also be hoped that plastic properties can be retained in the product complex. The present paper will deal with the electrical conductivity, ESR absorption and optical absorption of the charge transfer complexes between poly(*N*-vinyl carbazole) (abbreviated as PVCa) and antimony(V) chloride or iodine.

**Preparation.** — The PVCa used was Luvican M170 (Badische Anilin u. Soda Fabrik A. G.). The antimony(V) chloride was purified twice by distillation.

*Poly(N-vinyl Carbazole) - Antimony(V) Chloride Complexes.*—The preparation of sample No. 2 (Table I), which will serve as an example, was as follows. PVCa (0.4 g.) was dissolved in chloroform (20 cc.), and then 5 cc. of $1\times10^{-3}$ mol./l. antimony(V) chloride solution in chloroform was stirred in at room temperature. The solution turned green, and precipitation occured. The mixture was kept overnight in a desiccator, after which precipitated complex was filtered and washed repeatedly with chloroform in order to remove the excess antimony(V) chloride. The complex thus obtained was powdered and dried under reduced pressure until a constant weight was obtained. All procedures were carefully carried out free from moisture in order to avoid the decomposition of antimony(V) chloride. In the cases of samples No. 6 and 7, precipitation did not occur, although they turned green when the two components were mixed. The solution was evaporated to dryness to give the complex as a film, which was then washed repeatedly with chloroform and petroleum ether.

* Presented at the 16th Annual Meeting of the Chemical Society of Japan, Tokyo, 1963.

1) H. Akamatu, H. Inokuchi and Y. Matsunaga, This Bulletin, **29**, 213 (1956); H. Akamatu, Y. Matsunaga and H. Kuroda, ibid., **30**, 618 (1959); T. Uchida and H. Akamatu, ibid., **34**, 1015 (1961); **35**, 981 (1962).

2) J. Kommandeur and F. R. Hall, *J. Chem. Phys.*, **34**, 129 (1961); L. S. Singer and J. Kommandeur, ibid., **34**, 133 (1961).

3) G. E. Blomgren and J. Kommandeur, ibid., **35**, 1636 (1961).

4) H. Inoue, K. Noda, S. Takiuchi and E. Imoto, *J. Chem. Soc. Japan, Ind. Chem. Sec.* (*Kogyo Kagaku Zasshi*), **65**, 1286 (1962).

5) A. Mizoguchi, H. Moriga, T. Shimizu and Y. Amano, *National Technical Report*, **9**, 407, No. 5 (1963).

6) W. Slough, *Trans. Faraday Soc.*, **58**, 2360 (1962).

7) A. Taniguchi, S. Kanda, T. Nogaito, S. Kusabayashi, H. Mikawa and K. Ito, This Bulletin, **37**, 1386 (1964).

*N-Ethylcarbazole - Antimony(V) Chloride and Carbazole - Antimony(V) Chloride Complexes.*— The methods used were the same as those used in the case of PVCa. The complexes were soluble in chloroform.

*N*-Ethylcarbazole - antimony(V) chloride complexes; m. p. 129—132°C. Found: C, 29.8; H, 2.45; N, 2.40; Sb, 30.40. Calcd. for $(C_{14}H_{13}N)_2(SbCl_4)_3$: C, 28.4; H, 2.2; N, 2.37; Sb, 30.93%. Although the mole ratio of *N*-ethylcarbazole and antimony was found to be 2 : 3, Sb : Cl ratio was 1 : 4.

Carbazole - antimony(V) chloride complex; m. p. 179—183°C. Found: C, 44.38; H, 2.79; N, 4.40; Sb, 19.30. Calcd. for $(C_{12}H_9N)_2(SbCl_5)$: C, 45.54; H, 2.84; N, 4.40; Sb, 19.30%.

*Poly(N-vinyl Carbazole) - Iodine Complexes.*— PVCa and iodine in chloroform were mixed, the stirring was continued for two hours at room temperature, and then they were refluxed for another hour, after which the mixture was allowed to stand overnight. The green colored complex was then precipitated by petroleum ether.

*Electric Properties.* — Two disk electrodes, 0.2—0.3 mm. thick and 8 mm. in diameter, were prepared first by pressing graphite powder at $5\times10^3$ kg./cm$^2$. The powder of the material was packed between these two graphite electrodes in a mold with a diameter of 13 mm. and pressed at $6\times10^3$ kg./cm$^2$. The thickness of the specimen between the electrodes was about 0.7 mm. The d. c. conductivity was measured in the temperature range between 20 and 60°C.

An almost linear relationship was observed between the current and the applied voltage up to 4600—7000 V./cm. The temperature dependence of the resistivity obeyed the $\rho = \rho_0 \exp(\varepsilon/2kT)$ equation (Fig. 1). The resistivity at 20°C ($\rho_{20}$) and the apparent energy gap ($\varepsilon$) as calculated from the above equation are tabulated in Table I. The $\rho_{20}$ values of PVCa - antimony(V) chloride complexes and PVCa - iodine complexes were found to be $10^5$—$10^9$ and $10^{11}$—$10^{13}$ Ωcm. The $\varepsilon$ values were

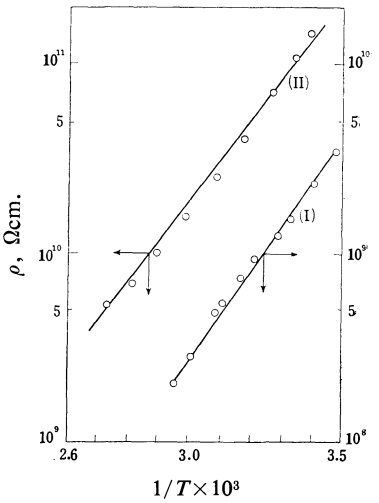



Fig. 1. Specific resistivity vs. $1/T\times10^3$.
Poly(*N*-vinyl carbazole) - $SbCl_5$ complex (I) (Sample No. 6)
Poly(*N*-vinyl carbazole) - $I_2$ complex (II) (Sample No. 10)

Table I. Properties of various complexes

| No. | Mole ratio between both components used in preparation | Mole ratio between carbazole monomer unit and $SbCl_5$ (or $I_2$) in the complex | Specific resistivity at room temperature $\rho_{20}$, Ωcm. | ε, eV. | spin/g. |
|---|---|---|---|---|---|
| Poly(*N*-vinyl carbazole) - $SbCl_5$ | | | | | |
| 1 | PVCa only | | $>10^{17}$ | | |
| 2 | 1 : 2.5 | 4.5 : 1 | $5.0\times10^7$ | 0.92 | $2\times10^{19}$ |
| 3 | 2 : 3 | | $2.0\times10^5$ | 0.50 | $6\times10^{19}$ |
| 4 | 1 : 1 | 7.3 : 1 | $8.0\times10^6$ | 0.62 | |
| 5 | 2 : 1 | 5.3 : 1 | $4.0\times10^5$ | 0.47 | $4\times10^{19}$ |
| 6 | 5 : 1 | 5.6 : 1 | $2.5\times10^9$ | 0.80 | $4\times10^{19}$ |
| 7 | 10 : 1 | 11.3 : 1 | $8.0\times10^7$ | 1.0 | |
| *N*-Ethylcarbazole - $SbCl_5$ | | | | | |
| 8 | 1 : 2.5 | 3.0 : 2 | $1.9\times10^6$ | 0.60 | $2\times10^{19}$ |
| Carbazole-$SbCl_5$ | | | | | |
| 9 | 1 : 2.5 | 2.0 : 1 | $1.5\times10^7$ | 1.18 | |
| Poly(*N*-vinyl carbazole) - $I_2$ | | | | | |
| 10 | 1 : 5 | 7.6 : 1 | $1.5\times10^{11}$ | 0.93 | $5\times10^{17}$ |
| 11 | 1 : 2 | 14 : 1 | $1.8\times10^{13}$ | 1.14 | $6\times10^{16}$ |
| 12 | 1 : 1 | 45 : 1 | $3.3\times10^{12}$ | 0.94 | $6\times10^{16}$ |
| 13 | 2 : 1 | 73 : 1 | $2.6\times10^{13}$ | 0.88 | $8\times10^{16}$ |

0.50—1.0 eV. for PVCa - antimony(V) chloride complexes and 0.88—1.22 eV. for PVCa - iodine complexes.

As a reference, the *N*-ethylcarbazole - antimony(V) chloride complex and the carbazole-antimony(V) chloride complex were also measured; there $\rho_{20}$ values were found to be $10^6$ and $10^7$ Ωcm. respectively.

**ESR Absorption.**—The ESR absorption was examined at room temperature with a Hitachi MPS-2C spectrometer. The observed values are shown in Table I in spin/g. All the measured samples showed ESR absorption, indicating the existence of unpaired electrons. In the PVCa - antimony(V) chloride complex the number of unpaired spins is about one-tenth of the number of antimony(V) chloride present in the complex. On the other hand, in the PVCa - iodine complex the number of unpaired spins is only $10^{-3}$—$10^{-4}$ of the number of iodine molecules in the complex.

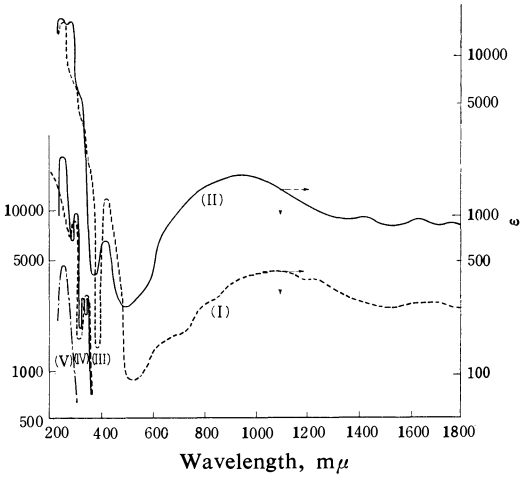



Fig. 2. Absorption spectra of some complexes.
(I) Poly(*N*-vinyl carbazole) - $SbCl_5$
(II) Ethyl carbazole - $SbCl_5$
(III) Poly(*N*-vinyl carbazole)
(V) Ethyl carbazole
(IV) $SbCl_5$

**Optical Absorption.**—The absorption spectra of the complexes are shown in Fig. 2. The absorption bands of the complexes in chloroform exist in four regions: <400, 420, 1000 and >1300 mμ of these, the <400 mμ bands are due to the components. The spectrum of antimony(V) chloride in chloroform did not show any absorption above 400 mμ. The 400, 1000 and >1300 mμ bands are, therefore, due to complexing between the components. The values of the energy gap as obtained from the temperature dependence of the resistivity are calculated to correspond to 1300—2500 mμ.

The authors wish to thank Mr. Takuzo Fujino and Mr. Tsuneyo Shishido for their elementary analyses.

*The Institute of Scientific and Industrial Reserch*
*Osaka University*
*Sakai, Osaka*

SHORT COMMUNICATIONS

# The Reactivities of Hydrated Electrons and OH Radicals in an Aqueous Hexacyanoferrate(II) Solution

By Shin-ichi OHNO

(Received June 28, 1965)

As has been reported previously,[1] the irradiation of aqueous hexacyanoferrate(II) solutions at 2537Å results in the formation of hexacyanoferrate(III) ions and hydrated electrons, $e^-_{aq}$:

$$Fe(CN)_6^{4-} \rightarrow Fe(CN)_6^{3-} + e^-_{aq} \quad (1)$$

The limiting quantum yield, obtained at high concentrations of an electron scavenger, $N_2O$ or $NO_3^-$, was 0.35 at 25°C. This communication will present some results of the investigations into the reactivities of hydrated electrons and OH radicals using the above photochemical system.

In the $Fe(CN)_6^{4-}-N_2O$ systems, the photochemical reaction 1 is followed by:

$$e^-_{aq} + N_2O \rightarrow N_2 + OH + OH^- \quad (2)[2]$$

$$Fe(CN)_6^{4-} + OH \rightarrow Fe(CN)_6^{3-} + OH^- \quad (3)$$

The addition of other solutes which compete efficiently with $N_2O$ for $e^-_{aq}$ reduces the $N_2$ yields:

$$e^-_{aq} + S \rightarrow S^- \quad (4)$$

Thus, the relative rates can be obtained. In those cases where the $S^-$ produced reduces the $Fe(CN)_6^{3-}$ ion, the ratio of the rate constants, $k_4/k_2$, can also be calculated from the measured hexacyanoferrate(III) yields. Some results obtained are shown in column a of Table I.

In the $Fe(CN)_6^{4-}-NO_3^-$ systems containing other electron acceptors, the observed yields of nitrite[1,3] permit us to calculate the rates relative to nitrate. Table I, column b, shows some of these results.

Table I. Relative reactivity of various solutes towards $e^-_{aq}$, normalized to $k(e^-_{aq}+N_2O)=100$ or $k(e^-_{aq}+NO_3^-)=100$

| a | | b | |
|---|---|---|---|
| $N_2O$ | =100 | $NO_3^-$ | =100 |
| $H^+$ | 220 | $N_2O$ | 35 |
| $NO_3^-$ | 286 | $O_2$ | 250 |
| $Fe(CN)_6^{3-}$ | 120 | $CO_2$ | 38 |
| Acetone | 150 | $H_2O_2$ | 210 |
| $H_2PO_4^-$ | 1.6 | Acetone | 45 |
| $HPO_4^{2-}$, $ClO_4^-$ | Unreactive | $Cl^-$, Methanol | Unreactive |

The solutes, RH, which compete with $Fe(CN)_6^{4-}$ in the reaction with OH to yield the reducing radicals, R;

$$RH + OH \rightarrow R + H_2O \quad (5)$$

$$Fe(CN)_6^{3-} + R \rightarrow Fe(CN)_6^{4-} + R^+$$

reduce the yields of hexacyanoferrate(III), and the rate constant ratios, $k_5/k_3$, can be calculated. Table II shows some of these results, $k(OH+Fe(CN)_6^{4-})$ being taken as 100.

Table II. Reactivity of some solutes towards OH radicals, normalized to $k(OH+Fe(CN)_6^{4-})=100$

| | |
|---|---|
| $Fe(CN)_6^{4-}$ | =100 |
| Methanol | 6.1 |
| Ethanol | 16 |
| 2-Propanol | 23 |
| $HCOO^-$ | 26 |
| $Br^-$ | 5.4 |
| Glycine | 2.8 |
| D-Glucose | ≈8 |

*Japan Atomic Energy Research Insitute*
*Tokai-mura, Ibaraki-ken*

1) S. Ohno and G. Tsuchihashi, This Bulletin, **38**, 1052 (1965).
2) F. S. Dainton and D. B. Peterson, *Proc. Roy. Soc.*, **A267**, 443 (1962).
3) A. Appleby, G. Scholes and M. Simic, *J. Am. Chem. Soc.*, **85**, 3891 (1963).

# The Non-catalytic Fusion Reaction of Acylated Sugars with Some Purines and Phenols[1]

By Yoshiharu ISHIDO, Teruo MATSUBA, Akira HOSONO, Kiyoshi FUJII
Hisayuki TANAKA, Koichi IWABUCHI, Sadanori ISOME, Akira MARUYAMA
Yasuhiko KIKUCHI and Tetsuo SATO

(Received July 12, 1965)

The authors wish to report on a new type of non-catalytic fusion of ordinary acylated sugars with some purines and phenols.

Helferich and Gootz[2] have reported that 1-*O*-trichloroacetyl-2, 3, 4, 6-tetra-*O*-acetyl-β-D-glucopyranose (I) is reactive enough in the non-catalytic fusion reaction with phenol to give phenyl 2′, 3′, 4′, 6′-tetra-*O*-acetyl-β-D-glucopyranoside.

When 2, 6-dichloropurine (II)[3] and theophylline (III) are applied to the reaction, only II gave 2, 6-dichloro-9-(2′, 3′, 4′, 6′-tetra-*O*-acetyl-β-D-glucopyranosyl)-purine (in a 57% yield) under the same conditions.[4] Moreover, II gave the corresponding 2′, 3′, 5′-tri-*O*-acetyl-β-D-ribofuranoside in a good yield[5] by the reaction with 1, 2, 3, 5-tetra-*O*-acetyl-β-D-ribofuranose (IV) in the presence of any catalyst, even though the reaction period was very short.[4]

These facts suggest that the non-catalytic reaction might be caused not only by the activation on the $C_{(1)}$-*O*-acyl group, as in the case of I, but also by that of the acidic hydrogen which is attached to the reaction center of such purines as II, as a result of the polar effect of the electron-withdrawing substituents, and that, therefore, the reactivity of purine derivatives can not simply be ascribed to their fusibility[1b] in the reaction with acylated sugars, as has been reported before.

6-Chloro-(V),[6] 6-iodo-,[6] 6-cyano-,[6] II, 2(6)-chloro-6(2)-iodo-,[6] and 2, 6, 8-trichloro-purine,[7] by non-catalytic fusion reaction with IV at 150—155°C in vacuo, gave the corresponding ribonucleosides in yields of 10,[8] 12,[8] 21,[9] 50,[10] 67,[10] and 64%[10] respectively. On the other hand, 6-methoxypurine[11] gave no corresponding product by the same reaction. In these cases, the fusibility of purine derivatives and their thermostability seem also to exert a considerable effect.

*p*-Nitrophenol, whose p*K*a value is almost the same as that of V,[12] also gave *p*-nitrophenyl 2′, 3′, 4′, 6′-tetra-*O*-acetyl-β-D-glucopyranoside[14] (in a 65% yield) by reaction with 1, 2, 3, 4, 6-penta-*O*-acetyl-β-D-glucopyranose at 175—195°C in vacuo. Similarly, IV gave two kinds of *p*-nitrophenyl tri-*O*-acetyl-D-ribofuranosides: *m*-Nitophenol gave *m*-nitrophenyl 2′, 3′, 4′, 6′-tetra-*O*-acetyl-β-D-glucopyranoside (m. p. 138—139.5°C, $[\alpha]_{578}^{27}$ −38.1°, $[\alpha]_{546}^{27}$ −40.1° in chloroform) in 47% yield, but neither *o*-nitro- nor 2, 4-dinitrophenol gave a corresponding product.

In view of these facts, the interpretation[15] of the polar effects of substituents on the reaction center requires further study. The fusion reaction of deoxy- and unsaturated-sugar derivatives with these purines and phenols is also under investigation.

A kinetic study of this reaction has been carried out by means of ultraviolet absorption spectroscopy; it has been found that the reaction of II with IV is of the second order. Detailed results will be published in the near future.

*Department of Chemistry*
*Tokyo Institute of Technology*
*Ookayama, Tokyo*
*(Y. I., T. M., A. H., K. F., H. T., K. I. & T. S.)*

*Tokyo Tanabe Co., Ltd.*
*Adachi-ku, Tokyo*
*(S. I., A. M. & Y. K.)*

1) A portion of this paper was presented at 18th Annual Meeting of the Chemical Society of Japan, Osaka, April, 1965. Previous papers: a) Y. Ishido, A. Hosono, S. Isome, A. Maruyama and T. Sato, This Bulletin, **37**, 1389 (1964); b) Y. Ishido, Y. Kikuchi and T. Sato, *J. Chem. Soc. Japan, Pure Chem. Sec.* (*Nippon Kagaku Zasshi*), **86**, 240 (1965).

2) B. Helferich and R. Gootz. *Ber.*, **62**, 2788 (1929).

3) J. A. Montgomery, *J. Am. Chem. Soc.*, **78**, 1928 (1956).

4) Y. Ishido, Doctoral Thesis, Tokyo Institute of Technology, Japan, March, 1963.

5) The yields range approximately from 50—80% of the theoretical yields.

6) G. B. Elion and G. H. Hitchings, *J. Am. Chem. Soc.*, **78**, 3508 (1956).

7) J. Davoll and B. A. Lowy, ibid., **73**, 2936 (1951).

8) Both products were isolated as adenosine by treating the acetylated products with methanolic ammonia (saturated at 0°C) in a sealed tube at 100°C.

9) The product was isolated as an equimolar adduct of ammonia by the deacetylation with methanolic ammonia mentioned above; m. p. 210—213°C.

10) These products were isolated as 2′, 3′, 5′-tri-*O*-acetate.

11) G. B. Brown and U. S. Welikey, *J. Biol. Chem.*, **204**, 1019 (1953).

12) A. Bendich, P. J. Russel, Jr., and J. J. Fox, *J. Am. Chem, Soc.*, **76**, 6073 (1954).

13) E. Glaser and W. Wulwek, *Biochem. Z.*, **145**, 514 (1934).

14) Y. Ishido, T. Matsuba, and T. Sato, *The Abstract of 17th Annual Meeting of the Chemical Society of Japan*, 253; (1964) quoted in Ref. 1b.

# Studies of the Absorption of Hydrogen on a Palladium Carbon Catalyst

By Sadao SUZUKI and Tsutomu SUZUKI

(Received July 20, 1965)

The platinum-carbon-hydrogen-system has been investigated by several groups[1-3] in recent years. The absorption of hydrogen on a palladium carbon catalyst (Pd-C) has been studied and some interesting information gained. It is known that hydrogen is only physically adsorbed on carbon at room temperature. Above 600°C hydrogen is chemisorbed on carbon.[4]

In this study, extraordinary absorption of hydrogen on Pd-C has been found. That is, the net amount absorbed on carbon (the amount absorbed on Pd-C minus that absorbed on palladium alone) is several hundred times that adsorbed physically at the same temperature. The measurements were made in a constant-volume apparatus. Carbon had been soaked in a 10% hydrofluolic acid solution in order to eliminate impurities. The required amount of palladium chloride solution was dispersed impartially over carbon to make a Pd-C catalyst. The catalyst, after it had been fully washed by ion-exchanged and distilled water, was put into the cell in a wet state and evacuated at 250°C.

The hydrogen for absorption measurements was made by the electrolysis of a 20% sodium hydroxide solution and purified by passing it through a palladium asbestos tube heated to 200°C.

A typical run of experiments is shown in Fig. 1. From this figure, it is evident that the amount absorbed on Pd-C is much larger than that which would be adsorbed phycically. The correlation between the over-all amount of hydrogen absorbed and the pressure at equilibrium is shown in Fig. 1 also.

Apparently the amount absorbed is proportional to the square root of the pressure at equilibrium over the range from 0 mmHg to 80. This pressure dependence indicates a dissociative absorption of hydrogen. The effect of the amount of palladium on the absorption rate is illustrated in Fig. 2. This figure suggests that the initial rate of absorption is

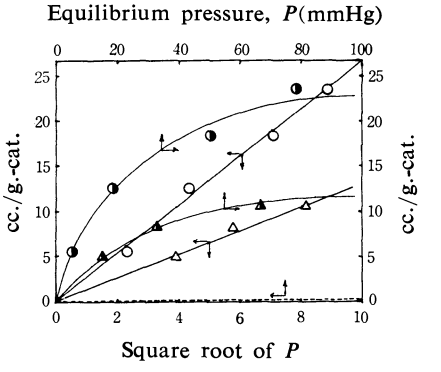



Fig. 1. Dependence of the amount absorbed on 5%Pd-C on equilibrium pressure.
Experimental results: ◑ at 150°C, ◭ at 200°C, ····· the amount physically absorbed on Pd only (the amount on C only is negligible). Avanged values with $\sqrt{P}$: ○ at 150°C, △ at 200°C.

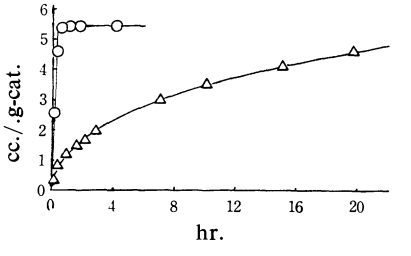



Fig. 2. Effect of the amount of Pd on the absorption rate at 150°C.
○ 5%Pd-C, △ 1%Pd-C

roughly proportional to the amount of palladium in the catalyst under the same initial pressure of hydrogen, and that the amounts absorbed at equilibrium are the same, irrespective of the palladium content.

The above information leads to several conclusions. The palladium in the catalyst plays the role of dissociating the hydrogen, which then migrates to the carbon surface and is stored there. The kinetic data predict that the rate-determining step of this absorption process is the diffusion of hydrogen from palladium to the carbon surface.

Gases other than hydrogen were found in the desorbed gas at 250°C.

*Research Laboratory of Resources Utilization*
*Tokyo Institute of Technology*
*Ookayama, Tokyo*

1) V. S. Boronin and O. M. Poltorak, *Vestn. Mosk. Univ., Ser. II, Khim.*, **18** (3), (1963).
2) A. J. Robbell, E. V. Ballou and M. Boudart, *J. Phys. Chem.*, **68**, 2748 (1964).
3) V. V. Sof'ina, *Pribory i Tekhn. Eksperim.*, **8** (4) 174 (1963).
4) R. M. Barrer, and E. K. Rideal, *Proc. Roy. Soc.*, **A149**, 231 (1935).

# The Photo-Ionization of *N*, *N*, *N'*, *N'*-Tetramethyl-*p*-phenylenediamine in Organic Matrices

By Hiroshi TSUBOMURA, Naoto YAMAMOTO, Katsumi KIMURA, Toru SATO Hikoichiro YAMADA, Masahiko KATO, Gentaro YAMAGUCHI and Yoshinori NAKATO

(Received August 13, 1965)

The photolytic formation of Wurster's blue cation from *N*, *N*, *N'*, *N'*-tetramethyl-*p*-phenylenediamine (TMPD) in an organic rigid matrix is well known after the pioneering research of Lewis and his collaborators.[1] Not much investigation has been made, however, into the behavior of the electron ejected in the matrix, except for the interesting work reported by Dolan and Albrecht.[2]

We have made flash-photolytic experiments of TMPD, using two argon-filled flash lamps, with a total discharge energy of 200—400 joules and the duration of which is less than 4 $\mu$sec. In deoxygenated liquid paraffin at room temperature, the flash photolysis of TMPD showed the transient absorption spectrum shown in Fig. 1a. From this result, although there is some difference in spectral position between the curves shown in Fig. 1, it seems certain that Wurster's blue cation is formed in the liquid paraffin solution at room temperature.

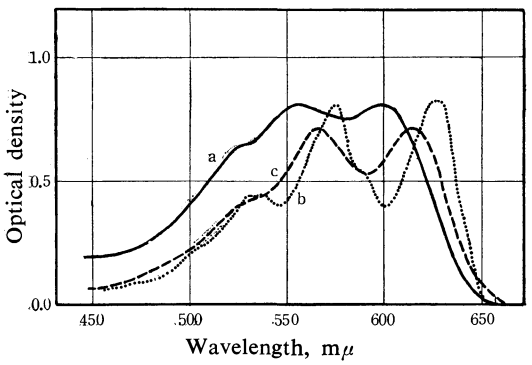



Fig. 1. Absorption spectra of Wurster's blue cation formed

a) by the fiash photolysis of TMPD in liquid paraffin at room temperature
b) by the ultraviolet illumination of TMPD in ethanol at 77°K.
c) Absorption spectrum of Wurster's blue perchlorate in ethanol at room temperature.

The transient spectrum decayed exponentially with $\tau_e = 82$ $\mu$sec. With deaerated *n*-heptane solutions, and also with aerated liquid paraffin solutions, no transient spectrum was obtained.

We have measured the fluorescence and phosphorescence spectra of TMPD at 77°K in ethanol, EPA and MP. These spectra, together with the absorption spectrum, may well be understood as those of the substituted benzenes.[3] In other words, no special band, such as the charge-transfer absorption band or the charge-transfer fluorescence band, appears at all in these solutions. The life-times of the phosphorescence spectrum for ethanol and MP solutions at 77°K have been found to be 1.57 and 2.12 sec. respectively. These life-times are also normal for substituted benzenes. From these results, we can conclude that, on excitation, TMPD goes first into its singlet excited level, and that then some of the molecules return to the ground state, either emitting fluorescence and phosphorescence or radiationlessly, while others are transferred into the ionized state.

The TMPD cation produced by the flash illumination of deoxygenated ethanol solutions has been found to have a surprisingly long life. It returns to the original state after two days, and the experiment can be repeated for several times. In aerated ethanol, only very few cations were formed by a flash with approximately the same energy as that used for deoxygenated solutions, and no transient absorption spectrum was photographed, even if the spectral flash lamp was fired at 10 $\mu$sec. after the photolysis flash.[4] We also photo-ionized the deoxygenated ethanol solution by the flash, and then introduced oxygen into the colored solution. The color did not change at all. These results show that oxygen quenches the photo-ionization at the initial stage.

*Department of Chemistry*
*Faculty of Engineering Science*
*Osaka University*
*Toyonaka, Osaka*

1) G. N. Lewis and D. Lipkin, *J. Am. Chem. Soc.*, **64**, 2801 (1942).
2) E. Dolan and A. C. Albrecht, *J. Chem. Phys.*, **37**, 1149 (1962); **38**, 567 (1963).
3) K. Kimura and H. Tsubomura, Unpublished results.
4) The cation in this case stays permanently.

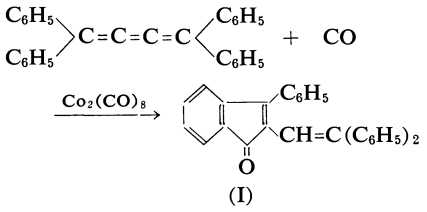
# The Carbonylation of Cumulenes

By Pu-Jun KIM and Nobue HAGIHARA

(Received August 16, 1965)

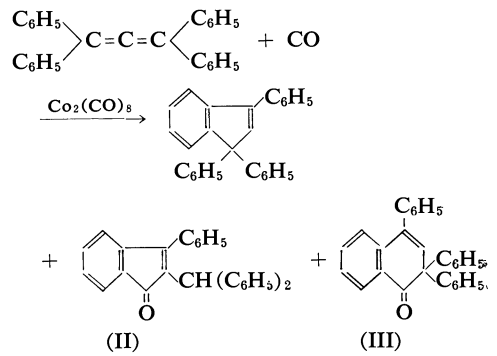
It has previously been shown that cumulenes interact with transition metal carbonyls to yield some new $\pi$-complexes.[1] In this paper we wish to describe the carbonylation of tetraphenyl-butatriene and -allene in the presence of dicobalt octacarbonyl.

Tetraphenylbutatriene (2.0 g.) in benzene (50 ml.) was treated with carbon monoxide (150 kg./cm$^2$) in the presence of dicobalt octacarbonyl (0.2 g.) at 230—250°C. Upon cooling after 6 hr., a red solution was obtained. The reaction mixture was separated by chromatography on alumina with benzene to give 1-diphenylmethylene-3-phenylindene[2] in a 0.04% yield and red prisms (I) (m. p. 147—148°C) in a 70% yield. The elemental analysis and molecular weight determination indicated that I has this composition: (tetraphenylbutatriene)·(CO), I (Found: C, 90.02; H, 5.55; mol. wt. (Rast), 365.5. Calcd. for $C_{29}H_{20}O$: C, 90.59; H, 5.24%; mol. wt., 384.5). The infrared spectrum of I showed the presence of a ketonic carbonyl group (1714 cm$^{-1}$). The NMR spectrum of I showed a singlet at 3.57$\tau$ and a multiplet at 2.67—3.08$\tau$, with a relative intensity of 1 : 19. I absorbed 2 mol. of hydrogen over a Raney-nickel catalyst and was oxidized with chromium trioxide in acetic acid to give *o*-benzoylbenzoic acid and benzophenone. On the basis of this evidence and the melting point described in the literature, I was shown to be 2-($\beta$, $\beta$-diphenylvinyl)-3-phenyl-indone (lit.[3] m. p. 147—148°C) as is shown below:




(I)

Analogously, tetraphenylallene in benzene was heated with carbon monoxide (150 kg./cm$^2$) in the presence of dicobalt octacarbonyl at 230—250°C for 6 hr. After the reaction, a yellow solution was obtained on cooling. The reaction mixture was separated by chromatography on alumina to give 1, 1, 3-triphenylindene (m. p. 133—134°C)[2] in a 41.5% yield, yellow plates (II) (m. p. 155.5—156.5°C) in a 23% yield, and yellow prisms (III) m. p. 172—174°C) in a 17% yield. These compounds were recrystallized from benzene and petroleum-ether. The elemental analyses and molecular weight determinations indicated that both II and III have this composition: (tetraphenylallene)·(CO), II (Found: C, 89.96; H, 5.33; mol. wt. (Rast), 367.0. Calcd. for $C_{28}H_{20}O$: C, 90.29; H, 54.1%; mol. wt., 372.4), III (Found: C, 89.80; H, 5.34%; mol. wt. (Rast), 367.4). The infrared spectra of II and III showed the presence of ketonic carbonyl groups (1714 and 1690 cm$^{-1}$ respectively in Nujol). The NMR spectrum of II showed a singlet at 4.81$\tau$ and a multiplet at 2.58—3.09$\tau$, with a relative intensity of 1 : 19. On the basis of this evidence and the melting point described in the literature, II was shown to be 2-diphenylmethyl-3-phenylindone (lit.[4] m. p. 154°C), while III, an isomer of II, seemed to be 2, 2, 4-triphenylnaphthalenone from its infrared spectrum, as is shown below:




(II) (III)

*The Institute of Scientific and Industrial Research*
*Osaka Univesity*
*Sakai, Osaka*

1) a) A. Nakamura, P.-J. Kim and N. Hagihara, This Bulletin, 37, 292 (1964); b) A. Nakamura, P.-J. Kim and N. Hagihara, *J. Organometal. Chem.*, 3, 7 (1965).

2) Identified with an authentic sample by comparing the infrared spectra.

3) C. F. Koelsch and H. J. Richter, *J. Org. Chem.*, 3, 471 (1938).

4) W. Baker, J. F. W. McOmie and T. L. V. Ulbricht, *J. Chem. Soc.*, 1957, 4031.

# The Anomalous Temperature Dependence of the Electrical Conductivity of Phenanthrene

By Shoichi MATSUMOTO and Tomomichi TSUKADA

(Received August 16, 1965)

A relatively large anisotropy in the electrical conductivity of the phenanthrene single crystal,[1] and the current-voltage characteristics of the single crystal,[2] characteristics which might be attributable to space-charge-limited currents phenomena, have previously been reported. In the course of an extensive study of the electrical properties of polycrystalline phenanthrene, the present authors have found an anomaly at around 64—71°C in the temperature dependence of the electrical conductivity. In this paper, the observed anomaly and a probable cause for it will be presented.

The powdered phenanthrene, purified by a combination of recrystallization and zone melting, was packed in a polytetrafluoroethylene cylinder with a small exhaust-path and compressed between the metal ends used as electrodes. The pressure of compression was 120 kg./cm$^2$, and the electrical measurements were carried out under a pressure of $10^{-3}-10^{-4}$ mmHg.

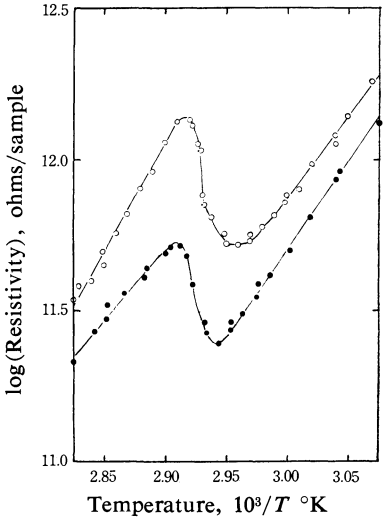



Fig. 1. One example of the temperature dependence (○ for heating, ● for cooling) of the electrical resistivity of phenanthrene, showing an anomaly at around 64—71°C.

A typical example of the temperature dependence of the electrical resistivity measured by the d. c. method is shown in Fig. 1, where an anomaly is observed at around 64—71°C. The linear relationship between the logarithm of resistivity and the reciprocal absolute temperature was broken in this temperature range, after which the resistivity increased abruptly with the rising temperature until it became approximately 6—7 times greater than that below 64°C. However, the linear relationship remained both below and above the anomaly, and there is no significant change in the slopes of each relationship. The anomalous phenomena were quite reversible. The reproducibility of the phenomena for different specimens is good within the range of experimental error.

Hence, the above-mentioned anomaly must be associated with a certain intrinsic property of phenanthrene itself. The large increase in resistivity at the anomalous point may be attributable to the influence of the differences in the molecular arrangement below and above the point; that is, it is probable that phenanthrene has a phase transition at around 64—71°C. However, this transition may not be great in itself, because the anomalous phenomena were quite reversible and no significant change of the activation energy for conduction can be admitted.

A preliminary investigation by differential thermal analysis showed an apparent endothermic peak at about 67°C on a thermogram. This may present evidence on a phase transition of phenanthrene suggested by the above-mentioned anomaly. This study is now in progress.

*Central Research Laboratory*
*Tokyo Shibaura Electric Co., Ltd.*
*Komukai, Kawasaki, Kanagawa*

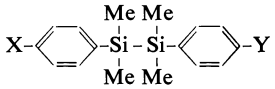
1) S. Matsumoto and T. Tsukada, This Bulletin, **37**, 1545 (1964).
2) S. Matsumoto, ibid., **38**, 997 (1965).

# The Substituent Effect on the Ultraviolet Spectrum of 1, 2-Diphenyltetramethyldisilane[1]

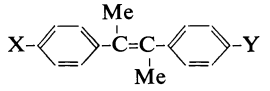
By Hideki SAKURAI, Hisayoshi YAMAMORI and Makoto KUMADA

(Received August 19, 1965)

It has previously been reported from this laboratory[2] that polysilanes with phenyl or vinyl groups, unlike monosilanes, have a very intense absorption in the ultraviolet region. This interesting ultraviolet property of polysilanes has been studied by several groups of workers in recent years.[3-5] These investigations are in accord with the view that the silicon-silicon bond is essential as a chromophore in making an enhanced conjugation with pi-electron systems.



(I)



(II)

TABLE I. UV SPECTRA OF SOME 1, 2-DIPHENYLTETRAMETHYLDISILANES[a]

| Substituent X | Substituent Y | $\lambda_{max}$ mμ | $\varepsilon \times 10^{-4}$ |
|---|---|---|---|
| none | | 238.0 | 1.85 |
| *p*-$CH_3$ | *p*-H | 238.5 | 2.11 |
| *p*-$CH_3$ | *p*-$CH_3$ | 239.0 | 2.49 |
| *p*-$CH_3O$ | *p*-$CH_3O$ | 242.0 | 3.26 |
| *p*-$CH_3O$ | *p*-H | 241.0 | 2.58 |
| *p*-$CH_3O$ | *p*-$CH_3$ | 241.5 | 2.82 |
| *p*-Cl | *p*-Cl | 242.5 | 2.80 |
| *p*-$CH_3$ | *p*-Cl | 240.5 | 2.46 |

a) Spectra were obtained in *n*-hexane with Shimadzu SV-50A automatic recording spectrophotometer.

We have now prepared several derivatives of 1, 2-diphenyltetramethyldisilane (I)[6] and examined their ultraviolet absorption spectra (Table I).

Bathochromic shifts of the first intense band of the parent compound are observed with all the available *para*-substituted derivatives; apparently the bathochromic effects of substituents are additive.

It is of considerable interest to compare the ultraviolet spectra of these compounds with those of the correspondingly-substituted *trans*-$\alpha, \alpha'$-dimethylstilbenes (II).[7] As may be seen in Fig. 1, there is a linear correlation between

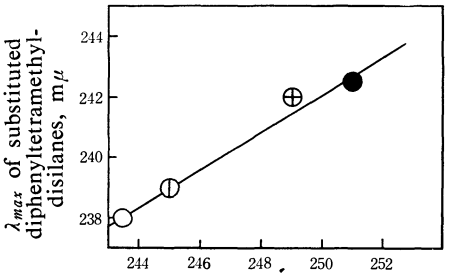



Fig. 1. Correlation of $\lambda_{max}$ of diphenyltetramethyldisilanes with $\lambda_{max}$ of trans-$\alpha, \alpha'$-dimethylstilbenes

○ Unsubstituted
ⓘ *p, p'*-Dimethyl
⊕ *p, p'*-Dimethoxy
● *p, p'*-Dichloro

the absorption maxima of the disilanes (I) and those of the stilbenes (II).

Further details will be published later.

*Department of Synthetic Chemistry*
*Kyoto University*
*Sakyo-ku, Kyoto*

1) Presented in part at the 18th Annual Meeting of the Chemical Society of Japan, Osaka, April, 1965.
2) H. Sakurai and M. Kumada, This Bulletin, **37**, 1894 (1964).
3) D. N. Hague and R. H. Prince, *Proc. Chem. Soc.*, **1962**, 300.
4) H. Gilman, W. H. Atwell and G. L. Schwebke, *Chem. & Ind.*, **1964**, 1063.
5) H. Gilman, W. H. Atwell and G. L. Schwebke, *J. Organometal. Chem.*, **2**, 369 (1964).
6) Details of preparations will be published elsewhere.
7) Y. Nagai, *J. Soc. Org. Synth. Chem. Japan*, **19**, 464 (1961).

# The Circular Dichroism of Tris(L-prolinato)cobalt(III)

By Takaji YASUI, Jinsai HIDAKA and Yoichi SHIMURA

(Received August 23, 1965)

It is shown by the construction of molecular models that the tris(L-prolinato)cobalt(III) molecule can not exist in any one of the mer-$\Delta$, mer-$\Lambda$ and fac-$\Delta$ configurations but only in the fac-$\Lambda$ configuration, as a result of the steric hindrance among the three coordinated L-prolinate ions. The complex was prepared as purplish-pink crystals by the reaction of diaquotetramminecobalt(III) perchlorate with L-proline in the presence of activated charcoal. Found: C, 44.17; H, 6.02; N, 10.37. Calcd. for $Co(C_5H_8NO_2)_3$: C, 44.88; H, 6.04; N, 10.47%. The absorption spectrum confirms that it is the facial form.[1]

The circular dichroism (CD) and the rotatory dispersion (ORD) curves,* shownin Fig. 1, confirm the absolute configuration ($\Lambda$) of the complex.[2] A similar CD behavior was observed in tris(L-hydroxyprolinato)cobalt(III).

*Department of Chemistry*
*Faculty of Science*
*Osaka University*
*Toyonaka, Osaka*

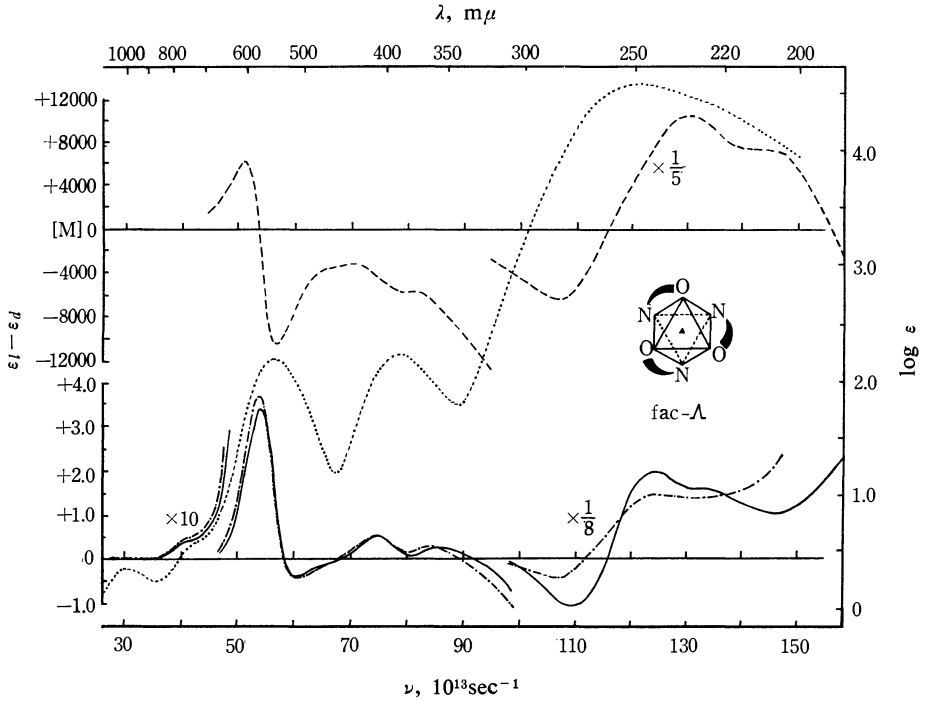



Fig. 1. CD curve (——), ORD curve (----) and absorption curve (····) of [Co(L-prol)$_3$], and CD curve (-·-·) of [Co(L-hydprol)$_3$] in 70% perchloric acid.

1) N. Matsuoka, Y. Shimura and R. Tsuchida, *J. Chem. Soc. Japan, Pure Chem. Sec. (Nippon Kagaku Zasshi)*, **82**, 1637 (1961).

2) A. J. McCaffery and S. F. Mason, *Mol. Phys.*, **6**, 359 (1963).

* These were measured by the spectropolarimeter model ORD/UV-5 of the Japan Spectroscopic Co.

# Aminocyclitols. IX. The Facile Synthesis of Streptamine

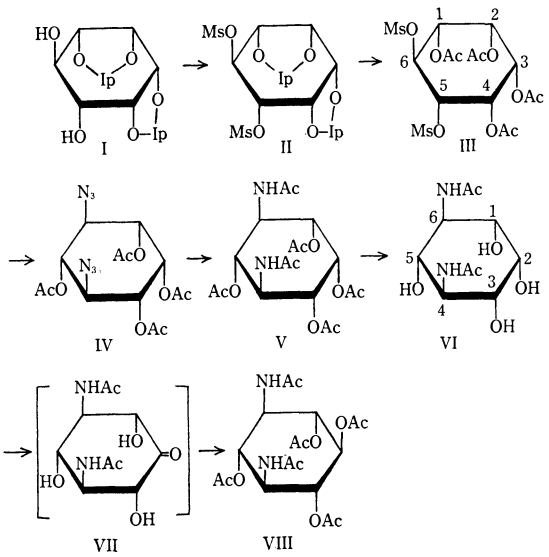
By Tetsuo SUAMI and Seiichiro OGAWA

(Received September 4, 1965)

In connection with the previous studies of this series,[1] a new synthetic route to streptamine has been established in our laboratory.

Streptamine has been found to be a component of the antibiotic streptomycin,[2] and its structure has been shown to be *scyllo*-inosadiamine-1, 3.[3] This compound has been synthesized by Wolfrom et al.[3] from natural glucosamine and by Heyns et al.[4] from *myo*-inositol.

(±)-1 : 2-3 : 4-Di-*O*-isopropylidene-*epi*-inositol (I) has been prepared by the method of Angyal et al.[5] from *epi*-inositol[6] and used as the starting material in the present experiment. When I is treated with an excess amount of methanesulfonyl chloride in pyridine, di-*O*-mesyl derivative (II), m. p. 147.5—148.5°C, is formed. Then II is heated in 50% acetic acid solution on a boiling water bath for 2 hr. in order to remove the acetone, and the product is acetylated to give (±)-5, 6-di-*O*-mesyl-*epi*-inositol tetraacetate (III), m. p. 166.5—168.5°C). When III is treated with sodium azide in boiling aqueous 2-methoxyethanol for 40 hr. and subsequently acetylated, 4, 6-diazido-4, 6-dideoxy-*myo*-inositol tetraacetate (IV), m. p. 147—149°C, is obtained as the main product in 28% yield. The catalytic hydrogenation of IV in ethanol and the acetylation of the reduction product give hexaacetyl-*myo*-inosadiamine-4, 6 (V), m. p. 290—292°C. The NMR spectrum of V in deuteriochloroform exhibits a sharp signal at 8.07 $\tau$ for two equatorial acetamido groups, and three sharp signals of a 2 : 1 : 1 relative intensity at 7.98, 7.92 and 7.79 $\tau$ for




Ac=$CH_3CO$- Ms=$CH_3SO_2$- Ip=isopropylidene

three equatorial groups and an axial acetoxy group respectively.

The selective deacetylation of V gives the di-*N*-acetyl derivative (VI). Now VI is expected to be oxidized at C-2 selectively, since there is only one axial hydroxyl group on C-2.[7] Therefore, VI is oxidized in the presence of platinum black in a stream of oxygen at 40°C for 24 hr.[8] Then the ketone (VII) is immediately reduced by sodium amalgam[9] in a slightly acidic solution. The reduction product is acetylated to give hexaacetyl-streptamine (VIII) in 12.5% yield. The transition point of VIII is 243—248°C. The infrared spectrum of VIII is superimposable on that of an authentic sample which has been prepared from streptomycin by the method of Peck et al.[2]

*Department of Applied Chemistry*
*Faculty of Engineering*
*Keio University*
*Koganei-shi, Tokyo*

1) T. Suami and S. Ogawa, This Bulletin, **37**, 1238 (1964); T. Suami and K. Yabe, ibid., **38**, 855 (1965); T. Suami, F. W. Lichtenthaler and S. Ogawa, ibid., in press.

2) M. G. Brink, F. A. Kuehl, Jr., and K. Folkers, *Science*, **102**, 506 (1945); H. E. Carter, R. K. Clark, Jr., S. R. Dickman, Y. H. Loo, J. S. Meek, P. S. Skell and W. A. Strong, ibid., **103**, 53 (1946); R. L. Peck, R. P. Graber, A. Walti, E. W. Peel, C. E. Hoffhine, Jr., and K. Folkers, *J. Am. Chem. Soc.*, **68**, 29 (1964); R. L. Peck, C. E. Hoffhine, Jr., E. W. Peel, R. P. Graber, F. W. Holly, R. Mozingo and K. Folkers, ibid., **68**, 776 (1946).

3) M. L. Wolfrom, S. M. Olin and W. J. Polglase, ibid., **72**, 1724 (1950); H. Straube-Rieke, H. A. Lardy and L. Anderson, ibid., **75**, 694 (1953).

4) K. Heyns and H. Paulsen, *Chem. Ber.*, **89**, 1152 (1956).

5) S. J. Angyal and C. G. Macdonald, *J. Chem. Soc.*, **1952**, 686; S. J. Angyal and P. T. Gilham, ibid., **1958**, 375.

6) T. Posternak, "Methods in Carbohydrate Chemistry," Vol. 1, Academic Press, New York (1962), pp. 289—291.

7) K. Heyns and H. Paulsen, *Chem. Ber.*, **86**, 833 (1953).

8) G. G. Post and L. Anderson, *J. Am. Chem. Soc.*, **84**, 471 (1962).

9) T. Posternak, *Helv. Chim. Acta*, **24**, 1045 (1941); G. R. Allen, Jr., *J. Am. Chem. Soc.*, **84**, 3128 (1962).

# The Photo-synthesis of Anemonin from Protoanemonin

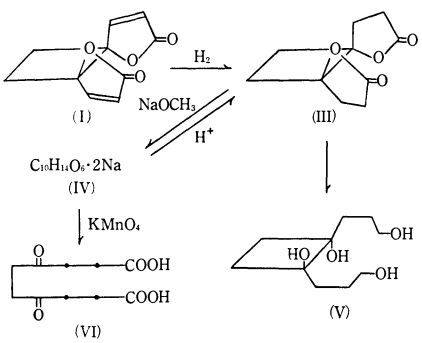
By Hiroshi KATAOKA, Kazutoshi YAMADA and Noboru SUGIYAMA

(Received September 7, 1965)

In 1914, Asahina proposed a structure for anemonin[1]; later he confirmed it by the dimerization of synthesized protoanemonin.[2] Later other authors[3] have not, however, paid any attention to the effect of light on the dimerization of protoanemonin.

We have attempted to dimerize protoanemonin to anemonin with radiation of light; we succeeded in getting anemonin in a much better yield than those of the previous reports. As the configuration of anemonin had never been described, we propose that anemonin has a configuration[4] (I).

A methanol solution of protoanemonin[5] (II) was irradiated at $-50°C$ by a high-pressure mercury lamp. The crystals of I deposited were collected (yield, 75%). Colorless needles (from ethanol; m. p. 153°C). IR: 1780, 1755, 935, 900, 810 $cm^{-1}$. I was catalytically reduced, and tetrahydroanemonin (III) was obtained (from hot water; m. p. 154.5°C). IR: 1775, 930, 900, 810 $cm^{-1}$. NMR: 7.30 $\tau$ (triplet, 4H), 7.89 $\tau$ (triplet, 4H), 7.48 $\tau$ (quartet, 4H). III was hydrolyzed with sodium methoxide to give sodium dicarboxylate (IV), which was again converted into the lactone III in an acidic solution. The permanganate oxidation of IV gave dilevulinic acid (VI). From these results it was clear that the photodimerization product was identical with Asahina's anemonin.




By letting a methanol solution of I stand at $-50°C$ without irradiation, the formation of I was observed, but the yield was very poor.

Tetrahydroanemonin III was further reduced with lithium aluminum hydride to a tetraol (V). V could not be oxidized by lead tetraacetate and was recovered quantitatively. V showed a shift of the stretching vibration bands of hydroxyl groups when treated by a dilution method. This suggest the existence of a weak inter-molecular hydrogen bond of hydroxyl groups. V had no signal less than 4 $\tau$ in the NMR spectrum, indicating the absence of a strong hydrogen bond. These data support the speculation that two hydroxyl groups on the cyclobutane ring of V have a trans configuration. From the trans configuration of V and the fact of the formation of VI, the configuration of I was concluded to be trans and head to head.

*Department of Chemistry*
*Tokyo Kyoiku University*
*Otsuka, Tokyo*

1) Y. Asahina, *Ber.*, **47**, 914 (1914).
2) Y. Asahina and A. Fujita, *Acta phytochim. Japan*, **1**, 1 (1922).
3) a) C. Grundman and E. Kober, *J. Am. Chem. Soc.*, **77**, 2332 (1955); b) G. F. D'alelio, C. J. Williams, Jr., and C. L. Wilson, *J. Org. Chem.*, **25**, 1025 (1960).
4) Immediately after our report of this result at the International Conference on Photochemistry, 1965, Tokyo, we received, *J. Am. Chem. Soc.*, **87** (1965), in this volume at page 3252, R. M. Moriarty, C. R. Romain, I. L. Karle and J. Karle described anemonin configuration determined by X-ray analysis.
5) E. Shaw, *J. Am. Chem. Soc.*, **68**, 2510 (1946).

# Altenin, a New Phytopathologically-toxic Metabolite from *Alternaria Kikuchiana*

By Noboru SUGIYAMA, Choji KASHIMA, Makoto YAMAMOTO and Ryotaro MOHRI[1]

(Received September 13, 1965)

*Alternaria Kikuchiana* Tanaka is a fungus which produces black spots on leaves and fruits of the pear, especially the improved species *Pyrus Ussuriensis var. Aromatica* Rehder (Japanese name *Nijusseiki*).[2] This fungus had been cultivated on a Czapek-Dox medium containing 4 per cent sucrose.[3] For the large-scale preparation it has now been cultivated in a 200-l. fermenter on a sucrose, ammonium phosphate, potassium phosphate and potassium chloride medium for 8 days at 30°C.

A factor which developed black spots on the leaf of the pear was isolated from the culture filtrate; this was designated "Altenin." Only one drop of an aqueous $2\times10^{-5}$ mg./ml. solution of altenin exhibited the phytopathologic effect. Thin-layer chromatography indicated that no other active substance was present in this filtrate. After the adjustment of the culture filtrate to pH 3.0, the active substance was adsorved on active charcoal and then eluted with acetone. The acetone was evaporated, and the altenin was purified by passing it through columns of silica gel and alumina.

One milligram of altenin was obtained from about 4 l. of the culture filtrate. Altenin is a yellow liquid, giving only one spot on silica-gel thin-layer chromatography with a benzene-acetone (1 : 1 v/v) mixture; the $R_f$ value is 0.76, while that of methyl red, a pilot dye, is 0.37. On alumina thin-layer chromatography with a methanol-water (5 : 1 v/v) mixture, the $R_f$ value is 0.87, while that of methyl red is 0.41.

Altenine is unstable at high temperatures and loses its biological activity in 10 min. at 80°C, or in an hour at 60°C. At 40°C, however, the activity continues for several hours, while at room temperature it is stable for 2 days, even when a stream of air is blown into the aqueous solution.

A molecular formula of $C_9H_{14}O_6$, (M. W. 218) was indicated by elementary analysis and mass spectrometry. Altenin is soluble in water, alcohol, ethyl ether, acetone and chloroform, and moderately soluble in benzene. It is extracted from acidic solutions with ethyl ether, but it is not extracted from alkaline solutions. A $pK_a$ value of 7.75 is indicated by potentiometry. The infrared absorption spectrum shows OH and carbonyl bands, but no carboxylic acid bands. The nuclear magnetic resonance spectrum shows a multiplet equivalent to two hydrogens, which disappears upon deuterium exchange. Altenin has a levo specific rotation at the D line.

Structural studies of altenin are now in progress; the details will be reported in the near furture.

*Department of Chemistry*
*Tokyo Kyoiku University*
*Otsuka, Tokyo*

1) The Liberal Art Department, Tottori University, Tachikawa-cho, Tottori City.

2) I. Hiroe, S. Nishimura and W. Sato, *Transactions of the Tottori Society of Agriculture Science (Tottori Nogei Kagaku Kai Shi)*, **11**, 291 (1958).

3) R. Mohri and S. Ikeda, *The Liberal Art Journal of Natural Science of Tottori University (Tottori Daigaku Gakugei Gakubu Kenkyu Hokoku)*, **10**, 38 (1959).

# 3,4-Benzotropolone and Related Compounds. IV.[1] Azo- and Hydroxy-3,4-benzotropolones*

By Seiji EBINE

(Received September 12, 1964)

There have been a few reports describing benzotropolones whose seven-membered ring carries an azo or hydroxy group, such as *x*-(*p*-tolylazo)-3,4-benzotropolone,[2] 3-(*p*-nitrophenylazo)-4,5-benzotropolone,[3] its 7-phenyl derivative,[4] and 3-hydroxy-4,5-benzotropolone.[5] The present work is undertaken in order to obtain such a type of compound by means of azo-coupling and the hydroxylation of 3,4-benzotropolone (I) and its halogen derivatives (II, III and IV).

It has been found that monocyclic tropolones, like phenols, undergo azo-coupling with ease to give 5-arylazotropolones in fair yields.[6] On the other hand, I, II, III, and IV reacted sluggishly with diazotized amines to afford azo-compounds or rearrangement products, along with a considerable amount of tar, as is summarized in Table I. An attempted azo-coupling of I in an alkaline solution gave only a resinous product, no definite product being isolated. The azo-coupling of I with diazotized aniline was effected in an acetic acid solution in the presence of sodium acetate to yield phenylazo-3,4-benzotropolone (V), whose infrared absorption spectrum exhibited a carbonyl band in the region below 1650 $cm^{-1}$ (Experimental), agreeing with a spectral feature of troponoid compounds.[7] V is either the 5- or the 7-phenylazo-compound, based upon the *o*, *p*-directing effect of its hydroxyl group; it seems more likely to be the former because its ultraviolet absorption spectrum resembles that of the 5-phenylazo-compound (VII, described below), as is shown in Fig. 1. The azo-coupling of I with diazotized aniline proceeded in a different mode when carried out in a pyridine solution; then it yielded an uncharacterized azo-compound (VI), the infrared absorption spectrum of which showed no carbonyl band (Experimental).

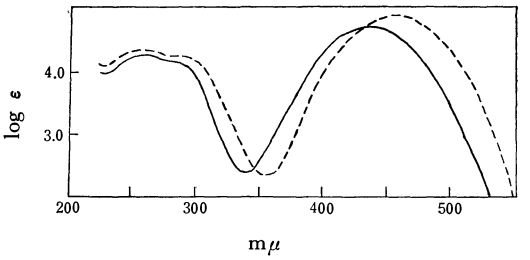



Fig. 1. Ultraviolet absorption spectra of 5-phenylazo-3,4-benzotropolone (V, ——) and 5-phenylazo-7-bromo-3,4-benzotropolone (VII, ----) in methanol.

The azo-coupling of 7-bromo-3,4-benzotropolone (IIa) with diazotized aniline in an acetic acid solution gave 5-phenylazo-7-bromo-3,4-benzotropolone (VII). However, when carried out in a pyridine solution, the same reaction resulted in the formation of rearrangement products, 2-phenyl-2*H*-benz[g]indazole-4,5-dione (VIIIa) and 2-phenylazo-1-naphthol (IX). Similarly, the azo-coupling of IIa with diazotized *p*-toluidine in a pyridine solution gave 2-(*p*-tolyl)-2*H*-benz[g]indazole-4,5-dione (VIIIb), but it did not produce an isolable amount of an azonaphthol. When the coupling component was *p*-methoxybenzenediazonium chloride, the products were 2-(*p*-anisylazo)- and 2,4-bis(*p*-anisylazo)-1-naphthols, no indazole derivative being produced. The azo-coupling of 7-chloro-3,4-benzotropolone (IIb) with diazotized aniline in a pyridine solution gave only IX, no indazole derivative again being isolated. The structure of VIII was established by the following reactions: (a) VIII was reduced to a leuco compound, which easily regenerated the original material on exposure to air; (b) VIII produced a diacetate (XII) on reductive acetylation and a quinoxaline derivative on treatment with *o*-phenylenediamine; (c) VIII was oxidized with peracetic acid to 1-phenyl- or 1-(*p*-tolyl)-3-(*o*-carboxyphenyl)pyrazole-4-carboxylic acid (XIIIa or XIIIb), and then XIIIa was decarboxylated by heating it with copper powder to give 1,3-diphenylpyrazole (XIV), whose melting point was undepressed on admixture with an authentic sample[8]; the infrared spectra of the two samples were also identical in all respects. Although it is not clear why the reaction of IIa with a diazotized amine gives rearrangement products

1) Part III: S. Ebine, This Bulletin, **35**, 122 (1962).

* Presented in part at the 14th Annual Meeting of the Chemical Society of Japan, Tokyo, April, 1961.

2) T. Nozoe, Y. Kitahara and T. Ando, *Proc. Japan Acad.*, **27**, 107 (1951).

3) D. S. Tarbell and J. C. Bill, *J. Am. Chem. Soc.*, **74**, 1234 (1952).

4) W. Davey and H. Gottfried, *J. Org. Chem.*, **26**, 3707 (1961).

5) H. Fernholz, E. Hartwig and J.-C. Salfeld, *Ann.*, **576**, 137 (1952).

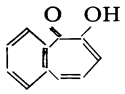
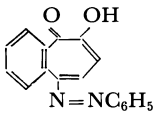
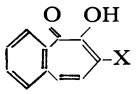
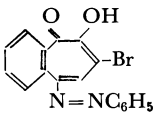
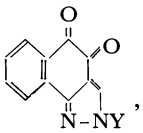
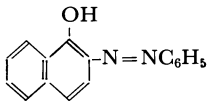
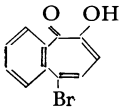
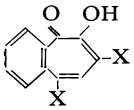
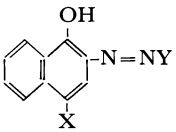
6) T. Nozoe, E. Sebe and S. Ebine, *Proc. Japan Acad.*, **26** (8), 24 (1950); W. von E. Doering and L. H. Knox, *J. Am. Chem. Soc.*, **73**, 829 (1951).

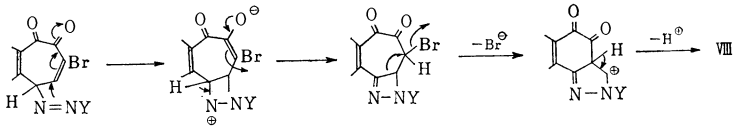
7) For the spectra of troponoid compounds, see M. Tsuboi, This Bulletin, **25**, 369 (1952); S. Kinumaki, K. Aida and Y. Ikegami, *Sci. Repts. Res. Inst. Tohoku Univ.*, **A-8**, 263 (1956); E. Kloster-Jensen, N. Tarkoy, A. Eschenmoser and E. Heilbronner, *Helv. Chim. Acta*, **39**, 780 (1956).

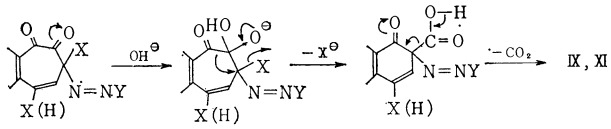
8) K. v. Awers and W. Schmidt, *Ber.*, **58**, 537 (1925).

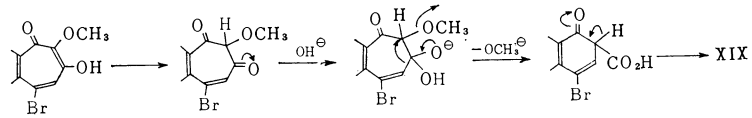
in a pyridine solution, whereas it gives a normal azo-coupling product in an acetic acid solution, possible courses for the formation of VIII and IX are tentatively illustrated by Schemes 1 and 2 respectively. III coupled with diazotized aniline to yield $C_{17}H_{11}O_2N_2Br$ (X), which showed an infrared absorption band at 1685 $cm^{-1}$, suggesting the presence of a non-troponoid carbonyl group. 5,7-Dibromo- and 5,7-dichloro-3,4-benzotropolones (IVa and IVb) reacted with diazotized aniline and *p*-toluidine, undergoing azo-coupling followed by rearrangement to the corresponding 2-arylazo-4-halogeno-1-naphthols (XI). This reaction is also illustrated by Scheme 2.

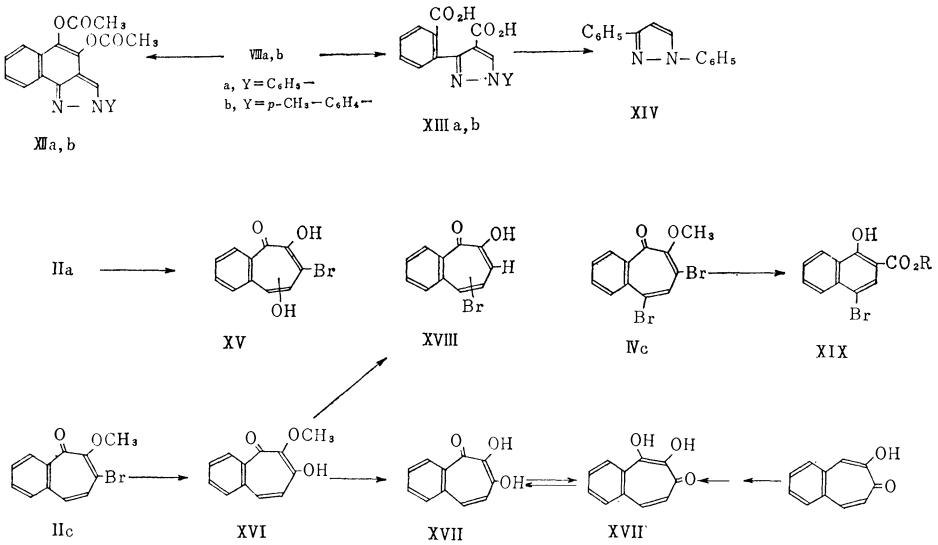
TABLE I. AZO-COUPLING PRODUCTS OF 3, 4-BENZOTROPOLONE AND ITS DERIVATIVES

| 3, 4-Benzotropolone and its derivative | Product (in acetic acid) | Product (in pyridine) |
|---|---|---|
|  I |  V | $C_{16}H_{12}ON_2$ VI |
|  IIa, X=Br IIb, X=Cl |  VII |  VIIIa, Y=$C_6H_5$ VIIIb, Y=*p*-$CH_3C_6H_4$ |  IX |
|  III | $C_{17}H_{11}O_2N_2Br$ X | X |
|  IVa, X=Br IVb, X=Cl |  XIa, X=Br, Y=$C_6H_5$ XIb, X=Cl, Y=$C_6H_5$ XIc, X=Br, Y=*p*-$CH_3C_6H_4$ | XI |

Scheme 1, IIa $\xrightarrow{YN_2Cl}$  VIII

Scheme 2, II, IV $\xrightarrow{YN_2Cl}$  IX, XI

Scheme 3, IVc $\xrightarrow{KOH}$  XIX




Attempts were then made to obtain hydroxybenzotropolones. According to the method of hydroxylation of monocyclic tropolones,[9] I and IIa were subjected to persulfate oxidation; the former failed to give a definite product, but the latter furnished 5(?)-hydroxy-7-bromo-3,4-benzotropolone (XV). 7-Bromo-3,4-benzotropolone methyl ether (IIc) reacted with methanolic alkali, affording 6-hydroxy-7-methoxy-2,3-benzotropone (XVI). The treament of IIc with alkali results in the hydrolysis of the bromine atom, giving XVI, whereas monocyclic 2-methoxy-7-bromotropone with alkali results in the hydrolysis of the methoxyl group, giving 3-bromotropolone.[10] Such a difference has been pointed out previously.[11] The further hydrolysis of XVI with concentrated hydrochloric acid gave 6,7-dihydroxy-2,3-benzotropone (XVII), which was identical with Fernholz and his co-workers' 3-hydroxy-4,5-benzotropolone (XVII'),[5] obtained by the bromination and subsequent hydrolysis of 4,5-benzotropolone. The bromination of XVI yielded 4(?)-bromo-6,7-dihydroxy-2,3-benzotropone (XVIII) or its tautomer. 5,7-Dibromo-3,4-benzotropolone methyl ether (IVc), unlike IIc, reacted with methanolic alkali to yield rearrangement products, 1-hydroxy-4-bromo-2-naphthoic acid and its methyl ether (XIX). It is of interest that 3,4-benzotropolone and its derivatives have a tendency to undergo azo-coupling and other reactions, accompanied with rearrangement.

## Experimental

**The Azo-coupling of 3,4-Benzotropolone (I).**—*5-Phenylazo-3,4-benzotropolone (V).*—A solution of 175 mg. of aniline in 2.3 ml. of 2.4 N hydrochloric acid was diazotized with 1.1 g. of 10% sodium nitrite. The benzenediazonium chloride solution was then dropped into an ice-cooled mixture of 250 mg. of I dissolved in 25 ml. of acetic acid and 4.5 g. of sodium acetate dissolved in 13.5 ml. of water. After the mixture had been stirred for 1 hr., the red precipitate was collected and crystallized from acetone to yield 120 mg. (30%) of V; red plates; m. p. 148—150°C; infrared spectrum in the 1800—1500 $cm^{-1}$ region (KBr): 1622, 1587, 1560 $cm^{-1}$.

Found: C, 73.59; H, 4.19; N, 9.95. Calcd. for $C_{17}H_{12}O_2N_2$: C, 73.90; H, 4.38; N, 10.14%.

*An Uncharacterized Azo-compound (VI).*—Aniline (350 mg.) dissolved in 4.6 ml. of 2.4 N hydrochloric acid was diazotized with 2.2 g. of 10% sodium nitrite; the resulting solution was dropped into an ice-cooled solution of 500 mg. of I in 15 ml. of pyridine. After standing overnight in an ice-chest, the solution was concentrated below 30°C under reduced pressure to give a dark red, tarry residue. The residue was then dissolved in benzene and chromatographed on silica gel, affording 100 ml. (14%) of VI; brownish red needles; m. p. 171.5—172.5°C after recrystallization from ethanol; infrared spectrum (Nujol): 3333, 1595, 1580, 1536, 1511, 1429, 1319, 1163, 1020, 821, 757 $cm^{-1}$.

Found: C, 77.61; H, 4.64; N, 11.44. Calcd. for $C_{16}H_{12}ON_2$: C, 77.40; H, 4.87; N, 11.28%.

**The Azo-coupling of 7-Bromo- and 7-Chloro-3,4-benzotropolones (IIa and IIb).**—*5-Phenylazo-7-bromo-3,4-benzotropolone (VII).*—A solution of 200 mg. of IIa and 2.5 g. of sodium acetate in 80 ml. of acetic acid was treated with a benzenediazonium chloride solution prepared from 96 mg. of aniline in a manner described above. The product was recrystallized from petroleum ether to yield 80 mg. (28%) of VII as brownish orange needles; m. p. 168—169°C; infrared spectrum in the 1800—1500 $cm^{-1}$ region (KBr): 1615, 1584, 1547, 1522 $cm^{-1}$.

9) T. Nozoe, S. Seto and S. Ito, *Proc. Japan Acad.*, **28**, 488 (1952); T. Nozoe, S. Seto, S. Ito, M. Sato and T. Katono, *Sci. Repts. Tohoku Univ., I*, **37**, 191 (1953).

10) T. Nozoe, Y. Kitahara and S. Masamune, *Proc. Japan Acad.*, **27**, 649 (1951).

11) S. Ebine, This Bulletin, **34**, 887 (1961).

Found: C, 57.55; H, 3.21; N, 7.62. Calcd. for $C_{17}H_{11}O_2N_2Br$: C, 57.48; H, 3.12; N, 7.89%.

*2-Phenyl- and 2-(p-Tolyl)-2H-benz[g]indazole-4, 5-diones (VIIIa and VIIIb).*—To an ice-cooled solution of 500 mg. of IIa in 15 ml. of pyridine there was added, drop by drop, a solution of benzenediazonium or *p*-toluenediazonium chloride prepared by the action of 1.4 g. of 10% sodium nitrite on 240 mg. of aniline or 280 mg. of *p*-toluidine dissolved in 3.2 ml. of 2.4 N hydrochloric acid. Dilution with an equal volume of water gave a precipitate, which was then filtered and recrystallized from ethanol to yield 160 mg. (29%) of VIIIa or 400 mg. (69%) of VIIIb, along with a 20% recovery of IIa. The pyridine filtrate contains azonaphthols as will be described below.

VIIIa; yellow needles; m. p. 251°C; infrared spectrum (Nujol): 3160, 1678, 1603, 1545, 1330, 1275, 1247, 910, 757, 700 $cm^{-1}$.

Found: C, 74.35; H, 3.85; N, 10.29. Calcd. for $C_{17}H_{10}O_2N_2$: C, 74.44; H, 3.68; N, 10.21%.

VIIIb; orangeish yellow needles; m. p. 273°C; infrared spectrum (Nujol): 3150, 1670, 1600, 1560, 1510, 1408, 1275, 1245, 1230, 957, 907, 863, 814, 772, 697 $cm^{-1}$.

Found: C, 74.78; H, 4.50; N, 9.98. Calcd. for $C_{18}H_{12}O_2N_2$: C, 74.99; H, 4.20; N, 9.72%.

*Azonaphthols.*—The pyridine filtrate obtained from VIIIa of the above experiment was concentrated under reduced pressure to a tarry residue; this was then dissolved in benzene and chromatographed on silica gel, yielding 45 mg. (9%) of 2-phenylazo-1-naphthol (IX). (Found: C, 77.59; H, 4.90; N, 11.44. Calcd. for $C_{16}H_{12}ON_2$: C, 77.40; H, 4.87; N, 11.28%; m. p. 134°C, the melting poing being undepressed on admixture with an authentic sample prepared by the condensation of 1, 2-naphthoquinone with phenylhydrazine.)

The pyridine filtrate from VIIIb, unlike that from VIIIa, gave no azonaphthol.

The azo-coupling of 500 mg. of IIa with a 1-mole equivalent of diazotized *p*-anisidine in a pyridine solution gave 65 mg. (12%) of 2-(*p*-anisylazo)-1-naphthol as red needles, m. p. 124°C (Found: C, 73.40; H, 4.99; N, 9.90. Calcd. for $C_{17}H_{14}O_2N_2$: C, 73.36; H, 5.07; N, 10.07%) and 30 mg. (3.6%) of 2, 4-bis(*p*-anisylazo)-1-naphthol as dark-brown fibrous needles, m. p. 182.5°C (Found: N, 13.40. Calcd. for $C_{24}H_{20}O_3N_4$: N, 13.59%), after the same work-up as above.

A pyridine solution of IIb (500 mg.) was coupled with benzenediazonium chloride in the same way as above, and the crude product was dissolved in benzene and chromatographed on silica gel to afford IX (85 mg., 14%), m. p. and mixed m. p. 134°C, with no benzindazoledione derivative.

**Reaction of VIIIa and VIIIb.**—*Hydrogenation.*—VIIIa or VIIIb (100 mg.) in 40 ml. of dioxane was hydrogenated over 50 mg. of 5% palladium-on-charcoal at atmospheric pressure until no further uptake of hydrogen was observed. The yellow solution faded during hydrogenation, but colored again on exposure to air. The removal of the catalyst and solvent left the original material (identified by a mixed melting point determination) in a quantitative recovery.

*Reductive Acetylation.*—A suspension of 100 mg. of VIIIa (or VIIIb) and 500 mg. of fused sodium acetate in 20 ml. of acetic anhydride was treated with 300 mg. of zinc powder. After the reaction mixture had become nearly colorless, the excess acetic anhydride was decomposed with water, the precipitate was extracted with boiling alcohol, the extract was concentrated, and the product was recrystallized from ethanol.

2-Phenyl-4, 5-diacetoxy-2*H*-benz[g]indazole (XIIa); colorless, fibrous needles; m. p. 191°C; yield 100 mg. (85%).

Found: C, 70.20; H, 4.20; N, 7.66. Calcd. for $C_{21}H_{16}O_4N_2$: C, 69.99; H, 4.48; N, 7.77%.

2-(*p*-Tolyl)-4, 5-diacetoxy-2*H*-benz[g]indazole (XIIb); colorless, fibrous needles; m. p. 167—168°C; yield 100 mg. (77%).

Found: C, 70.59; H, 4.95; N, 7.44. Calcd. for $C_{22}H_{18}O_4N_2$: C, 70.58; H, 4.85; N, 7.48%.

XIIa and XIIb underwent hydrolysis, followed by autoxidation, to regenerate VIIIa and VIIIb respectively when 10 mg. of the sample was heated in 1.5 ml. of ethanol containing 3 drops of concentrated hydrochloric acid.

*Reaction with o-Phenylenediamine.*—*o*-Phenylenediamine (120 mg.) and 80 mg. of VIIIa (or VIIIb) in 10 ml. of acetic acid were refluxed for 10 min.; the precipitate which separated on cooling was recrystallized from benzene.

Quinoxaline derivative of VIIIa; pale yellow needles; m. p. 233—234°C.

Found: C, 79.92; H, 3.90; N, 15.90. Calcd. for $C_{23}H_{14}N_4$: C, 79.75; H, 4.07; N, 16.18%.

Quinoxaline derivative of VIIIb; pale yellow needles; m. p. 252°C.

Found: C, 79.83; H, 4.52; N, 15.50. Calcd. for $C_{24}H_{16}N_4$: C, 79.98; H, 4.48; N, 15.55%.

*Oxidation with Permanganate.*—Aqueous potassium permanganate (10%, 15 ml.) was dropped into a solution of 200 mg. of VIIIa (or VIIIb) in 20 ml. of pyridine while the solution was being heated on a water bath. After 1 hr.'s heating, the pyridine was removed under reduced pressure, and the manganese dioxide was dissolved with sulfurous acid. The resulting solution was saturated with sodium chloride and extracted with ether. The evaporation of the solvent from the extract gave 90 mg. (74%) of phthalic acid, which was identified by converting it to phthalanil; m. p. and mixed m. p. 205—206°C.

*Oxidation with Peracetic Acid.*—To a solution of 200 mg. of VIIIa (or VIIIb) in 80 ml. of acetic acid containing 6 ml. of concentrated sulfuric acid there was added, drop by drop, 5 ml. of 30% hydrogen peroxide over a period of 1 hr. at 40°C. After being kept at the same temperature for another hour, the solution was concentrated to 10 ml. below 40°C under reduced pressure. Dilution with an equal volume of water gave a precipitate, which was then recrystallized from acetic acid.

1-Phenyl-3-(*o*-carboxyphenyl)pyrazole-4-carboxylic acid (XIIIa): colorless needles; m. p. 284—285°C (with decomposition); yield 180 mg. (80%).

Found: C, 66.34; H, 4.19; N, 9.09. Calcd. for $C_{17}H_{12}O_4N_2$: C, 66.23; H, 3.92; N, 9.09%.

1-(*p*-Tolyl)-3-(*o*-carboxyphenyl)pyrazole-4-carboxylic acid (XIIIb): colorless needles; m. p. 300—302°C (with decomposition); yield 160 mg. (71%).

Found: C, 66.94; H, 4.14; N, 8.80. Calcd. for $C_{18}H_{14}O_4N_2$: C, 67.07; H, 4.38; N, 8.69%.

*The Decarboxylation of XIIIa.*—A mixture of 200 mg. of XIIIa and 200 mg. of copper powder was heated at 285—295°C under 5-mmHg pressure for 10 min., the sublimate was then recrystallized from dilute ethanol to give 130 mg. (91%) of 1,3-diphenylpyrazole (XIV) melting at 84—84.5°C. (Found: C, 81.43; H, 5.70; N, 12.59. Calcd. for $C_{15}H_{12}N_2$: C, 81.79; H, 5.49; N, 12.72%.) The melting point was not depressed on admixture with an authentic sample, and infrared spectra of the two samples were superimposable.

**The Azo-coupling of 5-Bromo-3,4-benzotropolone (III).**—III (500 mg.) in acetic acid or pyridine was coupled with benzenediazonium chloride prepared from 240 mg. of aniline. After the same work-up as before, there was obtained an uncharacterized azo-compound (X) as red plates; m. p. 160—161°C; yields 150 mg. (21%) in an acetic acid solution and 110 mg. (16%) in a pyridine solution; infrared spectrum (KBr): 1685, 1614, 1587, 1506, 1459, 1384, 1192, 1168, 940, 758 $cm^{-1}$.

Found: C, 57.65; H, 2.99; N, 7.89. Calcd. for $C_{17}H_{11}O_2N_2Br$: C, 57.48; H, 3.12; N, 7.89%.

**The Azo-coupling of 5,7-Dibromo- and 5,7-Dichloro-3,4-benzotropolones (IVa and IVb).**—A solution of 500 mg. of IVa and 5 g. of sodium acetate in 75 ml. of acetic acid was treated with a diazonium chloride solution prepared from 185 mg. of aniline or 212 mg. of *p*-toluidine, and the azo-compound which resulted was recrystallized from ethanol. Azo-coupling carried out in a pyridine solution gave the same result. When IVb was substituted for IVa, the corresponding azo-compound was produced.

2-Phenylazo-4-bromo-1-naphthol (XIa); red needles; m. p. 178.5°C; yields 140 mg. (28%) in acetic acid, and 110 mg. (22%) in pyridine.

Found: C, 58.56; H, 3.43; N, 8.32. Calcd. for $C_{16}H_{11}ON_2Br$: C, 58.73; H, 3.39; N, 8.56%.

2-Phenylazo-4-chloro-1-naphthol (XIb): fibrous red needles; m. p. 160°C; yield 170 mg. (29%) in acetic acid.

Found: C, 68.04; H, 3.74; N, 9.50. Calcd. for $C_{16}H_{11}ON_2Cl$: C, 67.97; H, 3.92; N, 9.91%.

2-(*p*-Tolylazo)-4-bromo-1-naphthol (XIc): fibrous, reddish orange needles; m. p. 183—184°C; yield 150 mg. (29%) in a pyridine solution.

Found: C, 60.08; H, 3.97; N, 8.48. Calcd. for $C_{17}H_{13}ON_2Br$: C, 59.84; H, 3.84; N, 8.21%.

XIc showed no melting point depression on admixture with the sample (Found: C, 61.00; H, 4.05; N, 8.50%) prepared by the azo-coupling of 4-bromo-1-naphthol with *p*-toluenediazonium chloride in a pyridine solution.

The above azonaphthols were then subjected to reductive acetylation. To a suspension of 100 mg. of XIa or XIb and 500 mg. of fused sodium acetate in 3 ml. of acetic anhydride there was added 300 mg. of zinc powder in small portions. After the excess acetic anhydride had been decomposed with water, the precipitate was extracted with ethyl acetate. Upon cooling, the extrct gave the product, which was recrystallized from the same solvent.

1-Acetoxy-2-acetamino-4-bromonaphthalene: stout colorless needles; m. p. 232°C; yield 65 mg. (65%).

Found: C, 51.95; H, 3.85; N, 4.63. Calcd. for $C_{14}H_{12}O_3NBr$: C, 52.18; H, 3.75; N, 4.35%.

1-Acetoxy-2-acetamino-4-chloronaphthalene: fibrous colorless needles; m. p. 195—200°C; yield 67 mg. (68%).

Found: C, 60.20; H, 4.03; N, 4.70. Calcd. for $C_{14}H_{12}O_3NCl$: C, 60.55; H, 4.36; N, 5.04%.

**5(?)-Hydroxy-7-bromo-3,4-benzotropolone (XV).**—IIa (500 mg.) was dissolved in a mixture of 20 ml. of 0.4 N potassium hydroxide and 8 ml. of pyridine; to this there was added, drop by drop, a solution of 450 mg. of potassium persulfate in 15 ml. of water over a 2-hr. period with ice-cooling. After it had stood in an ice-chest for 3 days, the reaction mixture was strongly acidified with 100 ml. of concentrated hydrochloric acid to give a precipitate, whose recrystallization from ethanol gave 210 mg. of unchanged material (m. p. and mixed m. p. 147°C) and 150 mg. (28%) of XV; yellow needles; m. p. 317—320°C, with a darkening at 180°C; infrared spectrum in the 1800—1500 $cm^{-1}$ region (Nujol): 1616, 1606, 1585 $cm^{-1}$.

Found: C, 49.67; H, 2.87. Calcd. for $C_{11}H_7O_3Br$: C, 49.46; H, 2.64%.

**6-Hydroxy-7-methoxy-2,3-benzotropone (XVI).**—7-Bromo-3,4-benzotropolone methyl ether (IIc) (300 mg.) was dissolved in methanolic alkali prepared from 15 ml. of methanol and 1.2 g. of 50% potassium hydroxide, and then allowed to stand at room temperature for 10 hr. The reaction mixture was acidified with dilute hydrochloric acid and concentrated; after the inorganic salt had been removed by washing the mixture with water, the precipitate was recrystallized from dilute ethanol to give 165 mg. (86%) of pale yellow scales; m. p. 103.5—104.5°C; infrared spectrum in the 1800—1500 $cm^{-1}$ region (KBr): 1632, 1570, 1525 $cm^{-1}$; ultraviolet spectrum (MeOH): $m\mu$ (log $\varepsilon$), 260(4.55), 268(4.56), 350(3.90).

Found: C, 65.53; H, 5.56. Calcd. for $C_{12}H_{10}O_3 \cdot H_2O$: C, 65.44; H, 5.49%.

An anhydrous sample, m. p. 115—116°C, was obtained by drying over phosphorous pentoxide for 2 days at room temperature.

Found: C, 71.56; H, 5.06. Calcd. for $C_{12}H_{10}O_3$: C, 71.28; H, 4.99%.

Benzylamine salt: pale yellow scales; m. p. 165—169°C.

Found: C, 73.88; H, 6.32; N, 4.82. Calcd. for $C_{12}H_{10}O_3 \cdot C_7H_9N$: C, 73.76; H, 6.19; N, 4.53%.

**6,7-Dihydroxy-2,3-benzotropone (XVII).**—A solution of 100 mg. of XVI in 2 ml. of concentrated hydrochloric acid was heated in a sealed tube at 135—140°C for 5 hr. Dilution with an equal volume of water and the recrystallization of the precipitate from water yielded 65 mg. (70%) of yellow needles; m. p. 133.5°C; infrared spectrum in the 1800—1500 $cm^{-1}$ region (Nujol): 1640, 1595, 1522 $cm^{-1}$; ultraviolet spectrum (MeOH): $m\mu$ (log $\varepsilon$), 248(4.50), 270(4.56), 370(3.90); (Found: C, 70.07; H, 4.15. Calcd. for $C_{11}H_8O_3$: C, 70.21; H, 4.29%).

*4(?)-Bromo-6,7-dihydroxy-2,3-benzotropone (XVIII).*—Bromine (320 mg.) was dropped into a solution of 200 mg. of XVI in 2 ml. of acetic acid, whereupon a reddish-violet powder precipitated immediately. The whole was heated on a water bath for 1 hr. and then diluted with 20 ml. of water, giving 100 mg. (38%, after recrystallization from ethanol) of XVIII as yellow needles; m. p. 198.5°C; infrared spectrum in the 1800—1500 $cm^{-1}$ region (Nujol): 1604, 1540, 1510

$cm^{-1}$: ultraviolet spectrum (MeOH): $m\mu$ (log $\varepsilon$), 280(4.74), 328(3.70), 380(3.74).

Found: C, 49.33; H, 2.71. Calcd. for $C_{11}H_7O_3Br$: C, 49.46; H, 2.64%.

The reddish-violet powder described above was an intermediate product which regenerated XVI upon being heated with water.

Dimethyl ether: colorless needles from methanol; m. p. 73—75°C.

Found: C, 53.15; H, 3.75. Calcd. for $C_{13}H_{11}O_3Br$: C, 52.91; H, 3.76%.

**The Action of Alkali on 5, 7-Dibromo-3, 4-benzotropolone Methyl Ether (IVc).**—A solution of 300 mg. of IVc in 60 ml. of methanol containing 1.2 g. of 50% of potassium hydroxide was set aside overnight at room temperature. After acidification with dilute hydrochloric acid, the solvent was distilled, and the residue was then recrystallized from methanol to give 180 mg. (73%) of methyl 1-hydroxy-4-bromo-2-naphthoate (XIX, R=$CH_3$) (m. p. 120—121°C) (Found: C, 51.08; H, 3.42. Calcd. for $C_{12}H_9O_3Br$: C, 51.27; H, 3.23%); when treated with diazomethane, this gave methyl 1-methoxy-4-bromo-2-naphthoate, (m. p. 94°C) (Found: C, 53.09; H, 3.71. Calcd. for $C_{13}H_{11}O_3Br$: C, 52.90; H, 3.76%). When carried out under reflux, this reaction gave 1-hydroxy-4-bromo-2-naphthoic acid (XIX, R=H) (m. p. and mixed m. p. 237°C with decomposition).

Grateful acknowledgement is hereby made to Professor Tetsuo Nozoe of Tohoku University for his guidance throughout this work. Thanks are also due to Miss Ayako Iwanaga of Tohoku University for her microanalyses.

*Department of Chemistry*
*Saitama University*
*Urawa, Saitama*

# Compounds Related to Acridine. III.*,[1] The Formation of Acridone in the Reaction of 9-Methylacridine with *p*-Nitrosodimethylaniline

By Otohiko TSUGE and Minoru NISHINOHARA**

(Received July 23, 1965)

In a previous paper[2] dealing with the condensations of the acridine with an active methyl group and of the aromatic nitroso compound, it was shown that the presence of a catalytic amount of hydrochloric acid (HA) revealed interesting features regarding the yields and the amounts of the anil and of the nitrone compound relative to those in the presence of the alkaline catalyst usually used in such reactions.

It was also reported there that in the reaction of 9-methylacridine (I) with *p*-nitrosodimethylaniline (II), a higher-melting substance, m. p. over 300°C, whose structure was not identified, came to be formed as the amount of HA increased, and that its maximum yield was obtained when equimolar amounts of I and of HA were used.

Since the structure of the higher-melting substance has now been clarified, further investigation was undertaken in order to elucidate the course of the formation of the compound.

## Results and Discussion

After the higher-melting substance obtained in the previous paper[2] was washed with hydrochloric acid, recrystallization from a large amount of benzene or sublimation afforded pale yellow prisms, m. p. 354°C. This compound was proved, by the admixed melting point and by the infrared spectrum, to be identical with acridone (III), which was prepared from 9-chloroacridine.[3]

It may be supposed that *N*-(*p*-dimethylaminophenyl)-$\alpha$-(9-acridyl)nitrone (IV), which is the main product when a catalytic amount of HA was used, and acridine-9-carboxaldehyde *N*-(*p*-dimethylaminophenyl)anil (V) could be formed at an initial stage of the reaction when a sufficient amount of HA was used.

It is well known that both IV and V are almost quantitatively hydrolyzed by dilute hydrochloric acid to afford acridine-9-carboxaldehyde (VI), and we found that the nitroso compound (II) was also formed in the hydrolysis of IV. The treatment of IV with an equimolar amount of HA in ethanol, however, afforded III, and the similar treatment of V resulted only in the formation of VI. Further, III was formed not only from IV but also

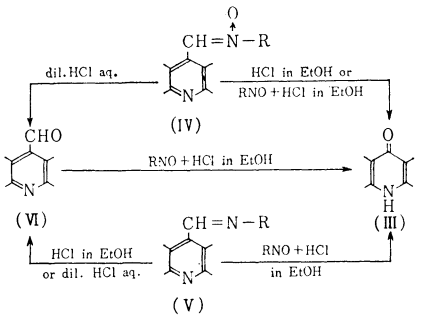
* Presented in part at the 17th Annual Meeting of the Chemical Society of Japan, Tokyo, April, 1964.

1) Part II: O. Tsuge and M. Nishinohara, *The Reports of the Research Institute of Science and Industry (Seisan Kagaku Kenkyusyo Hokoku), Kyushu University*, No. 37, 1 (1964).

** Present address: Textile Development Division, Research Institute, Nippon Rayon Co., Ltd., Uji, Kyoto.

2) O. Tsuge, M. Nishinohara and M. Tashiro, This Bulletin, **36**, 1477 (1963).

3) R. C. Elderfield, "Heterocyclic Compounds," John Wiley & Sons, New York (1952), p. 505.




R = *p*-$C_6H_4N(CH_3)_2$

Chart 1

from V in the heating with II in the presence of HA, as is depicted in Chart 1.

These observations indicate that both II and HA play an important role in the formation of III. It could be postulated that both IV and V will be hydrolyzed to afford VI in the presence of sufficient amounts of HA, and that III is formed from VI by a secondary reaction. In fact, it was found that the treatment of VI with II in the presence of HA in ethanol gave III in a high yield, besides a small amount of *p,p'*-bis(dimethylamino)azoxybenzene (VII). However, III was not formed from VI when treated with II or with HA alone.

On the basis of the facts mentioned above, the possible courses of the formation of III from VI are shown in Chart 2. It has been established that acridine *N*-oxide (VIII) rearranges to III in the heating with acetic anhydride.[4] As VIII was not rearranged to III under the reaction conditions, the possibility that VIII, which might be formed through the courses a and /or b by the oxidative property of II, may be rearranged to III was excluded. It was also recognized that III was not formed from either acridine-9-carboxlic acid (XI) or acridine (X) under similar conditions.

Now, the replacement of the formyl group by the hydroxyl group by the action of a peroxide has been known as the Dakin hydroxylation reaction, which proceeds through the formate.[5] If III is formed through 9-acridyl formate (XI), as is shown in the course c, the treatment of VI with a peroxide should give III.

The treatment of VI with hydrogen peroxide in ethanol or with perbenzoic acid in chloroform really gave III with a good yield. Furthermore, the formate (XI) was isolated when the reaction of VI with hydrogen peroxide was quenched after a short while. Although XI could not be isolated

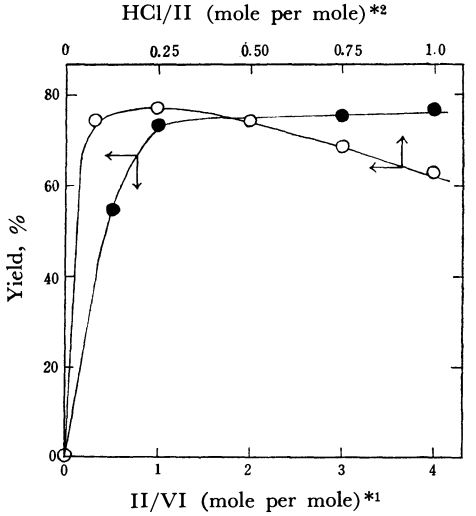



Fig. 1. Effects of hydrochloric acid and the nitroso compound (II) on the yield of acridone (III).

*1 Mixtures of the formyl compound VI (0.52 g.) and the specified amounts of II (II/HA=2) in ethanol (25 ml.) were refluxed for 3 hr.

*2 Mixtures of VI (0.52 g.), II (0.75 g.) and the specified amounts of HA in ethanol (25 ml.) were refluxed for 3 hr.

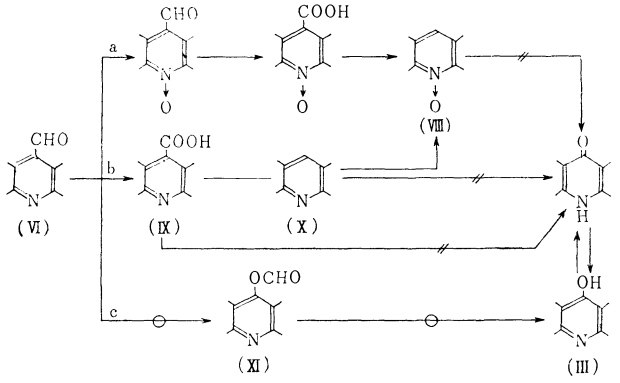
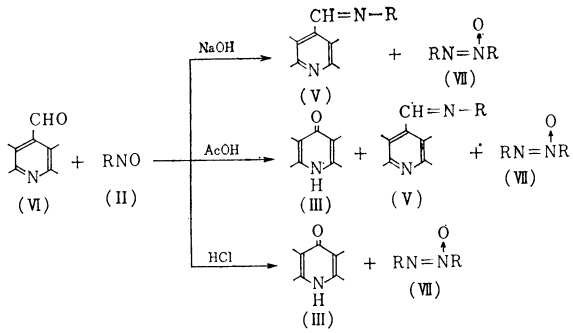



Chart 2

4) K. Kliegel and A. Fehrle, *Ber.*, **47**, 1629 (1914).

5) For example, 2-hydroxyphenyl formate was isolated in the reaction of salicylaldehyde with hydrogen peroxide. (A. v. Wacek and A. v. Bezard, *Ber.*, **74**, 845 (1941)).




R= $p$-$C_6H_4N(CH_3)_2$

Chart 3

in the reaction of VI with II in the presence of HA in ethanol, ethyl formate was identified by the gas chromatographic analysis of the distillate of the reaction mixture, as in the case of the reaction with hydrogen peroxide.

On the basis of these observations, it is reasonable to conclude that the formation of III from VI in the presence of II and HA proceeds through the course c.

The results of the effect of the amounts of II and of HA on the yield of III are shown in Fig. 1. It is notable that III was formed with a high yield even if an amount of II equimolar to VI and a catalytic amount of HA were used.

On the other hand, it was found that, in the treatment of VI with II in the presence of sodium hydroxide in ethanol, a small amount of the anil compound (V) was obtained, besides the azoxy compound (VII). Similar treatment in the presence of acetic acid in place of sodium hydroxide gave III, V and VII. The formation of V indicates that II was in part reduced to the corresponding amine in the reactions, since V can be formed only by the condensation of VI and the amine. Such a reduction of II to the amine would take place in the presence of HA. The above scheme is shown in Chart 3.

Further investigation of the oxidative property of II in the presence of HA will be published elsewhere in the near future.

## Experimental[6,7]

**The Reaction of 9-Methylacridine (I) with $p$-Nitrosodimethylaniline (II).**—A solution of 1.0 g. of I, 1.6 g. of II and 0.4 ml. of HA in 50 ml. of ethanol was refluxed for 2 hr. and then allowed to stand overnight. Filtration gave crystals which, on being washed with hot benzene (5 ml.×2), left 0.6 g. (35.4%) of the nitrone compound (IV) as reddish-brown prisms, m. p. 243°C (decomp.).[2] The benzene washings were then evaporated to give a small amount of the anil (V) as red prisms, m. p. 248°C.[2] The ethanol filtrate after the reaction was concentrated in vacuo, and then the residue was washed with concentrated hydrochloric acid to leave 0.46 g. of the higher-melting compound, m. p. over 300°C. Recrystallization from a large amount of benzene or sublimation gave pale yellow prisms, m. p. 354°C. This compound was proved, by the admixed melting point and by the infrared spectrum, to be identical with the acridone (III) which was obtained by the hydrolysis of 9-chloracridine.

Found: C, 79.93; H, 4.73; N, 7.05. Mol. wt. 191.[8] Calcd. for $C_{13}H_9ON$: C, 79.98; H, 4.65; N, 7.17%. Mol. wt. 195.2.

The results of other reactions under varying conditions have been reported in a previous paper.[2]

**The Formation of Acridone (III) from the Nitrone (IV) or Anil Compound (V).**—i) A mixture of 1.7 g. of IV and 0.4 ml. of HA in 50 ml. of ethanol was refluxed for 3 hr. After a large part of the ethanol had been evaporated in vacuo, the residue was washed with concentrated hydrochloric acid (5 ml.×2), aqueous ammonia, and then water to leave 0.38 g. (39%) of yellow crystals, m. p. 335—340°C. Recrystallization from a large amount of benzene gave yellow prisms, m. p. 354°C, whose infrared spectrum was superimposable on that of acridone.

The similar treatment of 0.8 g. of V and 0.2 ml. of HA in 30 ml. of ethanol afforded 0.37 g. (71%) of acridine-9-carboxaldehyde (VI), m. p. 147°C (lit.[9] 147°C).

ii) A mixture of 1.0 g. of IV, 1.0 g. of II and 0.3 ml. of HA in 30 ml. of ethanol was refluxed for 3 hr. and then cooled. Filtration gave 0.37 g. of brown crystals, m. p. 225—230°C, which, on recrystallization from benzene, afforded pale brown prisms, m. p. 240—241°C. This compound was proved by a study of its infrared spectrum to be identical with an authentic sample of $p,p'$-bis(dimethylamino)azoxybenzene (VII), m. p. 241—242°C.[10]

After the filtrate had been evaporated in vacuo, the residue was washed with hydrochloric acid, aqueous

6) All melting points are uncorrected.

7) HA used in this experiment: $d^{27}$ 1.1748.

8) Molecular weight was measured by the cryoscopic method, using dimethylsulfoxide (molecular depression constant=4.24) as the solvent.

9) L. Chardonnens and P. Heinrich, *Helv. Chim. Acta*, **32**, 656 (1949).

10) H. von Pechmann and W. Schmitz, *Ber.*, **31**, 295 (1898).

ammonia and then water to leave 0.34 g. (60%) of III.

A similar reaction of 0.5 g. of V with 0.5 g. of II in the presence of 0.15 ml. of HA in 20 ml. of ethanol afforded 0.18 g. (60%) of III and 0.18 g. of VII.

**The Reaciton of the Formyl Compound (VI) with II.**—*In the Presence of HA.*—A mixture of 0.52 g. of VI, 0.56 g. of II and 0.23 g. of the hydrochloride of II in 25 ml. of ethanol was refluxed for 3 hr., and then the ethanol was evaporated in vacuo. The residue was treated with hydrochloric acid, aqueous ammonia and water to give 0.37 g. (76%) of III, m. p. 350—353°C.

The results of other reactions under varying conditions are shown in Fig. 1.

*In the Presence of Sodium Hydroxide.* — A mixture of 0.52 g. of VI, 0.75 g. of II and 0.50 g. of sodium hydroxide in 25 ml. of ethanol was refluxed for 3 hr. and then allowed to stand overnight. Filtration gave 0.12 g. of crystals, m. p. 195—230°C, which were found to be a mixture of V and VII by a study of the infrared spectrum. The recrystallization of the crystals from ethanol gave a small amount of V, m. p. 248°C. From the filtrate, III was not isolated.

*In the Presence of Acetic Acid.* — A mixture of 0.52 g. of VI, 0.75 g. of II and 0.5 ml. of glacial acetic acid in 30 ml. of ethanol was refluxed for 3 hr. Treatment similar to that described above gave 0.10 g. of reddish brown crystals, m. p. 200—225°C, which were found to be a mixture of V and VII by a study of the infrared spectrum. From the filtrate, 0.13 g. of II was obtained.

**The Reaction of the Formyl Compound (IV) with Hydrogen Peroxide.**—*i*) To a solution of 0.52 g. of VI in 25 ml. of ethanol there was added 0.5 ml. of 30% of hydrogen peroxide. The refluxing of the reaction mixture resulted in the precipitation of yellow crystals in several minutes: then it turned into a complete solution. After it had been refluxed for 2 hr., the ethanol was evaporated in vacuo. The residue was washed with hydrochloric acid, aqueous ammonia and then water to obtain 0.44 g. (90%), m. p. 247—250°C, of III.

*ii*) *The Isolation of the Formate (XI).*—After a mixture of 0.25 g. of VI and 0.25 ml. of hydrogen peroxide in 25 ml. of ethanol had been refluxed for 10 min., 0.13 g. of yellow crystals, m. p. 254°C (decomp.), was obtained by filtration. Recrystallization from ethanol then afforded yellow prisms, m. p. 254°C (decomp.).

Found: C, 74.98; H, 4.39; N, 6.22. Calcd. for $C_{14}H_9O_2N$ (XI): C, 75.34; H, 4.04; N, 6.27%.

**The Reaction of the Formyl Compound (VI) with Perbenzoic Acid.**—To 30 ml. of a chloroform solution of perbenzoic acid,[11] 2.0 g. of VI was added under ice-cooling. After the reaction mixture had been stirred under ice-cooling for 3 hr., filtration gave 0.90 g. of III. The filtrate was not examined further.

The authers are deeply grateful to the staff of the Analytical Service Centre of this university of their elemental analyses.

*The Research Institute of Science and Industry*
*Kyushu University*
*Hakozaki, Fukuoka*

11) "Organic Syntheses," Coll. Vol. 1, 431 (1948).

# Compounds Related to Acridine. IV.[1,2] The Condensation of 9-Ethylacridine and *p*-Nitrosodimethylaniline

By Otohiko TSUGE, Minoru NISHINOHARA*[1] and Kunio SADANO[2]*

(Received July 23, 1965)

Recently[3] we found that the condensation of the acridine with an active methyl group and the aromatic nitroso compound, under the influence of a catalytic amount of hydrochloric acid (HA), afforded as condensation products an anil and a nitrone in fairly good yields compared with the yield when an alkaline catalyst is used.

Since, however, no informationn has been available regarding the condensation of the ethyl group and the aromatic nitroso compound, it appeared of interest to investigate whether 9-ethylacridine (I) can be condensed with *p*-nitrosodimethylaniline (II).

## Results and Discussion

The condensation of I and II did not take place in the presence of potassium carbonate, but a small amount of *p*,*p*'-bis(dimethylamino)azoxybenzene (III), m. p. 240—241°C (lit.[4] 241—242°C) was formed.

However, the presence of HA as a catalyst in

1) Preliminary communication: This Bulletin, **37**, 436 (1964).
2) Part III: O. Tsuge and M. Nishinohara, **38**, 2034 (1965).
*1 Present address: Textile Development Division, Research Institute, Nippon Rayon Co., Ltd., Uji, Kyoto.
*2 Present address: Research Division, Kobe Iron and Steel Co., Ltd., Kobe.
3) O. Tsuge, M. Nishinohara and M. Tashiro, This Bulletin, **36**, 1477 (1963).
4) H. von Pechmann and W. Schmitz, *Ber.*, **31**, 295 (1898).

place of an alkaline catalyst afforded condensation products (IV) as reddish crystals, m. p. about 260°C (decomp.).

The effect of different amounts of HA on the yield of IV was investigated; the results are shown in Table I. The maximum yield of IV was obtained when the molar ratio of HA to I was about 1.1 (0.2 ml. in Table I); a fairly large amount of HA was needed, in contrast with the case of the condensation of the 9-methylacridine and II. Also, acridone was not formed, even if the amount of HA was increased.

Table I. The effect of differents of HA on the yield of condensation products (IV)*

| HCl ml. | Yield g. | HCl ml. | Yield g. |
|---|---|---|---|
| 0.01 | trace | 0.3 | 1.05 |
| 0.03 | trace | 0.4 | 0.70 |
| 0.1 | 0.96 | 0.8 | 0.01 |
| 0.2 | 1.28 | | |

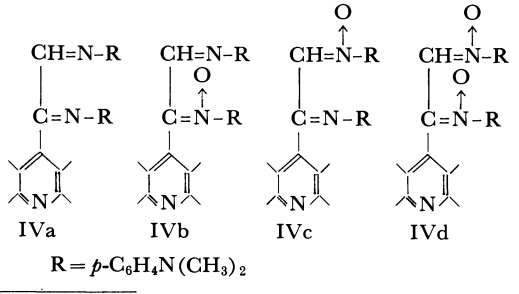
* Mixtures of I (1.0 g.), II (1.4 g.) and the specified amounts of HA in ethanol (20 ml.) were refluxed for 3 hr.

The hydrolysis of IV with 12% aqueous hydrochloric acid afforded acridine-9-carboxaldehyde (V), m. p. 147°C (lit.[5] 147°C), in a high yield. On the other hand, the treatment of IV with cold 10% aqueous sulfuric acid gave orange prisms (VI), m. p. 208°C (decomp.). The elemental analytical data of VI were in agreement with the formula $C_{23}H_{19}O_2N_3$, whose infrared spectrum exhibited the sharp bands at 1662 and 1604 $cm^{-1}$ ascribed to the carbonyl group and the C=N bond respectively. Also, the qualitative test for the formyl group by the Tollens reagent was positive.

Furthermore, VI was oxidized with silver oxide to give *N*-(*p*-dimethylaminophenyl)-$\alpha$-(9-acridyl)-nitrone (VII),[3] m. p. 243°C (decomp.), which was then easily hydrolyzed with dilute hydrochloric acid to V. VI was also easily hydrolyzed with the dilute acid to give V.

These observations indicate that VI is 9-acridylglyoxal-$\alpha$-*N*-(*p*-dimethylaminophenyl)nitrone.

In view of the fact that V and VI were obtained by the hydrolysis of IV, it seems most reasonable to assume that IV is either one of the compounds (IVa—IVd) whose structrues correspond with those of the condensation products of one mole of I and two moles of II, or a mixture of them.




R = *p*-$C_6H_4N(CH_3)_2$

The condensation of VI and *p*-aminodimethylaniline afforded 9-acridylglyoxal-$\alpha$-*N*-(dimethylaminophenyl)nitrone-$\beta$-*N*-(*p*-dimethylaminophenyl)anil (IVb), which was identified by an elemental analysis, as reddish-brown prisms, m. p. 265°C (decomp.). The infrared spectrum of IVb in KBr is given in Fig. 1.

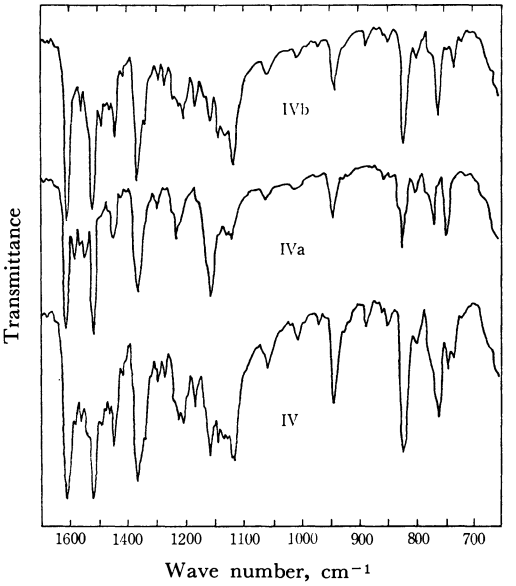



Fig. 1. Infrared spectra of IV, IVa and IVb in KBr.

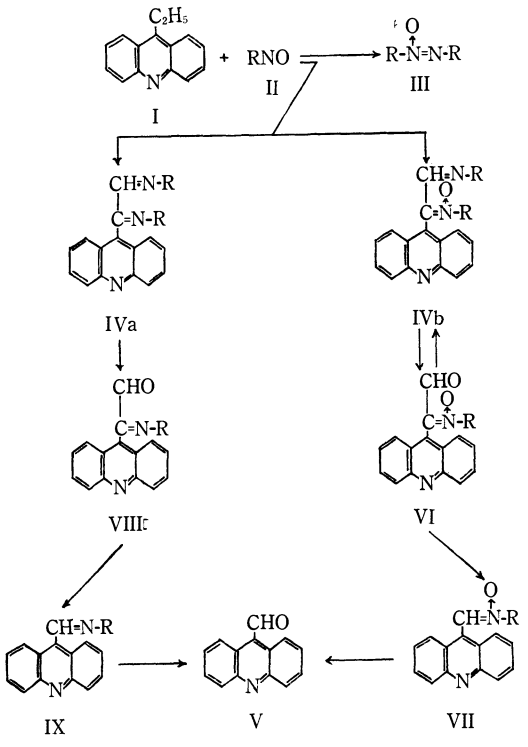
On the other hand, 9-acridylglyoxal-$\alpha$, $\beta$-*N*-(*p*-dimethylaminophenyl)dianil (IVa) was obtained as red prisms, m. p. 283°C (decomp.), by several fractional recrystallizations of IV from pyridine, or by the deoxygenation of IVb with triethyl phosphite. The infrared spectrum of IVa is also shown in Fig. 1.

On the basis of the infrared spectrum of IV, which revealed all the distinctive bands of IVa and IVb to be as shown in Fig. 1, and of the elemental analysis of IV,[6] it may be supposed that IV is a mixture of IVa and IVb only.

Moreover, it seems most reasonable to conclude that the hydrolysis of IV to V proceeds successively through the course depicted in Chart 1: IVa→VIII→IX→V; IVb→VI→VII→V, although 9-acridylglyoxal-$\alpha$-*N*-(*p*-dimethylaminophenyl)anil (VIII) and acridine-9-carboxaldehyde *N*-(*p*-dimethylaminophenyl)anil (IX) could not be isolated.

5) L. Chardonnens and P. Heinrich, *Helv. Chim. Acta*, **32**, 656 (1949).

6) As will be shown in the Experimental section, the elemental analysis of IV showed the intermediate values between those of IVa and IVb (or IVc), but these values were considerably different from those of IVd (C, 73.93; H, 5.80; N, 13.91%).




$R = p\text{-}C_6H_4N(CH_3)_2$

Chart 1

It is known that anil and nitrone compounds are difficult to separate. As the $\alpha$, $\beta$-dianil (IVa) and $\alpha$-nitrone-$\beta$-anil (IVb) have similarities in their chemical structures and properties, the separation was very difficult.

Although no chracteristic bands between IVa and IVb were observed in their infrared spectra, as is shown in Fig. 2, the quantitative estimation of IVa and IVb in IV was established by using of the ratio method,[7] which was carried out by the measurement of the absorbances $A_1$ and $A_2$ for the bands at 1120 and 1592 $cm^{-1}$ respectively.

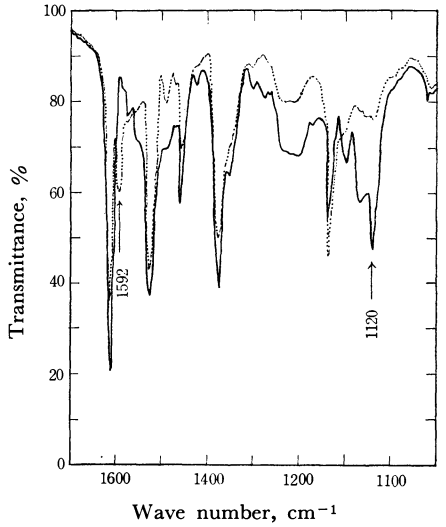



Fig. 2. Infrared spectra of IVa and IVb in chloroform.
..... IVa, —— IVb

Thus, samples of a mixture consisting of specified amounts of IVa and IVb were prepared and the absorbances $A_1$ and $A_2$ were measured according to the baseline method. The calibration curves plotting the relationship between $A_1/A_2$ or $A_2/A_1$ and the concentration (wt.%) of IVb are shown in Fig. 3.

According to the calibration curves thus obtained, the effect of reaction conditions on the yields of IVa and of IVb was examined. The results are given in Tables II and III.

When the molar ratio of HA to I was about 1.1 (Table III), the main product was the $\alpha$-nitrone-$\beta$-anil IVb, whose yield was increased with an increment in the nitroso compound II. While the

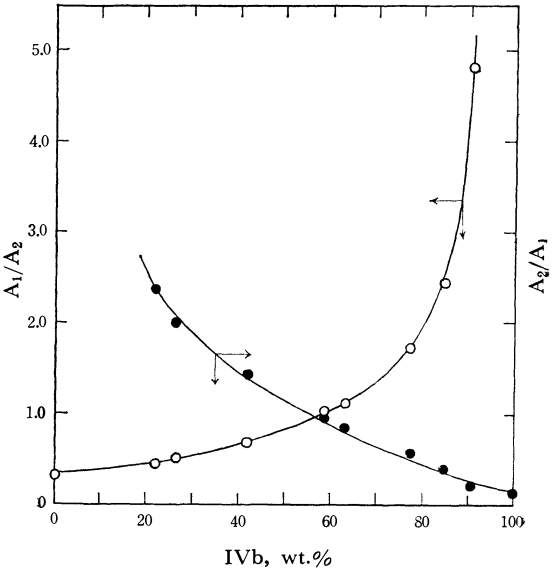



Fig. 3. Calibration curves.

Table II. Effect of HA*

| HA ml. | Product $A_1/A_2$ | IVb in IV wt.% | Yield IV g. | IVa % | IVb % |
|---|---|---|---|---|---|
| 0.03 | 2.04 | 80.5 | 0.15 | 2.6 | 10.4 |
| 0.1 | 2.11 | 81.5 | 0.65 | 10.6 | 45.3 |
| 0.2 | 0.80 | 49 | 0.35 | 15.8 | 14.7 |

* Mixtures of I (0.50 g.), II (0.70 g.) and the specified amounts of HA in ethanol (7 ml.) were refluxed for 3 hr.

7) S. Takagi, "Experiment and Calculation of Quantitative Analyses" (in Japanese), Vol. III, Kyoritsu, Tokyo (1961), p. 91.

Table III. Effect of II*1

| II*2 | Product | | | | |
|---|---|---|---|---|---|
| | $A_1/A_2$ | IVb in IV wt.% | Yield | | |
| | | | IV g. | IVa % | IVb % |
| 1 | 0.64 | 39 | 2.25 | 13.5 | 8.3 |
| 2 | 2.11 | 81.5 | 0.65 | 10.6 | 45.3 |
| 3 | 2.19 | 82 | 0.76 | 12.1 | 53.3 |
| 4 | 2.43 | 83 | 0.95 | 14.5 | 67.4 |

*1 Mixtures of I (0.50 g.), the specified amounts of II, and HA (0.1 ml.) in ethanol (7 ml.) were refluxed for 3 hr.
*2 Moles per mole I.

yield of $\alpha$, $\beta$-dianil IVa was little affected by II, it was low. In particular, it is interest that IVa and IVb were formed, even when an equimolar amount of II was used.

## Experimental[8]

9-Ethylacridine (I) was prepared by the condensation of diphenylamine and propionic acid in the presence of anhydrous zinc chloride, m. p. 116°C.[9]

**The Reaction of I with *p*-Nitrosodimethylaniline (II).**—To a solution of 1.0 g. of I and 1.4 g. of II in 20 ml. of ethanol, 0.20 ml. of HA was added.[10] After having been refluxed for 3 hr., the mixture was allowed to stand overnight. Filtration gave 1.28 g. of reddishbrown crystals (IV), m. p. 260—262°C (decomp.).

Found: C, 77.51, 77.74; H, 6.04, 6.10; N, 14.11, 14.36%.

Several fractional recrystallizations of IV from pyridine afforded a small amount of 9-acridylglyoxal-$\alpha$, $\beta$-*N*-(*p*-dimethylaminophenyl)dianil (IVa) as red prisms, m. p. 283°C (decomp.).

Found: C, 78.87; H, 6.19; N, 14.65. Calcd. for $C_{31}H_{29}N_5$: C, 78.95; H, 6.20; N, 14.85%.

The results of other reactions under varying conditions are shown in Tables I, II and III.

**The Hydrolysis of IV.** — *With Dilute Hydrochoric Acid.*—A mixture of 2.0 g. of IV in 7.5 ml. of 12% aqueous hydrochloric acid was heated on a water bath for several minutes. After the mixture had cooled, the precipitated crystals were filtered and washed with the saturated sodium chloride aqueous solution - dilute hydrochloric acid mixture. The insoluble crystals were dissolved in a large amount of hot water and then filtered. To the filtrate, a sodium acetate aqueous solution was then added to give yellow crystals. Filtration gave 0.95 g. of yellow crystals, m. p. 141—143°C. Recrystallization from the petroleum benzine - benzene mixture afforded yellow needles, m. p. 146—147°C. This compound was proved, by the admixed m. p. determination and its infrared spectrum, to be identical with an authentic sample of acridine-9-carboxaldehyde (V), m. p. 147°C.[4]

*With Cold 10% Aqueous Sulfuric Acid.*—Ten milliliters of 10% sulfuric acid was added to 0.5 g. of IV under ice-cooling. Immediately, the reaction mixture was filtered by suction to give yellow crystals, which, upon being washed with aqueous ammonia, afforded 0.12 g. of orange crystals, m. p. 204°C (decomp.). Recrystallization from benzene gave 9-acridylglyoxal-$\alpha$-*N*-(*p*-dimethylaminophenyl)nitrone (VI) as orange needles, m. p. 208°C (decomp.).

Found: C, 74.85; H, 5.18; N, 11.13. Calcd. for $C_{23}H_{19}O_2N_3$: C, 74.78; H, 5.18; N, 11.37%. IR (KBr): $\nu_{C=O}$ 1662 $cm^{-1}$.

**The Oxidation of VI with Silver Oxide.**—A mixture of 0.26 g. of VI in 170 ml. of the Tollens reagent was heated on a water bath for 4 hr. During the heating, the reaction mixture resulted in the precipitation of silver and yellow brown crystals. After it had been cooled, the mixture was extracted with chloroform. The chloroform solution was then evaporated in vacuo to give 0.10 g. of reddish-brown crystals, m. p. 239°C (decomp.). Recrystallization from chlorobenzene afforded reddish-brown prisms, m. p. 243°C (decomp.). This compound was proved, by a study of its infrared spectrum, to be identical with the *N*-(*p*-dimethylaminophenyl)-$\alpha$-(9-acridyl)-nitrone (VII)[3] obtained from the condensation of 9-methylacridine and II.

**9-Acridylglyoxal-$\alpha$-*N*-(*p*-dimethylaminophenyl)-nitrone-$\beta$-*N*-(*p*-dimethylaminophenyl)anil (IVb).**—A mixture of 0.1 g. of VI, 0.2 g. of *p*-aminodimethylaniline and 1 drop of acetic acid in 5 ml. of ethanol was refluxed for 2 hr. After the mixture had cooled, filtration afforded 0.12 g. (93%) of IVb as red crysals, m. p. 265°C (decomp.). Recrystallization from benzene gave red prisms, m. p. 265°C (decomp.).

Found: C, 76.67; H, 6.24; N, 14.10. Calcd. for $C_{31}H_{29}ON_5$: C, 76.36; H, 6.00; N, 14.36%.

**The Reaction of IVb with Triethyl Phosphite.**—A mixture of 0.5 g. of IVb and 2.0 g. of triethyl phosphite[11] was gently refluxed under a nitrogen atmosphere on an oil bath (160—165°C) for 20 hr. After the mixture had stood overnight, the precipitated crystals were filtered and then washed with ethanol to give 0.38 g. (80%) of red crystals, m. p. 279°C (decomp.). Recrystallization from pyridine gave red prisms, m. p. 283°C (decomp.), these were proved, by a study of their infrared spectrum, to be identical with the IVa obtained by the fractional recrystallization of IV from pyridine.

**The Spectroscopic Determination of IVa and IVb in IV.**—The infrared absorption measurements were made with a Koken IR-S double beam spectrophotometer with a sodium chloride prism.

Chloroform solutions containing IVa and IVb, in which the weight percentages of IVb were 0, 22.2, 26.3, 41.6, 58.8, 63.1, 77.4, 84.6, 90.2 and 100% respectively, were prepared. The absorbances $A_1$ and $A_2$ for the bands at 1120 and 1592 $cm^{-1}$ respectively were measured by the baseline method. The absorbances $A_1$ and $A_2$ in the order of the above concentrations of IVb were as follows. $A_1$: 0.064, 0.083, 0.085, 0.091, 0.135, 0.143, 0.166, 0.196, 0.207 and 0.238. $A_2$: 0.199, 0.192, 0.170, 0.161, 0.133, 0.127, 0.096, 0.080, 0.043 and 0.038.

8) All melting points are uncorrected.
9) O. Tsuge and M. Nishinohara, *The Reports of the Research Institute of Science and Industry (Seisan Kagaku Kenkyusho Hokoku), Kyushu University*, No. 37, 1 (1964).
10) HA used as a catalyst in this experiment: $d^{27}$ 1.1748.
11) "Organic Syntheses," **31**, 111 (1951).

The calibration curves obtained by the ratio method are shown in Fig. 3.

The authors wish to express their gratitude to the Kaisei Aid Association for providing the funds for this investigation. They indebted to the staff of the Analytical Service Centre of this university for the microanalyses.

*The Research Institute of Science and Industry*
*Kyushu University*
*Hakozaki, Fukuoka*

# Studies on Mixture Dyeing. III.[1] The Absorption Spectra of Direct Dye Mixtures in an Aqueous Solution

By Zenzo MORITA and Minoru SEKIDO

(Received December 22, 1964)

Since Neale and Stringfellow[2] discovered that most of the binary mixtures of dyes in an aqeous solution showed non-additive spectra, the interaction between molecules of different kinds of dyes in an aqueous solution has been studied extensively.[3-10]

Derbyshire and Peters[3] have investigated the interaction between Chrysophenine G and Sky Blue FF, for which pair Neale and Stringfellow[2] found the strongest interaction in an aqueous solution, measured the heat of the formation of the 1:1 complex of the two dyes to be −15 kcal./mol. by direct colorimetry, and concluded that the formation of the 1:1 complex occurred in an aqueous solution to an appreciable extent, even at 90°C.

Tanizaki, Kobayashi and Ando[4] have confirmed the non-additivity of the absorption spectra of a binary mixture with Sky Blue FF in an aqueous solution. Kobayshi Tanizaki and Ando,[5-7] and Kobayshi, Saito, Tanizaki and Ando[8] obtained the equilibrium constants for a 1:1 complex with many kind of two dyes. Inscore, Gould, Corning and Brode[9] observed the absorption spectra of binary dye mixtures in an aqueous solution and discussed qualitatively the relation between the structure of these dyes and the strength of the interaction between them. Very recently, Hoshi[10] has investigated spectroscopically the interaction in an aqueous solution between Chrysophenine G and the blue dyes derived from dianisidine as diazo components.

The investigations above quoted,[3-8,10] however, have some limitations in terms of the chemical structure of dyes. For the present paper, therefore, five typical dyes (cf. Table I) were selected in order to extend the scope of the study of the interaction, this study revealed that the interaction of Chrysophenine G and Sky Blue 6B is very strong and that the absorption spectra of the mixture of Chrysophenine G and Sirius Supra Blue BRR are almost additive.[2] Sirius Red 4B and Sirius Supra Blue BRR are typical unsymmetrical, direct dyes, and in terms of dyeability the other three dyes have been investigated as typical models of direct dyes. These five dyes may, then, be assumed to be representative so far as their shape, structure, dyeability, and molecular weight are concerned. In view of the above-mentioned reasons, the study of the interaction between every two of these five dyes would be helpful in obtaining a general idea of the combinations of most direct dyes commercially available.

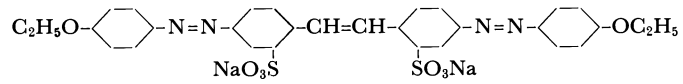
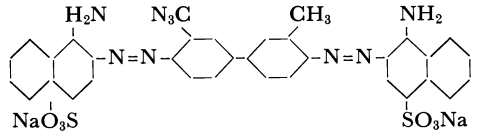
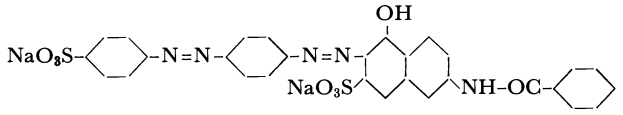
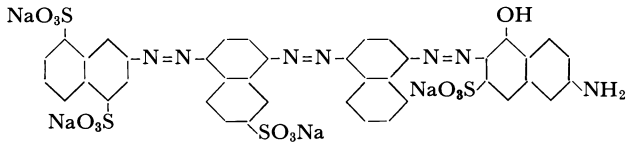
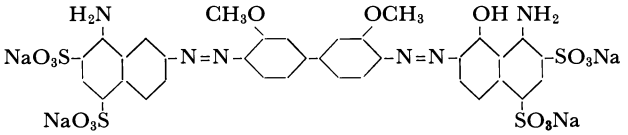
In the present paper the equilibrium constants for the complexes of six combinations among the ten will be obtained spectroscopically at room temperature. Because of the overlapping of their absorption spectra, the equilibrium constants of the other combinations were unobtainable.

## Experimental

Purified dyes were used throughout. The samples of Chrysophenine G, Benzopurpurine 4B, Sirius Red 4B and Sky Blue 6B were the same as those used before.[1,11]

1) Part II: M. Sekido and Z. Morita, This Bulletin, **36**, 1602 (1963).
2) S. M. Neale and W. A. Stringfellow, *J. Soc. Dyers Colourists*, **59**, 241 (1943).
3) A. N. Derbyshire and R. H. Peters, ibid., **72**, 268 (1956).
4) Y. Tanizaki, T. Kobayashi and N. Ando, This Bulletin, **32**, 119 (1956).
5) T. Kobayashi, Y. Tanizaki and N. Ando, ibid., **32**, 675 (1959).
6) T. Kobayashi, Y. Tanizaki and N. Ando, ibid., **32**, 680 (1959).
7) T. Kobayashi, Y. Tanizaki and N. Ando, ibid., **33**, 661 (1960).
8) T. Kobayashi, K. Saito, Y. Tanizaki and N. Ando, ibid., **35**, 935 (1962).
9) M. N. Inscore, J. H. Gould, M. E. Corning and W. R. Brode, *J. Res. Natl. Bur. of Std.*, **60**, 65 (1958).
10) T. Hoshi, Master's Dissertation, Tokyo Institute of Technology (1963).
11) M. Sekido and Z. Morita, This Bulletin, **35**, 1375 (1962).

Table I. Dye structures

| Name (C. I. Direct No.) | Structure |
|---|---|
| Chrysophenine G (Yellow 12) |  |
| Benzopurpurine 4B (Red 2) |  |
| Sirius Red 4B* (Red 81) |  |
| Sirius Supra Blue BRR* (Blue 71) |  |
| Sky Blue 6B (Blue 1) |  |

* Although Chlorazol Fast Red K and Chlorazol Fast Blue 2BN, used by Neale and Stringfellow,[2] are not listed in "Colour Index 2nd ed.," they are similar to Sirius Red 4B and Sirius Supra Blue BRR, respectively by "Colour Index 1 st ed." and "Schultz's Farbstofftabellen 7 th ed."

Sirius Supra Blue BRR were purified from commercial dyes (Sumilight Supra Blue BRR (NSK)) by the method of Robinson and Mills.[12] The absence of colored impurities was checked by paper chromatography.

All the concentrations were determined by weight. All of the absorption spectra were mesured in a 1.0 cm. cell by a Hitachi EPB-V type spectrophotometer at room temperature.

## Results and Discussion

The absorption spectra of two combinations among the six investigated are shown in Figs. 1 (Chrysophenine G - Sirius Supra Blue BRR) and 2 (Benzopurpurine 4B - Sky Blue 6B). These spectra show the same non-additivity as those early investigated,[2-9] but when the concentration of a component increases, no second isosbestic point, which corresponds to the formation of a 1:2 complex, is found.[7,10] It follows that only a 1:1 complex is formed in all the concentrations. Though the absorption spectra of the mixtures of Chrysophenine G and Sirius Supra Blue BRR were found to be almost additive by Neale and Stringfellow,[2] Fig. 2 shows the non-additive spectra and the presence of an isosbestic point.

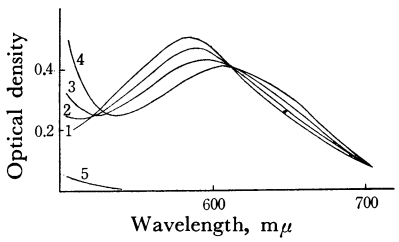



Fig. 1. Absorption spectra of the mixture of Chrysophenine G and Sirius Supra Blue BRR in aqueous solution at 16°C.

| | Sirius Supra Blue BRR | Chrysophenine G, mol./l. |
|---|---|---|
| 1 | $6.57_6\times10^{-6}$ | 0 |
| 2 | $6.57_6\times10^{-6}$ | $6.40_8\times10^{-6}$ |
| 3 | $6.57_6\times10^{-6}$ | $13.2_0$ |
| 4 | $6.57_6\times10^{-6}$ | $29.4_2$ |
| 5 | 0 | $10.0_0$ (calculated from molar extinction coefficient) |

In the determination of the equilibrium constants from spectroscopic measurements, the method of Benesi and Hildebrand[13] and modifications of it[14-16] have been most commonly employed. Some other methods have been proposed for the

12) C. Robinson and H. A. T. Mills, *Proc. Roy. Soc.*, **A131**, 576 (1931).

13) H. A. Benesi and J. H. Hildebrand, *J. Am. Chem. Soc.*, **71**, 2703 (1949).

14) V. J. A. Ketelaar, C. von de Stolpe, A. Goudsmit and W. Dzcubas, *Rec. trav. chim.*, **71**, 1104 (1952).

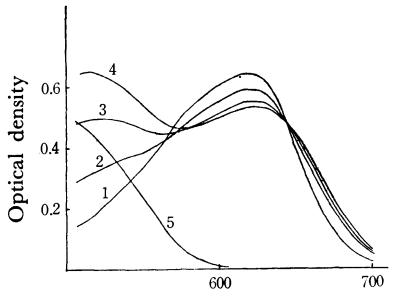



Fig. 2. Absorption spectra of the mixture of Benzopurpurine 4B and Sky Blue 6B in aqueous solution at 18°C.

| | Sky Blue 6B | Benzopurpurine, 4B mol./l. |
|---|---|---|
| 1 | $6.46_8\times10^{-6}$ | 0 |
| 2 | $6.46_8\times10^{-6}$ | $2.41_2\times10^{-6}$ |
| 3 | $6.46_8\times10^{-6}$ | $5.97_1$ |
| 4 | $6.46_8\times10^{-6}$ | $11.2_8$ |
| 5 | 0 | $10.0_0$ (calculated from molar extinction coefficient) |

determination of the equilibrium constants of dye-dye complexes.[5,10,17] In this paper Nash's method,[18] which permits a direct evaluation of the equilibrium constant with a minimum of computational labor, has been used.

Following Nash's presentation, it is assumed that there are chemical equilibria of the forms:

$$S + D = SD \quad (1)$$

$$SD + D = SD_2 \quad (2)$$

where D is any donor dye molecule; S, an acceptor substrate and SD and $SD_2$, 1:1 and 1:2 complexes respectively. The equilibrium constants appropriate to reactions 1 and 2 are given in concentration units by:

$$K_1=\frac{C_{SD}}{C_S\cdot C_D} \quad (3)$$

$$K_2=\frac{C_{SD_2}}{C_{SD}\cdot C_D} \quad (4)$$

where $C_{SD}$ and $C_{SD_2}$ are the equilibrium concentrations of SD and $SD_2$, and $C_S$ and $C_D$ are the final concentrations of S and D respectively.

In order to obtain the equilibrium constant of the complex between the S and D dyes, the spectroscopic measurement of mixture solutions containing a constant concentration of the S dye and various concentrations of the D dye is required. $A°$ denotes the optical density at a wavelength when the concentration of the D dye is zero, while $A$ denotes the optical density of the mixture solution when the final concentration of the D dye is $C_D$. When the reciprocal of the donor dye concentration is plotted against the reciprocal of (one minus the absorbance ratio) (i. e., $1/C_D$ vs. $A°/(A°-A)$), a straight line results if a 1 : 1 complex is formed. The intercept of this line is equal to the negative of the equilibrium constant.

However, it is necessary that the absorbance of the D dye at the wavelength be zero, and that the difference between $A°$ and $A$ be as large as possible. With these points in mind, the wavelength of 680 mμ was used. The results are shown in Figs. 3

Table II. Equilibrium constants for the complex between dyes

| Dye (1) | Dye (2) | $K_1$ l./mol. | Temp. °C |
|---|---|---|---|
| Sky Blue 6B | Chrysophenine G | $1.7\times10^7$ | 18 |
| | Benzopurpurine 4B | $1.8\times10^5$ | 18 |
| | Sirius Red 4B | $5.0\times10^4$ | 18 |
| Sirius Supra Blue BRR | Chrysophenine G | ca. $1.0\times10^4$ | 16 |
| | Benzopurpurine 4B | $5.0\times10^4$ | 16 |
| | Sirius Red 4B | $1.4\times10^5$ | 16 |

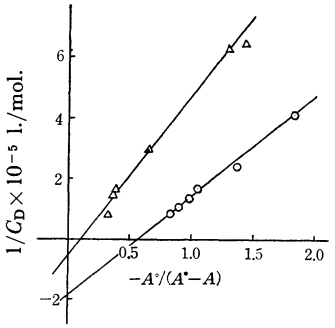



Fig. 3. The interaction of Sky Blue 6B with Benzopurpurine 4B (○) and Sirius Red 4B (△). The concn. of Sky Blue 6B=$6.46_8\times10^{-6}$ mol./l.; 680 mμ

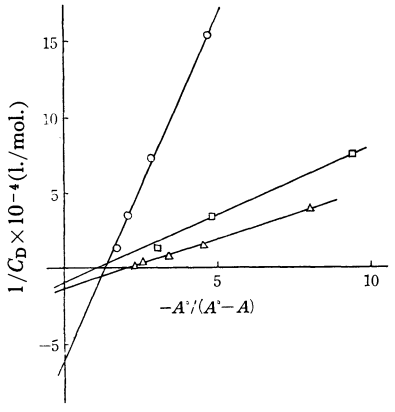



Fig. 4. The interaction of Sirius Supra Blue BRR with Chrysophenine G (□), Benzopurpurine 4B (○) and Sirius Red 4B (△).
The concn. of Sirius Supra Blue BRR=$6.57_6\times10^{-6}$ mol./l.; 680 mμ

15) R. L. Scott, ibid., **75**, 787 (1956).
16) R. M. Keefer and L. J. Andrews, *J. Am. Chem. Soc.*, **74**, 1891 (1952).
17) D. R. Lemin and T. Vickerstaff, *Trans. Faraday Soc.*, **43**, 491 (1947).
18) C. P. Nash, *J. Phys. Chem.*, **64**, 950 (1960).

and 4, while the equilibrium constant, $K_1$ is given in Table II. When the other wavelength was used, similar results were obtained.

The equilibrium constant for the complex of Chrysophenine G and Sky Blue 6B, as determined by Kobayashi, Tanizaki and Ando,[7] is different from that as determined by Hoshi;[10] this is due to the dissimilar concentrations of Sky Blue 6B. The absorption spectra of the mixture of Chrysophenine G and Sky Blue 6B are shown in Fig. 5. In this case, the equilibrium constant for the 1 : 1 complex could not be calculated by Nash's method because of the smaller concentration of Chrysophenine G (D) than of Sky Blue 6B (S), against the assumption $S \ll D$. Moreover, the equilibrium constants, $K_1$ and $K_2$, can be calculated by the method using the two isosbestic points corresponding to formations of 1 : 1 and 1 : 2 complexes.[10] The evaluation of the molar extinction coefficient of the $SD_2$ complex at the wavelength of the first isosbestic point is

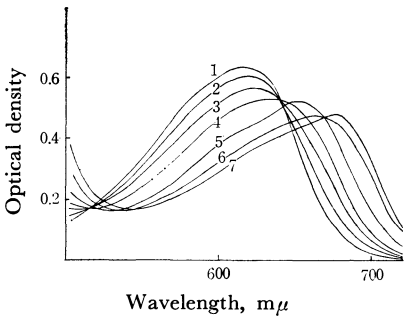



Fig. 5. Absorption spectra of the mixture of Chrysophenine G and Sky Blue 6B in aqueous solution at 18°C.

| | Sky Blue 6B | Chrysophenine G, mol./l. |
|---|---|---|
| 1 | $6.46_8\times10^{-6}$ | 0 |
| 2 | $6.46_8\times10^{-6}$ | $1.22_7\times10^{-6}$ |
| 3 | $6.46_8\times10^{-6}$ | $2.69_0$ |
| 4 | $6.46_8\times10^{-6}$ | $4.38_7$ |
| 5 | $6.46_8\times10^{-6}$ | $8.60_2$ |
| 6 | $6.46_8\times10^{-6}$ | $18.6_6$ |
| 7 | $6.46_8\times10^{-6}$ | $36.7_9$ |

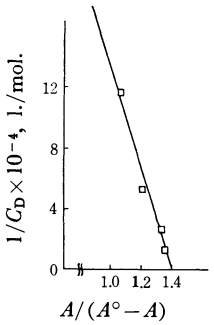



Fig. 6. The interaction of Sky Blue 6B with Chrysophenine G.
The concn. of Sky Blue 6B=$6.46_8\times10^{-6}$ mol./l.; 640 mμ

not easy by this method. At this wavelength, however, $K_2$ can be obtained with ease by Nash's method (Fig. 6). Here $A^\circ$ for Eq. 2 (the optical density of SD when the concentration of dye D is zero) corresponds to the first isosbestic point. $K_1$ and $K_2$ are $1.7_4\times10^7$ and $4.2_5\times10^5$ respectively, and they are in the range of values investigated earlier.[7,10]

The $K_1$ values for Chrysophenine G and Sky Blue 6B complexes are extremely large compared with those in Table II while the $K_1$ values for Chrysophenine G and Sirius Supra Blue BRR complexes are small. This can be supposed on the basis of the results reported earlier.[2] The strength of the interaction is of the following order: Chrysophenine G - Sky Blue 6B > Benzopurpurine 4B - Sky Blue 6B > Sirius Red 4B - Sirius Supra Blue BRR > Sirius Red 4B - Sky Blue 6B = Benzopurpurine 4B - Sirius Supra Blue BRR > Chrysophenine G - Sirius Supra Blue BRR. It follows that the combination of Chrysophenine G and Sky Blue 6B is a typical one in direct dyes, and that the equilibrium constants for dye-dye complexes in an aqueous solution at room temperature are in the $10^7$—$10^4$ range. The order of the magnitude of $K_1$ may confirm the qualitative observations by Inscore, Gould, Corning and Brode.[9]

Some factors influencing the interaction between dyes have been studied. The exact nature of the forces operative in the interaction and the manner how these dyes form complex have not yet been determined. However, since it is clear that the interaction between unlike dye molecules is stronger than that between like molecules, the aggregation of like dye molecules is less favorable than the complex formation between unlike molecules, such as Chrysophenine G and Sirius Supra Blue BRR. It follows that the equilibrium constant for a complex between like dye molecules is very much smaller than $10^4$.

## Summary

The absorption spectra of a binary mixture of five representative direct dyes in solution have been investigated. The equilibrium constants for complex formation are in the $10^7$—$10^4$ range and are in the order: Chrysophenine G - Sky Blue 6B > Benzopurpurine 4B - Sky Blue 6B > Sirius Red 4B - Sirius Supra Blue BRR > Sirius Red 4B - Sky Blue 6B = Benzopurpurine 4B - Sirius Supra Blue BRR > Chrysophenine G - Sirius Supra Blue BRR. The combination of Chrysophenine G and Sky Blue 6B is a typical one in direct dyes. The equilibrium constant for an aggregation of like dye molecules is very much smaller than the value of $10^4$ at room temperature.

*Division of Polymer Science*
*Tokyo Institute of Technology*
*Ookayama, Tokyo*

# Studies on Reactions of Polypropylene. V. On the Thermal Degradation Accelerated by Vinyl Polymers

By Yukio MIZUTANI, Seishiro MATSUOKA and Keiichi YAMAMOTO

(Received February 12, 1965)

A few drawbacks are encountered in the use of polypropylene, for example, the poor flow properties resulting from its very high molecular weight and the poor dyeability resulting from its nonpolarity and high crystallinity. The former drawback has been solved either by the improvement of the polymerization process,[1-3] in which the molecular weight of polypropylene can be controlled, or by the degradation of polypropylene in order to reduce its very high molecular weight.[4-9]

As for the latter drawback, the modification of polypropylene has been much studied: graft polymers have been prepared,[10-15] dyeable polymers have been blended,[16-18] and some functional groups have been introduced to the polypropylene chain.[19,20] Also, two thermally degradative methods have been proposed for the modification of polypropylene: the thermal degradation of polypropylene in the presence of vinyl monomers,[21] and the thermal treatment of polypropylene containing 5—95% specified polymers.[22]

For this paper, the thermal degradation of polypropylene accelerated by vinyl polymers was studied in an attempt to overcome the drawbacks described above. The fundamental idea of this study was as follows: A vinyl polymer generally degrades easily to a monomer by the chain reaction mechanism,[23] but polypropylene degrades by the random scission mechanism.[4,5] As a vinyl polymer is more susceptible to thermal degradation than polypropylene, if the mixture of polypropylene and a vinyl polymer is heated at an elevated temperature, the active radical generated by the scission of a vinyl polymer chain may be effective as an accelerator in the degradation of polypropylene and the modification of polypropylene may be expected because of the interaction among a vinyl monomer, a vinyl polymer radical, a polypropylene radical and a polypropylene molecule. The vinyl polymers used in this study were polystyrene, polymethyl methacrylate, the 2-methyl-5-vinylpyridine - styrene copolymer, and the acrylonitrile - styrene copolymer. As had been expected, it was proved that the vinyl polymers added were effective not only in accelerating the thermal degradation of polypropylene, but also in forming graft or block polymers.

## Experimental

**Polypropylene.** — Polypropylene (PP) was polymerized at 80°C in *n*-heptane by a catalyst consisting of titanium trichloride, dicyclopentadienyl titanium dichloride, sodium and hydrogen.[24] Polypropylene thus obtained was soaked in an excess methanol-isopropanol mixture (1:1) overnight after it had been separated from hot *n*-heptane under a nitrogen atmosphere, then it was filtered, washed with methanol, and soaked in methanol - concentrated hydrochloric acid mixture (10:1) overnight. Then polypropylene was

TABLE I. THE PROPERTIES OF POLYPROPYLENE

| Sample | Intrinsic viscosity* dl./g. | Ash content % | Specific gravity** | Grain size mesh |
|---|---|---|---|---|
| PP(A) | 6.60 | 0.03 | 0.914 | 60> |
| PP(B) | 9.1 | 0.02 | 0.913 | 30> |
| PP(C) | 4.75 | 0.02 | 0.913 | 30> |
| PP(D) | 5.78 | 0.05 | 0.913 | 30> |

* Values in tetraline at 135°C.
** Values at 23°C.

1) E. J. Vandenberg, Japanese Pat. 495 (1960).
2) E. Bua and L. Luciani, Japanese Pat. 3192 (1961).
3) J. M. Kelley Jr., and J. R. Lovett, Japanese Pat. 15541 (1961).
4) J. E. Davies, R. L. Tobias and E. B. Peterli, *J. Polymer Sci.*, **56**, 485 (1962).
5) F. Hamada, *Chem. High Polymers Japan (Kobunshi Kagaku)*, **19**, 402 (1962).
6) K. Machida, T. Yoshioka and H. Tamura, Japanese Pat. 14490 (1963).
7) R. Rado, *International Chem. Eng.*, **2**, 482 (1962).
8) D. Maragliano and R. Di Giulio, Ital. Pat. 555811; Japanese Pat. 6640 (1960).
9) T. Oshika, *J. Chem. Soc. Japan, Ind. Chem. Sec. (Kogyo Kagaku Zasshi)*, **64**, 1859 (1961).
10) S. Torikai and E. Mukoyama, *Chem. High Polymers Japan (Kobunshi Kagaku)*, **19**, 337 (1962); **19**, 344 (1962).
11) R. F. Stamm, E. F. Hosterman, C. D. Felton and C. S. Hsia Chen, *J. Appl. Polymer Sci.*, **7**, 753 (1963).
12) W. Kawai and S. Tsutsumi, *Chem. High Polymers Japan (Kobunshi Kagaku)*, **18**, 64 (1961).
13) W. Kawai and S. Tsutsumi, *J. Chem. Soc. Japan, Pure Chem. Sec. (Nippon Kagaku Zasshi)*, **80**, 92 (1959).
14) M. Lazar, R. Rado and J. Pavlinec, *J. Polymer Sci.*, **53**, 163 (1961).
15) G. Natta, E. Beati'and F. Seberini, ibid., **34**, 685 (1959).
16) P. Ginstiniani, G. Natta and G. Mazzanti, U. S. Pat. 3115478.
17) U. Riboni and L. Bartolucci, U. S. Pat. 3116966.
18) T. Tanekoda, K. Akamatsu, T. Okamoto and K. Matsui, Japanese Pat. 26284 (1963).
19) K. S. Minsker, I. Z. Shapiro and G. A. Razuvayev, *Polymer Sci. U. S. S. R.*, **4**, 1 (1963).
20) S. Morimoto, O. Ishiwari and S. Uchida, Japanese Pat. 4683; 4733 (1963).
21) M. Watanabe and Y. Arata, Japanese Pat. 18392 (1962).
22) H. W. Coover, Jr., M. A. McCall and J. E. Guillet, U. S. Pat. 3121070; Japanese Pat. 5593 (1962).
23) H. H. G. Jellinek, "The Degradation of Vinyl Polymers," Academic Press Inc., Publishers, New York (1955), p. 68.
24) K. Azuma and K. Takahashi, Japanese Pat. 12141 (1962).

filtered, washed with a methanol-water mixture (10:1) and methanol, and dried under a vacuum. Polypropylene used contained no stabilizer. The properties are shown in Table I.

**The Preparation of Samples.**—The vinyl polymers used were polystyrene [PSt; intrinsic viscosity in a benzene solution at 25°C : 1.05 dl./g.], polymethyl methacrylate [PMMA; intrinsic viscosity in an acetone solution at 25°C : 1.22 dl./g.], and the 2-methyl 5-vinylpyridine - styrene copolymer [P(MVP-St); (2-methyl-5-vinylpyridine/styrene) in the copolymer : 1.2 by weight], and the acrylonitrile-styrene copolymer [P(A-St); (acrylonitrile/styrene) in the copolymer : 1.4 by weight]. All the vinyl polymers used were purified by reprecipitation.

The samples were prepared as follows: PP powder was stirred into a PMMA-acetone solution, a P(MVP-St)-acetone solution, a P(A-St)-acetone solution or a PSt-toluene solution. In the case of the acetone solution, the acetone was evaporated by stirring under a vacuum. The slurry of PP powder and the PSt-toluene solution was poured into excess methanol in a mixer. The polymer precipitated was filtered, washed with methanol and dried under a vacuum. The quantity of PSt, PMMA, and P(MVP-St) added to polypropylene was regulated at 3% by weight, while the quantity of P(A-St) was 4.7% by weight.

**The Viscosity Measurements and the Calculation of the Scission Number.**—The viscosity of the tetraline solution of the polymer sample containing 0.2 g. of 2, 6-di-*t*-butyl *p*-cresol per 100 ml. of tetralin was determined at 135°C with an Ubbelohde viscometer under a nitrogen atmosphere. The intrinsic viscosity was determined from the three-point measurement by extrapolation. The scission number of the polypropylene chain ($S$) per molecule, with the molecular weight calculated by Parrini's equation[25] $[[\eta]=0.80\times10^{-4}M^{0.80}]$, was calculated by the following equation:

$$S=(1/0.524)\{([\eta]_0/[\eta]_t)^{1/0.80}-1\}$$

$[\eta]_0$: The intrinsic viscosity of a sample before thermal degradation

$[\eta]_0$: The intrinsic viscosity of a sample after thermal degradation for $t$ hr.

This equation was derived from Matsumoto's equation[26] and Parrini's equation,[25] and it was previously applied to the analysis of the thermal degradation of polypropylene by Oshika.[9]

**Thermal Degradation in a Glass Ampoule.**—The sample (0.3 g.) was transferred into an ampoule of 6 mm. in diameter and 10 cm. in length. The ampoule was then evacuated by the use of an oil diffusion pump for one hour after three cycles of evacuation-nitrogen substitution. The ampoule was sealed off and dipped into a salt bath of sodium nitrate - potassium nitrate. The hot ampoule was rapidly cooled in water, and the viscosity of the polymer was determined.

**Thermal Degradation by the Use of an Extruder.** — The thermal degradation by the use of an extruder was studied under a nitrogen stream in order to consider the practical utility of the thermal degradation of polypropylene accelerated by vinyl polymers. Figure 1 gives a rough sketch of the extruder. The extruder was a modification of type MK-1 from Modern Machinery Co., Ltd., the heating zone of which was divided into three parts.

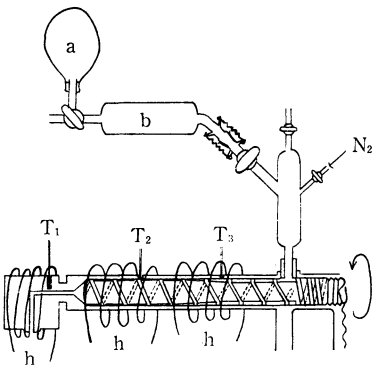



Fig. 1. The rough sketch of the extruder.
a : Nitrogen-balloon
b : Sample
$T_1$, $T_2$ and $T_3$: Thermo-couple
h : Heater

**Volatilization Curves.**—Volatilization curves of the samples were determined under a nitrogen stream with a differential thermal analysis apparatus DT-1A from Shimadzu Seisakusho, Ltd., in order to compare the thermal stability of the samples. The heating rate was 2°C/min.

**The Acetone-Extraction of Degraded Samples.**—The sample degraded by the use of the extruder was in the shape of a pellet. The sample was dissolved in *p*-xylene under a nitrogen atmosphere, and the hot solution was slowly cooled overnight, then the slurry obtained was poured into methanol [for the PP(A)-PSt sample, the PP(A)-PMMA sample, and the PP(D)-P(A-St) sample] or petroleum ether [for the PP(D)-P(MVP-St) sample] in a mixer. The precipitate was filtered, washed with methanol or petroleum ether, and dried under a vacuum. The powder obtained was extracted by acetone[12] with a Soxhlet extractor for 20 hr. under a nitrogen atmosphere. The residue was dried under a vacuum, and the vinyl polymer content of the residue was determined by infrared spectrum analysis, using a spectrophotometer, type AR-275, from Shimadzu Seisakusho Co., Ltd. The determination was carried out by the base-line method[27] using the following analytical wavelengths: PSt 14.4 $\mu$, PMMA 5.8$\mu$, and PMVP 13.6 $\mu$.

## Results and Discussion

**Volatilization Curves.**—Figures 2 and 3 show the volatilization curves of the PP(C), PP(D), PSt, PMMA, P(A-St), P(MVP-St), PP(C)-PSt, PP(C)-PMMA, PP(D)-P(A-St), and PP(D)-P(MVP-St)

25) P. Parrini, F. Selbastiano and G. Messina, *Makromol. Chem.*, **38**, 27 (1960).
26) S. Matsumoto, *Chem. High Polymers Japan (Kobunshi Kagaku)*, **6**, 77 (1949).
27) H. S. Szymanski, "IR Theory and Practice of Infrared Spectroscopy," Plenum Press, New York (1964), p. 320.

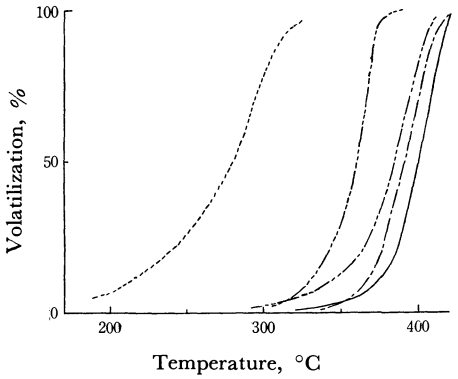



Fig. 2. Volatilization curves.
——: PP(C), ——: PSt, ----: PMMA,
——: PP(C)-PSt, ——: PP(C)-PMMA

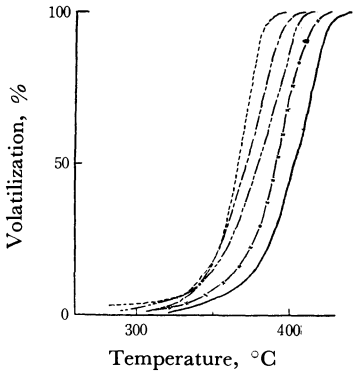



Fig. 3. Volatilization curves.
——: PP(D), ——: P(MVP-St),
----: P(A-St), —×—: PP(D)-P(MVP-St),
——: PP(D)-P(A-St)

samples. The volatilization curves of the PP(C)-PSt, PP(C)-PMMA, PP(D)-P(A-St), and PP(D)-P(MVP-St) samples were between the volatilization curves of PP(C) or PP(D) and those of PSt, PMMA, P(A-St), and P(MVP-St) respectively. These relations of the volatilization curves may be considered as suggesting the accelerating effect of vinyl polymers for the thermal degradation of polypropylene.

**Thermal Degradation in a Glass Ampoule.** —Figures 4—9 show the changes in the relative intrinsic viscosity with the reaction time at 280—345°C. Apparently, the changes in the relative intrinsic viscosity of the PP(A)-PSt, PP(A)-PMMA, PP(D)-P(A-St), and PP(D)-P(MVP-St) samples were larger than those of PP(A) and PP(D). Figures 10—15 show the changes in the scission number of the polypropylene chain with the reaction time, but it is necessary to note that the effect of addition of the vinyl ploymers was neglected. The scission rate was constant at a definite temperature, and the vinyl polymers were proved to be effective as accelerators for the thermal degradation of polypropylene. Judging from the fact that

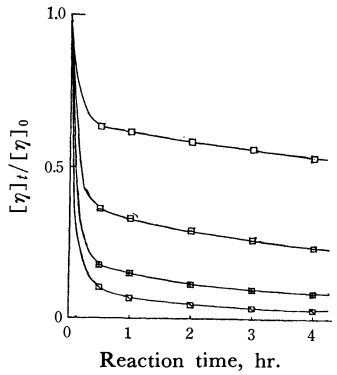



Fig. 4. The change in relative intrinsic viscosity of PP(A) with reaction time at various temperatures.
Reaction temperature;
-□-: 280°C, -⊟-: 300°C
-⊞-: 320°C, -▨-: 340°C

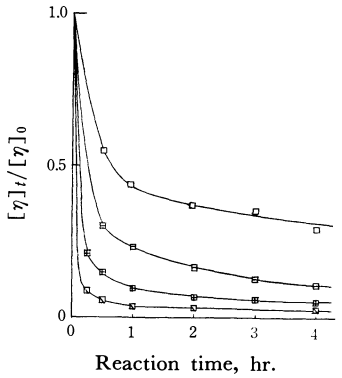



Fig. 5. The change in relative intrinsic viscosity of PP(A)-PMMA sample with reaction time at various temperatures.
Reaction temperature;
-□-: 280°C, -⊟-: 300°C
-⊞-: 320°C, -▨-: 340°C

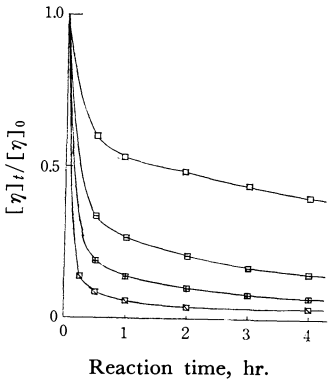



Fig. 6. The change in relative intrinsic viscosity of PP(A)-PSt sample with reaction time at various temperatures.
Reation temperatures;
-□-: 280°C, -⊟-: 300°C
-⊞-: 320°C, -▨-: 340°C

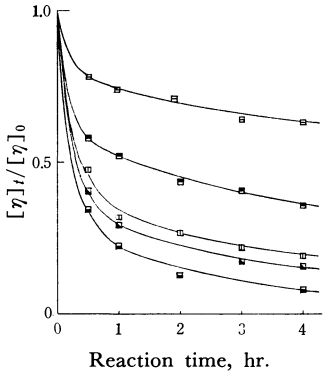



Fig. 7. The change in relative intrinsic viscosity of PP(D) with reaction time at various temperatures.
Reaction temperature;
-⊟-: 300°C, -■- 315°C, -◫- 330°C
-◪-: 334°C, -◨- 345°C

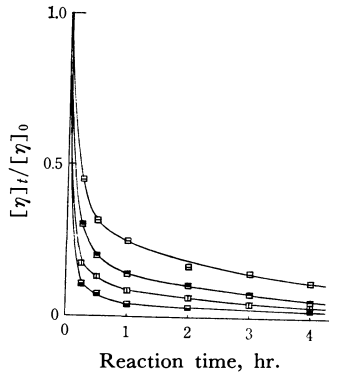



Fig. 8. The change in relative intrinsic viscosity of PP(D)-P(MVP-St) sample with reaction time at various temperatures.
Reaction temperature;
-⊟-: 300°C, -■-: 315°C
-◫-: 330°C, -◨-: 345°C

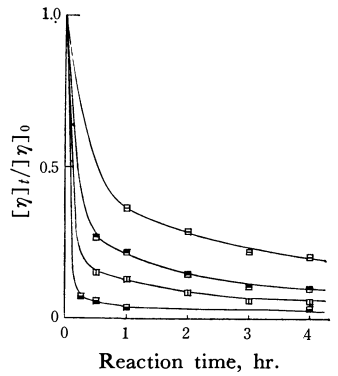



Fig. 9. The change in relative intrinsic viscosity of PP(D)-P(A-St) sample with reaction time at various temperatures.
Reaction temperature;
-⊟-: 300°C, -■-: 315°C
-◫-: 330°C, -◨-: 345°C

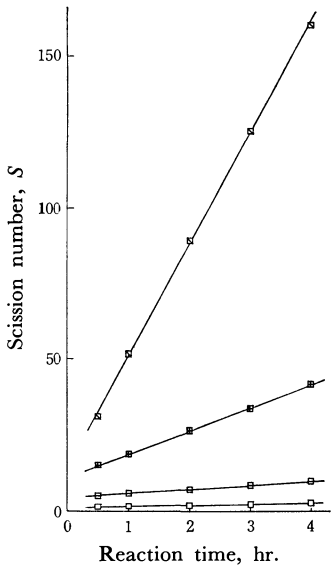



Fig. 10. Scission number of PP(A) vs. reaction time.
Reaction temperature;
-□-: 280°C, -⊟-: 300°C
-⊞-: 320°C, -▨-: 340°C

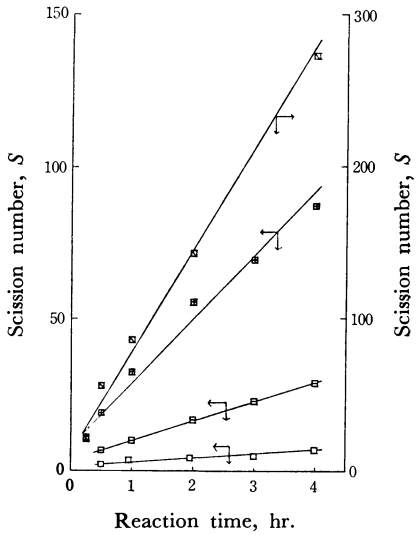



Fig. 11. Scission number of PP(A)-PMMA sample vs. reaction time.
Reaction temperature;
-□-: 280°C, -⊟-: 300°C
-⊞-: 320°C, -▨-: 340°C

the straight lines in Figs. 10—15 did not pass the origins, the scission rate at the initial step of the reaction should be larger than that at the stationary step of the reaction, and this should be attributed to the weak bond in the polymers.[5,9]

Figure 16 shows a plot of the logarithm of the scission rate versus the reciprocal of the absolute

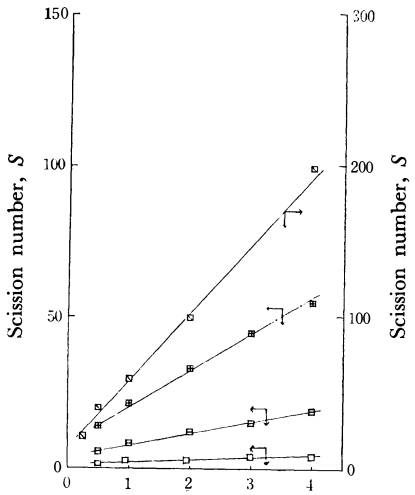



Fig. 12. Scission number of PP(A)-PSt sample vs. reaction time.
Reaction temperature;
-□-: 280°C, -⊟-: 300°C
-⊞-: 320°C, -▧-: 340°C

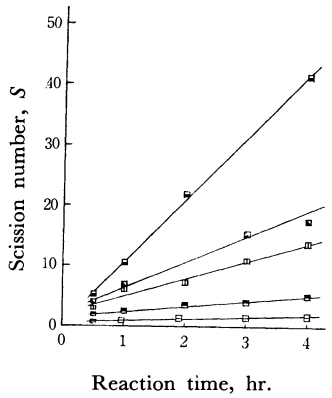



Fig. 13. Scission number of PP(D) vs. reaction time.
Reaction temperature;
-⊟-: 300°C, -■-: 315°C, -◫-: 330°C,
-◪-: 334°C, -▬-: 345°C

temperature, and the response to the Arrehenius law is considered to be good. From the gradient of the straight line as determined by the method of the least squares, the activation energies for the scission reaction of the samples were calculated to be as follows:

57.2 kcal./mol. for PP(A),
58.4 kcal./mol. for PP(D),
46.8 kcal./mol. for the PP(A)-PSt sample,
43.5 kcal./mol. for the PP(A)-PMMA sample,
46.9 kcal./mol. for the PP(D)-P(A-St) sample,
and 38.6 kcal./mol. for the PP(D)-P(MVP-St) sample.

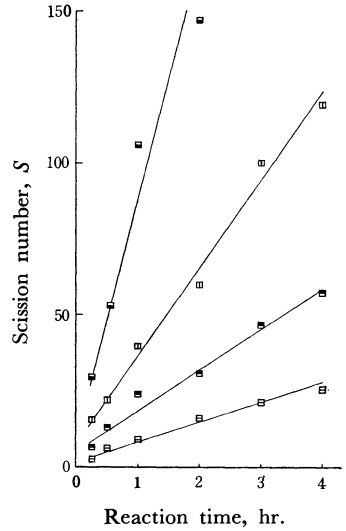



Fig. 14. Scission number of PP(D)-P(MVP-St) sample vs. reaction time.
Reaction temperature;
-⊟-: 300°C, -■-: 315°C
-◫-: 330°C, -▬-: 345°C

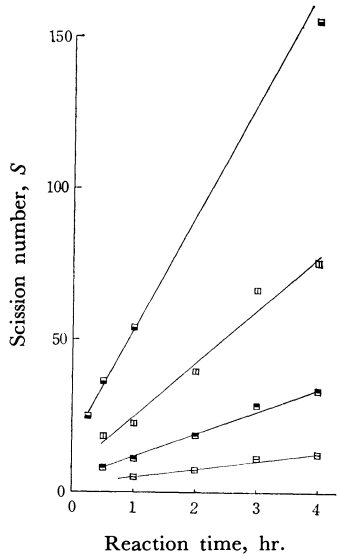



Fig. 15. Scission number of PP(D)-P(A-St) sample vs. reaction time.
Reaction temperature;
-⊟-: 300°C, -■-: 315°C
-◫-: 330°C, -▬-: 345°C

The activation energies for PP(A) and PP(D) could be cosidered to be consistent, but the reason for the difference between the scission rate of PP(A) and that of PP(D) is not clear. The values for PP(A) and PP(D) were larger than the value obtained by Hamada[5] (51.4 kcal./mol. at 250—320°C), while they were smaller than the value obtained by Davies et al.[4] (65 kcal./mol. at 250—300°C). The values for the PP - vinyl polymer

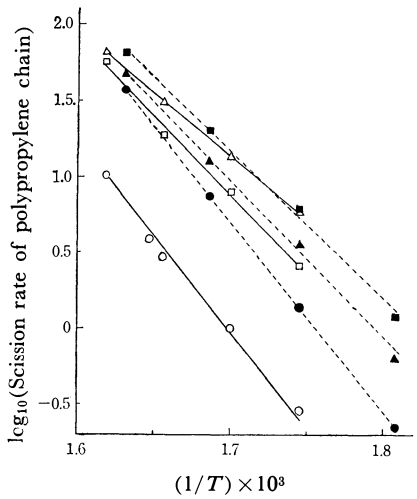



Fig. 16. $\log_{10}$(Scssion rate of polypropylene chain) vs. (1/T).
--●--: PP(A), --▲--: PP(A)-PSt,
--■--: PP(A)-PMMA, -○-: PP(D),
-△-: PP(D)P(MVP-St), -□-: PP(D)-P(A-St)

samples were smaller than the values for PP(A) and PP(D). This difference may be attributed to the accelerating effect of the vinyl polymers added.

The orders of the activation energies of the PP(A) series or the PP(D) series were consistent with the order of thermal stabilities, as is shown in Figs. 2 and 3 respectively.

The value of the PP(D)-P(A-St) sample could not be compared with the values of the other PP-vinyl polymer samples, because of the difference in the quantity of the vinyl polymers added.

In this study, the degradation process was regarded as only the scission process of the polypropylene chain. However, as the formation of graft or block polymers was observed, as will be described later, such reactions as the degradations of a vinyl polymer chain and of a polypropylene chain and the interaction among a vinyl monomer liberated by the thermal degradation, a vinyl polymer radical, a polypropylene radical, and a polypropylene molecule must be considered simultaneously. The study of these reactions would be an interesting theme in the future.

**Thermal Degradation by the Use of an Extruder and Acetone-Extraction.**—Table II shows the results of the thermal degradation of PP(C)-PMMA and PP(D)-P(MVP-St) samples by the use of an extruder. The accelerating effect of PMMA and P(MVP-St) may easily be observed from Table II. When these results are compared with those of the thermal degradation in the glass ampoule, it is clear that the reaction time needed here for modification to the appropriate intrinsic viscosity of polypropylene by the use of the extruder is shorter than that in the glass ampoule. As plausible reasons for this difference, the following factors may be listed: the mechanical shearing effect of the extruder, the mechanical mixing effect of the extruder, and the effect of a trace of oxygen which could not be eliminated because of the imperfect air-tightness of the extruder.

Regarding the mechanical shearing effect, it was well known that the mechanical degradation process has a negative temperature coefficient, since the bulk viscosity decreases and since, therefore, the degradative effect of the mechanical shear is reduced at higher temperatures until it finally become negligible. For example, the mechanical shearing effect is negligible for natural rubber at about 120°C.[28] In order to judge whether the mechanical shearing effect was negligible or not, PP([η]: 4.30 dl./g., specific gravity: 0.911) was extruded in a nitrogen atmosphere under these conditions: $T_1$: 190°C, $T_2$: 240°C, $T_3$: 200°C, and

TABLE II. THE RESULT OF THE THERMAL DEGRADATION BY THE USE OF THE EXTRUDER

| Sample | Quantity of vinyl polymer added % | Thermal degradative conditions: Temp. of the extruder, °C $T_1$ | $T_2$ | $T_3$ | Rotation speed of screwing shaft round/min. | Intrinsic viscosity dl./g. |
|---|---|---|---|---|---|---|
| PP(B)-PMMA | 0 | 220 | 340 | 330 | 7* | 3.15 |
| | 1 | 220 | 340 | 280 | 30*** | 1.60 |
| | 1 | 220 | 320 | 280 | 30 | 2.90 |
| | 3 | 220 | 320 | 280 | 30 | 2.15 |
| | 5 | 220 | 320 | 280 | 30 | 1.95 |
| | 5 | 220 | 320 | 280 | 20** | 1.46 |
| PP(D)-P(MVP-St) | 0 | 200 | 330 | 275 | 20 | 2.75 |
| | 3 | 200 | 330 | 275 | 10 | 1.58 |
| | 3 | 200 | 330 | 275 | 20 | 1.64 |
| | 3 | 200 | 330 | 275 | 34 | 1.75 |

* The retention time of a sample in the extruder was about 8 min.
** The retention time of a sample in the extruder was about 3.5 min.
*** The retention time of a sample in the extruder was about 2.3 min.

28) R. J. Ceresa, "Block and Graft Copolymers," Butterworths, London (1962), p. 69.

Table III. The result of acetone extraction

| Sample | Thermal degradation conditions: Temp. of the extruder, °C $T_1$ | $T_2$ | $T_3$ | Rotation speed of screwing shaft round/min. | Quantity of vinyl polymer added % | Intrinsic viscosity dl./g. | Content of vinyl polymer in the residue after acetone-extraction % | Vinyl polymer in the residue / Vinyl polymer added |
|---|---|---|---|---|---|---|---|---|
| PP(C)-PMMA | 220 | 340 | 320 | 30 | 3 | 1.79 | 0.23 | 0.08 |
| PP(C)-PSt | 220 | 335 | 315 | 35 | 3 | 1.75 | 1.47 | 0.49 |
| PP(D)-(MVP-St) | 200 | 330 | 275 | 10 | 3 | 1.58 | 0.50 {PMVP: 0.20 PSt: 0.30} | 0.17 {PMVP: 0.12 PSt: 0.22} |

rotation speed of the screwing shaft: 30 round/min. Since the thermal degradation under these conditions was found to be negligible and since no degradation was observed ([$\eta$] of PP extruded: 4.29 dl/g.), the mechanical shearing effect was judg ed to be negligible. Therefore, it is reasonable to say that the shearing effect was negligible for the degradation shown in Table II.

The effect of the trace of oxygen was negligible in the results described above, but this fact can not assure that the effect of the trace of oxygen is negligible for the degradation shown in Table II, as the temperature of the above experiment is considerably lower than that shown in Table II. Also, the mechanical mixing effect may be effective, because the diffusion of the active radicals generated in the viscous polymer phase will probably not be easy and so the mechanical mixing might be effective in promoting the diffusion and the reaction of active radicals.

Table III shows the results of acetone-extraction. The formation of graft or block polymers was confirmed from the fact that a considerable quantity of the vinyl polymers was detected in the residue after acetone-extraction, while, no vinyl polymer was detected in the residue from PP-P(MVP-St) and PP-PSt mixtures after acetone-extraction. Furthermore, the monomer unit ratio (MVP/St) in the residue from the PP(D)-P(MVP-St) sample was 0.67, smaller than that of P(MVP-St) itself (MVP/St=1.2). This interesting finding may be a key to a solution of the question of whether or not the vinyl polymers degrade to monomers in the thermal degradation process.

The thermal degradative process of the vinyl polymers to the monomers may, therefore, be considered to accelerate the polypropylene degradation. The details should be elucidated by a study using a fractionated vinyl copolymer with a narrow molecular weight distribution and a difinite monomer unit ratio.

**Dyeability.**—The fibers spun from the modified polymers showed a good dyeability by dispersed dyes, such as Celliton Blue Extra Type, Latyl Cerise B, and Diacelliton Fast Yellow G. It was established by the microscopic observation of the cross section of dyed fibers that the colored vinyl polymer was dispersed in the shape of a granule and that the dispersed state of the colored vinyl polymer in the modified polypropylene was finer and more preferable to that of polypropylene fibers blended only with the vinyl polymer. The graft or block polymers formed in the thermal degradation should play an important role in improving the dispersion state of the colored vinyl polymer in the modified polypropylene.

## Summary

The thermal degradation of polypropylene in the presence of such vinyl polymers as polystyrene, polymethyl methacrylate, the 2-methyl-5-vinylpyridine-styrene copolymer, and the acrylonitrile-styrene copolymer has been studied at 280—345°C by the use of glass ampoules and an extruder.

1) The vinyl polymers added were effective as accelerators for the thermal degradation of polypropylene. The activation energies for the scission reaction of the polypropylene chain were 57.2 and 58.4 kcal./mol. for the two polypropylene samples, and 46.8, 43.5, 46.9 and 38.6 kcal./mol. for polypropylenes containing 3% polystyrene, 3% polymethyl methacrylate, 4.7% the acrylonitrile-styrene copolymer, and 3% the 2-methyl-5-vinylpyridine-styrene copolymer respectively.

2) The reaction time needed for the modification of polypropylene to an appropriate intrinsic viscosity by the use of an extruder is shorter than that in glass ampoules.

3) Graft or block polymers have been detected in the residue after the acetone-extraction of the extruded polypropylene. They could be used in the modification of the polypropylene dyeability.

4) It has been concluded that the simple process of the thermal degradation of polypropylene accelerated by vinyl polymers can be used for the modification of polypropylene with a very high molecular weight and, simultaneously, for the preparation of graft or block polymers.

The authors wish to thank Professor Yoshinobu Takegami of Kyoto University and Mr. Senpachi Miyoshi, Director of Tokuyama Soda Co., Ltd., for their valuable advice and discussions.

The authors wish to thank Messrs. Shigeo Hisano and Hiroyuki Iwakura for their help.

*Tokuyama Soda Co., Ltd.*
*Tokuyama, Yamaguchi*

# Studies of the Decomposition Products of Ethereal Blue Perchromate by Ion-exchange Resins. II. The Open Bottle Decomposition Product

By B. S. RAJPUT and R. C. RAI

(Received February 19, 1965)

The blue perchromate decomposes in different manners, yielding different compounds under different conditions. Rai and Prakash[1] and Rajput and Rai[2] have shown, for instance, that in contact with water it gives $Cr_2(Cr_2O_7)_3$.

No serious attempt has, however, yet been made to ascertain the composition of and to assign a chemical formula to the decomposition product of the ethereal blue perchromate obtained when it is allowed to decompose in uncorked Erlenmeyer flasks (the open bottle decomposition product). According to Schwarz and Giese,[3] ethereal blue perchromate gives $CrO_3$ in presence of silver oxide. Rai, Rajput and Rai[4] have seen that if the ethereal blue perchromate is allowed to decompose under tightly-corked conditions (the closed bottle decomposition product), its titration value becomes nearly double when this product is oxidised with 30% hydrogen peroxide in a strongly alkaline medium (NaOH). They have thus tried to show that, under such conditions, a compound with the formula $CrCrO_4$ seems to be formed. The same compound has been reported by Vauquelin and others.[5]

In the present paper, the composition of the open bottle decomposition product of the ethereal blue perchromate will be studied, and, on the basis of the observations obtained, a chemical formula will be assigned to it. It will further be shown how the formation of this product supports the formula suggested by Rai for the ethereal blue perchromate.

## Experimental

Blue perchromate was prepared by mixing ice-cold solutions of 5% w/v potassium dichromate (50 ml.), 2 N sulphuric acid (5 ml.) and 6% hydrogen peroxide. The blue compound thus formed was then extracted with ice-cold ethyl ether (100 ml.), washed several times with ice-cold distilled water, and placed in a tightly-corked flask in the refrigerator in order to freeze out the water. After about three hours, it was transferred to a previously-dried and cooled flask and kept in ice. Five milliliters of it was then allowed to decompose in each of two dry, 100-ml. Erlenmeyer flasks; the rest of it was allowed to decompose in a 250-ml. Erlenmeyer flask under open conditions. After about 12 to 14 hr., only a brown residue was left in all the flasks. The contents of one of the 100-ml. Erlenmeyer flasks were titrated after potassium iodide and sulphuric acid had been added; that of the other was so titrated after the contents had been oxidised with 30% hydrogen peroxide in an alkaline medium (NaOH). The excess peroxide was then removed by prolonged boiling. The brown residue left in the third flask was dissolved in water with the aid of a few milliliters of dilute sulphuric acid.

Several columns (6/75 mm.) were prepared for the different ion-exchangers and washed thoroughly with distilled water. Cations and anions separated from the solution of the open bottle decomposition product prepared above. It was found, with the aid of a spot test, that chromium was present in cationic as well as in anionic portions of the product solution. The amount was then estimated quantitatively iodometrically. In the case of cationic chromium, it was oxidised with 30% hydrogen peroxide as above after elution and then titrated iodometrically. Anionic chromium was titrated iodometrically, as usual. In the case of anion exchangers, a final elution was made with a few milliliters of 1 N hydrochloric acid in order to elute any chromium formed due to some reaction[6] between the resin and the anion of the effluent. The elutriant so obtained did not liberate iodine with acid; hence it was oxidised as above with 30% hydrogen peroxide and titrated iodometrically after the excess peroxide had been removed. The titration value so obtained was added to the titration value of the anionic portion of the product solution. The experimental results are noted in Tables I—III:

## Discussion

According to Schwarz the ethereal blue perchromate decomposes in the presence of silver oxide, giving $CrO_3$:

$$CrO_5 \xrightarrow{Ag_2O} CrO_3 + 2O$$

When the ethereal blue perchromate is decomposed in an open bottle in the absence of any foreign substance, a brown substance is formed. It liberates iodine in the presence of acid; the

1) R. C. Rai and S. Prakash, *Z. anorg. u. allgem. Chem.*, **275**, 94 (1954).

2) B. S. Rajput and R. C. Rai, *J. Indian Chem. Soc.*, **42**, 277 (1965).

3) R. Schwarz and H. Giese, *Ber.*, **65B**, 871 (1932).

4) R. C. Rai, B. S. Rajput and R. C. Rai, Paper presented at the Annual convention of I. C. S. at Allahabad 1964 and paper communicated to *J. Indian Chem. Soc.*

5) L. N. Vauquelin et al., "A Comprehensive Treatise on Inorganic and Theoretical Chemistry," Vol. XI, Ed. by J. W. Mellor, Longmans, Green and Co., London (1931), p. 208.

6) O. Samuelson, "Ion-exchangers in Analytical Chemistry," John Wiley & Sons, Inc., New York (1953).

## Table I. Cation exchangers

Column : 6/75 mm.; Strength of thiosulphate solution used = N/97.58
Drop rate : 15 to 18 per minute ; Volume of the solution exchanged with resin each time = 5 ml.

| Name of resin | Vol. in ml. of thiosulphate solution used in titrating the open bottle decomposition product solution | | | | | Ratios | | | | | | |
|---|---|---|---|---|---|---|---|---|---|---|---|---|
| | 5 ml. unexchanged with resin and unoxidised | 5 ml. unexchanged with resin but oxidised | Effluent unoxidised | Effluent oxidised | Elutriant oxidised | $\frac{b}{a}$ ; | $\frac{a}{c}$ ; | $\frac{a}{d}$ ; | $\frac{d}{c}$ ; | $\frac{b}{c+e}$, $\frac{b}{d+e}$ or $\frac{b}{a+e}$; | $\frac{a}{e}$, $\frac{c}{e}$ or $\frac{d}{e}$ | |
| | a | b | c | d | e | f | g | h | i | j | k | |
| Amberlite | 8.25 | 13.95 | 7.80 | 8.00 | 5.80 | 1.69 | 1.05 | 1.03 | 1.02 | 1.02 | 1.42 | |
| IR 120(H) | 8.25 | 13.90 | 7.80 | 8.00 | 5.70 | 1.68 | 1.05 | 1.03 | 1.02 | 1.03 | 1.45 | |
| | 8.10 | 13.80 | 7.85 | 8.00 | 5.50 | 1.70 | 1.03 | 1.01 | 1.01 | 1.03 | 1.47 | |
| | 8.40 | 14.00 | 8.00 | 8.00 | 5.80 | 1.66 | 1.04 | 1.04 | 1.00 | 1.01 | 1.45 | |
| | 8.60 | 14.00 | 8.10 | 8.30 | 6.00 | 1.62 | 1.06 | 1.03 | 1.02 | 1.00 | 1.43 | |
| Dowex 50(H) | 8.10 | 13.80 | 8.00 | 8.20 | 5.50 | 1.70 | 1.01 | 0.99 | 1.02 | 1.02 | 1.47 | |
| | 8.10 | 13.75 | 8.00 | 8.15 | 5.45 | 1.70 | 1.01 | 0.99 | 1.01 | 1.02 | 1.47 | |
| | 8.40 | 14.00 | 8.15 | 8.30 | 5.80 | 1.66 | 1.01 | 1.01 | 1.01 | 1.00 | 1.45 | |
| | 8.25 | 13.95 | 8.10 | 8.40 | 5.75 | 1.69 | 1.01 | 0.98 | 1.03 | 1.00 | 1.42 | |
| | 8.30 | 13.95 | 8.10 | 8.20 | 5.75 | 1.69 | 1.01 | 1.01 | 1.01 | 1.00 | 1.42 | |

## Table II. Anion exchangers

Column : 6/75 mm.; Strength of thiosulphate solution used = N/97.58
Drop rate : 15 to 18 per minute ; Volume of the solution exchanged with resin each time = 5 ml.

| Name of resin | Vol. in ml. of thiosulphate solution used in titrating open decomposition product solution | | | | | Ratios | | | |
|---|---|---|---|---|---|---|---|---|---|
| | 5 ml. unexchanged with resin and unoxidised | 5 ml. unexchanged with resin but oxidised | Effluent oxidised | Elutriant (a) unoxidised | Elutriant (b) oxidised | $\frac{b}{a}$ or $\frac{b}{d+e}$ ; | $\frac{a}{c}$ or $\frac{d+e}{c}$ ; | $\frac{a}{d+e}$ ; | $\frac{b}{c+d+e}$ or $\frac{b}{a+c}$ |
| | a | b | c | d | e | f | g | h | i |
| Dowex-1(Cl) | 5.75 | 9.80 | 3.60 | 5.50 | 0.30 | 1.70 | 1.59 | 0.99 | 1.05 |
| | 8.30 | 13.90 | 5.75 | 7.50 | 0.60 | 1.67 | 1.44 | 1.02 | 1.00 |
| | 8.40 | 14.00 | 5.80 | 7.50 | 0.60 | 1.66 | 1.44 | 0.99 | 0.99 |
| | 8.40 | 14.00 | 5.80 | 7.90 | 0.40 | 1.66 | 1.44 | 1.01 | 1.00 |
| Dowex-21(Cl) | 5.75 | 9.80 | 3.60 | 5.45 | 0.40 | 1.70 | 1.59 | 0.99 | 1.03 |
| | 5.90 | 9.95 | 3.80 | 5.30 | 0.50 | 1.67 | 1.55 | 1.01 | 1.02 |
| | 5.85 | 9.90 | 3.80 | 5.35 | 0.40 | 1.69 | 1.53 | 1.02 | 1.03 |
| | 8.40 | 14.00 | 5.80 | 8.00 | 0.20 | 1.66 | 1.45 | 1.02 | 1.00 |
| Amberlite IR | 6.10 | 10.10 | 3.90 | 5.00 | 1.50 | 1.65 | 1.56 | 0.91 | 0.97 |
| 400(Cl) | 6.15 | 10.10 | 3.90 | 5.20 | 1.00 | 1.65 | 1.56 | 0.99 | 0.97 |
| | 5.75 | 9.80 | 3.55 | 4.00 | 1.30 | 1.70 | 1.60 | 1.08 | 1.10 |

TABLE III.

5% w/v $K_2Cr_2O_7$ solution=50 ml. 2N $H_2SO_4$=5 ml. Ethyl ether=100 ml.
6% $H_2O_2$=varying quantities Strength of $Na_2S_2O_3$ solution=N/40

| Sample No. | Vol. of 6% $H_2O_2$ used ml. | Vol. in ml. of $Na_2S_2O_3$ soln. used in titrating | | | Ratios | |
|---|---|---|---|---|---|---|
| | | Blue perchromate 5 ml. blue perchromate | Open decomp. product | | | |
| | | | unoxidised | oxidised | b/c | b/d |
| | a | b | c | d | e | f |
| 1 | 20 | 50.40 | 18.20 | 31.60 | 2.76 | 1.58 |
| 2 | 15 | 43.00 | 15.10 | 26.00 | 2.84 | 1.65 |
| 3 | 10 | 43.35 | 16.30 | 28.05 | 2.64 | 1.54 |
| 4 | 10 | 27.80 | 10.00 | 16.80 | 2.78 | 1.65 |
| 5 | 5 | 18.00 | 6.50 | 11.20 | 2.76 | 1.60 |

quantity of iodine liberated increases if the product is oxidised with 30% hydrogen peroxide in a strongly alkaline medium (NaOH) before the iodometric titration. This increase in titration value can be understood if the product is considered to have chromium in the cationic portion as well. In an attempt to verify this, the product was dissolved in water with the aid of dilute sulphuric acid, and then cationic and anionic portions were separated with the help of different ion-exchangers. Chromium was found to be present in both portions; when this was estimated quantitatively and iodometrically, it was found that the cationic and anionic chromium are present in the ratio of 1 : 1.5 (Tables II and III). The increase in the titration value of the unexchanged product solution may, therefore, be considered to be due only to the conversion of chromium(III) to chromium(VI).

On the basis of the above ratio (1 : 1.5) between cationic and anionic chromium, it can easily be found that the compound formed is $Cr_2(CrO_4)_3$, as otherwise this ratio can not be explained. Moreover, the insolubility of the compound in water also agrees with the known properties of $Cr_2(CrO_4)_3$.

An attempt will now be made to show how this product can be formed from the blue compound, and in what manner it is related to the parent compound (blue perchromate). It will also be seen which formula, the $CrO_5$ of Schwarz or the $Cr_2(Cr_2O_{10})_3$ and $CrCrO_8$ of Rai best explains the results obtained above.

If the blue perchromate is $CrO_5$, it is difficult to presume the formation of trivalent chromium from it without the presence of any reducing agent. However, omitting all this and admitting that it does happen, $CrO_5$ may be taken to decompose in the following manner to give chromium chromate:

$$10CrO_5 \rightarrow 2Cr_2(CrO_4)_3 + 26O \quad (1)$$

and the total oxidising capacity of the blue compound as expressed in the number of available oxygen atoms may be given in this case as:

$$10CrO_5 \rightarrow 5Cr_2O_3 + 35O \quad (2)$$

and from chromium chromate:

$$2Cr_2(CrO_4)_3 \rightarrow 5Cr_2O_3 + 9O \quad (3)$$

The ratio between the total available oxygen atoms from the blue perchromate and chromium chromate will, in this case, be 35 : 9, i. e., 3.88 : 1 (Eqs. 2 and 3). However, the ratio obtained in Table III, Column 'e' does not exceed 2.84 : 1.

On the contrary, if the formulae suggested by Rai are accepted, the above relation can be shown as follows:

$$5Cr_2(Cr_2O_{10})_3 \rightarrow 8Cr_2(CrO_4)_3 + 54O \quad (4)$$

and

$$20CrCrO_8 \rightarrow 8Cr_2(CrO_4)_3 + 64O \quad (5)$$

The total available oxygen atoms in these cases will be:

$$5Cr_2(Cr_2O_{10})_3 \rightarrow 20Cr_2O_3 + 90O \quad (6)$$

and

$$20CrCrO_8 \rightarrow 20Cr_2O_3 + 100O \quad (7)$$

and from chromium chromate:

$$8Cr_2(CrO_4)_3 \rightarrow 20Cr_2O_3 + 36O \quad (8)$$

The corresponding ratios in these cases will be 90 : 36 and 100 : 36, i. e., 2.5 : 1 and 2.77 : 1 (Eqs. 6, 7 and 8), values which agree fairly well with the ratios obtained in Table III, Column 'e' on the basis of experimental results.

When the open bottle decomposition product is oxidised with hydrogen peroxide in an alkaline medium, it is converted into sodium chromate:

$$8Cr_2(CrO_4)_3 + 80NaOH + 24H_2O_2 \rightarrow 40Na_2CrO_4 + 64H_2O \quad (9)$$

When titrated iodometrically, this gives:

$$40Na_2CrO_4 \rightarrow 40Na_2O + 20Cr_2O_3 + 60O \quad (10)$$

The ratios between the available oxygen atoms of the blue perchromate and those obtained from the sodium chromate so formed will be:

1) on the basis of $CrO_5$: 35 : 15, i. e., 2.33 : 1
2) on the basis of $Cr_2(Cr_2O_{10})_3$: 90 : 60, i. e., 1.50 : 1
3) on the basis of $CrCrO_8$: 100 : 60, i. e., 1.66 : 1

The values obtained in Column 'f' of Table III are, again, nearer to those obtained by Rai's formulae.

The formula, $Cr_2(Cr_2O_{10})_3$, suggested by Rai[7] for the blue perchromate has been shown by him[8] to be in equilibrium with the other formula, $CrCrO_8$:

$$Cr_2(Cr_2O_{10})_3 + 2H_2O_2 \rightleftarrows 4CrCrO_8 + 2H_2O$$

He has further shown that $CrCrO_8$ is formed when hydrogen peroxide is present in excess.

The observations noted above, therefore, prove that the ethereal blue perchromate gives chromium chromate, $Cr_2(CrO_4)_3$, when decomposed in an open bottle and that its formation can be explained on the basis of Rai's formulae for the blue perchromate.

7) R. C. Rai, *J. Indian Chem. Soc.*, **34**, 193 (1957).
8) R. C. Rai, D. Sc. Thesis, University of Allahabad, 1962 on 'On the Constitution of Blue Peroxy Chromic Acid,' page 214.

**Summary**

The composition of the open bottle decomposition product has been studied and a chemical formula $Cr_2(CrO_4)_3$ has been assigned to it. It has been shown that the formation of this product can be explained successfully if we accept the formula suggested by Rai for the ethereal blue perchromate.

*Chemical Laboratories*
*University of Saugar*
*Sagar (M.P.), India*

# The Dehydrogenation of All-*cis*-5, 11, 14-Eicosatrienoic Acid to Arachidonic Acid

By Toru TAKAGI

(Received March 5, 1965)

Early investigators have indicated, as a result of studying the feeding of linoleate concentrates to rats, that linoleate is transformed to arachidonate.[1] The transformation was confirmed by Mead and his co-workers using $^{14}C$-labeled linoleate.[2] The transformations of all-*cis*-6,9,12-octadecatrienoic acid[3] and all-*cis*-8,11,14-eicosatrienoic acid[4] to arachidonic acid were also confirmed by Mead and his co-workers.

Recently the present author reported that the unique fatty acid of *Podocarpus nagi* seed oil may be characterized as all-*cis*-5,11,14-eicosatrienoic acid.[5] The all-*cis*-acid was also found in *Ginko biloba*[6] and pinewood and tall oil.[7] The dehydrogenation of this acid to arachidonic acid in animals could be expected, because the structure of the acid differed from that of arachidonic acid only in lacking the double bond in the 8-position. Therefore, the metabolism of the eicosatrienoate has been investigated in our laboratory. This paper will present the results of the feeding experiments; an analysis of the fatty acid composition will follow.

## Results and Discussion

Twenty male rat weanlings (20 days old) of the Wister strain were kept on a basic fat-free-diet[8] obtained from the Nutrition Biochemical Co. After 100 days feeding, a gas chromatographic analysis of the fatty acids in the rat livers showed the presence of less than 1.1% linoleate and 2.0% arachidonate respectively of the total of the fatty acids. The rats were then divided into three groups of five rats in each. One gram portions of ethyl linoleate and ethyl all-*cis*-5,11,14-eicosatrienoate were fed daily intragastrically, by means of a syringe equipped with a round-end needle, to the first group and the second, respectivly. No fat was given to the third group. The fat-free-diet was fed to each group continuously. After 5 days, the rats were killed and the livers were quickly removed and immediately frozen. The fatty acid compositions of the liver lipids analyzed by the gas chromatographic method are given in Table I. A "shorthand designation" of the structure of each acid is included in the table; e.g., 18:2 is a C-18 acid with 2 double bonds, and 18:0 a saturated

1) L. C. A. Nunn and I. Smedley-MacLean, *Biochem. J.*, **32**, 2178 (1938); I. Smedley-MacLean and E. M. Hume, ibid., **35**, 990 (1941).
2) J. F. Mead, G. Steinberg and D. R. Howton, *J. Biol. Chem.*, **205**, 683 (1953).
3) J. F. Mead and D. R. Howton, ibid., **229**, 575 (1957).
4) D. R. Howton and J. F. Mead, ibid., **235**, 3380 (1960).
5) T. Takagi, *J. Am. Oil Chem. Soc.*, **41**, 516 (1964).
6) J. L. Gellerman and H. Shlenk, *Experientia*, **19** (19), 522 (1963).
7) T. Lehtinen, E. Elomaa and J. Alhojarvi, *Suomen. Kemistilehti B.*, **36** (7—8), 124 (1963); *Chem. Abstr.*, **57**, 9649 (1963).
8) J. G. Wooley and W. H. Sebrell, *J. Nut.*, **29**, 191 (1945).

Table I. Fatty acid compositions of liver lipids

| No. of rat group | I | II | III |
|---|---|---|---|
| Dietary ester | Linoleate | 5,11,14-Eicosatrienoate | None |
| Fatty acids found in liver lipids | | | |
| 16 : 0 | 22.7±2.0* | 25.4±0.2 | 25.6±2.0 |
| 16 : 1 | 5.3±0.5 | 6.5±1.0 | 14.4±0.5 |
| 18 : 0 | 17.7±1.2 | 15.8±0.9 | 10.4±1.4 |
| 18 : 1 | 25.5±2.1 | 25.1±3.5 | 40.6±1.5 |
| 18 : 2 | 14.2±0.9 | 2.4±0.3 | 1.0±0.1 |
| 20 : 3 | 2.6±0.9 | 15.9±1.5 | 6.2±1.2 |
| 20 : 4 | 12.2±0.5 | 9.0±1.6 | 1.8±0.2 |

* Standard deviation

** Small peaks corresponding those of myristate and others were disregarded in the calculation of the compositions.

C-18 acid. Each acid shown in the table was identified by internal standards. The low level of linoleate (18:2) and arachidonate (20:4) and the high level of eicosatrienoate in the fatty acid from the fat-free-diet group were consistent with the results of metabolic studies of the fatty acids reported by Mead and his co-workers.[9] The linoleate percentage was affected only to a slight degree by the dietary 5,11,14-eicosatrienoate, while it was significantly elevated by the dietary linoleate. On the contrary, the eicosatrienoate percentage was significantly elevated by the dietary 5,11,14-eicosatrienoate, while it was slightly decreased by the dietary linoleate. In spite of such differences, the arachidonate percentages were elevated in both cases. It is plausible that the dehydrogenation of 5,11,14-eicosatrienoate at the 8-position directly produced arachidonic acid in this experiment, because there was probably no other source for arachidonic acid except such dehydrogenation.

As the arachidonic acid detected by gas chromatography was identified only by the retention time, a structural confirmation was sought by a spectrophotometric analysis of alkali-isomerized products and by a gas chromatographic analysis of the degraded products. The eicosatrienoate and the eicosatetraenoate were therefore isolated from the liver lipids of rats fed with 5,11,14-eicosatrienoate by elution chromatography using silver-nitrate impregnated silicic acid as the stationary phase. The specific extinction coefficents at the maxima in the spectrophotometric absorption of the alkali-isomerized products of the eicosatrienoic acid and the eicosatetraenoic acid shown in Table II. The accordance of the specific extinction coefficients of the alkali-isomerized eicosatetraenoic acid with those of the alkali-isomerized arachidonic acid indicates that the greater part of the double bond in the

9) A. J. Fulco and J. F. Mead, *J. Biol. Chem.*, **234**, 1411 (1959).

Table II. Spectrophotometric absorption of alkali-isomerized products of the acids

| Wavelength mμ | Specific extinction coefficient | | |
|---|---|---|---|
| | Eicosatrienoic Found | Eicosatetraenoic | |
| | | Found | Reported* |
| 233 | 76.5 | 45.2 | 39.7 |
| 268 | 13.0 | 49.0 | 48.2 |
| 316 | 0 | 55.8 | 60.6 |

* Reported data for arachidonic acid in Ref. 14.

eicosatetraenoate belongs to the divinyl methylene system, for a double bond separated by more than 2 carbons can not be isomerized to the conjugated position with an adjacent double bond by alkali treatment. The oxidation of the eicosatrienoate by the periodate-permanganate reagent[10] gave mainly glutaric acid (96%) indicating the insertion of five carbon atoms between the carboxyl group and the first double bond in the eicosatetraenoate. The eicosatetraenoate fraction did not indicate the peak of a trans double bond in infrared spectrophotometric analysis. We may conclude, then, that the eicosatetraenoic acid from the liver lipids of rats of group II consists chiefly of arachidonic acid.

The data in Table II shows that more than 80% of the eicosatrienoate was changed to conjugated diene, not triene, by alkali isomerization; these data support the idea that the triene consisted chiefly unchanged 5,11,14-eicosatrienoate.

Further studies using the isotopic tracer technique are being planned in this laboratory in order to get direct evidence for the dehydrogenation and reliable knowledge concerning the effect of 5,11,14-eicosatrienoic acid as a new essential fatty acid.

## Experimental

**Materials.**—*Ethyl All-cis-5,11,14-Eicosatrienoic Acid.*—The ether extract (1.4 kg.) from *Podocarpus nagi* seeds was saponified with 4 l. of 10% ethanolic potassium hydroxide, and the free acids were esterified by refluxing them with 4 l. of 1% sulfuric acid - ethanol for 1 hr. The ethyl ester (1362 g.) was fractionally distilled through a glass column packed with stainless steel helices (1.5 cm. in diameter, 1 m. long) and with a heated jacket under 0.5—1 mmHg. Each fraction was analyzed by gas chromatography; a C-20 fraction (251 g.) containing less than 0.5% C-18 acid was collected. Further fractionation at 0—−20°C by the urea adduct method,[5] followed by distillation, yielded 70 g. of the eicosatrienoate, which was found to be 99.6% pure by gas chromatography.

*Ethyl Linoleate.* — Linoleate was prepared from safflower oil by the urea adduct method.[11] A gas

10) E. von Rudloff, *Can. J. Chem.*, **34**, 1413 (1956); C. G. Youngs, *J. Am. Oil Chem. Soc.*, **38**, 62 (1961).

11) J. G. Keppler, S. Sparreboom, J. B. A. Strorick and J. D. von Mikusch, *J. Am. Oil Chem. Soc.*, **36**, 38 (1959); A. R. Johnson and G. M. Ali, ibid., **38**, 453 (1961).

chromatographic analysis of the ester exhibited no peak other than that of linoleate.

*The Analysis of Fatty Acids.*—The livers were homogenized and extracted with chloroform-methanol (2:1 v/v) according to Folch's method.[12] The lipid extracted was then saponified by refluxing it for 1 hr. with 10% ethanolic potassium hydroxide. The fatty acids obtained from the saponified mixture were esterified by refluxing for 1 hr. with a 1% sulfuric acid - methanol solution. The esters obtained were then analyzed by gas chromatography using a stainless steel column, 6 min. in diameter and 2.25 m. long, packed with diethyleneglycol succinate-Celite 545 (60—80 mesh) (1 : 5 w/w) and with a hydrogen-flame-ionization detector. The remaining esters were separated according to column chromatography by the de Vries method.[13] The adsorbent was prepared by impregnating 100 g. of silicic acid with 200 ml. of 50% of an aqueous solution of silver nitrate. It was then filtered to remove the excess of the solution and activated at 120°C for 16 hr. Twenty grams of the adsorbent was packed into the glass tube using hexane and a hexane solution of the methyl ester (300 mg.) was added to the column. The sample was fractionated by step-by-step elution with 0—100% diethyl ether - hexane, and then the eicosatrienoate and the eicosatetraenoate were collected from the eluates. Their purities were found to be higher than 97% by gas chromatography. A portion was then isomerized by heating it with 11 g. of potassium hydroxide-ethyleneglycol for 15 min., after which the methanol solution of the products was subjected to spectrophotometric measurements according to the Herb method.[14] The other portion was oxidized by the periodate-permanganate method.[10] Ten milligrams of the sample in 20 ml. of *t*-butanol was added to 13.5 ml. of the periodate-permanganate reagent, which contained sodium periodate (284 mg.), potassium permanganate (1.10 mg.) and potassium carbonate (16.7 mg.), and the solution was refluxed for 1 hr. After the excess oxidizing reagent and *t*-butanol had been removed, the products were acidified and extracted with ether. The methyl esters were then analyzed by gas chromatography.

12) J. Folch, N. Lees and G. H. Sloane-Stanley, *J. Biol. Chem.*, **226**, 497 (1957).
13) B. De Vries, *Chem. & Ind.*, **1962**, 1049; *J. Am. Oil Chem. Soc.*, **40**, 184 (1963).
14) S. F. Herb and R. W. Riemenschneider, *Anal. Chem.*, **25**, 953 (1953).

## Summary

Ethyl 5,11,14-eicosatrienoate has been fed to fat-deficient rats. The gas chromatographic analysis of the fatty acids in the liver lipids and the alkali isomerization and oxidation scission of the eicosatetraenoate separated from the fatty acid has given evidence for the transformation of all-*cis*-5,11,14-eicosatrienoate to arachidonate.

The author wishes to thank Professor Emeritus Yoshiyuki Toyama of this university; Mr. Yoshito Koyama of the Food Research Institute, Aichi Prefecture for providing *Podocarpus nagi* seed oil; the Ono Pharmaceutical Co. for its financial support and for the sending an experimental assistant, and Dr. Kazuo Fukuzumi for his discussions.

*Department of Applied Chemistry*
*Faculty of Engineering*
*Nagoya University*
*Chikusa-ku, Nagoya*

# The Condensation Product of Monomethylammonium 6-Aminosalicylate with Acetone[1),*]

By Kazutoshi YAMADA and Noboru SUGIYAMA

(Received March 15, 1965)

In previous papers it has been demonstrated that the 8-quinolinecarboxylic acid derivative was obtained by the reaction between the ammonium salt of 6-amionsalicylic acid (II) and $\beta$-diketone at room temperature,[2)] and that the reaction of ammonium salt of II with ethyl acetoacetate gave 4,7-dihydroxy-2-methyl-8-quinolinecarboxylic acid as a major product.[3)]

While the reaction of ammonium or ethylammonium 6-aminosalicylate with acetone has been demonstrated to give a compound I (R=H or $C_2H_5$),[4,5] the reaction of methylammonium 6-aminosalicylate with acetone has not yet been

1) K. Yamada, Presented at the 15th Annual Meeting of the Chemical Society of Japan, Kyoto, April, 1962.

* Part III in the series of Condensation of Aminosalicylic Acid Salts.

2) K. Yamada, *Sci. Paper of the Inst. Pys. & Chem. Res.*, **56**, 101 (1962).

3) K. Yamada, ibid., **56**, 109 (1962).

4) K. Yamada and S. Seki, *J. Chem. Soc. Japan, Pure Chem. Soc. (Nippon Kagaku Zasshi)*, **82**, 1368 (1961).

5) K. Tamura, N. Sugiyama, S. Seki, K. Taya and K. Yamada, ibid., **80**, 662 (1959).

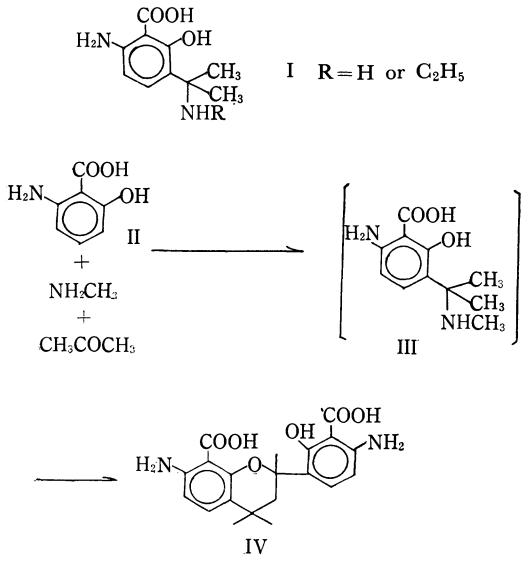



Fig. 1

studied. If the latter reaction proceeds as does the former, the III substance may be expected. Actually, however, the reaction product has not proved to be III.

Monomethylammonium 6-aminosalicylate was dissolved in acetone, and the solution was allowed to stand at room temperature. From this solution a solid was obtained. By purification with petroleum ether - ether, IV was obtained. IV could not be recrystallized from any solvents unless ether was added. IV was, however, readily susceptible to air-oxidation. The fact that flavan derivatives give a crystalline complex with ether is well-known.[6] This fact, plus the analogy of the reaction of ammonium or ethylammonium 6-amionsalicylate with acetone, suggests that this compound is a flavan derivative such as IV.

The structure of IV was established as follows. It showed positive ferric chloride and Ehrlich-Herter tests. In addition, it was soluble in a sodium bicarbonate solution. The ultraviolet absorption spectrum of IV in ethanol had two absorption maxima, at 285 and 312 m$\mu$, which indicates no radical change from the ultraviolet spectrum of I. The infrared absorption spectrum in the KBr disk contained an amino band (3350 cm$^{-1}$), a hydroxyl band (3500—3200 cm$^{-1}$), a carbonyl band (1695 cm$^{-1}$) and a C–H out-of-plane deformation vibration band of the benzene ring (with two adjacent hydrogen atoms) (820 cm$^{-1}$). Its p$K_a'$ values were 3.9 (COOH) and 7.2 (COOH) in 55% methanol.[7] By treatment with pyridine - acetyl chloride, it afforded a diacetyl derivative, the infrared absorption spectrum of which contained a $\nu$C=O (acetamido) band (1665 cm$^{-1}$). Therefore, it was presumed that the condensation product has no conjugated system except benzene, and that it has one hydroxyl, two amino and two carboxyl groups.

When IV was refluxed in 10% hydrochloric acid, V was obtained. Its infrared absorption spectrum contained bands of amino and hydroxyl groups (3350 cm$^{-1}$), and a C–H out-of-plane deformation vibration of the benzene ring (with one and two adjacent hydrogen atoms) (840 cm$^{-1}$), but the carbonyl band had disappeared. The Ferric chloride and Ehrlich-Herter tests were positive. Therefore, it was found to be a decarboxylated amino-hydroxyl compound. V was easily oxidized by air and changed to a sticky substance.

The diazotization of the amino-hydroxy compound V, followed by the Sandmeyer reaction,[8] resulted in the formation of the dichloro compound (VI). VI was then catalytically reduced with palladium black to a halogen-free compound (VII). The infrared absorption spectrum of VII showed a hydroxyl band (3300 cm$^{-1}$) and a C–H out-of-plane deformation band (with four adjacent hydrogen atoms) (750 cm$^{-1}$). The molecular weight of VII was 260 (by Rast method). Therefore, the compound IV is probably a dimer of 3-isopropenyl-6-aminosalicylic acid. The $\lambda_{max}$ value (282 m$\mu$) of VII in ethanol was shifted to 290 m$\mu$ in a 0.5 N sodium hydroxide solution. Since hindered or partially-hindered phenols usually show a bathochromic shift of 10—20 m$\mu$ in a 0.5 N alkaline solution,[9,10] the structure VII with a hindered hydroxyl group is sufficient to explain the 8 m$\mu$ shift. The NMR spectrum in carbon tetrachloride had a sharp singlet at 8.67 $\tau$ (6 : methyl protons of *gem*-dimethyl groups),[11,12] a singlet at 8.45 $\tau$ (3: methyl protons) and a singlet at 5.01 $\tau$ (hydroxyl proton), as well as complex multiplets at 8.2—8.4 $\tau$ (2: aliphatic protons) and 2.8—3.2 $\tau$ (8: aromatic protons).[13] Thus, the NMR data are consistent with the structure of 2'-hydroxy-2,4,4-trimethylflavan. The behavior of forming crystalline adducts with ether was characteristic of flavans.[14,15] The methylation of

6) K. Fries, *Ber.*, **41**, 371 (1908).
7) H. C. Brown, "Determination of Organic Structures by Physical Methods," Academic Press, New York (1955), p. 567.
8) T. Sandmeyer, *Ber.*, **17**, 1633 (1884).
9) N. D. Coggeshall and A. S. Glessner, *J. Am. Chem. Soc.*, **71**, 3150 (1949).
10) H. Hart, J. L. Corbin, C. R. Wagner and C. Y. Wu, ibid., **85**, 3269 (1963).
11) H. Hart, J. L. Corbin, C. R. Wagner and C. Y. Wu, ibid., **85**, 3270 (1963).
12) T. F. Wood, W. M. Easter, M. S. Carpenter and J. A. Angiolini, *J. Org. Chem.*, **28**, 2248 (1963).
13) J. A. Pople, "High-resolution Nuclear Magnetic Resonance," McGrow-Hill, New York (1959); E. J. Corey, E. M. Philbin and T. S. Wheeler, *Tetrahedron letters*, **1961**, 429.
14) W. Baker, R. F. Curtis and J. F. W. McOmie, *J. Chem. Soc.*, **1951**, 76; W. E. Noland, C. G. Richards, H. S. Desai and M. R. Venkiteswaran, *J. Org. Chem.*, **26**, 4254 (1961).
15) Many solvents are known to form the same adduct compounds with flavans. Since all such solvents are proton acceptors, salt formation or hydrogen bonding involving the 2'-hydroxyl group or ring oxygen may play a part in the formation of the 1 : 1 type adducts (over 40 examples are now known).

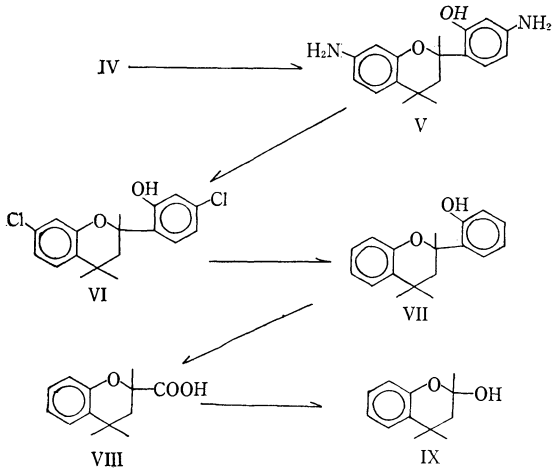



Fig. 2

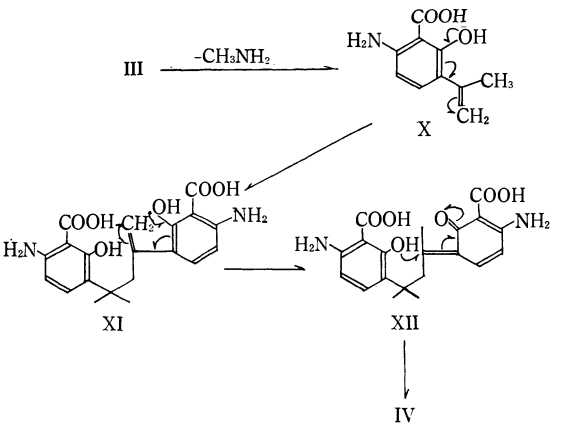



Fig. 3

VII with diazomethane gave a monomethoxy compound. Its infrared absorption spectrum did not show a hydroxyl band.

Compound VII was oxidized with potassium permanganate to an acid VIII. If the structure of VII is hydroxyflavan, the oxidized compound VIII should be chromancarboxylic acid. Its infrared absorption spectrum showed the group frequencies which characterize an acid carbonyl group, and a C–H out-of-plane deformation vibration of the benzene ring (with four adjacent hydrogen atoms). The ultraviolet absorption maxima in ethanol appeared at 226.5, 274.5 and 281.5 m$\mu$. The melting point of VIII coincided well with that of the literature.[16]

The decarboxylation of the acid VIII by the usual method was very difficult. When, however, a mixture of VIII and copper chromite in quinoline was heated, the compound $C_{12}H_{16}O_2$ (IX) was formed by the loss of carbon monoxide. The melting point and infrared absorption spectrum of this compound were identical with those of 2-hydroxy-2,4,4-trimethylchroman. The loss of carbon monoxide by heating in quinoline with copper chromite is frequently observed in this type of compound.[14] These degradation reactions and physical properties are consistent with the structure of IV, 7, 4'-diamino-2'-hydroxy-2, 4, 4-trimethylflavan-8, 3'-dicarboxylic acid.

It is known that the flavan derivative is obtained by the reduction of naturally-occurring flavon derivatives or by the cyclization of allyl ethers. The reaction of methylammonium 6-aminosalicylate with acetone presents another new method of preparing the flavan derivative.

The mechanism of the condensation reaction of monomethylammonium 6-aminosalicylate with acetone is considered to be following. Much as in the reaction of ammonium 6-aminosalicylate with acetone, it is probable that at the first stage 6-aminosalicylate produces an unstable intermediate III. III can readily lose its methylamino on account of its hyperconjugation by methyl group to give the 3-isopropenyl derivative X, which, in turn, can dimerize by means of proton transfer and electron rearrangement. The ready dimerization of 3-isopropenyl salicylic acid[5] and its derivatives would support this mechanism. The dimer XI (enol form), is probably in keto-enol equilibrium with the reactive form, XII, containing the more highly-substituted (and the more sterically-hindered) double bond. The process of cyclization is shown in Fig. 3. This is supported by the fact that the dimerization of the vinyl compound is promoted by an acid catalyst.

## Experimental

**4', 7-Diamino-2'-hydroxy-2, 4, 4-trimethylflavan-3', 8-dicarboxylic Acid (IV).**—A solution of methylammonium salt of 6-aminosalicylic acid,[17] which had been obtained from 10 g. of II, as has been described before,[2] in 50 ml. of dry acetone was allowed to stand at room temperature for one week. During this time, crystals were gradually separated. These crystals were then collected and dissolved in a 1 N sodium hydroxide solution. After neutralization with dilute hydrochloric acid, the solution was extracted with ether. The ether solution was dried with anhydrous sodium sulfate, and the ether was removed. The residue was recrystallized from petroleum ether with a small amount of ether. Pale yellow fine needles, m. p. 97°C (decomp.) were obtained. Yield, 3 g.

Found: C, 62.4; H, 6.98; N, 5.98. Calcd. for $C_{20}H_{22}O_6N_2 \cdot (C_2H_5)_2O$: C, 62.6; H, 7.01; N, 6.08%.

It was very sensitive to oxygen. Even in the crystalline state, it soon changed from colorless to red. A ferric chloride test was positive (dark red). Ehrlich-Herter and sodium nitroprusside tests were positive. UV: $\lambda_{max}^{EtOH}$ 265, 330 m$\mu$. IR: 3500—3200, 3350, 1695

16) W. Baker and J. C. McGowan, *J. Chem. Soc.*, **1952**, 1781; **1938**, 347.

17) K. Yamada, K. Taya and S. Seki, *J. Chem. Soc. Japan, Pure Chem. Sec.* (*Nippon Kagaku Zasshi*), **83**, 107 (1962).

820 $cm^{-1}$.[18] $pK_a'$: 3.9 (COOH) and 7.2 (COOH) in 55% methanol.[19] IV gave a diacetyl derivative with pyridine-acetyl chloride. IR: 1665 $cm^{-1}$ (acetamido carbonyl).

**4', 7-Diamino-2'-hydroxy-2, 4, 4-trimethylflavan (V).**—A suspension of 1.3 g. of IV in 20 ml. of 10% hydrochloric acid was refluxed for 5 hr. Carbon dioxide thus evolved vigorously. The neutralization of the resulting solution with a dilute sodium hydroxide solution separated precipitates, which were then recrystallized from petroleum ether-ether. Pale yellow needles, m. p. 177—180°C (decomp.), were obtained. Yield, 0.8 g.

Found: C, 70.6; H, 8.59; N, 7.30. Calcd. for $C_{18}H_{22}O_2N_2 \cdot (C_2H_5)_2O$: C, 71.0; H, 8.74; N, 7.41%.

Ferric chloride and Ehrlich-Herter tests were positive. UV: $\lambda_{max}^{EtOH}$ 235, 325 m$\mu$. IR: 3350, 840 $cm^{-1}$.

**4', 7-Dichloro-2'-hydroxy-2, 4, 4-trimethylflavan (VI).**—To a solution of 2 g. of V in a mixture of 15 ml. of concentrated hydrochloric acid and 15 ml. of water was dropped a solution of 0.6 g. of sodium nitrite in 2 ml. of water at 0—5°C with shaking. To the reaction mixture was then added a cuprous chloride solution, prepared from 9 g. of copper sulfate. After it had been kept at 60°C for 5 min., this solution was cooled in an ice bath. The precipitates were collected and recrystallized from light petroleum. Rhombic crystals, m. p. 135°C, were obtained. Yield, 1.1 g.

Found: C, 64.1; H, 5.3; Cl, 20.8. Calcd. for $C_{18}H_{18}O_2Cl_2$: C, 64.1; H, 5.3; Cl, 21.1%.

IR: 3380, 850 $cm^{-1}$. A ferric chloride test was positive.

**2'-Hydroxy-2, 4, 4-trimethylflavan (VII).**—A solution of 0.5 g. of dichloro-flavan (VI) in 10 ml. of methanol was reduced with hydrogen at an atmospheric pressure of 10 in the presence of 0.5 g. of palladium black and 0.3 g. of powdered anhydrous sodium acetate for 8 hr. To the filtered solution water was then added until all the precipitates had been separated. The recrystallization of the precipitates from petroleum ether gave prisms, m. p. 99°C. Yield, 0.25 g.

Found: C, 80.1; H, 7.6; mol. wt. (Rast), 260. Calcd. for $C_{18}H_{20}O_2$: C, 80.6; H, 7.5%; mol. wt. 268.

A ferric chloride test was positive. IR: 330, 750 $cm^{-1}$.

This compound was characterised as the $-OCOCH_3$ derivative; hexagonal prisms; m. p. 96°C.

Found: C, 81.8; H, 7.3. Calcd. for $C_{20}H_{22}O_2$: C, 81.6; H, 7.53%.

UV: $\lambda_{max}^{EtOH}$ 230, 282 m$\mu$.

**2, 4, 4-Trimethylchroman-2-carboxylic Acid (VIII).**—A solution of 1 g. of VII in 10 ml. of acetone was oxidized by the rapid addition of potassium permanganate in 300 ml. of acetone. The mixture boiled spontaneously, and the oxidation reaction was completed in 5 min. After the acetone had been removed, 50 ml. of water, 13 g. of sodium pyrosulfite and 13 ml. of 2 N hydrochloric acid were added to the residue. Sulfur dioxide was then passed in until the mixture became colorless. The mixture was extracted with ether. The ether solution was washed with water and extracted with four 5 ml. portions of a saturated sodium bicarbonate solution. The aqueous layer was washed with 10 ml. of ether and then acidified with hydrochloric acid. Pale yellow solid precipitates were collected at 0°C. Recrystallization from benzene gave an acid, VIII; 0.15 g.; rhombs; m. p. 172°C. UV: $\lambda_{max}^{EtOH}$ 226.5, 274.5, 281.5 m$\mu$. IR: 1695, 758 $cm^{-1}$. $pK_a'$: 4.6 (COOH) in 62% methanol. The structures of VIII and its methyl derivative were confirmed by their melting point infrared and ultraviolet absorption spectra.

**The Reaction of 2, 4, 4-Trimethylchroman-2-carboxylic Acid with Copper Chromite-Quinoline.**—A mixture of 0.3 g. of the acid VIII, 0.5 ml. of freshly-distilled quinoline, and 0.5 g. of copper chromite were refluxed for 20 min. The cooled mixture was then poured into 15 ml. of concentrated hydrochloric acid. After the mixture had been heated on a boiling water-bath for 15 min., 20 ml. of water was added. The solid precipitates which separated were filtered off through sand and washed with 30 ml. of ether. The aqueous layer was then extracted with three 10 ml. portions of ether. After the substance had been shaken with 10 ml. of a saturated sodium bicarbonate solution, the ether was removed. The oily residue, which soon solidified, was recrystallized from petroleum ether. Prisms, m. p. 90°C, were obtained. The melting point of IX was the same as that of the literature.[16]

Found: C, 75.5; H, 8.6. Calcd. for $C_{12}H_{16}O_2$: C, 75.0; H, 8.3%. UV: $\lambda_{max}^{EtOH}$ 274, 279 m$\mu$. IR: 3440, 750 $cm^{-1}$.

The authors wish to thank Professor Kunisaburo Tamura and Dr. Shigeo Seki for their helpful discussions.

*Department of Chemistry*
*Faculty of Science*
*Tokyo University of Education*
*Bunkyo-ku, Tokyo*

18) The IR absorption spectra were recorded with a Nihon Bunko Model DS 301 and Hitachi Model S-2 spectrophotometers. The UV absorption spectra were recorded with a Hitachi Model EPS-2 spectrophotometer; a pair of 1 cm. quartz cell was used. The NMR spectra were measured with a Nihon-denshi type NMR spectrometer equipped with a 60 Mc.

19) All p*Ka'* measurements were carried out at 25±1°C with a Radiometer (Copenhagen) type SBR-2/SBU-1/TTT-1/TTA-2 titration equipment.

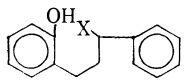
# The Condensation Products of Acetamidophenol with Acetone[1),*]

By Kazutoshi YAMADA and Noboru SUGIYAMA

(Received March 15, 1965)

In a previous paper,[2)] the reaction of methylammonium 6-aminosalicylate with acetone at room temperature was found to afford the aminoflavan derivative. The process of the formation of this derivative was explained by a dimerization mechanism of the intermediate isopropenyl compound.

Though it is known that flavan derivatives are synthesized through the dehydration of phenyl-(*o*-hydroxyphenylethyl)-carbinol derivatives (Ia) or through the dehydrohalogenation of halogen compounds such as Ib, these methods are accompanied by too many side reactions and too many difficulties for purification to be possible. In 1905 Fabinyi and Szeky obtained the so-call "Dragon's blood" by reacting phenols with acetone in an acidic medium.[3)] Their structures were studied by Baker



Ia X=OH
Ib X=halogen

Fig. 1.

and explained as flavan derivatives.[4)] Both of these projects, however, reported methods of obtaining flavan derivatives which are not satisfactory for practical purposes.

It has been found that aminoflavan derivatives are obtained easily by the acidic condensation of acetamidophenols with acetone. *m*-Acetamidophenol (II) was, therefore, dissolved in a large amount of acetone and heated at 50°C, and then dry hydrogen chloride gas was passed in. From the reaction mixture, a crystalline substance IV was obtained. Its ultraviolet absorption spectrum showed $\lambda_{max}$ 250, 287 m$\mu$. Compared with the absorption of II ($\lambda_{max}$ 246, 284 m$\mu$), no radical change was observed. Its infrared absorption spectrum showed absorptions at 1670 cm$^{-1}$ ($\nu$C=O, acetamido), 3380 cm$^{-1}$, and 3240 cm$^{-1}$ ($\nu$OH, $\nu$NH). As the ferric chloride test is positive, the existence of phenolic hydroxyl is evident. The position of each substituent can easily be estimated by the C–H out of plane deformation vibration band of the benzene ring (with one or two adjacent H atoms).[5)]

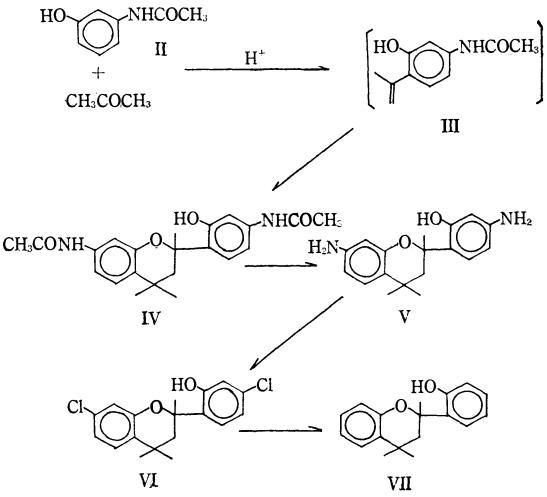


Fig. 2.

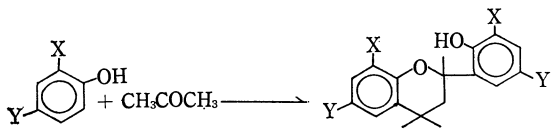
In order to determine the structure of IV, the following experiments were carried out. The refluxing of a suspension of IV in 10% hydrochloric acid for 5 hr. yielded a compound V. The ferric chloride test and Ehrlich-Herter test of V were positive, and its infrared absorption spectrum showed hydroxyl and amino groups. The ultraviolet absorption maximum of V coincided with that of 4', 7-diamino-2'-hydroxy-2, 4, 4-trimethylflavan. V was not stable in the air, however, it turned black at room temperature.

V was deaminated to a stable derivative as follows. It was diazotized, and then chlorinated to VI by the Sandmeyer method.[6)] VI was then catalytically dechlorinated to VII at room temperature with palladium black, which did not show any melting point depression when mixed with authentic 2'-hydroxy-2, 4, 4-trimethylflavan.[2)] Moreover, its infrared sbsorption spectrum also coincided completely with that of this authentic sample. Therefore, the structure of IV was identified as 4',7-diacetamido-2'-hydroxy-2, 4, 4-trimethylflavan. Furthermore, the NMR spectrum of IV in carbon tetrachloride had a sharp singlet at 8.67$\tau$ (6: methyl protons of *gem*-dimethyl groups), a singlet at 8.54$\tau$ (3: methyl protons), singlet at 5.01$\tau$ (a hydroxyl proton), a doublet at 7.85$\tau$ (6: methyl protons of *N*-acetyl groups),[7)] a multiplet at 8.3—8.5$\tau$ (2:

1) K. Yamada, Presented at the 16th Annual Meeting of the Chemical Society of Japan, Tokyo, April, 1963.
* Part IV in the series of Condensation of Aminosalicylic Acid Salts.
2) K. Yamada, This Bulletin, **38**, (1965).
3) I. Fabinyi and T. Széky, *Ber.*, **38**, 2307 (1905).
4) W. Baker and J. C. McGowan, *J. Chem. Soc.*, **1938**, 347.
5) W. West, "Chemical Application of Spectroscopy," Interscience Publications, New York (1956).
6) T. Sandmeyer, *Ber.*, **17**, 1633 (1884).
7) L. D. Roberts, "Nuclear Magnetic Resonance," Applications to Organic Chemistry, McGrow-Hill, New York (1960).

aliphatic protons) and complex multiplets at 2.8—3.2$\tau$(6: aromatic protons).[8] Thus, the NMR data also was consistent with the structure of 4', 7-diacetamido-2'-hydroxy-2, 4, 4-trimethylflavan.

A similar condensation reaction was applied to the *o*- and *p*-isomers of II. When *o*-acetamidophenol (VIII) and acetone were subjected to condensation by hydrogen chloride, a condensate (IX) was obtained. Its ultraviolet absorption maxima were at 248 and 286 m$\mu$. Infrared absorptions were observed at 1668 $cm^{-1}$ ($\nu$C=O), 3389 $cm^{-1}$ ($\nu$OH), and 3300 $cm^{-1}$ ($\nu$NH) respectively. From these results, IX was identified as 3', 8-diacetamido-2'-hydroxy-2, 4, 4-trimethylflavan.

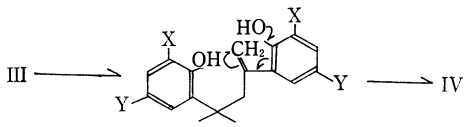


VIII X=NHCOCH$_3$, Y=H  IX X=NHCOCH$_3$, Y=H
X X=H, Y=NHCOCH$_3$  XI X=H, Y=NHCOCH$_3$

Fig. 3.

From *p*-acetamidophenol (X) and acetone 5', 6-diacetamido-2'-hydroxy-2, 4, 4-trimethylflavan (XI) was obtained. Its ultraviolet and infrared absorption were similar to those of IX.

As an intermediate product of the condensation reaction of II with acetone, III was considered. This process is supported by the formation of the flavan derivative from isopropenyl phenol in an acidic medium.[9] If Schnell's polymerization mechanism of vinyl compounds holds true, XII may be produced by the dimerization of III, and, further, will form a ring to yield IV. According to this mechanism, it is probable that isomeric acetamido-2-isopropenylphenol will be produced, however, due to the steric effect of the acetamido group, it is very difficult to produce it. The fact that the yields of the IX, IV, and XI condensates from *o*-, *m*- and *p*-acetamidophenol were 1.4, 5.2 and 4.7% respectively also supports the isopropenyl intermediate mechanism.



XII X=H or NHCOCH$_3$, Y=NHCOCH$_3$ or H

Fig. 4.

8) J. A. Pople W. G. Schneider and H. J. Bernstein "High-resolution Nuclear Magnetic Resonance," McGrow-Hill, New York (1959); E. J. Corey, E. M. Philbin and T. S. Wheeler, *Tetrahedron Letters*, **1961**, 429.

9) N. Sugiyama, K. Taya, *J. Chem. Soc. Japan, Pure Chem. Sec.* (*Nippon Kagaku Zasshi*), **80**, 673 (1959); W. Baker and D. M. Besly, *J. Chem. Soc.*, **1940**, 1103; W. E. Noland, C. G. Richards, H. S. Desai and M. R. Venkiteswaran, *J. Org. Chem.*, **26**, 4254 (1961).

## Experimental

**4', 7-Diacetamido-2'-hydroxy-2, 4, 4-trimethylflavan (IV).**—A mixture of *m*-acetamidophenol and 30 ml. of acetone was saturated with dry hydrogen chloride, and then kept at 50°C for 2 days. After the acetone had been removed, a dark red substance was obtained. After an excess of 20% sodium hydroxide solution had then been added to this substance, the mixture was stirred vigorously overnight. After filtration, the sodium hydroxide solution was acidified and next extracted with 250 ml. of ethyl acetate. The ethyl acetate solution was dried with sodium sulfate. After the distillation of ethyl acetate, the residue became a sodid. It was then purified by chromatography (alumina-acetone). After the acetone had been removed, the residual solid substance was recrystallized from ether-petroleum ether. Small rhombic crystals (IV), m. p. 165°C (decomp.), were obtained. Yield, 1.6 g.

Found: N, 6.01. Calcd. for $C_{22}H_{26}O_4N_2\cdot(C_2H_5)_2O$: N, 6.14%. This substance has 1 mol. of the ether of crystallization. It loses the ether of crystallization even upon standing in air, becoming opaque and sticky. UV: $\lambda_{max}^{EtOH}$ 250, 287 m$\mu$. IR: 3380, 3240, 1670, 870, 830 $cm^{-1}$.

**4', 7-Diamino-2'-hydroxy-2, 4, 4-trimethylflavan (V).**—A suspension of 1 g. of IV in 20 ml. of 10% hydrochloric acid was refluxed for 5 hr. Neutralization with an aqueous sodium hydroxide solution produced percipitates. Recrystallization from petroleum ether-ether then gave pale yellow needles (V), m. p. 179.5°C (decomp.). Yield, 0.3 g.

Found: N, 7.23. Calcd. for $C_{18}H_{22}O_2N_2\cdot(C_2H_5)_2O$: N, 7.41%. The ferric chloride test and Ehrlich-Herter test were positive. UV: $\lambda_{max}^{EtOH}$ 236, 325 m$\mu$. IR: 3400, 3100, 880, 830 $cm^{-1}$.

**2'-Hydroxy-2, 4, 4-trimethylflavan (VII).**—Diaminoflavan (V) was converted into a dichloro compound according to the method described in a previous paper.[2] The dichloroflavan in methanol was dechlorinated with hydrogen at an atmospheric pressure of 5 in the presence of palladium black and powdered anhydrous sodium acetate for 10 hr. The dechlorinated substance (VII) was then recrystallized from petroleum ether-ether. M. p. 98°C.

Found: C, 80.3; H, 7.4. Calcd. for $C_{18}H_{20}O_2$: C, 80.6; H, 7.5%. A mixed melting point determination with an authentic sample showed no depression (98°C), and its infrared and ultraviolet absorption spectra were identical with those of 2'-hydroxy-2, 4, 4-trimethylflavan.

**3', 8-Diacetamido-2'-hydroxy-2, 4, 4-trimethylflavan (IX).**—A mixture of 10 g. of *o*-acetamidophenol and 30 ml. of acetone was saturated with dry hydrogen chloride, and then kept at 50°C for a week, after which time the solution was treated in a manner similar to that described for IV. Yellow needles (IX), m. p. 146.5°C (decomp.), were obtained.

Found: N, 5.92. Calcd. for $C_{22}H_{26}O_4N_2\cdot(C_2H_5)_2O$: N, 6.14%. UV: $\lambda_{max}^{EtOH}$ 248, 286 m$\mu$. IR: 3340, 1668, 750 $cm^{-1}$. On standing in air, the crystals lost some of the ether of crystallization and became sticky. Yield, 0.4 g.

10) UV, IR, NMR and p$K_a'$ were measured with the same apparatus as the previous paper.[2]

**5′, 6-Diacetamido-2′-hydroxy-2, 4, 4-trimethylflavan (XI).**—The reaction of 5 g. of *p*-acetamidophenol with acetone under the same conditions as above afforded 5′,6-diacetamido-2′-hydroxy-2, 4, 4-trimethylflavan (XI), m. p. 85°C (decomp.). Yield, 0.7 g.

Found: N, 6.02. Calcd. for $C_{22}H_{26}O_4N_2 \cdot (C_2H_5)_2O$: N, 6.14%. UV: $\lambda_{max}^{EtOH}$ 250, 291 m$\mu$. IR: 3390, 1664, 875 (w.), 825 cm$^{-1}$.

The authers wish to thank Dr. Yoshimori Omote and Miss Yo Saiga for their helpful discussions.

*Department of Chemistry*
*Faculty of Science*
*Tokyo University of Education*
*Bunkyo-ku, Tokyo*

# Studies on Geometric Isomerism by Nuclear Magnetic Resonance. II.[1] Geometric Configurations of Alkylidenecyanoacetic Esters

By Toshio HAYASHI, Minoru IGARASHI, Shoichi HAYASHI and Hiroshi MIDORIKAWA

(Received March 30, 1965)

A number of studies of the mechanism of the Knoevenagel reaction has been published,[2-9] but little information is available concerning the stereochemistry of the reaction. Baker and Howes[10] have shown that the condensation of salicylaldehyde or its methyl ether with cyanoacetic acid or its ester gives only the isomers with the trans configuration.[11] However, this study has so far not been extended to alkylidenecyanoacetic esters.

In the preceding paper, the present authors have reported the successful application of the NMR technique to the configurational determinations of the compounds of the $R_1(R_2O)C=C(CN)\cdot COOR_3$ type. Therefore, it seems that it would be interesting to apply this technique to alkylidenecyanoacetic esters of the $R_1MeC=C(CN)COOR_2$ type.

For the present purpose, it is assumed that the $\beta$-methyl[12] signal of an isomer of these esters consists of only one peak, due to the absence of any resolved spin-spin coupling across the C=C bond. Hence, the esters of this type are believed to be a class of compounds which is suitable for studies of cis-trans isomerism. However, since no stereoisomer of a known configuration was available, the assignment of each of two signals for the $\beta$-methyl group to the correct stereoisomer had to be based on the previous assumption,[1] which states that the chemical shift for the $\beta$-methyl group occurs at a higher field in the trans- than in the cis-configuration with respect to the alkoxycarbonyl group, whereas the reverse is true for the $\gamma$-methyl group. The results obtained have been supported by the relative stability of the isomers.

## Experimental

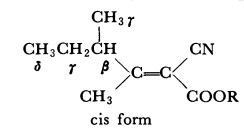
**Materials.**—All the alkylidenecyanoacetic esters examined were prepared according to the method of Cope.[9] Each compound was distilled under reduced pressure at least twice, and the boiling points and nitrogen contents were checked against the literature values.

An equilibrium mixture of cis-trans isomers was obtained by the addition of a trace amount of sodium ethoxide, after which the mixture was allowed to stand at room temperature for at least one week.

**NMR Spectra.**—All NMR spectra were taken with a JNM-C-60 high-resolution NMR spectrometer working

1) Part I: T. Hayashi, I. Hori, H. Baba and H. Midorikawa, *J. Org. Chem.*, **30**, 695 (1965). Presented partly at the 3rd Symposium on NMR, Osaka, November, 1963.
2) E. Knoevenagel, *Ann.*, **281**, 25 (1894).
3) A. C. O. Hann and A. Lapworth, *J. Chem. Soc.*, **85**, 46 (1904).
4) H. Rogerson and J. F. Thorpe, ibid., **87**, 1685 (1905).
5) V. J. Harding, W. N. Haworth and W. H. Perkin, ibid., **93**, 1943 (1908).
6) W. N. Haworth, ibid., **95**, 480 (1909).
7) C. K. Ingold, ibid., **119**, 329 (1921).
8) E. P. Kohler and B. B. Corson, *J. Am. Chem. Soc.*, **45**, 1975 (1923).
9) A. C. Cope, ibid., **59**, 2327 (1937).
10) W. Baker and C. S. Howes, *J. Chem. Soc.*, **1953**, 119.
11) By a trans isomer is meant the form in which the phenyl and carbonyl groups are on opposite sides of the C=C bond.

12) The notations used here to distinguish the various methyl and methylene groups are shown below, each group being referred to as cis or trans with respect to the alkoxycarbonyl group. The isomer in which the $\beta$-methyl group and alkoxycarbonyl groups are on the same side of the C=C bond is referred to as the isomer.



cis form

at 60 Mc. and at a temperature of 19—20°C. The samples were examined in a ca. 8 per cent (w/v) solution in carbon tetrachloride, using tetramethylsilane as an internal reference. The chemical shifts are given as p. p. m. downfield from tetramethylsilane.

The data recorded in Table II were obtained by averaging the results of at least three measurements. The values are accurate to ±0.025 p. p. m,; the relative values between *cis*- and *trans*-β-methyl protons are accurate to ±0.005 p. p. m.

Table I. Properties of alkylidencyanoacetic esters

| Compound $R_1MeC{=}C(CN)COOR_2$ | $R_1$ | $R_2$ | B. p. °C/mmHg | Formula | Calcd. | Found. | Yield[a] % |
|---|---|---|---|---|---|---|---|
| I | Me | Me[b] | 98—99/6 | $C_7H_9O_2N$ | 10.07 | 10.27 | — |
| II | Me | Et[c] | 104—105/6 (m. p. 31°C) | $C_8H_{11}O_2N$ | 9.14 | 9.21 | — |
| III | Et | Me[d] | 107—108/7 | $C_8H_{11}O_2N$ | 9.14 | 9.07 | — |
| IV | Et | Et[e] | 119—120/11 | $C_9H_{13}O_2N$ | 8.38 | 8.33 | — |
| V | *n*-Pr | Me[f] | 116—117/6 | $C_9H_{13}O_2N$ | 8.38 | 8.24 | — |
| VI | *n*-Pr | Et[g] | 135—136/11 | $C_{10}H_{15}O_2N$ | 7.73 | 7.90 | — |
| VII | *i*-Pr | Me | 107—108/6 | $C_9H_{13}O_2N$ | 8.38 | 8.26 | 80 |
| VIII | *i*-Pr | Et[h] | 121—124/7 | $C_{10}H_{15}O_2N$ | 7.73 | 7.53 | — |
| IX | *i*-Bu | Et[i] | 119—120/8 | $C_{10}H_{15}O_2N$ | 7.73 | 7.49 | — |
| X | *i*-Bu | Et[j] | 121—122/5 | $C_{11}H_{17}O_2N$ | 7.17 | 7.10 | — |
| XI | *t*-Bu | Me | 117—120/11 | $C_{10}H_{15}O_2N$ | 7.73 | 7.50 | 7 |
| XII | *t*-$BuCH_2$ | Me | 127—128/6 | $C_{11}H_{17}O_2N$ | 7.17 | 7.08 | 70 |
| XIII | *t*-$BuCH_2$ | Et | 140—141/10 | $C_{12}H_{19}O_2N$ | 6.69 | 6.67 | 75 |

a) Yield is shown only for a new compound. b) lit.,[9] b. p. 99—101°C/9 mmHg. c) lit., m. p. 27—28°C, F. S. Prout, *J. Org. Chem.*, **18**, 928 (1953). d) lit.,[9] b. p. 105—106°C/9 mmHg. e) lit., b. p. 116—118°C/11 mmHg, A. C. Cope, C, Wyckoff and E. Hardenbergh, *J. Am. Chem. Soc.*, **63**, 3452 (1941). f) lit.,[9] b. p. 116—118°C/9 mmHg. g) lit., b. p. 138—139°C/19 mmHg, Ref. e. h) lit., b. p. 115—120°C/8 mmHg, A. Brändström, *Acta Chem. Scand.*, **13**, 963 (1959). i) lit.,[9] b. p. 119—123°C/9 mmHg. j) b. p. 130—133°C/12 mmHg, Ref. e.

Table II. NMR spectra of alkylidenecyanoacetic esters (p. p. m. downfield from TMS)

Compound, $R_1MeC{=}C(CN)COOR_2$

| | $R_1$ | $R_2$ | β-$CH_3$ | | β-$CH_2$ | | γ-$CH_3$ | | $COOCH_3$ | $COOCH_2\underline{CH_3}$ | $COO\underline{CH_2}CH_3$ |
|---|---|---|---|---|---|---|---|---|---|---|---|
| Ia | Me | Me | 2.31 | 0.09 | | | | | 3.81 | | |
| Ib | Me | Me | 2.40 | | | | | | | | |
| IIa | Me | Et | 2.31 | 0.09 | | | | | | 1.33 | 4.23 |
| IIb | Me | Et | 2.40 | | | | | | | | |
| IIIa | Et | Me | 2.28 | 0.09 | 2.59 | 0.03 | 1.13 | 0.06 | 3.79 | | |
| IIIb | Et | Me | 2.37 | | 2.57 | | 1.19 | | | | |
| IVa | Et | Et | 2.26 | 0.08 | 2.59 | 0.03 | 1.14 | 0.06 | | 1.33 | 4.23 |
| IVb | Et | Et | 2.34 | | 2.57 | | 1.20 | | | | |
| Va | *n*-Pr | Me | 2.27 | 0.08 | 2.76 | 0.20 | 0.99[a] | 0.03 | 3.80 | | |
| Vb | *n*-Pr | Me | 2.35 | | 2.56 | | 1.02 | | | | |
| VIa | *n*-Pr | Et | 2.27 | 0.07 | 2.76 | 0.20 | 1.00[a] | 0.03 | | 1.34 | 4.23 |
| VIb | *n*-Pr | Et | 2.34 | | 2.56 | | 1.03 | | | | |
| VIIa | *i*-Pr | Me | 2.17 | 0.07 | 3.97[b] | 0.65 | 1.10 | 0.06 | 3.80 | | |
| VIIb | *i*-Pr | Me | 2.24 | | 3.32 | | 1.16 | | | | |
| VIIIa | *i*-Pr | Et | 2.17 | 0.07 | 3.95[b] | 0.65 | 1.10 | 0.06 | | 1.33 | 4.23 |
| VIIIb | *i*-Pr | Et | 2.24 | | 3.29 | | 1.16 | | | | |
| IXa | *i*-Bu | Me | 2.26 | 0.08 | 2.66 | 0.26 | 0.92[a] | 0.06 | 3.80 | | |
| IXb | *i*-Bu | Me | 2.34 | | 2.40 | | 0.99 | | | | |
| Xa | *i*-Bu | Et | 2.25 | 0.07 | 2.66 | 0.26 | 0.93[a] | 0.05 | | 1.33 | 4.23 |
| Xb | *i*-Bu | Et | 2.32 | | 2.40 | | 0.98 | | | | |
| XIa | *t*-Bu | Me | 2.18 | 0.07 | | | 1.11 | 0.08 | 3.81 | | |
| XIb | *t*-Bu | Me | 2.25 | | | | 1.19 | | | | |
| XIIa | *t*-$BuCH_2$ | Me | 2.28 | 0.07 | 2.86 | 0.32 | 0.98[a] | 0.08 | 3.81 | | |
| XIIb | *t*-$BuCH_2$ | Me | 2.35 | | 2.54 | | 1.06 | | | | |
| XIIIa | *t*-$BuCH_2$ | Et | 2.28 | 0.07 | 2.86 | 0.32 | 0.98[a] | 0.08 | | 1.33 | 4.23 |
| XIIIb | *t*-$BuCH_2$ | Et | 2.35 | | 2.54 | | 1.06 | | | | |
| XIV | H | Et | 2.21 | | 2.41[c] | | | | | 1.33 | 4.22 |

a) The chemical shift of the δ-methyl protons. b) The chemical shift of the β-methine proton.
c) The chemical shift of the β-proton.

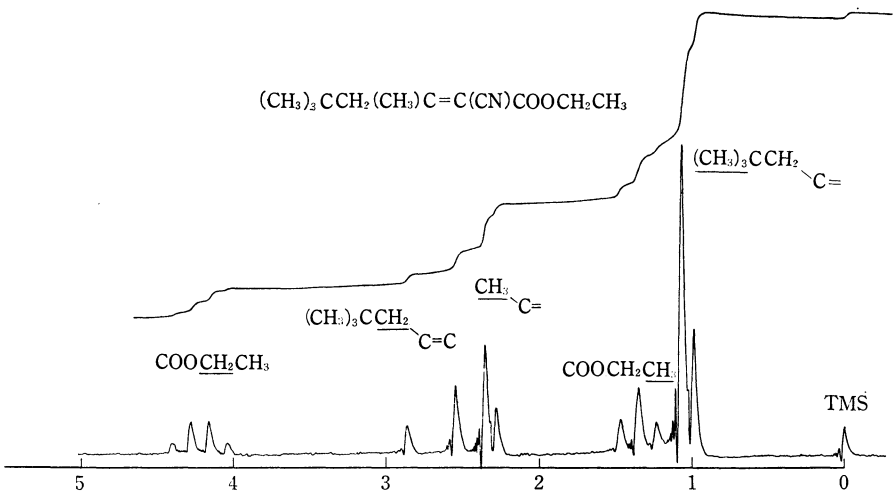



Fig. 1A. The NMR spectrum of a stereoisomeric mixture of ethyl $\alpha$-cyano-$\beta$-neopentylcrotonate at 19°C.

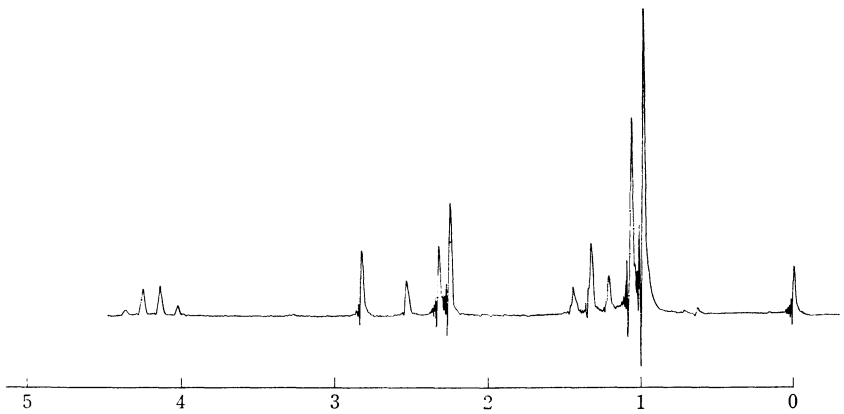



Fig. 1B. The NMR spectrum of a stereoisomeric mixture of ethyl $\alpha$-cyano-$\beta$-neopentylcrotonate at 71°C.

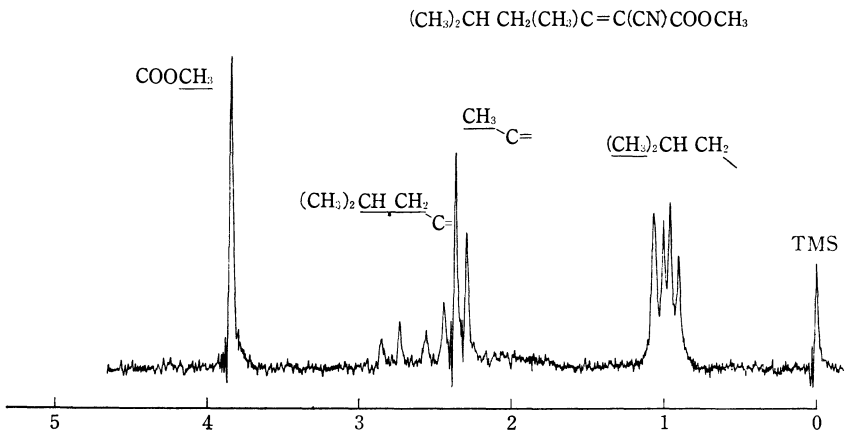



Fig. 2. The NMR spectrum of a stereoisomeric mixture of methyl $\alpha$-cyano-$\beta$-isobutylcrotonate at 19°C.

## Results and Discussion

The esters studied in this work are listed in Table I, together with the pertinent physical and chemical data, while the chemical shifts are shown in Table II. The isomeric compositions of fourteen esters are shown in Table III, together with the equilibrium ratios. Representative NMR spectra of the esters are shown in Figs. 1 and 2.

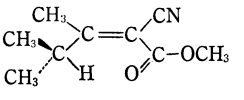
The resonance line-positions of the methyl protons of the methoxycarbonyl group were constantly located in the 3.80+0.01 p.p.m. range, while those of the methyl and methylene protons of the ethoxycarbonyl group always appeared in the 1.33+0.01 and 4.23+0.01 p.p.m. ranges respectively. The replacement of the methoxycarbonyl group by the ethoxycarbonyl group has practically no effect on the chemical shifts of the $\beta$-methyl and $\beta$-alkyl protons in the corresponding ester. This fact was often useful in assigning signals superimposed upon by signals of the alkoxycarbonyl group.

The fact that the spectra show two signals of an unequal intensity, separated by about 0.08 p.p.m., for the $\beta$-methyl group was ascribed to the co-existence of cis and trans isomers. As has been mentioned previously, the assignment of the configuration was made on the basis of a previous assumption.[1] This leads to the assignment of the $\beta$-methyl resonance at the higher field to the group which is in a position trans to the alkoxycarbonyl group.

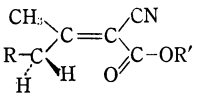
In the case of these esters, the relative stabilities of the stereoisomers may be expected to be determined by simple steric interactions between the $\beta$-alkyl substituent and the alkoxycarbonyl group. An examination of molecular models suggests that the cis configurations are to be favored over the trans. On the basis of this consideration, the more intense of the two signals of the $\beta$-methyl group is assigned to the cis isomer, and the less intense, to the trans. The conclusions reached by the two methods of assigning the peaks in the NMR spectrum are consistent with each other.

As a typical example, the present authors analyzed the spectrum of ethyl $\alpha$-cyano-$\beta$-neopentylcrotonate (XIII, Fig. 1A). The $\beta$-methyl signal appears as a doublet* of an unequal intensity, with the more intense signal at the lower field (2.28 and 2.35 p.p.m.). The $\beta$-methylene signal also appears as a doublet of an unequal intensity, with the more intense signal at the higher field (2.45 and 2.86 p.p.m.). On the basis of the arguments just given, the more intense signals are assigned to those of the cis isomer, and the weaker signals, to those of the trans. Since the $\beta$-methylene group of the cis isomer is in a position trans to the ethoxycarbonyl group, the results show that both the $\beta$-methyl and the $\beta$-methylene groups are more deshiedled by 0.08 p.p.m. in the cis- than in the trans-arrangement with respect to the ethoxycarbonyl group. The $\gamma$-methyl protons appear as a doublet of an unequal intensity, with the more intense signal at the lower field (0.98 and 1.06 p.p.m.), indicating that, contrary to the case of the $\beta$-methyl protons, the $\gamma$-methyl protons occur at the higher field when located cis to the ethoxycarbonyl group. Similar observations have already been made in the case of $\alpha$-cyano-$\beta$-alkoxy-$\beta$-alkylacrylic esters.[1]

It may be noticed in Table II that, in general, the peak separation of the $\beta$-methylene protons, except for III and IV, is much larger than that of the $\beta$-methyl protons, and that the peak separation of the $\beta$-methine proton (0.65 p.p.m. for VII and VIII) is much larger than that of the $\beta$-methylene protons. These facts suggest that the VIIa and XIIa conformations are heavily populated, as has been pointed out by Jackman and



(VIIa)



(XIIa)

TABLE III. CIS-TRANS COMPOSITION RATIOS OF THE CONDENSATION PRODUCTS

| Compound | Composition per cent of isomer | Equilibrium per cent of isomer |
|---|---|---|
| Ia | 50 | 50 |
| Ib | 50 | 50 |
| IIa | 50 | |
| IIb | 50 | |
| IIIa | 47 | |
| IIIb | 53 | |
| IVa | 46 | 44 |
| IVb | 54 | 56 |
| Va | 43 | |
| Vb | 57 | |
| VIa | 43 | 41 |
| VIb | 57 | 59 |
| VIIa | 38 | |
| VIIb | 62 | |
| VIIIa | 38 | 37 |
| VIIIb | 62 | 63 |
| IXa | 35 | 36 |
| IXb | 65 | 64 |
| Xa | 40 | |
| Xb | 60 | |
| XIa | 2 | |
| XIb | 98 | |
| XIIa | 47 | |
| XIIb | 53 | |
| XIIIa | 38 | 29 |
| XIIIb | 62 | 70 |

* In this discussion the terms "singlet" and "doublet" refer to multiplicity resulting from the co-existence of stereoisomers and not spin-spin coupling.

Wiley in the case of methyl β-methylglutaconate.[13]

The isomeric compositions of fourteen esters, as evaluated from the integration of the area under the appropriate NMR signals, are given in Table III. The composition is little affected by the temperature, as was determined by heating it to 71°C, except in the case of XIII. (As may be seen from Fig. 1B, the trans isomer of XIII was surprisingly much increased by heating it to 71°C (trans per cent, 61).) Attempts to separate the stereoisomers of these esters by gas chromatography were unsuccessful.

It seemed to be important to ascertain whether or not the isomeric compositions of the condensation products are the same in the equilibrium state. It is known that the isomerization of the esters is induced by a trace amount of base.[14,15] A sample which contained sodium ethoxide was allowed to stand at room temperature for a week and then distilled in vacuo. The results (Table III) show that the cis-trans ratios of the equilibrium mixtures are almost the same as those of the products ratios within the limit of experimental error, except for XIII. Accordingly, it is open to question whether or not the products were formed in these ratios. The present authors rather prefer the explanation that the products, once formed in some unidentified ratios, reached, by isomerization, a thermodynamic equilibrium. These circumstances would make it difficult to elucidate the steric course of the Knoevenagel reaction. However, these considerations are only tentative; they are now being investigated further.

It is interesting to note that the percentage of the cis isomer gradually increases with an increase in the size of the β-substituted alkyl group in the order; *t*-butyl > neopentyl > isobutyl > isopropyl > *n*-propyl > ethyl > methyl > hydrogen. This observation agrees with what would be expected on steric grounds, because this order is almost parallel with the magnitude of the steric requirement of the β-substituted alkyl group. Therefore, this finding supports the assumption suggested in Part I.[1]

## Summary

The Knoevenagel reaction of a methyl alkyl ketone with cyanoacetic ester gives a stereoisomeric mixture of α-cyano-β-alkylcrotonic ester. The NMR technique has been applied to the study of the geometric configurations of the mixture. It has been found that the isomer with a β-methyl group cis to the alkoxycarbonyl group always occurs predominantly. The magnitude of the cis-trans composition of the mixture is parallel to the steric requirement of the β-substituted alkyl group.

The authors wish to express their thanks to Mr. Jun Uzawa of this Institute for his measurements of the NMR spectra.

*The Institute of Physical and Chemical Research*
*Bunkyo-ku, Tokyo*

13) L. M. Jackman and R. H. Wiley, *J. Chem. Soc.*, **1960**, 2886.
14) S. Patai and Z. Rappoport, ibid., **1962**, 396.
15) Z. Rappoport, C. Degani and S. Patai, ibid., **1963**, 4513.

# Kinetic Studies of the Solution Polymerization of Trioxane Catalyzed by $BF_3 \cdot O(C_2H_5)_2$. I. The Effect of the Catalyst and the Water Concentration on the Rate of Polymerization

By Toshinobu HIGASHIMURA, Tetsuro MIKI and Seizo OKAMURA

(Received April 5, 1965)

It has been considered that, in the case of the cationic polymerization of cyclic oxygen compounds such as ethylene oxide, the chain carrier (active center) is a *t*-oxonium ion rather than a carbonium ion.[1-3] The reason for this is as follows: as the carbonium ion produced from cyclic monomers is generally unstable in comparison with that of vinyl monomer, the carbonium ion is transformed to the more stable oxonium ion by solvation at the ether group of the monomer whose concentration in the reaction system is very large. It is also inferred that, because of its stability, the oxonium ion is less reactive than the carbonium ion in vinyl polymerization.

Many patents on the cationic polymerization of trioxane (TO) have been presented, but only a few papers have been published on the kinetic study

1) H. Meerwein, E. Battenberg, H. Glod, E. Pfeil and G. Willfang, *J. Prakt. Chem.*, **154**, 83 (1939); K. Hamann, *Angew. Chem.*, **63**, 231 (1951).
2) J. B. Rose, *J. Chem. Soc.*, **1956**, 546.
3) D. J. Worsfold and A. M. Eastham, *J. Am. Chem. Soc.*, **79**, 897 (1957).

of the solution polymerization of TO catalyzed by cationic catalyst.[4-6] Recently, however, reports on the nature of the induction period of the solution polymerization[7] and on the kinetics of polymerization of molten TO[8-11] have been published, the results of the latter differing from those of solution polymerization. Kern et al.[4] suggested that the active center was a zwitter ion, unlike as in the usual polymerization mechanism of vinyl monomers.

In this series of reports we will try to establish the characteristics of the cationic polymerization of cyclic monomers. As such a monomer, trioxane was selected. Up to the present, none of the published papers on the cationic polymerization of TO has dealt with the quantitative relation between the polymerization condition and the rate of polymerization or the molecular weight of the resultant polymer. Therefore, we tried to mesaure the rate of polymerization and the molecular weight of the resultant polymer under various conditions, using $BF_3 \cdot O(C_2H_5)_2$ as the catalyst because it is most often used in cationic polymerizations. Even with the limitation of a single catalyst, the polymerizations in the different kinds of solvents were very dissimilar and it was difficult to infer the reaction mechanism.

In this first report the dependence of the rate of polymerization of the concentrations of the catalyst and the water will be discussed. In a non-polar solvent, a small amount of water acts as a co-catalyst. On the other hand, in a polar solvent water does not accelerate the polymerization reaction. It will also be found that the kinetic order of the catalyst concentration to the rate of polymerization varies with the kind of solvent in a complicated manner.

## Experimental

**Procedures.**—The polymerization was initiated by adding the catalyst solution from a syringe through a rubber stopper into a flask containing the monomer solution. Here the effects of air were not considered, and the polymerization solution was not stirred. In the course of the polymerization the polymers produced were suspended in the medium (when the water concentration was small) or precipitated (when the water concentration was large), and at longer times the whole reaction system gelled. The polymerization was stopped by adding methanol containing a small amount of ammonia to the reaction system. The resultant polymer was washed by methanol, dried in a vacuum at 40°C, and weighed. The initial rate of polymerization in this paper means the maximum rate at a range of 5—15% conversion. The induction period was determined from the intersection between the time axis and the extrapolated part of the maximum inclination of a time-conversion curve.

The water concentration in the reaction system was measured by the Karl-Fischer method. The reproducibility of the induction period and the rate of polymerization was fairly good as long as the water concentration was controlled.

**Materials.** — Trioxane (Celanese Co.) was twice recrylstallized in methylene chloride and stored in a desiccator over potassium hydroxide in a cool and dark place. The water content in the refined monomer was less than 0.008 wt.% (by the Karl-Fischer method), and the content of methylene chloride was less than 0.3% (by the gas chromatographic method).

The solvents were washed, dried, and distilled by the usual method; then they were refluxed and distilled on $CaH_2$ just before use. The water concentration was controlled by adding distilled water to a polymerizing solution.

$BF_3 \cdot O(C_2H_5)_2$ was refined by distilling commercial material.

## Results

**The Effects of the Catalyst Concentration.** —The effects of the catalyst concentration on the induction period and the rate of polymerization were studied at fixed concentrations of monomer and water.

Here benzene was used as the non-polar solvent, ethylene dichloride as the polar solvent, and nitrobenzene as the more polar solvent. As the polymerization in each solvent was characteristic and complicated, the time-conversion curves of each solvent are shown in the figures.

Figure 1 shows the time-conversion curve in benzene. The initial rate, as is shown in Fig. 2,

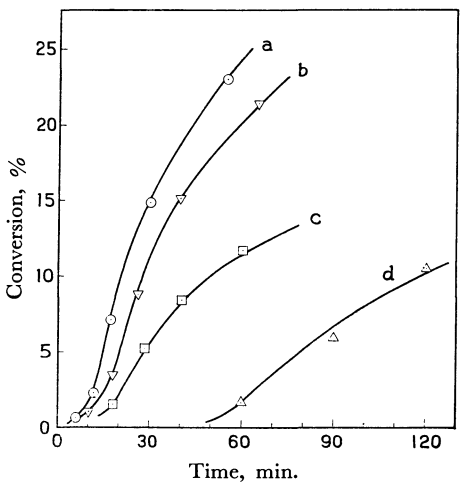



Fig. 1. Effect of the catalyst concentration on the rate of polymerization in benzene at 30°C. $[M]_0$; 3.3 mol./l., $[H_2O]$; 2.5 mmol./l., $[BF_3 \cdot O(C_2H_5)_2]$; a(○): 30, b(▽): 20, c(□): 10 and d(△): 5.0 mmol./l.

4) W. Kern and V. Jaacks, *J. Polymer Sci.*, **48**, 399 (1960).
5) V. Jaacks and W. Kern, *Makromol. Chem.*, **62**, 1 (1963).
6) S. Okamura, T. Higashimura and M. Tomikawa, *J. Chem. Soc. Japan, Ind. Chem. Sec.* (*Kogyo Kagaku Zasshi*), **65**, 712 (1962).
7) G. V. Rakova, L. M. Romanov and N. S. Enikolopyan, *Vysokomol. Soed.*, **6**, 2178 (1964).
8) M. Kučara and E. Spousta, *J. Polymer Sci.*, **A2**, 3431 (1964).
9) M. Kučera and E. Spousta, ibid., **A2**, 3443 (1964).
10) M. Kučera and E. Spousta, *Makromol. Chem.*, **76**, 183 (1964).
11) M. Kučera and E. Spousta, ibid., **76**, 190 (1964).

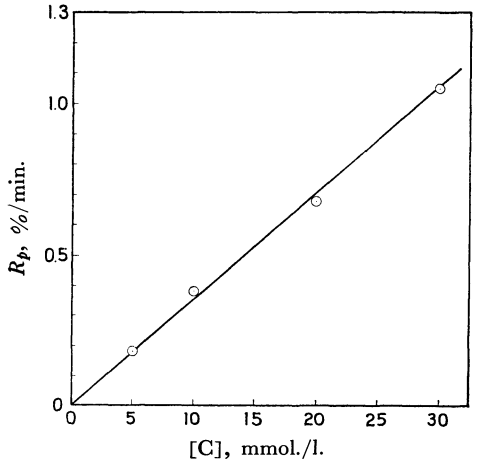



Fig. 2. Relationship between the catalyst concentration and the initial rate in benzene at 30°C. (Calculated from Fig. 1).

was proportional to the catalyst concentration. The decrease in the catalyst concentration increased the induction period. No simple relationship between the catalyst concentration and the induction period could be obtained.

Figure 3 shows the relation between the reaction time and conversion in the ethylene dichloride solvent. The initial rate was, as Fig. 4 shows, proportional to the square root of the catalyst concentration. No such phenomenon has been found in the cationic polymerization of vinyl monomers. When the catalyst concentration was more than the water concentration in the reaction system, the induction period of polymerization was less than 5 min. and was inversely proportional to the catalyst concentration, as is shown in Fig. 5.

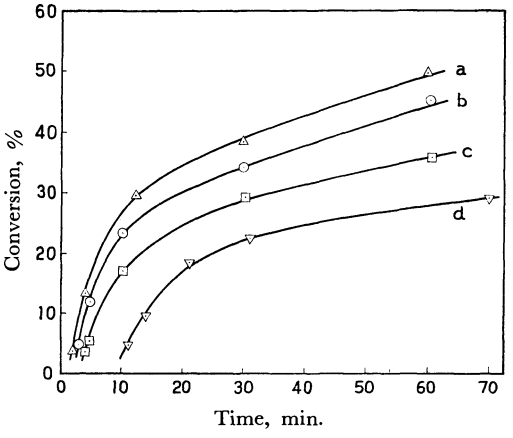



Fig. 3. Effect of the catalyst concentration on the rate of polymerization in ethylene dichloride at 30°C.
$[M]_0$; 3.3 mol./l, $[H_2O]$; 2.9 mmol./l., $[BF_3 \cdot O(C_2H_5)_2]$; a(△): 20, b(○): 10, c(□): 5.0 and d(▽): 2.5 mmol./l.

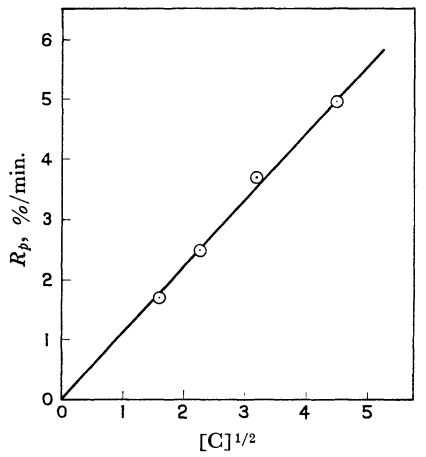



Fig. 4. Relationship between the catalyst concentration and the initial rate in ethylene dichloride at 30°C.
(Calculated from Fig. 3.)

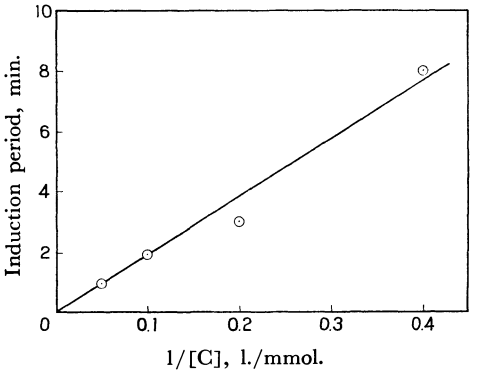



Fig. 5. Relationship between the reciprocal of the catalyst concentration and induction period in ethylene dichloride solution at 30°C.
(Calculated from Fig. 3.)

In the polymerization in nitrobenzene, the relation between the catalyst concentration and the polymerization rate was unusual. At a high monomer concentration, the polymerization reaction proceeded too fast for the rate of polymerization in nitrobenzene to be measured. Such an example is shown by the dotted line in Fig. 6. In order to ascertain the relation between the catalyst concentration and the polymerization rate, the polymerization was carried out at lower monomer concentrations. As Fig. 6 shows, the polymerization rate in nitrobenzene was almost independent of the catalyst concentration. The induction period tended to decrease with an increase in the catalyst concentration, being roughly proportional to the inverse square of the catalyst concentration.

**The Effects of the Water Concentration.**— At fixed concentrations of catalyst and monomer, the effects of the concentration of added water were

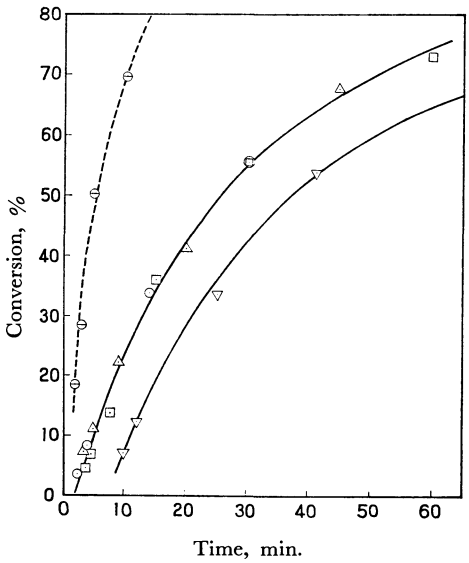



Fig. 6. Effect of the catalyst concentration on the rate of polymerization in nitrobezene at 30°C.
$[M]_0$; 1.1 mol./l., $[H_2O]$; 2.4 mmol./l., $[BF_3 \cdot O(C_2H_5)_2]$; (○): 20, (△): 10, (□): 5 and (▽): 2.5 mmol./l. Dotted line (—); $[M]_0$; 3.3 mol./l., $[H_2O]$; 1.8 mmol./l., $[BF_3 \cdot O(C_2H_5)_2]$; 1.0 mmol./l.

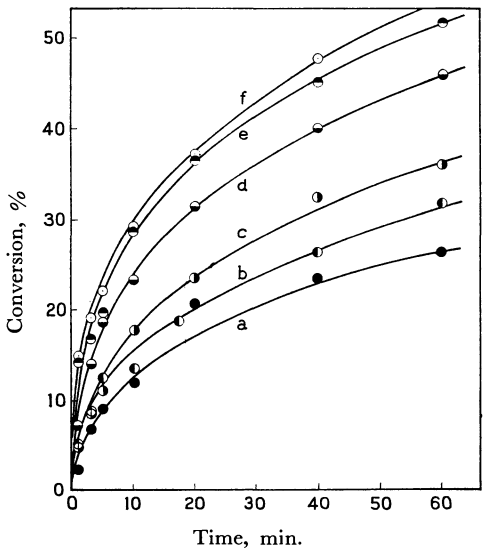



Fig. 7. Effect of the water concentration on the rate of polymerization in *n*-hexane at 30°C.
$[M]_0$; 0.37 mol./l., $[BF_3 \cdot O(C_2H_5)_2]$; 9.4 mmol./l., $[H_2O]$; a(●): 0.4, b(◐): 0.9, c(◑): 1.1, d(◒): 1.7, e(◓): 2.2 and f(○): 3.4 mmol./l.

studied. Here, *n*-hexane was used as the non-polar solvent, since it could dissolve less water than benzene.

Figure 7 shows the effects of water in *n*-hexane. At this range of water concentration, the polymerization proceeded entirely without an induction period, and even a small amount of water accelerated the reaction. However, the rate of polymerization decreases if more water is added.

Similar phenomena were found for the polymerization in the benzene solvent. A small amount of water accelerated the polymerization, but the rate of polymerization decreased upon the addition of a larger amount of water.

In the ethylene dichloride solvent, as is shown in Fig. 8, the induction period increased almost proportionally to the water concentration; the initial rate of polymerization reached its maximum at $[H_2O]/[BF_3 \cdot O(C_2H_5)_2] \simeq 1/2$.

As can be seen in Fig. 8, the time-conversion curve consisted of the initial part, where the rate of polymerization was large, and the subsequent part, where the rate was small. It is interesting that the initial part lasts longer at higher water concentrations.

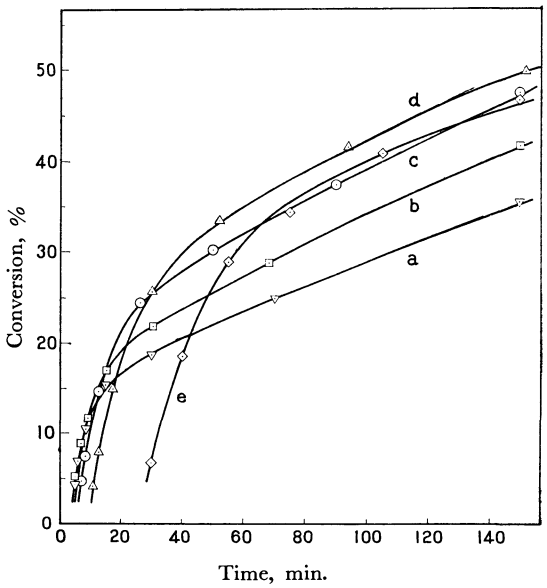



Fig. 8. Effect of the water concentration on the rate of polymerization in ethylene dichloride at 30°C.
$[M]_0$; 3.3mol./l., $[BF_3 \cdot O(C_2H_5)_2]$; 10mmol./l., $[H_2O]$; a(▽): 0.3, b(□): 1.6, c(○): 3.7, d(△): 5.9 and e(◇): 10.8 mmol./l.)

In nitrobenzene, where the water concentration was larger than that of the catalyst, the rate of polymerization was, as Fig. 9 shows, almost independent of the water concentration and only the induction period varied remarkably. On the other hand, where the water concentration was less than that of the catalyst, neither the induction period nor the rate of polymerization was affected, as is shown in Fig. 10.

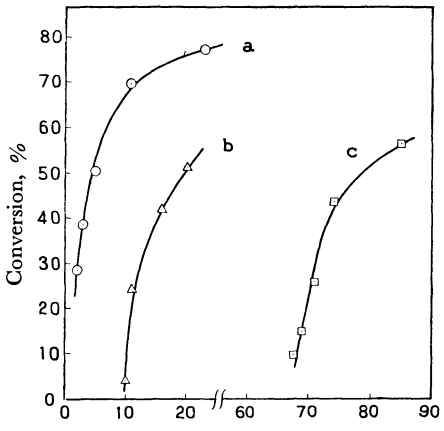



Fig. 9. Effect of the water concentration on the rate of polymerization in nitrobenzene at high concentrations of monomer and water at 30°C.
$[M]_0$; 3.3 mol./l., $[BF_3 \cdot O(C_2H_5)_2]$; 1.0 mmol./l., $[H_2O]$; a(○): 1.8, b(△): 4.7 and c(□): 8.3 mmol./l.

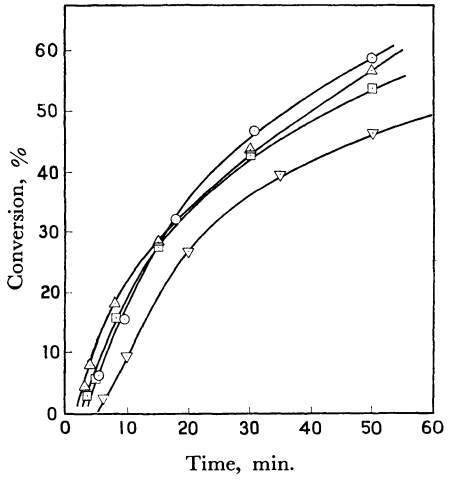



Fig. 10. Effect of the water concentration on the rate of polymerization in nitrobenzene at low concentrations of monomer and water at 30°C.
$[M]_0$; 1.1 mol./l., $[BF_3 \cdot O(C_2H)_2]$; 10 mmol./l., $[H_2O]$; (△): 2.2, (□): 4.0, (○): 5.9 and (▽): 7.8 mmol./l.

**The Effects of Added Methanol.**—As has been shown above, a small amount of water did not affect the polymerization in nitrobenzene. In order to clarify this point, the effects of the addition of methanol in nitrobenzene and in ethylene dichloride were compared.

In ethylene dichloride, as Fig. 11 shows, methanol equivalent to half the amount of the catalyst accelerated the polymerization, while an amount of methanol equal to the catalyst decreased the rate of polymerization. The addition of methanol

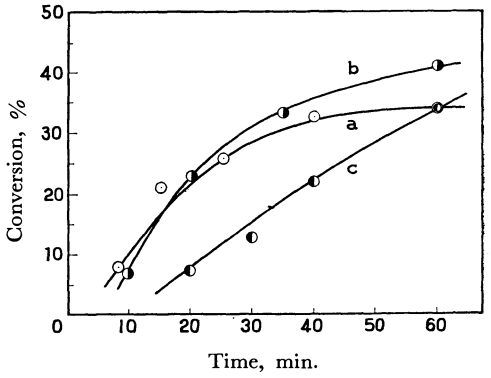



Fig. 11. Effect of the methanol concentration on the rate of polymerization in ethylene dichloride at 30°C.
$[M]_0$; 3.3 mol./l., $[BF_3 \cdot O(C_2H_5)_2]$; 20 mmol./l., $[H_2O]$; 2.7 mmol./l., $[CH_3OH]$; a(○): 0, b(◑): 10 and c(◑): 20 mmol./l..

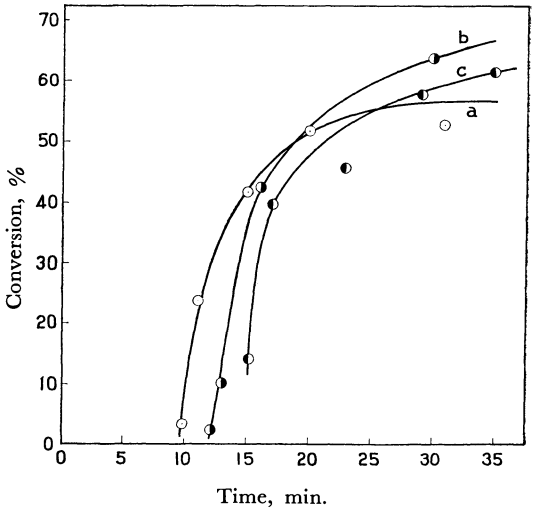



Fig. 12. Effect of the methanol concentration on the rate of polymerization in nitrobenzene at 30°C.
$[M]_0$; 3.3 mol./l., $[BF_3 \cdot O(C_2H_5)_2]$; 1.0 mmol./l., $[H_2O]$; 4.7 mmol./l., $[CH_3OH]$; a(○): 0, b(◑): 2.5 and c(◐): 5.0 mmol./l.

increased the induction period, as did the addition of water.

On the other hand, in nitrobenzene, as is shown in Fig. 12, even the addition of five times as much methanol to the catalyst tended to accelerate the rate, and its effect was very small, much as in the case of the addition of water.

## Discussion

Table I summarizes the effects of the catalyst concentration on the rate of polymerization. In Fig. 13 the effect of the water concentration on the rate of polymerization is schematically shown.

TABLE I. SUMMARY OF THE EFFECT OF CATALYST CONCENTRATION OF THE RATE OF POLYMERIZATION ($R_p$) IN VARIOUS SOLVENTS AT 30°C ($[BF_3 \cdot O(C_2H_5)_2] > [H_2O]$)

| Solvent | $R_p$ |
|---|---|
| $C_6H_6$ | $R_p \propto [C]^{1.0}$ |
| $(CH_2Cl)_2$ | $R_p \propto [C]^{0.5}$ |
| $C_6H_5NO_2$ | $R_p \propto [C]^0$ |

Figure 13 was obtained from the results of Figs. 7, 8 and 10. In a non-polar solvent such as *n*-hexane, the polymerization seems not to proceed when water is strictly excluded. Therefore, it may be concluded that water is necessary as a co-catalyst for the polymerization in a non-polar solvent. Even in this case, however, the rate of polymerization decreased when more water than a limited quantity was added. A similar tendency was found in the benzene solvent, also.

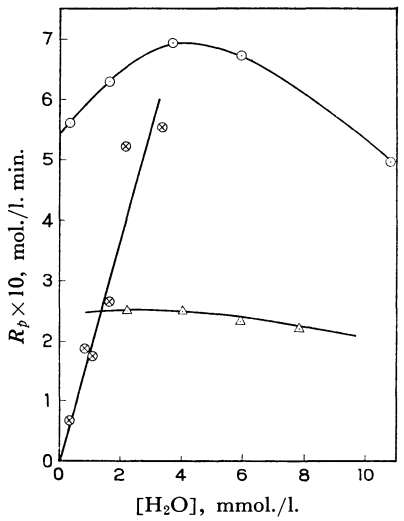



Fig. 13. Effect of the water concentration on the initial rate in various solvents at 30°C.
a(⊗); *n*-hexane solvent (from Fig. 7),
b(○); ethylene dichloride solvent (from Fig. 8),
c(△); nitrobenzene solvent (from Fig. 10)

On the other hand, in nitrobenzene the rate of polymerization was not affected by the water concentration within the range of our experiment, and water is not considered to act as a co-catalyst. In ethylene dichloride the rate of polymerization was slightly increased by a small amount of water, but the effect was very small and the polymerization seems to occur even without water.

In a polar solvent the catalyst $BF_3 \cdot O(C_2H_5)_2$, as is well known, dissociates according to Eq. 1, thus producing the ethyl cation.[12,13] The latter can initiate the polymerization of trioxane. On the contraty, in a non-polar solvent the catalyst $BF_3 \cdot O(C_2H_5)_2$ canont dissociate by itself according to Eq. 1; it needs water as a co-catalyst;

$$BF_3 \cdot O(C_2H_5)_2 \rightarrow BF_3 \cdot O(C_2H_5)^- \ (C_2H_5)^+ \quad (1)$$

$$BF_3 \cdot O(C_2H_5)_2 + H_2O \rightarrow (BF_3OH)^- \ H^+ + O(C_2H_5)_2 \quad (2)$$

as is shown in Eq. 2, to produce an ionizable species which has the ability to initiate the polymerization. In ethylene dichloride, it is inferred that the two processes (Eq. 1 and Eq. 2) took place simultaneously; and a behavior between that in *n*-hexane and that in nitrobenzene was observed. This consideration is supported by the thermodecomposition rate of the resultant polymer in each solvent, whose ends were not chemically treated and whose molecular weights ($\eta_{sp}/c$) were nearly equal. That is, the decomposition of the polymer obtained in *n*-hexane was 5 to 10 times faster than the rate of the polymer produced in nitrobenzene. The polymer obtained in ethylene dichloride had an intermediate value. The relationship between the co-catalytic effect of water and the thermodecomposition rate of the resultant polymer can be reasonably explained. The polymer produced in the presence of water as a co-catalyst, both of whose ends were –OH groups may be easily decomposed, while the polymer obtained by the initiation of the ethyl cation, one of whose ends was the ethoxyl radical, decomposes with more difficulty.

Kern et al.[4] have found that, in the cationic polymerization of trioxane by boron fluoride gas in methylene chloride, the rate of polymerization decreases with an increase in the concentration of added water; they have proposed that the polymerization of this system proceeds without a co-catalyst and that the active center is a zwitter ion. However, in the polymerization catalyzed by $BF_3 \cdot O(C_2H_5)_2$ the mechanism of the zwitter ion is considered to be impossible for the above-mentioned reasons; that is, a co-catalyst was necessary in the non-polar solvent, the thermodecomposition rate of polymers was affected by the kind of solvent, and the alkoxyl-end group was detected in the produced polymer.[14] On the other hand, it has been considered that water as a co-catalyst is necessary in the polymerization of trioxane by tin(IV) chloride.[5] The idea of the zwitter ion has also been rejected in the polymerization of 3, 3-bis-(chloromethyl)-oxetane by boron fluoride.[15] Therefore, it may be concluded that, under the conditions of our experiments, the polymerization reaction does not proceed through the zwitter ion. The above considerations also lead to the conclusion that the polymerization of trioxane catalyzed by $BF_3 \cdot O(C_2H_5)_2$ is initiated by the attack of the proton or the ethyl cation on trioxane.

12) J. D. Coombes and D. D. Eley, *J. Chem. Soc.*, **1957**, 3700.
13) J. P. Kennedy, *J. Polymer Sci.*, **38**, 263 (1959).
14) T. Miki, T. Higashimura and S. Okamura, unpublished data.
15) I. Penczek and S. Penczek, *Makromol. Chem.*, **67**, 213 (1963).

This interpretation of the co-catalysis was confirmed by the addition of not only water but also methanol. As is shown in Fig. 11 and Fig. 12, a small amount of methanol accelerated the polymerization in ethylene dichloride but scarcely affected that in nitrobenzene.

In the case of the cationic polymerization of vinyl monomers, the rate of polymerization is generally proportional to the catalyst concentration. As Table I shows, in the polymerization of trioxane in a non-polar solvent such as benzene, the polymerization rate is proportional to the catalyst concentration. However, it is difficult to explain the experimental fact that the kinetic order of the catalyst concentration to the rate of polymerization is equal to 0.5 in ethylene dichloride and to zero in nitrobenzene. It has been found that, in the polymerization of trioxane catalyzed by tin(IV) chloride, the final yield in both polar and non-polar solvents is not dependent on the catalyst concentration when the concentration of the catalyst is larger than that of water.[5] A similar result has been obtained in the polymerization of isobutene catalyzed by tin(IV) chloride[16] and aluminum chloride[17]. In our experiment, however, $BF_3 \cdot O(C_2H_5)_2$ can cause the polymerization reaction of trioxane in nitrobenzene without water as a co-catalyst; consequently, it is impossible to explain the above-mentioned phenomena only in terms of the relation between the water and catalyst concentrations.

Rose[2] has proposed, on the basis of the relation between the reaction rate and kinetic order of the concentration of the reagents, that, in the polymerization of cycloxabutane, the active center is an oxonium ion. However, in our experiment the relationship between the rate of polymerization and the catalyst concentration was very complicated; the nature of the active center can not be discussed on the basis of our kinetic results.

16) R. G. W. Norrish and K. E. Russell, *Trans. Faraday Soc.*, **48**, 91 (1952).
17) J. H. Beard, P. H. Plasch and P. P. Rutherford, *J. Chem. Soc.*, **1964**, 2566.

## Summary

In the solution polymerization of TO catalyzed by $BF_3 \cdot O(C_2H_5)_2$, water acted as a co-catalyst in *n*-hexane, a non-polar solvent; in ethylene dichloride, a polar solvent, water slightly accelerated the rate of polymerization, and in nitrobenzene, a more polar solvent, water did not affect the rate at all. The kinetic order of the catalyst concentration to the polymerization rate was 1.0 in benzene, 0.5 in ethylene dichloride, and zero in nitrobenzene. The induction period was very short when water was excluded as much as possible, but it increased with an increase in the water concentration and with a decrease in the catalyst concentration.

On the basis of these results, it may be concluded that the polymerization of TO by $BF_3 \cdot O(C_2H_5)_2$ is initiated by the attack of the proton or the ethyl cation on the monomer.

*Department of Polymer Chemistry*
*Kyoto University*
*Sakyo-ku, Kyoto*

# Investigations on Some Amine Complexes of Cobalt(II) Phthalimide. II. Infrared Spectroscopic Measurements

By Gopal NARAIN

(Received April 9, 1965)

The preparation of a series of amine complexes of cobalt(II) phthalimide and some preliminary investigations, such as their analysis and studies of their molecular weight and conductivity, have been reported in Part I.[1] It has there been pointed out that the non-electrolytic nature of the complexes shows that two phthalimide ions are co-ordinated along with the amine ligands, and that the co-ordination of the phthalimide ion to the metal can be either through the negatively-charged nitrogen or the oxygen of the carbonyl group. The present communication, related to infrared spectroscopic measurements, will attempt further to confirm and establish that both the amine and phthalimide ligands are co-ordinated to the cobalt atom.

## Experimental

The spectra were obtained on a small infracord, using potassium bromide prisms.

1) G. Narain, P. Shukla and L. N. Srivastava, Communicated to *J. Prakt. Chem.* for publication.

Table. I. Infraed absorpion band

| | Name | |
|---|---|---|
| 1 | Cobalt(II) phthalimide | 645w, 712s, 850w, 1055m, 1085w, 1140w, 1185w, 1310m, 1380s, 1465s, 1605m, 1725s, 1765m, 3140m. |
| 2 | Bi(phthalimido)-diaminocobalt(II) | 680m, 715s, 860m, 1130w, 1225w, 1305m, 1385s, 1470s, 1610w, 1715w, 3260m. |
| 3 | Bi(phthalimido)-ethylenediaminocobalt(II) | 675w, 712s, 850m, 935m, 975m, 1050s, 1130m, 1180s, 1210w, 1300m, 1380s, 1470s, 1610s, 1700s, 3240s. |
| 4 | Bi(phthalimido)-2, 2'-dipyridylcobalt(II) | 650w, 680m, 720s, 750w, 765m, 850m, 1020w, 1060w, 1175s, 1300m, 1313w, 1375w, 1470s, 1600s, 1624s, 1710w. |
| 5 | Bi(phthalimido)-*o*-phenanthrolinecobalt(II) | 650w, 680m, 725s, 750m, 855s, 870w, 960w, 1060w, 1105m, 1150m, 1230w, 1310w, 1360w, 1380s, 1430s, 1470s, 1500w, 1520m, 1575m, 1630m, 1714s. |

## Results

The spectra have been examined over the entire infrared range from 400—3500 $cm^{-1}$; the various bands obtained for individual complexes are listed in Table I.

## Discussion

The examination of the spectra shows that there are two interesting regions, the NH and C:O stretching frequency regions.

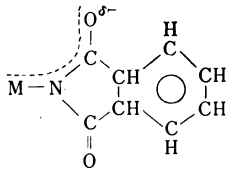
As has been mentioned earlier, the phthalimide ion has the possibility of being coordinated to the metal atom either through the nitrogen or through the oxygen of the carbonyl group. The infrared spectra cannot make a sharp distinction between these two conditions, because any change in phthalimide nitrogen, which is directly linked to the carbonyl group, will alter the molecular environment and, accordingly, the frequency of the latter, even if it is not co-ordinated.[2] However, on the basis of the Lewis concept, it may be expected that the nitrogen, which is negatively-charged, will have better possibilities of being co-ordinated than the oxygen.[3] In the co-ordination through oxygen, steric hindrance will be effective, as is exemplified by the unsuccessful attempt to prepare some metal complexes with phthalimide as the ligand, complexes which would be analogous to acetamide complexes.[4]

All complexes (except those prepared by using 2, 2-'dipyridyl or *o*-phenanthroline as the ligand) show a single sharp absorption band in the vicinity of 3300 $cm^{-1}$; this is taken to be the NH-stretching frequency band. In free ammonia the band occurs at 3414 $cm^{-1}$. This negative shift of the frequency is a result of the co-ordination of the amine to the cobalt atom, thus resulting in the formation of a highly covalent M–N bond, which weakens the NH bond order. In the case of the ethylene diamine complex also, there is a considerable shift; this is again because of the co-ordination of the amine. In the case of 2, 2'-dipyridyl and *o*-phenanthroline complexes, there is no band in the above region. However, a comparison of the positions of the various bands with those of free ligands[5,6] shows that the frequencies are shifted to higher values in complexes, which clearly shows that the ligands are co-ordinated.[5]

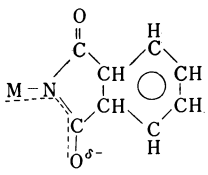
The band observed in the carbonyl-stretching frequency region is of interest. In phthalimide, the band occurs at 1745 $cm^{-1}$, and in cobalt phthalimide it shifts to 1725 $cm^{-1}$, while in complexes it shifts to 1700—1710 $cm^{-1}$. The cause of this negative shift of frequency appears to be the electron density of nitrogen. In the case of cobalt(II) phthalimide, which is supposed to possess a partial covalent character, exhibited by its low solubility in polar solvents, the band shifts by only 25 $cm^{-1}$. This negative nitrogen has an orbital covalently bonding to the metal and an orbital perpendicular to the plane to the phthalimide. This filled orbital on nitrogen would help to direct a greater electron density towards the C=O bond; this would tend to increase the frequency. However, other factors, such as the $\infty$-mass effect and hydrogen bonding, tend to decrease the frequency; hence, an intermediate value is obtained. In the case of complexes, the direction of the added electron density reaches a saturation point, beyond which any added electron density tends to reduce the C=O double bond to a single bond and reduce the frequency. The addition of additional ligands to the cobalt(II) ion causes the metal ions to attempt to "back donate" into the available orbitals on the nitrogen of phthalimide. The filled orbital of the phthalimide nitrogen is made available by a quasiaromatic delocalisation. Thus, the following formulae would give a lower bond

2) S. Krimm, *J. Chem. Phys.*, **23**, 1371 (1955).
3) J. C. Bailar, "Chemistry of Co-ordination Compounds," New York (1956), p. 180.
4) W. Bagnall, M. Deane, S. Robinson and A. Steward, *J. Chem. Soc.*, **1961**, 1611.
5) P. C. H. Mitchell, *J. Inorg. Nucl. Chem.*, **25**, 967 (1963).
6) P. C. H. Mitchell and R. J. P. Williams, *J. Chem. Soc.*, **1962**, 4570.

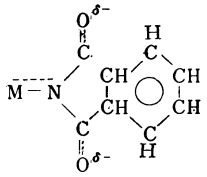
order to C=O and a lower frequency:



(I)



(II)



(III)

Another cause of the shift may be the ∝-mass effect.[7] In phthalimide, the nitrogen is linked to a very light hydrogen atom; hence, there is no hindrance in the normal motion of the CO group. In the case of complexes, the phthalimide nitrogen is linked to a heavy metal atom, which may cause a hindrance in its normal vibration, thus displacing the carbonyl frequency band to a lower value, although the magnitude of this shift would be small because, due to the cyclic nature of the ligand, the oxygen is vibrating against essentially the whole ligand. Hence, it appears that it is as a result of these factors that a negative shift of CO frequency is observed, although the oxygen of the carbonyl group is not co-ordinated.

7) G. F. Svatos, C. Kurran and J. V. Quagliano, *J. Am. Chem. Soc.*, **77**, 6159 (1955).

## Summary

Infrared measurements of a series of complexes prepared with cobalt(II) phthalimide and some amines of the $[Co(Phthalimide)_2(amine)_{2or1}]$ type have been made. The spectra confirm that both phthalimide ions and amine molecules are co-ordinated; they further suggest that the co-ordination of phthalimide is through the nitrogen.

The author is thankful to Dr. J. V. Quagliano, Florida State University, Tallahasse, Florida, for his valuable suggestions in the theoretical interpretation of I. R. data; and to Dr. L. N. Srivastava and Dr. P. R. Shukla, Chemistry Department, Lucknow University, for their help in the preparation of the manuscript. He is also indebted to the Council of Scientific and Industrial Research for the award of a senior research fellowship for this work.

*Department of Chemistry*
*Lucknow University*
*Lucknow, U.P., India,*

# An Isotopic Exchange Reaction between Oxygen and Carbon Dioxide on Zinc Oxide

By Toshizo TITANI, Tadamitsu KIYOURA and Akira ADACHI

(Received April 15, 1965)

Zinc oxide has been extensively studied by many investigators in terms of semiconductivity, and there are several works on the isotopic exchange between oxygen and zinc oxide.[1-6] However, only a little information is available on the isotopic exchange between oxygen and carbon dioxide on zinc oxide, or on that between carbon dioxide and zinc oxide. We have recently investigated the exchange reaction over the temperature range from 350 to 550°C in a rather qualitative way in order to provide preliminary data for further tracer studies. It appears worthwhile, therefore, to publish our results at this time. In this paper we shall discuss the general features of the isotopic exchange between carbon dioxide and zinc oxide, and that between oxygen and carbon dioxide on zinc oxide.

1) N. Morita, This Bulletin, **15**, 47 (1940).
2) E. R. S. Winter, *J. Chem. Soc.*, **1950**, 1170.
3) J. A. Barnard, E. R. S. Winter and H. V. A. Briscoe, ibid., **1954**, 1517.
4) T. J. Barry and F. S. Stone, *Proc. Roy. Soc.*, **A225**, 124 (1960).
5) G. K. Boreskov et. al., *Kinetika i Kataliz*, **4**, 388 (1963).
6) K. Hirota and M. Chono, *J. Catalysis*, **3**, 196 (1964).

## Experimental

Zinc oxide was prepared by the thermal decomposition of zinc oxalate at 500°C for 15 hr. in the presence of air; the B. E. T. area of the zinc oxide was 5.8 $m^2$/g. Zinc oxalate was obtained by the addition of an aqueous solution of ammonium oxalate to a solution of zinc chloride. The precipitate was washed so that it was free from chloride ions and then dried in the

air 110°C for 8 hr. prior to its thermal decomposition. Heavy oxygen, $O^{18}O$, was prepared in our laboratory by the thermal diffusion method;[7] its concentration was 1.81 atom.%. Carbon dioxide enriched in $^{18}O$, $CO^{18}O$ (3.01 atom.%) was obtained by equilibrating ordinary carbon dioxide with $^{18}O$ enriched water, $H_2{}^{18}O$. As the source of ordinary oxygen and carbon dioxide, commercial gases were used with some purification. All the gases used were dried through a train of traps at −78°C. The search for an impurity in the gases used was made by using a mass spectrometer up to mass 100. They contained about 0.3 to 0.5% of one impurity, giving rise to mass 28 (nitrogen); none other was found in any detectable amount.

The exchange reaction was studied by the static batch method. The reaction vessel was made of borosilicate glass. For the exchange between carbon dioxide and zinc oxide, an accurately-weighed 400 mg. portion of zinc oxide was placed in the reaction vessel and was then outgassed at 500°C for 3 hr., using a mercury diffusion pump, through a liquid nitrogen trap. Then the temperature of the reaction vessel was adjusted to the desired temperature, and 1.5 ml. (N. T. P.) of $^{18}O$-enriched carbon dioxide was introduced. The temperature range studied was from 350 to 550°C, with 50°C intervals. At desired time intervals, all the carbon dioxide was collected by a Toepler pump and the $^{18}O$ content of the carbon dioxide was analyzed by the use of a mass spectrometer. For the exchange between oxygen and carbon dioxide on zinc oxide, 2.7 ml. (N. T. P.) of the gas mixture of enriched oxygen and normal carbon dioxide or of normal oxygen and enriched carbon dioxide in a ratio of 1 to 1 was used. The amount of zinc oxide and the out-gassing and other procedures were the same as those in the exchange between carbon dioxide and zinc oxide. In order to maintain a constant pressure of the gas at each reaction temperature (14 cmHg for the $CO_2$-ZnO system and 25 cmHg for the $O_2$-$CO_2$-ZnO system), a reaction vessels of different volumes were chosen for the different temperatures; 19.0 ml. for 350°C, 20.0 for 400°C, 21.5 for 450°C, 23.0 for 500°C, and 25.0 for 550°C. The pressure change due to adsorption was ignored, since the accompanying pressure changes were less than 10% of the total pressure. In all the experiments, the pressure of the carbon dioxide was kept lower than the decomposition pressure of zinc carbonate (76 cmHg at 300°C).[8]

## Results and Discussion

First, the isotopic oxygen exchanges between carbon dioxide and the surface of the reaction vessel, and between oxygen and the surface, and also the catalytic action of the surface were examined. It was found that, within the limits of experimental error, the reaction vessel surface did not participate in the exchange reaction.

**Exchange between Carbon Dioxide and Zinc Oxide.**—The extent of the exchange reaction is shown in Fig. 1. The rate of the exchange was rapid, and within a few minutes after the introduction of the enriched carbon dioxide into the reaction vessel, the $^{18}O$ content of the carbon dioxide reached a definite value. This value was characteristic of the reaction temperature. At this stage of the reaction, an isotopic equilibrium was established between the carbon dioxide in the gas phase and a certain part of the zinc oxide. After the initial fast reaction had finished, there was a slow downward drift of the $^{18}O$ content of the carbon dioxide. From Fig. 1, we obtained the definite $^{18}O$ content by the extrapolation of the drift line to time zero. From these quantities, we obtained the amount of the rapidly-exchangeable oxygen of the zinc oxide, $n_s$ (gram atom per gram of zinc oxide). The calculation of $n_s$ was carried out using Eq. 1,[2] where $^{18}O_0$ and $^{18}O_\infty$ were the initial and the definite $^{18}O$ content of the carbon dioxide respectively; the numerical constant, 0.204, was the $^{18}O$ natural abundance; $n_g$ was the number of oxygen atoms in the amount of carbon dioxide used, and $w$ was the weight of the zinc oxide used.

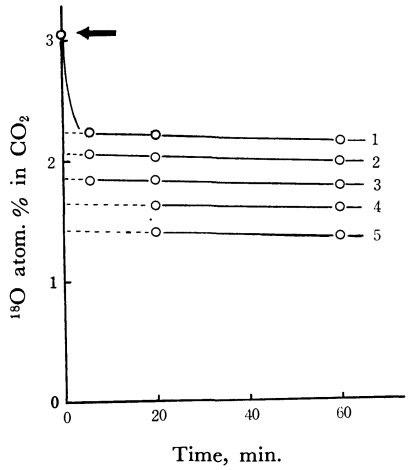



Fig. 1. Extent of the exchange reaction between $CO^{18}O$ and ZnO.
The arrow indicates the initial content of $^{18}O$ in $CO_2$.
1, 350°C 2, 400°C 3, 450°C 4, 500°C
5, 550°C

$$n_s w(^{18}O_\infty - 0.204) = n_g(^{18}O_0 - {}^{18}O_\infty) \quad (1)$$

The values of $n_s$ at various temperatures are listed in Table I. A random exposure of the crystalline face being assumed, the number of rapidly-exchangeable surface layers of the zinc oxide at various temperatures was obtained through the value of $n_s$, the surface area of zinc oxide, and the lattice constant of zinc oxide; they are also listed in Table I.

The pretreatment of the zinc oxide was changed from the normal evacuation at 500°C for 3 hr. to that at 600°C for 5 hr. However, no difference in the value of $n_s$ was observed after this change.

7) Y. Horibe, *Isotopes and Radiation*, **2**, 25 (1959).
8) K. Friedlich, *Stahl und Eisen*, **31**, 1901 (1911).

Table I. The value of $n_s$ and the number of rapidly-exchangeable surface layers of the zinc oxide

| Temp., °C | 350 | 400 | 450 | 500 | 550 |
|---|---|---|---|---|---|
| $n_s$ (g. atom./g.)·$10^5$ | 12.8 | 18.0 | 24.1 | 28.2 | 44.3 |
| Number of exchangeable layers | 0.7 | 0.9 | 1.2 | 1.5 | 2.3 |

Therefore, the rapidly-exchangeable oxygen of the zinc oxide was probably not a residual water nor a residual oxalate.

Below 400°C a part of the monolayer or the surface oxygen, between 400 to 450°C a monolayer, and above 450°C more than a monolayer participate in the fast initial exchange reaction.

**The Exchange between Oxygen and Zinc Oxide.**—The results are shown in Fig. 2. The experimental conditions were the same as those used with carbon dioxide.

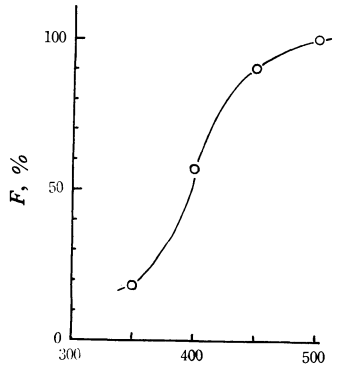



Fig. 2. Fractional attainment of the exchange between $O^{18}O$ and ZnO. Reaction time, 15 min.
$F=100(^{18}O_0-^{18}O_t)/(^{18}O_0-^{18}O_\infty)$
$^{18}O_0$ and $^{18}O_t$ are the initial and the after 15 min. $^{18}O$ content in $O_2$. $^{18}O_\infty$ is the equilibrium content of $^{18}O$ in $O_2$, calculated from the amounts of $O_2$ gas used and value of $n_s$.

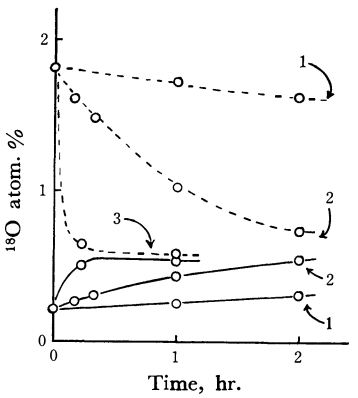



Fig. 3. Extent of the exchange reaction between $O^{18}O$ and $CO_2$.
Full line, increase of $^{18}O$ in $CO_2$
Broken line, decrease of $^{18}O$ in $O_2$
1, 450°C 2, 500°C 3, 550°C

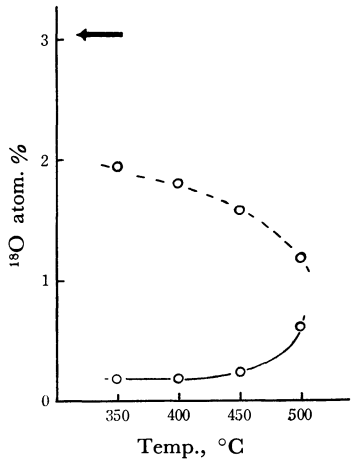



Fig. 4. $^{18}O$ in $CO_2$ and $O_2$. Reaction time, 1 hr.
Full line, $O^{18}O$. Broken line, $CO^{18}O$.
The arrow indicates the initial content of $^{18}O$ in $CO_2$.

**The Exchange between Oxygen and Carbon Dioxide on Zinc Oxide.**—The exchange of oxygen occurred at a measurable rate around 450°C. The decrease in the $^{18}O$ content in oxygen and the increase in carbon dioxide are shown in Fig. 3. The number of $^{18}O$'s that the carbon dioxide had gained was less than that which the oxygen had lost. This difference may be ascribed to the exchange with zinc oxide. In the above-mentioned experiments, $^{18}O$-enriched oxygen and normal carbon dioxide were used as the starting materials. The results of the exchange experiments, in which the $^{18}O$-enriched carbon dioxide and normal oxygen were used as the starting materials, are shown in Fig. 4. A considerable decrease in the $^{18}O$ content in the carbon dioxide was observed at 350°C, but no increase in the $^{18}O$ content of the oxygen was observed up to 400 to 450°C. This finding indicates that the $^{18}O$ which were transferred from carbon dioxide to zinc oxide were not transferred to oxygen up to 400 to 450°C. On the other hand, the exchange between oxygen and zinc oxide took place, even at 350°C, in the absence of carbon dioxide (see Fig. 2).

Schwab,[9] and Matsuura et al.[10] have reported that carbon dioxide inhibits the oxidation of carbon monoxide on zinc oxide. In our experiments also, carbon dioxide acts as an inhibitor of the exchange between oxygen and zinc oxide. For that reason, no exchange is observed up to 400 to 450°C in the presence of carbon dioxide. Figures. 1, 2, and

9) G. M. Schwab, *Z. Physik. Chem. (Neue Folge)*, **1**, 42 (1954).
10) I. Matsuura, Y. Kubokawa and O. Toyama, *J. Chem. Soc. Japan, Pure Chem. Sec. (Nippon Kagaku Zasshi)*, **81**, 997 (1960).

3 indicate that the rate of the isotopic exchange decreases in the following order;

$$CO_2\text{-}ZnO > O_2\text{-}ZnO > O_2\text{-}CO_2$$

According to these results, it was concluded that the isotopic exchange between oxygen and carbon dioxide takes place through the exchange between these gases and the oxygen atoms of zinc oxide, and that the limiting step is the exchange with oxygen.

## Summary

Isotopic oxygen exchange reactions between carbon dioxide and zinc oxide, and between oxygen and carbon dioxide on zinc oxide, have been studied by the static method in the temperature range from 350 to 550°C. At any temperature carbon dioxide exchanges its oxygen atoms with those of zinc oxide rapidly. Within a few minutes after the initiation of the reaction, an isotopic equilibrium is established between the carbon dioxide in the gas phase and a certain part of the zinc oxide. It has been found that the isotopic exchange between oxygen and carbon dioxide on zinc oxide takes place through the exchange between these gases and the oxygen atoms of the zinc oxide, that the limiting step is the exchange with oxygen, and that the carbon dioxide acts as an inhibitor of the exchange between oxygen and zinc oxide.

*Department of Chemistry*
*Faculty of Science*
*Tokyo Metropolitan University*
*Setagaya-ku, Tokyo*

# The Reaction of *C*-Substituted Ethylenediamine with the Ester of α-Halo Acid

By Kuniyoshi MASUZAWA, Mitsuo MASAKI and Masaki OHTA

(Received April 20, 1965)

In a previous report[1] it has been shown how 3,6-disubstituted 2-oxopiperazines were first synthesized by the reaction of α-chloro oximes with the esters of amino acids, followed by the reductive cyclization of the products. Recently Iwanami et al.[2] have described the synthesis of 3-ethoxycarbonylmethylene-6-methyl-2-oxopiperazine by the reaction of diethyl acetylenedicarboxylate with 1,2-propanediamine. 3-Substituted 2-oxopiperazines are usually synthesized by Aspinall's method,[3] which consists of the reaction of ethylenediamine with the ester of α-halo acid. The application of this method to the synthesis of disubstituted 2-oxopiperazine will involve the condensation of *C*-substituted ethylenediamine (III) with the ester of α-halo acid (IV). In such a case condensation may occur in one or both of two directions. Thus, the condensation of III with IV might give 3,6-disubstituted 2-oxopiperazine (V) or 3,5-disubstituted 2-oxopiperazine (VI), or a mixture of the two.

The present paper will describe the reaction of 1-phenylethylenediamine (IIIa) with ethyl α-bromo-β-phenylpropionate (IVa) and that of 1,2-propanediamine (IIIb) with ethyl α-bromopropionate (IVb), reactions yielding, as the main products, the corresponding 3,6-disubstituted 2-oxopiperazines (V). Although 1-phenylethylenediamine (IIIa) is usually prepared by reducing phenylaminoacetonitrile,[4] phenylglyoxime,[5] or phenylglycineamide,[6] these methods of preparation are troublesome or have defects in yield. The conversion of phenacylamine hydrochloride (I) to the oxime is usually in a low yield, because the former cyclizes rapidly to 2,5-diphenylpyrazine in the course of the reaction.[7] The oximination of α-halo and α-amino ketones have been known to be successfully carried out in the presence of acetic acid liberated from sodium acetate.[8] Phenacylamine hydrochloride (I) was converted to the oxime in a good yield by reaction with hydroxylamine hydrochloride and an excess of sodium acetate, and the resulting oxime was hydrogenated in the presence of Raney-nickel to IIIa. Ethyl α-bromo-β-phenylpropionate (IVa) was treated with an excess of IIIa in benzene to give, as the main product, crystals with a m. p. of 170—171.5°C

1) M. Masaki and M. Ohta, This Bulletin, **36**, 922 (1963).
2) Y. Iwanami, Y. Kenjo, K. Nishibe, M. Kajiura and S. Isoyama, This Bulletin, **37**, 1740 (1964).
3) S. R. Aspinall, *J. Am. Chem. Soc.*, **62**, 1202 (1940).
4) a) H. Reihlen, *Ann.*, **493**, 25 (1932); b) Z. Welvart, *Compt. rend.*, **239**, 1299 (1954).
5) Suzanne Ser, L. Piaux and P. Fréon, ibid., **229**, 376 (1949).
6) V. G. Yashunski, V. F. Vasil'eva, L. I. Tikhorova and M. N. Shchukina, *Zhur. Obshcheĭ. Khim.*, **29**, 2709 (1959).
7) a) S. Gabriel and G. Eschenbach, *Ber.*, **30**, 1126 (1897); b) S. Gabriel, ibid., **41**, 1127 (1908).
8) M. Masaki et al., unpublished work of this Laboratory.

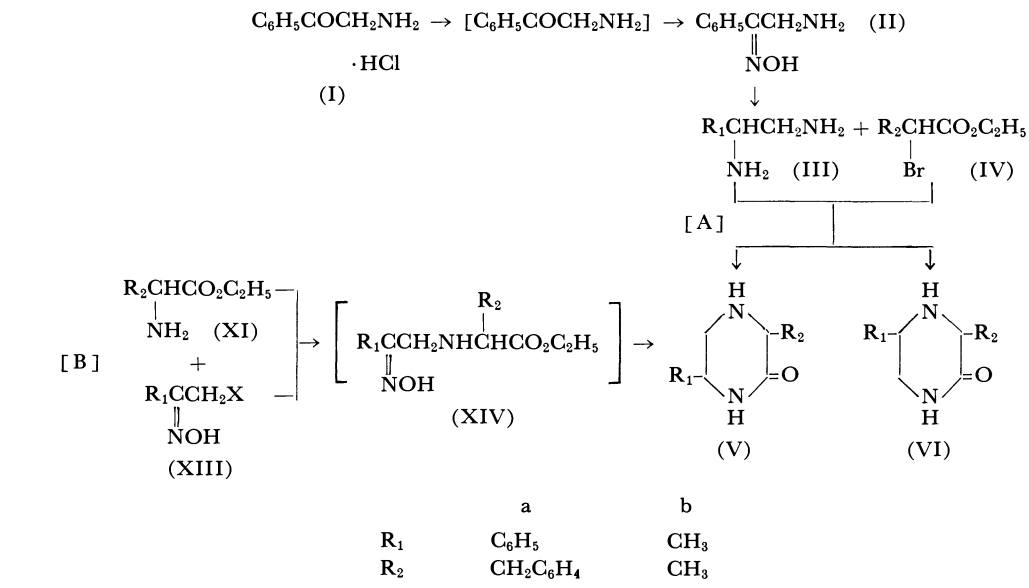
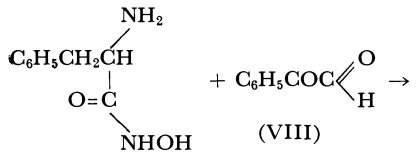
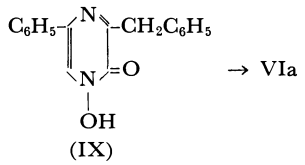



Fig. 1.

and a trace of a crystalline substance with an m. p. of 152—154°C, which was isolated from the mother liquor of the recrystallization of the former by means of column chromatography. The main product (m. p. 170—171.5°C) was easily identified as 3-benzyl-6-phenyl-2-oxopiperazine (Va) by a mixed



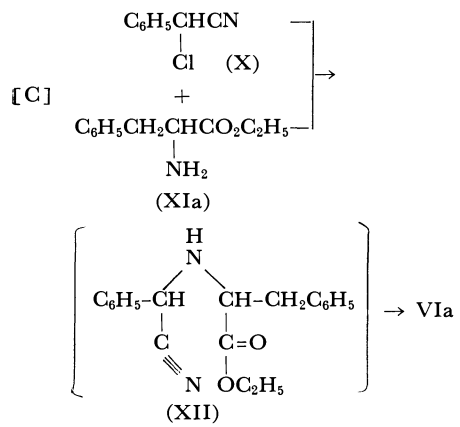




Fig. 2

melting point determination with an authentic sample.[10]

The structure of the substance with an m. p. of 152—154°C was indicated as being the 3,5-isomer by an elementary analysis of it and by its infrared spectrum. In order to confirm this, 3-benzyl-5-phenyl-2-oxopiperazine (VIa) was then synthesized through other two routes. It has been shown by Dutcher[9] that Aspergillic acid (1-hydroxy-3-isobutyl-6-*s*-butyl-2-pyrazinone) can be reduced to the corresponding 3,6-disubstituted 2-oxopiperazine by zinc and acetic acid. In a similar manner, 1-hydroxy-3-benzyl-5-phenyl-2-pyrazinone (IX) which had been synthesized by the reaction of DL-phenylalanylhydroxylamine (VII) with phenylglyoxal (VIII) was reduced, yielding the required 3-benzyl-5-phenyl-2-oxopiperazine (VIa), which was also synthesized by alternative route. By the treatment of α-chlorophenylacetonitrile (X) with DL-phenylalanine ethyl ester (XIa) in the presence of equimolar triethylamine, the *N*-(α-cyanobenzyl)-phenylalanine ethyl ester was obtained as an oily product. The product, without purification, was hydrogenated at 80°C in the presence of Raney-nickel; a simultaneous cyclization then occurred, giving VIa. The crystalline by-product with an m. p. of 152—154°C, which was obtained in the reaction of IIIa with IVa, showed no depression in a mixing test with the 3-benzyl-5-phenyl-2-oxopiperazine (VIa) prepared above.

In a manner analogous to the above case, the reaction of 1,2-propanediamine (IIIb) with ethyl α-bromopropionate (IVb) in benzene gave an oily product; this was converted to crystalline hydrochloride and a phenylureido derivative, which were

9) J. D. Dutcher, *J. Biol. Chem.*, **171**, 321 (1947).

characterized as 2-oxopiperazine derivatives by an elementary analysis of them and on the basis of their infrared spectra. These derivatives showed no depression in a mixing test with the corresponding derivatives of the 3,6-dimethyl-2-oxopiperazine (Vb) synthesized by an alternative method, which consisted of the reaction of $\alpha$-chloroacetone oxime (XIIIb) with the DL-alanine ethyl ester in ether, followed by the reductive cyclization of the product. In the case of the reaction of IIIb with IVb, the formation of the 3,5-isomer was not observed.

It is of interest that 3,6-disubstituted 2-oxopiperazine is formed exclusively either in the reaction of *C*-substituted ethylenediamine with the ester of $\alpha$-halo acid or in the reaction of 1,2-propanediamine with diethyl acetylenedicarboxylate.

## Experimental

**Phenacylamine Oxime (II).** — A hot solution of sodium acetate (24.8 g., 300 mmol.) in water (50 ml.) was added with stirring to solution of hydroxylamine hydrochloride (7.0 g., 100 mmol.) and I[10] (8.6 g., 50 mmol.) in water (50 ml.). The temperature was then raised from 20°C to 55°C. After it had been stirred for several hours, the pale yellow solution was allowed to stand overnight. The solution was made alkaline with a saturated solution of sodium carbonate in water under cooling by ice water, and then the crystals which separated from the solution were collected by filtration, washed with cold water, and recrystallized from ethanol to give colorless plates (5.3 g., 70.6%), m. p. 142—144°C (lit.[7a] m. p. 138—140°C).

**DL-1-Phenylethylenediamine (IIIa).** — To a solution of II (3.2 g., 21 mmol.) in ethanol (100 ml.) Raney-nickel (2 g.) which had previously been rinsed with ethanol (25 ml.) was added. The mixture was then stirred with hydrogen at an initial pressure of 40 kg./cm$^2$ at 70°C. Hydrogen absorption ceased after 2 hr.; the catalyst and the solvent were thereafter removed by the usual procedures. The residue was distilled under a nitrogen stream, yielding DL-1-phenylethylenediamine (2.1 g., 72.7%), b. p. 101—103°C/5.5 mmHg. Dry hydrogen chloride was introduced to the solution of IIIa in ethanol in order to precipitate crystalline solids which, after recrystallization from methanol, afforded pure dihydrochloride, m. p. 295—300°C (decomp., lit.[6] 300—301°C).

Found: C, 45.89; H, 6.95; N, 13.11. Calcd. for $C_8H_{12}N_2 \cdot 2HCl$: C, 45.94; H, 6.75; N, 13.39%.

**The Reaction of IIIa with IVa.**—A solution of IVa (3.6 g., 14 mmol.) in benzene (5 ml.) was vigorously stirred, drop by drop, into a solution of IIIa (5.7 g., 42 mmol.) in benzene (11 ml.), and the mixture was heated at 80°C for 4 hr. To the reaction mixture, a solution of potassium hydroxide (0.79 g.) in ethanol (15 ml.) was added, and the separated potassium bromide was filtered off, when the filtrate was concentrated under reduced pressure and the residue was dissolved in benzene (25 ml.), the insoluble crystals in the benzene were removed completely. The filtrate was then dried over anhydrous sodium sulfate and evaporated to dryness at 100°C under diminished pressure in order to recover the original IIIa and IVa. Carbon tetrachloride (6 ml.) was added to the residue; thereupon small needles slowly crystallized out. They were collected (1.4 g., 37.6%) and recrystallized from methanol to give colorless needles, m. p. 170—171.5°C, which showed no depression in a mixing test with authentic Va. After Va had separated, the above carbon tetrachloride was evaporated to dryness. The residue was dissolved in benzene (10 ml.), and the solution was dried over anhydrous sodium sulfate and passed through a column of activated alumina. The column was then washed with additional benzene (20 ml.). The evaporation of the combined benzene eluate yielded pale yellow solids, which were recrystallized from methanol to give the isomer of Va (0.06 g.) as colorless needles, m. p. 152—154°C. IR (KBr disk): 3430, 3300, 3180, 3050, 1655 and 1454 cm$^{-1}$.

Found: C, 76.80; H, 6.89; N. 10.79. Calcd. for $C_{17}H_{18}ON_2$: C, 76.66; H, 6.81; N, 10.52%.

**1-Hydroxy-3-benzyl-5-phenyl-2-pyrazinone (IX).** —IX was prepared by the use of the procedure of Dunn et al.[11] A solution of phenylglyoxal (2.68 g., 20 mmol.) in methanol (30 ml.) was added drop by drop to a suspension of DL-phenylalanylhydroxylamine[12] (3.6 g., 20 mmol) in methanol (30 ml.) and water (20 ml.) at −30°C. A sodium hydroxide solution (12.5 ml.; 2 N) was added during a 5—10 min. period, and then mixture was stirred at −30°C for 15 min. The temperature was raised to 0°C during the next 10 min., at the end of which period dissolution was complete. Stirring was continued at 5°C for 3 hr. The solution was acidified with a dilute solution of acetic acid to give yellow solids. These were collected, washed with water, and recrystallized from a small amount of ethyl acetate to yield yellowish needles (2.8 g., 50.0%), m. p. 165—166°C. The product gives a wine red color with a methanolic ferric chloride solution.

Found: N, 10.23. Calcd. for $C_{17}H_{14}O_2N_2$: N, 10.23%.

**The Reductions of IX.** — 1-Hydroxy-3-benzyl-5-phenyl-2-pyrazinone (IX) (1.25 g., 4.5 mmol.) was added to a solution of acetic acid (12.5 ml.) and water (12.5 ml.); zinc dust was then added in three 0.5 g. portions during 4 hr. of refluxing. The solution was cooled, and diluted with 70 ml. of water, and hydrogen sulfide was introduced to the solution until no more zinc sulfide precipitated. After the filtration of the zinc sulfide, the solution was neutralized with sodium hydroxide and extracted with three 30 ml. portions of benzene. The benzene was washed with water, dried over anhydrous sodium sulfate, and evaporated under reduced pressure, yielding crystalline, pale yellow solids. Carbon tetrachloride (4 ml.) was added to the solids, and insoluble crystals in carbon tetrachloride were collected (0.8 g., 66.7%) and recrystallized from methanol to yield colorless needles, m. p. 152—153°C (unchanged by admixture with VIa obtained by the reaction of X with XIa).

**3-Benzyl-5-phenyl-2-oxopiperazine (VIa).** — Triethylamine (2.1 g., 21 mmol.) was added to a solution of X (3.1 g., 20.5 mmol.) and XIa (4.0 g., 20.5 mmol.) in benzene (30 ml.), and the mixture was

10) C. Mannich and F. L. Hahn, *Ber.*, **44**, 1542 (1911).

11) G. Dunn, J. A. Elvidge, G. T. Newbalt, D. W. C. Ramsey, F. S. Spring and W. Sweeny, *J. Chem. Soc.*, **1949**, 2707.

12) K. G. Cunningham, G. T. Newbalt, F. S. Spring and J. Stark, ibid., **1949**, 2091.

heated at 80°C for 16 hr. The clear solution gradually became dark brown. After the mixture had been kept overnight, the triethylamine hydrochloride which had separated was filtrated off. The filtrate was washed twice successively with water with 3% hydrochloric acid, and twice more with water, and then dried over anhydrous sodium sulfate. After the solution of benzene had been saturated with hydrogen chloride under cooling, the resultant solution was allowed to stand for several hours. The separated crystals were collected, and dissolved in water (10 ml.), and the solution was filtered to remove a small amount of an insoluble substance. The filtrate was then neutralized with potassium carbonate, and the oily free base (XII) separated and it was extracted twice with benzene; the combined extracts were dried over anhydrous sodium sulfate and concentrated under reduced pressure to give XII as an brown residue (2.0 g.). A solution of crude XII (2.0 g.) in ethanol (100 ml.) was shaken with a Raney-nickel catalyst (1.0 g.) at an initial pressure of 100 kg./cm$^2$ of hydrogen at 70—80°C. The product was separated from the catalyst, the filtrate was evaporated to dryness under reduced pressure, and ligroin (5 ml.) was added to the residue. After several hours, 3-benzyl-5-phenyl-2-oxopiperazine precipitated; they were collected and washed with ligroin. The yield was 0.48 g. An analytical sample was obtained by recrystallization from methanol as colorless needles, m. p. 152—154°C. No depression of the melting point was observed on admixture with VIa synthesized by the reaction of IIIa with IVa. IR (KBr disk): 3400, 3300, 3180, 3060, 1660 and 1457 cm$^{-1}$.

Found: C, 76.63; H, 7.20; N, 11.10. Calcd. for $C_{17}H_{18}ON_2$: C, 76.66; H, 6.81; N, 10.52%.

**The Reaction of IIIb with IVb.**—A mixture of IIIb (14.8 g., 200 mmol.) and IVb (6.0 g., 33.2 mmol.) in benzene (50 ml.) was heated at 80°C for 3 hr. while being stirred. The mixture was concentrated to a half of the initial volume, and then a solution of potassium hydroxide (2.1 g.) in ethanol (30 ml.) was added. After the precipitate had separated, the solution was distilled under reduced pressure to yield a viscous liquid (2.0 g., 47%), b. p. 115—118°C/1 mmHg. The oil solidified spontaneously upon standing.

*Hydrochloride:* Colorless needles, m. p. 285—287°C (decomp.). IR (KBr disk): 3270, 2950, 2780—2250, 1685, 1465 and 1348 cm$^{-1}$.

Found: C, 44.10; H, 7.87; N, 17.02%.

*Phenylureido Derivative:* Colorless prisms, m. p. 202—203°C (unchanged by admixture with the phenylureido derivative synthesized by the reaction of XIb with XIIIb).

Found: N, 17.06%.

**3, 6-Dimethyl-2-oxopiperazine (Vb).**—A solution of chloroacetone oxime (8.3 g., 77 mmol.) in absolute ether (40 ml.) was added drop by drop to a solution of XIb (18 g., 154 mmol.) in absolute ether (180 ml.), after a few minutes amino acid ester hydrochloride began to precipitate. The mixture was then allowed to stand for 3 days at room temperature until the reaction was complete. The precipitated salt (11.1 g., 93.8%) was filtered off and washed with absolute ether. The combined ethereal solution, concentrated to about 100 ml., was extracted with 20 ml. of 3 N hydrochloric acid three times. The extracts were washed with ether, and then potassium carbonate was added until a yellow oil had separated completely. This oil was repeatedly extracted with ether, and then all the extracts were washed with saturated solution of sodium chloride and dried over anhydrous sodium sulfate. After the ether had been removed, a crude brown oil (7.0 g., 48.5% of the theoretical amount) was obtained; it was used for the next reduction step without further purification. A solution of crude XIVb (6.0 g., 32 mmol.) in ethanol (60 ml.) was shaken with Raney-nickel (2.0 g.) at an initial pressure of 100 kg./cm$^2$ of hydrogen. The reaction was then allowed to proceed for 5 hr. at room temperature. The catalyst was removed by filtration, and the brown oil was obtained by the concentration of the filtrate under reduced pressure. The oily products were distilled under a nitrogen stream to give 3,6-dimethyl-2-oxopiperazine (2.5 g., 61.0%), b. p. 129 — 132°C/2 mmHg.

*Hydrochloride:* Colorless needles, m. p. 285—286.5°C (decomp.). Its infrared spectrum in a potassium bromide pellet was superimposable with that of the hydrochloride of Vb obtained above.

Found: C, 43.90; H, 7.96; N, 17.12. Calcd. for $C_6H_{12}ON_2 \cdot HCl$: C, 43.77; H, 7.95; N, 17.02%.

**3, 6-Dimethyl-4-phenylcarbamoyl-2-oxopiperazine.**—Vb was treated with phenyl isocyanate, yielding the phenylureido derivative. This was crystallized from dilute ethanol to give colorless prisms; m. p. 202—203°C.

Found: N, 17.06 Calcd. for $C_{13}H_{17}O_2N_3$: N, 16.99%.

**The Thin-Layer Chromatography of Disubstituted 2-Oxopiperazines.**

Table I. $R_f$ Values of disubstituted 2-oxopiperazines

| Compound | Va | Va | VIa | VIa | Vb | Vb |
|---|---|---|---|---|---|---|
| Method* | A | B | A | C | A | B |
| $R_f$ | 0.75 | 0.76 | 0.82 | 0.83 | 0.31 | 0.31 |

* For details of the method, see Fig. 1 and Fig. 2.
Solvent system: *n*-Butylalcohol (4)-Acetic acid (1) - Water (2) (volume)
Adsorbent: Silica gel (Wakogel 10)
Sample: 2.5—5 μg. (0.01 ml. applied to plates)
Detection: $I_2$ vapor

*Laboratory of Organic Chemistry*
*Tokyo Institute of Technology*
*Ookayama, Tokyo*

# The Copolymerization of Cyclic Olefins with Maleic Anhydride*

By Shunsuke MURAHASHI, Shun'ichi NOZAKURA and Katsutoshi YASUFUKU

(Received April 23, 1965)

Olefins with an internal double bond are known to homopolymerize reluctantly. This is believed to be due to steric interaction, in the propagating transition state, between monomer substituents and the propagating polymer end.[1] It is conceivable that, in addition to steric effects, resonance and polar effects are also operative here, as in the case of vinyl polymerization. The present authors hope to elucidate the reactivities of internal olefins in terms of these and other unknown factors. Cyclic olefins are considered to be simple internal olefins, since both polar and resonance factors can be regarded as constant, with their relative reactivities governed mainly by steric factors.

Some polymerization reactions of cyclic olefins are known. It has been reported that cyclic olefins gave oily low polymers by a radical mechanism under high pressure.[2] Recently, a new type of the ring-opening polymerization of cyclopentene has been reported.[3] As for the copolymerization of cyclic olefins, the formation of polysulfones is a well-known example of radical polymerization.[4] The copolymerization of cyclic olefins with ethylene, using Ziegler catalysts, has also been reported.[5]

The reaction of cyclic olefins with maleic anhydride was reported, by Alder et al.[6] and by Barltrop and Robson[7], to give an 1:1 adduct. More recently, Imoto et al. described the copolymerization of butenes with maleic anhydride.[8]

The present paper will compare the reactivity of cyclic olefins and butene-2 isomers in the copolymerization with maleic anhydride (MAn). The kinetics of the formation of the cyclopentene-MAn copolymer will also be described.

## Experimental

**Materials.** — Cyclobutene was synthesized by the pyrolysis of the adduct of cycloöctatetraene and acetylenedicarboxylic acid according to a known method.[9] The yield of the pyrolysis, which was carried out at 220°C (10 mmHg), was 98%. The infrared spectrum of the product was identical to that reported in the literature.[10] Cyclopentene (b. p. 44—44.5°C), cyclohexene (b. p. 81.5—82.0°C) and cycloheptene (b. p. 115°C) were synthesized by the usual methods. *cis*-Cyclooctene (b. p. 73.5—74.5°C (85 mmHg)) was a commercial product and was purified by rectification. All the monomers were checked for purity by gas chromatography.

MAn was distilled and stored in a desiccator as a benzene solution. 2,2'-Azobis-isobutyronitrile was recrystallized from ethanol.

**Polymerization.** — Polymerization was carried out in a sealed tube and/or in a dilatometer. Into a 20 ml. glass ampoule was placed a known amount of a monomer solution in benzene, together with an initiator solution. The solution was then degassed, using three freeze-thaw cycles, and sealed under a vacuum, after which the sealed ampoule was kept in a thermostat at 60±0.05°C. In the case of the butenes, a known volume of liquified butene was distilled, under a vacuum, into the ampoule, which contained the other reactants and the solvent. The mixture after polymerization was dissolved in a small amount of dry acetone and reprecipitated with dry ether. This procedure was repeated three times. The polymer was then extracted with ether and dried in vacuo at room temperature.

Dilatometers had a capillary 2 mm. in inside diameter and a total volume of about 13 ml. The volume contraction was read to $10^{-2}$ mm. by a cathetometer, and the relation between the volume contraction and the conversion was obtained by precipitating the polymer after polymerization.

**The Esterification of Copolymers.** — When a cyclopentene-MAn copolymer (soft. p. 195—200°C) was refluxed in methanol for 3 days, the result was a homogeneous solution of half esters, which softened at 145—150°C. These half esters were soluble in methanol, acetone and dioxane, but insoluble in ether, benzene, haxane and water. A dioxane solution of the half ester was treated with an ether solution of diazomethane at room temperature to yield the dimethyl esters of the copolymer, which softened at 100—110°C. The dimethyl ester was soluble in acetone and benzene, and insoluble in ether. The infrared spectra of the anhydride copolymer and its dimethylester are shown in Fig. 1.

Found for cyclopentene-MAn copolymer: C, 64.15; H, 6.29. Calcd. for $C_5H_8 \cdot C_4H_2O_3$: C, 65.04; H, 6.06%.

* Paper V in a series on "The Polymerization of Internal Olefins." For the preceding paper, see *Chem. High Polymers (Kobunshi Kagaku)*, to be published. Presented at the Meeting of Polymer Science, Kobe, July, 1964.

1) T. Alfrey, J. J. Bohrer and H. Mark, "Copolymerization," Interscience Publishers, New York (1951), p. 51.

2) K. E. Weale, *J. Chem. Soc.*, **1955**, 2295.

3) G. Natta, G. Dall'Asta and G. Mazzanti, *Angew. Chem.*, **21**, 765 (1964).

4) J. E. Hazell and K. J. Ivin, *Trans. Faraday Soc.*, **58**, 176 (1962).

5) G. Dall'Asta and G. Mazzanti, *Makromol. Chem.*, **61**, 178 (1963).

6) K. Alder, G. Pascher and A. Schnitz, *Chem. Ber.*, **76**, 27 (1943).

7) J. A. Bartrop and R. Robson, *Tetrahedron Letter*, **1963**, 597.

8) T. Otsu, A. Shimizu and M. Imoto, *J. Polymer Sci.*, **B2**, 973 (1964).

9) A. C. Cope and A. C. Haven, *J. Am. Chem. Soc.*, **74**, 4867 (1952).

10) R. C. Lord and D. G. Rea, ibid., **79**, 2401 (1957).

Found for dimethyl ester of the copolymer: C, 62.43; H, 7.57. Calcd. for $C_5H_8 \cdot C_6H_8O_4$: C, 62.24; H, 7.59%.

**An Analysis of Copolymer Composition.**—The copolymers thus obtained were found to have been partly hydrolyzed because of unavoidable contact with moisture, and so the copolymer composition was calculated from an analysis of both carbon and hydrogen, using a calibrated composition formula: $[\text{cycloolefin}]_x [\text{MAn}]_y [\text{H}_2\text{O}]_z$.

The molecular weight of the copolymers was determined in acetone, and that of the dimethyl ester of the copolymer, in benzene, using a Mechrolab Vapor Pressure Osmometer.

## Results

**The Reactivity of Cyclic Olefins.**—In order to compare the reactivity of cyclic olefins in the copolymerization with MAn, copolymerization was carried out in benzene at an equimolar monomer concentration; the results are shown in Table I.

Table I. Copolymerization of cyclic olefins ($M_2$) with MAn ($M_1$)

$[\text{MAn}] = [\text{Olefin}] = 1.54$ mol./l.; $[\text{AIBN}] = 3.2 \times 10^{-2}$ mol./l. in benzene; 60±0.05°C

| $M_2$ | Time hr. | Yield % | %/hr. | Soft. p. °C | MW |
|---|---|---|---|---|---|
| Cyclobutene | 0.32 | 13.2 | 41.8 | 180—190 | Insol. |
| Cyclopentene | 1.25 | 26.2 | 21.0 | 190—195 | 1600 |
| Cyclohexene | 23 | 17.7 | 0.8 | 170—185 | 500 |
| Cycloheptene | 19 | 18.3 | 1.0 | 240—245 | 700 |
| Cyclooctene (*cis*) | 14 | 19.7 | 1.4 | 250—255 | 1600 |

The copolymers obtained in Table I were white brittle solids and were soluble in acetone, dioxane, dimethylformamide, dimethylsulfoxide, pyridine

Table II. Copolymerization of cyclic olefins ($M_2$) with MAn ($M_1$) in benzene, 60±0.05°C

| $M_2$ | $M_1$ mol. % | $M_2$ mol. % | Time hr. | Conversion % | Analysis C, % | Analysis H, % | $m_1$ mol. % | $m_2$ mol. % |
|---|---|---|---|---|---|---|---|---|
| Cyclobutene | 43.8 | 56.2 | 0.3 | 13.2 | 62.01 | 5.98 | 44.4 | 55.6 |
| | 65.0 | 35.0 | 0.3 | 2.2 | 61.57 | 5.06 | 53.7 | 46.3 |
| Cyclopentene | 11.1 | 88.9 | 1.1 | 3.7 | 64.21 | 5.81 | 52.3 | 47.7 |
| | 16.6 | 83.4 | 1.2 | 3.7 | 64.35 | 5.97 | 50.7 | 49.3 |
| | 33.3 | 66.7 | 1.5 | 4.1 | 64.10 | 5.93 | 50.4 | 48.6 |
| | 44.4 | 55.6 | 1.7 | 4.0 | 63.99 | 5.99 | 50.7 | 49.3 |
| | 50.0 | 50.0 | 1.9 | 3.3 | 63.47 | 5.97 | 51.2 | 48.8 |
| | 55.6 | 44.4 | 3.3 | 3.3 | 63.98 | 6.01 | 50.7 | 49.3 |
| | 66.7 | 33.3 | 3.4 | 2.2 | 62.71 | 6.09 | 50.9 | 49.1 |
| | 83.3 | 16.7 | 8.5 | 1.5 | 62.44 | 5.85 | 52.6 | 47.4 |
| Cyclohexene | 33.6 | 66.4 | 17.5 | 6.1 | 63.94 | 6.33 | 54.3 | 45.7 |
| | 50.0 | 50.0 | 17.5 | 10.6 | 63.34 | 6.32 | 54.8 | 45.2 |
| | 66.6 | 33.4 | 17.6 | 9.7 | 61.82 | 6.10 | 57.3 | 42.7 |
| | 80.0 | 20.0 | 17.6 | 9.6 | 59.72 | 6.09 | 58.7 | 41.3 |
| | 83.3 | 16.7 | 17.7 | 11.3 | 58.20 | 5.92 | 61.4 | 38.6 |
| Cycloheptene | 54.0 | 46.0 | 15.6 | 3.4 | 65.17 | 6.72 | 55.6 | 44.4 |
| | 67.4 | 32.6 | 15.6 | 4.9 | 63.55 | 6.52 | 57.8 | 42.2 |
| | 79.2 | 20.8 | 15.6 | 4.4 | 62.90 | 6.25 | 59.8 | 40.2 |
| | 81.0 | 19.0 | 15.6 | 4.0 | 62.61 | 6.25 | 60.0 | 40.0 |
| Cyclooctene (*cis*) | 16.6 | 83.4 | 24.4 | 4.6 | 67.64 | 7.60 | 51.5 | 48.5 |
| | 33.3 | 66.7 | 24.4 | 4.9 | 66.55 | 7.34 | 53.3 | 46.7 |
| | 50.0 | 50.0 | 24.5 | 5.0 | 65.56 | 7.17 | 55.4 | 44.6 |
| | 77.8 | 22.2 | 25.3 | 5.0 | 63.72 | 6.97 | 58.0 | 42.0 |
| | 83.3 | 16.7 | 27.0 | 5.6 | 62.47 | 6.98 | 58.5 | 41.5 |
| *cis*-Butene-2 | 28.5 | 71.5 | 14.8 | 9.2 | 61.51 | 6.50 | 50.2 | 49.8 |
| | 46.6 | 53.4 | 14.8 | 6.3 | 61.25 | 6.41 | 51.2 | 48.8 |
| | 60.8 | 39.2 | 14.8 | 9.0 | 60.99 | 6.38 | 51.2 | 48.8 |
| | 72.2 | 27.8 | 14.8 | 10.7 | 61.02 | 6.42 | 51.2 | 48.8 |
| *trans*-Butene-2 | 28.5 | 71.5 | 17.4 | 5.7 | 60.67 | 6.48 | 50.7 | 49.3 |
| | 46.6 | 53.4 | 17.4 | 4.2 | 61.04 | 6.39 | 51.5 | 48.5 |
| | 60.8 | 39.2 | 17.5 | 4.8 | 60.81 | 6.48 | 51.0 | 49.0 |
| | 72.2 | 27.8 | 17.6 | 4.8 | 59.98 | 6.27 | 52.8 | 47.2 |

and methanol (except for the copolymer of cyclobutene), but insoluble in hexane, benzene, chloroform and ether. The cyclobutene copolymer swelled in these solvents. Although a comparison of the relative overall reactivities of cyclic olefins can be made on the basis of these relative rate data, these data do not measure reactivity in propagation because of the inclusion of initiation and termination rates. To obtain a stricter measure of the reactivity in the propagation reaction, monomer reactivity ratios were calculated by the usual procedure from a set of copolymerizations for each monomer. Since cyclic olefins did not homopolymerize under these conditions, the following simplified copolymer composition equation can be used: $(m_1/m_2)-1=r_1M_1/M_2$, where $m_1$, $m_2$, $M_1$ and $M_2$ denote the concentrations of MAn and cyclic olefin in the copolymer and the monomer mixture respectively. The results are listed in Table II,

TABLE III. MONOMER REACTIVITY RATIOS IN THE COPOLYMERIZATION OF CYCLIC OLEFINS ($M_2$) WITH ($M_1$)

| $M_2$ | $r_1$ | $1/r_1$ |
|---|---|---|
| Cyclopentene | 0.010±0.003 | 100 |
| Cyclohexene | 0.083±0.005 | 12 |
| Cycloheptene | 0.068±0.002 | 14.5 |
| Cyclooctene (*cis*) | 0.067±0.006 | 15 |
| *cis*-Butene-2 | 0.016±0.005 | 63 |
| *trans*-Butene-2 | 0.030±0.009 | 33 |

together with data on butene-2 isomers. The $r_1$ values are summarized in Table III. The $1/r_1$ value measures the relative reactivity of cyclic olefins towards the MAn radical of the growing polymer end.

In calculating the copolymer composition from carbon and hydrogen analysis, a correction was made for the partial hydrolysis of the anhydride group. This treatment was found to give a better straight line with less standard deviation than that which did not consider partial hydrolysis. In fact, the infrared spectra of the copolymers showed a weak shoulder at 1720 $cm^{-1}$ indicating the existence of free acid. Even the same sample yielded different analyses after storage in air, but after correcting for hydrolysis the calculated compositions remained constant.

The copolymer composition curve should go through the point of origin if the simplified copolymer equation represents the system adequately. An intercept at the ordinate might indicate either the existence of a systematic error in the analysis or a penultimate effect.[11] In the present treatment, however, the slope was taken as $r_1$, with the small intercept at the ordinate ignored.

The data illustrate that *cis*-butene-2 is about twice as reactive as the trans-isomer. The relative reactivity is:

cis/trans = 1.91 from $1/r_1$ values

cis/trans = 1.84 from dilatometric measurements

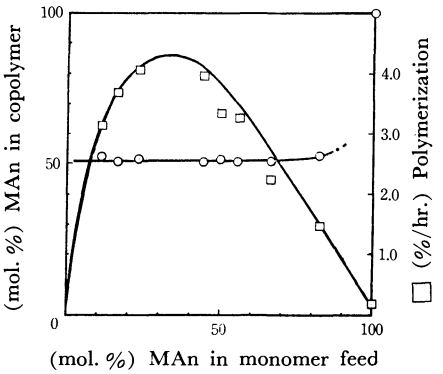



Fig. 2. Copolymer composition and rate in the cycloheptene-MAn copolymerization, 60°C in benzene.
[AIBN] = $1.05\times10^{-2}$ mol. $l^{-1}$
[MAn+Cyclopentene] = 1.72 mol. $l^{-1}$

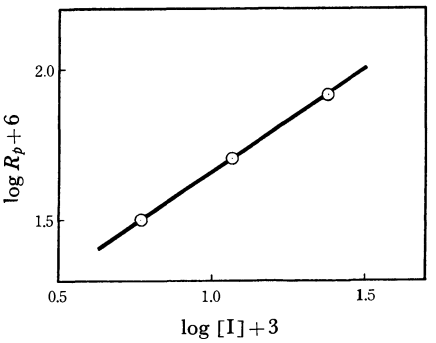



Fig. 3. Dependence of rate on initiator concentration in cyclopentene-MAn copolymerization, at 60°C in benzene.
[MAn] = [Cyclopentene] = 1.186 mol. $l^{-1}$

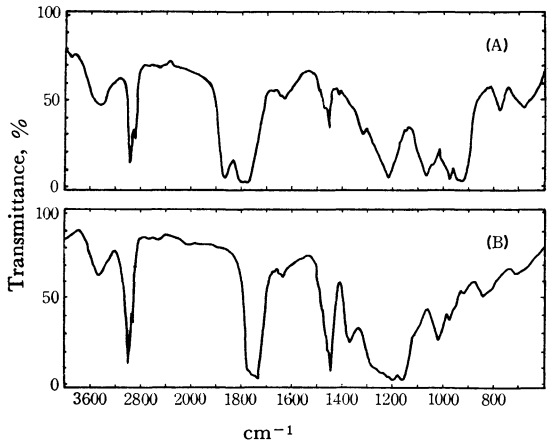



Fig. 1. IR spectra of cyclopentene-MAn copolymer (A), and its dimethyl-esterified product (B).

11) C. H. Bamford, W. G. Barb, A. D. Jenkins and P. F. Onyon, "The Kinetics of Vinyl Polymerization by Radical Mechanisms," Butterworth Scientific Pub., London (1958), p. 162.

The two values are in good agreement.

**The Kinetics of the Cyclopentene-MAn Copolymerization.**—The rate data for the copolymerization of cyclopentene and MAn, together with the copolymer composition curve, are shown in Fig. 2. MAn homopolymerizes slightly (0.18%/hr.) under the reaction conditions. A maximum rate was observed at 30 to 40 mol.% of MAn. The dependency of the rate on the initiator concentration (Fig. 3) and on the monomer concentration (Fig. 4) was measured, giving the expression:

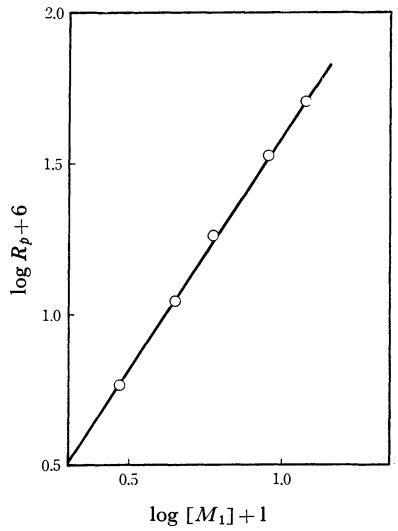



Fig. 4. Dependence of rate on the monomer concentration at 60°C in benzene.
[AIBM] = $1.14\times10^{-2}$ mol. $l^{-1}$
[MAn]/[Cyclopentene] = 1

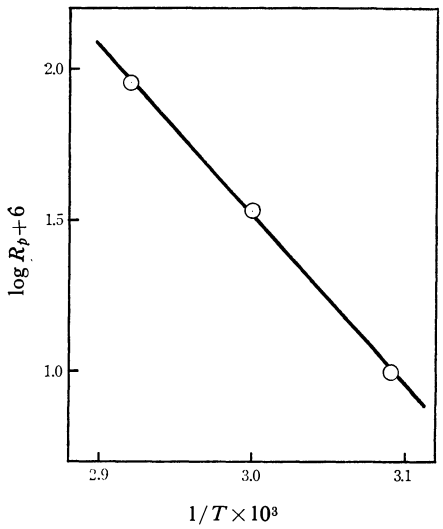



Fig. 5. Dependence of rate on temperature.
[MAn] = [Cyclopentene] = 0.895 mol. $l^{-1}$
[AIBN] = $1.14\times10^{-2}$ mol. $l^{-1}$

$$-(dM_1+dM_2)/dt=k[I]^{0.68\pm0.005}[M_1]^{1.54\pm0.018}$$

when $[M_1]=[M_2]$

$$k=(8.57\pm0.78)\times10^{-4}\ \text{mol.}\ l^{-1}\ \text{sec}^{-1}$$

An Arrhenius plot of the copolymerization rate data (Fig. 5) yielded an overall activation energy of 24.2±0.35 kcal./mol. Thus the overall rate constant, $k$, at 60°C is:

$$k=Ae^{-E/RT}=5.83\times10^{12}\,e^{-24.2kcal/RT}$$

No thermal polymerization was observed without the initiator for this monomer pair.

The molecular weights of the dimethylated copolymer were measured using a vapor pressure osmometer; values ranged from 3300 to 4400, i. e., the degree of polymerization was 30 to 40. Slight decreases in the molecular weight were observed with increasing monomer concentrations and initiator concentrations.

## Discussions

**The Copolymers of Cyclic Olefins and MAn.**—It may be seen from Table I that cyclobutene is much more reactive than the other cyclic olefins. Although the monomer reactivity ratio was not determined for cyclobutene because of insufficient data, Table II suggests that cyclobutene may add to its own radical. Cyclobutene has not been considered to homopolymerize by a radical mechanism.[5] It may also be noted that the copolymer was not soluble, and that even its dimethyl ester only swelled in organic solvents. This fact suggests that cross-linking had taken place during the polymerization, presumably due to opening of the cyclobutene ring.

Upon the dimethylation of the cyclopentene-MAn copolymer, the $\nu$C=O band at 1860 and 1780 $cm^{-1}$ and the $\delta$C–O–C band at 1220 $cm^{-1}$, which are due to the 5-membered cyclic acid anhydride group, disappeared; instead the $\nu$C=O of the ester appeared at 1720 $cm^{-1}$ (Fig. 1). The bands due to the cyclopentane ring at 970 and 920 $cm^{-1}$ became discernible in the dimethylated copolymer. There was a weak band at 1635 $cm^{-1}$; the fact that it increased in intensity upon methylation suggests that the $\nu$C=C band may be assigned to a double bond of the maleic anhydride type. The formation of that type of unsaturation may result from a chain transfer reaction. It has also been suggested by Joshi that the hydrogen atom of MAn is likely to be abstracted by a radical.[12] In fact, the molecular weight of the copolymer is always low, the degree of polymerization being at most 40.

**The Copolymerization of MAn ($M_1$) and Cyclopentene ($M_2$).**—Cyclopentene was chosen as representative of the cyclic olefins, and the kinetics

12) R. M. Joshi, *Makromol. Chem.*, **53**, 33 (1962).

of its copolymerization were sutdied. The rate of copolymerization was found to be of about the 0.7 th order with respect to the initiator. The value was significantly larger than one half, indicating some contribution of an unimolecular termination to the usual bimolecular one. The degradative chain transfer may partly account for the low molecular weight of the copolymers.

The rate was also found to be of the 1.5th order with respect to the monomer. A theoretical expression for the rate of copolymerization can be reduced to the following simple form in the case of $r_2=0$ and $[M_1]=[M_2]$:

$$R_p=kR_i^{1/2}[M_1]$$

The observed 1.5th order dependency might suggest that the monomer plays a role in the initiation reaction.

The monomer pair was found qualitatively to show a charge transfer band in the ultraviolet absorption spectrum.[13] In such an alternating copolymerization system, a question arises as to whether the two monomers behave as a complexed species in the propagation, as has been suggested in polysulfone formation.[14,15] If so, the rate of copolymerization should be at least of the second-order with respect to the monomer in the above expression, since the concentration of the complex molecule is low enough to be represented by $K_c[M_1][M_2]$.

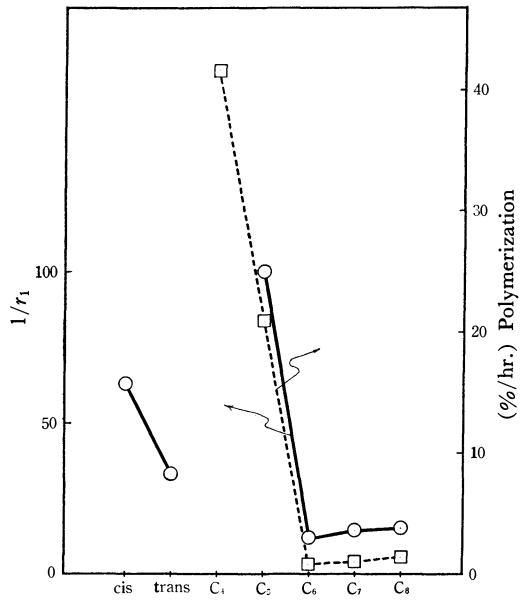



Fig. 6. Reactivities of cyclic olefins in the copolymerization with MAn.

$K_c$ denotes an equilibrium constant of the charge transfer reaction. The observed monomer dependency suggests that the present system is not such an extreme case.

**The Reactivity of Cyclic Olefins.**—The results listed in Tables I and III are reproduced in Fig. 6. The relative reactivity as determined by the $1/r_1$ value and the rate data are in good agreement. The features may be summarized as: i) The relative reactivities of cyclic olefins towards the growing MAn radical had a minimum at cyclohexene, higher members had slightly higher reactivities, and lower members had markedly higher reactivities.

ii) *cis*-Butene-2 is twice as reactive as the trans-isomer. *trans*-1, 2-Disubstituted ethylenes usually show higher reactivities than the cis-isomer.[16] This was rationalized by assuming that the resonance stabilization of the transition state is favored in the trans-isomers. The explanation could not, however, be applied to the present case.

iii) The reactivities of cyclohexene, cycloheptene and *cis*-cyclooctene were even lower than that of *trans*-butene-2, indicating that ring formation does not always activate the double bond.

The main factors which will control the reactivity of cyclic olefins are considered to be: 1) the difference in the strain energy in an olefin and the corresponding paraffin, 2) the strain energy of olefins, 3) steric hindrance due to ring bulkiness. Factors 1 and 2 will contribute to the activation energy of the propagation reaction, while factor 3 contributes mainly to the entropy term. If it is assumed that there is not much difference in the transition states for all the cyclic olefins, the difference between the strain energy in an olefin and that in the corresponding paraffin might reflect on the activation energy and, hence, on the relative reactivity. The energy difference can be approximated by the heat of the hydrogenation of these olefins.[17] Cyclohexene has the largest heat of hydrogenation, and so it should be the most reactive. However, this was not the case. Thus, factor 1 is not considered to be the predominant one.

A better correspondency was found between factor 2 and the observed reactivity. The strain energy of olefins is reproduced from the literature in Fig. 7.[18] The strain energy of *cis*-butene-2 is larger than that the of trans-isomer, and it is also in good agreement with the observed reactivity. Thus, the strain energy is considered to be one of the main factors which govern the reactivity of cyclic olefins.

Factor 3 may also make some contribution to

13) Unpublished data.
14) W. G. Barb, *Proc. Roy. Soc.*, **A212**, 66 (1952).
15) I. Ito, T. Saegusa and J. Furukawa, *J. Chem. Soc. Japan, Ind. Chem. Sec.* (*Kogyo Kagaku Zasshi*), **65**, 703 (1962).
16) C. Walling, "Free Radicals in Solution," John Wiley & Sons, New York (1957), p. 127.
17) J. Gresser, A. Rajbenbach and M. Szwarc, *J. Am. Chem. Soc.*, **83**, 3005 (1961).
18) J. G. Traynham and M. F. Sehnert, *J. Am. Chem. Soc.*, **78**, 4024 (1956).

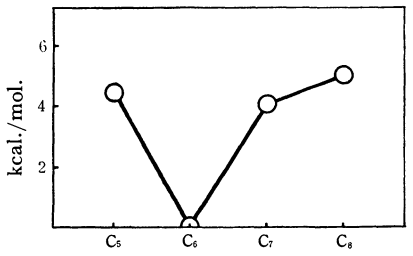



Fig. 7. Strain energy difference of cyclic olefin based on cyclohexene.[18]

the relative reactivity. In a study of methyl affinities,[17] cycloheptene and cyclooctene showed comparable reactivities to cyclopentene. In copolymerization with MAn, the attacking polymer radical is much larger than a methyl radical, and so the steric hindrance of higher cyclic olefins might have been enhanced in the copolymerization.

## Summary

The relative reactivities of cyclo-butene, -pentene, -hexene, -heptene, -octene(*cis*), *cis*- and *trans*-butene-2 have been compared in the copolymerization with MAn. The reactivity showed a minimum at cyclohexene, with the higher members having slightly higher reactivities and the lower members having markedly higher reativites than cyclohexene. *cis*-Butene-2 was found to be twice as reactive as the trans-isomer. These facts have been explained by a combination of the effects of the strain energy of olefins and of steric hindrance.

The kinetics of the copolymerization of cyclopentene and MAn was studied at 60°C in benzene, the overall rate being expressed by:

$$R_p = k[\mathrm{I}]^{0.7}[\mathrm{M}_1]^{1.5} \quad \text{when} \quad [\mathrm{M}_1]=[\mathrm{M}_2]$$

$$k = 5.83 \times 10^{12}\, e^{-24.2kcal/RT}$$

*Department of Polymer Science*
*Faculty of Science*
*Osaka University*
*Nakanoshima, Osaka (S. M. & S. N.)*

*The Institute of Physical & Chemical Research*
*Bunkyo-ku, Tokyo (K. Y.)*

# Studies of the Liquid-Liquid Partition Systems. IV. The Solvent Extraction Study of Europium(III) Adduct Chelate Complexes with Six Acetylacetone Derivatives and Tributylphosphate

By Tatsuya SEKINE and Masaru ONO

(Received April 24, 1965)

The enhancement of metal chelate extractions by the addition of a neutral organophilic ligand has attracted the attention of many authors and has very often been called the "synergic effect."

The synergic effect has been found in many metal extraction systems with various chelating acids and neutral ligands; the enhancement of the extraction has been explained by the adduct formation of the metal chelates with the neutral ligand in the organic phases. A short review of this problem is given in Ref. 1.

The synergic enhancement of the metal extraction has been most extensively studied in metal extraction systems with thenoyltrifluoroacetone (TTA) and various organic phosphate esters. Some of the results in the previous work may be summarized briefly as follows: (i) The TTA metal chelate extraction systems show a much larger synergic effect than many other metal chelate extraction systems. (ii) The synergic effect is larger when the neutral adduct-forming ligand is an organic phosphate ester than when it is any other neutral ligand. (iii) The synergic effect is quite different when the central metal ion in the TTA chelate is different. TTA chelates of trivalent lanthanides and actinides or uranyl ions show larger synergic effects than many other metal TTA chelates. (iv) The synergic effect is different in different inert organic solvents. The effect is usually larger when water has a smaller solubility in the solvent.

The mechanism of the synergic enhancement of the metal chelate extraction seems not to be very simple, and even though some discussion has been presented to explain this phenomenon, the details seem not to have been understood completely.

In our laboratory, a systematic study has been carried out to obtain further information on the synergic effect of metal chelates. For the present paper, the authors have studied the differences

in the adduct formation of europium(III) chelates with six acetylacetone derivatives and tributylphosphate (TBP) in chloroform. These six β-diketones were chosen in order to determine if the large synergic effect in the metal TTA extraction systems is a character of metal chelates with (a) common β-diketones, (b) β-diketones with a trifluoromethyl group, (c) β-diketones with a large organic group such as a thenoyl group, or (d) β-diketones with both a trifluoromethyl group and a thenoyl group.

Europium(III) was chosen as the central metal ion in the chelate, TBP was chosen as the adduct-forming ligand, and chloroform was chosen as the inert organic solvent. The choices were made in order to make it possible to compare the results with previous results.[1]

Acetylacetone and its five derivatives, benzoylacetone, trifluoroacetylacetone, benzoyltrifluoroacetone, froyltrifluoroacetone and thenoyltrifluoroacetone, were chosen as the chelating acids.

The chemical properties of these β-diketones and the previous work on the metal extraction with these β-diketones were summarized by Morrison and Freiser,[2] Poskanzer and Foreman,[3] and Stary.[4] In the present study, the aqueous phase was always 0.1 M sodium perchlorate solutions with a small amount of a buffer. The influence of the concentration of the electrolytes in the aqueous phase on the synergic enhancement will be reported in another paper of this series.

## Experimental

**Reagents.**—The europium 152+154 tracer was obtained from the Oak Ridge National Laboratory as europium chloride in a dilute hydrochloric acid solution. It was diluted with 0.1 M perchloric acid and used as the stock solution. The six β-diketones were obtained from the Dojin Yakukagaku Co. The other reagents were of reagent grade. Sodium perchlorate was prepared from perchloric acid and sodium carbonate. It was recrystallized two times from water. Tributylphosphate was washed with 0.1 M perchloric acid, water and 0.1 M sodium hydroxide respectively, and then several times with water until the washed solution gave a neutral color on an indicator paper. Chloroform was washed three times with water to remove the alcohol which had been added as the stabilizer.

**Procedures.**—All of the procedures were carried out in a thermostatted room at 25±0.5°C. The tracer solution, the buffer solution and 0.1 M sodium perchlorate solution were placed in stoppered glass tubes, and then chloroform solutions of the chelating acid and TBP were added to the tubes. The aqueous phase was buffered with sulfanilate, acetate, or triethanolamine. The initial concentration of the buffer was 0.01 M. The initial volumes of the organic and the aqueous phases were 5.0 ml., and the volume of the glass tubes was about 20 ml. All of the solutions were left standing overnight before use. The two phases in the tubes were agitated by a mechanical rotator at 20 r. p. m. for about two hours and centrifuged. Two-milliliter portions were pipetted from both phases and transferred into small test tubes. The γ-radioactivity of the solutions was measured with a well-type (NaI) scintillation counter. A small portion of the aqueous phase was transferred into a small vessel, and the hydrogen ion concentration was determined potentiometrically using a 0.010 M $HClO_4$+0.090 M $NaClO_4$ solution as the standard ($-\log[H^+]=2.00$).

The net distribution ratio of europium(III) was calculated as follows:

$$D=\frac{\gamma\text{-count-rate per 2 ml. of org. phase}}{\gamma\text{-count-rate per 2 ml. of aq. phase}} \quad (1)$$

## Statistical Treatment

In the present paper, the subscript "org" denotes a species in the organic phase, while the absence of a subscript denotes a species in the aqueous phase. The suffix "0" denotes the distribution ratio or the extraction constant when no adduct is formed in the organic phase.

**Metal Extraction with a Chelating Acid.**—The extraction of a trivalent metal ion $M^{3+}$ with an organophilic chelating acid, HA, can be described as follows:

$$M^{3+}+3HA(org)\rightleftarrows MA_3(org)+3H^+ \quad (2)$$

$$K_0=([MA_3]_{org}/[M^{3+}])[H^+]^3[HA]^{-3}{}_{org} \quad (3)$$

The net distribution ratio obtained by Eq. 1 is generally described as:

$$D=[M(III)]_{org,\ total}/[M(III)]_{total} \quad (4)$$

From the organic phase, a small amount of the chelating acid is distributed into the aqueous phase, and the metal ion in the aqueous phase may form chelate complexes, $MA^{2+}$, $MA_2{}^+$,… The total metal ion content in the aqueous phase is generally described as:

$$[M(III)]_{total}=[M^{3+}]+[MA^{2+}]+[MA_2{}^+]+\cdots \quad (5)$$

and Eq. 4 is described as:

$$D_0=[MA_3]_{org}/([M^{3+}]+[MA^{2+}]+[MA_2{}^+]+\cdots) \quad (6)$$

When the aqueous chelate complexes are negligible, the distribution ratio is :

$$D_0=[MA_3]_{org}/[M^{3+}] \quad (7)$$

Then the extraction constant in Eq. 3 is expressed as:

1) T. Sekine and D. Dyrssen, *J. Inorg. Nucl. Chem.*, **26**, 1727 (1964). Three more papers on this subject are to be published in the same journal.

2) G. H. Morrison and H. Freiser, "Solvent Extraction in Analytical Chemistry," John Wiley & Sons Inc., New York (1957).

3) A. M. Poskanzer and B. M. Foreman, Jr., *J. Inorg. Nucl. Chem.*, **16**, 323 (1961).

4) J. Stary, "The Solvent Extraction of Metal Chelates," Pergamon Press, Oxford (1964).

$$K_0 = D_0[H^+]^3[HA]^{-3}_{org} \quad (8)$$

or:

$$D_0 = K_0[HA]^3_{org}[H^+]^{-3} \quad (9)$$

Thus when aqueous complexes are negligible, Eq. 8 or 9 describes the distribution equilibrium of the metal ion.

The aqueous chelate complexes in Eq. 6 can be treated as follows. When the distribution constant and the dissociation constant of a chelating acid are defined as:

$$K_D = [HA]_{org}/[HA] \quad (10)$$

$$K_a = [H^+][A^-]/[HA] \quad (11)$$

then the following equation can be introduced:

$$[A^-] = (K_a/K_D) \times ([HA]_{org}/[H^+]) \quad (12)$$

When the stability constants of the aqueous chelates are defined as:

$$\beta_{aq,n} = [MA_n^{3-n}]/[M^{3+}][A^-]^n \quad (13)$$

then the following equation is introduced on the basis of Eqs. 6, 12 and 13:

$$D_0 = [MA_3]_{org}[M^{3+}]^{-1} \times \{1 + \sum_1^n \beta_{aq,n}(K_a/K_D)^n([HA]_{org}/[H^+])^n\}^{-1} \quad (14)$$

From Eqs. 7 and 9, Eq. 14 can be written as:

$$D_0 = K_0[HA]^3_{org}[H^+]^{-3} \times \{1 + \sum_1^n \beta_{aq,n}(K_a/K_D)^n([HA]_{org}/[H^+])^n\}^{-1} \quad (15)$$

When we can assume that

$$[HA]_{org} - ([HA] + [A^-]) \cong [HA]_{org}$$

we can use the initial concentration of the chelating acid in Eqs. 14 and 15 instead of the concentration at the equilibrium.

**The Adduct Formation of a Metal Chelate with a Neutral ligand.**—When a metal chelate complex, $MA_3$, in the organic phase forms adduct complexes with an organophilic neutral ligand, L, the equilibrium is described as:

$$MA_3(org) + n\,L(org) \rightleftarrows MA_3L_n(org) \quad (16)$$

$$\beta_n = [MA_3L_n]_{org}/[MA_3]_{org}[L]^n_{org} \quad (17)$$

The distribution ratio in Eq. 4 is then:

$$D = ([MA_3]_{org} + [MA_3L]_{org} + [MA_3L_2]_{org} + \cdots)/([M^{3+}] + [MA^{2+}] + \cdots) \quad (18)$$

From Eqs. 17 and 18 we can introduce:

$$D = [MA_3]_{org}(1 + \sum_1^n \beta_n[L]^n_{org})/([M^{3+}] + [MA^{2+}] + \cdots) \quad (19)$$

then from Eqs. 6 and 19 we can introduce:

$$D/D_0 = 1 + \sum_1^n \beta_n[L]^n_{org} \quad (20)$$

Here the $D_0$ is the distribution ratio of the metal ion when no adduct is formed in the system.

When we can assume that there is no chelate formation in the aqueous phase, we can define the extraction constant, $K$, when the concentration of the neutral ligand is $[L]_{org}$ as:

$$K = D[H^+]^3[HA]^{-3}_{org} \quad (21)$$

$$= \{1 + \sum_1^n \beta_n[L]^n_{org})[MA_3]_{org}/[M^{3+}]\} \times [H^+]^3[HA]^{-3}_{org} \quad (22)$$

We can then obtain the following equation from the extraction constant, $K_0$, in Eq. 8:

$$K/K_0 = 1 + \sum_1^n \beta_n[L]^n_{org} \quad (23)$$

## Graphical Expression

**Metal Extraction with a Chelating Acid.**—When no complexes are formed in the aqueous phase, Eq. 9 is valid and the $D_0$ vs. $-\log[H^+]$ plot ($[HA]_{org}$ is constant) is a straight line with a slope of $+3$. The plot of $\log D_0[H^+]^3[HA]^{-3}_{org}$ vs. $\log[HA]_{org}$ or vs. $\log[H^+]^{-1}$ should be a straight line parallel to the abscissa.

On the other hand, when chelate complexes are formed in the aqueous phase, Eq. 6 or 15 is valid and the plot deviates downward from the straight line with a slope of $+3$. The plot of $\log D[H^+]^3 \cdot [HA]^{-3}_{org}$ vs. $\log[H^+]^{-1}$ or vs. $\log[HA]_{org}$ deviates downward from the straight line parallel to the abscissa, as we can see from Eq. 15.

**Adduct Chelate Complex Formation in the Organic Phase.**—When adduct chelate complexes with an organophilic neutral ligand are formed, Eqs. 18 and 19 are valid. The increase in the extraction with the increase in the ligand concentration can be expressed by Eq. 20.

When the formation of chelate complexes in the aqueous phase is negligible, Eq. 23 can also be used.

The formation constants of the adduct complexes, $\beta_1, \beta_2, \cdots$ can be determined graphically by a curve-fitting method.[1,5,6] It may be possible to describe the problem generally, but in the present study the description will be limited to the $MA_3L$- and the $MA_3L_2$-type complexes because we have encountered only these two complexes in the present study.

(i) When only the $MA_3L$ complex exists in the porganic hase, Eq. 20 can be described as:

$$\log D/D_0 = \log(1 + \beta_1[L]_{org}) \quad (24)$$

When a parameter

$$v = \beta_1[L]_{org}$$

is introduced, Eq. 24 can be described as:

$$\log D/D_0 = \log(1 + v) \quad (25)$$

This plot can be fitted with a standard curve:

5) D. Dyrssen and L. G. Sillén, *Acta Chem. Scand.*, **7**, 663 (1953).
6) L. G. Sillén, ibid., **10**, 186 (1956).

$$Y=\log(1+v) \qquad (26)$$
$$X=\log v$$

Equation 24 has two asymptotes:

$$[L]_{org}\to\infty \qquad Y=\log\beta_1+\log[L]_{org} \qquad (27)$$
$$[L]_{org}\to 0 \qquad Y=0 \qquad (27')$$

From the intersect of these two asymptotes, $Y=0$ and $X=\log x_1$, the $\beta_1$ can be determined as:

$$\log\beta_1=-\log x_1$$

(ii) When both the $MA_3L$ and the $MA_3L_2$ complexes are formed in the organic phase, Eq. 20 is described as:

$$\log D/D_0=\log(1+\beta_1[L]_{org}+\beta_2[L]^2_{org}) \qquad (28)$$

When we introduce two parameters:

$$v=\beta_2^{1/2}[L]_{org}$$

and

$$p=\beta_1\beta_2^{1/2}$$

Equation 28 can be described as:

$$\log D/D_0=\log(1+pv+v^2) \qquad (29)$$

and Eq. 28 can be fitted with a family of standard curves:

$$Y=\log(1+pv+v^2) \qquad (30)$$
$$X=\log v$$

Equation 28 has two asymptotes:

$$[L]_{org}\to\infty \qquad Y=\log\beta_2+2\log[L]_{org} \qquad (31)$$
$$[L]_{org}\to 0 \qquad Y=0 \qquad (31')$$

When the intersects of these two asymptotes is $Y=0$ and $X=\log x_2$, the $\beta_2$ can be determined as:

$$\log\beta_2=-2\log x_2$$

Figure 1 gives the standard curves obtained by Eq. 30 when the $p$ values are 0, 1, 2, 3, 5, 10, 20, and 50 respectively.

When the plot in Eq. 28 is fitted with one of the standard curves, the $\beta_1$ can be obtained from the $p$ and from the $\beta_2$ as:

$$\beta_1=p\beta_2^{1/2}$$

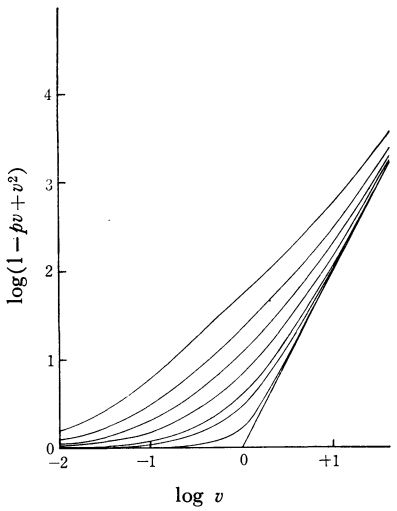



Fig. 1. Standard curves used for the graphical determination of the formation constants of the adducts, $Y=\log(1+pv+v^2)$, $X=\log v$. Each of the curves corresponds to the value of $p$, 50, 20, 10, 5, 3, 2, 1 and 0 respectively.

## Results

Figure 2 gives the plot of $\log D$ vs. $\log[H^+]^{-1}$ when the organic phase contained 0.1 M (initial) of the chelating acids.

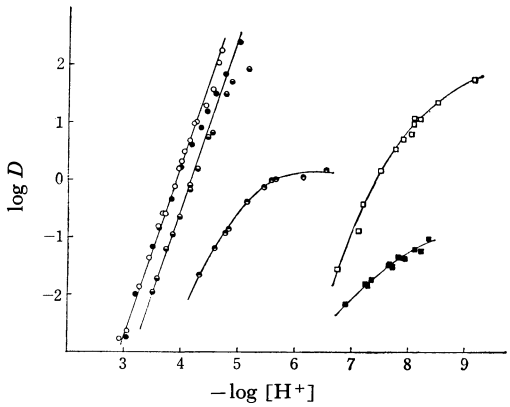



Fig. 2. The hydrogen ion concentration dependence of the distribution of europium(III). Aqueous phase: 0.1 M $NaClO_4$; Organic phase: Chloroform with 0.1 M of acetylacetone(■), benzoylacetone(□), trifluoroacetylacetone(◓), benzoyltrifluoroacetone(◒), froyltrifluoroacetone(●) and thenoyltrifluoroacetone(○).

Figures 3 to 8 give the plot of $\log D/D_0$ vs. $\log[TBP]_{org}$ when the chelating acid was acetylacetone (AA), benzoylacetone (BZA), trifluoroacetylacetone (TAA), froyltrifluoroacetone (FTA), or thenoyltrifluoroacetone (TTA) respectively.

The extraction constants of europium(III) with

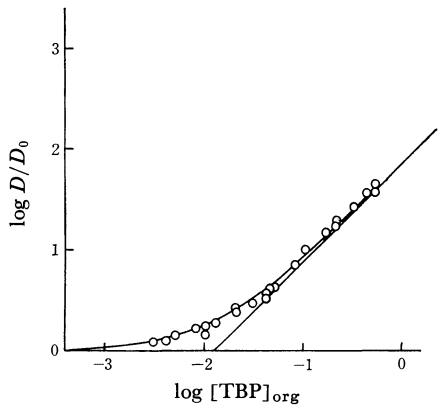


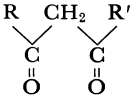

Fig. 3. 0.1 M acetylacetone - TBP system. The curve fitted is $Y=\log(1+v)$, $X=\log v$. The intersect of the two asymptotes is (−1.90, 0).

Table I. Equilibrium constants of europium(III) extraction with six acetylacetone derivatives and the adduct formation of the metal chelates with tributylphosphate (TBP)

| | AA | BZA | TAA | BFA | FTA | TTA[8] |
|---|---|---|---|---|---|---|
| R-[1] | $CH_3$- | $CH_3$- | $CF_3$- | $CF_3$- | $CF_3$- | $CF_3$- |
| R'-[1] | $CH_3$- | benzoyl | $CH_3$- | benzoyl | froyl | thenoyl |
| pH of 50% extraction | —[5] | 7.5 | 5.8 | 4.2 | 3.9 | 3.8 |
| log $K_0$[2] | —[6] | ca. −1[6] | —[6] | −9.47 | −8.73 | −8.68 |
| log $\beta_1$[3] | 1.90 | 1.60 | 3.32 | 3.64 | 3.50 | 3.34 |
| log $\beta_2$[4] | —[7] | —[7] | 4.64 | 5.28 | 5.00 | 5.28 |

Organic phase: 0.1 M of chelating ligand in $CHCl_3$. Aqueous phase: 0.1 M $NaClO_4$.

1) R and R' indicate the functional group in the $\beta$-diketone as indicated in the figure.



2) $K_0=[MA_3]_{org}[H^+]^3/[M^{3+}][HA]^3_{org}$

3) $\beta_1=[MA_3L]_{org}/[MA_3]_{org}[L]_{org}$

4) $\beta_2=[MA_3L_2]_{org}/[MA_3]_{org}[L]^2_{org}$ HA: a chelating ligand L: TBP

5) The extraction is always less than 10% over the entire pH range.

6) Metal chelate complexes are also formed in the aqueous phase and the $K_0$ cannot be determined definitely.

7) No evidence of the second adduct $EuA_3L_2$ is observed.

8) The concentration of TTA is 0.05 M for the experiments of the adduct formation.

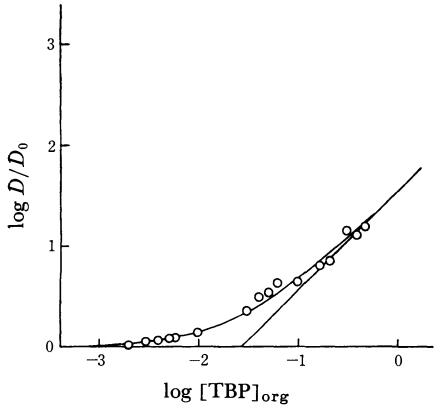



Fig. 4. 0.1 M benzoylacetone - TBP system. The curve fitted is $Y=\log(1+v)$, $X=\log v$. The intersect of the two asymptotes is (−1.60, 0).

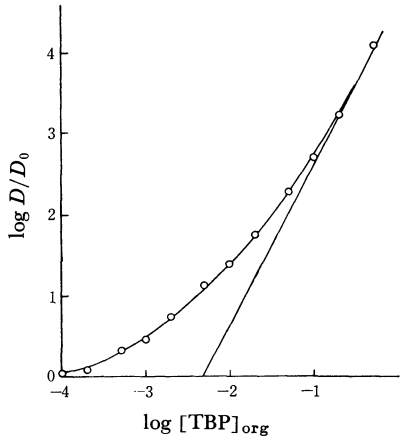


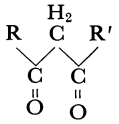

Fig. 5. 0.1 M trifluoroacetylacetone - TBP system. The curve fitted is $Y=\log(1+10v+v^2)$, $X=\log v$. The intersect of the two asymptotes is (−2.32, 0).

these chelating acids were calculated from the distribution data. The formation constants of the TBP adducts were obtained by the curve-fitting method.

The constants thus determined are given in Table I.

## Discussion

The six $\beta$-diketones in the present study can be described as:



In this discussion, the $\beta$-diketones will be classified into two groups and will be called the $CH_3$-group $\beta$-diketones and the $CF_3$-group $\beta$-diketones.

| | $\beta$-Diketone | R | R' |
|---|---|---|---|
| $CH_3$-group | Acetylacetone (AA) | $CH_3$- | $CH_3$- |
| | Benzoylacetone (BZA) | $CH_3$- | Benzoyl |
| $CF_3$-group | Trifluoroacetylacetone (TAA) | $CF_3$- | $CH_3$- |
| | Benzoyltrifluoroacetone (BFA) | $CF_3$- | Benzoyl |
| | Froyltrifluoroacetone (FTA) | $CF_3$- | Froyl |
| | Thenoyltrifluoroacetone (TTA) | $CF_3$- | Thenoyl |

A $\beta$-diketone exists in the keto form and in the enol form. A metal ion is extracted into the organic

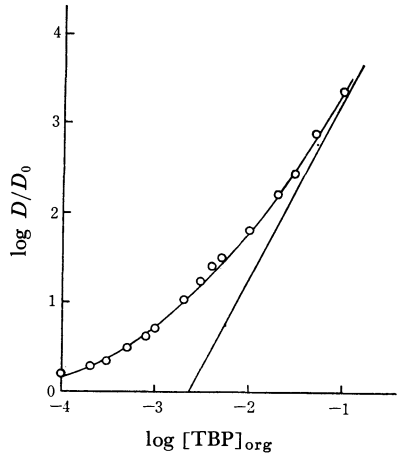



Fig. 6. 0.1 M benzoyltrifluoroacetone-TBP system. The curve fitted is $Y=\log(1+10v+v^2)$, $X=\log v$. The intersect of the two asymptotes is $(-2.64, 0)$.

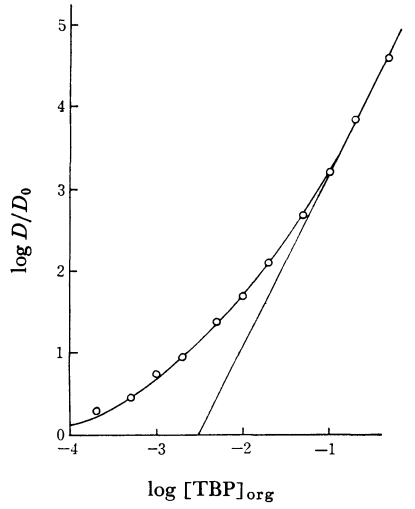



Fig. 7. 0.1 M froyltrifluoroacetone-TBP system. The curve fitted is $Y=\log(1+10v+v^2)$, $X=\log v$. The intersect of the two asymptotes is $(-2.50, 0)$.

phase as a metal chelate with only the enol-form ligand.

Adduct chelate complexes are sometimes also formed with the undissociated chelating acid, HA, as:

$$MA_3(org)+n\,HA(org)\rightleftarrows MA_3(HA)_n(org)$$

However, the formation of adducts of this type may be negligible when the concentration of the chelating acid is 0.1 M in chloroform (cf. Ref. 1, Paper III).

**Metal Extraction with Chelating Acids.**— The pH of 50% extraction increases in the following order:

$$TTA\cong FTA<BFA<TAA<BZA<(AA)$$

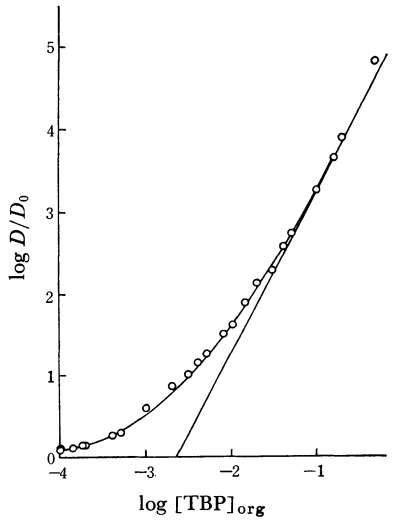



Fig. 8. 0.1 M thenoyltrifluoroacetone-TBP system. The curve fitted is $Y=\log(1+5v+v^2)$, $X=\log v$. The intersect of the two asymptotes is $(-2.64, 0)$.

Acetylacetone showed the least extraction of europium(III). With it the extraction was always less than 10%. The low extraction of trivalent lanthanide ions with this reagent has been reported by several authors.[7]

Benzoylacetone extracts europium(III) much better than acetylacetone, but the pH of 50% extraction is higher than that of the $CF_3$-group $\beta$-diketones. This agrees with previous observations.[8]

The extraction with thenoyltrifluoroacetone seems to agree with the results of the previous work.[1-4,9]

Most of the plots in Fig. 2 deviate from the straight line with a slope of +3. The deviation may be explained as resulting from the formation of aqueous complexes, as is shown in Eq. 15.

In the figure we can see that the deviation is larger in the order:

AA>TAA>BZA>FTA>BFA>TTA

In Eq. 15 we can see that the formation of aqueous complexes at a certain $[HA]_{org}/[H^+]$ is larger when the stability constants, $\beta_{aq,n}$, are larger and /or the $K_a/K_D$ ratio is larger.

Tables II and III summarize some data of the distribution constants and the dissociation constants of these $\beta$-diketones in the literature. In the tables we can see that the dissociation constants of the protons of acetylacetone and benzoylacetone are

7) W. B. Brown, J. F. Steinbach and W. F. Wagner, *J. Inorg. Nucl. Chem.*, **13**, 119 (1960); J. Stary and E. Hladky, *Anal. Chim. Acta*, **28**, 227 (1963); J. Rydberg, *Arkiv för Kemi*, **9**, 95 (1955).

8) I. P. Jefimov and V. M. Peshkova, *Vestnik Moskov. Univ., Ser. Khim.*, **17**, No. 3, 62 (1962); J. Stary, *Zhur. Neorg. Khim.*, **4**, 2412 (1959); J. Stary, *Coll, Czech. Chem. Comm.*, **25**, 86 (1960).

9) T. Sekine and D. Dyrssen, *Talanta*, **11**, 867 (1964).

Table II. Distribution constants of β-diketones between the organic and the aqueous phase[4]

$K_D = [HA]_{org}/[HA]$

| | log $K_a$ | Solvent | Remarks | Ref. |
|---|---|---|---|---|
| Acetylacetone | 1.37 | $CHCl_3$ | 25°C $\mu=0.1$ | 11 |
| | 0.54 | $C_6H_6$ | 25°C $\mu=1.0$ | 12 |
| Benzoylacetone | 3.44 | $CHCl_3$ | 25°C $\mu=0.1$ | 13 |
| | 2.79 | $C_6H_6$ | 25°C $\mu=1.0$ | 14 |
| Trifluoroacetylacetone | 0.18 | $C_6H_6$ | 2 M $HClO_4$ | 15 |
| Froyltrifluoroacetone | 0.87 | $C_6H_6$ | 2 M $HClO_4$ | 15 |
| Thenoyltrifluoroacetone | 1.84 | $CHCl_3$ | 25°C $\mu=0.1$ | 1 |
| | 2.12 | $C_6H_6$ | 25°C $\mu=1.0$ | 16 |

Table III. Dissociation constants of β-diketones as an acid[4]

$K_a = [H^+][A^-]/[HA]$

| | $-\log K_a$ | Remarks | Ref. |
|---|---|---|---|
| Acetylacetone | 8.82 | 25°C $\mu=0.1$ | 11 |
| | 8.76 | 25°C $\mu=0.1$ | 12 |
| Benzoylacetone | 8.74 | 20°C $\mu=1.0$ | 17 |
| | 8.24 | 25°C $\mu=1.0$ | 14 |
| | 8.96 | 25°C $\mu=1.0$ | 13 |
| Trifluoroacetylacetone | 6.3 | 25°C | 18 |
| Benzoyltrifluoroacetone | 6.3 | 25°C | 18 |
| Thenoyltrifluoroacetone | 6.23 | 25°C $\mu=0.1$ | 19 |

nearly the same, but that the distribution constant of acetylacetone is much smaller than that of benzoylacetone (this can easily be understood in terms of the higher organophilic tendency of the larger organic group). We can also see in the tables that the dissociation constants of the $CF_3$-group β-diketones are nearly the same, but that the distribution constant of trifluoroacetylacetone is much lower than those of the others. This shows that the $K_a/K_D$ value of acetylacetone or trifluoroacetylacetone is larger than that of their homologues; we can thus understand why these two β-diketones form much more aqueous chelate complexes and show a lower ability of metal extraction.*

From these results, we may assume that the $K_0$ values (cf. Eq. 3) for the metal extraction with these two β-diketones are not very far from those of their homologues, even though the apparent metal extraction is quite different.

**Adduct Formation of the Metal Chelates with TBP.**—The formation constants of the adduct chelate complexes in Table I may be summarized as follows:

1) The formation constants of the first adducts of the metal chelates with the $CH_3$-group β-diketones are much lower than those of the metal chelates with the $CF_3$-group β-diketones.

2) The metal chelates with the $CH_3$-group β-diketones do not form the second adduct, $MA_3 \cdot (TBP)_2$, but the metal chelates with the $CF_3$-group β-diketones form the second adducts.

3) There is no large difference in the formation constants between the adducts of the acetylacetone chelate and those of the benzoylacetone chelate. There is also no large difference in the formation constants among the adducts of the four metal chelates with the $CF_3$-group β-diketones.

Thus the substitution of a methyl group in a metal chelate with a trifluoromethyl group changes the stability of the metal chelates, as we can see in Fig. 2; this substitution should change the interaction between the central metal ion and the ligands.

When the interaction between the metal ion and the chelating ligand is changed, the residual coordination power of the metal ion which makes the adduct formation possible may be changed. However, as the mechanism of the adduct formation in a synergic extraction system has not yet been clarified, further information on the structrue of the complexes seems to be necessary before this problem can be discussed in more detail.

## Conclusion

From the results of this study, we may conclude the following for the extraction of europium(III) in 0.1 M sodium perchlorate with the six β-diketones in chloroform and the adduct formation of these chelates in the organic phase with tributylphosphate:

1) The substitution of a methyl group in acetylacetone or trifluoroacetone with a benzoyl, froyl or thenoyl group increases the possibility of metal extraction, because the substitution increases the organophilic tendency of the molecules and prevents the formation of metal chelates in the aqueous phase. However, the substitution does not seem to change the metal extraction equilibrium,

$$M^{3+} + 3\,HA(org) \rightleftarrows MA_3(org) + 3\,H^+,$$

very much.

2) The β-diketones with one trifluoromethyl group extract the metal ion from aqueous solutions at a lower pH than those without a trifluoromethyl group.

* In the synergic extraction systems, the deviation caused by the formation of aqueous complexes becomes smaller. The details of this have been discussed in another paper.[10]

10) T. Sekine, M. Sakairi, F. Shimada and Y. Hasegawa, This Bulletin, **38**, 847 (1965).
11) J. Rydberg, *Svensk Kem. Tidskr.*, **65**, 37 (1953).
12) V. M. Peshkova and Pen-An, *Zhur. Neorg. Khim.*, **6**, 2083 (1961).
13) A. P. Zozulya, N. N. Mezentseva, V. M. Peshkova and Yu. K. Yuriev, *Zhur. Analit. Khim.*, **14**, 17 (1959).
14) V. M. Peshkova, N. V. Mel'chakova and S. G. Zhemchuzhin, *Zhur. Neorg. Khim.*, **6**, 1233 (1961).
15) E. M. Larsen and G. Terry, *J. Am. Chem. Soc.*, **75**, 1560 (1953).
16) V. M. Peshkova and Pen-An, *Zhur. Neorg. Khim.*, **7**, 1484 (1962).
17) J. Stary and Rudenko, Nauch. Doklady Vyshey Skholy, *Khim. i Khim. Tekhnol.*, **1**, 624 (1958).
18) J. C. Reid and M. Calvin, *J. Am. Chem. Soc.*, **72**, 2948 (1950).
19) D. Dyrssen, *Svensk. Kem. Tidskr.*, **68**, 212 (1956).

3) The substitution of one methyl group in acetylacetone or benzoylacetone with one trifluoromethyl group increases the ability of metal chelates with these β-diketones to form adduct complexes with TBP in chloroform.

4) The substitution of one methyl group in acetylacetone chelate or that in trifluoroacetylacetone chelate with one benzoyl, froyl or thenoyl group does not change the adduct formation with TBP very much.

5) The high stability of TBP adducts observed in the metal TTA chelates seems to be similar to that in the TBP adducts of metal chelates with β-diketones which have a trifluoromethyl group.

## Summary

The extraction of europium(III) in 0.1 M sodium perchlorate with acetylacetone, benzoylacetone, trifluoroacetylacetone, benzoyltrifluoroacetone, froyltrifluoroacetone and thenoyltrifluoroacetone in chloroform and the adduct formation of these metal chelates with tributylphosphate have been studied at 25°C.

It has been concluded that: (i) The β-diketones which have one trifluoromethyl group extract europium(III) better than those which have no trifluoromethyl group. The difference in the metal extraction with acetylacetone or trifluoroacetylacetone and the metal extraction with the homologues of these β-diketones seems to be mainly due to the aqueous chelate complex formation. (ii) A metal chelate with a β-diketone which has a trifluoromethyl group is a much better acceptor of tributylphosphate to form adduct complexes than a metal chelate with a β-diketone which has no trifluoromethyl group. (iii) The ability of the acetylacetone chelate or the trifluoroacetylacetone chelate to form an adduct is not very much changed by the replacement of the methyl group with a benzoyl, froyl, or thenoyl group.

Some part of this work was carried out at the Laboratory of Nuclear Chemistry, Institute of Physical and Chemical Research, Tokyo. The authors are so grateful to Professor Nobufusa Saito, the head of the laboratory. Some of the experiments were made by Miss Tomoe Taira and by Messers Tatsuo Sato and Mitsuo Sakairi. The authors are also grateful to them.

*Department of Chemistry*
*Tokyo College of Science*
*Kagurazaka, Shinjuku-ku, Tokyo*

# The Catalytic Hydrogenation of Aniline[1)]

By Hiroshi HAGIHARA and Etsuro ECHIGOYA

(Received April 24, 1965)

A few reports and a number of patents have previously been published on the hydrogenation of aniline, but most of them have reported on the catalytic hydrogenation in the liquid phase.[2-4)] The present authors have investigated this subject, using a number of types of catalysts, and this report will describe the development of the catalysts, and their selectivity in the vapor-phase hydrogenation of the benzene nucleus of aniline.

Catalysts consisting of single or mixed metals, or of supported metals, were used for this reaction. The catalyzed main reaction is the hydrogenation of aniline to cyclohexylamine:

$$C_6H_5NH_2 + 3H_2 \rightarrow C_6H_{11}NH_2$$

The side reactions of cyclohexylamine or aniline occur as follows:

$$2C_6H_{11}NH_2 \rightarrow (C_6H_{11})_2NH + NH_3$$

$$C_6H_{11}NH_2 + C_6H_5NH_2 \rightarrow C_6H_5NHC_6H_{11} + NH_3$$

Also, on a smaller scale, the hydrogenolysis reactions of cyclohexylamine to cyclohexane and ammonia, and of aniline to benzene and ammonia, took place under 250°C, as follows:

$$C_6H_{11}NH_2 \xrightarrow{H_2} C_6H_{12} + NH_3$$

$$C_6H_5NH_2 \xrightarrow{H_2} C_6H_6 + NH_3$$

## Experimental

**Procedure of Catalyst Preparation.**—Reagents of a chemically-pure grade were used as starting materials in the preparation of the catalysts. The

1) Presented in part at the 15th Discussion Meeting on Catalysis of the Catalysis Society of Japan, Osaka, November, 1964.
2) C. F. Winans and H. Adkins, *J. Am. Chem. Soc.*, **54**, 306 (1932).
3) J. C. Jungers and G. Debus, *Chem. Abstr.*, **48**, 6975 (1954).
4) H. Yamamoto and T. Kwan, presented at the 16th Annual Meeting of the Chemical Society of Japan, Tokyo, April, 1963.

catalysts were prepared by co-precipitation, by impregnation followed by subsequent precipitation, by mixing, by impregnation, and by precipitation followed by hydrothermal treatment under pressure in an autoclave.

*The Catalyst Preparation of Single or Mixed Metal Oxide.*[5]—Single or mixed metal catalysts were precipitated by slowly adding, with rapid agitation, a dissolved equivalent quantity of ammonium carbonate to a solution of nitrates at 20°C. After washing the filtered precipitates, they were dried at 100°C and calcined at 500°C, for 2 hr.

*Catalyst Preparation by the Impregnation Method with Subsequent Precipitation.*—The powdered support was added to a solution of nickel or cobalt nitrate. The slurry was stirred for some time, and then a solution of ammonium carbonate was slowly added to it until there was a slight excess at 20°C. After the precipitate had been filtered and washed, it was dried at 100°C and then calcined at 500°C for 2 hr.

*Catalyst Preparation by the Co-precipitation Method.*—The catalysts were prepared by co-precipitation with vigorous stirring from a mixed solution of nickel, or cobalt, and aluminum nitrate, or sodium silicate, and ammonium carbonate at 20°C. The precipitates were washed with distilled water, dried at 100°C, powdered, and calcined at 500°C for 2 hr. in an electric furnace.

*Catalyst Preparation by the Impregnation Method.*—The powdered support was added to a solution of nickel or cobalt nitrate and was in the solution for 5 hr. The slurry was then evaporated to dryness on a water bath, and the residue was dried in an oven at 100°C, washed with distilled water to remove nitrate ions, and dried again at 100°C. Then it was calcined at 500°C for 2 hr. in an electric furnace.

*Catalyst Preparation by the Mixing Method.*—The powdered support and the slurry of nickel or cobalt-basic carbonate were mixed mechanically in a beaker. The mixture was vacuum-filtered, and then it was dried at 100°C and calcined at 500°C for 2 hr.

*Catalyst Preparation by Hydrothermal Treatment.*[6]—Basic nickel carbonate or basic cobalt carbonate (prepared from a nickel or cobalt nitrate solution and an ammonium carbonate solution at 20°C) was mixed with silica gel or aluminum oxide gel and then heated in an autoclave to 250°C for 25 hr. with water. It was then cooled, filtered, washed with distilled water, dried at 100°C, and then calcined at 550°C for 2 hr.

**Experimental Method of the Hydrogenation of Aniline.**—The hydrogenation experiments were performed in a fixed-bed apparatus of the flow type in the temperature range from 150°C to 300°C. Figure 1 shows its flow diagram. The mixture of aniline and hydrogen was introduced into a reactor which was immersed in a fluidized thermal bath.

The gaseous products leaving from the reaction zone were caught in a condenser trap cooled with dry ice-methanol, from which trap condensates were drawn every thirty minutes for gas chromatographic analyses.

The oxide catalysts (5 ml.) were in the same fixed-bed apparatus used for the reaction, reduced to the metals in hydrogen according to a definite reduction

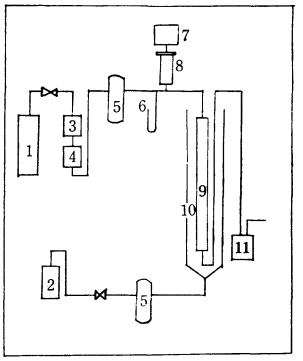



Fig. 1. Flow sheet for the hydrogenation reaction of aniline.
1. Hydrogen cylinder 2. Air compressor 3. Oxygen eliminator 4. Drier 5. Orifice flow meter 6. Manometer 7. Moter feeder 8. Feeder of aniline 9. Reactor 10. Fluidized thermal bath 11. Trap

schedule. The flow rate of hydrogen was 250 ml./min. The temparature of the catalyst bed was raised to 200°C in one hour, and then raised at the rate of 2.5°C per minute until 400°C or 450°C was reached. After the temperature had been held at 400°C or 450°C for two hours, the catalyst was cooled in the hydrogen stream to the reaction temperature, and then a run of the hydrogenation of aniline was carried out.

After a steady state of activity was achieved, the activity of the catalyst was estimated as follows:

$$\text{Conversion} = \frac{\text{The amount of reacted aniline (mol./hr.)}}{\text{Total aniline introduced (mol./hr.)}}$$

$$\text{Selectivity} = \frac{\text{Cyclohexylamine yield (mol./hr.)}}{\text{Reacted aniline (mol./hr.)}}$$

$$\text{Yield of benzene} = \frac{\text{Benzene yield (mol./hr.)}}{\text{Total aniline used (mol./hr.)}}$$

$$\text{Yield of secondary amine} = \frac{\text{Secondary amine yield (mol./hr.)}}{\text{Total aniline used (mol./hr.)}}$$

## Results

**The Activity of Various Metals for This Reaction.**—The catalysts were reduced by hydrogen at 400°C. The results of the activity tests are shown in Fig. 2. The single-metal catalysts are sharply divided into three classes. Ruthenium is active at low temperatures. Cobalt is more active than nickel. Iron and copper are inactive in this reaction.

It must be emphasized that the inactivity of iron or copper is not due to insufficient reduction or to the sintering of the metal. Especially in the case of copper, the reduction was carried out at a low temperature (about 200°C) to prevent it from sintering. It was found through experiments that the activity of a metal prepared by reduction

5) G. Natta, "Handbuch der Katalyse", Vol. V, Springen, Wien (1957), p. 269.
6) J. J. B. van Eijk van Voorthuijsen and P. Franzen, *Rec. Trav. Chim.*, **70**, 793 (1951).

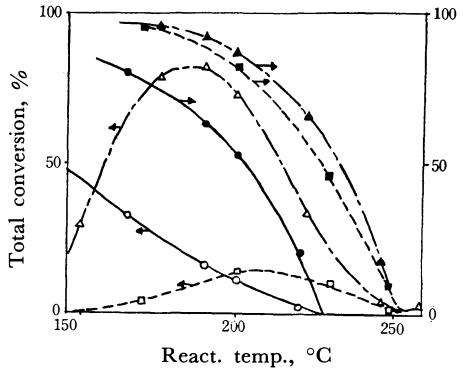



Fig. 2. The activity and selectivity of metallic catalysts in the hydrogenation.
—— Ru, ---- Co, ---- Ni
LHSV=1.0 $hr^{-1}$, $H_2$/aniline 10 (mole ratio)

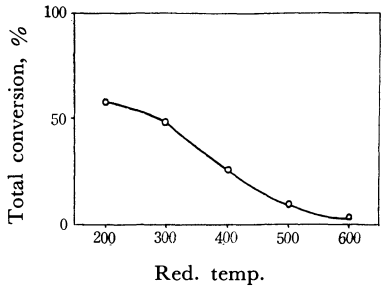



Fig. 3. Relative activity of Co vs. temp. of reduction.
LHSV=2 $hr^{-1}$, $H_2$/aniline 10 (mole ratio)

from the oxide is dependent on the length of the reduction time and on the temperature. The effects of the reduction temperature of cobalt on the activity were also investigated. The results are shown in Fig. 3.

**The Activity of the Mixed Metal Catalysts.**—The catalysts were reduced by hydrogen at 400°C. The results of the activity tests are shown in Fig. 4. The activity of the Co-Ni series showed a decrease as the nickel content increased. However, in the Co-Fe series, when the Fe content became 50%, the Co-Fe catalyst lost its activity almost completely. A similar results was obtained by Long et al.[7,8] in the hydrogenation of benzene.

Long et al. ascribed this to the different crystsl structures of mixed metal catalysts. They found that as the mixture becomes richer in cobalt, the more probable it is that the catalyst will have more of a face-centered cubic lattice, and will hence be active.

**The Activity of Supported Metal Catalysts.**—The activities of metal catalysts supported on the same oxide carrier, although prepared by different methods, show almost the same tendency in the relative abundance of the various products.

7) J. H. Long, W. Frazer and E. Ott, *J. Am. Chem. Soc.*, **50**, 1101 (1934).
8) F. Lihl, H. Wagner and P. Zemisch, *Z. Elek. Chem.*, **56**, 612, 619, (1952); **57**, 58 (1953).

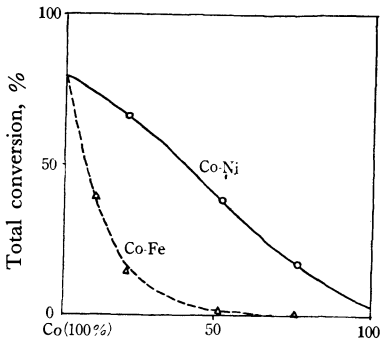



Fig. 4. The activity of Co-Ni and Co-Fe catalysts for the hydrogenation.
Reaction temp. 200°C
$H_2$/aniline 10 (mole ratio)

The activity of the catalysts prepared by the impregnation method with subsequent precipitation is shown in Figs. 6 to 9.

**The Effect of the Reduction Temperature on the Activity of the Catalyst.**—The catalyst

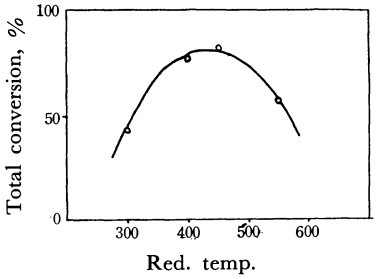



Fig. 5. Relative activity of Co-$Al_2O_3$ (50% cobalt) vs. temp. of reduction.
React. temp. 200°C, LHSV=1.0 $hr^{-1}$
$H_2$/aniline 10 (mole ratio)

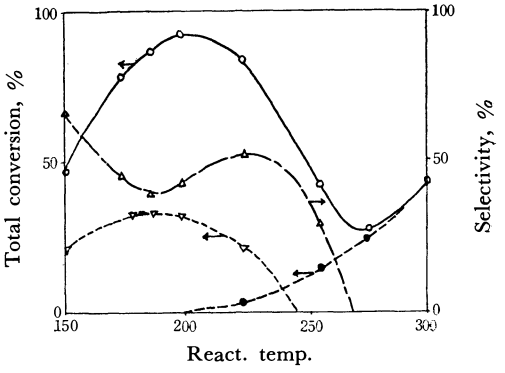



Fig. 6. The activity and selectivity of Ni-$Al_2O_3$ (30% nickel) for the hydrogenation.
LHSV=1.0 $hr^{-1}$, $H_2$/aniline 10 (mole ratio)
-▽- yield of dicyclohexylamine
-●- yield of benzene

samples were reduced for 2 hr. at various temperatures. Some of the results are presented in Fig. 5. Generally the catalyst which was reduced for 2 hr. at 400 to 450°C had the highest activity.

**The Activity of Supported Nickel Catalysts.**—The catalysts were reduced by hydrogen at 450°C. The results of the activity tests are shown in Figs. 6 and 7. From the results, it can be concluded that:

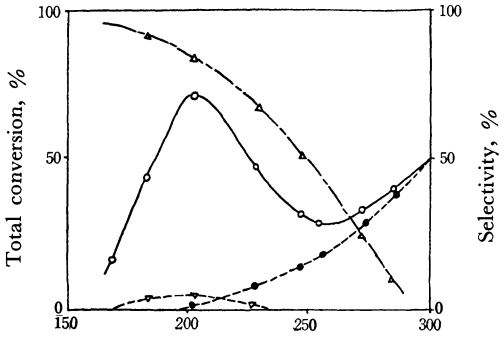



Fig. 7. The activity and selectivity of Ni-MgO (50% nickel) for the hydrogenation.
LHSV=1.0 $hr^{-1}$, $H_2$/aniline 10 (mole ratio)
-▽- yield of dicyclohexylamine
-●- yield of benzene

1) The maximum activity of catalysts for the hydrogenation reaction was obtained in the temperature range from 180 to 200°C, and 2) The production of secondary amine was affected by the kind of carrier-oxide used.

**The Activity of Supported Cobalt Catalysts.**—The catalysts were reduced by hydrogen at 450°C for 2 hr. The results of the activity tests are presented in Figs. 8 and 9.

From these data, it may be concluded that:

1) The maximum activity of catalysts for the hydrogenation reaction was obtained in the temperature range from 180 to 200°C, and 2) The production of secondary amine was less with a cobalt catalyst than with nickel catalysts. 3) The selectivity of this reaction was influenced by the kind of carrier-oxide.

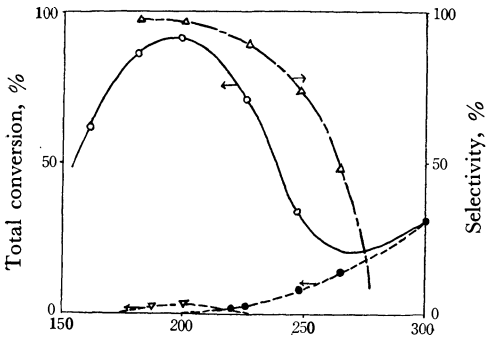



Fig. 8. The activity and selectivity of Co-$Al_2O_3$ (50% cobalt) for the hydrogenation.
LHSV=1.0 $hr^{-1}$, $H_2$/aniline 10 (mole ratio)
-▽- yield of dicyclohexylamine
-●- yield of benzene

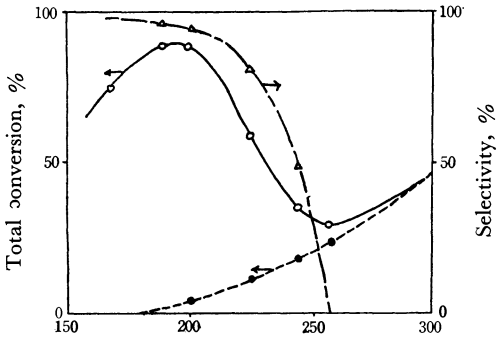



Fig. 9. The activity and selectivity of Co-MgO-Kieselguhr (45 : 10 : 45) for the hydrogenation.
LHSV=1.0 $hr^{-1}$ $H_2$/aniline 10 (mole ratio)
-●- yield of benzene

On the basis of the above data, we have concluded that the kind of carrier-oxide used has an effect on the activity of nickel, as well as on the cobalt. The production of dicyclohexylamine is especially affected by the kind of carrier used.

**The Activity of Catalysts Prepared by the Hydrothermal Treatment.**—The catalyst were reduced by hydrogen at 550°C. The results are presented in Fig. 10. It may be concluded that the catalysts produced by the hydrothermal treatment are less active.

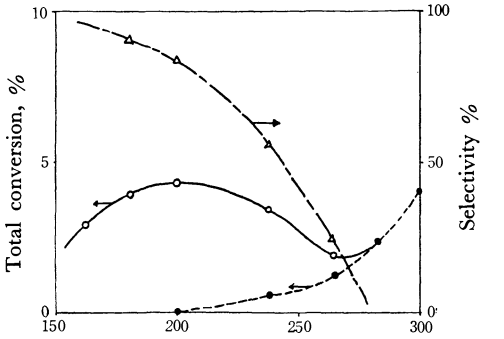



Fig. 10. The activity and selectivity of Co-$SiO_2$* cat. (20% cobalt) for the hydrogenation.
* The catalyst was treated at 250°C in an autoclave in the presence of water.
LHSV=1.0 $hr^{-1}$, $H_2$/aniline 10 (mole ratio)
-●- yield of benzene

**The Effect of the Carrier-oxide Content of Metallic Catalysts on the Hydrogenation Reaction of Aniline.**—The results are summarized

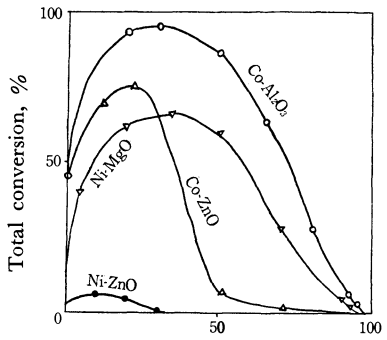



Fig. 11. Effect of the oxide carrier contents of metallic catalysts on the hydrogenation.
Reaction temp. 200°C
LHSV=1.0 $hr^{-1}$, $H_2$/aniline 10 (mole ratio)

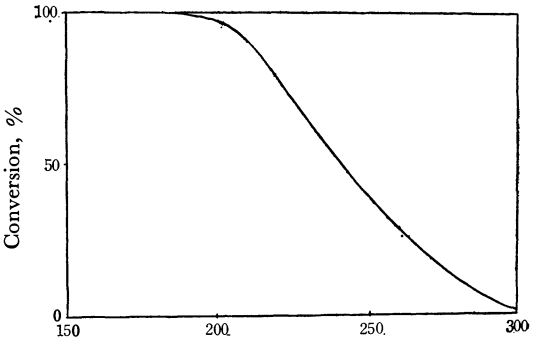



Fig. 12. Relation between temperature and equilibrium conversion.
$H_2$: aniline=10 : 1

in Fig. 11. The activity of the catalysts was found to be influenced by its carrier-oxide, and their activity is highest at a certain metal-to-carrier ratio.

In the Co-ZnO and Ni-ZnO series, the activity was found to be very low. This was attributed to the formation of a complex between the metal and its carrier. From X-ray analysis, it was concluded that $ZnCo_2O_4$ was formed.

**The Relationship between the Activity and the Metal Content of the Catalyst in the Hydrogenolysis Reaction of Aniline.**—Table I shows the relation between the conversion and the metal content of the catalyst in the hydrogenolysis reaction. From the data presented, it may be concluded that the rate of the hydrogenolysis reaction of aniline is related to the amount of metal on the oxide carrier, the activity of the catalyst was found to be proportional to the metal content of the catalyst.

TABLE I. THE RELATION BETWEEN CONVERSION AND THE METAL CONTENT OF THE CATALYST IN THE HYDROGENOLYSIS REACTION

Reaction temp. 300°C, LHSV=1.0 $hr^{-1}$
$H_2$/aniline 10 (mole ratio)

| Metal content, % | Catalyst | |
|---|---|---|
| | Ni-MgO | Co-$Al_2O_3$ |
| 10 | 11% | 14% |
| 20 | 19% | 17% |
| 30 | 28% | 24% |

## Discussion

**The Relationship between the Activity and the Reaction Temperature.**—As is shown in Figs. 6—9, in the hydrogenation reaction of aniline in the vapor phase the highest conversion of aniline into cyclohexylamine was obtained in the temperature range from 180 to 200°C. At high temperatures, the degree of hydrogenation decreased. This phenomenon of a negative temperature coefficient can be explained in terms of the thermodynamic chemical equilibrium calculated using the Nernst equation at the $H_2$ to aniline mole ratio of 10 to 1.

Since the hydrogenation is carried out in a dynamic (flow) system, the conversion is most probably controlled not only by the equilibrium constant, but also by the rate of the surface reaction. It was concluded from the kinetic study with cobalt and nickel of the vapor-phase hydrogenation of aniline that the results obtained may be expressed satisfactorily by the following rate equation in the 150—210°C temperature range.

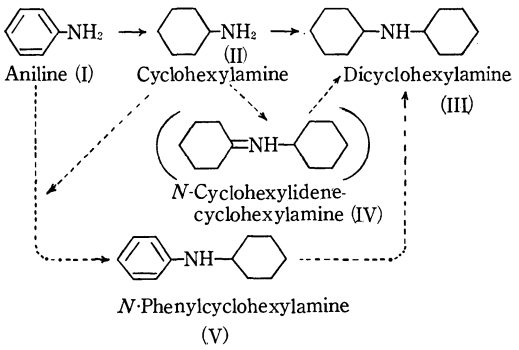
$$r=k\theta_A\theta_H^3$$

$r$: reaction rate
$k$: reaction rate constant
$\theta_A$: the fractions of the surface covered by the aniline
$\theta_H$: the fractions of the surface covered by hydrogen

A more detailed report of the kinetic study will be presented later.

**A Relationship between the Activity and the Structrue of the Catalyst.**—The chemical states of metal on the supported catalyst may be classified into two types. The one is the type in which the metal is not combined with the carrier but remains free on the surface of the carrier. In the other type, the metal oxide forms a complex with the carrier resists reduction by hydrogen. Generally speaking, catalysts of the first type (supported free metal) show a higher activity for the hydrogenation and hydrogenolysis reaction of aniline. A more detailed report on this will be presented in the near future.

**The Mechanism of the Production of Secondary Amine.**—In the course of the hydrogenation reaction, dicyclohexylamine and phenylcyclohexylamine are also found in the product. The course of the formation of those products may be described as follows.




(The main course is presented by a full line, the less important course is presented by dotted lines)

The cyclohexaneimine was not found in the product, but *N*-cyclohexylidene-cyclohexylamine could be isolated. However the quantity of IV found is small compared with that of III.

The main course of the production of dicyclohexylamine may consist of two paths, the one through *N*-cyclohexylidene-cyclohexylamine, and the other through the condensation of two cyclohexylamine molecules. We also found that the rate of the condensation of two cyclohexylamines into dicyclohexylamine is fast compared with the rate of the condensation of aniline and cyclohexylamine.

**The Properties of the Carrier-oxides.**—We have found that the properties of the carrier-oxides have a great influence on the selectivity of the catalyst.

According to Sanderson,[9] oxides have thier own partial charge on oxygen and this value is an important parameter for determining the acidic character of oxides. We used the values given by Sanderson for $Al_2O_3$, $SiO_2$, MgO, CaO, ZnO, and $K_2O$ and correlated these values with the $-\Delta H_0°$ values of the oxides given by Tamaru[10]

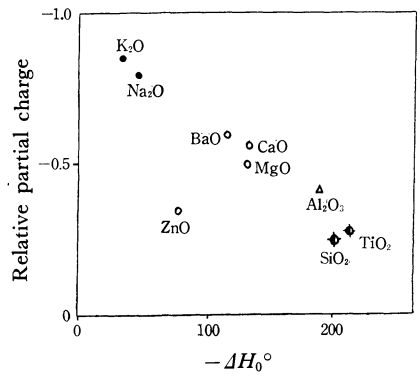



Fig. 13. Correlation between R.P.C. and $-\Delta H_0°$ of oxide.

9) R. T. Sanderson, "Chemical Periodicity," Reinhold Pub. Comp., N. Y. (1960), p. 106.

10) K. Tamaru and K. Tanaka, *Shokubai* (*Catalyst*), **4**, 328, (1962).

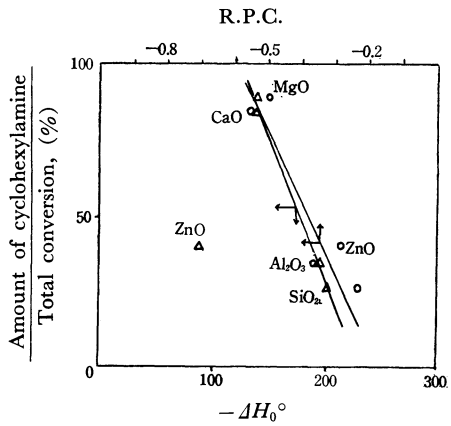



Fig. 14. Relationship between selectivity and oxide carrier of nickel catalysts (50% nickel). Reaction temp. 200°C, LHSV=1.0 $hr^{-1}$ SV=3000 $hr^{-1}$, $H_2$/aniline 10 (mole ratio)

(see Fig. 13).

There is a relationship between the r. p. c. and $-\Delta H_0°$ values. As Fig. 14 shows, the selectivity of the catalysts was proportional to the value of $-\Delta H_0°$. Thus, we have concluded that the acidic and basic property of the carriers has a great influence on the production of secondary amine. The property of the oxide carrier is probably related to the elimination of ammonia from the cyclohexylamine and aniline molecules. The electron-donating property of the nitrogen of the amino group suggests that the amino group strongly interacts with the metal surface.[11] This effect may be considered to play an important role in the formation of the secondary amine. The adsorption of amine may be weakened on that metal which is supported by basic oxides.

## Summary

1) The order of the activity of a metal catalyst for the hydrogenation of aniline is Co>Ni>Fe, Cu. The order of their selectivity is Co>Ni.

2) The activity of the mixed metals (Co-Ni, Co-Fe) is lower than that of a cobalt single catalyst.

3) The rate of hydrogenation increases with the temperature up to 180—200°C, and then decreases at higher temperatures. This phenomenon may be explained in terms of the kinetics of the reaction.

4) The catalyst which consists of a complex between the metal and its carrier-oxide is less active than the free metal catalyst for the hydrogenation reaction, and it almost completely loses its activity for the hydrogenolysis reaction.

5) The production of cyclohexylamine is affected by the property of the carrier oxide.

6) The main course of the production of dicyclohexylamine is considered to proceed through the

11) Y. Y. Yao, *J. Phys. Chem.*, **67**, 2055 (1963).

condensation of two cyclohexylamine molecules and through *N*-cyclohexylidene-cyclohexylamine.

Notation: r. p. c.=relative partial charge on the oxygen of oxide (reported by R. T. Sanderson)
$-\Delta H_0°$=standard heat of formation of the highest oxide per metal g.-atm.

The authors wish to thank Professor Kiyoshi Morikawa for his guidance and discussions in the course of this study.

*Yoshitomi Pharmaceutical Co., Ltd.*
*Yoshitomi, Fukuoka (H. H.)*

*Research Laboratory of Resources Utilization*
*Tokyo Institute of Technology*
*Oookayama, Tokyo (E. E.)*

# Phosphorylation by Means of Ethyl Phosphorodimorpholidite and $\alpha$-Bromoamides

By Oyo MITSUNOBU, Teisuke OBATA, Yoshiharu SUGAYA and Teruaki MUKAIYAMA

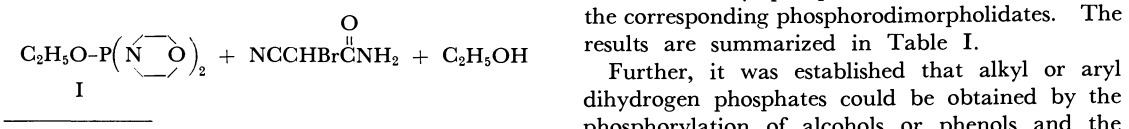
(Received April 24, 1965)

Preceding papers[1,2] have described a selective phosphorylation of alcohols and phosphates by means of monobromocyanoacetamide or monobromomalonamide with trialkyl phosphites, thus forming mixed esters of phosphoric acid and unsymmetrical pyrophosphates.

When this phosphorylation method was applied to the preparation of some naturally-occurring phosphorus compounds, tribenzyl phosphite was employed[3] since the benzyl group can be readily removed from the resulting phosphates by catalytic hydrogenation after phosphorylation has been performed.

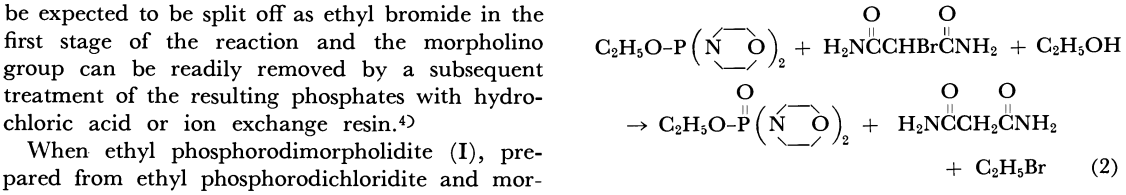
In the present study, another phosphite, ethyl phosphorodimorpholidite (I), was prepared and treated with monobromocyanoacetamide and alcohols. The ethyl group of the phosphite would be expected to be split off as ethyl bromide in the first stage of the reaction and the morpholino group can be readily removed by a subsequent treatment of the resulting phosphates with hydrochloric acid or ion exchange resin.[4]

When ethyl phosphorodimorpholidite (I), prepared from ethyl phosphorodichloridite and morpholine, was reacted with monobromocyanoacetamide in ethanol at $-40°C$, ethyl phosphorodimorpholidate (II) was obtained in a 46% yield by fractionation (Eq. 1).



(1)

Since a small amount of cyanoacetamide contaminates the fraction of ethyl phosphorodimorpholidate, monobromomalonamide was used in place of monobromocyanoacetamide in the above reaction. In this case, the resulting malonamide may be expected to be removed more readily than cyanoacetamide from the reaction mixture, while pure phosphate may be isolated by distillation. Actually, when ethyl phosphorodimorpholidite was reacted with monobromomalonamide in ethanol at room temperature, ethyl phosphorodimorpholidate was obtained in a 54% yield (Eq. 2).



(2)

Similarly, methyl alcohol, *n*-propyl alcohol, isopropyl alcohol, phenol and *p*-nitrophenol were phosphorylated by means of monobromomalonamide and ethyl phosphorodimorpholidite to yield the corresponding phosphorodimorpholidates. The results are summarized in Table I.

Further, it was established that alkyl or aryl dihydrogen phosphates could be obtained by the phosphorylation of alcohols or phenols and the subsequent hydrolysis of the reaction mixture with Amberlite IR-120 ($H^+$ form) ion exchange resin. For example, phenol was reacted with monobromocyanoacetamide and ethyl phosphorodimorpholidite

1) T. Hata and T. Mukaiyama, This Bulletin, **35**, 1106 (1962).
2) T. Mukaiyama, T. Hata and K. Tasaka, *J. Org. Chem.*, **28**, 481 (1963).
3) T. Hata and T. Mukaiyama, This Bulletin, **37**, 103 (1964).
4) H. A. C. Montgomery and J. H. Turnbull, *J. Chem. Soc.*, **1958**, 1963.

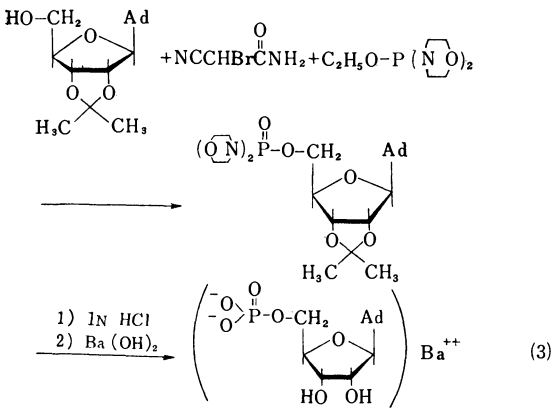
Table I. Phosphorylation of alcohols, phenols and morpholine by means of ethyl phosphorodimorpholidite and monobromomalonamide

| Alcohol, phenol or morpholine RH | Product $R-P(N\,O)_2$ | Yield % | B. p., °C/mmHg | N, % Found | N, % Calcd. |
|---|---|---|---|---|---|
| $CH_3OH$ | $CH_3O$ | 49 | 127—128/0.035 | 10.81 | 11.20 |
| $C_2H_5OH$ | $C_2H_5O$ | 54 | 130—132/0.01 | 10.48 | 10.61 |
| *n*-$C_3H_7OH$ | *n*-$C_3H_7O$ | 52 | 140—142/0.045 | 10.02 | 10.06 |
| *iso*-$C_3H_7OH$ | *iso*-$C_3H_7O$ | 21 | 125—127/0.02 | | |
| $C_6H_5OH$ | $C_6H_5O$ | 69 | 168—169/0.005 | 9.00 | 8.97 |
| *p*-$O_2NC_6H_4OH$ | *p*-$O_2NC_6H_4O$ | 87 | M. p. 118—120 | 12.03 | 11.77 |
|  |  | 32 | M. p. 185—186 | 13.48 | 13.76 |

at −40°C. After the cyanoacetamide had been removed by filtration, the filtrate was subsequently treated with Amberlite IR-120 ($H^+$ form) ion exchange resin, and phenyl dihydrogen phosphate was isolated as anilinium salt in a 47% yield.

Similarly, ethyl dihydrogen phosphate and *p*-nitrophenyl dihydrogen phosphate were obtained by the reaction of either ethanol or *p*-nitrophenol with monobromocyanoacetamide and ethyl phosphorodimorpholidite.

Further, this method of preparing monoesters of phosphoric acid was applied to the synthesis of adenosine 5′-phosphate. A mixture of 2′,3′-isopropylidene adenosine, monobromocyanoacetamide and ethyl phosphorodimorpholidite in dimethyl formamide was kept standing for 3 days at room temperature. After the solvent, had been promoved, the residue was treated with 1 N hydrochloric acid in order to remove protecting groups from the resulting 2′,3′-isopropylidene adenosine 5′-phosphorodimorpholidate. Adenosine 5′-phosphate was isolated as barium salt in a 54% yield and identified by paper chromatography and paper electrophoresis with an authentic sample. In the course of the hydrolysis, the glycosyl linkage was cleaved and a small amount of adenine was formed (as detected by paper chromatography).




(3)

## Experimental

Monobromocyanoacetamide,[1] monobromomalonamide,[2] ethyl phosphorodichloridite[5] and 2′,3′-isopropylidene adenosine[6] were prepared by the literature procedures.

**The Preparation of Ethyl Phosphorodimorpholidite.**—A solution of ethyl phosphorodichloridite (73.5 g., 0.5 mol.) in 100 ml. of ether was added drop by drop over a period of 1 hr. to a solution of triethylamine (101 g., 1 mol.) and morpholine (87.1 g., 1 mol.) in 500 ml. of ether cooled in an ice bath. The reaction mixture was refluxed for an additional 30 min. and triethylamine hydrochloride was removed by filtration. After the ether had been removed from the filtrate, 81 g. (65%) of ethyl phosphorodimorpholidite was obtained by fractionation, b. p. 120—124°C/5 mmHg. Redistillation gave an analytical sample, b. p. 118°C/0.35 mmHg.

Found: N, 11.37. Calcd. for $C_{10}H_{21}N_2O_3P$: N, 11.33%.

**The Phosphorylation of Ethanol by Means of Ethyl Phosphorodimorpholidite and Monobromocyanoacetamide.** — A solution of ethyl phosphorodimorpholidite (2.48 g., 0.01 mol.) in 5 ml. of ethanol was added drop by drop to a solution of monobromocyanoacetamide (1.63 g., 0.01 mol.) in 15 ml. of ethanol at −70°C. After the reaction mixture had been kept standing overnight at room temperature, ethanol was removed under reduced pressure. Chloroform was added to the residue and undissolved cyanoacetamide was filtered off, 0.76 g., 91%; m. p. 99—112°C. The filtrate was then concentrated to a syrup. This syrup was distilled to give 1.20 g. (46%) of ethyl phosphorodimorpholidate, b. p. 129—131°C/0.008 mmHg, along with a small amount of cyanoacetamide.

**The Phosphorylation of Ethanol by Means of Ethyl Phosphorodimorpholidite and Monobromomalonamide.**—To a suspension of monobromomalonamide (1.81 g., 0.01 mol.) in 13 ml. of ethanol was added, drop by drop, a solution of ethyl phosphorodimorpholidite (2.48 g., 0.01 mol.) in 3 ml. of ethanol at room temperature. The reaction started soon with the liberation of heat and a white precipitate, malonamide, appeared. After the reaction mixture

5) N. Menshutkin, *Ann.*, **139**, 343 (1866).
6) A. Hampton, *J. Am. Chem. Soc.*, **83**, 3640 (1961).

had been kept standing overnight, malonamide was removed by filtration. From the filtrate, ethyl phosphorodimorpholidate was obtained by fractionation; 1.54 g. (58%), b. p. 130—132°C/0.01 mmHg. When this stood at room temperature, the product solidified.

Found: N, 10.02. Calcd. for $C_{10}H_{21}N_2O_4P$: N, 10.06%.

Similarly, methyl alcohol, *n*-propyl alcohol and isopropyl alcohol were phosphorylated to give the corresponding alkyl phosphorodimorpholidates, as is shown in Table I.

**The Phosphorylation of Phenol by Means of Ethyl Phosphorodimorpholidite and Monobromomalonamide.**—To a suspension of monobromomalonamide (1.81 g., 0.01 mol.) and phenol (0.93 g., 0.01 mol.) in 15 ml. of ether there was added a solution of ethyl phosphorodimorpholidite (2.48 g., 0.01 mol.) in 5 ml. of ether at room temperature. The reaction started soon with the liberation of heat, and a white crystalline compound, malonamide, appeared. After the reaction mixture had been kept standing overnight, the malonamide was removed by filtration. From the filtrate, phenyl phosphorodimorpholidate was obtained by fractionation; 2.16 g. (69%), b. p. 168—169°C/0.005 mmHg.

Found: N, 9.00. Calcd. for $C_{14}H_{21}N_2O_4P$: N, 8.97%.

**The Phosphorylation of *p*-Nitrophenol by Means of Ethyl Phosphorodimorpholidite and Monobromomalonamide.**—A solution of ethyl phosphorodimorpholidite (2.48 g., 0.01 mol.) in 5 ml. of tetrahydrofuran (THF) was added drop by drop to a solution of monobromomalonamide (1.81 g., 0.01 mol.) and *p*-nitrophenol (1.39 g., 0.01 mol.) in 15 ml. of THF cooled in a water bath. After the reaction mixture had been kept standing overnight, the malonamide was removed by filtration; 1.00 g., 97%, m. p. 151—164°C. The removal of the solvent from the filtrate gave 3.80 g. of a solid residue which was recrystallized from ethyl acetate to give 3.10 g. (87%) of *p*-nitrophenyl phosphorodimorpholidate, m. p. 118.5—120°C.

Found: N, 12.09. Calcd. for $C_{14}H_{20}N_3O_6P$: N, 11.76%.

**The Phosphorylation of Morpholine by Means of Ethyl Phosphorodimorpholidite and Monobromomalonamide.**—A solution of ethyl phosphorodimorpholidite (2.48 g., 0.01 mol.) in 5 ml. of THF was added drop by drop to a solution of monobromomalonamide (1.81 g., 0.01 mol.) and morpholine (0.87 g., 0.01 mol.) in 15 ml. of THF at room temperature. After the reaction mixture had been kept standing overnight, the malonamide was removed by filtration. The filtrate was concentrated under reduced pressure, and 15 ml. of chloroform was added to the residue. A small amount of undissolved malonamide was filtered off. The removal of the solvent from the filtrate gave a solid residue which was recrystallized from acetone to give 0.98 g. (32%) of phosphorotrimorpholidate, m. p. 185—186°C.

Found: N, 13.48. Calcd. for $C_{12}H_{24}N_3O_4P$: N, 13.76%.

**The Preparation of Ethyl Dihydrogen Phosphate.**—A solution of ethyl phosphorodimorpholidite (2.48 g., 0.01 mol.) in 5 ml. of ethanol was added drop by drop to a solution of monobromocyanoacetamide (1.63 g., 0.01 mol.) in 10 ml. of ethanol cooled at −40—−30°C. After the reaction mixture had been kept standing overnight, the ethanol was removed under reduced pressure. Chloroform (20 ml.) was added to the residue, and the undissolved cyanoacetamide was removed by filtration. The filtrate was concentrated to a syrup, which was then dissolved in 30 ml. of water. The solution was passed slowly (1 hr.) through a column (18×150 mm.) of Amberlite IR-120 resin ($H^+$ form) at 60°C, and the column was washed with 100 ml. of water. After the water had been removed from the eluate under reduced pressure, the residue was dissolved in acetone and 1.4 ml. of cyclohexylamine was added to the solution, giving 0.88 g. (27%) of bis cyclohexylammonium ethyl phosphate. Recrystallization from *n*-propyl alcohol gave an analytical sample, m. p. 201—203°C (decomp.).

Found: N, 8.35. Calcd. for $C_{14}H_{33}N_2O_4P$: N, 8.63%.

**The Preparation of *p*-Nitrophenyl Dihydrogen Phosphate.**—The mixture which resulted from the reaction of *p*-nitrophenol (2.78 g., 0.02 mol.), ethyl phosphorodimorpholidite (4.96 g., 0.02 mol.) and monobromocyanoacetamide (3.26 g., 0.02 mol.) in 30 ml. of THF at −40°—−30°C was concentrated to give a solid residue. Chloroform (40 ml.) was then added, and the undissolved cyanoacetamide was removed by filtration. The removal of chloroform from the filtrate under reduced pressure gave a crystalline compound; this was then dissolved in acetonitrile (15 ml.) and water (30 ml.). The solution was passed through a column of Amberlite IR-120 resin ($H^+$ form), as in the above experiment, and the column was washed with a mixture of acetonitrile (50 ml.) and water (10 ml.). By a manner analogous to that mentioned above, bis(anilinium) *p*-nitrophenyl phosphate was obtained in a 49% (1.05 g.) yield. An analytical sample was obtained by recrystallization from acetone and water, m. p. 165—167°C.

Found: N, 10.41. Calcd. for $C_{18}H_{20}N_3O_6P$: N, 10.35%.

Similarly, anilinium phenyl hydrogen phosphate was obtained in a 47% yield, m. p. 180—182°C.

**The Preparation of Adenosine 5′-Phosphate.**—A solution of ethyl phosphorodimorpholidite (0.25 g., 0.001 mol.) in 0.4 ml. of dimethyl formamide (DMF) was added drop by drop to a suspension of 2′,3′-isopropylidene adenosine (0.15 g., 0.0005 mol.; dried over phosphorus(V) oxide at 115°C, 0.05 mmHg for 11 hr.) and monobromocyanoacetamide (0.16 g., 0.001 mol.; dried over phosphorus(V) oxide at room temperature, 20 mmHg for 11 hr.) in 1.8 ml. of DMF. The reaction started soon, with the liberation of heat. The reaction mixture was then kept standing for 3 days at room temperature. After the solvent had been removed under reduced pressure, 3 ml. of 1 N hydrochloric acid was added to the residue and it was heated at 40°C for 8.5 hr. in order to remove the protecting groups. After the pH had been adjusted to 7.5 with 1 N ammonium hydroxide, the water was removed under reduced pressure (50°C/4 mmHg). Ammonium hydroxide was added to the residue to pH 10, and then a saturated solution of barium chloride was added. After the mixture had been kept standing in a refrigerator, the precipitate was collected by centrifugation, washed with two portions of water

(5 ml.) and dried over phosphorus(V) oxide at room temperature to give 0.14 g. (54%) of the barium salt of adenosine 5′-phosphate. The product was found to be identical with an authentic adenosine 5′-phosphate by a comparison of $R_f$ values; 0.70 (5% $Na_2HPO_4$, isoamyl alcohol, 1 cm.: 0.5 cm.), and 0.33 (1% ammonium sulfate - isopropyl alcohol, 1 : 2 V/V). By paper electrophoresis, the product was also identified with an authentic sample (citrate buffer, pH 3.5, 4 hr. at 800 V.).

## Summary

The phosphorylation of alcohols or phenols by means of ethyl phosphorodimorpholidite and either monobromocyanoacetamide or monobromomalonamide has been studied. Further, adenosine 5′-phosphate has been prepared by the reaction of ethyl phosphorodimorpholidite and monobromocyanoacetamide with 2′,3′-isopropylidene adenosine.

The authors wish to thank Dr. Tsujiaki Hata for his helpful discussion, and also Miss Toshiko Aoyagi for her microanalyses.

*Laboratory of Organic Chemistry*
*Tokyo Institute of Technology*
*Ookayama, Tokyo*

# The Kinetics of the Acid-Catalyzed Formation of Peracetic Acid from Acetic Acid and Hydrogen Peroxide*

By Yasuhiko SAWAKI and Yoshiro OGATA

(Received April 30, 1965)

It has been established that the formation and hydrolysis of peracetic acid is acid-catalyzed,[1] and also that the equilibrium constant for reaction 1 increases with an increase in the concentration of catalytic acid.[2,3]

$$CH_3CO_2H + H_2O_2 \underset{k_{-1}}{\overset{k_1}{\rightleftarrows}} CH_3CO_3H + H_2O \quad (1)$$

In order to clarify these phenomena, the dependence of the rate and equilibrium constants on the concentration of mineral acid over a wider range has been studied, and the dependence has been correlated with Hammett's acidity function.

## Experimental

**Materials.**—Commercal aetic acid was refluxed with potassium permanganate and rectified over phosphorus pentoxide; b. p. 117—118°C. Hydrogen peroxide (30%) and sulfuric acid were both of guaranteed grade. *p*-Nitro- and *o*-nitroanilines were recrystallized from water containing a small amount of methanol.

**Kinetic Measurements.** — A definite amount of aqueous acetic acid of a known concentration containing an appropriate amount of surfuric acid was thermostated and the reaction was started by adding 30% hydrogen peroxide. (Water had been added previously in order to prevent the evolution of the heat of neutralization when 30% hydrogen peroxide was added.)

Aliquots were taken out at appropriate intervals of time and analyzed for hydrogen peroxide and peracid by means of an unique method. The aliquot was poured into ca. 50 ml. of ice-cooled ca. 0.4 N sulfuric acid containing three drops of 1% aqueous manganese sulfate. The hydrogen peroxide was quickly titrated with potassium permanganate until a pink color appeared, and then the remaining peracid was titrated iodometrically after the addition of potassium iodide. The peracid content was calculated from the ratio of the titres of permanganate and thiosulfate consumed, since the decomposition of hydrogen peroxide and peracid was found to be negligible under these reaction conditions. This novel method, which does without the weighing of aliquots, gave an adequate accuracy in a blank test.

**The Calculation of Rate Constants.**—Since the decomposition of hydrogen peroxide and peracid under these conditions was unappreciable, the rate constants may be calculated as follows. By representing the initial concentrations of acetic acid, hydrogen peroxide and water as $a$, $b$ and $c$, respectively, and the concentration of the peracid produced as $x$, the rate of the formation of peracetic acid may be expressed as:

$$v = k_1(a-x)(b-x) - k_{-1}(c+x)x$$

This equation is transformed to:

$$v = k_1(1-1/K_1)(\alpha-x)(\beta-x) \quad (2)$$

Here, $K_1 = k_1/k_{-1}$ and

$$\alpha, \beta = \frac{1}{2(1-1/K_1)}\left\{(a+b+c/K_1) \pm \sqrt{(a+b+c/K_1)^2 - 4ab(1-1/K_1)}\right\}$$

The rate constant $k_1$ thus calculated, has a good constancy, as is shown in Table I.

* Contribution No. 78.

1) D. Swern, *Chem. Revs.*, **45**, 1 (1949).
2) S. Havel and J. A. Weigner, *Chem. Prumysl*, **10**, 293 (1960).
3) T. Suzuki, I. Iwamoto and S. Suzuki, *J. Chem. Soc. Japan, Pure Chem. Sec.* (*Nippon Kagaku Zasshi*), **83**, 1212 (1962).

Table I. A typical rate constant for the formation of peracetic acid in 80 vol.% acetic acid at 25°C

Initial concn.: $a=[CH_3CO_2H]=13.77$ M; $b=[H_2O_2]=1.014$ M; $c=[H_2O]=9.831$ M; $[H_2SO_4]=0.30$ M.

| Time min. | $x=[CH_3CO_3H]$ M | $k_1\times10^6$ a) $M^{-1}\,sec^{-1}$ |
|---|---|---|
| 10 | 0.115 | 15.9 |
| 17 | 0.186 | 16.0 |
| 27 | 0.272 | 15.8 |
| 40 | 0.358 | 15.3 |
| 50 | 0.421 | 15.4 |
| 60 | 0.483 | 16.0 |
| 75 | 0.530 | 15.0 |
| 100 | 0.612 | 15.3 |
| 1800 | 0.800 | —b) |

a) $\alpha=26.04$; $\beta=0.777$
b) Calculated equilibrium constant ($K_1$) was 3.045.

**The Measurement of $H_0$.** — Hammett's acidity function of the reaction media (water was added in place of hydrogen peroxide) was measured using *o*- and *p*-nitroanilines as indicators. The absorption peaks were measured at 410 mμ for *o*-nitroaniline and at 370—380 mμ for *p*-nitroaniline; the shift of $\lambda_{max}$ was observed upon varying the ratio of acetic acid to water. The $H_0$'s were calculated from the equation; $H_0=pK_{BH^+}-\log(c_{BH^+}/c_B)$, where $pK_{BH^+}$ is an indicator constant and $c_{BH^+}$ is the concentration of the conjugate acid of the indicator and $c_B$ is that of the neutral form of the same indicator. The values of $pK_{BH^+}$ cited are −0.29 for *o*-nitroaniline and 0.99 for *p*-isomer.[4] These results are listed in Tables II and III.

## Results and Discussion

**The Rate Law.**—The acid-catalyzed formation of peracetic acid follows Rate Eq. 2, while a typical run is shown in Table I. The rate law coincides with the data reported previously in the literature.[3,5] The rate of peracid formation in the absence of mineral acid was too slow to measure.

**The Effect of the Acidity of the Media.**—The rates and equilibrium constants for the formation of peracetic acid are shown in Table II, where it is obvious that they increase with an increase in the concentration of sulfuric acid. These facts have been reported as the proportionalities of rate and equilibrium constants to the concentration (<0.5 M) of mineral acid.[2-4] However, this is not true at higher concentrations of mineral acid (>0.5 M), and the polts of $k_1$ or $K_1$ vs. $[H_2SO_4]$ lie not on a straight line but on a curve (Fig. 1).

This departure from linearity may be corrected for by plotting log $k_1$ or log $K_1$ against Hammett's acidity function; the plots then give a straight line with a solpe of 0.82 for log $k_1$ and 0.22 for log $K_1$ (Fig. 2).

Table II. The effect of acidity on the rate and equilibrium constants for the peracid formation in 80 vol.% acetic acid at 25°C[a)]

| $[H_2SO_4]$ M | $-H_0$[b)] | $K_1$ | $k_1\times10^6$ $M^{-1}\,sec^{-1}$ |
|---|---|---|---|
| 3.0 | 2.43 | 12.81 | 1030 |
| 2.0 | 1.68 | 7.635 | 353 |
| 1.5 | 1.20 | 6.016 | 175 |
| 1.2 | 0.91 | 5.146 | 116 |
| 1.0 | 0.80 | 4.517 | 80.0 |
| 0.80 | 0.58 | 3.944 | 52.3 |
| 0.60 | 0.30 | 3.528 | 34.9 |
| 0.50 | 0.15 | 3.405 | 27.7 |
| 0.40 | 0.00 | 3.224 | 20.1 |
| 0.30 | −0.15 | 3.045 | 15.1 |
| 0.20 | −0.33 | 2.870 | 9.04 |
| 0.10 | −0.63 | 2.708 | 4.25 |

a) Initial concn.: $[CH_3CO_2H]=11.5$—13.9 M; $[H_2O_2]=1.014$ M; $[H_2O]=9.831$ M
b) *o*-Nitroaniline was used as an indicator.

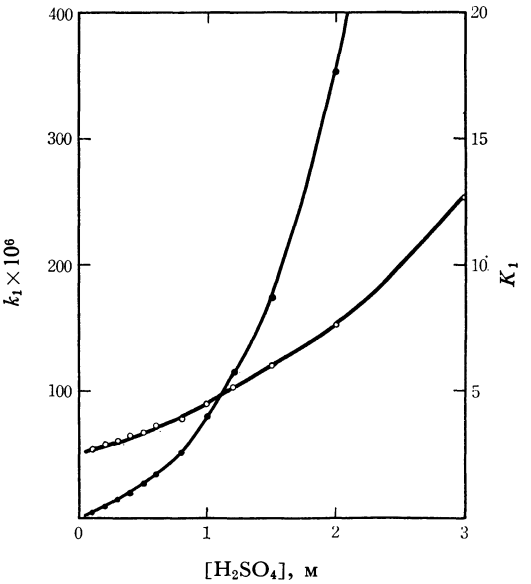



Fig. 1. Plots of $k_1$ and $K_1$ vs. $[H_2SO_4]$ in 80 vol.% acetic acid at 25°C.
—●— $k_1$ vs. $[H_2SO_4]$
—○— $K_1$ vs. $[H_2SO_4]$

**The Effect of the Ratios of the Concentrations of Acetic Acid and Water.**—The rate of peracid formation was found to increase with an increase in the ratio of concentrations of acetic acid and water at a constant concentration of sulfuric acid (Table III). The plots of log $k_1$ vs. $-H_0$ give a straight line with a slope of 1.10 or ca. unity, a considerably larger value than that in the

4) M. A. Paul and F. A. Long, *Chem. Revs.*, 57, 1 (1957).
5) K. Murai, G. Akazome and Y. Murakami, *J. Chem. Soc. Japan, Ind. Chem. Sec.* (*Kogyo Kagaku Zasshi*), **63**, 1233 (1960).

former slope (0.82). It should be noted that different indicators are used for the determination of the acidity function, and that this may cause a small difference in the observed acidity function.

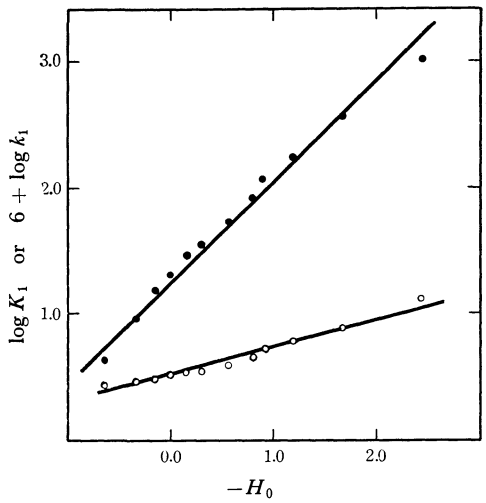



Fig. 2. Plots of $\log k_1$ and $\log K_1$ against the Hammett's acidity function in 80 vol.% acetic acid at 25°C.

—●— $\log k_1$ vs. $-H_0$
—○— $\log K_1$ vs. $-H_0$

Table III. Effect of the ratio of $[CH_3CO_2H]$: $[H_2O]$ at 25°C[a)]

| Acetic acid Vol.% | $-H_0$[b)] | $K_1$ | $k_1\times10^6$ M$^{-}$ sec$^{-1}$ |
|---|---|---|---|
| 90 | +0.065 | 3.551 | 28.6 |
| 80 | −0.339 | 3.053 | 9.21 |
| 70 | −0.607 | 2.909 | 7.01 |
| 60 | −0.770 | 2.563 | 3.30 |
| 40 | −0.871 | 2.080 | 1.76 |

a) Initial concn.: $[H_2SO_4]=0.20$ M; $H_2O_2=0.9350$ M.
b) *p*-Nitroaniline was used as an indicator.

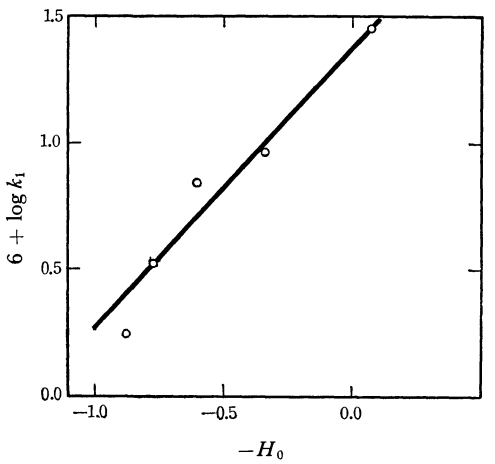



Fig. 3. Plots of $\log k_1$ vs. $-H_0$ in various ratio of $[CH_3CO_2H]$: $[H_2O]$ at 25°C.

**Temperature Dependence.**—The effect of the temperature on the rate was studied in 60 and 80 vol.% acetic acid; the results, together with the calculated activation parameters, are summarized in Table IV. The change in the energy and entropy of activation is unappreciable in going from 60% to 80% acetic acid.

Table IV. Apparent energies and entropies of activation for the acid-catalyzed formation of peracetic acid

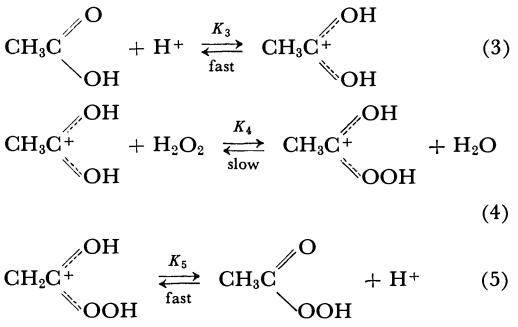
| Acetic acid vol.% | Temp. °C | $K_1$ | $k_1\times10^6$ M$^{-1}$ sec$^{-1}$ | $E_a$ kcal.·mol$^{-1}$ | $\Delta S^{\neq}$ e. u. |
|---|---|---|---|---|---|
| 80[a)] | 18.0 | 2.948 | 5.04 | 15.0 | −35.7 |
| | 25.0 | 2.907 | 9.54 | | |
| | 18.0 | 2.828 | 16.5 | | |
| 60[b)] | 18.0 | 2.589 | 1.84 | 15.1 | −33.2 |
| | 25.0 | 2.537 | 3.36 | | |
| | 32.0 | 2.453 | 6.10 | | |

a) Initial concn.: $[H_2SO_4]=0.20$ M; $[CH_3CO_2H]=12.36$ M; $[H_2O_2]=1.014$ M; $[H_2O]=9.831$ M.
b) Initial concn.: $[H_2SO_4]=0.20$ M; $[CH_3CO_2H]=8.611$ M; $[H_2O_2]=2.028$ M; $[H_2O]=19.66$ M.

The value for the entropy of activation (−33—−36 e.u.) implies a mechanism similar to that in the case of acid-catalyzed second-order esterification (−15——30 e.u.).[6)] The value for the energy activation (15.1 kcal. mol$^{-1}$) also suggests a second-order mechanism resembling the ester hydrolysis. Both the energy and the entropy of activation are close to the activation parameters in an oxygen-exchange reaction between water and benzoic acid (16 kcal. mol$^{-1}$ and −30 e.u. respectively).[7)]

**The Reaction Mechanism.**—The logarithm of the rate constant for peracid formation is proportional to $-H_0$. The energy and the entropy of activation are close to those in acid-catalyzed esterification. The substituent effect in acetic acid in dioxane was found to depend mostly on the steric factor, and to be little affected by the polar factor of the substituents.[8)] Tracer studies of the hydrolysis of peracid also reveal that the mechanism is analogous to the acyl-oxygen fission mechanism of ester hydrolysis.[9)] These facts suggest this probable mechanism for the peracid formation:

6) L. L. Schaleger and F. A. Long, "Advances in Physical Organic Chemistry," Vol. I, Academic Press, New York (1963), p. 23.
7) C. A. Bunton, D. H. James and J. B. Senior, *J. Chem. Soc.*, **1960**, 3364.
8) Y. Ogata and Y. Sawaki, *Tetrahedron*, in press.
9) C. A. Bunton, T. A. Lewis and D. R. Liewellyn, *J. Chem. Soc.*, **1956**, 1226.



The position of the protonation of the carboxyl group has been found to be mainly at carbonyl oxygen,[10] as has been described above. The rate-determining step is Eq. 4; hence, the rate of peracid formation should be proportional to the product of the concentrations of acetic acid and hydrogen peroxide, the logarithm of the rate constant being proportional to $-H_0$; this is indeed the case. The reaction of acetic acid with hydrogen peroxide in the absence of catalytic mineral acid was too slow to measure; hence, the reaction path through unprotonated acetic acid may be considered to be negligible.

Although the details of the mechanism are still unknown on the basis of the above results alone, a mechanism similar to those in the acid-catalyzed esterification may be assumed. Our data, together with those in the literature,[7,11] show a similarity of mechanisms in the esterification, the oxygen-exchange, and the peracid formation. Hence, a nucleophilic attack of hydrogen peroxide on protonated carboxylic acid is a probable course for the reaction.

**The Effect of the Acidity on the Equilibrium Constants.** — The equilibrium constant increased with an increase in the concentration of sulfuric acid. The plots of log $K_1$ vs. $-H_0$ gave a straight line, with a slope of 0.22 (Fig. 2). This fact may well be explained by assuming the elimination of free water from the reaction system by the protonation, since water is the strongest base among the components in Eq. 1.

$$K_1=\frac{[CH_3CO_3H][H_2O]}{[CH_3CO_2H][H_2O_2]}$$

It is known that water is a thousandfold stronger as a base than hydrogen peroxide;[12] hence, the protonation occurs only to water. The stoichiometric concentration of water is the sum of the free and the protonated water, the latter having little ability to make a uncleophilic attack on carboxyl carbon. The net concentration of free water, an effective nucleophile, decreases with an increase in the acidity much more rapidly than hydrogen peroxide does. Hence, the appearent equilibrium constant should increase with an increase in the acidity of the medium.

The protonation of acetic acid has been reported,[13] but no data is available on the protonation of peracetic acid. However, the extent of the protonation of acetic and peracetic acids should be much smaller than that of water and hydrogen peroxide, both of which are stronger as bases. Therfore, the protonation of these acids may be neglected in examining the effect of the acidity on the equilibrium constant, $K_1$.

## Summary

The sulfuric acid-catalyzed reversible formation of peracetic acid from acetic acid and hydrogen peroxide in aqueous acetic acid has been studied kinetically. The rate of peracid formation is proportional to the product of the concentrations of acetic acid and of hydrogen peroxide, increasing with an increase in the concentration of sulfuric acid. The plot of the logarithm of the rate constant vs. $-H_0$ gives a straight line, with a slope of 0.82 and 1.10. The mechanism has been discussed in connection with the analogous acid-catalyzed esterification. The equilibrium constants for the present reaction also increase with an increase in the acidity, and the similar plot of log $K_1$ vs. $-H_0$ gives a straight line with a slope of 0.22. These facts are explicable by considering the protonation of water.

*Department of Applied Chemistry*
*Faculty of Engineering*
*Nagoya University*
*Chikusa-ku, Nagoya*

10) R. Stewart and K. Yates, *J. Am. Chem. Soc.*, **82**, 4059 (1960).
11) I. Roberts and C. Urey, ibid., **61**, 2580 (1939).
12) M. G. Evans and N. Uri, *Trans. Faraday Soc.*, **49**, 410 (1953).
13) For quantitative estimation, see N. C. Deno, C. U. Pittman, Jr., and M. J. Wisotsky, *J. Am. Chem. Soc.*, **86**, 4370 (1964).

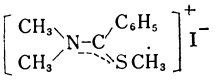
# Reactions of the Iodomethylate of *N, N*-Dimethylthiobenzamide with Nucleophilic Reagents

By Teruaki MUKAIYAMA, Tatsuaki YAMAGUCHI and Hiroyuki NOHIRA

(Received April 30, 1965)

It has been reported that α-dialkylaminomethylene compounds can be prepared by the condensation of *N,N*-dialkylformamide acetals[1,2] with active hydrogen compounds, such as active methylene compounds. In the present study, the preparation of various α-dimethylaminobenzylidene compounds by reactions of the iodomethylate (I) of *N,N*-dimethylthiobenzamide with nucleophilic reagents will be examined.

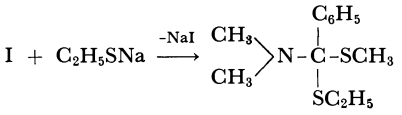
Recently, Böttcher and Bauer have isolated the iodomethylate (I) of *N,N*-dimethylthiobenzamide by treating *N*-methylisothiobenzamide-*S*-methylether with methyl iodide.[3] The iodomethylate (I) is easily hydrolyzed with alkali to give *N,N*-dimethylbenzamide and methyl mercaptan.



(I)

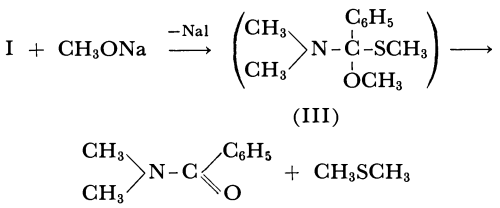
This result suggests that the iodomethylate (I) would yield condensation products when it is treated with nucleophilic reagents, such as sodium ethylmercaptide, potassium cyanide, amines, and the monosodium salts of active methylene compounds.

With this in mind the reaction of sodium ethylmercaptide with the iodomethylate (I) was attempted first. Sodium ethylmercaptide easily reacted with the iodomethylate (I) in dry ether at room temperature, and *N,N*-dimethylbenzamide methylethylmercaptol (II) was obtained in a fairly good yield.



(II)

On the other hand, sodium methoxide could hardly react at all with the iodomethylate (I) at room temperature. When they were refluxed in dry benzene for 1 hr., however, *N,N*-dimethylbenzamide was obtained in a 41.5% yield, along with dimethyl sulfide, instead of the expected product, *N,N*-dimethylbenzamide monothioketal (III).



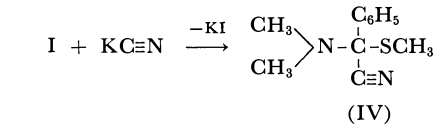
(III)

The results of the reactions of other sodium alkoxides with the iodomethylate (I) are listed in Table I.

Table I. Reactions of I with sodium alkoxides

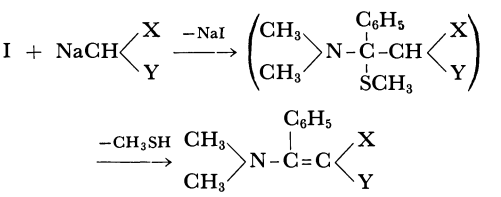
| Sodium alkoxide | Reaction condition | | | Yield, % | |
|---|---|---|---|---|---|
| | Solvent | Temp. °C | Time hr. | Amide | Sulfide |
| Methoxide | Benzene | 80 | 1.0 | 41.5 | — |
| Ethoxide | Benzene | 80 | 1.0 | 46 | — |
| Cyclohexyloxide | Toluene | 110 | 2.0 | 33 | 16 |
| Benzyloxide | Dioxane | 100 | 3.0 | 79 | 65 |

In addition, when potassium cyanide and the iodomethylate (I) were refluxed in dry benzene for 1 hr., α-dimethylamino-α-methylthiobenzyl cyanide (IV) was obtained in a 64% yield, while potassium iodide was eliminated.



(IV)

Next, it was found that α-dimethylaminobenzylidene malonate was produced in a 56% yield, with the evolution of methyl mercaptan, when a suspension of the iodomethylate (I) and the monosodium salt of ethyl malonate in dry dioxane was stirred at 80°C for 2 hr. Similar results were obtained by treating the iodomethylate (I) with the monosodium salts of other active methylene compounds, such as ethyl acetoacetate, ethyl cyanoacetate, acetylacetone and nitromethane (see Table II).



(V)

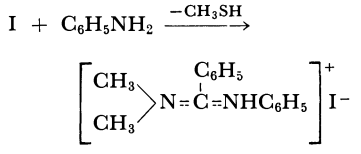
1) H. Meerwein, W. Florian, N. Schön and G. Stopp, *Ann.*, **641**, 1 (1961).
2) H. Eilingsfeld, M. Seefelder and H. Weidinger, *Chem. Ber.*, **96**, 2671 (1963).
3) B. Böttcher and F. Bauer, *Ann.*, **568**, 218 (1950).

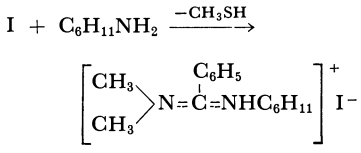
TABLE II. THE YIELDS, PHYSICAL PROPERTIES AND ANALYSES FOR α-DIMETHYLAMINOBENZYLIDENE DERIVATIVES OF ACTIVE METHYLENE COMPOUNDS

| Active Methylene Compound | Yield % | B. p. °C/mmHg | M. p. °C | Found % | Calcd. % |
|---|---|---|---|---|---|
| Ethyl Malonate | 56 | 136—137/0.11 | | C, 65.84 | C, 65.95 |
| | | | | H, 7.38 | H, 7.27 |
| | | | | N, 5.00 | N, 4.81 |
| Ethyl Acetoacetate | 60 | 144—145/0.06 | | C, 67.94 | C, 68.44 |
| | | | | H, 7.75 | H, 7.33 |
| | | | | N, 5.25 | N, 5.36 |
| Ethyl Cyanoacetate | 72 | 164—166/0.02 | 87—88[a] | C, 68.67 | C, 68.83 |
| | | | | H, 6.86 | H, 6.60 |
| | | | | N, 11.72 | N, 11,47 |
| Acetylacetone | 52 | | 115—117[b] | C, 72.45 | C, 72.70 |
| | | | | H, 7.41 | H, 7.41 |
| | | | | N, 6.26 | N, 6.06 |
| Nitromethane | 57 | | 128—129[c] | C, 62.37 | C, 62.48 |
| | | | | H, 6.54 | H, 6.29 |
| | | | | N, 14.66 | N, 14.58 |

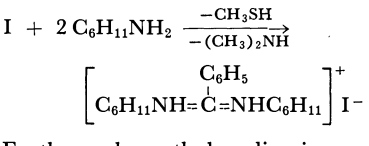
a) Recrystallized from benzene-ligroin. b) from ethyl acetate. c) from ethanol or benzene.

Further, the reactions of the iodomethylate (I) with primary amines were examined. When an ethanol solution of aniline was added to a suspension of the iodomethylate (I) in ethanol at room temperature, the evolution of methyl mercaptan was observed, and after stirring had been continued for 3 hr., *N*, *N*-dimethyl-*N'*-phenylbenzamidine hydroiodide was obtained in a 68% yield. Similarly, cyclohexylamine reacted with the iodomethylate (I) at room temperature to give *N*,*N*-dimethyl-*N'*-cyclohexylbenzamidine hydroiodide in a high yield.

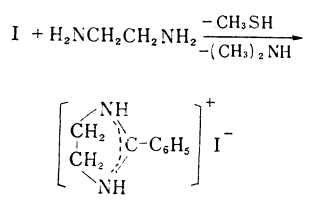




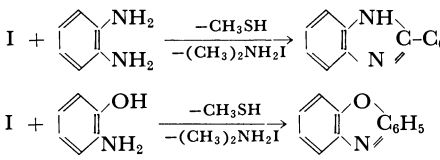
On the other hand, when a mixture of 2 mol. of cyclohexylamine and 1 mol. of the iodomethylate (I) was refluxed in ethanol for 2 hr., *N*, *N'*-dicyclohexylbenzamidine hydroiodide was given in a 49% yield, along with methyl mercaptan and dimethylamine.



Further, when ethylenediamine and the iodomethylate (I) were refluxed in ethanol for 2 hr., 2-phenylimidazoline hydroiodide was produced in a high yield. Free 2-phenylimidazoline was obtained by treating the hydroiodide with alkali.



*o*-Phenylenediamine reacted with the iodomethylate (I) at room temperature in ethanol to give 2-phenylbenzimidazole in a good yield, with the elimination of methyl mercaptan and dimethylamine hydroiodide. In a similar way, 2-phenylbenzoxazole was prepared in a good yield by the reaction between *o*-aminophenol and the iodomethylate (I).



## Experimental[4]

**The Iodomethylate (I) of *N*, *N*-Dimethylthiobenzamide.**—This compound was prepared by the following method. A solution of 83 g. (0.5 mol.) of *N*, *N*-dimethylthiobenzamide and 100 g. (0.7 mol.) of methyl iodide in 400 ml. of acetone was refluxed on a water-bath for 1 hr. After the mixture had then been cooled, the iodomethylate (I) was separated and recrystallized from acetone. Yield, 140 g. (92%); m. p. 148—149°C.

4) All melting points and boiling points are uncorrected.

**The Reaction of I with Sodium Ethylmercaptide.**—A suspension of 28 g. (0.1 mol.) of I and 9.8 g. (0.11 mol.) of sodium ethylmercaptide in 150 ml. of dry ether was stirred at room temperature for 1 hr. The precipitate of sodium iodide was then removed by filtration and washed with dry ether. After ether had been evaporated from the filtrate, the residual liquid was distilled in vacuo to give 11.1 g. (52%) of *N*, *N*-dimethylbenzamide methylethylmercaptol (II). B. p. 94—97°C/0.08 mmHg.

Found: C, 59.93; H, 8.14; N, 6.08. Calcd. for $C_{11}H_{19}NS_2$: C, 59.73; H, 7.94; N, 5.81%.

**The Reaction of I with Sodium Methoxide.**—A suspension of 3.0 g. (0.01 mol.) of I and 0.6 g. (0.01 mol.) of sodium methoxide in 20 ml. of dry benzene was refluxed for 1 hr. Then the reaction mixture was filtered to remove the precipitate of sodium iodide. After the benzene had been removed from the filtrate, the residual liquid was distilled under reduced pressure to give 0.62 g. (41.5%) of *N*, *N*-dimethylbenzamide. B. p. 133°C/12 mmHg.

By similar procedures, *N*, *N*-dimethylbenzamide and sulfides were obtained by the reactions of I with sodium ethoxide, sodium cyclohexyloxide and sodium benzyloxide (see Table I).

**The Reaction of I with Potassium Cyanide.**—A suspension of 3.0 g. (0.01 mol.) of I and 0.65 g. (0.01 mol.) of potassium cyanide in 20 ml. of dry benzene was refluxed for 1 hr. After the solution had cooled, the precipitated potassium iodide was filtered off and the benzene was removed from the filtrate in vacuo. The distillation of the residue under reduced pressure gave 1.33 g. (64%) of $\alpha$-dimethylamino-$\alpha$-methylthiobenzyl cyanide (IV). B. p. 93—94°C/2 mm Hg.

Found: C, 63.82; H, 7.13; N, 13.55. Calcd. for $C_{11}H_{14}N_2S$: C, 64.06; H, 6.84; N, 13.58%.

The infrared spectrum showed an absorption at 2230 $cm^{-1}$(C≡N).

**The Reactions of I with the Monosodium Salts of Active Methylene Compounds.**—Into a solution of an excess amount of an active methylene compound in 20 ml. of dry dioxane, 0.23 g. (0.01 mol.) of sodium metal was added in portions. Then the mixture was heated to the boiling point, when all the sodium parts disappeared. To the resulting suspension of the monosodium salt of the active methylene compound in dioxane was then added 3.0 g. (0.01 mol.) of I and the mixture was stirred for 2 hr. at 80°C. The $\alpha$-dimethylaminobenzylidene derivatives (V) of the active methylene compounds obtained were purified by distillation or recrystallization. Their properties are listed in Table II.

**The Reaction of I with Aniline.**—A solution of 0.9 g. (0.01 mol.) of aniline in 20 ml. of ethanol was added to a suspension of 3.0 g. (0.01 mol.) of I in 20 ml. of ethanol. Soon the evolution of methyl mercaptan was observed and the suspended I was dissolved. After the solution had been stirred for 3 hr. at room temperature, the ethanol was removed in vacuo, giving *N*, *N*-dimethyl-*N'*-phenylbenzamidine hydroiodide as a white crystal; this was then recrystallized from ethanol-ether. Yield, 2.3 g. (68%). m. p. 122—124°C. Free *N*, *N*-dimethyl-*N'*-phenylbenzamidine (m. p. 72°C) was obtained by treating the hydroiodide with a 20% aqueous solution of potassium hydroxide.

**The Reaction of 1 mol. of I with 1 mol. of Cyclohexylamine.**—A suspension of 3.0 g. (0.01 mol.) of I and 1.0 g. (0.01 mol.) of cyclohexylamine in 20 ml. of ethanol was stirred at room temperature. The suspended I was soon dissolved completely, and the evolution of methyl mercaptan was observed. After stirring had been continued for 3 hr., the ethanol was evaporated and *N*, *N*-dimethyl-*N'*-cyclohexylbenzamidine hydroiodide was obtained as a white crystal. The hydroiodide was then recrystallized from ethanol-ether. Yield, 3.4 g. (91.5%); m. p. 189—190°C.

Found: C, 50.33; H, 6.17; N, 7.85. Calcd. for $C_{15}H_{23}N_2I$: C, 50.37; H, 6.41; N, 7.81%.

**The Reaction of 1 mol. of I with 2 mol. of Cyclohexylamine.**—A suspension of 3.0 g. (0.01 mol.) of I and 2.0 g. (0.02 mol.) of cyclohexylamine in 20 ml. of ethanol was refluxed for 3 hr. Then the ethanol was removed from the reaction mixture, and the resulting *N*, *N'*-dicyclohexylbenzamidine hydroiodide was recrystallized from ethanol-ether. Yield, 2.0 g. (49%); m. p. 173—174°C.

Found: C, 55.50; H, 7.04; N, 7.02. Calcd. for $C_{19}H_{29}N_2I$: C, 55.34; H, 7.08; N, 6.79%.

**The Preparation of 2-Phenylimidazoline from I and Ethylenediamine.** — Into a suspension of 3.0 g. (0.01 mol.) of I in 20 ml. of ethanol was added a solution of 0.6 g. (0.01 mol.) of ethylenediamine in 10 ml. of ethanol; the mixture was then refluxed on a water-bath. Soon the I was dissolved completely, and the evolution of methyl mercaptan was observed. After 2 hr., the solvent was removed and the resulting 2-phenylimidazoline hydroiodide monohydrate was recrystallized from acetonitrile-ether. Yield, 2.4 g. (89%); m. p. 105—107°C.

Found: C, 37.44; H, 4.50; N, 9.89. Calcd. for $C_9H_{13}N_2OI$: C, 37.00; H, 4.45; N, 9.59%.

Free 2-phenylimidazoline (m. p. 100—101°C) was obtained by treating the hydroiodide with a 10% aqueous solution of potassium hydroxide.

**The Preparations of 2-Phenylbenzimidazole and 2-Phenylbenzoxazole from I.**—A suspension of 3.0 g. (0.01 mol.) of I and 1.0 g. (0.01 mol.) of *o*-phenylenediamine in 20 ml. of ethanol was stirred at room temperature. The suspended I was thus dissolved completely, and methyl mercaptan was evolved. After stirring had been continued for 4 hr., about 50 ml. of water was added to the reaction mixture giving 1.45 g. (74.5%) of 2-phenylbenzimidazole. This was then recrystallized from acetonitrile. M. p. 285—286°C.

Similarly, when a suspension of 3.0 g. (0.01 mol.) of I and 1.1 g. (0.01 mol.) of freshly-refined *o*-aminophenol in 20 ml. of ethanol was stirred for 3 hr. at room temperature, 1.3 g. (67%) of 2-phenylbenzoxazole was obtained; it was then recrystallized from ethanol-ether. M. p. 101—102°C.

## Summary

The reactions of the iodomethylate (I) of *N*, *N*-dimethylthiobenzamide with nucleophilic reagents have been examined. The iodomethylate I reacted with sodium ethylmercaptide and potassium

cyanide to give *N*,*N*-dimethylbenzamide methylethylmercaptol and α-dimethylamino-α-methylthiobenzyl cyanide respectively. When primary amines and the monosodium salts of active methylene compounds were treated with the iodomethylate I, benzamidine hydroiodides and α-dimethylaminobenzylidene derivatives of the active methylene compounds were, respectively, obtained, and methyl mercaptan was eliminated. Further, it has been found that diamines, such as *o*-phenylenediamine, easily condensed with the iodomethylate I to yield such heterocyclic compounds as 2-phenylbenzimidazole, while methyl mercaptan and dimethylamine were eliminated.

*Laboratory of Organic Chemistry*
*Tokyo Institute of Technology*
*Ookayama, Tokyo*

# A Study of the Charge-Transfer Complexes. II. The Complexes of Pyromellitic Dianhydride with Polycyclic Aromatic Compounds*

By Taku MATSUO

(Received May 4, 1965)

Many interesting properties of the solid complexes formed between pyromellitic dianhydride and polymethylbenzenes were reported in the preceding paper of this series.[1] In fact, pyromellitic dianhydride is characterized by the special ease with which it forms solid complexes with many aromatic compounds. Relatively few papers have, however, been published on the spectroscopic study of such charge-transfer complexes in the solid state.[2] In studying the complexes in solution, it has been quite common to consider the variation in the absorption maximum of the charge-transfer band as changing the donor molecule for a given acceptor. The results of such experiments are generally used to estimate the electron affinity of the acceptor molecule.[3] Dewar and Lepley showed that essentially the same technique can be fruitfully applied to the case of solid complexes.[4] The same type of experimental results will be presented here on charge-transfer complexes with pyromellitic dianhydride employed as the common acceptor. Polycyclic aromatic compounds were used as donors in order to cover a wide range of ionization potential for the donor molecule. Some other aromatic compounds were also used in the experiment in order to observe the donor dependence of the charge-transfer band in more detail. It may be adequate to mention here that the KBr disk method or something similar has been the most popular technique for measuring the absorption spectra of solid complexes.[2,4,5] In the present experiment, use was made of the diffuse reflectance method, which had been proven to be quite successful in studying solid molecular complexes.[6]

## Experimental

**Materials.**—Naphthalene and anthracene were purchased from the Wako Pure Chemical Industry Co., while chrysene, pyrene and phenanthrene were provided by the Tokyo Kasei Organic Chemicals Co. All of these compounds were purified by repeated recrystallization from various solvents, such as ethanol, acetic acid and toluene. The m. p.'s and ultraviolet spectra agreed well with those reported in the literature. *trans*-Stilbene was synthesized from benzaldehyde through benzoin.[7] $\alpha$-Methylnaphthalene was made by catalytic dehydrogenation following the dehydration of 1-methyltetralol.[8] Anisole was purchased from the Wako Pure Chemical Co. *para*-Methylanisole and *p*-dimethoxybenzene were synthesized by the usual method from the corresponding sodium phenolate and dimethylsulfate. All the liquid samples were found pure by gas chromatography and were identified by means of the infrared and NMR spectra. Reagent-grade ethylacetate was washed with a saturated aqueous sodium carbonate solution and then dried over calcium chloride. Further purification was made by repeated fractional distillation in the presence of phosphorus pentoxide. Pyromellitic dianhydride was obtained by dehydrating pyromellitic acid, as supplied by the Tokyo Kasei Organic Chemicals Co., in boiling acetic anhydride; it was then recrystallized from purified ethylacetate before use (m. p. 299.8—300.0°C).[1]

**Spectroscopic Measurements.**—Solutions of the complexes were prepared by dissolving pyromellitic

* Contribution No. 86 from the Department of Organic Synthesis, Faculty of Engineering, Kyushu University, Fukuoka.

1) Y. Nakayama, Y. Ichikawa and T. Matsuo, This Bulletin, **38**, 1674 (1965).

2) J. W. Eastman, G. M. Androes and M. Calvin, *J. Chem. Phys.*, **36**, 1197 (1962).

3) G. Briegleb, *Angew. Chem.*, **76**, 326 (1964).

4) M. J. S. Dewar and A. R. Lepley, *J. Am. Chem. Soc.*, **83**, 4560 (1961).

5) R. Foster and T. J. Thomson *Trans. Faraday Soc.*, **59**, 296 (1962).

6) G. Kortüm and W. Braun, *Z. Phys. Chem., N. F.*, **18**, 242 (1958).

dianhydride ($10^{-2}$ mol./l.) and the donor compounds into ethylacetate. The donor concentration varied from $10^{-2}$ to $10^{-1}$ mol./l., depending on the stability and on the solubility of the complex. The spectra were measured in 1 cm. cells in the visible range on a Hitachi model EPS-2U recording spectrophotometer. Solid molecular complexes were prepared by the method described in the previous paper.[1] The complex was dispersed in talcum powder, and it relative diffuse reflectance was measured with a Hitachi model EPU-2A photoelectric spectrophotometer equipped with an integrating sphere.[1]

## Results and Discussion

Examples of the appearance of the charge-transfer absorption band of the complex in an ethyl acetate solution are shown in Fig. 1 for the cases of $\alpha$-methylnaphthalene and anthracene. The spectra were measured using ethyl acetate as the reference; the absorptions due to the components are not substracted from the data. The absorption of pyromellitic dianhydride (abbreviated as PMDA hereafter) itself, however, is small enough to be neglected in the visible region.[1] The bands indicated by the arrows in Fig. 1 may, then, be easily identified as the charge-transfer absorption, as they are clearly separated from the bands mainly due to the donor absorption on the higher frequency side. There are cases, however, where the charge-transfer band appears as just a weak shoulder superimposed on the tail of a strong absorption on the higher frequency side. Such overlapping bands were resolved graphically, as is illustrated in Fig. 2 for the case of a PMDA-stilbene complex. The absorption maxima obtained by these methods for various donors are summarized in Table I, together with the errors involved in the resolution.

By definition, the Kubelka-Munk remission function, $f(R)$, is the ratio of the absorption to the scattering coefficients, $k/S$, of the powdered sample;

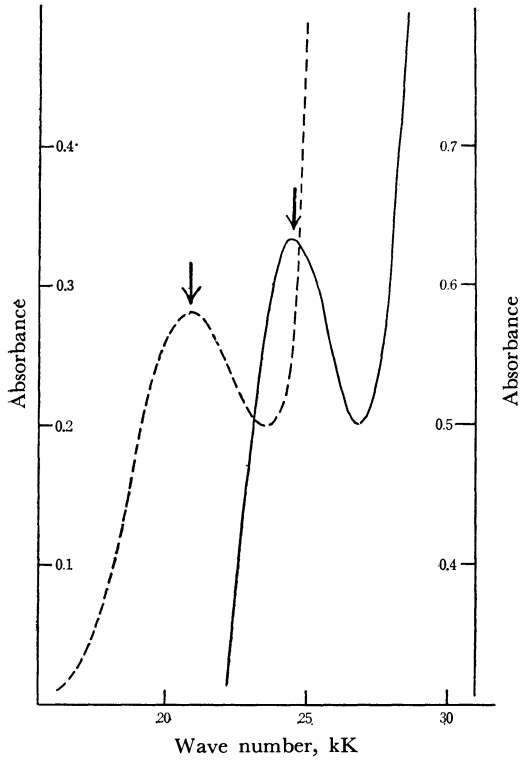



Fig. 1. The appearances of charge-transfer absorption bands of PMDA complexes with $\alpha$-methylnaphthalene (solid line) and anthracene (broken line) in ethyl acetate. The left scale is used for anthracene, and the right scale for $\alpha$-methylnaphthalene.
The following concentrations were used in the experiments:
$\alpha$-Methylnaphthalene; $6.67\times10^{-2}$ mol./l.
Anthracene ; $2.0\times10^{-2}$ mol./l.
PMDA ; $1.0\times10^{-2}$ mol./l.

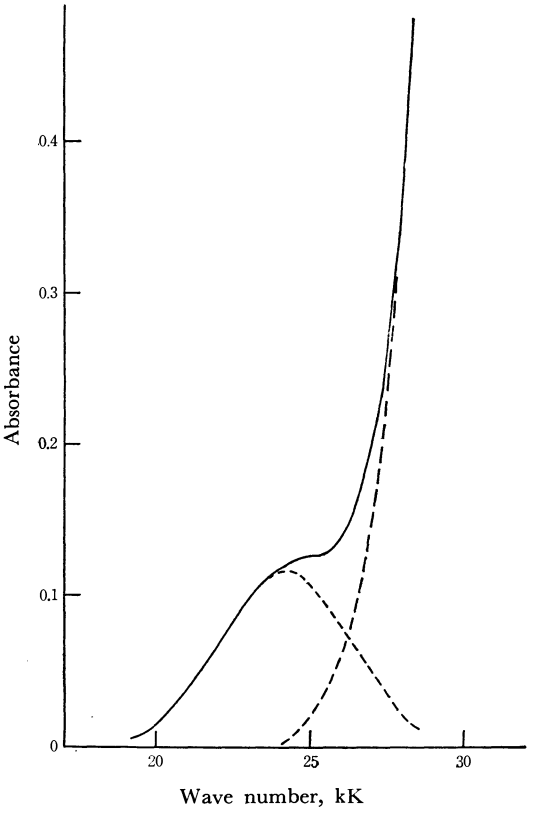



Fig. 2. Resolution of the charge-transfer absorption illustrated by the case of *trans*-stilbene-PMDA complex. The observed absorption curve (solid line) consists of two components shown by the dotted lines.
PMDA; $1.15\times10^{-2}$ mol./l.,
*trans*-Stilbene; $1.38\times10^{-1}$ mol./l.

7) R. L. Shriner and A. Berger, "Organic Synthesis," Coll. Vol. III, 786 (1955).
8) The author is indebted to Mr. Shinji Isatake for preparing the authentic sample of $\alpha$-methylnaphthalene by this method.

Table I. The charge-transfer absorption bands of PMDA complexes with various donors and the energy levels of the highest occupied MO of the donor molecules

| Donor | $m$ | $\tilde{\nu}_{CT}$ in EtOAc kK | $\tilde{\nu}_{CT}$ in solid kK |
|---|---|---|---|
| Anthracene | 0.414 | 20.9±0.1 | 19.6±0.1 |
| Pyrene | 0.445 | 21.3±0.1 | 20.1±0.1 |
| *trans*-Stilbene | 0.504 | 24.2±0.3 | 22.0±0.1 |
| Chrysene | 0.520 | 23.1±0.3 | 22.5±0.2 |
| *p*-Dimethoxy-benzene | (0.520) | 23.5±0.2 | |
| α-Methylnaph-thalene | (0.565) | 24.6±0.1 | |
| *p*-Methylanisole | (0.591) | 25.0±0.3 | |
| Phenanthrene | 0.605 | 25.0±0.3 | 24.8±0.3 |
| Naphthalene | 0.618 | 25.8±0.1 | 24.7±0.1 |
| Anisole | (0.690) | 27.1±0.5 | |

The $m$ values in parentheses are estimated from the charge-transfer bands of chloranil complexes with the same donor as explained in the text.

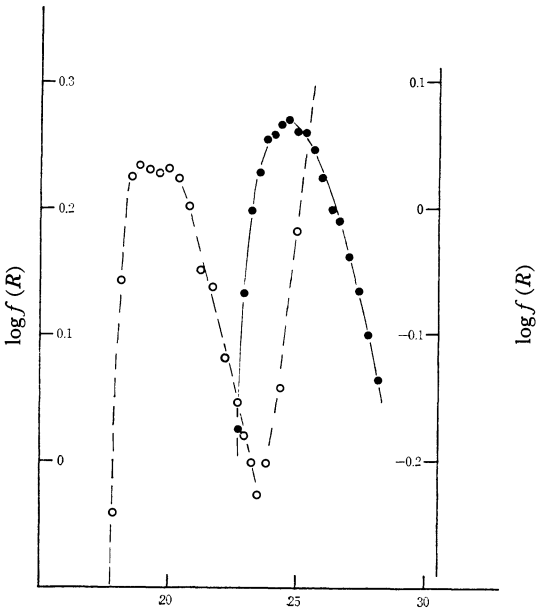



Fig. 3. Remission functions of the solid PMDA complexes with naphthalene (filled circle) and anthracene (open circle).
The right scale is for the case of naphthalene only.
Naphthalene-PMDA complex (45 mg.) in talcum powder (389 mg.)
Anthracene-PMDA complex (34 mg.) in talcum powder (402 mg.).

it is expressed in terms of the measured diffuse reflectance, $R$, by the following equation:[9]

$$f(R)=\frac{k}{S}=\frac{(R-1)^2}{2S} \quad (1)$$

Assuming that the scattering coefficient, $S$, is independent of the wavelength, $f(R)$ is taken to reproduce the absorption band in the region under investigation. This treatment is not entirely valid from the theoretical point of view. Experimental observation has, however, shown that the remission function is good enough to estimate the absorption maxima of molecular complexes in the solid state.[1,6] In addition, no violent treatment is applied to the molecular complexes in preparing the sample for diffuse reflectance measurement, in contrast to the KBr disk method. The remission functions of PMDA complexes with anthracene and naphthalene are shown in Fig. 3. The absorption maxima thus obtained for the solid complexes are given in the fourth column of Table I. The frequency of the charge-transfer absorption band is correlated with the electron affinity of an acceptor, $E_A$, and the ionization potential of the donor, $I_P$, by the following well-known equation:

$$h\nu_{CT}=I_p-E_A+\Delta \quad (2)$$

where $\Delta$ stands for a correction mainly due to the Coulombic interaction in the complex. The ionization potentials of polycyclic aromatic compounds are known to be linearly dependent on the energy level of the highest-occupied MO's, as calculated by the Hückel MO method.[10] Thus the following equation may be expected to hold:

$$h\nu_{CT}=am-E_A+\Delta \quad (3)$$

where the energy of the highest occupied MO is expressed as:

$$E=\alpha+m\beta \quad (4)$$

If the correction factor, $\Delta$, is assumed to be the same for a series of complexes with a common acceptor, Eq. 3 may be rewritten as:

$$h\nu_{CT}=am+b \quad (5)$$

The relationship expressed by Eq. 5 has been verified to hold in various series of complexes.[4,11] An attempt will be made here to treat the data of PMDA complexes given in Table I by the same method. The energies of the highest-occupied MO's in $\beta$ units are given in the second column of Table I. The values for ordinary polycyclic aromatic compounds are those calculated with the Hückel MO. The values for the substituted compounds were estimated by using the relationship $\tilde{\nu}_{CT}$ and $m$ for the chloranil complexes of polycyclic aromatic hydrocarbons reported by Kuboyama.[11g] The method of estimation is illustrated in Fig. 4.

9) G. Schreyer, *Z. Phys. Chem., N. F.*, **12**, 359 (1957) and the references quoted therein.

10) A. Streitwieser, Jr., "Molecular Orbital Theory," Wiley & Sons, Inc., New York (1961), p. 192.

11) a) M. J. S. Dewar and H. Rogers, *J. Am. Chem. Soc.*, **84**, 395 (1962); b) A. R. Lepley, ibid., **84**, 3577 (1962); c) A. Kuboyama, *J. Chem. Soc. Japan, Pure Chem. Sec.* (*Nippon Kagaku Zasshi*), **83**, 375 (1962).

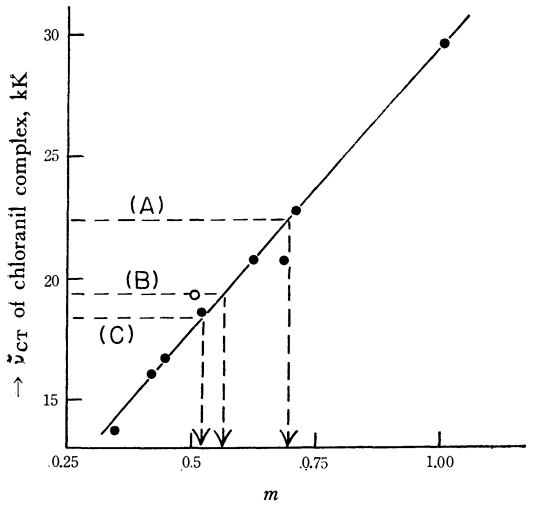



Fig. 4. Estimation of the energy level of the highest occupied MO. The experimental points and the solid line are as reported by Kuboyama.[11e]
(A) Anisole, (B) α-Methylnaphthalene and (C) *p*-Dimethoxybenzene.
The open circle represents the data of chloranil - *trans*-stilbene complex.

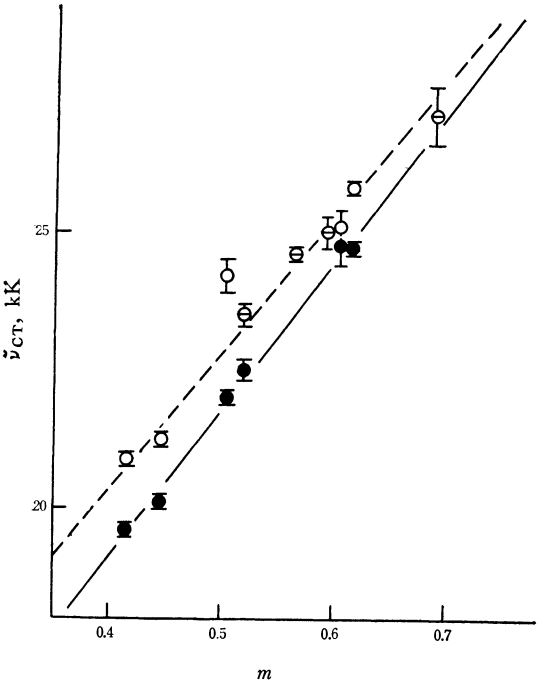



Fig. 5. Correlation of $\tilde{\nu}_{CT}$ and $m$ in the cases of the PMDA complexes with aromatic compounds.
● Solid complex,
○ Complex in solution ($m$ as calculated by Hückel MO)
⊖ Complex in solution ($m$ as estimated from Fig. 4)

The data in Table I are used in Fig. 5 to illustrate the close correlation between $\tilde{\nu}_{CT}$ and $m$ for the PMDA complexes of aromatic compounds, both solution and in the solid state. The charge-transfer band shows a bathochromic shift going from the solution to the solid state. The extent of the shift varies depending on the particular donor in question. The overall linear relationships observed between $\tilde{\nu}_{CT}$ and $m$ in both phases, however, are almost parallel each other.

The PMDA complex of *trans*-stilbene presents an anomalous example. In contrast to the fact that the experimental point for the solid complex rests exactly on the line, the corresponding $\tilde{\nu}_{CT}$ in the solution is located at much higher frequency than might be expected from the $m$ value. A similar situation is also met in the chloranil complex of stilbene, as is shown in Fig. 4. A part of the reason for this anomalous behavior may be that the $m$ value is calculated by means of the Hückel MO. The calculation is made by assuming that all the $\alpha$'s and $\beta$'s are the same in the conjugate system. It is obvious from the structure that the assumption would hold to a lesser extent in the case of *trans*-stilbene than in the cases of ordinary polycyclic aromatic hydrocarbons. In addition, the suggestion may be made that *trans*-stilbene can be slightly twisted around its essential single bond in a solution. As a result, the conjugation in the molecule is reduced and the energy level of the highest-occupied MO is lower than expected. In the solid state, a coplanar structure would be restored for *trans*-stilbene to enable it to form a strong molecular complex with PMDA. Other donor molecules attached to a conjugate group through an essential single bond seem to show behavior more or less similar to that of *trans*-stibene.

The linear relationships between $\tilde{\nu}_{CT}$ and $m$ observed above (excluding the point for the *trans*-stilbene complex in a solution) are expressed by the following equations:

in a solution,

$$\tilde{\nu}_{CT}=24.6\,m+10.5 \quad \text{(in kK)}, \tag{6}$$

and in the solid state,

$$\tilde{\nu}_{CT}=26.5\,m+\ 8.5 \quad \text{(in kK)}. \tag{7}$$

By comparing Eqs. 6 and 7 with Eq. 5 and by also remembering that

$$b=-E_A\ +\ \Delta, \tag{8}$$

one may estimate that the electron affinity of PMDA in ethyl acetate is lower than that in the solid state by 0.25 eV. The value can not be taken too seriously because an assumption is made here that the correction factor, $\Delta$, is the same for both phases. It should be remembered at this point that all of the molecules and the complexes under consideration are solvated at both their

ground and excited states. Due to this solvation effect, the equilibrium and the Franck-Condon states concerning the charge-transfer absorption will not be the same in various media. Consequently, it is quite unlikely that the correction factor, $\Delta$, is the same for an ethyl acetate solution and solid state. The parallel relation observed between Eqs. 6 and 7 indicates, however, that the difference in $\Delta$ value between the complexes in the two phases is almost constant in this series and nearly independent of the donor property. Thus, it appears that the electron affinity of PMDA in the solid state is higher than that in ethyl acetate by the before-mentioned amounts. As is clear from the above discussion, 0.25 eV. is the upper limit of the value of the change in the electron affinity of PMDA since the solvent effects on the donor and complex are also included in that number. No attempt will be made here to estimate the latter effects because too many unknown factors are involved for a successful reasoning to be carried out. A similar zero-order treatment suggests that PMDA in ethyl acetate behaves as an electron acceptor weaker by 0.53 eV. than chloranil in carbon tetrachloride.[11c] The difference in the electron affinity of these compounds has previously been given by Briegleb as 0.52 eV.[3] The agreement between these two results is surprisingly close in spite of the possible difference in the media.

**Summary**

The frequency of the charge-transfer absorption of the PMDA complex has been found to be linearly dependent on the energy level of the highest-occupied MO of the aromatic donor as estimated by the Hückel MO method. The behavior of the complex in the solid state is almost parallel to that in a solution. On the basis of these linear relationships, it has been suggested that PMDA in ethyl acetate behaves as if it is an electron acceptor weaker than that in a solid complex and chloranil in carbon tetrachloride by about 0.2 eV. and 0.53 eV. respectively in the zero order approximation.

Another suggestion has been made that *trans*-stilbene may be slightly twisted around its essential single bond in a solution but not in the solid complex.

The author wishes to express his gratitude to Mrs. Katsumi Aoyagi for measuring the spectra. He is also grateful to Miss Mizue Moritomo for both operating the spectrometer and for helping in the preparation of the manuscript.

*Department of Organic Synthesis*
*Faculty of Engineering*
*Kyushu University*
*Hakozaki, Fukuoka*

# The Reaction of Ions in the Radiolysis of *n*-Butane in the Gas Phase

By Tetsuo MIYAZAKI and Shoji SHIDA

(Received May 7, 1965)

The reaction of ions produced in the radiolysis of *n*-butane has been reported in previous papers by the present authors. In the first paper[1] it was shown, from a comparison of the results of radiolysis, photolysis and mass spectrum study, that the fragmentation of the excited butane ion is quite different from that of the excited butane molecule. In the second paper[2] the deactivation of the excited butane ion was discussed from the point of view of the effect of density in the radiolysis. The present work will concern the role of several ions in the radiolysis of *n*-butane in the gas phase. Since excited molecules and radicals are produced by irradiation in addition to ionic species, the role of ions in radiation chemistry is sometimes obscure. Futrell[3] explained the distribution of products in the radiolysis of *n*-hexane by using the mass-spectrometric cracking pattern, working on the assumption that the fragment ions form the products by hydride-ion transfer reactions with *n*-hexane. Ausloos et al.[4] studied the radiolysis of a $n$-$C_4H_{10}$ - $n$-$C_4D_{10}$ - $I_2$ mixture and found that $C_3H_7D$ and $C_3D_8$ were produced in comparable amounts. They concluded that 95% of propane is formed by hydride ion transfer reaction, and they assumed that hot radicals were not produced in the radiolysis.

In the present study ammonia was used as a proton transfer reagent, since ammonia has a high proton affinity (202 kcal./mol.)[5] and since products from ammonia by irradiation can be discriminated

1) T. Miyazaki, S. Arai, S. Shida and S. Sunohara, This Bulletin, **37**, 1352 (1964).
2) T. Miyazaki and S. Shida, This Bulletin, **38**, 716 (1965).
3) J. Futrell, *J. Am. Chem. Soc.*, **81**, 5921 (1959).
4) R. P. Borkowski and P. J. Ausloos, *J. Chem. Phys.*, **39**, 818 (1963).
5) A. P. Altshuller, *J. Am. Chem. Soc.*, **77**, 3480 (1955).

from those from *n*-butane. Ammonia is expected to react with ions to give alkene by the following proton transfer reaction:

$$C_nH_{2n+1}^+ + NH_3 \rightarrow C_nH_{2n} + NH_4^+$$

In the absence of ammonia, an alkyl ion forms alkane by hydride-ion transfer reaction with *n*-butane:

$$C_nH_{2n+1}^+ + n\text{-}C_4H_{10} \rightarrow C_nH_{2n+2} + C_4H_9^+$$

## Experimental

The *n*-Butane was the same as that used before.[1] The $C_5H_{10}$-1 was 99.99% pure. The water and ammonia were also of high purity. The samples were irradiated with $\gamma$-rays from Co-60 of 16000 c. at a total dose of $2.5\times10^{21}$ eV. $g^{-1}$. Most of the analytical procedures were identical with those described before.[1,2] The $C_2$—$C_4$ hydrocarbon products were analyzed by gas chromatography (benzyl ether column, 20 m.).

## Results and Discussion

The effect of ammonia in the radiolysis of *n*-butane in the gas phase is shown in Table I. The yields given in the table are expressed in moles per 1000 mol. of *n*-butane. This value is proportional to the *G*-value, and for Run 2-1 the yields are given also in *G*-value units. Since iodine has the unfavorable property[6] of reacting with unsaturated products, $C_5H_{10}$-1 was used as a radical scavenger in spite of its low reactivity to radicals. The yield of $C_4H_8$-1 was determined in Run 2-1 and Run 4-1 by separating *n*-butane before the analysis, since the peak of $C_4H_8$-1 in the gas chromatography was not separated from a large peak of *n*-butane. The electron fraction of ammonia in Table I indicates that the direct absorption of radiation energy by ammonia is small compared with that of *n*-butane.

The effect of ammonia is clearly shown in Fig. 1. Each product is affected in quite different ways. The effects may be classified into three types: A) $C_2$-products and $C_3H_8$ decrease upon

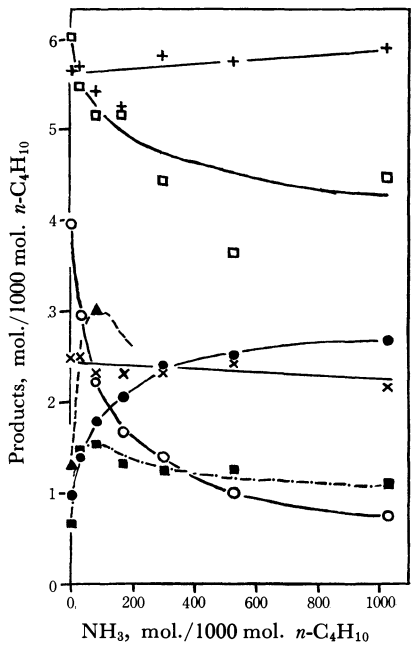



Fig. 1. Effect of ammonia in the radiolysis of *n*-butane at low pressure.
+ $H_2$ □ $C_2$ ● $C_3H_6$ ▲ $C_4H_8$
× $CH_4$ ○ $C_3H_8$ ■ $C_4H_8$-2

TABLE I. EFFECT OF AMMONIA IN THE RADIOLYSIS OF *n*-BUTANE AT LOW PRESSURE
Yields of Products[a] at 250 mmHg of $n$-$C_4H_{10}$ and 12.5 mmHg of $C_5H_{10}$-1

| | | Run | | | | | | |
|---|---|---|---|---|---|---|---|---|
| | | 2-1 | 3-1 | 4-1 | 5-1 | 6-1 | 8-1 | 1-1 |
| $NH_3$, mol.[b] | 0 | | 27.4 | 81.5 | 167 | 298 | 528 | 1030 |
| Electron fraction | 0 | | 0.008 | 0.023 | 0.047 | 0.081 | 0.13 | 0.23 |
| Products, mol.[b] | | (*G*-value) | | | | | | |
| $H_2$ | 5.66 | (2.33) | 5.70 | 5.43 | 5.24 | 5.81 | 5.75 | 5.87 |
| $CH_4$ | 2.49 | (1.03) | 2.50 | 2.31 | 2.31 | 2.31 | 2.41 | 2.13 |
| $C_2$ | 6.02 | (2.48) | 5.47 | 5.15 | 5.16 | 4.43 | 3.63 | 4.46 |
| $C_3H_8$ | 3.96 | (1.63) | 2.95 | 2.23 | 1.66 | 1.39 | 0.99 | 0.72 |
| $C_3H_6$ | 0.98 | (0.40) | 1.39 | 1.78 | 2.04 | 2.34 | 2.42 | 2.65 |
| $C_4H_8$-1 | 0.6 | (0.2) | | 1.5 | | | | |
| *trans*-$C_4H_8$-2 | 0.42 | (0.17) | 0.88 | 0.85 | 0.74 | 0.75 | 0.75 | 0.64 |
| *cis*-$C_4H_8$-2 | 0.26 | (0.10) | 0.54 | 0.68 | 0.57 | 0.49 | 0.50 | 0.43 |

a) Room temperature. The total dose is $2.5\times10^{21}$ eV. $g^{-1}$ and the dose rate is $1.44\times10^{19}$ eV. $g^{-1}$ $hr^{-1}$. The volume of reaction cell is about 50 cc.
b) Mol. per 1000 mol. of $n$-$C_4H_{10}$.
c) $C_2$ represents the sum of $C_2H_6+C_2H_4$.

6) T. Kudo and S. Shida, Symposium on Radiation Chemistry, Nagoya (1964).

the addition of ammonia: the latter decreases more markedly.

B) $C_3H_6$ and $C_4H_8$ increase upon the addition of ammonia. The latter increases sharply upon the addition of a small amount of ammonia, and then gradually decreases in the high concentrations.

C) $H_2$ and $CH_4$ are not significantly affected by ammonia. Although methane and propane are formed by the rupture of the first C–C bond, only propane is affected by ammonia. This shows that the methyl radical produced by the fragmentation of the butane ion does not react with ammonia, while $C_3H_7^+$ does react with it.

**The Reaction of $C_3H_7^+$.**—The rate of the non-radical formation of $C_3H_8$ decreases sharply upon the addition of ammonia (Fig. 1). One the contrary, the yield of $C_3H_6$ increases complementally. This may be due to the high proton affinity of ammonia, which has been described above. Similar phenomena were observed in the radiolysis of mixtures of isobutane and some organic compounds, such as nitromethane, acetone or methyl iodide.[7]

$$n\text{-}C_4H_{10} \xrightarrow{I'(C_3H_7^+)_0} C_3H_7^+ + CH_3 + e \qquad (1)$$

$$C_3H_7^+ + n\text{-}C_4H_{10} \xrightarrow{k_2} C_3H_8 + C_4H_9^+ \qquad (2)$$

$$C_3H_7^+ + NH_3 \begin{cases} \xrightarrow{k_3} C_3H_6 + NH_4^+ & (3) \\ \xrightarrow{k_4} C_3H_7NH_3^+ & (4) \end{cases}$$

N. B. $I'(C_3H_7^+)_0$: Rate of reaction 1, expressed in moles per 1000 mol. of *n*-butane.

$k$: Rate constant

$C_3H_7^+$ produced by irradiation forms propane via the hydride-ion transfer reaction with *n*-butane, but in the presence of ammonia it forms propylene via the proton transfer reaction. Since the increment of propylene is smaller than the decrement of propane, the condensation reaction 4 with ammonia may also occur. Though this type of ion-molecule reaction is seldom observed with a low pressure mass spectrometer, it is possible in the present use because of the deactivation of the condensed ion at 250 mmHg. The steady-state treatment leads to Eq. 1 for the decrease in propane and to Eq. 2 for the increase in propylene:

$$\frac{[NH_3]}{-\Delta G'(C_3H_8)} = \frac{k_2[C_4H_{10}]}{(k_3+k_4)I'(C_3H_7^+)_0} + \frac{1}{I'(C_3H_7^+)_0}[NH_3] \qquad \text{(Eq. 1)}$$

$$\frac{[NH_3]}{\Delta G'(C_3H_6)} = \frac{k_2[C_4H_{10}]}{k_3 I'(C_3H_7^+)_0} + \frac{(k_3+k_4)}{k_3 I'(C_3H_7^+)_0}[NH_3] \qquad \text{(Ep. 2)}$$

N. B. $G'$ is expressed in moles per 1000 mol. of *n*-butane: it is proportional to *G*-value. $\Delta G'$ represents the increment in the product.

Thus, there must be a linear relationship between $[NH_3]/-\Delta G'(C_3H_8)$ and $[NH_3]$, and between $[NH_3]/\Delta G'(C_3H_6)$ and $[NH_3]$. As may be seen in Fig. 2 and Fig. 3, satisfactory straight lines are obtained. From the slopes and the intercepts

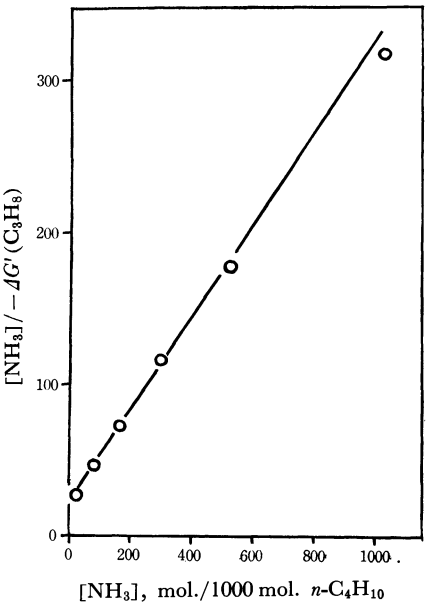



Fig. 2. Relation between $[NH_3]/-\Delta G'(C_3H_8)$ and $[NH_3]$.

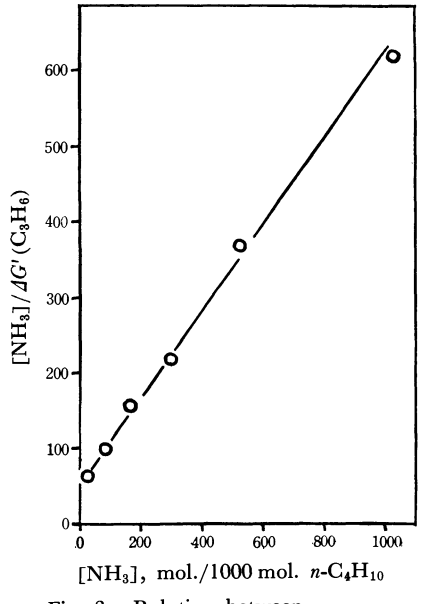



Fig. 3. Relation between $[NH_3]/\Delta G'(C_3H_6)$ and $[NH_3]$.

7) R. P. Borkowski and P. J. Ausloos, *J. Chem. Phys.*, **40**, 1128 (1964).

of Fig. 2 and Fig. 3, the following relationships are obtained:

$$\frac{1}{I'(C_3H_7^+)_0}=0.306$$

1000 mol. of $n$-$C_4H_{10}$/mol. (Eq. 3)

$$\frac{k_2[C_4H_{10}]}{I'(C_3H_7^+)_0(k_3+k_4)}=20 \quad \text{(Eq. 4)}$$

$$\frac{(k_3+k_4)}{k_3I'(C_3H_7^+)_0}=0.574$$

1000 mol. of $n$-$C_4H_{10}$/mol. (Eq. 5)

$$\frac{k_2[C_4H_{10}]}{k_3I'(C_3H_7^+)_0}=52 \quad \text{(Eq. 6)}$$

From the above four equations, we get $k_3=6.0k_2$ and $k_4=7.1k_2$ as the average values.

**The Reaction of $C_4H_9^+$.**—As is shown in Fig. 1, $C_4H_8$ increases sharply upon the addition of a small amount of ammonia, and then it decreases gradually upon any further addition. This increase may be due to the proton transfer reaction between $C_4H_9^+$ and $NH_3$. Since the following fragmentation is not known to occur from the mass spectrum of $n$-butane:

$$C_4H_{10}^{+*} \rightarrow C_4H_9^+ + H \quad (5)$$

the $C_4H_9^+$ in the radiolysis may be formed by the following secondary reactions:

$$C_4H_{10} \xrightarrow{I(Fr^+)_0} Fr^+ + N + e \quad (1)$$

$$Fr^+ + C_4H_{10} \xrightarrow{k_6} FrH + C_4H_9^+ \quad (6)$$

$$C_4H_9^+ \rightarrow P \quad (7)$$

$$C_4H_9^+ + NH_3 \begin{cases} \xrightarrow{k_8} C_4H_8 + NH_4 & (8) \\ \xrightarrow{k_9} C_4H_9NH_3^+ & (9) \end{cases}$$

$$Fr^+ + NH_3 \rightarrow \text{Products} \quad (10)$$

N. B. $Fr^+$: Fragment ions from the excited butane ion, such as $C_2H_5^+$ and $C_3H_7^+$.
N: Neutral fragments from the excited butane ion
P: A product
Reaction 10 represents the reaction of fragment ions and ammonia; cf., for example, reactions 3 and 4.

While the yield of $C_4H_8$ is increased by reaction 8 in a low concentration of ammonia, in a high concentration the reactions of ammonia with fragment ions cause a decrease in $C_4H_9^+$ (cf. reactions 10 and 6), that is, a depression of reaction 8.

We are able to estimate the life time of $C_4H_9^+$. As seen in Fig. 1, the concentration of ammonia where the rate of reaction 7 is about the same magnitude as that of reaction 8 is 5—10 mol./1000 mol. $n$-$C_4H_{10}$. Assuming that

$R(7)\simeq R(8)$ at $[NH_3]=7.5$ mol./1000 mol. $n$-$C_4H_{10}$
$=7.5$ mol./$7.42\times10^4$ l.

the life time of $C_4H_9^+$ is given as follows;

$$t(C_4H_9^+)=\frac{1}{k_8[NH_3]} \quad \text{(Eq. 7)}$$

If $k_8$ is assumed to be equal to $k_3$ and if $k_2$ is taken as $1.3\times10^{-9}$ cc. molec$^{-1}$ sec$^{-1}$,[8] we get $t(C_4H_9^+)=2.1\times10^{-9}$ sec., a value which is much shorter than the time of neutralization ($10^{-2}$—$10^{-3}$ sec.) in the gas-phase radiolysis.[9] Therefore, it seems that $C_4H_9^+$ reacts with $n$-butane or with the unsaturated products, including $C_5H_{10}$-1, before the neutralization.

**The Yields of $C_4H_{10}^{+*}$.**—One of the most important problems in the radiolysis is how to estimate the relative importance of the excited ion and the molecule. Their importance in the C–C rupture of $n$-butane will, therefore, now be considered in spite of some uncertainty.

We get, from Eq. 3, Eq. 4, Eq. 5 and Eq. 6: $I'(C_3H_7^+)_0=3.52$ mol./1000 mol. $n$-$C_4H_{10}$, which is the initial yield of $C_3H_7^+$. Since $-\Delta G'(C_3H_8)=3.24$ at the concentration of 1030 mol./1000 mol. $n$-$C_4H_{10}$ of ammonia, more than 90% of the ions react with ammonia at this concentration. Now we may assume that all of the fragment ions are eliminated by the proton transfer and condensation reactions with ammonia at 1030 mol./1000 mol. $n$-$C_4H_{10}$, and that the rate constants of the two reactions are the same. Since the total decreases in the $C_2$ and $C_3$ products upon the addition of ammonia are due to the condensation reaction, the yields of ions which react with ammonia should be twice the decrement:

$$-\Delta G'(C_3)=1.58 \text{ at } 1030 \text{ mol. } NH_3/1000 \text{ mol. } n\text{-}C_4H_{10}$$

$$-\Delta G'(C_2)=1.56 \text{ at } 1030 \text{ mol. } NH_3/1000 \text{ mol. } n\text{-}C_4H_{10}$$

Thus, $G'(C_4H_{10}^{+*})_{C_3}=3.2$ and $G'(C_4H_{10}^{+*})_{C_2}=3.1$ respectively. Therefore, $G'(C_4H_{10}^{+*})=6.3$ or $G(C_4H_{10}^{+*})=2.6$, as expressed in usual $G$-value units.

Most of the fragment ions form $C_4H_9^+$ via the hydride-ion transfer reaction with $n$-butane (cf. reaction 6); therefore, the yields of $C_4H_9^+$ may be considered to be approximately equal to that of $C_4H_{10}^{+*}$. The increment in $C_4H_8$ in Fig. 1 represents that of reaction 8. Assuming that $k_8/k_9\simeq k_3/k_4\simeq1$ as before, the yields of $C_4H_9^+$ are twice the increment of $C_4H_8$ (cf. reactions 8 and 9):

$$G(C_4H_9^+)=2\Delta G(C_4H_8)_{at\ [NH_3]=81.5}/0.6 \quad \text{(Eq. 8)}$$

The denominator is the correction factor as calculated from the decrease in $C_3H_8$ at 81.5 mol. $NH_3$/

8) F. H. Field and F. W. Lampe, *J. Am. Chem. Soc.*, **80**, 5587 (1958).
9) D. P. Stevenson, *J. Phys. Chem.*, **61**, 1453 (1957).

1000 mol. $n$-$C_4H_{10}$, since some of the fragment ions are lost by the reaction with ammonia at this concentration. Therefore, we get $G(C_4H_9^+)=2.4$. The agreement with $G(C_4H_{10}^{+*})$, as estimated from the decrement of products, is satisfactory.

Since the total $G$-value of the products from the C–C rupture, that is, $G(\sum C_1—C_3, C_5—C_7)$, is 6.5 (as determined by a previous study by the present authors[1]), the contribution of the excited molecule to the C–C rupture can be estimated by using $G(C_4H_{10}^{+*})$. As may be seen in Table II, the ionic C–C rupture is important in the radiolysis of gaseous $n$-butane. This result supports the conclusion of previous studies.[1,4]

TABLE II. THE CONTRIBUTION OF EXCITED ION AND MOLECULE IN THE C–C RUPTURE REACTION

| | A | B | C |
|---|---|---|---|
| $G(C_4H_{10}^{+*})$ | 2.6 | 2.4 | 2.6 |
| $G(C_4H_{10}^{*})$ | 0.7 | 0.9 | 0.8 |

A: Estimated from the reaction between fragment ions and $NH_3$.
B: Estimated from the reaction between $C_4H_9^+$ and $NH_3$.
C: Estimated from the analysis of products in the radiolysis of $n$-$C_4H_{10}$ - $n$-$C_4D_{10}$ - $I_2$ mixture.[4]

**$C_4H_{10}^+$ at High Pressure.**—Williams[10] used $ND_3$ as a proton scavenger in studying the ionic processes in the radiolysis of liquid cyclohexane. Since the saturation solubility of $ND_3$ in liquid cyclohexane is limited to a small percentage, however, he could not succeed in discussing the mechanism in detail. The present authors reported in a previous paper[2] that the radiolysis of $n$-butane near the critical state is similar to that in the liquid phase. Since we can get homogeneous mixtures of $n$-butane and the additive (water or ammonia) at any arbitrary concentration near the critical state, the effect of water or ammonia in high concentrations (up to 20%) has been studied near the critical state. The results in Table III show that all products by the C–C rupture decreases upon the addition of water or ammonia. Methane decreases to 70% upon the addition of 200 mol./1000 mol. $n$-$C_4H_{10}$ of ammonia though it does not decrease upon the addition of even 500 mol./1000 mol. $n$-$C_4H_{10}$ in the radiolysis at a low pressure (cf. Fig. 1). This fact suggests that the C–C rupture near the critical state may occur from the $C_4H_{10}^+$ produced by the deactivation of the excited butane ion:

$$C_4H_{10}^{+*} + C_4H_{10} \longrightarrow C_4H_{10}^+ + C_4H_{10} \quad (11)$$

$$C_4H_{10}^+ \xrightarrow[\text{or neutralization}]{\text{Thermal cracking}} CH_4, C_2H_6, \text{etc.} \quad (12)$$

$$C_4H_{10}^+ + NH_3 \longrightarrow Q \quad (13)$$

A more detailed study will be needed in order to discuss the mechanism of the effect of water or ammonia at high pressures.

TABLE III. EFFECT OF AMMONIA (OR WATER) IN THE RADIOLYSIS OF $n$-BUTANE AT HIGH PRESSURE

Yields of Products[a] at the density of 0.12 g. $cc^{-1}$ of $n$-butane

| Additive mol.[b] | Product, mol.[b] | | | |
|---|---|---|---|---|
| | $H_2$ | $CH_4$ | $C_2H_6$ | $C_3H_8$ |
| None | 11.10 | 3.71 | 4.26 | 0.93 |
| None | 11.40 | 3.82 | 4.40 | 1.02 |
| $H_2O$ | | | | |
| 9.8 | 11.08 | 3.45 | 4.13 | 0.71 |
| 49.8 | 12.52 | 3.49 | 3.83 | 0.55 |
| 112 | 13.21 | 3.19 | 3.55 | 0.42 |
| 276 | 13.60 | 2.57 | 2.80 | 0.28 |
| $NH_3$ | | | | |
| 101 | 12.65 | 2.98 | 3.67 | 0.47 |
| 198 | 14.30 | 2.62 | 2.88 | 0.24 |

a) 200°C, The total dose is $2.5\times10^{21}$ eV. $g^{-1}$.
b) Mol. per 1000 mol. of $n$-$C_4H_{10}$.

## Summary

The effect of ammonia in the radiolysis of $n$-butane has been investigated. In low pressure radiolysis, $C_3H_8$ and $C_2$-products decrease upon the addition of ammonia while $C_3H_6$ increases. $C_4H_8$ increases sharply upon the addition of a small amount of ammonia, but it gradually decreases upon further addition. $CH_4$ and $H_2$ are not significantly affected by ammonia. These results have been interpreted in terms of the proton transfer reaction of ammonia with ions, and their rate constants have been estimated. The contribution of the excited ion to the C–C rupture has been concluded to be much more important than that of the excited molecule in low-pressure radiolysis.

In high-pressure radiolysis all the products from the C–C rupture, including $CH_4$, decrease upon the addition of ammonia (or water).

We appreciate the help of the Japan Atomic Energy Institute in performing the irradiation.

*Laboratory of Physical Chemistry*
*Tokyo Institute of Technology*
*Ookayama, Tokyo*

10) F. Williams, *J. Am. Chem. Soc.*, **86**, 3954 (1964).

# The Hydroxide-Blacks of Ruthenium and Rhodium as Catalysts for the Hydrogenation of Organic Compounds. I. Their Catalytic Activity and Selectivity in the Hydrogenation of Some Aromatic Compounds*[1]

By Yuzuru TAKAGI, Takatoshi NAITO and Shigeo NISHIMURA*[2]

(Received May 7, 1965)

Recently it has been shown in many studies that ruthenium and rhodium catalysts or those containing these metals are outstanding in catalytic activity and selectivity in the hydrogenation of various organic compounds. High activities and/or high selectivities have been reported, for instance, in the hydrogenation of aromatic and heterocyclic compounds,[1] olefins,[2] carbonyl compounds,[1c,1e,3] nitriles,[4] and carboxylic acids to alcohols,[5] in the selective production of alicyclic primary amines,[6] in the selective hydrogenation of the compounds susceptible to hydrogenolysis,[1e,4,7] and in the selective cis-hydrogenation of substituted aromatic compounds.[8] There are also many other examples in which these catalysts have been shown to be useful.

The hydrogenations mentioned above are mostly concerned with the use of either the catalysts from the oxides of ruthenium and rhodium, those prepared by the reduction of the chlorides of ruthenium and rhodium with sodium borohydride, or the ruthenium and rhodium catalysts supported on various carriers. It appears that no study has yet been concerned with the use of the hydroxide-black catalysts of ruthenium and rhodium. The hydroxide of ruthenium or rhodium is easily prepared as, respectively, a black or a yellow precipitate, by adding a slight excess of a sodium hydroxide solution to a hot aqueous solution of ruthenium or rhodium chloride. The hydroxides of ruthenium and rhodium thus prepared have been found to exhibit excellent catalytic activity in the hydrogenation of various organic compounds when they are reduced to the metals in the presence of the compounds to be hydrogenated.

In this paper the activity and/or the selectivity of these hydroxide-black catalysts have been studied in the hydrogenation of toluene, benzoic acid, *o*-xylene, hydroquinone dimethyl ether and phenyl ether. The results are summarized in Tables I to V, along with those obtained with the oxides of ruthenium and rhodium. The mixed ruthenium-rhodium hydroxides were also prepared from mixtures of ruthenium chloride and rhodium chloride by the same method; the results with these catalysts are also included in the tables.

The hydroxide-catalyzed hydrogenations of the aromatic compounds proceed rapidly at 85 to 100°C under a high hydrogen pressure. Usually only a very small amount of the hydroxide is required for hydrogenation to be completed within a short time. Though a small amount of acetic acid was added in each hydrogenation in order to neutralize the trace of alkaline substances remaining in the catalysts, the hydroxide-catalyzed hydrogenations generally proceed smoothly without the addition of acetic acid (see the example shown in Table I). This fact, together with other observations,*[3] suggests that the hydroxides of ruthenium and rhodium

*[1] Presented at the 17th Annual Meeting of the Chemical Society of Japan, Tokyo, April, 1964.

*[2] Present address: Department of Industrial Chemistry, Faculty of Technology, Tokyo University of Agriculture and Technology, Koganei, Tokyo.

1) a) E. F. Rosenblatt, U. S. Pat. 2675390 (1954). b) L. D. Freedman, G. O. Doak and E. L. Petit, *J. Am. Chem. Soc.*, **77**, 4262 (1955). c) G. Gilman and G. Cohn, "Advances in Catalysis," Vol. 9, Academic Press Inc., New York (1957), p. 733. d) A. Amano and G. Parravano, ibid., Vol. 9 (1957), p. 716. e) S. Nishimura, This Bulletin, **33**, 566 (1960); **34**, 32 (1961). f) M. Freifelder and G. R. Stone, *J. Org. Chem.*, **26**, 3805 (1961); M. Freifelder, R. M. Robinson and G. R. Stone, ibid., **27**, 284 (1962).

2) O. Beeck, *Discussions Faraday Soc.*, **8**, 118 (1950); G. C. A. Schuit and L. L. van Reijen, "Advances in Catalysis," Vol. 10, Academic Press Inc., New York (1958), p. 242; H. C. Brown and C. A. Brasn, *J. Am. Chem. Soc.*, **84**, 1494 (1962).

3) G. G. Boyers, U. S. Pat. 2868847 (1959) (*Chem. Abstr.*, **53**, 9084d (1959)); A. A. Balandin, N. A. Vasyunina, G. A. Barysheva and S. V. Chepigo, *Izvest. Akad. Nauk S. S. S. R., Otdel. Khim. Nauk*, **1957**, 392 (*Chem. Abstr.*, **51**, 14260f (1957)); E. Breitner, E. Roginski and P. N. Rylander, *J. Org. Chem.*, **24**, 1855 (1959).

4) M. Freifelder, *J. Am. Chem. Soc.*, **82**, 2386 (1960).

5) J. E. Carnahan, T. A. Ford, W. F. Gresham, W. E. Grigsby and G. F. Hager, ibid., **77**, 3766 (1955).

6) L. C. Behr, J. E. Kirby, R. N. MacDonald and C. W. Todd, ibid., **68**, 1296 (1946); G. M. Whitman, U. S. Pat. 2606925 (1952) (*Chem. Abstr.*, **47**, 3874i (1953)); A. E. Barkdoll, D. C. England, H. W. Gray, W. Kirk, Jr. and G. M. Whitman, *J. Am. Chem. Soc.*, **75**, 1156 (1953); M. Freifelder and G. R. Stone, *J. Org. Chem.*, **27**, 3568 (1962); Abbott Laboratories, Brit. Pat. 881512 (1961) (*Chem. Abstr.*, **56**, 11465f (1962)); S. Nishimura and H. Taguchi, This Bulletin, **36**, 873 (1963).

7) a) H. A. Smith and R. G. Thompson, "Advances in Catalysis," Vol. 9, Academic Press Inc., New York (1957), p. 727; S. Nishimura et al., This Bulletin, **33**, 1356 (1960); **36**, 318, 353 (1963); J. H. Stocker, *J. Org. Chem.*, **27**, 2288 (1962); H. W. Arnold, U. S. Pat. 2555912 (1951) (*Chem. Abstr.*, **46**, 3074f (1952)); G. E. Ham and W. P. Coker, *J. Org. Chem.*, **29**, 194 (1964). b) Y. Takagi, T. Naito and S. Nishimura, This Bulletin, **37**, 585 (1964).

8) A. W. Burgstahler and Z. J. Bithos, *J. Am. Chem. Soc.*, **82**, 5466 (1960); "Organic Syntheses," Vol. 42, 62 (1962); S. Nishimura and H. Taguchi, This Bulletin, **36**, 353 (1963); F. Hartog and P. Zwietering, *J. Catalysis*, **2**, 79 (1963).

*[3] A marked difference in selectivity in the hydrogenation of nitriles and aniline was observed between the hydroxides and the oxides; this difference may be attributed to the difference in the alkali contents of the catalysts (to be described in following papers).

TABLE I. HYDROGENATION OF TOLUENE[a]

| Catalyst | Amount mg. | Additive, ml. | Time for hydrogenation[b] min. |
|---|---|---|---|
| Ru hydroxide | 25 | AcOH, 0.05 | 28 |
| Ru hydroxide | 10 | $H_2O$, 1 | 9 |
| Ru hydroxide | 10 | $H_2O$, 3 | 6 |
| Ru hydroxide | 10 | $H_2O$, 6 | 4 |
| Ru hydroxide | 5 | $H_2O$, 1 + AcOH, 0.05 | 12 |
| Ru hydroxide | 1 | $H_2O$, 1 + AcOH, 0.05 | 17 |
| Rh hydroxide | 5 | $H_2O$, 1 + AcOH, 0.05 | 11 |
| Ru dioxide | 5 | $H_2O$, 1 + AcOH, 0.05 | 18 |
| Rh oxide | 5 | $H_2O$, 1 + AcOH, 0.05 | 11 |

a) Toluene (9.2 g.) was hydrogenated at 85°C and 80 to 100 kg./cm² of hydrogen pressure.
b) The product consisted exclusively of methylcyclohexane throughout the runs, containing neither toluene nor any other compound.

TABLE II. HYDROGENATION OF BENZOIC ACID[a]

| Catalyst | Amount mg. | Solvent ml. | Time for hydrogenation[b] min. |
|---|---|---|---|
| (1:1) Ru-Rh hydroxide | 4 | $H_2O$, 15 | 180 |
| Rh hydroxide | 4 | $H_2O$, 15 | 130 |
| Rh oxide | 4 | $H_2O$, 15 | 120 |

a) Benzoic acid (12 g.) was hydrogenated at 100°C and 70 to 100 kg./cm² of hydrogen pressure.
b) The product (cyclohexanecarboxylic acid) was not isolated, but the hydrogen uptake was quantitative in each run.

contain much less alkali than do the oxides of ruthenium and rhodium, even though the hydroxides were precipitated from an alkaline solution.

The promoting action of water reported in the hydrogenation with a supported ruthenium catalyst[9] was also observed in the ruthenium hydroxide-catalyzed hydrogenations (see Tables I and IV). In the presence of water the ruthenium hydroxide was nearly as active as or even more active than the rhodium hydroxide in the hydrogenation of toluene and *o*-xylene, whereas the addition of water slightly retarded the hydrogenation of hydroquinone dimethyl ether with rhodium hydroxide. Generally the catalytic activity of ruthenium hydroxide is considerably greater than that of ruthenium dioxide,*4 and rhodium hydroxide is nearly as active as the rhodium oxide of the Adams type.[11] No appreciable co-activation effect of ruthenium and rhodium was observed in hydrogenation with the mixed ruthenium-rhodium hydroxides, although such an effect was reported with a supported ruthenium-rhodium catalyst.[12]

As may be seen from Tables III and IV, ruthenium hydroxide is more selective than the rhodium catalysts in the cis-hydrogenation of *o*-xylene*5 and hydroquinone dimethyl ether. It should be noted that the presence of water increases the yield of *cis*-1, 4-dimethoxycyclohexane in the hydrogenation of hydroquinone dimethyl ether. Both ruthenium and rhodium hydroxides give good yields of the corresponding saturated ethers in the hydrogenation of hydroquinone dimethyl ether and phenyl ether, which are both very easily susceptible to the hydrogenolysis of the C–O linkage (Table

TABLE III. HYDROGENATION OF *o*-XYLENE

| Catalyst | Amount, mg. | Additives, ml. | Time for hydrogenation min. | cis/trans ratio of 1,2-dimethylcyclohexane[b] |
|---|---|---|---|---|
| Ru hydroxide | 5 | $H_2O$, 1 + AcOH, 0.05 | 16 | 12.3 |
| (3:1) Ru-Rh hydroxide | 5 | $H_2O$, 1 + AcOH, 0.05 | 16 | 10.3 |
| (1:1) Ru-Rh hydroxide | 5 | $H_2O$, 1 + AcOH, 0.05 | 16 | 10.2 |
| (1:3) Ru-Rh hydroxide | 5 | $H_2O$, 1 + AcOH, 0.05 | 18 | 9.3 |
| Rh hydroxide | 5 | $H_2O$, 1 + AcOH, 0.05 | 23 | 9.5 |
| Ru dioxide | 5 | $H_2O$, 1 + AcOH, 0.05 | 26 | 11.2 |

a) *o*-Xylene (10.6 g.) was hydrogenated at 85°C and 80 to 100 kg./cm² of hydrogen pressure.
b) The yield of 1,2-dimethylcyclohexane was quantitative in each run.

9) P. N. Rylander, N. Rakoncza, D. Steele and M. Bollinger, *Engelhard Ind. Tech. Bull.*, **4**, 95 (1963).

*4 The ruthenium dioxide used in this study was prepared by the method of Pichler and Buffleb.[10] The oxide of ruthenium may also be prepared by the Adams method (cf. G. C. Bond and D. E. Webster, *Proc. Chem. Soc.*, **1964**, 398), but the resulting catalyst was far less active than the oxide of Pichler and Buffleb in the hydrogenation of toluene. The oxide obtained by the Adams method shows peaks at $2\theta = 28°$ and 35° in the X-ray diffraction analysis using Cu-$K\alpha$ radiation; these peaks are consistent with those of ruthenium dioxide reported in the literature. Pichler's dioxide and ruthenium hydroxide do not show any distinct diffraction patterns corresponding to the oxide of ruthenium. The oxide obtained by the Adams method does not dissolve in hot concentrated hydrochloric acid, whereas Pichler's dioxide partly, and ruthenium hydroxide rather easily, dissolve in the acid. These facts suggest that Pichler's dioxide is probably a mixture of the oxide and the hydroxide of ruthenium.

10) H. Pichler and H. Buffleb, *Brennstoff-Chem.*, **21**, 257 (1940).

11) S. Nishimura, This Bulletin, **34**, 1544 (1961).

12) P. N. Rylander and D. R. Steele, *Engelhard Ind. Tech. Bull.*, **3**, 91 (1962).

*5 Since rhodium oxide gives a better yield of *cis*-1, 2-dimethylcyclohexane than platinum oxide under similar conditions (unpublished; cf. Ref. 8), the order of selectivity in the cis-hydrogenation of *o*-xylene will be as follows: ruthenium>rhodium>platinum.

Table IV. Hydrogenation of hydroquinone dimethyl ether[a)]

| Catalyst | Amount, mg. | Additives, ml. | Time for hydrogenation min. | 1,4-Dimethoxycyclohexane | |
|---|---|---|---|---|---|
| | | | | % yield[b)] | cis/trans ratio |
| Ru hydroxide | 20 | AcOH, 0.05 | 80% hydrogenation/80 min. | — | 3.0 |
| Ru hydroxide | 20 | $H_2O$, 5 + AcOH, 0.05 | 19 | 78 | 4.0 |
| (3:1) Ru-Rh hydroxide | 20 | AcOH, 0.05 | 23 | 86 | 3.3 |
| (3:1) Ru-Rh hydroxide | 20 | $H_2O$, 5 + AcOH, 0.05 | 13 | 78 | 3.6 |
| (1:1) Ru-Rh hydroxide | 20 | AcOH, 0.05 | 19 | 91 | 3.0 |
| (1:1) Ru-Rh hydroxide | 20 | $H_2O$, 5 + AcOH, 0.05 | 11 | 78 | 3.6 |
| (1:3) Ru-Rh hydroxide | 20 | AcOH, 0.05 | 16 | 89 | 3.1 |
| (1:3) Ru-Rh hydroxide | 20 | $H_2O$, 5 + AcOH, 0.05 | 12 | 78 | 3.3 |
| Rh hydroxide | 20 | AcOH, 0.05 | 8 | 98 | 2.8 |
| Rh hydroxide | 20 | $H_2O$, 5 + AcOH, 0.05 | 12 | 76 | 3.2 |
| Rh oxide | 20 | AcOH, 0.05 | 8 | 97 | 2.8 |
| Ru dioxide | 20 | AcOH, 0.05 | 10% hydrogenation/60 min. | — | — |

a) Hydroquinone dimethyl ether (14 g.) was hydrogenated at 85°C and 80 to 100 kg./cm$^2$ of hydrogen pressure.
b) Smaller yields in the presence of water result from partly hydrolysis during the hydrogenation.

Table V. Hydrogenation of phenyl ether[a)]

| Catalyst | Amount, mg. | Additive, ml.[b)] | Time for hydrogenation min. | % yield of cyclohexyl ether |
|---|---|---|---|---|
| Ru hydroxide | 50 | AcOH, 0.05 | 120 | 77.5 |
| (3:1) Ru-Rh hydroxide | 50 | AcOH, 0.05 | 95 | 79.0 |
| (1:1) Ru-Rh hydroxide | 50 | AcOH, 0.05 | 25 | 84.0 |
| (1:3) Ru-Rh hydroxide | 50 | AcOH, 0.05 | 27 | 83.0 |
| Rh hydroxide | 50 | AcOH, 0.05 | 12 | 86.5 |
| Ru dioxide | 50 | AcOH, 0.05 | 42% hydrogenation/200 min. | — |
| Rh oxide | 50 | AcOH, 0.05 | 8 | 84.5 |

a) Phenyl ether (10 g.) was hydrogenated at 85°C and 80 to 100 kg./cm$^2$ of hydrogen pressure.
b) Addition of water caused the hydrolysis of phenyl ether to a large extent.

IV and V). The rhodium hydroxide is somewhat more selective than the ruthenium hydroxide in these hydrogenations, the results with it being consistent with those reported previously for the oxides of ruthenium and rhodium.[7b)] As can be seen from Tables III to V, the selectivities of the mixed ruthenium-rhodium hydroxides are generally those which would be expected from their compositions and not greater than that of either ruthenium hydroxide or rhodium hydroxide.

The results described above show that the hydroxide-black catalysts of ruthenium and rhodium are excellent catalysts in their activity and selectivity in the hydrogenation of the aromatic compounds. The method of preparing the hydroxides is very simple, and the resulting catalysts are nearly as active as or even more active than the corresponding oxide catalysts. Moreover, the catalysts containing much less alkali than the oxides may easily be obtained. Further studies will be reported in following papers.

## Experimental

**Catalysts.**—The hydroxides of ruthenium, rhodium, and ruthenium-rhodium were prepared by vigorously stirring a slight excess of a 10% sodium hydroxide solution into an about 1% aqueous solution of the metal chloride at 85 to 90°C. The precipitate thus formed was collected on a filter paper, washed with distilled water many times until the pH of the filtrate finally became 7.8, and then dried in a vacuum at room temperature. The yields were quantitative as judged on the basis of the metal contents of the hydroxides (see below). Ruthenium dioxide was

prepared according to the method of Pichler and Buffleb[10] by the fusion of ruthenium metal powder with potassium hydroxide and potassium nitrate, followed by reduction with methyl alcohol. Rhodium oxide was prepared by a modified Adams method[11] by the fusion of rhodium chloride with sodium nitrate at 460 to 480°C. The metal contents of the hydroxides and the oxides were estimated from the decrease in their weights when they were reduced to the metals in an atmosphere of hydrogen, using a thermobalance. The metal contents of ruthenium hydroxide, ruthenium dioxide, rhodium hydroxide, and rhodium oxide were 65, 75, 57, and 69% respectively.

**Hydrogenation.** — A 100 ml. bomb of an electromagnetically-stirring-type was used in all the hydrogenations. The bomb was charged with a 100 kg./cm$^2$ pressure of hydrogen and immersed in water maintained at 85°C during the hydrogenation, except in the case of benzoic acid. The hydrogenation of benzoic acid was carried out at 100°C with the use of water as the solvent, because at temperatures below 100°C the rate was too slow, probably because of the low solubility of benzoic acid in water. All the products, except cyclohexanecarboxylic acid, were analyzed by means of gas chromatography using a column containing PEG-6000.

The authors wish to express their gratitude to Professor Kozo Hirota of this Institute for his continued encouragement. The authors are also indebted to the Mitsubishi Chemical Industries Co., Ltd., for its financial support.

*The Institute of Physical and Chemical Research*
*Bunkyo-ku, Tokyo*

# Electrochemical Syntheses. V. The Direct Synthesis of Methyl Esters of $\alpha, \beta$-Unsaturated Carboxylic Acids from Some Arylated Olefins and Carbon Monoxide*

By Tadao INOUE and Shigeru TSUTSUMI

(Received May 12, 1965)

Although various reactions of olefins with carbon monoxide in the presence of proton-catalysts[1] and/or metal-carbonyls[2] or their-complexes[3] have been reported, the synthesis of $\alpha, \beta$-unsaturated carboxylic acids or esters from olefins and carbon monoxide has been unsuccessful as yet.

The present investigation deals with the first direct synthesis of methyl esters of $\alpha, \beta$-unsaturated carboxylic acids from olefins and carbon monoxide by a unique electrochemical method in the presence of a certain platinum carbonyl compound.

In the last previous paper[7] in this series,[4-7] the present authors have shown that the anodic oxidation of methanol in the presence of arylated olefins produced $\alpha, \beta$-dimethoxylated derivatives, and that the reaction involved a methoxy radical as an intermediate. In order to utilize the radicals produced in the electrolysis for organic synthesis, the electrolysis was carried out in these systems in the presence of carbon monoxide; consequently, we have observed that the platinum used as a cathode was easily dissolved into the solution during the electrolysis of methanol containing sodium methoxide, thus giving a certain platinum carbonyl compound. We have also found that this carbonyl compound reacted with olefins catalytically as well as electrolytically in the presence of carbon monoxide to give a methyl ester of the corresponding $\alpha, \beta$-unsaturated carboxylic acid as the main product. In order to provide some information with regard to the reaction mechanism and the synthetic usefulness of this curious electrochemical reaction, various experiments were carried out regarding the formation of the platinum carbonyl compound, its catalytic action on carboxylations of olefins, the influence of the concentration of the carbonyl compound, and the effect of the steric factor in olefins. Thus, styrene, $\alpha$-methylstyrene and 1, 1-diphenylethylene were chosen as the starting olefins.

## Results and Discussion

**1) The Carbomethoxylation of Olefins (Method A).**—The electrolyses were carried out

* Reported at the 18th Annual Meeting of the Chemical Society of Japan, Osaka, April, 1965.

1) M. Orchin and I. Wender, "Catalysis," Vol. V, Reinhold Publ. Corp., New York, N. Y. (1957), p. 6.

2) C. W. Bird, *Chem. Revs.*, **62**, 283 (1962); W. Reppe, *Ann.*, **582**, 38 (1953).

3) M. A. Bennett, *Chem. Revs.*, **62**, 611 (1962); N. Kutepof and H. Kindler, *Angew. Chem.*, **72**, 802 (1960).

4) T. Inoue, K. Koyama, T. Matsuoka, K. Matsuoka and S. Tsutsumi, *J. Chem. Soc. Japan, Ind. Chem. Sec.* (*Kogyo Kagaku Zasshi*), **66**, 1659 (1963).

5) T. Inoue, K. Koyama and S. Tsutsumi, This Bulletin, **37**, 1597 (1964).

6) T. Inoue, K. Koyama, T. Matsuoka, K. Matsuoka and S. Tsutsumi, *Tetrahedron Letters*, No. **21**, 1409 (1963).

7) T. Inoue and S. Tsutsumi, This Bulletin, **38**, 661 (1965).

by using two platinum-plate electrodes in a cylindrical glass cell placed in an autoclave under a pressure of 70 kg./cm² of carbon monoxide. The apparatus used is shown in Fig. 1. The current was controlled at nearly 1.0 amp., the temperature being kept at −10——15°C. The electrolysis of a methanolic solution containing sodium methoxide and styrene for 9 hr. gave methyl *trans*-cinnamate (I) as the main product in a 14% yield based on the styrene used; it also gave methyl β-methoxy-β-phenyl propionate (II) (3.6%), methyl β-phenyl propionate (III) (3.1%), dimethyl *meso*-β, γ-diphenyl adipate (IV) (a trace) and styrene glycol dimethyl ether (V) (5.6%), and unreacted styrene (57%). However, during the course of this electrolysis, the platinum plate used as a cathode (1.3 g.) was dissolved into the solution, and the electrolyzed solution turned a greenish-blue. The results obtained under various conditions are summarized in Table I, where the yield is calculated from the results of gas chromatographic analysis. When the electrolysis was carried out by using copper or carbon as the cathode and a platinum plate as the anode, styrene glycol dimethyl ether (V) was obtained as the sole product (23%), as is shown in Table I.

The electrolysis in the presence of α-methylstyrene instead of styrene for 9 hr. gave methyl *trans*-β-methyl cinnamate (VI) (14.8%), methyl 3-phenyl-3-butenoate (VII) (4.9%), methyl β-methyl-β-phenyl propionate (VIII) (1%) and α-methylstyrene glycol dimethyl ether (IX) (2.2%). When 1, 1-diphenylethylene was used, methyl β-phenyl cinnamate (X) was also obtained in a 17.2% yield as the main product, as is shown in Table II. In these electrolyses, the platinum used as a cathode was also dissolved into the electrolyzed solution.

**2) One Platinum Compound.**—When the electrolysis of methanol containing sodium methoxide was carried out by using two platinum-plate electrodes in the absence of olefins under the pressure of carbon monoxide, the platinum used as the cathode was also easily dissolved into the solution, giving a certain platinum carbonyl compound; this compound was then isolated by the removal

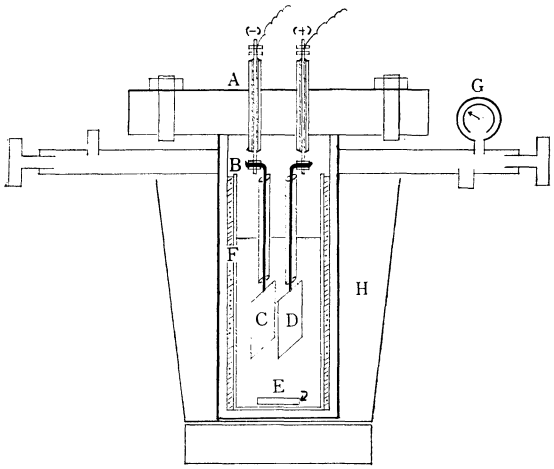



Fig. 1. Apparatus.
A: Autoclave (500 cc.)
B: Cylindrical glass cell
C: Cathode, Pt (2×3 cm²) or Cu (2×3 cm²)
D: Anode, Pt (2×3 cm²)
E: Magnetic stirrer
F: Methanol solution
G: Gauge
H: Ice-salt

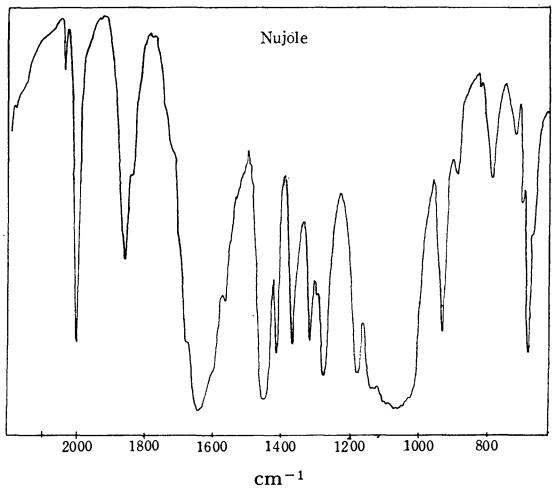



Fig. 2. IR spectrum of platinum carbonyl compound isolated.

Table I. Carbomethoxylation of styrene by method A

| Expt. No. | $C_6H_5CH=CH_2$ g. (mol.) | CO kg./cm² | Cathode material | Amp.·hr. | Wt. of Pt lost from cathode g. | Product, g. I | II | III | V |
|---|---|---|---|---|---|---|---|---|---|
| 1 | 52 (0.5) | 70 | Pt | 9.6 | 1.95 | 3.5 | 0.6 | 0.5 | 1.8 |
| 2 | 26 (0.25) | 70 | Pt | 9.6 | 1.77 | 3.5 | 0.7 | 0.5 | 2.1 |
| 3a) | 15.6 (0.15) | 70 | Pt | 8.6 | 1.32 | 3.4 | 1.0 | 0.7 | 1.4 |
| 4 | 52 (0.5) | 45 | Pt | 9.3 | 0.34 | 1.8 | 0.3 | 0.2 | 3.3 |
| 5 | 52 (0.5) | 45 | C | 9.2 | — | — | — | — | 4.2 |
| 6 | 26 (0.25) | 70 | C | 12.2 | — | — | — | — | 9.3 |

* $CH_3OH$, 80 g. (2.5 mol.); metallic sodium, 1.0 g.; anode, Pt, 2×3 cm².
** A current was controlled at nearly 1.0±0.1 amp.
a) Metallic sodium, 0.5 g. was used.

Table II. Carbomethoxylation of arylated olefins by method A

| $C_6H_5CR=CH_2$, g. (mol.) | R=H 15.6 (0.15) | $R=CH_3$ 17.7 (0.15) | $R=C_6H_5$ 18.0 (0.1) |
|---|---|---|---|
| Wt. of Pt lost from cathode, g. | 1.32 | 3.31 | 1.74 |
| Amp.·hr. | 8.6 | 8.4 | 8.6 |
| Product, g. (%)[a] | | | |
| $C_6H_5CR=CHCOOCH_3$ | 3.4 (14.0) | 3.9 (14.8) | 4.1 (17.2) |
| $C_6H_5CR(OCH_3)-CH_2COOCH_3$ | 1.0 (3.6) | — | — |
| $CH_2=C(C_6H_5)-CH_2COOCH_3$ | | 1.3 (4.9) | |
| $C_6H_5CHRCH_2COOCH_3$ | 0.7 (3.0) | trace | trace |
| $C_6H_5(R)C(OCH_3)-CH_2OCH_3$ | 1.4 (5.6) | 0.6 (2.2) | 1.8 (7.4) |

* $CH_3OH$, 80 g. (2.5 mol.); metallic sodium, 0.5 g.; anode and cathode, $2\times3$ cm$^2$; CO, 70 kg./cm$^2$; current, $1.0\pm0.1$ amp.; temperature, $-10$——$-15$°C.
a) Based on olefins used.

Table III. Carbomethoxylation of arylated olefins by method B

| Expt. No. | $C_6H_5CR=CH_2$ g. (mol.) | Pt-carbonyl compound g. (wt. of Pt) | Amp.·hr. | $RCOOCH_3$ (total) | Product, %[a] V | I | II | III |
|---|---|---|---|---|---|---|---|---|
| | R=H | | | | | | | |
| 1 | 15.6 (0.15) | 0.9 | 16.4 | 23 | 32 | 14 | 8 | 1 |
| 2 | 15.6 (0.15) | 1.5 | 16.6 | 35 | 23 | 21 | 13 | 1 |
| 3 | 15.6 (0.15) | 2.8 | 16.8 | 43 | 10 | 17 | 16 | 10 |
| | $R=CH_3$ | | | | IX | VI | VII | VIII |
| 4 | 17.7 (0.15) | 0.9 | 16.5 | 24 | 33 | 16 | 7 | 1 |
| 5 | 17.7 (0.15) | 2.9 | 16.8 | 31 | 9.3 | 18 | 11 | 2 |
| | $R=C_6H_5$ | | | | XI | X | | |
| 6 | 18.0 (0.10) | 1.0 | 16.4 | | 25 | 30 | | |

* $CH_3OH$, 90 g.; metallic sodium, 0.5 g.; anode, Pt, $2\times3$ cm$^2$; cathode, copper plate, $2\times3$ cm$^2$; current, $1.0\pm0.1$ amp.; time, 16 hr.; CO, 70 kg./cm$^2$; temperature, $-10$——$-15$°C.
a) Based on olefins used.

of methanol from the electrolyzed solution under a dry nitrogen atmosphere. This carbonyl compound was very sensitive to air and was greenish-blue. Its infrared spectrum has the characteristic absorption bands at about 2015 (v. s.) and 2145 cm$^{-1}$ (w.) (terminal carbonyl group), and at about 1860 (m. s.) and 1840 cm$^{-1}$ (m. s.) (the bridged carbonyl group); it also has strong absorption bands at about 1642, 1280 and 1180 cm$^{-1}$, as is shown in Fig. 2. Although the structure of this carbonyl compound has not yet been completely elucidated, the latter strong absorption bands may be due to the ester group attached to platinum metal, as has been reported in other metal-carbonyl compounds.[8]

**3) The Carbomethoxylation of Olefins in the Presence of the Platinum Carbonyl Compound (Method B).**—At first, the platinum carbonyl compound was produced in methanol containing sodium methoxide by electrolysis in a cylindrical glass cell in a manner similar to the procedure described above 2); then, after the plate of cathode had changed to copper($2\times3$ cm$^2$), electrolyses were carried out in the presence of olefins and carbon monoxide for 16 hr. (1.0 amp., $-10$——$-15$°C).

In these electrolyses, methyl esters of $\alpha,\beta$-unsaturated carboxylic acids were also obtained as the main products. Examples of the yields of these unsaturated esters and of other products are given in Table III.

**4) The Carbomethoxylation of Styrene in the Presence of Platinous Potassium Chloride.**—When the electrolysis was carried out in the presence of platinous potassium chloride or sodium cholride under similar conditions 3), it gave as products I (1%), II (3.3%) and V (18%).

The products obtained from these reactions were identified by the infrared spectroscopic, gas chromatographic and elemental analysis and, some of them, by NMR data; they were also identified as free acids by mixed melting points determinations with authentic specimens.

8) T. Kruck and M. Noack, *Chem. Ber.*, **97**, 1693 (1964).

*The Participation of the Platinum Carbonyl Compound.*—In these electrochemical reactions, the formation of unsaturated esters proceeds by the catalytic action of the platinum carbonyl compound, which is cathodically generated from the platinum used as the cathode and from sodium methoxide in the presence of carbon monoxide. The above statement was supported by the following experimental results: (a) Without the platinum carbonyl compound, the electrolysis of styrene using copper or carbon as the cathode and platinum as the anode gave styrene glycol dimethyl ether (V), and the formation of esters I—IV was not observed, as is shown in Table I (R-5 and 6); on the other hand, in the presence of the platinum carbonyl compound, these esters were mainly obtained, as Tables I—III show. (b) The electrolysis under a nitrogen atmosphere with catholyte and anolyte which contained the platinum carbonyl compound and styrene in each separated compartment resulted in the formation of the esters I and II from the anode compartment, although no product was detected from the cathode compartment. (c) With the increase in the concentration of the platinum carbonyl compound, the yield of these esters increased. On the contrary, the yield of styrene glycol dimethyl ether (V) decreased, as is shown in Table III. (d) The formation of these esters may proceed catalytically as well as electrolytically in the presence of the platinum carbonyl compound and carbon monoxide, for the electrolysis of styrene (0.15 mol.) give I (0.031 mol.), II (0.020 mol.) and III (0.003 mol.) in the presence of a catalytic amount of the platinum carbonyl compound (0.007 mol.), as Table III-R-2 shows.

Thus, it can be considered that the esters I and II are produced by the anodic reaction of styrene with the platinum carbonyl compound and carbon monoxide:

$$C_6H_5CH{=}CH_2 + CO + CH_3O^- \xrightarrow[[Pt_x(CO)_y]^n]{\text{anode}} C_6H_5CH{=}CHCOOCH_3\ (\textit{trans}\text{-})\ \text{(I)} + C_6H_5\underset{\displaystyle OCH_3}{\underset{|}{C}}HCH_2COOCH_3\ \text{(II)} \quad (1)$$

*Other Products.*—Styrene glycol dimethyl ether (V) is produced by the reaction of the methoxy radical, which is formed by the anodic oxidation of methanol as an intermediate, with styrene, as has been reported before.[7] Methyl $\beta$-phenyl propionate (III) and dimethyl *meso*-$\beta$, $\gamma$-diphenyl adipate (IV) are probably produced by the cathodic reduction of the methyl cinnamate (I) generated in the first step at a low concentration of the platinum carbonyl compound, since I was partly reduced to III and IV in, respectively, the absence of and presence of the platinum carbonyl compound under conditions similar to those described above 3), and since it is well known that cinnamic acid or its derivatives are easily reduced to propionic acid and adipic acid or their derivatives at mercury cathode.[9]

*Mechanistic Aspects.*—In this new electrochemical reaction, the above-mentioned carbomethoxy platinum carbonylate was assumed to be the active species for the carboxylation, preserving the olefinic double bond, of olefins. The experimental evidence for the above assumption included the facts that the carbomethoxy platinum carbonylate was isolated in the solid state, the infrared spectrum of which showed the presence of the ester group attached to platinum-metal, the terminal and the bridged carbonyl group, and that it reacted with olefins upon electrolysis to give methyl esters of $\alpha$, $\beta$-unsaturated carboxylic acids. Although the precise mechanism of the formation of this carbomethoxy platinum carbonylate is still open to question, it may be considered, as a possible rationalization, that the cathodically-generated platinum carbonyl compound immediately reacts with the methoxy radical or sodium methoxide via the anodic process to give the carbomethoxy platinum carbonylate (Eq. 2 or 3):

$$CH_3O^- \xrightarrow[\text{anode}]{-e} CH_3O\cdot \quad (2)$$

$$[Pt_x(CO)_y]^n + CH_3O\cdot \longrightarrow Pt_x(CO)_{y-1}COOCH_3$$
or
$$[Pt_x(CO)_y]^n \xrightarrow[\text{anode}]{-e} [Pt_x(CO)_y]^{n-1} \xrightarrow{CH_3ONa} \uparrow \quad (3)$$

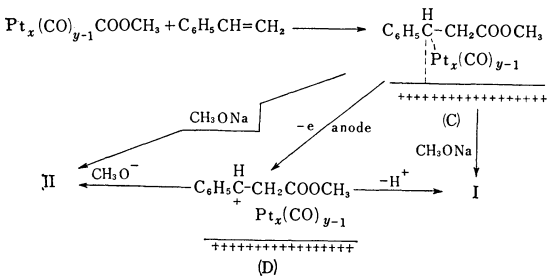
Equation 2 may be expected, since the environment around the electrode might have a particularly high concentration of the methoxy radical. The reaction scheme of Eq. 3 may be analogous to the formation of carbomethoxy manganese and rhenium carbonyl compound using manganese or rhenium carbonyl and sodium methoxide,[8] but in our case the reaction of Eq. 3 proceeded via the anodic process.[10] In any case, it is interesting that the platinum carbonyl or its derivatives, the preparation of which by other methods was difficult, was easily prepared by the electrochemical method.[11]

Thus, the esters of $\alpha$, $\beta$-unsaturated carboxylic acids may be considered to be produced by the addition of the Pt–$COOCH_3$ group in the platinum carbonyl compound to the olefinic double bond via the electrode process, followed by further anodic oxidation or decomposition with sodium methoxide, as is indicated below:

9) C. L. Wilson and K. B. Wilson, *Trans. Electrochem. Soc.*, **84**, 153 (1943); C. L. Wilson, ibid., **92**, 369 (1947).

10) This statement is supported by the experiment in which nickel carbonyl was easily oxidized at the anode surface by the electrolysis of methanol containing sodium methoxide.

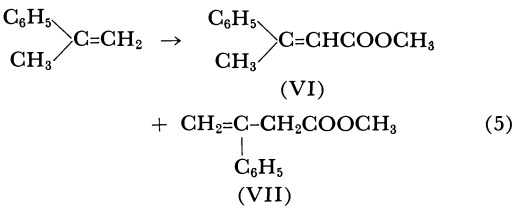
11) For example, the synthesis of manganese cyclopentadienyl tricarbonyls has been reported by the electrolysis of a mixture of a manganese compound, a cyclopentadiene, carbon monoxide and a transition metal-carbonyl. (Ethyl Corp., Brit 845074 (1960); *Chem. Abstr.*, **55**, 4205 (1961).)



The addition of the metal-carbon $\sigma$-bond to the olefinic double bond has recently been reported by several workers. For example, acyl and alkyl cobalt- and manganese-carbonyl compounds react with olefins,[12] diene[13] and fluoro-olefins.[14]

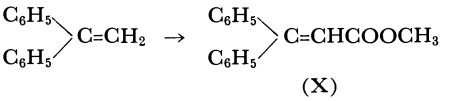
The complex C may be decomposed in the presence of sodium methoxide to give I and II as final products, as has been shown in other metal-carbonyl complexes.[12,13] Alternatively, the possibility of the oxidation of C to carbonium ions, which are then converted to I and II as final products, cannot be excluded, since it has been reported that benzylic carbonium ions can be easily produced as intermediates in electrolysies.[15,16]

*The Electrolyses of α-Methylstyrene or* 1, 1-*Diphenylethylene.*—When $\alpha$-methylstyrene was used instead of styrene, methyl 3-phenyl-3-butenoate (VII), besides methyl *trans*-$\beta$-methyl cinnamate (VI) as the main product, was obtained in a fairly high yield, as Table III shows. The NMR spectrum of



(5)

VII ($CCl_4$ as the solvent) showed peaks at 2.75 ($C_6H_5$), 4.55 ($CH_2$=), 4.85 ($CH_2$=), 6.47 ($OCH_3$) and 6.59 $\tau$ (-$CH_2$-); the peak areas were in the ratio of 5 : 1 : 1 : 3 : 2, as was to be expected from the presumed structure. In addition, VII could be easily hydrolyzed with an aqueous alkali solution to give *trans*-$\beta$-methyl cinnamic acid in the same way as methyl vinyl acetate.[17] The formation of these esters of unsaturated products VI and VII can be reasonably explained by $\alpha$- or $\gamma$-proton elimination from the intermediate complex C or the carbonium ion D in according to the hypothetical scheme described above. Similar electrolysis in the presence of 1, 1-diphenylethylene gave methyl $\beta$-phenyl cinnamate (X) and 1, 1-diphenylethylene glycol dimethyl ether (XI).



(6)

In these electrolyses, however, the corresponding methyl $\beta$-methoxy carboxylates were not detected in the products from $\alpha$-methylstyrene or in 1, 1-diphenylethylene, while methyl $\beta$-methoxy-$\beta$-phenyl propionate (II) was obtained from styrene, as has been mentioned above, and the corresponding dimethyl ether derivatives were obtained from these olefins. This may be due to the steric factor ($CH_3$-, $C_6H_5$-) with methoxide ions approaching the complex C or carbonium ion D as intermediates. More confirmations, however, are required with respect to this matter.

It is interesting to note that methyl esters of $\alpha$, $\beta$-unsaturated carboxylic acids were directly synthesized from olefins and carbon monoxide in fairly high yields in the presence of the platinum carbonyl compound.

## Experimental

All melting points and boiling points are uncorrected. The electrolyses were carried out with the apparatus shown in Fig. 1.

**Materials.** — Styrene and $\alpha$-methylstyrene were carefully purified in a usual manner,[18] stored in an ice-box, and distilled before use. 1, 1-Diphenylethylene was prepared by the dehydration of the alcohol formed by the action of phenylmagnesium bromide and ethyl acetate[19]; b. p. 97—97.5°C/0.5 mmHg, $n_D^{15}$= 1.6098. Methanol was purified in a manner described earlier.[4] These materials were confirmed to be pure by gas chromatography. Carbon monoxide (99.5% pure) was purchased from the Takatiho Co. The platinum plate (99.99% pure, 2×3 $cm^2$, 0.3 mm. thick) used as an electrode was prepared by carefully treating commercial material with dilute nitric acid and with distilled water; it was weighed before and after use. Commercially-available platinous potassium chloride was used.

**The Anodic Oxidation of Methanol in the Presence of Styrene and Carbon Monoxide (Method A).**—The reaction conditions and the yields of the products are summarized in Table I. R-3 may be illustrated as follows: Metallic sodium (0.5 g., 0.022 mol.) was dissolved in 80 g. of absolute methanol (2.5 mol.) in a cylindrical glass cell, and then 15.6 g. of freshly distilled styrene (0.15 mol.) was added to the mixture. After dry nitrogen had been bubbled through the mixture for about 1 hr., the cell was placed in an autoclave and the platinum plate as cathode was weighed. Carbon monoxide was then introduced (70 kg./$cm^2$), and the mixture was electrolyzed at −10—−15°C for 9 hr., with the current

12) R. F. Heck, *J. Am. Chem. Soc.*, **85**, 3116 (1963).
13) R. F. Heck, ibid., **85**, 3383 (1963).
14) J. B. Wilford, P. M. Treichel and F. G. A. Stone, *J. Organometallic Chem.*, **2**, 119 (1964); J. B. Wilford and F. G. A. Stone, *Inorg. Chem.*, **4**, 93 (1965).
15) W. A. Bonner and F. D. Mango, *J. Org. Chem.*, **29**, 430 (1964).
16) E. J. Corey, N. L. Bauld, R. T. Lalonde, J. Casanova and E. T. Kaiser, *J. Am. Chem. Soc.*, **82**, 2645 (1960); F. D. Mango and W. A. Bonner, *J. Org. Chem.*, **29**, 1367 (1964).
17) R. P. Linstead and E. G. Noble, *J. Chem. Soc.*, **1934**, 614.
18) A. Weissberger, "Technique of Organic Chemistry," Vol. VII, Interscience Publ., New York (1955), p. 331.
19) "Organic Syntheses," Coll. Vol. I (1956), p. 226.

maintained at nearly 1.0 amp. (current density, ca. 8.3 amp./cm$^2$). The electrolyzed solution turned a greenish-blue, and 1.32 g. of the platinum used as a cathode was dissolved into the electrolyzed solution. After the methanol had been removed from the reaction mixture under 25—30 mmHg pressure, the residue was poured into water (50 ml.), neutralized with 3 N hydrochloric acid, and extracted with ether; the extract was then dried over magnesium sulfate. After the ether had been removed, the oily residue (17.5 g.) was fractionated by distillation under diminished pressure into the following fractions:

| Fraction | B. p. | Weight, g. |
|---|---|---|
| 1 | ~50°C/25—28 mmHg | 4.1 |
| 2 | 70—120°C/0.7 mmHg | 6.9 |
| 3 | 120—150°C/0.7 mmHg | 1.0 |
| 4 | Residue | 2.0 |

By gas chromatographic analysis (conditions: column, Poly Ethylene Glycol 6000, 3 m. and Poly Ester DA., 3 m.; column temperature, 190°C; carrier gas, $H_2$), it was shown that Fraction 1 was unreacted styrene, while Fractions 2 and 3 were mixtures of styrene glycol dimethyl ether, methyl β-methoxy-β-phenyl propionate, methyl β-phenyl propionate, and methyl *trans*-cinnamate. The total amounts of these products were as follows: styrene glycol dimethyl ether, 1.4 g.; methyl β-methoxy-β-phenyl propionate, 1.0 g.; methyl β-phenyl propionate, 0.7 g.; methyl *trans*-cinnamate, 3.4 g. (14% yield based on the styrene used.)

Fraction 2 was submitted to preparative gas chromatography (column, Poly Ethylene Glycol 6000, 3 m.; column temperature, 190°C; carrier gas, $N_2$), and the respective products were isolated:

(a) methyl *trans*-cinnamate, m. p. 35—36°C.

Founds: C, 74.25; H, 6.46. Calcd. for $C_{10}H_{10}O_2$: C, 74.05; H, 6.22%.

The infrared spectrum of this ester showed the chracteristic bands at about 1735 (C=O) and 1640 cm$^{-1}$ (C=C), and it was identical with that of an authentic sample. The hydrolysis of this ester with an aqueous alkali solution gave *trans*-cinnamic acid (m. p. 132—133°C) from ligroin; a mixed melting point determination with an authentic sample showed no depression.

Found: C, 72.67; H, 5.57. Calcd. for $C_9H_8O_2$: C, 72.96; H, 5.44%.

(b) Methyl β-methoxy-β-phenyl propionate, b. p. 125—127°C/12—13 mmHg. The infrared spectrum of this compound showed the characteristic bands at about 1750 (C=O) and 1100 cm$^{-1}$ (C-O-C), and it was identical with that of an authentic sample prepared as described below; the hydrolysis of this ester with a cold 3 N potassium hydroxide solution gave β-methoxy-β-phenyl propionic acid, m. p. 98—98.5°C, from ligroin. A mixed melting point determination with an authentic sample showed no depression.

Found: C, 66.66; H, 6.77. Calcd. for $C_{10}H_{12}O_3$: C, 66.65; H, 6.71%.

With a boiling aqueous alkali solution, this ester was easily hydrolyzed to give *trans*-cinnamic acid, m. p. 132—133°C; a mixed melting point determination with an authentic sample showed no depression.

(c) Methyl β-phenyl propionate, b. p. 132—135°C/30 mmHg, $n_D^{15}=1.4997$. The hydrolysis of this compound with a boiling alkali solution gave β-phenyl propionic acid, m. p. 47.5—48°C, from petroleum ether; a mixed melting point determination with an authentic sample showed no depression.

Found: C, 72.18; H, 6.75. Calcd. for $C_9H_{10}O_2$: C, 71.98; H, 6.71%.

The infrared spectrum of this acid showed the characteristic band at about 1730 cm$^{-1}$ (C=O), and it was identical with that of an authentic sample.

(d) Styrene glycol dimethyl ether, b. p. 75—76°C/2 mmHg.

Found: C, 72.49; H, 8.88. Calcd. for $C_{10}H_{14}O_2$: C, 72.26; H, 8.49%.

The infrared spectrum of this ether showed the characteristic absorption band at 1105 cm$^{-1}$ (C-O-C), it was identical with that of an authentic sample prepared as described earlier.[7]

Fraction 3 was chromatographed over silica gel (2.5×45 cm). After the elusion of methyl *trans*-cinnamate (0.1 g.) with benzene, elusion with methanol gave a material which was then hydrolyzed with a methanolic alkali solution to give *meso*-β,γ-diphenyl adipic acid, m. p. 270—272°C, from methanol; a mixed melting point determination with an authentic sample prepared as described below showed no depression.

Found: C, 72.48; H, 6.14. Calcd. for $C_{18}H_{18}O_4$: C, 72.46; H, 6.08%.

The infrared spectrum of this acid was identical with that of an authentic sample.

**The Anodic Oxidation of Methanol in the Presence of Styrene, Carbon Monoxide and the Platinum Carbonyl Compound (Method B).**—The reaction conditions and the yields of the products are summarized in Table III.

R-2 may be illustrated as follows: Metallic sodium (0.5 g., 0.022 mol.) was dissolved in 90 g. of absolute methanol in a cylindrical glass cell, and dry nitrogen was bubbled through the mixture for about 1 hr. The cell was placed in an autoclave, carbon monoxide was introduced (70 kg./cm$^2$), and then the mixture was electrolyzed at −10—−15°C for 5 hr. (1.0 amp., 16—45 V.), using two weighed platinum plates. The platinum used as a cathod (1.5 g.) was dissolved into the solution in order to give a certain platinum carbonyl compound; the solution then turned to greenish-blue. After the carbon monoxide had been removed, the plate of cathode was changed to a copper one (2×3 cm$^2$), and then 15.6 g. of freshly-distilled styrene (0.15 mol.) was added to the electrolyzed solution. Carbon monoxide was again introduced (70 kg./cm$^2$) and the mixture was electrolyzed for 16 hr. under the conditions described above. The electrolyzed solution was worked up in a manner similar to the procedure described above (method A), and the oily residue was fractionated by distillation under reduced pressure into the following fractions:

| Fraction | B. p. | Weight, g. |
|---|---|---|
| 1 | ~39°C/15—17 mmHg | 2.5 |
| 2 | 64—75°C/0.3 mmHg | 3.5 |
| 3 | 75—85°C/0.3 mmHg | 10.5 |
| 4 | 85—125°C/0.3 mmHg | 1.8 |
| 5 | Residue | 3—4 |

By gas chromatographic analysis (conditions: described above), it was shown that Fraction 1 was unreacted styrene, while Fractions 2—4 were mixtures of

styrene glycol dimethyl ether (5.7 g.), methyl β-phenyl propionate (0.4 g.), methyl β-methoxy-β-phenyl propionate (3.9 g.) and methyl *trans*-cinnamate (5.0 g., 21% yield). The hydrolysis of the Fraction 5 (residue) with an aqueous alkali solution gave a small amount of *meso*-β,γ-diphenyl adipic acid (0.1 g.).

**The Anodic Oxidation of Methanol in the Presence of α-Methylstyrene, Carbon Monoxide and Platinum Carbonyl Compound (Method B).**—According to the procedure described above, the platinum carbonyl compound (2.9 g., wt. of Pt) was produced in a methanol solution containing sodium methoxide (metallic sodium (0.5 g.) in 90 g. of methanol) by electrolysis for 13.5 hr., and then freshly-distilled α-methylstyrene (17.7 g., 0.15 mol.) was added to the mixture. The electrolysis of the mixture was carried out, by using copper copper plate as a cathode, under the pressure of carbon monoxide (70 kg./cm²) for 16 hr. (1.0 amp., −10—−15°C). The electrolyzed solution was worked up in a manner similar to the procedure described above (method A), and the oily residue was fractionated by distillation under reduced pressure into the following fractions:

| Fraction | B. p. | Weight, g. |
|---|---|---|
| 1 | ~49°C/12—13 mmHg | 4.9 |
| 2 | 65—85°C/2—3 mmHg | 2.0 |
| 3 | 85—125°C/2—3 mmHg | 7.4 |
| 4 | 125—185°C/2—3 mmHg | 1.0 |
| 5 | Residue | 5.9 |

By gas chromatographic analysis (conditions: column, Poly Ester DA, 3 m.; temperature, 182°C; carrier gas, $H_2$), it was shown that Fractions 1—4 were mixtures of methyl *trans*-β-methyl cinnamate, methyl 3-phenyl-3-butenoate, methyl β-methyl-β-phenyl propionate, α-methylstyrene glycol dimethyl ether and acetophenone and that the total amount of these products were as follows: methyl *trans*-β-methyl cinnamate, 4.5 g. (18% yield, based on the α-methylstyrene used); methyl 3-phenyl-3-butenoate, 2.7 g.; methyl β-methyl-β-phenyl propionate, 0.6 g.; α-methyl-styrene glycol dimethyl ether, 2.5 g.; acetophenone, 1.1 g. Fractions 3 and 4 were chromatographed over silica gel (2.5×45 cm.). Elusion with benzene led to the isolation of the following products:

(a) Methyl *trans*-β-methyl cinnamate, b. p. 80—81°C/0.8 mmHg, m. p. 28—29°C; from ligroin.

Found: C, 74.88; H, 6.97. Calcd. for $C_{11}H_{12}O_2$: C, 74.97; H, 6.86%.

The infrared spectrum of this unsaturated ester showed the characteristic absorption bands at about 1735 (C=O) and 1642 $cm^{-1}$ (C=C), and it was identical with that of an authentic sample. The hydrolysis of this ester with an aqueous alkali solution gave *trans*-β-methyl cinnamic acid, m. p. 96.5—97.5°C, from ligroin; a mixed melting point determination with an authentic sample prepared as described below showed no depression.

Found: C, 74.22; H, 6.22. Calcd. for $C_{10}H_{10}O_2$: C, 74.05; H, 6.22%.

(b) Methyl 3-phenyl-3-butenoate, b. p. 125—126°C/12—13 mmHg.

Found: C, 75.17; H, 6.89. Calcd. for $C_{11}H_{12}O_2$: C, 74.97; H, 6.86%.

The infrared spectrum of this ester showed the characteristic absorption bands at about 1755 (C=O) and 1645 $cm^{-1}$ (C=C), and the NMR spectrum of this unsaturated ester ($CCl_4$ as solvent) showed peaks at 2.75($C_6H_5$), 4.55($CH_2$=), 4.85($CH_2$=), 6.47($OCH_3$) and 6.59 τ(−$CH_2$−); the peak areas were in the ratio of 5 : 1 : 1 : 3 : 2, as would be expected from the structure. The hydrolysis of this ester with a 3 N potassium hydroxide solution gave *trans*-β-methyl cinnamic acid, m. p. 96.5—97.5°C; a mixed melting point determination with an authentic sample showed no depression.

(c) α-Methylstyrene glycol dimethyl ether, b. p. 67—69°C/1.5 mmHg, $n_D^{14}$=1.5022.

Found: C, 73.57; H, 9.27. Calcd. for $C_{11}H_{16}O_2$: C, 73.39; H, 8.95%.

The infrared spectrum of this dimethyl ether showed the characteristic absorption bands at about 1110 and 1128 $cm^{-1}$ (C-O-C), and it was identical with that of an authentic sample prepared as earlier.[7]

Methyl β-methyl-β-phenyl propionate was identified by gas chromatographic analysis (conditions as described above). From Fraction 2, acetophenone was identified as its 2,4-dinitrophenylhydrazone: m. p. 237—238°C; a mixed melting point determination with an authentic sample was not depressed.

Found: C, 56.17; H, 3.93. Calcd. for $C_{14}H_{12}N_4O_4$: C, 56.00; H, 4.03%.

**The Anodic Oxidation of Methanol in the Presence of 1, 1-Diphenylethylene, Carbon Monoxide and the Platinum Carbonyl Compound (Method B).**—After the platinum carbonyl compound (1.0 g., wt. of Pt) had been produced in methanol containing sodium methoxide (metallic sodium 0.5 g in 90 g. of methanol) by electrolysis for 3 hr., 18.0 g. of freshly-distilled 1,1-diphenylethylene was added to the mixture; then the mixture was electrolyzed by using copper plate as the cathode for 16 hr. under carbon monoxide pressure (70 kg./cm²). The electrolyzed solution was worked up in a manner similar to that described above, and the oily residue was fractionated by distillation under diminished pressure into the following fractions:

| Fraction | B. p. | Weight, g. |
|---|---|---|
| 1 | ~125°C/0.2 mmHg | 2.5 |
| 2 | 125—145°C/0.2 mmHg | 17.3 |
| 3 | Residue | 2—3 |

10.0 g. of a mixture of Fractions 1 and 2 was chromatographed over silica gel (2.5×50 cm.). Elution with benzene led to the isolation of methyl β-phenyl cinnamate (4.0 g.), 1, 1-diphenylethylene glycol dimethyl ether (2.5 g.), unidentified products (3.5 g.) and unreacted 1,1-diphenylethylene (0.5 g.): (a) methyl β-phenyl cinnamate, b. p. 133—134°C/0.3 mmHg.

Found: C, 80.83; H, 6.19. Calcd. for $C_{16}H_{14}O_2$: C, 80.64; H, 5.92%.

The infrared spectrum of this ester showed the characteristic absorption bands at about 1745 (C=O) and 1625 $cm^{-1}$ (C=C). The hydrolysis of this ester with an alcoholic alkali solution gave β-phenyl cinnamic acid, m. p. 161—162°C, from methanol; a mixed melting point determination with an authentic sample prepared as described below showed no depression.

Found: C, 80.54; H, 5.15. Calcd. for $C_{15}H_{12}O_2$: C, 80.33; H, 5.39%.

(b) 1,1-Diphenylethylene glycol dimethyl ether, m. p. 64.5—65.5°C, from ligroin; a mixed melting point determination with an authentic sample prepared as described earlier[7] showed no depression.

Found: C, 79.06; H, 7.25. Calcd. for $C_{16}H_{18}O_2$: C, 79.31; H, 7.49%.

9.5 g. of the mixture of Fractions 1 and 2 was hydrolyzed with a 10% potassium hydroxide - ethanol solution to give 3.5 g. of β-phenyl cinnamic acid with a m. p. of 158—161°C.

**The Anodic Oxidation of Methanol in the Presence of Styrene, Carbon Monoxide and Platinous Potassium Chloride.** — Metallic sodium (0.5 g.) was dissolved in 90 g. of absolute methanol in a cylindrical glass cell, and then 3.0 g. of platinous potassium chloride and 33 g. of freshly-distilled styrene were added to the mixture. The mixture was electrolyzed by using carbon as the cathode and platinum as the anode for 17 hr. under a carbon monoxide pressure of 70 kg./cm². The reaction mixture was worked up in a manner similar to the procedure described above, and the oily residue was distilled under diminished pressure to give the following fractions:

| Fraction | B. p. | Weight, g. |
|---|---|---|
| 1 | ~49°C/20 mmHg | 8.7 |
| 2 | ~75°C/1 mmHg | 6.2 |
| 3 | 75—100°C/1 mmHg | 5.8 |
| 4 | 100—145°C/1 mmHg | 2.5 |
| 5 | Residue | 5.5 |

By gas chromatographic analysis (conditions: column, Poly Ethylene Glycol 6000, 3 m.; column temperature, 177°C; carrier gas, $H_2$), it was shown that the total amount of the products were as follows: styrene-glycol dimethyl ether, 9.3 g.; methyl β-methoxy-β-phenyl propionate, 1.8 g.; methyl *trans*-cinnamate, 0.4 g.; unidentified products, 3.5 g.

Fraction 3 was hydrolyzed with a cold 3 N potassium hydroxide solution to give 1.7 g. of β-methoxy-β-phenyl propionic acid with a m. p. of 97—98.5°C from ligroin; a mixed melting point determination with an authentic sample showed no depression.

**The Syntheses of the Authentic Samples.**— *trans*-Cinnamic acid and β-phenyl propionic acid or their esters were commercial; they were then purified from ligroin.

Methyl β-methoxy-β-phenyl propionate was prepared by the reaction of methyl α-acetoxymercury-β-methoxy-β-phenyl propionate, which had been prepared by the action of methyl *trans*-cinnamate with mercury acetate in methanol,[20] with hydrogen sulfide and ammonia[20]; b. p. 125—127°C/12—13 mmHg. β-Methoxy-β-phenyl propionic acid was obtained by the hydrolysis of methyl β-methoxy-β-phenyl propionate with a cold aqueous alkali solution; m. p. 97—98°C (lit.,[20] m. p. 98°C). *meso*-β,γ-Diphenyl adipic acid was prepared by the electrolytic reduction of *trans*-cinnamic acid at the mercury cathode[21]; m. p. 270—272°C (lit.,[21] m. p. 270—273°C). *trans*-β-Methyl cinnamic acid was synthesized from *t*-butyl acetate[22] and acetophenone by the action of lithium amide[23]; m. p. 97.5—98°C (lit.,[23] m. p. 98—98.5°C). Methyl β-methyl-β-phenyl propionate was prepared by the electrolytic reduction of methyl *trans*-β-methyl-cinnamate[24]; b. p. 133—134°C/22 mmHg. β-Phenyl cinnamic acid was prepared by the reaction of 1,1-diphenylethylene with oxalyl chloride[25]; m. p. 161—162°C (lit.,[25] m. p. 162°C).

We should like to thank Dr. Yoshinobu Odaira and Dr. Menbo Ryang for their useful suggestions and encouragement.

*Department of Chemical Technology*
*Faculty of Engineering*
*Osaka University*
*Miyakojima-ku, Osaka*

20) W. Schrauth, W. Schoeller and R. Struensee, *Ber.*, **44**, 1433 (1911).
21) C. L. Wilson and K. B. Wilson, *Trans. Electrochem. Soc.*, **84**, 11 (1943).
22) "Organic Syntheses," Vol. 24, 19 (1944).
23) C. R. Hauser and W. H. Puterbaugh, *J. Am. Chem. Soc.*, **75**, 1068 (1953).
24) "Organic Syntheses," Coll. Vol. 1, 311 (1948).
25) M. S. Kharasch, *J. Am. Chem. Soc.*, **64**, 333 (1942).

# The Optical Properties of Colored Colloidal Systems. III. A Theory of Spherical Particles, with Especial Attention to Systems Dispersed in Colored Media*

By Masayuki NAKAGAKI

(Received April 14, 1965)

In a previous paper,[1] the extinction, scattering and absorption of light by a colloidal sytem of colored spherical particles dispersed in a colorless medium was studied theoretically; it was concluded that the scattering is affected by the absorption, and that the absorption is affected by the scattering. In another paper,[2] the apparent refractive index of the same system was studied theoretically, and the results were applied to a solution of dye, Acid Orange R, the system being treated as a dispersed system of infinitesimally small particles. In the present paper, the theoretical treatment will be extended to cases where either the particle or the medium is colored, or both; the results will be discussed in detail for the case of a relatively small absorption.

## Theoretical

**Complex Refractive Index.**—The refractive index of a colored phase is usually expressed by a complex quantity. For the dispersion medium;

$$\mu_1 = \mu_{10}(1 - ik_2) \tag{1}$$

and for the dispersed phase;

$$\mu_2 = \mu_{20}(1 - ik_2) \tag{2}$$

may be used, where $\mu_{10}$ and $\mu_{20}$ are the usual refractive indices of the respective bulk phases, while $k_1$ and $k_2$ are related to the optical densities per unit of thickness, $E_i'$, of the respective bulk phases by the following equation,[3] with $i=1$ or 2;

$$E_i' = -[\ln(I_i'/I_0')]/l_i' = 4\pi\mu_{i0}k_i/\lambda_0 \tag{3}$$

Here $l_i'$ is the thickness of the phase $i$, $I_0'$ and $I_i'$ are the intensities of the incident and transmitted light, and $\lambda_0$ is the wavelength of the light in a vacuum.

When phase 2 is dispersed as small spherical particles in phase 1, the optical properties of the dispersed system are determined by the relative radius, $\alpha$, the relative refractive index, $m$, the number of particles in a unit volume, $N$, and the wavelength of light in the medium, $\lambda$. The relative radius is defined by:

$$\alpha = 2\pi a/\lambda \tag{4}$$

where $a$ is the radius of the sphere and where

$$\lambda = \lambda_0/\mu_{10} \tag{5}$$

If the concentration $c$ (g./ml.) is used instead of $N$;

$$c = \alpha^3\lambda^3\rho_2 N/6\pi^2 \tag{6}$$

where $\rho_2$ is the density of the dispersed phase.

The relative refractive index, $m$, defined by:

$$m = \mu_2/\mu_1 \tag{7}$$

is also a complex quantity in our case; it is separated into real and imaginary parts as follows:

$$m = m_0 - ik_0 \tag{8}$$

where $i$ is $\sqrt{-1}$ and

$$m_0 = (\mu_{20}/\mu_{10})(1+k_1k_2)/(1+k_1^2) \tag{9}$$

$$k_0 = (\mu_{20}/\mu_{10})(k_2-k_1)/(1+k_1^2) \tag{10}$$

or

$$k = k_0/m_0 = (k_2-k_1)/(1+k_1k_2) \tag{11}$$

If the medium is colorless and the particles are colored,

$$\left.\begin{array}{l} m_0 = \mu_{20}/\mu_{10} \\ k_0 = m_0k_2 \text{ or } k = k_2 \end{array}\right\} \text{ (if } k_1=0) \tag{12a}$$

Therefore, $m_0$ is equal to the ratio of the usual refractive indices and $k_0$ is positive. This is the case discussed in the previous papers.[1,2]

On the contrary, if the medium is colored and the particles are colorless,

$$\left.\begin{array}{l} m_0 = (\mu_{20}/\mu_{10})/(1+k_1^2) \\ k_0 = -m_0k_1 \text{ or } k = -k_1 \end{array}\right\} \text{ (if } k_2=0) \tag{12b}$$

Therefore, $m_0$ is smaller than the ratio of the usual refractive indices $(\mu_{20}/\mu_{10})$ and $k_0$ is negative. Finally, if both the medium and the particles are colored, the situation is different depending on whether $k_1$ or $k_2$ is the greater. If $k_1<k_2$, then $m_0>(\mu_{20}/\mu_{10})$ and $k_0>0$, but if $k_1>k_2$, then $m_0>(\mu_{20}/\mu_{10})$ and $k_0<0$. The case when $k_1=k_2$ is especially interesting because $m_0=\mu_{20}/\mu_{10}$ and $k_0=0$. This means that the effect of the particles on the optical properties of the dispersed system for which $k_1=k_2$ can be treated theoretically as if the system is colorless, although actually the system is colored.

* Presented at the 16th Colloid Symposium held by the Chemical Society of Japan, Osaka, November, 1963; and the 17th Annual Meeting of the Chemical Society of Japan, Tokyo, April, 1964.

1) M. Nakagaki, This Bulletin, **31**, 980 (1958).

2) M. Nakagaki and T. Fujii, ibid., **34**, 433 (1961).

3) The optical density is usually defined by a common logarithm, but the natural logarithm is used throughout this paper.

**Optical Density, Absorption and Scattering.**—The optical density per unit layer thickness of the colored colloidal system is set as $E_0$, which may be measured, for example, by a Beckman-type photometer, using distilled water as the reference for an aqueous colloidal system. The difference in the optical densities per unit layer thickness between the colored colloidal system, $E_0$, and the colored medium, $E_1$, is set at $E$, which may be measured by using the colored medium (instead of distilled water) as the reference solution. Therefore,

$$E=E_0-E_1=-[\ln(I/I_1)]/l \tag{13}$$

where $l$ is the layer thickness, $I$ is the transmitted light through the colloidal system, and $I_1$ is the transmitted light through the dispersion medium. On the other hand,

$$E_0=-[\ln(I/I_0)]/l=E+4\pi k_1/\lambda \tag{14}$$

where $I_0$ is the intensity of the incident light and where the last term is obtained from Eqs. 3 and 5. The quantity $E$ means the increment in the optical density as a result of the existence of the colloidal particles.' In the special case where the medium is colorless ($k_1=0$), $E$ is equal to $E_0$. When $k_0<0$ (that is, $k_2<k_1$), $E$ will take a negative value, as will be shown later, except when the effect of scattering is sufficiently large.

The optical density increment per particle, $E/N$, is considered to be the sum of the scattering, $R$, and the absorption, $A$.

$$E/N = R + A \tag{15}$$

The parameters $\varepsilon$, $\kappa$, and $\varepsilon_a$ will, however, be used because the concentration, $c$, is experimentally more convenient than the number of particles, $N$. Here,

$$\left.\begin{aligned}\varepsilon &= E/c\\ \kappa &= RN/c\\ \varepsilon_a &= AN/c\end{aligned}\right\} \tag{16}$$

The parameters $x$, $y$ and $z$ will be used, as in a previous paper.[1]

$$\left.\begin{aligned}x &= (\lambda\rho_2/3\pi)\varepsilon\\ y &= (\lambda\rho_2/3\pi)\kappa\\ z &= (\lambda\rho_2/3\pi)\varepsilon_a=x-y\end{aligned}\right\} \tag{17}$$

The theoretical values of the parameters $x$, $y$ and $z$ can be calculated according to the Mie theory.[4] The equations expanded in a power series of $\alpha$ and $k_0$ have already been given in a previous paper.[1] Numerical calculations according to these equations have been made for $\alpha=0$ (0.2) 0.8, $m_0=0.50$ (0.05) 1.50 and $k_0=-0.3$ (0.1) 0.3. The $m_0$-values smaller than 1.00 were included because, first, those values may be smaller than unity if $k_1$ is sufficiently greater than $k_2$ (cf. Eq. 9), even when $(\mu_{20}/\mu_{10})$ is greater than unity, and, second, $(\mu_{20}/\mu_{10})$ itself may be smaller than unity in such a case, as when, for examples, bubbles are dispersed in a liquid. The negative $k_0$-values were included because sometimes the medium is colored, as has been mentioned before. The results are shown in Fig. 1 for $x$, in Fig. 2 for $y$, and in Fig. 3 for $z$, although only the results for $m_0=1.50$, 1.00,

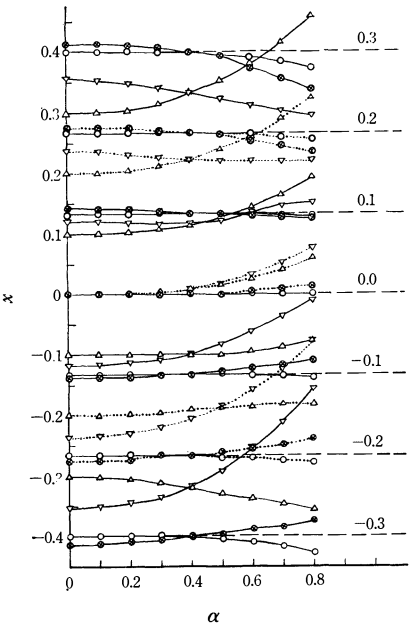



Fig. 1. Relation between $x$ and $\alpha$.
Parameter: $k_0$. $m_0=1.50(\triangle)$, $1.00(\bigcirc)$, $0.8165(\otimes)$ and $0.50(\triangledown)$. $k_0=0$ and $\pm 0.2(\cdots)$; $\pm 0.1$ and $\pm 0.3(—)$

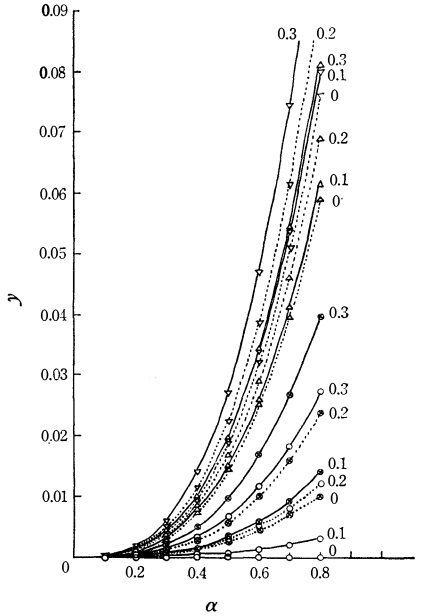



Fig. 2. Relation between $y$ and $\alpha$.
Parameter: $|k_0|$. $m_0=1.50(\triangle)$, $1.00(\bigcirc)$, $0.8165(\otimes)$ and $0.50(\triangledown)$. $|k_0|=0$ and $0.2(\cdots)$, 0.1 and $0.3(—)$

4) G. Mie, *Ann. Phys.*, (4), **25**, 377 (1908).

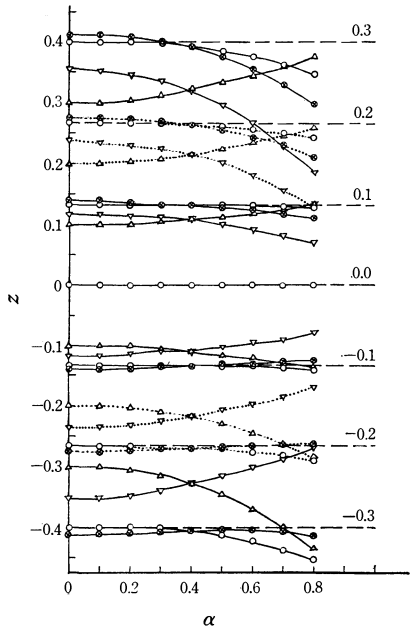



Fig. 3. Relation between $z$ and $\alpha$.
Parameter: $k_0$. $m_0=1.50(\triangle)$, $1.00(\bigcirc)$, 0.8165 ($\otimes$) and $0.50(\triangledown)$. $k_0=0$ and $\pm$ 0.2(···), $\pm$ 0.1 and $\pm$ 0.3(—)

0.8165 (corresponding to the maximum of $\zeta_0$, as will be discussed later) and 0.5 will be shown in order to keep the figures simple. The horizontal broken lines in Figs. 1 and 3 are the limitting values where $m_0$ is 1.00 and $\alpha$ is sufficiently small; that is:

$$\left.\begin{aligned} x(m_0=1.00;\ \alpha=0)=z(m_0=1.00;\ \alpha=0)=(4/3)k_0 \\ y(m_0=1.00;\ \alpha=0)=0 \end{aligned}\right\} \tag{18}$$

When the medium is colorless, these values are equal to the values for the bulk phase of the dispersed material;

$$\left.\begin{aligned} x_2(\text{bulk})=z_2(\text{bulk})=(4/3)\,(\mu_{20}/\mu_{10})k_2 \\ y_2(\text{bulk})=0 \end{aligned}\right\} \tag{19}$$

but when the medium is colored, the limiting value of Eq. 18 is not equal to the values of Eq. 19 for the bulk phase.

After the author had published a previous paper,[1] Chromey[5] made computations based on the exact Mie theory for $\alpha=0.2$ (0.2) 2.0; $m_0=0.50$ (0.25) 3.00, and $k=(k_0/m_0)=0.0$ (0.1) 1.0. The results agree with each other in the range discussed in the present paper as far as comparison is possible, although Chromey never treated the case of $k_0<0$.

The effect of $k_0$ on the quantities $x$, $y$ and $z$

5) F. C. Chromey, *J. Optical Soc. Am.*, **50**, 730 (1960). The symbols $\Omega$, $(\Omega-\Omega')$, $\Omega'$ and $x$ in his paper correspond, respectively, to $x$, $y$, $z$ and $k$ in our notation, although he erroneously states that $\Omega'$ is pure scattering.

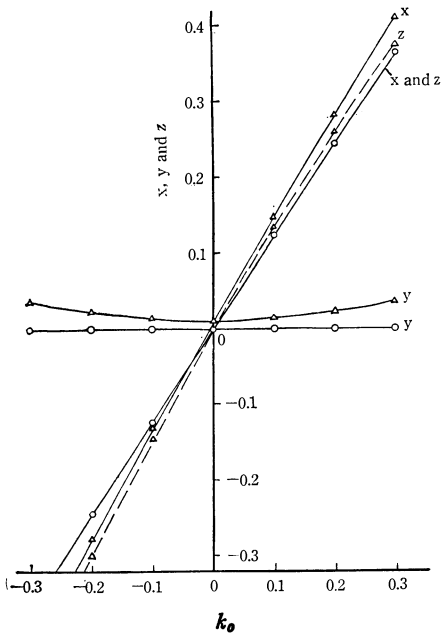



Fig. 4. Relation between $x$, $y$ and $z$ vs. $k_0$
$\alpha=0(\bigcirc)$ and $0.8(\triangle)$; $m_0=1.20$

can be seen from Fig. 4. The figure illustrates the case of $m_0=1.20$, which is close to the $m_0$-values for a polymer latex dispersed in an aqueous solution. In the range of small $k_0$-values, both $x$ and $z$ are approximately linear with regard to $k_0$. The line for $z$ passes the origin, but the line for $x$ does not, because $x$ is the sum of $y$ and $z$, and $y$ is not zero, even when $k_0$ is zero, if $\alpha\neq 0$.

If $k_0$ is small, the value of $z$ is proportional to $k_0$. The proportionality constant, $\zeta$, is defined by:

$$\zeta = \lim_{k_0\to 0}(z/k_0) \tag{20}$$

If there were no effect of scattering, $\zeta$ should be equal to 4/3, as is shown in Eq. 18. The actual

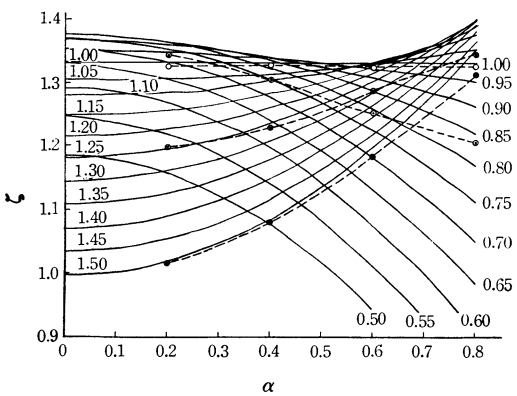



Fig. 5. Relation between $\zeta$ and $\alpha$.
Parameter: $m_0$. Chromey's date for $m_0=0.75$ ($\odot$), $1.00(\bigcirc)$, $1.25(\otimes)$, $1.50(\bullet)$

$\zeta$-value, however, depends on both the relative particle size, $\alpha$, and the relative refractive index, $m_0$, as is shown in Fig. 5. The results of the numerical calculation may be compared with the values obtained by extrapolating Chromey's data.[6] Fairly good agreement is observed, except when $\alpha$ exceeds 0.6. The value of $\zeta$ for very small particles, $\zeta_0$, depends on $m_0$, as is shown in Fig. 6. $\zeta_0$ takes a maximum value ($\zeta_0(\max)=1.377838$)

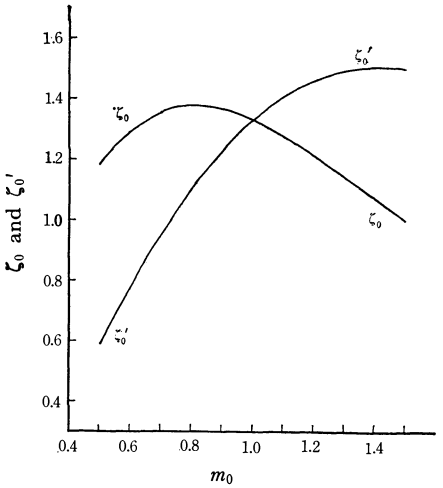



Fig. 6. Relation between $\zeta_0$ and $\zeta_0'$ vs. $m_0$.

at $m_0=\sqrt{2/3}$. Sometimes the quantity $k$, instead of $k_0$, is taken as the variable. Then:

$$\zeta_0' = \lim_{\substack{k\to 0 \\ \alpha\to 0}} (z/k) \tag{21}$$

should be used instead of $\zeta_0$. The value of $\zeta_0'$, too, is shown in Fig. 6, which takes a maximum value ($\zeta_0'(\max)=3/2$) at $m_0=\sqrt{2}$. The values of $\zeta_0$ and $\zeta_0'$ are the same and are equal to 4/3 at $m_0=1$, since $k_0=m_0k$.

The scattering (expressed by the quantity $y$ as has already been shown in Fig. 2) is proportional to the cube of the relative particle radius, as far as the present approximation is concerned.

$$y = Y\alpha^3 \tag{22}$$

The coefficient $Y$ depends on both $m_0$ and $k_0$, as is shown in Fig. 7, and its value is the greater, the greater $|m_0-1|$ is and the greater $|k_0|$ is. The scattering is, thus, caused by the refraction and absorption. The $Y$-value for $k_0=0$ is considered to represent the scattering caused by the refraction and is expressed by $Y_m$, while the $Y$-value for $m_0=1$ is considered to represent the scattering caused by the absorption and is expressed by $Y_k$. The actual $Y$-value is, however, not equal to the sum of $Y_m$ and $Y_k$; a cross term, $Y_{mk}$, is also required.

$$Y = Y_m+Y_k+Y_{mk} \tag{23}$$

6) His data for $m_0=1.25$, $k=0.2$ and $\alpha=0.2$ are in error. These values were, therefore, disregarded in the extrapolation.

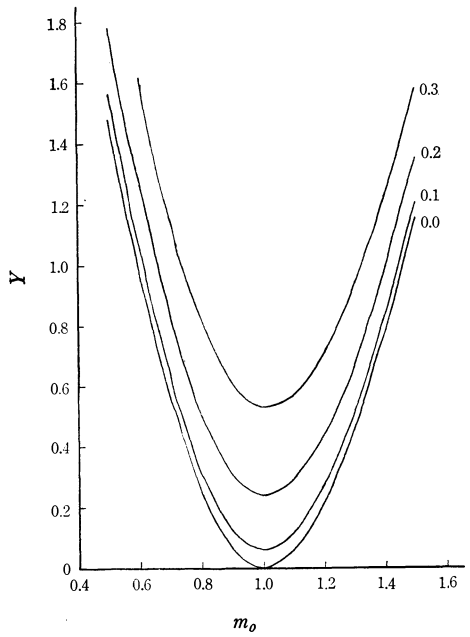



Fig. 7. Relation between $Y$ and $m_0$. Parameter: $|k_0|$

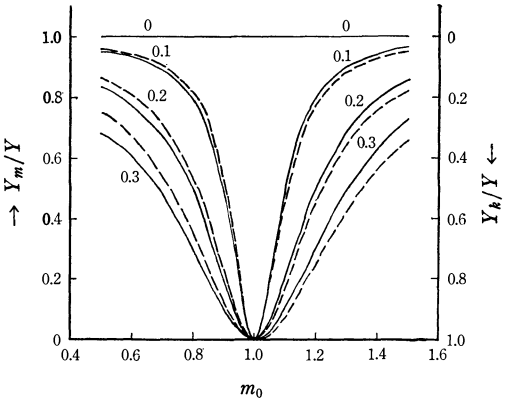



Fig. 8. Dependence of $Y_m/Y(-)$ and $Y_k/Y(\cdots)$ on $m_0$. Parameter: $|k_0|$

In Fig. 8, the ratio $Y_m/Y$ (solid lines) is shown on the left ordinate in an upward direction, while the ratio $Y_k/Y$ (broken lines) is shown on the right ordinate in a downward direction. It may be seen from Fig. 8 that the cross term, $Y_{mk}$, is negative when $m_0>1$ and positive when $m_0<1$. The value of $Y_{mk}/Y$ is not large, although it is not equal to zero except when $m_0=1$ or $k_0=0$.

**The Refractive Index of the Dispersed System.**—It has been well established experimentally that the refractive index of a dispersed system, $\mu_{12}$, is linear to the concentration, $c$, (g./ml.), at least within the concentration range of the usual experimental conditions. This can be explained by the mixture rule:

$$\mu_{12} = \mu_{10}\varphi_1 + \mu_{20}'\varphi_2 \quad (24)$$

because the rule yields the following equation, which states that $\partial\mu_{12}/\partial c$ is constant:

$$\partial\mu_{12}/\partial c = (\mu_{20}'-\mu_{10})/\rho_2 \quad (25)$$

where $\varphi_1$ and $\varphi_2$ are the volume fractions of the medium and the dispresed phase respectively, and where $\rho_2$ is the density of the dispersed phase. The apparent refractive index of the particle $\mu_{20}'$ is, however, not equal to the refractive index of the dispersed phase, $\mu_{20}$ (the real part of the complex refractive index as defined by Eq. 2) because the refractive index is affected by light scattering, as has already been stated by the author and Heller.[7]

The value of the apparent relative refractive index

$$m' = \mu_{20}'/\mu_{10} \quad (26)$$

can be calculated on the basis of the Mie theory, as has been stated in previous papers.[2,7] In the case of $\alpha \ll 1$ and $|k_0| \ll m_0$, the equation was expanded in a power series of $k_0$ and the coefficients of the power series were expressed[2] as known functions of $m_0$ and $\alpha$. Numerical calculation has been made for $\alpha=0$ (0.1) 0.8, $m_0=0.85$ (0.05) 1.50 and $k_0=-0.3$ (0.1)$+0.3$. The $m_0$-values smaller than unity and the negative $k_0$-values were included in order to consider the case where the medium is colored. Only some of the results, for $k_0=-0.3$, 0 and $+0.3$, are shown in Fig. 9 in order to keep the figure simple. When $k_0$ is equal to zero, or when the system is colorless, the value of $m'$ increases[8] with the $\alpha$, and the increment is the greater, the greater $|m_0-1|$ is. When $k_0$ is not equal to zero, or when the system is colored, the value of $m'$ increases or decreases with $\alpha$, depending on the values of $m_0$ and $k_0$. When $\alpha$ approaches zero, the value of $m'$ depends on the absolute value of $k_0$. When $\alpha$ is not so small, the value of $m'$ depends not only on the absolute value but also on the sign of $k_0$. If $k_0$ is so small that the term $k_0^2$ can be neglected, then:

$$m' = m_0'(1-fk_0) \quad (27)$$

where $m_0'$ is the $m'$-value for $k_0=0$. The value of the coefficient $f$ is shown in Fig. 10. The value of $f$ is positive for $m_0>1$ and negative for $m_0<1$, and the absolute value of $f$ increases with the $\alpha$.

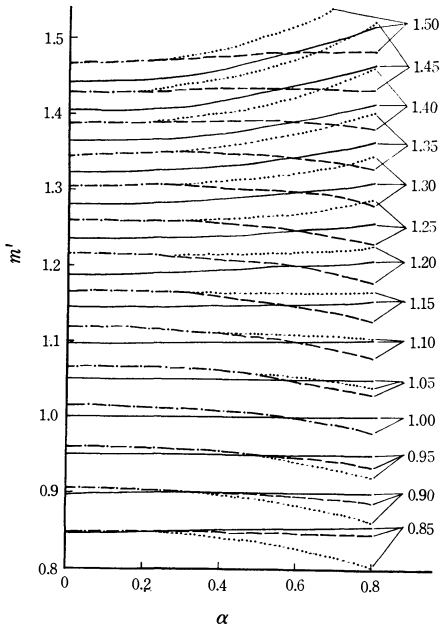



Fig. 9. Relation between $m'$ and $\alpha$.
Parameter: $m_0$. $k_0=+0.3$(---), 0(—), $-0.3$(···)

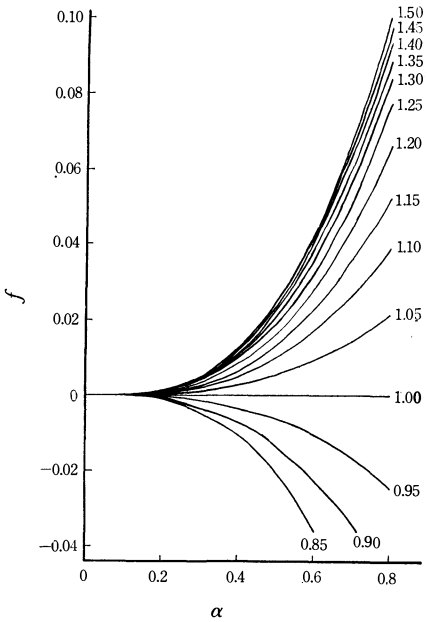



Fig. 10. Relation between $f$ and $\alpha$.
Parameter: $m_0$

**A Note on the Usual Experimental Conditions for the System of a Colored Medium.**— The value of $k_0$ may be very large if the particles are colored. It may even be infinitely large if the particles are made of a good conductor, but the extinction of the dispersed system as a whole can be made as small as possible in experimental work by diluting the dispersed system. If, however, the medium is colored and the particles are colorless, the absolute value of $k_0$ cannot be very large, because a certain detectable amount of light must pass through the layer of the dispersed system. If $k_0$ is not small, an extremely strong light source is needed.

Considering a layer of a colored medium, the value of, for example, $k_1=0.76\times10^{-4}$ is obtained

7) M. Nakagaki and W. Heller, *J. Appl. Phys.*, **27**, 975 (1956).

8) The value of $m'$ passes a maximum point when $\alpha$ increases further. (Cf. Ref. 7)

according to Eq. 3, if the optical density $-\log(I_1'/I_0')$ is 3.00, the layer thickness is 0.30 cm., the refractive index of the medium is $\mu_{10}=1.333$ (water), and the wavelength of the light is $\lambda_0=555\,\mathrm{m}\mu$ (the most sensitive wavelength for the human eye). This gives the result that $k_0=-0.91\times10^{-4}$ if $k_2=0$ and if $\mu_{20}/\mu_{10}=1.20$. Therefore, extremely small $k_0$-values are interesting experimentally.

The scattered-light intensity of a colored colloidal system, of course, decreases by the term $\exp.(-E_0l)$ according to the Lambert law, where $l$ is the path length of light in the colloidal system. However, after this decrease in light intensity ash been corrected properly, the scattered-light intensity of a colored colloidal system should be almost exactly equal to that of a colorless system which has the same $m_0$ and $\alpha$ values. This is obvious because, according to Fig. 4, the $x$, $y$ and $z$ values for such small $k_0$ value as $10^{-4}$ are practically equal to those for $k_0=0$. According to Eq. 27 and the $f$ value shown in Fig. 10, it is obvious that the value of the refractive index of the colored system is also practically equal to that of the colorless system if $k_0$ is as small as $10^{-4}$.


## Summary

In the expression of the complex refractive index of a colored colloidal system ($m=m_0-ik_0$), the value of $m_0$ may be smaller than unity and $k_0$ may be negative if the medium is colored. Including these cases, the values of $x$ (corresponding to the optical density), $y$ (scattering) and $z$ (absorption) have been calculated for relatively small $\alpha$ and $k_0$ values. The values of the apparent relative refractive index, $m'$, have been calculated also. These results have been discussed in detail in order to show the effect of the scattering and absorption on the scattering, absorption and apparent refractive index. It has been concluded that the data of a system in which colorless particles are dispersed in a colored medium will be practically equal to those in a colorless medium if the extinction of light according to the Lambert law is corrected properly.



*Faculty of Pharmaceutical Sciences*
*Kyoto University*
*Sakyo-ku, Kyoto*

# The Determination of Micro Amounts of Polythionates. II.* A Photometric Method for the Determination of Hexathionate by Means of Its Cyanolysis[1]

By Tomozo Koh and Iwaji Iwasaki

(Received May 18, 1965)

In the preceding paper[2] of this series, the methods in current use for analyzing polythionates have been reviewed. So far, there has not been any procedure for the determination of micro quantities of hexathionate. One of the present authors (T. K.)[2] has, however, reported an excellent method for the determination of a small amount of pentathionate, a method which depends upon the reaction:

$$S_5O_6^{2-}+4CN^-+H_2O=$$
$$S_2O_3^{2-}+SO_4^{2-}+2HCN+2SCN^-$$

followed by the photometric measurement of the thiocyanate thus formed with ferric iron. The above study establishes the feasibility of a method for the determination of hexathionate, because the higher polythionate, hexathionate, reacts more easily with cyanide to form thiocyanate.

The present authors have investigated, in detail, a photometric method for the determination of a micro amount of hexathionate, a method which is based on the reactions:

$$S_6O_6^{2-}+5CN^-+H_2O=$$
$$S_2O_3^{2-}+SO_4^{2-}+2HCN+3SCN^-$$
$$SCN^-+Fe^{3+}=FeSCN^{2+}$$

they have established an excellent method, finding the most suitable conditions for the reaction of hexathionate with cyanide to proceed completion by varying the cyanide amount, the pH, the reaction time, and the temperature.

In the present investigation, it was observed that hexathionate also is quantitatively converted

* Part I: This Bulletin, **38**, 1510 (1965)

1) Presented at the Scientific Meeting on Chemistry, Tokyo, November, 1964.

2) T. Koh, This Bulletin, **38**, 1510 (1965).

into thiocyanate under the same conditions as are used for the determination of pentathionate.

The proposed method is sufficiently rapid, precise, and accurate to be used for the determination of a small amount of hexathionate.

## Experimental

**Apparatus and Materials.**—Unless stated particularly, the apparatus and materials used in this investigation are the same as those described in the previous paper.[2]

*Potassium Hexathionate.*—This salt was prepared according to the directions of Goehring and Feldmann.[3] The hexathionate obtained was then recrystallized twice with 2 N hydrochloric acid and dried at room temperature for 6 days.

In order to obtain pure hexathionate, it is of great importance to recrystallize the raw hexathionate as fast as possible, because it undergoes thermal decomposition easily, even in a strong acid solution. In the present study, much purer hexathionate could be obtained than that described in the literature (96%).[3]

The water content physically adsorbed on the hexathionate was estimated to be 1.2% by the Karl Fischer method.

*The Purity of the Potassium Hexathionate.*—The purity of this salt was estimated by determining the total potassium and sulfur contents as follows.

The potassium hexathionate was decomposed into potassium sulfate by heating it at around 800°C; $K_2S_6O_6 \rightarrow K_2SO_4$. The potassium was determined by weighing[4] the potassium sulfate thus formed.

As for the sulfur, the hexathionate was oxidized[4,5] by bromine in an alkaline medium on heating and, the sulfate ion content formed was determined by the usual gravimetric method. Tables I and II show that

Table I. Determination of K for the potassium hexathionate* used in the present study

| Sample taken mg. | As $K_2S_6O_6$ mg. | Found as $K_2SO_4$ mg. | K found for $K_2S_6O_6$ % | K calcd. for $K_2S_6O_6$ % |
|---|---|---|---|---|
| 179.2 | 177.0 | 83.7 | 21.23 | 21.33 |
| 237.0 | 234.1 | 111.7 | 21.41 | |

Table II. Determination of S for the potassium hexathionate* used in the present study

| Sample taken mg. | As $K_2S_6O_6$ mg. | Found as $BaSO_4$ mg. | S found for $K_2S_6O_6$ % | S calcd. for $K_2S_6O_6$ % |
|---|---|---|---|---|
| 212.0 | 209.4 | 796.1 | 52.22 | 52.48 |
| 173.4 | 171.3 | 651.0 | 52.20 | |

* Water content was estimated to be 1.2%.

the results obtained are within the limits of experimental error and that this potassium hexathionate is pure enough for the purposes of this study.

3) M. Goehring and U. Feldmann, *Z. anorg. Chem.*, **257**, 223 (1948).
4) F. Martin and L. Metz, *Z. anorg. u. allgem. Chem.*, **127**, 83 (1923).
5) C. Mishima, *Bull. Tokyo Inst. Tech.*, No. 1, 27 (1951).

*The Standard Hexathionate Solution.*—The standard solution, a $1.0 \times 10^{-3}$ M concentration of hexathionate, was prepared by dissolving 185.6 mg. of the potassium hexathionate (water content: 1.2%) in redistilled water and by then diluting it to 500 ml. This stock solution proved to be stable; even after two months, no measurable change was found by the present method when it was kept at 5±2°C in a refrigerator. The working standard solutions were prepared by then diluting this stock solution properly.

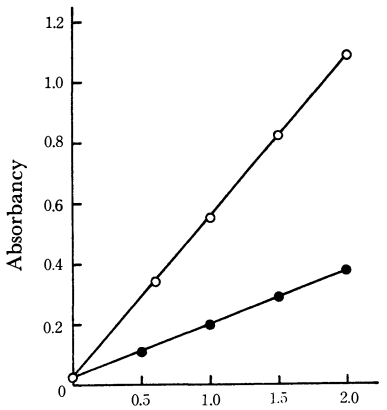
**Procedure.**—A standard hexathionate solution of 10.0 ml. is placed in a 25 ml. volumetric flask. To this solution are added first 4.0 ml. of the buffer solution of pH 7.4, and then 2.6 ml. of 0.05 M sodium cyanide, whereupon the pH of the solution is brought to 8.6.

The volumetric flask is kept in the thermostat at 40±1°C for 30 min.; hexathionate is thus converted into thiocyanate quantitatively. Then 3.0 ml. of a 1.5 M ferric nitrate - perchloric acid solution is added. After the flask has been filled to the mark with redistilled water, its contents are mixed well. The absorbancy of the solution of the ferric-thiocyanate complex thus formed is measured at the wavelength of 460 mμ, using distilled water as a reference.

## Results and Discussion

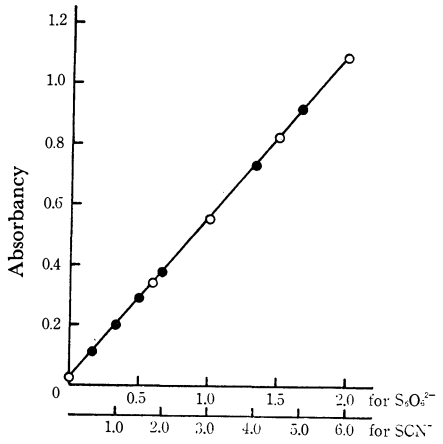
**Calibration Curves.**—The solutions containing various amounts of hexathionate and thiocyanate were treated by the procedure mentioned above; the experimental results are plotted in Figs. 1 and 2.

As can be seen in Figs. 1 and 2, the absorbancy and concentration were in a good linear relationship. When one ion of hexathionate undergoes cyanolysis, three ions of thiocyanate are formed. Consequently, if the hexathionate is pure enough and if it is, moreover, converted into thiocyanate quantitatively, the sensitivity of hexathionate should be just three times as high as that of thiocyanate when plotted by the mole concentration for hexathionate and thiocyanate. In fact, Fig. 1 shows that the calibration curve for hexathionate is three




Concn. of $S_6O_6^{2-}$ and $SCN^-$, $\times 10^{-4}$ M

Fig. 1. Calibration curves.
○ Hexathionate ● Thiocyanate



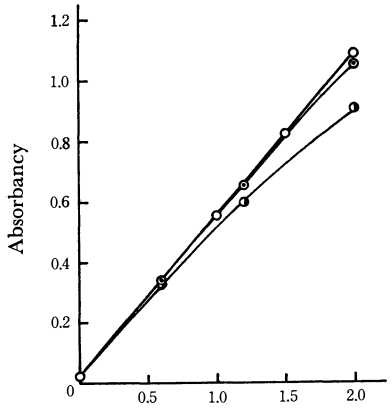

Concn. of $S_6O_6^{2-}$ and $SCN^-$, $\times 10^{-4}$ M

Fig. 2. Calibration curves.
○ Hexathionate ● Thiocyanate

times as sensitive as that for thiocyanate. As can also be seen in Fig. 2, the calibration curve of hexathionate exactly coincides with that of thiocyanate when the scale of the thiocyanate concentration is made one-third of that of the hexathionate concentration, demonstrating that the stoichiometric reaction has occurred.

**The Effect of the Amount of Sodium Cyanide.**—The preliminary experiments led the authors to the conclusion that pH has a great effect on the cyanolysis and that hexathionate, just like pentathionate,[2] undergoes a partial alkaline decomposition as a result of the higher pH caused by the addition of the cyanide.

As will be described below, it was observed that the optimum pH for the reaction of hexathionate with cyanide is over the range of 7.8 to 8.9 under the conditions of the preceding procedure. 0.5 ml. of 0.025 M sodium cyanide and 0.5 to 4.0 ml. of 0.05 M sodium cyanide were employed, and in all cases the solution was buffered to the optimum pH value. The resulting effect of the amount of sodium cyanide on the cyanolysis is shown in Fig. 3.




Concn. of hexathionate, $\times 10^{-4}$ M

Fig. 3. Effect of sodium cyanide amount. The pH was adjusted to the range from 7.8 to 8.9 in all cases.
Cyanolysis time: 30 min. at 40°C
◑ 0.025 M NaCN 0.5 ml. (I)
⊙ 0.05 M NaCN 0.5 ml. (II)
○ 0.05 M NaCN 1.0, 2.0, 2.6 and 4.0 ml. (III)

The calibration curves with 0.5 ml. portions of 0.025 and 0.05 M sodium cyanide solutions do not form straight lines (see I and II), indicating that hexathionate is not quantitatively converted into thiocyanate because of insufficient amounts of cyanide. It can be concluded from Fig. 3 that 1.0 ml. of a 0.05 M sodium cyanide solution is sufficient for the quantitative conversion of hexathionate into thiocyanate, and that the amount of sodium cyanide does not have any effect on the method, so long as it is sufficient and the pH is adjusted to an optimum value.

**The Effect of pH.**—At higher pH levels, hexathionate undergoes an alkaline decomposition besides cyanolysis; therefore, the procedure should be carried out below a pH value of 8.9. Figure 4 shows the dependence of the rate of cyanolysis on the pH of the solution at 20°C.

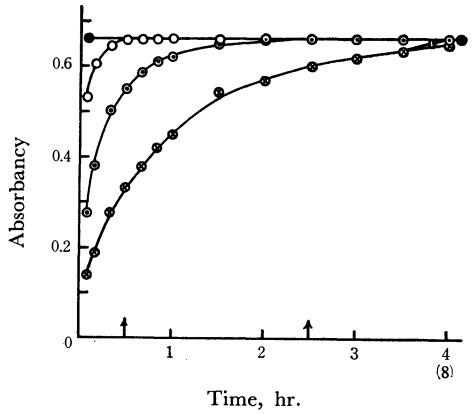



Fig. 4. Effect of pH on the rate of cyanolysis at 20°C.
● $3.6\times10^{-4}$ M $SCN^-$
○ pH 8.7 (I)
⊙ pH 8.0 (II) } $1.2\times10^{-4}$ M $S_6O_6^{2-}$
⊗ pH 7.5 (III)

The maximum absorbancy, which corresponds to the complete and stoichiometric reaction of hexathionate with cyanide, is reached in 30 min. at pH 8.7; it then remains constant (see I), while the reaction at pH 8.0 goes to completion in two hours and a half (see II). On the other hand, the reaction at pH 7.5 does not go to completion even within 4 hr.; however, it goes stoichiometrically to completion in 8 hr. (see III).

In order to accelerate the rate of cyanolysis, the reaction temperature was raised from 20°C to 40°C and 70°C. Figure 5 shows how the pH

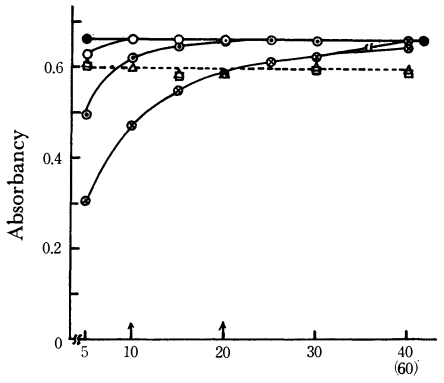



Fig. 5. Effect of pH on the rate of cyanolysis.
—●— $3.6\times10^{-4}$ M $SCN^-$
—○— pH 8.7 (I) } at 40°C
—⊙— pH 8.0 (II) } at 40°C
—⊗— pH 7.5 (III) } at 40°C
--△-- pH 8.7 (IV) } at 70°C
--□-- pH 8.0 (IV) } at 70°C
$1.2\times10^{-4}$ M $S_6O_6^{2-}$

of the solution affects the rate of cyanolysis at 40°C and 70°C.

At 40°C, the reaction goes well to completion and is stoichiometric in 10 min. at pH 8.7 (see I), while the reactions at pH 8.0 and 7.5 go to completion in 20 min. and 1 hr. respectively (see III). At 70°C, the thermodecomposition occurs in addition to cyanolysis, so hexathionate is not completely converted into thiocyanate (see IV).

The reaction of hexathionate with cyanide at various pH values was carried out, both at 20°C for 60 min. and at 40°C for 30 min., for the purpose of studying the effect of pH on the cyanolysis. The results are shown in Fig. 6, where the reaction

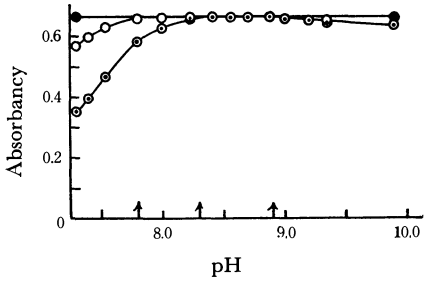



Fig. 6. Effect of pH.
● $3.6\times10^{-4}$ M $SCN^-$
○ 30 min. at 40°C (II) } $1.2\times10^{-4}$ M $S_6O_6^{2-}$
⊙ 60 min. at 20°C (I) }

at 20°C for 60 min. gives maximum absorbancies over the pH range from 8.9 to 8.3 (see I), and that at 40°C, for 30 min. over the pH range from 8.9 to 7.8 (see II). The decrease in absorbancy above the pH value of 9.0 may be attributed to the alkaline decomposition of hexathionate. The optimum pH range for the stoichiometric reaction can be extended from both 7.8 and 8.3 to a lower pH value by making the cyanolysis time longer, because the rate of cyanolysis decreases with the lowering of the pH.

A similar method which is available for the determination of micro amounts of tetrathionate under the same conditions as those used here for the determination of pentathionate and hexathionate will be reported on in another paper.

## Summary

A photometric method for the determination of a small amount of hexathionate has been developed, a method depending on the formation of thiocyanate equivalent to the hexathionate, and on the determination of thiocyanate with an excess of ferric iron. A buffer solution is first added to a standard hexathionate solution in order that the pH of the mixed solution after the addition of the cyanide solution may be within an optimum range; otherwise the hexathionate undergoes alkaline decomposition as a result of the higher pH value caused by the addition of the cyanide. The conditions under which the reaction of hexathionate with cyanide is rapid and proceeds well to completion, have been established by varying the cyanide amount, the pH, the reaction time, and the temperature. Hexathionate can be determined by exactly the same procedure as that used for phentathionate.

The authors wish to thank Dr. Satori Utsumi of Nihon University, and Mr. Takejiro Ozawa and Dr. Minoru Yoshida of the Tokyo Institute of Technology, for their many valuable discussions and suggestions during the course of this study. Thanks are also due to Dr. Kaname Muroi, Central Research Laboratory of the Mitsubishi Chemical Industries, Ltd., for estimating the water content in the hexathionate by the Karl Fischer method.

*Laboratory of Analytical Chemistry and Geochemistry*
*Tokyo Institute of Technology*
*Ookayama, Tokyo*

# Studies of Peptide Antibiotics. III. Cyclo-(L-valyl-L-ornithyl-L-leucyl-D-phenylalanylglycyl)$_2$[1]

By Haruhiko Aoyagi, Tetsuo Kato, Motonori Ohno, Michio Kondo
Michinori Waki, Satoru Makisumi and Nobuo Izumiya

(Received May 24, 1965)

Certain peptide antibiotics, such as gramicidin S,

L-Val-L-Orn-L-Leu-D-Phe-L-Pro
↑ ↓
L-Pro-D-Phe-L-Leu-L-Orn-L-Val
Gramicidin S

possess several characteristic features in common. These features include a cyclic structure, D-amino acid residues, and a basic character due to the presence of diamino acid residues. The necessity of a cyclic structure for antibacterial activity is indicated by the finding that the activity of a synthetic linear decapeptide, with the same sequence of amino acid residues as that found in gramicidin S, is markedly less than that of gramicidin S.[2] In a previous paper from this laboratory,[3] a cyclic hexapeptide, cyclo-L-valyl-L-ornithyl-L-leucyl-D-phenylalanyl-L-prolyl-glycyl, which contains a partial sequence found in gramicidin S, was prepared and its antibacterial activity was tested. The cyclic hexapeptide was, however, found to be devoid of antibacterial activity. Recently, another cyclic hexapeptide, cyclo-L-valyl-D-ornithyl-L-prolyl-D-phenylalanyl-D-leucyl-L-ornithyl, has been synthesized; it also was found to possess no antibacterial activity.[4] From these findings, it appears that, in addition to the characteristics mentioned above, other structural features, such as a ring size larger than that of the cyclic hexapeptide and/or specific amino acid sequence, are necessary in this type of molecule for an activity to be exhibited. Therefore, it became of interest to examine the effect on bacterial growth of a larger synthetic cyclic peptide than the cyclic hexapeptide.

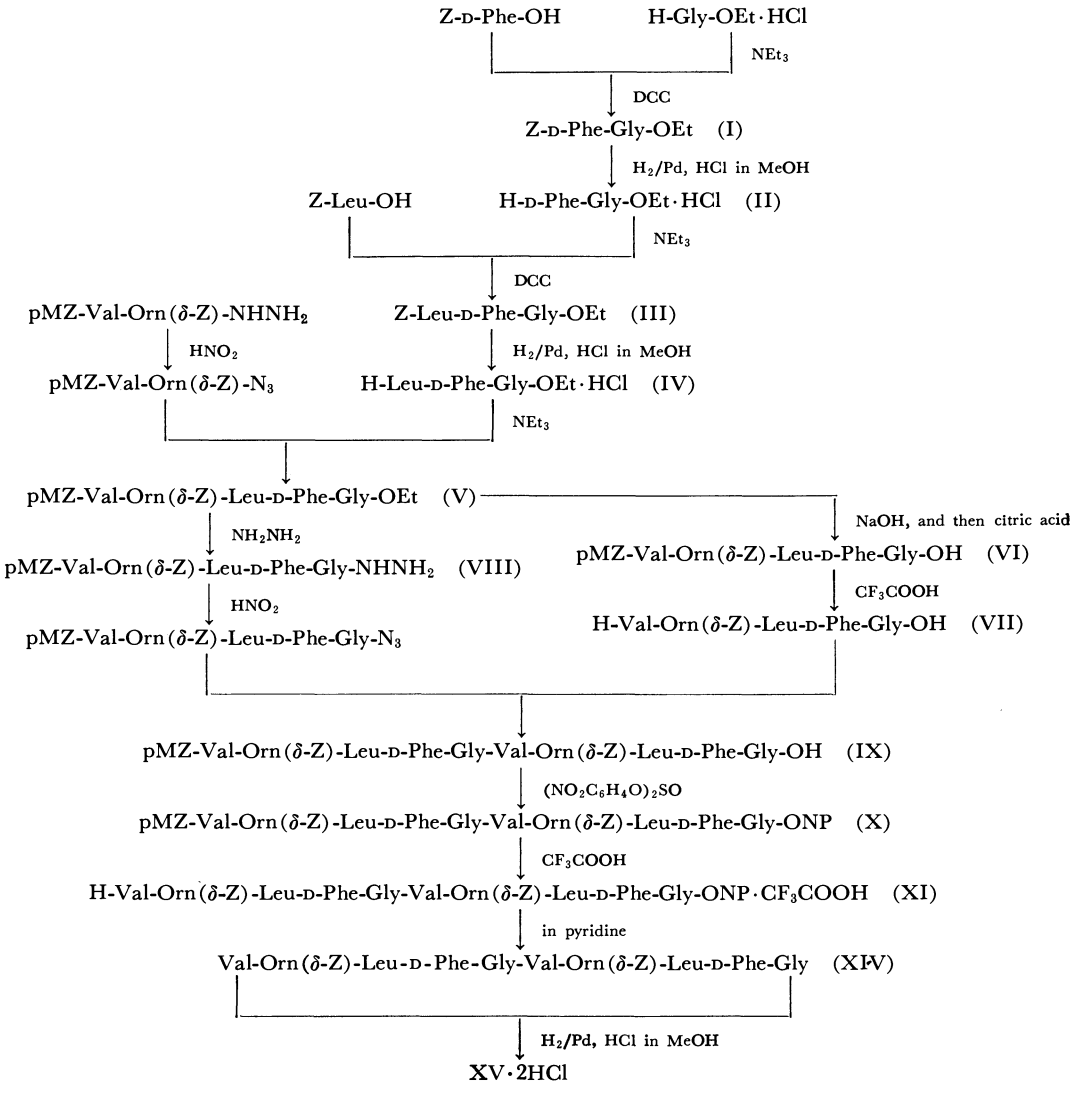
Syntheses of relatively large cyclic peptides have been reported from several laboratories in recent years. Cyclic hepta-[5] and octapeptide[6] related to polymyxin have been synthesized from the respective linear peptide via the carbodiimide. However, cyclic decapeptides have generally been obtained in better yields from the respective linear decapeptide active ester.[7,8] Furthermore, the cyclization reaction of linear pentapeptide active esters, wherein proline residues are C-terminuses, gave cyclic decapeptide in good yields by the dimerization reaction.[9,10] For these reasons, we have decided to attempt the synthesis of a cyclic decapeptide with the appropriate amino acid sequence.

It is well known that, in many polypeptides, a proline residue causes a kink in a peptide chain.[11] It has been reported that, in gramicidin S, the presence of proline might facilitate the formation of a stable conformation.[10] Therefore, it appeared of interest to synthesize an analog (XV) of the cyclic decapeptide gramicidin S, wherein proline residues are replaced by glycines, in order to determine to what degree the proline side chains contribute to the biological activity.

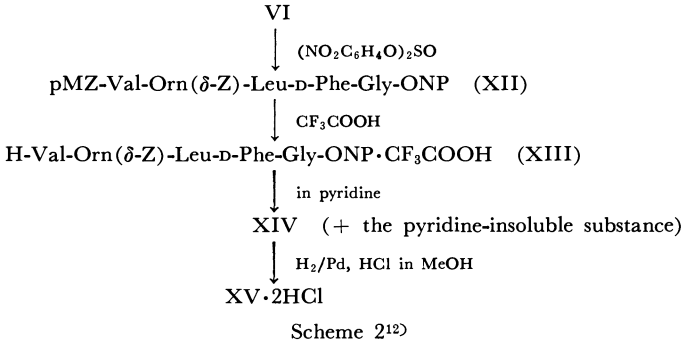
L-Val-L-Orn-L-Leu-D-Phe-Gly
↑ ↓
Gly-D-Phe-L-Leu-L-Orn-L-Val
XV

The reaction sequences employed for the synthesis of XV are shown in Schemes 1 and 2. The cyclic benzyloxycarbonyl-substituted decapeptide (XIV) was obtained both by the cyclization reaction of the decapeptide active ester (XI) (Scheme 1) and by the dimerization reaction of the pentapeptide active ester (XIII) (Scheme 2). It was found that the yield of XIV by the cyclization of XI was satisfactory, but that that by the dimerization reaction was only 10—15%, because a considerable amount of the unidentified pyridine insoluble product was formed. It should be noted that Schwyzer and Sieber, by the dimerization reaction, obtained tosyl-substituted gramicidin S in a satisfactory yield for the pertinent pentapeptide active ester, wherein a proline residue is the C-

1) A part of this work has already been briefly communicated: H. Aoyagi, T. Kato, M. Ohno, M. Kondo and N. Izumiya, *J. Am. Chem. Soc.*, **86**, 5700 (1964).
2) B. F. Erlanger and L. Goode, *Nature*, **174**, 80 (1954); *Science*, **131**, 669 (1960).
3) T. Kato, M. Kondo, M. Ohno and N. Izumiya, This Bulletin, **38**, 1202 (1965).
4) T. Kato and N. Izumiya, unpublished.
5) R. O. Studer, W. Lergier and K. Vogler, *Helv. Chim. Acta*, **46**, 612 (1963); K. Vogler, R. O. Studer, P. Lanz, W. Lergier, E. Bohni and B. Fust, ibid., **46**, 2823 (1963).
6) K. Vogler, R. O. Studer, W. Lergier and P. Lanz, ibid., **43**, 175 (1960); R. O. Studer, K. Vogler and W. Lergier, ibid., **44**, 131 (1961).
7) R. Schwyzer and P. Sieber, ibid., **40**, 624 (1957).
8) R. Schwyzer and P. Sieber, ibid., **41**, 1582 (1958).
9) German Patent, *Chem. Abstr.*, **57**, 949 (1962).
10) R. Schwyzer and P. Sieber, *Helv. Chim. Acta*, **41**, 2186 (1958).
11) A. F. Cullis, H. Muirhead, M. F. Perutz, M. G. Rossmann and A. C. T. North, *Proc. Roy. Soc.*, **A265**, 161 (1962); M. F. Perutz, *Nature*, **194**, 914 (1962).




Scheme 1[12]




Scheme 2[12]

12) The abbreviations used are: pMZ, *p*-methoxybenzyloxycarbonyl; Z, benzyloxycarbonyl; DCC, dicyclohexylcarbodiimide; ONP, *p*-nitrophenoxy ester. An amino acid residue except Gly and D-Phe is of L-configuration.

terminus.[10] The final product (XV) was obtained as colorless crystals with six moles of the water of crystallization, and its homogeneity was demonstrated by chromatography in many solvent systems.

The cyclic decapeptide (XV) was found to be much more active than gramicidin S against *B. subtilis* in a synthetic medium (Table I). This finding shows that the replacement of the proline residues by glycines in the sequence of gramicidin S does not reduce the activity, demonstrating that not all the original amino acid sequences in the natural peptide are necessary for the full activity; e.g., the side chain of proline is not required. It should be noted that homo-gramicidin S, wherein the ornithine residues are replaced by lysines, exhibits an activity nearly equal to that of the natural gramicidin S.[10] On the other hand, it appears that the valine residues in gramicidin S are of importance in the activity.[13]

In order to extend further the study of the relationship between the chemical structure and the biological activities of peptide antibiotics, experiments on the preparation of and studies in the properties of several cyclic and linear peptides are in progress in this laboratory.

## Experimental

All melting points are uncorrected.

**Benzyloxycarbonyl-D-phenylalanylglycine Ethyl Ester (I).** — To a solution of benzyloxycarbonyl-D-phenylalanine (2.99 g.) and glycine ethyl ester hydrochloride (1.40 g.) in chloroform (40 ml.), triethylamine (1.4 ml.) and dicyclohexylcarbodiimide[14] (2.06 g.) were added at 0°C. After it had been permitted to stand overnight at 0°C, the mixture was evaporated in vacuo, the residue diluted with ethyl acetate (50 ml.), and the dicyclohexylurea formed was filtered off. The filtrate was washed successively with 4% sodium bicarbonate, 3% hydrochloric acid, and water and dried over anhydrous sodium sulfate. The filtered solution was evaporated in vacuo. The residual oil solidified after ether and petroleum ether had been added. Recrystallization from ethyl acetate - petroleum ether gave 3.18 g. (83%); m. p. 109—110°C; $[\alpha]_D^{18}$ +20.5° (*c* 2, methanol).

Found: C, 65.86; H, 6.56; N, 7.33. Calcd. for $C_{21}H_{24}O_5N_2$: C, 65.61; H, 6.29; N, 7.29%.

This compound had been previously obtained by the acid chloride method; m. p. 109—111°C.[15]

**D-Phenylalanylglycine Ethyl Ester Hydrochloride (II).**—I (2.69 g.) was subjected to hydrogenolysis in the presence of palladium black and 0.31 N methanolic hydrogen chloride (24.8 ml.). The filtrate from the catalyst was then evaporated to dryness in vacuo. The product was obtained as a hygroscopic powder; yield, 2.01 g. (100%); $R_f$ 0.88[16] and 0.74[17].

**Benzyloxycarbonyl-L-leucyl-D-phenylalanylglycine Ethyl Ester (III).**—Benzyloxycarbonyl-L-leucine (1.86 g.) was coupled with II (2.01 g.) by dicyclohexylcarbodiimide (1.44 g), following the procedure described for the preparation of I. Recrystallization from ethyl acetate - ether gave 2.79 g. (80%); m. p. 122—124°C; $[\alpha]_D^{25}$ +13.0° (*c* 2, methanol).

Found: C, 64.75; H, 7.07; H, 7.07; N, 8.33. Calcd. for $C_{27}H_{35}O_6N_3$: C, 65.17; H, 7.09; N, 8.45%.

**L-Leucyl-D-phenylalanylglycine Ethyl Ester Hydrochloride (IV).**—III (1.99 g.) was subjected to hydrogenolysis in the presence of palladium black and 0.46 N methanolic hydrogen chloride (9.6 ml.), and then treated as described in the preparation of II. Yield of oily product: 1.61 g. (100%); $R_f$ 0.90[16] and 0.77[17].

***p*-Methoxybenzyloxycarbonyl-L-valyl-δ-benzyloxycarbonyl-L-ornithyl-L-leucyl-D-phenylalanylglycine Ethyl Ester (V).**—The following operations were carried out in a cold room. Into a chilled solution of *p*-methoxybenzyloxycarbonyl-L-valyl-δ-benzyloxycarbonyl-L-ornithine hydrazide[3] (0.98 g.) in glacial acetic acid (12 ml.), N hydrochloric acid (4 ml.) and sodium nitrite (136 mg.) in water (2 ml.) were stirred. After 6 min., cold water (100 ml.) was added to the solution. The azide which precipitated as a white mass was collected by filtration and washed with water, 4% sodium bicarbonate, and water, and then dried under a vacuum in a desiccator. The azide was added to a solution of IV (0.72 g.) and triethylamine (0.25 ml.) in dimethylformamide (20 ml.), and then the mixture was stirred for 3 days at 0°C. The precipitate which formed upon the addition of water (300 ml.) to the solution was collected, washed with 4% sodium bicarbonate, 0.5 M citric acd and water, and dried. The product was recrystallized from dioxane-ether; yield, 1.30 g. (83%); m. p. 206—208°C; $[\alpha]_D^{25}$ −23.5° (*c* 1, acetic acid); $R_f$ 0.87.[17]

Found: C, 63.02; H, 7.15; N, 9.94. Calcd. for $C_{46}H_{62}O_{11}N_6$: C, 63.14; H, 7.14; N, 9.61%.

***p*-Methoxybenzyloxycarbonyl-L-valyl-δ-benzyloxycarbonyl-L-ornithyl-L-leucyl-D-phenylalanylglycine (VI).**—To a solution of V (872 mg.) in a mixture of methanol (50 ml.) and dioxane (20 ml.), N sodium hydroxide (1.5 ml.) was added; the solution was then allowed to stand overnight at room temperature. After the addition of 0.5 M citric acid (6 ml.) under cooling, the solution was concentrated in vacuo at low temperature, and the residue was treated with water (100 ml.). After they had been stored in a refrigerator, the crystals were collected by filtration, washed with water, and dried. Recrystallization from dioxane-ether gave 712 mg. (84%) of VI; m. p. 214—215°C; $[\alpha]_D^{25}$ −21° (*c* 1, acetic acid); $R_f$ 0.82.[17]

Found: C, 61.95; H, 6.88; N, 10.00. Calcd. for $C_{44}H_{58}O_{11}N_6$: C, 62.39; H, 6.90; N, 9.92%.

13) T. Kato, M. Ohno, M. Kondo, Y. Fujita and N. Izumiya, 6th International Congress of Biochemistry, New York, N. Y. (1964), p. 159.

14) J. C. Sheehan and G. P. Hess, *J. Am. Chem. Soc.*, **77**, 1067 (1955).

15) O. K. Behrens, D. G. Doherty and M. Bergmann, *J. Biol. Chem.*, **136**, 61 (1940).

16) The $R_f$ of the paper chromatography with Toyo Roshi No. 52 refers to the *n*-butanol - acetic acid - pyridine - water (4 : 1 : 1 : 2, v./v.) system.

17) The $R_f$ of the thin layer chromatography with Merck silica gel G refers to the *n*-butanol - acetic acid - pyridine - water (4 : 1 : 1 : 2, v./v.) system. Compounds possessing a free amino group were detected by spraying with ninhydrin, and those with blocked amino groups, by spraying with 47% hydrobromic acid, and then ninhydrin.

**L-Valyl-δ-benzyloxycarbonyl-L-ornithyl-L-leucyl-D-phenylalanylglycine (VII).**—To a mixture of VI (434 mg.) and anisole (0.16 ml.) trifluoroacetic acid (2 ml.) was added at 0°C.[18] After being permitted to stand for 20 min. at 0°C, the solution was evaporated in vacuo. The residue was triturated with ether (20 ml.) and washed repeatedly with ether by decantation. The residual crystals were dissolved in water. After triethylamine (1 ml.) had been added, the solution was evaporated to dryness in vacuo. The crystalline product was collected by filtration with the aid of water; yield, 260 mg. (76%); m. p. 191—192°C; $[\alpha]_D^{25}$ −4.2° (*c* 1, acetic acid); $R_f$ 0.85.[17]

Found: C, 60.96; H, 7.37; N, 12.05. Calcd. for $C_{35}H_{50}O_8N_6 \cdot 1/2H_2O$; C, 60.76; H, 7.43; N, 12.15%.

***p*-Methoxybenzyloxycarbonyl-L-valyl-δ-benzyloxycarbonyl-L-ornithyl-L-leucyl-D-phenyalanylglycine Hydrazide (VIII).**—To a solution of V (440 mg.) in dimethylformamide (4 ml.) hydrazine hydrate (0.5 ml.) was added; the solution was allowed to stand for 2 days at room temperature. The reaction mixture was evaporated in vacuo. The hydrazide which precipitated upon the addition of water (20 ml.) was filtered, washed with water, and dried. It was recrystallized from methanol-ethyl acetate-ether; yield, 372 mg. (87%); m. p. 217—219°C; $[\alpha]_D^{25}$ −20° (*c* 1, acetic acid); $R_f$ 0.91.[17]

Found: C, 60.84; H, 7.15; N, 12.89. Calcd. for $C_{44}H_{60}O_{10}N_8$: C, 61.38; H, 7.02; N, 13.02%.

***p*-Methoxybenzyloxycarbonyl-L-valyl-δ-benzyloxycarbonyl-L-ornithyl-L-leucyl-D-phenylalanylglycyl-L-valyl-δ-benzyloxycarbonyl-L-ornithyl-L-leucyl-D-phenylalanylglycine (IX).**—Into a solution of VIII (345 mg.) in dimethylformamide (7 ml.), N hydrochloric acid (1.2 ml.) and sodium nitrite (30 mg.) in water (0.5 ml.) were stirred. After 5 min., cold water (100 ml.) was added to the solution. The azide which precipitated was filtered and treated as described in the preparation of V. The azide was added to a solution of VII (273 mg.) in a mixture of dimethylformamide (8 ml.) and triethylamine (0.055 ml.), and then the mixture was stirred for 3 days at 0°C. The insoluble material was removed by by filtration, and the filtrate was concentrated in vacuo. The precipitate which was formed upon the addition of ethyl acetate (10 ml.) and ether (4 ml.) to the concentrated filtrate was collected, washed with 0.5 M citric acid and water, and dried. Recrystallization from dimethylformamide-ethyl acetate-ether did not raise the melting point. The yield was 495 mg. (82%); m. p. 253—257°C; $[\alpha]_D^{25}$ −48° (*c* 0.5, acetic acid); $R_f$ of hydrogenated product of IX, 0.60.[17]

Found; C, 61.77; H, 7.18; N, 10.94. Calcd. for $C_{79}H_{106}O_{18}N_{12} \cdot H_2O$; C, 62.02; H, 7.12; N, 10.99%.

**Cyclo-(L-valyl-δ-benzyloxycarbonyl-L-ornithyl-L-leucyl-D-phenylalanylglycyl)$_2$ (XIV).**—*XIV (from deca).*—To a solution of IX (612 mg., 0.4 mmol.) in a mixture of dimethylformamide (3 ml.) and pyridine (0.95 ml.) di-*p*-nitrophenyl sulfite[19] (1.30 g., 4 mmol.) was added; the reaction mixture was then allowed to stand for 24 hr. at room temperature. After evaporation, the oily product was triturated with petroleum ether and washed repeatedly with a mixture of ether and petroleum ether (1:1) by decantation until no yellow color could be discerned on the addition of a sodium hydroxide solution to the washings. The product was filtered, washed with a mixture of ether and petroleum ether (1:1), and dried. It weighed 648 mg. This product was dissolved in dimethylformamide-N sodium hydroxide (1:1 v./v.), and the content of *p*-nitrophenyl ester was estimated by measuring the optical density of the solution at 412 mμ.[7] The purity of the compound was estimated to be 70%.

To the *p*-nitrophenyl ester X (638 mg.) anisole (0.5 ml.) and trifluoroacetic acid (3.5 ml.) were added at 0°C. The solution was evaporated in vacuo at 0°C, and the residue was triturated with ether. The decapeptide *p*-nitrophenyl ester trifluoroacetate (XI) was collected, washed with ether, and dissolved in dimethylformamide (12 ml.) containing glacial acetic acid (0.1 ml.). The solution was then stirred drop by drop into pyridine (120 ml.) which had been kept at 55—60°C over a period of 5 hr.; the stirring was then continued for an additional 2 hr. at the same temperature. After the solvent had been removed, the residual oil was dissolved in a mixture of methanol (150 ml.) and water (60 ml.). The insoluble substance was removed by filtration, and the filtrate was passed successively through columns of Dowex 1 ($OH^-$ form, 2.7×11 cm.) and Dowex 50 ($H^+$ form, 2.5×10 cm.). The columns were then washed with the same solvent (200 ml.), the combined effluent was evaporated to dryness in vacuo, and the product was suspended in water (30 ml.), filtered, and dried (246 mg.). The product was recrystallized from methanol-ether; yield, 211 mg. (38%) (named as XIV (from deca)); m. p. 248—250°C; $[\alpha]_D^{17}$ −127° (*c* 0.5, acetic acid); $R_f$ 0.93.[17]

Found: C, 60.62; H, 7.40; N, 12.25. Calcd. for $C_{70}H_{96}O_{14}N_{12} \cdot 3H_2O$: C, 60.76; H, 7.43; N, 12.15%.

The molecular weight of XIV (from deca) was determined by a Model 301A osmometer, Mechrolab Inc. solvent methanol).

Found: 1420. Calcd. for $C_{70}H_{96}O_{14}N_{12} \cdot 3H_2O$: 1384.

The air-dried compound lost 3.4% of its weight after it had been dried over phosphorus pentoxide for 2 hr. at 100°C; 2 mmHg. Calcd. for $3H_2O$: 3.9%.

*XIV (from penta).*—To a solution of VI (508 mg., 0.6 mmol.) in dimethylformamide (2 ml.) pyridine (0.2 ml.) and di-*p*-nitrophenyl sulfite (778 mg., 2.4 mmol.) were added. The reaction mixture was allowed to stand for 24 hr. at room temperature and treated as has been described above. The product (XII) obtained weighed 548 mg. The purity of the compound was estimated to be 78%.

To the *p*-nitrophenyl ester XII (538 mg.) anisole (0.5 ml.) and trifluoroacetic acid (3 ml.) were added. The solution was evaporated in vacuo, and the residue was triturated with ether. The pentapeptide *p*-nitrophenyl ester trifluoroacetate (XIII) was filtered, and then dissolved in dimethylformamide (10 ml.) containing glacial acetic acid (0.1 ml.). The solution was stirred drop by drop into pyridine (100 ml.) at 55—60°C as has been described above. During the stirring a crystalline precipitate appeared. After the completion of the reaction, the mixture was cooled to room temperature, and the crystals were filtered and washed with pyridine. It weighed 173 mg.[20] The filtrate was

18) F. Weygand and K. Hunger, *Chem. Ber.*, **95**, 1 (1962).
19) B. Iselin and R. Schwyzer, *Helv. Chim. Acta*, **43**, 1760 (1960).
20) Experiments on the properties of this pyridine-insoluble substance are in progress in this laboratory.

evaporated in vacuo. The residue was dissolved in a mixture with methanol (120 ml.) and water (40 ml.), and the solution was treated with the columns of Dowex 1 and 50 as has been described above. Recrystallization from methanol-ether gave 40 mg. (10%); m. p. 247—251°C[21]; $[\alpha]_D^{17}$ −123° (*c* 0.5, acetic acid); $R_f$ 0.93.[17]

Found: C, 61.31; H, 7.30; N, 12.20. Calcd. for $C_{70}H_{96}O_{14}N_{12}\cdot 3H_2O$: C, 60.76; H, 7.43; N, 12.15%.

When the procedure with the same scale was repeated, the yields of XIV (from penta) and the pyridine-insoluble substance were 62 mg. (15%) and 170 mg. respectively.

**Cyclo-(L-valyl-L-ornithyl-L-leucyl-D-phenylalanylglycyl)$_2$ Dihydrocloride (XV).** — *XV (from deca).*— XIV (from deca) (82 mg., 0.06 mmol.), dissolved in methanol (1 ml.) and 0.065 N methanolic hydrogen chloride (2 m.), was subjected to hydrogenolysis in the presence of palladium black. After it had been filtered from the catalyst, the solution was evaporated to dryness in vacuo, The crystals which remained were then filtered with the aid of a mixture of acetone and ether (4: 1); yield of air-dried product, 66 mg. (88%); m. p. 227—230°C; $[\alpha]_D^{17}$ −190° (*c* 0.5, ethanol); $R_f$ 0.90,[16] 0.77,[17] 0.91[22] and 0.78[23].

Found: C, 52.06; H, 7.98; N, 13.28. Calcd. for $C_{54}H_{86}O_{10}N_{12}Cl_2\cdot 6H_2O$: C, 52.20; H, 7.95; N, 13.53%.

The air-dried product lost 2.9% of its weight when it was left in a desiccator with calcium chloride at room temperature. Calcd. for $2H_2O$: 2.9%. The air-dried product lost 8.8% of its weight after it had been dried over phosphorus pentoxide for 2 hr. at 120°C; 2 mmHg. Calcd. for $6H_2O$: 8.7%. The product was treated with dinitrofluorobenzene in the usual manner.[24] After the hydrolysis of the dinitrophenylated compound (DNP-XV), only one DNP-amino acid identified as δ-DNP-ornithine was detected on the paper chromatogram; $R_f$ 0.64.[16]

*XV (from penta).* — XIV (from penta) (6.9 mg., 5 μmol.) was dissolved in methanol (0.5 ml.) and 0.05 N methanolic hydrogen chloride (0.22 ml.) and treated as has been mentioned above. Crystals were obtained; yield, 4.5 mg. (80%). $R_f$ values of the crystals (XV (from penta)) were identical with those of XV (from deca). 0.90,[16] 0.77,[17] 0.91[22] and 0.77[23]. Furthermore, the identity of XV (from deca) with XV (from penta) was confirmed by paper electrophoresis carried out with 500 V. for 2 hr., using a solvent of formic acid - acetic acid - methanol - water (1: 3: 6: 10, v./v.; pH 1.8) and Toyo Roshi No. 52 paper.

**The Amino Acid Analysis of XV.**—Quantitative amino acid analysis was performed as follows. XV (ca. 0.6 mg.) was hydrolyzed with 6 N hydrochloric acid at 110°C for 48 hr. Each of the hydrolysates of XV from deca and penta was dissolved in 0.1 ml. of

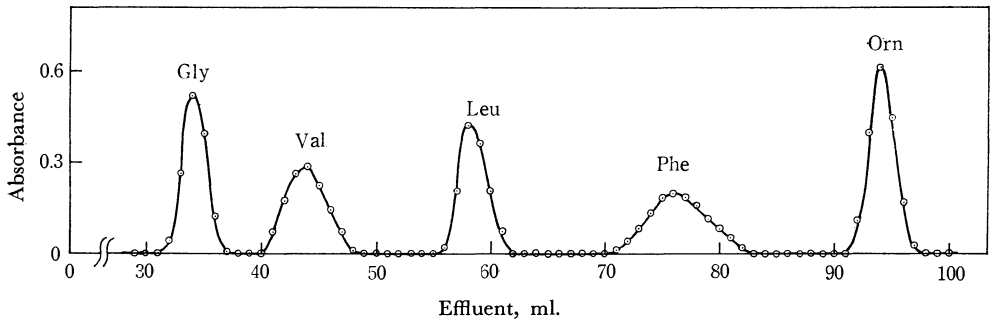



Fig. 1. Chromatogram of the hydrolysate of XV (from deca).

Table I. Amount of compound necessary for complete inhibition of growth (μg./ml.)

| Compound | Synthetic medium[a] | | Bouillon agar medium[b] | |
|---|---|---|---|---|
| | *E. coli*[c] | *B. subtilis*[d] | *E. coli*[c] | *B. subtilis*[d] |
| XV (from deca) | >100 | 1> | <100 | 20 |
| XV (from penta) | >100 | 1> | <100 | 20 |
| Gramicidin S sulfate[e] | >100 | 10 | <100 | 10 |

a) Stephenson-Whetham's medium (modified); $KH_2PO_4$ 1g., NaCl 1 g., $FeSO_4\cdot 7H_2O$ 0.7 g., Na-glutamate 4 g., glucose 5 g./1000 ml. and agar 20 g.
b) Usual bouillon agar medium, pH 7.0.
c) *Escherichia coli IRO 3044.*
d) *Bactllus subtilis PCI 219.*
e) A product of Astra Co., U. S. A. This contains eight moles of water of crystallization.

21) The melting point was not depressed by admixture with XIV (from deca).
22) The $R_f$ of the paper chromatography with Toyo Roshi No. 52 refers to the *t*-butanol - formic acid - water (75 : 15 : 10, v./v.) system.
23) The $R_f$ of the thin layer chromatography with Merck silica gel G refers to the *t*-butanol - formic acid - water (75 : 15 : 10, v./v.) system.
24) F. Sanger and E. O. P. Thompson, *Biochem. J.*, **53**, 353 (1953).

a 0.1 M citrate buffer (pH 3.1),[25] the solution was applied to a column (0.9×15 cm.) with Aminex Q-150 (31—45 microns, $Na^+$ form), and development was continued with the same solvent. Elution was carried out at about 20°C, the flow rate was 20—25 ml. per hr., and 1-ml. fractions were collected. The eluting solvent was replaced with a 0.1 M citrate buffer of pH 4.25[26] at fraction 35, and with a 0.2 N buffer of pH 9.2[26] at fraction 75. The amino acid contents in the fractions were determined by the modified ninhydrin reagent described by Yemm and Cocking.[27] A typical chromatogram is shown in Fig. 1. Quantitative amino acid determinations of XV from deca and penta gave the molar ratios of 1.0: 1.1: 1.0: 1.1: 1.1 and 1.0: 0.9: 1.0: 1.0: 1.0 for valine, ornithine, leucine, phenylalanine and glycine respectively.

**Microbiological Assays.**—The microrganisms employed are shown in Table I. A minimum amount of the compounds necessary for the complete inhibition of growth was determined by a dilution method with a bouillon agar medium and with a synthetic medium. As is shown in Table I, the cyclodecapeptide was found to be much more active than natural gramicidin S against *B. Subtilis* in a synthetic medium.

## Summary

A cyclic decapeptide, cyclo-(L-valyl-L-ornithyl-L-leucyl-D-phenylalanylglycyl)$_2$, has been synthesized in an attempt to obtain information about the relation of the structure to the antibacterial activity of gramicidin S.

The synthesis of the cyclic decapeptide was achieved in two ways. The condensation of *p*-methoxybenzyloxycarbonyl-L-valyl-δ-benzyloxycarbonyl-L-ornithyl-L-leucyl-D-phenylalanylglycine azide with L-valyl-δ-benzyloxycarbonyl-L-ornithyl L-leucyl-D-phenylalanylglycine afforded the corresponding N-blocked decapeptide, which was converted to the *p*-nitrpohenyl ester by the action of di-*p*-nitrophenyl sulfite. After the *p*-methoxybenzyloxycarbonyl group had been removed with trifluoroacetic acid, the decapeptide *p*-nitrophenyl ester was transformed to the cyclic benzyloxycarbonyl-substituted decapeptide by treatment with pyridine. On the other hand, this compound was also obtained by a dimerization reaction of L-valyl-δ-benzyloxycarbonyl-L-ornithyl-L-leucyl-D-phenylalanylglycine *p*-nitrophenyl ester. In the latter case, however, the yield was poor. The cyclic benzyloxycarbonyl-substituted decapeptide was hydrogenated in the presence of palladium black to give the desired cyclic decapeptide dihydrochloride.

The effects of the synthesized cyclic decapeptide on bacterial growth have also been examined. It was observed that the compound was about ten times as active as gramicidin S against *B. subtilis* in a synthetic medium; however, it showed silghtly less activity than gramicidin S in a bouillon agar medium.

The authors wish to express their thanks to Dr. Motoo Shibata of the Takada Chemical Industries, Ltd., for his microbiological assays. Thanks are also due to Ajinomoto Co., Inc., and Kyowa Hakko Kogyo Co., Ltd., for supplying some amino acids.

*Laboratory of Biochemistry*
*Faculty of Science*
*Kyushu University*
*Fukuoka*

25) S. Moore and W. H. Stein, *J. Biol. Chem.*, **211**, 893 (1954).
26) S. Moore and W. H. Stein, ibid., **192**, 663 (1951).
27) E. W. Yemm and E. C. Cocking, *Analyst*, **80**, 209 (1955); *Biochem. J.*, **58**, xii (1954).

# The Electronic Structure of Some Hydrides, Halides and Alkyl Compounds of Boron and Aluminum. I. Monomers and Ions

By Hiroshi KATO, Kaichiro YAMAGUCHI, Teijiro YONEZAWA and Kenichi FUKUI

(Received May 24, 1965)

Boron and aluminum atoms are known as typical group III elements of the periodic table which are very electro-positive and which are strong electron acceptors. Many experimental studies have been performed on compounds containing these two elements,[1] and theoretical investigations have been performed, especially on the basis of the valency theory.[2]

In the present paper, some boron and aluminum compounds, i.e., hydrides, halides, alkyl compounds, and their related ions will be treated by

1) "Organometallic Chemistry," Ed. by H. Zeiss, Reinhold Pub., New York (1960).

2) E. g., C. A. Coulson, "Valence," Oxford (1952), II (1961).

Table I. The values of the Coulomb integrals (eV.) and the effective nuclear charges ($Z^*$)

| | | H | B | C | F | Al | Cl |
|---|---|---|---|---|---|---|---|
| | $Z^*$ | 1.00 | 2.60 | 3.25 | 5.20 | 3.50 | 6.10 |
| $H_{ii}$[a] | $s$ | −13.60 | −15.15 | −21.43 | −40.16 | −12.74 | −25.26[b] |
| | $p$ | — | − 8.53 | −11.42 | −20.98 | − 6.67 | −15.09 |

a) H. A. Skinner and H. O. Pritchard, *Chem. Revs.*, **53**, 745 (1955).
b) Estimated value by the observed atomic spectra (C. E. Moore, "Atomic Energy Levels").

the extended Hückel method proposed by Hoffmann.[3] The electronic structures and some physico-chemical properties of these compounds, such as their electron-accepting characters, and the stabilities of these monomers will be investigated. In addition, a problem of stereochemical interest—the two configurations of the $B_2Cl_4$ molecule—will be briefly discussed.

The electronic structure of the dimers will be treated in Part II, while the aspects of the chemical behavior which are important in the synthetic process will be discussed in Part III.

## The Parameters Used

In the present method, the values of the Coulomb integral, $H_{ii}$ are given by changing the sign of the valence-state ionization potentials of valence electrons, and the values of the resonance integral, $H_{ij}$, are evaluated by the following equation:[3]

$$H_{ij}=0.875(H_{ii}+H_{jj})S_{ij}$$

where $S_{ij}$ is the overlap integral between the $i$th and the $j$th atomic orbitals (AO). The adopted values of the Coulomb integrals and the effective nuclear charges of various AO's are collected in Table I, where the notations $s$ and $p$ denote the values of $H_{ii}$ of the 2s and 2p orbitals for the second row elements and of the 3s and 3p orbitals for the third row elements of the periodic table respectively.

The bond distances and the bond angles are determined with reference to those cited in Ref. 4. Those values which have not yet been measured are estimated on an assumption that, for example, the B–H bond distance in the monomeric $BH_3$ is equal to the terminal B-H distance in the dimer. These values are cited in Table II, together with their symmetry groups.

Table II. The adopted values of the bond distances, bond angles and symmetries of various compounds

| Compounds | Sym. | Bond distance (Å) and bond angle (deg.)* |
|---|---|---|
| $BH_3$ | $C_{3v}$ | B-H=1.187 |
| $BH_4^-$ | $T_d$ | B-H=1.25 |
| $BCl_3$ | $D_{3h}$ | B-Cl=1.75 |
| $BF_3$ | $D_{3h}$ | B-F=1.30 |
| $BF_4^-$ | $T_d$ | B-F=1.40 |
| $B_2Cl_4$ | $D_{2d}$, $D_{2h}$ | B-B=1.77, B-Cl=1.73, ∠ClBCl=120 |
| $BH(CH_3)_2$ | $C_{2v}$ | B-H=1.20, B-C=1.56, ∠HBC=120 |
| $B(CH_3)_3$ | $C_{3v}$ | B-C=1.56 |
| $BC_2H_3(CH_3)_2$ / $B(C_2H_3)_2CH_3$ | $C_{2v}$ | B-C=1.56, ∠CBC=120 |
| $B(C_2H_3)_3$ | $C_{3v}$ | B-C=1.56, ∠CBC=120 |
| $AlH_3$ | $C_{3v}$ | Al-H=1.65 |
| $AlH_4^-$ | $T_d$ | Al-H=1.70 |
| $AlCl_3$ | $D_{3h}$ | Al-Cl=2.10 |
| $AlCl_4^-$ | $T_d$ | Al-Cl=2.13 |
| $Al(CH_3)_2Cl$ | $C_{2v}$ | Al-Cl=2.1, Al-C=2.0, ∠ClAlC=∠CAlC=120 |
| $Al(CH_3)_3$ | $C_{3v}$ | Al-C=2.0 |
| $Al(C_2H_5)_3$ | $C_{3v}$ | Al-C=2.0 |

* As to the methyl, ethyl and vinyl groups, the used values are as same as ones in these parent molecules.

## Results and Discussion

The calculated values of the atomic population of an atom X, $M(X)$, and the atom bond populations between X atoms and Y atoms, $M(X–Y)$, for various monomers and ions are summarized in Fig. 1.

**The Charge Distribution in Monomers.**—By referring to the values of $M(X)$ in Fig. 1, it may be seen that boron atoms have positive charges and that aluminum atoms are more positive in these monomers. That is to say, even in the $BH_3$ and $AlH_3$ molecules, each hydrogen atom bears more than one unit charge, and, in their alkyl compounds, the boron-carbon and aluminum-carbon bond are polarized in such a way as $B^{+\delta}$–$C^{-\delta}$ and $Al^{+\delta}$–$C^{-\delta}$. The atomic population of the methylene carbon atom in triethyl aluminum, 4.897, is larger than that of the methyl carbon atom, 4.386. This finding agrees with that of the NMR study described in Ref. 1. In the halides of boron and aluminum, the polarization of M–X bonds (M=boron or aluminum and X=halogens) is more remarkable than in alkyl compounds. An example is presented by the aluminum trichloride monomer, in which the value of $M(Al)$ is calculated to be 1.029 and that of $M(Cl)$ as 7.657. In this connection the result of Casabella et al. is worth our attention. They estimated, by the PQR

3) R. Hoffmann, *J. Chem. Phys.*, **39**, 1397 (1963); ibid., **40**, 2474 (1964).

4) A. D. Mitchell, L. C. Cross L. E. Sutton and D. G. Jenkin, "Table of Interatomic Distances and Configuration in Molecules and Ions," The Chemical Society, London (1958).

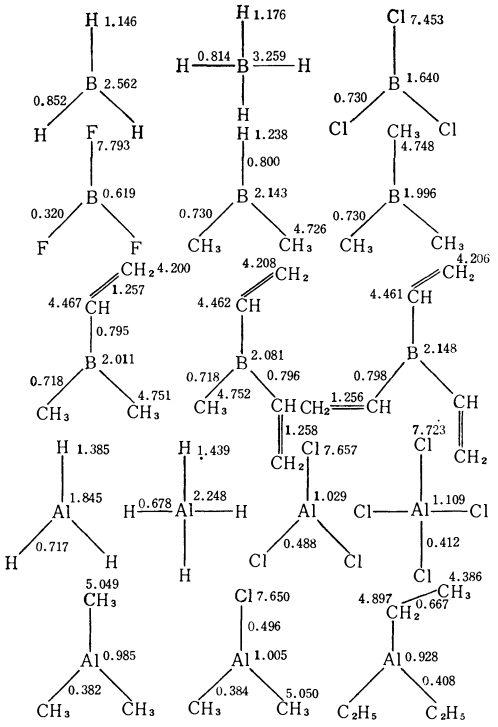


Fig. 1. The $M(X)$ and $M(X\text{-}Y)$ values of various compounds.

measurement, that the total electronic densities of various atoms in the aluminum tribromide dimer are 1.26 on the aluminum atom, 7.65 on the terminal bromine atom, and 7.44 on the bridged bromine atom.[5] With these values in mind, our results are not very extreme.

TABLE III. THE $N(r)$ VALUES ON THE BORON AND ALUMINUM ATOMS IN VARIOUS MONOMERS

| | $N$(s) | $N$(x) | $N$(y) | $N$(z) |
|---|---|---|---|---|
| (a) B-Compounds | | | | |
| $BH_3$ | 0.912 | 0.825 | 0.825 | 0.0 |
| $BF_3$ | 0.295 | 0.122 | 0.122 | 0.082 |
| $BH(CH_3)_2$ | 0.861 | 0.546 | 0.624 | 0.113 |
| $B(CH_3)_3$ | 0.812 | 0.522 | 0.522 | 0.140 |
| $BC_2H_3(CH_3)_2$ | 0.818 | 0.509 | 0.534 | 0.150 |
| $B(C_2H_3)_2CH_3$ | 0.823 | 0.553 | 0.526 | 0.175 |
| $B(C_2H_3)_3$ | 0.833 | 0.556 | 0.553 | 0.207 |
| $BCl_3$ | 0.646 | 0.387 | 0.387 | 0.220 |
| (b) Al-Compounds | | | | |
| $AlH_3$ | 0.850 | 0.497 | 0.497 | 0.0 |
| $Al(CH_3)_3$ | 0.603 | 0.165 | 0.165 | 0.052 |
| $Al(CH_3)_2Cl$ | 0.569 | 0.176 | 0.187 | 0.073 |
| $AlCl_3$ | 0.505 | 0.206 | 0.206 | 0.111 |
| $Al(C_2H_5)_3$ | 0.594 | 0.142 | 0.142 | 0.042 |

(s: 2s or 3s AO; x, y, z: 2px or 3px, 2py or 3py, 2pz or 3pz AO's)

5) P. A. Casabella, P. J. Bray and R. G. Barnes, *J. Chem. Phys.*, **30**, 1393 (1959).

The atomic orbital populations of the $r$th AO, $N(r)$, are collected in Table III(a) for the boron atoms and in Table III(b) for the aluminum atoms in various monomers, where the pz orbitals of these atoms consist of the $p\pi$ orbitals of these monomers. In $BH_3$ and $AlH_3$ molecules, the values of $N$(s) (the s denotes the 2s orbital on boron or the 3s orbital on aluminum) are almost comparable to those of $N$(x) and $N$(y), and $N$(z) is zero at both atoms (x, y, and z denote 2px, 2py, and 2pz AO's on boron or 3px, 3py, and 3pz AO's on aluminum). This result may be interpreted as meaning that in these atoms the promotion of the valence eletrons occurs from the $s^2p$ ground state to the $sp^2$ valence state. The strong electron-accepting ability of these compounds may also partly be attributed to the existence of pure, or almost-unfilled $\pi$ orbitals on the metal atom.

**The Energy Levels of Monomers.**—The calculated energy values of the highest-occupied orbitals (HO) and the lowest-vacant orbitals (LV) are presented in Table IV(a) for the boron compounds and in Table IV(b) for the aluminum compounds. The LV energies fall in a definite range, i. e., $-9$——$-6$ eV. for the boron compounds and $-7$——$-5$ eV. for the aluminum compounds; these values are considerably lower than those of the carbon atoms of saturated bonds. (The LV energies calculated by Hoffmann[3] are $+3.13$ eV. for the ethane and $-8.23$ eV. for the ethylene molecule.) Thus, these compounds might easily accept the electrons of donors and are very liable to the attack of nucleophilic reagents. Furthermore, these LV orbitals are $p\pi$ type orbitals, and the electron in them is almost localized on the $p\pi$ orbital of the boron or aluminum atom. For example, the atomic orbital population in the LV orbital is calculated to be 1.00 on the boron or aluminum atom in the hydrides (a pure $p\pi$ orbital), 0.97 on the aluminum atom in trimethylaluminum, and 0.94 on the aluminum atom in the aluminum trichloride monomer.

TABLE IV. THE HO AND LV ORBITAL ENERGY (eV.) OF VARIOUS MONOMERS

| | HO | LV |
|---|---|---|
| (a) B-Compounds | | |
| $BH_3$ | $-13.91$ | $-8.53$ |
| $BF_3$ | $-20.71$ | $-6.25$ |
| $BH(CH_3)_2$ | $-12.50$ | $-6.97$ |
| $B(CH_3)_3$ | $-12.36$ | $-6.23$ |
| $BC_2H_3(CH_3)_2$ | $-12.08$ | $-8.91$ |
| $BCl_3$ | $-14.58$ | $-5.91$ |
| (b) Al-Compounds | | |
| $AlH_3$ | $-13.86$ | $-6.67$ |
| $Al(CH_3)_3$ | $-12.14$ | $-5.01$ |
| $Al(C_2H_5)_3$ | $-11.54$ | $-5.08$ |
| $Al(CH_3)_2Cl$ | $-12.12$ | $-4.91$ |
| $AlCl_3$ | $-14.94$ | $-4.73$ |

With regard to the value of the HO energy, unfortunately, there seem to be no experimental results available to compare it with.

**$\pi$-Conjugation in Monomers.**—The magnitude of the $\pi$-conjugation has been supposed to be a measure of the stability of these monomer molecules. For instance, Mulliken described how the existence of trimethyl and trihalogenated boron monomers depends on the extent of stabilization due to $\pi$-conjugation in these monomers (hyperconjugation in the trimethylborane monomer).[6] Similarly, Ritter and his co-workers discussed the relation between the $\pi$-conjugation energy and the acid strength or the rate of disproportionation in vinyl boron derivatives.[7]

According to Table III, the orders of the magnitude of the $N(z)$ of boron atoms in various monomers are $BCl_3 > B(C_2H_3)_3 > B(C_2H_3)_2(CH_3) > BC_2H_3(CH_3)_2 > B(CH_3)_3 > BH(CH_3)_2 > BF_3 > BH_3$. Except for $BF_3$,* this order is reasonable, since it is known that $BH_3$ and $BH(CH_3)_2$ exist as in the dimeric form, and trimethyl boron and trihalogenated boron, as in the monomeric form.[6] The magnitude of $N(z)$ in aluminum compounds is smaller than that of the respective boron compounds, and the $N(z)$ of aluminum in the $AlCl_3$ monomer, which is the largest of the aluminum compound monomers presented here, is comparable to the $N(z)$ of boron in the $BH(CH_3)_2$ monomer; in fact, these two compounds are known to form dimers at room temperature.

Good and Ritter[7] treated the $\pi$ systems of vinyl boron compounds by a simple LCAO method. The calculated total $\pi$ electron densities for the $C_1{=}C_2{-}B$ system (dimethylvinylborane) are 0.84 on atom $C_1$, 1.05 on $C_2$, and 0.11 on the boron atom, whereas the $N(r)$ values of these $\pi$ orbitals in the present treatment are 0.941, 1.003, and 0.150 respectively. Furthermore, they obtained the $\pi$ densities of the boron atom as 0.21 in monomethyl divinylborane and as 0.29 in trivinylborane, while our values are 0.175 in the former and 0.207 in the latter.

The $\pi$-conjugation energies were also calculated by Good and Ritter.[7] These values were 4 kcal./mol. in dimethylvinylborane, 8.0 kcal/mol. in monomethyl divinylborane, and 11.8 kcal./mol. in trivinylborane. The results of our calculations are 2.4, 7.4, and 15.0 kcal./mol. respectively (our values are obtained as the differences between the $\pi$ orbital energy of the isolated ethylene molecule and those in methyl vinylboranes.). These two sets of results seem to be comparable with one other. The $\pi$-conjugation energies of the $BCl_3$, $BF_3$ and $AlCl_3$ monomers are obtained as 18.2, 6.7, and 7.4 kcal./mol. respectively. In $BF_3$, the value seems somewhat too small.

**The Electronic Structure of the Monomer and the Ion.**—Now the change in the electronic structure between the monomer ($MX_3$) and its ion ($MX_4^-$) will be discussed. A remarkable difference is indicated in the following two points. One is concerned with the LV orbital energy, and the other, with the $N(z)$ value of the boron and aluminum atoms. The energies of HO and LV orbitals are listed in Table V, while the $N(r)$ values of the boron and aluminum atoms in various compounds are given in Table VI.

Table V. The HO and LV orbital energies of some monomers ($MX_3$) and corresponding ions ($MX_4^-$)

| | HO | LV |
|---|---|---|
| $BH_3$ | −13.91 | − 8.53 |
| $BH_4^-$ | −13.71 | +10.02 |
| $BF_3$ | −20.71 | − 6.25 |
| $BF_4^-$ | −20.71 | + 8.82 |
| $AlH_3$ | −13.86 | − 6.67 |
| $AlH_4^-$ | −13.71 | + 6.98 |
| $AlCl_3$ | −14.94 | − 4.73 |
| $AlCl_4^-$ | −14.81 | +13.21 |

Table VI. The $N(r)$ values of boron and aluminum atoms in monomers and ions

| | $N$(s) | $N$(x) | $N$(y) | $N$(z) |
|---|---|---|---|---|
| $BH_3$ | 0.912 | 0.825 | 0.825 | 0.0 |
| $BH_4^-$ | 0.847 | 0.816 | 0.816 | 0.816 |
| $BF_3$ | 0.295 | 0.122 | 0.122 | 0.082 |
| $BF_4^-$ | 0.298 | 0.110 | 0.110 | 0.110 |
| $AlH_3$ | 0.850 | 0.497 | 0.497 | 0.0 |
| $AlH_4^-$ | 0.808 | 0.480 | 0.480 | 0.480 |
| $AlCl_3$ | 0.505 | 0.206 | 0.206 | 0.111 |
| $AlCl_4^-$ | 0.504 | 0.202 | 0.202 | 0.202 |

(s: 2s or 3s AO; x, y, z: 2px or 3px, 2py or 3py, 2pz or 3pz AO's)

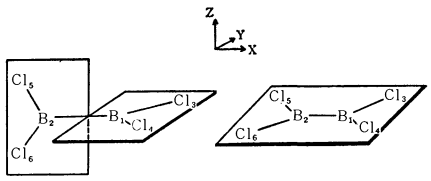
The difference in HO orbital energy between the monomer and its ion is small, whereas the LV level of ions lies much higher than that of the monomers, corresponding to the weak electron-accepting ability of these ions. The most important change in $N(r)$ value between the monomer and its ion occurs on the pz orbital of the boron and aluminum atoms. The $N(z)$ value of the ions is much larger than that of the corresponding monomers, naturally indicating that the electron-accepting abilities of monomers disappears in ions.

These saturation phenomena can be recognized from the charge migrations. In the $MX_3 + X^- \rightarrow MX_4^-$ (M = boron or aluminum) process, for instance the magnitude of the charge migration from $X^-$ to $MX_3$ may be roughly estimated by the unit charge in $X^-$ minus the net charge of X

6) R. S. Mulliken, *Chem. Revs.*, **41**, 207 (1947).
7) C. D. Good and D. M. Ritter, *J. Am. Chem. Soc.*, **84**, 1162 (1962).
* The calculated $\pi$ overlap values are 0.179 for the B-F bond in $BF_3$ and 0.124 for B-Cl in $BCl_3$, but the obtained $\pi$ charge of the boron atom in $BF_3$ is smaller than that of $BCl_3$.

in $MX_4^-$. This quantity is calculated as 0.824e in $BH_3$, as 0.157e in $BF_3$, as 0.561e in $AlH_3$ and as 0.277e in $AlCl_3$. Many of these transferred electrons enter into the vacant $p\pi$ orbitals of the boron or aluminum atom, as has been shown above.

**The Electronic Structures of the Two Configurations of the $B_2Cl_4$ Molecule.**—Two configurations of the tetrachlorodiborine, $B_2Cl_4$, have been considered.[8] The one is the planar configuration belonging to the symmetry group, $D_{2h}$, while the other has a $D_{2d}$ configuration in which two $BCl_2$ planes are perpendicular to each other. These two configurations are shown in Fig. 2. The molecule with the $D_{2d}$ symmetry exists in liquid and gas phases, and the $D_{2h}$ molecule, in the crystal form.[8]




$D_{2d}$ $D_{2h}$

Fig. 2. The $D_{2d}$ and $D_{2h}$ configurations of $B_2Cl_4$.

TABLE VII. ENERGY (eV.) OF SEVERAL LEVELS AND THEIR IRREDUCIBLE REPRESENTATION OF $D_{2d}$ AND $D_{2h}$ $B_2Cl_4$ MOLECULES

| $D_{2d}$ | | $D_{2h}$ | |
|---|---|---|---|
| e* | −6.46 | $b_{3g}$ | −4.39 |
| | −6.46 | $b_{2u}$* | −8.03 |
| $a_1$** | −11.19 | $a_g$** | −11.32 |
| e | −14.54 | $b_{2g}$ | −14.47 |
| | −14.54 | $b_{3u}$ | −14.60 |
| $a_2$*** | −14.96 | $a_u$*** | −14.95 |
| $b_1$*** | −14.99 | $b_{1g}$*** | −15.01 |
| $b_2$ | −15.27 | $b_{1u}$ | −15.09 |
| e | −15.33 | $b_{2g}$ | −15.17 |
| | −15.33 | $b_{3g}$ | −15.44 |
| e | −15.55 | $b_{3u}$ | −15.56 |
| | −15.55 | $b_{2u}$ | −15.58 |
| $a_1$ | −15.74 | $a_g$ | −15.85 |
| $b_2$ | −16.52 | $b_{1u}$ | −16.52 |
| $a_1$ | −17.39 | $a_g$ | −17.39 |
| e | −25.04 | $b_{2g}$ | −24.86 |
| | −25.04 | $b_{3u}$ | −25.22 |
| $b_2$ | −26.85 | $b_{1u}$ | −26.78 |
| $a_1$ | −27.54 | $a_g$ | −27.59 |

* The LV levels.
** The HO levels.
*** The lone pair orbitals of the chlorine atoms.

The energies of all of the occupied orbitals and lowest-unoccupied orbitals of the molecules in these two configurations are listed in Table VII, together with their irreducible representations. The correspondence of irreducible representations between these two groups is as follows:

| $D_{2d}$ (perpendicular) | $D_{2h}$ (planar) |
|---|---|
| $a_1$ | $a_g$ |
| $b_2$ | $b_{1u}$ |
| e | $b_{2g}$, $b_{3g}$, $b_{2u}$, $b_{3u}$ |

The differences between the corresponding orbital energies of these two groups are seen to be very small. (The same values of the bond distances are adopted for these two forms as is shown in Table II.) The energy of the e orbital in the $D_{2d}$ may be compared with the sum of the two split orbital energies in the $D_{2h}$. The LV orbital is the e orbital in the $D_{2d}$, while the lowest is $b_{2u}$ and the next is $b_{3g}$ in the $D_{2h}$ molecule. The difference in the LV orbital energy between these two forms will be discussed later, again from the point of view of the electronic structrue.

The $M(X)$, $N(r)$ and $M(X\text{-}Y)$ values for the two forms are collected in Table VIII. The corresponding data for these two are almost equal to each other. The atomic orbital bond population between the $r$th and $s$th AO's is here denoted by $N(r\text{-}s)$. The $N(z(B_1)\text{-}z(B_2))$ value is −0.001 in the $D_{2d}$ form and +0.002 in the $D_{2h}$, while the $N(y(B_1)\text{-}y(B_2))$ value is −0.001 in the $D_{2d}$ form and −0.009 in the $D_{2h}$ form. Accordingly, the B–B bond in these two configurations is almost purely of a $\sigma$ type and does not exhibit the double-bond character. This result leads to the conclusion that the rotation about the B–B bond is very easy and that the conversion between two forms may be carried out without a great hindrance.

However, as was discussed above, the situation is remarkably different in the LV orbitals. That is, the LV e orbital of the $D_{2d}$ molecule splits into $b_{2u}$ and $b_{3g}$ in the $D_{2h}$ molecule, where $b_{2u}$ is the lowest. The calculated coefficients of the AO's in these orbitals are collected in Table IX, together with those of the HO orbitals. It may be seen from the table that the LV orbitals in the $D_{2d}$ molecule, which is twofold degenerate, are nonbonding orbitals localized on the $B_1$ and

TABLE VIII. THE $M(X)$, $N(r)$ AND $M(X\text{-}Y)$ VALUES OF THE $D_{2d}$ AND $D_{2h}$ MOLECULES

| | $M(B_1)$ | $N(r)$ of $B_1$ | | | | $M$(B-B) | $M$(B-Cl) | $M$(Cl) |
|---|---|---|---|---|---|---|---|---|
| | | s | x | y | z | | | |
| $D_{2d}$ | 2.137 | 0.815 | 0.744 | 0.400 | 0.178 | 0.836 | 0.708 | 7.432 |
| $D_{2h}$ | 2.133 | 0.819 | 0.739 | 0.397 | 0.178 | 0.830 | 0.712 | 7.433 |

8) E. g., "Progress in Boron Chemistry," Ed. by H. Steinberg and A. L. McClossey, Vol. I, Pergamon Press, New York (1964).

TABLE IX. THE HO AND LV ORBITALS IN THE $D_{2d}$ AND $D_{2h}$ $B_2Cl_4$ MOLECULES

(a) The $D_{2d}$ molecule

LV e $1.03z_{B1}+0.02z_{B2}-0.33(z_{C13}+z_{C14})-0.06(s_{C15}-s_{C16})-0.09(x_{C15}-x_{C16})+0.04(z_{C15}+z_{C16})$

LV e $1.03y_{B2}+0.02y_{B1}-0.33(y_{C15}+y_{C16})-0.06(s_{C12}-s_{C14})+0.09(x_{C12}-x_{C14})+0.04(y_{C12}+y_{C14})$

HO $a_1$ $0.23(s_{B1}+s_{B2})-0.44(x_{B1}-x_{B2})+0.32(x_{C13}+x_{C14}-x_{C15}-x_{C16})-0.07(s_{C13}+s_{C14}+s_{C15}+s_{C16})$
$+0.05(y_{C13}-y_{C14}+y_{C15}-y_{C16})$

(b) The $D_{2h}$ molecule

$b_{3g}$ $0.84(z_{B1}-z_{B2})-0.23(z_{C13}+z_{C14}-z_{C15}-z_{C16})$

LV $b_{2u}$ $0.65(z_{B1}+z_{B2})-0.25(z_{C13}+z_{C14}+z_{C15}+z_{C16})$

HO $a_g$ $0.24(s_{B1}+s_{B2})-0.44(x_{B1}-x_{B2})+0.31(x_{C13}+x_{C14}-x_{C15}-x_{C16})-0.07(s_{C13}+s_{C14}+s_{C15}+s_{C16})$
$+0.07(y_{C13}-y_{C14}+y_{C15}-y_{C16})$

$B_2$ atoms respectively, whereas the LV orbital of the $D_{2h}$ molecule is a $\pi$ type B–B bonding and the next LV is a $\pi$ type B–B anti-bonding. Thus, if a $D_{2d}$ molecule receives two electrons, these will enter into the LV orbitals, localizing on the 2pz orbital of the $B_1$ atom and on the 2py orbital of the $B_2$ atom, so that this compound will behave like a biradical. In the $D_{2h}$ molecule, these added electrons will serve to strengthen the B–B $\pi$ conjugation, behaving like tetrachloroethylene.

It is hoped that these results will be examined by future experiments.

The calculations have been carried out on an IBM 7090 computer at Japan IBM Co., with the permission of the UNICON committee, whom the authors wish to thank.

*Faculty of Engineering*
*Kyoto University*
*Sakyo-ku, Kyoto*

# Intramolecular Hydrogen Bonds. V.[1] Aliphatic Hydroxy-carboxylates*1

By Nobuo Mori, Satoshi Ōmura,*2 Norihiko Kobayashi and Yojiro Tsuzuki

(Received May 24, 1965)

In a previous paper,[2] it was reported that an intramolecular hydrogen bond is formed in some $\alpha$- and $\beta$-hydroxy-carboxylates in a dilute carbon tetrachloride solution, mainly on to the carbonyl-oxygen atom, rather than to the ether-oxygen of the ester group; the bonded OH-stretching frequencies were about 3540 $cm^{-1}$ in the $\alpha$-hydroxy esters and about 3559—3586 $cm^{-1}$ in the $\beta$-hydroxy esters. In addition to this strong band, a completely resolved or an unresolved weak band or shoulder appeared in the range from ca. 3610 to 3625 $cm^{-1}$ in both cases. It has, however, not yet been settled whether this band or shoulder is due to the free OH group or to the OH group bonded to the ether-oxygen atom. Flett[3] has suggested that it comes from the free OH group and has attributed the lowering in frequency (by ca. 10 to 20 $cm^{-1}$ from the free OH frequencies of alcohols) to the electron-attracting effect of the ester group. This point has now been elucidated with reference to the rotational isomerism around the C–OH bond, by means of infrared measurements of a series of $\alpha$- and $\beta$-hydroxy-carboxylates. Further, this paper will report on the limitation of intramolecular hydrogen bonding through the length of an alkylene chain intervening between the hydroxyl and the ester group in the $\omega$-hydroxy $HO(CH_2)_nCOOR$ series, as well as in isomeric hydroxycyclohexane-carboxylates.

## Experimental

**Samples.**—All the esters used are listed in Table I. The esters 1, 3, 5, 7, 9, 15, 16, 19 and 21 were those previously[2] used, while the esters 2, 4, 6, 8, 18 and 20 were prepared in similar manners. Ester No. 10 was prepared by Reformatsky reaction from acetone and methyl bromoacetate; No. 11 by the reduction of

*1 Presented at the 17th Annual Meeting of the Chemical Society of Japan, Osaka, April, 1965.

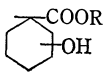
*2 Present address: The Kitasato Institute, Minato-ku, Tokyo.

1) Part IV: N. Mori, S. Ōmura and Y. Tsuzuki, This Bulletin, **38**, 1631 (1965).

2) N. Mori, S. Ōmura, O. Yamamoto, T. Suzuki and Y. Tsuzuki, ibid., **36**, 1401 (1963).

3) M. St. C. Flett, *Spectrochimica Acta*, **10**, 21 (1957).

Table I. Summary of infrared data

| No. | Ester | B. p., °C/mmHg ($n_D^{25}$) | Band* | $\nu_{OH}$ cm$^{-1}$ | $D$** | $\Delta\nu_{1/2}$ cm$^{-1}$ | $D_{II}/D_I$ |
|---|---|---|---|---|---|---|---|
| 1 | $HOCH_2COOEt$[2] | | I | 3550[a] | 0.68 | 46 | |
| | | | II | 3618[a] | 0.13 | 25 | 0.19 |
| 2 | $CH_3CHCOOMe$ (OH) | 68/46 | I | 3549 | 0.74 | 43 | |
| | | | II | 3616 | 0.17 | 32 | 0.23 |
| 3 | $CH_3CHCOOEt$[2] (OH) | | I | 3543 | 0.88 | 44 | |
| | | | II | 3613 | 0.19 | 18 | 0.22 |
| 4 | $CH_3CHCOO(i\text{-}Pr)$ (OH) | 74/40 | I | 3544 | 0.74 | 44 | |
| | | | II | 3614 | 0.15 | 21 | 0.20 |
| 5 | $(CH_3)_2CCOOEt$[2] (OH) | | I | 3544 | 0.43 | 48 | |
| | | | II | 3606 | 0.09 | 21 | 0.21 |
| 6 | $CH_2CH_2COOMe$ (OH) | 74/15 | I | 3586 | 0.42 | 87 | |
| | | | IIIa | 3621 | 0.04 | 18 | |
| | | | IIIb | 3638 | 0.14 | 20 | |
| 7 | $CH_2CH_2COOEt$[2] (OH) | | I | 3584[a] | 0.46 | 110 | |
| | | | IIIa | 3624[a] | 0.04 | 16 | |
| | | | IIIb | 3640[a] | 0.17 | 24 | |
| 8 | $CH_3CHCH_2COOMe$ (OH) | 67/13 | I | 3559 | 0.49 | 82 | |
| | | | II | 3592 | 0.08 | 32 | |
| | | | IIIab | 3622 | 0.16 | 30 | |
| 9 | $CH_3CHCH_2COOEt$[2] (OH) | | I | 3560 | 0.58 | 82 | |
| | | | II | 3590[a] | 0.08 | 37 | |
| | | | IIIab | 3626[a] | 0.11 | 39 | |
| 10 | $(CH_3)_2CCH_2COOMe$ (OH) | 67/15 | I | 3537 | 0.59 | 54 | |
| | | | II | 3588 | 0.04 | 20 | |
| | | | IIIab | 3613 | 0.06 | 22 | |
| 11 | $CH_3CH(CH_2)_2COOEt$ (OH) | 85—87/2 | I | 3544 | 0.12 | 74 | |
| | | | IIIa | 3618 | weak | | |
| | | | IIIab | 3628 | 0.13 | 41 | |
| 12 | $HO(CH_2)_5COOEt$ | 138/20[4] | I | 3542 | 0.12 | 72 | |
| | | | IIIa | 3624 | 0.20 | 14 | |
| | | | IIIb | 3640 | 0.62 | 26 | |
| 13 | $HO(CH_2)_6COOEt$ | 145/15[4] | IIIa | 3624 | 0.12 | 14 | |
| | | | IIIb | 3639 | 0.47 | 25 | |
| 14 | $HO(CH_2)_8COOEt$ | 131—132/2[5] | IIIa | 3620 | 0.09 | 13 | |
| | | | IIIb | 3638 | 0.33 | 25 | |
| 15 | $HO(CH_2)_9COOEt$[6] | | IIIa | 3626[a] | 0.07 | 16 | |
| | | | IIIb | 3641 | 0.36 | 24 | |
| 16 | $HO(CH_2)_{10}COOEt$[6] | | IIIa | 3620[a] | 0.13 | 18 | |
| | | | IIIb | 3638 | 0.48 | 24 | |
| |  | | | | | | |
| | R Position of OH | | | | | | |
| 17 | Me 1 | 87/10 (1.4585) | I | 3540 | 0.78 | 42 | |
| | | | II | 3609 | 0.22 | 32 | 0.31 |
| 18 | Me cis-2 | 103/14[7] (1.4637) | I | 3544 | 0.60 | 80 | |
| | | | IIIab | 3624 | 0.13 | 40 | |
| 19 | Et cis-2[2] | | I | 3536[a] | 0.55 | 76 | |
| | | | IIIab | 3620[a] | 0.08 | 40 | |
| 20 | Me trans-2 | 112.5/14[7] (1.4634) | I | 3530 | 0.19 | 108 | |
| | | | II | 3596 | 0.41 | 55 | |
| | | | IIIab | 3620 | 0.14 | 20 | |
| 21 | Et trans-2[2] | | I | 3534[a] | 0.28 | 102 | |
| | | | II | 3596[a] | 0.36 | 63 | |
| | | | IIIab | 3624[a] | 0.08 | 19 | |

(Continued Table I)

| No. | R | Position of OH | B. p., °C/mmHg ($n_D^{25}$) | Band* | $\nu_{OH}$ cm$^{-1}$ | $D$** | $\Delta\nu_{1/2}$cm$^{-1}$ | $D_{II}/D_I$ |
|---|---|---|---|---|---|---|---|---|
| 22 | Me | cis-3 | 113—115/5[8] (1.4658) | IIIab | 3620 | 0.72 | 24 | |
| 23 | Me | trans-3 | 111—112/6[8] (1.4657) | IIIab | 3624 | 0.70 | 26 | |
| 24 | Me | cis-4 | 128/12[9,10] (1.4684) | IIIab | 3624 | 0.76 | 28 | |
| 25 | Me | trans-4 | 125/12[9,10] (1.4669) | IIIab | 3626 | 0.78 | 26 | |

a) The frequencies are different from those previously[2] reported, but more exact.

* Band I denotes the band of the OH group bonded to the carbonyl-oxygen atom as in form I shown in Fig. 2, band II that of the OH group bonded to the ether-oxygen atom as in form II, and bands IIIa and IIIb are of the free OH groups as in forms IIIa and IIIb, respectively, and band IIIab consists of both the bands IIIa and IIIb.

** $D=\log I_0/I$

ethyl levulinate with sodium borohydride; Nos. 12 and 13 by the oxidation of the corresponding cycloalkanones with potassium persulfate in ethanol; No. 14 by the Bouveault-Blanc reduction of the corresponding $\alpha,\omega$-dicarboxylic acid monoester, followed by esterification; No. 17 by the hydrolysis of cyclohexanone-cyanohydrin followed by esterification, and Nos. 22 to 25 by the catalytic hydrogenation of the corresponding methyl hydroxybenzoates. The $\gamma$-hydroxyvalerate (11) was considerably contaminated by its lactone, which was formed during vacuum distillation. The physical constants of these esters agreed with those reported in the literature (cf. Table I).

**Infrared Measurements.**—These were carried out with solutions of ca. 0.004 mol./l.*3 in carbon tetrachloride at 25°C, in the OH-stretching region from 3300 to 3700 cm,$^{-1}$ using a Perkin-Elmer 21 spectrophotometer equipped with a lithium fluoride prism and with a cell 3 cm. in length. The slit width was constantly 0.029 mm. The observed frequencies were calibrated against that of the atmospheric vapor. The OH spectra observed were apparently those of an unresolved or a resolved doublet or triplet and were graphically separated*4 into two or three symmetric components, assuming that they consist of symmetric bands. The infrared data of the separated band-components are summarized in Table I.*5 The frequencies of the peaks of the components were identical with those of the apparent bands, but most of their absorbances were somewhat or much lower than those of the latter bands.

## Results and Discussion

The infrared data of the esters investigated are listed in Table I.

**$\alpha$-Hydroxy Esters.**—All the esters, without exception, show a strong symmetric band at 3540—3550 cm$^{-1}$ (band I) and a weak symmetric band at 3606—3618 cm$^{-1}$, as Fig. 1 shows. The

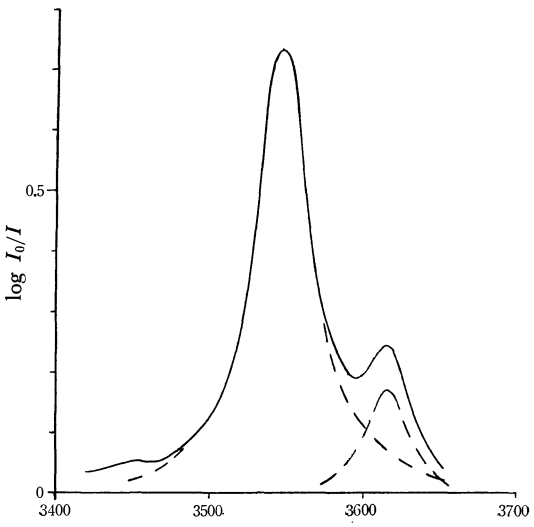



Fig. 1. OH spectrum of methyl lactate (2).

4) R. Robinson and L. H. Smith, *J. Chem. Soc.*, **1937**, 373.

5) P. Chuit and J. Hausser, *Helv. Chim. Acta*, **12**, 466 (1929). Me ester: b. p. 137—139°C/3 mmHg.

6) N. Mori, S. Ōmura and Y. Tsuzuki, This Bulletin, **38**, 1037 (1965).

7) H. B. Henbest and B. B. Millward, *J. Chem. Soc.*, **1960**, 3575; J. Pascual, J. Sistaré and A. Regàs, ibid., **1949**, 1943.

8) H. L. Goering and C. Serres, *J. Am. Chem. Soc.*, **74**, 5908 (1952); D. S. Noyce and D. B. Denney, ibid., **74**, 5912 (1952); S. Siegel, ibid., **75**, 1317 (1953).

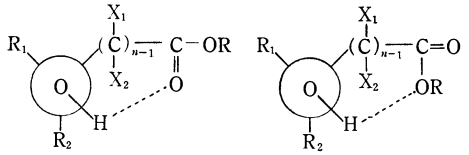
9) D. S. Noyce and H. I. Weingarten, ibid., **79**, 3098 (1957).

10) N. R. Campbell and J. H. Hunt, *J. Chem. Soc.*, **1950**, 1379.

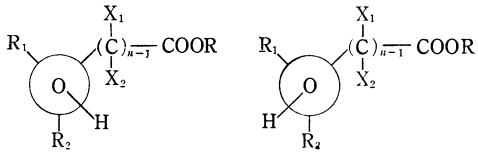
*3 At this concentration, intermolecular hydrogen bonding was entirely absent; a very weak band due to the overtone of a carbonyl group appeared in all the spectra at ca. 3445 cm$^{-1}$, in addition to the strong bands listed in Table I.

*4 The graphical separation was made by reflecting the major component of a doublet or a triplet about the ordinate at the apparent maximum and by subtracting the mirror image from the observed spectrum. In the triplet, the residual minor part, unsymmetric on the lower or on the higher frequency side, was then similarly separated into two. The process was repeated by the trial and error method, until the components were symmetric.

*5 Each ester in the cyclohexane series herein investigated can take two interconvertible chair-conformations; therefore, the OH band should consist of two bands due to the axial and the equatorial OH group, which are somewhat different in frequency (see A. R. H. Cole, P. R. Jefferies and G. T. A. Müller, *J. Chem. Soc.*, **1959**, 1222 and previous papers). This difference in frequency is too small to separate the observed OH band into the two components, and, at any rate, such separation is not very significant in this investigation. Accordingly, such a distinction has not drawn herein.



Form I Form II



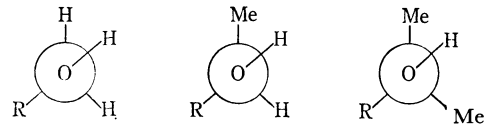
Form IIIa Form IIIb

| $n$ | Ester No. | $R_1$ | $R_2$ | $X_1$ | $X_2$ |
|---|---|---|---|---|---|
| 1 | 1 | H | H | | |
| 1 | 2—4 | Me(or H) | H(or Me) | | |
| 1 | 5 | Me | Me | | |
| 1 | 17 | $R_1$ and $R_2$ together form the pentamethylene group | | | |
| 2 | 6, 7 | H | H | H | H |
| 2 | 8, 9 | Me(or H) | H(or Me) | H | H |
| 2 | 10 | Me | Me | H | H |
| 2 | 18, 19 | $R_1$ and $X_1$ together form the tetramethylene group, and $R_2$ and $X_2$ are hydrogens. | | | |
| 2 | 20, 21 | $R_1$ and $X_2$ together form the tetramethylene group, and $R_2$ and $X_1$ are hydrogens. | | | |
| 3 | 11 | Me(or H) | H(or Me) | H | H |
| 3 | 22 | $R_1$ and $X_1$ on the $C_1$ atom together form the trimethylene group, and $R_2$, $X_2$ and the other $X_1$ are hydrogens. | | | |
| 3 | 23 | $R_1$ and $X_2$ on the $C_1$ atom together form the trimethylene group, and $R_2$, $X_1$ and the other $X_2$ are hydrogens. | | | |
| 4 | 24, 25 | The same with ester Nos. 22 and 23, respectively, except the trimethylene group is replaced by the ethylene group. | | | |
| 5 or more | 12—16 | H | H | H | H |

Fig. 2. Possible rotational isomers around the C-OH axis.

frequency of the latter band decreases with the increasing number of methyl groups attached to the $\alpha$-carbon atom. In assigning this band, it is convenient to take into account the rotational isomers possible by rotation around the $C_\alpha$–O axis, as is shown with the four possible forms, I—IIIa,b, and their mirror images, in Fig. 2. In this figure, form I is hydrogen-bonded with the carbonyl-oxygen atom, and form II, with the ether-oxygen atom, while forms IIIa and IIIb do not form any hydrogen bond.

According to the infrared study of alcohols by Ōki and Iwamura,[11] the OH frequency depends on the number of methyl groups skew to the OH group with respect to the C–O bond, as is shown by forms A—C:



$\nu_{OH}$ cm$^{-1}$ Form A: 3640 Form B: 3627 Form C: 3617

wherein R represents a hydrogen atom or an alkyl group.

As examples of compounds capable of taking a hydrogen-bonded form such as form I ($n$=1 in the figure) we may mention such $\alpha$-ketols as acylmethyl carbinol[12] and 2-hydroxycyclohexanones[13], whose bonded and free OH frequencies are ca. 3490 and 3615 cm$^{-1}$ respectively. The latter frequency is lower by 12 cm$^{-1}$ than the OH frequency of 3627 cm$^{-1}$ in form B of alcohols; this lowering in frequency may be caused by the electron-attracting effect of the ketone group.

In the case of the $\alpha$-hydroxy esters, the electron-attracting effect of the ester group exercised on the OH frequency, if there is any at all, is probably much smaller than that of the ketone group. The weak band of glycolate 1 appears at 3618 cm$^{-1}$, lower by 22 cm$^{-1}$ than the OH frequency of 3640 cm$^{-1}$ in form A of alcohols; therefore, it can not be due to the free OH group in form IIIb corresponding to form A. This indicates, further, the absence of the non-bonded form IIIa, which should be thermodynamically less stable than IIIb. Accordingly, the band must be assigned to the bonded OH group in the residual form II. In this case, the lowering in frequency is 9 cm$^{-1}$ from the OH frequency of 3627 cm$^{-1}$ in form B, corresponding to form II.

In the lactates 2, 3 and 4, similarly, the weak band whose frequency is lower by ca. 13 cm$^{-1}$ than the 3627 cm$^{-1}$ of the OH band for form B and lower by ca. 3 cm$^{-1}$ than the 3617 cm$^{-1}$ for form C, may consist of a major component due to the bonded OH group in form II and a minor component due to one in the less stable rotational isomer II ($R_1$=H; $R_2$=Me). With $\alpha$-hydroxyisobutyrate 5 and 1-hydroxycyclohexane-carboxylate 17, since the lowering in the frequency of the weak band is ca. 10 cm$^{-1}$ from the 3617 cm$^{-1}$ in form C, comparable to the above cases, this band may be predominantly due to the bonded OH group in form II. Consequently, the OH group other than that in form I may hydrogen-bond with the ether-oxygen atom to a much larger extent than it remains free.

Further evidence for this assignment is provided by the fact that the frequencies of the esters 1,

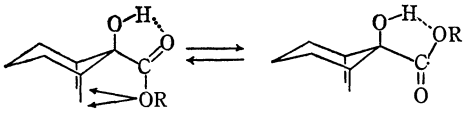
11) M. Ōki and H. Iwamura, This Bulletin, **32**, 950 (1959).

12) M. C. Duculot, *Compt. rend.*, **241**, 1738 (1955).

13) A. R. H. Cole and G. T. A. Müller, *J. Chem. Soc.*, **1959**, 1224; N. H. Cromwell and R. E. Bambury, *J. Org. Chem.*, **26**, 997 (1961), and the references therein cited.

2—4 and 17 are in good agreement with the bonded OH frequencies of 3622, 3614 and 3607 $cm^{-1}$, respectively, of the monoacetates[14] of ethylene glycol, *trans*-cyclohexane-1, 2-diol and 1-hydroxy-cyclohexylcarbinol in a hydrogen-bonded form such as form II. These frequencies are higher by 10—21 $cm^{-1}$ than the bonded OH frequencies of 3612,[15] 3602[15] and 3586[14] of the respective free diols; this rise in frequency may be attributed to the decreased electron-density on the ether-oxygen atom resulting from the resonance of the ester group. A similar finding is afforded in the case of diaxial *cis*-cyclohexane-1, 3-diols and their monoacetates.[16]

The ratio of the absorbance of the weak band to that of the strong band ($D_{II}/D_I$) is substantially constant in the esters, 1—5, except 17, irrespective of the number of methyl groups on the $\alpha$-carbon atom, but it tends to decrease as the alcoholic alkyl portion of the ester group increases in bulk or in number of carbon atoms, as is positively shown for lactates 2, 3 and 4, The relatively high ratio of the ester 17 may be explained in terms of the possible steric repulsion between the axial hydrogens on $C_2$ and $C_6$ and the alkoxy group in form I; by this means this form can be partially converted into form II, as is shown, e. g., by the following equilibrium between conformations containing an OH group axial:



Form I Form II

**β-Hydroxy Esters.**—The β-hydroxy-propionates and -butyrates 6—9 show, in each case, a strong band in the range from 3559 to 3586 $cm^{-1}$; this band is considerably broadened on the higher frequency side, and it also has a shoulder at ca. 3620—3640 $cm^{-1}$ on this side, as is shown in Fig. 3. On the other hand, the isovalerate 10 shows a strong, almost symmetric band at 3537 $cm^{-1}$, with a broad shoulder on the bottom of the band on the higher frequency side; the latter can be separated into two components, as is shown in Fig. 4. However, the spectra of the cyclic esters 18—21 are somewhat different; the cis esters show a strong band at 3544 $cm^{-1}$, with a weak shoulder on the higher frequency side, and the trans isomers, an unresolved triplet with a maximum at 3596 $cm^{-1}$, as is shown in Figs. 5 and 6.

In a previous paper,[2] which dealt with ethyl β-hydroxy-propionate and -butyrate (7 and 9), it could not be concluded whether the shoulder of the band was due to the free OH group. This point has now been solved by separating each of the complicated bands into three components, as is shown in Fig. 3. The separated components have maxima at 3585, 3622 and 3639 $cm^{-1}$ in the case of the esters 6 and 7; the lowest frequency

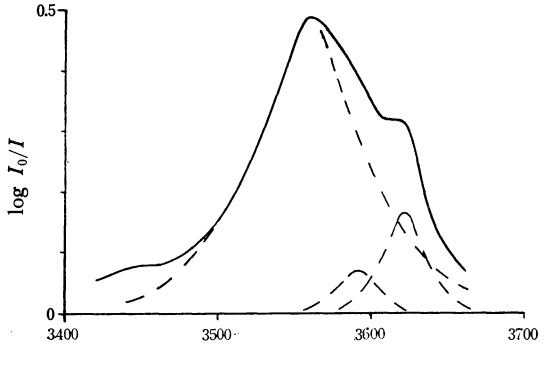



Fig. 3. OH spectrum of methyl 2-hydroxybutyrate (8).

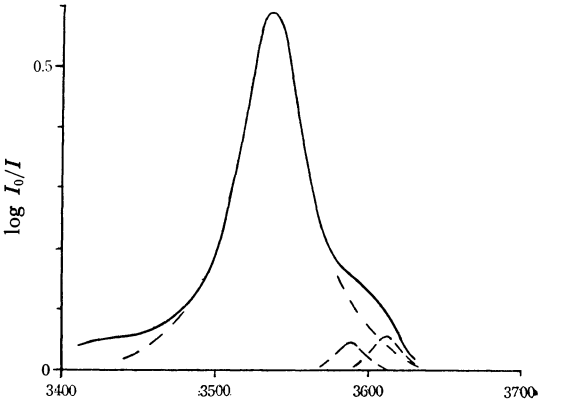



Fig. 4. OH spectrum of methyl 2-hydroxyisovalerate (10).

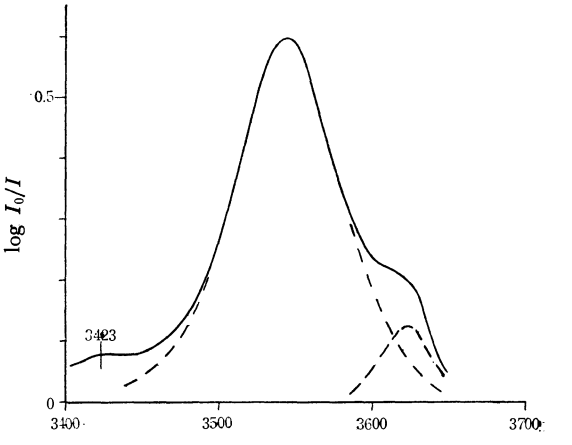



Fig. 5. OH spectrum of methyl *cis*-2-hydroxy-cyclohexane-carboxylate (18).

14) N. Mori, unpublished data.
15) L. P. Kuhn, *J. Am. Chem. Soc.*, **74**, 2492 (1952).
16) H. B. Henbest and B. J. Lovel, *J. Chem. Soc.*, **1959**, 1965; H. B. Henbest and J. McEntee, ibid., **1961**, 4478.

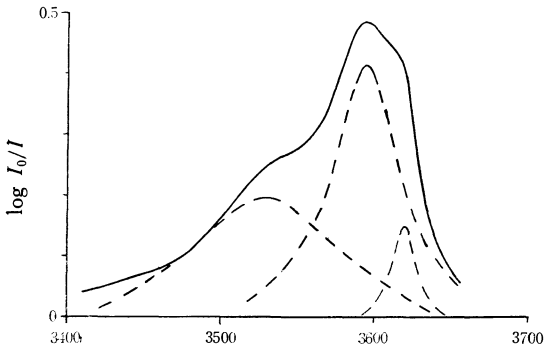



Fig. 6. OH spectrum of methy *trans*-2-hydroxy-cyclohexane-carboxylate (20).

band may be due to the bonded OH group in form I (band I). The other two may be assigned to the free OH groups in forms IIIa and IIIb, rather than to the bonded OH group in form II, because their relative intensities and frequencies are comparable to those of the other $\omega$-hydroxy esters 12—16.

In the $\beta$-hydroxybutyrates 8 and 9, the band at 3624 $cm^{-1}$ may consist predominantly of two bands due to the free OH groups in forms IIIa ($R_1$=Me ; $R_2$=H) and IIIb, probably with a weaker band due to the free OH in another form IIIa ($R_1$=H ; $R_2$=Me), because the frequency is comparable to the 3627 $cm^{-1}$ of the OH group in form B corresponding to the former two forms, while it is higher than the 3617 $cm^{-1}$ of the OH group in form C corresponding to the latter IIIa. Subsequently, the band at 3590 $cm^{-1}$ may be due to the bonded OH group in form II. This assignment can be supported also by the fact that the intensity of this band relative to the band IIIab of 3624 $cm^{-1}$ is higher than those of the band IIIa to IIIb for all the $\omega$-hydroxy esters. The same assignments can be given for the separated band-components in the cyclic series, 18—21. In this series, it is of interest that the cis-esters almost exclusively take form I, while the trans-isomers prefer form II, though the reason for this is not clear.

In the $\beta$-hydroxyisovalerate 10, the three bands can similarly be assigned to two bonded groups and one free OH group, as Table I shows.

Further evidence for the assignment of band I is given by the fact[3] that diacetone-alcohol and hydroacetylacetone, capable of forming a ring similar to form I through intramolecular hydrogen-bonding, exhibit the bonded OH frequencies of 3532 and 3557 $cm^{-1}$ respectively; these frequencies are comparable to those of the esters 10 and 8. A hydrogen-bonded form similar to form II can be realized in the diaxial conformations of *cis*-1, 3-diol monoacetates in cyclohexane systems; the bonded OH frequencies are lower by ca. 20 $cm^{-1}$ than the corresponding free OH ones;[16] this affords additional support for the assignment of band II.

From the above informations and reasoning, we are led to the conclusion that the methyl groups on the $\beta$-carbon atom sterically serve to make the hydroxyl and the ester group closer together; the non-bonded forms, IIIa and IIIb, thereby decrease in proportion, and instead the hydrogen-bonded form, II, comes into existence. Further, this effect results in strengthening the hydrogen bond in form I, as is indicated by the facts that the degree of the lowering in frequency of band I resulting from the introduction of one or two methyl groups is unexpectedly large (i. e., ca. 30 $cm^{-1}$ per methyl group) and that, simultaneously, the relative intensity of band I tends to increase. Such an effect is, however, not observed in the $\alpha$-hydroxy esters.

**The Other Esters.**—Higher $\omega$-hydroxy esters do not form a hydrogen bond with the ether-oxygen atom in form II. However, some of them are hydrogen-bonded with the carbonyl-oxygen atom. In the $\gamma$-hydroxyvalerate 11, the bonded OH band I has almost the same intensity as that of the free OH band, but in the $\varepsilon$-hydroxy ester 12 (see Fig. 7) it is very weak, and in the other $\omega$-hydroxy esters, it entirely disappears. It is interesting that the ester 12 is hydrogen-bonded and a nine-mumbered ring is formed, although the largest ring hitherto known contains at most eight members (in 5-methoxypentanol[17] and 5-phenylpentane-1,5-diol[18]). In addition to this, these esters have, in cach case, a strong free OH band broadened on the lower frequency side; the two components separated may be due to the free OH groups in forms IIIa and IIIb respectively.

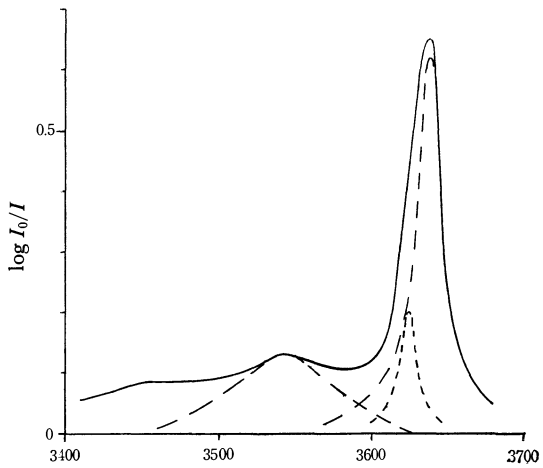



Fig. 7. OH spectrum of ethyl 5-hydroxycapronate (12).

17) A. B. Foster, A. H. Haines and M. Stacey, *Tetrahedron*, **16**, 177 (1961).
18) N. Mori, S. Ōmura and Y. Tsuzuki, This Bulletin, **38**, 1631 (1965).

In the case of the ester 11, the lower frequency band is due to the free OH group in form IIIa ($R_1$=H ; $R_2$=Me), while the higher frequency band is due to that in forms IIIa ($R_1$=Me; $R_2$=H) and IIIb. The intensity ratios of band IIIa to band IIIb (or IIIab) are ca. 0.25.

3- and 4-Hydroxycyclohexane-carboxylates (22—25) are not internally hydrogen-bonded. The absence of any hydrogen bonding in the *cis*-4-hydroxy ester 24 can be explained in view of the fact that even if the hydrogen bonding were possible, the stabilization*6 resulting from it would be much lower than the instabilization*7 resulting from taking the boat or twist conformation required for ordinary hydrogen-bondings between 1- and 4- cis groups.[19] In the case of the *cis*-3-hydroxy ester 22, the reason for the absence of hydrogen-bonding seems to be that the orientation of the ester group in its 1, 3-diaxial chair-conformation is unfavorable for hydrogen-bonding. If the ester group could take an orientation favorable for hydrogen-bonding with the OH group, the stabilization*6 resulting from the hydrogen-bonding could exceed the difference in free energy (ca. 2.0 kcal./mol.*8) between the non-bonded diaxial and the diequatorial chair-conformation and, therefore, molecules taking the diaxial conformation which is hydrogen-bonded should be present to a considerable extent.

**Comparison with Other Hydrogen-bonded Systems.**—As has been described above, the bonded OH frequencies may reasonably be assigned on the basis of a comparison with those of some ketols and alkane-diol monoacetates. In this paragraph, they will be compared with those of $\alpha$, $\omega$-alkane-diols[15,17] and $\omega$-methoxyalkanols[17] of the series $RO(CH_2)_nOH$, wherein R is a hydrogen atom or a methyl group. As is shown in Table II, only when the number of members in a ring to be formed through hydrogen-bonding is equal to 5, the bonded OH frequncies I in the $\alpha$-hydroxy esters are much lower, but the frequencies II are slightly higher than those of the other series. This seems to indicate this decreasing order in proton-accepting power: ester C=O>MeO>HO>ester –O–,† if the distances between the hydroxyl-hydrogen and the proton-accepting oxygen atoms in all the series are almost equal in such probable geometries that the OH and the ester group in the esters are oriented as in forms I and II (in I, the C=O bond almost eclipses the $C_\alpha$–O bond and the C–OR bond is situated between the $C_\alpha$–$R_1$ and the $C_\alpha$–$R_2$ bond, while in II, the C=O bond almost eclipses the $C_\alpha$–$R_1$ bond and the C–OR bond is skew to the $C_\alpha$–O and the $C_\alpha$–$R_2$ bond.); the OH and the OR group in both the alkanol series are skew to one another with respect to the $C_\alpha$–$C_\beta$ axis.

Table II. A comparison of bonded OH frequencies ($\nu_{bonded OH}$ $cm^{-1}$)

| Number of ring-memers | Hydroxy ester: Ester No. | Band I | Band II | $RO(CH_2)_nOH$[17]: R=H | R=Me |
|---|---|---|---|---|---|
| 5 | 1 | 3550 | 3618 | 3619, 3612[15] | 3610 |
| | 3 | 3543 | 3613 | | |
| 6 | 7 | 3584 | — | 3565, 3558[15] | 3554 |
| | 9 | 3560 | 3590 | | |
| 7 | 11 | 3544 | — | 3484, 3478[15] | 3460 |
| 8 | | | | — | 3500 |
| 9 | 12 | 3542 | — | — | — |

When the ring consists of six members or more, however, the frequencies I and II of the ester series are higher than those of both the alkanol series; this indicates that the OH group in the former series is more apart from the proton-accepting atoms than in the case of the latter. Further, in the hydrogen-bonded esters with $n$=1—5 (except 2,) the OH–O=C distances are almost equal and with $n$=2 it is longer, if the bonded OH frequencies directly reflect the distances, as has been recognized in the alkane-diol system.[15]

We thank Mr. Teruo Kajiura and Mr. Tadao Tamura, Government Chemical Industrial Research Institute, Tokyo, for infrared measurements.

*Department of Chemistry*
*Tokyo College of Science*
*Kagurazaka, Shinjuku-ku, Tokyo*

*6 Compared with the enthalpies of 2—3 kcal./mol. for ordinary OH-O type intramolecular hydrogen bondings.[20]

*7 Compared with the free energy difference between the chair and the twist conformations of the cyclohexane of 4 kcal./mol.[21]

*8 Approximated by adding the corresponding values of 0.9 and 1.1 kcal./mol.[22] for an OH and an ethoxycarbonyl group, since such summation has been verified to be approximately correct in some cases.[23,24] This value is comparable to the 1.9 kcal./mol.[23] for *cis*-cyclohexane-1, 3-diol, which is strongly internally hydrogen-bonded.[15]

† This order can be supported also by the 3622 $cm^{-1}$ of ethyleneglycol monoacetate (see Ref. 14).

19) R. D. Stolow, P. M. McDonagh and M. M. Bonaventure, *J. Am. Chem. Soc.*, **86**, 2165 (1964), and references therein cited.
20) H. Buc and J. Néel, *Compt. rend.*, **255**, 2947 (1962); L. P. Kuhn and R. A. Wires, *J. Am. Chem. Soc.*, **86**, 2161 (1964).
21) E. L. Eliel, "Stereochemistry of Carbon Compounds," McGraw-Hill Book Co., New York, N. Y. (1962), p. 206.
22) Ref. 21, p. 236.
23) S. J. Angyal and D. J. McHugh, *Chem. & Ind.*, **1956**, 1147.
24) N. L. Allinger and M. A. Miller, *J. Am. Chem. Soc.*, **83**, 2145 (1961); E. L. Eliel and H. Haubenstock, *J. Org. Chem.*, **26**, 3503 (1961).

# The Metal-catalyzed Autoxidation of Tetralin. V. The Effect of Fatty Acid Solvents

By Yoshio KAMIYA

(Received May 31, 1965)

Recently, the solvent effect on the autoxidation of hydrocarbons has attracted much attention. Hendry and Russell,[1] and Howard and Ingold[2,3] have studied the several hydrocarbons and tried to correlate the rate constant value of $k_3/k_6^{1/2}$ with the dielectric function, $(D-1)/(2D+1)$. The present author, in a previous paper,[4] derived $k_3/k_6^{1/2}$ from the limiting rate of the metal-catalyzed oxidation of tetralin. Mostly, his values showed good agreement with those obtained by a quite different method, that is, azobisisobutyronitrile-catalyzed oxidation.

For this paper the effect of fatty acid solvents, from acetic to myristic acids, on the rate of the cobalt-catalyzed oxidation of tetralin, and also the effect of small amounts of stronger organic acids, were studied.

A possible kinetic scheme[5] describing the overall reaction is:

$$\mathrm{ROOH} + n\mathrm{Me} \xrightarrow{k_1'} \text{radical} \xrightarrow{\mathrm{RH}} \mathrm{R}\cdot \quad (1)$$

$$\mathrm{R}\cdot + \mathrm{O_2} \rightarrow \mathrm{RO_2}\cdot \quad (2)$$

$$\mathrm{RO_2}\cdot + \mathrm{RH} \xrightarrow{k_3} \mathrm{ROOH} + \mathrm{R}\cdot \quad (3)$$

$$\mathrm{RO_2}\cdot + \mathrm{RO_2}\cdot \xrightarrow{k_6} \text{non-radical} + \mathrm{O_2} \quad (4)$$

Under stationary conditions:

$$-\mathrm{dO_2}/\mathrm{d}t = k_3(k_1'/2k_6)^{1/2}(\mathrm{ROOH})^{1/2}(\mathrm{Me})^{n/2}(\mathrm{RH}) - k_1'(\mathrm{ROOH})(\mathrm{Me})^n/2 \quad (5)$$

When the rate of the decomposition of hydroperoxide equals its rate of formation, the limiting rate of oxidation is given by:

$$-\mathrm{dO_2}/\mathrm{d}t = k_3^2(\mathrm{RH})^2/2k_6 \quad (6)$$

## Experimental

The purification of tetralin and the oxygen absorption apparatus have been described previously.[5,6] All the experiments described in this work were performed at 50°C. The cell-cleaning procedure was that of Chalk and Smith.[7] Tetralin hydroperoxide was prepared and analyzed by the method of Woodward and Mesrobian.[8]

Cobalt decanoate prepared by the method of Heaton and Uri[9] was used as a catalyst. The fatty acids used as solvents were acetic, propionic, butyric, pentanoic, octanoic, nonanoic, decanoic, lauric and myristic acids.

## Results and Discussion

**The Decomposition of Tetralin Hydroperoxide by Cobalt Salt in Fatty Acid Solvents.** —The decomposition of tetralin hydroperoxide by cobalt decanoate was carried out in a fatty acid-benzene solution (1 : 1 by volume); its rate was found to be first order with respect to hydroperoxide and second order with respect to cobalt, regardless of fatty acids, from acetic to myristic, which were used, at cobalt concentrations from $5\times10^{-4}$ to $5\times10^{-3}$ mol./l.; i. e.:

$$-\mathrm{dROOH}/\mathrm{d}t = k_1'(\mathrm{Co})^2(\mathrm{ROOH}) \quad (7)$$

The values of $k_1'$, as Table I shows, increased markedly with the increase in the carbon number of the fatty acid.

Table I. The rate constants of the cobalt-catalyzed decomposition of tetralin hydroperoxide in a 1 : 1 by volume fatty acid - benzene solution

| Fatty acid | $k_1'$ mol$^{-2}$ l$^2$ sec$^{-1}$ | $k''$ sec$^{-1}$ |
|---|---|---|
| Acetic | 244 | 18600 |
| Propionic | 495 | 22000 |
| Butyric | 754 | 22100 |
| Pentanoic | 963 | 20500 |
| Heptanoic | 1440 | 18000 |
| Nonanoic | 2440 | 20000 |

However, further experiments confirmed that the decomposition rate is inversely proportional to the square of the concentration of acid, as has been shown in the case of acetic acid;[5] i. e.:

$$-\mathrm{dROOH}/\mathrm{d}t = k''(\mathrm{CO})^2(\mathrm{ROOH})/(\mathrm{Acid})^2 \quad (8)$$

The most interesting feature of this experiments

1) D. G. Hendry and G. A. Russell, *J. Am. Chem. Soc.*, **86**, 2368 (1964).
2) J. A. Howard and K. U. Ingold, *Can. J. Chem.*, **42**, 1044 (1964).
3) J. A. Howard and K. U. Ingold, ibid., **42**, 1250 (1964).
4) Y. Kamiya and K. U. Ingold, ibid., **42**, 2424 (1964).
5) Y. Kamiya, K. U. Ingold, S. Beaton and A. Lafortune, ibid., **41**, 2020 (1963).
6) Y. Kamiya, K. U. Ingold, S. Beaton and A. Lafortune, ibid., **41**, 2034 (1963).
7) A. J. Chalk and A. H. Smith, *Trans. Faraday Soc.*, **53**, 1214 (1957).
8) A. E. Woodward and R. B. Mesrobian, *J. Am. Chem. Soc.*, **72**, 1942 (1950).
9) F. W. Heaton and N. Uri, *J. Lipid. Res.*, **2**, 152 (1956).

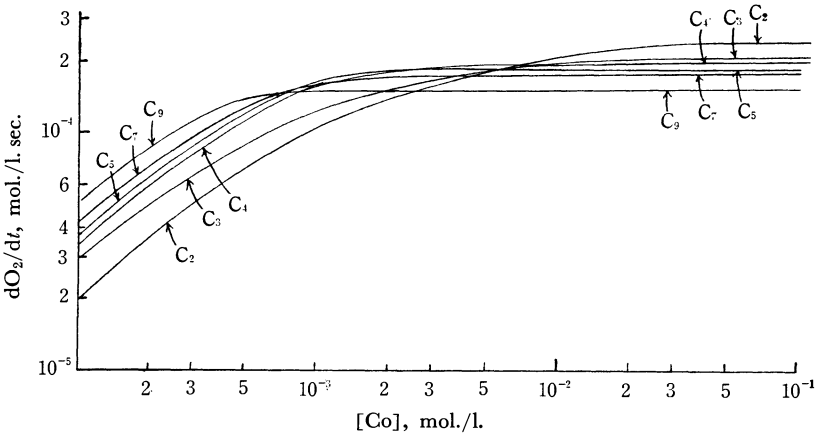
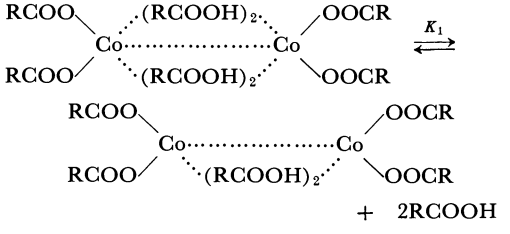



Fig. 1. The rate of oxidation of tetralin in the fatty acid as a function of cobalt concentration.

is that the calculated rate constant, $k''$, of Eq. 8 was nearly $2\times10^4$ $sec^{-1}$; it was independent of the molecular weight of the acid given in Table I. Each cobalt salt in an acid solvent may be complexed with two molecules of acids, and the active form of cobalt might be written as follows:




Thus,

$$\text{Active cobalt}=K_1(\text{Co})^2/(\text{acid})^2$$

Therefore, it can be concluded that the rate constant of the decomposition of tetralin hydroperoxide in an acid solvent may be attributed mainly to the kind of metal[2] and very little to the acid.

**The Oxidation of Tatralin in the Fatty Acid Solvent.**—Previously,[4,5] it was proved that the rate of the oxidation of tetralin reaches a limiting rate at high catalyst concentrations; this was explained by the mechanism suggested by Tobolsky;[10]

$$-dO_2/dt=k_3^2(RH)^2/2k_6$$

The rates of the oxidation of tetralin against the cobalt concentration in several fatty acids are shown in Fig. 1. At cobalt concentrations higher than $5\times10^{-2}$ mol./l., the rate reaches a limiting value according to the solvent used. The lower the dielectric constant of the acid, the lower the limiting rate. In contrast, the order of the rate of oxidation was completely reversed at low catalyst concentrations; this is due to the effect of the higher initiation rate caused by the solvent. Recently, the rate of autoxidation has been correlated as a dielectric function by several workers.[1,2,11] Hendry showed that the oxidation rate could be roughly correlated with the dielectric constant ($D$) of the solvent by means of the function $(D-1)/(2D+1)$, which describes the bulk effect of solvents on dipole-forming reactions.

That is, the rate constant, $k'$, for a reaction in a solution[13] is given by:

$$\ln k'=\ln k_0'-\frac{1}{kT}\frac{D-1}{2D+1}\left(\frac{\mu^2_A}{a^3_A}+\frac{\mu^2_B}{a^3_B}-\frac{\mu^2_{M^*}}{a^3_{M^*}}\right)+\frac{\phi_A+\phi_B-\phi_{M^*}}{kT}$$

$k_0'$ is the specific rate constant in a solvent with a unit dielectric constant, while $\mu$ and $a$ are the dipole moment and the radius of the reactants (A and B) and transition state (M). $\phi$ is a correction factor for non-electrostatic forces between the solvent and the reactants, and the solvent and transition state (e. g., dipole quadruple forces, van der Waals forces, and other specific solvation effects). Provided the non-electrostatic terms are small enough to be neglected, a plot of $\log k'$ against $(D-1)/(2D+1)$ should be linear.

Howard and Ingold[2] obtained a rather more linear correlation with styrene than was obtained by Hendry[1] with cyclohexene, but there was still the same sharp increase in the rate for the solvents with very high dielectric constants. The correlation between $\log(k_3/k_6^{1/2})$ and $(D-1)/(2D+1)$ is not significantly improved by multiplying the dielectric function by the ratio of the density

10) A. V. Tobolsky, D. J. Metz and R. B. Mesrobian, *J. Am. Chem. Soc.*, **72**, 1942 (1950).

11) G. E. Zaikov and Z. K. Maizus, *Inst. Chem. Phys. Acad. Sci. USSR*, **1962**, 1102.

12) Y. Kamiya and K. U. Ingold, *Can. J. Chem.*, **42**, 1027 (1964).

to the molecular weight of the solvent. Later, Howard and Ingold also studied the oxidation of $\alpha$-methylstyrene, tetralin, 4-methyl cyclohexene and cumene, and plotted the $k_3/k_6^{1/2}$ values for the first three hydrocarbons against the $k_3/k_6^{1/2}$ value for styrene. They concluded that the increase in the oxidation rate with an increase in the solvent dielectric constant results mainly from the interaction of the solvent with the dipolar transition state of the propagation reaction.

The values of $k_3/k_6^{1/2}$ calculated in this work from the limiting rate of the oxidation of tetralin in the fatty acid solution, are plotted against $(D-1)/(2D+1)$ in Fig. 2; an excellent linear correlation is obtained. The very good result in the case of the fatty acid solvent can be attributed to the lack of any deactivation of the catalyst and also, presumably, to little difference in the correction factor, $\phi$, upon a change in solvent.

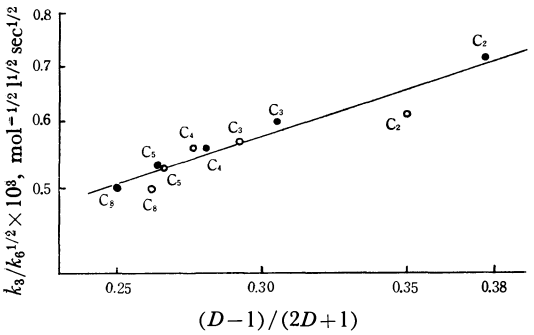



Fig. 2. Plot of $k_3/k_6^{1/2}$ for the oxidation of tetralin in the fatty acid against dielectric function, $(D-1)/(2D+1)$.
$C_n$: $n$ represents the carbon number of fatty acid.
● Tetralin 1.22 mol./l.
○ Tetralin 3.67 mol./l.

As a result, the limiting rate of the oxidation of tetralin in an acid solvent can easily and accurately be estimated when its dielectric constant is known.

At low catalyst concentrations, the rate of oxidation can be written by Eq. 5. When the hydroperoxide concentration is high enough compared with cobalt, the term $(Co)(ROOH)^{1/2}$ nearly equals (Co), because, as has been suggested by many workers,[5] cobalt and hydroperoxide form an intermediate complex. Therefore, Eq. 5 can be simplified as follows:

$$-dO_2/dt = k_3(k_1'/k_6)^{1/2}(RH)(Me) - k_1'(Me)^2/2$$

$k'_1$ can be obtained by the direct determination of the decomposition rate of hydroperoxide, or from $k''$, which is nearly $2\times10^4$ sec$^{-1}$, while $k_3/k_6^{1/2}$ can be obtained from the dielectric constant or the limiting rate of oxidation. The rate of oxidation calculated by Eq. 5 and the observed values at cobalt concentrations of $3\times10^{-4}$ and $1\times10^{-4}$ mol./l. in the six fatty acids are shown in Table II.

Table II. The calculated and observed values of the rate of oxidation of tetralin

| Solvent | $-dO_2/dt\times10^5$ (mol./l. sec.) | | | |
|---|---|---|---|---|
| | $CoDe_2$ $3\times10^{-4}$ mol./l. | | $CoDe_2$ $1\times10^{-4}$ mol./l. | |
| | Calcd. | Obs. | Calcd. | Obs. |
| Acetic | 6.1 | 5.2 | 2.3 | 2.0 |
| Propionic | 7.6 | 6.5 | 3.0 | 2.9 |
| Butyric | 8.0 | 8.5 | 3.4 | 3.2 |
| Pentanoic | 8.4 | 9.0 | 3.8 | 3.5 |
| Heptanoic | 8.8 | 10.1 | 4.7 | 4.1 |
| Nonanoic | 11.0 | 12.0 | 5.2 | 5.1 |

The calculated values showed an excellent agreement with the experimental results, thus justifying the limiting-rate theory.

It may be concluded that not only the limiting rate of tetralin oxidation, but also the rate of tetralin oxidation at low catalyst concentrations, can be estimated with very good accuracy.

**The Effect of Stronger Organic Acids on the Rate of Oxidation.**—When dichloro- or trichloro-acetic acids were used as solvents, the oxidation of tetralin did not proceed at all at cobalt concentrations lower than $5\times10^{-2}$. However, monochloroacetic acid gave a limiting rate of $2.62\times10^{-4}$ mol./l. sec., as compared with that of $2.5\times10^{-4}$ mol./l. sec. in acetic acid, which is a quite reasonable value in view of its dielectric constant. In the case of monochloroacetic acid, a slow but steady deactivation of the catalyst took place, probably due to the formation of an inactive complex between cobalt and monochloroacetic acid. Incidentally, no oxygen absorption was observed at $5\times10^{-3}$ mol./l. (Co) in a monochloroacetic acid solution. Even a small amount of monochloroacetic acid reduced the rate of the cobalt-catalyzed oxidation of tetralin in acetic acid. The effect of a small amount of various organic acids on the oxidation rate of tetralin in acetic acid was studied in the limiting-rate region, i. e., $5\times10^{-2}$ mol./l. (Co).

Benzene carboxylic acids produced in a slight decrease of the rate of oxidation, but oxalic acid, which showed the strongest effect of all acids tested, was found to deactivate an equimolar amount of cobalt. The solvent effect of chloroacetic acids was studied by Ohta[14] for $p$-xylene and by Levanevskii[15] for $n$-decane; they found a marked increase in the rate of oxidation compared with the rate in acetic acid. The difference between their results and those of experiment can be attributed to the strong temperature-dependency of the metal-deactivating effect of chloroacetic acids.

13) K. J. Laidler and H. Eyring, *Ann. N. Y. Acad. Sci.*, **39**, 303 (1940).
14) N. Ohta, E. Takahashi and H. Horikiri, *J. Chem. Soc. Japan, Ind. Chem. Sec.* (*Kogyo Kagaku Zasshi*), **63**, 768 (1960).
15) O. E. Levanevskii and T. Zhumabylov, *Neftkhim*, **1963**, 264; *Chem. Abstr.*, **60**, 13111 (1963).

**The True Limiting Rate of the Oxidation of Tetralin.**—The limiting rate of the oxidation of tetralin was, in the previous paper, calculated from the limiting rate of the oxidation in acetic acid to be $1\times10^{-3}$ mol./l. sec.; just the dilution effect due to the $(RH)^2$ term was considered. It was concluded that it showed an excellent agreement with the theoretical value of $1\times10^{-3}$ mol./l. sec. However, as has been described above, the dielectric effect should be taken into consideration. After correcting for the dielectric effect, the measured limiting rate of the oxidation of tetralin is $7.8\times10^{-4}$ mol./l. sec. The difference between the theoretical rate and observed rate after the correction may be attributed to the non-radical decomposition of hydroperoxide. The products of the decomposition of tetralin hydroperoxide by cobalt salt have been shown by gas chromatography to be composed of 50% $\alpha$-tetralone and 50% a mixture of $\alpha$-tetralol and dihydronaphthalene. Dyer et al.[16] obtained similar results by chemical analysis.

In the limiting-rate region, as has been described previously, the expected ratio of alcohol to ketone is 2 : 1. The non-radical decomposition of hydroperoxide may yield $\alpha$-tetralone as follows:

$$ROOH + n\text{Me} \xrightarrow{k^*} \alpha\text{-tetralone} + H_2O + n\text{Me}$$

Therefore, the radical-producing decomposition may be calculated to be 75%; i. e.: $k_1'/k_1'+k^*=0.75$

Accordingly, the limiting rate of the oxidation of tetralin at 50°C becomes $0.75\times10^{-3}=7.5\times10^{-4}$, which agrees excellently with the theoretical value of $7.8\times10^{-4}$.

16) E. Dyer K. R. Carle and D. E. Weiman, *J. Org. Chem.*, **23**, 1464 (1958).

## Summary

The rate of the cobalt-catalyzed decomposition of tetralin hydroperoxide in fatty acid solvents was first order with respect to hydroperoxide and second order with respect to the cobalt, and it was inversely proportional to the square of the acid concentration; i. e., $-\mathrm{dROOH}/\mathrm{d}t=k''(\mathrm{Co})^2\cdot(\mathrm{ROOH})/(\mathrm{Acid})^2$. The rate constant, $k''$, was found to be almost constant, regardless of the molecular weight of the acid. The values of $k_3/k_6^{1/2}$ obtained from the limiting rate of the oxidation showed an excellent linear correlation against the dielectric function of $(D-1)/(2D+1)$. The rate of the oxidation of tetralin calculated by $-\mathrm{dO}_2/\mathrm{d}t=k_3(k_1'/2k_6)^{1/2}(\mathrm{RH})(\mathrm{Co})-k_1'(\mathrm{Co})^2/2$ showed an excellent agreement with the value observed at cobalt concentrations lower than $3\times10^{-4}$ mol./l. Strong organic acids such as chloroacetic acids deactivated the cobalt catalyst, and oxalic acid, which has shown the strongest deactivating effect of all the acids tested, deactivated equimolar cobalt salt.

The author wishes to express his thanks to Professor Shingo Ando and Dr. K. U. Ingold for their continued advice and encouragement in this work.

*Department of Fuel*
*Faculty of Engineering*
*The University of Tokyo*
*Hongo, Tokyo*

# Studies of Halogenoacetato Cobalt(III) Complexes. III.*,[1] The Preparation and Some Properties of Trifluoroacetato Cobalt(III) Complexes

By Kashiro KURODA and Philip S. GENTILE

(Received June 7, 1965)

In the preceding communications[1,2] the present authors have reported on the preparation of and some properties of pentammine-, tetrammine- and bis(ethylenediamine)-cobalt(III) complexes with chloroacetato and bromoacetato ligands—$[Co(halac)(NH_3)_5]X_2$, *cis*- and *trans*-$[Co(halac)_2(NH_3)_4]X$ and *cis*- and *trans*-$[Co(halac)_2(en)_2]X$, where halac$=CH_3CO_2$, $CH_2ClCO_2$, $CHCl_2CO_2$, $CCl_3CO_2$, $CH_2BrCO_2$ and $CHBr_2CO_2$. There we pointed out several regularities found in their properties. It was there considered to be very interesting that in each series of complexes the basicity of the halogenoacetato ligands is the main factor determining the maxima of their absorption spectra, and that the volume of the ligands and the sort of halogen in the halac's are minor ones.

* This work was mostly done in the laboratory of Chemistry Department, Fordham University, New York 58, N. Y., U. S. A., when the former of the authors was a visiting chemist to the university.

1) Parts I and II of this series: K. Kuroda and P. S. Gentile, This Bulletin, **38**, 1362, 1368 (1965).

2) K. Kuroda and P. S. Gentile, *J. Inorg. Nucl. Chem.*, **27**, 155 (1965).

Although the trifluoroacetato-pentammine-cobalt(III) complex, $[Co(CF_3CO_2)(NH_3)_5]X_2$, has previously been studied,[3,4] bis(trifluoroacetato)-cobalt(III) complexes have so far not been prepared. Since trifluoroacetic acid is a stronger acid than any other halogenoacetic acid (it is virtually a strong electrolyte), the basicity of the trifluoroacetato ligand is the smallest among all of the halogenoacetato ligands, the spectral features of trifluoroacetato complexes should be the most extreme in each member of the above series. With such an expectation, several new cobalt complexes with trifluoroacetato ligand, *cis*-$[Co(CF_3CO_2)_2(NH_3)_4]ClO_4$, *trans*-$[Co(CF_3CO_2)_2(NH_3)_4]Cl$, *cis*-$[Co(CF_3CO_2)_2(en)_2]ClO_4$ and *trans*-$[Co(CF_3CO_2)_2(en)_2]ClO_4$, have been prepared, and some physical and chemical properties have been examined. In consequence, the expected results have been obtained, and also a few special noteworthy phenomena have been observed.

## Experimental

**Materials.** — Trifluoroacetic acid (K & K Laboratories, Inc.) and all the other reagent-grade chemicals were used without further purification.

**Analysis.**—Cobalt was analyzed by EDTA direct titration, using murexide as an indicator,[5] after a complex had been decomposed with hot concentrated sulfuric and nitric acids. The other elements were analyzed microquantitatively by the Schwarzkopf Microanalytical Laboratory (Woodside, New York, U. S. A.).

**Apparatus and Measurements.**—The visible and ultraviolet absorption spectra of the complexes were measured with a Cary 15 spectrophotometer, using a pair of one-cm. quartz cells. The measurements were carried out in a way which has been described previously.[1] The infrared spectra were also taken with a Perkin-Elmer Infracord in order to help verify the composition of the compounds. All of the complexes showed the characteristic absorptions of CO and $ClO_4$ (except for 3) below). The procedure of the solubility measurement, as well as that of the precipitation test, have also been described previously.[1]

**The Assignment of Configuration.**—It has been settled both experimentally[6,7] and theoretically[8,9] that the 1st band of a trans-isomer splits much more significantly than that of the corresponding cis-isomer. As may be seen in Fig. 1, two isomers exhibited such absorption curves; by this means geometrical configurations were assigned.

**Preparations.** — *1) Trifluoroacetato-pentammine-cobalt(III) Perchlorate, $[Co(CF_3CO_2)(NH_3)_5](ClO_4)_2$.*—The nitrate was prepared by a procedure similar to that used for the acetato-complex described in "Inorganic Syntheses."[10] The nitrate was transformed to the perchlorate by the addition of perchloric acid to its solution.

*2) cis-Bis(trifluoroacetato)-tetrammine-cobalt(III) Perchlorates, cis-$[Co(CF_3CO_2)_2(NH_3)_4]ClO_4$.*—A mixture of $[CoCO_3(NH_3)_4]ClO_4$ (2 g.), $CF_3CO_2H$ (1.7 g.) and water (2 ml.) was evaporated to almost complete dryness at 65°C. To the reaction product was then added 5 ml. of a 20% sodium perchlorate solution; the precipitate thus formed was collected and washed with the sodium perchlorate solution. The product was recrystallized from 20 ml. of warm (~40°C) water, and the resulting crystals were collected on a glass filter and washed with ether in order to remove the attached aqueous phase mechanically as completely as possible, and then with an ethanol (80%) - ether mixture and with ether. (The complex is very soluble in ethanol, especially when it is wet.) Yield: 0.5 g.

Found: Co, 12.76; C, 10.85; H, 2.83; N, 12.14. Calcd. for *cis*-$[Co(CF_3CO_2)_2(NH_3)_4]ClO_4$: Co, 13.02; C, 10.62; H, 2.67; N, 12.38%.

*3) trans-Bis(trifluoroacetato)-tetrammine-cobalt(III) Chloride, trans-$[Co(CF_3CO_2)_2(NH_3)_4]Cl$.*—A product was obtained by the evaporation of a mixture of $[CoCO_3(NH_3)_4]ClO_4$ (3 g.), $CF_3CO_2H$ (9.5 g.) and water (5 ml.) at 75—80°C. Ten milliliters of a 20% sodium perchlorate solution was added to the cooled product, and the precipitate formed was separated and extracted by 10 ml. of warm water. After combining the extracted solution with the first filtrate, 20 ml. of a 6 N hydrochloric acid was added and the mixture was kept at 0°C for an hour. The light brownish-violet crystals which formed, which were the acidic chloride of the complex *trans*-$[Co(CF_3CO_2)_2(NH_3)_4]Cl \cdot HCl$, were then washed with a cold 6 N hydrochloric acid until the filtrate became colorless. To convert to a neutral salt, the crystals were dissolved in 10 ml. of ethanol containing a few drops of water; then 10 ml. of ether was added to the solution. The resulting pale violet precipitate was washed with an ethanol (50%) - ether mixture and with ether. The neutral salt can also be obtained if the *dry* acidic chloride is treated with absolute ethanol, but the *wet* one is very soluble in ethanol. Yield: 0.5 g.

Found: Co, 14.94; C, 12.23; H, 3.46; N, 14.07. Calcd. for *trans*-$[Co(CF_3CO_2)_2(NH_3)_4]Cl$: Co, 15.17; C, 12.36; H, 3.34; N, 14.42%.

*4) cis-Bis(trifluoroacetato)-bis(ethylenediamine)-cobalt-(III) Perchlorate, cis-$[Co(CF_3CO_2)_2(en)_2]ClO_4$.* — This complex was prepared by a procedure similar to 2). The yield of the recrystallized product was 1 g. from 2 g. of $[CoCO_3(en)_2]ClO_4$.

Found: Co, 11.50; C, 18.91; H, 3.66; N, 10.93. Calcd. for *cis*-$[Co(CF_3CO_2)_2(en)_2]ClO_4$: Co, 11.68; C, 19.04; H, 3.20; N, 11.10%.

*5) trans-Bis(trifluoroacetato)-bis(ethylenediamine)-cobalt-(III) Perchlorate, trans-$[Co(CF_3CO_2)_2(en)_2]ClO_4$.*—A mixture of $[CoCO_3(en)_2]ClO_4$ (3 g.), $CF_3CO_2H$ (10 g.) and water (5 ml.) was evaporated at 75°C to a small volume; the solution was then carefully boiled for a few minutes with a small flame until the color suddenly changed from dark red to deep reddish-violet. As soon as this process had finished, the mixture was

3) F. Basolo, J. G. Bergmann and R. G. Pearson, *J. Phys. Chem.*, **56**, 22 (1952).
4) C. B. Riolo and T. Soldi, *Gazz. Chim. Ital.*, **86**, 282 (1956).
5) H. Flaschka, *Microchemie ver. Microchim. Acta*, **39**, 38 (1952).
6) M. Linhard and M. Weigel, *Z. anorg. Chem.*, **264**, 321 (1952).
7) Y. Shimura, This Bulletin, **25**, 49 (1952).
8) C.J. Ballhausen and C.K. Jørgensens, *Kgl. Danske Videnskab. Selskab. Mat. Fys. Medd.*, **29**, No. 14 (1955).
9) H. Yamatera, This Bulletin, **31**, 95 (1958).
10) J. C. Bailar, "Inorganic Syntheses," Vol. IV, 175 (1953).

cooled. The resulting solid was crushed, and 20 ml. of a dilute sodium perchlorate solution was added and thoroughly mixed in. The precipitate which formed, after being washed with a cold sodium perchlorate solution, was recrystallized from 40 ml. of warm water. A concentrated solution which contained 2 g. of sodium perchlorate was added in order to complete the precipitation. The pale violet crystals which formed were washed with ethanol and ether. Yield: 1.5 g.

Found: Co, 11.64; C, 18.84; H, 2.86; N, 11.45. Calcd. for *trans*-$[Co(CF_3CO_2)_2(en)_2]ClO_4$: Co, 11.68; C, 19.04; H, 3.20; N, 11.10%.

## Results and Discussion

Table I shows the solubilities of the complexes prepared and their precipitation reactions with various common anions. The salts are, in general, readily soluble in water; this is in contrast to the corresponding trichloroacetato-complexes.[1] On the other hand, they are soluble in ethanol or even in an ethanol-ether mixture, especially when they are wet, as are the trichloroacetato-complexes.[1] One must take remember this quality in washing the complexes in preparing them.

Among the reactions with various anions, the precipitation of *cis*-$[Co(CF_3CO_2)_2(en)_2]^+$ with acetate ions is considered to be the most important, because there is as yet no precipitant for acetate ions. It has already been reported[11] that this reaction may be used as a new method for detecting acetate in the qualitative analysis of anions. The reactions in which trichloroacetic acid makes precipitates with the trans-isomers but not with the cis-isomers are similar to those with other halogenoacetato-complexes already reported.[1]

Table II and Fig. 1 show the absorption spectra of the complexes. Previously,[1] it has been pointed out that, in the absorption spectra of each series of halogenoacetato-complexes—the pentammine-, *cis*- and *trans*-tetrammine- and *cis*- and *trans*-bis-(ethylenediamine)-series of complexes—, the basicity of halogenoacetato ligands is the predominant factor in determining spectral characteristics, and that the other factors—the volume of the ligands and the oxidation-reduction property of halogen atoms—are minor.

Thus, the relative position of $CF_3CO_2$ in the spectrochemical series is expected to be:

$$I < \cdots < CH_3CO_2 < \left\{ \begin{array}{c} \\ CH_2ClCO_2 < CHCl_2CO_2 < CCl_3CO_2 \\ CH_2BrCO_2 < CHBr_2CO_2 \end{array} \right\} < \cdots < CN$$

($CF_3CO_2$ above $CCl_3CO_2$)

(increasing ligand field)

since the basicity of $CF_3CO_2^-$ is the smallest of

Table I. Sulubilities and precipitation reactions of trifluoroacetato cobalt(III) complexes

| | HCl 6 N | $NH_4Cl$ 2 N | $HNO_3$ 6 N | $NH_4NO_3$ 2 N | KI 2 N | $CH_3CO_2Na$ N | $K_2Cr_2O_7$ sat | $CCl_3CO_2H$ 2 N | Solubility ml. $H_2O$/g. |
|---|---|---|---|---|---|---|---|---|---|
| $[Co(CF_3CO_2)(NH_3)_5](ClO_4)_2$ | — | — | 3 | 1 | 2 | — | 4 | 1 | 153 |
| *cis*-$[Co(CF_3CO_2)_2(NH_3)_4]ClO_4$ | — | — | — | — | — | — | — | — | ~10 |
| *trans*-$[Co(CF_3CO_2)_2(NH_3)_4]Cl$ | 4 | — | — | — | — | — | — | 1 | v.s. |
| *cis*-$[Co(CF_3CO_2)_2(en)_2]ClO_4$ | — | — | — | — | — | 4 | — | — | ~18 |
| *trans*-$[Co(CF_3CO_2)_2(en)_2]ClO_4$ | — | — | — | — | 1 | — | 3 | 4 | 25 |

— No precipitation
1 A small amount of deposit observable on the surface of the test tube
2 A small amount of precipitate
3 A large amount of precipitate (the liquid phase has still the color of the complex)
4 Almost complete precipitation (the liquid phase is almost colorless)
v.s. Very soluble
The following reagents do not precipitate with any of the above complexes: 6 N $H_2SO_4$, 2 N $(NH_4)_2SO_4$, 2 N NaBr, N $Na_2SO_3$, N $Na_2S_2O_3$, N $NaNO_2$, N $Na_2CO_3$, sat-$Na_2C_2O_4$, N KSCN, N $K_2CrO_4$, sat-$Na_2HPO_4$.

Table II. Absorption spectra of trifluoroacetato cobalt(III) complexes

| | 1st band | | | | 2nd band | |
|---|---|---|---|---|---|---|
| | Ia | | Ib | | | |
| | $\nu_{1a}$ ($10^{13}$/sec.) | log $\varepsilon_{1a}$ | $\nu_{1b}$ ($10^{13}$/sec.) | log $\varepsilon_{1b}$ | $\nu_2$ ($10^{13}$/sec.) | log $\varepsilon_2$ |
| $[Co(CF_3CO_2)(NH_3)_5]^{2+}$ | 60.1 | 1.799 | | | 86.2 | 1.697 |
| *cis*-$[Co(CF_3CO_2)_2(NH_3)_4]^+$ | 58.5 | 1.894 | | | 83.5 | 1.713 |
| *trans*-$[Co(CF_3CO_2)_2(NH_3)_4]^+$ | 53.7 | 1.672 | 66.0 | 1.40 | 84.5 | 1.702 |
| *cis*-$[Co(CF_3CO_2)_2(en)_2]^+$ | 60.6 | 2.061 | | | 83.3 | 1.903 |
| *trans*-$[Co(CF_3CO_2)_2(en)_2]^+$ | 54.5 | 1.650 | 68.6 | 1.49 | 85.2 | 1.728 |

11) K. Kuroda, *J. Chem. Soc. Japan, Pure Chem. Sec.* (*Nippon Kagaku Zasshi*), **85**, 515 (1964).

all of the halogenoacetate ions. This expectation was statisfactorily verified by the experimental results that the absorption maxima of the present complexes (except for the split 1st bands of the trans-isomers) were found at the highest frequencies in each series of complexes.[1]

The splitting of the 1st bands of the *trans*-isomers is worth noticing because of its magnitude. As may be clear from a comparison of Fig. 1 and Figs. 1 and 2 in Part II (Ref. 1), the degree of the splitting of the present trans-isomers is rather larger than that of trichloroacetato complexes. This result confirms the previous suggestion that the distance in the spectrochemical series between the "a" and "b" of a complex *trans*-$[Coa_4b_2]$ is not the sole factor determining the magnitude of the splitting.

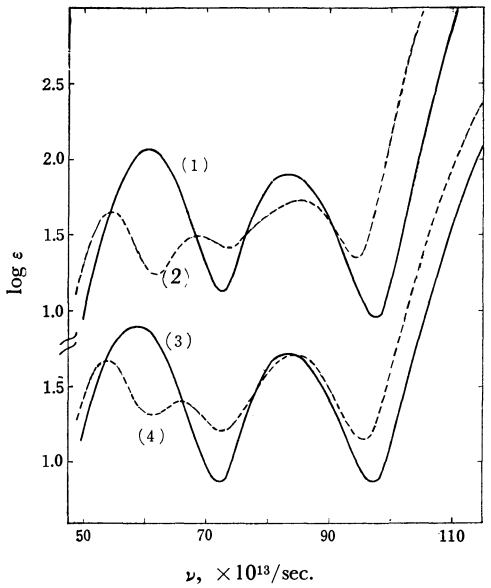



Fig. 1. Absorption spectra of trifluoroacetato cobalt(III) complexes.

(1) *cis*-$[Co(CF_3CO_2)_2(en)_2]ClO_4$
(2) *trans*-$[Co(CF_3CO_2)_2(en)_2]ClO_4$
(3) *cis*-$[Co(CF_3CO_2)_2(NH_3)_4]ClO_4$
(4) *trans*-$[CO(CF_3CO_2)_2(NH_3)_4]Cl$

The shape of the 2nd band of *trans*-$[Co(CF_3CO_2)_2(en)_2]^+$ is considered to be noteworthy. It is well known[12] that, in a pure single band, the half-width of the left branch, $\delta$-, is usually about 10% smaller than that of the right branch, $\delta_+$; this generality is preserved in the lst and 2nd bands of $[Co(CF_3CO_2)(NH_3)_5]^{2+}$, *cis*-$[Co(CF_3CO_2)_2(NH_3)_4]^+$, and *cis*-$[Co(CF_3CO_2)_2(en)_2]^+$ and in Ia bands of the trans-isomers, as in the bands of many other cobalt complexes. Contrary to this rule, however, the 2nd band of *trans*-$[Co(CF_3CO_2)_2(en)_2]^+$ is abnormally asymmetric in a direction the reverse of the ordinary cases, as may be observed in Fig. 1. Indeed, the right branch of the Ib band might influence the left branch of the 2nd band, but because Ib is so small and so separated from the 2nd that it is not possible to deform for it the band to such a large extent. A similar deformation can be observed in the spectra of the *trans*-$[Co(halac)_2(en)_2]^+$ series previously reported[1]; that is, the left branch of the 2nd band broadens steadily with an increase in the chlorine content of the halac-ligands, and the deformation of *trans*-$[Co(CCl_3CO_2)_2(en)_2]^+$ is as large as that of *trans*-$[Co(CF_3CO_2)_2(en)_2]^+$. The same trend, but to a lesser degree, is also observable in the *trans*-$[Co(halac)_2(NH_3)_4]^+$ series. These facts may indicate a splitting of the 2nd bands.

It has been pointed out[13] that the 2nd band of a *trans*-$[Coa_4b_2]$-type complexes should split into two parts by the tetragonal distortion of the ligand field, as the 1st band does. However, no cobalt complex has ever been found which exhibits such splitting in the band. The reasons for this are considered to be that, in many cases, the 2nd band is greatly influenced by adjacent bands and/or ligand specific bands; there have been very few examples in which both the branches of the band could be compared over a sufficient frequency range free from the influence of other bands. Fortunately, the 2nd bands of the present complexes are satisfactorily pure and can be examined with accuracy. A precise analysis of the spectral curves is undoubtedly necessary for a decision on the splitting phenomena; this research will be reported on shortly in a separate paper.

The authors are grateful for the support provided for this research by the Atomic Energy Commission of U. S. A. under Contract No. AT(30-1)-906.

*Department of Chemistry*
*Kyoto-Gakugei University*
*Fushimi-ku, Kyoto (K. K.)*

*Department of Chemistry*
*Fordham University*
*New York 58, N. Y., U. S. A. (P. S. G)*

12) C. K. Jørgensen, *Acta Chem. Scand.*, 8, 1495 (1954).

13) J. S. Griffith and L. E. Orgel, *J. Chem. Soc.*, **1956**, 4981.

# The Structure and Properties of Supported Cobalt Catalysts

By Hiroshi HAGIHARA and Etsuro ECHIGOYA

(Received June 8, 1965)

In experiments previously reported by the present same authors[1], it was observed that the catalytic activity of supported metal catalysts in the hydrogenation reaction of aniline varied greatly for different types of catalyst. In order to understand this phenomenon, it is necessary to know the structure and properties of these catalysts.

Many reports[2-5] have been published with respect to the structure and properties of supported nickel catalysts, but few regarding supported cobalt catalysts. Anderson et al.[6] have reported on the structure and properties of the catalyst for Fisher-Tropsch synthesis. However, their study was restricted to the chemical properties of a cobalt-diatomaceous earth system.

The present investigation has been undertaken in an attempt to obtain some information about the structure and properties of cobalt oxide as supported on various kinds of oxide carriers, and also on the relationship between the hydrogenation activity and the catalyst structure.

## Experimental

**The Preparation of Catalysts.** — The standard procedures of catalyst preparation were as follows:

*The Impregnation Method:* The powdered support was added to a solution of cobalt nitrate. The slurry was stirred for some time, and then to it was slowly added, at 20°C, a quantity of dissolved ammonium carbonate in a slight excess. After the precipitate has been filtered and washed, it was dried at 100°C and then calcined at 500°C for 2 hr.

*The Coprecipitation Method:* The catalyst was prepared by coprecipitation, from a mixed solution of cobalt nitrate and aluminum nitrate or sodium silicate, by ammonium carbonate solution at 20°C with vigorous stirring. The slurry was stirred for some time, and then it was vacuum-filtered. The precipitate was washed with distilled water on the filter, dried in a drying cabinet at 100°C, powdered, and calcined at 500°C for 2 hr. in air.

*The Hydrothermal Treatment:* Basic cobalt carbonate (prepared from cobalt nitrate and ammonium carbonate solutions at 20°C) was mixed with silica gel or aluminum oxide gel, and then heated with water in an autoclave at 200°C for 25 hr. It was then cooled, filtered, washed with distilled water, dried at 100°C, and calcined at 550°C for 2 hr.

*The Mixing Method:* The powdered silica gel and cobalt basic carbonate were mechanically mixed in water in a beaker. The mixture was vacuum filtered, and then it was dried at 100°C and calcined at 500°C for 2 hr.

**Surface Area Measurements.**—The area of the samples was estimated by the BET method.

**The Reduction of the Catalysts in Hydrogen.**—*Hydrogen consumption measurement.*—The volumetric apparatus shown in Fig. 1 was used for this attempt. Hydrogen was continuously circulated through the catalyst at the flow rate of 100 cc./min., and the water produced by reduction was removed using a dry-ice methanol trap and a silica gel drier placed behined the catalyst bed. The pressure was held manually at one atmosphere by adjusting the leveling (L). Thus the pressure difference of the manometer showed directly the volume of hydrogen consumed; this volume was then plotted as a function of the heating-up temperature and of the time (Fig. 1). The apparent $H_2$ consumption as measured as described above was then corrected for the changes in volume caused by heating.

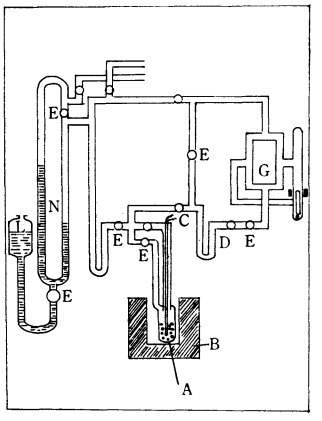



Fig. 1. Apparatus for hydrogen consumption measurements.

A: Catalyst bed
B: Electric heater
C: Themocouple
D: Drying agent
E: Stop-cock
G: Circulation pump
L: Leveling
N: Manometer

1) H. Hagihara and E. Echigoya, *Shokubai (Catalyst)*, **6**, 345 (1964).
2) J. J. B. van Eijk van Voorthujsen and P. Franzen, *Rec. Trav. Chim.*, **70**, 793 (1951).
3) W. O. Milligan and L. Merten, *J. Phys. Chem.*, **50**, 465 (1946).
4) G. C. A. Schuit and L. L. van Reijen, *Adv. in Catalysis*, **X**, 242 (1958).
5) K. Morikawa and F. Nozaki, *J. Chem. Soc. Japan, Ind. Chem. Sec. (Kogyo Kagaku Zasshi)*, **64**, 1568 (1962).
6) R. B. Anderson, W. K. Hall and L. J. E. Hofer, *J. Am. Chem. Soc.*, **69**, 3114 (1947).

TABLE I. SAMPLES

| No. | Catalyst | Metal-content Wt.% | Metal-content Mol.% | Preparation method | Color | |
|---|---|---|---|---|---|---|
| 1 | Co-$Al_2O_3$ | 20 | 30 | Impregnation | Black | 20 Co-$Al_2O_3$-p |
| 2 | Co-$Al_2O_3$ | 49 | 64 | Impregnation | Black | 49 Co-$Al_2O_3$-p |
| 3 | Co-$Al_2O_3$ | 25 | 30 | Coprecipitation | Black | 25 Co-$Al_2O_3$-cp |
| 4 | Co-$Al_2O_3$ | 18 | 27 | Hydrothermal treatment | Black-yellow | 18 Co-$Al_2O_3$-ht |
| 5 | Co-$SiO_2$ | 20 | 21 | Impregnation | Black | 20 Co-$SiO_2$-p |
| 6 | Co-$SiO_2$ | 51 | 53 | Impregnation | Black | 51 Co-$SiO_2$-p |
| 7 | Co-$SiO_2$ | 26 | 27 | Mixing | Black | 26 Co-$SiO_2$-m |
| 8 | Co-$SiO_2$ | 20 | 21 | Hydrothermal treatment | Blue | 20 Co-$SiO_2$-ht |
| 9 | Co-Celite | 50 | 52 | Impregnation | Black | 50 Co-Celite-p |
| 10 | Co-MgO | 46 | 37 | Impregnation | Black | 46 Co-MgO-p |
| 11 | Co-ZnO | 45 | 39 | Impregnation | Grey | 45 Co-ZnO-p |

* The color is given for the catalyst which was calcined at 500°C for 2 hr.

*The change in the X-ray diffraction pattern of the catalyst upon being reduced in a stream of $H_2$, using a high temperature X-ray camera.* The heating unit of this X-ray camera consists of a Pt-Rh plate, which serves as a support for the powdered sample and also as a heating element by means of the passage of the electric current through it. The sample temperature was measured by a alumel-chromel thermocouple inserted in the center of the Pt-Rh plate. The whole assembly was placed inside a container, through which $H_2$ gas was then passed. The X-ray tube irradiates the specimen attached to the Pt-Rh plate, as in the ordinary powder method, and produces an overlapping X-ray pattern of the specimen and platinum. After a one-hour reduction with a 50 cc./min. flow rate of $H_2$ at a definite temperature, X-ray diffraction pattern was obtained. This technique was previously described by Kubo[7]; it was only slightly modified in this investigation.

**Differential Thermal Analysis.**—The differential thermal analysis was performed in air at a heating rate of 7—10°C/min. The reference junction of the differential couple was embedded in an inserted fused quartz. Fifty milligrams of the sample was sandwiched between two 200 mg. layers, of the fused quartz or $\alpha$ alumina, each in a platinum cell. The thermocouple employed was alumel-chromel.

**Infrared Spectra.** — The infrared spectra in the NaCl and KBr prism regions (5000—600 $cm^{-1}$) were obtained by using a Hitachi EPI-2G infrared spectrophotometer. The wavelength calibration was made with polystyrene. Spectra were measured by the KBr disk and Nujol methods.

**The Solubility of the Catalysts in 2 N Hydrochloric Acid.**—0.2 g. of the powdered catalyst was added to 50 ml. of 2 N hydrochloric acid. The slurry was then stirred vigorously at 30°C for 8 hr. by a magnetic stirrer. The resulting slurry was decanted, and 50 cc. of 2 N hydrochloric acid was added to the remaining slurry. After this process had been repeated three times, the filtered solution was collected and the amount of cobalt oxide was determined by EDTA titration. The fraction dissolved was calculated as follows:

$$\text{Dissolved (\%)} = \frac{\text{the amount of Co in the soln. (g.)}}{\text{the initial amount of Co in the cat. (g.)}}$$

**Activity Test.**—The experiments were performed in a fixed bed apparatus of the flow type in the temperature range from 150 to 300°C.

## Results and Discussion

**Surface Area Data.**—The surface areas of the unreduced and reduced catalysts are given in Fig. 2 and in Table II. From these data, it can be seen that the surface area of all the catalysts studied decreased by upon reduction. The areas of the cobalt-silica, cobalt-alumina and cobalt-celite catalysts decreased to 90%, to 80—70% and to 60% of those before reduction respectively. It was shown, however, that the area of celite did not change appreciably when it was subjected to the usual reduction procedures[8]. From the data in Table II and Fig. 2, silica or alumina carriers appear to be more effective in preventing the sintering of Co during reduction than diatomaceous earth (celite). This may be attributed to the

TABLE II

| Catalyst | Surface area $m^2/g.$ |
|---|---|
| $Co_3O_4$ | 90 |
| NiO | 42 |
| Co-Celite (50%) | 140 |
| Co-Celite 450°C, 2 hr. red. | 95 |
| Co-MgO (46%) | 85 |
| Co-ZnO (45%) | 200 |
| Co-$SiO_2$-ht (20%) | 190 |
| Co-$Al_2O_3$-ht (18%) | 140 |

7) K. Kubo and M. Kato, *J. Chem. Soc. Japan, Ind. Chem. Sec.* (*Kogyo Kagaku Zasshi*), **64**, 63 (1961); **66**, 403 (1963).

8) R. B. Anderson, W. K. Hall and L. J. E. Hofer, *J. Am. Chem. Soc.*, **70**, 2465 (1948).

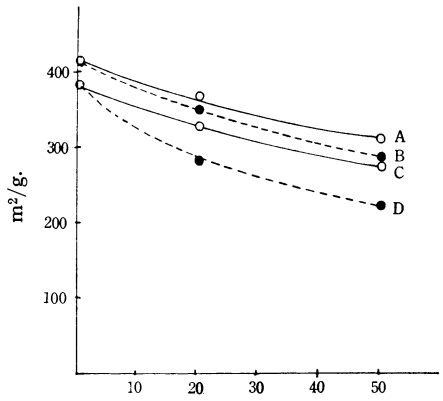



Fig. 2. Surface area of catalysts.
A: Co-$SiO_2$-p (unreduced)
B: Co-$SiO_2$-p (reduced at 450°C, 2 hr.)
C: Co-$Al_2O_3$-p (unreduced)
D: Co-$Al_2O_3$-p (reduced at 450°C, 2 hr.)

state of cobalt oxide on the carriers, i. e., to the oxide distribution on the carrier-surface and to the nature of the carrier-oxide bond. The decrease in the surface area of the catalysts produced by hydrothermal treatment during reduction was comparatively small. This may be caused by the low reducibility of cobalt oxide in the catalyst (i. e., the small fraction reduced to the metal.)

**Reducibility by $H_2$.**—The reduction curves are presented in Figs. 3, 4, and 5. The method of preparation bears a direct relationship to the reducibility of the supported cobalt oxide. For the cobalt diatomaceous earth system, Craxford[9] reported a decreasing reducibility as the formation of hydrosilicates progresses. The same phenomenon was reported for supported Ni-oxide by Van Eijk van Voorthujsen[2] and Morikawa et al.[5] Taking all these facts into consideration, it seems that an interaction has most probably occured between cobalt oxide and alumina or silica gel.

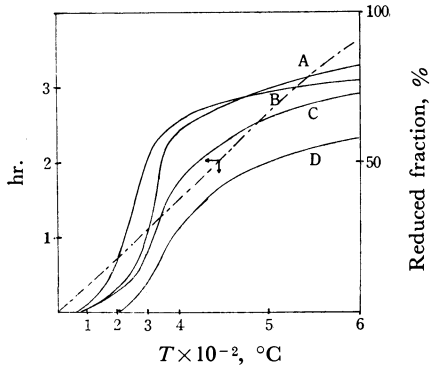



Fig. 3. Reduction curves of Co-$Al_2O_3$ catalysts.
A: 20 Co-$Al_2O_3$-p B: 49 Co-$Al_2O_3$-p
C: 25 Co-$Al_2O_3$-cp D: 18 Co-$Al_2O_3$-h

9) S. R. Craxford and A. Poll, *J. Chim. Phys.*, **47**, 253 (1950).

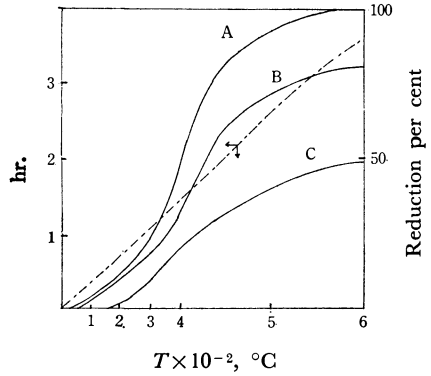



Fig. 4. Reduction curves of Co-$SiO_2$ catalysts.
A: 26 Co-$SiO_2$-m B: 51 Co-$SiO_2$-p
C: 20 Co-$SiO_2$-h

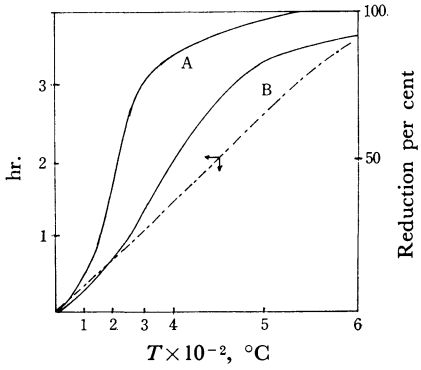



Fig. 5. Reduction curves of Co-MgO, Co-Celite.
A: 50 Co-Celite-p B: 46 Co-MgO-p

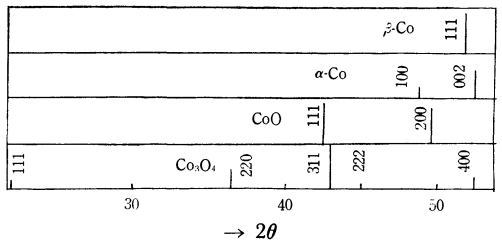



Fig. 6. The X-ray diffraction pattern of related materials.

In cobalt oxide - alumina catalysts,[10] prepared by the various methods described above, the degree of the formation of a complex structure was found to decrease in the following sequence: the hydrothermal > coprecipitation > impregnation methods. The same conclusion was obtained from a study of the effect of the hydrothermal treatment, which brought about an improvement in the complex structure. From the curves (Figs. 3 and 4), it is also apparent that the reducibility of cobalt oxide and the supported compounds decreases

10) J. T. Richardson and L. W. Vernon, *J. Phys. Chem.*, **62**, 1153 (1958).

with an increase in the quantity of the carrier. This may be related to the high degree of dispersion and to the strong interaction between the metal and carrier used.

**The Course of Catalyst Reduction in $H_2$, Seen by Using an X-Ray Camera.**—As Figs. 7 and 8 show, the temperatures of the reduction to cobalt(II) oxide and cobalt-metal varied greatly with the cobalt oxide contents, the methods of preparation, and the kinds of carriers used. In cobalt-alumina catalysts, cobalt-metal was first observed in the temperature range from 300°C to 500°C. The different temperature of the formation of the cobalt-metal on the carrier is related to the structure and to the cobalt-oxide content of the catalyst. The preparation by the coprecipitation methods results in an improvement of the formation of the complex between cobalt oxide and the carrier. In the cobalt-silica system, the catalyst produced by impregnation and the coprecipitation method also showed a high resistance to reduction by $H_2$. The cobalt metal was first observed at 500°C. This phenomenon suggested a complex formation between cobalt-oxide and silica gel. In cobalt-celite, the temperature of the reduction to cobalt-metal was about 300°C. This may be related to the low degree of dispersion of cobalt oxide and to the less complex formation in this case. In the range from 200 to 300°C, the cobalt-(II, III) oxide in the catalyst is mainly reduced to cobalt(II) oxide; later it is reduced to $\beta$-cobalt between 300 and 500°C (Fig. 9).

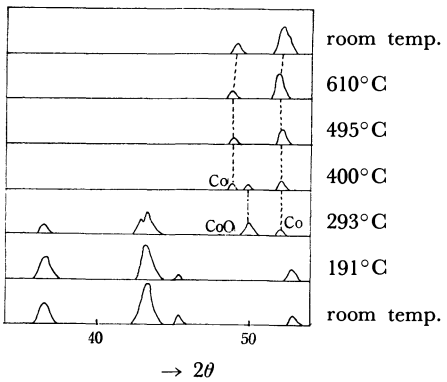



Fig. 7. X-Ray diffraction pattern in a stream of $H_2$. Sample: 49% Co-$Al_2O_3$-p

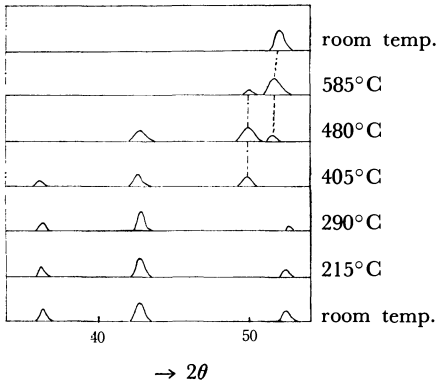



Fig. 8. X-Ray diffraction pattern in a stream of $H_2$. Sample: 25% Co-$Al_2O_3$-cp

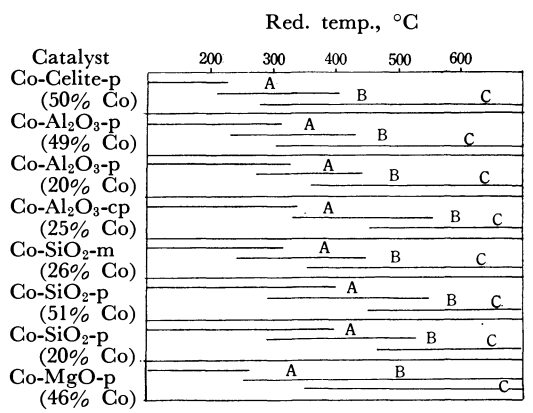



Fig. 9. Summary of the X-ray diffraction pattern of the catalyst being reduced in a stream of $H_2$. A: $Co_3O_4$, B: CoO, C: $\beta$-Co

**Differential Thermal Analysis.**—All the thermograms of cobalt oxide catalysts are given in Fig. 10 for purposes of comparison. The basic cobalt carbonate exhibited two endothermal and one exothermal peaks. The endotherm at 100—150°C refers principally to dehydration, when most of the water is lost without any changes in structure. The endotherm at 250—350°C corresponds to the decarboxylation and dehydration which results in the change in structure from basic carbonate to cobalt monoxide. The exotherm at 350—400°C corresponds to the oxidation from cobalt(II) oxide to cobalt(II, III) oxide. Thus the changes in basic cobalt carbonate upon heating follow each other in the following manner:

$$2CoCO_3 \cdot 3Co(OH)_2 \cdot nH_2O \xrightarrow{100-150^\circ C} 2CoCO_3 \cdot 3Co(OH)_2$$

$$2CoCO_3 \cdot 3Co(OH)_2 \xrightarrow{250-300^\circ C} CoO \xrightarrow{350-400^\circ C} Co_3O_4 \longrightarrow CoO^{11)}$$

Except for the Co-$SiO_2$ catalyst produced by the coprecipitation method, the DTA curves exhibited by the various supported cobalt-oxide catalysts were almost identical with that of the basic cobalt-carbonate. For the Co-$SiO_2$ catalyst prepared by coprecipitation, however, only one broad endothermal peak was clearly observed between 500 and 700°C above the dehydration temperature. This may be attributed to the decomposition of hydrosilicate (orthotype) into cobalt oxide, silica and water.

**The Infrared Spectrum.**—Several applications of this technique to the study of catalyst

11) K. Kubo and M. Kato, *J. Chem. Soc. Japan, Ind. Chem. Sec.* (*Kogyo Kagaku Zasshi*), **67**, 1502 (1964).

structures have been reported.[12-15] The results of our investigation are shown in Fig. 11. In the spectral region examined, three bands were found: near 3400 cm,$^{-1}$ 1600 cm,$^{-1}$ and 1000 cm$^{-1}$. The 3400 cm$^{-1}$ and 1600 cm$^{-1}$ bands are attributed to the O-H bond. The band near 1000 cm$^{-1}$ may generally be attributed to the silicon oxide or aluminum oxide.[16] In the catalysts produced by hydrothermal treatment, these three bands diminished in intensity or were shifted compared with

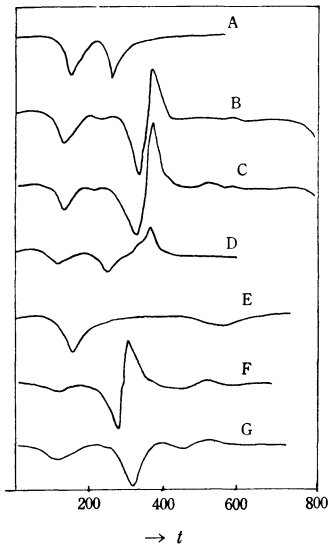



Fig. 10. DTA curves of dried catalysts.
A: $NiCO_3 \cdot Ni(OH)_2$ B: $CoCo_3 \cdot Co(OH)_2$
C: 49 $Co\text{-}Al_2O_3$-p D: 50 Co-Celite-p
E: 30 $Co\text{-}SiO_2$-cp F: 25 $Co\text{-}Al_2O_3$-cp
G: 18 $Co\text{-}Al_2O_3$-h

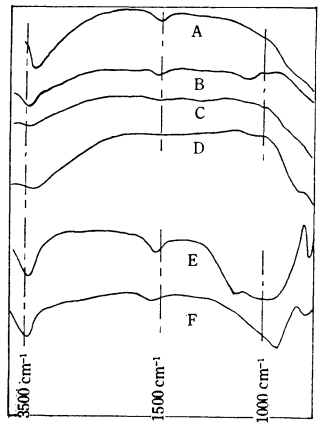


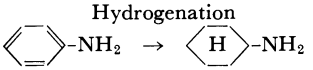
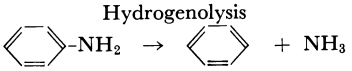

Fig. 11. IR spectra of catalysts.
A: 20 $Co\text{-}Al_2O_3$-p B: 49 $Co\text{-}Al_2O_3$-p
C: 18 $Co\text{-}Al_2O_3$-h D: $CoAl_2O_4$
E: 26 $Co\text{-}SiO_2$-m F: 20 $Co\text{-}SiO_2$-h

Table III. List of properties

| Catalyst | Preparation method | Reducibility (at 500°C) | Main compound from X-ray (reduced at 500°C) | DTA main peeks | | Solubility in 2 H HCl | Suggested structure after calcined at 500°C for 2 hr. |
|---|---|---|---|---|---|---|---|
| $Co\text{-}Al_2O_3$ (20%) | Impregnation | 73% | β-Co | ① 120°C<br>② 310<br>③ 360 | endo<br>endo<br>exo | 60% | $Co_3O_4$<br>$CoAl_2O_4$ |
| $Co\text{-}Al_2O_3$ (25%) | Coprecipitation | 65% | β-Co<br>CoO | ① 120°C<br>② 290<br>③ 310 | endo<br>endo<br>exo | 54% | $Co_3O_4$<br>$CoAl_2O_4$ |
| $Co\text{-}Al_2O_3$ (18%) | Hydrothermal | 50% | | ① 100°C<br>② 300 | endo<br>endo | 38% | $CoAl_2O_4$<br>$Co_3O_4$ |
| $Co\text{-}SiO_2$ (26%) | Mixing | 93% | β-Co | | | 100% | $Co_3O_5$ |
| $Co\text{-}SiO_2$ (20%) | Impregnation | 70% | CoO<br>β-Co | ① 150°C | endo | 98% | $Co_3O_4$<br>Cobalt-hydro-silicate (ortho type) |
| $Co\text{-}SiO_2$ (20%) | Hydrothermal | 40% | | | | 45% | $Co_3O_4$<br>Cobalt-hydro-silicate (meta type) |
| Co-Celite (50%) | Impregnation | 96% | β-Co | ① 120°C<br>② 250<br>③ 360 | endo<br>endo<br>exo | 100% | $Co_3O_4$ |
| Co-MgO (46%) | Impregnation | 85% | β-Co<br>CoO | | | | $Co_3O_4$ |

12) J. M. Hund, M. P. Wisherd and L. C. Bonham, *Anal. Chem.*, **22**, 1478 (1950).
13) E. A. Miller and C. H. Wilkins, ibid, **24**, 1253 (1952).
14) L. D. Frederickson, *Anal. Chem.*, **26**, 1883 (1954).
15) K. Morikawa and F. Nozaki, *J. Chem. Soc. Japan, Ind. Chem. Sec.* (*Kogyo Kagaku Zasshi*), **58**, 64 (1961).
16) K. Kumata and K. Aizawa, *Kagaku no Ryoiki*, Nankodo, (Tokyo) **40**, 21 (1959).

TABLE IV. ACTIVITY OF CATALYSTS

| Reaction / Experimental condition | Hydrogenation  Reaction temp. 200°C $H_2$/aniline mol. ratio 10 LHSV=1.0 $\pi$=1 atm. | | Hydrogenolysis  Reaction temp. 300°C $H_2$/aniline mol. ratio 10 LHSV=1.0 $\pi$=1 atm. | |
|---|---|---|---|---|
| | Conversion | Yield of aniline | Conversion | Yield of benzene |
| 20% Co-$Al_2O_3$ (Impreg.) | 48% | 42% | 17% | 15.5% |
| 18% Co-$Al_2O_3$ (Hydrother.) | 8.5% | 5.5% | 4% | 2.8% |
| 26% Co-$SiO_2$ (Mixing) | 27% | 22% | 12% | 10% |
| 20% Co-$SiO_2$ (Hydrother.) | 3% | 2.5% | 3.2% | 3.0% |
| 50% Co-Celite (Impreg.) | 85% | 73% | 43% | 35% |

those of catalysts prepared by impregnation. These changes may also be due to the complex formation between cobalt oxide and the carriers.

**Solubility in 2 N Hydrochloric Acid.**—Applications of this test to the supported nickel catalysts have been reported by Morikawa and Nozaki. They found that only the free metal in the catalyst is soluble in 2 N hydrochloric acid. This technique was then applied to the supported cobalt-oxide in order to find the chemical state of cobalt oxide in the catalyst. The results are summarized in Table III. The catalysts which dried at 100°C were fully soluble in 2 N hydrochloric acid. In the cobalt-alumina system, when it was calcined at 700°C for 2 hr. the cobalt(II, III) oxide in the catalyst almost became insoluble. This shows that the interaction between cobalt oxide and alumina carrier progressed further as the calcining temperature was raised. The structure of the complex was probably that of cobalt aluminate ($CoAl_2O_4$) and a solid solution. In the cobalt-silica catalyst prepared by coprecipitation, the cobalt oxide was fully soluble in 2 N hydrochloric acid, even after calcination. This may be attributed to the formation of a soluble compound, like ortho hydrosilicate.[17]

**The Relationship between Activity and Structure.**—The results of activity tests are summarized in Table IV. From the data given above, generally speaking, the catalysts of the supported free-metal type showed a higher activity in the hydrogenation and hydrogenolysis reaction of aniline. For example, in the cobalt alumina series, the activity of the catalyst produced by hydrothermal treatment is about one-fifth that of that made by the impregnation method.

17) J. A. A. Ketelaar, "Chemical Constitution," Elsvier (1958), p. 61.

## Summary

1) The chemical states of cobalt in the supported catalysts may be classified into two types. One is the type in which the cobalt is not combined with the carrier but remains free on its surface. In the other type, cobalt oxide forms a complex with the carrier and resists reduction by hydrogen.

2) The ratio of the amounts of the two types varied both with the kind of carrier and with the method of preparation used.

3) The hydrothermally-formed cobalt-alumina and cobalt-silica catalysts form $CoAl_2O_4$ and cobalt hydrosilicate compounds respectively.

4) The course of the reduction of cobalt oxide in the catalyst is as follows: In the temperature range from 200 to 300°C, the cobalt(II, III) oxide is mainly reduced to cobalt(II) oxide, and later cobalt(II) oxide is reduced to $\beta$-Co between 300 and 500°C. The reduction temperature of cobalt(II, III) oxide is different for the various types of catalysts.

5) The catalyst which consists of a complex between the metal and its carrier-oxide is less active than the free metal catalyst for the hydrogenation reaction, and it is almost completely inactive in the hydrogenolysis reaction.

6) The results of the various analyses of the supported cobalt catalysts are in good agreement with one other.

The authors wish to thank Professor Kiyoshi Morikawa for his valuable discussion, and Mr. Masaki Kato, Mr. Kaku Ishizima, Miss Keiko Irie, and Mr. Daiziro Ohata for their kind assistance.

*Yoshitomi Phramaceutical Co., Ltd.*
*Yoshitomi, Fukuoka (H. H.)*
*Research Laboratory of Resources Utilization*
*Tokyo Institute of Technology*
*Ookayama, Tokyo (E. E.)*

# Studies of Cycloheximide-Related Compounds. II. The Acid-catalyzed Condensation of Glutarimide-β-acetaldehyde with Ketones*

By Yoshiyuki EGAWA and Sumio UMEZAWA

(Received June 14, 1965)

Cycloheximide, a mold metabolite, has been known for many years, having been first isolated from the culture of streptomycin-producing Streptomyces griseus by Whiffen et al.[1] The antibiotic has been used as an agricultural fungicide and possesses antitumor and rodent-repellent activities. We have now undertaken a program of synthesis with the intention of preparing new compounds related to cycloheximide, meanwhile improving the biological activities of the antibiotic.

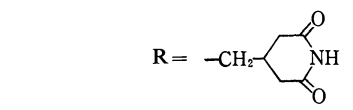
One approach to the synthesis of cycloheximide-related compounds is to condense carbonyl compounds with glutarimide-β-acetaldehyde (GAA) by aldol reaction. Lawes[2] successfully synthesized anhydrocycloheximide by condensing 2,4-dimethyl-6-formylcyclohexanone with GAA in the presence of potassium carbonate. However, since our preliminary experiments showed that basic catalysts, such as sodium hydroxide, carbonate, bicarbonate and cyanides of sodium and potassium, caused a cleavage of the imide ring in GAA during the aldol reaction, it was thought advisable to investigate condensation by the aid of acid catalysts.

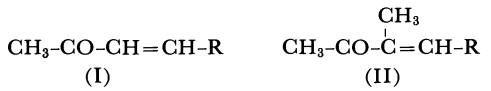
We have successfully condensed GAA with ketones by the use of dry hydrogen chloride (method A) or concentrated sulfuric acid in acetic acid (method B) to give cycloheximide-related compounds. When GAA is sparingly soluble in ketone component, method B is preferable to A.

The glutarimide-β-acetaldehyde was prepared from diethyl β-ketoglutarate and cyanoacetic acid by way of diethyl β-cyanomethylglutarate by the method of Egawa et al.[3]

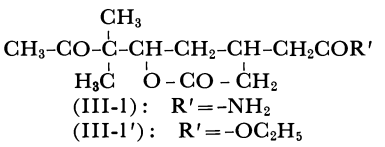
The condensation of acetone and ethyl methyl ketone with GAA by method A gave 3-(4-oxo-2-*n*-pentenyl)glutarimide (I) and 3-(3-methyl-4-oxo-2-*n*-pentenyl)glutarimide (II) respectively. Woodward's ultraviolet rule[4] predicted the values of the absorption maxima of I and II.

The reaction of methyl isopropyl ketone with GAA by method A resulted in the formation

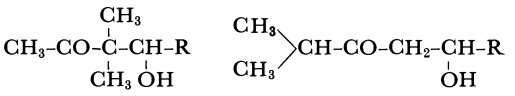




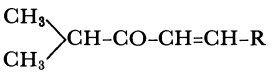
(I) (II)



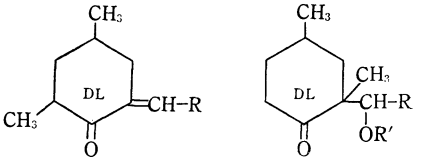
(III-1): R′=-NH₂
(III-1′): R′=-OC₂H₅



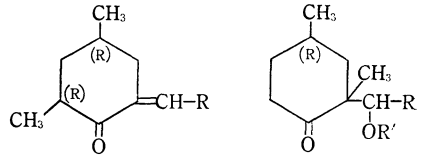
(III-2) (III-3)



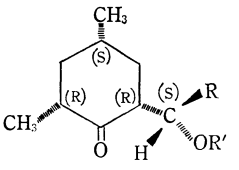
(III-4)



(IV-1) (IV-2), (IV-3): R′=H
(IV-2′), (IV-3′): R′=COCH₃



(V-1) (V-2), (V-3): R′=H
(V-2′), (V-3′): R′=COCH₃



(VI): R′=H
(VI′): R′=COCH₃

Chart 1.

* This constitutes Part XXIII of a series entitled "Studies of Antibiotics and Related Substances," by S. Umezawa; a portion of this paper was presented at the 16th Annual Meeting of the Chemical Society of Japan, Tokyo, March, 1963.

1) A. J. Whiffen, N. Bohonos and R. L. Emerson, *J. Bacteriol.*, **52**, 610 (1946).
2) B. C. Lawes, *J. Am. Chem. Soc.*, **82**, 6413 (1960).
3) Y. Egawa, M. Suzuki and T. Okuda, *Chem. Pharm. Bull. (Tokyo)*, **11**, 598 (1963).
4) R. B. Woodward, *J. Am. Chem. Soc.*, **64**, 76 (1942).

TABLE I. CYCLOHEXIMIDE-RELATED COMPOUNDS

| Compound | M. p. °C | UV absorption* mμ (ε) | Formula | Analyses, % Calcd. C | H | N | Found C | H | N | Yield % (Method) |
|---|---|---|---|---|---|---|---|---|---|---|
| I | 112.5—113 | 223(15560) | $C_{10}H_{13}O_3N$ | 61.51 | 6.67 | 7.18 | 61.39 | 6.46 | 7.21 | 34 (A), 5(B) |
| II | 81—81.5 | 230(8210) | $C_{11}H_{15}O_3N$ | 63.14 | 7.23 | 6.69 | 63.02 | 7.05 | 6.73 | 28 (A), 5(B) |
| III-1 | 164—164.5 | — | $C_{12}H_{19}O_4N$ | 59.73 | 7.94 | 5.81 | 59.90 | 7.73 | 5.89 | 37 (A) |
| III-2 | 112.5—113 | — | $C_{12}H_{19}O_4N$ | 59.73 | 7.94 | 5.81 | 59.75 | 7.79 | 5.70 | 2.7(A),16(B) |
| III-2′ | 143.5—144 | — | $C_{14}H_{21}O_5N$ | 59.35 | 7.49 | 4.49 | 59.42 | 7.32 | 4.86 | — |
| III-3 | 96.5—97 | — | $C_{12}H_{19}O_4N$ | 59.73 | 7.94 | 5.81 | 59.75 | 7.72 | 5.91 | 1.0 |
| IV-1 | 113—114 | 240(6700) | $C_{15}H_{21}O_3N$ | | | | — | | | 1.1(B) |
| IV-2 | 142.5—143 | — | $C_{15}H_{23}O_4N$ | 64.03 | 8.24 | 4.98 | 64.23 | 7.97 | 4.90 | 1.5(B) |
| IV-2′ | 174—175 | — | $C_{17}H_{25}O_5N$ | | | | — | | | — |
| IV-3 | 182—182.5 | — | $C_{15}H_{23}O_4N$ | 64.03 | 8.24 | 4.98 | 63.90 | 8.10 | 4.94 | 10 (B) |
| IV-3′ | 207—208 | — | $C_{17}H_{25}O_5N$ | 63.14 | 7.79 | 4.33 | 63.01 | 7.62 | 4.49 | — |
| V-1 | 135—136 | 242(7360) | $C_{15}H_{21}O_3N$ | | | | — | | | 1.0(B) |
| V-2 | 156—156.5 | — | $C_{15}H_{23}O_4N$ | 64.03 | 8.24 | 4.98 | 63.81 | 8.14 | 4.86 | 4 (B) |
| V-2′ | 145—147 | — | $C_{17}H_{25}O_5N$ | | | | — | | | — |
| V-3 | — | — | $C_{15}H_{23}O_4N$ | | | | — | | | 9 (B) |
| V-3′ | 164.5—165 | — | $C_{17}H_{25}O_5N$ | | | | — | | | — |

* Methanol solution

of δ-(1, 1-dimethyl-2-oxo-*n*-propyl)-β-carbamoylmethyl-δ-valerolactone (III-1) and 3-(2-hydroxy-3, 3-dimethyl-4-oxo-*n*-pentyl)glutarimide (III-2) in yields of 37 and 2.7% respectively. When the reaction was carried out by method B, III-2 was obtained as the main product. The ultraviolet spectrum of III-1 indicated the absence of the α, β-unsaturated ketone system. The infrared spectrum of III-1 showed the disappearance of bands at 3200 and 3100 $cm^{-1}$ characteristic of glutarimide moiety and the appearance of new bands at 3442, 3225 and 1630 $cm^{-1}$ and at 1737 $cm^{-1}$ which indicate the presence of primary amide and of a δ-lactone ring respectively. The presence of a terminal $CH_3CO$-group in III-1 was demonstrated by a positive iodoform reaction. In order to further establish that III-1 contains the carbamoyl group, the ethanolysis of III-1 in the presence of a catalytic amount of concentrated sulfuric acid was carried out; an ester derivative (III-1′) was thus obtained.

It is noteworthy that either method, A or B, resulted in the formation of an isomer (III-2) of 3-(2-hydroxy-5-methyl-4-oxo-*n*-hexyl)glutarimide (III-3), the product which was obtained by Nielsen's aldol condensation procedure.[3] The latter (III-3) easily afforded an anhydro-derivative, 3-(5-methyl-4-oxo-2-*n*-hexenyl)glutarimide (III-4) on dehydration with phosphorus pentoxide in dry benzene and showed a negative iodoform reaction, while the former (III-2) resisted dehydration, showed a positive iodoform reaction, and afforded an *O*-acetate derivative (III-2′) by the usual acetylation.

In a preliminary attempt to synthesize cycloheximide,[5] DL-2, 4-dimethylcyclohexanone was caused to react with GAA by method B, however no stereoisomers of cycloheximide were obtained, while DL-anhydrocycloheximide (IV-1) and two stereoisomers (IV-2, IV-3) of DL-*gem*-cycloheximide were produced in poor yields. An analogous condensation of (2R : 4R)-2, 4-dimethylcyclohexanone[6] prepared from natural cycloheximide by alkaline degradation with GAA afforded anhydrocycloheximide[2] (V-1) and two stereoisomers (V-2, V-3) of *gem*-cycloheximide.

The resorcinol color reactions[7] of IV-2, IV-3, V-2 and V-3 were negative, suggesting the presence of the –CO–C(OH)–CH(OH)– ketol system, while those of IV-1 and V-1 were positive, indicating the presence of the –CO–C=CH– anhydro-system, which was further judged to be present by the absorption band near 240 mμ in the ultraviolet spectra. The melting points of these compounds corresponded well to those previously reported for the substances prepared by an alternative method.[3,8] The ketol compounds (IV-2, IV-3, V-2, V-3) were additionally characterized by having been led to their acetates. The identities were ascertained by analyses, by infrared spectra determination and by their failure to depress the melting points of authentic samples respectively.

Table I lists the melting point, absorption maxima, analyses and yields of the above-mentioned products.

5) The total synthesis of cycloheximide was recently achieved by F. Johnson, N. A. Starkovsky, A. C. Paton and A. A. Carlson, *J. Am. Chem. Soc.*, **86**, 118 (1964).
6) T. Okuda, *Chem. Pharm. Bull.* (*Tokyo*), **7**, 659 (1959).
7) M. Takeshita, H. Takahashi and T. Okuda, ibid., **10**, 304 (1962).
8) M. Suzuki, Y. Egawa and T. Okuda, ibid., **11**, 582 (1963).

In connection with the above synthesis, several attempts were made to effect the hydration of the ethylene linkage of the anhydrocycloheximide (V-1); however, this attempt resulted in no more than the formation of a small quantity of *α-epi*-isocycloheximide[8] (VI).

The results of preliminary screening studies of the antimicrobial, antitumor and rodent-repellent activities of the above-mentioned compounds will be reported elsewhere.

## Experimental

**General Procedures.**—*Method A* (Condensation by hydrogen chloride). — Glutarimide - β - acetaldehyde (GAA) was dissolved in excess ketone saturated with dry hydrogen chloride at room temperature, and then the mixture was allowed to stand overnight. After the excess ketone and hydrogen chloride had been removed by evaporation under reduced pressure, the residue was washed with ether and further purified by chromatography.

*Method B* (Condensation by concentrated sulfuric acid in acetic acid).—A large excess of a ketone and GAA (5—10 mmol.) were dissolved in glacial acetic acid (2—4 ml.). Into the solution, concentrated sulfuric acid (0.3 ml.) was added drop by drop under stirring at room temperature, and the mixture was allowed to stand overnight. Volatile ketones were removed by evaporation under reduced pressure. In the case of nonvolatile ketones, the reaction mixture was diluted with water, and, after neutralization with sodium carbonate, the solution was extracted with ethyl acetate. The removal of the solvent after drying over anhydrous sodium sulfate, gave a residue; this residue was then washed with *n*-hexane and further purified by chromatography.

**Acetylation.**—By the usual procedure, using acetic anhydride and pyridine at room temperature overnight.

**3-(4-Oxo-2-*n*-pentyl)glutarimide (I).**—The crude product (2.83 g.) obtained from GAA (1.55 g., 10 mmol.) and acetone (14 g.) by method A was dissolved in acetone (2 ml.), poured onto a column of acid-treated alumina (42 g.), and eluted with 3% methanol-benzene. After the eluate had been concentrated, dry ether was added and the mixture was kept standing in a refrigerator; thereupon separated crude crystals, which were washed with a small quantity of ether (yield 658 mg. (34%)). Recrystallization from ethyl acetate gave colorless prisms, m. p. 112.5—113°C. Infrared bands (Nujol): 3210, 3100 (NH), 1732, 1700, 1685 (C=O), 1652 $cm^{-1}$ (conjugated C=C).

2, 4-*Dinitrophenylhydrazone*: Red prisms, m. p. 203.5—205°C. Found: C, 50.90; H, 4.60; N, 18.50. Calcd. for $C_{16}H_{17}O_4N_5$; C, 51.20; H, 4.53; N, 18.67%.

**3-(3-Methyl-4-oxo-2-*n*-pentenyl)glutarimide (II).**—The crude product (806 mg.) obtained from GAA (775 mg., 5 mmol.) and ethyl methyl ketone (14.4 g., 0.5 mol.) by method A was dissolved in benzene (3 ml.) and chromatographed over acid-treated alumina (16 g.) using 3% methanol-benzene as a solvent. After the solvent had been removed by evaporation, the resulting syrup (642 mg.) was mixed with ether and allowed to stand in a refrigerator to give crude crystals (288 mg., 28%). Recrystallization from ethyl acetate gave colorless prisms, m. p. 81—81.5°C. Infrared bands (Nujol): 3200, 3100 (NH), 1732, 1702, 1675 (C=O), 1650 $cm^{-1}$ (conjugated C=C).

2, 4-*Dinitrophenylhydrazone*: Red prisms, m. p. 242—244°C (decomp.). Found: C, 52.74; H, 4.88; N, 17.99. Calcd. for $C_{17}H_{19}O_4N_5$: C, 53.00; H, 4.76; N, 17.75%.

**δ-(1, 1-Dimethyl-2-oxo-*n*-propyl)-β-carbamoylmethyl-δ-valerolactone (III-1).**—GAA (1.55 g., 10 mmol.) in acetic acid (2 ml.) was added drop by drop into methyl isopropyl ketone (8.6 g., 100 mmol.) containing hydrogen chloride (1.8 g., 51 mmol.) and stirred at room temperature. The crude product (3.65 g.) was then dissolved in acetone-benzene (1 : 1), poured onto a column of acid-treated alumina (50 g.), and eluted with 3% methanol-benzene. The viscous residue (985 mg.) obtained was caused to crystallize from acetone; yield 890 mg. (37%). Two recrystallizations from hot acetone gave colorless prisms, m. p. 164—164.5°C. Infrared bands (Nujol): 3442, 3225 (NH), 1737, 1685, 1665 (C=O), 1630 $cm^{-1}$ (NH).

Found: C, 59.90; H, 7.73; N, 5.87. Calcd. for $C_{12}H_{19}O_4N$: C, 59.73; H, 7.94; N, 5.81%.

**δ-(1, 1-Dimethyl-2-oxo-*n*-propyl)-β-ethoxycarbonylmethyl-δ-valerolactone (III-1′).**—A sample (120 mg.) of III-1 was dissolved in 95% ethanol (4 ml.). A solution of concentrated sulfuric acid (0.4 ml.) in 95% ethanol (2 ml.) was then added to the solution, and the mixture was allowed to stand at room temperature. After evaporation under reduced pressure, the resulting residue was diluted with a small amount of water, neutralized with 5% aqueous sodium carbonate, and extracted with ethyl acetate. Washing this with water, drying it over anhydrous sodium sulfate, and evaporating it left a syrup, which was then dissolved in *n*-hexane and allowed to stand in a refrigerator. There were deposited colorless prisms of III-1′ (35 mg.), m. p. 52—53°C. The infrared spectrum (Nujol) contained bands at 1750, 1740, 1715 (C=O), 1245, 1130 $cm^{-1}$ (C-O).

Found: C, 62.32; H, 8.68. Calcd. for $C_{14}H_{22}O_5$: C, 62.20; H, 8.20%.

2, 4-*Dinitrophenylhydrazone*: Red prisms, m. p. 166—166.5°C (decomp.).

Found: C, 53.11; H, 5.82; N, 12.15. Calcd. for $C_{20}H_{26}O_8N_4$: C, 53.33; H, 5.82; N, 12.44%.

**3-(2-Hydroxy-3,3-dimethyl-4-oxo-*n*-pentyl)glutarimide (III-2).**—*By Method A.*—A syrup (810 mg.) obtained by the evaporation of the mother liquor left after isolation of III-1 was chromatographed over acid-treated alumina (16 g.) with 3% methanol-benzene. After concentration under reduced pressure, the resulting syrup (450 mg.) was dissolved in ethyl acetate - ether and kept standing in a refrigerator to give crude crystals of III-2 (150 mg., 2.7%). Recrystallization from ethyl acetate gave colorless prisms, m. p. 112—112.5°C.

*By Method B.*—The crude product (660 mg.) obtained from GAA (775 mg., 5 mmol.) and methyl isopropyl ketone (4.3 g., 50 mmol.) was dissolved in acetone-benzene (1 : 1) and chromatographed on acid-treated alumina (16 g.). Elution with 3% methanol-benzene gave crude crystals of III-3 (190 mg., 16%). Recrystallization from ethyl acetate gave colorless prisms, m. p. 112.5—113°C. No depression in melting point

was observed upon its admixture with the sample prepared by method A.

*2, 4-Dinitrophenylhydrazone*: Red prisms, m. p. 227—227.5°C (decomp.). Found: C, 51.59; H, 5.56; N, 16.75. Calcd. for $C_{18}H_{23}O_7N_5$: C, 51.30; H, 5.50; N, 16.62%.

**Acetate of III-2 (III-2′).**—A crude sample (28 mg.) of III-2 was acetylated to give the acetate (11 mg.). Recrystallization from isopropanol gave colorless prisms, m. p. 143.5—144°C.

**3-(2-Hydroxy-5-methyl-4-oxo-*n*-hexyl) glutarimide (III)-3.**—The ethyl acetate solution obtained from *N*-methylanilinomagnesium bromide (33 mmol.), methyl isopropyl ketone (3.01 g., 35 mmol.) and GAA (1.86 g., 12 mmol.) by the procedure previously[3] reported was concentrated to give a syrup; this syrup was then washed with *n*-hexane to remove the unchanged ketone. The insoluble residue (900 mg.) was chromatographed on acid-treated alumina (18 g.). Elution with 3% methanol-benzene again gave a syrup (150 mg.); when this syrup was taken up in dry ether and kept in a refrigerator, it gave crude crystals (28 mg., 1.0%). Recrystallization from ethyl acetate afforded colorless prisms, m. p. 96.5—97°C. The ultraviolet spectrum in methanol showed end absorption. The infrared spectrum (Nujol) contained bands at 3540 (OH), 3220, 3110 (NH), 1733, 1708 and 1685 $cm^{-1}$ (C=O).

**3-(5-Methyl-4-oxo-2-*n*-hexenyl) glutarimide (III-4) (Anhydro-derivative of III-3).**—A sample of III-3 (20 mg.) dissolved in benzene (5 ml.) was mixed with phosphorus pentoxide (100 mg.), slowly heated to boiling, and then cooled. Evaporation under reduced pressure gave a residue which was recrystallized from dry ether to afford colorless prisms (3 mg.), m. p. 46—48°C. The ultraviolet spectrum in methanol showed a maximum at 224 mμ (ε 15200). The infrared spectrum (KBr) contained bands at 3200, 3080 (NH), 1737 sh, 1715, 1675 (C=O) and 1630 $cm^{-1}$ (conjugated C=C).

**DL-Anhydrocycloheximide (IV-1).**—A crude product (2.84 g.) prepared from DL-2, 4-dimethylcyclohexanone[9] (6.3 g., 50 mmol.) and GAA (1.55 g., 10 mmol.) by method B was dissolved in benzene-methanol (8 : 1), and the solution was poured onto acid-treated alumina (56 g.) and eluted with 3% methanol-benzene. When a syrup obtained from the early fractions was taken up in dry ether and allowed to stand in a refrigerator, it afforded crude IV (yield 30 mg., 1.1%). Recrystallization from ethyl acetate gave colorless prisms (12 mg.), m. p. 113—114°C. No depression in melting point was observed in admixture with an authentic specimen (m. p. 114—115°C) previously[3] reported.

**DL-*gem*-Cycloheximide I (IV-2).**—The mother liquor left after the isolation of IV-1 was concentrated under reduced pressure. The resulting syrup (1.01 g.) was charged on a column of silica gel (50 g.) and eluted with isopropyl ether - ethyl acetate (9 : 1, 7 : 3, 1 : 1 and 1 : 3) and ethyl acetate successively. The early fractions obtained with 30% ethyl acetate - isopropyl ether were concentrated to give a syrup which was caused to crystallize from ether; yield, 40 mg., m. p. 112—113°C. The product was identical with VI-1 in all respects.

A syrup (108 mg.) obtained from the early fractions with 50% ethyl acetate - isopropyl ether was caused to crystallize from ethyl acetate to give crude IV-2 (42 mg., 1.5%). Two recrystallizations from the same solvent gave colorless prisms, m. p. 142.5—143°C, which showed a negative resorcinol reaction.[7] The product has a higher melting point than that of a sample of DL-*gem*-cycloheximide I previously obtained,[3] which has now been found to be impure. The identity was ascertained by both samples leading to the same acetate, as will be described below.

**Acetate of IV-2 (IV-2′).**—A sample of IV-2 (15 mg.) was acetylated to give colorless prisms (10 mg.), m. p. 174—175°C. The acetate was found to be identical with the DL-*gem*-cycloheximide I acetate (reported m. p. 174—175°C) previously reported[3] by a mixed melting point determination and by a comparison of the infrared spectra.

**DL-*gem*-Cycloheximide II (IV-3).**—The later fractions with 3% methanol - benzene and all fractions with 5% methanol - benzene (see DL-anhydrocycloheximide (IV-1)) were collected and concentrated to dryness, and the residue (783 mg.) was caused to crystallize from ethyl acetate to give crude crystals of IV-3 (280 mg., 10%). Recrystallization from methanol gave colorless prisms, m. p. 182—182.5°C, which showed a negative resorcinol reaction. The product has a higher melting point than that of DL-*gem*-cycloheximide II previously obtained,[3] a product which has now been found to be impure. The identity was confirmed by both products leading to acetate, as will be described below.

**Acetate of IV-3 (IV-3′).**—A sample of IV-3 (26 mg.) was acetylated to give crude acetate (22 mg.). Recrystallization from isopropanol gave colorless prisms (15 mg.), m. p. 207—208°C, undepressed by admixture with an authentic specimen (m. p. 200—202°C) previously obtained.[3]

**Anhydrocycloheximide (V-1).**—The crude product (1.93 g.) obtained by the reaction of optically-active (2R : 4R)-2, 4-dimethylcyclohexanone (3.2 g., 25 mmol.) with GAA (775 mg., 5 mmol.) was chromatographed over acid-treated alumina (38 g.) with 3% methanol - benzene. The eluate was then evaporated under reduced pressure, and the resulting residue (481 mg.) was dissolved in ethyl acetate, poured onto a column of silica gel (25 g.) and eluted with the same solvent systems as were used for the isolation of IV-1. A syrup obtained from the early fractions with ethyl acetate - isopropyl ether (1 : 1) was caused to crystallize from ether; crude crystals (12 mg.) (1.0%). Recrystallization from methanol gave colorless prisms, m. p. 135—136°C. The product was found to be identical with anhydrocycloheximide (reported m. p. 136.5—138°C) by a mixed melting point determination. Additionally, they had identical ultraviolet and infrared spectra.

***gem*-Cycloheximide II (V-2) and Its Acetate (V-2′).**—When a residue (197 mg.) obtained from the middle fractions with 50% ethyl acetate - isopropyl ether in the above chromatography was taken up in ether and allowed to stand at room temperature, there separated crystals of V-2 (60 mg., 4%). Recrystallization from ethyl acetate afforded colorless prisms, m. p. 156—156.5°C. The product showed a negative resorcinol color reaction, indicating that the product

9) H. E. Ungnada and A. D. McLaren, *J. Org. Chem.*, **10**, 29 (1945).

was a diastereoisomer[10] of the *gem*-cycloheximide. The product has been led to its acetate (colorless prisms; m. p. 145—147°C) by the general procedure. The infrared spectrum (KBr) contained bands at 3270, 3100w (NH), 1745sh, 1715, 1700 (C=O) and 1250 $cm^{-1}$ (C-O).

***gem*-Cycloheximide (V-3) and Its Acetate (V-3′).** —The mother liquor left after the isolation of V-2 was evaporated to give crude V-3, which could not be caused to crystallize. Then, the residue (50 mg.) was acetylated by the general procedure to give a crude solid (20 mg.). Recrystallization from isopropanol gave colorless prisms of V-3′ (10 mg.), m. p. 164.5—165°C. The product was found to be identical in all respects with the *gem*-cycloheximide I acetate (reported m. p. 166—166.5°C) previously[8] reported.

***α-epi*-Isocycloheximide (VI) and Its Acetate (VI′) (The Hydration of Anhydrocycloheximide).** —Into a mixture of anhydrocycloheximide (V-1) (4.21 g., 16 mmol.) and acetic acid (12 ml.), 75% sulfuric acid (2.34 g., 17.6 mmol.) was added drop by drop and stirred at room temperature. Stirring was continued for 2 hr. to give a clear solution, and then the mixture was stirred for an additional 3 hr. The reaction mixture was diluted with water (12 ml.) and neutralized with sodium carbonate, followed by extraction with ethyl acetate. After it had been washed with water, aqueous 5% sodium bicarbonate and water, and dried over anhydrous sodium sulfate, the extract was evaporated to remove the solvent. The resulting yellow syrup was treated with ether in order to precipitate unchanged anhydrocycloheximide (2.2 g., m. p. 133—135°C). The ethereal solution was evaporated to give a residue (2.45 g.), which was then taken up in dry benzene, poured onto acid-treated alumina (60 g.), and eluted with 3% methanol-benzene. The later fractions showed a significant activity in reaction to *Saccharomyces sake*. The resulting residue (950 mg.) was similarly rechromatographed to afford crude VI (240 mg.), which was taken in ethyl acetate and again chromatographed over silica gel (32 g.) with ethyl acetate - isopropyl ether (1 : 1). The evaporation of the later fractions again afforded a gummy solid (210 mg.). The minimum inhibitory concentration of the product against *S. sake* was found to be 30 mg./ml. by a dilution method.

Found: C, 63.95; H, 8.06; N, 4.95. Calcd. for $C_{15}H_{23}O_4N$: C, 64.03; H, 8.24; N, 4.98%.

10) M, Suzuki et al. described a diastereomer with a m. p. of 141—145°C. See Ref. 8.

The product (100 mg.) was acetylated by the general procedure. The crude acetate was purified by chromatography over silica gel (3 g.) with 30% ethyl acetate - isopropyl ether. Recrystallizations from ether and isopropyl ether gave colorless prisms, 30 mg., m. p. 177.5—178°C. No depression in melting point was observed upon admixture with an authentic specimen of *α-epi*-isocycloheximide acetate.[8] Additionally, the product was identical in infrared spectra with the authentic specimen.

## Summary

1) Glutarimide-β-acetaldehyde has been condensed with several aliphatic ketones by acid-catalysts to give mainly α, β-unsaturated keto-derivatives. The condensation with methyl isopropyl ketone has given δ-(1, 1-dimethyl-2-oxo-*n*-propyl)-β-carbamoylmethyl-δ-valerolactone (III-1) and 3-(2-hydroxy-3, 3-dimethyl-4-oxo-*n*-pentyl)-glutarimide (III-2). It has been found that the latter is an isomer of the product prepared by Nielsen's aldol condensation procedure.

2) An analogous condensation with DL-2,4-dimethylcyclohexanone has given DL-anhydrocycloheximide and two stereoisomers of DL-*gem*-cycloheximide. The condensation with (2R:4R)-2, 4-dimethylcyclohexanone has given a similar result.

3) It has been shown that the acid-catalyzed hydration of anhydrocycloheximide affords *α-epi*-isocycloheximide.

The authors are grateful to Dr. Tomoharu Okuda. Director of the Microbial Chemistry Research Laboratories of Tanabe Seiyaku Co., for his helpful advice. The authors also wish to thank Mr. Saburo Nakada for his microanalyses and Mr. Hajime Miki and Mr. Tatsuo Hasue for their technical assistance. The support of this work by a cancer research grant of the Ministry of Education is hereby gratefully acknowledged.

*Department of Applied Chemistry*
*Faculty of Engineering*
*Keio University*
*Koganei-shi, Tokyo*

# The Cross-linking Reaction of the Polybutadiene Binder for Composite Propellants

By Kiroku YAMAZAKI and Harusuke TOKUI

(Received June 14, 1965)

The monomer or prepolymer of the fuel binder should have a suitable fluidity at an ambient temperature in order to secure a high holding capacity of solid ingredients and a high castability. On the other hand, a propellant grain should have good mechanical and combustion characteristics. Polyurethane is an excellent binder, one which fulfills such requirements; its physical properties can be widely controlled by means of the reaction conditions and the type of starting materials.[1] Polybutadiene also seems to give a grain with a high ballistic performance and a good low temperature property due to its low heat of formation, its high hydrogen/carbon ratio and its low second-order transition point.

In view of these points, a polybutadiene fuel binder with good mechanical properties was studied using "telechelic polybutadiene" (carboxy-terminated polybutadiene) as the starting material.[2] "Telechelic polybutadiene" has a relatively uniform molecular weight distribution and is cross-linked with terminal groups, so that the resultant polymer network will be essentially uniform, containing no terminal sections. Unlike conventionally-vulcanized rubbers, which are randomly cross-linked, the strain would be distributed uniformly upon each elastic chain of the cross-linkage and the mechanical strength might be improved remarkably. Moreover, it is possible to control to some extent the reaction of the chain extension and the cross-linking because this compound functions as a dicarboxylic acid.

Tris[1-(2-methyl)aziridinyl] phosphine oxide [MAPO] was used as the cross-linking agent in this work.[3] Usually a curing temperature as high as 100—150°C is recommended; however, we preferred here to suppress the temperature as much as possible toward the ambient temperature in view of the volume contraction of the cured material and the inferior heat resistance of the additives. An effective accelerator was found which enables cross-linkage even at the relatively low temperatures of 50—70°C without the sacrifice of the properties of the cured products.

1) K. Yamazaki, A. Iwama, S. Aoyagi, T. Sofue, M. Hayashi and K. Kishi, *J. Chem. Soc. Japan, Ind. Chem. Sec.* (*Kogyo Kagaku Zasshi*), **66**, 1630 (1963).
2) C. A. Uraneck, H. L. Hsieh and O. G. Buck, *J. Pol. Sci.*, **46**, 535 (1960).
3) U. S. Pat. 3087844.

## Raw Materials

"Telechelic polybutadiene" HC-434 (Thiokol Chem.) and Butarez CTL (Phillips Pet. Co.) were used as received. The number-average molecular weights were 3770 and 5500 respectively.

## Experimental Results

**An Accelerator for the Curing Reaction.**— Reaction mixtures were poured into a 40×40×5 mm. glass cell, made of two 40×40 mm. glass plates standing face to face with a 5 mm. spacer with tin foils lining the inside surfaces; these plates served as a pair of electrodes. The loaded cell was put into a constant temperature oven, and the specific resistivity at 50°C was measured continuously. Figure 1 shows the curve of the specific resistivity versus the reaction time. The time required until the specific resistivity become constant is cut by the addition of the accelerator.

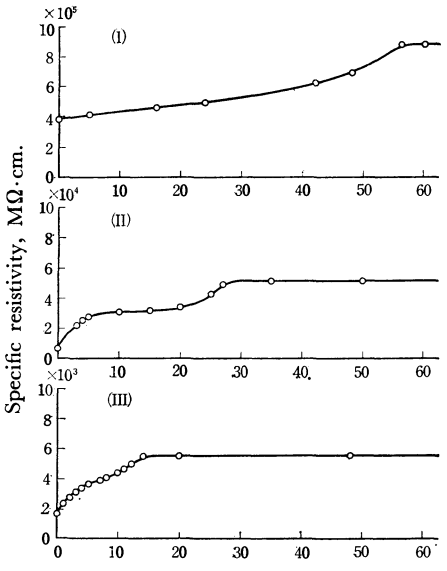



Fig. 1. Specific resistivity versus reaction time (50°C cure).
(I) HC-434 100 g.-MAPO 9.7 g.
(II) HC-434 100 g.-MAPO 9.7 g.-Accelerator 5 g.
(III) HC-434 100 g.-MAPO 9.7 g.-Accelerator 10 g.

Table I. Physical properties of HC-434 - MAPO - Accelerator elastomers

| Cross-linking agent [MAPO] (Equiv.) | Ultimate tensile strength kg./cm² | Elongation % | 100% Modulus kg./cm² | 300% Modulus kg./cm² | Hardness | $M_c$ | Sol-fraction % |
|---|---|---|---|---|---|---|---|
| Accelerator 5 phr. 50°C cure | | | | | | | |
| 2.0 | 10.9 | 360 | 5.1 | 10.0 | 34 | 9540 | 9.28 |
| 2.5 | 10.3 | 330 | 5.4 | — | 36 | 8140 | 8.46 |
| 3.0 | 13.8 | 400 | 5.8 | 11.5 | 38 | 7670 | 8.21 |
| 4.0 | 8.1 | 470 | 2.9 | 5.7 | 24 | 16890 | 21.12 |
| Accelerator 10 phr. 50°C cure | | | | | | | |
| 2.0 | 10.8 | 510 | 3.7 | 7.1 | 19 | 14640 | 31.1 |
| 2.5 | 16.7 | 510 | 5.5 | 10.5 | 28 | 13560 | 16.7 |
| 3.0 | 15.0 | 440 | 6.1 | 11.8 | 39 | 7680 | 18.1 |
| 4.0 | 13.9 | 450 | 4.9 | 10.1 | 42 | 7030 | 7.3 |
| Accelerator 5 phr. 70°C cure | | | | | | | |
| 1.0 | | | (undercured) | | | | |
| 1.5 | 13.0 | 300 | 6.9 | — | 36 | 11540 | 8.14 |
| 2.0 | 14.0 | 260 | 7.8 | — | 43 | 5880 | 3.06 |
| 2.5 | 11.9 | 260 | 7.1 | — | 36 | 7030 | 5.19 |
| 3.0 | 11.3 | 310 | 5.7 | — | 33 | 6800 | 5.31 |
| 4.0 | 7.7 | 540 | 2.4 | 4.8 | 19 | 14900 | 14.91 |

Table II. Physical properties of Butarez CTL-MAPO-Accelerator elastomer

| Cross-linking agent [MAPO] (Equiv.) | Ultimate tensile strength kg./cm² | Elongation % | 100% Modulus kg./cm² | 300% Modulus kg./cm² | Hardness | $M_c$ | Sol-fraction % |
|---|---|---|---|---|---|---|---|
| Accelerator 5 phr. 50°C cure | | | | | | | |
| 2.0 | 7.0 | 730 | — | — | 12 | 14540 | 10.07 |
| 3.0 | 11.1 | 390 | — | — | 27 | 10900 | 8.87 |
| 4.0 | — | — | — | — | — | 14130 | 14.67 |

Even though the changes of the electric property could not indicate the degree of the chemical cross-linking exactly, it may be expected that the increase in specific resistivity is still be related to the process of the curing reaction; it is evident that the addition of the accelerator is very effective.

However, the time required for a perfect cure is remarkably affected by the type of vessel used for the curing. For example, the composition shown on Fig. 1 was cast and cured at 50°C in a 60 mm.$\phi \times$90 mm.H polyethylene cup, and the progress of the curing reaction was followed by hardness measurements with a durometer. The hardness increased as the reaction proceeded, but more than 2 weeks were required for a perfect cure. It is reasonable for the heat transfer to the inside of the reaction mixture in a large vessel to be slower than in a smaller one, but this difference alone can not explain the result. Although no decisive interpretation can yet be made, the difference may be attributed to the differences in the area of contact with the atmosphere from vessel to vessel. However, the addition of an accelerator was effective in both cases. In the end, for the purpose of lowering the curing temperature for the carboxy-terminated polybutadiene-MAPO system, some effective accelerators were found.

**The Elastomer Preparation.**—The required amounts of the ingredients were mixed manually at 75—80°C, degassed, and cast into the cavity formed by two parallel glass plates in order to form elastomer sheets about 2—3 mm. thick. After some preliminary tests, the curing time of 7 days was taken.

**The Measuring Process.**—The tensile stress-strain data were obtained using "Tensilon" with dumbbell-shaped specimens. Following the standard "Physical Testing Methods for Vulcanized Rubber" (JIS-K-6301), a strain rate of 500 mm./min., a cross-head distance of 50 mm. and No. 3 type dumbbell-shaped specimens die-cut from the elastomer were used.

The hardness was measured using an Asker durometer J.

All the experiments were performed in an air-conditioned room at a constant temperature of 20°C and at a constant relative humidity of 60%.

The data are shown in Tables I and II.

**Equilibrium Swelling.**—If a two-functional carboxy-terminated polybutadiene reacts quantitatively with an equivalent amount of a three-functional cross-linking agents [MAPO], the resultant network will have no terminal sections. In this case, each segment of the network structure

acts in an elastic manner, and the length of each segment should be same as that of the initial two-functional polybutadiene molecule. However, the actual curing reaction will be more complicated because of some undesirable side reactions. The average molecular weight for the chain of the network and the degree of cross-linking are very important factors in describing a three-dimensional polymer network model; therefore, the equilibrium swelling was measured in order to clarify these indexes.

When the volume fraction, $Q_m$, of the polymer present in the swollen gel is rather small, it can be approximately represented by Eq. 1.[4]

$$Q_m=[(1/2-\mu)M_c/\rho_2 V_1]^{3/5} \quad (1)$$

where $\rho_2$ : the polymer density
$V_1$ : the molar volume of the solvent
$\mu$ : the polymer-solvent interaction constant
$M_c$ : the average molecular weight between cross-links

$Q_m$ can be determined directly by Eqs. 2 and 3.

$$W=W_1+W_2 \quad (2)$$

$$Q_m=1+(\rho_2/\rho_1)(W'/W_1-1) \quad (3)$$

where $\rho_1$ : the density of the solvent
$W$ : the weight of the specimen before swelling
$W_1$ : the weight of gel in the specimen
$W_2$ : the weight of sol in the specimen
$W'$ : the weight of the specimen on equilibrium swelling

The calibration term for terminal chains could be neglected because its fraction would be very small from the standpoint of the reaction scheme.

Small pieces of elastomers about 0.4—0.5 g. were immersed in carbon tetrachloride at 20°C. After 7 days, the swollen gel was removed from the solvent, quickly blotted with dry filter paper, and reweighed in a stoppered weighing bottle. The specimen was then transferred to an electric oven at 50°C in order to remove the imbibed solvent; the $W_1$ was thus determined. The weight difference, $W_2$, between $W$ and $W_1$ was taken as the weight of the sol. It is impossible for all of the sol to be extracted by such a simple procedure; however, the measured value is useful as a semi-quantitative measure of the sol fraction.

The polymer density at 20°C was measured by the pycnometer method, using distilled water as the sealant.

The $Q_m$ was determined from Eq. 3; then $M_c$ was calculated by Eq. 1. The data obtained are shown in Table I and Table II, together with the sol fraction, which was measured by the procedure described.

4) J. Furukawa and S. Yamashita, *J. Soc. Rubber Ind. Japan (Nippon Gomu Kyokai-shi)*, **30**, 955 (1957).

The polymer-solvent interaction parameter, $\mu$, was calculated as 0.264 (at 20°C) by means of the data shown by Shvarts.[5]

## Discussion

From the data illustrated on Table I and Table II, it is evident that the chain length between cross-links, $M_c$, is strongly influenced by the cross-linking agent, the accelerator and the curing temperature. In general, as the addition of the cross-linking agent increases, the tensile strength and the modulus of the elastomer pass through a maximum. Namely, there is a peak in the curve of the tensile modulus versus the quantity of the cross-linking agent added. If this was due to only the "dilution effect" of an excess cross-linking agent, $M_c$ would not decrease even if the tensile modulus decreased.

Though the data observed are negative for such a relation, $M_c$ was inversely proportional to the tensile modulus; and this shows that the optimum molar ratio of the cross-linking agent should be determined with the maximum tensile modulus and it was found that a 100—200% excess of equivalence is required.

Assuming that the ideally cross-linked HC-434 polymer has a network model as has been described previously, its $M_c$ should be same as the average molecular weight 3800 of the HC-434 polymer. However, the minimum $M_c$ value obtained is about 6000, which is about one and a half times the chain length for an ideal network. Therefore, it is reasonable to assume that a considerable chain extending reaction occurs inevitably; this may be the reason why an excess of the cross-linking agent is required in order to obtain the maximum tensile modulus.

The kinetic theory of rubber elasticity predicts that the tensile stress-strain will be given by Flory's equation:

$$S=\nu \boldsymbol{R} T(\alpha-1/\alpha^2) \quad (4)$$

where $S$ : the stress based on the original cross-sectional area
$\nu$ : moles of effective chain per unit volume
$\boldsymbol{R}$ : the gas constant
$T$ : the absolute temperature
$\alpha$ : the principal extension ratio

In Eq. 4 $\nu$ can be replaced by $1/M_c$, for the polymer density is almost equal to 1.00; the tensile stress, $S$, should then be inversely proportional to the chain length, $M_c$. As $\boldsymbol{R}$ and $T$ are known quantities, the tensile stress at 100% elongation ($\alpha=2$) can be calculated by means of Eq. 5:

$$S_{100}=0.426\times 10^5(1/M_c) \text{ kg./cm}^2 \quad (5)$$

Figure 2 shows the relationship between the tensile stress at 100% elongation and the chain length, $M_c$.

5) A. G. Shvarts, *Rubber Chem. and Tech.*, **31**, 691 (1958).

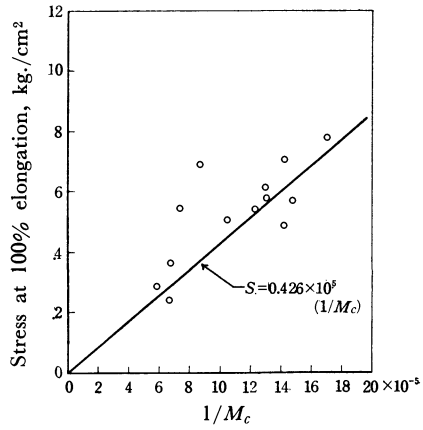



Fig. 2. Plot of tensile stress at 100% elongation versus $M_c$ (HC-434 - MAPO - Accelerator).

Although there are a few exceptions, in general, the observed data agree well with the theoretical quantities.

It can readily be assumed that the quantity of an ingredient which makes no contribution to the cross-linking reaction (which would be proportional to the sol fraction) might be at a minimum at the optimum mixing ratio of the polybutadiene, the cross-linking agent and the accelerator for the maximum tensile modulus of an elastomer. The longer the chain length, the greater the quantity of the sol fraction. These relationships are illustrated in Fig. 3.

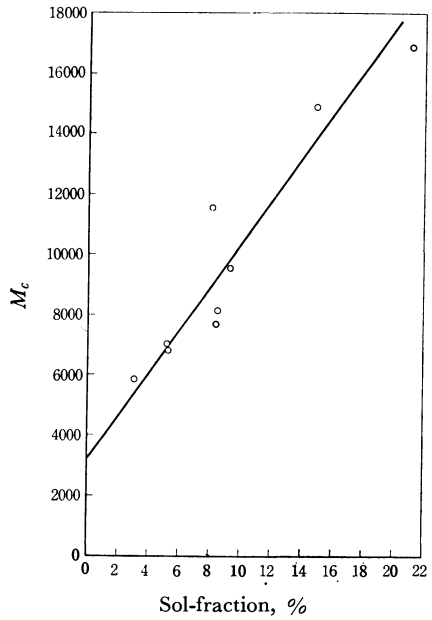



Fig. 3. Plot of sol fraction versus $M_c$ (HC-434 - MAPO - Accelerator 5 phr.).

Figure 4 shows the chain length, $M_c$, versus the elongation at the break point of the elastomer.

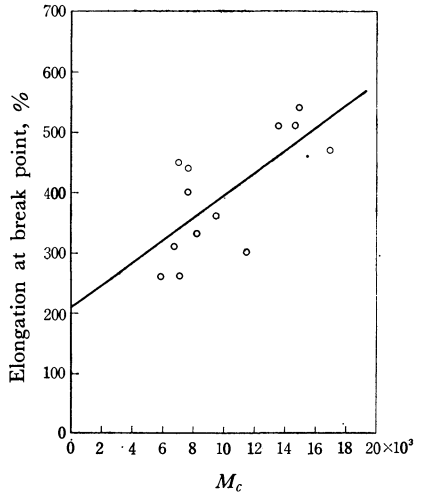



Fig. 4. Plot of elongation at break point versus $M_c$ (HC-434 - MAPO - Accelerator).

Breaking phenomena can scarcely give reliable data, because they are strongly influenced by the internal defects in the molecular structure of the specimens. However, it is shown that the elongation at the break point increases with the chain length, $M_c$. As the cross-linking reaction proceeds so effectively that the chain length, $M_c$, becomes short, the internal stress per unit of the chain of the network should be increased; this may be what happens in the breaking of the elastomer.

Equation 4 shows that the stress, $S$, should be proportional to $(\alpha - 1/\alpha^2)$ and that the slope of this line, $\nu RT$, equals the shear modulus. These relationships are illustrated in Fig. 5 and Fig. 6; plots of $S$ versus $(\alpha - 1/\alpha^2)$ show a good linearity.

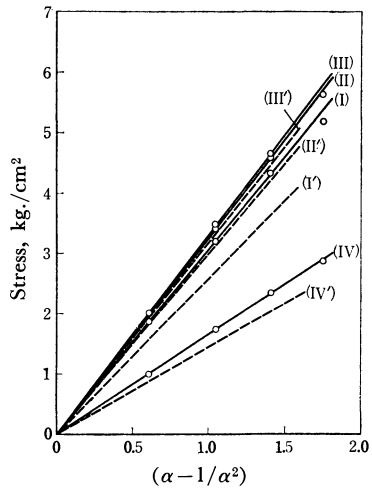



Fig. 5. Stress-strain data for some elastomers (HC-434 - MAPO - Accelerator 5 phr., 50°C cure).
(I) MAPO 2.0 eq. (III) MAPO 3.0 eq.
(II) MAPO 2.5 eq. (IV) MAPO 4.0 eq.

TABLE III. COMPARISON OF $M_c$ AND SOL-FRACTION OF CURED BUTAREZ CTL AND HC-434

| Cured condition | MAPO added | HC-434 | | | Butarez CTL | | |
|---|---|---|---|---|---|---|---|
| | | $M_c$ | $M_c/M$ | Sol-fraction | $M_c$ | $M_c/M$ | Sol-fraction |
| 50°C, 7 days | 2.0 eq. | 9540 | 2.53 | 9.28 | 14540 | 2.65 | 10.07 |
| 50°C, 7 days | 3.0 eq. | 7670 | 2.03 | 8.21 | 10900 | 1.98 | 8.87 |

(Accelerator 5 phr.)
$M$: Average molecular weight of raw materials

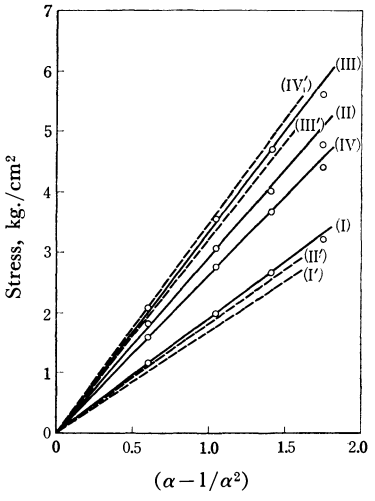



Fig. 6. Stress-strain data for some elastomers (HC-434 - MAPO - Accelerator 10 phr., 50°C cure).
(I) MAPO 2.0 eq. (III) MAPO 3.0 eq.
(II) MAPO 2.5 eq. (IV) MAPO 4.0 eq.

On the other hand, as $M_c$ was determined from swelling data, the stress-strain data could be calculated by means of Eq. 4. These are represented in Fig. 5 and Fig. 6 with dotted lines. (The polymer density was assumed to be 1.00.)

Of course, there is a considerable amount of sol occluded in the network structure, and if the sol fraction has no role to play in the networks, the tensile stress can be calculated by considering the term of the "dilution effect" for the swelling data; however, the observed value is higher than that calculated from $M_c$. Therefore, a dilution effect of the sol fraction is not conceivable, while a reinforcing effect such as chain entanglement is plausible.

Table I shows the effects of the curing temperature. As is shown by the table, the increase in the temperature for the cross-linking reaction from 50°C to 70°C causes a decrease in the sol fraction, the chain length, $M_c$, and the quantity of cross-linking agent required for the maximum tensile modulus. These tendencies seem quite reasonable, since the reactivity and the mobility of the ingredients would increase with the reaction temperature.

Table III compares the cross-linking reactions of the Butarez CTL and HC-434 polymers. The average molecular weight of Butarez CTL is larger than that of HC-434, so the $M_c$ of the cured products of the former is longer than that of those of the latter. However, not only are the ratios of $M_c$ divided by the average molecular weight of respective raw materials almost the same; the sol fractions are also almost the same. Hence, it may be concluded that there is no noticeable difference between the reactivities of these two raw materials.

## Conclusion

The cross-linking reactions of "telechelic polybutadiene" at relatively low temperatures have been studied, and some kinds of accelerator have been found to be effective.

In general, a 100—200% excess of cross-linking agent was required in order to obtain cured elastomers of the maximum tensile modulus.

As the curing temperature rose, the excess quantity of the cross-linking agent was diminished.

The measured stress-strain data of the elastomers closely fit Flory's equation for the rubber elasticity theory. The swelling data were in line with the stress-strain data.

## Summary

The cross-linking reactions of carboxy-terminated polybutadiene with tris[1-(2-methyl)aziridinyl] phosphine oxide have been studied in order to obtain an excellent fuel binder of good mechanical properties as well as good combustion characteristics.

The tensile strength and elongation at the break point, as shown by the elastomer studied, were about 10—15 kg./cm.² and 250—500% respectively. For high tensile modulus of the elastomer, an 100—200% excess of the cross-linking agent over the equivalent ratio was required.

The reaction temperature for cross-linking was lowered to the 50—70°C range by the addition of a suitable accelerator.

The stress-strain curve of the elastomer closely fit the equation for the rubber elasticity theory, and these stress-strain data was in accordance with the measured swelling data.

*Institute of Space and Aeronautical Science*
*The University of Tokyo*
*Komaba, Meguro-ku, Tokyo (K. Y.)*

*Dai-Nippon Celluloid Co. Ltd.*
*Yuraku-cho, Chiyoda-ku, Tokyo (H. T.)*

# Palladium(II) Complexes of β-Ketoamines Derived from Acetylacetone and Amines

By Emiko YOSHIDA and Shoichiro YAMADA

(Received June 14, 1965)

In previous papers from this laboratory,[1] transition metal complexes of Schiff bases derived from salicylaldehyde and various amines were discussed. A similar study was then made of nickel(II) and copper(II) complexes of β-ketoamines[2] derived from acetylacetone and amines in order to compare the results with those of the corresponding salicylideneimine complexes previously studied.[3,4] Most of the papers about this and similar topics were, however, concerned mainly with complexes of the first transition elements, such as cobalt, nickel and copper. It seemed, therefore, worthwhile to study the corresponding complexes of the second or the third transition elements and to compare them with those of the first transition elements. The present paper will describe palladium(II) complexes of β-ketoamines derived from acetylacetone and monoamines. No palladium(II) complexes of these ketoamines have yet been described in the literature.

## Experimental

**Materials.** — The palladium(II) complexes, Pd(Aca.R)$_2$, were prepared according to either of the following two methods. (A) To a solution of bis(acetylacetonato)palladium(II)[5] in ethanol, a calculated amount or a slight excess of one of the amines was added. The mixture was then stirred while being heated at about 50—60°C for five hours. (B) To a solution of a β-ketoamine in ethanol there was gradually added an aqueous solution of potassium tetrachloropalladate(II) and potassium hydroxide. The mixture was then stirred while being heated at about 40—50°C for about five hours. The yield was generally higher by the method B than by the method A. The method B was, therefore, applied to the preparation of the complexes with aryl amines, ammonia, methyl amine and benzyl amine. Since, however, it was difficult to prepare the β-ketoamines by condensation in the case of alkyl amines (with the exception of methyl amine), the metal complexes with alkyl amines were prepared according to the method A.

A typical example of preparation by the method A is that for bis(*N*-methyl-acetylacetoneaminato)palladium(II), Pd(Aca.$CH_3$)$_2$. To 1.0 g. (1/300 mol.) of Pd(acac)$_2$ in 10 ml. of ethanol, was added 0.67 g. of a 30% solution of methyl amine (2/300 mol.).[6] The reaction mixture was then stirred while being heated at abbut 60°C for about five hours. The coluor of the solution gradually changed from yellow to reddish brown. Then the solution was filtered and allowed to stand at room temperature. Reddish-brown crude crystals were obtained and recrystallized from chloroform.

A typical example of preparation by the method B is that for bis(*N*-phenyl-acetylacetoneaminato)palladium(II), Pd(Aca.$C_6H_5$)$_2$. To a slight excess of a β-ketoamine in 10 ml. of ethanol were added 1.0 g. (1/300 mol.) of potassium tetrachloropalladate(II) in 10 ml. of water and 0.38 g. of potassium hydroxide in 5 ml. of water. An orangish-yellow precipitate was produced at once, but the resulting mixture was incessantly stirred at 45—50°C for five hours. Then it was allowed to stand at room temperature. The product was filtered, washed with ether, and recrystallized from benzene-ethanol.

These palladium(II) complexes are all yellow or yellow-orange, with the exception of the *N*-methyl-substituted complex, for which two isomers were obtained as pure crystals, one being yellow and the other orange-red. The yellow form was prepared by the method B, and the orange-red form, by the method A. All the complexes prepared were stable in the atmosphere and were readily soluble in benzene and chloroform and moderately soluble in acetone, ethanol and methanol. The solvents used for the recrystallization of the complexes are shown in Table I, together with elemental analyses of the compounds.

**Measurements.**—The visible and ultraviolet absorption spectra of the complexes in solution were determined with a Shimadzu QR-50 spectrophotometer and a Beckman DU spectrophotometer. The infrared spectra of the compounds were determined with a Hitachi EPU-2A infrared spectrophotometer. The X-ray diffraction diagrams were obtained with a Toshiba ADX-103 X-ray diffractometer.

## Results and Discussion

Many new palladium(II) complexes have been synthesized in the present work with β-ketoamines

1) S. Yamada, H. Nishikawa and K. Yamasaki, This Bulletin, **36**, 483 (1963); S. Yamada and H. Nishikawa, ibid., **36**, 755 (1963); S. Yamada, H. Nishikawa and E. Yoshida, *Proc. Japan* Academy, **40**, (1964); etc.

2) As a matter of convenience, these ligands will be referred to as β-ketoamines, although their electronic state in the metal complexes may be somewhere between the ketoamine and the enolimine.

3) These metal complexes are abbreviated in this paper as M(Sal. R)$_2$ and M(Aca. R)$_2$, R being an alkyl or an aryl group attached to the nitrogen atom.

4) S. Yamada, H. Nishikawa and E. Yoshida, Proceedings 8. I. C. C. C. (International Conference on Co-ordination Chemistry), Vienna (1964), p. 373.

5) Bis(acetylacetonato)palladium(II) was prepared according to the method of A. A. Grinberg and L. K. Simonova (*Zhur. Priklad. Khim.*, **26**, 880 (1953)).

6) The symbol *acac* denotes an acetylacetonate anion.

Table I. Elemental analyses of palladium(II) complexes of β-ketoamines, $Pd(Aca.R)_2$

| R | Analyses Calcd., % C | H | N | Found, % C | H | N | Solvents for recrystalliz. |
|---|---|---|---|---|---|---|---|
| H | 39.42 | 5.91 | 9.20 | 40.0 | 5.38 | 9.10 | Chloroform |
| $CH_3$* | 43.60 | 6.05 | 8.47 | 43.70 | 6.22 | 8.32 | Methanol |
| $CH_3$** | 43.60 | 6.05 | 8.47 | 43.10 | 6.00 | 8.51 | Chloroform |
| $C_2H_5$ | 46.90 | 6.70 | 7.81 | 46.34 | 6.59 | 8.00 | Chloroform |
| $n$-$C_3H_7$ | 49.71 | 7.24 | 7.24 | 49.16 | 7.28 | 7.41 | Chloroform |
| $n$-$C_4H_9$ | 52.14 | 7.72 | 6.75 | 51.54 | 7.67 | 6.65 | Chloroform |
| $CH_2C_6H_5$ | 59.70 | 5.80 | 5.80 | 59.18 | 5.82 | 5.66 | Ethanol |
| $C_6H_5$ | 58.10 | 5.28 | 6.16 | 58.21 | 5.31 | 5.95 | Benzene-ethanol |
| $o$-tolyl | 59.70 | 5.80 | 5.80 | 58.52 | 5.70 | 5.71 | Benzene-ethanol |
| $m$-tolyl | 59.70 | 5.80 | 5.80 | 59.87 | 5.77 | 5.77 | Benzene-ethanol |
| $p$-tolyl | 59.70 | 5.80 | 5.80 | 59.84 | 5.75 | 5.69 | Benzene |
| $o,o'$-xylidyl | 61.13 | 6.27 | 5.48 | 60.50 | 6.11 | 5.39 | Benzene-ethanol |

* Yellow form ** Orange-red form

derived from acetylacetone and alkyl amines. The elemental analysis of the complexes, which agrees with the general formula of $Pd(Aca.R)_2$, definitely excludes the formation of the sexa-co-ordinate complexes of $Pd(acac)_2(RNH_2)_2$, as may also be inferred from the property of palladium(II) of being generally reluctant to take a co-ordination number exceeding four. This is borne out by the infrared spectra of the complexes, which show no absorption due to the CO-group of the acetylacetonate ion co-ordinated with the metal ion, but instead absorption peaks at about 1510—1520 and 1590—1600 $cm^{-1}$. These two peaks are most probably due to the β-ketoamines in the metal complexes[7]. Of the three possible forms for the β-ketoamines (Fig. 1), the structure B was considered to be most likely.[8] For the metal complexes of the β-ketoamines, however, the structures corresponding to the complexes of A and B may be surmized.[7] The

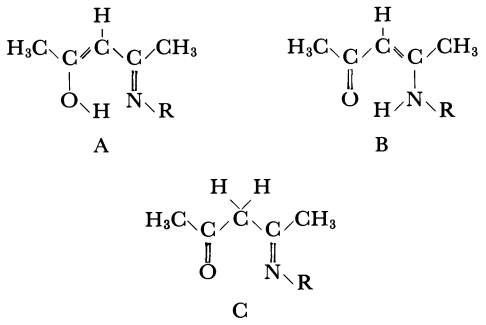


Fig. 1. Possible structures for the condensation products from acetylacetone and an amine, $RNH_2$: A, enolimine; B, ketoamine; c, ketoimine.

7) H. F. Holtzclaw, Jr., J. P. Collman and R. M. Alire, *J. Am. Chem. Soc.*, **80**, 1100 (1958).

8) N. H. Cromwell, F. A. Miller, A. R. Johnson, R. L. Frank and D. J. Wallace, ibid., **71**, 3337 (1949); etc.

extent of the contribution of these forms in the metal complexes has not been determined in the present work.

It should be noted that the palladium(II) complexes, $Pd(Aca.R)_2$ (R being $n$-propyl and $n$-butyl), have been prepared as crystals, although the free ligands have never been isolated as pure substances. This is regarded as an example of the stabilization of the otherwise unstable ligands through co-ordination with a metal ion. No reaction of a similar type with nickel(II), which also has a $d^8$ configuration, was found to take place at all; that is, the color of the mixed solution did not show any sign of the reaction taking place. The difference in this respect between palladium(II) and nickel(II) seems to be in agreement with the current view that the palladium(II)-ligand bond is generally stronger than the nickel(II)-ligand bond.

It is most likely that the palladium(II) complexes prepared in the present work are square-planar in non-donor solvents as well as in the solid state, since it is known that the palladium(II) ion strongly demands the quadri-co-ordinate square-planar configuration. A recent X-ray study has revealed that $Pd(Aca.H)_2$ takes a trans-square-planar configuration.[9] However, it has not yet been definitely concluded whether the complexes reported here belong to a trans- or a cis-series.

For $Pd(Aca.CH_3)_2$, two kinds of crystals were obtained according to the method of the preparation, one being yellow and the other a brownish orange. The X-ray powder patterns of the two forms are difinitely different. Furthermore, the electronic spectrum of the one is quite different from the spectrum of the other in solution, the red form displaying an absorption band in a far lower frequency region than the yellow form (Fig. 2).

9) G. E. Gurr, *Inorg. Chem.*, **3**, 614 (1964).

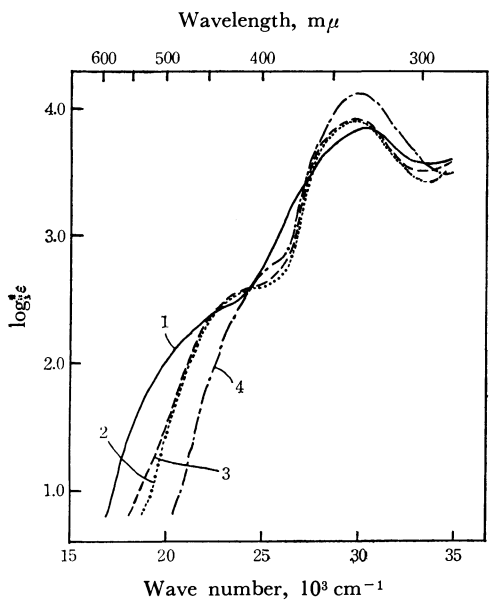



Fig. 2. Electronic spectra of ketoamine complexes of palladium(II) in chloroform: 1, Pd(Aca.-$CH_3$)$_2$, orange-red form (——); 2, Pd(Aca.-$CH_3$)$_2$, yellow form (----); 3, Pd(Aca.*n*-$C_4H_9$)$_2$ (— — —); 4, Pd(Aca.H)$_2$ (—·—·—).

Consequently, the difference in color between the two is not due to the difference in the mere effect of the packing of the molecules in the crystal, but to the difference in the molecular configuration. The two forms presumably correspond to cis- and trans-isomers. No definite conclusion has been reached in the present work about which is the cis- and which the trans-form.[10]

Judging from the similarity in the electronic spectrum (Fig. 2), the compounds prepared in the present work, which have the general formula of Pd(Aca.R)$_2$, R being ethyl, *n*-propyl and *n*-butyl, probably have the same geometrical configuration as the yellow form of Pd(Aca.$CH_3$)$_2$. The absorption band at about $24\times10^3$ cm$^{-1}$ is presumably due to an electronic transition between an orbital in the ligand and a d-orbital in the metal ion. The strong absorption band at about $30\times10^3$ cm$^{-1}$ may be due to an electronic transition within the ligand combined with the palladium(II) ion.

Many new complexes of palladium(II) β-ketoamines derived from acetylacetone and aryl amines have been prepared in the present work. As in the case of the corresponding alkyl complexes, the elemental analysis indicates that these palladium(II)-complexes are quadri-co-ordinate, with the formula of Pd(Aca.R)$_2$, while the infrared spectra show the formation of the ligands, Aca.R, combined with the metal ion.

10) A reaction similar to that employed in the preparation of the orange-red isomer does not yield the corresponding orange-red complex in the case of the aryl-substituents.

The free ligands can be isolated in the pure form with aryl group for R, while the isolation of the corresponding compounds in the pure form is possible only with methyl or ethyl for R throughout the alkyl series. The preparation of the metal complexes, therefore, is generally easier with the aryl than with the alkyl group for R.

As has been discussed in connection with the alkyl-derivatives, these palladium(II) complexes may also be considered square-planar. It is not certain at the present stage whether they should take a cis- or a trans-configuration. It might be argued that Pd(Aca.*o*,*o*'-xylidyl)$_2$ would take a configuration distorted from the square-plane due to the possible steric hindrance of the two methyl groups at the *o*- and *o*'-carbon atoms. However, this complex is also considered to be square-planar, since the formation of the corresponding nickel(II) complex with a square-planar configuration indicates that the probable steric hindrance of the two methyl groups is not so serious as to prohibit the square-planar configuration,[4] and since palladium(II) generally demands the square-planar configuration more strongly than nickel(II). This seems to be borne out by the electronic spectrum of this complex in non-donor solvents, (cf. Fig. 3); the spectrum is nearly superposable upon the spectra of Pd(Aca.tolyl)$_2$, which are all presumed to be square-planar since no steric hindrance is present in these complexes.

The capacity of nickel(II) in a square-planar

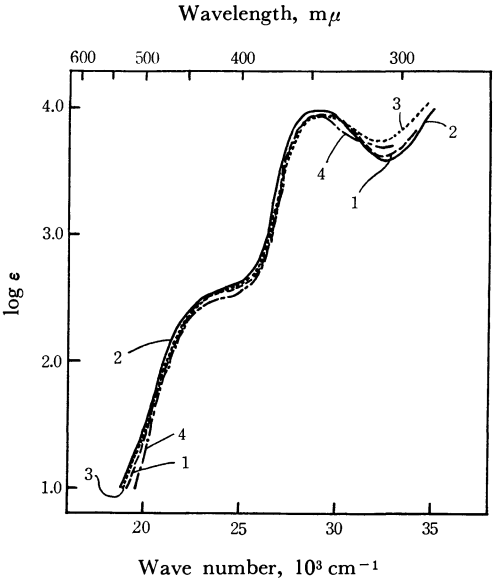



Fig. 3. Electronic spectra of ketoamine complexes of palladium(II): 1, Pd(Aca. *o*-tolyl)$_2$ in chloroform (----); 2, Pd(Aca. *m*-tolyl)$_2$ in chloroform (——); 3, Pd(Aca.*o*,*o*'-xylidyl)$_2$ in chloroform (----); 4, Pd(Aca.*o*,*o*'-xylidyl)$_2$ in pyridine (—·—·—).

complex to take the six-co-ordination by combining additional ligands was formerly examined, with pyridine used as the ligand.[4] In order to compare palladium(II) with nickel(II) in this respect, the electronic spectra were examined with the palladium(II) complexes prepared in the present work. The present measurements reveal that the spectra of these palladium(II) complexes in pyridine are almost superposable upon the spectra of the same compounds in non-donor solvents. This fact shows that these complexes keep the square-planar configuration, taking up no additional pyridine molecules at the fifth or the sixth site, even in pyridine. The corresponding nickel(II) complexes, $Ni(Aca.R)_2$ (R being aryl radicals), are found to form sexa-co-ordinated complexes by combining two pyridine molecules in the pyridine solution[4] (with the exception of Ni(Aca. *o*, *o'*-xylidyl)$_2$, which is square-planar in pyridine). It is found again that the palladium(II) has less of a tendency to form sexa-co-ordination than has nickel(II), as was also observed with other ligands.

No difference was observed in this property of the nickel(II) and palladium(II) complexes between the corresponding $\beta$-acetylacetoneamines and the salicylideneimines. A similar result was obtained with the corresponding complexes of salicylideneimines. The palladium(II) complexes of the $Pd(Sal.R)_2$ type (R being *o*, *o'*-xylidyl, *o*-, *m*- and *p*-tolyl, and phenyl) are all square-planar in pyridine as well as in non-donor solvents,[11] while the corresponding nickel(II) complexes, $Ni(Sal.R)_2$, are sexa-co-ordinated in pyridine (with the exception of Ni(Sal. *o*, *o'*-xylidyl)$_2$).[4]

11) S. Yamada and K. Fujita, unpublished.

## Summary

Numerous new palladium(II) complexes, $Pd(Aca.R)_2$, have been synthesized with $\beta$-ketoamines derived from acetylacetone and amines, where R represents methyl, ethyl, *n*-propyl, *n*-butyl, benzyl, phenyl, *o*-, *m*- and *p*-tolyl, and *o*, *o'*-xylidyl. It should be noted that when R denotes *n*-propyl or *n*-butyl, the palladium(II) complexes have been prepared successfully, although the free ligands can not be isolated in a pure form. This may be regarded as an example of the stabilization of a molecular configuration through co-ordination with a metal ion. The visible and ultraviolet spectra indicate that the palladium(II) complexes prepared in the present paper, which are considered to be square-planar in non-donor solvents as well as in the solid state, combine no additional pyridine molecules, even in pyridine. This is contrary to the previous observation that $Ni(Aca.R)_2$ complexes combine two molecules of pyridine to form a sexa-co-ordinated complex in pyridine.

The present authors wish to thank Professor Mitsue Koizumi and Dr. Shoichi Kume of the Institute of Geological Sciences of the College of General Education, Osaka University, for their X-ray diffraction diagrams. This investigation was supported in part by the Ministry of Education.

*Institute of Chemistry*
*College of General Enducation*
*Osaka University*
*Toyonaka, Osaka*

# The Selective Halogenation of Methylhydropolysiloxanes : Syntheses of Methylhalopolysiloxanes and Their Derivatives

By Minoru SAKIYAMA,† Yukinori NISHIZAWA and Rokuro OKAWARA

(Received June 18, 1965)

Toward nucleophilic reagents, the silicon-hydrogen bond is less reactive than Si–Cl, but more reactive than C–H. Thus, the hydrolysis of methylhydrochlorosilanes gives silicon-oxygen compounds with hydrogen still bonded to the silicon. Recently, we have reported on the synthesis of many organosiloxane polymers prepared by the co-hydrolysis of dimethylchlorosilane or methyldichlorosilane with other methylchlorosilanes.[1] The reaction of some of these compounds with cupric oxide has also been reported on.[2] In this

† Present address: Department of Chemistry, Faculty of Science, Osaka University, Kita Toneyama, Toyonaka.

1) a) R. Okawara and M. Sakiyama, This Bulletin, **29**, 236, 547 (1956). b) R. Okawara, U. Takahashi and M. Sakiyama, ibid., **30**, 608 (1957). See also, R. Okawara and M. Sakiyama, *Technol, Rept. Osaka Univ.*, **7**, 459 (1957).

2) M. Sakiyama and R. Okawara, *J. Organometal. Chem.*, **2**, 473 (1964).

Table I. Linear and cyclic methylbromopolysiloxanes

| | | Starting material: Methylhydropolysiloxane g. (mol.) | Starting material: $Br_2$ g. (mol.) | Starting material: Pyridine g. (mol.) | Product: Compound | Product: wt. g. | Product: % yield | Product: B. p. °C/mmHg | Product: %Br(-Si) Found (Calcd.) | Product: $n_D^{20}$ |
|---|---|---|---|---|---|---|---|---|---|---|
| I | $M'_2$ | 40(0.3) | 96(0.6) | 48(0.6) | $Br(CH_3)_2Si-O-Si(CH_3)_2Br$ | 30 | 70 | 167/760 | 53.3 (54.7) | — |
| II | $M'_2$ | 40(0.3) | 48(0.3) | 24(0.3) | $Br(CH_3)_2Si-O-Si(CH_3)_2H$ | 14 | 22 | 122/760 | 35.1 (37.5) | — |
| III | MD'M | 89(0.4) | 64(0.4) | 32(0.4) | $(CH_3)_3Si-O-Si(Br)(CH_3)-O-Si(CH_3)_3$ | 32 | 28 | 77/28 | 26.2 (26.6) | — |
| IV | $MD'_2M$ | 16(0.06) | 18(0.12) | 9(0.12) | $(CH_3)_3Si-O-Si(Br)(CH_3)-O-Si(Br)(CH_3)-O-Si(CH_3)_3$ | 7 | 28 | 114/12 | 35.2 (36.4) | — |
| V | $D'_4$ | 30(0.125) | 20(0.125) | 10(0.125) | $[-O-Si(H)(Br)-]_4$ | 5 | 13 | 59—60/15 | 22.3 (24.8) | 1.4113 |

Table II. Co-hydrolysis of methyldichlorosilane and dimethyldichlorosilane

| Expt. | Starting material: $CH_3SiHCl_2$ mol. | Starting material: $(CH_3)_2SiCl_2$ mol. | Starting material: mole ratio | Product: Tetramer g. | Product: Tetramer %yield | Product: Pentamer g. | Product: Pentamer % composition: $D'_5$ | $DD'_4$ | $D_2D'_3$ | $D_3D'_2$ | $D_4D'$ | $D_5$ |
|---|---|---|---|---|---|---|---|---|---|---|---|---|
| 1 | 0.8 | 2.4 | 1/3 | 180 | 80 | 24 | 0 | 0 | 0 | 38 | 44 | 17 |
| 2 | 1.6 | 1.6 | 1/1 | 190 | 88 | 34 | 0 | 11 | 37 | 40 | 9 | 3 |
| 3 | 2.4 | 0.8 | 3/1 | 155 | 77 | 27 | — | — | — | — | — | — |
| 4 | 3.2 | 0.0 | — | 85 (not decomposed thermally) | 44 | 14 | 100 | 0 | 0 | 0 | 0 | 0 |

Table III. Methylhydrocyclopentasiloxanes

| Compound | B. p. °C/mmHg | $n_D^{20}$ | $d_4^{20}$ | $MR_D$[c] Found (Calcd.) | %H(-Si) Found (Calcd.) |
|---|---|---|---|---|---|
| $D'_5$[a] | 168.7 | 1.3912 | 0.9985 | 71.54(71.35) | — |
| $DD'_4$ | — | — | — | — | — |
| $D_2D'_3$ | 81/18 | 1.3942 | 0.9794 | 80.32(80.09) | 0.92(0.92) |
| $D_3D'_2$ | 88/18 | 1.3957 | 0.9726 | 84.62(84.46) | 0.60(0.57) |
| $D_4D'$ | 96/18 | 1.3970 | 0.9662 | 88.92(88.83) | 0.27(0.28) |
| $D_5$[b] | 210 | 1.3982 | 0.9593 | 93.40(93.20) | — |

a) R. O. Sauer, W. J. Scheiber and S. D. Brewer, *J. Am. Chem. Soc.*, **68**, 962 (1946).
b) W. I. Patnode and D. F. Wilcock, ibid., **68**, 358 (1946).
c) Calculated from bond refractivities by E. L. Warrick, ibid., **68**, 2455 (1946).

Table IV. Bromination of methylhydrocyclotetra- and -pentasiloxanes

| Expt. | Starting material: Main component | Starting material: B. p. °C/mmHg | Starting material: $n_D^{20}$ | Starting material: %H(-Si) | Starting material: wt. g. | Product: wt. g. | Product: % yield |
|---|---|---|---|---|---|---|---|
| 1 | $D_3D'$ | 64—66/20 | 1.3935—1.3940 | 0.53—0.45 | 25.5 | 18.1 | 39 |
| 2 | $D_2D'_2$ | 56—60/20 | 1.3918—1.3822 | 0.84—0.72 | 23.4 | 10.3 | 29 |
| 3 | $DD'_3$ | 48—55/20 | 1.3901—1.3911 | 1.02—0.94 | 23.0 | 17.0 | 45 |
| 4 | $D'_4$ | 132/760 | 1.3870 | 1.67 | 13.0 | 6.7 | 17 |
| 5 | $D_4D'$ | 92—99/20 | 1.3969—1.3972 | 0.19—0.44 | 13.8 | 8.6 | 38 |

paper, we will report on the preparation of methylhalopolysiloxanes obtained by the halogenation of these polymers.

In these reactions, it is necessary to use a reagent which will halogenate the silanic hydrogen without reacting with the C–H and Si–O bonds. Photochlorination in a cooled carbon tetrachloride was applied successfully to $D'_n$ ($n$=4—7)* in order to chlorinate the silanic hydrogen.[3] However, this method brings about the chlorination of the methyl hydrogen when applied to the methylchlorosilanes, $M_2$ and $D_4$.[4] Moreover, in the case of $M_2$, the Si–O bond cleaved by hydrogen chloride. Elemental bromine readily reacts with alkylsilanes, for example, diethylsilane, to form alkylsilyl bromides.[5] However, bromine is unreactive toward hexamethyldisiloxane or alkylchlorosilanes not containing Si–H, except under forcing conditions.[6] Thus, bromine seemed a good choice as a reagent for the selective bromination of methylhydropolysiloxanes.

Photo-chlorination by chlorine gas by the method of Sokolov et al.[3] was first examined. $M'_2$ reacted with chlorine, but an aqueous layer soon separated, and much more chlorine was absorbed than had been calculated. It is evident that the carbon-hydrogen and silicon-oxygen bonds were attacked by, respectively, the chlorine and hydrogen chloride formed, in contrast to the case of $D'_n$. Bromine did not react with $M_2$ and $D_4$, even when refluxed, but did react violently with $M'_2$, the brown color disappearing soon after the addition. $D'_4$ also reacted with bromine, though less vigorously than $M'_2$. In both cases, however, the corresponding silicon-brominated compounds were obtained in only poor yields. A cleavage of the silicon-oxygen bond by hydrogen bromide probably takes place in these cases.

Pyridine forms crystalline adducts with bromine. The adducts are so unstable, however, that they decompose into bromine and pyridine when exposed to air.[7] Thus, pyridine may be expected to be utilized successfully in order to prevent the cleavage of the silicon-oxygen bond resulting from the attack of hydrogen bromide by forming pyridine hydrobromide. When bromine was added to a mixture of methylhydropolysiloxane and pyridine dissolved in carbon tetrachloride, the reaction took place smoothly and the corresponding bromo - compounds were obtained. The reaction scheme is as follows:

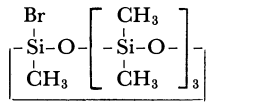
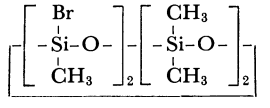
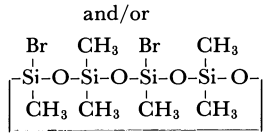
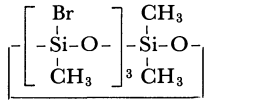
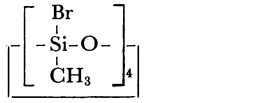
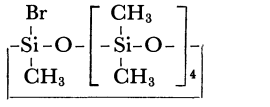


$$HBr + C_5H_5N \rightarrow C_5H_5NH^+Br^-$$

By this method the bromine-substituted methylpolysiloxanes given in Table I were synthesized. Iodine and iodine chloride were found to react neither with $M'_2$ nor with $D'_4$.

In the preceding paper, the isolation of methylhydrocyclotetrasiloxanes, $D_3D'$, $D_2D'_2$, $DD'_3$ as well as $D'_4$, was reported from the co-hydrolysis of methyldichlorosilane and dimethyldichlorosilane.[1b] In the present experiments, the isolation of methylhydrocyclopentasiloxanes was attempted, and $D_4D'$, $D_3D'_2$, and $D_2D'_3$ were obtained. Details of the reaction and the properties of these polysiloxanes are presented on Tables II and III. Fractions of the above-mentioned co-hydrolyzate, fractions which are composed mainly of $D'_4$, $DD'_3$, $D_2D'_2$, $D_3D'$, and $D_4D'$ respectively, were perfectly brominated in the presence of pyridine. Details of the reactions and properties of the methylbromopolysiloxanes thus obtained are given in Tables IV and V.

TABLE V. CYCLIC METHYLBROMOPOLYSILOXANES

| Compound | B. p. °C/mmHg | M. p. °C | %Br(-Si) Found (Calcd.) |
|---|---|---|---|
|  | 68/18 | — | 21.2 (22.1) |
|  and/or  | 107/20 | 49 | 37.2 (37.5) |
|  | 92/55 | 58—59 | 47.4 (48.8) |
|  | 112/ 4 | 97—98 | 56.8 (57.5) |
|  | 90/ 4 | — | 18.2 (18.4) |

Mono-bromine- or -chlorine-substituted methylpolysiloxanes synthesized as described above, or by the analogous method of Sokolov et al.,[3] were hydrolyzed or co-hydrolyzed with trimethylchlorosilane and dimethylchlorosilane in a large amount of water. Details of the experiments are given in Table VI. In the co-hydrolysis experiments,

* In order to show the structural units of methylpolysiloxanes, short-hand notations, which have been used frequently, will be used in this paper as follows:
$(CH_3)_3SiO_{1/2}$: M, $O_{1/2}Si(CH_3)_2O_{1/2}$: D,
$H(CH_3)_2SiO_{1/2}$: M', $HSi(CH_3)O_{2/2}$: D'.

3) N. N. Sokolov, K. A. Andrianov and S. M. Akimova, *Zhur. Obshchei Khim.*, **26**, 933 (1956).
4) F. C. Whitmore and L. H. Sommer, *J. Am. Chem. Soc.*, **68**, 481 (1946); R. H. Krieble and J. R. Elliott, ibid., **67**, 1810 (1945); B. A. Bluestain, ibid., **70**, 3068 (1948).
5) P. A. McCusker and E. L. Reilly, ibid., **75**, 1583 (1953).
6) J. R. Speier, Jr., ibid., **73**, 826 (1951).
7) P. F. Trowbridge and O. C. Diehl, ibid., **19**, 562 (1898).

TABLE VI. HYDROLYSIS OF HALOGEN SUBSTITUTED METHYLPOLYSILOXANES

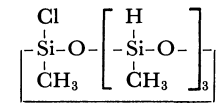
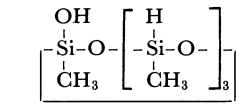
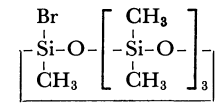
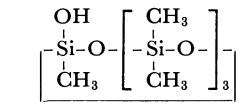
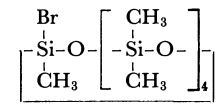
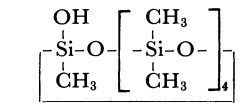
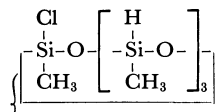
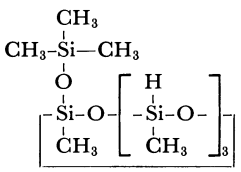
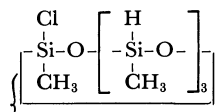
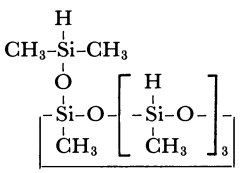
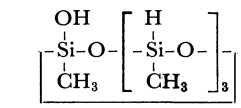
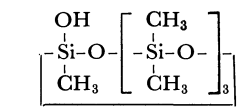
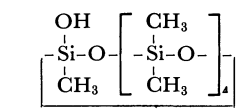
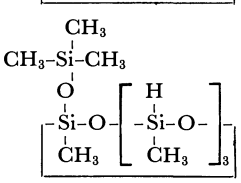
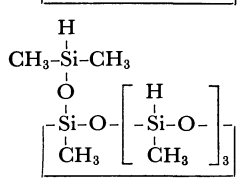
| Starting material | | Product | | | | |
|---|---|---|---|---|---|---|
| Compound | wt. g. | Compound | wt. g. | Yield % | %OH Found (Calcd.) | %H(—Si) Found (Calcd.) |
|  | 33 |  | 3 | 10 | — | 1.16 (1.16) |
|  | 14 |  | 5 | 41 | 5.69 (5.70) | — |
|  | 3.4 |  | 1.5 | 50 | 4.58 (4.56) | — |
|  | 20 |  | 2 | 8 | — | 0.90 (0.91) |
| $(CH_3)_3SiCl$ | 40 | | | | | |
|  | 27 |  | 9 | 29 | — | 1.25 (1.27) |
| $H(CH_3)_2SiCl$ | 40 | | | | | |

TABLE VII. PROPERTIES OF METHYLHYDROXYPOLYSILOXANES

| Compound | B. p. °C/mmHg | $n_D^{20}$ | $d_4^{20}$ | $MR_D$* Found (Calcd.) |
|---|---|---|---|---|
|  | 76/10 | 1.4040 | — | — |
|  | 80/ 9 | 1.4076 | 1.0404 | 70.76 (70.47) |
|  | 92/3.8 | 1.4077 | 1.0273 | 89.46 (89.11) |
|  | 68/10 | 1.3963 | — | — |
|  | 67/10 | 1.3922 | — | — |

* See Ref. c of Table III.

hydroxy-substituted methylcyclotetrasiloxanes were also formed. The properties of the siloxanols thus obtained are given in Table VII.

## Experimental

**Starting Materials.**—The preparation of the methylhydropolysiloxanes used in these experiments has already been reported on.[1]

**Bromination.**—Into a mixture of methylhydropolysiloxane and pyridine, dissolved in carbon tetrachloride and placed in a three-necked flask equipped with an efficient stirrer, a reflux condenser and a dropping funnel, bromine, diluted with carbon tetrachloride was stirred. After the addition, the mixture was refluxed for 30 to 60 min. in order to complete the reaction. Pyridine hydrobromide was then filtered off, and the filtrate was fractionally distilled. Hydrolyzable bromine was analyzed by neutralizing the hydrogen bromide formed from the hydrolysis of the methylbromopolysiloxanes.

**Co-hydrolysis.** — Methylhalogenopolysiloxanes or mixtures of them with methylchlorosilanes, diluted with dry ether, was added to cooled water. In the case of siloxanol formation, a buffer solution was used, and the mixture was neutralized by a dilute alkaline solution in the course of the reaction. The ethereal layer was separated, and, after the ether had been distilled off, the residue was fractionated by the column described in the previous papers. The hydroxyl content was determined with a Karl Fischer reagent.

## Summary

Bromine was utilized in the presence of stoichiometric amount of pyridine to brominate silanic hydrogen of methylhydropolysiloxanes. Methylbromopolysiloxanes thus obtained and methylchloropolysiloxanes prepared from photo-chlorination of methylhydropolysiloxanes were hydrolyzed with or without methylchlorosilanes to yield new methylhydroxypolysiloxanes and branched methylpolysiloxanes. Preparation of methylhydrocyclopentasiloxanes was also reported.

*Department of Applied Chemistry*
*Osaka University*
*Miyakojima, Osaka*

# NOTES

## An Iodometric Assay of Some Derivatives of 7-Aminocephalosporanic Acid

By Sachiko OKADA, Kiyoshi HATTORI and Tadayoshi TAKANO

(Received February 20, 1965)

The hydroxylamine method[1] and the iodometric assay are widely used for the determination of the purity of penicillins. Cephalosporin-C (II) is an antibiotic with a structure similar to penicillin; Alicino has reported an iodometric assay of this substances.[2]

An iodometric assay for some derivatives of 7-aminocephalosporanic acid (I) has now been studied. As the $\beta$-lactum ring of these derivatives is generally more stable than that of penicillins upon acidic and basic hydrolyses, only the conditions of the basic hydrolysis have been changed in the iodometric assay.

In Fig. 1, the time of hydrolysis is shown against the consumption of iodine. The experimental method has been standardized as follows: a sample

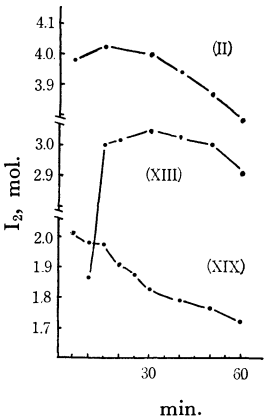
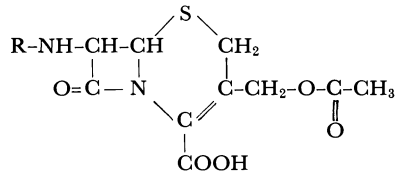



Fig. 1. The relation between $I_2$ consumption and time of basic hydrolysis; the number of derivative indicated in Table I.

1) J. H. Ford, *Ind. Eng. Chem., Anal. Ed.*, **19**, 1004 (1947).
2) J. F. Alicino, *Anal. Chem.*, **33**, 648 (1961).

(3—5 mg.) is dissolved in 5 ml. of a phosphate buffer (pH 6.0). To this solution is then added the same volume of N sodium hydroxide, and the mixture is kept at 23—25°C for fifteen minutes. Five milliliters of 1.2 N hydrochloric acid and 10 ml. of a 0.01N iodine solution are then added in order. Fifteen minutes later the residual iodine is titrated with 0.01 N sodium thiosulfate.

TABLE I. IODINE COMSUMPTION OF 7-AMINOCEPHALOSPORANIC ACID DERIVATIVES



| No. (derivatives) | R- (substituents) | Iodine consumption mol. |
|---|---|---|
| I | Hydrogen | 2.90 |
| II | δ-Aminoadipoyl | 4.01 |
| III | 10-Undecenoyl | 3.62 |
| IV | α-Chlorobutyroyl | 3.59 |
| V | Phenylacetyl | 4.18 |
| VI | *p*-Tolylacetyl | 3.98 |
| VII | *p*-Anisylacetyl | 4.76 |
| VIII | α-Thienylacetyl | 3.95 |
| IX | *p*-Chlorophenoxyacetyl | 4.15 |
| X | *o*-Nitrophenoxyacetyl | 3.68 |
| XI | Cinnamoyl | 3.88 |
| XII | β-(5-Nitro-2-furyl)acryloyl | 4.10 |
| XIII | α, β-Dichloro-β-phenylpropionoyl | 3.10 |
| XIV | α-Phenyl-β-(*p*-anisyl)propionoyl | 4.54 |
| XV | *N*-Benzyloxycarbonyl-*C*-phenylglycyl | 4.63 |
| XVI | Ethoxycarbonyl | 4.01 |
| XVII | Phenoxycarbonyl | 4.63 |
| XVIII | Phenylcarbamoyl | 3.86 |
| XIX | α-Naphthylcarbamoyl | 1.97 |

The results are listed in Table I.

The *N*-acylation of the 7-amino group gives evidence of an iodine consumption differing from that of the original 7-aminocephalosporanic acid (I); this behavior is similar to that between penicillin and 6-aminopenicillanic acid. Under these conditions, iodine consumption is not observed for the substituent parts—i. e., cinnamic acid, β-(5-nitro-1-furyl)acrylic acid, phenylacetic acid, *p*-chlorophenoxyacetic acid and 10-undecenoic acid.

Even when the substituents are sturcturally classified, there is no regular relationship between the iodine consumption and any of the groups. However, the reproducibility of the iodine consumption in this assay is high with respect to each of the derivatives. Hence, this assay might be useful for the inspection of the purity of each compound. The decreasing curves of iodine consumption in Fig.1 indicate that some destruction of the active structure or some formation of a reductive substance might occur during a long basic hydrolysis. The nature of the active structure in this assay remains to be studied, however.

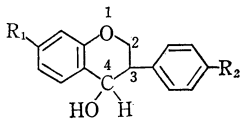
*Research Laboratories*
*Fujisawa Pharm. Co., Ltd.*
*Higashiyodogawa, Osaka*

# The Stereochemistry of Isoflavan-4-ols

By Shozo YAMAGUCHI, Shoei ITO, Asao NAKAMURA* and Naoto INOUE

(Received March 16, 1965)

One of the present authors, Inoue, obtained isoflavan-4-ol (I), 7-methoxyisoflavan-4$\alpha$-ol (II), 7-methoxyisoflavan-4$\beta$-ol (III) and 7, 4'-di methoxyisoflavan-4-ol (IV) by the reduction of the corresponding isoflavanones; he tentatively assigned a trans configuration to II and cis configurations to I, III and IV, mainly on the basis of the mechanism of the reduction and on that of the reactions of those compounds.[1]




(I): $R_1=R_2=H$
(II), (III): $R_1=OMe$, $R_2=H$
(IV): $R_1=R_2=OMe$

The NMR spectra of hydroxyflavans have been measured by Clark-Lewis and Jackman[2] and by other authors[3], who have reported that spin-spin

* Present address: The Ajinomoto Co., Ltd., Kawasaki, Japan.

1) N. Inoue, This Bulletin, **37**, 601 (1964).
2) J. W. Clark-Lewis and L. M. Jackman, *Proc. Chem. Soc.*, **1961**, 165; J. W. Clark-Lewis, T. M. Spotswood and L. R. Williams, ibid., **1963**, 20; J. W. Clark-Lewis, L. M. Jackman and L. R. Williams, *J. Chem. Soc.*, **1962**, 3858.
3) C. P. Lillya, D. Kehoe, E. M. Philbin, M. A. Vickars and T. S. Wheeler, *Chem. & Ind.*, **1963**, 84; C. P. Lillya, ibid., **1963**,

TABLE I. NMR SPECTRA OF 4-HYDROXYISOFLAVANES AND THEIR DERIVATIVES

| | Position of peaks in c. p. s. | No. of protons | Assignment | Remark | Configuration |
|---|---|---|---|---|---|
| Isoflavan-4-ol (I)*4 | 181—201 | 1 | $H_3$ | Sextet | |
| | 240—283 | 2 | $H_2$ | Multiplet | |
| | 274.5, 277.4*1 | 1 | $H_4$ | Doublet $J_{3,4}=2.9$ c. p. s. | 3(ax), 4(eq) cis |
| Acetate of I | 368.2, 371.0 | 1 | $H_4$ | Doublet $J_{3,4}=3.0$ c. p. s. | 3(ax), 4(eq) cis |
| 7-Methoxy-isoflavan-4$\alpha$-ol (II) | 175.5—195.5 | 1 | $H_3$ | Sextet | |
| | 242—266 | 2 | $H_2$ | Multiplet | |
| | 288.6, 296.0 | 1 | $H_4$ | Doublet $J_{3,4}=7.4$ c. p. s. | 3(ax), 4(ax) trans |
| Acetate of II | 364.3, 369.3 | 1 | $H_4$ | Doublet $J_{3,4}=5.0$ c. p. s. | 3(ax), 4(ax) trans |
| 7-Methoxy-isoflavan-4$\beta$-ol (III) | 186.5—205 | 1 | $H_3$ | Sextet*3 | |
| | 249.3—286.8 | 2 | $H_2$ | Multiplet*3 | |
| | 282.1, 285.1*2 | 1 | $H_4$ | Doublet $J_{3,4}=3.0$ c. p. s. | 3(ax), 4(eq) cis |
| Acetate of III | 364.9, 368.1*2 | 1 | $H_4$ | Doublet $J_{3,4}=3.2$ | 3(ax), 4(eq) cis |
| 4-Isopropoxy-7-methoxy-isoflavan[6] | 264.0, 271.0 | 1 | $H_4$ | Doublet $J_{3,4}=7.0$ | 3(ax), 4(ax) trans |
| 7,4'-Dimethoxy-isoflavan-4-ol (IV)*4 | 278.0, 280.9 | 1 | $H_4$ | Doublet $J_{3,4}=2.9$ | 3(ax), 4(eq) cis |

*1 Long range coupling ($J_{2,4}=1.0$ c. p. s.) was observed.
*2 Long range coupling ($J_{2,4}=1.2$ c. p. s.) was observed.
*3 The following values were calculated from the ABX pattern[7]:
$J_{AB}=10.4$ c. p. s., $J_{AX}=11.9$ c. p. s., $J_{BX}=3.0$ c. p. s., $\delta_{AB}=16.7$ c. p. s.
*4 These compounds[1] were also prepared from the corresponding isoflavones by reduction with sodium borohydride at room temperature.[8]

coupling constants between the 2- and 3-, and the 3- and 4- protons define the stereochemistry and conformation of the heterocyclic ring.

On the other hand, the NMR spectrum of only one 4-hydroxyisoflavan, 2-methyl-4-hydroxy-7, 4'-diacetoxyisoflavan, has been reported[4]; the spectra of pterocarpin and similar compounds have also been discussed,[5] but the simple 4-hydroxyisoflavans have not been investigated.

With this in mind, the NMR spectra of I, II, III, IV and their derivatives were measured out in order to determine their configurations and to decide whether relationships similar to those found in the case of the hydroxyflavans exist between the coupling constants and the configurations of the isoflavan-4-ols.

The experimental results are summarized in Table I.

A consideration of the dependence of the proton vicinal coupling constants on the dihedral angle, as in the Karplus equation,[9] leads unambiguoulsy to the assignment of the same configuration as was proposed in the preceding paper. The relationship between the 3, 4-coupling constants and the configurations which was observed with hydroxyisoflavans is the same as that seen in the case of the hydroxyflavans.[2,3] Therefore, it may be concluded that the configuration of a 4-hydroxyisoflavan can be determined from the coupling constant of the 3- and 4-protons.

Furthermore, the *S*-methylxanthates of II and III were submitted to thermal elimination in order to confirm the stereochemical relations obtained by NMR measurements. The *S*-methylxanthates

TABLE II

| Heating time min. | Yield of isoflavene, % | |
|---|---|---|
| | Xanthate of II | Xanthate of III |
| 10 | 20 | 4 |
| 20 | 30 | 7 |
| 40 | 37 | 22 |
| 60 | 43 | 31 |

783; E. J. Corey, *Tetrahedron Letters*, **1961**, 429.
4) R. A. Micheli, A. N. Booth, A. L. Livingston and E. M. Bickoff, *J. Med. & Pharm. Chem.*, **5**, 321 (1962).
5) J. B. Bredenberg and J. N. Shoolery, *Tetrahedron Letters*, **1961**, 285; D. R. Perrin, ibid., **1964**, 29; D. D. Perrin and D. R. Perrin, *J. Am. Chem. Soc.*, **84**, 1922 (1962).
6) N. Inoue, S. Yamaguchi and S. Fujiwara, This Bulletin, **37**, 588 (1964).
7) H. J. Bernstein, J. A. Pople and W. G. Schneider, *Can. J. Chem.*, **35**, 65 (1957).
8) After this work had been completed, a report appeared by L. R. Row, A. S. R. Anjaneyulu and C. S. Krishna (*Curr. Sci.*, **32**, 67 (1963)) in which 7-methoxy and 7,4'-dimethoxyisoflavanones were reduced to isoflavan-4-ols by the same procedure.
9) M. Karplus, *J. Chem. Phys.*, **30**, 11 (1959).

of II and III were prepared by Corey's method[10] and were subjected to elimination reactions at 180°C. The rate of the formation of the corresponding isoflavene was determined by measuring the extinction of the product at 332.5 mμ (Table II).

From the results summarized in Table II, it is apparent that the xanthate of II decomposes faster than that of III, consequently, II has the cis, and III has the trans, configuration.

## Experimental

The NMR spectra were determined with a Varian A-60 spectrometer, at 60 Mc., using deuterochloroform as the solvent and tetramethylsilane as the internal reference.

**Isoflavan-4-ol (I) and 7,4'-Dimethoxyisoflavan-4-ol (IV).** — A solution of isoflavone (0.7 g.) and sodium borohydride (0.3 g.) in methanol (130 ml.) was stirred for 2 days at room temperature. The methanol was then distilled off under reduced pressure, and the residue was decomposed with 70% acetic acid. The resulting solution was diluted with water and extracted with ether. The ether layer was washed once with a sodium bicarbonate solution and twice with water, then dried over anhydrous sodium sulfate and evaporated. The residue crystallized from petroleum ether as prisms (0.4 g.); m. p. 75°C.

7,4'-Dimethoxyisoflavan-4-ol (37%) m.p. 143—144°C was similarly prepared from the corresponding isoflavone.

***S*-Methylxanthates of II (V) and III (VI).**—A dimethyl sulfoxide solution (10 ml.) of sodium methylsulfinylcarbanion (prepared from 0.3 g. of sodium hydride and 20 ml. of dimethyl sulfoxide) was added to a stirred solution of II (0.25 g.) in dimethyl sulfoxide (5 ml.); the mixture was then stirred for 30 min. Then carbon disulfide (0.16 g.) was added and, after 30 min., 0.29 g. of methyl iodide, after which stirring was continued for 2.5 hr. All of these operations were carried out at room temperature under an atmosphere of nitrogen. Finally, the resulting solution was diluted with water and extracted with ether. The evaporation of the ether gave pale yellow crystals, which were treated with 5 ml. of methanol. The insoluble solid was collected and recrystallized from ethanol - ethyl acetate to give the *S*-methylxanthate of II (0.15 g.), m. p. 136—137.5°C.

Found: C, 62.17; H, 5.14. Calcd. for $C_{18}H_{18}O_3S_2$: C, 62.42; H, 5.24%.

*S*-Methylxanthate of III, m. p. 93—95°C (after recrystallization from ethanol - ethyl acetate), was similarly prepared from the corresponding isoflavan-4-ol.

Found: C, 62.31; H, 5.08. Calcd. for $C_{18}H_{18}O_3S_2$: C, 62.42; H, 5.24%.

**The Decomposition of the Xanthates.**—The weighed xanthates (ca. 0.1 mg.) described above were placed in separate glass tubes (4×150 mm.) under a nitrogen atmosphere; the tubes were then clamped vertically in an oil bath at 180°C. At the end of a given time, the tubes were removed from the bath, the reaction product was dissolved in methanol, and the extinction at 332.5 mμ for each solution was measured in order to determine the yield of isoflavene by reference to a previously-prepared calibration curve.

The authors wish to express their gratitude to Assistant Professor Ichiro Murata of Tohoku University for his valuable advice.

*The College of General Education*
*Tohoku University*
*Kawauchi, Sendai*

10) E. J. Corey and H. Uda, *J. Am. Chem. Soc.*, **85**, 1790 (1963).

# The Isomerization and Pyrolysis of Cyclopropane in a Single-Pulse Shock Tube*

By Hajime MIYAMA and Tetsu TAKEYAMA

(Received April 22, 1965)

The isomerization of cyclopropane has been studied by several researchers.[1,2] However, no data at high temperatures (above 900°K) have been reported so far. Therefore, we have studied the isomerization and pyrolysis of cyclopropane over the temperature range from 1020 to 1660°K by using a single-pulse shock tube developed at Cornell University.[3]

The shock tube was fabricated from stainless steel tubing of 2.5 cm. i. d. The length of the driver section could be varied from 50 to 200 cm. by a piston mounted on a screw. A quick valve, placed at a distance of 22 cm. from the end-plate, was used to prevent the mixing and diffusion

* Presented at the 18th Annual Meeting of the Chemical Society of Japan, Osaka, April, 1965.

1) T. S. Chambers and G. B. Kistiakowsky, *J. Am. Chem. Soc.*, **56**, 399 (1934).

2) B. R. Davis and D. S. Scott, *Ind. Eng. Chem., Fundamentals*, **3**, 20 (1964).

3) A. Lifshitz and S. H. Bauer, *J. Chem. Phys.*, **38**, 2056 (1963).

Table I. The experimental conditions and results

The composition of gas mixture is 88% Ar, 10% cyclo-$C_3H_6$, and 2% Ne[a)]

| $T$ °K | $P$ mmHg | $t$ μsec. | Conversion of product, %[b)] | | | | | | $k$ $10^3$ sec$^{-1}$ |
|---|---|---|---|---|---|---|---|---|---|
| | | | Cyclo-$C_3H_6$ | $C_3H_6$ | $CH_4$ | $C_2H_6$ | $C_2H_4$ | $C_2H_2$ | |
| 1047 | 3060 | 425 | 77.2 | 1.7 | 0.0 | 0.0 | 0.0 | 0.0 | 0.608 |
| 1097 | 3390 | 435 | 58.3 | 23.8 | 0.0 | 0.0 | 0.0 | 0.0 | 1.240 |
| 1173 | 3950 | 520 | 45.9 | 34.9 | 0.5 | 0.0 | 1.0 | 0.0 | 1.498 |
| 1226 | 2140 | 540 | 46.4 | 44.1 | 1.5 | Trace | 2.2 | 0.0 | 1.422 |
| 1271 | 4630 | 440 | 41.9 | 35.4 | 2.6 | Trace | 3.6 | 1.1 | 1.978 |
| 1279 | 2340 | 465 | 35.6 | 29.1 | 2.8 | Trace | 4.3 | Trace | 2.222 |
| 1294 | 4800 | 430 | 42.1 | 32.3 | 3.8 | 0.0 | 5.0 | 2.1 | 2.012 |
| 1493 | 3180 | 355 | 31.4 | 30.7 | 7.6 | Trace | 8.9 | 6.4 | 3.263 |
| 1657 | 3920 | 200 | 31.6 | 23.5 | 8.5 | 0.0 | 9.6 | 8.3 | 5.762 |

a) Used as an internal standard.

b) Conversions of $C_1$, $C_2$ and $C_3$ hydrocarbons are obtained by multiplying the molar percentages of those products to the initial concentration of cyclo-$C_3H_6$ by 1/3, 2/3 and 1, respectively.

Table II. The experimental conditions and results

The composition of gas mixture is 93% Ar, 5% cyclo-$C_3H_6$, and 2% Ne[a)]

| $T$ °K | $P$ mmHg | $t$ μsec. | Conversion of product, %[b)] | | | | | | $k$ $10^3$ sec$^{-1}$ |
|---|---|---|---|---|---|---|---|---|---|
| | | | Cyclo-$C_3H_6$ | $C_3H_6$ | $CH_4$ | $C_2H_6$ | $C_2H_4$ | $C_2H_2$ | |
| 1021 | 2090 | 615 | 84.4 | 0.0 | 0.0 | 0.0 | 0.0 | 0.0 | 0.276 |
| 1046 | 2226 | 650 | 83.9 | 13.5 | 0.0 | 0.0 | 0.0 | 0.0 | 0.270 |
| 1053 | 4480 | 695 | 61.8 | 8.9 | 0.0 | 0.0 | 0.0 | 0.0 | 0.693 |
| 1106 | 2476 | 580 | 46.6 | 33.8 | 0.0 | 0.0 | 0.0 | 0.0 | 1.317 |
| 1140 | 2640 | 670 | 47.4 | 43.7 | Trace | 0.0 | Trace | 0.0 | 1.115 |
| 1156 | 2725 | 500 | 34.0 | 47.7 | 0.6 | 0.0 | 1.0 | 0.0 | 2.158 |
| 1187 | 4680 | 640 | 50.4 | 19.5 | 0.0 | 0.0 | 0.0 | 0.0 | 1.070 |
| 1245 | 6220 | 735 | 35.6 | 34.5 | 1.8 | 0.0 | 2.8 | Trace | 1.406 |
| 1364 | 3730 | 580 | 25.0 | 26.6 | 5.3 | 0.3 | 6.0 | 3.5 | 2.391 |
| 1432 | 4080 | 480 | 28.8 | 20.4 | 7.0 | Trace | 7.5 | 6.4 | 2.593 |
| 1540 | 4605 | 405 | 26.7 | 20.5 | 8.1 | Trace | 9.1 | 11.5 | 3.513 |
| 1598 | 4966 | 325 | 22.7 | 22.8 | 7.7 | Trace | 8.2 | 13.1 | 3.659 |
| 1602 | 4930 | 490 | 27.6 | 17.2 | 9.1 | Trace | 7.9 | 11.6 | 2.628 |

of gases in the cold and hot regions. Five piezogauges were placed in a line over 90 cm. upstream of the endplate in order to measure incident shock velocities, and an additional piezogauge on the endplate, to record the reaction times. Matheson cyclopropane (99.5% pure), Takachiho propylene (99.90% pure) Nippon Sanso argon (99.999% pure), and Takachiho neon (99.9% pure) were used without further purification.

After each run, a 5 cc. sample was taken from the end section and analyzed by a gas chromatograph (Yanagimoto GCG-2) at 55°C by using columns of silica gel (1 m.) and β, β'-oxydipropionitrile (2 m.) for the analysis of $C_2$ and $C_3$ hydrocarbons and a column of molecular sieve 5A (1 m.) for the analysis of methane, with helium as the carrier. The other details of the experiment and calculation were almost the same as those described in Ref. 3, except that the incident shock velocities were used for the calculation of shock parameters.

The experimental conditions and results are shown in Tables I and II, where $T$, $P$, $t$ and $k$

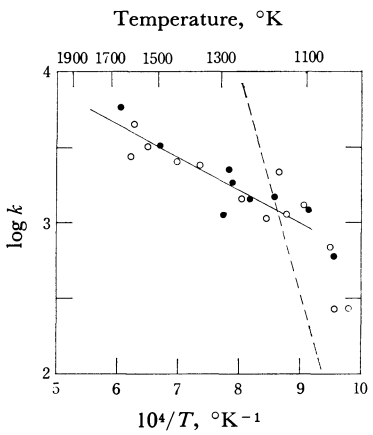



Fig. 1. Arrhenius plot of first-order rate constant. Open and solid circles are, respectively, obtained from mixtures, 93% Ar, 2% Ne, and 5% cyclo-$C_3H_6$ and 88% Ar, 2% Ne, and 10% cyclo-$C_3H_6$. Solid line is the least-squares fit to the points above 1200°K.
Dashed line represents the following relation[2)] obtained at lower temperatures.
$2.303 \log k = 35.431 - 65570/RT$

Table III. The experimental conditions and results
The composition of gas mixture is 88% Ar, 10% $C_3H_6$, and 2% Ne

| $T$, °K | $P$, mmHg | $t$, $\mu$sec. | Conversion of product, % | | | | |
|---|---|---|---|---|---|---|---|
| | | | $C_3H_6$ | $CH_4$ | $C_2H_6$ | $C_2H_4$ | $C_2H_2$ |
| 1268 | 4600 | 385 | 88.7 | 0.2 | 0.0 | 0.5 | 0.0 |
| 1283 | 2360 | 550 | 80.8 | 0.5 | 0.0 | 0.7 | 0.0 |
| 1291 | 2430 | 440 | 80.1 | 0.7 | 0.0 | 0.9 | 0.0 |
| 1346 | 5130 | 410 | 85.3 | 1.0 | 0.0 | 2.0 | Trace |
| 1374 | 2710 | 560 | 78.6 | 1.6 | Trace | 2.5 | Trace |
| 1420 | 2880 | 380 | 69.3 | 2.3 | Trace | 4.0 | 1.8 |
| 1582 | 3560 | 510 | 53.8 | 5.6 | 0.3 | 6.8 | 4.5 |
| 1615 | 3680 | 210 | 59.4 | 5.4 | 0.4 | 7.2 | 5.6 |
| 1638 | 3800 | 370 | 52.0 | 6.6 | 0.4 | 7.9 | 6.8 |
| 1649 | 3920 | 220 | 60.5 | 5.3 | 0.3 | 7.2 | 5.8 |

Table IV. The experimental conditions and results
The composition of gas mixture is 93% Ar, 5% $C_3H_6$, and 2% Ne

| $T$, °K | $P$, mmHg | $t$, $\mu$sec. | Conversion of product, % | | | | |
|---|---|---|---|---|---|---|---|
| | | | $C_3H_6$ | $CH_4$ | $C_2H_6$ | $C_2H_4$ | $C_2H_2$ |
| 1161 | 2720 | 610 | 95.6 | 0.0 | 0.0 | 0.0 | 0.0 |
| 1219 | 5980 | 590 | 83.7 | 0.4 | 0.0 | 0.6 | 0.0 |
| 1384 | 3830 | 580 | 72.5 | 3.3 | 0.0 | 5.5 | 2.5 |
| 1422 | 4020 | 575 | 72.9 | 3.7 | 0.3 | 6.7 | 3.2 |
| 1436 | 4080 | 645 | 68.0 | 3.7 | 0.0 | 0.0 | 2.8 |
| 1577 | 4790 | 575 | 52.6 | 7.0 | Trace | 8.4 | 8.4 |
| 1582 | 4860 | 500 | 52.9 | 6.1 | Trace | 8.7 | 8.8 |
| 1616 | 5030 | 535 | 46.9 | 6.6 | Trace | 7.0 | 11.2 |
| 1683 | 5380 | 540 | 44.9 | 7.0 | Trace | 7.2 | 9.6 |

are the reaction temperature, the pressure, the time, and the first-order rate constant respectively.

The first-order rate constant was calculated by the following equation:

$$k=\ln (C_0/C_f)/t$$

Here $C_0$ and $C_f$ are the initial and final concentrations of cyclopropane. An Arrhenius plot of the rate constants is shown in Fig. 1; it may be compared with the dashed-line extrapolated from the results obtained at lower temperatures.[2] There is apparently a bend at about 1200°K. The points of the low-temperature region fall somewhat above the extrapolated line; this seems due to the experimental difference between the shock-tube and conventional techniques.[4] Those of the high-temperature region fall below it and present a straight line with an apparent activation energy of 9.2 kcal./mol.

A comparison of Tables I and II with Fig. 1 would suggest that the production of methane and $C_2$ hydrocarbons affects the bend of $k$ values at 1200°K, although the materials recovered after each run are deficient; this deficiency can not be explained by the present study, because not all species in the reaction products could be analyzed in terms of the columns described above. A pyrolysis experiment with propylene under the same conditions as in the present study gave almost the same dependence of the composition of the reaction products upon the temperature, as is shown in Tables III and IV.

Therefore, it may be concluded that, at higher temperatures, the isomerization of cyclopropane occurs first, followed by pyrolysis, and that some of reaction products inhibit the isomerization. However, further experimentation will be necessary in order to establish a more detailed mechanism.

We are grateful to Messrs Akio Sawa and Kazutoshi Sugiyama for their help in the experiments.

*Basic Research Laboratories*
*Toyo Rayon Company, Ltd.*
*Tebiro, Kamakura, Kanagawa*

4) A. Lifshitz, H. F. Carroll and S. H. Bauer, ibid., **39**, 1661 (1963).

# Diffusion Coefficients for Aqueous Solutions of Benzene and α-Naphthalene Sulfonates at 25°C*

By Hatsuho UEDAIRA and Hisashi UEDAIRA

(Received April 26, 1965)

Aromatic sulfonate ions consist of two distinct parts, a hydrophilic part (sulfonic group) and a hydrophobic part (aromatic ring). These two parts interact differently with water. The effect of these interactions on the limiting conductance of four kinds of sulfonates has been reported on previously.[1]

It now seems to be important to investigate the effect of these interactions on the other physicochemical properties of aromatic sulfonates. In this paper, the diffusion coefficients of sodium benzenesulfonate (BSNa) and sodium α-naphtalenesulfonate (NSNa) in water at 25°C were measured by the magnetically-stirred porous diaphragm method, and their apparent molar volumes were obtained by a density method. From the measured cell integral diffusion coefficients, the integral and differential diffusion coefficients were calculated by Stokes method.[2]

## Experimental

**Materials.**—The BSNa and NSNa were purified as before.[1] The potassium chloride was of an analytical grade (Merck) and was used without further purification. The conductance water was boiled before use in order to make it air-free. Its specific conductance was less than $1\times10^{-6}\,\mathrm{cm^{-1}\,\Omega^{-1}}$.

**Diffusion Cell.**—The diaphragm-cell was the same type as has been described by Stokes.[3] Modifications were, however, made in the lower stopper and in the magnet. In order to avoid disturbing the liquid in the diaphragm upon withdrawing or inserting the lower stopper, grooves were cut in both the stopper and the neck of the lower compartment, as is shown in the figure. The lower compartment was completely closed by rotating the stopper. When the cell was dipped in the thermostat water, the lower stopper was sealed by air.

A ring ferrite magnet was used instead of a horseshoe magnet. This magnet is so strong and light that it can be rotated smoothly by a small induction motor (Yokogawa SM-Q; output 2W) at a rate of 30 or 50 r.p.m.

**The Calibration of Cell and Measurements of the Diffusion Coefficient and Density.**—The cell

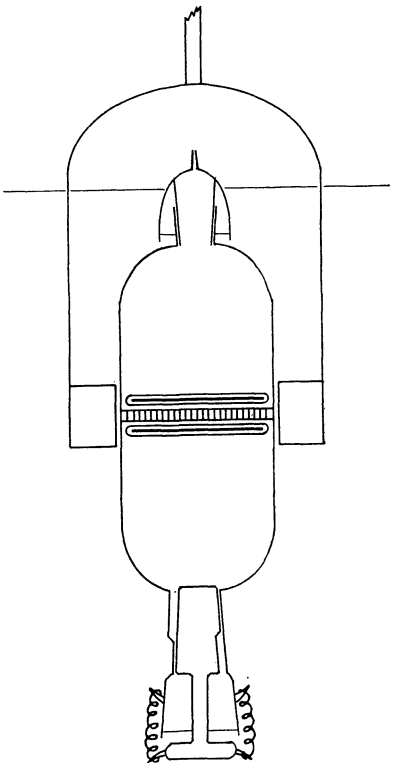


Fig. 1. The diaphragm cell.

integral diffusion coefficient, $\overline{D}$, is given by:

$$\overline{D}=\frac{1}{\beta t}\ln\frac{c_1-c_2}{c_3-c_4} \qquad (1)$$

where $\beta$ is the cell constant and $t$ is the duration of the experiment (sec.). $c_2$ (invariably zero, as recommended by Stokes[2]) and $c_4$ are the initial and the final molar concentrations in the upper compartment respectively, while $c_3$ is the final concentration in the lower compartment. The initial lower concentration, $c_1$ (mol./l.), is obtained by the Stokes method.[4]

The cell constant, $\beta$, was determined by the measurement of the diffusion of 0.08—0.1 N potassium chloride in water and by comparing the results with the data of Stokes.[2,4] The concentrations of potassium chloride were determined by measuring the conductances of the solutions, using the conductance data

* Presented at the 16th Annual Meeting of the Chemical Society of Japan, Tokyo, April, 1963.

1) H. Uedaira and H. Uedaira, This Bulletin, **37**, 1885 (1964).

2) R. H. Stokes, *J. Am. Chem. Soc.*, **72**, 2243 (1950); **73**, 3527 (1951).

3) B. R. Hammond and R. H. Stokes, *Trans. Faraday Soc.*, **51**, 1641 (1955).

4) R. A. Robinson and R. H. Stokes, "Electrolye Solutions," 2nd. ed. Butterworths Scientific Publns., London (1959), Chap. 10.

obtained by Shedlovsky[5] and Stokes[6].

The time necessary for the concentration gradient in the diaphram to attain a steady state was estimated by Gordon's equation.[7]

The molar concentrations of BSNa and NSNa were determined by measuring the conductance of the solution. The conductance-concentration relation had been measured peviously.

The apparent molar volume, $\phi_v$, was calculated from the density, which was determined with a springel pycnometer 30 ml. in capacity. $\phi_v$ is expressed in the dilute solution by the following Masson relation:[8]

$$\phi_v = \phi_v^\circ + S_v c^{1/2} \quad (2)$$

where $\phi_v^\circ$ is the $\phi_v$ at an infinite dilution and $S_v$ is the limiting slope.

## Results and Discussion

The experimental equation of the density for a BSNa solution calculated by the method of least squares at 25°C is ($c < 1.0$ mol./l.):

$$d = 0.99707 + (0.0837 \pm 0.0013)c - (0.0106 \pm 0.0015)c^{3/2} \quad (3)$$

while the equation for NSNa is: ($c < 0.25$ mol./l.)**

$$d = 0.99707 + (0.09443 \pm 0.00056)c - (0.0076 \pm 0.0013)c^{3/2} \quad (4)$$

Thus, from Eqs. 2, 3 and 4, the apparent molar volumes for BSNa and NSNa solutions can be given by the following equations:

$$\phi_v = 96.70 + 10.61c^{1/2} \quad (5)$$

$$\phi_v = 136.2 + 7.620c^{1/2} \quad (6)$$

The cell integral diffusion coefficients, $\overline{D}$, for BSNa and NSNa solutions are shown in Tables I and II. The limiting diffusion coefficients at the infinite dilution, $D^\circ$, as calculated by Nernst's limiting law are $10.97 \times 10^{-6}$ and $9.840 \times 10^{-6}$ ($cm^2 sec^{-1}$) for BSNa and NSNa respectively, where the limiting equivalent conductances of sodium, $BS^-$ and $NS^-$ ions were 50.10,[4] 34.99[9] and 29.31[1] ($cm^2 \Omega^{-1}$ equiv$^{-1}$) respectively. The integral diffusion coefficients, $\overline{D}^\circ$, at the concentration $c_m$, where $c_m = (c_1 + c_3)/2$, could then be calculated from Stokes' equation[4]; they are shown in Tables I and II.

The differential diffusion coefficient, $D$, is calculated from $\overline{D}^\circ$ by Stokes' equation. The equations obtained for the $D$ of BSNa and NSNa solutions are as follows:

Table I. Diffusion coefficients for BSNa

| | | | | |
|---|---|---|---|---|
| $c_1$, mol./l. | 0.16223 | 0.23577 | 0.33732 | 0.49813 |
| $c_1^{1/2}$ | 0.4027 | 0.4856 | 0.5808 | 0.7058 |
| $c_m^{1/2}$ | 0.3917 | 0.4704 | 0.5627 | 0.6845 |
| $\overline{D} \times 10^6$ $cm^2 sec^{-1}$ | $10.5_4$ | $10.5_1$ | $10.3_9$ | $10.2_9$ |
| $\overline{D}^\circ(c_m) \times 10^6$ $cm^2 sec^{-1}$ | $10.5_6$ | $10.5_4$ | $10.4_2$ | $10.3_2$ |

Table II. Diffusion coefficients for NSNa

| | | | |
|---|---|---|---|
| $c_1$, mol./l. | 0.086599 | 0.15603 | 0.20588 |
| $c_1^{1/2}$ | 0.2943 | 0.3950 | 0.4537 |
| $c_m^{1/2}$ | 0.2859 | 0.3850 | 0.4406 |
| $\overline{D} \times 10^6$ $cm^2 sec^{-1}$ | $9.70_5$ | $9.60_4$ | $9.57_5$ |
| $\overline{D}^\circ(c_m) \times 10^6$ $cm^2 sec^{-1}$ | $9.71_1$ | $9.61_4$ | $9.58_2$ |

$$D \times 10^6 = 10.96 - 0.476c^{1/2} \quad (7)$$

$$D \times 10^6 = 9.840 - 0.280c^{1/2} \quad (8)$$

The integral and differential diffusion coefficients for BSNa and NSNa solutions decrease linearly with the square root of the concentration, whereas for most aqueous inorganic electrolyte systems, $D$ initially decreases rapidly with the concentration passes through a broad minimum at $c \approx 0.2-0.5$ mol./l., and thereafter increases slowly.

The concentration dependence of the diffusion coefficient and the apparent molar volume for NSNa are smaller than those for BSNa. The limiting slopes of the equivalent conductances for BSNa and NSNa solutions show a similar tendency.[10]

The experimentally-found values of the slopes for $D$ versus $c^{1/2}$ curves do not agree exactly with that predicted by the Harned theory;[11] nevertheless, the agreement is good with regard to the sign and the order of magnitude. The discrepancy for NSNa is larger.[12]

In a previous paper,[1] it was shown that the effect of the hydrophobic part-water interaction on the mobilities of aromatic sulfonate ions was larger for the $NS^-$ ion. Wen and Saito[13] showed that, in the case of the aqueous solutions of tetraalkylammonium salts, the value of $S_v$ for the more hydrophobic ion was smaller. The parallel relation between the conductances and the diffusion coefficients for BSNa and NSNa may be caused by the water interaction.

*The Textile Research Institute of Japanese Government*
*Sawatari, Kanagawa-ku, Yokohama*

5) T. Shedrovsky, *J. Am. Chem. Soc.*, **54**, 1411 (1932).
6) J. F. Chamber, J. M. Stokes and R. H. Stokes, *J. Phys. Chem.*, **60**, 985 (1956).
7) A. R. Gordon, *Ann. N. Y. Acad. Sci.*, **46**, 285 (1945).
8) D. O. Masson, *Phil. Mag.*, (7) **8**, 219 (1929).
** As the saturate concentration of NSNa is low, measurement at higher concentration was not made.
9) M. Yokoi and G. Atkinson, *J. Am. Chem. Soc.*, **83**, 4367 (1961).
10) The limiting slopes for BSNa and NSNa solutions are respectively, 79.56 and 78.32 at 25°C.
11) H. S. Harned and B. B. Owen, "The Physical Chemistry of Electrolyte Solutions," 3rd. ed., Reinhold, New York (1958), Chap. 6.
12) The limiting slopes for BSNa and NSNa solutions are respectively, $0.670 \times 10^{-6}$ and $0.639 \times 10^{-6}$.
13) W.-Y. Wen and S. Saito, *J. Phys. Chem.*, **68**, 2639 (1964).

# Two Types of Water Contained in Transient Aluminas

By Hiroaki YANAGIDA, Goro YAMAGUCHI and Joe KUBOTA

(Received April 30, 1965)

All the polymorphs of alumina except the well-crystallized alpha modification have only a little water. The behavior of the water has, however, hardly been clarified at all. The water remaining after being heated at temperatures of 100—120°C has been simply explained as being combined with the oxygen atoms on the surface or in the lattice of alumina. The amount of the water depends either on the type of alumina[1] or on the forming conditions. For example, in gamma alumina the amount of water and the degree of the splitting of the 400-reflection in the powder pattern vary in accordance with the conditions of preparation.

Through an investigation into thermal effects on the lattices of gamma and eta alumina, the present authors have previously pointed out there should exist a certain type of water within only the former, one which causes a change in the lattice dimensions.[2]

For the present work, the behavior of the water within transient aluminas was investigated quantitatively with the help of a precise thermobalance.

Gamma alumina was prepared from the dehydration of well-crystallized boehmite in air at 750°C, and the delta, from the dehydration of the same boehmite under a water vapor of 1 atm. at

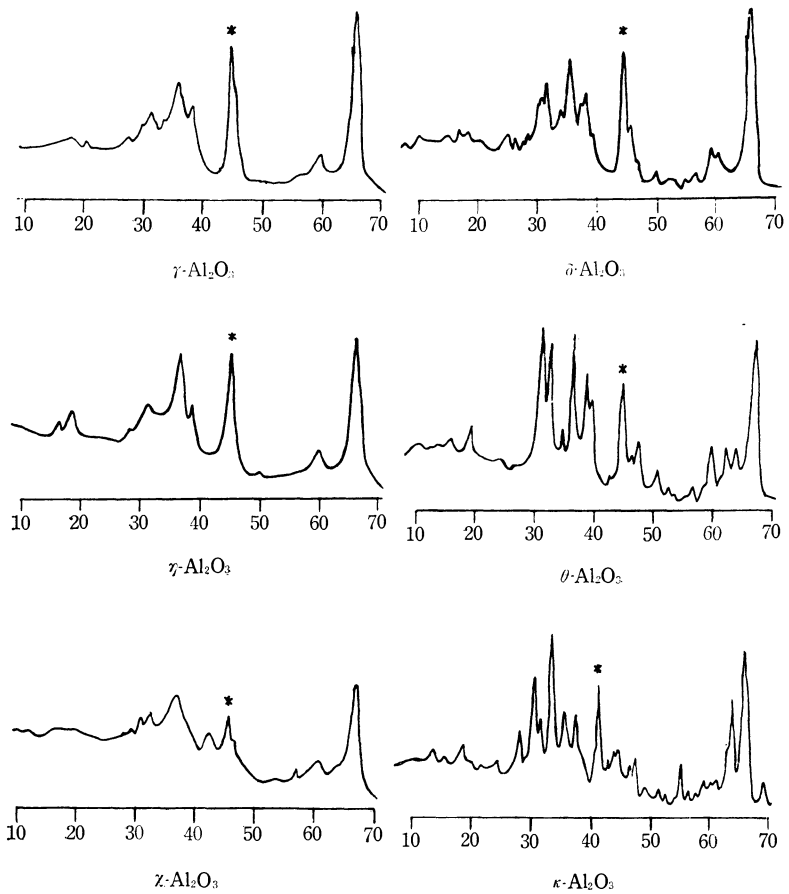



Fig. 1. X-Ray powder diffraction pattern of six transient aluminas using Cu$K\alpha$ radiation.

1) B. C. Lippens, Thesis, "Structure and Texture of Aluminas."

2) H. Yanagida and G. Yamaguchi, This Bulletin, **37**, 1229 (1964).

950°C. Eta and theta forms were obtained from the dehydration of bayerite in air, at 750°C and at 1100°C respectively. Chi and kappa forms were prepared from the dehydration of micro-crystalline gibbsite in air, at 750°C and at 1100°C respectively. The X-ray powder diagrams of these six aluminas are shown in Fig. 1.

The total amount of water (except that physisorbed ($W_0$ mg./g. $Al_2O_3$)) and the amount of water remaining in or on an alumina denoted as $W_t$ (mg./g. $Al_2O_3$) at a temperature were determined as follows; after being heated at 120°C for 24 hr. in air in order to remove the physisorbed water, each alumina was held at each given temperature in air or under a water vapor pressure of 1 atm. until the loss in weight could no longer be observed at that temperature in determining an ignition loss under the quasi-equilibriumic conditions. The weighings were made with a model LB-Shimazu direct vision balance (sensitivity; 0.1 mg.).

The typical d-spacings of each alumina, marked in Fig. 1. by an asterisk are measured by the Cu-$K\alpha$ irradiation X-ray powder diffraction method, after heat treatments at 120°C, 400°C, and 600°C.

The total amount of water, $W_0$, on transient aluminas and their specific surface areas as measured by the nitrogen adsorption method are summarized in Table I. They seem considerably different from each other. However, after plotting the ratio of $W_t$ to $W_0$, the present authors found the following rules.

Table I. The total amount of water except that physisorbed and specific surface area

| Transient alumina | Water content $W_0$ mg./g. $Al_2O_3$ | Specific surface area $m^2/g.$ |
|---|---|---|
| $\gamma$-$Al_2O_3$ | 11.0 | 44.8 |
| $\delta$-$Al_2O_3$ | 5.6 | 32.7 |
| $\eta$-$Al_2O_3$ | 34.0 | 183.7 |
| $\theta$-$Al_2O_3$ | 17.3 | 119.7 |
| $\chi$-$Al_2O_3$ | 25.2 | 126.3 |
| $\kappa$-$Al_2O_3$ | 6.7 | 74.6 |

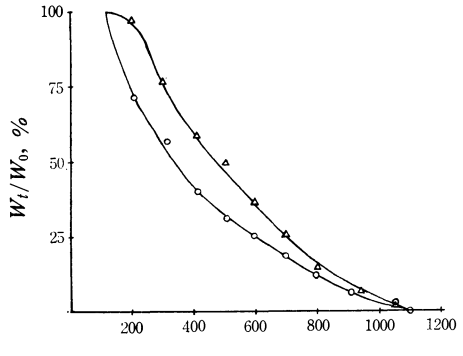



Fig. 2. Relation between heating temperature and ratio of remaining water to the total amount of water ($W_t/W_0$) on eta, ○; in air, △; in a water vapor of 1 atm.

Figure 2 shows the $W_t/W_0$ curve vs. the temperature for eta alumina in air and under a water vapor pressure of 1 atm. Theta, chi and kappa aluminas show curves approximately identical with that of eta when the $W_t/W_0$ ratios are plotted. As is shown in Table II, the typical d-spacings of these four aluminas are hardly changed at all by the thermal treatments. The present authors classify this type of water as the water not affecting the lattice dimensions and name it "non-lattice water."

Figure 3 shows the $W_t/W_0$ curve vs. the temperature for gamma alumina in air and under a water vapor pressure of 1 atm. Here the curve becomes quite different if the vapor pressure of the water is changed. The curve for delta alumina is identical with that for gamma. Table II shows that the removal of this type of water causes a change in the d-spacings. The present authors classify this as the water affecting the lattice dimensions and name it "lattice water."

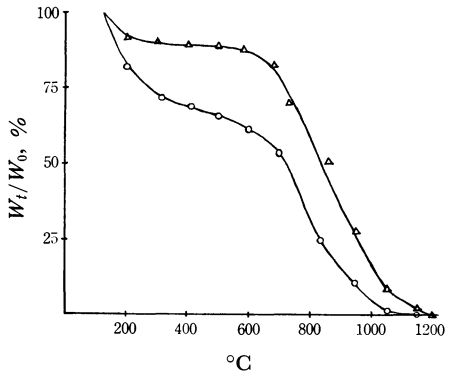



Fig. 3. Relation between heating temperature and ratio of remaining water to the total amount of water ($W_t/W_0$) on gamma, ○; in air, △; in a water vapor of 1 atm.

Table II. The change of the typical d-spacing of transient aluminas by thermal treatments measured at 25°C

| Transient alumina | Heating temperature 120°C | 400°C | 600°C | $d_{120}-d_{600}$ |
|---|---|---|---|---|
| $\gamma$-$Al_2O_3$ | 1.9867 Å | 1.9835 Å | 1.9810 Å | 0.0057 Å |
| $\delta$-$Al_2O_3$ | 1.9899 | 1.9879 | 1.9867 | 0.0032 |
| $\eta$-$Al_2O_3$ | 1.9790 | 1.9787 | 1.9787 | 0.0003 |
| $\theta$-$Al_2O_3$ | 2.0183 | 2.0186 | 2.0183 | 0.0000 |
| $\chi$-$Al_2O_3$ | 1.9909 | 1.9909 | 1.9909 | 0.0000 |
| $\kappa$-$Al_2O_3$ | 2.1195 | 2.1186 | 2.1186 | 0.0009 |

With the infrared absorption method, Peri showed that there are several types of water on the surface but not within the lattice of gamma-type

alumina.[3] The present results, however, show a certain type of water exists in the lattice of gamma and delta aluminas.

The present authors will report the results of further investigation into these types of water and the effects on the thermal conversions of transient aluminas in a later paper.

*Department of Industrial Chemistry*
*Faculty of Engineering*
*The University of Tokyo*
*Hongo, Tokyo*

3) J. B. Peri and R. B. Hannan, *J. Phys. Chem.*, **64**, 1526 (1960).

# The Effect of Ionizing Radiations on the Adsorption Rate of Hydrogen on Manganese Dioxide

By Toshizo TITANI and Tadamitsu KIYOURA

(Received May 25, 1965)

Kolarov and Kirilov[1] determined the temperature at which the reduction of differently-treated samples of manganese dioxide in a stream of hydrogen started; they found that this temperature was 234°C for the original manganese dioxide, whereas it was 217°C after the oxide had been ground for half an hour and 239°C after the irradiation of the oxide with ultraviolet light for half an hour. From these experimental results, they concluded that the grinding caused an activation, whereas the ultraviolet light caused an aging, of the oxide. We found a similar inactivation of manganese dioxide caused by the irradiation of ionizing radiations; the rate of hydrogen adsorption decreased for the oxide previously irradiated with radiations from a reactor or with $^{60}$Co $\gamma$-rays.

The manganese dioxide was prepared by the thermal decomposition of manganous nitrate, and the surface area of the oxide was measured by the B. E. T. method and found to be 10 $m^2/g$. The pile-irradiation of the oxide was carried out in the experimental hole of a swimming pool reactor of the Tokyo Atomic Industrial Research Laboratory. The flux of thermal and fast neutrons in the experimental hole was $1.7\times10^{12}$n/cm$^2$ sec. and $0.7\times10^{12}$n/cm$^2$ sec. respectively, and the dose rate of $\gamma$-rays was $1.1\times10^6$ r./hr. The oxide was irradiated in the hole for 15 hr. in the presence of air. The irradiation of the oxide by $^{60}$Co $\gamma$-rays was carried out in the hot cell of the Tokyo Metropolitan Isotope Research Center, under conditions similar to those of the pile-irradiation; the oxide was irradiated for 15 hr. in the presence of air, and the dose rate of $\gamma$-rays was $1.0\times10^6$ r./hr.

The oxide (400 mg.) was placed in the adsorption apparatus; after it had been evacuated at 100°C for 1 hr. the temperature of the apparatus was raised and kept costant at 175, 200, or 250°C respectively, and 1.6 ml. (N. T. P.) of the hydrogen gas was introduced. Then the pressure of the hydrogen in the apparatus was measured from time to time by a mercury manometer attached to the apparatus through a liquid nitrogen trap.

An example of the experimental results is graphically shown in Fig. 1, where the ordinate represents the logarithm of the manometric reading of the hydrogen pressure. As will be seen from Fig. 1, a rapid stage in the decrease of hydrogen pressure, shown by dotted lines, is followed by a slow stage of pressure decrease, shown by full lines in the figure. The slow stage proceeds as a first-order reaction rather than as a Zeldowitch[2] form. From the slope of the straight line, the rate

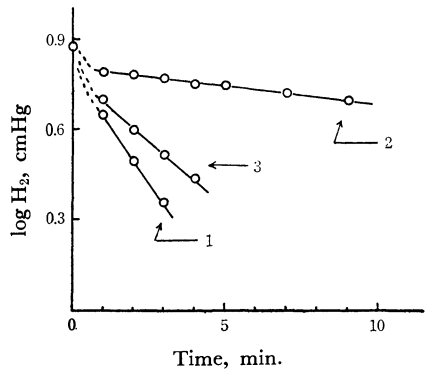



Fig. 1. The decrease of the pressure of hydrogen with time at 200°C.
1 Original
2 Irradiated in a reactor
3 Irradiated by $^{60}$Co $\gamma$-rays

1) N. Kolarov and M. Kirilov, *Bulgar. Akad. Nauk. Geol.-Geograf. i Khim. Nauk. Izvest. Inst.*, **1**, 205 (1951).

2) J. Zeldowitch, *Acta Physicochim. U. S. S. R.*, **1**, 449, 554, 559 (1934).

TABLE I. ADSORPTION RATE CONSTANTS UNDER VARIOUS CONDITIONS

| Samples of $MnO_2$ | Adsorption temp., °C: Rate const., $min^{-1}$ 175 | 200 | 250 | Activation energy, kcal./mol. |
|---|---|---|---|---|
| Original | 0.16 | 0.34 | | 12.5±0.5 |
| Irradiated in a reactor | | 0.033 | 0.12 | 12.8±0.5 |
| Irradiated by $^{60}Co$ $\gamma$-rays | 0.092 | 0.19 | | 12.0±0.5 |

constant can be obtained. The adsorption rate constants thus obtained under various conditions are tabulated in Table I, where the activation energy in the last column was calculated from the rate constants obtained at two different temperatures.

From Fig. 1 and Table I we can see that the adsorption rate of hydrogen on manganese dioxide is decreased by the preirradiation of the oxide with ionizing radiations. The decrease is especially significant in the case of the pile-irradiation, where the rate constant for the adsorption decreases to about one-tenth of the original one. If this decrease in the activity of the oxide is wholly due to the increase in the activation energy, the activation energy of the irradiated oxide must be about 2 kcal./mol. higher than that of the original one. However, as will be seen from Table I, the activation energy of the original and the irradiated oxide agree with each other within the limits of experimental error (±0.5 kcal./mol.). Therefore, it must be concluded that the decrease in the adsorption rate on the pile-irradiated manganese dioxide is solely due to the decrease in the number of active sites on the surface of the oxide. A part of the active sites on the surface of the manganese dioxide may be sintered by the irradiation with ionizing radiations. This sintering effect of the ionizing radiations from a reactor, if any, must be mainly due to the neutrons, because the decrease in the adsorption rate on the oxide irradiated with $^{60}Co$ $\gamma$-rays is far smaller than that on the oxide irradiated in a reactor, as may be seen from Fig. 1 and Table I, in spite of the fact that the dose rate of $\gamma$-rays was almost the same in both cases.

*Department of Chemistry*
*Faculty of Science*
*Tokyo Metropolitan University*
*Setagaya-ku, Tokyo*

# A Microcell for NMR Spectral Measurements

By Shô Itô and Iwao Miura

(Received May 10, 1965)

The necessity of handling the minute amounts of substances encountered by many chemsits has lead to the invention of a few micro- and semimicro-cells.[1] Some of them, however, can not be used at an elevated temperature, and they are usually expensive. We have been using a convenient and simple microcell made from a glass-capillary for measurements with a Varian A-60 spectrometer.

The sample tube consists of a capillary, 1 to 2 mm. in outside diameter and about 19 cm. long (similar to a normal melting point tube), which is fixed inside a standard-size NMR tube by means of two cylindrical plugs.[2] These plugs have concentric holes with a diameter slightly larger than that of the capillary. The sample solution, usually prepared from about 3 mg. of the substance and about 30 $\mu$l. of a solvent containing a trace of the internal reference, is introduced into the capillary tube (one end sealed) either by a process of warming and cooling or with the aid of a micro-syringe. The open end is then sealed. One of the plugs is placed at the bottom, and the other, about 50 mm. from the bottom of the NMR tube; the capillary is inserted into the tube and through the hole in each plug. The upper end of the capillary tube is stabilized by inserting it through a hole bored in the center of a plastic cap, which is then fitted over the mouth of the NMR tube. The

1) As far as we know, three types of these cells are commercially available, those made by Varian Associates, U. S. A., Nuclear Magnetic Specialities Inc., Canada, and Japan Electron Optics Laboratory Co., Japan.

2) For the sake of convenience, we have been using sections of the nylon upper-plug of a Varian microcell or the insulating cover of electric wire for measurements at room temperature, and sections of Teflon tubing at elevated temperatures (up to 130°C).

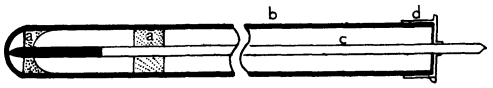



Fig. 1. Cross-section of the micro-cell.

a Nylon plugs
b Standard-size NMR sample tube
c Capillary
d Plastic cap

completely-assembled micro-cell is illustrated in Fig. 1.

The measurement of the NMR spectra is carried out in the normal way. The spectra obtained with the use of this cell are usually as good as those obtained with 5 to 10 times the amount of sample in an ordinary 5-mm. cell. Examples of spectra obtained with the use of this microcell and of those with the use of a standard cell are shown in Figs.

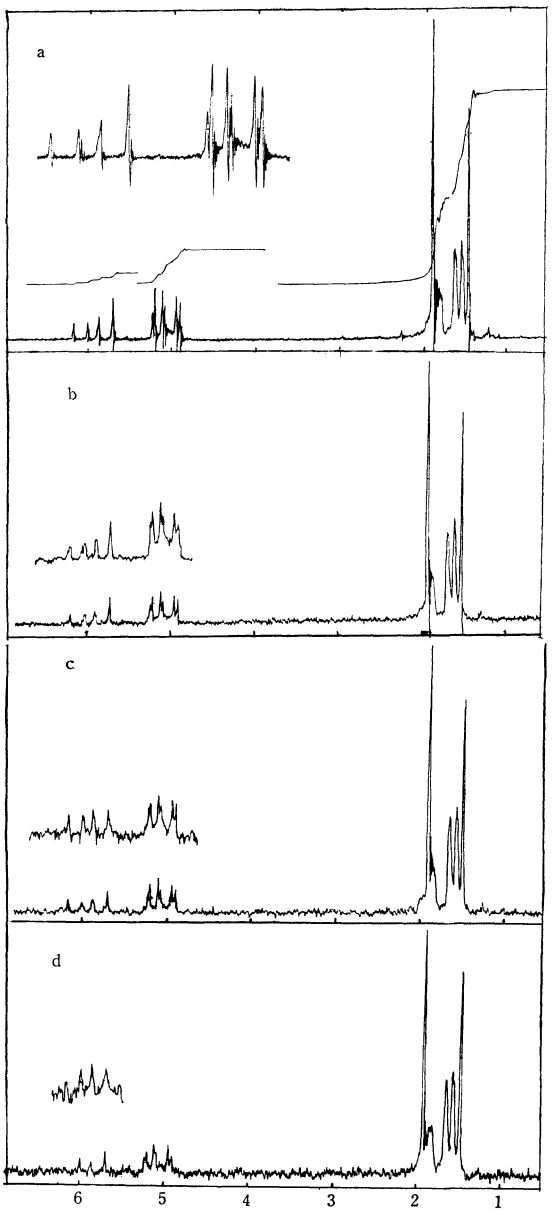



Fig. 2. NMR spectra of linalool in carbon tetrachloride

a 30 mg. in standard cell
b 8 mg. in microcell
c 5 mg. in microcell
d 3 mg. in microcell

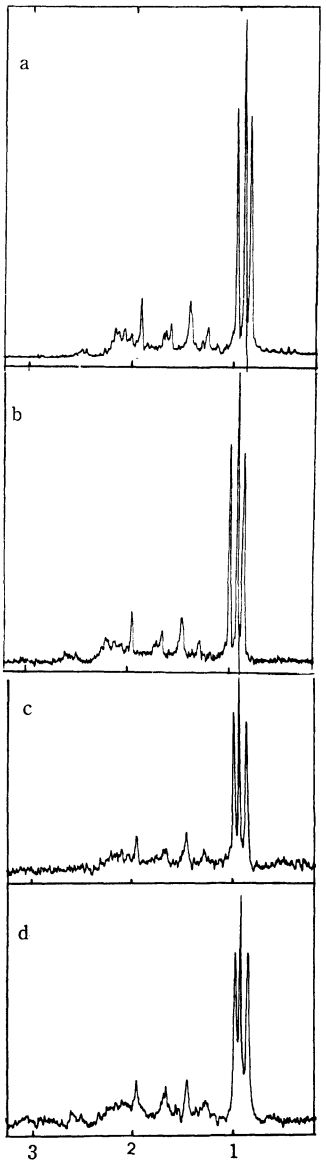



Fig. 3. NMR spectra of camphor in carbon tetrachloride.

a 30 mol.% in standard cell
b 30 mol.% in the microcell
c 10 mol.% in the microcell
d 3.2 mol.% in the microcell

2 and 3 in order to illustrate the limitations of this micro-cell.

In the case of linalool, the one proton quartet, due to the X part of the ABX system, is visible with 3 mg. of sample in about a 8 mol.% solution, whereas in the case of the methyl protons of camphor, the signal can be clearly recognized when 1.1 mg. of the sample (ca. 3.2 mol.% solution), or even as little as 0.35 mg. of the sample (1 mol.% solution), is used.

Although a certain degree of sensitivity is sacrificed because of the large diameter of the receiver coil, which has been designed for use with the larger standard NMR tubes, this cheap and simple micro-cell is very useful when only small quantities of sample are available.

*Department of Chemistry*
*Faculty of Science*
*Tohoku University*
*Katahira-cho, Sendai*

# Intramolecular Hydrogen Bonds. VI.[1] The Characteristic Infrared OH Spectra of Isomeric Ethyl $\alpha$, $\beta$-Dihydroxy-carboxylates and Their Geometries

By Nobuo MORI, Satoshi ŌMURA* and Yojiro TSUZUKI

(Received May 24, 1965)

The threo and the erythro isomers of any compound of the RCH(OH)CH(A)R′ series, wherein R and R′ are alkyl groups and A is a proton-accepting group, show characteristic infrared OH spectra in a dilute carbon tetrachloride solution; the apparent relative intensities of the bonded and the free OH bands[2] and, in some cases, also the separations between the two bands $(\Delta\nu)$[3,4] are useful as important criteria for the configurational assignment. Such characteristic features, however, are not observed in ethyl dextro- and meso-tartrates, in which the apparent OH spectra are almost identical.[5]

In this investigation, we have found that isomeric $\alpha$, $\beta$-dihydroxy-carboxylates of the $CH_3(CH_2)_n$-CH(OH)CH(OH)COOEt series, wherein $n$ is an integer of 0, 1 and 2, exhibit some characteristic features which differ from the above statement in their OH spectra. The spectra were measured at 25°C according to a method previously[1] described. The concentrations were ca. 0.004 mol./l. in carbon tetrachloride, at which point intermolecular hydrogen bonding was absent. The erythro esters show identical OH spectra, composed of two peaks with nearly the same intensities, the higher frequency band being broadened on the higher frequency side. The threo isomers show a partially-resolved doublet with an additional shoulder at ca. 3625 $cm^{-1}$. In addition to these bands, both the isomers show a very weak band at ca. 3445 $cm^{-1}$ due to the overtone of a carbonyl group.[6] Typical spectra are shown in Fig. 1, while the data on the apparent OH bands are summarized in Table I.

As is shown in the table, the lowest frequencies

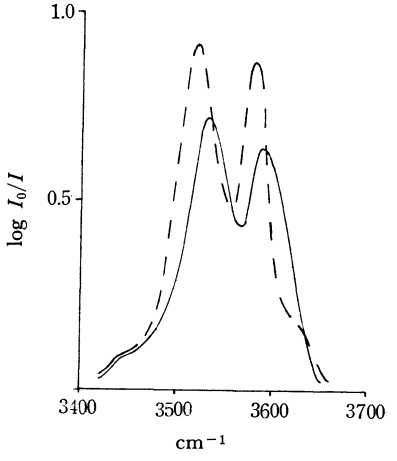



Fig. 1. OH spectra of ethyl $\alpha$, $\beta$-dihydroxyvalerates.
Threo: ----; Erythro: ——

1) Part V: N. Mori, S. Ōmura, N. Kobayashi and Y. Tsuzuki, This Bulletin, **38**, 2149 (1965).

* Present address: The Kitasato Institute, Minato-ku, Tokyo.

2) J. Sicher, M. Cheresty, Y. Gault and H. Felkin, *Coll. Czechoslov. Chem. Commun.*, **28**, 72 (1963).

3) L. P. Kuhn, *J. Am. Chem. Soc.*, **80**, 5950 (1958).

4) G. Chiurdoglu, R. de Groote, W. Masschelein and M. H. van Risseghem, *Bull. soc. chim., Belges*, **70**, 342 (1961); G. Drefahl and G. Heublein, *Chem. Ber.*, **94**, 922 (1961); N. Mori, S. Ōmura and Y. Tsuzuki, This Bulletin, **38**, 1037 (1965),; also, A. Mosher and N. D. Heindel, *J. Org. Chem.*, **28**, 2154 (1963).

5) N. Mori, S. Ōmura, O. Yamamoto, T. Suzuki and Y. Tsuzuki, This Bulletin, **36**, 1401 (1963).

6) R. W. Jones and C. Sandorfy, "Chemical Application of Spectroscopy," Vol. IX of A. Weissberger's "Technique of Organic Chemistry," Interscience Publishers, New York, N. Y. (1956), p. 424.

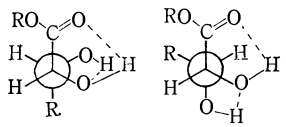
TABLE I. SUMMARY OF INFRARED DATA OF THE ESTERS $CH_3(CH_2)_nCH(OH)CH(OH)COOEt$

| | $n$ | B. p. °C/mmHg | $\nu_{OH}$ cm$^{-1}$ ($D$)*1 I | II | III | IV | $\Delta\nu$ cm$^{-1}$ (II−I) | $D_I/D_{II}$ |
|---|---|---|---|---|---|---|---|---|
| Threo | 0 | 116/17 | 3522 (0.83) | 3585 (0.79) | — | 3622*2 | 63 | 1.05 |
| Threo | 1 | 99.5/5 | 3520 (0.94) | 3579 (0.88) | — | 3626*2 | 59 | 1.07 |
| Threo | 2 | 95/7 | 3521 (0.87) | 3581 (0.76) | — | 3626*2 | 60 | 1.14 |
| Erythro | 0 | 113.5/10 | 3533 (0.91) | 3588 (0.83) | weak*3 | — | 55 | 1.09 |
| Erythro | 1 | 115/8 | 3532 (0.73) | 3588 (0.64) | weak*3 | — | 56 | 1.14 |
| Erythro | 2 | 114—115/6 | 3532 (0.63) | 3589 (0.60) | weak*3 | — | 57 | 1.05 |
| Butane-2, 3-diol[3] | | | | | | | | |
| Threo | | | — | 3583 | — | 3632 | | |
| Erythro | | | — | 3591 | — | 3633 | | |
| Ethyl lactate[1] | | | 3543 (0.88) | — | 3613 (0.19) | — | | |
| Ethyl β-hydroxybutyrate[1] | | | 3560 (0.58) | — | 3590 (0.09) | 3626 (0.09) | | |

*1 $D=\log I_0/I$ for the apparent bands.
*2 These are of the shoulder of band.
*3 Presumed from the broadening on the higher frequency side of band II.

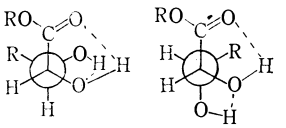
(ca. 3521 and 3532 cm$^{-1}$ (band I)) and the separations between the strong peaks (ca. 61 and 56 cm$^{-1}$) are characteristic of the threo and the erythro esters respectively, but their relative intensities are indiscriminate. The additional OH absorption on the higher frequency side is, in both cases, very weak, yet it can serve as another indicator for a configurational assignment.

The α-OH group and the β-OH group can form hydrogen-bonds with one another and with the carbonyl- and the ether-oxygen atom of the ester group. According to the findings on intramolecular hydrogen bonding in α- and β-hydroxycarboxylates previously[1] reported, the hydrogen bond with the carbonyl-oxygen atom is stronger in the α-series than in the β-series; the extent of this hydrogen-bonding is very high compared with that of the hydrogen-bonding with the ether-oxygen atom in both series. Evidence for the type of hydrogen-bonding between the OH groups has already been given for ethylene-glycols.[3] On the basis of this, band I may almost exclusively be due to the α-OH group bonded to the carbonyl-oxygen, and band II may be due to the β-OH group bonded to the oxygen atom of the above bonded α-OH group, since the free OH band IV does not appear or is only slightly present. In the erythro esters, the broadening on the higher frequency side of band II may be caused by an additional weak absorption of OH groups bonded to the ether-oxygen atom. Accordingly the OH groups assigned to bands I and II must be skew to one another in respect to the $C_\alpha$–$C_\beta$ bond, as is shown in geometries I—IV:



I II

Threo form



III IV

Erythro form

In the NMR spectra* of the threo and the erythro ester with $n=1$ in solutions of 5 v.% in carbon tetrachloride, the resonance line of the α-methine proton appears at −3.98 p.p.m. from TMS as a doublet ($J_{\alpha\beta}=2.3$ c.p.s.) for the threo ester and at −4.09 p. p. m. as a doublet ($J_{\alpha\beta}=3.8$ c. p. s.) for the erythro isomer. The $J$ values indicate in each case that the two methine-hydrogens are skew to one another in respect to the $C_\alpha$–$C_\beta$ bond.[7] Since such an orientation of the hydrogens is considered to be probable also in a concentration

* The spectra were measured at ca. 25°C in the concentration range from 5 to 20 v.% in carbon tetrachloride, using a Varian A-60 spectrometer on pre-calibrated chart paper; TMS was used as the internal standard. The $\delta$ values of the α-methine protons in both the esters were somewhat dependent on the concentrations, but the $J$ values were not.

7) K. Karplus, *J. Chem. Phys.*, **30**, 11 (1959); *J. Phys. Chem.*, **64**, 1793 (1960).

as low as 0.004 mol./l., form I seems to be most favorable for the threo esters in a dilute carbon tetrachloride solution, and form III and/or form IV for the erythro isomers.

## Experimental

The threo and the erythro esters were prepared by Fischer's method of esterification from the respective $\alpha$, $\beta$-dihydroxy-carboxylic acids,[8] which had been obtained by the oxidation of the corresponding *trans*-olefinic acids[9] with silver chlorate in the presence of osmium tetroxide and with perbenzoic acid respectively. The threo forms of the free dihydroxy-acids with $n=$ 0, 1 and 2 melted at 74, 75 and 107°C respectively, and the erythro isomers, at 80, 105 and 98°C. The boiling points of the ethyl esters are shown in Table I.

We thank Mr. Teruo Kajiura and Mr. Tadao Tamura, Government Chemical Industrial Research Institute, Tokyo, for infrared measurements.

*Department of Chemistry*
*Tokyo College of Science*
*Kagurazaka, Shinjuku-ku, Tokyo*

8) G. Braun, *J. Am. Chem. Soc.*, **51**, 228 (1929); **52**, 3188 (1930); W. E. Glattfeld and W. G. Straitiff, ibid., **60**, 1384 (1938).
9) A. A. Goldberg and R. P. Linstead, *J. Chem. Soc.*, **1928**, 2343.

# The Electrical Conductivities of Aromatic Diamine-Chloranil and -Tetracyanoethylene Charge-Transfer Complexes*

By Hideaki KUSAKAWA and Shun-ichiro NISHIZAKI

(Received June 22, 1965)

We have reported in previous papers[1,2] on the electrical conductivities of the iodine complexes of several kinds of aromatic diamines. Since then we have obtained aromatic diamine, *p*-, *m*-, and *o*-phenylenediamine (*p*-, *m*-, *o*-PDA), 1,5-naphthylenediamine (NDA), benzidine (BEN), *o*-tolidine (TOL) and *p*, *p'*-diaminodiphenylmethane (APM) complexes, in which chloral (CHL) or tetracyanoethylene (TCNE) was used as the electron acceptor. In this report we will present the results obtained from a comparison of the electrical conductivities of CHL and TCNE complexes with those of iodine complexes.

These CHL and TCNE specimens were prepared by mixing the equivalent donor and acceptor solutions. The complex crystals precipitated rapidly by cooling or from a highly concentrated solution were not suited to the observation of their electrical properties.

The chemical analysis for these CHL and TCNE complexes indicated that TCNE specimens scarcely include the solvent at all, but that CHL specimens contain a respectable amount of the solvent; the ratio between the donor and the acceptor in these complexes was 1 : 1. These CHL and TCNE complexes showed the absorption bands arising from the NH stretching vibration in the wave number region between 3455 $cm^{-1}$ and 3140 $cm^{-1}$, and the signals of the electron-spin resonance at room temperature.

The magnitude and the temperature dependence of the resistivities and energies of the charge-transfer transitions obtained by previous methods[1,3] are summarized in Table I for CHL complexes and in Table II for TCNE complexes. Some of these crystals were given needle-shaped forms (about $3 \times 0.05 \times 0.01$ mm.). Therefore, the lattice constants along the crystal growth axis could be found for such crystals by applying an oscillation method. These results are listed in the last column in both tables.

The following results are obtained from the data shown in Tables I and II:

1) The energy of the charge-transfer transition is more than twice the activation energy of the resistivity for the aromatic-diamine-complex specimens.

2) In the case of CHL complexes, the order of resistivity, *p*-PDA:CHL, TOL:CHL and NDA:CHL, agrees with that of the lattice constant along the crystal growth axis. On the other hand, the resistivity of BEN:TCNE, the lattice constant of which is smaller than that of NDA:TCNE, is not as low as the resistivity of NDA:TCNE.

3) The donor character of an aromatic diamine is dependent on what the acceptor molecule is; e. g., BEN is the strongest donor for an iodine acceptor, *p*-PDA is for CHL, and NDA is for TCNE.

* This paper was presented in part at the 18th Annual Meeting of the Chemical Society of Japan, Osaka, April, 1965.

1) S. Nishizaki and H. Kusakawa, This Bulletin, **36**, 1681 (1963).

2) H. Kusakawa and S. Nishizaki, ibid., **38**, 313 (1965).

3) H. Kusakawa and S. Nishizaki, ibid., **38**, 783 (1965).

Table I. Physical properties of aromatic diamine-chloranil complexes

| Donor | Resistivity at 20°C | Activation energy | Energy of c. t. transition | Lattice constant along crystal growth axis |
|---|---|---|---|---|
| | Ω cm. | eV. | eV. | *A* |
| *p*-PDA | $1.5\times10^{7}$ | 0.46 | 1.42 | 6.36 |
| *m*-PDA | Complex in solution only | | | |
| *o*-PDA | Complex in solution only | | | |
| NDA | $1.2\times10^{11}$ | 0.58 | 1.46 | 7.63 |
| BEN | Nonstoichiometrical composition | | | |
| TOL | $3.8\times10^{9}$ | 0.53 | 1.23 | 7.35 |
| APM | Complex in solution only | | | |

Table II. The phisical properties of aromatic diamine-tetracyanoethylene complexes

| Donor | Resistivity at 20°C | Activation energy | Energy of c. t. transition | Lattice constant along crystal growth axis |
|---|---|---|---|---|
| | Ω cm. | eV. | eV. | *A* |
| *p*-PDA | $2\times10^{15}$ | 0.78 | 2.26 | 8.73 |
| *m*-PDA | $6\times10^{14}$ | 0.93 | 2.11 | |
| *o*-PDA | $10^{16}$ | | 2.22 | |
| NDA | $1.0\times10^{7}$ | 0.40 | 1.14 | 6.75 |
| BEN | $1\times10^{14}$ | 0.71 | | 6.11 |
| TOL | $10^{16}$ | | | |
| APM | $>10^{16}$ | | | |

4) Among the three isomers of phenylenediamine (PDA), the para substituent is the best donor; for instance, *m*-PDA and *o*-PDA do not form complex crystals with CHL, and the resistivity of the *p*-PDA-iodine system is $10^{5}$ Ωcm., while those of *m*-PDA-isodine and *o*-PDA-iodine are $10^{7}$ Ωcm. and $10^{9}$ Ωcm.[4] respectively.

5) It cannot be expected that the charge-transfer complex the donor of which is nonconjugated aromatic amine, APM, will have a conductivity as good as that of conjugated amine complexes.

*The Central Research Laboratories*
*Mitsubishi Electric Corporation*
*Amagasaki, Hyogo*

4) H. Kusakawa, unpublished.

## SHORT COMMUNICATIONS

# Infrared Absorption Spectra of Photochromic and Piezochromic Systems of the Dimers of Triarylimidazolyls

By Taro HAYASHI and Koko MAEDA

(Received August 14, 1965)

The compounds, such as $C_{42}H_{30}N_4$, (A) (m. p. 199—200°C), $C_{48}H_{42}N_4$ (B) (m. p. 194—195°C), $C_{42}H_{24}N_4Cl_6$ (C) (m. p. 213—214°C) and $C_{42}H_{28}N_4Cl_2$ (D) (m. p. 219—220°C), produced by the oxidation of corresponding 2, 4, 5-triarylimidazoles, have previously been found[1] to exhibit photochromism, thermochromism and piezochromism. It was then determined that these compounds were the dimers of triarylimidazolyl radicals[2,3] and that the colors exhibited by the

1) T. Hayashi, K. Maeda, S. Shida and K. Nakada, *J. Chem. Phys.*, **32**, 1568 (1960).

2) T. Hayashi and K. Maeda, This Bulletin, **35**, 2057 (1962).

3) T. Hayashi, K. Maeda and M. Morinaga, ibid., **37**, 1563 (1964); T. Hayashi, K. Maeda and M. Takeuchi, ibid., **37**, 1717 (1964); T. Hayashi and K. Maeda, ibid., **38**, 685 (1965).

TABLE I. THE INFRARED ABSORPTION BANDS OF THE DIMERS OF TRIARYLIMIDAZOLYLS IN THE 1620—1480 $cm^{-1}$ REGION (KBr pellet)

| Compound | Wave number, $cm^{-1}$ |
|---|---|
| A | 1617 (sh), 1603 (s), 1577 (m), 1565 (m), 1554 (s), 1526 (sh), 1501 (m), 1485 (s) |
| B | 1622 (sh), 1604 (s), 1574 (sh), 1568 (m), 1551 (sh), 1520 (w), 1501 (s) |
| C | 1616 (sh), 1600 (s), 1572 (w), 1560 (sh), 1553 (m), 1519 (w), 1495 (sh), 1484 (s) |
| D | 1618 (sh), 1604 (m), 1575 (w), 1565 (m), 1556 (m), 1525 (sh), 1501 (m), 1484 (s) |

(s, strong; m, medium; w, weak; sh, shoulder)

TABLE II. THE INFRARED ABSORPTION BANDS CHARACTERISTIC OF TRIARYLIMIDAZOLYL RADICALS PRODUCED PHOTOCHROMICALLY OR PIEZOCHROMICALLY

| Triarylimidazolyl | Wave number, $cm^{-1}$ |
|---|---|
| 2,4,5-triphenyl- | 870 (sh) |
| 2,4,5-tri-*p*-tolyl- | 551, 881 (sh), 1359 |
| 2,4,5-tri-*p*-chlorophenyl- | 882 (sh) |
| 2-*p*-chlorophenyl-4,5-diphenyl- | 610 (sh), 812, 877 (sh), 883 (sh), 1142 |

photochromism, thermochromism or piezochromism are due to the triarylimidazolyl radicals produced by the dissociation of the dimers by irradiation, heating or grinding respectively.[3]

The infrared absorption spectra of the compounds mentioned above and of the photochromic and piezochromic systems (KBr pellet) have now been observed with a Perkin-Elmer 521 grating infrared spectrophotometer.

The absorption bands of the dimers of triarylimidazolyls in the 1620—1480$cm^{-1}$ region are shown in Table I.

As was to be expected from the mechanism,[3] the spectra of the photochromic systems of these compounds were similar to those of the respective piezochromic systems. One or several new weak bands were observed in the spectra of the photochromically- and piezochromically-colored systems, as is shown in Table II.

Recently, White and Sonnenberg[4] showed that, in the 1620—1480 $cm^{-1}$ region, aryl-2*H*-imdazoles exhibit the characteristic bands at approximately 1615(w) and 1550 $cm^{-1}$(m-s), while arylimidazoles do not exhibit such bands and tetraphenyl-4*H*-imidazole exhibits strong bands at 1594 and 1563 $cm^{-1}$, along with the 1616 $cm^{-1}$ band. Since in the 1620—1480 $cm^{-1}$ region the absorption bands of the dimers of triarylimidazolyls were very similar to the characteristic bands of the aryl-2*H*-imidazoles, as is shown in Table I, the results may suggest that the structures of the dimers of triarylimidazolyls are not the hexaaryl-*N*, *N'*-biimidazolyls which were previously reported,[3] but rather hexaaryl-2, 2'-bi-2*H*-imidazolyls produced by the dimerization of the 2, 4, 5-triarylimidazolyl radicals at the 2-position, and that the homolytic dissociation of the C–C bond of hexaaryl-2, 2'-bi-2*H*-imidazolyls into 2, 4, 5-triarylimidazolyl radicals is the more probable mechanism of the photochromism, thermochromism and piezochromism of the dimers of triarylimidazolyls than the dissociation of the N–N bond of hexaaryl-*N*, *N'*-biimidazolyls. In order to determine more exactly the constitution of the dimers and the mechanism of the photochromism, thermochromism and piezochromism, further investigations are now being carried out.

*Department of Chemistry*
*Faculty of Science*
*Ochanomizu University*
*Bunkyo-ku, Tokyo*

4) D. M. White and J. Sonnenberg, *J. Org. Chem.*, **29**, 1926 (1964).

# A New Method for the Determination of Nitrate Ions by Atomic Absorption Spectrophotometry

By Takahiro KUMAMARU, Eiji TAO, Nobuko OKAMOTO and Yuroku YAMAMOTO

(Received August 24, 1965)

In the course of our studies of the solvent extraction of anions with metal chelate cations,[1] it was found that a small amount of nitrate could be extracted into methyl isobutyl ketone (MIBK) when neo-cuproine* was contained in the organic phase and when copper(I) ions were present in the aqueous phase. This paper is concerned with the determination of nitrate ions by atomic absorption spectrophotometry. Figure 1 shows the

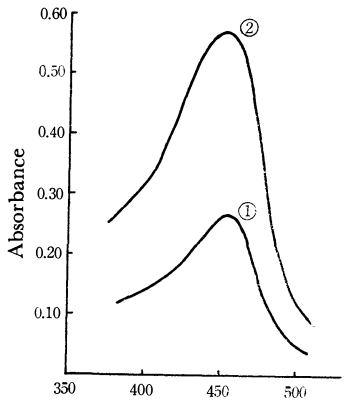



Fig. 1. Absorption spectra.

| | | |
|---|---|---|
| Water phase | $Cu^{2+}$ | $8\times10^{-4}$ M |
| | Hydroxylamine | 0.4% |
| | Phosphate | $5\times10^{-2}$ M |
| | $NO_3^-$ | $4\times10^{-5}$ M |
| | pH | 4.0 |

MIBK phase: Neo-cuproine $1\times10^{-4}$ M
① Extracts by MIBK without nitrate ions
② Extracts by MIBK with nitrate ions
Reference: MIBK

absorption spectra in the organic phase. It may be observed that the presence of nitrate leads to a considerable increase in the extraction. The absorbance maximum of the extracted species is at 456 mμ. The chemical formula of the extracted species was determined to be $[Cu(Neocup.*)_2NO_3]$. It was also found that there is a linear relationship between the concentration of nitrate in the aqueous solution and the absorbance at 456 mμ of the organic phase. These facts suggest that it may be possible to determine the nitrate ions by spraying the extracted MIBK solution into the flame of an atomic absorption spectrophotometer using a copper hollow-cathode lamp (3247Å). The recommended procedure for the calibration curve is given below.

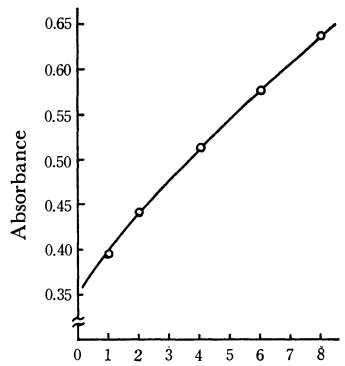



Fig. 2. Calibration curve (Reference: MIBK).

Two milliliters of the cupric sulfate solution ($1\times10^{-2}$ M), 2 ml. of the hydroxylamine sulfate solution (5%), 5 ml. of the buffer solution (0.25 M phosphate), and varying amounts of the standard nitrate solution ($2\times10^{-4}$ M, 1—8 ml.) were mixed. After the solution had been diluted with water to 25 ml., it was shaken for 2 min. with 10.0 ml. of a MIBK solution containing neo-cuproine ($2\times10^{-3}$ M). The atomic absorption measurements of the organic phase were made by using a Hitachi model 139—0420 atomic absorption spectrophotometer equipped with a copper hollow-cathode source. In atomic absorption spectrophotometry, it has generally been considered that the special spectral line issuing from the same metal as the element to be determined should be used. This has been a fairly great disadvantage in some cases because of the necessity of a special light source. Moreover, it has not been possible to apply the atomic absorption method to most non-metals. In this paper, we have suggested the possibility of determining some anions such as nitrate by solvent extraction with a metal chelate cation using a proper solvent and an appropriate hollow-cathode source.

*Department of Chemistry*
*Faculty of Science*
*Hiroshima University*
*Higashisenda, Hiroshima*

1) Y. Yamamoto et al., This Bulletin, **37**, 434, 594, 785 (1964); **38**, 499, 1494 (1965).

* Neocup=neo-cuproine=2, 9-dimethyl-1, 10-phenanthroline.

# The Zeeman Effect of $^{35}Cl$ Nuclear Quadrupole Resonance Spectra in *p*-Chlorophenol

By Masahiko SUHARA, Tadashi YONEMITSU and Tokuzo TONOMURA

(Received August 27, 1965)

The Zeeman effect of the $^{35}Cl$ nuclear quadrupole resonance spectrum was studied on a single crystal of *p*-chlorophenol in order to obtain information about the crystal and molecular structures in the solid state and in order to explain the doublet separation of the spectrum.[1]

A commercial product was distilled and then purified by zone-melting before use; the single crystal was prepared by Bridgeman's method. The Zeeman effect was observed at room temperature by means of a superregenerative spectrometer and a goniometer equipped with a Helmholtz coil.

Two zero-splitting loci, for each element of the doublet, $\nu_1$ and $\nu_2$, were obtained. This suggests that the unit cell is composed of four molecules.

The asymmetry parameters obtained are listed in Table I. Asymmetry parameters in several chlorobenzene derivatives have been obtained by the studies of the Zeeman effect: for example, 0.08 in *p*-dichlorobenzene,[2] 0.06 in *p*-chloroaniline,[3] and 0.08 in *p*-chlorobenzoic acid.[4] In comparison with these values, the $\eta_1$ value of the present molecule is considerably larger. This indicates that two of the four chlorine nuclei in the unit cell are placed in an unusual intermolecular interaction, such as hydrogen bonding.

The double-bond character, the ionic-bond character, and the single-bond character of the C–Cl bond in *p*-chlorophenol were evaluated by the method proposed by Townes and Dailey[5] and developed by Bersohn,[6] from the asymmetry parameter, $\eta_2$, and the resonance frequency, $\nu_2$, extrapolated to 0°K. In this calculation, we used the values of 0.15[5] for the *s*-characters of the $\sigma$ and $\pi$ bonds, and of 0.15[7] for the screening correction for a positive formal charge at the chlorine atom. The results are shown in Table I.

The double-bond character thus evaluated is plotted against Hammett's $\sigma$-value in Fig. 1, together with the findings for other chlorobenzene derivatives without an ortho substituent. It may be concluded from the linear correlation in the figure that the double-bond character becomes larger as the substituent is more electron-attractive. A future study of the electronic structure of chlorobenzene derivatives with reference to this correlation seems of interest. A similar correlation has already been obtained for iodobenzene derivatives.[8]

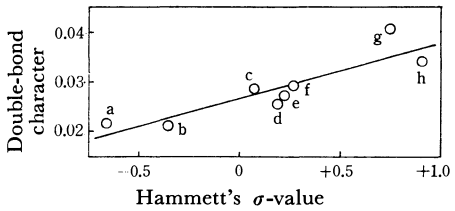



Fig. 1. Relation between double-bond character and Hammett's $\sigma$-value

a) *p*-Chloroaniline: Ref. 3. b) *p*-Chlorophenol: Present work. c) 2, 5-Dichloroaniline: T. Sakurai, M. Sundaralingam and G. A. Jeffrey, *Acta Cryst.*, **16**, 354 (1963). d) *p*-Chlorobenzyl chloride: Ref. 3. e) *p*-Dichlorobenzene: Ref. 2. f) *p*-Chlorobenzoic acid: Ref. 4. g) 1, 3, 5-Trichlorobenzene: Y. Morino and M. Toyama, *J. Phys. Soc. Japan*, **15**, 288 (1960). h) 1, 4-Dichloro-2-nitrobenzene: V. Nagarajan and C. R. Murty, *Current Science*, **6**, 254 (1963)

TABLE I

| | | |
|---|---|---|
| Resonance frequency (17°C) | $\nu_1$=34.367 Mc./s. | $\nu_2$=34.145 Mc./s. |
| $\lvert e^2 Qq \rvert$ (0°K) | — | 69.565 Mc./s. |
| Asymmetry parameter | $\eta_1$=0.223±0.035 | $\eta_2$=0.058±0.013 |
| Double-bond character | — | 0.021 |
| Ionic-bond character | — | 0.243 |
| Single-bond character | — | 0.736 |

*Department of Chemistry*
*Faculty of Science*
*Kanazawa University*
*Kanazawa*

1) C. Dean and R. V. Pound, *J. Chem. Phys.*, **20**, 195 (1952).
2) C. Dean, *Phys. Rev.*, **86**, 607 (1952).
3) H. C. Meal, *J. Chem. Phys.*, **24**, 1011 (1956).
4) S. Ogawa and K. Ohi, *J. Phys. Soc. Japan*, **15**, 1064 (1960).
5) C. H. Townes and B. P. Dailey, *J. Chem. Phys.*, **17**, 782 (1949).
6) R. Bersohn, ibid., **22**, 2078 (1954).
7) C. H. Townes and A. L. Schawlow, "Microwave Spectroscopy," McGraw-Hill Co., Inc., New York (1955), p. 239.
8) M. Kubo and Y. Kurita, *Kagaku (Chemistry)*, **12**, 566 (1957)) obtained the correlation by using the data given by G. W. Ludwig (*J. Chem. Phys.*, **25**, 159 (1956)).

# Copper and Nickel Chelates of Pyridine-2-carboxamide*

By Kazuo YAMASAKI and Masao SEKIZAKI

(Received September 2, 1965)

The metal chelates of pyridine-2-carboxamide, picolinic acid amide, have scarcely been studied at all; only a copper chelate containing two moles of the ligand was known.[1] Recently another chelate of copper with 1 mol. of the same ligand was reported.[2] The present communication deals with the syntheses of copper and nickel chelates of this ligand and with studies of their properties. In the following the ligand, pyridine-2-carboxamide, $C_5H_4NCONH_2$, will be abbreviated as "piaH."

The chelates prepared were: (1), $Cu(pia)_2 \cdot 5H_2O$; (2), $Cu(piaH)_2Cl_2 \cdot 2H_2O$; (3), $Ni(pia)_2 \cdot 2H_2O$ and (4), $Ni(piaH)_2Cl_2 \cdot 2H_2O$.

1) $Cu(pia)_2 \cdot 5H_2O$. This chelate was prepared after the method of Emmert and Brandl[1] by adding 1 g. of the ligand to a solution containing 2 g. of tetramminecopper(II) sulfate. Reddish-violet crystals were produced; they were soluble in cold water and chloroform only with difficulty. Emmert and Brandl reported the anhydrous compound, but the chelate prepared by the present authors had the formula, $C_{12}H_{10}O_2N_4Cu \cdot 5H_2O$.

Found: Cu, 16.06; N, 13.76; $H_2O$ 23.13%, Calcd. for $C_{12}H_{10}O_2N_4Cu \cdot 5H_2O$: Cu, 16.05; N, 14.15; $H_2O$, 22.76%.

2) $Cu(piaH)_2Cl_2 \cdot 2H_2O$. If 0.7 g. of copper(II) chloride was used instead of tetramminecopper(II) sulfate in the above preparation and if the mixed solution was concentrated on a water-bath, fine blue crystals of this chelate were crystallized.

Found: Cu, 15.34; N, 13.81; $H_2O$, 8.97%. Calcd. for $C_{12}H_{12}O_2N_4CuCl_2 \cdot 2H_2O$: Cu, 15.32; N, 13.51; $H_2O$, 8.69%.

3) $Ni(pia)_2 \cdot 2H_2O$. To an aqueous solution containing 2 g. of the ligand, 0.75 g. of sodium hydroxide dissolved in a small amount of water and then 2 g. of nickel chloride dissolved in 20 ml. of water were added. Fine orange-red crystals were precipitated; they were soluble in chloroform and ethanol only with difficulty and were insoluble in water.

Found: Ni, 17.44; N, 16.88; $H_2O$, 10.43%. Calcd. for $C_{12}H_{10}O_2N_4Ni \cdot 2H_2O$: Ni, 17.32; N, 16.63; $H_2O$, 10.63%.

4) $Ni(piaH)_2Cl_2 \cdot 2H_2O$. Prepared in a way similar to that used for 2). Blue crystals.

Found: Ni, 14.20; N, 14.01; $H_2O$ 9.10%. Calcd. for $C_{12}H_{12}O_2N_4NiCl_2 \cdot 2H_2O$: Ni, 14.32; N, 13.67; $H_2O$, 8.79%.

In the solution of pH 8.2 of $Ni(piaH)_2^{2+}$ the bands are at 602 and 995 m$\mu$, and while in a more alkaline solution they shift to a shorter wavelength, with the precipitation of insoluble $Ni(pia)_2$. In an acid solution of pH 0.9, the bands are at 645 and $>1050$ m$\mu$, rather close to those of the nickel aquo ion.[3] These facts suggest that, in a strongly acid solution, the nickel chelate (4) dissociates into the nickel aquo ion and the ligand, while in an alkaline solution the chelate (3) is formed. The copper chelates show a similar change in absorption spectra.

The infrared absorption bands of these chelates are listed in Table I, together with the tentative assignments.

TABLE I

| Chelate | C=O Str. vibr. | C-N Str. vibr. | M-N Str. vibr. | Magnetic moment |
|---|---|---|---|---|
| | | | $-(cm^{-1})$ | |
| piaH | 1659 | 1390 | | — |
| $Cu(pia)_2 \cdot 5H_2O$ | 1624 | 1395 | 567 | 1.87 (B.M.) |
| $Cu(piaH)_2Cl_2 \cdot 2H_2O$ | 1667 | 1440 | 510 | 1.90 |
| $Ni(pia)_2 \cdot 2H_2O$ | 1640 | 1400 | 592 | diamagnetic |
| $Ni(piaH)_2Cl_2 \cdot 2H_2O$ | 1660 | 1433 | 518 | 3.25 |

The ligand molecule in these chelates seems to be coordinated to the metal by nitrogen atoms, acting as a bidentate ligand.[4] Of these four chelates chelate (3) is diamagnetic, while the other three are paramagnetic; the magnetic moments are as shown in Table I. It is well known that nickel often forms, with the same ligand, paramagnetic and diamagnetic chelates of different colors. The present chelates add another example of this class of compounds.

*Inorganic Chemistry Laboratory*
*Faculty of Science*
*Nagoya University*
*Chikusa-ku, Nagoya*

* Presented at the Symposium on Coordination Chemistry of the Chemical Society of Japan, Fukuoka, November, 1964.

1) B. Emmert and F. Brandl, *Ber.*, **60**, 2211 (1927).

2) K. Nagano, H. Kinoshita and A. Hirakawa, *Chem. Pharm. Bull.*, **12**, 1198 (1964).

3) H. Ito, *J. Chem. Soc. Japan, Pure Chem. Sect.* (*Nippon Kagaku Zasshi*), **77**, 1385 (1956).

4) The crystal structures of these nickel chelates are now under investigation by Professer Y. Saito of the Universiy of Tokyo.

# The Bromination of Tris(3-phenyl-2, 4-pentanediono)chromium(III)*

By Yukito MURAKAMI and Teruomi WAKABAYASHI

(Received September 13, 1965)

In connection with the quasiaromatic nature of a chelate ring in the metal acetylacetonates, the electrophilic substitution reactions of these complexes have been systematically investigated.[1] In order to understand further the characteristic properties of a metal-chelate ring formed with $\beta$-diketones, the chromium(III) chelate of 3-phenyl-2, 4-pentanedione was prepared in this study.

Into a mixture of tris(3-phenyl-2,4-pentanediono)-chromium(III) and pyridine in carbon tetrachloride, there was added bromine dissolved in the same solvent at around 0°C over a period of 20—25 min. The bromination product was then fractionated into five components by means of liquid-chromatography with a combination of silica gel (60—80 mesh) and benzene. The fraction which came off first from a column was re-crystallized from ligroin as green crystals; m. p. 237—239°C (decomp.).

Found: C, 39.16; H, 3.11; Br, 43.94; Cr, 5.0%. An infrared spectrum of this product is illustrated in Fig. 1, together with that of the starting material.

The absorption peaks characteristic of the starting chromium(III) chelate, i. e., 1452, 1357, 1343, and 928 $cm^{-1}$, disappeared in the brominated material, while new bands were observed in the latter at 1388 and 1240 $cm^{-1}$. In addition, absorption bands at 771 and 764 $cm^{-1}$ in the unbrominated chelate spread further to 785 and 758 $cm^{-1}$ in the product. Among these infrared absorption peaks, the 1240 $cm^{-1}$ band in the brominated chelate may be assigned to $CH_2$ wagging vibration in the $CH_2Br$ group;[2] while the 928 $cm^{-1}$ band in the unsubstituted chelate may be attributed to the coupled stretching vibration of C–$CH_3$ and CO.[3] Therefore, the infrared spectrum of the brominated chelate provides evidence for a substitution reaction through which all the methyl groups in tris(3-phenyl-2, 4-pentanediono)chromium(III) were brominated to the monobromomethyl ($CH_2Br$).

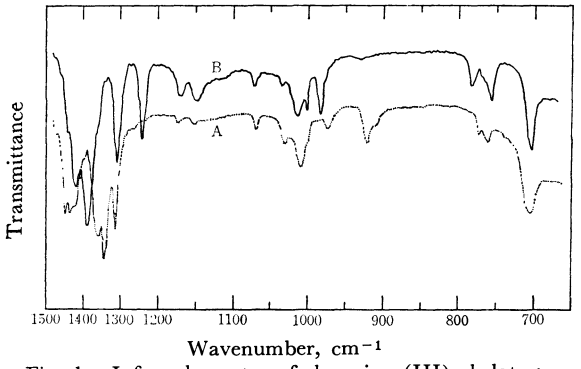



Fig. 1. Infrared spectra of chromium(III) chelates: A, tris(3-phenyl-2, 4-pentanediono)chromium(III); B, a bromination product of tris(3-phenyl-2, 4-pentanediono)chromium(III). (KBr disk method).

Calcd. for $C_{33}H_{27}O_6Br_6Cr$ (hexabromochelate): C, 37.71; H, 2.59; Br, 45.62; Cr, 4.95; and for $C_{33}H_{28}O_6Br_5Cr$ (pentabromochelate): C, 40.77; H, 2.90; Br, 41.17; Cr, 5.35%.

Thus, the possibility of the coexistence of pentabrominated chelate in the first fraction from the column may not be excluded, as its elemental analysis has indicated.

The later fractions from the chromatographic column were identified as less-brominated and unreacted chelates.

An attempt has been made to brominate 3-phenyl-2, 4-pentanedione under similar conditions in the absence of pyridine, but this attempt failed to afford the corresponding bromination product. Thus, the occurrence of the present reaction with the chromium chelate may be said to be due primarily to the chelate ring.

Since the bromination of tris(2, 4-pentanediono)-chromium(III) resulted only in the substitution of the $\gamma$-hydrogen,[1,4] the $\pi$-electronic interaction of a phenyl ring with the chelate ring in the present chromium chelate[5] seems to activate the methyl groups in the reaction process.

*Department of Organic Synthesis*
*Faculty of Engineering*
*Kyushu University*
*Hakozaki, Fukuoka*

* Contribution No. 95 from the Department of Organic Synthesis, Faculty of Engineering, Kyushu University.

1) For a general review, see J. P. Collman, "Reactions of Coordinated Ligands and Homogeneous Catalysis," (Advances in Chemistry Series, 37), American Chemical Society (1963), p. 78; *Angew. Chem., Internat. Edit.*, **4**, 132 (1965).

2) N. B. Colthup, L. H. Daly and S. E. Wiberley, "Introduction to Infrared and Raman Spectroscopy," Academic Press, New York (1964), p. 317.

3) K. Nakamoto, P. J. McCarthy, A. Ruby and A. E. Martell, *J. Am. Chem. Soc.*, **83**, 1066 (1961).

4) J. P. Collman, R. A. Moss, H. Maltz and C. C. Heindel, ibid., **83**, 531 (1961).

5) Y. Murakami and K. Nakamura, This Bulletin, in press.

# The Transient Absorption of Irradiated α-Methylstyrene

By Meiseki KATAYAMA

(Received September 15, 1965)

A new transient absorption was observed at 5461Å in extremely dried α-methylstyrene by means of pulse radiolysis.

We have proposed previously[1,2] that the important intermediate in the radiation-induced polymerization of α-methylstyrene was the anion radical, which exhibited an absorption maximum at about 3500Å which was observed by a photographic method of pulse radiolysis.

It has been reported[3] that an absorption at 5100Å, as well as one at 3275Å, usually assigned to the anion radical, appeared when α-methylstyrene was brought into contact with alkalimetals. Therefore, irradiated α-methylstyrene may be expected to show an absorption maximum anywhere between 5000 to 6000 Å, in addition to that at 3500Å, if our proposal is correct.

The experimental details may be briefly explained as follows: An electron linear accelerator was used as the source of radiation. It provided a 1.6 μsec. pulse. A mercury lamp was used as the source of analytical light for spectroscopy. For recording the absorption, the photoelectric method was employed. The monomer was eventually dried by using a mirror of alkali metal. All the measurements were conducted at 15°C.

A typical synchroscope trace for the decay of absorption in dried α-methylstyrene is shown in Fig. 1. The arrow in the figure indicates the time of the irradiation of the sample with a pulse. The rate of the decay of the intermediate obeyed

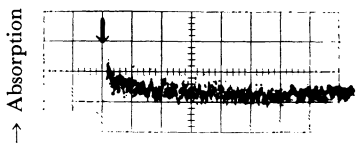



Fig. 1. Decay of absorption in extremely dried α-methylstyrene at 5461 Å (mean dose of 3 k. rads). Absorption: 1.6% per large division Sweep speed: 50 μ sec. per large division

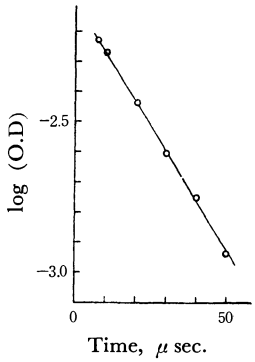



Fig. 2. The first-order plot of the decay of the absorption at 5461 Å (mean dose of 3 k. rads).

the first-order reaction kinetics (Fig. 2.) and had a half-life of about 25 μsec.

The transient absorption observed here at 5461Å behaves exactly like the one at 3500Å previously reported.[1] Thus, the addition of water or DPPH in a minute amount caused the intermediate to decay at a much faster rate. The decays with the additives were, actually, both too fast to be measured* with the same time scale as in Fig. 1. This is in conformity with the fact[2] that the polymerization is practically inhibited by the addition of these compounds. The first-order decay of the intermediate strongly suggests that it is reacting with the monomer molecules:

$$(\alpha\text{-MS})^{\ominus} + \alpha\text{-MS} \rightarrow \text{Polymerization}$$

It should be mentioned that the rate of the decay observed at 5461Å in the dried monomer quantitatively agreed with that at 3500Å.[4]

In conclusion, further support for the proposed anion radical mechanism in the radiation-induced polymerization of α-methylstyrene has been obtained by the present investigation.

*Department of Chemistry*
*Faculty of Science*
*Hokkaido University*
*Sapporo*

1) M. Katayama, M. Hatada, K. Hirota, H. Yamazaki and Y. Ozawa, This Bulletin, **38**, 851 (1965).
2) K. Hirota and M. Katayama, *Annual Report of Japanese Association for Rad. Res. Polymers*, **5**, 205 (1963—64).
3) K. Hirota, K. Kuwata, H. Togawa and S. Ishida, *J. Chem. Soc. Japan, Pure Chem. Sec.* (*Nippon Kagaku Zassi*), **79**, 602 (1958).

* The momentary effects of Cerenkov radiation, make it difficult to observe the decays quantitatively with a shorter time scale.
4) M. Katayama, et al., to be published in *J. Chem. Soc. Japan, Pure Chem. Sec.* (*Nippon Kagaku Zasshi*), January (1966).

# The Electron Spin Resonance of the Anion Radicals Formed on Metal Oxides*

By Kozo HIROTA, Keiji KUWATA and Yasaburo AKAGI

(Received September 20, 1965)

The formation of cationic species adsorbed on surfaces has been established by studies[1-3] of the adsorption of hydrocarbons on silica-alumina catalysts. It is also probable that an anionic species will be formed on an adsorbent of an electron donor if a strong electron acceptor is used as the adsorbate.[4]

The present authors will here report on the formation of such anionic species in the cases of tetracyanoethylene and benzophenone adsorbed on zinc oxide or alumina.

Tetracyanoethylene[5] and benzophenone, which are known to be strong electron acceptors and which can easily form stable anion radicals,[6,7] were adsorbed on zinc oxide or alumina in vacuo.

All the samples gave ESR signals which were stable for a week or more. The signals quickly dissappeared, however, upon the introduction of air.

A fairly well-resolved hyperfine structure of the ESR spectrum of tetracyanoethylene was observed when tetracyanoethylene was adsorbed on alumina from a benzene solution with a $10^{-1}$ mol. concentration and evacuated under a high vacuum (Fig. 1.)

The spectrum is the same as that for the anion of a solid state, and shows the characteristic feature of a nine-line hyperfine structrue for the solution of the anion.[4]

In the case of benzophenone, the hyperfine structure was not resolved so well and so was not

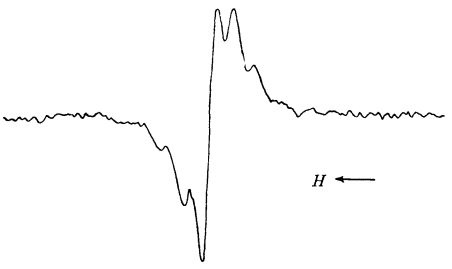



Fig. 1. ESR spectrum of tetracyanoethylene adsorbed on alumina.

confirmative evidence for the formation of aion radicals; however, the most probable paramagnetic species formed from benzophenone is its anion radical.

In an attempt to accelerate the electron transfer from donor to acceptor, the samples were exposed for several tens of minutes to a strong illumination of ultraviolet light from a high pressure mercury lamp. An increase in the signal intensity was observed in both cases upon irradiation.

A transfer of the trapped electrons from oxides to adsorbates will decrease the paramagnetic centers in the oxides; experimental evidence of this was, however, obtained only in the case of zinc oxide by the decrease of the signal at $g=1.96$.

It is interesting to observe the anion radical of tetracyanoethylene on alumina in contrast to the fact that aromatic hydrocarbons are easily oxidized into cation radicals on silica-alumina.[1-3] The milder treatment of the alumina samples in this experiment (evacuation for 3 hr. at 350°C) may be a reason for its poor oxidative tendency.

*Department of Chemistry*
*Faculty of Science*
*Osaka University*
*Toyonaka, Osaka*

---

* Presented to the 18th Annual Meeting of Chemical Society of Japan, Osaka, April, 1965.

1) D. M. Brouwer, *Chem. Ind.*, **1961**, 177.
2) J. J. Rooney and R. C. Pink, *Proc. Chem. Soc.*, **1961**, 70
3) W. K. Hall, *J. Catalysis*, **1**, 53 (1962).
4) Cf. T. H. Wolkenstein, "Advances in Catalysis," Vol. 12, Academic Press, New York (1960).
5) R. E. Merrifield and W. D. Phillips, *J. Am. Chem. Soc.*, **80**, 2778 (1958).
6) W. D. Phillips, J. C. Rowell and S. I. Weissman, *J. Chem. Phys.*, **33**, 626 (1960).
7) R. C. Adam and S. I. Weissman, *J. Am. Chem. Soc.*, **80**, 1518 (1958).

# On the Isothermal Decay of Trapped Electrons Formed in a Rigid $\gamma$-Irradiated Medium

By Hideo TSUJIKAWA, Kenji FUEKI and Zenichiro KURI

(Received September 29, 1965)

The study of trapped electrons formed by the $\gamma$-irradiation of organic glasses is of great significance in the elucidation of the primary processes in radiation chemistry. The isothermal decay of trapped electrons in 2-methyltetrahydrofuran (MTHF)[1] and in 3-methylpentane[2] at low temperatures has recently been observed by spectroscopic methods. It does not appear, however, that the mechanism for the isothermal decay of trapped electrons has been established.

As a theoretical approach to this problem, we have made a calculation of the tunneling of an electron from an electron-trapping center to a positive hole in MTHF. In the calculation the following formula has been used; it is similar to that used in the calculation of the tunneling of F-center electrons in alkali halides[3]:

$$\lambda(R)=-\frac{E_0}{\boldsymbol{h}}\exp\left[-\frac{4\pi}{\boldsymbol{h}}\int_{r_0}^{r^*}\sqrt{2\boldsymbol{m}\{U(r)-E_0\}}\,dr\right]$$

where $\lambda$ is the decay constant; $R$, the distance between a trapping center and a positive hole; $E_0$, the ground-state energy of the trapped electron; $\boldsymbol{m}$, the electron mass, and $\boldsymbol{h}$, the Planck constant. $U(r)$, the potential function, is given by;

$$U(r)=-\frac{\boldsymbol{e}^2}{\varepsilon(R-r)}, \qquad R>r\geq r_0$$

where $r$ is the distance from the trapping center; $r_0$, the radius of the trapping center[4]; $r^*$, the distance at which the kinetic energy of the trapped electron becomes negative and equal to $R-(\boldsymbol{e}^2/\varepsilon E_0)$, and $\varepsilon$, the dielectric constant of the medium. In the numerical computation we have used the values of $E_0=-1$ eV.[5] and $\varepsilon=4.6$ for MTHF.

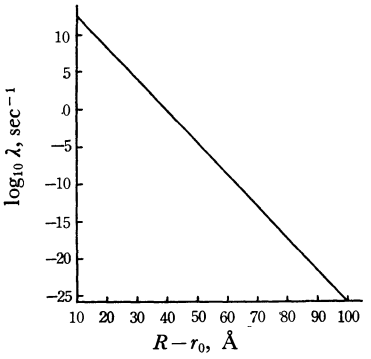



Fig. 1. Decay constant of trapped electrons in MTHF as a function of the ion-pair separation distance.

Figure 1 shows the decay constant of trapped electrons in MTHF, calculated as a function of the ion-pair separation distance. The decay constants of trapped electrons measured by Smith and Pieroni[1] are of the order of $10^{-4}$—$10^{-5}$ sec$^{-1}$ in this system. From Fig. 1 the corresponding ion-pair separation distance is obtained as $\sim$50 Å, in good agreement with the average distance ascertained experimentally.[1] Thus the tunneling of electrons is a possible mechanism for the isothermal decay of trapped electrons formed in rigid $\gamma$-irradiated media.

*Department of Synthetic Chemistry*
*Faculty of Engineering*
*Nagoya University*
*Chikusa-ku, Nagoya*

1) D. R. Smith and J. J. Pieroni, *Can. J. Chem.*, **43**, 876 (1965).
2) M. Burton, M. Dillon and R. Rein, *J. Chem. Phys.*, **41**, 2228 (1964).
3) D. L. Dexter, *Phys. Rev.*, **93**, 985 (1954).
4) The radius of the trapping center, $r_0$, would be about 3 Å. It should be noted that the value of $r_0$ is not explicitly required for the present purpose.
5) This value corresponds to the electronic transition energy at the absorption maximum, which is believed to be close to the binding energy of the trapped electron in the ground state. W. H. Hamill, J. P. Guarino, M. R. Ronayne and J. A. Ward, *Discussions Faraday Soc.*, **36**, 169 (1963).

# The Dielectric Constant of Triethanolamine Borate

By Seiichi KONDO

(Received October 5, 1965)

The nearly spherical triptich or cage-type structure proposed for triethanolamine borate by Brown and Fletcher[1] suggested the possibility of molecular rotation in the crystalline state. Although Westrum[2] concluded, from his thermal measurements, that such rotation was unlikely, this paper will present a study of the dielectric properties in the crystalline state in an endeavor to shed further light on the nature of this transition.

The raw material synthesized from triethanolamine and boric acid was provided by the courtesy of the U. S. Borax Co.*; it was vacuum-sublimed four successive times at 180°C and $10^{-3}$ mmHg. The melting point of the purified sample was 513°K, in good accord with the literature values of 508°K[1] and 512°K[2]. The sample was put into the measuring electrode under streaming nitrogen gas. A bridge with a frequency range from $3\times10^2$ to $3\times10^4$ c. p. s., as described elsewhere,[3] was used. Temperatures over the range from 10°C to 238°C were determined with a copper-constantan thermocouple attached firmly to the electrode cell. The dielectric constant versus temperature curves obtained are shown in Fig. 1.

No frequency dependency of the dielectric constant was noted over the available range studied. At lower temperatures the dielectric loss is approximately $10^{-2}$ to $10^{-3}$. However, the resistance of the sample decreased very rapidly to $10^5$ ohm or less as the melting point was approached; hence, it was beyond the range of the bridge. Only a large and abrupt increase in the dielectric constant at the melting point could be observed; the dielectric constant of the liquid state was not obtained.

As is shown in Fig. 1, a small change in the dielectric constant may be noted at 474°K. The dielectric transition point presumably corresponds to the phase transition point, 466.54°K, found by Westrum.[2] Since both the increment in the dielectric constant and the entropy of transition are relatively small, the change in chemical bonding from a triptich to a cage-type structure is probably not involved in the mechanism of the phase transition. Moreover, there is no evidence of a rotational transition of the molecular dipole at this temperature; presumably dipolar rotation commences only at the melting temperature.

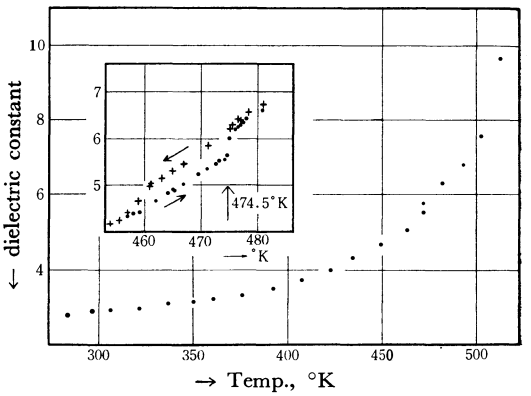



Fig. 1. The dielectric constant versus temperature curves of triethanolamine borate. The dotted and crossed points of the upper figure show the measured values in increasing and decreasing temperatures, respectively, near the phase transition.

These results thus confirm the conclusion by Westrum that this material is not plastically crystalline.

*Laboratory of Physical Chemistry*
*Osaka University of Liberal Arts and Education*
*Tennoji-ku, Osaka*

1) H. C. Brown and E. A. Fletcher, *J. Am. Chem. Soc.*, **73**, 2808 (1951).
2) H. L. Clever, W. Wong, C. A. Wulff and E. F. Westrum, Jr., *J. Phys. Chem.*, **68**, 1967 (1964).
* This sample was obtained by the kind help of Professor Edgar F. Westrum, Jr., University of Michigan.
3) S. Kondo and M. Matsumoto, This Bulletin, **31**, 319 (1958).

# Novel Dialkyl Cobalt Derivatives

By Hiroshi YAMAZAKI and Nobue HAGIHARA

(Received October 7, 1965)

Previously, we have reported[1] some stable alkyl nickel derivatives, with a formula of $\pi$-$C_5H_5Ni(PPh_3)R$, in which nickel metal attained the electronic configuration of krypton. The surprising stabilities of these compounds have now prompted us to prepare isoelectronic compounds of cobalt. Here we wish to report the preparation of the some dialkyl cobalt derivatives.

The treatment of a slurry of triphenylphosphine-$\pi$-cyclopentadienylcobalt diiodide[2,3] in benzene with a solution of methyl magnesium iodide in ether at room temperature gave an orange-red solution.* After the hydrolysis and evaporation of the solvent, the residue was separated on an alumina column, using benzene as the eluant. From the first red fraction, air-stable orange-red crystals of triphenylphosphine-$\pi$-cyclopentadienyl dimethylcobalt (I) ($\pi$-$C_5H_5Co(PPh_3)(CH_3)_2$) were obtained. (Yield, 54%. M. p. 142—143°C (decomp.). PMR (in $CS_2$)**: 2.65 $\tau$ ($C_6\underline{H}_5$), doublet ($J$=5 c. p. s.); 5.67 $\tau$ ($C_5\underline{H}_5$), sharp singlet; 10.02 $\tau$ ($C\underline{H}_3$), doublet ($J_{PH}$=6 c. p. s.).

Found: C, 71.80; H, 6.42. Calcd. for $C_{25}H_{26}PCo$: C, 72.11; H, 6.30%.) I is very stable in air, especially in the solid state, and it is soluble in most organic solvents.

From the second brown fraction, fine dark brown crystals of triphenylphosphine-$\pi$-cyclopentadienylmethylcobalt iodide (II) ($\pi$-$C_5H_5Co(PPh_3)(CH_3)I$) were obtained. (Yield, 1.3%. M. p. 112°C (decomp. without melting). Found: C, 54.35; H, 4.41. Calcd. for $C_{24}H_{23}IPCo$: C, 54.57; H, 4.39%.) Another experiment which was carried out employing an amount of methyl magnesium iodide equivalent to the diiodide and by the reverse addition method gave I in a 8% yield and II in a 13% yield.

According to the results of a similar procedure using benzyl magnesium chloride, dark red crystals of triphenylphosphine-$\pi$-cyclopentadienyldibenzylcobalt (III) ($\pi$-$C_5H_5Co(PPh_3)(CH_2Ph)_2$) were obtained. (Yield, 68%. M. p. 102°C (decomp.). PMR (in $C_6D_6$)***: 2.7 $\tau$ (P-$C_6\underline{H}_5$); 2.9 $\tau$ ($CH_2$-$C_6\underline{H}_5$); 5.67 $\tau$ ($C_5\underline{H}_5$); 6.85 and 7.15 $\tau$ (-$C\underline{H}_2$-), broad. Found: C, 77.96; H, 6.03. Calcd. for $C_{37}H_{34}PCo$: C, 78.16; H, 6.03%.)

The reaction of II with benzyl magnesium chloride resulted in the formation of triphenylphosphine - $\pi$ - cyclopentadienylmethylbenzylcobalt (IV) ($\pi$-$C_5H_5Co(PPh_3)(CH_3)(CH_2Ph)$) as red crystals. (Yield, 51%. M. p. 112—113°C (decomp.). PMR (in $C_6D_6$)***: 2.5 $\tau$ (P-$C_6\underline{H}_5$); 2.95 $\tau$ ($CH_2$-$C_6\underline{H}_5$); 5.72 $\tau$ ($C_5\underline{H}_5$); 6.75 and 8.30 $\tau$ (-$C\underline{H}_2$-), broad; 9.17 $\tau$ ($CH_3$), doublet ($J_{PH}$= 6 c. p. s.). Found: C, 76.07; H, 6.13. Calcd. for $C_{31}H_{30}PCo$: C, 75.60; 6.14%.) This is the first example of a compound with two different alkyl groups bonded to a cobalt metal. The air sensitivities of I, IV and III increase in this order.

The proton magnetic resonance spectra of III and IV show that the methylenic protons of the benzyl group are not equivalent, suggesting the inhibition of the free rotation of the benzyl group. Attempts to isolate other dialkyl and diaryl derivatives were unsuccessful. The steric factor is essential for their stabilities.

*The Institute of Scientific and Industrial Research*
*Osaka University*
*Sakai, Osaka*

1) H. Yamazaki and N. Hagihara, This Bulletin, **37**, 907 (1964).
2) R. B. King, *Z. Naturforch.*, **19b**, 1160 (1964).
3) R. F. Heck, *Inorg. Chem.*, **4**, 855 (1965).
* The reactions were all carried out under a nitrogen atmosphere, and melting points were measured in a nitrogen-filled capillary.

** Varian A 60. $Si(CH_3)_4$ was used as the external standard.
*** Japan Electron Optics, 100 Mc. $Si(CH_3)_4$ was used as the internal standard.

# Organic Syntheses by Means of Noble Metal Compounds. XIX. The Hydroformylation Reaction Catalyzed by Metallic Palladium.[1]

By Jiro Tsuji, Nobuo Iwamoto and Masanobu Morikawa

(Received October 19, 1965)

It is known that the syntheses of aldehydes from olefins, carbon monoxide and hydrogen (Oxo reaction) are catalyzed by cobalt carbonyl. In addition, some other metal carbonyls, such as rhodium and ruthenium carbonyls, are known to be active in the reaction.

In the course of our studies of the catalytic action of metallic palladium on the carbonylation of various olefins thus, forming saturated and unsaturated carboxylic esters,[2,3] we have found that palladium chloride or metallic palladium is also active in the hydroformylation of olefins.

A typical example will be described below. In order to avoid the effect of the metal surface of an autoclave, the reaction was carried out in a glass vessel equipped with a gas-inlet capillary. Benzene (15 ml.), toluene (for the gas chromatographic determination, 2 ml.) and palladium chloride (2 g.) were mixed in the glass vessel, which was then placed in a 100-ml. autoclave. Ethylene and synthesis gas were introduced (50 and 100 kg./cm$^2$ respectively), and the autoclave was shaken at 100°C for 15 hr.; a 55 kg./cm$^2$ pressure drop was observed during this period. The amount of propionaldehyde formed was gas chromatographically determined to be 1.2 g. The conversion was not very high in general. It was confirmed that a considerable amount of ethylene was consumed by hydrogenation, thus forming ethane. Such a metallic palladium as palladium black was equally active; it seems likely, therefore, that metallic palladium is the true catalyst. The recovered palladium could be used repeatedly. The reaction procedure is simple, because metallic palladium can be used and then recovered quantitatively. The application of the method to other olefins and the reaction mechanism will be reported in a forthcoming paper.

*Basic Research Laboratories*
*Toyo Rayon Company, Ltd.*
*Kamakura*

1) Part XVIII: J. Tsuji, T. Nogi and M. Morikawa, This Bulletin, in preparation.
2) J. Tsuji, Morikawa and J. Kiji, *Tetrahedron Letters*, No. 22, **1963**, 1437.
3) J. Tsuji, J. Kiji, S. Imamura and M. Morikawa, *J. Am. Chem. Soc.*, **86**, 4350 (1964).

# The Catalytic Action of Binary Metal-Polyphthalocyanine Complexes on the Oxidation of Acetaldehyde Ethylene Acetal

By Hiroo INOUE, Yasuji KIDA and Eiji IMOTO

(Received October 28, 1965)

We wish to report in this communication our recent findings that acetaldehyde ethylene acetal is effectively oxidized with oxygen to ethylene glycol monoacetate in the presence of some metal-phthalocyanine complexes, which may act as catalysts. The catalytic activities of the phthalocyanine complexes are remarkably dependent on the type of complex involved. The acetal is not oxidized with oxygen at 30°C by copper- or iron-phthalocyanine, nor by copper- or iron-polyphthalocyanine. However, the acetal is quickly oxidized with oxygen at 30°C by binary copper-iron-polyphthalocyanine, although the acetal is not oxidized in the presence of the mixture of copper- and iron-polyphthalocyanines.

Similar phenomena have also been observed in the case of iron- and molybdenum-phthalocyanine complexes. The binary complex which contains iron and molybdenum ions together in polyphthalocyanine was active in the oxidation of the acetal with oxygen, but the mixture of iron- and molybdenum-polyphthalocyanines was not active. The meaning of the need for two kinds of metal ions in the complexes is not clearly understood. However, one could speculate that two kinds of metal ions may play different roles in the catalytic oxidation. For example, one kind of metal ion serves to produce the hydroperoxide of the acetal, and the other, to decompose it, while the conjugated system in the complexes would contribute to the electron transfer between two kinds of metal ions.

All of the metal-phthalocyanines used in this investigation were synthesized by a modification of the methods described by Epstein and Wildi,[1] and Drinkard and Bailar.[2] Acetaldehyde ethylene acetal was purified by repeated distillation over sodium. The oxidation of the acetal was carried out by stirring 0.05 g. of the catalyst in 5 ml. of the acetal under an atmosphere of oxygen at 30°C.

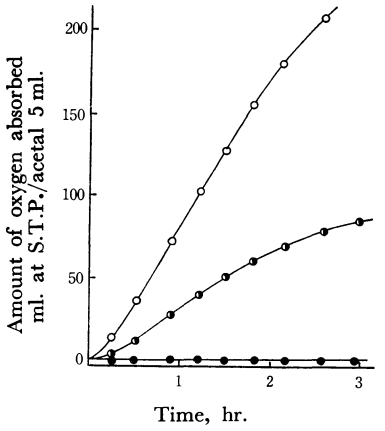



Fig. 1. Effects of metal-polyphthalocyanine complexes on the rate of the oxygen absorption: ◑ Cu-Fe-, ○ Mo-Fe-polyphthalocyanines, and ● Cu-, Fe-, Mo-, Cu- and Fe-, Mo- and Fe-polyphthalocyanines.

The amounts of oxygen absorbed and the reaction times were measured by using the equipment described in a previous paper.[3] The results are shown in Fig. 1. As the reaction products, ethylene glycol monoacetate and diacetate were identified and were determined by gas chromatography. In the case of binary iron-molybdenum-polyphthalocyanine, the yields of ethylene glycol monoacetate and diacetate, based on the amount of acetaldehyde ethylene acetal, were 41.2% and 1.3% respectively at the reaction time of 3.5 hr.; 58.5% of the acetal was recovered. A detailed report of this experiment will be published later.

*Department of Applied Chemistry*
*College of Engineering*
*The University of Osaka Prefecture*
*Sakai, Osaka*

1) A. Epstein and B. S. Wildi, *J. Chem. Phys.*, **32**, 324 (1960).
2) W. C. Drinkard and J. C. Bailar, *J. Am. Chem. Soc.*, **81**, 4795 (1959).
3) H. Inoue, Y. Kida and E. Imoto, This Bulletin, in press.